

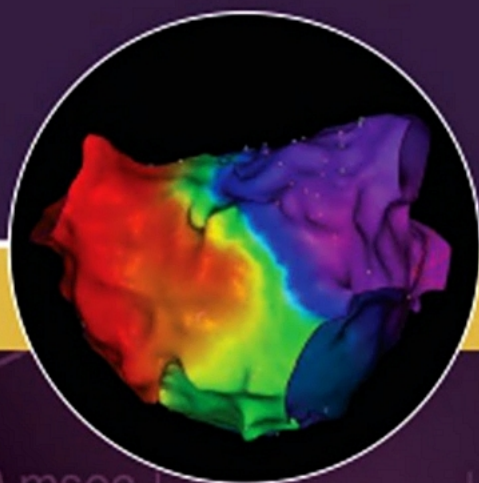
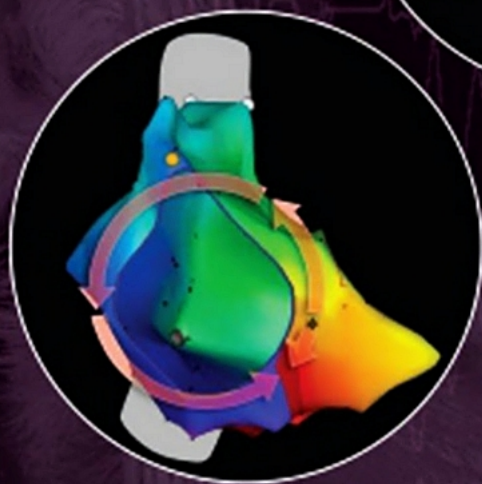
ZIAD F. ISSA
JOHN M. MILLER
DOUGLAS P. ZIPES



CLINICAL ARRHYTHMOLOGY AND ELECTROPHYSIOLOGY


A COMPANION TO **BRAUNWALD'S**
HEART DISEASE

THIRD EDITION




ELSEVIER

— 300 msec —



CLINICAL ARRHYTHMOLOGY AND ELECTROPHYSIOLOGY

A COMPANION TO **BRAUNWALD'S HEART DISEASE**



CLINICAL ARRHYTHMOLOGY AND ELECTROPHYSIOLOGY

A COMPANION TO **BRAUNWALD'S HEART DISEASE**

THIRD EDITION

ZIAD F. ISSA, MD

Executive Director
Cardiac Electrophysiology
Prairie Heart Institute of Illinois
Medical Director
Cardiac Electrophysiology Laboratory
HSHS St. John's Hospital
Springfield, Illinois

JOHN M. MILLER, MD

Professor of Medicine
Krannert Institute of Cardiology
Indiana University School of Medicine
Director
Clinical Cardiac Electrophysiology
Indiana University Health
Indianapolis, Indiana

DOUGLAS P. ZIPES, MD

Distinguished Professor
Professor Emeritus of Medicine, Pharmacology, and Toxicology
Director Emeritus
Division of Cardiology and the Krannert Institute of Cardiology
Indiana University School of Medicine
Indianapolis, Indiana

ELSEVIER

ELSEVIER

1600 John F. Kennedy Blvd.
Ste 1600
Philadelphia, PA 19103-2899

CLINICAL ARRHYTHMOLOGY AND ELECTROPHYSIOLOGY:
A COMPANION TO BRAUNWALD'S HEART DISEASE, THIRD EDITION

ISBN: 978-0-323-52356-1

Copyright © 2019 by Elsevier, Inc. All rights reserved.

No part of this publication may be reproduced or transmitted in any form or by any means, electronic or mechanical, including photocopying, recording, or any information storage and retrieval system, without permission in writing from the publisher. Details on how to seek permission, further information about the Publisher's permissions policies and our arrangements with organizations such as the Copyright Clearance Center and the Copyright Licensing Agency, can be found at our website: www.elsevier.com/permissions.

This book and the individual contributions contained in it are protected under copyright by the Publisher (other than as may be noted herein).

Notices

Knowledge and best practice in this field are constantly changing. As new research and experience broaden our understanding, changes in research methods, professional practices, or medical treatment may become necessary.

Practitioners and researchers must always rely on their own experience and knowledge in evaluating and using any information, methods, compounds, or experiments described herein. In using such information or methods they should be mindful of their own safety and the safety of others, including parties for whom they have a professional responsibility.

With respect to any drug or pharmaceutical products identified, readers are advised to check the most current information provided (i) on procedures featured or (ii) by the manufacturer of each product to be administered, to verify the recommended dose or formula, the method and duration of administration, and contraindications. It is the responsibility of practitioners, relying on their own experience and knowledge of their patients, to make diagnoses, to determine dosages and the best treatment for each individual patient, and to take all appropriate safety precautions.

To the fullest extent of the law, neither the Publisher nor the authors, contributors, or editors, assume any liability for any injury and/or damage to persons or property as a matter of products liability, negligence or otherwise, or from any use or operation of any methods, products, instructions, or ideas contained in the material herein.

Previous editions copyrighted 2012 and 2009.

Library of Congress Control Number: 2018945138

Publishing Director: Dolores Meloni
Senior Content Development Manager: Katie DeFrancesco
Publishing Services Manager: Catherine Jackson
Book Production Specialist: Kristine Feeherty
Design Direction: Renee Duenow

Printed in China

Last digit is the print number: 9 8 7 6 5 4 3 2 1



Working together
to grow libraries in
developing countries

www.elsevier.com • www.bookaid.org

As always, we would like to thank our families for their support during the writing of this book,
since it meant time away from them:

Ziad F. Issa:

My wife, Dana, and my sons, Tariq and Amr

John M. Miller:

My wife, Jeanne, and my children, Rebekah, Jordan, and Jacob

Douglas P. Zipes:

My wife, Joan, and my children, Debbie, Jeff, and David

We also thank the Elsevier support team that helped bring this edition to fruition.

Disturbances in cardiac rhythm occur in a large proportion of the population. Arrhythmias can have sequelae that range from life-shortening to inconsequential. Sudden cardiac deaths and chronic disability are among the most frequent serious complications resulting from arrhythmias.

The eleventh edition of *Braunwald's Heart Disease: A Textbook of Cardiovascular Medicine* includes an excellent section on rhythm disturbances carefully edited and largely written by Douglas Zipes and Gordon Tomaselli, the most accomplished and respected investigators and clinicians in this field. However, there are many subjects that simply cannot be discussed in sufficient detail, even in a 2000-page, densely packed book. For this reason, the current editors and I decided to commission a series of companions to the parent title. We were extremely fortunate to enlist Dr. Zipes' help in editing and writing *Clinical Arrhythmology and Electrophysiology*. Dr. Zipes, in turn, enlisted two talented collaborators, Drs. Ziad F. Issa and John M. Miller, to work with him to produce this excellent volume.

This third edition is superbly illustrated, with the number of figures and tables increasing substantially from its predecessor. What has not changed, however, is the very high quality of the content, which is accurate, authoritative, and clear; second, it is as up-to-date as last month's journals; and third, the writing style and illustrations are consistent throughout with little, if any, duplication. As this important branch of cardiology has grown, so has this book.

The first seven chapters ("Molecular Mechanisms of Cardiac Electrical Activity," "Cardiac Ion Channels," "Electrophysiological Mechanisms of Cardiac Arrhythmias," "Electrophysiological Testing: Tools and Techniques," "Conventional Intracardiac Mapping Techniques," "Advanced Mapping and Navigation Modalities," and "Ablation Energy Sources") provide a superb introduction to the field. This is followed by 24 chapters on individual arrhythmias, each following a similar outline. Here, the authors lead us from a basic understanding of the arrhythmia to its clinical recognition, natural history, and management. The latter is moving rapidly from being largely drug-based to device-based, although many patients receive combination device-drug therapy. These options, as well as ablation therapy, are clearly spelled out as they apply to each arrhythmia. The final chapter discusses the complications of catheter ablation of cardiac arrhythmias.

We are proud to include *Clinical Arrhythmology and Electrophysiology* as a companion to *Braunwald's Heart Disease*, and we are fully confident that it will prove to be valuable to cardiologists, internists, investigators, and trainees.

Eugene Braunwald, MD
Peter Libby, MD
Robert Bonow, MD
Douglas Mann, MD
Gordon Tomaselli, MD

PREFACE

The third edition of *Clinical Arrhythmology and Electrophysiology* maintains its unique style, written by just the three of us. Once again, we can “explain, integrate, coordinate, and educate in a comprehensive, cohesive fashion while avoiding redundancies and contradictions.” We liken it to a comprehensive travel guide written by an expert who has actually stayed in that unique hotel or eaten in that special restaurant. We have experienced the progress first-hand, from basic science to clinical application, and are able to pass on our experiences to you. In addition, as before, readers have the opportunity to delve deeper into basic mechanisms or invasive procedures...or not...depending on the level of interest.

We have thoroughly revised and updated all chapters. In addition, we have greatly expanded the book by increasing the total number of

pages from 700 to over 1100 and increased the number of figures to almost 1000 in print and over 200 online. A unique feature of our book are 74 new videos that take the reader into our electrophysiology labs to become a “fly on the wall” observing electrophysiology procedures. We believe the adage that “one picture is worth a thousand words,” and we invite you to learn with us during actual procedures.

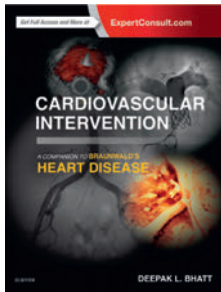
Our textbook, written as a companion to the *Braunwald’s Heart Disease* series, is for learners of all stages. We hope you enjoy, learn, and expand your care of arrhythmia patients.

Ziad F. Issa
John M. Miller
Douglas P. Zipes

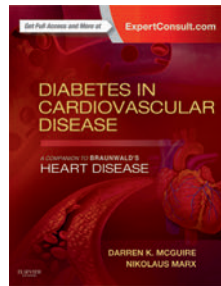
- 1 **Molecular Mechanisms of Cardiac Electrical Activity**, 1
- 2 **Cardiac Ion Channels**, 15
- 3 **Electrophysiological Mechanisms of Cardiac Arrhythmias**, 51
- 4 **Electrophysiological Testing: Tools and Techniques**, 81
- 5 **Conventional Intracardiac Mapping Techniques**, 125
- 6 **Advanced Mapping and Navigation Modalities**, 155
- 7 **Ablation Energy Sources**, 206
- 8 **Sinus Node Dysfunction**, 238
- 9 **Atrioventricular Conduction Abnormalities**, 255
- 10 **Intraventricular Conduction Abnormalities**, 286
- 11 **Focal Atrial Tachycardia**, 305
- 12 **Typical Atrial Flutter**, 339
- 13 **Macroreentrant Atrial Tachycardia**, 375
- 14 **Atrial Tachyarrhythmias in Adults With Congenital Heart Disease**, 407
- 15 **Atrial Fibrillation**, 421
- 16 **Inappropriate Sinus Tachycardia**, 549
- 17 **Atrioventricular Nodal Reentrant Tachycardia**, 560
- 18 **Typical Atrioventricular Bypass Tracts**, 599
- 19 **Atypical Bypass Tracts**, 677
- 20 **Paroxysmal Supraventricular Tachycardias**, 697
- 21 **Wide Complex Tachycardias**, 730
- 22 **Ventricular Arrhythmias in Ischemic Heart Disease**, 748
- 23 **Idiopathic Focal Ventricular Tachycardia**, 816
- 24 **Fascicular Ventricular Tachycardia**, 858
- 25 **Ventricular Tachycardia in Nonischemic Dilated Cardiomyopathy**, 869
- 26 **Bundle Branch Reentrant Ventricular Tachycardia**, 897
- 27 **Epicardial Ventricular Tachycardia**, 907
- 28 **Arrhythmias in Hypertrophic Cardiomyopathy**, 925
- 29 **Ventricular Tachycardia in Arrhythmogenic Right Ventricular Cardiomyopathy**, 942
- 30 **Ventricular Arrhythmias in Adults With Congenital Heart Disease**, 968
- 31 **Ventricular Arrhythmias in Inherited Channelopathies**, 976
- 32 **Complications of Catheter Ablation of Cardiac Arrhythmias**, 1042
- Index**, 1068

BRAUNWALD'S HEART DISEASE FAMILY OF BOOKS

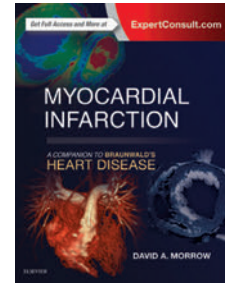
BRAUNWALD'S HEART DISEASE COMPANIONS



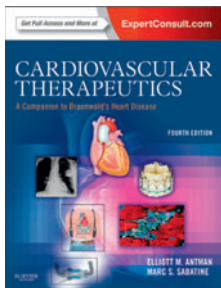
BHATT
Cardiovascular Intervention



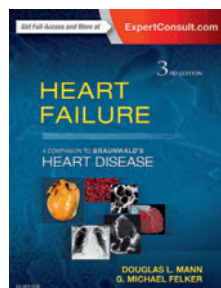
MCGUIRE AND MARX
Diabetes in Cardiovascular Disease



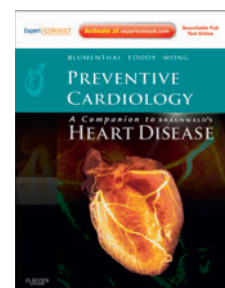
MORROW
Myocardial Infarction



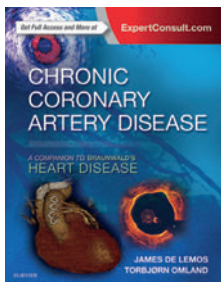
ANTMAN AND SABATINE
Cardiovascular Therapeutics



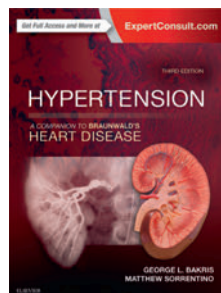
MANN AND FELKER
Heart Failure



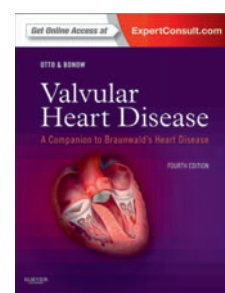
BLUMENTHAL, FOODY, AND WONG
Preventive Cardiology



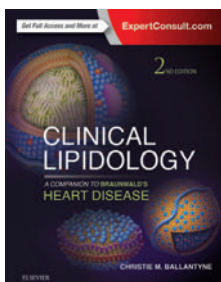
DE LEMOS AND OMLAND
Chronic Coronary Artery Disease



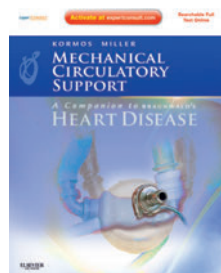
BAKRIS AND SORRENTINO
Hypertension



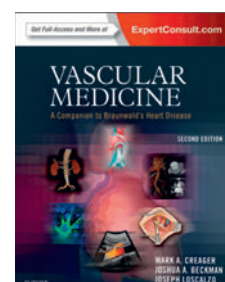
OTTO AND BONOW
Valvular Heart Disease



BALLANTYNE
Clinical Lipidology

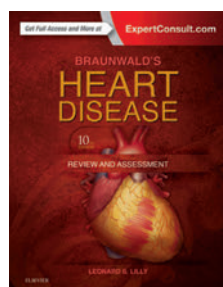


KORMOS AND MILLER
Mechanical Circulatory Support



CREAGER, BECKMAN, AND LOSCALZO
Vascular Medicine

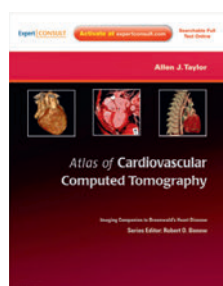
BRAUNWALD'S HEART DISEASE REVIEW AND ASSESSMENT



LILLY

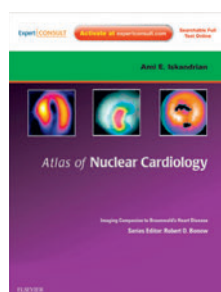
Braunwald's Heart Disease Review and Assessment

BRAUNWALD'S HEART DISEASE IMAGING COMPANIONS



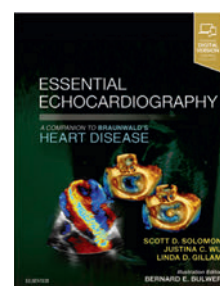
TAYLOR

Atlas of Cardiovascular Computed Tomography



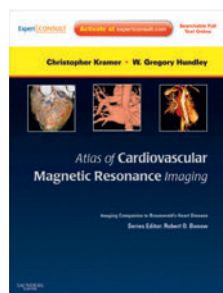
ISKANDRIAN AND GARCIA

Atlas of Nuclear Cardiology



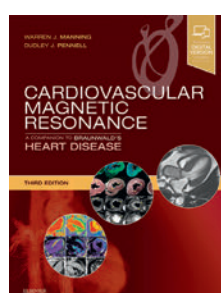
SOLOMON, WU, AND GILLAM

Essential Echocardiography



KRAMER AND HUNDLEY

Atlas of Cardiovascular Magnetic Resonance Imaging



MANNING AND PENNELL

Cardiovascular Magnetic Resonance

Molecular Mechanisms of Cardiac Electrical Activity

OUTLINE

Ionic Equilibrium, 1

Transmembrane Potentials, 1

Cardiac Action Potential, 2

Fast Response Action Potential, 3

Slow Response Action Potential, 8

Excitability, 8

Refractoriness, 9

Propagation, 10

Intracellular Propagation, 10

Intercellular Propagation, 10

Anisotropic Conduction, 11

Source-Sink Relationship, 11

Safety Factor for Conduction, 12

Excitation-Contraction Coupling, 12

IONIC EQUILIBRIUM

The lipid bilayer of the cell membrane is hydrophobic and impermeable to water-soluble substances such as ions. Hence, for the hydrophilic ions to be able to cross the membrane, they need hydrophilic paths that span the membrane (i.e., pores), which are provided by transmembrane proteins called ion channels. Once a hydrophilic pore is available, ions move passively across the membrane, driven by two forces: the electrical gradient (voltage difference) and chemical gradient (concentration difference). The chemical gradient forces the ions to move from a compartment of a higher concentration to one of lower concentration. The electrical gradient forces ions to move in the direction of their inverse sign (i.e., cations [positively charged ions] move toward a negatively charged compartment, whereas anions [negatively charged ions] move toward a positively charged compartment). Because the chemical and electrical gradients can oppose each other, the direction of net ion movement will depend on the relative contributions of chemical gradient and electrical potential (i.e., the net electrochemical gradient), so that ions tend to move spontaneously from a higher to a lower electrochemical potential.¹

The movement of an ion down its chemical gradient in one direction across the cell membrane results in build-up of excess charge carried by the ion on one side of the membrane, which generates an electrical gradient that impedes (repels) continuing ionic movement in the same direction. When the driving force of the electrical gradient across the membrane becomes equal and opposite to the force generated by the chemical gradient, the ion is said to be in electrochemical equilibrium, and the net transmembrane flux (or current) of that particular ion is zero. In this setting, the membrane electrical potential is called the equilibrium potential (E_{ion}) ("reversal potential" or "Nernst potential") of that individual ion. Any further current flow would reverse the balance of forces and therefore reverse the current direction until equilibrium is restored, hence the name "reversal potential."² The E_{ion} for a given ion measures the voltage that the ion concentration gradient generates when it acts as a battery, and it depends on its concentration on either side of the membrane and the temperature. At membrane voltages more positive to the reversal potential of the ion, passive ion movement is outward, whereas it is inward at a membrane potential (E_m) more negative to the Nernst potential of that channel.¹

When multiple ions across a membrane are removed from their electrochemical equilibrium, each ion will tend to force the E_m toward

its own E_{ion} . The contribution of each ion type to the overall E_m at any given moment is determined by the instantaneous permeability of the plasma membrane to that ion. The larger the membrane conductance to a particular ion, the greater is the ability of that ion to bring the E_m toward its own E_{ion} . Hence the E_m is the average of the E_{ion} of all the ions to which the membrane is permeable, weighed according to the membrane conductance of each individual ion relative to the total ionic conductance of the membrane.¹

TRANSMEMBRANE POTENTIALS

All living cells, including cardiomyocytes, maintain a difference in the concentration of ions across their membranes. There is a slight excess of positive ions on the outside of the membrane and a slight excess of negative ions on the inside of the membrane, resulting in a difference in the electrical charge (i.e., voltage, potential difference, or electrical gradient) across the cell membrane, called the E_m (also known as membrane voltage or transmembrane potential). A membrane that exhibits an electrical gradient is said to be polarized.

In nonexcitable cells, and in excitable cells in their baseline states (i.e., not conducting electrical signals), the E_m is held at a relatively stable value, called the resting E_m . All cells have a negative resting E_m (i.e., the cytoplasm is electrically negative relative to the extracellular fluid), which arises from the interaction of ion channels and ion pumps embedded in the membrane that maintain different ion concentrations on the intracellular and extracellular sides of the membrane.

When an ion channel opens, it allows ion flux across the membrane that generates an electrical current (I). This current affects the E_m , depending on the membrane resistance (R), which refers to the ratio between the E_m and electrical current, as shown in Ohm's law: $E = I \times R$, or $R = E/I$. Resistance arises from the fact that the membrane impedes the movement of charges across it; hence the cell membrane functions as a *resistor* (i.e., when current is passed through the membrane, there is a voltage drop that is predictable from Ohm's law). Conductance describes the ability of a membrane to allow the flux of charged ions in one direction across the membrane. The more permeable the membrane is to a particular ion, the greater is the conductance of the membrane to that ion (Table 1.1). Membrane conductance (g) is the reciprocal of resistance: $g = 1/R$.

Because the lipid bilayer of the cell membrane is very thin, accumulation of charged ions on one side gives rise to an electrical force

TABLE 1.1 Definitions Related to Electrical Properties of Cell Membranes

Term	Unit	Definition
Charge (electric charge, Q)	Coulombs	<ul style="list-style-type: none"> The physical property of matter that causes it to experience a force (electrostatic attraction or repulsion) in the presence of other matter.
Voltage (potential difference, V)	Volt (V)	<ul style="list-style-type: none"> There are two types of electric charges: positive and negative. Like charges repel and unlike attract. A separation of unlike charge in space; the greater the amount of charge separated, the larger the voltage, and the greater the tendency for the charges to flow toward each other. Voltage is always measured at one point with respect to another point. There cannot be a voltage at one point in space. Voltage is the ability to drive an electric current across a resistance.
Current (I)	Amperes (A)	<ul style="list-style-type: none"> A flow of electrical charges.
Resistance (R)	Ohm (Ω)	<ul style="list-style-type: none"> A measure of the difficulty with which current flows in a circuit; the greater the difficulty, the greater the resistance.
Conductance (g)	Siemen (S)	<ul style="list-style-type: none"> A measure of the ease with which current flows in a circuit. Conductance is the reciprocal of the resistance.
Capacitance (C)	Farad	<ul style="list-style-type: none"> The ability of a body to store an electrical charge. A material with a large capacitance holds more electric charge at a given voltage, than one with low capacitance.
Membrane potential (transmembrane potential, membrane voltage, E_m)	Volt (V)	<ul style="list-style-type: none"> The difference in electrical potential between the interior and the exterior of a biological cell.
Equilibrium potential of an ion (E_{ion}) (reversal potential, Nernst potential)	Volt (V)	<ul style="list-style-type: none"> The value of the E_m at which diffusive and electrical gradients for a particular ion counterbalance, so that there is no net ion flow across the membrane (i.e., electrochemical equilibrium). In other words, equilibrium potential is the membrane potential necessary to maintain a given concentration difference or the membrane potential that will result from maintenance of a given concentration difference. An ion will be in electrochemical equilibrium if $E_m = E_{ion}$.
Ionic current (I_{ion})	Amperes (A)	<ul style="list-style-type: none"> Electrical current generated by the flux of charged ions across the cell membrane.
Capacitive current (nonfaradaic current, double-layer current)		<ul style="list-style-type: none"> The electric current generated by the movement of electrons toward and away from the surfaces of the cell membrane. This current does not involve movement of charged ions across the cell membrane, it only causes accumulation (or removal) of electrical charges on membrane surface.

(potential) that pulls oppositely charged particles toward the other side. Hence the cell membrane functions as a *capacitor* (i.e., capable of separating and storing charge). Although the absolute potential differences across the cell membrane are small, they give rise to enormous electrical potential gradients because they occur across a very thin surface. As a consequence, apparently small changes in E_m can produce large changes in potential gradient and powerful forces that are able to induce molecular rearrangement in membrane proteins, such as those required for opening and closing ion channels embedded in the cell membrane. The capacitance of the membrane is generally fixed and unaffected by the molecules that are embedded in it. In contrast, membrane resistance is highly variable and depends on the conductance of ion channels embedded in the membrane.³

The sodium (Na^+), potassium (K^+), calcium (Ca^{2+}), and chloride (Cl^-) ions are the major charge carriers, and their movement across the cell membrane creates a flow of current that generates excitation and signals in cardiac myocytes. The electrical current generated by the flux of an ion across the membrane is determined by the membrane conductance to that ion (g_{ion}) and the potential (voltage) difference across the membrane. The potential difference represents the potential at which there is no net ion flux (i.e., the E_{ion}) and the actual E_m : current = $g_{ion} \times (E_m - E_{ion})$.

By convention, an inward current increases the electropositivity within the cell (i.e., causes depolarization of the E_m [to become less negative]) and can result from either the movement of positively charged ions (most commonly Na^+ or Ca^{2+}) into the cell or the efflux of nega-

tively charged ions (e.g., Cl^-) out of the cell. An outward current increases the electronegativity within the cell (i.e., causes hyperpolarization of the E_m [to become more negative]) and can result from either the movement of anions into the cell or the efflux of cations (most commonly K^+) out of the cell.

Opening and closing of ion channels can induce a departure from the relatively static resting E_m , which is called *depolarization* if the interior voltage rises (becomes less negative) or *hyperpolarization* if the interior voltage becomes more negative. The most important ion fluxes that depolarize or repolarize the membrane are passive (i.e., the ions move down their electrochemical gradient without requiring the expenditure of energy), occurring through transmembrane ion channels. In excitable cells a sufficiently large depolarization can evoke a short-lasting all-or-none event called an *action potential*, in which the E_m very rapidly undergoes specific and large dynamic voltage changes.

Both resting E_m and dynamic voltage changes such as the action potential are caused by specific changes in membrane permeabilities for Na^+ , K^+ , Ca^{2+} , and Cl^- , which, in turn, result from concerted changes in functional activity of various ion channels, ion transporters, and ion exchangers.

CARDIAC ACTION POTENTIAL

During physiological electrical activity, the E_m is a continuous function of time. The current flowing through the cell membrane, at each instant, is provided by multiple channels and transporters carrying charge in

opposite directions because of their different ion selectivity. The algebraic summation of these contributions is referred to as net transmembrane current.

The cardiac action potential reflects a balance between inward and outward currents. When a depolarizing stimulus (typically generated by an electric current from an adjacent cell) abruptly changes the E_m of a resting cardiomyocyte to a critical value (the threshold level), the properties of the cell membrane and ion conductances change dramatically, precipitating a sequence of events involving the influx and efflux of multiple ions that together produce the action potential of the cell. In this fashion an electrical stimulus is conducted from one cell to the cells adjacent to it.⁴

Unlike skeletal muscle, cardiac muscle is electrically coupled so that the wave of depolarization propagates from one cell to the next, independent of neuronal input. The heart is activated by *capacitive currents* generated when a wave of depolarization approaches a region of the heart that is at its resting potential. Unlike ionic currents, which are generated by the flux of charged ions across the cell membrane, capacitive currents are generated by the movement of electrons toward and away from the surfaces of the membrane. These electrotonic potential changes are passive and independent of membrane conductance. The resulting decrease in positive charge at the outer side of the cell membrane reduces the negative charge on the intracellular surface of the membrane. These charge movements, which are carried by electrons, generate a capacitive current. When an excitatory stimulus causes the E_m to become less negative and beyond a threshold level (approximately -65 mV for working atrial and ventricular cardiomyocytes), Na^+ channels activate (open) and permit an inward Na^+ current (I_{Na}), resulting in a rapid shift of the E_m to a positive voltage range. This event triggers a series of successive opening and closure of selectively permeable ion channels. The direction and magnitude of passive movement (and the resulting current) of an ion at any given transmembrane voltage are determined by the ratio of the intracellular and extracellular concentrations and the reversal potential of that ion, with the net flux being larger when ions move from the more concentrated side.

The “threshold potential” is the lowest E_m at which opening of enough Na^+ channels (or Ca^{2+} channels in the setting of nodal cells) is able to initiate the sequence of channel openings needed to generate a propagated action potential. Small (subthreshold) stimuli depolarize the membrane in proportion to the strength of the stimulus and cause only local responses because they do not open enough Na^+ channels to generate depolarizing currents large enough to activate nearby resting cells (i.e., insufficient to initiate a regenerative action potential). On the other hand, when the stimulus is sufficiently intense to reduce the E_m to a threshold value, regenerative action potential results, whereby intracellular movement of Na^+ depolarizes the membrane more, a process that increases conductance to Na^+ more, which allows more Na^+ to enter, and so on. In this fashion the extent of subsequent depolarization becomes independent of the initial depolarizing stimulus, and more intense stimuli do not produce larger action potential responses; rather, an all-or-none response results.⁴

Electrical changes in the action potential follow a relatively fixed time and voltage relationship that differs according to specific cell types. Although the entire action potential takes only a few milliseconds in nerve cells, the cardiac action potential lasts several hundred milliseconds. The course of the action potential can be divided into five phases (numbered 0 to 4). Phase 4 is the resting E_m , and it describes the E_m when the cell is not being stimulated.

During the cardiac action potential, membrane voltages fluctuate in the range of -94 to $+30$ mV (Fig. 1.1). With physiological external K^+ concentration, the reversal potential of K^+ (E_K) is approximately -94 mV, and passive K^+ movement during an action potential is out of

the cell. On the other hand, because the calculated reversal potential of a cardiac Ca^{2+} channel (E_{Ca}) is $+64$ mV, passive Ca^{2+} flux is into the cell.

In normal atrial and ventricular myocytes and in His-Purkinje fibers, action potentials have very rapid upstrokes, mediated by the fast inward I_{Na} . These potentials are called *fast response* potentials. In contrast, action potentials in the normal sinus and atrioventricular (AV) nodal cells and many types of diseased tissues have very slow upstrokes, mediated by a slow inward, predominantly L-type voltage-gated Ca^{2+} current (I_{CaL}), rather than by the fast inward I_{Na} (Fig. 1.2). These potentials have been termed *slow response* potentials.

Fast Response Action Potential

Phase 4: The Resting Membrane Potential

The E_m of resting atrial and ventricular cardiomyocytes remains steady throughout diastole. The resting E_m is caused by the differences in ionic concentrations across the membrane and the selective membrane permeability (conductance) to various ions. Large concentration gradients of Na^+ , K^+ , Ca^{2+} , and Cl^- across the cell membrane are maintained by the ion pumps and exchangers (Table 1.2).⁴

Under normal conditions, the resting membrane is most permeable to K^+ and relatively impermeable to other ions. K^+ has the largest resting membrane conductance (g_K is 100 times greater than g_{Na}) because of the abundance of open K^+ channels at rest, whereas Na^+ and Ca^{2+} channels are generally closed. Thus K^+ exerts the largest influence on the resting E_m . As a consequence, the resulting E_m is almost always close to the K^+ reversal potential (E_m approximates E_K). The actual resting E_m is slightly less negative than E_K because the cell membrane is slightly permeable to other ions.

The inwardly rectifying K^+ (Kir) channels underlie an outward K^+ current (I_{K1}) responsible for maintaining the resting potential near the E_K in atrial, His-Purkinje, and ventricular cells, under normal conditions. Kir channels preferentially allow currents of K^+ ions to flow into the cell with a strongly voltage-dependent decline of K^+ efflux (i.e., reduction of outward current) on membrane depolarization. As such, I_{K1} is a strong rectifier that passes K^+ currents over a limited range of E_m . At a negative E_m , I_{K1} conductance is much larger than that of any other current; thus it clamps the resting E_m close to the reversal potential for K^+ (E_K) (see Chapter 2 for detailed discussion on the concept of rectification). I_{K1} density is much higher in ventricular than in atrial myocytes, a feature that largely prevents the ventricular cell from having diastolic membrane depolarization and pacemaker activity. By contrast, I_{K1} is almost absent in sinus and AV nodal cells, thus allowing for relatively more depolarized resting diastolic potentials compared with atrial and ventricular myocytes (Table 1.3). The effect of outward K^+ current to resist membrane depolarization (keeping voltage fixed) is sometimes referred to as a voltage clamping effect.²

A unique property of Kir currents is the unusual dependence of rectification on extracellular K^+ concentration. Specifically, with an

TABLE 1.2 Intracellular and Extracellular Ion Concentrations and Equilibrium Potentials in Cardiomyocytes

Ion	Extracellular Concentration (mM)	Intracellular Concentration (mM)	Equilibrium Potential (mV)
Na^+	135–145	10	+70
K^+	3.5–5.0	155	−94
Ca^{2+}	2	0.0001	+132
Cl^-	87	30	−28

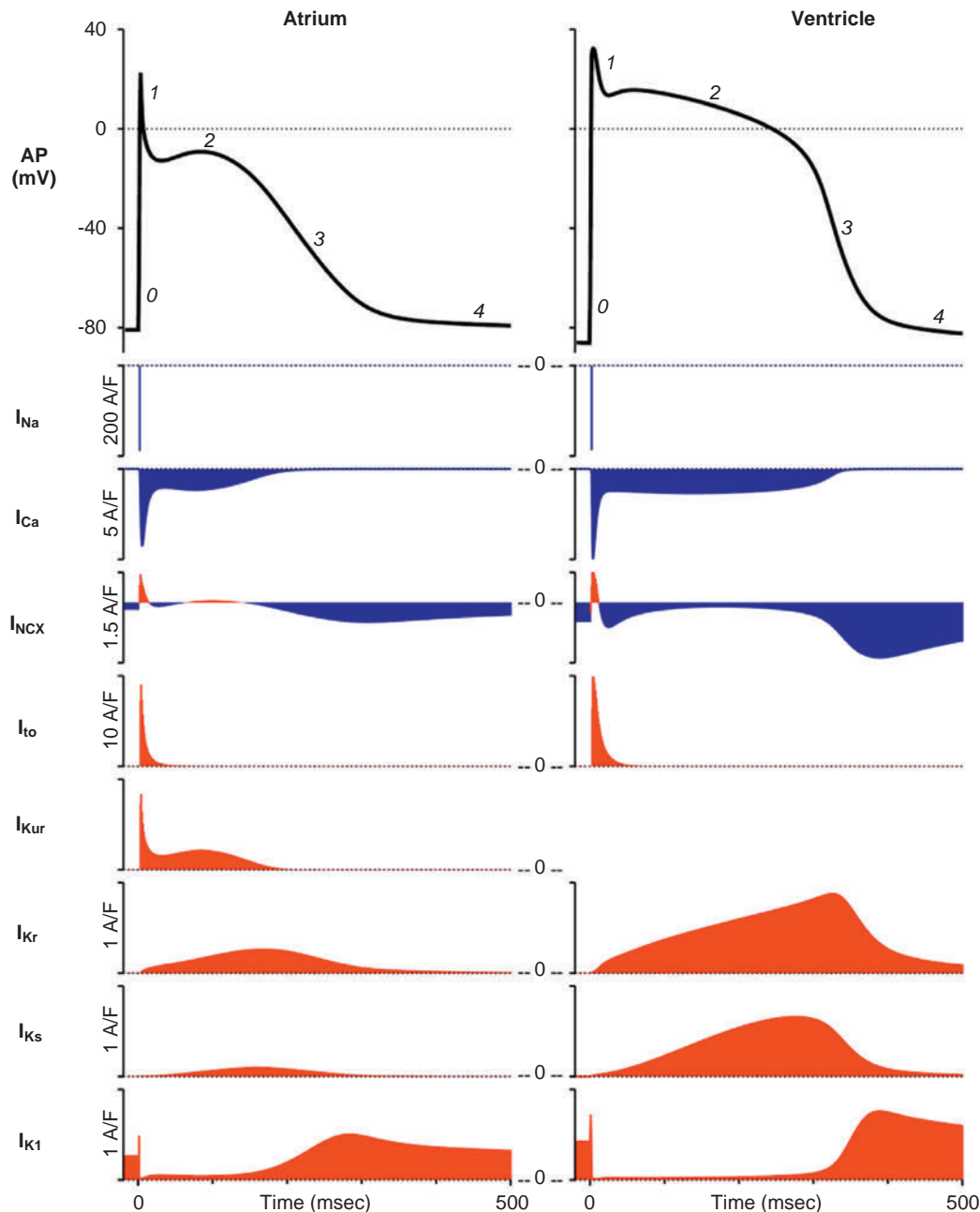


Fig. 1.1 Contribution of Depolarizing Inward and Repolarizing Outward Currents to the Atrial and Ventricular Action Potential (AP). The top panel from the atrial (*left*) and ventricular (*right*) myocytes. The five phases of the AP are labeled: 0 = upstroke of the AP represents depolarization of the membrane; 1 = initial repolarization; 2 = plateau phase; 3 = late repolarization; 4 = the resting (diastolic) phase. The rate of change of the AP is directly proportional to the sum of the underlying transmembrane ion currents (*lower panels*). Inward currents (*blue*) depolarize the membrane, whereas outward currents (*red*) contribute to repolarization. Compared with an atrial AP, the ventricular AP typically has longer duration, higher plateau potential (phase 2), and more negative resting membrane potential (phase 4). I_{Ca} , L-type Ca^{2+} current; I_{Na} , Na^+ current; I_{NCX} , Na^+ - Ca^{2+} exchanger; I_{Kr} , rapidly activating delayed rectifier K^+ current; I_{Ks} , slowly activating delayed rectifier K^+ current; I_{Kur} , ultrarapidly activating delayed rectifier K^+ current; I_{K1} , inward rectifier K^+ current; I_{to} , transient outward K^+ current. (With permission from Oudit GY, Backx PH. Voltage-gated potassium channels. In: Zipes DP, Jalife J, eds. *Cardiac Electrophysiology: From Cell to Bedside*. 7th ed. Philadelphia: Elsevier; 2018.)

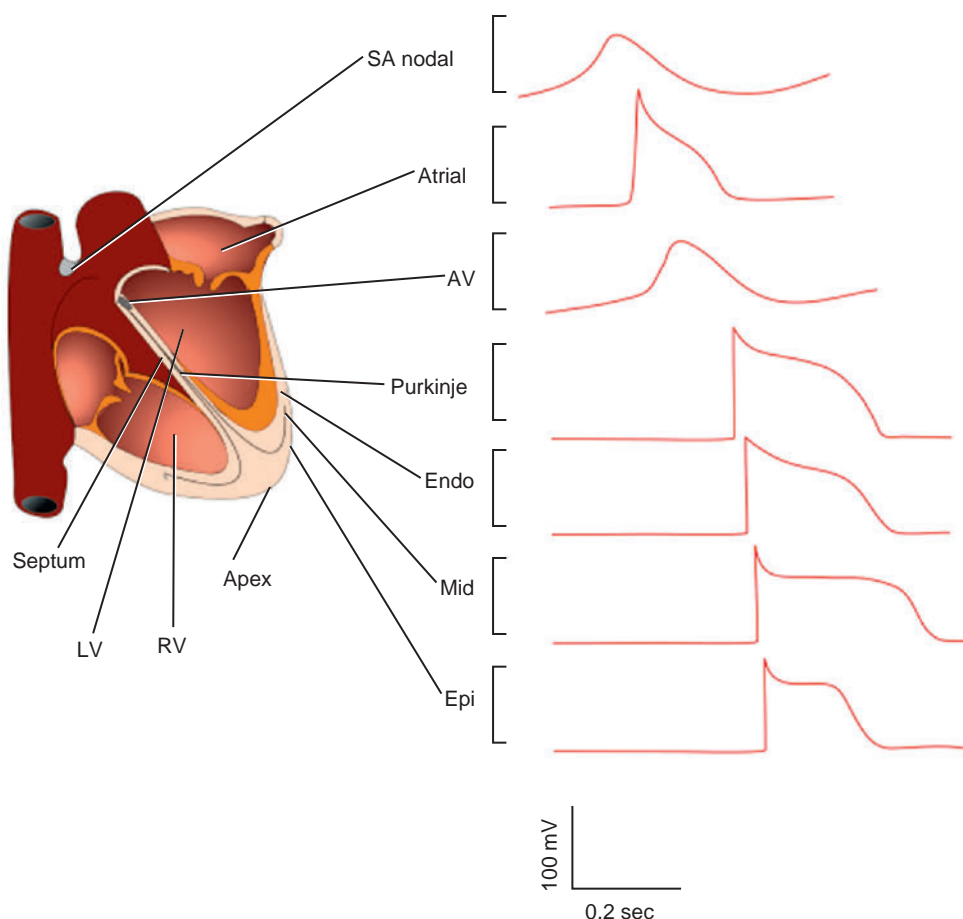


Fig. 1.2 Action Potential Waveforms, Displaced in Time to Reflect the Temporal Sequence of Propagation, Vary in Different Regions of the Heart. AV, Atrioventricular (node); Endo, endocardial; Epi, epicardial; LV, left ventricle; Mid, midmyocardial; RV, right ventricle; SA, sinoatrial. (Modified with permission from Nerbonne JM. Heterogeneous expression of repolarizing potassium currents in the mammalian myocardium. In Zipes DP, Jalife J, eds. *Cardiac Electrophysiology: From Cell to Bedside*. 5th ed. Philadelphia: Saunders; 2009:293–305.)

TABLE 1.3 Regional Differences in Cardiac Action Potential

Property	Sinus Nodal Cell	Atrial Muscle Cell	AV Nodal Cell	Purkinje Fiber	Ventricular Muscle Cell
Resting potential (mV)	–50 to –60	–80 to –90	–60 to –70	–90 to –95	–80 to –90
Action potential amplitude (mV)	+60 to +70	+110 to +120	+70 to +80	+120	+110 to +120
Action potential duration (msec)	100 to 300	100 to 300	100 to 300	300 to 500	200 to 300

AV, Atrioventricular.

increase in extracellular K^+ , the I_{K1} current-voltage relationship shifts nearly in parallel with the E_K and leads to a crossover phenomenon. One important consequence of such behavior is that at potentials positive to the crossover, K^+ conductance increases rather than decreases, against an expectation based on a reduced driving force for K^+ ions as a result of elevated extracellular K^+ concentration.⁵

The resting E_m is also powered by the Na^+ - K^+ adenosine triphosphatase (ATPase) (the Na^+ - K^+ pump), which helps to establish concentration gradients of Na^+ and K^+ across the cell membrane. Under physiological conditions, the Na^+ - K^+ pump transports two K^+ ions into the cell against its chemical gradient and three Na^+ ions outside against

its electrochemical gradient at the expense of one ATP molecule. Because the stoichiometry of ion movement is not 1:1, the Na^+ - K^+ pump is electrogenic and generates a net outward movement of positive charges (i.e., an outward current). At faster heart rates, the rate of Na^+ - K^+ pumping increases to maintain the same ionic gradients, thus counteracting the intracellular gain of Na^+ and loss of K^+ with each depolarization.

Ca^{2+} does not contribute directly to the resting E_m because the voltage-activated Ca^{2+} channels are closed at the hyperpolarized resting E_m . However, changes in intracellular free Ca^{2+} concentration can affect other membrane conductance values. Increases in intracellular Ca^{2+}

levels can stimulate the $\text{Na}^+\text{-Ca}^{2+}$ exchanger ($I_{\text{Na-Ca}}$), which exchanges three Na^+ ions for one Ca^{2+} ion; the direction depends on the Na^+ and Ca^{2+} concentrations on the two sides of the membrane and the E_m difference. At resting E_m and during a spontaneous sarcoplasmic reticulum Ca^{2+} release event, this exchanger would generate a net Na^+ influx, possibly causing transient membrane depolarizations.

Phase 0: The Upstroke—Rapid Depolarization

On excitation of an atrial, ventricular, or Purkinje cardiomyocyte by electrical stimuli from adjacent cells, its resting E_m (approximately -85 mV) depolarizes, leading to opening (activation) of Na^+ channels from its resting (closed) state and enabling a large and rapid influx of Na^+ ions (inward I_{Na}) into the cell down their electrochemical gradient. As a consequence of increased Na^+ conductance, the excited membrane no longer behaves like a K^+ electrode (i.e., exclusively permeable to K^+) but more closely approximates an Na^+ electrode, and the E_m moves toward the E_{Na} (see Table 1.2). Once an excitatory stimulus depolarizes the E_m beyond the threshold for activation of Na^+ channels (approximately -65 mV), the activated I_{Na} is regenerative and no longer depends on the initial depolarizing stimulus. As a consequence, the influx of Na^+ ions further depolarizes the membrane and thereby increases conductance to Na^+ more, which allows more Na^+ to enter the cell (thus “regenerative”).⁶

Normally, activation of Na^+ channels is transient; fast inactivation (closing of the channel pore) starts simultaneously with activation, but because inactivation is slightly delayed relative to activation, the channels remain transiently (less than 1 millisecond) open to conduct I_{Na} during phase 0 of the action potential before it closes. In addition, the influx of Na^+ into the cell increases the positive intracellular charges and reduces the driving force for Na^+ . When the E_{Na} is reached, no further Na^+ ions enter the cell.

The rate at which depolarization occurs during phase 0 (i.e., the maximum rate of change of voltage over time [dV/dt_{max}]) is a reasonable approximation of the rate and magnitude of Na^+ entry into the cell and a determinant of conduction velocity for the propagated action potential (see later).

The threshold for activation of I_{CaL} is approximately -30 to -40 mV. Although I_{CaL} is normally activated during phase 0 by the regenerative depolarization caused by the fast I_{Na} , I_{CaL} is much smaller than the peak I_{Na} . Furthermore, the amplitude of I_{CaL} is not maximal near the action potential peak because of the time-dependent nature of I_{CaL} activation, as well as the low driving force ($E_m - E_{\text{Ca}}$) for I_{CaL} . Therefore I_{CaL} contributes little to the action potential until the fast I_{Na} is inactivated, after completion of phase 0. As a result, I_{CaL} affects mainly the plateau of action potentials recorded in atrial and ventricular muscle and His-Purkinje fibers. On the other hand, I_{CaL} plays a prominent role in the upstroke of slow response action potentials in partially depolarized cells in which the fast Na^+ channels have been inactivated.

Phase 1: Early Repolarization

Phase 0 is followed by phase 1 (early repolarization), during which the membrane repolarizes rapidly and transiently to almost 0 mV (early notch), partly because of the inactivation of I_{Na} and concomitant activation of several outward currents. The transient outward K^+ current (I_{to}) is mainly responsible for phase 1 of the action potential. I_{to} rapidly activates (with time constants less than 10 milliseconds) by depolarization and then rapidly inactivates (25 to 80 milliseconds for the fast component of I_{to} [$I_{\text{to,f}}$], and 80 to 200 milliseconds for the slow component of I_{to} [$I_{\text{to,s}}$]). The influx of K^+ ions via I_{to} channels partially repolarizes the membrane, thus shaping the rapid repolarization (phase 1) of the action potential and setting the height of the initial plateau (phase 2) (see Fig. 1.1). In addition, an Na^+ outward current through

the $\text{Na}^+\text{-Ca}^{2+}$ exchanger operating in reverse mode likely contributes to this early phase of repolarization.⁴

Phase 2: The Plateau

Phase 2 (plateau) represents a delicate balance between the depolarizing inward currents (I_{CaL} and a small residual component of inward I_{Na}) and the repolarizing outward currents (ultrarapidly [I_{Kur}], rapidly [I_{Kr}], and slowly [I_{Ks}] activating delayed outward rectifying currents) (see Fig. 1.1). Phase 2 is the longest phase of the action potential, lasting tens (atrium) to hundreds of milliseconds (His-Purkinje system and ventricle). The plateau phase is unique among excitable cells and marks the phase of Ca^{2+} entry into the cell. It is the phase that most clearly distinguishes the cardiac action potential from the brief action potentials of skeletal muscle and nerve.^{4,7,8}

I_{CaL} is activated by membrane depolarization, is largely responsible for the action potential plateau, and is a major determinant of the duration of the plateau phase. I_{CaL} also links membrane depolarization to myocardial contraction. L-type Ca^{2+} channels activate on membrane depolarization to potentials positive to -40 mV. I_{CaL} peaks at an E_m of 0 to $+10$ mV and tends to reverse at $+60$ to $+70$ mV, following a bell-shaped current-voltage relationship.

Na^+ channels also make a contribution, although minor, to the plateau phase. After phase 0 of the action potential, some Na^+ channels occasionally fail to inactivate or exhibit prolonged opening or reopening repetitively for hundreds of milliseconds after variable and prolonged latencies, resulting in a small inward I_{Na} (with a magnitude of less than 1% of the peak I_{Na}). This persistent or “late” I_{Na} (I_{NaL}), along with I_{CaL} , helps to maintain the action potential plateau.⁹

I_{Kr} and I_{Ks} are activated at depolarized membrane potentials. I_{Kr} activates relatively fast (in the order of tens of milliseconds) on membrane depolarization, thus allowing outward diffusion of K^+ ions in accordance with its electrochemical gradient, but voltage-dependent inactivation thereafter is very fast. Hence only limited numbers of channels remain in the open state, whereas a considerable fraction resides in the nonconducting inactivated state. The fast voltage-dependent inactivation limits outward current through the channel at positive voltages and thus helps to maintain the action potential plateau phase that controls contraction and prevents premature excitation. However, as the voltage becomes less positive at the end of the plateau phase of repolarization, the channels recover rapidly from inactivation; this process leads to a progressive increase in I_{Kr} amplitudes during action potential phases 2 and 3, with maximal outward current occurring before the final rapid declining phase of the action potential.¹⁰

I_{Ks} , which is approximately 10 times larger than I_{Kr} , also contributes to the plateau phase. I_{Ks} activates in response to membrane depolarization to potentials positive to -30 mV and gradually increases during the plateau phase because its time course of activation is extremely slow, slower than any other known K^+ current. In fact, steady-state amplitude of I_{Ks} is achieved only with extremely long membrane depolarization. Hence the contribution of I_{Ks} to the net repolarizing current is greatest late in the plateau phase, particularly during action potentials of long duration. Importantly, although I_{Ks} activates slowly compared with action potential duration, it is also slowly inactivated. As heart rate increases, I_{Ks} increases because channel deactivation is slow and incomplete during the shortened diastole. This allows I_{Ks} channels to accumulate in the open state during rapid successive action potentials and mediate the faster rate of repolarization. Hence I_{Ks} plays an important role in determining the rate-dependent shortening of the cardiac action potential.⁵

I_{Kur} is detected only in human atria but not in the ventricles, such that it is the predominant delayed rectifier current responsible for atrial repolarization and is a basis for the much shorter duration of the action

potential in the atrium. I_{Kur} activates rapidly on depolarization in the plateau range and displays outward rectification, but it inactivates slowly during the time course of the action potential.

The Na^+ - Ca^{2+} exchanger operating in forward mode (three Na^+ ions in for one Ca^{2+} ion out) and the Na^+ - K^+ pump provide minor current components during phase 2.

Importantly, during the plateau phase, membrane conductance to all ions falls to rather low values. Thus less change in current is required near plateau levels than near resting potential levels to produce the same changes in E_m . In particular, K^+ conductance falls during the plateau phase as a result of inward rectification of I_{K1} (i.e., voltage-dependent decline of K^+ efflux and hence reduction of outward current) on membrane depolarization, in spite of the large electrochemical driving force on K^+ ions during the positive phase of the action potential (phases 0, 1, and 2). This property allows membrane depolarization following Na^+ channel activation, slows membrane repolarization, and helps to maintain a more prolonged cardiac action potential. This also confers energetic efficiency in the generation of the action potential.^{11,12}

Phase 3: Final Rapid Repolarization

Phase 3 is the phase of rapid repolarization that restores the E_m to its resting value. Phase 3 is mediated by the increasing conductance of the delayed outward rectifying currents (I_{Kr} and I_{Ks}), the inwardly rectifying K^+ currents (I_{K1} and acetylcholine-activated K^+ current [I_{KACH}]), and time-dependent inactivation of I_{CaL} (see Fig. 1.1). Final repolarization during phase 3 results from K^+ efflux through the I_{K1} channels, which open at potentials negative to -20 mV.⁴

Phase 4: Restoration of Resting Membrane Potential

During the action potential, Na^+ and Ca^{2+} ions enter the cell and depolarize the E_m . Although the E_m is quickly repolarized by the efflux of K^+ ions, restoration of transmembrane ionic concentration gradients to the baseline resting state is necessary. This is achieved by the Na^+ - K^+ ATPase (Na^+ - K^+ pump, which exchanges two K^+ ions inside and three Na^+ ions outside) and by the Na^+ - Ca^{2+} exchanger ($I_{\text{Na-Ca}}$) which exchanges three Na^+ ions for one Ca^{2+} ion).⁴

Reduction of cytosolic Ca^{2+} concentration during diastole is achieved by the reuptake Ca^{2+} by the sarcoplasmic reticulum via activation of the sarco/endoplasmic reticulum calcium-ATPase calcium pump (SERCA), in addition to extrusion across the sarcolemma via the Na^+ - Ca^{2+} exchanger. In the human heart under resting conditions, the time required for cardiac myocyte depolarization, contraction, relaxation, and recovery is approximately 600 milliseconds.

Regional Heterogeneity of the Action Potential

Substantial differences in expression levels of ion channels underlie the considerable heterogeneity in action potential duration and configuration between cardiomyocytes located in different regions of the heart. The characteristics of the action potential differ in atrial versus ventricular myocardium, as well as across the ventricular myocardial wall from endocardium, midmyocardium, to epicardium (see Fig. 1.2).

Atrioventricular Heterogeneity of the Action Potential

Compared with the atrium, ventricular myocytes maintain a slightly more hyperpolarized resting E_m (approximately -85 mV vs. -80 mV). In addition, the action potential duration is longer, the plateau phase reaches a more depolarized E_m (approximately $+20$ mV), and phase 3 repolarization curve is steeper in ventricular myocytes as compared with the atrial action potential (see Table 1.3).

The differences in action potential configuration between atria and ventricles are mainly related to differences in ionic current densities and ion channel expression (especially K^+ channels) between ventricular

and atrial myocytes. Although I_{Kr} and I_{Ks} densities are similar in atrial and ventricular myocytes, I_{Kur} is detected only in human atria and not in the ventricles. In fact, I_{Kur} is the predominant delayed rectifier current responsible for human atrial repolarization, with only small contribution of I_{Kr} and I_{Ks} .

Furthermore, the density of I_{to} is twofold higher in the atria compared with ventricular myocytes. In addition, I_{to} subtypes ($I_{to,f}$ and $I_{to,s}$) are differentially expressed in the heart. $I_{to,f}$ is the principal subtype expressed in human atrium. Conversely, $I_{to,s}$ is larger and $I_{to,f}$ is smaller in the ventricles compared with atrial tissue.⁸

The markedly higher densities of $I_{to,f}$ together with the expression of I_{Kur} accelerate the early phase of repolarization and lead to lower plateau potentials and shorter action potential durations in atrial as compared with ventricular cells.¹³

I_{K1} density is much higher in ventricular than in atrial myocytes, and this explains the steep repolarization phase in the ventricles (where the more abundant I_{K1} plays a larger role in accelerating the terminal portion of repolarization) and the shallower phase in the atria. Furthermore, the higher I_{K1} channel expression underlies the hyperpolarized resting E_m in ventricular myocytes, and prevents the ventricular cell from exhibiting pacemaker activity.¹⁴

Several other K^+ channels are atrial selective and potentially contribute significantly to the atrial, but not ventricular, action potential. These include I_{KACH} , two-pore K^+ channels (K_{2P}), and small-conductance Ca^{2+} -activated K^+ (SK) channels.

Ventricular Regional Heterogeneity of the Action Potential

Action potential differences exist among the different layers across the ventricular wall, between the left and right ventricles, and from the apical region to the base.

Three distinct action potential waveforms have been distinguished from three predominant cell types contributing to the transmural heterogeneity of ventricular repolarization: the epicardial, midmyocardial, and endocardial cardiomyocytes. The most notable differences among these three layers are the prominent phase 1 notch and the spike and dome morphology of epicardial and midmyocardial action potentials compared with endocardium. The action potential duration of epicardial myocytes is shorter than that of endocardial myocytes. The duration of the action potential is longest in midmyocardial myocytes.^{8,14}

The distinct notch phase in the action potential waveform of epicardial myocytes has mainly been attributed to the regional differences in I_{to} density across the myocardial wall. In human ventricles, I_{to} densities are much higher in the epicardium and midmyocardium than in the endocardium. Furthermore, although both $I_{to,f}$ and $I_{to,s}$ are expressed in the ventricle, $I_{to,f}$ is more prominent in the epicardium and midmyocardium than in the endocardium, whereas $I_{to,s}$ is mainly present in the endocardium and Purkinje cells. A prominent I_{to} -mediated action potential notch in ventricular epicardium but not endocardium produces a transmural voltage gradient during early ventricular repolarization that registers as a J wave or J point elevation on the electrocardiogram (ECG).^{8,14}

Some experimental studies in wedge preparations strongly suggest the presence of a subpopulation of cells in the midmyocardium (referred to as the M cells) that exhibits distinct electrophysiological (EP) properties, although the presence of M cells has not been consistently confirmed by intact heart experiments. The putative M cells appear to have the longest action potential duration across the myocardial wall, largely attributed to their weaker I_{Ks} current but stronger late I_{Na} and Na^+ - Ca^{2+} exchanger currents. Hence the M cells have been proposed to underlie the EP basis for transmural ventricular dispersion of repolarization and the T wave on the surface ECG, with the peak of the T wave (in wedge preparations) coinciding with the end of epicardial repolarization and

the end of the T wave coinciding with the end of repolarization of the M cells. Although the role of M cells under physiological conditions remains controversial, these cells appear to have a significant role in arrhythmogenesis under a variety of pathological conditions, such as the long QT and Brugada syndromes, secondary to exaggeration of transmural repolarization gradients.

In addition to the transmural action potential gradient that exists across the three layers of myocardium in the left and right ventricles, the right ventricular (RV) action potential duration overall is shorter and the spike and dome morphology is more pronounced compared with that of the left ventricle (LV). These differences have been attributed to higher I_{to} densities in the right than in the left ventricular myocytes.¹⁴

Evidence also suggests an apicobasal ventricular action potential heterogeneity. Action potential duration appears to be shorter in LV base compared with the apex. Larger I_{to} and I_{Ks} in apical compared with basal myocytes likely underlie those observations.¹⁴

Slow Response Action Potential

In normal atrial and ventricular myocytes and in the His-Purkinje fibers, action potentials have very rapid upstrokes mediated by the fast inward I_{Na} . These potentials are called fast response potentials. In contrast, action potentials in the normal sinus and AV nodal cells and many types of diseased tissue have very slow upstrokes, mediated predominantly by the slow inward I_{CaL} , rather than by the fast inward I_{Na} (see Fig. 1.2). These potentials have been termed *slow response potentials*.⁴

As noted, action potentials of pacemaker cells in the sinus and AV nodes are significantly different from those in working atrial and ventricular myocardium. Slow response action potentials are characterized by a more depolarized E_m at the onset of phase 4 (–50 to –65 mV), slow diastolic depolarization during phase 4, and reduced action potential amplitude. Furthermore, the rate of depolarization in phase 0 is much slower than that in the working myocardial cells, resulting in reduced conduction velocity of the cardiac impulse in the nodal regions (see Table 1.3). Cells in the His-Purkinje system can also exhibit phase 4 depolarization under special circumstances (when Na^+ channels are inactivated by pathological processes).

Phase 4: Diastolic Depolarization

The sinus and AV nodal cells lack the inward rectifier K^+ current (I_{K1}), which acts to stabilize the resting E_m in the normal working atrial and ventricular myocardium and Purkinje fibers. Sinus and AV nodal excitable cells exhibit a spontaneous, slow, and progressive decline in the E_m during diastole (spontaneous diastolic depolarization or phase 4 depolarization) that underlies normal automaticity and pacemaking function. Once this spontaneous depolarization reaches threshold (approximately –40 mV), a new action potential is generated.¹⁵

The ionic mechanisms responsible for diastolic depolarization and normal pacemaker activity in the sinus node are still controversial. Originally, a major role was attributed to the decay of the delayed K^+ conductance (an outward current) activated during the preceding action potential (the I_K -decay theory). This model of pacemaker depolarization lost favor upon the discovery of the “funny” current (I_f), sometimes referred to as the pacemaker current. I_f is a hyperpolarization-activated inward current that is carried largely by Na^+ and, to a lesser extent, K^+ ions. Once activated, I_f depolarizes the membrane to a level where the Ca^{2+} current activates to initiate an action potential.^{15,16}

Other ionic currents gated by membrane depolarization (i.e., I_{CaL} and T-type Ca^{2+} current [I_{CaT}]), nongated and nonspecific background leak currents, and a current generated by the Na^+ - Ca^{2+} exchanger have also been proposed to be involved in pacemaking. The “membrane

clock” (also referred to as the “voltage clock” or “ion channel clock”) refers to the time- and voltage-dependent membrane ion channels underlying pacemaking activity, including the decay of the outward rectifier K^+ current and the activation of several inward currents (I_f , I_{CaL} , I_{CaT} , and I_{Na}).

Newer evidence suggests that the sarcoplasmic reticulum, a major Ca^{2+} store in sinus nodal cells, can function as a physiological clock (the so-called calcium clock) within the cardiac pacemaker cells and has a substantial impact on late diastolic depolarization.^{15,17}

There remains some degree of uncertainty about the relative role of I_f versus that of intracellular Ca^{2+} cycling in controlling the normal pacemaker cell automaticity. Furthermore, the interactions between the membrane clock and the intracellular calcium clock and cellular mechanisms underlying this internal Ca^{2+} clock are not completely elucidated. A further debate has arisen around their individual (or mutual) relevance in mediating the positive and negative chronotropic effects of neurotransmitters. Nevertheless, these interactions are of fundamental importance for understanding the integration of pacemaker mechanisms at the cellular level (see Chapter 3 for detailed discussion on the mechanisms of automaticity and pacemaker activity).¹⁴

Phase 0: The Upstroke—Slow Depolarization

I_{K1} is almost absent in sinus and AV nodal cells, thus allowing for relatively more depolarized resting diastolic potentials (–50 to –65 mV) compared with atrial and ventricular myocytes and facilitating diastolic depolarization mediated by the inward currents (e.g., I_f). At the depolarized level of the maximum diastolic potential of pacemaker cells, most Na^+ channels are inactivated and unavailable for phase 0 depolarization. Consequently, action potential upstroke is mainly achieved by I_{CaL} .¹⁵

L-type Ca^{2+} channels activate on depolarization to potentials positive to –40 mV, and I_{CaL} peaks at 0 to +10 mV. The peak amplitude I_{CaL} is less than 10% that of I_{Na} , and the time required for activation and inactivation of I_{CaL} is approximately an order of magnitude slower than that for I_{Na} . As a consequence, the rate of depolarization in phase 0 (dV/dt) is much slower and the peak amplitude of the action potential is less than that in the working myocardial cells.

EXCITABILITY

Excitability of a cardiac cell describes the ease with which the cell responds to a stimulus with a regenerative action potential. A certain minimum charge must be applied to the cell membrane to elicit a regenerative action potential (i.e., the stimulus should be sufficiently intense to reduce the E_m to the threshold value). Excitability is inversely related to the charge required for excitation.

Excitability of a cardiac cell depends on the passive and active properties of the cell membrane. The passive properties include the membrane resistance and capacitance and the intercellular resistance. The most important determinant of reduced excitability is the reduced availability of Na^+ channels. The more negative the E_m is, the more Na^+ channels are available for activation, the greater the influx of Na^+ into the cell during phase 0, and the greater the conduction velocity. In contrast, membrane depolarization to levels of –60 to –70 mV can inactivate half the Na^+ channels, and depolarization to –50 mV or less can inactivate all the Na^+ channels, thereby rendering Na^+ channels unavailable for mediating an action potential upstroke and thus reducing tissue excitability (Fig. 1.3).

Reduced excitability is physiologically observed during the relative refractory period (occurring during phase 3 of the action potential, before full recovery of E_m). At less negative potentials of the cell membrane, a portion of Na^+ channels will still be inactivated and unavailable

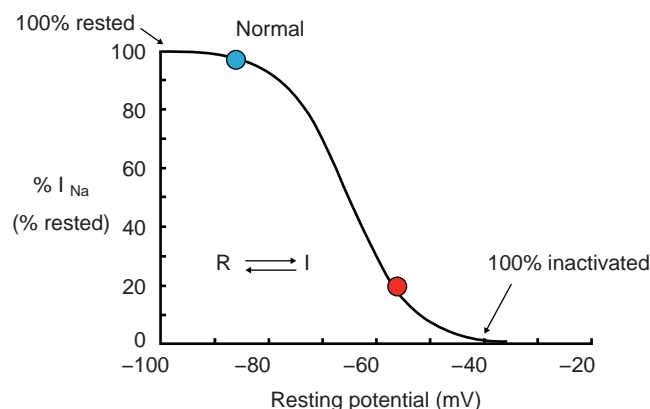


Fig. 1.3 Cellular Excitability. Relationship between transmembrane action potential from single ventricular muscle fiber and excitability of fiber to cathodal stimulation. Amplitudes of peak sodium current (I_{Na}) and proportion of Na^+ channels in the resting state are depicted as a function of resting membrane potential. *I*, Inactivation of Na^+ channels; *R*, recovery of Na^+ channels. (Redrawn from Rosen MS, Wit AL, Hoffman BF. Electrophysiology and pharmacology of cardiac arrhythmias. I. Cellular electrophysiology of the mammalian heart. *Am Heart J*. 1974;88:380.)

for activation. As a result, initiation of a propagating action potential will require a larger-than-normal stimulus. Even then, I_{Na} and phase 0 of the resulting action potential are reduced, and conduction of a premature stimulus occurring during that period is slowed.

On the other hand, supernormal excitability can be observed during a brief period at the end of phase 3 of the action potential. During the supernormal period, excitation is possible in response to an otherwise subthreshold stimulus; that same stimulus fails to elicit a response earlier and later than the supernormal period. Two factors are responsible for supernormality: the availability of fast Na^+ channels and the proximity of the E_m to threshold potential. During the supernormal phase of excitability, the cell has recovered enough to respond to a stimulus (i.e., an adequate number of Na^+ channels is available for activation). At the same time, because the E_m is still reduced, it requires only a little additional depolarization to bring the fiber to threshold; thus a stimulus that is smaller than is normally required is now able to elicit an action potential. However, because Na^+ channels are still not fully activated, the resulting action potential is still somewhat reduced from normal in amplitude and propagation velocity.¹⁸ In general, the later the second stimulus comes, the more the Na^+ channels are reactivated, and the more rapid the upstroke of the second action potential.

Reduced membrane excitability can occur in certain pathophysiological conditions, including genetic mutations that result in loss of Na^+ channel function, Na^+ channel blockade with class I antiarrhythmic drugs, and acute myocardial ischemia.¹⁹

Action potentials with reduced upstroke velocity resulting from partial inactivation of Na^+ channels are called “depressed fast responses.” Importantly, refractoriness in cells with reduced E_m can outlast voltage recovery of the action potential (i.e., the cell can still be refractory or partially refractory after the resting E_m returns to its most negative value).

REFRACTORINESS

During a cardiac cycle, once an action potential is initiated, the cardiomyocyte becomes inexcitable to stimulation (i.e., unable to initiate another action potential in response to a stimulus of threshold intensity) for some duration of time (which is generally slightly shorter than the duration of the “true” action potential duration) until its membrane

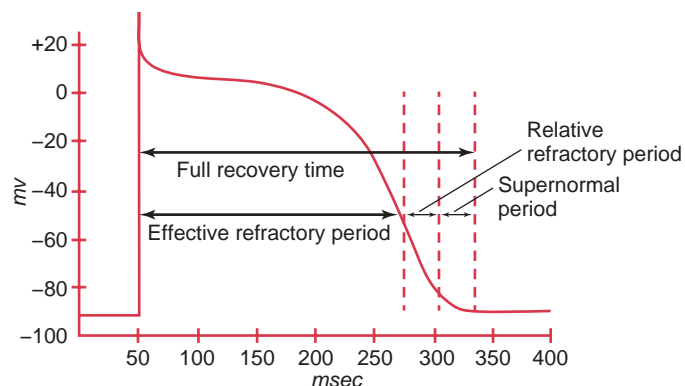


Fig. 1.4 Cellular Refractory Periods. See text for details. (Redrawn from Rosen MS, Wit AL, Hoffman BF. Electrophysiology and pharmacology of cardiac arrhythmias. I. Cellular electrophysiology of the mammalian heart. *Am Heart J*. 1974;88:380.)

has repolarized to a certain level. With repolarization, Na^+ channels normally recover rapidly from inactivation (within 10 milliseconds) and are ready to open again. Refractoriness is determined, in part, by the action potential duration and the E_m , and the degree of refractoriness primarily reflects the number of Na^+ channels that have recovered from their inactive state. The period of refractoriness to stimulation is physiologically necessary for the mechanical function of the heart; it allows only gradual recovery of excitability, thus permitting relaxation of cardiac muscle before subsequent activation. In addition, the refractory period acts as a protective mechanism by preventing multiple, compounded action potentials from occurring (i.e., it limits the frequency of depolarization and heart rate). Therefore refractoriness is a determinant of susceptibility to arrhythmias. In general, shorter refractoriness facilitates reentry and arrhythmias.⁹

There are different levels of refractoriness during the action potential (Fig. 1.4). During the *absolute refractory period* (which extends over phases 0, 1, 2, and part of phase 3 of the action potential), no stimulus, regardless of its strength, can reexcite the cell. After the absolute refractory period, a stimulus can cause some cellular depolarization, but it does not lead to a propagated action potential. The sum of this period (which includes a short interval of phase 3 of the action potential) and the absolute refractory period is termed the *effective refractory period* (ERP, ending during phase 3 at an E_m of approximately -60 mV). The ERP is followed by the *relative refractory period*, which extends over the middle and late parts of phase 3 (at an E_m of approximately -60 mV during phase 3) to the end of phase 3 of the action potential. During the relative refractory period, initiation of a second action potential is more difficult but not impossible; a larger-than-normal stimulus can result in activation of the cell and lead to a propagating action potential (Fig. 1.5). However, the upstroke of the new action potential is less steep and of lower amplitude and its conduction velocity is reduced compared with normal. As noted, there is a brief period in phase 3, the supernormal period, during which excitation is possible in response to an otherwise subthreshold stimulus (supernormal excitability).¹⁸

In pacemaking tissues, I_{Na} is predominantly absent and excitability is mediated by the activation of I_{CaL} . After inactivation, the transition of Ca^{2+} channels from the inactivated to the closed resting state (i.e., recovery from inactivation) is relatively slow. The time constant for recovery from inactivation depends on both the E_m and the intracellular Ca^{2+} concentration (typically 100 to 200 milliseconds at -80 mV and low intracellular Ca^{2+} concentration). This means that I_{CaL} must recover from inactivation between action potentials. As a result, excitability in

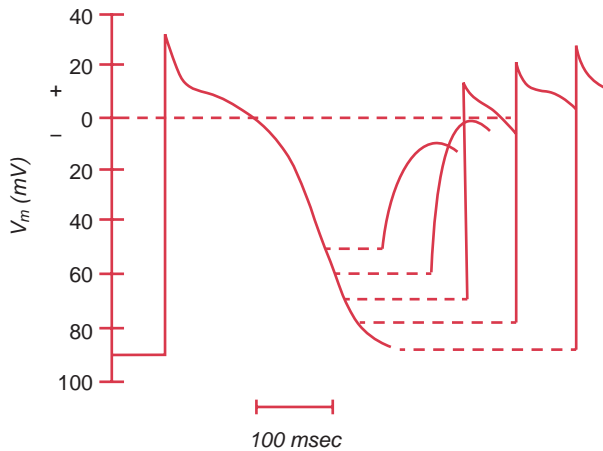


Fig. 1.5 Excitability as a Function of Latency. The changes in action potential amplitude and shape of the upstroke as action potentials are initiated at different stages of the relative refractory period of the preceding excitation. (Redrawn from Rosen MS, Wit AL, Hoffman BF. Electrophysiology and pharmacology of cardiac arrhythmias. I. Cellular electrophysiology of the mammalian heart. *Am Heart J*. 1974;88:380.)

pacemaking cells may not be recovered by the end of phase 3 of the action potential and full restoration of maximum diastolic potential because L-type Ca^{2+} channels require longer time to recovery from inactivation to be able to mediate the upstroke of a new action potential. In other words, sinus and AV nodal cells remain refractory for a time interval that is longer than the time it takes for full membrane repolarization to occur, a phenomenon termed *postrepolarization refractoriness*. This can also occur in working myocardium during some disease states such as myocardial infarction.

PROPAGATION

Cardiac excitation involves generation of the action potential by individual cells, followed by propagation of the electrical impulse along the cardiac muscle fiber and rapidly from cell to cell throughout the cardiac tissue. Conduction velocity refers to the speed of propagation of the action potential through cardiac tissue. The conduction velocity varies in cardiac tissues, ranging from 0.05 m/s in the atrioventricular node (AVN), to 0.5 m/s in atrial and ventricular working myocardium, 2 m/s in the bundle branches, and up to 4 m/s in Purkinje fibers.²⁰ In most regions of the heart, conduction does not occur as a continuous process; rather, the propagating electrical wavefronts interact with structural boundaries that exist at the cellular level (cell membranes, intercellular gap junctions, the three-dimensional [3-D] arrangement of cardiomyocytes), as well as at the more macroscopic level (microvasculature, connective tissue barriers, trabeculation).^{21,22}

Intracellular Propagation

Once initiated, the action potential propagates along the cell membrane until the entire cardiomyocyte is depolarized. The velocity of propagation increases with increasing cell diameter, action potential amplitude, and the initial rate of the rise of the action potential.

An action potential traveling along a cardiac muscle fiber is propagated by local circuit currents, much as it does in nerve and skeletal muscle. Conduction velocity along the cardiac fiber is directly related to the action potential amplitude (i.e., the voltage difference between the fully depolarized and the fully polarized regions) and the rate of change of potential (i.e., the rate of rise of phase 0 of the action potential

[dV/dt]). These factors depend on the amplitude of I_{Na} , which, in turn, is directly related to the E_m at the time of stimulation, the availability of Na^+ channels for stimulation, and the size of the Na^+ electrochemical potential gradient across the cell membrane.

Normally, the charge flow across depolarizing ion channels (I_{Na}) is significantly larger than the charge needed to excite the same cell, providing sufficient extra stimulatory current to drive propagation forward. This property (referred to as “propagation reserve” or “safety of propagation”) helps to maintain action potential propagation under different physiological and pathophysiological conditions.²³ Working atrial and ventricular myocardium and, in particular, Purkinje fibers have high concentrations of Na^+ channels (Purkinje fibers contain up to 1 million Na^+ channels per cell), which help to generate a large depolarizing current flow (I_{Na}) during the action potential. The large I_{Na} spreads quickly within and between cells to support rapid conduction.

Reduction of membrane excitability leads to a reduction in the rate or amplitude of depolarization (I_{Na}) during phase 0 of the action potential. Conduction velocity decreases monotonically with progressive reduction of membrane excitability. When the safety factor for conduction falls to less than 1 (i.e., the source current becomes less than the current necessary for excitation of downstream tissue), conduction can no longer be sustained, and failure (conduction block) occurs.

In tissues with slow response action potentials (sinus and AV nodes), the upstroke of the action potential is formed by I_{CaL} instead of I_{Na} . Because I_{CaL} has lower amplitude and slower activation kinetics than I_{Na} , slow response action potentials exhibit reduced amplitudes and upstroke velocities. Hence slow conduction (approximately 0.1 to 0.2 m/s) and prolonged refractoriness are characteristic features of nodal tissues. These cells also have a reduced safety factor for conduction, which means that the stimulating efficacy of the propagating impulse is low, and conduction block occurs easily.

Intercellular Propagation

Propagation of action potentials from one cell to adjacent cells is achieved by direct ionic current spread (without electrochemical synapses) via specialized, low resistance intercellular connections (gap junctional channels) located mainly in arrays within the intercalated disks. Gap junctions facilitate impulse propagation throughout the heart, so that the heart behaves electrically as a functional syncytium, resulting in a coordinated mechanical function.²²

Gap junctional channels connect neighboring cells and allow biochemical and low-resistance electrical coupling. Although the resistivity of the gap junctional membrane for the passage of ions and small molecules and for electrical propagation is several orders of magnitude lower compared with uncoupled cell membranes, gap junction coupling provides a resistance pathway that is several orders of magnitude higher than the cytoplasmic intracellular resistivity (conduction delay is approximately 0.21 to 0.27 milliseconds at gap junctions, and 0.05 to 0.1 milliseconds at the cell membrane).²⁴ As a consequence, impulse propagation along single cell chains of cardiomyocytes is saltatory, in which the high-resistance intercellular junctions alternate with the low cytoplasmic resistance. However, this feature is lost in intact multicellular tissue due to lateral gap junctional coupling which serves to average local small differences in activation times of individual cardiomyocytes at the excitation wavefront.¹⁹

The number, size, and molecular composition of the gap junction channels contribute to the specific propagation properties of a given tissue. Tissue-specific connexin expression and gap junction spatial distribution, as well as the variation in the structural composition of gap junction channels, allow for a greater versatility of gap junction physiological features and enable disparate conduction properties in cardiac tissue.²⁵

Three different connexins are prominently expressed in the atrial and ventricular myocardium: connexin 40 (Cx40), connexin 43 (Cx43), and connexin 45 (Cx45), named for their molecular masses. A fourth connexin has been described in the AVN (Cx31.9). Cx40 gap junction channels exhibit the largest conductance and Cx45 the smallest. The myocytes of the sinus node and AVN are equipped with small, sparse, and dispersed gap junctions containing Cx45, a connexin that forms low conductance channels, thus underlying the relatively poor intercellular coupling in nodal tissues, a property that is linked to slowing of conduction. In contrast, atrial myocardium gap junctions consist mainly of Cx43 and Cx40, ventricular myocardium of Cx43, and the Purkinje fibers of Cx40.^{24,25}

Importantly, there is a high redundancy in connexin expression in the heart with regard to conduction of electrical impulse, and a large reduction of intercellular coupling is required to cause major slowing of conduction velocity. It has been shown that a 50% reduction in Cx43 does not alter ventricular impulse conduction. Cx43 expression must decrease by 90% to affect conduction, but even then conduction velocity is reduced only by 20%.^{25,26}

Similar to its behavior during reduced membrane excitability, conduction velocity decreases monotonically with reduction in intercellular coupling. Of note, partial gap junctional uncoupling was shown to result in conduction velocities that are over an order of magnitude slower than those obtained during a maximal reduction of excitability before conduction failure develops.^{19,23}

An alternative to the generally accepted understanding of gap junction-mediated intercellular impulse propagation is the electric field mechanism (also referred to as “ephaptic transmission”). Electrical field coupling (ephaptic coupling) refers to the initiation of an action potential in a nonactivated downstream cell by the electrical field caused by an activated upstream cell. This model postulates that activation spreads along tracts of cardiac cells in a saltatory fashion driven by the negative potential that develops in the restricted cleft space between cells when an action potential develops in the prejunctional membrane. The large I_{Na} in the proximal side of an intercellular cleft at the intercalated disks (where Na^+ channels are concentrated) generates a negative extracellular potential within the cleft, which depolarizes the distal membrane and activates its Na^+ channels. Thus propagation can continue downstream in the absence of gap junctions, provided there is a large I_{Na} at the intercalated disk and a narrow (2 to 5 nm) intercellular cleft that separates the two opposing cells. Computer simulation studies suggest that, under certain conditions, ephaptic coupling may play a role in cardiac impulse propagation, and that ephaptic transmission can explain the insensitivity of conduction velocity to reduced intercellular gap junction coupling. However, the importance and contribution of ephaptic transmission to action potential propagation in normal cardiac tissue are currently unclear and remain difficult to define.^{22,24,25}

Anisotropic Conduction

Anisotropy refers to directionally dependent conduction velocity. Isotropic conduction is uniform in all directions; anisotropic conduction is not. Anisotropy is a normal feature of heart muscle and is related to the differences in longitudinal and transverse conduction velocities, which are attributable to the lower resistivity of myocardium in the longitudinal (parallel to the long axis of the myocardial fiber bundles) versus the transverse direction (eFig. 1.1).²⁵

In normal adult working myocardium, a given cardiomyocyte is electrically coupled to an average of approximately 11 adjacent cells, with gap junctions being predominantly localized at the intercalated discs at the ends of the rod-shaped cells. Lateral (side-to-side) gap junctions in nondisc lateral membranes of cardiomyocytes are much less abundant and occur more often in atrial than ventricular tissues.

This particular subcellular distribution of gap junctions is a main determinant of anisotropic conduction in the heart; a wavefront must traverse more cells in the transverse direction than over an equivalent distance in the longitudinal direction because cell diameter is much smaller than cell length. In addition, less intercellular gap junctional coupling occurs and hence greater resistance and slower conduction transversely than longitudinally.^{19,24}

A further level of anisotropy exists in the normal working myocardium secondary to discontinuities of 3-D myocyte architecture at the tissue scale. The myocardium is not a continuum. Distinct layers or bundles of myocytes are evident in the atria and ventricles, at dimensions ranging from approximately 100 μ m to several millimeters.²² The myocardial tissue is not uniformly connected transverse to the myofiber direction. Ventricular myocytes are arranged in layers four to six cells thick (referred to as sheets, myolaminae, or sheetlets) that are separated by clefts of connective tissue, across which there is little direct cell-to-cell coupling. These layers form a branching network. In addition to the laminar myocyte architecture, transmural myofiber rotation adds further complexity to cellular organization. In a normal heart, myocardial fiber direction changes (gradually) from the endocardium to the epicardium by nearly 90 degrees. A lower axial resistivity in the longitudinal myofiber and myolaminar orientation than in the transverse direction further exacerbates electrical anisotropy.²²

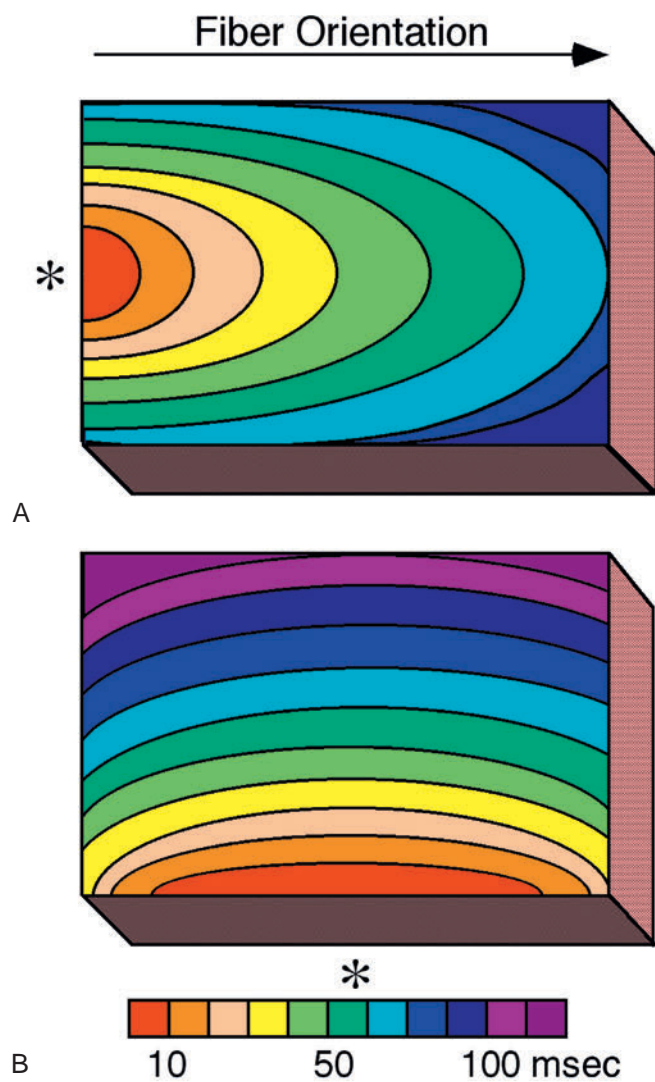
Source-Sink Relationship

Source-sink relationships reflect the interplay between the main factors influencing source current (the rate of rise of the upstroke and amplitude of the action potential) and those that influence the current requirements of the sink (the membrane resistance, the difference between the resting and threshold potentials, cell-to-cell coupling, and tissue geometry).

During action potential propagation, an excited cell serves as a source of electrical charge for depolarizing neighboring unexcited cells. The requirements of adjacent resting cells to reach the threshold E_m constitute an electrical sink (load) for the excited cell. For propagation to succeed, the excited cell must provide sufficient charge to bring the E_m at a site in the sink from its diastolic value to the threshold. Once threshold is reached and an action potential is generated, the load on the excited cell is removed, and the newly excited cell switches from being a sink to being a source for the downstream tissue, thus perpetuating the process of action potential propagation. Action potentials are “regenerative” because they can be conducted over large distances without attenuation. Propagation will continue to be successful as long as the active sources can generate enough current to satisfy local sinks. Alternatively, if the sink overwhelms the source, propagation will fail.²⁷

The current provided by the source must reach the sink. The pathway between the source and the sink includes intracellular resistance (provided by the cytoplasm) and intercellular resistance (provided by the gap junctions). Extracellular resistance plays a role, but it can often be neglected. The coupling resistance is mainly determined by resistance of the gap junctions. Therefore the number and distribution of gap junctions, as well as the conductance of the gap junction proteins (connexins) and the geometry of the source-sink relationship, are important factors for propagation of the action potential.^{21,28}

A major cause for source-sink mismatch is an abrupt change in the structure of the cellular network, such as that which occurs at the Purkinje fiber-ventricular muscle junction. Each Purkinje fiber (source) transfers the impulse to hundreds or thousands of ventricular cardiomyocytes (sink). This mismatch can potentially result in dispersion of the source current to many neighboring cells (sink), and in each of these the accumulated charge may be too low to trigger an action potential, leading to conduction failure.^{12,29} Nonetheless, in a



eFig. 1.1 Anisotropic Conduction. Progression of activation wavefronts in blocks of ventricular myocardium with longitudinal fiber orientation are shown. A wavefront stimulated (*asterisk*) at the left edge progresses more rapidly (wider isochrone spacing, [A]) than one starting perpendicularly (B) because of more favorable conduction parameters in the former direction.

normal heart, the local structure of the cellular network and abrupt changes in geometric properties are not of magnitude to provide sufficient sink-source mismatch and cause conduction block of the normal action potential because the safety factor for conduction is large (i.e., there is a large excess of activating current over the amount required for propagation). However, when the action potential is abnormal, the unexcited area has decreased excitability (e.g., in the setting of acute ischemia), or both, anatomical impediments can result in conduction block.^{19,30}

Reduction of intercellular coupling can improve the safety of propagation despite the presence of significant source-sink mismatch. For example, this is realized in the sinus node, where a small current source (sinus node) meets a large sink (atrium). At the sinus node/atrium border, there is only little expression of connexins, which protects the excitatory current generated in the sinus node from downstream dissipation.²⁴

Importantly, such tissue structures can exhibit directional asymmetry in source-sink relationships. The source is smaller than the sink in the orthodromic direction but larger than the sink in the opposite direction. Depending on the size of the source-sink mismatch, this results in either local conduction delay or conduction block at the junction during orthodromic conduction.^{27,31,32}

Furthermore, the shape of the wavefront is a major determinant of efficiency of propagation. Due to source-sink balance, conduction velocity is dependent on wave curvature (Fig. 1.6). A convex wavefront, as might be observed after point stimulation, has a smaller source and a larger sink because the local excitatory current supplied by the cells in the front of a convex wave diverges into a larger membrane area downstream. Conversely, a concave activation front produces a source-sink mismatch that favors the source, resulting in a high safety factor and more rapid impulse transmission. Hence, as wavefront curvature increases, conduction velocity decreases.^{24,33}

Safety Factor for Conduction

The safety factor for conduction predicts the success of action potential propagation and is based on the source-sink relationship. The *safety factor* is defined as the ratio of the current generated by the depolarizing ion channels of a cell (source) to the current consumed during the excitation cycle of a single cell in the tissue (sink). Thus the safety factor

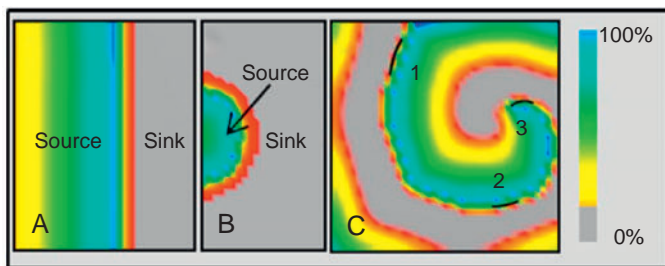


Fig. 1.6 Wave Curvature and Source-Sink Balance. (A) Flat wavefronts have source-sink balance, whereas (B) convex wavefronts have a smaller source and a larger sink. (C) The curvature of a spiral wave increases as one moves along the wavefront toward the spiral center (the curvature at point 3 is greater than at point 2, which is greater than at point 1). At the innermost aspect of the wavefront, the source is too small to excite the adjacent sink; the result is a core of unexcited cells around which rotation occurs. Color bar indicates percentage depolarization; gray indicates subthreshold voltage. (From Spector P. Principles of cardiac electric propagation and their implications for re-entrant arrhythmias. *Circ Arrhythmia Electrophysiol.* 2013;6:655–661.)

for propagation is proportional to the excess of source current over the sink needs. By this definition, conduction fails when the safety factor drops to less than 1 and becomes increasingly stable as it rises to more than 1.

Membrane excitability, intercellular coupling, and tissue structure have a huge influence on the safety of propagation. The safety factor decreases monotonically as membrane excitability is reduced. In addition, the safety factor tends to be low for propagation that occurs from a smaller cell to a larger cell or from a relatively small number of cells to a larger number of cells.

On the other hand, although reduction of intercellular coupling between the source cell and the sink leads to slowing of conduction, it is associated with improved safety of conduction. Uncoupling the source cells from neighboring cells prevents the source from becoming overwhelmed by sink demand. As cells become less coupled, there is greater confinement of depolarizing current to the depolarizing source cell, with less electrotonic load and axial flow of charge to the downstream “sink” cells. As a result, individual cells depolarize with a high margin of safety, but conduction proceeds with long intercellular delays. At such low levels of coupling, conduction is very slow but, paradoxically, very robust. Due to the high safety factor, extremely slow conduction velocities can be sustained in tissue with greatly reduced intercellular coupling.^{25,27,31,34}

EXCITATION-CONTRACTION COUPLING

Excitation-contraction coupling describes the physiological process by which electrical stimulation of the cardiomyocytes (the action potential) results in a mechanical response (muscle contraction). The contraction of a cardiac myocyte is governed primarily by intracellular Ca^{2+} concentration (Fig. 1.7). Ca^{2+} enters the cell during the plateau phase of the action potential through the L-type Ca^{2+} channels that line areas of specialized invaginations known as transverse (T) tubules. Although the rise in intracellular Ca^{2+} is small and not sufficient to induce contraction, the small amount of Ca^{2+} entering the cell via I_{CaL} triggers a massive release of Ca^{2+} from the sarcoplasmic reticulum (the major store for Ca^{2+}) into the cytosol by opening the ryanodine receptor 2 (RyR2) channels (present in the membrane of the sarcoplasmic reticulum) in a process known as *calcium-induced calcium release* (CICR). Approximately 75% of Ca^{2+} present in the cytoplasm during contraction is released from the sarcoplasmic reticulum.

Each junction between the sarcolemma (T tubule) and sarcoplasmic reticulum, where 10 to 25 L-type Ca^{2+} channels and 100 to 200 RyRs are clustered, constitutes a local Ca^{2+} signaling complex (called a “couplon”). When a Ca^{2+} channel opens, local cytosolic Ca^{2+} concentration rises in less than 1 millisecond to 10 to 20 μM in the junctional cleft, and this activates RyR2 to release Ca^{2+} from the sarcoplasmic reticulum. The close proximity of the RyR2 to the T tubule enables each L-type Ca^{2+} channel to activate four to six RyR2s and generate a “ Ca^{2+} spark.” Ca^{2+} influx via I_{CaL} simultaneously activates approximately 10,000 to 20,000 couplons in each ventricular cardiomyocyte with every action potential.³⁵

CICR raises cytosolic Ca^{2+} levels from approximately 10^{-7} M to approximately 10^{-5} M. The free Ca^{2+} binds to troponin C, a component of the thin filament regulatory complex, and thus causes a conformational change in the troponin-tropomyosin complex, such that troponin I exposes a site on the actin molecule that is able to bind to the myosin ATPase located on the myosin head. This binding results in ATP hydrolysis that supplies energy for a conformational change to occur in the actin-myosin complex. The result of these changes is a movement (ratcheting) between the myosin heads and the actin, such that the actin and myosin filaments slide past each other and thereby shorten

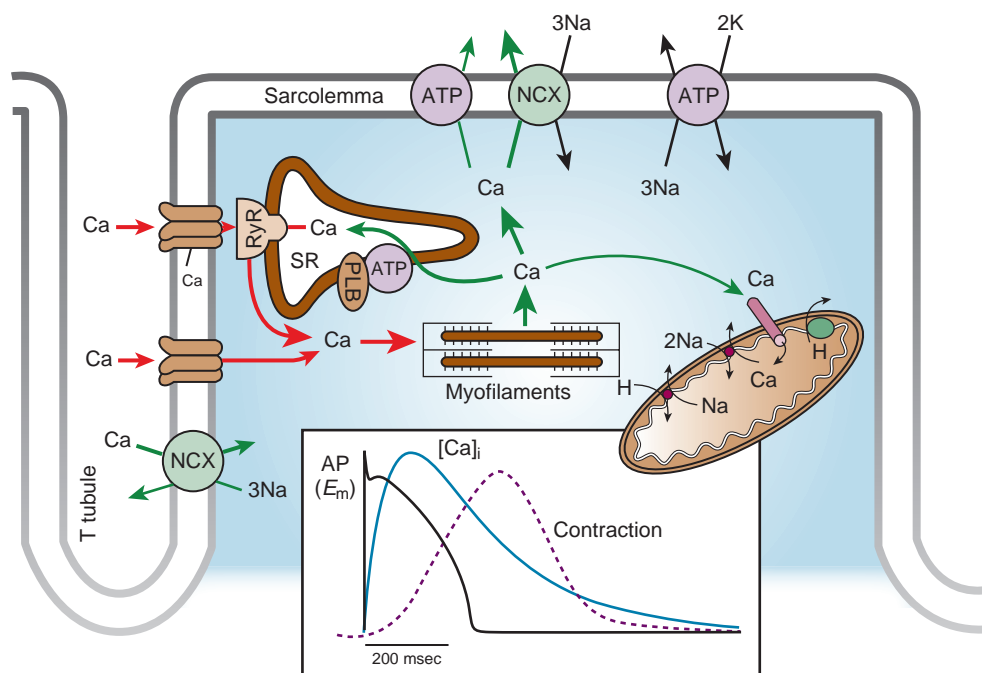


Fig. 1.7 Excitation-Contraction Coupling. *Inset:* Diagram showing relationship between transmembrane action potential (AP), Ca^{2+} transient, and the contractile response in a ventricular muscle cell. See text for details. ATP, Ca^{2+} adenosine triphosphatase; NCX, $\text{Na}^{+}\text{-Ca}^{2+}$ exchanger; PLB, phospholamban; RyR, ryanodine receptor channel; SR, sarcoplasmic reticulum. (Modified with permission from Bers DM. Cardiac excitation-contraction coupling. *Nature*. 2002;415:198–205.)

the sarcomere length. Ratcheting cycles continue to occur as long as cytosolic Ca^{2+} levels remain elevated.

CICR typically induces release of approximately 50% to 60% of sarcoplasmic reticulum Ca^{2+} content. RyR2 channels are inactivated by a feedback mechanism from the rising Ca^{2+} concentration in the cleft and, more importantly, by the decline of sarcoplasmic reticulum Ca^{2+} content (a process referred to as luminal Ca^{2+} -dependent deactivation). This process ensures that the sarcoplasmic reticulum never is fully depleted of Ca^{2+} physiologically.

Relaxation requires the removal of Ca^{2+} from the cytosol, a process vital for enabling cardiac chamber relaxation and filling, as well as for prevention of arrhythmias. At the end of phase 2 of the action potential, Ca^{2+} entry into the cell slows, and most of the surplus Ca^{2+} in the cytosol is resequenced into the sarcoplasmic reticulum by the SERCA, the activity of which is controlled by the phosphoprotein phospholamban. In addition, some of the Ca^{2+} is extruded from the cell by the sarcolemmal $\text{Na}^{+}\text{-Ca}^{2+}$ exchanger and, to a minor degree, the cell membrane Ca^{2+} ATPase, to balance the Ca^{2+} that enters the cell via I_{CaL} . As the cytosolic Ca^{2+} concentration drops, Ca^{2+} dissociates rapidly from the myofilaments, thus inducing a conformational change in the troponin complex leading to troponin I inhibition of the actin binding site. At the end of the cycle, a new ATP binds to the myosin head and displaces the adenosine diphosphate, and the initial sarcomere length is restored, thus ending contraction. Recurring Ca^{2+} release-uptake cycles provide the basis for periodic elevations of cytosolic Ca^{2+} concentration and contractions of myocytes, hence for the orderly beating of the heart.

REFERENCES

1. Zaza A. Control of the cardiac action potential: the role of repolarization dynamics. *J Mol Cell Cardiol*. 2010;48:106–111.
2. Spector P. Principles of cardiac electric propagation and their implications for re-entrant arrhythmias. *Circ Arrhythmia Electrophysiol*. 2013;6:655–661.
3. Grant AO. Cardiac ion channels. *Circ Arrhythmia Electrophysiol*. 2009;2:185–194.
4. Grant AO. Basic electrophysiology. *Card Electrophysiol Clin*. 2010;2:325–340.
5. Nerbonne JM. Molecular basis of functional myocardial potassium channel diversity. *Card Electrophysiol Clin*. 2016;8:257–273.
6. Adler A, Gollob MH. A practical guide to early repolarization. *Curr Opin Cardiol*. 2015;30:8–16.
7. Chen L, Sampson KJ, Kass RS. Cardiac delayed rectifier potassium channels in health and disease. *Card Electrophysiol Clin*. 2016;8:307–322.
8. Voigt N, Dobrev D. Atrial-selective potassium channel blockers. *Card Electrophysiol Clin*. 2016;8:411–421.
9. Belardinelli L, Giles WR, Rajamani S, et al. Cardiac late Na^{+} current: proarrhythmic effects, roles in long QT syndromes, and pathological relationship to CaMKII and oxidative stress. *Heart Rhythm*. 2015;12:440–448.
10. Wu W, Sanguinetti MC. Molecular basis of cardiac delayed rectifier potassium channel function and pharmacology. *Card Electrophysiol Clin*. 2016;8:275–284.
11. Boyden PA, Dun W, Robinson RB. Cardiac Purkinje fibers and arrhythmias; The GK Moe Award Lecture 2015. *Heart Rhythm*. 2016;13:1172–1181.
12. Boyden PA, Hirose M, Dun W. Cardiac Purkinje cells. *Heart Rhythm*. 2010;7:127–135.
13. Workman AJ, Marshall GE, Rankin AC, et al. Transient outward K^{+} current (ITO) reduction prolongs action potentials and promotes afterdepolarisations: a dynamic-clamp study in human and rabbit cardiac atrial myocytes. *J Physiol*. 2012;17:4289–4305.
14. Bartos DC, Grandi E, Ripplinger CM. Ion channels in the heart. *Compr Physiol*. 2015;5:1423–1464.

15. Murphy C, Lazzara R. Current concepts of anatomy and electrophysiology of the sinus node. *J Interv Card Electrophysiol*. 2016;46:9–18.
16. DiFrancesco D, Noble D. The funny current has a major pacemaking role in the sinus node. *Heart Rhythm*. 2012;9:299–301.
17. DiFrancesco D, Noble D. Rebuttal: ‘The funny current in the context of the coupled clock pacemaker cell system. *Heart Rhythm*. 2012;9:457–458.
18. Elizari MV, Schmidberg J, Atenza A, et al. Clinical and experimental evidence of supernormal excitability and conduction. *Curr Cardiol Rev*. 2014;10:202–221.
19. Kléber AG, Rudy Y. Basic mechanisms of cardiac impulse propagation and associated arrhythmias. *Physiol Rev*. 2004;84:431–488.
20. Temple IP, Inada S, Dobrzynski H, et al. Connexins and the atrioventricular node. *Heart Rhythm*. 2012;10:297–304.
21. Dhillon PS, et al. Relationship between gap-junctional conductance and conduction velocity in mammalian myocardium. *Circ Arrhythmia Electrophysiol*. 2013;6:1208–1214.
22. Smaill BH, Zhao J, Trew ML. Three-dimensional impulse propagation in myocardium: Arrhythmogenic mechanisms at the tissue level. *Circ Res*. 2013;112:834–848.
23. Kleber AG. Role of the cardiac sodium current in excitability and conduction. *Card Electrophysiol Clin*. 2014;6:657–664.
24. Dhein S, et al. Remodeling of cardiac passive electrical properties and susceptibility to ventricular and atrial arrhythmias. *Front Physiol*. 2014;5: 1–13.
25. Kleber AG, Saffitz JE. Role of the intercalated disc in cardiac propagation and arrhythmogenesis. *Front Physiol*. 2014;5:404.
26. Hulsmans M, et al. Macrophages facilitate electrical conduction in the heart. *Cell*. 2017;169:510–522.e20.
27. Unudurthi SD, Wolf RM, Hund TJ. Role of sinoatrial node architecture in maintaining a balanced source-sink relationship and synchronous cardiac pacemaking. *Front Physiol*. 2014;5:446.
28. Delmar M, Liang FX. Connexin43 and the regulation of intercalated disc function. *Heart Rhythm*. 2012;9:835–838.
29. Syed FF, Hai JJ, Lachman N, et al. The infrahisian conduction system and endocavitary cardiac structures: Relevance for the invasive electrophysiologist. *J Interv Card Electrophysiol*. 2014;39: 45–56.
30. Rohr S, et al. Role of gap junctions in the propagation of the cardiac action potential. *Cardiovasc Res*. 2004;62:309–322.
31. Nikolaidou T, Aslanidi OV, Zhang H, et al. Structure-function relationship in the sinus and atrioventricular nodes. *Pediatr Cardiol*. 2012;33:890–899.
32. Majumder R, Pandit R, Panfilov AV. Turbulent electrical activity at sharp-edged inexcitable obstacles in a model for human cardiac tissue. *Am J Physiol Heart Circ Physiol*. 2014;307: H1024–H1035.
33. Ciaccio EJ, Coromilas J, Wit AL, et al. Formation of functional conduction block during the onset of reentrant ventricular tachycardia. *Circ Arrhythm Electrophysiol*. 2016;9:e004462.
34. Kléber AG. Gap junctions and conduction of cardiac excitation. *Heart Rhythm*. 2011;8:1981–1984.
35. Wu P, et al. Structural basis for the gating mechanism of the type 2 ryanodine receptor RyR2. *Science*. 2016;80:354. aah5324.

Cardiac Ion Channels

OUTLINE

Sodium Channels, 16

- Structure and Physiology, 16
- Function, 18
- Regulation, 18
- Pharmacology, 18
- Inherited Channelopathies, 19
- Acquired Diseases, 22

Potassium Channels, 22

- Structure and Physiology, 22
- Function, 24
- Transient Outward Potassium Current, 24
- Ultrarapidly Activating Delayed Outward Rectifying Current, 27
- Rapidly Activating Delayed Outward Rectifying Current, 27
- Slowly Activating Delayed Outward Rectifying Current, 29
- Inward Rectifying Current, 31
- Acetylcholine-Activated Potassium Current, 32
- Adenosine Triphosphate-Sensitive Potassium Current, 33
- Two-Pore Potassium Channels, 36
- Small-Conductance Calcium-Activated Potassium Channels, 36

Calcium Channels, 37

- Structure and Physiology, 37
- The α_1 Subunit, 38
- The β Subunit, 38
- The $\alpha_2\delta$ Subunit, 38
- The γ Subunit, 39

Cardiac L-Type Calcium Current, 39

T-Type Calcium Current, 41

Cardiac Pacemaker Current, 42

- Structure and Physiology, 42
- Function, 42
- Regulation, 43
- Pharmacology, 43
- Inherited Channelopathies, 43
- Acquired Diseases, 43

Sarcoplasmic Reticulum Calcium Release Channels (Ryanodine Receptor 2), 43

- Structure and Physiology, 43
- Function, 44
- Regulation, 45
- Pharmacology, 45
- Inherited Channelopathies, 46
- Acquired Diseases, 46

Cardiac Gap Junctions, 46

- Structure and Physiology, 46
- Function, 47
- Regulation, 48
- Pharmacology, 48
- Inherited Channelopathies, 48
- Acquired Diseases, 48

Ion channels are pore-forming membrane proteins that regulate the flow of ions passively down their electrochemical gradient across the membrane. Ion channels are present on all membranes of cells (plasma membrane) and intracellular organelles (nucleus, mitochondria, endoplasmic reticulum). There are more than 300 types of ion channels in a living cell. The channels are not randomly distributed in the membrane but tend to cluster at the intercalated disc in association with modulatory subunits.

Ion channels are distinguished by two important characteristics: ion permeation selectivity and gating kinetics. Ion channels can be classified by the strongest permeant ion (sodium [Na^+], potassium [K^+], calcium [Ca^{2+}], and chloride [Cl^-]), but some channels are less selective or are not selective, as in gap junctional channels. Size, valency, and hydration energy are important determinants of selectivity. Na^+ channels have a selectivity ratio for Na^+ to K^+ of 12:1. Voltage-gated K^+ and Na^+ channels exhibit more than 10-fold discrimination against other monovalent and divalent cations, and voltage-gated Ca^{2+} channels exhibit more than 1000-fold discrimination against Na^+ and K^+ ions and are impermeable to anions. Ions move through the channel pore at a very high rate (more than 10^6 ions/s).

Gating is the mechanism of opening and closing of ion channels and represents time-dependent transitions among distinct conformational states of the channel protein resulting from molecular movements, most commonly in response to variations in voltage gradient across the plasma membrane (termed voltage-dependent gating) and, less commonly, in response to specific ligand molecules binding to the extracellular or intracellular side of the channel (ligand-dependent gating) or in response to mechanical stress such as stretch, pressure, shear, or displacement (mechanosensitive gating).

Importantly, channel opening and closing are not instantaneous but usually take time. The transition from the resting (closed) state to the open state is called activation. Once opened, channels do not remain in the open state, but instead they undergo conformational transition in a time-dependent manner to a stable nonconducting (inactivated) state. Inactivated channels are incapable of reopening and must undergo recovery or reactivation process back to the resting state to regain their ability to open. Inactivation curves of the various voltage-gated ion channel types differ in their slopes and midpoints of inactivation and can overlap, in which case a steady-state or noninactivating current flows.

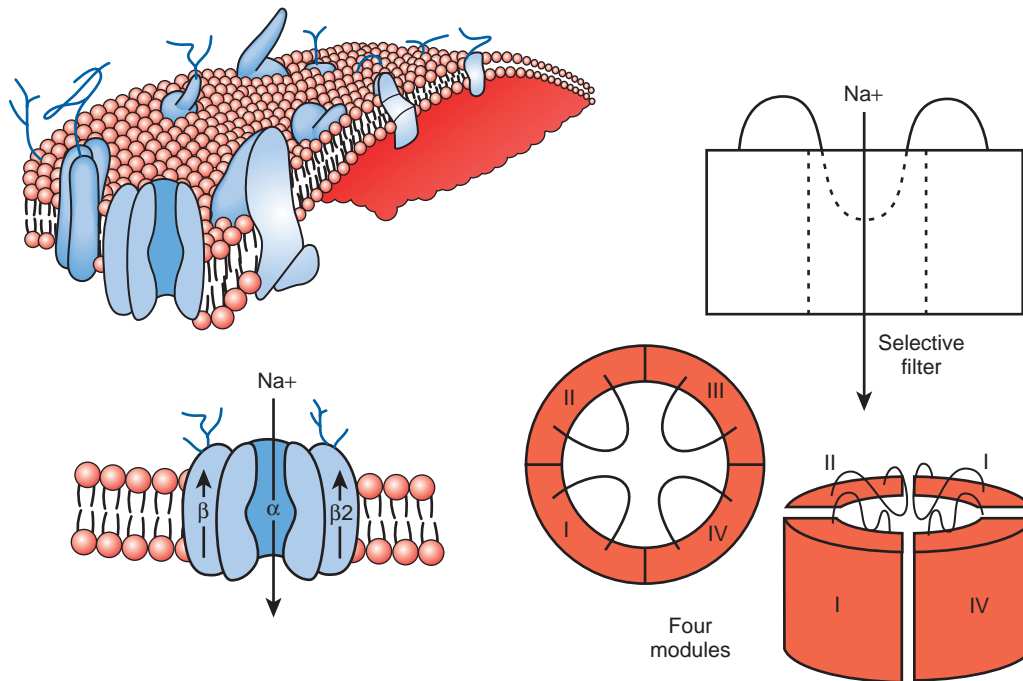


Fig. 2.1 The Sodium Channel Macromolecular Complex. See text for discussion. (From Boussy T, Paparella G, de Asmundis C, et al. Genetic basis of ventricular arrhythmias. *Heart Fail Clin.* 2010;6:249–266.)

Ion channels differ with respect to the number of subunits of which they are composed and other aspects of structure. Many ion channels function as part of macromolecular complexes in which many components are assembled at specific sites within the membrane. For most ion channels, the pore-forming subunit is called the α subunit, whereas the auxiliary subunits are denoted β , γ , and so on. Most ion channels have a single pore; however, some have two.

It is important to note that although cardiomyocytes generally last the entire human lifetime, the half-lives of ion channels at the membrane are on the order of hours. The life cycle of cardiac ion channels encompasses many processes, starting from DNA transcription to translation into proteins, protein modification, protein oligomerization, channel transport to specific subdomains of the cell membrane (a process known as forward trafficking), and finally internalization for degradation or recycling (i.e., retrograde trafficking). Given the quick turnover of channels, the intracellular forward trafficking of channels constitutes a key regulatory step in controlling the current density of specific channels and offers targets for therapeutic manipulation of channel function in the treatment of heart disease. In addition, genetic channelopathies can result not only from mutations affecting channel structure and function but also from mutations leading to perturbation of any of the molecular processes involved in channel trafficking.

SODIUM CHANNELS

Structure and Physiology

The cardiac Na^+ channel complex is composed of a primary α and multiple ancillary β subunits. The approximately 2000-amino-acid α subunit contains the channel's ion-conducting pore and controls channel selectivity for Na^+ ions and voltage-dependent gating machinery. This subunit contains all the drug and toxin interaction sites identified to date.

Nine genes encode the α subunit of the Na^+ channel in humans ($\text{Na}_v1.1$ through $\text{Na}_v1.9$). $\text{Na}_v1.5$ is the principal cardiac isoform. $\text{Na}_v1.8$

and $\text{Na}_v1.9$ are primarily expressed peripheral sensory neurons, $\text{Na}_v1.4$ in skeletal muscle, and $\text{Na}_v1.6$ in the central nervous system.

$\text{Na}_v1.5$, encoded by the *SCN5A* gene, consists of four internally homologous domains (I to IV) that are connected to each other by cytoplasmic linkers (Fig. 2.1). Each domain consists of six membrane-spanning segments (S1 to S6), connected to each other by alternating intracellular and extracellular peptide loops. The four domains are arranged in a fourfold circular symmetry to form the channel. The extracellular loops between S5 and S6 (termed the P segments) have a unique primary structure in each domain (Fig. 2.2). The P segments curve back into the membrane to form an ion-conducting central pore whose structural constituents determine the selectivity and conductance properties of the Na^+ channel.¹

Four auxiliary β subunits ($\text{Na}_v\beta1$ to $\text{Na}_v\beta4$, encoded by the genes *SCN1B* to *SCN4B*, respectively) have been identified; each is a glycoprotein with a single membrane-spanning segment. The β subunits modulate density, kinetics, voltage dependence of activation and inactivation, as well as surface expression of the Na^+ channel.¹

Na^+ channels are the typical example of voltage-gated ion channels. Na^+ channels switch among three functional states: deactivated (closed), activated (open), and inactivated (closed), depending on the membrane potential (E_m). These channel states control Na^+ ion permeability through the channel into the cardiomyocyte. Na^+ channel activation allows Na^+ ion influx into the cell, and inactivation blocks the entry of Na^+ ions.

On excitation of the cardiomyocyte by electrical stimuli from adjacent cells, its resting E_m (approximately -85 mV) depolarizes. The positively charged S4 segment of each domain of the α subunit functions as the sensor of the transmembrane voltage; these segments are believed to undergo rapid structural conformational changes in response to membrane depolarization, thus leading to channel opening (activation) from its resting (closed) state and enabling a large and rapid influx of Na^+ (inward Na^+ current, I_{Na}) during the rapid upstroke (phase 0) of the action potential in atrial, ventricular, and Purkinje cardiomyocytes.²

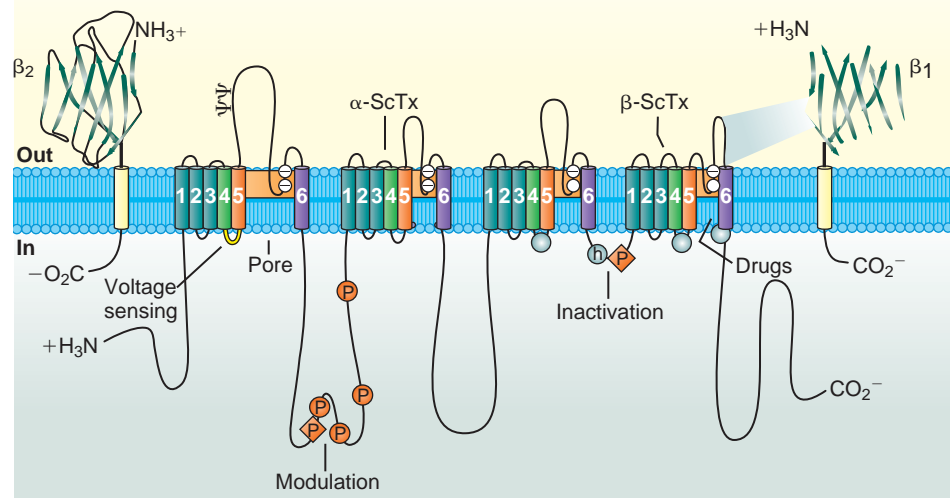


Fig. 2.2 Transmembrane Organization of Sodium Channel Subunits. The primary structures of the subunits of the voltage-gated ion channels are illustrated as transmembrane folding diagrams. Cylinders represent probable α -helical segments: S1 to S3, blue; S4, green; S5, orange; S6, purple; outer pore loop, shaded orange area. Bold lines represent the polypeptide chains of each subunit, with length approximately proportional to the number of amino acid residues in the brain sodium channel subtypes. The extracellular domains of the β 1 and β 2 subunits are shown as immunoglobulin-like folds. ψ shows sites of probable N-linked glycosylation. P represents sites of demonstrated protein phosphorylation by protein kinase A (red circles) and protein kinase C (red diamonds); h in the blue circle signifies an inactivation particle in the inactivation gate loop; the empty blue circles represent sites implicated in forming the inactivation gate receptor. The structure of the extracellular domain of the β subunits is illustrated as an immunoglobulin-like fold based on amino acid sequence homology to the myelin P0 protein. Sites of binding of α and β scorpion toxins (α -ScTx, β -ScTx) and a site of interaction between α and β 1 subunits also are shown. H_3N and NH_3 , Ammonia. (From Caterall WA, Maier SK. Voltage-gated sodium channels and electrical excitability of the heart. In Zipes DP, Jalife J, eds. *Cardiac Electrophysiology: From Cell to Bedside*. 5th ed. Philadelphia: Saunders; 2009:9–17.)

Normally, activation of Na^+ channels is transient; fast inactivation (closing of the pore) starts simultaneously with activation, but because inactivation is slightly slower than activation, the channels remain transiently open to conduct I_{Na} during phase 0 of the action potential before it closes. Each Na^+ channel opens very briefly (less than 1 millisecond) during phase 0 of the action potential; collectively, activation of the channels lasts a few milliseconds and is followed by fast inactivation.

Na^+ channel inactivation comprises different conformational states, including fast, intermediate, and slow inactivation. Fast inactivation is at least partly mediated by rapid occlusion of the inner mouth of the pore by the cytoplasmic interdomain linker between domains III and IV of the α subunit, which has a triplet of hydrophobic residues that likely functions as a hinged “latch” that limits or restricts Na^+ ions from passing through the pore. The carboxyl terminus (C-terminus) also plays an important role in the control of Na^+ channel inactivation and stabilizing the channels in the inactivated state by interacting with the loop linking domains III and IV. Of note, although most Na^+ channels open before inactivating, some actually inactivate without ever opening (a process known as closed-state inactivation).

Once inactivated, Na^+ channels do not conduct any more current and cannot be reactivated (reopened) until after recovery from inactivation. The recovery of the Na^+ channel to reopen is voltage dependent. Channel inactivation is removed when the E_m of the cell repolarizes during phase 4 of the action potential. The recovery of channels from inactivation is also time dependent; Na^+ channels typically activate

within 0.2 to 0.3 milliseconds and inactivate completely within 2 to 5 milliseconds.

Following recovery, Na^+ channels enter a closed state that represents a nonconducting conformation, which allows the channels to be activated again during the next action potential. The fraction of channels available for opening varies from almost 100% at a membrane potential of -90 mV and 50% at an E_m of -75 mV to almost 0% at $+40$ mV. Consequently, highly polarized (-80 to -90 mV) cell membranes can be depolarized rapidly by stimuli because more Na^+ channels reopen, whereas partially depolarized cells with potentials close to threshold -70 mV generate a much slower upstroke because of the inactivation of a proportion of Na^+ channels. Given that Na^+ channels are major determinants of conduction velocity, this velocity generally slows at a reduced E_m .

Na^+ channel activation, inactivation, and recovery from inactivation occur within a few milliseconds. At the end of phase 1 of the action potential, more than 99% of Na^+ channels transit from an open (activated) state to an inactivated state. However, very few Na^+ channels are not inactivated and may reactivate (reopen) during phase 3 of the action potential. The small current produced by these channels (less than 1% of the peak I_{Na}) is called the “window current” because it arises when the sarcolemma reaches a potential that is depolarized sufficiently to reactivate some channels, but not enough to cause complete inactivation. The voltage range for the window current is very restricted and narrow in healthy hearts, thus granting it a small role during the cardiac action potential.

In addition to these rapid gating transitions, Na^+ channels are also susceptible to slower inactivating processes (slow inactivation) if the membrane remains depolarized for a longer time. These slower events can contribute to the availability of active channels under various physiological conditions. Whereas fast-inactivated Na^+ channels recover rapidly (within 10 milliseconds) during the hyperpolarized interval between stimuli, slow inactivation requires much longer recovery times (ranging from hundreds of milliseconds to many seconds). The molecular movements leading to slow inactivation are less well understood. The P segments seem to play a key role in slow inactivation.

Some Na^+ channels occasionally show alternative gating modes consisting of isolated brief openings occurring after variable and prolonged latencies and bursts of openings, during which the channel opens repetitively for hundreds of milliseconds. The isolated brief openings are the result of occasional failure of inactivation. Prolonged opening or reopening of some Na^+ channels during phases 2 and 3 can result in a small late Na^+ current (I_{NaL}). Despite its minor contribution in healthy hearts, I_{NaL} can potentially play an important role in diseased hearts.³

Function

Na^+ channels play a pivotal role in the initiation, propagation, and maintenance of the normal cardiac rhythm. The I_{Na} determines excitability and conduction in atrial, His-Purkinje system (HPS), and ventricular myocardium. On membrane depolarization, the voltage-gated Na^+ channels respond within a millisecond by opening, thus leading to the very rapid depolarization of the cardiac cell membrane (phase 0 of the action potential), reflected by the fast (within tenths of a microsecond) subsequent opening of Na^+ channels triggering the excitation-contraction coupling. Na^+ entry during phase 0 of the action potential also modulates intracellular Na^+ levels and, through Na^+ - Ca^{2+} exchange, intracellular Ca^{2+} concentration and cell contraction.

Na^+ channel also plays a crucial role in the propagation of action potentials throughout the atrium, HPS, and ventricles. The opening of Na^+ channels in the atria underlies the P wave on the electrocardiogram (ECG), and in the ventricles I_{Na} underlies the QRS complex and enables a synchronous ventricular contraction. Because the upstroke of the electrical potential primarily determines the speed of conduction between adjacent cells, Na^+ channels are present in abundance in tissues where speed is of importance. Cardiac Purkinje cells contain up to 1 million Na^+ channels, a finding that illustrates the importance of rapid conductance in the heart.

Na^+ channels also make a contribution in the plateau phase (phase 2) and help determine the duration of the action potential. After phase 0 of the action potential, I_{Na} decreases to less than 1% of its peak value over the next several milliseconds because of voltage-dependent inactivation. This persistent or “late” inward I_{Na} (I_{NaL}), along with the L-type Ca^{2+} current (I_{CaL}), helps maintain the action potential plateau.

Furthermore, inactivation of the Na^+ channel is very important, as it prevents cells from being prematurely reexcited. With repolarization, the Na^+ channel normally recovers rapidly from inactivation (within 10 milliseconds) and is ready to open again. Hence Na^+ channels help determine the frequency of action potential firing. To a lesser extent, cardiac Na^+ channels are also present in the sinus node and the atrioventricular node (AVN), where they contribute to pacemaker activity.

Regulation

The regulatory proteins interacting with $\text{Na}_v1.5$ (Fig. 2.3) can be classified as follows: (1) anchoring-adaptor proteins (e.g., ankyrin-G, syntrophin proteins, multicopy suppressor of *gsp1* [MOG1]), which play roles only in trafficking and targeting the channel protein in specific membrane compartments; (2) enzymes interacting with and modifying

the channel structure (posttranslational modifications), such as protein kinases or ubiquitin ligases; and (3) proteins modulating the biophysical properties of $\text{Na}_v1.5$ on binding (e.g., caveolin-3, calmodulin, glycerol 3-phosphate dehydrogenase 1-like [G3PD1L], telethonin, Plakophilin-2). Coexpression of $\text{Na}_v1.5$ with its β subunits induces acceleration in the recovery from inactivation and enhancement of I_{Na} amplitude.⁴

The cardiac Na^+ channels are subject to phosphorylation and dephosphorylation by kinases or phosphatases. The intracellular linker between domains I and II contains eight consensus sites for cyclic adenosine monophosphate (cAMP)-dependent protein kinase A (PKA) phosphorylation. cAMP-dependent PKA and G protein stimulatory α subunit ($\text{Gs}\alpha$) modulate the function of expressed cardiac Na^+ channels on β -adrenergic stimulation and enhance I_{Na} .

In contrast, the activation of α -adrenergic stimulating protein kinase C (PKC) results in the attenuation of I_{Na} . The effect of PKC is largely attributable to phosphorylation of a highly conserved serine in the linker between domains III and IV. PKC reduces the maximal conductance of the channels and alters gating. Na^+ channels exhibit a hyperpolarizing shift in the steady-state availability curve, suggesting an enhancement of inactivation from closed states.

All subunits of the Na^+ channel are modified by glycosylation. The $\beta 1$ and $\beta 2$ subunits are heavily glycosylated, with up to 40% of the mass being carbohydrate. In contrast, the α subunit is only 5% sugar by weight. Sialic acid is a prominent component of the N-linked carbohydrate of the Na^+ channel. The addition of such a highly charged carbohydrate has predictable effects on the voltage dependence of gating through alteration of the surface charge of the channel protein.

Pharmacology

Na^+ channels are the targets for the action of class I antiarrhythmic drugs. Na^+ channel blockers bind to a specific receptor within the channel's pore. The binding blocks ion movement through the pore and stabilizes the inactivated state of Na^+ channels. Blockade of Na^+ channels tends to decrease tissue excitability and conduction velocity (by attenuating peak I_{Na}) and can shorten action potential duration (by attenuating late I_{Na}).

One important component in the action of antiarrhythmic drugs is a voltage-dependent change in the affinity of the drug-binding site (i.e., the channel is a modulated receptor). In addition, restricted access to binding sites can contribute to drug action, a phenomenon that has been called the guarded receptor model. Open and inactivated channels are more susceptible to block than resting channels, likely because of a difference in binding affinity or state-dependent access to the binding site. Consequently, binding of antiarrhythmic drugs occurs primarily during the action potential (known as use-dependent block), and the block dissipates after repolarization (i.e., in the interval between action potentials). When the time interval between depolarizations is insufficient for block to recover before the next depolarization occurs (secondary to either abbreviation of the interval between action potentials during fast heart rates or slow kinetics of the unbinding of the Na^+ channel blocker), block of Na^+ channels accumulates (resulting in an increased number of blocked channels and enhanced blockade). A drug with rapid kinetics produces less channel block with the subsequent depolarization than a drug with slower recovery. Use-dependent block is important for the action of antiarrhythmic drugs because it allows strong drug effects during fast heart rates associated with tachyarrhythmias but limits Na^+ channel block during normal heart rates. This property is known as use-dependence and is seen most frequently with the class IC agents, less frequently with the class IA drugs, and rarely with the class IB agents. Importantly, drug recovery kinetics can potentially be slowed by pathophysiological conditions such as membrane depolarization, ischemia, and acidosis.

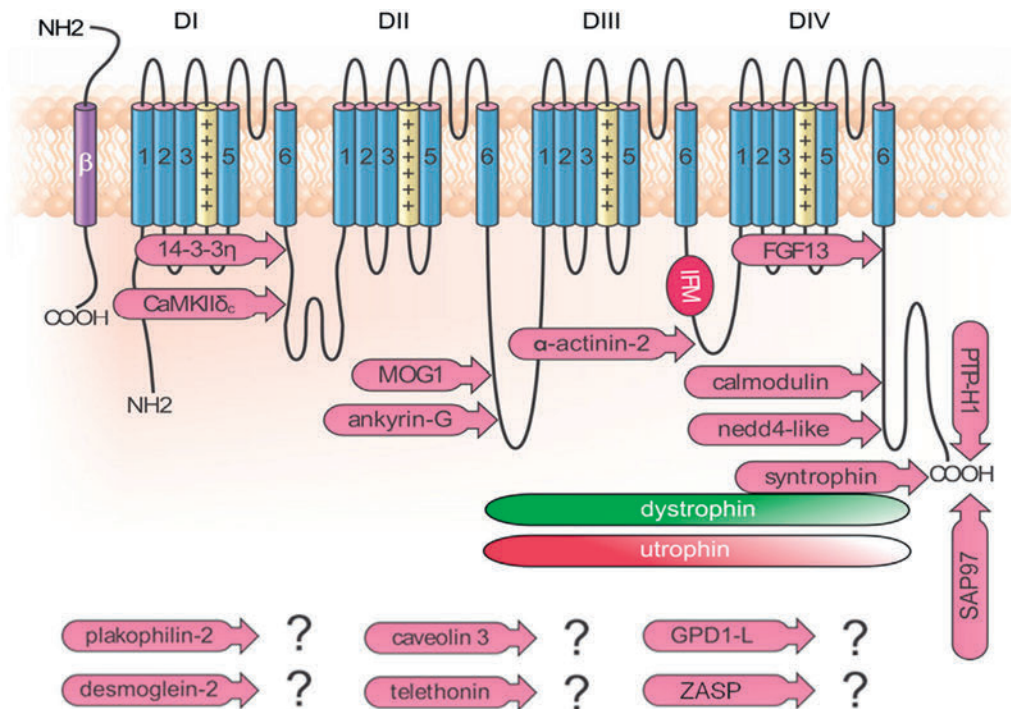


Fig. 2.3 Topology of Na_v1.5 and Its Interaction With Various Regulatory Proteins. The pore-forming α subunit of Na_v1.5 consists of four homologous domains (DI to DIV), connected together by intracellular and extracellular loops. Several regulatory proteins for Na_v1.5 are identified and their sites of interaction have been mapped on the α subunit of the Na_v1.5 channel. Many of these interactions are shown to take place at the intracellular loops or the C-terminus of Na_v1.5. For a few proteins that have been shown to associate with Na_v1.5, the sites of interaction on the Na_v1.5 channel are still unknown. *CaMKII*, Ca²⁺-calmodulin-dependent kinase II; *FGF13*, fibroblast growth factor 13; *GPD1-L*, glycerol-3-phosphate dehydrogenase 1-like; *MOG1*, multicopy suppressor of gsp1. (From Shy D, Gillet L, Abriel H. Cardiac sodium channel Na_v1.5 distribution in myocytes via interacting proteins: the multiple pool model. *Biochim Biophys Acta*. 2013;1833: 886–894.)

Class I antiarrhythmic drugs are classified into three groups according to rates of drug binding to and dissociation from the channel receptor. Class IC drugs (flecainide and propafenone) block both the open and inactivated Na⁺ channels (which is induced by membrane depolarization) and have the slowest kinetics of unbinding during diastole. The results are prolongation of conduction at normal heart rates and a further increase in the effect at more rapid rate (use-dependence).

The class IB agents (lidocaine, mexiletine, and tocainide) block both open and inactivated Na⁺ channels and dissociate from the channel more rapidly than other class I drugs. As a consequence, class IB drugs exhibit minimal or no effects on the Na⁺ channels in normal tissue but cause significant conduction slowing in depolarized tissue, especially at faster depolarization rates. Furthermore, class IB drugs are less effective in the atrium, where the action potential duration is so short that the Na⁺ channel is in the inactivated state only briefly compared with the relatively long diastolic recovery times; thus accumulation of block is less likely to result from the rapid recovery of block.

Class IA drugs (quinidine, procainamide, and disopyramide) exhibit open state block, have intermediate effects on Na⁺ channels, and generally only cause significant prolongation of conduction in cardiac tissue at rapid heart rates. Because the open state block is dominant and recovery from block is slow, these drugs are effective in both the atrium (where action potential duration is short) and the ventricle.

Importantly, class IA drugs also have moderate K⁺ channel blocking activity (which tends to slow the rate of repolarization and prolong the action potential duration) and anticholinergic activity, and they tend to depress myocardial contractility. At slower heart rates, when use-

dependent blockade of I_{Na} is not significant, K⁺ channel blockade becomes predominant (reverse use-dependence), leading to prolongation of the action potential duration and QT interval and increased automaticity. Flecainide and propafenone also have K⁺ channel blocking activity and can increase the action potential duration in ventricular myocytes. Propafenone has significant β -adrenergic blocking activity.

The late I_{Na} (I_{NaL}) also can be a target for blockade. Several drugs exhibit relative selectivity for block of I_{NaL} over peak I_{NaS} including mexiletine, flecainide, lidocaine, amiodarone, and ranolazine.

Inherited Channelopathies

Mutations in genes that encode various subunits of the cardiac Na⁺ channel or proteins involved in regulation of the inward I_{Na} have been linked to several types of electrical disorders (Table 2.1). Depending on the mutation, the consequence is either a gain of channel function (with consequent prolongation of action potential duration because more positive ions accumulate in the cell) or an overall loss of channel function that influences the initial depolarizing phase of the action potential (with consequent decrease in cardiac excitability and electrical conduction velocity). It is noteworthy that a single mutation can cause different phenotypes or combinations thereof. The pathophysiology and clinical presentation of those channelopathies are discussed in detail in Chapter 31.⁵

Long QT Syndrome

Type 3 congenital long QT syndrome (LQTS; LQT3), which accounts for approximately 5% to 10% of congenital LQTS cases, is caused by

TABLE 2.1 Inherited Cardiac Sodium Channelopathies

Clinical Phenotype	Gene	Protein	Functional Effect
Long QT Syndrome (LQTS)			
LQT3	SCN5A	Na _v 1.5	↑ late or sustained I _{Na}
LQT9	CAV3	Caveolin-3	↑ sustained I _{Na}
LQT10	SCN4B	Na _v β4	↑ sustained I _{Na}
LQT12	SNTA1	α1-syntrophin	↑ sustained I _{Na}
Brugada Syndrome (BrS)			
BrS1	SCN5A	Na _v 1.5	↓ I _{Na}
BrS2	GPD1L	G3PD1L	↓ I _{Na}
BrS5	SCN1B	Na _v β1	↓ I _{Na}
BrS7	SCN3B	Na _v β3	↓ I _{Na}
BrS11	RANGRF	MOG1, Na _v 1.5 cofactor	↓ I _{Na}
BrS12	SLAMP	Sarcolemmal associated protein	↓ I _{Na}
BrS14	SCN2B	Na _v β2	↓ I _{Na}
BrS15	PKP2	Plakophilin-2	↓ I _{Na}
BrS16	FGF12	Fibroblast growth factor homologous factor-1	↓ I _{Na}
BrS17	SCN10A	Na _v 1.8	↓ I _{Na}
BrS18	HEY2	Transcriptional factor	↑ I _{Na}
Early Repolarization Syndrome (ERS)			
ERS6	SCN5A	Na _v 1.5	↓ I _{Na}
ERS7	SCN10A	Na _v 1.8	↓ I _{Na}
Progressive Cardiac Conduction Disease			
	SCN5A	Na _v 1.5	↓ I _{Na}
	SCN1B	Na _v β3	↓ or ↑ I _{Na}
Congenital Sick Sinus Syndrome			
	SCN5A	Na _v 1.5	↓ I _{Na}
Atrial Standstill			
	SCN5A	Na _v 1.5	↓ I _{Na}
Familial Atrial Fibrillation			
	SCN5A	Na _v 1.5	Different and discordant molecular phenotypes
	SCN1B	Na _v β1	Different and discordant molecular phenotypes
	SCN2B	Na _v β2	Different and discordant molecular phenotypes
Dilated Cardiomyopathy			
	SCN5A	Na _v 1.5	Different and discordant molecular phenotypes
Sudden Infant Death Syndrome			
	SCN5A	Na _v 1.5	↓ I _{Na}
	CAV3	Caveolin-3	↓ I _{Na}
	GPD1L	G3PD1L	↑ late I _{Na}
SCN5A Overlap Syndromes			
	SCN5A	Na _v 1.5	↓ or ↑ I _{Na}

I_{Na}, Sodium current.

gain-of-function mutations in the *SCN5A* gene, which encodes the α subunit of the Na⁺ channel (Na_v1.5), *SCN5A*. More than 200 mutations have been identified in *SCN5A*, with most being missense mutations mainly clustered in Na_v1.5 regions that are involved in fast inactivation (i.e., S4 segment of domain IV, the domain III–domain IV linker, and the cytoplasmic loops between the S4 and S5 segments of domain III and domain IV), or in regions that stabilize fast inactivation (e.g., the C-terminus).⁵

Several mechanisms have been identified to underlie ionic effects of *SCN5A* mutations in LQT3 (see eFigs. 31.1 and 31.2). Most *SCN5A* mutations cause a gain of function through disruption of fast inactivation, thus allowing repeated reopening during sustained depolarization and resulting in an abnormal, small, but functionally important sustained (or persistent) noninactivating Na⁺ current (I_{Na}) during action potential plateau. Because the general membrane conductance is small during the action potential plateau, the presence of a persistent inward I_{Na},

even of small amplitude, can potentially have a major impact on the plateau duration and can be sufficient to prolong repolarization and QT interval. QT prolongation and the risk of developing arrhythmia are more pronounced at slow heart rates, when the action potential duration is longer, thereby allowing more I_{Na} to enter the cell.⁶

Other less common mechanisms of *SCN5A* mutations to cause LQT3 include increased window current, which results from delayed inactivation of mutant Na^+ channels, occurring at more positive potentials and widening the voltage range during which the Na^+ channel may reactivate without inactivation. In addition, some mutations cause slower inactivation, which allows longer channel openings and causes a slowly inactivating I_{Na} . This current is I_{NaL} and is to be distinguished from I_{sus} (which does not inactivate). Comparable to I_{sus} , both the window current and I_{NaL} exert their effects during phases 2 and 3 of the action potential, in which normally no or very little I_{Na} is present. Other mutations induce prolonged action potential duration by enhancing recovery from inactivation, an effect that leads to larger peak I_{Na} by increasing the fraction of channels available for activation (because of faster recovery) during subsequent depolarizations. Finally, some mutations can cause increased expression of mutant $Na_v1.5$ through enhanced messenger RNA (mRNA) translation or protein trafficking to the sarcolemma, decreased protein degradation, or altered modulation by β subunits and regulatory proteins. These effects lead to larger I_{Na} density during phase 0 of the action potential. Importantly, one single *SCN5A* mutation can potentially cause several changes in the expression and/or gating properties of the resulting Na^+ channels.

Regardless of the mechanism, increased Na^+ current (I_{sus} , window current, I_{NaL} , or peak I_{Na}) upsets the balance between depolarizing and repolarizing currents in favor of depolarization. The resulting delay in the repolarization process triggers early afterdepolarizations (EADs) by reactivation of the L-type Ca^{2+} channel during phase 2 or 3 of the action potential, especially in Purkinje fiber myocytes, in which action potential durations are intrinsically longer. Compared with other LQT subtypes, patients with LQT3 are particularly at risk for sudden cardiac death (SCD), and cardiac arrest is often the first clinical event.

LQT9 is caused by gain-of-function mutations on the *CAV3* gene, which encodes caveolin-3, a plasma membrane scaffolding protein that interacts with $Na_v1.5$ and plays a role in compartmentalization and regulation of channel function. Mutations in *CAV3* induce kinetic alterations of the $Na_v1.5$ current that result in persistent Na^+ current (I_{sus}) and have been reported in cases of sudden infant death syndrome (SIDS).

LQT10 is caused by loss-of-function mutations on the *SCN4B* gene, which encodes the β subunit ($Na_v\beta4$) of the $Na_v1.5$ channel. These mutations likely cause a shift in the inactivation of the I_{Na} toward more positive potentials, resulting in increased window currents at an E_m corresponding to phase 3 of the action potential.

LQT12 is caused by mutations on the *SNTA1* gene, which encodes $\alpha1$ syntrophin, a cytoplasmic adaptor protein that enables the interaction among $Na_v1.5$, nitric oxide synthase, and the sarcolemmal Ca^{2+} adenosine triphosphatase (ATPase) complex that appears to regulate ion channel function. By disrupting the interaction between $Na_v1.5$ and the sarcolemmal Ca^{2+} ATPase complex, *SNTA1* mutations cause increased $Na_v1.5$ nitrosylation with consequent reduction of channel inactivation and enhanced I_{sus} densities.

Brugada Syndrome

Brugada syndrome is an autosomal dominant inherited channelopathy characterized by an elevated ST segment or J wave appearing in the right precordial leads. This syndrome is associated with a high incidence of SCD secondary to a rapid polymorphic ventricular tachycardia (VT) or ventricular fibrillation (VF). Approximately 65% of mutations identified in the *SCN5A* gene are associated with the Brugada syndrome

phenotype (Brugada syndrome type 1), and they account for approximately 11% to 28% of cases of Brugada syndrome. So far, more than 300 Brugada syndrome-associated loss-of-function (i.e., reduced peak I_{Na}) mutations have been described in *SCN5A*. Some of these mutations result in loss of function secondary to impaired channel trafficking to the cell membrane (i.e., reduced expression of functional Na^+ channels), disrupted ion conductance (i.e., expression of nonfunctional Na^+ channels), or altered gating function. Altered gating properties comprise delayed activation (i.e., activation at more positive potentials), earlier inactivation (i.e., inactivation at more negative potentials), faster inactivation, and enhanced slow inactivation.^{2,7}

Most of the mutations are missense mutations, whereby a single amino acid is replaced by a different amino acid. Missense mutations commonly alter the gating properties of mutant channels. Because virtually all reported *SCN5A* mutation carriers are heterozygous, mutant channels with altered gating may cause up to a 50% reduction of I_{Na} . Different *SCN5A* mutations can cause different degrees of I_{Na} reduction and therefore different degrees of severity of the clinical phenotype of Brugada syndrome.⁷

In addition to *SCN5A* mutations, reduction in I_{Na} can be caused by mutations in *SCN1B* (encoding the $\beta1$ and $\beta1b$ subunits of the Na^+ channel), *SCN2B* (encoding the $\beta2$ subunit), and *SCN3B* (encoding the $\beta3$ subunit), resulting in the clinical phenotype of Brugada syndrome.⁷ Recently, *SCN10A* (which encodes $Na_v1.8$, a neuronal Na^+ channel that appears to play a role in the heart) was identified as a major susceptibility gene for Brugada syndrome (identified in 16.7% of probands). Loss-of-function mutations in *SCN10A* lead to significant reduction in I_{Na} .⁸

Furthermore, mutations in *GPD1L* (which encodes the protein G3PD1L protein) affect the trafficking of the cardiac Na^+ channel to the cell surface, resulting in reduction of I_{Na} and Brugada syndrome. The Brugada phenotype associated with *GPD1L* mutations is characterized by progressive conduction disease, low sensitivity to procainamide, and a relatively good prognosis.⁸

Mutations in several other genes have been reported to cause reduction in I_{Na} and lead to the Brugada phenotype, including *HEY2* (encoding the transcriptional factor HEY2), *FGF12* (encoding for a fibroblast growth factor homologous factor-1, which exerts modulatory effects on cardiac Na^+ and Ca^{2+} channels), *PKP2* (encoding the desmosomal protein plakophilin-2, a known susceptibility gene for arrhythmogenic right ventricular cardiomyopathy [ARVC]), *RANGRF* (encoding MOG1, a protein known to modulate the Na^+ channel), and *SLMAP* (encoding the sarcolemmal membrane-associated protein, SLMAP, a component of T-tubules and sarcoplasmic reticulum).⁸

Early Repolarization Syndrome

Loss-of-function mutations in the $\alpha1$ subunit of $Na_v1.5$ and $Na_v1.8$ (*SCN5A*, *SCN10A*) have been reported in patients with early repolarization syndrome.^{9,10}

Familial Progressive Cardiac Conduction Disease

Loss-of-function *SCN5A* mutations have been linked to familial forms of progressive cardiac conduction disease (referred to as hereditary Lenègre disease, primary cardiac conduction system disease, and familial AV block). This disease is characterized by slowing of electrical conduction through the atria, AVN, His bundle, Purkinje fibers, and ventricles, accompanied by an age-related degenerative process and fibrosis of the cardiac conduction system, in the absence of structural or systemic disease. It is often reflected by varying degrees of AV block and bundle branch block. Whether the age-dependent fibrosis of the conduction system is a primary degenerative process in progressive cardiac conduction disease or a physiological process that is accelerated by I_{Na} reduction

remains to be established. A single loss-of-function *SCN5A* mutation can cause isolated progressive cardiac conduction disease or can be combined with the Brugada syndrome (overlap syndrome). Loss-of-function mutations in *SCN1B* also have been identified in patients with progressive cardiac conduction disease who carried no mutation in *SCN5A*.

Congenital Sick Sinus Syndrome

Although I_{Na} does not play a prominent role in sinus node activity, mutations in *SCN5A* have been linked to sick sinus syndrome, manifesting as sinus bradycardia, sinus arrest, sinoatrial block, or a combination of these conditions, which can progress to atrial inexcitability (atrial standstill). Loss-of-function *SCN5A* mutations result in reduced peak I_{Na} density, hyperpolarizing shifts in the voltage dependence of steady-state channel availability, and slow recovery from inactivation. These effects likely cause reduced automaticity, decreased excitability, and conduction slowing or block of impulses generated in the sinus node to the surrounding atrial tissue. Sinus node dysfunction can also manifest concomitantly with other phenotypes that are linked to *SCN5A* loss-of-function mutations such as Brugada syndrome and progressive cardiac conduction disorders.¹¹

Familial Atrial Fibrillation

Loss-of-function mutations, gain-of-function mutations, and common polymorphisms on the *SCN5A* gene have been identified in some cases of atrial fibrillation (AF) occurring in young patients with structurally normal hearts. It is speculated that I_{Na} reduction can predispose to AF by slowing the electrical conduction velocity and thereby facilitating reentry. On the other hand, gain-of-function mutations can potentially predispose to AF by increasing atrial excitability. AF can occur in patients with other phenotypes of Na^+ channelopathies, including LQT3, Brugada syndrome, dilated cardiomyopathy, and sinus node dysfunction. Furthermore, mutations in the *SCN1B* gene (encoding the $\beta 1$ subunit of the Na^+ channel) and the *SCN2B* gene (encoding the $\beta 2$ subunit of the Na^+ channel) have been identified in patients with AF, many of whom displayed ECG patterns suggestive of the Brugada syndrome.¹²

Dilated Cardiomyopathy

Some cases of familial dilated cardiomyopathy have been linked to *SCN5A* mutations. Dilated cardiomyopathy-linked *SCN5A* mutations cause diverse loss-of-function and gain-of-function changes in the gating properties, but how such changes evoke contractile dysfunction is not understood. It is speculated that *SCN5A* mutations disrupt the interactions between the mutant Na^+ channels and intracellular (or extracellular) proteins that are essential for normal cardiomyocyte structure and architecture. Notably, dilated cardiomyopathy with *SCN5A* mutations often display atrial or ventricular arrhythmias (including AF, VT, and VF), sinus node dysfunction, AV block, and intraventricular conduction delay.¹³

Sudden Infant Death Syndrome

Gain-of-function mutations in *SCN5A* may be the most prevalent genetic cause of SIDS. *SCN5A* mutations in SIDS commonly increase I_{sus} . Less frequently, loss-of-function mutations in *SCN5A* or *CAV3* and gain-of-function mutations in *GPD1-L* have also been found in infants with SIDS. However, it is possible that in these patients SIDS represents a malignant form of LQT3 or Brugada syndrome that manifests during infancy.¹⁴

Overlap Syndrome

A single *SCN5A* mutation can result in multiple clinical phenotypes and rhythm disturbances within the same family, a phenomenon now

referred to as “cardiac sodium channel overlap syndrome.” Not surprisingly, loss-of-function *SCN5A* mutations have often been associated with overlapping phenotypes of Brugada syndrome, sinus node dysfunction, and progressive cardiac conduction disorders, which all share similar underlying mechanisms that implicate I_{Na} reduction. More surprisingly, some *SCN5A* mutations are associated with both BrS1 (I_{Na} loss-of-function) and LQT3 (I_{Na} gain-of-function). Carriers of these mutants present with BrS1, LQT3, or a mixed ECGs with both ST-segment abnormalities and QT elongation. These mutations are likely associated with altered gating properties in a manner that results in both reduction of the peak I_{Na} and augmentation of the persistent I_{Na} . Furthermore, it is likely that genetic background and clinical and environmental factors play a role in the variable disease expressivity and severity.^{5,15}

Acquired Diseases

In heart failure, peak I_{Na} is reduced (likely secondary to reduced *SCN5A* expression), whereas I_{NaL} is increased (likely because of increased phosphorylation of Na^+ channels). $Na_v1.5$ expression is reduced in the surviving myocytes in the border zone of the myocardial infarct. Importantly, Na^+ channel blockers can increase the risk for SCD in patients with ischemic heart disease, possibly by facilitating the initiation of reentrant excitation waves. In addition, I_{NaL} increases during myocardial ischemia, explaining why I_{NaL} inhibition may be an effective therapy for chronic stable angina. $Na_v1.5$ expression is reduced in response to persistent atrial tachyarrhythmias as part of the “electrical remodeling” process, leading to attenuation of I_{Na} .

Furthermore, mutations in *SCN5A* can predispose affected individuals to acquired LQTS induced by a variety of drugs such as antihistamines or antibiotics. These mutations result in changes in channel activity that exert a significant impact on action potential duration only when combined with drug-induced alteration of other channels.

POTASSIUM CHANNELS

Structure and Physiology

Cardiac K^+ channels are membrane-spanning proteins that allow the passive movement of K^+ ions across the cell membrane along its electrochemical gradient. The ion-conducting or pore-forming subunit is generally referred to as the α subunit. The backbone carbonyl oxygen contributed by tripeptide sequence glycine-tyrosine-glycine plus the side-chain oxygens from threonine in the sequence TXGYG (where X represents a variable residue) is common to the pore of all K^+ channels and constitutes the signature motif for determining K^+ ion selectivity. A gating mechanism controls switching between open-conducting and closed-nonconducting states.

K^+ channels represent the most diverse class of cardiac ion channels (Fig. 2.4). The diversity of K^+ currents in native tissues exceeds the number of K^+ channel genes identified. The explanations for this diversity include alternative splicing of gene products, posttranslational modification, and heterologous assembly of β subunits within the same family and assembly with accessory β subunits that modulate channel properties. Even small differences in channel composition give rise to significant functional diversity.¹⁶

Cardiac K^+ channels can be categorized as voltage-gated (K_v) and ligand-gated channels. In K_v channels, pore opening is coupled to the movement of a voltage sensor within the membrane electric field, and they include the rapidly activating and inactivating transient outward current (I_{to}); the ultrarapid (I_{Kur}), rapid (I_{Kr}), and slow (I_{Ks}) components of the delayed rectifier current; and the inward rectifier current (I_{K1}). In contrast, pore opening in ligand-gated channels is coupled to the binding of an organic molecule, including channels activated by a

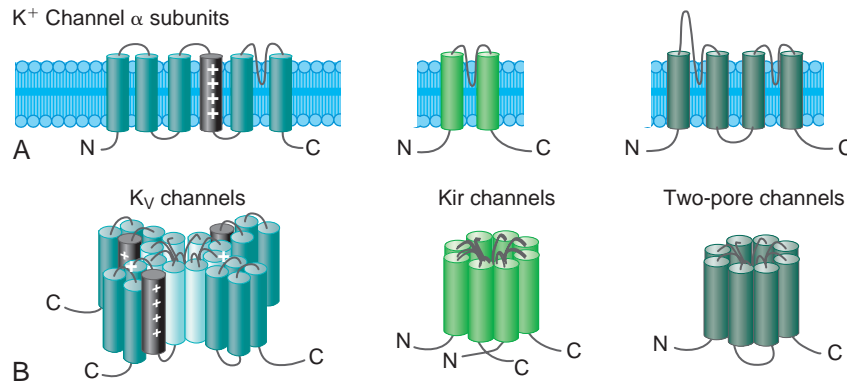


Fig. 2.4 Molecular Compositions of Cardiac Potassium (K^+) Channels. Amino termini (N) and carboxyl termini (C) are indicated. (A) Voltage-gated (K_v), inward rectifier (K_{ir}), and two-pore α subunits are integral membrane proteins with six, two, and four membrane-spanning domains, respectively. (B) These α subunits assemble as tetramers or dimers to form K^+ -selective pores. (Modified from Oudit GY, Backx PH. Voltage-regulated potassium channels. In Zipes DP, Jalife J, eds. *Cardiac Electrophysiology: From Cell to Bedside*. 5th ed. Philadelphia: Saunders; 2009:29–42.)

decrease in the intracellular concentration of adenosine triphosphate (K_{ATP}) or by acetylcholine (K_{ACh}). Other classes of K^+ channels respond to different stimuli, including changes in intracellular Ca^{2+} concentration and G proteins.¹⁷

On the basis of the primary amino acid sequence of the α subunit, K^+ channels have been classified into three major families (Table 2.2):

1. Channels containing six transmembrane segments and a single pore. This architecture is typical of K_v channels.
2. Channels containing two transmembrane segments (M1 and M2) and a single pore. This architecture is typical of inward rectifier K^+ (K_{ir}) channels, including K_1 , K_{ATP} , and K_{ACh} channels. These channels conduct K^+ currents more in the inward direction than the outward and play an important role in setting the resting potential close to the equilibrium potential for K^+ and in repolarization. Kir channels form either homotetramers or heterotetramers.
3. Channels containing four transmembrane segments and two pores (K_{2P}). These channels exist as homodimers or heterodimers. K_{2P} currents display little time or voltage dependence.

Each voltage-gated K^+ channel (K_v family) is formed by the coassembly of four identical (homotetramers) or a combination of four different (from the same subfamily, heterotetramers) α subunits ($K_v\alpha$). A total of 38 genes has been cloned and assigned to 12 subfamilies of $K_v\alpha$ (K_v1 to K_v12) on the basis of sequence similarities. Most K_v subfamilies contain many individual channel members (e.g., K_v1 has eight members, identified as $K_v1.1$ to $K_v1.8$, with gene designations *KCNA1* to *KCNA8*, respectively).

Each $K_v\alpha$ contains one domain consisting of six membrane-spanning segments (S1 to S6), connected to each other by alternating intracellular and extracellular peptide loops (similar to one of the four domains of voltage-gated Na^+ and Ca^{2+} channels), with both the amino terminus (N-terminus) and the C-terminus located on the intracellular side of the membrane. The central ion-conducting pore region is formed by the S5 and S6 segments and the S5-S6 linker (P segment); the S5-S6 linker is responsible for K^+ ion selectivity. The S4 segment serves as the voltage sensor.

$K_v\alpha$ can generate voltage-dependent K^+ current when expressed in heterologous systems. However, the assembly of a functional tetramer can occur only in the presence of multiple auxiliary units (see Table 2.2). In many cases, auxiliary subunits coassociate with $K_v\alpha$ and likely modulate cell surface expression, gating kinetics, and drug sensitivity of the α subunit complex. Most K^+ channel β subunits assemble with

α subunits and give rise to an $\alpha\beta_4$ complex. K^+ channel β subunits represent a diverse molecular group, which includes (1) cytoplasmic proteins ($K_v\beta1$ to $K_v\beta4$, $KChIP$, and $KChAP$) that interact with the intracellular domains of $K_v\alpha$; (2) single transmembrane spanning proteins (e.g., $minK$ and $minK$ -related proteins [$MiRPs$]) encoded by the *KCNE* gene family; and (3) large ATP-binding cassette (ABC) transport-related proteins (e.g., the sulfonylurea receptors [$SURs$]).

Similar to voltage-dependent Na^+ (Na_v) and Ca^{2+} (Ca_v) channels, K_v channels typically fluctuate among distinct conformational states because of molecular movements in response to voltage changes across the cell membrane (voltage-dependent gating). The K_v channel activates (opens) on membrane depolarization, thus allowing the rapid passage of K^+ ions across the sarcolemma. After opening, the channel undergoes conformational transition in a time-dependent manner to a stable nonconducting (inactivated) state. Inactivated channels are incapable of reopening, even if the transmembrane voltage is favorable, unless they “recover” from inactivation (i.e., enter the closed state) on membrane repolarization. Closed (preopen) channels are nonconducting but can be activated on membrane depolarization.¹⁸

Four mechanistically distinct types of K_v channel inactivation that are associated with distinct molecular domains have been identified: N-type, C/P-type, AG-type, and U-type. N-type (“ball and chain”) inactivation involves physical occlusion of the intracellular mouth of the channel pore through binding of a small group of amino acids (“inactivation ball tethered to a chain”) at the extreme N-terminus.¹⁸

C/P-type inactivation involves conformational changes in the external mouth of the pore. C/P-type inactivation exists in almost all K^+ channels and may reflect a slow constriction of the pore. This inactivation process is thought to be voltage independent, coupled to channel opening, and is usually slower than N-type inactivation. Recovery from C/P-type inactivation is relatively slow and weakly voltage dependent. Importantly, the rate of C/P-type inactivation and recovery can be strongly influenced by other factors. C/P-type inactivation is strongly accelerated by N-type inactivation, and is promoted by extracellular H^+ ions. Unlike N-type inactivation, C/P-type inactivation is prevented by extracellular K^+ ions binding to the face of the pore. These interactions render C/P-type inactivation an important biophysical process in regulating repetitive electrical activity and determining certain physiological properties such as refractoriness, drug binding, and sensitivity to extracellular ions.

AG-type inactivation involves conformational changes in S4 that inactivate K_v channels directly from the closed (preopen) state. In

TABLE 2.2 Genetic and Molecular Basis of Cardiac Potassium Currents

Current	α Subunit	α Subunit Gene	β Subunit/Accessory Proteins	β Subunit Gene
Voltage-Gated Channels (K_v)				
$I_{to,f}$	$K_v4.2$	KCND2	MiRP1	KCNE2
	$K_v4.3$	KCND3	MiRP2	KCNE3
			KChIP1	KCNIP1
			KChIP2	KCNIP2
			DPP6	DPP6
$I_{to,s}$	$K_v1.4$	KCNA4	$K_v\beta 1$	KCNB1
	$K_v1.7$	KCNA7	$K_v\beta 2$	KCNB2
			$K_v\beta 3$	KCNB3
			$K_v\beta 4$	KCNB4
I_{Kur}	$K_v1.5$	KCNA5	$K_v\beta 1$	KCNAB1
			$K_v\beta 2$	KCNAB2
			$K_v\beta 3$	KCNB3
I_{Kr}	$K_v11.1$ (HERG)	KCNH2	minK	KCNE1
			MiRP1	KCNE2
			MiRP2	KCNE3
I_{Ks}	$K_v7.1$ (K_vLQT1)	KCNQ1	minK	KCNE1
			MiRP1	KCNE2
			MiRP2	KCNE3
			MiRP3	KCNE4
			MiRP4	KCNE5
Inward Rectifier Channels (K_{ir})				
I_{K1}	Kir2.1	KCNJ2	AKAP5	AKAP5
	Kir2.2	KCNJ12		
	Kir2.3	KCNJ14		
I_{KACH}	Kir3.1 (GIRK1)	KCNJ3		
	Kir3.4 (GIRK4)	KCNJ5		
I_{KATP}	Kir6.1	KCNJ8	SUR1	ABCC8
	Kir6.2	KCNJ11	SUR2	ABCC9
Two-Pore Channels (K_{2p})				
ITWIK-1	$K_{2p}1.1$ (TWIK-1)	KCNK1		
ITASK-1	$K_{2p}3.1$ (TASK-1)	KCNK3		
ITASK-3	$K_{2p}9.1$ (TASK-3)	KCNK9		
ITALK-2	$K_{2p}17.1$ (TALK-2)	KCNK17		
Calcium-Activated Channels (SK, KCa)				
ISK	KCa2.1 (SK1)	KCNN1		
	KCa2.2 (SK2)	KCNN2		
	KCa2.3 (SK3)	KCNN3		

addition, some K_v channels also show another type of inactivation (U-type), which exhibits a U-shaped voltage dependence with prolonged stimulation rates. Those channels appear to exhibit preferential inactivation at intermediate depolarizing voltages (corresponding to pre-activated closed state) than at more positive voltages (corresponding to the open state). The exact conformational changes underlying U-type inactivation remain unclear. Importantly, there is extreme diversity in the kinetic and potentially molecular properties of K_v channel inactivation, particularly of C/P-type inactivation.

Function

K^+ channels are a diverse and ubiquitous group of membrane proteins that regulate K^+ ion flow across the cell membrane on the electrochemi-

cal gradient and regulate the resting E_m , the frequency of pacemaker cells, and the shape and duration of the cardiac action potential. Because the concentration of K^+ ions outside the cell membrane is approximately 25-fold lower than that in the intracellular fluid, the opening of K^+ channels generates an outward current resulting from the efflux of positively charged ions that offers a mechanism to counteract, dampen, or restrict the depolarization front (phases 1 through 4 of the action potential) triggered by an influx of cations (Na^+ and Ca^{2+}).

The variation in the level of expression of K^+ channels that participate in the genesis of the cardiac action potential explains the regional differences of the configuration and duration of cardiac action potentials from sinus node and atrial to ventricular myocytes and across the myocardial wall (endocardium, midmyocardium, and epicardium). Moreover, the expression and properties of K^+ channels are not static; heart rate, neurohumoral state, pharmacological agents, cardiovascular diseases (cardiac hypertrophy and failure, myocardial infarction [MI]), and arrhythmias (e.g., AF) can influence those properties, and they underlie the change in action potential configuration in response to variation in heart rate and various physiological and pathological conditions.

Transient Outward Potassium Current

Structure and Physiology

Cardiac I_{to} channels are macromolecular protein complexes, comprising four pore-forming $K_v\alpha$ subunits and a variety of K_v channel accessory (β) subunits (see Fig. 2.4). Two major types of I_{to} have been characterized: (1) I_{to1} generated by voltage-dependent, Ca^{2+} -independent K_v channels; and (2) I_{to2} generated by Ca^{2+} -activated Cl^- channels. In human atrial and ventricular myocytes, the presence of I_{to2} has not been clearly demonstrated.

I_{to1} (which is referred to as I_{to}) displays two phenotypes with distinct recovery kinetics: a rapid or fast I_{to} ($I_{to,fast}$ or $I_{to,f}$) phenotype and a slower phenotype ($I_{to,slow}$ or $I_{to,s}$). The transient nature of I_{to} is secondary to its rapid activation (with time constants of less than 10 milliseconds for both $I_{to,f}$ and $I_{to,s}$) and rapid inactivation (25 to 80 milliseconds for $I_{to,f}$ and 80 to 200 milliseconds for $I_{to,s}$). However, whereas $I_{to,f}$ recovers rapidly from inactivation (60 to 100 milliseconds), $I_{to,s}$ recovers slowly (with time constants on the order of seconds).¹⁷

K_v channels mediating $I_{to,s}$ are formed by the coassembly of four α subunits from the $K_v1.x$ subfamily (primarily $K_v1.4$, and possibly $K_v1.7$), whereas those mediating $I_{to,f}$ are formed by the coassembly of four α subunits from the $K_v4.x$ subfamily (primarily $K_v4.3$, and possibly $K_v4.2$) (see Table 2.2). Among the various accessory subunits identified, a crucial role has been definitively demonstrated only for KChIP2, and potentially for MiRP2.¹⁶

Function

I_{to} is a prominent repolarizing current; it partially repolarizes the membrane, shapes the rapid (phase 1) repolarization of the action potential, and sets the height of the initial plateau (phase 2). Thus the activity of I_{to} channels influences the activation of voltage-gated L-type Ca^{2+} channels and the balance of inward and outward currents during the plateau (mainly the L-type Ca^{2+} current [I_{CaL}] and the delayed rectifier K^+ currents), thereby mediating the duration and the amplitude of phase 2.

The density of I_{to} varies across the myocardial wall and in different regions of the heart. In human ventricles, I_{to} densities are much higher in the epicardium and midmyocardium than in the endocardium. Furthermore, $I_{to,f}$ and $I_{to,s}$ are differentially expressed in the myocardium, thus contributing to regional heterogeneities in action potential waveforms. $I_{to,f}$ is the principal subtype expressed in human atrium. The markedly higher densities of $I_{to,f}$ together with the expression of the ultrarapid delayed rectifier K^+ current, accelerate the early phase of repolarization and lead to lower plateau potentials and shorter action

potentials in atrial as compared with ventricular cells. Due to its slow recovery kinetics, $I_{to,s}$ plays a limited role in repolarization compared to $I_{to,f}$, especially at faster heart rates.¹⁹

Although both $I_{to,f}$ and $I_{to,s}$ are expressed in the ventricle, $I_{to,f}$ is more prominent in the epicardium and midmyocardium (putative M cells) than in the endocardium, whereas $I_{to,s}$ is mainly present in the endocardium and Purkinje fiber cells. These regional differences are responsible for the shorter duration and the prominent phase 1 notch and the “spike-and-dome” morphology of epicardial and midmyocardial compared with endocardial action potentials. A prominent I_{to} -mediated action potential notch in ventricular epicardium but not endocardium produces a transmural voltage gradient during early ventricular repolarization that registers as a J wave or J point elevation on the ECG. I_{to} densities are also reportedly higher in right than in left (midmyocardial and epicardial) ventricular myocytes, consistent with the more pronounced spike-and-dome morphology of right, compared with left, ventricular action potentials, particularly in the epicardium.

Furthermore, variations in cardiac repolarization associated with I_{to} regional differences strongly influence intracellular Ca^{2+} transient by modulating Ca^{2+} entry via the I_{CaL} and Na^+ - Ca^{2+} exchanger, thereby regulating excitation-contraction coupling and regional modulation of myocardial contractility and hence synchronizing the timing of force generation between different ventricular regions and enhancing mechanical efficiency.

Regulation

I_{to} channels are subject to α - and β -adrenergic regulation. α -Adrenergic stimulation reduces I_{to} ; concomitant β -adrenergic stimulation appears to counteract the α -adrenergic effect, at least in part. The effects of α - and β -adrenergic stimulation are exerted by phosphorylation of the $K_v1.4$, $K_v4.2$, and $K_v4.3$ α -subunits by PKA as well as PKC. Calmodulin-dependent kinase II, on the other hand, has been shown to be involved in enhancement of I_{to} . Adrenergic stimulation is also an important determinant of transient outward channel downregulation in cardiac disease. Chronic α -adrenergic stimulation and angiotensin II reduce I_{to} channel expression, which explains channel downregulation in many types of chronic heart disease.

KChIP2, when coexpressed with $K_v4.3$, increases surface channel density and current amplitude, slows channel inactivation, and markedly accelerates the recovery from inactivation. In the ventricle, KChIP2 mRNA is 25-fold more abundant in the epicardium than in the endocardium. This gradient parallels the gradient in I_{to} expression, whereas $K_v4.3$ mRNA is expressed at equal levels across the ventricular wall. Thus transcriptional regulation of the *KChIP2* gene is the primary determinant of I_{to} expression in the ventricular wall.

Observations suggest that MiRP2 is required for the physiological functioning of human $I_{to,f}$ channels and that gain-of-function mutations in MiRP2 predispose to Brugada syndrome through augmentation of $I_{to,f}$.

I_{to} is strongly rate dependent. I_{to} fails to recover from previous inactivation at very fast heart rates; thus tachycardia is associated with reduction of I_{to} , which can be manifest as a decrease in the magnitude of the J wave on the surface ECG. Hence abrupt changes in rate and pauses have important consequences for the early repolarization of the membrane.

I_{to} can be enhanced by aging, low sympathetic activity, high parasympathetic activity, bradycardia, hypothermia, and drugs. Estrogen suppresses the expression of the $K_v4.3$ channel and results in reduced I_{to} and a shallow phase 1 notch.

Phase 1 notch of the action potential modulates the kinetics of slower activating ion currents and consequently the later phases of the action potential. Initial enhancement of phase 1 notch promotes phase 2 dome and delays repolarization, presumably by delaying the peak of

I_{CaL} . However, further enhancement of phase 1 notch prevents the rising of phase 2 dome and abbreviates action potential duration, presumably by deactivation or voltage modulation that reduces I_{CaL} . Thus progressive deepening of phase 1 notch can cause initial enhancement followed by sudden disappearance of phase 2 dome and corresponding prolongation followed by abbreviation of action potential duration. On the other hand, modulators that decrease I_{to} lead to a shift of the plateau phase into the positive range of potentials, thus increasing the activation of the delayed rectifier currents, promoting faster repolarization, and reducing the electrochemical driving force for Ca^{2+} and hence I_{CaL} . Phase 1 notch also affects the function of the Na^+ - Ca^{2+} exchanger and subsequently intracellular Ca^{2+} handling and Na^+ channel function.

Pharmacology

Quinidine, 4-aminopyridine, flecainide, and propafenone produce an open channel blockade and accelerate I_{to} inactivation. Quinidine, but not flecainide or propafenone, produces a frequency-dependent block of I_{to} that results from a slow rate of drug dissociation from the channel. Quinidine has relatively strong I_{to} blocking effect, whereas flecainide mildly blocks I_{to} .

I_{to} blockers can potentially prolong the action potential duration in the atrium and in ischemic ventricular myocardium. However, because the net effects of I_{to} blockade on repolarization depend on secondary changes in other currents, the reduction of I_{to} density can result in a shortening of the ventricular action potential. Moreover, heterogeneous ventricular distribution of I_{to} can cause marked dispersion of repolarization across the ventricular wall that, when accompanied by prominent conduction delays related to Na^+ channel blockade, results in extrasystolic activity through a phase 2 reentrant mechanisms.

Currently no cardioselective and channel-specific I_{to} openers or blockers are available for clinical use. Development of an I_{to} -selective drug is expected to be beneficial in patients with primary abnormality in the I_{to} or in other channels, such as the Brugada syndrome, in which heterogeneity in the expression of I_{to} between epicardium and endocardium in the RV results in the substrate responsible for reentry and ventricular arrhythmias.^{20,21}

Inherited Channelopathies

Gain-of-function mutations in *KCNQ3* (which encodes the α -subunit of the I_{to} channel [$K_v4.3$]) and *KCNE3* (which encodes the auxiliary β subunit [MiRP2]) result in an increase in I_{to} density and cause Brugada syndrome. Furthermore, gain-of-function mutations in *SCN1B* (which encodes the auxiliary $\beta 1$ subunit of the Na^+ channel), in addition to reducing I_{Na} , can also increase I_{to} . Mutations in *SEMA3A* (which encodes semaphorin) were also implicated in Brugada syndrome by increasing I_{to} .⁸

In addition, gain-of-function mutations in *KCNQ3* and *KCNE3* have been linked to familial AF. *KCNE3* mutations were found to increase $I_{to,f}$ and were postulated to cause AF by shortening action potential duration and facilitating atrial reentrant excitation waves (Table 2.3).

A genome-wide haplotype-sharing study associated a haplotype on chromosome 7, harboring DPP6, with idiopathic VF in three distantly related families. Overexpression of *DPP6*, which encodes dipeptidyl-peptidase 6, a putative component of the I_{to} channel complex, was proposed as the likely pathogenetic mechanism. DPP6 significantly alters the inactivation kinetics of both $K_v4.2$ and $K_v4.3$ and promotes expression of these α subunits in the cell membrane.

Importantly, the normally functioning I_{to} channels play an important role in the electrophysiological consequences of the ionic current abnormalities in the Brugada and J wave syndromes. Heterogeneity in the distribution of I_{to} channels across the myocardial wall, being more prominent in ventricular epicardium than endocardium, and particularly

TABLE 2.3 Inherited Cardiac Potassium Channelopathies

Clinical Phenotype	Gene	Protein	Functional Effect
Long QT Syndrome (LQTS)			
LQT1	KCNQ1 (K_v LQT1)	$K_v7.1$	↓ I_{Ks}
LQT2	KCNH2 (HERG)	$K_v11.1$	↓ I_{Kr}
LQT5	KCNE1	MinK	↓ I_{Ks}
LQT6	KCNE2	MiRP1	↓ I_{Kr}
LQT7 (Andersen-Tawil syndrome)	KCNJ2	Kir2.1	↓ I_{K1}
LQT11	AKAP9	Yotiao	↓ I_{Ks}
LQT13	KCNJ5	Kir3.4 (GIRK4)	↓ I_{KACH}
Brugada Syndrome (BrS)			
BrS6	KCNE3	MiRP2	↑ I_{to}
BrS8	KCNJ8	Kir6.1	↑ I_{KATP}
BrS10	KCND3	$K_v4.3$	↑ I_{to}
BrS13	ABCC9	SUR2A	↑ I_{KATP}
BrS19	SEMA3A	Semaphorin	↑ I_{to}
Short QT Syndrome (SQTs)			
SQT1	KCNH2 (HERG)	$K_v11.1$	↑ I_{Kr}
SQT2	KCNQ1 (K_v LQT1)	$K_v7.1$	↑ I_{Ks}
SQT3	KCNJ2	Kir2.1	↑ I_{K1}
Early Repolarization Syndrome (ERS)			
ERS1	KCNJ8	Kir6.1	↑ I_{KATP}
ERS 5	ABCC9	SUR2A	↑ I_{KATP}
Catecholaminergic Polymorphic Ventricular Tachycardia Phenocopy			
	KCNJ8	Kir2.1	↓ I_{K1}
Familial Atrial Fibrillation			
	KCNE1	MinK	↑ I_{Ks}
	KCNE2	MiRP1	↑ I_{Kr}
	KCNE3	MiRP2	↑ I_{to} /↑ I_{Kr}
	KCNQ1 (K_v LQT1)	$K_v7.1$	↑ I_{Ks}
	KCND3	$K_v4.3$	↑ I_{to}
	KCNJ2	Kir2.1	↑ I_{K1}
	KCNA5	$K_v1.5$	↓ K_{ur}
	KCNJ5	Kir3.4 (GIRK4)	↓ K_{ACH}
	ABCC9	SUR2A	↓ K_{ATP}
	KCNK3	$K_{2p3.1}$ (TASK-1)	↓ ITASK-1

I_{K1} , Inward rectifier K^+ current; I_{KACH} , acetylcholine-activated inward rectifier K^+ current; I_{Kr} , rapidly activating delayed rectifier K^+ current; I_{Ks} , slowly activating delayed rectifier K^+ current; I_{to} , transient outward K^+ current.

in the RV, results in the shorter duration and the prominent phase 1 notch and the spike-and-dome morphology of the epicardial action potential as compared with the endocardium. The resultant transmural voltage gradient during the early phases (phases 1 and 2) of the action potential is thought to be responsible for the inscription of the J wave on the surface ECG. An increase in net repolarizing current, secondary to either a decrease in the inward currents (I_{Na} and I_{CaL}) or an increase in the outward K^+ currents (I_{to} , I_{Kr} , I_{Ks} , acetylcholine-activated potassium current [I_{KACH}], ATP-sensitive potassium current [I_{KATP}]), or both, can

accentuate the action potential notch and lead to augmentation of the J wave or the appearance of ST segment elevation on the surface ECG. An outward shift of currents that extends beyond the action potential notch not only accentuates the J wave but also can lead to partial or complete loss of the dome of the action potential, thus resulting in a protracted transmural voltage gradient that manifests as greater ST segment elevation and gives rise to J wave syndromes. The type of the ion current affected and its regional distribution in the ventricles determine the particular phenotype (including the Brugada syndrome, early repolarization syndrome, hypothermia-induced ST segment elevation, and MI-induced ST segment elevation). The degree of accentuation of the action potential notch leading to loss of the dome depends on the magnitude of I_{to} . These changes are more prominent in regions of the myocardium exhibiting a relatively large I_{to} , such as the RV epicardium; this explains the appearance of coved ST segment elevation, characteristic of Brugada syndrome, in the right precordial ECG leads.¹⁹

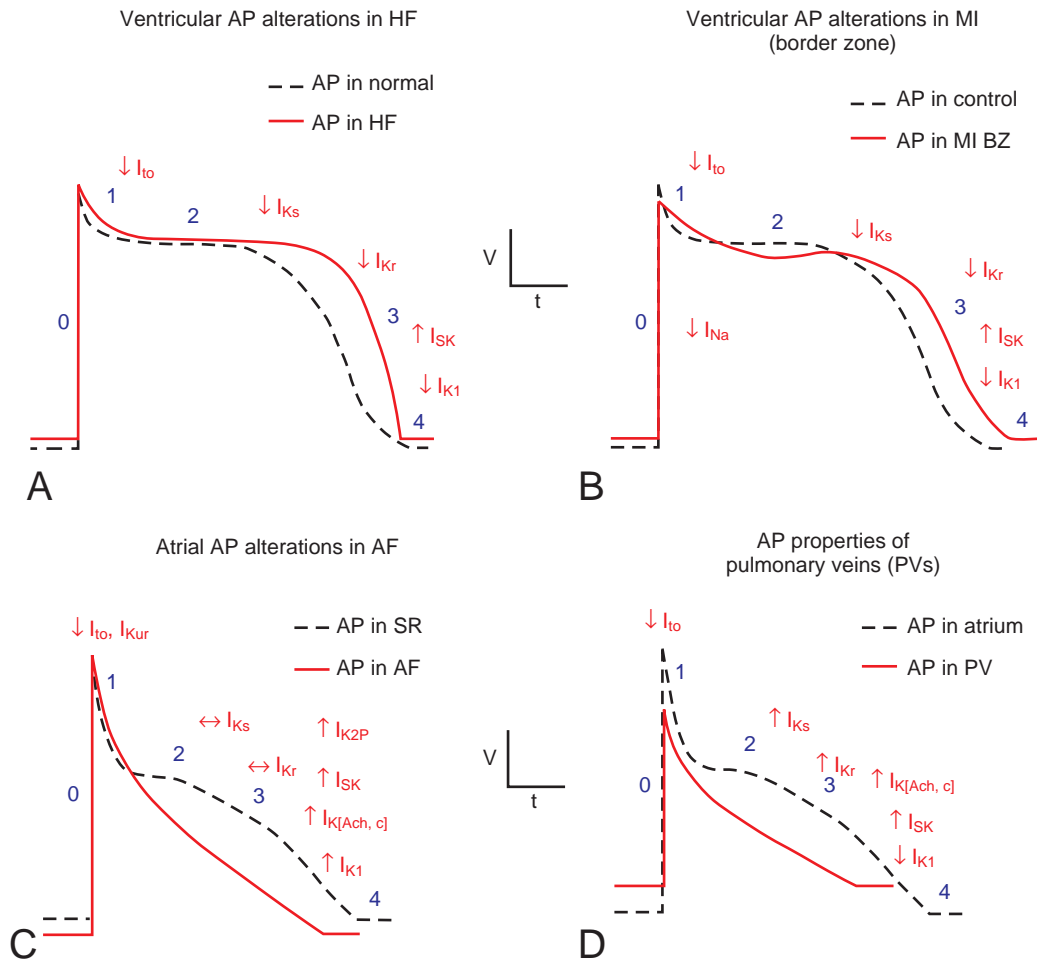
In this context, factors that influence the kinetics of I_{to} or the other repolarization currents can modify the manifestation of the J wave on the ECG. Na^+ channel blockers (procainamide, pilsicainide, propafenone, flecainide, and disopyramide), which reduce the inward I_{Na} , can accentuate the J wave and ST segment elevation in patients with concealed J wave syndromes. Quinidine, which inhibits both I_{to} and I_{Na} , reduces the magnitude of the J wave and normalizes ST segment elevation. In addition, acceleration of the heart rate, which is associated with reduction of I_{to} (because of slow recovery of I_{to} from inactivation), results in a decrease in the magnitude of the J wave. Male predominance can potentially result from larger epicardial I_{to} density versus I_{to} in women.

The increased transmural heterogeneity of ventricular repolarization (i.e., dispersion of repolarization between epicardium and endocardium), which is responsible for J point elevation and early repolarization pattern on the surface ECG, is also responsible for the increased vulnerability to ventricular tachyarrhythmias. A significant outward shift in current can cause partial or complete loss of the dome of the action potential in regions where I_{to} is prominent (epicardium), with the consequent loss of activation of I_{CaL} . The dome of the action potential then can propagate from regions where it is preserved (midmyocardium endocardium) to regions where it is lost (epicardium), thus giving rise to phase 2 reentry, which can generate premature ventricular complexes that in turn can initiate polymorphic VT or VF.

Acquired Diseases

An alteration in the expression and distribution of I_{to} is observed in various pathophysiological conditions (eFig. 2.1). Adrenergic effects seem to be involved in at least some of these I_{to} -regulating processes during heart disease.²²

In general, myocardial ischemia, MI, dilated cardiomyopathy, and end-stage heart failure cause downregulation of I_{to} . In fact, I_{to} downregulation is the most consistent ionic current change in the failing heart. The reduction in I_{to} results in attenuation of early repolarization (phase 1) and affects the level of plateau (phase 2) of the action potential and other currents involved in delayed repolarization (phase 3), with resulting prolongation and increased heterogeneity of action potential duration. The prominent epicardial I_{to} contributes to the selective electrical depression of the epicardium. This process leads to the development of a marked dispersion of repolarization between normal and abnormal epicardium and between epicardium and endocardium, which provides the substrate for reentrant arrhythmias and may underlie the increased predisposition to ventricular arrhythmias and SCD in patients with heart failure and ischemic heart disease. In addition, downregulation of I_{to} in advanced heart failure likely slows the time course of force generation, thereby contributing to reduced myocardial performance.



eFig. 2.1 Potassium Channel Remodeling in Heart Disease. Schematic summarizing the principal alterations in the action potential (AP) and corresponding K^+ currents alterations in four situations: heart failure (HF; A), border zone (BZ) of the myocardial infarction (MI; B), atrial fibrillation (AF; C) and pulmonary veins (D). Blue numbers indicate AP phases. Red are changes in pathology (A to C) or differences in pulmonary vein versus atrium (D). Numbers (0 to 4) indicate phases of the action potential. SR, Sarcoplasmic reticulum. (From Algalarrondo V, Nattel S. Potassium channel remodeling in heart disease. *Card Electrophysiol Clin*. 2016;8:337–347.)

On the other hand, compensatory ventricular hypertrophy preceding heart failure is associated with upregulation of I_{to} . The prolongation of the action potential, concomitant with an increase in I_{to} , presumably results from the more negative level of the plateau with less I_{CaL} inactivation and probably less delayed rectifier activation. In contrast, progression of hypertrophy to heart failure is associated with a clear reduction in I_{to} .

Chronic AF reduces atrial I_{to} density and $K_v4.3$ mRNA levels. Hypothyroidism reduces the expression of *KCND2* ($K_v4.2$) genes. In addition, I_{to} may also be reduced and contribute to QT interval prolongation in diabetes. Importantly, with some delay, insulin therapy partially restores I_{to} , possibly by enhancing $K_v4.3$ expression.¹⁹

Ultrarapidly Activating Delayed Outward Rectifying Current

Structure and Physiology

The ion-conducting pore of I_{Kur} channels is formed by four $K_v1.5$ α subunits (encoded by *KCNA5*), whereas the ancillary β subunits $K_v\beta1.2$, $K_v\beta1.3$, and $K_v\beta2.1$ control channel trafficking and plasma membrane integration as well as activation and inactivation kinetics.

I_{Kur} activates rapidly on depolarization in the plateau range and displays outward rectification, but it inactivates very slowly during the time course of the action potential. Inactivation accelerates when $K_v1.5$ is coexpressed with its β subunits.

Function

I_{Kur} is detected only in human atria and not in the ventricles, so that it is the predominant delayed rectifier current responsible for human atrial repolarization and is a basis for the much shorter duration of the action potential in the atrium.

Regulation

β -Adrenergic stimulation enhances I_{Kur} , whereas α -adrenergic stimulation inhibits it, effects likely mediated by PKA and PKC, respectively. Membrane depolarization and elevated extracellular K^+ concentrations reduce $K_v1.5$ expression. In addition, cAMP, mechanical stretch, hyperthyroidism, and dexamethasone increase $K_v1.5$ expression, whereas extracellular acidosis, phenylephrine, and hypothyroidism decrease it.

Coexpression of $K_v\beta1.3$ with $K_v1.5$ induces a fast inactivation and a hyperpolarizing shift in the activation curve (i.e., $K_v\beta1.3$ subunit converts $K_v1.5$ from a delayed rectifier with a modest degree of slow inactivation to a channel with both fast and slow components of inactivation). Data suggest that $K_v\beta1.2$ and $K_v\beta1.3$ subunit modification of $K_v1.5$ currents requires phosphorylation by PKC or a related kinase.

Pharmacology

I_{Kur} is relatively insensitive to class III antiarrhythmic drugs of the methane-sulfonanilide group, but it is highly sensitive to 4-aminopyridine. Selective inhibition of I_{Kur} by 4-aminopyridine prolongs the human atrial action potential duration.

Because I_{Kur} is atrium specific, $K_v1.5$ channels are a promising target for the development of new, safer antiarrhythmic drugs to prevent AF without risk of inducing QT prolongation and ventricular arrhythmias. However, although several selective I_{Kur} blockers have been evaluated, the clinical value of “pure” I_{Kur} blockers for antiarrhythmic therapy in AF remains unproven. Because $K_v1.5$ is downregulated in AF, the beneficial effect of I_{Kur} blockade becomes less certain. Furthermore, because $K_v1.5$ is also expressed in other organs (e.g., brain), discovery of drugs that selectively inhibit cardiac $K_v1.5$ channels remains necessary.¹⁸

Vernakalant, an I_{Kur} blocker, has been shown effective for the acute termination of AF and was approved in Europe. The efficacy of vernakalant in acute cardioversion of AF is likely due to multiple-channel

block. Vernakalant inhibits two atrial-specific K^+ channels (I_{Kur} and I_{KACH}) at low concentration, and is able to block I_{to} and I_{Na} at higher concentration.^{20,23,24}

Although selective I_{Kur} block would be expected to specifically prolong atrial action potential duration, such effects were not observed in healthy subjects at physiological atrial rates. Simulated inhibition of I_{Kur} was shown to increase plateau height, leading to additional activation of I_{Kr} and no net change in action potential duration.

Physiologically, rapid activation of I_{Kur} in the positive potential range following the action potential upstroke can offset depolarizing I_{CaL} and hence lead to the less positive plateau phase in atrial compared with ventricular cardiomyocytes. Conversely, block of I_{Kur} produces a more pronounced spike-and-dome configuration and therefore shifts the potential into a more positive range in which I_{CaL} activation enhances systolic Ca^{2+} influx during a free-running action potential. Such an indirect effect on I_{CaL} should be shared by all I_{Kur} blockers and is expected to result in a positive atrial inotropic effect.¹⁸

Inherited Channelopathies

KCNA5 mutations have been reported in individuals with familial AF. Heterologous expression of these mutations revealed complete I_{Kur} loss of function (see Table 2.3). Absence of I_{Kur} can excessively prolong atrial action potential duration with an enhanced risk of EADs that can trigger or maintain AF.

Acquired Diseases

A prolonged period of rapid activation of the atria as occurs during AF leads to a decrease in I_{Kur} . In addition, I_{Kur} may be affected in myocardial ischemia (see eFig. 2.1). Decreased $K_v1.5$ mRNA levels were reported for the epicardial border zone of infarcted hearts. Moreover, ischemic damage disrupted the normal location of $K_v1.5$ in the intercalated discs.

Rapidly Activating Delayed Outward Rectifying Current

Structure and Physiology

I_{Kr} is formed by coassembly of four pore-forming α subunits ($K_v11.1$, encoded by *KCNH2*) and β subunits (MiRP1, encoded by *KCNE2*). *KCNH2* is also known as the human-ether-a-go-go-related gene (*HERG*), so-named because the mutation in the *Drosophila* fruit fly caused it to shake like a go-go dancer. The current generated by *HERG* channels shows unusual voltage dependence. In contrast to I_{Ks} , I_{Kr} activates relatively rapidly (on the order of 10s of milliseconds) on membrane depolarization. Activation of I_{Kr} occurs with steep voltage dependence and reaches half-maximum activation at membrane voltage of approximately -20 mV. The magnitude of I_{Kr} increases as a function of E_m up to approximately 0 mV, but it declines with stronger depolarization (higher than 0 mV), resulting in a negative slope conductance of the current-voltage relationship. During repolarization of the action potential, I_{Kr} rapidly recovers from inactivation, thus causing the current to peak at -40 mV. The amplitude of the tail current on repolarization exceeds that of the current during the depolarizing pulse.²³

The unusual voltage dependence of I_{Kr} results from a fast, voltage-dependent C/P-type inactivation process, which limits outward K^+ flow at positive voltages. The large tail current on repolarization from positive voltages results from the rapid recovery of inactivated channels into a conducting state. On repolarization, *HERG* channels deactivate (close) via a slow, voltage-independent process (in contrast to the voltage-dependent inactivation process).

Unlike most K_v channels, *HERG* channels exhibit inward rectification. Rectification describes the property of an ion channel to allow currents preferentially to flow in one direction or limit currents from flowing in the other direction. In other words, conductivity of channels

carrying such currents is not constant but is altered at a different E_m . A channel that is inwardly rectifying is one that passes current (positive charge) more easily into the cell. This property is critical for limiting outward K^+ conductance during the plateau phase of the cardiac action potential. Unlike typical K_{ir} channels, in which rectification derives from blockade of the channel pore by intracellular polyamines (see later discussion), the mechanism of *HERG* inward rectification is a very rapid inactivation that develops at far more negative potentials (-85 mV) than channel activation (-20 mV).

The inactivation of *HERG* channels resembles the C/P-type inactivation of other K_v channels in its sensitivity to extracellular cations (including K^+ and Na^+) and tetraethyl ammonium (TEA), and to mutations in the P segment. However, the gating behavior is distinctive. First, channel inactivation is much faster than voltage-dependent activation, thus resulting in its characteristic rectification. Second, *HERG* inactivation displays intrinsic voltage dependence. Similar to the classic C/P-type inactivation, raising the concentration of extracellular K^+ slows *HERG* channel C/P-type inactivation, an effect that appears to result from occupancy of the pore selectivity filter by K^+ .

Function

I_{Kr} presents the principal repolarizing current at the end of the plateau phase in most cardiac cells and plays an important role in governing the cardiac action potential duration and refractoriness. I_{Kr} is differentially expressed, with high levels in left atrial and in ventricular endocardium.

I_{Kr} activates relatively fast on membrane depolarization and allows outward diffusion of K^+ ions in accordance with its electrochemical gradient, but voltage-dependent inactivation thereafter is very fast. Hence only limited numbers of channels remain in the open state, while a considerable fraction resides in the nonconducting inactivated state. The fast voltage-dependent inactivation limits outward current through the channel at positive voltages and thus helps maintain the plateau phase that controls contraction and prevents premature excitation. However, as the voltage becomes less positive at the end of the plateau phase of repolarization, the channels recover rapidly from inactivation, thus leading to a progressive increase in I_{Kr} amplitudes during action potential phases 2 and 3, with maximal outward current occurring before the final rapid declining phase of the action potential. The large resurgent I_{Kr} outward current repolarizes the membrane potential. Next, the channel deactivates (closes) slowly. The resulting large and transient outward current adds considerably to the ongoing repolarization and makes *HERG* especially suitable for robust control of the repolarization phase.^{23,25}

Regulation

β -Adrenergic stimulation and elevation of intracellular cAMP levels enhance I_{Kr} amplitude both through PKA-mediated effects and by direct interaction with the protein. α -Adrenergic stimulation is inhibitory. Coexpression of *HERG* with its β subunit (*KCNE1* or *KCNE2*) accentuates the cAMP-induced voltage shift. The net result of these effects is a reduction in I_{Kr} .

Extracellular Na^+ potentially inhibits I_{Kr} by binding to an outer pore site, and it also speeds recovery from inactivation. The inhibitory effect of Na^+ is potentially relieved by physiological levels of extracellular K^+ . Competition with external K^+ for a binding site near the external pore explains the finding that elevation of extracellular K^+ concentration paradoxically enhances I_{Kr} despite the decrease in the electrochemical driving force. Hypokalemia causes prolongation of the action potential duration as a result of reduced K^+ conductance. Low extracellular K^+ levels accelerate fast inactivation of the *HERG* channel and increase channel blockade by extracellular Na^+ .²⁶

Pharmacology

I_{Kr} is the target of class III antiarrhythmic drugs of the methanesulfonanilide group (almokalant, dofetilide, D-sotalol, E-4031, ibutilide, and MK-499). These drugs produce a voltage- and use-dependent block, shorten open times in a manner consistent with open channel block, and exhibit low affinity for closed and inactivated states. I_{Kr} blockers prolong atrial and ventricular action potential duration (and the QT interval) and refractoriness in the absence of significant changes in conduction velocity (AH, HV, and PR intervals do not prolong). Although selective I_{Kr} blockers exhibit antiarrhythmic properties against reentrant arrhythmias, they are probably not effective against triggered activity or increased automaticity.

Selective I_{Kr} blockers have several disadvantages. These drugs tend to prolong the action potential duration in the Purkinje and midmyocardial cells more than in the subepicardial or subendocardial cells, thus resulting in increased dispersion of repolarization across the ventricular wall and, as a consequence, increased arrhythmogenesis. Moreover, the effects of these drugs increase with decreasing heart rate. This reverse frequency-dependent nature of I_{Kr} blockers can potentially result in excessive prolongation of the QT interval during bradycardia, potentially precipitating torsades de pointes, whereas this prolongation is much less marked or even absent following β -adrenergic stimulation or during sustained tachycardia. This phenomenon limits the efficacy of these drugs in terminating tachyarrhythmias, while maximizing the risk of torsades de pointes during slow heart rates, such as during sinus rhythm after termination of AF. Reverse use-dependence has been attributed, at least in part, to the incomplete deactivation (accumulation) of I_{Kr} during fast heart rates that leads to a progressive increase in current amplitude, which counteracts the action potential prolongation effects of I_{Kr} blockers.

Azimilide blocks I_{Kr} , I_{Ks} , and I_{CaL} , whereas amiodarone exhibits a complex mechanism of action because it blocks I_{Na} , I_{Ca} , I_{Kr} , I_{Ks} , I_{to} , and I_{KATP} . Quinidine, a class IA agent, also blocks I_{Kr} at concentrations lower than those required to block I_{Ks} , I_{to} , and I_{K1} .

Furthermore, *HERG* channels display an unusual susceptibility to blockade by a variety of drugs compared with other voltage-gated K^+ channels. Increasing numbers of drugs with diverse chemical structures (including some antihistaminics, antipsychotics, and antibiotics) decrease I_{Kr} by depressing *HERG* channel gating, delay ventricular repolarization, prolong the QT interval (acquired LQTS), and induce torsades de pointes. In fact, almost all drugs that cause acquired LQTS target *HERG* channels, likely because of unique structural properties rendering this channel unusually susceptible to a wide range of different drugs. Compared with other cardiac K^+ channels, the *HERG* channel has a large, funnel-like vestibule that allows many small molecules to enter and block the channel. The more spacious inner cavity results from a lack of the S6 helix bending Pro-X-Pro sequence, which presumably facilitates access of drugs to the pore region from the intracellular side of the channel to block the channel current. In addition, the *HERG* channel contains two aromatic residues located in the S6 domain facing the channel vestibule (not present in most other K^+ channels) that provide high-affinity binding sites for a wide range of structurally diverse compounds. The accessory β subunit (*MiRP1*, *KCNE2*) also determines the drug sensitivity. Interaction of these compounds with the channel's pore causes functional alteration of its biophysical properties or occlusion of the permeation pathway.^{18,23}

One novel mechanism for acquired LQTS involves compounds interfering with *HERG* trafficking (i.e., moving the *HERG* protein from the endoplasmic reticulum to the cell membrane), rather than direct pore blocking. These compounds include arsenic trioxide, pentamidine, probucol (a cholesterol-lowering therapeutic compound), and cardiac glycosides.²³

Some drugs (almokalant, norpropoxyphene, azimilide, candesartan, and E3174, the active metabolite of losartan) can enhance I_{Kr} . Flufenamic acid and niflumic acid also increase I_{Kr} by accelerating channel opening. These observations open the possibility of developing new I_{Kr} openers for the treatment of patients with congenital (LQT2) or drug-induced LQTS.

Inherited Channelopathies

Long QT syndrome. The LQTS variants in which I_{Kr} is dysfunctional include LQT2 (caused by *KCNH2* [*HERG*] loss-of-function mutations) and LQT6 (caused by *KCNE2* [*MiRP1*] mutations; see Table 2.3). LQT2 is the second most prevalent type of LQTS. More than 200 putative disease-causing mutations have been identified for *KCNH2*; most appear to disrupt the maturation and trafficking of I_{Kr} α subunit ($K_{v11.1}$) to the sarcolemma, thereby reducing the number of functional ion channels at the cell surface membrane. Mutations involving the pore region of the *HERG* channel are associated with a significantly more severe clinical course than nonpore mutations; most pore mutations are missense mutations with a dominant negative effect. Attenuation of I_{Kr} results in prolongation of the action potential and the QT interval and can potentially generate EADs and torsades de pointes.²³

The trafficking of some mutant channels into the sarcolemma can be restored by *HERG* channel blockers (e.g., cisapride, terfenadine, astemizole, E-4031), even when fexofenadine rescues mutant *HERG* channels at concentrations that do not cause channel block. However, because I_{Kr} blockers failed to rescue other trafficking-defective mutants, it is likely that multiple mechanisms underlie the pharmacological rescue of LQT2 mutations.

Proarrhythmia induced by conditions associated with reduction of I_{Kr} (acquired and congenital LQTS) is related to excessive prolongation of action potential duration near plateau voltages, especially those that favor the development of EADs. It is also related to a more marked prolongation of the action potential duration in midmyocardial than in subepicardial or subendocardial ventricular cells, possibly because of the relative scarcity of I_{Ks} and hence less “repolarization reserve” in the midmyocardial cells. Thus triggered focal activity and ventricular reentry associated with an increased heterogeneity of repolarization across the ventricular wall would lead to the development of torsades de pointes.²⁷

Short QT syndrome. Short QT syndrome (SQTS) is a rare disease associated with short QT intervals and increased risk for AF and VF. A gain-of-function mutation in *KCNH2* (*HERG*) is linked to SQTS type 1 (SQT1). The *KCNH2* mutation causes a shift of voltage dependence of inactivation of I_{Kr} to more depolarized potentials (by +90 mV) out of the range of the action potential, leading to less inward rectification at physiological potentials and a significant increase of I_{Kr} during the action potential plateau at the expense of the magnitude of the repolarizing tail current. The resulting I_{Kr} increase achieved by altered gating hastens repolarization, thereby shortening action potential duration and facilitating reentrant excitation waves to induce atrial and ventricular arrhythmia.^{23,27}

Familial AF. Gain-of-function mutations in *KCNE2* (*MiRP1*) have been found in two families with AF. MI can result in reduction in $K_{v11.1}$ mRNA levels and I_{Kr} with consequent prolongation of the action potential duration (see eFig. 2.1). Conversely, I_{Kr} density increases in subendocardial Purkinje cells in the infarcted heart at 48 hours, which can potentially increase the proarrhythmic effects of I_{Kr} blockers in patients with MI. In addition, during acute ischemia, I_{Kr} is increased and action potential duration is shortened. Such changes can be arrhythmogenic. I_{Kr} is unchanged in patients with chronic AF and is homogeneously distributed in failing canine hearts.

ATP, derived from either glycolysis or oxidative phosphorylation, is critical for *HERG* channel function. Both hyperglycemia and hypoglycemia depress I_{Kr} and can cause QT prolongation and ventricular arrhythmias. In diabetes, $K_{v11.1}$ levels are downregulated, leading to reduction in I_{Kr} and contributing to QT interval prolongation. Importantly, insulin therapy restores I_{Kr} function and shortens QT intervals.

Unlike with most other K^+ currents, I_{Kr} amplitude increases on elevation of extracellular K^+ concentrations and decreases after removal of extracellular K^+ . Elevation of extracellular K^+ concentration reduces C/P-type inactivation and increases the single channel conductance of *HERG* channels. This explains why the action potential durations are shorter at higher extracellular K^+ concentrations and longer at low concentrations, and it clarifies the associations among hypokalemia, action potential duration prolongation, and induction of torsades de pointes in patients treated with I_{Kr} blockers. In contrast, modest elevations of extracellular K^+ concentrations using K^+ supplements and spironolactone in patients given I_{Kr} blockers or with LQT2 significantly shorten the QT interval and may prevent torsades de pointes. Moreover, the antiarrhythmic actions of I_{Kr} blockers can be reversed during ischemia, which is frequently accompanied by elevations of the extracellular K^+ concentrations in the narrow intercellular spaces and by catecholamine surges that occur with exercise or other activities associated with fast heart rates.

Slowly Activating Delayed Outward Rectifying Current Structure and Physiology

I_{Ks} is formed by coassembly of four pore-forming α subunits ($K_{v7.1}$, also known as K_{vLQT1} , encoded by the *KCNQ1* gene) and β subunits (minK, encoded by the *KCNE1* gene). I_{Ks} is a K^+ -selective current that activates very slowly in response to membrane depolarization to potentials greater than −30 mV and reaches half-maximum activation close to +20 mV. I_{Ks} has a linear current-voltage relationship, its time course of activation is extremely slow, slower than any other known K^+ current, and steady-state amplitude is achieved only with extremely long membrane depolarization.²³

Inactivation of *KCNQ1* channels is half-maximal at −18 mV. At its maximum, inactivation reduces fully activated current by approximately 35%. In addition, unlike inactivation of other K_v channels, the onset of I_{Ks} inactivation occurs after a delay (a delay of approximately 75 milliseconds at +40 mV). In contrast, when inactivation is induced after transient recovery of channels to open states, the onset of inactivation is 10 times faster. The molecular mechanism of *KCNQ1* channel inactivation is unknown, but in contrast to a classical C/P-type inactivation, *KCNQ1* inactivation is independent of extracellular K^+ concentration.

Function

I_{Ks} contributes to human atrial and ventricular repolarization, particularly during action potentials of long duration. I_{Ks} gradually increases during the plateau phase of the action potential because its activation is delayed and very slow. As a consequence, the contribution of I_{Ks} to the net repolarizing current is greatest late in the cardiac action potential plateau phase. I_{Ks} is expressed in all cell types, but it is reduced in midmyocardial cells. The midmyocardial cells have the longest action potential duration across the myocardial wall.

I_{Ks} plays an important role in determining the rate-dependent shortening of the cardiac action potential and QT interval. As heart rate increases, I_{Ks} increases because channel deactivation is slow and incomplete during the shortened diastole. This allows I_{Ks} channels to accumulate in the open state during rapid heart rates and contribute to the faster rate of repolarization.

Importantly, I_{Ks} is functionally upregulated when other repolarizing currents (e.g., I_{Kr}) are reduced, potentially serving as a safeguard against

loss of repolarizing power. As such, several redundant mechanisms contribute to repolarization constituting the repolarization reserve, in which I_{Ks} plays an important role.

Regulation

I_{Ks} is markedly enhanced by β -adrenergic stimulation through channel phosphorylation by PKA (requiring A-kinase anchoring protein 9 [AKAP9, also known as Yotiao]) and PKC (requiring minK). This produces a rate-dependent shortening of the action potential duration, such as seen during exercise-induced sinus tachycardia. I_{Ks} is also modulated by α -adrenergic receptors through the PKC pathway. Lowering extracellular K^+ and Ca^{2+} concentrations increases I_{Ks} .²⁸

Coexpression of $K_{v7.1}$ with minK regulates α subunit trafficking and behavior and results in a sevenfold increase in I_{Ks} magnitude, marked slowing of the time course of activation, and removal (or significant slowing) of inactivation of $K_{v7.1}$ channels.

As noted, I_{Kr} and I_{Ks} are functionally linked; when I_{Kr} is reduced, the action potential is prolonged, causing I_{Ks} activation to increase to prevent excess repolarization delay. Hence the duration of the action potential is very tightly tuned via I_{Ks} and I_{Kr} regulation.

Pharmacology

I_{Ks} is resistant to methanesulfonanilides (almokalant, dofetilide, D-sotalol, E-4031, ibutilide, and MK-499), but it is selectively blocked by chromanols, indapamide, thiopentone, propofol, and benzodiazepines. I_{Ks} is also blocked, although nonselectively, by amiodarone, dronedarone, and azimilide. β subunits (minK) modulate the effects of I_{Ks} blockers and agonists. In fact, coexpression of $K_{v7.1}$ with minK confers 6- to 100-fold higher affinity for some I_{Ks} blockers than $K_{v7.1}$ channels.

Selective I_{Ks} blockers prolong the cardiac action potential duration and QT interval and suppress electrically induced ventricular tachyarrhythmias in animals with acute coronary ischemia and exercise superimposed on a healed MI.

I_{Ks} blockade seems to have less proarrhythmic potency as compared with I_{Kr} blockade, likely the result of less drug-induced dispersion in repolarization. In addition, because I_{Ks} accumulates at fast driving rates because of its slow deactivation, I_{Ks} blockers can be expected to be more effective in prolonging action potential duration and refractoriness tachyarrhythmias, with lesser effects at normal sinus rates. Furthermore, since I_{Ks} activation occurs at approximately 0 mV and this voltage is more positive than the Purkinje fiber action potential plateau voltage, I_{Ks} blockade should not be expected to prolong the action potential duration at this level. Conversely, in ventricular muscle, the plateau voltage is more positive (approximately +20 mV), thus allowing I_{Ks} to be substantially more activated, so that I_{Ks} blockade would be expected to markedly increase action potential duration.²⁰

β -Adrenergic agonists increase I_{Ks} density and produce a rate-dependent shortening of the action potential duration, and can also decrease the antiarrhythmic effects of I_{Ks} blockers. In addition, in the presence of I_{Ks} blockade, isoproterenol seems to abbreviate the action potential duration of epicardial and endocardial, but not midmyocardial, cells, an effect that can accentuate transmural dispersion of repolarization and precipitate torsades de pointes. These observations may explain the therapeutic actions of beta-blockers in patients with LQTS syndromes linked to attenuation of I_{Ks} and the increased risk of fatal cardiac arrhythmias under physical activity or stressful situations that increase sympathetic activity in these patients.

Inherited Channelopathies

KCNQ1 and *KCNE1* mutations can lead to a defective protein and several forms of inherited arrhythmias, including LQTS (comprising

the autosomal dominant Romano-Ward syndrome and the autosomal recessive Jervell and Lange-Nielsen syndrome), SQTs, and familial AF.

Long QT syndrome. The most common type of LQTS, LQT1, is caused by loss-of-function mutations on the *KCNQ1* gene (*K_vLQT1*). To date, more than 200 mutations of this gene have been reported. They comprise many Romano-Ward (autosomal dominant) syndromes and account for approximately 45% of all genotyped LQTS families. Individuals with the less prevalent LQTS type 5 (LQT5) carry loss-of-function autosomal dominant mutations in *KCNE1* and display a phenotype similar to that seen in patients with LQT1.²³

Loss-of-function mutations in both alleles of *KCNQ1* or *KCNE1* (i.e., inherited from both parents, autosomal recessive) cause the very rare Jervell and Lange-Nielsen syndrome type 1 or 2, respectively. Jervell and Lange-Nielsen syndrome is characterized by severe QT interval prolongation, high risk of sudden death, and congenital deafness; the deafness results from deficient endolymph secretion (*KCNQ1* and *KCNE1* are also expressed in the inner ear, where they enable endolymph secretion).²⁷

LQT11 is caused by loss-of-function mutations on the *AKAP9* gene, which encodes an A-kinase anchoring protein (Yotiao), shown to be an integral part of the I_{Ks} macromolecular complex. The presence of Yotiao is necessary for the physiological response of the I_{Ks} channel to β -adrenergic stimulation. A mutation in *AKAP9* (Yotiao) in the I_{Ks} channel ($K_{v7.1}$) binding domain reduces the interaction between the I_{Ks} channel and Yotiao. This, in turn, reduces the cAMP-induced phosphorylation of the channel and prevents the functional response of the I_{Ks} channel to cAMP and adrenergic stimulation (i.e., prevents the increase in magnitude of I_{Ks} and the shortening of action potential duration in response to sympathetic stimulation). The final result is an attenuation of I_{Ks} , resulting in a delay in ventricular repolarization and QT interval prolongation.²³

Mutations in LQT1, LQT5, and LQT11 result in attenuation of I_{Ks} , which causes prolongation of repolarization, action potential duration, and QT interval, which may be especially notable during periods of increased sympathetic activity, such as exercise, when I_{Ks} becomes the predominant repolarization current rather than I_{Kr} . In LQT1, ventricular arrhythmias are usually triggered by emotional or physical stress, probably because mutant I_{Ks} does not increase sufficiently (i.e., has less repolarization reserve) during β -adrenergic stimulation. Accordingly, β -adrenergic blocking drugs suppress arrhythmic events in LQT1.

Short QT syndrome. SQT2 is caused by mutations on the *KCNQ1* gene (*K_vLQT1*). A gain-of-function *KCNQ1* mutation causes a shift of voltage dependence of activation of I_{Ks} by -20 mV and acceleration of activation kinetics, leading to enhancement of I_{Ks} and shortening of the action potential duration and QT interval. *KCNQ1* gain-of-function mutations likely predispose to AF and VF by shortening refractoriness and facilitating reentry.²³

Familial AF. *KCNQ1* gain-of-function mutations have been linked to familial AF, with or without the SQTs phenotype. In addition, gain-of-function mutations in the *KCNE1*, *KCNE2*, and *KCNE5*, which encode β subunits of I_{Ks} , have been linked to familial AF. Of note, a few loss-of-function mutations have been identified in patients with familial AF. The explanation of how gain- and loss-of-function mutations in the same channel could result in the same type of arrhythmia remains unclear.²⁷

Acquired Diseases

Heart failure reduces I_{Ks} in atrial, ventricular, and sinus node myocytes. Given that I_{Kr} is unchanged, I_{Ks} reduction may largely account for the prolonged action potential duration in heart failure (see eFig. 2.1).

I_{Ks} density and *KCNQ1/KCNE1* mRNA levels are reduced in myocytes from infarcted border zones 2 days after MI. However, *KCNQ1*

expression is restored 5 days after MI, whereas *KCNE1* expression remains decreased.

Inward Rectifying Current

Structure and Physiology

Kir family is categorized into seven subfamilies (Kir1-Kir7). Kir2 subfamily is responsible for the human I_{K1} . The Kir2 subfamily consists of six members (Kir2.1-Kir2.6), of which only three are expressed in human cardiac myocytes (Kir2.1, Kir2.2, and Kir2.3, encoded by *KCNJ2*, *KCNJ12*, and *KCNJ4*, respectively).²⁹

The Kir channels are formed by the coassembly of four α subunits (see Fig. 2.4). Each α subunit (Kir2.x) of I_{K1} consists of two transmembrane domains (M1 and M2) connected by a pore-forming P loop (H5) along with cytoplasmic N- and C-termini. The tetrameric Kir2 channel complex can be formed by identical (homotetramers) or different (heterotetramers) α subunits.²⁹

Kir channels exhibit a strong inward rectification property because conductance to K^+ ions alters at a different E_m . As noted, rectification describes the property of an ion channel to allow currents preferentially to flow in one direction or limit currents from flowing in the other direction. A channel that is inwardly rectifying is one that passes current (positive charge) more easily into the cell. In the case of Kir channels, inward rectification is a strongly voltage-dependent decline of K^+ efflux (i.e., reduction of outward current) on membrane depolarization that produces a characteristic region of so-called “negative slope conductance” (Fig. 2.5). At E_m more negative to the reversal potential for K^+ ($E_K = -90$ mV), I_{K1} conductance is much larger than that of any other current, and so it clamps the resting E_m close to E_K . On depolarization, I_{K1} channels close almost immediately and thus limit K^+ efflux at membrane potentials more positive than the E_K , remain closed throughout the plateau of the action potential, and open again at potentials negative to -20 mV. As such, I_{K1} channels also conduct a substantial outward current at an E_m between -40 and -90 mV. Within this voltage range, outward I_{K1} is larger at more negative potentials. Thus I_{K1} also contributes to terminal phase 3 of repolarization. Because an E_m negative to E_K is not reached in cardiomyocytes, only the outward I_{K1} plays a role in action potential formation.

The phenomenon of inward rectification of I_{K1} channels results from high-affinity and strongly voltage-dependent blockade of the inner

channel pore (at a site provided by a ring of negative charges) by cytosolic Mg^{2+} , Ca^{2+} , and positively charged polyamines (spermine, spermidine, putrescine), which plug the channel pore at depolarized potentials, resulting in a decline in outward currents, but are displaced by incoming K^+ ions at hyperpolarized potentials. This voltage-dependent block by polyamines causes currents to be conducted well only in the inward direction. As such, I_{K1} channels are voltage regulated despite the lack of the classic voltage-sensing mechanism of K_v channels.²⁰

Reducing overall membrane conductance and limiting K^+ efflux during the action potentials by inward rectification is an important energy-saving mechanism, since restoration of resting membrane state requires influx of the extruded K^+ ions by the Na^+-K^+ pump at the expense of ATP hydrolysis.²⁹

A unique property of I_{K1} is the unusual dependence of rectification on extracellular K^+ concentration. Specifically, on increase in extracellular K^+ , the I_{K1} current-voltage relationship shifts nearly in parallel with the E_K and leads to a crossover phenomenon (Fig. 2.6). One important consequence of such behavior is that at potentials positive to the crossover, K^+ conductance increases rather than decreases. This is against an expectation of a depolarization of the cell membrane based on a reduced driving force for K^+ ions (due to a less negative E_K) as a result of elevated extracellular K^+ concentration.¹⁷

Function

I_{K1} sets and stabilizes the resting E_m and regulates cellular excitability of atrial and ventricular myocytes during phase 4. It also contributes to the terminal portion of phase 3 repolarization. In addition to the contribution of I_{K1} to the T wave on surface ECG, data suggest that the U wave is strongly modulated by I_{K1} .

I_{K1} channels close on depolarization. The strong inward rectification of the I_{K1} limits the outward current during the positive phase of the action potential (phases 0, 1, and 2), thus allowing membrane depolarization following Na^+ channel activation, slowing membrane repolarization, and helping maintain a more prolonged cardiac action potential. This also confers energetic efficiency in the generation of the action potential.

I_{K1} density is much higher in ventricular than in atrial myocytes, a finding that explains the steep repolarization phase in the ventricles (where more abundant I_{K1} plays a larger role in accelerating the terminal portion of repolarization) and the shallower phase in the atria. The higher I_{K1} channel expression in the ventricle protects the ventricular cell from pacemaker activity. By contrast, I_{K1} is almost absent in sinus

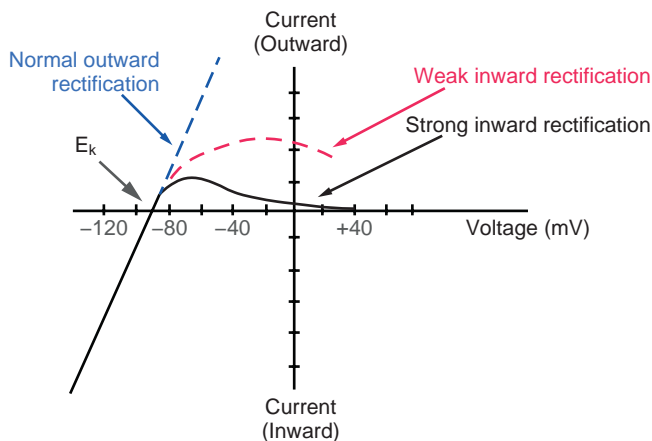


Fig. 2.5 Idealized Current-Voltage Relation of Strong and Weak Kir Channels. Both conduct inward currents significantly at diastolic membrane potentials more negative to the reversal potential for K^+ ($E_K = -90$ mV). However, but strong inward rectifiers pass little or no current at action potential plateau potentials.

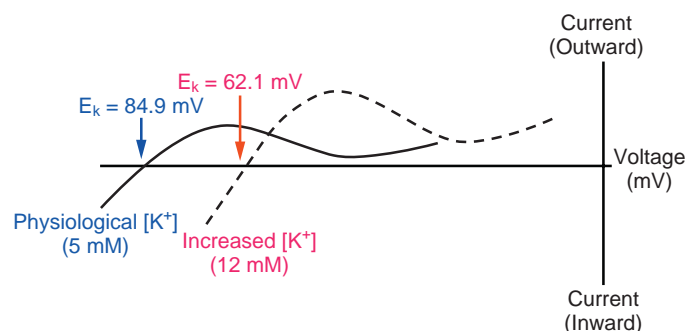


Fig. 2.6 Current-Voltage Relationship for Kir Channels at Two Different Extracellular K^+ Concentrations. E_K is calculated from the Nernst equation using extracellular $[K^+]$ of 5 or 12 mM and intracellular $[K^+]$ of 130 mM. (From Sorensen CM, Braunstein TH, Holstein-Rathlou N-H, Salomonsson M. Role of vascular potassium channels in the regulation of renal hemodynamics. *AJP Ren Physiol*. 2012;302:F505–F518.)

node and AVN cells, thus allowing for relatively more depolarized resting diastolic potentials compared with atrial and ventricular myocytes. In addition, location-dependent expression of specific Kir2 isoforms (Kir2.1, Kir2.2, Kir2.3) has been observed.

Fast heart rates increase K^+ concentration in the narrow intercellular space to several millimolars (secondary to K^+ efflux via I_{Kr} and I_{Ks} during repetitive action potentials) and augments I_{K1} , which results in a shortening of the action potential duration that may offset the ability of I_{Kr} blockers to prolong the action potential duration under these conditions.

Regulation

β -Adrenergic stimulation inhibits I_{K1} in ventricular myocytes via PKA-mediated phosphorylation of the channel. In atrial myocytes, α 1-adrenergic stimulation reduces I_{K1} via PKC-dependent pathways.

Kir2 overexpression increases I_{K1} density, shortens the action potential duration, and hyperpolarizes the resting E_m . In contrast, suppression of I_{K1} prolongs the action potential duration and disrupts effective clamping of the resting E_m , thus precipitating spontaneous pacemaker activity in otherwise nonpacemaking atrial and ventricular cardiomyocytes.

The phospholipid phosphatidylinositol 4,5-bisphosphate (PIP2) enhances I_{K1} and modulates various properties of Kir2 channels, such as pH sensitivity. In addition, increased levels of cholesterol in the membrane reduce I_{K1} . Various intracellular cations can block Kir2 channels, such as Ca^{2+} and H^+ (i.e., intracellular pH).

Pharmacology

Barium (Ba^{2+}) is a potent I_{K1} blocker. Blocking of I_{K1} by extracellular Ba^{2+} results in depolarization of the resting potential and mild action potential prolongation. Terikalant and chloroquine (an antimalarial drug) are strong I_{K1} inhibitors but can also block other K^+ channels.

Selective blockers of Kir2 channels are available only for experimental purposes. I_{K1} blockers prolong atrial and ventricular action potential duration and are effective against various types of experimental reentrant VTs. Moreover, I_{K1} blockers produce membrane depolarization, an effect that slows conduction velocity as a result of voltage-dependent inactivation of Na^+ channels, and prolongs the QT interval; both actions are proarrhythmic.²⁰

I_{K1} agonists include flecainide, arachidonic acid, tenidap (an anti-inflammatory agent), and zacopride (a gastrointestinal prokinetic agent).

Inherited Channelopathies

Long QT syndrome. Loss-of-function mutations of *KCNJ2* (encoding Kir2.1) result in dominant negative effects on the current and have been linked to Andersen-Tawil syndrome (LQT7), a rare autosomal dominant disorder characterized by the triad of skeletal developmental abnormalities, periodic paralysis, and usually ventricular arrhythmias (Kir2.1 channels are expressed primarily in skeletal muscle, heart, and brain). Compared with other types of LQTS, LQT7 is associated with more prominent U waves, a milder degree of QT interval prolongation, as well as a lesser risk of malignant ventricular arrhythmias.

Disruption of the I_{K1} function can potentially lead to prolongation of the terminal repolarization phase and QT interval, which can predispose to the generation of EADs and delayed afterdepolarizations (DADs) that cause ventricular arrhythmias. However, unlike other types of LQTS in which the afterdepolarizations arise from reactivation of L-type Ca^{2+} channels, the EADs and DADs generated in LQT7 are likely secondary to Na^+ - Ca^{2+} exchanger-driven depolarization. It is believed that the differential origin of the triggering beat is responsible for the observed discrepancy in arrhythmogenesis and the clinical features compared with other types of LQTS. In addition, it is likely that pro-

longation of the action potential duration in LQT7 is somewhat homogeneous across the ventricular wall (i.e., transmural dispersion of repolarization is less prominent than in other types of LQTS), and this can potentially explain the low frequency of torsades de pointes.

Catecholaminergic polymorphic ventricular tachycardia. Loss-of-function mutations of *KCNJ2* have been found in patients with catecholaminergic polymorphic ventricular tachycardia (CPVT) and may represent a CPVT phenocopy. These patients had prominent U waves, ventricular ectopy, and polymorphic VT, but no dysmorphic features or skeletal muscle abnormalities.

I_{K1} reduction can trigger arrhythmia by allowing inward currents, which are no longer counterbalanced by the strong outward I_{K1} , to depolarize the E_m gradually during phase 4. Membrane depolarization during phase 4 induces arrhythmia by facilitating spontaneous excitability.

Short QT syndrome. A gain-of-function mutation of *KCNJ2* has been identified and linked to SQTs type 3 (SQT3) (see Table 2.3). The mutation causes a significant increase in the outward I_{K1} at potentials between -75 mV and -45 mV, thus leading to acceleration of the terminal phase of repolarization and, as a consequence, shortening the action potential duration and QT interval and asymmetrical T waves with a rapid terminal phase.

Familial AF. A gain-of-function *KCNJ2* mutation has been linked to familial AF. The affected members had normal QT intervals. The mutation was speculated to cause AF by shortening atrial action potential duration and facilitating reentrant excitation waves.

Acquired Diseases

I_{K1} is downregulated in patients with severe heart failure and cardiomyopathy (see eFig. 2.1). The downregulation of I_{K1} produces membrane depolarization and prolongation of the action potential duration, and it can facilitate spontaneous excitability and trigger arrhythmia (both EADs and DADs). Ventricular myocytes from patients with idiopathic dilated cardiomyopathy exhibit decreased channel activity, longer action potential duration, and a lower resting E_m than those from patients with ischemic cardiomyopathy. Upregulation of I_{K1} can be observed in ventricular hypertrophy.

Atrial I_{K1} is upregulated in patients with chronic AF, resulting in more negative resting potentials and, together with reduced I_{CaL} , accounting for action potential shortening in AF.

Acetylcholine-Activated Potassium Current

Structure and Physiology

I_{KACH} results from a heterotetrameric complex of two Kir3.1 (GIRK1, encoded by *KCNJ3*) and two Kir3.4 (GIRK4, encoded by *KCNJ5*) α subunits. I_{KACH} is a receptor-activated Kir channel; it has large cytoplasmic domains that harbor specific binding sites for cytosolic effectors (G proteins). The channel conducts I_{KACH} in response to the stimulation of G protein-coupled muscarinic (M2) and adenosine (A1) receptors. Because channel gating requires a G protein, Kir3.1/ Kir3.4 are considered a type of KG channel (hence the terminology GIRK1/GIRK4).

Cardiac I_{K1} and I_{KACH} are the major K^+ currents displaying classical strong inward rectification with membrane depolarization, a unique property that is critical for their roles in cardiac excitability.

Function

I_{KACH} has generally an opposite distribution to that of I_{K1} . I_{KACH} is more prominent in atrial tissue, as well as in the sinus node and AVN, and is largely absent in the ventricles. The regional distribution of I_{KACH} is also heterogeneous within and between the atria.¹⁷

I_{KACH} mediates vagal influences on sinus rate and atrial repolarization, as well as AVN conduction. Activation I_{KACH} by acetylcholine

hyperpolarizes the E_m and shortens action potential duration. These effects result in slowing of phase 4 depolarization, reduction in the spontaneous firing rate of the pacemaker cells of the sinus node, and slowing of AVN conduction. These effects explain why vagal maneuvers or IV adenosine can terminate reentrant supraventricular tachycardias using the AVN.

Regulation

Vagal stimulation produces a nonuniform shortening of the atrial action potential duration and refractoriness mediated by activation of $I_{K_{ACH}}$, an effect that can contribute to the perpetuation of AF.²⁸

$I_{K_{ACH}}$ is also increased by purinergic stimulation. Adrenergic stimulation via β_1 -receptor-mediated signaling increases the amplitude of constitutively active current, whereas α_1 -stimulation decreases $I_{K_{ACH}}$.

Atrial $I_{K_{ACH}}$ is inhibited by membrane stretch, possibly serving as a mechanoelectrical feedback pathway, a property conferred by the Kir3.4 subunit.

Pharmacology

$I_{K_{ACH}}$ activity can be stimulated by intracellular ATP, PIP2, ETA endothelin, A opioid, and α_2 -adrenergic agonists. α_1 -Adenosine receptor agonists stimulate $I_{K_{ACH}}$, whereas methylxanthines, such as theophylline and aminophylline, antagonize the effects of adenosine. Dipyridamole prolongs the action of adenosine by disturbing the action of the cell membrane transporter of adenosine.

$I_{K_{ACH}}$ is inhibited by several antiarrhythmic drugs, including amiodarone, dronedarone, dofetilide, ibutilide, sotalol, terikalant, disopyramide, procainamide, flecainide, and propafenone. Disopyramide and procainamide mainly block the muscarinic receptors, whereas flecainide and propafenone act as open channel blockers. Blockade of $I_{K_{ACH}}$ by dronedarone is approximately 100 times more potent than that of amiodarone.²⁰

$I_{K_{ACH}}$ is regarded as an atrial-selective drug target. A potent $I_{K_{ACH}}$ blocking property can be of a particular therapeutic value for treatment of AF, because $I_{K_{ACH}}$ plays a prominent role in vagally induced AF and has been shown to be constitutively active in chronic AF. In fact, several newer compounds targeting $I_{K_{ACH}}$ are currently being evaluated in pre-clinical and clinical studies for AF therapy. Inhibition of $I_{K_{ACH}}$ in the setting of AF can potentially produce proportionally greater action potential duration prolongation than under control conditions and can even terminate experimental atrial tachyarrhythmias and AF without ventricular side effects.²⁴

Inherited Channelopathies

LQT13 is caused by loss-of-function mutations on the *KCNJ5* gene. The *KCNJ5* mutation exerts dominant-negative effects on Kir3.1/Kir3.4 channel complexes by disrupting membrane targeting and stability of Kir3.4.

Acquired Diseases

Evidence indicates that constitutively active $I_{K_{ACH}}$ channels develop during AF as part of the electrical remodeling processes (i.e., these channels become activated despite the absence of stimulating acetylcholine). This increase in functionally uncoupled $I_{K_{ACH}}$ in human AF is possibly the result of increased phosphorylation of Kir3 channels by PKC or a reduction in inhibitory G α_i -3 subunits (see eFig. 2.1). Constitutively active $I_{K_{ACH}}$ can hyperpolarize the membrane and hence contribute to AF-related electrical remodeling and to the persistence of AF by stabilization of rotors. Therefore selectively targeting constitutively active $I_{K_{ACH}}$ channels only may preserve physiological stimulation by vagal nerves and could serve as a promising remodeling-related drug target.²⁰

Adenosine Triphosphate–Sensitive Potassium Current Structure and Physiology

Cardiac ATP-sensitive K^+ (K_{ATP}) channels (also termed the adenosine diphosphate [ADP]–activated K^+ channel) are formed by the unique combination of two dissimilar proteins: four pore-forming α subunits (Kir6) and four regulatory ABC proteins (SUR subunits). Two Kir6 genes, *KCNJ8* (encoding Kir6.1) and *KCNJ11* (encoding Kir6.2), and 2 SUR genes, *ABCC8* (encoding SUR1) and *ABCC9* (encoding SUR2), encode mammalian K_{ATP} subunits (Fig. 2.7). Alternative splicing of mRNA products give rise to multiple SUR variants (e.g., SUR2A and SUR2B), which confer distinct functional and pharmacologic properties on K_{ATP} channels.¹⁶

K_{ATP} channels are found in virtually every kind of cardiac tissue and, to a lesser extent, vascular smooth muscle. Current evidence suggests that K_{ATP} channels in ventricular myocytes are composed primarily of Kir6.2 and SUR2A isoforms, whereas K_{ATP} channels in atrial myocytes are composed primarily of Kir6.2 and SUR1 subunits. Kir6.1 subunits may contribute to the formation of K_{ATP} channels in SAN, AVN, and Purkinje fiber cells.¹⁶

The Kir6 subunits have two transmembrane domains (M1, M2) bridged by an extracellular loop that generates the narrow portion of the pore and controls ion selectivity, and large cytoplasmic domains that provide the binding sites for ATP.

The ATP-binding cassette transporter family consists of seven subfamilies (ABCA to ABCG) with 48 subfamily members. Most of the ABC proteins transport various molecules across cell membranes at the expense of ATP hydrolysis. The SUR subunits are much larger than Kir6 subunits and have 17 transmembrane regions, arranged in three transmembrane domains (TMD0, TMD1, and TMD2). TMD1 and TMD2 each contain six transmembrane segments and nucleotide-binding domains on the cytoplasmic side (known as nucleotide-binding folds [NBFs] that contain the characteristic Walker A and B motifs). TMD0 contains five transmembrane segments and is critical for trafficking and gating of the channel complex. The SUR subunits allow for nucleotide-mediated regulation of K_{ATP} and are critical in its role as a sensor of metabolic status. The SUR2A subunits are also sensitive to sulfonylureas, Mg-ATP, Mg-ADP, and some other pharmacological channel openers. In addition, SUR2A subunit harbors an ATPase for ATP hydrolysis, which gates the K^+ permeation through the Kir6.2 α subunit. Kir6 subunits are unique among the K^+ channel subunits since the presence of an auxiliary SUR subunit is an absolute requirement to form a functional channel. The details of the physical connection between Kir6 and SUR subunits remain unclear.^{29,30}

K_{ATP} is a receptor-activated weak inward rectifier channel, regulated by intracellular ATP and ADP concentrations. An increase in the ratio of ATP to ADP closes the channel, and a decrease opens it, linking the metabolic state to the cellular E_m . Further, physiological levels of intracellular Na^+ and Mg^{2+} and naturally occurring intracellular polyamines (e.g., spermine, spermidine, and putrescine) contribute to K_{ATP} channel inward rectification.

Function

$I_{K_{ATP}}$ is inhibited by intracellular ATP and activated by Mg-ADP, so that the channel activity is regulated by the ATP/ADP ratio, coupling cell metabolism to the E_m . In responding to cytoplasmic nucleotide levels, K_{ATP} channel activity provides a unique link between cellular energetics and electrical excitability and hence contractility. Under normal metabolic conditions, sarcolemmal K_{ATP} channels are predominantly closed (inhibited by intracellular ATP), and they do not significantly contribute to the cardiac action potential, resting E_m , or cell excitability. However, when exposed to a severe metabolic stress such as anoxia, metabolic

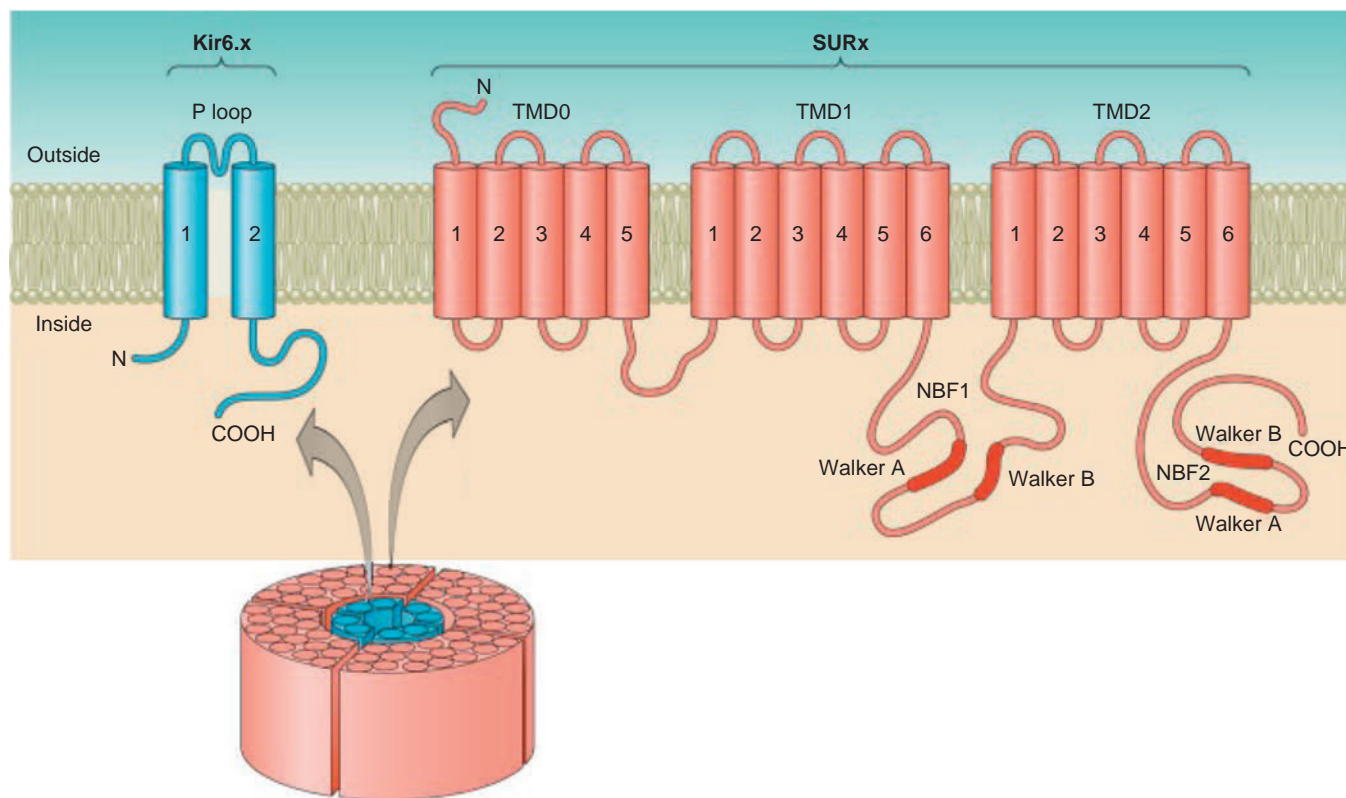


Fig. 2.7 Membrane Topology and Structural Organization of the Subunits of the Adenosine Triphosphate-Sensitive Potassium Channel. The channel consists of four members of the Kir6 subfamily members (Kir6.1 and/or Kir6.2) and four members of the sulfonylurea receptor family (SUR1 and/or SUR2; or splice variants of these subunits). The Kir6.x subunit has two membrane-spanning regions (M1 and M2) with intracellular NH₂ and COOH termini. The SURx subunit has 17 transmembrane regions, arranged in three domains: TMD0, TMD1, and TMD2. An intracellular nucleotide binding fold (NBF1), with Walker A and Walker B domains, exists between TMD1 and TMD2. A second intracellular nucleotide binding fold (NBF2) exists in the COOH terminus region of the protein. It is thought that NBF1 binds (and hydrolyzes) Mg-ATP, whereas Mg-ADP binds primarily to NBF2 to stimulate channel activity. ATP blocks the channel by direct binding to Kir6.x intracellular domains, whereas Mg²⁺-complexes of nucleotides regulate the channel activity by binding to intracellular nucleotide binding folds (NBF1 and NBF2) of the SURx subunits. ADP, Adenosine diphosphate; ATP, adenosine triphosphate; Mg, magnesium. (From Foster MN, Coetzee WA. K_{ATP} channels in the cardiovascular system. *Physiol Rev.* 2016;96:177–252.)

inhibition, or ischemia, K_{ATP} channels become activated (secondary to reduced intracellular ATP levels) and conduct an outward repolarizing K⁺ current (I_{KATP}), which results in abbreviation of the action potential duration and reduction of Ca²⁺ influx through L-type Ca²⁺ channels. By reducing Ca²⁺ entry, I_{KATP} depresses muscle contractility, thereby conserving scarce energy resources, and prevents the damaging effects of intracellular Ca²⁺ overload.^{17,28}

Accordingly, cardiac K_{ATP} channels act as membrane-based metabolic sensors that receive energetic signals of cellular distress and provide adaptive response to acute stress capable of controlling cardiac action potential duration and associated cellular functions and adjusting cellular excitability to match demand.^{29,30}

In addition, activation of I_{KATP} plays an important role in ischemic preconditioning; brief periods of myocardial ischemia confer protection against subsequent prolonged ischemia, reducing MI size, severity of myocardial stunning, and the risk of cardiac arrhythmias. Experimental studies found that K_{ATP} channel openers reproduce the effects of preconditioning, while I_{KATP} blockers prevent the protective effects of ischemic preconditioning. However, the role of sarcolemmal I_{KATP} channels in ischemic preconditioning versus that of mitochondrial I_{KATP} channels

(which appear to be pharmacologically distinct from sarcolemmal I_{KATP}) has been debated.^{28,31}

On the other hand, activation of I_{KATP} also results in shortening of the action potential duration, accumulation of extracellular K⁺, membrane depolarization, and slowed conduction velocity—effects that render the ischemic heart vulnerable to reentrant arrhythmias.

K_{ATP} channels have been further implicated in the adaptive cardiac response to chronic pathophysiological hemodynamic load. K_{ATP} channel deficiency affects structural remodeling, renders the heart vulnerable to Ca²⁺-dependent maladaptation, and predisposes to heart failure.

In the vasculature, activation of K_{ATP} channels results in hyperpolarization of the membrane potential, leading to inhibition of voltage-sensitive Ca²⁺ channels and lowering of intracellular Ca²⁺, with consequent vasodilation.³⁰

Regulation

ATP (with or without Mg²⁺) inhibits I_{KATP} by interacting directly with Kir6.2 and stabilizing the closed state of the channel. In addition, in the presence of Mg²⁺, ATP and ADP can activate the channel through interaction with the SUR2A subunit. Inhibition by ATP binding to

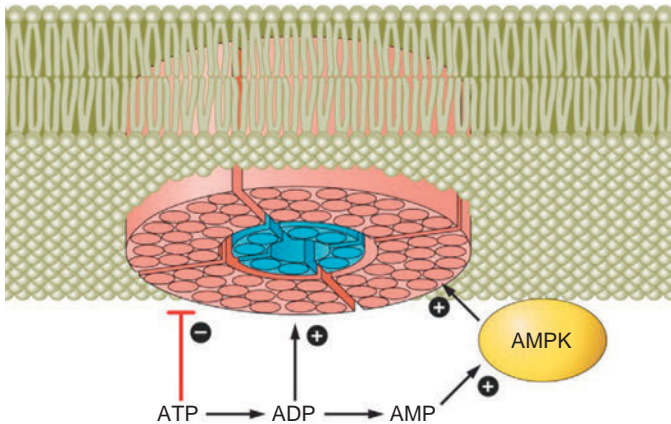


Fig. 2.8 Regulation of ATP-sensitive potassium (K_{ATP}) Channels by Intracellular Nucleotides. The K_{ATP} channel is composed of four Kir6.x and four SURx subunits (respectively color coded in blue and orange). Channel activity is inhibited by intracellular adenosine triphosphatase (ATP). In the presence of magnesium (Mg)-ATP, adenosine diphosphate (ADP) stimulates K_{ATP} channel opening, such that the channel is regulated by the ADP-to-ATP ratio. Even a small decrease in ATP levels during metabolic stress translates to a relatively large increase in adenosine monophosphate (AMP) levels, which may indirectly further stimulate K_{ATP} channel opening and promote surface trafficking through the actions of the trimeric AMP-activated protein kinase (AMPK) and adenylate kinase. (From Foster MN, Coetzee WA. K_{ATP} channels in the cardiovascular system. *Physiol Rev.* 2016;96:177–252.)

Kir6.2 and activation by Mg-nucleotides is the primary physiological regulatory mechanism (Fig. 2.8).

K_{ATP} channel's sensitivity to ATP is not fixed, and it can be modulated by other cellular factors. Nucleotide diphosphates, lactate, oxygen-derived free radicals, and adenosine α_1 receptor stimulation desensitize K_{ATP} to inhibition by intracellular ATP. In addition, the phospholipid PIP2 directly interacts with Kir6.2 subunit stabilizing the open state of the channel and antagonizes ATP inhibition of I_{KATP} .

Pharmacology

K_{ATP} channels can be inhibited or activated by a variety of drugs, all acting on the SUR subunit. K_{ATP} channel openers (pinacidil, cromakalim, rimakalim, and nicorandil) bind at two distinct regions of SUR2A subunits and can exert cardioprotective effects in patients with acute MI. However, K_{ATP} channel openers also activate vascular K_{ATP} (Kir6.1/SUR2B) and produce hypotensive effects that limit their use in the treatment of myocardial ischemia. Moreover, because I_{KATP} density is larger in the epicardium, K_{ATP} channel openers produce a more marked shortening of action potential duration in epicardial cells, thus leading to a marked dispersion of repolarization and to the development of extrasystolic activity via a mechanism of phase 2 reentry. On the other hand, K_{ATP} channel openers shorten the action potential duration (and QT interval), reduce transmural dispersion of repolarization, and suppress EADs and DADs induced in patients with LQT1. Thus K_{ATP} channel openers can potentially prevent spontaneous torsades de pointes when congenital or acquired LQTS is secondary to reduced I_{Kr} or I_{Ks} . K_{ATP} channel openers may be useful in simulating ischemic preconditioning and may be protective in the setting of acute ischemia.

I_{KATP} blockers (e.g., sulfonylureas and various antiarrhythmic drugs) prevent the shortening of the action potential duration and can potentially prevent VF during myocardial ischemia. Nonetheless, they can also be arrhythmogenic. Moreover, because K_{ATP} channels are present

in pancreatic β cells and vascular smooth muscle, I_{KATP} blockers can produce hypoglycemia and coronary vasoconstriction, effects that may preclude their potential benefit as antiarrhythmic agents.

On the other hand, cardioselective I_{KATP} blockers (clamikalant, HMR 1098) inhibited hypoxia-induced shortening of the action potential duration and prevented VF induced by coronary artery occlusion in postinfarction conscious dogs at doses that had no effect on insulin release, blood pressure, or coronary blood flow. Thus these drugs may represent a new therapeutic approach to the treatment of ventricular arrhythmias in patients with coronary heart disease.

It is still unclear whether the opening of K_{ATP} channels has completely proarrhythmic or antiarrhythmic effects. Increased K^+ conductance should stabilize the E_m during ischemic injury and reduce the extent of infarct and ectopic pacemaker activity. On the other hand, K_{ATP} channel opening accelerates repolarization of the action potential, possibly promoting reentry.

Inherited Channelopathies

Gain-of-function mutations in *KCNJ8* (Kir6.1) and *ABCC9* (SUR2A) have been linked to J wave syndromes (Brugada and early repolarization syndromes). K_{ATP} channel-pore polymorphisms have also been linked to SCD.¹⁷

Mutations in *ABCC9* resulting in reduced intrinsic channel ATPase activity, metabolic sensing deficit, and dysfunctional K_{ATP} channels have been found in patients with idiopathic dilated cardiomyopathy and rhythm disturbances. These mutations confer susceptibility to Ca^{2+} -dependent maladaptive remodeling, progressing to cardiomyopathy and congestive heart failure. In addition, a loss-of-function *ABCC9* mutation has been linked to predisposition to adrenergic AF.

Gain- and loss-of-function mutations in *KCNJ11* (Kir6.2) and *ABCC8* (SUR1), which encode the predominant K_{ATP} channel subunits in pancreatic cells and in neurons, have now been identified as causal in human neonatal diabetes mellitus and congenital hyperinsulinism, respectively. Although cardiac K_{ATP} channels (Kir6.2/SUR2A) have the same Kir6.2 subunit as that in pancreatic K_{ATP} channels (Kir6.2/SUR1), there are no reports of any cardiac abnormalities in patients with neonatal diabetes mellitus; this finding suggests that factors other than nucleotide sensitivity play an important role.³⁰

More recently, gain-of-function mutations in *KCNJ8* (Kir6.1) and *ABCC9* (SUR2A) have been linked to Cantu syndrome (hypertrichosis-osteochondrodysplasia-cardiomegaly syndrome), a rare multiorgan disease characterized by multiple cardiovascular abnormalities (cardiac enlargement, ventricular hypertrophy, pericardial effusion, pulmonary hypertension secondary to partial pulmonary venous obstruction, patent ductus arteriosus, and bicuspid aortic valves with and without stenosis). In addition, these patients typically exhibit congenital hypertrichosis, distinctive acromegaly facial appearance (including broad nasal bridge, wide mouth with full lips, and macroglossia), and skeletal abnormalities (thickening of the calvaria, broad ribs, scoliosis, and flaring of the metaphyses). Of note, K_{ATP} channel openers, such as diazoxide and minoxidil, can also result in side effects such as hypertrichosis, pericardial effusion, edema, and even coarsening of the facial features.³⁰

Acquired Diseases

Metabolic dysregulation of I_{KATP} created by disease-induced structural remodeling appears to contribute to the dysfunction of heart failure.

The effects of Kir6.2 modulation in AF have not extensively been studied. However, evidence indicates a reduction of I_{KATP} in patients with chronic AF, a finding suggesting that regulation of this current may not contribute importantly to AF-related ionic remodeling.

Two-Pore Potassium Channels

Structure and Physiology

K_{2P} channels are composed of four transmembrane domains and two pore-forming P loops arranged in tandem, one between the first and second transmembrane domains and the other between the third and fourth domains (see Fig. 2.4). The presence of two pores enables K_{2P} channels to form homodimers or heterodimers instead of tetramers like other K^+ channels.¹⁶

K_{2P} channels are characterized by their lack of voltage sensitivity, their open state at all membrane potentials, and their regulation by numerous chemical and physical stimuli (such as pH, oxygen, phospholipids, neurotransmitters, G protein-coupled receptors, temperature, and stretch). These features allow these channels to play a role in regulating membrane potential and excitability in various cell types under a range of physiological and pathological situations.

Based on their functional properties, K_{2P} channels are classified into six different subfamilies: (1) two-pore domain in a weakly Kir channel (TWIK); (2) TWIK-related K^+ channel (TREK); (3) TWIK-related acid-sensitive K^+ channel (TASK); (4) TWIK-related alkaline-sensitive K^+ channel (TALK); (5) tandem pore domain halothane-inhibited K^+ channel (THIK); and (6) TRESK TWIK-related spinal cord K^+ channel (TRESK).

TASK channels exhibit sensitivity to variations in extracellular pH over a narrow physiological range. TASK-1 (*KCNK3*) and TASK-3 (*KCNK9*) subunits are functional when associated as homodimers or heterodimers. TASK channels display strong basal currents with very fast activation and inactivation kinetics.

TREK channels, which comprise TREK-1 (*KCNK2*), TREK-2 (*KCNK10*), and TRAAK (*KCNK4*), display low basal activity, but are stimulated by stretch of the cell membrane, lysophospholipids, and arachidonic acid and are inactivated by hypo osmolarity and phosphorylation by PKA and PKC.

Several members of the K_{2P} channel family are expressed in the heart and in the systemic or pulmonary circulations, and some contribute to background K^+ currents and the control of E_m in vascular smooth muscle cells. Of the 15 known different K_{2P} α subunits, TWIK-1 ($K_{2P}1.1$, encoded by *KCNK1*); TASK-1 ($K_{2P}3.1$, encoded by *KCNK3*); TASK-3 ($K_{2P}9.1$, encoded by *KCNK9*); TALK-2 ($K_{2P}17.1$, encoded by *KCNK17*) channels are found in human heart and are recognized to play a role in cardiac electrophysiology and some inherited forms of arrhythmias. Evidence suggest a role for TASK-1 in atrial repolarization and for TALK-2 in AVN conduction.^{16,20}

Function

There is clear evidence for TREK-1 and TASK-1 in the heart, and these channels likely modulate cardiac action potential duration through their regulation by stretch, polyunsaturated fatty acids, pH, and neurotransmitters. TREK-1 may also have a critical role in mediating the vasodilator response of resistance arteries to polyunsaturated fatty acids, thus contributing to their protective effect on the cardiovascular system. TASK-1, on the other hand, is a strong candidate for a role in hypoxic vasoconstriction of pulmonary arteries.

In working atrial and ventricular myocytes, background K^+ currents are crucial for stabilizing the E_m at a hyperpolarized value toward the K^+ equilibrium potential (E_K) and regulating action potential duration in various physiological and pathological conditions. The background current is mainly carried by inward rectifier channels (including I_{K1} , $I_{K_{ACH}}$, and $I_{K_{ATP}}$). Several K_{2P} channels have been proposed to contribute to the cardiac background or “leak” K^+ current through all phases of the cardiac action potential, thereby stabilizing the resting potential near the equilibrium potential of K^+ during phase 4, ensuring the

availability of Na^+ channels during phase 0 and facilitating repolarization during phase 1 to 3 of the action potential. Among them, TREK-1 and TASK-1 have been the most extensively studied.¹⁶

TREK-1, as an outwardly rectifying current, can potentially participate in balancing the E_m and action potential duration. Indeed, on a beat-to-beat basis, it could be involved in a negative feedback loop, hyperpolarizing the E_m in response to a stretch stimulus following the stretch activation of nonselective cation channels. The expression of TREK-1 appears to be nonuniform in the heart, with stronger TREK-1 mRNA expression in endocardial cells compared with epicardial cells. This finding possibly reflects different amounts of stretch experienced by muscle cells in different parts of the ventricular wall, leading to differential mechanoelectrical feedback and thereby reducing action potential repolarization in areas of the myocardium where conduction velocity is slower. Mechanoelectric feedback following an increase in atrial volume may be arrhythmogenic, changing the shape of the action potential. Physiological evidence of the direct involvement of TREK-1 current in mechanoelectric feedback in the heart is still to be provided.

Pharmacology

Data are limited regarding the pharmacology of K_{2P} channels. Theoretically, blockade of K_{2P} channels is expected to prolong action potential duration; however, whether K_{2P} channels could be promising antiarrhythmic drug targets remains to be investigated. Human cardiac $K_{2P}3.1$ (TASK-1) channels appear to be blocked by amiodarone. Other antiarrhythmic drugs, including mexiletine, propafenone, carvedilol, and dronedarone, also block TASK-1 at high therapeutic plasma concentration, indicating a possible contribution to their therapeutic effect.²⁰

Inherited Channelopathies

Mutations in *KCNK3* (encoding $K_{2P}3.1$ channels) resulting in attenuation of the TASK-1 current have been linked to familial AF.

Acquired Diseases

TREK-1 activity may have some importance in pathological conditions such as ischemia, when released purinergic agonists such as ADP and ATP lead to arachidonic acid production. Activation of TREK-1 by ATP during ischemia may contribute to electrophysiological disturbances in the ventricular wall. As a stretch-activated K^+ channel in atrial cells, TREK-1 could additionally be involved in regulating the release of atrial natriuretic peptide, which is released by a stretch-induced increase in intracellular Ca^{2+} concentration. Further work will be necessary to clarify the possible role of TREK or other stretch-dependent channels in the pathological heart.

Small-Conductance Calcium-Activated Potassium Channels

Structure and Physiology

Calcium-activated K^+ channels (KCa) are categorized into three subfamilies according to their single-channel K^+ conductance properties: big-conductance (BK, $KCa1.1$), intermediate-conductance (IK, $KCa3.1$), and small-conductance (SK, $KCa2.x$). To date, only small-conductance channels have been identified as functional in the cell membranes of cardiac myocytes.¹⁶

The subfamily of SK channels consists of three members with differential sensitivity to apamin: SK1 (or $KCa2.1$ encoded by *KCNN1*) with the least sensitivity; SK2 (or $KCa2.2$ encoded by *KCNN2*) with the highest sensitivity; and SK3 (or $KCa2.3$ encoded by *KCNN3*) with intermediate sensitivity.³²

Four α subunits ($KCa2.1$, $KCa2.2$, or $KCa2.3$) coassemble to form a functional homotetrameric or heterotetrameric SK channel. Each α

subunit consists of six transmembrane domains and one pore-forming loop between the fifth and sixth domains responsible for K^+ selectivity. Unlike K_v channels, the transmembrane segment S4 in the SK α subunit is uncharged. Also, SK channels do not coassemble with β subunits.

SK channels are activated by submicromolar concentrations of cytoplasmic Ca^{2+} . The Ca^{2+} sensitivity is ascribed to the association with calmodulin, which is constitutively bound to the proximal C-terminus of each α subunit and mediates gating in response to Ca^{2+} binding. SK channels play an important role in linking fluctuations in intracellular Ca^{2+} concentration with membrane K^+ conductance. Like in vascular smooth muscle, the physiologic function of SK channels in the heart is probably to limit excessive Ca^{2+} entry.¹⁶

The SK channel-mediated current (ISK or ISK,Ca) shows inward rectification, thereby limiting the physiological relevant outward current branch. Similar to the classic inward-rectifier K^+ currents, divalent cations such as Ca^{2+} or Mg^{2+} may account for this inward rectification.

Function

SK channels are highly expressed in a range of tissues including vascular endothelium, smooth and skeletal muscle, and neural tissue. Recent evidence suggests that SK channels are abundantly expressed in the atrium, while ventricular expression is relatively scarce. The three subtypes of SK channels display variable spatial distribution; SK1 and SK2 are predominantly expressed in the atrium, while SK3 is equally expressed in the atrium and the ventricle. However, the heterogeneous expression of SK channels in the heart is not completely defined.

Owing to their predominant expression in the atria, SK channels are attributed with atrial electrophysiology and have been proposed to play a role in the pathophysiology of AF. However, although multiple studies have reported that SK channels are important mediators of proarrhythmogenic electrical remodeling in the atria, the role of atrial SK channels in AF patients remains controversial; both ISK upregulation and downregulation have been reported in patients with persistent and permanent AF.^{16,32}

In the ventricles, SK channels do not appear to contribute significantly to repolarization under normal physiological circumstances; however, SK channels have been implicated as potentially important mediators of ventricular repolarization in failing hearts. ISK is upregulated in patients with heart failure, which can potentially increase ventricular repolarization reserve and provide an antiarrhythmic benefit.

Pharmacology

SK channels are selectively blocked by apamin (the active peptide neurotoxin in bee venom). The highly selective blockade by apamin is the signature of SK channels that enables verification of the molecular identity of SK channels in mammalian brain. Several other peptides from scorpion venom (such as scyllatoxin, tamapin, and BmSKTx1) block SK channels.^{24,32,33}

SK channels represent potentially attractive therapeutic targets for AF. The preferential atrial expression of SK channels may offer a unique therapeutic strategy to target atria without interfering with ventricular function. However, while some SK channel-modulating drugs in animal models have been demonstrated to suppress AF, others are associated with a negligible antiarrhythmic or indeed proarrhythmogenic effect, especially in the setting of heart failure.³³ Currently there is no general consensus of whether block of SK channels provides protection against or facilitates atrial or ventricular arrhythmias.²⁰

Regulation

SK channels are unique in that they are insensitive to membrane voltage and are gated solely by changes in intracellular Ca^{2+} . Calmodulin binds to a domain within the C-terminus of the SK channels. Binding of Ca^{2+}

to calmodulin results in changes in the conformation of the channels leading to channel activation. Calmodulin not only is essential for Ca^{2+} sensitivity but also is critical to the trafficking and cell surface expression of SK channels.³²

In addition to calmodulin, α -actinin2, filamin A, and myosin light chain-2 appear to play a role in the gating, regulation, and membrane trafficking of the SK channels in cardiomyocytes.³²

Inherited Channelopathies

Genome-wide association analysis revealed an association between single nucleotide polymorphism in *KCNN3* with lone AF.³²

Acquired Diseases

Both upregulation and downregulation of SK channels and ISK have been reported in patients with chronic AF, and the exact role of these channels in atrial remodeling and the pathophysiology of AF remains debated. ISK is upregulated in the failing heart, which could potentially enhance ventricular repolarization reserve and reduce the risk of DADs and triggered activity (eFig. 2.1).²⁰

CALCIUM CHANNELS

Structure and Physiology

Functional voltage-gated Ca^{2+} channels (Ca_v) are composed of pore-forming α_1 subunit proteins, encoded by the *CACNA1x* genes, of which there are 10 isoforms in the mammalian genome. Based on amino acid sequence similarity, $Ca_v\alpha_1$ channels are divided into three subfamilies: Ca_v1 , Ca_v2 , and Ca_v3 .

The Ca_v1 subfamily conducts the L-type Ca^{2+} current and includes four isoforms: $Ca_v1.1$ (α_1S), $Ca_v1.2$ (α_1C), $Ca_v1.3$ (α_1D), and $Ca_v1.4$ (α_1F), encoded by *CACNA1S*, *-C*, *-D*, and *-F*, respectively. Tissue expression of $Ca_v1.1$ and $Ca_v1.4$ is more restricted than that of $Ca_v1.2$ and $Ca_v1.3$. $Ca_v1.1$ is mainly expressed in skeletal muscle, while $Ca_v1.4$ is primarily restricted to the retina. $Ca_v1.2$ is the main isoform in cardiac muscle, and is also present in smooth muscle cells, secretory tissue, and the nervous system. $Ca_v1.3$ plays a major role in sinoatrial node tissue, and in the auditory system, and is also present in the brain. Both isoforms ($Ca_v1.2$ and $Ca_v1.3$) are often even expressed in the same cell, such as in neurons, adrenal chromaffin cells, and sinoatrial node and atrial cardiomyocytes.³⁴

The Ca_v2 subfamily conducts the P/Q-, N-, and R-type Ca^{2+} currents and includes three isoforms: $Ca_v2.1$ (α_1A , also termed P/Q-type), $Ca_v2.2$ (α_1B , also termed N-type), and $Ca_v1.2$ (α_1E , also termed R-type), encoded by *CACNA1A*, *-B*, and *-E*, respectively. The $Ca_v2.x$ channels are mainly expressed in the nervous system.³⁴

The Ca_v3 subfamily conducts the T-type Ca^{2+} current and includes three isoforms: $Ca_v3.1$ (α_1G), $Ca_v3.2$ (α_1H), and $Ca_v3.3$ (α_1I), encoded by *CACNA1G*, *-H*, and *-I*, respectively. The Ca_v3 channels are extensively distributed in neurons and other excitable cells. They have important roles in neuronal and cardiac excitability and in cardiac and neuronal pacemaker activity.³⁴

Although the α_1 subunit ($Ca_v\alpha_1$) is the principal component of voltage-gated Ca^{2+} channels and is responsible for their unique biophysical and pharmacological properties, a functional Ca^{2+} channel requires coassembly of the α_1 subunit with auxiliary subunits (β subunit and $\alpha_2\delta$ subunits; Fig. 2.9).³⁵ These accessory subunits enhance the expression of the α_1 subunit and modify its properties.

Both the Ca_v1 and Ca_v2 subfamilies are able to form a heteromeric complex, coassembling with one of four β subunits ($Ca_\beta1$ – β_4 , encoded by *CACNB1*–*4*), and one of four $\alpha_2\delta$ subunits (encoded by *CACNA2D1*–*4*). For the Ca_v3 channels, the α_1 subunits can form functional channels alone, but may also associate with other proteins.

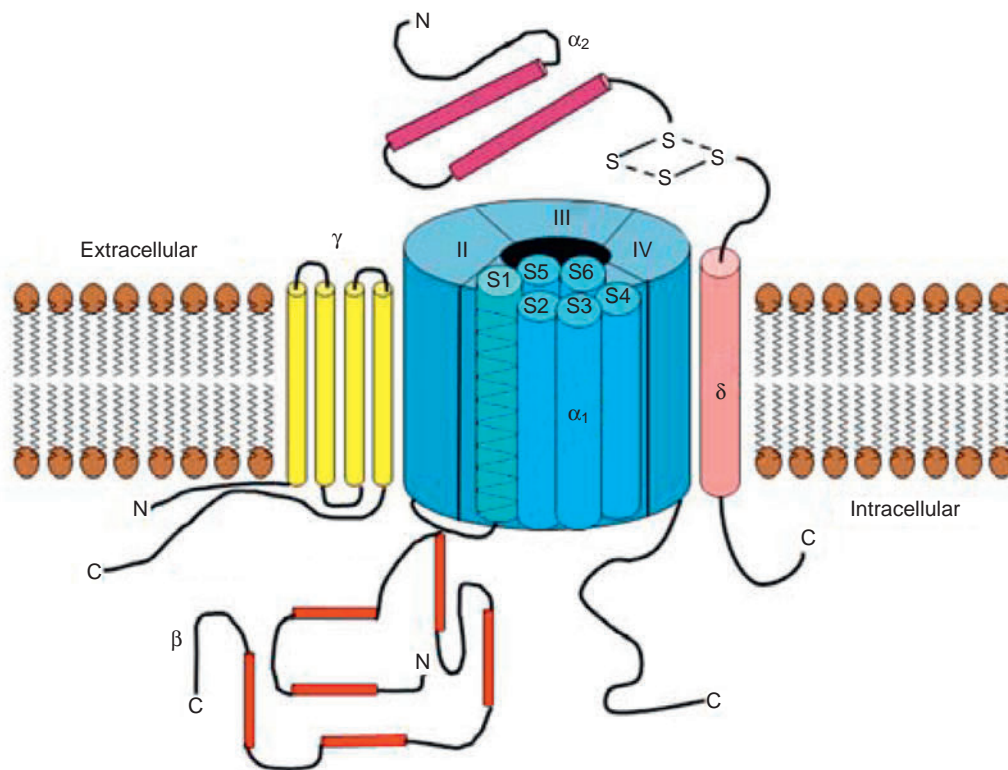


Fig. 2.9 Membrane Topology and Structural Organization of the Subunits of the Cardiac L-Type Calcium Channel. The α_1 is the pore-forming subunit that contains voltage-sensing machinery and the binding sites of channel blockers. The α_1 subunit contains four homologous domains (I to IV), each containing six transmembrane helices (S1 to S6). The $\alpha_2\delta$ and β subunits enhance expression and modulate the voltage dependence and gating kinetics of the channel. (Modified from Gurkoff G, Shahlaie K, Lyeth B, Berman R. Voltage-gated calcium channel antagonists and traumatic brain injury. *Pharmaceuticals*. 2013;6:788–812.)

A γ subunit also forms part of the skeletal muscle Ca^{2+} channel complex. Eight γ subunit isoforms (γ_1 – γ_8 , encoded by *CACNG1*–*8*) have been identified. Only γ_4 , γ_6 , γ_7 , and γ_8 are expressed in human heart. However, no γ subunits have been shown to form an integral part of cardiac or neuronal Ca^{2+} channels.

For some Ca_v1 and Ca_v2 channels, the tight binding of calmodulin to an isoleucine-glutamine domain (the so-called “IQ” motif) in their C-terminal tail allows calmodulin to be considered as a quasi-subunit. Several other proteins interact with the channel complex, including kinases, phosphatases, scaffold proteins, caveolin-3, among others.

The α_1 Subunit

The α_1 subunit ($\text{Ca}_v\alpha_1$) has a structure similar to that of the Na^+ channel: four homologous domains (I to IV), each consisting of six transmembrane segments (S1 to S6). The S5 and S6 segments and the membrane-associated pore loop (P loop) between them form the central pore through which ions flow down their electrochemical gradient. The P loop contains four negatively charged glutamate residues (EEEE) that are required for the Ca^{2+} selectivity of the channel. S4 in each homologous domain contains a highly conserved positively charged residue (arginine or lysine) at every third or fourth position. This segment serves as the voltage sensor for gating.

The $\alpha_1\text{C}$ subunit is the main and largest component of Ca_v and it dictates the principal biophysical and pharmacological properties of these channels because it harbors the ion-selective pore, voltage sensor, gating apparatus, and the majority of drug- and toxin-binding sites.

The β Subunit

The β subunit ($\text{Ca}_v\beta_1$, encoded by the *CACNB* gene) is entirely intracellular and is tightly bound to a highly conserved motif in the cytoplasmic linker between domains I and II of the $\alpha_1\text{C}$ subunit (termed the α -interacting domain, AID). Coexpression of the β subunit modulates the biophysical properties of the $\alpha_1\text{C}$ subunit. The β subunit has a prominent role in channel expression, trafficking, and regulation. Sites possible for phosphorylation by various protein kinases (PKA, PKC, protein kinase G [PKG]) have been identified in these subunits. The β subunits are also involved in channel regulation by β -adrenergic stimulation and in response to the changes of the pH of the cell. In addition, the β subunit can dramatically enhance Ca^{2+} current amplitude, change the voltage dependence and kinetics of channel activation and inactivation, and alter pharmacological properties of the channel.

The $\alpha_2\delta$ Subunit

The α_2 and δ proteins are encoded by a single mRNA; the mature forms of the $\alpha_2\delta$ subunits are derived by posttranslational proteolytic cleavage of α_2 and δ , but they remain associated through a disulfide bond. The α_2 subunit is completely extracellular, whereas the δ subunit has a single membrane-spanning segment with a very short intracellular part that anchors the $\alpha_2\delta$ subunit complex to the $\alpha_1\text{C}$ subunit.

The $\alpha_2\delta$ subunit complex has less influence on channel function than the β subunit. The $\alpha_2\delta$ subunit slightly increases Ca^{2+} current amplitude and accelerates channel inactivation and can change the

properties of Ca^{2+} channel activation. It can also affect channel density trafficking.

The γ Subunit

The γ subunit is composed of four transmembrane segments and intracellular N- and C-termini. The γ subunits have variable effects on channel function, depending on the partnered $\text{Ca}_v\alpha_1$ and $\text{Ca}_v\beta$ subunits.

Cardiac L-Type Calcium Current

Structure and Physiology

In cardiac muscle, two types of voltage-dependent Ca^{2+} channels, the L-type and the T-type, transport Ca^{2+} into the cells. The L-type channel (L for long-lasting because of its slow kinetics of current decay as compared with Na^+ channels) is found in all cardiac cell types. The T-type channel (T for tiny and transient) is found principally in pacemaker, atrial, and Purkinje cells. The term “ Ca^{2+} channels” is used to refer to the L-type channel.

Cardiac L-type Ca^{2+} channels are composed of four polypeptide subunits (α_1 , β , α_2 , δ) and form a heterotetrameric complex. Both $\text{Ca}_v1.2$ ($\alpha_1\text{C}$ encoded by the *CACNA1C*) and $\text{Ca}_v1.3$ ($\alpha_1\text{D}$ encoded by the *CACNA1D*) isoforms are expressed in the heart, but their contribution to L-type current (I_{CaL}) varies in different regions.³⁶

L-type Ca^{2+} channels are characterized by a large single channel conductance. The channels are closed at the resting potential, but they activate on depolarization to potentials positive to -40 mV. I_{CaL} peaks at 0 to $+10$ mV, and tends to reverse at $+60$ to $+70$ mV, following a bell-shaped current-voltage relationship.

Although I_{CaL} is normally activated during phase 0 by the regenerative depolarization caused by the fast I_{Na} , I_{CaL} is much smaller than the peak I_{Na} . In addition, the amplitude of I_{CaL} is not maximal near the action potential peak because of the time-dependent nature of I_{CaL} activation as well as the low driving force ($E_m - E_{\text{Ca}}$, where E_{Ca} is reversal potential of a cardiac Ca^{2+} channel) for I_{CaL} .

The decay of I_{CaL} during depolarization (i.e., time-dependent inactivation) is very slow and depends on two mechanisms: voltage-dependent inactivation and Ca^{2+} -dependent inactivation. These two mechanisms control Ca^{2+} influx into cardiomyocytes and hence regulate signal transduction to sarcoplasmic reticulum Ca^{2+} channels (ryanodine receptor 2 [RyR2]) and ensure normal contraction and relaxation of the heart.

Fast Ca^{2+} -dependent inactivation serves as a negative feedback for Ca^{2+} to limit further Ca^{2+} entry via L-type Ca^{2+} channels. The slow voltage-dependent inactivation (induced by membrane depolarization) prevents a premature rise in I_{CaL} when intracellular Ca^{2+} concentration decreases and Ca^{2+} -dependent inactivation terminates during maintained depolarization. Although still under dispute, the relative contribution of Ca^{2+} -dependent inactivation to total inactivation of I_{CaL} appears to be greater at negative potentials when voltage-dependent inactivation, which typically exhibits a U-shaped availability curve, is weak. After β -adrenergic stimulation, Ca^{2+} -dependent inactivation becomes the main inactivation mechanism as a result of a slowing down of voltage-dependent inactivation.³⁵

The Ca^{2+} -dependent inactivation mechanism depends primarily on Ca^{2+} released from the sarcoplasmic reticulum. The Ca^{2+} -binding protein calmodulin functions as a critical sensor mediating Ca^{2+} -induced inactivation of L-type Ca^{2+} channels. Calmodulin binds to two $\alpha_1\text{C}$ subunit amino acid sequences (called domains L and K). When local intracellular Ca^{2+} concentration increases (secondary to influx Ca^{2+} via I_{CaL} , as well as Ca^{2+} -induced Ca^{2+} release from the sarcoplasmic reticulum), more Ca^{2+} ions bind to calmodulin, which harbors four Ca^{2+} -binding sites. When saturated with Ca^{2+} , conformational change of both calmodulin and $\alpha_1\text{C}$ subunit leads to blockage of the channel pore.

Voltage steady-state activation and inactivation are sigmoidal, with an activation range over -40 to $+10$ mV (with a half-activation potential near -15 mV) and a half-inactivation potential near -35 mV. However, a relief of inactivation for voltages positive to 0 mV leads to a U-shaped voltage curve for steady-state inactivation. Overlap of the steady-state voltage-dependent inactivation and activation relations defines a window current near the action potential plateau, within which transitions from closed and open states can occur that may participate in action potential repolarization and may play a major role in the initiation of EADs.

After inactivation, the transition of Ca^{2+} channels from the inactivated to the closed resting state (i.e., recovery from inactivation [reactivation, restoration, or repriming]) is also Ca^{2+} and voltage dependent. Reduction of intracellular Ca^{2+} concentration in the immediate vicinity of the channel allows recovery from Ca^{2+} -dependent inactivation. Acceleration of Ca^{2+} channel reactivation, as may occur secondary to reuptake of Ca^{2+} by the sarcoplasmic reticulum during prolonged depolarization, can result in the recovery from Ca^{2+} -dependent inactivation and enable secondary depolarization. This leads to instability of the cell E_m during repolarization and may be the basis for the EADs that are capable of initiating torsades de pointes.

Voltage-dependent recovery of I_{CaL} from inactivation between action potentials is slow at low (depolarized) E_m , and it becomes very fast as the action potential repolarization is nearly complete. As a consequence, I_{CaL} declines in response to repetitive stimulation at a partially depolarized E_m between pulses (resulting from Ca^{2+} channel incomplete recovery from inactivation), and a negative staircase of contractility is observed.

In contrast, at normal resting membrane potentials, recovery of I_{CaL} from inactivation is fast, and I_{CaL} can increase progressively during repetitive stimulation. This positive staircase or rate-dependent potentiation of contractility is Ca^{2+} dependent and likely is the result of diminished Ca^{2+} -dependent inactivation at frequencies with less sarcoplasmic reticulum Ca^{2+} release. In addition, similar to Ca^{2+} -dependent inactivation, Ca^{2+} -dependent facilitation requires high-affinity binding of calmodulin to the C-terminal tail of the $\text{Ca}_v1.2$ channel and can be facilitated by calmodulin kinase II-dependent phosphorylation. Calmodulin kinase II is a Ca^{2+} /calmodulin-dependent serine/threonine kinase that is activated by low intracellular Ca^{2+} concentration. The facilitatory effect of Ca^{2+} entry on subsequent I_{CaL} is distinct from, but coexistent with, Ca^{2+} -dependent inactivation.

Function

Both $\text{Ca}_v1.2$ and $\text{Ca}_v1.3$ isoforms are expressed in the heart. In the working myocardium, the $\text{Ca}_v1.2$ channels predominate, with no (ventricular myocytes) or minimal (atrial myocytes) expression of $\text{Ca}_v1.3$. In contrast, $\text{Ca}_v1.3$ is the predominant isoform in the sinus node and AVN, and plays an important role in pacemaking function.³⁶

In atrial and ventricular cardiomyocytes, $\text{Ca}_v1.2$ channels trigger contraction. I_{CaL} is activated by membrane depolarization, is largely responsible for the action potential plateau, and is a major determinant of the duration of the plateau phase and hence of the action potential duration and refractoriness. I_{CaL} also links membrane depolarization to myocardial contraction and constitutes the dominant factor in mediating positive inotropy in cardiac tissue.

L-type Ca^{2+} channels are the principal portal of entry of Ca^{2+} into the cells during depolarization. Ca^{2+} influx during the action potential plateau triggers more massive Ca^{2+} release (Ca^{2+} transients) from the sarcoplasmic reticulum into the cytosol via activation of Ca^{2+} -release channels (e.g., RyR2). This amplifying process, termed Ca^{2+} -induced Ca^{2+} release (CICR), causes a rapid increase in intracellular Ca^{2+} concentration (from approximately 100 nM to approximately 1 μM) to a

level required for optimal binding of Ca^{2+} to troponin C and induction of contraction. Most of the L-type Ca^{2+} channels in the adult myocyte are localized in the transverse tubules (T tubules) facing the sarcoplasmic reticulum junction and the RyR2, organized as a “complex” that ensures coordinated Ca^{2+} release during excitation-contraction coupling.

Cytosolic Ca^{2+} concentration decreases during diastole: contraction is followed by Ca^{2+} release from troponin C and its reuptake by the sarcoplasmic reticulum via activation of the sarcoplasmic reticulum Ca^{2+} -ATPase Ca^{2+} pump, in addition to extrusion across the sarcolemma via the Na^{+} - Ca^{2+} exchanger. Intracellular Ca^{2+} -dependent inactivation limits Ca^{2+} influx during action potential.

For maintenance of intracellular Ca^{2+} homeostasis and balanced cardiac activity, Ca^{2+} influx into cytoplasm via I_{CaL} has to be terminated. This is achieved by Ca^{2+} -dependent inactivation of I_{CaL} . This inactivation serves as a negative feedback mechanism for regulating Ca^{2+} entry into the cell and as a physiological safety mechanism against a harmful Ca^{2+} overload in the cell, which can cause both arrhythmias and cell death. Ca^{2+} -dependent inactivation is also a major determinant of action potential duration, and it ensures that contraction and relaxation cycles of the heart muscle fiber are coordinated. A failure to deactivate I_{CaL} completely may possibly be an essential mechanism underlying EADs caused by suppression of the K^{+} delayed rectifier currents.³⁶

Inhibition of $\alpha 1\text{C}$ subunit binding to calmodulin eliminates Ca^{2+} -dependent inactivation, thus promoting Ca^{2+} -dependent facilitation, which contributes to a force-frequency relationship in the heart.

In addition, I_{CaL} is responsible for the upstroke (phase 0) of slow response action potentials (in pacemaking cardiomyocytes and regions of depressed resting E_m) and contributes to physiological frequency regulation in the sinus node.

In sinus node cells, both $\text{Ca}_v1.2$ and $\text{Ca}_v1.3$ channel isoforms are required for proper function. $\text{Ca}_v1.2$ support the sinus node action potential. $\text{Ca}_v1.3$ channels activate at more negative threshold (activation) potential than $\text{Ca}_v1.2$. This property facilitates pacemaking function, since $\text{Ca}_v1.3$ channels are activated earlier during the diastolic depolarization phase. Further, $\text{Ca}_v1.3$ closely co-localizes with sarcomeric RyRs, which may allow it to contribute to RyR-mediated Ca^{2+} release during diastolic depolarization. $\text{Ca}_v1.3$ is also the prominent L-type channel in AVN cells and contributes to AVN conduction and pacemaking.³⁶

Regulation

Phosphorylation of the pore-forming $\alpha 1$ subunits by different kinases is one of the most important pathways to change the activity of the L-type Ca^{2+} channel. Phosphorylation by PKA is the main mechanism of Ca^{2+} channel activation, because it increases the probability and duration of the open state of the channels and consequently increases I_{CaL} .

Several different agonists (e.g., catecholamines, glucagon, histamine, serotonin) can activate PKA-mediated phosphorylation and activation of the L-type Ca^{2+} channel via an intracellular signaling cascade. Once one of these agonists binds to its receptor, receptor stimulation activates guanosine triphosphate (GTP)-binding protein (Gs), which activates adenylyl cyclase and in turn mediates the conversion of ATP into cAMP. The increased cAMP levels stimulate cAMP-dependent PKA phosphorylation of $\text{Ca}_v\alpha 1$ and result in an increase in I_{CaL} amplitude and a shift in activation to a more negative E_m . cAMP is degraded by cAMP phosphodiesterases, and the signaling cascade is then suppressed, limiting cAMP-dependent phosphorylation; in addition, the signaling cascade is terminated by serine/threonine phosphatases that remove a phosphate group from kinase-phosphorylated proteins.

The suppression of adenylyl cyclase activity is one of the most common pathways to interrupt PKA-dependent Ca^{2+} channel stimulation. Adenylyl cyclase is usually suppressed (and cAMP synthesis is blocked) by activation of Gi proteins. Stimulation of various Gi protein-coupled receptors (e.g., M2 muscarinic receptors, adenosine A1 receptors, opiates, and atrial natriuretic peptides) does not change basal I_{CaL} in most cases, but reduces I_{CaL} increased via stimulation of β -adrenergic receptors. Activation of phosphodiesterases is another way to reduce PKA-dependent channel phosphorylation. Phosphodiesterases hydrolyze cAMP and cyclic guanosine monophosphate (cGMP) and decrease their intracellular concentrations.

The physiological functions of cardiac L-type Ca^{2+} channels are under control of catecholamines of circulating and neurohumoral origin. The effects of adrenergic stimulation are exerted by phosphorylation of the L-type Ca^{2+} channel subunits by PKA, PKC, and PKG. $\beta 1$ -Adrenergic receptors couple exclusively to the Gs protein, thus producing a widespread increase in cAMP levels in the cell, whereas $\beta 2$ -adrenergic receptors couple to both Gs and Gi, thus producing a more localized activation of L-type Ca^{2+} channels.

The effect of PKC-mediated phosphorylation on I_{CaL} can be highly diverse. PKC can either increase or decrease I_{CaL} . Activation of Gq subunits by Gq protein-coupled receptors (e.g., α -adrenergic receptors, endothelin, angiotensin II, and muscarinic receptors) stimulates phospholipase C, which hydrolyzes PIP2 to inositol 1,4,5-triphosphate (InsP3) and diacylglycerol (DAG). DAG activates PKC, which, in turn, phosphorylates L-type Ca^{2+} channels. The mechanism of the effect of PKC on the activity of cardiac L-type Ca^{2+} channels is not exactly known. PKC phosphorylates the N-terminus of $\text{Ca}_v\alpha 1$, and the effect on the channel can be either stimulating or suppressive.

Activation of soluble guanylate cyclase (primarily by nitric oxide) results in the conversion of GTP into cGMP. cGMP activates PKG, which phosphorylates $\text{Ca}_v\alpha 1$, with a resulting inhibition of I_{CaL} . Besides direct phosphorylation of the L-type Ca^{2+} channel, it is also possible that PKG activates a protein phosphatase, which dephosphorylates the channel, or that cGMP activates phosphodiesterase 2, which reduces cAMP levels. Thus stimulation of I_{CaL} by PKA is inhibited. However, besides an inhibition of I_{CaL} , stimulatory effects of the PKG pathway have been shown.

I_{CaL} is blocked by several cations (such as Mg^{2+} , nickel [Ni^{2+}], zinc [Zn^{2+}]) and drugs (including dihydropyridines, phenylalkylamines, benzothiazepines). In addition, coexpression of the β -subunit increases I_{CaL} amplitude, accelerates the kinetics of Ca^{2+} channel activation, and alters pharmacological properties of the channel.

Pharmacology

Cardiac L-type Ca^{2+} channels are the targets for class IV antiarrhythmic drugs. The three classes of Ca^{2+} channel blockers include dihydropyridines (e.g., nifedipine, nicardipine, amlodipine, felodipine), phenylalkylamines (verapamil), and benzothiazepines (diltiazem). They all preferentially target the $\text{Ca}_v1.2$ channels that initiate excitation-contraction coupling in cardiac and vascular smooth muscle. Each drug type binds specifically to separate binding sites on the channel's $\alpha 1\text{C}$ subunit. The combined use of Ca^{2+} channel blockers can enhance or weaken the block effect because, at least in part, of the different binding sites for those drugs. It is noteworthy that increased extracellular Ca^{2+} concentrations inhibit the binding of phenylalkylamines and dihydropyridines to their receptors on $\text{Ca}_v\alpha 1\text{C}$.

Verapamil and diltiazem preferentially block open and inactivated states of the channel. Thus repeated opening of the channel pore in rapidly firing cells allows more rapid access of the drugs to their receptor site and increases the fraction of Ca^{2+} channels that are blocked. Hence these drugs cause use-dependent block of conduction in cells

with Ca^{2+} -dependent action potentials such as those in the sinus node and AVN. This explains their preferential effect on nodal tissue in paroxysmal SVT.

Dihydropyridines stabilize and induce inactivated channel states, and they likely act as gating modifiers rather than pore blockers. Those drugs exhibit high affinity to the inactivated channel state. Since the inactivated channel state is more prevalent in vascular smooth muscle, due to the depolarized resting membrane potential, dihydropyridines preferentially block $\text{Ca}_v1.2$ in vascular smooth muscle, leading to vasodilation. The kinetics of recovery from block is sufficiently fast that these drugs produce no significant cardiac effect.³⁷

Inherited Channelopathies

Long QT syndrome. Gain-of-function mutations of the *CACNA1C* gene encoding the $\alpha_1\text{C}$ subunit ($\text{Ca}_v1.2$) result in nearly complete elimination of voltage-dependent inactivation of $\text{Ca}_v1.2$ channels, thus leading to inappropriate continuation of the depolarizing I_{CaL} and lengthening the plateau phase of the action potential. The resultant sustained Ca^{2+} influx, action potential (and QT interval) prolongation, and Ca^{2+} overload promote EADs and DADs (Table 2.4). These mutations have been

linked to Timothy syndrome, a rare disease with QT interval prolongation (LQT8). Because the $\text{Ca}_v1.2$ is abundant in many tissues, patients with Timothy syndrome have many clinical manifestations, including congenital heart disease, autism, syndactyly, and immune deficiency. However, the exact pathophysiology of hypertrophic cardiomyopathy, congenital heart defects, and extracardiac manifestations of Timothy syndrome and their relation to *CACNA1C* mutations remain unclear.

Recently, multiple nonsyndromic LQTS-causative mutations in *CACNA1C* (nonsyndromic LQT8) were described in patients with isolated QT prolongation and propensity to ventricular arrhythmias in the absence of congenital heart defects and extracardiac manifestations that define Timothy syndrome.³⁸ Other *CACNA1C* mutations were found to cause cardiac-only Timothy syndrome (COTS), characterized by the concomitant but variably expressed phenotypes of LQTS (QT prolongation), hypertrophic cardiomyopathy, congenital heart defects, and SCD in the absence of any extracardiac symptoms.^{38,39}

Brugada syndrome. Approximately 13% of cases of the Brugada syndrome are attributable to loss-of-function mutations in the cardiac Ca^{2+} channel, resulting in a reduction of the depolarizing I_{CaL} . These include *CACNA1C* (which encodes $\text{Ca}_v1.2$), *CACNB2* (which encodes $\text{Ca}_v\beta_2$), and *CACNA2D1* (which encodes the $\alpha_2\delta$ subunit of $\text{Ca}_v1.2$). In this setting, the mechanism of Brugada syndrome involves a reduction of the depolarizing I_{CaL} .⁴⁰

Short QT syndrome. SQT4 is caused by mutations of the *CACNA1C* gene (encoding $\text{Ca}_v1.2$), SQT5 is caused by mutations of the *CACNB2* gene (encoding the $\text{Ca}_v\beta_2\text{b}$ subunit of $\text{Ca}_v1.2$), and SQT6 is caused by mutations of the *CACNA2D1* gene (encoding the $\alpha_2\delta_1$ subunit of $\text{Ca}_v1.2$). Loss-of-function mutations of those genes result in major attenuation in I_{CaL} amplitude, leading to shortening of the action potential duration.⁴¹

Early repolarization syndrome. Loss-of-function mutations in the $\alpha_1\text{C}$, β_2 , and $\alpha_2\delta$ subunits of the cardiac L-type Ca^{2+} channel (encoded respectively by the *CACNA1C*, *CACNB2*, *CACNA2D1* genes) have been reported in patients with early repolarization syndrome.

Acquired Diseases

Abnormalities in Ca^{2+} currents or intracellular Ca^{2+} transients in acquired diseases may induce both arrhythmia and contractile dysfunction. In AF, $\text{Ca}_v1.2$ mRNA and protein levels are downregulated, resulting in I_{CaL} reduction, which contributes to action potential shortening.

In heart failure, the membrane density of I_{CaL} channels is reduced. However, channel phosphorylation is increased, leading to reduced response to phosphorylating interventions and causing increased single channel open probability that compensates for the reductions in channel density. Despite unchanged I_{CaL} , sarcoplasmic reticulum Ca^{2+} transients are smaller and slower in heart failure, and they cause contractile dysfunction.

T-Type Calcium Current

Structure and Physiology

The cardiac T-type Ca^{2+} channel (originally called low-voltage-activated channels) is composed of a single α_{11} subunit. $\text{Ca}_v3.1$ ($\alpha_{1\text{G}}$ subunit encoded by *CACNA1G*) and $\text{Ca}_v3.2$ ($\alpha_{1\text{H}}$ subunit encoded by *CACNA1H*) isoforms are major candidates for the cardiac T-type Ca^{2+} channel. The structure of the $\alpha_{1\text{H}}$ and $\alpha_{1\text{G}}$ subunits is similar to that involved in the L-type Ca^{2+} channels. However, unlike L-type Ca^{2+} channels, T-type Ca^{2+} channels lack AID and IQ motifs, and do not require β subunits or calmodulin for appropriate function.

T-type Ca^{2+} channels can be distinguished from L-type channels on the basis of their distinctive gating and conductance properties. Compared with L-type Ca^{2+} channels, T-type channels have a smaller conductance and transient openings, generating small currents that quickly

TABLE 2.4 Inherited Channelopathies Related to Calcium Regulation

Clinical Phenotype	Gene	Protein	Functional Effect
Long QT Syndrome (LQTS)			
LQT8 (Timothy syndrome)	CACNA1C	$\text{Ca}_v1.2$	$\uparrow I_{\text{CaL}}$
LQT14	CALM1	Calmodulin 1	$\uparrow I_{\text{CaL}}$
LQT15	CALM2	Calmodulin 2	$\uparrow I_{\text{CaL}}$
LQT16	CALM3	Calmodulin 3	$\uparrow I_{\text{CaL}}$
LQT17 (Triadin knockout syndrome)	TRDN	Triadin	$\uparrow I_{\text{CaL}}$
Brugada Syndrome (BrS)			
BrS3	CACNA1C	$\text{Ca}_v1.2$	$\downarrow I_{\text{CaL}}$
BrS4	CACNB2B	$\text{Ca}_v\beta_2$	$\downarrow I_{\text{CaL}}$
BrS9	CACNA2D1	$\text{Ca}_v\alpha_2\delta_1$	$\downarrow I_{\text{CaL}}$
Short QT Syndrome (SQTS)			
SQT4	CACNA1C	$\text{Ca}_v1.2$	$\downarrow I_{\text{CaL}}$
SQT5	CACNB2B	$\text{Ca}_v\beta_2\text{b}$	$\downarrow I_{\text{CaL}}$
SQT6	CACNA2D1	$\text{Ca}_v\alpha_2\delta_1$	$\downarrow I_{\text{CaL}}$
Early Repolarization Syndrome (ERS)			
ERS2	CACNA1C	$\text{Ca}_v1.2$	$\downarrow I_{\text{CaL}}$
ERS3	CACNB2B	$\text{Ca}_v\beta_2\text{b}$	$\downarrow I_{\text{CaL}}$
ERS4	CACNA2D1	$\text{Ca}_v\alpha_2\delta$	$\downarrow I_{\text{CaL}}$
Catecholaminergic Polymorphic Ventricular Tachycardia (CPVT)			
CPVT1	RyR2	Ryanodine receptor	
CPVT2	CASQ2	Calsequestrin	
CPVT4	CALM1	Calmodulin	
CPVT5	TRDN	Triadin	
Idiopathic Ventricular Fibrillation			
	RyR2	Ryanodine receptor	
	CALM1	Calmodulin	

I_{CaL} , L-type Ca^{2+} current.

decay (within 10s of milliseconds) because of inactivation. Also, T-type channels open at the significantly more negative E_m that overlaps the pacemaker potentials of sinus node cells. The threshold for activation of I_{CaT} is -70 to -60 mV, and I_{CaT} is fully activated at -30 to -10 mV at physiological Ca^{2+} concentration. Membrane depolarization also causes inactivation of I_{CaT} . The inactivation threshold is near -90 mV, with half-maximal inactivation at -60 mV. In contrast to L-type Ca^{2+} channels, T-type Ca^{2+} channels do not inactivate in a Ca^{2+} -dependent manner. The activation and steady-state inactivation overlap near the activation threshold (-60 to -30 mV), thus providing a constant inward current (a window current). This window component may help facilitate the slow diastolic depolarization in sinus node cells and contribute to automaticity.

Function

Ca_v3 channels conduct the T-type Ca^{2+} current (I_{CaT}), which is important in a wide variety of physiological functions, including neuronal firing, hormone secretion, smooth muscle contraction, cell proliferation of some cardiac tissues, and myoblast fusion. In the heart, T-type channels are abundant in sinus node pacemaker cells and Purkinje fibers of many species and are important for maintenance of pacemaker activity by setting the frequency of action potential firing.

T-type Ca^{2+} channels are functionally expressed in embryonic hearts, but they are almost undetectable or markedly reduced in postnatal ventricular myocytes, although some reports described substantial amplitude of I_{CaT} . In the adult heart, the largest I_{CaT} densities are seen in pacemaker cells located in the conduction system.

Because T-type Ca^{2+} channels are most prevalent in the conduction system in the adult heart and the activation range of I_{CaT} overlaps the pacemaker potential, it has been suggested that T-type Ca^{2+} channels play a role in generating pacemaker depolarization and contribute to automaticity. However, experimental evidence indicates that I_{CaT} is not a primary pacemaker current; rather, it can modify depolarization frequency to a small extent. Although organic T-type Ca^{2+} channel blockers (e.g., mibefradil) result in marked decrease in firing frequency of sinus node cells in clinical studies, the possibility that these blockers affect other ionic currents, including I_{CaL} , cannot be entirely excluded. Further studies are necessary to clarify the role of T-type Ca^{2+} channels in the human heart.

Pharmacology

Unlike L-type channels, T-type Ca^{2+} channels are relatively insensitive to dihydropyridines. Mibefradil preferentially block Ca_v3 , as compared with Ca_v2 , but is also capable of blocking several other ion channels, including Na^+ and K^+ channels.

Acquired Diseases

Interestingly, the T-type Ca^{2+} channels are reexpressed in atrial and ventricular myocytes in animal models under various pathological conditions such as cardiac hypertrophy, MI, and heart failure. These findings reflect a reversion to a fetal or neonatal pattern of gene expression, and I_{CaT} contributes to abnormal electrical activity and excitation-contraction coupling. It is possible that similar remodeling occurs in the hypertrophied human heart; however, to date, T-type Ca^{2+} channels have not been detected in normal or diseased human myocardial cells.

Furthermore, experimental evidence suggests that T-type Ca^{2+} channels can be of functional importance in arrhythmogenesis in cardiomyocytes in the pulmonary veins, which can initiate paroxysmal AF. I_{CaT} may directly and indirectly participate in pacemaker depolarization in sinoatrial and other regions of the heart, and this mechanism may become more important in failing hearts.

CARDIAC PACEMAKER CURRENT

Structure and Physiology

Channels responsible for the pacemaker current (I_f ; also called the funny current because it displays unusual gating properties) are named hyperpolarization-activated cyclic nucleotide-gated (HCN) channels. HCN channels are members of the voltage-gated cation channel superfamily and, based on sequence homology, are most closely related to the cyclic nucleotide-gated (CNG) channel and ether-a-go-go (EAG) K^+ channel families.

Four α -subunit isoforms are described (HCN1 to HCN4, encoded by *HCN1* to *HCN4*), which are preferentially expressed in sinus and AVN myocytes and Purkinje fibers. HCN isoforms differ in the extent of voltage-dependent gating and sensitivity to cAMP, and they have different relative rates of activation and deactivation, with HCN1 the fastest, HCN4 the slowest, and HCN2 and HCN3 intermediate. HCN4 is the isoform primarily expressed in the sinus node, AVN, and ventricular conducting system, but low levels of HCN1 and HCN2 have also been reported.⁴²

It is likely that the HCN channel is formed by the coassembly of four either identical (homotetramers) or nonidentical (heterotetramers) α subunits that create an ion-conducting pore. Each α subunit comprises six transmembrane segments (S1 to S6), with a voltage sensor domain in the S4 segment and a pore-forming region between S5 and S6 carrying the GYG triplet signature of K^+ -permeable channels. Their intracellular C-terminus contains cyclic nucleotide-binding domains, which enable direct cAMP binding. A potential auxiliary subunit of HCN channels is MiRP1 (encoded by *KCNE2*).⁴³

I_f is a mixed Na^+ - K^+ current, with a threefold higher selectivity for Na^+ than for K^+ . Despite the GYG amino acid motif, HCN channels are more permeable to Na^+ than K^+ ions. Unlike most voltage-gated channels, which are activated on membrane depolarization, HCN channels are activated on hyperpolarization. The HCN channel activates slowly on hyperpolarization (at voltages lower than approximately -40 to -45 mV) and inactivate slowly in a voltage-independent manner on depolarization. The speed of channel opening is strongly dependent on E_m and is faster at more negative potentials. I_f conducts an inward current during phases 3 and 4 of the action potential and may underlie slow membrane depolarization in cells with pacemaker activity (i.e., cells with I_f and little or no I_{K1}).

Function

I_f is a major player in both generation of spontaneous activity and rate control of cardiac pacemaker cells, and it is sometimes referred to as the “pacemaker current.”

HCN channels are deactivated during the action potential upstroke and the initial plateau phase of repolarization, but they begin to activate at the end of the action potential as repolarization brings the E_m to levels more negative than -40 to -50 mV, and they are fully activated at approximately -100 mV. Once activated, I_f depolarizes the membrane back toward a level at which the Ca^{2+} current activates to initiate the action potential. In its range of activation, which quite properly comprises the voltage range of diastolic depolarization in sinus node cells (approximately -40 to -65 mV), the current is inward, and its reversal occurs at approximately -10 to -20 mV. At the end of the repolarization phase of an action potential, because I_f activation occurs in the background of a decaying outward (K^+ time-dependent) current, current flow quickly shifts from outward to inward, giving rise to a sudden reversal of voltage change (from repolarizing to depolarizing) at the maximum diastolic potential. Hence I_f first opposes and then stops the repolarization process (at the maximum diastolic potential) and finally initiates the diastolic depolarization.⁴³

The I_f contribution terminates when, in the late part of diastolic depolarization, Ca^{2+} -dependent processes take over, and the threshold for L-type Ca^{2+} current activation and action potential firing is reached. Although deactivation of I_f at depolarized voltages is rapid, complete switch off of the current occurs only during the very early fraction of the action potential, which provides a brief time interval during which I_f carries an outward current at positive voltages.

I_f is not only involved in principal rhythm generation but also plays a key role in heart rate regulation. The degree of activation of I_f determines, at the end of an action potential, the steepness of phase 4 depolarization and hence the frequency of action potential firing. In addition, I_f represents a basic physiological mechanism mediating autonomic regulation of heart rate. I_f is regulated by intracellular cAMP and is thus activated and inhibited by β -adrenergic and muscarinic M2 receptor stimulation, respectively.

However, given the complexity of the cellular processes involved in rhythmic activity, exact quantification of the extent to which I_f and other mechanisms contribute to pacemaking is still a debated issue.

Regulation

The voltage dependence of I_f activation is regulated by cAMP direct binding to the cyclic nucleotide-binding domain in the HCN channel and not via phosphorylation-dependent activation mechanisms. Direct interaction of cAMP to the channel shifts the activation curve to more depolarized voltages and strongly accelerates channel activation kinetics. Sympathetic stimulation activates I_f and hence accelerates heart rate via β -adrenoceptor-triggered cAMP production, whereas low-level vagal stimulation lowers heart rate via inhibition of cAMP synthesis and an ensuing inhibition of I_f activity. High vagal tone most likely lowers the heart rate, mainly via the activation of I_{KACH} .

HCN channels are inhibited by increased intracellular acidity (e.g., during myocardial ischemia). Protons shift the activation of I_f to more hyperpolarized potentials and slow pacemaker activity.

Pharmacology

Given the key role of HCN channels in cardiac pacemaking, I_f has become a pharmacological target for the development of novel and more specific heart rate-reducing agents in patients with ischemic heart disease, systolic heart failure, and inappropriate sinus tachycardia. Whereas current heart rate-lowering drugs adversely affect cardiac contractility, selective I_f inhibition is believed to lower heart rate without impairing contractility. In the past, several agents inhibiting cardiac I_f were developed. Early drugs identified as pure negative chronotropic agents include zatebradine and cilobradine, which are derived from the L-type Ca^{2+} channel blocker verapamil.⁴³

Ivabradine is a selective inhibitor of I_f . Ivabradine blocks HCN4 and HCN1 channels by accessing the channels from their intracellular side and by exerting a use- and current-dependent block. Interestingly, ivabradine acts as open channel blocker in HCN4 (as in sinus nodal I_f), whereas block of HCN1 requires channels either to be closed or in a transitional state between an open and closed configuration. Unlike ivabradine, other HCN channel blockers are not specific enough for sinus nodal (mainly HCN4-mediated) I_f ; they also block neuronal HCN channels (I_h current) in several regions of the nervous system, and this has prevented their clinical utility. The principal action of all these substances is to reduce the frequency of pacemaker potentials in the sinus node by inducing a reduction of the diastolic depolarization slope.⁴⁴⁻⁴⁶

Ivabradine induces heart rate reduction without any modification in cardiac contractility and atrioventricular and intraventricular conduction times. Blockade of the I_f current induced by ivabradine is dose and heart rate dependent, resulting in greater effects during fast heart

rates and limiting the risk of symptomatic bradycardia. Clinical trials have demonstrated ivabradine to be an effective antianginal agent in patients with ischemic heart disease and to offer significant hemodynamic benefits in patients with systolic heart failure and higher baseline heart rates. Several smaller studies also suggest a potential benefit of ivabradine in the treatment of patients with inappropriate sinus tachycardia.⁴⁴⁻⁴⁷

Clonidine, an α_2 -adrenergic agonist, was shown to block sinus nodal I_f . Clonidine produces a shift in the voltage dependence of the channel by 10 to 20 mV to more hyperpolarizing potentials.

Inherited Channelopathies

Heterozygous loss-of-function *HCN4* mutations have been identified in individuals with familial sinus bradycardia AV block, early-onset AF, tachycardia-bradycardia syndrome. Also, severe bradycardia resulting from *HCN4* mutations can potentially result in QT prolongation and torsades de pointes or lead to accentuation or unmasking of the Brugada syndrome phenotype. HCN mutations slow channel activation kinetics or, when located in cyclic nucleotide-binding domains, abolish sensitivity of HCN channels to cAMP, thus attenuating I_f and reducing the speed of diastolic depolarization. Recently a gain-of-function mutation in *HCN4* was linked to familial inappropriate sinus tachycardia.^{48,49}

Acquired Diseases

HCN2/HCN4 expression is upregulated in the atria of patients with AF and in ventricular tissues in cardiac hypertrophy and congestive heart failure. This response may contribute to the arrhythmias observed in these disease states. Enhancement of I_f in these pathological conditions can potentially initiate arrhythmia by triggering spontaneous excitation of nonpacemaker cardiomyocytes.

SARCOPLASMIC RETICULUM CALCIUM RELEASE CHANNELS (RYANODINE RECEPTOR 2)

Structure and Physiology

The Ca^{2+} release channel is a macromolecular complex, formed by the cardiac ryanodine receptor isoform (RyR2, encoded by the *RYR2* gene) homotetramer and certain proteins localized on both the cytosolic and the luminal side of the sarcoplasmic reticulum membrane. Cardiac RyR2, by far the largest protein of the complex, operates as a Ca^{2+} -conducting channel. RyR2 channels are approximately 10 times larger than voltage-gated Ca^{2+} and Na^{+} channels.

Each RyR2 monomer contains a transmembrane domain, the pore-forming region that is composed of an even but still undetermined number (likely 6 to 8) of transmembrane segments. This domain encompasses only approximately 10% of the protein clustered at the C-terminus, but it has a critical functional role because it contains sequences that control RyR2 localization and oligomerization and is sufficient to form a functional Ca^{2+} release channel. The remaining 90% of the protein at the N-terminus comprises an enormous cytoplasmic domain that serves as a cytosolic scaffold that interacts with regulatory molecules (including Ca^{2+} , ATP) and proteins (including FKBP12.6, calmodulin). On the luminal (sarcoplasmic reticulum) side, RyR2 forms a part of a large quaternary complex with calsequestrin (CASQ2), triadin, and junctin. Together these four proteins form the core of the Ca^{2+} release channel complex (Fig. 2.10).⁵⁰

Cardiac RyR2 functions as a ligand-activated ion channel that activates (opens) on Ca^{2+} binding. However, the exact structural determinants of RyR gating are as yet unknown. RyR2 is normally closed at low cytosolic Ca^{2+} concentrations (approximately 100 to 200 nM) during diastole. At submicromolar cytosolic Ca^{2+} concentrations, Ca^{2+} binds to high-affinity binding sites on RyR2 and thus increases the open

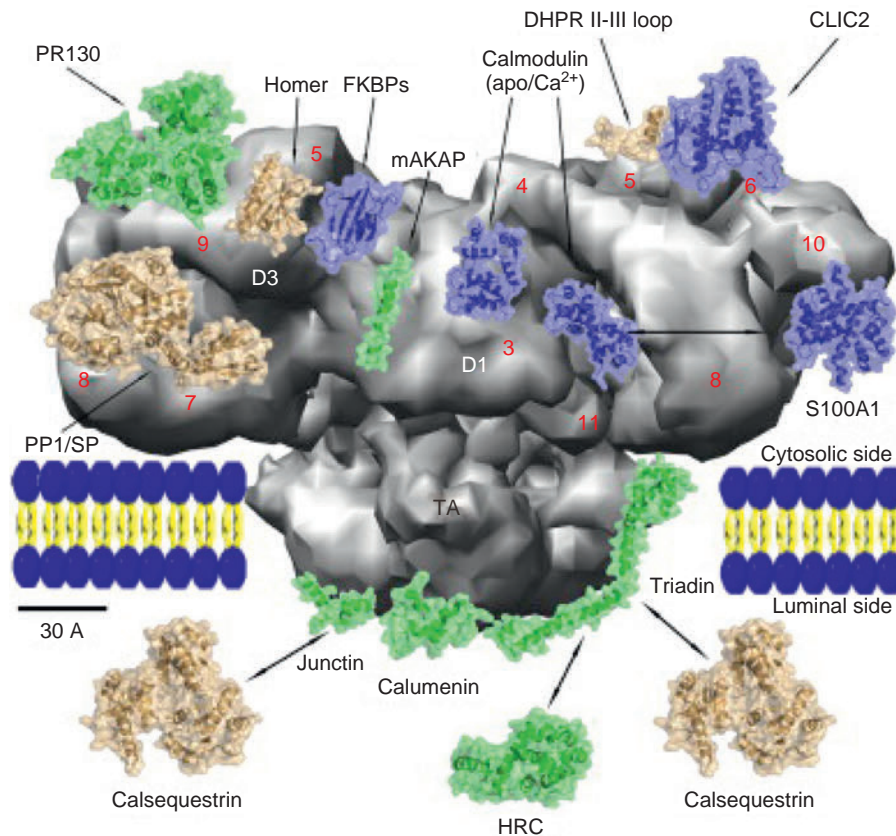


Fig. 2.10 Three-Dimensional Map of Ryanodine Receptor (RyR) Assembly. The large gray structure shows a side view of the RyR homotetramer. In order to show the interactions between sarcoplasmic reticulum membrane-bound RyR and its associated proteins, the single particle cryo-electron microscope reconstruction map of rabbit RyR1 in the closed state at resolution of 10 Å was used. Location of each domain is labeled in red. D1–3 (white) and transmembrane assembly (TA) (brown) indicate the divergent region and transmembrane assembly domain, respectively. D2 is located in the groove hidden by domains 5 and 6. CLIC2, Chloride intracellular channel protein 2; DHPR, dihydropyridine receptor; FKBP, FK506-binding protein; HRC, histidine-rich Ca^{2+} -binding protein; mAKAP, muscle A-kinase anchor protein; PP, protein phosphatase; SP, spinophilin; S100A1, S100 calcium binding protein A1. (From Song DW, Lee J-G, Youn H-S, et al. Ryanodine receptor assembly: a novel systems biology approach to 3D mapping. *Prog Biophys Mol Biol.* 2011;105:145–161.)

probability of the channel (two Ca^{2+} ions are required to open the RyR2 channel) and allows Ca^{2+} release from the sarcoplasmic reticulum into the cytosol.

The precise juxtaposition of the sarcolemmal specialized invaginations (known as T tubules) and sarcoplasmic reticulum forms specific junctional microdomains, creating a 10- to 12-nM gap, known as the dyadic cleft. RyR2s are assembled in a paracrystalline lattice in each dyad, containing 80 to 260 channels, where the RyR2 cytoplasmic region resides, and its transmembrane region spans the sarcoplasmic reticulum membrane to immerse the luminal portion into the sarcoplasmic reticulum Ca^{2+} store. Each array of RyR2s is faced by 10 to 25 L-type Ca^{2+} channels in the sarcolemmal T tubule. Hence each dyad constitutes a local Ca^{2+} signaling complex, or “couplon,” whereby these proteins are coordinately regulated via the changing concentrations of Ca^{2+} , Na^+ , and K^+ within the dyadic cleft.

After approximately 10 milliseconds of RyR2 channel opening, Ca^{2+} release from the sarcoplasmic reticulum terminates, and the Ca^{2+} spark signal starts to decay, mostly owing to diffusion of Ca^{2+} away from its source. RyR2 channel activity is maximal at cytosolic Ca^{2+} concentrations of approximately 10 μM . Elevating cytosolic Ca^{2+} concentrations beyond this point leads to a reduction in the open probability of the

channel, possibly because of Ca^{2+} binding to low-affinity inhibitory binding sites on the RyR2 channel.

Inactivation of Ca^{2+} release is not well understood. It is likely mediated by Ca^{2+} -induced inactivation of RyR2, thus extinguishing of CICR by stochastic attrition, or by Ca^{2+} depletion of the sarcoplasmic reticulum, or both.

RyR2 open probability increases by elevation of sarcoplasmic reticulum Ca^{2+} concentration. When levels of Ca^{2+} in the sarcoplasmic reticulum reach a critical threshold, spontaneous Ca^{2+} release (spillover) can occur even in the presence of normal channels (store overload–induced Ca^{2+} release [SOICR]). Ca^{2+} concentration in the sarcoplasmic reticulum is physiologically increased as an effect of adrenergic (sympathetic) stimulation.

Function

The RyR2 channels are an essential component of the excitation-contraction coupling and act as sentinels to the large sarcoplasmic reticulum Ca^{2+} store. Excitation-contraction coupling describes the physiological process of converting an electrical stimulus (action potential) to a mechanical response (muscle contraction). The contraction of a cardiac myocyte is governed primarily by intracellular Ca^{2+} concentration

(see Fig. 1.7). Ca^{2+} enters the cell during the plateau phase of the action potential through L-type Ca^{2+} channels that line the sarcolemmal T tubules. However, the rise in intracellular Ca^{2+} is small and not sufficient to induce contraction. Nonetheless, the small amount of Ca^{2+} entering the cell via I_{CaL} triggers a rapid mobilization of Ca^{2+} from the sarcoplasmic reticulum into the cytosol by opening the RyR2 channels in the CICR process. Approximately 75% of Ca^{2+} present in the cytoplasm during contraction is released from the sarcoplasmic reticulum. The close proximity of the RyR2 to the T tubule enables each L-type Ca^{2+} channel to activate 4 to 6 RyR2s and generate a Ca^{2+} spark. Ca^{2+} influx via I_{CaL} simultaneously activates approximately 10,000 to 20,000 couplons in each ventricular myocyte with every action potential. Such sophisticated coordination in opening and closing is required to ensure that Ca^{2+} release occurs during the systolic phase of the cardiac cycle and functional silence during diastole.

Luminal Ca^{2+} -dependent deactivation of RyR2 is a process by which the decline in sarcoplasmic reticulum Ca^{2+} that follows sarcoplasmic reticulum Ca^{2+} release renders RyR2s functionally inactive. This results in termination of CICR and induction of a refractory state that suppresses Ca^{2+} release during the diastole, which is an important determinant of the mechanical refractoriness required for efficient relaxation and refilling of the heart.

Regulation

Many proteins interact directly and indirectly with the N-terminal cytoplasmic domain of RyR2, including FK506-binding protein (calstabin2 or FKBP12.6), PKA, Ca^{2+} -calmodulin-dependent kinase II (CaMKII), phosphodiesterase 4D3, calmodulin, protein phosphatases 1 and 2A, and sorcin. CASQ2, junctin, and triadin bind with the luminal (sarcoplasmic reticulum) C-terminus of RyR2.

Calsequestrin

CASQ2 is a low-affinity, high-capacity Ca^{2+} -binding protein, which serves as a Ca^{2+} storage reservoir that is able to bind luminal Ca^{2+} (40 to 50 Ca^{2+} ions per molecule) during diastole, thus buffering Ca^{2+} within the sarcoplasmic reticulum (i.e., preventing Ca^{2+} precipitation and lowering luminal free Ca^{2+} concentration) and preventing diastolic Ca^{2+} release via RyR2 to cytosol. CASQ2 presumably serves as a luminal Ca^{2+} sensor that modulates the responsiveness of the RyR2 to luminal Ca^{2+} . At low luminal Ca^{2+} concentrations, CASQ2 interacts with RyR2 via binding to triadin and junctin and inhibits the activity of the RyR2. When sarcoplasmic reticulum Ca^{2+} levels increase, Ca^{2+} binds to CASQ2, resulting in weakened interactions or complete dissociation of CASQ2 from triadin. This process relieves the inhibitory action of CASQ2 on the RyR2 complex, allows Ca^{2+} release to the cytosol, and hence normalizes sarcoplasmic reticulum Ca^{2+} load. Triadin and junctin not only mediate functional interactions of CASQ2 and RyR2 but also modulate RyR2 function by themselves by increasing the activity of the RyR2 channel. This Ca^{2+} -dependent modulation of RyR2s by triadin, junctin, and CASQ2 may contribute to deactivation and refractoriness of RyR2 channels after sarcoplasmic reticulum Ca^{2+} release.

FK506-Binding Protein

FKBP12.6 (the 12.6-kDa cytosolic FK506-binding protein), also known as calstabin2 (Ca^{2+} channel-stabilizing binding protein), stabilizes the closed conformational state of the RyR2 channel, thus enabling the channel to close completely during diastole (at low intracellular Ca^{2+} concentrations), preventing aberrant Ca^{2+} leakage from the sarcoplasmic reticulum, and ensuring muscle relaxation. PKA phosphorylation of RyR2 decreases the binding affinity of FKBP12.6 to RyR2 and thereby increases the probability of an open state and amplifies the response to Ca^{2+} -dependent activation.

Calmodulin

Calmodulin is a Ca^{2+} -binding protein with ubiquitous expression that has a regulatory function for numerous Ca^{2+} -dependent processes. The main binding partner of calmodulin in cardiac cells is RyR2. Calmodulin has four Ca^{2+} -binding sites and four sites that bind to RyR2 monomers. Calmodulin preferentially inhibits RyR2 at Ca^{2+} concentrations lower than 10 μM by binding to a region on RyR2. Calmodulin may function to assist closing RyR2 following sarcoplasmic reticulum Ca^{2+} release in excitation-contraction coupling.

Protein Kinase A

Stimulation of β -adrenergic receptors results in an increase in cAMP and consequent PKA activation. PKA interacts with the RyR2 channel via binding to the muscle A kinase anchoring protein (mAAP). PKA phosphorylation of RyR2 activates the channel, at least in part by increasing the sensitivity of RyR2 to cytosolic Ca^{2+} and a transient decrease in the binding affinity of calstabin2. This allows for increased sarcoplasmic reticulum Ca^{2+} release on Ca^{2+} influx via I_{CaL} as a part of the fight-or-flight mechanism. By contrast, chronic PKA hyperphosphorylation of RyR2 can result in incomplete channel closure and Ca^{2+} leak during diastole, which causes depletion of the sarcoplasmic reticulum Ca^{2+} store and reduced Ca^{2+} release on receptor activation.

Calcium-Calmodulin-Dependent Protein Kinase II

CaMKII is a dodecameric holoenzyme activated by Ca^{2+} -bound calmodulin, possibly at high cellular Ca^{2+} loads. CaMKII phosphorylation increases RyR2 channel open probability, but to a smaller extent than PKA phosphorylation. CaMKII activity increases at faster heart rates (typically mediated by β -adrenergic stimulation and PKA activation and associated with increased cytosolic Ca^{2+}) and phosphorylates RyR2 to enhance sarcoplasmic reticulum Ca^{2+} release, which helps maintain the positive force-frequency relationship (i.e., cardiac contractility increases as a function of heart rate). Increased CaMKII activity also phosphorylates phospholamban to help accelerate diastolic filling of the ventricles at higher heart rates. Physiologically, sympathetic activation stimulates both PKA and CaMKII, which thus function synergistically. CaMKII is typically considered to be downstream of PKA and elevated Ca^{2+} transients.

Pharmacology

RyR2s are targets of multiple experimental drugs. However, thus far, no compounds in clinical use are known to target RyR2 directly.

The plant alkaloid ryanodine binds the RyR2 channel with high affinity in a Ca^{2+} -dependent and use-dependent fashion, thus making it an important tool for biochemical characterization of the channel. Two ryanodine-binding sites, a high-affinity site and a low-affinity one, have been described at the C-terminus of RyR2. At the high-affinity site, ryanodine induces long-lasting channel openings at a subconductance state, whereas high concentrations block the channel.

Caffeine, in high concentrations (5 to 20 mM), increases the RyR2 sensitivity to Ca^{2+} and ATP and results in increased RyR2 mean open time and open probability. Caffeine is used experimentally to measure sarcoplasmic reticulum Ca^{2+} content indirectly, because its application causes emptying of the sarcoplasmic reticulum Ca^{2+} store.

JTV-519, also known as K201, is a benzothiazepine derivative (an analogue of diltiazem) and an L-type Ca^{2+} channel blocker and stabilizer. JTV-519 can increase the binding affinity of calstabin2 for RyR2, thus stabilizing the closed conformational state of the RyR2 channel and hence preventing diastolic sarcoplasmic reticulum Ca^{2+} leak. JTV-519 can potentially offer an antiarrhythmic benefit in a variety of pathological conditions that lead to destabilization of the RyR2 channel's closed

state, such as RyR2 mutations, hyperphosphorylation of the RyR2 during heart failure, and sarcoplasmic reticulum Ca^{2+} overload.

Among class I antiarrhythmic drugs, only flecainide and propafenone were found to inhibit RyR2 channels (by inducing brief closures of open RyR2 to subconductance states), suppress arrhythmogenic Ca^{2+} sparks, and prevent CPVT in experimental studies. The potency of RyR2 channel inhibition rather than Na^+ channel blockade appears to determine the efficacy of class I agents for the prevention of CPVT. Flecainide has been demonstrated to prevent lethal ventricular arrhythmias in patients with familial CPVT.

Several toxins (e.g., the scorpion toxins imperatoxin A and imperatoxin I), some anticancer drugs (e.g., doxorubicin), and some immunosuppressants (e.g., rapamycin) can potentially cause cardiac adverse events likely related to effects on the gating kinetics of RyR2 channels.

Inherited Channelopathies

Mutations in genes that encode for four key Ca^{2+} regulatory proteins other than L-type Ca^{2+} channels have been implicated in the pathogenesis of CPVT, idiopathic VF, and LQTS (see Table 2.4).

Mutations Related to Ryanodine Receptor

CPVT1, an autosomal-dominant trait, is the most common genetic variant (50% to 70%) of familial CPVT and is caused by mutations in the *RyR2* gene. CPVT mutant RyR2s typically shows gain-of-function defects following channel activation by PKA phosphorylation (in response to β -adrenergic stimulation or caffeine), resulting in uncontrolled Ca^{2+} release from the sarcoplasmic reticulum during electrical diastole, which facilitates the development of DADs and triggered arrhythmias.⁵¹

Missense mutations in *RyR2* also have been linked to a form of arrhythmogenic cardiomyopathy (ARVC-2) characterized by exercise-induced polymorphic VT that does not appear to have a reentrant mechanism, occurring in the absence of significant structural abnormalities. These patients do not develop characteristic features of ARVC on the 12-lead ECG or signal-averaged ECG, and global RV function remains unaffected. ARVC-2 shows a closer resemblance to familial CPVT in both etiology and phenotype; its inclusion under the umbrella term of ARVC remains controversial.

Recently, two different heterozygous mutations in the *RYR2* gene have been identified in a family with multiple idiopathic VF victims. Those mutations resulted in a phenotype distinct from classic RYR2-related CPVT.^{52,53}

Mutations Related to Calsequestrin

CPVT2, an autosomal-recessive disease, is associated with homozygous mutations in the *CASQ2* gene. Heterozygous carriers of one *CASQ2* mutation are usually healthy. While some *CASQ2* mutations are thought to compromise *CASQ2* synthesis and result in reduced expression or complete absence of *CASQ2* in the heart, other mutations seem to cause expression of defective *CASQ2* proteins with abnormal regulation of cellular Ca^{2+} homeostasis. *CASQ2* mutations result in disruption of the control of RyR2s by luminal Ca^{2+} required for effective termination of sarcoplasmic reticulum Ca^{2+} release and prevention of spontaneous Ca^{2+} release during diastole, leading to diminished Ca^{2+} signaling refractoriness and generation of arrhythmogenic spontaneous Ca^{2+} releases.⁵¹

Mutations Related to Calmodulin (Calmodulinopathy)

Three different genes (*CALM1*–*3*) in the human genome encode the exact same calmodulin protein. Recent genetic studies have identified several calmodulin mutations associated with CPVT, LQTS, and idiopathic VF. Defective calmodulin–RyR2 binding results in impaired calmodulin inhibition of RyR2 function with consequent dysregulation of sarcoplasmic reticulum Ca^{2+} release.

CPVT4, an autosomal-dominant trait, is caused by a mutation of *CALM1*. In addition, a familial form of idiopathic VF was linked to mutations of the *CALM1* gene, with autosomal-dominant transmission. Further, de novo mutations in *CALM1*, *CALM2*, or *CALM3* genes were found to disrupt Ca^{2+} -dependent inactivation of the cardiac L-type Ca^{2+} channel ($\text{Ca}_v1.2$), which leads in augmentation of I_{CaL} , prolongation of the plateau phase of action potential, and LQTS phenotype (LQT14–16).^{54,55}

Mutations Related to Triadin

CPVT5, an autosomal-recessive disease, is caused by mutations of the *TRDN* gene (encoding triadin). In addition, homozygous or compound heterozygous loss-of-function mutations in *TRDN* likely reduce triadin-mediated negative feedback on the L-type Ca^{2+} channel, resulting in augmentation of I_{CaL} , prolonged action potential duration, and the recessively inherited LQTS phenotype (LQT17). Intracellular Ca^{2+} overload and increases in spontaneous sarcoplasmic reticulum Ca^{2+} release, particularly in the setting of β -adrenergic stimulation, result in ventricular arrhythmias. LQT17 is characterized by extensive T-wave inversions in the precordial leads V1 through V4, with either persistent or transient QT prolongation, exercise-induced cardiac arrest in early childhood (2 to 6 years of age), and mild-to-moderate proximal skeletal muscle weakness. Because all *TRDN*-null patients display a strikingly similar phenotype, it has been proposed that either triadin knockout syndrome or *TRDN*-mediated autosomal-recessive LQTS should be used rather than LQT17.^{38,56}

Acquired Diseases

RyR2 dysfunction is a key factor leading to arrhythmias in heart failure. Chronic β -adrenergic stimulation results in PKA hyperphosphorylation of RyR2. This process causes the dissociation of the channel-stabilizing protein calstabin and leads to diastolic Ca^{2+} leak from the sarcoplasmic reticulum and the generation of spontaneous Ca^{2+} waves, which can be maintained despite a reduced Ca^{2+} gradient, thus underlying DAD-induced triggered arrhythmias in heart failure.

Importantly, in the setting of digitalis poisoning, the abnormal RyR2 behavior leading to spontaneous Ca^{2+} release and DADs is secondary to the elevation of the sarcoplasmic reticulum Ca^{2+} content (SOICR). In CPVT, on the other hand, spontaneous Ca^{2+} release and DADs can occur without Ca^{2+} overload. Mutations in *RyR2* or *CASQ2* lead to defective Ca^{2+} signaling lowering of the sarcoplasmic reticulum Ca^{2+} threshold for spontaneous Ca^{2+} release below the normal baseline level (“perceived” Ca^{2+} overload). A similar mechanism may underlie triggered arrhythmias in other disease conditions, including heart failure and ischemic heart disease, in which sarcoplasmic reticulum Ca^{2+} release regulation is compromised because of acquired defects in components of the RyR2 channel complex.

CARDIAC GAP JUNCTIONS

Structure and Physiology

Cardiomyocytes make contact with each other via multiple intercalated discs, which mediate the transmission of force, electrical continuity, and chemical communication between adjacent cells. Three types of specialized junctions exist in the intercalated disc: (1) fascia adherens, (2) macula adherens (desmosome), and (3) gap junction (nexus). The fascia adherens is an anchoring site for myofibrils, facilitating the transmission of mechanical energy between neighboring cells. The desmosomes link to the cytoskeleton of adjacent cells to provide strong localized adhesion sites that resist shearing forces generated during contraction. Gap junctions are assemblies of intercellular channels that provide electrical continuity and chemical communication between adjacent cells.⁵⁷

In addition to the end-to-end and side-to-side gap junctions localized at the intercalated discs, lateral (side-to-side) gap junctions can exist in nondisc lateral membranes of cardiomyocytes, but they are much less common, occurring more in atrial than ventricular myocardium.⁵⁸

Each gap junction channel is constructed of two hemichannels (connexons) aligned head-to-head in mirror symmetry across a narrow extracellular gap, one provided by each of the adjoining cells. Each connexon is composed of six integral membrane proteins called connexins (Cx) hexagonally arranged around the pore. Each connexin consists of four membrane-spanning domains (M1 to M4), two extracellular loops (E1, E2), one intracellular loop, and cytoplasmic N- and C-termini. The extracellular loops mediate the docking of the two hemichannels.^{59,60}

Up to 24 different connexin types have been identified. They are named after their theoretical molecular weight in daltons. Three different connexins are prominently expressed in the atrial and ventricular myocardium: Cx40, Cx43, and Cx45. A fourth connexin has been described in the AVN (Cx31.9). Cx40 gap junction channels exhibit the largest conductance and Cx45 the smallest. Although each connexin exhibits a distinct tissue distribution, most cardiomyocytes express more than one connexin isoform. Cx43 is by far the most abundant and is expressed in atrial and ventricular myocytes and distal parts of the Purkinje system. Cx40 is mainly expressed in the atrial myocytes, AVN, and HPS. Cx45 appears to be primarily expressed in nodal tissue (the sinus and compact AVNs), and more weakly in the atrium, HB, bundle branches, and Purkinje fibers.⁶⁰⁻⁶²

Connexons can be composed by the oligomerization of a single connexin type (homomeric) or of different types (heteromeric). In addition, the gap junction channel as a whole may be formed of two matching hemichannels (homotypic) or nonmatching hemichannels (heterotypic; Fig. 2.11).

The different cardiac connexins exhibit distinctive biophysical properties; hence, the connexin composition of a gap junction channel determines its unitary conductance, voltage sensitivity, and ion selectivity. Cx40 gap junctions express the largest conductance, and Cx45 expresses

the smallest. Both Cx40 and Cx45 are highly cation selective, and their conductance is voltage dependent. Cx43 has an intermediate conductance and is nonselective.⁶³

The individual gap junction channels allow exchange of nutrients, metabolites, ions (e.g., Na^+ , Cl^- , K^+ , Ca^{2+}) and small molecules (e.g., cAMP, cGMP, inositol triphosphate [IP3]) with molecular weights up to approximately 1000 Da.

Function

Gap junctions maintain direct cell-to-cell communication in the heart by providing biochemical and low-resistance electrical coupling between adjacent cardiomyocytes. Thus gap junctions are responsible for propagation of the electrical current from one cardiac cell to another and are crucial in myocardial synchronization and heart function. Gap junctions also provide biochemical coupling, which allows intercellular movement of second-messenger substances (e.g., ATP, cyclic nucleotides, and IP3) and hence enables coordinated responses of the myocardial syncytium to physiological stimuli.

The role of gap junction channels in action potential propagation and conduction velocity in cardiac tissue depends primarily on static factors of the channels (e.g., the number of channels, channel conductance, and voltage sensitivity) and dynamic factors (e.g., channel gating kinetics), as well as on properties of the propagated action potential, structural aspects of the cell geometry, and tissue architecture. Tissue-specific connexin expression and gap junction spatial distribution, as well as the variation in the structural composition of gap junction channels, allow for a greater versatility of gap junction physiological features and for disparate conduction properties in cardiac tissue. The myocytes of the sinus and AVNs are equipped with small, sparse, dispersed gap junctions containing Cx45, a connexin that forms low conductance channels; this feature underlies the relatively poor intercellular coupling in nodal tissues, a property that is linked to slowing of conduction. In contrast, ventricular muscle expresses predominantly Cx43 and Cx45, which have larger conductance. Atrial muscle and Purkinje fibers express all three cardiac connexins.^{63,64}

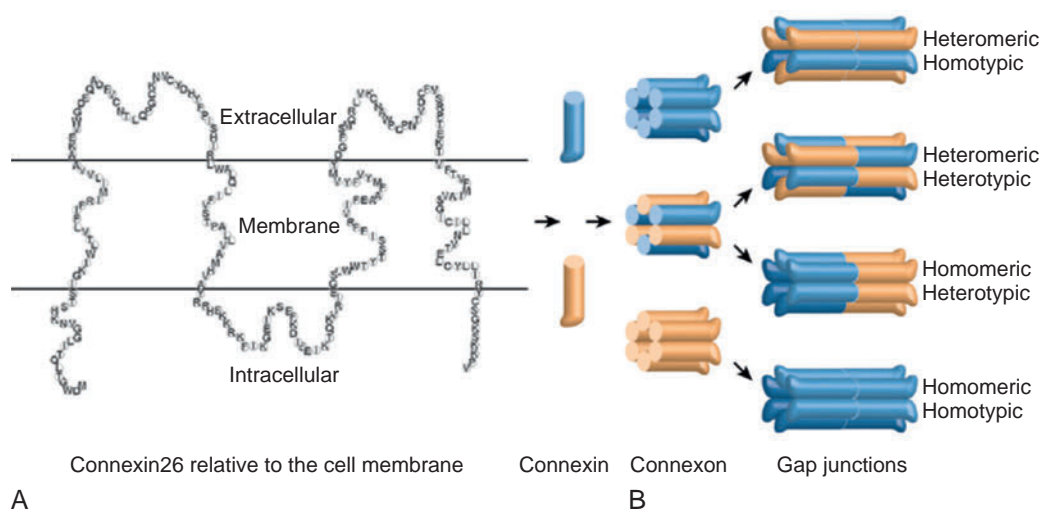


Fig. 2.11 Schematic Representation of Connexins and Gap Junction Channels. (A) Connexins have four transmembrane domains, two extracellular loops, a cytoplasmic loop, and cytoplasmic N- and C-termini. (B) Six connexins oligomerize to form hemichannels called “connexons,” which then align in the extracellular space to complete the formation of gap junction channels. Different connexins can selectively interact with each other to form homomeric, heteromeric, and heterotypic channels, which differ in their content and spatial arrangement of connexin subunits. (From Meşe G, Richard G, White TW. Gap junctions: basic structure and function. *J Invest Dermatol.* 2007;127:2516–2524.)

Under physiological conditions, a given cardiomyocyte in the adult working myocardium is electrically coupled to an average of approximately 11 adjacent cells, with gap junctions predominantly localized at the intercalated discs at the ends of the rod-shaped cells. Lateral (side-to-side) gap junctions in nondisc lateral membranes of cardiomyocytes are much less abundant and occur more often in atrial than ventricular tissues. Thus intercellular current flow occurs primarily at the cell termini, although propagation can occur both longitudinally and transversely. This particular subcellular distribution of gap junctions underlies uniform anisotropic impulse propagation throughout the myocardium, whereby conduction in the direction parallel to the long axis of the myocardial fiber bundles is approximately three to five times more rapid than that in the transverse direction. This property is attributable principally to the lower resistivity of myocardium provided by the gap junctions in the longitudinal versus the transverse direction.^{65,66}

Cx43 hemichannels can occur as free, nonjunctional channels in the plasma membrane. These hemichannels are normally closed but may open in response to various pathological (rather than physiological) triggers.

Regulation

Gap junction channels have a voltage-dependent gating mechanism, depending primarily on transjunctional voltage (i.e., the potential difference between the cytoplasm of the two adjacent cells). At rest, when the junctional voltage is zero, the channels usually are open. During the course of a propagated action potential, the channels tend to close in a voltage- and time-dependent manner. Gap junction channel gating can also be altered by specific changes in intracellular ions and by posttranslational modifications ("loop" gating). Cytosolic Na^+ and Ca^{2+} overload, acidosis, and reduced ATP levels decrease gap junction channel function. Unlike the voltage gate, which closes rapidly and incompletely, the chemical gate closes slowly and completely.

Cx43 gap junction proteins have a short life span (half-life in the order of hours). The life cycle of Cx43 involves connexon delivery to the cell plasma membrane (forward/anterograde trafficking), connexon movement within the plasma membrane (lateral diffusion), and connexon internalization from the plasma membrane (retrograde trafficking). Given the short life span, regulation of gap junction trafficking, assembly and disassembly, and degradation is likely to be critical in the control of intercellular communication.

Phosphorylation also appears to play a key role in channel gating that determines channel conductance and has been implicated in the regulation of the connexin "life cycle" at several stages. Gap junction coupling also is regulated by certain endogenous mediators (e.g., acetylcholine, norepinephrine, and angiotensin), likely via phosphorylation-mediated mechanisms. Importantly, channels composed of different connexins possess different properties and are susceptible to different regulation.

Pharmacology

Several agents have been found to decrease gap junction channel coupling, including long-chain alcohols (e.g., heptanol, octanol), fatty acids (myristoleic acid, decanoic acid, palmitoleic acid), general anesthetics (e.g., halothane, isoflurane), carbachol (an acetylcholine analogue), α -adrenergic agonists (phenylephrine), angiotensin, insulin, insulin-like growth factor, and the nonsteroidal agents fenamates (e.g., flufenamic acid, meclofenamic acid). The mechanisms of action of those agents remain largely unknown.

Antimalarial drugs, particularly quinine and quinine derivatives such as mefloquine, can reduce gap junction channel conductance, and their effects seem to be connexin subtype specific. In addition, it has been

suggested that the cardiac glycosides strophanthidin, ouabain, and digitoxin decrease intercellular coupling.

Experimental evidence suggests that optimization of gap junction conductance can potentially confer an antiarrhythmic effect by ensuring more homogeneous propagation of activation wavefronts and minimizing opportunities for reentrant arrhythmias to develop.⁶³

Some compounds, including antiarrhythmic peptides and their derivatives (e.g., AAP10, ZP123, rotigaptide), can upregulate Cx43 via modulation either synthesis or degradation and enhance gap junctional communication and were found to reduce conduction slowing and prevent AF and ischemic reentrant VT in various cell and animal models. These peptides presumably act by modulating Cx43 phosphorylation.⁶⁷

Inherited Channelopathies

Studies have demonstrated an association between changes in the primary sequence of Cx43, or Cx40 and arrhythmias. Rare single nucleotide polymorphism in the atrial-specific Cx40 gene (*GJA5*) has been found to increase the risk of idiopathic AF.⁶³ *GJA5* mutations have also been linked to progressive cardiac conduction disease.⁶⁸

Cx43 gene (*GJA1*) amino acid substitutions have been described in SIDS and familial AF. Of note, *GJA1* mutations also cause the pleiotropic phenotype of oculodentodigital dysplasia, an autosomal dominant syndrome characterized by craniofacial and limb dysmorphisms, as well as neurologic manifestations. Surprisingly, this phenotype does not include cardiac arrhythmias.⁶⁸

Mutations in desmosomal proteins underlying ARVC can also impair expression of interacting proteins at the intercalated disk (e.g., gap junction or Na^+ channel proteins), giving rise to impairment of intercellular conductance and promoting ventricular arrhythmogenesis, even in the absence of fibrofatty tissue replacement. In particular, Cx43 remodeling in the gap junctions, which contributes to delayed conduction and ventricular arrhythmogenesis, is often observed in ARVC patients. Abnormal electrical coupling and ion channel dysfunction, leading to electrical instability, can promote arrhythmias and predispose patients to high risk of SCD, even in the early disease stages, prior to the development of significant ventricular dysplasia and scarring.⁶⁹⁻⁷¹

Acquired Diseases

Given highly dynamic and active turnover of connexons, remodeling of gap junction coupling can occur rapidly after insult. Modification of cell-to-cell coupling occurs in numerous pathophysiological settings (e.g., acute myocardial ischemia, hypertrophic cardiomyopathies, dilated cardiomyopathies, ischemic cardiomyopathies, and clinical congestive heart failure) as a consequence of acute changes in the average conductance of gap junctions secondary to ischemia, hypoxia, acidification, or an increase in intracellular Ca^{2+} , or it can be produced by changes in expression or cellular distribution patterns of gap junctions.⁶⁰

Remodeling includes a decrease in the number of gap junction channels resulting from the interruption of communication between cells by fibrosis and downregulation of Cx43 formation or of trafficking to the intercalated disc. In addition, gap junctions can become more prominent along lateral membranes of myocytes (so-called structural remodeling). The mislocalization of Cx43 during disease reflects impaired forward trafficking to the intercalated discs. Lateralized Cx43 likely represents protein that is not functional junctions. Influences of Cx43 lateralization on impulse propagation have not yet been well defined.⁶³

Changes in function or remodeling of connexins occur in almost all major arrhythmogenic cardiac disorders. Inactivation of gap junctions decreases transverse conduction velocity to a greater degree than longitudinal conduction, thus resulting in exaggeration of anisotropy and providing a substrate for reentrant activity and increased susceptibility to arrhythmias. Importantly, there is a high redundancy in

connexin expression in the heart with regard to conduction of electrical impulse. It has been shown that a 50% reduction in Cx43 does not alter ventricular impulse conduction. Cx43 expression must decrease by 90% to affect conduction, but even then conduction velocity is reduced only by 20%.

AF is associated with abnormal expression and distribution of atrial Cx40, which can potentially lead to inhomogeneous electrical coupling and abnormal impulse formation and conduction, and thereby provide the substrate for atrial arrhythmias.⁶³

REFERENCES

- Bao Y, Isom LL. Na_v1.5 and regulatory β subunits in cardiac sodium channelopathies. *Card Electrophysiol Clin*. 2014;6:679–694.
- Varga Z, et al. Direct measurement of cardiac Na⁺ channel conformations reveals molecular pathologies of inherited mutations. *Circ Arrhythm Electrophysiol*. 2015;8:1228–1239.
- Belardinelli L, Giles WR, Rajamani S, et al. Cardiac late Na⁺ current: proarrhythmic effects, roles in long QT syndromes, and pathological relationship to CaMKII and oxidative stress. *Heart Rhythm*. 2015;12:440–448.
- Shy D, Gillet L, Abriel H. Cardiac sodium channel Na_v1.5 distribution in myocytes via interacting proteins: the multiple pool model. *Biochim Biophys Acta*. 2013;1833:886–894.
- Peters CH, Abdelsayed M, Ruben PC. Triggers for arrhythmogenesis in the Brugada and long QT 3 syndromes. *Prog Biophys Mol Biol*. 2016;120:77–88.
- Greer-Short A, George SA, Poelzing S, et al. Revealing the concealed nature of long-QT type 3 syndrome. *Circ Arrhythm Electrophysiol*. 2017;10:e004400.
- Buch T, et al. Mutations in SCN10A are responsible for a large fraction of cases of Brugada syndrome. *J Am Coll Cardiol*. 2014;64:66–79.
- Antzelevitch C, Patocskaï B. Brugada syndrome: clinical, genetic, molecular, cellular, and ionic aspects. *Curr Probl Cardiol*. 2016;41:7–57.
- Adler A, Gollob MH. A practical guide to early repolarization. *Curr Opin Cardiol*. 2015;30:8–16.
- Antzelevitch C, Yan GX. J-wave syndromes: Brugada and early repolarization syndromes. *Heart Rhythm*. 2015;12:1852–1866.
- Abe K, et al. Sodium channelopathy underlying familial sick sinus syndrome with early onset and predominantly male characteristics. *Circ Arrhythm Electrophysiol*. 2014;7:511–517.
- Lieve KV, et al. Gain-of-function mutation in SCN5A causes ventricular arrhythmias and early onset atrial fibrillation. *Int J Cardiol*. 2017;236:187–193.
- Mizusawa Y, Tan HL. Sodium current disorders. *Card Electrophysiol Clin*. 2014;6:819–824.
- Crotti L, Ghidoni A, Insolia R, et al. The role of the cardiac sodium channel in perinatal early infant mortality. *Card Electrophysiol Clin*. 2014;6:749–759.
- Remme CA. Cardiac sodium channel overlap syndrome. *Card Electrophysiol Clin*. 2014;6:761–776.
- Amin AS, Wilde AAM. Genetic control of potassium channels. *Card Electrophysiol Clin*. 2016;8:285–306.
- Nerbonne JM. Molecular basis of functional myocardial potassium channel diversity. *Card Electrophysiol Clin*. 2016;8:257–273.
- Wu W, Sanguinetti MC. Molecular basis of cardiac delayed rectifier potassium channel function and pharmacology. *Card Electrophysiol Clin*. 2016;8:275–284.
- Workman AJ, Marshall GE, Rankin AC, et al. Transient outward K⁺ current (ITO) reduction prolongs action potentials and promotes afterdepolarizations: a dynamic-clamp study in human and rabbit cardiac atrial myocytes. *J Physiol*. 2012;17:4289–4305.
- Skibbye L, Ravens U. Mechanism of proarrhythmic effects of potassium channel blockers. *Card Electrophysiol Clin*. 2016;8:395–410.
- Nguyen TP, Singh N, Xie Y, et al. Repolarization reserve evolves dynamically during the cardiac action potential: effects of transient outward currents on early afterdepolarizations. *Circ Arrhythm Electrophysiol*. 2015;8:694–702.
- Algalarrondo V, Nattel S. Potassium channel remodeling in heart disease. *Card Electrophysiol Clin*. 2016;8:337–347.
- Chen L, Sampson KJ, Kass RS. Cardiac delayed rectifier potassium channels in health and disease. *Card Electrophysiol Clin*. 2016;8:307–322.
- Voigt N, Dobrev D. Atrial-selective potassium channel blockers. *Card Electrophysiol Clin*. 2016;8:411–421.
- Altomare C, et al. I_{Kr} Impact on repolarization and its variability assessed by dynamic clamp. *Circ Arrhythm Electrophysiol*. 2015;8:1265–1275.
- Roden DM. Pharmacogenetics of potassium channel blockers. *Card Electrophysiol Clin*. 2016;8:385–393.
- Adler A, Viskin S. Clinical features of genetic cardiac diseases related to potassium channelopathies. *Card Electrophysiol Clin*. 2016;8:361–372.
- Tomson TT, Arora R. Modulation of cardiac potassium current by neural tone and ischemia. *Card Electrophysiol Clin*. 2016;8:349–360.
- Foster MN, Coetzee WA. K_{ATP} channels in the cardiovascular system. *Physiol Rev*. 2016;96:177–252.
- Nichols CG. Adenosine triphosphate-sensitive potassium currents in heart disease and cardioprotection. *Card Electrophysiol Clin*. 2016;8:323–335.
- Zhou L, et al. Effects of regional mitochondrial depolarization on electrical propagation: implications for arrhythmogenesis. *Circ Arrhythm Electrophysiol*. 2014;7:143–151.
- Zhang XD, Lieu DK, Chiamvimonvat N. Small-conductance Ca²⁺-activated K⁺ channels and cardiac arrhythmias. *Heart Rhythm*. 2015;12:1845–1851.
- Mahida S. Expanding role of SK channels in cardiac electrophysiology. *Heart Rhythm*. 2014;11:1233–1238.
- Dolphin AC. Voltage-gated calcium channels and their auxiliary subunits: physiology and pathophysiology and pharmacology. *J Physiol*. 2016;594:5369–5390.
- Gurkoff G, Shahlaie K, Lyeth B, et al. Voltage-gated calcium channel antagonists and traumatic brain injury. *Pharmaceuticals (Basel)*. 2013;6:788–812.
- Zamponi GW, Striessnig J, Koschak A, et al. The physiology, pathology, and pharmacology of voltage-gated calcium channels and their future therapeutic potential. *Pharmacol Rev*. 2015;67:821–870.
- Catterall WA, Swanson TM. Structural basis for pharmacology of voltage-gated sodium and calcium channels. *Mol Pharmacol*. 2015;88:141–150.
- Giudicessi JR, Ackerman MJ. Calcium revisited. *Circ Arrhythm Electrophysiol*. 2016;9:e002480.
- Boczek NJ, et al. Identification and functional characterization of a novel CACNA1C-mediated cardiac disorder characterized by prolonged QT intervals with hypertrophic cardiomyopathy, congenital heart defects, and sudden cardiac death. *Circ Arrhythm Electrophysiol*. 2015;8:1122–1132.
- Antzelevitch C, et al. J-Wave syndromes expert consensus conference report: emerging concepts and gaps in knowledge. Endorsed by the Asia Pacific Heart Rhythm Society (APHRS), the European Heart Rhythm Association (EHRA), the Heart Rhythm Society (HRS), and the Latin American S. *Heart Rhythm*. 2016;13:e295–e324.
- Khera S, Jacobson JT. Short QT syndrome in current clinical practice. *Cardiol Rev*. 2015;24:1–17.
- Li N, et al. Molecular mapping of sinoatrial node HCN channel expression in the human heart. *Circ Arrhythm Electrophysiol*. 2015;8:1219–1227.
- Sartiani L, Romanelli MN, Mugelli A, et al. Updates on HCN channels in the heart: function, dysfunction and pharmacology. *Curr Drug Targets*. 2015;16:868–876.
- Ptaszynski P, et al. Ivabradine in combination with metoprolol succinate in the treatment of inappropriate sinus tachycardia. *J Cardiovasc Pharmacol Ther*. 2013;18:338–344.
- Kumar Goyal V, Godara S, Chandra Sadasukhi T, et al. Management of inappropriate sinus tachycardia with ivabradine in a renal transplant recipient. *Drug Discov Ther*. 2014;8:132–133.
- Ptaszynski P, Kaczmarek K, Ruta J, et al. Ivabradine in the treatment of inappropriate sinus tachycardia in patients after successful radiofrequency

- catheter ablation of atrioventricular node slow pathway. *Pacing Clin Electrophysiol.* 2013;36:42–49.
47. Page RL, et al. 2015 ACC/AHA/HRS guideline for the management of adult patients with supraventricular tachycardia. *Circulation.* 2016;133:e506–e574.
48. Duhme N, et al. Altered HCN4 channel C-linker interaction is associated with familial tachycardia-bradycardia syndrome and atrial fibrillation. *Eur Heart J.* 2013;34:2768–2775.
49. Baruscotti M, et al. A gain-of-function mutation in the cardiac pacemaker HCN4 channel increasing cAMP sensitivity is associated with familial inappropriate sinus tachycardia. *Eur Heart J.* 2017;38:280–288.
50. Wu P, et al. Structural basis for the gating mechanism of the type 2 ryanodine receptor RyR2. *Science.* 2016;80:354, aah5324.
51. Györke S. Molecular basis of catecholaminergic polymorphic ventricular tachycardia. *Heart Rhythm.* 2009;6:123–129.
52. Marsman RF, et al. A mutation in CALM1 encoding calmodulin in familial idiopathic ventricular fibrillation in childhood and adolescence. *J Am Coll Cardiol.* 2014;63:259–266.
53. Paech C, et al. Ryanodine receptor mutations presenting as idiopathic ventricular fibrillation: a report on two novel familial compound mutations, c.6224T>C and c.13781A>G, with the clinical presentation of idiopathic ventricular fibrillation. *Pediatr Cardiol.* 2014;35:1437–1441.
54. Nomikos M, et al. Altered RyR2 regulation by the calmodulin F90L mutation associated with idiopathic ventricular fibrillation and early sudden cardiac death. *FEBS Lett.* 2014;588:2898–2902.
55. Søndergaard MT, et al. Arrhythmogenic calmodulin mutations affect the activation and termination of cardiac ryanodine receptor-mediated Ca²⁺ release. *J Biol Chem.* 2015;290:26151–26162.
56. Altmann HM, et al. Homozygous/compound heterozygous triadin mutations associated with autosomal-recessive long-QT syndrome and pediatric sudden cardiac arrest: elucidation of the triadin knockout syndrome. *Circulation.* 2015;131:2051–2060.
57. Desplantez T, et al. Relating specific connexin co-expression ratio to connexon composition and gap junction function. *J Mol Cell Cardiol.* 2015;89:195–202.
58. Smaill BH, Zhao J, Trew ML. Three-dimensional impulse propagation in myocardium: arrhythmogenic mechanisms at the tissue level. *Circ Res.* 2013;112:834–848.
59. Leo-Macias A, Agullo-Pascual E, Delmar M. The cardiac connexome: non-canonical functions of connexin43 and their role in cardiac arrhythmias. *Semin Cell Dev Biol.* 2016;50:13–21.
60. Basheer WA, Shaw RM. Connexin 43 and Ca_v1.2 ion channel trafficking in healthy and diseased myocardium. *Circ Arrhythm Electrophysiol.* 2016;9:e001357.
61. Jassim A, Aoyama H, Ye WG, et al. Engineered Cx40 variants increased docking and function of heterotypic Cx40/Cx43 gap junction channels. *J Mol Cell Cardiol.* 2016;90:11–20.
62. Meşe G, Richard G, White TW. Gap junctions: basic structure and function. *J Invest Dermatol.* 2007;127:2516–2524.
63. Lambiase PD, Tinker A. Connexins in the heart. *Cell Tissue Res.* 2015;360:675–684.
64. Temple IP, Inada S, Dobrzynski H, et al. Connexins and the atrioventricular node. *Heart Rhythm.* 2012;10:297–304.
65. Kléber AG, Rudy Y. Basic mechanisms of cardiac impulse propagation and associated arrhythmias. *Physiol Rev.* 2004;84:431–488.
66. Dhein S, et al. Remodeling of cardiac passive electrical properties and susceptibility to ventricular and atrial arrhythmias. *Front Physiol.* 2014;5:1–13.
67. Wit AL, Peters NS. The role of gap junctions in the arrhythmias of ischemia and infarction. *Heart Rhythm.* 2012;9:308–311.
68. Delmar M, Makita N. Cardiac connexins, mutations and arrhythmias. *Curr Opin Cardiol.* 2012;27:236–241.
69. Sawant AC, Calkins H. Relationship between arrhythmogenic right ventricular dysplasia and exercise. *Card Electrophysiol Clin.* 2015;7:195–206.
70. Shaw RM. Reduced sodium channels in human ARVC. *Heart Rhythm.* 2013;10:420–421.
71. Noorman M, et al. Remodeling of the cardiac sodium channel, connexin43, and plakoglobin at the intercalated disk in patients with arrhythmogenic cardiomyopathy. *Heart Rhythm.* 2013;10:412–419.

Electrophysiological Mechanisms of Cardiac Arrhythmias

OUTLINE

Automaticity, 51

- Enhanced Normal Automaticity, 51
- Abnormal Automaticity, 55
- Overdrive Suppression of Automatic Rhythms, 56
- Arrhythmias Caused by Automaticity, 57

Triggered Activity, 58

- Delayed Afterdepolarizations and Triggered Activity, 58

Reentry, 63

- Basic Principles of Reentry, 63
- Requisites of Reentry, 63

Types of Reentrant Circuits, 65

- Excitable Gaps in Reentrant Circuits, 68
- Resetting Reentrant Tachycardias, 69
- Entrainment of Reentrant Tachycardias, 73
- Mechanism of Slow Conduction in the Reentrant Circuit, 74
- Anisotropy and Reentry, 76
- Mechanism of Unidirectional Block in the Reentrant Circuit, 78

The mechanisms responsible for cardiac arrhythmias are generally divided into categories of disorders of impulse formation (automaticity or triggered activity), disorders of impulse conduction (reentry), or combinations of both. Automaticity is the property of cardiac cells to initiate an impulse spontaneously, without need for prior stimulation. Triggered activity is impulse initiation in cardiac fibers caused by depolarizing oscillations in membrane voltage (known as afterdepolarizations) that occur consequent to one or more preceding action potentials. Reentry occurs when a propagating action potential wave fails to extinguish after initial tissue activation; instead, it blocks in circumscribed areas, circulates around the zones of block, and reenters and reactivates the site of original excitation after it recovers excitability. Reentry is the likely mechanism of most recurrent clinical arrhythmias.¹

Diagnosis of the underlying mechanism of an arrhythmia can be of great importance in guiding appropriate treatment strategies. Spontaneous behavior of the arrhythmia, mode of initiation and termination, and response to programmed electrical stimulation are the most commonly used tools to distinguish among the different mechanisms responsible for cardiac arrhythmias. However, our present diagnostic tools do not always permit unequivocal determination of the electrophysiological (EP) mechanisms responsible for many clinical arrhythmias or their ionic bases. In particular, it can be difficult to distinguish among several mechanisms that appear to have a focal origin with centrifugal spread of activation (automaticity, triggered activity, and microreentry). This is further complicated by the fact that some arrhythmias can be started by one mechanism and perpetuated by another.

AUTOMATICITY

Automaticity, or spontaneous impulse initiation, is the ability of cardiac cells to depolarize spontaneously, reach threshold potential, and initiate a propagated action potential, in the absence of external electrical stimulation. Altered automaticity can be caused by enhanced normal automaticity or by abnormal automaticity.

Enhanced normal automaticity refers to the accelerated generation of an action potential by normal pacemaker tissue and is found in the

primary pacemaker of the heart, the sinus node, as well as in certain subsidiary or latent pacemakers that can become the functional pacemaker under certain conditions. Impulse initiation is a normal property of the primary and latent pacemakers.

Abnormal automaticity occurs in cardiac cells only when there are major abnormalities in their transmembrane potentials, in particular in steady-state depolarization of the membrane potential. This property of abnormal automaticity is not confined to any specific latent pacemaker cell type but can occur almost anywhere in the heart.

The discharge rate of normal or abnormal pacemakers can be influenced by drugs, various forms of cardiac disease, reduction in extracellular potassium (K^+), or alterations of autonomic nervous system tone.

Enhanced Normal Automaticity Pacemaker Mechanisms

Normal automaticity involves a spontaneous, slow, progressive decline in the transmembrane potential (i.e., the membrane voltage becomes less negative) during diastole. This process is known as “spontaneous diastolic depolarization” or “phase 4 depolarization.” Once this spontaneous depolarization reaches threshold (approximately -40 mV), a new action potential is generated (Fig. 3.1) (see Chapter 1).

The ionic mechanisms responsible for normal pacemaker activity in the sinus node are still controversial. The fall in membrane potential during phase 4 seems to arise from a changing balance between positive inward currents, which favor depolarization, and positive outward currents, with a net gain in intracellular positive charges during diastole (i.e., a net inward depolarizing current) (Fig. 3.2).¹

I_K -decay theory. The sinus node lacks the inward rectifier K^+ current (I_{K1}), which acts to stabilize the resting membrane potential (E_m) in the normal working atrial and ventricular myocardium. The outward K^+ currents are carried by the delayed rectifier K^+ channels (I_{Kr} and I_{Ks}), which are responsible for repolarization of the sinus node action potential; those currents decay following repolarization and channel inactivation, allowing the membrane potential to drift toward the more positive equilibrium potentials of other ions (Na^+ , Ca^{2+} , and Cl^-). The decay of the delayed K^+ conductance activated during the preceding action

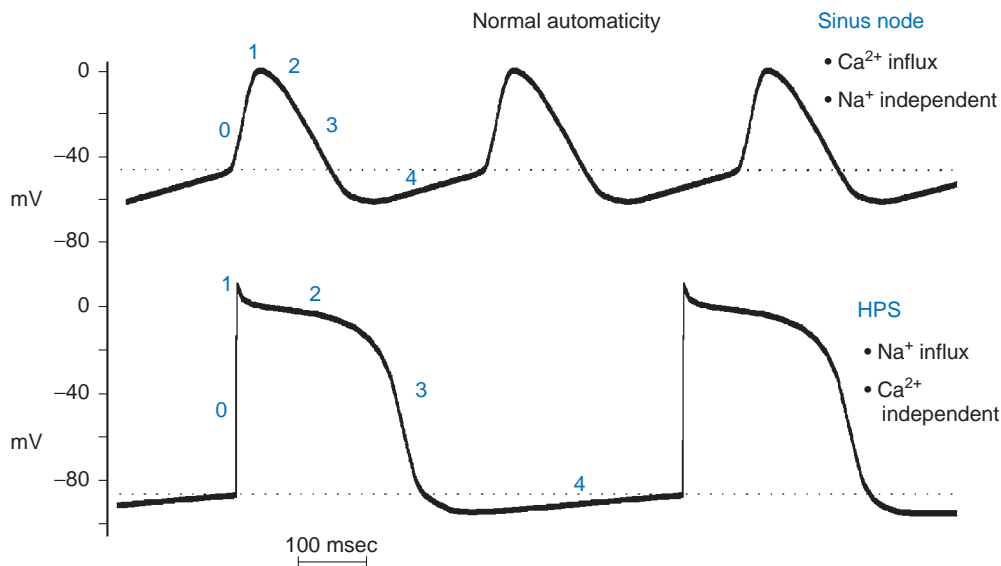


Fig. 3.1 Normal Cardiac Automaticity. Action potentials from typical sinus nodal and His-Purkinje cells are shown with the voltage scale on the vertical axes; dashed lines are threshold potential, and numbers on the figure refer to phases of the action potential. Note the qualitative differences between the two types of cells, as well as different rates of spontaneous depolarization. Ca^{2+} , Calcium; *HPS*, His-Purkinje system; Na^+ , sodium.

potential was initially thought to play a major role in pacemaker activity (the I_K -decay theory). This model of pacemaker depolarization lost interest after the discovery of the pacemaker current (I_f). Nonetheless, I_K -decay is still believed to contribute to diastolic depolarization (especially the earliest part of the pacemaker potential) by allowing other inward currents to depolarize the myocyte during diastole. Other ionic currents gated by membrane depolarization (i.e., L-type [I_{CaL}] and T-type [I_{CaT}] Ca^{2+} currents), nongated and nonspecific background leak currents, and a current generated by the Na^+ - Ca^{2+} exchanger (I_{Na-Ca}), were also proposed to be involved in pacemaking.²

Membrane clock. Evidence suggests that I_f (named the “funny” current because, unlike most voltage-sensitive currents, it is activated by hyperpolarization rather than depolarization) is one of the most important ionic currents involved in the rate regulation of cardiac pacemaker cells, hence its designation as the pacemaker current. I_f is an inward current carried largely by Na^+ and, to a lesser extent, K^+ ions. I_f channels are deactivated during the action potential upstroke and the initial plateau phase of repolarization. However, they begin to activate at the end of the action potential as repolarization brings the membrane potential to levels more negative than -40 to -50 mV, and I_f is fully activated at approximately -100 mV. Once activated, I_f depolarizes the membrane to a level where the Ca^{2+} current activates to initiate the action potential. In its range of activation, which quite properly comprises the voltage range of diastolic depolarization, the current is inward, and its reversal occurs at approximately -10 to -20 mV because of the mixed Na^+ - K^+ permeability of I_f channels. At the end of the repolarization phase of an action potential, because I_f activation occurs in the background of a decaying outward (K^+ time-dependent) current, the current flow quickly shifts from outward to inward, thus giving rise to a sudden reversal of voltage change (from repolarizing to depolarizing) at the maximum diastolic potential. The major role of I_f has been reinforced by the findings that drugs such as ivabradine targeted to block I_f slow heart rate and mutations in the I_f channel are associated with slowed heart rate.³⁻⁵

The “membrane clock” (also referred to as the “voltage clock” or “ion channel clock”) refers to the time- and voltage-dependent mem-

brane ion channels underlying pacemaking activity, including the decay of the outward rectifier K^+ current and the activation of several inward currents (I_f , I_{CaL} , I_{CaT} , and I_{Na}).

Calcium clock. Several studies have recently demonstrated that I_f is not the only current that can initiate the diastolic depolarization process in the sinus node. In addition to voltage and time, the electrogenic and regulatory molecules on the surface membrane of sinus nodal cells are strongly modulated by Ca^{2+} and phosphorylation, a finding suggesting that intracellular Ca^{2+} is an important player in controlling pacemaker cell automaticity. Newer evidence points to a substantial impact of another current on the late diastolic depolarization; that is, the Na^+ - Ca^{2+} exchanger current (I_{Na-Ca}) activated by submembrane spontaneous rhythmic local Ca^{2+} releases from the sarcoplasmic reticulum (a major Ca^{2+} store within sinus node cells) via the ryanodine receptors (RyR2). Activation of the local oscillatory Ca^{2+} releases is independent of membrane depolarization and is driven by a high level of basal state phosphorylation of Ca^{2+} cycling proteins. Critically timed Ca^{2+} releases occur during the later phase of diastolic depolarization and instantaneously trigger Ca^{2+} extrusion from the cytosol by the Na^+ - Ca^{2+} exchanger operating in the forward mode (one Ca^{2+} out for three Na^+ in). This generates a net inward membrane current that causes the late diastolic depolarization to increase exponentially, thus driving the membrane potential to the threshold to activate a sufficient number of voltage-gated L-type Ca^{2+} channels and leading to generation of the rapid upstroke of the next action potential (see Fig. 1.7). Although regulated by membrane potential and submembrane Ca^{2+} , the Na^+ - Ca^{2+} exchanger does not have time-dependent gating, as do ion channels, but generates an inward current almost instantaneously when submembrane Ca^{2+} concentration increases.^{3,5,6}

Such rhythmic, spontaneous intracellular Ca^{2+} cycling has been referred to as an intracellular “calcium clock.” Phosphorylation-dependent gradation of the speed at which calcium clock cycles is the essential regulatory mechanism of normal pacemaker rate and rhythm. The robust regulation of pacemaker function is ensured by tight integration of the calcium clock and the membrane clock to form the overall “pacemaker clock.” The action potential shape and ion fluxes are tuned by

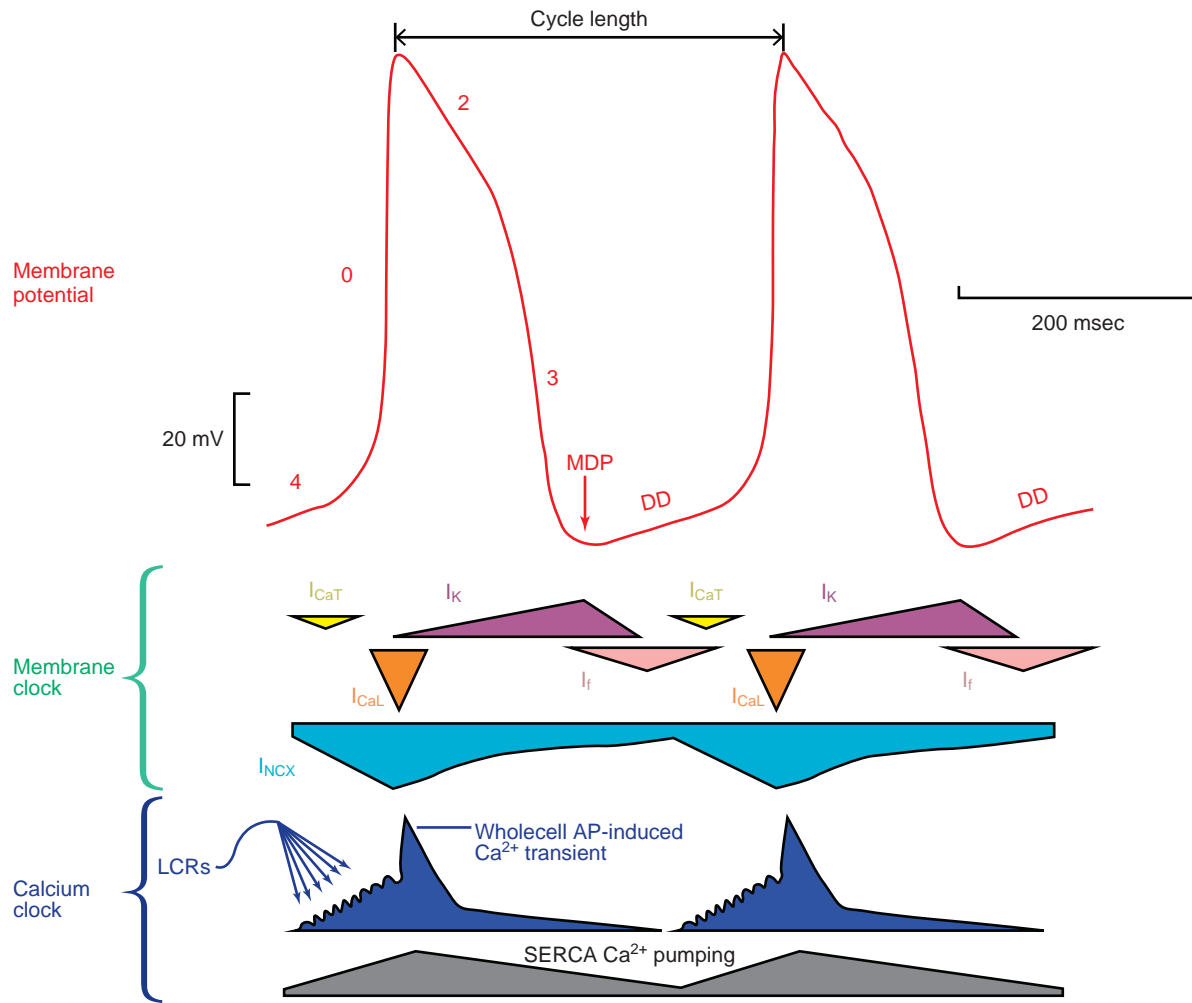


Fig. 3.2 Ionic Currents Involved in Producing the Sinus Node Pacemaker Potential. A typical action potential of spontaneously beating rabbit sinus node is shown on the top (red trace). The different phases are labeled, with phase 4 representing diastolic depolarization, the defining feature of pacemaking cells. The timing and magnitude of the components of the “membrane clock” is shown in the middle (green bracket). There is voltage-dependent decay of the outward rectifier K^+ current I_K , and voltage-dependent activation of inward currents: I_f , I_{CaL} , and I_{CaT} . The timing and magnitude of the components of the “calcium clock” are shown at the bottom (dark blue bracket). Ca^{2+} entry into the cell via I_{CaL} and I_{CaT} results in spontaneous local Ca^{2+} release (LCR) from the sarcoplasmic reticulum (SR) through RyR2 channels. During phase 4, this rise in total intracellular Ca^{2+} activates the Na^+ - Ca^{2+} exchanger (NCX1) which generates the net inward I_{NCX} (or I_{Na-Ca}) current. Toward the end of diastole, activation of L-type Ca^{2+} channels causes Ca^{2+} -induced Ca^{2+} release from the SR via RyR2, resulting in the whole cell Ca^{2+} transient. Cytoplasmic Ca^{2+} is then removed by the SR Ca^{2+} pump sarcoplasmic/endoplasmic reticulum calcium adenosine triphosphatase (SERCA) and by the sarcolemmal Na^+ - Ca^{2+} exchanger. AP, Action potential; DD, diastolic depolarization; I_{CaL} , L-type voltage-dependent Ca^{2+} current; I_{CaT} , T-type voltage-dependent Ca^{2+} current; I_f , funny current; I_K , delayed rectifier potassium current; I_{NCX} , sodium-calcium exchange current; LCRs, local Ca^{2+} releases; MDP, maximum diastolic potential. (From Murphy C, Lazzara R. Current concepts of anatomy and electrophysiology of the sinus node. *J Interv Card Electrophysiol*. 2016;46:9–18.)

membrane clocks to sustain operation of the calcium clock, which produces timely and powerful ignition of the membrane clocks to effect action potentials.^{3,7,8}

There remains some degree of uncertainty about the relative role of I_f versus that of intracellular Ca^{2+} cycling in controlling the normal pacemaker cell automaticity and their individual (or mutual) relevance in mediating the positive-negative chronotropic effect of neurotransmitters. Furthermore, the interactions between the membrane ion channel clock and the intracellular calcium clock and the cellular mechanisms underlying this internal calcium clock are not completely elucidated.⁵

Automaticity in subsidiary pacemakers appears to arise via a mechanism similar to that occurring in the sinus node.

Hierarchy of Pacemaker Function

Automaticity is not limited to the cells within the sinus node. Under physiological conditions, cells in parts of the atria and within the atrio-ventricular node (AVN) and the His-Purkinje system (HPS) also possess pacemaking capability. However, the occurrence of spontaneous activity in these cells is prevented by the natural hierarchy of pacemaker function that causes these sites to be latent or subsidiary pacemakers. The

spontaneous discharge rate of the sinus node normally exceeds that of all other subsidiary pacemakers (see Fig. 3.1). Therefore the impulse initiated by the sinus node depolarizes subsidiary pacemaker sites and keeps their activity depressed before they can spontaneously reach threshold. However, slowly depolarizing and previously suppressed pacemakers in the atrium, AVN, or ventricle can become active and assume pacemaker control of the cardiac rhythm if the sinus node pacemaker becomes slow or unable to generate an impulse (e.g., secondary to depressed sinus node automaticity) or if impulses generated by the sinus node are unable to activate the subsidiary pacemaker sites (e.g., sinoatrial exit block or atrioventricular [AV] block). The emergence of subsidiary or latent pacemakers under such circumstances is an appropriate fail-safe mechanism, which ensures that ventricular activation is maintained. Because spontaneous diastolic depolarization is a normal property, the automaticity generated by these cells is classified as *normal*.⁴

There is also a natural hierarchy of the intrinsic rates of subsidiary pacemakers that have normal automaticity, with atrial pacemakers having faster intrinsic rates than AV junctional pacemakers, and AV junctional pacemakers having faster rates than ventricular pacemakers.

Subsidiary Pacemakers

Subsidiary atrial pacemakers. Subsidiary pacemakers have been identified in the atrial myocardium, especially in the crista terminalis, at the junction of the inferior right atrium (RA) and inferior vena cava (IVC), near or on the eustachian ridge, near the coronary sinus (CS) os, in the atrial muscle that extends into the tricuspid and mitral valves, and in the muscle sleeves that extend into the cardiac veins (venae cavae and pulmonary veins).⁴

Latent atrial pacemakers can contribute to impulse initiation in the atrium if the discharge rate of the sinus node is reduced temporarily or permanently. In contrast to the normal sinus node, these latent or ectopic pacemakers usually generate a fast action potential (referring to the rate of upstroke of the action potential [dV/dt]) mediated by Na⁺ fluxes. However, when severely damaged, the atrial tissue may not be able to generate a fast action potential (which is energy dependent) but rather generates a slow, Ca²⁺-mediated action potential (which is energy independent). Automaticity of subsidiary atrial pacemakers can also be enhanced by myocardial ischemia, chronic pulmonary disease, or drugs such as digitalis and alcohol, possibly overriding normal sinus activity.

Subsidiary AV junctional pacemakers. Some data suggest that the AVN itself has pacemaker cells, but that concept is controversial. However, it is clear that the AV junction, which is an area that includes atrial tissue, the AVN, and His-Purkinje tissue, does have pacemaker cells and is capable of exhibiting automaticity.

Subsidiary ventricular pacemakers. In the ventricles, latent pacemakers are found in the HPS, where Purkinje fibers have the property of spontaneous diastolic depolarization. Isolated cells of the HPS discharge spontaneously at rates of 15 to 60 beats/min, whereas ventricular myocardial cells do not normally exhibit spontaneous diastolic depolarization or automaticity. The relatively slow spontaneous discharge rate of the HPS pacemakers, which further decreases from the His bundle (HB) to the distal Purkinje branches, ensures that pacemaker activity in the HPS will be suppressed on a beat-to-beat basis by the more rapid discharge rate of the sinus node and atrial and AV junctional pacemakers. However, enhanced Purkinje fiber automaticity can be induced by certain situations, such as myocardial infarction (MI). In this setting, some Purkinje fibers that survive the infarction develop moderately reduced maximum diastolic membrane potentials and therefore accelerated spontaneous discharge rates.

Regulation of Pacemaker Function

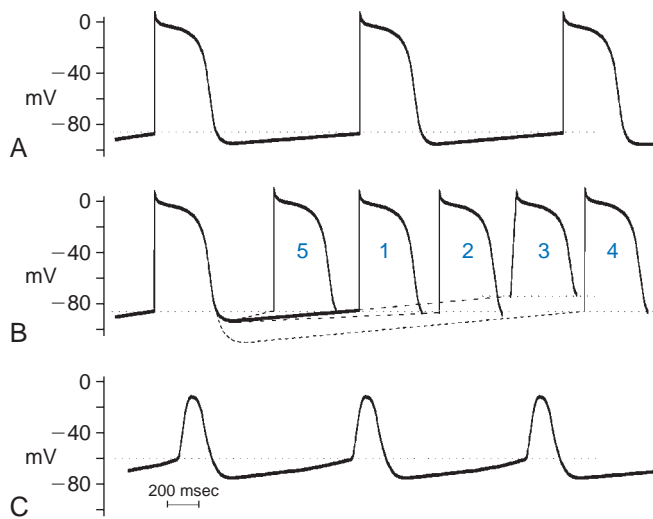
The intrinsic rate at which the sinus node pacemaker cells generate impulses is determined by the interplay of three factors: the maximum diastolic potential, the threshold potential at which the action potential is initiated, and the rate (slope) of phase 4 depolarization (eFig. 3.1). A change in any one of these factors will alter the time required for phase 4 depolarization to carry the membrane potential from its maximum diastolic level to threshold and thus alter the rate of impulse initiation.

The sinus node is innervated by the parasympathetic and sympathetic nervous systems, and the balance between these systems importantly controls the pacemaker rate. The classic concept has been that of a reciprocal relationship between sympathetic and parasympathetic inputs. However, more recent investigations stress dynamic, demand-oriented interactions, and the anatomical distribution of fibers that allows both autonomic systems to act quite selectively. Muscarinic cholinergic and beta₁-adrenergic receptors are nonuniformly distributed in the sinus node, and they modulate both the rate of depolarization and impulse propagation.

Parasympathetic activity. Parasympathetic tone reduces the spontaneous discharge rate of the sinus node, whereas its withdrawal accelerates sinus node automaticity. Acetylcholine, the principal neurotransmitter of the parasympathetic nervous system, inhibits spontaneous impulse generation in the sinus node by increasing K⁺ conductance. Acetylcholine acts through M₂ muscarinic receptors to activate the G_i protein, which subsequently results in activation of I_{KACH} (an acetylcholine-activated subtype of inward rectifying current) in tissues of the sinus node and AVN, as well as of the atria, Purkinje fibers, and ventricles. The increased outward repolarizing K⁺ current leads to membrane hyperpolarization (i.e., the resting potential and the maximum diastolic potential become more negative). The resulting hyperpolarization of the membrane potential lengthens the time required for the membrane potential to depolarize to threshold and thereby decreases the automaticity of the sinus node (see eFig. 3.1). In addition, activation of the G_i protein results in inhibition of beta receptor-stimulated adenylate cyclase activity, thus reducing cyclic adenosine monophosphate (cAMP) and inhibiting protein kinase A, with subsequent inhibition of the inward L-type Ca²⁺ current (I_{CaL}). This results in reduction of the rate of diastolic depolarization because of less Ca²⁺ entry and subsequent slowing of the pacemaker activity. Inhibition of beta receptor-stimulated adenylate cyclase activity can also inhibit the inward I_f current.³

Sympathetic activity. Increased sympathetic nerve traffic and the adrenomedullary release of catecholamines increase sinus node discharge rate. Stimulation of beta₁ receptors by catecholamines enhances I_{CaL} by increasing cAMP and activating the protein kinase A system. The increment in I_{CaL} increases the slope of diastolic depolarization and enhances pacemaker activity (see eFig. 3.1). The redistribution of Ca²⁺ can also increase the completeness and the rate of deactivation of the rapid (I_{Kr}) and slow (I_{Ks}) components of the delayed rectifier K⁺ current. The ensuing decline in the opposing outward current results in a further net increase in inward current. Catecholamines can also enhance the inward I_f current by shifting the voltage dependence of I_f to more positive potentials, thus augmenting the slope of phase 4 and increasing the rate of sinus node firing.³

In addition to altering ionic conductance, changes in autonomic tone can produce changes in the rate of the sinus node by shifting the primary pacemaker region within the pacemaker complex. Mapping of activation indicates that, at faster rates, the sinus node impulse usually originates in the superior portion of the sinus node, whereas at slower rates, it usually arises from a more inferior portion of the sinus node. The sinus node can be insulated from the surrounding atrial myocytes, except at a limited number of preferential exit sites. Shifting pacemaker



eFig. 3.1 Abnormalities of Automaticity. (A) Normal His-Purkinje action potential. (B) Modulation of rate of depolarization from baseline (1) by slowing rate of phase 4 depolarization (2), increasing threshold potential (3), starting from a more negative resting membrane potential (4), all of which slow discharge rate, or by increasing rate of phase 4 depolarization (5), thus yielding a faster discharge rate. (C) Abnormal automaticity with change in action potential contour (resembling sinus nodal cell) when resting membrane potential is less negative, inactivating most sodium channels.

sites can select different exit pathways to the atria. As a result, autonomically mediated shifts of pacemaker regions can be accompanied by changes in the sinus rate. Vagal fibers are denser in the cranial portion of the sinus node, and stimulation of the parasympathetic nervous system shifts the pacemaker center to a more caudal region of the sinus node complex, thus resulting in slowing of the heart rate. In contrast, stimulation of the sympathetic nervous system or withdrawal of vagal stimulation shifts the pacemaker center cranially, resulting in an increase in heart rate.

Atrial, AV junctional, and HPS subsidiary pacemakers are also under similar autonomic control, with the sympathetic nervous system enhancing pacemaker activity through β_1 -adrenergic stimulation and the parasympathetic nervous system inhibiting pacemaker activity through muscarinic receptor stimulation.

Other influences. Adenosine binds to A1-receptors, thus activating $I_{K_{ACH}}$ and increasing outward I_K in a manner similar to that of marked parasympathetic stimulation. It also has similar effects on I_f channels.

Digitalis exerts two effects on the sinus rate. It has a direct positive chronotropic effect on the sinus node, resulting from depolarization of the membrane potential caused by inhibition of the Na^+ - K^+ exchange pump. The reduction in the maximum diastolic membrane potential shortens the time required for the membrane to depolarize to threshold and thereby accelerates the spontaneous discharge rate. However, digitalis also enhances vagal tone, which decreases spontaneous sinus discharge.

Enhanced subsidiary pacemaker activity may not require sympathetic stimulation. Normal automaticity can be affected by certain other factors associated with heart disease. Inhibition of the electrogenic Na^+ - K^+ exchange pump results in a net increase in inward current during diastole because of the decrease in outward current normally generated by the pump, and therefore it can increase automaticity in subsidiary pacemakers sufficiently to cause arrhythmias. This can occur when adenosine triphosphate (ATP) is depleted during prolonged hypoxia or ischemia or in the presence of toxic amounts of digitalis. Hypokalemia can reduce the activity of the Na^+ - K^+ exchange pump, thereby reducing the background repolarizing current and enhancing phase 4 diastolic depolarization. The end result would be an increase in the discharge rate of pacemaking cells. In addition, the flow of current between partially depolarized myocardium and normally polarized latent pacemaker cells can enhance automaticity. This mechanism has been proposed to be a cause of some of the ectopic complexes that arise at the borders of ischemic areas in the ventricle. Slightly increased extracellular K^+ can reduce the maximum diastolic potential (i.e., becomes less negative), thereby also increasing the discharge rate of pacemaking cells. However, a greater increase in extracellular K^+ renders the heart inexcitable by depolarizing the membrane potential and inactivating the Na^+ current (I_{Na}).

Evidence indicates that active and passive changes in the mechanical environment of the heart provide feedback to modify cardiac rate and rhythm and are capable of influencing both the initiation and spread of cardiac excitation. This direction of the crosstalk between cardiac electrical and mechanical activity is referred to as mechanoelectric feedback and is thought to be involved in the adjustment of heart rate to changes in mechanical load, which would help to explain the precise beat-to-beat regulation of cardiac performance. Acute mechanical stretch enhances automaticity, reversibly depolarizes the cell membrane, and shortens the action potential duration. Feedback from cardiac mechanics to electrical activity involves mechanosensitive ion channels and ATP-sensitive K^+ channels. In addition, Na^+ and Ca^{2+} entering the cells via nonselective ion channels are thought to contribute to the genesis of stretch-induced arrhythmia.

Abnormal Automaticity

In the normal heart, automaticity is confined to the sinus node and other specialized conducting tissues. Working atrial and ventricular myocardial cells do not normally exhibit spontaneous diastolic depolarization and do not initiate spontaneous impulses, even when they are not excited for long periods of time by propagating impulses. Although these cells do have an I_f , the range of activation of this current in these cells is much more negative (-120 to -170 mV) than in Purkinje fibers or in the sinus node. As a result, during physiological E_m (-85 to -95 mV), the I_f is not activated and ventricular cells do not depolarize spontaneously. However, when the resting potentials of these cells are depolarized sufficiently, to approximately -70 to -30 mV, spontaneous diastolic depolarization can occur and cause repetitive impulse initiation, a phenomenon called depolarization-induced automaticity or abnormal automaticity (see eFig. 3.1). Similarly, cells in the Purkinje system, which are normally automatic at high levels of membrane potential, show abnormal automaticity when the membrane potential is reduced to approximately -60 mV or less, as can occur in ischemic regions of the heart. When the steady-state membrane potential of Purkinje fibers is reduced to levels more positive to -60 mV, the I_f channels that participate in normal pacemaker activity in Purkinje fibers are closed and nonfunctional, and automaticity is therefore not caused by the normal pacemaker mechanism. However, it can be caused by an “abnormal” mechanism. In contrast, enhanced automaticity of the sinus node, subsidiary atrial pacemakers, or the AVN caused by a mechanism other than acceleration of normal automaticity has not been demonstrated clinically.^{1,9}

A low level of membrane potential is not the only criterion for defining abnormal automaticity. If this were so, the automaticity of the sinus node would have to be considered abnormal. Therefore an important distinction between abnormal and normal automaticity is that the membrane potentials of fibers showing the abnormal type of activity are reduced from their own normal level. For this reason, automaticity in the AVN (e.g., where the membrane potential is normally low) is not classified as abnormal automaticity.

Several different mechanisms probably cause abnormal pacemaker activity at low membrane potentials, including activation and deactivation of the delayed rectifier I_K , intracellular Ca^{2+} release from the sarcoplasmic reticulum that causes activation of inward Ca^{2+} current as well as I_{Na} (through the Na^+ - Ca^{2+} exchanger), and a potential contribution by I_f . It has not been determined which of these mechanisms are operative in the different pathological conditions in which abnormal automaticity can occur.

The upstroke of the spontaneously occurring action potentials generated by abnormal automaticity can be caused by Na^+ or Ca^{2+} inward currents or possibly a combination of the two. In the range of diastolic potentials between approximately -70 and -50 mV, repetitive activity is dependent on extracellular Na^+ concentration and can be decreased or abolished by Na^+ channel blockers. In a diastolic potential range of approximately -50 to -30 mV, Na^+ channels are predominantly inactivated; repetitive activity depends on extracellular Ca^{2+} concentration and is reduced by L-type Ca^{2+} channel blockers.

The intrinsic rate of a focus with abnormal automaticity is a function of the membrane potential. The more positive the membrane potential, the faster the automatic rate (see eFig. 3.1). Abnormal automaticity is less vulnerable to suppression by overdrive pacing (see later). Therefore even occasional slowing of the sinus node rate can allow an ectopic focus with abnormal automaticity to fire without a preceding long period of quiescence. Catecholamines can increase the rate of discharge caused by abnormal automaticity and therefore can contribute to a shift in the pacemaker site from the sinus node to a region with abnormal automaticity.

The decrease in the membrane potential of cardiac cells required for abnormal automaticity to occur can be induced by a variety of factors related to cardiac disease, such as ischemia and infarction. However, the circumstance under which membrane depolarization occurs can influence the development of abnormal automaticity. For example, an increase in extracellular K^+ concentration, as occurs in acutely ischemic myocardium, can reduce membrane potential; however, normal or abnormal automaticity in working atrial, ventricular, and Purkinje fibers usually does not occur because of an increase in K^+ conductance (and hence net outward current) that results from the increase in extracellular K^+ concentration.

Overdrive Suppression of Automatic Rhythms

The sinus node maintains its dominance over subsidiary pacemakers in the AVN and the Purkinje fibers likely by several mechanisms. During sinus rhythm in a normal heart, the intrinsic automatic rate of the sinus node is faster than that of the other potentially automatic cells. Consequently, the latent pacemakers are excited by propagated impulses from the sinus node before they have a chance to depolarize spontaneously to threshold potential. The higher frequency of sinus node discharge also suppresses the automaticity of other pacemaker sites by a mechanism called overdrive suppression. The diastolic (phase 4) depolarization of the latent pacemaker cells with the property of normal automaticity is actually inhibited because the cells are repeatedly depolarized by the impulses from the sinus node. Electrotonic interaction between the pacemaker cells and the nonpacemaker cells in the surrounding myocardium via intercalated discs and gap junctions can also hyperpolarize the latent pacemakers and contribute to their suppression (Fig. 3.3).

The mechanism of overdrive suppression is mediated mostly by enhanced activity of the Na^+-K^+ exchange pump that results from driving a pacemaker cell faster than its intrinsic spontaneous rate. During normal sinus rhythm (NSR), latent pacemakers are depolarized at a higher frequency than their intrinsic rate of automaticity. The increased frequency of depolarizations leads to an increase in intracellular Na^+ , which enters the cell with every action potential. The increased intracellular Na^+ stimulates the Na^+-K^+ exchange pump. Because the Na^+-K^+ exchange pump is electrogenic (i.e., moves more Na^+ outward than K^+ inward), it generates a net outward (hyperpolarizing) current across the cell membrane. This drives the membrane potential more negative, thereby offsetting the depolarizing I_f being carried into the cell and slowing the rate of phase 4 diastolic depolarization. This effectively prevents the I_f from depolarizing the cell to its threshold potential and thereby suppresses spontaneous impulse initiation in these cells.

When the dominant (overdrive) pacemaker is stopped, suppression of subsidiary pacemakers continues because the Na^+-K^+ exchange pump continues to generate the outward current as it reduces the intracellular Na^+ levels toward normal. This continued Na^+-K^+ exchange pump-generated outward current is responsible for the period of quiescence,

which lasts until the intracellular Na^+ concentration, and hence the pump current, becomes low enough to allow subsidiary pacemaker cells to depolarize spontaneously to threshold. Intracellular Na^+ concentration decreases during the quiescent period because Na^+ is constantly being pumped out of the cell and little is entering. The spontaneous rate of the suppressed cell remains lower than it would be otherwise until the intracellular Na^+ concentration has a chance to decrease. Intracellular Na^+ concentration and pump current continue to decline even after spontaneous discharge begins because of the slow firing rate, thus causing a gradual increase in the discharge rate of the subsidiary pacemaker. At slower rates and shorter overdrive periods, the Na^+ load is of lesser magnitude, as is the activity of the Na^+-K^+ pump, resulting in a progressively rapid diastolic depolarization and warm-up. The higher the overdrive rate or the longer the duration of overdrive, the greater the enhancement of pump activity will be, so that the period of quiescence after the cessation of overdrive is directly related to the rate and duration of overdrive.

The sinus node itself also is vulnerable to overdrive suppression. However, when overdrive suppression of the normal sinus node occurs, it is generally of lesser magnitude than that of subsidiary pacemakers overdriven at comparable rates. The sinus node action potential upstroke is largely dependent on the slow inward current carried by I_{CaL} , and far less Na^+ enters the fiber during the upstroke than occurs in latent pacemaker cells such as the Purkinje fibers. As a result, the accumulation of intracellular Na^+ and enhancement of Na^+-K^+ exchange pump activity occur to a lesser degree in sinus node cells after a period of overdrive; therefore there is less overdrive suppression caused by enhanced Na^+-K^+ exchange pump current. The relative resistance of the normal sinus node to overdrive suppression is important in enabling it to remain the dominant pacemaker, even when its rhythm is perturbed transiently by external influences such as transient shifts of the pacemaker to an ectopic site. However, the diseased sinus node can be much more easily overdrive suppressed, such as in the so-called tachycardia-bradycardia syndrome.

Abnormally automatic cells and tissues at reduced levels of membrane potential are less sensitive to overdrive suppression than are cells and tissues that are fully polarized, with enhanced normal automaticity. The amount of overdrive suppression of spontaneous diastolic depolarization that causes abnormal automaticity is directly related to the level of membrane potential at which the automatic rhythm occurs. At low levels of membrane potential, Na^+ channels are inactivated, decreasing the fast inward I_{Na} ; therefore there are reductions in the amount of Na^+ entering the cell during overdrive and the degree of stimulation of the Na^+-K^+ exchange pump. The more polarized the membrane is during phase 4, the larger the amount will be of Na^+ entering the cell with each action potential and the more overdrive suppression will occur. As a result of the lack of overdrive suppression of abnormally automatic cells, even transient sinus pauses can permit an ectopic focus

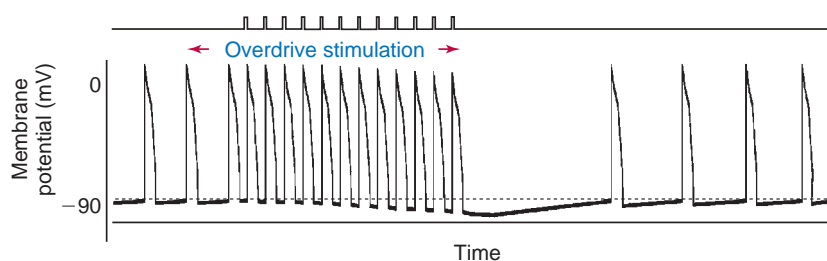


Fig. 3.3 Overdrive Suppression of Automaticity. A spontaneously firing cell is paced more rapidly, resulting in depression of resting membrane potential; after pacing is stopped, spontaneous depolarization takes longer than usual and gradually resumes baseline rate. *Dashed line*, Threshold potential.

with a slower rate than the sinus node to capture the heart for one or more beats. However, even in situations in which the cells can be sufficiently depolarized to inactivate the I_{Na} and limit intracellular Na^+ load, overdrive suppression can still be observed because of increased intracellular Ca^{2+} loading. Such Ca^{2+} loading can activate Ca^{2+} -dependent K^+ conductance (favoring repolarization) and promote Ca^{2+} extrusion through the Na^+ - Ca^{2+} exchanger and Ca^{2+} channel phosphorylation, thus increasing Na^+ load and thus Na^+ - K^+ exchange pump activity. The increase in intracellular Ca^{2+} load can also reduce the depolarizing I_{CaL} by promoting Ca^{2+} -induced inactivation of the Ca^{2+} current.

In addition to overdrive suppression being of paramount importance for maintenance of NSR, the characteristic response of automatic pacemakers to overdrive is often useful to distinguish automaticity from triggered activity and reentry.

Arrhythmias Caused by Automaticity

Inappropriate Sinus Node Discharge

Examples of these arrhythmias include inappropriate sinus bradycardia, sinus arrest, inappropriate sinus tachycardia, and inappropriate respiratory sinus arrhythmia. Such arrhythmias result simply from an alteration in the rate of impulse initiation by the normal sinus node pacemaker, without a shift of impulse origin to a subsidiary pacemaker at an ectopic site, although there can be shifts of the pacemaker site within the sinus node itself during alterations in sinus rate. These arrhythmias are often a result of the actions of the autonomic nervous system on the sinus node.

Escape Ectopic Automatic Rhythms

Impairment of the sinus node can allow a latent pacemaker to initiate impulse formation. This would be expected to happen when the rate at which the sinus node overdrives subsidiary pacemakers falls considerably below the intrinsic rate of the latent pacemakers or when the inhibitory electrotonic influences between nonpacemaker cells and pacemaker cells are interrupted.

The rate at which the sinus node activates subsidiary pacemakers can be decreased in certain situations, including sinus node dysfunction, with depressed sinus automaticity (secondary to increased vagal tone, drugs, or intrinsic sinus node disease), sinoatrial exit block, AV block, and parasystolic focus. The sinus node and AVN are most sensitive to vagal influence, followed by atrial tissue, with the ventricular conducting system being least sensitive. Moderate vagal stimulation allows the pacemaker to shift to another atrial site, but severe vagal stimulation suppresses the sinus node and blocks conduction at the AVN and therefore can allow a ventricular escape pacemaker to become manifest.

Interruption of the inhibitory electrotonic influences between nonpacemaker cells and pacemaker cells allows those latent pacemakers to fire at their intrinsic rate. Uncoupling can be caused by fibrosis or damage (e.g., infarction) of the tissues surrounding the subsidiary pacemaker cells or by reduction in gap junction conductance secondary to increased intracellular Ca^{2+} , which can be caused by digitalis. Some inhibition of the sinus node is still necessary for the site of impulse initiation to shift to an ectopic site that is no longer inhibited by uncoupling from surrounding cells because the intrinsic firing rate of subsidiary pacemakers is still slower than that of the sinus node.

Accelerated Ectopic Automatic Rhythms

Accelerated ectopic automatic rhythms are caused by enhanced normal automaticity of subsidiary pacemakers. The rate of discharge of these latent pacemakers is then faster than the expected intrinsic automatic rate. Once the enhanced rate exceeds that of the sinus node, the enhanced ectopic pacemaker prevails and overdrives the sinus node and other

subsidiary pacemakers. A premature impulse caused by enhanced automaticity of latent pacemakers comes *early* in the normal rhythm. In contrast, an escape beat secondary to relief of overdrive suppression occurs *late* in normal rhythm.

Enhanced automaticity is usually caused by increased sympathetic tone, which steepens the slope of diastolic depolarization of latent pacemaker cells and diminishes the inhibitory effects of overdrive. Such sympathetic effects can be localized to subsidiary pacemakers in the absence of sinus node stimulation. Other causes of enhanced normal automaticity include periods of hypoxemia, ischemia, electrolyte disturbances, and certain drug toxicities. There is evidence that in the subacute phase of myocardial ischemia, increased activity of the sympathetic nervous system can enhance automaticity of Purkinje fibers, thus enabling them to escape from sinus node domination.

Parasystole

Parasystole is a result of interaction between two fixed rate pacemakers having different discharge rates. Parasystolic pacemakers can exist in either the atrium or the ventricle. The latent pacemaker is protected from being overdriven by the dominant rhythm (usually NSR) by intermittent or constant entrance block (i.e., impulses of sinus origin fail to depolarize the latent pacemaker secondary to block in the tissue surrounding the latent pacemaker focus).

Various mechanisms have been postulated to explain the protected zone surrounding the ectopic focus. It is possible that the depolarized level of membrane potential at which abnormal automaticity occurs can cause entrance block, leading to parasystole. This would be an example of an arrhythmia caused by a combination of an abnormality of impulse conduction and impulse initiation. However, such block must be unidirectional, so that activity from the ectopic pacemaker can exit and produce depolarization whenever the surrounding myocardium is excitable. The protected pacemaker is said to be a parasystolic focus. In general, under these conditions, a protected focus of automaticity of this type fires at its own intrinsic frequency, and the intervals between the discharges of each pacemaker are multiples of its intrinsic discharge rate (sometimes described as *fixed parasystole*). Therefore on the surface electrocardiogram (ECG) the coupling intervals of the manifest ectopic beats wander through the basic cycle of the sinus rhythm. Accordingly, the traditional ECG criteria used to recognize the fixed form of parasystole include: (1) the presence of variable coupling intervals of the manifest ectopic beats; (2) interectopic intervals that are simple multiples of a common denominator; and (3) the presence of fusion beats. Occasionally, the parasystolic focus can exhibit exit block, during which it may fail to depolarize excitable myocardium.¹⁰

Although the parasystolic focus is protected, it may not be totally immune to the surrounding electrical activity. The effective electrical communication that permits the emergence of the ectopic discharges can also allow the rhythmic activity of the surrounding tissues to electrotonically influence the periodicity of the pacemaker discharge rate (described as *modulated parasystole*). Electrotonic influences arriving during the early stage of diastolic depolarization result in a delay in the firing of the parasystolic focus, whereas those arriving late accelerate the discharge of the parasystolic focus. As a consequence, the dominant pacemaker can entrain the partially protected parasystolic focus and force it to discharge at periods that may be faster or slower than its own intrinsic cycle and give rise to premature discharges whose patterns depend on the degree of modulation and the basic heart rate, occasionally mimic reentry, and occur at fixed coupling intervals. Therefore appropriate diagnosis of modulated parasystole relies on the construction of a phase response curve as theoretical evidence of modulation of the ectopic pacemaker cycle length (CL) by the electrotonic activity generated by the sinus discharges across the area of protection.

All these features of abnormal automaticity can be found in the Purkinje fibers that survive in regions of transmural MI and cause ventricular arrhythmias during the subacute phase.

Arrhythmias Caused by Abnormal Automaticity

There appears to be an association between abnormal Purkinje fiber automaticity and the arrhythmias that occur during the acute phase of MI (e.g., an accelerated idioventricular rhythm). However, the role of abnormal automaticity in the development of ventricular arrhythmias associated with chronic ischemic heart disease is less certain. In addition, isolated myocytes obtained from hypertrophied and failing hearts have been shown to manifest spontaneous diastolic depolarization and enhanced I_b findings, suggesting that abnormal automaticity can contribute to the occurrence of some arrhythmias in heart failure and ventricular hypertrophy.¹⁰

Abnormal automaticity can underlie atrial tachycardia, accelerated idioventricular rhythms, and ventricular tachycardia (VT), particularly that associated with ischemia and reperfusion. It has also been suggested that injury currents at the borders of ischemic zones can depolarize adjacent nonischemic tissue, thus predisposing to automatic VT.

Although automaticity is not responsible for most clinical tachyarrhythmias, which are usually caused by reentry or triggered activity, normal or abnormal automaticity can lead to arrhythmias caused by nonautomatic mechanisms. Premature beats, caused by automaticity, can initiate reentry. Rapid automatic activity in sites such as the cardiac veins can cause fibrillatory conduction, reentry, and atrial fibrillation (AF).

TRIGGERED ACTIVITY

Triggered activity is impulse initiation in cardiac fibers caused by afterdepolarizations that occur consequent to a preceding impulse or series of impulses. Afterdepolarizations are depolarizing oscillations in membrane potential that follow the upstroke of a preceding action potential. Afterdepolarizations can occur early during the repolarization phase of the action potential (early afterdepolarization [EAD]) or late, after completion of the repolarization phase (delayed afterdepolarization [DAD]) (Fig. 3.4). When either type of afterdepolarization is large enough to reach the threshold potential for activation of a regenerative inward current, a new action potential is generated, which is referred to as *triggered*.¹

Unlike automaticity, triggered activity is not a self-generating rhythm. Instead, triggered activity occurs as a response to a preceding impulse (the trigger). Automatic rhythms, on the other hand, can arise *de novo* in the absence of any prior electrical activity.

Delayed Afterdepolarizations and Triggered Activity

DADs are oscillations in membrane voltage that occur after completion of repolarization of the action potential (i.e., during phase 4). The

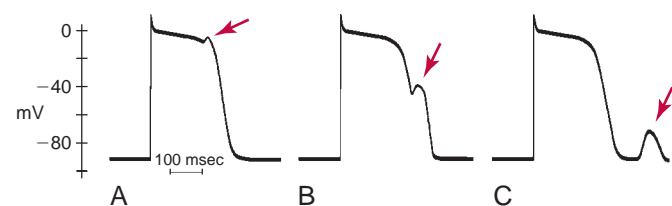


Fig. 3.4 Types of Afterdepolarizations. Afterdepolarizations are indicated by arrows. Purkinje cell action potentials are shown with phase 2 early afterdepolarizations (EADs) (A) and phase 3 EADs (B), as well as delayed afterdepolarizations (C), which occur after full repolarization.

transient nature of the DAD distinguishes it from normal spontaneous diastolic (pacemaker) depolarization, during which the membrane potential declines almost monotonically until the next action potential occurs. DADs may or may not reach threshold. Subthreshold DADs do not initiate action potentials or trigger arrhythmias. When a DAD does reach threshold, only one triggered action potential occurs (Fig. 3.5). The triggered action potential can also be followed by a DAD that, again, may or may not reach threshold and may or may not trigger another action potential. The first triggered action potential is often followed by a short or long train of additional triggered action potentials, each arising from the DAD caused by the previous action potential.¹⁰

Ionic Basis of Delayed Afterdepolarizations

DADs usually occur under a variety of conditions in which Ca^{2+} overload develops in the cytoplasm and sarcoplasmic reticulum. During the plateau phase of the normal action potential, Ca^{2+} flows through voltage-dependent L-type Ca^{2+} channels (I_{CaL}). Although the rise in intracellular Ca^{2+} is small and not sufficient to induce contraction, the small amount of Ca^{2+} entering the cell via I_{CaL} triggers a massive release of Ca^{2+} from the sarcoplasmic reticulum (the major store for Ca^{2+}) into the cytosol by opening the RyR2 channels (present in the membrane of the sarcoplasmic reticulum) in a process known as calcium-induced calcium release (CICR). During electrical diastole, most of the surplus Ca^{2+} in the cytosol is resealed into the sarcoplasmic reticulum by the sarcoplasmic/endoplasmic reticulum calcium adenosine triphosphatase (SERCA), the activity of which is controlled by the phosphoprotein phospholamban. In addition, some of the Ca^{2+} is extruded from the cell by the $\text{Na}^+/\text{Ca}^{2+}$ exchanger to balance the Ca^{2+} that enters via I_{CaL} . Recurring Ca^{2+} release-uptake cycles provide the basis for periodic elevations of the cytosolic Ca^{2+} concentration and contractions of myocytes, hence for the orderly beating of the heart (Fig. 3.6).^{10,11}

Under various pathological conditions, Ca^{2+} concentration in the sarcoplasmic reticulum can rise to a critical level during repolarization (i.e., Ca^{2+} overload), at which time a secondary spontaneous release of Ca^{2+} from the sarcoplasmic reticulum occurs after the action potential, rather than as a part of excitation-contraction coupling. This secondary release of Ca^{2+} results in inappropriately timed Ca^{2+} transients and

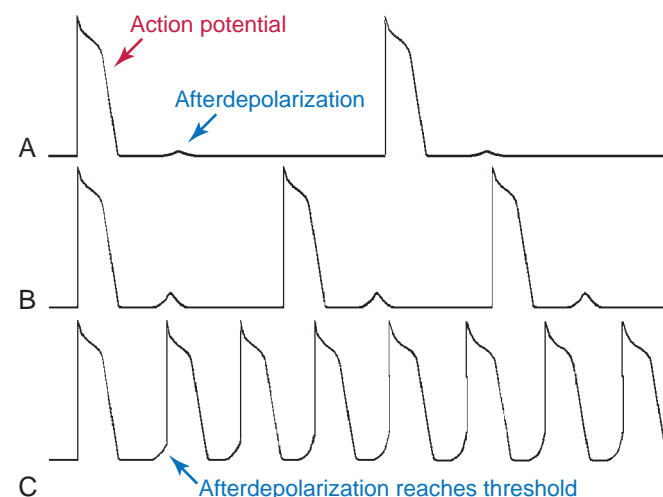


Fig. 3.5 Behavior of Delayed Afterdepolarizations (DADs). (A) The DAD is seen following the action potential at slow rates. (B) At faster rates, the DAD occurs slightly earlier and increases in amplitude. (C) At still more rapid rates, the DAD occurs even earlier and eventually reaches threshold, resulting in sustained firing.

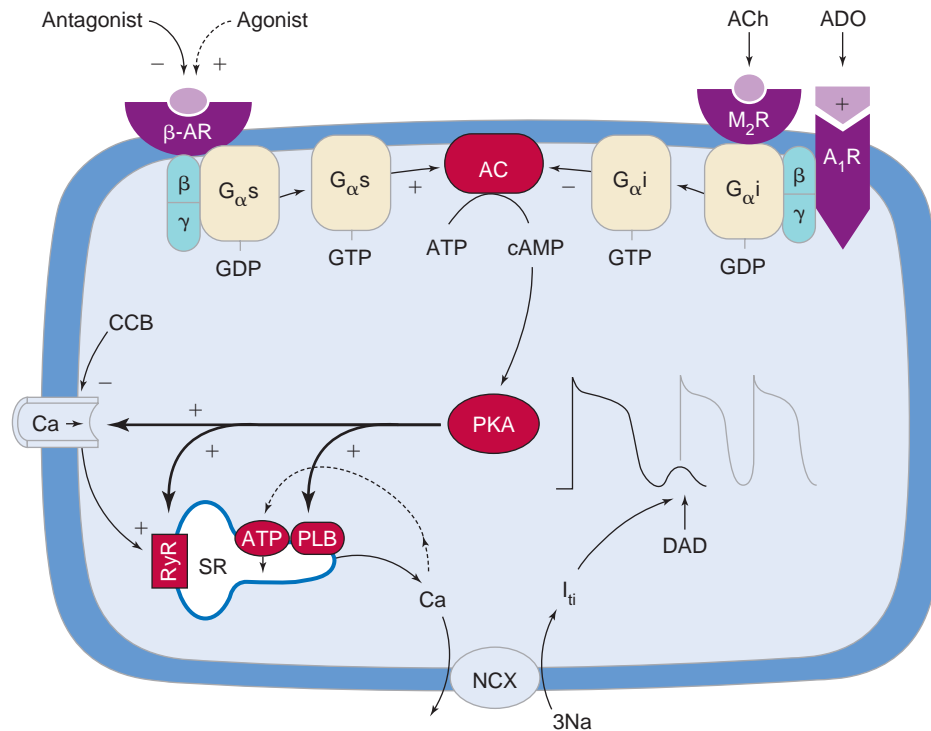


Fig. 3.6 Signal Transduction Schema for Initiation and Termination of Cyclic Adenosine Monophosphate (cAMP)-Mediated Triggered Activity. See text for discussion. *A1R*, α_1 -adenosine receptor; *AC*, adenylyl cyclase; *ACh*, acetylcholine; *ADO*, adenosine; *ATP*, adenosine triphosphate; *Ca*, calcium; *CCB*, calcium channel blocker; *DAD*, delayed afterdepolarization; *GDP*, guanosine diphosphate; *GTP*, guanosine triphosphate; *Gai*, inhibitory G protein; *Gas*, stimulatory G protein; *I_{ti}*, transient inward current; *M2R*, muscarinic receptor; *Na*, sodium; *NCX*, sodium (Na^+)-calcium (Ca^{2+}) exchanger; *PKA*, protein kinase A; *PLB*, phospholamban; *RyR*, ryanodine receptor; *SR*, sarcoplasmic reticulum; β -*AR*, β -adrenergic receptor. (From Lerman BB. Mechanism of outflow tract tachycardia. *Heart Rhythm*. 2007;4:973.)

contractions. Spontaneous Ca^{2+} waves can be arrhythmogenic; they induce Ca^{2+} -dependent depolarizing membrane currents (transient inward current [I_{ti}]), mainly by activation of the Na^+ - Ca^{2+} exchanger. Increases in intracellular Ca^{2+} levels can stimulate the Na^+ - Ca^{2+} exchanger ($I_{\text{Na-Ca}}$), which exchanges three Na^+ ions for one Ca^{2+} ion; the direction depends on the Na^+ and Ca^{2+} concentrations on the two sides of the membrane and the E_m difference. At resting E_m and during a spontaneous sarcoplasmic reticulum Ca^{2+} release event, this exchanger operates in the forward mode (three Na^+ ions in for one Ca^{2+} ion out) and generates a net Na^+ influx, causing transient oscillations of the membrane potential (DADs). After one or several DADs, myoplasmic Ca^{2+} can decrease because the Na^+ - Ca^{2+} exchanger extrudes Ca^{2+} from the cell, and the membrane potential stops oscillating.^{12,13}

When the DADs are of low amplitude (*subthreshold* DAD), they usually are not apparent or clinically significant. However, during pathological conditions (e.g., myocardial ischemia, acidosis, hypomagnesemia, digitalis toxicity, and increased catecholamines), the amplitude of the Ca^{2+} -mediated membrane depolarization is increased and can reach the stimulation threshold (*suprathreshold* DAD) and an action potential is triggered (called *triggered activity*). If this process continues, sustained tachycardia will develop. Triggered action potentials can also initiate reentry when they encounter a vulnerable tissue substrate.

Probably the most important influence that causes subthreshold DADs to reach threshold is a decrease in the initiating CL because that increases both the amplitude and rate of the DADs. Therefore initiation of arrhythmias triggered by DADs can be facilitated by a spontaneous or pacing-induced increase in the heart rate.

Subthreshold DADs can also play a role in arrhythmogenesis by partially depolarizing the cell membrane and hence inactivating a portion of Na^+ channels and reducing their availability during the subsequent (triggered or nontriggered) action potential. The resultant regional dispersion of excitability or refractoriness can generate a tissue substrate vulnerable to unidirectional conduction block and reentry.¹⁴

Role of Delayed Afterdepolarizations in Arrhythmogenesis

A suprathreshold DAD can trigger an action potential and generate triggered activity, which can cause focal, nonreentrant arrhythmias (triggered activity atrial or ventricular ectopic beats or tachycardia) or, when it encounters a vulnerable tissue substrate, the triggered action potential can act as a trigger for initiation of reentrant arrhythmias.¹²

Both suprathreshold and subthreshold DADs can potentially generate a vulnerable substrate and promote reentry by regionally decreasing excitability sufficiently to cause regional conduction block of a subsequent nontriggered action potential. In addition, when both subthreshold and suprathreshold DADs coexist in the same tissue, the combination of triggers and a vulnerable substrate can lead directly to reentry initiation. DADs can potentially generate both a vulnerable substrate that promotes reentry, as well as a trigger for initiation of reentrant arrhythmias. In some regions, suprathreshold DADs can trigger an action potential, whereas in other regions, subthreshold DADs promoting regional conduction block. Once the triggered action potential propagates to the region of conduction block, it may initiate reentry.^{14,15}

DAD-related triggered activity is thought to be a mechanism for tachyarrhythmia associated with MI, reperfusion injury, digitalis toxicity,

and some idiopathic VTs, as well as some arrhythmias associated with inherited channelopathies. DADs are more likely to occur with fast spontaneous or paced rates or with increased premature beats.⁹

Digitalis. Digitalis causes DAD-dependent triggered arrhythmias by inhibiting the $\text{Na}^+\text{-K}^+$ exchange pump. In toxic amounts, this effect results in the accumulation of intracellular Na^+ and consequently an enhancement of the $\text{Na}^+\text{-Ca}^{2+}$ exchanger in the reverse mode (three Na^+ ions out for one Ca^{2+} ion in) and an accumulation of intracellular Ca^{2+} . Spontaneously occurring accelerated ventricular arrhythmias that occur during digitalis toxicity are likely to be caused by DADs. Triggered ventricular arrhythmias caused by digitalis also can be initiated by pacing at rapid rates. As toxicity progresses, the duration of the trains of repetitive responses induced by pacing increases.

Catecholamines. Catecholamines can facilitate the development of DADs by increasing intracellular Ca^{2+} overload via several mechanisms, including (1) increasing the I_{CaL} through stimulation of beta-adrenergic receptors and increasing cAMP, which results in an increase in transsarcolemmal Ca^{2+} influx and intracellular Ca^{2+} overload (see Fig. 3.6); (2) enhancing the activity of the $\text{Na}^+\text{-Ca}^{2+}$ exchanger, thus increasing the likelihood of DAD-mediated triggered activity; (3) enhancing the uptake of Ca^{2+} by the sarcoplasmic reticulum, leading to increased Ca^{2+} stored in the sarcoplasmic reticulum and the subsequent release of an increased amount of Ca^{2+} from the sarcoplasmic reticulum during contraction; and (4) increasing the heart rate.

Sympathetic stimulation can potentially cause triggered atrial and ventricular arrhythmias and possibly underlies some of the ventricular arrhythmias that accompany exercise and those occurring during ischemia and infarction.

Myocardial ischemia. Elevations in intracellular Ca^{2+} in the ischemic myocardium are also associated with DADs and triggered arrhythmias. Accumulation of lysophosphoglycerides in the ischemic myocardium, with consequent Na^+ and Ca^{2+} overload, has been suggested as a mechanism for DADs and triggered activity. Cells from damaged areas or surviving the infarction can display spontaneous release of Ca^{2+} from sarcoplasmic reticulum, which can generate waves of intracellular Ca^{2+} elevation and arrhythmias.

Genetic mutations. DADs can be caused by genetic defects that impair the ability of the sarcoplasmic reticulum to sequester Ca^{2+} during diastole. Mutations in the cardiac RyR2, the sarcoplasmic reticulum Ca^{2+} release channel in the heart, have been identified in kindreds with the syndrome of catecholaminergic polymorphic VT and ventricular fibrillation (VF) with short QT intervals. It seems likely that perturbed intracellular Ca^{2+} and perhaps also DADs underlie arrhythmias in this syndrome (see Fig. 3.6).¹⁶

Drugs. Several drugs can inhibit DAD-related triggered activity via different mechanisms, including reduction of the inward Ca^{2+} current and intracellular Ca^{2+} overload (Ca^{2+} channel blockers, beta-adrenergic blockers), reduction of Ca^{2+} release from the sarcoplasmic reticulum (caffeine, ryanodine, thapsigargin, cyclopiazonic acid), and reduction of the inward I_{Na} (tetrodotoxin, lidocaine, phenytoin).

Properties of Delayed Afterdepolarizations

The amplitude of DADs and the possibility of triggered activity are influenced by the level of membrane potential at which the action potential occurs. The reduction of the membrane potential during DADs may also result in Na^+ channel inactivation and hence slowing of conduction.

The duration of the action potential is a critical determinant of the presence of DADs. Longer action potentials, which are associated with more transsarcolemmal Ca^{2+} influx, are more likely to be associated with DADs. Drugs that prolong action potential duration (e.g., class IA antiarrhythmic agents) can increase DAD amplitude, whereas drugs

that shorten action potential duration (e.g., class IB antiarrhythmic agents) can decrease DAD amplitude.

The number of the action potentials preceding the DAD affects the amplitude of the DAD (i.e., after a period of quiescence, the initiation of a single action potential can be followed by either no DAD or only a small one). With continued stimulation, the DADs increase in amplitude, and triggered activity can eventually occur.

The amplitude of DADs and the coupling interval between the first triggered impulse and the last stimulated impulse that induced them are directly related to the drive CL at which triggered impulses are initiated. A decrease in the basic drive CL (even a single drive cycle; i.e., premature impulse), in addition to increasing the DAD amplitude, results in a decrease in the coupling interval between the last drive cycle and the first DAD-triggered impulse, with respect to the last driven action potential, and an increase of the rate of DADs. Triggered activity tends to be induced by a critical decrease in the drive CL, either spontaneous, such as in sinus tachycardia, or pacing induced. The increased time during which the membrane is in the depolarized state at shorter stimulation CLs or after premature impulses increases Ca^{2+} in the myoplasm and the sarcoplasmic reticulum (because of repeated activation of I_{CaL}), thus increasing the I_{ti} responsible for the increased DAD amplitude, causing the current to reach its maximum amplitude more rapidly, and decreasing the coupling interval of triggered impulses. This characteristic property can help to distinguish triggered activity from reentrant activity because the relationship for reentry impulses initiated by rapid stimulation is often the opposite (i.e., as the drive CL is reduced, the first reentrant impulse occurs later with respect to the last driven action potential because of rate-dependent conduction slowing in the reentrant pathway).

In general, triggered activity is markedly influenced by overdrive pacing. These effects are dependent on both the rate and the duration of overdrive pacing. When overdrive pacing is performed for a critical duration of time and at a critical rate during a catecholamine-dependent triggered rhythm, the rate of triggered activity slows until the triggered rhythm stops, because of enhanced activity of the electrogenic $\text{Na}^+\text{-K}^+$ exchange pump induced by the increase in intracellular Na^+ caused by the increased number of action potentials. When overdrive pacing is not rapid enough to terminate the triggered rhythm, it can cause overdrive *acceleration* (in contrast to overdrive suppression observed with automatic rhythms). Single premature stimuli also can terminate triggered rhythms, although termination is much less common than it is by overdrive pacing.

EADs and triggered activity. EADs are oscillations in membrane potential that occur during the action potential and interrupt the orderly repolarization of the cardiomyocyte. EADs manifest as an abrupt change in the time course of repolarization of an action potential such that the membrane voltage suddenly shifts in a depolarizing direction.^{12,17}

Ionic Basis of Early Afterdepolarizations

Normal cardiac repolarization relies on a critical balance between depolarizing inward currents and repolarizing outward currents during the action potential plateau. Repolarization has built-in redundancy (“repolarization reserve”) to protect against excessive prolongation of the action potential duration. The plateau of the action potential is a time of high membrane resistance (i.e., membrane conductance to all ions falls to rather low values), when there is little current flow. Consequently, small changes in repolarizing or depolarizing currents can have profound effects on the action potential duration and profile. Normally, during phases 2 and 3, the net membrane current is outward. Any factor that transiently shifts the net current in the inward direction can potentially overcome and reverse repolarization (a condition termed “reduced

repolarization reserve”) and lead to EADs and EAD-related arrhythmias. Such a shift can arise from decreased outward (repolarizing) currents (mostly carried by K^+ at that time), increased inward (depolarizing) currents (carried by Na^+ or Ca^{2+} at that time), or both. However, although reduced repolarization reserve is sufficient to prolong action potential duration, it is not sufficient to produce EADs. Other conditions are required to generate the voltage oscillations pathognomonic of EADs, which arise from different causes. The most critical to the dynamics of EAD oscillations include window I_{CaL} , late I_{Na} , and I_{Ks} . In addition, EADs can also be promoted by intracellular Ca^{2+} oscillations or by prolonged Ca^{2+} transients via Na^+-Ca^{2+} exchanger current (I_{Na-Ca}).¹²

EADs have been classified as phase 2 (occurring at the plateau level of membrane potential) and phase 3 (occurring during phase 3 of repolarization) (see Fig. 3.4). The ionic mechanisms of phase 2 and phase 3 EADs and the upstrokes of the action potentials they elicit can

differ. At the depolarized membrane voltages of phase 2, Na^+ channels are inactivated; hence the I_{CaL} and I_{Na-Ca} are the major currents potentially responsible for EADs. Voltage steady-state activation and inactivation of the L-type Ca^{2+} channels are sigmoidal, with an activation range over -40 to $+10$ mV (with a half-activation potential near -15 mV) and a half-inactivation potential near -35 mV. However, a relief of inactivation for voltages positive to 0 mV leads to a U-shaped voltage dependence for steady-state inactivation. Overlap of the steady-state voltage-dependent inactivation and activation relations defines a “window” current near the action potential plateau, within which transitions from closed and open states can occur. As the action potential repolarizes into the window region, I_{CaL} increases and can potentially be sufficient to reverse repolarization, thus generating the EAD upstroke (Fig. 3.7).¹¹

The cardiac Na^+-Ca^{2+} exchanger exchanges three Na^+ ions for one Ca^{2+} ion; the direction is dependent on the Na^+ and Ca^{2+} concentrations

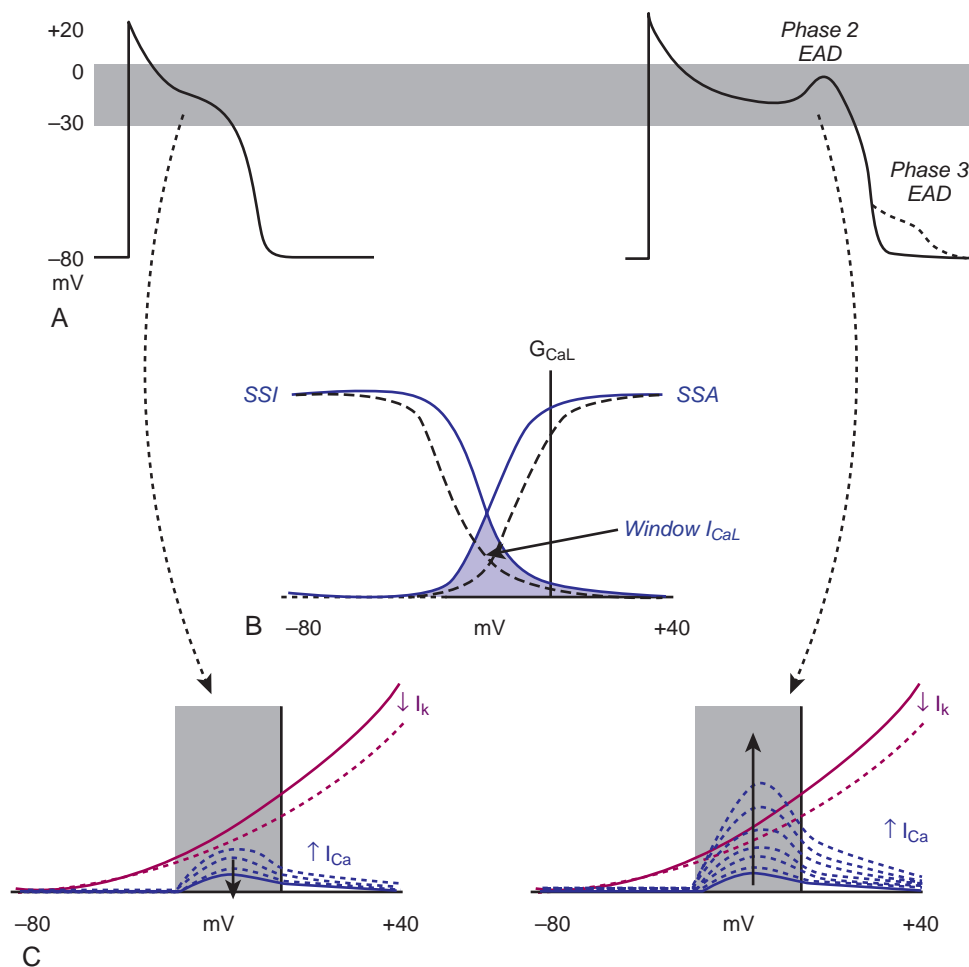


Fig. 3.7 Mechanisms Underlying Early Afterdepolarization (EADs). (A) Normal action potential (left) and an action potential with phase 2 EAD (solid line) or phase 3 EAD (dashed line) (right). (B) Schematic plot of L-type calcium (Ca^{2+}) channel conductance (G_{CaL}) versus membrane voltage (mV) showing the window L-type inward Ca^{2+} current (I_{CaL}) region (purple area) where the steady-state activation (SSA) and steady-state inactivation (SSI) curves overlap and a fraction of Ca^{2+} channels remain continuously open. Dashed lines show a potential therapeutic intervention that shifts the SSA and SSI curves to reduce the overlapping window current region. (C) Schematic diagram illustrating the interaction between time-dependent I_{CaL} reactivation (dashed blue lines) and time-dependent deactivation of repolarizing currents (I_K) (dashed red lines) in the window voltage range during action potential repolarization. For the normal action potential (left), the repolarization rate is too fast for I_{CaL} to grow larger than I_K . However, if the repolarization rate is too slow, I_{CaL} can grow larger than I_K , thereby reversing repolarization to cause an EAD (right). (From Weiss JN, Garfinkel A, Karagueuzian HS, et al. Early afterdepolarizations and cardiac arrhythmias. *Heart Rhythm*. 2010;7:1891–1899.)

on the two sides of the membrane and the transmembrane potential difference. When operating in forward mode, this exchanger generates a net Na^+ influx, thereby resisting repolarization. The increase in the window I_{CaL} results in Ca^{2+} influx into the cell, which further increases $I_{\text{Na-Ca}}$ in the forward mode, thus possibly facilitating EAD formation and increasing the probability of an EAD-triggered action potential.

After opening, most Na^+ channels quickly inactivate to prevent passage of Na^+ and remain inactivated throughout the duration of the plateau phase of the action potential. However, under pathophysiological conditions (e.g., type 3 long-QT syndrome [LQTS], heart failure, cardiomyopathy, ischemia, drugs), Na^+ channel inactivation may be either delayed or reversed to allow channel reopenings before repolarization of the action potential, resulting in a small residual inward current (called “late I_{Na} ,” I_{NaL}) that persists throughout the action potential plateau. The inward late I_{Na} acts to slow repolarization and prolong the action potential duration and hence promotes EADs. Besides late I_{Na} , increased “window I_{Na} ” (due to delayed inactivation or shifts in the voltage dependence of activation/inactivation) may also promote EADs. The role of the late I_{Na} and window I_{Na} in EAD genesis is similar to the window I_{CaL} .^{17,18}

It was traditionally thought that, unlike DADs, EADs do not depend on a rise in intracellular Ca^{2+} ; instead, action potential prolongation and reactivation of depolarizing currents are fundamental to their production. More recent experimental evidence suggested a previously unappreciated interrelationship between intracellular Ca^{2+} loading and EADs. Cytosolic Ca^{2+} levels can increase when action potentials are prolonged. This situation, in turn, appears to enhance I_{CaL} (possibly via Ca^{2+} -calmodulin kinase activation), thus further prolonging the action potential duration as well as providing the inward current driving EADs. Intracellular Ca^{2+} loading by action potential prolongation can also enhance the likelihood of DADs. The interrelationship among intracellular Ca^{2+} , DADs, and EADs can be one explanation for the susceptibility of hearts that are Ca^{2+} loaded (e.g., in ischemia or congestive heart failure) to develop arrhythmias, particularly on exposure to action potential-prolonging drugs.

EADs occurring late in repolarization develop at membrane potentials more negative than -60 mV in atrial, ventricular, or Purkinje cells that have normal resting potentials. Normally, a net outward membrane current shifts the membrane potential progressively in a negative direction during phase 3 repolarization of the action potential. Despite fewer data, it has been suggested that current through the Na^+ - Ca^{2+} exchanger and possibly the I_{Na} can participate in the activation of phase 3 EADs. Nevertheless, this concept was questioned by a study suggesting that phase 2 EADs appear to be responsible for inducing phase 3 EADs through electrotonic interactions and that a large voltage gradient related to heterogeneous repolarization is essential for phase 3 EADs.^{19,20}

The upstrokes of the action potentials elicited by phase 2 and phase 3 EADs also differ. Phase 2 EAD-triggered action potential upstrokes are exclusively mediated by Ca^{2+} currents. Even when these triggered action potentials do not propagate, they can substantially exaggerate heterogeneity of the time course of repolarization of the action potential (a key substrate for reentry) because EADs occur more readily in some regions (e.g., Purkinje fibers, mid left ventricular [LV] myocardium, right ventricular outflow tract [RVOT] epicardium) than others (e.g., LV epicardium, endocardium). Action potentials triggered by phase 3 EADs arise from more negative membrane voltages. Therefore the upstrokes can be caused by Na^+ and Ca^{2+} currents and are more likely to propagate.²¹

Under certain conditions, when an EAD is large enough, the decrease in membrane potential leads to an increase in net inward (depolarizing) current and a second upstroke or an action potential is *triggered* before complete repolarization of the first. The triggered action potential also can be followed by other action potentials, all occurring at the low level

of membrane potential characteristic of the plateau or at the higher level of membrane potential of later phase 3 (eFig. 3.2). The sustained rhythmic activity can continue for a variable number of impulses and terminates when repolarization of the initiating action potential returns membrane potential to a high level. As repolarization occurs, the rate of the triggered rhythm slows because the rate is dependent on the level of membrane potential. Sometimes repolarization to the high level of membrane potential may not occur, and membrane potential can remain at the plateau level or at a level intermediate between the plateau level and the resting potential. The sustained rhythmic activity then can continue at the reduced level of membrane potential and assumes the characteristics of abnormal automaticity. However, in contrast to automatic rhythms, without the initiating action potential, there can be no triggered action potentials.

The ability of the triggered action potentials to propagate is related to the level of membrane potential at which the triggered action potential occurs. The more negative the membrane potential, the more Na^+ channels are available for activation, the greater the influx of Na^+ into the cell during phase 0, and the higher the conduction velocity. At more positive membrane potentials of the plateau (phase 2) and early during phase 3, most Na^+ channels are still inactivated, and the triggered action potentials most likely have upstrokes caused by the inward I_{CaL} . Therefore those triggered action potentials have slow upstrokes and are less able to propagate. Increased dispersion of repolarization facilitates the ability of phase 2 EADs to trigger propagating ventricular responses.

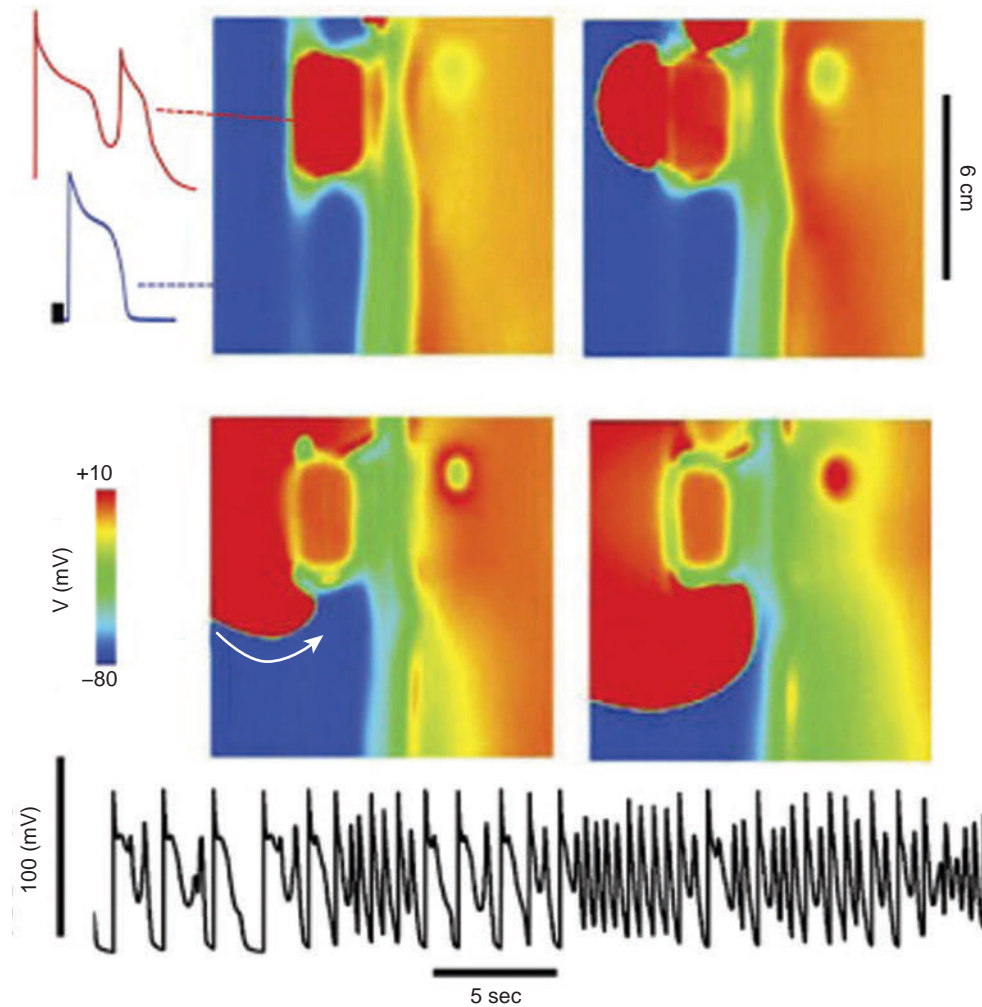
Role of Early Afterdepolarizations in Arrhythmogenesis

Both suprathreshold and subthreshold EADs can create dispersion of refractoriness and a tissue substrate vulnerable to reentry. When EADs reach the threshold to propagate, they generate triggers that initiate reentry in the vulnerable substrate. Therefore, depending on the cellular and tissue properties, EADs can result in purely reentrant arrhythmias, multiple shifting foci, and a mixture of multiple shifting foci and reentry.^{12,22}

A fundamental condition that underlies the development of EADs is action potential prolongation, which is manifest on the surface ECG by QT prolongation. An EAD occurs when the repolarization phase is prolonged either in acquired conditions (e.g., heart failure) and inherited diseases (e.g., LQTS). Other conditions that can contribute to a prolongation of the action potential and lead to EADs include electrolyte abnormalities (e.g., hypokalemia, hypomagnesemia, acidosis), bradycardia, catecholamines, and drugs that block K^+ currents.^{22,23}

Drugs. Drugs are the most common cause of EAD-mediated arrhythmias. Class IA and III antiarrhythmic agents prolong the action potential duration and the QT interval, effects intended to be therapeutic but frequently causing proarrhythmia. Noncardiac drugs such as some phenothiazines, some nonsedating antihistamines, and some antibiotics can also prolong the action potential duration and predispose to EAD-mediated triggered arrhythmias, particularly when there is associated hypokalemia or bradycardia.²⁴ Decreased extracellular K^+ concentration paradoxically decreases some membrane I_{K} (particularly the I_{Kr}) in the ventricular myocyte. This finding explains why hypokalemia causes action potential prolongation and EADs. Of note, EADs are opposed by ATP-dependent K^+ channel (I_{KATP}) openers (pinacidil, cromakalim, rimakalim, and nicorandil), magnesium, alpha-adrenergic blockade, tetrodotoxin, nitrendipine, and antiarrhythmic drugs that shorten action potential (e.g., lidocaine and mexiletine). Alpha-adrenergic stimulation can exacerbate EADs.^{25,26}

Long QT syndromes. EAD-mediated triggered activity likely underlies initiation of the characteristic polymorphic VT, torsades de pointes, seen in patients with congenital and acquired forms of LQTS (see Chapter 31). Although the genesis of ventricular arrhythmias in these patients



eFig. 3.2 Early Afterdepolarizations (EADs) and Cardiac Arrhythmias. Mixed focal reentrant polymorphic ventricular tachycardia as a result of EAD-mediated premature ventricular complexes (PVCs) arising from EAD islands in simulated two-dimensional homogeneous tissue. The tissue was paced from the left edge at a slow rate. Four successive voltage snapshots show an EAD (red in upper left quadrant) that generates a PVC (red blob). The PVC then initiates reentry by reentering (white arrow) the receding wave back of the region without EADs (blue blob). The voltage trace below from a representative cell shows multiple EADs followed by rapid tachycardia resulting from a mixture of triggered activity and reentry. (From Weiss JN, Garnkel A, Karagueuzian HS, et al. Early afterdepolarizations and cardiac arrhythmias. *Heart Rhythm*. 2010;7: 1891–1899.)

is still unclear, marked transmural dispersion of repolarization can create a vulnerable window for development of reentry. EADs arising from these regions can underlie the premature complexes that initiate or perpetuate the tachycardia.¹²

Structural heart disease. Structural heart disease such as cardiac hypertrophy and failure can also delay ventricular repolarization—so-called electrical remodeling—and predispose to arrhythmias related to abnormalities of repolarization. The abnormalities of repolarization in hypertrophy and failure are often magnified by concomitant drug therapy or electrolyte disturbances.²⁷

Properties of Early Afterdepolarizations

EAD-triggered arrhythmias exhibit rate dependence. In general, the amplitude of an EAD is augmented at slow rates when action potentials are longer in duration. Pacing-induced increases in rate shorten the action potential duration and reduce EAD amplitude. Action potential shortening and suppression of EADs with increased stimulation rate are likely the result of augmentation of delayed rectifier I_K and perhaps hastening of Ca^{2+} -induced inactivation of I_{CaL} . Once EADs have achieved a steady-state magnitude at a constant drive CL, any event that shortens the drive CL tends to reduce their amplitude. Hence the initiation of a single premature depolarization, which is associated with an acceleration of repolarization, will reduce the magnitude of the EADs that accompany the premature action potential; as a result, triggered activity is not expected to follow premature stimulation. The exception is when a long compensatory pause follows a premature ventricular complex. This situation can predispose to the development of an EAD and can be the mechanism of torsades de pointes in some patients with the LQTS. Thus EADs are more likely to trigger rhythmic activity when the spontaneous heart rate is slow because bradycardia is associated with prolongation of the QT interval and action potential duration (e.g., bradycardia- or pause-induced torsades de pointes). Similarly, catecholamines increase heart rate and decrease action potential duration and EAD amplitude, despite the effect of beta-adrenergic stimulation to increase I_{CaL} .

REENTRY

Basic Principles of Reentry

During each normal cardiac cycle, at the completion of normal cardiac excitation, the electrical impulse originating from the sinus node becomes extinct, and the subsequent excitation cycles originate from new pacemaker impulses. Physiological excitation waves vanish spontaneously after the entire heart has been activated because of the long duration of refractoriness in the cardiac tissue compared with the duration of the excitation period; therefore, after its first pass, the impulse, having no place to go, expires. Reentry occurs when a propagating impulse fails to die out after normal activation of the heart and persists to reexcite the heart after expiration of the refractory period. In pathological settings, excitation waves can be blocked in circumscribed areas, rotate around these zones of block, and reenter the site of original excitation in repetitive cycles. The wavefront does not extinguish but rather propagates continuously and thus continues to excite the heart because it always encounters excitable tissue.¹⁰

Reentrant tachycardia (also called reentrant excitation, reciprocating tachycardia, circus movement, or reciprocal or echo beats) is a continuous repetitive propagation of the activation wave in a circular path, returning to its site of origin to reactivate that site. Traditionally, reentry has been divided into two types: (1) anatomical reentry, when there is a distinct relationship of the reentry pathway with the underlying tissue structure; and (2) functional reentry, when reentrant circuits occur at random locations without clearly defined anatomical boundaries

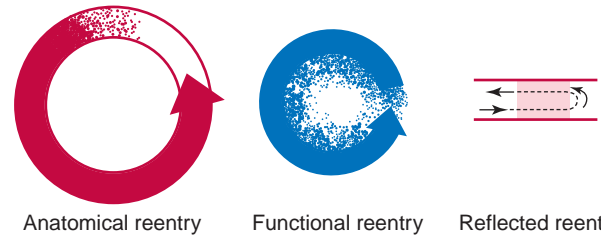


Fig. 3.8 Models of Reentry. The solid area is completely refractory tissue, and mottled area is partially refractory. In anatomical reentry, the circuit is determined by structures or scar in the heart, and a portion of the circuit that has fully recovered excitability can be stimulated while it awaits the next cycle. However, in functional reentry, the rate is as rapid as it can be and still allow all portions of the circuit to recover.

BOX 3.1 Criteria for Diagnosis of Reentrant Tachycardia

1. Mapping activation in one direction around the continuous loop
2. Correlation of continuous electrical activity with occurrence of tachycardia
3. Correlation of unidirectional block with initiation of reentry
4. Initiation and termination by premature stimulation
5. Dependence of initiation of the arrhythmia on the site of pacing
6. Inverse relationship between the coupling interval of the initiating premature stimulus and the interval to the first tachycardia beat
7. Resetting of the tachycardia by a premature beat, with an inverse relationship between the coupling interval of the premature beat and the cycle length of the first or return beat of the tachycardia
8. Fusion between a premature beat and the tachycardia beat followed by resetting
9. Transient entrainment (with external overdrive pacing, the ability to enter the reentrant circuit and capture the circuit, resulting in tachycardia at the pacing rate with fused complexes)
10. Abrupt termination by premature stimulation
11. Dependence of initiation on critical slowing of conduction in the circuit
12. Similarity with experimental models in which reentry is proven and is the only mechanism of tachycardia

(Fig. 3.8). Although this distinction has a historical background and is useful for didactic purposes, both the anatomical and functional forms can coexist in a given pathological setting and share many common basic biophysical mechanisms.²⁸

The original three criteria for reentry proposed by Mines still hold true: (1) unidirectional block is necessary for initiation; (2) the wave of excitation should travel in a single direction around the pathway, returning to its point of origin and then restarting along the same path; and (3) the tachycardia should terminate when one limb of the pathway is cut or temporarily blocked. The 12 conditions that were proposed to prove or identify the existence of reentrant tachycardia in the EP laboratory are listed in Box 3.1.

Requisites of Reentry

Substrate

The initiation and maintenance of a reentrant arrhythmia require the presence of myocardial tissue with adjacent tissue or pathways having different EP properties, conduction, and refractoriness, and that they be joined proximally and distally, forming a circuit. These circuits can be stationary or can move within the myocardial substrate.

The reentrant circuit can be an anatomical structure, such as a loop of fiber bundles in the Purkinje system or accessory pathways, or a

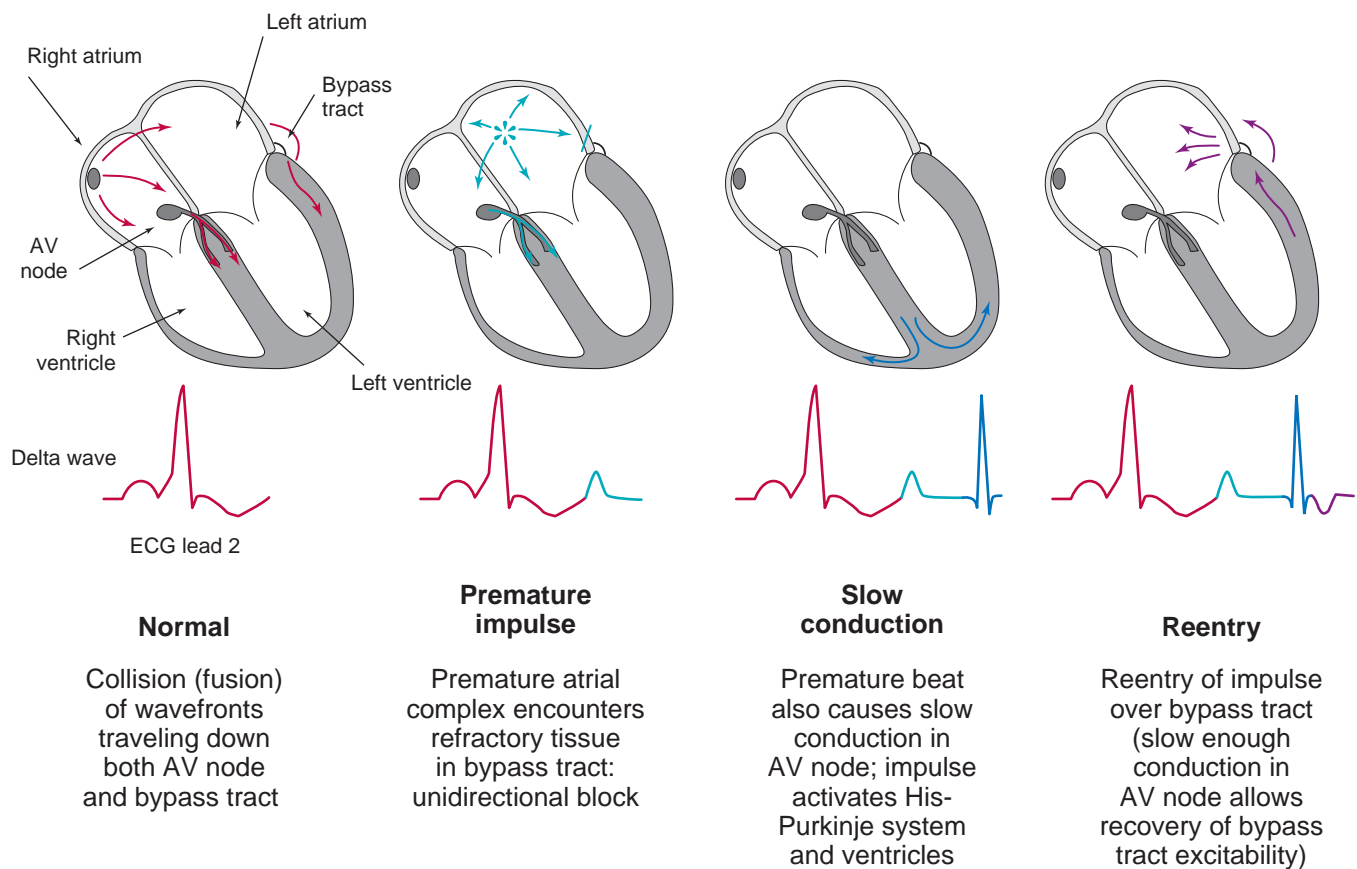


Fig. 3.9 Reentry in the Wolff-Parkinson-White Syndrome. AV, Atrioventricular; ECG, electrocardiographic.

functionally defined pathway, with its existence, size, and shape determined by the EP properties of cardiac tissues in which the reentrant wavefront circulates. The circuit can also be an anatomical-functional combination. The cardiac tissue that constitutes the substrate for reentrant excitation can be located almost anywhere in the heart. The reentrant circuit can be a variety of sizes and shapes and can include different types of myocardial cells (e.g., atrial, ventricular, nodal, Purkinje) (Fig. 3.9).

Central Area of Block

A core of inexcitable tissue around which the wavefront circulates is required to sustain reentry. Without this central area of block, the excitation wavefront will not necessarily be conducted around the core of excitable tissue; rather, it could take a shortcut, permitting the circulating excitation wavefront to arrive early at the site where it originated. If it arrives sufficiently early, the tissue at the site of origination will still be refractory, and reentrant excitation will not be possible.

As mentioned earlier, the area of block can be anatomical, functional, or a combination of the two. Anatomical block is the result of a non-conductive medium in the center of the circuit, such as the tricuspid annulus in typical atrial flutter (AFL). Functional block at the center of a circuit occurs when there is block of impulses in otherwise excitable cardiac muscle. The central area of functional block develops during the initiation of the reentrant circuit by the formation of a line of block that most likely is caused by refractoriness. When the reentrant circuit forms, the line of block then is sustained by centripetal activation from the circulating wavefront that, by repeatedly bombarding the central area of block, maintains the state of refractoriness of this region. A combination of an anatomical and a functional central area of block

in the reentrant circuit has been described in some models of AFL such as the orifice of one or both venae cavae and an area of functional block continuous with or adjacent to either or both caval orifice(s). In addition, it has now been shown that a functional extension of an anatomical line of block can occur such that it plays a role in creating the necessary or critical substrate for reentry. Thus a surgical incision in the RA made to repair a congenital heart lesion can, under certain circumstances, develop a functional extension to one or both of the venae cavae, such that the substrate to create and sustain AFL develops.¹⁹

Unidirectional Conduction Block

Transient or permanent unidirectional block is usually a result of heterogeneity of EP properties of the myocardium and is essential for the initiation of reentry. The excitation wavefront propagating in the substrate must encounter unidirectional block; otherwise, the excitation wavefronts traveling down both limbs of the reentrant circuit will collide and extinguish each other.

Area of Slow Conduction

In a successful reentrant circuit, the wavefront of excitation must encounter excitable cells or the tachycardia will terminate. Therefore a condition necessary for reentry is the maintenance of excitable tissue ahead of the propagating wavefront. In other words, the tissue initially activated by the excitation wavefront should have sufficient time to recover its excitability by the time the reentrant wavefront returns. Thus conduction of the circulating wavefront must be sufficiently delayed in an alternate pathway to allow for expiration of the refractory period in the tissue proximal to the site of unidirectional block, and there must always be a gap of excitable tissue (fully or partially excitable) ahead

of the circulating wavefront (i.e., the length of the reentrant pathway must equal or exceed the reentrant wavelength; see later). This is facilitated by a sufficiently long reentrant pathway (which is especially important when conduction is normal along the reentrant path), sufficiently slow conduction in all or part of the alternative pathway (because sufficiently long pathways are usually not present in the heart), sufficient shortening of the refractory period, or a combination of these factors.

Critical Tissue Mass

An additional requisite for random reentry is the necessity of a critical mass of tissue to sustain the one or usually more simultaneously circulating reentrant wavefronts. Thus it is essentially impossible to achieve sustained fibrillation of ventricles of very small, normal, mammalian hearts and equally difficult to achieve sustained fibrillation of the completely normal atria of humans or smaller mammals.

Initiating Trigger

Another prerequisite for reentrant excitation to occur is often, but not always, the presence of an initiating trigger, which invokes the necessary EP milieu for initiation of reentry. Susceptible patients with appropriate underlying substrates usually do not suffer from incessant tachycardia because the different EP mechanisms required for the initiation and maintenance of a reentrant tachycardia are infrequently present at exactly the same time. However, changes in heart rate or autonomic tone, ischemia, electrolyte or pH abnormalities, or the occurrence of a premature depolarization can be sufficient to initiate reentrant tachycardia.

The trigger frequently is required because it elicits or brings to a critical state one or more of the conditions necessary to achieve reentrant excitation. In fact, premature depolarizations frequently initiate these tachyarrhythmias because they can cause slow conduction and unidirectional block. Thus a premature impulse initiating reentry can arrive at one site in the potential reentrant circuit sufficiently early that it encounters unidirectional block because that tissue has had insufficient time to recover excitability after excitation by the prior impulse. Furthermore, in the other limb of the potential reentrant circuit, the premature arrival of the excitation wavefront causes slow conduction or results in further slowing of conduction of the excitation wavefront through an area of already slow conduction. The resulting increase in conduction time around this limb of the potential reentrant circuit allows the region of unidirectional block in the tissue in the other limb activated initially by the premature beat to recover excitability. It should be noted that the mechanism causing the premature impulse can be different from the reentrant mechanism causing the tachycardia. Thus the premature impulse can be caused by automaticity or triggered activity.

Types of Reentrant Circuits

Anatomical Reentry

In anatomically determined circuits, a discrete inexcitable anatomical obstacle creates a surrounding circular pathway, resulting in a fixed length and location of the reentrant circuit. Because the length and location of the reentrant pathway are relatively fixed, the characteristics of the reentrant circuit are determined by the characteristics of the anatomical components of that circuit.¹⁰

A reentrant tachycardia is initiated when an excitation wavefront splits into two limbs after going around the anatomical obstacle and travels down one pathway and not the other, thus creating a circus movement. Tachycardia rates are determined by the wavelength and by the length of the reentrant pathway (the path length). The initiation and maintenance of anatomical reentry depend on conduction velocity and refractory period. Thus, as long as the extension of the refractory zone behind the excitation wave, the so-called wavelength of excitation,

is smaller than the entire length of the anatomically defined reentrant pathway, a zone of excitable tissue, the so-called excitable gap, exists between the tail of the preceding wave and the head of the following wave. In essence, circus movements containing an excitable gap are stable with respect to their frequency of rotation and can persist at a constant rate for hours. In the setting where the wavelength of excitation exceeds the path length, the excitation wavefront becomes extinct when it encounters the not yet recovered inexcitable tissue. A special case is present in the intermediate situation, when the head of the following wavefront meets the partially refractory tail of the preceding wavefront (i.e., the wavelength approximates the path length). This situation is characterized by unstable reentrant CLs and complex dynamics of the reentrant wavefront. There is often a long excitable gap associated with anatomical reentry.¹⁰

Anatomical circuits therefore are associated with ordered reentry. Examples of this type of reentry are atrioventricular reentrant tachycardia, atrioventricular nodal reentrant tachycardia, AFL, VT originating within the HPS (bundle-branch reentry VT), and post-MI VT.

Functional Reentry

In functionally determined circuits, the reentrant pathway depends on the intrinsic heterogeneity of the EP properties of the myocardium, not by a predetermined anatomical circuit (i.e., without involvement of an anatomical obstacle or anatomically defined conducting pathway). Such heterogeneity involves dispersion of excitability or refractoriness and conduction velocity, as well as anisotropic conduction properties of the myocardium.²⁹

Functional circuits typically tend to be small and unstable; the reentrant excitation wavefront can fragment, generating other areas of reentry. The location and size of these tachycardias can vary. The circumference of the leading circle around a functional obstacle can be as small as 6 to 8 mm and represents a pathway in which the efficacy of stimulation of the circulating wavefront is just sufficient to excite the tissue ahead, which is still in its relative refractory phase. Therefore conduction through the functional reentrant circuit is slowed because impulses are propagating in partially refractory tissue. Consequently, this form of functional reentry has a partially excitable gap. The reentry CLs are therefore significantly dependent on the refractory period of the involved tissue.²⁹

The mechanisms for functionally determined reentrant circuits include the leading circle type of reentry, anisotropic reentry, and spiral wave reentry. Functional circuits can be associated with ordered reentry (the reentrant circuit remains in the same place) or random reentry (the reentrant circuit changes size and location). Random reentry can occur when leading circle reentry causes fibrillation.

Leading circle concept. To explain the properties of a single functional reentrant circuit, Allesie and colleagues formulated the leading circle concept (see Fig. 3.8). It was postulated that during wavefront rotation in tissue without anatomical inexcitable obstacles, the wavefront impinges on its refractory tail and travels through partially refractory tissue. The interaction between the wavefront and the refractory tail determines the properties of functional reentry. In this model, functional reentry involves the propagation of an impulse around a functionally determined region of inexcitable tissue or a refractory core and among neighboring fibers with different EP properties. The tissue within this core is maintained in a state of refractoriness by constant centripetal bombardment from the circulating wavefront. The premature impulse that initiates reentry blocks in fibers with long refractory periods and conducts in fibers with shorter refractory periods and eventually returns to the initial region of block after excitability has recovered there. The impulse then continues to circulate around a central area that is kept refractory because it is bombarded constantly by wavelets propagating toward it from the circulating wavefront. This central area provides a

functional obstacle that prevents excitation from propagating across the fulcrum of the circuit.¹²

The leading circle was defined as “the smallest possible pathway in which the impulse can continue to circulate” and “in which the stimulating efficacy of the wavefront is just enough to excite the tissue ahead which is still in its relative refractory phase.” Thus the “head of the circulating wavefront is continuously biting its tail of refractoriness” and the length of the reentrant pathway equals the wavelength of the impulse; as a result, there is usually no fully excitable gap. Because the wavefront propagates through partially refractory tissue, the conduction velocity is reduced.²⁹

The velocity value and the length of the circuit depend on the excitability of the partially refractory tissue and on the stimulating efficacy of the wavefront, which is determined by the amplitude and upstroke velocity of the action potential and by the passive electrical properties of the tissue (e.g., gap junctional conductance). The partially refractory tissue determines the revolution time period. Because of the absence of a fully excitable gap, this form of reentry is less susceptible to resetting, entrainment, and termination by premature stimuli and pacing maneuvers. Leading circle reentry is thought to be the underlying mechanism of AF and VF and of at least some of the ventricular arrhythmias associated with acute ischemia.

Anisotropic reentry. Anisotropy refers to directionally dependent conduction velocity. Isotropic conduction is uniform in all directions; anisotropic conduction is not. Anisotropy is a normal feature of heart muscle and is related to the differences in longitudinal and transverse conduction velocities, which are attributable to the lower resistivity of myocardium in the longitudinal (parallel to the long axis of the myocardial fiber bundles) versus the transverse direction (see eFig. 1.1). Anisotropy in myocardium composed of tissue with structural features different from those of adjacent tissue results in heterogeneity in conduction velocities and repolarization properties (see later discussion), which can lead to conduction slowing or block, thereby setting the stage for reentry (referred to as anisotropic reentry).

Unlike the functional characteristic that leads to the leading circle type of reentry (differences in refractoriness in adjacent areas caused by local differences in membrane properties), the functional characteristic that is important in functional reentry caused by anisotropy is the difference in effective axial resistance to impulse propagation dependent on fiber direction. In its pure form, the unidirectional conduction block and slow conduction in the reentrant circuit result from anisotropic, discontinuous propagation, and there is no need for variations in membrane properties, such as regional differences in refractoriness or depression of the resting and action potentials.

Anisotropic circuits are elliptical or rectangular because of the directional differences in conduction velocities, with the long axis of the ellipse in the fast longitudinal direction and a central line of functional block parallel to the long axis of fibers. Circuits with this shape can have a smaller dimension than circular circuits, such as the leading circle. Reentrant circuits caused by anisotropy also can occur without well-defined anatomical pathways and may be classified as functional.

Anisotropic reentrant circuits usually remain in a fixed position and cause ordered reentry. The degree of anisotropy (i.e., the ratio of longitudinal to transverse conduction velocity) varies in different regions of the heart, and the circuit can reside only in a region in which the conduction transverse to the longitudinal axis is sufficiently slow to allow reentry. Stability of anisotropic reentrant circuits is also assisted by the presence of an excitable gap, which does not occur in the leading circle functional circuit. The excitable gap is caused by the sudden slowing of conduction velocity and a decrease in the wavelength of excitation as the reentrant impulse turns the corner from the fast longitudinal direction to the slow transverse direction and from the slow

transverse direction to the fast longitudinal direction. Anisotropic reentry is typically initiated by a premature stimulus that blocks in the direction of propagation parallel to the long axis of the cells and then propagates slowly in the transverse direction of fiber orientation because of high axial resistance (see later).

Anisotropic reentry can potentially provide the substrate for sustained VT that occurs in the epicardial border zone region of healed infarcts, where viable normal myocytes are intermingled with islands of fibrous connective tissue that separate muscle fiber bundles preferentially in the longitudinal direction and decrease the density of side-to-side junctional connections, therefore creating nonuniform anisotropy.

Figure-of-8 reentry. The model of “figure-of-8” or “double-loop” reentry involves two concomitant excitation wavefronts circulating in opposite directions, clockwise and counterclockwise, around a long line of functional conduction block rejoining on the distal side of the block. The wavefront then breaks through the arc of block to reexcite the tissue proximal to the block. The single arc of block is thus divided into two, and reentrant activation continues as two circulating wavefronts that travel clockwise and counterclockwise around the two arcs in a pretzel-like configuration. This form of reentry has been shown in atrial and ventricular myocardia.¹²

Figure-of-8 reentry can also occur when two adjacent anatomical obstacles are located transverse to the direction of propagation, with only a small gap (isthmus) of low excitability in between. The activation wavefront blocks anterogradely in the gap and bifurcates into two distinct activation wavefronts skirting the two anatomical obstacles in clockwise and counterclockwise directions. The two wavefronts coalesce at the opposite side of the gap; the convergence increases the source/sink ratio, allowing the activation to propagate retrogradely through the gap and initiate reentry (Fig. 3.10; Video 3.1).^{30,31}

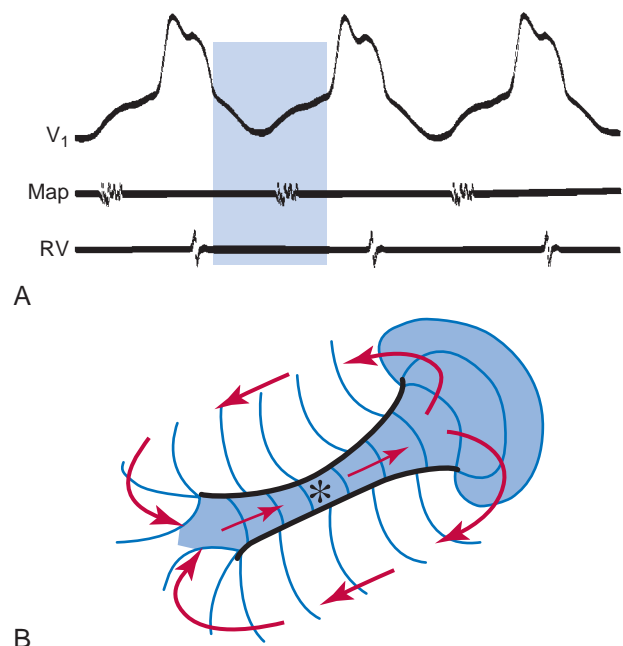
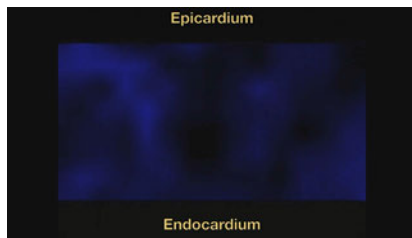


Fig. 3.10 Figure-of-8 Reentry. (A) Electrocardiographic and intracardiac recordings from a left ventricular mapping catheter (*Map*) and the right ventricle (*RV*) are shown during scar-based ventricular tachycardia. (B) A stylized tachycardia circuit is shown in which propagation proceeds through a central common pathway (*small arrows and asterisk*) constrained by scar or other barriers and then around the outside of these same barriers. Activation in the circuit during electrical diastole is shaded (also in A).



Video 3.1 Reentrant Ventricular Tachycardia. Optical Mapping. Optical mapping of sustained reentrant ventricular tachycardia in an isolated wedge of ventricular wall from a dog with a previous infarct. The presence of transmural dispersion of excitability and refractoriness provided the substrate for transmural reentry during epicardial stimulation. Activation initiated in the epicardium blocks laterally in the epicardium, conducts transmurally to the endocardium, propagates laterally in the endocardium, and returns to the epicardium to complete reentrant loops (figure-of-8 reentry).

Reflection. Reflection is a special subclass of reentry in which the excitation wavefront does not require a circuit but appears to travel back and forth in a linear segment of tissue (e.g., trabecula or Purkinje fiber) containing an area of conduction block (see Fig. 3.8). In such a situation an action potential propagates toward, but not through, the inexcitable zone. Subsequently, an electrotonic current conducts passively (i.e., without eliciting an action potential) through the inexcitable zone toward the distal portion of the pathway. If the inexcitable zone is sufficiently small and the magnitude of the electrotonic current is sufficiently large, the segment of tissue distal to the blocked area will be excited (i.e., an action potential is elicited) but with a significant delay. The action potential generated in the distal portion of the pathway will then cause electrotonic current to flow back through the inexcitable zone toward the proximal region. Provided the proximal portion of the conduction pathway recovers quickly enough, this current may be sufficient to elicit a second action potential on the proximal side of the inexcitable zone, which propagates in the opposite direction to the first action potential, thus giving the appearance that the inexcitable zone has reflected the initial action potential.

A different model of reflection (“expansion-type reflection”) was recently demonstrated, whereby the activation wavefront propagates through a narrow isthmus region to stimulate a larger number of cells in the expanded distal region. The source-sink mismatch causes the direction of electrotonic currents to be reversed, and the delayed depolarization in the distal region provides enough time to generate an action potential in the proximal region, and hence acts as the source of reflection.^{1,32}

Because reflection can occur within areas of tissue as small as 1 to 2 mm², it is likely to appear of focal origin. Its identification as a mechanism of arrhythmia may be difficult even with very high spatial resolution mapping of the electrical activity of discrete sites. Reflections may be responsible for premature cardiac contractions and may initiate fatal cardiac arrhythmias such as VT and VF.

Phase 2 reentry. As discussed in Chapter 1, substantial differences in the expression levels of ion channels underlie the substantial heterogeneity in action potential duration and configuration between cardiomyocytes across the ventricular wall. Heterogeneity in the distribution of the transient outward I_K (I_{to}) channels across the myocardial wall, being more prominent in ventricular epicardium than endocardium, results in the shorter duration and the prominent phase 1 notch and the “spike and dome” morphology of the epicardial action potential as compared with the endocardium. The resultant transmural voltage gradient during the early phases (phases 1 and 2) of the action potential is thought to be responsible for the inscription of the J wave on the surface ECG (see Fig. 31.9). A significant outward shift of currents, secondary to either a decrease in the inward currents (I_{Na} and I_{CaL}) or an increase in the outward I_K (I_{to} , I_{Kr} , I_{Ks} , I_{KACH} , I_{KATP}), or both, can cause partial or complete loss of the dome of the action potential in the epicardium that leads to exaggeration of transmural voltage gradient and dispersion of repolarization between the epicardium and endocardium. The type of the ion current affected and its regional distribution in the ventricles determine the particular phenotype (including the Brugada syndrome, early repolarization syndrome, hypothermia-induced ST segment elevation, and infarction-induced ST segment elevation).¹⁰

In this setting the phase 2 dome (plateau) of the action potential can potentially propagate from regions where it is preserved (midmyocardium and endocardium) to regions where it is abolished (epicardium), thus causing local reexcitation (phase 2 reentry) and the generation of a closely coupled extrasystole that, in turn, can initiate VT or VF (see Fig. 31.10).

Spiral wave (rotor) activity. The leading circle concept was based on properties of impulse propagation in a one-dimensional tissue that forms a closed pathway (e.g., a ring). The concept was a major breakthrough in the understanding of the mechanisms of reentrant excitation. However, it became evident that these considerations alone do not fully describe wave rotation in two- and three-dimensional cardiac tissue.^{10,33}

Spiral waves typically describe reentry in two dimensions. The three-dimensional representation of the spiral wave is called a “scroll wave.” The center of the spiral wave is called the core, and the distribution of the core in three dimensions is referred to as the filament, which is formed by the revolving trajectory of the spiral tip. The term *rotor* initially described the rotating source, and the spiral wave defined the shape (i.e., curvature) of the wave emerging from the rotating source. In many publications, this difference has been blurred, and terms used in the literature include *rotors*, *vortices*, and *reverberators*.^{12,34,35}

Propagation of two- and three-dimensional waves depends on wavefront curvature, a property that is not present in one-dimensional preparations (Fig. 3.11). The curvature of an activation wavefront influences the source-sink balance; convex wavefronts have a smaller source and a larger sink, whereas flat wavefronts have source-sink balance. As a result, a planar wavefront propagates faster than a convex wavefront. As curvature of a wavefront increases, conduction velocity decreases; with sufficient curvature, propagation fails. Because the maximal velocity of a convex rotating wavefront can never exceed the velocity of a planar wavefront and the period of rotation remains constant in a stable rotating wave, the velocity has to decrease from the periphery (where the highest value corresponds to linear velocity) to the center of a rotating wave. As a consequence, any freely rotating wave in an excitation-diffusion system has to assume a spiral shape.¹⁹

The curvature of the rotating spiral waves progressively increases (and the conduction velocity progressively decreases) toward the tip near the spiral center (the core). At the tip the convex curvature reaches a critical value, forming a singularity point (rotor) that organizes the reentrant spiral wave activity. At the singularity point the curvature is so extreme that makes it impossible for the activity to invade the core. Therefore, instead of moving farther into the center, the rotor spins in the myocardium at high speed around a core of unexcited (rather than refractory) tissue, organizing the electrical activity around it in the form of spiral waves.^{28,34,35}

A prominent curvature of the spiral wave is generally encountered following a wave break, a situation in which a planar wave encounters an anatomical or functional obstacle with sharp edges and breaks up into two or more daughter waves (so-called vortex shedding). Because it has the greatest curvature, the broken end of the wave moves most slowly along a complex trajectory and radiates waves into the surrounding medium. Activation waves propagate radially from the rotor core producing a spiral wave. If the edge of this spiral wave encounters unexcitable tissue, then it will break, giving rise to daughter spirals. As the spinning rate increases, the turbulence and spiral wave fractionation around the rotor increase. This can exhibit complex reentry patterns in which multiple meandering spiral waves divide to form daughter waves while others are simultaneously annihilated, resulting in disorganized electrical activity.^{28,30,34}

Because the slow activation by a rotor is not dependent on conduction in relatively refractory myocardium, an excitable gap can exist, despite the functional nature of reentry. This type of functional reentrant excitation does not require any inhomogeneities of refractory periods as in leading circle reentry, inhomogeneities in conduction properties as in anisotropic reentry, or a central obstacle, whether functional or anatomical. The heterogeneity that allows initiation can result from a previous excitation wave and the pattern of recovery from that wave. Even though nonuniform dispersions of refractoriness or anisotropy

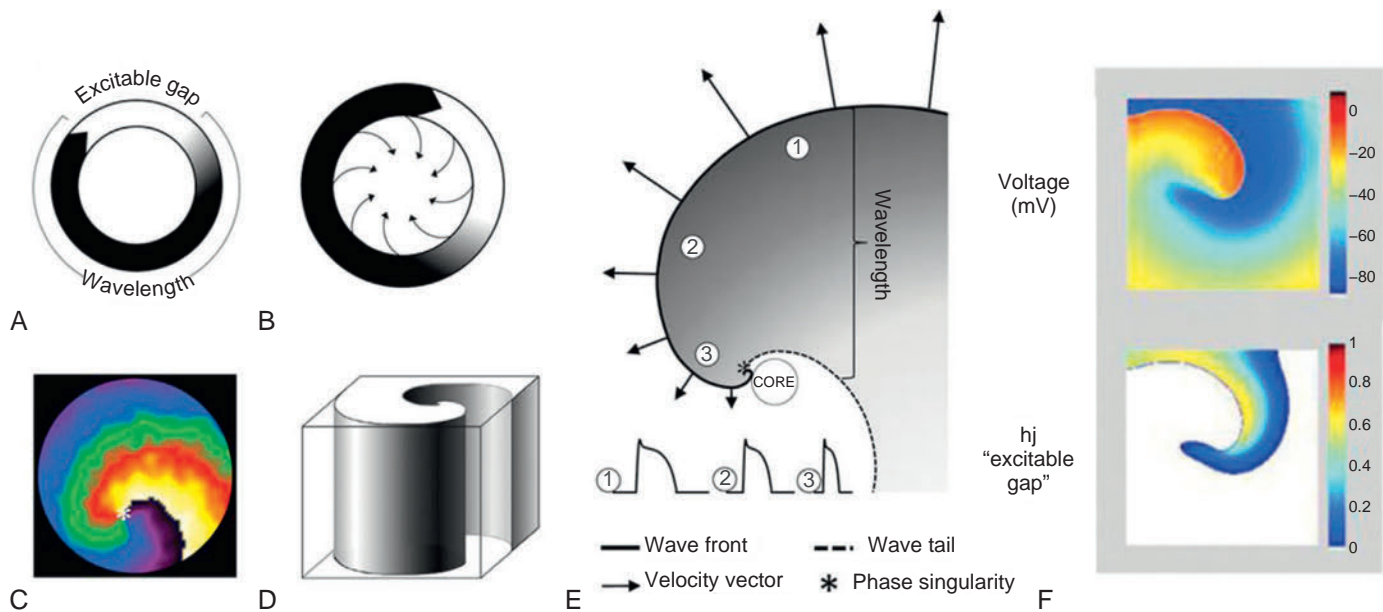


Fig. 3.11 Rotors and Spirals, Basic Concepts. (A) Schematic representation of reentry around a ringlike anatomic obstacle where the wavelength (black) is shorter than the path length, allowing for a fully excitable gap (white). (B) Leading circle reentry, in which activation propagates around a functionally refractory core. (C) Color phase map of a two-dimensional spiral wave, along with the rotor tip at the center (asterisk). (D) Schematic of a three-dimensional scroll wave. (E) Snapshot of the spiral wave: electrotonic effects of the core decrease conduction velocity (arrows), action potential duration (representative examples shown from positions 1, 2, and 3), and wavelength (the distance from the wavefront [black line] to the wave tail [dashed line]). Conduction velocity decreases and wavefront curvature becomes more pronounced, near the rotor, which is a phase singularity at the point where the wavefront and the wave tail meet (asterisk). (F) Computer simulation of reentry. *Top*, Snapshot of the transmembrane voltage distribution during simulated reentry in chronic atrial fibrillation conditions in a two-dimensional sheet incorporating human atrial ionic math models. *Bottom*, Snapshot of inactivation variables of sodium current (h_j) during reentry. (From Pandit SV, Jalife J. Rotors and the dynamics of cardiac fibrillation. *Circ Res*. 2013;112:849–862.)

are not necessary for the initiation of reentrant excitation caused by rotors in excitable media, the myocardium, even when normal, is never homogeneous, and anisotropy and anatomical obstacles can modify the characteristics and spatiotemporal behavior of the spiral. Because cells at the core are unexcited, a voltage gradient develops and establishes a continuous electronically mediated repolarizing influence on excited cells in the immediate core vicinity, shortening their action potential duration.^{28,35}

The location of the rotor can occur wherever the second stimulated excitation encounters the wake of the first excitation with the appropriate characteristics. Rotors can be stationary, continuously drift or migrate away from their origin, or anchored, initially drifting and then becoming stationary by anchoring to an anatomical obstacle. This depends on the electrical (e.g., wavelength) and structural (e.g., fibrosis) properties of the tissue in which they occur.²⁸

In the heart, both two-dimensional spiral waves and three-dimensional scroll waves have been implicated in the mechanisms of reentry in atrial and VT and fibrillation.¹⁹ Monomorphic VT results when the spiral wave is anchored within the ventricular myocardium and cannot drift away from its origin. In contrast, a polymorphic VT, such as the torsades de pointes encountered with LQTS, is thought to be caused by a meandering or drifting spiral wave. VF seems to be the most complex representation of rotating spiral waves in the heart. VF develops when the single spiral wave responsible for VT breaks up, leading to the development of multiple spirals that are continuously extinguished and recreated.^{34–36}

Excitable Gaps in Reentrant Circuits

Wavelength Concept

The *wavelength* is defined as the product of the conduction velocity of the circulating excitation wavefront and the refractory period of the tissue in which the excitation wavefront is propagating. The wavelength quantifies how far the impulse travels relative to the duration of the refractory period. The wavelength of the reentrant excitation wavefront must be shorter than the length of the pathway of the potential reentrant circuit for reentrant excitation to occur; that is, the impulse must travel a distance during the refractory period that is less than the complete reentrant path length to give myocardium ahead of it sufficient time to recover excitability. Slowing of impulse conduction or shortening of refractoriness shortens the wavelength and increases the excitable gap.

For almost all clinically important reentrant arrhythmias resulting from ordered reentry and in the presence of uniform, normal conduction velocity along the potential reentrant pathway, the wavelength would be too long to permit reentrant excitation. Thus almost all these arrhythmias must have, and do have, one or more areas of slow conduction as a part of the reentrant circuit. The associated changes in conduction velocity, as well as associated changes in refractory periods, actually cause the wavelength to change in different parts of the circuit. However, the presence of one or more areas of slow conduction permits the average wavelength of reentrant activation to be shorter than the path length.

The wavelength concept is a good predictive parameter of arrhythmia inducibility. A decrease in conduction velocity or shortening of

refractoriness results in a decrease in the wavelength or lessening of the amount of tissue needed to sustain reentry. This situation favors initiation and maintenance of reentry. In contrast, an increase in conduction velocity or prolongation of refractoriness prolongs the wavelength of excitation, and in this situation a larger anatomical circuit is necessary to sustain reentry. If a larger circuit is not possible, initiation or maintenance of tachycardia cannot occur.

Excitable Gaps

The excitable gap in a reentrant circuit is the region of excitable myocardium that exists between the head of the reentrant wavefront and the tail of the preceding wavefront and, at any given time, is no longer refractory (i.e., is capable of being excited) if the excitation wavelength is shorter than the length of the reentrant circuit (Fig. 3.12).

The occurrence of an excitable gap is dependent on the recovery of excitability of the myocardium from its previous excitation by the reentrant wavefront. A fully excitable gap is defined as the segment of the reentrant circuit in which the tail of the preceding wavefront does not affect the head and velocity of the following wavefront (i.e., absence of head-tail interaction). A partially excitable gap is defined as the zone where the rotating wave can be captured by local stimulation in the presence of head-tail interaction. Although the excitable gap denotes a length of a segment within the reentrant circuit, the fully or partially excitable period denotes the time period during which a segment within the reentrant circuit is fully or partially excitable, respectively (see Fig. 3.12).

There are two different measurements of the excitable gap. The spatial excitable gap is the distance (in millimeters) of excitability occupied at any moment of time in the circuit ahead of the reentrant wavefront. On the other hand, the temporal excitable gap is the time interval (in milliseconds) of excitability between the head of activation of one impulse and the tail of refractoriness of the prior impulse. Both the spatial and temporal gaps can be composed of partially excitable or fully excitable myocardium, depending on the time interval between successive excitations of the circuit. The size of the spatial gap and the duration of the temporal gap vary in different parts of the circuit as the wavelength of the reentrant impulse changes because of changes in conduction velocity, refractory periods, or both.

The characteristics of the excitable gap can be different in different types of reentrant circuits. Many anatomically determined reentrant circuits have large excitable gaps with a fully excitable component, although the gap can sometimes be only partially excitable. On the other hand, functional reentrant circuits caused by the leading circle

mechanism have very small gaps that are only partially excitable, although parts of some functionally determined reentrant circuits (anisotropic reentrant circuits) can have fully excitable gaps. An excitable gap has been shown to occur during AF, VF, and AFL; these are examples of arrhythmias caused by functional reentrant mechanisms, possibly including spiral waves. The relationship between the excitable gap and the excitable period can be complex if the velocity of propagation changes within the reentry circuit.

The existence and extent of an excitable gap in a reentrant circuit have important implications. The presence of an excitable gap enables modulation of the frequency of a reentrant tachycardia by a locally applied stimulus or by field stimulation; the longer the excitable gap, the more likely an extrastimulus will be able to enter the reentrant circuit and reset or terminate the arrhythmia. Termination of arrhythmias by stimulation would be expected to be much more difficult when the reentrant circuit has only a small partially excitable gap. In addition, the excitable gap can influence the effects of drugs on the reentrant circuit, so that reentry with a partially excitable gap and mainly functional components may respond more readily to drugs that prolong repolarization, without slowing conduction. In contrast, fixed anatomical reentry with a large excitable gap responds to drugs that decrease conduction velocity, preferentially at pivot points.

The properties of the excitable gap influence the characteristics of arrhythmias caused by reentry. Arrhythmias caused by leading circle reentry, in which the wavefront propagates in the just-recovered myocardium of the refractory tail and in which there is only a small partially excitable gap, are inherently unstable and often terminate after a short period or go on to fibrillation. On the other hand, the reentrant wavefront in anatomical and nonuniform anisotropic reentry circuits generally is not propagating in myocardium that has just recovered excitability, and the excitable gap can be large. This property can contribute to the stability of these reentrant circuits.

Resetting Reentrant Tachycardias

Basic Principles of Resetting

Resetting is the interaction of a premature wavefront with a tachycardia, resulting in either advancement (acceleration) or delay of the subsequent tachycardia beat. The extrastimulus is followed by a pause that is less (or more) than fully compensatory before resumption of the original rhythm. The tachycardia complexes that return first should have the same morphology and CL as the tachycardia before the extrastimulus, regardless of whether single or multiple extrastimuli are used. The resetting phenomenon can easily be recognized by comparing the intervals encompassing the extrastimuli with the tachycardia cycle length (TCL). If they differ from twice the TCL (in the case of a single extrastimulus) or from 3 times the TCL (in the case of double extrastimuli) the tachycardia has been reset.^{37,38}

The introduction of a single extrastimulus (S_2) during a tachycardia yields a return cycle (S_2X_3) if the tachycardia is not terminated (Fig. 3.13). If S_2 does not affect the arrhythmogenic focus, the coupling interval (X_1S_2) plus the return cycle (S_2X_3) will be equal to twice the tachycardia cycle ($2 \times [X_1X_1]$); that is, a fully compensatory pause will occur. Resetting of the tachycardia occurs when a less than fully compensatory pause occurs. In this situation, $X_1S_2 + S_2X_3$ will be less than $2 \times (X_1X_1)$, as measured from the surface ECG. TCL stability should be taken into account when the return cycle is measured. To account for any TCL instability, at least a 20-millisecond shortening of the return cycle is required to demonstrate resetting.

When more than a single extrastimulus is used, the relative prematurity should be corrected by subtracting the coupling interval or intervals from the spontaneous tachycardia cycles when the extrastimuli are delivered.

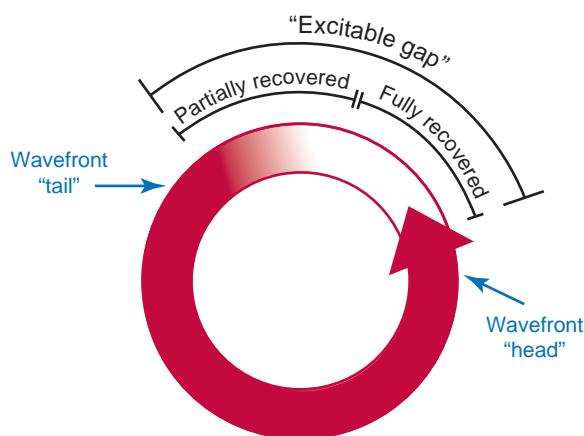


Fig. 3.12 Excitable Gap of Recovered Tissue in Anatomically Determined Reentry.

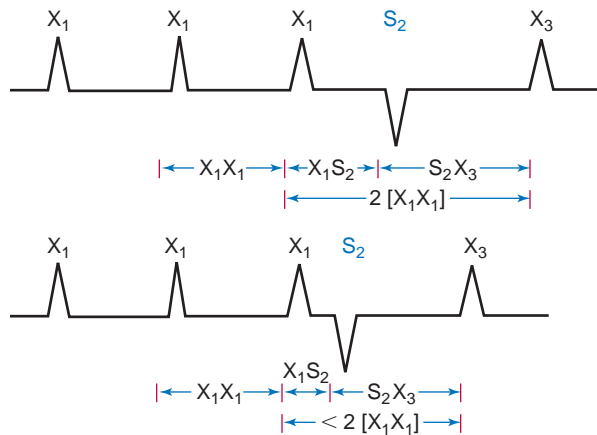


Fig. 3.13 Response of Tachycardia to a Single Extrastimulus (S_2). The tachycardia cycle length is $[X_1X_1]$. The coupling interval of the extrastimulus is $[X_1S_2]$. The return cycle length of the first complex of tachycardia after the extrastimulus is $[S_2X_3]$. In the top portion of the figure, the extrastimulus does not affect the tachycardia circuit, and a compensatory pause occurs. Resetting (i.e., advancement) of the tachycardia is shown at the bottom of the figure. (From Frazier DW, Stanton MS. Resetting and transient entrainment of ventricular tachycardia. *Pacing Clin Electrophysiol.* 1995;18:1919.)

To reset a reentrant tachycardia, the stimulated wavefront must reach the reentrant circuit, encounter excitable tissue within the circuit (i.e., enter the excitable gap of the reentrant circuit), collide in the antidromic (retrograde) direction with the previous tachycardia impulse, and continue in the orthodromic (anterograde) direction to exit at an earlier than expected time and perpetuate the tachycardia (Fig. 3.14). If the extrastimulus encounters fully excitable tissue, which commonly occurs in reentrant tachycardias with large excitable gaps, the tachycardia will be advanced by the extent that the stimulated wavefront arrives at the entrance site prematurely. If the tissue is partially excitable, which can occur in reentrant tachycardias with small or partially excitable gaps or even in circuits with large excitable gaps when the extrastimulus is very premature, the stimulated wavefront will encounter some conduction delay in the orthodromic direction within the circuit (see Fig. 3.14). Therefore the degree of advancement of the next tachycardia beat depends on both the degree of prematurity of the extrastimulus and the degree of slowing of its conduction within the circuit. The reset tachycardia beat consequently can be early, on time, or delayed.^{37,38}

Termination of the tachycardia occurs when the extrastimulus collides with the preceding tachycardia impulse antidromically and blocks in the reentrant circuit orthodromically (see Fig. 3.14). This occurs when the extrastimulus enters the reentrant circuit early in the relative refractory period; it fails to propagate in the anterograde direction because it encounters absolutely refractory tissue. In the retrograde direction, it encounters increasingly recovered tissue and can propagate until it encroaches on the circulating wavefront and terminates the arrhythmia.

Resetting does not require that the pacing site be located within the reentrant circuit. However, the closer the pacing site is to the circuit, the less premature a single extrastimulus can be and reach the circuit without being extinguished by collision with a wave emerging from the circuit. The longest coupling interval for an extrastimulus to be able to reset a reentrant tachycardia depends on (1) the TCL; (2) the duration of the excitable gap of the tachycardia; (3) refractoriness at the pacing site; and (4) the conduction time from the pacing site to the reentrant circuit.

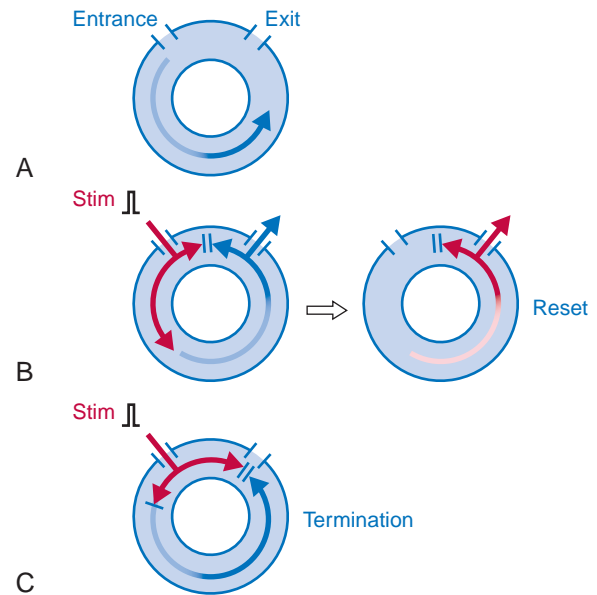


Fig. 3.14 Response of Reentrant Tachycardia to Premature Stimulation. (A) Schematic representation of the reentrant circuit is illustrated with separate entrance and exit sites. During tachycardia, a wavefront is shown propagating through the tissue of the reentrant circuit (arrow). The dark portion of the arrow represents fully refractory tissue, and the fading portion represents partially refractory tissue. (B) A premature stimulus (Stim) introduced during the tachycardia results in a wavefront of depolarization (red arrow), which enters the reentrant circuit and conducts anterogradely over fully excitable tissue while it collides retrogradely with the already propagating wavefront (blue arrow). The premature wavefront (red arrow) then propagates around the circuit to the exit site, thus leading to the less than compensatory pause and resetting of the tachycardia. (C) A more premature extrastimulus (Stim) results in a wavefront of depolarization (red arrow), which enters the circuit at a time when it collides retrogradely with the previously propagating wavefront (blue arrow) and encounters anterograde tissue incapable of sustaining further propagation. As a result, circus movement in the circuit is extinguished, and tachycardia terminates. (From Rosenthal ME, Stamato NJ, Almendral JM, et al. Coupling intervals of ventricular extrastimuli causing resetting of sustained ventricular tachycardia secondary to coronary artery disease: relation to subsequent termination. *Am J Cardiol.* 1988;61:770.)

When refractoriness of the intervening tissue between the pacing site and the reentrant circuit limits the ability of an extrastimulus to reach the reentrant circuit with adequate prematurity, the use of double extrastimuli can be helpful. The first extrastimulus, although it does not reset the tachycardia, it does shorten the local refractory period at the stimulus site and reverse the activation sequence in part of the intervening tissue, allowing the second extrastimulus to access and interact with the reentrant circuit with a greater degree of prematurity at comparable coupling intervals. Another advantage of using double extrastimuli is that it allows the longest potential coupling interval of the second extrastimulus to be delivered following the first (conditioning) extrastimulus, so that it interacts with the circuit with the lowest possible prematurity.^{37,39}

Resetting zone and excitable gap. For an extrastimulus to be able to reset the reentrant circuit, it has to penetrate the circuit during its excitable gap. The difference between the longest and shortest coupling intervals resulting in resetting is defined as the *resetting interval* or *resetting zone*. Thus the coupling intervals over which resetting occurs, the resetting zone, can be considered a measure of the duration of the temporal excitable gap existing in the reentrant circuit. Hence the entire

extent of the fully excitable gap would be the zone of coupling intervals from the onset of tachycardia resetting until tachycardia termination. However, the excitable gap can be underestimated by using only a single extrastimulus or by using single or double extrastimuli in the absence of tachycardia termination by the extrastimuli.³⁷

All tachycardias reset by a single extrastimulus can be reset by double extrastimuli, unless tachycardia termination occurs. Double extrastimuli produce resetting over a longer range of coupling intervals and should therefore be used to characterize the excitable gap of the reentrant circuit more fully. During EP testing, only the temporal excitable gap of the entire circuit can be evaluated. It is impossible to assess the conduction velocity and refractoriness at any point in the circuit, which certainly must vary, with available technology.

Return cycle. The return cycle is the time interval from the resetting stimulus to the next excitation of the pacing site by the new orthodromic wavefront. This corresponds to the time required for the stimulated impulse to reach the reentrant circuit, conduct through the circuit, exit the circuit, and travel back to the pacing site. The noncompensatory pause following the extrastimulus and the return cycle are typically measured at the pacing site; however, they may also be measured to the onset of the tachycardia complex on the surface ECG.

When the return cycle is measured from the extrastimulus producing resetting to the onset of the first return tachycardia complex on the surface ECG, conduction time into the tachycardia circuit is incorporated into that measurement. Conduction time between the pacing site and the tachycardia circuit may or may not be equal to that from the circuit to the pacing site. Differences in location of the site of stimulation, as well as the tachycardia circuit entrance and exit, can result in differences in conduction time to and from the pacing site.

Orthodromic and antidromic resetting

Orthodromic resetting. Orthodromic resetting occurs when the premature stimulus traverses the reentrant circuit, including the zone of slow conduction, in the same direction as the spontaneous tachycardia impulse and with an identical exit site. Intracardiac areas that are orthodromically reset are advanced by the premature extrastimulus but retain the same morphology because they are activated from the impulse emerging from the same reentrant circuit exit site. The conduction interval from the pacing stimulus to the orthodromically captured electrogram exceeds the TCL by the time required for the extrastimulus to travel from the pacing site to the reentrant circuit. Thus an orthodromic resetting response implies that the pacing site is located proximal to a region of slow conduction in the reentry circuit and that the recording site is located distal to this region. The ability to demonstrate orthodromic resetting is critically dependent on the location of pacing and recording electrodes relative to the region of slow conduction in the circuit. Therefore failure to demonstrate an orthodromic resetting response does not exclude reentry with an excitable gap as a possible tachycardia mechanism.³⁷

Antidromic resetting. Antidromic resetting occurs when intracardiac sites are directly captured by the premature stimulus without traversing the reentrant circuit and the zone of slow conduction. Therefore antidromic resetting of intracardiac sites occurs with a conduction interval from the pacing stimulus to the captured electrogram that is less than the TCL and with differing morphology of the captured as compared with the spontaneous electrogram. Although demonstration of an antidromic resetting response can indicate a tachycardia mechanism other than reentry, an antidromic resetting pattern can also be observed during reentry with an excitable gap if the pacing site is located distal to a region of slow conduction in the reentry circuit. Conversely, if the recording sites are located in regions activated proximal to a region of slow conduction, an antidromic resetting response will be observed.

Resetting Response Curves

Response patterns during resetting are characterized by plotting the coupling interval of the extrastimulus producing resetting versus the return cycle measured at the pacing site. Alternatively, the return cycle is measured to the onset of the first tachycardia complex following stimulation on the surface ECG; then, qualitatively similar but quantitatively different response curves are obtained. Demonstration of a noncompensatory pause following the extrastimulus is required, and the interval encompassing the extrastimulus should be 20 or more milliseconds earlier than the expected compensatory pause following a single extrastimulus and 20 or more milliseconds less than three TCLs when double extrastimuli are used. As always, it is important to establish the stability of TCL before assessing any perturbation in tachycardia presumed to be caused by resetting.^{37,38}

Four resetting response patterns are possible (Fig. 3.15):

1. Flat response pattern: The return cycle is constant (less than a 10-millisecond difference) over a 30-millisecond range of coupling intervals.

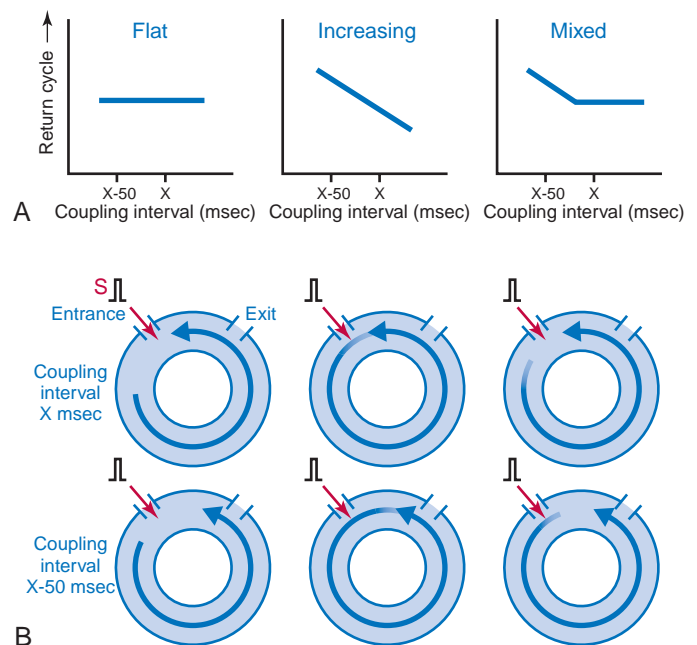


Fig. 3.15 Mechanisms of Various Resetting Response Patterns. (A) Schemas of three types of resetting response curves. (B) A theoretical mechanism of resetting patterns in response to extrastimuli at coupling intervals of X and X-50 milliseconds. The reentrant circuit is depicted as having a separate entrance and exit in each pattern. Each tachycardia wavefront is followed by a period of absolute refractoriness (blue arrow), which is then followed by a period of relative refractoriness (fading tail of the arrow) of variable duration. On the left side, a flat curve results when the stimulated wavefront reaches the tachycardia circuit and finds a fully excitable gap between the head and tail of the tachycardia wavefront. The gap is still fully excitable at a coupling interval of X-50. Therefore the conduction time from the entrance to exit is the same. An increasing curve is shown in the middle; this results when the initial stimulated wavefront enters the reentrant circuit when the excitable gap is partially refractory. The curve continues to increase at a coupling interval of X-50 because the tissue is still in a relative refractory state. A mixed curve (right side) results when the less premature extrastimuli find the reentrant circuit fully excitable, whereas the more premature one (at coupling intervals of X-50) finds it in the relative refractory period. (From Josephson ME. Recurrent ventricular tachycardia. In: Josephson ME, ed. *Clinical Cardiac Electrophysiology*. 3rd ed. Philadelphia: Lippincott Williams & Wilkins; 2004:425–610.)

2. Increasing response pattern: The return cycle increases as the coupling interval increases.
3. Decreasing response pattern: The return cycle decreases as the coupling interval increases.
4. Mixed response pattern: This pattern meets the criteria for a flat response at long coupling intervals and for an increasing response at shorter coupling intervals.

Triggered rhythms secondary to DADs usually have a flat or decreasing response. A flat response can be observed in automatic, triggered, or reentrant rhythms.

Occasionally, a response pattern to a single extrastimulus cannot be characterized because resetting occurs over too narrow a range of coupling intervals as a result of significant variability of the baseline TCL or of variability in the return cycle. In all cases in which a single extrastimulus resets the tachycardia, double extrastimuli from the same pacing site produce an identical or expected resetting curve. Thus, if a single extrastimulus produces a flat curve, double extrastimuli will produce a flat or mixed curve. If a single extrastimulus produces an increasing or mixed curve, double extrastimuli will produce the same curve.

The types of resetting curves can vary depending on the site of stimulation. Extrastimuli from different pacing sites likely engage different sites in the reentrant circuit that are in different states of excitability or refractoriness and therefore result in different conduction velocities and resetting patterns.

Flat response curves in reentrant rhythms. A flat resetting curve implies the presence of a fully excitable gap within the reentrant circuit over a range of coupling intervals. The total duration of the excitable gap should exceed the range of coupling intervals that produce resetting with a flat response. Large excitable gaps are more likely to result in flat response curves, because the increasingly premature extrastimuli are less likely to encroach on the trailing edge of refractoriness and encounter decremental conduction (see Fig. 3.15). The flat return cycle also suggests the presence of fixed sites of entrance and exit from the circuit and fixed conduction time from the stimulation site through the reentrant circuit over a wide range of coupling intervals.

If a single extrastimulus produced resetting with a flat response, the response to double extrastimuli would also be flat. However, because the use of double extrastimuli allows engagement of the reentrant circuit at relatively long coupling intervals with greater prematurity, resetting will begin at longer coupling intervals and will continue over a greater range of coupling intervals than observed with a single extrastimulus. Therefore double extrastimuli can produce a flat and then increasing response curve.

Increasing response curves in reentrant rhythms. Increasing resetting curves result from progressively longer return cycles in response to increasingly premature extrastimuli and indicate a zone of decremental slow conduction, usually located within the reentrant circuit. The most probable mechanism underlying the decremental conduction is encroachment of the advancing wavefront from the premature extrastimuli on an increasingly more refractory tissue within the reentrant circuit, most likely within the zone of slow conduction (see Fig. 3.15). This response pattern is possible only for reentrant arrhythmias and is not observed in triggered or automatic rhythms.

Mixed response curves in reentrant rhythms. In a mixed response curve, the initial coupling intervals demonstrate a flat portion of the curve of variable duration (but less than 30 milliseconds), followed by a zone during which the return cycle increases (see Fig. 3.15). Occasionally, a flat curve is seen with a single extrastimulus; it is only by using double extrastimuli that an increasing response can be observed.

Decreasing response curves in reentrant rhythms. Decreasing reset curves are not observed in reentry but can be seen in triggered

rhythms, although flat responses are the most common response for triggered activity. The return cycle in triggered activity is typically 100% to 110% of the TCL.

Resetting With Fusion

Fusion of the stimulated impulse can be observed on surface ECG or intracardiac recordings if the stimulated impulse is intermediate in morphology between a fully paced complex and the tachycardia complex. The ability to recognize ECG fusion requires a significant mass of myocardium to be depolarized by both the extrastimulus and the tachycardia. With early extrastimuli, the paced antidromic wavefront captures all or most of the myocardium prior to the orthodromic wavefront of the tachycardia impulse exiting from the reentrant circuit. Thus no ECG fusion is present, although resetting can occur. With later coupled extrastimuli, the orthodromic wavefront exits from the reentrant circuit, thus capturing a certain portion of myocardium before colliding with the paced antidromic wavefront. In this situation, ECG fusion occurs. Resetting with ECG fusion requires wide separation of the entrance and exit of the reentrant circuit, with the stimulus wavefront preferentially engaging the entrance.³⁷

If presystolic activity in the reentrant circuit is recorded before delivery of the extrastimulus that resets the tachycardia, one must consider this to represent local fusion (eFig. 3.3). Thus an extrastimulus that is delivered after the onset of the tachycardia complex and enters and resets the circuit always demonstrates local fusion. Resetting with local fusion and a totally paced complex morphology provides evidence that the reentrant circuit is electrocardiographically small.

The farther the pacing site from the reentrant circuit, the less likely resetting with ECG fusion will occur because the extrastimulus should be delivered at a shorter coupling interval to reach the circuit with adequate prematurity. Consequently, the stimulated impulse is more likely to capture both the exit and entrance sites and therefore have a purely paced ECG complex morphology without fusion.

Reentrant circuits reset with fusion have a higher incidence of flat resetting curves, longer resetting zones, and significantly shorter return cycles measured from the stimulus to the onset of the tachycardia complex. Resetting with fusion is a potential indication that the pacing site is located proximal to the zone of slow conduction (i.e., prior to the entrance site) within the reentrant circuit, whereas resetting without fusion potentially suggests pacing distal to the zone of slow conduction, because pacing closer to the exit is more likely to capture both the exit and entrance sites and produce resetting without fusion.^{37,38}

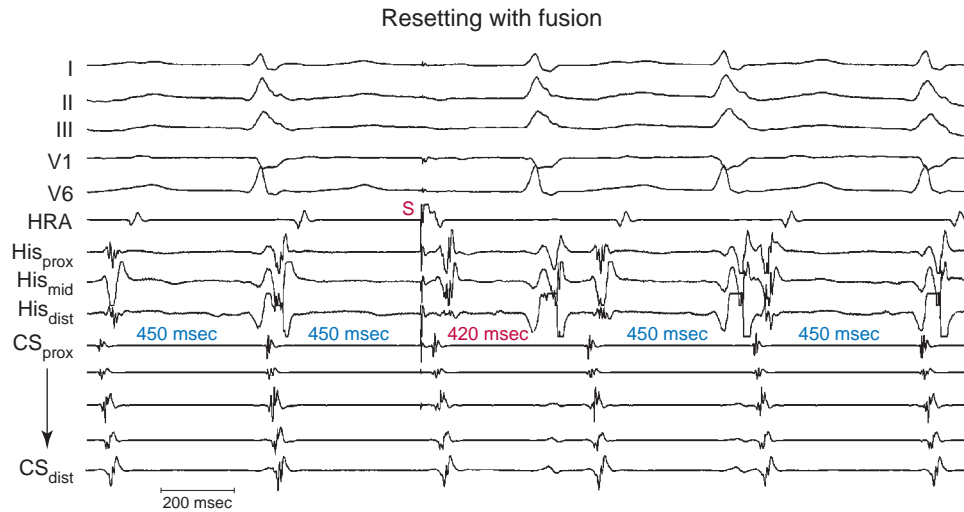
Resetting of Tachycardias With Diverse Mechanisms

Resetting can be demonstrated for tachycardias based on different mechanisms, including reentry, normal or abnormal automaticity, and triggered activity. Although the ability to reset an arrhythmia is not helpful in distinguishing the underlying mechanism, certain features of the resetting response can be useful for the differential diagnosis.

Site specificity of resetting. Triggered activity and automaticity do not demonstrate site specificity for resetting, whereas reentry can. The closer the stimulus to the entrance site in the reentrant tachycardia circuit, the easier it is to reset the tachycardia. Site specificity for resetting is decreased with the use of multiple extrastimuli.

Resetting response curves. Triggered rhythms secondary to DADs usually have a flat or decreasing resetting curve. A flat resetting curve can be seen in automatic, triggered, or reentrant rhythms. Reentrant rhythms never demonstrate a decreasing resetting curve to single or double extrastimuli.

Resetting with fusion. The ability to reset tachycardia after it has begun activating the myocardium (i.e., resetting with fusion) is diagnostic of reentry and excludes automatic and triggered mechanisms.



eFig. 3.3 Resetting With Fusion. An atrial tachycardia is shown with a stable cycle length (450 milliseconds). A single extrastimulus (*S*) is delivered from the high right atrium (*HRA*) that resets or advances the timing of the next cycle (420 milliseconds); however, the coronary sinus (*CS*) electrogram occurs on time when the extrastimulus is delivered. Thus intracardiac fusion is evident when resetting occurs, signifying macroreentry. *dist*, Distal; *mid*, middle; *prox*, proximal.

In automaticity or triggered activity, resetting of the arrhythmia by an extrastimulus requires depolarization of the site of origin by the paced wavefront. Because the entrance and exit sites of focal rhythms (automatic or triggered) are not separate, a tachycardia wavefront cannot exit the focus once the exit or entrance site has already been depolarized and rendered refractory by the paced wavefront.^{37,38}

During automatic or triggered tachycardias, when an extrastimulus is delivered late in the tachycardia cycle, it can collide with the tachycardia impulse exiting the tachycardia focus and produce fusion of a single beat on the surface ECG or intracardiac recordings. However, in this case, resetting cannot occur because the surrounding myocardium is refractory to the advancing extrastimulus (i.e., entrance block occurs). This produces a fully compensatory pause.

Entrainment of Reentrant Tachycardias

Basic Principles of Entrainment

Entrainment of reentrant tachycardias by external stimuli was originally defined in the clinical setting as “an increase in the rate of a tachycardia to a faster pacing rate, with resumption of the intrinsic rate of the tachycardia upon either abrupt cessation of pacing or slowing of pacing beyond the intrinsic rate of the tachycardia” and taken to indicate an underlying reentrant mechanism. The ability to entrain a tachycardia also establishes that the reentrant circuit contains an excitable gap.^{37,38}

Orthodromic resetting and transient entrainment are manifestations of the same phenomenon (i.e., premature penetration of a tachycardia circuit by a paced wavefront), and the ability to demonstrate resetting is a strong indication that entrainment can occur from that specific pacing site. Entrainment is the continuous resetting of a reentrant circuit by a train of capturing stimuli. However, following the first stimulus of the pacing train that penetrates and resets the reentrant circuit, the subsequent stimuli interact with the reset circuit, which has an abbreviated excitable gap.³⁷

During entrainment, each pacing stimulus creates two activation wavefronts, one in the orthodromic direction and the other in the antidromic direction. The wavefront in the antidromic direction collides with the existing tachycardia wavefront. The wavefront that enters the reentrant circuit in the orthodromic direction (i.e., the same direction as the spontaneous tachycardia wavefront) conducts through the reentrant pathway, resets the tachycardia, and emerges through the exit site to activate the myocardium and collide with the antidromically paced wavefront from the next paced stimulus. This sequence continues until cessation of pacing or block somewhere within the reentrant circuit develops. The first entrained stimulus results in retrograde (antidromic) collision between the stimulated and tachycardia wavefronts, whereas for all subsequent stimuli, the collision occurs between the currently stimulated wavefront and the one stimulated previously. Depending on the degree to which the excitable gap is preexcited (and abbreviated) by the first resetting stimulus, subsequent stimuli fall on fully or partially excitable tissue.^{37,38}

Entrainment is said to be present when two consecutive extrastimuli conduct orthodromically through the circuit with the same conduction time while colliding antidromically with the preceding paced wavefront. Because all pacing impulses enter the tachycardia circuit during the excitable gap, each paced wavefront advances and resets the tachycardia. Thus, when pacing is terminated, the last paced impulse will continue to activate the entire tachycardia reentrant circuit orthodromically at the pacing cycle length (PCL) and also will activate the entire myocardium orthodromically on exiting the reentrant circuit.^{37,38}

Overdrive pacing at long PCLs (approximately 10 to 20 milliseconds shorter than the TCL) can almost always entrain reentrant circuits with large flat resetting curves and a postpacing interval (PPI) equal to the return cycle observed during the flat part of the resetting curve. During

overdrive pacing, once the n th pacing stimulus resets the circuit, the following pacing stimulus ($n + 1$)th will reach the circuit more prematurely. Depending on how premature it is, this ($n + 1$)th extrastimulus may produce no change in the return cycle (compared with that in response to the n th extrastimulus), encounter progressive conduction delay (until a fixed, longer return cycle is reached), or terminate the tachycardia. The larger the flat curve observed during resetting and the longer the PCL, the more likely the return cycle of the n th and ($n + 1$)th extrastimuli will be the same. In this case, no matter how many subsequent extrastimuli are delivered, the return cycle will be the same and equal to that observed during the flat portion of the resetting curve. However, if the flat portion of the resetting curve is small or the PCL is short, the ($n + 1$)th extrastimulus will fall on partially refractory tissue and the return cycle will increase. Continued pacing at the same PCL will result in a stable but longer return cycle than the n th extrastimulus or termination of the tachycardia. Consequently, circuits with large fully excitable gaps (i.e., large flat resetting curves) can demonstrate prolonged return cycles or even termination at PCLs equal to coupling intervals of a single extrastimulus demonstrating a fully excitable gap.

Entrainment Response Curves

During entrainment, the orthodromic wavefront of the last extrastimulus propagates around the circuit to become the first complex of the resumed tachycardia. The conduction time of this impulse to the exit site of the circuit is termed the *last entrained interval*, and it characterizes the properties of the reset circuit during entrainment. Measurement of the interval between the last paced extrastimulus to the first nonpaced tachycardia complex (on the surface ECG or presystolic intracardiac electrogram) during entrainment at progressively shorter PCLs characterizes an entrainment response curve, analogous but not identical to resetting response curves with single extrastimuli. In the setting of entrainment the return cycle depends critically on the number of extrastimuli delivered that reset the circuit before the return cycle is measured because following the first extrastimulus producing resetting (the n th extrastimulus), subsequent extrastimuli are relatively more premature and can lead to a different return cycle.³⁷

During entrainment, the return cycle measured at an orthodromically captured presystolic electrogram should equal the PCL regardless of the site of pacing, as long as the presystolic electrogram is orthodromically activated at a fixed stimulus-to-electrogram interval (i.e., fixed orthodromic conduction time). This would not be observed if the electrogram were captured antidromically. If the time from the orthodromically activated electrogram to the onset of the return cycle on the surface ECG remains constant, which is a requirement to prove that the electrogram is within or attached to the reentrant circuit proximal to the exit site, then the interval from the stimulus to the surface ECG complex will remain constant. The same is true for the electrogram measured at the stimulation site. In the absence of recording of a presystolic electrogram, other measurements may be used to characterize the last entrained interval at any PCL. Therefore, during entrainment, curves relating the PCL to the last entrained interval can be measured from the stimulus to the orthodromic presystolic electrogram, to the onset of the surface ECG of the first tachycardia (nonpaced) complex, or to the local activation time at the pacing site of the first tachycardia (nonpaced) complex. These measurements will be qualitatively identical but have different absolute values. As always, it is important to establish the stability of TCL and document the presence of entrainment before assessing the return cycle and PPI.³⁷

Termination is the usual response to overdrive pacing of circuits that demonstrate an increasing curve in response to resetting by a single extrastimulus. However, if the number of extrastimuli following the n th extrastimulus is limited to one or two (especially at long PCLs),

termination may not occur, although the return cycle will be progressively longer following each extrastimulus. Entrainment is not present until two consecutive PPIs are identical. In such cases, when termination does not occur, the return cycle will be longer than that observed if pacing were discontinued following the *n*th extrastimulus at that PCL. Thus, if only the return cycle following entrainment is used to analyze the excitable gap, an increasing curve suggesting decremental conduction can result, even though a flat curve is observed with single or double extrastimuli. Therefore only resetting phenomena describe the characteristics of the reentrant circuit. Entrainment analyzes a reset circuit that has a shorter excitable gap. Flat, mixed (flat and increasing), and increasing curves can be seen during entrainment of macroreentrant circuits. Increasing curves are almost always observed during entrainment of small or microreentrant circuits.

Relationship of Pacing Site and Cycle Length to Entrainment

As with resetting, entrainment does not require the pacing site be located in the reentrant circuit. However, the closer the pacing site is to the circuit, the less premature a single stimulus can be and reach the circuit and, with pacing trains, the fewer the number of stimuli required before a stimulated wavefront reaches the reentrant circuit without being extinguished by collision with a wave emerging from the circuit.

Overdrive pacing can almost always entrain reentrant tachycardias. However, the number of pacing stimuli required to entrain the reentrant circuit depends on the TCL, the PCL, the duration of the excitable gap of the tachycardia, refractoriness at the pacing site, and the conduction time from the stimulation site to the reentrant circuit.

Diagnostic Criteria of Entrainment

Entrainment is the continuous resetting of a tachycardia circuit. Therefore, during constant rate pacing, entrainment of tachycardia results in the activation of all myocardial tissue responsible for maintaining the tachycardia at the PCL, with the resumption of the intrinsic tachycardia morphology and rate after cessation of pacing. Unfortunately, it is almost impossible to document the acceleration of all tissues responsible for maintaining the reentrant circuit to the PCL. Therefore certain criteria have been proposed for establishing the presence of entrainment: (1) fixed fusion of the paced complexes at a constant PCL; (2) progressive fusion or different degrees of fusion at different PCLs (i.e., the surface ECG and intracardiac morphology progressively look more like the purely paced configuration and less like the pure tachycardia complex in the course of pacing at progressively shorter PCLs); (3) when overdrive pacing at a constant PCL during tachycardia results in tachycardia termination, there is the demonstration of localized conduction block to a site (or sites) for one paced beat associated with interruption of the tachycardia, followed by activation of that site (or sites) by the next paced P wave from a different direction and with a shorter conduction time; and (4) during overdrive pacing at two different rates during tachycardia, there is change in conduction time to and electrogram morphology at the electrode recording site.³⁷⁻³⁹ These criteria are discussed in more detail in **Chapter 5**.

Mechanism of Slow Conduction in the Reentrant Circuit

As mentioned earlier, a condition necessary for reentry is that the impulse be delayed sufficiently in the alternative pathway or pathways to allow tissues proximal to the site of unidirectional block to recover excitability. All types of reentrant arrhythmias have a basic feature in common—the wavefront must encounter a zone of tissue where local electrical inhomogeneity is present. This inhomogeneity can be related to electrical properties of the individual cardiac myocyte that generates the action potential (inhomogeneity in electrical excitability or refractoriness), passive properties governing the flow of current among cardiac cells

(cell-to-cell coupling and tissue geometry), or combinations of those conditions. Such changes can be permanent (e.g., in remodeling after ventricular hypertrophy or infarction), or they can be purely functional (e.g., inhomogeneity of refractoriness in acutely ischemic tissue). In addition, some of those changes are needed only to set the initial condition for the deviation of the impulse, the so-called unidirectional conduction block. Once the disturbance is initiated, an arrhythmia can develop in a perfectly homogeneous electrical medium.

Slow conduction within the reentrant circuit is also an important determinant of the size of the reentrant circuit. A decrease in conduction velocity results in a reduction in the wavelength and a lessening of the amount of tissue needed to sustain reentry. In contrast, an increase in conduction velocity prolongs the wavelength of excitation, and hence a larger anatomical circuit is necessary to sustain reentry. If a larger circuit is not possible, initiation or maintenance of tachycardia cannot occur.

In some cardiac tissues (e.g., the AVN), slow conduction is normal physiology. Slow conduction also can be secondary to pathophysiological settings (e.g., MI) or caused by functional properties that can develop as a result of premature stimulation or evolve during a rapid transitional rhythm.

As discussed in **Chapter 1**, action potential propagation and conduction velocity in cardiac tissue are determined by source-sink relationships, which reflect the interplay between the active membrane properties of cardiac cells (the source generating the action potential) and the passive properties determined by architectural features of the myocardium (sink), as well as the coupling resistance between source and sink. The current provided by the source must reach the sink. The pathway between the source and sink includes intracellular resistance (provided by the cytoplasm) and intercellular resistance (provided by the gap junctions). Extracellular resistance plays a role, but it can often be neglected. The coupling resistance is mainly determined by resistance of the gap junctions. Therefore the number and distribution of gap junctions, as well as the conductance of the gap junction proteins (connexins), are important factors for conduction of the action potential.

The safety factor for conduction predicts the success of action potential propagation and is defined as the ratio of the current generated by the depolarizing ion channels of a cell (source) to the current consumed during the excitation cycle of a single cell in the tissue (sink). Thus the safety factor for propagation is proportional to the excess of source current over the sink needs. By this definition, conduction fails when the safety factor drops to less than 1 and becomes increasingly stable as it rises to more than 1. This concept of propagation safety provides information about the dependence of propagation velocity on the state of the ion channels, cell-to-cell coupling, and tissue geometry. In essence, local source-sink relationships determine the formation of conduction heterogeneities and provide conditions for the development of slow conduction, unidirectional block, and reentry.

Reduced Membrane Excitability

Excitability of a cardiac cell describes the ease with which the cell responds to a stimulus with a regenerative action potential, and it depends on the passive and active properties of the cell membrane. The passive properties include the membrane resistance and capacitance and the intercellular resistance. The most important determinant of reduced excitability is the reduced availability of Na⁺ channels. The more negative the membrane potential is, the more Na⁺ channels are available for activation, the greater the influx of Na⁺ into the cell during phase 0, and the greater the conduction velocity. In contrast, membrane depolarization to levels of −60 to −70 mV can inactivate half the Na⁺ channels, and depolarization to −50 mV or less can inactivate all the Na⁺ channels.

Reduced membrane excitability occurs in numerous physiological and pathophysiological conditions. When stimulation occurs during phase 3 (e.g., premature stimulation during the relative refractory period), before full recovery and at less negative potentials of the cell membrane, a portion of Na^+ channels will still be refractory and unavailable for activation (due to prolonged recovery of Na^+ channels from inactivation). As a result, I_{Na} and phase 0 of the next action potential are reduced, and conduction of the premature stimulus is slowed, facilitating reentry. Reduced membrane excitability is also present in cardiac cells with persistently low levels of resting potential caused by disease (e.g., acute ischemia, certain electrical remodeling processes), genetic mutations that result in loss of Na^+ channel function (e.g., Brugada syndrome), tachycardia, and treatment with class I antiarrhythmic agents.¹⁹

Action potentials with reduced upstroke velocity resulting from partial inactivation of Na^+ channels are called “depressed fast responses.” These action potential changes are likely to be heterogeneous, with unequal degrees of Na^+ inactivation that create areas with minimally reduced velocity, more severely depressed zones, and areas of complete block. In addition, refractoriness in cells with reduced membrane potentials can outlast voltage recovery of the action potential; that is, the cell can still be refractory or partially refractory after the E_m returns to its most negative value. With progressive reduction of excitability, less Na^+ source current is generated, and conduction velocity and the safety factor decrease monotonically. When the safety factor falls to less than 1, conduction can no longer be sustained, and failure (conduction block) occurs.

Thus, in a diseased region with partially depolarized fibers, there can be some areas of slow conduction and some areas of conduction block, depending on the level of resting potential and the number of Na^+ channels that are inactivated. This combination can create a substrate for reentry. The chance for reentry in such fibers is even greater during premature activation or during rhythms at a rapid rate, because slow conduction or the possibility of block is increased even further.

Notably, reduced membrane excitability does not support very slow conduction; rather, it leads to a transition to abrupt conduction failure from conduction velocities that are relatively fast (Fig. 3.16). The safety factor decreases very slowly and is relatively insensitive to moderate changes in membrane excitability. Only when there is extreme (90%) reduction in Na^+ channel availability, the generated depolarizing charge is not sufficient to depolarize the membrane to excitation threshold, and the safety factor drops precipitously toward 1 (in a nonlinear “all-or-none” behavior of the cell membrane and the threshold phenomenon that characterizes the excitation process).

Reduced Cellular Coupling

Intercellular communication is maintained by gap junctional channels that connect neighboring cells and allow biochemical and low-resistance electrical coupling. Although the resistivity of the gap junctional membrane for the passage of ions and small molecules and for electrical propagation is several orders of magnitude higher than the cytoplasmic intracellular resistivity, gap junction coupling provides a resistance pathway that is several orders of magnitude lower compared with uncoupled cell membranes.

In normal adult working myocardium, a given cardiomyocyte is electrically coupled to an average of approximately 11 adjacent cells, with gap junctions being predominantly localized at the intercalated discs at the ends of the rod-shaped cells. Lateral (side-to-side) gap junctions in nondisc lateral membranes of cardiomyocytes are much less abundant and occur more often in atrial than ventricular tissues. This particular subcellular distribution of gap junctions is a main determinant of anisotropic conduction in the heart; a wavefront must traverse more cells in the transverse direction than over an equivalent distance

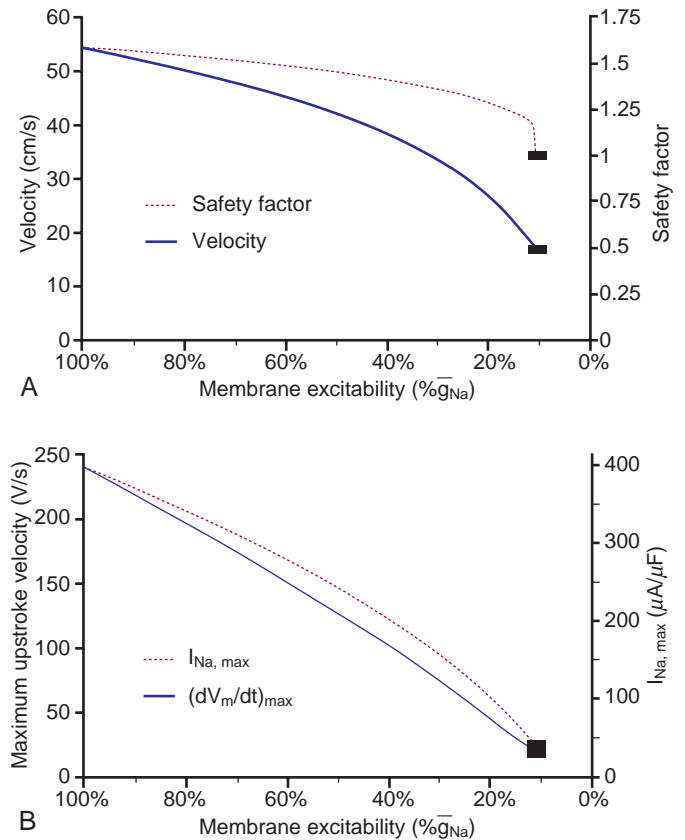


Fig. 3.16 Computer Simulation of the Effects of a Gradual Reduction of Membrane Excitability on the Characteristics of Impulse Propagation. (A) Dependence of conduction velocity and of the safety factor for conduction on membrane excitability. Conduction velocity (solid line) and safety factor of conduction (dashed line) versus Na^+ channel availability (% \bar{g}_{Na}). Both velocity and safety factor decrease monotonically as membrane excitability is reduced. Horizontal bars indicate conduction failure, which occurs when the safety factor decreases to less than 1. (B) Dependence of maximal upstroke velocity and maximal sodium inward current on membrane excitability. (From Rohr S. Role of gap junctions in the propagation of the cardiac action potential. *Cardiovasc Res*. 2004;62: 309–322.)

in the longitudinal direction because cell diameter is much smaller than cell length. In addition, with less intercellular gap junctional coupling, greater resistance and slower conduction occurs transversely than longitudinally.¹⁹

Modification of intercellular coupling occurs in numerous physiological and pathophysiological conditions. Physiologically, cell-to-cell coupling is reduced in atrial and ventricular myocardium in the transverse direction to the main fiber axis relative to the longitudinal direction. Reduced intercellular coupling also likely contributes to slow impulse conduction in the AVN. In pathophysiological settings (e.g., myocardial ischemia, ventricular hypertrophy, cardiomyopathy), modification of intercellular coupling can occur as a consequence of acute changes in the average conductance of gap junctions secondary to ischemia, hypoxia, acidosis, or increase in intracellular Ca^{2+} , or it can be produced by changes in expression or cellular distribution patterns of gap junctions. Changes in the distribution and number of gap junctions (gap junction remodeling) have been reported in almost all cardiac diseases predisposing to arrhythmias. Remodeling includes a decrease in some gap junction channels resulting from the interruption of communication between cells by fibrosis and downregulation of connexin 43 (Cx43)

formation or trafficking to the intercalated disc. In addition, gap junctions can become more prominent along lateral membranes of myocytes (so-called structural remodeling).⁴⁰

Similar to its behavior during reduced membrane excitability, conduction velocity decreases monotonically with reduction in intercellular coupling. However, partial gap junctional uncoupling was shown to result in conduction velocities that are over an order of magnitude slower than those obtained during a maximal reduction of excitability.¹⁹ In fact, very slow electrical propagation, necessary to explain very small local reentry circuits, cannot occur with reduced membrane excitability alone, and it necessitates the presence of either very low levels of intercellular coupling or highly discontinuous architecture of the myocytes network.⁴¹

Importantly, the changes in the safety factor resulting from intercellular uncoupling are opposite to those observed with reduction in membrane excitability (Fig. 3.17). The safety factor increases to a maximum as coupling is reduced and velocity is significantly slowed. Electrical coupling between adjacent cells is an important determinant of source-sink balance. As cells become less coupled, there is greater confinement of depolarizing current to the depolarizing “source” cell, with less electrotonic load and axial flow of charge to the downstream “sink” cells (the source is less likely to become overwhelmed by the demand from neighboring cells). As a result, individual cells depolarize with a high margin of safety, but conduction proceeds with long intercellular delays. At such low levels of coupling, conduction is very slow but paradoxically very robust. Due to the high safety factor, extremely slow conduction velocities can be sustained in tissue with greatly reduced intercellular coupling. Only at extreme levels of uncoupling do propagation block occur.^{30,40,42,43}

Importantly, there is a high redundancy in connexin expression in the heart with regard to conduction of electrical impulse, and a large reduction of intercellular coupling is required to cause major slowing of conduction velocity. It has been shown that a 50% reduction in Cx43 does not alter ventricular impulse conduction. Cx43 expression must

decrease by 90% to affect conduction, but even then conduction velocity is reduced only by 20%.⁴⁰

Tissue Structure and Geometry

Tissue geometry can influence action potential propagation and conduction velocity. In contrast to an uncoupled cell strand, in which the high resistance junctions alternate with the low cytoplasmic resistance of the cells, a high degree of discontinuity can be produced by large tissue segments (consisting of a segment with side branches) alternating with small tissue segments having a small tissue mass (connecting segments without branches).¹⁹

When a small mass of cells has to excite the large mass (the so-called tissue expansion), transient slowing of the conduction velocity can be observed at the junction. This occurs, for instance, with an impulse passing abruptly from a narrow bundle of myocardial fibers into a large tissue layer or propagating into a region where there is an abrupt increase in branching of the myocardium). In this setting, conduction slowing or block can occur because of sink-source mismatch; the current provided by the excitation wavefront (current source) is insufficient to charge the capacity and thus excite the much larger volume of tissue ahead (current sink).^{19,41,44}

In a normal heart, abrupt changes in geometric properties are not of magnitude to provide sufficient sink-source mismatch and cause conduction block of the normal action potential because the safety factor for conduction is large; that is, there is a large excess of activating current over the amount required for propagation. However, when the action potential is abnormal, the unexcited area has reduced excitability (e.g., in the setting of acute ischemia), or both, anatomical impediments can result in conduction block.

Furthermore, the fibrosis that accompanies aging, heart disease, and heart failure increases the extent and heterogeneity of structural discontinuity. Fibrotic myocardium exhibits slow, inhomogeneous, and strongly anisotropic conduction, likely secondary to reduced intercellular coupling, discontinuous branching architecture, and zigzagging circuits. Fibrotic strands typically occur between the cardiomyocytes, running parallel to their longitudinal axis, thus separating laterally neighbored cardiomyocytes, with reduced transverse conduction velocity. Fibroblasts, although nonexcitable, may allow electrotonic spread of activation, but with considerable delay. Of note, experimental studies suggest that fibroblasts might couple via gap junctions to cardiomyocytes; however, it remains unclear whether fibroblast-myocyte coupling occurs *in vivo*.⁴⁵

Anisotropy and Reentry

The anisotropic cellular structure of the myocardium is important for the understanding of normal propagation and arrhythmogenesis. Structural anisotropy can relate to cell shape and to the cellular distribution pattern of proteins involved in impulse conduction, such as gap junction connexins and membrane ion channels. The anisotropic architecture of most myocardial regions, consisting of elongated cells forming strands and layers of tissue, leads to a dependence of propagation velocity on the direction of impulse spread.¹⁹ In normal ventricular myocardium, conduction in the direction parallel to the long axis of the myocardial fiber bundles is approximately 3 to 5 times more rapid than that in the transverse direction. This is attributable principally to the lower resistivity of myocardium in the longitudinal versus the transverse direction; hence intercellular current flow occurs primarily at the cell termini (although propagation also occurs transversely). As discussed previously, the gap junctions of the intercalated discs form a major source of intercellular resistance to current flow between fiber bundles. Therefore the structure of the myocardium that governs the extent and distribution of these gap junctions has a profound influence on axial resistance and conduction.

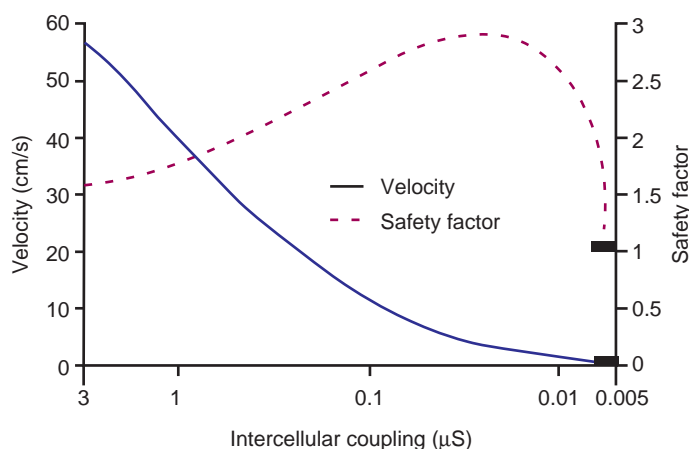


Fig. 3.17 Computer Simulation of the Effects of a Gradual Reduction of Gap Junctional Coupling on the Characteristics of Impulse Propagation. Conduction velocity (solid line) and safety factor for conduction (dashed line) versus gap junction conductance. Velocity decreases monotonically as coupling is reduced. In contrast, the safety factor first “paradoxically” increases to a maximum and then decreases sharply to the point of conduction block (horizontal bar at safety factor of 1). (From Rohr, S. Role of gap junctions in the propagation of the cardiac action potential. *Cardiovasc Res.* 2004;62:309–322.)

Cellular Coupling: Gap Junctional Organization

The anisotropic conductive properties of ventricular myocardium are dependent on the geometry of the interconnected cells and the number, size, and location of gap junction channels between them. In addition, gap junctions vary in their molecular composition, degree of expression, and distribution pattern, whereby each of these variations can contribute to the specific propagation properties of a given tissue. Tissue-specific connexin expression and gap junction spatial distribution, as well as the variation in the structural composition of gap junction channels, allow for a greater versatility of gap junction physiological features and enable disparate conduction properties in cardiac tissue.⁴⁰

Three different connexins are prominently expressed in the atrial and ventricular myocardium: Cx40, Cx43, and Cx45, named for their molecular masses. A fourth connexin has been described in the AVN (Cx31.9). Cx40 gap junction channels exhibit the largest conductance and Cx45 the smallest. The myocytes of the sinus node and AVN are equipped with small, sparse, dispersed gap junctions containing Cx45, a connexin that forms low conductance channels, thus underlying the relatively poor intercellular coupling in nodal tissues, a property that is linked to slowing of conduction. In contrast, atrial myocardium gap junctions consist mainly of Cx43 and Cx40, ventricular myocardium of Cx43, and the and Purkinje fibers of Cx40.⁴⁰

Alterations in distribution and function of cardiac gap junctions are associated with conduction delay or block. Inactivation of gap junctions decreases transverse conduction velocity to a greater degree than longitudinal conduction, thereby resulting in exaggeration of anisotropy and providing a substrate for reentrant activity and increased susceptibility to arrhythmias.

Myocyte Packing and Tissue Geometry

Discontinuities in myocardial architecture exist at several levels. In addition to discontinuities imposed by cell borders, microvessels and connective tissue sheets separating bundles of excitable myocytes can act as resistive barriers. A propagating impulse is expected to collide with such barriers and travel around them wherever it encounters excitable tissue.

In some regions of the myocardium (e.g., the papillary muscles), connective tissue septa subdivide the myocardium into unit bundles, each composed of 2 to 30 cells surrounded by a connective tissue sheath. Within a unit bundle, cells are tightly connected or coupled to each other longitudinally and transversely through intercalated discs that contain the gap junctions and are activated uniformly and synchronously as an impulse propagates along the bundle. Adjacent unit bundles also are connected to each other. Unit bundles are coupled better in the direction of the long axis of its cells and bundles (because of the high frequency of the gap junctions within a unit bundle) than in the direction transverse to the long axis (because of the low frequency of interconnections between the unit bundle). This is reflected as a lower axial resistivity in the longitudinal direction than in the transverse direction in cardiac tissues composed of many unit bundles. In addition, anisotropy on a macroscopic scale can influence conduction at sites at which a bundle of cardiac fibers branches or separate bundles will coalesce. Marked slowing can occur when there is a sudden change in the fiber direction, causing an abrupt increase in the effective axial resistivity. Conduction block, which sometimes can be unidirectional, can occur at such junction sites, particularly when membrane excitability is reduced.

Uniform Versus Nonuniform Anisotropy

Uniform anisotropy is characterized by smooth wavefront propagation in all directions, and measured conduction velocity changes monotonically on moving from fast (longitudinal) to slow (transverse) axes, thus indicating relatively tight coupling between groups of fibers in all direc-

tions. However, this definition is based on the characteristics of activation at a macroscopic level, where the spatial resolution encompasses numerous myocardial cells and bundles, and therefore it describes the behavior of the myocardial syncytium. In contrast, when the three-dimensional network of cells is broken down into linear single-cell chains, gap junctions can be shown to limit axial current flow and induce saltatory conduction because of the recurrent increases in axial resistance at the sites of gap junctional coupling; that is, conduction is composed of rapid excitation of individual cells followed by a transjunctional conduction delay. In two- and three-dimensional tissue, these discontinuities disappear because of lateral gap junctional coupling, which serves to average local small differences in activation times of individual cardiomyocytes at the excitation wavefront.⁴⁴

In multicellular tissue, saltatory conduction reappears only under conditions of critical gap junctional uncoupling, which leads to a functional unmasking of the cellular structure and induces ultraslow and meandering conduction, well known to be a key ingredient in arrhythmogenesis. Change in the characteristics of anisotropic propagation at the macroscopic scale from uniform to nonuniform strongly predisposes to reentrant arrhythmias. Nonuniform anisotropy has been defined as tight electrical coupling between cells in the longitudinal direction but uncoupling to the lateral gap junctional connections. Therefore there is disruption of the smooth transverse pattern of conduction characteristic of uniform anisotropy, which results in a markedly irregular sequence or zigzag conduction, producing the fractionated extracellular electrograms characteristic of nonuniform anisotropic conduction (Fig. 3.18). In nonuniformly anisotropic muscle, there also can be an abrupt transition in conduction velocity from the fast longitudinal direction to the slow transverse direction, unlike the case with uniform anisotropic muscle, in which intermediate velocities occur between the two directions.³⁰

Nonuniform anisotropic properties can exist in normal cardiac tissues secondary to separation of the fascicles of muscle bundles in the transverse direction by fibrous tissue that proliferates with aging to form

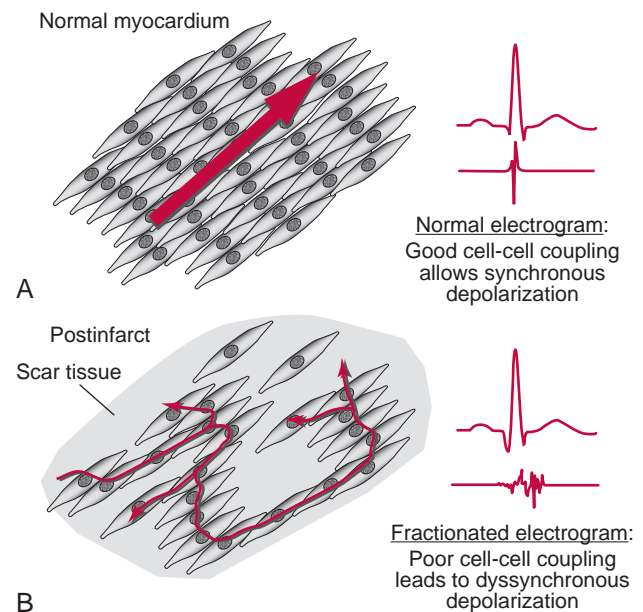


Fig. 3.18 Effect of Scar on Electrical Propagation. (A) A homogeneous sheet of myocardium conducts an electrical wavefront rapidly, with synchronous activation of a large number of cells that leads to a sharp electrogram. (B) Myocardial scarring produces disordered propagation, resulting in a low-amplitude electrogram, with multiple fragmented peaks.

longitudinally oriented insulating boundaries (e.g., crista terminalis, interatrial band in adult atria, or ventricular papillary muscle). Similar connective tissue septa cause nonuniform anisotropy in pathological situations such as chronic ischemia or a healing MI, in which fibrosis in the myocardium occurs (see Fig. 3.18).⁴⁶

Mechanism of Unidirectional Block in the Reentrant Circuit

Unidirectional block occurs when an impulse cannot conduct in one direction along a bundle of cardiac fibers but can conduct in the opposite direction. As mentioned earlier, this condition is necessary for the occurrence of classic reentrant rhythms. Several mechanisms, involving active and passive electrical properties of cardiac cells, can cause unidirectional block. Expression of ion channels and associated flow of depolarizing currents (I_{Na} and I_{CaL}), cell-to-cell electrical coupling, and microscopic tissue structure all interact to define local propagation and risk of unidirectional propagation block in tissues with a discontinuous structure such as occurs in the heart.⁴⁰

Inhomogeneity of Membrane Excitability and Refractoriness

Unidirectional block develops when the activation wavefront interacts with the repolarization phase (tail) of a preceding excitation wave. There is a critical or vulnerable window during the relative refractory period of a propagating action potential within which unidirectional block occurs (Fig. 3.19). When a premature stimulus is delivered outside this window, the induced action potential propagates or blocks in both directions; specifically, a stimulus delivered too early fails to induce a propagating action potential in either direction (bidirectional block), whereas a late stimulus results in bidirectional conduction (no block). In contrast, when a stimulus is applied within the vulnerable window,

the induced action potential propagates incrementally in the retrograde direction because the tissue is progressively more recovered as the distance from the window increases in this direction, but it blocks in the anterograde direction following a short distance of decremental conduction because the tissue is progressively less excitable as the distance from the window increases in this direction.¹⁹

The size of the vulnerable window provides an index of the vulnerability to the development of reentrant arrhythmias. Therefore the probability that a premature stimulus will fall inside the window and induce reentry is high when the vulnerable window is large. In contrast, precise timing of a premature stimulus is required to induce reentry in a small window, and the probability of such an event is low. In normal tissue the vulnerable window is very small and inducibility of unidirectional block and reentry is negligible. The width of the vulnerable window can be affected by changes in the availability of Na^+ channels for depolarization, cell-to-cell coupling, and repolarizing I_K . In addition, the size of the vulnerable window can be widened (and reentry facilitated) by factors that increase the spatial inhomogeneity of refractoriness or decrease cellular coupling via gap junctions.

Unidirectional conduction block in a reentrant circuit also can be persistent and independent of premature activation, in which case it often occurs in a region of depressed and heterogeneous excitability (as occurs in acute ischemia); this leads to a widening of the vulnerable window. Asymmetry in excitability, which can occur because of asymmetrical distribution of a pathological event, can lead to an abrupt rise in the threshold for excitation in one direction and to a more gradual rise in the other. Conduction fails when the wavefront encounters the least depressed site first and is successful in the direction in which it encounters the most depressed site first. In addition, impulses are conducted more easily from a rapidly conducting tissue to a slowly conducting tissue than in the opposite direction.⁴⁷

Local dispersion of refractory periods is a normal feature of ventricular myocardium. Critical increases in the dispersion of refractoriness (i.e., the difference between the shortest and longest refractory periods) can result in the local widening of the vulnerability window and an increased probability for the generation of unidirectional block and reentry. Increased heterogeneity of repolarization and dispersion of refractoriness can be caused by acute or prolonged ischemia, the LQTS, or electrical remodeling in the setting of ventricular hypertrophy and failure, and in the setting of MI. When differences in the duration of the refractory periods occur in adjacent areas, conduction of an appropriately timed premature impulse can be blocked in the region with the longest refractory period, which then becomes a site of unidirectional block, whereas conduction continues through regions with a shorter refractory period.

Anisotropy and Unidirectional Block

The anisotropic properties of cardiac muscle can contribute to the occurrence of unidirectional block. As mentioned earlier, in the anisotropic muscle, the safety factor for conduction is lower in the longitudinal direction of rapid conduction than in the transverse direction of slow conduction. The low safety factor longitudinally is a result of a large current load on the membrane associated with the low axial resistivity and a large membrane capacitance in the longitudinal direction. This low safety factor can result in a preferential conduction block of premature impulses in the longitudinal direction while conduction in the transverse direction continues. The site of block in the longitudinal direction can become a site of unidirectional block that leads to reentry. In contrast to the propensity of premature impulses to block in the longitudinal direction in nonuniformly anisotropic myocardium because of the decreased depolarizing current and low safety factor, when coupling resistance between cells is increased, conduction of all impulses

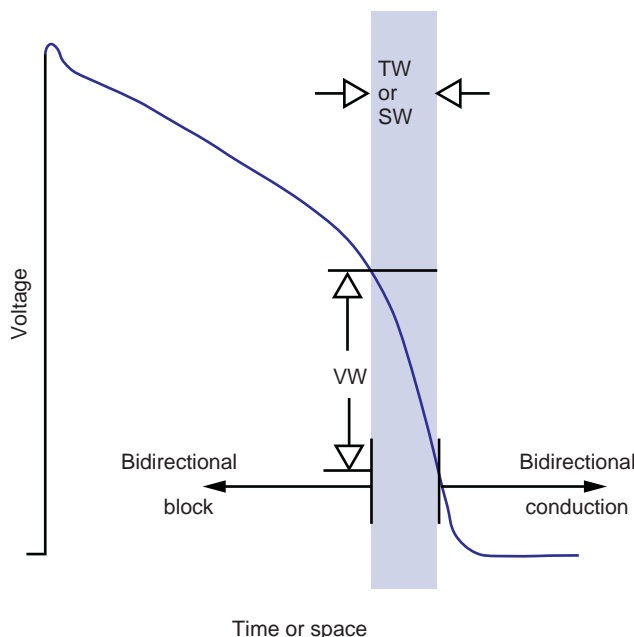


Fig. 3.19 Schematic Representation of the Vulnerable Window During the Refractory Period of a Propagating Action Potential. The critical or vulnerable window within which unidirectional block occurs can be characterized as a time interval or window (TW), or alternatively, it can be represented as a distance in the space domain (SW) or as a range of membrane potentials in the voltage domain (VW). (From Kléber AG, Rudy Y. Basic mechanisms of cardiac impulse propagation and associated arrhythmias. *Physiol Rev.* 2004;84:431–488.)

will block first in the transverse direction. Preferential block in this direction occurs because an increase in coupling resistance will reduce the safety factor to less than the critical level needed to maintain transverse conduction before the safety factor for longitudinal conduction is reduced to this critical level.

Discontinuities in Tissue Structure and Geometry

Geometric factors related to tissue architecture also can influence impulse conduction and, under certain conditions, lead to unidirectional block. Structural discontinuities exist in the normal heart in the form of trabeculations of the atrial and ventricular walls, sheets interconnected by small trabeculae, or myocardial fibers with different diameters packed in a connective tissue matrix. Structural discontinuities can also be secondary to pathophysiological settings, such as the connective tissue septa characteristic of aging, infarcted, hypertrophic, and failing myocardium. The propagating excitation wave is expected to interact with these normal and abnormal structural discontinuities. These structural features influence conduction by affecting the axial currents that flow ahead of the propagating wavefront.⁴⁷ Therefore an impulse conducting in one direction can encounter a different sequence of changes in fiber diameter, branching, and frequency and distribution of gap junctions than it does when traveling in the opposite direction. The configuration of pathways in each direction is not the same.⁴⁶

Such tissue structures can exhibit directional asymmetry in source-sink relationships. Depending on the size of the source-sink mismatch, this results in either local conduction delays or conduction blocks at the junction during anterograde conduction, where the source is smaller than the sink. On the other hand, conduction remains preserved in the opposite direction, where the source is larger than the sink. As a consequence, unidirectional block develops. Similar phenomena occur at other types of structural discontinuities such as pivot points and isthmuses.^{28,42,43,48}

Importantly, discontinuities in propagation are very sensitive to the state of underlying electrical cell-to-cell coupling. Although a reduction of gap junctional conductance (e.g., during ischemia) can promote arrhythmogenesis by slowing conduction velocities, partial gap junctional uncoupling has the capacity to remove unidirectional conduction blocks and therefore act, at least over a certain range of partial uncoupling, in an antiarrhythmogenic fashion. Partial uncoupling of cells at the junction of source-sink mismatch decrease in the current sink and hence reduces dissipation of local (source) current. Reduced dispersion of the source current protects the impulse from being blocked at the point of abrupt expansion of cardiac tissue. As a consequence, partial cell-to-cell uncoupling can reverse the unidirectional block and allow bidirectional propagation.

VIDEOS

The following video accompanies this chapter:

Video 3.1. Reentrant Ventricular Tachycardia: Optical Mapping

REFERENCES

- Anumonwo JM, Pandit SV. Ionic mechanisms of arrhythmogenesis. *Trends Cardiovasc Med*. 2015;25:487–496.
- Rosen MR, Nargeot J, Salama G. The case for the funny current and the calcium clock. *Heart Rhythm*. 2012;9:616–618.
- Murphy C, Lazzara R. Current concepts of anatomy and electrophysiology of the sinus node. *J Interv Card Electrophysiol*. 2016;46:9–18.
- Mangoni ME, Nargeot J. Genesis and regulation of the heart automaticity. *Physiol Rev*. 2008;88:919–982.
- Bartos DC, Grandi E, Ripplinger CM. Ion channels in the heart. *Compr Physiol*. 2015;5:1423–1464.
- Lakatta EG, Maltsev VA. Rebuttal: What If the shoe doesn't fit? 'The funny current has a major pacemaking role in the sinus node'. *Heart Rhythm*. 2012;9:459–460.
- Yaniv Y, et al. Synchronization of sinoatrial node pacemaker cell clocks and its autonomic modulation impart complexity to heart beating intervals. *Heart Rhythm*. 2014;11:1210–1219.
- Maltsev VA, Lakatta EG. The funny current in the context of the coupled-clock pacemaker cell system. *Heart Rhythm*. 2012;9:302–307.
- Boyden PA, Dun W, Robinson RB. Cardiac Purkinje fibers and arrhythmias; The GK Moe Award Lecture 2015. *Heart Rhythm*. 2016;13:1172–1181.
- Tse G. Mechanisms of cardiac arrhythmias. *J Arrhythm*. 2016;32:75–81.
- Song Z, et al. Calcium-voltage coupling in the genesis of early and delayed afterdepolarizations in cardiac myocytes. *Biophys J*. 2015;108:1908–1921.
- Qu Z, Weiss JN. Mechanisms of ventricular arrhythmias: from molecular fluctuations to electrical turbulence. *Annu Rev Physiol*. 2015;77:29–55.
- Kim JJ, Némec J, Li Q, et al. Synchronous systolic subcellular Ca²⁺-elevations underlie ventricular arrhythmia in drug-induced long QT type 2. *Circ Arrhythmia Electrophysiol*. 2015;8:703–712.
- Liu MB, De Lange E, Garfinkel A, et al. Delayed afterdepolarizations generate both triggers and a vulnerable substrate promoting reentry in cardiac tissue. *Heart Rhythm*. 2015;12:2115–2124.
- Weiss JN, et al. Perspective: a dynamics-based classification of ventricular arrhythmias. *J Mol Cell Cardiol*. 2015;82:136–152.
- Padfield GJ, et al. Flecainide monotherapy is an option for selected patients with catecholaminergic polymorphic ventricular tachycardia intolerant of β -blockade. *Heart Rhythm*. 2016;13:609–613.
- Qu Z, et al. Early afterdepolarizations in cardiac myocytes: beyond reduced repolarization reserve. *Cardiovasc Res*. 2013;99:6–15.
- Belardinelli L, Giles WR, Rajamani S, et al. Cardiac late Na⁺ current: proarrhythmic effects, roles in long QT syndromes, and pathological relationship to CaMKII and oxidative stress. *Heart Rhythm*. 2015;12:440–448.
- Kléber AG, Rudy Y. Basic mechanisms of cardiac impulse propagation and associated arrhythmias. *Physiol Rev*. 2004;84:431–488.
- Antzelevitch C, Yan GX. J-wave syndromes: Brugada and early repolarization syndromes. *Heart Rhythm*. 2015;12:1852–1866.
- Xie Y, Liao Z, Grandi E, et al. Slow [Na]⁺i Changes and positive feedback between membrane potential and [Ca]²⁺i underlie intermittent early afterdepolarizations and arrhythmias. *Circ Arrhythmia Electrophysiol*. 2015;8:1472–1480.
- Nguyen TP, Singh N, Xie Y, et al. Repolarization reserve evolves dynamically during the cardiac action potential: effects of transient outward currents on early afterdepolarizations. *Circ Arrhythmia Electrophysiol*. 2015;8:694–702.
- Maruyama M, et al. Genesis of phase 3 early afterdepolarizations and triggered activity in acquired long-QT syndrome. *Circ Arrhythmia Electrophysiol*. 2011;4:103–111.
- Eijkemans MJC, et al. Predicting the unpredictable. *Anesthesiology*. 2010;112:41–49.
- Nichols CG. Adenosine triphosphate-sensitive potassium currents in heart disease and cardioprotection. *Card Electrophysiol Clin*. 2016;8:323–335.
- Weiss JN, Qu Z, Shivkumar K. Electrophysiology of hypokalemia and hyperkalemia. *Circ Arrhythmia Electrophysiol*. 2017;10:e004667.
- Coronel R, et al. Electrophysiological changes in heart failure and their implications for arrhythmogenesis. *Biochim Biophys Acta*. 2013;1832:2432–2441.
- Spector P. Principles of cardiac electric propagation and their implications for re-entrant arrhythmias. *Circ Arrhythmia Electrophysiol*. 2013;6:655–661.
- Allessie MA, Bonke FI, Schopman FJ. Circus movement in rabbit atrial muscle as a mechanism of tachycardia. III. The "leading circle" concept: a new model of circus movement in cardiac tissue without the involvement of an anatomical obstacle. *Circ Res*. 1977;41:9–18.

30. Dhein S, et al. Remodeling of cardiac passive electrical properties and susceptibility to ventricular and atrial arrhythmias. *Front Physiol.* 2014;5:1–13.
31. Ciaccio EJ, Coromilas J, Wit AL, et al. Formation of functional conduction block during the onset of reentrant ventricular tachycardia. *Circ Arrhythmia Electrophysiol.* 2016;9:e004462.
32. Kandel SM, Roth BJ. The mechanism of reflection type reentry: a simulation study. *J Cardiovasc Electrophysiol.* 2015;26:1370–1375.
33. Zaman JAB, Peters NS, Narayan SM. Rotor mapping and ablation to treat atrial fibrillation. *Curr Opin Cardiol.* 2015;30:24–32.
34. Pandit SV, Jalife J. Rotors and the dynamics of cardiac fibrillation. *Circ Res.* 2013;112:849–862.
35. Filgueiras-Rama D, Jalife J. Structural and functional bases of cardiac fibrillation differences and similarities between atria and ventricles. *JACC Clin Electrophysiol.* 2016;2:1–13.
36. Jalife J. Dynamics and molecular mechanisms of ventricular fibrillation in structurally normal hearts. *Card Electrophysiol Clin.* 2016;8:601–612.
37. Josephson ME, Almendral J, Callans DJ. Resetting and entrainment of reentrant ventricular tachycardia associated with myocardial infarction. *Heart Rhythm.* 2014;11:1239–1249.
38. Almendral J, Caulier-Cisterna R, Rojo-Álvarez JL. Resetting and entrainment of reentrant arrhythmias: part I: concepts, recognition, and protocol for evaluation: surface ECG versus intracardiac recordings. *Pacing Clin Electrophysiol.* 2013;36:508–532.
39. Almendral J. Resetting and entrainment of reentrant arrhythmias: part II: informative content and practical use of these responses. *Pacing Clin Electrophysiol.* 2013;36:641–661.
40. Kleber AG, Saffitz JE. Role of the intercalated disc in cardiac propagation and arrhythmogenesis. *Front Physiol.* 2014;5:404.
41. Kleber AG. Role of the cardiac sodium current in excitability and conduction. *Card Electrophysiol Clin.* 2014;6:657–664.
42. Unudurthi SD, Wolf RM, Hund TJ. Role of sinoatrial node architecture in maintaining a balanced source-sink relationship and synchronous cardiac pacemaking. *Front Physiol.* 2014;5:446.
43. Nikolaidou T, Aslanidi OV, Zhang H, et al. Structure-function relationship in the sinus and atrioventricular nodes. *Pediatr Cardiol.* 2012;33:890–899.
44. Rohr S, et al. Role of gap junctions in the propagation of the cardiac action potential. *Cardiovasc Res.* 2004;62:309–322.
45. Smaill BH, Zhao J, Trew ML. Three-dimensional impulse propagation in myocardium: arrhythmogenic mechanisms at the tissue level. *Circ Res.* 2013;112:834–848.
46. Ciaccio EJ, et al. Model of bipolar electrogram fractionation and conduction block associated with activation wavefront direction at infarct border zone lateral isthmus boundaries. *Circ Arrhythmia Electrophysiol.* 2014;7:152–163.
47. Segal OR, Chow AWC, Peters NS, et al. Mechanisms that initiate ventricular tachycardia in the infarcted human heart. *Heart Rhythm.* 2010;7:57–64.
48. Majumder R, Pandit R, Panfilov AV. Turbulent electrical activity at sharp-edged inexcitable obstacles in a model for human cardiac tissue. *Am J Physiol Heart Circ Physiol.* 2014;307.

Electrophysiological Testing: Tools and Techniques

OUTLINE

Indications, 81

Periprocedural Management, 81

- Preprocedure Evaluation, 81
- Consent, 81
- Procedural Sedation, 82
- Oxygen and Carbon Dioxide Monitoring, 83
- Blood Pressure Monitoring, 83
- Defibrillator Pads, 83
- Urinary Problems, 83
- Antiarrhythmic Drugs, 83
- Anticoagulation, 83

Catheterization Techniques, 84

- Electrode Catheters, 84
- Catheter Positioning, 84
- Transcaval Approach, 85
- Transaortic Approach, 87
- Transseptal Approach, 87
- Subxiphoid Epicardial Approach, 95

Signal Acquisition and Processing, 101

- Analog Versus Digital Recordings, 101
- Signal Amplification, 101
- Signal Clipping, 101
- Signal Filtering, 102

Intracardiac Electrograms, 103

- Unipolar Recordings, 103
- Bipolar Recordings, 104
- Timing of Local Events, 105
- Choices of Surface and Intracardiac Signals, 105

Baseline Intervals, 107

- P Wave–Atrial Interval, 107
- Interatrial Conduction, 108
- Atrial–His Bundle Interval, 109
- His Potential, 109
- His Bundle–Ventricular Interval, 109

Programmed Electrical Stimulation, 109

- Stimulators, 109
- Pacing Techniques, 109
- Conduction and Refractoriness, 110

Atrial Stimulation, 112

- Technical Aspects, 112
- Normal Response to Rate-Incremental Atrial Pacing, 112
- Normal Response to Atrial Premature Stimulation, 114
- Repetitive Atrial Responses, 115

Ventricular Stimulation, 115

- Technical Aspects, 115
- Normal Response to Rate-Incremental Ventricular Pacing, 117
- Normal Response to Ventricular Premature Stimulation, 117
- Repetitive Ventricular Responses, 118

Miscellaneous Electrophysiological Phenomena, 120

- Concealed Conduction, 120
- Gap Phenomenon, 121
- Supernormality, 122

Complications of Electrophysiological Testing, 122

- Risks and Complications, 122
- Iatrogenic Problems Encountered During Electrophysiological Testing, 123

INDICATIONS

Invasive electrophysiological (EP) testing involves recording a portion of cardiac electrical activity and programmed cardiac electrical stimulation via multipolar catheter electrodes positioned percutaneously strategically at various locations within the cardiac chambers. EP testing is used predominantly in patients with suspected or documented cardiac arrhythmias when the precise EP diagnosis is required for management decisions or when catheter ablation is planned. In addition, EP testing is of value in selected groups of patients for risk stratification of life-threatening arrhythmias. The role of EP testing in specific cardiac electrical and structural cardiac diseases is discussed in subsequent chapters.

PERIPROCEDURAL MANAGEMENT

Preprocedure Evaluation

Heart failure, myocardial ischemia, and electrolyte abnormalities should be treated and adequately controlled before any invasive EP testing is

undertaken. Patients with critical aortic stenosis, severe hypertrophic cardiomyopathy, left main or severe three-vessel coronary artery disease, or decompensated heart failure are at higher than average risk of complications. Induction of sustained tachyarrhythmias in these patients can cause rapid and severe hemodynamic deterioration. In addition, assessment of the risks for sedation and anesthesia must be performed prior to the procedure.

Consent

Patients generally are not as familiar with EP procedures as they are with other invasive cardiac procedures such as coronary angiography. Therefore patient education is an essential part of the procedure, and is best delivered in the outpatient setting before the procedure day. The patient should be informed about the value of the EP study, its risks, and the expected outcome. Patients should also have a realistic idea of the benefit that they can derive from undergoing EP studies, including the possibility that the study result can yield negative or equivocal results.¹

Obtaining an informed consent is an integral part of the procedure and is not only a legal requirement but also an ethical obligation. The discussion should take place out of the procedure room and be in a language that the patient adequately understands. Common risks, even if not considered serious, should be discussed, as should serious risks that are potentially life threatening, even if exceedingly rare. All aspects of the procedure that can be reasonably anticipated should be included in the discussion. Patients should be given ample opportunity to discuss their concerns about the procedure and to have their questions answered satisfactorily.¹

Procedural Sedation

Some degree of sedation is required in most patients undergoing invasive EP procedures to relieve anxiety, discomfort, and pain. Also, sedation is often necessary to prevent patient movements during long and potentially painful procedures. Patient movement can expose the patient to potential risk during transseptal puncture, pericardial access, or catheter dislocation during ablation in close proximity to critical structures. In addition, large shifts in reconstructed geometry on the electroanatomical map resulting from patient movement can hinder mapping and ablation efforts.^{2,3}

Sedation and anesthetic practices vary dramatically among different institution and operators. There is variation in the selection of patients for sedation or general anesthesia, the personnel administering sedation, the agents employed, and the technique for monitoring sedation.¹

Several patient factors warrant consultation with an anesthesiologist, such as increased risk for airway obstruction or difficult mask ventilation (e.g., obesity, obstructive sleep apnea, anatomical factors) and high risk for sedation complications (e.g., pulmonary disease, heart failure, hemodynamic instability, psychiatric or neuromuscular disorders, previous problems with anesthesia or sedation, and medication or substance use that complicates the administration of sedative agents, such as chronic opioid or benzodiazepine use, alcohol abuse).⁴

Types of Anesthesia

The anesthetic plan must be individually tailored, depending on the nature of procedure, patient characteristics, hospital resources, patient preference, and anesthesia skill/training of the EP team. Furthermore, changes in the level of sedation and in the type of drugs used can be necessary during the course of the procedure and must be aligned with the needs of the interventional procedures. For example, the optimal degree of anesthesia may vary from minimal (during induction of arrhythmias) to deep (during painful ablation or electrical cardioversion). Also, the anesthesiologist should be asked to avoid or minimize nondepolarizing muscle relaxants when the evaluation of phrenic nerve function is required during ablation. Therefore close communication and collaboration between the electrophysiologists and anesthesia providers are crucial to perform EP procedures safely and successfully.^{5,6}

One of following anesthesia techniques or their combinations may be used: (1) local anesthesia at the site of vascular access; (2) conscious (moderate) sedation with intravenous (IV) sedatives; (3) deep sedation with IV sedatives; and (4) general anesthesia.²

Local anesthesia. Infiltration of the site of vascular access with local anesthetics is commonly used. Lidocaine is the local anesthetic of choice given its fast onset of action and safety profile. Bupivacaine offers longer periods of analgesia after procedure completion, but it is not preferred due to its cardiac toxicity. Local anesthesia may be preferred to IV sedation when arrhythmia induction is expected to be adversely affected by sedation (e.g., automatic or triggered-activity tachycardias). This approach requires a well-informed and cooperative patient who can cope with lying still during the procedure.² Of note, injecting large

amounts of lidocaine can result in systemic levels that might affect arrhythmia induction.

Conscious sedation. Mild to moderate conscious sedation, in conjunction with local anesthesia, is utilized in most EP procedures. The combination of a benzodiazepine and a narcotic are typically used to provide analgesia, sedation, and amnesia. Midazolam and fentanyl are preferred because of their rapid onset, titratability, reversibility, and very wide therapeutic window.²

It is important to recognize that sedation and general anesthesia are part of a continuum, and there is a danger of patients unintentionally slipping into anesthesia with the loss of spontaneous ventilation, requiring immediate airway intervention. The transition from moderate to deeper levels of sedation can occur suddenly and unexpectedly. In fact, oversedation, loss of airway, necessity of airway intervention, or conversion to general anesthesia is reported to occur in 40% of non-general anesthesia EP procedures. Therefore even when mild to moderate levels of sedation are targeted with only benzodiazepine and narcotics, the electrophysiologist and EP staff performing the procedure must be knowledgeable and trained to promptly recognize and treat sedation-related adverse events in the absence of a specialist anesthesiologist. Hence, some operators prefer to have anesthesia providers (anesthesiologists or nurse anesthetists working with anesthesiologists) provide monitored anesthesia care (MAC) during such procedures, especially given the fact that an unplanned need for deep sedation (e.g., for electrical cardioversion of induced atrial fibrillation [AF] or ventricular tachycardia [VT]) or unpredicted complications (e.g., cardiac perforation, worsening heart failure) not infrequently arise during the course of the procedure. The latter approach allows the electrophysiologist to focus solely on the technical aspects of the procedure and share the responsibility for the patient with the anesthesia care team. The decision to involve an anesthesiologist ideally should be made before the start of the procedure. The practice of calling the anesthesia team only as needed during the course of the procedure to provide deeper levels of sedation or to rescue a deteriorating patient or manage airway emergencies is suboptimal for patient care and is not recommended.^{3,7,8}

Deep sedation. Deep levels of sedation can be required for longer procedures, such as for AF or VT ablation, and during electrical cardioversion. Deep sedation is administered under the supervision of an anesthesiologist. Although the combination of midazolam and fentanyl is commonly utilized, the use of propofol for cardiac procedures has recently been reported in several large series. Propofol has rapid onset and offset of action and an excellent safety profile; however, it also has profound respiratory depressant actions as well as vasodilatory and myocardial depressant effects, which can cause hypotension, particularly when used with other anesthetics. Propofol offers significant advantages over benzodiazepines, including more rapid induction, better acute intraprocedural control of sedation level, and more rapid recovery. Continuous infusions of IV sedatives are preferred to repeated boluses to avoid waxing and waning levels of consciousness.^{7,9}

Other options include a low dose of ketamine or etomidate. Ketamine has minimal respiratory and stimulatory effects on blood pressure and heart rate, a significant advantage in patients with preexisting hypotension or bradycardia. Etomidate also has a stable hemodynamic profile but a high incidence of transient myoclonus and nausea.^{2,10}

When deep sedation is required for only a brief period (e.g., for direct current cardioversion), IV anesthetics (such as methohexital, propofol, or etomidate) may be considered.²

General anesthesia. General anesthesia has increasingly been used for complex EP procedures. Advantages of general anesthesia include optimal airway management, pain control, and patient immobilization, as well as enhanced tolerance of esophageal temperature probes. However, this requires the additional expense and time of a dedicated anesthetic

team in the laboratory, and turn around between patients is prolonged by induction of anesthesia and recovery. In addition, the use of general anesthesia is associated with an increased risk of trauma during intubation and esophageal complications, as well as the delay in recognition of and intervention for thromboembolic complications.⁴ Furthermore, general anesthetics can suppress inducibility of various arrhythmias or render them hemodynamically unstable by the abolition of sympathetic tone for compensatory vasoconstriction.^{5,11}

Propofol or etomidate is commonly used for induction. Midazolam is often administered to patients upon arrival in EP laboratory for its anxiolytic and amnesic effects. Rocuronium is a preferred muscle relaxant to facilitate the intubation. Anesthesia is usually maintained by an inhalation agent (nitrous oxide, isoflurane, sevoflurane, or desflurane), combined with IV narcotics.² Importantly, if there is concern about phrenic nerve stimulation or injury, the anesthesiologist should be asked to avoid or minimize nondepolarizing muscle relaxants to verify the preservation of diaphragmatic function.¹²

Jet Ventilation

Using high-frequency ventilation during general anesthesia decreases the regular chest wall motion associated with standard mechanical ventilation, thus minimizing respiration-related cardiac movement. Recent data suggest that the use of jet ventilation in the EP laboratory can enhance catheter stability during mapping and ablation and potentially improve the efficacy and safety of the ablation procedure, especially when a stable field needs to be established.^{1,8}

On the other hand, several disadvantages of high-frequency jet ventilation have been reported, including the lack of airtight sealing of airway to decrease secretions, the inability to use inhaled anesthesia, and the difficult measurement of resulting ventilator parameters and efficiency of gas exchange. Furthermore, the risk of barotrauma (e.g., volutrauma, pneumothorax, mediastinal emphysema) is increased, especially in patients with chronic obstructive pulmonary disease. Mucosal damage, especially necrotizing tracheobronchitis, has been reported, and can be prevented by adequate humidification of the ventilator circuit.³

Electrophysiological Effects of Anesthetic Medications

The exact influences anesthetics have on cardiac EP in the clinical setting are not entirely certain. In general, sedation of any kind decreases endogenous catecholamine release, potentially suppressing arrhythmic activity, which can impede the mapping and ablation procedure. Nonetheless, some anesthetics (e.g., ketamine) induce sympathetic stimulation, which can potentially facilitate or induce arrhythmias.

Benzodiazepines reduce blood pressure by decreasing peripheral vascular resistance leading to reflex tachycardia. Opioids, especially at high doses, have a central vagotonic effect with resultant bradycardia. Propofol can trigger vagally mediated bradycardia and inhibit spontaneous ventricular arrhythmias.

Inhalational anesthetics enhance automaticity of latent atrial pacemakers relative to the sinus node, promoting ectopic atrial rhythms and wandering atrial pacemakers. In addition, these agents demonstrate varying effects on the atrioventricular node (AVN) and His-Purkinje system (HPS). Isoflurane prolongs the atrial refractory period and delays ventricular repolarization, but the clinical significance of these effects appears minimal.

Neuromuscular relaxants modulate autonomic tone; some agents can precipitate vasodilatation and reflex tachycardia while others can cause bradycardia, particularly if used in combination with other vagotonic drugs. Ketamine can increase heart rate and blood pressure by increasing central sympathetic outflow. Also, ketamine is a direct myocardial depressant.^{2,3,10}

Oxygen and Carbon Dioxide Monitoring

Continuous pulse-oximetry to monitor oxygen saturation is mandatory. Supplemental oxygen is generally administered to help prevent arterial desaturation and to increase the margin of safety during sedation. End-tidal CO₂ monitoring (capnography) is a noninvasive method for monitoring respiratory rate and pattern and can help detect airway obstruction and hypoventilation, and is recommended during cases involving moderate and deep sedation and general anesthesia. Monitoring oxygen saturation alone can be misleading, especially in patients receiving supplemental oxygen. The elevated baseline arterial oxygen concentration allows a longer period of apnea to ensue before arterial desaturation falls low enough to prompt airway intervention. Capnography, on the other hand, provides instantaneous information about ventilation, perfusion, and metabolism.²⁻⁴

Blood Pressure Monitoring

Accurate monitoring of blood pressure is vital. Noninvasive automated cuff blood pressure devices are usually adequate in most EP procedures performed under minimal or moderate sedation. Invasive arterial pressure monitoring should be considered for unstable patients, those with severely compromised cardiac function, when periods of deep sedation are expected or planned, and during procedures with higher risk of complications with serious hemodynamic consequences (e.g., procedures involving transseptal left atrium [LA] access, scar-related VT ablation).²

Defibrillator Pads

A functioning cardioverter-defibrillator should be available at the patient's side throughout the EP study. Using preapplied adhesive defibrillator pads is preferred to avoid disrupting the sterile field in the event that electrical defibrillation or cardioversion is needed during the procedure. Biphasic devices are more effective than devices with monophasic waveforms.

Urinary Problems

Urinary retention can occur during lengthy EP procedures, particularly in combination with sedation, fluid administration, and tachycardia-related diuresis. When such situations are anticipated, it is useful to insert a urinary drainage catheter before the procedure.

Antiarrhythmic Drugs

Antiarrhythmic drugs are usually, but not always, stopped for at least five half-lives prior to EP testing. In selected cases, antiarrhythmic drugs can be continued if an arrhythmic event occurred while the patient was taking a specific agent.

Anticoagulation

Therapeutic levels of oral anticoagulation for 4 weeks before the procedure or transesophageal echocardiography (TEE) (to exclude the presence of intracardiac thrombus) are required before studying patients who have persistent AF and atrial flutter (AFL) who may have sinus rhythm restored intentionally or inadvertently (i.e., cardioversion of VT).

Periprocedural anticoagulation for catheter ablation of persistent AFL or AF is necessary to minimize thromboembolic stroke risk; LA stunning and increased spontaneous echo contrast within the LA can occur following cardioversion or ablation of these arrhythmias. Similarly, patients with a mechanical valvular prosthesis require uninterrupted anticoagulation.

A perception of increased bleeding risks of invasive procedures in patients taking therapeutic doses of oral anticoagulants led many operators to adopt a "bridging" strategy of conversion to enoxaparin

to allow ablation and subsequent hemostasis to be performed during a pause in anticoagulation. An alternative strategy of uninterrupted oral anticoagulation during these procedures was found to be safe and feasible and more cost-effective for ablation of typical AFL or AF, without increasing hemorrhagic complications. This anticoagulation strategy can potentially be used routinely for EP studies and ablation of other arrhythmias when interruption of anticoagulation poses a significant risk.

Anticoagulation with heparin (or bivalirudin in patients allergic to heparin) is necessary for all left heart procedures, even in patients on uninterrupted oral anticoagulation. For right heart procedures, there is no evidence favoring routine use of anticoagulation, unless in individual patients at particularly high risk for thromboembolism.¹

CATHETERIZATION TECHNIQUES

Electrode Catheters

Electrode catheters are used during EP testing for recording and pacing. These catheters consist of insulated wires; at the distal tip of the catheter, each wire is attached to an electrode, which is exposed to the intracardiac surface. At the proximal end of the catheter, each wire is attached to a plug, which can be connected to an external recording device. Electrode catheters are generally made of woven Dacron or newer synthetic materials, such as polyurethane. The Dacron catheters have the advantage of stiffness, which helps maintain catheter shape with enough softness at body temperature to allow formation of loops. Catheters made of synthetic materials cannot be easily manipulated and change shape within the body, but they are less expensive and can be made smaller. Some manufacturers use braided metal strands to enhance torque control.

Electrode catheters come in different sizes (3 to 8 Fr). In adults, sizes 5, 6, and 7 Fr catheters are the most commonly used. Recordings derived from electrodes can be unipolar (one pole) or bipolar (two poles). The electrodes are typically 1 to 2 mm in length. The interelectrode distance can range from 1 to 10 mm or more; catheters with a 2- or 5-mm interelectrode distance are most commonly used.

Many multipolar electrode catheters have been developed to facilitate placement of the catheter in the desired place and to fulfill various recording requirements. Bipolar or quadripolar electrode catheters are used to record and pace from specific sites of interest within the atria or ventricles. These catheters come with a variety of preformed distal curve shapes and sizes (eFig. 4.1). Multipolar recording electrode catheters are placed within the coronary sinus (CS) or along the crista terminalis in the right atrium (RA). The Halo catheter is a multipolar catheter used to map atrial electrical activity around the tricuspid annulus during atrial tachycardias, as well as for locating right-sided bypass tracts (BTs) (Fig. 4.1). A multipolar catheter with a distal ring configuration is used to record electrical activity from the pulmonary veins (PVs) (Fig. 4.2). The star-shaped multielectrode PentaRay is a 7 Fr steerable catheter with 20 electrodes distributed over 5 soft, radiating spines, allowing for rapid and high-density mapping (see Fig. 4.2). Basket catheters capable of conforming to the chamber size and shape have also been used for mapping atrial and ventricular arrhythmias (Fig. 4.3). Special catheters are also used to record LA and left ventricular (LV) epicardial activity from the CS branches.

Catheters can have a fixed or deflectable tip. Steerable catheters allow deflection of the tip of the catheter in one or two directions in a single plane; some of these catheters have asymmetrical bidirectional deflectable curves (eFig. 4.2).

Ablation catheters have tip electrodes that are conventionally 4 mm long and are available in sizes up to 10 mm in length (eFig. 4.3). The larger tip electrodes on ablation catheters reduce the resolution of a map obtained using recordings from the distal pair of electrodes.

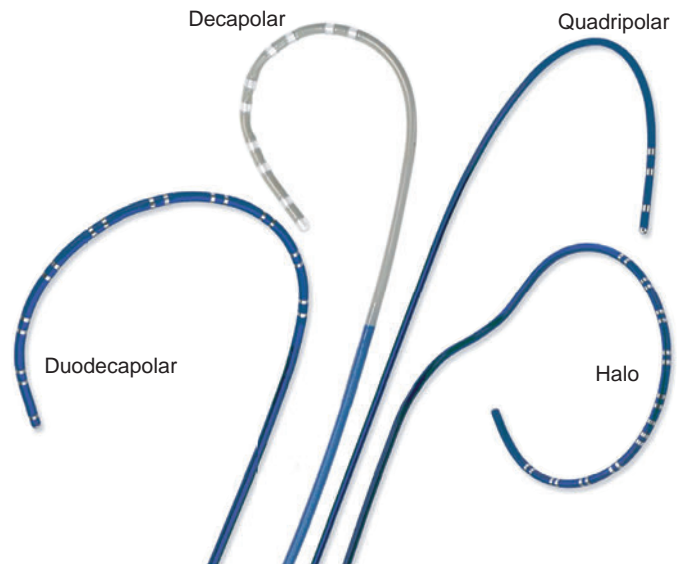


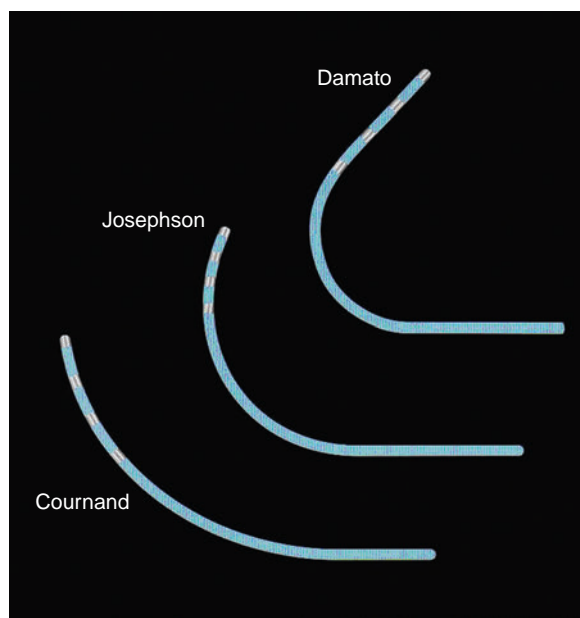
Fig. 4.1 Multipolar Electrode Catheters With Different Electrode Numbers and Curve Shape. *Left to right*, Duodecapolar catheter, decapolar catheter, quadripolar catheter, and Halo catheter. (Image provided courtesy of Boston Scientific. © 2018 Boston Scientific Corporation or its affiliates. All rights reserved.)



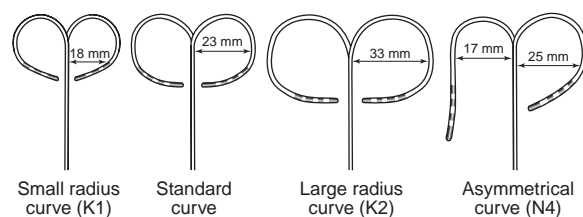
Fig. 4.2 Multipolar Ring (Lasso, *Left*) and Star-Shaped PentaRay (*Right*) Mapping Catheters. (Courtesy Biosense Webster, Inc., Diamond Bar, CA, United States.)

Catheter Positioning

The percutaneous technique is used almost exclusively. RA, His bundle (HB), and right ventricular (RV) electrograms are most commonly recorded using catheters inserted via a femoral vein. Some other areas (e.g., the CS) are more easily reached through the superior vena cava (SVC), although the femoral approach can be adequate in most cases. Insertion sites can also include the internal jugular and subclavian veins. Femoral arterial access can be required for mapping of the LV or mitral annulus or for invasive blood pressure monitoring. Occasionally, an epicardial approach is required to map and ablate certain VTs and BTs as well as the sinus node. For this purpose, the epicardial surface is accessed via the CS and its branches or percutaneously (subxiphoid puncture).



eFig. 4.1 Multipolar Electrode Catheters With Different Preformed Curve Shapes. (Courtesy Boston Scientific, Boston, MA, United States.)



eFig. 4.2 Deflectable Multipolar Electrode Catheters With Different Curve Sizes and Shapes. (Courtesy Boston Scientific, Boston, MA, United States.)



eFig. 4.3 Ablation Catheters With Different Tip Electrode Sizes and Shapes. *Left to right*, Peanut 8-, 4-, 8-, and 10-mm tip electrodes. (Courtesy Boston Scientific, Boston, MA, United States.)

Fluoroscopy is conventionally used to guide intracardiac positioning of the catheters. It is important to remember that catheters can be withdrawn without fluoroscopy (an exception being when permanent pacemaker or implantable cardioverter-defibrillator [ICD] leads are in place), but they should always be advanced under fluoroscopic guidance. More recently, newer navigation systems have been tested to guide catheter positioning in an effort to limit radiation exposure (see Chapter 6).

Transcaval Approach

The modified Seldinger technique is used to obtain multiple venous accesses. The femoral approach is most common, but the subclavian, internal jugular, or brachial approaches may be used, most often for the placement of a catheter in the CS.



Fig. 4.3 Basket Catheters. *Left*, Basket catheter (Constellation) with eight equidistant, flexible, self-expanding splines; each spline contains eight 1.5-mm electrodes. *Right*, Mini-basket catheter (Orion) with eight splines, each containing eight very small electrodes (surface area, 0.4 mm²). (Image provided courtesy of Boston Scientific. © 2018 Boston Scientific Corporation or its affiliates. All rights reserved.)

Ultrasound guidance is recommended for cannulation of the internal jugular veins. Recent studies have also shown potential benefit of ultrasound-guidance for femoral vein puncture in reducing vascular complications, particularly in the setting of anticoagulation. Ultrasound imaging allows direct visualization of peripheral arterial and venous anatomy and assessment of variations in the spatial relationship between the common femoral vein and the adjacent common femoral artery.^{13–15}

The femoral access should be avoided in patients with any of the following: known or suspected femoral vein or inferior vena cava (IVC) thrombosis, active lower extremity thrombophlebitis or postphlebotic syndrome, groin infection, bilateral leg amputation, extreme obesity, or severe peripheral vascular disease resulting in nonpalpable femoral arterial pulse. IVC umbrella filters are not necessarily a contraindication to the femoral approach.

Typically, the RA, HB, and RV catheters are introduced via the femoral veins. It is advisable to use the left femoral vein for diagnostic EP catheters and to save the right femoral vein for potential ablation or mapping catheter placement, which then would be easier to manipulate because it would be on the side closer to the operator. Multiple venous punctures and single vascular sheaths may be used for the different catheters. Alternatively, a single triport 12 Fr sheath can be used to introduce up to three EP catheters (usually the RA, HB, and RV catheters). The CS catheter is frequently introduced via the right internal jugular or subclavian vein, but also via the femoral approach.

Right Atrial Catheter

A fixed-tip, 5 or 6 Fr quadripolar electrode catheter is typically used. The RA may be entered from the IVC or SVC. The femoral veins are the usual entry sites. Most commonly, stimulation and recording from the RA is performed by placing the RA catheter tip at the high posterolateral wall at the SVC-RA junction in the region of the sinus node or in the RA appendage (Fig. 4.4).

Right Ventricular Catheter

A fixed-tip, 5 or 6 Fr quadripolar electrode catheter is typically used. All sites in the RV are accessible from any venous approach. The RV apex is most commonly chosen for stimulation and recording because of stability and reproducibility (see Fig. 4.4).

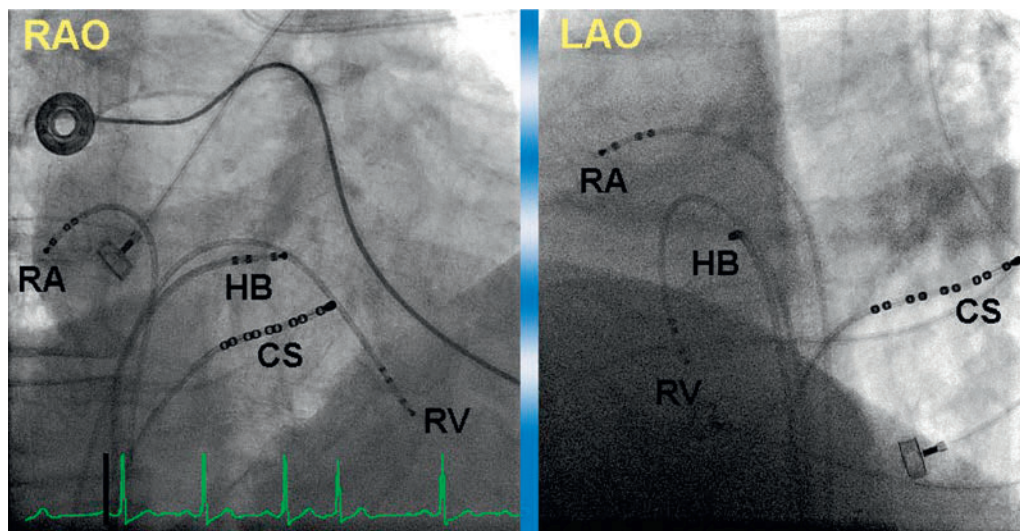


Fig. 4.4 Fluoroscopic Views of Catheters in Study for Supraventricular Tachycardia. Catheters are labeled high right atrium (RA), right ventricle (RV), and coronary sinus (CS); the CS catheter was inserted from a jugular venous approach. HB, His bundle; LAO, left anterior oblique; RAO, right anterior oblique.

His Bundle Catheter

A fixed- or deflectable-tip, 6 Fr quadripolar electrode catheter is typically used. The catheter is passed via the femoral vein into the RA and across the tricuspid annulus until it is clearly in the RV (under fluoroscopic monitoring, using the right anterior oblique [RAO] view) (see Fig. 4.4). It is then withdrawn across the tricuspid orifice while maintaining a slight clockwise torque for good contact with the septum until a His potential is recorded. Initially, a large ventricular electrogram can be observed; then, as the catheter is withdrawn, the right bundle (RB) potential can appear (manifesting as a narrow spike less than 30 milliseconds before the ventricular electrogram). When the catheter is further withdrawn, the atrial electrogram appears and grows larger. The His potential usually appears once the atrial and ventricular electrograms are approximately equal in size and is manifest as a biphasic or triphasic deflection interposed between the local atrial and ventricular electrograms. If the first pass was unsuccessful, the catheter should be passed again into the RV and withdrawn with a slightly different rotation. If, after several attempts, a His potential cannot be recorded using a fixed-tip catheter, the catheter should be withdrawn and reshaped, or it may be exchanged with a deflectable-tip catheter. Once the catheter is in place, a stable recording can usually be obtained. Occasionally, continued clockwise torque on the catheter shaft is required to obtain a stable HB recording, which can be accomplished by looping the catheter shaft remaining outside the body and fixing the loop by placing a couple of towels on it, or by twisting the connection cable in the opposite direction so that it maintains a gentle torque on the catheter.

When the access is from the SVC, it is more difficult to record the His potential because the catheter does not lie across the superior margin of the tricuspid annulus. In this case, a deflectable-tip catheter is typically used, advanced into the RV, positioned near the HB region by deflecting the tip superiorly to form a J shape, and then withdrawing the catheter so that it lies across the superior margin of the tricuspid annulus. Alternatively, the catheter can be looped in the RA (“figure-of-6” position); then the body of the loop is advanced into the RV so that the tip of the catheter is pointing toward the RA and lying on the septal aspect of the RA. Gently withdrawing the catheter can increase the size of the loop and allow the catheter tip to rest on the HB location.

Recording of the HB electrogram can also be obtained via the retrograde arterial approach. Using this approach, the catheter tip is positioned in the noncoronary sinus of Valsalva (just above the aortic valve) or in the left ventricular outflow tract (LVOT), along the interventricular septum (just below the aortic valve).

Coronary Sinus Catheter

A femoral, internal jugular, or subclavian vein can be used to access the CS. It is easier to cannulate the CS using the right internal jugular or left subclavian vein versus the femoral vein because the CS valve is oriented anterosuperiorly and, when prominent, can prevent easy access to the CS from the femoral venous approach. A fixed-tip, 6 Fr decapolar electrode catheter is typically used for access from the SVC, whereas a deflectable-tip catheter is preferred for CS access from the femoral veins.

The standardized RAO and left anterior oblique (LAO) fluoroscopic views are used to guide placement of catheters in the CS. Although the CS cannot be directly visualized with standard fluoroscopy, the epicardial fat found in the posteroseptal space just posterior to the CS ostium (os) can be visualized as a characteristic radiolucency on cine fluoroscopy in the RAO projection, where the cardiac and diaphragmatic silhouettes meet.

When cannulating the CS from the SVC approach, the LAO view is used, the catheter tip is directed to the left of the patient, and the catheter is advanced with some clockwise torque to engage the CS os; electrodes should resemble rectangles rather than ovals when the catheter tip is properly oriented to advance into the CS. Once the CS os is engaged, the catheter is further advanced gently into the CS, so that the most proximal electrodes lie at the CS os (see Fig. 4.4).

During cannulation of the CS from the IVC approach, the tip of the catheter is first placed into the RV, in the RAO fluoroscopy view, and flexed downward toward the RV inferior wall. Subsequently, the catheter is withdrawn until it lies at the inferoseptal aspect of the tricuspid annulus. In the LAO or RAO view, the catheter is then withdrawn gently with clockwise rotation until the tip of the catheter drops into the CS os. Afterward, the catheter is advanced into the CS concomitantly with gradual release of the catheter curve (Fig. 4.5). Alternatively, the tip of the catheter is directed toward the posterolateral RA wall and

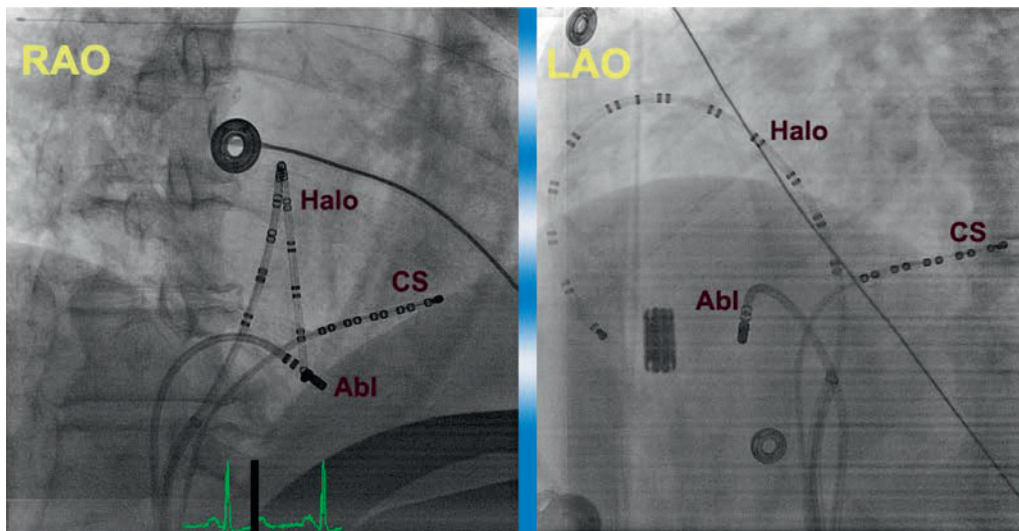


Fig. 4.5 Fluoroscopic Views of Catheters in a Study of Typical Atrial Flutter. A 20-pole Halo catheter is positioned along the tricuspid annulus. The coronary sinus (CS) catheter was introduced from a femoral venous approach. The ablation catheter (Abl) is at the cavotricuspid isthmus. LAO, Left anterior oblique; RAO, right anterior oblique.

advanced with a tight curve to form a loop in the RA, in the LAO view, with the tip directed toward the inferomedial RA. The tip is then advanced with gentle up-down, right-left manipulation using the LAO and RAO views to cannulate the CS. In the RAO view, the atrioventricular (AV) fat pad (containing the CS) appears as more radiolucent than surrounding heart tissue.

When attempting CS cannulation, the catheter can enter the RV, and premature ventricular complexes (PVCs) or VT can be observed. Catheter position in the right ventricular outflow tract (RVOT) can be misleading and simulate a CS position. Confirming appropriate catheter positioning in the CS can be achieved by fluoroscopy and recorded electrograms. In the LAO view, further advancement in the CS directs the catheter toward the left heart border, where it curves toward the left shoulder. Conversely, advancement of a catheter lying in the RVOT leads to an upward direction of the catheter toward the pulmonary artery. In the RAO view, the CS catheter is directed posteriorly, posterior to the AV sulcus, whereas the RVOT position is directed anteriorly. Recording from the CS catheter shows simultaneous atrial and ventricular electrograms, with the atrial electrogram falling in the later part of the P wave, whereas a catheter lying in the RVOT records only a ventricular electrogram. The catheter can also pass into the LA via a patent foramen ovale, in which case it takes a straight course toward the left shoulder, and all recordings are atrial.

If used, the CS catheter should be placed first because its positioning can be impeded by the presence of other catheters. It is also recommended that the CS catheter sheath be sutured to the skin to prevent displacement of the catheter during the course of the EP study.

Transaortic Approach

This approach is generally used for mapping the LV and mitral annulus (for VT and left-sided BTs). The right femoral artery is most commonly used. The mapping-ablation catheter is passed to the descending aorta. If any resistance to catheter advancement occurs, it should not be forced; the tip can be withdrawn a few centimeters, deflected and torqued slightly, and another attempt made at advancing it. If several attempts do not allow access to the descending aorta, this approach should be abandoned, since even if one is able to manipulate the catheter through tortuous vessels, torque control of the tip within the LV is likely to be severely restricted. A solution is use of a long vascular sheath; the catheter is removed from the short sheath, and a long guidewire placed in it to ascertain if it passes smoothly into the distal aorta. If so, a long sheath can be advanced over the guidewire and the catheter can then be safely passed through the sheath into the aorta. If access to the aorta via the right femoral artery is impossible or unsafe, the left femoral artery can be used.

Once the catheter tip is in the central aorta, movement proximally toward the heart is usually relatively smooth (although side branches and atheromas can be encountered). In this position, a tight J curve is formed with the catheter tip before passage to the aortic root to minimize catheter manipulation in the arch. In a 30-degree RAO view, the curved catheter is advanced through the aortic valve with the J curve opening to the right, so the catheter passes into the LV oriented anterolaterally (eFig. 4.4). The straight catheter tip must never be used to cross the aortic valve because of the risk of leaflet damage or perforation and also because the catheter tip can slip into the left or right coronary artery or a coronary bypass graft, thus mimicking entry to the LV and causing damage to these structures.

In addition to facilitating catheter passage through a tortuous iliac artery, the use of a long sheath (e.g., SL0 or SL1; 81 cm; St. Jude Medical, St. Paul, MN, United States), with the tip of the sheath placed through the aortic valve into the LV, can provide added catheter stability and limit catheter dislodgement out of the LV.

Anticoagulation with IV heparin should be started once the LV is accessed or before, to maintain the activated clotting time (ACT) between 250 and 350 seconds.

Transseptal Approach

The atrial transseptal approach is utilized for mapping and ablation in the LA and has also been increasingly used for accessing the LV. A search for a patent foramen ovale, which is present in 15% to 20% of normal subjects, is initially performed by probing the septum from the inferior approach. If no opening is found, atrial septal puncture is performed. Several approaches have been described to achieve a safe and successful transseptal puncture. The challenge for a successful atrial septal puncture is positioning the Brockenbrough needle at the thinnest aspect of the atrial septum, the membranous fossa ovalis, guided by fluoroscopy or intracardiac echocardiography (ICE).

Anatomical Considerations

Knowledge of septal anatomy and its relationship with adjacent structures is essential to ensure safe and effective access to the LA. Many apparent atrial septal structures are not truly septal. The true interatrial septum is limited to the floor of the fossa ovalis (primary septum), the flap valve, and the anteroinferior rim of the fossa. Therefore the floor of the fossa (with an average diameter of 18.5 ± 6.9 mm [vertically] and 10.0 ± 2.4 mm [horizontally] and 1 to 3 mm in thickness) is the target for atrial septal crossing (Fig. 4.6). The area between the superior border of the fossa and the mouth of the SVC is an infolding of the atrial musculature filled with adipose tissue (corresponding to the pericardial transverse sinus and the anterosuperior interatrial groove). Although this area is often described incorrectly as the “septum

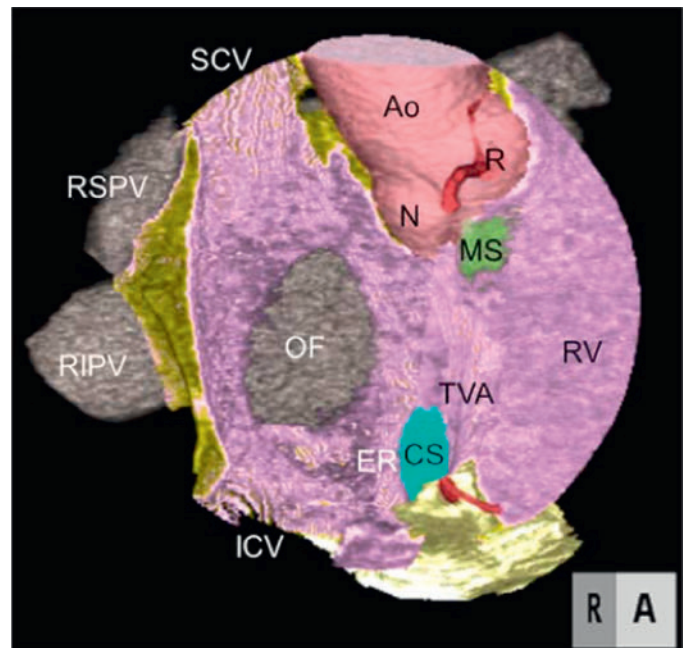
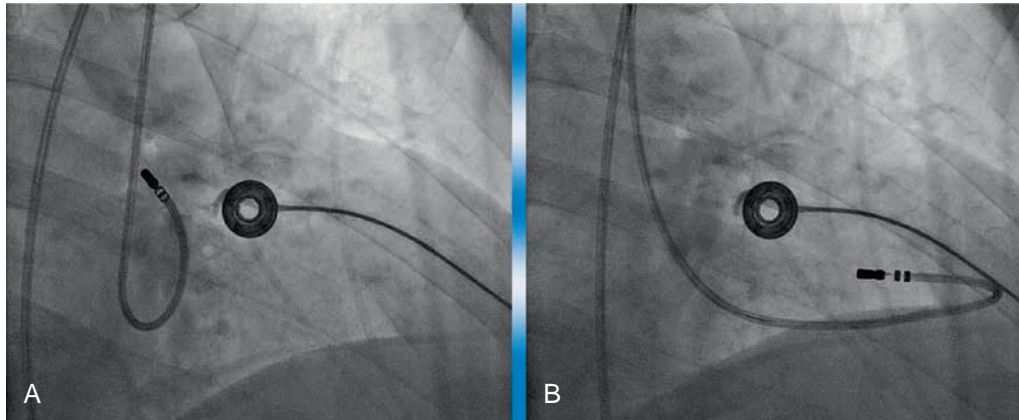


Fig. 4.6 Anatomy of the Atrial Septum. En face view of the atrial septum, observed from a 35 right anterior oblique view. Ao, Ascending aorta; CS, coronary sinus; ER, eustachian ridge; ICV, inferior caval vein; MS, membranous septum; N, noncoronary aortic sinus; OF, oval fossa; R, right coronary aortic sinus; RIPV, right inferior pulmonary vein; RSPV, right superior pulmonary vein; RV, right ventricle; SCV, superior caval vein; TVA, tricuspid valve attachment. (From Mori S, Fukuzawa K, Takaya T, et al. Clinical cardiac structural anatomy reconstructed within the cardiac contour using multidetector-row computed tomography: atrial septum and ventricular septum. *Clin Anat*. 2016;29:342–352.)



eFig. 4.4 Fluoroscopic Views of a Mapping-Ablation Catheter Introduced Into the Left Ventricle (LV) via the Retrograde Transaortic Approach. In a 30-degree right anterior oblique view, the curved catheter (A) is prolapsed across the aortic valve into the LV (B).

secundum,” it is not really a true septum, and puncture in this region would lead to exiting the heart. The infolded groove ends at the superior margin (superior rim) of the fossa ovalis. The anteroinferior muscular buttress anchors the primary septum to the muscular ventricular septum and attaches to the central fibrous body (which is composed of the right fibrous trigone and the AV portion of the membranous septum) just beneath the noncoronary aortic sinus. Anterior and superior to the fossa ovalis, the RA wall overlies the aortic root. Advancing the transseptal needle in this area can puncture the aorta.¹⁶

Understanding the attitudinal anatomical relationships of the atrial septum and adjacent structures as well as the fluoroscopic anatomy based on conventional landmarks is critical for a safe and successful transseptal puncture procedure. When the heart is viewed in an attitudinally correct orientation (as it lies within the chest), the RA lies rightward and anterior, while the LA lies posterior, leftward, and slightly superior in relation to the RA. The aortic root runs along the anterior aspect of the interatrial septum (Fig. 4.7). The fossa ovalis is located inferior and posterior relative to the noncoronary aortic sinus, and posterior to the triangle of Koch. The plane of the interatrial septum is slanted from left anterior to right posterior, with a mean orientation of 37 degrees, but can vary from 19 to 53 degrees. The orientation of the atrial septum orientation was found to strongly correlate with the direction of the CS, despite a wide range of variability in our patient population. Hence, typically the interatrial septum is almost perpendicular to the plane of the screen in the LAO 50- to 60-degree projection angle, and horizontal in the RAO 30- to 40-degree projection angle. However, adjustment of the RAO and LAO projection angles can be required to account for

rotation of the interatrial septum observed in some patients. This can be facilitated by aligning the RAO projection to an angle where the proximal part of CS catheter lies perpendicular to the screen or a His recording catheter is pointing directly toward the screen.¹⁷

Anticoagulation

Anticoagulation is essential for prevention of thromboembolism during any left-sided heart catheterization. Current recommendations advocate that IV heparin bolus be administered immediately after or, preferably, just before puncturing the atrial septum, followed by intermittent boluses or continuous heparin infusion to maintain an elevated ACT (300 to 400 seconds), even in patients on uninterrupted therapeutic doses of oral anticoagulation. However, recent evidence found that unfractionated heparin displays unexpected slow anticoagulation kinetics in a significant proportion of patients for up to 20 minutes after infusion (reflected in ACTs less than 300 seconds). Hence, some investigators have suggested administering IV heparin at least 10 minutes *before* transseptal puncture and assessing ACT at 10 minutes with an additional unfractionated heparin infusion in patients with subtherapeutic ACT.^{18,19}

Fluoroscopy-Guided Transseptal Catheterization

Equipment required for atrial septal puncture includes the following: an 8 Fr transseptal sheath for LA cannulation (e.g., SR0, SL series, Mullins, or Agilis NxT Steerable sheath, St. Jude Medical, Minnetonka, MN, United States), a 0.032-inch J guidewire, a Brockenbrough needle (e.g., BRK, St. Jude Medical), and a 190-cm, 0.014-inch guidewire. The transseptal sheaths and Brockenbrough needles are available in two

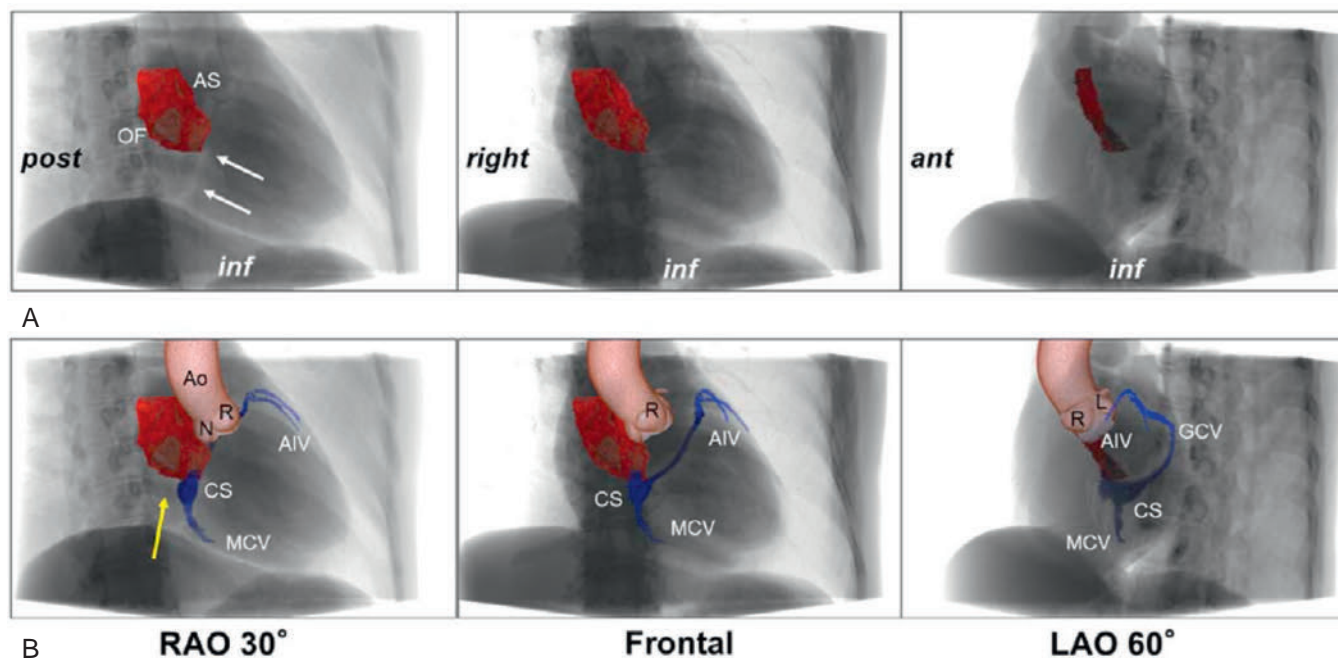


Fig. 4.7 Volume-Rendered Images of the Atrial Septum. (A) The “atrial septum” (AS) is merged with the fluoroscopy-like image. White arrows show the radiolucent band. Note that the oval fossa (OF), interatrial fold, and anteroinferior muscular buttress were reconstructed as one piece (red). Only the OF and muscular buttress are the true AS. (B) The ascending aorta (Ao), coronary sinus (CS), and middle coronary vein (MCV) are added. The yellow arrow indicates where the inferior free wall of the right atrium directly faces the inferior pyramidal space. AIV, Anterior interventricular vein; GCV, great cardiac vein; L, left coronary aortic sinus; LAO, left anterior oblique; N, noncoronary aortic sinus; R, right coronary aortic sinus; RAO, right anterior oblique. (From Mori S, Fukuzawa K, Takaya T, et al. Clinical cardiac structural anatomy reconstructed within the cardiac contour using multidetector-row computed tomography: atrial septum and ventricular septum. *Clin Anat*. 2016;29:342–352.)

different lengths; it is important to ensure that the length of needle matches that of the sheath.

Venous access is obtained via the femoral vein, preferably the right femoral vein because it is closer to the operator. The sheath, dilator, and guidewires are flushed with heparinized saline. The transseptal sheath-dilator assembly is advanced over a 0.032-inch J guidewire under fluoroscopy guidance into the SVC (to the level of the tracheal carina). The guidewire is then withdrawn, thus leaving the sheath and its dilator locked in place. The dilator within the sheath is flushed and attached to a syringe to avoid introduction of air into the RA.

Attention is then directed to preparing the transseptal needle. The Brockenbrough needle comes prepackaged with an inner stylet, which may be left in place to protect it as it is advanced within the sheath. Alternatively, the inner stylet may be removed and the needle connected to a pressure transducer line (pressure monitoring through the Brockenbrough needle will be required during the transseptal puncture); continuous flushing through the Brockenbrough needle is used while advancing the needle into the dilator. A third approach, when the use of contrast injection is planned, is to attach the Brockenbrough needle to a standard three-way stopcock via a freely rotating adapter. A 10-mL syringe filled with radiopaque contrast is attached to the other end of the stopcock while a pressure transducer line is attached to the third stopcock valve for continuous pressure monitoring. The entire apparatus should be vigorously flushed to ensure that no air bubbles are present within the circuit.

Before making an attempt at puncturing the atrial septum, it is important to ensure that all equipment is working properly, especially the pressure transducer attached to the needle. If this detail is not attended to prior to the septal puncture attempt, it becomes difficult to interpret a flat pressure tracing when the needle tip is supposedly in the LA cavity. This may mean the needle is in fact in the LA but the stopcock on the pressure tubing is turned incorrectly, or that the wrong tubing was connected to the needle hub, or that the needle tip is not in the LA. Assuring that the pressure system is working properly by “flicking” the needle shaft and seeing its corresponding pressure reverberation waveform obviates uncertainty as to whether the connections are correct. In addition, taking note of baseline blood pressure and appearance of the left heart border on fluoroscopy are important for reference; unanticipated decreases in blood pressure or decreased motion of the left heart border, compared to baseline, may be early clues to a developing pericardial effusion.

Engaging the fossa ovalis. The Brockenbrough needle is advanced into the dilator until the needle tip is within 1 to 2 cm of the dilator tip. The needle tip must be kept within the dilator at all times, except during actual septal puncture. This can be ensured by holding the sheath-dilator assembly by the left hand, and holding the needle by the right hand, while minding a safe distance of the proximal needle hub from the dilator. The curves of the dilator, sheath, and needle (as indicated by the side port of the sheath and the pointer on the proximal hub of the needle) should be aligned so that they are all in agreement and not contradicting each other. The sheath, dilator, and needle assembly is then rotated leftward and posteriorly (usually with the Brockenbrough needle arrow pointing at the 3 to 6 o'clock position relative to its shaft) and retracted caudally as a single unit (while maintaining the relative positions of its components) to engage the tip of the dilator into the fossa ovalis. Under fluoroscopy monitoring (30-degree LAO view), the dilator tip moves slightly leftward on entering the RA and then leftward again while descending below the aortic root. A third abrupt leftward movement (“jump”) below the aortic root indicates passage over the limbus into the fossa ovalis (Fig. 4.8). This jump generally occurs at the level of the HB region (marked by an EP catheter recording the HB potential). If the sheath and dilator assembly is pulled back farther than

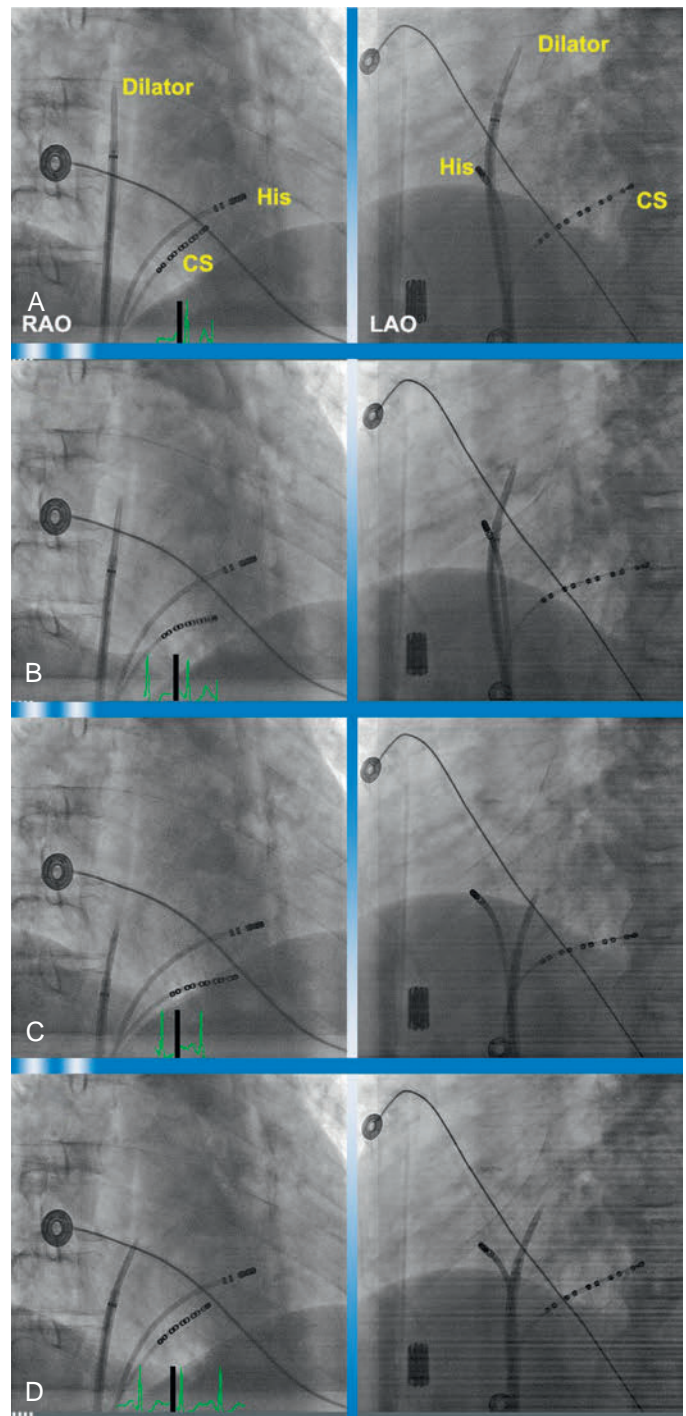


Fig. 4.8 Fluoroscopic Views During Transseptal Catheterization. Right anterior oblique (RAO, left panels) and left anterior oblique (LAO, right panels) are shown. (A) Initially, the transseptal sheath-dilator assembly is advanced into the superior vena cava. (B) The transseptal assembly is withdrawn into the high right atrium. (C) With further withdrawal, the dilator tip abruptly moves leftward, indicating passage over the limbus into the fossa ovalis at the level of the His bundle catheter. At the fossa ovalis, the dilator tip has an anteroposterior orientation in the RAO view and a leftward orientation in the LAO view. (D) The transseptal assembly is advanced across the atrial septum. CS, Coronary sinus.

intended (i.e., below the level of the fossa and HB region), the needle should be withdrawn and the guidewire placed through the dilator into the SVC. The sheath and dilator assembly is then advanced over the guidewire into the SVC and repositioning attempted, as described earlier. The sheath and dilator assembly should never be advanced without the guidewire at any point during the procedure.

Confirming position at the fossa ovalis. Several fluoroscopic markers are used to confirm the position of the dilator tip at the fossa ovalis. As noted, an abrupt leftward movement (jump) of the dilator tip below the aortic knob is observed (in the LAO view) as the tip passes under the muscular atrial septum onto the fossa ovalis. In addition, the posterior extent of the aortic root can be marked by a pigtail catheter positioned through the femoral artery in the noncoronary cusp or by the HB catheter (recording a stable proximal HB potential), which lies at the level of the fibrous trigone opposite and caudal to the noncoronary aortic cusp. When the dilator tip lies against the fossa ovalis, it is directed posteroinferiorly to the proximal HB electrode (or pigtail catheter) in the RAO view and to the left of the proximal HB electrode (or pigtail catheter) in the LAO view (see Fig. 4.8). Another method that can be used to ensure that the tip is against the fossa ovalis is injection of 3 to 5 mL of radiopaque contrast through the Brockenbrough needle to visualize the interatrial septum. The contrast stains the fossa and the needle tip then can be seen tenting the fossa ovalis

membrane with small movements of the entire transseptal apparatus. Typically, septal staining remains visible after contrast injection, which allows for real-time septal visualization while monitoring the pressure during transseptal puncture.

Puncturing the septum. Once the position of the dilator tip is confirmed at the fossa ovalis, the sheath-dilator-needle assembly is pushed slightly against the interatrial septum, and the needle is then briskly advanced to protrude outside the dilator in the LAO view during continuous pressure monitoring. If excessive force is applied without a palpable “pop” to the fossa, then the Brockenbrough needle likely is not in proper position. Occasionally, pushing the sheath-dilator-needle assembly against the fossa ovalis results in sliding of the whole assembly up the interatrial septum rather than tenting of the fossa ovalis. Increasing the “reach” of the transseptal needle tip by curving the shaft 15 to 20 back from the tip (achieved by manual adjustment) or of the sheath (when a deflectable transseptal sheath is utilized) can help mitigate this problem.

Confirming position in the LA. After passage through the fossa ovalis and before advancing the dilator and sheath, an intraatrial position of the needle tip within the LA, rather than the ascending aorta or posteriorly into the pericardial space, needs to be confirmed. Recording an LA pressure waveform from the needle tip confirms an intraatrial location (Fig. 4.9). An arterial pressure waveform indicates intraaortic

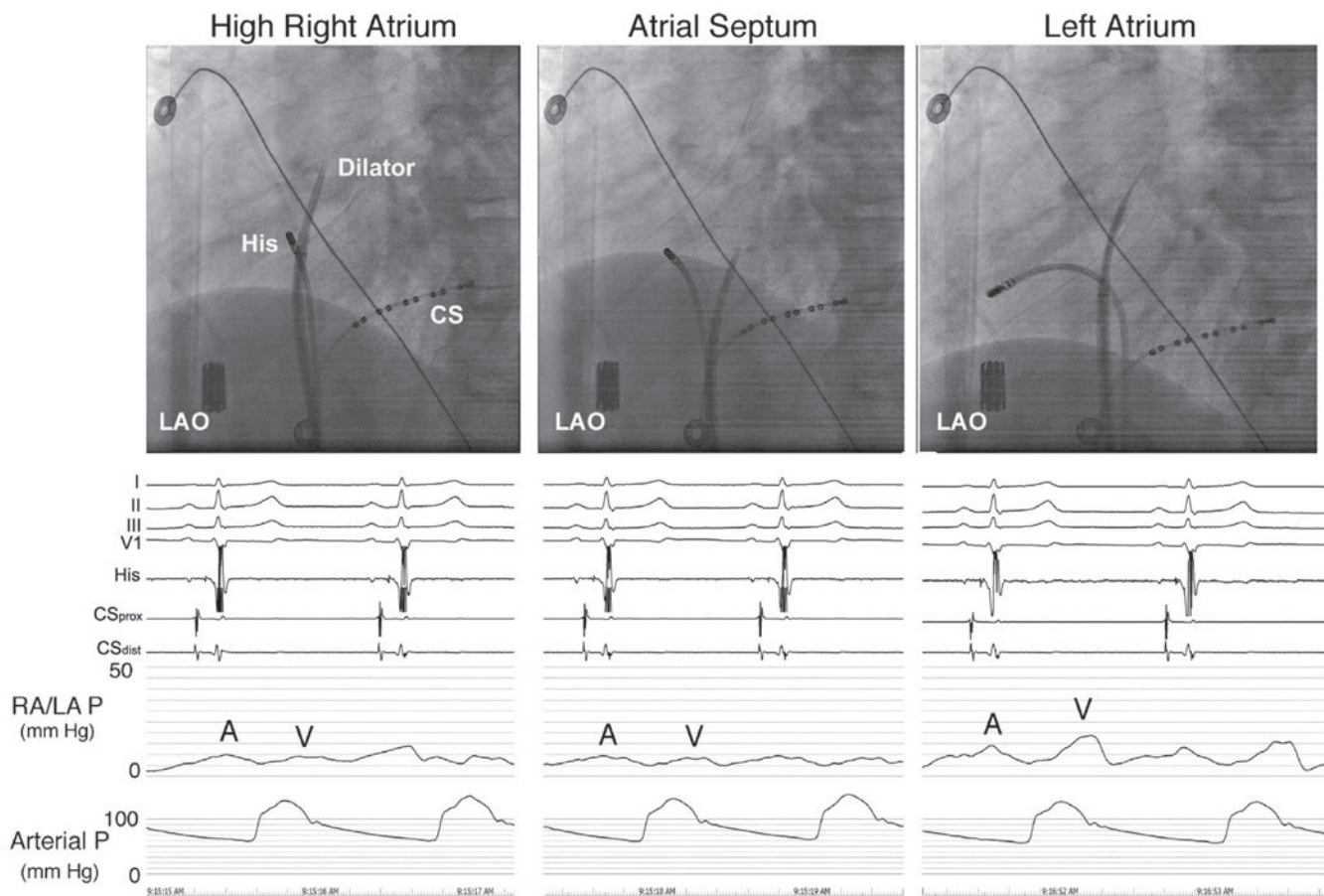


Fig. 4.9 Fluoroscopic Views and Simultaneous Electrical and Pressure Recordings During Transseptal Catheterization. *Left*, The transseptal assembly is in the right atrium (RA), indicated by typical A and V waves of right-heart pressure tracing. *Middle*, The pressure waveform is dampened somewhat as the catheter tip abuts the septum. *Right*, The needle is across the atrial septum, and characteristic waves (V larger than A) are seen. CS, Coronary sinus; CS_{dist}, distal coronary sinus; CS_{prox}, proximal coronary sinus; LA, left atrium; LAO, left anterior oblique; P, pressure.

position of the needle. Absence of a pressure wave recording can indicate needle passage into the pericardial space or sliding up and not puncturing through the atrial septum. A second method is injection of contrast through the needle to assess the position of the needle tip. Opacification of the LA (rather than the pericardium or the aorta) verifies the successful transseptal access. Alternatively, passing a 0.014-inch floppy guidewire through the Brockenbrough needle into a left-sided PV (beyond the cardiac silhouette in the LAO fluoroscopy view) helps verify that needle tip position is within the LA. If the guidewire cannot be advanced beyond the fluoroscopic border of the heart, atrial free-wall puncture with pericardial needle location should be suspected. In addition, aortic puncture should be suspected if the guidewire seems to follow the course of the aorta. In these situations, contrast should be injected to assess the position of the Brockenbrough needle before advancing the transseptal dilator. Sometimes, the guidewire enters the LA appendage rather than a PV; in this setting, a clockwise torque of the sheath and dilator assembly can help direct the guidewire posteriorly toward the ostium of the left superior or left inferior PV.

Once the position of the needle tip is confirmed to be in the LA, both the sheath and dilator are advanced as a single unit over the needle by using one hand while fixing the Brockenbrough needle in position with the other hand (to prevent any further advancement of the needle). Preferably, the sheath-dilator assembly is advanced into the LA over a guidewire placed distally into a left-sided PV, which helps direct the path of the assembly as it enters the LA and minimize the risk of inadvertent puncture of the LA free wall, especially in the presence of an elastic or redundant septum that can suddenly release, resulting in a significant forward lurch of the dilator and sheath. Once the dilator tip is advanced into the LA over the needle tip, the needle and dilator are firmly stabilized as a unit—to prevent any further advancement or withdrawal of the needle and dilator—and the sheath is advanced over the dilator into the LA. It is important to keep the needle across the septum at this time to facilitate advancement of the sheath through the puncture site. In some cases, the septum is very stiff (after prior transseptal procedures, especially) and attempts to advance the sheath into the LA result in bowing of the assembly in the RA, risking “backing out” of the dilator from the LA. In such cases, rotating the entire apparatus such that the dilator points toward the head or right superior PV can facilitate passage of the sheath through the septum, since the pushing force administered along the long axis of the assembly is now transmitted in line with the intended direction of the sheath tip (as opposed to pushing from the groin and hoping the sheath advances more sideways, toward the left shoulder). Once the transseptal sheath tip is within the LA, the dilator and needle are withdrawn slowly during continuous flushing through the needle or while suction is maintained through a syringe placed on the sheath side port to minimize the risk of air embolism and while fixing the sheath with the other hand to prevent dislodgment outside the LA. The sheath should be aspirated until blood appears without further bubbles; this usually requires aspiration of approximately 5 mL and sometimes “flicking” the sheath hub with a finger is needed to dislodge trapped air. The sheath is then flushed with heparinized saline at a flow rate of 3 mL/min during the entire procedure.

The mapping-ablation catheter is advanced through the sheath into the LA. This is safely done by advancing the catheter tip to the tip of the sheath, and while holding the catheter steady, withdrawing the sheath slightly over the catheter, exposing about 2 cm of the catheter tip. In so doing, one ensures that the catheter (stiffened by being inside the sheath) does not perforate the atrial wall. Flexing the catheter tip and applying clockwise and counterclockwise torque to the sheath help confirm free movement of the catheter tip within the LA, rather than possibly in the pericardium. It is important to recognize that merely recording atrial electrograms does not confirm an LA catheter location

because an LA recording can be obtained from the epicardial surface of the LA, from the RA, or even the aortic root.

Second transseptal puncture. When two transseptal accesses are required, the second access can be obtained through a separate transseptal puncture performed in a fashion similar to that described for the first puncture. Alternatively, the first transseptal puncture can be used for the second sheath. This technique entails passing a guidewire or thin catheter through the first transseptal sheath into the LA, preferably into the left inferior or superior PV, and then the sheath is pulled back into the RA. Subsequently, a deflectable tip catheter is used through the second transseptal sheath to interrogate the fossa ovalis and to try to access the LA through the initial puncture site. Once this is accomplished, the first sheath is advanced back into the LA, and the guidewire is replaced with the mapping catheter. It is also possible to advance two guidewires through the first transseptal sheath into the LA (preferably into the left inferior or superior PV). The sheath is then pulled out, and a separate transseptal sheath is advanced over each of the two guidewires. This requires both sheaths to go through the same femoral puncture site, which can increase bleeding in the presence of significant anticoagulation.

Intracardiac Echocardiography–Guided Transseptal Catheterization

Although fluoroscopy provides sufficient information to allow safe transseptal puncture in most cases, variations in septal anatomy, atrial or aortic root dilation, the need for multiple punctures, and the desired ability to direct the catheter to specific locations within the LA can make fluoroscopy inadequate for complex LA ablation procedures. Intraoperative TEE allows identification of the fossa ovalis and its relation to surrounding structures and provides real-time evaluation of the atrial septal puncture procedure, with demonstration of tenting of the fossa prior to entry into the LA and visualization of the sheath advancing across the septum. However, the usefulness of TEE is limited by the fact that the probe obstructs the fluoroscopic field, and it is impractical in the unanesthetized patient. ICE, which provides similar information on septal anatomy, can be used for the conscious patient and does not impede fluoroscopy.

The intent of ICE-guided transseptal catheterization is to image intracardiac anatomy and identify the exact position of the distal aspect of the transseptal dilator along the atrial septum—in particular, to assess for tenting of the fossa ovalis with the dilator tip.

Two types of ICE imaging systems are currently available: the electronic phased-array ultrasound catheter and the mechanical ultrasound catheter. The phased-array ultrasound catheter sector imaging system (AcuNav, Siemens Medical Solutions, Malvern, PA, United States) uses an 8 or 10 Fr catheter that has a forward-facing 64-element vector phased-array transducer scanning in the longitudinal plane. The catheter has a four-way steerable tip (160 degree anteroposterior or left-right deflections). The catheter images a sector field oriented in the plane of the catheter. The mechanical ultrasound catheter radial imaging system (Ultra ICE, EP Technologies, Boston Scientific, San Jose, CA, United States) uses a 9-MHz catheter-based ultrasound transducer contained within a 9 Fr (110-cm length) catheter shaft. It has a single rotating crystal ultrasound transducer that images circumferentially for 360 degrees in the horizontal plane. The catheter is not freely deflectable.

When using the mechanical radial ICE imaging system, a 9 Fr sheath (preferably a long, preshaped sheath) for the ICE catheter is advanced via a femoral venous access. To enhance image quality, all air must be eliminated from the distal tip of the ICE catheter by flushing vigorously with 5 to 10 mL of sterile water. The catheter then is connected to the ultrasound console and advanced until the tip of the rotary ICE catheter images the fossa ovalis. Satisfactory imaging of the fossa

ovalis for guiding transseptal puncture is viewed from the mid-RA (Fig. 4.10).

The AcuNav ICE catheter is introduced under fluoroscopy guidance through a 23-cm femoral venous sheath. Once the catheter is advanced into the mid-RA with the catheter tension controls in neutral position (the ultrasound transducer oriented anteriorly and to the left), the RA, tricuspid valve, and RV are viewed. This is called the home view (Fig. 4.11A). Gradual clockwise rotation of a straight catheter from the home view allows sequential visualization of the aortic root and the pulmonary

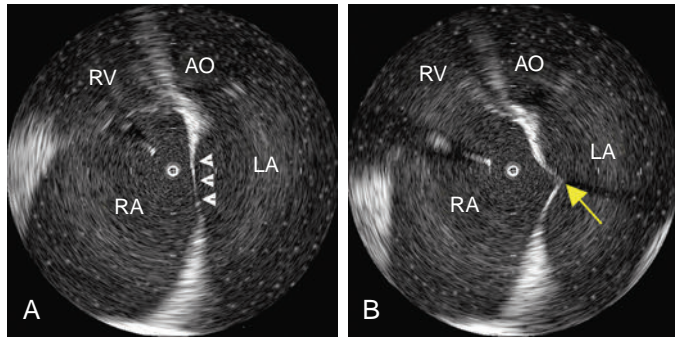


Fig. 4.10 Intracardiac Echocardiography (ICE)-Guided Transseptal Puncture Using the Ultra-ICE Catheter. These ICE images are obtained with the transducer placed in the right atrium (RA). (A) The RA, fossa ovalis (arrowheads), left atrium (LA), and aorta (AO) are visualized. (B) The transseptal needle is properly positioned, with tenting (yellow arrow) against the mid-interatrial septum at the fossa ovalis. RV, Right ventricle.

artery (see Fig. 4.11B), followed by the CS, the mitral valve, the LA appendage orifice, and a cross-sectional view of the fossa ovalis (see Fig. 4.11C and D). The mitral valve and interatrial septum are usually seen in the same plane as the LA appendage. Posterior deflection or right-left steering of the imaging tip in the RA, or both, is occasionally required to optimize visualization of the fossa ovalis; the tension knob (lock function) can then be used to hold the catheter tip in position. Further clockwise rotation beyond this location demonstrates images of the left PV ostia (see Fig. 4.11E). The optimal ICE image to guide transseptal puncture demonstrates adequate space beyond the interatrial septum on the LA side and clearly identifies adjacent structures, but it does not include the aortic root because it would be too anterior for the interatrial septum to be punctured safely. In patients with an enlarged LA, a cross-sectional view that includes the LA appendage is also optimal if adequate space exists beyond the atrial septum on the LA side.

The sheath-dilator-needle assembly is introduced into the RA, and the dilator tip is positioned against the fossa ovalis, as described earlier. Before advancing the Brockenbrough needle, continuous ICE imaging should direct further adjustments in the dilator tip position until ICE confirms that the tip is in intimate contact with the middle of the fossa, confirms proper lateral movement of the dilator toward the fossa, and excludes inadvertent superior displacement toward the muscular septum and aortic valve. With further advancement of the dilator, ICE demonstrates tenting of the fossa (Figs. 4.10 and 4.12). If the distance from the tented fossa to the LA free wall is small, minor adjustments in the dilator tip position can be made to maximize the space. The Brockenbrough needle is then advanced. With successful transseptal puncture, a palpable pop is felt, and sudden collapse of the tented fossa is observed (see Fig. 4.12). Advancement of the needle is then

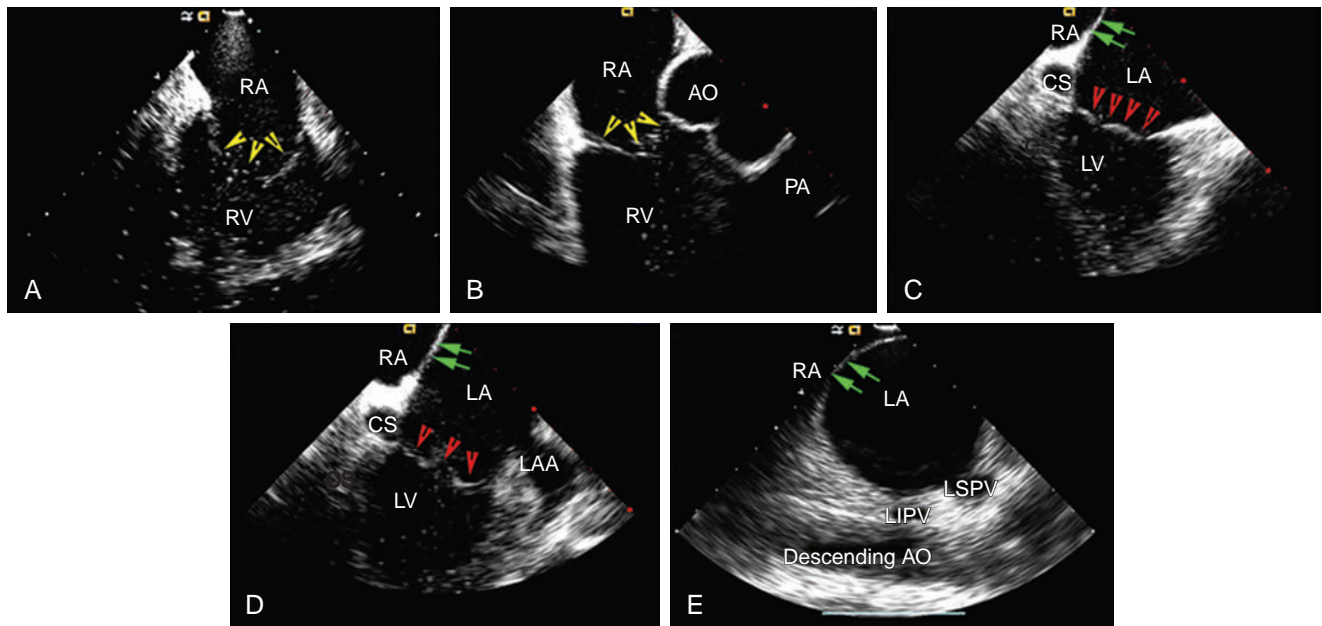


Fig. 4.11 Phased-Array Intracardiac Echocardiography (ICE). Phased-array ICE (AcuNav) serial images with the transducer placed in the middle right atrium (RA) demonstrate serial changes in tomographic imaging views following clockwise rotation of the transducer. Each view displays a left-right orientation marker to the operator's left side (i.e., craniocaudal axis projects from image right to left). (A) Starting from the home view, the RA, tricuspid valve (yellow arrowheads), and right ventricle (RV) are visualized. (B) Clockwise rotation brings the aorta (AO) into view. (C) Further rotation allows visualization of the interatrial septum (green arrows), left atrium (LA), coronary sinus (CS), left ventricle (LV), and mitral valve (red arrowheads). (D) Subsequently, the left atrium appendage (LAA) becomes visible. (E) The ostia of the left superior pulmonary vein (LSPV) and left inferior PV (LIPV) can be visualized with further clockwise rotation. PA, Pulmonary artery. (Courtesy AcuNav, Siemens Medical Solutions, Malvern, PA, United States.)

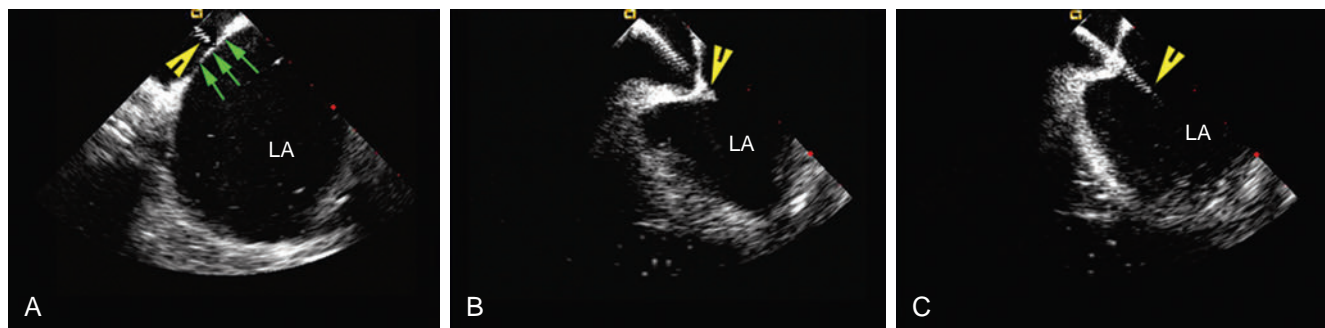


Fig. 4.12 Phased-Array Intracardiac Echocardiography (ICE)-Guided Transseptal Puncture. (A) These ICE images, with the transducer placed in the right atrium (RA), show a transseptal dilator tip (yellow arrow-head) lying against the interatrial septum (green arrows). (B) With further advancement of the dilator, ICE demonstrates tenting of the interatrial septum at the fossa ovalis. (C) Advancement of the transseptal needle is then performed, with the needle tip visualized in the left atrium (LA), and tenting of the interatrial septum is lost.

immediately stopped. Saline infusion through the needle is visualized on ICE as microbubbles in the LA, thus confirming successful septal puncture. With no change in position of the Brockenbrough needle, the transseptal dilator and sheath are advanced over the guidewire into the LA, as described earlier.

Alternative Methods for Difficult Transseptal Catheterization

In some cases, the conventional approach using a Brockenbrough needle sheath fails to pierce the septum because of the presence of a small fossa area, a thick interatrial septum, fibrosis and scarring of the septum from previous interventions, or an aneurysmal septum with excessive laxity. Applying excessive force to the needle-dilator-sheath assembly against a resistant septum (which can be seen as bending and buckling of the assembly in the RA) can lead to building pressure of the needle tip on the septum, which can potentially lead to an uncontrolled sudden jump of the assembly once across the fossa ovalis, thus perforating the opposing lateral LA wall. Similarly, excessive tenting of the interatrial septum (beyond halfway into the LA) can bring it in close proximity to the lateral LA wall, so that the needle can potentially puncture the lateral LA wall once across the septum. Some of these difficulties can be overcome by manual reshaping of the curvature of the Brockenbrough needle tip, applying slight rotation on the needle and sheath assembly to puncture a different point on the fossa ovalis, or using a sharper transseptal needle type (BRK-1 extra sharp).²⁰

Other tools designed specifically for transseptal puncture, including the SafeSept Transseptal Guidewire and the radiofrequency (RF)-powered needle, can help minimize pressure application to the needle as it crosses the septum and tenting of the septum, which can potentially reduce the chances of sudden advancement through the lateral LA as the needle crosses the septum.

SafeSept Transseptal Guidewire. The SafeSept Transseptal Guidewire (Pressure Products, San Pedro, CA, United States) is a 135-cm long, 0.014-inch diameter nitinol guidewire, tipped with a flexible J-curve needle specifically designed for transseptal puncture. Once the sheath-dilator-needle assembly is appropriately positioned at the fossa, and tenting of the fossa is seen on ICE, the SafeSept guidewire is advanced through the Brockenbrough needle to puncture the floor of the fossa with minimal force. The flexible J-curve needle then forms a loop (J curve) in the LA once it crosses the septum and is exposed out of the dilator, rendering it incapable of further tissue penetration. The transseptal needle, dilator and sheath are then sequentially advanced over the SafeSept wire into the LA.

A second iteration of this technique uses a 150-cm long, 0.032-inch diameter nitinol guidewire (SafeSept Needle Free Transseptal Guidewire) with a very sharp tip specifically designed to easily perforate and cross the fossa ovalis in conjunction with a transseptal sheath and dilator, but without the need for a transseptal needle. When the tip of the introducer has reached the fossa ovalis and tenting is seen on ICE, the guidewire is advanced, tapping on the interatrial septum until it pushes through the septum into the LA. Once across the septum, unsupported by the dilator and sheath, the tip of the guidewire assumes a J shape, rendering it incapable of further tissue penetration. The wire is then advanced into the left superior PV under fluoroscopic guidance, and the transseptal sheath-dilator assembly is advanced over the guidewire into the LA. A limitation of this technique, when compared to the Brockenbrough needle, is the lack of an open lumen to easily inject contrast or measure pressure.²¹

RF-powered needle. A specialized, electrically insulated RF-powered needle (Baylis Medical Company, Montreal, Canada) has been developed to facilitate transseptal puncture. The needle is connected to a proprietary RF generator (RFP-100 RF Puncture Generator, Baylis Medical), which delivers RF energy to the blunt, closed tip of the needle positioned at the atrial septum. Once septal tenting is visualized on ICE, RF energy is applied at 10 W for 2 seconds (unipolar mode). The RF perforation generators apply a high-voltage/low-power RF current from a small surface area of the embedded needle tip for short bursts, resulting in a high-energy electric field and an almost instantaneous temperature rise to 100°C, leading to steam popping and septal perforation with minimal collateral tissue damage (similar to the cut-mode of a surgical electrocautery unit). This can facilitate needle passage through atrial muscle with minimal—or at least reduced—mechanical pressure. This in contrast to conventional RF generators, which deliver a higher power with a lower voltage and impedance range for longer periods of time, with resulting thermal destruction of the local tissue around the needle tip, rather than perforation. The needle is also equipped with two distal side ports for measuring pressure and injecting contrast and fluids. The blunt tip of the RF needle offers an additional benefit. In contrast to the standard transseptal needle, advancing the blunt-tipped RF needle through the dilator is not associated with shaving off pieces of plastic from the inside of the dilator, which can potentially enter the patient's vascular system.^{22,23}

Other techniques to facilitate transseptal puncture include the application of pulses of electrosurgical cautery or RF energy to the proximal end of the Brockenbrough needle. Once the position of the dilator tip

is confirmed at the fossa ovalis (under ICE guidance), the needle is advanced beyond the tip of the dilator in contact with the septum until resistance is met. RF energy (5 to 30 W for 1 to 11 seconds) can be applied through a conventional ablation catheter electrode brought manually in contact with the proximal hub of the transseptal needle. Typically, the fossa is punctured almost instantaneously (within 1 to 2 seconds) following RF application. Alternatively, electrosurgical cautery (set to 15 to 20 W for a 1- to 2-second pulse of cut-mode cautery) is applied to the proximal hub of the needle as its tip is advanced out of the dilator. Importantly, the cautery should be initiated on the needle handle prior to pushing the needle tip beyond the dilator tip to help minimize the power needed to puncture the septum, and it should be stopped as soon as the needle is pushed out fully.²⁴

A potential disadvantage of using RF-assisted transseptal puncture is that it is more traumatic at the puncture site than a standard needle, and it is possible that the transseptal puncture site is less likely to close spontaneously after the procedure. Similarly, inadvertent cardiac perforation occurring in the setting of powered needles can potentially be associated with serious consequences. This is of a lesser concern when using the RF-powered Baylis needle, since it results in less tissue damage than that when applying electrosurgical cautery or standard RF energy to the Brockenbrough needle. Whether RF is more likely to cause a thrombus at the puncture site compared with a standard needle is unknown.

Another potential complication of applying electrocautery or RF energy to a standard open-ended Brockenbrough needle is coring (entrapment of a small plug) of septal atrial tissue into the tip of the open-ended Brockenbrough needle, which can lead to systemic embolization. In contrast, the Baylis needle is specifically designed with side holes, rather than an end-hole, to prevent coring.²⁵

Transseptal Puncture in the Presence of Atrial Septal Defect Repair

Transseptal catheterization is feasible and safe in most patients with prior surgical repair of an atrial septal defect or a patent foramen ovale. Nonetheless, because of the altered anatomical landmarks after repair, fluoroscopic guidance for transseptal puncture is not as reliable, and the procedure can be challenging. In these patients, an understanding of the method of repair and utilization of ICE guidance are essential.²⁰

In patients with a septal stitch or pericardial or Dacron patch, puncture can be achieved through the thickened septum or the patch. However, transseptal access is typically not achievable through a Gore-Tex patch (W.L. Gore & Associates, Flagstaff, AZ, United States) because of its resistant texture; instead, puncture can be performed directly through neighboring native interatrial tissue. However, when the patch is wide, sufficient free septal tissue for transseptal puncture may not be available, in which setting transseptal access to the LA may not be feasible.

In patients with atrial septal defect closure devices, puncture is preferably performed at the portion of the septum located inferior and posterior to the closure device and not through the device itself (eFig. 4.5). When areas of native septum are not available for transseptal access, recent reports described successful LA access through a direct puncture of the closure device.^{26,27}

Complications of Atrial Transseptal Puncture

Injury to cardiac and extracardiac structures is the most feared complication. Because of its stiffness and large caliber, the transseptal dilator should never be advanced until the position of the Brockenbrough needle is confirmed with confidence. Advancing the dilator into an improper location, such as the aortic root, can be fatal. Therefore many operators recommend the use of ICE-guided transseptal puncture, especially for patients with normal LA chamber size.²⁰

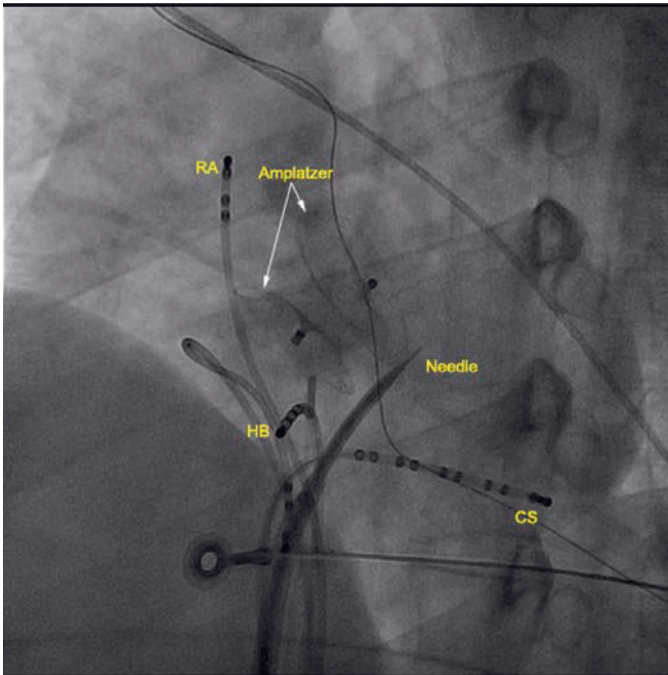
Cardiac perforation. Cardiac perforation, hemopericardium, and cardiac tamponade can result from puncturing the atrial wall outside the region of the fossa ovalis. In addition, perforation of the opposing posterior or lateral LA wall can occur once the transseptal assembly crosses the atrial septum, especially in the setting of excessive stiffness of the septum. Similarly, excessive tenting of the interatrial septum (beyond halfway into the LA) can bring it in close proximity to the lateral LA wall, so that the needle can potentially puncture the lateral LA wall once across the septum.²⁸ It is possible to puncture the RA free wall above the fossa and continue forward with the apparatus, puncturing back into the LA. In such a situation, sheath and catheter will be in the LA, but having achieved that position by exiting the heart and reentering it. This may not be noticed immediately, as the sheath may effectively occlude the holes it has traversed in the atrial walls, but will become evident when sheaths are withdrawn at the end of the procedure, leaving a hole in each atrium.

It is important to recognize that successful atrial septal puncture is a painless procedure for the patient. If the patient experiences significant discomfort, careful assessment should be made of the catheter and sheath locations (pericardial space, aorta).

Prompt recognition and management of cardiac perforation are critical to prevent the development of cardiac tamponade. Assessment of the cardiac silhouette fluoroscopically can provide the first clue, especially if a careful assessment was made at baseline. Decreased excursion of the lateral heart border on fluoroscopy in the LAO projection, indicating accumulating pericardial effusion, usually can be seen well before a decrease in blood pressure and prior to progression to cardiac tamponade. It is reasonable to obtain a baseline LAO cine image at the outset of a procedure to serve as a reference for comparison during the procedure, followed by intermittent evaluation of the same fluoroscopic projection during the procedure. Similarly, when ICE is utilized to guide transseptal puncture, it can be used to obtain baseline images of the LV and pericardial space before transseptal puncture and then monitor for the development of pericardial effusion afterwards. Importantly, bleeding into the pericardial space may develop only after the transseptal sheath has been removed. This may occur especially when the transseptal puncture is performed too superiorly or posteriorly, crossing the pericardial space (the anterosuperior interatrial groove) before entering the LA, as noted above.

The management of pericardial effusion is largely determined by its relative size and hemodynamic effect. Trivial pericardial effusions, if recognized early during the procedure, should be monitored continuously but do not warrant termination of the procedure. For larger effusions, the procedure should be terminated and anticoagulation, if administered, should be reversed. Protamine is used to reverse the effects of heparin, and activated factor VII, fresh frozen plasma, and vitamin K can be used in patients with therapeutic anticoagulation with warfarin. Immediate pericardiocentesis is required for large, rapidly expanding, or hemodynamically significant effusions.

Aortic puncture. When the aorta is adventerly punctured by the Brockenbrough needle—an arterial waveform is recorded from the needle tip and dye injected through the needle is carried away from the heart—the needle should be withdrawn back into the dilator. If only the needle enters the aorta and this is recognized before advancing the dilator and sheath, the needle can be withdrawn and the patient monitored for stability of vital signs and with echocardiography. The procedure can usually be continued if there is no accumulation of pericardial fluid after 15 to 30 minutes of monitoring. Advancing the dilator and sheath assembly into the aorta can lead to catastrophic consequences. If the dilator and sheath have been advanced into the aortic root before the error is recognized, it is imperative that the sheath not be removed immediately, as this can result in immediate and perhaps



eFig. 4.5 Transseptal Puncture in a Patient With Atrial Septal Defect Closure Device. A left anterior oblique fluoroscopic view shows the transseptal needle crossing the atrial septum at a site inferior to an Amplatzer occluder device, in a portion of the native interatrial septum not covered by the closure device. CS, Coronary sinus catheter; HB, His bundle catheter; RA, right atrial catheter.

irretrievable hemodynamic collapse due to intractable bleeding into the pericardial space. Once surgical intervention is readily available, and after reversal of anticoagulation, it may be feasible to pull the sheath back, leaving a wire in the aorta. Under careful hemodynamic and echocardiographic observation, this wire may be also pulled back 30 minutes later. In general, the need for closing device or open heart surgery is rare.²⁹

Systemic embolism. Another potential complication is embolism of thrombus or air. To avoid air embolism, catheters must be advanced and withdrawn slowly so as not to introduce air into the assembly. Sheaths must be aspirated with a syringe on a stopcock to the amount of their volume (e.g., an 8 Fr sheath contains 5 mL when filled) to remove any retained air each time a catheter is removed and prior to reintroduction. Thromboembolic complications can be avoided by flushing all sheaths and guidewire with heparinized saline and maintaining the ACT at longer than 300 seconds. In addition, a guidewire should not be left in the LA for more than 1 minute, especially if no systemic heparin has been administered. As noted earlier, administration of heparin before, rather than after, the atrial septal puncture can also help reduce thromboembolism. Importantly, the presence of an LA thrombus is an absolute contraindication for transseptal catheterization.^{18,19}

Occasionally, ST segment elevation in the inferior electrocardiogram (ECG) leads (with or without transient bradycardia or AV block) can occur following transseptal catheterization, potentially secondary to air embolism in coronary arteries, although a Bezold-Jarisch–like reflex mechanism can also be implicated.

Interatrial shunt. Iatrogenic atrial septal defects have been described in up to 20% to 30% of patients following transseptal atrial interventions, though about two thirds of these disappear with the first 12 months of follow-up.³⁰ Predictors of developing a persistent iatrogenic atrial septal defect include the size of the transseptal sheath, LA pressure, RV systolic pressure, and the presence of severe mitral or tricuspid regurgitation. The location of the transseptal puncture (fossa ovalis vs. inferior limbus), the use of RF-powered transseptal needles, and the anatomy of the interatrial septum (e.g., aneurysmal septum) have been suggested to predict a higher risk for the development of persistent iatrogenic atrial septal defects. The clinical significance of persistent iatrogenic atrial septal defects is not clear, but can potentially result in hemodynamically significant interatrial shunts in some patients.^{31–33}

Subxiphoid Epicardial Approach

Coronary veins can be used to perform epicardial mapping, but manipulation of the mapping catheter is limited by the anatomical distribution of these vessels. In contrast, the subxiphoid percutaneous approach to the epicardial space allows for unrestricted mapping of wide areas of the epicardial surfaces of the ventricles and most part of the epicardial atria surface. Percutaneous epicardial access has become an increasingly important tool for mapping and ablation of complex ventricular arrhythmias and for LA appendage exclusion using an epicardial ligation system like the Lariat device. More recently, investigators have applied the technique to manage supraventricular arrhythmias, including inappropriate sinus tachycardia, AT arising from the LA appendage, BTs, and AF.³⁴

Anatomical Considerations

The pericardium is a double-walled sac that contains the heart and the roots of the great arteries, SVC, and PVs. By separating the heart from its surroundings—the descending aorta, lungs, diaphragm, esophagus, trachea, and tracheobronchial lymph nodes—the pericardial space allows complete freedom of cardiac motion within this sac.³⁵

The pericardium consists of two sacs intimately connected with one another: an outer fibrous envelope (the fibrous pericardium) and an

inner serous sac (the serous pericardium). The fibrous pericardium (0.8 to 2.5 mm in thickness) consists of fibrous tissue and forms a flask-shaped bag, the neck of which is closed by its fusion with the adventitia of the great vessels, while its base is attached by loose fibroareolar tissue to the central tendon and to the muscular fibers of the left side of the diaphragm. The fibrous pericardium is also attached to the posterior sternal surface by superior and inferior sternopericardial ligaments. These attachments are essential to maintain the normal cardiac position in relation to the surrounding structures, to restrict the volume of the thin-walled cardiac chambers (RA and ventricle), and also to serve as direct protection against injuries.³⁶

The serous pericardium is a delicate membrane that lies within the fibrous pericardium and lines its walls; it is composed of two layers: the parietal pericardium and the visceral pericardium. The parietal pericardium is fused to and inseparable from the fibrous pericardium. On the other hand, the visceral pericardium, which is composed of a single layer of mesothelial cells, is part of the epicardium (i.e., the layer immediately outside of the myocardium) and covers the heart and the great vessels except for a small area on the posterior wall of the atria. The visceral layer extends to the beginning of the great vessels, and is reflected from the heart onto the parietal layer of the serous pericardium along the great vessels in tube-like extensions. This happens at two areas: where the aorta and pulmonary trunk leave the heart and where the SVC, IVC, and PVs enter the heart.^{34–37}

The pericardial cavity or sac is a continuous virtual space that lies between the parietal and visceral layers of serous pericardium. The heart invaginates the wall of the serous sac from above and behind, and practically obliterates its cavity, the space being merely a potential one. The pericardial sac normally contains 20 to 40 mL of clear fluid that occupies the virtual space between the two layers and serves as a lubricant.^{34,36}

The lateral surfaces of the heart are predominantly covered by the lungs, prohibiting a direct percutaneous access to the pericardial space. The anterior borders of the lungs extend vertically downward along the midsternal line. The right lung anterior border curves laterally and downward at the level of the sixth costal cartilage on the right side. On the left side, however, the anterior border of the lung diverges laterally at an earlier point (at the level of the fourth costal cartilage), forming the cardiac notch, and reaches the parasternal line at the fifth costal cartilage (about 1 inch from the sternal border) before turning medially and downward (as the lingula) to the sixth sternocostal junction (eFig. 4.6). Thus, the subxiphoid region offers a window for direct pericardial access without traversing the lungs. Nonetheless, even with the subxiphoid approach, a needle angulated too far in the lateral direction can potentially puncture the left lung and result in pneumothorax.^{38,39}

In the subxiphoid pericardial access approach, the needle traverses the skin, subcutaneous tissue, and rectus abdominis, and then travels above the dome of the diaphragm before arriving to the fibrous pericardium. In the vicinity of the path of the needle lie several important structures that can be vulnerable to damage, including the diaphragm and diaphragmatic vessels, left internal mammary artery, lung, left lobe of the liver, stomach, and transverse colon.

The diaphragm is a dome-shaped muscular structure that separates the thoracic cavity from the abdomen. The muscle fibers of the diaphragm emerge from the circumference of the inferior thoracic aperture and converge in a *central tendon*, which forms the crest of the dome. The pericardium rests on the central tendon, an almost flat area of the dome of the diaphragm (the cardiac plateau). Anteriorly, the muscle fibers of the diaphragm emerge from the xiphoid process and along the costal margin and arch back in a “parachute” shape to a maximum height equivalent to the xiphisternal junction at the midline. The left

hemidiaphragm conforms to the left lobe of the liver, the fundus of the stomach, the spleen, and the left kidney.³⁶ The left lobe of the liver is near the xiphoid process and can be particularly at risk in patients with hepatomegaly. Manual pressure over the right upper quadrant can help displace the liver and abdominal contents posteriorly away from the path of the needle.³⁸

The internal mammary (thoracic) artery arises from the subclavian artery and descends vertically 1 to 1.5 cm lateral to the sternal border, behind the first six costal cartilages, accompanied by the internal thoracic vein. After passing the sixth intercostal space, the internal mammary artery bifurcates into the superior epigastric artery (which continues downward into the abdominal wall) and the musculophrenic artery (which roughly follows the costal margin). The risk of puncturing the internal mammary artery is increased when the needle entry or trajectory is too lateral.

Technical Considerations

The subxiphoid approach procedure may be performed under conscious sedation, deep sedation with the support of an anesthesiologist, or general anesthesia. General anesthesia allows better control of respiratory motion, which can potentially reduce the chance of unintentional RV puncture, as well as better pain control, given the fact that epicardial RF ablation is usually associated with significant pain and discomfort. IV antibiotics are routinely administered within an hour prior to the procedure. Previous heparin administration should be reversed before pericardial access; this is accomplished by protamine infusion.

Advancing the needle. The pericardial space is accessed using a 17- or 18-gauge, blunt-tipped Tuohy needle (6 inches in length), which is also used to enter the epidural space when administering epidural anesthesia. The puncture is performed at the angle between the left border of the subxiphoid process and the lower left rib. A small incision on the skin at the puncture site helps reduce the resistance when introducing the pericardial access needle and enhance tactile feedback upon puncturing the fibrous pericardium. The needle is then introduced aiming toward the left midclavicle or the left shoulder and at a shallow angle (less than 20 degrees) in order to penetrate the skin and slide under the left rib cage, above and parallel to the dome of the diaphragm, while avoiding injury to diaphragmatic vessels and subdiaphragmatic organs. Occasionally, manual pressure over the epigastrium is required to push away the liver from the path of the needle.^{38,40}

Once over the dome of the diaphragm, the needle can be angled to a steeper degree (according to whether an anterior or posterior approach is preferred, see below) and advanced under fluoroscopic guidance (40-degree LAO view or, preferably, biplane RAO and LAO projections) until close to the cardiac silhouette. Directing the needle superiorly at a relatively shallow angle (passing just posterior to the sternum on a steep lateral fluoroscopy projection), aiming for the RV apex in the RAO projection, generally allows entry into the pericardial space anteriorly over the RV and facilitates access to the anterior aspect of the RV and LV. Directing the needle more posteriorly and toward the left shoulder allows it to enter the pericardium over the diaphragmatic portion of the heart, such that the sheath typically tracks along the posterior aspect of the LV, as observed in the LAO projection. The medial third of the RV is the preferred entry region because of the absence of major coronary vessels in this region.^{34,37}

Puncturing the parietal pericardium. As the needle approaches the cardiac silhouette on the LAO view, the needle stylet is removed and a 10-mL syringe containing a saline-contrast mixture is attached to the proximal port of the needle. In the 40-degree LAO view, injection of a minimal amount of contrast (less than 1 mL) can help assess the relation of the needle to the parietal pericardium. If the diaphragm has not been reached, the contrast will be seen in the subdiaphragmatic

area. On the other hand, pooling of contrast in the mediastinal space indicates that the needle has not reached the pericardial space. Puncture of the diaphragmatic attachments before accessing the pericardial space sometimes can be misinterpreted as the puncturing the parietal pericardium; in the former setting, contrast will pool in the mediastinum outside the parietal pericardium. A needle directed too laterally can result in patchy contrast in the pleural space.

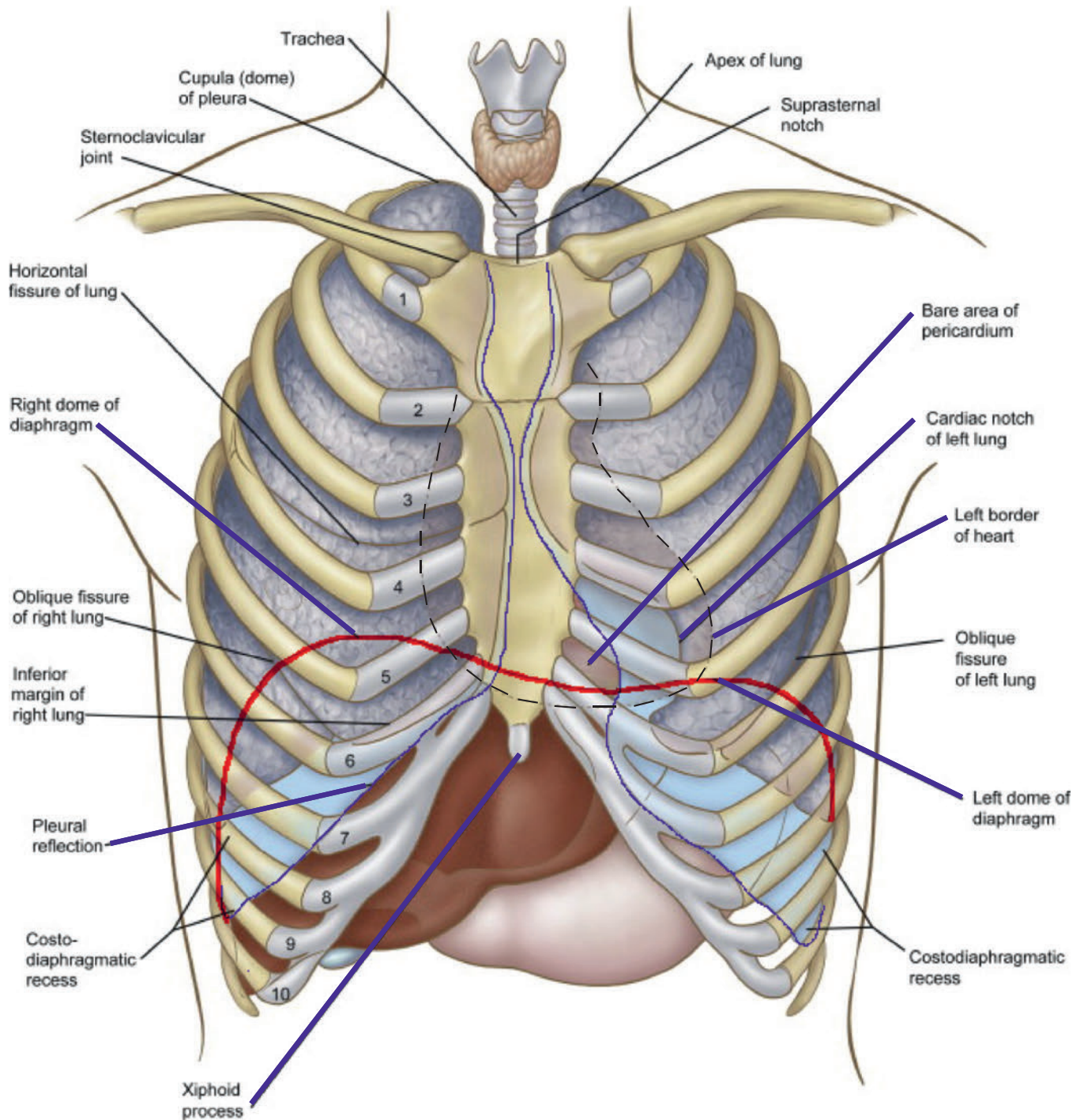
When the needle arrives at the fibrous pericardium, the contrast is seen at the heart border and, with a slight advance of the needle, tenting of the pericardium can be observed. Care must be taken not to inject too much contrast that can potentially obscure the fluoroscopic image. If too much contrast is injected, the operator may consider waiting to allow the contrast to dissipate before attempting a second puncture.^{34,37}

Once tenting of the pericardium is seen, holding the needle still against the respiratory downward movement of the diaphragm or gentle forward pressure on the needle achieves entry into the pericardial space, and often one can feel a sensation of “give” as the needle penetrates the fibrotic parietal pericardial wall (i.e., release of resistance on the needle), coupled with the disappearance of tenting of the pericardium on the LAO fluoroscopic view (Fig. 4.13).^{37,41}

Needle entry into the pericardial space and contact with the myocardium can be suggested by tactile feedback, occurrence of ventricular ectopy, or observation of a current of injury from an alligator clip attached to the shaft of the needle. At this point, further advancement of the needle can result in ventricular puncture and should be avoided.^{34,37}

Confirming intrapericardial position of the needle. When the needle reaches the pericardial sac, aspiration without blood indicates that the needle has not entered the RV, and injected contrast will spread in a thin outline of the pericardium around the heart, restricted to its silhouette. At this point, a long soft J tip guidewire is advanced far enough so that it loops in the pericardial space. Confirmation that the wire is intrapericardial and has not been inadvertently inserted into a cardiac chamber is obtained by observing the course of the wire in multiple fluoroscopic projections confirming that it crosses multiple cardiac chambers and crosses the midline, hugging the edge of the cardiac silhouette in the 40-degree LAO view (circumferential to both the right and left heart), and without induction of PVCs (see Fig. 4.13). In the LAO fluoroscopic view, the guidewire will not cross the spine and outline the left cardiac border if it is in the RV. Observation in the RAO or anterior-posterior projection alone can be misleading, as a wire that enters the RV and passes into the RA or pulmonary artery can be misinterpreted as intrapericardial.^{42,43}

Inadvertent puncture of the RV is relatively common, but usually is not associated with serious consequences (less than 80 mL of pericardial bleeding) if only the needle or guidewire has entered the chamber. Therefore it is critical to recognize RV perforation before introducing the dilator and sheath. Crossing the RV myocardium by the needle can be indicated by aspiration of blood through the needle. In addition, RV perforation can be easily recognized by observation of the ejection of contrast injected through the needle into the pulmonary artery rather than forming a thin-walled contrast lining of the pericardium. If RV perforation could not be identified, and a guidewire is advanced through the needle, stimulation of the RV or RVOT by the wire typically induces PVCs or VT. In addition, the LAO fluoroscopy view will reveal a course of guidewire (usually passing through the RVOT into the pulmonary artery) different from that of the expected pericardial course described above. If the needle is confirmed to be within the RV, it should be slightly retracted (rather than completely withdrawn) and then a little more contrast can be injected until it is observed to layer within the pericardial space. At this point, the guidewire may be successfully advanced into the pericardial space, and the position reconfirmed



eFig. 4.6 Anatomic Relationship of the Heart and Surrounding Structures. (From Smith SE, Darling GE. Surface anatomy and surface landmarks for thoracic surgery: part II. *Thorac Surg Clin.* 2011;21:139–155.)

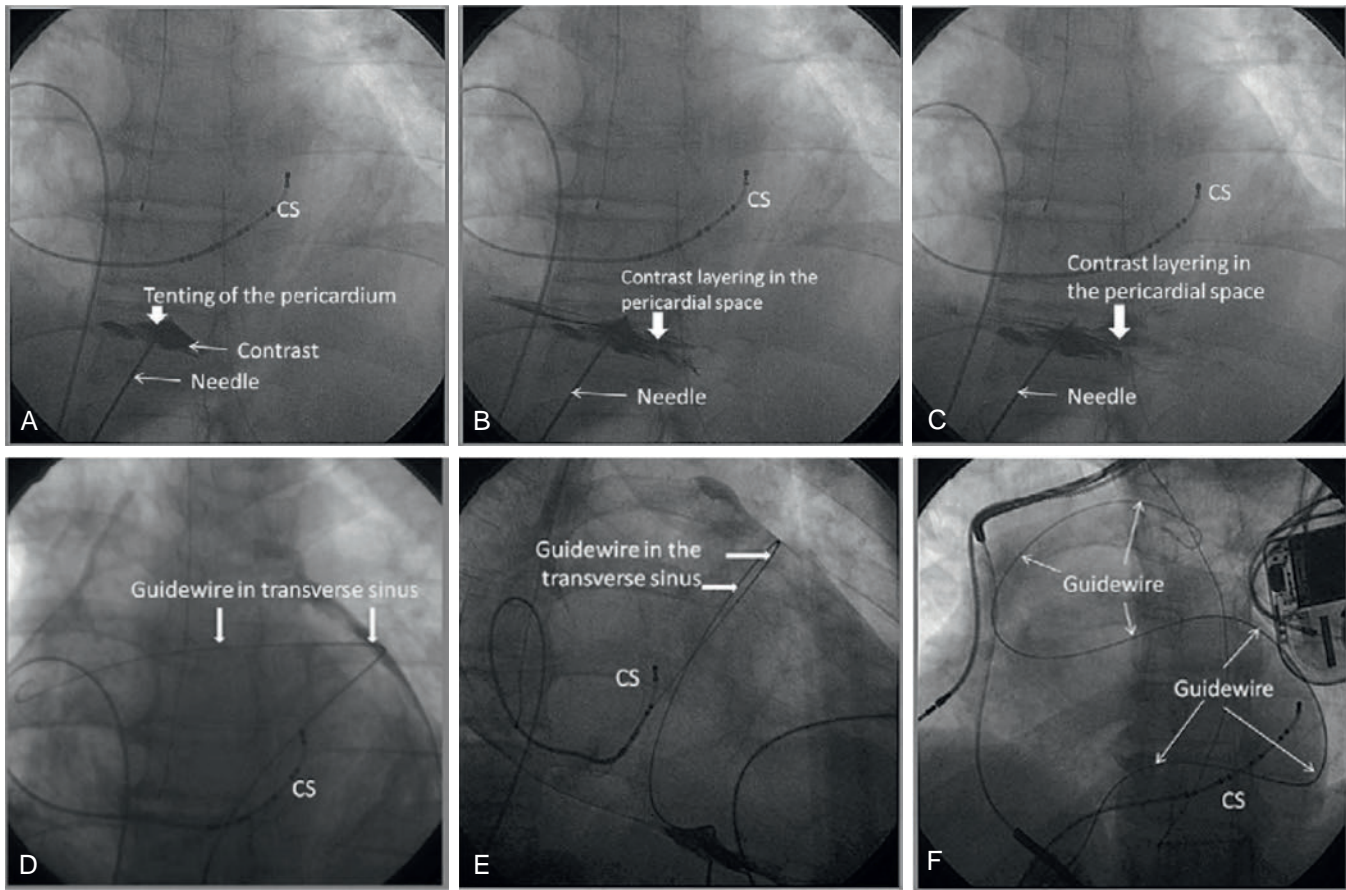


Fig. 4.13 Sequential Fluoroscopic Images of an Epicardial Access Procedure. A decapolar catheter is placed into the coronary sinus (CS) through a femoral venous approach. (A) Left anterior oblique (LAO) fluoroscopic view. Contrast injection through the Tuohy needle demonstrates tenting of the pericardium before puncture. (B and C) LAO view. As the needle is advanced, additional contrast is injected. Layering of contrast in the pericardial space confirms successful entry into the desired space. (D) LAO view. A guidewire is present in the pericardial space and traverses the transverse sinus. Note that the guidewire abuts the outer fluoroscopic border of the heart, thereby confirming its location in the proper space. (E) Right anterior oblique view. The guidewire remains within the transverse sinus. (F) LAO view of a different patient showing the position of the guidewire. (From Garikipati NV, Paruchuri V, Mittal S. How to learn epicardial intervention techniques in electrophysiology. *Card Electrophysiol Clin*. 2010;2:35–43.)

with the above criteria.^{37,42} If the guidewire is in the pericardial space, it should advance easily (in the absence of adhesions); if resistance is met, further efforts to advance the wire are discouraged as this will only result in distortion of the wire end, making it less useful for subsequent use.

Once an intrapericardial location of the guidewire is confirmed, the puncture needle is withdrawn and gradual dilatation of the puncture site is performed over the guidewire, followed by insertion of the desired sheath. Serial dilators are used to dilate the epicardial access route and then the epicardial sheath is advanced into the pericardial space. Dilators should be advanced carefully to avoid compression of the RV or kinking of the guidewire. Using a guidewire with a very soft tip but a relatively stiff proximal segment can help support advancing the dilators and sheath through the tough fibrous pericardium. Before removing the dilator out of the sheath, the sheath must be pushed against the chest to ensure that the tip of the sheath is placed well inside the pericardial sac to prevent loss of access. Although using a standard 15 cm, 8 Fr sheath may suffice, the use of longer sheaths (e.g., Agilis, St. Jude Medical, St. Paul, MN, United States) should be considered, especially in patients with a larger thoracic anteroposterior dimension.³⁷

It is preferred to maintain the option for a second pericardial access. This can provide access for a second pericardial sheath when needed (e.g., for a balloon to protect the phrenic nerve), but also can become important in the setting of inadvertent loss of the initial epicardial access or when repeated aspiration of pericardial fluid becomes necessary during the epicardial procedure. A second guidewire can be advanced through the pericardial sheath; the sheath is then removed, leaving two guidewires inside the pericardial space. Subsequently, the sheath desired for introducing the catheter is advanced over one guidewire, while the second guidewire is secured in place or a second sheath is introduced when necessary.

Before introducing the mapping-ablation catheter, the pericardial sheath must be aspirated to check for bleeding. When bleeding is under control, the mapping-ablation catheter can be introduced. Once it is inside the pericardial sac, the catheter can usually be easily moved, allowing exploration of the entire epicardial surface. Adhesions from prior pericardial entries (surgical, prior catheter ablation procedures) or idiopathic pericarditis (sometimes subclinical) can limit access to all portions of the epicardium.

EpiAccess Smart Needle. Recently, a novel epicardial access needle with an integrated needle tip pressure transducer has been developed (EpiAccess Smart Needle, EpiEP, New Haven, CT, United States). The system includes a proprietary needle (similar to the Tuohy needle in shape and size) with a fiber optic pressure sensor mounted permanently at the distal tip. The EpiAccess device provides real-time pressure frequency data designed to detect the extrapericardial, pericardial, and ventricular transitions to provide immediate adjunctive confirmation of the needle tip location during its introduction into the pericardial space.⁴⁴

The needle tip pressure frequency signal (along with an arterial line signal) is displayed as a raw waveform on the graphical user interface, and a proprietary algorithm conducts a beat-to-beat analysis of the needle tip pressure frequency and graphs the pulsatile pattern within the needle tip pressure signal. The arterial pressure signal is used by the system as a reference to compare with the pulsed pressure signal pattern of the needle tip. Consistent pulsatile pressure is also displayed in a bar graph format to provide an additional visual notification that the needle has or is about to enter the pericardial sac (Fig. 4.14).

As the needle is advanced towards the heart, no pressure is detected from the entry site in the epigastrium to the parietal pericardium. Once the needle is in contact with the parietal pericardium, a transition signal is observed, which correlates with tenting of the fibrous and parietal pericardium on fluoroscopy. Upon entering the pericardial space, the pressure monitor displays a real-time amplitude shift in frequency and a pressure signal ranging from 15 to 25 mm Hg (see Fig. 4.14). When the needle is touching the RV wall or is inside the RV cavity, the needle tip tracing displays a significantly higher pressure signal oscillating between 120 and 220 mm Hg.

“Needle-in-needle” technique. The use of a 21-gauge micropuncture needle (instead of the 18-gauge Tuohy needle) has been suggested for epicardial access to help reduce the risk of pericardial bleeding. Inadvertent cardiac or vascular puncture with the finer needle is less likely to result in significant bleeding, as compared to the larger Tuohy needle. However, it is often challenging to direct the thin micropuncture needle under the sternum because it tends to flex over the course of insertion. The “needle-in-needle” technique utilizes a short (7-cm) 18-gauge stiff needle to navigate the subcutaneous tissue and provide the proximal stability and support necessary to guide the longer (20-cm) micropuncture needle through the subcutaneous tissue and gain entry into the pericardial space (telescoping approach).^{45,46}

The “needle-in-needle” technique replaces the Tuohy needle with two needles: an 18-gauge, 7-cm Cook needle and a 21-gauge micropuncture or a long spinal (21-gauge, 20-cm) needle. Initially, the 18-gauge short needle is advanced via the subxiphoid puncture site (in a fashion similar to that described using the Tuohy needle). Once the tip of the needle arrives under the rib cage, and well before it reaches the cardiac silhouette, the micropuncture needle is inserted through the 18-gauge needle. The 21-gauge needle alone is used to puncture the parietal

pericardium and enter the pericardial space (with the aid of contrast, fluoroscopy, and tactile sensation, as described for the Tuohy needle technique). Once an intrapericardial location of the needle tip is confirmed, an 0.018-inch floppy-tip guidewire is advanced through the 21-gauge needle into the pericardial space. Once an intrapericardial location of the wire is confirmed (as described above), both needles are removed and a micropuncture dilator is advanced into the pericardial space over the guidewire and then exchanged for a 6 Fr dilator. The 0.018-inch guidewire is then exchanged for a floppy-tip 0.35-inch guidewire.^{45,46}

The “needle-in-needle” technique was found to offer several advantages over the conventional Tuohy needle technique. The micropuncture needle is able to penetrate tough fibrous pericardium and with less resistance, requiring less force and torque. This helps a more controlled needle entry to the pericardial space and avoids an “overshoot” of the needle after crossing the parietal pericardium. Even when the RV wall is inadvertently punctured, the likelihood of auto-seal of the puncture site is higher with the small-caliber needle, which translates into lesser risk of significant pericardial bleeding and subsequent need of surgical repair.^{45,46}

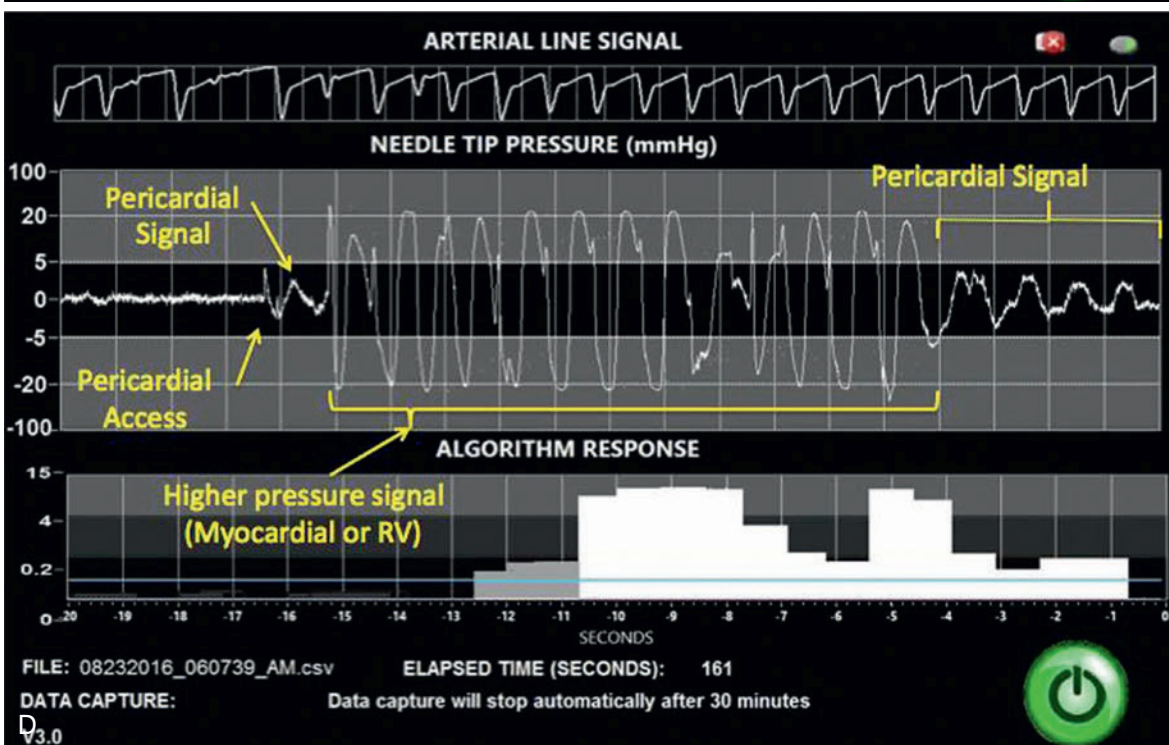
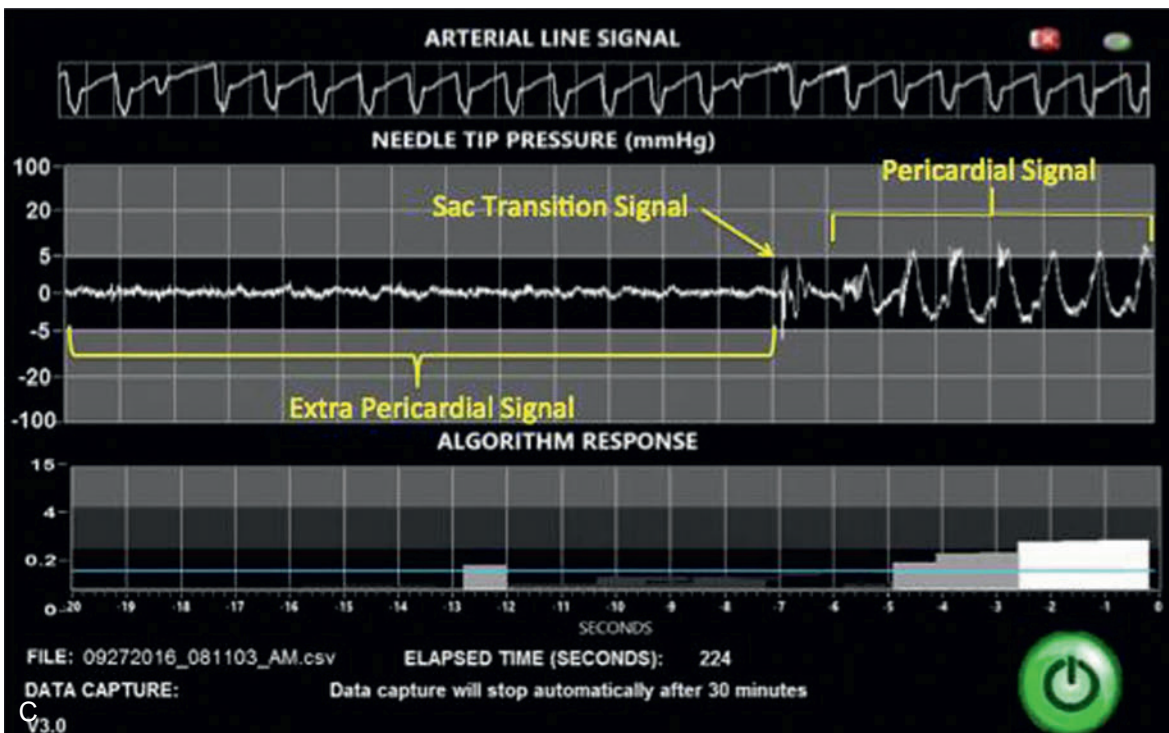
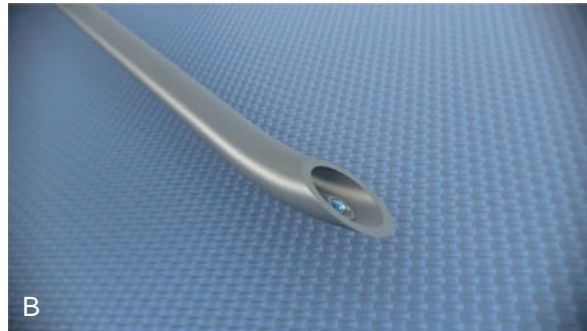
A disadvantage of this technique is the limited tactile feedback transmitted by the micropuncture needle upon crossing the parietal pericardium. In addition, the 0.018-inch guidewire may be difficult to visualize with low-quality fluoroscopy.^{45,46}

Anterior versus posterior approach for epicardial access. Depending on the anatomical region of interest, either an anterior or a posterior (inferior) approach to pericardial puncture may be chosen (Fig. 4.15). The anterior or posterior approach allows access to the anterior surface of the ventricles and LA appendage, and also allows access to the posterior and inferior regions of the heart (by looping the ablation catheter around the IV). On the other hand, the posterior approach allows easier access to the inferior ventricular walls and posterior LA walls. In addition, the posterior approach may be preferred in patients with prior cardiac surgery, since the pericardial adhesions are typically more extensive anteriorly, limiting the anterior approach.

For the anterior approach, the pericardial needle is advanced at a shallow angle (20 to 30 degrees in the LAO view), and closer to the midline, which allows entry to the pericardial space anteriorly over the RV. In contrast, for the posterior approach, once the needle passes over the dome of the diaphragm, it is directed more posteriorly at a steeper angle (greater than 45 degrees), aiming toward the basal portion of the heart (marked by the CS catheter in the LAO view), and slightly more leftward (to minimize the risk of injury to the posterior descending artery), which allows entry to the pericardial space under the inferior aspect of the ventricles.⁴⁷

When the curved-tip Tuohy needle is used, the needle bevel is pointed away from the myocardium (upward during the anterior approach and downward during the posterior approach) to minimize the risk of cardiac perforation and point the guidewire in the desired direction.³⁷

Fig. 4.14 The EpiAccess Needle. (A) The EpiAccess needle is depicted at the entry site in the subxiphoid area. Note that this needle is connected to a cable in order to transmit the pressure data into a screen monitor. (B) EpiAccess needle with a distal tip fiber optic sensor. (C and D) EpiAccess monitor screen. Arterial blood pressure and needle tip pressure tracings are displayed in the monitor of the EpiAccess System. (C) EpiAccess waveform showing transition from the extrapericardial to the pericardial space. (D) EpiAccess waveform showing transition from the myocardium or right ventricle to the pericardial space. Note the higher amplitude signals once the needle tip is against the right ventricular (RV) free wall. The needle is gently retracted into the pericardial space with signals ranging from 15 to 25 mm Hg. (Modified from Di Biase L, Burkhardt JD, Reddy V, et al. Initial international multicenter human experience with a novel epicardial access needle embedded with a real time pressure/frequency monitoring to facilitate epicardial access: feasibility and safety. *Heart Rhythm*. 2017;14:981–988.)



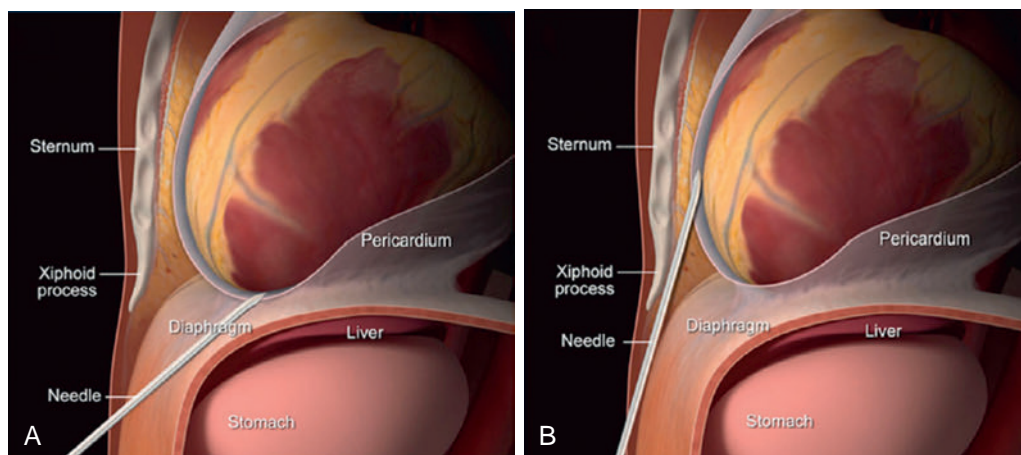


Fig. 4.15 Anterior Versus Posterior Approach for Epicardial Access. Diagrammatic representation of needle entry utilized in inferior (A) and anterior (B) approach epicardial access, respectively. Note the “bevel-out” needle tip position. (From Killu AM, Wan SH, Munger TM, et al. Pericardial effusion following drain removal after percutaneous epicardial access for an electrophysiology procedure. *Pacing Clin Electrophysiol.* 2015;38:383–390.)

Generally, the anterior approach is considered safer than the posterior approach, and is preferred, whenever possible. The shallow angle of the needle trajectory used for the anterior approach directs the needle above and parallel to the dome of the diaphragm directly toward the fibrous pericardium, obviating injury to diaphragmatic vessels and subdiaphragmatic organs. Conversely, a steeply angled needle (as used for the inferior approach) is more likely to pass through the diaphragm and can potentially puncture subdiaphragmatic structures (vessels, liver, colon). Furthermore, with the posterior approach, there is potential risk, although small, of damage to the posterior descending artery; this risk can be mitigated by directing the needle away from the septum.³⁸

Pericardial adhesions. Attempted epicardial access fails in approximately 10% of patients, primarily due to the presence of pericardial adhesions (e.g., following cardiac surgery or pericarditis). Even when epicardial access is possible, the presence of pericardial adhesions can significantly limit catheter maneuverability within the pericardial space.⁴²

In postsurgical patients, the adhesions are mostly concentrated in the anterior portion of the heart (the area where the pericardial sac was opened during sternotomy); therefore the puncture must be directed toward the diaphragmatic area (posterior approach). In this setting, contrast pooling along the inferior wall (instead of spreading around the cardiac silhouette) and restricted intrapericardial maneuverability of the guidewire often are observed, indicating the presence of pericardial adhesions. Conversely, adhesions can be more diffuse in postpericarditis patients, severely limiting percutaneous access to the pericardium.^{37,42,48}

In patients with pericardial adhesions, the curve of the deflected ablation catheter can be used to gently disrupt the adhesions; however, care must be taken to avoid cardiac perforation with the catheter tip in these cases. A hybrid procedure involving surgical access with a sub-xiphoid pericardial window or a limited anterior or lateral thoracotomy combined with manual dissection and lysis of the adhesions can facilitate access to the epicardial region of interest. However, access to other areas may still be limited.^{47–49}

Complications of Pericardial Access

Pericardial bleeding. Pericardial bleeding related to the epicardial access procedure is most commonly related to myocardial injury. The coronary arteries are covered by epicardial fat along the AV groove and the interventricular septum, located away from the typical path of the

access needle and therefore are less vulnerable to injury. Occasionally, disruption of epicardial fat can result in limited bleeding.

The anterior wall of the RV is the cardiac structure most vulnerable to perforation during the anterior approach. RV puncture is not rare, and usually occurs when the needle inadvertently overshoots into the RV myocardium after crossing the tough fibrous pericardium. RV puncture is usually benign if only the needle or guidewire has entered the chamber in a patient who is not anticoagulated. When the RV is inadvertently entered with the needle (indicated by aspiration of blood or contrast injection passing to the pulmonary artery), the needle can be withdrawn slightly (reentering the pericardial space after exiting the ventricle); contrast injection can then show silhouetting of the heart, and at that point the guidewire is advanced into the pericardial space. The small hole in the RV generally seals without incident. If the dilator and sheath have been passed into the RV, the larger hole may require surgical repair. In this setting, it may be preferable to leave the sheath in the RV and obtain a pericardial access and carry out the intended epicardial procedure. After completion of the procedure, the RV sheath may be removed when the surgical team is prepared to intervene immediately if required.^{38,42,46} Alternatively, the surgical consultant may prefer a limited thoracotomy or even sternotomy prior to sheath removal to ensure control of bleeding.

The use of the “needle-in-needle” technique can help reduce the risk of significant bleeding in the setting of inadvertent RV puncture.^{45,46} In addition, when the curved-tip Tuohy needle is used, directing the needle bevel away from the myocardium can help minimize the risk of cardiac perforation.³⁷

Approximately 10% to 20% of patients experience pericardial bleeding, particularly if inadvertent RV puncture has occurred. Bleeding is managed by frequent aspiration from the pericardial access sheath. Continued bleeding may require urgent surgical intervention. It is not uncommon to aspirate 10 to 30 mL of bloody drainage from the pericardial sheath early in the procedure. At this point, anticoagulation should not have been administered; therefore any bleeding should be self-limited and is generally considered a minor complication because it is not necessary to interrupt the procedure. Systemic anticoagulation with IV heparin is started when subsequent LV endocardial mapping is desired, but only after verifying the absence of continued pericardial bleeding.³⁷

There is concern that abrasion or laceration of pericardial structures can occur by the edges of a stiff sheath if the sheath is left in the pericardium without a catheter protruding from the lumen. Therefore it is recommended not to leave a large sheath in the pericardial space without a catheter in place. Also, it is important to lead with a wire or ablation catheter before advancing or moving the curl of the sheath to avoid damaging epicardial structures.⁴²

Intraabdominal bleeding. Infrequently (0.5% in one case series), intraabdominal bleeding can occur during the epicardial access procedure. Hemoperitoneum secondary to injury to the subdiaphragmatic vessels (e.g., epigastric artery) or abdominal viscera (liver and colon) can occur when the angle of the needle is too steep (during the posterior approach to pericardial access) or if the subxiphoid entry site is too caudal. The risk is higher in obese patients and in the presence of hepatomegaly, bowel distension, or left diaphragmatic paralysis.^{37,42,50} Also, the presence of a large hiatal hernia can predispose to inadvertent perforation (and subsequent mediastinal infections) during cannulation attempts.

Although perforation of the liver and intrahepatic bleeding can be well tolerated, more severe degrees of abdominal bleeding can result in acute hemodynamic decompensation and refractory hypotension and can necessitate immediate surgical intervention. Importantly, significant intraabdominal bleeding can develop only upon sheath withdrawal (and removal of the tamponading effect of the sheath) after the completion of the procedure.^{37,42,50}

Recognition of this complication can be difficult and requires a high index of suspicion. Abdominal pain (in unanesthetized patients), rebound tenderness, progressive hypotension in the absence of a pericardial effusion, and unexplained decrease in hemoglobin should prompt evaluation with abdominal ultrasound or (in hemodynamically stable patients) computed tomography (CT) imaging.

Adequate palpation of the xiphoid process, manual pressure over the epigastrium to push the liver away from the path of the needle, using a shallow needle angle, and avoiding sideways movements of the needle can help prevent injury to subdiaphragmatic structures. Also, avoiding general anesthesia at the time of epicardial access can help early recognition of this complications as it can manifest as abdominal pain.^{37,42,50}

Pneumopericardium. Air can be introduced into the pericardial space during the exchange of sheaths and catheters. Although pericardial air rarely causes cardiac tamponade, it can increase the transthoracic defibrillation threshold. Air in the pericardial space tends to stay around the cardiac apex (which is located most anteriorly located in the supine position) and is easily detected on fluoroscopy. Once detected, pericardial air should be evacuated, especially before the induction of ventricular arrhythmias that may require electrical cardioversion.³⁷ Careful sheath management to prevent air aspiration is important.⁴² On the other hand, air or an air-saline mixture may be introduced into the pericardial space intentionally (in a controlled manner) to physically displace a phrenic nerve from an epicardial ablation target site.

SIGNAL ACQUISITION AND PROCESSING

Cardiac electrograms are generated by the potential (voltage) differences recorded at two electrodes during the cardiac cycle. All clinical electrogram recordings are differential recordings from one source that is connected to the anodal (positive) input of the recording amplifier and a second source that is connected to the cathodal (negative) input.⁵¹

Whereas the surface ECG records a summation of the electrical activity of the entire heart, intracardiac electrograms recorded by the electrode catheter represent only the electrical activity (phase 0 of the action potential) of the local cardiac tissue in the immediate vicinity of the catheter's electrodes.

Unipolar electrograms represent the potential difference between the electrode in close association with cardiac tissue (the exploring electrode) and a distant *indifferent* (reference) electrode which is placed at a distance from the heart (so that the indifferent electrode has little or no cardiac signal). In practice, the Wilson central terminal is used to approximate the indifferent electrode. The precordial ECG leads, for example, are unipolar recordings that use an indifferent electrode created by connecting the arms and left leg electrodes through high-impedance resistors. Bipolar electrograms represent the potential difference between two electrodes and are calculated as the algebraic difference between the two unipolar electrograms at the two sites (using the same reference electrode).⁵²

The electrode is an electrical conductor which is used to make contact with the heart and convert ionic currents into electrical currents that can be detected by electronic devices. These currents are typically very small and, hence, must be processed and displayed in an easily understandable manner. This involves amplification and filtering of the signals.

Analog Versus Digital Recordings

Intracardiac electrograms are recorded with amplifiers that have high-input impedances (greater than 1010 Ω), to reduce unwanted electrical interference and ensure high-quality recordings. Analog recording systems directly amplify the potential from the recording electrodes, plot the potential on a display oscilloscope, and write it to recording paper or store it on magnetic tape.⁵¹

Analog systems have largely been replaced by digital recording systems that use an analog to digital (A/D) converter that converts the amplitude of the potential recorded at each point in time to a number that is stored. The quality of digital data is influenced by the sampling frequency and precision of the amplitude measurement. The most common digital recording systems sample the signal approximately every 1 millisecond (i.e., 1000 Hz), which is generally adequate for practical purposes of activation mapping. However, higher sampling frequencies can be required for high-quality recording of high-frequency, rapid potentials that can originate from the Purkinje system or areas of infarction. The faster sampling places greater demands on the computer processor and increases the size of the stored data files.⁵¹

Signal Amplification

The amplitude of intracardiac electrograms is usually small, ranging from 25 μV (recorded from scarred myocardium) to 5 mV (from a surface ECG lead). Therefore signal amplification (voltage gain) is necessary and is achieved by electronic amplifiers (voltage amplifiers), which can amplify recorded signals (up to 10,000 times) to a large enough voltage to be displayed and easily visualized. However, the recorded signal is often contaminated with noise, and signal amplification can also amplify the noise. Therefore signal filtering is required. To further enhance the signal-to-noise ratio, a type of electronic amplifier (differential amplifier or instrumentation amplifier) amplifies the difference between two voltages while rejecting any signal common to both inputs.⁵³ Of note, excessive electrogram amplification can result in electrogram saturation and signal cutting.⁵⁴

Signal Clipping

Electrogram clipping is useful when the intracardiac electrogram of interest (e.g., His potential) is small relative to the size of surrounding electrograms (e.g., ventricular signal), and the gain must be markedly increased to produce a measurable deflection. In this setting, clipping the signals can help eliminate the highly amplified surrounding signals (that do not need to be visualized to their full extent) and allow focusing on the deflection of interest (Fig. 4.16). It is important to recognize, however, that clipping eliminates the ability to determine the amplitude

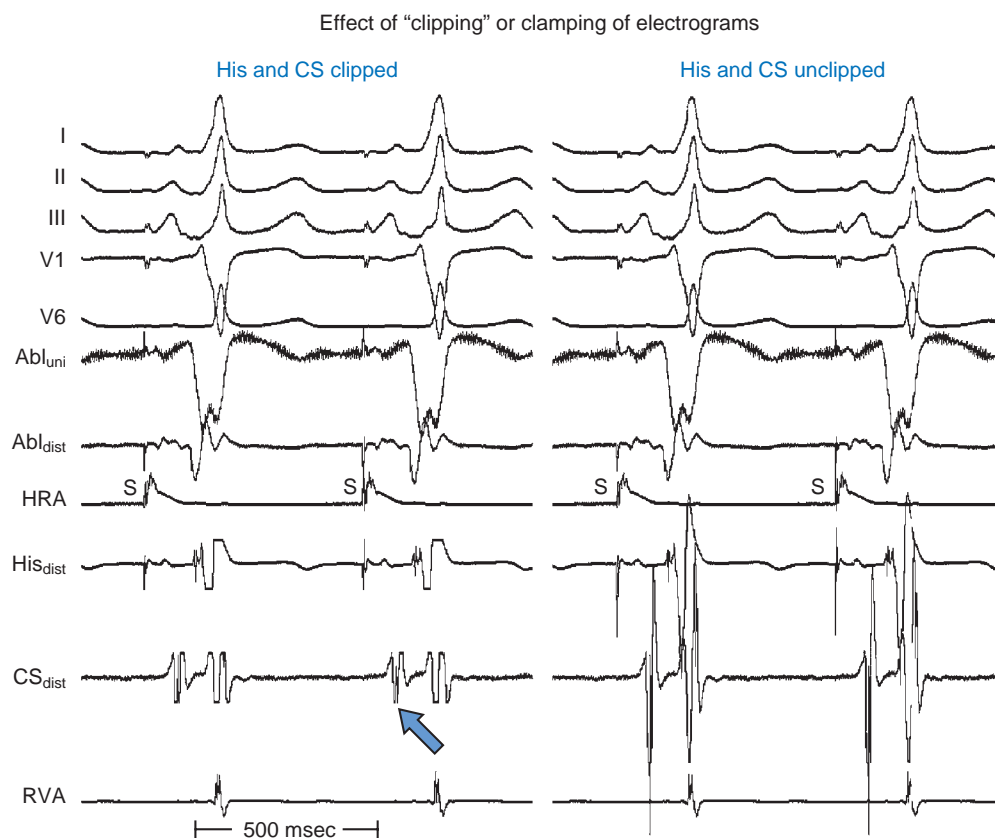


Fig. 4.16 Effect of Electronic Clipping on Recordings. The same two complexes are shown in both panels. *Left*, Both His and coronary sinus (CS) recordings are electronically attenuated (clipped) to reduce excursions on the display. The CS atrial and ventricular signals appear to have equal amplitude, and the ventricular electrogram in the His recording is small. *Right*, Without clipping, the true signal amplitudes are seen, showing a very large ventricular signal in the His recording and a larger atrial than ventricular signal in the CS recording. *Abl_{dist}*, Distal ablation; *Abl_{uni}*, unipolar ablation; *CS_{dist}*, distal coronary sinus; *His_{dist}*, distal His bundle; *HRA*, high right atrium; *RVA*, right ventricular apex.

and timing of the intrinsic deflection (local timing) of the signals being clipped.⁵⁴

Signal Filtering

Filtering enhances certain portions of the frequency spectrum while rejecting unwanted portions of the spectrum. The range of frequencies not filtered out is frequently called the band pass. The high-pass filter allows frequencies higher than a certain limit to remain in the signal (i.e., it filters out lower frequencies), while the low-pass filter allows frequencies lower than a certain limit to remain in the signal.⁵³

Surface ECG signals and intracardiac electrograms contain different frequencies and therefore require different filtering parameters. Bipolar intracardiac electrograms are usually filtered at 30 to 500 Hz, whereas unipolar electrograms are filtered at 0.05 to 500 Hz.

Diagnostic-quality surface ECG signals are usually filtered at 0.05 to 100.0 Hz. Although the bulk of the energy is in the 0.1- to 20.0-Hz range, the lower frequency cutoff of 0.05 Hz is a better reproduction of the ST segments (but at the expense of more baseline drift) and the upper cutoff frequency of 100 Hz is a better reproduction of high-frequency components in the P-QRS (but at the expense of increased susceptibility to interference at the power-line frequency of 50 to 60 Hz). An upper cutoff frequency of 100 Hz enables detailed analysis of the morphology of the P wave and QRS complex (which is of importance

during arrhythmia mapping) as well as identification of high-frequency fragmented P-QRS components (e.g., Epsilon waves). Because of interference from alternating current (AC), muscle twitches, and similar relatively high-frequency interference, it is sometimes necessary to record the surface ECG over a lower frequency range or to use notch filters. An optional notch filter is provided at 50/60 Hz to further reject line frequency interference. Monitor-quality ECGs are usually filtered at 0.5 to 40 Hz.^{53,54}

High-Pass Filtering

High-pass filtering allows signals faster than a specified frequency (the cutoff frequency or corner frequency) to be transmitted unchanged while rejecting or significantly attenuating the amplitude of signals slower than the cutoff frequency. If intracardiac recordings were not filtered, the signal would wander up and down as this potential fluctuates with respiration, catheter movement, and variable catheter contact.⁵³

For bipolar electrograms, high-pass filters with corner frequencies between 10 and 50 Hz are commonly used for rejection of baseline drift. Filtering can distort the electrogram morphology and reduce its amplitude. The bipolar signal becomes more complex, and additional peaks are introduced. In general, high-pass filtering can be viewed as differentiating the signal, so that the height of the signal is proportional to the rate of change of the signal, rather than only the amplitude.⁵²

Unipolar signals are commonly filtered at 0.05 to 0.5 Hz to remove baseline drift and DC voltages (which, by definition, have a frequency of 0 Hz). Filtering at higher corner frequencies (e.g., 30 Hz) alters the morphology of the signal so that the morphology of the unipolar signal is no longer an indication of the direction of wavefront propagation and the presence or absence of a QS complex cannot be used to infer proximity to the site of earliest activation. However, filtering the unipolar signal does not affect its usefulness as a measure of the local activation time. During mapping of areas with infarcts or scars, where local electrograms can have very low amplitude and can be masked by larger far-field signals, high-pass filtering of a unipolar signal (at 30 Hz) can help reduce the far-field signal and improve detection of the lower amplitude local signals.⁵²

Low-Pass Filtering

Low-pass filters attenuate frequencies that are faster than the specified corner frequency (usually 250 to 500 Hz). This approach is useful for reducing high-frequency noise without substantially affecting electrograms recorded with clinical systems where most of the signal content is lower than 300 Hz.⁵² A reduction of the low-pass filter to less than 250 Hz is not recommended because of attenuation of high-frequency electrogram contents that are essential for near-field signals recorded from the HB, HPS, and PVs, as well as scar-containing slow-conduction sites with fractionated high-frequency electrograms.^{53,54}

Band-Pass Filtering

Defining a band of frequencies to record, such as setting the high-pass filter to 30 Hz and the low-pass filter to 300 Hz, defines a band of frequencies from 30 to 300 Hz that are not attenuated (i.e., band-pass filtering).

Notch Filtering

A notch filter is a special case of band-pass filtering, with specific attenuation of frequencies at 50 or 60 Hz to reduce electrical noise introduced by the frequency of common AC current. Importantly, notch filtering can significantly attenuate certain local intracardiac signals, such as near-field PV potentials or rapidly varying fractionated potentials.⁵³ In addition, notch filtering can introduce “ringing” to sharp simple bipolar signals, making them appear fractionated. This is a particular concern when targeting fractionated potentials during VT and AF.¹

INTRACARDIAC ELECTROGRAMS

Recorded intracardiac electrograms can provide three important pieces of information: (1) the local activation time (i.e., the time of activation of the myocardium immediately adjacent to the recording electrode relative to a reference), (2) the direction of propagation of electrical activation within the field of view of the recording electrode, and (3) the complexity of myocardial activation within the field of view of the recording electrode.

Significant differences exist between unipolar and bipolar recording in terms of spatial resolution (i.e., ability to locate the discrete area of excited tissue generating the recorded potentials), temporal resolution (i.e., ability to identify the local activation time which coincides best with the arrival of the depolarization wavefront), and directionality (i.e., ability to provide information regarding the direction and the origin of wavefronts). Those differences can be utilized to assist in mapping by simultaneously recording bipolar and unipolar signals from the mapping catheter.⁵¹ Although bipolar recordings provide sufficient information for most mapping purposes in clinical EP laboratories, simultaneous unipolar recordings can provide an indication of the

direction of wavefront propagation and a more precise measure of the timing of local activation.

Unipolar Recordings

A unipolar electrogram is the voltage difference recorded between an intracardiac electrode in close association with cardiac tissue (the exploring electrode) and a distant *indifferent* (reference) electrode which is placed at a distance from the heart (so that the indifferent electrode has little or no cardiac signal), such as at the Wilson central terminal or an electrode positioned in the IVC. The amplitude of the unipolar signal is directly proportional to the area of the wavefront of depolarization and inversely proportional to the square of its distance from the exploring electrode. Poor electrode contact manifests as a slow (low rate-of-change) signal instead of the expected rapid positive-to-negative polarity change.^{52,55}

Spatial Resolution

Unipolar recordings have poor signal-to-noise ratio and contain substantial far-field signal generated by depolarization of tissue remote from the recording electrode because the unipolar electrode records a potential difference between widely spaced electrodes. Therefore distant activity can be difficult to separate from local activity. This is especially true when recording from areas of scarred myocardium, where the fractionated ventricular potentials are ubiquitous and it is often impossible to select a rapid negative dV/dt when the entire QS potential is slowly inscribed—that is, cavity potential.

Noise can be reduced by using an indifferent electrode in the IVC instead of the Wilson central terminal. In addition, filtering the unipolar electrograms can help eliminate far-field signals; however, the filtered unipolar recordings lose the ability to provide directional information. The unipolar electrograms are generally unfiltered (0.05 to 300 Hz or more). When an abnormal tissue (scars or infarct areas) is studied, where local electrograms can have very low amplitude and can be masked by larger far-field signals, the unipolar recordings can be filtered at settings comparable to those of bipolar electrograms (10 to 40 to 300 Hz or more).

Temporal Resolution

Unipolar recordings provide a more precise measure of the timing of local activation than bipolar recordings. This is true for filtered and unfiltered unipolar electrograms.⁵¹ By convention, the exploring electrode in contact with the cardiac tissue is connected to the positive input of the recording amplifier. In this configuration, a wavefront propagating toward the exploring electrode generates a positive deflection, whereas a wavefront traveling away from the electrode generates a negative deflection. Thus, an approaching wavefront creates a positive deflection that quickly reverses itself as the wavefront travels past the electrode, thus generating an RS complex. The transition from positive to negative occurs when the wavefront is immediately beneath the exploring electrode and is marked by the steepest negative slope of the signal. In normal homogeneous tissue, the maximum negative slope (dV/dt) of the signal coincides with the arrival of the depolarization wavefront directly beneath the electrode because the maximal negative dV/dt corresponds to the maximum sodium (Na⁺) channel conductance (Fig. 4.17). This is true for filtered and unfiltered unipolar electrograms.⁵⁶

Directionality

The morphology of the unfiltered unipolar electrogram provides information about the direction of impulse propagation (and therefore its origin); positive deflections (R waves) indicate propagation towards the recording electrode, and negative deflections (S waves) indicate

Unipolar recordings: local vs. remote events



Fig. 4.17 Unipolar and Bipolar Recordings. Two complexes from different sites are shown in a patient with Wolff-Parkinson-White syndrome. The dashed line denotes onset of the delta wave. In site A, the unfiltered unipolar recording shows a somewhat blunted “QS” complex and small atrial component, but the filtered (30- to 300-Hz) bipolar signal shows a very large atrial signal and very small ventricular signal (arrow), suggesting a poor choice for ablation site. Site B shows a sharper “QS” in the unipolar signal, with a larger ventricular than atrial electrogram, and the initial nadir of bipolar recording coincides with the maximal negative dV/dt of the unipolar recording. Ablation at this site was successful. *Abl_{dist}*, Distal ablation; *Abl_{uni}*, unipolar ablation; *CS_{dist}*, distal coronary sinus; *His_{dist}*, distal His bundle; *HRA*, high right atrium; *RVA*, right ventricular apex.

propagation away from the electrode. A biphasic electrogram (positive then negative, RS complex) indicates a wavefront of depolarization traveling past the electrode, representing the approach and recession of the activation wavefront. If the wavefront originates immediately below the exploring electrode, it spreads away from the electrode in all directions simultaneously, producing a negative deflection (QS) with no R wave. Importantly, a QS electrogram configuration has a low spatial resolution and relatively low specificity, being attainable in an area of more than 1 cm in diameter from the real site of origin of the arrhythmia.^{52,57}

As noted, filtering the unipolar electrogram at higher corner frequencies (e.g., 30 Hz) alters its morphology so that it no longer indicates the direction of wavefront propagation and, then, the presence or absence of a QS complex cannot be used to infer proximity to the site of earliest activation.

Bipolar Recordings

Bipolar recordings are obtained by connecting two electrodes that are exploring the area of interest to the recording amplifier. At each point in time, the potential generated is the sum of the potential from the positive input and the potential at the negative input. The potential at the negative input is inverted; this is subtracted from the potential at the positive input so that the final recording is the difference between the two.⁵¹

Spatial Resolution

Bipolar recordings provide an improved signal-to-noise ratio. In addition, high-frequency components are more accurately seen, which facilitates identification of local depolarization, especially in abnormal areas of infarction or scar.

Unlike unipolar recordings, bipolar electrodes with short interelectrode distances are relatively unaffected by far-field events and mainly reflect the local electrical activity produced by the area of tissue in contact with and between the two electrodes. The bipolar electrogram is simply the difference between the two unipolar electrograms recorded at the two poles. Because the far-field signal is similar at each instant in time, it is largely subtracted out, thus leaving the local signal. Therefore compared with unipolar recordings, bipolar recordings provide an improved signal-to-noise ratio, and high-frequency components are more accurately seen. This allows more accurate visualization of high frequency components of the electrogram. As the distance from the recording site increases, amplitude and frequency of the recorded signal decrease depending on the interelectrode distance.

To acquire true local electrical activity, a bipolar electrogram with an interelectrode distance of less than 1 cm is desirable. Smaller interelectrode distances record increasingly local events (as opposed to far-field). Elimination of far-field noise is usually accomplished by filtering the intracardiac electrograms, typically at 30 to 500 Hz.

Temporal Resolution

Algorithms for detecting local activation time from bipolar electrograms have been more problematic, partly because of generation of the bipolar electrogram by two spatially separated recording poles. Multiple methods were proposed. In a homogeneous sheet of tissue, the initial peak of a filtered (30 to 300 Hz) bipolar signal coincide with depolarization beneath the recording electrode and appears to correlate most consistently with local activation time, corresponding to the maximal negative dV/dt of the unipolar recording (see Fig. 4.17). However, in the setting of complex multicomponent bipolar electrograms, such as those with marked fractionation and prolonged duration seen in regions with complex conduction patterns (e.g., in regions of slow conduction in macroreentrant AT or VT), determination of local activation time becomes challenging, and the decision about which activation time is most appropriate needs to be made in the context of the particular rhythm being mapped.^{51,58}

Directionality

In contrast to unipolar electrograms, the direction of wavefront propagation cannot be reliably inferred from the morphology of a single bipolar signal (direction can, however, be inferred from the relative timing of two adjacent bipolar recordings).

Several factors can affect bipolar electrogram morphology and amplitude, including: (1) the orientation of the bipolar recording axis to the direction of propagation of the activation wavefront; (2) electrode size; (3) interelectrode distance; (4) electrode-tissue contact (i.e., the distance between the source of the potential and the recording electrode); (5) conduction velocity (the greater the velocity, the higher the peak amplitude of the filtered bipolar electrogram); and (6) the mass of the activated tissue. A wavefront that is propagating in the direction exactly perpendicular to the axis of the recording dipole produces no difference in potential between the electrodes and hence no signal is recorded.

Nevertheless, a change in morphology can provide important clues about the activation pattern of the propagating wavefront.

Timing of Local Events

As noted, with an unfiltered unipolar electrogram, a wavefront of depolarization that is propagating toward the exploring electrode generates a positive deflection (an R wave). As the wavefront reaches the electrode and propagates away, the deflection sweeps steeply negative. This rapid reversal constitutes the intrinsic deflection of the electrogram and represents the timing of the most local event (i.e., at the site of the electrode). The maximum downslope (dV/dt) of the unipolar electrogram coincides with the arrival of the depolarization wavefront directly beneath

the electrode and is now considered the most accurate marker of local tissue activation (see Fig. 4.17).^{52,55}

Filtering the unipolar signal does not affect its usefulness as a measure of the local activation time. The slew rate or dV/dt of the filtered electrogram is so rapid in normal heart tissue that the difference between the peak and the nadir of the deflection is 5 milliseconds or less. Identification of the local event is therefore easy with filtered or unfiltered electrograms in normal tissue. On the other hand, diseased myocardium can conduct very slowly with fractionated electrograms, and this makes local events harder to identify.

To acquire true local electrical activity, a bipolar electrogram with an interelectrode distance of less than 1 cm is preferable. Smaller interelectrode distances record increasingly local events. In normal homogeneous tissue, the initial peak of a filtered (30 to 300 Hz or more) bipolar recording coincides with depolarization beneath the recording electrode and corresponds to the maximal negative dV/dt of the unipolar recording (see Fig. 4.17). However, in the setting of complex multicomponent bipolar electrograms, such as those with marked fractionation and prolonged duration seen in regions with complex conduction patterns, determination of local activation time becomes problematic.

Choices of Surface and Intracardiac Signals

Baseline recordings obtained during a typical EP study include several surface ECG leads and several intracardiac electrograms, all of which are recorded simultaneously. Timing of events with respect to onset of the QRS complex or P wave on the surface ECG is often important during the EP study, but it is cumbersome to display all 12 leads of the regular surface ECG. It is more common to use leads I, II, III, V1, and V6, which provide most of the information required to determine the frontal plane axis, presence and type of intraventricular conduction abnormalities, and P wave morphology.

Intracardiac leads can be placed strategically at various locations within the cardiac chambers to record local events in the region of the lead. A classic display would include three to five surface ECG leads, high RA recording, HB recording, CS recording, and RV apex recording (Fig. 4.18). Depending on the type of study and information sought, stimulation and recording from other sites can be appropriate and can include RB recording, LV recording, transseptal LA recording, and atrial and ventricular mapping catheter tracings for EP mapping and ablation.⁵²

The intracardiac electrograms are generally displayed in the order of normal cardiac activation. The first intracardiac tracing is a recording from the high RA close to the sinus node. The next intracardiac tracing is the HB recording, obtained from a catheter positioned at the HB, which shows low septal RA, HB, and high septal RV depolarizations. One to nine recordings may be obtained from the CS, which reflects LA activation, followed by a recording from the RV catheter (see Fig. 4.18).

Right Atrial Electrogram

Depending on the exact location of the RA catheter, the high RA electrogram typically shows a local sharp, large atrial electrogram and a smaller, far-field ventricular electrogram. The catheter is usually positioned in the RA appendage because of stability and reproducibility. The recorded atrial electrogram is earlier in the P wave when the catheter is positioned close to the sinus node. Recordings from this site also help determine the direction of atrial activation (e.g., high-low versus low-high, and right-left versus left-right). Pacing at this position allows evaluation of sinus node function and AV conduction, as well as the induction of supraventricular, and occasionally ventricular, arrhythmias.

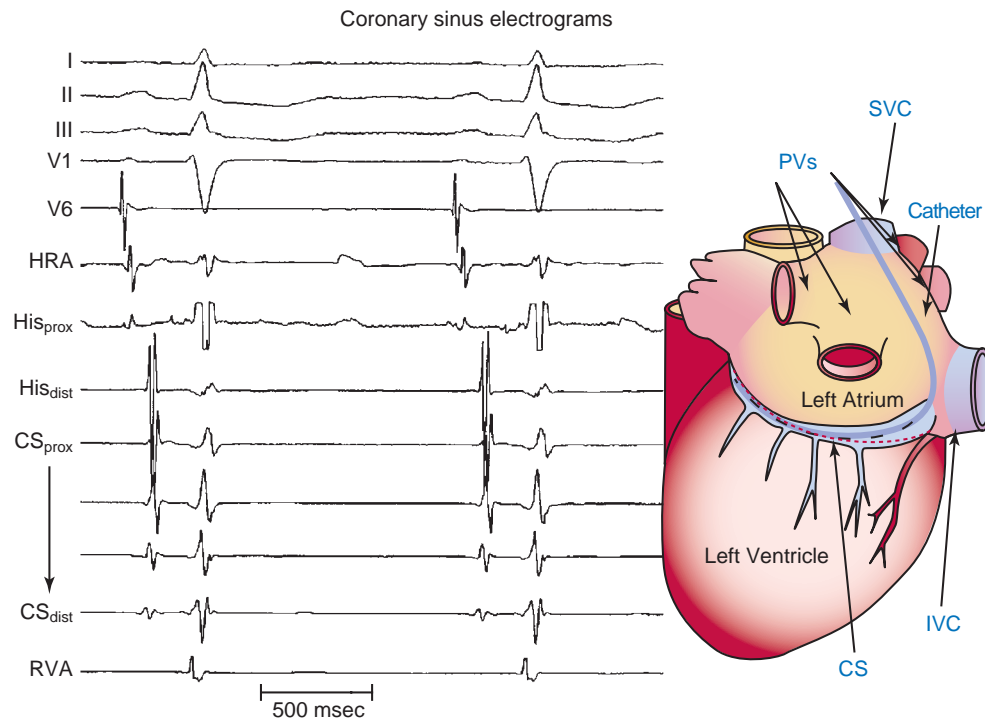


Fig. 4.18 A Classic Display of Surface ECG and Intracardiac Recordings During an Electrophysiology Study of Supraventricular Tachycardia. *Left*, Included are four surface ECG leads, high right atrium (HRA) recording, two His bundle recordings (proximal and distal His [His_{prox} and His_{dist}]), five coronary sinus (CS) recordings (in a proximal-to-distal sequence), and a right ventricular apex (RVA) recording. The relative amplitudes of atrial and ventricular electrograms in CS recordings are also shown. *Right*, The back of the heart is shown with a CS catheter in position. The distal portion of the CS (CS_{dist}) is closer to the ventricle (originating as the great cardiac vein on the anterior wall); the CS crosses the atrioventricular groove at the lateral margin and becomes an entirely atrial structure as it empties into the right atrium. Thus, proximal CS (CS_{prox}) recordings show large atrial and small ventricular signals, whereas more distal recordings show small atrial, large ventricular signals. IVC, Inferior vena cava; PVs, pulmonary veins; SVC, superior vena cava.

His Bundle Electrogram

The HB catheter is positioned at the junction of the RA and RV. Therefore it records electrograms from local activation of the adjacent atrial, HB, and ventricular tissues (Fig. 4.19). Using a 5- to 10-mm bipolar recording, the His potential appears as a rapid biphasic spike, 15 to 25 milliseconds in duration, interposed between local atrial and ventricular electrograms. The use of a quadripolar catheter allows simultaneous recording of three bipolar pairs.

Before measuring conduction intervals within the HB electrogram, it is important to verify that the spike recorded between the atrial and ventricular electrograms on the HB catheter actually represents activation of the most proximal HB and not the distal HB or RB. The most proximal electrodes displaying the His potential should be chosen. Anatomically, the proximal portion of the HB originates in the atrial side of the tricuspid annulus; thus, the most proximal HB deflection is the one associated with the largest atrial electrogram. Recording a His potential associated with a small atrial electrogram can reflect a recording of the distal HB or RB and therefore would miss important intra-His conduction abnormalities and falsely shorten the measured His bundle–ventricular (HV) interval (see Fig. 4.19). Therefore even if a large His potential is recorded in association with a small atrial electrogram, the catheter should be withdrawn to obtain a His potential associated with a larger atrial electrogram. Using a multipolar electrode catheter to record simultaneously proximal and distal HB electrograms (e.g., a quadripolar catheter records three bipolar

electrograms over a 1.5-cm distance) can help evaluate intra-His conduction.

Validation of the HB recording can be accomplished by assessment of the HV interval and establishing the relationship between the His potential and other electrograms. The HV interval should be 35 milliseconds or longer (in the absence of preexcitation). In contrast, the RB potential invariably occurs within 30 milliseconds before ventricular activation. Atrial pacing can be necessary to distinguish a true His potential from a multicomponent atrial electrogram. With a true His potential, the AH interval should increase with incremental pacing rates. HB pacing can also be a valuable means for validating HB recording. The ability to pace the HB through the recording electrode and obtain HB capture (i.e., QRS identical to that during normal sinus rhythm [NSR] and stimulus-to-QRS interval identical to the HV interval during NSR) provides the strongest evidence validating the His potential. However, this technique is inconsistent in accomplishing HB capture, especially at low current output. Higher output can result in nonselective HB capture. The use of closely spaced electrodes and the reversal of current polarity (i.e., anodal stimulation) can facilitate HB capture. Failure to capture the HB selectively does not necessarily imply that the recorded potential is from the RB.

Other measures that can be used, although rarely required, to validate the HB recording include recording of pressure simultaneously with a luminal electrode catheter (which should reveal atrial pressure wave when the catheter is at the proximal His electrogram position) and simultaneous left and right recording of the His potential. The His

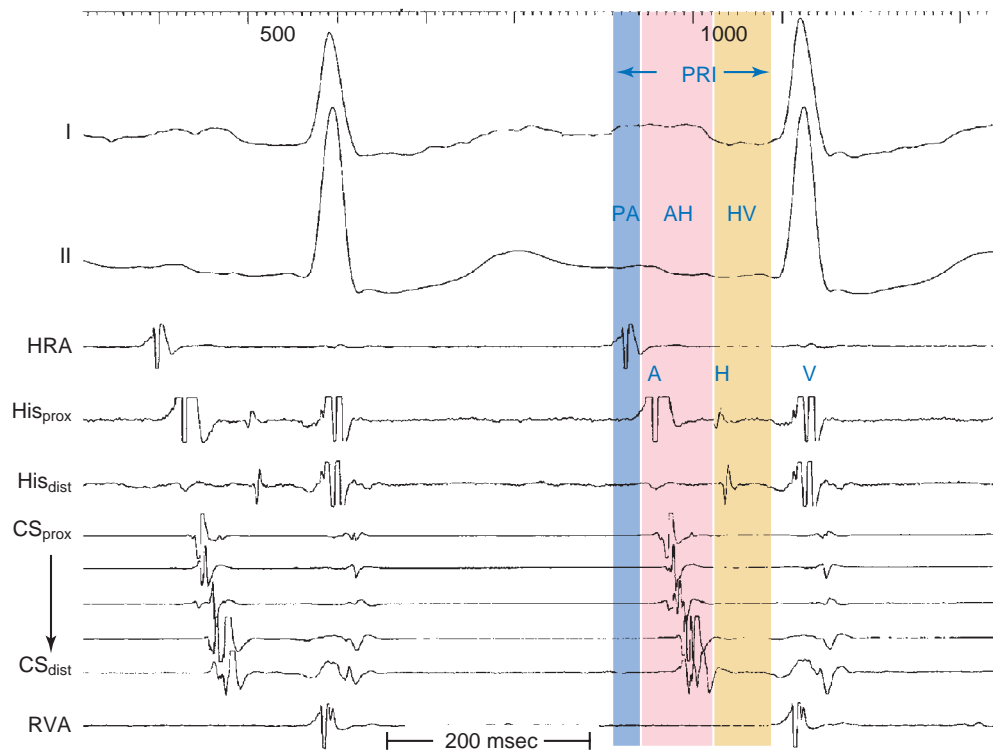


Fig. 4.19 Intracardiac Intervals. Shaded areas represent the P wave–atrial (PA) (blue), atrial–His bundle (AH) (pink), and His bundle–ventricular (HV) (yellow) intervals. It is important that the HV interval be measured from the onset of the His potential in the recording showing the most proximal (rather than the most prominent) His potential (His_{prox}) to the onset of the QRS on the surface ECG (rather than the ventricular electrogram on the His bundle recording). CS_{dist} , Distal coronary sinus; CS_{prox} , proximal coronary sinus; His_{dist} , distal His bundle; HRA , high right atrium; PRI , PR interval; RVA , right ventricular apex.

potential can be recorded in the noncoronary sinus of Valsalva (just above the aortic valve) or in the LVOT along the interventricular septum (just below the aortic valve). Because these sites are at the level of the central fibrous body, the proximal penetrating portion of the HB is recorded and can be used to time the His potential recorded via the standard venous route. Recording the HB from the noncoronary cusp (versus the LVOT) is preferred because only a true His potential can be recorded from that site.

Coronary Sinus Electrogram

Because the CS lies in the AV groove, in close contact to both the LA and the LV, the CS catheter records both atrial and ventricular electrograms. However, the CS has a variable relationship with the mitral annulus. The CS lies 2 cm superior to the annulus as it crosses from the RA to the LA. More distally, the CS frequently overrides the LV. Consequently, the most proximal CS electrodes (located at the CS os) are closer to the atrium and typically show a local sharp, large atrial electrogram and a smaller, far-field ventricular electrogram. The more distal CS electrodes, lying closer to the LV than the LA, record progressively smaller, less sharp, far-field atrial electrograms and larger, sharper, near-field ventricular electrograms (see Fig. 4.18).

During NSR, the atrial activation sequence proceeds from the proximal CS electrodes (positioned at the CS os) toward the distal CS electrodes. However, if the CS catheter is deeply seated in the CS, so that the most proximal electrodes are distal to the CS os and the most distal electrodes are anterolateral on the mitral annulus, then both proximal and distal electrodes can be activated at the same time (Fig. 4.20).

Right Ventricular Electrogram

The RV electrogram typically shows a local sharp and large ventricular electrogram and generally no atrial electrogram. The closer the RV catheter tip position is to the apex, the closer it is to the RB myocardial insertion site and the earlier the ventricular electrogram timing to the onset of the QRS. The catheter is usually positioned in the RV apex because of stability and reproducibility.

BASELINE INTERVALS

The accuracy of measurements made at a screen speed of 100 mm/s is ± 5 milliseconds, and at a speed of 400 mm/s is ± 1 millisecond. In dealing with large intervals (e.g., sinus node recovery time), a speed of 50 to 100 mm/s is adequate. For refractory periods, a speed of 150 to 200 mm/s is adequate, but for detailed mapping, a speed of 200 to 400 mm/s is required.

P Wave–Atrial Interval

The PA interval is measured from the first evidence of sinus node depolarization, whether on the intracardiac or surface ECG, to the atrial deflection recorded in the HB lead. It represents conduction through the RA to the inferoposterior atrial septum (i.e., the region of the AVN and HB; see Fig. 4.19).

The PA interval reflects conduction time from the sinus node to the AVN. A prolonged PA interval suggests abnormal atrial conduction and can be a clue to the presence of biatrial disease or disease confined to the RA. The normal range of the PA interval is 20 to 60 milliseconds. Rarely, diseased atrial conduction can underlie first-degree AV block,

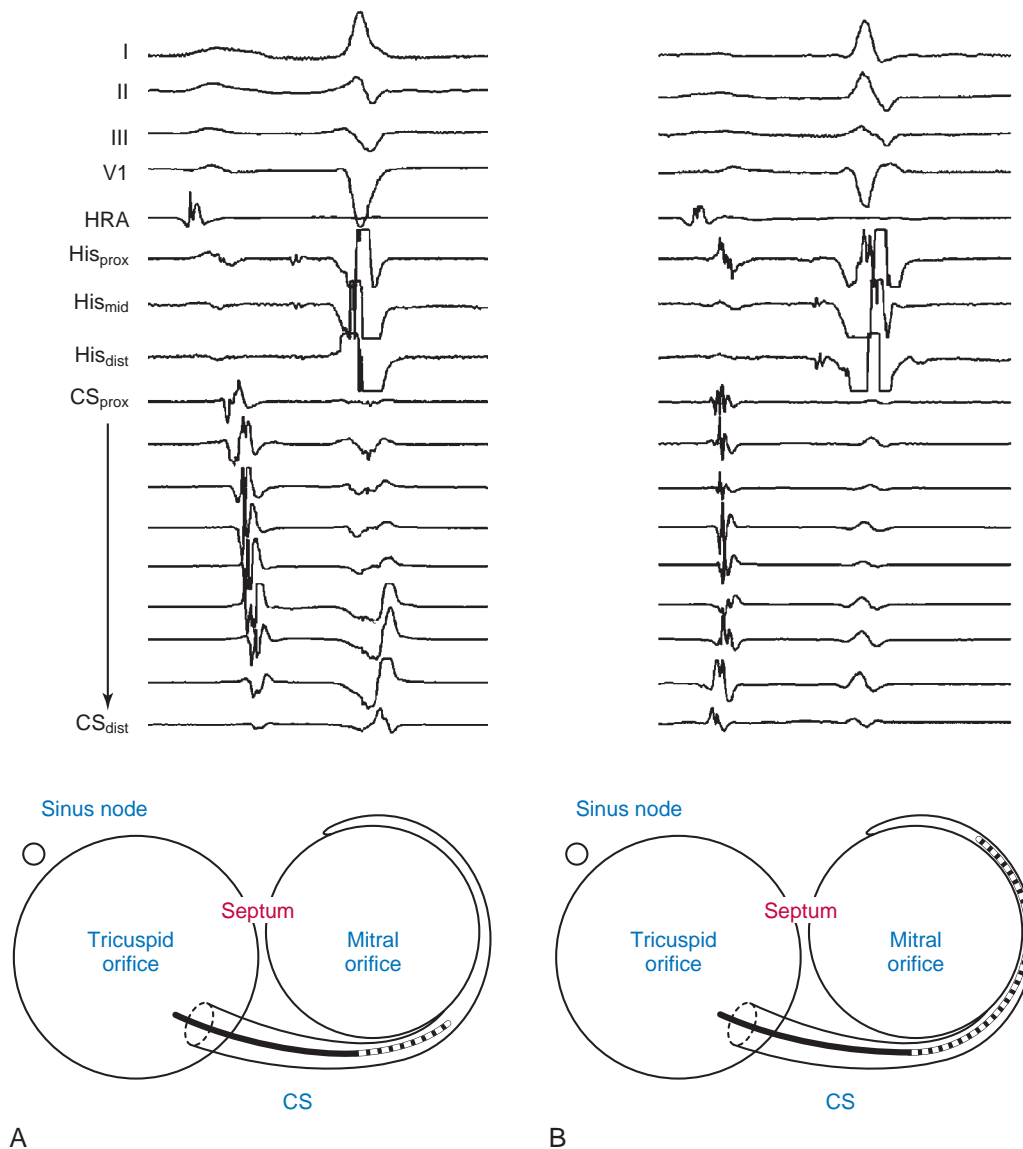


Fig. 4.20 Influence of Catheter Position on Coronary Sinus (CS) Atrial Electrograms. Two different CS atrial activation sequences are shown from different patients. (A) A proximal-to-distal sequence is shown. (B) The latest activation is in the mid-CS electrodes. The diagrams at the bottom show relative positions of the CS catheter in each instance (atrioventricular grooves viewed from above). With more proximal CS position (CS_{prox}), propagation is proximal-distal, indicating relative distance from the sinus node. With a more distal CS position (CS_{dist}), the mid-CS electrodes are farthest from the sinus node. His_{dist} , Distal His bundle; His_{mid} , middle His bundle; His_{prox} , proximal His bundle; HRA , high right atrium.

indicated by a prolonged PA interval. A short PA interval suggests an ectopic source of atrial activation.

Interatrial Conduction

Normal atrial activation begins in the high or mid-lateral RA (depending on the sinus rate), and spreads from there to the atrial septum, low RA and AV junction.

Activation of the LA is mediated by three possible routes. Superiorly, activation proceeds through the Bachman bundle; this can be seen in 50% to 70% of patients and can be demonstrated by CS os activation followed by distal CS and then mid-CS activation. Activation also propagates through the mid-atrial septum at the fossa ovalis and at the region of the central fibrous trigone at the apex of the triangle of Koch. The latter provides the most consistent amount of LA activation.

Interatrial conduction is measured by the interval between the atrial electrogram in the high RA lead and that in the CS lead. LA-to-RA activation during LA pacing appears primarily to cross the fossa and low septum and not the Bachman bundle, as reflected by relatively late high RA activation.

Normal retrograde atrial activation proceeds over the AVN. The earliest atrial activation is recorded in the AV junction (HB recording), then in the adjacent RA and CS os, and finally in the high RA and LA. More detailed mapping reveals atrial activation to start at the HB recording, with secondary breakthrough sites in the CS (reflecting activation over the LA extension of the AVN) or the posterior triangle of Koch. At faster ventricular pacing rates, the earliest atrial activation typically shifts to the posterior portion of the triangle of Koch, the CS os, or within the CS itself.

Atrial–His Bundle Interval

The AH interval is measured from the first rapid deflection of the atrial deflection in the HB recording to the first evidence of HB depolarization in the HB recording (see Fig. 4.19). The AH interval is an approximation of the AVN conduction time because it represents conduction time from the low RA at the interatrial septum through the AVN to the HB.

The AH interval can vary according to the site of atrial pacing. During LA or CS os pacing, the impulse can enter the AVN at a different site that bypasses part of the AVN, or it can just enter the AVN earlier in respect to the atrial deflection in the HB electrogram. Both mechanisms can give rise to a shorter AH interval.

The response of the AH interval to atrial pacing or drugs often provides more meaningful information about AVN function than an isolated measurement of the AH interval. Autonomic blockade with atropine (0.04 mg/kg) and propranolol (0.02 mg/kg) can be used to evaluate AVN function in the absence of autonomic influences. Not enough data, however, are available to define normal responses under these circumstances.

The AH interval has a wide range in normal subjects (50 to 120 milliseconds) and is markedly influenced by the autonomic nervous system. Short AH intervals can be observed in cases of increased sympathetic tone, reduced vagal tone, enhanced AVN conduction, and preferential LA input into the AVN, as well as unusual forms of preexcitation (atrio-His BTs).

Long AH intervals are usually caused by negative dromotropic drugs (such as digoxin, beta-blockers, calcium channel blockers, and antiarrhythmic drugs), enhanced vagal tone, and intrinsic disease of the AVN. Artificially prolonged AH intervals can result from an improperly positioned catheter or the incorrect identification of an RB potential as a His potential. This situation needs to be distinguished from true AH interval prolongation.

His Potential

His potential duration reflects conduction through the short length of the HB that penetrates the fibrous septum. Disturbances of HB conduction can manifest as fractionation, prolongation (longer than 30 milliseconds), or splitting of the His potential.

His Bundle–Ventricular Interval

The HV interval is measured from the onset of the His potential to the onset of the earliest registered surface or intracardiac ventricular activation. It represents conduction time from the proximal HB through the distal HPS to the ventricular myocardium (see Fig. 4.19).

The HV interval is not significantly affected by the autonomic tone, and it usually remains stable under normal conditions. The range of HV intervals in normal subjects is narrow, 35 to 55 milliseconds. A prolonged HV interval is consistent with diseased distal conduction in all fascicles or in the HB itself. A validated short HV interval suggests ventricular preexcitation via a BT. A falsely shortened HV interval can occur during sinus rhythm with PVCs or an accelerated idioventricular rhythm that is isorhythmic with the sinus rhythm, or when an RB potential rather than a His potential is inadvertently recorded.

PROGRAMMED ELECTRICAL STIMULATION

Stimulators

Cardiac stimulation is carried out by delivering a pulse of electrical current through the electrode catheter from an external pacemaker (stimulator) to the cardiac surface. Such an electrical impulse depolarizes cardiac tissue near the pacing electrode, which then propagates

through the heart. The paced impulses (stimuli) are introduced in predetermined patterns and at precise timed intervals using a programmable stimulator.

A typical stimulator has a constant current source and is capable of pacing at a wide range of cycle lengths (CLs), variable current strengths (0.1 to 10 mA), and pulse widths (0.1 to 10 milliseconds). In addition, current stimulators have at least two different channels of stimulation (preferably four) and allow delivery of multiple extrastimuli (three or more) and synchronization of the pacing stimuli to selected electrograms during intrinsic or paced rhythms.

Pacing Techniques

Pacing Output

Stimulation is usually carried out using an isolated constant current source that delivers a rectangular impulse. Pacing output at twice (2×) diastolic threshold is generally used. *Pacing threshold* is defined as the lowest current required for consistent capture determined in late diastole with a stimulus of a given duration. The pacing threshold can be influenced by the pacing cycle length (PCL); therefore the threshold should be determined at each PCL used. In general, refractory periods are somewhat longer when determined using 2× threshold (as opposed to higher outputs), and this can reduce the incidence of induction of nonclinical tachyarrhythmias. In addition, diastolic excitability can be influenced by drug administration; reevaluation of the pacing threshold and adjustment of the pacing output (2× threshold) are therefore required in such situations. A pulse duration of 1 or 2 milliseconds is generally used.

High current strength is generally used for determination of strength-interval curves to overcome drug-induced prolongation of refractoriness, assess the presence and mechanism of antiarrhythmic therapy, and overcome the effect of decreased tissue excitability (e.g., pace mapping in scar-related arrhythmias).

Cycle Length

During EP testing, CLs often change from beat to beat, so that these measures are more relevant than an overall rate expressed in beats per minute. The use of rates in beats per minute is retained mostly to facilitate communication with physicians who are more comfortable with this terminology. Pacing rate (per min) is determined by dividing 60,000 (milliseconds/min) by the CL (in milliseconds).

Incremental Versus Decremental

The terms *incremental* and *decremental* can have opposite meaning, depending on whether one is considering the pacing rate in beats per minute or the PCL in milliseconds. The term *incremental pacing rate* is derived from stimulators controlled by an analog dial. Digitally controlled devices often increase the rate by choosing a sequence of CL decrements, but the term *incremental pacing* may still be used.

Overdrive Pacing (“Straight Pacing”)

Pacing stimuli are delivered at a constant pacing rate (constant PCL) throughout the duration of the stimulation. The pacing rate is faster than the rate of the baseline rhythm to ensure capture of the spontaneous rhythm.

Burst Pacing

Pacing stimuli are delivered at a constant rate for a relatively short duration, but at successively faster rates with each burst until a predetermined maximum rate (or minimum PCL) has been reached. This technique is generally used for induction or termination of tachycardias.

Stepwise Rate-Incremental Pacing

After pacing at a given rate for a predetermined number of stimuli or seconds, the rate is increased (with intervening pauses) in a series of steps until predetermined endpoints are reached. It is important to maintain the pacing at any given rate for at least 15 seconds (period of accommodation) before increasing the pacing rate. Otherwise, the initial stimuli at any given rate can produce effects different from those observed several seconds later because the ability of a tissue to conduct is affected by the baseline rate or CL of the preceding beats. A disadvantage for this technique is the prolonged pacing required at each rate, which is time-consuming.

Ramp Pacing

Ramp pacing implies a smooth change in the interval between successive stimuli, with gradual decrease of the PCL every several paced complexes (without intervening pauses). Ramps are often used as an alternative to the stepwise method for assessment of conduction. The pacing rate is slowly increased at 2 to 4 beats/min every several paced beats until block occurs. This method is particularly useful when multiple assessments of conduction are planned (e.g., after therapeutic interventions) and in the assessment of retrograde conduction. Because each successive paced interval differs from its predecessor by only a few milliseconds, the interval at which block occurs can be determined more precisely using the ramp method. However, prolonged episodes of continuous high-rate pacing can provoke significant hypotension, and close monitoring of blood pressure is important while performing these maneuvers.

For tachycardia induction or termination, the ramp is decreased in duration, but the inter-stimulus intervals are decreased more rapidly. Ramp pacing is generally used in antitachycardia pacing algorithms in ICDs. Programmed rate-incremental ramps are also known as *auto-decremental pacing*.

Extrastimulus Technique

S_1 - S_1 drive stimuli. The heart is paced, or driven, at a specified rate and duration (typically eight paced beats) after which a premature extrastimulus is delivered. The eight drive beats are each termed S_1 stimulus. The S_1 - S_1 drive stimuli are sometimes called trains. These S_1 drive stimuli can be followed by first, second, third, and n th premature extrastimuli, which are designated as S_2 , S_3 , S_4 , and S_N . When the extrastimuli follow a series of sinus beats, the sinus beats can also be designated as S_1 .

S_1 , S_2 , S_3 , ..., S_N . S_2 is the first extrastimulus, with the S_1 - S_2 interval almost always shorter than the S_1 - S_1 interval. S_3 , S_4 , ..., S_N are the second, third, ..., n th extrastimuli. When stimulation is performed in the atrium, capture of S_1 , S_2 , S_3 , ..., S_N results in atrial depolarizations, termed A_1 , A_2 , A_3 , ..., A_N , respectively, and when stimulation is performed in the ventricle, they are termed V_1 , V_2 , V_3 , ..., V_N , corresponding to the resultant ventricular depolarizations, respectively.

One or more extrastimuli (designated S_2 , S_3 , and S_N) are introduced at specific coupling intervals based on previous S_1 drive stimuli or spontaneous beats. Thereafter, the S_1 - S_2 interval is altered, usually in 10- to 20-millisecond steps, until an endpoint is reached, such as tissue refractoriness or termination or induction of a tachycardia. It is usual to begin late in diastole and successively decrement the S_1 - S_2 interval. A second extrastimulus (S_3) can then be introduced, with the S_2 - S_3 interval altered similarly to that used for S_1 - S_2 .

Two methods are in common clinical use for decreasing the coupling intervals during delivery of multiple extrastimuli. In the simple sequential method, the S_1 - S_2 coupling interval is decreased until it fails to capture, at which time the coupling interval is increased until it captures (usually within 10 to 20 milliseconds). The S_1 - S_2 coupling interval is then held

constant while the S_2 - S_3 interval is decreased similarly to that used for S_1 - S_2 , and then the same is done for S_3 - S_4 . In the tandem method, the S_1 - S_2 coupling interval is decreased until S_2 fails to capture, and then the S_1 - S_2 coupling interval is increased by 40 to 50 milliseconds and held there. S_3 is then introduced and the S_2 - S_3 interval decreased until S_3 fails to capture. At that point, the S_1 - S_2 interval is decreased, and S_3 is retested to see whether it captures. From that point on, the S_1 - S_2 and S_2 - S_3 intervals are decreased in tandem until refractory. As compared with the simple sequential method, the tandem method allows relatively longer intervals and provides a larger number of stimulation runs before moving on to the next extrastimulus. Prospective studies comparing the two methods have shown no differences between the two methods in any of the outcomes assessed.⁵⁹

Ultrarapid Train Stimulation

Pacing at very short CLs (10 to 50 milliseconds) is rarely performed, mainly for induction of ventricular fibrillation (VF), to test defibrillation threshold during implantation of a cardioverter-defibrillator.

Conduction and Refractoriness

Conduction

During depolarization, the electrical impulse spreads along each cardiac cell, and rapidly from cell to cell, because each myocyte is connected to its neighbors through low resistance gap junctions. As discussed in **Chapter 1**, conduction velocity refers to the speed of propagation of an electrical impulse through cardiac tissue, which is dependent on both the active membrane properties of the individual cardiac myocyte that generates the action potential (i.e., electrical excitability and refractoriness) and passive properties governing the flow of current between cardiac cells (cell-to-cell coupling and tissue geometry).⁶⁰

Conduction can be assessed by observing the propagation of wavefronts during pacing at progressively incremental rates. Rate-incremental pacing is delivered to a selected site in the heart while propagation to a selected distal point is assessed. Conduction velocity is assessed by measuring the time it takes for an impulse to travel from one intracardiac location to another. During tests of conduction, it is usual for capture to be maintained at the site of stimulation and block to occur at a distal point.

Refractoriness

As discussed in **Chapter 1**, during a cardiac cycle, once an action potential is initiated, the cardiac cell is inexcitable to stimulation (i.e., unable to initiate another action potential in response to a stimulus of threshold intensity) for some duration of time (which is slightly shorter than the "true" action potential duration) until its membrane has repolarized to a certain level.⁶⁰⁻⁶²

There are different levels of refractoriness during the action potential. During the *absolute refractory period* (which extends over phases 0, 1, 2, and part of phase 3 of the action potential), the tissue is completely inexcitable and a second action potential absolutely cannot be initiated, no matter how large a stimulus is applied, because of the inactivation of the majority of Na^+ channels. After the absolute refractory period, a stimulus may cause some cellular depolarization but does not lead to a propagated action potential. The sum of this period (which includes a short interval of phase 3 of the action potential) and the absolute refractory period is termed the *effective refractory period* (ERP).

The ERP is followed by the *relative refractory period* (RRP), which extends over the middle and late parts of phase 3 of the action potential. During the RRP, initiation of a second action potential is *repressed* but not impossible; a larger-than-normal stimulus can result in activation of the cell and lead to a propagating action potential. However, the

upstroke of the new action potential is less steep and of lower amplitude and its conduction velocity slower than normal. Of note, there is a brief period in phase 3 of the action potential, the *supernormal period*, during which excitation is possible in response to an otherwise subthreshold stimulus; that same stimulus fails to elicit a response earlier or later than the supernormal period (see later).

Measurements of Refractory Periods

Refractoriness or, more appropriately, *excitability* is defined by the response of a tissue to premature stimulation. Refractory periods are analyzed by the extrastimulus technique, with progressively premature extrastimuli delivered after a train of 8 to 10 paced beats at a fixed PCL to allow for reasonable (more than 95%) stabilization of refractoriness, which is usually accomplished after 3 or 4 paced beats.

Several variables are considered in the assessment of refractory periods, including the stimulus amplitude and the basic drive CL. Longer drive CLs are generally associated with longer refractory periods. However, refractory periods of different parts of the conducting system do not respond comparably with changes in the drive CLs.⁶³

In addition, the measured ERP is invariably related to the current used. Thus, standardization of the pacing output is required. In most laboratories, it is arbitrarily standardized at twice the diastolic threshold. A more detailed method of assessing refractoriness is to define the strength-interval curves at these sites. The steep portion of that curve defines the ERP of that tissue. The use of increasing current strengths to 10 mA usually shortens the measured ERP by approximately 30 milliseconds. However, such a method does not offer a useful clinical advantage, except when the effects of antiarrhythmic drugs on ventricular excitability and refractoriness are to be characterized. Moreover, the safety of using high current strengths, especially when multiple extrastimuli are delivered, is questionable because fibrillation is more likely to occur in such situations.

It is important that measurements of refractory periods be taken at specific sites. Measurements of atrial and ventricular ERP are taken at the site of stimulation. Measurements of AVN ERP and HPS ERP are taken from responses in the HB electrogram.

Effective refractory period. The ERP is the longest premature coupling interval (S_1 - S_2) at a designated stimulus amplitude (usually $2\times$ diastolic threshold) that results in failure of propagation of the premature impulse through a tissue (i.e., fails to capture). ERP therefore must be measured proximal to the refractory tissue.

Relative refractory period. The RRP is defined as the longest premature coupling interval (S_1 - S_2) that results in prolonged conduction of the premature impulse (an increase in stimulus to distal response time) compared with the conduction of the stimulus delivered during the basic drive train. Conduction is slowed when a wavefront

encounters tissue that is not completely repolarized. Thus, the RRP marks the end of the full recovery period (i.e., the zone during which conduction of the premature and basic drive impulses is identical). The RRP is generally slightly longer than the ERP by an amount called the *latency period*. During the latency period, the tissue is excitable, but the excitation wavefront conducts with slower or even decremental conduction.

Functional refractory period. The functional refractory period (FRP) is the shortest interval between two consecutively conducted impulses out of a cardiac tissue resulting from any two consecutive input impulses into that tissue (i.e., the shortest output interval that can occur in response to *any* input interval in a particular tissue). Because the FRP is a measure of output from a tissue, it is described by measuring points distal to that tissue. It is helpful to think of the FRP as a response-to-response measurement (in contrast, the ERP is a stimulus-to-stimulus measurement). Therefore the FRP is a measure of both refractoriness *and* conduction velocity of a tissue. The definitions of anterograde ERP and FRP of the AV conduction system are given in Table 4.1.

Cycle Lengths Responsiveness of Refractory Periods

Normally, refractoriness of the atrial, HPS, and ventricular tissue is directly related to the basic drive CL (i.e., the ERP shortens with decreasing drive CL). This phenomenon results from rate-related shortening of the action potential duration and is most marked in the HPS. Abrupt changes in the CL also affect refractoriness of these tissues. A change from a long to short CL (e.g., with introduction of an extrastimulus [S_2] following a pacing drive [S_1] with a long CL) shortens the ERP of the HPS and atrium, whereas a change from a short to a long drive CL markedly prolongs the HPS ERP but alters the ventricular ERP little, if at all. Refractoriness of the atrial, HPS, and ventricular tissue appears relatively independent of autonomic tone; however, data have shown that increased vagal tone can potentially shorten atrial ERP and prolong ventricular ERP.⁶³ CL shorting can affect different structures differently. For example, normally at relatively long cycle lengths, the RB ERP exceeds that of the left bundle (LB), so that functional right bundle branch block (RBBB) is common. At short CLs, the LB ERP exceeds that of the RB so that left bundle branch block (LBBB) is more common.

In contrast, the AVN ERP increases with increasing drive CL in response to the fatigue phenomenon, which most likely results because AVN refractoriness is time-dependent and exceeds its action potential duration (unlike HPS refractoriness). In addition, AVN refractory periods are labile and can be markedly affected by the autonomic tone. On the other hand, the response of AVN FRP to changes in PCL is variable, but it tends to decrease with decreasing PCL. This paradox occurs because the FRP is not a true measure of refractoriness encountered by an atrial

TABLE 4.1 Definition of Refractory Periods

	ERP	RRP	FRP
Atrium	Longest S_1 - S_2 interval that fails to achieve atrial capture	Longest S_1 - S_2 interval at which S_2 - A_2 is $>S_1$ - A_1	Shortest A_1 - A_2 interval (recorded at a designated site, often the HB region) in response to any S_1 - S_2
AVN	Longest A_1 - A_2 interval (measured at the HB region) that fails to propagate to the HB	Longest A_1 - A_2 interval at which A_2 - H_2 is $>A_1$ - H_1	Shortest H_1 - H_2 interval in response to any A_1 - A_2
HPS	Longest H_1 - H_2 interval that fails to propagate to the ventricles	Longest H_1 - H_2 interval at which H_2 - V_2 is $>H_1$ - V_1 or generates an aberrant QRS complex	Shortest V_1 - V_2 interval in response to any H_1 - H_2
Ventricle	Longest S_1 - S_2 interval that fails to achieve ventricular capture	Longest S_1 - S_2 interval at which S_2 - V_2 is $>S_1$ - V_1	Shortest V_1 - V_2 interval (recorded at a designated site or) in response to any S_1 - S_2

AVN, Atrioventricular node; ERP, effective refractory period; FRP, functional refractory period; HB, His bundle; HPS, His-Purkinje system; RRP, relative refractory period.

TABLE 4.2 Normal Refractory Periods in Adults

Study ^a	ERP Atrium (ms)	ERP AVN (ms)	FRP AVN (ms)	ERP HPS (ms)	ERP Ventricle (ms)
Denes et al. (1974)	150–360	250–365	350–495	—	—
Akhtar et al. (1975)	230–330	280–430	320–680	340–430	190–290
Josephson (2002)	170–300	230–425	330–525	330–450	170–290

^aStudies performed at 2× threshold.

AVN, Atrioventricular node; ERP, effective refractory period; FRP, functional refractory period; HPS, His-Purkinje system.

Data from Denes P, Wu D, Dhingra R, et al. The effects of cycle length on cardiac refractory periods in man. *Circulation*. 1974;49:32; Akhtar M, Damato AN, Batsford WP, et al. A comparative analysis of anterograde and retrograde conduction patterns in man. *Circulation*. 1975;52:766; and Josephson ME. Electrophysiologic investigation: general aspects. In: Josephson ME, ed. *Clinical Cardiac Electrophysiology*. 3rd ed. Philadelphia: Lippincott Williams & Wilkins; 2002:19–67.

extrastimulus (atrial extrastimulus [AES]; A₂); it is significantly determined by the AVN conduction time of the basic drive beat (A₁-H₁); the longer the A₁-H₁ is, the shorter the calculated FRP will be at any A₂-H₂.

Limitations of Tests of Conduction and Refractoriness

It is unusual to be able to collect a complete set of measurements. With refractory period testing, the atrial ERP is often longer than the AVN ERP, so that atrial refractoriness is encountered before AVN refractoriness, thus limiting the ability to assess the latter. Moreover, an AES cannot be used to test the HPS if conduction is blocked at the AVN level. This is a limitation that applies to most patients undergoing conduction or refractory period testing. On the other hand, it is possible to assess anterograde conduction and refractoriness distal to the AVN by direct pacing of the HB. This is not part of the routine EP evaluation, however, and is reserved for cases in which the information is particularly desired.

It is important to note that atrial conduction can materially affect the determination of refractory periods. Therefore refractory periods should not be timed from the site of stimulation, but from the point in the conduction cascade that is being assessed. For example, if the high RA is stimulated in a patient with a left lateral BT, an early AES can encounter the RRP of the atrium, so that intraatrial conduction time is prolonged. Thus, the timing of the S₁-S₂ stimuli in the high RA would be shorter than the timing of the propagated impulse when it arrives at the region of the BT as the local A₁-A₂ interval.

A wide range of normal values has been reported for refractory periods (Table 4.2). However, it is difficult to interpret these so-called normal values because they come from pooled data using different standards (different PCLs, stimulus strengths, and pulse widths).

ATRIAL STIMULATION

Technical Aspects

Atrial stimulation provides a method for evaluation of the functional properties of the sinus node and AV conduction system and of the means of induction of different arrhythmias (supraventricular and, occasionally, ventricular arrhythmias). Atrial stimulation from different atrial sites can result in different patterns of AV conduction. Thus, stimulation should be performed from the same site if the effects of drugs and physiological maneuvers are to be studied. Atrial stimulation is usually performed from the high RA and CS.

Rate-incremental atrial pacing is usually started at a PCL just shorter than the sinus CL, with progressive shortening of the PCL (by 10- to 20-millisecond decrements) until 1:1 atrial capture is lost, Wenckebach AVN block develops, or a PCL of 200 to 250 milliseconds is reached. Ramp atrial pacing is equivalent to rate-incremental pacing if AVN Wenckebach CL is all that is required. Stepwise rate-incremental pacing,

however, also allows evaluation of sinus node recovery time at each drive CL. Atrial pacing should always be synchronized because alteration of the coupling interval of the first paced beat of the pacing drive can affect subsequent AV conduction.

During stepwise rate-incremental pacing, pacing should be continued long enough (usually 15 to 60 seconds) at each PCL to ensure stability of conduction intervals and to overcome two factors that significantly influence the development of a steady state: the phenomenon of accommodation and the effects of autonomic tone. During rate-incremental pacing, if the coupling interval of the first beat of the drive is not synchronized, it can be shorter, longer, or equal to the subsequent PCL. Therefore one can observe an increasing, decreasing, or stable AH interval pattern for several cycles, and the initial AH interval can be different from the steady-state AH interval. Oscillations of the AH interval, which dampen to a steady level, or the AVN Wenckebach can occur under these circumstances. Regarding the influence of the autonomic tone on AVN conduction, rapid pacing can produce variations in AVN conduction, depending on the patient's immediate autonomic state. Rapid pacing can also provoke symptoms or hypotension in patients who then produce neurohumoral responses that can alter results. Therefore for assessment of AV conduction, ramp pacing is often an attractive alternative to the stepwise method. The pacing rate is slowly increased at 2 to 4 beats/min per second (or the PCL is decreased by 10 milliseconds every several paced beats) until block occurs.

AES is used to assess of atrial and AVN refractory periods and to induce arrhythmias. During programmed stimulation, a sequence of eight paced stimuli is delivered at a constant rate (the S₁ drive), which allows stable AVN conduction. Following these eight beats, an AES (S₂) is delivered. This stimulation sequence is repeated at progressively shorter S₁-S₂ coupling intervals, thus allowing the response of the sinus node and AVN to be recorded across a range of premature test stimuli.

Normal Response to Rate-Incremental Atrial Pacing Sinus Node Response to Atrial Pacing

The sinus node is the prototype of an automatic focus. Automatic rhythms are characterized by spontaneous depolarization, overdrive suppression, and post-overdrive warm-up to baseline CL. Rapid atrial pacing results in overdrive suppression of the sinus rate, with prolongation of the return sinus CL following termination of the pacing train. Longer pacing trains and faster pacing rates further prolong the return cycle. After cessation of pacing, the sinus rate resumes discharge at a slower rate and gradually speeds up (warms up) to return to the pre-pacing sinus rate.

Sinus node recovery time is the interval between the end of a period of pacing-induced overdrive suppression of sinus node activity and the return of sinus node function, manifested on the surface ECG by a post-pacing sinus P wave.

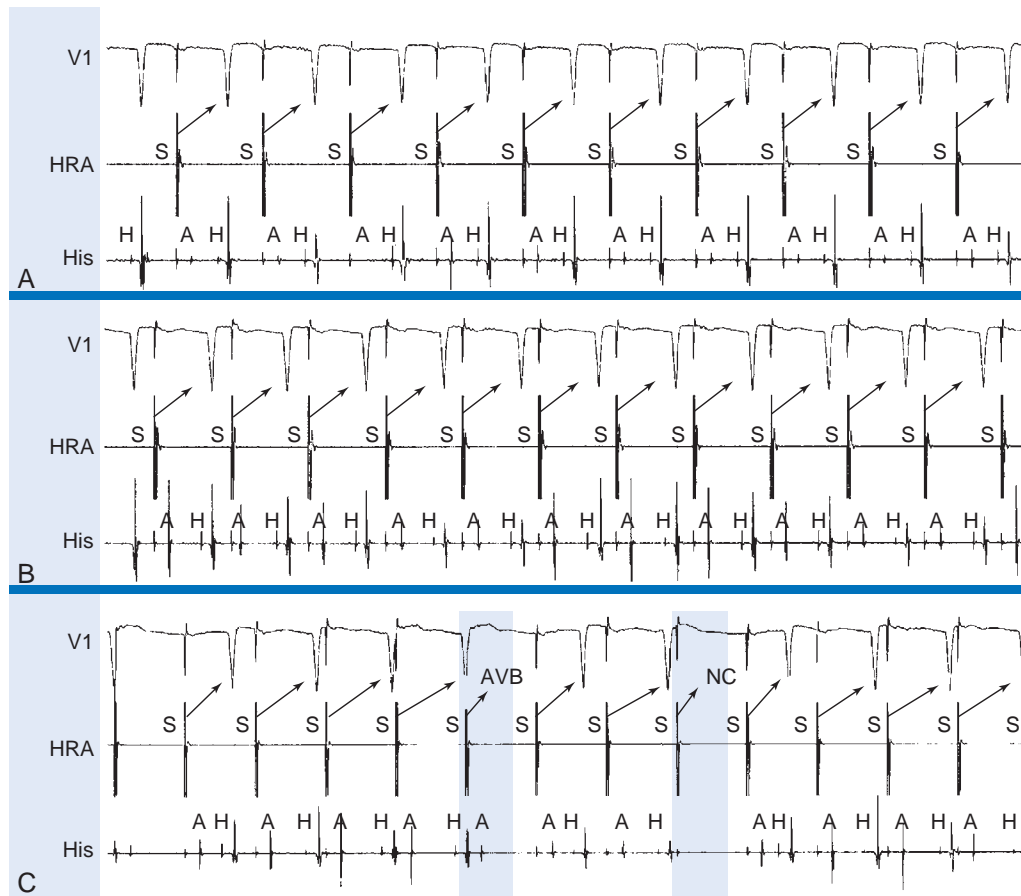


Fig. 4.21 Normal Atrioventricular Node (AVN) Response to Rate-Incremental Atrial Pacing. (A) Fixed-rate high right atrial (HRA) pacing (S) at a cycle length (CL) of 600 milliseconds. (B) Decreasing the pacing CL to 500 milliseconds results in prolongation of the atrial–His bundle (AH) interval, as illustrated in the His bundle recording (His). Infranodal conduction (His bundle–ventricular interval) remains unaffected. (C) Further decrement of the pacing CL results in progressive prolongation of the AH interval until block occurs in the AVN (AVB), followed by resumption of conduction, indicating Wenckebach CL. The site of block is in the AVN because no His bundle deflection is present after the nonconducted atrial stimulus. Of note, apparent block of another atrial stimulus is observed (pseudoblock) because of failure of the atrial stimulus to capture (NC), which is confirmed by the absence of an atrial electrogram on the His bundle recording after the stimulus artifact.

Atrioventricular Node Response to Atrial Pacing

The normal AVN response to rate-incremental atrial pacing is for the PR and AH intervals to increase gradually as the PCL decreases until AVN Wenckebach block appears (Fig. 4.21). With further decrease in the PCL, higher degrees of AV block (2:1 or 3:1) can appear. Infranodal conduction (HV interval) generally remains unaffected.

Wenckebach block is frequently atypical; that is, the AH interval does not increase gradually in decreasing increments but stabilizes for several beats before the block, or it can show its greatest increment in the last conducted beat. The incidence of atypical Wenckebach periodicity from Mobitz II AV block. In addition, it is important to ensure that the ventricular pauses observed during atrial pacing are not secondary to loss of atrial capture or the occurrence of AVN echo beats (pseudoblock; see Fig. 4.21).

AVN Wenckebach CL is the longest PCL at which Wenckebach block in the AVN is observed. Normally, Wenckebach CL is 500 to 350 milliseconds, but it is sensitive to the autonomic tone. There is a correlation between the AH interval during NSR and the Wenckebach CL; patients

with a long AH interval during NSR tend to develop Wenckebach block at a longer PCL, and vice versa.

At short PCLs (less than 350 milliseconds), infranodal block can occasionally occur in patients with normal baseline HV interval and QRS complex. This occurs especially when atrial pacing is started during NSR with the first or second paced impulses acting as a long-short sequence. The HPS can also show accommodation following the initiation of pacing. Prolongation of the HV interval or infranodal block at a PCL longer than 400 milliseconds is abnormal and indicates infranodal conduction abnormalities.

Atrial Response to Atrial Pacing

It is usually possible to maintain 1:1 atrial capture with rate-incremental pacing techniques to a PCL of 200 to 300 milliseconds. Pacing threshold normally tends to increase at faster rates. Rate-incremental pacing can result in prolongation of the intraatrial (PA interval) and interatrial conduction. At rapid pacing rates, induction of AF is not rare and is not necessarily an abnormal response. Vagal tone and medications such as adenosine and edrophonium can slow the sinus rate, but they tend

to shorten the atrial ERP, which makes the atrium more vulnerable to induction of AF.

Normal Response to Atrial Premature Stimulation

Sinus Node Response to Atrial Extrastimulation

Four zones of response of the sinus node to AES have been identified: the zone of collision, the zone of reset, the zone of interpolation, and the zone of reentry (Fig. 4.22).

Zone I. A late-coupled AES with very long A_1 - A_2 intervals (with A_2 falling in the last 20% to 30% of the sinus CL) collides with the impulse already emerging from the sinus node, resulting in fusion of atrial activation (fusion between the AES [A_2] with the spontaneous sinus impulse [A_1]) or paced-only atrial activation sequence; it fails to affect the timing of the next sinus beat, thus producing a fully compensatory pause. This zone, also known as the zone of collision, zone of interference, and nonreset zone, is defined by the range of A_1 - A_2 at which A_2 - A_3 is fully compensatory (see Fig. 4.22).

Zone II. An earlier coupled AES results in penetration of the sinus node with resetting so that the resulting pause is less than compensatory (i.e., A_1 - A_3 is $< 2 \times [A_1$ - $A_1]$), but without changing sinus node automaticity. The range of A_1 - A_2 at which resetting of the sinus pacemaker occurs, resulting in a less than compensatory pause, defines zone II, also known as the zone of reset (see Fig. 4.22). This zone is typically of long duration (40% to 50% of the sinus CL). In most patients, A_2 - A_3 remains constant throughout zone II, thus producing a plateau in the curve because, although A_2 penetrates and resets the sinus node, it does so without changing the sinus pacemaker automaticity. Hence, A_2 - A_3 should equal the spontaneous sinus CL (A_1 - A_1) plus the time it takes the AES (A_2) to enter and exit the sinus node. The difference between A_2 - A_3 and A_1 - A_1 therefore has been taken as an estimate of total sinoatrial conduction time.

Zone III. A very early coupled AES encounters a refractory sinus node (following the last sinus discharge) and fails to enter or reset the sinus node. The next sinus discharge is on time because the atrium is already fully recovered following that early AES. The range of A_1 - A_2 coupling intervals at which A_2 - A_3 is less than A_1 - A_1 , and A_1 - A_3 is less than $2 \times (A_1$ - A_1), defines zone III, also known as the zone of interpolation (see Fig. 4.22). The A_1 - A_2 coupling intervals at which incomplete interpolation is first observed define the RRP of the perinodal tissue. Some refer to this as the sinus node refractory period. In this case, A_3 represents delay of A_1 exiting the sinus node, which has not been affected. The A_1 - A_2 coupling interval at which complete interpolation is observed probably defines the ERP of the most peripheral of the perinodal tissue because the sinus impulse does not encounter refractory tissue on its exit from the sinus node. In this case, $(A_1$ - A_2) + $(A_2$ - A_3) = A_1 - A_1 and sinus node entrance block is said to exist.

Zone IV. This zone, also known as the zone of reentry, is defined as the range of A_1 - A_2 at which A_2 - A_3 is less than A_1 - A_1 , $(A_1$ - A_2) + $(A_2$ - A_3) is less than A_1 - A_1 , and the atrial activation sequence and P wave morphology are identical to those of the sinus. The incidence of single beats of sinus node reentry is approximately 11% in the normal population.

Atrioventricular Nodal Response to Atrial Extrastimulation

Progressively premature AES results in prolongation of PR and AH intervals, with inverse relationship between the AES coupling interval (A_1 - A_2) and the AH interval (A_2 - H_2). The shorter the coupling interval of the AES is, the longer the A_2 - H_2 interval will be (see Fig. 4.22). More premature AES can block in the AVN with no conduction to the ventricle (defining AVN ERP). Occasionally, conduction delay and block occur in the HPS, especially when the AES is delivered following long basic drive CLs, because HPS refractoriness frequently exceeds the AVN FRP at long PCLs.

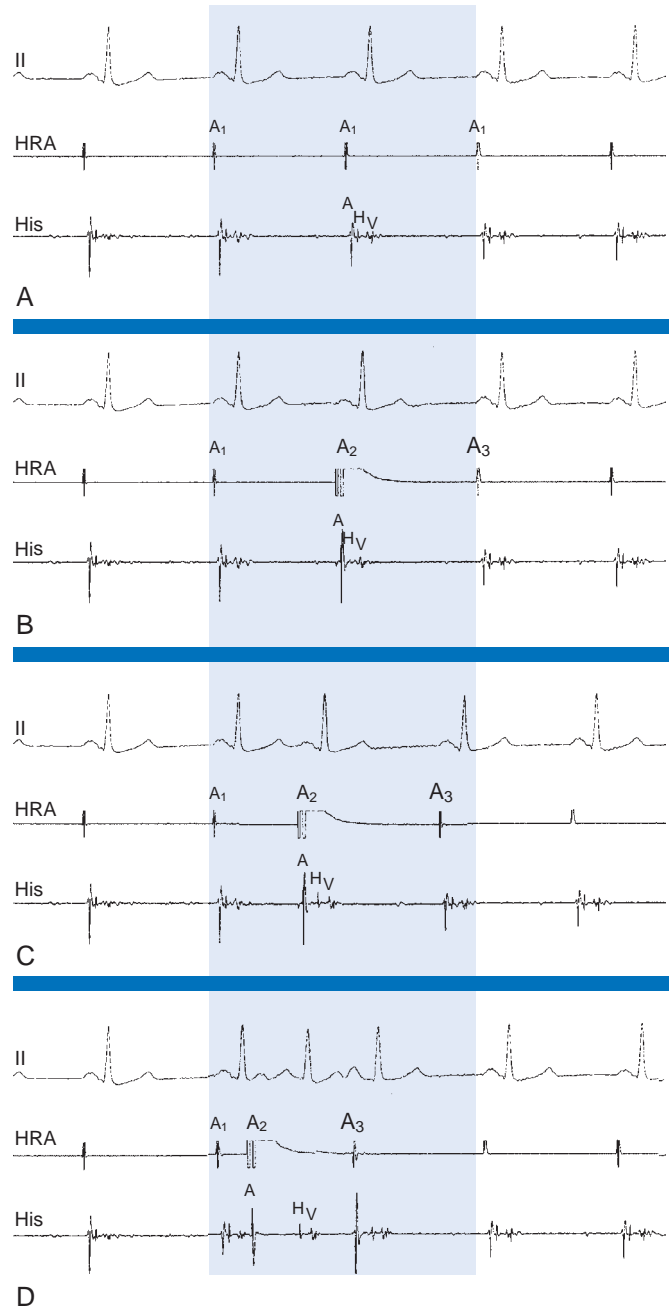


Fig. 4.22 Normal Sinus Node and Atrioventricular Node Response to Atrial Extrastimulation. (A) Baseline sinus rhythm shown in surface ECG lead II, high right atrium (HRA) recording, and His bundle (His) recording. The shaded area represents two sinus cycle lengths ($2 \times [A_1$ - $A_1]$). (B) A late coupled atrial extrastimulus (AES; A_2) collides with the exiting sinus impulse and therefore does not affect (or reset) the sinus pacemaker (zone of collision). The next sinus impulse (A_3) occurs at exactly twice the baseline sinus cycle length. (C) An early coupled AES is able to penetrate and reset the sinus node (zone of resetting). (D) An even earlier coupled AES reaches refractory tissue around the sinus node and is thus unable to penetrate the sinus node (entrance block); therefore it does not affect sinus node discharge. The next spontaneous sinus beat (A_3) arrives exactly at the sinus interval (zone of interpolation). The atrial-His bundle interval progressively prolongs with progressively premature coupling intervals (B to D). In contrast, the His bundle-ventricular (HV) interval remains constant.

The patterns of AV conduction can be expressed by plotting refractory period relating the A_1 - A_2 interval to the responses of the AVN and HPS. Plotting the A_1 - A_2 interval versus the H_1 - H_2 and V_1 - V_2 intervals illustrates the functional input-output relationship between the basic drive beat and the AES and provides an assessment of the FRP of the AV conduction system. In contrast, plotting the A_2 - H_2 interval (AVN conduction time of the AES) and the H_2 - V_2 interval (HPS conduction time of the AES) versus the A_1 - A_2 interval (the AES coupling interval) allows determination of the conduction times through the various components of the AV conduction system.

Type I response. In this type, the progressively premature AES encounters progressive delay in the AVN without any changes in the HPS. Therefore refractoriness of the AVN determines the FRP of the entire AV conduction, and the ERP of the AV conduction system is determined at the atrial or AVN level. This response is characterized by initial shortening of the H_1 - H_2 and V_1 - V_2 intervals as the AES coupling interval (A_1 - A_2) shortens, whereas AVN conduction (A_2 - H_2) and HPS conduction (H_2 - V_2) remain stable (eFig. 4.7). With further shortening of the A_1 - A_2 interval, the RRP of the AVN is encountered, resulting in progressive delay in AVN conduction (manifesting as progressive prolongation of the A_2 - H_2 interval) accompanied by stable HPS conduction (H_2 - V_2) and a progressive but identical prolongation of both the H_1 - H_2 and V_1 - V_2 intervals, until the AES is blocked within the AVN (AVN ERP) or until the atrial ERP is reached. The minimum H_1 - H_2 and V_1 - V_2 intervals attained define the FRP of the AVN and entire AV conduction system. AVN conduction (A_2 - H_2) usually increases by 2 to 3× baseline values before block.

Type II response. In type II response, conduction delay occurs initially in the AVN; however, with further shortening of the AES coupling interval, progressive delay develops in the HPS. Therefore refractoriness of the HPS determines the FRP of the entire AV conduction system, and the ERP of the AV conduction system is determined at any level. At longer A_1 - A_2 intervals, type II response is similar to type I response; however, as the A_1 - A_2 interval shortens, conduction delay develops initially in the AVN (manifesting as progressive prolongation of the A_2 - H_2 interval) but then in the HPS (manifesting as aberrant QRS conduction and progressive prolongation of the H_2 - V_2 interval) as the RRP of the HPS is encountered. Therefore in contrast to type I response, both A_2 - H_2 and H_2 - V_2 intervals prolong in response to progressively shorter A_1 - A_2 , resulting in divergence in the H_1 - H_2 and V_1 - V_2 curves until the AES is blocked within the AVN (AVN ERP), in the HPS (HPS ERP), or until the atrial ERP is reached (see eFig. 4.7). Block usually occurs in the AVN, but it can occur in the atrium and occasionally in the HPS (modified type II response). AVN conduction (A_2 - H_2) usually increases only modestly (by less than 2× baseline values before block).

Type III response. In type III response, conduction delay occurs initially in the AVN; however, at a critical AES coupling interval, sudden and marked delay develops in the HPS. Therefore refractoriness of the HPS determines the FRP of the entire AV conduction system, and the ERP of the AV conduction system is determined at any level. However, in contrast to type II response, the HPS is invariably the first site of block. At longer A_1 - A_2 intervals, type II response is similar to type I response; however, as the A_1 - A_2 interval shortens, progressive delay is noted initially in the AVN (manifest as progressive prolongation in the A_2 - H_2 interval), but then a sudden delay of conduction in the HPS occurs (manifesting as aberrant QRS conduction and a sudden jump in the H_2 - V_2 interval). This results in a break in the V_1 - V_2 curve, which subsequently descends until, at a critical A_1 - A_2 interval, the impulse blocks in the AVN or HPS (see eFig. 4.7). The FRP of the HPS occurs just before the marked jump in H_2 - V_2 . AVN conduction (A_2 - H_2) usually increases by less than 2× baseline values before block.

Type I response is the most common pattern, whereas type III response is the least common. The pattern of AV conduction (type I, II, or III), however, is not fixed in any patient. Drugs (e.g., atropine, isoproterenol) or changes in CL can alter the refractory period relationship among different tissues so that one type of response can be switched to another. For example, atropine can decrease the FRP of the AVN and allow the impulse to reach the HPS during its RRP, changing type I response to type II or III.

Not infrequently, the ERP of the atrium is reached earlier than that of the AVN, especially when the basic drive is slow (which increases atrial ERP and decreases AVN ERP) or when the patient is agitated, which increases sympathetic tone and decreases AVN ERP. The first site of block is in the AVN in most patients (45%), in the atrium in 40%, and in the HPS in 15%.

Atrial Response to Atrial Extrastimulation

Early AESs can impinge on the atrial RRP, with resulting local latency (i.e., long interval between the pacing artifact and the atrial electrogram on the pacing electrode). A very early AES delivered during the atrial ERP fails to capture the atrium. The atrial ERP can be longer or shorter than the AVN ERP, especially at long basic drive CLs or in cases of enhanced AVN conduction secondary to autonomic influences.

As with rate-incremental pacing, AES can result in prolongation of intraatrial and interatrial conduction, which is more pronounced in patients with a history of atrial arrhythmias. Development of a fractionated atrial electrogram is more often observed in patients who have a history of AF. Intraatrial block in response to AES is unusual. Occasionally, double or triple AESs induce AF in patients with no history of such arrhythmia. Such episodes usually terminate spontaneously and are not clinically relevant in the absence of a history of known or suspected atrial arrhythmias.

Repetitive Atrial Responses

Atrial stimulation can trigger extraatrial complexes or echo beats. Those complexes can be caused by different mechanisms; the most common are intraatrial reentrant beats and AVN echo beats.

Intraatrial reentrant beats usually occur at short coupling intervals. They can originate anywhere in the atrium, and atrial activation sequence depends on the site of origin of the beat. The incidence of these responses increases with increasing the number of AESs, the number of drive PCLs, and the number of stimulation sites used.

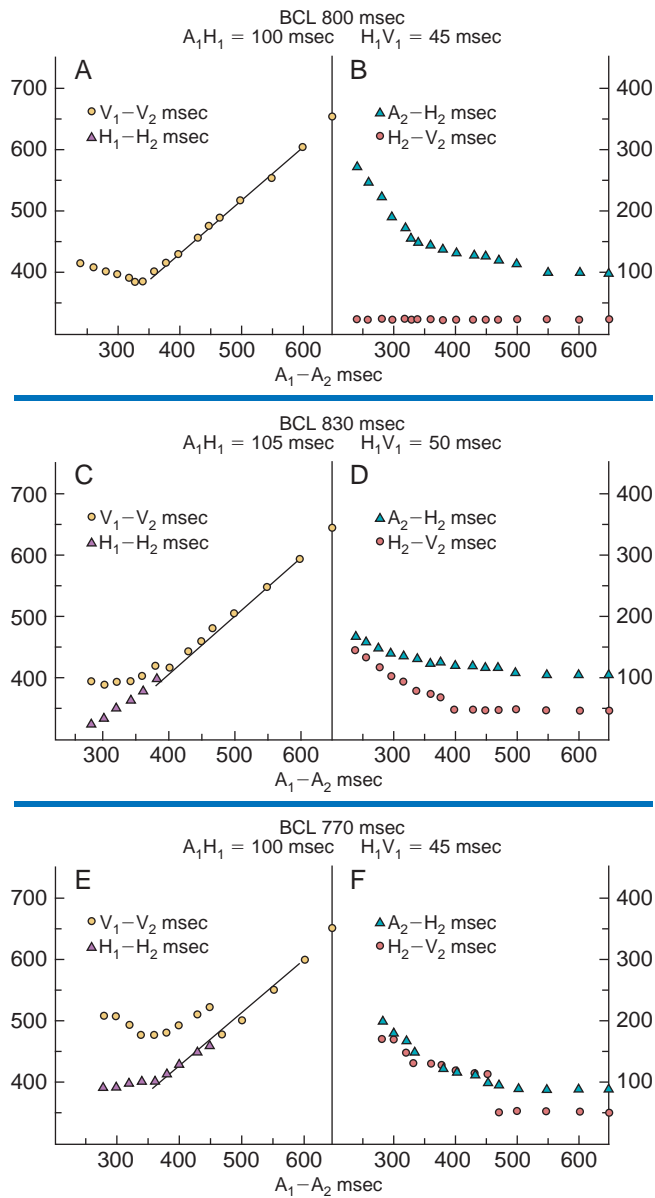
Repetitive atrial responses can also be caused by reentry in the AVN. These patients have anterograde dual AVN physiology, and the last paced beat conducts slowly down the slow AVN pathway and then retrogradely up the fast pathway to produce the echo beat (Fig. 4.23). Atrial activation sequence is consistent with retrograde conduction over the fast AVN pathway, earliest in the HB catheter recording. Atrial and ventricular activations occur simultaneously.

VENTRICULAR STIMULATION

Technical Aspects

Ventricular stimulation is used to assess retrograde ventricular-atrial (VA) conduction and refractory periods, retrograde atrial activation patterns, including sequences that can indicate the presence of a BT, and vulnerability to inducible ventricular arrhythmias.

Stepwise rate-incremental ventricular pacing or ramp pacing is used in the assessment of VA conduction. It is unusual to provoke ventricular arrhythmias with these tests, even in patients with known ventricular arrhythmia. Rate-incremental ventricular pacing is usually started at a PCL just shorter than the sinus CL, and the PCL is then gradually decreased (in 10- to 20-millisecond decrements) down to 300



eFig. 4.7 Patterns of Atrioventricular Conduction Response to Atrial Extrastimulation (AES). (A and B) Type I pattern of atrioventricular node response to AES. (C and D) Type II pattern of response to AES. (E and F) Type III pattern of response to AES. *BCL*, Basic cycle length. (From Josephson ME. Electrophysiologic investigation: general aspects. In: Josephson ME, ed. *Clinical Cardiac Electrophysiology*. 3rd ed. Philadelphia: Lippincott Williams & Wilkins; 2002:19–67.)

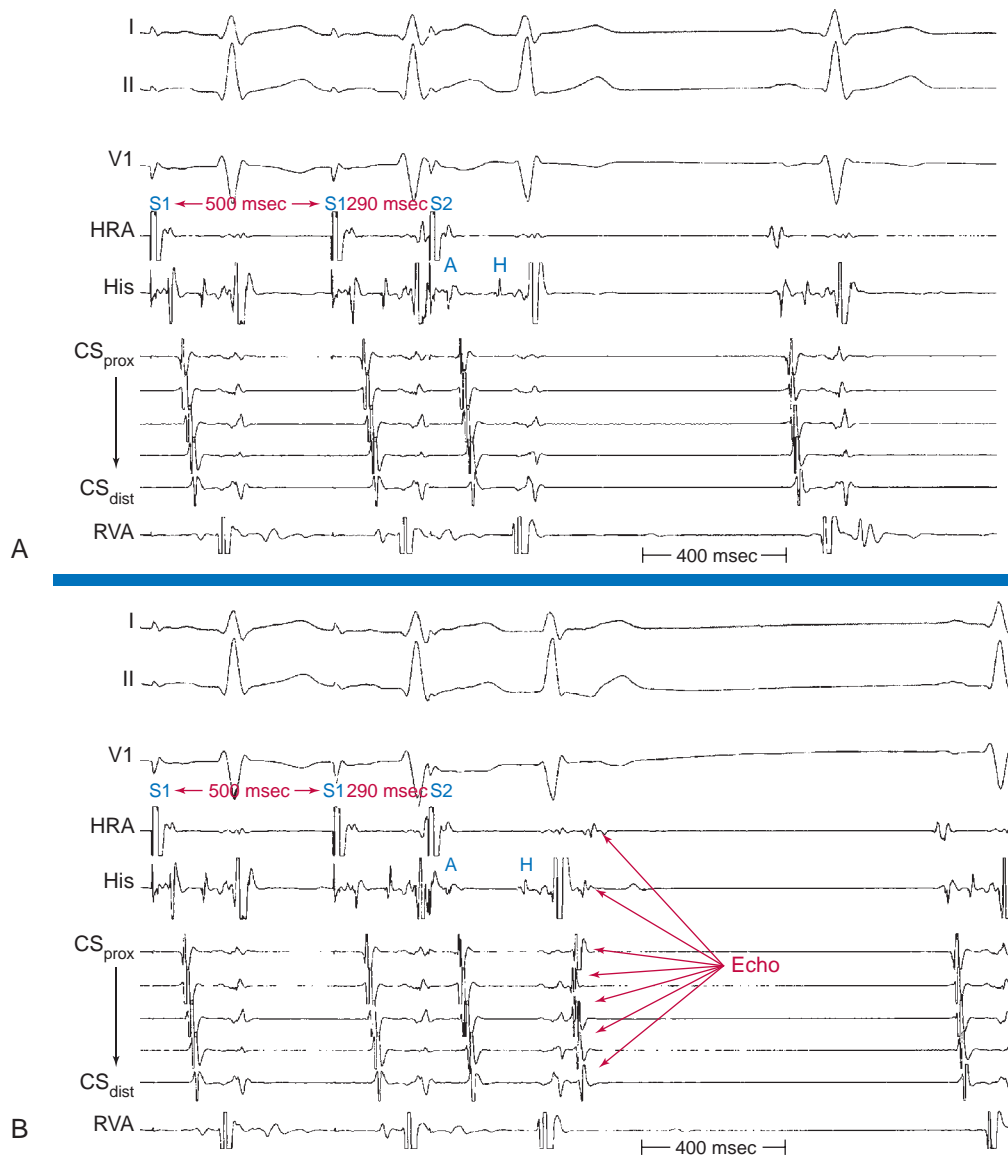


Fig. 4.23 Anterograde Dual Atrioventricular Nodal Pathways. *Top*, A single extrastimulus is introduced from the high right atrium (HRA; S_2) at 290 milliseconds after the last drive stimulus (S_1). This results in an atrial-His bundle (AH) interval of 140 milliseconds. *Bottom*, An extrastimulus is delivered 10 milliseconds earlier than above (280 milliseconds), resulting in marked prolongation of the AH interval to 202 milliseconds and an atrial echo. CS_{dist}, distal coronary sinus; CS_{prox}, proximal coronary sinus; HRA, high right atrium; RVA, right ventricular apex.

milliseconds. Shorter PCL may be used to assess rapid conduction in patients with supraventricular tachycardia (SVT) or to induce VT. With ramp pacing, the pacing rate is slowly increased at 2 to 4 beats/min per second (or the PCL is decreased by 10 milliseconds every several paced beats) until VA block occurs.

Ventricular extrastimulus (VES) testing is used to assess ventricular, HPS, and AVN refractory periods and to induce arrhythmias. During programmed stimulation, a sequence of eight paced stimuli is delivered at a constant rate (the S_1 drive), which allows stable VA conduction. Following these eight beats, a VES (S_2) is delivered. This stimulation sequence is repeated at progressively shorter S_1 - S_2 intervals, thus allowing the response of the HPS and AVN to be recorded across a range of premature test stimuli.

During ventricular stimulation, the HB electrogram shows a retrograde His potential in 85% of patients with a normal QRS during NSR. Ventricular pacing at the base of the heart close to the AV junction

facilitates recording a retrograde His potential because it allows the ventricles to be activated much earlier relative to the HB (Fig. 4.24). The VH or stimulus-HB (S-H) interval always exceeds the anterograde HV interval by the time it takes for the impulse to travel from the stimulation site to the ipsilateral bundle branch. In patients with normal HV intervals, a retrograde His potential can usually be seen before the ventricular electrogram in the HB recording during RV apical pacing. In contrast, when ipsilateral bundle branch block (BBB) is present, especially with long HV intervals, a retrograde His potential is less frequently seen; when it is seen, it is usually inscribed after the QRS when pacing from the ipsilateral ventricle (eFig. 4.8).

Ventricular stimulation is relatively safe; however, induction of clinically irrelevant serious arrhythmias, including VF, can occur in patients with normal hearts and those who have not had spontaneous ventricular arrhythmias. The induction of these arrhythmias is directly related to the aggressiveness of the ventricular stimulation protocol. Thus, the

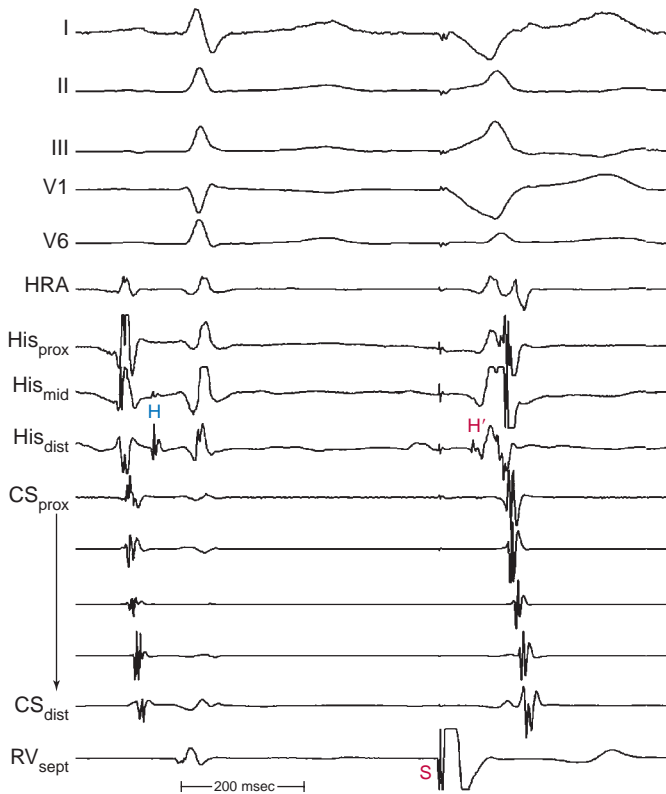


Fig. 4.24 Retrograde Activation With Right Ventricular (RV) Septal Pacing. Sinus and RV septal paced complexes (S) are shown. Retrograde atrial activation is concentric, following a retrograde His potential (H'). CS_{dist}, Distal coronary sinus; CS_{prox}, proximal coronary sinus; His_{dist}, distal His bundle; His_{mid}, middle His bundle; His_{prox}, proximal His bundle; HRA, high right atrium; RV_{sept}, RV septum.

stimulation protocol is usually limited to single or double VES in patients without a clinical history consistent with malignant ventricular arrhythmias. The use of high pacing output can also increase the risk of such arrhythmias. Therefore ventricular stimulation at 2× diastolic threshold and 1-millisecond pulse width is preferable.

Normal Response to Rate-Incremental Ventricular Pacing

Ventricular pacing provides information about VA conduction, which is present in 40% to 90% of patients, depending on the population studied. Absence of VA conduction at any paced rate is common and normal. There is no difference in the capability of VA conduction regarding the site of ventricular stimulation in patients with a normal HPS. When present, normal VA conduction uses the normal AV conduction system, with the earliest atrial activation site usually in the septal region in proximity to the AVN. In some cases, the slow posterior AVN pathway is preferentially engaged so that the earliest atrial activation site is somewhat posterior to the AVN, closer to the CS os.

The normal AVN response to rate-incremental ventricular pacing is a gradual delay of VA conduction (manifest as gradual prolongation of the HA interval) as the PCL decreases. Retrograde VA Wenckebach block and a higher degree of block appear at shorter PCLs. Occasionally, VA Wenckebach cycles are terminated with ventricular echo beats secondary to retrograde dual AVN physiology. When a retrograde His potential is visible, a relatively constant VH interval at a rapid pacing rate, despite the development of retrograde VA block, localizes the site of block to the AVN (Fig. 4.25). When a retrograde His potential is not visible during ventricular pacing, the site of VA block, when it occurs,

must be inferred from the effect of paced impulses on conduction of spontaneous or stimulated atrial beats (i.e., by analyzing the level of retrograde concealment; see Fig. 4.25). If the AH interval of the atrial beat is independent of the time relationship of the paced impulse, the site of block is in the HPS (infranodal). On the other hand, if the AH interval varies according to the coupling interval of the atrial beat to the paced QRS, or if the atrial beat fails to depolarize the HB, the site of block is in the AVN. Moreover, drugs that enhance AVN (but not HPS) conduction (e.g., atropine) improve VA conduction if the site of block is in the AVN, but they do not affect VA conduction if the site of block is in the HPS.

At comparable PCLs, anterograde AV conduction is better than retrograde VA conduction in most patients. AVN conduction is the major determinant of retrograde VA conduction. Patients with prolonged PR intervals are much less likely to demonstrate retrograde VA conduction. Furthermore, patients with prolonged AVN conduction are less capable of VA conduction than patients with infranodal conduction delay. Anterograde AV block in the AVN is almost universally associated with retrograde VA block. On the other hand, anterograde AV block in the HPS is associated with some degree of VA conduction in up to 40% of cases. However, the exact comparison between anterograde and retrograde AVN conduction can be limited by the absence of a visible retrograde His potential during ventricular stimulation. Consequently, localization of the exact site of conduction delay or block (AVN vs. HPS) may not be feasible. The response to rate-incremental pacing at two different PCLs may differ because of the opposite effects of the PCL on AVN and HPS refractoriness.

Rapid ventricular pacing can result in ipsilateral retrograde BBB, with subsequent impulse propagation across the septum, retrogradely up the contralateral bundle branch, and then to the HB. Such an event can manifest as sudden prolongation of the VH interval during pacing. This can be followed by resumption of VA conduction after a period of VA block in the AVN when the VH interval is short because the delay in the HPS allows recovery of the AVN (the gap phenomenon). This occurrence can permit better visualization of the His potential, and, by comparing the ventricular electrogram in the HB recording when the His potential is clearly delayed with that with normal retrograde ipsilateral bundle branch conduction, a previously unappreciated His potential within that electrogram can then be visualized (see Fig. 4.25).

To exclude the presence of a nondecremental retrogradely conducting BT, the VES technique is usually more effective than rate-incremental ventricular pacing for demonstrating normal prolongation of the VA interval. If uncertainty continues to exist, adenosine can be extremely helpful, which is much more likely to block AVN conduction than BT.

Normal Response to Ventricular Premature Stimulation

Because a retrograde His potential may not be visible in 15% to 20% of patients during ventricular pacing, evaluation of the HPS, and consequently VA conduction, is often incomplete. In addition, in the absence of a visible His potential during ventricular pacing, the FRP of the HPS (theoretically, the shortest H₁-H₂ interval at any coupling interval) must be approximated by the S₁-H₂ interval (S₁ being the stimulus artifact of the basic drive CL), so that the S₁-H₂ interval approximates the H₁-H₂ interval, but exceeds it by a fixed amount, the S₁-H₁ interval. Retrograde AVN conduction time (H₂-A₂) is best measured from the end of the His potential to the onset of the atrial electrogram on the HB tracing.

Typically, VA conduction proceeds over the RB or LB, and then to the HB, AVN, and atrium. With a progressively premature VES, the initial delay occurs in the HPS, and the most common site of retrograde VA block is in the HPS. Delay or block in the AVN can occur but is less common.

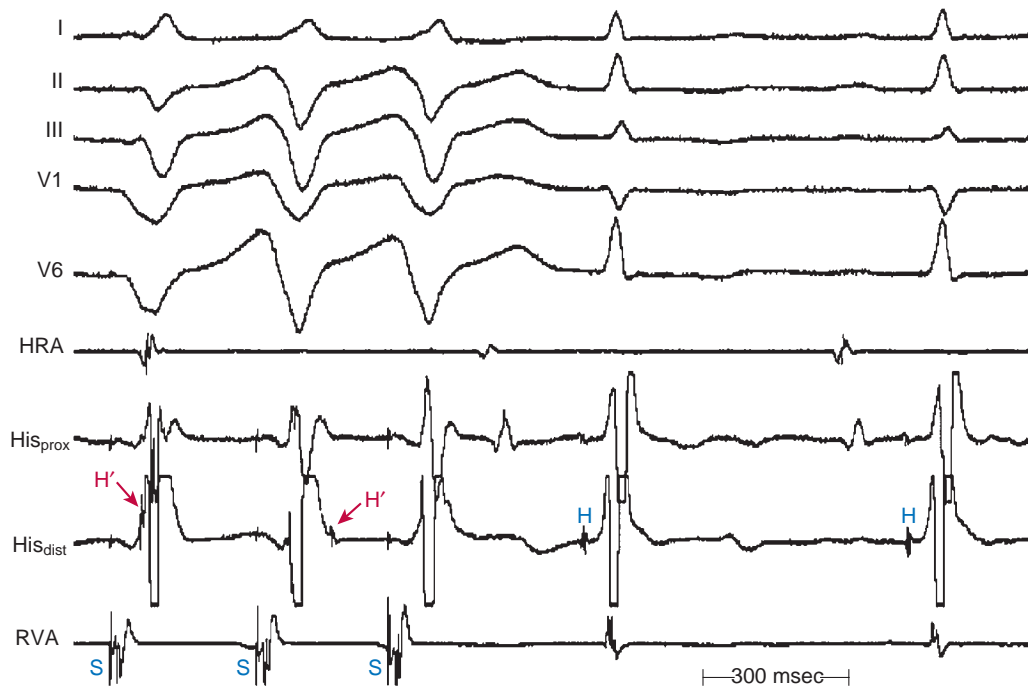


Fig. 4.25 Complete Retrograde Ventricular-Atrial (VA) Block in the Atrioventricular Node (AVN). Three ventricular paced complexes are shown, the first two of which have a clear retrograde His potential (H') and no retrograde atrial activation (sinus rhythm in atria), suggesting the AVN as the site of VA block. However, the site of VA block (AVN vs. His-Purkinje system) following the third ventricular complex is not obvious because there is no His potential visible following that ventricular stimulus. The site of VA block, however, can be inferred from the effect of paced impulses on conduction of the sinus complex after cessation of pacing. The atrial-His bundle (AH) interval of the conducted sinus complex after the last paced ventricular complex is longer than the baseline AH interval (at right), consistent with retrograde penetration of the AVN by the ventricular stimulus (resulting in concealed conduction) and therefore suggesting the AVN as the site of VA block. His_{dist} , Distal His bundle; His_{prox} , proximal His bundle; HRA , high right atrium; RVA , right ventricular apex.

The typical response to VES can be graphically displayed by plotting the S_1 - S_2 interval versus S_2 - H_2 , S_2 - A_2 , and H_2 - A_2 intervals, as well as the S_1 - S_2 interval versus S_1 - H_2 and A_1 - A_2 intervals. At long S_1 - S_2 intervals, no delay occurs in the retrograde conduction (S_2 - A_2). Further shortening of the S_1 - S_2 intervals results in prolongation in the S_2 - A_2 intervals, and localization of the exact site of S_2 - A_2 delay may not be feasible unless a retrograde His potential is visible (Fig. 4.26A and B). During RV pacing, the initial delay usually occurs in retrograde RB conduction. At a critical coupling interval (S_1 - S_2), block in the RB occurs, and retrograde conduction proceeds over the LB. A retrograde His potential (H_2) eventually becomes visible after the ventricular electrogram in the HB recording (see Fig. 4.26D). Once a retrograde His potential is seen, progressive prolongation in the S_2 - H_2 interval (HPS conduction delay) occurs as the S_1 - S_2 interval shortens, and the VA conduction time (S_2 - A_2) is determined by the HPS conduction delay (S_2 - H_2), as demonstrated by parallel S_2 - A_2 and S_2 - H_2 curves. The degree of prolongation of the S_2 - H_2 interval varies, but it can exceed 300 milliseconds.

In patients with preexistent BBB, retrograde block in the same bundle is common. This is suggested by a prolonged VH interval during a constant paced drive CL or late VES from the ventricle ipsilateral to the BBB, so that a retrograde His potential is usually seen after the ventricular electrogram in the HB tracing (see eFig. 4.8).

In most cases, once a retrograde His potential is visible, the S_1 - H_2 curve becomes almost horizontal because the increase in the S_2 - H_2 interval is similar to the decrease in the S_1 - S_2 interval. This response results in a relatively constant input to the AVN (as determined by measuring the S_1 - H_2 interval) and consequently a fixed H_2 - A_2 interval.

Occasionally, the increase in the S_2 - H_2 interval greatly exceeds the decrease in the S_1 - S_2 interval, thus giving rise to an ascending limb on the curve, with a subsequent decrease in the AVN conduction time (H_2 - A_2) because of decreased input to the AVN. As the S_1 - S_2 interval is further shortened, block within the HPS appears, or ventricular ERP is reached.

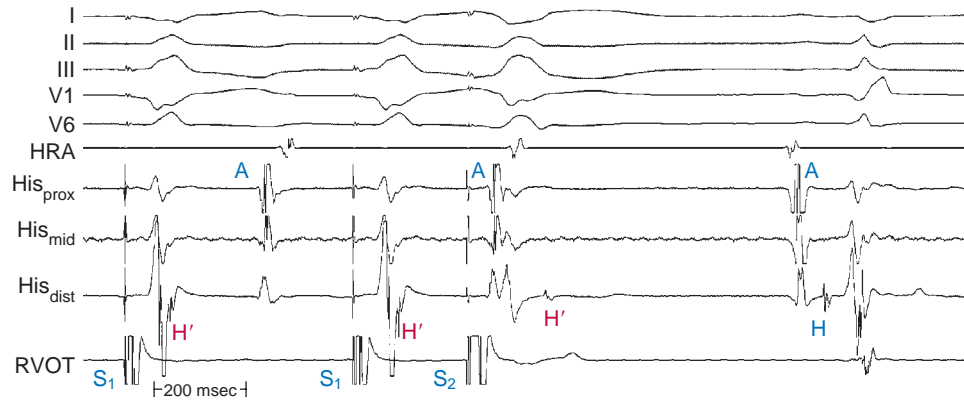
HPS refractoriness depends markedly on the CL, and shortening of the basic drive CL shortens the FRP and ERP of the HPS and ventricle. The general pattern, however, remains the same, with an almost linear increase in the S_2 - H_2 interval as the S_1 - S_2 interval is shortened. The curves for S_2 - H_2 versus S_1 - S_2 are shifted to the left, and the curves for S_1 - S_2 versus S_1 - H_2 are shifted down.

Repetitive Ventricular Responses

Ventricular stimulation can trigger extra ventricular beats. Those beats can be caused by different mechanisms; the most common are bundle branch reentry (BBR) beats, ventricular echo beats, and intraventricular reentrant beats. Multiple mechanisms may be responsible for repetitive responses in the same patient. Almost always, one of these responses is BBR.

Bundle Branch Reentry Beats

BBR beats are the most common ventricular response and can occur in up to 50% of normal individuals. In patients with normal hearts, BBR is rarely sustained and is usually self-limiting in one or two complexes. The occurrence of nonsustained BBR in patients with or without structural heart disease is not related to the presence of spontaneous ventricular arrhythmias.



eFig. 4.8 His Recordings in the Presence of Right Bundle Branch Block (RBBB). Two right ventricular drive complexes (S_1) and an extrastimulus (S_2) are shown, with a subsequent sinus complex with typical RBBB. Retrograde His activation (H') cannot traverse the blocked right bundle branch and must occur over the left bundle branch following transseptal ventricular activation, resulting in a long S- H' interval. The S- H' interval prolongs further following the extrastimulus (S_2). Of note, S_2 is associated with retrograde ventricular-atrial block in the atrioventricular node. His_{dist} , Distal His bundle; His_{mid} , middle His bundle; His_{prox} , proximal His bundle; HRA , high right atrium; $RVOT$, right ventricular outflow tract.

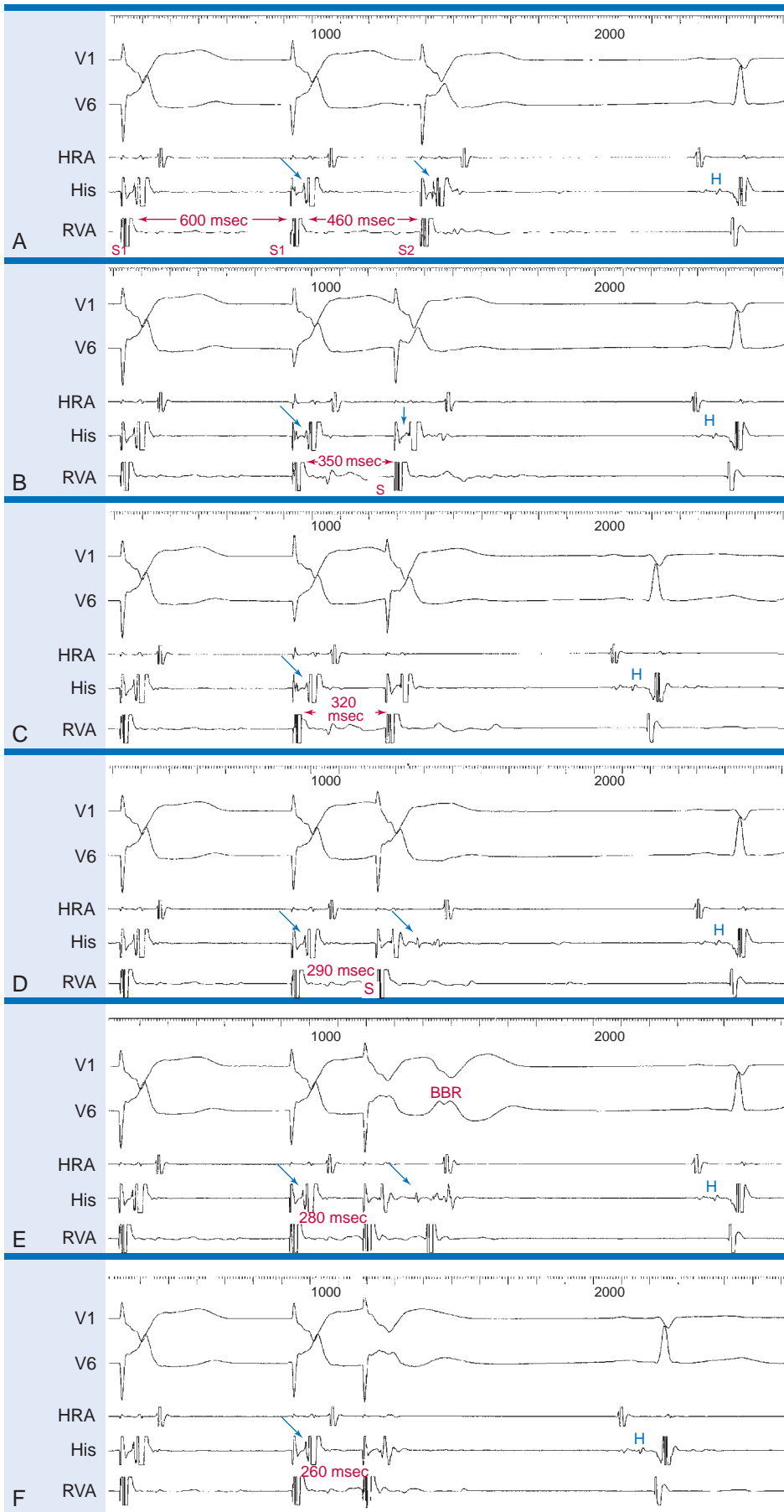


Fig. 4.26 Normal Response to Progressively Premature Ventricular Stimulation. Following a drive stimulus (S₁) at a cycle length of 600 milliseconds, a progressively premature ventricular extrastimulus (VES; S₂) is delivered from the right ventricular apex (RVA). (A) At a VES coupling interval of 460 milliseconds, retrograde His potential (arrows) is visible just before the local ventricular electrogram on the His bundle (HB) tracing, and ventricular-atrial (VA) conduction is intact. (B) An earlier VES is followed by some delay in VA conduction and prolongation of the His bundle-atrial interval. (C) A short coupled VES is followed by VA block. A retrograde His potential is not clearly visible. (D) An earlier VES is associated with retrograde block in the right bundle branch (RBB), followed by transseptal conduction and retrograde conduction up the left bundle branch (LBB) to the HB (the retrograde His potential is now visible well after the local ventricular electrogram). VA conduction now resumes because of proximal delay (in the His-Purkinje system), allowing distal recovery in the atrioventricular node (the gap phenomenon). (E) Further decrement in the VES coupling interval results in progressive delay in retrograde HPS conduction (and further prolongation of the S₂-H₂ interval), allowing for anterograde recovery of the RBB, so that the impulse can return down the initially blocked RBB, producing a QRS with a typical LBB block pattern (bundle branch reentry beat). (F) A very early VES is followed by ventricular-atrial block secondary to retrograde block in both the RBB and LBB; therefore no His potential is visible. HRA, High right atrium.

The longest refractory periods in the HPS are found most distally, at or near the Purkinje-myocardial junction. This creates a distal gate that inhibits retrograde conduction of early VES. Thus, when an early VES is delivered to the RV apex, the nearby distal gate of the RB can still be refractory. The results are progressive retrograde conduction delay and block occurring in the distal RB, with subsequent transseptal conduction of the impulse to the LV, leading to retrograde conduction up the LB to the HB (see Fig. 4.26D). At this point, the His potential usually follows the local ventricular electrogram in the HB recording, and retrograde atrial stimulation, if present, follows the His potential. Further decrease in the VES coupling interval produces progressive delay in retrograde HPS conduction. When a critical degree of HPS delay (S_2 - H_2) is attained, the impulse can return down the initially blocked RB, thus producing a QRS with a typical LBBB pattern and left-axis deviation, because ventricular activation originates solely from conduction over the RB (see Fig. 4.26E). This beat is called a BBR beat or V_3 phenomenon.

The HV interval of the BBR beat usually approximates that during anterograde conduction. However, it can be shorter or longer, depending on the site of HB recording relative to the turnaround point and on anterograde conduction delay down the RB.

Ventricular Echo Beats

This is the second most common response and can occur in 15% to 30% of normal individuals. It is caused by reentry in the AVN, and it appears when a critical degree of retrograde AVN delay is achieved. These patients have retrograde dual AVN physiology, and the last paced beat conducts slowly retrogradely up the slow AVN pathway and then anterogradely down the fast pathway to produce the echo beat (eFig. 4.9). In most cases, this delay is achieved before the appearance of a retrograde His potential beyond the local ventricular electrogram. At a critical H_2 - A_2 interval (or V_2 - A_2 interval, when the His potential cannot be seen), an extra beat with a normal anterograde QRS morphology results. Atrial activity also precedes the His potential before the echo beat.

This phenomenon can occur at long or short coupling intervals and depends only on the degree of retrograde AVN conduction delay. The presence of block within the HPS prevents its occurrence, as does block within the AVN. If a retrograde His potential can be seen throughout the zone of coupling intervals, a reciprocal relationship between the H_2 - A_2 and A_2 - H_3 intervals can often be noted.

Intraventricular Reentrant Beats

This response usually occurs in the setting of a cardiac pathological condition, especially coronary artery disease with a prior myocardial infarction (MI). It usually occurs at short coupling intervals and can have any morphology, but more often RBBB than LBBB in patients with a prior MI. Such beats occur in fewer than 15% of normal patients with a single VES at $2\times$ diastolic threshold and in 24% with double VESs. In contrast, intraventricular reentrant beats occur following single or double VESs in 70% to 75% of patients with prior VT or VF and cardiac disease. The incidence of this response increases with increasing the number of VESs, basic drive CLs, and stimulation sites used. These responses are usually nonsustained (1 to 30 complexes) and typically polymorphic. In patients without prior clinical arrhythmias, such responses are of no clinical significance.

MISCELLANEOUS ELECTROPHYSIOLOGICAL PHENOMENA

Concealed Conduction

Concealed conduction can be defined as the propagation of an impulse within the specialized conduction system of the heart that can be

recognized only from its effect on the subsequent impulse, interval, or cycle. This phenomenon can occur in any portion of the AV conduction system.

As long as the cardiac impulse is traveling in the specialized conduction system, the amount of electrical current generated is too small to be recorded on the surface ECG. However, if this impulse travels only a limited distance—incomplete anterograde or retrograde penetration—within the system, it can interfere with the formation or propagation of another impulse. When this interference can be recognized in the tracing because of an unexpected behavior of the subsequent impulse, unexpected in the sense that the event cannot be explained on the basis of readily apparent physiological or pathophysiological processes, it is known as concealed conduction.

The effect on subsequent events is an important part of the definition of concealed conduction because it differentiates the concept of concealed conduction from other forms of incomplete conduction, such as block of conduction at the level of the AVN or HPS. Ideally, a diagnosis of concealed conduction is supported by evidence in other areas of the same tracing where, given the opportunity and proper physiological setting, an impulse that is occasionally concealed can be conducted and become manifest. However, this condition cannot always be satisfied, nor is it absolutely necessary for the diagnosis of concealed conduction. Following are descriptions of the most frequent clinical circumstances in which concealed conduction can be observed.

Ventricular Response During Atrial Fibrillation

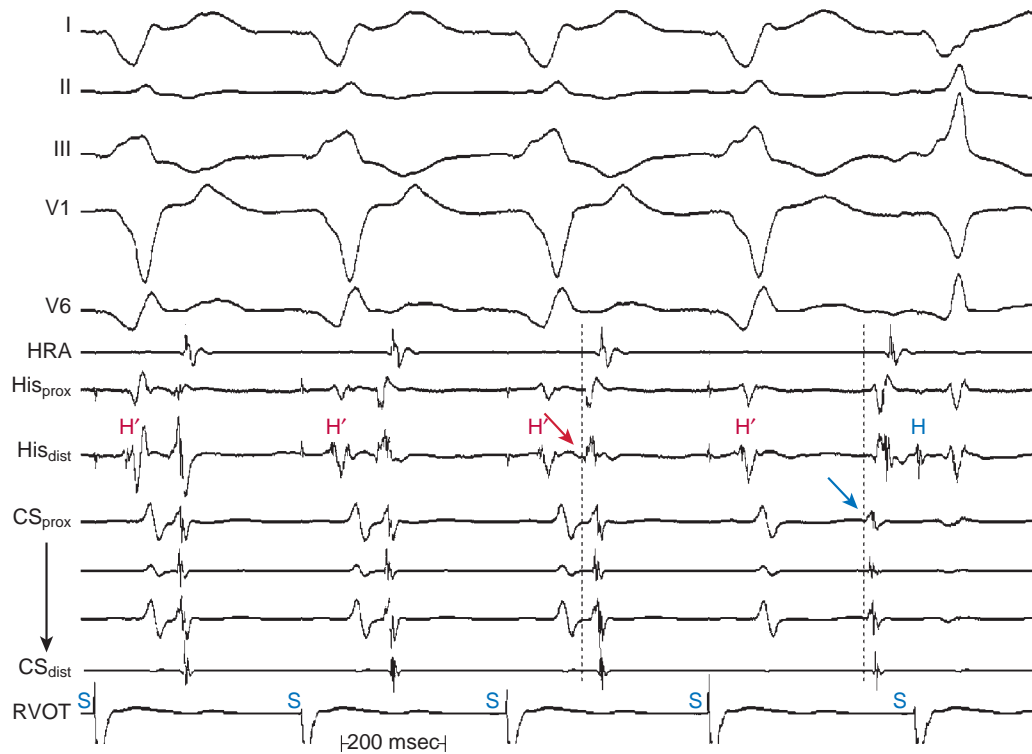
Repetitive concealed conduction is the mechanism of a slow and irregular ventricular rate during AF, with varying degrees of atrial penetration into the AVN. During AF, the irregular ventricular response is caused by the varying depth of penetration of the numerous atrial wavefronts approaching the AVN. Although the AVN would be expected to conduct whenever it recovers excitability after the last conducted atrial impulse, which would then be at regular intervals, the ventricular response is irregularly irregular because some fibrillatory impulses penetrate the AVN incompletely and block, thus leaving it refractory in the presence of subsequent atrial impulses.

Unexpected Prolongation or Failure of Conduction

Prolongation of the PR (and AH) interval or AVN block can occur secondary to a nonconducted premature depolarization of any origin (atrium, ventricle, or HB). The premature impulse incompletely penetrates the AVN (anterogradely or retrogradely), resets its refractoriness, and renders it fully or partially refractory at the time of the next sinus beat, which may then be blocked or may conduct with longer PR interval (see Fig. 4.25). For example, concealed junctional (HB) impulses can manifest as isolated PR interval prolongation, pseudo-type I AV block, or pseudo-type II AV block. ECG clues to concealed junctional extrasystoles causing such unexpected events include abrupt unexplained prolongation of the PR interval, the presence of apparent type II AV block in the presence of a normal QRS, the presence of types I and II AV block in the same tracing, and the presence of manifest junctional extrasystoles elsewhere in the tracing.

Unexpected Facilitation of Conduction

When a premature impulse penetrates the AV conduction system, it can result in facilitation of AV conduction and normalization of a previously present AV block or BBB by one of two mechanisms: (1) pre-exciting parts of the conduction system so that its refractory period ends earlier than expected (i.e., peeling back the refractory period of that tissue, thus allowing more time to recover excitability), or (2) causing CL-dependent shortening of refractoriness of tissues (i.e., atria, HPS, and ventricles) by decreasing the CL preceding the subsequent



eFig. 4.9 Retrograde Dual Atrioventricular Pathways. Fixed-rate ventricular pacing results in retrograde conduction; retrograde His potential is labeled H'. The first three complexes are conducted over a fast atrioventricular nodal (AVN) pathway; with the fourth complex, the fast AVN pathway conduction is blocked and retrograde conduction proceeds up the slow pathway (longer ventricular-atrial interval), followed by a fused QRS complex, partially paced and partially conducted to the His bundle anterogradely over the fast pathway. The two AVN pathways have different earliest atrial activation sites, indicated by colored arrows and dashed lines. CS_{dist}, Distal coronary sinus; CS_{prox}, proximal coronary sinus; His_{dist}, distal His bundle; His_{prox}, proximal His bundle; HRA, high right atrium; RVOT, right ventricular outflow tract.

spontaneous impulse. Abrupt normalization of the aberration by a PVC, the finding of which proves retrograde concealment as the mechanism for perpetuation of aberration, is based on these principles.

Perpetuation of Aberrant Conduction During Supraventricular Tachycardias

The most common mechanism (70%) of perpetuation of aberrant conduction during tachyarrhythmias is retrograde penetration of the blocked bundle branch subsequent to transseptal conduction. For example, a PVC from the LV during an SVT can activate the LB early and then conduct transseptally and later penetrate the RB retrogradely. Subsequently, the LB recovers in time for the next SVT impulse, whereas the RB remains refractory. Therefore the next SVT impulse travels to the LV over the LB (with an RBBB pattern, phase 3 aberration). Conduction subsequently propagates from the LV across the septum to the RV. By this time, the distal RB has recovered, thereby allowing retrograde penetration of the RB by the transseptal wavefront and rendering the RB refractory to each subsequent SVT impulse (see Fig. 10.8). This scenario is repeated and RBBB continues until another, well-timed PVC preexcites the RB (and either peels back or shortens its refractoriness), so that the next impulse from above finds the RB fully recovered and conducts without aberration (see Fig. 10.4). This phenomenon may persist even when the PCL is prolonged, until the site of collision in

the affected bundle branch has recovered adequately for anterograde propagation (Fig. 4.27).

Gap Phenomenon

The term *gap* in AVN conduction was originally used to define a zone in the cardiac cycle during which PACs failed to evoke ventricular responses, whereas PACs of greater or lesser prematurity conducted to the ventricles. The physiological basis of the gap phenomenon depends on a distal area with a long refractory period and a proximal site with a shorter refractory period. During the gap phenomenon, initial block occurs distally. With earlier impulses, proximal conduction delay is encountered, which allows the distal site of early block to recover excitability and resume conduction.

The gap phenomenon is not an abnormality, but reflects the interplay between conduction velocity and refractory periods at two different levels in the AV conduction system. Demonstration of the gap phenomenon can be enhanced or eliminated by any intervention that alters the relationship between the EP properties of those structures (e.g., changes in the neurohumoral tone created by drugs or changes in the heart rate by pacing).

An example of the most common type of gap phenomenon is an AES (A_2) conducting with modest delay through the AVN that finds the HB still refractory, thus causing block. With increasing prematurity

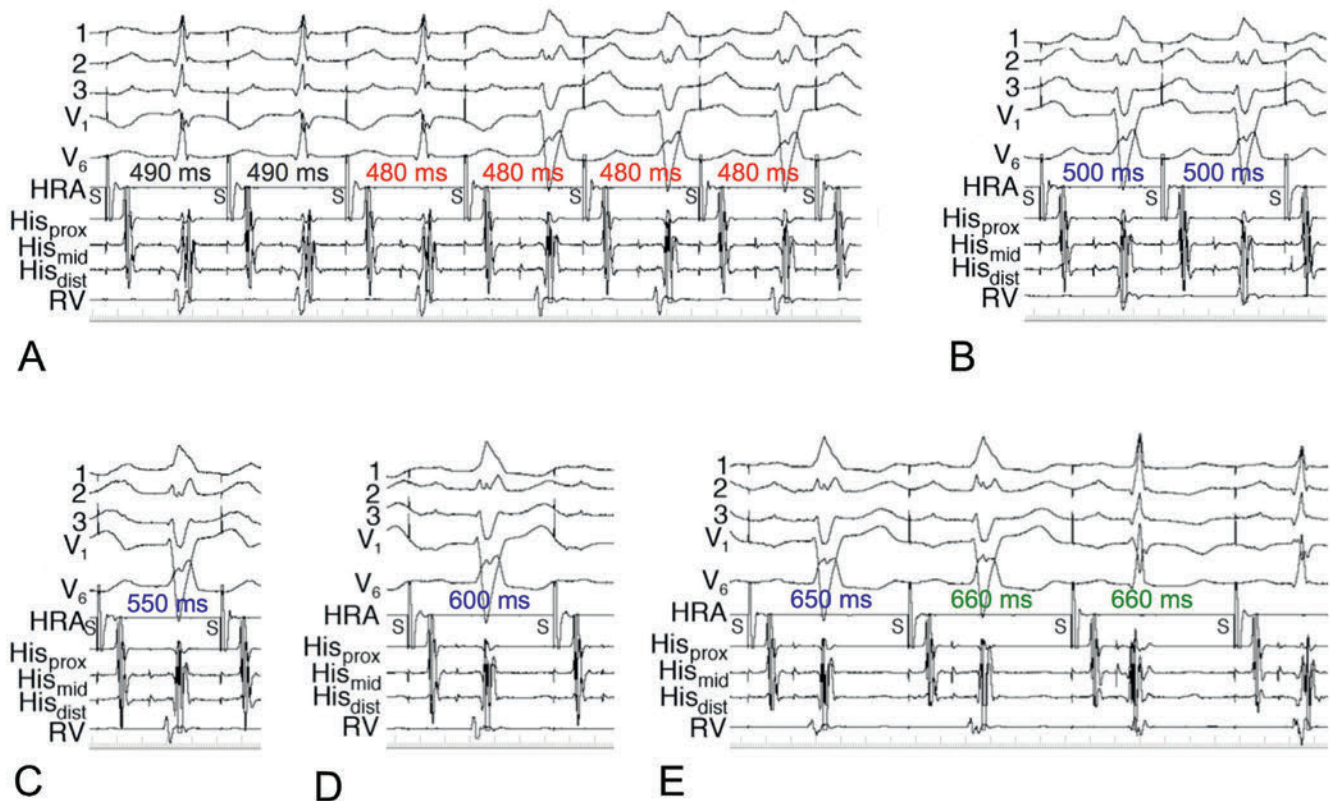


Fig. 4.27 Perpetuation of Concealed Conduction in the Left Bundle Branch (LB). Segments of a continuous run of atrial pacing are shown, starting at 490 milliseconds (A). At 480 milliseconds pacing cycle length (PCL), LB block develops (red numbers) and persists despite gradually increasing the PCL to 500 milliseconds (B), 550 milliseconds (C), 600 milliseconds (D) and 650 milliseconds (E) (blue numbers). Finally, at 660 milliseconds (E), the site of block in the LB has migrated distally enough that conduction in the LB can resume. This is an extreme example of linking or concealed perpetuation of block, over a range of PCLs of 180 milliseconds. *His_{dist}*, Distal His bundle; *His_{mid}*, middle His bundle; *His_{prox}*, proximal His bundle; *HRA*, high right atrium; *RV*, right ventricular.

of the AES, the AES travels more slowly through the AVN (i.e., the A_2 - H_2 interval prolongs further), so that the H_1 - H_2 interval now exceeds the refractory period of the HB. By the time the impulse traverses the AVN, the HB has completed its ERP and conduction resumes (Fig. 4.28).

Other types of the gap phenomenon are described in which the required conduction delay is in the HB, proximal AVN, or atria. The gap phenomenon depends on the relationship between the EP properties of two sites; any pair of structures in the AV conduction system that has the appropriate physiological relationship can exhibit the gap phenomenon (e.g., AVN-HB, HB-HPS, atrium-AVN, atrium-HPS, proximal AVN-distal AVN, proximal HPS-distal HPS), and gap can occur during anterograde or retrograde stimulation. Therefore there are almost endless possibilities for gaps, all based on the fundamental precept of “proximal delay allows distal recovery” (see Fig. 4.26C and D).

Supernormality

Supernormal conduction implies conduction that is better than anticipated or conduction that occurs when block is expected. Electrocardiographically, however, supernormal conduction is not better than normal conduction, only better than expected. When an alteration in conduction can be explained in terms of known physiological events, true supernormal conduction need not be invoked.⁶⁴

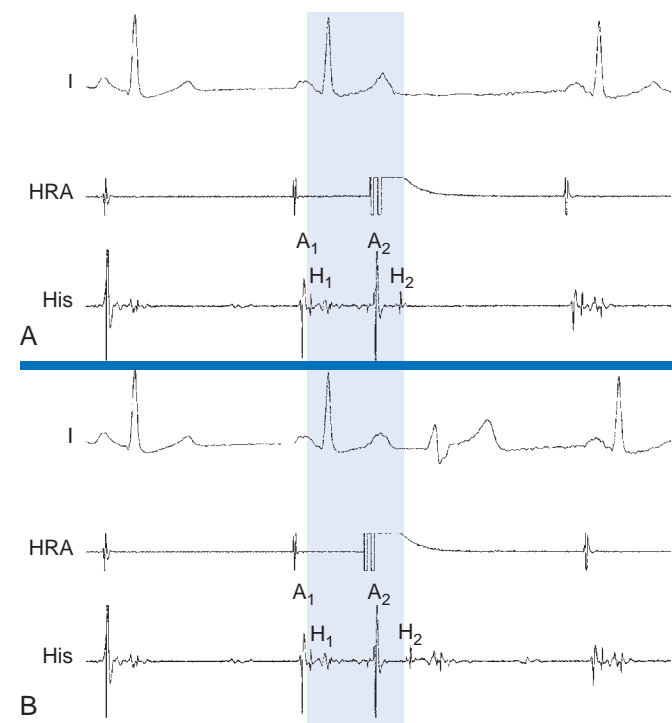


Fig. 4.28 Anterograde Atrioventricular (AV) Gap Phenomenon. (A) An atrial extrastimulus (AES; A_2) conducting with modest delay through the atrioventricular node (AVN) finds the His bundle (HB) still refractory, causing atrioventricular block. (B) An earlier AES results in further prolongation of the A_2 - H_2 interval and the subsequent H_1 - H_2 interval (shaded area). The longer H_1 - H_2 interval now exceeds the refractory period of the HB, and, by the time the impulse traverses the AVN, the HB has completed its effective refractory period and conduction resumes; however, the conducted QRS has a left bundle branch block morphology and a longer HV interval because the left bundle is still refractory. HRA, High right atrium.

Supernormal conduction is dependent on supernormal excitability, a condition that exists during a brief period of repolarization, at the end of phase 3. During the supernormal period, excitation is possible in response to an otherwise subthreshold stimulus; that same stimulus fails to elicit a response earlier or later than the supernormal period. Two factors are responsible for supernormality: the availability of fast Na^+ channels and the proximity of the membrane potential to threshold potential. During the supernormal phase of excitability, the cell has recovered enough to respond to a stimulus. However, because the membrane potential is still reduced, it requires only a little additional depolarization to bring the fiber to threshold; thus, a smaller stimulus than is normally required elicits an action potential. Supernormality has been demonstrated in the HPS, Bachmann's bundle in the dog, and working myocardium of the atrium and ventricle, but not in the AVN.⁶⁴

Supernormal excitability is diagnosed when the myocardium responds to a stimulus that is ineffective when applied earlier or later in the cycle. Some ECG manifestations of supernormality include the following:

1. Paradoxical normalization of bundle branch conduction at an R-R interval shorter than that associated with BBB. This can occur with a PAC conducting with a normal QRS during baseline NSR with BBB or with acceleration-dependent BBB that normalizes at even faster rates.
2. Intermittent AV conduction during periods of high-degree AV block. Only the P waves falling on or just after the terminal part of the T wave are conducted, whereas other timed P waves fail to conduct.
3. A poorly sensing pacemaker captures just at the end of the T wave, but not elsewhere in the cardiac cycle.

Although supernormal conduction is a proven property of the HPS and has been demonstrated in vitro, it is uncertain whether true supernormal conduction is a clinically important phenomenon. Other physiological mechanisms can be invoked to explain almost all reported examples of supernormal conduction in humans. Causes of apparent or pseudo-supernormal conduction include the gap phenomenon (the most common mechanism of pseudo-supernormal conduction), peeling back of refractoriness, shortening of refractoriness by changing the preceding CL, Wenckebach phenomena in the bundle branches, bradycardia-dependent (phase 4) block, summation, dual AVN physiology, reentry with ventricular echo beats, and concealed junctional extrasystoles.^{64,65}

COMPLICATIONS OF ELECTROPHYSIOLOGICAL TESTING

Risks and Complications

The complication rate of EP testing is relatively low (less than that of coronary arteriography) when only right-heart catheterization is performed, with almost negligible mortality. The risk of complications increases significantly in patients with severe or decompensated cardiac disease. The addition of left-heart access or therapeutic maneuvers (e.g., ablation) to the procedure increases the incidence of complications, especially with the increasing use of extensive ablation to treat AF and ischemic VT.

Complications of EP testing include vascular injury (hematoma, pseudoaneurysm, and arteriovenous fistula), bleeding requiring transfusion, deep venous thrombosis and pulmonary embolism, systemic thromboembolism, infection at catheter sites, systemic infection, pneumothorax, hemothorax, pericarditis, cardiac perforation and tamponade, MI, worsening heart failure, stroke, complete AV block, and BBB. Although potentially lethal arrhythmias such as rapid VT or VF can occur in the EP laboratory, they are not necessarily regarded as complications, but are often expected and anticipated. Complications following specific ablation procedures are discussed in subsequent chapters.

Iatrogenic Problems Encountered During Electrophysiological Testing









Mechanical irritation from catheters during placement inside the heart, even when they are not being manipulated, can cause arrhythmias and conduction disturbances, including induction of atrial, junctional, and ventricular ectopic beats or tachyarrhythmias, AV block, and BBB. AV block can occur especially during RV catheterization in patients with preexisting LBBB, and occasionally secondary to mechanical trauma of the compact AVN. Ventricular stimulation can also occur from physical movement of the ventricular catheter coincident with atrial contraction, thus producing patterns of ventricular preexcitation on the surface ECG. Recognition of all these iatrogenic patterns is important for avoiding misinterpretation of EP phenomena and determining the significance of findings in the laboratory.

AF and VF are to be avoided unless they are the subject of the study. AF obviously does not permit study of any other form of SVT, and VF requires prompt defibrillation. If AF must be initiated for diagnostic purposes (e.g., to assess ventricular response over an AV BT), it is preferably induced at the end of the diagnostic portion of the study. Patients with a prior history of AF are more prone to the occurrence of sustained AF in the EP laboratory. Frequently, this occurs during initial placement of catheters; excessive manipulation of catheters in the atria should therefore be avoided.

Another iatrogenic problem is catheter trauma resulting in abolition of BT conduction or injury to the focus of a tachycardia or to the reentrant pathway, which can make the mapping and curative ablation difficult or impossible.

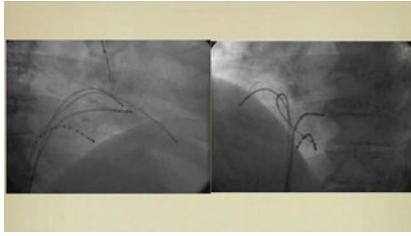
VIDEOS

The following videos accompany this chapter:

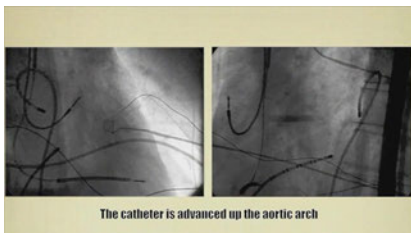
-  **Video 4.1.** Placement of the Coronary Sinus Catheter via the Inferior Vena Cava (IVC): Fluoroscopy
-  **Video 4.2.** Transaortic Left Ventricular (LV) Access: Fluoroscopy
-  **Video 4.3.** Atrial Transseptal Puncture: Guided by Fluoroscopy
-  **Video 4.4.** Atrial Transseptal Puncture: Guided by Intracardiac Echocardiography (ICE)
-  **Video 4.5.** Atrial Transseptal Puncture: Guided by Transesophageal Echocardiography
-  **Video 4.6.** Atrial Transseptal Puncture Using the Radiofrequency (RF)-Powered Needle
-  **Video 4.7.** Atrial Transseptal Puncture (in the Presence of Atrial Septal Defect Closure Device [CD])
-  **Video 4.8.** Pericardial Access: Technique

REFERENCES

- Haines DE, et al. Heart Rhythm Society expert consensus statement on electrophysiology laboratory standards: process, protocols, equipment, personnel, and safety. *Heart Rhythm*. 2014;11:e9–e51.
- Lü F, Lin J, Benditt DG. Conscious sedation and anesthesia in the cardiac electrophysiology laboratory. *J Cardiovasc Electrophysiol*. 2013;24:237–245.
- Haddy S. Anesthesia for structural heart interventions. *Cardiol Clin*. 2013;31:455–465.
- Anderson R, Harukuni I, Sera V. Anesthetic considerations for electrophysiologic procedures. *Anesthesiol Clin*. 2013;31:479–489.
- de Bono J. Propofol: a safe drug for physician-led procedures? *Europace*. 2012;14:303–305.
- Thomas SP, Thakkar J, Kovoov P, et al. Sedation for electrophysiological procedures. *Pacing Clin Electrophysiol*. 2014;37:781–790.
- Rozner MA, McKay RE. Components of safe propofol sedation: defining the formula. *Heart Rhythm*. 2012;9:347–348.
- Trentman TL, Fassett SL, Mueller JT, et al. Airway interventions in the cardiac electrophysiology laboratory: a retrospective review. *J Cardiothorac Vasc Anesth*. 2009;23:841–845.
- Salukhe TV, et al. Propofol sedation administered by cardiologists without assisted ventilation for long cardiac interventions: an assessment of 1000 consecutive patients undergoing atrial fibrillation ablation. *Europace*. 2012;14:325–330.
- Wutzler A, et al. Effects of deep sedation on cardiac electrophysiology in patients undergoing radiofrequency ablation of supraventricular tachycardia: impact of propofol and ketamine. *Europace*. 2013;15:1019–1024.
- Nazer B, et al. Importance of ventricular tachycardia induction and mapping for patients referred for epicardial ablation. *Pacing Clin Electrophysiol*. 2015;38:1333–1342.
- Gaitan BD, Trentman TL, Fassett SL, et al. Sedation and analgesia in the cardiac electrophysiology laboratory: a national survey of electrophysiologists investigating the who, how, and why? *J Cardiothorac Vasc Anesth*. 2011;25:647–659.
- Tanaka-Esposito CC, et al. Real-time ultrasound guidance reduces total and major vascular complications in patients undergoing pulmonary vein antral isolation on therapeutic warfarin. *J Interv Card Electrophysiol*. 2013;37:163–168.
- Errahmouni A, Bun SS, Latcu DG, et al. Ultrasound-guided venous puncture in electrophysiological procedures: a safe method, rapidly learned. *Pacing Clin Electrophysiol*. 2014;37:1023–1028.
- Rodríguez Muñoz D, et al. Wireless ultrasound guidance for femoral venous cannulation in electrophysiology: impact on safety, efficacy, and procedural delay. *Pacing Clin Electrophysiol*. 2015;38:1058–1065.
- Mori S, et al. Clinical cardiac structural anatomy reconstructed within the cardiac contour using multidetector-row computed tomography: left ventricular outflow tract. *Clin Anat*. 2016;29:353–363.
- Sun H, Wang Y, Zhang Z, et al. Predicting interatrial septum rotation: is the position of the heart or the direction of the coronary sinus reliable? *Pacing Clin Electrophysiol*. 2015;38:514–519.
- Gabus V, et al. Short-term heparin kinetics during catheter ablation of atrial fibrillation. *Pacing Clin Electrophysiol*. 2015;38:1142–1150.
- Briceno DE, Natale A, Di Biase L. Heparin kinetics: the ‘holy grail’ of periprocedural anticoagulation for ablation of atrial fibrillation. *Pacing Clin Electrophysiol*. 2015;38:1137–1141.
- Tzeis S, Andrikopoulos G, Deisenhofer I, et al. Transseptal catheterization: considerations and caveats. *Pacing Clin Electrophysiol*. 2010;33:231–242.
- Giudici MC, Mickelsen SR, Bhavne PD, et al. A safe, simple technique for transseptal catheterization. *Pacing Clin Electrophysiol*. 2015;38:295–296.
- Esch JJ, Triedman JK, Cecchin F, et al. Radiofrequency-assisted transseptal perforation for electrophysiology procedures in children and adults with repaired congenital heart disease. *Pacing Clin Electrophysiol*. 2013;36:607–611.
- Winkle RA, Mead RH, Engel G, et al. The use of a radiofrequency needle improves the safety and efficacy of transseptal puncture for atrial fibrillation ablation. *Heart Rhythm*. 2011;8:1411–1415.
- Knecht S, et al. Radiofrequency puncture of the fossa ovalis for resistant transseptal access. *Circ Arrhythm Electrophysiol*. 2008;1:169–174.
- Greenstein E, Passman R, Lin AC, et al. Incidence of tissue coring during transseptal catheterization when using electrocautery and a standard transseptal needle. *Circ Arrhythm Electrophysiol*. 2012;5:341–344.
- Santangeli P, et al. Transseptal access and atrial fibrillation ablation guided by intracardiac echocardiography in patients with atrial septal closure devices. *Heart Rhythm*. 2011;8:1669–1675.
- Li X, et al. Safety and feasibility of transseptal puncture for atrial fibrillation ablation in patients with atrial septal defect closure devices. *Heart Rhythm*. 2014;11:330–335.
- Katritsis GD, Siontis GCM, Giazitzoglou E, et al. Complications of transseptal catheterization for different cardiac procedures. *Int J Cardiol*. 2013;168:5352–5354.
- Wasmer K, et al. Incidence and management of inadvertent puncture and sheath placement in the aorta during attempted transseptal puncture. *Europace*. 2017;19:447–457.



Video 4.1 Placement of the Coronary Sinus Catheter via the Inferior Vena Cava (IVC): Fluoroscopy. Simultaneous left anterior oblique (LAO) and right anterior oblique (RAO) fluoroscopy projections are acquired during catheterization of the coronary sinus (CS) via the IVC. Electrophysiological (EP) catheter are positioned in the right atrial (RA) appendage, right ventricular (RV) apex, and at the His bundle (HB) region. The CS catheter is advanced via the IVC. The tip of the catheter is first placed into the RV, using the RAO fluoroscopy view, and flexed downward toward the RV inferior wall. Subsequently, the catheter is withdrawn until it lies at the inferoseptal aspect of the tricuspid annulus. Using the LAO or RAO view, the catheter is then withdrawn gently with clockwise rotation until the tip of the catheter drops into the CS ostium (CS os). Afterward, the catheter is advanced into the CS concomitantly with gradual release of the catheter curve.



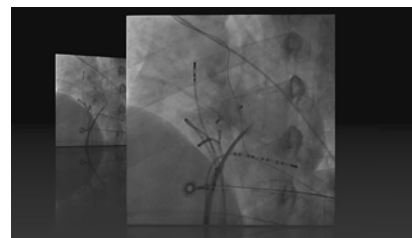
Video 4.2 Transaortic Left Ventricular (LV) Access. Fluoroscopy. Simultaneous left anterior oblique (LAO) and right anterior oblique (RAO) fluoroscopy projections are acquired during retrograde LV access. Leads of an implantable cardioverter-defibrillator (ICD) are visualized in the right atrial (RA) appendage and right ventricular (RV) apex. A multipolar electrophysiological (EP) catheter is positioned at the His bundle (HB) region. The ablation catheter is initially advanced to the descending aorta, where a tight J curve is formed with the catheter tip before passage to the aortic root to minimize catheter manipulation in the arch. The curved catheter is advanced through the aortic valve. A long vascular sheath is used in this case to provide added catheter stability during LV mapping.



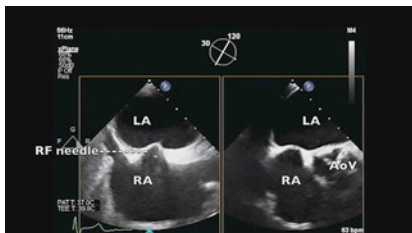
Video 4.3 Atrial Transseptal Puncture: Guided by Fluoroscopy. Simultaneous left anterior oblique (LAO) right anterior oblique (RAO) fluoroscopy projections are acquired during atrial septal puncture. Initially, the sheath-dilator-needle assembly is visualized in the superior vena cava (SVC), with curves of the dilator, sheath, and needle aligned so that they are all in agreement, the Brockenbrough needle tip positioned within 1 to 2 cm of the dilator tip, and the assembly rotated leftward and posteriorly. Also visualized are an electrophysiological (EP) catheter positioned at the His bundle (HB) region (to mark the root of the aorta), an intracardiac echocardiography (ICE) catheter positioned in the mid right atrium (RA), and a guidewire in the SVC. The assembly is retracted caudally as a single unit (while maintaining the relative positions of its components). Note that, in the LAO view, the dilator tip moves slightly leftward upon entering the RA and then leftward again while descending below the aortic root. A third abrupt leftward movement ("jump") at the level of the HB region (marked by an EP catheter) indicates passage over the limbus into the fossa ovalis. This latter jump generally occurs at the level of the HB region. In the RAO view, the dilator tip is directed posteriorly to the His bundle region. Once the dilator tip is confirmed at the fossa ovalis, the needle is extended across the interatrial septum. A 0.014 angioplasty wire is advanced through the Brockenbrough needle into the LA. Initially, the wire coils at the LA roof. The wire is then withdrawn and advanced into the left superior pulmonary vein, as it is visualized extending outside the cardiac silhouette. The sheath-dilator assembly is advanced as a single unit over the needle and angioplasty wire into the LA, while holding the needle in a stable position. Subsequently, the sheath is advanced over the dilator while holding the needle and dilator in a stable position. Note that some resistance at the interatrial septum meets advancing the sheath over dilator, and force build-up causes a sudden jump of the dilator-sheath assembly toward the LA lateral wall. Having the angioplasty wire deeply seated in a left-sided pulmonary vein helps direct the path of the assembly as it enters the LA and minimizes the risk of inadvertent injury to the opposing LA wall. A second atrial septal puncture is performed using the same technique for the first puncture. A lasso catheter is positioned in the LA at the ostium of the left superior pulmonary vein (PV). Again, advancing the sheath across the septum is met by resistance and causes a jump of the sheath-dilator assembly, which is controlled and directed in a safe path over the guidewire.



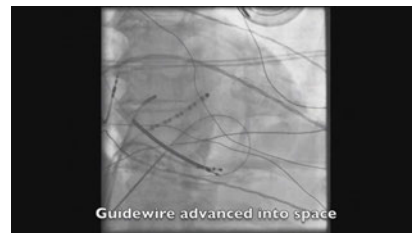
Video 4.4 Atrial Transseptal Puncture: Guided by Intracardiac Echocardiography (ICE). The interatrial septum is visualized by the ICE phased array catheter positioned in the mid-right atrium. As demonstrated, the optimal ICE image to guide transseptal puncture will demonstrate adequate space behind the interatrial septum on the left atrial (LA) side, but will not include the aortic root because it would be too anterior for the interatrial septum to be punctured safely. Advancement of sheath-dilator-needle assembly against the interatrial septum causes tenting of the septum. The Brockenbrough needle is then advanced while saline is infused continuously through the needle. With successful transseptal puncture, sudden collapse of the tented fossa is observed, and saline infusion through the needle is visualized on ICE as bubbles in the LA.



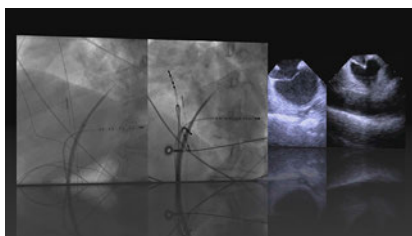
Video 4.7 Atrial Transseptal Puncture (in the Presence of Atrial Septal Defect Closure Device [ASD]). Fluoroscopic images are shown in the left anterior oblique projection are acquired during atrial septal puncture in a patient with prior device closure of an atrial septal defect. Initially, the needle is erroneously advanced within the inferior portion of the device, and the closure device is observed on fluoroscopy to be pushed by the needle as it is advanced across the atrial septum. While a 0.014 angioplasty wire could be advanced through the Brockenbrough needle into the left atrium (LA), the dilator and sheath could not be advanced across the device. Then, the needle was withdrawn out of the LA, and a site on the atrial septum more caudal and posterior to the closure device was successfully punctured. CS, Coronary sinus catheter.



Video 4.5 Atrial Transseptal Puncture: Guided by Transesophageal Echocardiography. The left atrium (LA) is visualized on top, and the right atrium (RA) is visualized at 7 o'clock. Advancement of the sheath-dilator-needle assembly against the interatrial septum causes tenting of the septum. The Brockenbrough needle is then advanced while saline is infused continuously through the needle. Bubbles of saline infusion are visualized in the LA once the needle tip crosses the septum. AoV, Aortic valve.



Video 4.8 Pericardial Access: Technique. Initially, catheters are positioned in the coronary sinus (CS), right ventricular apex (RVA), and the His bundle (HB) region through the femoral approach. The leads of a dual-chamber implantable cardioverter-defibrillator are visualized in the right atrial appendage (RAA) and RVA. The puncture needle is introduced at the angle between the left border of the subxiphoid process and the lower left rib, with the needle pointing to the left shoulder. The needle is then advanced under fluoroscopy guidance until close to the cardiac silhouette, and then a small amount of contrast is injected through the needle to assess the relation of the needle to the parietal pericardium. Once tenting of the pericardium is seen, a slight advance achieves entry into the pericardial space. When the needle reaches the pericardial sac, injected contrast will spread around the heart, restricted to its silhouette. After reaching the pericardial space, a long soft J tip guide wire is advanced far enough to silhouette the pericardial space. The puncture needle is then withdrawn and an 8 Fr dilator is advanced over the guide wire under fluoroscopic guidance for pre-dilatation, followed by insertion of a standard 8 Fr sheath.



Video 4.6 Atrial Transseptal Puncture Using the Radiofrequency (RF)-Powered Needle. The tip of the needle can be easily visualized on fluoroscopy (both inside or outside the dilator) and intracardiac echocardiography (ICE). Once septal tenting is observed on ICE, RF energy is delivered to the blunt, closed tip of the needle, resulting in steam popping and septal perforation.

30. Singh SM, Douglas PS, Reddy VY. The incidence and long-term clinical outcome of iatrogenic atrial septal defects secondary to transseptal catheterization with a 12F transseptal sheath. *Circ Arrhythm Electrophysiol*. 2011;4:166–171.
31. Alkhouli M, Sarraf M, Zack CJ, et al. Iatrogenic atrial septal defect following transseptal cardiac interventions. *Int J Cardiol*. 2016;209:142–148.
32. Aznaouridis K, Hobson N, Rigg C, et al. Emergency percutaneous closure of an iatrogenic atrial septal defect causing right-to-left shunt and severe refractory hypoxemia after pulmonary vein isolation. *JACC Cardiovasc Interv*. 2015;8:e179–e181.
33. Davies A, et al. Persistent iatrogenic atrial septal defects after pulmonary vein isolation: long-term follow-up with contrast transesophageal echocardiography. *J Interv Card Electrophysiol*. 2017;48:99–103.
34. Garikipati NV, Paruchuri V, Mittal S. How to learn epicardial intervention techniques in electrophysiology. *Card Electrophysiol Clin*. 2010;2:35–43.
35. Syed F, et al. The pericardial space: obtaining access and an approach to fluoroscopic anatomy. *Card Electrophysiol Clin*. 2010;2:9–23.
36. Ernst S, Sanchez-Quintana D, Ho SY. Anatomy of the pericardial space and mediastinum: relevance to epicardial mapping and ablation. *Card Electrophysiol Clin*. 2010;2:1–8.
37. Lim HS, et al. Safety and prevention of complications during percutaneous epicardial access for the ablation of cardiac arrhythmias. *Heart Rhythm*. 2014;11:1658–1665.
38. Swale M, et al. Epicardial access: patient selection, anatomy, and a stepwise approach. *J Innov Card Rhythm Manag*. 2011;2:239–249.
39. Smith SE, Darling GE. Surface anatomy and surface landmarks for thoracic surgery: part II. *Thorac Surg Clin*. 2011;21:139–155.
40. Bradfield JS, Tung R, Boyle NG, et al. Our approach to minimize risk of epicardial access: standard techniques with the addition of electroanatomic mapping guidance. *J Cardiovasc Electrophysiol*. 2013;24:723–727.
41. Boyle NG, Shivkumar K. Epicardial interventions in electrophysiology. *Circulation*. 2012;126:1752–1769.
42. Yamada T, Kay GN. Recognition and prevention of complications during epicardial ablation. *Card Electrophysiol Clin*. 2010;2:127–134.
43. Koneru JN, Badhwar N, Ellenbogen KA, et al. LAA ligation using the LARIAT suture delivery device: tips and tricks for a successful procedure. *Heart Rhythm*. 2014;11:911–921.
44. Di Biase L, et al. Initial international multicenter human experience with a novel epicardial access needle embedded with a real time pressure/frequency monitoring to facilitate epicardial access: feasibility and safety. *Heart Rhythm*. 2017;14:981–988.
45. Kumar S, et al. ‘needle-in-needle’ epicardial access: preliminary observations with a modified technique for facilitating epicardial interventional procedures. *Heart Rhythm*. 2015;12:1691–1697.
46. Gunda S, et al. Differences in complication rates between large bore needle and a long micropuncture needle during epicardial access. *Circ Arrhythm Electrophysiol*. 2015;8:890–895.
47. D’Avila A, Koruth JS, Dukkupati S, et al. Epicardial access for the treatment of cardiac arrhythmias. *Europace*. 2012;14:13–18.
48. Tschabrunn CM, et al. Percutaneous epicardial ventricular tachycardia ablation after noncoronary cardiac surgery or pericarditis. *Heart Rhythm*. 2013;10:165–169.
49. Killu AM, et al. Percutaneous epicardial access for mapping and ablation is feasible in patients with prior cardiac surgery, including coronary bypass surgery. *Circ Arrhythm Electrophysiol*. 2015;8:94–101.
50. Killu AM, et al. Atypical complications encountered with epicardial electrophysiological procedures. *Heart Rhythm*. 2013;10:1613–1621.
51. Stevenson WG, Soejima K. Recording techniques for clinical electrophysiology. *J Cardiovasc Electrophysiol*. 2005;16:1017–1022.
52. Tedrow UB, Stevenson WG. Recording and interpreting unipolar electrograms to guide catheter ablation. *Heart Rhythm*. 2011;8:791–796.
53. Venkatachalam KL, Herbrandson JE, Asirvatham SJ. Signals and signal processing for the electrophysiologist: part I: electrogram acquisition. *Circ Arrhythm Electrophysiol*. 2011;4:965–973.
54. Jadidi AS, Lehrmann H, Weber R, et al. Optimizing signal acquisition and recording in an electrophysiology laboratory. *Card Electrophysiol Clin*. 2013;5:137–142.
55. Cantwell CD, et al. Techniques for automated local activation time annotation and conduction velocity estimation in cardiac mapping. *Comput Biol Med*. 2015;65:229–242.
56. Venkatachalam KL, Herbrandson JE, Asirvatham SJ. Signals and signal processing for the electrophysiologist: part II: signal processing and artifact. *Circ Arrhythm Electrophysiol*. 2011;4:974–981.
57. van der Does LJME, de Groot NMS. Inhomogeneity and complexity in defining fractionated electrograms. *Heart Rhythm*. 2017;14:616–624.
58. Sorgente A, et al. Negative concordance pattern in bipolar and unipolar recordings: an additional mapping criterion to localize the site of origin of focal ventricular arrhythmias. *Heart Rhythm*. 2016;13:519–526.
59. Almendral J, Caulier-Cisterna R, Rojo-Álvarez JL. Resetting and entrainment of reentrant arrhythmias: Part I: Concepts, recognition, and protocol for evaluation: surface ECG versus intracardiac recordings. *Pacing Clin Electrophysiol*. 2013;36:508–532.
60. Noorman M, et al. Cardiac cell-cell junctions in health and disease: electrical versus mechanical coupling. *J Mol Cell Cardiol*. 2009;47:23–31.
61. Nerbonne JM, Kass RS. Molecular physiology of cardiac repolarization. *Physiol Rev*. 2005;85:1205–1253.
62. Michael G, Xiao L, Qi X-Y, et al. Remodelling of cardiac repolarization: how homeostatic responses can lead to arrhythmogenesis. *Cardiovasc Res*. 2009;81:491–499.
63. Hanson B, et al. Interaction of activation-repolarization coupling and restitution properties in humans. *Circ Arrhythm Electrophysiol*. 2009;2:162–170.
64. Elizari MV, Schmidberg J, Atienza A, et al. Clinical and experimental evidence of supernormal excitability and conduction. *Curr Cardiol Rev*. 2014;10:202–221.
65. Ho RT. An uncommon manifestation of atrioventricular block: what is the mechanism? *Pacing Clin Electrophysiol*. 2014;37:900–903.

Conventional Intracardiac Mapping Techniques

OUTLINE

Activation Mapping, 125

Fundamental Concepts, 125

Mapping Procedure, 127

Limitations, 135

Entrainment Mapping, 135

Fundamental Concepts, 135

Mapping Procedure, 144

Clinical Implications, 144

Limitations, 146

Pace Mapping, 146

Fundamental Concepts, 146

Mapping Procedure, 152

Clinical Implications, 152

Limitations, 152

Cardiac mapping refers to the process of identifying the temporal and spatial distributions of myocardial electrical potentials during a particular heart rhythm. Cardiac mapping is a broad term that covers several modes of mapping such as body surface, endocardial, and epicardial mapping, in order to characterize the timing and/or amplitude (voltage) of signals relative to each other. Mapping during tachycardia aims at elucidation of the mechanism or mechanisms of the tachycardia, description of the propagation of activation from its initiation to its completion within a region of interest, and identification of the site of origin or a critical site of conduction to serve as a target for catheter ablation.

ACTIVATION MAPPING

Fundamental Concepts

Essential to the effective management of any cardiac arrhythmia is a thorough understanding of the mechanisms of its initiation and maintenance. Conventionally this has been achieved by careful study of the surface electrocardiogram (ECG) and correlation of the changes therein with data from intracardiac electrograms recorded by catheters at various key locations within the cardiac chambers (i.e., activation mapping). A record of these electrograms documenting multiple sites simultaneously is studied to determine the mechanisms of an arrhythmic event.

The main value of intracardiac and surface ECG tracings consists of the comparative timing of electrical events and the determination of the location and direction of impulse propagation. In addition, electrogram morphology can be of significant importance during mapping. Establishing electrogram criteria, which permit accurate determination of the moment of myocardial activation at the recording electrode, is critical for the construction of an area map of the activation sequence. Bipolar recordings are generally used for activation mapping. Unipolar recordings are used to supplement the information obtained from bipolar recordings.¹

Unipolar Recordings

Timing of local activation. The major component of the unipolar electrogram allows for the determination of the local activation time, although there are exceptions. The point of maximum amplitude, the zero crossing, the point of maximum slope (maximum first derivative),

and the minimum second derivative of the electrogram have been proposed as indicators of underlying myocardial activation (Fig. 5.1). The maximum downslope (i.e., maximum change in potential, dV/dt) of the unipolar electrogram coincides best with the arrival of the depolarization wavefront directly beneath the electrode and is now considered the most accurate marker of local tissue activation. Using this fiducial point, errors in determining the local activation time as compared with intracellular recordings have typically been less than 1 millisecond. This is true for filtered and unfiltered unipolar electrograms.¹⁻⁴

Direction of local activation. The morphology of the unfiltered unipolar recording indicates the direction of wavefront propagation. By convention, the mapping electrode that is in contact with the myocardium is connected to the positive input of the recording amplifier. In this configuration, positive deflections (R waves) are generated by propagation *toward* the recording electrode, and negative deflections (QS complexes) are generated by propagation *away* from the electrode (Figs. 5.2 and 5.3). If a recording electrode is at the source from which all wavefronts propagate (at the site of initial activation), depolarization will produce a wavefront that spreads away from the electrode, thus generating a monophasic QS complex.

It is important to recognize that a QS complex can be recorded when the mapping electrode is floating in the cavity and not in contact with the myocardium. In that situation, the initial negative slope of the recording is typically slow, suggesting that the electrogram is a far-field signal, generated by tissue at some distance from the recording electrode.

Filtering at higher corner frequencies (e.g., 30 Hz) alters the morphology of the signal, so that the morphology of the unipolar electrogram is no longer indicative of the direction of wavefront propagation, and the presence or absence of a QS complex cannot be used to infer proximity to the site of earliest activation (Fig. 5.4).^{1,5}

Advantages of unipolar recordings. One important value of unipolar recordings is that they provide a more precise measurement of the timing of local activation. This is true for filtered and unfiltered unipolar electrograms. In addition, unfiltered unipolar recordings provide information about the direction of impulse propagation. Furthermore, unipolar recordings allow pacing and recording at the same location while eliminating a possible anodal contribution to depolarization that is sometimes seen with bipolar pacing at high output. This generally facilitates the use of other mapping modalities—namely pace mapping.^{1,2,5}

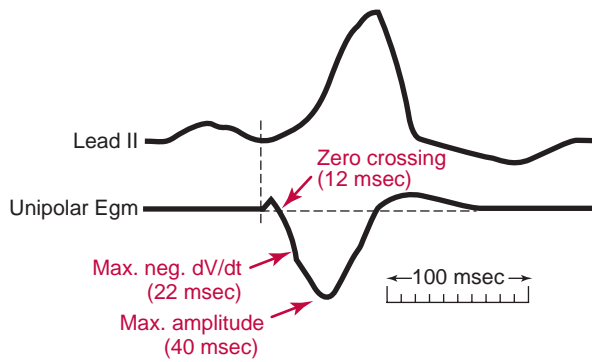


Fig. 5.1 Unipolar Electrogram Activation Times. A lead II electrocardiogram and a unipolar electrogram (Egm) from the ventricle of a patient with Wolff-Parkinson-White syndrome are shown. The vertical dashed line denotes the onset of the delta wave; the horizontal dotted line is the baseline of the unipolar recording. Several candidates for the timing of unipolar activation are labeled with corresponding activation times relative to delta wave onset.

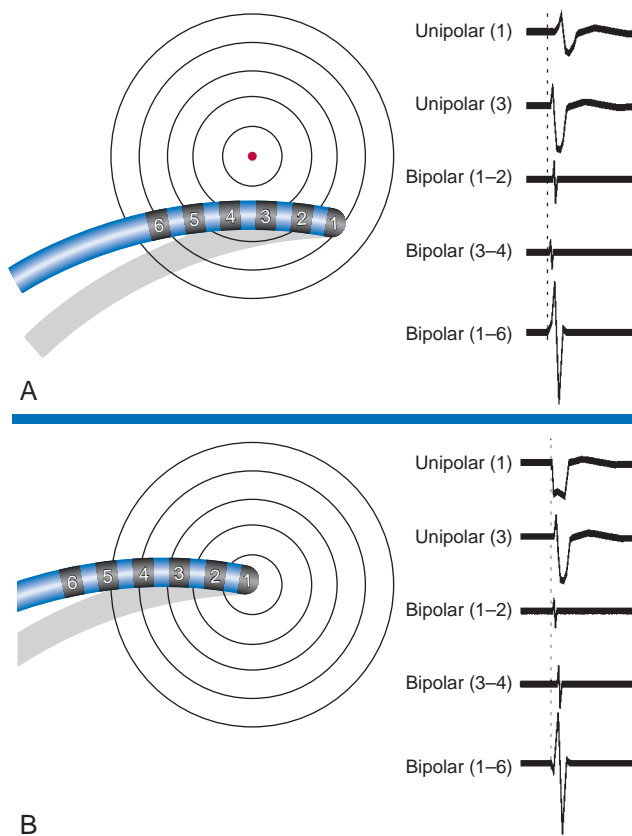


Fig. 5.2 Hypothetical Recordings From a Multipolar Electrode Catheter. (A) The electrodes are near a point source of activation (red dot in center of concentric rings). Note the timing and shape of the resultant electrogram patterns based on distance from point source, unipolar or bipolar recording, and width of bipole. (B) The tip electrode (1) is at the point source of activation. Note the differences in timing and shape of the electrograms compared with A.

Disadvantages of unipolar recordings. The major disadvantage of unipolar recordings is that they have poor signal-to-noise ratio and contain substantial far-field signal generated by depolarization of tissue remote from the recording electrode. Therefore distant activity can be difficult to separate from local activity. This is especially true when

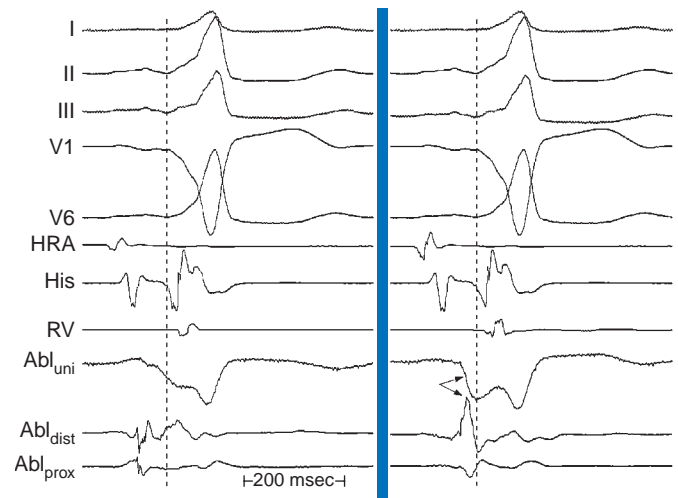


Fig. 5.3 Unipolar and Bipolar Recordings From a Patient With Wolff-Parkinson-White Syndrome. The dashed line denotes the onset of the QRS complex (delta wave). *Right panel*, Recordings at the successful ablation site, characterized by QS in the unipolar recording. The most rapid component precedes the delta wave onset by 22 milliseconds, has the same timing as the peak of the ablation distal electrode recording, and precedes the ablation proximal electrode recording (arrows). *Left panel*, Recordings from a poorer site, with an rS in the unipolar recording; most of the bipolar recordings are atrial. *Abl_{dist}*, Distal ablation; *Abl_{prox}*, proximal ablation; *Abl_{uni}*, unipolar ablation; *HRA*, high right atrium; *RV*, right ventricle.

recording from areas of prior myocardial infarction (MI), where the fractionated ventricular potentials are ubiquitous, and it is often impossible to select a rapid negative dV/dt when the entire QS potential is slowly inscribed—that is, cavity potential. Furthermore, a QS electrogram configuration has a low spatial resolution and relatively low specificity, being attainable in an area of more than 1 cm in diameter from the real site of origin of the arrhythmia or when the exploring electrode has poor contact with the myocardium.⁶ Another disadvantage is the inability to record an undisturbed electrogram during or immediately after pacing. This is a significant disadvantage when entrainment mapping is to be performed during activation mapping because the recording of the return tachycardia complex on the pacing electrode immediately after cessation of pacing is required to interpret entrainment mapping results. There is also some baseline drift of the unipolar recording in some recording systems that makes interpretation difficult.^{1,5,7}

Bipolar Recordings

Timing of local activation. Algorithms for detecting local activation time from bipolar electrograms have been more problematic, partly because of generation of the bipolar electrogram by two spatially separated recording poles. In a homogeneous sheet of tissue, the initial peak of a filtered (30 to 300 Hz) bipolar signal coincides with depolarization beneath the recording electrode and appears to correlate most consistently with local activation time, corresponding to the maximal negative dV/dt of the unipolar recording (see Fig. 5.3).

A bipolar electrogram is the sum of two unipolar electrograms with a time delay due to the interelectrode distance. When a bipolar electrogram with an interelectrode distance is recorded in a homogeneous sheet of tissue, activation time delay between the two poles is usually minimal. In the setting of inhomogeneous conduction, however, a significant time delay can exist between two unipolar electrograms, resulting in a fractionated electrogram when converted to a bipolar electrogram (Figs. 5.5 and 5.6).⁸

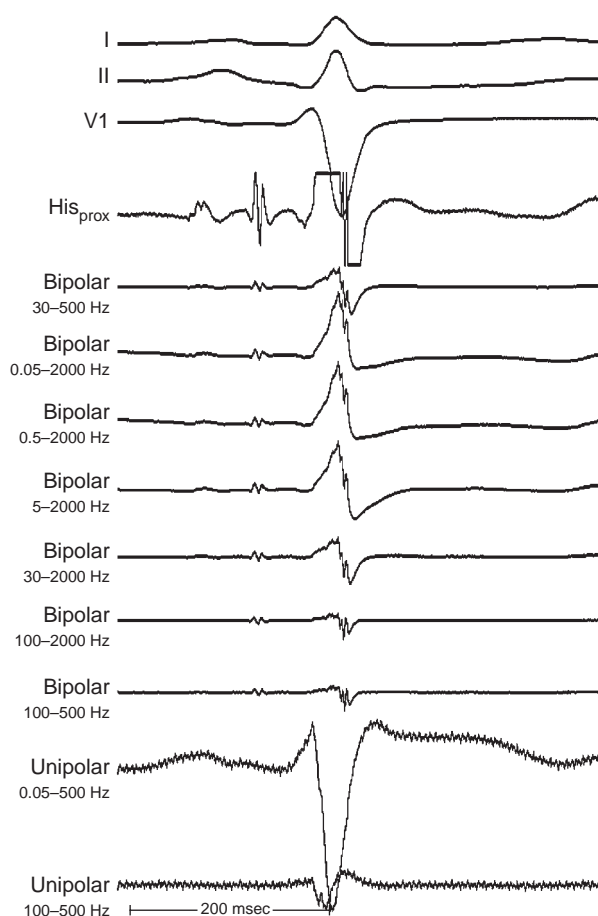


Fig. 5.4 Effect of Filtering on Intracardiac Recordings. The signal labeled “Bipolar 30–500 Hz” is the same signal as the proximal His bundle signal (His_{prox}) above it, displayed at lower gain. All signals beneath this are of the same gain but different filter bandwidths, and they illustrate progressive loss of signal amplitude as the bandwidth is narrowed. Unipolar signals below are of the same gain.

In the setting of complex multicomponent bipolar electrograms, such as those with marked fractionation and prolonged duration seen in regions with complex conduction patterns (e.g., in regions of slow conduction in macroreentrant atrial tachycardia [AT] or ventricular tachycardia [VT]), determination of local activation time becomes challenging, and the decision about which activation time is most appropriate needs to be made in the context of the particular rhythm being mapped. Therefore, during mapping procedures, the onset (rather than the peak or nadir) of high-frequency components of a local bipolar electrogram is often used because it is easier to determine reproducibly, especially when measuring heavily fractionated, low-amplitude local electrograms. The onset of the bipolar electrogram likely precedes the maximal $-dV/dt$ in unipolar electrogram by 15 to 30 milliseconds.³

To acquire true local electrical activity, a bipolar electrogram with an interelectrode distance of less than 1 cm is desirable. Smaller interelectrode distances record increasingly local events (as opposed to far-field). Elimination of far-field noise is usually accomplished by filtering the intracardiac electrograms, typically at 30 to 500 Hz.^{1,5,6}

Direction of local activation. The morphology and amplitude of bipolar electrograms are influenced by many factors, including (1) the orientation of the bipolar recording axis to the direction of propagation of the activation wavefront; (2) electrode size; (3) interelectrode distance; (4) electrode-tissue contact (i.e., the distance between the source of the

potential and the recording electrode); (5) anisotropic conduction; and (6) intrinsic characteristics of the recorded medium (e.g., normal myocardial tissue versus scar). A wavefront that is propagating in the direction exactly perpendicular to the axis of the recording dipole produces no difference in potential between the electrodes and hence no signal.^{2,5}

Although the direction of wavefront propagation cannot be reliably inferred from the morphology of the bipolar signal, a change in morphology can provide important clues about the activation pattern of the propagating wavefront. The change in polarity in bipolar electrograms recorded across an ablation line is consistent with complete line conduction block. For example, when recording from the lateral aspect of the cavotricuspid isthmus (CTI) during pacing from the coronary sinus (CS), a reversal in the bipolar electrogram polarity from positive to negative at the ablation line indicates complete isthmus block. Similarly, if bipolar recordings are obtained with the same catheter orientation parallel to the atrioventricular (AV) annulus during retrograde bypass tract (BT) conduction, an RS configuration electrogram will be present on one side of the BT, where the wavefront is propagating from the distal electrode toward the proximal electrode, and a QR morphology electrogram will be present on the other side, where the wavefront is propagating from the proximal electrode toward the distal electrode (eFig. 5.1).^{1,5}

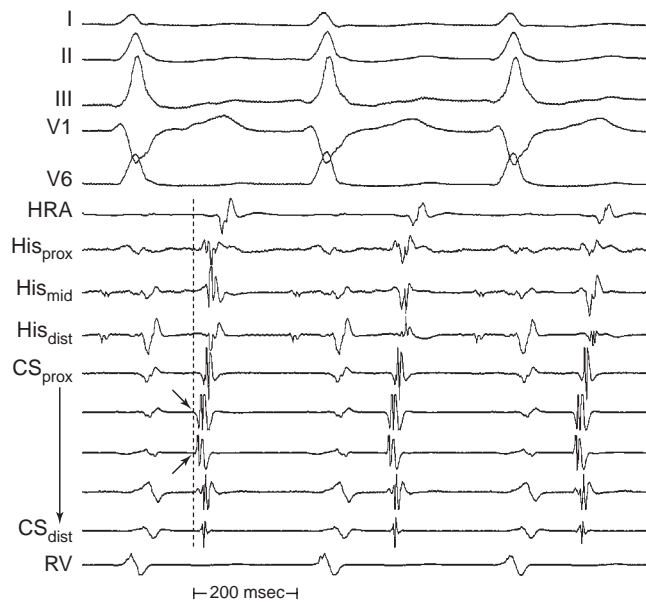
Furthermore, the “bipolar” electrogram can be considered as a “mini-unipolar” recording with the proximal electrode simulating the indifferent remote electrode in the unipolar electrogram configuration, and thus the bipolar electrogram morphology may also be helpful in localizing the site of origin of focal arrhythmias. Hence, when the distal electrode of the mapping catheter is positioned at the site of origin of a focal tachycardia (e.g., premature ventricular contractions [PVCs]), an early negative deflection in the initial component of the bipolar electrogram reflects the wavefront propagation opposite to the recording dipole vector (i.e., depolarization reaches electrode 1 before electrode 2). A recent report found that a negative concordance in the initial forces of both unipolar and bipolar electrograms (in addition to the electrogram temporal relationship assessment) may be considered a reliable criterion to identify the site of origin of focal ventricular arrhythmias.^{2,6}

Advantages of bipolar recordings. Bipolar recordings provide an improved signal-to-noise ratio. In addition, high-frequency components are more accurately seen, which facilitates the identification of local depolarization, especially in abnormal areas of infarction or scar.^{2,5}

Disadvantages of bipolar recordings. In contrast to unipolar signals, the direction of wavefront propagation cannot be reliably inferred from the morphology of a single bipolar signal; however, with two adjacent bipolar recordings, the recording that occurs first is closer to the wavefront source. Furthermore, bipolar recordings do not allow simultaneous pacing and recording from the same location. To pace and record simultaneously in bipolar fashion at endocardial sites as close together as possible, electrodes 1 and 3 of the mapping catheter are used for bipolar pacing, and electrodes 2 and 4 are used for recording. The precision of locating the source of a particular electrical signal depends on the distance between the recording electrodes, because the signal of interest can be beneath the distal or proximal electrode (or both) of the recording pair.^{2,5}

Mapping Procedure

Several factors are important for the success of activation mapping, including inducibility of tachycardia at the time of electrophysiology (EP) testing, hemodynamic stability of the tachycardia, and stable tachycardia morphology. In addition, determinations of an electrical reference point, of the mechanism of the tachycardia (focal vs. macroreentrant), and subsequently of the goal of mapping are essential prerequisites.



eFig. 5.1 Recordings From a Patient With a Left Lateral Bypass Tract During Orthodromic Atrioventricular Reentrant Tachycardia. Note electrogram inversion at the middle of the coronary sinus (CS) (arrows), where the earliest retrograde atrial activation (over the bypass tract) occurs (dashed line). CS_{dist}, Distal coronary sinus; CS_{prox}, proximal coronary sinus; His_{dist}, distal His bundle; His_{mid}, middle His bundle; His_{prox}, proximal His bundle; HRA, high right atrium; RV, right ventricle.

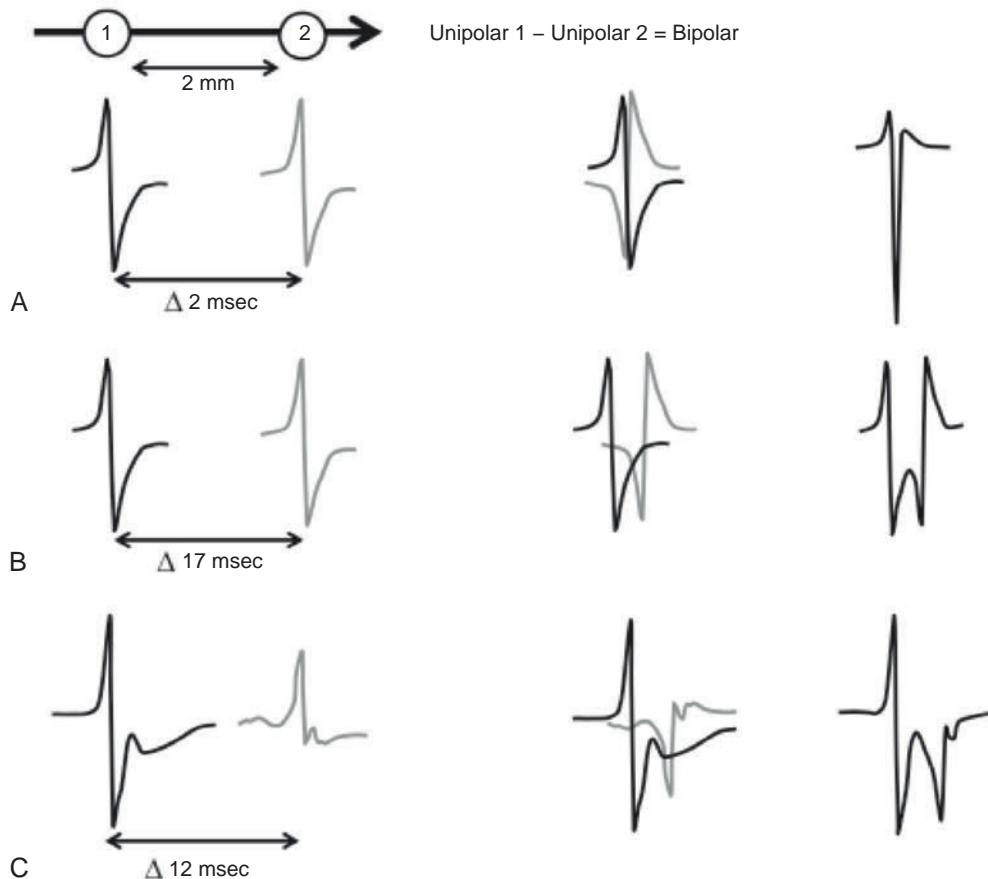


Fig. 5.5 Fractionation in Bipolar Electrograms (EGMs). A depolarizing wavefront travels from electrode 1 to electrode 2, which are separated by an interelectrode distance of 2 mm. (A) The wavefront passes the electrodes with a time delay of 2 milliseconds, which results in a simple bipolar EGM. (B) The time delay is increased to 17 milliseconds due to either increased electrode spacing or decreased velocity of the wavefront. This results in an extra negative and increased positive bipolar deflections. (C) Example of two real unipolar EGMs recorded during atrial fibrillation by electrodes with a diameter of 0.45 mm and 2-mm interelectrode spacing and filtered from 0.5 to 400 Hz. The time delay is 12 milliseconds, and conversion to a bipolar EGM gives rise to a fractionated EGM. (From van der Does LJME, de Groot NMS. Inhomogeneity and complexity in defining fractionated electrograms. *Heart Rhythm*. 2017;14:616–624.)

Selection of the Electrical Reference Point

Local activation times must be relative to some external and consistent fiducial marker (such as the onset of the P wave or QRS complex on the surface ECG) or a reference intracardiac electrode. For VT, the QRS complex onset should be assessed using all surface ECG leads to search for the lead with the earliest QRS onset. This lead should then be used for subsequent activation mapping. Similarly, the P wave during AT should be assessed using multiple ECG leads, choosing the one with the earliest P onset. However, determining the onset of the P wave can be impossible if the preceding T wave or QRS is superimposed. To facilitate visualization of the P wave, a ventricular extrastimulus (VES) or a train of ventricular pacing can be delivered to anticipate ventricular activation and repolarization and permit careful distinction of the P wave onset (Fig. 5.7). After determining P wave onset, a surrogate marker, such as right atrial (RA) or CS electrogram indexed to the P wave onset, where it is clearly seen, can be used rather than the P wave onset.

Defining the Goal of Mapping

Determination of the mechanism of the tachycardia (focal vs. macroreentrant) is essential to define the goal of activation mapping. For

focal tachycardias, activation mapping entails localizing the site of origin of the tachycardia focus. This is reflected by the earliest presystolic activity that precedes the onset of the P wave (during focal AT) or QRS (during focal VT) by an average of 10 to 40 milliseconds because only this short amount of time is required after the focus discharges to activate enough myocardium and begin generating a P wave or QRS complex (Fig. 5.8). For mapping macroreentrant tachycardias, the goal of mapping is identification of the critical isthmus of the reentrant circuit, as indicated by finding the site with a continuous activity spanning diastole or with an isolated mid-diastolic potential (see Fig. 5.8). One caveat is that focal tachycardias can occur in patients with scar, and the focus can be imbedded in scar tissue; in this setting, propagation from the source to a site at which enough atrium (or ventricle) is activated to generate a P (or QRS complex) can be significantly delayed, such that the timing of the earliest site may be considerably longer than 50 milliseconds.

Epicardial Versus Endocardial Mapping

Activation mapping is predominantly performed endocardially. Occasionally, epicardial mapping is required because of an inability to ablate

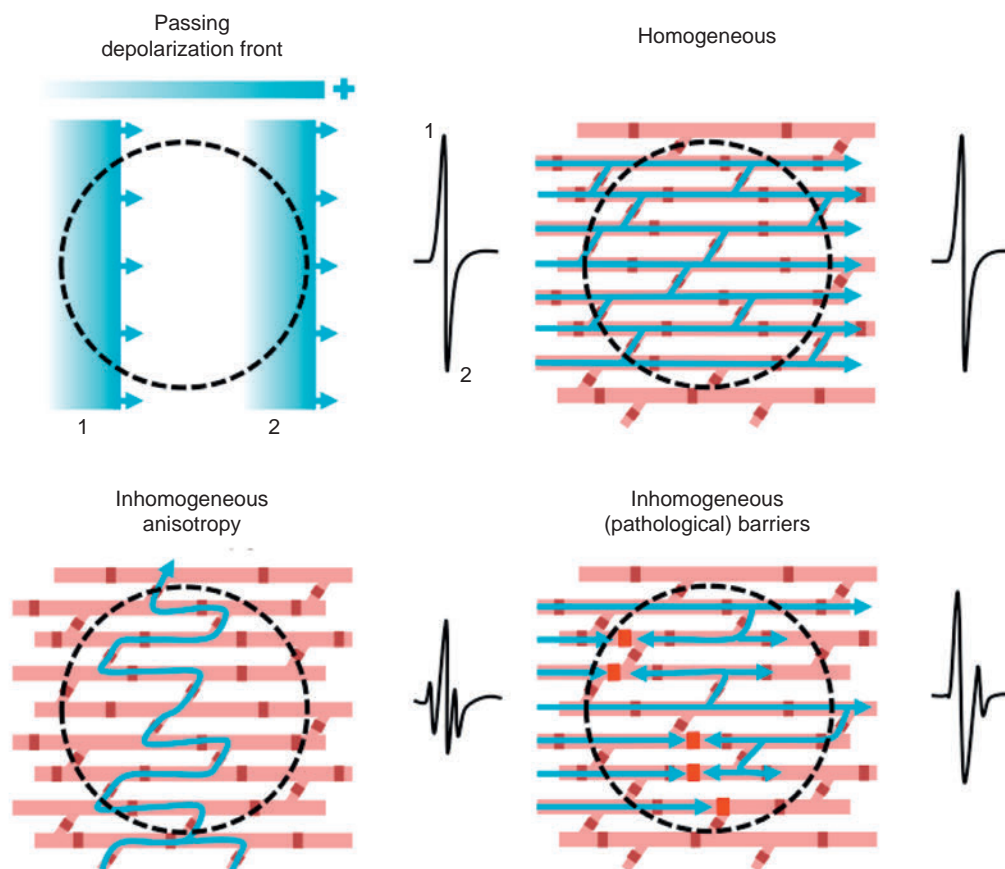


Fig. 5.6 Myocardial Activation Patterns of Simple and Fractionated Electrograms. *Top panels*, Homogeneous activation front across myocardial cells results in a simple electrogram. *Bottom panels*, Inhomogeneous activation front, in which the direction of the activation front changes, due to either the direction of propagation and coupling structure of myocardial fibers (anisotropy) or the functional or pathological barriers between myocardial fibers, will result in a complex electrogram with multiple deflections. (From van der Does LJME, de Groot NMS. Inhomogeneity and complexity in defining fractionated electrograms. *Heart Rhythm*. 2017;14:616–624.)

some VTs, ATs, or AV BTs by using the endocardial approach. Limited epicardial mapping can be performed with special recording catheters that can be steered in the branches of the CS. This technique has been used for mapping VTs and AV BTs, but its scope is limited by the anatomy of the coronary venous system.

A more common epicardial mapping technique utilizes the subxiphoid percutaneous approach for accessing the epicardial surface. This technique has become an important adjunctive strategy to ablate a diverse range of cardiac arrhythmias, especially in patients with scar-related VT, in whom more reentrant circuits with vulnerable isthmuses are on the epicardial surface. The same fundamental principles of activation mapping are used for both endocardial mapping and epicardial mapping.⁹

Mapping Catheters

The simplest form of mapping is achieved by moving the mapping catheter sequentially to sample various points of interest on the endocardium to measure local activation. The precision of locating the source of a particular electrical signal depends on the distance between the recording electrodes on the mapping catheter. For ablation procedures, recordings between adjacent electrode pairs are commonly used (e.g., between electrodes 1 and 2, 2 and 3, and 3 and 4), with 1- to 5-mm interelectrode spacing. In some studies, wider bipolar recordings (e.g.,

between electrodes 1 and 3 and 2 and 4) have been used to provide an overlapping field of view. For bipolar recordings, the signal of interest can be beneath the distal or the proximal electrode of the recording pair. As noted, this is germane in that ablation energy can be delivered only from the distal (tip) electrode (Fig. 5.9). Because of this, many operators display the unipolar recordings from each component of the distal bipole, in order to determine which electrode is actually recording the earliest activity.

Mapping Focal Tachycardias

The goal of activation mapping of focal-appearing tachycardias (automatic, triggered activity, or microreentrant) is identifying the site of origin, defined as the site with the earliest presystolic bipolar recording in which the distal electrode shows the earliest intrinsic deflection and QS unipolar electrogram configuration (Figs. 5.10 and 5.11). Local activation at the site of origin precedes the onset of the tachycardia complex on the surface ECG by an average of 10 to 40 milliseconds. Earlier electrograms occurring in mid-diastole, as in the setting of macroreentrant tachycardias, are not expected and do not constitute a target for mapping.¹

Endocardial activation mapping of focal tachycardias can trace the origin of activation to a specific area, from which it spreads centrifugally. There is generally an electrically silent period in the tachycardia cycle

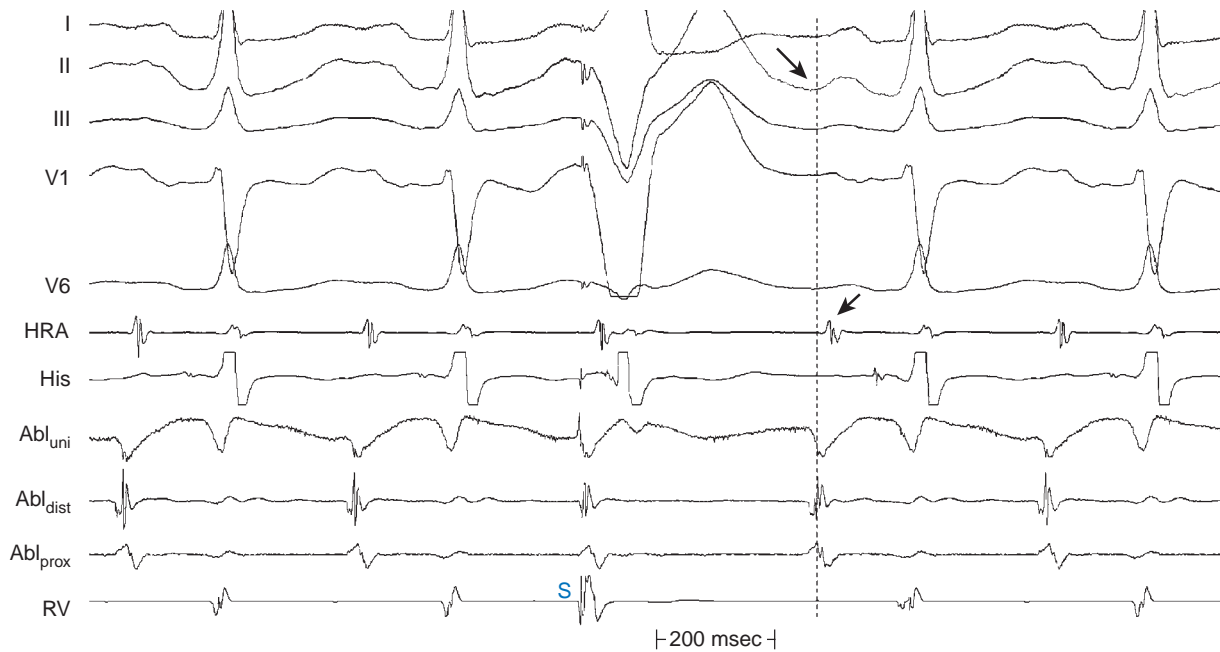


Fig. 5.7 Use of Ventricular Extrastimulus (VES) to Clarify Onset of the P Wave During Atrial Tachycardia (AT). A single VES (S) delivered during AT advances the timing of ventricular activation to show the P wave (long arrow) by itself without the overlying ST segment and T wave, which made it difficult to determine P wave onset during ongoing tachycardia. The dashed line denotes onset of the P wave; timing of the reference electrogram (high right atrium [HRA]; short arrow) can thereafter be used as a surrogate for P wave onset. Abl_{dist}, Distal ablation; Abl_{prox}, proximal ablation; Abl_{uni}, unipolar ablation; RV, right ventricle.

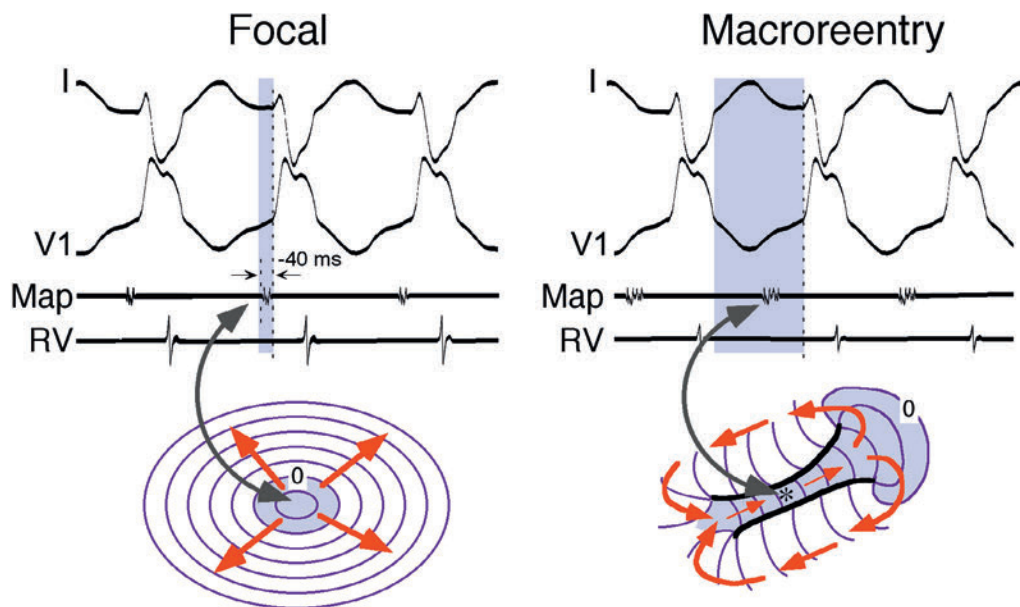


Fig. 5.8 Focal Versus Macroreentrant Ventricular Tachycardia (VT). Top, Electrocardiogram (ECG) and intracardiac electrograms from the mapping (Map) and right ventricle (RV) catheters. Bottom, Depictions of events at sites where mapped electrograms are obtained. Left, VT focus fires and activation spreads to normal myocardium within 30 to 40 milliseconds, generating a QRS complex. Thus the electrogram at the site of the focus is generally 40 milliseconds or less prior to the QRS onset. Right, In contrast, in a macroreentrant VT, some myocardium is being activated at each instant in the cardiac cycle. During surface ECG diastole, only a few cells are activating (too few to cause surface ECG deflections). The area of a protected diastolic corridor, often cordoned off by scar, contains mid-diastolic recordings and is an attractive ablation site. The 0 isochrone indicates the time at which the QRS complex begins.

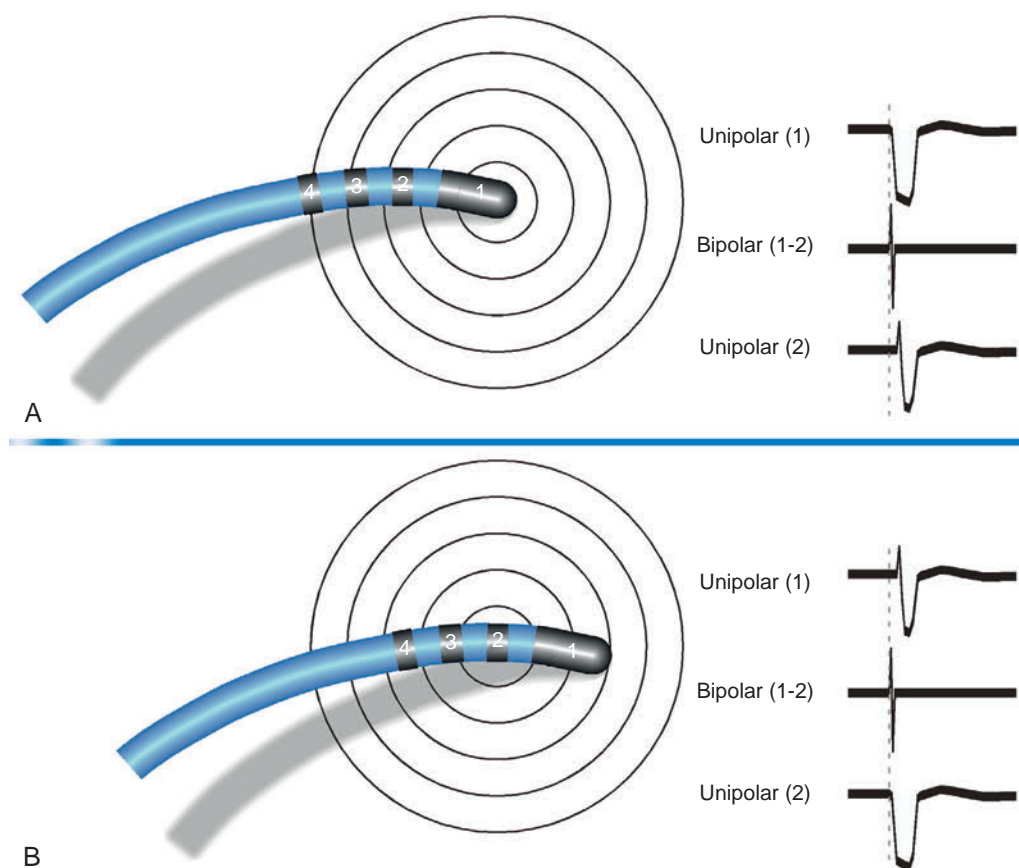


Fig. 5.9 Hypothetical Recordings Showing Complimentary Information From Unipolar and Bipolar Electrograms. A point source of activation is at the center of the concentric rings (that depict radial spread of activation from the source). (A) The ablation electrode (1) is directly over the source; its unipolar electrogram shows a QS configuration with a steep downstroke coincident with the moment of depolarization (*dashed line*). The bipolar electrogram (electrodes 1 and 2) is likewise early and the bipolar and unipolar recordings "agree." (B) The catheter has been moved such that electrode 2 is now directly over the point source. While bipolar recording 1-2 is the same as before (since 1 of its electrodes is over the source), now electrode 1 (the tip, through which ablation energy is delivered) is no longer as early in timing as 1-2 nor is there a QS configuration (both of which features are found in unipolar 2). Here, unipolar 1 and bipolar 1-2 "disagree."

length (TCL) that is reflected on the surface ECG by an isoelectric line between tachycardia complexes. Intracardiac mapping shows significant portions of the TCL without recorded electrical activity, even when recording from the entire cardiac chamber of tachycardia origin. However, in the presence of complex intramyocardial conduction disturbances, activation during focal tachycardias can extend over a large proportion of the TCL, and conduction spread can follow circular patterns suggestive of macroreentrant activation.¹⁰

Technique of activation mapping of focal tachycardias. Initially one should seek the general region of the origin of the tachycardia as indicated by the surface ECG. In the EP laboratory, additional data can be obtained by placing a limited number of catheters within the heart in addition to the mapping catheter or catheters; these catheters are frequently placed at the right ventricle (RV) apex, His bundle region, high RA, and CS. During initial arrhythmia evaluation, recording from this limited number of sites allows a rough estimation of the site of interest. Mapping simultaneously from as many sites as possible greatly enhances the precision, detail, and speed of identifying regions of interest.

Subsequently, a single mapping catheter is moved under fluoroscopic guidance over the endocardium of the chamber of interest to sample

bipolar signals. Using standard equipment, mapping a tachycardia requires recording and mapping performed at several sites, based on the ability of the investigator to recognize the mapping sites of interest from the morphology of the tachycardia on the surface ECG and baseline intracardiac recordings.

Local activation time is then determined from the filtered (30 to 300 Hz) bipolar signal recorded from the distal electrode pair on the mapping catheter; this time is determined and compared with the timing reference (fiducial point). Activation times are generally measured from the onset of the first rapid deflection of the bipolar electrogram to the onset of the tachycardia complex on the surface ECG or surrogate marker (see Fig. 5.7). Using the onset (rather than the peak or nadir) of a local bipolar electrogram is often preferable because it is easier to determine reproducibly, especially when measuring heavily fractionated, low-amplitude local electrograms.

Once an area of relatively early local activation is found, small movements of the catheter tip in the general target region are undertaken until the site is identified with the earliest possible local activation relative to the tachycardia complex. Recording from multiple bipolar pairs from a multipolar electrode catheter is helpful in that if the proximal

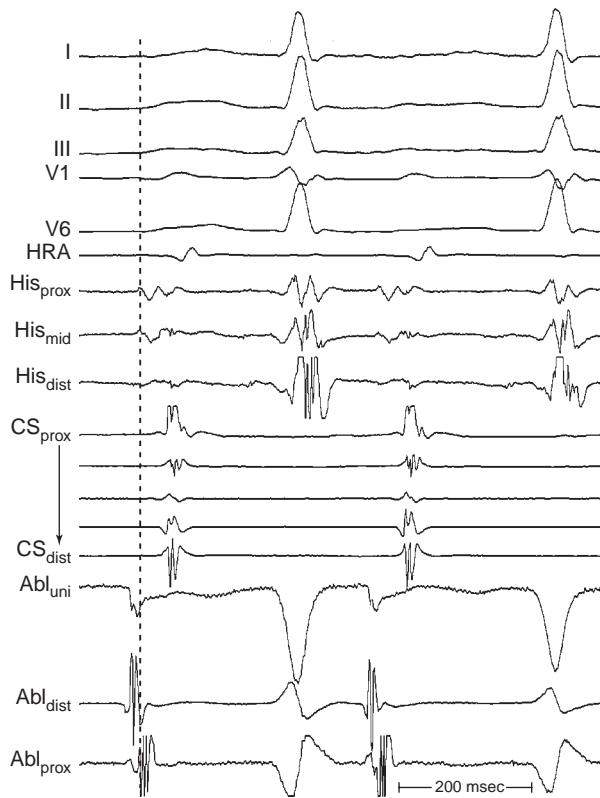


Fig. 5.10 Focal Atrial Tachycardia. The unipolar electrogram recorded by the distal ablation electrode (Abl_{uni}) shows a QS configuration, and its timing coincides with the distal ablation (Abl_{dist}) recording at the site of successful ablation. The dashed line marks the onset of the P wave on the surface electrocardiogram. Abl_{prox} , proximal ablation; CS_{dist} , distal coronary sinus; CS_{prox} , proximal coronary sinus; His_{dist} , distal His bundle; His_{mid} , middle His bundle; His_{prox} , proximal His bundle; HRA , high right atrium.

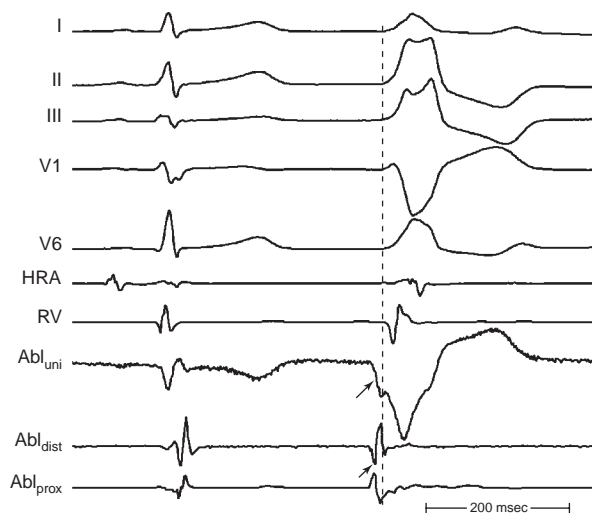


Fig. 5.11 Sinus Rhythm and a Single Premature Ventricular Complex From a Patient With Focal Ventricular Tachycardia. The unipolar ablation site (Abl_{uni}) show a QS configuration, the most rapid slope of which times with the initial peak in the distal ablation (Abl_{dist}) recording (arrows) at the site of successful ablation. The dashed line marks the onset of the QRS complex on the surface electrocardiogram. Abl_{prox} , proximal ablation; HRA , high right atrium; RV , right ventricle.

pair has a more attractive electrogram than the distal, the catheter may be withdrawn slightly to achieve the same position with the distal electrode.

Once the site with the earliest bipolar signal is identified, the unipolar signal from the distal ablation electrode should be used to supplement bipolar mapping. The unfiltered (0.05 to 300 Hz) unipolar signal morphology should show a monophasic QS complex with a rapid negative deflection if the site was at the origin of impulse formation (see Figs. 5.10 and 5.11). However, the size of the area from which a QS complex can be larger than the tachycardia focus, exceeding 1 cm in diameter. Thus a QS complex should not be the only mapping finding used to guide ablation. Successful ablation is unusual, however, at sites with an RS complex on the unipolar recording because these are generally distant from the focus (see Fig. 5.2). Concordance of the timing of the onset of the bipolar electrogram with that of the filtered or unfiltered unipolar electrogram (with the rapid downslope of the S wave of the unipolar QS complex coinciding with the initial peak of the bipolar signal) helps ensure that the tip electrode, which is the ablation electrode, is responsible for the early component of the bipolar electrogram. A tissue contact force measuring 10 to 20 g, as well as the presence of slight ST elevation on the unipolar recording and the ability to capture the site with unipolar pacing, are used to indicate good electrode-tissue contact.⁶

Furthermore, a negative concordance of the vector of the initial (first 20 milliseconds) forces of both unipolar and bipolar electrograms (both being negative deflections), in conjunction with electrogram temporal relationship assessment, further improves the accuracy of conventional mapping to localize the site of origin of PVCs (Fig. 5.12). In a recent report, the presence of this criterion ("negative concordance") at sites fulfilling other conventional criteria used to guide focal PVC ablation highly predicted the acute success rate of radiofrequency ablation with a sensitivity and specificity of 94% and 95%, respectively. Furthermore, its positive predictive value was significantly superior to those of all other conventional criteria (76% vs. 33% to 43%).⁶

Mapping Macroreentrant Tachycardias

The main goal of activation mapping of macroreentrant tachycardias (e.g., post-MI VT, macroreentrant AT) is identification of the isthmus critical for maintenance of the macroreentrant circuit. The site of origin of a tachycardia is the source of electrical activity producing the tachycardia complex; although this is a discrete site of impulse formation in focal rhythms, during macroreentry it can represent the exit site from the diastolic pathway (i.e., from the critical isthmus of the reentrant circuit) to the myocardium that gives rise to the ECG deflection. During macroreentry, an isthmus is defined as a corridor of conductive myocardial tissue bounded by nonconductive tissue (barriers) through which the depolarization wavefront must propagate to perpetuate the tachycardia. These barriers can be scar areas or naturally occurring anatomical or functional (present only during tachycardia, but not in sinus rhythm) obstacles. The earliest presystolic electrogram closest to mid-diastole is the most commonly used definition for the site of origin of the reentrant circuit. However, recording continuous diastolic activity or bridging of diastole at adjacent sites, or mapping a discrete diastolic pathway, is more specific. Therefore the goal of activation mapping during macroreentry is finding the site, or sites, with continuous electrical activity spanning diastole or with an isolated mid-diastolic potential; once such a site has been located, further testing should be done to ensure that the tissue generating that electrogram is in fact integral to the tachycardia rather than a bystander. Unlike focal tachycardias, a presystolic electrogram preceding the tachycardia complex by 10 to 40 milliseconds is not adequate in defining the site of origin of a macroreentrant tachycardia (see Figs. 5.8, 5.13, and 5.14).¹¹

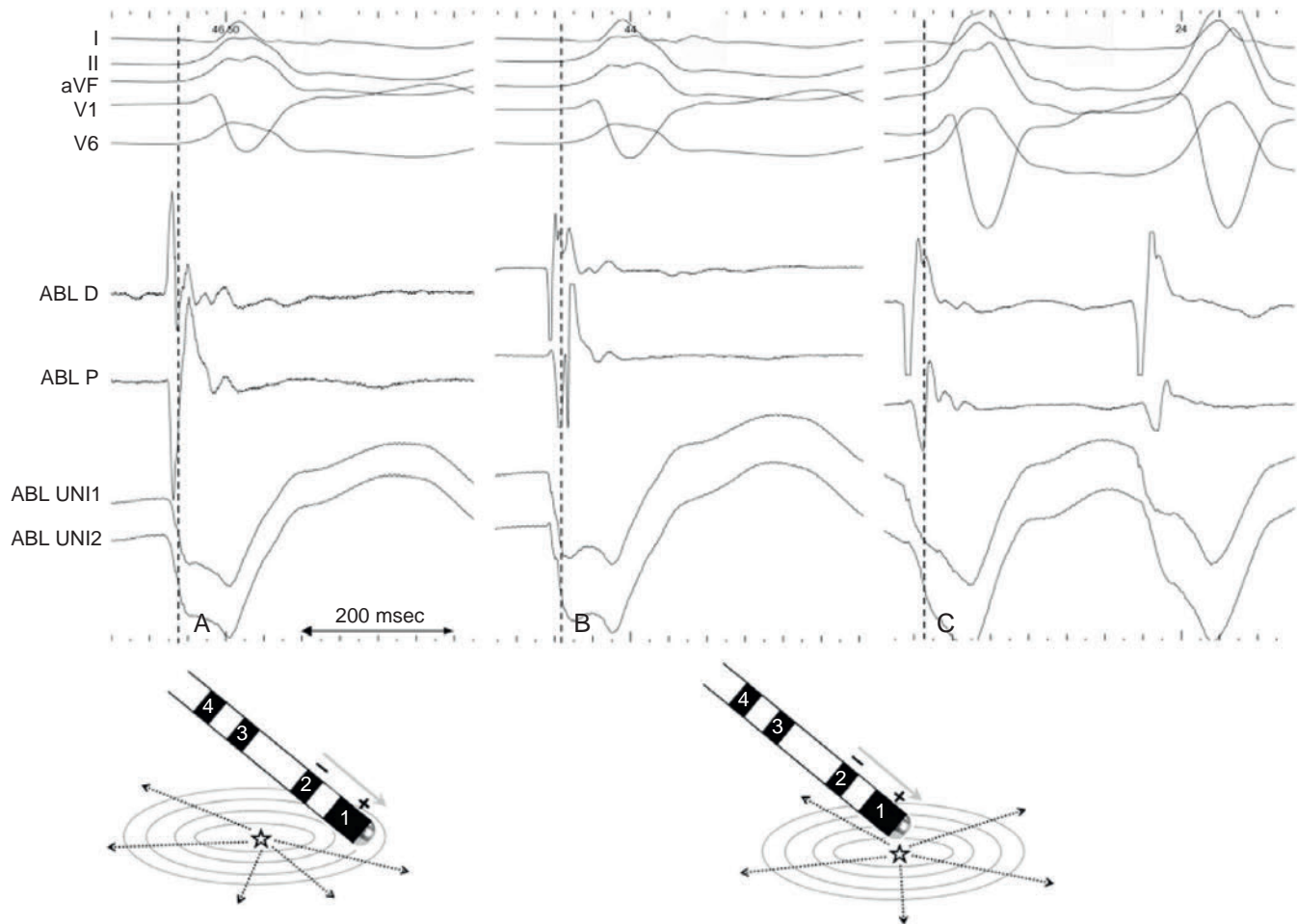


Fig. 5.12 Negative Concordance in the Initial Forces of Unipolar and Bipolar Electrograms. Surface electrocardiogram and intracardiac recordings during spontaneous (A and B) and mechanical (C) premature ventricular contractions (PVCs) in the same patient. The bottom diagrams show the presumed corresponding positions of the ablation catheter relative to the site of origin (*star*). An initially positive bipolar electrogram is recorded at the unsuccessful ablation site (A) where the catheter tip is not precisely at the site of origin (the *bottom left* diagram). A negative concordance in the initial (first 20 milliseconds) forces of both bipolar and unipolar recordings is observed at the successful ablation site (B) and during mechanical PVCs (C) where the catheter tip is touching the site of origin (the *bottom right* diagram). Note that in all cases there is a QS pattern in the unipolar electrogram and a discrete prematurity relative to the QRS onset (*dotted vertical lines*). The mechanical PVC (C) has a different QRS morphology as compared with the spontaneous PVCs (A and B). ABL, Ablation catheter; D and P, bipolar recordings from the distal (1-2) and proximal (3-4) electrode pairs, respectively; UNI1 and UNI2, unipolar recordings from the distal (1) and proximal (2) electrodes of the ablation catheter, respectively. (From Sorgente A, Epicoco G, Ali H, et al. Negative concordance pattern in bipolar and unipolar recordings: an additional mapping criterion to localize the site of origin of focal ventricular arrhythmias. *Heart Rhythm*. 2016;13:519–526.)

However, identification of critical isthmuses is often challenging. The abnormal area of scarring, where the isthmus is located, is frequently large and contains side branch pathways (bystanders) that confound mapping. In addition, multiple potential reentry circuits can be present, giving rise to multiple different tachycardias in a single patient. Furthermore, in abnormal regions such as infarct scars, the tissue beneath the recording electrode can be small relative to the surrounding myocardium outside the scar; thus a large far-field signal can obscure the small local potential. For this reason, bipolar recordings are preferred in scar-related VTs because the noise is removed and high-frequency components are more accurately seen. Unipolar recordings are usually of little help when mapping arrhythmias associated with regions of

scar, unless the recordings are filtered to remove far-field signal; even so, signal amplitude in the unipolar recording is often extremely small and may be difficult to distinguish from noise. Much of the far-field signal in a unipolar recording consists of lower frequencies than the signal generated by local depolarization because the high-frequency content of a signal diminishes more rapidly with distance from the source than the low-frequency content. Therefore high-pass filtering of unipolar signals (at 30 or 100 Hz) is generally used when mapping scar-related arrhythmias to reduce the far-field signal and improve detection of lower amplitude local signals from abnormal regions.

Although activation mapping alone is usually inadequate for defining the critical isthmus of a macroreentrant tachycardia, it can help

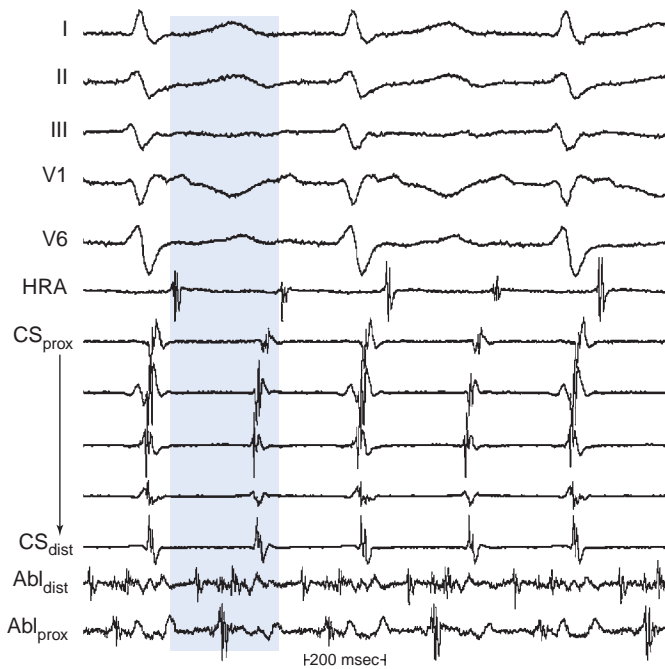


Fig. 5.13 Macroeentrant Atrial Tachycardia. Electrical activity spans the tachycardia cycle length (*shaded*); thus a merely presystolic electrogram is a poor indicator of optimal ablation site. *Abl_{dist}*, Distal ablation; *Abl_{prox}*, proximal ablation; *CS_{dist}*, distal coronary sinus; *CS_{prox}*, proximal coronary sinus; *HRA*, high right atrium.

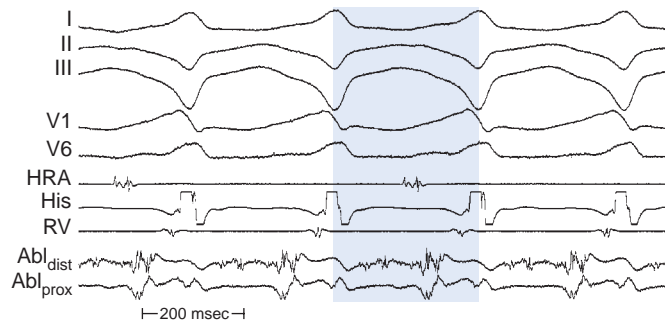


Fig. 5.14 Macroeentrant Post-Myocardial Infarction Ventricular Tachycardia. Electrical activity spans diastole and nearly the tachycardia cycle length (*shaded*); thus a simply presystolic electrogram is a poor indicator of the optimal ablation site. *Abl_{dist}*, Distal ablation; *Abl_{prox}*, proximal ablation; *HRA*, high right atrium; *RV*, right ventricle.

guide other mapping modalities (e.g., entrainment or pace mapping, or both) to the approximate region of the isthmus.

Continuous electrical activity. Theoretically, if reentry were the mechanism of the tachycardia, electrical activity should occur throughout the tachycardia cycle. For example, in macroreentrant AT, the recorded electrical activity at different locations in the atrium should span the TCL (see Fig. 5.13).¹²

For macroreentrant VT, conduction during diastole is extremely slow and is in a small area so that it is not recorded on the surface ECG. The QRS complex is caused by propagation of the wavefront from the exit of the circuit from that isthmus to the surrounding myocardium. After leaving the exit of the isthmus, the circulating wavefront propagates through a broad path (loop) along the border of the scar, back to the

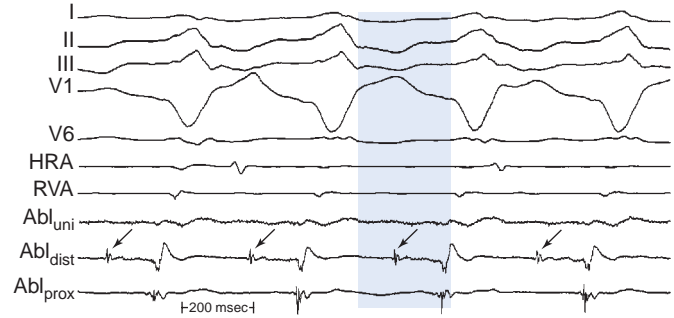


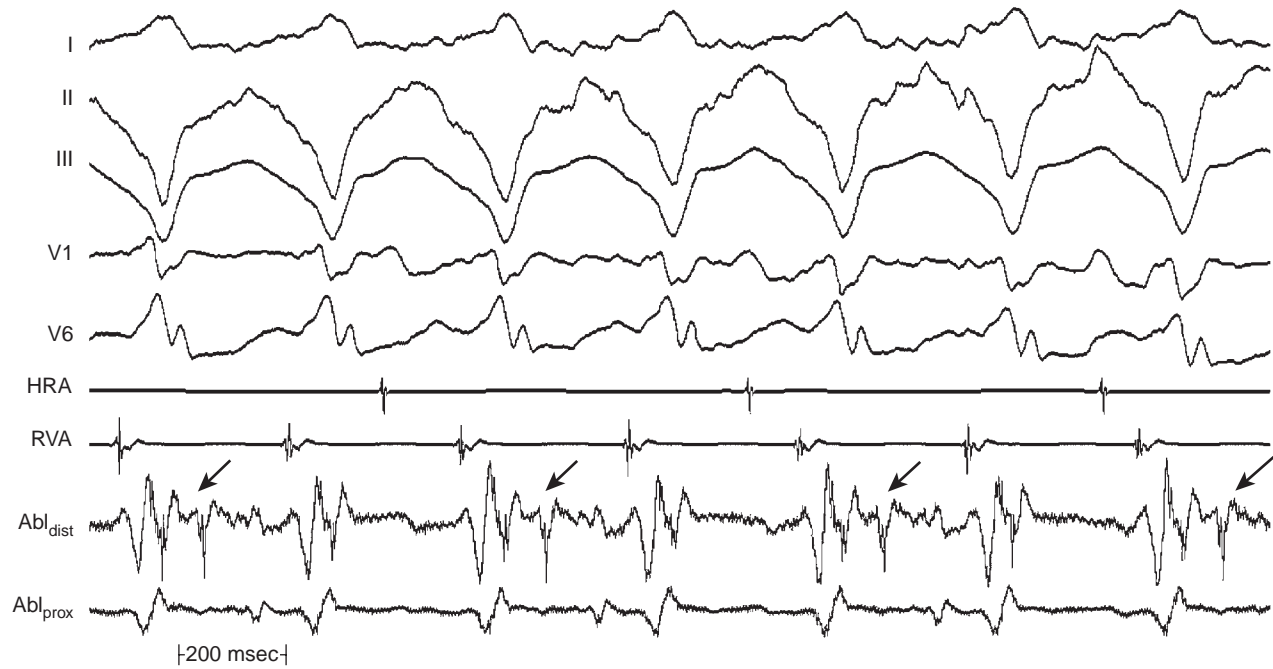
Fig. 5.15 Mid-Diastolic Potential During Ventricular Tachycardia (VT). Duration of diastole (*shaded area*), with isolated mid-diastolic potential from the site at which ablation eliminated VT (*arrows*). *Abl_{dist}*, Distal ablation; *Abl_{prox}*, proximal ablation; *Abl_{uni}*, unipolar ablation; *HRA*, high right atrium; *RVA*, right ventricular apex.

entrance of the isthmus (see Fig. 5.8). Continuous diastolic activity is likely to be recorded only if the bipolar pair records from a small circuit; if a large circuit is present (i.e., the reentrant circuit is larger than the recording area of the catheter, or the catheter is not covering the entire circuit), non-holodiastolic activity will be recorded. In such circuits, repositioning of the catheter to other sites may allow visualization of what is termed *bridging of diastole*; electrical activity in these adjacent sites spans diastole.

All areas from which diastolic activity is recorded are not necessarily part of the reentrant circuit. Such sites can reflect late activation of sites that may not be related to the tachycardia circuit. Analysis of the response of these electrograms to spontaneous or induced changes in TCL is critical in deciding their relationship to the tachycardia mechanism. In addition, electrical signals that come and go throughout diastole should not be considered continuous (eFig. 5.2). For continuous activity to be consistent with reentry, it must be demonstrated that such electrical activity is required for initiation and maintenance of the tachycardia, so that termination of the continuous activity, either spontaneously or following stimulation, without affecting the tachycardia, would exclude such continuous activity as requisite for sustaining the tachycardia. It is also important to verify that an electrogram that extends throughout diastole is not just a broad electrogram whose duration equals the TCL. This can be achieved by analyzing the local electrogram during pacing at a pacing cycle length (PCL) comparable to TCL; if pacing produces continuous diastolic activity in the absence of tachycardia, the continuous electrogram may have no mechanistic significance. Furthermore, the continuous activity should be recorded from a circumscribed area, and motion artifact should be excluded.

Mid-diastolic activity. An isolated mid-diastolic potential is defined as a low-amplitude, high-frequency diastolic potential separated from the preceding and subsequent electrograms by an isoelectric segment (Fig. 5.15). Sometimes these discrete potentials provide information that defines a diastolic pathway, which is believed to be generated from a narrow isthmus of conduction critical to the reentrant circuit. Localization of this pathway is critical for guiding catheter-based ablation.

Detailed mapping usually reveals more than one site of presystolic activity, and mid-diastolic potentials can be recorded from bystander sites attached to the isthmus. Therefore, regardless of where in diastole the presystolic electrogram occurs (early, middle, or late), its timing and appearance on initiation of the tachycardia, although necessary, does not confirm its relevance to the tachycardia mechanism. One must always confirm that the electrogram is required to maintain, and cannot be dissociated from, the tachycardia. Thus, during spontaneous changes



eFig. 5.2 Diastolic Recordings During Ventricular Tachycardia (VT). Note that the diastolic electrograms (arrows) during VT have a 2:1 conduction ratio. Cells causing these recordings are clearly not integrally involved in the ongoing arrhythmia. They are not atrial because atrial ventricular dissociation is evident in the high right atrium (HRA) recording. *Abl_{dist}*, Distal ablation; *Abl_{prox}*, proximal ablation; *RVA*, right ventricular apex.

in the TCL or those produced by programmed stimulation, the electrogram, regardless of its timing in diastole, should show a fixed relationship with the subsequent tachycardia complex (and not the preceding one). Very early diastolic potentials (in the first half of diastole) can represent an area of slow conduction at the entrance of a protected isthmus. These potentials remain fixed to the prior tachycardia complex (exit site from the isthmus), and a delay between this complex and the subsequent tachycardia complex would reflect a delay in entering or propagating through the protected diastolic pathway. Although such potentials that are related to the prior QRS complex can in fact be integral to the tachycardia (e.g., if the variability in cycle length [CL] is due to varying delay in the diastolic corridor “downstream” from the recording site), this is not guaranteed as it is when the electrogram is tightly related to the subsequent QRS complex.

If after very detailed mapping the earliest recorded site is not at least 50 milliseconds presystolic, this suggests that the map is inadequate (most common), the mechanism of tachycardia is not macroreentry, or the diastolic corridor is deeper than the subendocardium (in the midmyocardium or subepicardium).

Limitations

Standard catheter endocardial mapping, as performed in the EP laboratory, is limited by the number, size, and type of electrodes that can be placed within the heart. Therefore these methods do not simultaneously cover a vast area of the endocardial surface. Time-consuming, point-by-point maneuvering of the catheter is required to trace the origin of an arrhythmic event and its activation sequence in the neighboring areas.

The success of roving point mapping depends on the sequential beat-by-beat stability of the activation sequence being mapped and the ability of the patient to tolerate sustained arrhythmia. Therefore it can be difficult to perform activation mapping in poorly inducible tachycardias, in hemodynamically unstable tachycardias, and in tachycardias with unstable morphology. Sometimes poorly tolerated rapid tachycardias can be slowed by antiarrhythmic agents to allow for mapping. Alternatively, mapping can be facilitated by starting and stopping the tachycardia after data acquisition at each site. In addition, newer techniques (e.g., basket catheter, electroanatomic mapping, and noncontact mapping) can facilitate activation mapping in these cases by simultaneous multipoint mapping.

Although activation mapping is adequate for defining the site of origin of focal tachycardias, it is insufficient by itself in defining the critical isthmus of macroreentrant tachycardias, and adjunctive mapping modalities (e.g., entrainment mapping, pace mapping) are required. Moreover, the laborious process of precise mapping with conventional techniques can expose the electrophysiologist, staff, and patient to undesirable levels of radiation from the extended fluoroscopy time.

Using conventional activation mapping techniques, it is difficult to conceive the three-dimensional orientation of cardiac structures because a limited number of recording electrodes guided by fluoroscopy is used. Although catheters using multiple electrodes to acquire data points are available, the exact location of an acquired unit of EP data is difficult to ascertain because of inaccurate delineation of the location of anatomical structures. The inability to accurately associate the intracardiac electrogram with a specific endocardial site accurately also limits the reliability with which the roving catheter tip can be placed at a site that was previously mapped. This results in limitations when the creation of long linear ablation lesions is required to modify the substrate, as well as when multiple isthmuses or channels are present. The inability to identify, for example, the site of a previous ablation increases the risk of repeated ablation of areas already dealt with and the likelihood that new sites can be missed.

ENTRAINMENT MAPPING

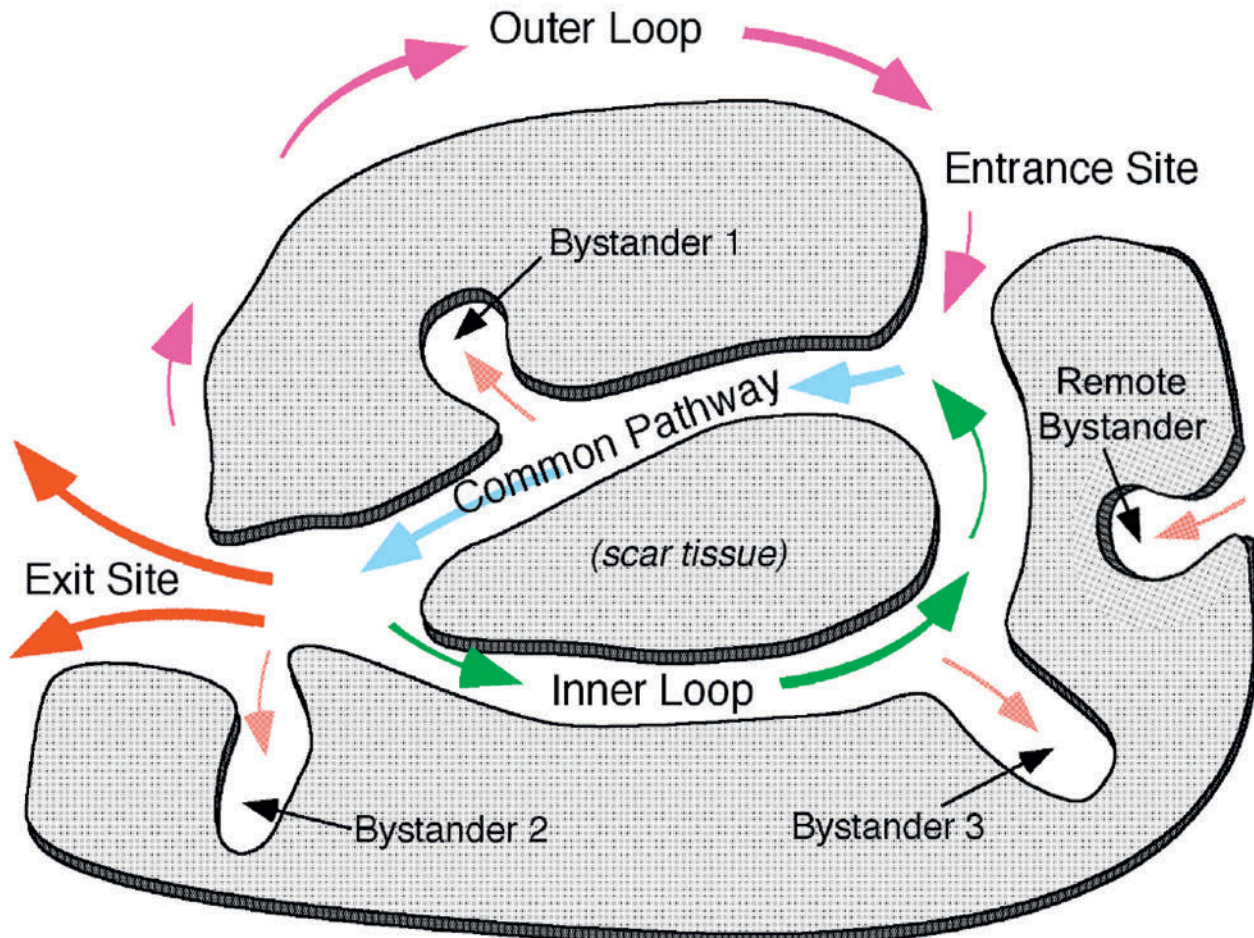
Fundamental Concepts

To help understand the concept of entrainment, a hypothetical reentrant circuit is shown in Fig. 5.16. This reentrant circuit has several components—a common pathway, an exit site, an outer loop, an inner loop, an entry site, and bystander sites.

- The reentrant wavefront propagates through the common central pathway (protected critical isthmus) during electrical diastole. Because this zone of slow conduction is usually composed of a small amount of myocardium and is bordered by anatomical or functional barriers preventing the spread of the electrical signal except in the orthodromic direction, propagation of the wavefront in the protected isthmus is electrocardiographically silent.
- The exit site is the site at which the reentrant wavefront exits the protected isthmus to start activation of the rest of the myocardium, including the outer loop. Activation of the exit site corresponds to the onset of the tachycardia complex on the surface ECG.
- The entrance is where the reentrant wavefront enters the critical isthmus.
- The outer loop is a pathway outside the scars connecting to the common central pathway and forming a circuit, and at the same time communicating with the main body of myocardium. The reentrant wavefront propagates through the outer loop while at the same time activating the rest of the myocardium. Activation of the outer loop corresponds to electrical systole (P wave during AT and QRS during VT) on the surface ECG.
- An inner loop is a conduction pathway within scars, communicating with the common central pathway forming a circuit. The inner loop can serve as an integral part of the reentrant circuit or function as a bystander pathway; the timing of activation, like the outer loop, is typically during electrical systole.
- The dominant loop is the circuit loop outside the common central pathway with the shortest conduction time. If conduction through the inner loop is slower than conduction from the exit to entrance sites (through the outer loop), the inner loop will serve as a bystander, and the outer loop will be the dominant loop. If conduction through the inner loop is faster than conduction through the outer loop, it will form an integral component of the reentrant circuit and is designated the dominant inner loop; ablation of the inner loop in this case may cause an abrupt change in TCL without change in QRS because the inner loop is no longer operative and the outer loop now becomes the default pathway.
- Bystander sites are sites that are activated by the reentrant wavefront but are not an essential part of the reentrant circuit. These sites can be remote, adjacent, or attached to the circuit. An attached bystander site represents a dead-end pathway (or a blind pouch) that communicates with the common central pathway or any inner loop and has no other exits.¹³

Understanding the concepts associated with resetting is critical to understanding entrainment. When a premature stimulus is delivered to sites remote from the reentrant circuit, it can interact with the circuit in different ways. When the stimulus is late-coupled, it may reach the circuit after it has just been activated by the reentrant wavefront. Consequently, although the extrastimulus may have resulted in activation of part of the myocardium, it fails to affect the reentrant circuit, and the reentrant wavefront continues to propagate in the critical isthmus and through the exit site to produce the next tachycardia complex on time. Fusion can be observed, but not resetting.

To reset a reentrant tachycardia, the paced wavefront must reach the reentrant circuit (entry site), encounter excitable tissue within the circuit (i.e., enter the excitable gap of the reentrant circuit), collide in



Site	Electrogram Timing in VT	Entrainment with Concealed Fusion	Entrained [S-QRS] – [Egm-QRS]	[S-QRS] TCL	PPI – TCL	Sinus Rhythm Pacemap QRS vs. VT
Entrance Site	Early diastolic	Present*	≤20 ms	51%–70%	≤30 ms	Different
Common Pathway	Mid diastolic	Present	≤20 ms	31%–50%	≤30 ms	Same [†]
Exit Site	Late diastolic	Present	≤20 ms	≤30%	≤30 ms	Same
Inner Loop	Systolic	Present	≤20 ms	>70%	≤30 ms	Same [†]
Bystander 1	Mid-diastolic*	Present	>20 ms	>70%	>30 ms	Same
Bystander 2	Late diastolic*	Present	>20 ms	>70%	>30 ms	Same
Bystander 3	Early diastolic*	Present*	>20 ms	>70%	>30 ms	Same [†]
Outer Loop	Systolic	Absent	≤20 ms	Variable	≤30 ms	Different
Remote Bystander	Systolic	Absent	>20 ms	Variable	>30 ms	Different

*Variable

[†]Depends on whether captured orthodromically or antidromically

Fig. 5.16 Representation of a Ventricular Tachycardia (VT) Circuit. The illustration shows a common diastolic pathway, entrance and exit sites, inner and outer loops, adjacent bystander dead-end paths in three locations, and remote bystander sites. The accompanying table describes the behavior of each of these locations during VT, as well as pacing during VT and sinus rhythm. Egm, Electrogram; S, stimulus; PPI, post pacing interval; TCL, tachycardia cycle length.

the antidromic (retrograde) direction with the previous tachycardia complex, and propagate in the orthodromic (anterograde) direction through the same tachycardia reentrant path (critical isthmus) to exit at an earlier than expected time and perpetuate the tachycardia (Fig. 5.17). If the extrastimulus encounters fully excitable tissue, as commonly occurs in reentrant tachycardias with large excitable gaps, the tachycardia is advanced by the extent that the paced wavefront arrives

at the entrance site prematurely. If the tissue is partially excitable, as can occur in reentrant tachycardias with small or partially excitable gaps, or even in circuits with large excitable gaps when the extrastimulus is very premature, the paced wavefront will encounter some conduction delay in the orthodromic direction within the circuit. Consequently, the degree of advancement of the next tachycardia complex depends on both the degree of prematurity of the extrastimulus and

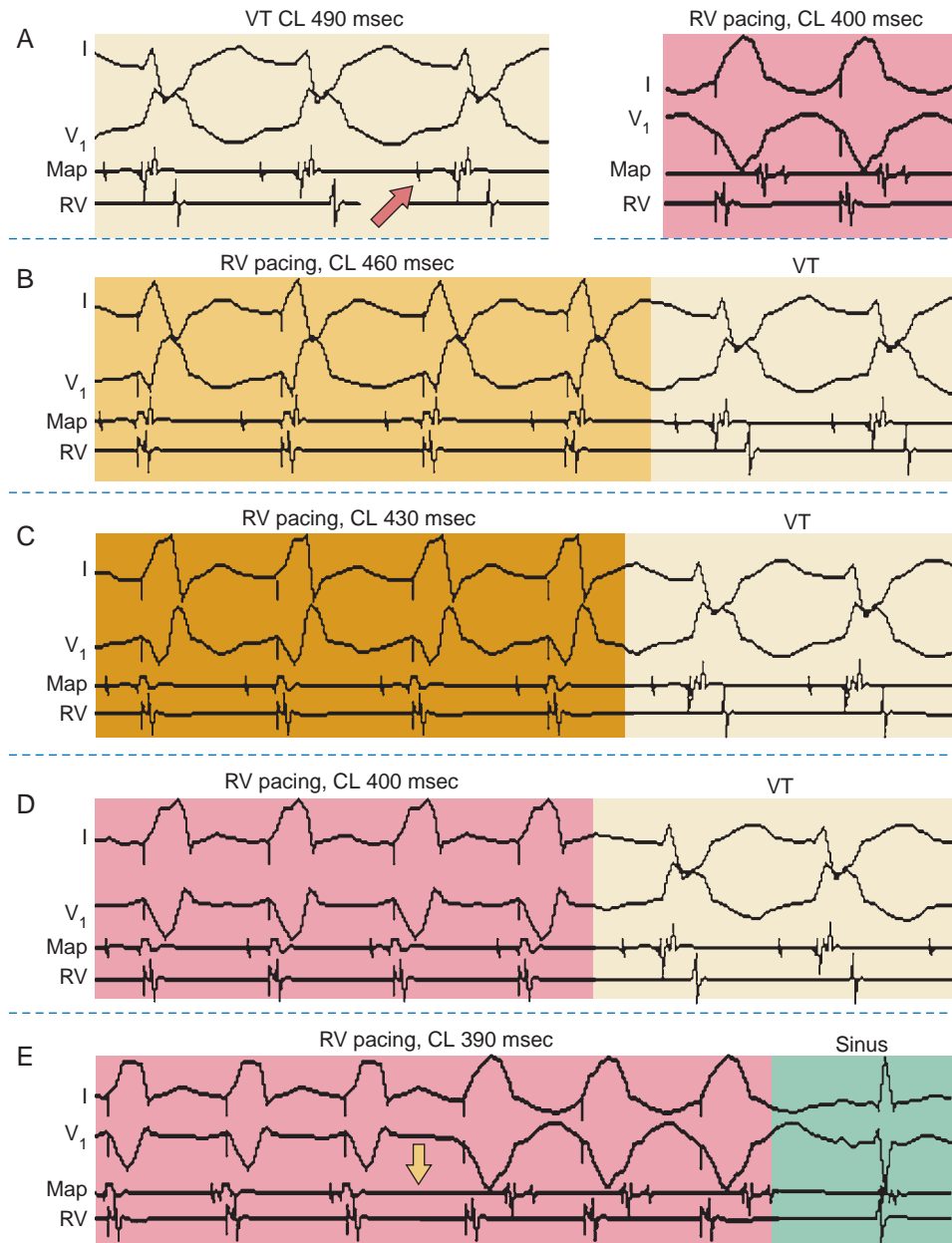


Fig. 5.17 Entrainment of Ventricular Tachycardia (VT). (A) Pure VT is shown in yellow (*right bundle branch block, right axis*), pure right ventricle (RV) pacing in red (*left bundle branch block, left axis*). A mid-diastolic potential during VT (*arrow*) is recorded by the mapping catheter. (B) Pacing the RV at 460 milliseconds (30 milliseconds faster than VT), each paced complex is a stable blend of pacing and VT (*gold*). This illustrates fixed fusion. After cessation of pacing, VT resumes. (C) Pacing the RV faster (430 milliseconds), all complexes are again identical to each other but different than with pacing at 460 milliseconds; they look slightly more like pure RV pacing (*deeper gold shading*). (D) Pacing the RV faster still (400 milliseconds), QRS complexes again are identical to each other (fixed fusion) but look progressively more like fully paced (progressive fusion). (E) Finally, with pacing rapidly enough, an antidromic wavefront captures the diastolic potential, QRS complexes become fully paced, and when pacing ceases, sinus rhythm resumes. This figure demonstrates all established entrainment criteria (fixed fusion at a given paced cycle length [CL], progressive fusion over a range of paced CLs, and antidromic capture of critical circuit elements leading to termination of the tachycardia).

the degree of slowing of its conduction within the circuit. Therefore the reset tachycardia complex may be early, on time, or later than expected.^{13,14}

Termination of the tachycardia occurs when the extrastimulus collides with the preceding tachycardia impulse antidromically and blocks in the reentrant circuit orthodromically. This occurs when the premature

impulse enters the reentrant circuit early enough in the relative refractory period because it fails to propagate in the anterograde direction, given that it encounters absolutely refractory tissue (see Fig. 5.17). In the retrograde direction, it encounters increasingly recovered tissue and is able to propagate until it meets the incoming circulating wavefront and terminates the arrhythmia.

Entrainment is the continuous resetting of a reentrant circuit by a train of capturing stimuli. However, following the first stimulus of the pacing train that penetrates and resets the reentrant circuit, the subsequent stimuli interact with the “reset circuit,” which has an abbreviated excitable gap. The first entrained complex results in retrograde collision between the stimulated and the tachycardia wavefronts, whereas in all subsequent beats, the collision occurs between the currently stimulated wavefront and that stimulated previously. Depending on the degree that the excitable gap is preexcited (shortened) by the first resetting stimulus, subsequent stimuli can fall on fully or partially excitable tissue. Entrainment is said to be present when two consecutive extrastimuli conduct orthodromically through the circuit with the same conduction time while colliding antidromically with the preceding paced wavefront.¹³

During entrainment, each pacing impulse creates two activation wavefronts—one in the orthodromic direction and the other in the antidromic direction. The wavefront in the antidromic direction collides with the existing tachycardia wavefront. The wavefront that enters the reentrant circuit in the orthodromic direction (i.e., the same direction as the spontaneous tachycardia wavefront) conducts through the critical isthmus, resets the tachycardia, and emerges through the exit site to activate the myocardium and collide with the antidromically paced wavefront from the next paced stimulus. This sequence continues until cessation of pacing or development of block somewhere within the reentrant circuit. Because all pacing impulses enter the tachycardia circuit during the excitable gap, each paced wavefront advances and resets the tachycardia. Thus when pacing is terminated, the last paced impulse continues to activate the entire tachycardia reentrant circuit orthodromically at the PCL and also activates the entire myocardium orthodromically on exiting the reentrant circuit (as this time there is no paced antidromic wavefront with which to collide).¹⁴

Entrainment does not require that the pacing site be located in the reentrant circuit. The closer the pacing site is to the circuit, however, the less premature a single stimulus needs to be to reach the circuit and, with pacing trains, the fewer stimuli will be required before a stimulated wavefront reaches the reentrant circuit without being extinguished by collision with a wave emerging from the circuit. Overdrive pacing at relatively long PCLs (i.e., 10 to 30 milliseconds shorter than the TCL) can almost always entrain reentrant tachycardias. However, the number of pacing stimuli required to entrain the reentrant circuit depends on the TCL, the duration of the excitable gap of the tachycardia, refractoriness at the pacing site, and the conduction time from the stimulation site to the reentrant circuit.¹⁵

Entrainment Criteria

During constant-rate pacing, entrainment of a reentrant tachycardia results in the activation of all myocardial tissue responsible for maintaining the tachycardia at the PCL, with the resumption of the same tachycardia morphology following cessation of pacing and the first postpacing ECG tachycardia complex displaying no fusion but occurring at a return cycle equal to the PCL. Unfortunately, it is almost impossible to document the acceleration of all the tissue responsible for maintaining the reentrant circuit to the PCL. Importantly, the mere acceleration of the tachycardia to the pacing rate and the subsequent resumption of the original tachycardia after the cessation of pacing do not establish the presence of entrainment; these can be seen with any type of tachycardia, including focal automatic tachycardias. Therefore several surface ECG and intracardiac electrogram criteria have been proposed for establishing the presence of entrainment (see Fig. 5.17; Box 5.1), largely dealing with the phenomenon of fusion during pacing.¹⁶

Demonstration of one or more of the four criteria proves the presence of entrainment and supports a reentrant mechanism, but their absence does not exclude entrainment or reentry. Pacing at different

BOX 5.1 Criteria for Entrainment

1. Constant fusion during overdrive pacing at a given cycle length, except for the last captured P wave which is entrained but not fused.
2. Progressive fusion during overdrive pacing from the same site at different cycle lengths.
3. When overdrive pacing at a constant rate during tachycardia results in tachycardia termination, there is the demonstration of localized conduction block to a site (or sites) for one paced beat associated with interruption of the tachycardia, followed by activation of that site (or sites) by the next paced P wave from a different direction and with a shorter conduction time.
4. During overdrive pacing at two different rates during tachycardia, there is change in conduction time to and electrogram morphology at the electrode recording site.

endocardial sites and at multiple PCLs and recording activation sequence from multiple intracardiac locations (especially in the setting of macroreentrant AT) is often required to demonstrate one or more of the entrainment criteria and hence establish the diagnosis of macroreentrant tachycardia.¹⁷

Of note, the third “entrainment criterion” seems to be a paradox, since it is based on tachycardia termination by overdrive pacing, invalidating the presence of “entrainment” which, by definition, requires “resumption of the same tachycardia morphology following cessation of pacing.” Nevertheless, this criterion demonstrates that the mechanism of tachycardia termination is related to block of an orthodromic wavefront after it has entered the circuit. When localized block to a recording site occurs and the same site is activated in subsequent beats with a shorter conduction time, it means that such a site had been originally activated orthodromically.¹³

Fusion During Entrainment

A stimulated impulse is said to be fused when its morphology is a hybrid between that of a fully paced complex morphology (when pacing is performed at identical site and rate but in the absence of tachycardia) and a tachycardia complex morphology (in the absence of pacing). Fusion can be observed on the surface ECG, intracardiac recordings, or both. For fusion to be observed on the surface ECG, the tachycardia and stimulated wavefronts must collide within the reentrant circuit after the tachycardia wavefront has exited from the isthmus. This requires the paced wavefront to have access to an entrance site of the reentrant circuit that is anatomically distinct from the exit site. If the antidromically stimulated wavefront penetrates the reentrant circuit and collides with the tachycardia wavefront (or the previously stimulated orthodromic wavefront) before the point at which the tachycardia wavefront would be exiting to the mass of the myocardium, then no fusion will be evident on the surface ECG, and the surface ECG will appear entirely paced (Fig. 5.18).^{13,18}

The ability to demonstrate surface ECG fusion requires that a significant mass of myocardium be depolarized by both the extrastimulus and the tachycardia. The degree of fusion represents the relative amount of myocardium depolarized by the two separate wavefronts. The relative degree of myocardium antidromically activated by the paced wavefront depends on the site of pacing relative to the reentrant circuit, the PCL, and the degree of conduction delay within the reentrant circuit. With a single extrastimulus, the farther the stimulation site is from the reentrant circuit, the less likely ECG fusion will be to occur, because the extrastimulus must be delivered at a shorter coupling interval (well before the tachycardia wavefront exits the circuit) in order to reach the circuit with adequate prematurity. Therefore, by the time the tachycardia

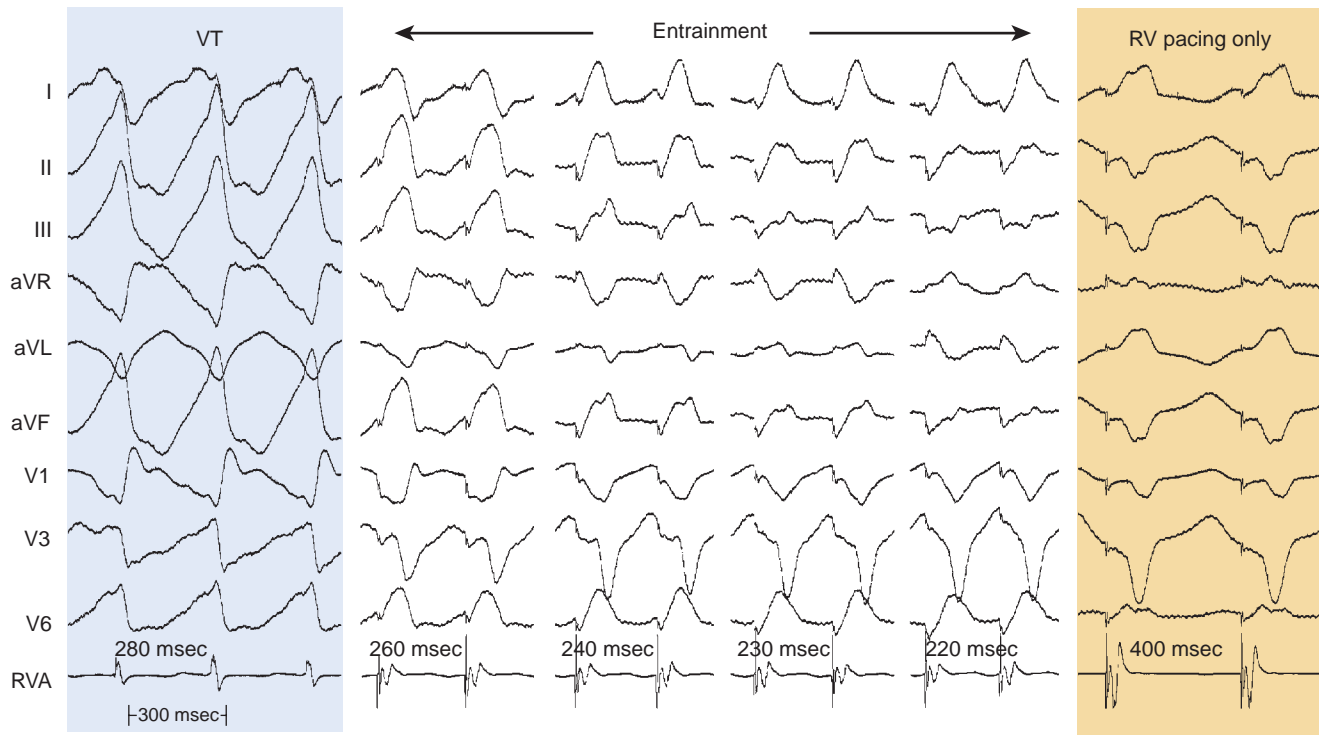


Fig. 5.19 QRS Fusion During Entrainment of Ventricular Tachycardia (VT). Progressive electrocardiogram fusion is shown over a range of paced cycle lengths (CLs). Pure tachycardia complexes are shown on the left; fully paced complexes are shown on the right. As the paced CL shortens, complexes gradually appear more like those that are fully paced. RV, Right ventricle; RVA, right ventricular apex.

fusion and more fully paced morphology. Such phenomena (referred to as “variable fusion”) should be distinguished from “constant fusion” and “progressive fusion” characteristic of entrainment, and sometimes this distinction requires pacing for long intervals to demonstrate variable degrees of fusion. Moreover, overdrive pacing frequently results in suppression (automatic) or acceleration (triggered activity) of focal tachycardias, rather than resumption of the original tachycardia with an unchanged TCL.^{13,17}

During entrainment, varying degrees of fusion at different pacing rates are caused by a progressive increase in the amount of myocardium activated by the antidromic wavefront at progressively shorter PCLs; although fusion remains fixed at each of the PCLs, a different degree of fixed fusion is manifest at different PCLs (see Figs. 5.17 and 5.19). At slower PCLs, a larger amount of the myocardium is activated by the orthodromic wavefront exiting from the reentrant circuit prior to its intracardiac collision, with the subsequent antidromic wavefront incoming from the pacing site. With a faster pacing rate, more myocardium is antidromically activated because the orthodromic wavefront must continue to traverse the zone of slow conduction within the reentrant circuit, thus creating progressive fusion with changing PCLs. In the extreme situation, the antidromic wavefront can capture the exit site of the reentrant circuit (i.e., capture of the presystolic electrogram during tachycardia) and produce a fully paced complex on the surface ECG. Once this occurs, pacing at shorter PCLs does not cause further progressive fusion, although entrainment is still present. As noted, progressive fusion at decreasing PCLs during entrainment of tachycardia excludes the possibility of automaticity or triggered activity as the mechanism of the tachycardia. In those cases, overdrive pacing would yield solely the morphology of the pacing stimulus for a nonprotected focus or would yield varying (not progressive) degrees of fusion for a

protected focus with entrance block. Of note, a microreentrant circuit with entrance block could also yield variable fusion during overdrive pacing; thus this finding would not exclude reentry as the underlying mechanism.¹³

The traditional definition of entrainment states that following cessation of pacing, the same tachycardia morphology resumes, with the first postpacing ECG tachycardia complex displaying no fusion but occurring at a *return cycle equal to the PCL*. On cessation of pacing, the last paced wavefront traverses the protected isthmus and exits the circuit to produce a normal (nonfused) tachycardia ECG complex because there is no paced antidromic wavefront with which to fuse. The wavefront continues around the reentrant circuit to maintain the tachycardia. However, demonstration of the first return cycle (measured at the onset of the ECG complex) that is equal to the PCL is difficult. This response is rare and occurs only when the pacing stimulus occurs after the onset of the tachycardia ECG complex (P wave or QRS), whereby the initial part of the fused complex is activated by the orthodromic wavefront exiting the tachycardia circuit. Then, the first nonpaced complex will occur at the PCL because it will really be orthodromically activated by the last paced beat. More commonly, constant fusion of the surface ECG occurs without the first nonpaced beat occurring at the PCL. When surface ECG fusion occurs, the initial portion of the ECG complex usually reflects activation of the myocardium by the paced wavefront, whereas the terminal portion represents the orthodromically activated wavefront exiting from the tachycardia circuit. The point at which this wavefront exits the circuit can be late in the surface ECG complex. The degree to which the first ECG complex postpacing interval (PPI) exceeds the PCL is primarily a reflection of the time from the onset of the paced surface ECG complex to the exit of the orthodromic wavefront from the reentrant circuit. This represents the period of time during which

the myocardium is depolarized by the stimulated wavefront before the activation of any portion of the myocardium by the wavefront exiting the tachycardia circuit. Therefore, constant fusion occurring in the absence of the first ECG PPI being equal to the PCL can be a valid manifestation of entrainment. In this situation, appropriate placement of intracardiac electrodes demonstrates orthodromic entrainment of some intracardiac recording sites occurring at the PCL, even though the last entrained ECG complex occurred at an interval longer than the PCL.¹³

Entrainment with manifest fusion. Entrainment with manifest fusion demonstrates surface ECG evidence of constant fusion at a constant pacing rate and progressive fusion with incremental-rate pacing (see Fig. 5.19). When entrainment is manifest, the last captured wave is entrained at the PCL but does not demonstrate fusion.¹³

Demonstration of the presence of manifest fusion during entrainment requires knowledge of the tachycardia surface ECG complex morphology as well as that of pure pacing (at the same site and rate) in the absence of tachycardia. However, in the setting of macroreentrant AT, P wave morphology during tachycardia or pure pacing may not be easily visualized in the presence of overlapping ST-T waves; hence intraatrial activation sequence can be utilized as a surrogate to ECG morphology to demonstrate fusion. Manifest fusion is said to be present when the ECG morphology (or intracardiac activation sequence) is a hybrid of the tachycardia complex morphology and that observed during pure pacing (see Figs. 5.17 and 5.19).

Sometimes fusion is difficult to recognize in the surface ECG because the morphology of the purely paced ECG complex may not be readily available. This can occur, for example, in patients presenting with persistent macroreentrant tachycardia, whereby pacing during NSR is not feasible. In this setting, the presence of manifest fusion can be inferred by one of the following observations:

1. The surface ECG complex (QRS/P wave) during entrainment is different from pure tachycardia morphology, and the onset of the QRS/P wave precedes the pacing stimulus artifact of each paced beat by a fixed interval (see Figs. 12.12 and 13.7). This observation provides evidence that the tachycardia wavefront has exited from the circuit, and that the initial portion of the QRS/P wave (inscribed before the pacing stimulus artifact) is activated orthodromically by the tachycardia wavefront while the latter portion is activated by the paced wavefront.
2. The surface ECG complex morphology (or intracardiac activation sequence) is different from the pure tachycardia morphology but is inconsistent with the expected morphology during pure pacing at a particular site (e.g., VT entrainment from the ventricular inferior wall producing QRS vector that is positive in inferior leads, or AT entrainment from the distal CS producing a proximal-to-distal CS activation sequence).
3. The demonstration of shortening of conduction time to (and change in electrogram morphology at) an intracardiac electrode recording site in response to increasing pacing rates during entrainment. Since *conduction velocity* with increasing rate is expected to either stay the same or decrease, but not increase, a decrease in *conduction time* (same paced site, same recorded site) in relation to faster pacing rate demonstrates that there are two routes of activation and that the faster one can only conduct to the recording site at faster pacing rates. This represents the fourth entrainment criterion and is the intracardiac equivalent of the second entrainment criterion (progressive fusion). The amount of tissue antidromically captured is critically dependent on the pacing rate. If the recording site is located in an area activated orthodromically at a slower rate and antidromically at a faster rate, the conduction time will dramatically shorten at the faster pacing rate.¹⁴

Entrainment with concealed fusion. Entrainment with concealed fusion (sometimes also referred to as “concealed entrainment” or “exact entrainment”) is defined as entrainment with orthodromic capture and a surface ECG complex (and intracardiac activation sequence) identical to that of the tachycardia (see Figs. 12.12 and 13.7).¹³

Entrainment with concealed fusion suggests that the pacing site is within a protected isthmus, either inside the reentrant circuit or outside the circuit but attached to its diastolic pathway (see Fig. 5.16). It is important to recognize that entrainment with concealed fusion can occur by pacing not only from the critical isthmus of the reentrant circuit, but also from bystander pathways, such as a blind alley, alternate pathway, or nondominant inner loop, that are attached to the protected isthmus that forms the diastolic pathway of the circuit but are not critical to the maintenance of reentry.

Pacing in a protected isthmus, either inside or outside (but attached to) the reentrant circuit isthmus, forces the paced wavefront to travel in one (orthodromic) direction through the same reentrant pathway as the tachycardia wavefront. Propagation of the paced wavefront in the opposite (antidromic) direction is prevented by either a dead-end (when one end of the protected pathway being paced is attached to the circuit and the other end is a dead end) or by colliding with the previous reentrant wavefront propagating orthodromically through the reentrant circuit (when both ends of the protected isthmus are attached to the circuit’s diastolic pathway, whether the isthmus is critical to the circuit or just a bystander). In either situation, the paced wavefront is forced to utilize the same reentry circuit exit to stimulate the rest of the myocardium and is prevented from stimulating the myocardium by propagating in any other direction. Hence the entrained ECG morphology is identical to that of the tachycardia.^{13,19}

Since only tissue near the pacing site within the critical isthmus is antidromically activated, evidence of fusion may be lacking. Compared with the intrinsic tachycardia, this antidromic capture may result in earlier intracardiac recordings from sites located adjacent to the pacing region. The morphological appearance of the ECG, however, is the same during entrainment as during the tachycardia.¹⁴

Entrainment with inapparent fusion. Entrainment with inapparent fusion (also referred to as “local” or “intracardiac” fusion) is said to be present when a fully paced morphology (with no ECG fusion) results, even when the tachycardia impulse exits the reentrant circuit (i.e., orthodromic activation of the presystolic electrogram is present). Fusion is limited to a small area and does not produce surface ECG fusion, and only intracardiac (local) fusion is recognized (Fig. 5.20; see Fig. 13.7).

Local fusion can occur only when the presystolic electrogram is activated orthodromically by the tachycardia wavefront. Collision with the last paced impulse must occur distal to the presystolic electrogram, either at the exit from the circuit or outside the circuit. In such cases, the return cycle measured at this local electrogram equals the PCL. Therefore a stimulus delivered after the onset of the tachycardia complex on the surface ECG during entrainment always demonstrates local fusion. This is to be distinguished from entrainment with antidromic capture. As noted, when antidromic (retrograde) capture of the local presystolic electrogram occurs, the return cycle, even when measured at the site of the presystolic electrogram, exceeds the PCL.

Entrainment with antidromic capture. During entrainment with a PCL pacing that is significantly shorter than the TCL, the paced impulse can penetrate the circuit antidromically and retrogradely capture the presystolic electrogram (exit site of the reentry circuit). In other words, the paced wavefront collides with the tachycardia wavefront within the diastolic pathway (protected isthmus) of the circuit. As a result, tachycardia wavefront cannot exit from the reentrant circuit and thus cannot contribute to myocardial activation. Therefore the ECG morphology

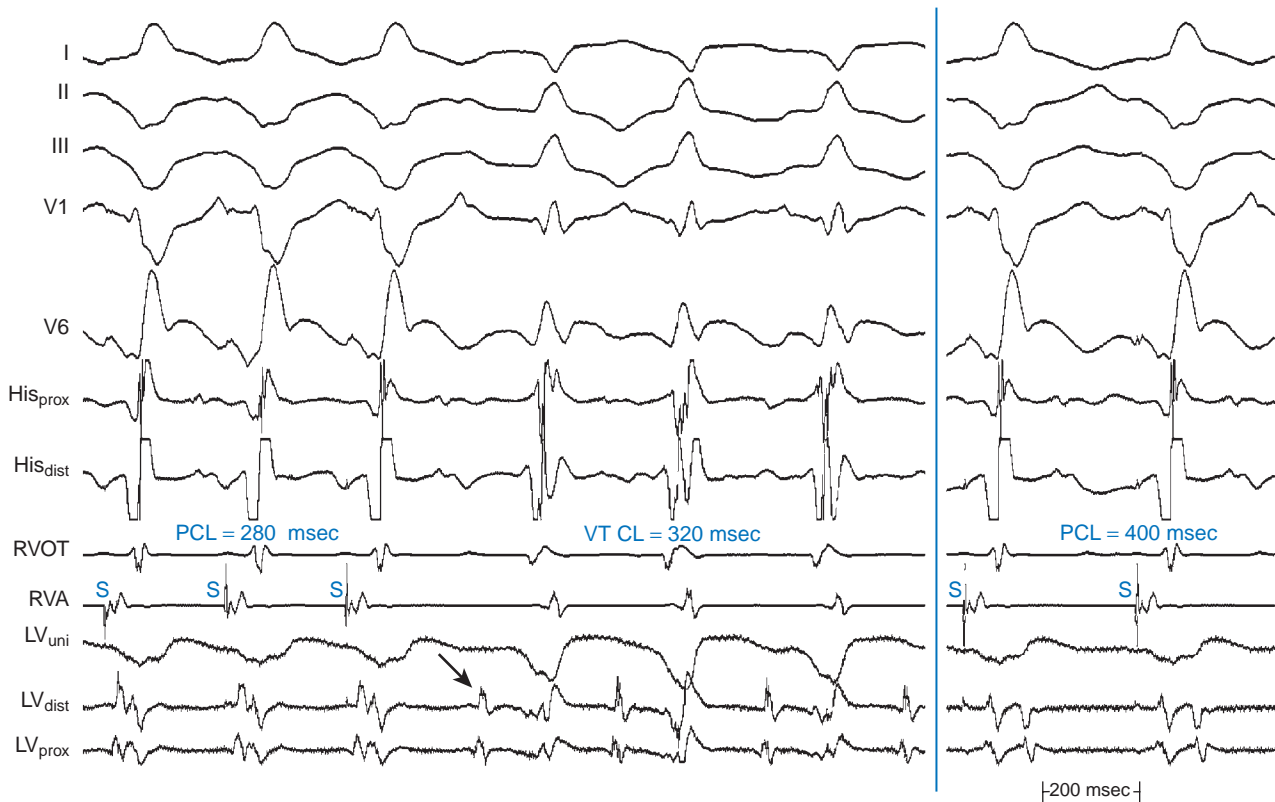


Fig. 5.20 Inapparent Fusion. The last three complexes paced from the right ventricular apex during ventricular tachycardia (VT) are shown; VT resumes on cessation of pacing. Fusion is not evident on the surface electrocardiogram because these complexes are identical to fully paced QRS complexes at the far right, yet fusion is present on the distal ablation recording (mid-diastolic potential at arrow seen during pacing as well). CL, Cycle length; PCL, pacing cycle length; His_{dist}, distal His bundle; His_{prox}, proximal His bundle; LV_{dist}, distal left ventricle; LV_{prox}, proximal left ventricle; LV_{uni}, unipolar left ventricle; RVA, right ventricular apex; RVOT, right ventricular outflow tract.

during entrainment will be identical to that of pacing in the absence of tachycardia (fully paced QRS or P wave) and no fusion.

When pacing is stopped, the impulse that conducts antidromically also conducts orthodromically to reset the reentrant circuit with orthodromic activation of the presystolic electrogram. When antidromic (retrograde) capture of the local presystolic electrogram occurs, the return cycle, even when measured at the site of the presystolic electrogram, exceeds the PCL by the difference in time from when the electrogram is activated retrogradely (i.e., preexcited antidromically) and when it would have been activated orthodromically.¹⁴

Postpacing Interval

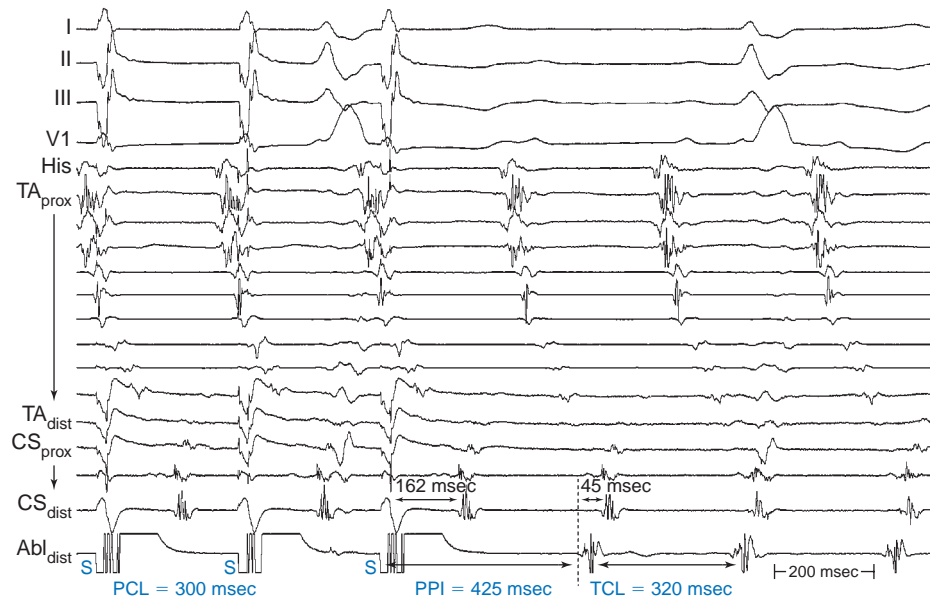
The PPI is the time interval from the last pacing stimulus that entrained the tachycardia to the next nonpaced recorded electrogram at the pacing site (eFig. 5.4).

During entrainment from sites within the reentrant circuit, the orthodromic wavefront from the last stimulus propagates through the reentry circuit and returns to the pacing site, following the same path as the circulating reentry wavefronts. The conduction time required is the revolution time through the circuit. Thus the PPI (measured from the pacing site recording) should be equal (within 30 milliseconds) to the TCL, given that conduction velocities and the reentrant path did not change during pacing (see Fig. 5.16). At sites remote from the circuit, stimulated wavefronts propagate to the circuit, then through the circuit, and finally back to the pacing site. Thus the PPI should

equal the TCL (representing one complete revolution through the reentry circuit) plus the time required for the stimulus to propagate from the pacing site to the tachycardia circuit and back. Given that the TCL is stable (which is a prerequisite for entrainment assessment), and that there is no decremental conduction between the pacing site and the reentry circuit, the PPI should remain relatively stable when entrainment of a macroreentrant tachycardia is performed at the same site, regardless of the length of the pacing drive.

The greater the physical (or electrical) distance will be between the pacing site and the circuit, the longer the conduction time will be between the pacing site and reentry circuit, and the greater the difference is between the PPI and the TCL (PPI–TCL; see Figs. 12.12 and 13.7). The PPI–TCL value is highly reproducible during repeated entrainment attempts at the same PCL.^{19,20}

Several factors have to be considered when evaluating the PPI. The PPI should be measured to the near-field potential that indicates depolarization of tissue at the pacing site. However, assessment of the PPI can be problematic when the electrograms from the pacing site are not discernible, especially in regions of scar, where local near-field potentials are small and often difficult to distinguish or separate from far-field potentials. In addition, recordings of local activation at the pacing site may not be obtainable or interpretable due to electrical noise and signal saturation after the stimulus artifact. In these situations, the PPI can be measured from electrograms recorded by electrodes adjacent to those used for pacing (e.g., the proximal electrodes on the mapping catheter),



eFig. 5.4 Bystander Site During Left Atrial (LA) Flutter. The last three complexes of pacing from the posterior LA are shown in a patient with LA macroreentry. Although the timing of the electrogram at the pacing site is in early mid-diastole and the paced activation sequence is similar to tachycardia, thereby giving the appearance of an attractive ablation site, the results of entrainment indicate otherwise, with a large difference between the stimulus–coronary sinus (CS) electrogram interval (162 milliseconds) and the ablation recording–CS electrogram interval (45 milliseconds), as well as a large difference between the post-pacing interval (PPI) (425 milliseconds) and tachycardia cycle length (TCL, 320 milliseconds). *Abl_{dist}*, Distal ablation; *CS_{dist}*, distal coronary sinus; *CS_{prox}*, proximal coronary sinus; *PCL*, pacing cycle length; *TA_{dist}*, distal tricuspid annulus; *TA_{prox}*, proximal tricuspid annulus.

but this does introduce potential error, particularly in regions of abnormal conduction.¹³

It is important to recognize that the PPI–TCL value can be misleadingly long despite pacing from sites within the reentrant circuit. This is likely a result of rate-related decremental conduction in a zone of slow conduction within the reentry circuit, and is more likely to occur at rapid pacing rates or when the reentry circuit involves a slow conduction zone with a decremental conduction property such as the atrioventricular node (AVN). In one report in patients with typical atrial flutter (AFL), long PPI–TCL values (more than 30 milliseconds) after entrainment from the CTI were observed in 18% of patients despite a PCL within 20 milliseconds of the TCL, and more frequently when the PCL was more than 30 milliseconds shorter than the TCL and in patients on amiodarone therapy. The long PPI–TCL values are likely caused by rate-dependent slowing of conduction or alterations of the activation path. These findings likely also apply to other macroreentrant tachycardias.^{21–23}

On the other hand, an erroneously short PPI interval (shorter than the TCL) can result from far-field capture of downstream tissue distal to the local electrogram recorded at the pacing site. This results in shortening the path of the return cycle. A short PPI may also be encountered during delayed local capture, as indicated by latency between the stimulus artifact and local electrogram. In addition, transient acceleration of tachycardia can yield a seemingly short PPI.

In summary, the PPI–TCL value serves as an approximate measure of the distance from the pacing site to the reentry circuit. During pacing at a site that is in the circuit, the conduction time between the pacing site and the circuit is 0, and the PPI equals the TCL, provided that three fundamental assumptions are true. First, pacing must capture and entrain the tachycardia. Second, the electrograms used for measurement of the PPI are because of depolarization at the pacing site. Third, conduction through the reentry circuit must not be slowed or altered by pacing.^{22,24}

Stimulus–Electrocardiogram Complex Interval During Entrainment

During entrainment of reentrant tachycardia, the interval between the pacing stimulus and the onset of the tachycardia complex on the surface ECG (QRS or P wave) reflects the conduction time from the pacing site to the exit of the reentrant circuit (stimulus-exit interval), regardless of whether the pacing site is inside or outside the reentrant circuit. This is because activation starts at the pacing site and propagates in sequence to the circuit exit site.

Pacing from outer loop and remote bystander sites generates very short stimulus-exit intervals because the myocardium outside the circuit is directly activated by the pacing stimulus. In contrast, pacing from protected sites, such as the diastolic pathway (isthmus) of the reentry circuit or attached bystander or inner loop sites (communicating with the isthmus of the circuit and sharing the same exit) produces longer stimulus-exit intervals that reflect the conduction time from the pacing site through the protected pathway to the exit site of the circuit. Pacing from inner loop sites generates very long stimulus-exit intervals (>70% of TCL). On the other hand, pacing from the entrance, central isthmus, and exit site of the reentry circuit produces long (51% to 70% of TCL), intermediate (31% to 50% of TCL), and short (\leq 30% of TCL) stimulus-exit intervals, respectively.

During tachycardia, the interval between the local electrogram at a given mapping site and circuit exit site (electrogram-exit interval) can reflect the true conduction time between those two sites if they are activated in sequence (as occurs when the mapping site is located directly within the reentrant pathway), or it may be shorter than the true conduction time if those two sites are activated in parallel (which occurs

when the mapping site is located outside the reentrant circuit; see Fig. 5.16 and eFig. 5.4).^{13,19} Consequently, when mapping along the diastolic pathway of the reentry circuit, the electrogram-exit interval becomes progressively shorter as the mapping catheter is sequentially moved from the entrance toward the central isthmus and then the exit site of the circuit. Electrograms from the isthmus are generally fractionated and low amplitude, and occur during diastole resulting in early- (entrance), mid- (central), and late- (exit) diastolic (or presystolic) potentials. In contrast, mapping sites located at bystander sites attached to the isthmus of the circuit are activated in parallel with the exit site, resulting in a shortened electrogram-exit interval (i.e., a “pseudo-interval” that does not represent a true conduction time between the two locations).

Because a diastolic electrogram is not specific for the critical isthmus but can be recorded from bystander sites, comparing the stimulus-exit interval during entrainment to the electrogram-exit interval during tachycardia (both intervals are measured at the pacing site) can help distinguish the critical isthmus sites from attached bystander and non-dominant inner loop sites. At isthmus sites, activation from those sites to the exit of the circuit follows the same pathway during both tachycardia and entrainment. In contrast, attached bystander and nondominant inner loop sites are activated in parallel with the exit site during tachycardia but in sequence during entrainment, resulting in a significantly shorter (by more than 20 milliseconds) electrogram-exit interval than stimulus-exit interval. On the other hand, at any given pacing site, an electrogram-exit interval that is equal (\pm 20 milliseconds) to the stimulus-exit interval indicates that the pacing site lies within the reentry circuit and excludes the possibility that the site is a dead-end pathway attached to the circuit (i.e., not a bystander).

This measurement is essentially similar to PPI–TCL during concealed entrainment, but obviates some of the problems of PPI measurement since the electrogram-exit interval does not have to be measured in the first beat after pacing. However, the electrogram-exit interval may not be exactly equal to the stimulus-exit interval at sites within the reentrant circuit. Several factors can explain this. First, decremental conduction properties of the zone of slow conduction can potentially produce lengthening of the stimulus-exit interval during pacing; however, this appears to occur rarely, and can largely be obviated by measuring the stimulus-exit interval during pacing at the slowest PCL that reliably entrains the tachycardia. Second, stimulus latency in an area of diseased tissue can account for a delay in the stimulus-exit interval compared with the electrogram-QRS interval. Third, failure of the recording electrodes to detect low-amplitude depolarizations at the pacing site can account for a mismatch of the stimulus-exit and electrogram-exit intervals.¹⁹

This criterion helps verify the relationship of pacing sites demonstrating entrainment with concealed fusion to the reentry circuit. This measurement can produce conflicting results in cases of manifest ECG fusion or when the onset of the surface ECG complex (as is the case for many macroreentrant ATs) is not discernable. Therefore this criterion is of little value at pacing sites not exhibiting concealed fusion.¹⁷ This pitfall can be mitigated measuring the interval between the last stimulus entraining the tachycardia and a timing reference during the second beat after the stimulus (the N+1 beat), and then subtracting this interval from a comparable interval between the electrogram (at the pacing site) in any following beat (the so-called N+1 difference).

Number of Pacing Stimuli Needed to Entrain

As noted, the number of pacing stimuli required to entrain the reentrant circuit depends on the TCL, the duration of the excitable gap of the tachycardia, refractoriness at the pacing site, and the conduction time from the stimulation site to the reentrant circuit. Overdrive pacing

begins to advance a reentrant tachycardia precisely when the total pacing prematurity exceeds the PPI–TCL value after correcting for conduction velocity changes associated with the shorter PCL.¹⁵

The “number needed to entrain” assesses the number of captured pacing stimuli required to accelerate the tachycardia to the PCL. Recording electrograms at widely separated endocardial sites and properly timed initiation of the entrainment pacing (the coupling interval of the first paced stimulus is identical to the PCL) are required to measure the number needed to entrain. A short number of pacing stimuli needed to entrain indicates close proximity to the reentry circuit and agrees with a short PPI.²⁵

The number needed to entrain is associated with the time for the wavefront to reach the circuit. It becomes smaller at shorter PCLs (and greater TCL–PCL value) as the paced wavefronts arrive earlier to reentrant circuits. Therefore the number of pacing stimuli needed to entrain is predictable in proportion to the distance between the pacing site and reentrant circuit when the TCL–PCL value is taken into account.²⁵

A recent report evaluated this criterion in patients with macroreentrant AT. The number needed to entrain measured with a TCL–PCL value of 16 to 30 milliseconds is most accurate, where a number needed to entrain ≤ 2 is consistent with pacing site being within the reentry circuit, and greater than 3 is consistent with outside-the-circuit sites. Nevertheless, the number needed to entrain still has diagnostic value even when the TCL–PCL value did not fall within this range. A number needed to entrain ≤ 2 is highly specific for in-the-circuit for a TCL–PCL value of 5 to 15 milliseconds, whereas a number needed to entrain greater than 4 with a TCL–PCL value of 5 to 15 milliseconds and number needed to entrain greater than 3 with a TCL–PCL value of 31 to 50 milliseconds can exclude an in-the-circuit pacing site.²⁵

An advantage of this criterion is that it does not require continuation of tachycardia after pacing for assessment and remains valid even when the tachycardia terminates or changes. The number needed to entrain is also useful when electrograms for assessment of the PPI are difficult to define. Also, the number needed to entrain does not increase at shorter PCLs, likely because the conduction velocity in the intervening myocardium (between the pacing site and the reentry circuit) is less susceptible to changes in the PCL. This is in contrast to the slow conduction zone within the reentry circuit, which can display decremental conduction properties at PCLs shorter than the TCL, resulting in misleading long PPIs.²⁵

Mapping Procedure

Before attempting to use entrainment methods for mapping, it is necessary to demonstrate that the tachycardia can be entrained (fulfilling entrainment criteria discussed above), by providing strong evidence that it is caused by reentry rather than by triggered activity or automaticity. Proof of entrainment is best obtained by pacing from sites remote from the circuit, which most readily demonstrate manifest fusion.

Then, entrainment mapping is directed to sites identified by other mapping modalities, such as activation mapping and pace mapping, as potentially related to the reentrant circuit. These include areas of slow conduction (manifest as fractionated electrograms), sites with mid-diastolic electrograms, or those displaying long delays between the pacing stimulus and the captured surface ECG complex (see Fig. 5.16).

Entrainment mapping can be reliably carried out only if one can record and stimulate from the same area (e.g., for 2-5-2-mm spacing catheters, record from the second and fourth poles and stimulate from the first and third poles). Pacing is usually started at a PCL just shorter (10 to 20 milliseconds) than the TCL. Pacing should be continued for a long enough duration to allow for entrainment; short pacing trains are usually not helpful. Pacing is then repeated at progressively shorter PCLs.¹⁴

After cessation of each pacing drive, the presence of entrainment should be verified by demonstrating one or more of the entrainment criteria discussed previously. It is important to understand that the mere acceleration of the tachycardia to the pacing rate and then resumption of the original tachycardia after cessation of pacing do not establish the presence of entrainment. Evaluation of the PPI or other criteria is meaningless when the presence of true entrainment has not been established. Moreover, it is important to verify the absence of termination and reinitiation of the tachycardia during the same pacing drive.

Once the presence of entrainment is verified, several criteria can be used to indicate the relation of the pacing site to the reentrant circuit (Fig. 5.21). The first entrainment criterion to be sought is concealed fusion. Entrainment with concealed fusion indicates that the pacing site is in a protected isthmus located within or attached to the reentrant circuit. Whether this protected isthmus is crucial to the reentrant circuit or is just a bystander site needs to be verified by other criteria, mainly comparing the PPI with the TCL and comparing the stimulus-exit interval with the electrogram-exit interval. Furthermore, the ratio of the stimulus-exit interval to the TCL can provide information regarding the location of the pacing site within the diastolic pathway of the reentry circuit. Long (51% to 70% of TCL), intermediate (31% to 50% of TCL), and short ($\leq 30\%$ of TCL) stimulus-exit intervals are observed during pacing from the entrance, central isthmus, and exit site of the reentry circuit, respectively. Features of entrainment when pacing from different sites are listed in Box 5.2 (see Figs. 5.16, 5.20, and eFig. 5.4).¹⁹

A graphical representation of entrainment mapping can be constructed by plotting the PPI–TCL values on an electroanatomical mapping system (CARTO, Biosense Webster, Diamond Bar, CA, United States; or NavX, St. Jude Medical, St. Paul, MN, United States) to generate color-coded three-dimensional entrainment maps (see Chapter 6 for discussion).^{26,27}

Clinical Implications

1. **CONFIRMATION OF REENTRY AS THE TACHYCARDIA MECHANISM.** Achievement of entrainment of a tachycardia establishes

BOX 5.2 Entrainment Mapping of Reentrant Tachycardias

Pacing From Sites *Outside* the Reentrant Circuit (Remote Bystanders)

- Manifest fusion on surface ECG or intracardiac recordings
- PPI–TCL > 30 ms

Pacing From Sites *Outside* the Reentrant Circuit (Attached Bystanders)

- Concealed fusion
- PPI–TCL > 30 ms
- Stimulus-exit interval $>$ electrogram-exit interval

Pacing From Sites *Inside* the Reentrant Circuit (Outer Loop)

- Manifest fusion on surface ECG or intracardiac recordings
- PPI–TCL < 30 ms

Pacing From a Protected Isthmus *Inside* the Reentrant Circuit

- Concealed fusion
- PPI–TCL < 30 ms
- Stimulus-exit interval = electrogram-exit interval (± 20 ms)

PPI, Postpacing interval; TCL, Tachycardia cycle length.

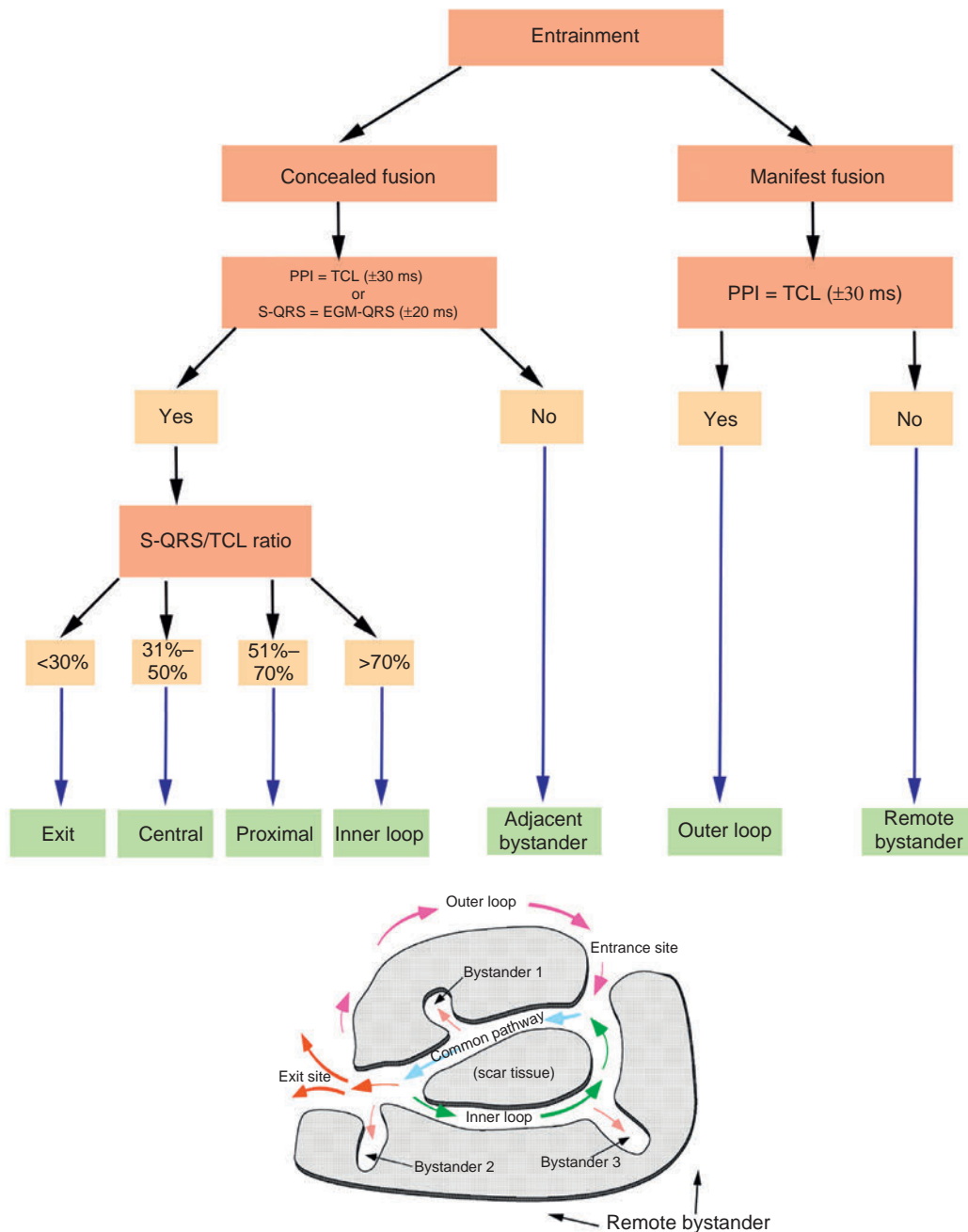


Fig. 5.21 Entrainment Mapping of Macroreentrant Ventricular Tachycardia. Surface electrocardiogram fusion, postpacing interval (*PPI*), and stimulus-QRS interval (*S-QRS*) during entrainment help identify the relation of the pacing site to the reentrant circuit. *EGM*, Electrogram; *TCL*, tachycardia cycle length.

reentry as the mechanism of the tachycardia and excludes triggered activity and abnormal automaticity as potential mechanisms. Furthermore, entrainment with fusion excludes microreentry, and establishes the diagnosis of macroreentry (with spatially separate entrance and exit sites).¹³

2. **APPROXIMATION OF THE LOCATION OF THE REENTRANT CIRCUIT.** Entrainment is commonly used to estimate how far the reentrant circuit is from the pacing site qualitatively. Pacing at multiple sites and measuring the difference between the *PPI* and *TCL* provide an indication of how far or near the pacing site is from the circuit (Fig. 5.22). The smaller the *PPI*–*TCL* value, the closer the pacing site to the reentry circuit. For example, entrainment of an

AT from multiple sites in the RA with a *PPI* significantly longer than the *TCL* can help identify an LA origin of the AT before attempting LA access (see Fig. 13.7).^{19,28}

3. **IDENTIFICATION OF THE CRITICAL ISTHMUS OF THE REENTRANT CIRCUIT.** Entrainment mapping is the gold standard for ablation of reentrant circuits generating hemodynamically well-tolerated tachycardias (macroreentrant VT or AT). Focal ablation of all sites defined as within the reentrant circuit may not result in a cure of reentrant tachycardia. Cure requires ablation (transection) of an isthmus bordered by barriers on either side, which is critical to the reentrant circuit. Entrainment mapping helps identify this critical part of the reentrant circuit to guide ablation. Sites

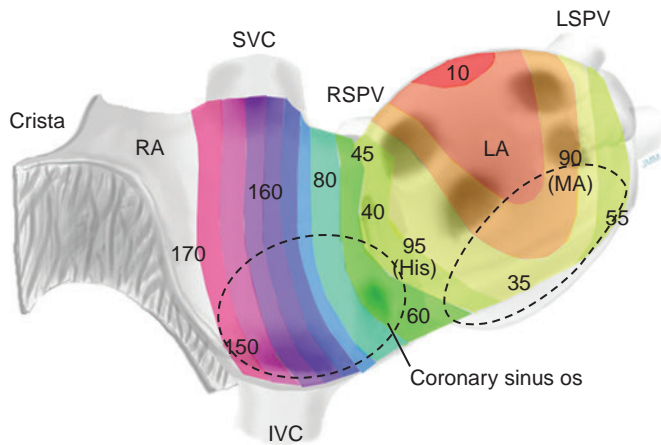


Fig. 5.22 The Postpacing Interval (PPI). PPI-TCL interval as an indicator of distance from the pacing site to the reentrant circuit (located in the dome of the left atrium [LA], near 10). In this representation of both atria viewed from the front, colors indicate isochrones of the difference between PPI and TCL in milliseconds at various pacing sites (indicated by numbers). IVC, Inferior vena cava; LSPV, left superior pulmonary vein; MA, mitral annulus; os, ostium; RA, right atrium; RSPV, right superior pulmonary vein; SVC, superior vena cava; TCL, tachycardia cycle length.

demonstrating entrainment with concealed fusion are initially sought. Once these sites are identified, their relationship to the reentrant circuit is verified using the PPI or stimulus-exit interval (see earlier). Sites demonstrating (1) concealed fusion, (2) PPI equal to the TCL (± 30 milliseconds), and (3) stimulus-exit interval equal to the electrogram-exit interval (± 20 milliseconds) have a very high positive predictive value for successful ablation.¹³

Limitations

One of the limitations of entrainment mapping is the requirement of the presence of sustained, hemodynamically well-tolerated tachycardia of stable morphology and TCL. Furthermore, attempts at entrainment can result in termination, acceleration, or transformation of the index tachycardia into a different one, thus making further mapping challenging. Bipolar pacing at relatively high stimulus strengths used during entrainment can result in the capture of an area larger than the local area, decreasing the specificity of the results.

Errors can be introduced by the decremental conduction properties of the zone of slow conduction that may cause a rate-dependent lengthening of the PPI. This is more likely to occur at rapid pacing rates or when the reentry circuit involves a slow conduction zone with a decremental conduction property such as the AVN.^{21–23}

An erroneously short PPI interval (shorter than the TCL) can result from far-field capture of myocardium tissue distal to the local electrogram recorded at the pacing site or delayed local capture. Therefore the differentiation between near- and far-field responses during pacing is critical to entrainment mapping.

Pacing and recording from the same area are required for entrainment mapping. This requirement is usually satisfied by pacing from electrodes 1 and 3 and recording from electrodes 2 and 4 of the mapping catheter. However, this technique has several limitations:

1. There are differences, albeit slight, of the area from which the second and fourth electrodes record as compared with the first and third. When the local electrogram is not recorded from the same pair of electrodes used for pacing, errors can be introduced when comparing the PPI with the TCL.

2. The bipolar pacing technique has the potential for anodal (proximal electrode) contribution to local capture.
3. The total area captured by the pacing stimulus can exceed the local area from which the electrogram is recorded, especially when high currents (more than 10 mA) are required for stimulation.
4. The pacing artifact can obscure the early part of the captured local electrogram. In such a case, a comparable component of the electrogram can be used to measure the PPI.
5. Far-field electrical signals generated by depolarization of adjacent tissue can cause false-positive entrainment criteria at some sites.¹⁷

As noted, the “number needed to entrain” criterion can overcome some of the disadvantages mentioned above, since it does not require continuation of tachycardia after pacing and is not affected by decremental conduction properties within the reentrant circuit.²⁵

PACE MAPPING

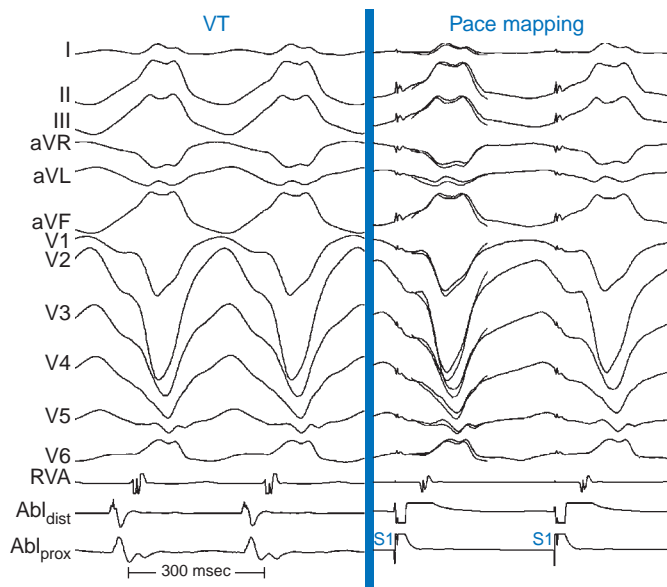
Fundamental Concepts

Pace mapping is a technique designed to help locate tachycardia sources by pacing at different endocardial sites to reproduce the ECG morphology of the tachycardia. Pace mapping is based on the principle that pacing from the site of origin of a focal tachycardia at a PCL similar to the TCL results in the same activation sequence as that during the tachycardia.

When myocardial activation originates from a point-like source, such as during focal tachycardia or during pacing from an electrode catheter, ECG configuration of the resultant tachycardia or paced complex (QRS or P wave) is determined by the sequence of myocardial activation, which is largely determined by the initial site of myocardial depolarization, assuming no conduction abnormalities from that site. Analysis of specific surface ECG configurations in multiple leads allows for the estimation of the pacing site location to within several square centimeters, and comparing the paced complex configuration with that of tachycardia can be used to locate the arrhythmia focus (eFig. 5.5). However, differences in spatial resolution within different cardiac chambers has been demonstrated.²⁹

On the other hand, reentry circuits in healed infarct scars often extend over several square centimeters and can have a variety of configurations. In many circuits, the excitation wavefront circulates through surviving myocytes within the scar, the depolarization of which is not detectable on the standard surface ECG. The QRS complex is then inscribed after the reentry wavefront exits the scar and propagates across the ventricles. At sites at which the reentrant wavefront exits the scar, pace mapping is expected to produce a QRS configuration similar to that of the VT (Fig. 5.23). Pace mapping at sites more proximally located in the isthmus should also produce a similar QRS complex, but with a longer S-QRS interval. The S-QRS interval lengthens progressively as the pacing site is moved along the isthmus, consistent with pacing progressively farther from the exit.

In infarct-related VT, however, a paced QRS configuration different from that during VT does not reliably indicate that the pacing site is distant from the reentry circuit. At many reentry circuit sites, pacing during NSR can produce a QRS configuration different from that during VT. It is rather uncommon to have similar or even almost identical morphology result from pacing from a known isthmus determined by mapping. Several factors can explain this mismatch. First, the pattern of ventricular activation and hence resultant QRS depends on how the wavefront propagates from the exit of the isthmus to the remainder of the heart, which can be totally different during VT than during pacing from the same site during NSR (see Fig. 5.23). In fact, such pacing would be expected to produce a different QRS than the VT because the paced wavefront may spread roughly centrifugally to the heart while



eFig. 5.5 Pace Mapping of Ventricular Tachycardia (VT). At left, 12 electrocardiogram (ECG) leads and intracardiac recordings during idiopathic right ventricular outflow tract VT are shown (cycle length [CL], 280 milliseconds). At right, pace mapping from the site of earliest ventricular activation at CL 350 milliseconds produces an identical 12-lead ECG configuration (the VT complex superimposed on the first paced complex). *Abl_{dist}*, Distal ablation; *Abl_{prox}*, proximal ablation; *RVA*, right ventricular apex.

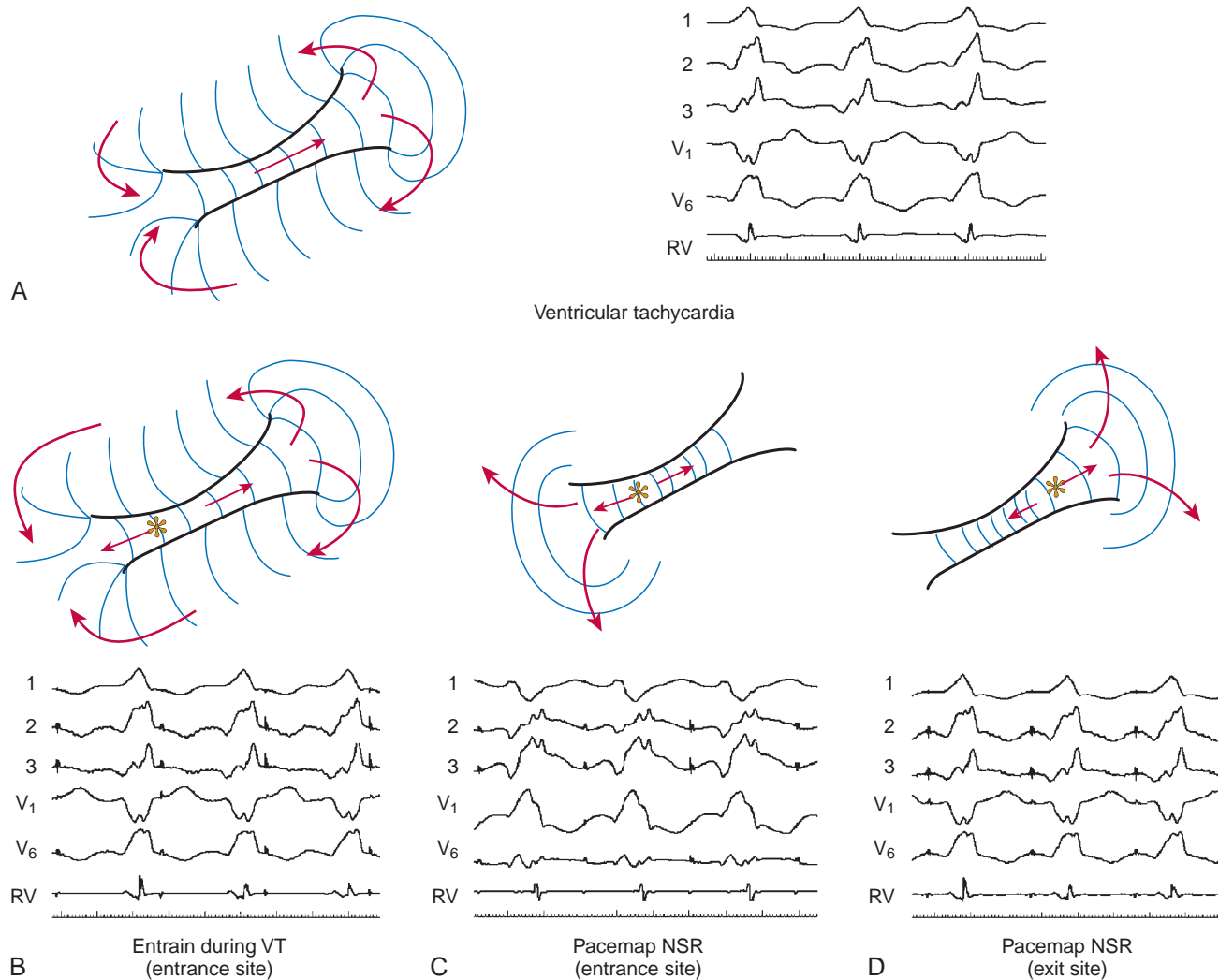


Fig. 5.23 Pacing to Verify Ablation Sites in Reentrant Ventricular Tachycardia (VT). (A) Five electrocardiogram leads of VT are shown with a figure-of-eight circuit with propagation of the reentrant wavefront (arrows); the protected diastolic corridor is also shown (short straight arrow). (B) Pacing is performed during VT from a site near the entrance to the diastolic corridor (asterisk); the impulse must traverse a significant slow conduction zone before exiting to generate a QRS complex, resulting in a long S-QRS as shown. (C) Pacing is performed at the same site as in B, but during sinus rhythm; the impulse exits in the opposite direction from B because it takes less time to propagate in this direction (short S-QRS). The resulting QRS complex is completely different, despite pacing at the same site. (D) Pacing is performed during sinus rhythm from a site closer to the exit of the diastolic corridor. The QRS is the same as VT because the path taken is the same as in VT, and the S-QRS is short. NSR, Normal sinus rhythm; RV, right ventricle.

the VT wavefront spreads in one direction (i.e., orthodromically). This observation is one of the important limitations of the use of pace mapping to identify the critical isthmus of post-MI VT. Propagation in the diseased myocardium is not homogeneous, and small differences in catheter location can cause grossly different propagation wavefronts and resultant QRS complexes. Even small differences in the angle of contact of catheter to the ventricular wall and site of initial ventricular activation can alter the precise QRS configuration. The relationship between conduction time, pacing site location in the isthmus, and conduction block determines whether pace mapping in an isthmus produces a QRS that resembles that of VT. When pace mapping in a defined isthmus is performed, the stimulated wavefront can only follow along its course, which occurs in at least two directions—orthodromic and antidromic (relative to the direction of VT propagation). The wavefront

is only detected on the surface ECG when it leaves this protected channel. If the isthmus is long and the catheter is positioned in the distal part, near the exit, the orthodromic wavefront leaves the exit and rapidly depolarizes the region along the infarct, colliding with and preventing emergence of the antidromic wavefront from the infarct region. The resulting QRS complex is then similar to that of VT. If the isthmus is short, or the catheter is positioned more proximally, the stimulated antidromic wavefront leaves the protected isthmus at the entrance, propagating to the surrounding myocardium and producing a different QRS morphology (see Fig. 5.23). If the orthodromic wavefront reaches the exit, a fusion QRS is produced that includes depolarization from both the antidromic and orthodromic wavefronts.

A second explanation is that the process whereby VT is generated in patients with structural heart disease usually involves the development

of an area of functional block to conduction. Such functional block, by definition, is not fixed and varies in its extent. When formed, it combines with an area of fixed conduction block caused by, for example, the infarct scar, to create a protected channel for conduction that allows reentry to occur. Regions of functional block, present during VT, can define propagation paths during tachycardia but not during pace mapping in NSR. Therefore, if block defining an isthmus is present only during VT and is absent during pace mapping in NSR, the stimulated wavefront produced by pacing at the isthmus site would propagate in all directions, resulting in a different QRS morphology (see Fig. 22.26). This is further exaggerated by the fact that pace mapping is usually performed at rates slower than the VT to avoid VT induction during the mapping process, which can reduce the likelihood of development of a line of functional block. In addition, the area over which the current is delivered, especially where high current is required for relatively inexcitable tissue, can influence the pattern of subsequent ventricular activation, presumably by capturing more distant (far-field) tissue. When this occurs, it can indicate pacing in a region of a protected isthmus, where pacing at low output would capture only the isthmus, whereas pacing at a higher output can capture both the isthmus and far-field tissue, resulting in different QRS morphologies and S-QRS intervals (see Fig. 22.27). Finally, some circuits can have more than one exit, with wavefronts emerging from the scar at multiple locations. Different exits can participate preferentially during VT but not during pace mapping, and vice versa.

On the other hand, pacing during NSR from sites attached to the reentrant circuit but not part of the circuit can occasionally produce QRS morphology identical to that of the VT, because the stimulated wavefront can be physiologically forced to follow the same route of activation as the VT as long as pacing is carried out between the entrance and exit of the protected isthmus. Although this strategy can result in

the identification of irrelevant nondominant inner loop and adjacent bystander sites as well as the desired isthmus sites, it still can be helpful in gross identification of the region of the VT circuit.

Conduction away from the pacing site (and the resultant QRS morphology) potentially can be influenced by the pacing output, pacing rate, and antiarrhythmic drugs. To minimize the impact of rate-related changes in conduction, pacing is performed at a relatively slow rate. Pacing slower than the rate of the VT, however, can further reduce the relationship of the paced QRS morphology to that of the VT target area. During bipolar pacing, capture at the proximal electrode (anode) rather than uniquely at the distal electrode can also modify the QRS morphology. Further, the sequence of ventricular activation can vary during pacing at different stimulus strengths. This phenomenon is more pronounced with bipolar than unipolar pacing, likely because of anodal capture at higher stimulus strengths (see Fig. 22.25). This potential problem can be avoided by using unipolar pacing and by limiting the current output to 10 mA and 2 milliseconds, which is within the range of routine programmed stimulation.

The same principles used in pace mapping in VT apply to AT, but in this case, matching of a paced intracardiac activation sequence with that of tachycardia is used. This is because while the P wave can be difficult to discern on the ECG, it is possible to have a large number of electrode recordings representing much of the atrial mass, with which to compare paced versus tachycardia activation sequences.

Pace Map Matching

The greater the degree of concordance between the morphology during pacing and that during tachycardia, the closer the catheter will be to the site of origin of the tachycardia. Pace maps with identical or nearly identical matches of the tachycardia morphology in all 12 surface ECG leads can be indicative of the site of origin of the tachycardia (Fig. 5.24).

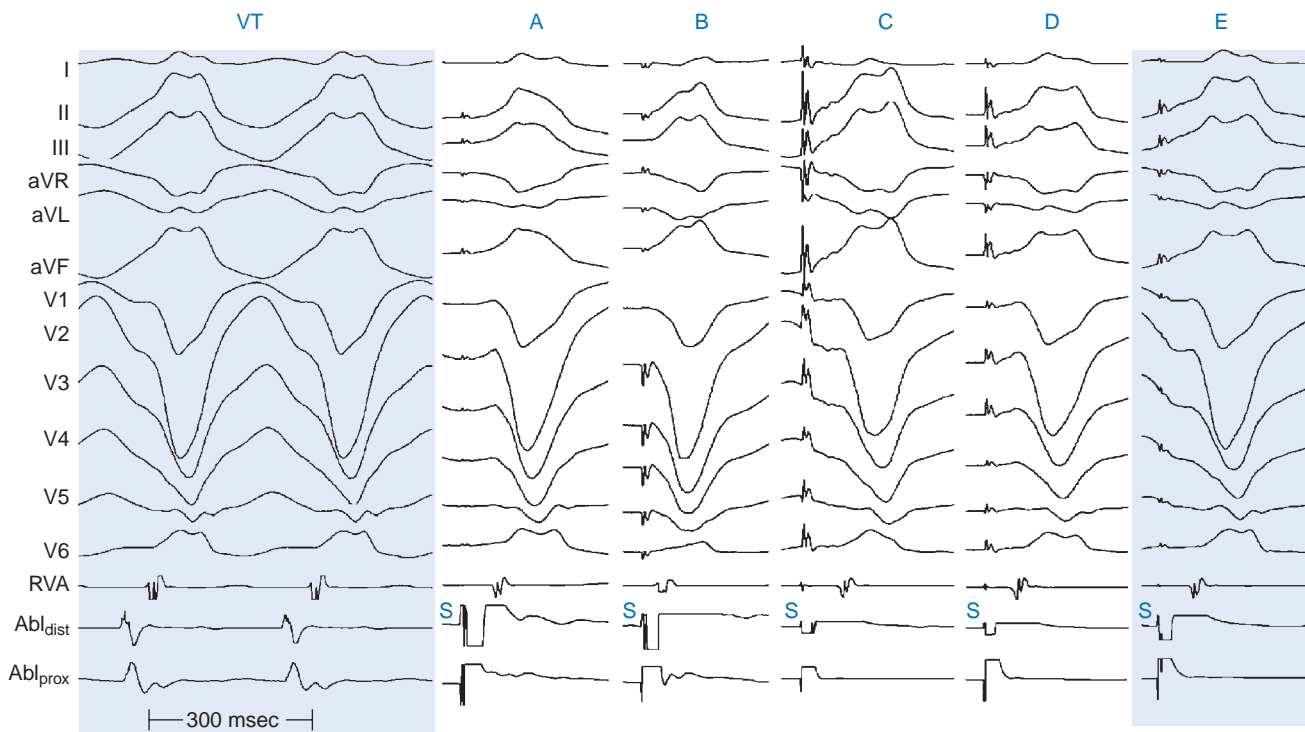


Fig. 5.24 Pace Mapping of Right Ventricular Outflow Tract Tachycardia. Pace mapping at various sites in the right ventricular outflow tract produces QRS configurations (A to D) with less or more similarity to the ventricular tachycardia (VT) QRS (left panel); E shows an exact match. *Abl_{dist}*, Distal ablation; *Abl_{prox}*, proximal ablation; *RVA*, right ventricular apex.

Differences in the morphology between pacing and spontaneous tachycardia in a single lead can be critical. For VT, pacing at a site 5 mm from the index pacing site results in minor differences in QRS configuration (e.g., notching, new small component, change in amplitude of individual component, or overall change in QRS shape) in at least one lead in most patients. In contrast, if only major changes in QRS morphology are considered, pacing sites separated by as much as 15 mm can produce similar QRS morphologies.

Although qualitative comparison of the 12-lead ECG morphology between a pace map and VT is frequently performed, there are few objective criteria for quantifying the similarity between two 12-lead ECG waveform morphologies. Such comparisons are frequently completely subjective or semiquantitative, such as a “10/12 lead match.” Discrepancies in VT ablation outcome can result, in part, from subjective differences in opinion regarding the closeness of a pace map match to the clinical VT. In addition, a common human error in analyzing a pace map is not appreciating subtle amplitude or precordial lead transition differences between two ECG patterns.

To overcome these limitations, two mathematical waveform comparison metrics, the correlation coefficient (CORR) and the mean absolute deviation (MAD), have been developed to quantify the similarity of 12-lead ECG waveforms during VT/PVC and pace mapping objectively.

It has been suggested that an automated objective interpretation can have some advantage to qualitative interpretation. Although CORR is more commonly used, MAD is more sensitive to differences in waveform amplitude. The MAD score grades 12-lead ECG waveform similarity as a single number ranging from 0% (identical) to 100% (completely different). A MAD score of up to 12% was 93% sensitive and 75% specific for a successful ablation site (eFig. 5.6). It is not surprising that the MAD score is more sensitive than specific; characteristics other than a 12-lead ECG match are necessary for successful ablation, including catheter-tissue contact, catheter orientation, and tissue heating.

More recently, an automated waveform comparison algorithm using CORR has been implemented in the Boston Scientific LabSystem PRO EP recording system (Boston, MA, United States) (Fig. 5.25). A template matching software is also currently available and integrated into the CARTO 3-D mapping systems (PaSo, Biosense Webster) (Fig. 5.26). These automated algorithms process digital images to match the target QRS complex (template signal) and the paced QRS complex (test signal), and they provide a score according to the similarity between the two QRS morphologies. The software “slides” the reference over the incoming data until the best local match is found by using a correlation calculation. For each lead-to-lead comparison, both the polarity and

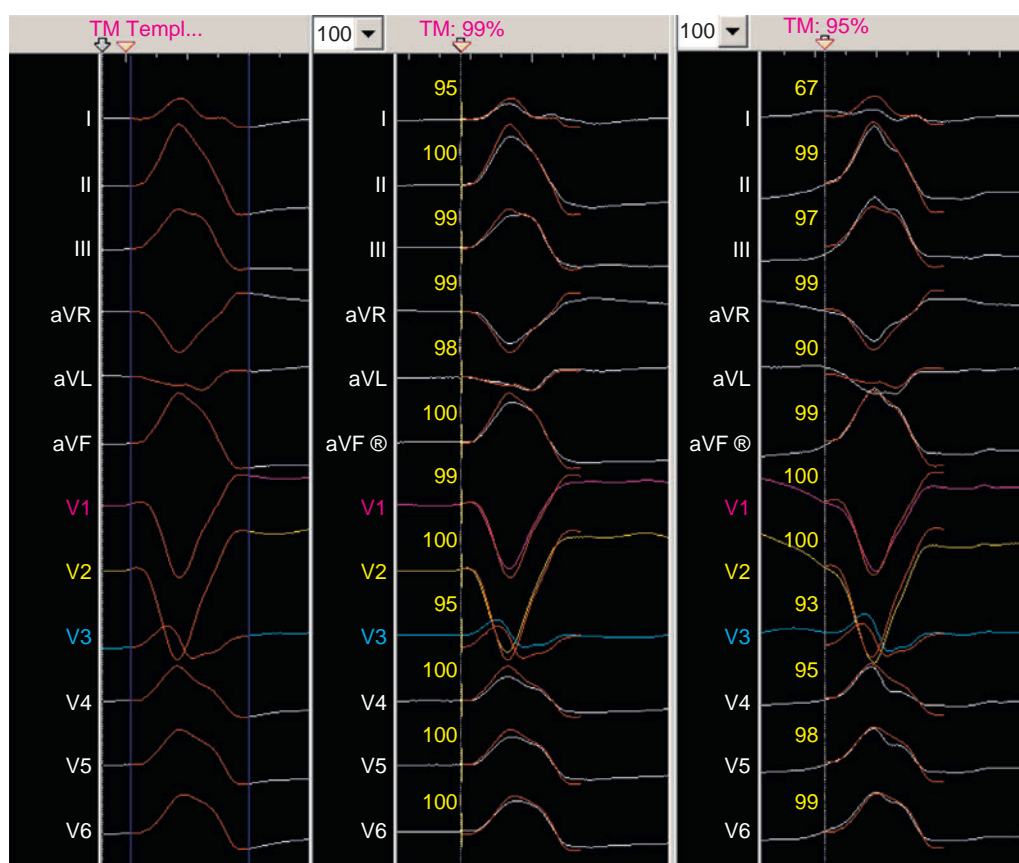
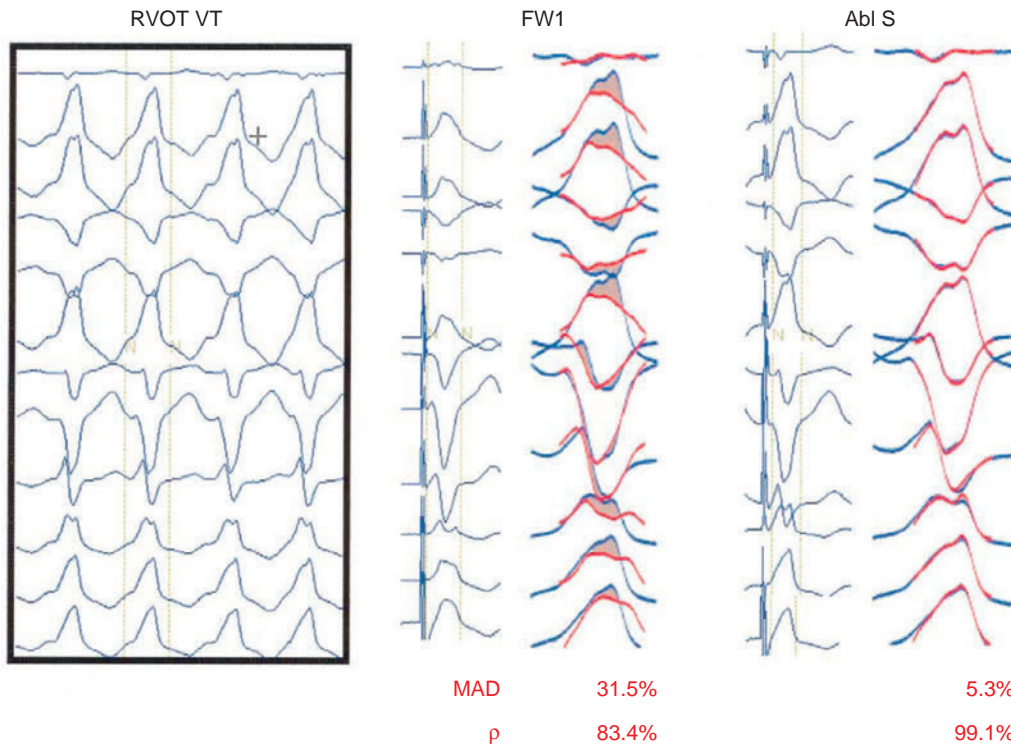


Fig. 5.25 Automated Pace Map Matching. Pace mapping using an automated waveform comparison algorithm implemented in the Boston Scientific LabSystem PRO EP recording system (Boston, MA, United States). *Left*, Surface 12-lead electrocardiogram (ECG) QRS morphology of the spontaneous premature ventricular complex (PVC) is saved as a template. *Middle*, A score is calculated (yellow numbers) according to QRS morphology similarity between the template PVC morphology (red) and the paced QRS morphology (white) in each surface ECG lead, and is averaged at 99%, indicating an almost perfect pace match. *Right*, Pace match is averaged at 95%, with the largest discrepancy occurring in lead I (QRS similarity of only 67%).



eFig. 5.6 The Mean Absolute Deviation (MAD) Score. (A) Example of right ventricular outflow tract (RVOT) ventricular tachycardia (VT). The second VT complex has been identified as the target waveform by the annotation markers placed on either side of this complex. (B) Pace map from a free wall site 1 (FW1) next to the superimposed VT and pace map waveforms after automatic computer alignment. There are substantial differences between these two waveforms (highlighted in gray), resulting in an MAD score of 31.5%. (C) Pace map from the successful ablation site (Abl S) near the posterior septum and the superimposed pace map and VT waveform. Note in the Abl S panel that when these two waveforms are aligned they are nearly superimposable, and result in a very low MAD score of 5.3%. Correlation coefficients for these comparisons are also shown. (From Gerstenfeld EP, Dixit S, Callans DJ, et al. Quantitative comparison of spontaneous and paced 12-lead electrocardiogram during right ventricular outflow tract ventricular tachycardia. *J Am Coll Cardiol.* 2003;41:2046.)

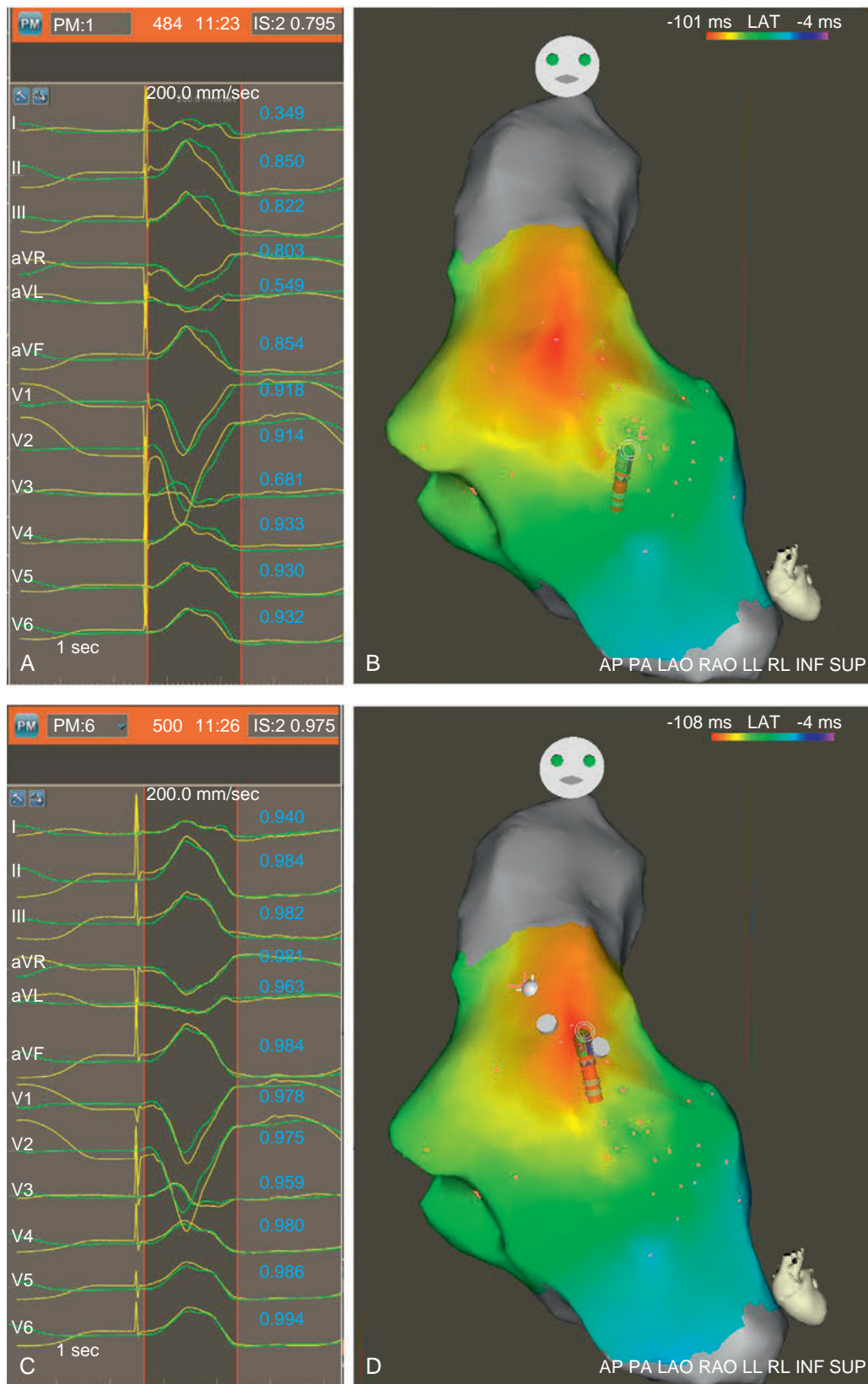


Fig. 5.26 Automated Pace Mapping Integrated Into the Electroanatomical Mapping System. *Left panels* (A and C), The template matching software integrated into the CARTO-3 mapping systems (PaSo, Biosense Webster, Diamond Bar, CA, United States) processes digital images to match the premature ventricular complex (PVC) QRS complex (green) and the paced QRS complex (yellow), and provides a score between 0 and 1 (blue numbers) according to the similarity between the two QRS morphologies. *Right panels* (B and D), CARTO electroanatomical activation map (color-coded) of the focus of the PVCs in the right ventricular outflow tract (anterior view). *Upper panels* (A and B), Pacing performed from the tip of the ablation catheter (visualized on the activation map) about 18 mm away from the site of earliest local activation (red on the activation map) produced a paced QRS morphology with an 80% pace match. *Lower panels* (C and D), Pacing closer to the site of earliest local activation resulted in a higher degree of degree of correlation (98%).

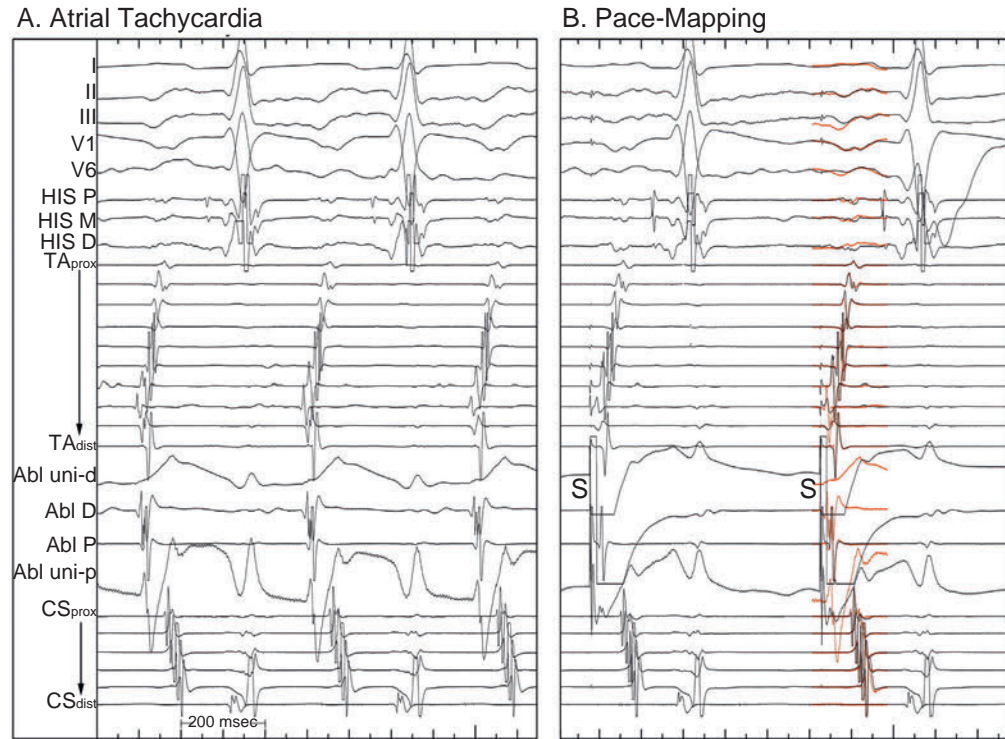


Fig. 5.27 Pace Map Matching in Focal Atrial Tachycardia. (A) Intracardiac activation sequence during a focal inferolateral right atrial tachycardia. (B) Pacing at the site with the earliest local activation time shows a nearly exact match with tachycardia (superimposed in red) in intracardiac recordings. P wave matching is more problematic. *Abl D*, Distal ablation; *Abl P*, proximal ablation; *Abl uni*, unipolar ablation; *CS_{dist}*, distal coronary sinus; *CS_{prox}*, proximal coronary sinus; *HIS D*, distal His bundle; *HIS M*, middle His bundle; *HIS P*, proximal His bundle; *TA_{dist}*, distal tricuspid annulus; *TA_{prox}*, proximal tricuspid annulus.

the amplitude of the QRS complexes play an important role as to the resulting value of the percentage of correlation calculated by the software. The site that yields the highest average correlation (value toward 99% to 100%) across all of ECG leads means a perfect match between two 12-lead ECG morphologies. Generally, an average template-matching score above 90% is considered sensitive for the identification of successful versus unsuccessful ablation sites. The Boston Scientific LabSystem PRO also has an algorithm for matching intracardiac activation sequences, but its performance does not seem as good as the QRS matching algorithm (Fig. 5.27).^{30–32}

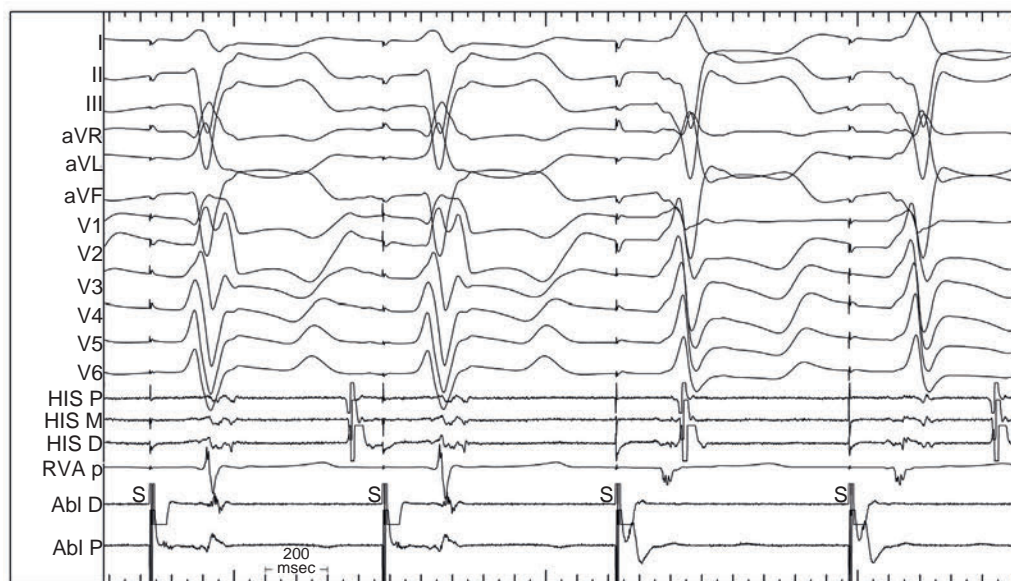
Stimulus–QRS Interval During Pace Mapping

Ventricular pacing in normal myocardium is associated with an S–QRS interval shorter than 20 milliseconds. On the other hand, an S–QRS interval longer than 40 milliseconds is consistent with slow conduction from the pacing site and is typically associated with abnormal fractionated electrograms recorded from that site during sinus rhythm. Thus pace mapping can provide a measure of slow conduction, as indicated by the S–QRS interval. It is likely that pacing sites with long S–QRS delays are in an isthmus adjacent to regions of conduction block. However, this isthmus can be part of the reentrant circuit or a bystander.

For post-MI VTs, at sites at which the reentrant wavefront exits the scar, pace mapping is expected to produce a QRS configuration similar to that of the VT. Pace mapping at sites located more proximally in the isthmus should also produce a similar QRS complex, but with a longer S–QRS interval. The S–QRS interval lengthens progressively as the pacing

site is moved along the isthmus, a finding consistent with pacing progressively farther from the exit. Therefore parts of VT reentry circuit isthmuses can be traced during NSR by combining both the QRS morphology and the S–QRS delay from pace mapping in anatomical maps. This works well when pacing is performed during tachycardia, at which time wavefront propagation is constrained in one direction through a corridor bounded by barriers that can be anatomically or functionally determined. However, pace mapping at the same sites during sinus rhythm can yield different results because the barriers may not exist then, and the preferential direction of propagation may not be the same as during tachycardia. This is especially true for pacing at circuit entrance sites (see Fig. 5.23).

When pacing during sinus rhythm at sites within a protected isthmus area, as the electrode is moved more proximally (relative to the direction of propagation during VT), the paced QRS complex matches that of VT but the S–QRS interval progressively increases. As the pacing site continues to move, when there is an abrupt change in QRS configuration, the site at which this occurs has been correlated with an attractive ablation site, indicating that the pacing site is now closer to another outlet from the isthmus (the entrance) than it is to the exit. A corollary of this is the so-called multiple exit site phenomenon, in which continued pacing from one location (at the same or varied outputs) yields two or more QRS morphologies (eFig. 5.7). Ablation at such sites may eliminate multiple VT morphologies that use the same isthmus, but with either different exit sites or different directions of propagation in the isthmus.



eFig. 5.7 Pacing at One Site Within Scar Yields Different QRS Configurations. Stimulation at the same site throughout the figure shows different QRS configurations, with a similar delay from stimulus to QRS onset. *Abl D*, Distal ablation; *Abl P*, proximal ablation; *HIS D*, distal His bundle; *HIS M*, middle His bundle; *HIS P*, proximal His bundle; *RVA p*, right ventricular apex.

Mapping Procedure

Initially the exact morphology of the tachycardia complex should be determined and used as a template for pace mapping. For VT, QRS morphology during the tachycardia should be inspected in all 12 surface ECG leads. For AT, determining the morphology of the P wave during the tachycardia can be challenging, and proper interpretation of discrete changes in P wave shape is limited by its low voltage and distortion or masking by the superimposed ST segment and T wave. Therefore the P wave during AT should be assessed using multiple ECG leads in addition to the intracardiac electrogram activation sequence. Delivery of a VES (or a train of ventricular pacing) to advance ventricular activation and repolarization can allow careful distinction of the P wave onset and morphology. Paced activation sequence mapping can be used as an alternative to P-wave morphology, but requires the use of multiple electrodes (e.g., Halo and CS catheters) to assess atrial activation sequence.

Pace mapping during tachycardia (at a PCL 20 to 40 milliseconds shorter than the TCL) is preferable whenever possible, because it facilitates rapid comparison of tachycardia and paced complexes at the end of the pacing train in a simultaneously displayed 12-lead ECG. If only nonsustained tachycardia or ectopic beats are inducible, pacing is performed during NSR. In this setting, the PCL and coupling intervals of the extrastimuli should match those of spontaneous ectopy. This seems to be more relevant for ventricular arrhythmias. For ATs, pacing at exactly the TCL does not seem as critical to reproduce a similar atrial sequence.

Pace mapping is preferably performed with unipolar stimuli (≤ 10 mA, 2 milliseconds) from the distal electrode of the mapping catheter (cathode) and an electrode in the inferior vena cava (anode), or with closely spaced bipolar pacing at twice diastolic threshold to eliminate far-field stimulation effects.

The resulting 12-lead ECG morphology is compared with that of the tachycardia. ECG recordings should be reviewed at the same gain and filter settings, and at a paper-sweep speed of 100 mm/sec. It is often helpful to display all 12 ECG leads side by side in review windows on screen, as well as a printout of regular 12-lead ECGs for side-by-side comparison on paper. The greater the degree of concordance between the morphology during pacing and tachycardia, the closer the catheter will be to the site of origin of the tachycardia. Exact concordance occurring in 12 of 12 leads on the surface ECG is predictive of the site of origin of the tachycardia. Also, automated waveform comparison algorithms offer a significant advantage for template matching during pace mapping.³³

For mapping macroreentrant VT circuits, it is important to evaluate the S-QRS interval, the interval from the pacing stimulus to the onset of the earliest QRS on the 12-lead ECG. The reentry circuit exit, which is more likely to be at the border of the infarct and close to the normal myocardium, often has a short S-QRS interval during pace mapping during NSR, even though it is a desirable target for ablation. A delay between the pacing stimulus and QRS onset is consistent with slow conduction away from the pacing site; this can indicate a greater likelihood that the pacing site is in a reentry circuit. This method can be useful for initially screening sites during NSR.

Clinical Implications

Pace mapping is used as an adjunct to other methods of mapping to corroborate putative ablation sites. It can be of great help, especially when the tachycardia is difficult to induce. Although there are some limitations to this technique, many studies have demonstrated efficacy using pace mapping to choose ablation target sites. The highest benefit of pace mapping has been found in focal tachycardias, especially in idiopathic VT. Pace mapping of focal ATs is more limited due to

difficulties in precisely comparing P wave morphologies, and intracardiac activation sequences limit the applicability of pace mapping.

For macroreentrant VT, pace mapping remains at best a corroborative method of localizing the isthmus critical to the reentrant circuit. It can be used to focus initial mapping efforts to regions likely to contain the reentrant circuit exit or abnormal conduction, but it is sufficiently specific or sensitive to be the sole guide for ablation. Pace mapping can also be used in conjunction with substrate mapping when other mapping techniques are not feasible. Pace mapping has advantages over activation mapping in that induction of VT is not required; thus it allows for the identification of the site of origin when the induced VT is poorly tolerated or when VT is not inducible by EP techniques but the QRS morphology from a prior 12-lead ECG during VT is available.

Limitations

An optimal spatial pace mapping resolution requires a short maximum distance between two points generating a similar ECG configuration. Usually the spatial resolution is best for unipolar stimulation, and deteriorates with large electrodes, bipolar stimulation, and pacing at pathological areas. Spatial resolution worsens with bipolar stimulation by inducing electrical capture at both electrodes with variable contribution of the proximal electrode (anode) to depolarization. Such changes in paced ECG morphology that are potentially induced by bipolar pacing can be minimized by low pacing outputs and a small interelectrode distance (5 mm or less). Importantly, the rapid electrical propagation within the right ventricular outflow tract (RVOT) limits the spatial resolution of pace mapping. In one report, the spatial resolution of a good pace map for targeting RVOT VT was about 1.8 cm² and was inferior to that of an activation map for locating the exact site of origin at which ablation would eradicate the arrhythmia.³⁴


Current strengths up to 10 mA have little effect on unipolar paced ECG configuration. In contrast, bipolar pacing can introduce some variability in the paced ECG; a significantly large amount of local myocardium is captured, which, combined with varying degrees of anodal capture, can be detrimental to mapping accuracy.

It is important to understand that the morphology of single paced complexes can vary, depending on the coupling interval, and the paced complex morphology during overdrive pacing is affected by the PCL. Therefore the coupling interval or TCL of the template arrhythmia should be matched during pace mapping, especially during mapping of isolated PVCs. In this case, a single VES at a coupling interval matching that of the PVC can provide a more accurate match than fixed-rate pacing at the same site (Fig. 5.28). Also, spontaneous couplets from the same focus can have slight variations in QRS morphology that must be considered when seeking a pace match.

Pace mapping during post-MI VT has several other limitations. Some areas of conduction block are not anatomically determined but can be functional. Therefore pacing within the diastolic corridor of the VT circuit during NSR can generate a completely different QRS complex from that of the VT (see Fig. 5.24). Consequently, during pace mapping, a QRS configuration different from VT does not reliably indicate that the pacing site is distant from the reentry circuit. On the other hand, pacing during NSR from sites attached to the reentrant circuit but not part of the circuit can occasionally produce a QRS morphology identical to that of the VT. At best, a pace map that matches the VT would identify only the exit site to the normal myocardium, and this site can be distant from the critical sites of the circuit required for ablation.

VIDEOS

The following video accompanies this chapter:

See Video 3.1. Reentrant Ventricular Tachycardia: Optical Mapping. 

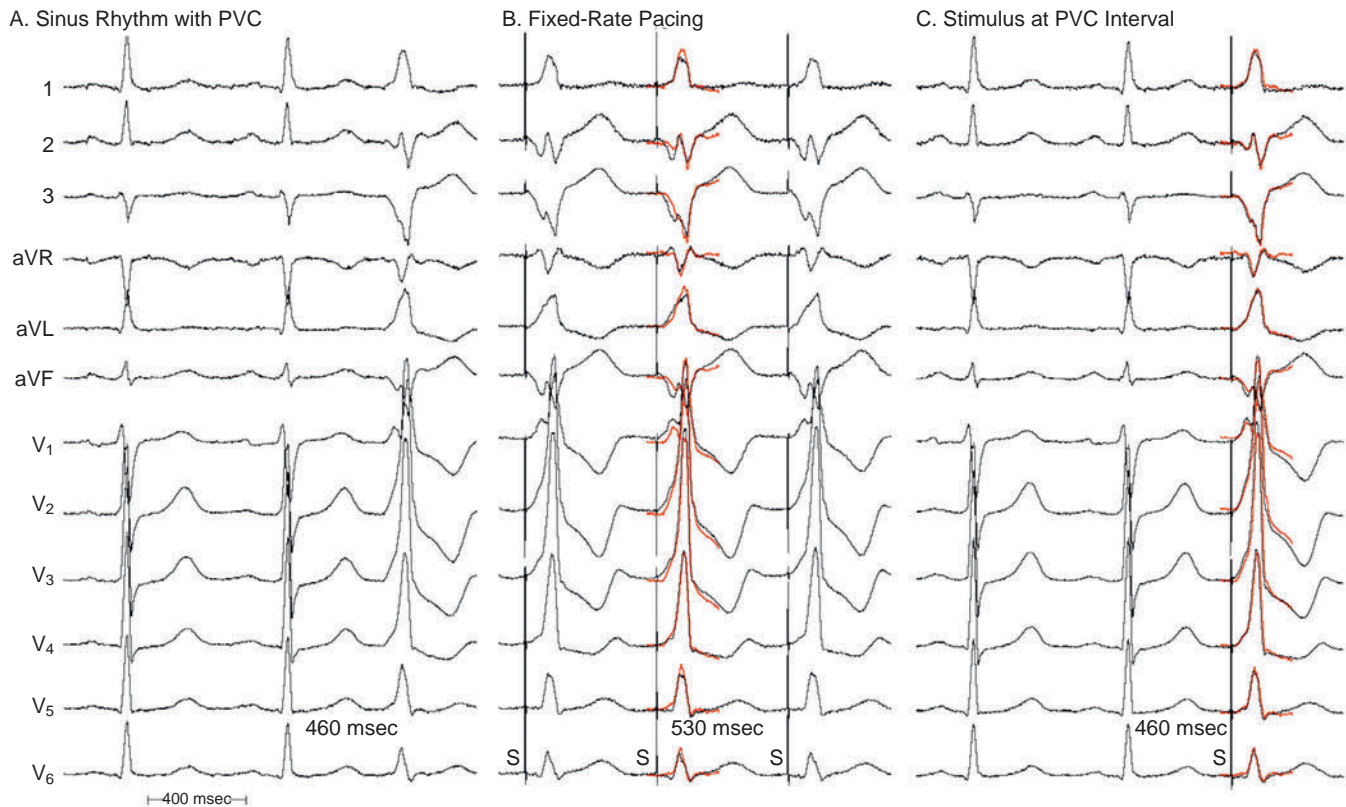


Fig. 5.28 Use of Ventricular Extrastimuli (VES) as Opposed to Fixed-Rate Pacing When Matching Morphology of a Premature Ventricular Complex (PVC). (A) The target PVC is shown that has a coupling interval from the prior QRS 460 milliseconds. (B) Fixed-rate pacing is performed at a site of presystolic activation; the match with the PVC (superimposed in red) is good but not perfect. (C) A single VES delivered at the same site with the same coupling interval as the PVC yields a much better match with the PVC.

REFERENCES

- Stevenson WG, Soejima K. Recording techniques for clinical electrophysiology. *J Cardiovasc Electrophysiol.* 2005;16:1017–1022.
- Jadidi AS, Lehrmann H, Weber R, et al. Optimizing signal acquisition and recording in an electrophysiology laboratory. *Card Electrophysiol Clin.* 2013;5:137–142.
- El Haddad M, et al. Novel algorithmic methods in mapping of atrial and ventricular tachycardia. *Circ Arrhythmia Electrophysiol.* 2014;7:463–472.
- Cantwell CD, et al. Techniques for automated local activation time annotation and conduction velocity estimation in cardiac mapping. *Comput Biol Med.* 2015;65:229–242.
- Venkatachalam KL, Herbrandson JE, Asirvatham SJ. Signals and signal processing for the electrophysiologist: part I: electrogram acquisition. *Circ Arrhythmia Electrophysiol.* 2011;4:965–973.
- Sorgente A, et al. Negative concordance pattern in bipolar and unipolar recordings: an additional mapping criterion to localize the site of origin of focal ventricular arrhythmias. *Heart Rhythm.* 2016;13:519–526.
- Tedrow UB, Stevenson WG. Recording and interpreting unipolar electrograms to guide catheter ablation. *Heart Rhythm.* 2011;8:791–796.
- van der Does LJME, de Groot NMS. Inhomogeneity and complexity in defining fractionated electrograms. *Heart Rhythm.* 2017;14:616–624.
- Pisani CF, Lara S, Scanavacca M. Epicardial ablation for cardiac arrhythmias: techniques, indications and results. *Curr Opin Cardiol.* 2014;29:59–67.
- Wong MCG, et al. Left septal atrial tachycardias: electrocardiographic and electrophysiologic characterization of a paraseptal focus. *J Cardiovasc Electrophysiol.* 2013;24:413–418.
- Asirvatham SJ, Stevenson WG. Electrocardiogram mapping-reentry final frontier. *Circ Arrhythmia Electrophysiol.* 2014;7:760–761.
- Asirvatham SJ, Stevenson WG. Reentry, pseudo-reentry, and pseudo-pseudo-reentry. *Circ Arrhythmia Electrophysiol.* 2014;7:557–558.
- Josephson ME, Almendral J, Callans DJ. Resetting and entrainment of reentrant ventricular tachycardia associated with myocardial infarction. *Heart Rhythm.* 2014;11:1239–1249.
- Almendral J, Caulier-Cisterna R, Rojo-Álvarez JL. Resetting and entrainment of reentrant arrhythmias: part I: concepts, recognition, and protocol for evaluation: surface ECG versus intracardiac recordings. *Pacing Clin Electrophysiol.* 2013;36:508–532.
- Kaiser DW, et al. The precise timing of tachycardia entrainment is determined by the postpacing interval, the tachycardia cycle length, and the pacing rate: theoretical insights and practical applications. *Heart Rhythm.* 2016;13:695–703.
- Tung R. Challenges and pitfalls of entrainment mapping of ventricular tachycardia. *Circ Arrhythmia Electrophysiol.* 2017;10:e004560.
- Almendral J. Resetting and entrainment of reentrant arrhythmias: part II: informative content and practical use of these responses. *Pacing Clin Electrophysiol.* 2013;36:641–661.
- Benito B, Josephson ME. Ventricular tachycardia in coronary artery disease. *Rev Esp Cardiol (Engl Ed).* 2012;65:939–955.
- Deo R, Berger R. The clinical utility of entrainment pacing. *J Cardiovasc Electrophysiol.* 2009;20:466–470.
- Derejko P, Podziemski P, Zebrowski JJ, et al. Effect of the restitution properties of cardiac tissue on the repeatability of entrainment mapping response. *Circ Arrhythmia Electrophysiol.* 2014;7:497–504.
- Vollmann D, et al. Misleading long post-pacing interval after entrainment of typical atrial flutter from the cavotricuspid isthmus. *J Am Coll Cardiol.* 2012;59:819–824.

22. Wong KCK, Rajappan K, Bashir Y, et al. Entrainment with long postpacing intervals from within the flutter circuit: what is the mechanism? *Circ Arrhythm Electrophysiol.* 2012;5:e90–e92.
23. Kinjo T, et al. Long postpacing interval after entrainment of tachycardia including a slow conduction zone within the circuit. *J Cardiovasc Electrophysiol.* 2016;27:923–929.
24. Asirvatham SJ, Stevenson WG. Mapping reentry. *Circ Arrhythmia Electrophysiol.* 2016;9:e003609.
25. Maruyama M, et al. Number needed to entrain: a new criterion for entrainment mapping in patients with intra-atrial reentrant tachycardia. *Circ Arrhythmia Electrophysiol.* 2014;7:490–496.
26. Esato M, et al. Color-coded three-dimensional entrainment mapping for analysis and treatment of atrial macroreentrant tachycardia. *Heart Rhythm.* 2009;6:349–358.
27. Santucci PA, et al. Electroanatomic mapping of postpacing intervals clarifies the complete active circuit and variants in atrial flutter. *Heart Rhythm.* 2009;6:1586–1595.
28. Miyazaki H, Stevenson WG, Stephenson K, et al. Entrainment mapping for rapid distinction of left and right atrial tachycardias. *Heart Rhythm.* 2006;3:516–523.
29. Li A, et al. Relationship between distance and change in surface ECG morphology during pacemapping as a guide to ablation of ventricular arrhythmias implications for the spatial resolution of pacemapping. *Circ Arrhythm Electrophysiol.* 2017;10:e004447.
30. Lüker J, et al. Automated template matching correlates with earliest activation during mapping of idiopathic premature ventricular contractions. *IJC Heart Vessel.* 2014;4:25–29.
31. Luther V, Qureshi N, Kanagaratnam P, et al. Automated activation and pace-mapping to guide ablation within the outflow tract. *J Cardiovasc Electrophysiol.* 2016;27:127–128.
32. Kuteszko R, et al. Utility of automated template matching for the interpretation of pace mapping in patients ablated due to outflow tract ventricular arrhythmias. *Europace.* 2015;17:1428–1434.
33. Hutchinson MD, Garcia FC. An organized approach to the localization, mapping, and ablation of outflow tract ventricular arrhythmias. *J Cardiovasc Electrophysiol.* 2013;24:1189–1197.
34. Zhang F, et al. Noncontact mapping to guide ablation of right ventricular outflow tract arrhythmias. *Heart Rhythm.* 2013;10:1895–1902.

Advanced Mapping and Navigation Modalities

OUTLINE

Electroanatomic Mapping, 156

- Fundamental Concepts, 156
- Electroanatomic Activation Mapping, 161
- Electroanatomic Voltage Mapping, 169
- High-Resolution Electroanatomic Mapping, 171
- Ripple Mapping, 172
- Anatomical Mapping, 172
- Clinical Implications, 174
- Choice of Electroanatomic Mapping System, 175

EnSite Noncontact Mapping System, 176

- Fundamental Concepts, 176
- Technology Application, 177
- Clinical Implications, 180
- Limitations, 180

Basket Catheter Mapping, 180

- Fundamental Concepts, 180
- Technology Application, 181
- Clinical Implications, 181
- Limitations, 181

Focal Impulse and Rotor Mapping, 182

- Technology Application, 182
- Clinical Implications, 182
- Limitations, 182

Stereotaxis Magnetic Navigation System, 183

- Fundamental Concepts, 183
- Technology Application, 184
- Clinical Implications, 185
- Limitations, 185

Sensei Robotic Navigation System, 186

- Fundamental Concepts, 186
- Technology Application, 186

- Clinical Implications, 186

- Limitations, 187

Mediguide Navigation System, 187

- Fundamental Concepts, 187
- Technology Application, 187
- Clinical Implications, 188
- Limitations, 188

Body Surface Potential Mapping, 188

- Fundamental Concepts, 188
- Clinical Implications, 190
- Limitations, 190

Electrocardiographic Mapping, 190

- Fundamental Concepts, 190
- Technology Application, 191
- Clinical Implications, 192
- Limitations, 193

Intracardiac Echocardiography, 193

- Catheter Design, 193
- Imaging Technique, 193
- Clinical Implications, 195

Computed Tomography and Magnetic Resonance Imaging, 197

- Fundamental Concepts, 197
- Image Integration Technique, 198
- Clinical Implications, 199
- Limitations, 201

Three-Dimensional Rotational Angiography, 202

- Fundamental Concepts, 202
- Imaging Technique, 202
- Clinical Implications, 203
- Limitations, 203

Conventional radiofrequency (RF) ablation has revolutionized the treatment of many supraventricular as well as ventricular arrhythmias. Success in stable arrhythmias with predictable anatomical locations or characteristics identifying endocardial electrograms, such as idiopathic ventricular tachycardia (VT), atrioventricular nodal reentrant tachycardia (AVNRT), atrioventricular reentrant tachycardia (AVRT), or typical atrial flutter (AFL), has approached 90% to 99%. However, as interest has turned to a broad array of more complex arrhythmias, including some atrial tachycardias (ATs), many forms of intraatrial reentry, most VTs, and atrial fibrillation (AF), ablation of such arrhythmias continues to pose a major challenge. This stems in part from the limitations of fluoroscopy and conventional catheter-based mapping techniques to localize arrhythmogenic substrates that are removed from fluoroscopic landmarks and the lack of characteristic electrographic patterns for ablation targets.

The use of fluoroscopy for these purposes can be problematic for several reasons: (1) intracardiac electrograms cannot be associated accurately with their precise location within the heart; (2) the endocardial surface is invisible using fluoroscopy, and target sites may be approximated only by their relationship with nearby structures, such as ribs, blood vessels, and the position of other catheters; (3) fluoroscopy-guided catheter navigation is not exact, is time-consuming, and requires multiple views to estimate the three-dimensional (3-D) location of the catheter; (4) the catheter cannot accurately and precisely be returned to a previously mapped site; and (5) the patient and medical team are exposed to radiation.

Newer mapping systems have transformed the clinical electrophysiology (EP) laboratory, have enabled physicians to overcome some of the limitations of conventional mapping, and have offered new insights into arrhythmia mechanisms. These systems are aimed at improving

mapping resolution, 3-D spatial localization, and rapidity of acquisition of cardiac activation maps. The application of these various techniques for mapping specific arrhythmias is described elsewhere in this text, as are the details of the diagnosis, mapping, and treatment of specific arrhythmias.

However, to date, the integration of anatomical, EP, and software information by an experienced physician is an indispensable prerequisite to accomplish a safe and successful procedure. At most, such systems must be used as an adjunctive tool to facilitate mapping and ablation. The operator should understand the advantages and shortcomings of each system, and should recognize that these systems can be misleading and confusing, providing inaccurate information as a result of either incorrect data acquisition or inherent limitations of the technology.¹

ELECTROANATOMIC MAPPING

Electroanatomic mapping systems use novel approaches to determine the 3-D location of the mapping catheter accurately, while local electrograms are acquired using conventional methods. Recorded data of the catheter location and associated intracardiac electrogram at that location are used to reconstruct in real time a representation of the 3-D geometry of the cardiac chamber, color-coded with relevant EP information (local activation time and electrogram amplitude), as well as purely anatomical chamber mapping.

At the present time, three electroanatomic mapping systems are in clinical use: (1) CARTO (Biosense Webster, Diamond Bar, CA, United States); (2) EnSite NavX (St. Jude Medical, St. Paul, MN, United States); and (3) Rhythmia (Boston Scientific, Cambridge, MA, United States). These systems use electromagnetic or impedance-based catheter location methods, or a hybrid of both.¹

Fundamental Concepts

CARTO Electroanatomic Mapping System

The CARTO mapping system consists of an ultralow magnetic field emitter, a magnetic field generator locator pad (placed beneath the operating table), an external reference patch (fixed on the patient's back), a deflectable 7 Fr quadripolar mapping-ablation catheter with a 4- or 8-mm tip and proximal 2-mm ring electrodes, location sensors inside the mapping-ablation catheter tip (the three location sensors are located orthogonally to each other and lie just proximal to the tip electrode, totally embedded within the catheter), a reference catheter, a data processing unit, and a graphic display unit to generate the electroanatomic model of the chamber being mapped.²

The CARTO electroanatomic mapping is based on the premise that a metal coil generates an electrical current when it is placed in a magnetic field. The magnitude of the current depends on the strength of the magnetic field and the orientation of the coil in it. The CARTO mapping system uses a triangulation algorithm similar to that used by a global positioning system (GPS). The magnetic field emitter, mounted under the operating table, consists of three coils that generate a low-intensity magnetic field (5×10^{-6} to 5×10^{-5} T) that is a very small fraction of the magnetic field intensity inside a magnetic resonance imaging (MRI) machine (Fig. 6.1).²

The sensor embedded proximal to the tip of a specialized mapping catheter detects the intensity of the magnetic field generated by each coil and allows for the determination of its distance from each coil. These distances determine the area of theoretical spheres around each coil, and the intersection of these three spheres determines the exact position and orientation of the tip of the catheter, in relation to a reference sensor on the skin. The accuracy of the determination of the location is highest in the center of the magnetic field; therefore it is important to position the location pad under the patient's chest. In

addition to the x , y , and z coordinates of the catheter tip, the CARTO system can determine three orientation determinants—roll, yaw, and pitch—for the electrode at the catheter tip. The position and orientation of the catheter tip can be seen on the screen and monitored in real time as the catheter moves within the electroanatomic model of the chamber mapped. The catheter icon has four color bars (green, red, yellow, and blue), enabling the operator to view the catheter as it turns clockwise or counterclockwise. In addition, because the catheter always deflects in the same direction, each catheter will always deflect toward a single color. Hence, to deflect the catheter to a specific wall, the operator should first turn the catheter so that this color faces the desired wall.²

The unipolar and bipolar electrograms recorded by the mapping catheter at each endocardial site are archived within that positional context. Using this approach, local tissue activation at each successive recording site produces activation maps within the framework of the acquired surrogate geometry.

When mapping the heart, the system can deal with four types of motion artifacts: cardiac motion (the heart is in constant motion; thus the location of the mapping catheter changes throughout the cardiac cycle), respiratory motion (intrathoracic change in the position of the heart during the respiratory cycle), patient motion, and system motion. Several steps are taken by the CARTO mapping system to compensate for these possible motion artifacts, and to ensure that the initial map coordinates are appropriate, including using a reference electrogram and an anatomical reference.

CARTO-3. The CARTO-3 system is the third-generation platform from Biosense Webster that offers two additional features: Advanced Catheter Location Technology and Fast Anatomical Mapping (FAM). Advanced Catheter Location technology is a hybrid technology that combines magnetic location technology and current-based visualization data to provide accurate visualization of multiple catheter tips and curves on the electroanatomic map. It allows the visualization of up to five EP catheters (with and without the magnetic sensors) simultaneously with clear distinction of all electrodes. In addition to the previously noted magnetic field, CARTO-3 uses an electrical field created by two sets of patches (three on the patient's back, three on the chest). The system sends a low-intensity current at a unique frequency that is emitted by various catheter electrodes, and the strength of the current emitted by each electrode is measured at each patch; this creates a current ratio unique to each electrode's location. The magnetic technology calibrates the current-based technology and thereby minimizes distortions at the periphery of the electrical field. Visualization of catheters is confined into a 3-D virtual area called the "matrix," which can be built only by using a magnetic sensor-equipped manufacturer-specific catheter (Figs. 6.1 and 6.2).²

Mapping is performed in two steps. Initially the magnetic mapping permits precise localization of the catheter with the sensor. This is associated with the current ratio of the electrode closest to the sensor. As the catheter with the sensor moves around a chamber, multiple locations are acquired and stored by the system. The system integrates the current-based points with their respective magnetic locations, resulting in a calibrated current-based field that permits accurate visualization of other catheters and their locations. Since each electrode emits a unique frequency, individual electrode locations are distinct, even when they are close to each other. FAM is a feature that permits rapid creation of anatomical maps by movement of a sensor-based catheter throughout the cardiac chamber. Unlike point-by-point electroanatomic mapping, volume data can be collected with FAM (see Fig. 6.1).

CARTO-Merge. The CARTO-Merge Module allows for images from preacquired computed tomography (CT) angiogram or MRI volume data sets to be integrated on the electroanatomic image of the cardiac

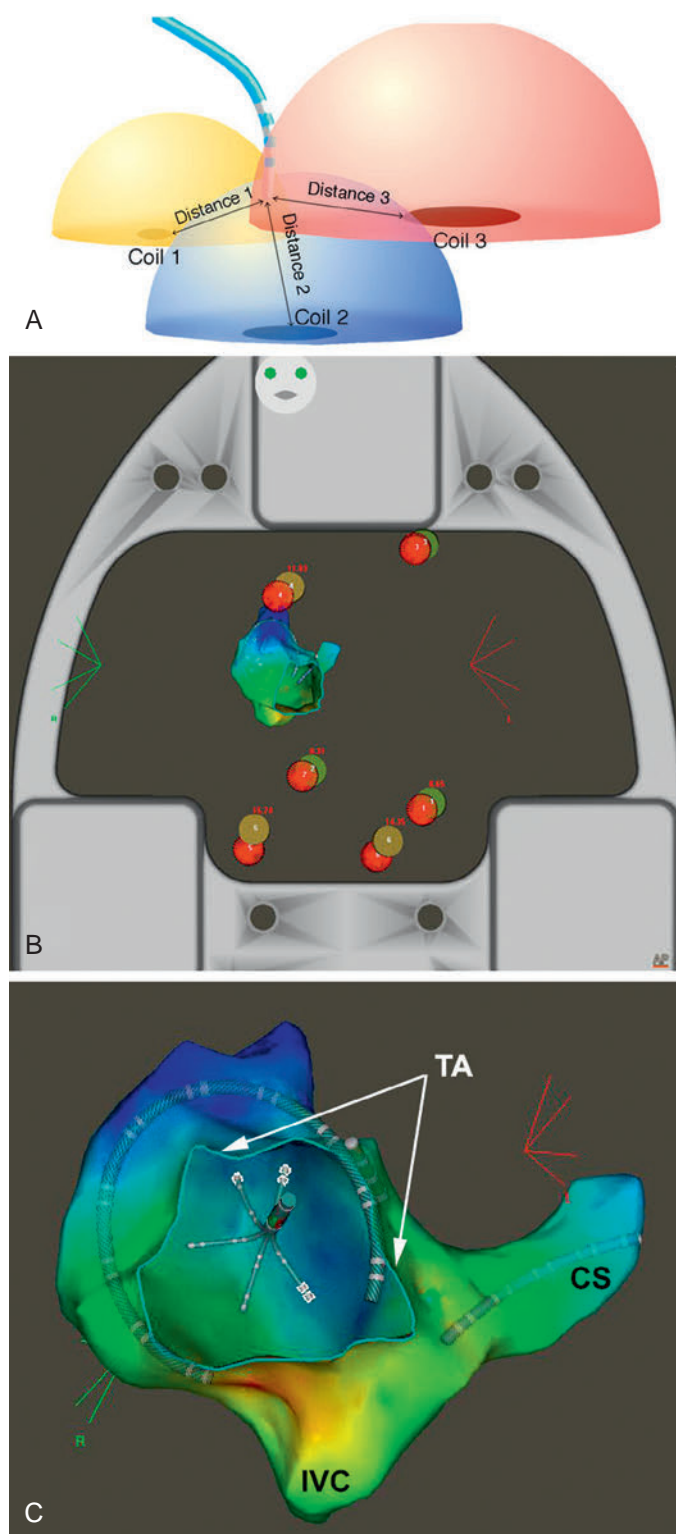


Fig. 6.1 The CARTO Electroanatomic Mapping System. (A) The three hemispheres represent fields from three different electromagnets situated beneath the patient. The catheter tip contains an element that is sensed by these fields, and this triangulating information is used to monitor the location and orientation of the catheter tip in the heart. (B) The magnetic field emitter, mounted under the operating table, is shown in relation to six electrode patches positioned at the patient's back and chest monitor (to create an electrical field and allow current-based visualization of catheters not equipped by magnetic sensors). The electroanatomic map is shown in the middle. (C) Color-coded activation map superimposed on the virtual anatomical geometry of the right atrium (left anterior oblique view) during mapping and ablation of typical atrial flutter using the CARTO-3 electroanatomic mapping system. Three standard diagnostic catheters are visualized on the electroanatomic map: Halo catheter positioned around the tricuspid annulus (TA); decapolar catheter positioned in the coronary sinus (CS); and multielectrode PentaRay catheter positioned at the right atrial posterior wall. The PentaRay and decapolar catheters are equipped with magnetic sensors and can be used to collect electroanatomic data. Current-based data are used to enable visualization of the Halo catheter. IVC, Inferior vena cava.

coronary circulation is a concern, such an overlay of the coronary angiogram allows RF energy application without the need for repeated coronary angiography. It is important to recognize, however, that the fluoroscopy or angiographic images are not gated to the electrocardiogram (ECG) or respiratory cycle, and any shift in of the prerecorded image during the course of the study requires the acquisition of new x-ray images.³

CARTO-Sound. The CARTO-Sound Image Integration Module incorporates the electroanatomic map to a map derived from intracardiac echocardiography (ICE), and allows for 3-D reconstruction of the cardiac chambers using real-time ICE. ICE is performed using a phased-array transducer catheter incorporating a navigation sensor (SoundStar, Biosense Webster) that records individual 90-degree sector image planes of the cardiac chamber of interest, including their location and orientation, to the CARTO workspace. A 3-D volume-rendered image is created by obtaining ECG-gated ICE images of the endocardial surface of the cardiac chamber of interest (Fig. 6.4). Three-second segments of 2-D ICE images are acquired during ECG gating to the P wave during sinus rhythm and to the R wave during AF. Since ICE images are not automatically gated to respiration by the system, images used in the analysis are acquired in the late-expiration to the midexpiration phase. Following optimizing each image by adjusting frequency (5 to 10 MHz) and contrast, the chamber endocardial surfaces are identified (based on differences in the echo intensity of blood and tissue), and their contours are traced automatically, and overwritten by hand as necessary, using the CARTO-Sound software. The contour lines for the chamber of interest are drawn below the border to prevent image bloating. The software then resolves each contour into a series of discrete spatial points, with an interpoint spacing of up to 3 mm (closer spacing on curved contours or at angulations). The CARTO software interpolates these points to create models of the chamber endocardial surface in the CARTO workspace. CARTO-Sound allows for detailed real-time visualization of the cardiac chamber and of its adjacent structures, and elimination of the chamber deformity that often happens with contact mapping.^{4,5}

CARTO-Sound has been successfully utilized to facilitate AF catheter ablation by incorporating a real-time ICE volume map of the left atrium (LA) and pulmonary veins (PVs) with the electroanatomic map, either as a stand-alone tool to guide navigation and ablation or as a facilitator of CT/MRI image integration. In addition, studies have shown the

chamber created with the CARTO system and simultaneously display them within the same coordinate system (Fig. 6.3). This can be very valuable in guiding real-time catheter ablation using the detailed cardiac chamber anatomy acquired from the CT/MRI.

CARTO-Univu. The CARTO-Univu module permits overlaying of the 3-D anatomic map and catheter visualization on prerecorded x-ray images or cine loops. When proximity of the ablation target to the

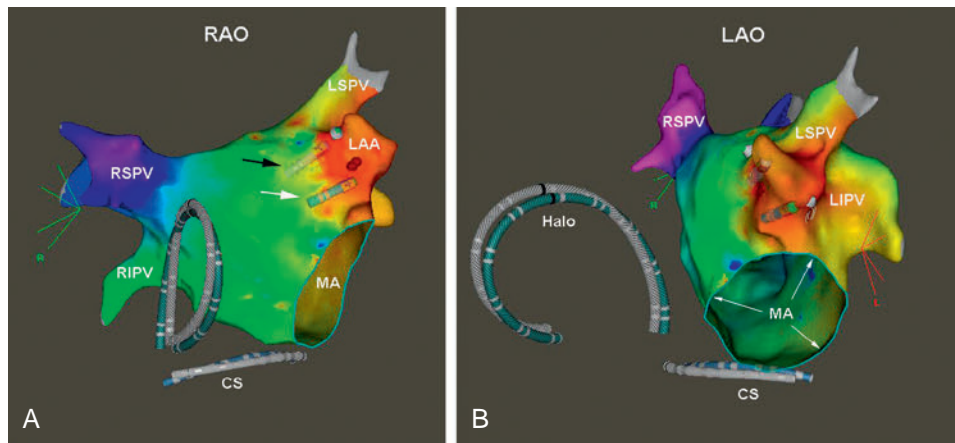


Fig. 6.2 CARTO-3 Color-Coded Activation Map of Focal Atrial Tachycardia Originating From the Left Atrial Appendage (LAA). The ablation catheter is positioned at the roof of the LAA (*black arrow*). A shadow of the position of the ablation catheter at the successful ablation site is marked (*white arrow*). A multipolar Halo catheter is positioned in the right atrium around the tricuspid annulus and a decapolar catheter is positioned in the coronary sinus (CS). Shadows of the original position of each of the catheters are marked for reference. Both Halo and CS catheters are not equipped with magnetic sensors and cannot be used to collect electroanatomic data. Visualization of these catheters is enabled by current-based data and is confined into a 3-D virtual area called the “matrix,” which can be built only by using a magnetic sensor-equipped manufacturer-specific catheter. Red dots indicate radiofrequency ablation lesions. LAO, Left anterior oblique view; LIPV, left inferior pulmonary veins; LSPV, left superior pulmonary veins; MA, mitral annulus; RAO, right anterior oblique view; RIPV, right inferior pulmonary veins; RSPV, right superior pulmonary veins.

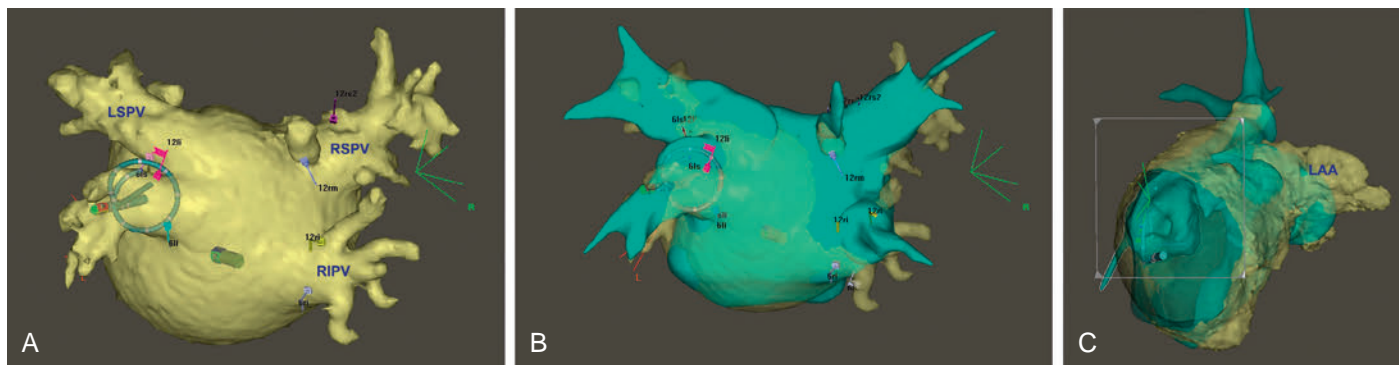


Fig. 6.3 The CARTO-Merge Image Integration Module. (A) Posterior view of preacquired segmented three-dimensional (3-D) CT images of the left atrium (LA) registered on the CARTO-3 electroanatomic system (CARTO-Merge Module). The ring catheter is visualized in the left inferior pulmonary vein (PV). (B) Integration of the preacquired CT images (shown in A) with 3-D reconstruction of the LA (posterior view) using the CARTO-3 (fast anatomical mapping [FAM]). (C) Cardioscopic view of the integrated CT and surface reconstructions of the LA. LAA, Left atrial appendage; LSPV, left superior PV; RIPV, right inferior PV; RSPV, right superior PV.

feasibility of using CARTO-Sound to define scar boundaries in the left ventricle (LV; identified on ICE imaging by both by wall thickness and motion) to facilitate substrate mapping and ablation of ischemic VT. Of note, when AF ablation is guided by 3-D ICE-derived images, ablation points fall beyond the 3-D ICE-derived surface contour more often than when guided by FAM or merged 3-D ICE-CT volume rendering.⁴

EnSite NavX Electroanatomic Mapping System

The EnSite NavX system consists of a set of three pairs of skin patches—a system reference patch, ECG electrodes, a display workstation, and a patient interface unit. The reference patch is placed on the patient's abdomen and serves as the electrical reference for the system.

The EnSite NavX combines catheter location and tracking features of the Localisa system (Medtronic, Minneapolis, MN, United States) with the ability to create an anatomical model of the cardiac chamber using only a single conventional EP catheter and skin patches. This mapping modality is based on currents across the thorax, developed as originally applied in the Localisa system. In contrast to the NavX system, Localisa does not allow the generation of 3-D geometry of the heart cavity because catheters and desired anatomical landmarks are displayed in a Cartesian frame of reference. This technology has undergone substantial additional development in the NavX iteration.²

For 3-D navigation, six electrodes (skin patches) are placed on the patient's skin to create electrical fields along three orthogonal axes (x,

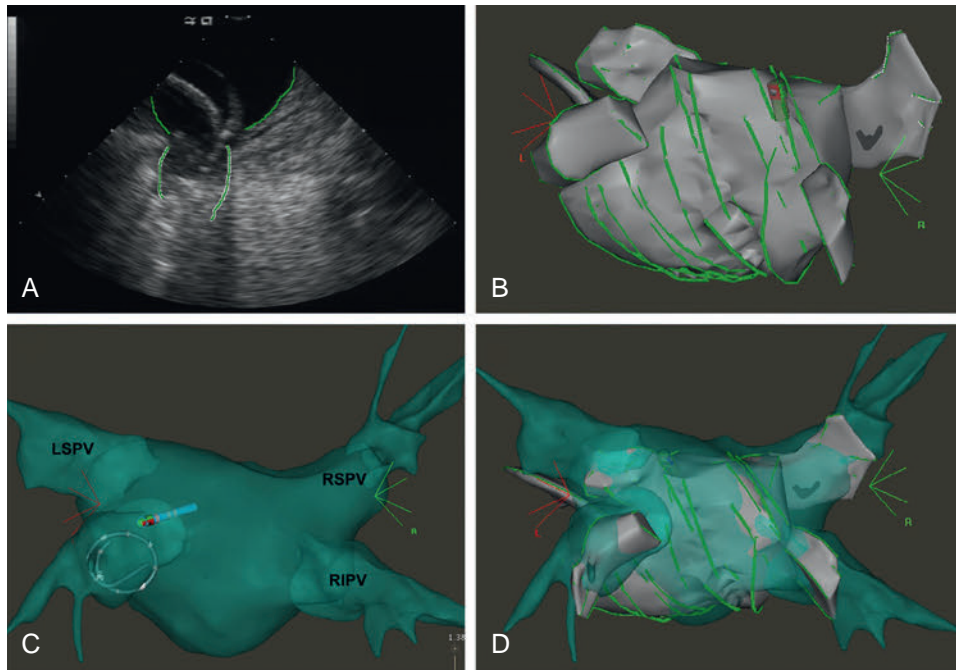


Fig. 6.4 The CARTO-Sound Image Integration Module. (A) Intracardiac echocardiographic image showing the left atrium (LA) and left inferior pulmonary vein (PV) obtained using a 10 Fr phased-array transducer catheter. The endocardial surfaces of the LA and PV are traced. (B) Three-dimensional geometry of the LA is reconstructed by interpolation of points on the traced endocardial surface from multiple ICE images. (C) CARTO-3 anatomical reconstruction of the LA (posterior view). Note that the circular and ablation catheters are visualized in the left inferior PV. (D) Integration of the CARTO-Sound volume and the electroanatomic maps of the LA. LSPV, Left superior PV; RIPV, right inferior PV; RSPV, right superior PV.

y, and z). The patches are placed on both sides of the patient (x-axis), the chest and back (y-axis), and the back of the neck and inner left thigh (z-axis). Analogous to the Frank lead system, the three orthogonal electrode pairs are used to send three independent, alternating, low-power currents of 350 mA at a frequency of 5.7 kHz through the patient's chest in three orthogonal (x, y, and z) directions, with slightly different frequencies of approximately 30 kHz used for each direction, to form a 3-D transthoracic electrical field with the heart at the center. The absolute range of voltage along each axis varies from each other, depending on the volume and type of tissue subtended between each surface-electrode pair. The voltage gradient is divided by the known applied current to determine the impedance field that has equal unit magnitudes in all three axes. Each level of impedance along each axis corresponds to a specific anatomical location within the thorax. As standard catheter electrodes are maneuvered within the chambers, each catheter electrode senses the corresponding levels of impedance, derived from the measured voltage. The mixture of the 30-kHz signals, recorded from each catheter electrode, is digitally separated to measure the amplitude of each of the three frequency components. The three electrical field strengths are calculated automatically via the difference in amplitudes measured from neighboring electrode pairs with a known interelectrode distance for three or more different spatial orientations of that dipole. Timed with the current delivery, NavX calculates the x-y-z impedance coordinates at each catheter electrode by dividing each of the three amplitudes (V) by the corresponding electrical field strength (V/cm), and expresses them in millimeters to locate the catheters graphically in real time to enable nonfluoroscopic navigation. The NavX system allows real-time visualization of the position and motion of up to 128 electrodes on both ablation and standard catheters positioned elsewhere in the heart (Fig. 6.5). Importantly, the relative positions of the electrodes are

calculated by assuming that changes in the recorded field potential are only caused by changes in catheter position. Therefore changes in thoracic impedance can cause the system to "drift."²

The NavX system also allows for rapid creation of detailed models of cardiac anatomy. Sequential positioning of a catheter at multiple sites along the endocardial surface of a specific chamber establishes that chamber's geometry. The system automatically acquires points from a nominated electrode at a rate of 96 points/s. Chamber geometry is created by several thousand points. The algorithm defines the surface by using the most distant points in any given angle from the geometry center, which can be chosen by the operator or defined by the system. In addition, the operator is able to specify fixed points that represent contact points during geometry acquisition; the algorithm that calculates the surface cannot eliminate these points. In addition to mapping at specific points, there is additional interpolation, providing a smooth surface onto which activation voltages and times can be registered (see Fig. 6.5). To control for variations related to the cardiac cycle, data acquisition can be gated to any electrogram. Also, electrode positions are averaged over a few seconds to minimize the effect of cardiac motion. Respiratory compensation is collected just before mapping. The algorithm records the movement that occurs with respiration and correlates it with changes in transthoracic impedance to filter low-frequency cardiac shift associated with the breathing cycle.

After creating chamber geometry, a scaling algorithm (field scaling) is applied to compensate for variations in impedance between the heart chambers and venous structures, which can otherwise result in a distortion of the x-y-z coordinates when a "roving" catheter is maneuvered among the differing regions of impedance (Fig. 6.6). Field scaling is based on the measured interelectrode spacing for all locations within the geometry. Adjustments to the local strength of the navigation fields

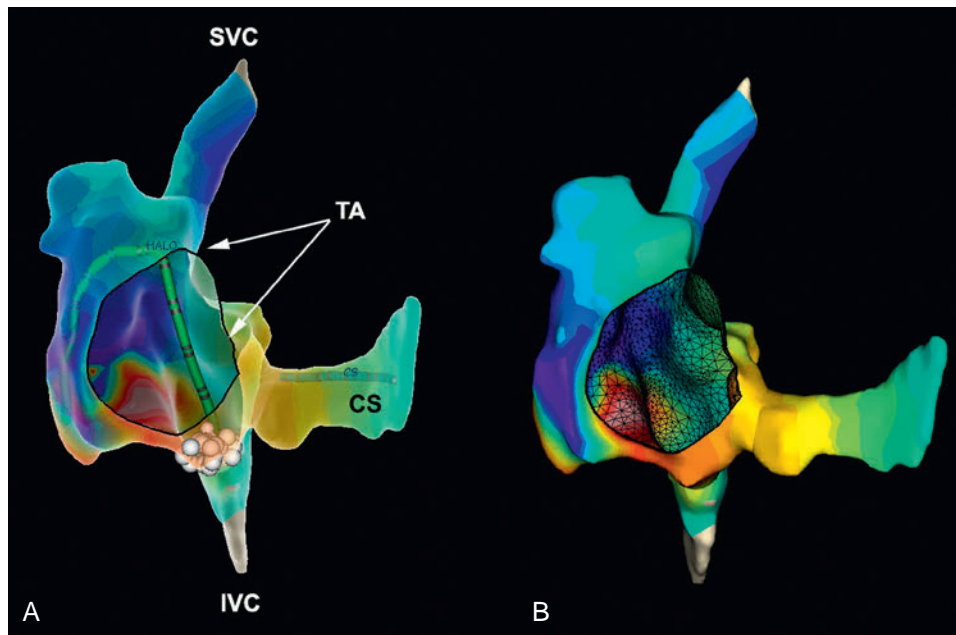


Fig. 6.5 Electroanatomic Activation Mapping Using the NavX System. (A) Color-coded activation map superimposed on the virtual anatomical geometry of the right atrium (left anterior oblique view) during mapping and ablation of typical atrial flutter using the NavX electroanatomic mapping system. Two standard diagnostic catheters (a Halo catheter positioned around the tricuspid annulus [TA], and a decapolar catheter positioned in the coronary sinus [CS]) as visualized by the NavX system during mapping. White dots denote RF ablation points across the cavotricuspid isthmus. (B) The same color-coded activation map is viewed after changing transparency and removing diagnostic catheters. IVC, Inferior vena cava; SVC, superior vena cava.

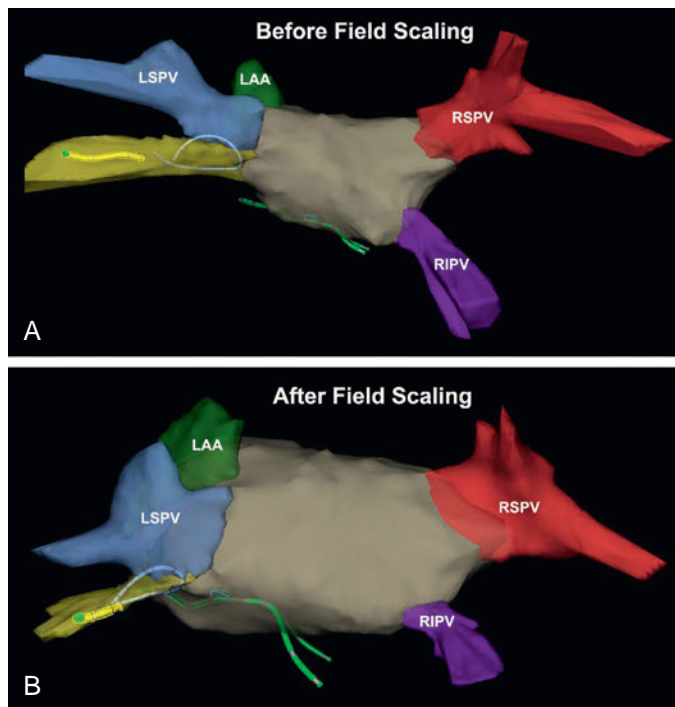


Fig. 6.6 Field Scaling in the NavX Mapping System. Three-dimensional geometry model (posterior view) of the left atrium (LA) and pulmonary veins (PVs) created by the NavX electroanatomic mapping system. Ablation and circular catheters are visualized in the left inferior PV. A decapolar catheter is visualized in the coronary sinus (CS). (A) The LA geometry model before field scaling. (B) The same geometry model is shown after applying the field scaling algorithm to compensate for variations in impedance between the LA and PVs. LAA, Left atrial appendage; LSPV, left superior PV; RIPV, right inferior PV; RSPV, right superior PV.

are made so that the computed catheter electrode positions match the known interelectrode spacing of the catheters used to create the geometry.

The NavX system works with most manufacturers' ablation catheters, RF generators, or cryogenerators. Sites of ablation energy application can be tagged, thus facilitating the creation of lines of block with considerable accuracy by serial placement of energy applications and allowing verification of the continuity of the ablation line.

The EnSite Fusion iteration has the capability to integrate images from a preacquired CT/MRI scan on the real-time electroanatomic image the cardiac chamber created with the NavX system to facilitate anatomically based ablation procedures. To allow local adjustment of the EnSite System model, the registration module comes with Dynamic Registration. The system has the ability to mold the created geometry dynamically into the CT/MRI image (see later discussion).

The EnSite Precision iteration adds magnetic navigation capability. Magnetic points are collected with several new magnet-enabled catheters. Magnetic-field stability reduces the effects of "impedance drift," corrects impedance distortion, and helps optimize catheter navigation and creation of a precise, accurate geometry model.

Rhythmia Electroanatomic Mapping System

Rhythmia is a novel 3-D electroanatomic mapping platform that is paired to a mini-basket array catheter with 64 mini-electrodes (Orion, Boston Scientific) and is capable of generating ultra-high-density electroanatomic maps. This system uses a hybrid location technology that combines impedance and magnetic location. The magnetic field is generated by a localization generator positioned under the patient's table and is capable of locating catheters with magnetic sensors. The impedance location technology is used to track catheters that are not equipped with a magnetic sensor. The system then maps the impedance field measurements to the magnetic location coordinates and creates

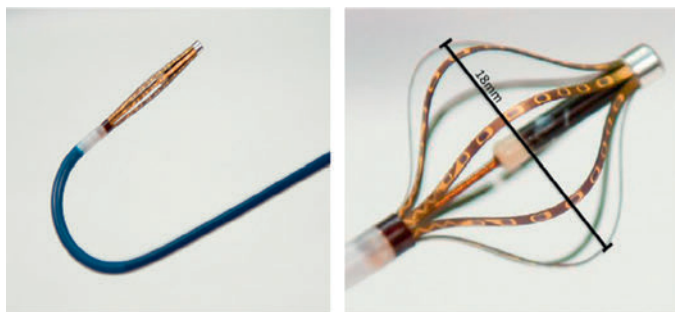


Fig. 6.7 The Orion Mini-Basket Catheter. The 8-F bidirectional mini-basket catheter is 27 mm long from the catheter shaft to the distal tip of the basket. It consists of 8 splines, each with 8 electrodes. The nominal diameter of the basket is 18 mm when measured at its equator. (From Anter E, Tschabrunn CM, Contreras-Valdes FM, Li J, Josephson ME. Pulmonary vein isolation using the Rhythmia mapping system: verification of intracardiac signals using the Orion mini-basket catheter. *Heart Rhythm*. 2015;12:1927–1934.)

an impedance field map. This map is used to enhance the accuracy of the impedance location.^{6,7}

Orion is an 8.5 Fr bidirectional deflectable catheter with a mini-basket electrode array containing eight splines, each spline containing eight small electrodes (Fig. 6.7). The surface area of each electrode is 0.4 mm², and the interelectrode spacing is 2.5 mm (measured from center to center). The basket can be deployed into a spherical configuration through mechanical flexion of the splines to varying diameter (minimum 3 mm, nominal 18 mm, maximum 22 mm, when measured at its equator). The location of each electrode is determined using a combination of magnetic sensor located at the tip of the catheter and impedance sensing at each of the electrodes. A flushing mechanism is present at the catheter tip to prevent thrombus formation. Other catheters are tracked by an impedance-based system.^{6–9}

Two data acquisition modes are available with the Orion catheter: continuous and manual. In the continuous data acquisition mode, operator-defined criteria for accepting cardiac beats are applied for automated map construction during uninterrupted movement of the catheter, without immediate input from the operator. The electrograms from collected beats are automatically annotated by the system. In the manual data acquisition mode, the operator collects data in an “area-by-area” manner, and manually accepts and annotates selected points.

During continuous, automated data acquisition, points are accepted only if they meet user predefined acceptance criteria such as cycle length (CL) stability, stable timing difference between two reference electrodes, respiration gating (the respiratory cycle is tracked by measuring impedance change across the chest), stable catheter location, stability of catheter signal compared with adjacent points, and morphology matching. The automated algorithms filter out points with discrepancy in comparison to those of close proximity. Far-field components are reduced by combining unipolar and bipolar electrograms.

The setup for the mapping window is automatic. The system calculates the mean CL of the rhythm over 10 seconds and consequently sets 100% of the CL equally before and after the timing reference electrode (usually one of the coronary sinus [CS] electrograms, or the QRS interval of one of the surface ECG leads for ventricular rhythms). For annotation of the local activation time of each acquired electrogram, the system combines unipolar (maximum negative dV/dt) and bipolar (maximum amplitude) electrogram. For electrograms with multiple potentials, the system selects the potential that best matches the timing of electrograms in the surrounding area.^{6–8} The very small size of the

electrodes on the Orion catheter minimizes far-field signals and background noise, and allows accurate detection of very small amplitude signals.^{10,11}

The anatomical shell is gradually constructed with every accepted beat based on the location of the outermost electrodes of the basket catheter. Inclusion or exclusion of electrograms into the group of surface electrograms is based on the distance from the surface geometry (1 to 5 mm), which can be set by the operator. The system will automatically delete inner electrogram points as more signals are recorded from a spatially outside location.^{6–8}

All electrograms are stored for later review. Maps can be edited by the operator after data acquisition is complete. The software allows for visualization of the electrogram associated with each anatomic point, facilitating re-annotation or removal of inaccurate data.⁷ By selecting individual electrograms with a virtual roving probe, it is possible to determine and mark a region of interest (e.g., His bundle [HB] region). In addition, a cutout of anatomical structures such as the tricuspid annulus can be performed based on the corresponding electrograms in review mode (Fig. 6.8).^{12,13}

Electroanatomic Activation Mapping

Anatomical Reference

Once the mapping catheter (or any electroanatomically tracked electrode) is placed inside the heart, its location can be determined in relation to a fixed anatomical reference. This reference catheter is positioned inside the heart or on the body surface, and its location must remain stable throughout the procedure to prevent distortion of the electroanatomic map. The movement of the mapping catheter is then tracked relative to the position of this reference. An intracardiac reference catheter has the advantage of moving with the patient's body and with the heart during the phases of respiration. However, the intracardiac reference catheter can change its position during the course of the procedure, especially during manipulation of the other catheters.

In the CARTO mapping system, locations of magnetically enabled catheters are displayed in relation to the fixed magnetic field sensors placed under the patient. The CARTO system continuously calculates the position of the mapping catheter in relation to this array of sensors, thus solving the problem of any possible motion artifacts. The movement of the ablation catheter is then tracked relative to the position of this reference. Slight movement of the patient relative to the location reference pad may distort the map; significant patient movement or dislocation of the location pad can lead to uncorrectable map shifts.

In the NavX system, the 3-D localization of all EP catheters is based on an impedance gradient-calculation system in relation to a reference electrode placed on the patient's body or inside the heart (e.g., CS catheter). Since the reference electrodes and catheters are placed either on the patient's skin or in the patient's cardiac chambers, they move simultaneously with the patient, preventing map shifts and rendering the NavX largely insensitive to potential patient movements.² The Rhythmia system also uses an anatomical sensor attached to patient's back.

The Rhythmia mapping system uses a hybrid location technology that combines impedance location with magnetic location technology and uses two location references, one for each localization technology. The magnetic technology uses a location reference attached to the patient's back, while the impedance technology uses a stationary intracardiac electrode (e.g., a CS electrode) selected by the user.

Electrical Reference

The electrical reference is the fiducial marker on which the entire mapping procedure is based. The timing of the fiducial point is used to determine the activation timing in the mapping catheter in relation to the acquired points and to ensure collection of data during the same part of the

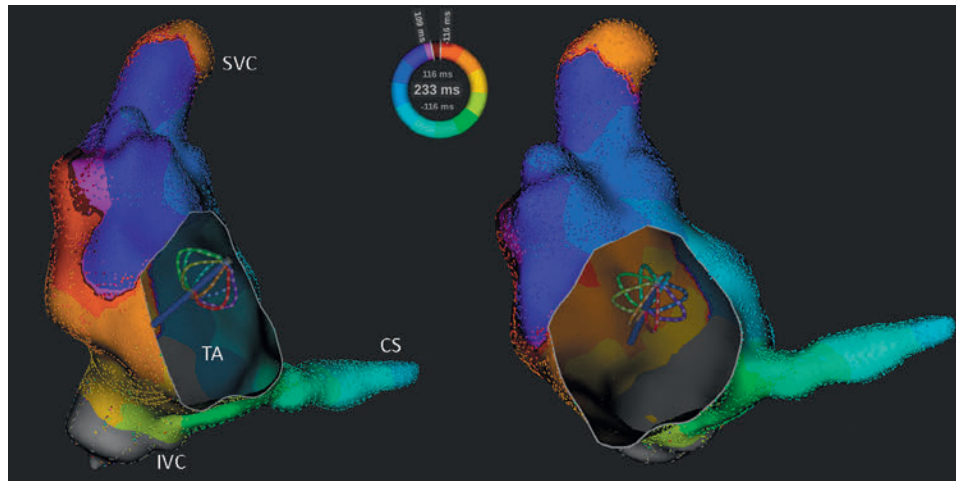


Fig. 6.8 Rhythmia Color-Coded Activation Map of Typical Counterclockwise Atrial Flutter (AFL). Three-dimensional electroanatomic activation map of the right atrium in the right anterior oblique (*left*) and left anterior oblique (*right*) views constructed during counterclockwise typical AFL. During tachycardia, the depolarization wavefront travels counterclockwise around the tricuspid annulus (TA), as indicated by a continuous progression of colors (from red to purple) with close proximity of earliest and latest local activation. The mini-basket (Orion) catheter is visualized on the map. CS, Coronary sinus; IVC, inferior vena cava; SVC, superior vena cava.

cardiac cycle. It is therefore vital to the performance of the system. All the local activation timing information recorded by the mapping catheter at different anatomical locations during mapping (displayed on the completed 3-D map) is relative to this fiducial point, with the acquisition gated so that each point is acquired during the same part of the cardiac electrical signal. It is important that the rhythm being mapped is monomorphic and the fiducial point is reproducible at each sampled site.

The fiducial point is defined by the user by assigning a reference channel and an annotation criterion. The system has a great deal of flexibility in terms of choosing the reference electrogram and gating locations. Any surface ECG lead or intracardiac electrogram in bipolar or unipolar mode can serve as a reference electrogram. For the purpose of stability when intracardiac electrograms are selected, CS electrograms are usually chosen for mapping supraventricular rhythms, and a right ventricle (RV) electrode or a surface ECG lead is commonly chosen as the electrical reference during mapping ventricular rhythms. Care must be taken to ensure the reference electrogram is distinct and stable, and that automatic sensing of the reference is reproducible and is not subject to oversensing in the case of annular electrograms (e.g., oversensing of a ventricular electrogram on the CS reference electrode during mapping an atrial rhythm). Any component of the reference electrogram may be chosen for a timing reference, including maximum (peak positive) deflection, minimum (peak negative) deflection, maximum upstroke (dV/dt), or maximum downslope.¹

Window of Interest

Defining an electrical window of interest is a crucial aspect in ensuring the accuracy of the initial map coordinates. The window of interest is defined as the time interval relative to the fiducial point during which the local activation time is determined (Fig. 6.9). Within this window, activation is considered early or late relative to the reference. Timing and voltage of electrograms falling outside this window are excluded from the map and cannot be tagged without altering the window. The total length of the window of interest should not exceed the tachycardia cycle length (TCL; generally 10 or 20 milliseconds less than the TCL). The boundaries are set relative to the reference electrogram. Thus the

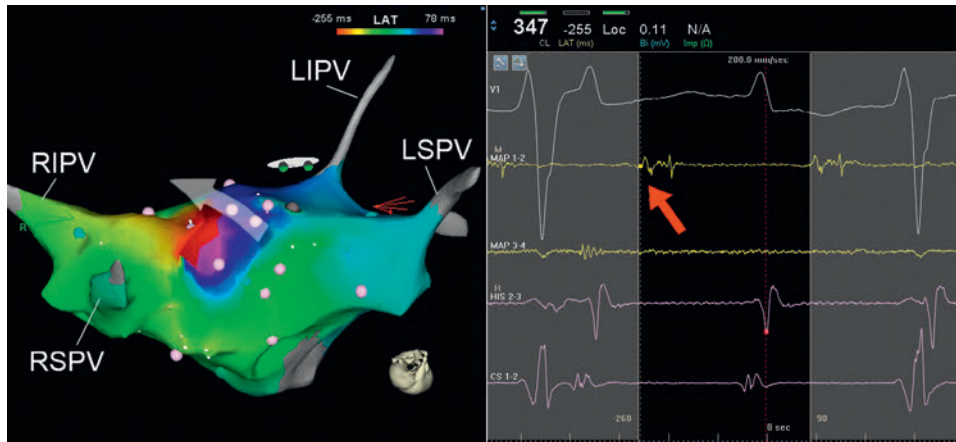
window is defined by two intervals—one extending before the reference electrogram and the other after it. For focal tachycardias, the window of interest is usually selected so that it starts about 50 milliseconds before the onset of the tachycardia complex on the surface ECG (P wave or QRS), regardless of the timing of the electrical reference. For macroreentrant tachycardias, the sensing window should approximate the TCL, and designating activation times in a circuit as early or late is arbitrary. If the activation window spans more than one tachycardia cycle, the resulting map can be ambiguous, lack coherency, and give rise to a spurious pattern of adjacent regions of early and late activation (Figs. 6.9 and 6.10). In theory, a shift in the window or electrical reference would not change a macroreentrant circuit but only result in a phase shift of the map (Fig. 6.11).¹

Local Activation Time

Once the reference electrogram, anatomical reference, and window of interest have been chosen, the mapping catheter is moved from point to point along the endocardial surface of the cardiac chamber being mapped. These points can be acquired in a unipolar or bipolar configuration. These electrograms are analyzed using the principles of activation mapping discussed in Chapter 5. The local activation time at each sampled site is calculated as the time interval between the fiducial point on the reference electrogram and the corresponding local activation determined from the unipolar or bipolar local electrogram recorded from that site.

In general, the local activation time at each site is determined from the intracardiac bipolar electrogram and is measured in relation to the fixed reference electrogram. For bipolar electrograms, the initial peak of a filtered (30 to 300 Hz) bipolar signal coincides with depolarization beneath the recording electrode and appears to correlate most consistently with local activation time, corresponding to the maximal negative dV/dt of the unipolar recording. However, in the setting of complex multicomponent or fractionated bipolar electrograms, the determination of local activation time becomes challenging, and the decision about which activation time is most appropriate needs to be made in the context of the particular rhythm being mapped. Therefore, during mapping procedures, the onset (rather than the peak or nadir) of a

A. Correct window width



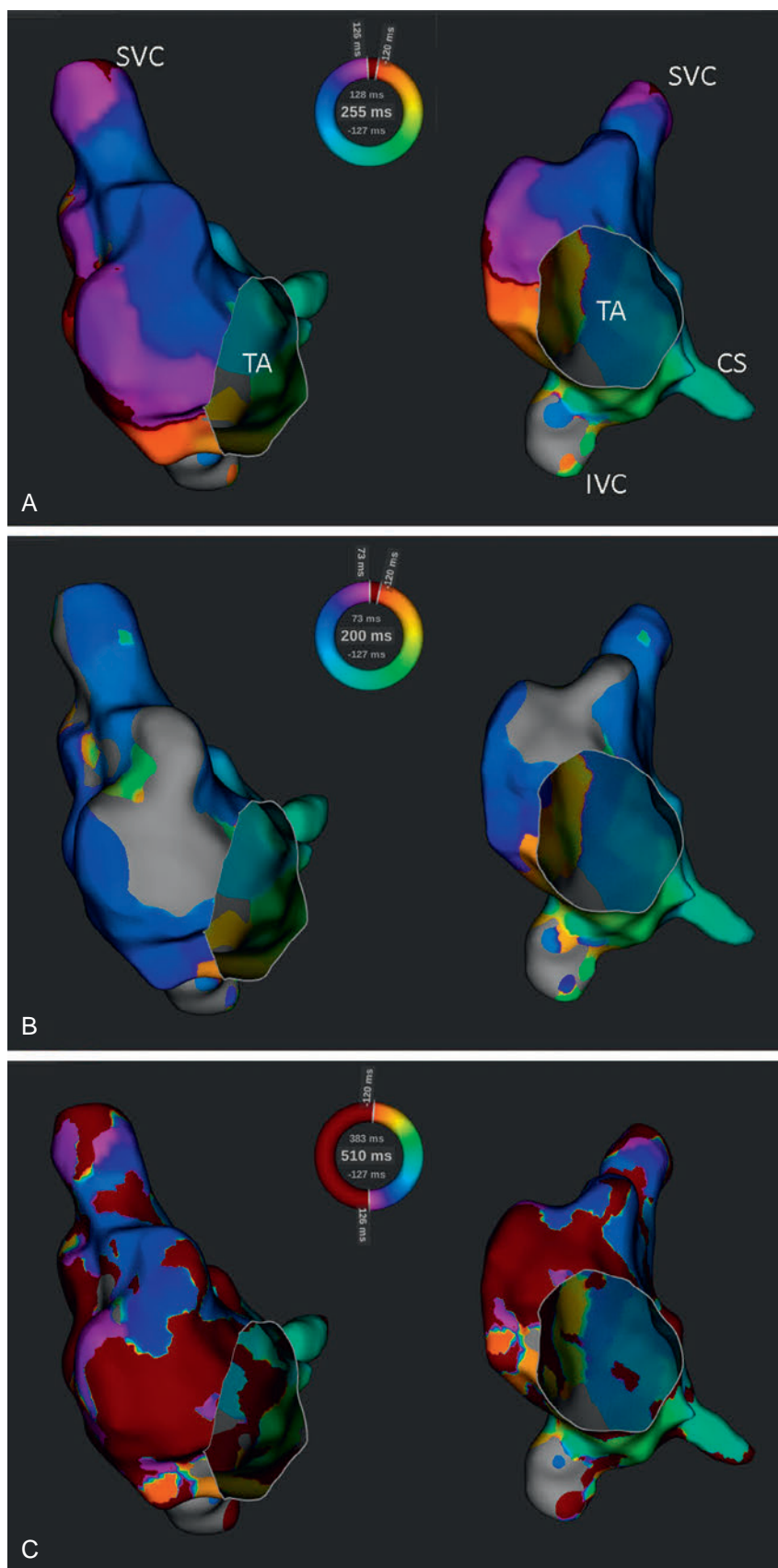
B. Window too wide



C. Window too narrow



Fig. 6.9 Influence of Window of Interest on Activation Mapping. CARTO-3 activation map of a macro-reentrant left atrial tachycardia is shown (anterior-cranial view). In (A) the correct window of interest width was chosen encompassing one complete cardiac cycle. A mid-diastolic potential (*red arrow*) is recorded from the top of the left atrium, with its timing at the left portion of the window (*darker vertical panel*), giving rise to an activation map at left with direction of propagation as indicated by the white arrow. In (B) the window of interest is too wide, including portions of two cardiac cycles. It is possible for the activation at this same site to be assigned as indicated by the red arrow, yielding a completely different activation map at left, seeming to show splitting of wavefronts going around the right pulmonary veins (PVs). In (C) the window is too narrow, and while no actual electrogram occurs within the window, the system is obligated to take an activation time (noise, at *red arrow*). This again yields a very different activation map as shown at left. LSPV, Left superior PV; LIPV, left inferior PV; RSPV, right superior PV; RIPV, right inferior PV.



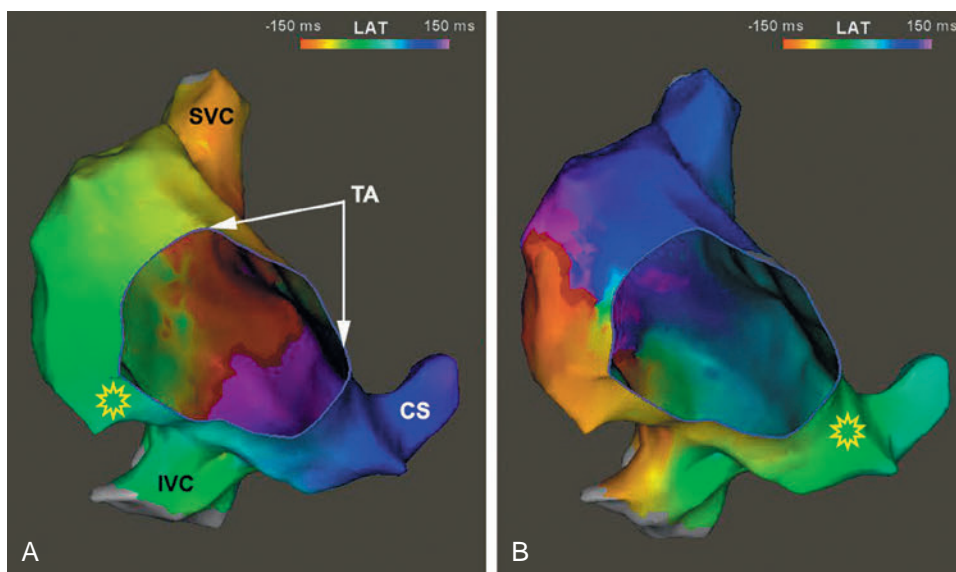


Fig. 6.11 Influence of the Electrical Reference on Activation Mapping. CARTO-3 activation map of the right atrium (left anterior oblique view) constructed during typical atrial flutter (cycle length [CL], 310 milliseconds) with “counterclockwise” rotation around the tricuspid annulus (TA). (A) The distal bipole of a Halo catheter (positioned at the lateral aspect of the TA, indicated by *yellow star*) was selected as the electrical reference (fiducial point) of the activation map. Note that the early-meets-late zone is located at the septal aspect of the right atrium. The window of interest was set at 300 milliseconds (150 milliseconds before to 150 milliseconds after the timing of the electrical reference). (B) The proximal bipole of the coronary sinus (CS) catheter (positioned at the CS ostium, indicated by *yellow star*) was selected as the electrical reference for activation mapping of the same tachycardia. Again, the window of interest was set at 150 milliseconds before to 150 milliseconds after the timing of the electrical reference. Now, the early-meets-late zone is located at the lateral aspect of the RA. In both maps, there is continuous progression of colors (from *red* to *purple*) with close proximity of earliest and latest local activation (*red* meeting *purple*), consistent with counterclockwise peritricuspid reentry. The change in the electrical reference did not cause a change a macro-reentrant circuit but only resulted in a phase shift of the map. Note that the early-meets-late zone in both maps does not localize the ablation target (which is the cavotricuspid isthmus in these cases); rather, it is merely a function of where the offset and onset of the window of interest are defined relative to the timing of the selected electrical reference. IVC, Inferior vena cava; SVC, superior vena cava.

high frequency component of the local bipolar electrogram often is used because it is easier to determine reproducibly, especially when measuring heavily fractionated, low-amplitude local electrograms. The onset of the bipolar electrogram likely precedes the maximal $-dV/dt$ in unipolar electrogram by 15 to 30 milliseconds.¹⁴

For filtered and unfiltered unipolar electrograms, the maximum negative slope (i.e., maximum change in potential, dV/dt_{\max}) of the signal coincides best with the arrival of the depolarization wavefront directly beneath the electrode.^{14–16}

Contemporary mapping systems offer automatic data acquisition and timing annotation of accepted points. Using these automated algorithms, timing of local activation is annotated at the point of maximum amplitude of the bipolar signal or the maximum negative dV/dt of the unipolar signal. For electrograms with multiple potentials, the system selects the potential that best matches the timing of electrograms in the surrounding area. When automated timing annotation is used, it is important to utilize the same parameters for the timing of local activation when additional points are acquired manually or during the editing of automatically acquired data.

Data Acquisition

Following selection of the reference electrogram, positioning of the anatomical reference, and determination of the window of interest, the mapping catheter is positioned in the cardiac chamber of interest.

The CARTO and Rhythmia systems require the use of proprietary catheters with a location sensor to collect mapping data. In contrast, NavX-guided procedures are performed using the same catheter setup as conventional approaches. Any electrode can be used to gather data, create static isochronal and voltage maps, and perform ablation procedures. Standard EP catheters of choice are introduced into the heart; up to 128 electrodes can be viewed simultaneously. The NavX system can locate the position of the catheters from the moment that they are inserted in the vein. Therefore all catheters can be navigated to the heart under guidance of the EnSite NavX system, and the use of fluoroscopy can be minimized for preliminary catheter positioning. However, interrupted fluoroscopy must be used repeatedly when an obstacle to catheter advancement is encountered. Once in the heart, one intracardiac catheter is used as a reference for geometry reconstruction. A shadow (to record original position) is placed over this catheter to recognize displacement during the procedure, in which case the catheter can be returned easily to its original location under the guidance of NavX. A shadow can also be displayed on each of the other catheters to record that catheter's exact spatial position at some particular time (e.g., where PV potentials are best seen).

The mapping catheter is initially positioned (using fluoroscopy) at known anatomical points that serve as landmarks in the chamber of interest for the electroanatomic map. For example, to map the right atrium (RA), points such as the superior vena cava (SVC), inferior vena

cava (IVC), HB, tricuspid annulus, and CS os are marked. The catheter is then advanced slowly around the chamber walls to sample multiple points along the endocardium, thus sequentially acquiring the location of its tip together with the local electrogram.

Points are selected only when the catheter is in stable contact with the wall. The system continuously monitors the quality of catheter-tissue contact and local activation time stability to ensure the validity and reproducibility of each local measurement. The stability of the catheter and contact is evaluated at every site by examining the following: (1) local activation time stability, defined as a difference between the local activation calculated from two consecutive beats of less than 2 milliseconds; (2) location stability, defined as a distance between two consecutive gated locations of less than 2 mm; (3) morphological super-impositioning of the intracardiac electrogram recorded on two consecutive beats; and (4) CL stability, defined as the difference between the CL of the last beat and the median CL during the procedure. Furthermore, contact force measurement at the tip of the mapping electrode (when available) can help optimize electrode-tissue contact and improve mapping accuracy.

Contemporary mapping systems enable automated data acquisition from the designated mapping catheter. The algorithm automatically accepts and annotates activation times for points that fulfill an operator-defined set of acceptance criteria. Beats are included in the map based on CL stability, relative timing of reference electrograms, electrode location stability, and respiratory gating, among other optional criteria. These algorithms help streamline the mapping and validation process and reduce overall mapping and manual annotation time.

Because respiratory excursions can cause significant shifts in apparent catheter location, respiratory compensation is collected just before mapping to filter low-frequency cardiac shift associated with the breathing cycle. The current iteration of the CARTO mapping system allows for automatic gating to the respiratory cycle.¹

Each selected point is tagged on the 3-D map. Lines of block (manifest as double potentials) are tagged for easy identification because they can serve as boundaries for the subsequent design of ablation strategies. Electrically silent areas (defined as having an endocardial potential amplitude less than 0.05 mV [the baseline noise in the mapping system], and the absence of capture at 20 mA) and surgically related scars are tagged as “scar” and therefore appear in gray on the 3-D maps and are not assigned an activation time (see Figs. 14.1 and 14.2). The map can also be used to catalog sites at which pacing maneuvers are performed during assessment of the tachycardia.¹

Sampling the location of the catheter together with the local electrogram is performed from multiple endocardial sites. Catheters other than the ablation catheter, such as the multipolar Lasso or Penta-Ray, can further enhance the collection of points, increase the mapping speed, and improve map resolution. The points sampled are connected by lines to form several adjoining triangles in a global model of the chamber. Next, gated electrograms are used to create an activation map, which is superimposed on the anatomical model. The acquired local activation times are then color-coded and superimposed on the anatomical map, with red indicating early-activated sites, blue and purple indicating late-activated areas, and yellow and green indicating intermediate activation times (see Figs. 6.5 and 6.11). Between these points, the mapping systems assign an activation time over the area around each acquired point, and the adjoining triangles are colored with these interpolated values. The size of this area is determined by setting the triangle “fill threshold” or “interpolation threshold,” which is adjustable. If the points are spaced widely apart (beyond the fill threshold), no interpolation is done. As each new site is acquired, the reconstruction is updated in real time to create a 3-D chamber geometry color progressively encoded with activation time.¹

Sampling an adequate number of homogeneously distributed points is necessary. If inadequate numbers of points are taken and the fill threshold allows interpolation over a large area, the colors assigned to the poorly mapped areas will not be representative of the actual conduction pattern and activation timing. Thus bystander sites can be mistakenly identified as part of a reentrant circuit, and lines of conduction block can be missed. In addition, low-resolution mapping can obscure other interesting phenomena, such as the second loop of a dual-loop tachycardia. Some arrhythmias, such as complex reentrant circuits, require more than 80 to 100 points to obtain adequate resolution. Other tachycardias can be mapped with fewer points, including focal tachycardias and some less complex reentrant arrhythmias, such as isthmus-dependent AFL. The use of multielectrode mapping catheters can improve map resolution and expedite the mapping process.¹

It is also important to identify areas of scar or central obstacles to conduction; failure to do so can confuse an electroanatomic map because interpolation of activation through areas of conduction block can give the appearance of wavefront propagation through, rather than around, those obstacles. This occurrence precludes identification of a critical isthmus in reentrant arrhythmias to target for ablation. A line of conduction block can be inferred if there are adjacent regions with wavefront propagation in opposite directions separated by a line of double potentials or dense isochrones.

The electroanatomic model, which can be viewed in a single view or in multiple views simultaneously and freely rotated in any direction, forms a reliable road map for navigation of the ablation catheter. Any portion of the chamber can be seen in relation to the catheter tip in real time, and points of interest can easily be revisited even without fluoroscopy. The electroanatomic maps can be presented in two or three dimensions as activation, isochronal, propagation, or voltage maps.

Activation Map

During mapping, the electrogram obtained at a given site is stored and the activation time catalogued as compared with the designated reference electrogram. The accrued points in the map are assigned to an isochronal color scale based on their respective activation times. The activation maps display the local activation time, color-coded and overlaid on the reconstructed 3-D geometry (see Figs. 11.21 and 12.14). Each color shift represents a temporal fraction of the entire TCL. Activation mapping is performed to define the activation sequence. A reasonable number of points homogeneously distributed in the chamber of interest must be recorded. The selected points of local activation time are color-coded.

The electroanatomic maps of focal tachycardias demonstrate radial spreading of activation, from the earliest local activation site in all directions, and in these cases, activation time is markedly shorter than TCL (Fig. 6.2). In contrast, a continuous progression of colors around the mapped chamber, with close proximity of earliest and latest local activation (“early-meets-late” zone), suggests the presence of a macroreentrant tachycardia (see Fig. 6.11). Importantly, the early-meets-late zone should not be used as an indicator of the location of the critical isthmus of the macroreentrant circuit (which is the usual ablation target). Rather, it is merely a function of where the offset and onset of the window of interest are defined relative to the timing of the selected reference electrogram. As noted previously, the early-meets-late zone can shift in location and timing in response to shifts in the window of interest or electrical reference (see Figs. 6.8 and 6.11).¹

It is also important to recognize that a focal tachycardia can produce an electroanatomic activation map that mimics reentry when anatomical or functional barriers to conduction close to the site of origin of the tachycardia (such as anisotropic conduction, scars, incisions, or prior ablation lines) cause the delay of wavefront propagation to span the

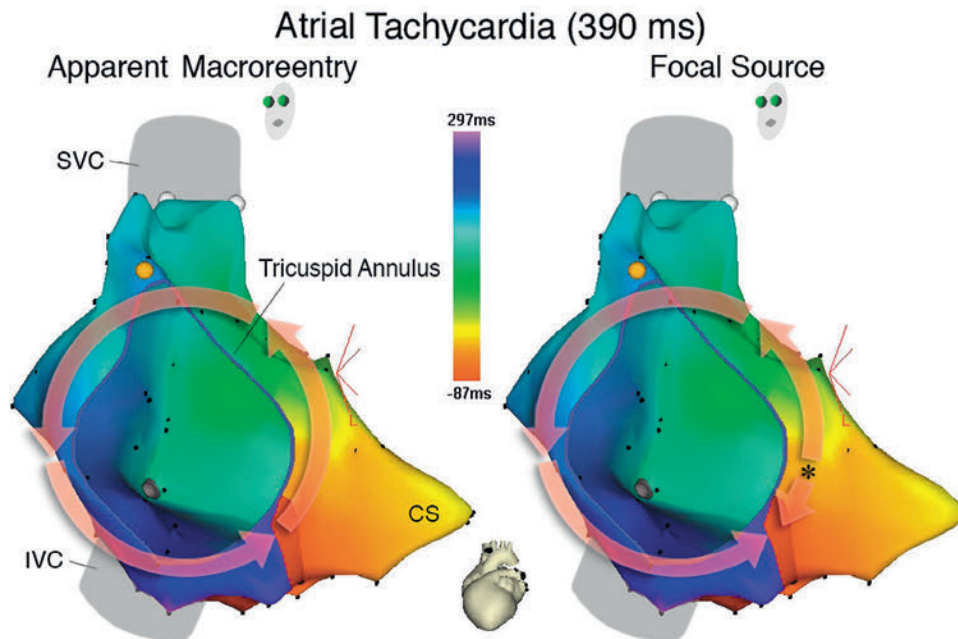


Fig. 6.12 Focal Versus Macroreentrant Atrial Tachycardia (AT) in a Patient With Prior Cavotricuspid Isthmus Ablation. A right atrial electroanatomic map during AT (tachycardia cycle length [TCL] 390 milliseconds) is shown. At left, the activation pattern (arrows) suggests typical counterclockwise atrial flutter; mapped sites account for 384 milliseconds (98% of TCL). Overdrive pacing had suggested a focal automatic process; additional mapping showed a focal site at the coronary sinus (CS) ostium (right panel, asterisk) where ablation terminated AT. A revised pattern of activation shows propagation in both directions from the focus. IVC, Inferior vena cava; SVC, superior vena cava.

entire TCL and arrive late to sites close to the focus of the tachycardia. For example, a focal AT originating from the coronary sinus ostium (CS os) in a patient with prior cavotricuspid isthmus (CTI) ablation can produce an electroanatomic map mimicking that of peritricuspid macroreentry (counterclockwise typical AFL; Fig. 6.12). When the “early-meets-late zone” is observed in an activation map that does not span the entire TCL, inadequate mapping should be suspected and more detailed mapping should be performed before concluding macroreentry as the mechanism of the tachycardia.

On the other hand, a macroreentrant tachycardia can produce an electroanatomic activation map that mimics a focal mechanism. If an insufficient number of activation points is obtained, it may be falsely concluded through the interpolation of activation times that the wavefront propagates from a focal source (see Fig. 13.11).¹⁷ This is frequently encountered when the macroreentrant tachycardia originates from the chamber contralateral to the one being mapped. In the latter situation, the activation map will localize the site of the earliest local activation to the earliest breakthrough of conduction into the chamber being mapped. Notably this breakthrough location, although showing the earliest recorded activation timing relative to the intracardiac electrical reference, may not be presystolic (as compared with the onset of the P wave or QRS on the surface ECG) and, hence, cannot be the site of origin of a focal tachycardia. This provides an additional clue to help interpret the activation map and should prompt more detailed mapping. Similarly, a focal pattern can be observed during endocardial mapping when significant parts of the macroreentry circuits are located intramurally or epicardially.

Isochronal Map

The electroanatomic mapping system can generate isochrones of electrical activity as color-coded static maps. The isochronal map depicts

all the points with an activation time within a specific range (e.g., 10 milliseconds) with the same color. Depending on conduction velocity, each color layer is of variable width; isochrones are narrow in areas of slow conduction and broad in areas of fast conduction. Displaying information as an isochronal map helps demonstrate the direction of wavefront propagation, which is perpendicular to the isochronal lines, along the vector of the color changes. Furthermore, isochronal crowding (i.e., multiple colors evident over a small distance) indicating a conduction velocity of 0.033 cm/msec (slower than 0.05 cm/msec) is considered a zone of slow conduction, whereas a collision of two wavefronts traveling in different directions separated temporally by 50 milliseconds is defined as a region of local block. Spontaneous zones of block or slow conduction (less than 0.033 cm/msec) may have a major role in the stabilization of certain arrhythmias.

Propagation Map

Activation mapping data can be displayed in a color-coded animated dynamic map of activation wavefront (propagation map; see Figs. 11.21 and 12.13). Propagation of electrical activation is visualized superimposed on the 3-D anatomical reconstruction of the cardiac chamber in relation to the anatomical landmarks and barriers. Analysis of the propagation map can allow estimation of the conduction velocity along the reentrant circuit and identification of areas of slow conduction.

EnSite Precision enables the visualization of propagation of the activation wavefront over voltage maps, which better illustrate activation patterns in relation to regions of electrical scar (Fig. 6.13).

Entrainment Map

A graphical representation of entrainment mapping can be constructed by plotting values of the differences between the postpacing intervals (PPIs) and the TCLs (PPI–TCL) on the electroanatomic mapping system

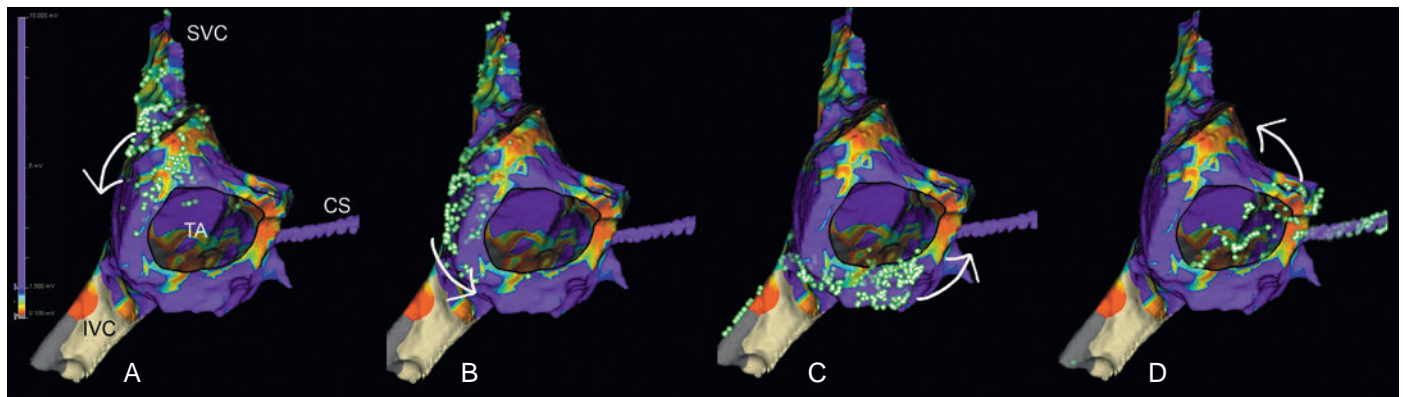


Fig. 6.13 Propagation Map of Typical Atrial Flutter (AFL). Activation and voltage maps of the right atrium are acquired during typical counterclockwise AFL using the EnSite Precision mapping system. Voltage maps are shown in the left anterior oblique projection. Red color corresponds to endocardial atrial bipolar potentials with an amplitude of ≤ 0.1 mV; purple color corresponds to electrogram amplitude of ≥ 1 mV. (A to D) Propagation of the activation wavefront is visualized over the voltage map as bright green dots (“sparkles”) traveling in a counterclockwise direction around the tricuspid annulus (TA), as indicated by the white arrows. CS, Coronary sinus; IVC, inferior vena cava; SVC, superior vena cava.

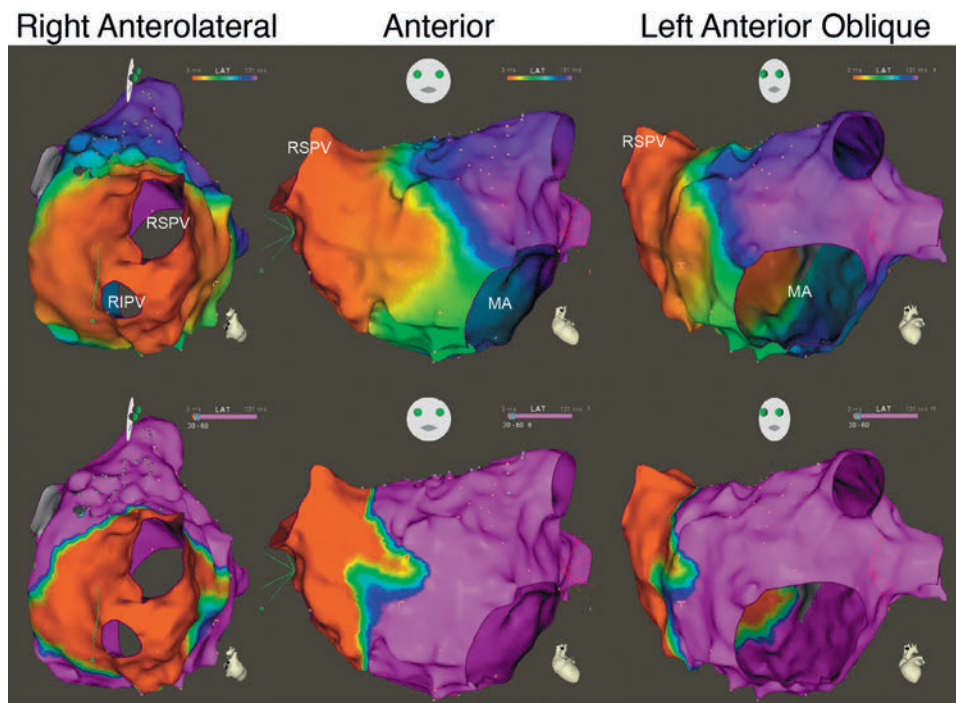


Fig. 6.14 Electroanatomic Color-Coded Entrainment Mapping. Left atrial (LA) electroanatomic color-coded entrainment map in a patient with atrial tachycardia following pulmonary vein isolation for treatment of atrial fibrillation. The LA is shown in various attitudes as indicated. The colors represent the difference between the postpacing interval (PPI) at each site following entrainment pacing and the tachycardia cycle length (TCL): the less the difference, the closer to the circuit. In the top row, red and orange areas have minimal difference between the PPI and TCL (i.e., in or near circuit), while purple areas have large differences (i.e., remote from circuit). Bottom row shows the same data with the timing scale set such that 0 to 30 milliseconds is red (i.e., in peri-right pulmonary veins circuit). Note that not all areas that are in the circuit are reasonable ablation target areas. MA, Mitral annulus; RIPV, right inferior pulmonary veins; RSPV, right superior pulmonary veins.

to generate color-coded 3-D entrainment maps (Fig. 6.14). This approach can potentially help accurately determine and visualize the 3-D location of the entire reentrant circuit, even though the area of slow conduction of the tachycardia is not specified. Because none of the electroanatomic mapping systems contain an algorithm for color-coding of entrainment

information, the modus for activation mapping is altered manually. At each 3-D location of the catheter tip stored on the electroanatomic mapping system, entrainment stimulation is performed, and the difference between PPI and TCL is calculated and associated with that site on the electroanatomic mapping system (as if it were an “activation

time”). For that, the local electrogram stored at the 3-D location is completely disregarded. The annotation marker is manually moved into a position where the numeric timing information equals the entrainment information (PPI–TCL). That timing information then is displayed in a color-coded fashion as if it were activation time, but instead it represents information on the length of the entrainment return cycle. With the color range, red represents points closest to the reentrant circuit (i.e., sites with smaller PPI–TCL differences, approaching 0, signifying their inclusion in the reentrant circuit) and purple represents points far away from the circuit (i.e., sites with the largest PPI–TCL differences).

Color-coded 3-D entrainment mapping allows determination of the full active reentrant circuit (vs. passively activated regions of the chamber) and the obstacle around which the tachycardia is circulating, and it provides very useful information on the location of potential ablation sites (see Fig. 6.14). However, ablation will not terminate reentry at all these sites. (Just as, although the circuit in orthodromic supraventricular tachycardia includes the ventricle, ablation at one or two sites in that ventricle will not eliminate reentry.) The final choice is determined by the location of anatomical barriers and width of putative isthmuses, so that strategic ablation lines, mainly connecting anatomical barriers, can be applied to transect the circuit and treat the arrhythmia.

Limitations of Electroanatomic Activation Mapping

Although 3-D mapping systems with image integration have been widely adopted for ablation procedures, many of their theoretical benefits remain to be proven. Therefore these systems should remain just one type among the tools facilitating complex catheter ablation procedures and should not distract the electrophysiologist from established EP principles and endpoints.¹⁸

The sequential data acquisition required for map creation remains very time-consuming because the process of creation of an electroanatomic map requires tagging many points, depending on the spatial details needed to analyze a given arrhythmia. Because the acquired data are not coherent in time, multiple beats are required, and stable, sustained, or frequently repetitive arrhythmia is usually needed for creation of the activation map. Given that these points do not provide real-time, constantly updated information, more time may be needed for making new maps to see a current endocardial activation sequence, detect a change in arrhythmia, or fully visualize multiple tachycardias. In addition, rapidly changing or transient arrhythmias are not easily recorded and may be mapped only if significant substrate abnormalities are present. For macroreentrant tachycardias, variation of the TCL by more than 10% can prevent complete understanding of a circuit, and it decreases the confidence in the electroanatomic activation map. Single premature ventricular complexes (PVCs) or premature atrial complexes (PACs) or nonsustained events may be mapped, although at the expense of an appreciable amount of time. The use of multielectrode catheters for data acquisition helps address many of these issues.

One difficulty with current methods is that incorrect assignment of activation for a few electrograms can invalidate the entire activation map, and manual adjustment is often required to achieve the optimal representation. This is the major drawback of mapping with multipolar electrode catheters; although data from a large number of sites can be acquired quickly, unless all electrograms are adjudicated to ensure correct designation of activation time by the mapping system, the map may be very misleading. In addition, data interpolation between mapped points is used to improve the quality of the display; however, areas of unmapped myocardium are then assigned simple estimates of timing and voltage information that may not be accurate.

If highly fractionated and wide potentials are present, it can be difficult to assign an activation time. In some macroreentrant circuits,

much of the TCL is occupied by fractionated low-amplitude potentials. Furthermore, the assignment of a single time value to a multicomponent electrogram does not represent the quality of the electrogram and dismisses important information about the potential role of the recorded potential in the arrhythmia circuit. The subjective selection of an individual local potential within a multicomponent electrogram can drastically alter a propagation map. If these potentials are dismissed or assigned relatively late activation times, a macroreentrant tachycardia may mimic a focal arrhythmia, and it will appear as if substantially less than 90% of the TCL is mapped.

Electroanatomic Voltage Mapping

Voltage mapping is performed to delineate the region of electrical scar that can harbor the arrhythmogenic substrate or can potentially serve as a boundary for the subsequent design of ablation strategies. This can be of significant value in the setting of unstable or unsustainable tachycardias, especially scar-related VT. Substrate mapping helps identify the VT substrate and facilitates ablation of multiple VTs, pleomorphic VTs, and VTs that are unmappable because of hemodynamic instability or poor inducibility. Substrate mapping is also of value even in well-tolerated VTs because it can help focus activation and entrainment mapping efforts on a small region harboring the VT substrate, and therefore help minimize the duration during which the patient is actually in VT. In addition, superimposition of the voltage map on the activation map can help focus auditing of the activation map to areas where low amplitude potentials are recorded.

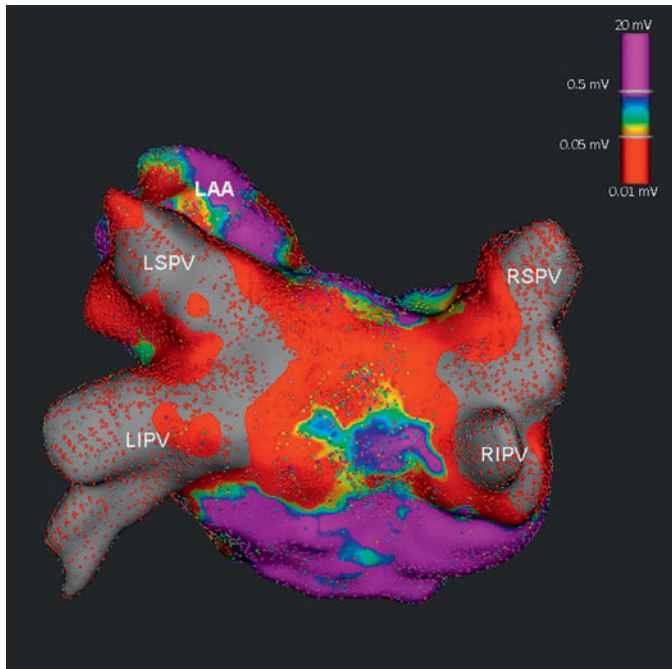
Bipolar voltage mapping has been correlated with dense scar defined by histopathology and cardiac MRI. Electrical scar is defined by low amplitude of local electrograms and tissue inexcitability during high-output pacing. Although the true range of normal electrogram amplitude is often difficult to define, endocardial ventricular bipolar electrogram amplitude less than 1.5 mV has been accepted as an abnormally low voltage, with a cutoff of 0.5 mV as the signal amplitude that best defines the anatomical region of dense scar (Table 6.1). A pacing threshold greater than 10 mA has been used to define inexcitable scar, provided electrode-tissue contact is adequate.¹⁹ For the atrium, endocardial bipolar potentials with an amplitude of 0.5 mV or less are typically considered abnormal and termed low voltage areas (eFig. 6.1). Silent areas (scars) are defined as having an atrial bipolar potential amplitude of less than 0.05 mV and the absence of atrial capture at 20 mA.^{20–24}

A more rigid voltage cutoff criterion is used when analyzing bipolar signals on the ventricular epicardium to limit the influence of epicardial fat and coronary vasculature (see Table 6.1). As epicardial fat overlying normal myocardium insulates the underlying tissue, attenuated low-amplitude signals can be mistaken for abnormal myocardial tissue. Normal epicardial electrogram amplitude is defined as greater than 1.0 mV. Dense scar is defined as confluent areas with bipolar electrogram amplitude less than 0.5 mV, and border zone in regions with bipolar

TABLE 6.1 Voltage Criteria to Define Abnormal Myocardial Substrate

Electrogram Amplitude	Low Voltage	Dense Scar
RV and LV endocardial bipolar	<1.5 mV	<0.5 mV
RV and LV epicardial bipolar	<1.0 mV	<0.5 mV
LV endocardial unipolar	<8.3 mV	<7.0 mV
RV endocardial unipolar	<5.5 mV	<3.5 mV
RA and LA endocardial bipolar	<0.5 mV	<0.05 mV

LA, Left atrium; LV, left ventricle; RA, right atrium; RV, right ventricle.



eFig. 6.1 Rhythmia Voltage Map of the Left Atrium (LA). A postero-anterior view of the LA is shown. The patient had prior catheter ablation for atrial fibrillation. Endocardial atrial bipolar potentials with an amplitude of ≥ 0.5 mV are considered normal (*purple color*). Silent areas (scars) are defined as having an atrial bipolar potential amplitude of less than 0.05 mV (*red color*). Gray color indicates electrogram amplitudes below the threshold of detection by the mapping system. Note the low voltage zones in the posterior LA wall and pulmonary vein (PV) regions consequent to prior ablation. LAA, Left atrial appendage; LIPV, left inferior PV; LSPV, left superior PV; RIPV, right inferior PV; RSPV, right superior PV.

electrogram amplitude between 0.5 and 1.0 mV. Because epicardial fat may decrease signal amplitude, low-voltage areas during epicardial mapping should also show abnormal electrogram configuration.^{19,21,22}

A limitation of bipolar recordings is that they have a limited field of view such that the amplitude of the bipolar electrogram is primarily driven by local tissue activity, while far-field activity is subtracted out. Therefore, although voltage properties of the endocardium are well-represented in the bipolar signal, intramural or epicardial scar that can potentially harbor the arrhythmogenic substrate can be missed by purely endocardial bipolar voltage mapping. In contrast, unipolar electrograms reflect the voltage difference between the exploring electrode in contact with myocardium and a second electrode that is distant from the heart (usually Wilson's central terminal). Thus the unipolar electrode has a wide field of view, and unipolar electrogram amplitude primarily represents more remote, far-field tissue depolarization.²² Therefore unipolar voltage mapping has recently been proposed to improve myocardial sensing with a wider field of view to detect the presence of midmyocardial and epicardial scar. A voltage cutoff of 8.3 mV is used to distinguish normal from abnormal LV unipolar endocardial electrogram amplitude (eFig. 6.2).¹⁹ A lower cutoff value of less than 5.5 mV defined normal unipolar voltage for the thinner free wall of the RV (see Fig. 25.4).^{21,25–27}

Electroanatomic voltage mapping can be performed during sinus, paced, or any other rhythm. The voltage map displays the peak-to-peak amplitude of the electrogram within the sampling time window at each site and is measured automatically by the mapping system. This value is color-coded and superimposed on the anatomical model (see eFig. 6.2). The gain on the 3-D color display allows the user to concentrate on a narrow or wide range of potentials. By diminishing the color scale, larger amplitude signals are eliminated.

Embedded within or between areas of dense fibrosis, isolated bundles of viable myocardium (called *conducting channels*) can potentially form protected the diastolic isthmuses necessary to support the arrhythmia circuit. Conduction through these bundles is typically slow and anisotropic, resulting in low-amplitude, multipotential, fractionated bipolar electrograms. Abnormal low-voltage electrograms can be recorded throughout extensive areas of scar that are not sufficiently specific for the components of the reentrant circuit. Thus the identification of the conducting channels within the low voltage zones helps refine the area that potentially supports the tachycardia circuit. Conducting channels can be identified on the electroanatomic voltage map as corridors of voltage preservation (voltage channels) within denser regions of scar, or as corridors between a dense scar and a valvular annulus. Careful step-by-step manual adjustment of voltage upper and lower limits on the color-coded electroanatomic voltage map (scar thresholding) can help maximize the color contrast between adjacent myocardium with different electrogram voltage levels within the 0.5-mV scar and thus unmask channels of viable myocardium within a dense scar (see eFig. 22.14 and Fig. 22.28).^{3,26}

Pacing provides complementary information to electrogram amplitude; only 2% of sites with amplitude more than 0.5 mV have a pacing threshold more than 10 mA, whereas a substantial number of very low amplitude sites have high pacing thresholds, and many sites in reentry circuit isthmuses have very low amplitudes. A dense scar is defined by the lack of electrical excitability during high-output pacing.¹⁹

Factors Influencing Voltage Mapping Resolution

Bipolar electrogram amplitude is influenced by multiple variables that can affect the accuracy and resolution of the voltage map. These include the electrode size, interelectrode distance, conduction velocity between the bipolar electrodes, vector of activation, and the angle at which the electrode engages the tissue, and signal filtering, among others.^{28–30}

Electrode size. The resolution of voltage mapping is influenced electrode size and interelectrode spacing. The spatial resolution of the standard mapping catheter is limited due to the large electrode surface area and wide interelectrode spacing. These catheters record signals produced by relatively large tissue mass and, hence, are more likely to exhibit larger bipolar electrogram amplitudes. Furthermore, low-amplitude signals produced by smaller mass of viable tissue can be lost when recorded with large electrodes. Therefore, while voltage mapping likely identifies large unexcitable areas of scar, small strands of fibrosis, which could harbor the arrhythmogenic substrate, may escape detection amidst the background of high-amplitude far-field signals. Similarly, small strands of surviving myocardium within an area of dense scar may not be detected during voltage mapping.

Smaller electrodes with closer interelectrode spacing record signals from smaller tissue mass and are subjected to less signal averaging and cancellation effects. As a result, data acquisition with smaller electrodes allows for the accurate detection of very small amplitude signals while limiting the effects of far-field signals and background noise. This can be of particular advantage in the low-voltage zones and areas of heterogeneous scar distribution, where the increased mapping resolution offered by the multielectrode catheters allows identifying surviving myocardial bundles channels, otherwise considered dense scar by standard linear catheters (Fig. 6.15).^{9,28,31}

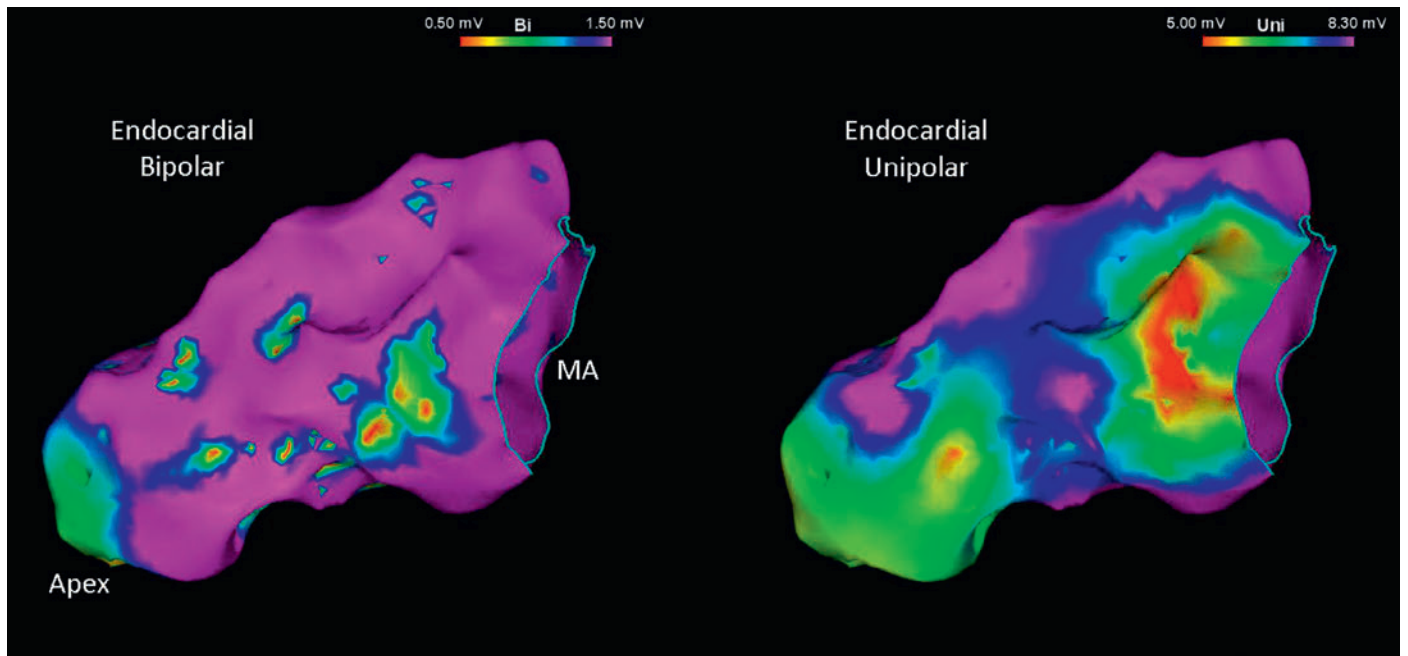
It is important to note that a minimal electrogram amplitude to identify an unexcitable scar has not yet been strictly defined. As different catheters with various electrode sizes and interelectrode spacings are becoming available, individualized validation is required, and catheter-specific thresholds are needed to improve scar characterization.

Vector of activation. The vector of propagation of the activation wavefront in relation to the two recording electrodes, and orientation of the recording electrode relative to the tissue, influences the degree of signal cancellation and therefore the resultant bipolar signal amplitude.²⁸

In multiple studies, significant differences in bipolar and unipolar low-voltage characterization of ventricular scar were frequently observed by varying the wavefront of ventricular activation. Activation within viable neighboring tissue can allow for greater variability in myocardial activation, resulting in wavefront fusion (additive to electrogram) and cancellation (subtractive from electrogram). Furthermore, local conduction delay or block and uncoupling between near- and far-field signals can potentially account for these observations. Mismatches between low bipolar voltage regions appear to occur most frequently in areas with predominantly mixed scar tissue (areas with electrogram amplitudes in the range of 0.5 to 1.5 mV) and in septal regions. Dense scar appears to be less sensitive to wavefront changes compared with mixed scars, likely due to lesser available mass of normal far-field myocardium to contribute to the electrogram signal within the field of view of the mapping catheter. Therefore voltage mapping during more than one activation sequence (e.g., during normal sinus rhythm [NSR] and ventricular pacing) can potentially increase the sensitivity to detect arrhythmogenic substrate.³²

Tissue contact. Voltage mapping relies heavily on consistent catheter contact. If catheter contact is suboptimal and falsely low voltage measurements are recorded, the voltage map will erroneously suggest a scar. The use of ICE and contact force sensors can help ensure adequate catheter contact.²⁸

Mapping density. Low mapping density is associated with the significant interpolation of data between sampled points. The use of multielectrode catheters enables rapid high-density voltage mapping through simultaneous multiple-point acquisition, which reduces interpolation of data between points and improves mapping accuracy.²⁸



eFig. 6.2 Endocardial Left Ventricular (LV) Electroanatomic Voltage Mapping. *Left*, Endocardial bipolar voltage map of the LV (left lateral view) showing low voltage areas (peak-to-peak bipolar amplitude less than 1.5 mV) in the basal lateral and apical walls. *Right*, Endocardial unipolar voltage map reveals more diffuse low voltage areas (unipolar amplitude of <8.3 mV) consistent with more extensive epicardial distribution of fibrosis. MA, Mitral annulus. Apex.

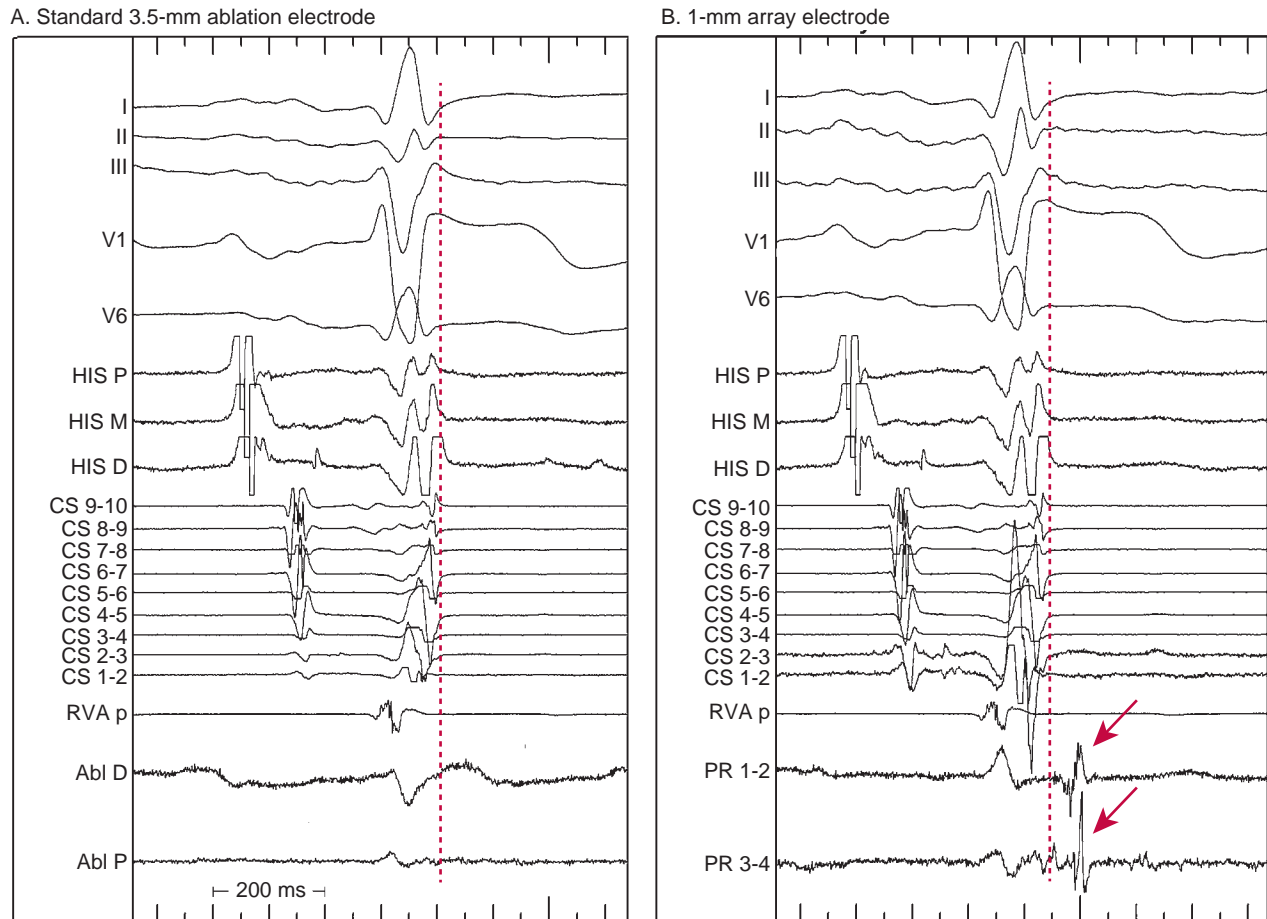


Fig. 6.15 Standard Electrode Versus Small Electrode for Delineation of Late Potentials in a Patient With Cardiomyopathy. Endocardial recordings from the inferolateral left ventricular free wall are shown from approximately the same location at almost the same time (two catheters in left ventricle). In (A) with a standard 3.5 mm distal tip, only far-field signals are recorded. In (B) with much smaller electrodes on a multipolar catheter, discrete high-frequency late potentials (red arrows) are observed (after end of QRS complex, red dotted line). Abl, Ablation; CS, coronary sinus.

Limitations of Electroanatomic Voltage Mapping

Electrogram amplitude is annotated to the electrogram peak. In regions of scar, far-field signals are frequently of larger amplitude than local electrograms. Therefore automated voltage annotation of the larger far-field electrograms can introduce errors in the voltage map, especially in scar regions (Fig. 6.16). Manual tagging of abnormal potentials or manual annotation of near-field electrogram voltage can help improve the map accuracy, but this can be challenging with high-density point acquisition.

Voltage mapping during NSR depends on the assumption that the arrhythmogenic substrate is limited to fixed myocardial scar and anatomical barriers. It is now well known that functional lines of block (present during tachycardia but not in NSR) play an important role in arrhythmogenesis, and these barriers cannot be detected by substrate mapping performed in NSR. Therefore conducting channels developing during arrhythmias and surrogates of channels and conduction barriers identified by substrate mapping in NSR may not correspond.³³

Even when conducting channels within the scar area can be identified by voltage mapping, their relationship to the arrhythmia circuit remains to be assessed by other mapping methods (e.g., entrainment mapping). Voltage mapping does not distinguish abnormal bystander

areas that are not involved in a tachycardia circuit from clinically relevant channels.³⁴

It is also important to recognize that the transmural distribution of the scar may not be reliably represented by voltage mapping from either the endocardial or epicardial surface. In particular, identifying septal or mid-myocardial substrates can be challenging.¹⁹

High-Resolution Electroanatomic Mapping

Current iterations of electroanatomic mapping systems allow the construction of high-resolution electroanatomic maps through catheters with multiple electrodes. These multielectrode mapping catheters facilitate the creation of high-density maps through simultaneous acquisition of points from multiple closely spaced electrodes. The rapid acquisition of a large quantity of data facilitates the generation of detailed, high-density, high-resolution activation and voltage maps. Further, the use of multielectrode mapping catheters helps expedite the process of data acquisition during electroanatomic mapping and decrease fluoroscopy and procedure times. Automated data acquisition and annotation can further facilitate the mapping process (with the previously noted caveats).^{10,20,29}

Several multielectrode catheters with varying configurations have been described. The EnSite NavX system can utilize any multielectrode catheter

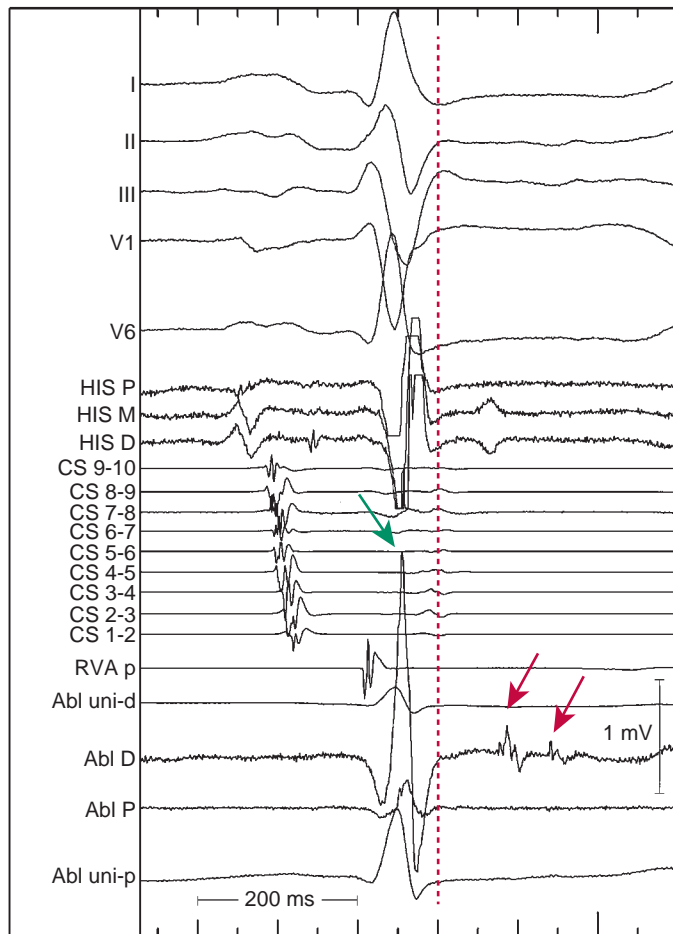


Fig. 6.16 Epicardial Late Potential Obscured by Far-Field Signal in a Patient With Dilated Cardiomyopathy. The ablation catheter is on the epicardial surface after percutaneous pericardial access; a very large potential within the QRS complex (green arrow) will be taken by the mapping system to characterize the site as being “normal,” whereas distinct high-frequency late (red arrows) are evident well after the end of the QRS complex (dotted red line). Abl, Ablation; CS, Coronary sinus.

for data acquisition. The multipolar Lasso, PentaRay, and DecaNav catheters (Biosense Webster) are equipped with the electromagnetic sensor and can be used with the CARTO system, allowing for electroanatomical data acquisition. The circular Lasso catheter has 10 or 20 electrodes, each with a surface area of 1.0 mm², recording bipolar electrograms with an interelectrode spacing of 3 mm, and maximal diameter of 25 mm. The star-shaped multielectrode PentaRay is a 7 Fr steerable catheter (180 degrees of unidirectional flexion) with 20 electrodes distributed over five soft, radiating spines (1-mm electrodes separated by 4-4-4 or 2-6-2 mm edge-to-edge interelectrode spacing), thus allowing splaying of the catheter to cover a surface diameter of 3.5 cm (see Fig. 6.1; see Fig. 4.2). The spines have been given alphabetical nomenclature (A to E), and spines A and B are recognized by radiopaque markers. These multielectrode catheters have smaller electrodes (0.8 mm²) and closer interelectrode spacing (as compared with ablation catheters), which allow for recording bipolar signals from smaller tissue diameters that are less vulnerable to averaging and cancellation effects.^{20,31,35}

The Rhythmia system utilizes a mini-basket catheter (Orion), which has 64 very small electrodes (0.4 mm²) with interelectrode spacing of 2.5 mm (see Fig. 6.7). This catheter allows for the construction of ultra-high resolution activation and voltage maps.^{29,36}

Ripple Mapping

Ripple mapping is a novel visualization technique that displays time-voltage data as dynamic bars on the cardiac surface. Ripple mapping software requires incorporation of a 3-D electroanatomic mapping system (CARTO). Each electrogram component is visualized at its corresponding 3-D coordinate on the CARTO-generated chamber geometry as a dynamic surface bar that varies in height and color according to the electrogram voltage–time relationship that is time-gated to a selected fiduciary reference electrogram. Both positive and negative electrogram deflections are shown protruding outward from the surface. The height of each bar correlates with the voltage amplitude of the electrogram at that time point, without the need for annotation of local activation timing (Fig. 6.17).³⁷

When multiple points are collected over an area, adjacent bars move up and down (according to the local voltage) in a sequential fashion (in time relative to a chosen fiducial reference electrogram). As a result, a “ripple” effect is seen as the movement traverses from one bar to the next, creating a “ripple map.” Propagation of activation is visualized by the direction of the “ripple” on the map (Fig. 6.18). Ripple activation maps can be superimposed on a conventional bipolar voltage map, thereby displaying the surface geometry with both voltage and activation simultaneously.³⁸

Ripple mapping is designed to overcome some of the limitations of existing electroanatomic activation and voltage mapping. Electroanatomic mapping requires the accurate annotation of local activation time of electrograms within the window of interest. In the region of scar, annotation as a single activation time often is suboptimal, due to the presence of fractionated or multiple late potentials. Incorrect annotation of only a small number of electrograms can invalidate the entire activation map. Furthermore, the assignment of a single time value to an individual local potential within a multicomponent electrogram without indication of signal quality often ignores the information contained within complex fractionated electrograms that can be valuable for the identification of the arrhythmogenic substrate and ablation targets. Voltage mapping can also be challenging in the region of scar. Voltage annotation to the electrogram peak can erroneously incorporate far-field electrograms, which are frequently larger than the local signal. In addition, interpolation of data within unmapped regions can lead to the display of false information.

In contrast, ripple mapping preserves all components of the electrogram. Instead of assigning each point as a single time value to create a color-coded map, ripple mapping preserves and represents all the components of the electrogram (voltage, waveform, and timing) at its corresponding 3-D coordinate as a bar that rises perpendicular to the surface of the cardiac chamber that varies in height according to the underlying voltage amplitude, without the need for manual or automatic annotations of local activation timing or setting a window of interest (see Fig. 6.17). As a result, a sequence of small potential changes in a fractionated electrogram can be temporally linked to its adjacent neighbors, and delayed low-amplitude local activation within scar is seen distinct from an initial far-field electrogram occurring in tandem with activation in the surrounding healthy myocardium. Also, the system does not interpolate within unmapped regions; thus interpolation errors are avoided as only “real” data is displayed on the ripple map.^{38,39}

Although data are limited, several small studies demonstrated the potential value ripple mapping in determining activation patterns in both simple and complex cardiac rhythms.^{39,40}

Anatomical Mapping

All the recorded catheter locations are aggregated and used to create a shell (anatomical map) of the cardiac chamber. Modern electroanatomic

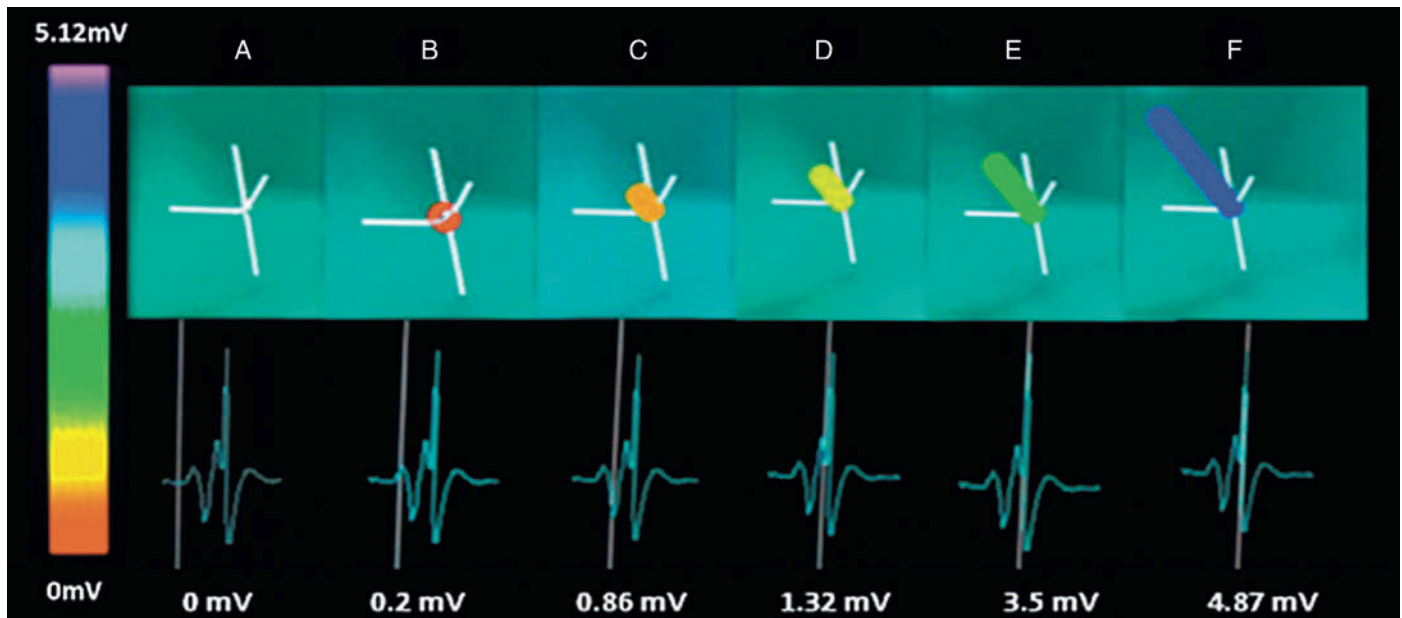


Fig. 6.17 Ripple Bar Height Versus Electrogram Voltage. The top panels (A to F) show increasing ripple bar height in correlation to the increasing magnitude of the corresponding electrogram voltage in the annotation window (*lower window*). Panel A shows the time-cursor (*white bar*) at an isoelectric point of the chosen electrogram (*lower panel*) with no visible corresponding ripple bar (*upper panel*). As the time-cursor moves along the electrogram, the bar always moves outward from the cardiac shell irrespective of whether it is a negative or positive bipolar electrogram polarity. Panel C represents deflection of the electrogram below the isoelectric line corresponding to a negative bipolar value (-0.86 mV); however, the bar is clearly protruding outward from the shell. The color can be correlated to the reference color bar seen to the left of the panel with low voltage represented by red and high voltage represented by purple. (From Jamil-Copley S, Linton N, Koa-Wing M, et al. Application of ripple mapping with an electroanatomic mapping system for diagnosis of atrial tachycardias. *J Cardiovasc Electrophysiol*. 2013;24:1361–1369.)

mapping systems incorporate utilities enabling computer-automated multipoint model creation while the mapping catheter is maneuvered around the anatomical structure (CARTO-3 Fast Anatomic Map Module and EnSite NavX Velocity One-Model Module). A virtual anatomical intracardiac geometry is obtained by moving the catheter in all directions throughout the cardiac chamber of interest, keeping contact with the endocardial wall to outline the structures. Points at the outermost boundaries are used to depict the outer geometry (shell), while points inbound to the outer shell are automatically removed. Acquired *activation* or *voltage* mapping points internal or external to the outer shell are included only if they fall within a *threshold* distance (defined by the user) from the outer surface. A purely anatomical map and catheter navigation capabilities are particularly suitable for ablation of arrhythmias with well-known substrates that can be treated by an anatomically based ablation approach, such as AFL and linear LA ablation for AF.

Electroanatomic maps represent the same anatomical map with an overlay of color-coded electrical data. Acquired *activation* or *voltage* mapping points internal or external to the outer shell are included only if they fall within a *threshold* distance (defined by the user) from the outer surface.

Acquired *activation* or *voltage* mapping points internal or external to the outer shell are included only if they fall within a *threshold* distance (defined by the user) from the outer surface. A purely anatomic map and catheter navigation capabilities are particularly suitable for ablation of arrhythmias with well-known substrates that can be treated by an anatomically based ablation approach, such as AFL and linear LA ablation for AF.

It is important to move the mapping catheter carefully and minimize inconsistency in the contact force on the catheter tip to avoid excessive

anatomical distortion and expansion of the virtual image. Such anatomical distortion can misrepresent the local fiducial sites, which should be taken into consideration when mapping and ablation are guided by fast anatomical maps.^{4,41}

Characteristic anatomical landmarks and sites of interest in the cardiac chamber are acquired and tagged. Valvular annuli, thoracic veins, and other structures can be marked and *carved* out of the electroanatomic map. If a CT reconstruction of the mapped cardiac chamber is available, the image can be visualized on a split screen and used to guide finer anatomical definition with the ablation catheter. On completion, maps can be edited to eliminate “false space” (i.e., geometry with sparse acquired points) and erroneous structure definition. Additional tagging of sites of interest and ablation points can be done during the procedure. Point-to-point activation mapping is carried out to create static isochronal, voltage, and activation maps (see Fig. 6.5).

Respiratory compensation is collected just before mapping to filter low-frequency cardiac shift associated with the breathing cycle. The CARTO-3 system enables automatic respiratory-gating for data acquisition through thoracic impedance measurement. With other systems, volume sampling with catheter movement during the exhalation phase can help reduce respiratory artifacts.

With the NavX system, a scaling algorithm (field scaling) can be applied to the completed detailed geometry to compensate for variations in impedance between the heart chambers and venous structures (which can otherwise result in a distortion of the *x-y-z* coordinates when a “roving” catheter is maneuvered among the regions of differing impedance). Field scaling is based on the measured interelectrode spacing for all locations within the geometry. Adjustments to the local strength of the navigation fields are made so that the computed catheter electrode

LEFT ATRIAL FOCAL TACHYCARDIA

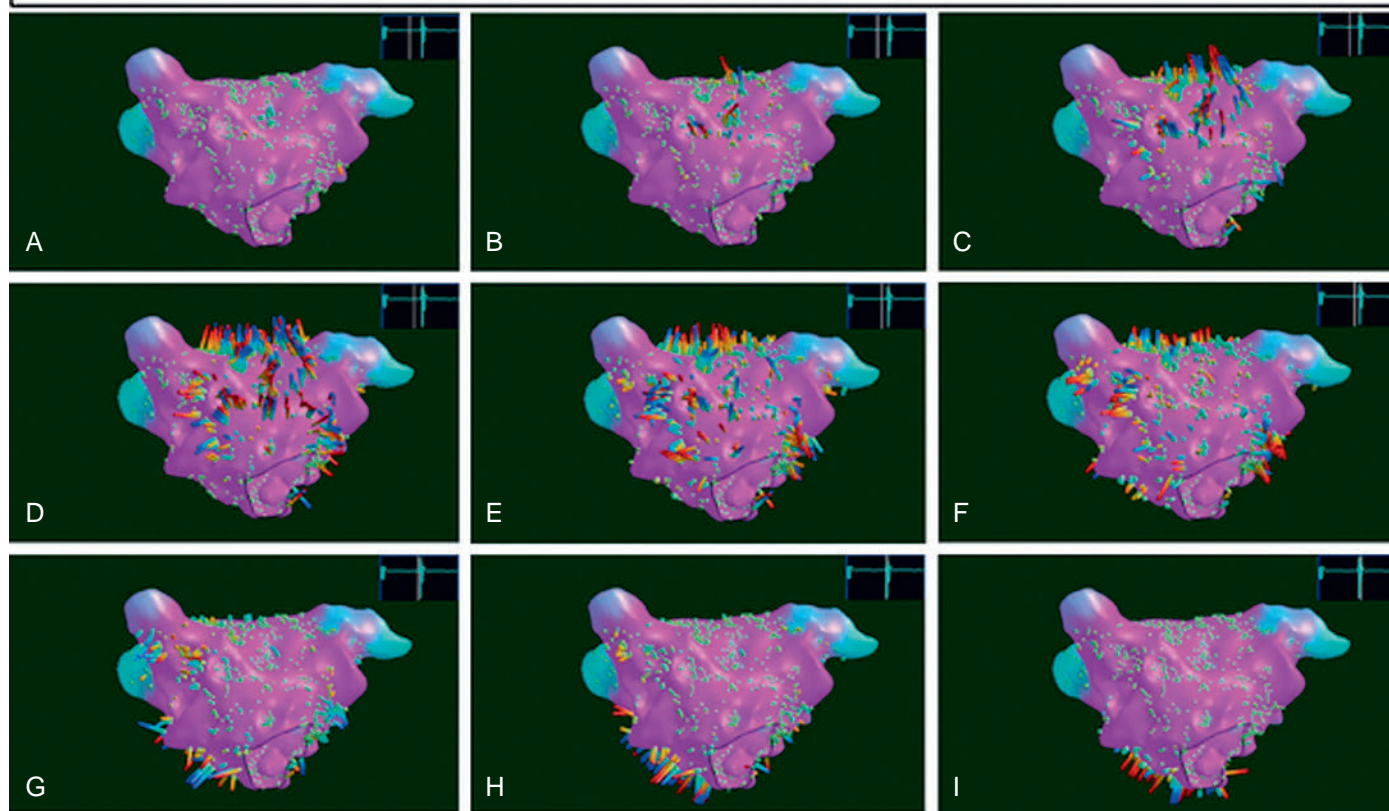


Fig. 6.18 Ripple Map of Focal Atrial Tachycardia. Panels A to I demonstrate the centrifugal ripple bar propagation during a focal atrial tachycardia originating from the anterior wall of the left atrium. The map was created using CARTO and 1433 points collected in the left atrium. (From Jamil-Copley S, Linton N, Koa-Wing M, et al. Application of ripple mapping with an electroanatomic mapping system for diagnosis of atrial tachycardias. *J Cardiovasc Electrophysiol.* 2013;24:1361–1369.)

positions match the known interelectrode spacing of the catheters used to create the geometry.

The CARTO and Rhythmia systems require the use of proprietary catheters with a location sensor to collect mapping data and depict cardiac geometry. In contrast, NavX-guided procedures can be performed using any EP catheter.

Limitations of Anatomical Mapping

Significant anatomical distortions in complex structures can occur with low-density mapping, whereby individual interpolation schemes in the region of curvature do not depict the accurate geometry, especially at areas of exvaginations (e.g., the PVs, atrial appendages). This can be mitigated by (1) the acquisition of a larger number of points (increased density) to reduce the extent of interpolation; (2) the acquisition of a set of points at the critical junctions between the different anatomical structures; and (3) creating geometric shells of these structures in separate maps and then combining them into the main chamber.

In addition, a change in rhythm during the mapping procedure can alter cardiac geometry to the extent that anatomical points acquired during one rhythm cannot be relied on after a change in rhythm (Fig. 6.19). This is relevant during the mapping of PVCs (especially PVCs originating from the RV and those with short coupling intervals), because electrical and spatial information acquired during the arrhythmia can potentially be spatially separated from the same locations when they

are assigned during normal rhythm (e.g., at the time of RF delivery after tachycardia termination). Therefore, after termination of the arrhythmia, revisiting the site of early activation tagged during PVCs or tachycardia may not be feasible and can potentially be misleading as a target for ablation. This can be mitigated by annotating the site of interest after tachycardia termination before moving the mapping catheter from its original location.⁴²

Furthermore, electroanatomic mapping systems do not provide real-time correlation of catheter position and heart border motion. Therefore localizing the catheter tip against the virtual anatomical shell does not establish catheter tip-tissue contact, and other methods to confirm adequate electrode-tissue contact should be utilized (e.g., pacing and recording data at the catheter tip, intermittent fluoroscopic imaging, ICE, and force contact sensors). In fact, geometric reconstructions of the cardiac chamber during the same procedure can vary depending on the method used. For example, the 3-D ICE-derived LA geometric reconstruction was found to be smaller than reconstructions derived from electroanatomic mapping and merged CT images. During procedures lasting several hours, chamber sizes may change based on the accrual of 1 or more liters of saline infused.^{4,43}

Clinical Implications

Contemporary electroanatomic mapping systems provide the ability to visualize and navigate a complete set of intracardiac catheters in any

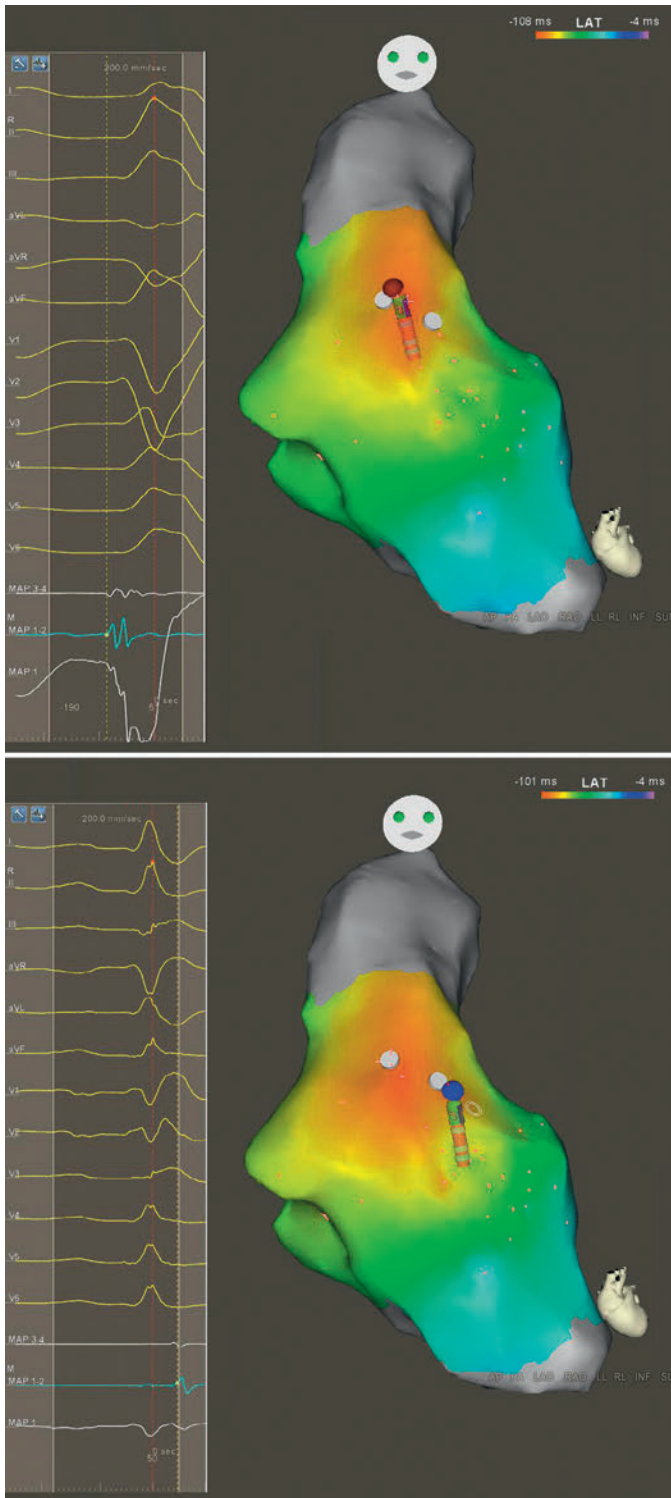


Fig. 6.19 Alteration of Cardiac Geometry by a Change in Cardiac Rhythm. CARTO electroanatomic activation map (color-coded) of the focus of the premature ventricular complexes (PVCs) in the right ventricular outflow tract (anterior view). The acquisition reference is set to the peak of the R wave in the surface ECG lead II. *Upper panel*, Electrical information (local activation time) is acquired by the CARTO system during activation mapping during the PVC. Spatial location of that point is acquired simultaneously (as indicated by the catheter location visualized on cardiac geometry, *red dot*). *Lower panel*, When the spatial location is acquired by the CARTO system during sinus rhythm (*blue dot*), the location of the ablation catheter is assigned to a spatially removed location of the virtual chamber model of the right ventricular outflow tract (RVOT; distance between the two points is 9 mm). Although the tip of the ablation catheter is maintained at the same anatomical location, the spatial information annotated on the virtual chamber model of the RVOT during sinus rhythm is removed and then tagged during the PVC. Therefore when the target of ablation is identified during PVCs, revisiting that target during sinus rhythm may not be accurate unless the acquired electroanatomical location during the PVC is also annotated (before moving the catheter from the identified ablation target) during sinus rhythm.

origin and macroreentrant tachycardia, precisely describing macroreentrant circuits and the sequence of activation during the tachycardia, understanding the reentrant circuit in relation to native barriers and surgical scars, identifying all slow-conducting pathways, rapidly visualizing the activation wavefront (propagation maps), and identifying appropriate sites for entrainment and pace mapping.

In addition, these systems provide a highly accurate geometric rendering of the cardiac chamber, with a straightforward geometric display having the capability to determine the 3-D location and orientation of the ablation catheter accurately. The position of the mapping electrode at any instant is readily apparent. The catheter can anatomically and accurately revisit a critically important recording site (e.g., sites with double potentials or those with good pace maps) identified previously during the study, even if the tachycardia is no longer present or inducible and map-guided catheter navigation is no longer possible. This accurate repositioning provides significant advantages over conventional techniques and is of great value in ablation procedures.

Sites of ablation energy application can be tagged, thus facilitating the creation of lines of block with considerable accuracy by serial RF lesion placement and allowing verification of the continuity of the ablation line and anatomical visualization of the remaining gaps, where additional RF applications can be delivered. This is of particular value after incomplete ablations caused by catheter dislocation, especially if these ablations had caused interruption of the target tachycardia. Additional RF applications can be delivered closely around an apparently successful ablation site to ensure elimination of the arrhythmogenic area. It also helps avoid repeated ablations at the same location.¹

Furthermore, fluoroscopy time and radiation exposure to the operator, the patient, and the laboratory staff can be substantially reduced (or even eliminated entirely) via electroanatomical catheter navigation, and the catheter can be accurately guided to positions removed from fluoroscopic markers.

Choice of Electroanatomic Mapping System

The choice of a specific mapping system for a particular interventional procedure is shaped by the importance of a specific characteristic in the mapping process, as well as the skill and experience of the operator. Advanced mapping systems have a limited role in the ablation of typical AFL, AVNRT, or bypass tracts (BTs), given the high success rate of the

cardiac chamber for diagnostic and therapeutic applications. Electroanatomic mapping systems integrate 3-D catheter localization with sophisticated complex arrhythmia maps and help associate relevant EP information with the appropriate spatial location in the heart and the ability to study activation patterns with high spatial resolution during tachycardia in relation to normal anatomical structures and areas of scar. This significantly facilitates defining the mechanisms underlying the arrhythmia, making a rapid first-pass distinction between a focal

conventional approach. However, for more complex arrhythmias, such as AT, AF, and VT, advanced mapping modalities offer a clear advantage. In addition, electroanatomic mapping systems can potentially shorten procedural time, reduce radiation exposure, and enhance the success rate for the ablation of wide spectrum of arrhythmias.

All three systems perform well for mapping of sustained arrhythmias and for substrate-based ablation procedures. On the other hand, mapping nonsustained arrhythmias, PACs, or PVCs can be tedious with each of these three mapping systems because of the need for sequential data acquisition. However, differences in methods of map acquisition between systems may affect procedure length and radiation use. The use of multielectrode mapping catheters (e.g., PentaRay or Orion) can expedite the mapping process.⁴⁴

Nonetheless, it is important for the electrophysiologist to be cognizant of the distinct advantages and shortcomings of each system.

CARTO

Although all three electroanatomic mapping systems demonstrate a high level of intrinsic accuracy, the magnetic field localization technology of CARTO appears to have superior accuracy at point localization performance and fewer problems with interstructure delineation as compared with impedance-based systems. Another advantage of using magnetic fields for catheter localization is that the fields remain stable over time and are unaffected by biological material; hence the localization accuracy of CARTO is less subject to inhomogeneous tissue characteristics. Electrical field distortions seen with EnSite NavX do not occur with CARTO.^{44,45}

A limitation of the CARTO system is the requirement of a special Biosense Webster catheter with a location sensor embedded proximal to its tip. No other catheter types may be used for electroanatomical data acquisition. Furthermore, the magnetic signal necessary for the CARTO system can potentially create interference with other EP laboratory recording systems. Defibrillators and pacemakers are safe with the system, but the magnetic field can prevent device communication with its programmer, and the magnetic field may need to be disabled temporarily to allow device programming. Percutaneous LV assist devices can cause interference and distortion on the mapping system. Magnetic fields used with the Stereotaxis remote magnetic navigation system are not problematic for the CARTO system.

Although CARTO-3 allows current-based visualization of EP catheters without magnetic sensors, the visualization of catheters is confined into a 3-D virtual area (matrix) that can be built only by using a magnetic sensor-equipped manufacturer-specific catheter. Furthermore, the system still cannot process electrical or location data from the nonproprietary catheters (i.e., catheters without magnetic sensors) to build the virtual geometry or for mapping purposes.²

Importantly, the coordinates of the magnetic field of CARTO are linked to the table and not the patient's body. Therefore significant movement of the patient can cause uncorrectable shifts requiring remapping.

EnSite NavX

One of the principal advantages of this system is its open platform. EnSite NavX enables the display in real time up to 128 electrodes simultaneously on multiple EP catheters with almost every commercially available catheter, including pacemaker leads. This system works with most manufacturers' ablation catheters, RF generators, and cryogenerators. The EnSite System can also be integrated with the Sensei robotic catheter system (Hansen Medical, Mountain View, CA, United States), allowing completely remote catheter navigation.

Also, unlike with the CARTO and Rhythmia, anatomic and electrical data (voltage or activation) can be acquired simultaneously by the EnSite

NavX system from multiple poles on all catheters utilized during the study (and not just catheters with magnetic sensors). Data acquisition can be augmented by the addition of a multielectrode array (MEA) for noncontact mapping.

A unique advantage of the EnSite system is that it can locate the position of the catheters from the puncture site to the final destination in the heart. Therefore all catheters can be navigated to the heart under guidance of the EnSite NavX system, and the use of fluoroscopy can be minimized for preliminary catheter positioning. This contrasts with CARTO-3 that enables visualization of EP catheters without magnetic sensors only when positioned within the 3-D matrix built only by using a magnetic sensor-equipped catheter.

Furthermore, NavX technology is partially insensitive to potential patient movements, as the coordinate system (patches) are linked to the patient, and therefore they move simultaneously with the patient, preventing map shifts.²

On the other hand, the impedance-based localization system used by EnSite is subject to changes in tissue properties. Changes in the respiration pattern and volume shifts during the course of the procedure (e.g., secondary to saline infusion when using an irrigated ablation) can cause impedance changes inside the body and potentially impact the localization accuracy of the EnSite system.^{44,45} The newer version of EnSite (EnSite Precision) now uniquely combines impedance and magnetics, which can enhance navigation and model creation.

Rhythmia

The main advantage of Rhythmia is the ability to create ultra-high-resolution activation and voltage maps using rapid and accurate automated data acquisition and annotation. The very small size of the electrodes on the Orion catheter minimizes far-field signals and background noise and allows accurate detection of very small amplitude signals. Also, this system offers the ability to change the mapping window in retrospect (see Fig. 6.10).

Similar to the EnSite system, Rhythmia can acquire electroanatomical data from magnetically enabled catheters (Orion and ablation catheters) as well as catheter without magnetic sensors. Data acquisition from catheters without magnetic sensors can be acquired only after construction of the electromagnetic field using magnetically enabled catheters. Notably, Rhythmia does not allow for integration with CT or MRI.^{6,36}

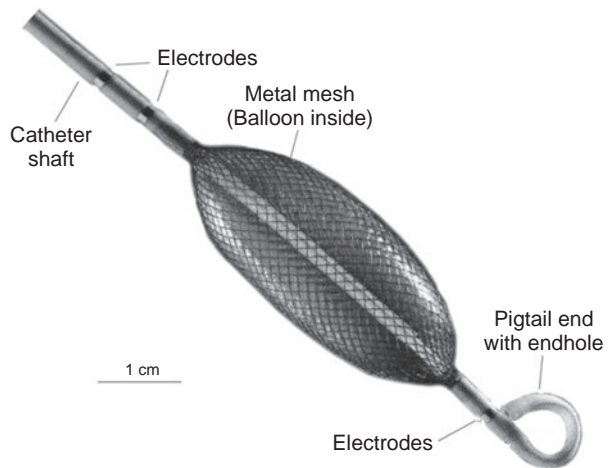
This mapping technology is preferentially designed for complex cardiac arrhythmias like AF, macroreentrant atrial tachycardia (MRAT), and scar-related VT, especially for substrate analysis (voltage maps), and analysis of conduction pattern (activation maps), but also for maps promoting effective catheter ablation (e.g., mapping gap in ablation lines). However, further studies are required to explore the potential clinical benefits gained from such ultra-high-density mapping.¹²

ENSITE NONCONTACT MAPPING SYSTEM

Fundamental Concepts

The noncontact mapping system (EnSite Array, St. Jude Medical) consists of a catheter-mounted MEA, which serves as the probe, a custom-designed amplifier system, a computer workstation used to display 3-D maps of cardiac electrical activity, and a conventional ablation catheter.⁴⁶

The MEA catheter consists of a 7.5-mL ellipsoid balloon mounted on a 9 Fr catheter around which is woven a braid of 64 insulated 0.003-mm-diameter wires (eFig. 6.3). Each wire has a 0.025-mm break in insulation that serves as a noncontact unipolar electrode. The system acquires more than 3000 noncontact unipolar electrograms from all points in the chamber simultaneously. The unipolar signals are recorded using a ring electrode located on the shaft of the array catheter as a



eFig. 6.3 Multielectrode Array for Noncontact Endocardial Mapping.

reference. The raw far-field EP data acquired by the array catheter are fed into a multichannel recorder and amplifier system that also has 16 channels for conventional contact catheters, 12 channels for the surface ECG, and pressure channels. Using data from the 64-electrode array catheter suspended in the heart chamber, the computer uses sophisticated algorithms to compute an inverse solution to determine the activation sequence on the endocardial surface.^{46,47}

The EnSite 3000 mapping system is based on the premise that endocardial activation creates a chamber voltage field that obeys the Laplace equation. Therefore when one 3-D surface of known geometry is placed within another of known geometry, if the electrical potential on one surface is known, then the potential on the other can be calculated. Because the geometry of the balloon catheter is known, and the geometry of the cardiac chamber can be reconstructed during the procedure (see later), endocardial surface potential can then be determined once the potentials over the balloon catheter are recorded. Using this concept, the raw far-field EP data acquired by the array catheter, which are generally lower in amplitude and frequency than the source potential of the endocardium itself and therefore have limited usefulness, are mathematically enhanced and resolved. The inverse solution to Laplace equation using the boundary element method predicts how a remotely detected signal by the MEA would have appeared at its source, the endocardial surface, so that electrograms are reconstructed at endocardial sites in the absence of physical electrode contact at those locations (“virtual electrograms”). Once the potential field has been established, more than 3000 activation points can be displayed as computed electrograms or as isopotential maps. The activation time at each endocardial site is determined by taking the time instant with maximum negative time derivative ($-dV/dt$) on the electrogram.⁴⁸

The system can locate any conventional mapping-ablation catheter in space with respect to the array catheter (and thus with respect to the cardiac chamber being mapped). A low-current (5.68 kHz) locator signal is passed between the contact catheter electrode being located and reference electrodes on the noncontact MEA. This creates a potential gradient across the array electrodes, which is then used to position the source. This locator system is also used to construct the 3-D computer model of the endocardium (virtual endocardium) that is required for the reconstruction of endocardial electrograms and isopotential maps. This model is acquired by moving a conventional contact catheter around the endocardial surface of the cardiac chamber; the system collects the location information, thus building up a series of coordinates for the endocardium and generating a patient-specific, anatomically contoured model of its geometry. During geometry creation, only the most distant points visited by the roving catheter are recorded to ignore those detected when the catheter is not in contact with the endocardial wall.

Using mathematical techniques to process potentials recorded from the array, the system can reconstruct more than 3000 unipolar electrograms simultaneously and superimpose them onto the virtual endocardium, thus producing isopotential maps with a color range representing voltage amplitudes. In addition, the locator signal can be used to display and track the position of any catheter on the endocardial model (virtual endocardium) and allows the marking of anatomical locations identified using fluoroscopy and electrographic characteristics. During catheter ablation procedures, the locator system is used in real time to navigate the ablation catheter to sites of interest identified from the isopotential color maps, catalog the position of RF energy applications on the virtual endocardium, and facilitate revisitation of sites of interest by the ablation catheter.

In addition, the EnSite software provides the capability of point-to-point contact mapping, to allow the creation of activation and voltage maps by acquiring serial contact electrograms and displaying them on

the virtual endocardium (see later). This is useful for adding detail, familiarity, and validation of the information obtained by the noncontact method.

Technology Application

The EnSite 3000 system requires placing a 9 Fr MEA and a mapping-ablation catheter. To create a map, the balloon catheter is advanced over a 0.035-inch guidewire under fluoroscopic guidance into the cardiac chamber of interest. For RA arrhythmias, the guidewire is advanced into the SVC, and the balloon is deployed in the upper third of the RA for tachycardia originating in the SVC, in the middle third for ectopic AT, and in the lower third for typical AFL. For LA arrhythmias, the guidewire is advanced into the left superior PV, and the balloon is deployed in the middle of the LA. For RV arrhythmias, the guidewire is advanced into the pulmonary artery, and the balloon is deployed close to the right ventricular outflow tract (RVOT) or in the middle of the RV. The balloon can be filled with contrast dye, thus permitting it to be visualized fluoroscopically (see Chapter 23, eFig. 23.9). Except in the RVOT, the balloon is positioned in the center of the cardiac chamber of interest and does not come in contact with the walls of the chamber being mapped. In addition, the position of the array in the chamber must be secured to avoid significant movement that would invalidate the electrical and anatomical information. The array must be positioned as closely as possible (and in direct line of sight through the blood pool) to the endocardial surface being mapped, because the accuracy of the map is sensitive to the distance between the center of the balloon and the endocardium being mapped.⁴⁶

During the use of this mapping modality, systemic anticoagulation is critical to avoid thromboembolic complications. Intravenous (IV) heparin is usually given to maintain the activated clotting time longer than 250 seconds for right-sided and longer than 300 seconds for left-sided mapping.

A conventional (roving) deflectable mapping catheter is also positioned in the chamber being mapped and used to collect geometry information. The mapping catheter is initially moved to known anatomical locations, which are tagged. A detailed geometry of the chamber is then reconstructed by moving the mapping catheter and tracing the contour of the endocardium (using the locator technology). To create detailed geometry, attempts must be made to make contact with as much endocardium as possible. This requires maneuvering on all sides of the array, which can be challenging and can require decreasing the profile of the balloon by withdrawing a few milliliters of fluid. This results in the rapid formation of a relatively accurate 3-D geometric model of the cardiac chamber. The creation of chamber geometry can be performed during sinus rhythm or tachycardia.

Once the chamber geometry has been delineated, tachycardia is induced and mapping is started. The data acquisition process is performed automatically by the system, and all data for the entire chamber are acquired simultaneously. Following this, the segment must be analyzed by the operator to find the early activation during the tachycardia (Fig. 6.20).⁴⁶

The noncontact mapping system is capable of simultaneously reconstructing more than 3360 unipolar electrograms and superimposing them onto the virtual endocardium. From these electrograms, isopotential or isochronal maps can be reconstructed (see Fig. 6.20). In isopotential mapping, unlike isochronal mapping, activation is assumed to occur when the electrogram voltage reaches a predefined magnitude. Because of the high density of data, color-coded isopotential maps are used to depict graphically regions that are depolarized, and wavefront propagation is displayed as a user-controlled 3-D “movie” (Fig. 6.21). The color range represents the voltage or timing of onset of the electrogram. The highest chamber voltage is at the site of origin of the

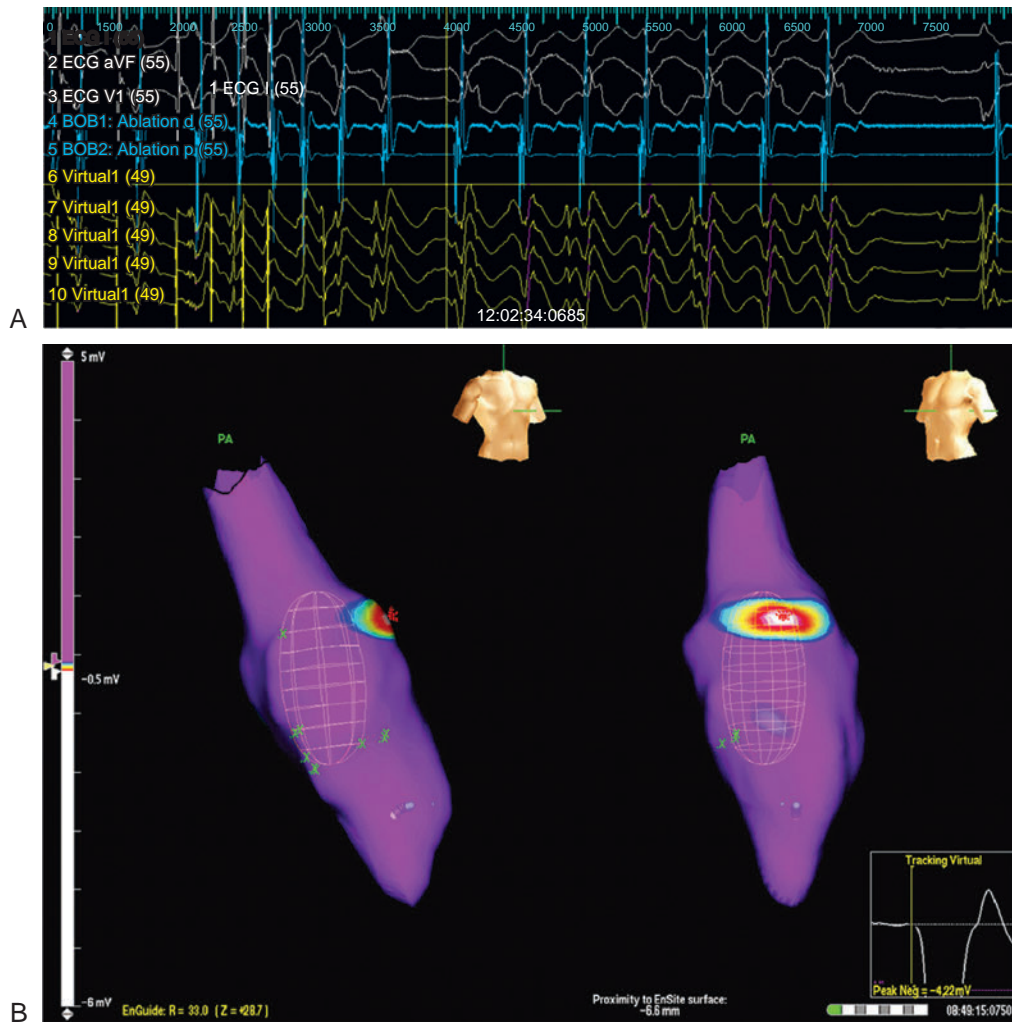


Fig. 6.20 Noncontact Mapping of Idiopathic Right Ventricular Outflow Tract (RVOT) Tachycardia. (A) Right anterior oblique and right lateral views of color-coded isopotential map of RVOT activation during a single premature ventricular complex (PVC). (B) Surface electrocardiographic (white) and intracardiac contact (blue) and virtual noncontact (yellow, V_1 - V_1 through V_1 - V_4) electrograms are shown during the PVC. Inset, Virtual electrograms at the site of earliest activation (note the QS pattern).

electrical impulse. Although the electrode closest to the origin of the impulse is influenced the most, all the electrodes on the array catheter are influenced, with the degree of influence diminishing with the distance between the electrode and each endocardial point.⁴⁶

In addition, the system can simultaneously display as many as 32 electrograms as waveforms (see Fig. 6.20). Unipolar or bipolar electrograms (virtual electrograms) can be selected at any given interval of the tachycardia cycle by using the cursor from any part of the created geometry and displayed as waveforms as if from point, array, or plaque electrodes. The reconstructed electrograms are subject to the same electrical principles as contact catheter electrograms because they contain far-field electrical information from the surrounding endocardium, as well as the underlying myocardium signal vector, and distance from the array may affect the contribution to the electrogram. These selected unipolar waveforms are used to augment information obtained from the 3-D map by demonstrating the slope of depolarization, the presence of double potentials or fractionation, and differentiation of far-field signals from more relevant endocardial activation.

In the unipolar electrogram, signals associated with high conduction velocity (e.g., the His-Purkinje system) possess a greater slope ($-dV/dt$), and thus are characterized by high-frequency spectral components

(more than 32 Hz). Electrograms recorded in normally conducting atrial or ventricular myocardium possess spectral components in the midrange from 4 to 16 Hz, whereas electrograms in regions of slow conduction are composed of lower frequency spectral components from 1 to 4 Hz. Thus the high-pass filter must be adjusted between 1 and 32 Hz, helping modulate the extent to which low-frequency signals are visible on the 3-D display. The identification of true local activation and its differentiation from the far-field signals are essential to the successful utilization of noncontact mapping. The true local activation always shows advancement of isopotential lines, but far-field signals would show retraction of isopotential lines on the 3-D display when electrograms are traced in their entirety.

When analyzing noncontact activation map data to locate the site of origin of a focal arrhythmia, two distinct sites can be marked at the onset of electrical activity: earliest activation and breakout sites. The earliest activation site is defined as the site with the earliest unipolar deflection from baseline during tachycardia, forming a single spot on the isopotential map, as well as characterized by a QS pattern of non-contact unipolar electrogram. The breakout site is marked as the site

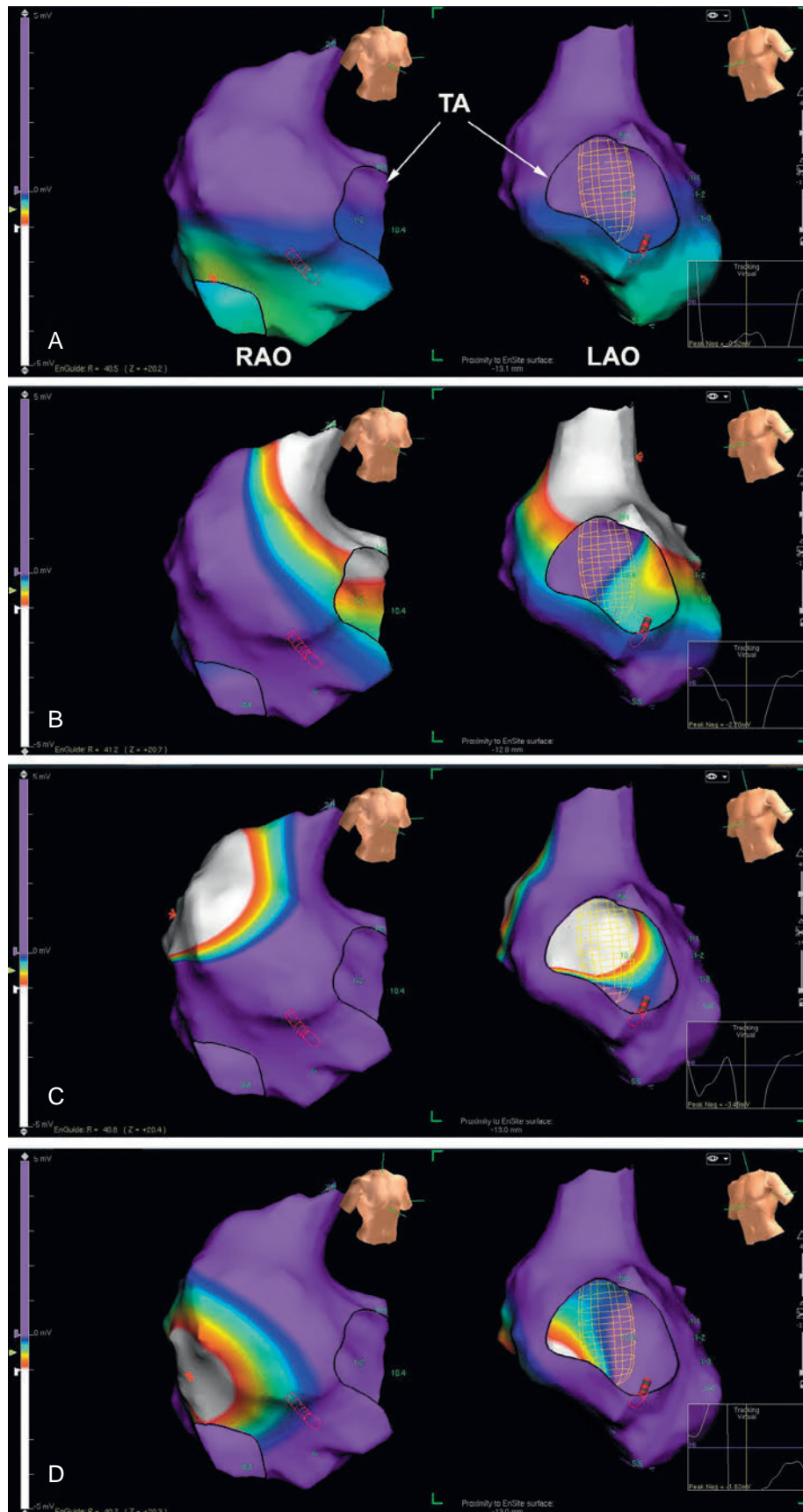


Fig. 6.21 Noncontact Isopotential Maps of Typical Atrial Flutter. Right atrial shell is displayed in right anterior oblique (RAO, left panels) and left anterior oblique projections (LAO, right panels). Wavefront activation sequence is tracked on the isopotential map throughout the tachycardia cycle (burning red star surrounded by white and red circles) propagating in a counterclockwise pattern (from A to D) around the tricuspid annulus (TA).

along the depolarization pathway identified by the color-coded activation map where rapid centrifugal electrical propagation originated from and local unipolar electrograms exhibited the maximum $-dV/dt$. For the identification of earliest activation and breakout sites, a broad color band setting is used with color high (defined as unipolar electrogram baseline) at -0.1 mV and color low at -2 mV. The virtual unipolar high-pass filter is set to 4 Hz. While earliest activation and breakout sites (that may be separated by ≥ 1 cm) appear to be associated with similar pace map scores and endocardial bipolar activation prematurity in relation to the onset of the tachycardia complex, one study found that the earliest activation site was a more sensitive marker for the true site of origin of the VT/PVC, as evident by the greater likelihood of achieving acute ablative success.⁴⁹

Substrate mapping based on scar or diseased tissue has been introduced to the noncontact mapping technology. High-density voltage mapping of the atrial substrate is performed using the peak negative voltage of the reconstructed unipolar electrograms. Areas with slow conduction are identified along the reentrant circuit of the atypical AFL. An atrial substrate characterized by an abnormally low peak negative voltage can potentially predict areas with slow conduction during macroreentrant tachycardias, which would provide a substrate for reentry.

Clinical Implications

The MEA has been successfully deployed in all four cardiac chambers by using a transvenous, transeptal, or retrograde transaortic approach to map atrial and ventricular tachyarrhythmias.⁴⁸

The biggest advantage of noncontact endocardial mapping is its ability to recreate the endocardial activation sequence from simultaneously acquired multiple data points over a few (theoretically one) tachycardia beats, without requiring sequential point-to-point acquisitions, thus obviating the need for prolonged tachycardia episodes that the patient might tolerate poorly. This technique can be used to map non-sustained arrhythmias; PACs; PVCs; rhythms that are not hemodynamically stable, such as very rapid VT (see Fig. 6.20); and possibly irregular rhythms such as AF or polymorphic VT. The system generates isopotential maps of the endocardial surface at successive cross sections of time, and when these are animated, the spread of the depolarization wave can be visualized. These maps are particularly useful for identifying rapid breakthrough points and slowly conducting macroreentrant pathways, such as the critical slow pathways in ischemic VT or reentrant AT in patients with surgically corrected congenital heart disease. In macroreentrant tachycardias such as typical AFL or VT, the reentry circuit can be fully identifiable, along with other aspects, such as the slowing, narrowing, and splitting of activation wavefronts in the isthmus (see Chapter 12, eFig. 12.5; Fig. 6.21). The system can also map multiple cardiac cycles in real time, a method that discloses changes in the activation sequence from one beat to the next. Because mapping data are acquired without direct contact of conventional electrode catheters with the endocardium, the use of noncontact mapping can help avoid the mechanical induction of ectopic activity that is frequently seen during conventional mapping. An additional advantage of this system is that any catheter from any manufacturer can be used in conjunction with this mapping platform. Other useful features include radiation-free catheter navigation, revisitation of points of interest, and cataloging ablation points on the 3-D model.⁴⁶

In complex substrate-related arrhythmias, the use of activation mapping alone may not be sufficient for rhythm analysis or identifying ablation targets. Substrate mapping based on scar or diseased tissue is of value in these cases. Although substrate mapping used to be relatively limited with the noncontact mapping technology (very low amplitude signals may not be detected, particularly if the distance between the center of the balloon catheter and endocardial surface exceeds 40 mm),

dynamic substrate mapping allows the creation of voltage maps from a single cardiac cycle (in contrast to the contact mapping system, in which the mapping catheter is moved point to point over the endocardial surface). Dynamic substrate mapping also provides the capability of identifying low-voltage areas, as well as fixed and functional block, on the virtual endocardium through noncontact methods, provided that points more than 40 mm from the electrode array are excluded from analysis. Combining substrate mapping with the ability of the noncontact system to assess activation over a broad area from a single beat may facilitate the ablation of hemodynamically unstable or nonsustained macroreentrant tachycardias.

Limitations

The overall accuracy of the reconstructed electrograms decreases with the distance of the area mapped from the array catheter, thus creating problems in mapping large cardiac chambers. Virtual electrogram quality deteriorates at a distance exceeding 4 cm from the array catheter and at polar regions. Therefore the array must be positioned as closely as possible to the endocardial area of interest, and at times it can be necessary to reposition the array catheter to acquire adequate isopotential maps.

Only data segments up to a maximum of 10 seconds in length can be stored retroactively by the EnSite system once the record button has been pushed. Thus continuous recording and storage of all segments of an arrhythmia are not possible at the time of evaluation of the arrhythmia maps. Therefore some isolated PACs or PVCs that can be of interest during evaluation and mapping could be missed. In addition, the acquired geometry with the current version of software is somewhat distorted, requiring multiple set points to establish the origin and shape of complicated structures such as the LA appendage or PVs clearly. Otherwise these structures can be lost in the interpolation among several neighboring points. In addition, synchronized mapping of multiple chambers requires multiple systems. Importantly, maps are highly sensitive to the changes in filtering frequencies used in postprocessing analysis.⁴⁸

Because the geometry of the cardiac chamber is contoured at the beginning of the study during sinus rhythm, changes of the chamber size and contraction pattern during tachycardia or administration of medications (e.g., isoproterenol) can adversely affect the accuracy of the location of the endocardial electrograms. Moreover, because isopotential maps are predominantly used, ventricular repolarization must be distinguished from atrial depolarization and diastolic activity. Early diastole can be challenging to map during VT.

Sometimes it is difficult to manipulate the ablation catheter around the outside of the balloon, especially during mapping in the LA. Special attention and care also are necessary during the placement of the large balloon electrode in a relatively small cardiac chamber. Another disadvantage is that the balloon catheter cannot be moved after the completion of geometry creation because it will change the activation localization and result in distortion of isopotential maps.

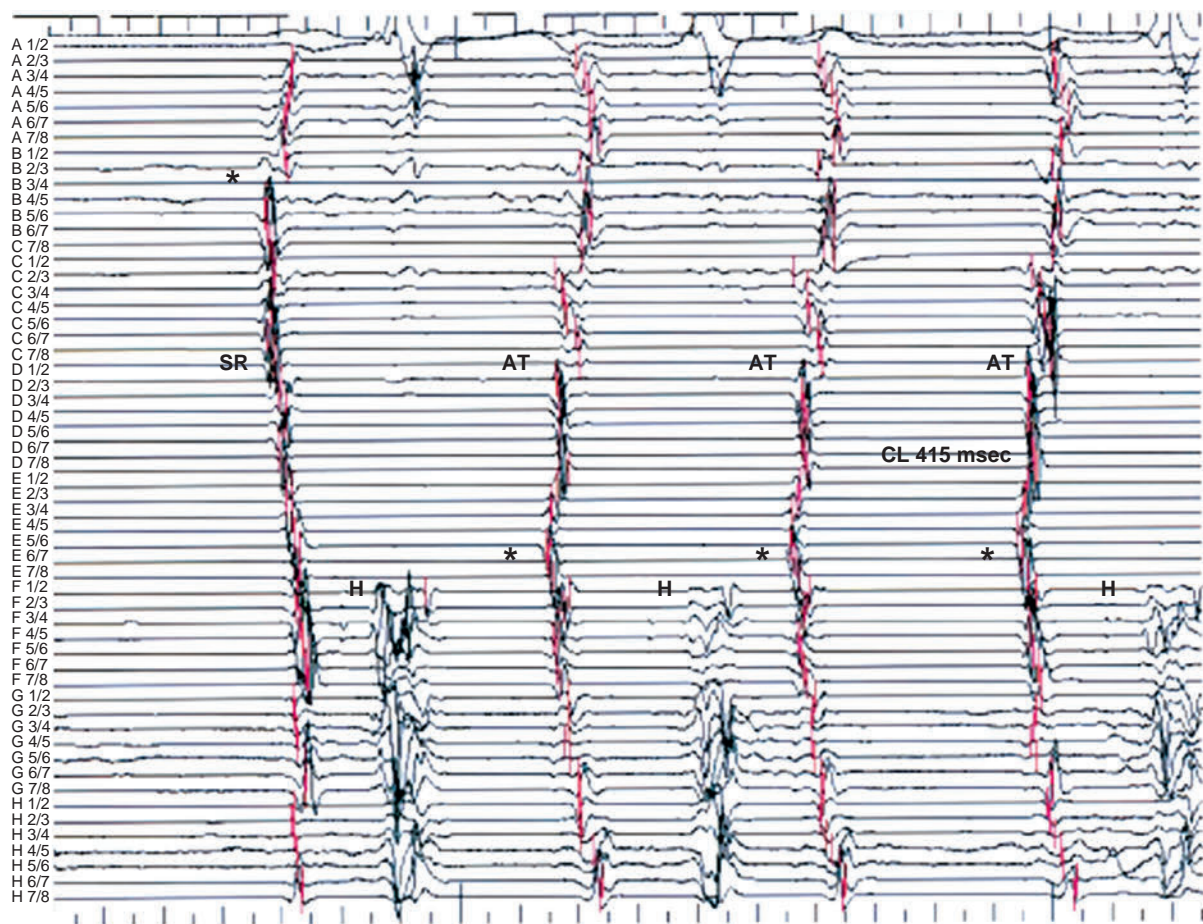
Although the risk of complications is low, aggressive anticoagulation measures because of balloon deployment in the cardiac chamber expose patients to potential bleeding complications.

BASKET CATHETER MAPPING

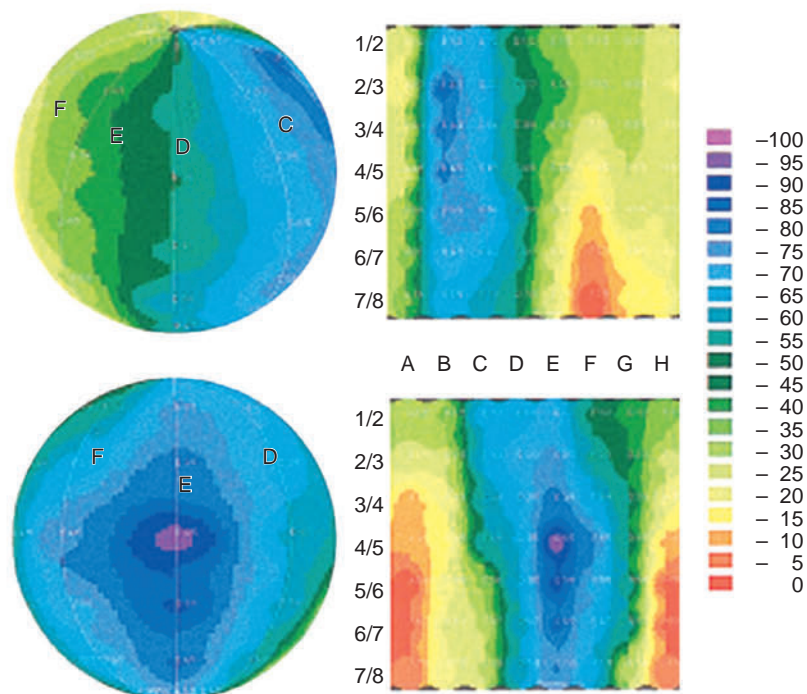
Fundamental Concepts

The basket catheter mapping system consists of a basket catheter (Constellation, Boston Scientific, Natick, MA, United States), a conventional ablation catheter, the Astronomer (Boston Scientific), and a mapping system.

The basket catheter consists of an open-lumen catheter shaft with a collapsible, basket-shaped, distal end. Currently, baskets are composed



A



B

eFig. 6.4 Basket Catheter Mapping During Focal Atrial Tachycardia (AT). (A) Simultaneous recordings of the surface ECG leads I and aVF and 56 bipolar electrograms from the basket catheter in a patient with focal AT. The first beat is a sinus beat. The next three beats are tachycardia beats. His bundle (H) potential is recorded in electrode pairs F2/3 and F3/4. The earliest spot of activation during sinus rhythm (SR) and AT is shown (asterisks). Spline A was located in the anterolateral right atrium (RA), splines B and C in the lateral region, splines D and E in the posterior region, and splines G and H across the tricuspid valve. The activation times are marked with red bars. (B) *Upper panel*, Animated map of the SR beats. *Lower panel*, Animated map of the AT beats. Planar and three-dimensional options are shown. During SR, the impulse emerged in the high lateral area (spline B1-B2) and propagated rapidly down the lateral wall. The complete activation of the RA took 85 milliseconds. During focal AT, the earliest activity emerged in the midposterior wall (spline E4-E5). The activation sequence of the RA was entirely different from that of SR. The complete activation of the RA took 95 milliseconds. CL, Cycle length. (From Zrenner B, Ndrepepa G, Schneider M, et al. Computer-assisted animation of atrial tachyarrhythmias recorded with a 64-electrode basket catheter. *J Am Coll Cardiol*. 1999;34:2051.)

of 64 platinum-iridium ring electrodes mounted on eight equidistant, flexible, self-expanding nitinol splines (metallic arms; see Fig. 4.3). Each spline contains eight 1.5-mm electrodes equally spaced at 4 or 5 mm apart, depending on the size of the basket catheter used. Each spline is identified by a letter (from A to H) and each electrode by a number (distal 1 to proximal 8). The basket catheter is constructed of a superelastic material to allow passive deployment of the array catheter and optimize endocardial contact. The size of the basket catheter used depends on the dimensions of the chamber to be mapped, and it requires antecedent evaluation (usually by echocardiogram) to ensure proper size selection.

The mapping system consists of an acquisition module connected to a computer, which is capable of simultaneously processing bipolar electrograms from the basket catheter, 16 bipolar-unipolar electrogram signals, a 12-lead ECG, and a pressure signal. Color-coded activation maps are reconstructed online. The color-coded animation images simplify the analysis of multielectrode recordings and help establish the relation between activation patterns and anatomical structures (eFig. 6.4). The electrograms and activation maps are displayed on a computer monitor, and the acquired signals can be stored on optical disk for off-line analysis. Activation marks are generated automatically with a peak or slope (dV/dt) algorithm, and activation times are then edited manually as needed.

Technology Application

The size of the cardiac chamber of interest is initially evaluated, usually with echocardiography, to help select the appropriate size of the basket catheter. The collapsed basket catheter is advanced under fluoroscopic guidance through a long sheath into the chamber of interest; the sheath is then withdrawn to expose several electrodes at the tip of the catheter (such that the exposed portion is flexible rather than stiff) and the catheter is then advanced and allowed to expand. Electrical-anatomical relations are determined by fluoroscopically identifiable markers (spline A has one marker and spline B has two markers located near the shaft of the basket catheter) and by the electrical signals recorded from certain electrodes (e.g., ventricular, atrial, or HB electrograms), which can help identify the location of those particular splines (Fig. 6.22).

From the 64 electrodes, 64 unipolar signals and 32 to 56 bipolar signals can be recorded (by combining electrodes 1-2, 3-4, 5-6, 7-8, or

1-2, 2-3 until 7-8 electrodes on each spline). Color-coded activation maps can be reconstructed (see eFig. 6.4). The concepts of activation mapping discussed earlier are then used to determine the site of origin of the tachycardia.

The electrograms recorded from the basket catheter can be used to monitor changes in the activation sequence in real time and thereby indicate the effects of ablation as energy applications are made. The capacity of pacing from most basket electrodes allows the evaluation of activation patterns, pace mapping, and entrainment mapping.

Clinical Implications

The multielectrode endocardial mapping system allows simultaneous recording of electrical activation from multiple sites and fast reconstruction of endocardial activation maps. This can limit the time endured in tachycardia compared with single point-mapping techniques without the insertion of multiple electrodes. It also facilitates the endocardial mapping of hemodynamically unstable or nonsustained tachycardias. Importantly, the recording of only a single beat can be sufficient to enable analysis of the arrhythmogenic substrate.

Endocardial mapping with a multielectrode basket catheter has been shown to be feasible and safe for various arrhythmias, including AT, AFL, VT, and PV isolation (see eFig. 11.8). However, in view of more advanced mapping systems, and because of significant limitations of the current basket catheters, its use has been limited.

Limitations

Because of its poor spatial resolution, the basket catheter in its current iteration has demonstrated only limited clinical usefulness for guiding ablation of reentrant atrial or ventricular arrhythmias. The relatively large interelectrode spacing in available catheters prevents high-resolution reconstruction of the tachycardia and is generally not sufficient for a catheter-based ablation procedure, given the small size and precise localization associated with RF lesions. In addition, the quality of recordings is critically dependent on proper selection of the basket size. Resolution is limited to the proportion of electrodes in contact with the endocardium and by unequal deployment and spacing of the splines; in addition, electrodes are not evenly distributed on the splines (no electrodes on the proximal 30% of each spline). Unfortunately the electrode array does not expand to provide adequate contact with the

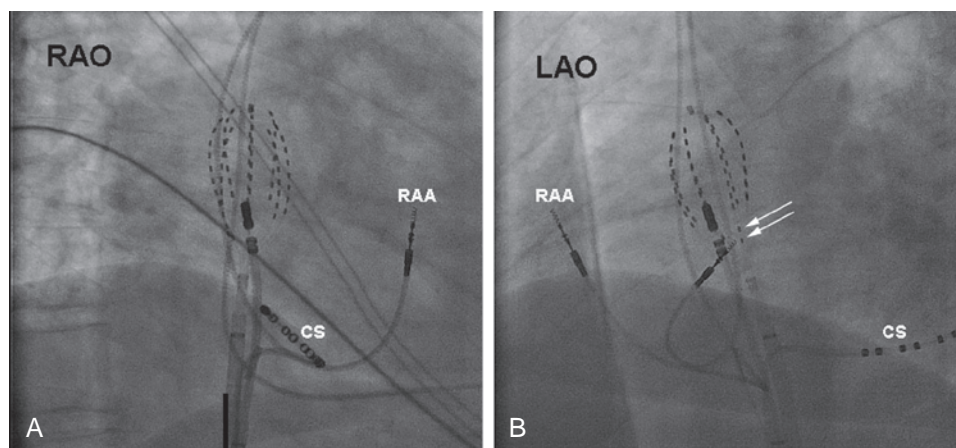


Fig. 6.22 Fluoroscopic Appearance of the Constellation Basket Catheter in the Superior Vena Cava. (A) Right anterior oblique view (RAO). (B) Left anterior oblique view (LAO). A decapolar catheter is positioned in the coronary sinus (CS). Dual chamber pacemaker leads are implanted in the right atrial appendage (RAA) and right ventricle. Note the radiopaque electrodes on the splines of the basket catheter. Spline B can be identified on fluoroscopy by the two markers located near the shaft of the basket catheter (arrows). An ablation catheter is positioned at the proximal aspect of spline A.

entire cardiac chamber; therefore good electrode contact at all sites on the endocardium is difficult to ensure because of irregularities in the cardiac chamber surface, so that areas crucial to arrhythmia circuit or focus may not be recorded. Moreover, regions such as the right and left atrial appendages and CTI are incompletely covered by the basket catheter. As a result, arrhythmia substrates involving these structures are not recorded by the basket catheter.

Voltage, duration, and late potential maps are not provided by this mapping approach. In addition, basket catheter mapping does not permit immediate correlation of activation times to precise anatomical sites, and a second mapping-ablation catheter is still required to be manipulated to the site identified for more precise mapping and localization of the target for ablation, as well as for RF energy delivery. Basket catheters also have limited torque capabilities and limited maneuverability, which hamper correct placement, and they can abrade the endocardium.

Carbonizations occasionally observed after ablation on the splines of the basket catheter can potentially cause embolism. Carbonization, which appears as dark material attached to the basket catheter electrodes or splines, are thought to be caused by the concentration of RF energy on the thin splines that results in very high local temperatures that induce the denaturation of proteins. Carbonization can be greatly diminished with the use of an irrigated tip catheter, as opposed to conventional ablation catheters; complete avoidance is difficult if the basket is deployed in the region of interest for ablation.

FOCAL IMPULSE AND ROTOR MAPPING

Focal impulse and rotor modulation (FIRM) mapping is a novel spatiotemporal mapping system (RhythmView, Abbott, Chicago, IL, United States) that uses a 64-electrode basket catheter (eight splines with eight electrodes per spline) for biatrial panoramic contact mapping of AF.

FIRM mapping has been used to identify patient-specific AF drivers—that is, regions in the atrium that may be responsible for maintaining AF, to design tailored ablation strategies. FIRM mapping records AF unipolar electrograms in a wide field-of-view across the majority of both atria and then employs physiologically directed computational methods to create activation trails, which can identify putative regions of recurrent organized rotational activity (rotors) and focal sources (focal drivers) within the atria, which appear to have a mechanistic role in sustaining human AF.^{50,51}

Wide-area contact mapping uses monophasic action potentials to separate potentially reproducible elements (principal components) of activation in AF from bystander disorganized activation in a clinically meaningful fashion. Basket catheter data are exported to RhythmView, which filters out QRS complexes and T waves and analyzes the unipolar atrial electrograms, taking into account rate-dependent refractoriness (“restitution”) and conduction slowing to determine physiologically plausible activation paths. The resulting computational phase maps depict putative propagation of electric activity during AF, displayed as a gray-scale animation. Rotors are defined as phase singularities with emanating spiral waves that disorganize in surrounding tissue. Repetitive focal drivers are defined as activation emanating centrifugally from a source region. Clinically rotors or focal drivers observed in FIRM maps are diagnosed as AF sources only if they lie in a spatially reproducible location (i.e., showing spatial stability) for minutes (i.e., showing temporal stability). This definition excludes transient or migratory activity that would be difficult to target for ablation.^{52,53}

Technology Application

Initially, atrial geometry is constructed using an electroanatomic mapping system (EnSite NavX or CARTO). Then the 64-pole basket catheter (Constellation, Boston Scientific; or FIRMap, Abbott, Chicago, IL, United

States) is advanced through a long sheath from the femoral vein sequentially into the RA and then (transseptally) into the LA. The size of the basket catheter is selected according to LA dimensions (as measured on preprocedural imaging or intraprocedural ICE). The basket catheter is manipulated to ensure good electrode contact and electrode locations are verified within the atrial geometry using fluoroscopy or electroanatomic mapping. Upsizing the basket catheter needs to be considered when optimal endocardial coverage (greater than 75% of either atrial surface) by basket catheter electrodes cannot be achieved. Downsizing the basket size should be considered when excessive basket distortion or insufficient basket expansion occurs. IV heparin is infused to achieve an activated clotting time of more than 350 seconds.⁵⁴

FIRM mapping is performed during spontaneous or induced AF. Unipolar and bipolar atrial electrograms from the basket catheter are filtered at 0.05 to 500 Hz and recorded at 1-kHz sampling frequency. Unipolar electrograms are recorded during AF for 1 minute and exported to a dedicated proprietary mapping system (RhythmView). Multiple 1-minute recordings are typically analyzed over a period of 5 to 10 minutes. Using phase-based algorithms, RhythmView software provides 2-D maps of AF propagation (isopotential movies and isochronal activation maps) projected onto grids. AF (FIRM) maps are analyzed intra-procedurally to guide ablation.

Electrical rotors are defined as phase-mapped rotation around a center of rotation, while focal impulses showed centrifugal activation from a source, both with precession (“wobble”) and complex surrounding breakdown that obscure fibrillatory sources on simple activation maps (Fig. 6.23). Rotors and focal impulses are considered AF sources only if they lay in reproducible regions, with precession, on repeated analysis for thousands of cycles.^{50,54,55}

Based on basket grid coordinates, referenced to electrode positions on electroanatomic shells, the ablation catheter is manipulated within the area indicated by the FIRM map as the center of rotation (for rotors) or focal impulse origins that are targeted by RF application. Following ablation, remapping is performed to confirm rotor elimination.⁵⁰

Clinical Implications

Initial studies using FIRM showed that rotors and focal sources are present in the vast majority of patients with AF.⁵¹ Ablation of AF drivers as guided by FIRM, in the form of small number of stable rotors or focal sources distributed in both atria and frequently located outside the PV ostia, resulted in high rates of acute termination and long-term freedom from recurrent AF. However, subsequent studies failed to replicate the findings of initial reports with some reporting a low acute procedural success in nonparoxysmal AF population after targeting the FIRM-identified rotors and very high long-term arrhythmia recurrence as compared with conventional approaches to AF ablation. Other reports with more extensive experience are more encouraging. Therefore the strategy of rotor ablation as guided by FIRM remains controversial, given the lack of randomized data supporting its efficacy and safety.⁵⁴

Limitations

FIRM mapping has several limitations. The basket catheter may provide inadequate coverage of both atria, although catheters chosen for LA mapping generally work well in the RA. Rotors arising in appendages and PVs could appear as foci at breakout sites. Interpretation of maps for targeting sources can be challenging, and there are as yet no standards for geographic extent of ablation or endpoints (i.e., complete elimination of electrograms vs. amplitude reduction).

Furthermore, studies showed that FIRM-identified rotor sites did not differ quantitatively or mathematically from other atrial sites, and did not appear to exhibit distinctive EP characteristics that would allow for prediction of ablation success.⁵²

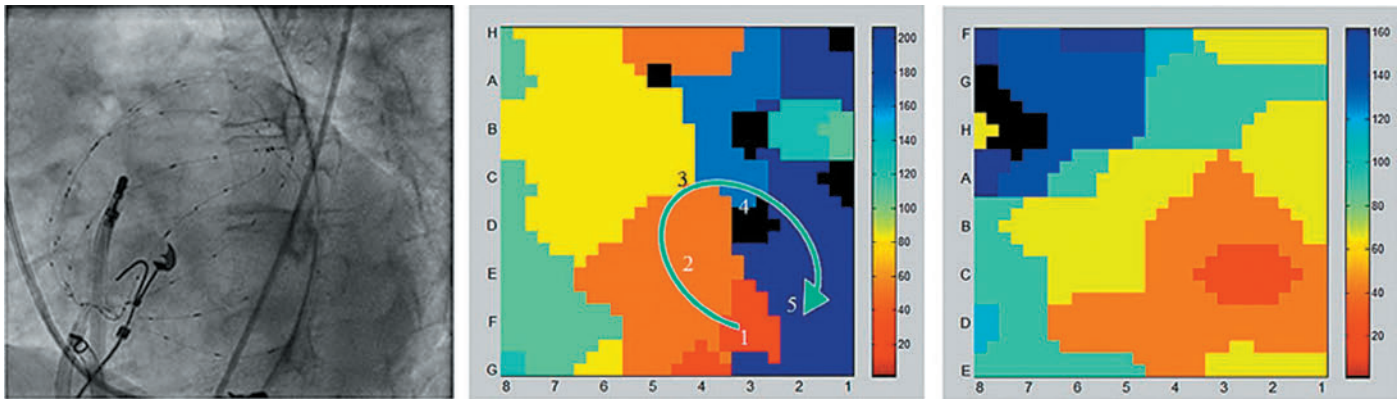


Fig. 6.23 Focal Impulse and Rotor Modulation Mapping. *Left*, Basket deployment in the left atrium (LA). *Middle*, LA rotor showing counter-clockwise rotation (from red to blue on the activation time scale with red representing early activation). *Right*, LA focal impulse originating from electrodes 2 and 3 spline C and D (red represents early activation with a centrifugal pattern). (From Sommer P, Kircher S, Rolf S, et al. Successful repeat catheter ablation of recurrent longstanding persistent atrial fibrillation with rotor elimination as the procedural endpoint: a case series. *J Cardiovasc Electrophysiol.* 2016;27:274–280.)

STEREOTAXIS MAGNETIC NAVIGATION SYSTEM

Fundamental Concepts

Catheter navigation by magnetic force was initially introduced in the early 1990s for diagnostic studies in neonates. However, the development of conventional steerable electrodes with integrated pull wires to deflect the catheter tip facilitated the current technique for catheter ablation. This conventional technique is limited by the fixed maximal catheter deflection and relies mostly on the skill of the operator to ensure stable catheter positioning. A novel magnetic navigation system (MNS; 0.15 T, Telstar, Stereotaxis, St. Louis, MO, United States) was introduced to clinical practice. It was proven to be a safe and feasible tool for catheter ablation, although it did not allow remote catheter ablation. The second-generation MNS (Niobe, Stereotaxis) now allows complete, remote RF catheter ablation.

The Niobe MNS consists of two permanent neodymium-iron-boron magnets (inside fixed housings positioned on either side of the single-plane fluoroscopy table); their orientations relative to each other are computer controlled. While positioned in the “navigate” position, the magnets create a 360-degree omnidirectional rotation of the device by a uniform magnetic field (0.08 Tesla) within an approximately spherical navigation volume 20 cm in diameter (NaviSphere), sufficient to encompass the heart when the patient is properly positioned. The combination of rotation, translation, and tilt movements of the magnets adjusts the magnetic field to any desired orientation within the NaviSphere.

The mapping and ablation catheters are extremely flexible distally, especially the distal shaft of the catheter, and have three tiny magnets distributed along the distal shaft and tip of the catheter to increase responsiveness of the catheter to the magnetic field generated (eFig. 6.5). The catheter magnets align themselves with the direction of the externally controlled magnetic field to enable the catheter tip to be steered effectively. By changing the orientation of the outer magnets relative to each other, the orientation of the magnetic field changes, thereby leading to deflection of the catheter.

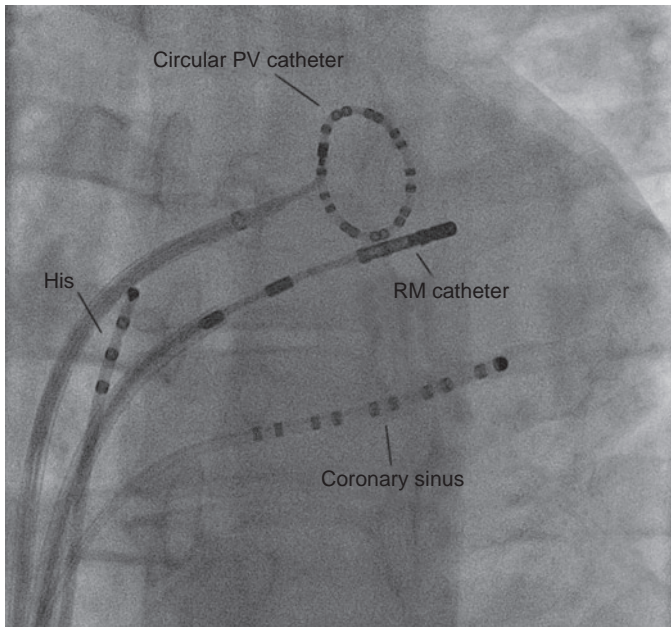
The system is integrated with a modified C-arm digital x-ray system, mainly a single-plane unit because of the physical limitations imposed by the magnets, although a biplane system can be installed and used when the magnets are stowed and not in use. Because of the magnets, the rotation of the imaging system is limited to an approximately 30-degree right anterior oblique view (RAO) and left anterior oblique

(LAO) in Niobe I and almost a 45-degree view with Niobe II. In the Niobe I iteration, the magnets can be swung only in (active navigation) or stowed, whereas in the Niobe II the magnets have a different housing and can also be tilted to allow for more angulation of the single-plane C-arm imaging system.

It is important to emphasize that the external magnetic field does not pull or push the tiny magnets and the catheters or guidewires in which they are contained. The position of the magnetic catheter within the heart is controlled by manual advancement or retraction of the catheter through a vascular sheath. A computer-controlled catheter advancer system (Cardiodrive unit, Stereotaxis) is used to allow truly remote catheter navigation without the need for manual manipulation. The operator is positioned in a separate control room, at a distance from the x-ray beam and the patient’s body. The graphic workstation (Navigant II, Stereotaxis), in conjunction with the Cardiodrive unit, allows precise orientation of the catheter by 1-degree increments and by 1-mm steps in advancement or retraction. The system is controlled by a joystick or mouse and allows remote control of the ablation catheter from inside the control room. In addition, the x-ray image data can be transferred from the x-ray system to the user interface of the MNS system to provide an anatomical reference.

Directional catheter navigation is accomplished by drawing a desired magnetic field vector on orthogonal fluoroscopic views with a digitization tablet (Fig. 6.24). A control computer then calculates the appropriate currents to each of the superconducting magnets. The resultant composite magnetic field interacts with the magnets in ablation catheter and deflects it to align parallel to the magnetic field. Magnetic field orientations corresponding to specific map points can be stored on the MNS and reapplied to return repeatedly and accurately to previously visited locations on the map. Navigation to a particular target often requires two or three manipulations of the magnetic field to refine the catheter position. Each magnetic field manipulation requires less than 5 seconds to activate. By changing the orientation of the outer magnets, the orientation of the magnetic field changes, thereby leading to the deflection of the catheter in parallel.

The MNS has become integrated with the CARTO RMT (Biosense Webster) electroanatomic mapping system. The CARTO RMT system is similar to the standard CARTO system but is able to localize the ablation catheter without interference from the magnetic field. CARTO RMT is able to send real-time catheter tip location and orientation



eFig. 6.5 Stereotaxis Catheters. Anteroposterior fluoroscopic view of the Stereotaxis remote magnetic (*RM*) catheter in the left atrium. Multipolar circular mapping, coronary sinus, and His bundle catheters are also shown. The RM catheter has a large distal mapping and ablation electrode; this and three other opaque regions more proximally on the catheter shaft contain magnetic elements that conform to changes in direction of an externally applied magnetic field. *PV*, Pulmonary vein.

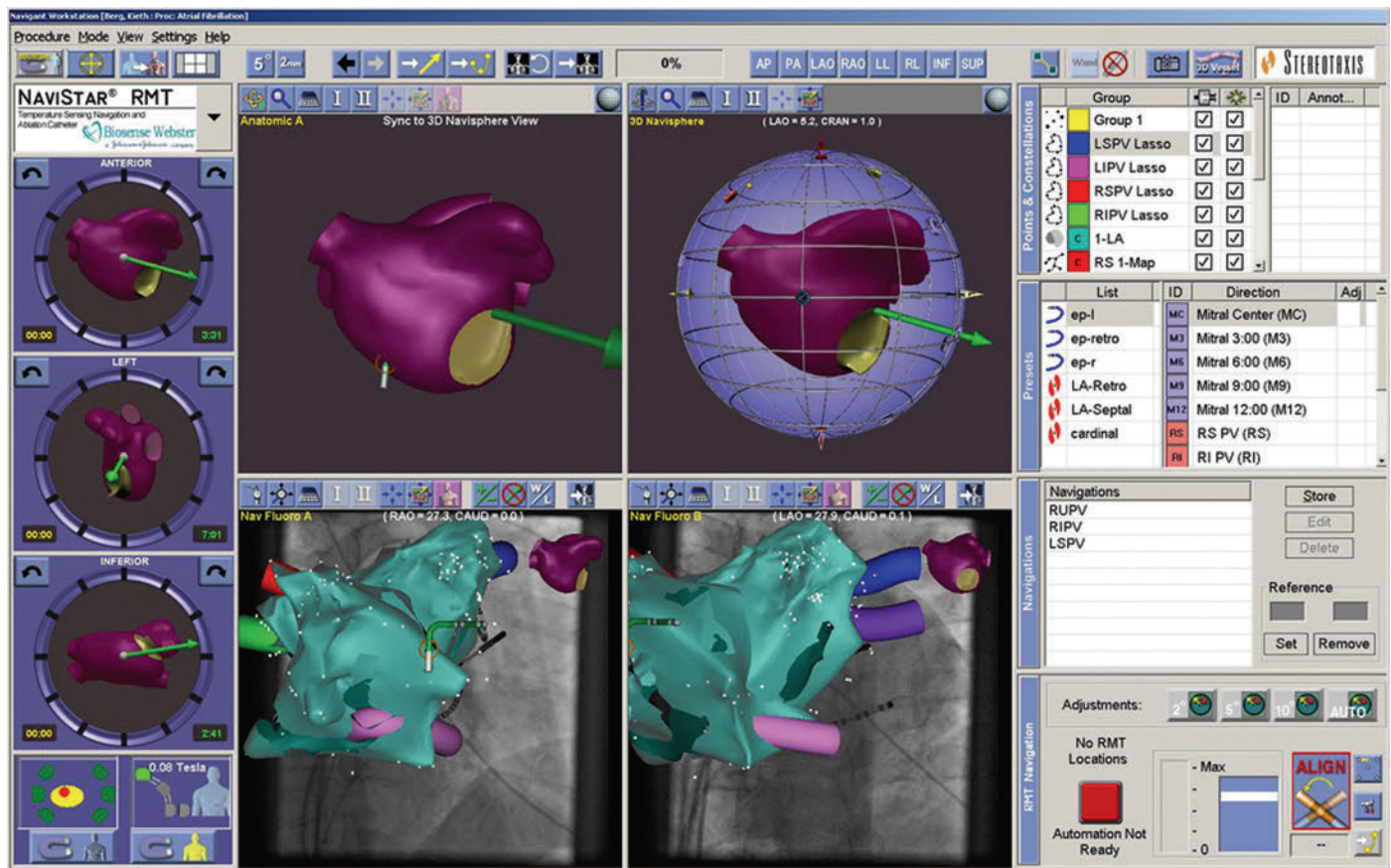


Fig. 6.24 Stereotaxis Remote Magnetic Guidance System. *Top two central panels*, Representation of idealized left atrium shells with a green arrow (“vector”) that can be pointed in any direction with a computer mouse, commanding the magnetic steering mechanism to deflect the catheter tip in that direction. *Bottom two central panels*, Shell generated by electroanatomic mapping, integrated with the images on the Stereotaxis unit. These overlie the patient’s initial right anterior oblique and left anterior oblique fluoroscopic images. Tubular structures are the pulmonary veins and coronary sinus (pink). Other panels on the screen are various controls and indicators for the Stereotaxis manipulation.

data to the MNS. It also sends target locations, groups of points, and anatomical surface information from the electroanatomic map to the MNS.

The system has options for controlling deflectable ring (for PV mapping) and ICE catheters remotely, using a device into which the catheter handle is mounted and clamped. All functions (advancement/withdrawal; deflection in any direction; changing diameter of a ring catheter loop) are available via operator use of a joystick in the control room.

Technology Application

All the components of the MNS, as well as the x-ray, ablator, and stimulator, can be operated from the control room. Therefore, after initial placement of sheaths and catheters, the entire ablation procedure can be performed remotely from the control room. The Navigant system is the computerized graphical user interface system. It includes the software used for image integration and for control of the magnetic fields that orient the catheter within the heart, and allows the operator to direct the movement of the tip of the catheter to access the region of interest (see Fig. 6.24).

After synchronizing with respiratory and cardiac cycles, such as inspiration and the end-diastolic period, a pair of best-matched RAO-LAO images is transferred and kept in the Navigant screen as background references for orientation and navigation (see Fig. 6.24).

Thus the real-time catheter location information can be displayed on the Navigant reference x-ray images, thus enabling continuous real-time monitoring of the catheter tip position, even without acquiring a fresh x-ray image.

The operator can access an area of interest by using vector-based or target-based navigation. In vector-based navigation, the operator tells the system, by drawing a vector in virtual 3-D space on the computer, what orientation of the magnetic field is required. In target-based navigation, a target is placed on a specified point using the stored orthogonal fluoroscopic views; the user marks the support or base of the catheter (the distal portion of the sheath) on the pair of x-ray images. This provides Navigant with the data needed to compute field orientations corresponding to particular targets. Each time a vector is selected or a target is marked, the computer sends information to the magnets, which changes their relative orientation, and with it the orientation of the uniform magnetic field in the chest, so that catheter orientation is then changed within a few seconds (see Fig. 6.24). A target can also be defined by selecting a preset magnetic field vector based on a selected study protocol from the list on the Navigant. The software contains several preset vectors selected by the manufacturer, after careful appraisal of multiple CT images and reconstructions, for positioning the catheter at various anatomical landmarks. When a preset vector is applied, it can steer the catheter near the approximate region indicated. In addition, the software can be used to map various chambers

of the heart automatically. Once the tip electrode is at the desired location, the magnetic field keeps it in stable contact throughout the cardiac cycle; contact force (maximum 10 to 15 gm) is less than what can be applied with a manually directed catheter, but this is largely offset by the consistency of contact.

The magnetic catheter is advanced to target positions in the cardiac chamber of interest and guided by using the x-ray system, user interface monitors, and catheter advancer (Cardiodrive) system, which allows precise orientation of the catheter in extremely small increments (1-degree increments, by 1-mm steps) within the heart and vessels in advancement or retraction, thus making mapping more accurate. All vectors and targets selected can be saved, as can relative positions of the catheter advancer system, to allow specific areas in the heart or side branches of vessels to be revisited reproducibly.⁵⁶

CARTO RMT has also been integrated with the MNS and has been specifically redesigned to work in the magnetic environment of Stereotaxis. CARTO RMT includes all the latest updates such as CARTO-Merge, in which a 3-D reconstruction of a CT or MRI image can be integrated into the electroanatomic map. With the CARTO integration, communication between the two systems allows for real-time catheter orientation and positioning data to be sent from CARTO to the Stereotaxis system, and for the catheter tip to be displayed on the saved images stored on the Navigant system. This permits tracking of the ablation catheter without having to update the radiographic image as often. Magnetic vectors can also be applied from the CARTO screen. A feature called “design line” can be used to send a line of points, either for mapping a specific area or potentially as a line of ablation points. “Click and go” is a tool allowing for an area of the map to be clicked on to set a target and have the system guide the catheter to this point. Because Stereotaxis and CARTO have feedback integration, the CARTO system can feed back to the Stereotaxis system if the exact point is not reached, thus allowing for further automatic compensation by the software until the desired point is reached. The combined system has the capability of automatically mapping chambers (anatomy and activation times) by using predetermined scripts. The accuracy of such automaps is highly dependent on the anatomy, as well as where in the heart the operator designates the starting point for mapping. At present, standard 4- and 8-mm-tip and irrigated 3.5-mm-tip RF catheters are available.

Clinical Implications

Precise target localization and catheter stability are prerequisites for successful RF applications and to minimize risks of potential complications. Stiff, manually deflectable catheters with a unidirectional or bidirectional deflection radius, which deflect in a single plane, have several inherent limitations because stable electrode-tissue contact can be difficult to achieve, particularly in regions of complex cardiac anatomy. This is much less problematic using the MNS. For example, in repaired congenital heart disease, such as Mustard procedures, the pulmonary venous atrium can be accessed retrogradely (via the aorta), obviating the need for baffle puncture. Another strength of the current MNS lies in the precision of catheter movement and the ability to steer the flexible distal portion of the catheter in any direction in 3-D space.

The MNS has been used for ablation of AVNRT, BTs, AFL, idiopathic and scar-related VT, and especially AF.⁵⁷ Intracardiac electrograms and stimulation thresholds are not significantly different from those recorded with a standard, manually deflected ablation catheter, and the safety of standard EP procedures has not been compromised by use of the MNS.^{56,58} For AF ablation, efficacy outcomes were accomplished with use of MNS when compared with conventional manual navigation. MNS was associated with significant reduction of fluoroscopy time but a slightly longer total procedure time.^{59,60} Because of the flexibility of the catheters, cardiac perforation is extremely unlikely.

Although the current MNS may not offer a distinct advantage over conventional catheters for navigation to targets that are easily reached, it has potential advantages for complex catheter maneuvers and navigation to sites that are exceptionally difficult to reach with a standard catheter. In addition, catheter mobility and endocardial stability can be superior by virtue of the compliance of the distal catheter and lack of constraints on the magnetic vector used to steer the catheter. Cardiac and respiratory motion can be buffered by the catheter compliance, thereby contributing to endocardial contact stability.

After the diagnostic catheters are positioned, the EP study and ablation process can be performed completely from inside the control room. This offers several potential advantages, including reducing fluoroscopic exposure time for the operator, reducing the strain from standing next to the bed for long periods while wearing a lead apron, and facilitating simultaneous catheter navigation and electrogram analysis.

A unique feature of the current MNS is that the magnetic vector coordinates used to navigate the magnetic catheter to a particular site can be stored and reused later in the study to return to a site of interest. The integration of a stable magnetic catheter with the CARTO electroanatomic mapping system is useful to reconstruct an accurate electroanatomic map by acquiring many more points than are possible manually for successful ablation, even of challenging areas.

For certain procedures, notably AF ablation, MNS can decrease fluoroscopy time significantly. Although the use of MNS may increase total procedure duration, procedure times decrease with increasing operator experience.

Limitations

A potential limitation of the MNS is the interference induced by the magnetic field in the surface ECG. The origin of the induced potentials is thought to be attributable to blood flow within the magnetic field. Blood is an electrolyte solution that can induce the potential because of motion within the magnetic field. The magnetic field strength used for catheter manipulation is approximately one order of magnitude less than that associated with MRI. The interaction of the magnetic field with the surface ECG is therefore less in magnitude compared with MRI and is restricted to the ST segment, and the temporal distribution of the interfering signal component probably would not compromise cardiac rhythm analysis or analysis of the P wave or QRS morphology. However, the interpretation of changes in the ST segment would be predictably compromised by this interference. Whether this distortion will affect arrhythmia analysis is currently being investigated.

Claustrophobia and morbid obesity are contraindications for using the MNS because of the restricted space within the system; deep sedation or anesthesia obviate this problem. The next generation of the MNS features an open design that is more comfortable for obese patients and those with claustrophobia. Patients with pacemakers or defibrillators had been excluded because of possible electromagnetic interference, although few problems have been observed, even with very old devices. In addition, the MNS requires monitoring instruments that are compatible with magnetic fields.

The angulation of the fluoroscopic system is limited to 30 degrees to 45 degrees for both LAO and RAO projections when the magnets are in the “navigate” position. Although this may not be important in simple ablations, addressing more complex substrates can be more challenging.

The MNS is an evolving technology. Further technical development through the availability of additional catheter designs (e.g., number of recording electrodes) is necessary to address more complex arrhythmias in the future.

The use of the MNS for ablation of AF, MRAT, and typical AFL was associated with slightly longer procedure times as compared with

conventional catheter navigation. The preparation for the procedure (registration and positioning of the magnets for MNS) is still time-consuming. Furthermore, the use of the MNS for catheter ablation of typical AFL resulted in a lower overall success rate (achievement of cavotricuspid isthmus block and freedom from AFL recurrence during follow-up). A lower success rate of PV electrical isolation was also observed when a standard 4-mm-tip ablation catheter was used. Some reports also expressed concern about a higher incidence of char formation during MNS-guided ablation of AF and AFL using solid tip catheters. Irrigated magnetic catheters are now used and appear to the risk of char formation, and increase lesion efficacy during MNS-guided ablation.

SENSEI ROBOTIC NAVIGATION SYSTEM

Fundamental Concepts

The Sensei robotic navigation system (Hansen Medical) is an electro-mechanical system that realizes catheter navigation by two concentric steerable sheaths (Artisan, Hansen Medical) incorporating an ablation catheter. The outer sheath (14 Fr) and the inner sheath (10.5 Fr) are both manipulated via a pull-wire mechanism by a sheath-carrying robotic arm that is fixed at the foot of the patient's table. The robot arm obeys the commands of the central workstation (master console) positioned in the control room.⁶¹

Catheter navigation is realized using a 3-D joystick (Instinctive Motion Control, Hansen Medical) and allows a broad range of motion in virtually any direction. At the master console, fluoroscopic images, ICE images, and other 3-D representations (electroanatomic maps) are displayed, providing immediate feedback to the operator. Seamless instinctive integration and interpreted motion logic allow the physician to direct catheter movement in 3-D regardless of image orientation or perspective. To provide a representation of tactile feedback, the system continuously monitors the contact force that is exerted by the catheter tip by using a specially designed algorithm (IntelliSense, Hansen Medical). If the contact force exceeds a preset limit, an optical alarm is displayed, and catheter advancement is rendered virtually impossible.

In general, all catheters and all electroanatomic mapping systems may be used. Apart from the different navigational approach, the technical aspects of the ablation are identical to the manual ones. Integration of this robotic system with available mapping systems (CARTO and EnSite NavX) is feasible.

Technology Application

Both the inner and the outer sheaths should be flushed with heparinized normal saline before insertion and continuously throughout the procedure to prevent clot formation and air embolism. The steerable guide sheath is manually inserted via a 14 Fr sheath in the right femoral vein and advanced manually into the inferior RA under fluoroscopy guidance. To minimize the risk of vascular complications, it is advisable to obtain venous access under ultrasound guidance, initially insert an 8 Fr sheath and upsize to 11 Fr and then 14 Fr, and then insert a long, 30-cm 14 Fr sheath that usually ends at the level of the liver. Through this, the steerable sheath is inserted with the ablation catheter leading by at least 10 cm into the RA. At this level, the ablation catheter is withdrawn into the steerable sheath with only the distal electrodes protruding. Failure to leave the ablation catheter out beyond the end of the Artisan sheath and to observe the catheter system advance up to the RA increases the risk of vascular injury.

Subsequently, the position of the sheath is registered into the robotic catheter remote control system. The registration process involves the use of two orthogonal fluoroscopic views of the heart (anteroposterior

and lateral) to allow saving the position of the guide sheath in 3-D space. Following registration, the remote control system is used to steer the tip of the ablation catheter to the desired targets; all four cardiac chambers are accessible.

For ablation in the LA, transseptal puncture is usually performed manually with a standard transseptal sheath and needle system. If a second atrial septal puncture is required, the guidewire or EP catheter placed in the LA through the first transseptal puncture is used as a marker, and the second transseptal puncture is performed with the Sensei system. A custom-made transseptal needle (Hansen Medical) is advanced through a transseptal sheath and dilator (Hansen Medical) under fluoroscopy and ICE guidance. After the septum is punctured, the steerable guide sheath and dilator are advanced robotically in the LA, and the dilator is replaced with the ablation catheter, which is then inserted into the guide sheath with approximately 1 cm of the ablation catheter exposed from the tip of the guide sheath.⁶¹

The steerable sheath containing the ablation catheter is remotely controlled by a physician at the master console. Manipulation of other catheters, including the circular mapping catheter, however, is performed manually by a second operator at the procedure tableside.

The required amount of energy applied during remote navigation cases is generally lower than that of manual cases, likely because of enhanced catheter contact and stability throughout the cardiac cycle afforded by the robotic sheath. As a result, the rate of steam pop and potential thermal complications may be higher if compensatory energy-lowering strategies are not implemented.

Clinical Implications

Endocardial navigation using conventional manual steerable diagnostic and ablation catheters can be challenging and time-consuming, and require certain skills and experience. The robotic catheter remote control system was designed to facilitate control and allow precise and stable positioning of catheters within the cardiovascular system. This technology has the potential to overcome some of the limitations of manual control by combining the ease of navigation with a readily available wide navigational field.⁶²

An additional advantage of remote navigation is the ability to reduce the operator's radiation exposure because of the remote location of the workstation from the fluoroscopy unit. Furthermore, because of better catheter stability and easier navigation with the robotic system, total fluoroscopy time and patient and staff radiation exposure can potentially be reduced; however, this remains to be determined.⁶¹

Several studies have shown that robotic navigation and ablation of AF are as safe and effective as manual ablation. Furthermore, the use of the robotic catheter remote control system for transseptal puncture and endocardial navigation is safe and feasible. However, its usefulness in decreasing procedure time and improving procedural efficacy and safety compared with current approaches (which continue to evolve) requires further evaluation in randomized clinical trials. In addition, a comparison between this technology and remote magnetic navigation may be warranted.

In contrast to the magnetic guidance system (Niobe, Stereotaxis), which requires specific compatible magnetic-guided catheters, the Sensei robotic navigation system is an open platform system whereby almost any mapping or ablation catheter of appropriate size can be introduced into the remotely steerable catheter or sheath. In addition, the MNS requires continuous alteration and adjustment of the magnetic field and then advancement of the catheter in that direction. With the use of the Sensei robotic navigation system, a continuous uninterrupted motion of the ablation catheter can be achieved with the use of the instinctive motion controller. Finally, the Sensei robotic system is, at least in principle, portable and could be transported from one

laboratory to another in the facility, whereas the remote MNS requires large magnets permanently installed in one location.^{61,62}

Limitations

Although the remote location of the workstation from the fluoroscopy can significantly reduce radiation exposure to the physician, there is a need for a second physician or operator to manipulate the circular mapping catheter at the bedside during a PV isolation procedure. Radiation exposure is not reduced to this operator or to the patient. With the use of other AF ablation strategies, such as anatomically based ablation, however, there would be no need for a separate mapping catheter. In the future, it is possible that both the ablation and mapping catheters will be controlled in tandem with two coordinated robotic steerable guides, though likely at increased procedural cost.

The steerable robotic sheath is inherently stiff to make it pushable and mechanically steerable, and it must be advanced through a 14 Fr vascular sheath. The size of the introducer sheath itself increases the likelihood of complications, and advancing the steerable sheath into the vein may cause dissection. The amount of force required to advance the Artisan through the hemostatic valve of the sheath at the groin is significant. Therefore insertion of the 14 Fr sheath and the Artisan catheter does require special care to avoid retroperitoneal vascular complications.

Infrequent cases of cardiac perforations and PV stenosis were reported in several studies using the Sensei robotic navigation system for catheter ablation of AF. Some of those events were thought to be consequent to the use of high power output during RF ablation. Therefore it is important to recognize that with better catheter contact and stability offered by the robotic sheath, the effectiveness of ablation is increased, and less power is probably needed to achieve adequate attenuation of electrograms. Further studies will be required to evaluate adequate and optimal tissue contact during navigation mapping and ablation, as well as the optimal ablation energy parameters while using a robotic system at different pressure levels, and compare those with the parameters used with conventional manually operated catheters.

During catheter ablation of AF, the major advantage of robotic navigation with respect to stability as compared with manual navigation is along the LA roof. However, at the anterior inferior portion along the lateral circumferential ablation line, catheter stability is suboptimal in almost 50% of the cases despite robotic navigation. This may be explained by the fact that this is the most distant location from the transeptal puncture site. This limitation can be partially compensated for by a “deeper” LA position of the outer sheath and the application of a distal bend. In addition, electrical isolation of the right inferior PV is challenging using this system. Because of the large outer diameter of the sheath, robotic navigation to the distal CS is discouraged. This may limit its use in ablation procedures for long-lasting persistent AF or perimitral LA macroentrant tachycardias, which frequently require epicardial ablation via the CS.

Certain ablation catheters with flat wire deflection mechanisms are not compatible with the Sensei robotic navigation system. The flat wire mechanism allows the catheter to only bend along a 2-D plane described by the flat surface of the wire without causing tension. When the robotic sheath moves in a direction that is not along the 2-D plane of the flat wire, tension is created, resulting in an uncontrolled rebound rapid correction of the system, which can potentially cause cardiac perforation. This rarely happens with manual manipulation of the catheter alone because the operator rotates the catheter appropriately to achieve the desired position.

Although the robotic system affords greater stability at ablation targets, complications that occur with the manual approach can also occur with the robotic system. Given the stability of the system and

also the stiffness and rigidity of the sheath, it is crucial that the operator understands the anatomy of the LA and adjacent structures. Even more so with the robotic navigation system, it is very important that the operator is cognizant of possible complications and is able to manage such complications effectively.

MEDIGUIDE NAVIGATION SYSTEM

Fundamental Concepts

The guided medical positioning system (MediGuide Technology, St. Jude Medical, St. Paul, MN, United States) is a novel nonfluoroscopic, sensor-based electromagnetic catheter visualization system. This technology enables real-time tracking of the catheter tip that is displayed on a prerecorded cine loop and is constantly visible during the procedure.^{63,64}

The MediGuide technology consists of three components: (1) a transmitter generating a 3-D electromagnetic field (installed within the fluoroscopy detector of a conventional flat panel x-ray imaging system); (2) a miniaturized (less than 1 mm³) single coil sensor (MediGuide Enabled Livewire, St. Jude Medical) embedded within an intracardiac device such as a conventional EP or ablation catheters, sheaths, and wires; and (3) a magnetic field reference sensor attached to the patient's chest (which functions as an anchor for the system and continuously scans patient position within the tracking space).^{63,64}

MediGuide combines the x-ray system with electromagnetic tracking on the hardware level. The transmitter unit is installed within the fluoroscopy detector of a conventional x-ray imaging system. This assembly enables aligning the fluoroscopic and electromagnetic 3-D working spaces and allows for the auto-registration of sensor tracking into dynamic x-ray imaging. As a result, the sensor-equipped EP catheter can be either visualized on fluoroscopy or tracked nonfluoroscopically at the identical position by the electromagnetic sensor field (Fig. 6.25). The use of prerecorded cine loops instead of live fluoroscopy allows for nonfluoroscopic tracking of catheters within the x-ray environment and helps reduce radiation exposure. The speed of the cine loop is matched to the real-time ECG signal to adjust for cardiac cycle dependent changes in catheter position. Furthermore, the reference sensor attached to the patient's chest helps compensate for respiration and for movement of the patient or the table, as well as changes in C-arm angulation.^{63–65}

Technology Application

Initially, before EP catheter introduction, two cine loops with a length of three cardiac cycles are recorded in standard RAO 30-degree and LAO 60-degree projections. A simultaneous display of these two pre-acquired cine loops in a continuous pseudo-biplane mode constitutes the background for the nonfluoroscopic placement of the sensor-equipped diagnostic and ablation catheters. Contrast-enhanced background angiograms (e.g., LA or PV angiography), as opposed to native cine loops, further enhances orientation within complex anatomies (Fig. 6.26). The sensor-enabled catheters then are positioned into the appropriate cardiac chambers using MediGuide for nonfluoroscopic catheter tracking within prerecorded cine loops.

MediGuide technology can be used in conjunction with the EnSite NavX electroanatomic mapping system (see Fig. 6.26). One of the sensor-equipped catheters can be used to acquire the electroanatomic map. The use of MediGuide data improves impedance-based field adjustment (“field scaling”) of the EnSite NavX system, resulting in more realistic chamber reconstructions. Furthermore, using the sensor-equipped catheters as the positional reference for the EnSite system allows for the detection and correction of reference catheter dislocations, thereby preventing catheter shifts, which necessitate repeated reconstruction and registration processes.^{63–65}

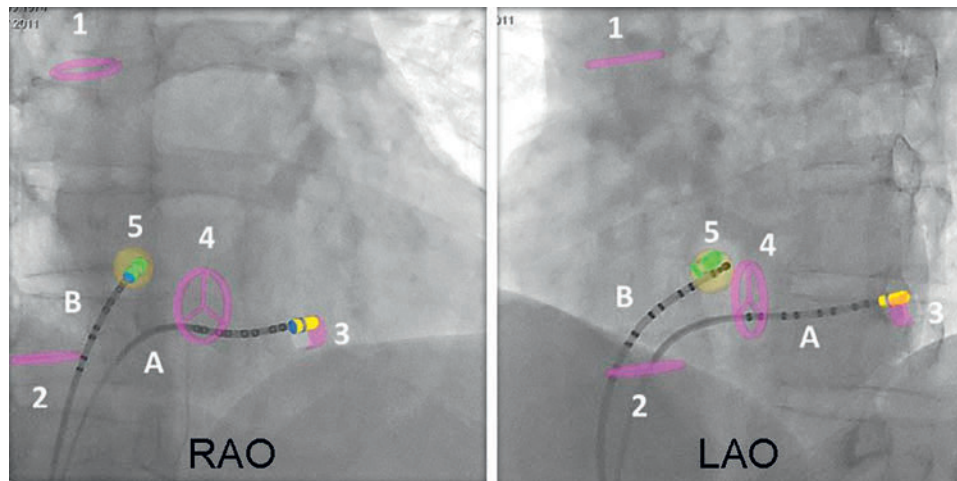


Fig. 6.25 MediGuide-Enabled Catheter Visualization. Two decapolar diagnostic catheters are visualized by both the MediGuide system (green and yellow tip) and real-time fluoroscopy (right anterior oblique [RAO] and left anterior oblique [LAO] views). In addition, different landmarks are set: ostium of the superior vena cava (1), ostium of the inferior vena cava (2), tip of the coronary (CS) catheter (3), ostium of the CS (4), and fossa ovalis (5). (From Sommer P, Wojdyla-Hordynska A, Rolf S, et al. Initial experience in ablation of typical atrial flutter using a novel three-dimensional catheter tracking system. *Europace*. 2013;15:578–581.)

Clinical Implications

The MediGuide tracking platform enables excellent 3-D orientation for spatial catheter positioning based on underlying prerecorded cine loops. This system can be used as a “stand-alone system” for simple catheter ablations, such as AVNRT, BT, and CTI ablation, where it can potentially allow almost complete nonfluoroscopic procedures, except the acquisition of the two cine loops that can be taken prior catheter insertion (see Fig. 6.25). This catheter tracking technology can also be combined with a 3-D electroanatomic mapping system for more complex ablations (e.g., AF; see Fig. 6.26). The option to use contrast-enhanced background angiograms further improves catheter visualization in relation to cardiac anatomy.

Initial studies using MediGuide demonstrated significant (more than 50%) reduction of radiation exposure to both the patient and the operator, which was found to be its most prominent measurable benefit. These effects were achieved with minor adaptations of established workflows and without excessive procedure duration or complication rates.

Limitations

One of the limitations of the MediGuide system is that catheter shaft and transseptal sheaths are not visualized on MediGuide screens. Therefore additional fluoroscopy can be required when catheter orientation is not entirely clear. Also, fluoroscopy is required during manipulation of EP catheter lacking the magnetic sensors and during atrial septal puncture. Another limitation is the limited selection of EP catheters being equipped with MediGuide sensor technology. A broader variety of sensor-equipped catheters in addition to sensor markers on the transseptal sheath would offer a greater variability in the application of this technology.

BODY SURFACE POTENTIAL MAPPING

Fundamental Concepts

Although the conventional 12-lead ECG is extensively used, its limitations for optimal detection of cardiac abnormalities are widely appreciated. The main deficiency in the 12-lead approach is that only six chest

electrodes are incorporated, and they cover a relatively constrained area of the precordium. The main reason for the choice of the location of the conventional precordial electrodes, suggested by Wilson in the 1940s, was the need to adopt some standard, which to this day has remained relatively unchallenged. In the years since then, the growing appreciation for the limitations of the conventional precordial electrode positions and the increase in understanding of the localization of various cardiac abnormalities on the body surface have led to the suggestion of various alternatives.

One of the most widely studied alternatives to the 12-lead ECG in clinical and experimental electrocardiology has been body surface potential mapping (BSPM). In this approach, 32 to 256 electrodes are used in an attempt to sample all ECG information as projected onto the body's surface. The merits of this enhanced spatial sampling are obvious, in that localized abnormalities that may be difficult to detect using the 12-lead approach can readily be picked up with the additional electrodes.⁶⁶

BSPM is defined as the temporal sequence of potential distributions observed on the thorax throughout one or more electrical cardiac cycles. BSPM is an extension of the conventional ECG aimed at refining the noninvasive characterization and use of cardiac-generated potentials. The improved characterization is accomplished by increased spatial sampling of the body surface ECG, recorded as tens or even hundreds of unipolar ECGs, simultaneously or individually, with subsequent time alignment.

BSPMs provide much more electrical and diagnostic information than the 12-lead ECG. They contain all the electrical information that can be obtained from the surface of the body, and they reveal diagnostically significant electrical features in areas that are not sampled by the 12-lead ECG systems. In addition, BSPMs often show distinct electrical manifestations of two or more events simultaneously evolving in the heart; they make it possible to compute any ECG that would be obtained from any pair or combination of body surface electrodes (i.e., from any current or future lead system). In addition, the recorded data can be displayed as a sequence of contour maps, thus allowing for the isolation of significant ECG events in both space and time.

BSPMs can be used to reconstruct epicardial and, in some cases, endocardial potential distributions, excitation times, and electrograms

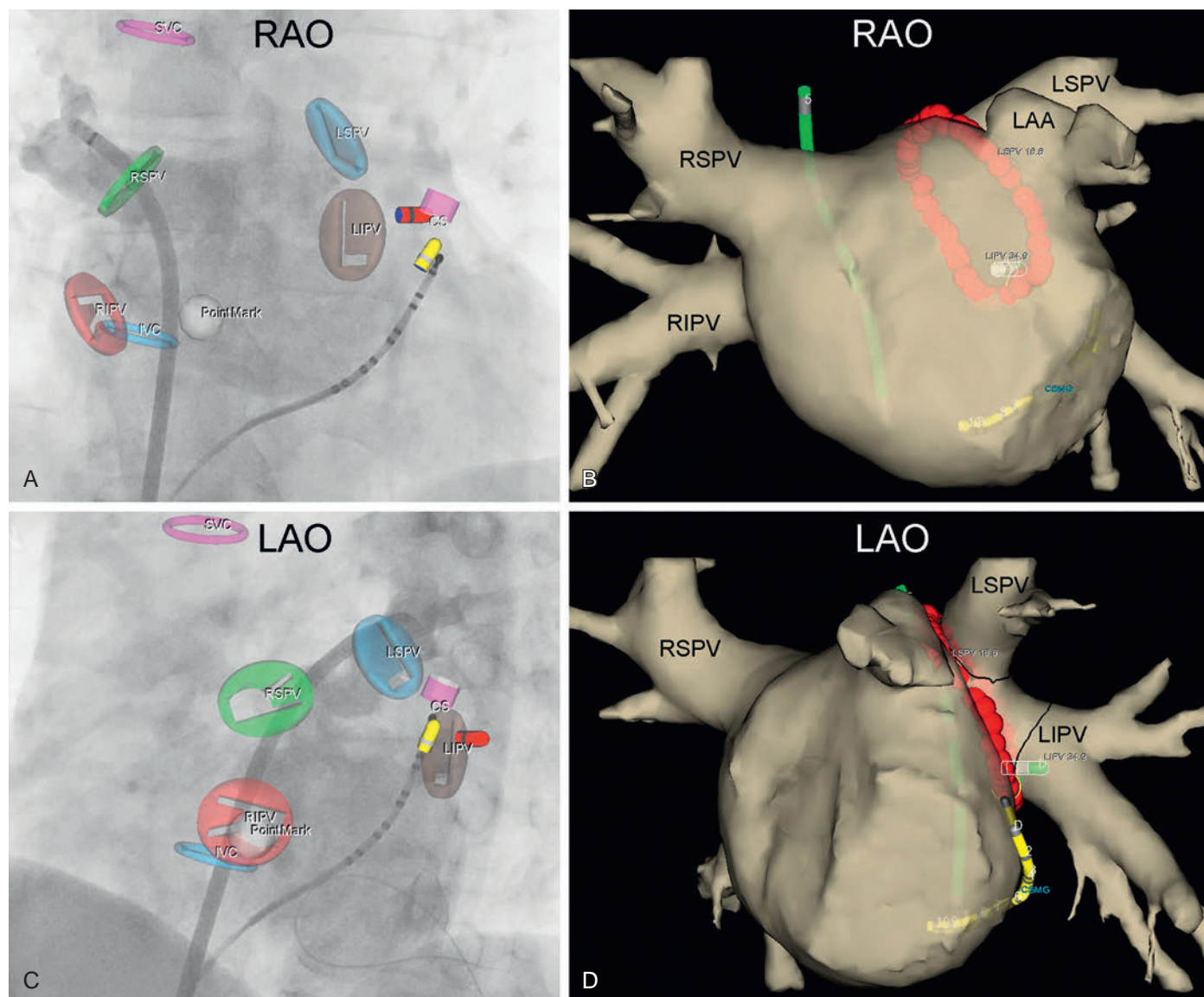


Fig. 6.26 Nonfluoroscopic Tracking of the MediGuide-Enabled Ablation Catheter During Circumferential Left Pulmonary Vein (PV) Isolation. Snapshots show MediGuide screens (A and C) with PV angiographic background loop, three-dimensional MediGuide technology markers (SVC, IVC CS, PV ostia, and oval fossa), and sensor icons of diagnostic catheter (yellow) and ablation catheter (red). Respective Ensite NavX screens are also displayed (B and D). CS, Coronary sinus; IVC, inferior vena cava; LAA, left atrial appendage; LAO, left anterior oblique views; LIPV, left inferior PV; LSPV, left superior PV; RAO, right anterior oblique; RIPV, right inferior PV; RSPV, right superior PV; SVC, superior vena cava. (From Rolf S, et al. Catheter ablation of atrial fibrillation supported by novel nonfluoroscopic 4D navigation technology. *Heart Rhythm*. 2013;10: 1293–1300.)

noninvasively, by means of inverse procedures, which help transform the ECG into an imaging method of electrical activity. This yields 3-D images that depict anatomical features with superimposed activation isochrones or excitation and recovery potentials, isochrones, and electrograms.

In BSPM measurements, unipolar potentials of single heartbeats are acquired simultaneously at more than 60 locations covering the whole thorax. A Wilson central terminal is used as a reference for the unipolar leads. Lead sites in the array are arranged in columns and rows, and the electrodes are attached to flexible plastic strips, attached to dozens of thoracic sites vertically, with the highest electrode density

at the left anterior thorax. Recordings are band pass-filtered at 0.16 to 300 Hz and digitized with a sampling frequency of 1 kHz.

BSPMs depict the spatial distribution of heart potentials on the surface of the torso. Initially, all lead tracings are visually screened to reject poor-quality signals. The amplitude of every electrogram is measured at a given time instant during the cardiac cycle and plotted on a chart representing the torso surface. Several analytical procedures are used to convert the grid of data points into map contours. The time interval between successive instantaneous maps (frames) is generally 1 to 2 milliseconds. A sequence of 400 to 800 frames shows the evolution of the potential pattern during the cardiac cycle. Often 20 to 50

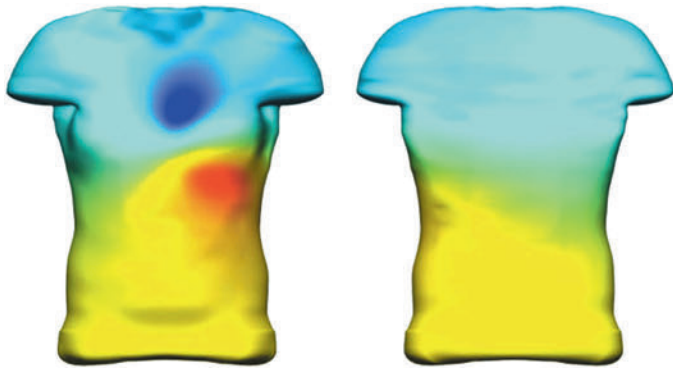


Fig. 6.27 Body Surface Potential Mapping. Body surface potential distribution at the peak of the R-wave during sinus rhythm. Potentials are displayed on a realistic human torso model with anterior (*left*) and posterior (*right*) views. Positive potentials are represented in red and negative in blue. (From Bear L, Cuculich PS, Bernus O, Efimov I, Dubois R. Introduction to noninvasive cardiac mapping. *Card Electrophysiol Clin.* 2015;7:1–16.)

properly selected maps are sufficient to show the essential features of the time-varying surface field.

Localization of the site of origin of focal tachycardia, pacing site, or myocardial insertion site of a BT relates to the thoracic site of greatest negativity in the isointegral map. An activation wavefront moving away from such sites yields a negative body surface identifier because of the dominant effect of activating the remainder of the myocardial mass away from the stimulus site (Fig. 6.27).

Clinical Implications

BSPM has been used in both experimental and clinical setting for the detection and diagnosis of various pathological conditions. BSPM has been used for patients with conditions such as pulmonary embolism, aortic dissection, and acute coronary syndromes. It has also been used for diagnosing an old myocardial infarction (MI), recognizing ventricular hypertrophy, and ascertaining the location, size, and severity of MI and the effects of different interventions designed to reduce the infarct size.⁶⁶

From an EP standpoint, BSPM has been studied for the discrimination of clockwise and counterclockwise AFL, localization of the earliest retrograde atrial activation site in dogs with simulated Wolff-Parkinson-White syndrome and orthodromic AVRT, localization of the ventricular insertion site of BTs during preexcitation, localization of sites of origin of ATs and VTs, and localization of endocardial or epicardial pacing sites.

Many studies have demonstrated higher diagnostic and prognostic value of BSPM as compared with the 12-lead ECG; nonetheless, BSPM has not been adopted in clinical practice. Although ongoing research continues to address the role of BSPM, and how BSPM addresses many of the inadequacies associated with the conventional 12-lead ECG approach, the clinical effectiveness of this procedure has not been established and the incremental value of BSPM over traditional 12-lead ECG have not justified the additional procedural complexity and expense. Hence, BSPM is mostly used as a research tool, rather than a routine diagnostic method because of significant limitations.^{66,67}

Limitations

The ability to determine precise details of cardiac electrical activity from BSPM is limited by the filtering effects of the torso cavity—that

is, body surface potentials are a smoothed representation of the underlying global cardiac electrical activity. A second limitation of BSPM is the complexity of the recording, which requires many leads from each patient, sophisticated instrumentation, and dedicated personnel. Complexity of the interpretation is another limitation because it is mostly based on pattern recognition and knowledge of variability in normal subjects and in patients—features that are difficult to memorize. Therefore, visual inspection and measurement of BSPMs cannot result, *per se*, in direct localization of single or multiple electrical events as they occur in the heart. Furthermore, BSPMs do not offer a picture of the heart, but they show an attenuated and distorted projection of epicardial and intracardiac events on the body surface. In addition, the method of interpolating maps from acquired data is vulnerable to the precision of localization of the electrode sites and to the assurance that each electrode is receiving a true signal.^{66,67}

ELECTROCARDIOGRAPHIC MAPPING

Fundamental Concepts

Body surface electrocardiographic imaging (ECGI), also called electrocardiographic mapping (ECM), is a noninvasive technique providing global electroanatomic maps of cardiac chambers by projecting body surface potentials onto the cardiac epicardial geometry derived from a thoracic CT scan or MRI.⁶⁸

The ECM system has three main components: a multielectrode ECG vest, a multichannel mapping system for ECG signal acquisition, and an anatomical imaging modality to determine the heart-torso geometry.⁶⁹ ECM requires two sets of data: ECG unipolar potentials measured over the body surface and the heart-torso geometrical relationship relating the epicardial surface to the location of the recording body surface ECG electrodes. The body surface ECG unipolar potentials are measured using a 252-electrode ECG vest (Fig. 6.28). With the vest remaining in the same position, the precise anatomic relation between the cardiac geometry and the torso electrodes is determined using noncontrast thoracic CT. The electrode positions and 3-D epicardial geometry are obtained via segmentation from the CT images.^{69,70}

Using mathematical algorithms (the inverse problem of electrocardiography), the ECM noninvasively computes and reconstructs 1500 epicardial unipolar electrograms from measured torso potentials for each beat per cycle. This is achieved by solving the inverse solution to Laplace's equation (the forward problem computes body surface potentials from epicardial potentials). Laplace's equation describes the electric potential field in the volume between the heart surface and the body surface. Accordingly, when one 3-D surface of known geometry is placed within another of known geometry, if the electrical potential on one surface is known, the potential on the other can be calculated. Because the 3-D geometry of the torso and that of the epicardial surface of the heart can be reconstructed from segmental CT images, and body surface unipolar potentials are recorded by the ECG vest (the relative positions of body surface electrodes can be visualized on the torso geometry), unipolar potentials on the cardiac epicardium can be computed. The inverse solution to Laplace's equation using the boundary element method predicts how a remotely detected signal by the ECG vest would have appeared at its source, the epicardial surface, so that electrograms are reconstructed at epicardial sites in the absence of physical electrode contact at those locations (virtual electrograms). Importantly, the inverse problem is ill-posed—that is, small errors in the input data (noise on the ECGs, inaccurate electrode locations, and inaccurate conductivity values)—can cause large errors in the solution. Therefore ECGI employs regularization techniques that impose physiologically based constraints or iterative schemes to stabilize the solution in the presence of these inaccuracies.^{70,71–73}

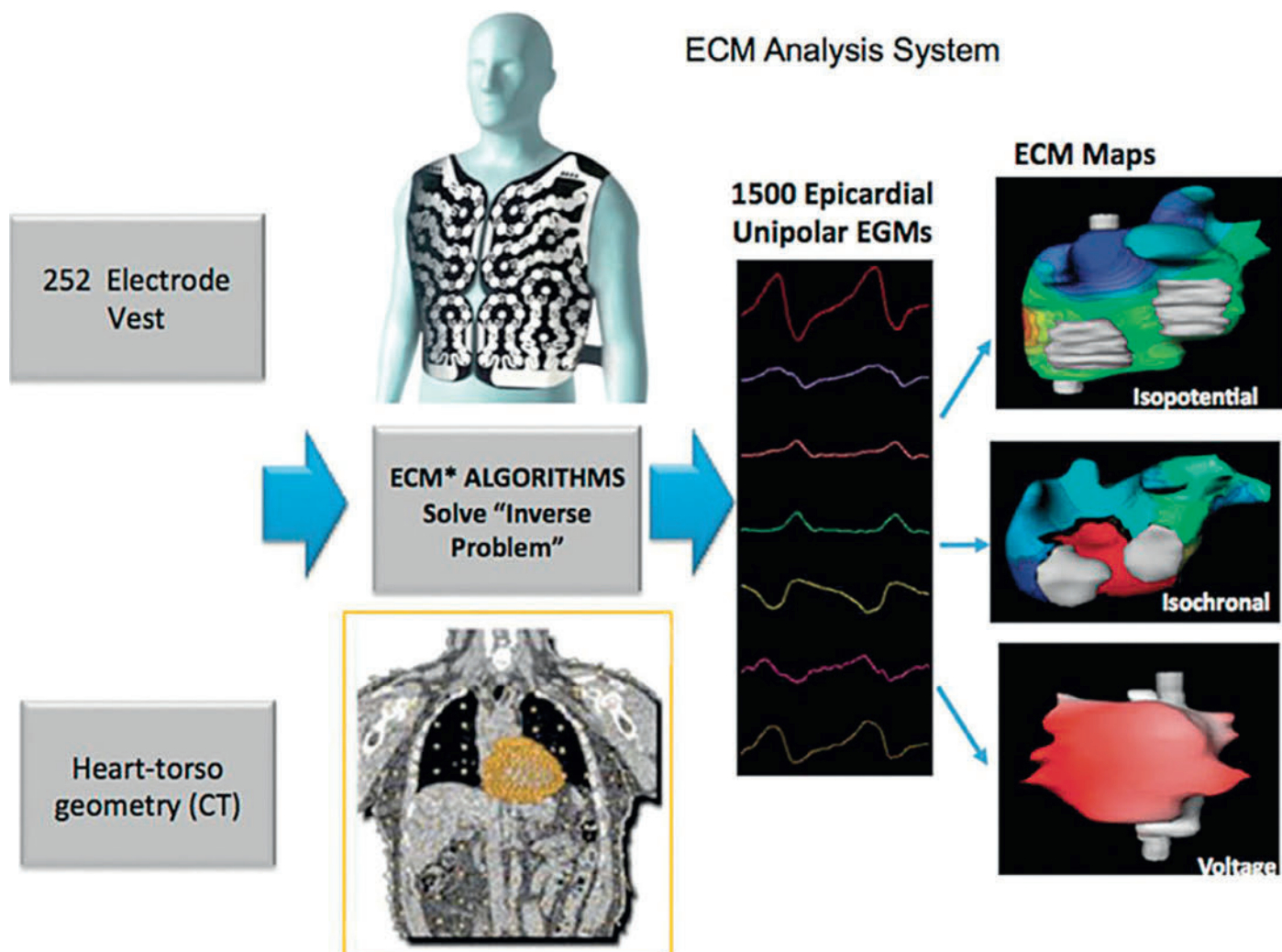


Fig. 6.28 Electrocardiographic Mapping (ECM) Procedure. Body surface potential mapping (BSPM) is recorded using a multichannel (256-electrode) mapping system embedded in a vest that can easily be placed on a patient torso. Noncontrast computed tomographic (CT) scan of the chest is performed with the body surface electrodes applied simultaneously to record the precise anatomic relation between the 252 electrodes on the vest (shining dots in CT images) and the geometry of the epicardial surface of the heart. By combining the BSPM and heart-torso geometry information, ECM reconstructs 1500 unipolar electrograms from the 252 electrodes. Out of these 1500 unipolar electrograms, isopotential, isochronal, and voltage maps can then be reconstructed. EGM, Electrogram. (From Cakulev I, Sahadevan J, Arruda M, et al. Confirmation of novel noninvasive high-density electrocardiographic mapping with electrophysiology study: implications for therapy. *Circ Arrhythm Electrophysiol.* 2013;6:68–75.)

Once the potential field has been established, more than 1500 activation points can be displayed as computed electrograms or as color-coded isopotential maps for each heartbeat. The activation time at each epicardial site is determined by taking the time instant with maximum negative time derivative ($-dV/dt$) on the virtual unipolar electrogram, allowing the generation of activation sequences (isochronal maps). Activation movies (propagation maps) can be constructed by animating the activation wavefront on the patient-specific CT-derived epicardial surface. The reconstruction is performed during a single beat and does not require accumulating data from many beats.^{66,70,72–76}

It is important to understand that ECGI is not BSPM. BSPM is only an extension of the body surface 12-lead ECG, accomplished through the application of a large number of electrodes to the torso surface. The output of BSPM is potentials on the body surface, not on the heart.

In contrast, ECGI overcomes some of the limitations of BSPM by solving the “electrocardiographic inverse problem” to estimate the equivalent cardiac sources from body surface potentials, which then are projected onto the cardiac epicardial geometry.^{67,74}

Technology Application

ECM can be performed preprocedurally or periprocedurally. The 252-electrode vest is fitted to the patient’s torso, and recording of the arrhythmia is acquired. In patients with infrequent or intermittent arrhythmias (e.g., PVCs or PACs, paroxysmal AF with focal triggers), patients may be allowed to ambulate, and the vest can be applied for several hours to help capture the culprit arrhythmia.⁷⁷

Once the index arrhythmia is recorded, the exact geometry of the epicardial and torso surfaces and vest electrode positions is obtained

by anatomical imaging modalities, such as noncontrast thoracic CT or MRI. Scans are usually set to an axial resolution between 0.6 and 1 mm and are typically gated at the R wave of the ECG to obtain diastolic volume (geometry for reconstruction of activation). Systolic volume, gated during the T wave of the ECG, is also measured to obtain suitable geometry for reconstruction during the repolarization phase. The transverse slices are segmented slice by slice to obtain heart geometry (as epicardial contours on each slice) and torso geometry (described by body surface electrode positions, seen as bright dots on the images; see Fig. 6.28). The geometry of the heart and torso surfaces is then assembled in a common x - y - z coordinate system to provide the geometrical heart-torso relationship.

ECM reconstructs an epicardial electroanatomic map noninvasively by combining a 252-electrode body surface ECG with a CT scan of the heart-torso geometry. The ECM images can be presented as 3-D color-coded, epicardial isopotential, isochronal, propagation, and voltage maps. Characteristics of activation can be analyzed at any point in the cardiac cycle, and atrial and ventricular patterns can be displayed.⁶⁸

Four modes of display are typically used. Epicardial potential maps depict the spatial distributions of potentials on the epicardium (see Fig. 6.28). Each map depicts one instant of time; maps are computed at 1-millisecond intervals during the entire cardiac cycle. The electrograms depict the variation of potential with respect to time at a single point on the epicardium. The electrograms are computed at many points (more than 1500 sites) around the epicardium. In isopotential maps, activation is assumed to occur when the electrogram voltage reaches a predefined magnitude and can be displayed as a moving image over the surface (eFig. 6.6). Isochrone maps depict the sequence of epicardial activation based on local activation time, taken as the point of maximum negative derivative ($-dV/dt_{\max}$) of the QRS segment in each electrogram (Fig. 6.29). Recovery times are assigned as the point of maximum derivative (dV/dt_{\max}) of the T wave segment. Activation times are determined as the time of maximum negative derivative in the epicardial electrograms. Information from neighboring electrograms is used to edit activation times in electrograms with multiple large negative derivatives.

Lines of block are drawn to separate sites with activation time differences more than 30 milliseconds.

Clinical Implications

Noninvasive diagnosis of arrhythmias is currently based on the standard 12-lead ECG, BSPMs, or paced body surface QRS integral mapping. Standard diagnostic techniques such as the ECG provide only low-resolution projections of cardiac electrical activity on the body surface and cannot provide detailed information on regional electrical activity in the heart, such as the origin of arrhythmogenic activity, sequence of arrhythmic activation, or existence and location of an abnormal EP substrate. Recently ECM (ECVUE, CardioInsight Technologies, Cleveland, OH, United States) has emerged as a tool of substantially greater clinical value than the 12-lead ECG in the diagnostic and therapeutic management of cardiac rhythm disorders.⁷⁸

ECGI has been investigated in experimental and clinical studies in normal cardiac EP and various atrial and ventricular arrhythmias, ventricular conduction abnormalities, as well as repolarization disorders. Several studies demonstrated the value of ECM for diagnosing the mechanism of arrhythmia (focal vs. macroreentrant), identifying the chamber of interest, localizing the origin of focal AT and VT (see eFig. 6.6 and Fig. 6.29; see eFig. 11.1), and evaluating the arrhythmogenic substrate (e.g., low voltage and fractionated electrograms in post MI scar). Such information can provide necessary guidance to facilitate planning management strategies, including EP testing and catheter ablation.^{69,72–74,77,79}

ECGI is capable of recording and displaying global electrical activation of any single beat and, unlike invasive contact electroanatomic mapping systems, does not require accumulating data from many beats. This property is particularly useful in patients with PACs or PVCs that are not of sufficient frequency to allow sequential mapping. This also allows for prolonged bedside noninvasive monitoring in patients with transient events or scarcely inducible arrhythmias and those with multiple arrhythmias. In addition, in patients with paroxysmal AF, identification, and localization of triggering PACs can potentially identify

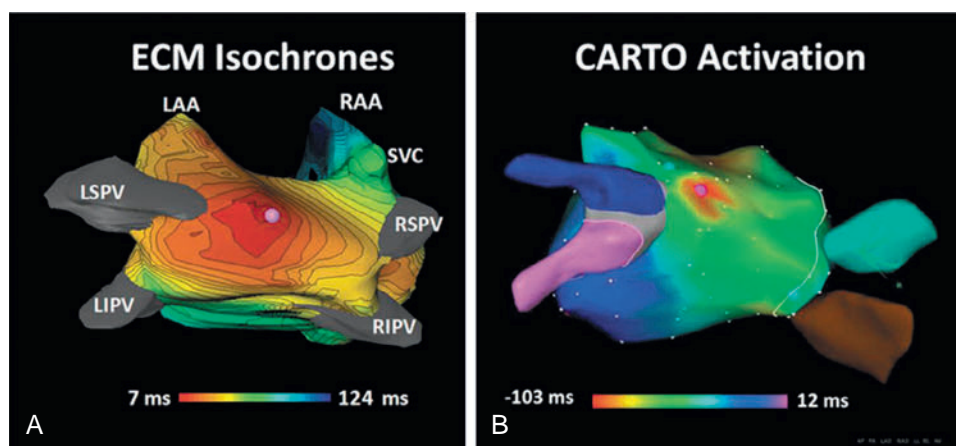
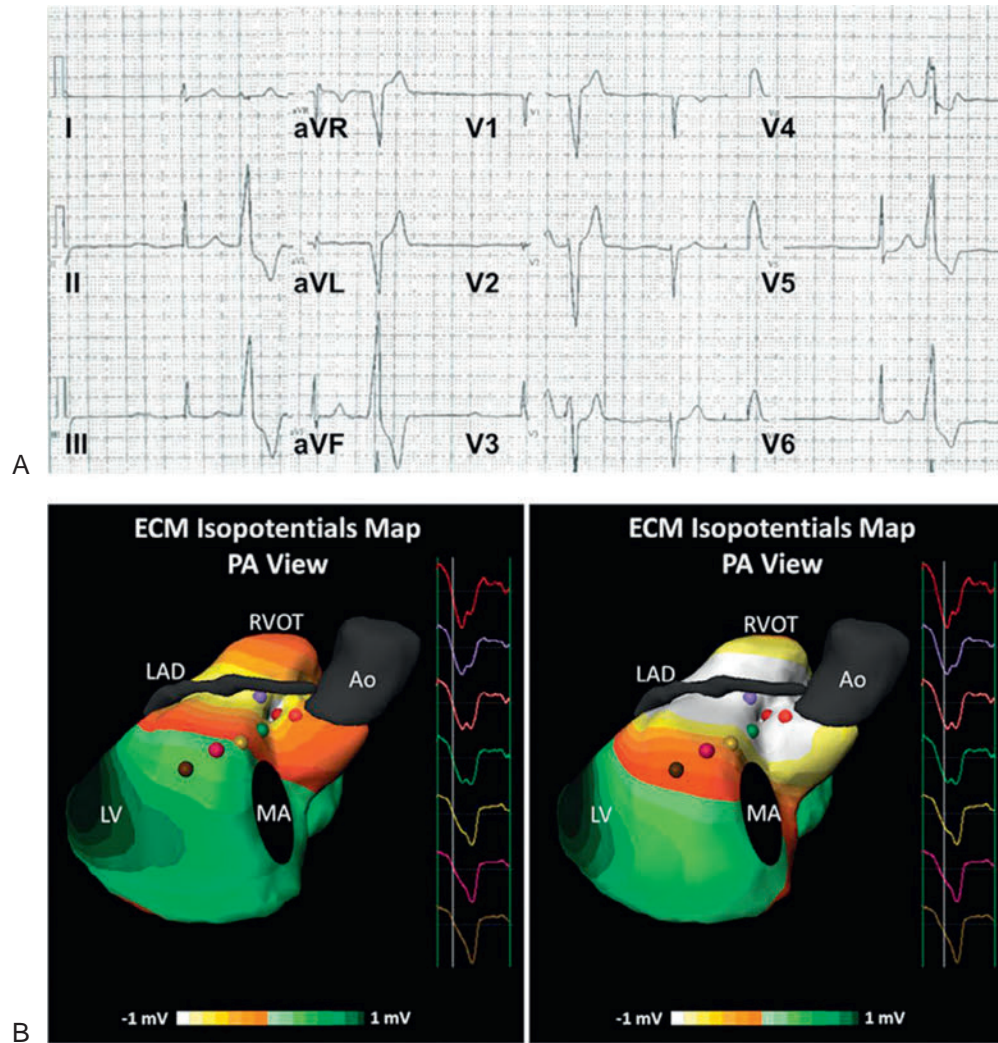


Fig. 6.29 Electrocardiographic Mapping (ECM) of Focal Atrial Tachycardia. (A) ECM isochronal map demonstrates focal activation of the left atrium (LA), with the earliest site of activation on the LA roof. This area was close to the atrial incision that was made during the left lung transplant. (B) CARTO electroanatomic activation map showing the successful site of ablation which correlates with the ECM site of earliest activation. LAA, Left atrial appendage; LIPV, left inferior pulmonary vein; LSPV, left superior pulmonary vein; RAA, right atrial appendage; RSPV, right superior pulmonary vein; RIPV, right inferior pulmonary vein; SVC, superior vena cava. (From Cakulev I, Sahadevan J, Arruda M, et al. Confirmation of novel noninvasive high-density electrocardiographic mapping with electrophysiology study: implications for therapy. *Circ Arrhythm Electrophysiol.* 2013;6:68–75.)



eFig. 6.6 Electrocardiographic Mapping (ECM) of Premature Ventricular Complexes (PVCs). (A) Surface ECG showing sinus rhythm with PVCs. The PVC QRS morphology suggests an origin from the right ventricular outflow tract (RVOT). (B) Two ECM isopotential maps show the propagation of the depolarizing wavefront. The first panel on the left shows the location of the earliest activation (*white color*) of the PVC in the vicinity of the proximal left anterior descending (LAD) coronary artery, but on the left side of the ventricular septum. The electrograms with a QS complex morphology (shown in both panels of [B] on the right side of each ECM) indicate an epicardial origin. The electrograms around, but not at, the focus, lack the sharp negative deflection of the focal electrogram, and exhibit more slurring of the downslope. The vertical lines across the electrograms show the time point at which the potential was measured. Ao, Aorta; LV, left ventricle; MA, mitral annulus; PA, posteroanterior. (From Yamashita S, Sacher F, Mahida S, et al. Role of high-resolution image integration to visualize left phrenic nerve and coronary arteries during epicardial ventricular tachycardia ablation. *Circ Arrhythm Electrophysiol*. 2015;8:371–380.)

important targets for ablation. However, the impact of ECM on the success, safety, and efficiency of the subsequent ablation procedure remains to be evaluated.^{68,74–76,80–82}

Noninvasive mapping has demonstrated the ability to image arrhythmogenic substrate having EP characteristics of low voltage, electrogram fragmentation, and presence of late potentials. In addition, ECM can potentially image the reentry pathway and its key components in atrial and ventricular macroreentrant tachycardias, including the critical isthmus, its entry and exit sites, lines of block, and regions of slow and fast conduction. Although clinical reentry usually occurs in the endocardium, the subepicardium plays an important role in the maintenance of reentry in a small proportion of patients undergoing ablation therapy. Interpretation of intramural arrhythmogenic activity can be further enhanced by direct catheter mapping or noncontact catheter reconstruction of EP information on the endocardial surface simultaneously with noninvasive epicardial ECM. The combination of epicardial and endocardial EP information, with knowledge of the intramural anatomical organization of the myocardium, can provide an unprecedented ability to localize arrhythmogenic activity within the myocardial depth by using only noninvasive or minimally invasive procedures.^{76,77,83}

ECGI can possibly be used to quantify ventricular dyssynchrony, identify potential responders/nonresponders to cardiac resynchronization therapy, and guide electrode placement for effective resynchronization therapy. Furthermore, ECGI's ability to noninvasively image regions of dispersion of repolarization in the form of QRST integral maps (or other metrics of repolarization dispersion) during a single beat provides a feasible and computationally efficient method for evaluating the severity of the substrate in patients at risk of developing arrhythmias. Noninvasive reconstruction of epicardial measures of repolarization dispersion can therefore provide a tool for rapid screening of patients at high risk of life-threatening arrhythmias. The significance of applying ECM for risk stratification is amplified by the lack of sensitivity of body surface measures (e.g., QT dispersion) at reflecting any underlying dispersion of repolarization.

Limitations

ECM provides EP information about the heart's epicardial surface; it does not directly reconstruct endocardial information in the 3-D myocardium. This is of lesser importance in relatively thin atrial tissue as opposed to ventricular. Septal arrhythmia sources, of great importance in scar-based ventricular arrhythmias, are thus less well characterized with ECM. Computation of endocardial activation is not yet possible because the electrical signal amplitude from the midwall and endocardium is much smaller. Nevertheless, in contrast to BSPMs, epicardial potentials provide high-resolution reflection of underlying intramural activity.

In addition, ECM can have limited success in defining components of arrhythmia pathways that involve small volumes of tissue, such as microreentry. Furthermore, the need to use CT limits the clinical application of ECM during intervention in the EP laboratory, where CT is not available. To render the ECM procedure more practical for mainstream adoption, newer methods for obtaining patient-specific geometry using biplane fluoroscopy or pseudo-3-D ultrasound have been developed and successfully tested in the context of ECM in the EP laboratory.

The need for CT scanning and associated radiation exposure should be weighed against value of ECM in the management of the individual patient and the potential reduction in subsequent procedural and fluoroscopic time, which warrant further studies. Nonetheless, ECM requires noncontrast CT at very low radiation (mean 148 mGy/cm). Also, cardiac geometry acquisition using an alternative technique (e.g., MRI) can help reduce radiation exposure.^{68,84}

INTRACARDIAC ECHOCARDIOGRAPHY

Catheter Design

Two types of ICE imaging systems are currently available: the mechanical ultrasound catheter radial imaging system and the electronic phased-array catheter sector imaging system.

Mechanical Ultrasound Catheter Radial Imaging System

In the mechanical ultrasound catheter (Ultra ICE) radial imaging system (EP Technologies, Boston Scientific, Sunnyvale, CA, United States), the ultrasound transducer is mounted at the end of a nonsteerable 9 Fr (110-cm length) catheter and has a single, rotating, crystal ultrasound transducer. An external motor drive unit rotates the crystal at 1800 rpm within the catheter to provide an imaging plane that is 360 degrees circumferential and perpendicular to the long axis of the catheter, with the catheter located centrally. Mechanical ICE uses imaging frequencies of 9 to 12 MHz, which provide near-field clarity (within 5 to 7 cm of the transducer) but poor tissue penetration and far-field resolution. As a result, these systems have not allowed clear imaging of the LA and PVs, except when they are introduced directly into the LA (transseptally). This technology lacks Doppler capability, and the catheter is not freely deflectable.

Electronic Phased-Array Catheter Sector Imaging System

In the electronic phased-array ultrasound catheter (AcuNav) sector imaging system (Acuson Corporation, Siemens Medical Solutions, Malvern, PA, United States), the ultrasound transducer is mounted on the distal end of an 8 or 10 Fr (90-cm length) catheter and has a forward-facing 64-element vector phased-array transducer scanning in the longitudinal plane. The catheter has a four-way steerable tip (160-degree anteroposterior and left-right deflections). The catheter images a sector (wedge-shaped) field in a plane in line with the catheter shaft and oriented in the plane of the catheter. Imaging capabilities include 90-degree sector 2-D, M-mode, and Doppler imaging (pulsed-wave, continuous-wave, color, and tissue Doppler), with tissue penetration up to 16 cm, and variable ultrasound frequency (5.5, 7.5, 8.5, and 10 MHz).

Imaging Technique

Using the Mechanical Radial Intracardiac Echocardiographic Catheter

Initially, all air must be eliminated from the distal tip of the ICE catheter by flushing vigorously with 5 to 10 mL of sterile water to optimize the ultrasound image. The ICE catheter is introduced through a long femoral venous sheath. Because the catheter is not deflectable, preshaped angled long sheaths are preferred to allow some steerability. The mechanical radial ICE catheter generates a panoramic 360-degree image perpendicular to the catheter, with the tip as a central reference point. The catheter is connected to the ultrasound console and advanced until the tip of the rotary ICE catheter image is in the RA.

When the transducer is advanced into the SVC, the ascending aorta, the right pulmonary artery, and occasionally the right superior PV are viewed. Withdrawing the catheter into the mid-RA brings the fossa ovalis and LA in view; the crista terminalis and aortic valve are usually visible in this view (Fig. 6.30). The LA, left PV orifices, and aortic root are imaged by positioning the transducer at the fossa ovalis. However, visualization of the LA and PV ostia is limited because of limited penetration depth. Withdrawing the catheter to the low RA allows visualization of the eustachian valve, lateral crista terminalis, and CS ostium (see Fig. 6.30). When the transducer is placed in the RV through the tricuspid valve and further advanced into the RVOT, both ventricles and the pulmonary artery can be visualized.

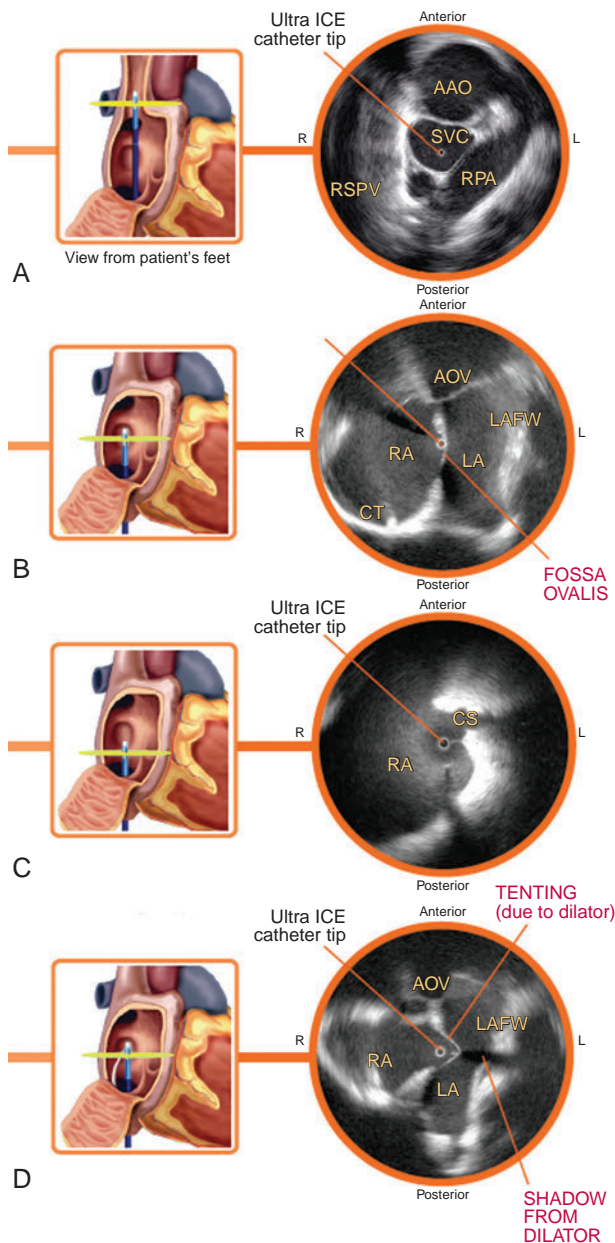


Fig. 6.30 Mechanical Radial Intracardiac Echocardiographic (ICE) Images From Different Levels in the Right Atrium (RA) and Superior Vena Cava (SVC). (A) With the transducer tip in the SVC, typical structures visible in this plane are the ascending aorta (AAO), right pulmonary artery (RPA), and right superior pulmonary vein (RSPV). (B) Withdrawing the ICE catheter into the mid-RA brings the fossa ovalis into view. Typical structures visible in this plane are the left atrium (LA), LA free wall (LAFW), aortic valve (AOV), and crista terminalis (CT). (C) Withdrawing the ICE catheter down to the RA floor visualizes the coronary sinus (CS) and inferior vena cava. (D) During transseptal puncture, tenting of the fossa is observed on the ICE. (Image provided courtesy of Boston Scientific. © 2018 Boston Scientific Corporation or its affiliates. All rights reserved.)

Using the AcuNav Catheter

A femoral venous approach is used for the insertion of the ICE catheter. The catheter is advanced to the RA under fluoroscopy guidance. ICE 90-degree sector scanning demonstrates a cross-sectional anatomical view oriented from the tip to the shaft of the imaging catheter's active face. The left-right (L-R) orientation marker indicates the catheter's

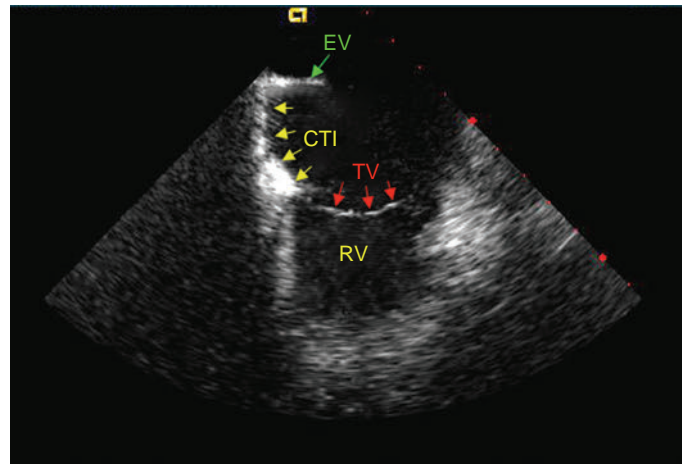


Fig. 6.31 Intracardiac Echocardiographic (ICE) Image of the Cavotricuspid Isthmus (CTI). The CTI (yellow arrows) is shown between the eustachian valve (EV, green arrow) and the tricuspid valve (TV, red arrows). RV, Right ventricle.

shaft side. When the L-R orientation marker is set to the operator's right, the craniocaudal axis projects left to right from the image and the posterior to anterior axis projects from the image top to bottom. Changing the L-R marker to the left side inverts the image but does not change the top-to-bottom image orientation. Image orientation can be adjusted to visualize targeted structures by simple catheter advancement or withdrawal, by tip deflection in four directions (anteroposterior and left-right), or by catheter rotation.

The AcuNav ICE catheter includes variable ultrasound frequency (5.5, 7.5, 8.5, and 10 MHz). Increasing ultrasound frequency improves axial image resolution; however, tissue penetration decreases and reduces imaging depth. An ultrasound frequency of 7.5 MHz is useful for imaging most cardiac structures. Frequency can then be increased (to 8.5 or 10 MHz) for imaging near-field structures, or decreased (to 5.5 MHz) for imaging far-field structures.

RA targets. All RA targets are visualized by advancing or withdrawing the ICE catheter to an appropriate level within the RA and rotating the catheter to bring the target into view. The best resolution of near-field and mid-field structures is obtained at an 8.5-MHz frequency. Once the catheter is advanced into the mid-RA with the catheter tension controls in neutral position (the ultrasound transducer oriented anteriorly and to the left), the RA, tricuspid valve, and RV are viewed. This is called the home view (see Fig. 4.11), and it can serve as a starting point; whenever the operator loses orientation, he or she can go back to the home view and start over. From the home view, counterclockwise rotation of the catheter brings the RA appendage into view, whereas anterior deflection of the catheter tip toward the RV allows visualization of the tricuspid valve and CTI (Fig. 6.31). The superior crista terminalis is visualized when the catheter is advanced to the RA-SVC junction in an anterior direction.

Interatrial septum. Gradual clockwise rotation of a straight catheter from the home view allows sequential visualization of the aortic root and the pulmonary artery, followed by the CS, mitral valve, the LA appendage orifice, and a cross-sectional view of the fossa ovalis (see Fig. 4.11). The mitral valve and interatrial septum are usually seen in the same plane as the LA appendage. Posterior deflection, right-left steering, or both, of the imaging tip in the RA, is occasionally required to optimize visualization of the fossa ovalis; the tension knob (lock function) can then be used to hold the catheter tip in position. Further

clockwise rotation beyond this location demonstrates images of the left PV ostia (see Fig. 4.11). The optimum ICE image to guide transeptal puncture demonstrates adequate space behind the interatrial septum on the LA side and clearly identifies adjacent structures (see Fig. 4.12).

LA structures. A 7.5- or 8.5-MHz imaging frequency optimizes visualization of LA structures and PVs beyond the interatrial septum. PV imaging is possible by first visualizing the membranous fossa from a mid-RA to low-RA catheter tip position. With clockwise catheter rotation, the LA appendage can be visualized, followed by long-axis views of the left superior and inferior PVs (Fig. 6.32; see Fig. 4.12). Further clockwise rotation of the catheter brings the orifices of the right superior and inferior PVs into view. The ostia of these veins are typically viewed en face, yielding an owl's eyes appearance at the vein's orifice. The LA appendage can also be visualized with the transducer positioned in the CS.

LV and RV targets. Imaging of each targeted LV structure at depths of 6 to 15 cm is accomplished with the catheter tip in a low-RA position. When the catheter transducer is placed near the fossa and oriented anteriorly and to the left, the left ventricular outflow tract (LVOT) and truncated LV are imaged. With clockwise rotation and slight adjustment of the transducer level, the mitral valve and LV apex can be viewed. To image the mitral valve in a long-axis, two-chamber view (LA, mitral valve, and LV), a mild degree of apically directed catheter tip deflection can be required. The RVOT, LVOT, and aortic root with coronary artery ostia can be imaged by advancing the catheter in the RA to the level of the outflow tracts (mid-RA), with an appropriate deflection to the right. The aortic valve can also be imaged in its cross section from this region (Fig. 6.33). A long-axis view of the LV can also be visualized by advancing the catheter with its anteriorly deflected tip into the RV and clockwise rotation against the interventricular septum (Fig. 6.34). Further clockwise rotation or right-left steering of the catheter tip allows a short-axis view of the LV, as well as the mitral valve (see Fig. 6.34). Pericardial effusions usually can be readily identified from these views. Withdrawing the catheter back to the base of the RVOT and rotating the shaft allow the RVOT to be visualized in its long axis, with a cross-sectional view of the pulmonic valve.

Clinical Implications

Transesophageal imaging has been used to guide ablation of VT and BTs, as well as transeptal catheterization, and for the closure of atrial septal defects or cardiac biopsy. This approach, however, has been limited in the interventional arena by aspiration risk and patient discomfort accompanying prolonged esophageal intubation, and it requires a second ultrasound operator to complete the study.

Previous human applications of ICE have been limited to those generated by the mechanical rotation of a single piezoelectric element in 6 to 10 Fr catheters. Miniaturization of these elements required the use of higher 10- to 20-MHz transducer frequencies, thus limiting ultrasound penetration to surrounding cardiac tissues. This technology has been applied to the imaging of RA structures in humans and animals, membranous fossa ovalis, crista terminalis, eustachian ridge, tricuspid annulus, and the SVC-RA junction in the region of the sinus node. However, visualization of the LA and PV ostia is limited using this system because of limited penetration depth, except when it is introduced directly into the LA (transseptally).

The electronic phased-array ultrasound system offers a deeper field of view, standard intracardiac visualization of specific right- and left-sided cardiac structures, as well as color flow and pulsed-wave and continuous-wave Doppler imaging by a single operator. These features have been of significant value for PV isolation procedures and LA linear ablation for AF.

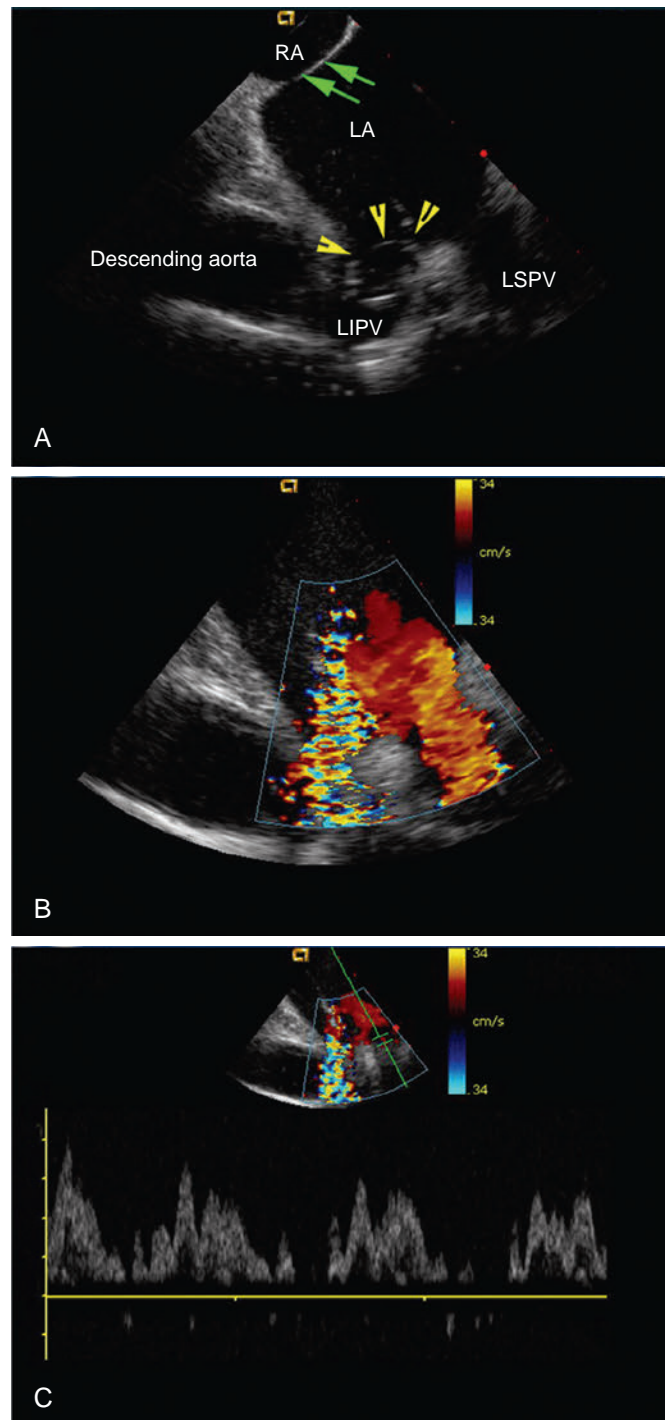


Fig. 6.32 Intracardiac Echocardiographic (ICE) Images of the Left Pulmonary Veins With Transducer Placed in the Right Atrium (RA). (A) The RA, interatrial septum (green arrows), left inferior pulmonary vein (LIPV), left superior pulmonary vein (LSPV), and descending aorta are visualized. The Lasso catheter (yellow arrowheads) is visualized at the ostium of the LIPV. Color Doppler images of both LIPV and LSPV (B) and a pulsed-wave Doppler tracing (C) obtained from the LSPV are shown. LA, Left atrium.

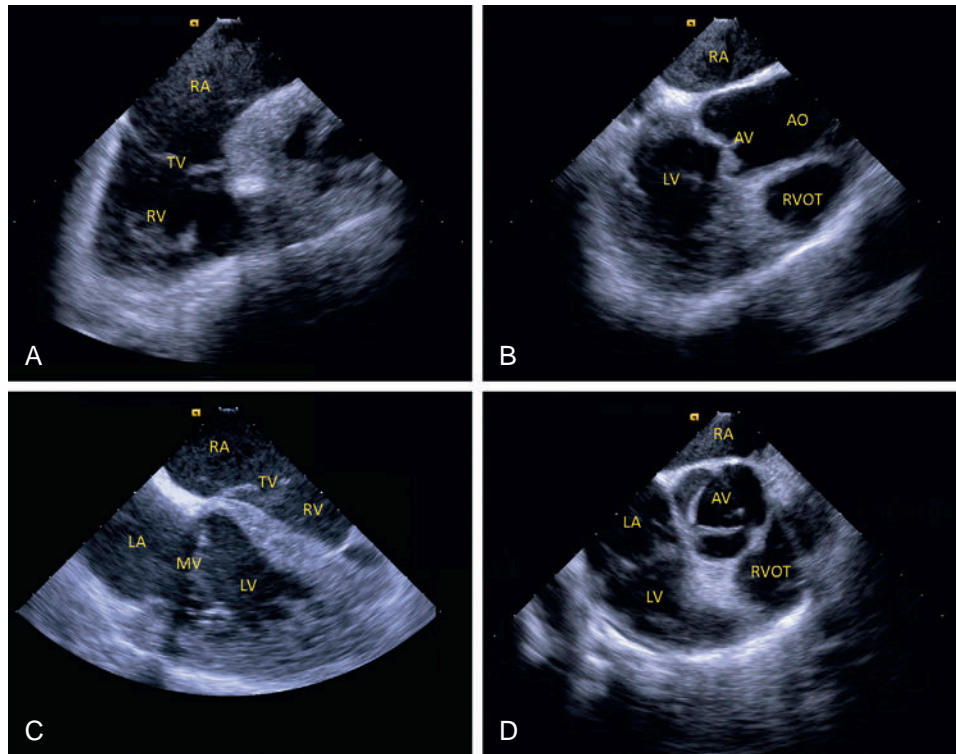


Fig. 6.33 Several Intracardiac Echocardiographic (ICE) Views Obtained From ICE Transducer Positioned in the Low Right Atrium and at the Tricuspid Annulus. AO, Aortic root; AV, aortic valve; LA, left atrium; LV, left ventricle; MV, mitral valve; RA, right atrium; RV, right ventricle; RVOT, right ventricular outflow tract; TV, tricuspid valve.

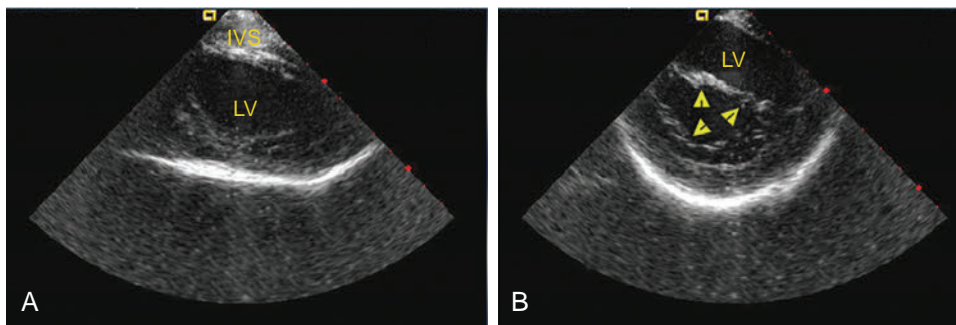


Fig. 6.34 Intracardiac Echocardiographic Images of the Left Ventricle (LV). The transducer is placed in the right ventricle against the interventricular septum (IVS). (A) Long-axis view of the LV. (B) Short-axis view of the LV at the level of the mitral valve (arrowheads).

Several practical uses for ICE have emerged in the setting of EP procedures, including the following: (1) assessment of catheter contact with cardiac tissues; (2) determination of catheter location relative to cardiac structures (specifically useful in otherwise difficult to localize areas; e.g., the PVs, papillary muscle); (3) guidance of atrial septal puncture, particularly in the setting of complex or unusual anatomy; (4) facilitation of deployment of mapping or ablation systems (e.g., PV encircling devices, noncontact mapping systems, and basket technologies); (5) visualization of evolving lesions during RF energy delivery (both changing tissue echogenicity and microbubbles reflect tissue heating, with the latter providing a signal for energy termination); (6) defining LV scar to guide substrate-based ablation of scar-related VT (Fig. 6.35); (7) evaluation of cardiac structures before and after intervention (e.g., cardiac valves and PVs); (8) assessment of PV anatomy,

dimensions, and function via 2-D anatomical imaging and Doppler physiological measurements; (9) assessment of complications (e.g., tamponade, electromechanical dissociation, or thrombus formation; see Fig. 32.1); (10) identification of the anatomical origin of certain arrhythmias (e.g., ICE can facilitate ablation of inappropriate sinus tachycardia or sinus nodal reentrant tachycardia); (11) definition of the proximity of the catheter tip and coronary arteries (during mapping and ablation of arrhythmias originating from the aortic cusp); and (12) identification of esophageal location.⁸⁵

As mentioned previously, the CARTO-Sound Image Integration Module incorporates the electroanatomic map to an ICE volume map of the cardiac chamber derived from a phased-array transducer catheter incorporating a position sensor (Sound-Star, Biosense Webster), which may be used as a stand-alone tool to guide navigation and ablation or

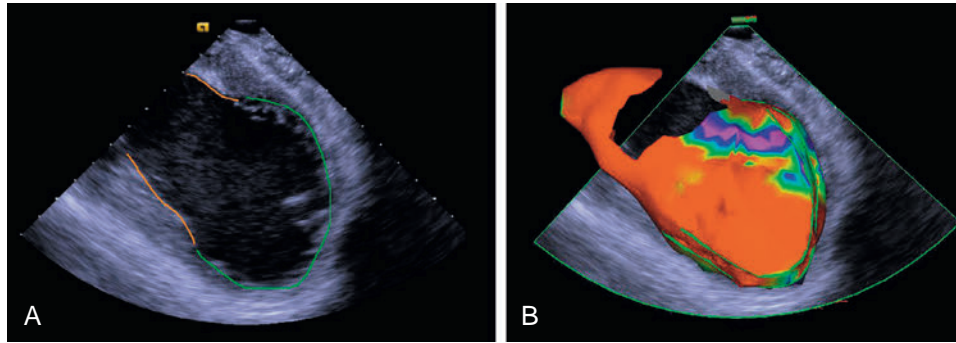


Fig. 6.35 The CARTO-Sound Image Integration Module to Guide Scar-Related Ventricular Tachycardia Ablation. (A) Intracardiac echocardiographic (ICE) image showing a long-axis view of the left ventricle (LV) using a 10 Fr phased-array transducer catheter. The endocardial surface of the LV is traced. Note aneurysmal wall thinning of the anteroapical of the LV (traced in green) as compared with normal wall thickness in the LV base (traced in red). (B) Integration of the CARTO-Sound volume and the electroanatomic voltage map of the LV (modified anterior view).

as a facilitator of CT/MRI image integration (see Fig. 6.4). This navigation approach has been successfully utilized for catheter ablation of AF. In addition, 3-D ultrasound images can potentially yield anatomically accurate chamber geometries and identify scar in the LV (both by wall thickness and motion) to facilitate substrate mapping and ablation of post-infarct VT (see Fig. 6.35).

COMPUTED TOMOGRAPHY AND MAGNETIC RESONANCE IMAGING

Fundamental Concepts

During catheter ablation procedures, the catheters are usually manipulated under the guidance of fluoroscopy. However, fluoroscopy does not provide adequate depiction of cardiac anatomy because of its poor soft tissue contrast and the 2-D projective nature of the formed image, which hinders its application for complex procedures such as AF ablation. On the other hand, CT and MRI images offer anatomical detail in 3-D. However, these images are presented out of the context of the ablation catheter, thus greatly diminishing their potential value. An optimal strategy would therefore be to integrate the 3-D images generated by CT or MRI with the electrical and navigational information obtained by an interventional system. This can be achieved through the process of integration. Image integration refers to the process of aligning the preprocedural cardiac CT and MRI images with the real-time 3-D electroanatomic maps reconstructed from multiple endocardial locations. The process of image integration consists of three steps: preprocedural CT and MRI image acquisition, image segmentation and extraction, and image registration.

Image Acquisition

Cross-sectional or axial CT or MRI scans are acquired at sufficient resolution to delineate cardiac structures less than 1 to 2 mm in thickness. Images at 0.625-mm thickness can be reconstructed from images obtained at 1.25-mm intervals with currently available multirow helical scanners. A simultaneous ECG is recorded to assign the source images retrospectively to the respective phases of the cardiac cycle. MRI images are similarly obtainable, although at a slightly lower spatial resolution. Reconstructing any cardiac chamber in 3-D from the axial images is performed using any one of various software packages.

Image Segmentation

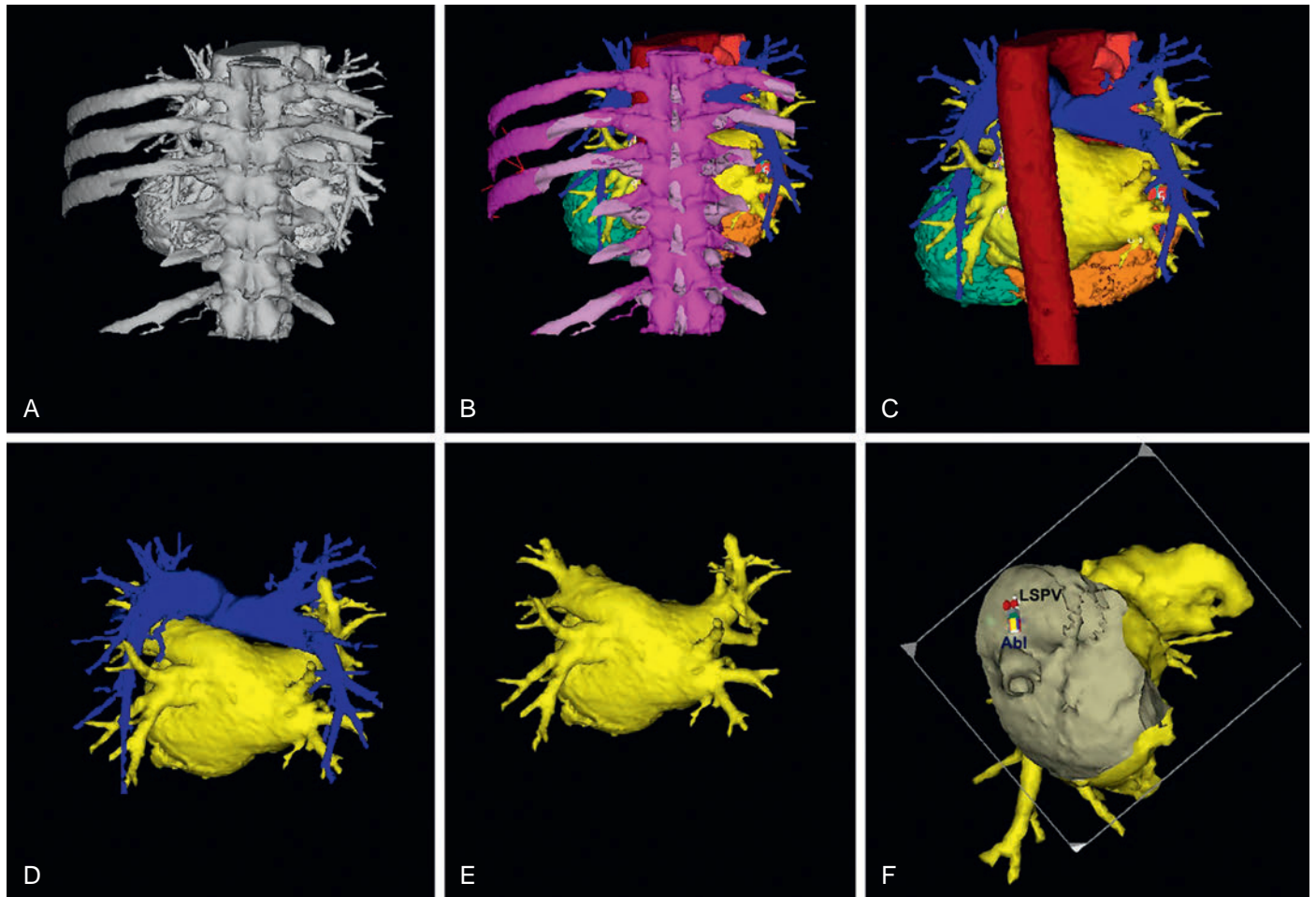
Image segmentation refers to the process of extracting the 3-D anatomy of individual cardiac structures from its surrounding structures. Methods

of image segmentation include thresholding, boundary detection, and region identification. Thresholding involves assigning pixels with intensities lower than a threshold to one class and the remaining pixels to a different class. Connecting adjacent pixels of the same class then forms regions. Boundary differentiation methods use information about intensity differences between adjacent regions to separate the regions from each other. Region identification techniques then form regions by combining pixels of similar properties. For cardiac ablation procedures, the volume of cardiac structures is extracted from the whole-volume data set using a computerized algorithm that differentiates the boundary between the blood pool (which is high in contrast) and the endocardium (which is not contrast enhanced). This allows for clear differentiation between the chamber lumen and endocardial wall (eFig. 6.7). Subsequently, the volumes of individual cardiac structures are separated from each other with the use of another algorithm capable of detecting their boundaries. Using a third algorithm, the segmented volumes for individual cardiac structures are extracted as 3-D surface reconstructions. The segmented volumes can be viewed from an external perspective or from within the chamber using virtual endoscopic or cardioscopic displays. These images, in addition to providing a road map for ablation, can also be used for registration.

Image Registration

Although the segmented structures are highly useful for visualizing the cardiac structures and characteristics of the tissue forming that structure, they do not convey the physiology of an arrhythmia. Integrating that physiology, as captured by electroanatomic or noncontact mapping with the spatial information contained in the CT or MRI images, requires the registration of activation or voltage data to an appropriate location on a 3-D representation of a chamber. This is of critical importance in that it establishes the relationship between anatomy and physiology as required for the structure- and activity-based understanding of arrhythmias and for enabling image-guided intervention. Image registration refers to superimposing the 3-D CT/MRI surface reconstruction onto the real-time electroanatomic maps yielded by the 3-D mapping system (see Fig. 6.3).⁸⁶

During registration, the assumption is made that the anatomy of the organ being registered has not changed. Two computerized algorithms are used to accomplish the image registration process: landmark registration and surface registration. Landmark registration aligns the 3-D CT/MRI image reconstruction with corresponding electroanatomic maps through linking two sets of corresponding fiducial points in each set of the images to be registered. Under the guidance of fluoroscopy



eFig. 6.7 CT Image Segmentation and Integration With Electroanatomic Mapping (CARTO) Data. (A) Three-dimensional reconstruction of the heart and part of the spine from the two-dimensional CT image (posteroanterior view). (B and C) Individual cardiac chambers are segmented from each other using computerized algorithms capable of detecting their boundaries (aorta, *red*; left atrium [LA], *yellow*; left ventricle, *green*; pulmonary artery, *blue*; right atrium, *orange*). (D) and (E) The cardiac chamber is selected (LA in this case), and others are deleted. (F) Integration of CT and electroanatomic mapping (CARTO) data. Shown is a left lateral cardioscopic view of the ostia of the left pulmonary veins (PVs) during PV electrical isolation. Radiofrequency applications (*small red circles*) were deployed at the posterior aspect of the ostium of the left superior PV (LSPV). The ablation (*Abl*) catheter tip is positioned at the inferior aspect of the LSPV.

or ICE, or both, at least three landmark pairs are created by real-time catheter tip locations on the interventional system being used for registration and then placed on their estimated locations on the 3-D CT/MRI image reconstructions. Using more landmark points increases the accuracy of the registration process. Surface registration is an algorithm that attaches the acquired endocardial points to the closest CT/MRI surface to compose the best fit of the two sets of images by minimizing the average distance between the landmarks, and the distance from multiple endocardial locations, to the surface of 3-D CT/MRI image reconstructions. Surface registration complements landmark registration to improve the registration accuracy. However, because of surface indentation and potentially missed areas during mapping, the acquired electroanatomic map does not represent the perfect anatomy of the cardiac chamber.⁸⁶

Computed Tomography Overlay

A novel application (EP Navigator prototype, Philips Healthcare, Best, The Netherlands) has been developed to superimpose a preacquired segmented 3-D CT image of the LA over real-time fluoroscopy system (“CT overlay”) to help in guiding ablation of atrial arrhythmias, particularly AF. This application can be used on monoplane or biplane fluoroscopy. It permits fluoroscopy-directed guiding of an ablation catheter and diagnostic catheters in a virtual 3-D model of the LA, and subsequent tagging of ablation sites on the registered 3-D image without the simultaneous use of an electroanatomic mapping system, thus facilitating the creation of continuous lines and returning to critical ablation sites. Furthermore, it is feasible to identify and segment the esophagus on the CT scan, which can subsequently be overlaid on the fluoroscopic images along with the cardiac structures.

Image Integration Technique

Image Registration Using CARTO-Merge

The preacquired CT/MRI digital imaging data are imported by a CD into the CARTO system equipped with commercially available software (CARTO-Merge image integration software module) that allows structures of interest to be easily and quickly segmented and reconstructed in 3-D. The segmented images are then imported into the real-time mapping system. Once created using the CARTO system (as described previously), the electroanatomic map of the cardiac chamber is “fused” to the CT/MRI. The most frequently used registration technique is a combination of landmark registration and surface registration. Landmark registration involves the 3-D orientation of the imported CT/MRI image on the *x*, *y*, and *z* axes, and requires the acquisition of at least three noncollinear endocardial landmark points using the mapping-ablation catheter. The precise location of these on the 3-D image is a critical factor in this technique and remains challenging. Biplane fluoroscopy, angiography, and ICE can be used to facilitate identification of the landmark point. Catheter contact is ensured by fluoroscopy visualization of the catheter mobility in relation to the cardiac motion and by a discrete electrogram. The estimated corresponding locations of these endocardial landmark points are then marked on the imported 3-D CT/MRI image, thus creating a landmark pair, with one landmark point on the real-time electroanatomic map and the other on the 3-D CT/MRI image.

Landmark registration approximates the electroanatomic map to the 3-D CT/MRI surface reconstruction by matching the landmark pair. Surface registration fits the 3-D CT/MRI surface reconstruction with the electroanatomic map points by rendering the smallest average distance of the two datasets. Although the registration of surface points should improve alignment of the two images, registering points from the entire surface of the cardiac chamber involves the risk of incorporating errors related to potential indentation of the chamber wall and

distortion of chamber geometry resulting from the pressure of the mapping catheter on the most mobile regions. The mapping system then provides an average tip-to-surface distance, which ideally should be less than 2 mm. While manipulating the catheter during ablation, the projected catheter distance to the surface is used as an additional guide to assess catheter contact. This can be complemented by information from electrograms recorded by the catheter, fluoroscopy, and ICE.

Image Registration Using CARTO-Sound

Real-time ICE images can provide accurate chamber geometries. The CARTO-Sound utilizes an 8 or 10 Fr phased-array ICE catheter with an embedded navigation sensor (SoundStar, Biosense Webster), which records individual 90-degree sector image planes of the cardiac chamber of interest, including their location and orientation, to the CARTO workspace. To correct for respiratory phase, all ICE images should be acquired during expiratory breath-hold. Once the CARTO-Sound volume map of the cardiac chamber is created, registration is performed using CARTO-Merge software. First, the CT/MRI image is visually aligned with the ICE-created cardiac chamber anatomical shell. Second, landmark registration is performed whereby three echocardiographically discrete anatomical sites identified with ICE (landmark points) are tagged on the ICE contour and matched to a corresponding location on the CT/MRI image. Finally, the CARTO-Merge surface registration algorithm is performed. This algorithm attempts optimally to juxtapose, or integrate, the CT/MRI image spatially with the CARTO-Sound model to minimize the average distance between each point on the ICE-created anatomical rendering of the cardiac chamber and the corresponding CT/MRI image, thus permitting the CT model to guide navigation.⁸⁵

Registration is based on the best fit between the cardiac chamber surface reconstruction obtained with each ICE contour and the corresponding CT/MRI image, and it is not based on the LA volume obtained with ICE and the corresponding CT/MRI image. ICE-guided focused endocardial surface registration seems to be superior to landmark registration in achieving a better alignment between the CT/MRI image and the electroanatomic map. The 3-D ultrasound images can help create anatomically accurate, real-time chamber geometries, and eliminate chamber deformity (as often happens with contact mapping), potentially to yield more accurate CT/MRI registration.

Image Registration Using NavX Fusion

The cardiac chamber of interest is segmented and reconstructed in 3-D from CT/MRI slices using EnSite Verismo software. The 3-D virtual anatomical geometry of the cardiac chamber is created using NavX Fusion (as described previously). The CT/MRI reconstruction of the mapped cardiac chamber is displayed on a split screen and used to guide finer anatomical definition with the ablation catheter and help edit the virtual 3-D geometry to eliminate “false space.” Subsequently, “field scaling” is applied to the geometry to compensate for variations in impedance between the heart chambers and venous structures, and render the geometry and navigational space more physiologically relevant and to more closely resemble the CT/MRI image. The field scaled geometry is fused to the CT/MRI in two stages, termed *primary (rigid) fusion* and *secondary (dynamic) fusion*. Primary fusion uses three fiducial (i.e., landmark) corresponding points on the created geometry and the CT/MRI image to superimpose, or lock together, both images (Fig. 6.36). These points are chosen to ensure reasonable 3-D anatomical separation and allow orientation of the CT/MRI, but the registration error is high. Therefore secondary fusion points or fiducials are applied to the primary fused geometry at sites of local mismatch between the two superimposed geometries.

In this unique component of image fusion, the created geometry surface is molded to the CT/MRI surface while also “bending” the 3-D

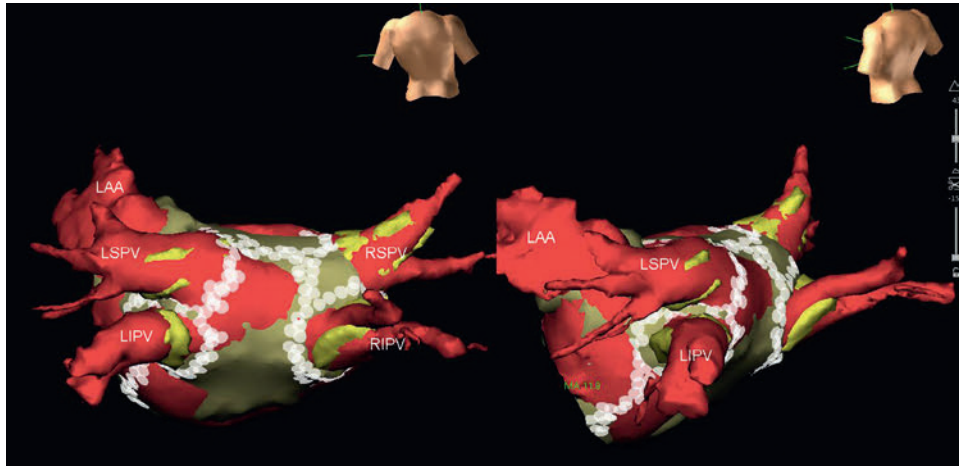


Fig. 6.36 Integration of CT and EnSite NavX Electroanatomic Mapping Data. Shown are posteroanterior (*left*) and left lateral views (*right*) of the electroanatomic contour acquired with catheter manipulation in the left atrium (LA) during atrial fibrillation ablation overlaid on a CT image of the left atrium acquired several days earlier. Small white circles are tagged sites at which radiofrequency energy was applied. Circumferential LA ablation, as well as linear ablation across the LA roof and later mitral annulus, were performed. LAA, Left atrial appendage; LIPV, left inferior pulmonary veins; LSPV, left superior pulmonary veins; RIPV, right inferior pulmonary veins; RSPV, right superior pulmonary veins.

navigation space within the geometry. This process is continued, adding supplemental (usually more than 15) fiducial point pairs until good correspondence between the NavX geometry and CT/MRI models is achieved. For example, if the anterior wall of the geometry is fused anteriorly to the CT/MRI, the catheter location also will be moved so that when the catheter is repositioned on the anterior wall after fusion, it should be visualized on the CT/MRI surface and not within the bounds of the original perfusion geometry.

Although the principle of CT/MRI image integration is common to both the EnSite NavX Fusion and CARTO-Merge systems, there is a significant difference in how registration is achieved. As described previously, the EnSite system uses a dynamic registration process (with four or more fiducial points) to optimize both rotation and stretching of the surface of the NavX geometry to match the CT/MRI. With the CARTO-Merge system, the whole registration process is rigid with rotation of the CT/MRI to minimize the distance between the surface of the anatomical model generated and that of the CT, but no stretching of the model itself. Despite this difference, the registration error is similar with both techniques (CARTO-Merge, 2.3 ± 1.8 mm, vs. EnSite NavX Fusion, 3.2 ± 0.9 mm).

Image Registration Using Fluoroscopy (Computed Tomography Overlay)

The preacquired CT data set is imported into the software, the cardiac chamber of interest is automatically segmented, and a 3-D volume of the LA and PVs is constructed. Before CT registration is performed, the patient must be properly positioned, and the structure of interest must be isocentered in two orthogonal fluoroscopic projections. Initial registration is based on the heart contour to allow for quick alignment of the CT-rendered volume with the fluoroscopic image. On an antero-posterior fluoroscopic projection (without contrast injection), the CT volume overlay is aligned by first using the right lateral atrial contour. The rest of the cardiac contour then is superimposed on the fluoroscopic image, based on the best visual estimate. Subsequently, fluoroscopic identification of intracardiac landmarks by catheter manipulation within the LA and PVs improves the overlay accuracy (e.g., caudal drop of the catheter when withdrawing from a PV into the LA helps identify the

PV ostium; insertion of the ablation catheter into readily identifiable anatomical landmarks such as PV branches immediately connected to PV ostium, accessory PVs; and looping of the ablation catheter in the LA resulting in circumferential catheter-endocardium contact). Finally, angiography of the right and left superior PVs (sequentially or simultaneously) in two orthogonal views is performed to adjust the CT image further and improve registration by matching the superior border of the LA and the superior PV ostia, as well as certain landmarks, such as PV bifurcations, between 3-D image and fluoroscopy.

After registration and locking, the 3-D CT image is always depicted at the same angle as the fluoroscopy (i.e., the CT-generated volume rotates on the screen following the rotation of the C-arm), thus allowing for constant visualization of the CT and fluoroscopic images under the same viewing angle. The transparency of the overlaid CT 3-D volume is adjustable, to allow visualization of the catheters in the fluoroscopic image. In addition, the 3-D image can be clipped with a customizable cutting plane, to permit internal (endoscopic) views. Moreover, tags can be placed on the surface of the registered 3-D image to mark ablation sites and other sites of interest.

Clinical Implications

The 21st century has also seen the rapid development of integrated, anatomically based atrial and ventricular mapping and ablation. This progress has been driven by a realization of both the critical coupling and dependence of arrhythmias on their underlying anatomy and the limitations of surrogate geometries of contemporary mapping systems for reflecting that anatomy. Over this same time frame, rapid CT and MRI imaging systems have emerged as the mainstays of imaging in the EP laboratory and have been used to plan or guide ablation. Helical 16- to 64-row CT and MRI studies provide a broad anatomy library of an individual patient at one point in time. Segmented CT volumes can be downloaded on the CARTO and NavX platforms. These systems are able to register the surrogate map fully onto actual CT and MRI anatomy; they also enable the integration of electroanatomic mapping with preacquired CT and MRI images, and allow real-time visualization of the location and orientation of the catheter tip within the registered CT anatomical framework (see Fig. 6.3; eFig. 6.7).

The use of registered CT and MRI images to guide catheter ablation presents a significant advantage over the less detailed surrogate geometry created by previously available 3-D mapping systems. Because it provides detailed anatomical information on the catheter tip location in relation to the true cardiac anatomy, the image integration technique has the potential to facilitate many ablation procedures, especially anatomically based ablation strategies, such as AF ablation and ablation of intraatrial reentrant tachycardias following corrective surgery for congenital heart diseases. Initial experience has shown that the registered CT and MRI of LA reconstructions can provide accurate information on the catheter tip location in relation to the important LA structures, such as the PV ostium and LA appendage. The real-time update of the catheter tip location and the marking of ablation lesions on the detailed 3-D image can potentially improve the quality of lesion sets, reduce complications, and shorten procedure and fluoroscopy times.

In addition, CT and MRI integration has been increasingly used to guide substrate-based ablation procedures for scar-related VT (see Fig. 6.37, eFig. 6.8, and Fig. 6.38). Ventricular scar and its border zone represent the target of “substrate modification” VT ablations; therefore, an exact anatomical delineation is critical. Multiple imaging modalities detailing the LV or RV substrate in a 3-D format can be visualized and displayed simultaneously with the electroanatomic 3-D ventricular voltage

map. These imaging approaches can be used to correctly predict abnormal voltage locations in advance of the mapping procedure, which may allow the electrophysiologist to concentrate on areas of likely myocardial scar, obviate the need to perform a complete point-by-point voltage mapping, identify falsely low-voltage recordings in areas of normal perfusion due to suboptimal catheter contact, as well as reduce procedure time and fluoroscopic exposure. In addition, some imaging modalities are able to characterize the transmural extent and intramyocardial location of scar tissue, which can potentially help identify intramural and epicardial arrhythmia substrate, overcoming a limitation of endocardial voltage mapping.^{86,87} In addition, real-time integration of CT images of the phrenic nerve and coronary arteries can help guide epicardial ablation and minimize the risk of injury to these structures.^{88,89}

Registration of a preacquired 3-D CT image on fluoroscopy potentially combines the accuracy of CT with the real-time fluoroscopy to guide catheter ablation of AF. Compared with an established and widely used electroanatomic mapping technique for PV antrum isolation, procedural duration can be shortened significantly without a concomitant increase in radiation burden. An additional advantage to CT overlay is the ability to perform a quick repeat registration in case of major changes in a patient's position. However, unlike the CARTO system, which provides notification for significant patient movements, the

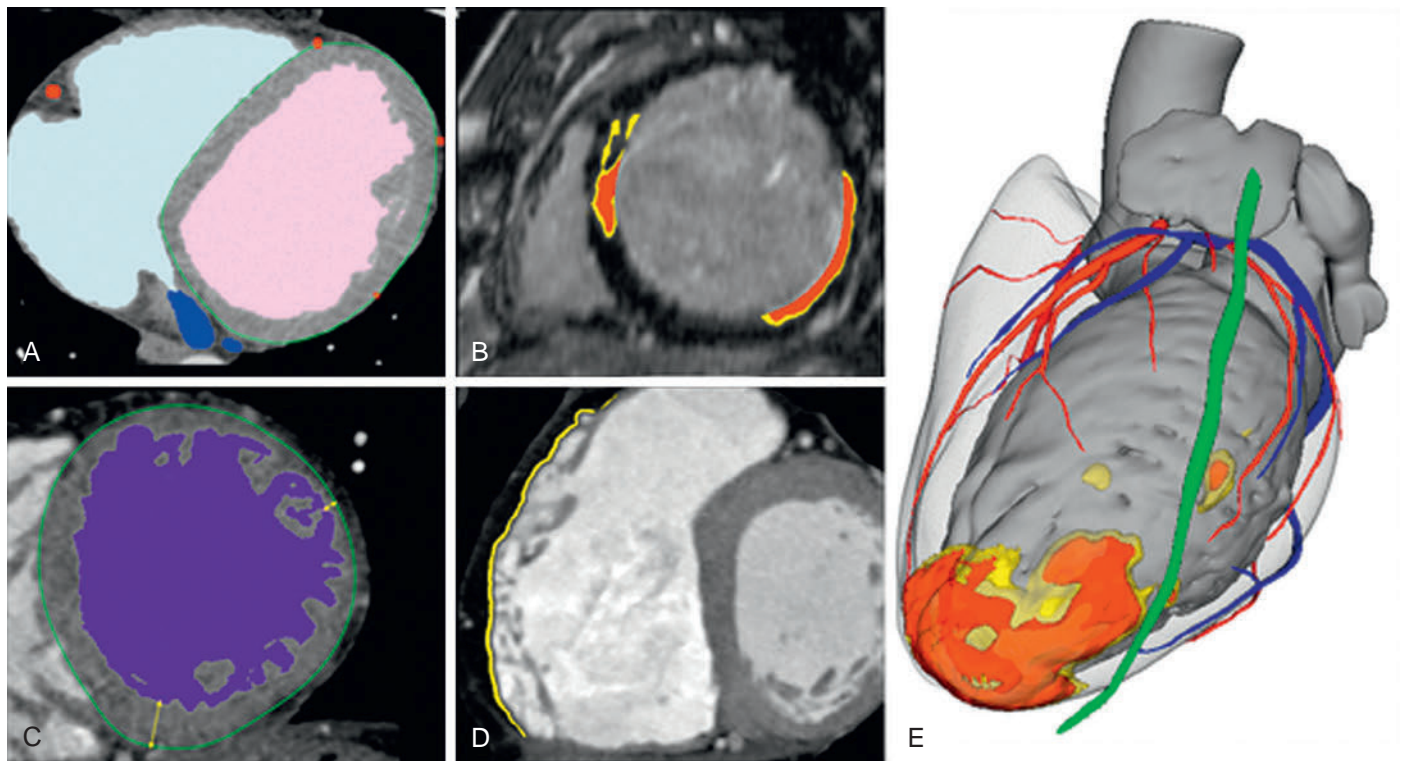
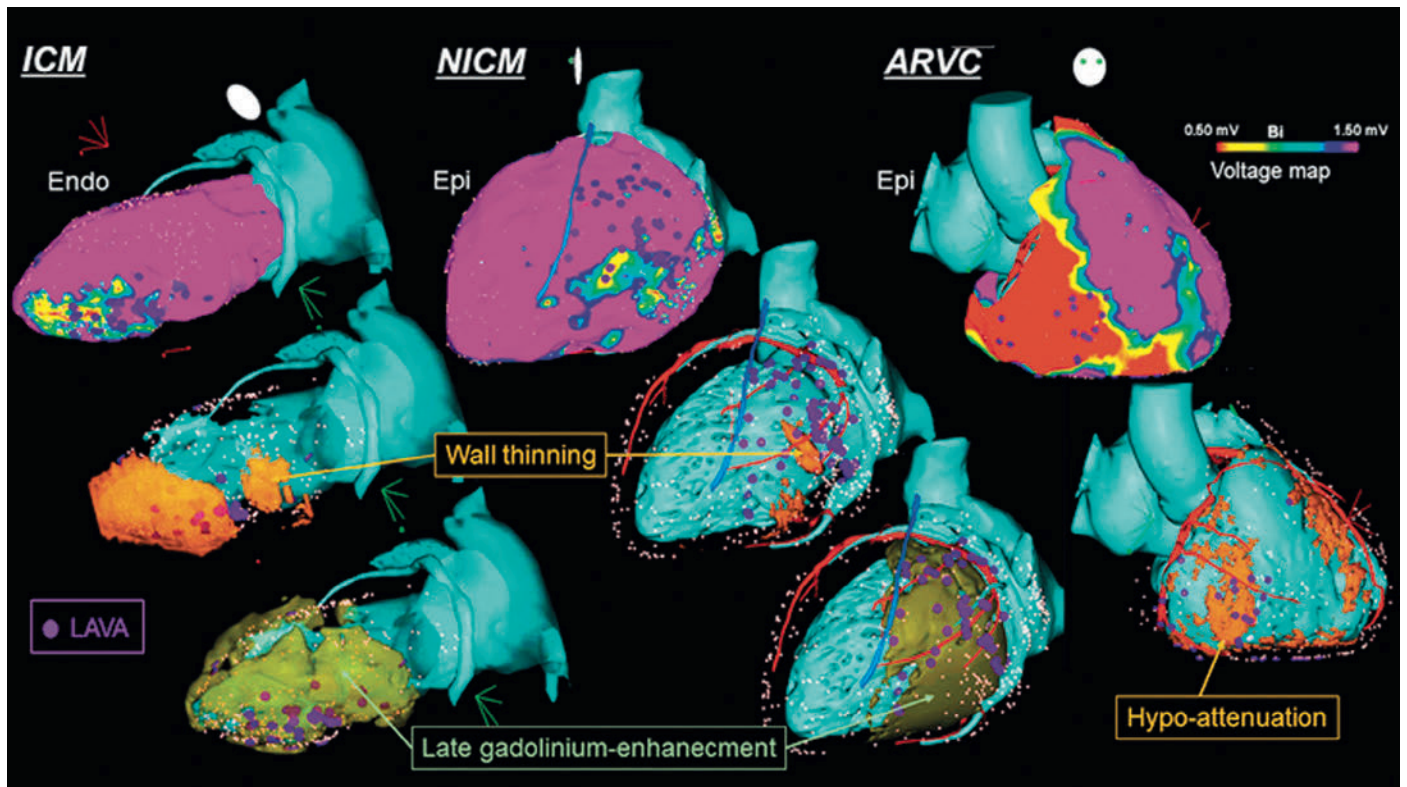


Fig. 6.37 Image Integration to Guide Catheter Ablation in Scar-Related Ventricular Tachycardia (VT). (A) Imaging is used to segment the cardiac chambers, epicardium, coronary sinus, as well as coronary arteries and left phrenic nerve to facilitate ablation of scar-related VT. In patients with ischemic or nonischemic cardiomyopathy, the structural substrate is segmented on imaging as areas of late gadolinium enhancement on cardiac magnetic resonance images (MRI) (B), and/or areas of wall thinning (less than 5 mm, note double arrows) on multidetector CT scans (C). In patients with arrhythmogenic right ventricular cardiomyopathy, the structural substrate is segmented as areas of myocardial hypo-attenuation on multidetector CT (D). All segmentations are used to compute a 3-D cardiac model (E; cardiac MRI and CT fusion: left ventricular endocardium is shown in gray, epicardium in translucent white, dense scar from cardiac MRI in orange, gray zone in yellow, coronary arteries in red, coronary sinus in blue, left phrenic nerve course in green). (From Yamashita S, Sacher F, Mahida S, et al. Image integration to guide catheter ablation in scar-related ventricular tachycardia. *J Cardiovasc Electrophysiol*. 2016;27:699–708.)



eFig. 6.8 Image Integration in Ventricular Tachycardia (VT) Ablation. Examples of image-guided VT ablation in patients with ischemic cardiomyopathy (ICM, left panels), nonischemic cardiomyopathy (NICM, middle panels), and arrhythmogenic right ventricular cardiomyopathy (ARVC, right panels). Bipolar voltage maps are shown on the top row, detector computed tomography-derived substrate in orange on the second row, and cardiac magnetic resonance-derived substrate in green on the third row. Blue dots indicate local abnormal ventricular activity (LAVA). Blue line in the second column indicates the course of the left phrenic nerve. *Endo*, Endocardial; *Epi*, epicardial. (From Yamashita S, Sacher F, Mahida S, et al. Image integration to guide catheter ablation in scar-related ventricular tachycardia. *J Cardiovasc Electrophysiol*. 2016;27:699–708.)

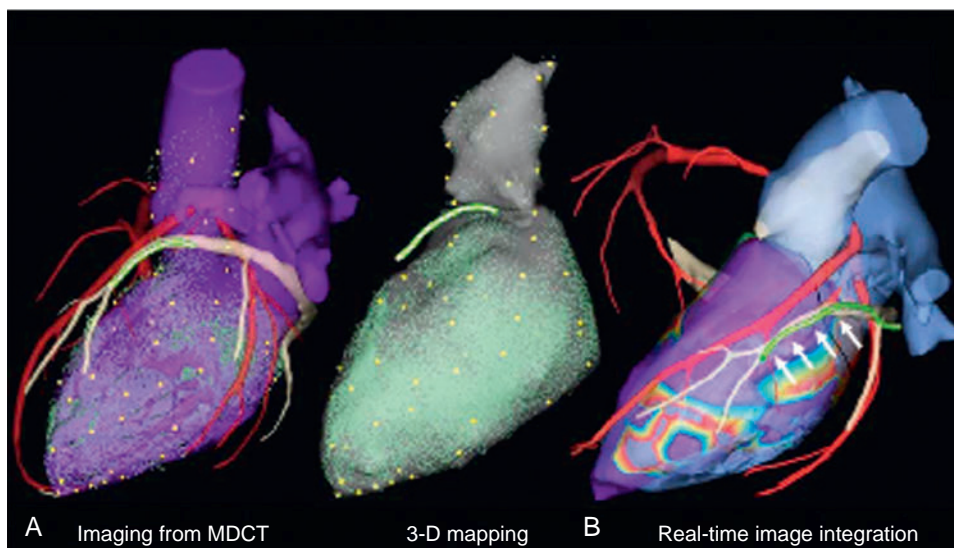


Fig. 6.38 Computed Tomography Integration on NavX Electroanatomic Mapping System. (A) After field scaling and registration with four points (left ventricular apex, mitral annulus, aortic root, and coronary sinus), additional fusion points on the local mismatch sites (yellow points) were applied. (B) Real-time integrated image can be monitored with a catheter position in the coronary sinus during procedure (white arrows). 3-D, Three-dimensional; MDCT, multidetector computed tomography. (From Yamashita S, Sacher F, Mahida S, et al. Role of high-resolution image integration to visualize left phrenic nerve and coronary arteries during epicardial ventricular tachycardia ablation. *Circ Arrhythm Electrophysiol.* 2015;8:371–380.)

operator needs to be alert on discrepancies between catheters and anatomy, and must check registration in case of suspected movement. In addition, with the CARTO system, one can return to the catheter-based LA reconstruction without Merge, which may be more accurate than the CT image.

Limitations

Although CT and MRI provide exquisite images of the underlying structures relevant in arrhythmogenesis, they are limited by the requirement of off-line generation of the CT and MRI libraries and the inability to reflect all phases of the cardiac cycle during an arrhythmia. Because CT and MRI are performed prior to the ablation procedure, registration error can arise from interval changes in the heart size because of differences in rhythm, rate, contractility, or fluid status. Performing image registration and ablation procedures within 24 hours after CT and MRI scans and CT and MRI image acquisition and image registration during the same rhythm may help limit interval changes. This situation is confounded by the inevitable imperfection of the created virtual geometry of the cardiac chamber. These factors can impede the clinical utility of image integration in approximately 25% of patients.

Furthermore, the static images of the registered CT and MRI reconstructions provide little information on true catheter-tissue contact. In addition, because the initial landmark points are picked up by the operator using fluoroscopy, the exact location of these points in the 3-D space can be deceptive, and registration errors in the identification of these points are very common, even when angiography and ICE are used for guidance. In addition, because multiple points are needed for surface registration, the accuracy of chamber reconstruction is directly dependent on the number of points taken and the position of the catheter, thus adding a significant amount of time and a manual component to the process.

To overcome some of these limitations, fusion of real-time ICE images with those generated by CT and MRI scans is becoming

available and can provide a more real-time interactive display, as well as real-time information on catheter-tissue contact and RF lesion formation. In addition, it is highly likely that subsequent generations of CT or MRI scanners will be sufficiently fast to permit real-time or almost real-time imaging for interventional guidance. Studies have demonstrated the ability to merge the 3-D CT and MRI images with real-time 2-D fluoroscopy images for navigation on virtual anatomy, because the images can be corrected against the background of real-time fluoroscopy as needed.

The accuracy of registration remains the subject of investigation. 3-D image integration aims at improving the operator's perception of the catheter spatial location in relation to the patient's cardiac structures. However, the success of this approach is primarily dependent on the accuracy of the image integration process. Even if the 3-D cardiac chamber image provides an accurate model of a matched phase of the chamber volume at the time of the procedure, it needs to be accurately registered to the procedural chamber orientation to provide reliable navigation. Current registration algorithms depend on accurate catheter geometry; this requires an accurate update of 3-D coordinates of the catheter tip, as recorded and displayed on the computer image. The exact location of the initial fiducial points picked by the operator using fluoroscopy in the 3-D space can be deceptive. Movement of the catheter tip is complex and is affected by wall motion and respiration. Point collection should therefore be gated to the same phase of the cardiac and respiratory cycle as the CT or MRI scan. In addition, catheter tip pressure can cause tenting of the chamber wall, thereby distorting the chamber geometry. Stability of catheter contact with the endocardial wall should also be optimized. Catheter contact can vary with the type of ablation catheter and introducer sheath, as well as the degree of regional wall motion; for example, the mitral annulus and appendage are more dynamic than the posterior atrial wall. Ideally, geometry points should be collected from stable catheter positions. The operator can then accept good points or delete bad points. This process can be aided by

fluoroscopy, electrogram morphology, and confirmation of the catheter tip location on ICE. However, the process still remains a subjective art.

Several studies of AF catheter ablation have reported success using different integration modalities with CT or MRI, by using either non-contact mapping or fluoroscopy as a second integrated image. The registration technique has also varied, including three- or four-point registration or surface registration. Alternatively, a single point and the surface have been used as well (visual alignment). Different techniques for point localization have been reported, including fluoroscopy alone, angiography, or ICE for direct visualization of the catheter at the designated site. The mean error for surface registration in most studies varied between 1.8 and 2.7 mm; one study that compared the landmark registration with and without surface registration found that surface registration increases the accuracy of image integration. On the other hand, a more recent study found that the most accurate landmark registration is achieved when posterior points are acquired at the PV-LA junction, whereas points acquired on the anterior wall, LA appendage, or other structures outside the LA, such as the CS or SVC, afford less accuracy. In addition, surface registration usually results in shifting the landmark points away from the initially acquired position on the corresponding PVs using ICE. Furthermore, accurate surface registration does not guarantee accurate alignment with the important anatomical structures. Another report found that serious inaccuracies of the CARTO-Merge image integration algorithms still exist, despite using the precautions discussed earlier.

It is important to recognize that the registered CT model still is prone to subjective inaccuracies and should remain only a guide, and a combination of fluoroscopy and the electrogram appearance is frequently used in assessing contact with the endocardial surface and the true position of the catheter. Further, registration quality has not yet been shown necessarily to correlate with ablation accuracy.

THREE-DIMENSIONAL ROTATIONAL ANGIOGRAPHY

Fundamental Concepts

Three-dimensional rotational angiography combines the accuracy of direct angiography with the benefits of computer animation and supplements conventional 2-D fluoroscopy to provide real-time representation of cardiac structures. Its feasibility and clinical utility in the setting of LA imaging and AF ablation have been described. This method provides rapid intraprocedural visualization of LA anatomy and of important nearby structures such as the esophagus. Prior studies have demonstrated that the diagnostic value of 3-D rotational angiography is comparable to that of CT imaging.⁹⁰

The principle of 3-D rotational angiography is similar to the CT scan, in which images acquired from different angles are reconstructed to a 3-D image. The C-arm x-ray system is rotated around the patient over 240 degrees to create a circumferential run of many exposure images of the region of interest distributed over the 360-degree (or similar) trajectory. To improve differentiation of the cardiac structures, the cardiac chamber of interest can be opacified with a contrast medium injected either directly into the LA or indirectly into the right side of the heart, in which case rotation of the fluoroscopic system is started after passage of the contrast medium through the lungs. The esophagus can be opacified using a barium paste prior to the image acquisition. The rotational angiographic images of the LA, PVs, esophagus, and other surrounding structures can be segmented and registered with the fluoroscopy on a specialized computer system (EP Navigator; or DynaCT Cardiac, Siemens, Forchheim, Germany). The latest version of the software allows registration of the segmented 3-D volume on a live fluoroscopy screen.^{90,91}

Imaging Technique

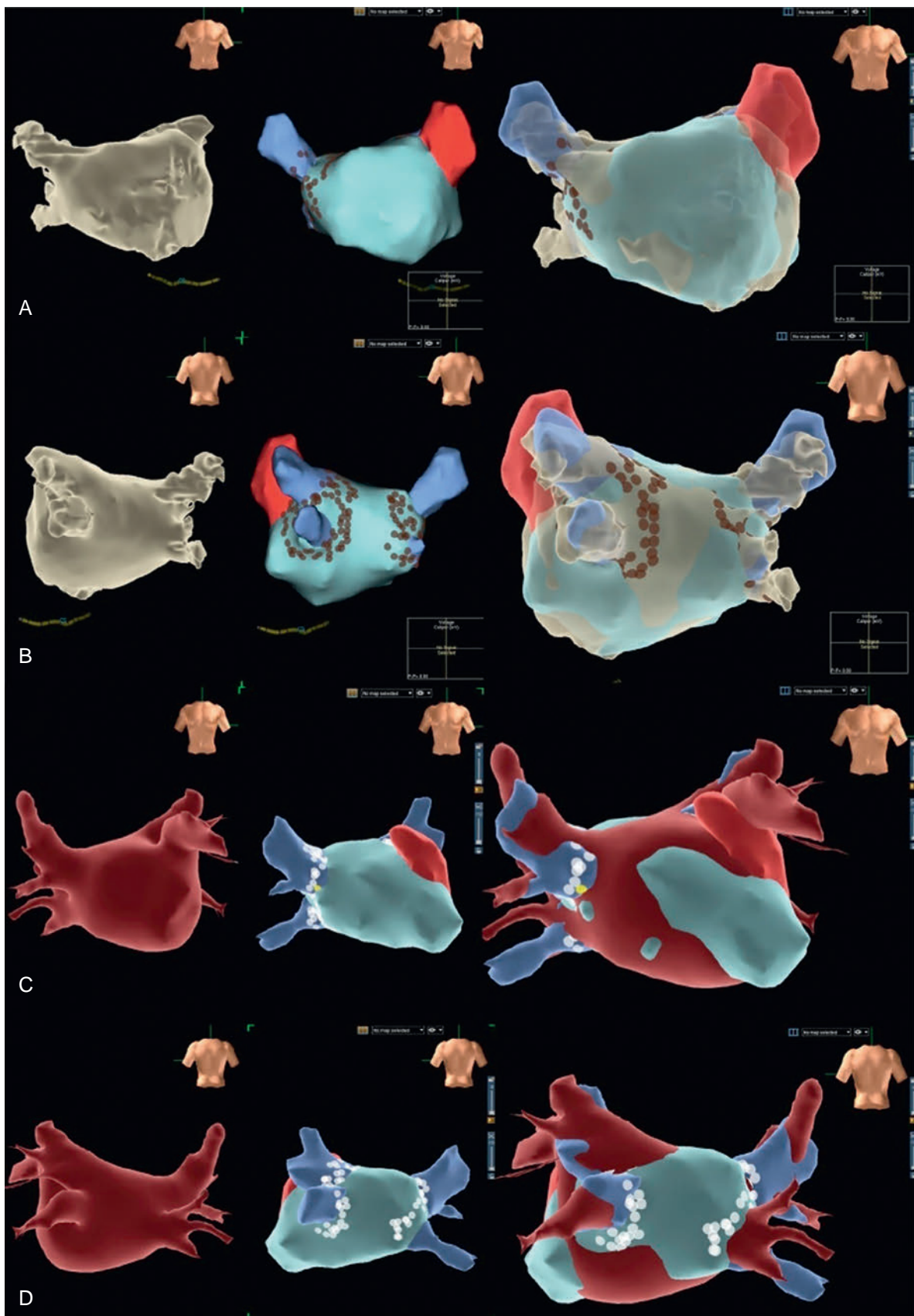
First, the patient must be properly positioned, and the structure of interest must be isocentered. The patient's arms may be extended above the head to reduce mass artifact. Oral contrast (5 mL barium sulfate esophageal cream) is administered immediately prior to initiation of the rotational run, and once it is visualized in the esophagus, IV contrast may be injected into the main pulmonary artery, RV, RA, or IVC via a 6 Fr pigtail catheter to obtain adequate levophase opacification of the LA. In general, contrast injection at the IVC-RA junction results in adequate LA and PV opacification in most patients. In addition, this method is technically simpler and potentially safer than more downstream injections. Higher amounts of contrast and longer injection time are generally used with RA and IVC injections than with main pulmonary artery injection. Direct contrast injection into the LA was described and seemed to provide great detail of LA and PV anatomy, but it required a high-dose (30 to 50 mg) adenosine injection immediately prior to the rotational run. Transient cessation of contractions prevents anterograde washout of contrast from the PVs, thus keeping them opacified during the rotational run. Deep sedation, intubation, and RV pacing are usually needed to counteract apnea and asystole produced by adenosine. In addition, high doses of adenosine are not tolerated by the conscious patient because of the induced flush and dyspnea. Given such complexities, this method can be more difficult to implement in clinical practice.⁹⁰

For injection at the RA-IVC junction, 80 to 100 mL of contrast is injected over 4 seconds via a pigtail catheter using a power injector. The C-arm is rotated over a 240-degree arc (120-degree RAO to 120-degree LAO view) in a 4.1-second period. The x-ray acquisition speed is 30 frames per second, which results in a total of 120 frames in the rotational run. Continuous fluoroscopic monitoring for contrast appearance in the LA is used to trigger the rotational run, based on visual guidance rather than on an empirically determined delay. The patient is instructed to stop breathing immediately prior to initiation of the rotational run to prevent respiratory movement of the structure of interest and inadequate reconstruction. Normal breathing can be resumed immediately on the completion of rotation.

The rotational angiogram is judged to be adequate when the LA is filled with contrast during most of the run and antral portions of all PVs are opacified without truncation. A resultant movie file is then transferred to an EP Navigator workstation to be segmented and overlaid on a live fluoroscopy screen. After the catheters are advanced into the LA, the 3-D image is used for navigation. With registration of the 3-D volume, all movements of the C-arm are translated into the appropriate rotation or shift, thus keeping the relationship between the fluoroscopic heart shadow and reconstructed image unchanged.

Image integration of intraprocedural rotational angiography-based 3-D reconstructions of LA and PVs into the electroanatomic mapping system (EnSite Velocity or CARTO-Merge) has become feasible. The images of the segmented LA are saved on a compact disc and transferred to the electroanatomic mapping system by using custom-designed software and integrated without further segmentation (eFig. 6.9).

Theoretically, no registration for 3-D rotational angiography image overlay is necessary if the original x-ray table position and the patient's position during the rotational run are maintained. However, moving the x-ray table is often required after 3-D rotational angiography, especially given the fact that intracardiac catheters should be placed only after the rotational run to prevent artifacts. Therefore registration is often necessary because in its current iteration, overlay movement is linked only to C-arm rotation and not to x-ray table repositioning. Several registration methods using different primary landmarks, such as catheter placement, heart contour, and PV angiography, have been



eFig. 6.9 Integration of Rotational Angiography With Electroanatomic Mapping and CT. (A and B) Rotational angiography three-dimensional (3-D) reconstruction (*left*) and NavX electroanatomic map (*middle*) of the LA shown in the anterior-posterior (A) and posterior-anterior (B) views before and after (*right*) merging. Also shown are a multipolar coronary sinus catheter (*both panels*, left side) and ablation lesion set. Pulmonary veins are shown in gray in both panels. The left atrium (LA) body is shown in gray for rotational angiography 3-D reconstruction and in blue for NavX in both images. Left atrial appendage surface is shown in red. (C and D), CT image (*left*) and NavX map (*middle*) of the LA shown in the anterior-posterior (C) and posterior-anterior (D) views before and after (*right*) merging. The ablation lesions are also shown in both panels. The fused LA shell is constructed from the CT surface data (*red*) and NavX surface data (*blue*). The left atrial appendage is shown in red in both panels. Note a more realistic appearance of the merged map with both imaging modalities. (From Anand R, Gorev MV, Poghosyan H, et al. Prospective randomized comparison of rotational angiography with three-dimensional reconstruction and computed tomography merged with electro-anatomical mapping: a two center atrial fibrillation ablation study. *J Interv Card Electrophysiol*. 2016;46:1–9.)

evaluated. These methods are particularly useful when registering previously obtained CT images on live fluoroscopy (i.e., CT overlay), which is another imaging input available in the EP Navigator (as discussed previously).^{90,91}

The current software version allows for the inner surface of the LA and PVs to be visualized (endoscopic view), further aiding the physician when navigating around the LA. Ablation points can be marked on the overlaid 3-D rotational angiography model to track the completeness of lesions. LA proximity to the esophagus can be evaluated and catheter ablation modified as necessary to avoid ablation near the esophagus.

Clinical Implications

One of the advantages of 3-D rotational angiography over conventional 2-D fluoroscopy is the capability of depth perception and volume appreciation. 3-D rotational angiography provides direct visualization of cardiac structures, whereas electroanatomic methods require either operator imagination or confirmation via other imaging modalities, such as CT. Although preprocedure CT/MRI images provide visualization of the LA and the PVs, and facilitate integration with the electroanatomic mapping systems, a significant drawback is the time lag to the actual procedure. Interval changes in volume status, respiratory phase, and cardiac rhythm can result in temporal changes in the size and location of the anatomical structures between the time of image acquisition and the registration process. These limitations can be overcome by intraprocedural acquisition of the LA volume and PV anatomy; 3-D rotational angiography can be performed immediately before ablation using the same fluoroscopic imaging system, thus providing realistic anatomical detail at the time of the intervention.⁹⁰

Other advantages of 3-D rotational angiography technology include quick and accurate repeat registration of the 3-D volume in case of patient movement not requiring a new map, as is frequently the case with electroanatomic methods.

Despite exclusively fluoroscopic guidance of the ablation catheter using the 3-D rotational angiography technology, total fluoroscopy time and fluoroscopy time for PV isolation have been comparable to reported times for AF ablation procedures performed with different nonfluoroscopic mapping systems. In addition, 3-D rotational angiography has the potential to eliminate the need for preprocedural CT/MRI imaging, and the radiation exposure is less than that of CT scanning (estimated at 2.2 ± 0.2 mSv exposure with one rotational angiography run).

Imaging by 3-D rotational angiography should not be confined to the LA and PVs. Other cardiac structures (current possibilities include RA and RVOT) can be easily visualized by timing the rotational run with the passage of contrast through the structures. The possibility of “whole heart” imaging has been reported.

Limitations

The use of contrast makes 3-D rotational angiography a less appealing option for patients with heart failure or renal insufficiency. In addition, the technique is sensitive to patient movements during the study period.

One shortfall of 3-D rotational angiography is the absence of streaming electrogram data. In addition, because of the lack of respiratory compensation in the 3-D rotational angiography-fluoroscopy fusion, the end-expiratory phase is used as a reference for monitoring the position of the ablation catheter tip during RF application.

Proper isocentering is important to obtain adequate 3-D rotational angiography. Concerns have been raised about the frequent difficulty in fitting the LA and PVs into one rotational run with the commonly used detector. However, with proper isocentering, even a dilated LA and the PV anatomy can be adequately imaged; truncation can occur more easily if the structures of interest are not at the center of rotation.

3-D rotational angiography is evolving into a true online imaging tool; however, further refinements are needed before it can be widely adopted. These include incorporation of respiratory and cardiac motion compensation and the ability to display electrogram data on the 3-D shell (activation timing, scar and voltage maps, and dominant frequency). Further development is likely to involve several aspects of the method: automation of the workflow, injection protocols, and software; imaging of cardiac structures other than the LA and development of methods to visualize highly mobile structures such as the ventricles; and integration of anatomical 3-D rotational angiography information with electrogram data.

VIDEOS

The following videos accompany this chapter:

Video 6.1. Focal Atrial Tachycardia (Originating From the Left Atrial Posterior Wall): CARTO Activation and Propagation Maps

Video 6.2. Focal Atrial Tachycardia (Originating From the Inferolateral Tricuspid Annulus): EnSite Precision Activation, Propagation, and Voltage Maps

Video 6.3. Focal Atrial Tachycardia (Originating From the Left Atrial Appendage): EnSite NavX Activation and Propagation Maps

Video 6.4. Fast Anatomical Mapping (FAM): CARTO-3

Video 6.5. CARTO-Sound: Mapping of Ventricular Tachycardia

Video 6.6. Typical Atrial Flutter: Rhythmia Batrial Propagation Maps

Video 6.7. Clockwise and Counterclockwise Typical Atrial Flutter: Rhythmia and CARTO Activation and Propagation Maps

Video 6.8. Typical Atrial Flutter: EnSite Precision Activation, Voltage, and Propagation Maps

Video 6.9. Electroanatomic Activation Mapping of Typical Atrial Flutter: Effects of the Window of Interest

Video 6.10. Electroanatomic Activation Mapping of Typical Atrial Flutter: Effects of the Electrical Reference

Video 6.11. Macroreentrant Atrial Tachycardia (Related to Gaps in Left Atrium [LA] Roof Ablation Line): CARTO Activation and Propagation Maps

Video 6.12. Macroreentrant Atrial Tachycardia (Involving the Left Atrium [LA] Posterior Wall): Rhythmia Activation and Propagation Maps

Video 6.13. Small Atrial Macroreentry: Rhythmia Activation and Propagation Maps

Video 6.14. Ripple Mapping: Mapping Gaps in Ablation Line

Video 6.15. Electrical Isolation of the Pulmonary Veins and Left Atrial Posterior Wall: Rhythmia Voltage Mapping

Video 6.16. Outflow Tract Ventricular Tachycardia: Noncontact Mapping

Video 6.17. Typical Atrial Flutter: Noncontact Mapping

Video 6.18. Intracardiac Echocardiography: Home View

Video 6.19. Intracardiac Echocardiography Imaging of the Left Ventricle and Aortic Valve

Video 6.20. Intracardiac Echocardiography for Visualization of the Papillary Muscle

See **Video 4.4.** Atrial Transseptal Puncture: Guided by Intracardiac Echocardiography (ICE)

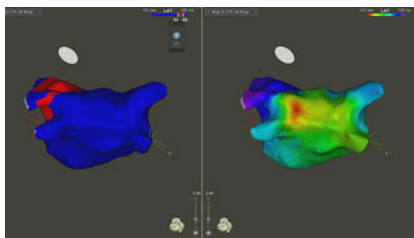
Video 6.21. CARTO Sound: Ablation of Atrial Fibrillation

Video 6.22. Cardiac Anatomy (Segmented Computed Tomography)

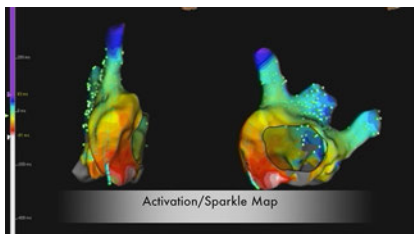
Video 6.23. Segmented Computed Tomography of the Left Atrium and Pulmonary Veins (PVs)

REFERENCES

1. Del Carpio Munoz F, Buescher TL, Asirvatham SJ. Three-dimensional mapping of cardiac arrhythmias: what do the colors really mean? *Circ Arrhythmia Electrophysiol.* 2010;3:e6–e11.



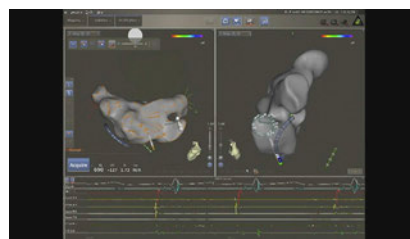
Video 6.1 Focal Atrial Tachycardia (Originating From the Left Atrial Posterior Wall): CARTO Activation and Propagation Maps. Electroanatomic (CARTO-3) activation and propagation maps of a focal atrial tachycardia (AT) originating from the left atrial (LA) posterior wall. *LIPV*, Left inferior pulmonary veins; *LSPV*, left superior pulmonary veins; *MA*, mitral annulus; *RIPV*, right inferior pulmonary veins; *RSPV*, right superior pulmonary veins.



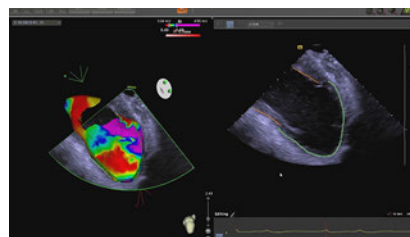
Video 6.2 Focal Atrial Tachycardia (Originating From the Inferolateral Tricuspid Annulus): EnSite Precision Activation, Propagation, and Voltage Maps. Electroanatomic (EnSite Precision) activation, propagation, and voltage maps of a focal atrial tachycardia (AT) originating from the inferolateral aspect of the tricuspid annulus (TA). Radiofrequency (RF) ablation at the AT focus results in termination of the tachycardia. *CS*, Coronary sinus; *IVC*, inferior vena cava; *SVC*, superior vena cava.



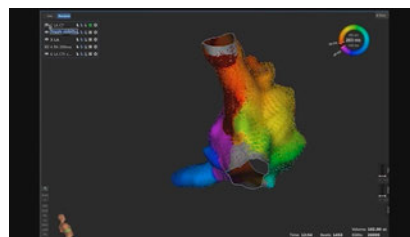
Video 6.3 Focal Atrial Tachycardia (Originating From the Left Atrial Appendage): EnSite NavX Activation and Propagation Maps. Electroanatomic (EnSite NavX) activation and propagation maps of a focal atrial tachycardia (AT) originating from the left atrial appendage (LAA). Radiofrequency (RF) ablation at the AT focus results in termination of the tachycardia. *LIPV*, Left inferior pulmonary veins; *LSPV*, left superior pulmonary veins; *MA*, mitral annulus; *RIPV*, right inferior pulmonary veins; *RSPV*, right superior pulmonary veins.



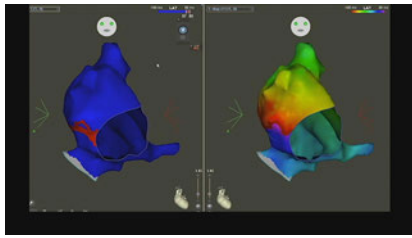
Video 6.4 Fast Anatomical Mapping (FAM): CARTO-3. “FAM” is a feature of CARTO-3 that permits rapid creation of anatomical maps by movement of sensor-based catheter throughout the cardiac chamber. In addition, catheters besides the ablation catheter can be visualized (the Lasso [ring], coronary sinus [CS], ablation [ABL], and right ventricular [RV] catheters are visualized in this case). Catheters besides the ablation catheter can be used for data collection. As in this case, the use of the multipolar ring catheter to collect volume data of the left atrial (LA) enhances the mapping speed. The catheter is moved with the LA cavity and pulmonary veins (PVs). *LIPV*, Left inferior PV; *LSPV*, left superior PV; *RIPV*, right inferior PV; *RSPV*, right superior PV.



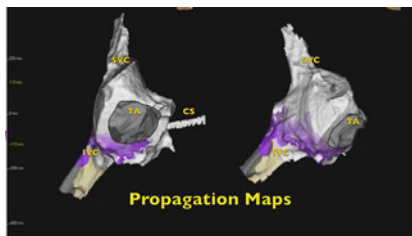
Video 6.5 CARTO-Sound: Mapping of Ventricular Tachycardia. The CARTO-Sound module is used to construct three-dimensional shell of the LV during mapping and ablation of ventricular tachycardia in a patient with prior anteroapical myocardial infarction. To visualize the LV, the ICE transducer is positioned across the tricuspid valve at the right ventricular septum. The acquired ICE images are gated to the same phase of the cardiac cycles (to the QRS). The LV endocardium is traced manually or automatically. ICE contours can be revisited and revised. The CARTO-Sound volume map of the LV is merged with the electroanatomic shell obtained during voltage mapping. Note the large LV apical scar evident as wall thinning on ICE, which correlates to scar zone (electrogram amplitude less than 0.5 mV; [red] on the voltage map). *ICE*, Intracardiac echocardiography; *LV*, left ventricle.



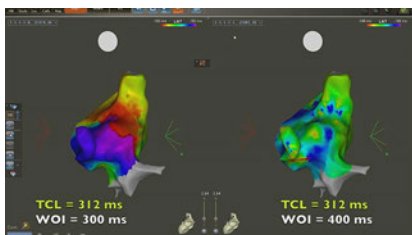
Video 6.6 Typical Atrial Flutter: Rhythmia Biatrial Propagation Maps. Electroanatomic (Rhythmia) activation and propagation maps of both atria during typical counterclockwise atrial flutter. In the right atrium, the activation wavefront propagates around the tricuspid annulus, consistent with macroreentry. In the left atrium (LA), activation starts at the interatrial septum and CS os, and activation of the whole LA chamber usually comprises only a portion of the tachycardia cycle length. *CS*, Coronary sinus; *LAA*, left atrial appendage; *MA*, mitral annulus; *SVC*, superior vena cava; *TA*, tricuspid annulus.



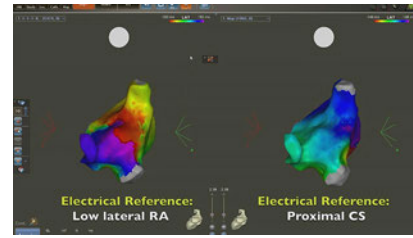
Video 6.7 Clockwise and Counterclockwise Typical Atrial Flutter: Rhythmia and CARTO Activation and Propagation Maps. Shown are electroanatomic activation and propagation maps of the right atrium during counterclockwise atrial flutter (Rhythmia) and during clockwise atrial flutter (CARTO) in two different patients. CS, Coronary sinus; IVC, inferior vena cava; SVC, superior vena cava; TA, tricuspid annulus.



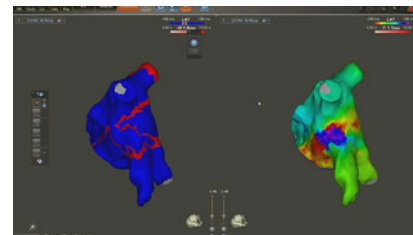
Video 6.8 Typical Atrial Flutter: EnSite Precision Activation, Voltage, and Propagation Maps. Shown are electroanatomic (EnSite Precision) activation, voltage, and propagation maps of the right atrium during counterclockwise atrial flutter. CS, Coronary sinus; IVC, inferior vena cava; SVC, superior vena cava; TA, tricuspid annulus.



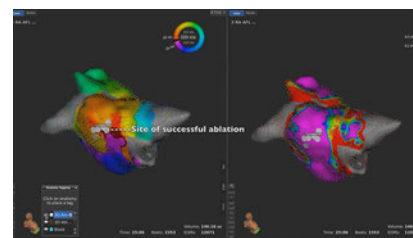
Video 6.9 Electroanatomic Activation Mapping of Typical Atrial Flutter: Effects of the Window of Interest. Shown are two electroanatomic (CARTO) activation maps of the right atrium during counterclockwise atrial flutter (tachycardia cycle length [TCL] = 312 milliseconds) in the same patient. At left, with the window of interest (WOI) set at 300 milliseconds (about 96% of the TCL), the activation map demonstrates a continuous progression of colors around the tricuspid annulus with close proximity of earliest and latest local activation and an activation time in a similar range to TCL, consistent with macroreentry. At right, the WOI is set at 400 milliseconds (which spans more than one tachycardia cycle); this resulted in ambiguous activation map with incoherent activation patterns. CS, Coronary sinus; IVC, inferior vena cava; SVC, superior vena cava; TA, tricuspid annulus.



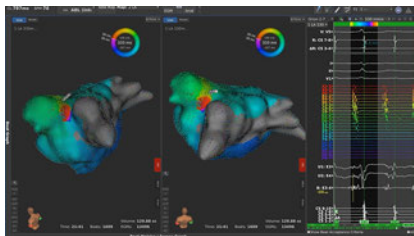
Video 6.10 Electroanatomic Activation Mapping of Typical Atrial Flutter: Effects of the Electrical Reference. Shown are two electroanatomic (CARTO) activation maps of the right atrium during counterclockwise atrial flutter (tachycardia cycle length [TCL] = 312 milliseconds) in the same patient. At left, with the electrical reference assigned to the electrogram recorded at the low lateral right atrial wall, the early-meets-late zone occurs at the septal aspect of the atrial septum. At right, the electrical reference is assigned to the electrogram recorded at the proximal coronary sinus (CS), and the early-meets-late zone at the lateral right atrial wall. Note that the location of the early-meets-late zone is merely a function of where the offset and onset of the window of interest are defined relative to the timing of the selected reference electrogram, and can shift in location and timing in response to shifts in the window of interest or electrical reference. In addition, early-meets-late zone should not be used as an indicator of the location of the critical isthmus of the macroreentrant circuit or the ablation target (the cavotricuspid isthmus in this case). IVC, Inferior vena cava; SVC, superior vena cava; TA, tricuspid annulus.



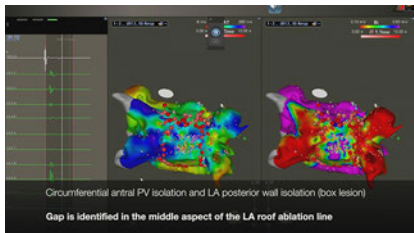
Video 6.11 Macroreentrant Atrial Tachycardia (Related to Gaps in Left Atrium [LA] Roof Ablation Line): CARTO Activation and Propagation Maps. Three electroanatomic (CARTO-3) activation maps of the LA acquired during sustained atrial tachycardia (AT) in three different patients with prior history of catheter ablation of atrial fibrillation (circumferential pulmonary vein [PV] isolation and LA roof linear ablation). Propagation and activation maps demonstrate atrial macroreentry involving a gap in the previous LA roof ablation line. LAA, Left atrial appendage; LIPV, left inferior PV; LSPV, left superior PV; MA, mitral annulus; RIPV, right inferior PV; RSPV, right superior PV.



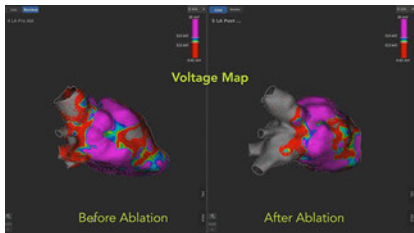
Video 6.12 Macroreentrant Atrial Tachycardia (Involving the Left Atrium [LA] Posterior Wall): Rhythmia Activation and Propagation Maps. Electroanatomic (Rhythmia) activation and propagation maps of the LA acquired during sustained atrial tachycardia (AT) in a patient with prior history of catheter ablation of atrial fibrillation (circumferential antral pulmonary vein [PV] isolation) and electrical isolation of the LA posterior wall (with linear ablation across the LA roof and floor). Propagation and activation maps demonstrate atrial macroreentry involving a gap in the previous LA posterior wall. A few radiofrequency ablation lesions (white dots) transecting the isthmus of the reentry circuit in the LA posterior wall successfully terminate the tachycardia. LIPV, Left inferior PV; LSPV, left superior PV; RIPV, right inferior PV; RSPV, right superior PV.



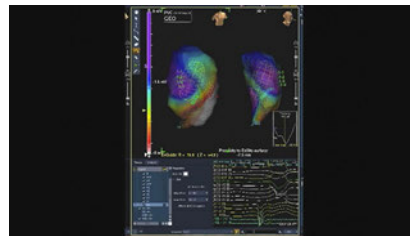
Video 6.13 Small Atrial Macroreentry: Rhythmia Activation and Propagation Maps. Electroanatomic (Rhythmia) activation and propagation maps of the left atrium (LA) acquired during sustained atrial tachycardia (AT) in a patient with prior history of catheter ablation of atrial fibrillation (circumferential antral pulmonary vein [PV] isolation) and electrical isolation of the LA posterior wall (with linear ablation across the LA roof and floor). Propagation and activation maps demonstrate a small atrial macroreentry circuit involving a gap in the ridge between the LA appendage (LAA) and left-sided PVs. Local electrograms at the isthmus of the reentry circuit are fractionated and occupy a large proportion of the tachycardia cycle length. Radiofrequency (RF) ablation at that site results in termination of the tachycardia. *LIPV*, Left inferior PV; *LSPV*, left superior PV; *MA*, mitral annulus; *RIPV*, right inferior PV; *RSPV*, right superior PV.



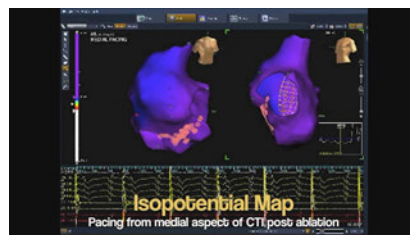
Video 6.14 Ripple Mapping: Mapping Gaps in Ablation Line. An electroanatomic (CARTO-3) activation map of the LA (posteroanterior view) acquired during pacing from the mid CS after performing circumferential antral pulmonary vein isolation and electrical isolation of the LA posterior wall (with linear ablation across the LA roof and floor, box lesion). Ablation lesions are shown as red dots. The ripple map is projected over an activation map (*at left*) and over a voltage map (*at right*). The ripple map reveals late activation of the LA posterior wall via a gap in the mid region of the LA roof line. *CS*, Coronary sinus; *LA*, left atrium.



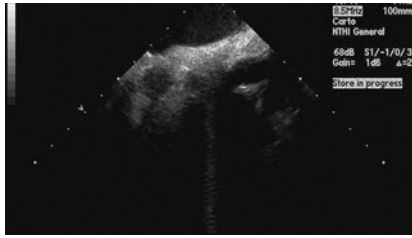
Video 6.15 Electrical Isolation of the Pulmonary Veins and Left Atrial Posterior Wall: Rhythmia Voltage Mapping. Three-dimensional reconstruction of the LA using the Rhythmia electroanatomic system before and after catheter ablation of atrial fibrillation. Small white circles are tagged sites at which RF energy was applied. Circumferential antral PV isolation is performed with a single circumferential ablation lesion around the antrum of the LCPV and separate encircling lesions around the right-sided PVs. Electrical isolation of the LA posterior wall (box isolation) is performed by an ablation line joining the two superior PVs (LA roof line) and a second ablation line joining the two inferior PVs (LA floor line). Sites with voltage lower than 0.1 mV are red on the map, and those with voltage higher than 0.5 mV are purple, with interpolation of color for intermediate amplitudes. The gray area denotes no detectable signal (scar). Note the voltage abatement encompassing all PVs and the whole LA posterior wall within the box lesion. *LA*, Left atrium; *LCPV*, left common pulmonary vein; *PV*, pulmonary vein; *RIPV*, right inferior pulmonary vein; *RSPV*, right superior pulmonary vein.



Video 6.16 Outflow Tract Ventricular Tachycardia: Noncontact Mapping. Mapping of premature ventricular complexes (PVCs) originating from the right ventricular outflow tract (RVOT) using the EnSite 3000 non-contact mapping system. The balloon catheter (*yellow shadow*) is positioned in the RVOT. A detailed geometry of the RVOT is reconstructed by moving a conventional mapping-ablation catheter around the atrium. Color-coded isopotential map of RVOT activation sequence (burning red star surrounded by *white* and *red circles*) during a single PVC is superimposed on the reconstructed three-dimensional shell of the RVOT. Wavefront propagation spreads radially from a small focus. The location of the His bundle is marked (HBE). The inset shows a virtual unipolar electrogram at the site of earliest activation (note QS pattern) with the bar indicating the timing of activation during the PVC. Surface ECG leads and intracardiac contact (ABL) and virtual unipolar electrograms (V_1 - V_4) are shown during mapping of PVCs (*lower panel*). Note the timing of the ABL distal electrogram preceding the onset of the QRS during PVC on all surface ECG leads and coinciding with the downslope of the QS unipolar virtual electrograms.



Video 6.17 Typical Atrial Flutter: Noncontact Mapping. Noncontact mapping (EnSite 3000, St. Jude Medical, St. Paul, MN, United States) during typical atrial flutter (AFL). The multielectrode array surrounding the balloon catheter (*yellow shadow*) is positioned in the center of the atrium and does not come in contact with the atrial walls being mapped. A detailed geometry of the right atrium (RA, shown in *purple*) is reconstructed by moving a conventional mapping-ablation catheter (*red shadow*) around the atrium. RA shell is displayed in right and left anterior oblique (RAO and LAO, respectively) projections. Surface ECG (*white*), contact intracardiac electrograms recorded by the distal and proximal electrodes of the ablation catheter (*red*), and virtual intracardiac electrograms (*yellow*) are shown in the panel in the bottom of the screen, and the yellow vertical line tracks the timing of the activation wavefront displayed on top. Noncontact unipolar electrograms are acquired simultaneously and superimposed onto the virtual endocardium, producing isopotential maps with a color range representing voltage amplitude. **Part 1:** During counter-clockwise typical AFL, wavefront activation sequence is tracked on the isopotential map throughout the tachycardia cycle (burning red star surrounded by *white* and *red circles*). **Part 2:** Before ablation of the cavotricuspid isthmus (CTI), atrial pacing from the medial aspect of the CTI results in two wavefronts: one propagating up the septum and a second propagating across the CTI (viewed clearly in the RAO projection). The two wavefronts converge in the lateral RA wall. This indicates intact conduction through the CTI in the clockwise direction. Note that an initial white activation artifact is caused by the pacing stimulus saturation artifact and precedes the activation wavefront through the RA. **Part 3:** After successful ablation of the CTI (indicated by the *pink dots* across the CTI), atrial pacing from the medial aspect of the CTI results in a single wavefront that propagates cranially up the septum and caudally down the RA free wall in a counterclockwise direction around the tricuspid annulus. No conduction is observed via the CTI, suggesting clockwise block in the CTI. **Part 4:** After successful ablation of the CTI, atrial pacing from the lateral aspect of the CTI results in a single wavefront that propagates cranially up RA free wall and caudally down the septum the in a clockwise direction around the tricuspid annulus. No conduction is observed via the CTI, suggesting counterclockwise block in the CTI.



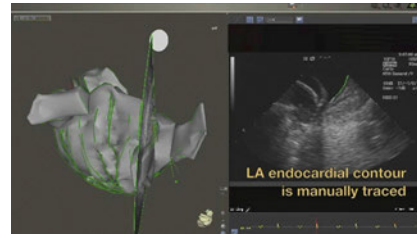
Video 6.18 Intracardiac Echocardiography: Home View. The “home view” obtained by the intracardiac echocardiography (ICE) catheter. Initially, the catheter is positioned in the mid-right atrium (RA) with the catheter tension controls in neutral position (the ultrasound transducer oriented anteriorly and to the left), the RA, tricuspid valve (TV), and right ventricle (RV) are viewed. Gradual clockwise rotation of a straight catheter from the home view allows sequential visualization of the aortic root and aortic valve (AoV), followed by the coronary sinus (CS) and the left atrium (LA), and a cross-sectional view of the interatrial septum.



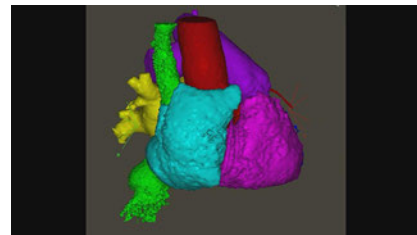
Video 6.19 Intracardiac Echocardiography Imaging of the Left Ventricle and Aortic Valve. The “home view” obtained by the ICE catheter. Initially, the catheter is positioned in the mid RA with the catheter tension controls in neutral position (the ultrasound transducer oriented anteriorly and to the left), the RA, TV, and RV are viewed. Gradual clockwise rotation of a straight catheter from the home view allows sequential visualization of the AO and AoV, followed by the LA, and a cross-sectional view of the interatrial septum. From that point, forward flexion of the ICE catheter into the RV brings the LV and MV in view. Slight counter-clockwise rotation (while maintaining forward flexion) of the ICE catheter enables cross sectional imaging of the AoV. Ao, Aortic root; AoV, aortic valve; ICE, intracardiac echocardiography; LA, left atrium; LAA, left atrial appendage; LV, left ventricle; RA, right atrium; RV, right ventricle; RVOT, right ventricular outflow tract; TV, tricuspid valve.



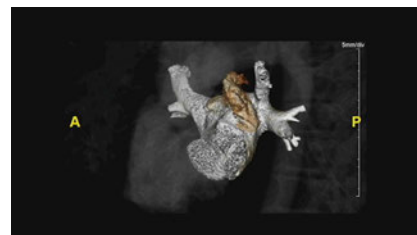
Video 6.20 Intracardiac Echocardiography for Visualization of the Papillary Muscle. The ICE catheter is advanced to the right atrium then flexed across the tricuspid valve and positioned at the RV septum. A longitudinal view of the LV is obtained, and the ablation catheter can be seen in contract with the lateral papillary muscle. ICE, Intracardiac echocardiography; LV, left ventricle; RV, right ventricle.



Video 6.21 CARTO-Sound: Ablation of Atrial Fibrillation. The CARTO-Sound utilizes a phased-array intracardiac echocardiography (ICE) catheter with an embedded navigation sensor (SoundStar, Biosense Webster), which records individual 90-degree sector image planes of the cardiac chamber, including their location and orientation, to the CARTO workspace. **Part 1:** ICE images are acquired before atrial septal puncture and are gated to the same phase of the cardiac cycles (to the QRS). The endocardial surfaces of the left atrium (LA) and pulmonary veins (PVs) are traced manually. A three-dimensional (3-D) geometry of the LA and PVs is reconstructed by interpolation of points the traced endocardial surface from multiple ICE images. **Part 2:** ICE images are acquired after access to the LA. A transseptal sheath can be visualized in the LA. LA endocardial surface can be traced automatically. However, verification of traced endocardial surfaces is required. In this case, the transseptal sheath was erroneously marked as an endocardial surface, and manual overwriting is required. **Part 3:** The ICE probe can be advanced into the LA across the atrial septum to obtain higher quality images of the endocardial border of the LA and PVs. **Part 4:** A 3-D geometry of the LA and PVs is reconstructed by interpolation of points the traced endocardial surface from multiple ICE images. The CARTO-Sound volume map of the cardiac chamber can be used as a stand-alone tool to guide navigation and ablation. **Part 5:** All contours can be revisited and revised.



Video 6.22 Cardiac Anatomy (Segmented Computed Tomography). Ao, Aorta; IVC, inferior vena cava; LAA, left atrial appendage; LIPV, left inferior pulmonary vein; LPA, left pulmonary artery; LSPV, left superior pulmonary vein; LV, left ventricle; PA, pulmonary artery; RA, right atrium; RIPV, right inferior pulmonary vein; RPA, right pulmonary artery; RV, right ventricle; RSPV, right superior pulmonary vein; SVC, superior vena cava.



Video 6.23 Segmented Computed Tomography of the Left Atrium and Pulmonary Veins (PVs). LAA, Left atrial appendage; LIPV, left inferior PV; LSPV, left superior PV; RIPV, right inferior PV; RSPV, right superior PV.

2. Koutalas E, et al. Contemporary mapping techniques of complex cardiac arrhythmias—identifying and modifying the arrhythmogenic substrate. *Arrhythmia Electrophysiol Rev.* 2015;4:19.
3. Kumar P, Mounsey JP, Chung EH. Adjusting voltage criteria can unmask conducting channels in a patient with arrhythmogenic right ventricular cardiomyopathy and ventricular tachycardia. *Heart Case Reports.* 2015;1:275–278.
4. Okumura Y, et al. Effect of catheter tip-tissue surface contact on three-dimensional left atrial and pulmonary vein geometries: potential anatomic distortion of 3D ultrasound, fast anatomical mapping, and merged 3D CT-derived images. *J Cardiovasc Electrophysiol.* 2013;24:259–266.
5. Kimura M, et al. Validation of accuracy of three-dimensional left atrial CartoSound™ and CT image integration: influence of respiratory phase and cardiac cycle. *J Cardiovasc Electrophysiol.* 2013;24:1002–1007.
6. Mantziari L, et al. Utility of a novel rapid high-resolution mapping system in the catheter ablation of arrhythmias an initial human experience of mapping the atria and the left ventricle. *JACC Clin Electrophysiol.* 2015;1:411–420.
7. Ptaszek LM, et al. Rapid acquisition of high-resolution electroanatomical maps using a novel multielectrode mapping system. *J Interv Card Electrophysiol.* 2013;36:233–242.
8. Thajudeen A, et al. Correlation of scar in cardiac MRI and high-resolution contact mapping of left ventricle in a chronic infarct model. *Pacing Clin Electrophysiol.* 2015;38:663–674.
9. Anter E, Tschabrunn CM, Contreras-Valdes FM, et al. Pulmonary vein isolation using the Rhythmia mapping system: verification of intracardiac signals using the Orion mini-basket catheter. *Heart Rhythm.* 2015;12:1927–1934.
10. Bun S-S, et al. Ultra-high-definition mapping of atrial arrhythmias. *Circ J.* 2016;80:579–586.
11. Gabriel D, Bun S, Viera F. Selection of critical isthmus in scar-related atrial tachycardia using a new automated ultrahigh resolution mapping system. *Circ Arrhythmia Electrophysiol.* 2017;10:pii:e004510.
12. Bollmann A, Hilbert S, John S, et al. Initial experience with ultra high-density mapping of human right atria. *J Cardiovasc Electrophysiol.* 2016;27:154–160.
13. Schaeffer B, et al. Characterization, mapping, and ablation of complex atrial tachycardia: initial experience with a novel method of ultra high-density 3D mapping. *J Cardiovasc Electrophysiol.* 2016;27:1139–1150.
14. El Haddad M, et al. Novel algorithmic methods in mapping of atrial and ventricular tachycardia. *Circ Arrhythmia Electrophysiol.* 2014;7:463–472.
15. Stevenson WG, Soejima K. Recording techniques for clinical electrophysiology. *J Cardiovasc Electrophysiol.* 2005;16:1017–1022.
16. Jadidi AS, Lehrmann H, Weber R, et al. Optimizing signal acquisition and recording in an electrophysiology laboratory. *Card Electrophysiol Clin.* 2013;5:137–142.
17. De Ponti R, et al. Electroanatomic mapping and ablation of macroreentrant atrial tachycardia : comparison between successfully and unsuccessfully treated cases. *J Cardiovasc Electrophysiol.* 2010;21:155–162.
18. Heist EK, et al. Comparison of electroanatomical mapping systems: accuracy in left atrial mapping. *Pacing Clin Electrophysiol.* 2013;36:626–631.
19. Tanawuttiwat T, Nazarian S, Calkins H. The role of catheter ablation in the management of ventricular tachycardia. *Eur Heart J.* 2016;37:594–609.
20. Anter E, Tschabrunn CM, Josephson ME. High-resolution mapping of scar-related atrial arrhythmias using smaller electrodes with closer interelectrode spacing. *Circ Arrhythmia Electrophysiol.* 2015;8:537–545.
21. Berte B, et al. VT recurrence after ablation: incomplete ablation or disease progression? A multicentric European study. *J Cardiovasc Electrophysiol.* 2016;27:80–87.
22. Berte B, et al. Characterization of the left-sided substrate in arrhythmogenic right ventricular cardiomyopathy. *Circ Arrhythmia Electrophysiol.* 2015;8:1403–1412.
23. Casella M, et al. Feasibility of combined unipolar and bipolar voltage maps to improve sensitivity of endomyocardial biopsy. *Circ Arrhythmia Electrophysiol.* 2015;8:625–632.
24. Tzou WS, et al. Core isolation of critical arrhythmia elements for treatment of multiple scar-based ventricular tachycardias. *Circ Arrhythmia Electrophysiol.* 2015;8:353–361.
25. Santangeli P, Marchlinski FE. Substrate mapping for unstable ventricular tachycardia. *Heart Rhythm.* 2016;13:569–583.
26. Fernández-Armenta J, et al. Sinus rhythm detection of conducting channels and ventricular tachycardia isthmus in arrhythmogenic right ventricular cardiomyopathy. *Heart Rhythm.* 2014;11:747–754.
27. Philips B, et al. Outcomes and ventricular tachycardia recurrence characteristics after epicardial ablation of ventricular tachycardia in arrhythmogenic right ventricular dysplasia/cardiomyopathy. *Heart Rhythm.* 2015;12:716–725.
28. Anter E, Josephson ME. Bipolar voltage amplitude: what does it really mean? *Heart Rhythm.* 2016;13:326–327.
29. Josephson ME, Anter E. Substrate mapping for ventricular tachycardia assumptions and misconceptions. *JACC Clin Electrophysiol.* 2015;1:341–352.
30. Gianni C, Natale A. Voltage mapping for ventricular tachycardia ablation: we can work it out. *Heart Rhythm.* 2016;13:2003.
31. Tung R, Ellenbogen KA. Emergence of multielectrode mapping. *Circ Arrhythmia Electrophysiol.* 2016;9:e004281.
32. Tung R, Josephson ME, Bradfield JS, et al. Directional influences of ventricular activation on myocardial scar characterization: voltage mapping with multiple wavefronts during ventricular tachycardia ablation. *Circ Arrhythmia Electrophysiol.* 2016;9:e004155.
33. Proietti R, et al. A historical perspective on the role of functional lines of block in the re-entrant circuit of ventricular tachycardia. *Pacing Clin Electrophysiol.* 2016;39:490–496.
34. Mountantonakis SE, et al. Relationship between voltage map ‘channels’ and the location of critical isthmus sites in patients with post-infarction cardiomyopathy and ventricular tachycardia. *J Am Coll Cardiol.* 2013;61:2088–2095.
35. Rav-Acha M, et al. A novel annotation technique during mapping to facilitate the termination of atrial tachycardia following ablation for atrial fibrillation. *J Cardiovasc Electrophysiol.* 2016;[Epub ahead of print].
36. Proietti R, Roux J-F, Essebag V. Recent advances in ablation of ventricular tachycardia associated with structural heart disease. *Curr Opin Cardiol.* 2016;31:64–71.
37. Jamil-Copley S, et al. Application of ripple mapping with an electroanatomic mapping system for diagnosis of atrial tachycardias. *J Cardiovasc Electrophysiol.* 2013;24:1361–1369.
38. Koa-Wing M, et al. A diagnostic algorithm to optimize data collection and interpretation of ripple maps in atrial tachycardias. *Int J Cardiol.* 2015;199:391–400.
39. Luther V, et al. A prospective study of ripple mapping in atrial tachycardias. *Circ Arrhythmia Electrophysiol.* 2016;9:e003582.
40. Jamil-Copley S, et al. Application of ripple mapping to visualize slow conduction channels within the infarct-related left ventricular scar. *Circ Arrhythmia Electrophysiol.* 2015;8:76–86.
41. Bunch TJ, Day JD. The atrial fibrillation ablation theory of relativity. *J Cardiovasc Electrophysiol.* 2013;24:267–268.
42. Andreu D, et al. Displacement of the target ablation site and ventricles during premature ventricular contractions: relevance for radiofrequency catheter ablation. *Heart Rhythm.* 2012;9:1050–1057.
43. Romero J, et al. Electroanatomic mapping systems (CARTO/EnSite NavX) vs. conventional mapping for ablation procedures in a training program. *J Interv Card Electrophysiol.* 2016;45:71–80.
44. Kapa S, Asirvatham SJ. You can’t know where you’re going until you know where you’ve been: the clinical relevance of differences in accurate assessment of catheter location with mapping technologies. *J Cardiovasc Electrophysiol.* 2014;25:84–86.
45. Bourier F, et al. Accuracy assessment of catheter guidance technology in electrophysiology procedures: a comparison of a new 3D-based fluoroscopy navigation system to current electroanatomic mapping systems. *J Cardiovasc Electrophysiol.* 2014;25:74–83.
46. Zhang F, et al. Noncontact mapping to guide ablation of right ventricular outflow tract arrhythmias. *Heart Rhythm.* 2013;10:1895–1902.

47. Yamabe H, Kanazawa H, Ito M. Prevalence and mechanism of rotor activation identified during atrial fibrillation by noncontact mapping: lack of evidence for a role in the maintenance of atrial fibrillation. *Heart Rhythm*. 2016;13:2323–2330.
48. Dixit S, et al. Noncontact electroanatomic mapping to characterize typical atrial flutter: participation of right atrial posterior wall in the reentrant circuit. *J Cardiovasc Electrophysiol*. 2011;22:422–430.
49. Zhang F, et al. Noncontact mapping to guide ablation of right ventricular outflow tract arrhythmias. *Heart Rhythm*. 2013;10:1895–1902.
50. Sommer P, et al. Successful repeat catheter ablation of recurrent longstanding persistent atrial fibrillation with rotor elimination as the procedural endpoint: a case series. *J Cardiovasc Electrophysiol*. 2016;27:274–280.
51. Zaman JAB, Peters NS, Narayan SM. Rotor mapping and ablation to treat atrial fibrillation. *Curr Opin Cardiol*. 2015;30:24–32.
52. Benharash P, et al. Quantitative analysis of localized sources identified by focal impulse and rotor modulation mapping in atrial fibrillation. *Circ Arrhythmia Electrophysiol*. 2015;8:554–561.
53. Schricker AA, Lalani GG, Krummen DE, et al. Rotors as drivers of atrial fibrillation and targets for ablation. *Curr Cardiol Rep*. 2014;16:509.
54. Mohanty S, et al. Impact of rotor ablation in non-paroxysmal AF patients: results from a randomized trial (OASIS). *J Am Coll Cardiol*. 2016;68:274–282.
55. Narayan SM, et al. Ablation of rotor and focal sources reduces late recurrence of atrial fibrillation compared with trigger ablation alone: extended follow-up of the CONFIRM trial (Conventional Ablation for Atrial Fibrillation With or Without Focal Impulse and Rotor Modulation). *J Am Coll Cardiol*. 2014;63:1761–1768.
56. Kim JJ, et al. Magnetic versus manual catheter navigation for ablation of free wall accessory pathways in children. *Circ Arrhythmia Electrophysiol*. 2012;5:804–808.
57. Kim SH, et al. Long-term outcomes of remote magnetic navigation for ablation of supraventricular tachycardias. *J Interv Card Electrophysiol*. 2015;43:187–192.
58. Zhang F, et al. Magnetic versus manual catheter navigation for mapping and ablation of right ventricular outflow tract ventricular arrhythmias: a randomized controlled study. *Heart Rhythm*. 2013;10:1178–1183.
59. Shurrab M, et al. Robotically assisted ablation of atrial fibrillation: a systematic review and meta-analysis. *Int J Cardiol*. 2013;169:157–165.
60. Jin Q, Pehrson S, Jacobsen PK, et al. Impact of catheter ablation with remote magnetic navigation on procedural outcomes in patients with persistent and long-standing persistent atrial fibrillation. *J Interv Card Electrophysiol*. 2015;44:197–204.
61. Wong KCK, et al. Mitral isthmus ablation is feasible, efficacious, and safe using a remote robotic catheter system. *Pacing Clin Electrophysiol*. 2013;36:1364–1373.
62. Luther V, et al. Non-randomised comparison of acute and long-term outcomes of robotic versus manual ventricular tachycardia ablation in a single centre ischemic cohort. *J Interv Card Electrophysiol*. 2015;43:175–185.
63. Rolf S, et al. Catheter ablation of atrial fibrillation supported by novel nonfluoroscopic 4D navigation technology. *Heart Rhythm*. 2013;10:1293–1300.
64. Sommer P, et al. Initial experience in ablation of typical atrial flutter using a novel three-dimensional catheter tracking system. *Europace*. 2013;15:578–581.
65. Sommer P, et al. MediGuide in supraventricular tachycardia: initial experience from a multicentre registry. *Europace*. 2013;15:1292–1297.
66. Bear L, Cuculich PS, Bernus O, et al. Introduction to noninvasive cardiac mapping. *Card Electrophysiol Clin*. 2015;7:1–16.
67. Cakulev I, Sahadevan J, Waldo AL. Noninvasive diagnostic mapping of supraventricular arrhythmias (Wolf-Parkinson-White syndrome and atrial arrhythmias). *Card Electrophysiol Clin*. 2015;7:79–88.
68. Jamil-Copley S, et al. Noninvasive electrocardiographic mapping to guide ablation of outflow tract ventricular arrhythmias. *Heart Rhythm*. 2014;11:587–594.
69. Ploux S, et al. Noninvasive electrocardiographic mapping to improve patient selection for cardiac resynchronization therapy: beyond QRS duration and left bundle branch block morphology. *J Am Coll Cardiol*. 2013;61:2435–2443.
70. Rudy Y. Noninvasive electrocardiographic imaging of arrhythmogenic substrates in humans. *Circ Res*. 2013;112:863–874.
71. Rudy Y. The forward problem of electrocardiography revisited. *Circ Arrhythmia Electrophysiol*. 2015;8:526–528.
72. Cakulev I, et al. Confirmation of novel noninvasive high-density electrocardiographic mapping with electrophysiology study: implications for therapy. *Circ Arrhythmia Electrophysiol*. 2013;6:68–75.
73. Bear LR, et al. Forward problem of electrocardiography: is it solved? *Circ Arrhythmia Electrophysiol*. 2015;8:677–684.
74. Rudy Y, Lindsay BD. Electrocardiographic imaging of heart rhythm disorders. From bench to bedside. *Card Electrophysiol Clin*. 2015;7:17–35.
75. Shah AJ, et al. Validation of novel 3-dimensional electrocardiographic mapping of atrial tachycardias by invasive mapping and ablation: a multicenter study. *J Am Coll Cardiol*. 2013;62:889–897.
76. Scheinman M, Gerstenfeld E. Mapping of complex atrial tachycardia circuits by 3-dimensional body surface mapping: the first step in the dawn of a new era. *J Am Coll Cardiol*. 2013;62:898–899.
77. Shah AJ, et al. Noninvasive mapping of ventricular arrhythmias. *Card Electrophysiol Clin*. 2015;7:99–107.
78. Shah AJ, Hocini M, Jais P, et al. Advent of noninvasive mapping of atrial tachycardias. *Card Electrophysiol Clin*. 2013;5:265–270.
79. Sapp JL, Dawoud F, Clements JC, et al. Inverse solution mapping of epicardial potentials: quantitative comparison with epicardial contact mapping. *Circ Arrhythmia Electrophysiol*. 2012;5:1001–1009.
80. Erkapic D, et al. Clinical impact of a novel three-dimensional electrocardiographic imaging for non-invasive mapping of ventricular arrhythmias—a prospective randomized trial. *Europace*. 2015;17:591–597.
81. Ernst S, et al. Utility of noninvasive arrhythmia mapping in patients with adult congenital heart disease. *Card Electrophysiol Clin*. 2015;7:117–123.
82. Shah A, Hocini M, Haissaguerre M, et al. Non-invasive mapping of cardiac arrhythmias. *Curr Cardiol Rep*. 2015;17:1–11.
83. Zhang J, et al. Electrophysiologic scar substrate in relation to VT: noninvasive high-resolution mapping and risk assessment with ECGI. *Pacing Clin Electrophysiol*. 2016;39:781–791.
84. Leong KMW, Lim PB, Kanagaratnam P. Comparative analysis of diagnostic 12-lead electrocardiography and 3-dimensional noninvasive mapping. *Card Electrophysiol Clin*. 2015;7:71–78.
85. Hussein A, et al. Assessment of ventricular tachycardia scar substrate by intracardiac echocardiography. *Pacing Clin Electrophysiol*. 2014;37:412–421.
86. Yamashita S, et al. Impact of new technologies and approaches for post-myocardial infarction ventricular tachycardia ablation during long-term follow-up. *Circ Arrhythmia Electrophysiol*. 2016;9:e003901.
87. Komatsu Y, et al. Regional myocardial wall thinning at multidetector computed tomography correlates to arrhythmogenic substrate in postinfarction ventricular tachycardia: assessment of structural and electrical substrate. *Circ Arrhythmia Electrophysiol*. 2013;6:342–350.
88. Yamashita S, et al. Role of high-resolution image integration to visualize left phrenic nerve and coronary arteries during epicardial ventricular tachycardia ablation. *Circ Arrhythmia Electrophysiol*. 2015;8:371–380.
89. Yamashita S, et al. Image integration to guide catheter ablation in scar-related ventricular tachycardia. *J Cardiovasc Electrophysiol*. 2016;27:699–708.
90. Anand R, et al. Prospective randomized comparison of rotational angiography with three-dimensional reconstruction and computed tomography merged with electro-anatomical mapping: a two center atrial fibrillation ablation study. *J Interv Card Electrophysiol*. 2016;46:1–9.
91. Carpen M, et al. First experience of 3D rotational angiography fusion with NavX electroanatomical mapping to guide catheter ablation of atrial fibrillation. *Heart Rhythm*. 2013;10:422–427.

Ablation Energy Sources

OUTLINE

Radiofrequency Ablation, 206

- Biophysics of Radiofrequency Energy, 206
- Biophysics of Cooled Radiofrequency Ablation, 210
- Pathophysiology of Radiofrequency Lesion Formation, 211
- Determinants of Radiofrequency Lesion Size, 212
- Monitoring Radiofrequency Lesion Formation, 215
- Titration of Standard Radiofrequency Energy, 217
- Titration of Cooled Radiofrequency Energy, 217
- Optimizing Catheter-Tissue Contact, 218
- Prevention of Steam Pops, 221
- Clinical Applications of Standard Radiofrequency Ablation, 222
- Clinical Applications of Cooled Radiofrequency Ablation, 222
- Phased Radiofrequency Ablation, 223
- nMARQ Ablation System, 225

Cryoablation, 225

- Biophysics of Cryothermal Energy, 225
- Pathophysiology of Lesion Formation by Cryoablation, 226

Determinants of Cryogenic Lesion Size, 228

- Technical Aspects of Cryoablation, 229
- Clinical Advantages of Cryoablation, 230
- Clinical Applications of Cryoablation, 230

Laser Energy, 231

- Biophysics of Laser Energy, 231
- Clinical Applications of Laser Energy, 231

Ultrasound Energy, 232

- Biophysics of Ultrasound Energy, 232
- Pathophysiology of Lesion Formation by Ultrasound Energy, 232
- Clinical Applications of Ultrasound Energy, 233

Microwave Ablation, 233

- Biophysics of Microwave Energy, 233
- Pathophysiology of Lesion Formation by Microwave Ablation, 234
- Clinical Applications of Microwave Ablation, 234

Electroporation, 235

RADIOFREQUENCY ABLATION

Biophysics of Radiofrequency Energy

Radiofrequency (RF) refers to the portion of the electromagnetic spectrum in which electromagnetic waves can be generated by alternating current (AC) fed to an antenna. Electrosurgery (coagulation, cauterization, and ablation) currently uses hectomeric wavelengths found in band 6 (300 to 3000 kHz), which are similar to those used for broadcast radio. However, the RF energy is electrically conducted, not radiated, during catheter ablation. The RF current is similar to low-frequency AC or direct current (DC) with regard to its ability to heat tissue and create a lesion, but it oscillates so rapidly that cardiac and skeletal muscles are not stimulated, thereby avoiding induction of arrhythmias and decreasing the pain perceived by the patient. RF current rarely induces rapid polymorphic arrhythmias; such arrhythmias can, however, be observed in response to low-frequency (60-Hz) stimulation. Frequencies higher than 1000 kHz are also effective in generating tissue heating; however, such high frequencies are associated with considerable energy loss along the transmission line. Therefore frequencies of the RF current commonly used are in the range of 300 to 1000 kHz, a range that optimizes efficacy and safety.

Radiofrequency Energy Delivery

Delivery of RF energy depends on the establishment of an electrical circuit involving the human body as one of its in-series elements. The RF current is applied to the tissue via a metal electrode at the tip of the ablation catheter and is generally delivered in a unipolar fashion between the tip electrode and a ground pad applied to the patient's skin. Bipolar RF systems also exist, in which the current flows between

two closely apposed small electrodes, thus limiting the current flow to small tissue volumes interposed between the metal conductors. Bipolar systems, partly because of their relative safety, are now the preferred tools in electrosurgery (oncology, plastic surgery, and ophthalmology), and have been increasingly utilized for catheter ablation of cardiac arrhythmias.

Unipolar RF systems. Unipolar systems apply RF energy between the ablation catheter tip electrode and a large dispersive electrode (indifferent electrode, or ground pad) applied to the patient's skin. The polarity of connections from the electrodes to the generator is not important because the RF current is an AC. The system impedance comprises the impedance of the generator, transmission lines, catheter, electrode-tissue interface, dispersive electrode-skin interface, and interposed tissues. As electricity flows through a circuit, every point of that circuit represents a drop in voltage, and some energy is dissipated as heat. The point of greatest drop in line voltage represents the area of highest impedance and is where most of the electrical energy becomes dissipated as heat. Therefore with excessive electrical resistance in the transmission line, the line actually warms up and power is lost. Currently used electrical conductors from the generator all the way through to the patient and from the dispersive electrode back to the generator have low impedance, to minimize power loss.

Flow of the RF current from the ablation electrode through the myocardium to the indifferent electrode results in resistive tissue heating and lesion formation. With normal electrode-tissue contact, only a fraction of all power is effectively applied to the tissue. The rest is dissipated in the blood pool and elsewhere in the patient. With an ablation electrode in contact with the endocardial wall, part of the electrode contacts tissue and the rest contacts blood, and the RF current flows

through both the myocardium and the blood pool surrounding the electrode. The distribution between both depends on the impedance of both routes and also on how much electrode surface contacts blood versus endocardial wall. Whereas tissue heating is the goal of power delivery, the blood pool is the most attractive route for RF current because blood is a better conductor and has significantly lower impedance than tissue and because the contact between electrode and blood is often better than with tissue. Therefore with normal electrode-tissue contact, much more power is generally delivered to blood than to cardiac tissue.

After leaving the electrode-blood-tissue interface, the current flows through the thorax to the ground pad. Part of the RF power is lost in the patient's body, including the area near the ground pad. However, because the surface area of the ablation electrode (approximately 12 mm²) is much smaller than that of the dispersive electrode (approximately 100 to 250 cm²), the current density is higher in the immediate vicinity of the ablation electrode, and heating occurs preferentially at that site, with no significant heating occurring at the dispersive electrode. Nonetheless, when RF energy delivery is power-limited, dissipation of energy can occur at the dispersive electrode site (at the contact point between the ground pad and the skin) to a degree that can limit lesion formation at the ablation electrode.¹

The dispersive electrode may be placed on any convenient skin surface. The geometry of the RF current field is defined by the geometry of the ablation electrode and is relatively uniform in the region of volume heating. Thus, the position of the dispersive electrode (on the patient's back or thigh) has little effect on impedance, voltage, current delivery, catheter tip temperature, or geometry of the resulting lesion. The size of the dispersive electrode, however, is important. Sometimes it is advantageous to increase the surface area of the dispersive electrode. This increase leads to lower impedance, higher current delivery, increased catheter tip temperatures, and more effective tissue heating. This is especially true in patients with baseline system impedance greater than 100 Ω . Moreover, when the system is power limited, as with a 50-W generator, heat production at the catheter tip varies with the proportion of the local electrode-tissue interface impedance to the overall system impedance. If the impedance at the skin-dispersive electrode interface is high, then a smaller amount of energy is available for tissue heating at the electrode tip. Therefore when ablating certain sites, adding a second dispersive electrode or optimizing the contact between the dispersive electrode and skin should result in relatively more power delivery to the target tissue. In addition, meticulous skin preparation is imperative to optimize skin-patch contact and minimize impedance at the skin interface with the dispersive electrode.¹

A large surface area, and good skin contact, is required at the indifferent electrode patch not only to effectively dissipate heat but also to prevent skin burns. The skin temperature beneath the patch is inversely proportional to patch surface area in contact with the skin and the distance between the patch and the active electrode. If ablation is performed with a high-amplitude current (more than 50 W) and skin contact by the dispersive electrode is poor, skin temperatures can potentially rise above 45°C which, even when short lasting, can result in significant skin burns, especially at the "leading edge" of the patch (the side closest to the RF catheter electrode) (eFig. 7.1).¹

Bipolar RF systems. Bipolar RF ablation uses two adjacent ablation electrodes between which the RF flows, leading to lesion formation between electrodes. Although used in cardiac surgery, bipolar RF ablation has not been widely adopted as a catheter-based treatment for clinical arrhythmias.

Recent studies have demonstrated that bipolar RF ablation using two ablation catheter tips (at opposite sides of the myocardial wall) as the active and ground poles, can potentially create deeper, transmural

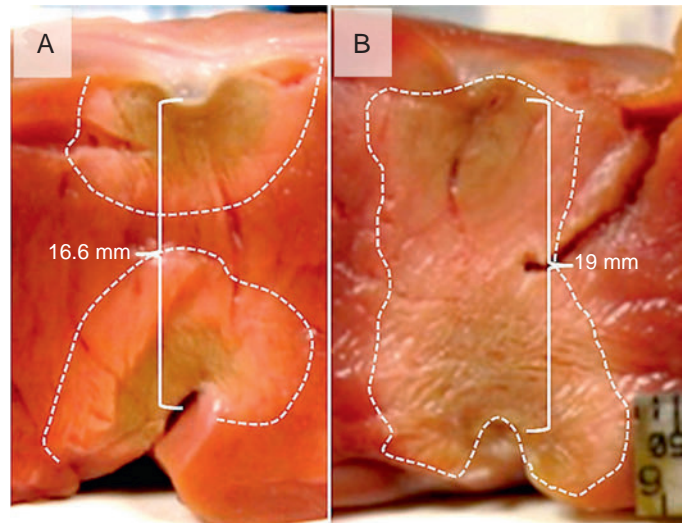


Fig. 7.1 Bipolar Versus Sequential Unipolar Radiofrequency Ablation. Representative image of gross lesion following ablation with (A) sequential unipolar lesion showing nontransmural lesion (tissue thickness of 16.6 mm) and (B) bipolar lesion showing a transmural lesion (tissue thickness of 19 mm). (From Koruth JS, Dukkupati S, Miller MA, et al. Bipolar irrigated radiofrequency ablation: a therapeutic option for refractory intramural atrial and ventricular tachycardia circuits. *Heart Rhythm*. 2012;9:1932–1941.)

lesions (Fig. 7.1). Simultaneous tissue heating and increased current density result in the concentration of thermal injury within the zone between the two closely spaced ablation electrodes and improve efficacy of ablation, as compared with sequential or even simultaneous unipolar RF ablation.² In one report, transmural lesions with bipolar RF ablation could be realized in tissues as thick as 25 mm, in contrast to sequential unipolar RF, which was unable to achieve transmural lesions when thicknesses are greater than 15 mm. This can offer a significant advantage for ablation of septal atrial tachycardia (AT) or ventricular tachycardia (VT) circuits (with one ablation catheter positioned on one side of the septum and the second catheter positioned at the opposite side, Fig. 7.2) or intramural free wall VT circuits (with one ablation catheter positioned endocardially and the second catheter positioned epicardially).^{2,3}

In another design, bipolar RF ablation is used to create contiguous lesions between adjacent electrodes mounted on a multielectrode ablation catheter positioned at one side of the myocardial wall. A multi-channel duty-cycled RF ablation generator (GENius MultiChannel RF Generator, Medtronic, Minneapolis, MN, United States) contains 12 independently controlled RF generators, and is capable of delivering RF energy to each electrode independently. RF energy can be delivered in either bipolar (between the electrodes) and unipolar (from the electrode to the ground pad) current by a phase difference between the channels (thus the term, "phased RF"). During unipolar ablation, current flow is provided between the electrodes and an indifferent electrode attached to the patient's skin, while in the bipolar energy mode, current flows between adjacent electrodes. In this design, bipolar RF ablation lesions are longer, but shallower than unipolar RF lesions. To improve lesion depth, RF energy can also be delivered in a unipolar mode from each electrode to a dispersive electrode.^{4–6}

A second atrial fibrillation (AF) ablation system (nMARQ, Biosense Webster, Diamond Bar, CA, United States) employs a multichannel RF generator capable of independently delivering unipolar or bipolar RF energy to a maximum of 10 electrodes simultaneously. The nMARQ catheter is a decapolar mapping and ablation catheter with individually



eFig. 7.1 Second-Degree Skin Burns at the Site of Ablation Ground Pad Contact. Skin burns occurred on the patient's thigh secondary to poor contact between the skin and the ground pad during radiofrequency ablation of atrial fibrillation.

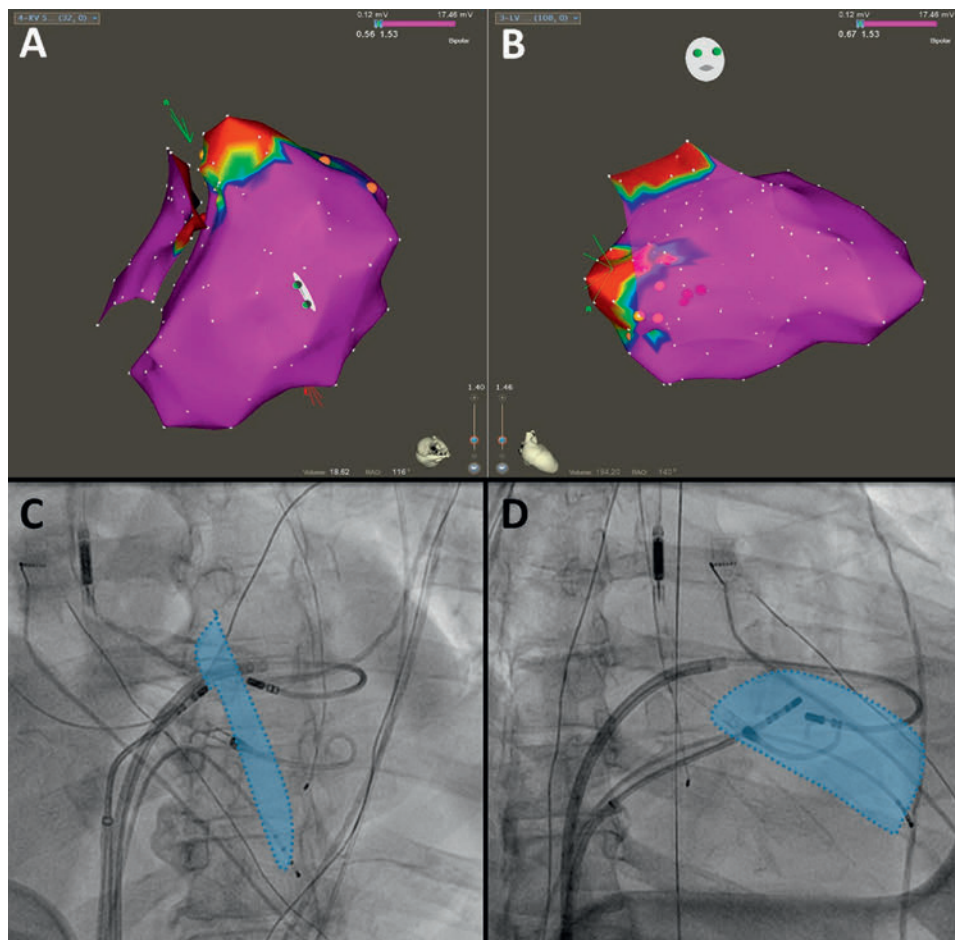


Fig. 7.2 Ventricular Septal Bipolar Radiofrequency Ablation. (A and B) Voltage maps of left ventricle. (C and D) Fluoroscopic views of catheter positions on either side of the septum at the site of successful termination of ventricular tachycardia. (From Koruth JS, Dukkipati S, Miller MA, et al. Bipolar irrigated radiofrequency ablation: a therapeutic option for refractory intramural atrial and ventricular tachycardia circuits. *Heart Rhythm*. 2012;9:1932–1941.)

irrigated platinum electrodes. Each electrode possesses a thermocouple and holes for irrigation. RF energy is applied in a temperature-controlled mode and energy delivery can be individually arranged over each combination of the 10 electrodes in unipolar mode or bipolar mode between two adjacent electrodes.^{7–9}

Tissue Heating

While free electrons serve as charge carriers inside the RF generator, cables, and RF electrode, the electric current inside tissue is carried by charged ions (such as Na^+ , K^+ , and Cl^-). During AC flow, charged carriers in tissue (ions) attempt to follow the changes in the direction of the AC. For a typical frequency of 500 kHz, the direction of the current (and ion movement) changes a million times per second. Ion oscillations generate heat due to friction, thus converting electromagnetic (current) energy into molecular mechanical energy or heat. This type of electric current-mediated heating is known as ohmic (resistive) heating. Using Ohm's law, with resistive heating, the amount of power (= heat) per unit volume equals the square of current density times the specific impedance of the tissue. With a spherical ablation electrode, the current flows outward radially, and current density therefore decreases with the square of distance from the center of the electrode. As a consequence, power dissipation per unit volume decreases with the fourth power of distance. The thickness of the electrode eliminates the first

steepest part of this curve, however, and the decrease in dissipated power with distance is therefore somewhat less dramatic.

Approximately 90% of all RF power that is delivered to the tissue is absorbed within the first 1 to 1.5 mm from the ablation electrode surface. Therefore only a thin rim of tissue in immediate contact with the RF electrode is directly heated (within the first 2 mm of depth from the electrode). The remainder of tissue heating occurs as a result of heat conduction from this rim to the surrounding tissues. On initiation of fixed-level energy application, the temperature at the electrode-tissue interface rises monoexponentially to reach steady state within 7 to 10 seconds, and the steady state is usually maintained between 80°C and 90°C. However, whereas resistive heating starts immediately with the delivery of RF current, conduction of heat to deeper tissue sites is relatively slow and requires 1 to 2 minutes to equilibrate (thermal equilibrium). Therefore the rate of tissue temperature rise beyond the immediate vicinity of the RF electrode is much slower, resulting in a steep radial temperature gradient as tissue temperature decreases radially in proportion to the distance from the ablation electrode, and deep tissue temperatures continue to rise for several seconds after interruption of RF delivery (the so-called thermal latency phenomenon). Therefore RF ablation requires at least 30 to 60 seconds to create full-grown lesions. In addition, when temperature differences between adjacent areas develop because of differences in local current density or local heat capacity,

heat conducts from hotter to colder areas, thus causing the temperature of the former to decrease and that of the latter to increase. Furthermore, heat loss to the blood pool at the surface and to intramyocardial blood vessels determines the temperature profile within the tissue.

At steady state, the lesion size is proportional to the temperature measured at the interface between the tissue and the electrode, as well as to the RF power amplitude. By using higher powers and achieving higher tissue temperatures, the lesion size can be increased. Tissue temperatures of up to 110°C can be achieved. Above this temperature, tissue vaporization ensues and prevents any further heating by RF current due to the electrically insulating properties of vapor. Also, boiling of the plasma at the electrode-tissue interface can cause tissue carbonization (“charring”) at the site of very high RF current densities (typically very close to the RF electrode), producing an electrically insulating coagulum, which is accompanied by a sudden increase in electrical impedance that prevents further current flow into the tissue and further heating.

The range of desired tissue temperatures during RF ablation is 50°C to 90°C. Within this range, relatively uniform desiccation of tissue can be expected. If the temperature is lower than 50°C, no or only minimal tissue necrosis results. Temperatures above 100°C are associated with tissue vaporization, including steam pops, and charring. Because the rate of temperature rise at deeper sites within the myocardium is slow, a continuous energy delivery of at least 60 seconds is often warranted to maximize depth of lesion formation.

Convective Cooling

At the site of endocardial ablation, tissues heated directly by RF energy start losing heat into deeper layers of myocardium as well as into the circulating blood pool and the metal ablation electrode (Fig. 7.3). Heat conduction into deeper myocardial layers helps increase the size of the ablation lesion. Heat conduction to the ablation electrode helps indirect monitoring of tissue temperature via the embedded temperature sensors. On the other hand, convective heat loss from the endocardium at the site of ablation into the circulating blood pool results in cooling of the endocardial surface, and constitutes the dominant factor opposing

effective myocardial heating and lesion formation. Because the tissue surface is cooled by the blood flow, the highest temperature during RF delivery occurs slightly below the endocardial surface. Consequently, the width of the endocardial lesion matures earlier than the intramural lesion width (20 seconds vs. 90 to 120 seconds). Hence, the maximum lesion width is usually located intramurally, and the resultant lesion is usually teardrop shaped, with less necrosis of the superficial tissue.

As the magnitude of convective cooling increases (e.g., unstable catheter position, poor catheter-tissue contact, or high blood flow in the region of catheter position), there is decreased efficiency of heating as more energy is carried away in the blood and less energy is delivered to the tissue. When RF power is limited and insufficient to overcome the heat lost by convection, lesion size is reduced. On the other hand, when RF power delivery is not limited, convective cooling allows for more power to be delivered into the tissue (as long as adequate electrode-tissue contact is maintained), increasing the depth of direct resistive heating and intramural tissue temperatures (and hence larger ablation lesion size), while avoiding very high endocardial surface temperatures (and temperatures measured by the catheter tip sensors) that can otherwise result in blood boiling and coagulum formation at the electrode tip, with consequent sudden rise in electrical impedance and reduction of further power delivery.

The concept of convective cooling can explain why there are few coronary arterial complications with conventional RF ablation. Coronary arteries act as a heat sink; substantive heating of vascular endothelium is generally prevented by heat dissipation in the high-velocity coronary blood flow, even when the catheter is positioned close to the vessel. Although this is advantageous, because coronary arteries are being protected, it can limit success of the ablation lesion if a large perforating artery is close to the ablation target and can protect the target tissue from ablation by transferring heat away from it.¹⁰

The effects of convective cooling have been exploited to increase the size of catheter ablative lesions. Active electrode cooling by ablation electrode irrigation is currently used to largely eliminate the risk of overheating at the electrode-tissue contact point and increase the magnitude of power delivery and the depth of volume heating.

Of note, standard RF ablation is not as effective when delivered to the epicardium compared with lesions delivered to the endocardium for a number of reasons, one of which is the lack of convective cooling (by the circulating blood) of the ablation electrode in the epicardial space. This results in high electrode temperatures at low-power settings (≤ 10 W), limiting power delivery in the pericardial space and hindering lesion formation. Therefore active electrode cooling is required in this setting.¹¹

Catheter Tip Temperature

Ablation catheter tip temperature depends on tissue temperature, tissue contact of the ablation electrode, convective cooling by the surrounding blood, heat capacity of the electrode material, and type and location of the temperature sensor.

Catheter tip temperature is measured by a sensor located in the ablation electrode. There are two different types of temperature sensors: thermistors and thermocouples. Thermistors require a driving current, and the electrical resistance changes as the temperature of the electrical conductor changes. More frequently used are thermocouples, which consist of copper and constantan wires and are incorporated in the center of the ablation electrode. Thermocouples are based on the so-called “Seebeck effect”; when two different metals are connected (sensing junction), a voltage can be measured at the reference junction that is proportional to the temperature difference between the two metals.

The electrode temperature rise is an indirect process—the ablation electrode is not heated by RF energy, but it heats up because it happens

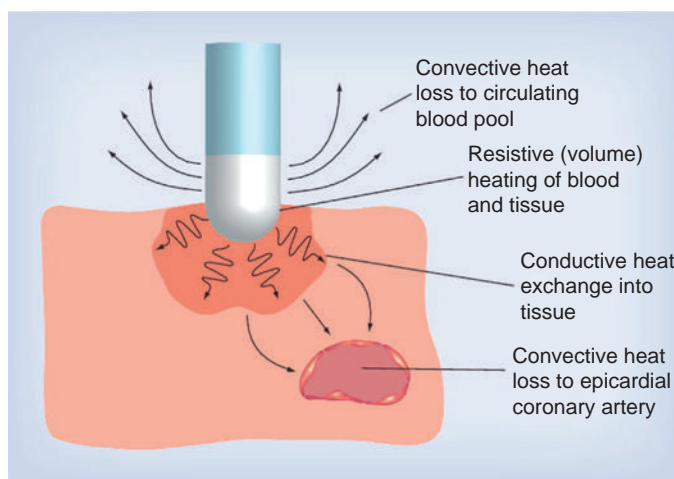


Fig. 7.3 Biophysics of Radiofrequency Heating. This illustration represents the regions of resistive and conductive heating of tissue, and convective heat loss from tissue into the circulating blood pool and epicardial coronary arteries when delivering radiofrequency current to the endocardium using a conventional 4-mm-tip electrode catheter. (From Houmsse M, Daoud EG. Biophysics and clinical utility of irrigated-tip radiofrequency catheter ablation. *Expert Rev Med Devices*. 2012;9: 59–70.)

to touch heated tissue. Consequently, the catheter tip temperature is always lower than, or ideally equal to, the superficial tissue temperature. Conventional electrode catheters with temperature monitoring report the temperature only from the center of the electrode mass with one design, or from the apex of the tip of the catheter with another design. It is likely that the measured temperature underestimates the peak tissue temperature (which occurs slightly below the endocardial surface).

Several other factors can increase the disparity between catheter tip temperature and tissue temperature, including catheter tip irrigation, large ablation electrode size, and poor electrode-tissue contact. Catheter tip irrigation increases the disparity between tissue temperature and electrode temperature because it results in cooling of the ablation electrode, but not the tissue. With a large electrode tip, a larger area of the electrode tip is exposed to the cooling effects of the blood flow than with standard tip lengths, thus resulting in lower electrode temperatures. Similarly, with poor electrode-tissue contact, less electrode material is in contact with the tissue, and heating of the tip by the tissue occurs at a lower rate, resulting in relatively low tip temperatures.

Biophysics of Cooled Radiofrequency Ablation

There are two methods of active electrode cooling by irrigation: internal and external (Fig. 7.4). With the internal (closed-loop) system (Chilli, Boston Scientific, Natick, MA), cooling of the ablation electrode is achieved by circulating fluid within the electrode. In contrast, with the external (open-loop) system (Celsius or Navistar ThermoCool, Biosense Webster, Diamond Bar, CA, United States; and Therapy Cool Path, St. Jude Medical, St. Paul, MN, United States), electrode cooling is performed by flushing saline through openings in the porous-tipped electrode (showerhead-type system). Another cooling system is sheath-based open irrigation, which uses a long sheath around the ablation catheter for open irrigation. The latter system was found to provide the best results, but this type of catheter tip cooling is not clinically available.

Active electrode cooling by irrigation can produce higher tissue temperatures and create larger lesions, compared with standard RF

ablation catheters, because of a reduction in overheating at the tissue-electrode interface, even at sites with low blood flow. This allows the delivery of higher amounts of RF power for a longer duration to create relatively large lesions with greater depth but without the risk of coagulum and char formation. Unlike with standard RF ablation, the area of maximum temperature with cooled ablation is within the myocardium, rather than at or just below the electrode-myocardial interface. Higher power results in greater depth of volume heating, but if the ablation is power limited, power dissipation into the circulating blood pool can actually result in decreased lesion depth (Fig. 7.5). Compared with large-tip catheters, active cooling has been shown to produce equivalent lesions with energy delivery via smaller irrigated electrodes, with less dependence on catheter tip orientation and extrinsic cooling, whereas larger electrodes have significant variability in their electrode-tissue interface, depending on catheter orientation (see Fig. 7.5). For the nonirrigated catheter, greater lesion volumes are observed with a horizontal orientation of the RF electrode compared with a vertical orientation. In contrast, for irrigated catheters, lesion volume increased with a perpendicular electrode orientation compared with the horizontal orientation.

Lesion depth seems to be similar between closed-loop and open-irrigation electrodes. However, open irrigation is more effective in cooling the electrode-tissue interface, as reflected by lower interface temperature, lower incidence of thrombus, and smaller lesion diameter at the surface (with the maximum diameter produced deeper in the tissue). These differences between the two electrodes are greater in low blood flow, presumably because the flow of saline irrigation out of the electrode provides additional cooling of the electrode-tissue interface (external cooling). Ablation with internal electrode cooling in low blood flow regions frequently results in high electrode-tissue interface temperature (despite low electrode temperature) and coagulum formation.¹²

When maximum power and temperature parameters that did not result in any evidence of excessive heating (including popping, boiling, or impedance rise) for each catheter type were selected, closed-irrigation

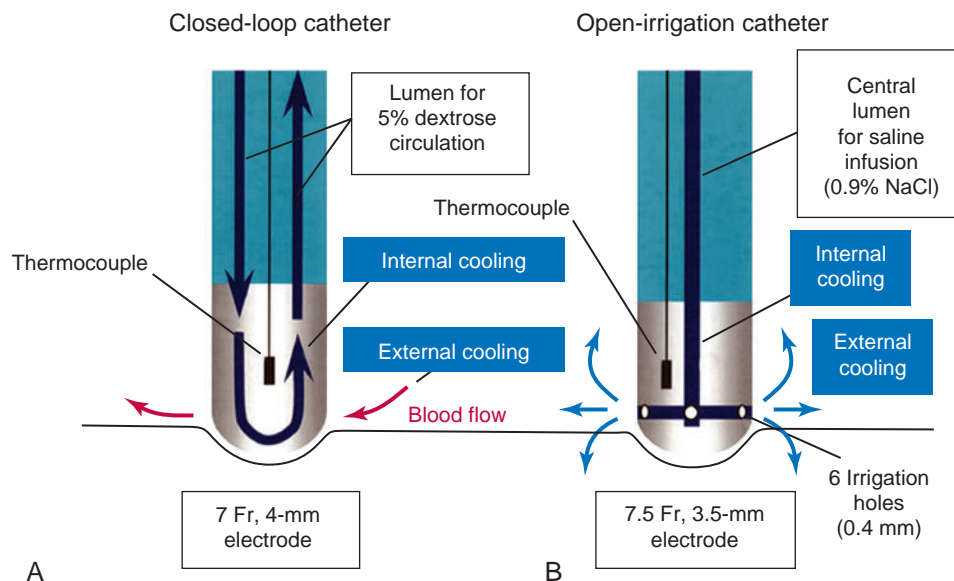


Fig. 7.4 Schematic Representation of Irrigated Electrode Catheters. (A) The closed-loop irrigation catheter has a 7 Fr, 4-mm-tip electrode with an internal thermocouple. (B) The open-irrigated catheter has a 7.5 Fr, 3.5-mm-tip electrode with an internal thermocouple and six irrigation holes (0.4-mm diameter) located around the electrode, 1.0 mm from the tip. NaCl, Sodium chloride. (From Yokoyama K, Nakagawa H, Wittkamp FH, et al. Comparison of electrode cooling between internal and open irrigation in radiofrequency ablation lesion depth and incidence of thrombus and steam pop. *Circulation*. 2006;113:11.)

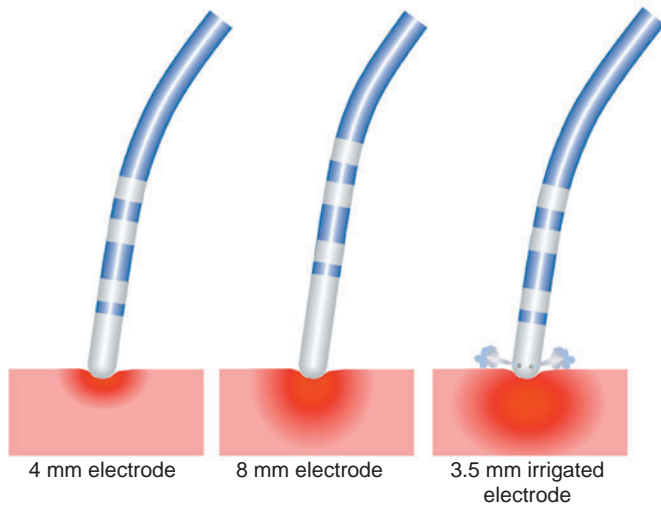


Fig. 7.5 Effect of Electrode Type on Lesion Size. Representative blocks of myocardium are shown with lesions (*dark shading*) resulting from optimal radiofrequency energy delivery for each electrode type. A 4-mm electrode makes a small shallow lesion (*left*). An 8-mm electrode makes a larger, deeper lesion (*center*). The open-irrigated electrode makes a larger, deeper lesion, with a maximum width at some tissue depth (*right*).

catheters resulted in slightly larger lesion volumes and greater lesion depths than the open-irrigation catheters. Both cooled catheters fared better than the standard 4-mm-tip and large 10-mm-tip catheters with larger lesions achieved within the range of safe energy delivery.

Pathophysiology of Radiofrequency Lesion Formation

Cellular Effects of Radiofrequency Ablation

The primary mechanism of tissue injury by RF ablation is likely to be thermally mediated. Hyperthermic injury to the myocyte is both time- and temperature-dependent, and it is likely the result of changes in the cell membrane, protein inactivation, cytoskeletal disruption, nuclear degeneration, as well as other potential mechanisms. The cell membrane, in particular, is very sensitive to thermal injury. Hyperthermia results in potential phase change in membrane fluidity, kinetic and structural changes in membrane ion channels and ion pumps, inhibition of transport proteins, and formation of nonspecific ionic membrane pores.

Experimentally, the resting membrane depolarization is related to temperature. In the low hyperthermic range (37°C to 45°C), little tissue injury occurs, and a minor change can be observed in the resting membrane potential and action potential amplitude. However, action potential duration shortens significantly, and conduction velocity becomes greater than at baseline. In the intermediate hyperthermic range (45°C to 50°C), progressive depolarization of the resting membrane potential occurs, and action potential amplitude decreases. In addition, abnormal automaticity is observed, reversible loss of excitability develops, and conduction velocity progressively decreases. In the high temperature ranges (higher than 50°C), marked depolarization of the resting membrane potential occurs, and permanent loss of excitability is observed. Temporary (at temperatures of 49.5°C to 51.5°C) and then permanent (at 51.7°C to 54.4°C) conduction block develops, and fairly reliable irreversible myocardial injury occurs with a short hyperthermic exposure.

In the clinical setting, the success of ablation is related to the mean temperature measured at the electrode-tissue interface. Block of conduction in an atrioventricular (AV) bypass tract (BT) usually occurs at 62°C \pm 15°C. During ablation of the AV junction, an accelerated junctional rhythm, which is probably caused by thermally or electrically induced

cellular automaticity or triggered activity, is observed at temperatures of 51°C \pm 4°C, whereas reversible complete AV block occurs at 58°C \pm 6°C, and irreversible complete AV block occurs at 60°C \pm 7°C.

RF ablation typically results in high temperatures (70°C to 90°C) for a short time (up to 60 seconds) at the electrode-tissue interface, but significantly lower temperatures at deeper tissue sites. This leads to rapid tissue injury within the immediate vicinity of the RF electrode but relatively delayed myocardial injury with increasing distance from the RF electrode. Therefore, although irreversible loss of electrophysiological (EP) function can usually be demonstrated immediately after successful RF ablation, this finding can be delayed because tissue temperatures continue to rise somewhat after cessation of RF energy delivery (thermal latency phenomenon). This effect can account for the observation that patients undergoing atrioventricular node (AVN) modification procedures who demonstrate transient heart block during RF energy delivery can progress to persisting complete heart block, even if RF energy delivery is terminated immediately. Reversible loss of conduction can be demonstrated within seconds of initiating the RF application, which can be caused by an acute electrotonic effect. On the other hand, there can be late recovery of EP function after an initial successful ablation.

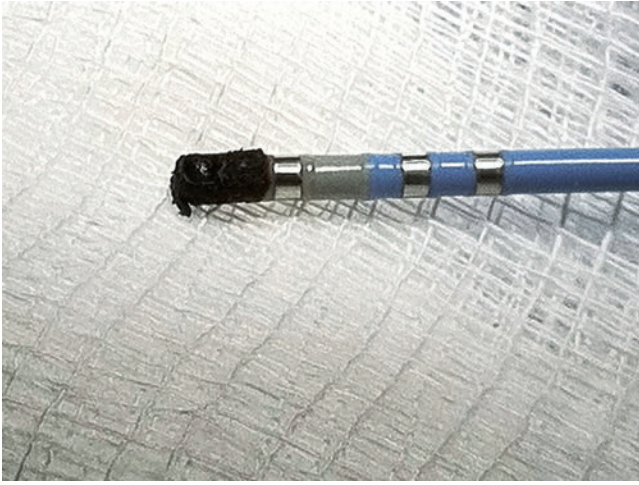
In addition to the dominant thermal effects of RF ablation, some of the cellular injury has been hypothesized to be caused by a direct electrical effect, which can result in dielectric breakdown of the sarcolemmal membrane with creation of transmembrane pores (electroporation), resulting in nonspecific ion transit, cellular depolarization, calcium overload, and cell death. Such an effect has been demonstrated with the use of high-voltage electrical current. However, it is difficult to examine the purely electrical effects in isolation of the dominant thermal injury.

Tissue Effects of Radiofrequency Ablation

Changes in myocardial tissue are apparent immediately on completion of the RF lesion. Pallor of the central zone of the lesion is attributable to denaturation of myocyte proteins (principally myoglobin) and subsequent loss of the red pigmentation. Slight deformation, indicating volume loss, occurs at the point of catheter contact in the central region of lesion formation. The endocardial surface is usually covered with a thin fibrin layer and, occasionally, if a temperature of 100°C has been exceeded, with char and thrombus (eFig. 7.2). In addition, a coagulum (an accumulation of fibrin, platelets, and other blood and tissue components) can form at the ablation electrode because of the boiling of blood and tissue serum.

On sectioning, the central portion of the RF ablation lesion shows desiccation, with a surrounding region of hemorrhagic tissue and then normal-appearing tissue. Histological examination of an acute lesion shows typical coagulation necrosis with basophilic stippling consistent with intracellular calcium overload. Immediately surrounding the central lesion is a region of hemorrhage and acute monocellular and neutrophilic inflammation.

The progressive changes seen in the evolution of an RF lesion are typical of healing after any acute injury. Within 2 months of the ablation, the lesion shows fibrosis, granulation tissue, chronic inflammatory infiltrates, and significant volume contraction. The lesion border is well demarcated from the surrounding viable myocardium without evidence of a transitional zone. This likely accounts for the absence of proarrhythmic side effects of RF catheter ablation. As noted, because of the high-velocity blood flow within the epicardial coronary arteries, these vessels are continuously cooled and are typically spared from injury, despite nearby delivery of RF energy. Nonetheless, high RF power delivery in small hearts, such as in pediatric patients, or in direct contact with the vessel can potentially cause coronary arterial injury.¹⁰



eFig. 7.2 Standard Radiofrequency Ablation Catheter With Char Formed on the Tip.

The border zone around the acute pathological RF lesion accounts for several phenomena observed clinically. The border zone is characterized by marked ultrastructural abnormalities of the microvasculature and myocytes acutely, as well as a typical inflammatory response later. The most thermally sensitive structures appear to be the plasma membrane and gap junctions, which show morphological changes as far as 6 mm from the edge of the pathological lesion. The border zone accounts for documented effects of RF lesion formation well beyond the acute pathological lesion. The progression of the EP effects after completion of the ablation procedure can be caused by further inflammatory injury and necrosis in the border zone region that result in late progression of physiological block and a delayed cure in some cases. On the other hand, initial stunning and then early or late recovery of function can be demonstrated in the border zone, thus accounting for the recovery of EP function after successful catheter ablation in the clinical setting, which can be caused by healing of the damaged, but surviving, myocardium.

Coagulum Formation

Excessive tissue heating can lead to high temperatures at the electrode-tissue interface. Once the peak tissue temperature exceeds the threshold of 100°C, boiling of blood and tissue serum at the electrode-tissue interface can ensue. When boiling occurs, denatured serum proteins and charred tissue form a thin film that adheres to the electrode, thus producing an electrically insulating coagulum (an accumulation of fibrin, platelets, and other blood and tissue components). The coagulum can detach and embolize. Of note, unlike typical thrombi, a coagulum is not formed by activation of clotting factors, and its formation is not prevented by anticoagulation.

In temperature-controlled RF ablation, electrode temperature does not reach the boiling point. Nonetheless, the true tissue temperature can be significantly higher than the measured electrode temperature. In addition, serum proteins denature at temperatures well below the interfacial boiling temperature. Therefore coagulum can still form even when the electrode temperature is limited to 65°C with a 4-mm ablation electrode, and 55°C with an 8-mm electrode. Open irrigation cools the electrode and its direct environment (blood, and catheter-tissue interface), reducing (but not eliminating) the risk of interfacial boiling and coagulum formation. Also, the irrigant helps wash away denatured proteins as it forms.¹³

Usually, coagulum adheres to the electrode tip, which is accompanied by a sudden increase in electrical impedance that prevents further current flow into the tissue and further heating, at which point the ablation catheter needs to be withdrawn from the body and cleaned to remove the adhering coagulum. However, when the coagulum attaches to the tissue surface rather than to the electrode tip, electrode temperature or impedance may not be affected, and coagulum formation can continue unnoticed. Therefore the absence of impedance rise during ablation does not guarantee the absence of coagulum formation on the tissue contact site.

Steam Pop

High RF power application (especially in the setting of cooled RF ablation) can cause superheating within the tissue (with subendocardial tissue temperatures exceeding 100°C), which can result in boiling of water within the tissue under the electrode. Consequently, evaporation and rapid steam expansion can occur intramurally, and a gas bubble can develop in the tissue under the ablation electrode. Continued application of RF energy causes the bubble to expand and its pressure to increase, which can lead to eruption of the gas bubble (causing a popping sound) through the path with the least mechanical resistance that can leave behind a gaping hole (the so-called “steam pop”). This often occurs

toward the heat-damaged endocardial surface (leading to crater formation) or, infrequently, across the myocardial wall (resulting in myocardial perforation).

The consequence of a steam pop depends on the area of the heart being ablated. The risk of cardiac perforation is low in areas of dense ventricular scar. The risk of perforation and cardiac tamponade is likely to be higher for ablation in the thin-walled right ventricular outflow tract (RVOT) and in the atria. Therefore it is reasonable to take a more conservative approach to power application in these areas.

Steam pops are often associated with a sudden, although small (less than 10 Ω) impedance rise and a sudden drop in electrode temperature. When steam pops burst toward the endocardial surface, a shower of microbubbles is often detected on intracardiac echocardiography (ICE).

The risk of steam pops is relatively low with temperature-controlled standard 4-mm-tip RF catheter ablation, since the electrode temperature, which approximates tissue temperature, is limited to a safe level. However, when there is significant discrepancy between tissue and electrode temperature, due to passive or active electrode cooling, tissue temperature can reach the boiling point without being detected by the monitoring electrode temperature.

Electrode orientation also seems to affect the significance of steam pops; pops that occur when the electrode tip is perpendicular to the tissue are more likely to cause cardiac perforation than those that occur when the electrode is lying horizontally on the tissue. Therefore one should try to avoid high-pressure perpendicular tissue contact, especially at higher RF power outputs. RF applications preceding steam pops have a greater and more rapid decrease in impedance and occur at a higher maximum RF power than applications without pops. Because of the considerable overlap of impedance changes in lesions with and without steam pops, it is not possible to advocate a general limit for impedance decrease for all RF lesions. However, when ablation is performed in areas at risk for perforation (i.e., especially in thin-walled structures), reducing power to achieve an impedance decrease of less than 18 Ω is a reasonable strategy to reduce the chance of a pop.

Determinants of Radiofrequency Lesion Size

It is axiomatic that successful ablation occurs when an adequate amount of ablation energy is delivered for an adequate amount of time, with adequate electrode-tissue contact, at an appropriate target site. Many of the elements of this statement relate to formation of an effective ablation lesion. Lesion size is defined as the total volume or dimensions (width and depth) of the lesion. The size of the lesion created by RF power is determined by the amount of tissue heated to more than the critical temperature for producing irreversible myocardial damage (50°C). Tissue heating is a function of the magnitude of RF power that is converted into heat in the tissues. As noted, only a thin rim (1 to 2 mm) of tissue immediately under the ablating electrode is directly heated. This heat then radiates to adjacent tissue; however, conduction of heat to deeper tissue sites is relatively slow and very inefficient. The distance at which temperature drops to less than 50°C delimits the depth of lesion formation. The use of higher power output to achieve higher tissue temperatures results in larger lesions by raising the temperature of the rim of resistively heated tissue to substantially more than 50°C for deeper tissue to reach the 50°C threshold required for tissue necrosis. However, the rim of heated tissue in direct contact with the ablating electrode conducts not only to deeper tissue but also to the electrode tip itself. Higher electrode temperatures either limit further energy delivery (in temperature-controlled power delivery mode) or increase electrode impedance as a result of coagulum formation; these effects potentially limit lesion size. Furthermore, tissue temperatures higher than 100°C are unsafe because they are associated with a higher risk of steam pops. Cooling of the ablating electrode (passively by using a

TABLE 7.1 Determinants of Radiofrequency Lesion Size

Electrode temperature	Lesion size increases with higher electrode temperature unless a coagulum is formed or power output is limited
RF power amplitude	Lesion size increases with higher RF power delivery given adequate tissue contact
Duration of RF application	Lesion size increases with increasing duration of RF application (up to 30–60 s for 4-mm tip standard RF, or up to 60–120 s for large or irrigated RF electrodes)
Electrode-tissue contact	Lesion size increases with improved tissue contact, unless RF power output is limited by increasing electrode temperatures and lack of electrode cooling
Electrode length	Lesion size increases with larger electrode length, unless RF power output is limited
Electrode orientation	With the same total power, perpendicular electrode orientation yields larger lesion volumes than parallel electrode orientation. When RF power level is unrestricted and is increased to maintain a constant current density, lesion size will increase proportionally to the electrode-tissue contact area, which is larger with parallel tip orientation
Electrode material	Gold electrodes have greater thermal conductivity than platinum, allowing for more RF power to be applied at constant temperature
Reference patch electrode size	Lesion size increases with increasing ground pad size and optimizing skin contact
Convective cooling	At any given power output (with no temperature restriction), RF lesion size decreases with increasing passive or active convective cooling
RF system polarity	At any given electrode temperature (with no power restriction), RF lesion size increases with increasing convective cooling
Electrode flexibility	Unipolar RF ablation produces narrower but deeper lesions. Bipolar RF ablation produces longer but shallower lesions
	Electrode flexibility improves tissue contact and can increase lesion size, unless RF power output is limited by increasing electrode temperatures and lack of electrode cooling

RF, Radiofrequency.

larger electrode length or actively by using catheter irrigation) can help diminish electrode heating, allowing for greater power delivery and creation of larger lesions. Several other factors can influence RF lesion size (Table 7.1).

Ablation Electrode Temperature

The relationship between lesion size and the recorded catheter tip temperature is complex and subject to several confounding factors. When electrode tip temperature closely resembles tissue temperature (the main determinant of lesion formation), lesion size appears to increase directly with electrode temperature up until the point of coagulum formation at the electrode-tissue interface, when further power delivery becomes limited. However, with good contact between catheter tip and tissue and low cooling of the catheter tip, the target temperature can be reached with little power, thus resulting in fairly small lesions although a high catheter tip temperature is being measured.

Furthermore, catheter tip temperature is not a reliable measure of tissue temperature, as it is also influenced by convective cooling, electrode-tissue contact, and type and location of the temperature sensor. A low catheter tip temperature can be caused by a high level of convective cooling, which allows a higher amount of RF power to be delivered to the tissue (because it is no longer limited by temperature rise of the ablation electrode) and yields relatively large lesions. This is best illustrated with active cooling of the ablation electrode using irrigation during RF energy delivery; the tip temperature is usually less than 40°C, which allows the application of high-power output for longer durations.

Radiofrequency Power Amplitude

Lesion size is proportional to the amount of RF power delivered *effectively* into the tissue. Higher RF power delivery increases the amount of directly heated tissue as well as tissue temperatures, resulting in greater depth of thermal injury and larger lesion size. However, the mere amplitude of RF power application does not necessarily translate to a larger amount of power delivered into the tissue, since RF power can be wasted into the surrounding blood pool due to poor electrode-tissue contact.

Duration of Radiofrequency Application

The RF lesion is predominantly generated within the first 10 seconds of target energy delivery and tissue temperatures, and it reaches a maximum after 30 seconds. Extension of RF application beyond 45 to 60 seconds during power-controlled RF delivery does not generally seem to increase lesion size further. However, lesions created using large or irrigated RF electrodes have a longer half time of lesion growth, and extended ablation (60 to 120 seconds) can potentially help create larger lesions.

Electrode-Tissue Contact

Catheter electrode-tissue contact pressure is a major determinant of lesion size. Data indicate that increasing the firmness of contact (contact force) is comparable to increasing RF power; that is, the same tissue temperatures and lesion size can be reached at a much lower power level when tissue contact is optimized.^{14,15}

The efficiency of energy transfer to the myocardium (i.e., temperature rise per watt of applied power) largely depends on the electrode-tissue contact. Increasing contact force can improve the efficiency of RF lesion formation by several mechanisms: (1) expanding the area of the contact footprint of the electrode on myocardial tissue by embedding it deeper within the soft myocardium, which leads to a higher amount of RF power that can be effectively delivered to the tissue; (2) reducing the electrode surface exposed to surrounding blood pool and, hence, reducing RF current shunting into the low-impedance blood pool; (3) improving stability of the electrode-tissue contact and reducing catheter sliding with cardiac motion, which improves the efficiency of lesion formation; and (4) stretching of the myocardium, bringing the epicardium closer to the ablation electrode and, hence, improving transmural of the RF lesion.¹⁶

However, at a certain moderate contact force, further increase in contact firmness results in progressively smaller lesions because a lesser amount of RF power is required to reach target temperature. The temperature rise of the ablation electrode signals excessive tissue heating and limits power delivery in a temperature-controlled system. Reduced convective cooling of the ablation electrode (because of lesser interface

with the blood pool) results in higher electrode temperatures and can further reduce RF current delivery.

Electrode Length

Ablation catheters have tip electrodes that are conventionally 4 mm long and are available in sizes up to 10 mm long (see eFig. 4.3). An increased electrode size reduces the interface impedance with blood and tissue, but the impedance through the rest of the patient remains the same. Hence, the ratio between interface impedance and the impedance through the rest of the patient is lower with an 8-mm electrode than with a 4-mm electrode, which reduces the efficiency of power transfer to the tissue. Therefore with the same total power, lesions created with a larger electrode are always smaller than lesions created with a smaller electrode (Fig. 7.6). A larger electrode size also creates a greater variability in power transfer to the tissue because of greater variability of tissue contact, and tissue contact becomes much more dependent on catheter orientation with longer electrodes. Consequently, an 8-mm electrode may require a 1.5 to 4 times higher power level than a 4-mm electrode to create the same lesion size.

On the other hand, when the power is not limited, catheters with large distal electrodes create larger lesions, both by increasing the ablation electrode surface area in contact with the bloodstream (resulting in an augmented convective cooling effect) and by increasing the volume of tissue directly heated because of an increased surface area at the electrode-tissue interface (see Fig. 7.6). However, this assumes that the electrode-tissue contact, tissue heat dissipation, and blood flow are uniform throughout the electrode-tissue interface. As the electrode size increases, the likelihood that these assumptions are true diminishes because of variability in cardiac chamber trabeculations and curvature, tissue perfusion, and intracardiac blood flow, which affect the heat dissipation and tissue contact. These factors result in unpredictable lesion size and uniformity for electrodes more than 8 mm long.

There is a potential safety concern with the use of long ablation electrodes because of nonuniform heating, with maximal heating occurring at the electrode edges. Thus, large electrode-tipped catheters with

only a single thermistor can underestimate maximal temperature and allow char formation and potential thromboembolic complications. Catheter tips with multiple temperature sensors at the electrode edges are preferable for temperature feedback. In addition, the greater variation in power delivered to the tissue and the greater discrepancy between electrode and tissue temperature make it difficult to avoid steam pops and char formation. Another point of concern is that the formation of char may only minimally affect electrode impedance by covering a much smaller part of the electrode surface. Therefore the lower electrode temperature and the absence of any impedance rise may erroneously suggest a safer ablation process.

The principal limitations of a large ablation electrode (8 to 10 mm in length) are the reduction in mobility and the flexibility of the catheter (which can impair positioning of the ablation electrode) and a reduction in the resolution of recordings from the ablation electrode, thus making it more difficult to identify the optimal ablation site. A larger electrode dampens the local electrogram, especially that of the distal electrode. With an 8- or 10-mm long distal and a 1-mm short proximal ring electrode, the proximal electrode can be the main source for the bipolar electrogram; this then confuses localization of the optimal ablation site. In contrast, a smaller electrode improves mapping accuracy and feedback of tissue heating; its only drawback is the limited power level that can be applied to the tissue.

Electrode Orientation

The effect of catheter orientation on lesion size depends on the presence of passive or active cooling, whether or not power delivery is restricted, the length of the ablation electrode, as well as the placement of the temperature sensors relative to the portion of the electrode in contact with tissue. Lesion size is only slightly affected by catheter tip orientation using 4- or 5-mm-long tip catheters; the effects of catheter orientation become more pronounced for larger ablation electrodes.

When the catheter tip is perpendicular to the tissue surface, a much smaller surface area is in contact with the tissue (resulting in increased current density at the electrode-tissue interface) and larger area exposed to the circulating blood pool (resulting in augmented convective cooling) than when the catheter electrode tip is lying on its side. On the other hand, parallel tip orientation provides larger electrode-tissue contact area (resulting in less power waste into the blood stream and less current density at the electrode-tissue interface). Therefore with the same total power, perpendicular electrode orientation yields larger lesion volumes than parallel electrode orientation. However, if the RF power level is unrestricted and is increased to maintain a constant current density, lesion size will increase proportionally to the electrode-tissue contact area, which is larger with parallel tip orientation.

Furthermore, the character of the lesion created with temperature control depends on the placement of the temperature sensors relative to the portion of the electrode in contact with tissue. Thus, the orientation of the electrode and its temperature sensors determines the appropriate target temperature required to create maximal lesions while avoiding coagulum formation caused by overheating at any location within the electrode-tissue interface.

Electrode Material

Although platinum-iridium electrodes have been the standard for most RF ablation catheters, gold exhibits excellent electrical conductive properties, as well as a more than four times greater thermal conductivity than platinum (300 vs. 70 W/m K), although both materials have similar heat capacities (130 and 135 J/kg K). The higher thermal conductivity of gold can potentially lead to a higher mean rate of power delivery because of better heat conduction at the tissue-electrode interface and to enhanced cooling as a result of heat loss to the surrounding blood

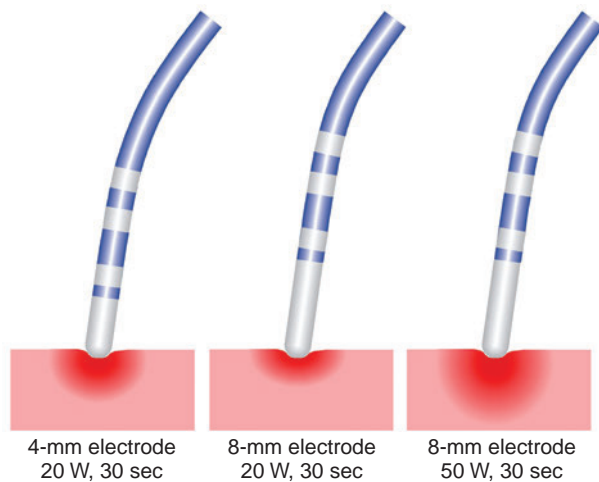


Fig. 7.6 Effect of Electrode Size and Power Delivery on Lesion Size. Representative blocks of myocardium are shown with lesions (dark shading) resulting from optimal radiofrequency energy delivery for each electrode type. The effect of 20 W delivered for 30 seconds is shown for a 4-mm electrode (left) and an 8-mm electrode (center). The larger electrode dissipates more of the energy into the blood pool and thus paradoxically creates a smaller lesion. Because of electrode cooling from its larger surface area, the same 8-mm electrode can deliver more power than the 4-mm electrode and could create a larger lesion (right).

with this electrode material. Therefore gold electrodes allow for greater power delivery to create deeper lesions at a given electrode temperature without impedance increases. Enhanced electrode cooling allows for more RF power to be applied at constant temperature, before the temperature limit is reached or before the impedance of the electrode rises. However, the higher thermal conductivity of gold electrodes is no longer an advantage in areas of low blood flow (e.g., between myocardial trabeculae), where convective cooling at the electrode tip is minimal. Under these circumstances, electrode materials with a low thermal conductivity can produce larger lesions.¹⁷

Conflicting results were observed in clinical studies comparing 8-mm gold-tip with platinum-iridium-tip catheters for ablation of the cavotricuspid isthmus (CTI). During catheter ablation of the slow AVN pathway in patients with atrioventricular nodal reentry tachycardia (AVNRT), no significant differences were observed between 4-mm gold-tip and platinum-iridium-tip catheters in the primary endpoint or in the increases of power or temperature at any of the measured time points. However, ablation with gold electrodes seemed to be safe and well tolerated and specifically did not increase the risk of AV block. Interestingly, a significant reduction of charring on gold tips was observed, compared with platinum-iridium material, a finding suggesting a possible advantage of this material beyond its better conduction properties.

An irrigated gold-tip ablation catheter was recently tested and found to allow for improved energy delivery at lower catheter-tip temperatures and at lower irrigation flow rate compared to irrigated platinum-iridium-tip catheters.^{17,18}

Reference Patch Electrode Location and Size

The RF current path and skin reference electrode interface present significant impedance for the ablation current flow, thereby dissipating part of the power. Increasing patch size (or using two patches) and optimizing skin contact reduce electrical impedance at skin-patch interface (and minimize power dissipation) and provide for increased heating at the electrode-endocardium interface and thus increase ablation efficiency and increase lesion size. On the other hand, the position of the dispersive electrode (on the patient's back or thigh) has little effect on the size of the resulting lesion.

Convective Cooling

The ablation electrode temperature is dependent on the opposing effects of heating from the tissue and cooling by the blood flowing around the electrode. Because ablation lesion size is primarily dependent on the RF power delivered to the tissue, lesion size varies with the magnitude of convective cooling of the ablation electrode. Electrode cooling can be achieved passively (by local blood flow) or actively (by electrode irrigation).

At any given electrode temperature, the RF power delivered to the tissue is significantly reduced in areas of low local blood flow (e.g., deep pouch in the CTI, dilated and poorly contracting atria, between myocardial trabeculae). The reduced cooling associated with low blood flow causes the electrode to reach the target temperature at lower power levels, and if the ablation lesion is temperature-controlled, power delivery will be limited. In these locations, increasing electrode temperature to 65°C or 70°C only minimally increases RF power but it does increase the risk of thrombus formation and impedance rise. Conversely, increasing local blood flow is associated with increased convective cooling of the ablation electrode. Passive electrode cooling can be promoted by using large electrode length or electrode material with high thermal conductivity. Convective cooling can also be achieved by internal or external saline irrigation of the ablation electrode.

With enhanced convective cooling, more power is delivered to the tissue to reach and maintain target temperature, thus resulting in larger

lesion volumes. However, when RF power output is limited, increased convective cooling curtails tissue heating due to increased heat loss into the blood pool. Therefore at any given power output (with no temperature restriction), RF lesion size decreases with increasing convective cooling. Conversely, at any given electrode temperature (with no power restriction), RF lesion size increases with increasing convective cooling.

Radiofrequency System Polarity

Most RF lesions are created by applying energy in a unipolar fashion between an ablating electrode touching the myocardium and a grounded reference patch electrode placed externally on the skin. Bipolar energy delivery produces larger lesions than unipolar delivery. In general, the unipolar configuration creates a highly localized lesion, with the least amount of surface injury (i.e., narrower but deeper lesions), while bipolar RF ablation produces longer but shallower lesions.

Electrode Flexibility

An irrigated catheter with a flexible tip design (Cool Flex, St. Jude Medical) allows the ablation tip to flex and provide more uniform distribution of force and a larger, more stable tissue-contact (nonperpendicular orientations) in beating hearts, regardless of catheter orientation relative to targeted tissue (eFig. 7.3). This design also enhances cooling of the catheter-tissue interface through open irrigation with numerous slits that are uniformly spread throughout the electrode for radial cooling, which also creates preferential flow toward the tissue when the catheter tip is flexed, as in a drag lesion. Four additional ports are built into the distal tip for cooling of the target tissue when the catheter is in a perpendicular orientation.¹⁹

In one report, the Cool Flex flexible-tip catheter was associated with larger ablation lesions at similar depths compared to the rigid-tip catheter. This was mainly related to enhanced cooling of the catheter tip-tissue interface which allowed more power delivery to targeted tissue, especially in nonperpendicular catheter orientation which would also result in a larger contact area during RF applications with the flexible tip. The performance of the rigid-tip catheter seemed to be significantly affected by catheter orientation which was not the case with the flexible-tip catheter.¹⁹

Monitoring Radiofrequency Lesion Formation

The goal of optimizing RF ablation is to create an adequate-sized lesion while minimizing the chance of coagulum formation at the electrode itself and steam formation within the tissue. As discussed previously, for ablation to be effective, RF power must be increased sufficiently to achieve temperatures substantially higher than 50°C at the tissue directly in contact with the ablating electrode in order to achieve tissue necrosis. At the same time, for ablation to be safe, the highest tissue temperature must be maintained at less than 100°C to prevent steam pops and coagulum formation. Monitoring of RF energy delivery is therefore very important to help achieve successful as well as safe ablation.

RF lesion creation is influenced by many factors, some of which can be controlled, whereas others are variable and can be unpredictable. With standard RF ablation, power delivery is titrated to electrode temperature, typically at 55°C to 65°C. Higher temperatures can increase the chance of reaching 100°C at edges of the ablation electrode (away from the temperature sensor), thus resulting in coagulum formation. An increase in tissue temperature is accompanied by a decrease in impedance, also a reliable marker of tissue heating. Impedance reduction and temperature rise correlate with both lesion width and depth; maximum temperature rise is best correlated with lesion width, and maximum impedance reduction is best correlated with lesion depth.

The efficiency of tissue heating (i.e., the temperature per watt of applied power) is dependent on several variables, including catheter



eFig. 7.3 Ablation Catheter With a Flexible Tip Design. Cool Flex irrigated-tip ablation catheter. (Courtesy St. Jude Medical, Minneapolis, MN, United States.)

stability, electrode-tissue contact pressure, electrode orientation relative to the endocardium, effective electrode contact area, convective heat loss into the blood pool, and target location. Thus, applied energy, power, and current are poor indicators of the extent of lesion formation, and the actual electrode-tissue interface temperature remains the only predictor of the actual lesion size. Currently, although less than ideal, monitoring temperature and impedance are used to help ensure adequate but not excessive heating at the electrode-tissue interface. Newer technologies may be implemented in the future to monitor tissue temperatures during RF delivery, including infrared sensors and ultrasound transducers.

Impedance Monitoring

The magnitude of the current delivered by the RF generator used in ablation is largely determined by the impedance between the ablation catheter and the dispersive electrode. This impedance is influenced by several factors, including intrinsic tissue properties, catheter contact pressure, catheter electrode size, dispersive electrode size, presence of coagulum, and body surface area. Impedance measurement does not require any specific catheter-based sensor circuitry and can be performed with any catheter designed for RF ablation.²⁰

As tissue temperature rises during RF energy application, ions within the tissue being heated become more mobile, resulting in a decrease in impedance to current flow. Hence a drop in impedance resulting from RF ablation can serve as a real-time marker of tissue heating. Although the impedance drop during RF ablation occurs mainly because of a reversible phenomenon, rather than from an irreversible myocardial tissue damage secondary to ablation, lesion diameter and depth have been shown to correlate well with impedance decrease, with an even more direct relationship than measured temperature.²¹

Typically, the impedance associated with firm catheter contact (before tissue heating has occurred) is 90 to 120 Ω . When catheter contact is poor, the initial impedance is 20% to 50% less, because of the lower resistivity of blood. Moreover, larger electrodes have larger contact area and consequently lower impedance. A 5- to 10- Ω reduction in impedance is usually observed in clinically successful RF applications, it correlates with a tissue temperature of 55°C to 60°C, and it is rarely associated with coagulum formation. Larger decrements in impedance reflect excessive tissue heating and are noted when coagulum formation is imminent. Once a coagulum is formed, an abrupt rise in impedance to more than 250 Ω is usually observed.²⁰

To titrate RF energy using impedance monitoring alone, the initial power output is set at 20 to 30 W and is then gradually increased to target a 5- to 10- Ω decrement in impedance. When target impedance is reached, power output should be manually adjusted throughout the RF application to maintain the impedance in the target range. A larger decrement of impedance should prompt reduction in power output. Lack of impedance drop during RF energy application can reflect inefficient energy delivery to the tissue due to poor catheter-tissue or catheter instability, and should prompt catheter repositioning and verification of adequate tissue contact.

The drop in impedance as a monitoring tool has several limitations. When blood flow rates are low, blood can also be heated, and electrode impedance drops accordingly. Moreover, a large rise in tissue temperature at a small contact area and a smaller rise with better tissue contact can result in a similar drop in impedance. Inversely, similar tissue heating with different tissue contact can result in a different change in impedance. In addition, resistive heating nearby is fast, whereas conductive heating to deeper layers is relatively slow. The former, at close distance, has a much greater effect on impedance than the latter, which occurs at greater distance. Therefore the drop in impedance during RF

application is not a reliable parameter for estimating deep tissue heating and lesion growth.

Although coagulum formation is usually accompanied by an abrupt rise in impedance, the absence of impedance rise during ablation does not guarantee the absence of coagulum formation on the tissue contact site, which can unnoticeably be created on the tissue surface rather than on the ablation electrode. In addition, with large ablation electrodes, formation of blood clots may only minimally affect electrode impedance by covering a much smaller part of the electrode surface. Any increase in impedance during RF application can, however, indicate the beginning of coagulum formation or unintended catheter movement; in either case, RF application is discontinued.

Electrode Temperature Monitoring

Temperature monitoring utilizes dedicated sensors within the catheter tip. Two types of sensors are available: thermistor and thermocouple. No catheter or thermometry technology has been demonstrated to be superior in clinical use. Conventional electrode catheters with temperature monitoring report the temperature only from the center of the electrode mass with one design or from the apex of the tip of the catheter with another design, and it is likely that the measured temperature underestimates the peak tissue temperature. Therefore it is best if target temperatures no higher than 70°C are selected in the clinical setting.

Monitoring of catheter tip temperature and closed-loop control of power output are useful to accomplish effective heating at the target area while avoiding excessive heating at the tissue surface that can lead to coagulum formation. However, catheter tip temperature is influenced by cooling effects and electrode-tissue contact and, thus, correlates poorly with lesion size. Tissue temperature can be markedly higher than catheter tip temperature; a higher target temperature can increase the incidence of tissue overheating associated with coagulum formation and steam pops. High-flow areas are associated with more efficient cooling of the ablation electrode; hence, more RF power is delivered to the tissue to reach target temperature, thus resulting in relatively large lesions and vice versa.

The discrepancy between monitored electrode temperature and tissue temperature is significantly exaggerated by active cooling of the ablation electrode. The thermal effects on the electrode temperature are dependent on electrode heating from the tissue, internal cooling by the irrigation fluid, and external cooling from blood flow or open irrigation. With high irrigation flow rates, catheter tip temperature is no longer representative of tissue temperature, and therefore feedback cannot be used to guide power output. The difference between the electrode temperature and tissue-electrode interface temperature is greater with the closed-loop electrode than with the open-irrigation electrode. The discrepancy is likely to be increased in areas of high blood flow, by increasing the irrigation flow rate, or by cooling the irrigant. Saline-irrigated catheters result in peak tissue heating several millimeters from the electrode-tissue interface. Because maximum tissue heating does not occur at the electrode-tissue interface, the value of temperature and impedance monitoring is limited with this type of catheter.

Therefore monitoring lesion formation and optimizing power delivery during cooled RF ablation remain challenging. Appropriate energy titration is important to allow greater power application and to produce large lesions while avoiding overheating of tissue with steam formation leading to pops. Moreover, the inability to assess tissue heating, and hence to titrate power to an objective endpoint, prevents the operator from determining whether unsuccessful applications are caused by inadequate mapping or inadequate heating. In general, temperatures exceeding 42°C to 45°C with power greater than 30 W during open-irrigation RF ablation can be associated with a greater risk of steam

pops and impedance rises, particularly during long RF applications, exceeding 60 seconds. Steam pops are often, but not always, audible. A sudden decrease in temperature, sudden catheter movement (as a consequence of the pop blowing the catheter out of position), and a sudden change in impedance are all potential indications that a pop has occurred.

Electrophysiological Effects of Ablation

In addition to impedance and catheter tip temperature monitoring, effects of tissue heating on recorded electrograms or the arrhythmia are important indicators for monitoring lesion formation. Interruption of tachycardia (VT, atrial flutter [AFL], supraventricular tachycardia) or block in conduction over a pathway (AVN or BT) during the process of ablation provide immediate feedback about the disruption of tissue integrity. In addition, an increase in pacing threshold and a decrease in electrogram amplitude can indicate tissue damage. These factors, however, are not easily monitored during the RF application, particularly the change in pacing threshold. Moreover, the decrease in electrogram amplitude is often not visible during RF application because of superimposed electrical artifact.²²

Of note, reductions in amplitude and steepness of the local electrogram as indicators of tissue heating apply only to the unipolar distal electrogram. With a bipolar recording, the signal from the ring electrode may dominate the electrogram, and the bipolar amplitude can theoretically even rise during ablation because of a greater difference between the signals from both electrodes.

Tissue Temperature Monitoring

Technologies to directly measure tissue temperature during RF ablation (which is the primary determinant of lesion formation) are currently not available for clinical use. Novel technologies are being evaluated, including microwave radiometry, near-field ultrasound thermal strain imaging, and magnetic resonance thermometry.

Direct monitoring of tissue temperature enables titration of RF power output, duration of energy application, and active cooling to optimize lesion formation. Maintaining temperatures during ablation in a “safe and effective” zone (50°C to 80°C) helps achieve adequate RF lesion and prevent steam pops.¹³

Titration of Standard Radiofrequency Energy

Monitoring catheter tip temperature and closed-loop control of power output are useful to accomplish effective heating at the target area while avoiding excessive heating at the tissue surface that can lead to coagulum formation. However, catheter tip temperature is influenced by cooling effects and electrode-tissue contact and, thus, correlates poorly with lesion size.

Titration of RF energy using temperature monitoring is usually done automatically by a closed-loop temperature monitoring system. When manual power titration is directed by temperature monitoring, the power initially is set to 20 to 30 W and then is gradually increased until the target temperature is achieved. With both manual and automatic power titration, a change in power output is frequently required throughout the RF application to maintain the target temperature. Application of RF energy is continued if the desired clinical effect is observed within 5 to 10 seconds after the target temperature or impedance is achieved. If the desired endpoint does not occur within this time, the failed application is probably because of inadequate mapping. If the target temperature or impedance is not achieved with maximum generator output within 20 seconds (the time it takes to achieve sub-endocardial steady-state temperature), the RF application can be terminated, and catheter adjustment should be considered to obtain better tissue contact.

The target ablation electrode temperature varies according to the arrhythmia substrate. For AVNRT, target temperature is usually 50°C to 55°C. For BT, AV junction, AT, and VT, higher temperatures (55°C to 60°C) are usually targeted.

When using 4-mm-tip catheters, the target temperature should be lower than 80°C. In high-flow areas in the heart, the disparity between tip temperature and tissue temperature is large and a lower cutoff temperature (e.g., 60°C) should be considered. Conversely, in low flow areas tissue temperature is much better reflected by tip temperature and a higher target temperature can be considered (e.g., 70°C to 80°C). The duration of RF application is usually limited to 30 to 60 seconds for nonirrigated 4-mm-tip electrodes. The lesion is predominantly formed within the first 30 seconds. A longer duration does not create larger lesions.

When using 8-mm-tip catheters, a larger portion of the ablation electrode is exposed to the blood and thus cooled by blood flow, and a relatively large difference between catheter tip temperature and tissue temperature can be expected. Consequently, a moderate target temperature (e.g., 60°C) should be chosen; the RF power may be limited to 50 to 60 W to avoid tissue overheating and coagulum formation.

It is important to recognize that prevention of coagulum formation is difficult, even with temperature and impedance monitoring. The clot first adheres to the tissue because that is the site with the highest temperature and may only loosely attach to the cooler electrode. The denatured proteins probably have higher electrical impedance than blood, but the contact area with the electrode can be small, and RF impedance may not rise noticeably. The absence of flow inside the coagulum and its presumed higher impedance accelerate local heating and, because of some contact with the electrode, also accelerate heating of the electrode. Desiccation and adherence to the electrode then lead to coagulum formation on the metal electrode and impedance rise. Automatic power reduction by temperature-controlled RF ablation compensates for the reduction of electrode cooling and may prevent desiccation and impedance rise. The coagulum, however, can still be formed as demonstrated by experimental *in vivo* studies, and this can remain unnoticeable until it detaches from the tissue. Therefore the absence of thermal and electrical phenomena does not imply that the ablation has been performed safely.

Titration of Cooled Radiofrequency Energy

Active cooling of the ablation electrodes makes lesion formation more difficult to monitor and control. As noted, the discrepancy between monitored electrode temperature and tissue temperature is significantly exaggerated by active electrode cooling; as a result, electrode temperature is no longer a reliable predictor of lesion formation. Several other indicators of tissue heating can be monitored, including impedance and EP effects of ablation. Adjustment of RF power output, duration of RF application, and irrigant flow rate help modulate lesion formation.

The most easily controllable factors are the power output and duration of RF application. Although the optimal method for adjusting power during saline-irrigated RF ablation is not yet clearly defined, some useful guidelines have emerged. The most commonly recommended approach is to perform ablation in a power-controlled mode, typically starting at 20 to 30 W and gradually increasing power to achieve evidence of tissue heating or damage. An impedance fall likely indicates tissue heating, similar to that observed with conventional RF ablation. When catheter temperature is between 28°C and 31°C, power can be ramped up, watching for a 5- to 10- Ω impedance fall. Measured electrode temperature will generally increase, and electrode temperatures of 37°C to 40°C are commonly achieved. Power levels typically used during open-irrigation ablation depend on the site of ablation: 25 to

30 W in the left and right atrial free wall, 35 to 40 W for CTI and mitral isthmus ablation, 50 W in the LV, and 20 W in the coronary sinus (CS).

Also, instead of increasing the power (which increases the likelihood of steam pops) to achieve the desired EP effect, the duration of energy application may be increased. A moderate power of 20 to 35 W with a relatively long RF duration of 60 to 300 seconds may be considered to achieve relatively large lesions, with a limited risk of crater formation.

The flow rate of the irrigant determines the degree of cooling. Faster flow rates likely allow greater power application without impedance rises, increase the difference between tissue and electrode temperature, and thereby potentially increase the risk of steam pops if temperature is used to guide ablation. With the internally irrigated ablation system, the approved flow rate is fixed at 36 mL/min and is not currently manipulated. With the externally irrigated ablation system, an irrigation flow rate of 10 to 17 mL/min during RF application (and 2 mL/min during all other times to maintain patency of the pores in the electrode) may be selected in a power-controlled mode with a delivered power of up to 30 W. The irrigation flow rate should be increased to 20 to 30 mL/min with delivery of more than 30 W, to avoid excessive heating of the superficial tissue layers. Using a lower irrigation flow rate (10 mL/min) in the left atrium (LA) can help maintain some temperature feedback, with a cutoff temperature of 43°C. The temperature is usually set at 40°C to 45°C. If the temperature at the tip is lower than 40°C, the flow rate may be reduced. If the desired power is not met because the target temperature is reached at a lower power, the irrigation flow rate may be increased to a maximum of 60 mL/min. Parameters for epicardial ablation are similar to those used for endocardial ablation. New catheter designs employing lower irrigation flow rates (e.g., ThermoCool SF, Biosense Webster), in order to maintain adequate electrode cooling but with less total fluid load during long procedures, are also available.

In addition, the temperature of the irrigant can be manipulated. Cooling the irrigant can potentially allow power delivery to be increased without coagulum formation. However, the cooled irrigant is warmed as it passes through the tubing to reach the catheter and through the length of the catheter, and the impact of cooling the irrigant has not been well studied. In most studies, the irrigant that enters the catheter is at room temperature.

Temperatures exceeding 42°C to 45°C with power greater than 30 W during open-irrigation RF ablation can be associated with a greater risk of steam pops and impedance rises, particularly during long RF applications, exceeding 60 seconds. Steam pops are often, but not always, audible. A sudden decrease in temperature, a sudden catheter movement (as a consequence of the pop blowing the catheter out of position), and a sudden change in impedance are all potential indications that a pop has occurred. Whether the catheter is maintained in a stable position, as opposed to dragging it across the tissue during linear ablation, also likely influences tissue heating. High power can be applied continuously during dragging with little risk of excessive heating, although the duration of time to spend at each site to create an effective lesion may be difficult to ascertain. As a rule, the lowest effective power setting, shortest duration, and fewest applications should be employed whenever possible.

During open-irrigation RF ablation, initiation of irrigation results in a drop of electrode temperature by several degrees. Failure of electrode temperature to decrease indicates a lack of irrigant flow. When power delivery begins, catheter tip temperature should rise to 36°C to 42°C (the presence of rising temperature, not the magnitude, reflects tissue heating). Temperatures higher than 40°C achieved with low power (less than 20 W) can indicate that the electrode is in a location with

little or no cooling from the surrounding circulating blood, or that there is a failure of the catheter cooling system that requires attention. In contrast, the absence of any increase in tip temperature should raise the possibility of poor catheter contact.

With the internally irrigated system, the room temperature irrigant flowing at 36 mL/min typically cools the measured electrode temperature to 28°C to 30°C. During RF application, the electrode temperature increases; temperatures of 50°C can indicate that cooling is inadequate or has stopped, which warrants termination of RF application. The measured impedance typically decreases during cooled RF ablation by 5 to 10 Ω , in a manner similar to that observed during standard RF ablation.

Optimizing Catheter-Tissue Contact

Optimizing catheter-tissue contact and minimizing catheter motion are critical for achieving safe and effective lesion formation. Poor or unstable contact leads to ineffective tissue heating and lesion formation as well as potential collateral injury to adjacent structures. Suboptimal contact can also result in partially successful ablation lesions, which can transiently interrupt the arrhythmia or eliminate its inducibility but without permanent destruction of the arrhythmogenic substrate. This outcome hinders further mapping and ablation efforts and predicts higher risk of arrhythmia recurrence. In addition, repetitive RF applications with inconsistent contact can result in tissue edema that can prevent effective lesion formation during later RF energy applications (even with optimized tissue contact). Therefore stable catheter contact should be ensured before each and every ablation lesion.²³

On the other hand, excess catheter pressure against the cardiac wall during RF ablation can cause tissue compression and thinning and, as a result, increase the risk of steam pop and cardiac perforation. Excessive contact force can also result in stretching and potential disruption of the chamber wall, even without RF ablation. Tenting of the chamber wall can potentially bring the tip of the ablation catheter in closer proximity to adjacent extracardiac structures (e.g., esophagus, phrenic nerve), increasing the risk of collateral damage during RF ablation.¹⁶

Several methods to both optimize catheter contact and minimize catheter motion have been developed. General anesthesia and high-frequency jet ventilation have been used to optimize catheter stability and minimize the degree of respiratory effects on catheter contact during AF ablation. In addition, the use of steerable sheaths facilitates achieving stable and firm tissue contact, at least partly by increasing the column rigidity of the catheter-sheath combination. Furthermore, several approaches have been employed to ensure adequate catheter-tissue contact during RF ablation (Table 7.2). Most of those approaches utilize indirect measures that represent imperfect surrogate of catheter-tissue contact. In addition, while those methods can potentially suggest inadequate tissue contact, they are far less reliable in estimating the force applied by the catheter tip on the chamber wall. More recently, real-time measurement of tissue contact and contact force has become available in several irrigated ablation catheters, and can potentially improve RF ablation efficacy and safety.¹⁶

Record Electrograms

Local electrogram characteristics (sharp, near-field electrogram vs. far-field electrogram), beat-to-beat stability of recorded electrograms, and pacing capture threshold provide some information about tissue contact. However, electrograms only provide transient contact information and have been shown to be imprecise in judging contact. Also, assessing contact with abnormal myocardial tissue (e.g., infarct scar) can be difficult, since local electrograms are frequently low amplitude and local capture may not be achievable.^{16,20,23}

TABLE 7.2 Strategies to Optimize Electrode-Tissue Contact and Stability

Recorded electrograms	Local electrogram demonstrating sharp, near-field signals with beat-to-beat stability and low pacing capture threshold
Fluoroscopy	Catheter shaft and tip move congruent to chamber wall movement
Tactile feedback	Tactile sensation by operator can provide some feedback regarding catheter contact to chamber wall, resistance of catheter advancement, as well as movement with cardiac wall
Intracardiac echocardiography	Visualization of the catheter tip in contact with tissue
Temperature monitoring	Increased electrode-tissue contact results in higher tissue temperatures, and the plateau is achieved later
Impedance monitoring	Firm tissue contact is modestly correlated with increased initial impedance levels and a larger initial drop of impedance during RF application
Contact force monitoring	Maintaining adequate contact can be guided by contact force sensors
Electrogram-gated pulsed RF delivery	Gating pulsed RF power delivery to recorded electrogram can potentially compensate for cardiac motion
Steerable sheaths	Using steerable sheaths facilitates achieving stable and firm tissue contact

RF, Radiofrequency.

Fluoroscopy

Fluoroscopy can be useful to assess contact by monitoring catheter shaft and tip movement relative to the heart. However, utilization of fluoroscopy for this purpose significantly increases radiation exposure to both the patient and operator. In addition, fluoroscopic monitoring is difficult to titrate and is not helpful for avoiding the application of excess catheter pressure against the cardiac wall.²³

Tactile Feedback

Tactile feedback is often used as an indirect surrogate to catheter contact to the chamber wall. Tactile feedback, however, is subjective, a function of the operator's experience, and is difficult to titrate. The use of steerable introducer sheaths can help improve catheter stability and contact, but such a technique often dampens the tactile feedback.²⁰

Data suggest that relying on tactile feedback alone is not sufficient, and stronger effort should be made to gather as much information as possible about contact from as many different sensing modalities as possible. Furthermore, the use of three-dimensional (3-D) mapping systems alone, without the aid of fluoroscopy, to supplement tactile feedback may not be adequate.²⁴

Intracardiac Echocardiography

Visualization of the catheter tip with ICE can help confirm tissue contact. However, catheter visualization with ICE at all endocardial locations and throughout the cardiac cycle usually is not feasible.

Temperature Monitoring

During RF energy delivery, increased electrode-tissue contact results in higher tissue temperatures, and the plateau is achieved later. Thus, failure of electrode temperature to increase despite high RF energy output suggests poor tissue contact. Nevertheless, several factors can cause discrepancies between the real tissue temperature and the catheter tip temperature, including catheter tip orientation, cooling effect of blood flow, and electrode irrigation.

Impedance Monitoring

Baseline electrode impedance and changes in electrode temperature and impedance during RF application provide information regarding the degree of electrode-tissue contact. Higher baseline impedance with greater contact is thought to be due to increasing the electrode-tissue interface area and reducing the interface area between the electrode and the low-resistivity blood pool. In animal studies, firm tissue contact was associated with increased baseline impedance levels (by a mean of 22%), and a larger initial drop of impedance (within the first 20 seconds of RF application).^{20,14} However, clinical studies using real-time contact force measurements showed that impedance measurements (both

baseline levels and subsequent impedance fall) have poor to modest efficacy as surrogate markers for catheter-tissue contact force and, hence, may not be useful in predicting catheter-tissue contact force in humans.^{25,26}

Electroanatomical Catheter Localization

Modern electroanatomic mapping systems enable the creation of a virtual anatomical intracardiac geometry by moving the catheter in all directions throughout the cardiac chamber of interest. Points at outermost boundaries are used to depict the outer geometry (shell), while points inside to the outer shell are automatically removed. Also, pre-acquired cardiac magnetic resonance or computed tomography (CT) images and intraprocedural ICE images can be registered on the real-time 3-D electroanatomic maps. Those systems also estimate the proximity of the ablation electrode to the virtual shell.

However, anatomical distortion and expansion of the virtual image are common due to the inconsistent contact force on the catheter tip during the process geometry creation. Therefore the 3-D anatomical geometries generated by different mapping methods are not reliable to establish catheter tip-tissue contact. Of note, studies evaluating the fidelity of those technologies in AF ablation procedures have showed that the 3-D ICE-derived LA geometric reconstruction is smaller than reconstructions derived from electroanatomic virtual shell and merged 3-D ICE or CT images.^{27–29}

Contact Force Monitoring

Two different designs of open-irrigation ablation catheters have been developed to measure real-time catheter-tissue contact force during catheter mapping and ablation (Fig. 7.7). The first design (ThermoCool SmartTouch CF, Biosense Webster, Diamond Bar, CA, United States) uses a small spring connecting the ablation tip electrode to the catheter shaft, with a magnetic transmitter and location sensors to measure microdeflections of the spring. The second design (TactiCath, Endosense, St. Jude Medical, St. Paul, MN, United States) incorporates a force sensor between the second and third electrode, consisting of a deformable body and three optical fibers to measure microdeformations that correlate with the force applied to the catheter tip.^{14,30–33}

Contact force ablation catheters show promise for improving the outcome of complex catheter ablation procedures. Contact force sensing may also improve the safety of catheter ablation by avoiding excessive contact force and, hence, decreasing the risk of perforation or steam pops. Contact force catheters may also enhance operators' catheter manipulation skills by providing real-time feedback of catheter-tissue contact.¹⁴

Nevertheless, the range of contact forces that are both effective and safe is yet to be determined. Clinical studies suggested that at least 10 g

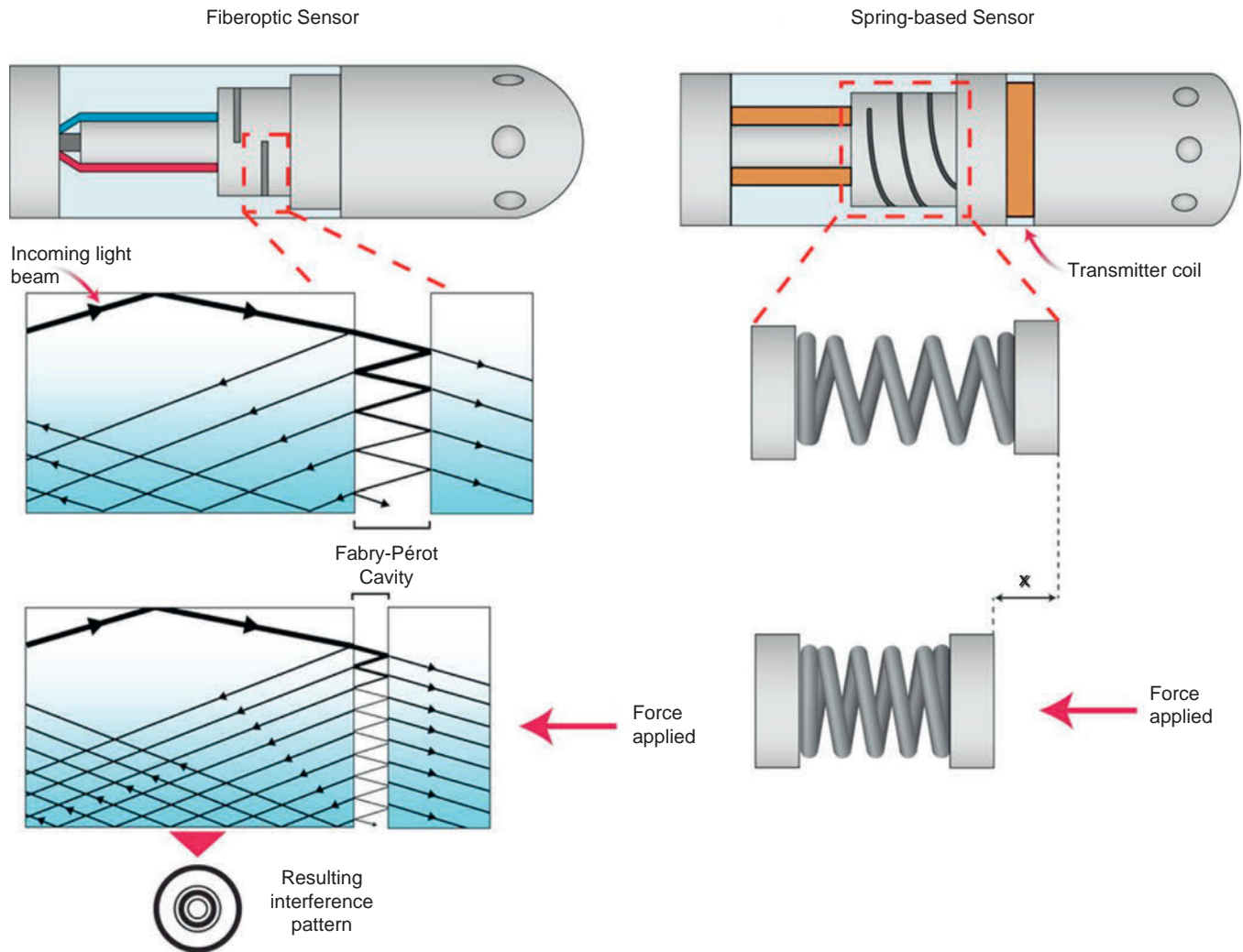


Fig. 7.7 Comparison of Fiberoptic and Spring-Based Contact Force Sensors for Radiofrequency Ablation. Two different technologies are currently used to measure contact force. One catheter uses a sensor based on a Fabry-Pérot interferometer (*left*). Force on the distal catheter tip changes the length of an air cavity, altering the reflection pattern of light shining through two adjacent semireflective mirrors. This changes the interference pattern of the light, and this pattern is transmitted back to the operating system to calculate the contact force. A second catheter uses a spring-based sensor (*right*). Force on the distal tip of the catheter compresses a precision spring. Deflection (x) of the spring is determined by measuring micromovements of a transmitter coil distal to the spring, and the contact force is calculated using the known spring characteristics (k). (From Barnett AS, Bahnson TD, Piccini JP. Recent advances in lesion formation for catheter ablation of atrial fibrillation. *Circ Arrhythm Electrophysiol*. 2016;9:e003299.)

of contact force is required to optimize lesion formation. The average contact force used in these studies was greater than 10 g (range 10 to 40 g). Above 10 g, there is a wide margin of safety.^{31,34,35} Experimental studies showed that, at constant RF power and application time, increasing contact force (2 to 40 g) significantly increased tissue temperature (at depths of 3 to 7 mm) with significant increases in RF lesion depth, diameter, and volume. Lesion size was more dependent on contact force than on power. However, higher contact force is associated with increases in the frequency of steam pop and coagulum formation.¹⁴ On the other hand, in another study, low-force ablation (less than 10 g) resulted in RF ablation lesion size, quality, and transmuralty equivalent to those of high-force ablation (greater than 20 g) in an atrial ablation model. During temperature-controlled RF energy delivery, higher RF power output appeared to compensate for reduced catheter-myocardium energy transfer at low contact force.^{34,36,37}

More recently, a novel automated ablation lesion tagging technology based on catheter stability information (CARTO 3, VisiTag Module, Biosense Webster, Diamond Bar, CA, United States) was developed to provide real-time feedback on catheter stability. This system uses an algorithm for the automated annotation of RF ablation applications based on objective, predefined parameters that incorporates catheter stability range of motion, catheter stability duration, impedance drop, and contact force measured at the catheter tip. Those parameters are recorded and updated 60 times/s throughout each energy application, and ablation tags are displayed accurately on the electroanatomic map on the basis of the locating coordinates of the catheter at each individual stable ablation site (Fig. 7.8). In addition, the tags are color-coded to provide the biophysical information of each individual ablation site. The ideal settings for an effective ablation lesion with this technique, however, have not been confirmed.^{38,39}

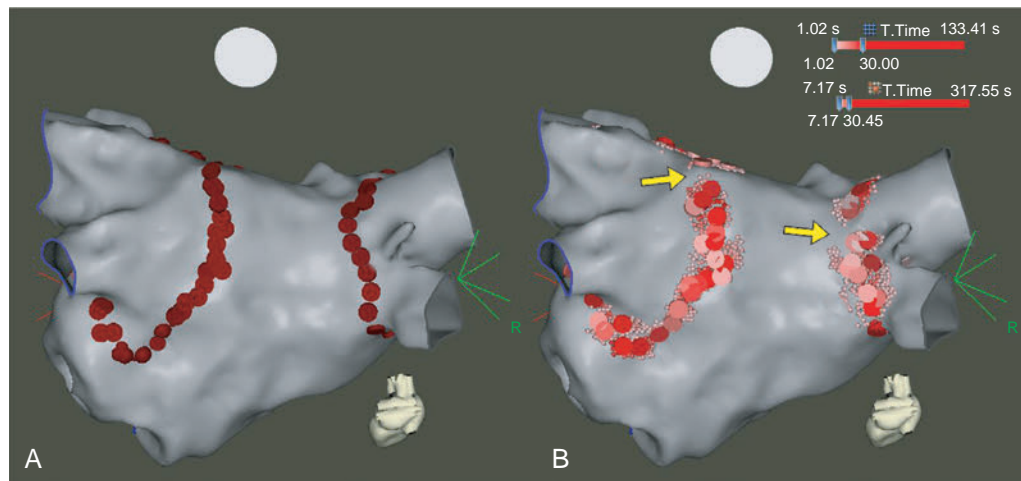


Fig. 7.8 Use of VisiTag Indicators of Tissue Contact During Ablation. The left atrium is shown from a posterior view in a case of circumferential pulmonary vein (PV) isolation for atrial fibrillation. (A) Manually designated standard dark red tags indicate sites of presumed ablation (where energy was delivered, but not necessary where a lesion was made). (B) Automated VisiTag markers indicate duration of catheter tip dwell at each site (*darker shades* = longer contact) and very small dots indicate where the catheter was at any time during radiofrequency energy delivery. No tag will be placed unless at least 20 seconds of consistent contact has been made. Note areas indicated by yellow arrows where VisiTag did not register enough ablation contact/time to warrant a tag, yet the operator believed an adequate lesion had been made. PV isolation was incomplete in both sets of PVs due to ablation gaps in these regions, that were subsequently effectively ablated.

TABLE 7.3 Strategies to Prevent Steam Pops During Cooled Radiofrequency Ablation

Ablation electrode temperature	Limiting electrode temperature to 40°C (for internally irrigated catheters) and 42°C–45°C (for externally irrigated catheters)
RF power output	Limiting RF power output especially in areas with firm tissue contact or thin chamber wall
Impedance monitoring	Titrating power output to prevent rapid or large (>15 Ω) reductions impedance during RF application
Contact force monitoring	Avoiding excessive catheter-tissue contact force
Intracardiac echocardiography	Visualization of microbubbles on ICE has been used as an indication of excessive tissue heating
Tissue temperature monitoring	Microwave radiometer-enabled catheter enables monitoring intramyocardial tissue temperature (investigational)
High-frequency ultrasound transducer	High-frequency ultrasound transducer integrated into the ablation catheter enables visualization of acute lesion formation in real time (investigational)

ICE, Intracardiac echocardiography; RF, radiofrequency.

Another method of trying to ensure atrial transmural lesions during pulmonary vein (PV) isolation is the force-time integral (FTI—St. Jude Medical, Sunnyvale, CA, United States), the product of the average contact force and time over which it was delivered at a given site. Some data suggest that a FTI of less than 400 gs was associated with recovery of venoatrial conduction after PV electrical isolation and thus a target of more than 400 gs appears to be useful. This does not account for the amount of power delivered, nor the contiguity of lesions. Other data suggest that tissue thickness is another variable to consider, and that 100 gs/mm tissue thickness is a more appropriate target. It should be pointed out that none of the methods used to try to ensure adequate ablation have been shown to decrease potential complications (such as collateral damage from too-deep ablation).

Electrogram-Gated Ablation

Even when catheter contact to target tissue appears stable, ablation catheter tip often slides along the cardiac tissue surface during regular heart motion. This lateral sliding motion spread delivered RF energy during a conventional ablation over a larger surface area of endocardium, reducing the efficiency of heating (less heating per unit area of tissue)

and limiting lesion depth. Studies in patients undergoing PV isolation showed that contact force remains highly variable during RF applications in spite of optimizing contact because of the ventricular (rather than atrial) contraction and respiratory movements of the heart.⁴⁰

A recent study described a novel method to compensate for cardiac motion by gating pulsed RF delivery to the sensed local electrogram, whereby RF energy delivery is limited to when the catheter is in contact with the local target (as judged by the quality of local electrogram) as opposed to the remainder of the cardiac cycle when the catheter may be sliding against the underlying myocardium. This method can potentially help improve lesion formation and avoid inappropriate energy delivery to surrounding tissue while the catheter is in motion. Nonetheless, electrogram gating can be difficult when the local electrogram is low amplitude or fractionated, when the electrogram changes in response to RF ablation, and when electric noise develops during energy delivery.⁴¹

Prevention of Steam Pops

Several approaches have been proposed to reduce the incidence of pop formation (Table 7.3).¹³

Ablation Electrode Temperature

For internally cooled catheters, it is recommended to limit electrode temperature to less than 40°C to prevent pop formation. In the setting of open irrigated catheters, however, electrode temperatures have shown to be correlate poorly with steam pop occurrence.

Power Output

Higher RF power output increases the risk of steam pops. However, a safe cut-off output has not been established, and power output limits have to be considered in relation with other factors, such as the degree of electrode cooling, catheter-tissue contact force, and cardiac wall thickness.

Impedance Monitoring

Large drops in impedance (greater than 15 Ω) during RF ablation are associated with increased risk of steam pops. In particular, the rate of impedance drop (greater than 1 Ω /s) appears to be a good predictor of steam pops. Power titration to prevent rapid reductions impedance can help improve safety.

Contact Force Monitoring

Increasing catheter-tissue contact force is associated with increased risk of steam pops, especially at thin target tissues that are not structurally well supported (such as the posterior LA wall). In one report, steam pops occurred with contact force of 40 g or more at RF output of 30 W, but with much lower contact force (10 g) at 50 W.

Intracardiac Echocardiography

Visualization of microbubbles on ICE has been used as an indication of excessive tissue heating that is predictive of char formation and steam pops during ablation and that warrants reduction or termination of RF energy. The presence of microbubbles on ICE is typically associated with a tissue temperature higher than 60°C and increased lesion size, and continued RF application after the appearance of the bubbles is usually followed by an increase in impedance. Of note, steam pops can be seen well on ICE, often with a sudden explosion of echocardiographic contrast.

Microbubble formation, however, is not a straightforward surrogate for tissue heating. The absence of microbubble formation clearly does not indicate that tissue heating is inadequate or that the power level should be increased, nor does the presence of scattered microbubbles indicate safe tissue heating. This marker is fairly specific for tissue heating as judged by tissue temperatures but is not routinely sensitive. Specifically, scattered microbubbles can occur over the entire spectrum of tissue temperatures, whereas dense showers of microbubbles appear only at tissue temperatures higher than 60°C. Scattered microbubbles can represent an electrolytic phenomenon, whereas dense showers of microbubbles suggest steam formation, with associated tissue disruption and impedance rises.

Furthermore, while identification of microbubbles on ICE as an indication of excessive tissue heating can potentially be helpful during ablation with nonirrigated and internally irrigated catheters, external irrigation produces visible bubbles, precluding the use of this method.

Tissue Temperature Monitoring

A novel microwave radiometer-enabled catheter is currently being tested for monitoring intramyocardial tissue temperature. The volume circumscribed by its radiometric antenna encompassed tissue present to a depth of 3 mm, which is the point of highest attained temperature during irrigated RF ablation. "Volumetric" temperature correlated well with tissue temperature measured at 3 mm depth. No steam pops occurred below a volumetric temperature of 89°C, especially when

associated with rapid temperature rise (greater than 1.5°C/s). Therefore limiting temperatures to less than 80°C can potentially prevent steam pop formation.¹³

High-Frequency Ultrasound

Recently, a high-frequency ultrasound transducer integrated into a novel RF ablation catheter enabled visualization of acute lesion formation in real-time. In experimental studies, the integrated near-field ultrasound was able to accurately visualize intramyocardial gas formation, which develops several seconds prior to a rise in tissue impedance measured from the ablation catheter. Therefore ultrasound can potentially detect steam formation prior to a potential pop, and if power delivery is terminated, intramyocardial steam can dissipate within the tissue without venting to the surface. Clinical evaluation is still pending.^{42,43}

Clinical Applications of Standard Radiofrequency Ablation

RF is the most frequently used mode of ablation energy and has become a widely accepted treatment for most atrial and ventricular arrhythmias. Studies have demonstrated the effectiveness of RF current in producing precise and effective lesions. Standard RF ablation catheters have tip electrodes with lengths ranging from 4 mm long and are available in sizes up to 10 mm long.

Nonetheless, several limitations exist, many of which center on how RF creates the tissue lesion. Current flow and energy delivery are critically dependent on a low-impedance electrode-tissue junction, but tissue desiccation, coagulation, and charring around the electrode can result in marked falls in conductivity. Temporal evolution of ablation lesions can potentially alter the immediate postablation substrate, by producing either lesion expansion (mediated in part by secondary myocyte loss from disrupted microcirculation) or lesion regression (resolution of edema and healing).

A major limitation of RF ablation is the relatively small depth of tissue injury produced by this technique. This can be attributed to the precipitous fall-off of direct tissue heating (volume heating) by the RF energy as the distance from the electrode-tissue interface increases. Deeper tissue layers can be ablated by heat conduction from the volume-heated source, but the maximum lesion depth is limited.

Because the success of RF catheter ablation in the clinical setting is sometimes limited by the relatively small size of the lesion, attempts have been made to increase the size of those lesions reliably and safely. One approach is to increase the size and surface area of the electrode. The RF power needs to be increased comparably to achieve a similar current density and temperature at the electrode-tissue interface, and the results are greater depth of volume heating and a larger lesion. In addition, using an electrode material with high thermal conductivity (such as gold) enhances passive cooling of the ablation electrode by the circulating blood pool, allowing for greater power delivery to create deeper lesions. Modifications to the RF energy delivery mechanism, including cooled catheters and pulsed energy, have also helped address some of these limitations. Moreover, investigation into alternative energy sources appears to be more promising, including microwave, ultrasound, laser, and cryoablation.

Delivery of RF energy on the epicardial surface generally requires an irrigated-tip catheter because there is otherwise no passive cooling of the electrode (outside the blood pool) and relatively little power can be delivered without being limited by temperature increases.

Clinical Applications of Cooled Radiofrequency Ablation

Several designs of the number and distribution of the holes around the open-irrigated electrode tip are currently available, aiming to provide

more homogeneous cooling over the tip surface and improve irrigation efficiency. Conventional open-irrigated electrodes have six irrigation holes circumferentially arranged at the distal end of the electrode. Another design adds another set of six ports at the proximal electrode end. A third design (ThermoCool SF, Biosense Webster) has 56 very small holes positioned along the entire distal electrode. A fourth design (Cool Flex, St. Jude Medical) involves laser-cut irrigation slits in a zigzag pattern in addition to four ports at the distal end of the tip.

However, from a clinical perspective, changing the electrode tip design of open-irrigated ablation catheters does not appear to have a significant impact on efficacy (lesion size) or safety.⁴⁴ Nonetheless, high irrigation rates during RF catheter ablation can be disadvantageous for patients with heart failure. Thus, catheter designs employing lower irrigation flow rates (e.g., ThermoCool SF) can be of particular value in these patients.⁴⁵

Potential Advantages of Cooled Radiofrequency Ablation

Excessive tissue surface heating invites coagulum formation and carbonization. These adverse effects can limit the RF lesion formation, thus making it difficult to produce lesions of sufficient depth in scar tissue or thickened ventricular walls. Active cooling of the ablation electrode by saline irrigation can help prevent overheating of the endocardium while allowing sufficient energy delivery to achieve a larger lesion size and depth.

Cooled tip catheters have several advantages. First, they allow the desired power to be delivered independent of local blood flow, and that results in increased lesion size. Second, they reduce the temperature of the ablation electrode as well as the temperature at the tissue interface, especially with the open-irrigation system, and that helps spare the endocardium and reduce the risk of coagulum and charring. Third, when compared with standard 8-mm-tip ablation catheters, a 3.5- to 4-mm irrigated electrode offers higher mapping accuracy while providing comparable ablation lesion size.

Cooled tip catheters are preferred (1) for long linear ablations (in the right or left atrium) and complex atrial arrhythmias (macroreentrant atrial tachycardia or AF), (2) when there is a high probability of encountering thick or trabeculated tissue, (3) for specific areas with low local blood flow (including the CS, particularly CS aneurysms, and pericardial space), (4) when ablating in the arterial circulation (to minimize the likelihood of arterial thromboembolism), and (5) for targets resistant to previous conventional ablation. Clinical trials have found irrigated tip catheters to be more effective than and as safe as conventional catheters for CTI ablation. Irrigated tip catheters also were found to be safe and effective in eliminating BT conduction resistant to conventional catheters, irrespective of the location, and they have been successfully used for PV isolation for treatment of AF. Irrigated tip catheters also

offer an advantage over conventional RF catheters in the case of scar-related VTs, by facilitating creation of larger and deeper lesions that can help eliminate intramyocardial or subepicardial reentrant pathways necessary for the VT circuit.

Internally cooled RF ablation is an attractive choice for use in pericardial ablation because no fluid is infused, and one need not worry about accumulation of pericardial fluid causing cardiac tamponade throughout the ablation procedure, although drainage of irrigant during open-irrigation RF ablation can be managed in this setting.

Potential Risks of Cooled Radiofrequency Ablation

Although creation of larger ablation lesions can improve the efficacy of ablation for some patients, particularly when the targeted arrhythmia originates deep to the endocardium and when large areas require ablation, it is associated with increased risk of damage to tissue outside the target region (Table 7.4). While increasing power delivery and convective cooling can create large lesions, lesion production is somewhat difficult to control. Active electrode cooling does not allow the temperature at the tip to be monitored, and thus some feedback about lesion formation is lost.

These concerns can be more pronounced with internal cooling as compared with open irrigation. Open irrigation cools the electrode and its direct environment, blood, and tissue surface. In contrast, with internal cooling, the main parameter affected by cooling is the temperature of the electrode, which further exaggerates the disparity between electrode and tissue temperatures. There can be minimal cooling of the direct electrode-tissue interface, but only at the true contact site between metal and tissue. A coagulum can also be formed, but it can go unnoticed because it does not adhere to a cool electrode and does not cause an impedance rise.

With open-irrigation catheters, extensive ablation often performed for AF and scar-related VT can result in substantial saline administration. Therefore management of the patient's volume status before, during, and after the procedure is crucial. This is also important during epicardial ablation, in which an obligatory fluid volume enters the pericardial sac and, if not intermittently or continuously evacuated, gradually results in cardiac tamponade. This complication can be prevented by having the side port of the introducer sheath attached to a suction bottle or gravity drain or by intermittent aspiration of accumulated fluid. Internal irrigation, on the other hand, has the advantages that no fluid is infused into the vasculature or pericardial space, and there is no possibility of embolization from the irrigation system.

Phased Radiofrequency Ablation

The phased RF AF ablation catheter family (Medtronic, Minneapolis, MN, United States) consists of three anatomically designed, multielectrode

TABLE 7.4 Comparison of Features of Ablation Electrodes

Feature	4-mm Standard RF	8-mm Standard RF	4-mm Cooled RF (Closed)	4-mm Cooled RF (Open)	6-mm Cryoablation
Electrogram resolution	+++	+	++++	++++	++
Lesion depth	+	+++	+++	+++	++
Lesion surface area	++	++++	++++	++++	+++
Usefulness of temperature monitoring	+++	++	0	0	0
Risk of steam pop	+	++	+++	+++	0
Thrombus risk	++	++++	+++	+	0
Time efficiency of ablation ^a	++	++++	++++	++++	+

^aInverse function of duration of energy application for effective lesion (higher efficiency = best).
0, None; +, least, worst; ++, minimal; +++, moderate; +++, most, best; RF, radiofrequency.

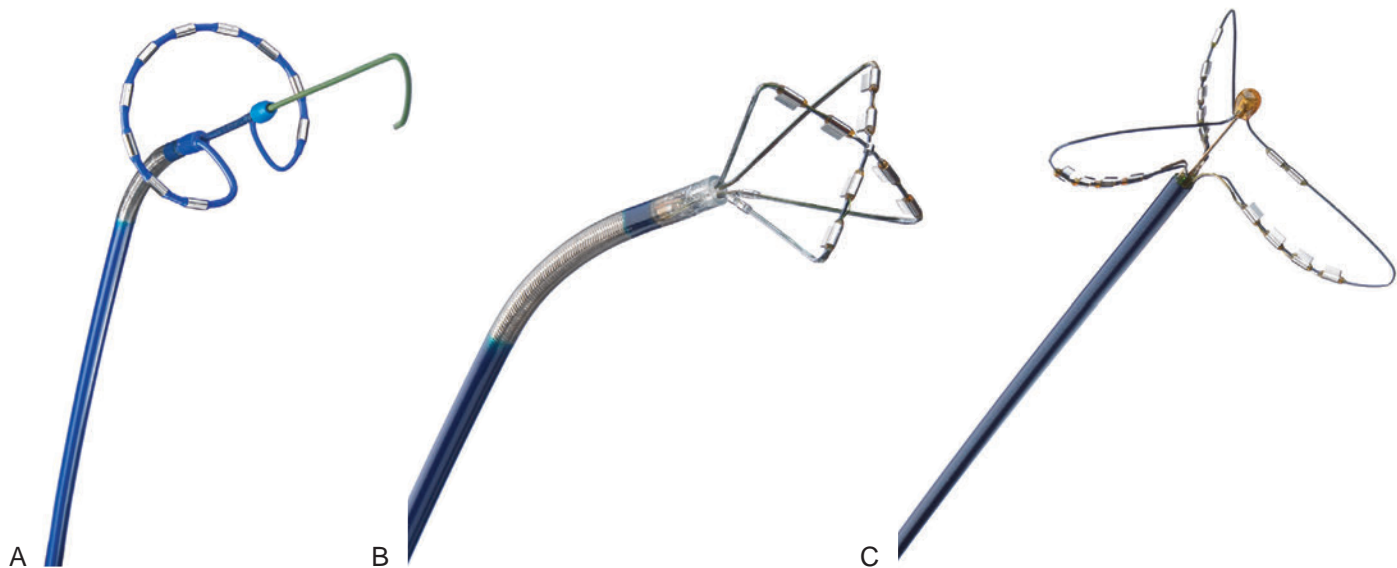


Fig. 7.9 Novel Multipolar Electrode Catheters Using Duty-Cycled Radiofrequency. (A) The Pulmonary Vein Ablation Catheter is a multielectrode catheter used to map, ablate, and verify isolation of the pulmonary veins. (B) The Multi-Array Ablation Catheter is a multielectrode catheter designed to map and ablate complex fractionated atrial electrograms in the left atrial body. (C) The Multi-Array Septal Catheter is a multielectrode catheter designed to map and ablate complex fractionated atrial electrograms along the left atrial septum. (Courtesy Medtronic, Minneapolis, MN, United States.)

catheters that deliver duty-cycled bipolar and unipolar RF energy: (1) the circular-shaped PV ablation catheter (PVAC, 10 platinum or 9 gold electrodes), used to create contiguous lesions in the PV antrum; (2) the Multi-Array Ablation Catheter (MAAC, 8 platinum electrodes), used to create linear lesions in the LA and to target fractionated electrograms; and (3) the Multi-Array Septal Catheter (MASC, 12 platinum electrodes), used to ablate tissue along the interatrial septum (Fig. 7.9). Each platinum electrode has a thermocouple on the side of the electrode in contact with the tissue.^{4-6,33}

A multichannel duty-cycled RF ablation generator (GENius Multi-Channel RF Generator, Medtronic) contains 12 independently controlled RF generators, and is capable of delivering RF energy to each electrode independently. RF energy can be delivered in either bipolar (between contiguous electrodes) or unipolar (from the electrode to the ground pad) current by a phase difference between the channels (Fig. 7.10). When “in phase,” there is no voltage difference and, thus, no current flow between neighboring electrodes, so only unipolar energy is delivered between each electrode and the ground pad. When the voltages for the two adjacent electrodes are “out of phase,” interelectrode voltage difference results in bipolar RF delivery.⁴⁻⁶

Power regulation is achieved through cycling the RF energy on and off (duty-cycled RF), rather than voltage control (see Fig. 7.10). The time period with no RF delivery allows accurate temperature monitoring and provides time for the electrode to cool between RF bursts. Unipolar RF delivery results in deeper lesions, while bipolar application creates shallower but longer and contiguous lesions between electrodes. The generator has five preset energy settings: bipolar, unipolar, and three ratios of bipolar/unipolar energy: 4:1 (80% bipolar, 20% unipolar), 2:1 (66% bipolar, 34% unipolar), and 1:1 (50% bipolar, 50% unipolar). The choice of bipolar-to-unipolar energy delivery ratio is based on desired lesion depths (determined by the unipolar energy ratio) and fill in between adjacent electrodes (determined by bipolar RF ratio). Unipolar RF delivery creates the deepest lesions, followed by 1:1, 2:1,

4:1 and bipolar RF application, with the latter causing the shallowest lesions.

A maximum of 10 W of RF energy is delivered (using a closed-loop power control generator) to individual electrodes in a temperature controlled mode to achieve a target temperature (nominally 60°C). Cooling of the nonirrigated electrodes (in order to deliver sufficient power for lesion generation without producing char or coagulum) is facilitated by the combined effect of energy duty cycling, convective blood flow, and increased temperature accuracy to maintain adequate electrode cooling.⁴⁶ In addition, gold electrodes (for PVAC-Gold catheter) offer more than four times better thermal conductivity than that of platinum, thereby providing faster cooling and more precise temperature control.

One advantage of this approach is the simultaneous application of RF energy across an electrode array, intended to create contiguous lesions near an anatomical structure. In addition, the multielectrode catheters allow selective mapping and ablation through any or all electrodes as required.

The majority of available data relate to PV isolation with the PVAC in patients with paroxysmal AF. The PVAC isolation technique demonstrated high acute procedural success and significantly shorter procedure and fluoroscopy times relative to other AF ablation methods, without the need for a 3-D mapping system. However, initial reports showed an alarmingly high incidence of asymptomatic cerebral embolism when using PVAC (fivefold greater as compared with conventional irrigated RF delivery or cryoballoon for PV isolation).^{4,47,48} This is likely related to electrode overheating, which was predominantly found when electrodes 1 and 10 were in close proximity during ablation (especially bipolar current) and lack of tissue contact. The incidence of manifest and silent cerebral complications has fallen significantly in recent reports, after implementation of aggressive periprocedural anticoagulation regime (uninterrupted anticoagulation with warfarin and activated clotting time greater than 350 seconds), disconnection of either electrode 1 or

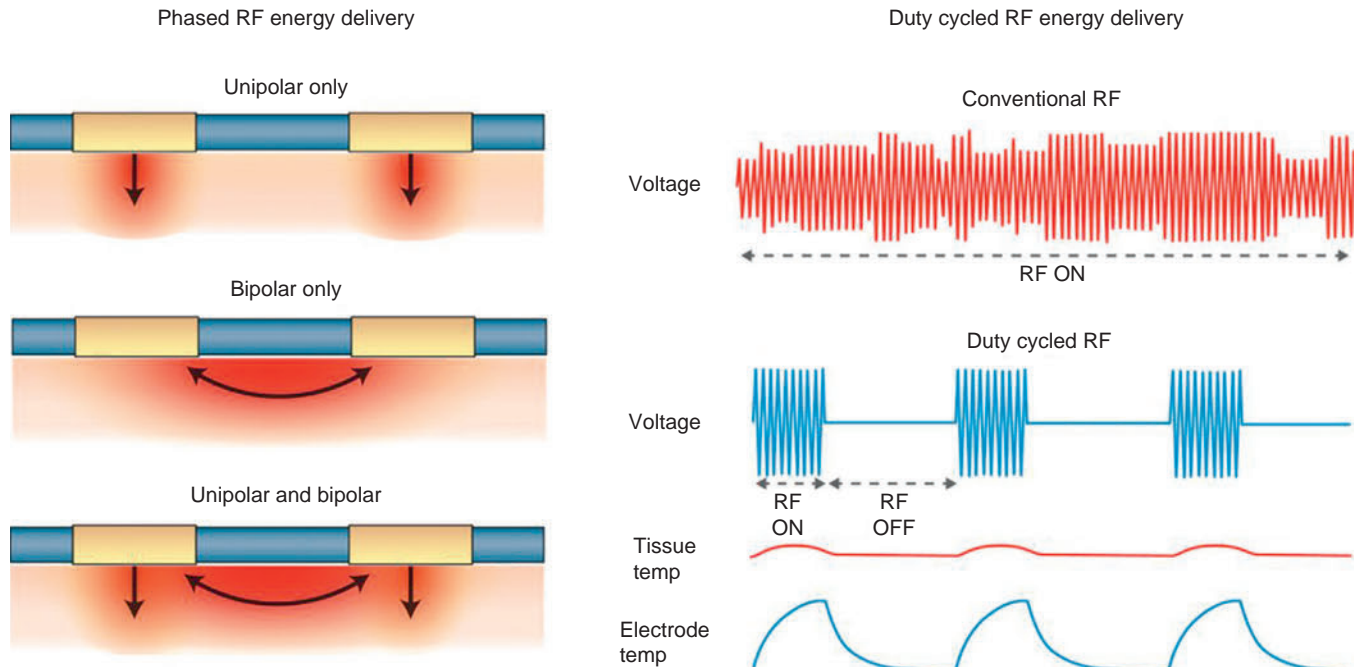


Fig. 7.10 Phased and Duty-Cycled Radiofrequency (RF) Ablation. In phased RF (*left*), energy can be delivered in a unipolar mode, a bipolar mode, or a combination. In the unipolar mode, energy is delivered between the catheter electrodes and a ground electrode on the patient's back, providing lesion depth. In the bipolar mode, energy is delivered between adjacent catheter electrodes, providing lesion continuity. A combination of the two modes can be used to create lesions of varying size. In duty-cycled RF energy delivery (*right*), RF energy is cycled on and off to allow the catheter electrodes to cool without saline irrigation. The length of the "on" time is regulated to reach and maintain the target temperature. The time period with no RF delivery allows accurate temperature monitoring and provides time for the electrode to cool between RF bursts. (From Barnett AS, Bahnson TD, Piccini JP. Recent advances in lesion formation for catheter ablation of atrial fibrillation. *Circ Arrhythm Electrophysiol*. 2016;9:e003299.)

10, and improvements in catheter design and software regulations of the RF generator.^{49–51} More recently, the second-generation phased RF catheter, PVAC Gold, was introduced, which eliminates electrode 10 (to avoid the formation of emboli through the interaction of electrodes 1 and 10) and uses gold electrode material instead of platinum (to improve electrode cooling) (Fig. 7.11).^{4,52,53}

nMARQ Ablation System

The nMARQ catheter (Biosense Webster, Diamond Bar, CA, United States) is a decapolar mapping and ablation catheter with individually irrigated platinum electrodes (3 mm long, with interelectrode spacing of 4 mm). Each electrode possesses a thermocouple and holes for irrigation. The multichannel RF generator (nMARQ, Biosense Webster) is capable of delivering independently unipolar or bipolar RF energy to a maximum of 10 electrodes simultaneously (Fig. 7.12).

RF energy is applied in a temperature-controlled mode and energy delivery can be individually arranged over each combination of the 10 electrodes in unipolar mode (maximum 25 W and 45°C) or bipolar mode between two adjacent electrodes (maximum 15 W and 45°C). During ablation, a continuous flow of heparinized saline fluid is provided by a cooling pump with 60 mL/min for irrigation of all electrodes.^{7–9}

The conceptual advantage of the nMARQ ablation system over the previous multielectrode ablation systems is the presence of irrigation, which theoretically provides the same benefit that it brought to focal RF ablation: lowering the electrode temperature to reduce charring and allow higher power delivery. However, the risk of deep RF lesions and consequent esophageal injury remains a concern. The nMARQ catheter

was recalled from clinical use due to issues with the thermocouple and reporting of three deaths, of which two were confirmed to be due to atrioesophageal fistula.^{54,55}

CRYOABLATION

Biophysics of Cryothermal Energy

If a gas is compressed at high pressure and then is allowed to expand suddenly in region of low pressure, the temperature of the gas decreases. This phenomenon is known as the Joule-Thomson effect. Compression of the gas decreases intermolecular distances and, as a result, the forces of attraction between the molecules become appreciable. During expansion, gas molecules move far away from each other, but energy is required to counteract the intermolecular attraction forces. Heat energy of the molecules of the gas is utilized for this purpose, a process that results in reduction of gas temperature.⁵⁶

For intravascular cryoablation, a precooled, compressed liquid refrigerant (nitrous oxide) is delivered under constant pressure from the console to the tip of the ablation catheter. Cryoablation catheters have a terminal segment with sudden luminal widening (expansion chamber) (Fig. 7.13). In cryoballoon catheters, the balloon acts as the expansion chamber. Decompression and expansion of the liquefied nitrous oxide (accelerated liquid-to-gas phase change) as it passes into the expansion chamber absorbs heat from the surrounding tissue (based on the Joule-Thomson effect), thereby cooling the surface. The vaporized refrigerant then is vacuumed back to the console via a second coaxial return lumen within the shaft of the catheter. Nitrous oxide has a boiling

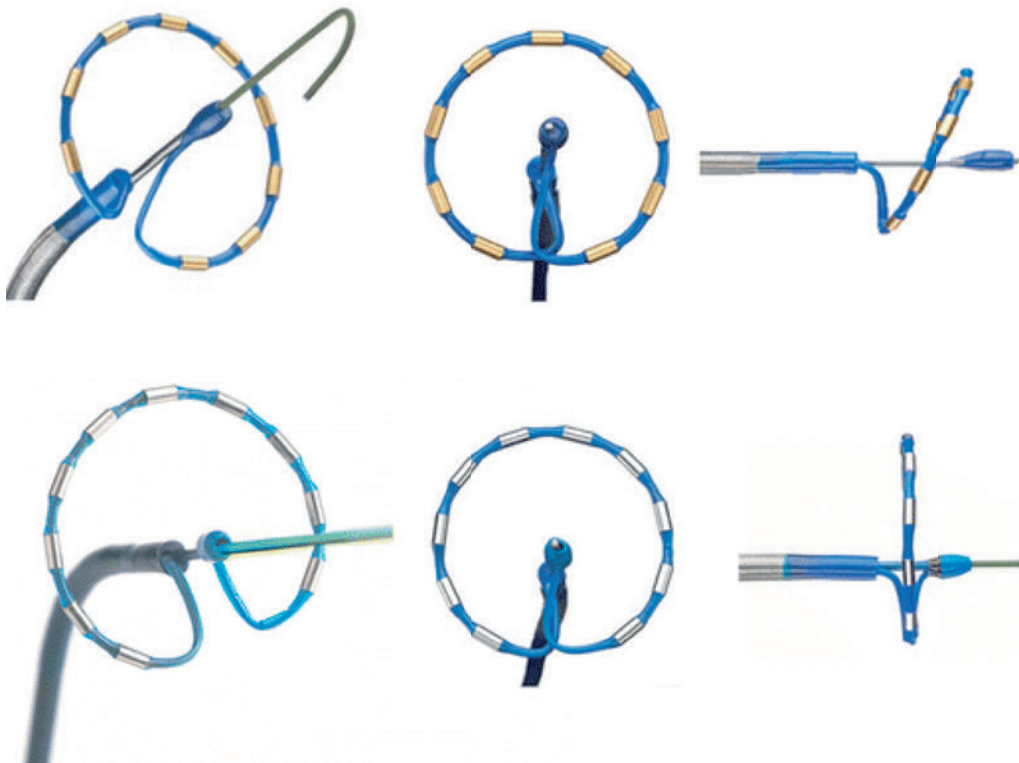


Fig. 7.11 Pulmonary Vein Ablation Catheter (PVAC) Design. Design differences between PVAC Gold (*top panel*) and PVAC (*lower panel*) are shown. Electrodes were switched to gold from platinum, number of electrodes reduced to 9 for PVAC Gold from 10 with PVAC, interelectrode spacing increased from 3.00 to 3.75 for PVAC Gold, and PVAC Gold includes a 20-degree forward tilt of the array. (From Weber S, Höher M, Schultes, D. First results and follow-up of a second-generation circular mapping and ablation catheter. *J Interv Card Electrophysiol.* 2016;47:213–219.)

temperature of -88.4°C , and is capable of rapid cooling of the catheter tip to below -75°C .^{56,57}

The effect produced by cryothermal ablation is the result of a temperature gradient occurring at the electrode-tissue interface (i.e., heat is extracted from the tissue by the cooled catheter tip), which causes tissue freezing and ice formation, both intracellularly and extracellularly. Whereas extracellular ice yields destruction due to solute effects (see below), damage caused by intracellular ice is mediated mainly by shearing force. The degree of tissue freezing and formation of ice only extracellularly versus both inside and outside the cell greatly depend on the minimum temperature reached, the duration of energy application, and the temperature time constant. The temperature time constant indicates the course of the descent of temperature to the target temperature, and a shorter value (expressed in seconds) identifies a more effective application. Important modulatory variables that can affect tissue damage produced by cryoablation include firmness of the catheter-tissue contact, tip temperature, freeze duration, and blood flow.⁵⁶

Initially, mild hypothermia (32°C) impacts the transport capacity of the ion pumps and, consequently, decreases action potential amplitude, prolongs action potential duration, and impairs conduction. With mild freezing temperatures (-10°C to -25°C), extracellular ice forms, resulting in cell dehydration, more acidic intracellular pH, and ionic imbalances, leading to membrane injury and cessation of cardiac electrical activity. The degree of permanent cellular damage at these tissue temperatures is directly related to duration of freezing. On the other hand, rapid extreme freezing (tissue temperatures colder than -50°C) results in intracellular ice formation and near instantaneous permanent tissue injury.^{56,57}

At the electrode-tissue interface, the coldest area is the one adjacent to the catheter tip, where functional effects of energy delivery are observed early (Fig. 7.14). Conversely, the less cooled area is the one at the periphery of the cryolesion, whose dimensions can also vary according to the duration of freezing. Because of limited cooling of the outer limit of the lesion (both in time and temperature), this region is less likely to incur irreversible damage. As a consequence, the effects obtained late during cryothermal energy application are likely to be reversible early on rewarming, and therefore any expected functional modification induced by cryoenergy should occur early (usually within the first 30 seconds of the application) to obtain a successful and permanent ablation of a given arrhythmogenic substrate.

Pathophysiology of Lesion Formation by Cryoablation

The mechanisms underlying lesion formation by cryoenergy are twofold: direct cell injury caused by ice formation and vascular-mediated tissue injury. The mechanisms of cellular death associated with tissue freezing involve immediate cellular effects, as well as late effects that determine the lesion produced.⁵⁷

Extracellular Ice Formation (Solution Effect Injury)

Direct cellular injury results from ice formation. Ice forms only extracellularly when the tissue is cooled to mild temperatures (0°C to -20°C) and results in hypertonic stress (the extracellular environment becomes hyperosmotic) through freeze concentration of solutes. This creates a diffusion gradient that causes shift of water from the intracellular to the extracellular space, net movement of H^{+} ions out of the cell, and the migration of solute ions into the cell. These changes ultimately

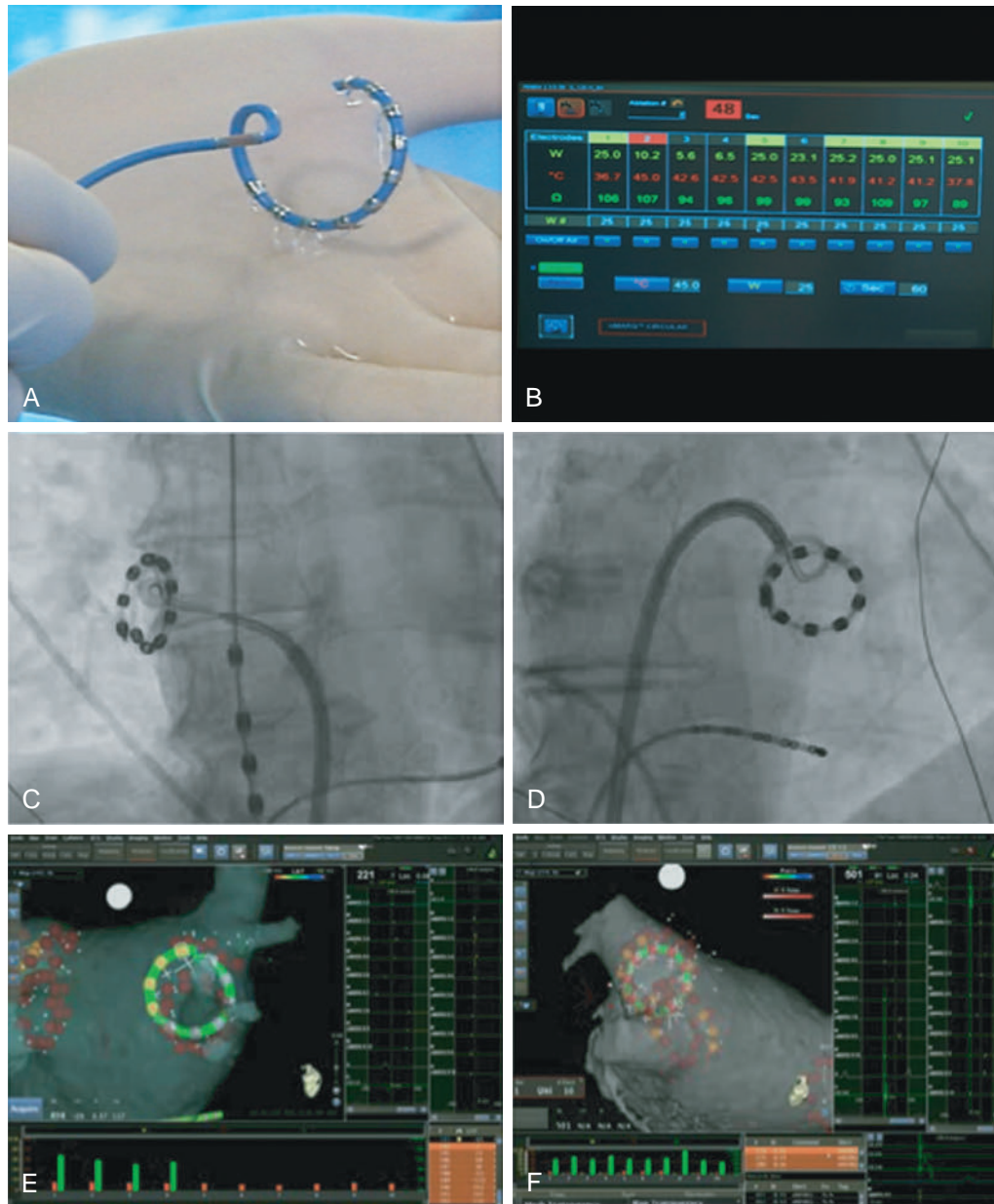


Fig. 7.12 The nMARQ Ablation System. (A) nMARQ ablation catheter with 10 irrigated 3-mm electrodes and 4-mm interelectrode spacing. (B) nMARQ Multi-Channel Ablation System during RF application indicating energy (W), electrode temperature (°C) and local impedance for each of the 10 electrodes during unipolar ablation. (C and D) Fluoroscopic image of the nMARQ catheter in the right superior pulmonary vein (PV) (C, posteroanterior view) and the left inferior PV (D, right anterior oblique view). (E and F) CARTO-3 electro-anatomic images during PV isolation with the nMARQ catheter positioned in the antrum of the right inferior PV (E) and the left superior PV (F). Red-colored electrodes indicate RF ablation on. CS, Coronary sinus catheter; Eso, esophageal temperature probe. (From Deneke T, Schade A, Müller P, et al. Acute safety and efficacy of a novel multipolar irrigated radiofrequency ablation catheter for pulmonary vein isolation. *J Cardiovasc Electrophysiol.* 2014;25:339–345.)

cause cell shrinkage, increased intracellular saline concentration with a reduction in intracellular pH, which result in damage to the plasma membrane cellular constituents and impairment of enzyme function.

These effects are reversible when rewarming is achieved within a short period (30 to 60 seconds). However, extended periods of extracellular freezing result in cellular death, and rewarming then results in cellular swelling sufficient to disrupt cellular membranes.⁵⁷

Intracellular Ice Formation

When the tissue is cooled to below -40°C , especially if cooling occurs rapidly, ice forms both extracellularly and intracellularly. Intracellular ice results in major and irreversible disruption of organelles, leading to cellular death. Although ice crystals do not characteristically destroy cell membranes, they compress and deform nuclei and cytoplasmic components. Mitochondria are particularly sensitive to ice crystals and

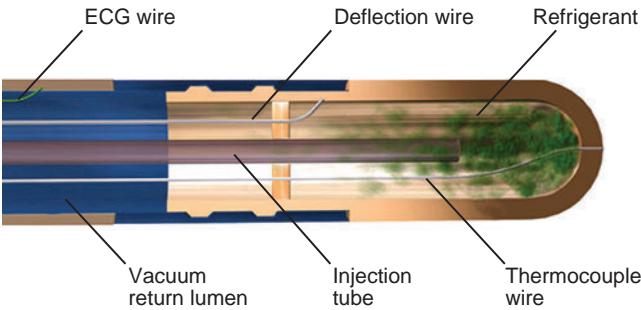


Fig. 7.13 Schematic Diagram Demonstrating the CryoCath Freezor Cryocatheter Internal Design. (Courtesy CryoCath Technologies, Montreal, Canada.)

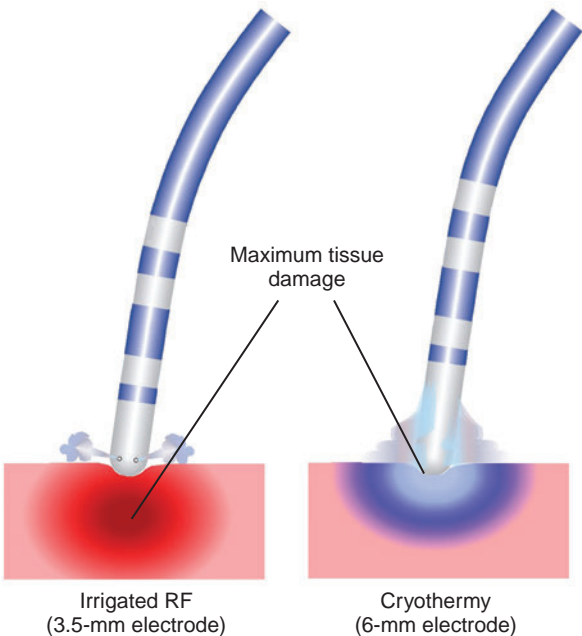


Fig. 7.14 Depth of Maximum Tissue Injury With Irrigated-Tip Radio-frequency (RF) Versus Cryotherapy. With irrigated RF (*left*), the maximum tissue heating occurs at some tissue depth because of cooling at the surface. With cryotherapy (*right*), the maximum effect is at the endocardial surface.

are the first structures to suffer irreversible damage. Furthermore, intracellular ice can propagate from one cell to another via intercellular channels, thus potentially resulting in lesion growth.

Importantly, cellular injury, disruption of membranous organelles in particular, is enhanced on cellular thawing. Rewarming causes recrystallization of ice (−20°C to −25°C), whereby intracellular ice crystals fracture and reform into larger crystals that extend mechanical shear forces and cellular destruction. Further, thawing of ice creates a transient hypotonic environment with consequent shift of water from the extracellular to the intracellular space, leading to severe swelling of the cell and membrane rupture. Cellular injury can be extended by repeated freeze-thaw cycles. Final rewarming evokes an inflammatory response to released cellular constituents and reperfusional hemorrhage, leading to tissue repair and eventual dense scarring. The size of ice crystals and their density depend on the proximity to the cryoenergy source, local tissue temperature achieved, rate of freezing, and surface area in contact with freezing temperatures.^{57,58}

TABLE 7.5 Determinants of Cryoablation Lesion Size

Ablation electrode temperature	Lesion size increases with lower electrode temperature
Freezing duration	Lesion size increases longer freezing duration
Freezing rate	Lesion size increases with faster freezing rate
Thawing rate	Lesion size increases slower thawing rate
Electrode-tissue contact	Lesion size increases with improved tissue contact
Electrode length	Lesion size increases with larger electrode length
Electrode orientation	Lesion size increases with parallel electrode orientation
Convective warming	Lesion size decreases with increased local blood flow due to increased convective warming

The zone of intracellular ice formation, the cornerstone of cryoablation and permanent tissue damage, is typically located within the core of the cryogenic lesion adjacent to the ablation electrode. Tissues located at a distance from the electrode are exposed to lesser degrees of cooling, resulting in a zone of only extracellular ice formation where incomplete tissue damage is experienced. Tissues farthest from the tip only experience hypothermia, resulting in reversible damage.

Vascular-Mediated Tissue Injury

Tissue freezing results in vasoconstriction, hypoperfusion, and ischemic necrosis. Subsequent tissue rewarming produces a hyperemic response with increased vascular permeability and edema formation. Endothelial disruption within the frozen tissue is also observed and results in platelet aggregation, microthrombi, and microcirculatory stagnation within the lesion.

Chronic Cryogenic Lesion Formation

In the final phase of cryoinjury, replacement fibrosis and apoptosis of cells near the periphery of frozen tissue give rise to a mature lesion within weeks. Typically, these lesions display a well circumscribed necrotic core (corresponding to the frozen volume within the critical isotherm), which eventually becomes replaced by dense homogeneous fibrosis, with sharply demarcated borders.⁵⁷ Characteristically, cryoablation does not cause collagen denaturation or contracture, which helps preserve tissue ultrastructural integrity, and matrix architecture tensile strength, and minimize tissue shrinkage. In addition, the degree of endothelial damage and overlying thrombus formation are substantially less than that associated with standard RF lesions. Of note, higher levels of biomarkers of necrosis (creatinine kinase [CK], CK-MB, and Troponin I) were observed in cryoablation when compared to RF ablation.^{59,60}

Determinants of Cryogenic Lesion Size

During cryoablation, lesion size and tissue temperature are related to convective warming, electrode orientation, electrode contact pressure, electrode size, refrigerant flow rate, and electrode temperature (Table 7.5). Lesion sizes during catheter cryoablation can be maximized by use of larger ablation electrodes with higher refrigerant delivery rates.

In contrast to RF ablation, cryoablation in areas of high blood flow can result in limited tissue cooling and smaller lesion sizes because of convective warming.⁵⁶ Conversely, cryoablation lesion size can be maximized in areas of low blood flow. A horizontal electrode orientation to the tissue and firm contact pressure also enhance lesion size, likely due

to increasing tissue contact area and reducing electrode exposure to the warming effect of the surrounding blood pool.

As noted, duration of freezing is an important determinant of the extent of tissue damage. Longer freezing durations not only enhance cell injury but also provide time for the tissues at the periphery of the cryolesion (exposed to slower cooling rate) to attain the lowest achievable temperature.⁶¹ Importantly, the rate of both freezing and thawing can affect lesion size. Rapid freezing rates are associated with larger volumes of cryoablation lesion. In addition, prolonged rewarming (i.e., slower thawing rate) increases the time of cell damage and lesion size. Slow thawing subjects the tissue to prolonged hypotonic stress, cellular edema, and ice recrystallization. The optimal freeze/thaw cycle employs fast freezing rate (approximately 100°C/min), followed by a slow thawing rate (optimally by allowing passive rewarming by natural body heat and blood flow) to maximize tissue injury. Repeating the freeze-thaw cycle also extends lesion boundaries.^{56,62}

Larger electrode sizes allow greater refrigerant flow rates as well as larger electrode surface area in contact with the tissue and, hence, larger lesions. The 6- and 8-mm electrode-tip cryocatheters produce ablation lesions of similar depth that are more than two- and threefold larger than 4-mm catheters, respectively. Despite larger lesions, endothelial cell layers remain intact and devoid of thrombosis.

Surface areas and volumes can be particularly sensitive to catheter tip-to-tissue contact angles with larger electrodes. As such, particular attention in catheter orientation is required with 8-mm electrode-tip cryocatheters to produce desired lesions.

Technical Aspects of Cryoablation

The cryoablation procedure is often performed in two steps. First, “cryomaps” are obtained by moderate cooling of tissue (electrode-tissue interface temperature approximately -28°C to -32°C), which is accompanied by reversible suppression of cellular electrical activity without inducing histologically identifiable damage. Second, cryoablation cools the selected cryomapped pathways to much lower temperatures (electrode-tissue interface temperature below -68°C) and causes intracellular ice formation and irreversible tissue injury.⁵⁷

Cryomapping

Cryomapping is designed to verify that ablation at the chosen site will have the desired effect and to ensure the absence of complications (i.e., to localize electrical pathways to be destroyed or spared). This procedure generally is performed using various pacing protocols that can be performed during cryomapping (or ice mapping) at -32°C . At this temperature, the lesion is reversible (for up to 80 seconds), and the catheter is stuck to the adjacent frozen tissue because of the presence of an ice ball that includes the tip of the catheter (cryoadherence). This permits programmed electrical stimulation to test the functionality of a potential ablation target during ongoing ablation and prior to permanent destruction. It also allows ablation to be performed during tachycardia without the risk of catheter dislodgment on termination of the tachycardia.

In the cryomapping mode, the temperature is not allowed to drop to less than -30°C , and the time of application is limited to 60 seconds. Formation of an ice ball at the catheter tip and adherence to the underlying myocardium are signaled by the appearance of electrical noise recorded from the ablation catheter's distal bipole. Once an ice ball is formed, programmed stimulation is repeated to verify achievement of the desired effect. If cryomapping does not yield the desired result within 20 to 30 seconds or results in unintended effect (e.g., AV conduction delay or block), cryomapping is interrupted, to allow the catheter to thaw and become dislodged from the tissue. After a few seconds, the catheter may be moved to a different site and cryomapping repeated.

Cryoablation

When sites of successful cryomapping are identified by demonstrating the desired effect with no adverse effects, the cryoablation mode is activated, in which a target temperature lower than -75°C is sought (a temperature of -75°C to -80°C is generally achieved). The application is then continued for 4 to 8 minutes, thus creating an irreversible lesion (although recent experimental evidence suggests that single 2-minute and 4-minute application times result in catheter ablation lesions of similar size using the modern cryoablation system) (eFig. 7.4).⁶²

If the catheter tip is in close contact with the endocardium, a prompt drop in catheter tip temperature should be observed as soon as the cryoablation mode is activated. A slow decline in catheter tip temperature or a very high flow rate of refrigerant during ablation suggests poor electrode-tissue contact. In such cases, cryoablation is interrupted, and the catheter is repositioned.

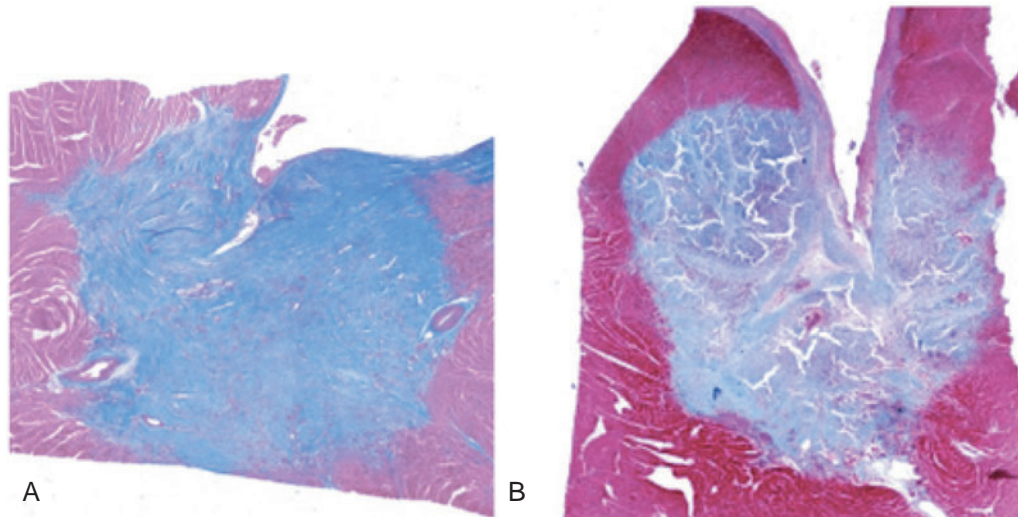
Cryoballoon Ablation

The cryothermal balloon ablation system (Arctic Front, Medtronic, Minneapolis, MN, United States) consists of a nondeflectable, 10.5 Fr catheter with distally mounted coaxial double inner-outer cooling balloons (“balloon within a balloon,” outer balloon maximum diameter, 23 or 28 mm) specifically designed for PV isolation (Fig. 7.15). The balloon acts as the expansion chamber as the liquid nitrous oxide converts to gas. During cryotherapy, temperature is monitored via a thermocouple located at the inner balloon.^{56,57,63}

The cryoballoon is deployed at the ostium of targeted PV and cryoenergy is delivered over the occluding balloon system to create circumferential lesions around the PV ostium. This design helps limit the convective warming effects of the high blood flow at the PV ostium (which can limit lesion size and ablation efficacy), as well as shorten the lengthy procedure times required for circumferential point-by-point cryoablation around the PV ostia with the standard steerable cryocatheters.^{56,57,63,64}



Fig. 7.15 Cryothermal Balloon Catheter. (Courtesy Medtronic, Inc., Minneapolis, MN, United States.)



eFig. 7.4 Cryoablation Lesions With 2-Minute and 4-Minute Application Times. Ablation lesions are shown 1 month after cryothermal applications in the left ventricle (in canine model) of 2-minute (A) and 4-minute (B) duration. Lesions were stained with Masson's trichrome and slides were scanned for visualization and analyses. The ablation lesions are sharply demarcated from the surrounding myocardium, with preserved ultrastructural tissue integrity. (From Bessière, F, Dubuc M, Andrade J, et al. Focal transcatheter cryoablation: is a four-minute application still required? *J Cardiovasc Electrophysiol.* 2017;28:559–563.)

Clinical Advantages of Cryoablation

The use of cryoablation in the EP laboratory provides some distinct advantages not seen with conventional RF ablation. The slow development of the cryolesion (approximately 240 seconds), although time-consuming, enables the creation of reversible lesions and modulation of lesion formation in critical areas. As noted, cryomapping allows functional assessment of the efficacy and safety of a putative ablation site during ongoing ablation and prior to permanent destruction. This offers a safety advantage when ablation is performed close to critical structures such as the AVN or His bundle (HB).

Compared with standard RF lesions, cryolesions are associated with substantially less endothelial disruption, less platelet activation, and lower thrombogenic tendency. Therefore the risk of coagulum formation or charring is less than with RF ablation (see Table 7.4). Furthermore, cryoablation results in dense homogeneous fibrotic lesions with a well-demarcated border zone and does not cause collagen denaturation or contracture (which helps preserve tissue ultrastructural integrity), in contrast to the RF hyperthermic effects. Therefore cryothermal energy application in close proximity to the coronary arteries (e.g., during epicardial ablation) or in venous vessels (CS, middle cardiac vein, and PVs) is less likely to result in damage, perforation, or chronic stenosis of their lumen.⁵⁷

The cryoadherence effect results in the formation of a very focal lesion because of fixed and stable tip electrode contact to adjacent frozen tissue throughout the whole application. This has a particular safety advantage, especially for ablation in the proximity of critical areas, such as the AVN and HB. In addition, cryoadherence augments catheter stability throughout the energy application, even when sudden changes in heart rhythm that can potentially displace the ablation catheter (e.g., tachycardia termination) occur. At the same time, cryoadherence does not compromise safety. On discontinuation of cryothermal application, the defrost phase is fast (within 3 seconds), and the catheter can be immediately disengaged from the ablation position.

Cryothermal energy application is characterized by the absence of pain perception in nonsedated patients, likely because hypothermic exposure desensitizes the nerves in the injured area secondary to decreased ion transport. In fact, cryoablation can be performed without analgesia. Occasionally, a light sense of cold or headache is perceived as minor discomfort. This characteristic can be particularly useful in younger and pediatric patients.

Clinical Applications of Cryoablation

Currently, two different types of cryoablation catheters are available: traditional-tip ablation catheters and balloon catheters. The traditional catheters (Freezor Max, Medtronic, Minneapolis, MN, United States) are used for focal ablation. These steerable catheters come with 4-, 6-, or 8-mm-long-tip electrodes, and have three additional proximal ring electrodes for EP recordings as well as a proximal thermocouple.⁶⁴

The cryoballoon catheter is specifically designed for PV isolation. The second generation of cryoballoon catheter offers twice the number of refrigerant spray ports and more homogeneous cooling effect on the distal hemisphere of the balloon (see Chapter 15).^{56,57,63}

As noted, catheter-based cryoablation can have specific advantages over RF catheter ablation, including greater safety as a result of greater catheter stability, reduced risk of systemic embolization, low propensity for thrombus formation and endothelial disruption, and preservation of ultrastructural tissue integrity. As a result, cryoablation has quickly been adapted for specific arrhythmogenic substrates in which RF has specific limitations that can potentially be overcome by cryotherapy. However, it is unlikely that cryoablation will replace standard RF ablation in unselected cases.

Atrioventricular Nodal Reentrant Tachycardia

So far, slow pathway ablation for AVNRT by cryothermal energy represents the largest experience in the clinical application of focal cryoablation. Cryoablation can be of particular safety advantage in patients with AVNRT. Not a single case of persistent AV block has been reported, even when using large-tip cryocatheters, and despite the fact that transient AV block occurs in up to 2% to 23% of patients during cryomapping at -30°C or during cryoablation at -75°C .⁶⁵ However, long-term success rates remain lower than that of RF ablation. In a meta-analysis of cryoablation versus RF ablation for AVNRT, cryoablation was associated with a lower risk of permanent AV block (0% vs. 0.75%) but higher risk of long-term AVNRT recurrence (9.7% vs. 3.8%) and longer total procedure time (111.7 minutes vs. 81.2 minutes).^{66–68}

According to current data, cryothermal energy is a valuable and useful alternative to RF energy to treat patients with AVNRT. The absence of permanent inadvertent damage of AV conduction makes this new technology particularly useful for patients with difficult anatomy, after an unsuccessful prior standard ablation procedure, in pediatric patients, and in patients in whom even the small risk of AV block associated with RF ablation is considered unacceptable. Cryoablation can be of particular advantage in several situations, including posterior displacement of the fast pathway or AVN, a small space in the triangle of Koch between the HB and the CS ostium, and the need for ablation to be performed in the midseptum. However, given the high success rate and low risk of RF slow pathway ablation, it can be difficult to demonstrate a clinical advantage of cryoablation over RF ablation in unselected AVNRT cases.

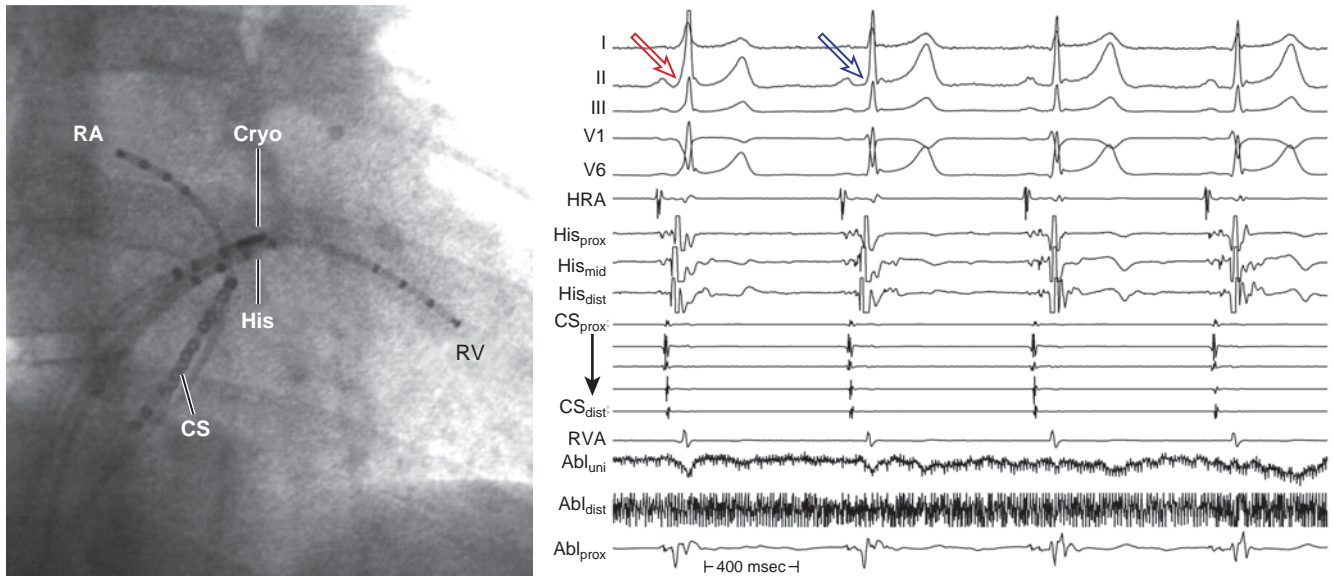
Bypass Tracts

Cryothermal ablation of BTs in the superoparaseptal and midseptal areas, both at high risk of complete permanent AV block when standard RF energy is applied, is highly safe and successful (eFig. 7.5). Cryoablation can also be successfully and safely used to ablate selected cases of epicardial left-sided BTs within the CS, well beyond the middle cardiac vein, once attempts using the transseptal and transaortic approaches have failed. However, the experience with cryoablation in unselected BTs is more limited and less satisfactory; this likely is related to multiple factors, including the learning curve and the smaller size of the lesion produced by cryoablation. Also, the cryocatheter is not yet as steerable as the conventional RF catheter. Catheter stiffness and limited maneuverability can limit proper positioning of the catheter tip and potentially result in tissue trauma and transient mechanical AV or BT block. Furthermore, the large electrode spacing decreases the specificity of mapping of the BT. In addition, all the distinguishing features of cryothermal energy, which are optimal for septal ablation, are less important for ablation of BTs located elsewhere.⁶⁹

In recent series, the acute success rate of cryoablation of BTs in the superoparaseptal and midseptal regions exceeded 90% (range, 60% to 100%). However, recurrence rates after initially successful cryoablation remain high (occurring in up to 20% of patients), and overall success rates have been lower than those with RF ablation of BTs. It is, however, important to note that alternatives for elimination of up to 17% of those BTs are limited by a prohibitive risk of AV block with RF ablation. Further, patients often prefer a strategy to minimize the risk of procedural AV block even when associated with a lower rate of procedural success.^{69–71}

Typical Atrial Flutter

Complete CTI block can be achieved by cryothermal ablation. An advantage of using cryothermal energy for the ablation of typical AFL is the absence of pain perception related to energy application. However, although the acute success rates of cryoablation appear comparable to



eFig. 7.5 Cryoablation of a Para-Hisian Bypass Tract (BT). Right anterior oblique fluoroscopic view of cryoablation catheter (*Cryo*) position and ECG and intracardiac recordings during cryoablation of para-Hisian BT. The first two QRS complexes at left are preexcited, with the second QRS complex (*blue arrow*) less so than the first (*red arrow*), as cryoablation begins to affect pathway conduction. Preexcitation disappears afterward. The ablation recordings at bottom are severely disrupted by the delivery of cryoenergy. *Abl_{dist}*, Distal ablation site; *Abl_{prox}*, proximal ablation site; *Abl_{uni}*, unipolar ablation site; *CS*, coronary sinus; *CS_{dist}*, distal coronary sinus; *CS_{prox}*, proximal coronary sinus; *His_{dist}*, distal His bundle; *His_{mid}*, middle His bundle; *His_{prox}*, proximal His bundle; *HRA*, high right atrium; *RA*, right atrium; *RV*, right ventricle; *RVA*, right ventricular apex.

those for RF ablation (89% vs. 91%), long-term cryolesion durability is inferior to that in patients treated with RF ablation, as evidenced by the higher recurrence rate of symptomatic, ECG-documented AFL (10.9% vs. 0%), and higher asymptomatic CTI conduction recurrence rates (23.4% vs. 15%). In addition, compared with RF ablation, cryoablation is associated with significantly longer procedure times, driven mainly by the longer duration of each cryoablation (4 minutes) compared with RF ablation (up to 60 seconds).

Pulmonary Vein Isolation

In view of the characteristics mentioned earlier, cryothermal energy ablation can be considered an ideal and safer energy source for PV isolation, and the incidence of PV stenosis and thromboembolic events is expected to be dramatically reduced compared with RF ablation. On the other hand, cryothermal injury is sensitive to surrounding thermal conditions. The high flow of the PVs can present a considerable heat load to cryothermal technologies, which can limit the size and depth of the lesion produced by cryothermal energy at the ostium of the PV. Unlike point-by-point RF ablation, cryoenergy cannot be modified selectively in different regions around the PVs. Also, variations in PV anatomy can influence the effectiveness of cryoballoon ablation, likely due to the difference in the venous seal obtained being dependent on the PV ostial shape and cryoballoon alignment.^{56,57,63,64}

Studies comparing cryoablation with open-irrigated RF ablation in the setting of paroxysmal AF ablation demonstrated statistical equivalence between the two technologies in terms of safety and efficacy. Limited data also suggest comparable outcomes in patients with persistent AF, with a comparable rate of freedom from AF at 1 year after a single RF procedure (42% to 67%). Phrenic nerve injury is significantly more common following second-generation cryoballoon ablation (approximately 3%) as compared to RF ablation. Nonetheless, this rate is much less than that observed with the first-generation cryoballoon system (up to 13%). Despite the hope that cryoablation would not cause significant esophageal damage and thus could prevent formation of atrioesophageal fistulae, these have nonetheless been reported with standard usage of the cryoballoon.^{72–76}

Focal Atrial Tachycardia

Cryoenergy can be particularly valuable in ablating atrial foci located close to the AVN or within venous structures.

Ventricular Tachycardia

Data regarding cryoablation for VT remain scant. Small reports described feasibility and success of cryoenergy for ablation of outflow tract VT. In addition, cryothermal energy can be of potential advantage in percutaneous subxiphoid epicardial ablation of VT because of less potential damage to the epicardial coronary arteries. The reduced heat load in the pericardial space related to the absence of blood flow limits RF energy delivery but can be to the advantage of cryoablation, with the possibility of producing larger transmural lesions.⁷⁷

LASER ENERGY

Biophysics of Laser Energy

Light amplification by stimulated emission of radiation (laser) produces a monochromatic (narrow-frequency range) phase-coherent beam at a specific wavelength (Fig. 7.16). This beam can be directed for a specific duration and intensity, and as it penetrates the tissue, it is absorbed and scattered. The photothermal effect occurs with the absorption of photon energy, thus producing a vibrational excited state in molecules (chromophores). By absorbing this energy, the tissue is heated and a lesion is created (i.e., tissue injury is thermally mediated).



Fig. 7.16 Laser Balloon Aiming Beam. (Courtesy CardioFocus, Marlborough, MA, United States.)

Laser energy can be delivered in a continuous or a pulsed mode. Laser energy is selectively absorbed by the tissues over several millimeters, and it decays exponentially as it passes through the tissue secondary to absorption and scatter, the extent of which depends on laser beam diameter and the optical properties of the tissue. Lesion size is determined by the extent of light diffusion and heat transport.

Three major laser systems are used: argon laser, neodymium:yttrium-aluminum-garnet (Nd:YAG) laser, and diode laser. Argon laser uses a gaseous lasing medium (argon), which emits light at a wavelength of 500 nm. With this system, the light energy is absorbed rapidly in the first few millimeters of tissue, with resulting surface vaporization with crater formation. Nd:YAG laser uses a solid lasing medium (Nd:YAG), which emits energy at a wavelength of 1060 to 2000 nm in the infrared spectrum. This system is associated with significant scatter in tissue. It causes more diffuse and deeper tissue injury and results in photo-coagulation necrosis. On the other hand, diode laser uses semiconductors and emits energy at a wavelength of 700 to 1500 nm (near-infrared). To an extent, diode lasers can be customized to effect different depths of damage (mid-myocardial vs. endo- or epicardial, for instance).

Clinical Applications of Laser Energy

Early studies of laser ablation used a high-energy laser that carried a high risk of crater formation and endothelial damage. These studies focused on the intraoperative use of lasers in the ultraviolet and visible range (308- to 755-nm wavelength), and they appeared to show effectiveness of the lesions placed. Laser energy can also be delivered along the entire length of a linear diffuser, which provides uniform linear laser ablation and a superior transmural lesion when compared with previous end-firing optical delivery systems. The use of the linear diffuser in combination with lasers in the infrared or near-infrared wavelength (800 to 1100 nm) is currently under investigation.

Laser energy is absorbed by blood; as a consequence, its application directly into blood results in thrombus formation. This limitation is obviated by application of laser energy through a fluid-filled balloon positioned against the tissue to provide a bloodless interface for ablation. Laser energy has been used with balloon technology for PV isolation. The most recent generation of this balloon catheter is a nonsteerable, variable-diameter, compliant balloon (HeartLight, CardioFocus, Marlborough, MA, United States). The central shaft of the balloon contains a 2-Fr endoscope that provides real-time visualization of the face of the balloon: both the tissue and blood in contact with the balloon. Also,

within the central shaft are additional lumens for circulating deuterium dioxide (D_2O) to cool the balloon, and a maneuverable optical fiber that generates a 30° arc/spot of both nonablative visible light and near-infrared ablative light energy.^{78–80}

The laser balloon is inserted at the PV antrum through a 12 Fr deflectable sheath. Varying balloon inflation pressure allows for adjustment to the individual PV anatomy to optimize PV occlusion and maximize balloon-tissue contact. The balloon is filled with a mixture of contrast and D_2O and irrigated internally at 20 mL/min to minimize absorption of laser energy. Once the balloon is deployed, the endoscope enables real-time visualization of the face of the balloon at the targeted PV antrum and monitoring for the intrusion of blood into the space between the balloon and the tissue.⁷⁹

The arc generator consists of an optical fiber located within the central shaft that projects a 30-degree arc of light onto regions of balloon-tissue contact guided by an endoscopic view of the PV antrum (areas of balloon-tissue contact are visualized as blanched white, whereas contact with blood is visualized as red). This arc serves as an aiming beam for laser delivery and can be maneuvered along the balloon face with endoscopic visualization, to facilitate individual lesion application in an anatomically flexible lesion design that adapts to the highly variable PV anatomy. Once the proper location is identified, a diode laser is used to deliver laser energy at 980 nm. The laser fiber can be advanced or withdrawn to shift the site of lasing along the longitudinal axis of the catheter, and can be rotated to any location on the face of the balloon. Lesions are deployed in a point-by-point fashion in a circumferential, contiguous, and overlapping manner around the PV; each individual ablation lesion covers 30 degrees of a circle.^{79,80}

Laser energy is delivered at power output of 5.5 to 12 W for 20 to 30 seconds, depending on the thickness of tissue or the proximity of the esophagus. To minimize thrombus formation risk, a 5.5-W energy is applied for 30 seconds when ablation is required in regions of overlapping moving blood along the periphery of the endoscopic view. Stagnant blood at the center of the endoscopic image represents blood from the target PV that is completely occluded by the balloon. Ablation is avoided in this region due to risk of thrombus formation at any laser energy dose.⁸⁰

The laser ablation catheter technology appears to be equivalent to RF ablation with respect to efficacy and safety in patients with paroxysmal AF. The initial clinical experience with this technology suggests the ability to achieve reliable and lasting PV electrical isolation in patients with highly variable PV shapes and sizes.^{79,80} Unlike other balloon catheters (cryoballoon and high-intensity focused ultrasound [HIFU]), the visually guided laser ablation is unique in that it uses a compliant, variable diameter balloon, thus allowing a single balloon catheter to accommodate multiple PV sizes and shapes. In addition, the endoscope provides real-time direct visualization of the target tissue. Another important feature is the ability to customize the ablation lesion and selectively titrate energy to each part of the circumferential lesion set, similar to point-by-point RF ablation. With other balloon catheters, the operator cannot choose which part of the balloon would deliver ablative energy or adjust the intensity of tissue destruction around the balloon. As a result, the portion of the LA adjacent to the esophagus or phrenic nerve receive the same energy as those areas where deeper lesions are desired.⁸¹

ULTRASOUND ENERGY

Biophysics of Ultrasound Energy

Sound is a propagation of cyclical (oscillatory) displacements of atoms and molecules around their average position in the direction of propagation. When the cyclical events occur at frequencies of more than

20,000 Hz (i.e., higher than those audible to humans), the sound is defined as ultrasound.

Ultrasound beams can be treated in a manner analogous to light beams, including focusing (ultrasonic lens) and minimization of convergence and divergence (collimation). These optical geometric manipulations allow for ultrasound to be directed toward confined distant (deep) tissue volumes. This is a pivotal capability of therapeutic ultrasound.⁸²

Ultrasound energy transmission is subject to attenuation with distance and medium, especially with air. The amount of ultrasound energy transferred to tissue is proportional to the intensity of the wave and the absorption coefficient of the tissue. Because of this property, ultrasound ablation does not require direct contact with the myocardium, in contrast to RF ablation. Ultrasound energy decreases proportionally with the distance ($1/r$), whereas RF ablation electrical conduction decreases with the square of the distance ($1/r^2$). This feature allows ultrasound energy to create deeper and transmural lesions. The duration of application and acoustic power used have a direct relationship with the lesion depth.

Pathophysiology of Lesion Formation by Ultrasound Energy

Tissue injury caused by ultrasound is mediated by thermal and non-thermal mechanisms. Ultrasound waves can propagate through living tissue and fluids without causing any harm to the cells. However, by focusing highly energetic ultrasound waves (HIFU) to a well-defined volume, local heating (achieving a tissue temperature of 65°C to 100°C) occurs and causes rapid tissue destruction by coagulative necrosis. Thermal energy results when the energy transported by an ultrasound beam becomes attenuated as it propagates through viscous (viscoelastic) media, such as human soft tissue. The attenuation partly represents conversion of ultrasound energy into heat.^{82–84}

Nonthermal mechanisms by which HIFU destroys tissue include ultrasonic cavitation, gas body activation, and mechanical stress. Mechanical agitation results from pressure waves (sound waves) propagating in gas-containing tissues as they cyclically expand (explode) and shrink (implode) microbubbles in the tissue (i.e., oscillation and collapse of gas microbubbles), a process known as microcavitation. This process of vibration of cellular structures causes local hyperthermia and mechanical stress by bubble formation because of rapid changes in local pressure, thus leading to cell death.⁸²

Previous studies showed that rapid, focused absorption of HIFU energy in noncardiac tissue produced a steep tissue temperature gradient (2°C to 5°C/s) between the focus and the surrounding tissue, thus allowing for the production of sharply demarcated lesions and reducing collateral damage. However, later studies using HIFU for PV isolation in canine hearts found that HIFU produced a dual temperature profile, probably because of immediate direct acoustic heating and subsequent conductive heating. In addition, the region of direct acoustic heating with HIFU energy *in vivo* was largely predictable from the distance of the target tissue to the HIFU balloon surface; actual tissue temperatures exceeding 50°C (the temperature at which permanent tissue damage is supposed to occur) were focused within a 7-mm width and 7.5-mm depth around the HIFU exit site (significantly larger than the 2- to 3-mm area of resistive heating observed with RF energy). However, the actual distribution of tissue temperatures during lesion generation can be affected by other factors, such as: blood circulation; location of different tissue thicknesses within the atrium, venoatrial junction, or PV; or energy attenuation at various interfaces between the target tissue and the energy source.

HIFU lesion depth increases with longer duration of energy delivery from 15 to 60 seconds, and there is a linear relationship between increasing power and depth of lesions. HIFU applications were found

to achieve transmural lesions and PV electrical isolation. However, although this can translate into increased effectiveness of ablation, it also can potentially lead to collateral damage, namely to the phrenic nerve and esophagus. HIFU ablation can produce damage to the phrenic nerve when it is located within 4 to 7 mm of HIFU exit from its balloon.

Clinical Applications of Ultrasound Energy

HIFU is an attractive alternative energy source. Because it can be focused at specific depths, ultrasound can be advantageous when considering epicardial ablation. The presence of epicardial fat makes the use of standard RF current difficult, both with catheter-based epicardial ablation and minimally invasive surgical ablation. Furthermore, the ability of ultrasound to be collimated through echolucent fluid medium (e.g., water, blood) makes it ideal for a balloon delivery system, which can potentially facilitate circumferential ablation at the PV orifice with a single energy delivery. Another potential advantage of ultrasound is that it does not rely on extensive heating on the vein surface. This can be of value in PV isolation procedures, to help prevent PV stenosis seen with RF ablation. Because HIFU is delivered at the beam convergence site rather than at the tissue surface, successful ablation is less dependent on absolute balloon-tissue contact than other balloon-based technologies. Furthermore, unlike other energy sources, HIFU can be deflected within the balloon to create a wide, focused zone of energy delivery outside the PV orifice, thereby mimicking current wide area circumferential ablative approaches. Currently, no HIFU catheters are available that can be used for linear ablation.

An 8-MHz cylindrical transducer mounted within a saline-filled balloon had been designed for PV isolation. The ablation system (Atrionix, Palo Alto, CA, United States) consists of a 0.035-inch-diameter luminal catheter with a distal balloon (maximum diameter, 2.2 cm) housing a centrally located ultrasound transducer. The system is advanced over a guidewire into the target PV. Tissue surface temperature monitoring is achieved by thermocouples on the balloon and the ultrasound transducer. Despite initial enthusiasm, the long-term report including 33 patients was disappointing, with a long-term cure rate of approximately 30%, although short-term electrical isolation was achieved in all but one of the PVs targeted. Surprisingly, several applications were required to achieve PV isolation. The variability of the PV anatomy was the main culprit for the system failure. In larger PV orifices, it was difficult to achieve adequate heating. The system delivered a narrow band of ultrasound energy radially from a centrally located transducer, and it was at times challenging to place the catheter in all PVs at the proximal portion. Therefore foci at the most proximal lip of a PV may not be ablated successfully.

Later on, a forward-projecting HIFU balloon catheter (ProRhythm, Ronkonkoma, NY, United States) was developed for circumferential PV isolation outside the PV ostia (to limit the risk of PV stenosis). Radially emitted ultrasound is reflected from the back of the balloon, thus resulting in forward projection of ultrasound energy, with a focal point at the balloon-endocardial interface (eFig. 7.6). This system has two noncompliant balloons. A 9-MHz ultrasound crystal is located in the distal balloon filled with contrast and water. The proximal balloon, filled with carbon dioxide, forms a parabolic interface with the distal balloon to reflect the ultrasound energy in the forward direction, by focusing a 360-degree ring (sonicating ring) of ultrasound energy 2 to 6 mm in front of the distal balloon surface. The distal balloon has three sizes—24, 28, or 32 mm in diameter—producing sonicating rings of 20, 25, or 30 mm in diameter. The acoustic power of the system is 45 W for all three balloons, with negligible loss of power in the balloon. The distal balloon is irrigated with contrast and water at 20 mL/min during ablation to keep the balloon cool (lower than 42°C). The

catheter has a central lumen used for insertion of a hexapolar, spiral mapping catheter (ProMap, ProRhythm) for real-time assessment of PV potentials.

Clinical application of this system for PV isolation was shown to be feasible. However, fatal esophageal injury was observed. A study of 28 patients using an esophageal temperature-guided power modulation algorithm to enhance procedural safety demonstrated that acute PV electrical isolation with HIFU ablation could be achieved in only 77% of PVs. Eight percent of PVs could not be isolated with HIFU as a result of excessive esophageal heating or balloon catheter dislodgment. In only 32% of patients, all PVs could be isolated using HIFU ablation only. Although power modulation did not negatively influence short-term success rates of PV electrical isolation, it also did not prevent esophageal temperature from exceeding levels higher than 40.0°C at the end of the ablation. Elevated esophageal temperature prompting cessation of energy delivery occurred in 9% of PVs. Despite use of the safety algorithm and continuous phrenic nerve pacing, transient and persistent phrenic nerve palsy occurred in 14% and 7% of patients, respectively. Even worse, use of the safety algorithm could not prevent occurrence of esophageal thermal damage and lethal atrioesophageal fistula. With mean PV isolation times of less than 15 seconds and a high number of complications, it is evident that the present energy source is too powerful in some patients.⁸⁵

Although PV isolation with HIFU had proven to be successful, it did not meet the safety standards required for treatment of AF, and this led to a halt of its clinical use. The problems of phrenic nerve palsy and atrioesophageal fistula occurrence remain unresolved. Still, the concept of the energy source and mode of energy delivery can be very interesting for future treatment of AF.⁸⁵

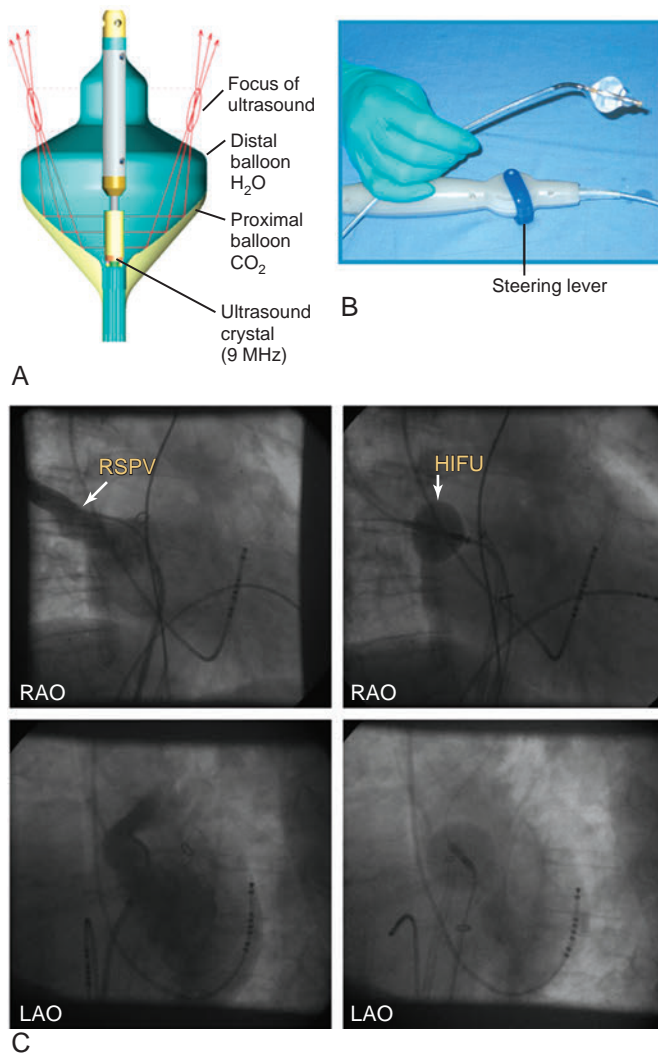
MICROWAVE ABLATION

Biophysics of Microwave Energy

Microwaves are the portion of the electromagnetic spectrum between 0.3 and 300 GHz. For the ablation of cardiac arrhythmias, microwave energy has been used at frequencies of 0.915 and 2.450 GHz. Similar to RF, microwave energy produces thermal cell necrosis. However, in contrast to heating by electrical resistance as observed during RF ablation, the mechanism of heating from a high-frequency microwave energy source is dielectrics. Dielectric heating occurs when high-frequency electromagnetic radiation stimulates the oscillation of dipolar molecules (e.g., water molecules) in the surrounding medium at a very high speed, thereby converting electromagnetic energy into kinetic energy. This high-speed vibration causes friction between water molecules within the myocardial wall that results in an increase of myocardial tissue heat. This mode of heating lends microwave ablation the potential for a greater depth of volume heating than RF ablation and should theoretically result in a larger lesion size.⁸⁶

Microwave energy is not absorbed by blood and can propagate through blood, desiccated tissue, or scar. It also can be deposited directly into the myocardial tissue at a distance, regardless of the intervening medium. The microwave energy field generated around the ablation catheter antenna can create myocardial lesions up to 6 to 8 mm in depth without overheating the endocardial surface, a feature that can potentially limit the risk of charring, coagulum formation, and intra-myocardial steam pops. Penetration depth achieved with microwave energy depends on several factors—dielectric properties of the tissue, frequency of the microwave energy, antenna design, and composition and thickness of the cardiac layers.⁸⁶

The effectiveness of microwave ablation depends on the radiating ability of the microwave antenna that directs the electric field and determines the amount transmitted into the myocardium, which is critical



eFig. 7.6 Circumferential Antral Pulmonary Vein (PV) Isolation Using the High-Intensity Focused Ultrasound (HIFU) Balloon Catheter. (A) Schematic representation of the HIFU balloon catheter designed to focus ultrasound energy circumferentially outside the PV (PV antrum). (B) HIFU balloon. (C) Right anterior oblique (RAO) and left anterior oblique (LAO) fluoroscopic views of the angiograms (right) and HIFU balloon positioning (left) in the right superior PV (RSPV). (From Schmidt B, Antz M, Ernst S, et al. Pulmonary vein isolation by high-intensity focused ultrasound: first-in-man study with a steerable balloon catheter. *Heart Rhythm*. 2007;4:575.)

for heating. An end-firing monopolar antenna has been used to produce lesions at depths of 1 cm without disruption of the endocardium in porcine ventricles. The depth of these lesions increased exponentially over time as compared with standard nonirrigated RF energy, which had minimal lesion expansion after 60 seconds of ablation. To concentrate more of the energy distribution near the electrode tip, circularly polarized coil antennas have been developed. Other configurations of the microwave antenna include helical, dipole, and whip designs; these have a large effect on the magnetic field created. However, many of these catheters are still under clinical investigation.⁸⁶

Pathophysiology of Lesion Formation by Microwave Ablation

Microwave energy produces thermal cell necrosis and transmural damage, with foci of coagulation necrosis of myocytes in the central part of the lesion. Hyperthermia (more than 56°C) causes protein denaturation and changes in myocardial cellular EP properties resulting from movement of mobile ions within the aqueous biological medium and altering membrane permeability. The acute myocyte changes include architectural disarray, loss of contractile filaments, and focal interruption of the plasma membrane, which are signs of irreversible injury. In addition, occlusion of the lumen of the small intramyocardial vessels and severe disruption of endothelial and adventitial layers are observed. Carbonization does not occur on tissue surfaces because of the good penetration of microwave energy. Fibrotic tissue eventually replaces the necrotic muscle, which typically becomes sharply demarcated from normal myocardium.

In vitro and in vivo experiments have demonstrated good uniformity in the distribution of the electromagnetic energy throughout the tissue and excellent penetration depth, with no areas of discontinuity over the length of the ablating probe. Energy distribution is maximal near the center of the ablating element, a finding indicating that depth of ablation is relatively deeper at the midpoint of a lesion. There is no indication of edge effect along the ablating tip, which can potentially produce overheating of the tissue surface and induce charring. The temperature at the tissue surface typically remains at less than 100°C over the time required to produce a 6-mm-deep lesion. This is a critical finding because the ability to raise the tissue temperature to 50°C while maintaining it at less than 100°C is paramount to effective and safe hyperthermic ablation.⁸⁷

In addition to the frequency of the microwave energy and length of antenna used, penetration of microwave into the tissue and lesion dimensions is proportional to the power and duration of energy application.⁸⁷

Although microwave ablation in theory should be less likely than RF to induce surface overheating, in vivo studies found that a higher targeted temperature of 90°C resulted in a surface temperature of more than 70°C and was associated with some tissue surface charring when compared with lower temperatures. Therefore the use of the temperature-controlled mode of microwave energy delivery to limit the targeted temperature to 80°C may prevent tissue overheating and reduce the risk of tissue charring. It should be noted that no coagulum formation and no steam pops were observed during any of the microwave ablations performed.⁸⁷

In contrast to RF energy, in which lesion expansion is maximal after 60 seconds, microwave lesion size continues to increase after 300 seconds of energy application. As compared with conventional 4-mm-tip RF ablation, microwave ablation creates a similar lesion depth and width. Lesion length created by a 10-mm antenna is comparable to that created by 8-mm-tip RF ablation. However, because of the lack of physical limitations on the length of the microwave antenna that can be made, microwave ablation may be more advantageous in creating long linear

lesions by using a longer antenna. Nevertheless, a parallel antenna orientation is needed for optimal energy delivery because the growth in lesion sizes is limited beyond the energy field as a result of the finite radial energy distribution of the microwave ablation antenna. Furthermore, the lesion depth created with an 8-mm-tip or saline-irrigated electrode catheter appears to be larger than the lesion depth created by microwave ablation. However, direct comparisons among these different ablation technologies are not available.⁸⁷

Clinical Applications of Microwave Ablation

Microwave ablation can be a promising technique that is potentially capable of treating a wide range of ventricular and supraventricular arrhythmias. The physics of the microwave energy source can be particularly useful for transmural ablation lesions of atrial tissue, as well as the treatment of tachyarrhythmias arising from deep foci of ventricular myocardium.⁸⁶

Microwave can potentially overcome several limitations of RF energy for linear ablation. In contrast to resistive heating produced by RF, microwave generates frictional heat by inducing oscillation of dipoles in a medium such as water. Tissue with higher water content, such as cardiac tissue, allows better energy transfer during the propagation of microwave energy deep into the tissue. Therefore microwave energy is capable of creating deeper lesions, to penetrate scar tissue and to reduce surface heating with less endocardial disruption or coagulation formation. Furthermore, delivery of microwave energy is not limited by electrode size as in RF, and microwave ablation can be applied over a larger surface by modifying antenna size and shape. Another theoretical advantage of microwave energy is that it provides sufficient lesions, independent of contact. However, experimental data have shown that penetration of electromagnetic fields into tissue declines exponentially, and the decline is steep when using frequencies in the microwave range; therefore distance is still an important consideration. Nevertheless, this theoretical advantage can potentially improve the versatility of microwave ablation, especially in areas where muscular ridges and valleys may pose problems for conventional RF ablation.⁸⁶

Currently, microwave ablation has been increasingly used intraoperatively (epicardially or endocardially) during surgical maze procedures. The ability to make microwave antennas into flexible linear applicators and place them parallel to the endocardium by means of clamps has increased the effectiveness of microwave as a tool in open-chest surgery and in minimally invasive surgery.⁸⁸

The development and manufacture of antennae for delivery of microwave energy is technically more complex than for RF electrodes because the efficacy of microwave energy transmission depends mainly on its delivery apparatus. Developments in the catheter-based microwave system may allow the transvenous delivery of microwave energy for endocardial ablation. Only a few case reports have described the successful use of transvenous catheter microwave ablation of the AV junction and CTI. Currently, only one transvenous microwave catheter system (MedWaves, San Diego, CA) is available for investigational use. This system includes a deflectable, 10 Fr catheter with 10-mm or 20-mm helical coil antenna with temperature monitoring, bipolar electrode recording, and a generator delivering microwave at 900 to 930 MHz. Microwave energy is delivered by using a temperature-controlled mode in which the generator automatically adjusts the power output to maintain the targeted temperature of the temperature sensor inside the antenna. For ablation of typical AFL, linear lesions are created with a point-by-point technique with gradual pullback of the microwave catheter across the CTI. Interestingly, microwave causes no perception of pain during ablation of the CTI with energy delivery in the inferior vena cava region.

ELECTROPORATION

DC ablation was investigated in the early 1980s but was abandoned shortly after RF energy emerged as a safer and more effective energy source for catheter ablation. DC ablation was associated with a high rate of serious complications, supposedly related to barotrauma and proarrhythmia. Barotrauma is caused by a high-pressure shock wave resulting from an electrically isolating vapor globe, leading to arcing (spark) and explosion at the catheter tip. Proarrhythmia was thought to result from the nonhomogeneous lesion formation by DC ablation. The effects of this technique were difficult to predict, ranging from no effect on the arrhythmia substrate, to successful ablation, to prolonged myocardial stunning with pulseless electrical activity.⁸⁹

Electroporation is a recent adaptation of low-energy DC catheter ablation. Electroporation uses large electrodes to reduce overall current density, thereby minimizing the risks associated with standard DC catheter ablation.

Tissue damage by electroporation is the result of an electric field-driven reorganization of the lipid structure of the cell membrane. Application of pulsed high-voltage electric field results in penetration of water molecules into the lipid bilayer of the membrane, causing reorientation of the adjacent lipids with their polar head groups toward these water molecules, which leads to the formation of small (nanoscale) pores in the cell membrane. The pores formed in the plasma membrane increase membrane permeability and electrical conductivity and provide a pathway for transport of a wide range of molecules, including DNA, into and out of the cell.

This effect—membrane electroporation—can be either reversible or irreversible. In the range of reversible electroporation, nanopores provide a temporary pathway for transport, but after the electric pulse they gradually reseal, the cells reconstitute their membrane integrity and function, and most cells retain their viability. In the range of irreversible electroporation, higher voltage electric field results in larger nanopores (beyond the reparative capability of the cell), leading to cell death. Other parts of the cell, such as DNA, collagen, or other proteins, are not directly affected by irreversible electroporation. The cutoff between reversible and irreversible electroporation is dependent on the electrical field threshold of the tissue.⁹⁰

The amount of damage caused by electroporation depends on the presence of cell membranes, the applied electrical field, and the electrical resistivity of the target tissue. Therefore tissues can vary in its vulnerability for electroporation, allowing for some degree of tissue specificity for lesion formation.⁹¹

In microbiology, reversible electroporation has been used to transiently increase the permeability of the cell membrane, allowing chemicals, drugs, or new coding DNA to be introduced into the cell (e.g., gene transfection). Irreversible electroporation has been successfully used in the treatment of selected cancers in multiple organs such as the liver, lung, pancreas, kidney, and prostate.


Irreversible electroporation is currently being investigated for catheter ablation of cardiac arrhythmias, and can potentially offer distinct advantages. Unlike other ablation energy sources (such as RF, cryotherapy, microwave, ultrasound, and laser), DC electroporation lesion formation is not thermally mediated.⁹² As a nonthermal therapy, irreversible electroporation is not be impeded by the cold/heat sink effect of local vascular system (which can be of advantage when the ablation target is adjacent to a major coronary artery), is less dependent on perfusion (which is well-suited for epicardial ablation), and is associated with reduced collateral thermal injury. Furthermore, reduced posttreatment inflammation promotes reduced scarring and preservation of the extracellular matrix and major tissue architectural components. In addition, coronary arteries are not or only minimally affected by irreversible

electroporation. The extensive connective tissue around the coronary arteries exhibits a relative reduction in large cell membranes, which makes them relatively invulnerable to irreversible electroporation.^{91,93}


Newer catheter designs (multipolar, large surface area electrodes in a circular arrangement) have been studied in porcine models and shown to produce desirable amounts of ablation on the epicardium without damaging coronary arteries, and in PVs without causing stenosis.⁹⁴


VIDEOS

The following videos accompany this chapter:

Video 7.1. Cryoballoon Positioning for Pulmonary Vein (PV) Isolation: Contrast PV Angiography 

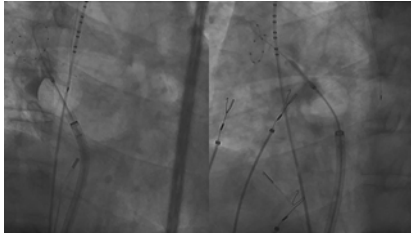
Video 7.2. Cryoballoon Pulmonary Vein (PV) Isolation: Contrast Angiography for Assessment of Vein Occlusion 

Video 7.3. Cryoballoon Positioning for Pulmonary Vein (PV) Isolation: Intracardiac Echocardiography (ICE) 

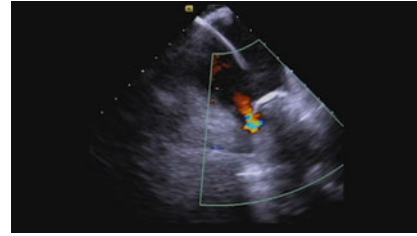
Video 7.4. Laser Balloon Pulmonary Vein (PV) Isolation 

REFERENCES

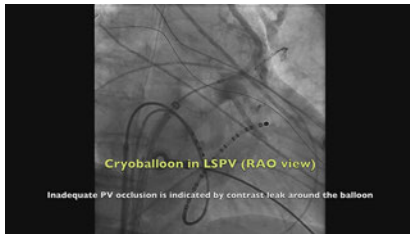
1. Dhillon PS, Gonna H, Li A, et al. Skin burns associated with radiofrequency catheter ablation of cardiac arrhythmias. *Pacing Clin Electrophysiol.* 2013;36:764–767.
2. Koruth JS, et al. Bipolar irrigated radiofrequency ablation: a therapeutic option for refractory intramural atrial and ventricular tachycardia circuits. *Heart Rhythm.* 2012;9:1932–1941.
3. Nguyen DT, et al. Clinical and biophysical evaluation of variable bipolar configurations during radiofrequency ablation for treatment of ventricular arrhythmias. *Heart Rhythm.* 2016;13:2161–2171.
4. Boersma IV, et al. Multielectrode pulmonary vein isolation versus single tip wide area catheter ablation for paroxysmal atrial fibrillation: a multinational multicenter randomized clinical trial. *Circ. Arrhythm. Electrophysiol.* 2016;9:1–8.
5. Greef YDE, et al. Impact of radiofrequency characteristics on acute pulmonary vein reconnection and clinical outcome after PVAC ablation. *J Cardiovasc Electrophysiol.* 2013;24:290–296.
6. Compier MG, et al. Duty-cycled bipolar/unipolar radiofrequency ablation for symptomatic atrial fibrillation induces significant pulmonary vein narrowing at long-term follow-up. *Europace.* 2013;15:690–696.
7. Shin DI, et al. Initial results of using a novel irrigated multielectrode mapping and ablation catheter for pulmonary vein isolation. *Heart Rhythm.* 2014;11:375–383.
8. Rosso R, et al. Radiofrequency ablation of paroxysmal atrial fibrillation with the new irrigated multipolar nMARQ ablation catheter: verification of intracardiac signals with a second circular mapping catheter. *Heart Rhythm.* 2014;11:559–565.
9. Stabile G, et al. Safety and efficacy of pulmonary vein isolation using a circular, open-irrigated mapping and ablation catheter: a multicenter registry. *Heart Rhythm.* 2015;12:1782–1788.
10. Garabelli PJ, Stavrakis S, Po SS. A case series and review of the literature regarding coronary artery complications associated with coronary sinus catheter ablation. *Heart Case Reports.* 2015;1:315–319.
11. Yamada T. Transthoracic epicardial catheter ablation. *Circ J.* 2013;77:1672–1680.
12. Nguyen DT, et al. Effect of irrigant characteristics on lesion formation after radiofrequency energy delivery using ablation catheters with actively cooled tips. *J Cardiovasc Electrophysiol.* 2015;26:792–798.
13. Koruth JS, et al. Occurrence of steam pops during irrigated RF ablation: novel insights from microwave radiometry. *J Cardiovasc Electrophysiol.* 2013;24:1271–1277.
14. Hoffmayer KS, Gerstenfeld EP. Contact force-sensing catheters. *Curr Opin Cardiol.* 2015;30:74–80.
15. Ikeda A, et al. Relationship between catheter contact force and radiofrequency lesion size and incidence of steam pop in the beating canine heart: electrogram amplitude, impedance, and electrode



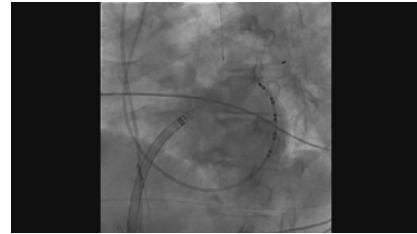
Video 7.1 Cryoballoon Positioning for Pulmonary Vein (PV) Isolation: Contrast PV Angiography. Fluoroscopic images are shown in the right anterior oblique (RAO) and Left anterior oblique (LAO) views during positioning of the cryoballoon at the antrum of the right superior PV (RSPV). Initially, contrast angiography through the balloon catheter reveals distal balloon location within the PV. The balloon is pulled back and maneuvered to optimize antral PV occlusion guided by PV angiography. Similarly, angiography of the right inferior pulmonary vein (RIPV) reveals distal balloon location within the PV. The balloon is pulled back and maneuvered to optimize antral PV occlusion guided by PV angiography. When suboptimal balloon contact with the superior aspect of the RIPV antrum is observed, two maneuvers can be used to facilitate adequate PV occlusion: the “hockey stick technique” and the “pull-down technique.”



Video 7.3 Cryoballoon Positioning for Pulmonary Vein (PV) Isolation: Intracardiac Echocardiography (ICE). ICE imaging is performed with the transducer positioned in the mid right atrium. The cryoballoon is positioned at the antrum of the left superior pulmonary vein (LSPV). Color Doppler imaging reveals persistent flow around the cryoballoon at the inferior aspect of the LSPV, indicating inadequate tissue contact and PV occlusion. Note that flow from the LIPV has to be distinguished from residual flow from the LSPV. LA, Left atrium; LIPV, left inferior pulmonary vein.



Video 7.2 Cryoballoon Pulmonary Vein (PV) Isolation: Contrast Angiography for Assessment of Vein Occlusion. Fluoroscopic images are shown in the right anterior oblique (RAO) projection during positioning of the cryoballoon at the antrum of the left superior pulmonary vein (LSPV). Initially, contrast angiography through the balloon catheter reveals sub-optimal occlusion of the PV antrum by the balloon, as indicated by leak of contrast around the balloon. Repositioning the mapping catheter in a different PV branch helps to change the orientation of the balloon at the PV ostium and achieve PV occlusion on repeat angiography.



Video 7.4 Laser Balloon Pulmonary Vein (PV) Isolation. Fluoroscopic images are shown in the left anterior oblique projection during laser balloon ablation of the left inferior pulmonary vein (LIPV). Initially, contrast angiography of the LIPV is performed via the transseptal sheath. Then, the deflated balloon is advanced into the LIPV and slowly inflated with a mixture of contrast and deuterium dioxide (D_2O). The inflated balloon is manipulated to optimize contact with the antrum of the LIPV. After laser ablation, the balloon catheter is replaced with a circular mapping catheter to confirm electrical isolation of the PV.

- temperature are poor predictors of electrode-tissue contact force and lesion. *Circ. Arrhythmia Electrophysiol.* 2014;7:1174–1180.
16. Shah DC, Namdar M. Real-time contact force measurement: a key parameter for controlling lesion creation with radiofrequency energy. *Circ. Arrhythmia Electrophysiol.* 2015;8:713–721.
 17. Akca F, et al. Radiofrequency ablation at low irrigation flow rates using a novel 12-hole gold open-irrigation catheter. *Pacing Clin Electrophysiol.* 2013;36:1373–1381.
 18. Akca F, et al. High-volume lesions using a new second-generation open irrigation radiofrequency catheter are associated with the development of inhomogeneous lesions. *Pacing Clin Electrophysiol.* 2014;37:864–873.
 19. Hussein AA, et al. Radiofrequency ablation with an enhanced-irrigation flexible-tip catheter versus a standard-irrigation rigid-tip catheter. *Pacing Clin Electrophysiol.* 2015;38:1151–1158.
 20. Reichlin T, et al. Initial impedance decrease as an indicator of good catheter contact: insights from radiofrequency ablation with force sensing catheters. *Heart Rhythm.* 2014;11:194–201.
 21. Chinitz JS, et al. Sites with small impedance decrease during catheter ablation for atrial fibrillation are associated with recovery of pulmonary vein conduction. *J Cardiovasc Electrophysiol.* 2016;27:1390–1398.
 22. Kosmidou I, Houde-Walter H, Foley L, et al. Loss of pace capture after radiofrequency application predicts the formation of uniform transmural lesions. *Europace.* 2013;15:601–606.
 23. Kapa S, Asirvatham SJ. Maintaining contact for effective mapping and ablation. *Circ. Arrhythmia Electrophysiol.* 2014;7:781–784.
 24. Di Biase L, et al. Visual, tactile, and contact force feedback: which one is more important for catheter ablation? Results from an in vitro experimental study. *Heart Rhythm.* 2014;11:506–513.
 25. Kumar S, et al. Predictive value of impedance changes for real-time contact force measurements during catheter ablation of atrial arrhythmias in humans. *Heart Rhythm.* 2013;10:962–969.
 26. Anter E, Tschabrunn CM, Contreras-Valdes FM, et al. Radiofrequency ablation annotation algorithm reduces the incidence of linear gaps and reconnection after pulmonary vein isolation. *Heart Rhythm.* 2014;11:783–790.
 27. Okumura Y, et al. Effect of catheter tip-tissue surface contact on three-dimensional left atrial and pulmonary vein geometries: potential anatomic distortion of 3D ultrasound, fast anatomical mapping, and merged 3D CT-derived images. *J Cardiovasc Electrophysiol.* 2013;24:259–266.
 28. Bunch TJ, Day JD. The atrial fibrillation ablation theory of relativity. *J Cardiovasc Electrophysiol.* 2013;24:267–268.
 29. Sasaki N, et al. Relations between contact force, bipolar voltage amplitude, and mapping point distance from the left atrial surfaces of 3D ultrasound - and merged 3D CT-derived images: implication for atrial fibrillation mapping and ablation. *Heart Rhythm.* 2015;12:36–43.
 30. Bourrier F, et al. Electromagnetic contact-force sensing electrophysiological catheters: how accurate is the technology? *J Cardiovasc Electrophysiol.* 2016;27:347–350.
 31. Afzal MR, et al. Use of contact force sensing technology during radiofrequency ablation reduces recurrence of atrial fibrillation: a systematic review and meta-analysis. *Heart Rhythm.* 2015;12:1990–1996.
 32. Koutalas E, et al. Contemporary mapping techniques of complex cardiac arrhythmias—identifying and modifying the arrhythmogenic substrate. *Arrhythmia Electrophysiol Rev.* 2015;4:19.
 33. Barnett AS, Bahnson TD, Piccini JP. Recent advances in lesion formation for catheter ablation of atrial fibrillation. *Circ Arrhythm Electrophysiol.* 2016;9:e003299.
 34. Andreu D, et al. Contact force threshold for permanent lesion formation in atrial fibrillation ablation: a cardiac magnetic resonance-based study to detect ablation gaps. *Heart Rhythm.* 2016;13:37–45.
 35. Reddy VY, et al. The relationship between contact force and clinical outcome during radiofrequency catheter ablation of atrial fibrillation in the TOCCATA study. *Heart Rhythm.* 2012;9:1789–1795.
 36. Williams SE, et al. The effect of contact force in atrial radiofrequency ablation electroanatomical, cardiovascular magnetic resonance, and histological assessment in a chronic porcine model. *JACC Clin Electrophysiol.* 2015;1:421–431.
 37. Reddy VY, et al. Relationship between catheter stability and 12-month success after pulmonary vein isolation. *JACC Clin Electrophysiol.* 2016;2:691–699.
 38. Fujiwara R, et al. The importance of catheter stability evaluated by VisiTag(TM) during pulmonary vein isolation. *J Interv Card Electrophysiol.* 2016;46:161–166.
 39. Okumura Y, et al. Clinical utility of automated ablation lesion tagging based on catheter stability information (VisiTag Module of the CARTO 3 System) with contact force-time integral during pulmonary vein isolation for atrial fibrillation. *J Interv Card Electrophysiol.* 2016;47:245–252.
 40. Sarkozy A, et al. Contact force in atrial fibrillation: role of atrial rhythm and ventricular contractions: co-force atrial fibrillation study. *Circ Arrhythmia Electrophysiol.* 2015;8:1342–1350.
 41. Chik WWB, et al. Electrogram-gated radiofrequency ablations with duty cycle power delivery negate effects of ablation catheter motion. *Circ Arrhythmia Electrophysiol.* 2014;7:920–928.
 42. Wright M, et al. Visualizing intramyocardial steam formation with a radiofrequency ablation catheter incorporating near-field ultrasound. *J Cardiovasc Electrophysiol.* 2013;24:1403–1409.
 43. Chung FP, Chen SA. Avoiding steam explosions during catheter ablation: ‘Stopping before popping’. *J Cardiovasc Electrophysiol.* 2013;24:1410–1411.
 44. Guerra JM, et al. Effects of open-irrigated radiofrequency ablation catheter design on lesion formation and complications: in vitro comparison of 6 different devices. *J Cardiovasc Electrophysiol.* 2013;24:1157–1163.
 45. Winterfield JR, et al. Lesion size and safety comparison between the novel flex tip on the FlexAbility ablation catheter and the solid tips on the ThermoCool and ThermoCool SF ablation catheters. *J Cardiovasc Electrophysiol.* 2016;27:102–109.
 46. Hocini M, Condie C, Stewart MT, et al. Predictability of lesion durability for AF ablation using phased radiofrequency: power, temperature, and duration impact creation of transmural lesions. *Heart Rhythm.* 2016;13:1521–1526.
 47. Wiczeorek M, et al. Investigation into causes of abnormal cerebral MRI findings following PVAC duty-cycled, phased RF ablation of atrial fibrillation. *J Cardiovasc Electrophysiol.* 2013;24:121–128.
 48. Debruyne P, et al. Formation of thermal coagulum on multielectrode catheters during phased radiofrequency energy ablation of persistent atrial fibrillation. *Pacing Clin Electrophysiol.* 2014;37:188–196.
 49. Kiss A, Sándorfi G, Nagy-baló E, et al. Phased RF ablation: results and concerns. *J Atr Fibrillation.* 2015;8:1240.
 50. Wiczeorek M, Hoeltgen R, Brueck M. Does the number of simultaneously activated electrodes during phased RF multielectrode ablation of atrial fibrillation influence the incidence of silent cerebral microembolism? *Heart Rhythm.* 2013;10:953–959.
 51. Mittal S, Steinberg JS. The last shot for ‘one shot’ pulmonary vein isolation with radiofrequency energy? *J Cardiovasc Electrophysiol.* 2014;25:346–348.
 52. Nagy-Balo E, et al. Predictors of cerebral microembolization during phased radiofrequency ablation of atrial fibrillation: analysis of biophysical parameters from the ablation generator. *Heart Rhythm.* 2014;11:977–983.
 53. Weber S, Höher M, Schultes D. First results and follow-up of a second-generation circular mapping and ablation catheter. *J Interv Card Electrophysiol.* 2016;47:213–219.
 54. Burri H, et al. Pulmonary vein isolation for paroxysmal atrial fibrillation using a circular multipolar ablation catheter: safety and efficacy using low-power settings. *J Cardiovasc Electrophysiol.* 2016;27:170–174.
 55. Rosso R, et al. Radiofrequency ablation of atrial fibrillation: nonrandomized comparison of circular versus point-by-point ‘smart’ ablation for achieving circumferential pulmonary vein isolation and curing arrhythmic symptoms. *J Cardiovasc Electrophysiol.* 2016;[Epub ahead of print].
 56. Avitall B, Kalinski A. Cryotherapy of cardiac arrhythmia: from basic science to the bedside. *Heart Rhythm.* 2015;12:2195–2203.

57. Andrade JG, Khairy P, Dubuc M. Catheter cryoablation: biology and clinical uses. *Circ Arrhythmia Electrophysiol.* 2013;6:218–227.
58. Kaszala K, Ellenbogen KA. Biophysics of the second-generation cryoballoon: cryobiology of the big freeze. *Circ Arrhythmia Electrophysiol.* 2015;8:15–17.
59. Hernández-Romero D, et al. Comparative determination and monitoring of biomarkers of necrosis and myocardial remodeling between radiofrequency ablation and cryoablation. *Pacing Clin Electrophysiol.* 2013;36:31–36.
60. Malmborg H, Christersson C, Lönnérholm S, et al. Comparison of effects on coagulation and inflammatory markers using a duty-cycled bipolar and unipolar radiofrequency pulmonary vein ablation catheter vs. a cryoballoon catheter for pulmonary vein isolation. *Europace.* 2013;15:798–804.
61. Ciconte G, et al. On the quest for the best freeze: predictors of late pulmonary vein reconnections after second-generation cryoballoon ablation. *Circ Arrhythmia Electrophysiol.* 2015;8:1359–1365.
62. Bessière F, et al. Focal transcatheter cryoablation: is a four-minute application still required? *J Cardiovasc Electrophysiol.* 2017;28:559–563.
63. Kenigsberg DN, Martin N, Lim HW, et al. Quantification of the cryoablation zone demarcated by pre- and postprocedural electroanatomic mapping in patients with atrial fibrillation using the 28-mm second-generation cryoballoon. *Heart Rhythm.* 2015;12:283–290.
64. Betts TR, et al. Feasibility of mitral isthmus and left atrial roof linear lesions using an 8 mm tip cryoablation catheter. *J Cardiovasc Electrophysiol.* 2013;24:775–781.
65. Kiplapinar N, et al. Assessment of atrioventricular conduction following cryoablation of atrioventricular nodal reentrant tachycardia in children. *Pacing Clin Electrophysiol.* 2014;37:712–716.
66. Pieragnoli P, et al. Cryoablation of typical AVNRT: younger age and administration of bonus ablation favor long-term success. *Heart Rhythm.* 2015;12:2125–2131.
67. Qureshi MY, Ratnasamy C, Sokoloski M, et al. Low recurrence rate in treating atrioventricular nodal reentrant tachycardia with triple freeze-thaw cycles. *Pacing Clin Electrophysiol.* 2013;36:279–285.
68. Hanninen M, et al. Cryoablation versus RF ablation for AVNRT: a meta-analysis and systematic review. *J Cardiovasc Electrophysiol.* 2013;24:1354–1360.
69. Karadeniz C, Akdeniz C, Turan O, et al. Cryoablation of septal accessory pathways in children: midterm results. *Pacing Clin Electrophysiol.* 2014;37:1095–1099.
70. Collins KK. Cryoablation, limited fluoroscopy, and more. *Pacing Clin Electrophysiol.* 2014;37:1093–1094.
71. Swissa M, et al. Cryotherapy ablation of parahisian accessory pathways in children. *Heart Rhythm.* 2015;12:917–925.
72. Cardoso R, et al. Cryoballoon versus radiofrequency catheter ablation in atrial fibrillation: a meta-analysis. *J Cardiovasc Electrophysiol.* 2016;27:1151–1159.
73. Liu X-H, Chen C-F, Gao X-F, et al. Safety and efficacy of different catheter ablations for atrial fibrillation: a systematic review and meta-analysis. *Pacing Clin Electrophysiol.* 2016;39:883–899.
74. Koektuerk B, et al. Cryoballoon ablation for pulmonary vein isolation in patients with persistent atrial fibrillation: one-year outcome using second generation cryoballoon. *Circ Arrhythm Electrophysiol.* 2015;8:1073–1079.
75. Guhl EN, et al. Efficacy of cryoballoon pulmonary vein isolation in patients with persistent atrial fibrillation. *J Cardiovasc Electrophysiol.* 2016;27:423–427.
76. Boveda S, et al. Outcomes after cryoballoon or radiofrequency ablation for persistent atrial fibrillation: a multicentric propensity-score matched study. *J Interv Card Electrophysiol.* 2016;47:133–142.
77. Di Biase L, et al. Safety and outcomes of cryoablation for ventricular tachyarrhythmias: results from a multicenter experience. *Heart Rhythm.* 2011;8:968–974.
78. Bordignon S, et al. Energy titration strategies with the endoscopic ablation system: lessons from the high-dose vs. low-dose laser ablation study. *Europace.* 2013;15:685–689.
79. Dukkupati SR, et al. Pulmonary vein isolation using a visually guided laser balloon catheter: the first 200-patient multicenter clinical experience. *Circ Arrhythm Electrophysiol.* 2013;6:467–472.
80. Dukkupati SR, et al. Pulmonary vein isolation using the visually guided laser balloon a prospective, multicenter, and randomized comparison to standard radiofrequency ablation. *J Am Coll Cardiol.* 2015;66:1350–1360.
81. Buch E, Shivkumar K. Catheter ablation of atrial fibrillation advent of second-generation technologies. *J Am Coll Cardiol.* 2015;66:1361–1363.
82. Miller DL, et al. Overview of therapeutic ultrasound applications and safety considerations. *J Ultrasound Med.* 2012;31:623–634.
83. Laughner JJ, Sulkin MS, Wu Z, et al. Three potential mechanisms for failure of high intensity focused ultrasound ablation in cardiac tissue. *Circ Arrhythmia Electrophysiol.* 2012;5:409–416.
84. Wu Z, Kumon RE, Laughner JJ, et al. Electrophysiological changes correlated with temperature increases induced by high-intensity focused ultrasound ablation. *Ultrasound Med Biol.* 2015;41:432–448.
85. Neven K, Metzner A, Schmidt B, et al. Two-year clinical follow-up after pulmonary vein isolation using high-intensity focused ultrasound (HIFU) and an esophageal temperature-guided safety algorithm. *Heart Rhythm.* 2012;9:407–413.
86. Brace CL. Microwave tissue ablation: biophysics, technology, and applications. *Crit Rev Biomed Eng.* 2010;38:65–78.
87. Tse H-F, et al. Determinants of lesion dimensions during transcatheter microwave ablation. *Pacing Clin Electrophysiol.* 2009;32:201–208.
88. Vicol C, et al. Long-term results after ablation for long-standing atrial fibrillation concomitant to surgery for organic heart disease: is microwave energy reliable? *J Thorac Cardiovasc Surg.* 2008;136:1156–1159.
89. DeSimone CV, Kapa S, Asirvatham SJ. Electroporation past and future of catheter ablation. *Circ Arrhythmia Electrophysiol.* 2014;7:573–575.
90. Kotnik T, et al. Electroporation-based applications in biotechnology. *Trends Biotechnol.* 2015;33:480–488.
91. Jiang C, Davalos RV, Bischof JC. A review of basic to clinical studies of irreversible electroporation therapy. *IEEE Trans Biomed Eng.* 2015;62:4–20.
92. van Driel VJHM, et al. Pulmonary vein stenosis after catheter ablation: electroporation versus radiofrequency. *Circ Arrhythmia Electrophysiol.* 2014;7:734–738.
93. Du Pré BC, et al. Minimal coronary artery damage by myocardial electroporation ablation. *Europace.* 2013;15:144–149.
94. Neven K, et al. Myocardial lesion size after epicardial electroporation catheter ablation after subxiphoid puncture. *Circ Arrhythmia Electrophysiol.* 2014;7:728–733.

Sinus Node Dysfunction

OUTLINE

Anatomy and Physiology of the Sinus Node, 238

- Anatomy, 238
- Histology, 238
- Physiology, 238
- Blood Supply, 239
- Innervation, 239

Pathophysiology of Sinus Node Dysfunction, 240

- Intrinsic Sinus Node Dysfunction, 240
- Extrinsic Sinus Node Dysfunction, 241

Clinical Presentation, 242

Epidemiology and Natural History, 242

Diagnostic Evaluation, 242

- Electrocardiogram and Ambulatory Monitoring, 242
- Autonomic Modulation, 243
- Exercise Testing, 243
- Electrophysiological Testing, 243

Electrocardiographic Features, 243

- Sinus Bradycardia, 243
- Sinus Arrest, 243

Sinoatrial Exit Block, 243

Chronotropic Incompetence, 243

Tachycardia-Bradycardia Syndrome, 244

Atrial Fibrillation With Slow Ventricular Response, 244

Carotid Sinus Hypersensitivity, 245

Atrial Standstill, 245

Sinus Arrhythmia, 245

Wandering Atrial Pacemaker, 246

Electrophysiological Testing, 246

Role of Electrophysiological Testing, 246

Sinus Node Recovery Time, 246

Sinoatrial Conduction Time, 248

Effects of Drugs, 250

Principles of Management, 251

Acute Management, 251

Chronic Management, 251

Pacemaker Device and Mode Selection, 251

ANATOMY AND PHYSIOLOGY OF THE SINUS NODE

Anatomy

The sinus node is a crescent-shaped, subepicardial specialized muscular structure located posterolaterally in the right atrium (RA) free wall. The sinus node lies within the epicardial groove of the sulcus terminalis, at the junction of the anterior trabeculated RA appendage with the posterior smooth-walled venous component (Fig. 8.1). The endocardial aspect of the sulcus terminalis is marked by the crista terminalis. Although the head and proximal body portion of the node usually is located subepicardially beneath the fatty tissues at the junction of the superior vena cava (SVC) and the RA appendage, the remaining nodal body and tail portions penetrate inferiorly and obliquely into the musculature of crista terminalis to end subendocardially almost to the inferior vena cava (IVC). The sinus node is a tadpole-shaped structure with a head, central body, and tail with nodal extensions representing multiple limbs. The head extends toward the interatrial groove, and the tail extends toward the orifice of IVC. In adults the sinus node measures 8 to 22 mm long and 2 to 3 mm wide and thick.¹⁻⁴

Histology

The sinus node appears to be a distributed complex of weakly coupled, heterogeneous cells, including mesh-like nests of densely packed specialized myocytes (the principal pacemaker cell) as well as nonpacemaker cells embedded in a dense supporting connective matrix (see Fig. 8.1).^{1,2,5}

Within the sinus node, pacemaker cells (referred to as P cells because of their relatively pale appearance on electron microscopy) vary by

size, shape, and electrophysiological (EP) properties and may be divided into three major classes: (1) “elongated spindle-shaped cells,” which are spindle shaped but with long cell dimension (extending up to 80 μm in length) and can be multinucleated; (2) “spindle cells,” which have a faintly striated spindle-shaped cell body, similar shape to that of elongated spindle cells, but are shorter in length (extending up to 40 μm) and are predominantly mononucleated; and (3) “spider cells,” which have irregularly shaped branches with blunt ends.^{6,7}

The nodal margins can be discrete, with fibrous separation from the surrounding atrial myocardium, or interdigitating with the atrium though a transitional zone. Commonly, prongs of nodal and transitional cells extend from the nodal central area toward the perinodal region and atrial myocardium. The transitional zone at the node periphery exhibits mosaic features with gradation of cellular structural and membrane EP properties from the primary pacemaker cells to atrial myocardium. Compared with atrial working myocytes, nodal cells are smaller and have fewer myofilaments, poorly developed sarcomeres and sarcoplasmic reticulum, lower cell-to-cell electrical coupling, and higher density of nuclei. A gradient in myofilament content is observed from center to periphery.⁷⁻⁹

Physiology

The sinus node is the dominant pacemaker of the heart. Its pacemaker function is determined by its reduced maximum diastolic membrane potential and steep phase 4 spontaneous depolarization. The molecular mechanisms of pacemaker function of the sinus node are discussed in detail in **Chapters 1 and 3**.

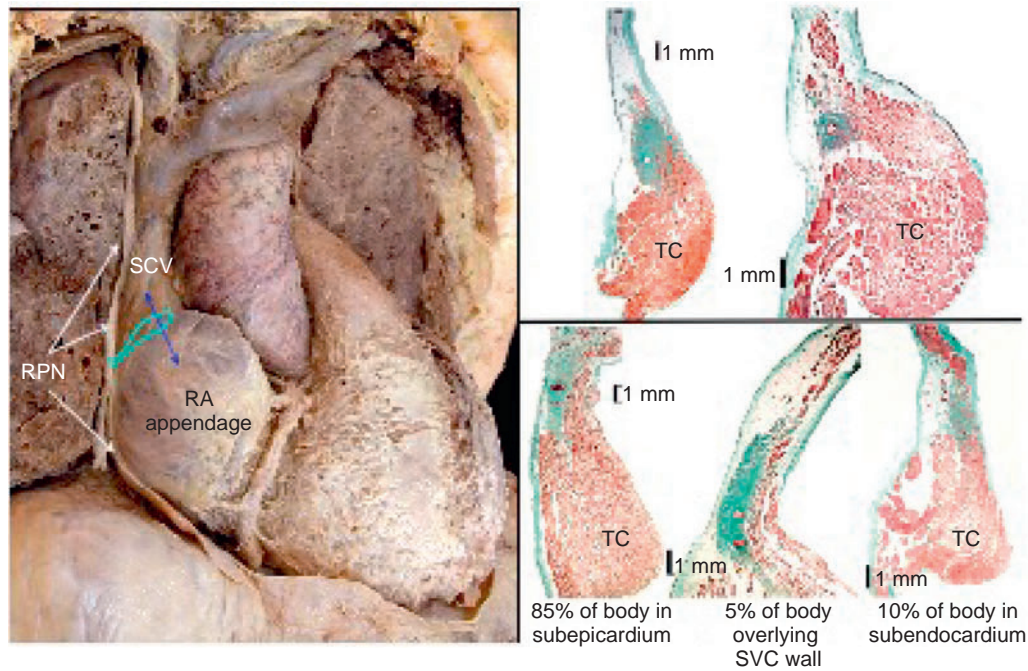


Fig. 8.1 Anatomy of the Sinus Node. Anterior view of the heart in a cadaver that has been dissected to show the course of the right phrenic nerve (RPN) relative to the right atrium (RA). The anticipated location of the sinus node outlined with the dots. The double-headed arrow represents the sectioning plane used for making the cross-sections through the sinus node and the terminal crest (TC) shown in the histological sections. The histological sections in the two upper panels show variations in sizes of the sinus node cross-section and the TC. With this stain (Masson trichrome), the node is recognizable by its fibrous matrix (green) and its artery. The lower panels show variations in nodal location relative to the epicardial and endocardial surfaces and to the superior caval vein (SCV). (From Ho SY, Sánchez-Quintana D. Anatomy and pathology of the sinus node. *J Interv Card Electrophysiol.* 2015;46:3–8, with permission.)

The pacemaker activity is not confined to a single cell in the sinus node; rather, nodal cells function as electrically coupled oscillators that discharge synchronously because of mutual entrainment. It is possible that sinus rhythm results from impulses originating at widely separated sites, with two or three individual wavefronts merging to form a single, widely disseminated wavefront. Mapping of electrograms in and around the node has disclosed a multicentric initiation of activation with irregular propagation to the atrial myocardium.

Current models involve the concept of a “pacemaker hierarchy” within the sinus node, with cells that depolarize at a higher frequency generating faster heart rates located at the superior compartments (head) of the sinus node, whereas slower firing cells are located at the inferior part (tail). The hierarchy mediates heart rate changes (in response to physiological stimuli) via a dynamic craniocaudal shift in the “leading pacemaker” site. For example, sympathetic stimulation shifts the leading pacemaker site superiorly, resulting in an increase in heart rate.³

The sinus node is insulated electrically from the surrounding atrial myocytes, except at a limited number of preferential exit sites that allow transmission of sinus impulses to atrial myocardium. Anatomical insulation (provided by substantial interstitial tissue, fat, and blood vessels) and functional barriers (poor electrical coupling between adjacent cells due to reduced expression of connexins) are critical for protecting the small cluster of pacemaker cells in the sinus node from the hyperpolarizing influence of the surrounding atrial myocardium and enabling “source” nodal cells to overcome the source-sink mismatch and depolarize the much larger surrounding atrial tissue (sink).^{3,6,7,10}

Blood Supply

The blood supply to the sinus node region predominantly comes from a large central artery, the sinus nodal artery, which is a branch of the right coronary artery in 55% to 60% of patients and from the circumflex artery in 40% to 45%. The sinus nodal artery typically passes centrally through the length of the sinus body, and it is disproportionately large, which is considered physiologically important in that its perfusion pressure can affect the sinus rate. Distention of the artery slows the sinus rate, whereas collapse causes an increase in sinus rate.³

Innervation

The sinus node is densely innervated with postganglionic adrenergic and cholinergic nerve terminals (threefold greater density of beta-adrenergic and muscarinic cholinergic receptors than adjacent atrial tissue). Neural and hormonal factors influence both the rate of spontaneous depolarization in pacemaker cells (likely via craniocaudal shift in the principal pacemaker site within the sinus node region) and the point of exit from the sinus node complex to the atrium. These changes often are associated with subtle changes in P wave morphology. The right vagus nerve predominantly affects sinus node function.^{2,5,11}

Enhanced vagal activity can produce sinus bradycardia, sinus arrest, and sinoatrial exit block, whereas increased sympathetic activity can increase the sinus rate and reverse sinus arrest and sinoatrial exit block. Sinus node responses to brief vagal bursts begin after a short latency and dissipate quickly. In contrast, responses to sympathetic stimulation begin and dissipate slowly. The rapid onset and offset of responses to vagal stimulation allow dynamic beat-to-beat vagal modulation of the

heart rate, whereas the slow temporal response to sympathetic stimulation precludes any beat-to-beat regulation by sympathetic activity.^{3,10}

Periodic vagal bursting (as may occur each time a systolic pressure wave arrives at the baroreceptor regions in the aortic and carotid sinuses) induces phasic changes in the sinus cycle length (CL) and can entrain the sinus node to discharge faster or slower at periods identical to those of the vagal burst. Because the peak vagal effects on sinus rate and atrioventricular node (AVN) conduction occur at different times in the cardiac cycle, a brief vagal burst can slow the sinus rate without affecting AVN conduction or can prolong AVN conduction time and not slow the sinus rate.

PATHOPHYSIOLOGY OF SINUS NODE DYSFUNCTION

Sinus node dysfunction (SND) refers to a wide range of abnormalities involving sinus node and atrial impulse generation and propagation, leading to the inability of the sinus node to generate heart rates that are appropriate for the physiological needs. Causes of SND can be classified as intrinsic (secondary to a pathological condition involving the sinus node proper, [Box 8.1](#)) or extrinsic (caused by depression of sinus node function by external factors such as drugs or autonomic influences, [Box 8.2](#)).

Not only automaticity of the individual nodal cells but also architectural factors at the tissue level are essential for normal pacemaking function. Defects in sinus node architecture can disrupt the normal source-sink balance, leading to SND. Structural changes (e.g., sinus nodal cell loss and fibrosis) and alterations in the normal gradient of EP properties in the sinus node complex likely underlie slowing of pacemaking with normal aging and cardiovascular disease (e.g., atrial fibrillation [AF], heart failure). Furthermore, autonomic modulation, adenosine, ischemia, and structural remodeling can potentially lead not only to depression of sinus pacemaker function but also to complete block of conduction through all nodal conduction pathways.^{6,12–14}

Intrinsic Sinus Node Dysfunction

Degenerative Diseases

SND is generally a disease of aging, and idiopathic degenerative disease is probably the most common cause of intrinsic SND. Aging-related

progressive fibrosis with cell loss and degeneration (structural remodeling), as well as EP remodeling of the sinus node (e.g., during AF), are important factors in the pathophysiology of SND. These degenerative changes are typically more diffuse, affecting surrounding atrial tissue (atrial remodeling or “atriopathy”), as well as other parts of the conduction system. The frequent lack of an effective escape rhythm in patients with SND and the long asystolic pauses are likely a manifestation of the diffuse nature of the conduction system disease.^{5,9,15}

Ischemic Heart Disease

Coronary artery disease is very common among SND patients. Although this can be coincidental, because both diseases tend to occur in older individuals, ischemic heart disease is thought to be responsible for as much as one-third of chronic SND. In addition, SND (sinus bradycardia or sinus arrest) is observed in up to 15% to 25% of patients with acute myocardial infarction (MI), most commonly in inferior and posterior infarctions.

SND after an acute MI is usually a transient phenomenon, most commonly related to increased vagal tone, and is generally associated with other signs of vagotonia, such as atrioventricular (AV) conduction delay, and is responsive to atropine and catecholamine stimulation. Possible mechanisms include neurological reflexes (Bezold-Jarisch reflex), coronary chemoreflexes (vagally mediated), humoral reflexes (enzymes, adenosine, potassium [K⁺]), and oxygen-conserving reflex (“diving” reflex). Pain and the use of vagotonic medications, such as morphine, can potentiate vagal tone and exacerbate SND. However, infarction or ischemia of the sinus node or the surrounding atrium (e.g., secondary to proximal occlusion of the right or the circumflex coronary artery) can also cause SND, which can be more persistent.⁹

BOX 8.1 Causes of Intrinsic Sinus Node Dysfunction

Idiopathic degenerative disorder (most common)
Ischemic heart disease
Genetic defects: mutations in *SCN5A*, *HCN4*, *GJA5*, *ANK2*, and *EMD* genes
Atrial tachyarrhythmias
Hypertensive heart disease
Cardiomyopathy
Congenital heart disease: sinus venosus atrial septal defect, left atrial isomerism
Surgical trauma: Mustard, Senning, Glenn, and Fontan procedures
Cardiac transplant
Inflammatory diseases: rheumatic fever, pericarditis, myocarditis
Infectious causes: Lyme disease, legionella, Q fever, typhoid, psittacosis, malaria, leptospirosis, Chagas disease
Collagen vascular disease: systemic lupus, scleroderma
Infiltrative diseases: amyloidosis, sarcoidosis, hemochromatosis, tumors
Neuromuscular disorders: Friedreich ataxia, myotonic dystrophy, Emery-Dreifuss muscular dystrophy

BOX 8.2 Causes of Extrinsic Sinus Node Dysfunction

Drugs

Antiarrhythmic agents
Class IA: quinidine, procainamide
Class IC: propafenone, flecainide
Class II: beta blockers
Class III: sotalol, amiodarone, dronedarone
Class IV: diltiazem, verapamil
Ivabradine
Digitalis
Sympatholytic antihypertensive agents: clonidine, reserpine, methyldopa
Parasympathomimetic agents: acetylcholine, carbachol, acetylcholinesterase inhibitors
Opioids: morphine
Antipsychotic agents: lithium, phenothiazines, amitriptyline
Chemotherapeutic agents: thalidomide, paclitaxel
Miscellaneous: cimetidine, phenytoin

Autonomic influences

Excessive vagal tone
Neurocardiogenic syncope (cardioinhibitory)
Carotid sinus hypersensitivity (cardioinhibitory)
Well-trained athletes

Hypothermia

Hyperkalemia
Increased intracranial pressure (the Cushing response)
Hypoxemia
Hypercapnia
Sleep apnea
Hypothyroidism

Atrial Arrhythmias

Atrial tachyarrhythmias can precipitate SND, likely secondary to sinus node remodeling. Although early studies implicated anatomical structural abnormalities in the sinus node, which suggested a fixed SND substrate, more recent evidence has implicated a functional, and potentially reversible, component involving remodeling of sinus node ion channel expression and function.¹¹ This finding is supported clinically by the observation that successful catheter ablation of AF and atrial flutter (AFL) can be followed by significant improvements in sinus node function. In particular, downregulation of the funny current (I_f) and malfunction of the calcium (Ca^{2+}) clock (characterized by reduced sarcoplasmic reticulum Ca^{2+} release and downregulated ryanodine receptors in the sinus node) seem to account largely for tachycardia-induced remodeling of sinus node.¹⁶ The remodeled atria are associated with more caudal activation of the sinus node complex, slower conduction time along preferential pathways, and only modest shifts within the functional pacemaker complex.^{17,18} Endogenous adenosine recently has been implicated in the pathophysiology of SND following termination of atrial tachyarrhythmias.^{5,19}

On the other hand, SND has been associated with an increased propensity for atrial tachyarrhythmias, AF in particular.²⁰ The mechanism leading to AF in patients with SND is unlikely to be bradycardia-dependent because AF was found to develop despite pacing in these patients. Importantly, patients with SND appear to have more widespread atrial changes beyond the sinus node, a finding indicating atrial myopathy with fibrosis and scar formation, as evidenced by increased atrial refractoriness, prolonged P wave duration, conduction slowing, electrogram fractionation, and regions of low voltage and scar.⁵ Furthermore, abnormal atrial electromechanical properties, chronic atrial stretch, and neurohormonal activation are likely contributors to SND and its related atrial myopathy. Atrial and sinus node remodeling in heart failure, hypertension, and aging have shown caudal shift of the pacemaker complex with loss of normal multicentric pattern of activation. Similar and often more severe atrial and sinus node remodeling has been observed in patients with intermittent atrial tachyarrhythmias. The diffuse atrial myopathy potentially underlies the increased propensity to both SND and atrial arrhythmias.^{10,21–25}

Familial Sinus Node Dysfunction

Genetic defects in ion channels and structural proteins have been shown to contribute to SND, many of which also exhibit an increased propensity to AF. Mutations in the *SCN5A* gene (which encodes the alpha subunit of the cardiac sodium [Na^+] channel [I_{Na}]), have been linked to sick sinus syndrome, manifesting as sinus bradycardia, sinus arrest, sinoatrial block, or a combination of these conditions, which can progress to atrial inexcitability (atrial standstill). Loss-of-function *SCN5A* mutations result in reduced peak I_{Na} density, hyperpolarizing shifts in the voltage dependence of steady-state channel availability, and slow recovery from inactivation. These effects likely cause reduced automaticity, decreased excitability, and conduction slowing or block of impulses generated in the sinus node to the surrounding atrial tissue. SND can also manifest concomitantly with other phenotypes that are linked to *SCN5A* loss-of-function mutations such as Brugada syndrome and progressive cardiac conduction disorders (Lev-Lenègre disease).^{8,9,26–29}

Heterozygous mutations in the *HCN4* gene (which encodes the protein that contributes to formation of I_f channels) have been identified in individuals with sinus bradycardia and chronotropic incompetence. Severe bradycardia, QT prolongation, and torsades de pointes have been described in another family. *HCN* mutations slow channel activation kinetics or, when located in cyclic nucleotide-binding domains, abolish sensitivity of HCN channels to cyclic adenosine monophosphate, thus reducing I_f and the rate of diastolic depolarization.^{8,30}

Several other mutations have been associated with familial forms of SND, including mutations in the *ANK2* gene (which encodes for ankyrin, which links the integral membrane proteins to the underlying cytoskeleton), the *MYH6* gene (which encodes for atrial myosin heavy chain), and the *EMD* gene (which encodes the nuclear membrane protein emerin). Mutations in the *GJA5* gene (which encodes for connexin 40, a gap junction protein), have been associated with individuals with atrial standstill and AF. In addition, mutations in the calsequestrin gene (*CASQ2*), which is involved in Ca^{2+} handling and is associated with catecholaminergic polymorphic ventricular tachycardia, have been linked to SND.^{8,26,27,31}

Congenital Heart Disease

Congenital heart disease, such as sinus venosus atrial septal defects, can be associated with SND, even though no surgery has been performed. Heterotaxy syndromes, particularly left atrial (LA) isomerism, can be associated with congenital absence of the sinus node.^{28,32}

A more common cause of SND in patients with congenital heart disease is sinus node injury caused by corrective cardiac surgery. Most commonly associated with this complication is the Mustard, Senning, Glenn, and Fontan operations, as well as repair of atrial septal defects, especially of the sinus venosus type. Surgical incisions, suture lines, and cannulation of the SVC can result in direct damage to the sinus node, its blood supply, or neural inputs.³² In addition, SND may develop as a consequence of longstanding hemodynamic perturbations or the atrial arrhythmias frequently observed in this patient population.

Other Causes

Cardiomyopathy and longstanding hypertension can result in SND. Orthotopic cardiac transplantation with atrial-atrial anastomosis is associated with a high incidence of SND in the donor heart (likely because of sinus nodal artery damage); this is far less likely with a caval-caval anastomosis. Musculoskeletal disorders such as myotonic dystrophy or Friedreich ataxia are rare causes of SND. Other causes of SND include a variety of infiltrative, infectious, and inflammatory disorders (see Box 8.1).

Extrinsic Sinus Node Dysfunction

In the absence of structural abnormalities, the predominant causes of SND are drug effects and autonomic influences (see Box 8.2).

Drugs

Drugs can alter sinus node function by direct pharmacological effects on nodal tissue or indirectly by neurally mediated effects. Drugs known to depress sinus node function include beta-blockers, calcium channel blockers (verapamil and diltiazem), digoxin, sympatholytic antihypertensive agents (e.g., clonidine), and antiarrhythmic agents.

Autonomic Influences

SND can sometimes result from excessive vagal tone in individuals without intrinsic sinus node disease. Hypervagotonia can be seen in hypersensitive carotid sinus syndrome and neurocardiogenic syncope.³³ Surges in vagal tone also can occur during Valsalva maneuvers, endotracheal intubation, vomiting, and coughing. Sinus slowing in this setting is characteristically paroxysmal and may be associated with evidence of AV conduction delay, secondary to effects of the enhanced vagal tone on both the sinus node and AVN.

Significant sinus bradycardia is very common in highly conditioned athletes and is usually correlated to type and intensity of training. Respiratory sinus arrhythmia, wandering pacemaker, junctional bradycardia, first-degree AV block, and Wenckebach second-degree AV block are also more common in this population. These changes, at least

in the initial stages, have been attributed to increased vagal tone. However, over time, endurance training does lead to intrinsic changes in the sinus node and the cardiac conduction system potentially related to dilatation and hypertrophy of the athlete's heart. Deconditioning of athletes can sometimes help to prevent symptomatic bradyarrhythmias; however, it is not uncommon that slow heart rates persist for many years after training has stopped.³⁴

Other Causes

Obstructive sleep apnea can be associated with significant sinus bradycardia and long sinus pauses during apneic episodes. Less common extrinsic causes of SND include electrolyte abnormalities such as hyperkalemia, hypothermia, increased intracranial pressure (the Cushing response), hypoxia, hypercapnia, hypothyroidism, and obstructive jaundice.

CLINICAL PRESENTATION

Patients with SND often are asymptomatic or have symptoms that are mild and nonspecific, and the intermittent nature of these symptoms makes documentation of the associated arrhythmia difficult at times. In addition, because most patients with SND are elderly, symptoms of the disease can erroneously be attributed to the aging process or other comorbidities.

Symptoms of SND include paroxysmal dizziness, presyncope, or syncope, which are predominantly related to prolonged sinus pauses. Episodes of syncope are often unheralded and can manifest in older patients as repeated falls. The highest incidence of syncope associated with SND probably occurs in patients with tachycardia-bradycardia syndrome, in whom syncope typically occurs secondary to a long sinus pause following cessation of the supraventricular tachyarrhythmia (usually AF). Occasionally, a stroke can be the first manifestation of SND in patients presenting with paroxysmal AF and thromboembolism.

Patients with sinus bradycardia or chronotropic incompetence often present with decreased exercise capacity or fatigue. Chronotropic incompetence is estimated to be present in 20% to 60% of patients with SND. Other symptoms include irritability, nocturnal wakefulness, memory loss, lightheadedness, and lethargy. More subtle symptoms include mild digestive disturbances, periodic oliguria or edema, and mild intermittent dyspnea. In addition, symptoms caused by the worsening of conditions such as congestive heart failure and angina pectoris can be precipitated by SND.

EPIDEMIOLOGY AND NATURAL HISTORY

SND is largely a disease of the elderly, and its incidence increases exponentially with age. Most SND patients are in their seventh or eighth decade of life and have frequent comorbid diseases. SND in young patients is often related to underlying heart disease. Although the exact incidence of SND is difficult to determine, a recent report estimated the incidence of SND at 0.8 per 1000 person-years. SND likely accounts for 50% or more of permanent pacemaker placements in the United States. With the aging population, it is projected that the annual incidence of SND cases in the United States will increase from 78,000 in 2012 to 172,000 in 2060 (Fig. 8.2). The most significant risk factor for SND is advancing age. Other risk factors include greater body mass index, longer QRS duration, hypertension, right bundle branch block, and cardiovascular disease. Blacks carry a 41% lower risk of SND than whites. Men and women appear equally affected.³⁵

The natural history of SND can be variable, but slow progression (over 10 to 30 years) is expected. The prognosis largely depends on the type of SND and the presence and severity of the underlying heart disease. SND does not appear to affect survival whether untreated or

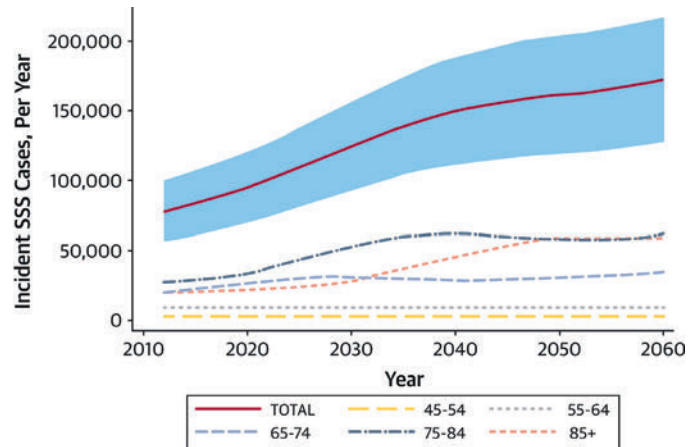


Fig. 8.2 Incidence of Sick Sinus Syndrome. Estimated number of incident sick sinus syndrome (SSS) cases per year, overall and by age group in the United States, 2012 to 2060. (From Jensen PN, Gronroos NN, Chen LY, et al. Incidence of and risk factors for sick sinus syndrome in the general population. *J Am Coll Cardiol*. 2014;64:531–538, with permission.)

treated with pacemaker therapy. The incidence of sudden death is extremely low; mortality in patients with SND is primarily determined by underlying heart disease. The worst prognosis is associated with the tachycardia-bradycardia syndrome (mostly because of the risk for thromboembolic complications), whereas sinus bradycardia is much more benign.

Up to 50% of SND patients experience episodes of AF over a lifetime. The incidence of new-onset AF in patients with SND is approximately 5.2% per year. Atrial-based pacing (AAI or DDD) in SND patients is associated with a 20% reduction in risk of AF and stroke as compared with single-chamber ventricular pacing.

The incidence of advanced AV conduction system disease in patients with SND is relatively low (5% to 10%), and, when present, its progression is slow. At the time of diagnosis of SND, approximately 17% of the patients have some degree of AV conduction system disease (PR interval longer than 240 milliseconds, BBB, HV interval prolongation, AV Wenckebach rate less than 120 beats/min, or second- or third-degree AV block). New AV conduction abnormalities develop at a rate of approximately 7% per year in patients with baseline BBB or bifascicular block but much less frequently (0.6% to 1.8% per year) in those without any evidence of AV or intraventricular conduction abnormalities. The incidence of advanced AV block during long-term follow-up is low (approximately 1% per year).³⁶

DIAGNOSTIC EVALUATION

In general, the noninvasive methods of electrocardiogram (ECG) monitoring, exercise testing, and autonomic testing are used first. However, if symptoms are infrequent and noninvasive evaluation is unrevealing, invasive EP testing can be considered.

Electrocardiogram and Ambulatory Monitoring

A 12-lead ECG needs to be obtained in symptomatic patients. However, the diagnosis of SND as the cause of the symptoms is rarely made from the ECG. In patients with frequent symptoms, 24- or 48-hour ambulatory Holter monitoring can be useful. Cardiac event monitoring or implantable loop recorders may be necessary in patients with less frequent symptoms. Documentation of symptoms in a diary by the patient while wearing the cardiac monitor is essential for correlation of symptoms

with the heart rhythm at the time. In some cases, ambulatory monitoring can exclude SND as the cause of symptoms if normal sinus rhythm (NSR) is documented at the time of symptom occurrence. In contrast, recorded sinus pauses may not be associated with symptoms.

Autonomic Modulation

An abnormal response to carotid sinus massage (pause longer than 3 seconds) can indicate SND, but this response can also occur in asymptomatic older individuals. Heart rate response to the Valsalva maneuver (normally decreased) or upright tilt (normally increased) can also be used to verify that the autonomic nervous system itself is intact. Complete pharmacological autonomic blockade is used to determine the intrinsic heart rate (see later).

Exercise Testing

Exercise testing to assess chronotropic incompetence is of value in patients with exertional symptoms (see later).

Electrophysiological Testing

In the majority of patients, noninvasive testing is adequate in establishing the diagnosis of SND and guiding subsequent therapy. However, invasive EP testing can be of value in symptomatic patients in whom SND is suspected but cannot be documented in association with symptoms. In addition to assessing the function of the sinus node, EP testing can be useful in evaluating other potential causes for symptoms of syncope and palpitations (e.g., AV block, supraventricular tachycardia, and ventricular tachycardia).

ELECTROCARDIOGRAPHIC FEATURES

Sinus Bradycardia

Sinus bradycardia (less than 60 beats/min) is considered abnormal when it is persistent, unexplained, and inappropriate for physiological circumstances. Sinus bradycardia slower than 40 beats/min (not associated with sleep or physical conditioning) is generally considered abnormal.

Sinus Arrest

The terms *sinus arrest* and *sinus pause* are often used interchangeably; sinus arrest is a result of total cessation of impulse formation within the sinus node. The pause is not an exact multiple of the preceding P-P interval but is random in duration (Fig. 8.3). Although asymptomatic pauses of 2 to 3 seconds can be seen in up to 11% of normal individuals and in one-third of trained athletes (especially during sleep), pauses longer than 3 seconds are rare in normal individuals and may or may not be associated with symptoms, but they are usually caused by underlying SND.

Sinoatrial Exit Block

Sinoatrial exit block results when a normally generated sinus impulse fails to conduct to the atria because of delay in conduction or block

within the sinus node itself or perinodal tissue. Sinoatrial exit block produces a pause that is eventually terminated by a delayed sinus beat or an atrial or junctional escape beat. In theory, sinoatrial exit block can be distinguished from sinus arrest because the exit block pause is an exact multiple of the baseline P-P interval. However, sinus arrhythmia causing normal beat-to-beat variations in the sinus rate often makes the distinction impossible. Establishing the diagnosis of sinoatrial exit block versus sinus arrest is often of academic interest only.

Sinoatrial exit block is classified into three types, analogous to those of AV block: first-degree, second-degree, and third-degree exit block. First-degree sinoatrial exit block is caused by abnormal prolongation of the sinoatrial conduction time (SACT). It occurs every time a sinus impulse reaches the atrium, but it is conducted with a delay at a fixed interval. This type of sinoatrial exit block is concealed on the surface ECG and can be diagnosed only by direct sinus node recording or indirect measurement of SACT during an EP study.

Second-degree sinoatrial exit block is marked by intermittent failure of the sinus impulse to exit the sinus node. Type I block is viewed as Wenckebach periodicity of the P wave on the surface ECG, and it manifests as progressive delay in conduction of the sinus-generated impulse through the sinus node to the atrium, finally resulting in a nonconducted sinus impulse and absence of a P wave on the surface ECG. Because the sinus discharge is a silent event on the surface ECG, this arrhythmia can be inferred only, because of a missing P wave and the signs of Wenckebach periodicity seen with this type of arrhythmia. The increment in delay in impulse conduction through the sinus node tissue is progressively less; thus the P-P intervals become progressively shorter until a P wave fails to occur. The pauses associated with this type of sinoatrial exit block are less than twice the shortest sinus cycle.

Type II block manifests as an abrupt absence of one or more P waves because of failure of the sinus impulse to exit the sinus node, without previous progressive prolongation of SACT (and without progressive shortening of the P-P intervals). Sometimes, two or more consecutive sinus impulses are blocked within the sinus node, thus creating considerably long pauses. The sinus pause should be an exact multiple of the immediately preceding P-P interval. However, normal variations in the sinus rate caused by sinus arrhythmia can obscure this measurement.

Third-degree or complete sinoatrial exit block manifests as absence of sinus P waves, with long pauses resulting in lower pacemaker escape rhythm. This type of block is impossible to distinguish from sinus arrest with certainty without invasive sinus node recordings.

Chronotropic Incompetence

The term *chronotropic incompetence* is used to denote an inadequate heart rate response to increases in metabolic demands. Although the resting heart rate can be normal, patients with chronic incompetence are unable to increase their heart rate during exercise or may have unpredictable fluctuations in the heart rate during activity. Some patients can initially experience a normal increase in the heart rate with exercise, which then plateaus or decreases inappropriately.

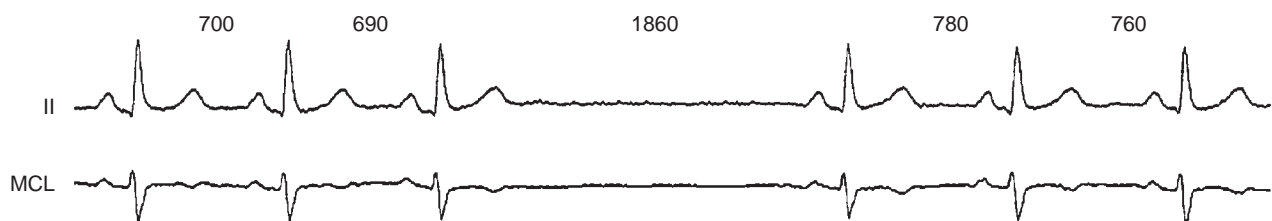


Fig. 8.3 Sinus Pause. Sinus pause is shown in two monitor leads. Although the sinus rate is slightly irregular, the pause significantly exceeds any two P-P intervals (excluding sinus exit block). *MCL*, Modified chest lead.

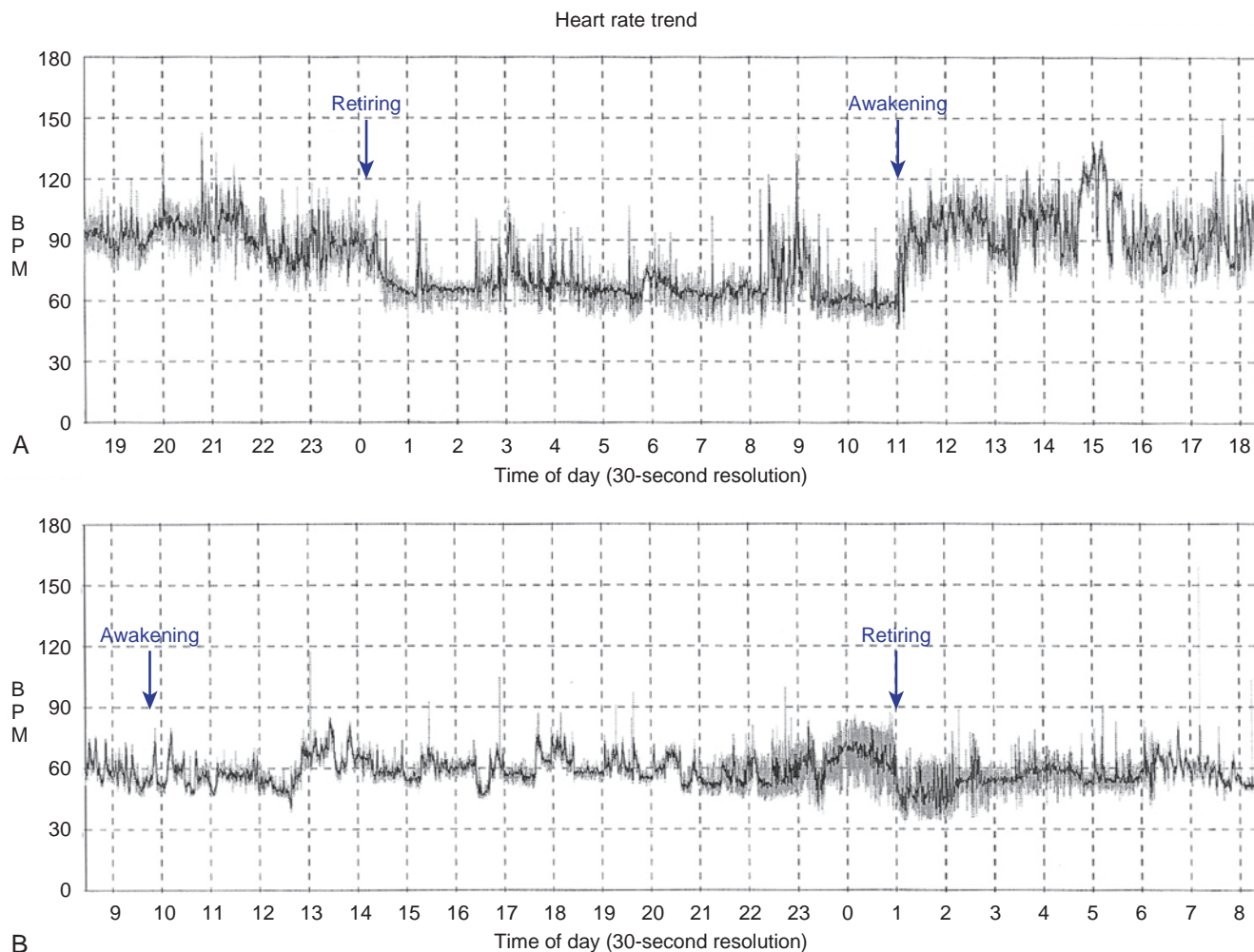


Fig. 8.4 Chronotropic Incompetence. (A) A 24-hour Holter recording in a normal subject showing normal sinus rate diurnal variation and response to activity. (B) A 24-hour Holter recording in a different patient with chronotropic incompetence and activity intolerance. Note the blunted response of the sinus rate to activity during waking hours and the slow average heart rate. *BPM*, Beats per minute.

On 24-hour ambulatory Holter monitoring, chronotropic incompetence commonly manifests as a monotonic daily heart rate profile in an ambulatory patient (Fig. 8.4). In addition, treadmill exercise testing can be of substantial value in assessing the chronotropic response (“competence”) to increases in physical activity in patients with sinus bradycardia who are suspected of having SND. Although the definition of chronotropic incompetence is not agreed on, it is reasonable to designate it as a blunted heart rate response to exercise manifesting as a less than normal increase in the sinus rate at each stage of exercise, with a plateau at less than 70% to 80% of the age-predicted maximum heart rate ($220 - \text{age}$) at peak exercise (having completed at least two stages of exercise testing using a modified Bruce protocol) or an inability to achieve a sinus rate of 100 to 120 beats/min at maximum effort. Irregular (and nonreproducible) increases, and even decreases, in the sinus rate during exercise, can also occur but are rare. Other patients with SND can achieve an appropriate peak heart rate during exercise but may have slow sinus rate acceleration in the initial stage or rapid deceleration of heart rate in the recovery stage.

Tachycardia-Bradycardia Syndrome

Tachycardia-bradycardia syndrome, frequently referred to as sick sinus syndrome, is a common manifestation of SND, and it refers to the

presence of intermittent sinus or junctional bradycardia alternating with atrial tachyarrhythmias (Fig. 8.5). The atrial tachyarrhythmia is most commonly paroxysmal AF, but AT, AFL, and occasionally atrio-ventricular nodal reentry tachycardia or AVRT can also occur.

Apart from underlying sinus bradycardia of varying severity, these patients often experience prolonged sinus arrest and asystole on termination of the atrial tachyarrhythmia, resulting from overdrive suppression of the sinus node and secondary pacemakers by the tachycardia. Long sinus pauses that occur following electrical cardioversion of AF constitute another manifestation of SND.

Therapeutic strategies to control the tachyarrhythmias often cause SND and result in the need for pacemaker therapy (Fig. 8.6). On the other hand, long sinus pauses occurring following tachycardia episodes can be reversible in some patients once the tachyarrhythmia is eliminated, thus obviating the need for pacing.

Atrial Fibrillation With Slow Ventricular Response

Persistent AF with a slow ventricular response in the absence of AVN blocking drugs is often present in patients with SND. These patients can demonstrate very slow ventricular rates at rest or during sleep and occasionally have long ventricular pauses. Occasionally, they can develop complete AV block with a junctional or ventricular escape rhythm.

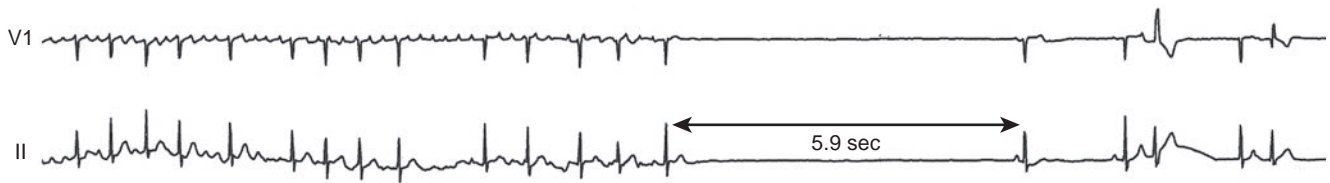


Fig. 8.5 Tachycardia-Bradycardia Syndrome. Two surface electrocardiogram leads showing atrial fibrillation that spontaneously terminates followed by a 5.9-second pause before sinus rhythm resumes. The patient became lightheaded during this period.

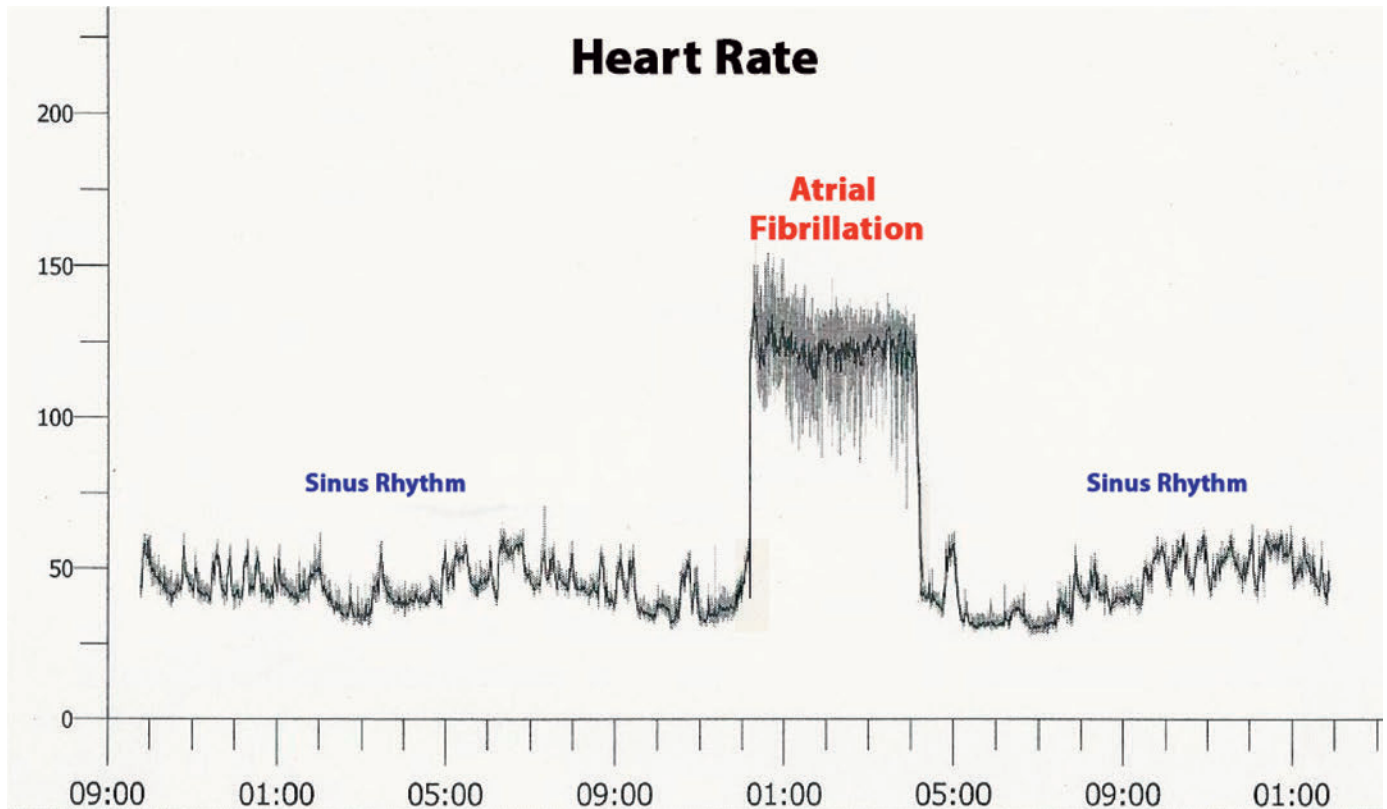


Fig. 8.6 Sinus Node Dysfunction and Atrial Fibrillation. A 24-hour Holter heart rate trend showing slow sinus bradycardia (average sinus rate <50 beats/min) alternating with rapid ventricular rates (averaging >120 beats/min) during a sustained episode of atrial fibrillation. Pacing was required in this patient to prevent symptomatic bradycardia and allow the use of drug therapy to control the tachycardia.

They can also conduct rapidly and develop symptoms caused by tachycardia during exercise. In some cases, cardioversion results in a long sinus pause or junctional escape rhythm before the appearance of sinus rhythm. Although a combination of sinus node and AV conduction disease can be present in many cases, examples of rapid ventricular responses during atrial tachyarrhythmias are frequently found.

Carotid Sinus Hypersensitivity

An abnormal response to carotid sinus massage (pause longer than 3 seconds) can indicate SND, but this response can also occur in asymptomatic older individuals (eFig. 8.1).³³

Atrial Standstill

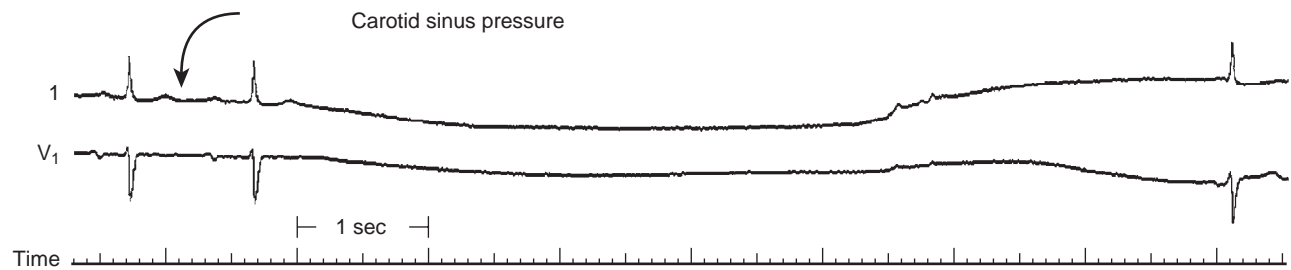
Atrial standstill is a rare clinical syndrome in which there is no spontaneous atrial activity and the atria cannot be electrically stimulated. The surface ECG usually reveals junctional bradycardia without atrial

activity (eFig. 8.2). The atria are generally fibrotic and without any functional myocardium. Lack of mechanical atrial contraction poses a high risk for thromboembolism in these patients.

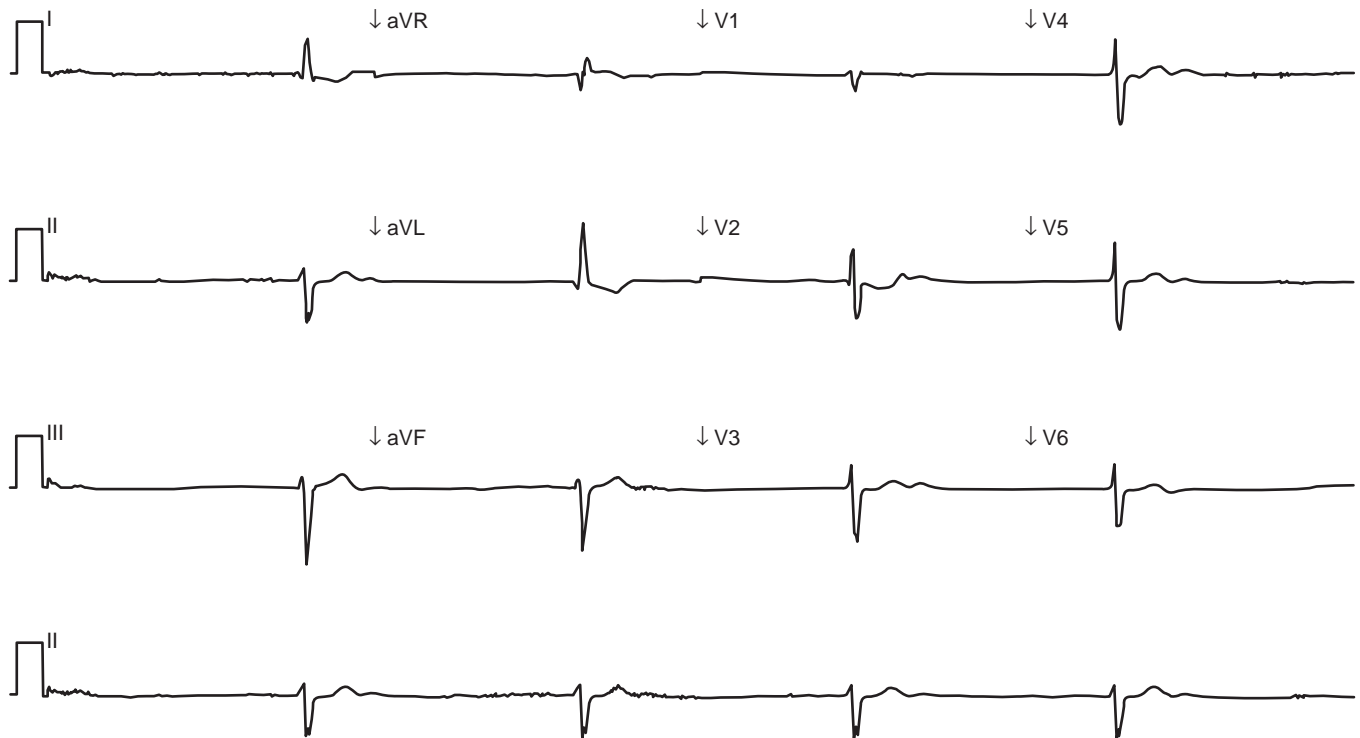
Sinus Arrhythmia

Sinus arrhythmia is present when the P wave morphology is normal and consistent and the P-P intervals vary by more than 120 milliseconds (or by more than 10% of the shortest P-P interval). The PR interval generally does not vary significantly (because of the consistent site of impulse generation, i.e., the sinus node).

Respiratory sinus arrhythmia is mediated by atrial stretch receptors, which respond to increased and decreased venous return during inspiration and expiration by speeding or slowing sinus rate, respectively. Respiratory sinus arrhythmia is not an abnormal rhythm and is most commonly seen in young healthy subjects, especially those with slower heart rates or with enhanced vagal tone.³⁴



eFig. 8.1 Carotid Sinus Hypersensitivity. Two surface electrocardiogram leads are shown during carotid sinus pressure, as indicated. The PR interval is prolonged, followed by a 7.5-second sinus pause ended by a P wave and probable junctional escape complex. The patient was nearly syncopal during this period.



eFig. 8.2 Atrial Standstill. Surface electrocardiogram showing sinus arrest with escape junctional rhythm in a patient with atrial standstill.

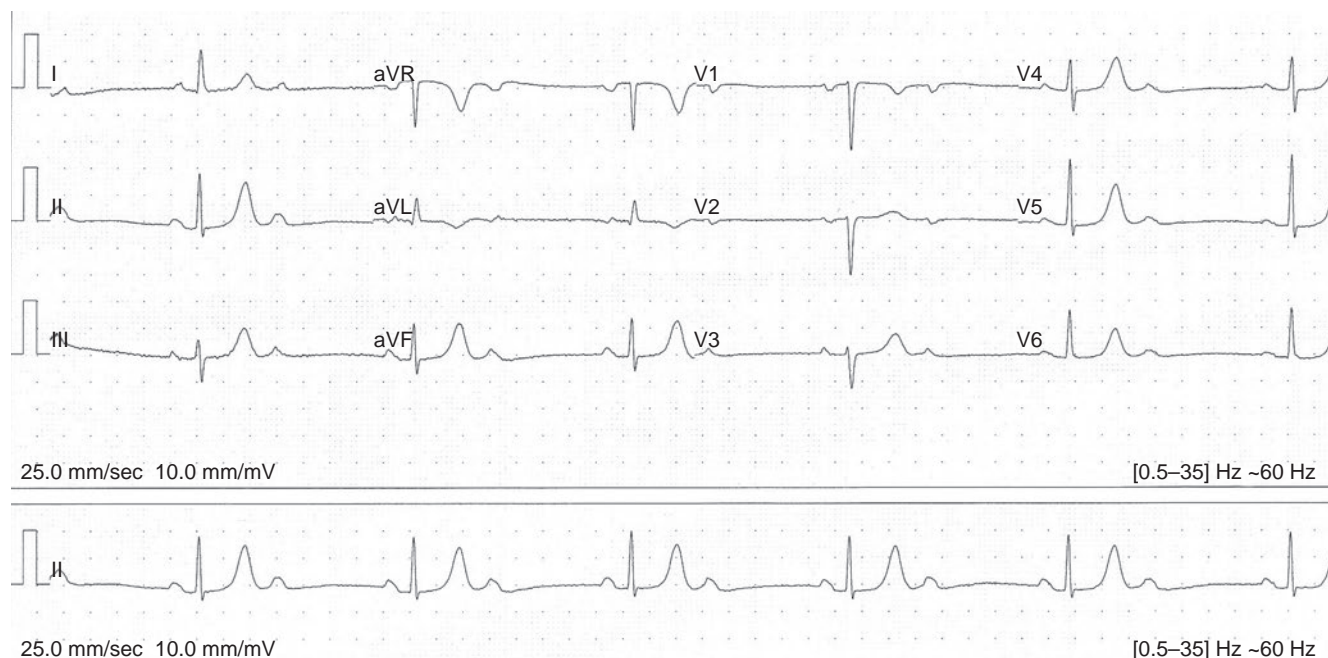


Fig. 8.7 Ventriculophasic Sinus Arrhythmia. Surface electrocardiogram during sinus rhythm with second-degree 2:1 atrioventricular block. Consecutive sinus P waves enclosing a QRS occur at shorter intervals than that of consecutive P waves without a QRS in between (ventriculophasic arrhythmia).

Nonrespiratory sinus arrhythmia, in which phasic changes in sinus rate are not related to the respiratory cycle, can be accentuated by the use of vagal agents such as digitalis and morphine; its mechanism is unknown. Patients with nonrespiratory sinus arrhythmia are likely to be older and to have underlying cardiac disease, although the arrhythmia itself is not a marker for structural heart disease. None of the sinus arrhythmias (respiratory or nonrespiratory) indicate SND. In addition, respiratory variation in the sinus P wave contour can be seen in the inferior leads and should not be confused with wandering atrial pacemaker, which is unrelated to breathing and therefore is not phasic.

Ventriculophasic sinus arrhythmia is an unusual rhythm that occurs when sinus rhythm and high-grade or complete AV block coexist; it is characterized by shorter P-P intervals when they enclose QRS complexes and longer P-P intervals when no QRS complexes are enclosed (Fig. 8.7). The mechanism is uncertain but may be related to the effects of the mechanical ventricular systole itself: ventricular contraction increases the blood supply to the sinus node, thereby transiently increasing its firing rate. Ventriculophasic sinus arrhythmia is not a pathological arrhythmia and should not be confused with premature atrial complexes or sinoatrial block.

Wandering Atrial Pacemaker

Wandering atrial pacemaker is characterized by multiple P waves of varying morphology with a relatively normal or slow rate, caused by shifting of the dominant pacemaker focus between the sinus node and latent pacemakers in other atrial and AV junctional sites (eFig. 8.3). The shift in pacemaker focus occurs gradually, over the course of several beats, so that only one pacemaker at a time controls the rhythm. In addition to a change in P wave morphology, the shift in pacemaker focus is usually associated with different PR intervals (depending on its proximity to the AVN) and R-R intervals. By definition, wandering atrial pacemaker has to have at least three distinctly different P wave morphologies and a ventricular rate of less than 100 beats/min. Wandering pacemaker is a normal phenomenon, usually caused by varying

vagal tone, and can be observed in young healthy subjects and athletes, especially during sleep or with enhanced vagal tone, but also in patients with SND. Wandering pacemaker is rarely symptomatic.

ELECTROPHYSIOLOGICAL TESTING

Role of Electrophysiological Testing

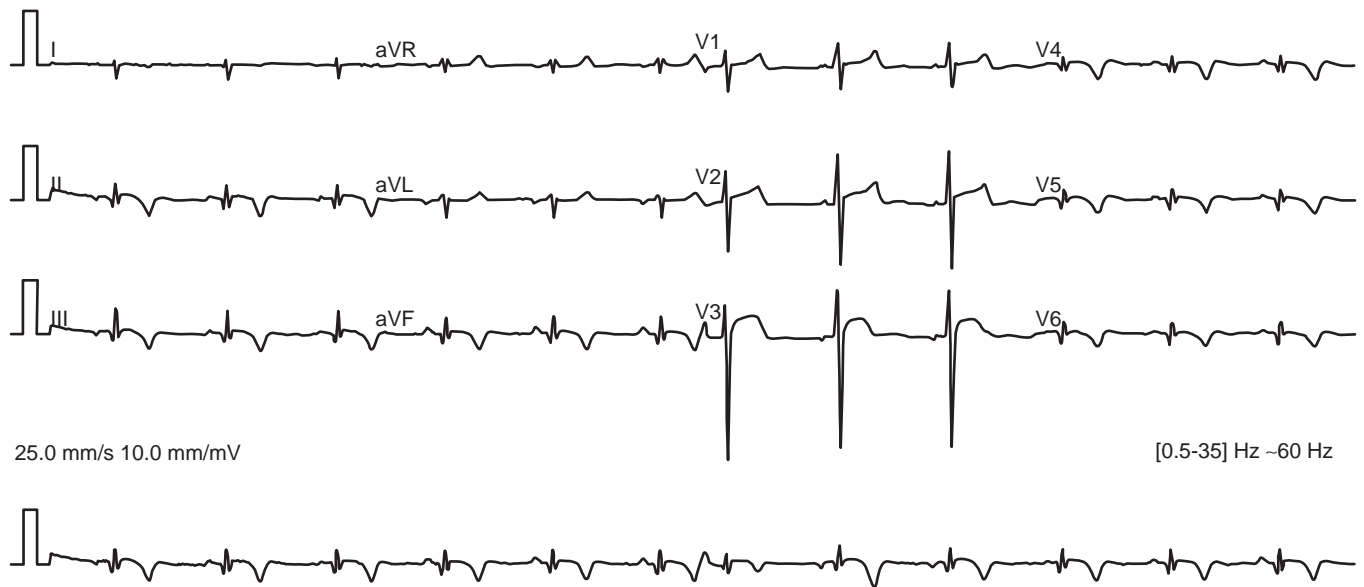
The diagnosis of SND usually can be made based on clinical and ECG findings, which are typically adequate for deciding subsequent treatment. After symptoms and SND are correlated with ECG findings, further documentation by invasive studies is not required. Similarly, asymptomatic patients with evidence of SND need not be tested because no therapy is indicated. However, EP testing can be important to assess sinus node function in patients who have had symptoms compatible with SND and in whom no documentation of the arrhythmia responsible for these symptoms has been obtained by prolonged monitoring. In these cases, EP testing can yield information that can be used to guide appropriate therapy. The most useful measures of the overall sinus node function are a combination of the responses to atropine and exercise and the sinus node recovery time (SNRT).³⁷

Sinus Node Recovery Time

The sinus node is the archetype of an automatic focus. Automatic rhythms are characterized by spontaneous depolarization, overdrive suppression, and post-overdrive warm-up (i.e., gradual return to baseline CL). SNRT is the interval between the end of a period of overdrive pacing and the return of sinus node function, manifest on the surface ECG by a postpacing sinus P wave. Clinically, SNRT is used to test sinus node automaticity.³⁷

Technique

Pacing site. Pacing is performed in the high RA at a site near the sinus node, to decrease the conduction time to and from the sinus node.



eFig. 8.3 Wandering Atrial Pacemaker. Surface electrocardiogram showing wandering atrial pacemaker with multiple P waves of varying morphology with a relatively normal rate.

Pacing cycle length. SNRT is preferably measured after pacing at multiple CLs. Pacing is started at a CL just shorter than the sinus CL. After a 1-minute rest, pacing is repeated at progressively shorter CLs (with 50- to 100-millisecond decrements) down to a pacing cycle length (PCL) of 300 milliseconds.

Pacing duration. Pacing is continued for 30 or 60 seconds at a time. Although pacing durations beyond 15 seconds usually have little effect on the SNRT in healthy subjects, patients with SND can manifest marked suppression after longer pacing durations. It is also preferable to perform pacing at each PCL for different durations (30, 60, or 120 seconds), to ensure that sinus entrance block has not obscured the true SNRT.

Measurements

Several intervals have been used as a measure of SNRT.³⁷

Sinus node recovery time. SNRT is the longest pause from the last paced beat to the first sinus return beat at a particular pacing CL. Normally, SNRT is less than 1500 milliseconds, with a scatter on multiple tests of less than 250 milliseconds (Fig. 8.8). SNRT tends to be shorter with shorter baseline sinus CLs, and therefore various corrections have been introduced.

Corrected SNRT. Corrected SNRT equals SNRT minus the baseline sinus CL. Normal values of corrected SNRT have been reported from 350 to 550 milliseconds, with 500 milliseconds most commonly used (see Fig. 8.8). However, the use of corrections at slow sinus rates can produce odd results. For example, in a patient with symptomatic bradycardia at a 1500-millisecond CL and an SNRT of 2000 milliseconds, the corrected SNRT is 500 milliseconds. For cases of severe bradycardia, an abnormal uncorrected SNRT of 2000 milliseconds is more accurate; in fact, one does not need SNRT to make the clinical diagnosis.

Maximum SNRT. Maximum SNRT is the longest pause from the last paced beat to the first sinus return beat at any pacing CL.

Ratio of SNRT to sinus CL. The ratio of $[(\text{SNRT}/\text{sinus CL}) \times 100\%]$ is lower than 160% in normal subjects.

Total recovery time. On cessation of atrial pacing, the pattern of subsequent beats returning to the basic sinus CL should be analyzed. Various patterns exist. Total recovery time equals the time to return to basic sinus CL (normal total recovery time is less than 5 seconds, usually by the fourth to sixth recovery beat).

Secondary pauses. Normally, following cessation of overdrive pacing, a gradual shortening of the sinus CL is observed until the baseline sinus CL is reached, typically within a few beats. Limited oscillations of

recovery CLs before full recovery can be observed, especially at faster pacing rates. Secondary pauses are identified when there is an initial shortening of the sinus CL after the SNRT, followed by an unexpected lengthening of the CL (see Fig. 8.8). Sudden and marked secondary pauses occurring during sinus recovery are abnormal. Sinoatrial exit block of variable duration is the primary mechanism of prolonged pauses, with a lesser component of depression of automaticity. Both may, and often do, coexist. However, secondary pauses can be a normal reflex following hypotension induced by pacing at rapid rates or in response to pressure overshoot in the first recovery beat resulting from the prolonged filling time. Because these secondary pauses represent SND and because they occur more frequently following rapid atrial pacing, overdrive pacing should be performed at rates up to 200 beats/min.

Limitations of Sinus Node Recovery Time

Many factors in addition to automaticity are involved in the measurement of SNRT, including proximity of the pacing site to the sinus node and conduction time from the pacing site to the sinus node and vice versa, as well as conduction time in and out of the sinus node. Sinus node entrance block during rapid atrial pacing can lead to a shorter SNRT, whereas sinus node exit block after cessation of pacing can result in marked prolongation of the SNRT. Moreover, sometimes SNRT cannot be measured because of atrial ectopic or junctional escape beats that preempt the sinus beat.

Some degree of atrial-nodal block should be suspected when SNRT shortens in response to an increment in the pacing rate or if there is marked variation (more than 250 milliseconds) in the SNRTs when multiple tests are performed at a constant pacing rate.

Despite these limitations, SNRT is probably the best and most widely used test for sinus node automaticity. The durations of the maximum SNRT and corrected SNRT are independent of age. Evaluation of the corrected SNRT following pharmacological denervation (see later) can increase the sensitivity of the test.

Sinus Node Recovery Time in Patients With Sinus Node Dysfunction

The sensitivity of a single SNRT measurement is approximately 35% in patients with SND. This rises to more than 85% when multiple SNRTs at different rates are recorded, along with scatter and total recovery time, with a specificity of more than 90%. A prolonged SNRT or corrected SNRT is found in 35% to 93% of patients suspected of having SND (depending on the population studied). The incidence is lowest in

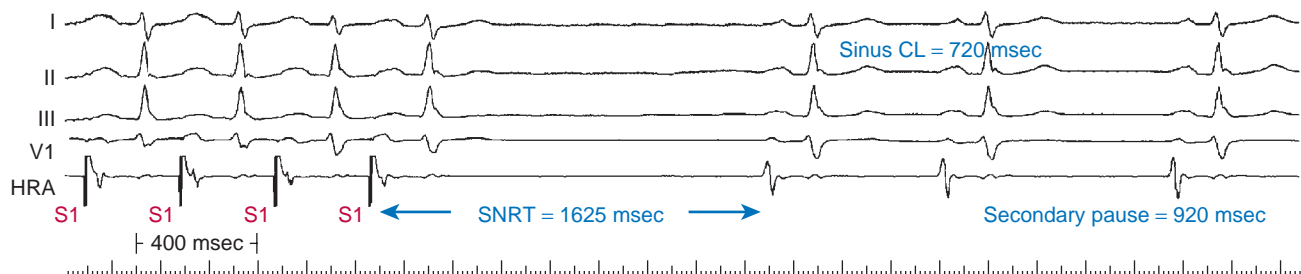


Fig. 8.8 Sinus Node Recovery Time. Surface electrocardiogram leads and high right atrial (HRA) recordings are shown at the end of a burst of atrial pacing, suppressing sinus node automaticity. The interval at which the first sinus complex returns (SNRT) is abnormally long at 1625 milliseconds. With a baseline sinus cycle length (CL) of 720 milliseconds, the corrected SNRT ($1625 - 720 = 905$ milliseconds) is also prolonged. In addition, there is a secondary pause after the first two sinus complexes.

patients with sinus bradycardia. Marked abnormalities in the corrected SNRT usually occur in symptomatic patients with clinical evidence of sinoatrial block or bradycardia-tachycardia syndrome.³⁷

The PCL at which maximum suppression occurs in patients with SND is unpredictable and, unlike in healthy subjects, tends to be affected by the duration of pacing. However, if sinus entrance block is present, the greatest suppression is likely to occur at relatively long PCLs. If the longest SNRT occurs at PCLs longer than 600 milliseconds, a normal value can reflect the presence of entrance block. In such cases a normal SNRT is an unreliable assessment of sinus node automaticity. The fact that the longest SNRT occurs at PCLs longer than 600 milliseconds is in itself a marker of SND.

Marked secondary pauses are another manifestation of SND and can occasionally occur in the absence of prolongation of SNRT, in which case sinoatrial block is the mechanism. Approximately 69% of patients with secondary pauses have clinical evidence of sinoatrial exit block, and 92% of patients with sinoatrial exit block demonstrate marked secondary pauses.

Sinoatrial Conduction Time

Although the sinus node is the dominant cardiac pacemaker, neither sinus node impulse initiation nor conduction is visible on the surface ECG or on the standard intracardiac recordings because depolarization within the sinus node is of very low amplitude. Therefore sinus node function has usually been assessed indirectly. Normal sinus node function is assumed when the atrial musculature is depolarized at a normal rate and in a normal temporal sequence—so-called *normal sinus rhythm*. In NSR the atrial rate is assumed to correspond to the rate of impulse formation within the sinus node; however, the time of impulse conduction from the sinus node to the atrium cannot be ascertained. Several methods have been developed for the assessment of SACT, either indirectly (the Strauss and Narula methods) or by directly recording the sinus node electrogram. Signal-averaging techniques have also been used to measure SACT noninvasively.³⁷

Direct Recordings

Sinus node depolarization can be recorded directly using high-gain unfiltered electrograms in approximately 50% of patients. A catheter with a 0.5- to 1.5-mm interelectrode distance is used. The catheter is placed directly at the SVC-RA junction, or a loop is formed in the RA and the tip of the catheter is then placed at the SVC-RA junction. Optimizing the filter setting can help to reduce baseline drift (0.1 to 0.6 Hz to 20 to 50 Hz), with signal gain at 50 to 100 mV/cm.

SACT is measured as the interval between the pacemaker prepotential on the local electrogram and the onset of the rapid atrial deflection (Fig. 8.9). When SACT is normal, a smooth upstroke slope merges into the atrial electrogram. When SACT is prolonged, an increasing amount of sinus node potential becomes visible before the rapid atrial deflection. Sinoatrial block is said to occur when the entire sinus node electrogram is seen in the absence of a propagated response to the atrium.

The sinus node electrogram can be validated by the ability to record the electrogram in only a local area, with loss of the upstroke potential during overdrive atrial pacing. In addition, persistence of the sinus node electrogram following carotid sinus massage, following induced pauses, or during pauses following overdrive suppression is an important method for validation.

Strauss Technique

The Strauss technique uses atrial premature stimulation to assess SACT. Baseline sinus beats are designated as A_1 . Progressively premature atrial extrastimuli (A_2) are delivered after every eighth to tenth A_1 , and the timing of the recovery beat (A_3) is measured. The Strauss method



Fig. 8.9 Direct Measurement of Sinoatrial Conduction Time (SACT). A schematic copy of a sinus node electrogram is shown. On the sinus node electrogram, high right atrial depolarization (A), ventricular depolarization (V), T wave (T), and the sinus node potential (SN) are identified. In the second beat, reference lines are drawn through the point at which the SN potential first becomes evident and the point at which atrial activation begins. SACT is the interval between these two reference lines. (From Reiffel JA, Gang E, Gliklich J, et al. The human sinus node electrogram: a transvenous catheter technique and a comparison of directly measured and indirectly estimated sinoatrial conduction time in adults. *Circulation*. 1980; 62:1324–1334.)

is useful as part of an overall EP study when information is also sought on conduction system refractoriness or possible dual AVN physiology or bypass tracts during sinus rhythm. Four zones of response of the sinus node to AES have been identified. SACT can be measured only in the zone of reset (Fig. 8.10).

Zone I: zone of collision. This zone (also referred to as the zone of interference or nonreset zone) is defined by the range of A_1 - A_2 intervals at which the A_2 - A_3 interval is fully compensatory (see Fig. 8.10). Very long A_1 - A_2 intervals (with A_2 falling in the last 20% to 30% of the sinus CL) generally result in collision of the AES (A_2) with the spontaneous sinus impulse (A_1). The sinus pacemaker and the timing of the subsequent sinus beat (A_3) are therefore unaffected by A_2 , and a complete compensatory pause occurs (i.e., A_1 - $A_3 = 2 \times [A_1$ - $A_1]$).

Zone II: zone of reset. The range of A_1 - A_2 intervals at which reset of the sinus pacemaker occurs, resulting in a less than compensatory pause, defines the zone of reset (see Fig. 8.10). Shorter A_1 - A_2 intervals result in penetration of the sinus node with resetting so that the resulting pause is less than compensatory— A_1 - $A_3 < 2 \times (A_1$ - $A_1)$ —but without changing sinus node automaticity. This zone typically occupies a long duration (40% to 50% of the sinus CL). In most patients the A_2 - A_3 interval remains constant throughout zone II, thus producing a plateau in the curve because A_2 penetrates and resets the sinus node, but it does so without changing the sinus pacemaker automaticity. Hence the A_2 - A_3 interval should equal the spontaneous sinus CL (A_1 - A_1) plus the time it takes the AES (A_2) to enter and exit the sinus node. The difference between the A_2 - A_3 and A_1 - A_1 intervals therefore has been taken as an estimate of total SACT (Fig. 8.11).³⁷

Conventionally, it is assumed that conduction times into and out of the sinus node are equal (i.e., $SACT = [A_2$ - $A_3 - A_1$ - $A_1]/2$). However, data suggest that conduction time into the sinus node is shorter than that out of the sinus node (see Fig. 8.11). Thus the Strauss method for assessment of SACT can be affected by the site of stimulation; the farther the site of stimulation is from the sinus node, the greater the overestimation of SACT will be (because conduction through more intervening atrial and perinodal tissue will be incorporated in the measurement). The value of SACT can also be affected by the prematurity of the AES (A_2); the more premature an A_2 is, the more likely it will be to encroach on perinodal or atrial refractoriness and slow conduction

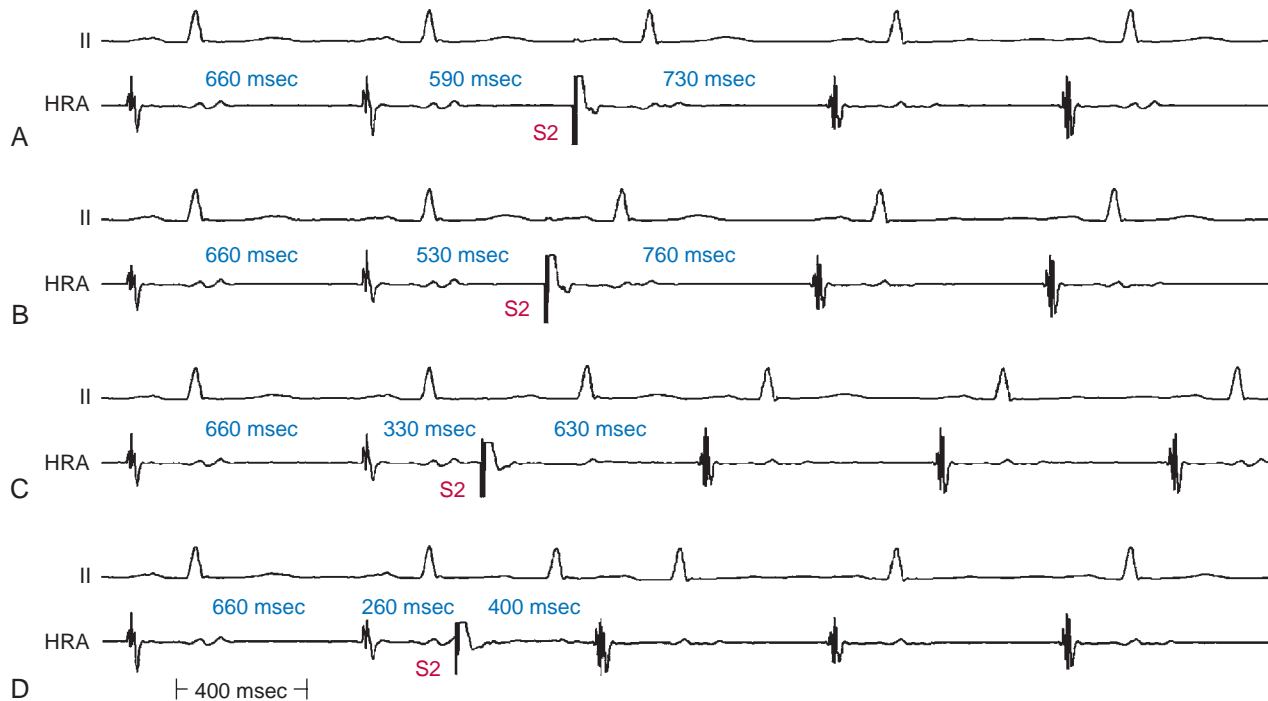


Fig. 8.10 Strauss Sinoatrial Conduction Time Zones. Leads 2 and recording from the high right atrium (HRA) are shown, with a single extrastimulus (S) delivered during sinus rhythm (cycle length, 660 milliseconds) at progressively shorter coupling intervals as indicated relative to the preceding sinus complex. The timing of the subsequent sinus P wave relative to when it would be expected if there were no extrastimulus determines the zone of effect: (A), collision; (B), reset; (C), interpolation; and (D), reentry. See text for details.

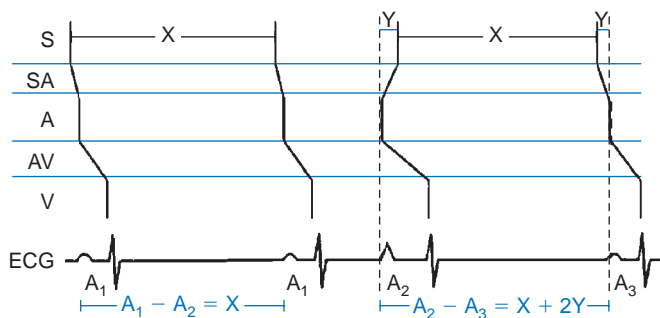


Fig. 8.11 Calculation of Sinoatrial Conduction Time (SACT) Using the Strauss Method. The baseline sinus cycle length (A_1-A_2) equals X . The third P wave represents an atrial extrastimulus (A_2) that reaches and discharges the sinoatrial (SA) node, which causes the next sinus cycle to begin at that time. Therefore the A_2-A_3 interval = $X + 2Y$ milliseconds, assuming no depression of sinus node automaticity. Consequently, $SACT = Y = ([A_2-A_3] - [X])/2$. AV, Atrioventricular; ECG, electrocardiogram. (From Olgin JE, Zipes DP: Specific arrhythmias: diagnosis and treatment. In: Libby P, Bonow RO, Mann DL, Zipes DP, eds. *Braunwald's Heart Disease: A Textbook of Cardiovascular Medicine*. 8th ed. Philadelphia, PA: Saunders; 2008:869.)

into the sinus node. In addition, an early AES commonly causes pacemaker shift to a peripheral latent pacemaker, which can exit the atrium earlier because of its proximity to the tissue, thus shortening conduction time out of the sinus node.

Despite those limitations, for practical purposes, the Strauss method is a reasonable estimate of functional SACT, provided that stimulation

is performed as closely as possible to the sinus node and the measurement is taken when a true plateau is present in zone II. SACT appears to be independent of the spontaneous sinus CL. However, marked sinus arrhythmia invalidates the calculation of SACT because it is impossible to know whether the return cycle is a result of spontaneous oscillation or is a result of the AES. To eliminate the effects of sinus arrhythmia, multiple tests need to be performed at each coupling interval. Alternatively, atrial pacing drive at a rate just faster than the sinus rate is used instead of delivery of AES during NSR (Narula method; see later). However, this latter method can result in depression of sinus node automaticity, pacemaker shifts, sinus entrance block, sinus acceleration (if the drive PCL is within 50 milliseconds of sinus CL), and shortening of sinus action potential and can lead to an earlier onset of phase IV; each of these actions can potentially yield misleading results.

In an occasional patient, in response to progressively premature AESs, the A_2-A_3 interval prolongs either continuously or after a brief plateau (in both cases the pause remains less than compensatory). This progressive prolongation of the A_2-A_3 interval during zone II can be caused by suppression of sinus node automaticity, a shift to a slower latent pacemaker, or an increase in conduction time into the sinus node because of encroachment of A_2 on perinodal tissue refractoriness. Thus it is recommended to use the first third of zone II to measure SACT because it is less likely to introduce such errors. Analysis of the A_3-A_4 interval may provide insights into changes in sinus node automaticity or pacemaker shift. If the A_3-A_4 interval is longer than the A_1-A_2 interval, depression of sinus node automaticity is suggested. Therefore the calculated SACT overestimates the true SACT, and correction of SACT is necessary (in which case the A_3-A_4 interval is used as the basic sinus CL with which the A_2-A_3 interval is compared).

Zone III: zone of interpolation. This zone is defined as the range of A_1 - A_2 intervals at which the A_2 - A_3 interval is less than the A_1 - A_1 interval and the A_1 - A_3 interval is less than twice the A_1 - A_1 interval (see Fig. 8.10). The A_1 - A_2 coupling intervals at which incomplete interpolation is first observed define the relative refractory period of the perinodal tissue. Some investigators refer to this as the *sinus node refractory period*. In this case, A_3 represents delay of A_1 exiting the sinus node, which has not been affected. The A_1 - A_2 coupling interval at which complete interpolation is observed probably defines the effective refractory period of the most peripheral of the perinodal tissue because the sinus impulse does not encounter refractory tissue on its exit from the sinus node. In this case, $(A_1-A_2) + (A_2-A_3) = A_1-A_1$, and sinus node entrance block is said to exist.

Zone IV: zone of reentry. This zone is defined as the range of A_1 - A_2 intervals at which the A_2 - A_3 interval is less than the A_1 - A_1 interval and $(A_1-A_2) + (A_2-A_3)$ is less than A_1-A_1 , and the atrial activation sequence and P wave morphology are identical to sinus beats. The incidence of single beats of sinus node reentry is approximately 11% in the normal population.

Narula Method

The Narula method for measuring SACT is simpler than the Strauss technique. Instead of atrial premature stimulation, atrial pacing at a rate slightly faster (10 beats/min or more) than the sinus rate is used as A_2 . It is assumed that such atrial pacing will depolarize the sinus node without significant overdrive suppression. The SACT is then calculated using the same formula as for the Strauss method. The Narula method is the quickest and easiest to perform, but it gives only SACT and does not provide information about the AV conduction system.³⁷

Kirkorian-Touboul Method

In contrast to the Strauss method, which uses progressively premature AESs delivered during NSR to evaluate SACT, the Kirkorian-Touboul method uses progressively premature AESs delivered following an eight-beat pacing train at a fixed rate. This method was designed to determine SACT independently of baseline sinus CL, which can normally be somewhat variable. It can have several advantages, especially for the study of drug effects at identical basic rates, but it is less widely used than the other methods.

Sinoatrial Conduction Time in Patients With Sinus Node Dysfunction

The normal SACT is 45 to 125 milliseconds. There is a good correlation between direct and indirect measurements of SACT in a patient with or without SND. However, SACT is an insensitive indicator of SND, especially in patients with isolated sinus bradycardia. SACT is prolonged in only 40% of patients with SND, and more frequently (78%) in patients with sinoatrial exit block or tachycardia-bradycardia syndrome. In patients with sinus pauses, corrected SNRT is more commonly abnormal than SACT (80% versus 53%). SACT appears to be directly related to the baseline sinus CL, and the sinus node refractory period is directly related to the drive CL.³⁷

Effects of Drugs

Autonomic Blockade (Intrinsic Heart Rate)

Autonomic blockade is the most commonly used pharmacological intervention for evaluation of SND, and it is used to determine the intrinsic heart rate. Autonomic blockade is accomplished by administering atropine, 0.04 mg/kg, and propranolol, 0.2 mg/kg (or atenolol, 0.22 mg/kg). The resulting intrinsic heart rate represents sinus node rate without autonomic influences. The normal intrinsic heart rate is age-dependent and can be calculated using the following equation:

intrinsic heart rate (beats/min) = $118.1 - (0.57 \times \text{age})$. Normal values are $\pm 14\%$ for age younger than 45 years and $\pm 18\%$ for age older than 45 years, and approximately 5 beats/min less for women at all ages. A low intrinsic heart rate is consistent with intrinsic SND. A normal intrinsic heart rate in a patient with known SND suggests extrinsic SND caused by abnormal autonomic regulation. Of note, autonomic blockade with atropine and propranolol also results in shortening of corrected SNRT, as well as sinus CL and SACT.

Atropine

The normal sinus node responses to atropine are an acceleration of heart rate to more than 90 beats/min and an increase over the baseline rate by 20% to 50%. Atropine-induced sinus rate acceleration is usually blunted in patients with intrinsic SND. Failure to increase the sinus rate to more than the predicted intrinsic heart rate following 0.04 mg/kg of atropine is diagnostic of impaired sinus node automaticity. Atropine (1 to 3 mg) markedly shortens SNRT and, in most cases, corrected SNRT. Atropine also abolishes the marked oscillations frequently observed following cessation of rapid pacing. Atropine occasionally results in the appearance of a junctional escape rhythm on cessation of pacing before sinus escape beats in normal subjects (especially in young men with borderline slow sinus rate) and, more commonly, in patients with SND. When this occurs, the junctional escape rhythm is usually transient (lasting only a few beats). Persistence of junctional rhythm and failure of the sinus rate to increase are indicative of SND. Atropine, with or without propranolol, shortens SACT (unrelated to its effects on the sinus rate).

Propranolol

Propranolol (0.1 mg/kg) produces a 12% to 22.5% increase in sinus CL in normal subjects. Patients with SND have a similar chronotropic response to propranolol, a finding suggesting that the sympathetic tone or responsiveness is intact in most patients with SND. Propranolol increases SNRT by 160% in approximately 40% of patients with SND and increases SACT in most patients with SND. The mechanism of these effects is unclear. Effects are minimal in normal subjects.

Isoproterenol/Epinephrine

Isoproterenol (1 to 3 $\mu\text{g}/\text{min}$) or epinephrine (0.05 $\mu\text{g}/\text{kg}$ per min) produces sinus acceleration of at least 25% in normal subjects. An impaired response to isoproterenol correlates well with a blunted chronotropic response to exercise observed in some patients with SND.

Digoxin

Digoxin shortens SNRT or corrected SNRT in some patients with clinical SND, probably because of increased perinodal tissue refractoriness with consequent sinus node entrance block.

Verapamil and Diltiazem

Verapamil and diltiazem have minimal effects on SNRT and SACT in normal persons. Effects in patients with SND have not been studied, but worsening of the SND is expected.

Antiarrhythmic Agents

Procainamide, quinidine, mexiletine, dronedarone, and amiodarone can adversely affect sinus node function in patients with preexisting SND. Severe sinus bradycardia and sinus pauses are the most common problems encountered. Amiodarone is the worst offender and has even caused severe SND in patients without prior evidence of SND. In general, other drugs have minimal effects on sinus node function in normal persons.

PRINCIPLES OF MANAGEMENT

Acute Management

Although pacing is the mainstay of treatment for symptomatic SND, identifying transient or reversible causes for SND is the first step in management. Withdrawal of any offending drugs, correction of any electrolyte abnormalities, and treatment of any extrinsic causes for SND (e.g., obstructive sleep apnea, hypothyroidism, hypoxemia) should be considered prior to permanent pacing therapy. In addition, the specific clinical circumstance in which SND occurred should be analyzed to document potential heightened vagal tone as a cause of sinus bradycardia or pauses. Hypervagotonia as a cause of SND is often suspected by its transient nature and by the symptoms associated with specific clinical circumstances associated with surges in vagal tone, such as vomiting, coughing, gagging, endotracheal intubation, nasogastric tube placement, airway suctioning, and neurocardiogenic syncope. Vagally induced SND may respond to atropine, but it needs to be treated only if the patient is symptomatic.^{33,38} Sinus bradycardia (as low as 30 beats/min) in conditioned athletes is typically benign and does not require further work-up or treatment.³⁴

Pharmacological therapy (atropine, isoproterenol) is effective only as a short-term emergency measure until pacing can be accomplished. Temporary percutaneous or transvenous pacing is necessary in patients with hemodynamically significant bradycardia to provide immediate stabilization prior to permanent pacemaker placement or to provide pacemaker support when the bradycardia is precipitated by what is presumed to be a transient event, such as electrolyte abnormality or drug toxicity.

Chronic Management

After all reversible causes are excluded or treated, correlation of symptoms with ECG evidence of SND is an essential part of the management strategy. Because of the episodic nature of symptomatic arrhythmias, ambulatory monitoring is often required. For the patient with asymptomatic bradycardia or sinus pauses, the long-term prognosis is generally benign, and no treatment is necessary. For symptomatic patients with nonreversible SND, pacing is the mainstay of treatment (Box 8.3). SND is currently the most common reported diagnosis for pacemaker implantation, and it accounts for 40% to 60% of new pacemaker implants.

For symptomatic patients with tachycardia-bradycardia syndrome, pacing may be required to prevent symptomatic bradycardia and allow the use of drug therapy for control of the tachycardia (see Fig. 8.6). These patients are at increased risk for thromboembolism, and the issue of long-term anticoagulation for stroke prevention should be addressed.³⁸ Importantly, in patients with symptomatic paroxysmal AF accompanied by prolonged sinus pauses on AF termination, catheter ablation of AF may be preferred to pacemaker implantation because it can potentially eliminate the arrhythmia as well as the need for permanent pacing.³⁹

No oral drugs with acceptable safety and efficacy profile are currently available for long-term treatment of sinus bradycardia. Chronotropic medications, such as theophylline or aminophylline, have limited efficacy.

Pacemaker Device and Mode Selection

After the decision to pace is made, choosing the optimal pacemaker prescription is essential. Single-chamber atrial or ventricular pacemakers and dual-chamber pacemakers will all prevent bradycardia in the patient with SND; however, each pacemaker type has inherent advantages and disadvantages (Box 8.4).³⁶

In patients with SND but normal AV conduction, physiological pacing can be accomplished with a single-chamber atrial pacemaker (AAI). As compared with dual-chamber pacemakers (DDD), AAI

BOX 8.3 ACCF/AHA/HRS Recommendations for Permanent Pacing in Sinus Node Dysfunction

Class I

- Documented symptomatic bradycardia, including frequent sinus pauses that produce symptoms
- Symptomatic chronotropic incompetence
- Symptomatic sinus bradycardia that results from required drug therapy for medical conditions

Class IIa

- SND with heart rate <40 beats/min when a clear association between significant symptoms consistent with bradycardia and the actual presence of bradycardia has not been documented
- Syncope of unexplained origin when clinically significant abnormalities of SND are discovered or provoked at electrophysiological studies

Class IIb

- Minimally symptomatic patients with chronic heart rate <40 beats/min while awake

Class III

- SND in asymptomatic patients
- SND in patients whose symptoms suggestive of bradycardia have been clearly documented to occur in the absence of bradycardia
- SND with symptomatic bradycardia caused by nonessential drug therapy

ACCF, American College of Cardiology Foundation; AHA, American Heart Association; HRS, Heart Rhythm Society; SND, sinus node dysfunction.

Modified from Epstein AE, DiMarco JP, Ellenbogen KA, et al. 2012 ACCF/AHA/HRS focused update incorporated into the ACCF/AHA/HRS 2008 guidelines for device-based therapy of cardiac rhythm abnormalities: a report of the American College of Cardiology Foundation/American Heart Association Task Force on Practice Guidelines and the Heart Rhythm Society. *J Am Coll Cardiol*. 2013;61:e6–75.

pacemakers offer several advantages: simpler implantation, less risk of lead dislodgement, lower initial cost, and avoidance of RV pacing.⁴⁰ However, unlike DDD systems, AAI pacemakers will not prevent ventricular bradycardia if AV block develops. In SND patients the incidence of high-grade AV block requiring ventricular pacing has been estimated at 0.6% to 1.8% per year in patients with apparently normal AV conduction at the time of initial pacemaker placement but significantly higher (7% per year) in those with a complete BBB or bifascicular block at presentation. In a recent report, 9.3% of patients with SND and single-chamber atrial pacemakers required upgrade to a DDD system over a mean follow-up of 5.4 years (1.7% per year), predominantly due to symptomatic AV block or AF with slow ventricular response, despite careful patient selection. Such reoperations were associated with significant complications in up to 16.7% of patients. Advanced age and LA enlargement were predictors for system upgrade.³⁶

Although DDD pacemakers have the capability to maintain AV synchrony and prevent bradycardia from all causes, they are associated with increased incidence of unnecessary RV pacing, which can be hemodynamically detrimental in many patients. Therefore the decision for which system to use is often based on implanting clinician preferences and evidence of baseline AV conduction abnormalities.

Although an AAI pacing system may be considered in the younger patient with SND and no evidence of AV or ventricular conduction abnormalities, in the United States, DDD pacing generally is preferred

BOX 8.4 HRS/ACCF Recommendations for Pacemaker Device and Mode Selection for SND

Class I

- DDD or AAI is recommended over VVI in patients with SND and intact AV conduction.
- Dual-chamber pacing is recommended over single-chamber atrial pacing in patients with SND.

Class IIa

- Rate adaptive pacing can be useful in patients with significant symptomatic chronotropic incompetence, and its need should be reevaluated during follow-up.
- In patients with SND and intact AV conduction, programming dual-chamber pacemakers to minimize ventricular pacing can be useful for prevention of AF.

Class IIb

- AAI pacing may be considered in selected patients with normal AV and ventricular conduction.
- Single-chamber VVI pacing may be considered in instances where frequent pacing is not expected or the patient has significant comorbidities that are likely to influence survival and clinical outcomes.

Class III

- Dual-chamber pacing or single-chamber atrial pacing should not be used in patients in permanent or longstanding persistent AF where efforts to restore or maintain sinus rhythm are not planned.

AAI, single-chamber atrial pacing; ACCF, American College of Cardiology Foundation; AF, atrial fibrillation; AV, atrioventricular; DDD, dual-chamber pacing; HRS, Heart Rhythm Society; SND, sinus node dysfunction; VVI, single-chamber ventricular pacing. Modified from Gillis AM, Russo AM, Ellenbogen KA, et al. HRS/ACCF expert consensus statement on pacemaker device and mode selection. *J Am Coll Cardiol*. 2012;60:682–703.

to single-chamber atrial pacemakers in SND patients due to the concern about progressive AV conduction disease and need for pacemaker upgrade, as well as the lack of evidence that AAI pacing has long-term clinical outcome beneficial effects compared with DDD pacing. In addition, patients who have evidence of abnormal AV conduction prior to pacemaker therapy (up to 20% of SND patients) are not candidates for single-chamber atrial pacing.

On the other hand, single-chamber ventricular pacemakers (VVI) have a limited role in patients with SND because of several disadvantages, including lack of AV synchrony, high burden of RV pacing and ventricular dyssynchrony, as well as increased risk of AF, stroke, and heart failure. Nonetheless, back-up VVI pacing may be considered in sedentary patients, those with significant morbidities and poor clinical prognosis, or when frequent pacing is not expected (e.g., carotid sinus hypersensitivity).³⁶

Pacemaker Syndrome

AV dyssynchrony or suboptimal AV synchrony can cause significant reduction in cardiac output, especially in patients who are particularly sensitive to loss of atrial contribution to ventricular filling, such as those with reduced ventricular compliance and diastolic dysfunction (due to aging or hypertensive, hypertrophic, or restrictive cardiomyopathy) and those with mitral stenosis. Atrial contraction against closed mitral and tricuspid valves (which is further promoted in patients with

intact retrograde ventriculoatrial conduction) can cause uncomfortable pulsation in the neck (cannon a waves) and abdomen, headache, cough, and jaw pain. The resultant increase in LA pressure and left ventricular filling pressure cause increased plasma levels of atrial natriuretic peptide and B-type natriuretic peptide, potent peripheral venous and arterial vasodilators. Furthermore, reduction of cardiac output causes reflex sympathetic activation.³⁶

The combination of detrimental hemodynamic consequences of AV dyssynchrony leads to a constellation of symptoms (including fatigue, weakness, effort intolerance, chest discomfort, dyspnea, confusion, dizziness, presyncope, or syncope) known as “pacemaker syndrome.” Although pacemaker syndrome can occur with any pacing mode, it occurs most commonly with VVI pacing in patients who are in sinus rhythm (reported in up to 83%). Severe symptoms warranting reprogramming from VVI to DDD pacing has been needed in 25% to 30% of these patients.⁴⁰

Minimizing Right Ventricular Pacing

A high percentage of RV pacing (>40%) can cause cardiomyopathy and heart failure secondary to ventricular dyssynchrony due to an abnormal activation sequence. In addition, frequent ventricular pacing, even in an AV synchronous pacing mode, increases the risk and burden of AF, likely secondary to ventricular dyssynchrony and systolic dysfunction. As compared with ventricular pacing, atrial or dual-chamber pacing significantly reduces AF, with relative risk reductions of 18% to 46%, as well as a significant reduction in the risk of stroke.^{36,41}

Therefore minimizing unnecessary RV pacing should be a goal in SND patients treated with pacemaker therapy. This can be achieved by programming longer AV delays or turning off rate response (in patients with single-chamber ventricular devices or in those with dual-chamber pacemakers in whom faster atrial pacing causes unacceptably long paced PR interval or AVB). In addition, contemporary pacemakers offer a variety of algorithms designed to give preference to intrinsic ventricular activation, thereby minimizing the adverse effects of unnecessary RV pacing, including AV search hysteresis (AVSH) and managed ventricular pacing (MVP).⁴²

AVSH, the most widely used algorithm, searches for intrinsic AV conduction by periodically and incrementally extending the AV interval to a prespecified maximum (which allows the avoidance of nonphysiologic AV delays). If intrinsic conduction is detected, the AV delay remains extended to give priority to intrinsic AV conduction; otherwise, the device returns to the baseline programmed AV delay.

The MVP algorithm provides functional AAIR pacing with ventricular monitoring and an automatic switch from AAIR to DDDR during episodes of AV block. However, in some patients the benefit of these algorithms in minimizing RV pacing can be counteracted by the deleterious effects of excessively long native or paced PR intervals or bradycardia. Severe first-degree AV conduction delay can potentially cause worsening of heart failure symptoms. Even in apparently healthy adults, prolongation of the PR interval was found to be associated with higher risk of AF and heart failure.⁴³ In addition, the timing cycles in the MVP algorithm can predispose to short-long-short ventricular sequences, which can be proarrhythmic in vulnerable patients. Therefore the use of these algorithms must be individualized.

Recently, a pacing mode that combines atrial preventive pacing and atrial antitachycardia pacing (DDDRP) plus MVP algorithms was found to effectively promote intrinsic ventricular activation, thereby minimizing the adverse effects of unnecessary RV pacing. This combination was associated with 61% reduction of the risk of progression to permanent AF on 2-year follow-up in patients with bradycardia and paroxysmal or persistent atrial tachyarrhythmias when compared with standard DDDR pacing mode.⁴⁴

These algorithms often produce unanticipated findings on ECG monitoring (i.e., varying AV intervals, occasional P waves that are neither conducted nor tracked with paced complexes). It is important for those reviewing monitor strips to know whether these algorithms are operative and interpret them correctly and thereby avoid unnecessary intervention (pacemaker revision) on a system that is functioning normally.

Rate Adaptive Programming

All contemporary pacemakers have rate-adaptive algorithms to mimic the physiological chronotropic response for patients with SND. Several parameters have been investigated to estimate metabolic need and heart rate requirements for rate-adaptive algorithms, including: (1) accelerometer; (2) minute ventilation; and (3) closed-loop stimulation, and they vary according to pacemaker manufacturer and model.

The most widely used rate-adaptive algorithms use an accelerometer coupled with piezoelectric sensors that increase pacing rate according to the amount and vigorousness of anterior to posterior thoracic motion. Certain pacemakers have the capacity to estimate minute ventilation (which correlates with oxygen consumption and cardiac output) by measuring transthoracic impedance from a rapid, low-amplitude current impulse applied between the lead tip and pulse generator. Measured changes in minute ventilation trigger changes in pacing rates. Pacemakers with closed-loop stimulation algorithms estimate cardiac sympathetic activation by measuring changes in the unipolar RV impedance, which correlates to changes of the RV contractility and reflects the level of cardiac sympathetic activity. An increase in intracardiac impedance (and cardiac contractility) is used to indicate a need for increased heart rate. Importantly, each algorithm is associated with inherent advantages and disadvantages, and none is able to accurately predict the physiological chronotropic response in all different physiological scenarios or to completely eliminate the risk of unnecessary pacing.³⁶

Although some studies found rate-responsive algorithms superior to fixed-rate pacing in improving exercise capacity in patients with chronotropic incompetence, other studies raised the concern of increased risk of heart failure and AF associated with a higher percentage of atrial pacing. In addition, in some patients, atrial pacing can cause excessive prolongation of PR intervals or second-degree AVB and as a result a high percentage of RV pacing. Furthermore, faster pacing rates, even at levels that are appropriate to the physiological need in normal subjects, can have detrimental effects in patients with ischemic heart disease or heart failure.⁴⁵ Hence rate-adaptive programming is recommended only for patients with chronotropic incompetence who experience symptomatic benefit in response to rate adaptive pacing. The need for rate-adaptive programming should be evaluated periodically to help minimize unnecessary pacing.

Mode Switch Algorithms

Automatic mode switching (AMS) algorithms reprogram the pacemaker from an atrial tracking (DDD or DDDR) to a nontracking mode (VVI, VVIR, DDI, or DDIR) on sensing an atrial tachyarrhythmia and back again to DDD or DDDR mode when a normal atrial rate is sensed. This helps to avoid rapid ventricular pacing in response to atrial tachyarrhythmias or other rapidly occurring signals sensed by the atrial channel.

The accurate detection of atrial tachyarrhythmias depends on the rate of the detected atrial arrhythmia compared with the programmed AMS rate, the length of the atrial blanking and refractory periods, and the programmed atrial sensitivity. Reduced sensitivity can occur due to AF with small electrogram amplitudes, slower atrial tachycardias, or blanked atrial waves during AFL. On the other hand, false-positive mode switching can result from oversensing of ventricular far-field signals or, rarely, myopotentials. Hence optimal pacemaker programming requires a thorough knowledge of the patient's arrhythmia history,

atrial electrogram amplitude (in sinus rhythm and atrial tachyarrhythmia), atrial rates during the arrhythmia, and the characteristics of the AMS algorithm used in the specific pacemaker make and model.³⁶

Overall, the performance of AMS algorithms has been quite satisfactory, and the data provided by these programs on the time of onset and duration of AMS episodes can generally be used as a reliable surrogate marker for the occurrence and burden of atrial tachyarrhythmias and help to guide clinical decisions regarding the need and efficacy of antiarrhythmic interventions or the risk of thromboembolic events. If clinical decisions are being contemplated based on these findings, interrogation and analysis of stored electrograms during available AMS episodes should be considered to verify the reliability of these algorithms.³⁶

REFERENCES

1. Sánchez-Quintana D, et al. Sinus node revisited in the era of electroanatomical mapping and catheter ablation. *Heart*. 2005;91:189–194.
2. Anderson RH, Yanni J, Boyett MR, et al. The anatomy of the cardiac conduction system. *Clin Anat*. 2009;22:99–113.
3. Murphy C, Lazzara R. Current concepts of anatomy and electrophysiology of the sinus node. *J Interv Card Electrophysiol*. 2016;46:9–18.
4. Ho SY, Sánchez-Quintana D. Anatomy and pathology of the sinus node. *J Interv Card Electrophysiol*. 2016;46:3–8.
5. Lau DH, Roberts-Thomson KC, Sanders P. Sinus node revisited. *Curr Opin Cardiol*. 2011;26:55–59.
6. Unudurthi SD, Wolf RM, Hund TJ. Role of sinoatrial node architecture in maintaining a balanced source-sink relationship and synchronous cardiac pacemaking. *Front Physiol*. 2014;5:446.
7. Nikolaidou T, Aslanidi OV, Zhang H, et al. Structure-function relationship in the sinus and atrioventricular nodes. *Pediatr Cardiol*. 2012;33:890–899.
8. Milanese R, Bucchi A, Baruscotti M. The genetic basis for inherited forms of sinoatrial dysfunction and atrioventricular node dysfunction. *J Interv Card Electrophysiol*. 2015;43:121–134.
9. Monfredi O, Dobrzynski H, Mondal T, et al. The anatomy and physiology of the sinoatrial node—a contemporary review. *Pacing Clin Electrophysiol*. 2010;33:1392–1406.
10. Fedorov VV, Glukhov AV, Chang R. Conduction barriers and pathways of the sinoatrial pacemaker complex: their role in normal rhythm and atrial arrhythmias. *Am J Physiol Heart Circ Physiol*. 2012;302:H1773–H1783.
11. Stiles MK, et al. High-density mapping of the sinus node in humans: role of preferential pathways and the effect of remodeling. *J Cardiovasc Electrophysiol*. 2010;21:532–539.
12. Lou Q, et al. Upregulation of adenosine A1 receptors facilitates sinoatrial node dysfunction in chronic canine heart failure by exacerbating nodal conduction abnormalities revealed by novel dual-sided intramural optical mapping. *Circulation*. 2014;130:315–324.
13. Luo M, et al. Diabetes increases mortality after myocardial infarction by oxidizing CaMKII. *J Clin Invest*. 2013;123:1262–1274.
14. Wolf RM, et al. Atrial fibrillation and sinus node dysfunction in human ankyrin-B syndrome: a computational analysis. *Am J Physiol Heart Circ Physiol*. 2013;304:H1253–H1266.
15. Csepe TA, Kalyanasundaram A, Hansen BJ, et al. Fibrosis: a structural modulator of sinoatrial node physiology and dysfunction. *Front Physiol*. 2015;6:37.
16. Chang H-Y, et al. Sinus node dysfunction in atrial fibrillation patients: the evidence of regional atrial substrate remodelling. *Europace*. 2013;15:205–211.
17. Joung B, et al. Mechanisms of sinoatrial node dysfunction in a canine model of pacing-induced atrial fibrillation. *Heart Rhythm*. 2010;7:88–95.
18. Yeh Y-H, et al. Funny current downregulation and sinus node dysfunction associated with atrial tachyarrhythmia: a molecular basis for tachycardia-bradycardia syndrome. *Circulation*. 2009;119:1576–1585.

19. Lou Q, et al. Tachy-brady arrhythmias: the critical role of adenosine-induced sinoatrial conduction block in post-tachycardia pauses. *Heart Rhythm*. 2013;10:110–118.
20. O'Neal WT, et al. Chronotropic incompetence and risk of atrial fibrillation: the Henry Ford Exercise Testing (FIT) project. *JACC Clin Electrophysiol*. 2016;2:645–652.
21. Tellez JO, et al. Ageing-dependent remodelling of ion channel and Ca²⁺ clock genes underlying sino-atrial node pacemaking. *Exp Physiol*. 2011;96:1163–1178.
22. Li G, et al. Atrial electrical remodeling in a canine model of sinus node dysfunction. *Int J Cardiol*. 2011;146:32–36.
23. Yanni J, et al. Changes in ion channel gene expression underlying heart failure-induced sinoatrial node dysfunction. *Circ Heart Fail*. 2011;4:496–508.
24. Medi C, et al. Atrial electrical and structural remodeling associated with longstanding pulmonary hypertension and right ventricular hypertrophy in humans. *J Cardiovasc Electrophysiol*. 2012;23:614–620.
25. Dimitri H, et al. Atrial remodeling in obstructive sleep apnea: implications for atrial fibrillation. *Heart Rhythm*. 2012;9:321–327.
26. Nof E, Glikson M, Antzelevitch C. Genetics and sinus node dysfunction. *J Atr Fibrillation*. 2009;1:328–336.
27. Park DS, Fishman GI. The cardiac conduction system. *Circulation*. 2011;123:904–915.
28. Brugada J, et al. Pharmacological and non-pharmacological therapy for arrhythmias in the pediatric population: EHRA and AEPC-Arrhythmia Working Group joint consensus statement. *Europace*. 2013;15:1337–1382.
29. Chiang DY, et al. Loss-of-function SCN5A mutations associated with sinus node dysfunction, atrial arrhythmias, and poor pacemaker capture. *Circ Arrhythm Electrophysiol*. 2015;8:1105–1112.
30. Verkerk AO, Wilders R. Pacemaker activity of the human sinoatrial node: an update on the effects of mutations in hcn4 on the hyperpolarization-activated current. *Int J Mol Sci*. 2015;16:3071–3094.
31. Ishikawa T, et al. Novel mutation in the α -myosin heavy chain gene is associated with sick sinus syndrome. *Circ Arrhythm Electrophysiol*. 2015;8:400–408.
32. Khairy P, et al. PACES/HRS Expert Consensus Statement on the Recognition and Management of Arrhythmias in Adult Congenital Heart Disease: developed in partnership between the Pediatric and Congenital Electrophysiology Society (PACES) and the Heart Rhythm Society (HRS). *Heart Rhythm*. 2014;11:e102–e165.
33. Sheldon RS, et al. Heart Rhythm Society expert consensus statement on the diagnosis and treatment of postural tachycardia syndrome, inappropriate sinus tachycardia, and vasovagal syncope. *Heart Rhythm*. 2015;12:e41–e63.
34. Uberoi A, et al. Interpretation of the electrocardiogram of young athletes. *Circulation*. 2011;124:746–757.
35. Jensen PN, et al. Incidence of and risk factors for sick sinus syndrome in the general population. *J Am Coll Cardiol*. 2014;64:531–538.
36. Gillis AM, et al. HRS/ACCF expert consensus statement on pacemaker device and mode selection. *J Am Coll Cardiol*. 2012;60:682–703.
37. Graff B, et al. Electrophysiological features in patients with sinus node dysfunction and vasovagal syncope. *Arch Med Sci*. 2011;7:963–970.
38. Epstein AE, et al. 2012 ACCF/AHA/HRS focused update incorporated into the ACCF/AHA/HRS 2008 guidelines for device-based therapy of cardiac rhythm abnormalities: a report of the American College of Cardiology Foundation/American Heart Association Task Force on Practice Guide. *Circulation*. 2013;127:e283–e352.
39. Chen YW, et al. Pacing or ablation: which is better for paroxysmal atrial fibrillation-related tachycardia-bradycardia syndrome? *Pacing Clin Electrophysiol*. 2014;37:403–411.
40. Kirkfeldt RE, Andersen HR, Nielsen JC. System upgrade and its complications in patients with a single lead atrial pacemaker: data from the DANPACE trial. *Europace*. 2013;15:1166–1173.
41. Auricchio A, Ellenbogen KA. Reducing ventricular pacing frequency in patients with atrioventricular block. *Circ Arrhythm Electrophysiol*. 2016;9:e004404.
42. Botto GL, et al. Managed ventricular pacing compared with conventional dual-chamber pacing for elective replacement in chronically paced patients: results of the Prefer for Elective Replacement Managed Ventricular Pacing randomized study. *Heart Rhythm*. 2014;11:992–1000.
43. Magnani JW, et al. Electrocardiographic PR interval and adverse outcomes in older adults: the Health, Aging, and Body Composition study. *Circ Arrhythm Electrophysiol*. 2013;6:84–90.
44. Padeletti L, et al. New-generation atrial antitachycardia pacing (reactive ATP) is associated with reduced risk of persistent or permanent atrial fibrillation in patients with bradycardia: results from the MINERVA randomized multicenter international trial. *Heart Rhythm*. 2015;12:1717–1725.
45. Swedberg K, et al. Ivabradine and outcomes in chronic heart failure (SHIFT): a randomised placebo-controlled study. *Lancet (London, England)*. 2010;376:875–885.

Atrioventricular Conduction Abnormalities

OUTLINE

Anatomy and Physiology of the Atrioventricular Junction, 255

- Internodal and Interatrial Conduction, 255
- Central Fibrous Body, 255
- Triangle of Koch, 256
- Atrioventricular Node, 257
- His Bundle, 257

Pathophysiology of Atrioventricular Block, 257

- Congenital and Inherited Atrioventricular Block, 257
- Acquired Atrioventricular Block, 258
- Paroxysmal Atrioventricular Block, 261

Clinical Presentation, 262

Natural History, 263

Diagnostic Evaluation, 264

- Electrocardiography, 264
- Autonomic Modulation, 264
- Exercise Testing, 264
- Electrophysiological Testing, 264

Electrocardiographic Features, 264

- First-Degree Atrioventricular Delay, 264
- Second-Degree Atrioventricular Block, 265
- Third-Degree (Complete) Atrioventricular Block, 270

Electrophysiological Testing, 270

- Role of Electrophysiological Testing, 270
- Normal Atrioventricular Conduction, 272
- Localization of the Site of Atrioventricular Block, 272
- Exclusion of Other Phenomena, 274

Principles of Management, 277

- Permanent Pacing Therapy, 277
- Pacemaker Device and Mode Selection for Atrioventricular Block, 280
- Ventricular Pacing Site, 281

ANATOMY AND PHYSIOLOGY OF THE ATRIOVENTRICULAR JUNCTION

Internodal and Interatrial Conduction

Evidence suggests the presence of preferential impulse propagation from the sinus node to the atrioventricular node (AVN) (i.e., higher conduction velocity between the nodes in some parts of the atrium than in other parts). However, whether preferential internodal conduction is caused by fiber orientation, size, or geometry or by the presence of specialized preferentially conducting pathways located between the nodes has been controversial. It is believed by many that there are three preferential anatomic conduction pathways from the sinus node to the AVN: anterior, posterior, and middle. However, ultrastructural evidence for discrete bands of rapidly conducting myocytes is sparse, and it is more likely that preferential conduction occurs over muscle bundles and not discrete internodal tracts. These groups of internodal tissue are best referred to as *internodal atrial myocardium*, not tracts, because they do not appear to be histologically recognizable specialized tracts, only plain atrial myocardium. In addition, detailed electroanatomic activation maps do not reveal more rapidly conducting tracts.¹

The anterior “internodal atrial myocardium” begins at the anterior margin of the sinus node, curves anteriorly around the superior vena cava (SVC) to the interatrial septum, and then splits into two bundles: one passes to the left atrium (LA) (Bachmann bundle), while the second bundle descends along the interatrial septum and connects to the superior margin of the AVN. The Bachmann bundle is a large, flat muscle bundle that appears to conduct the cardiac impulse preferentially from the right atrium (RA) to the LA. It connects the anterosuperior RA and

LA behind the ascending aorta, just beneath the epicardium, and is recognized as the preferential path of LA activation during sinus rhythm. Histologically, the Bachmann bundle has characteristics of atrial myocardium and is considered the main, but not the exclusive, route of interatrial conduction.² Three other interatrial conduction pathways have been described: muscular bundles on the inferior atrial surface near the coronary sinus (CS), transseptal fibers in the fossa ovalis, and posteriorly in the vicinity of the right pulmonic valves (PVs).^{3,4}

The middle “internodal atrial myocardium” begins at the superior and posterior margins of the sinus node, travels posteriorly behind the SVC to the crest of the interatrial septum, and descends within the interatrial septum to the superior margin of the AVN. The posterior “internodal atrial myocardium” starts at the inferoposterior margin of the sinus node, travels inferiorly through the crista terminalis to the eustachian ridge, and then into the interatrial septum above the CS os, where it joins the posterior portion of the AVN. Some fibers from all three pathways bypass the crest of the AVN and enter its more distal segment.

Central Fibrous Body

The cardiac skeleton consists of four rings of dense connective tissue that surround the AV canals (mitral and tricuspid) and extends to the origins of the aorta and the pulmonary trunk. The aortic valve occupies the central position with the other valve rings attached to it. The triangular formation between the aortic valve and the medial parts of the tricuspid and mitral valves is the right fibrous trigone, which represents the largest thickening and strongest portion of the cardiac skeleton (Fig. 9.1). The right fibrous trigone, together with the membranous

Atrioventricular Node

The AVN is an interatrial structure, measuring approximately 5 mm long, 5 mm wide, and 0.8 mm thick in adults. The AVN is located beneath the RA endocardium at the apex of the triangle of Koch, anterior to the CS os and directly above the insertion of the septal leaflet of the tricuspid valve, where the tendon of Todaro merges with the central fibrous body. Slightly more anteriorly and superiorly is where the His bundle (HB) penetrates the AV junction through the central fibrous body and the posterior aspect of the membranous AV septum. The compact node is adjacent to the central fibrous body on one side but is uninsulated by fibrous tissue on its other sides, thus allowing contiguity with the atrial myocardium. When traced inferiorly, toward the base of the triangle of Koch, the compact AVN area separates into two (rightward and leftward) posterior extensions, usually with the artery supplying the AVN running between them. These prongs bifurcate toward the tricuspid and mitral annuli, respectively. The rightward posterior extension has been implicated in the so-called slow pathway in the typical atrioventricular nodal reentry tachycardia (AVNRT) circuit.^{2,6,7}

The normal AV junctional area can be divided into distinct regions: the transitional cell zone (which represents the approaches from the working atrial myocardium to the AVN), the compact AVN, and the penetrating part of the HB. The AVN and perinodal area are composed of at least three electrophysiologically distinct cells: the atrionodal (AN), nodal (N), and nodal-His (NH) cells. The AN region corresponds to the cells in the transitional region that are activated shortly after the atrial cells.^{6,7} The N region corresponds to the region where the transitional cells merge with midnodal cells. The N cells represent the most typical of the N cells, which are smaller than atrial myocytes, are closely grouped, and frequently are arranged in an interweaving fashion. Sodium (Na^+) channel density is lower in the midnodal zone of the AVN than in the AN and NH cell zones, and the inward L-type calcium (Ca^{2+}) current is the basis of the upstroke of the N cell action potential. Therefore conduction is slower through the N region in the compact AVN than in the AN and NH cell zones. In addition, the N cells exhibit diastolic depolarization and are capable of automatic impulse formation.¹ The N cells in the compact AVN appear to be responsible for the major part of AV conduction delay and exhibit decremental properties in response to premature stimulation because of their slow rising and longer action potentials. They are likely the site of Wenckebach block and the site at which calcium channel blockers delay AV conduction. Fast pathway conduction through the AVN apparently bypasses many of the N cells by transitional cells, whereas slow pathway conduction traverses the entire compact AVN. Importantly, the recovery of excitability after conduction of an impulse is faster for the slow pathway than for the fast pathway, for reasons that are unclear.¹ The NH region corresponds to the lower N cells, typically distal to the site of Wenckebach block, connecting to the insulated penetrating portion of the HB. The action potentials of the NH cells are closer in appearance to the fast-rising and long action potentials of the HB.²

The AVN is the only normal electrical connection between the atria and the ventricles; the fibrous skeleton acts as an insulator to prevent electrical impulses from entering the ventricles by any other route. The main function of the AVN is modulation of atrial impulse transmission to the ventricles; it introduces a delay between atrial and ventricular systole, thereby allowing atrial systole and ventricular filling to complete prior to initiation of ventricular systole.¹ Another primary function of the AVN is to limit the number of impulses conducted from the atria to the ventricles. This function is particularly important during fast atrial rates (e.g., during AF or atrial flutter [AFL]), in which only a portion of impulses are conducted to the ventricles and the remaining

impulses are blocked in the AVN. In addition, fibers in the lower part of the AVN can exhibit automatic impulse formation, serving as a subsidiary pacemaker.^{6,7}

The AVN region is innervated by a rich supply of cholinergic and adrenergic fibers. Sympathetic stimulation shortens AVN conduction time and refractoriness, whereas vagal stimulation prolongs AVN conduction time and refractoriness. The negative dromotropic response of the AVN to vagal stimulation is mediated by activation of the inwardly rectifying potassium (K^+) current (IK_{ACh}), which results in hyperpolarization and action potential shortening of AVN cells, increased threshold of excitation, depression of action potential amplitude, and prolonged conduction time. The positive dromotropic effect of sympathetic stimulation arises as a consequence of activation of the L-type Ca^{2+} current.

The blood supply to the AVN predominantly comes via the AV nodal artery, a branch of the right coronary artery in approximately 90% of hearts and from the circumflex artery in 10%.

His Bundle

The HB connects with the distal part of the compact AVN and penetrates the central fibrous body (where it is called the “nonbranching” or “penetrating” bundle) in a leftward direction (away from the RA endocardium and toward the crest of the muscular interventricular septum). The HB then emerges on the crest of the ventricular septum and continues sandwiched between the muscular and the membranous components of the septum for 1 to 2 cm before dividing into the right and left bundle branches. Viewed from the aorta, the HB passes beneath the part of the membranous septum that adjoins the interleaflet fibrous triangle between the right and non-CSs. The HB is insulated from the atrial myocardium by the membranous septum and from the ventricular myocardium by connective tissue of the central fibrous body, thus preventing atrial impulses from bypassing the AVN. Proximal cells of the penetrating portion of the HB are heterogeneous and resemble those of the compact AVN; distal cells are larger, similar to cells in the proximal bundle branches and ventricular myocytes.^{1,8,9}

The HB is supplied by the AV nodal artery and the first septal branch of the left anterior descending artery. The dual blood supply makes the conduction system at this site less vulnerable to ischemic damage unless the ischemia is extensive.

The AVN and the HB region are innervated by a rich supply of cholinergic and adrenergic fibers, with a density exceeding that found in the ventricular myocardium. Although neither sympathetic stimulation nor vagal stimulation affects normal conduction in the HB, either can affect abnormal AV conduction.

PATHOPHYSIOLOGY OF ATRIOVENTRICULAR BLOCK

Block or delay of a cardiac impulse can take place anywhere in the heart or even within a single cell. AV block can be defined as a delay or interruption in the transmission of an impulse from the atria to the ventricles caused by an anatomical or functional impairment in the conduction system. The conduction disturbance can be transient or permanent.

Congenital and Inherited Atrioventricular Block

Congenital Atrioventricular Block

Congenital complete AV block is thought to result from embryonic maldevelopment of the AVN (and, much less frequently, the His-Purkinje system [HPS]), resulting in a lack of connection between the atria and the peripheral conduction system, with fatty replacement of the AVN and nodal approaches. The incidence of congenital complete AV block

varies from 1 in 15,000 to 1 in 22,000 live births. The defect usually occurs proximal to the HB and is associated with a stable escape rhythm (greater than 60 beats/min) with a narrow QRS complex.^{10,11}

In 60% to 90% of cases, congenital AV block is associated with neonatal lupus caused by passively acquired autoimmune disease in which maternal autoantibodies to the intracellular ribonucleoproteins Ro (SS-A) and La (SS-B) cross the placenta and injure the previously normal fetal heart. These antibodies can be seen with subclinical or clinical maternal lupus erythematosus, maternal Sjögren syndrome, and other maternal autoimmune diseases. The exact mechanism by which these autoantibodies can cause AV block or other cardiac abnormalities is uncertain. Involvement of the AV conduction system produces different degrees of AV block. Although first-degree AV delay can be transient, complete AV block is irreversible. The risk of the fetus developing congenital atrioventricular block (AVB) in a single anti-Ro- or anti-La-positive pregnancy is relatively low (1% to 2%), but the risk in the same mother increases significantly (12% to 20%) in subsequent pregnancies. Although the severity of AV block can vary, most cases diagnosed in utero present with second- or third-degree block.^{12,13}

Approximately one-third of patients with congenital AV block have concurrent congenital heart disease (e.g., congenitally corrected transposition of the great vessels, AV discordance, ventricular septal defects, AV canal defects, tricuspid atresia, anomalous left coronary artery arising from the pulmonary artery, or Ebstein anomaly of the tricuspid valve). The AV conduction system can be displaced if atrial and ventricular septa are malaligned, AV arrangements are discordant, or the heart is univentricular. In general, if the AV conduction system is displaced, it will also tend to be more fragile and susceptible to degeneration, thus placing patients at greater risk for AV block.¹⁴

Hereditary Cardiac Conduction Disease

Progressive cardiac conduction disorder is an inherited cardiac disease that can present as a primary electrical disease or be associated with structural heart disease. Mutations in genes encoding cardiac ion channels, ion channel-interacting proteins, cardiac transcription factors, and cytoskeletal elements have been described as a rare cause of familial forms of AV block (see Chapter 2). Disease can occur at any level of the cardiac conduction system and can manifest as sinoatrial exit block, AV block, or bundle branch block (BBB).^{15,16,17}

Loss-of-function mutations in the *SCN5A* gene (encoding the alpha subunit of the cardiac Na⁺ channel) cause the majority of familial forms of progressive cardiac conduction disease (referred to as hereditary Lenègre disease, primary cardiac conduction system disease, and familial AV block). This disease is characterized by slowing of electrical conduction through the atria, AVN, HB, Purkinje fibers, and ventricles, accompanied by an age-related degenerative process and fibrosis of the cardiac conduction system, in the absence of structural or systemic disease. It is often reflected by varying degrees of AV block and BBB. A single loss-of-function *SCN5A* mutation can cause isolated progressive cardiac conduction disease or can be combined with the Brugada syndrome (overlap syndrome). Furthermore, loss-of-function mutations in the *SCN1B* gene (encoding the beta₁ and beta_{1b} subunits of the Na⁺ channel) have been identified in patients with progressive cardiac conduction disease who carried no mutation in *SCN5A*.^{13,18}

Mutations in the gene *TRPM4* gene (encoding the calcium-activated nonselective cation channel of the transient receptor potential melastatin, which is highly expressed in cardiac Purkinje fibers) have been associated with isolated progressive cardiac conduction block.

Another channelopathy that has been associated with conduction system disorders is the LQT7, or Andersen-Tawil syndrome, caused by mutations in the *KCNJ2* gene (encoding the inward rectifier *Kr*2.1, a critical component of the cardiac inward K⁺ rectifier current, *I_{K1}*).

In addition, mutations in the *PRKAG2* gene (encoding the gamma₂ regulatory subunit of adenosine monophosphate-activated protein kinase) have been described in patients with Wolff-Parkinson-White syndrome and AV conduction block.¹⁸ Recently, mutations in *GJA5* gene (encoding for connexin 40 protein) were linked to progressive familial heart block and malignant ventricular arrhythmias.¹⁵

Neuromyopathies

Neuromuscular disorders represent a diverse collection of inherited diseases affecting skeletal muscle, frequently caused by mutations in genes encoding cytoskeletal, nuclear envelope (e.g., lamin A/C and emerin), or mitochondrial proteins. Cardiac involvement is common and usually manifests as dilated or hypertrophic cardiomyopathy (HCM), AV conduction abnormalities, and atrial and ventricular dysrhythmias. AV conduction disturbances are usually the major cardiac manifestation of Becker muscular dystrophy, peroneal muscular dystrophy, Kearns-Sayre syndrome, Erb dystrophy, and myotonic muscular dystrophy. Progression of AV block is unpredictable and can be an important cause of mortality in such cases.¹⁸

Long-QT Syndrome

In long-QT syndrome (LQTS) with a very long QT interval (e.g., in LQT2, LQT3, LQT8, and LQT9), functional block between the HB and ventricular muscle caused by prolonged ventricular refractoriness can lead to 2:1 AV block and severe bradycardia. In addition, conduction abnormalities of the HPS, including PQ prolongation and right bundle branch block (RBBB) or left bundle branch block (LBBB), can occur in some patients with LQTS.

Acquired Atrioventricular Block

Drugs

Various drugs can impair conduction and cause AV block. Digoxin and beta blockers act primarily indirectly on the AVN through their effects on the autonomic nervous system. Calcium channel blockers and other antiarrhythmic drugs, such as amiodarone and dronedarone, act directly to slow conduction in the AVN. Class I and III antiarrhythmic drugs can also affect conduction in the HPS and cause infranodal block. However, these effects typically occur in patients with preexisting conduction abnormalities. Patients with a normal conduction system function rarely develop complete heart block as a result of using antiarrhythmic agents. Other agents that can produce AV conduction disturbances include clonidine, lithium (in toxic concentrations), and fingolimod (usually transient).

Ischemic Heart Disease

AV block occurs in 12% to 25% of all patients with acute ST-elevation myocardial infarction (MI); first-degree AV delay occurs in 2% to 12%, second-degree AV block occurs in 3% to 10%, and third-degree AV block occurs in 3% to 7%.

First-degree AV delay and type 1 second-degree (Wenckebach) AV block occur more commonly in inferior MI, usually caused by increased vagal tone (Bezold-Jarisch reflex), rather than direct nodal ischemia, and generally associated with other signs of vagotonia, such as sinus bradycardia and responsiveness to atropine and catecholamine stimulation. Wenckebach AV block in the setting of acute inferior MI is usually transient (resolving within 48 to 72 hours of onset) and asymptomatic and rarely progresses to more advanced degrees of AV block. Wenckebach AV block occurring later in the course of acute inferior MI is less responsive to atropine and probably is associated with ischemia of the AVN.

Type 2 second-degree (Mobitz type II) AV block occurs in only 1% of patients with acute MI (more commonly in anterior than inferior

MI) and has a worse prognosis than type 1 second-degree block. Type 2 second-degree AV block occurring during acute anterior MI is typically associated with HB or bundle branch ischemia or infarction and frequently progresses to complete heart block.

The incidence of new-onset, high-grade AV block in patients complicating ST elevation MI has decreased in the reperfusion era from 5% to 7% with thrombolytic therapy to 2.2% with primary percutaneous coronary intervention. The risk is even less in non-ST elevation MI. Predictors of AV block in acute MI patients include older age, female gender, inferior acute MI, prior MI, smoking, hypertension, and diabetes. Furthermore, the risk is 2 to 4 times higher in acute inferior MI as compared with anterior MI (9.4% vs. 2.5% in the thrombolytic era). In patients undergoing primary percutaneous coronary intervention, the incidence of high-grade AV block is approximately 7% when the culprit lesion is in the right coronary artery, compared with 1% when the culprit lesion is in the left anterior descending artery.^{19,20,21}

High-degree AV block complicating acute MI is an ominous prognostic marker and is independently associated with 3 times higher in-hospital and 30-day mortality as compared with those with preserved AV conduction, irrespective of the site of the infarction or LV function. This markedly adverse prognostic impact of high-grade AV block has not been reduced by primary percutaneous coronary intervention as compared with thrombolytic therapy or even to prethrombolytic era.²² The negative prognostic impact of complete AV block is greater in patients with anterior than those patients with inferior ST elevation MI.²¹ The risk of death is higher in patients with occlusion of the left anterior descending artery as compared with those with right coronary artery occlusion (55% vs. 36%). Importantly, AV block itself is not responsible for the increased mortality but rather is a marker for a more extensive infarct size. Similar to observations from the prethrombolytic era, the occurrence of high-degree AV block during acute MI has no impact on 1-year mortality among 30-day survivors.^{19,20} Of note, new-onset intraventricular conduction disturbances complicate 10% to 20% of anterior MI (with or without AV block) and are usually associated with high mortality due to the extensive myocardial necrosis (rather than the conduction disturbance).

High-grade AV block develops upon hospital admission in more than half of patients with this complication and within 48 hours after admission in the majority patients. The block is typically transient, most often resolves spontaneously within a few days or weeks, with only 9% of these patients requiring pacemaker implantation prior to hospital discharge.^{19,20}

Of note, in the thrombolytic era, thrombolytic therapy frequently precipitated transient AV block, likely due to enhanced vagal tone secondary to reperfusion. Whether this effect is different when reperfusion is achieved by intracoronary stenting is unknown.

Acute Inferior Myocardial Infarction

In the setting of acute right coronary artery occlusion, AV block is almost always (90% of the patients) located above the HB. The block often progresses gradually (from first-degree, to type 1 second-degree, to complete AVB) and is associated with a junctional escape rhythm with a narrow QRS complex (in 70% of cases) and a rate of 40 to 60 beats/min. Complete AVB occurring in the early phase of acute inferior MI (within 6 hours of onset of symptoms) is more likely related to enhanced vagal tone, tends to be reversed by vagolytic drugs or catecholamines, and usually resolves within several days. In contrast, AV block developing later in the course of acute inferior MI tends to be more persistent and is more likely related to ischemia of the AVN (hypoperfusion of the AVN artery). Small areas of focal necrosis can occur; however, complete infarction and necrosis of the AVN or occlusion of the AVN artery are rare.^{23,20}

Acute Anterior Myocardial Infarction

Development of complete AV block in the setting of acute anterior MI is usually a marker of a large infarct area and hence is commonly associated with a higher risk of VT and VF, hypotension, pulmonary edema, and in-hospital mortality. Frequently, these patients have extensive infarction of the septum and anterior wall in the presence of severe multivessel disease involving both the left anterior descending artery and the right or a dominant left circumflex coronary artery.

In the setting of anterior MI, AV block is most often located below the AVN and is usually associated with ischemia or infarction of the HB or bundle branches (related to interruption of septal perfusion) and is less likely to be reversible. Complete AV block during acute anterior MI generally occurs abruptly during the first 24 hours after MI and often is preceded by the development of a new RBBB, fascicular block, or type 2 second-degree AV block. The escape rhythm usually originates from the bundle branch and Purkinje system, with a rate less than 40 beats/min and a wide QRS complex, with higher risk of ventricular asystole.^{23,20}

Chronic Ischemic Heart Disease

Chronic ischemic heart disease, with or without infarction, can result in persistent AV block secondary to fibrotic changes in the bifurcating HB and bundle branches. Transient AV block can occasionally occur during angina pectoris whether due to atherosclerosis or spasm in relatively normal caliber vessels (Prinzmetal angina).

Degenerative Diseases

Fibrosis and sclerosis of the conduction system are the most common causes of acquired conduction system disease. These disorders account for approximately half the cases of AV block in adults and can be induced by several different conditions, which often cannot be distinguished clinically.

Progressive cardiac conduction disease (including Lev disease or Lenègre disease) manifests as progressive slowing of electrical conduction through the atria, AVN, HB, Purkinje fibers, and ventricles, accompanied by an age-related degenerative process, in which fibrosis affects only the cardiac conduction system. Complete AV block can develop and cause syncope or sudden death. Lev disease is a result of proximal bundle branch calcification or fibrosis and is often described as senile degeneration of the conduction system. Its postulated cause is a hastening of the aging process by hypertension and arteriosclerosis of the blood vessels supplying the conduction system. Lenègre disease is a sclerodegenerative process that occurs in a younger population and involves the more distal portions of the bundle branches. As noted, an inherited form of progressive cardiac conduction disease has been identified, whereby conduction slowing may be attributed to loss-of-function mutations in the *SCN5A* gene. Whether the age-dependent fibrosis of the conduction system is a primary degenerative process in progressive cardiac conduction disease or a physiological process that is accelerated by I_{Na} reduction remains to be investigated.¹⁸

Calcification of the aortic or (less commonly) mitral valve annulus can extend to the nearby conduction system and produce AV block. As noted, the HB penetrates the central fibrous body adjacent to the fibrous continuity between the aortic and mitral valves that is the usual site of dystrophic calcification, and extension of calcification can directly involve the HB and the origin of the left bundle branch.

Rheumatic Diseases

AV block can occur in association with collagen vascular diseases such as scleroderma, rheumatoid arthritis, Reiter syndrome, systemic lupus erythematosus, ankylosing spondylitis, and polymyositis. Polyarteritis nodosa and Wegener granulomatosis also can cause AV block.

Infectious Diseases

Infective endocarditis (especially of the aortic valve) and myocarditis of various viral, bacterial, and parasitic causes (including Lyme disease, Chagas disease, rheumatic fever, tuberculosis, measles, and mumps) can cause varying degrees of AV block.

In the setting of infective endocarditis, AV block and BBB can develop due to perivalvular extension complicating aortic valve involvement and typically predict poor prognosis. Lyme disease involves the heart in 1% to 2% of cases. AV block (ranging from asymptomatic first-degree AV delay to complete AV block, typically intranodal) is the most common manifestation of Lyme carditis. The degree of AV block can fluctuate rapidly over minutes to hours and days. In the majority of patients, AV block is a transient phenomenon and typically resolves completely within 1 to 6 weeks. Resolution of AV block is usually gradual, from complete heart block, to Wenckebach AV block, to first-degree AV delay.²⁴ Although temporary pacing can be required in some patients, implantation of a permanent pacemaker is not recommended.²⁵ Hence Lyme disease should be excluded prior to considering permanent pacemaker implantation in young patients in endemic areas who present with complete AV block. In Chagas disease, conduction system abnormalities, most frequently RBBB or left anterior fascicular (LAF) block, and various degrees of AV block are observed in approximately 36% of patients. Complete AV block can develop in more than 8% and is correlated with increased mortality.²⁶

Infiltrative Processes

Infiltrative cardiomyopathies such as amyloidosis, sarcoidosis, hemochromatosis, and tumors can be associated with AV block. Cardiac involvement occurs in more than 25% of the patients with pulmonary/systemic sarcoidosis but frequently remains asymptomatic. Symptomatic cardiac involvement occurs in approximately 5% of sarcoidosis patients. Various conduction abnormalities can develop as a result of granulomatous infiltration (with inflammation and subsequent scarring) of the basal interventricular septum and conduction system or involvement of the nodal artery causing ischemia in the conduction system.²⁷ BBB (more commonly RBBB) has been observed 12% to 32% of cases of cardiac sarcoidosis and complete AV block in 23% to 30%.²⁸ AV block can manifest early or late in the course of the disease and occasionally can be the first clinical manifestation of sarcoidosis involving any organ. In early stages, before scar formation, AV block can be reversible with immunosuppression therapy. However, permanent pacing is frequently required. In these patients, because AV block likely signifies extensive cardiac disease and portends a higher risk of future ventricular arrhythmias, implantation of an implantable cardioverter-defibrillator (for the primary prevention of sudden cardiac death) instead of a pacemaker needs to be considered, regardless of left ventricular ejection fraction (LVEF) or prior occurrence of ventricular arrhythmias.²⁸ Cardiac sarcoidosis should be suspected in young patients (especially black patients) who present with complete AV block, even in those who do not carry a previous diagnosis of extracardiac sarcoidosis.

Atrioventricular Block in Athletes

AV block occurs in highly conditioned athletes, probably an expression of hypervagotonia related to physical training, and is usually correlated to type and intensity of training. First-degree AV delay has been observed in up to 40% of athletes and type 1 second-degree block in up to 22%. Other signs of hypervagotonia (e.g., sinus bradycardia, respiratory sinus arrhythmia, wandering pacemaker, and junctional bradycardia) are also more common in this population, but AV block can develop without significant sinus bradycardia because the relative effects of sympathetic and parasympathetic systems on the AVN and sinus node can differ. First-degree and Wenckebach AV block in athletes is usually benign,

asymptomatic, resolves with aerobic exercise (as vagal tone is withdrawn), and frequently disappears or decreases after deconditioning.²⁹ Therefore further diagnostic evaluation is not required. In contrast, AV block that does not respond to exercise or atropine, and type II second-degree and complete AV block are rare in athletes, and their presence should prompt careful evaluation and management.

Iatrogenic Atrioventricular Block

Intracardiac catheter manipulation can inadvertently produce varying degrees of heart block, which is usually temporary. Complete heart block can occur during right-sided heart catheterization in a patient with preexisting LBBB or during LV catheterization (LV angiography or ablation procedures) in a patient with preexisting RBBB. Catheter trauma has been reported to cause AV nodal block, as well as block in each of the fascicles of the conduction system; although most blocks are transient, catheter-induced LBBB may persist. AV block can also be a complication of catheter ablation of AVNRT, BTs, and ATs in the AVN vicinity, as well as VTs originating in the interventricular septum adjacent to the HB. Rarely, ablation on the left side of the interatrial septum can damage AVN conduction.

Cardiac surgery can be complicated by varying degrees of AV block caused by trauma and ischemic damage to the conduction system. Mechanical trauma to the conduction system is more common in valvular surgeries, septal myectomy for HCM, or repair of basal ventricular septal defect. Ischemic injury can occur as a result of inadequate myocardial protection during surgery. Not infrequently, the block is temporary and is thought to be secondary to postoperative local inflammation. However, AV block can appear years later, usually in patients who had transient block just after the operation.

AV block occurs with an overall incidence of 1% to 3% after surgical procedures for congenital heart disease and 0.8% to 2.1% after non-congenital cardiac surgeries. Significant risk factors for high-degree AVB include older age, preoperative AV and intraventricular conduction abnormalities, AF, valvular surgery (except pulmonic), and cardiopulmonary bypass time.^{14,30}

Congenital heart disease substrates associated with a relatively high prevalence of postoperative AV block include displaced AV conduction systems (congenitally corrected transposition of the great arteries, AV septal defects), ventricular septal defect, and subaortic stenosis. AV block resolves within 7 to 10 days in 50% of patients.^{14,31}

Complete or high-degree AVB requiring permanent pacing complicates approximately 0.6% of coronary bypass surgeries, 4.5% of cardiac transplant surgeries, and 1.5% after mitral valve repair or replacement surgeries. The incidence is higher (7.7%) after redo valve surgeries. In patients with HCM, persistent AV block complicates 14% to 22% septal alcohol ablation procedures and 2% of surgical myectomy.³²

The close anatomical proximity of the aortic valve annulus, AVN, and HB makes the AV conduction system especially vulnerable to injury during prosthetic aortic valve procedures. The incidence of AV block postsurgical aortic valve replacement is approximately 6%.³³ Predictors indicating the need for a permanent pacemaker in this patient population include aortic insufficiency, pulmonary hypertension, and prior MI. The incidence of AV block is doubled when aortic valve surgery is combined with mitral valve or coronary bypass surgery.³⁴

The overall rate of requirement of a permanent pacemaker is significantly higher (more than 17%) after transcatheter aortic valve replacement (TAVR). Several parameters indicate a high risk of requirement of a permanent pacemaker post TAVR, including male sex, pre-existing AV conduction abnormalities (including first-degree AV delay, LAF block, and RBBB), and intraprocedural AV block. In addition, the risk of pacemaker implantation is 2.5-fold higher in patients receiving the Medtronic CoreValve Revalving System (Medtronic, Minneapolis,

MN) than in those receiving the balloon-expandable Edwards SAPIEN valve (Edwards Lifesciences, Irvine, CA, United States; 19% to 42% vs. 7% to 22%). This is likely related to the valve design (self-expanding vs. balloon-expandable) and the potential of a deeper implantation into the left ventricular outflow tract, causing more injury to the AVN and left bundle branches, which may be delayed because of the self-expanding nature of the prosthesis and tissue edema. Other reported risk factors include advanced age, permanent AF, preoperative bradycardia, larger or oversized prosthesis, and postprocedural new-onset of LBBB.^{35,36}

New LBBB is the most common conduction abnormality observed after TAVR, occurring in 29% to 65% with the Medtronic CoreValve and in 6% to 30% with Edwards SAPIEN valve. It usually occurs during the procedure but can develop afterward in 2% to 8% of patients.³⁷ Although new-onset LBBB after TAVR can be transient and disappears within the first few days in 19% to 34% of patients, it persists in the majority of patients. The risk of progression from LBBB to complete AVB is relatively high. Furthermore, LBBB appears to be an independent predictor of all-cause mortality at 1 year. In the subgroup of patients with new-onset LBBB, the HV interval after TAVR was found to predict AV block with a reasonable diagnostic accuracy.^{35,36} However, whether the development of new LBBB without AV block warrants electrophysiological (EP) testing or prophylactic pacemaker implantation has not yet been validated.^{35,38,39}

Other Causes of Atrioventricular Block

AV block can also occur in a variety of other disorders including hyperkalemia, hypermagnesemia, hyperthyroidism, myxedema, and Addison disease.

Paroxysmal Atrioventricular Block

Three forms of paroxysmal AV block have been described: vagally mediated AV block, intrinsic AV block, and idiopathic AV block.^{40,41,42}

Paroxysmal Vagally Mediated Atrioventricular Block

Vagally mediated AV block is a paroxysmal form of AV block induced by surges of vagal discharge. It occurs in patients with or without heart disease, most of them with no prior evidence of AV or intraventricular

conduction abnormalities. AV block is localized within the AVN, is associated with a narrow QRS escape rhythm, and is generally benign.

The prevalence of vagally mediated AV block is unknown. Not infrequently, it is accidentally encountered as an asymptomatic event during cardiac monitoring, occurring more often during the night (commonly, but not always, precipitated by nocturnal apnea), and in most cases without ventricular asystole. However, prolonged ventricular pauses are common during syncope, typically preceded by identifiable triggering and predisposing factors suggesting a diagnosis of reflex syncope, such as vomiting, coughing, micturition, or phlebotomy, among others. In addition, transient AV block (Wenckebach, 2:1, high grade, or complete AV block) can occur secondary to enhanced vagal tone caused by hypersensitive carotid sinus syndrome and neurocardiogenic syncope. However, the cause of the vagal surge may not be evident in some patients.⁴⁰ Often, the episodes of syncope are preceded by a prodrome of symptoms of vagotonia (lightheadedness, diaphoresis, warm clammy feeling, and nausea). However, some patients experience no such warnings.

A classic vagal effect on the conduction system includes gradual slowing of the sinus rate (P-P interval) and AV conduction (first-degree or Wenckebach block), due to simultaneous vagal effect on both the sinus node and AVN, occasionally followed by sinus arrest or complete AV block. Not infrequently, a more prominent AV response with sudden AV block can occur with heightened vagal tone; nevertheless, slowing of the sinus rate and prolongation of PR interval in at least one beat typically precedes complete AV block. The sinus rate continues to slow down during ventricular asystole. This is followed by gradual resumption of AV conduction (with initial significant PR interval prolongation) and sinus acceleration.

Paroxysmal Intrinsic Atrioventricular Block

Paroxysmal intrinsic AV block is characterized by pause-dependent, abrupt, and sustained AV block occurring in diseased HPS. The change from apparently normal 1:1 AV conduction to complete heart block is sudden and unexpected. The block is usually initiated by conducted or nonconducted premature atrial complexes (PACs) or premature ventricular contractions (PVCs) or by a change of baseline heart rate, and it persists until another PAC or PVC or rate change terminates it (Fig. 9.3). Episodes of AV block are commonly associated with prolonged



Fig. 9.3 Paroxysmal Intrinsic Atrioventricular Block. Shown are two-channel rhythm strips during sinus rhythm with prolonged but stable PR interval and right bundle branch block. A premature ventricular complex (middle, top panel) occurs and is followed by a string of nonconducted P waves for almost 10 seconds until conduction resumes (at a faster sinus rate and with slightly shorter PR intervals, likely because of sympathetic discharge during the asystole).

periods of ventricular asystole (of unpredictable duration) precipitating presyncope or syncope and potentially sudden death. Long-term outcome is characterized by a rapid progression toward permanent AV block.^{43,44}

Paroxysmal AV block is a rare, unique disorder of the HPS, possibly caused by local phase 4 block in the HPS after a critical change in the H-H interval (see Chapter 10). Phase 4 or diastolic depolarization is a property of pacemaker cells of the heart; normal His-Purkinje fibers do not possess this property. However, diseased Purkinje cells can manifest phase 4 depolarization. During a long pause (prolonged diastolic period), the fibers of the often-diseased HPS spontaneously depolarize (membrane potential becomes less negative) and become less responsive to subsequent impulses due to Na⁺ channel inactivation. The critical prolongation of the input stimulus is typically initiated by a compensatory pause after a PAC or PVC, spontaneous slowing of the sinus rate, or overdrive suppression of sinus rhythm on termination of a fast supraventricular rhythm. Once a critical diastolic membrane potential is reached (at which sodium channel inactivation occurs), subsequent conduction may not resume until a well-timed escape beat or premature beat (sinus or ectopic) resets the transmembrane potential to its excitable state. It is important to note that, in some cases, pause-dependent block may be caused by other mechanisms (e.g., source-to-sink mismatch) that may not be related to phase 4 depolarization.^{43,44,45}

No specific or optimal tests exist to diagnose paroxysmal AV block. Patients with paroxysmal intrinsic AV block may or may not have structural heart disease at baseline, and conduction abnormalities may not be evident on resting electrocardiograms (ECGs), and when present, RBBB is the most common finding. The role of EP testing remains uncertain because there is no predictable marker for identifying patients at risk for paroxysmal AV block. Although paroxysmal AV block may be reproduced during EP testing via critically timed atrial or ventricular extrastimuli, a negative EP study result does not exclude the diagnosis of paroxysmal AV block.

Paroxysmal Idiopathic Atrioventricular Block

Paroxysmal “idiopathic” AV block is a recently described distinct form of paroxysmal AV block in patients with recurrent syncope. This form of AV block is unexplainable in terms of currently known mechanisms and has clinical and EP features distinct from those of the two other known types of paroxysmal AV block: intrinsic AV block due to AV conduction disease and extrinsic vagal AV block.⁴¹

Idiopathic paroxysmal AV block is characterized sudden onset of complete AV block causing one or multiple consecutive asystolic pauses and recurrent syncope, absence of cardiac and resting ECG abnormalities, and absence of progression to persistent forms of AV

block (Fig. 9.4). AV block occurs without P-P cycle lengthening or PR interval prolongation (unlike paroxysmal vagal AV block) and is not triggered by PACs or PVCs or by variations in the baseline heart rate (unlike paroxysmal intrinsic AV block).⁴¹

The mechanism of idiopathic AV block has not been elucidated yet. A possible role of adenosine has been suggested. Patients with this form of AV block have low baseline adenosine plasma level values as compared with controls or to patients with reflex (vagal) asystolic syncope. Furthermore, patients with idiopathic AV block frequently exhibit an increased susceptibility to exogenous adenosine; the rapid intravenous injection of 18 mg adenosine or 20 mg adenosine triphosphate (ATP) reproduced spontaneous AV block in the majority of patients. The adenosine response could be abolished by theophylline (an adenosine antagonist) but not by atropine (a vagal antagonist). However, the adenosine test does not appear to be specific, and its value in clinical practice requires further evaluation. Carotid sinus massage or tilt table testing did not reproduce AV block. Permanent pacing was successful in preventing syncopal recurrences during long-term follow-up in patients with idiopathic AV block.^{41,45,46}

Distinction between the three forms of paroxysmal AV block (vagally mediated, intrinsic, and idiopathic) has important prognostic and therapeutic implications. Table 9.1 lists features of each entity, although some of those characteristics can have limited sensitivity and/or specificity, as discussed previously.^{41,42}

CLINICAL PRESENTATION

Symptoms in patients with AV conduction abnormalities are generally caused by bradycardia and loss of AV synchrony. Symptoms caused by advanced AV block can range from exercise intolerance, easy fatigability, dyspnea on exertion, angina, mental status changes, dizziness, and near syncope to frank syncope. In patients with paroxysmal or intermittent complete heart block, symptoms are episodic, and routine ECGs may not be diagnostic. Importantly, acquired AV block can lead to prolongation of the QT interval and torsades de pointes, a potentially lethal complication.⁴⁷

Individuals with first-degree AV delay are usually asymptomatic; however, marked prolongation of the PR interval (longer than 300 milliseconds) can precipitate symptoms similar to those with pacemaker syndrome caused by loss of AV synchrony and atrial contraction against closed AV valves.⁴⁸ In addition, in patients with LV dysfunction, severe first-degree AV delay can lead to impaired hemodynamics, “diastolic” mitral regurgitation, and reduction in cardiac output, with consequent worsening of heart failure symptoms.⁴⁹

TABLE 9.1 Differential Diagnosis of Paroxysmal Atrioventricular Block			
	Paroxysmal Vagally Mediated AV Block	Paroxysmal Intrinsic AV Block	Paroxysmal Idiopathic AV Block
Triggers	Heightened vagal tone	PAC, PVC, change in heart rate	No identifiable triggers
Sinus rate before/during AVB	Slowing	Accelerating	Accelerating
First-degree and/or Wenckebach AV block before or after complete AV block	Common	Absent	Absent
Wide QRS	Uncommon	Common	Common
Level of block	AVN	HPS	HPS
Adenosine plasma level	High	Normal	Low
Sensitivity to Adenosine	Uncommon	Uncommon	Common
Response to pacing therapy	Modest	Good	Good

AV, Atrioventricular; AVB, atrioventricular block; AVN, atrioventricular node; HPS, His-Purkinje system; PAC, premature atrial complexes; PVC, premature ventricular contractions.



Fig. 9.4 Paroxysmal Idiopathic Atrioventricular Block. Implantable loop recorder documentation of syncope due to idiopathic atrioventricular (AV) block. (A) Heart rate trend during 4-minute loop recording. Initially, the heart rate is stable at 60 beats/min and suddenly falls at the time of syncope. (B) Expanded electrocardiogram. The five strips are continuous and show a blocked P wave followed by a complete AV block with an asystolic pause of 20 seconds. During AV block, the P-P cycle is initially constant and then progressively shortens, indicating compensatory reflex sympathetic activation. There is no apparent trigger of the onset of AV block. (From Brignole M, Guieu R, Tomaino M, et al. Mechanism of syncope without prodromes with normal heart and normal electrocardiogram. *Heart Rhythm*. 2016;14:234–239.)

On physical examination, the “a” to “c” wave interval in the jugular venous pulse prolongs and intensity of the first heart sound diminishes as the PR interval lengthens. These changes can be constant in first-degree AV delay, or dynamic, mirroring the changes in PR interval in type I second-degree AV block. In the latter setting, the “a” wave is intermittently not followed by “v” wave, indicating failure of conduction of the P wave to the ventricles. Wenckebach used an analysis of the jugular venous pulse to first describe the phenomenon of type I second-degree AV block.

Congenital AV block can be apparent in utero or at birth; however, many individuals have few or no symptoms and reach their teens or young adulthood before the diagnosis is made. Because of the presence of reliable subsidiary HB pacemakers with adequate rates (especially in the presence of catecholamines), syncope is rare with congenital complete AVN block. Some patients become symptomatic only when aging produces chronotropic incompetence of the escape rhythm.

NATURAL HISTORY

The natural history of patients with AV block depends on the underlying cardiac condition. In addition, the site of the block and the resulting rhythm disturbances themselves contribute to the prognosis. Healthy middle-aged subjects with first-degree AV delay have an excellent prognosis, even when associated with chronic bifascicular block, because the rate of progression to third-degree AV block is low. However, in older populations and in patients with underlying heart failure or coronary artery disease, prolongation of the PR interval was found to be an adverse prognostic marker and a predictor of higher risk of AF and heart failure.⁴⁹

Type 1 second-degree AV block is generally benign; however, when type 1 AV block occurs in association with bifascicular block, the risk of progression to complete heart block is significantly increased because of probable infranodal site of AV conduction delay. Type 2 second-degree

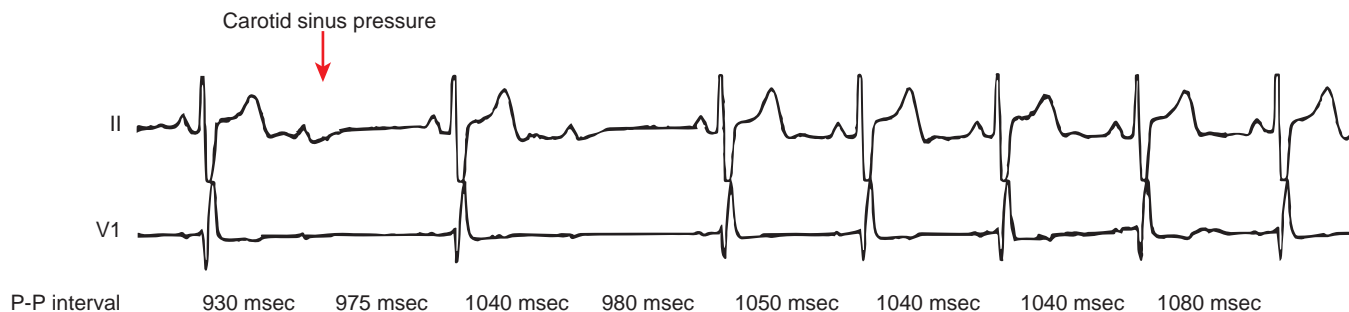


Fig. 9.5 Improvement of Atrioventricular (AV) Conduction With Carotid Sinus Pressure. Two ECG leads are shown in a patient with right bundle branch block, left axis deviation and 2:1 AV block. Carotid sinus pressure is applied (red arrow), P-P intervals shown at bottom gradual increase following this, allowing adequate time for His-Purkinje refractoriness to recover and restore 1:1 AV conduction (at right).

AV block carries a high risk of progression to advanced or complete AV block, which can occur suddenly. The prognosis of 2:1 AV block depends on whether the site of block is within or below the AVN.

The prognosis for patients with symptomatic acquired complete heart block is poor in the absence of pacing, regardless of the extent of the underlying heart disease. However, once appropriate pacing therapy has been established, the prognosis depends on the underlying disease process. As noted previously, high-degree AV block complicating acute MI is associated with high in-hospital and 30-day mortality but has no impact on 1-year mortality among 30-day survivors.^{19,20} In contrast, complete heart block secondary to idiopathic fibrosis of the conduction system in the absence of additional cardiac disease carries a more benign prognosis. AV block after valve surgery can recover; however, if conduction has not recovered by 48 hours after surgery, permanent pacing will likely be necessary.

Congenital complete AVB diagnosed in utero or at birth is associated with an approximately 30% mortality rate in utero or in the early postnatal life. Mortality is much lower during childhood and adolescence and increases slowly later in life. Many patients have few or no symptoms and reach their teens or young adulthood before the diagnosis is made. The outlook for patients with congenital heart block depends largely on the presence or absence of underlying structural heart disease. Patients with concomitant structural heart disease, a wide QRS complex, or LQTS are more likely to develop symptoms early and are at an increased risk for sudden death. Of all cases that have been recognized with congenital heart block, approximately two-thirds will have a pacemaker placed before reaching adulthood.^{10,12}

DIAGNOSTIC EVALUATION

Because the prognosis and, in some cases, the treatment of AV block differ depending on whether the block is within the AVN or is infranodal, determining the site of block is important. In most cases, this can be achieved noninvasively.

Electrocardiography

The QRS duration, PR interval, and ventricular rate on the surface ECG can provide important clues for localizing the level of AV block (see later).

Autonomic Modulation

Although the AVN is richly innervated and highly responsive to both sympathetic and vagal stimuli, the HPS is influenced less so by the autonomic nervous system. Carotid sinus massage increases vagal tone and worsens second-degree AVN block, whereas exercise and atropine

improve AVN conduction because of sympathetic stimulation or parasympathetic withdrawal. In contrast, carotid sinus massage can improve second-degree infranodal block by slowing the sinus rate and allowing HPS refractoriness to recover (Fig. 9.5). In addition, exercise and atropine worsen infranodal block because of the enhanced function of the sinus node and AVN and, as a consequence, the increased rate of impulses conducted to the HPS without changing HPS refractoriness.

Exercise Testing

Vagolysis and increased sympathetic drive that occur with exercise enhance AVN conduction. Thus patients with first-degree AV delay can have shorter PR intervals during exercise, and patients with type 1 second-degree AV block can develop higher AV conduction ratios (e.g., 3:2 at rest becoming 6:5 during exercise).

Exercise testing can be a useful tool to help confirm the level of block in second- or third-degree AV block associated with a narrow or wide QRS complex. Patients with presumed type 1 block or congenital complete heart block and a normal QRS complex usually have an increased ventricular rate with exercise, the former because of improved AVN conduction and the latter because of a faster escape rate. On the other hand, patients with acquired complete heart block and a wide QRS complex usually show minimal or no increase in ventricular rate. In addition, patients with 2:1 AV block in whom the site of conduction block is uncertain can benefit from exercise testing by observing whether the AV conduction ratio increases in a Wenckebach-like manner (e.g., to 3:2 or 4:3) or decreases (e.g., to 3:1 or 4:1). In the latter setting the increase in the sinus rate finds the HPS refractory, thus causing the higher degrees of block. This response is always abnormal, and it indicates intra-Hisian or infra-Hisian block, which requires permanent cardiac pacing.

Electrophysiological Testing

EP testing is usually not required for the diagnosis or treatment of AV block, because the previously described noninvasive measures are usually adequate. Nevertheless, EP testing can be of value in symptomatic patients in whom AV conduction abnormalities are suspected but cannot be documented or in patients with equivocal ECG findings.

ELECTROCARDIOGRAPHIC FEATURES

First-Degree Atrioventricular Delay

First-degree AV delay manifests on the surface ECG as a PR interval longer than 200 milliseconds following a normally timed (nonprematuring) P wave. All P waves are conducted but with delay; each P wave is followed by a QRS complex with a constant, prolonged PR interval.

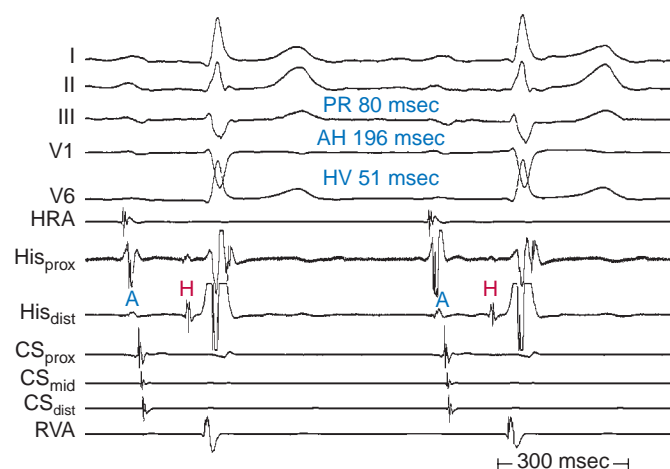


Fig. 9.6 First-Degree Atrioventricular Delay Caused by Intranodal Conduction Delay. The intranodal conduction delay is indicated by the prolonged atrial–His bundle (AH) and normal pulmonary artery and His bundle–ventricular (HV) intervals. *CS_{dist}*, Distal coronary sinus; *CS_{mid}*, middle coronary sinus; *CS_{prox}*, proximal coronary sinus; *His_{dist}*, distal His bundle; *His_{prox}*, proximal His bundle; *HRA*, high right atrium; *RVA*, right ventricular apex.

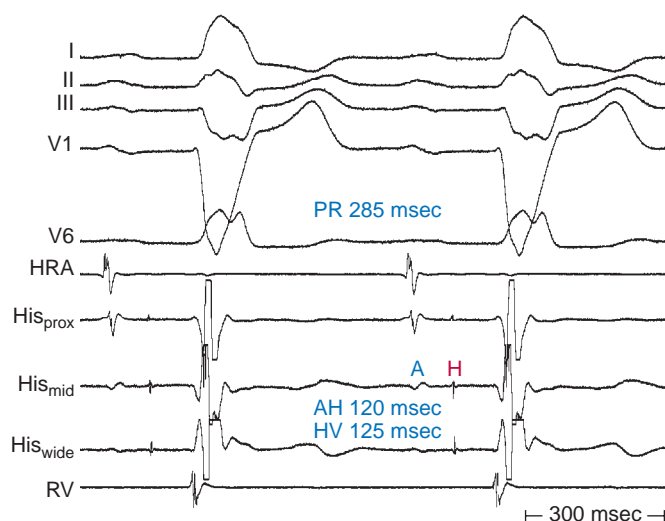


Fig. 9.7 First-Degree Atrioventricular Delay Secondary to His-Purkinje System Disease. The atrial–His bundle (AH) interval is normal but the His bundle–ventricular (HV) interval is markedly prolonged and associated with complete left bundle branch block. *His_{mid}*, Middle His bundle; *His_{prox}*, proximal His bundle; *His_{wide}*, wide His bundle; *HRA*, high right atrium; *RV*, right ventricle.

Site of Block

The degree of PR interval prolongation and QRS duration can help predict the site of conduction delay. Very long (more than 300 milliseconds) or highly variable PR intervals suggest involvement of the AVN. Normal QRS duration also suggests involvement of the AVN.

Atrioventricular node. Although conduction delay can be anywhere along the AVN–HPS, the AVN is the most common site of delay (87% when the QRS complex is narrow, and more than 90% when the PR interval is longer than 300 milliseconds; Fig. 9.6).

His-Purkinje system. Intra-Hisian conduction delay or HPS disease can cause prolongation of the PR interval. First-degree AV delay in the presence of BBB is caused by infranodal conduction delay in 45% of cases. A combination of delay within the AVN and in the HPS must also be considered (Fig. 9.7).

Atrium. Not infrequently, first-degree AV delay is caused by intraatrial or interatrial conduction delay. RA enlargement can prolong the PR interval (eFig. 9.1), as can be observed in certain cases of congenital structural heart disease, such as Ebstein anomaly of the tricuspid valve or endocardial cushion defects, or after surgical repair of congenital disease (e.g., Fontan repair of single ventricle, Mustard/Senning repairs of transposed great arteries). The presence of LA enlargement pattern on the ECG (i.e., prolonged P wave duration) reflects the presence of interatrial conduction delay and can be a clue to the underlying mechanism of first-degree AV delay.⁵⁰

Second-Degree Atrioventricular Block

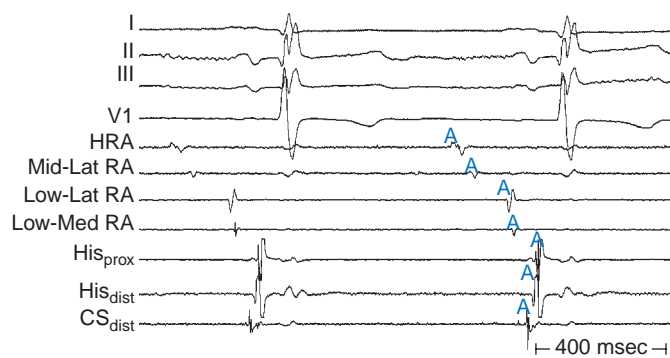
The term second-degree AV block is applied when intermittent failure of AV conduction is present (i.e., one or more atrial impulses that should be conducted fail to reach the ventricles). This term encompasses several conduction patterns. Types 1 and 2 AV block are ECG patterns that describe the behavior of the PR intervals (in sinus rhythm) in sequences (with at least two consecutively conducted PR intervals) in which a single P wave fails to conduct to the ventricles. The anatomical site of block should not be characterized as either type 1 or type 2 because these designations refer only to ECG patterns.⁵¹

Type 1 Second-Degree Atrioventricular Block

Type 1 second-degree AV block (Wenckebach or Mobitz type I block) manifests on the surface ECG as progressive prolongation of the PR interval before failure of an atrial impulse to conduct to the ventricles. The PR interval immediately after the nonconducted P wave returns to its baseline value, and the sequence begins again.

The behavior of Wenckebach block can be simplified by relating it to an abnormally long relative refractory period of the AVN. In this setting the rate of AVN conduction depends on the time that the impulse arrives at the AVN. The earlier it arrives at the AVN, the longer it takes to propagate through the AVN, and the longer the PR interval will be; the later it arrives, the shorter the conduction time, and the shorter the PR interval. Thus Wenckebach periodicity in part develops because each successive atrial impulse arrives earlier and earlier in the relative refractory period of the AVN, thus resulting in longer and longer conduction delay and PR interval, until one impulse arrives during the absolute refractory period and fails to conduct, with a consequent ventricular pause. In other words, the shorter the RP interval is, the longer the PR interval will be; and the longer the RP interval is, the shorter the PR interval will be; they are inversely related. This is referred to as RP-PR reciprocity or RP-dependent PR interval. Using this concept, it is easy to explain the behavior of the PR interval during the Wenckebach periodicity. The first atrial impulse conducting after the pause has an unusually long RP interval, whereas with the following atrial impulse, the RP interval dramatically shortens, thus resulting in prolongation of the PR interval. Although the following atrial impulses have shorter RP intervals, such shortening is not as dramatic, and consequently the progressive prolongation of the PR interval is of lesser degree. In other words, although each successive PR interval prolongs, it does so at a decreasing increment. So, for example, if the PR interval following the first conducted P wave in the cycle increased by 100 milliseconds, the PR interval of the next beat would increase by 50 milliseconds, and so forth.

Features of typical Wenckebach periodicity include the following: (1) progressive lengthening of the PR interval throughout the Wenckebach



eFig. 9.1 First-Degree Atrioventricular Delay Caused by Intraatrial Conduction Delay. The long PR interval (240 milliseconds) is caused by prolonged conduction in the right atrium (prolonged PA interval) in a patient who has undergone Fontan repair for complex congenital heart disease. *CS_{dist}*, Distal coronary sinus; *His_{dist}*, distal His bundle; *His_{prox}*, proximal His bundle; *HRA*, high right atrium; *Low-Lat RA*, low lateral right atrium; *Low-Med RA*, low medial right atrium; *Mid-Lat RA*, middle lateral right atrium.

cycle; (2) lengthening of the PR interval occurring at progressively decreasing increments, resulting in progressively shorter R-R intervals; (3) a pause between QRS complexes encompassing the nonconducted P wave that is less than the sum of R-R intervals of any two consecutively conducted beats; (4) shortening of the PR interval after block, compared with the PR interval just preceding the blocked cycle; and (5) group beating, which offers a footprint that identifies Wenckebach periodicity (eFig. 9.2). It is important to recognize that, during Wenckebach periodicity, the atrial impulse conducted to the ventricles is not always represented by the P wave that immediately precedes the QRS complex; the PR interval can be very long and exceed the P-P interval.

However, less than 50% of type 1 AV block cases follow this typical pattern. Typical Wenckebach periodicity is more frequently observed during pacing-induced AV block. Atypical patterns are more likely found with longer Wenckebach periods (more than 6:5 atrial/ventricular complexes). In patients with dual AVN physiology, Wenckebach cycles are almost always atypical; the greatest increment in the atrial–His bundle (AH) interval occurs when block occurs in the fast pathway, whichever beat this may be. Differentiating atypical from typical patterns is of

little clinical significance. However, an atypical pattern can be misdiagnosed as type 2 second-degree AV block. Some possible atypical features of Wenckebach periodicity include the following: (1) the second (conducted) PR interval (after the pause) often fails to show the greatest increment, and the increment may actually increase for the PR interval of the last conducted beat in the cycle (Fig. 9.8); (2) very little incremental conduction delay and no discernible change in the duration of the PR intervals for a few beats just before termination of a sequence (this is seen most often during long Wenckebach cycles and in association with increased vagal tone and is usually accompanied by slowing of the sinus rate; Fig. 9.9); (3) the PR interval can actually shorten and then lengthen in the middle of a Wenckebach sequence; and (4) a junctional escape beat can end the pause following a nonconducted P wave, resulting in an apparent shortening of the PR interval.

AVN block usually can be reversed completely or partially by altering the autonomic tone (e.g., with atropine). However, these measures fail occasionally, especially in the presence of structural damage to the AVN (e.g., congenital heart disease or inferior wall MI). In such cases, progression to complete AV block can occur, although such an event is more likely to occur with block in the HPS.

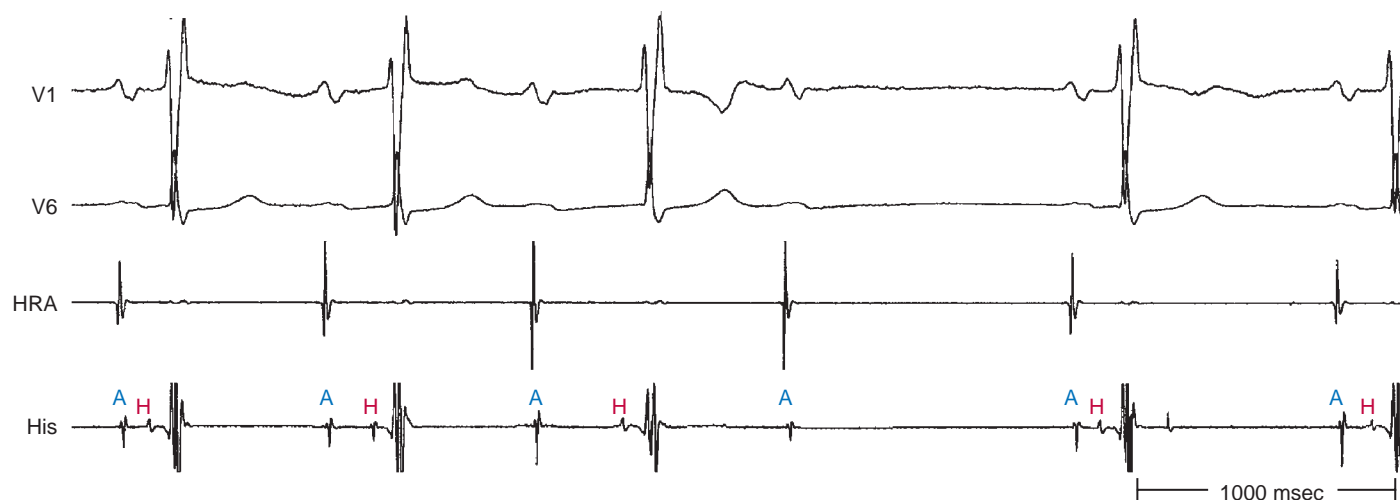


Fig. 9.8 Atypical Wenckebach Periodicity Due to Increased Vagal Tone. Type 1 second-degree atrioventricular (AV) block caused by heightened vagal tone. Note the greatest increment occurs in the PR interval of the last conducted beat in the cycle and not in the second PR interval after the pause. Also note the slowing in the sinus rate coinciding with significant prolongation in the PR interval and then AV block, a finding suggesting that increased vagal tone is responsible for both slowing of the sinus rate and atrioventricular nodal block. HRA, High right atrium.

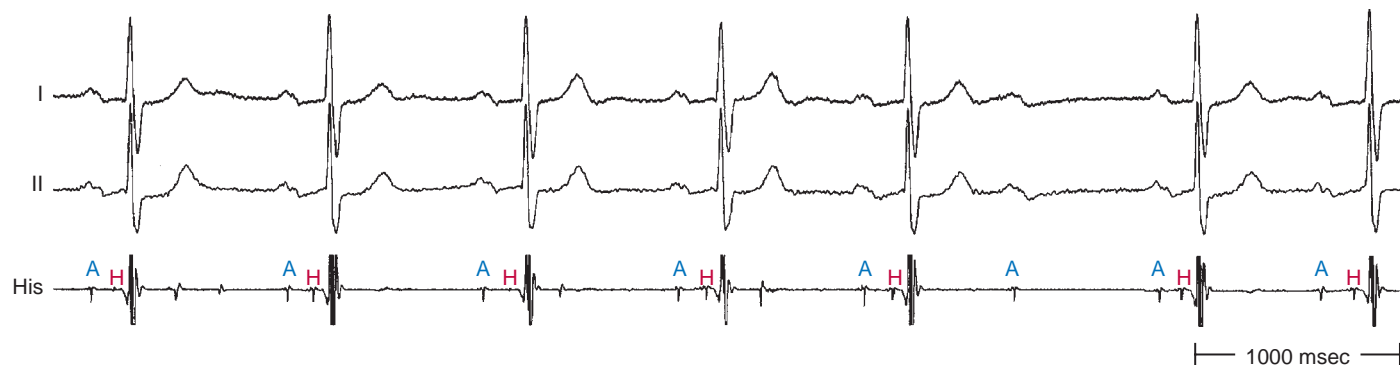
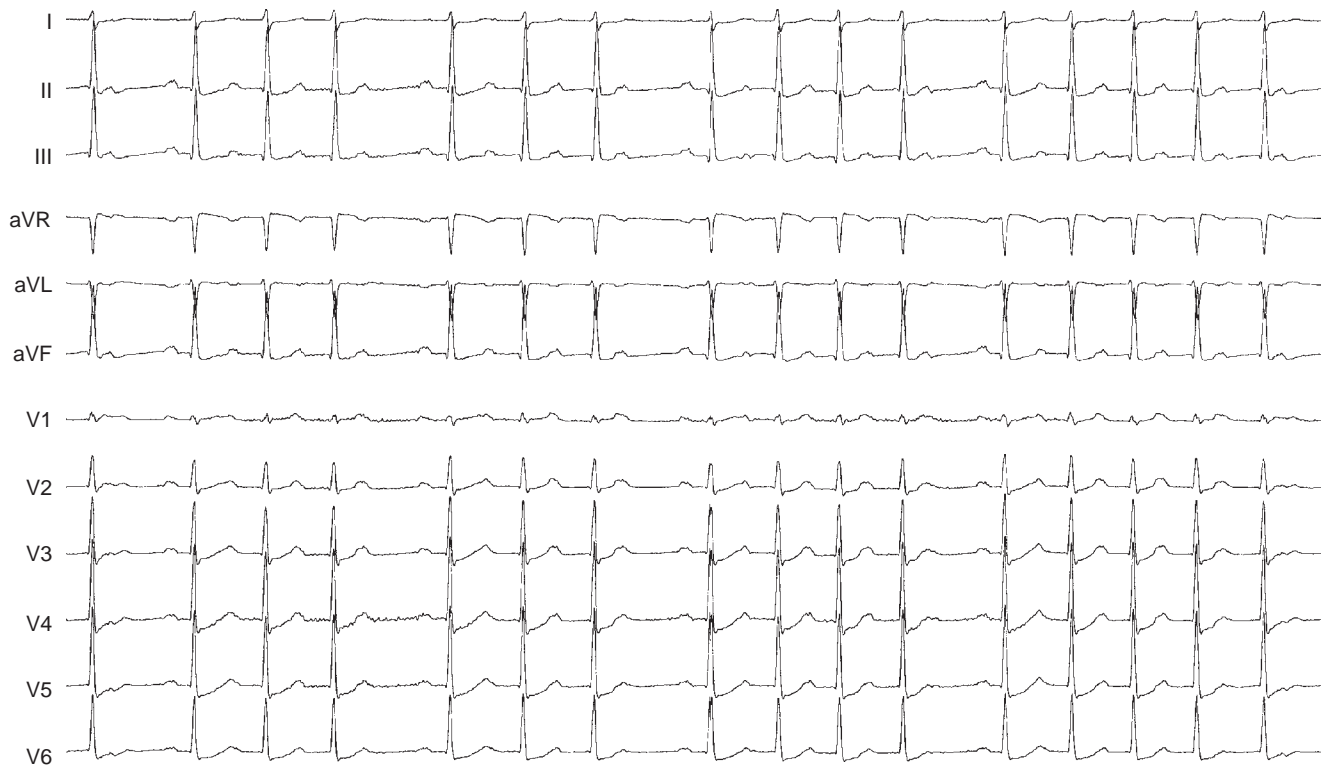


Fig. 9.9 Atypical Wenckebach Periodicity. Note the very small increments in the duration of the PR intervals for a few beats just before termination of a sequence. However, the first conducted P wave after the pause is associated with obvious shortening of the PR interval.



eFig. 9.2 Typical Wenckebach Periodicity. Normal sinus rhythm with type 1 second-degree atrioventricular block is characterized by progressive prolongation of the PR intervals preceding the nonconducted P wave and group beating.

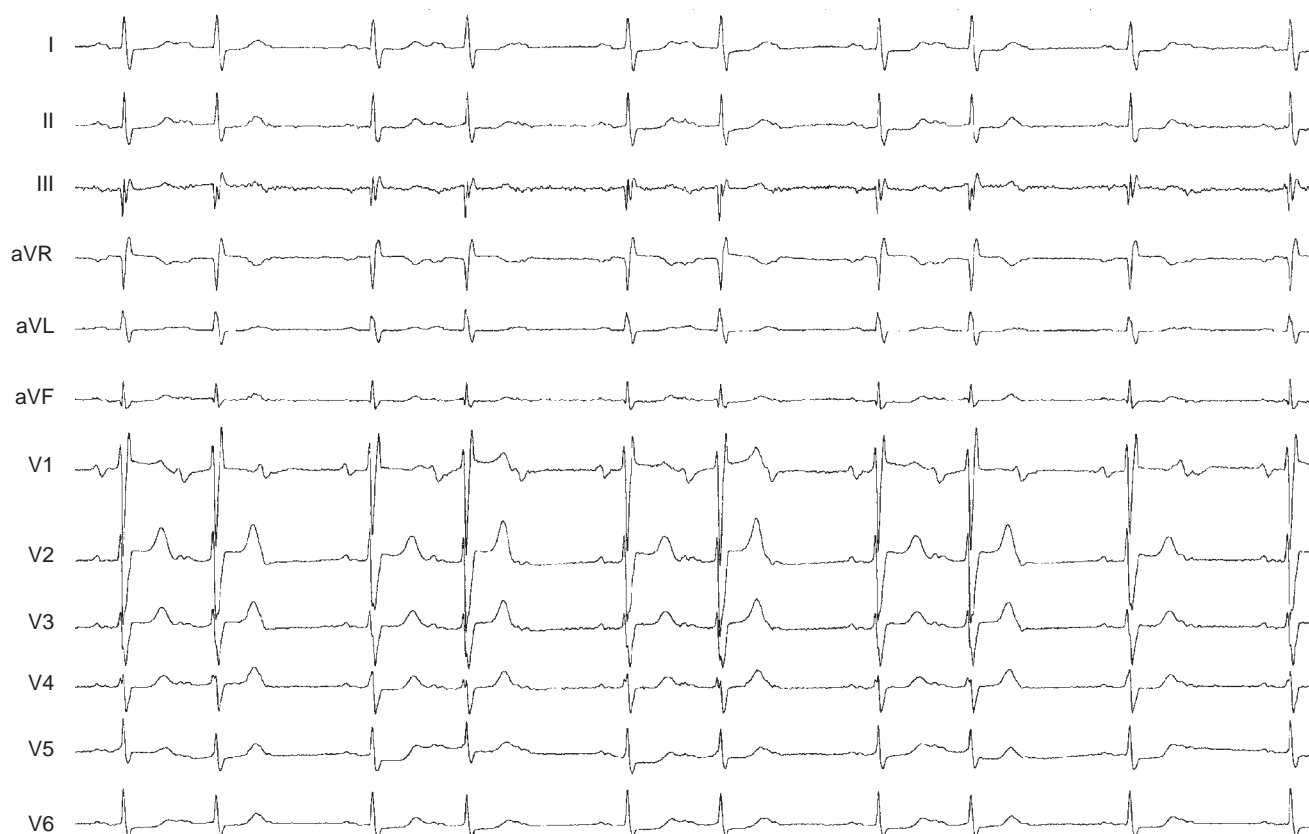


Fig. 9.10 Intranodal Second-Degree Atrioventricular Block. Normal sinus rhythm with type 1 second-degree atrioventricular (AV) block is characterized by progressive prolongation of the PR intervals preceding the nonconducted P wave and group beating. Despite the presence of His-Purkinje system disease (as indicated by incomplete right bundle branch block), Wenckebach AV block is more common in the atrioventricular node. At right, the last four P waves encountered 2:1 AV block.

Site of block. The degree of PR interval prolongation and QRS duration can help to predict the site of block. A normal QRS duration usually suggests AVN involvement, whereas the presence of BBB suggests (but does not prove) HPS involvement. Furthermore, a short baseline PR interval and small PR interval increments preceding the block suggest HPS involvement.

Atrioventricular node. Wenckebach block is almost always within the AVN (and rarely intra-Hisian) when a narrow QRS complex is present.

His-Purkinje system. When type 1 block is seen with the presence of BBB, the block is still more likely to be in the AVN (Fig. 9.10), but it can also be localized within or below the HB (Fig. 9.11). In this setting a very long PR interval is more consistent with AVN block.

Type 2 Second-Degree Atrioventricular Block

Type 2 second-degree (Mobitz type II) AV block is characterized on the surface ECG by a constant (normal or prolonged) PR interval of all conducted P waves, followed by sudden failure of a P wave to be conducted to the ventricles (eFig. 9.3). RP-PR reciprocity, the hallmark of type 1 block, is absent in type 2 block. Consequently, the PR interval following a long RP interval (immediately following the pause) is identical to that following a short RP interval (immediately preceding the pause). Type 2 block cannot be diagnosed if the first P wave after a blocked beat is absent or if the PR interval following the pause is shorter than all the other PR intervals of the conducted P waves, regardless of the number of constant PR intervals before the block (see Fig. 9.9). The P-P intervals remain constant, and the

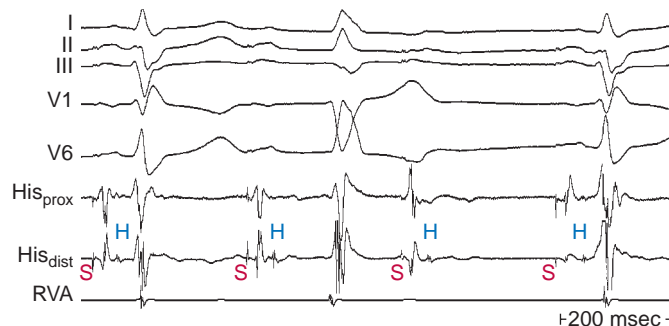
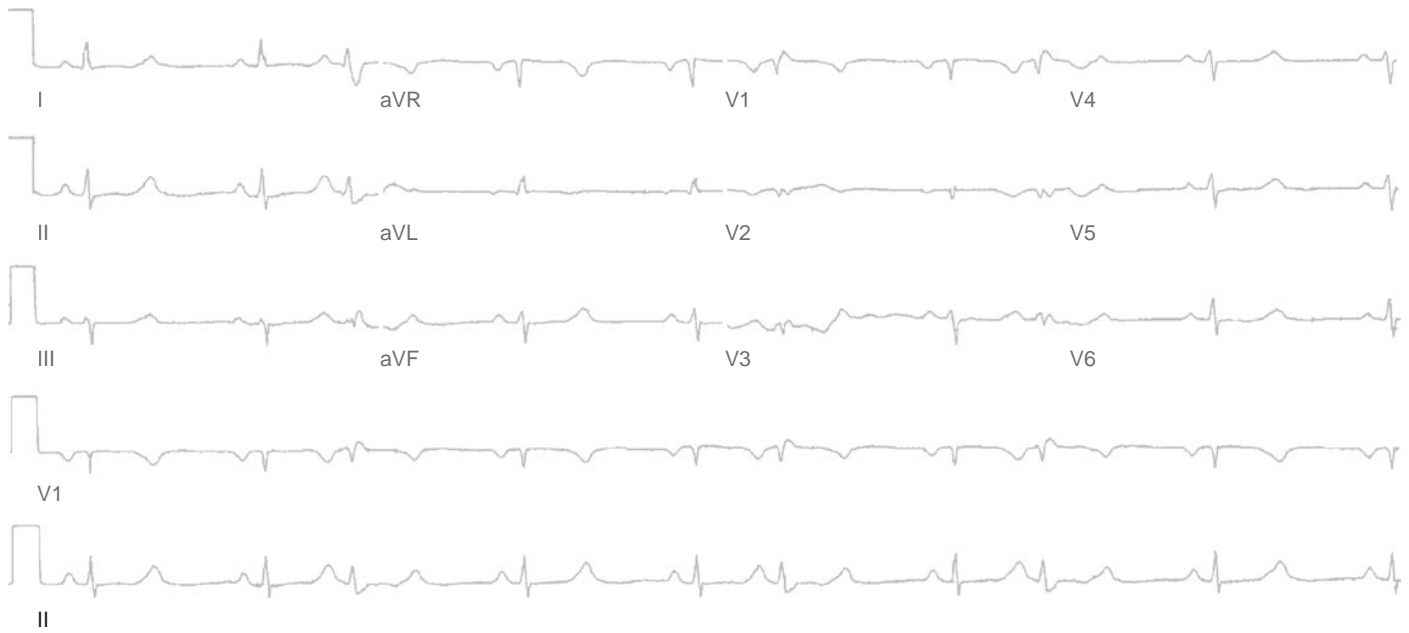


Fig. 9.11 Infra-Hisian Second-Degree Wenckebach Atrioventricular Block. Atrial pacing in a patient with a normal prolonged atrial-His bundle interval but prolonged His bundle-ventricular (HV) interval and right bundle branch block (RBBB). On the second complex, the HV is dramatically prolonged and left bundle branch block is present, suggesting very slow conduction over the right bundle branch. With the third paced complex, atrioventricular block occurs below the His bundle recording, and on the fourth complex, conduction with RBBB resumes, suggesting a Wenckebach cycle in the His-Purkinje system. *His_{prox}*, proximal His bundle; *RVA*, right ventricular apex.

pause encompassing the nonconducted P wave equals twice the P-P interval.⁵¹

A true Mobitz type II AV block in conjunction with a narrow QRS complex is relatively rare and occurs without sinus slowing and without the characteristic Wenckebach sequences. Atypical forms of



eFig. 9.3 Second-Degree Intra-Hisian Atrioventricular Block. Despite the presence of narrow QRS complexes, the site of block is likely intra-Hisian, as suggested by the short PR intervals on conducted beats and no increment in the PR intervals on 3:2 cycles. The P waves frequently are partially concealed within the preceding T waves (especially in view of the presence of long QT intervals) and are more obvious in lead V3. Note QRS aberrancy (right bundle branch block) resulting from the long-short R-R intervals.

Wenckebach block with only minimal PR interval variation should be excluded (see Fig. 9.9). Apparent type 2 second-degree AV block can be observed not infrequently under the influence of increased vagal tone during sleep, in which case Wenckebach block without discernible or measurable increments in the PR intervals is the actual diagnosis; sinus slowing with AV block essentially excludes Mobitz type II block. When an apparent Mobitz type II-like pattern with a narrow QRS complex alternating with periods of intermittent Wenckebach AV block sequences (as in Holter recordings), a true Mobitz type II block can be safely excluded because narrow QRS type 1 and type 2 second-degree AV blocks almost never coexist within the HB. On the other hand, sustained advanced second-degree AV block is far more common in association with true Mobitz type II block than with Wenckebach block or its variant.

Apparent Mobitz type II AV block can also be caused by concealed junctional extrasystoles (confined to the specialized conduction system

and not propagated to the myocardium) and junctional parasystole (Fig. 9.12).⁵² Exercise-induced second-degree AV block is most commonly infranodal and rarely is secondary to AVN disease or myocardial ischemia.

Site of block

His-Purkinje system. Type 2 second-degree AV block is almost always below the AVN, occurring in the HB in approximately 30% of cases and in the bundle branches in the remainder (Fig. 9.13). Infrequently, type 2 second-degree AV block is found with a narrow QRS complex and is caused by intra-Hisian block (see eFig. 9.3).

Atrioventricular node. Type 2 second-degree AV block has not yet been convincingly demonstrated in the body of the AVN or the N zone. Although multiple reports have described the occurrence of type 2 second-degree AV block in the AVN, in each case either the block could have been localized to the HPS, rather than the AVN, or the block probably was an atypical variant of Wenckebach block.

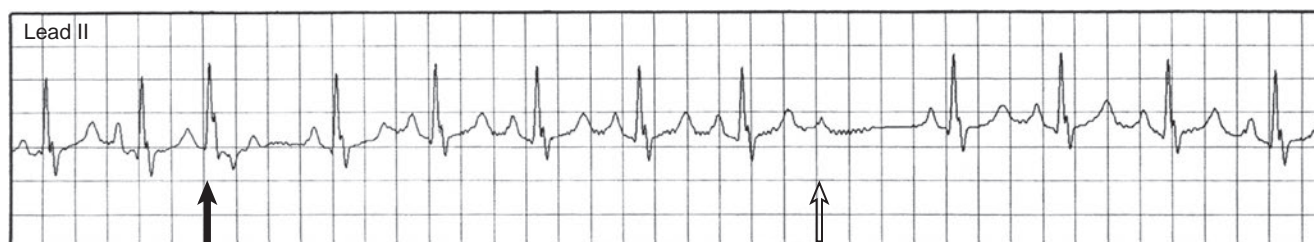


Fig. 9.12 Junctional Ectopy Mimicking Mobitz Type II Atrioventricular Block. The lead II rhythm strip shows sinus rhythm with normal atrioventricular conduction, but the second complex (*black arrow*) is a normal QRS not preceded by a P wave (thus His bundle extrasystole) with retrograde conduction (inverted P wave following QRS). The white arrow shows a nonconducted P wave that would ordinarily indicate Mobitz II block, but in this patient with known His bundle (junctional) extrasystoles, the P wave more likely fails to conduct because of concealed conduction into the atrioventricular node following a concealed His extrasystole (no resultant QRS or retrograde P wave). Note that the nonconducted P wave has a slightly different contour, perhaps as a result of fusion between the sinus P wave and retrograde atrial capture from the concealed His bundle extrasystole.

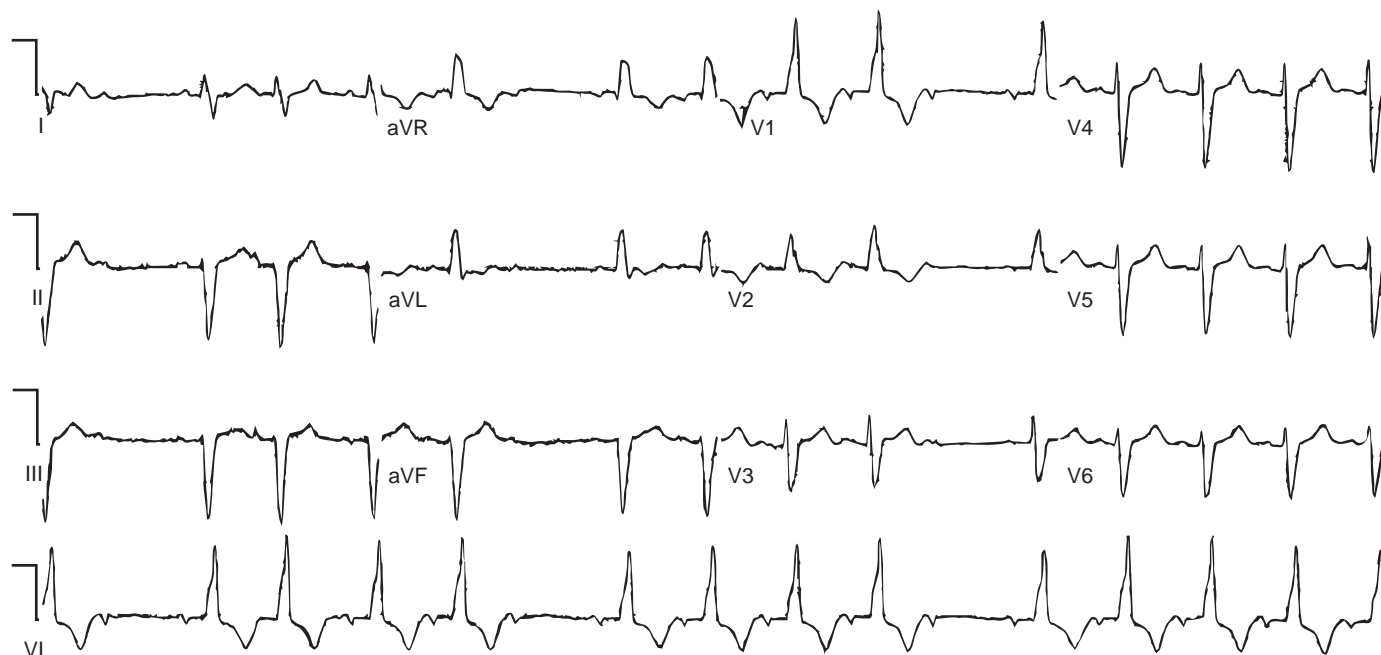


Fig. 9.13 Type II Second-Degree Infranodal Atrioventricular Block. Bifascicular block (right bundle branch block and left anterior fascicular block) and normal, constant PR intervals (196 milliseconds) are observed during conducted beats, consistent with infranodal block.

Second-Degree 2:1 Atrioventricular Block

When only alternate beats are conducted, resulting in a 2:1 ratio, the PR interval is constant for the conducted beats, provided that the atrial rhythm is regular (Fig. 9.14). A 2:1 AV block cannot be classified as type 1 or type 2; using the term type 1 to describe 2:1 AV block when the lesion is in the AVN or when there is evidence of decremental conduction and using the term type 2 to describe 2:1 AV block when it is infranodal or when there is evidence of all-or-none conduction should be discouraged because this practice violates the well-accepted traditional definitions of types 1 and 2 block based on ECG patterns,

not on the anatomical site of block. Both types 1 and 2 block can progress to a 2:1 AV block, and a 2:1 AV block can regress to type 1 or 2 block.⁵¹

Site of block. Fixed 2:1 AV block poses a diagnostic dilemma because it can be difficult to localize the site of block by the surface ECG alone. Several ECG features can help in the differential diagnosis:

1. A 2:1 AV block associated with a narrow QRS complex is likely to be intranodal, whereas that associated with a wide QRS complex is likely to be infranodal, but it could still be at the level of the AVN (Figs. 9.14 and 9.15).

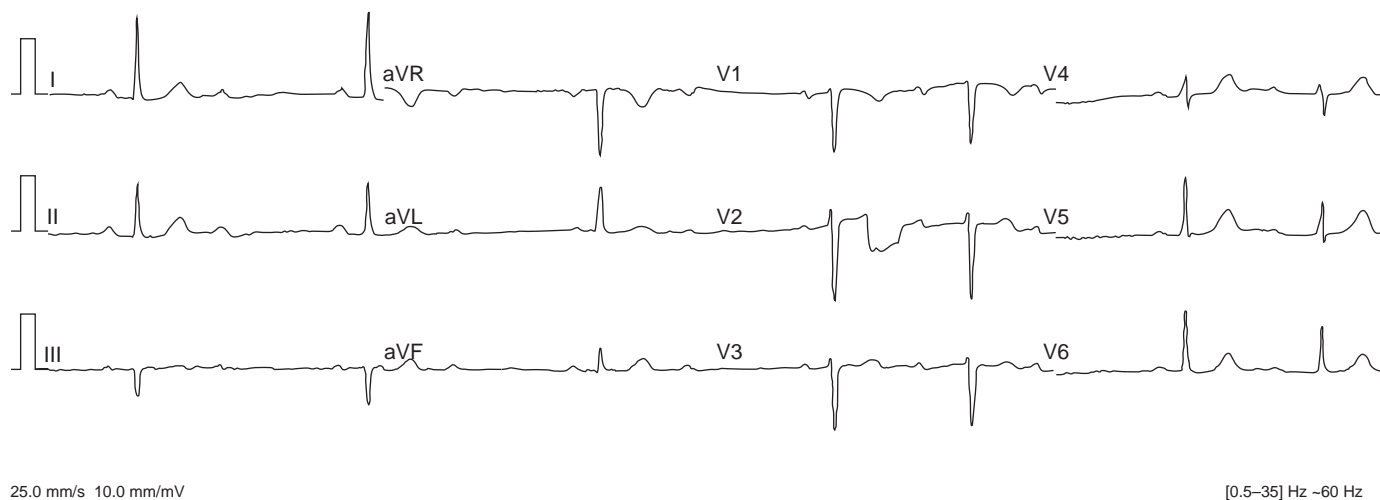


Fig. 9.14 Second-Degree Atrioventricular (AV) Block. Normal sinus rhythm with second-degree 2:1 AV block. At right, the conduction pattern changes from 2:1 AV block pattern to a Wenckebach pattern.

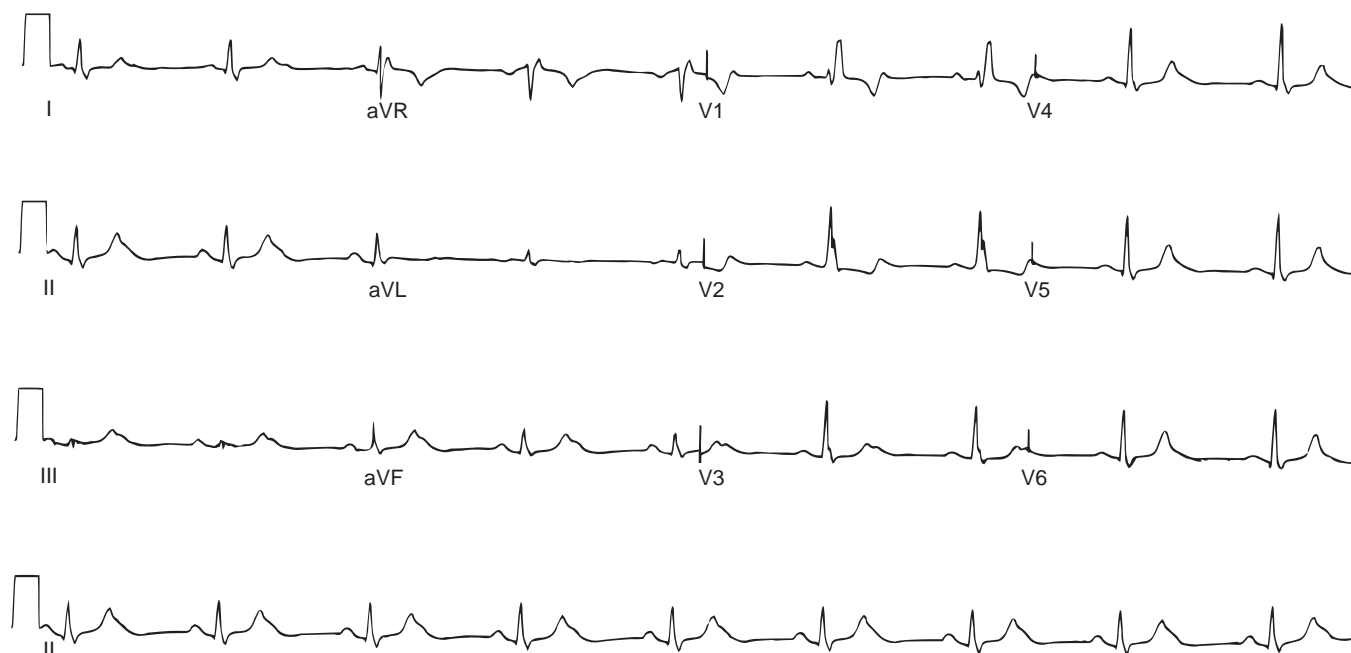


Fig. 9.15 Second-Degree 2:1 Infranodal Atrioventricular Block. Note the short PR interval during conducted complexes and the wide QRS complexes (right bundle branch block), suggesting block in the His-Purkinje system.

2. Fixed 2:1 AV block with PR intervals shorter than 160 milliseconds suggests intra-Hisian or infra-Hisian block, whereas very long PR intervals (more than 300 milliseconds) suggest AVN block.
3. If the PR interval of all the conducted complexes is constant despite a varying RP interval, infranodal block is likely.
4. The presence of Wenckebach block before or after episodes of 2:1 AV block is highly suggestive of block at the AVN level (see Figs. 9.10 and 9.14).
5. Improvement of block with atropine or exercise suggests AVN block; however, the absence of such response does not exclude intranodal block.

High-Grade Atrioventricular Block

Failure of conduction of two or more consecutive P waves when AV synchrony is otherwise maintained is sometimes termed high-grade AV block or advanced second-degree AV block (Fig. 9.16). This block must happen because of the existing block itself and not because of retrograde concealment in the AVN or HPS resulting from junctional or ventricular escape complexes that prevent conduction.

Site of block. The level of block can be at the AVN or the HPS. When high-degree AV block is caused by block in the AVN, QRS complexes of the conducted beats are usually narrow. Wenckebach periodicity can also be seen, and atropine administration produces lesser degrees of AV block. Features suggesting block in the HPS are conducted beats with BBB and no improvement in block with atropine.

Third-Degree (Complete) Atrioventricular Block

AV block is termed complete when all P waves fail to conduct, despite having ample opportunity for conduction. Therefore, if there is less than optimal opportunity for the AVN-HPS to conduct (e.g., a ventricular escape rate exceeding 40/min), it cannot be regarded as complete

AV block if a P wave does not conduct. Third-degree AV block is seen on the surface ECG as completely dissociated P waves and QRS complexes, each firing at its own pacemaker rate, with a continuously changing PR relationship as the P waves march through all phases of the ventricular cycle in the presence of a regular ventricular rhythm (Fig. 9.17). Every possible chance for conduction is afforded, with the P waves occurring at every conceivable RP interval, but the atrial impulse is never conducted to the ventricles. The atrial rate is always faster than the ventricular rate (Fig. 9.18).

Site of Block

Atrioventricular node. Most cases of congenital third-degree AV block are localized to the AVN (see Fig. 9.17), as are cases of transient AV block associated with acute inferior wall MI, beta blockers, calcium channel blockers, and digitalis toxicity. Complete AVN block is characterized by a junctional escape rhythm with a narrow QRS complex and a rate of 40 to 60 beats/min, which tends to increase with exercise or atropine. However, in 20% to 50% of patients with chronic AV block, a wide QRS escape rhythm may occur. Rhythms originating in the distal HB may have a wide QRS. Those rhythms are usually slower and non-responsive to atropine.

His-Purkinje system. Acquired complete heart block is usually associated with block in the HPS that results in an escape rhythm with a wide QRS complex with a rate of 20 to 40 beats/min (Fig. 9.19).

ELECTROPHYSIOLOGICAL TESTING

Role of Electrophysiological Testing

ECG diagnosis of AV block is usually adequate for deciding subsequent treatment. Once symptoms and AV block are correlated with ECG findings, further documentation by invasive studies is not required unless

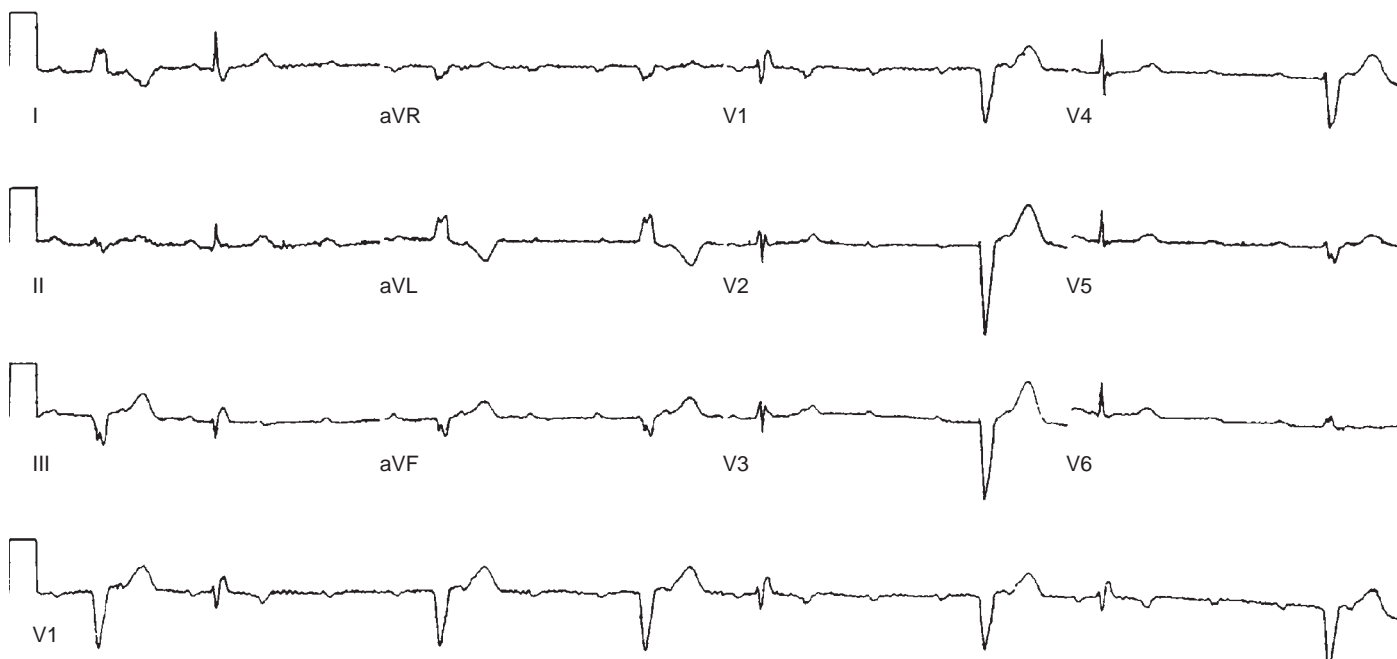


Fig. 9.16 High-Grade Atrioventricular Block. Note that only three P waves conducted to the ventricle in the whole tracing. Conducted P waves were associated with normal PR intervals and right bundle branch block, a finding suggesting infranodal block. All other P waves were blocked, and ventricular escape rhythm with a left bundle branch block pattern is observed. Note that the block is not caused by retrograde concealment in the atrioventricular node or His-Purkinje system from the ventricular escape complexes because the conducted P waves occurred at a short cycle following the escape complexes.

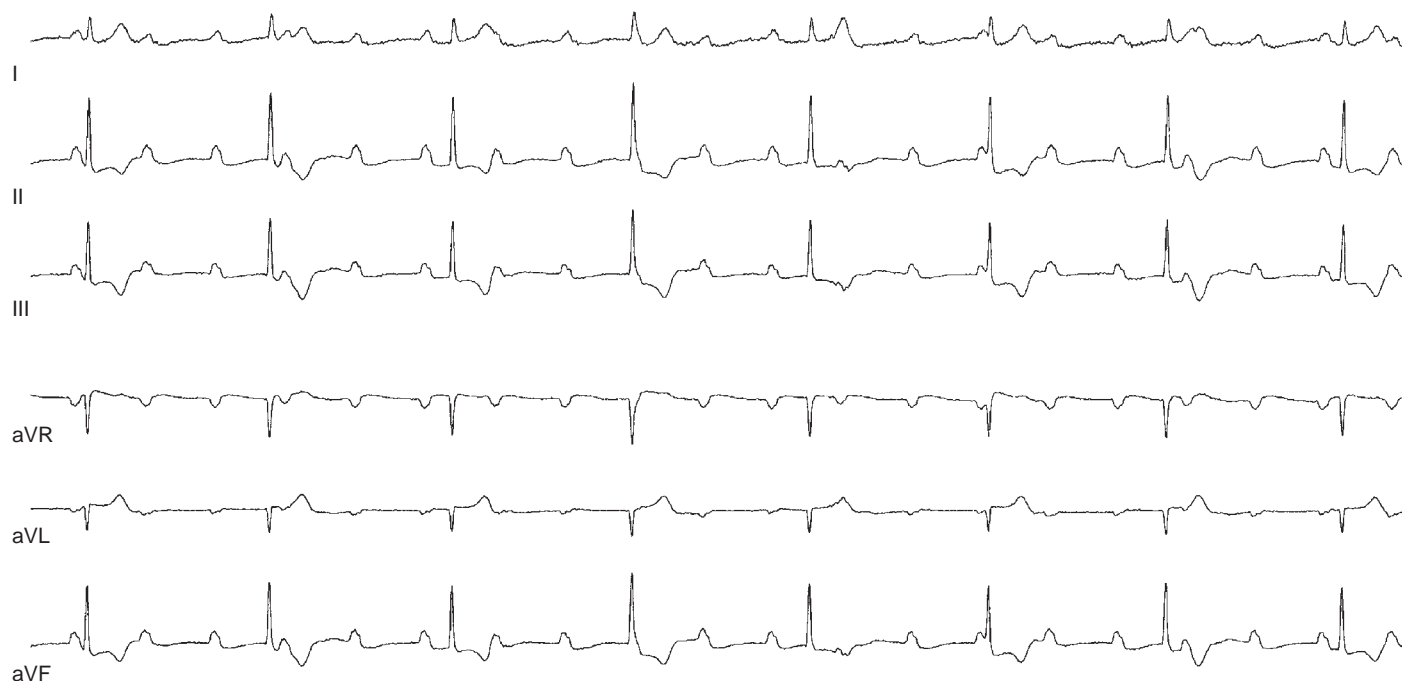


Fig. 9.17 Congenital Third-Degree Atrioventricular Block. Sinus rhythm with complete atrioventricular block and junctional escape rhythm with a narrow QRS are seen, consistent with intranodal block.

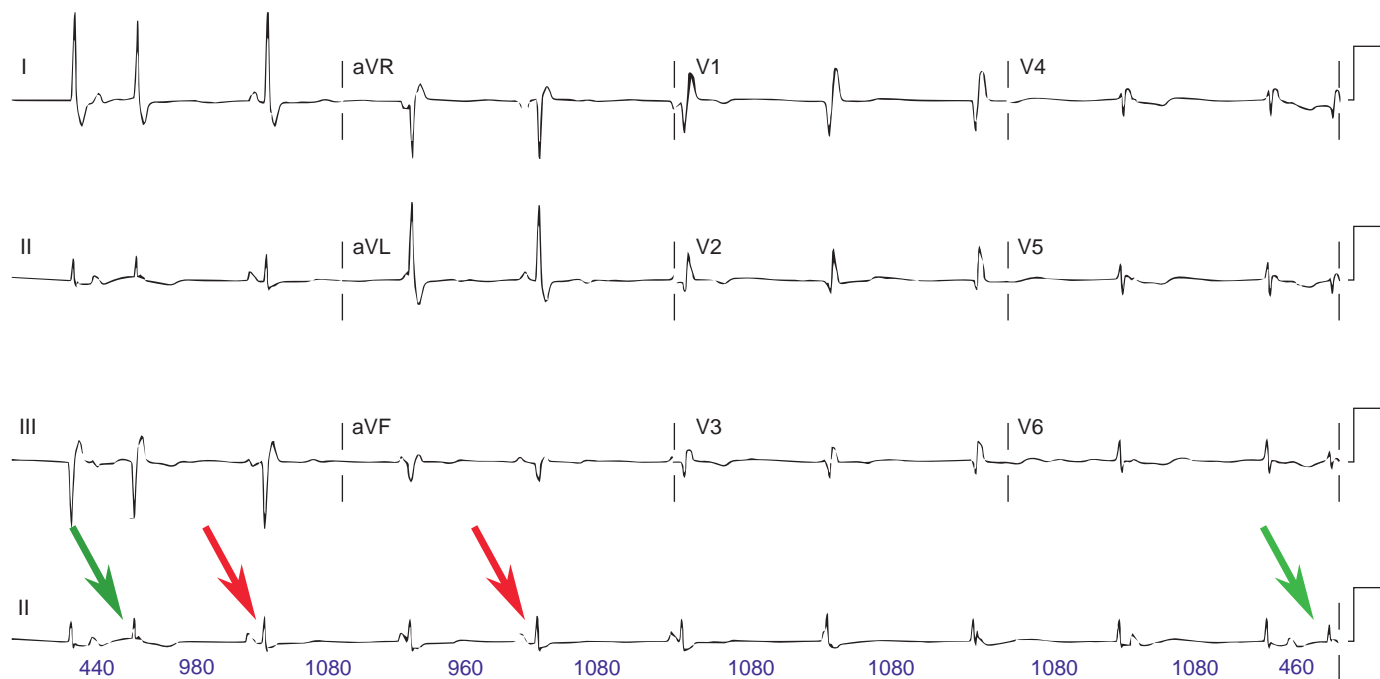


Fig. 9.18 Competing Sinus and Junctional Rhythms Mimicking Atrioventricular (AV) Block. Surface ECG of sinus bradycardia at a cycle length (CL) of 1180 milliseconds and junctional escape rhythm at a shorter CL (1080 milliseconds). Junctional impulses fail to conduct retrogradely to the atrium, thus setting the stage for AV dissociation, which is observed during most of the recording. Note that no pathological AV block is present; failure of AV conduction of several sinus impulses occurred secondary to the physiological refractoriness of the atrioventricular node (AVN) and His bundle (HB) caused by retrograde concealment by the escape junctional impulses. However, whenever sinus P waves occurred at appropriate timings, they did conduct to the ventricle (red and green arrows) and elicited QRS complexes at CLs shorter than the expected junctional rhythm CL. Note that retrograde concealment of the junctional impulses occurred in the AVN and not just the HB, evident by the prolonged PR intervals of conducted sinus P waves when they closely follow the preceding QRS complex (green arrows). Numbers denote R-R intervals in milliseconds.

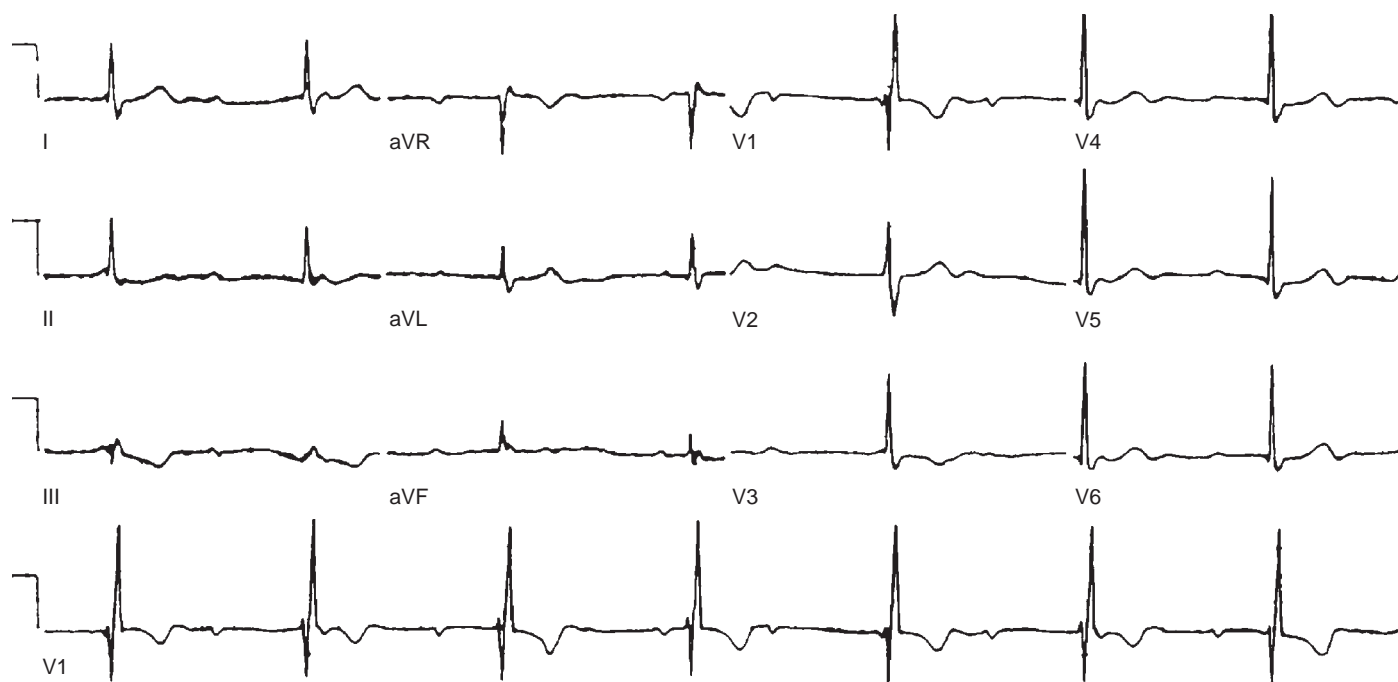


Fig. 9.19 Complete Infranodal Atrioventricular Block. Complete atrioventricular dissociation is observed, and all the P waves fail to conduct despite having ample opportunity for conduction. Note the slow ventricular escape rhythm with a wide QRS complex and a rate of 40 beats/min, consistent with block in the His-Purkinje system.

additional information is needed. Similarly, asymptomatic patients with transient Wenckebach block associated with increased vagal tone should not undergo EP testing.

Nevertheless, EP testing can help diagnose an equivocal ECG pattern or delineate the site of conduction abnormality, if that is required for therapeutic decision making. EP testing is indicated in a patient with suspected high-grade AV block as the cause of syncope or presyncope when documentation cannot be obtained noninvasively. Similarly, in patients with coronary artery disease, it can be unclear whether symptoms are secondary to AV block or VT; therefore EP testing can be useful in establishing the diagnosis. Some patients with known second- or third-degree block can benefit from an invasive study to localize the site of AV block to help determine therapy or assess prognosis.

Normal Atrioventricular Conduction

The normal PR interval is 120 to 200 milliseconds. This interval reflects the conduction time from the high RA to the point of earliest ventricular activation (i.e., QRS onset), and it includes activation of the atrium, AVN, HB, bundle branches and fascicles, and terminal Purkinje fibers. To measure the different components of the conduction system contained in the PR interval, intracardiac recordings from the high RA and HB region are required.

The PA interval, measured from the high RA electrogram to the low RA deflection in the HB recording, gives an indirect approximation of the intraatrial conduction time. The normal PA interval is 20 to 60 milliseconds.

The AH interval is measured from the first rapid deflection of the atrial deflection in the HB recording to the first evidence of HB depolarization in the HB recording. The AH interval is an approximation of AVN conduction time because it represents conduction time from the low RA at the interatrial septum through the AVN to the HB. The AH interval has a wide range in normal subjects (50 to 120 milliseconds) and is markedly influenced by the autonomic tone.

His potential duration reflects conduction through the short length of the HB that penetrates the fibrous septum. Disturbances of the HB conduction can manifest as fractionation, prolongation (more than 30 milliseconds), or splitting of the His potential (Fig. 9.20).

The HV interval is measured from the onset of the His potential to the onset of the earliest registered surface or intracardiac ventricular activation, and it represents conduction time from the proximal HB through the distal HPS to the ventricular myocardium. The most proximal electrodes displaying the His potential should be chosen, and a large atrial electrogram should accompany the proximal His potential. The HV interval is not significantly affected by the autonomic tone, and it usually remains stable over a wide range of heart rates (indicating differences in autonomic tone). The range of HV intervals in normal subjects is narrow, 35 to 55 milliseconds.

Localization of the Site of Atrioventricular Block

EP testing allows analysis of the HB electrogram, as well as providing atrial and ventricular pacing to uncover conduction abnormalities. A markedly prolonged HV interval (100 milliseconds or longer) is associated with a high incidence of progression to complete heart block. In addition, a His potential 30 milliseconds or longer in duration or that is frankly split into two deflections is indicative of intra-Hisian conduction delay.

When the His potential is recorded during atrial pacing at progressively shorter pacing cycle lengths (PCLs), the AH interval normally gradually lengthens until Wenckebach block develops. The HV interval normally remains constant despite different pacing rates. Abnormal AVN conduction produces Wenckebach block at slower atrial pacing rates than what is normally seen (i.e., at a PCL longer than 500 milliseconds). To determine whether AVN disease is truly present or whether AVN conduction is just under the influence of excessive vagal tone, atropine or isoproterenol may be administered to evaluate for improvement in conduction.

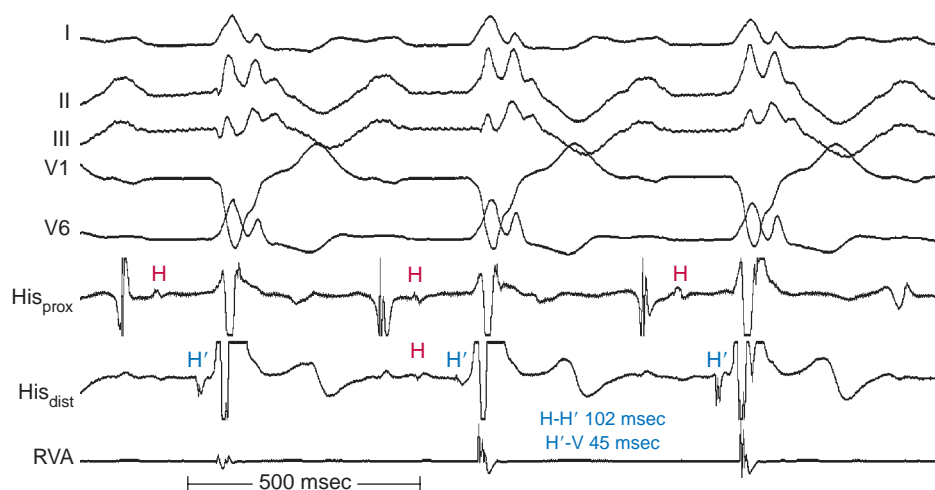


Fig. 9.20 Split His Potential. Split His potentials are observed on His catheter recording obtained in a patient with cardiomyopathy and left bundle branch block. Recording only the distal His signal (H') would give His_{dist} the false impression of normal infranodal conduction ($H'V = 42$ milliseconds). His_{dist} , Distal His bundle; His_{prox} , proximal His bundle; RVA , right ventricular apex.

Infranodal block is present when the atrial electrogram is followed by the His potential but no ventricular depolarization results. Block below the HB is abnormal unless it is associated with short PCLs (350 milliseconds or less) or after sudden increases in atrial rate. Block in the HB can be masked by prolonged AVN conduction time or refractoriness. When block in the AVN develops at a slow pacing rate, atropine may be administered to improve AVN conduction and allow evaluation of the HPS at faster pacing rates.

Selective pacing of the HB can help localize the site of infranodal block (intra- vs. infra-Hisian). HB capture with normal QRS duration is consistent with intra-Hisian site of conduction block, whereby HB pacing recruits fibers in the HB and bundle branches distal to the site of conduction block.⁵³

Site of First-Degree Atrioventricular Block

Atrioventricular node. An AH interval longer than 130 milliseconds with a normal HV interval indicates intranodal conduction delay (see Fig. 9.6). Dual AVN physiology can produce transient, abrupt, or alternating first-degree block caused by block in the fast AVN pathway and conduction down the slow pathway. The change in the PR interval seen on the surface ECG corresponds to a jump in the AH interval viewed on the HB electrogram.

His-Purkinje system. As long as at least one fascicle conducts normally, the HV interval should not exceed 55 milliseconds (or 60 milliseconds in the presence of LBBB). A prolonged HV interval (more than 55 to 60 milliseconds) with or without prolonged His potential duration (more than 30 milliseconds) or a split His potential is diagnostic for HPS disease, even in the presence of a normal PR interval (see Figs. 9.7 and 9.20). A prolonged HV interval is almost always associated with an abnormal QRS because the impairment of intra-Hisian conduction is not homogeneous. Most patients have an HV interval of 60 to 100 milliseconds but only occasionally more than 100 milliseconds. With pure intra-Hisian conduction delay, the AH interval and the distal His-to-ventricular ($H'-V$) interval are normal, whereas the duration of the His potential is longer than 30 milliseconds, with a notched, fragmented, or split His potential. In this case, verification of the origin of the “split H” from the HB (and not part of the atrial or ventricular electrograms) is critical. This can be achieved by dissociation of the His potential from atrial activation with atrial pacing,

adenosine, or vagal stimulation and dissociation of the His potential from ventricular activation by documenting that the HV interval is longer than 30 milliseconds.

Atrium. A prolonged PA interval with normal AH and HV intervals indicates intraatrial conduction delay (see eFig. 9.1).

Site of Type 1 Second-Degree Atrioventricular Block

Atrioventricular node. Wenckebach block in the AVN is characterized by progressive prolongation of the AH interval, until an atrial deflection is not followed by His and ventricular deflections (see Figs. 9.8 and 9.9).

His bundle. A prolonged His potential duration or a split His potential is indicative of intra-Hisian disease. Intra-Hisian Wenckebach block can occur between the two His deflections, characterized by progressive conduction delay until the first His deflection is not followed by the second one.

Bundle branches. In Wenckebach AV block secondary to block below the HB, progressive prolongation of the HV interval is followed by a His deflection without an associated ventricular activation (see Fig. 9.11).

Site of Type 2 Second-Degree Atrioventricular Block

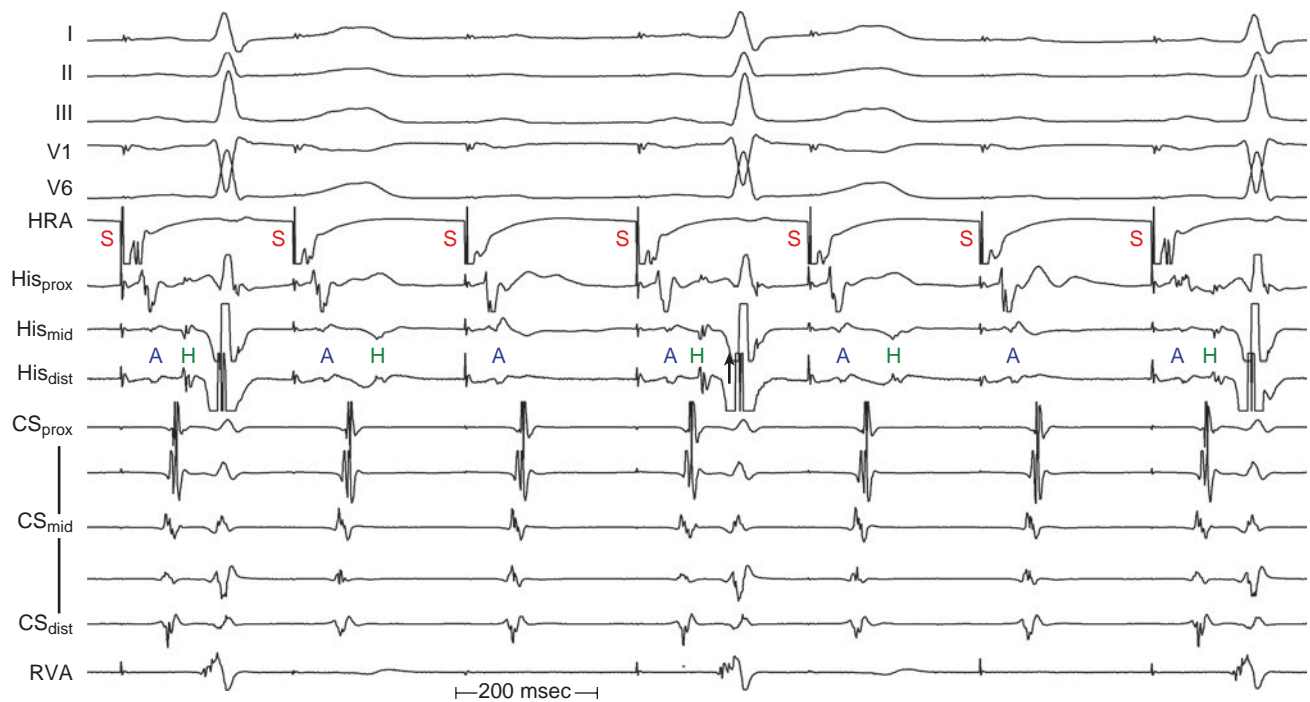
His-Purkinje system. The blocked cycle features atrial and HB deflections without ventricular depolarization (eFig. 9.4 and Fig. 9.21). The conducted beats usually show evidence of infranodal conduction system disease, with a prolonged HV interval, or even a split His potential, and BBB. Multilevel AV block (intranodal and infranodal) can also occur, especially during rapid atrial tachycardias or atrial pacing. Typically, infranodal AV block occurs in the presence of prolonged HPS refractoriness caused by antiarrhythmic agents or during Wenckebach cycles in the AVN (eFig. 9.5).

Site of Third-Degree Atrioventricular Block

Atrioventricular node. Complete heart block at the AVN level is usually seen on the intracardiac tracings as His potentials consistently preceding each ventricular electrogram. The atrial electrograms are dissociated from the HV complexes (Fig. 9.22). Most often, the escape rhythm originates in the HB (with normal QRS preceded by a His potential and normal HV interval); however, in 20% to 50% of patients



eFig. 9.4 Infranodal Block in a Patient With Persistent Atrial Fibrillation (AF) and Recurrent Syncope. (A) Surface electrocardiogram (ECG) recordings show AF with slow ventricular response and left bundle branch block. (B) Intracardiac recordings showing His potentials (*H*), some of which are conducted (HV interval, 124 milliseconds) and some are blocked.



eFig. 9.5 Multiple Levels of Atrioventricular Block. Rapid atrial pacing (at a cycle length of 330 milliseconds) from the high right atrium (*HRA*) shows repeating pattern of atrial impulses with normal AH intervals conducted to the ventricle, atrial impulses associated with AH interval prolongation with block below the His bundle, and atrial impulses associated with atrioventricular nodal block (no His potential). *CS_{dist}*, Distal coronary sinus; *CS_{mid}*, middle coronary sinus; *CS_{prox}*, proximal coronary sinus; *His_{dist}*, distal His bundle; *His_{mid}*, middle His bundle; *His_{prox}*, proximal His bundle; *RVA*, right ventricular apex.

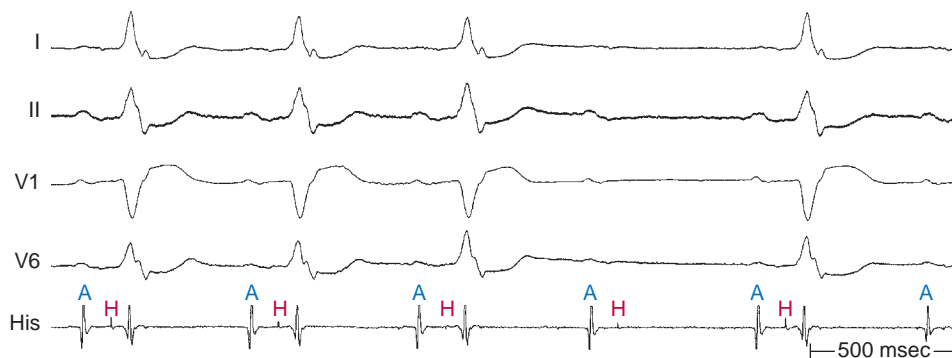


Fig. 9.21 Type 2 Second-Degree Atrioventricular Block. Sinus rhythm is observed with a wide QRS complex. The PR interval of all conducted P waves is constant and slightly prolonged (224 milliseconds). The fourth P wave fails to conduct to the ventricle but is followed by a His potential, suggesting that the level of AV block is infra-Hisian.

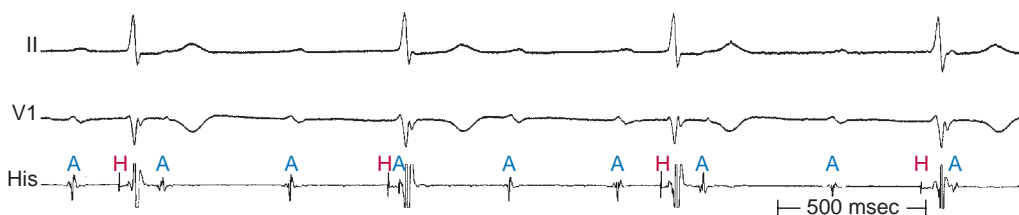


Fig. 9.22 Complete Intranodal Atrioventricular (AV) Block. Complete AV block with AV dissociation is observed, and all the P waves fail to conduct despite having ample opportunity for conduction. Note the junctional escape rhythm with a narrow QRS complex and a rate of 45 beats/min, consistent with block in the AVN. Note that the P waves surrounding a QRS complex occur at a faster rate when compared with the P waves that occur sequentially without an intervening QRS complex (ventriculophasic arrhythmia).

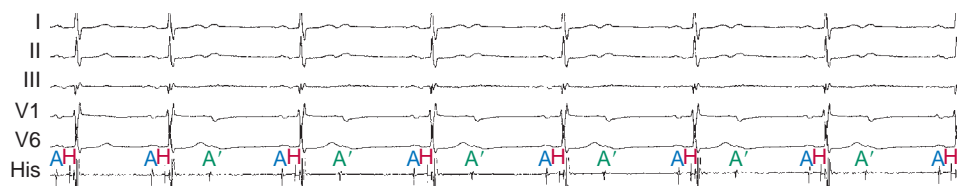


Fig. 9.23 Atrial Bigeminy Mimicking 2:1 Atrioventricular (AV) Block. Frequent premature atrial complexes (PACs; A') are observed in a bigeminal pattern. The PACs arrive at the atrioventricular node during the absolute refractory period and fail to conduct to the ventricle, thus mimicking 2:1 AV block. In contrast to 2:1 AV block, the nonconducted P waves are premature (compare with the first A-A interval, which is not interrupted by a PAC) and have different morphology than the conducted sinus P waves.

with chronic AV block, a wide QRS escape rhythm can occur. Rhythms originating in the distal HB can have a QRS preceded by a retrograde His potential or no His potential at all. Those rhythms are usually slower and nonresponsive to atropine. The stability of the HB rhythm can be assessed by noting the effects of overdrive suppression produced by ventricular pacing (in a manner analogous to testing sinus node function); prolonged pauses (i.e., the lack of HB escapes) herald subsequent complete failure of the escape rhythm.

His-Purkinje system. The intracardiac electrogram shows HB deflections consistently following atrial electrograms, but ventricular depolarizations are completely dissociated from the AH complexes. Block below the HB is thus demonstrated.

Exclusion of Other Phenomena

Nonconducted Premature Atrial Complexes

Early PACs can arrive at the AVN during the absolute refractory period and fail to conduct to the ventricle. This condition can be misdiagnosed

as type 1 or type 2 second-degree AV block. Similarly, atrial bigeminy, with failure of conduction of the PACs, can be misinterpreted as 2:1 AV block (Fig. 9.23). In type 2 second-degree AV block, the atrial rhythm is regular, the P-P interval is fairly constant (except for some variation caused by ventriculophasic arrhythmia), the nonconducted P wave occurs on time as expected, and P wave morphology is constant. On the other hand, in the setting of nonconducted PACs, the P wave occurs prematurely and usually has a different morphology from that of the baseline atrial rhythm. Nonconducted PACs can often be hidden in the preceding T wave (Figs. 9.24 and 9.25). In addition, the mere occurrence of PACs (even when conducted) in a trigeminal or quadrigeminal pattern can produce a pattern mimicking Wenckebach periodicity (see eFig. 9.5).

Concealed Junctional Ectopy

Ectopic beats arising from the HB that fail to conduct to both the atria and ventricles can result in retrograde concealment in the AVN, causing

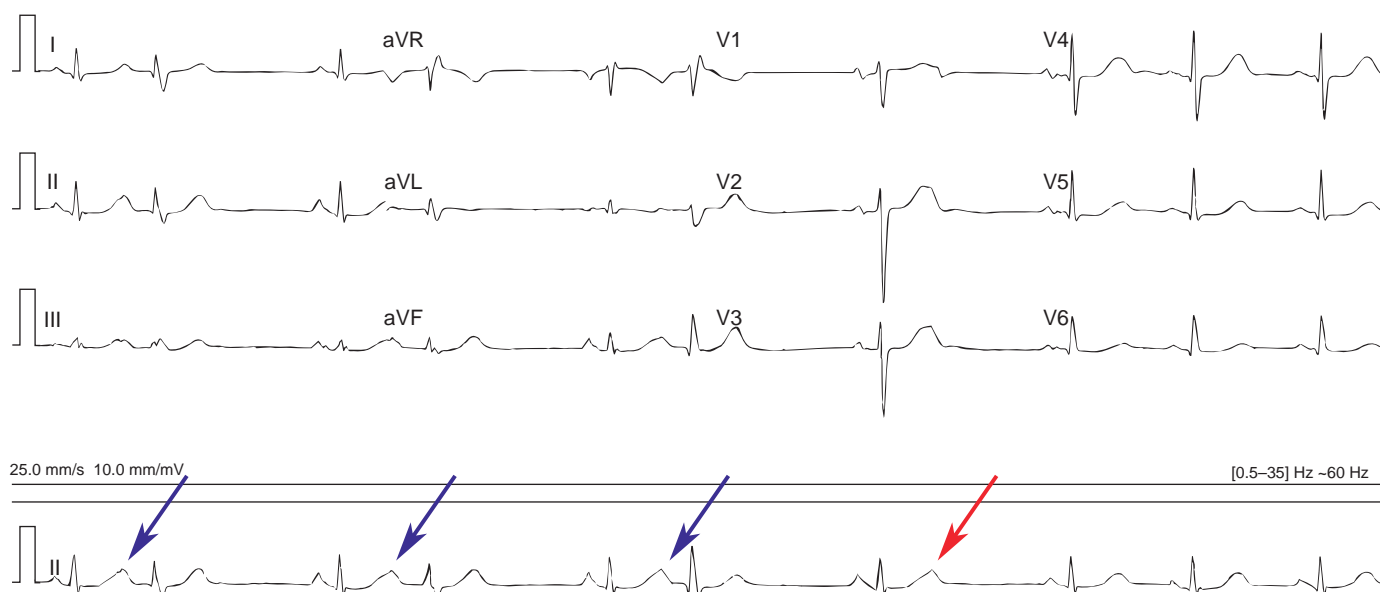


Fig. 9.24 Atrial Ectopy Mimicking Wenckebach Atrioventricular (AV) Block. The surface electrocardiogram shows normal sinus rhythm with four premature atrial complexes (PACs) occurring in a bigeminal pattern. The first three PACs (blue arrows) are conducted and give rise to a pattern that can mimic Wenckebach type I atrioventricular block. The fourth PAC (red arrow) is nonconducted. Note the premature P waves occur early and lie within the preceding T wave (arrows). The last three sinus P waves have no intervening PACs, and the T waves during those beats are clearly different from the ones harboring the PACs. All sinus P waves are conducted with a normal, constant PR interval.

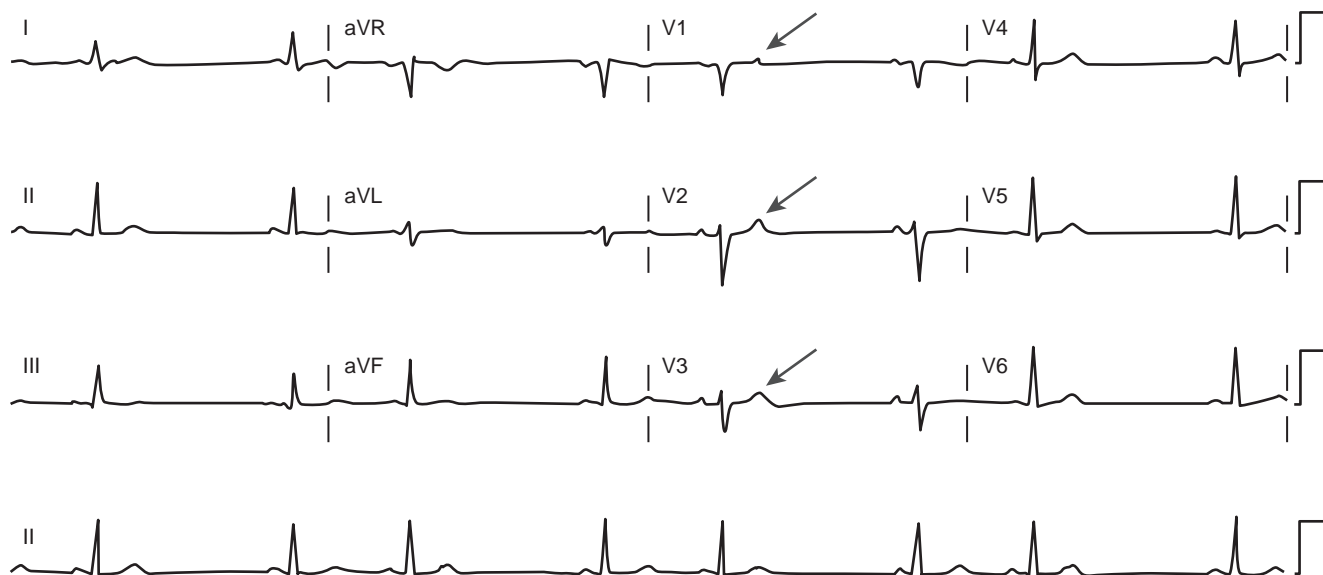


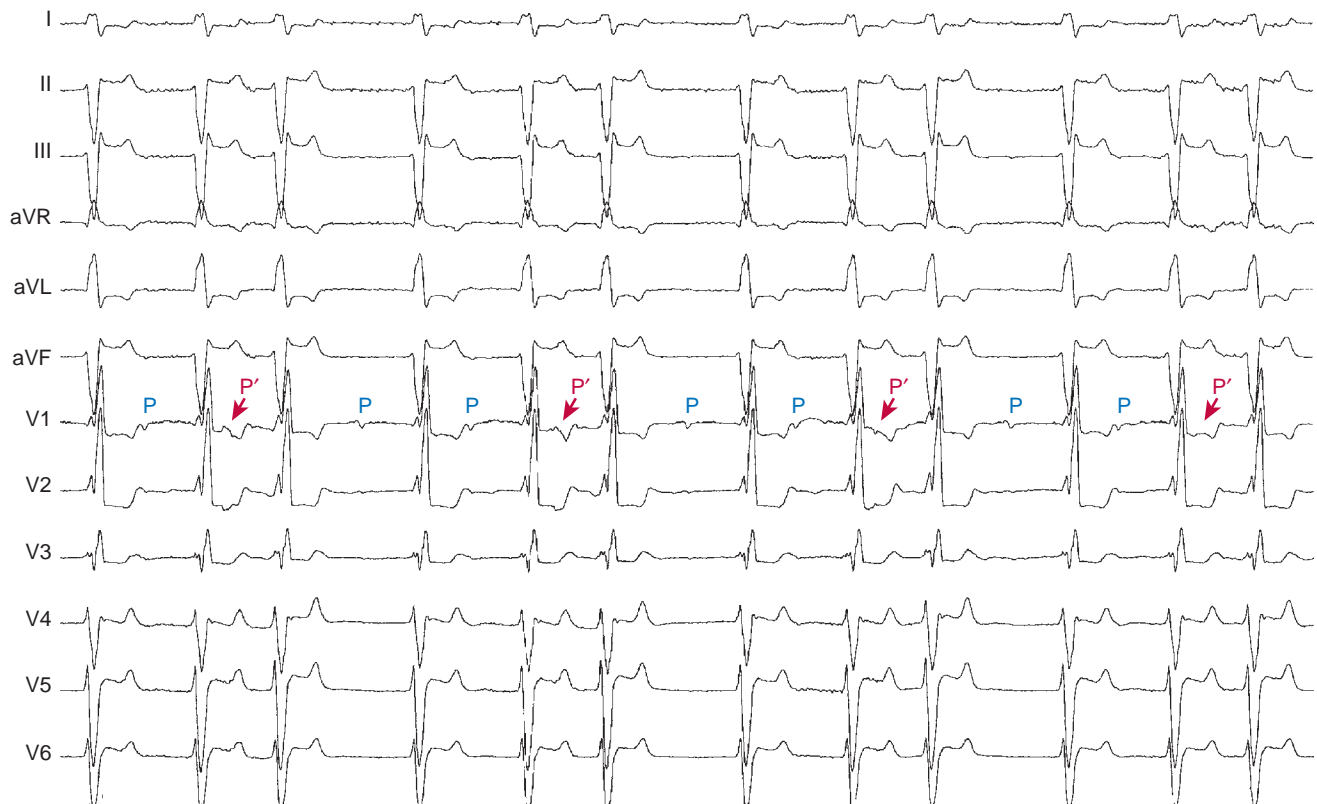
Fig. 9.25 Atrial Trigeminy Mimicking Mobitz Type II Atrioventricular Block. The blocked premature atrial complexes occur in a trigeminal pattern during sinus rhythm, resulting in a pattern that can mimic Mobitz type II atrioventricular block. Note the nonconducted P waves occur early (premature) and lie within the preceding T wave (arrows). All sinus P waves are conducted with a normal, constant PR interval.

either slowing of conduction or block of the following sinus P wave and hence mimicking type 2 second-degree AV block (eFig. 9.6). In this setting, AV block is physiological; however, it can be difficult to differentiate from pathological AV block without EP testing. ECG clues to concealed junctional extrasystoles causing such unexpected events include the following: (1) abrupt, unexplained prolongation of the PR interval; (2) the presence of apparent Mobitz type II block in the presence of a normal QRS; (3) the presence of apparent types 1 and 2 AV

block in the same tracing; and (4) the presence of manifest junctional extrasystoles elsewhere in the tracing (see Fig. 9.12).

Atrioventricular Dissociation

AV dissociation is present when the atria and ventricles depolarize independently of each other. The ventricles are activated by a nonatrial source and are uninfluenced by atrial activity. By definition, there is no retrograde conduction from the ventricles to the atria. AV dissociation



eFig. 9.6 Frequent Premature Atrial Complexes Mimicking Second-Degree Atrioventricular (AV) Block. Sinus rhythm with marked first-degree AV block and bifascicular block (right bundle branch block and left anterior fascicular block). Frequent premature atrial complexes (PACs; *P'*) are observed in a trigeminal pattern. The PACs are conducted to the ventricles; however, they produce a periodicity, thus mimicking Wenckebach AV block. Note that no P waves fail to conduct to the ventricle. Despite the presence of marked His-Purkinje system disease, the marked prolongation of the PR intervals (420 milliseconds) suggests the atrioventricular node as the site of AV conduction delay.

can occur secondary to complete AV block, atrial bradycardia with a faster independent junctional-ventricular escape rhythm, or increased discharge rate of a subsidiary pacemaker that takes control of the ventricular rhythm.

The distinction between AV dissociation and complete AV block is important. In complete AV block the atrial rate is faster than the ventricular rate. For AV block to be diagnosed, the P waves must fail to conduct, given every opportunity for optimal conduction. Thus failure of conduction of all the P waves, even those occurring at long RP intervals and throughout the phases of the ventricular cycle, has to be documented. Occasionally, the rate of the junctional or ventricular rhythm during AV dissociation is only slightly different from that of the atrial rhythm. In this setting the standard ECG may not provide a recording opportunity long enough to verify failure of conduction, because all the P waves recorded on a single ECG recording may not occur at an appropriate time to allow conduction. Thus obtaining ECG recording for an adequate length of time is important (Fig. 9.26). Regularity of both atrial and ventricular rhythms with constantly changing PR relationships, despite the fact that the P wave falls at every conceivable RP interval, and an independent ventricular rate of 40 beats/min or less (faster in congenital complete AV block) are diagnostic of complete AV block. On the other hand, some irregularity of the ventricular rhythm should immediately draw attention to the possibility of intermittent conduction of P waves, which may reflect lesser degrees of AV block or incomplete AV dissociation. Moreover, with complete AV block, the ventricular rate is almost always slower than the atrial rate, whereas in other forms of AV dissociation, the reverse is true. Therefore complete AV block with a junctional or ventricular escape rhythm is one form of AV dissociation. However, AV dissociation (complete or incomplete) can occur in the absence of AV block.

In the setting of atrial bradycardia, the atrial rate can become slower than a subsidiary escape focus from the AV junction or ventricle. When the faster junctional or ventricular escape rhythm is associated with VA block, it results in failure of the atrial impulses to conduct anterogradely secondary to retrograde concealment by the escape rhythm impulses (see Fig. 9.18).

An increase in the discharge rate of a subsidiary pacemaker, such as accelerated junctional rhythm, accelerated idioventricular rhythm, or VT, which then exceeds the normal sinus rate, can result in a competing junctional or ventricular rhythm, in which case the atrial rate is always slower than the ventricular rate (see Fig. 9.26).

AV dissociation can be complete or incomplete. In the setting of complete AV dissociation, both the atrial and ventricular rates remain constant and therefore the PR interval varies, with none of the atrial complexes conducted to the ventricles. In incomplete AV dissociation, ventricular capture beats occur because some of the atrial impulses arrive at the AV junction when the AV junction is no longer refractory. This phenomenon is common in advanced AV block with periodic capture beats.

Echo Beats

AVN echo beats can manifest as “group beating” and be misdiagnosed as Wenckebach block. Verification of constant P-P intervals and P wave morphology during the Wenckebach cycle can avoid such misinterpretation. On the other hand, in the presence of dual AVN physiology, not infrequently Wenckebach AV block can result in AVN echo beats.

Atrial Tachyarrhythmias

Failure of the AVN to conduct during fast atrial tachyarrhythmias (AT or AFL) should not be considered pathological AV block. One of the main physiological roles of the AVN is to safeguard the ventricles from rapid atrial rates. Therefore failure of the AVN to conduct every atrial impulse occurring at a fast rate should be considered a normal physiological finding caused by normal refractoriness. In such situations, terms such as 3:2 and 2:1 AV conduction are more appropriate than 3:2 or 2:1 AV block.

Atrial Fibrillation With Slow Ventricular Rate

AF with slow ventricular response can be misinterpreted as complete AV block. Verification of the regularity of the slow ventricular rhythm is critical. When AV block is present, the escape rhythm is regular, whereas in AF associated with very slow ventricular response, the

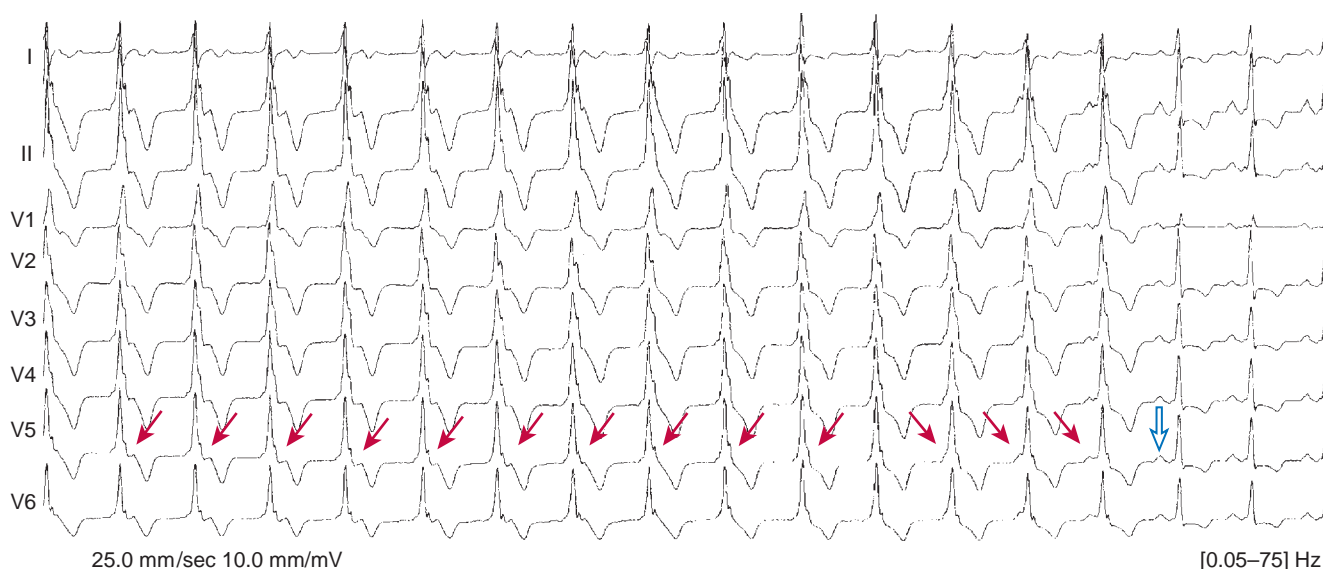


Fig. 9.26 Atrioventricular Dissociation. Slow ventricular tachycardia and normal sinus rhythm coexist with slightly different rates and ventricular-atrial dissociation. Sinus P waves are marked by red arrows. Note that no atrioventricular block is present and that, once the sinus P wave had the chance to conduct, it did (blue arrow).

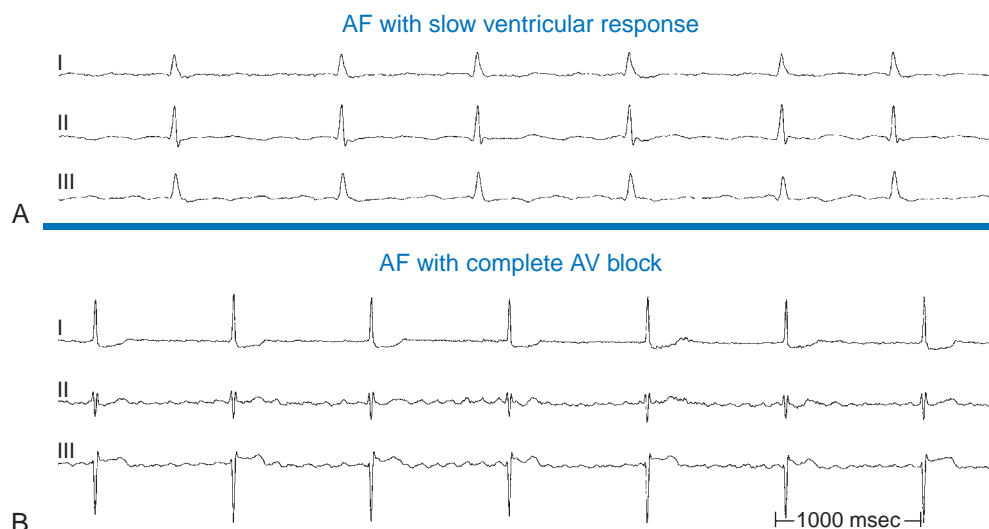


Fig. 9.27 Atrial Fibrillation (AF) With Slow Ventricular Rate. (A) The ventricular rhythm is irregular, indicating that it is the result of conducted atrial beats. (B) The ventricular rhythm is regular, consistent with the presence of complete atrioventricular (AV) block and a regular junctional escape rhythm.

ventricular rhythm is a result of conducted atrial beats and is irregular (Fig. 9.27).

Ventriculophasic Sinus Arrhythmia

Ventriculophasic sinus arrhythmia can be observed whenever there is second- or third-degree AV block, and it is manifest as intermittent differences in the P-P intervals based on their relationship with the QRS complex. The two P waves surrounding a QRS complex have a shortened interval or occur at a faster rate when compared with two P waves that occur sequentially without an intervening QRS complex (see Fig. 9.22). The mechanism of this phenomenon is not certain. However, it has been suggested that ventricular contractions enhance sinus node automaticity by increasing the pulsatile blood flow through the sinus nodal artery and by mechanical stretch on the sinus node.

PRINCIPLES OF MANAGEMENT

Identifying transient or reversible causes for AV conduction disturbances is the first step in management. Withdrawal of any offending drugs, correction of any electrolyte abnormalities, or treatment of any infectious processes (e.g., Lyme disease) or myocardial ischemia should be considered prior to permanent pacing therapy.

Pharmacological therapy (atropine, isoproterenol, epinephrine) can be effective in intranodal AV block but only as a short-term emergency measure until pacing can be accomplished.

Temporary percutaneous or transvenous pacing can be necessary in patients with hemodynamically significant AV block and bradycardia to provide immediate stabilization prior to permanent pacemaker placement or to provide pacemaker support when the block is precipitated by what is presumed to be a transient event, such as ischemia or drug toxicity.²⁵ However, it is important to recognize that transcutaneous pacing does not provide reliable ventricular capture and should be used sparingly. When used, careful hemodynamic and ECG monitoring is mandatory to verify effective ventricular stimulation. Similarly, due to the multitude of complications associated with temporary transvenous pacing (e.g., lead dislodgement, cardiac perforation, patient immobilization), this modality should be used only as a last resort and as briefly as possible. Unless there is a contraindication, positive chronotropic drug infusion is preferred.^{19,20}

Permanent Pacing Therapy

Pacing is the mainstay of treatment for symptomatic AV block (Box 9.1). After all reversible causes are excluded or treated, correlation of symptoms with ECG evidence of AV block is an essential part of the diagnostic strategy. In the setting of intermittent AV block or Wenckebach AV block, ambulatory monitoring often is required to correlate symptoms with the presence and severity of AV conduction abnormalities. As discussed previously, exercise testing can be a useful tool to help confirm the level of block in second- or third-degree AV block associated with a narrow or wide QRS complex. In addition, EP testing can be required in a patient with suspected high-grade AV block as the cause of syncope or presyncope when documentation cannot be obtained noninvasively. Similarly, in patients with coronary artery disease, in whom symptoms can be secondary to AV block or VT, EP testing can be useful in establishing the diagnosis. Some patients with known second- or third-degree block also can benefit from an invasive study to localize the site of AV block to help determine therapy or assess prognosis.²⁵

Third-Degree Atrioventricular Block

Permanent pacemaker implantation is indicated in patients with symptomatic complete AV block, regardless of the site of block. Permanent pacing is also recommended in asymptomatic patients with complete heart block, especially those with documented ventricular pauses longer than 3 seconds or a ventricular escape rhythm of less than 40 beats/min.²⁵

Second-Degree Atrioventricular Block

Permanent pacing is recommended in most patients with symptomatic second-degree AV block, regardless of the site of block. However, in asymptomatic patients, permanent pacemakers may be considered only in patients with infranodal (type 2) second-degree AV block but not those with intranodal type 1 second-degree AV block.²⁵

First-Degree Atrioventricular Block

Permanent pacing is not recommended for asymptomatic first-degree AV delay. However, dual-chamber pacing can be beneficial in some of these patients with marked PR prolongation (more than 300

BOX 9.1 ACCF/AHA/HRS Recommendations for Permanent Pacing in Acquired Atrioventricular Block in Adults

Class I

- Third-degree and advanced second-degree AV block at any anatomic level, associated with any one of the following:
 - Symptomatic bradycardia (including heart failure)
 - Ventricular arrhythmias presumed to result from AV block
 - Arrhythmias and other medical conditions that require drugs that result in symptomatic bradycardia
- Awake, symptom-free patients in sinus rhythm and documented periods of asystole ≥ 3.0 s or any escape rate < 40 beats/min, or with an escape rhythm that is below the AV node
- Average awake ventricular rates of 40 beats/min or faster if cardiomegaly or left ventricular dysfunction is present or if the site of block is below the AV node
- Awake, symptom-free patients with atrial fibrillation and bradycardia with one or more pauses of at least 5 s
- After catheter ablation of the AV junction
- Postoperative AV block that is not expected to resolve
- Neuromuscular diseases, such as myotonic muscular dystrophy, Kearns-Sayre syndrome, Erb dystrophy (limb-girdle muscular dystrophy), and peroneal muscular atrophy, with or without symptoms
- Second-degree AV block with associated symptomatic bradycardia regardless of type or site of block
- Second- or third-degree AV block during exercise in the absence of myocardial ischemia
- Persistent third-degree AV block at any anatomic site in asymptomatic patients with average awake ventricular rates of 40 beats/min or faster if cardiomegaly or LV dysfunction is present or if the site of block is below the AV node

Class IIa

- Persistent third-degree AV block with an escape rate > 40 beats/min in asymptomatic adult patients without cardiomegaly
- Asymptomatic second-degree AV block at intra-Hisian or infra-Hisian levels found at electrophysiological study
- First- or second-degree AV block with symptoms similar to those of pacemaker syndrome or hemodynamic compromise
- Asymptomatic type II second-degree AV block with a narrow QRS; when type II second-degree AV block occurs with a wide QRS, including isolated right bundle branch block, pacing becomes a class I recommendation

Class IIb

- Neuromuscular diseases such as myotonic muscular dystrophy, Erb dystrophy (limb-girdle muscular dystrophy), and peroneal muscular atrophy with any degree of AV block (including first-degree AV delay), with or without symptoms, because there may be unpredictable progression of AV conduction disease
 - AV block in the setting of drug use and/or drug toxicity when the block is expected to recur even after the drug is withdrawn

Class III

- Asymptomatic first-degree AV delay
- Asymptomatic type I second-degree AV block at the AV node level or that which is not known to be intra-Hisian or infra-Hisian
 - AV block that is expected to resolve and is unlikely to recur (e.g., drug toxicity, Lyme disease, or transient increases in vagal tone, or during hypoxia in sleep apnea syndrome in the absence of symptoms)

ACCF, American College of Cardiology Foundation; AHA, American Heart Association; AV, atrioventricular; HRS, Heart Rhythm Society. Modified from Epstein AE, DiMarco JP, Ellenbogen KA, et al. 2012 ACCF/AHA/HRS focused update incorporated into the ACCF/AHA/HRS 2008 guidelines for device-based therapy of cardiac rhythm abnormalities: a report of the American College of Cardiology Foundation/American Heart Association Task Force on Practice Guidelines and the Heart Rhythm Society. *J Am Coll Cardiol*. 2013;61:e6–75.

milliseconds) and symptoms similar to those of pacemaker syndrome (see later), as well as in patients with LV dysfunction and heart failure symptoms in whom a shorter AV interval is expected to lead to hemodynamic improvement, presumably by improving ventricular filling and reducing diastolic mitral regurgitation. Nonetheless, the benefit of pacing with optimized AV synchrony (with a shorter AV delay) should be weighed against the potentially detrimental effects of RV pacing and resultant ventricular dyssynchrony.^{25,19}

Atrioventricular Block Post Acute Myocardial Infarction

Temporary pacing is sometimes required in patients with acute MI (more often in anterior than inferior wall MI). Patients with asymptomatic first-degree or type 1 second-degree AV block do not require pacing. However, patients with type 2 second-degree or complete AV block, temporary pacing should be considered, even if they are asymptomatic. Isoproterenol should be used with extreme caution or not at all in patients with acute MI. Importantly, acute temporary transvenous pacing in these patients is associated with a 6% risk of cardiac tamponade. This should be carefully considered when determining optimal treatment strategy.^{19,20}

In patients with acute MI and high-grade AV block, the conduction abnormality is present upon hospital admission in more than 50% of patients and within 48 hours in the majority of patients. In patients treated by primary percutaneous coronary intervention, AV block is predominantly transient, most often resolves spontaneously within a

few days. Pacemaker implantation is required in only 9% patients. Importantly, these patients continue to have high mortality, despite pacing.^{19,20}

In the setting of acute MI, the criteria for permanent pacing depends less on the presence of symptoms (Box 9.2). If type 2 second-degree or complete AV block persists once past the periinfarct period, permanent pacing is indicated. Even if the type 2 or third-degree AV block was transient but associated with BBB that persists following resolution of the AV block, permanent pacing may improve long-term survival.²⁵

Iatrogenic Atrioventricular Block

Permanent pacing is recommended for persistent type 2 second- or third-degree AV block complicating cardiac interventional or surgical procedures (e.g., aortic valve replacement), even in the absence of symptoms. Importantly, early conduction abnormalities occurring after such procedures are often transient, caused by local inflammation near the AV conduction system. Hence, when the patient is hemodynamically stable or already has a functional temporary pacemaker, some delay before committing to a permanent pacemaker may be appropriate.³⁹ However, the duration of “watchful waiting” is not defined and can vary in different settings; therefore the decision for permanent pacing is at the physician’s discretion. In addition, patients with transient postoperative third-degree AV block that reverts to sinus rhythm with residual bifascicular block can occasionally develop high-degree AV block later

BOX 9.2 ACCF/AHA/HRS Recommendations for Permanent Pacing in Atrioventricular Block With Acute Myocardial Infarction

Class I

- Persistent second-degree AV block in the HPS with bilateral bundle branch block or third-degree AV block within or below the HPS after ST-segment elevation MI
- Transient advanced (second- or third-degree) infranodal AV block and associated bundle branch block; if the site of block is uncertain, an electrophysiology study may be necessary
- Persistent and symptomatic second- or third-degree AV block

Class IIb

- Persistent second- or third-degree AV block at the AV node level, even in the absence of symptoms

Class III

- Transient AV block in the absence of intraventricular conduction defects
- Transient AV block in the presence of isolated left anterior fascicular block
- New bundle branch block or fascicular block in the absence of AV block
- Persistent asymptomatic first-degree AV delay in the presence of bundle branch block or fascicular block

ACCF, American College of Cardiology Foundation; AHA, American Heart Association; AV, atrioventricular; HPS, His-Purkinje system; HRS, Heart Rhythm Society; MI, myocardial infarction.

Modified from Epstein AE, DiMarco JP, Ellenbogen KA, et al. 2012 ACCF/AHA/HRS focused update incorporated into the ACCF/AHA/HRS 2008 guidelines for device-based therapy of cardiac rhythm abnormalities: a report of the American College of Cardiology Foundation/American Heart Association Task Force on Practice Guidelines and the Heart Rhythm Society. *J Am Coll Cardiol*. 2013;61:e6–75.

in the postoperative course. Accordingly, extended cardiac monitoring might be reasonable in patients deemed to be at high risk. If unexplained syncope occurs in these patients, paroxysmal AV block should be suspected.^{25,19}

Congenital Atrioventricular Block

In children (beyond the first year of life) with congenital AV block, pacemaker implantation is recommended for those with symptomatic bradycardia or chronotropic incompetence. Permanent pacing is also recommended in asymptomatic patients who have a wide QRS escape rhythm, complex ventricular ectopy, ventricular dysfunction, inappropriately slow average ventricular rate (fewer than 50 beats/min), or abrupt pauses in ventricular rate that are two or three times the basic cycle length. The value of permanent pacing is questionable in asymptomatic patient with congenital third-degree AV block with an acceptable rate, a narrow QRS complex, and normal ventricular function (Box 9.3).²⁵

Vagally Mediated Atrioventricular Block

Vagally mediated AV block is localized within the AVN and generally is benign. When the AV block is associated with neurocardiogenic syncope, avoidance of triggering and predisposing factors and noninvasive therapy are effective and are preferred to pacing therapy. Nonetheless, permanent pacing may be considered highly selected patients, such as those significantly older than 40 years and patients who experience frequent recurrences associated with repeated injury, limited prodromes, and documented asystole (Fig. 9.28). Even in this subgroup of

BOX 9.3 ACCF/AHA/HRS Recommendations for Permanent Pacing for Atrioventricular Block in Children, Adolescents, and Patients With Congenital Heart Disease

Class I

- Advanced second- or third-degree AV block associated with symptomatic bradycardia, ventricular dysfunction, or low cardiac output
- Congenital third-degree AV block with a wide QRS escape rhythm, complex ventricular ectopy, or ventricular dysfunction
- Congenital third-degree AV block in the infant with a ventricular rate less than 55 beats/min or with congenital heart disease and a ventricular rate less than 70 beats/min
- Postoperative advanced second- or third-degree AV block that is not expected to resolve or that persists at least 7 days after cardiac surgery

Class IIa

- Congenital third-degree AV block beyond the first year of life with an average heart rate less than 50 beats/min, abrupt pauses in ventricular rate that are two or three times the basic cycle length, or associated with symptoms due to chronotropic incompetence
- Congenital heart disease and impaired hemodynamics due to sinus bradycardia or loss of AV synchrony
- Unexplained syncope in the patient with prior congenital heart surgery complicated by transient complete heart block with residual fascicular block after a careful evaluation to exclude other causes of syncope

Class IIb

- Transient postoperative third-degree AV block that reverts to sinus rhythm with residual bifascicular block
- Congenital third-degree AV block in asymptomatic children or adolescents with an acceptable rate, a narrow QRS complex, and normal ventricular function

Class III

- Transient postoperative AV block with return of normal AV conduction in the otherwise asymptomatic patient
- Asymptomatic bifascicular block with or without first-degree AV delay after surgery for congenital heart disease in the absence of prior transient complete AV block
- Asymptomatic type I second-degree AV block
- Asymptomatic sinus bradycardia with the longest relative risk interval less than 3 s and a minimum heart rate more than 40 beats/min

ACCF, American College of Cardiology Foundation; AF, atrial fibrillation; AHA, American Heart Association; AV, atrioventricular; HRS, Heart Rhythm Society.

Modified from Epstein AE, DiMarco JP, Ellenbogen KA, et al. 2012 ACCF/AHA/HRS focused update incorporated into the ACCF/AHA/HRS 2008 guidelines for device-based therapy of cardiac rhythm abnormalities: a report of the American College of Cardiology Foundation/American Heart Association Task Force on Practice Guidelines and the Heart Rhythm Society. *J Am Coll Cardiol*. 2013;61:e6–75.

patients, syncope continues to recur in up to 25% post pacemaker implantation, likely due to the coexistence of a vasodepressor reflex.⁴⁰

Permanent pacing is recommended for patients with syncope due to carotid sinus hypersensitivity or those with syncope without clear provocative events when carotid sinus massage precipitates a cardioinhibitory response of 3 seconds or longer. Pacemaker implantation is not indicated asymptomatic hypersensitive carotid sinus massage response.^{25,40,42}

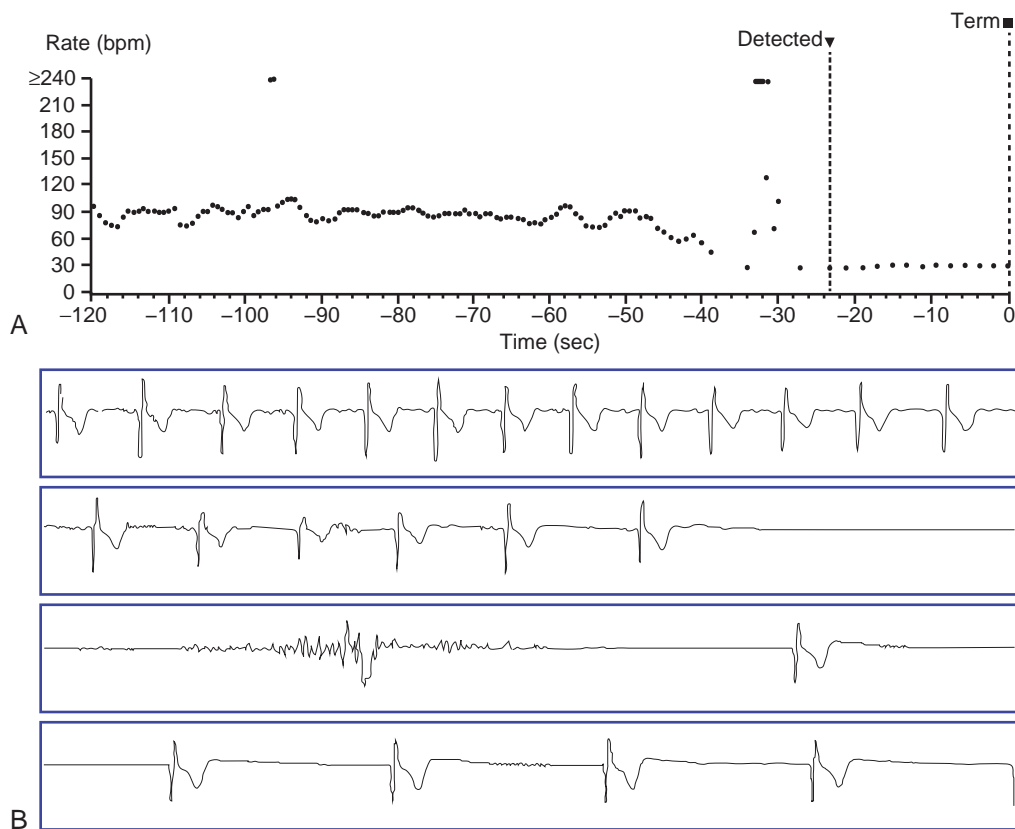


Fig. 9.28 Asystole Associated With Neurocardiogenic Syncope. Implantable loop recorder documentation of syncope due to vasovagal cardioinhibitory response. (A) Heart rate trend during 4-minute loop recording. Initially, the heart rate is stable at 90 beats/min and gradually falls at the time of syncope. (B) Expanded electrocardiogram. The four strips are continuous and show progressive slowing of the heart rate culminating in a long asystolic pause (greater than 10 seconds), followed by recovery of a slow rhythm.

Pacemaker Device and Mode Selection for Atrioventricular Block

In patients with persistent or intermittent AV block and those at risk of developing AV block requiring ventricular pacing, single-chamber ventricular (VVI), dual-chamber (DDD), or single-lead AV (VDD) pacemaker implantation may be considered (Box 9.4). In general, DDD pacing is the preferred pacing system in the majority of patients with AV block. In addition, regardless of the pacing system used, cardiac resynchronization therapy should be considered in patients with AV block and LV systolic dysfunction who are expected to require high percentage (more than 40%) of ventricular pacing.⁵⁴

DDD and VDD Pacing

Compared with VVI pacing, VDD and DDD pacemakers offer several advantages: First, both systems have the capability to maintain AV synchrony, which can be of significant hemodynamic benefit in patients with LV systolic or diastolic dysfunction, who depend on optimized preload, improved exercise time, functional status, and quality of life, especially in younger, active patients with few comorbidities. Second, in patients with AV block but normal sinus node function, both DDD and VDD pacemakers can preserve AV synchrony and physiological chronotropic response driven by the sinus node rather than by imperfect rate-adaptive algorithms. Third, in patients with only intermittent AV block, VDD and DDD pacemakers can help to promote intrinsic ventricular activation and minimize unnecessary RV pacing that can be

hemodynamically detrimental in many patients. Fourth, device diagnostics available in VDD and DDD pacemakers permit detection of episodes of atrial tachyarrhythmias, which may result in therapeutic interventions, including therapy for stroke prevention.⁵⁴

The VDD pacing systems use a single lead with a series of electrodes for atrial sensing and ventricular pacing and sensing and hence enables atrial-tracking ventricular pacing and restores AV synchrony without the need for an additional atrial lead. As compared with DDD pacemakers, VDD pacemakers offer the advantage of simpler implantation and less risk of procedure complications (in particular, less risk of lead dislodgement) and can be of particular advantage in the younger patient, such as the patient with congenital heart block who might expect multiple system revisions over his lifetime. Nonetheless, VDD pacemakers are used very infrequently (less than 1% of implanted pacemakers in the United States), mostly due to the concern of the potential need for atrial pacing if sinus node dysfunction (SND) develops and the relatively poor long-term performance of the atrial sensing ability of the lead.⁵⁴

VVI Pacing

VVI pacing has limited role in patients with AV block and normal sinus rhythm, given the lack of AV synchrony and the associated pacemaker syndrome (see later). However, VVI or VVIR pacing is adequate for patients with permanent AF and bradycardia and may also be considered post AV junction ablation in patients with intermittent AF who are expected to have high rate of progression to persistent or permanent AF and rhythm control strategies are no longer pursued. In patients

BOX 9.4 HRS/ACCF Recommendations for Pacemaker Device and Mode Selection for Atrioventricular Block

Class I

- Dual-chamber pacing is recommended in patients with AV block
- Single-chamber ventricular pacing is recommended as an acceptable alternative to dual-chamber pacing in patients with AV block who have specific clinical situations that limit the benefits of dual-chamber pacing. These include, but are not limited to, sedentary patients, those with significant medical comorbidities likely to impact clinical outcomes, and those in whom technical issues, such as vascular access limitations, preclude or increase the risk of placing an atrial lead
- Dual-chamber pacing is recommended over single-chamber ventricular pacing in adult patients with AV block who have documented pacemaker syndrome

Class IIa

- Single-lead, dual-chamber VDD pacing can be useful in patients with normal sinus node function and AV block (e.g., the younger patient with congenital AV block)
- VVI pacing can be useful in patients following AV junction ablation, or in whom AV junction ablation is planned, for rate control of AF due to the high rate of progression to permanent AF

Class III

- Dual-chamber pacing should not be used in patients with AV block in permanent or longstanding persistent AF in whom efforts to restore or maintain sinus rhythm are not planned

ACCF, American College of Cardiology Foundation; AF, atrial fibrillation; AV, atrioventricular; HRS, Heart Rhythm Society. Modified from Gillis AM, Russo AM, Ellenbogen KA, et al. HRS/ACCF expert consensus statement on pacemaker device and mode selection. *J Am Coll Cardiol*. 2012;60:682–703.

with permanent AF and AV block, rate-responsive pacing (VVIR) is generally preferred to fixed-rate VVI pacing because of the associated improvement of symptoms, exercise tolerance, and quality of life. Of note, setting the minimum pacing rate to 70 beats/min has been suggested to help to compensate for loss of active atrial filling.

In addition, back-up VVI pacing may be considered in patients with only “paroxysmal” AV block who are not expected to require frequent pacing, and can also be an appropriate choice for inactive or incapacitated patients and those with significant morbidities and poor clinical prognosis. Although atrial-based pacing was shown to significantly reduce the risk of AF and stroke compared with VVI in patients with SND, the benefit may not be of a similar magnitude in patients with AV block as the indication for pacing therapy because the incidence of AF in the latter population is lower compared with those with a SND indication for pacing. In addition, DDD pacing was not shown to reduce the risk of heart failure or the risk of death from all causes or from cardiovascular causes as compared with VVI pacing in the AV block patient population.⁵⁴

Pacemaker Syndrome

Suboptimal AV synchrony or AV dyssynchrony is associated with several detrimental hemodynamic consequences that lead to a constellation of symptoms (including fatigue, weakness, effort intolerance, chest discomfort, dyspnea, confusion, dizziness, presyncope, or syncope) known as the “pacemaker syndrome.”⁵⁴

AV dyssynchrony can cause significant reduction in cardiac output, especially in patients with reduced ventricular compliance and diastolic dysfunction (due to aging or hypertensive, hypertrophic, or restrictive cardiomyopathy), who are particularly sensitive to loss of atrial contribution to ventricular filling. Reduction of cardiac output causes reflex sympathetic activation. Furthermore, atrial contraction against closed mitral and tricuspid valves (which is further promoted in patients with intact retrograde ventriculoatrial conduction) can cause uncomfortable pulsation in the neck (cannon a waves) and abdomen, headache, cough, and jaw pain. The resultant increase in LA pressure and LV filling pressure cause increased plasma levels of atrial natriuretic peptide and B-type natriuretic peptide, potent peripheral venous, and arterial vasodilators.

Although pacemaker syndrome can occur with any pacing mode, it occurs most commonly with VVI pacing in patients who are in sinus rhythm (reported in up to 83%). However, pacemaker syndrome severe enough to warrant reprogramming from VVI to DDD pacing has been reported in only 25% to 30% of patients.⁵⁴

Ventricular Pacing Site

Right Ventricular Apical Pacing

The RV apex has been the traditional site of choice for permanent ventricular pacing, mainly due to technical aspects such as a stable lead position given the available electrode design. However, chronic apical RV pacing has been associated with deleterious hemodynamic effect on LV systolic function. Electrical and mechanical dyssynchrony induced by RV pacing can cause LV systolic dysfunction (“pacing-induced cardiomyopathy”) and heart failure. In fact, new-onset heart failure can be observed in approximately 9% of patients receiving RV pacing for acquired second- or third- degree AV block at 1-year follow-up and 20% after a median follow-up of nearly 10 years. It is important to note that pacing-induced cardiomyopathy can develop as early as 1 month and as late as 9 years after pacemaker implantation.⁵⁵

Male gender, prior heart failure hospitalization, low baseline LVEF, coronary artery disease, wider native QRS duration, wider paced QRS duration after implantation, and higher burden of RV pacing appear to predict a higher risk for developing pacing-induced cardiomyopathy. Although an RV pacing burden of 40% or more has been traditionally considered the cutoff at which risk for pacing-induced cardiomyopathy begins, accumulative pacing burdens as low as 20% have been found to precipitate cardiomyopathy, albeit with a lower incidence.⁵⁵

Nonapical Right Ventricular Pacing

Concern about RV apical pacing has driven an examination of nonapical RV sites, including the RVOT and RV mid or low septum. Although these sites can potentially provide more physiological LV activation and less cardiac dyssynchrony, presumably due to its closer proximity to the HPS, there is as yet no conclusive evidence that supports the superiority of these pacing sites (in terms of quality of life, functional tests, or morbidity and mortality) compared with RV apical pacing.^{56,57,58}

Most studies addressing this issue were limited by small sample sizes, limited follow-up intervals, different patient characteristics, and lack of standardization and verification of pacing site selection, which do not allow the advantages of septal pacing to be categorically determined. Nonetheless, no study has demonstrated inferiority of non-RV apical pacing, and many data point to the contrary. The subgroups benefiting the most from nonapical RV pacing were patients with LV systolic dysfunction.^{56,57,58,59}

Biventricular Pacing

Biventricular pacing can potentially prevent LV remodeling and heart failure caused by conventional RV pacing in patients abnormal LV systolic function and is currently recommended for in patients with LV

dysfunction (LVEF $\leq 50\%$) and advanced AV block and expected frequent (greater than 40%) ventricular pacing.⁶⁰

Although studies have suggested some value for prophylactic biven- tricular pacing in patients with AV block and normal LVEF, the benefit seems marginal and the evidence is not yet sufficiently strong to support widespread adoption of such strategy. No validated risk stratification system currently exists to identify who of these patients would benefit most from biven- tricular pacing. Currently, the best strategy seems to be to evaluate LVEF before pacemaker implantation.^{61,55}

His Bundle Pacing

Direct HB pacing (with the pacing electrode positioned in the mem- branous septum) or para-Hisian pacing can enable physiological pacing in patients without distal conduction disease by recruiting the native HPS, thus avoiding electrical dyssynchrony and potentially preventing pacing-induced cardiomyopathy and heart failure (Figs. 9.29 and 9.30).^{53,62}

However, HB pacing has not gained widespread acceptance in clinical practice because of perceived procedural complexity. Selective HB pacing

can be technically difficult to accomplish reliably and typically requires longer procedure and fluoroscopy times than traditional RV pacing. In addition, HB pacing can be associated with comparatively higher lead dislodgement rates and increasing pacing capture thresholds over time, which can lead to faster battery drain. Nonetheless, recent studies at experienced centers demonstrated safety and feasibility of such an approach in more than 80% of unselected patients referred for pace- maker implantation.^{62–65}

HB pacing is not applicable to patients with native block in the HPS. However, it is important to recognize that HB pacing can normal- ize intraventricular conduction in a large proportion of patients with infranodal AV block who previously had chronic BBB. Longitudinal dissociation of the HB with disease affecting the fibers destined to be right or left bundle branch (rather than disease in the bundle branch itself) may explain this observation. In this setting, HB pacing can recruit HB and bundle branches distal to the site of block and correct the conduction abnormalities. Other mechanisms also have been pro- posed to explain this observation.^{53,66}

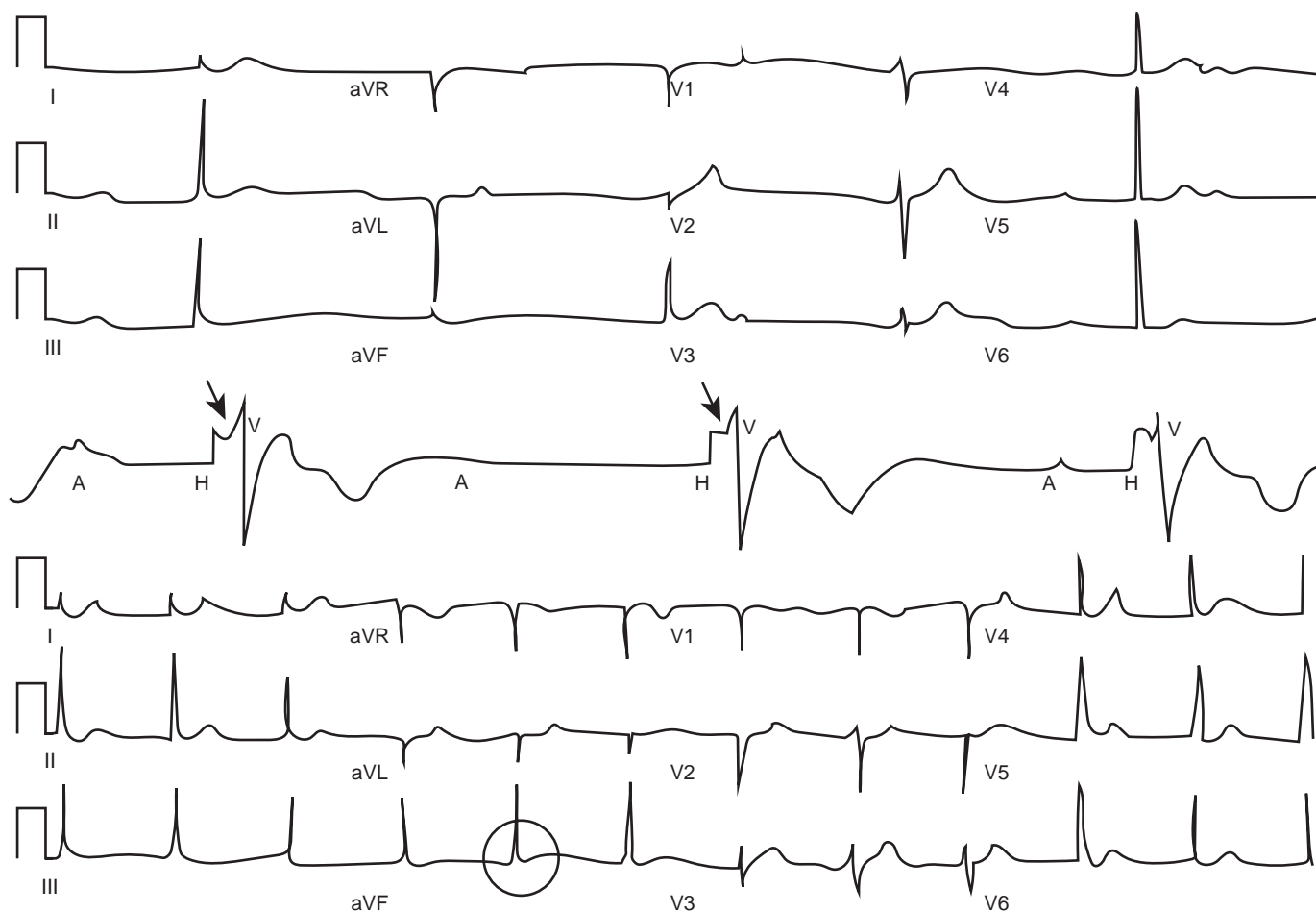


Fig. 9.29 Direct His Bundle Pacing. *Top*, The 12-lead electrocardiogram of a patient with complete heart block with narrow QRS escape rhythm. *Middle*, Intracardiac electrogram recorded from the permanent His bundle pacing lead at the time of implantation. Note the His bundle electrogram (H) with injury current (arrow) followed by ventricular electrogram (V). *Bottom*, His bundle pacing. The pacing spike (circle) is followed by an isoelectric interval of 40 milliseconds and QRS complexes identical to the intrinsic rhythm. (From Vijayaraman P, Naperkowski A, Ellenbogen KA, Dandamudi G. Electrophysiologic insights into site of atrioventricular block lessons from permanent His bundle pacing. *JACC Clin Electrophysiol*. 2015;1:571–581, with permission.)

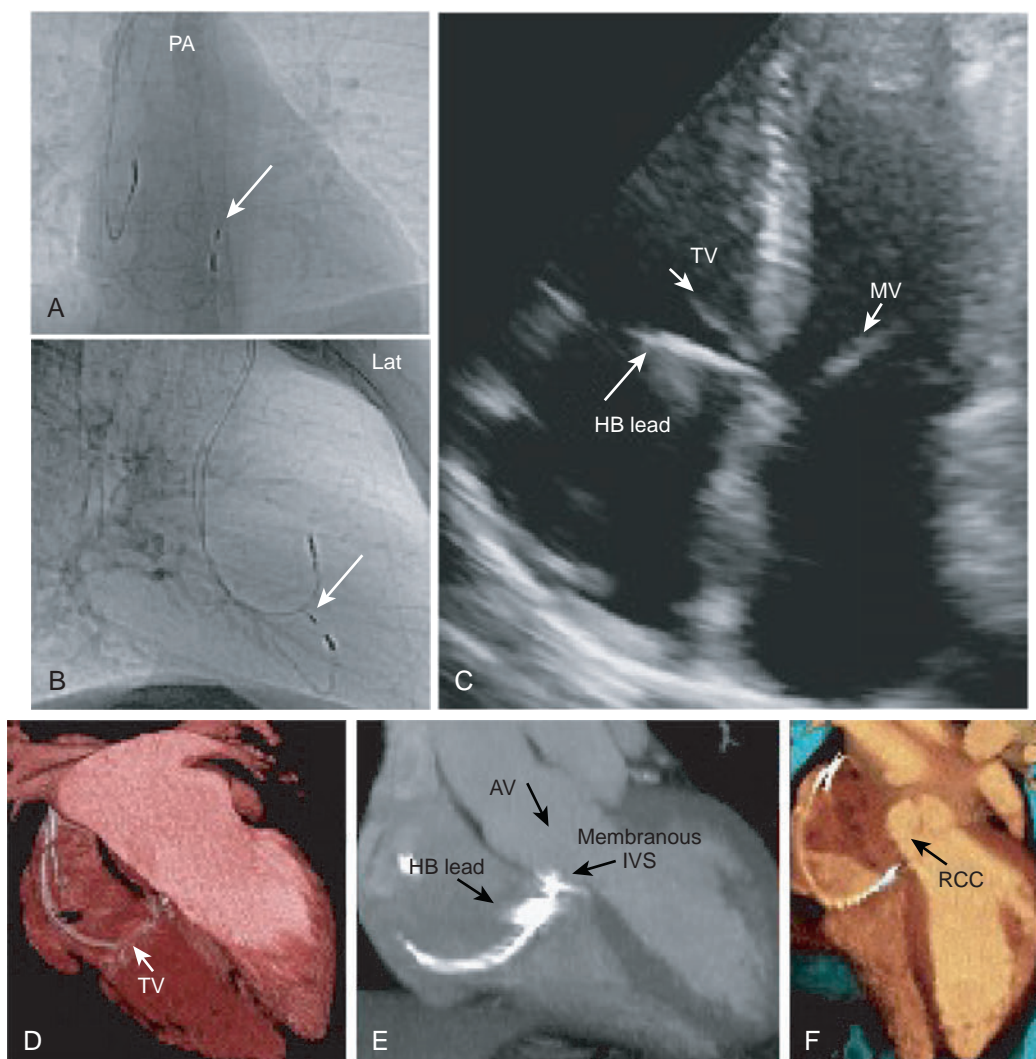


Fig. 9.30 Location of Direct His Bundle (HB) Pacing Lead. Images from chest x-ray (A–B), transthoracic echocardiography (C), and cardiac computed tomography (D–F) showing the location of the direct HB pacing lead. Note that the electrode position is above the plane of the tricuspid valve (TV), in the supraventricular portion of the membranous septum below the level of right coronary cusp of the aortic valve. AV, Atrioventricular; CT, computed tomography; IVS, interventricular septum; Lat, lateral; MV, mitral valve; PA, postero-anterior; RCC, right coronary cusp. (From Vijayaraman P, Dandamudi G, Bauch T, Ellenbogen KA. Imaging evaluation of implantation site of permanent direct His bundle pacing lead. *Heart Rhythm*. 2014;11:529–530, with permission.)

REFERENCES

1. Dobrzynski H, et al. Structure, function and clinical relevance of the cardiac conduction system, including the atrioventricular ring and outflow tract tissues. *Pharmacol Ther*. 2013;139:260–288.
2. Nikolaidou T, Aslanidi OV, Zhang H, et al. Structure-function relationship in the sinus and atrioventricular nodes. *Pediatr Cardiol*. 2012;33:890–899.
3. Chhabra L, Devadoss R, Chaubey VK, et al. Interatrial block in the modern era. *Curr Cardiol Rev*. 2014;10:181–189.
4. Teuwen CP, et al. Relevance of conduction disorders in Bachmann's bundle during sinus rhythm in humans. *Circ Arrhythm Electrophysiol*. 2016;9:e003972.
5. Faletra FF, Ho SY, Auricchio A. Anatomy of right atrial structures by real-time 3D transesophageal echocardiography. *JACC Cardiovasc Imaging*. 2010;3:966–975.
6. Lee P-C, Chen S-A, Hwang B. Atrioventricular node anatomy and physiology: implications for ablation of atrioventricular nodal reentrant tachycardia. *Curr Opin Cardiol*. 2009;24:105–112.
7. Kurian T, Ambrosi C, Hucker W, et al. Anatomy and electrophysiology of the human AV node. *Pacing Clin Electrophysiol*. 2010;33:754–762.
8. Syed FF, Hai JJ, Lachman N, et al. The infrahisian conduction system and endocavitary cardiac structures: relevance for the invasive electrophysiologist. *J Interv Card Electrophysiol*. 2014;39:45–56.
9. Dandamudi G, Vijayaraman P. The complexity of the His bundle: understanding its anatomy and physiology through the lens of the past and the present. *Pacing Clin Electrophysiol*. 2016;39:1294–1297.
10. Eliasson H, et al. Outcome in young patients with isolated complete atrioventricular block and permanent pacemaker treatment: a nationwide study of 127 patients. *Heart Rhythm*. 2015;12:2278–2284.
11. DE Caluwé E, et al. Long-term follow-up of children with heart block born from mothers with systemic lupus erythematosus: a retrospective

- study from the Database Pediatric and Congenital Heart Disease in University Hospitals Leuven. *Pacing Clin Electrophysiol.* 2016;39:935–943.
12. Lazzarini PE, Capecchi PL, Laghi-Pasini F. Isolated atrioventricular block of unknown origin in adults and anti-Ro/SSA antibodies: clinical evidence, putative mechanisms, and therapeutic implications. *Heart Rhythm.* 2015;12:449–454.
 13. Brugada J, et al. Pharmacological and non-pharmacological therapy for arrhythmias in the pediatric population: EHRA and AEPIC-Arrhythmia Working Group joint consensus statement. *Europace.* 2013;15:1337–1382.
 14. Khairy P, et al. PACES/HRS Expert Consensus Statement on the Recognition and Management of Arrhythmias in Adult Congenital Heart Disease: developed in partnership between the Pediatric and Congenital Electrophysiology Society (PACES) and the Heart Rhythm Society (HRS). *En. Heart Rhythm.* 2014;11:e102–e165.
 15. Baruteau A-E, Probst V, Abriel H. Inherited progressive cardiac conduction disorders. *Curr Opin Cardiol.* 2015;30:33–39.
 16. Milanesi R, Bucchi A, Baruscotti M. The genetic basis for inherited forms of sinoatrial dysfunction and atrioventricular node dysfunction. *J Interv Card Electrophysiol.* 2015;43:121–134.
 17. Priori SG, et al. HRS/EHRA/APHRS Expert Consensus Statement on the Diagnosis and Management of Patients with Inherited Primary Arrhythmia Syndromes. *Heart Rhythm.* 2013;10:1932–1963.
 18. Park DS, Fishman GI. The cardiac conduction system. *Circulation.* 2011;123:904–915.
 19. Brignole M, et al. ESC guidelines on cardiac pacing and cardiac resynchronization therapy: the task force on cardiac pacing and resynchronization therapy of the European Society of Cardiology (ESC). Developed in collaboration with the European Heart Rhythm Association. *Europace.* 2013;15:1070–1118.
 20. Gang UJO, et al. High-degree atrioventricular block complicating ST-segment elevation myocardial infarction in the era of primary percutaneous coronary intervention. *Europace.* 2012;14:1639–1645.
 21. Hari Krishnan P, et al. Complete heart block complicating ST-segment elevation myocardial infarction. *JACC Clin Electrophysiol.* 2015;1:529–538.
 22. Nguyen HL, et al. Thirty-year trends (1975–2005) in the magnitude and hospital death rates associated with complete heart block in patients with acute myocardial infarction: a population-based perspective. *Am Heart J.* 2008;156:227–233.
 23. Gorenk B, et al. Cardiac arrhythmias in acute coronary syndromes: position paper from the joint EHRA, ACCA, and EAPCI task force. *EuroIntervention.* 2015;10:1095–1108.
 24. Robinson ML, Kobayashi T, Higgins Y, et al. Lyme carditis. *Infect Dis Clin North Am.* 2015;29:255–268.
 25. Epstein AE, et al. 2012 ACCF/AHA/HRS focused update incorporated into the ACCF/AHA/HRS 2008 guidelines for device-based therapy of cardiac rhythm abnormalities: a report of the American College of Cardiology Foundation/American Heart Association Task Force on Practice Guide. *Circulation.* 2013;127:e283–e352.
 26. Nunes MCP, Dones W, Morillo CA, et al. Chagas disease: an overview of clinical and epidemiological aspects. *J Am Coll Cardiol.* 2013;62:767–776.
 27. Sekhri V, Sanal S, Delorenzo LJ, et al. Cardiac sarcoidosis: a comprehensive review. *Arch Med Sci.* 2011;7:546–554.
 28. Birnie DH, et al. HRS expert consensus statement on the diagnosis and management of arrhythmias associated with cardiac sarcoidosis. *Heart Rhythm.* 2014;11:1305–1323.
 29. Uberoi A, et al. Interpretation of the electrocardiogram of young athletes. *Circulation.* 2011;124:746–757.
 30. Gross GJ, Chiu CC, Hamilton RM, et al. Natural history of postoperative heart block in congenital heart disease: implications for pacing intervention. *Heart Rhythm.* 2006;3:601–604.
 31. Ayyildiz P, et al. Evaluation of permanent or transient complete heart block after open heart surgery for congenital heart disease. *Pacing Clin Electrophysiol.* 2015;39:160–165.
 32. Gersh BJ, et al. 2011 ACCF/AHA Guideline for the Diagnosis and Treatment of Hypertrophic Cardiomyopathy: a report of the American College of Cardiology Foundation/American Heart Association Task Force on Practice Guidelines. Developed in collaboration with the American Association for Thoracic Surgery, American Society of Echocardiography, American Society of Nuclear Cardiology, Heart Failure Society of America, Heart Rhythm Society, Society for Cardiovascular Angiography and Interventions, and Society of Thoracic Surgeons. *J Am Coll Cardiol.* 2011;58:e212–e260.
 33. Huynh H, et al. Permanent pacemaker implantation following aortic valve replacement: current prevalence and clinical predictors. *Pacing Clin Electrophysiol.* 2009;32:1520–1525.
 34. Leyva F, et al. Long-term requirement for pacemaker implantation after cardiac valve replacement surgery. *Heart Rhythm.* 2017;14:529–534.
 35. Siontis GCM, et al. Predictors of permanent pacemaker implantation in patients with severe aortic stenosis undergoing TAVR: a meta-analysis. *J Am Coll Cardiol.* 2014;64:129–140.
 36. Rivard L, et al. Electrocardiographic and electrophysiological predictors of atrioventricular block after transcatheter aortic valve replacement. *Heart Rhythm.* 2015;12:321–329.
 37. Dijk KB, et al. Predictors and permanency of cardiac conduction disorders and necessity of pacing after transcatheter aortic valve implantation. *Pace.* 2014;37:1–10.
 38. Ramazzina C, et al. Pacemaker implantation and need for ventricular pacing during follow-up after transcatheter aortic valve implantation. *Pacing Clin Electrophysiol.* 2014;37:1592–1601.
 39. Tovia-Brodie O, et al. The value of electrophysiologic study in decision-making regarding the need for pacemaker implantation after TAVI. *J Interv Card Electrophysiol.* 2017;48:121–130.
 40. Sheldon RS, et al. Heart Rhythm Society expert consensus statement on the diagnosis and treatment of postural tachycardia syndrome, inappropriate sinus tachycardia, and vasovagal syncope. *Heart Rhythm.* 2015;12:e41–e63.
 41. Brignole M, et al. Syncope due to idiopathic paroxysmal atrioventricular block: long-term follow-up of a distinct form of atrioventricular block. *J Am Coll Cardiol.* 2011;58:167–173.
 42. Brignole M, et al. Pacemaker therapy in patients with neurally mediated syncope and documented asystole: third international study on syncope of uncertain etiology (ISSUE-3): a randomized trial. *Circulation.* 2012;125:2566–2571.
 43. El-Sherif N, Jalife J. Paroxysmal atrioventricular block: are phase 3 and phase 4 block mechanisms or misnomers? *Heart Rhythm.* 2009;6:1514–1521.
 44. Lee S, Wellens HJJ, Josephson ME. Paroxysmal atrioventricular block. *Heart Rhythm.* 2009;6:1229–1234.
 45. Brignole M, Deharo JC, Guieu R. Syncope and idiopathic (paroxysmal) AV block. *Card Electrophysiol Clin.* 2013;5:487–493.
 46. Brignole M, et al. Mechanism of syncope without prodromes with normal heart and normal electrocardiogram. *Heart Rhythm.* 2016;14:234–239.
 47. Cho MS, et al. Electrocardiographic predictors of bradycardia-induced torsades de pointes in patients with acquired atrioventricular block. *Heart Rhythm.* 2015;12:498–505.
 48. Magnani JW, et al. Electrocardiographic PR interval and adverse outcomes in older adults: the Health, Aging, and Body Composition study. *Circ Arrhythm Electrophysiol.* 2013;6:84–90.
 49. Nikolaidou T, Ghosh JM, Clark AL. Outcomes related to first-degree atrioventricular block and therapeutic implications in patients with heart failure. *JACC Clin Electrophysiol.* 2016;2:181–192.
 50. Spodick DH, Ariyaratnam V. Interatrial block: the pandemic remains poorly perceived. *Pacing Clin Electrophysiol.* 2009;32:667–672.
 51. Nelson WP. Diagnostic and prognostic implications of surface recordings from patients with atrioventricular block. *Card Electrophysiol Clin.* 2016;8:25–35.
 52. Bonner AJ, Zipes DP. Lidocaine and His bundle extrasystoles. His bundle discharge conducted with functional right of left bundle-branch block, or blocked entirely (concealed). *Arch Intern Med.* 1976;136:700–704.
 53. Vijayaraman P, Naperkowski A, Ellenbogen KA, et al. Electrophysiologic insights into site of atrioventricular block: lessons from permanent His bundle pacing. *JACC Clin Electrophysiol.* 2015;1:571–581.
 54. Gillis AM, et al. HRS/ACCF expert consensus statement on pacemaker device and mode selection. *J Am Coll Cardiol.* 2012;60:682–703.

55. Khurshid S, et al. Incidence and predictors of right ventricular pacing-induced cardiomyopathy. *Heart Rhythm*. 2014;11:1619–1625.
56. Kaye GC, et al. Effect of right ventricular pacing lead site on left ventricular function in patients with high-grade atrioventricular block: results of the Protect-Pace study. *Eur Heart J*. 2015;36:856–862.
57. Hussain MA, Furuya-Kanamori L, Kaye G, et al. The effect of right ventricular apical and nonapical pacing on the short- and long-term changes in left ventricular ejection fraction: a systematic review and meta-analysis of randomized-controlled trials. *Pacing Clin Electrophysiol*. 2015;38:1121–1136.
58. Arenas IA, Jacobson J, Lamas GA. Routine use of biventricular pacing is not warranted for patients with heart block. *Circ Arrhythmia Electrophysiol*. 2015;8:730–737.
59. Kiehl EL, et al. Incidence and predictors of right ventricular pacing-induced cardiomyopathy in patients with complete atrioventricular block and preserved left ventricular systolic function. *Heart Rhythm*. 2016;13:2272–2278.
60. Curtis AB, et al. Biventricular pacing for atrioventricular block and systolic dysfunction. *N Engl J Med*. 2013;368:1585–1593.
61. Fang F, Sanderson JE, Yu CM. All heart block patients with a pacemaker indication should receive biventricular pacing: one move, double the gains? *Circ Arrhythmia Electrophysiol*. 2015;8:722–728.
62. Vijayaraman P, Dandamudi G, Bauch T, et al. Imaging evaluation of implantation site of permanent direct His bundle pacing lead. *Heart Rhythm*. 2014;11:529–530.
63. Sharma PS, et al. Permanent His-bundle pacing is feasible, safe, and superior to right ventricular pacing in routine clinical practice. *Heart Rhythm*. 2015;12:305–312.
64. Dandamudi G, Vijayaraman P. How to perform permanent His bundle pacing in routine clinical practice. *Heart Rhythm*. 2016;13:1–5.
65. Vijayaraman P, Dandamudi G. How to perform permanent His bundle pacing: tips and tricks. *Pacing Clin Electrophysiol*. 2016;39:1298–1304.
66. Sharma PS, Ellenbogen KA, Trohman RG. Permanent His bundle pacing: the past, present and future. *J Cardiovasc Electrophysiol*. 2017;28:458–465.

Intraventricular Conduction Abnormalities

OUTLINE

Transient Bundle Branch Block, 286

- Acceleration-Dependent Bundle Branch Block, 286
- Pause-Dependent Bundle Branch Block, 289
- Aberration Caused by Concealed Transseptal Conduction, 291

Chronic Bundle Branch Block, 293

- Anatomy and Physiology of the His-Purkinje System, 293
- Pathophysiology of His-Purkinje System Disease, 294
- Clinical Significance, 295

Electrocardiographic Features, 295

- Bundle Branch Block, 295
- Fascicular Block, 298
- Other Types of Intraventricular Conduction Abnormalities, 299

Electrophysiological Testing, 300

- Baseline Intervals, 300
- Diagnostic Maneuvers, 301
- Role of Electrophysiological Testing, 303

Normally, the entire mass of ventricular myocardium is depolarized in about 80 to 100 milliseconds. This requires highly synchronous electrical activation of the ventricular myocardium, which can be achieved only through the rapidly conducting His-Purkinje system (HPS). The term *intraventricular conduction disturbances* (IVCDs) refers to abnormalities in the intraventricular propagation of supraventricular impulses resulting in changes in the morphology and/or duration of the QRS complex. These changes in intraventricular conduction can be fixed and present at all heart rates, or they can be intermittent (transient). They can be caused by structural abnormalities in the HPS or ventricular myocardium, functional refractoriness in a portion of the conduction system (i.e., aberrant ventricular conduction), or ventricular preexcitation over a bypass tract.¹

TRANSIENT BUNDLE BRANCH BLOCK

The term *aberration* is used to describe transient bundle branch block (BBB) and usually does not include persistent QRS abnormalities caused by persistent BBB, preexcitation, or the effect of drugs. Transient BBB can have several mechanisms, including acceleration-dependent block, pause-dependent block, and concealed conduction. These mechanisms of aberration can occur anywhere in the HPS and, unlike in chronic BBB, the site of block during aberration can shift. Right bundle branch block (RBBB) is the most common pattern of aberration, perhaps in part due to the thin nature of its anatomy, occurring in 80% of patients with aberration and in up to 100% of cases of aberration in normal hearts.

Acceleration-Dependent Bundle Branch Block

Conduction velocity depends, in part, on the rate of rise of phase 0 (dV/dt) of the action potential and the height to which it rises. These factors, in turn, depend on the membrane potential at the time of stimulation. The more negative the membrane potential, the more sodium (Na^+) channels are available for activation, allowing for a greater influx of Na^+ into the cell during phase 0 and, hence, larger action potential amplitude, fast depolarizing Na^+ current, and faster conduction velocity.²

On the other hand, when stimulation occurs during phase 3 of the action potential, before full voltage recovery and at less negative

transmembrane potentials, a portion of Na^+ channels is still refractory and unavailable for activation. Consequently, the Na^+ current and phase 0 of the action potential are reduced, and the resulting action potential has slower conduction properties and is more susceptible to conduction block (Fig. 10.1).

“Phase 3 block” (also called “voltage-dependent block”) occurs when an impulse arrives at tissues that are still refractory due to incomplete repolarization. Functional or physiological phase 3 aberration can occur in normal fibers if the impulse is sufficiently premature to encroach on the physiological refractory period of the preceding beat. This is commonly seen with a premature atrial complex (PAC) with a very short coupling interval that attempts to depolarize the HPS during phase 3 of the action potential and, hence, is conducted aberrantly, most often with RBBB.²

Manifestations of phase 3 block include BBB and fascicular block, as well as complete atrioventricular (AV) block. Transient left bundle branch block (LBBB) is less common than RBBB (only 25% of phase 3 aberration is of the LBBB type). The block usually occurs in the very proximal portion of the right bundle (RB). Phase 3 block constitutes the physiological explanation of several phenomena, including aberration caused by premature excitation, Ashman phenomenon, and acceleration-dependent aberration.

Importantly, in the presence of HPS disease, the mechanism of acceleration-dependent aberration may no longer be related to phase 3 block. In this setting, aberration can be precipitated by premature or shorter-coupled impulses occurring well after completion of phase 3 of the action potential. This type of block or aberrancy is usually a sign of conduction system disease. In normal myocardial cells, recovery of electrical excitability coincides in time with voltage recovery, that is, the end of the action potential. The resting membrane potential remains polarized throughout diastole. In contrast, under pathological conditions (e.g., ischemia, hyperkalemia, hypoxemia, acidosis), cardiomyocytes can have a less negative resting membrane potential. Hence, a portion of Na^+ channels remains closed and unavailable for activation throughout diastole. This results in reduced upstroke velocity and smaller amplitude of the action potential. At more depolarized resting potentials, the Na^+ current cannot be activated, though a strong stimulus can still induce a “slow response” action potential carried out by the slowly depolarizing calcium current. The “slow response” is characterized by slow conduction

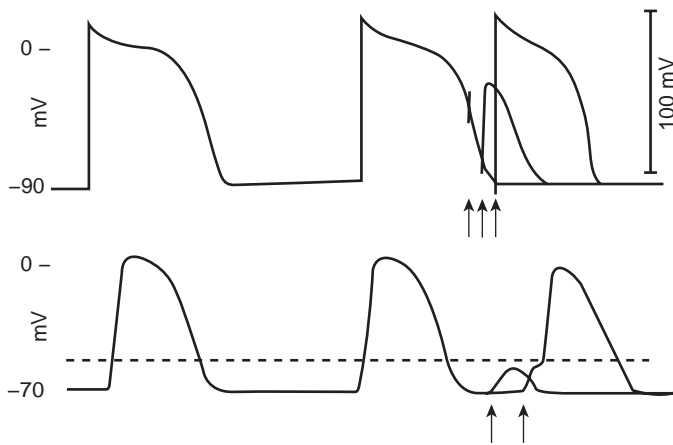


Fig. 10.1 Mechanisms of Transient Bundle Branch Block. Diagrammatic illustration of the responses of a normal ventricular myocyte action potential (AP, *top*) and a depressed AP (*bottom*) to premature stimulation. *Top*, So-called phase 3 or voltage-dependent refractoriness. The first stimulus (arrow) falls on an early phase 3 and fails to elicit a response. The second stimulus falls in late phase 3 and results in an abbreviated, slowly rising AP of low amplitude. The third stimulus that falls at the end of repolarization results in a full AP. The bottom recording illustrates postrepolarization refractoriness (arrows) in a depressed fiber. Because of delayed recovery of excitability, despite full repolarization after the second action potential, a depolarizing stimulus applied very early in diastole is incapable of bringing the cell to the threshold potential (broken horizontal line). Thus the stimulus fails, and only a subthreshold depolarization is seen. When a similar stimulus is applied later in diastole, the cell is activated after a substantial delay. (From El-Sherif N, Jalife J. Paroxysmal atrioventricular block: are phase 3 and phase 4 block mechanisms or misnomers? *Heart Rhythm*. 2009;6:1514–1521.)

properties and refractoriness that can extend beyond the end of the action potential, a phenomenon known as “post-repolarization refractoriness.” As a result, a premature stimulus occurring during the early phase of diastole may fail to trigger a propagating action potential and, hence, manifest as block or aberration. Furthermore, the diseased HPS cells with depressed resting membrane potential are vulnerable to the phenomenon of concealed conduction and rate-dependent repetitive conduction block (see below), which can also mediate, at least in part, acceleration-dependent block.^{2,3}

Aberration Caused By Premature Excitation

Premature excitation can cause aberration by encroaching on the refractory period of the bundle branch prior to full recovery of the action potential, namely during so-called voltage-dependent refractoriness (see Fig. 4.28). In normal hearts, this type of aberration is almost always in the form of RBBB (Fig. 10.2), whereas such aberration in the abnormal heart can be that of RBBB or LBBB.

At normal heart rates, the effective refractory period (ERP) of the RB exceeds that of the atrioventricular node (AVN), His bundle (HB), and left bundle (LB). At faster heart rates, the ERP of both bundle branches shortens. However, RB ERP shortens to a greater degree than LB ERP, so that the duration of the refractory periods of the two bundles crosses over, and LB ERP becomes longer than that of the RB. This explains the tendency of aberration to be in the form of RBBB when premature excitation occurs during normal heart rates and in the form of LBBB when it occurs during fast heart rates.

Ashman Phenomenon

The Ashman phenomenon refers to aberration occurring when a short cycle follows a long one (long-short cycle sequence) (Fig. 10.3). Aberrancy is caused by the physiological changes of the conduction system

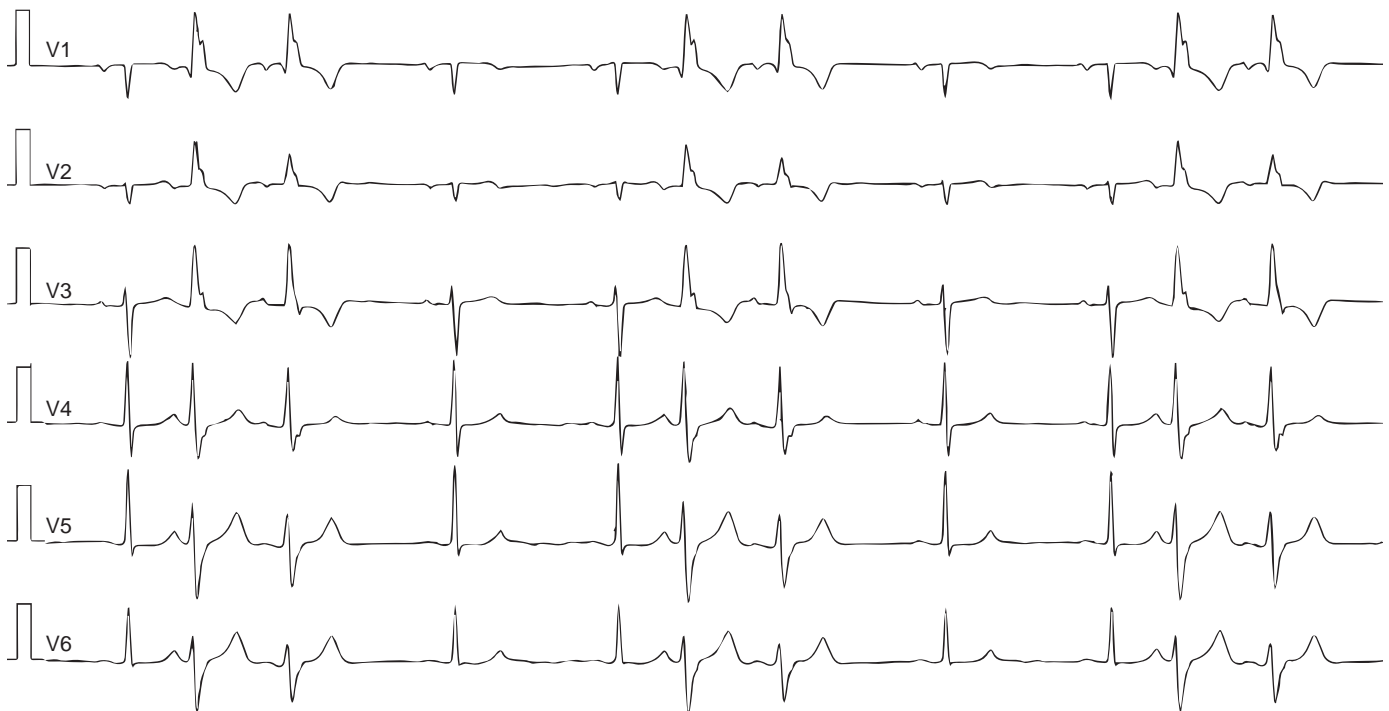


Fig. 10.2 Aberrantly Conducted Premature Atrial Complexes. Sinus rhythm with atrial couplets. Note that the premature atrial complexes are conducted with right bundle branch block aberrancy (phase 3 block).

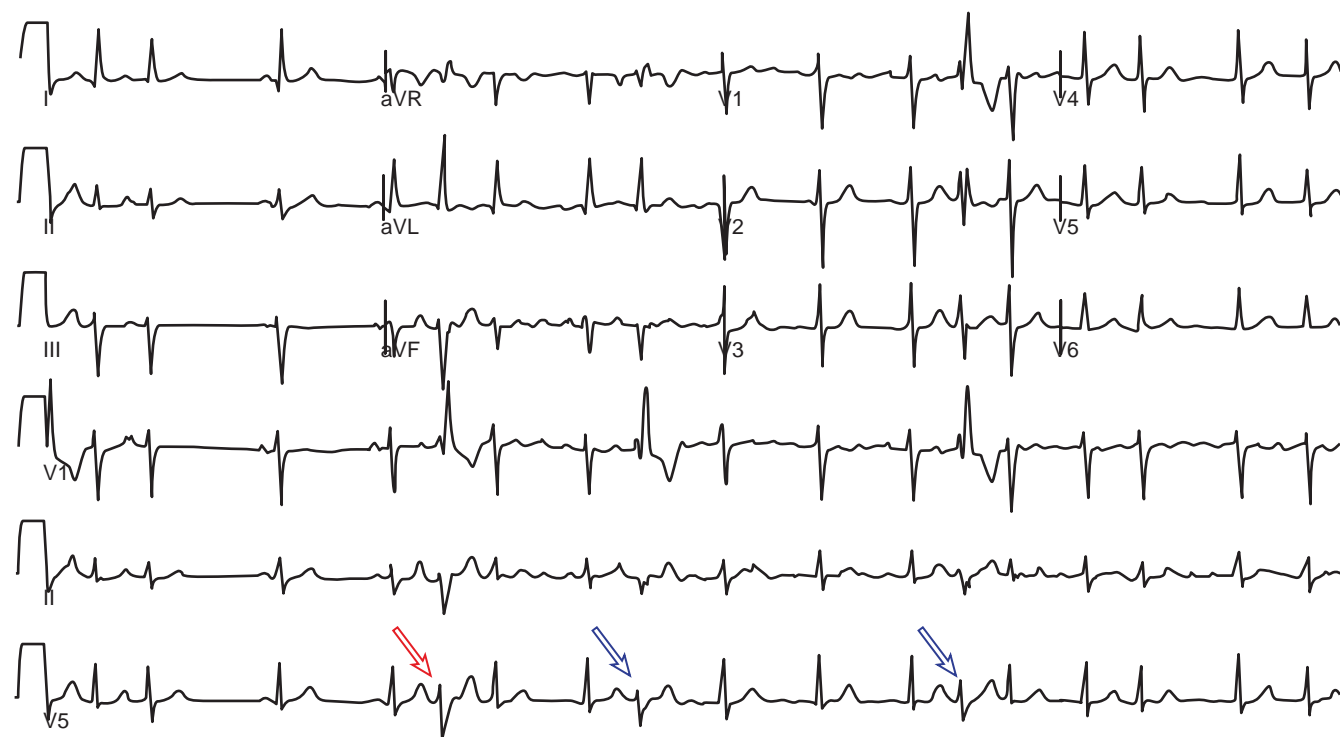


Fig. 10.3 Ashman Phenomenon. A premature atrial complex (PAC, red arrow) during sinus rhythm induces atrial fibrillation (AF). Note that the PAC is conducted with right bundle branch block (RBBB) aberrancy (phase 3 block). During AF, long-short cycle sequences occur repeatedly and are associated with RBBB aberrancy (Ashman phenomenon, phase 3 block). Note that the aberrantly conducted complex (blue arrows) during AF occurs at variable coupling intervals to the preceding beats.

refractory periods associated with the R-R interval. Normally, the refractory period of the HPS lengthens as the heart rate slows and shortens as the heart rate increases, even when heart rate changes are abrupt. Thus, aberrant conduction can result when a short cycle follows a long R-R interval. In this scenario, the QRS complex that ends the long pause (i.e., long R-R interval) is conducted normally but creates a prolonged ERP of the bundle branches. If the next supraventricular impulse approaches the bundle branches after a short coupling interval, it may be conducted aberrantly because one of the bundles is still refractory as a result of a lengthening of the refractory period following the immediately preceding QRS (phase 3 block) (eFig. 10.1). RBBB aberration is more common than LBBB in this setting because at heart rates usually present, the RB has a longer ERP than the LB.

The Ashman phenomenon can occur during second-degree AV block (see eFig. 9.3), but it is most common during atrial fibrillation (AF), in which it was originally described, whereby the irregularity of the ventricular response results in frequently occurring long-short cycle sequences. Of note, aberration caused by the Ashman phenomenon can persist for several cycles. The persistence of aberration can reflect a time-dependent adjustment of refractoriness of the bundle branch to the abrupt change in cycle length (CL), or it can be the result of concealed transseptal activation (see later).

The aberrancy can be present for one beat and have a morphology resembling a premature ventricular complex (PVC), or it can involve several sequential complexes, mimicking ventricular tachycardia (VT). In the setting of aberrancy during AF, the mere “long-short cycle sequence” characteristic of the Ashman phenomenon may not be helpful in differentiating aberration from ventricular ectopy. Although a long cycle (pause) sets the stage for the Ashman phenomenon, it also tends to precipitate ventricular ectopy. Furthermore, concealed conduction

TABLE 10.1 Distinguishing Aberrantly Conducted Complexes from Premature Ventricular Complexes During Atrial Fibrillation		
	Aberration	Premature Ventricular Complexes
Onset sequence	Long-short	Short-long
Rate parity between periods of wide versus narrow QRS complexes	Similar rates	Different rates
Coupling intervals from prior narrow QRS complexes	Variable over several occurrences	Same or similar over several occurrences
Regularity of consecutive wide QRS complexes	Irregular	Relatively regular
Fusion complexes	Absent	May be present

occurs frequently during AF and therefore it is never possible to know from the surface electrocardiogram (ECG) exactly when a bundle branch is activated. Thus, if an aberrant beat does end a long-short cycle sequence during AF, it can be because of refractoriness of a bundle branch secondary to concealed conduction into it, rather than because of changes in the length of the ventricular cycle.

Nevertheless, there are several features of ventricular ectopy that can help distinguish a PVC from an aberrantly conducted “Ashman beat” during AF (Table 10.1). PVCs are usually followed by a longer R-R cycle, indicating the occurrence of a compensatory pause, the result

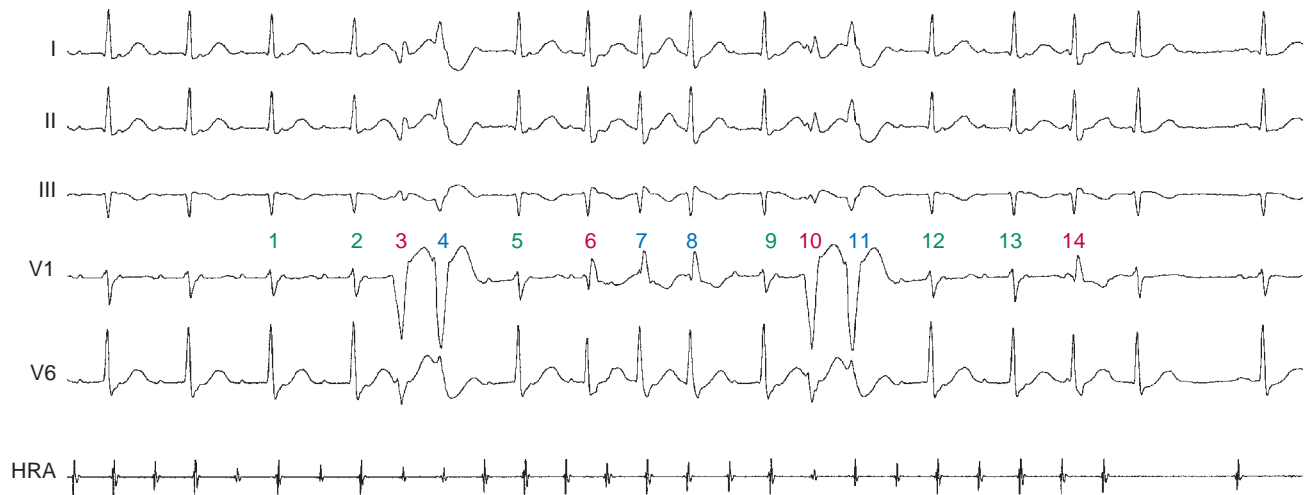


Fig. 10.1 Atrial Tachycardia With Variable Atrioventricular Conduction and Intermittent Aberrancy. Left, atrial tachycardia (AT) with 2:1 atrioventricular (AV) conduction and normal QRS morphology is observed. Once 1:1 AV conduction occurs (QRS 3), left bundle branch block (LBBB) aberration develops (caused by long-short cycle sequence, phase 3 block). LBBB aberration is also observed during QRS 4, likely secondary to concealed transseptal conduction causing perpetuation of aberration. After a pause, both bundle branches recover from refractoriness producing a normal QRS 5. Ashman phenomenon (long-short cycle sequence) explains phase 3 block during QRS 6, but this time it manifests as a right bundle branch block (RBBB) pattern. This is because activation during QRS 4 propagated down the right bundle branch (RB) and across the septum, thus activating the left bundle branch (LB) retrogradely after some delay (concealed transseptal conduction), so that the LB-LB interval (between QRS 4 and QRS 5) resulted in a shorter effective refractory period (ERP) of the LB following QRS 5. Conversely, the RB-RB interval (between QRS 4 and QRS 5) was longer and, consequently, the ERP of the RB was still prolonged following QRS 5, thereby setting the stage for a long-short cycle sequence of the RB but not the LB. Therefore, RBBB (rather than LBBB) aberration develops. RBBB aberration during QRS complexes 7 and 8 is secondary to either concealed transseptal conduction or rate-dependent aberration. However, because LBBB (rather than RBBB) was observed during QRS 4 (although QRS 4 occurred following a similar cycle length to that of QRS 8), concealed transseptal conduction is more likely to be the mechanism of aberration. After a pause, both bundle branches recover from refractoriness to produce a normal QRS 9. Long-short cycle sequence explains phase 3 block during QRS 10, but this time it manifests as LBBB. This is because activation during QRS 8 propagated down the LB and across the septum, thus activating the RB after some delay (concealed transseptal conduction). The result is that the RB-RB interval (following QRS 8) and ERP of the RB became shorter, whereas the LB-LB interval (following QRS 8) was longer. Consequently, the ERP of the LB was still prolonged following QRS 9, thereby setting the stage for a long-short cycle sequence and LBBB aberration. LBBB aberration during QRS 11 is caused by concealed transseptal conduction. The Ashman phenomenon (long-short cycle sequence) underlies RBBB aberration during QRS 14. *HRA*, High right atrium.

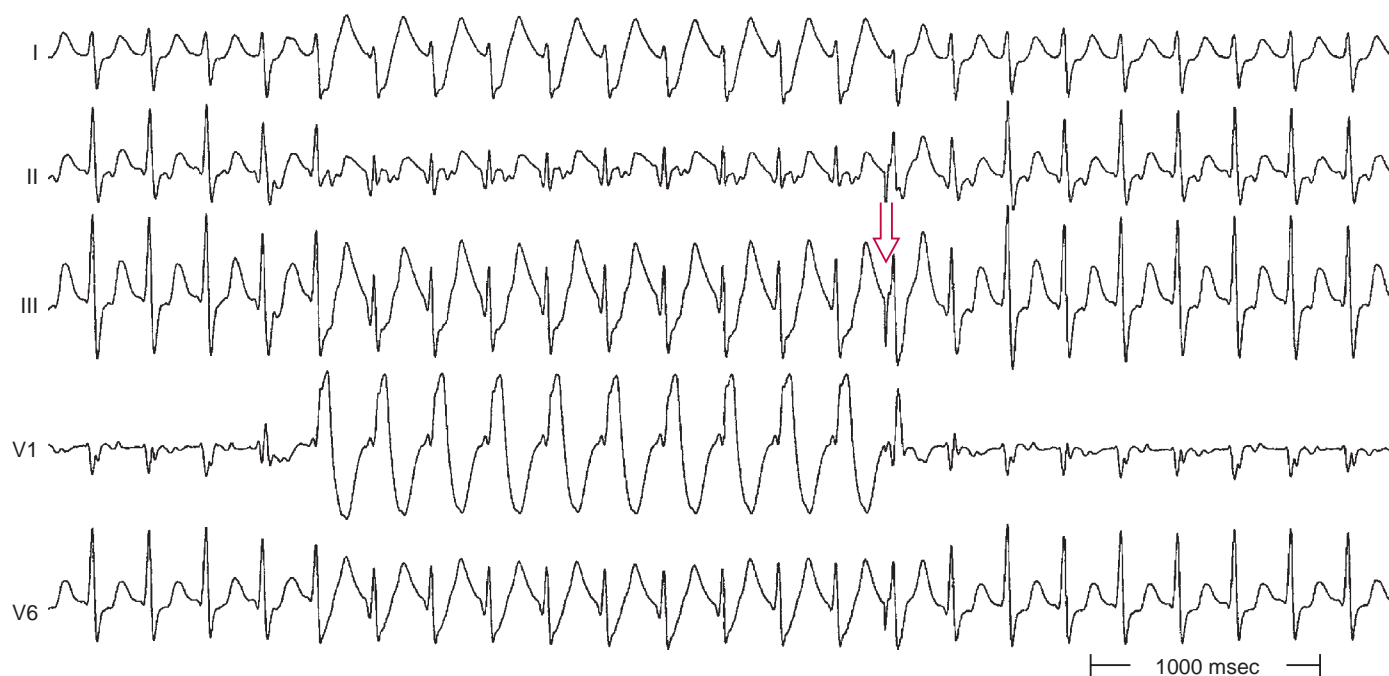


Fig. 10.4 Tachycardia-dependent (Phase 3) Block. The tracing shows sustained supraventricular tachycardia. Initially, the QRS is of normal morphology. Tachycardia-dependent (phase 3) right bundle branch block develops in the middle of the tracing and is sustained for a few beats. Delivery of a late ventricular extrastimulus (arrow) during the tachycardia preexcites the right bundle branch (and either peels back or shortens its refractoriness) and restores normal conduction.

of retrograde conduction into the AVN and anterograde block of the impulse originating in the atrium. Hence, the presence of consistently long R-R cycles after the aberrated beats is suggestive of PVCs. A ventricular origin is also likely when there is a fixed coupling cycle between the normal and aberrant QRS complexes. Additionally, the absence of aberrancy despite the presence of comparable long-short cycle sequences elsewhere in the rhythm recording argues against aberrancy and is more consistent with ventricular ectopy. Finally, QRS morphology inconsistent with LBBB or RBBB aberrancy argues against aberration and is consistent with ventricular origin of the QRS complex (eFig. 10.2).

Aberration Caused by Heart Rate Acceleration

As the heart rate accelerates, the HPS refractory period shortens allowing for normal 1:1 conduction at the faster atrial rate. However, refractoriness of the HPS eventually reaches a critical value beyond which it can no longer shorten in response to a further increase in the atrial rate; at this point, BBB or AV block can occur. Acceleration-dependent BBB is a result of failure of the action potential of the bundle branches to shorten in response to acceleration of the heart rate (Fig. 10.4). As noted previously, the ERP of the RB normally shortens at faster heart rates to a greater degree than that of the LB; this finding explains the more frequent RBBB aberration at longer CLs (i.e., at slower heart rates) and LBBB aberration at shorter CLs.

Notably, during slowing of the heart rate, intraventricular conduction often fails to normalize at the critical CL, and aberration persists at cycles longer than the critical cycle that initiated the aberration. Once acceleration-dependent BBB is established, the actual cycle for the blocked bundle does not begin until approximately halfway through the QRS complex because of concealed transseptal conduction (see later); thus, it is necessary for the heart rate to slow down more than would be expected to reestablish normal conduction.

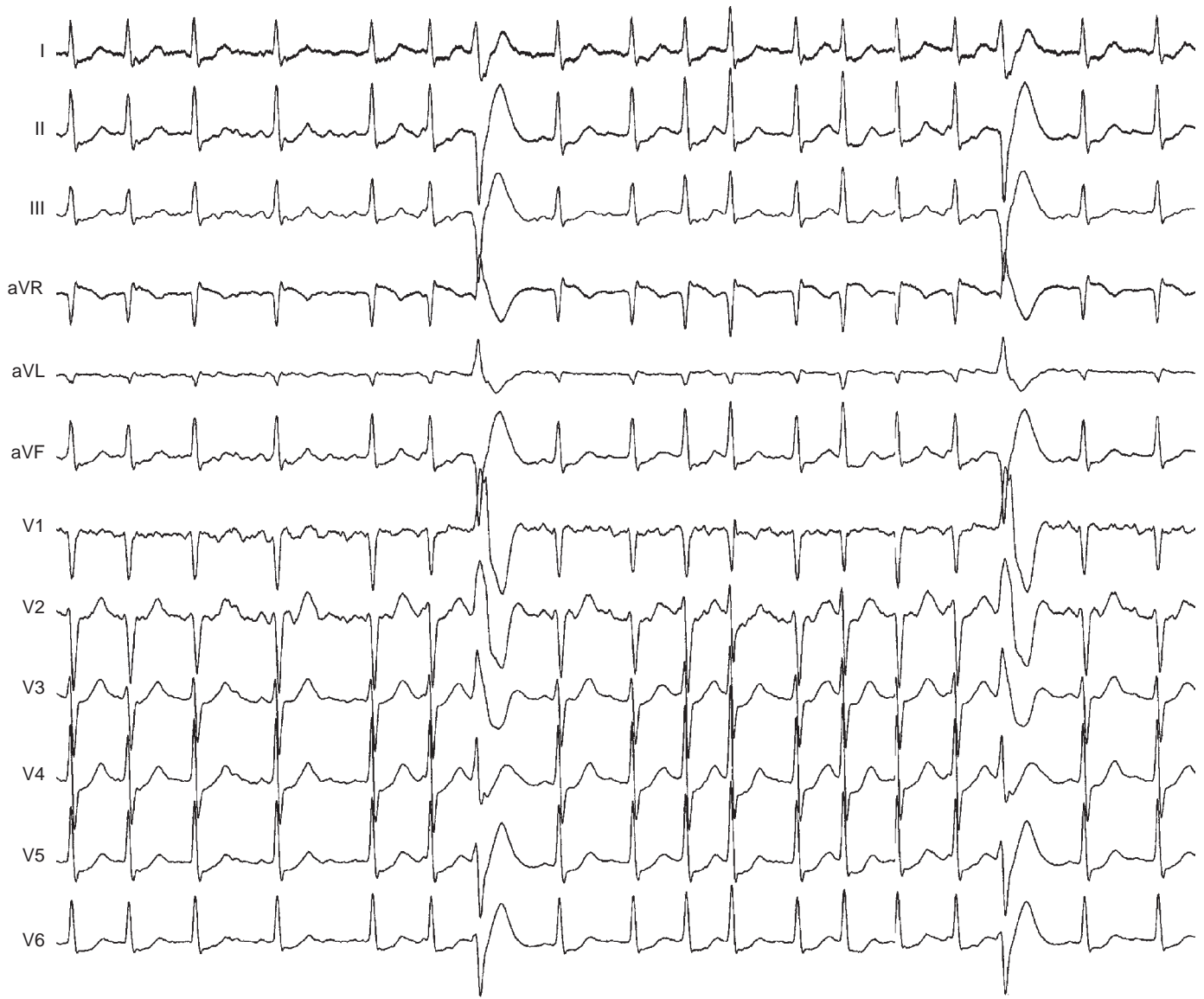
Occasionally, with increasing heart rate or persistence of fast heart rate, acceleration-dependent aberration can disappear. The normalization of a previously aberrant QRS complex can be explained by shortening of the ERP of the bundle branches to a greater degree than that of the AVN, by a time-dependent gradual shortening of the refractory period of the affected bundle branch (a phenomenon occasionally referred to as “restitution”), or by the loss of transseptal concealed conduction.

Importantly, acceleration-dependent aberration is a marker of a diseased HPS when it (1) appears at relatively slow heart rates (less than 70 beats/min); (2) displays LBBB (Fig. 10.5); (3) appears after several cycles of accelerated but regular rate; or (4) appears with gradual rather than abrupt acceleration of the heart rate.²

Pause-Dependent Bundle Branch Block

Pause-dependent (or bradycardia-dependent) block occurs when conduction of an impulse is blocked in tissues well after their normal refractory periods have ended. Phase 4 aberration is one explanation for the development of aberration at the end of a long cycle (i.e., after a pause). Phase 4 block is governed by the same physiological principles as those for phase 3 block. Membrane responsiveness is determined by the relationship of the membrane potential at excitation with the maximum rate of rise of phase 0. The availability of the Na⁺ channels is reduced at less negative membrane potentials, and activation at a reduced membrane potential is likely to cause aberration or block. The cause of membrane depolarization (i.e., reduction of membrane potential) in the setting of phase 4 block, however, is different from that in phase 3 block.^{2,4}

Phase 4 or diastolic depolarization is a property of pacemaker cells of the heart; normal His-Purkinje fibers do not possess this property at rates faster than 40 beats/min; however, diseased Purkinje cells can



eFig. 10.2 Premature Ventricular Complexes During Atrial Fibrillation. Several features suggest that the wide QRS complexes are caused by ventricular ectopy rather than aberration. QRS morphology is inconsistent with either left bundle branch block or right bundle branch block aberrancy. Additionally, there is a fixed coupling interval between the normal and aberrant QRS complex. The absence of a long-short cycle sequence associated with the wide QRS complex and the absence of aberrancy despite the presence of R-R cycle length combinations elsewhere in the tracing that are longer and shorter than those associated with the wide QRS complex also suggest ventricular ectopy.



Fig. 10.5 Acceleration-dependent Aberration. The lead II continuous rhythm strip demonstrates sinus rhythm with rate-related left bundle branch block (LBBB). Note that small changes in rate can result in acceleration-dependent aberration. LBBB develops at a sinus rate faster than 70 beats/min, and normal QRS complexes are observed at slower sinus rates. The LBBB and the slow rate at which aberration develops strongly suggest an abnormality in the left bundle branch (LB), rather than physiological aberration, which is often associated with underlying structural heart disease such as cardiomyopathy. Interestingly, the onset and offset of the LBBB demonstrate hysteresis in that the cycle length (CL) required to initiate the LBBB is shorter than the CL required to maintain it, probably because of retrograde concealed penetration of the LB.

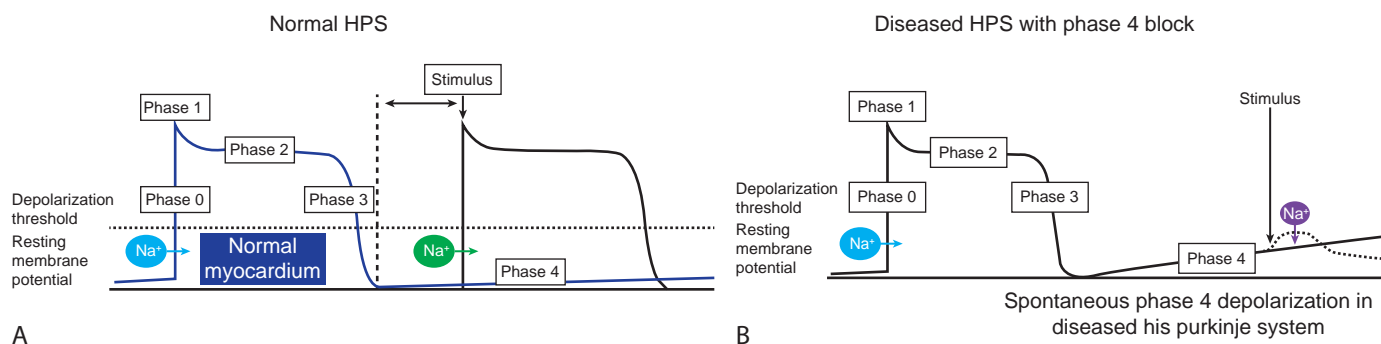


Fig. 10.6 Action Potentials in Normal (A) and Diseased (B) Conduction Systems Showing Phase 4 Block. Spontaneous diastolic depolarization during phase 4 in the diseased His-Purkinje system results in reduced availability of sodium channels during the next depolarization, and the resulting action potential cannot propagate the impulse. (From Divakara Menon SM, Ribas CS, Ribas Meneclier CA, Morillo CA. Intermittent atrioventricular block: what is the mechanism? *Heart Rhythm*. 2012;9:154–155, with permission.)

acquire the property of phase 4 depolarization at more rapid rates. Enhanced phase 4 depolarization within the bundle branches can be caused by enhanced automaticity or partial depolarization of injured myocardial tissue. In this setting, the maximum diastolic potential immediately follows repolarization, from which point the membrane potential steadily depolarizes (becomes less negative). This reduction in membrane potential, in turn, causes inactivation of some Na^+ channels. Thus, an action potential initiated early in the cycle (immediately after repolarization) would have a steeper and higher phase 0 and consequently better conduction than would an action potential initiated

later in the cycle when the membrane potential at the time of the stimulus is reduced, with resulting slower upstroke velocity and smaller amplitude of the action potential and, hence, slower conduction or block (Fig. 10.6). Phase 4 aberration is “pause-dependent” because the pause allows for spontaneous depolarization and, hence, the cell is activated from a less negative potential, and the result is impaired conduction (Fig. 10.7). The critical prolongation of the input stimulus is typically initiated by a compensatory pause after a PAC or PVC, spontaneous slowing of the sinus rate, or overdrive suppression of sinus rhythm upon termination of a fast supraventricular rhythm. Once such

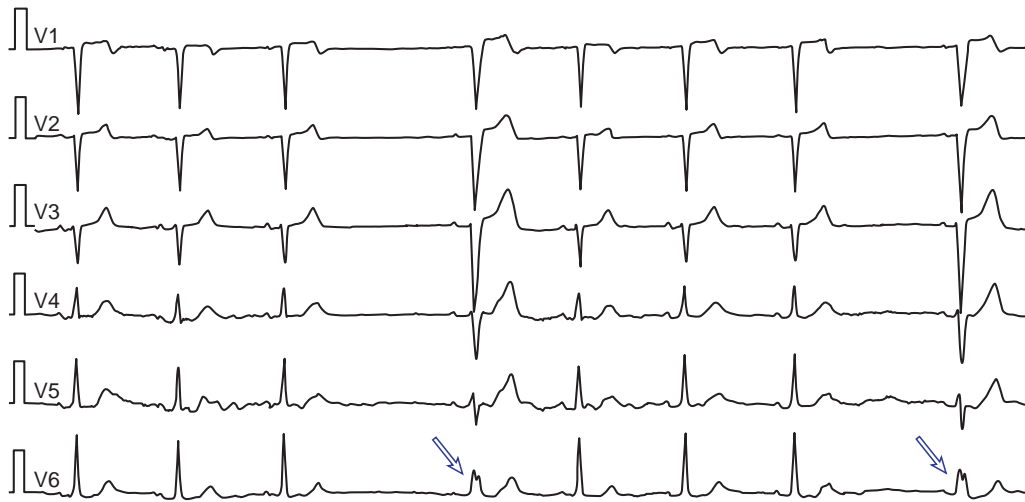


Fig. 10.7 Bradycardia-dependent Block. Normal intraventricular conduction is observed during sinus rhythm. Premature atrial complexes (hidden within the T waves) are not conducted to the ventricles, resulting in pauses. The sinus complex following the pause is conducted with left bundle branch block pattern (arrows) presumably secondary to phase 4 block.

critical diastolic membrane potential is reached (at which Na^+ channel inactivation occurs), subsequent conduction may no longer resume until a well-timed escape beat or premature beat (sinus or ectopic) resets the transmembrane potential to its excitable state. The extent of depolarization has to be significant because lesser amounts of depolarization improves excitability (membrane voltage closer to the threshold voltage) and should improve conduction.^{2,5,6}

Despite the fact that bradycardia is common and cells with phase 4 depolarization are abundant, phase 4 block is not commonly seen in normal myocardial tissue. In fact, most reported cases are associated with structural heart disease. One explanation for this phenomenon is that in normal fibers, conduction is well maintained at membrane potentials more negative than -70 to -75 mV. Significant conduction disturbances are first manifested when the membrane potential is less negative than -70 mV at the time of stimulation; local block appears at -65 to -60 mV. Because the threshold potential for normal His-Purkinje fibers is -70 mV, spontaneous firing occurs before the membrane can actually be reduced to the potential necessary for conduction impairment or block. In fact, in the latter setting, mild membrane depolarization can actually improve conduction because the membrane potential is moved closer to threshold potential. Phase 4 block is therefore pathological when it does occur, and it requires one or more of the following: (1) the presence of slow diastolic depolarization, which needs to be enhanced (i.e., occurring at rates faster than these cells normally spontaneously depolarize); (2) a decrease in excitability (a shift in threshold potential toward zero) so that, in the presence of significant bradycardia, sufficient time elapses before a new stimulus arrives, thus enabling the bundle branch fibers to reach a potential at which conduction is impaired; and (3) a deterioration in membrane responsiveness so that significant conduction impairment develops at -75 mV instead of -65 mV; this occurrence would also negate the necessity for such a long cycle before conduction fails. Also, it is important to recognize that, in some cases, pause-dependent aberrancy may be caused by other mechanisms (e.g., source-to-sink mismatch) that may not be related to phase 4 depolarization.^{2,5}

Pause-dependent or phase 4 block almost always manifests an LBBB pattern, likely because the left ventricle (LV) conduction system is more susceptible to ischemic damage and has a higher rate of spontaneous phase 4 depolarization than the right ventricular (RV). Both acceleration-

dependent and pause-dependent aberrancy can be seen in the same patient with an intermediate range of CLs associated with normal conduction. The prognosis of rate-dependent BBB largely depends on the presence and severity of the underlying heart disease. Its clinical implications are not clear, and it usually occurs in diseased tissue and in the setting of myocardial infarction (MI), especially inferior wall MI.⁵

Aberration Caused by Concealed Transseptal Conduction

Concealed transseptal conduction is the underlying mechanism of aberration occurring in several situations, including perpetuation of aberrant conduction during tachyarrhythmias, unexpected persistence of acceleration-dependent aberration, and alternation of aberration during atrial bigeminal rhythm.

Perpetuation of Aberrant Conduction During Tachyarrhythmias

During a supraventricular tachycardia (SVT) with normal ventricular activation, a PVC originating from the RV can retrogradely activate the RB early, whereas retrograde activation of the LB occurs later, following transseptal conduction of the PVC. Consequently, although the RB ERP expires in time for the next SVT impulse, the LB remains refractory because its actual cycle began later than the RB. Therefore the next SVT impulse traveling down the HB encounters an excitable RB and a refractory LB; thus it propagates to the RV over the RB (with an LBBB pattern, phase 3 aberration). Conduction subsequently propagates from the RV across the septum to the LV. By this time, the distal LB has recovered, allowing for retrograde penetration of the LB by the SVT impulse propagating transseptally, thereby rendering the LB refractory to each subsequent SVT impulse (Fig. 10.8). This process is repeated, and the LBBB pattern continues until another well-timed PVC preexcites the LB (and either “peels back” or shortens its refractoriness), so that the next impulse from above finds the LB fully recovered (see Fig. 10.4).²

More commonly, a PAC blocks anterogradely in the proximal portion of the RB to cause RBBB, conducts down the LB to activate the ventricle, crosses the septum to excite the RB retrogradely and make it refractory for the next supraventricular complex, thus perpetuating the RBBB (see below).



Fig. 10.8 Perpetuation of aberrant conduction during supraventricular tachycardia secondary to concealed transseptal conduction. At left, supraventricular tachycardia is associated with normal ventricular activation and narrow QRS complexes. Critically timed ventricular extrastimulus delivered from the right ventricle (*arrow*) precipitates left bundle branch block aberrancy during the tachycardia.

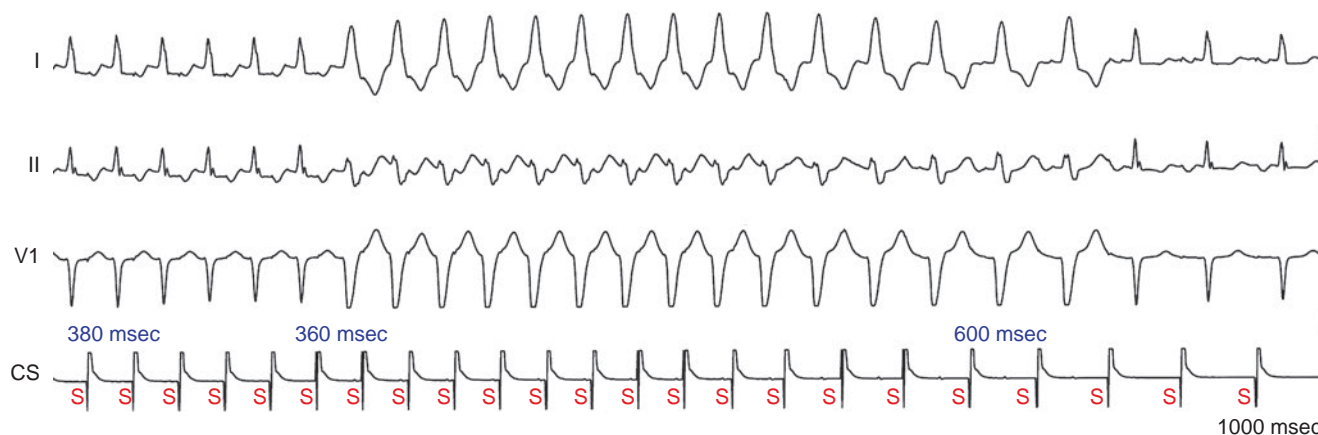


Fig. 10.9 Unexpected Persistence of Acceleration-dependent Aberration. During incremental-rate atrial pacing from the coronary sinus (CS), acceleration-dependent bundle branch block develops at a cycle length (CL) of up to 370 milliseconds. Aberrancy continues despite progressively increasing the pacing CL and disappears only when pacing at a CL of more than 600 milliseconds.

Unexpected Persistence of Acceleration-Dependent Aberration

Acceleration-dependent BBB develops at a critical rate faster than the rate at which it disappears (Fig. 10.9). This paradox is most commonly ascribed to concealed conduction from the contralateral conducting

bundle branch across the septum with delayed activation of the blocked bundle. Such concealed transseptal activation results in a bundle branch-to-bundle (RB-RB or LB-LB) interval shorter than the manifest R-R cycle. The reason is that the actual cycle for the blocked bundle does not begin until approximately halfway through the QRS complex because

it takes 60 to 100 milliseconds for the impulse to propagate down the RB and transeptally reach the blocked LB. Consequently, for normal conduction to resume, the cycle (R-R interval) during deceleration must be longer than the critical cycle during acceleration by at least 60 to 100 milliseconds.²

However, unexpected delay of normalization of conduction cannot always be explained by concealed conduction. Conduction sometimes normalizes with slowing of the heart rate, only to recur at cycles that are still longer than the critical cycle. Such a sequence excludes transeptal concealment as the mechanism of recurrence of the aberration. Similarly, when the discrepancy between the critical cycle and the cycle at which normalization finally occurs is longer than the expected transeptal activation time (approximately 60 milliseconds in the normal heart and 100 milliseconds in the diseased states), transeptal concealment alone cannot explain the delay (see Fig. 10.9). Fatigue and overdrive suppression have been suggested as possible mechanisms of the delayed normalization of conduction.

Alternation of Aberration During Atrial Bigeminal Rhythm

A bigeminal rhythm can be caused by atrial bigeminy, 3:2 AV block, or atrial flutter with alternating 2:1 and 4:1 AV conduction. The alternation can be between a normal QRS complex and BBB or between RBBB and LBBB.

When alternation occurs between a normal QRS complex and RBBB during atrial bigeminy, the ERP of both RB and LB starts simultaneously following the normally conducted PAC, and the ERP of both branches is relatively short because of the preceding short cycle. After the pause, the sinus beat conducts normally, and the ERP of both bundle branches starts simultaneously but is relatively long because of the preceding long cycle. However, because the RB ERP is relatively longer than that of the LB, the next PAC encroaches on the RB refractoriness and conducts with an RBBB pattern (phase 3 block). Subsequently, that PAC is conducted down the LB and across the septum. The PAC activates the RB retrogradely after some delay (concealed transeptal conduction), so that the RB-RB interval (during the following pause) and the RB ERP become shorter. As a result, by the time the next PAC reaches the RB, the RB is fully recovered because of its abbreviated ERP (reflecting the shorter preceding RB-RB interval, which is shorter than the manifest R-R interval during the preceding pause), and normal conduction occurs (see eFig. 10.1).⁷

The same phenomenon (concealed transeptal conduction) explains alternating RBBB and LBBB during bigeminal rhythms. In the presence of RBBB, transeptal concealed conduction from the LB to the RB shortens the RB-RB interval relative to the now longer LB-LB interval. As a result, the ERP of the LB is longer and conduction in the LB fails. In the presence of a refractory LB, conduction propagates through the RB. The delayed transeptal activation of the LB shortens the LB-LB interval. The ERP of the RB is now relatively longer because RB conduction is blocked.

CHRONIC BUNDLE BRANCH BLOCK

Anatomy and Physiology of the His-Purkinje System Cardiac Skeleton

The cardiac skeleton consists of four rings of dense connective tissue that surround the mitral and tricuspid valves and extend to the origins of the aorta and the pulmonary trunk. The aortic valve occupies the central position with the other valve rings attached to it. The right fibrous trigone is formed by the triangular junction between the aortic valve and the medial parts of the tricuspid and mitral valves, and it represents the largest thickening and strongest portion of the cardiac skeleton (see Fig. 9.1). Together with the membranous septum, the

right fibrous trigone constitutes the central fibrous body. The membranous interventricular septum is an inferior extension of the central fibrous body that attaches to the muscular interventricular septum. The membranous septum is crossed on its right aspect by the attachment of the tricuspid valve, dividing the septum into AV and interventricular components. The electrically inert central body and skeleton of the heart functions to electrically isolate the atria from the ventricles, except at the site of penetration of the AV conducting system.

His Bundle

The HB connects with the distal part of the compact AVN and penetrates the central fibrous body (where it is called the “nonbranching” or “penetrating” bundle) in a leftward direction (away from the RA endocardium and toward the crest of the muscular interventricular septum) (eFig. 10.3). The HB then emerges on the crest of the ventricular septum and continues sandwiched between the muscular and the membranous components of the septum for 1 to 2 cm before dividing into the right and left bundle branches. Viewed from the aorta, the HB passes beneath the part of the membranous septum that adjoins the interleaflet fibrous triangle between the right and noncoronary sinuses. The HB is insulated from the atrial myocardium by the membranous septum and from the ventricular myocardium by connective tissue of the central fibrous body, thus preventing atrial impulses from bypassing the AVN. Proximal cells of the penetrating portion are heterogeneous and resemble those of the compact AVN; distal cells are larger, similar to cells in the proximal bundle branches and ventricular myocytes.^{8,9}

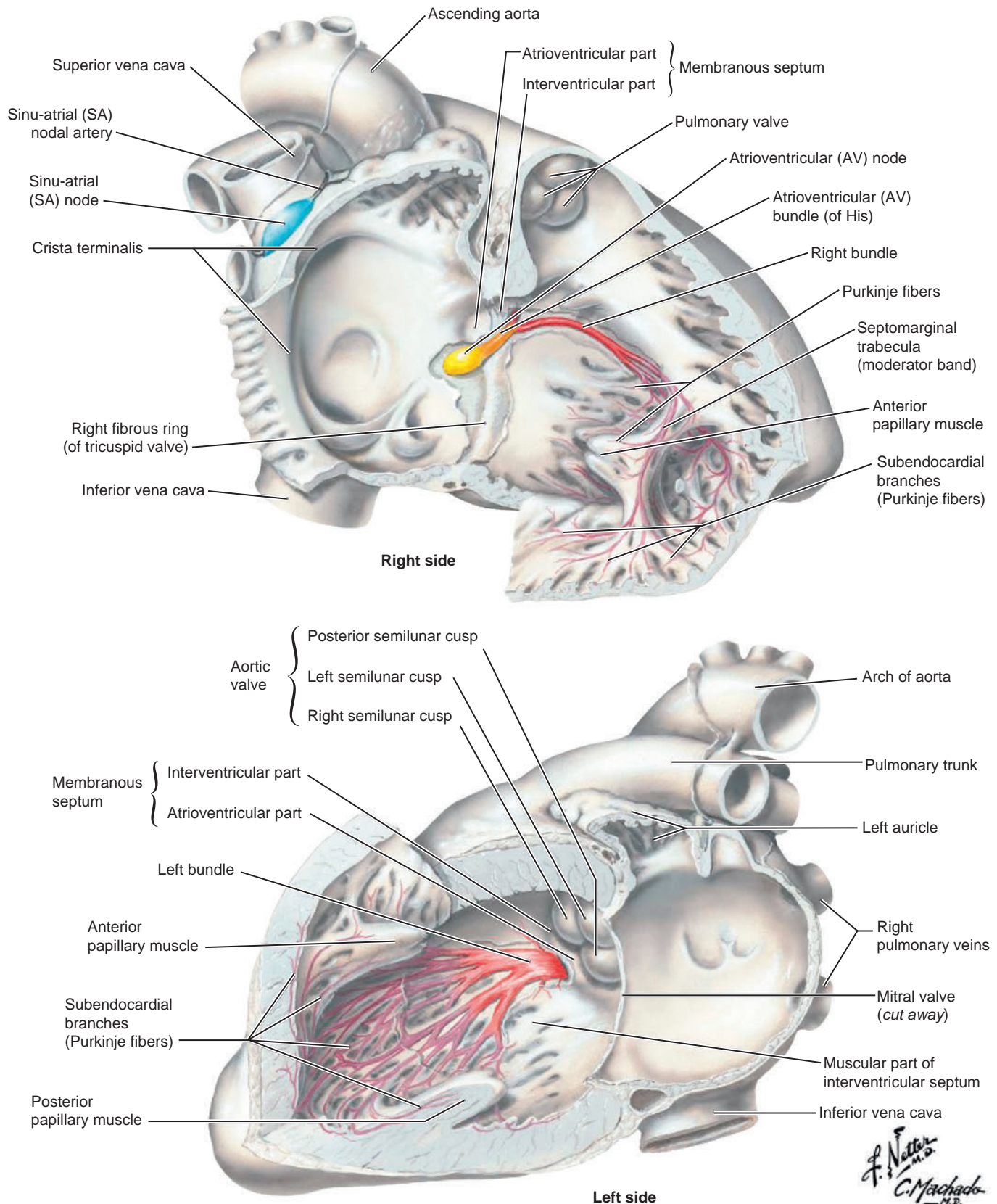
Right Bundle

The RB travels as a direct continuation of the HB down the right side of interventricular septum toward the RV apex. The RB is a narrow, cable-like structure, insulated by a fibrous sheath from surrounding myocardium and remains without ramifications for most of its length until it approaches the origin of the right anterior papillary muscle, where it divides profusely into a network of subendocardial fascicles spreading to the RV septal and free walls (see eFig. 10.3). In addition, free-running strands extend from the RB toward the apical trabeculated portion of the RV. The ventricular cavity is also bridged via connections through the moderator band (a muscular structure that crosses from the septum to the RV free wall and supports the anterior papillary muscle of the tricuspid valve). The RB runs subendocardially in its basal and apical thirds and deeper within the muscular portion of the septum in the middle third. This path renders the subendocardial segments vulnerable to stretch and trauma.¹⁰

Left Bundle

The LB at its origin is not a discrete branch of the HB, but arises as numerous fine, intermingling fascicles that leave the left margin of the branching HB through most of its course along the crest of the muscular ventricular septum. The predivisional portion of the LB penetrates the membranous portion of the interventricular septum under the aortic ring and then divides under the septal endocardium into two branches: the left anterior fascicle (LAF) and the left posterior fascicle (LPF). An estimated 65% of individuals have a third fascicle of the LB, the septal or left median fascicle (LMF). The fascicles cascade down the LV septum in a fan-like configuration with extensive interconnections. Unlike the cord-like RB, the LB and its divisions are diffuse, fan-like structures that branch out just beyond their origin (see eFig. 10.3). The LAF represents the superior (anterior) division of the LB, the LPF represents the inferior (posterior) division, and the LMF represents the septal (median) division.⁹

The LB subdivisions extend to the mid portion of the septum before they detach from the underlying endocardium and form free-running



eFig. 10.3 Anatomy of the Atrioventricular Conduction System. (From Netter Images, www.netterimages.com, with permission.)

false tendons that traverse the ventricular chamber, projecting predominantly toward the papillary muscles. The fascicles become ramified in the ventricular apex and extend back along the ventricular walls toward the cardiac base.⁸

The LAF crosses the anterobasal LV region toward the anterior papillary muscle and terminates in the Purkinje system of the anterolateral LV wall. The LPF appears as an extension of the main LB and is large in its initial course. It then fans out extensively toward the posterior papillary muscle and terminates in the Purkinje system of the posteroinferior LV wall. The LMF runs to the interventricular septum; it arises in most cases from the LPF, less frequently from the LAF, or from both, and in a few cases it has an independent origin from the central part of the main LB at the site of its bifurcation.

Purkinje Fibers

The bundle branches and fascicles consist of bundles of Purkinje cells insulated from the surrounding myocardium by a dense sheath of connective tissue. Insulation is lost distally as the Purkinje network connects the ends of the bundle branches to the ventricular myocardium. This design enables the transfer of action potentials to the ventricular apex without activating the ventricular myocardium at the base first, ensuring a synchronized and coordinated apex-to-base contraction pattern that optimizes ventricular ejection.⁸

A combination of subendocardial and free-running Purkinje fibers (false tendons) form complex three-dimensional mesh-like networks on the endocardial surface of both ventricles and penetrate only the inner third of the myocardium. Purkinje fibers tend to be less concentrated at the base of the ventricles and at the tips of the papillary muscle. The free-running false tendons traverse the ventricular chamber and reattach at the free wall myocardium, projecting predominantly toward the papillary muscles. This pattern promotes septal-free wall synchronization.⁸

Cardiac Purkinje cells exhibit structural and electrophysiological (EP) features that are distinct from nodal and working cardiomyocytes. Purkinje fibers are larger than working cardiomyocytes and are more often larger and more rod-shaped than sinus and AV nodal cells. Additionally, Purkinje cells have fewer myofibrils, which are different in composition of myosin from the cells of working myocardium. These myofibrils function only as passive cytoskeletal components. Purkinje cells contain a considerable amount of glycogen, and they exhibit more resistance to hypoxia than the ventricle myocardium cells. As compared to the working ventricular cardiomyocytes, the action potential in Purkinje fibers has a faster upstroke velocity (dV/dt), higher amplitude, more prominent early phase of rapid repolarization (phase 1), more negative plateau potential, and a significantly longer duration.^{11,12}

The Purkinje fiber network is critical for the almost simultaneous depolarization of the terminal HPS and propagation of the cardiac impulse to the entire RV and LV endocardium. Purkinje cells are specialized to conduct rapidly, at 2.3 m/s, much faster than working ventricular cardiomyocytes (0.75 m/s). This rapid conduction is facilitated by the high expression of Na^+ channels, resulting in action potential upstroke velocities of ~ 1000 V/s. Additionally, an exceptionally high enrichment of connexin proteins (Cx40, Cx43, Cx45) result in a very low intercellular resistance (as low as $100 \Omega/cm$). Purkinje fibers are connected to the working myocardial cells by intercalated disks. One Purkinje fiber transfers the impulse to thousands of ventricular cardiomyocytes.^{9,11}

The Purkinje fiber network arrangement guarantees a synchronous action of working cardiomyocytes during the contraction. Ventricular activation starts at the left side of the interventricular septum, followed by a wave of excitation traveling from the apex to the base (to ensure efficient and optimized ejection towards the basally located semilunar outlet valves), and from the endocardium to the epicardium.

Blood Supply

The HB, and predivisional portion of the LB, receive dual blood supply from the septal branches of the anterior and posterior descending coronary arteries. The RB and LAF are supplied by the septal perforating branches of the left anterior descending coronary artery. The LPF is supplied by the conus branch of the right coronary artery in the majority of the cases. Hence, RBBB or LAF block can result from occlusion of the left anterior descending artery, whereas the development of LBBB during acute MI usually indicates occlusion of both the right and the left anterior descending coronary arteries.¹³

Innervation

The AVN and the HB region are innervated by a rich supply of cholinergic and adrenergic fibers, with a density exceeding that found in the ventricular myocardium. Although neither sympathetic stimulation nor vagal stimulation affects normal conduction in the HPS, either can affect abnormal AV conduction.

Pathophysiology of His-Purkinje System Disease

The clinical presentation of conduction disturbances, in order of decreasing incidence, is LAF block, RBBB, LBBB, and LPF block. This rank depends not only on the intrinsic, anatomical and genetically determined differences among branches and fascicles, but also on the manner in which the intraventricular conduction system is exposed to the various pathological processes of the surrounding cardiac structures.

Right Bundle

The RB runs subendocardially in its basal (proximal) and apical (distal) thirds; this path renders the subendocardial segments vulnerable to stretch and trauma. Chronic RBBB pattern can result from three levels of conduction delay in the RV: proximal, distal, or terminal. Proximal RBBB is the most common site of conduction delay. Distal RBBB occurs at the level of the moderator band (or even more distally), and it is an unusual site of conduction delay unless there has been transection of the moderator band during surgery. Terminal RBBB involves the distal conduction system of the RB or, more likely, the ventricular muscle itself, and it can be produced by ventriculotomy or transatrial resection of parietal bands in repair of tetralogy of Fallot. In addition, RBBB can be caused by events in the HB because certain fibers of the HB are organized longitudinally and predestined to activate only one fascicle or bundle branch.¹⁴

RBBB can be an isolated ECG abnormality or associated with structural heart disease. Causes of RBBB include increased RV pressure, RV hypertrophy or dilatation, ischemic heart disease, acute MI, myocarditis, cor pulmonale, acute and chronic pulmonary embolism, hypertension, cardiomyopathies, congenital heart disease, and Lev and Lenègre diseases. Additionally, transient or permanent RBBB can result from mechanical trauma during right heart catheterization or catheter ablation in the vicinity of the RB and is very common following alcohol septal ablation for hypertrophic cardiomyopathy. Interestingly, in some patients with RBBB who are being considered for a pacemaker, pacing the HB eliminates the RBBB and may be the preferred site of pacing.¹⁵

Left Bundle

LBBB is usually caused by ischemic or mechanical factors, and the site of block is typically in the predivisional segment at the junction of the LB and HB. LBBB is usually encountered in patients with structural heart disease involving dilation, hypertrophy, or fibrosis of the LV such as ischemic heart disease, valvular heart disease, and various cardiomyopathies. Also, LBBB can be caused by Lev and Lenègre diseases.

The LAF can be injured by diseases that involve the LV basal septum, the anterior half of the ventricular septum, and the anterolateral LV

wall. Isolated LAF block is the most common type of IVCD seen in acute anterior MI. LAF block can also be a result of hypertension, cardiomyopathies, aortic valve disease, Lev and Lenègre diseases, or spontaneous or surgical closure of ventricular septal defect.¹⁶

In contrast, the LPF is the least vulnerable segment of the whole conduction system because it is short and wide and is located in the inflow tract of the LV, a less turbulent region than the outflow tract. Additionally, the LPF has a dual blood supply, from the anterior and posterior descending coronary arteries. Isolated LPF block is a rare finding, and rather nonspecific for cardiac disease. LPF block is almost always associated with RBBB.¹⁶

Despite ECG anatomical correlates, the site of block producing BBB patterns is not always certain. Conduction delay can be related to disease affecting the main bundle branch or fascicle, the distal conduction system, or even the working myocardium. Furthermore, data suggest that fibers to the RB and LB are already predestined within the HB and that lesions in the HB can produce characteristic BBB patterns. Longitudinal dissociation with asynchronous conduction in the HB can give rise to abnormal patterns of ventricular activation; hence, the conduction problem may not necessarily lie in the individual bundle branch. Moreover, it is not uncommon for intra-Hisian disease to be accompanied by BBB (especially LBBB). Importantly, the problem may not be actual block, because conduction *delay* within the bundle in the range of as little as 10 milliseconds can give rise to an ECG pattern of BBB.

Nonspecific Intraventricular Conduction Disturbances

The pathophysiology of nonspecific IVCD can be related to intraventricular parietal conduction disease (i.e., Purkinje fiber network or the working myocardium) in the presence of a preserved proximal conduction system (the branches of the HB and their main subdivisions). Nonspecific IVCDs can be observed in various cardiomyopathies and postinfarction. Widening of the QRS is also common in patients with significant LV hypertrophy, likely related to the increase in LV myocardial mass to be depolarized as well as an intramyocardial conduction disorder linked to modification in myofibrillar organization and possibly increased myocardial fibrosis. Additionally, patients with true LBBB or RBBB can have superimposed myocardial disease (e.g., infarction) that can alter the ECG pattern and result in a “nonspecific” IVCD pattern.¹⁷

Clinical Significance

BBB can result from either intrinsic conduction system degeneration or an extrinsic insult from a variety of cardiovascular diseases, and the prognosis of BBB is largely related to the presence, type, and severity of the underlying heart disease, and to the possible presence of other conduction disturbances.

Bifascicular block (especially RBBB and LAF block) is the most common ECG pattern preceding complete heart block in adults.¹⁸ Other forms of IVCD precede the bulk of the remaining cases of complete infranodal AV block. The incidence of progression to complete AV block is approximately 2% in asymptomatic patients with an IVCD and approximately 6% in patients with an IVCD and neurological symptoms (e.g., syncope). The risk of AV block is much higher (up to 70%) in patients with alternating BBB (see below).

Patients with BBB have an unusually high incidence of cardiac disease and sudden cardiac death (SCD). The highest incidence of SCD is among patients with LBBB and cardiac disease. However, many SCDs are caused by VT or ventricular fibrillation (VF), do not seem to be related to AV block, and are not prevented by pacemakers (although pacing can potentially relieve symptoms such as syncope). Complete EP testing and ventricular stimulation are therefore necessary in patients with syncope and BBB because VT can be found in up to 30% to 50%

of cases. Although the poor prognosis associated with BBB is related to myocardial dysfunction, heart failure, and VF rather than heart block, symptoms such as syncope are often related to heart block.^{19,20}

The prevalence of RBBB in the general population is estimated at between 0.2% and 0.8%.²¹ The prevalence increases with age and is two to three times higher in men than in women. RBBB has generally been considered a benign finding that does not imply increased risk when found in individuals free of heart disease. However, this has been challenged by two recent reports suggesting an increase in all-cause and cardiac mortality in individuals with RBBB.^{20,21} Additionally, new-onset RBBB does predict a higher rate of coronary artery disease, heart failure, and cardiovascular mortality. When cardiac disease is present, the coexistence of RBBB suggests advanced disease and is an independent predictor of all-cause mortality. In the setting of an acute MI, RBBB is associated with a significant increase in mortality.^{20–22}

The prevalence of LBBB in the general population ranges from 0.2% to 1.1%, and it increases with age (prevalence increases steadily from <1% at age 50 years to 6% by 80 years). In patients with LBBB associated with ischemic heart disease, hypertension, or cardiomyopathy, the prognosis depends on the severity of the underlying heart disease. Nevertheless, among patients with acute MI, cardiomyopathy, and heart failure, the presence of LBBB is associated with a worse prognosis. Additionally, LBBB can cause ventricular dyssynchrony, which can have detrimental effects on patients with LV dysfunction and heart failure. Importantly, the presence of LBBB can represent the first manifestation of a more diffuse myocardial disease; hence, a noninvasive assessment for structural heart disease and ischemia is reasonable in patients with LBBB and no prior heart disease, especially those with known cardiovascular risk factors.¹⁹ Once heart disease is excluded, the presence of isolated LBBB in young healthy individuals seems to carry no adverse prognostic significance.^{20,23}

LAF block is the most common IVCD in the general population (prevalence, 4.5%). Isolated LAF block does not itself imply a risk factor for cardiac mortality or morbidity, and in a healthy population it should be regarded as an incidental ECG finding. The prognosis of LAF block is primarily related to the underlying heart disease. LAF block in the setting of acute MI is probably associated with increased mortality.¹⁶

Isolated LPF block is a rare finding and rather nonspecific for cardiac disease. When present, LPF block is almost always associated with RBBB, in that LPF block and RBBB share cause, pathogenesis, and prognosis. The combination of LPF block and RBBB in acute MI is associated with a high mortality rate (80% to 87%) during the first weeks after the coronary event. Similarly, the risk of progression toward complete AV block (a form of trifascicular block) is also considerable (42%), and approximately 75% of these patients die of pump failure.

ELECTROCARDIOGRAPHIC FEATURES

Bundle Branch Block

The ECG criteria for different types of fascicular blocks and BBB are listed in [Box 10.1](#). The ECG pattern of BBB can represent either complete block or conduction delay (relative to the other fascicles) that produces asynchronous ventricular activation without necessarily implying complete failure of conduction in the diseased fascicle. Therefore, an ECG pattern of complete BBB can have varying degrees or alternate with contralateral complete BBB pattern. These phenomena can be explained by delay, rather than complete block, as the underlying pathophysiological feature of the ECG pattern.¹

BBB leads to prolongation of the QRS duration, the degree of which depends on the severity of the impairment. With complete BBB, the QRS is 120 milliseconds or longer in duration; with incomplete BBB, the QRS duration is 100 to 120 milliseconds. Also, the QRS vector can

BOX 10.1 Electrocardiogram Criteria for Fascicular and Bundle Branch Block

Complete Right Bundle Branch Block

- QRS duration ≥ 120 ms in adults
- Broad, notched secondary R waves (rsr', rsR', or rSR' patterns) in right precordial leads (V_1 and V_2); R' or r' deflection usually wider than the initial R wave; in a minority of patients, a wide and often notched R wave pattern may be seen in lead V_1 and/or V_2
- Wide, deep S waves (QRS pattern) of greater duration than R wave or greater than 40 ms in leads I and V_6
- Normal R wave peak time in leads V_5 and V_6 but >50 ms in lead V_1
- Of the foregoing criteria, the first three should be present to make the diagnosis; when a pure dominant R wave with or without a notch is present in V_1 , criterion 4 should be satisfied

Complete Left Bundle Branch Block

- QRS duration ≥ 120 ms in adults
- Broad notched or slurred R wave in leads I, aVL, V_5 , and V_6 and an occasional RS pattern in V_5 and V_6 attributed to displaced transition of QRS complex
- Absent q waves in leads I, V_5 , and V_6 , but in the lead aVL, a narrow q wave may be present in the absence of myocardial disease
- R wave peak time >60 ms in leads V_5 and V_6 but normal in leads V_1 , V_2 , and V_3 , when small initial r waves can be discerned in the above leads
- ST and T waves usually opposite in direction to QRS
- Positive T wave in leads with upright QRS may be normal (positive concordance)
- Depressed ST segment and/or negative T wave in leads with negative QRS (negative concordance) are abnormal
- Appearance of LBBB may change the mean QRS axis in the frontal plane to the right, to the left, or superiorly, in some cases in a rate-dependent manner

Left Anterior Fascicular Block

- Frontal plane axis between -45 and -90 degrees
- qR pattern in lead aVL
- R wave peak time in lead aVL ≥ 45 ms
- QRS duration <120 ms

Left Posterior Fascicular Block

- Frontal plane axis between 90 and 180 degrees in adults
- rS pattern in leads I and aVL
- qR pattern in leads III and aVF
- QRS duration <120 ms

be altered by BBB, and generally the last component of the QRS vector becomes oriented in the direction of the myocardial region in which depolarization is delayed (i.e., the region that is activated last).

BBB is characteristically associated with secondary repolarization (ST-T) abnormalities (LBBB more so than RBBB). The T wave is typically opposite in polarity to the last deflection of the QRS. This discordance is caused by the altered sequence of repolarization that occurs secondary to altered depolarization. This is often evident mainly in right precordial leads (leads V_1 , V_2 , overlying the RV) in RBBB, and all leads in LBBB since the bulk of ventricular myocardium is served by the LB.

Right Bundle Branch Block

Development of RBBB alters the activation sequence of the RV, whereas the LV is activated normally. Because the LB is not affected, the initial septal activation (the initial 30 milliseconds of the QRS complex), which

depends on the LB, remains normal, occurring from left to right, and results in septal q waves in leads I, aVL, and V_6 and r waves in leads V_1 , V_2 , and aVR. Thus, the Q wave of a prior MI remains unchanged.

Septal activation is followed by activation of the LV (within the subsequent 40 to 60 milliseconds), occurring over the LB in a leftward and posterior vector and resulting in R waves in the leftward leads (I, aVL, and V_6), as well as s (or S) waves in the anterior precordial leads (V_1 and V_2). This appearance is usually similar to that in normal subjects because the LV is normally electrically predominant during this phase of the QRS.¹

The asynchronous depolarization caused by RBBB is primarily manifested in the later portion of the QRS, beyond the first 80 milliseconds. During this time, RV activation spreads slowly by conduction through working muscle fibers rather than the specialized Purkinje system, and it occurs predominantly after activation of the LV has completed. The forces generated by the late, unopposed RV free wall activation result in a terminal rightward and anterior positivity, manifesting as a second positive deflection that can be small (r') or large (R') in the anterior precordial leads (V_1 and V_2) and S waves in the leftward leads (I, aVL, and V_6 ; Fig. 10.10). The QRS axis is unaffected by RBBB; left or right axis deviation can indicate concurrent LAF or LPF block, respectively (see Fig. 10.10).¹⁸

RBBB also results in abnormal repolarization of the RV myocardium. As a result, there are often secondary ST-segment and T-wave changes present in the right precordial leads. The ST segment change is usually small and, when present, is discordant (i.e., has an axis in the opposite direction) to the terminal mean QRS spatial vector. The T wave also tends to be discordant to the terminal conduction disturbance, resulting in inverted T waves in the right precordial leads (where there is a terminal R' wave) and upright T waves in the left precordial leads (where there is a terminal S wave).

The time interval necessary for full depolarization of the ventricular free wall (from the endocardium to the epicardium) beneath any given ECG electrode corresponds to the interval from the beginning of the QRS complex to the time of initial downstroke of the R wave after it has peaked (or to the time of initial upstroke of the S wave after it has reached its nadir). This interval is termed *R wave peak time* (in preference to the term *intrinsicoid deflection*). Normally, the upper limit of normal for R wave peak time is 35 milliseconds in the right precordial leads, and 45 milliseconds in the left precordial leads. In RBBB, the R wave peak time is delayed in the right precordial leads (more than 50 milliseconds).

Atypical RBBB. Atypical RBBB can be caused by attenuation or loss of posterior deflections in the anteroposterior leads, resulting in an rsR', qR, or M-shaped QRS pattern in lead V_1 . This pattern can be a normal variant, a consequence of a gain of mid-temporal anterior forces secondary to RV enlargement or concurrent LAF block, or the result of a loss of posterior forces caused by a posterior wall MI.

Incomplete RBBB. An incomplete RBBB can result from lesser degrees of conduction delay in the RB. The ECG pattern of incomplete RBBB is similar to that of complete RBBB, except that the QRS duration is between 110 and 120 milliseconds (see Fig. 10.10). An RBBB pattern with a QRS duration shorter than 100 milliseconds can be a normal variant, presumably reflecting a slight delay in the terminal posterobasal forces in some individuals.

The ECG pattern of incomplete or complete RBBB in association with a distinct ST segment elevation in the right precordial leads can be observed in the Brugada syndrome. The Brugada ECG pattern, however, is characterized by the absence of a wide terminal S wave in the left lateral leads (I, aVL, V_6) and no broad terminal R wave in lead aVR, findings indicating that true RBBB is not present (see Fig. 31.13).

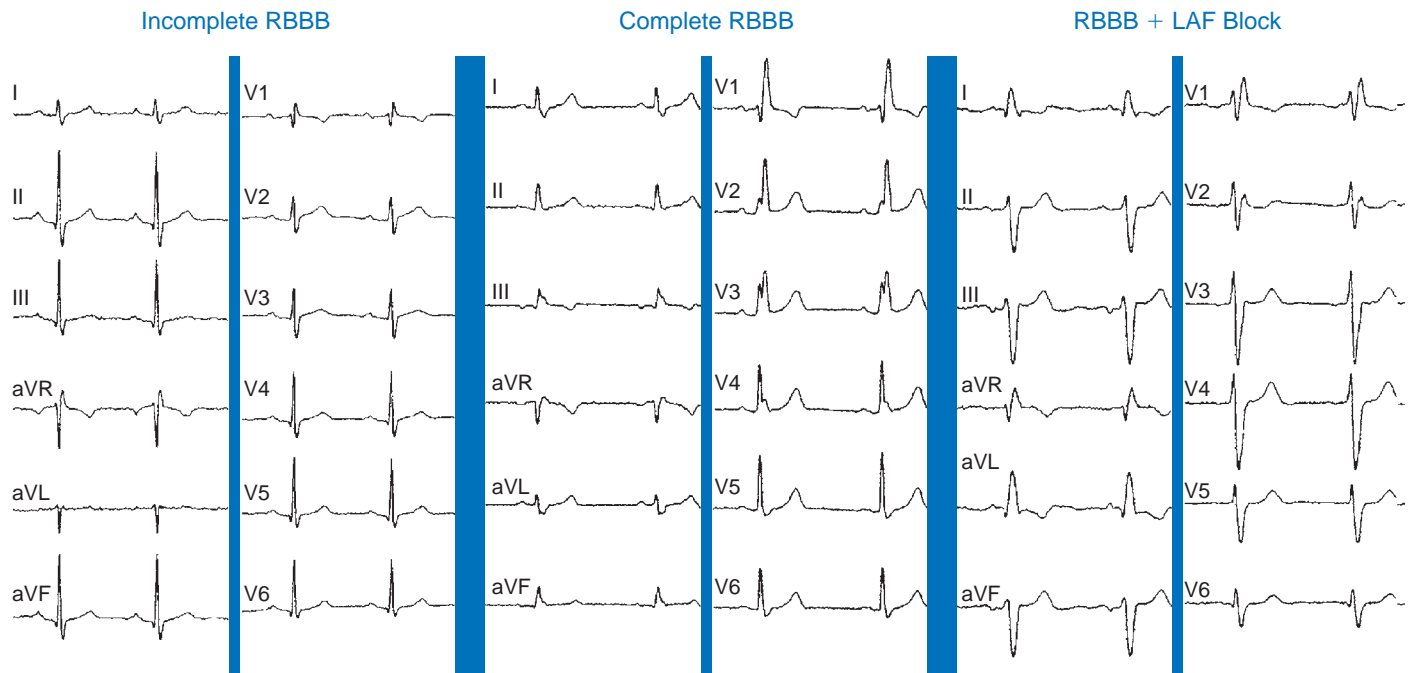


Fig. 10.10 Surface electrocardiogram of incomplete and complete right bundle branch block and bifascicular block. LAF, Left anterior fascicle; RBBB, right bundle branch block.

Additionally, the ECG manifestations of the Brugada syndrome are often dynamic or concealed and can be unmasked or modulated primarily by Na^+ channel blockers but also during a febrile state or with vagotonic agents.

Left Bundle Branch Block

The normal sequence of ventricular activation is altered dramatically in LBBB. Complete LBBB results in delayed and abnormal activation and diffuse slowing of conduction throughout the LV. During LBBB, activation of the LV originates from the RB in a right-to-left direction, in contrast to the normal situation in which the first part of the LV myocardium to be activated is the septum in a left-to-right direction via a small septal branch of the LB. Thus, LBBB results in reversal of the direction of the initial septal activation sequence (within the initial 30 milliseconds of the QRS complex), with the activation traveling from right to left and from apex to base as well as to the RV free wall. RV activation is typically completed within the first 45 milliseconds of the onset of the QRS, before the onset of LV activation. However, because the septum is a larger structure than the RV free wall, septal activation predominates, eliciting a leftward and usually anterior vector and resulting in loss of the normal small q waves and initiation of a wide, slurred R wave in leads I, aVL, and V_6 and an rS or QS pattern in lead V_1 (Fig. 10.11). As a consequence, Q waves of a prior MI may disappear, and new Q waves can emerge.¹

Following septal activation, LV activation (starting as late as 44 to 58 milliseconds into the QRS) spreads slowly by conduction through working muscle fibers rather than the HPS, with spatial vectors oriented to the left and posteriorly because the LV is a leftward and posterior structure. As a consequence, the delayed LV activation (unopposed by the now completed RV activation) produces large, broad, and notched or slurred R waves (without q or s waves) in the leftward leads (I, aVL, and V_6), with delayed R wave peak time in the left precordial leads (more than 60 milliseconds). The slowing and notching of the mid-QRS portion are caused by slow transseptal conduction. The terminal

activation vector results from depolarization of the anterolateral LV wall that produces a small vector that is also directed to the left and posteriorly.¹

LBBB may cause no shift or variable degrees of left and superior shift of the frontal plane QRS axis. Pronounced left axis deviation can be associated with additional delay in activation in the LV secondary to myocardial disease. Right axis deviation in the setting of LBBB is rare and may be caused by RV hypertrophy or MI. It has been suggested that a superior axis shift may occur in patients with predivisional LBBB with an additional delay in the LAF. A superior axis can also be observed in patients with RV enlargement.²⁴

The altered activation sequence also changes the sequence of repolarization. Both the ST segment and T wave vectors are discordant from the QRS complex.

Importantly, recent evidence has challenged the conventional ECG criteria for complete LBBB. In particular, the threshold of 120 milliseconds for QRS duration seems to be misleading, as experimental studies found that the QRS duration is usually prolonged by 70 to 80 milliseconds with the onset of LBBB, instead of the 40 milliseconds required by the conventional criteria.^{25,26} In fact, endocardial mapping studies have suggested that one-third of patients with “complete LBBB” diagnosed by conventional ECG criteria do not have endocardial activation consistent with LBBB but likely have a combination of LV hypertrophy and LAF block. Hence, more “strict” ECG criteria were proposed, including a terminal negative deflection in lead V_1 , mid-QRS notching/slurring in at least two of the leads V_1 , V_2 , V_5 , V_6 , I, and/or aVL, and a higher cutoff for QRS duration (140 milliseconds or longer for men and 130 milliseconds or longer for women). During true complete LBBB, mid-QRS notching or slurring (beginning after the first 40 milliseconds and ending at approximately two-thirds through the QRS duration) likely corresponds to the time of breakthrough of activation to the LV endocardium (first notch) and then to the LV posterolateral wall epicardium (second notch).²⁷ In a simulations study, these “strict” ECG criteria for LBBB were found to have greater specificity (100% vs.

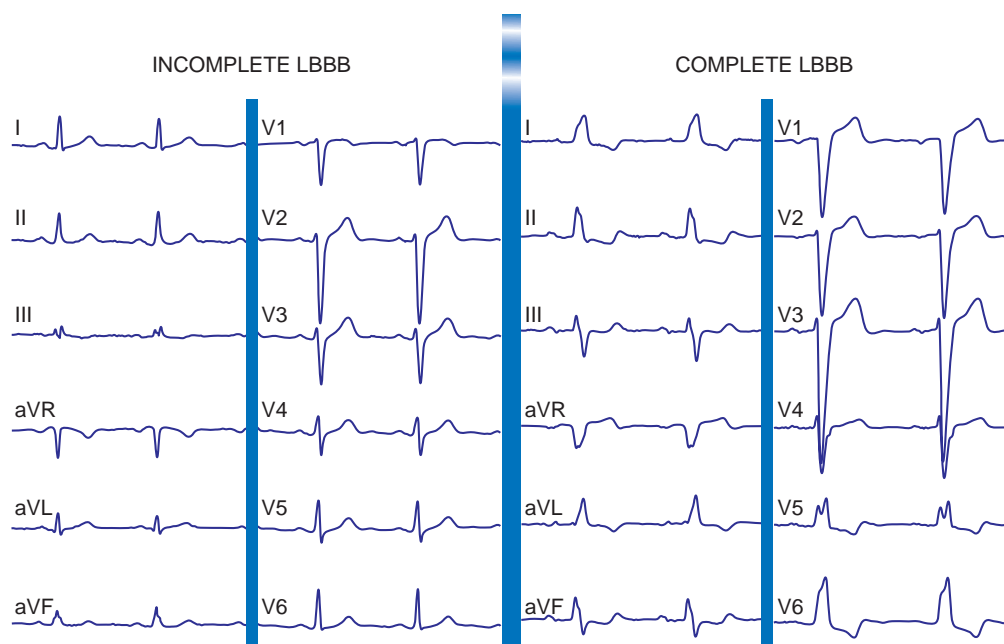


Fig. 10.11 Surface electrocardiogram of incomplete and complete left bundle branch block (LBBB).

48%) and equivalent sensitivity (100%) in diagnosing complete LBBB as compared to the conventional LBBB criteria.²⁸ These criteria were also found to predict better response to cardiac resynchronization therapy in patients with heart failure.^{23,29}

Atypical LBBB. Several atypical ECG patterns of LBBB have been identified. In a common atypical pattern, RS deflections are present in leads V₅ and V₆, likely secondary to leftward displacement of the precordial transitional zone, which may be caused by cardiac dilatation. In another atypical pattern, the small initial r wave in the right precordial leads is absent and in lead III, mimicking anterior or inferior MI pattern, respectively.

Incomplete LBBB. Incomplete LBBB can result from lesser degrees of conduction delay in the LB. Although LV activation begins abnormally on the right side of the septum (as in the setting of complete LBBB), much of the subsequent LV activation occurs via the normal conduction system. Incomplete LBBB is characterized by the following: (1) QRS duration of 110 to 119 milliseconds; (2) presence of an LV hypertrophy pattern; (3) R wave peak time longer than 60 milliseconds in leads V₄, V₅, and V₆; and (4) absence of q wave in leads I, V₅, and V₆ and frequent replacement by a slurred initial upstroke (pseudo-delta wave) (see Fig. 10.11). This entity can bear an ECG resemblance to a Wolff-Parkinson-White (WPW) ECG pattern secondary to the delayed upstroke of the R wave, although the PR interval is usually short in WPW syndrome, whereas it should be normal in cases of incomplete LBBB.¹

LV hypertrophy is often associated with delayed activation and prolongation of the QRS duration, mimicking complete or incomplete LBBB pattern, even in the absence of conduction abnormalities. However, in contrast to LV hypertrophy, LBBB is characterized by delayed R wave peak time in leads V₅ to V₆ to over 60 milliseconds.

Fascicular Block

Hemiblocks in the LB system affect the LAF, LPF, or LMF. Fascicular block generally does not substantially prolong QRS duration, but alters only the sequence of LV activation. The primary ECG change is a shift in the frontal plane QRS axis because the conduction disturbance primarily involves the early phases of activation. The QRS duration

is usually less than 100 milliseconds (unless complicated by BBB or hypertrophy), although some investigators allow a QRS duration of up to 120 milliseconds, or 20 milliseconds longer than the previous baseline.¹⁶

Left Anterior Fascicular Block

The LAF normally initiates activation in the upper part of the septum, the anterolateral LV free wall, and the left anterior papillary muscle. Delayed activation of these regions secondary to damage to the LAF causes unopposed activation wavefronts by the LPF and LMF early during the QRS complex and unopposed anterosuperior forces late during ventricular activation. All these changes occur with a QRS that widens no more than 20 milliseconds in pure and uncomplicated LAF block.¹⁶

As a consequence, the initial (first 20 milliseconds) QRS vector is normal in time, but it has an abnormal direction. Rather than proceeding superiorly and to the left, the QRS vector depicts an inferior and rightward shift in the frontal plane (frontal plane axis more than +120 degrees) that produces a small, sharp r wave in the inferior leads (II, III, and aVF) and a small q wave in leads I, aVL, V₅, and V₆. Additionally, the inferior and rightward shift in the initial QRS forces can occasionally result in a small, sharp q wave in leads V₂ and V₃ (mimicking old anteroseptal infarction patterns) when the electrodes are placed at the normal level and, in almost all cases, when they are placed in a higher position.¹

During the midportion of the QRS, the main forces of LV activation are oriented superiorly and to the left (frontal plane axis more leftward than -45 or -60 degrees), with a wide-open counterclockwise-rotated loop in the frontal plane caused by the delayed activation of the high lateral wall, which is normally activated by the LAF. This results in deep S waves in leads II, III, and aVF (S wave deeper in lead III than in lead II), and R waves in aVR and aVL. The net effect is an rS pattern in leads II, III, and aVF and a qR or R pattern in leads I, aVL, V₅, and V₆. Additionally, as a result of the superiorly directed forces, deeper S waves are recorded in leads V₅ and V₆; these waves tend to disappear when the electrodes are placed above the normal level and are deeper when the electrodes are placed below the normal level.¹⁶

Of note, the ECG pattern of LAF block can simulate LV hypertrophy in limb leads I and aVL. Conversely, it can conceal signs of LV hypertrophy in the left precordial leads, and it can also hide signs of inferior ischemia.

Left Posterior Fascicular Block

The early unopposed activation of the anterolateral wall of the LV by the normally conducting LAF and LMF causes the initial forces to be oriented superiorly and to the left, producing initial small r waves in leads I, aVL, V₁, and V₆ and small q waves in leads II, III, and aVF. However, the main and terminal forces of the QRS are directed posteriorly, inferiorly, and to the right with a wide-open clockwise-rotated loop, because of the late unopposed activation of the areas normally activated by the LPF (the inferoposterior LV free wall). This is responsible for the characteristic rightward frontal plane axis of +120 to +180 degrees. As a result, there is a qR morphology in leads II, III, and aVF and an rS morphology in leads I and aVL. In fact, the ECG pattern of LPF block is the exact mirror image of LAF block in the standard and unipolar leads. LPF block is almost always associated with RBBB. Isolated LPF block is extremely rare, and a firm diagnosis requires that other causes of right axis deviation have been excluded.^{1,16}

Left Median Fascicular Block

The ECG pattern seen with LMF block is probably determined by the differences in the sites of insertion of the LMF, LAF, and LPF. Functional block in the LMF can lead to the apparent loss of anterior forces and can result in the transient development of q waves in leads V₁ and V₂, which normally have a positive initial deflection caused by septal depolarization. These changes are similar to those that occur in septal MI. On the other hand, prominent R waves are seen in the right precordial leads when LMF block leads to a gain of anterior forces. These changes are similar to those caused by true posterior MI. The prominence of the R waves may be increased when LMF block occurs in association with RBBB.

Other Types of Intraventricular Conduction Abnormalities

Nonspecific Intraventricular Conduction Defects

A nonspecific IVCD is the result of diffuse slowing of impulse conduction involving the entire HPS that causes a generalized and uniform delay in activation of the ventricular myocardium. A nonspecific IVCD is diagnosed in the presence of a QRS duration longer than 120 milliseconds and a QRS morphology that does not resemble either LBBB or RBBB and may even resemble the normal QRS complex. Nonspecific IVCDs can be classified as LV or RV IVCD, depending on the site of delayed R wave peak time and the direction of the terminal forces.¹

Bifascicular Blocks

Bifascicular block refers to different combinations of fascicular block and BBB. Examples of bifascicular block include RBBB with LAF block (most common; see Fig. 10.10), RBBB with LPF block, and LAF block plus LPF block (which manifests as LBBB).

Trifascicular Blocks

Trifascicular block involves conduction delay in the RB and either the main LB or both the LAF and LPF. The resulting ECG pattern depends on the relative degree of conduction delay in the affected fascicles. Ventricular activation starts at the insertion site of the fastest conducting fascicle, with subsequent spread of activation from that site to the remainder of the ventricles. ECG documentation of trifascicular block during 1:1 AV conduction is rare. ECG manifestations of trifascicular block include the following: (1) complete AV block with a slow ven-

tricular escape rhythm with a wide, bizarre QRS; (2) alternating RBBB and LBBB; and (3) fixed RBBB with alternating LAF and LPF block.

The combination of bifascicular block (RBBB plus LAF block, RBBB plus LPF block, or LBBB) with first-degree AV block on the surface ECG (eFig. 10.4) cannot be considered as trifascicular block because the site of AV conduction delay can reside in either the AVN or HPS. Hence, such a pattern can reflect slow conduction in the AVN with concomitant bifascicular block rather than disease in the third fascicle. In such circumstances, the PR interval on the ECG does not appear to be helpful in selecting those individuals with a prolonged His bundle–ventricular (HV) interval because a normal PR interval can easily conceal a significantly prolonged HV interval and a prolonged PR interval can be caused by a prolonged AH interval. However, two criteria can be of value: (1) a short PR interval (less than 160 milliseconds) makes a markedly prolonged HV interval (i.e., more than 100 milliseconds) unlikely; and (2) a markedly prolonged PR interval (more than 300 milliseconds) almost always indicates that at least some of the AV conduction abnormality, if not all, is caused by AVN conduction delay.³⁰

Alternating Bundle Branch Block

Alternating RBBB and LBBB is manifested by QRS complexes with LBBB morphology coexisting with complexes with RBBB morphology (Fig. 10.12). Often, every other complex is an RBBB or LBBB. Spontaneous alternating BBB, especially when associated with a change in the PR interval, represents the most common ominous sign for progression to AV block (Fig. 10.13). In fact, 70% of these patients develop high-grade AV block within weeks of diagnosis. Beat-to-beat alternation is the most concerning, whereas a change in BBB noted on different days is less ominous.

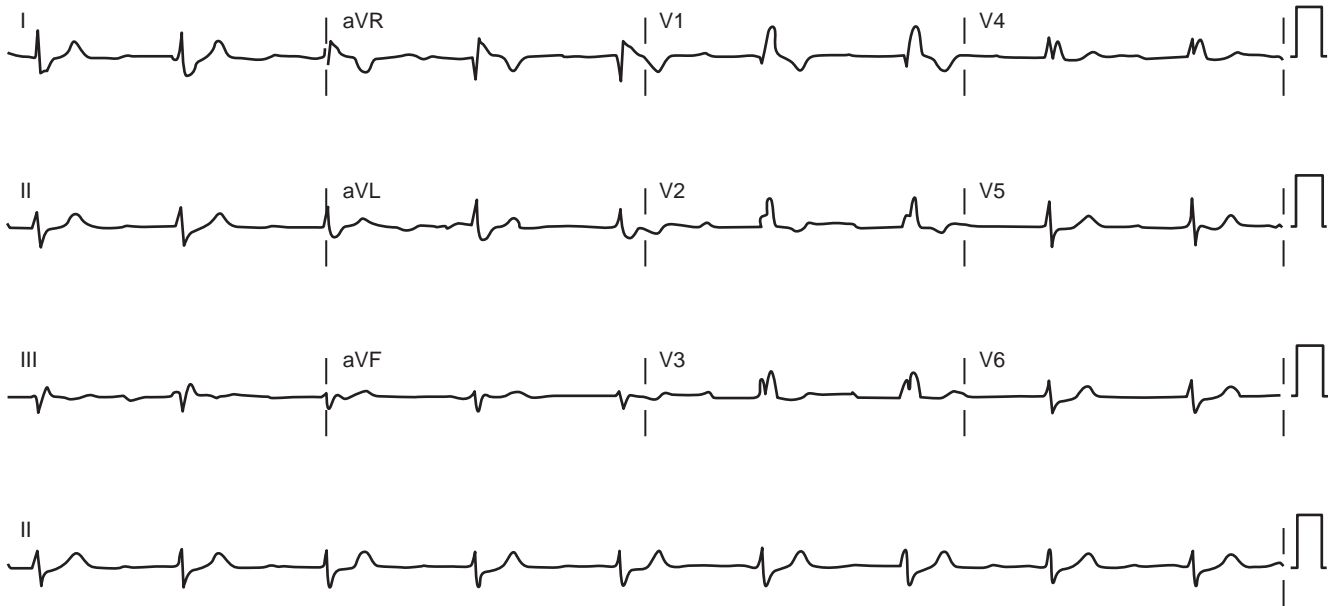
This phenomenon implies instability of the HPS and a disease process involving the HB or bundle branches. In most patients with diffuse HPS disease, delay or block in one of the bundle branches consistently predominates, and alternating BBB is uncommon. The HV interval in alternating BBB is almost universally prolonged and typically varies with the change in BBB. This group has the highest incidence of HV interval exceeding 100 milliseconds. As a rule, AV conduction delay or block can be assumed to be caused by BBB only in the presence of an alternating or intermittent RBBB and LBBB with a changing PR interval. Not infrequently, the bilateral BBB is caused by acceleration-dependent aberration.

Masquerading Bundle Branch Block

Some ECG features can potentially predict the presence of concomitant conduction delay or block in both the RB and LB. The finding of RBBB pattern (with or without LAF block) in the anterior precordial leads with absent S waves in leads I and aVL can be indicative of concomitant conduction delay or block in the LB (a pattern known as “masquerading BBB”). In typical RBBB, the activation of the RV occurs predominantly after activation of the LV has completed. The forces generated by the late, unopposed RV free wall activation manifest as S waves in the leftward leads (I, aVL, and V₆; see Fig. 10.10). Concurrent delay of the activation of the LV due to LBBB may result in disappearance of the S waves in leads I and aVL in patients with RBBB pattern since the late RV activation is no longer “unopposed.” A recent report identified this pattern of bilateral BBB in 1.5% of ECGs with “RBBB pattern,” and it was associated with high risk of AV block or syncope (24%).^{17,18}

Intermittent Bundle Branch Block

Intermittent BBB, either right or left, is diagnosed on the surface ECG when there are occasional QRS complexes with RBBB or LBBB morphology, interspersed with QRS complexes that have a normal morphology. Most often, the intermittent BBB is rate-related (as discussed



eFig. 10.4 Surface electrocardiogram (ECG) of sinus rhythm with first-degree atrioventricular block and bifascicular block (right bundle branch block and left anterior fascicular block). The PR interval is markedly prolonged (480 milliseconds), which suggests that at least some of the atrioventricular conduction delay, if not all, occurs in the atrioventricular node and is not exclusively in the His-Purkinje system. A diagnosis of trifascicular block cannot be made solely based on this ECG.

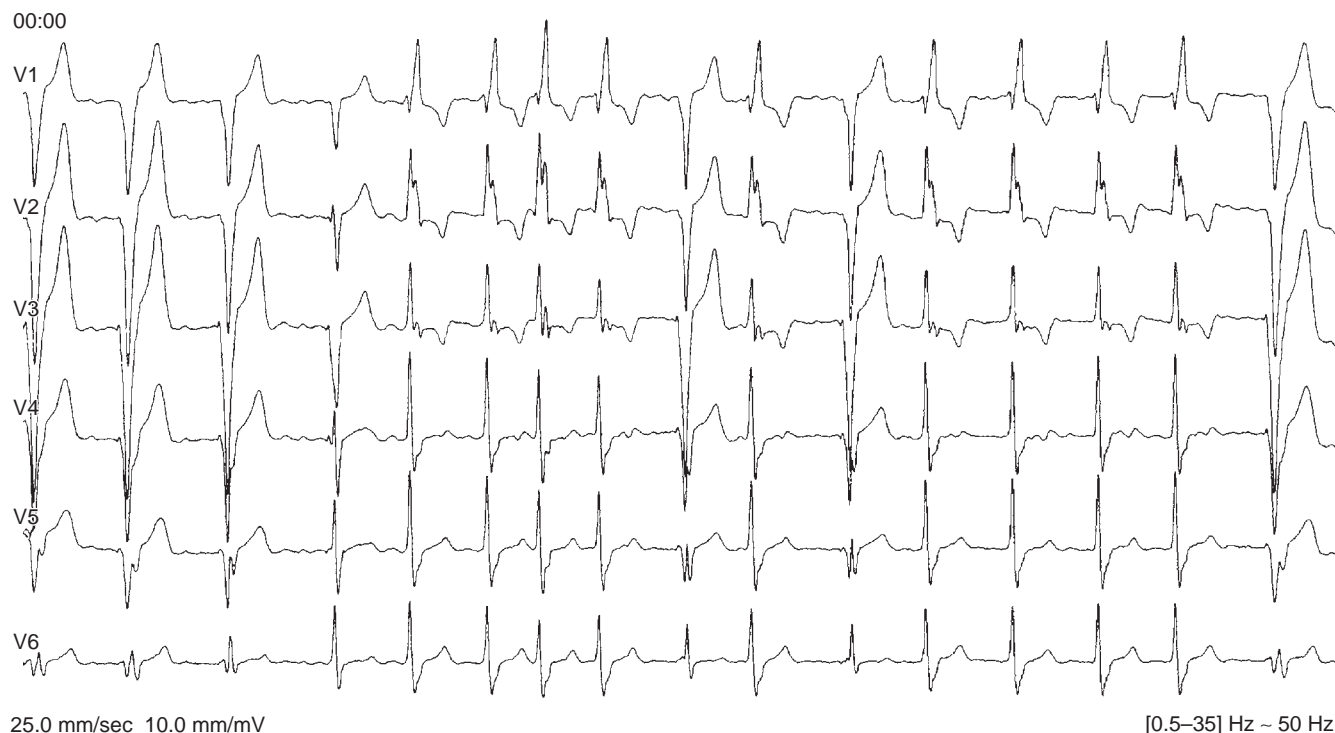


Fig. 10.12 Alternating Bundle Branch Block During Atrial Fibrillation. Surface electrocardiogram precordial leads during atrial fibrillation. QRS complexes with left bundle branch block configuration are observed mostly at long cycle lengths, and complexes with right bundle branch block configuration are observed mostly at shorter cycle lengths.

previously); thus, the R-R intervals of the QRS complexes manifesting the BBB are shorter when compared with the intervals of the normal QRS complexes. In other cases, there is no rate-related change in the QRS intervals, but the occurrence of the BBB is a random or sporadic event.

ELECTROPHYSIOLOGICAL TESTING

Baseline Intervals

His-Ventricular Interval

The use of multipolar catheters to record distal, middle, and proximal HB potentials can help localize the site of conduction delay or block within the HPS. The value of prolonged HV interval in predicting the risk of AV block is controversial. Studies have shown that an HV interval longer than 70 milliseconds predicts a higher risk of AV block, especially in symptomatic patients. An HV interval exceeding 100 milliseconds identifies a group of patients at a very high risk of AV block (25% over 22 months).¹⁰

In the presence of RBBB with or without additional fascicular block, the HV interval should be normal as long as conduction is unimpaired in the remaining fascicle (eFig. 10.5). However, 50% of patients with RBBB plus LAF block and 75% of those with LBBB have a prolonged HV interval. Thus, in these patients, a prolonged HV interval itself is nonspecific as a predictor of AV block.

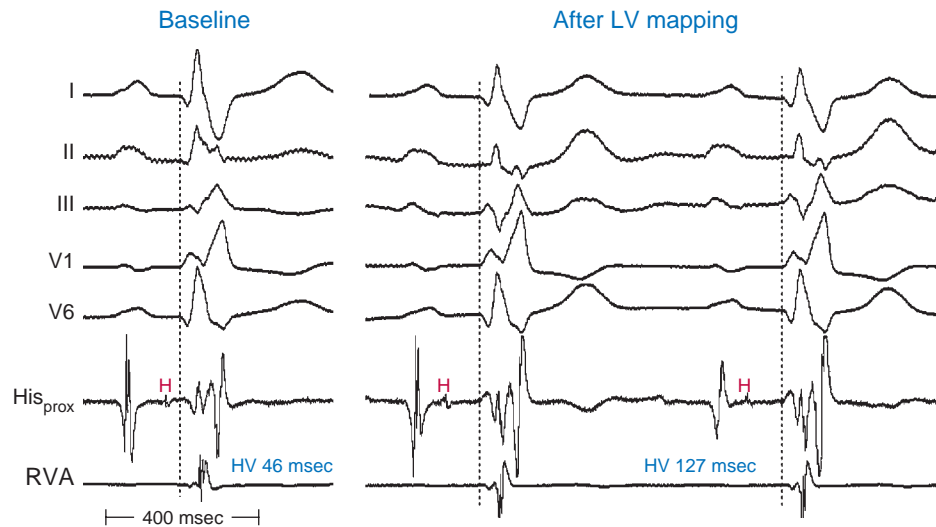
In the presence of LBBB, and in the absence of a change in the HB-RB and HB-RV intervals, the HV interval may be slightly prolonged because the earliest site of depolarization on the left side of the septum via the LB precedes activation of the RB by 5 to 15 milliseconds. Therefore an HV interval of up to 60 milliseconds in the presence of LBBB should be considered normal and does not by itself indicate associated RB or HB disease (eFig. 10.6).²³

Of note, catheter manipulation in the LV or RV can inadvertently produce prolongation of the HV interval and varying degrees of AV block or BBB, or both, usually temporarily (see eFigs. 10.5 and 10.6). Complete heart block can occur during right-sided heart catheterization in a patient with preexisting LBBB or during LV catheterization (LV angiography or ablation procedures) in a patient with preexisting RBBB. Among patients with chronic LBBB, the presence of an r wave of more than 1 mm in lead V₁ appears to identify a subgroup at lower risk for complete AV block in response to catheter trauma to the RB. This ECG sign likely suggests intact conduction over the septal fibers of the LB.³¹

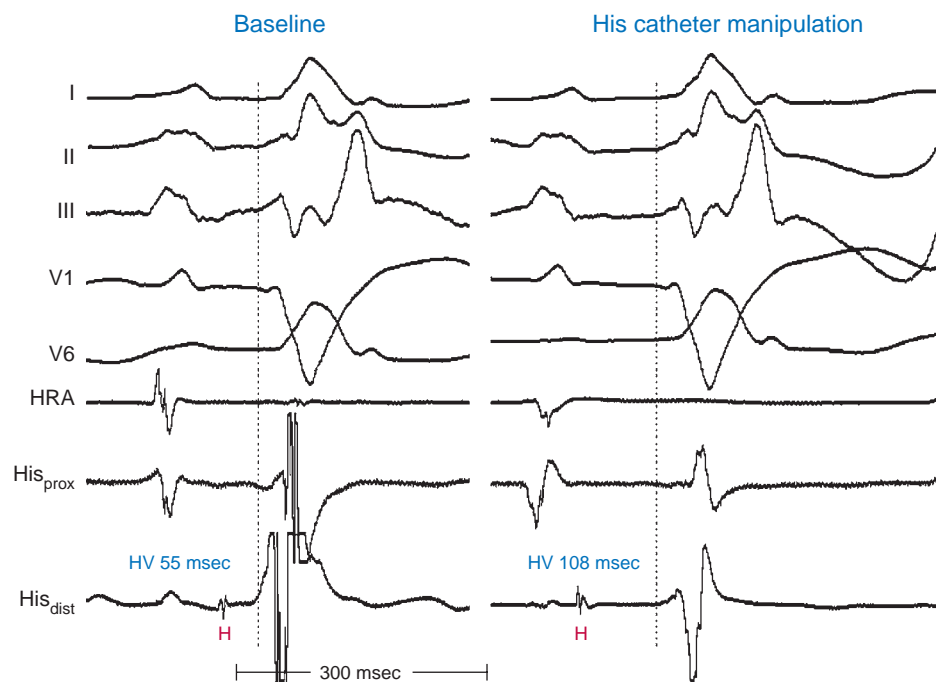
Localization of the Site of Block in Right Bundle Branch Block

Measurement of activation times at different areas of the RV (HB, proximal RB, RV apex, and right ventricular outflow tract [RVOT]) can help assess conduction properties of the RB and distinguish between proximal and distal RBBB (Fig. 10.14). With proximal RBBB, recording of the RB potential is not feasible beyond the site of block. Activation of the RV septum occurs via transeptal spread following LV activation. The transeptal activation begins at the apex and then sequentially activates the midanterior wall and base of the RV. Consequently, the mid and apical portions of the RV septum are activated at least 30 milliseconds after the onset of the QRS. This results in prolongation of the ventricular-right ventricular apical (V-RVA) interval (the interval from onset of the surface QRS to RV apical local activation) to more than 30 milliseconds.¹⁰

In the setting of distal RBBB, activation of the HB, proximal RB, and the RV midseptum and apex remains normal. RB potentials persist at the base of the moderator band but disappear at the midanterior wall (where the moderator band normally inserts). Activation of the free wall at the level of the moderator band is delayed, as is the



eFig. 10.5 Catheter-induced His Bundle–Ventricular (HV) Interval Prolongation. Right bundle branch block with a normal HV is present at baseline (*at left*). Prolongation of the HV interval is observed after introducing a mapping catheter into the left ventricle (LV) that traumatized a portion of the His–Purkinje system. The QRS is also slightly different from baseline. *His_{prox}*, Proximal His bundle; *RVA*, right ventricular apex.



eFig. 10.6 Catheter-induced Trauma to the His Bundle. Left bundle branch block (LBBB) and His bundle–ventricular (HV) interval at the upper limit of normal are observed at baseline (*at left*). Manipulation of the His bundle recording catheter results in prolongation of the HV interval. This is not an artifact of the location of His recording, because the PR interval is also prolonged. There is no change in the QRS complex (LBBB pattern), suggesting trauma to the right bundle (RB) or His fibers destined to the RB. *His_{dist}*, Distal His bundle; *His_{prox}*, proximal His bundle; *HRA*, high right atrium.

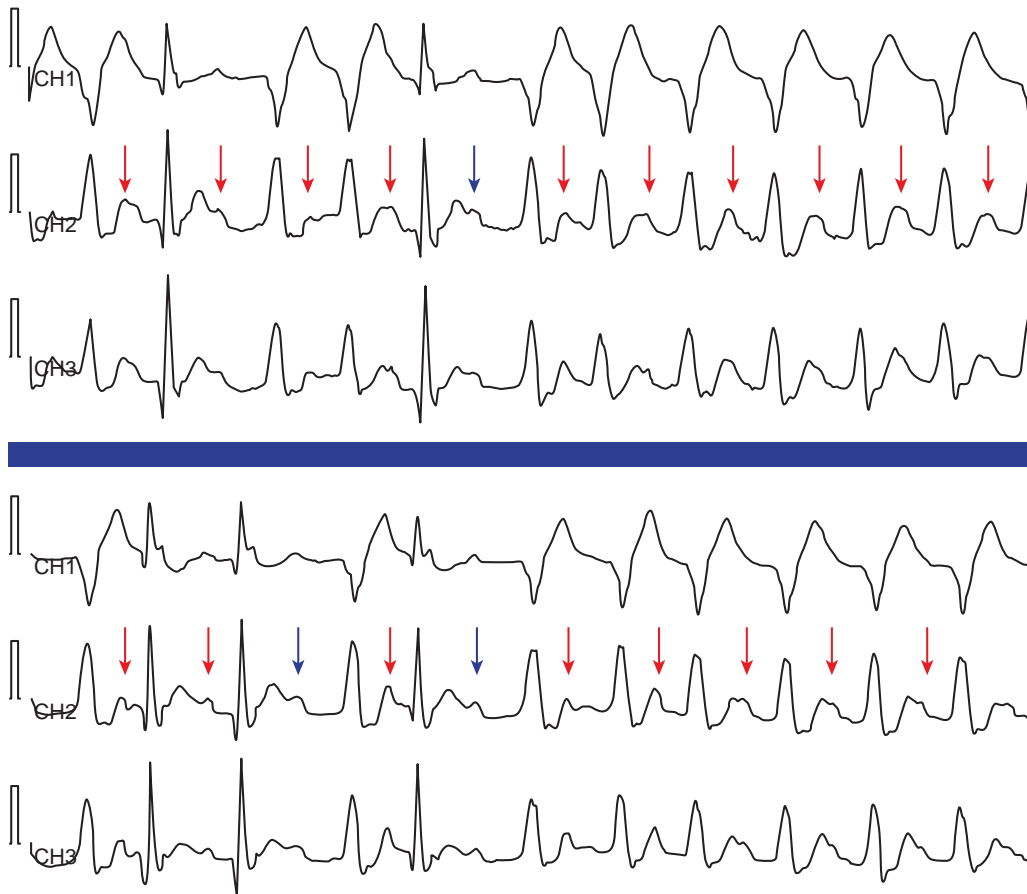


Fig. 10.13 Alternating Bundle Branch Block During Sinus Rhythm. Continuous Holter three-lead recordings demonstrating sinus rhythm with first-degree atrioventricular (AV) block and right bundle branch block (RBBB) alternating with left bundle branch block (LBBB). Arrows denote sinus P waves, which are commonly masked by the preceding T waves. Note that sinus beats conducted with RBBB are associated with shorter PR intervals compared with those conducted with LBBB. This suggests that conduction delay in the right bundle branch (RBB) is more severe than that in the left bundle branch (LBB); hence, the PR interval is longer when conduction occurs only over the RBB (i.e., with LBBB pattern), but shorter when conduction occurs only over the LBB (i.e., with RBBB pattern). The first sinus P waves to conduct with LBBB (blue arrows) are associated with the longest PR intervals, with subsequent P waves conducting with somewhat shorter PR intervals, resulting in gross irregularity of the QRS complexes despite relatively regular sinus P waves. These findings are suggestive of severe His-Purkinje system disease and high risk for complete AV block.

subsequent activation of the RVOT and the remaining RV. This results in prolongation of the V-RVOT interval, while the V-RVA intervals remain normal (less than 30 milliseconds).

Localization of the Site of Block in Left Bundle Branch Block

Because the LB and its fascicles rapidly fan out over the entire LV, endocardial activation mapping is of limited value for the assessment of conduction properties of the LB. Therefore, for practical reasons, clinical evaluation has primarily focused on the surface ECG pattern and the HV interval.

A common observation in patients with LBBB is a delay in transseptal activation. The pattern in which the LV is activated initially (i.e., the site of breakthrough) as well as the remainder of the LV endocardium and transmural activation depend critically on the nature of the underlying heart disease. The bizarreness of the QRS width and morphology is more a reflection of the underlying LV disease than of the primary conduction disturbance. Patients with normal hearts and those with cardiomyopathy appear to have an intact distal conducting system and,

hence, early engagement and rapid spread throughout the rest of the intramural myocardium. In patients with large infarcts, the bulk of their distal specialized conducting system has been destroyed; consequently, endocardial activation occurs via muscle-to-muscle conduction and thus is much slower.

Diagnostic Maneuvers

Atrial Extrastimulation

Atrial premature stimulation helps determine the ERP of HPS. Normally, the HPS ERP is 450 milliseconds or less and it decreases with decreasing pacing drive CL. Because the AVN functional refractory period usually exceeds the HPS ERP, it can be difficult to evaluate the HPS ERP. Administration of atropine or catecholamines such as epinephrine or isoproterenol can help decrease AVN refractoriness and allow impulses to reach the HPS earlier so that HPS ERP can be determined. A grossly prolonged HPS ERP or a paradoxical increase in the HPS ERP in response to shortening of the pacing drive CL indicates an abnormal HPS and predicts a higher risk for progression to AV block.

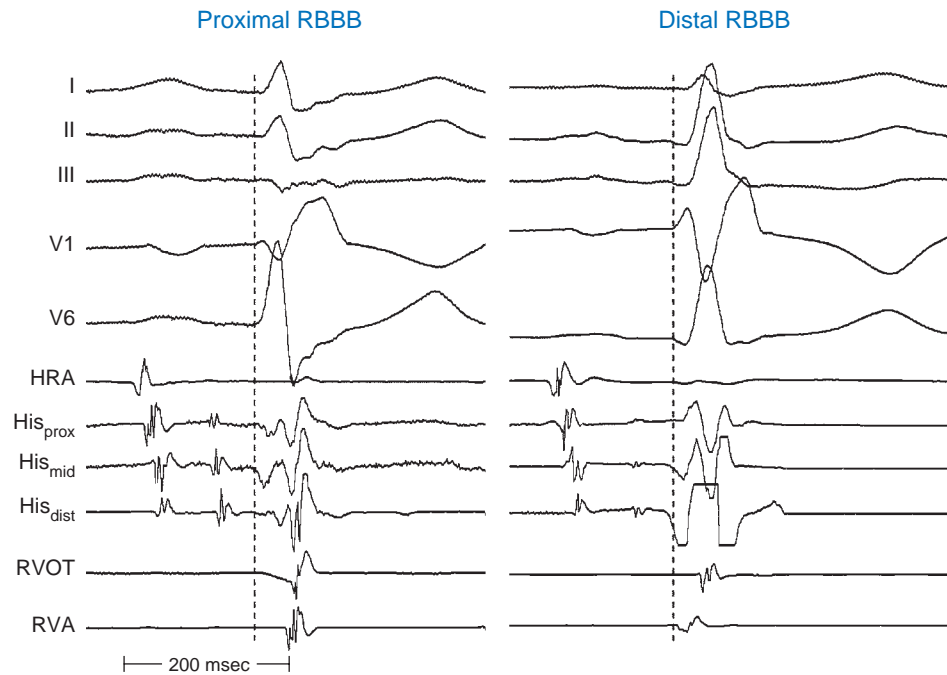


Fig. 10.14 Localization of the Site of Block in Right Bundle Branch Block (RBBB). Two complexes from different patients are shown, with proximal (left panel) and distal (right panel) RBBB, distinguished by the interval from QRS onset to right ventricle apical (RVA) recording. *His_{dist}*, Distal His bundle; *His_{mid}*, middle His bundle; *His_{prox}*, proximal His bundle; *RVA*, right ventricular apex; *RVOT*, right ventricular outflow tract.

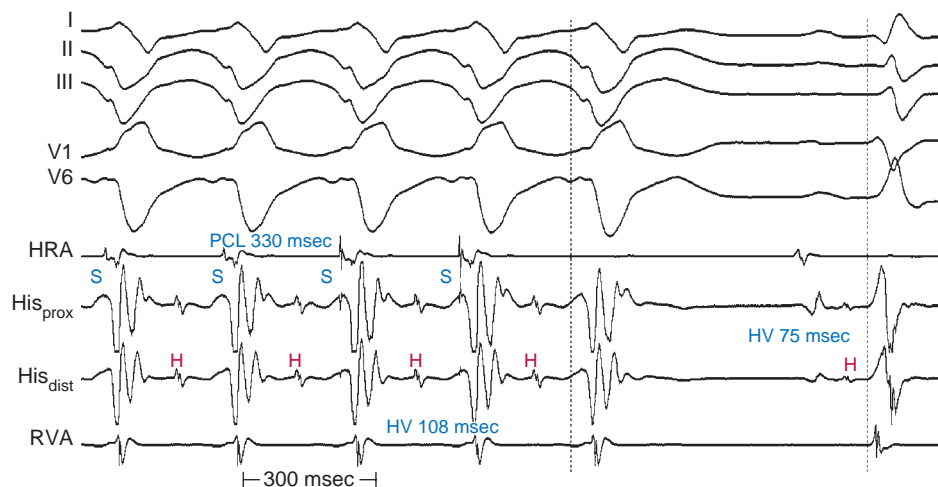


Fig. 10.15 His-Purkinje System (HPS) Disease. The PR interval is borderline (210 milliseconds), and the His bundle–ventricular (HV) interval is prolonged (75 milliseconds) during normal sinus rhythm (at right). Atrial pacing at a cycle length of 330 milliseconds results in stressing the HPS and further prolonging the HV interval (108 milliseconds). Right bundle branch block also develops during atrial pacing, a finding suggesting slower conduction over the right bundle than the left bundle. *His_{dist}*, Distal His bundle; *His_{prox}*, proximal His bundle; *HRA*, high right atrium; *PCL*, pacing cycle length.

Atrial Pacing

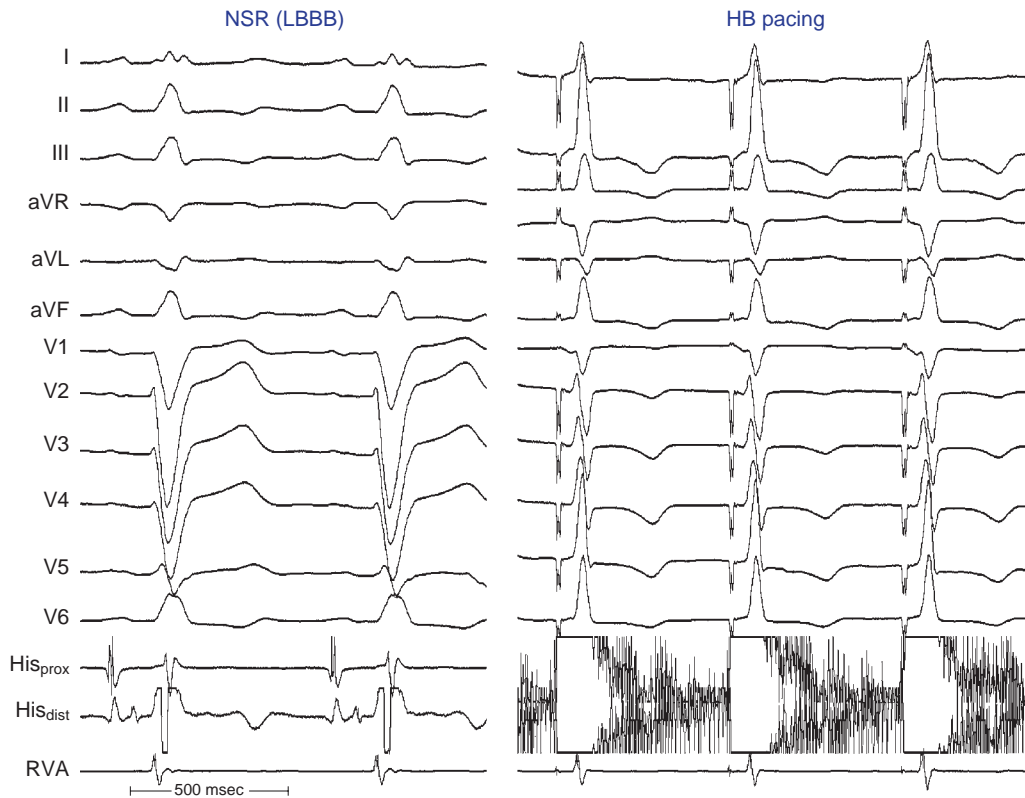
During incremental-rate atrial pacing, normal shortening of the HPS refractoriness at decreased pacing CLs facilitates 1:1 AV conduction. The development of second- or third-degree AV block within the HPS (in the absence of changing AH intervals) at pacing cycle lengths (PCLs) longer than 400 milliseconds is abnormal and suggests a high risk (50%) for progression to high-grade AV block (Fig. 10.15).

His Bundle Pacing

Selective pacing of the HB can help localize the site of bundle branch block. Normalization of the QRS during HB pacing is suggestive of HB disease proximal to the pacing site (eFig. 10.7).¹⁴

Ventricular Pacing

During RV pacing, retrograde RBBB is characterized by recording the His potential occurring after local ventricular activation in the HB



eFig. 10.7 Left Bundle Branch Block (LBBB) Secondary to Intra-Hisian Disease. Left, electrocardiogram leads and intracardiac recordings in a patient with complete LBBB. Right, pacing from the His bundle (HB) pacing normalizes the QRS complex, a finding suggesting that the LBBB is caused by HB disease proximal to the pacing site. *His_{dist}*, Distal His bundle; *His_{prox}*, proximal His bundle; *NSR*, normal sinus rhythm; *RVA*, right ventricular apex.

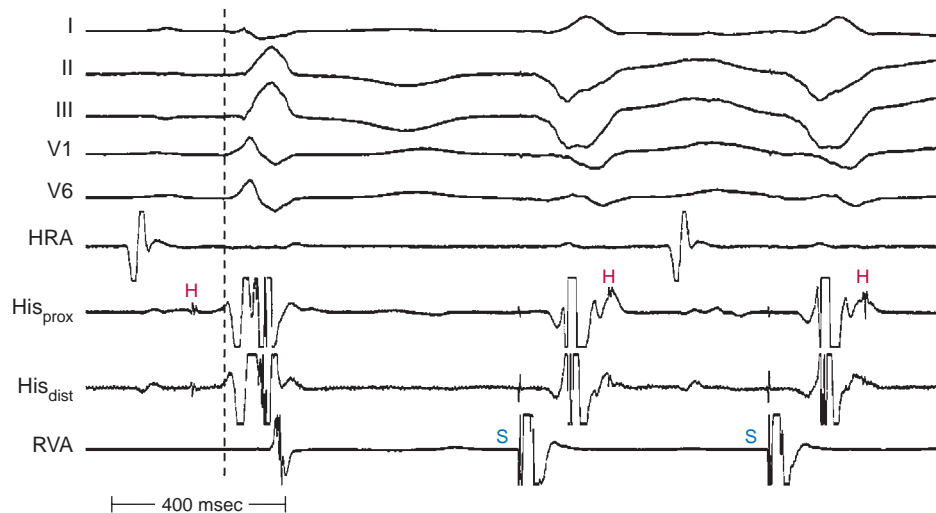


Fig. 10.16 Bidirectional right bundle branch block (RBBB). The sinus complex at left has proximal RBBB, indicated by a very prolonged ventricular–right ventricular apical (V–RVA) time (more than 100 milliseconds). RV pacing with the next two complexes show His activation following local ventricular activation in the His bundle (HB) recording, caused by propagation from the RV pacing site across the interventricular septum to the left bundle and then to the HB, rather than the more direct route retrogradely up the right bundle. This is consistent with both anterograde and retrograde proximal RBBB. *His_{dist}*, Distal His bundle; *His_{prox}*, proximal His bundle; *HRA*, high right atrium; *RVA*, right ventricular apex.

region (on the same catheter recording the His potential). The delay in HB activation is secondary to the longer route the paced impulse has to travel to reach the HB. The activation wavefront propagates from the RV pacing site across the interventricular septum to the LB and then to the HB, rather than the more direct retrograde route up the RB, which takes longer time than that required to activate the basal RV septum (Fig. 10.16).

Importantly, assessment of retrograde VH (or VA) conduction is not useful as an indicator of anterograde HPS reserve. Anterograde RBBB is usually proximal, whereas during RV stimulation, block usually occurs at the gate, which is at the distal HPS–myocardial junction.

Procainamide Challenge

The administration of drugs known to impair the HPS (e.g., procainamide) can unmask extraordinary sensitivity to the usual therapeutic doses of the drug, which itself can indicate poor HPS reserve. In normal individuals and in most patients with a moderately increased HV interval (55 to 80 milliseconds), procainamide typically produces a 10% to 20% increase in the HV interval. Abnormal HV interval responses to procainamide representing evidence of a higher risk for infra-Hisian AV block include any of the following: (1) doubling of the HV interval, (2) prolongation of the HV interval to more than 100 milliseconds, or (3) second- or third-degree infra-Hisian block.

Role of Electrophysiological Testing

EP testing is used to obtain information that could predict which patients are at risk for syncope, AV block, or SCD from a ventricular tachyarrhythmia (Box 10.2). Complete EP testing with programmed atrial and ventricular stimulation is necessary in patients with syncope and BBB because VT can be induced in 30% to 50% of such patients. Pacemaker therapy clearly can help prevent syncope in those patients in whom that event most likely was caused by transient bradyarrhythmia, but it has not been shown to prevent SCD or reduce cardiac mortality. The guidelines for permanent pacing therapy in chronic BBB are listed in Box 10.3.

BOX 10.2 Role of Electrophysiological Testing in Patients With Intraventricular Conduction Disturbances

EP Indicators of HPS Disease

- HV interval >55 ms
- Infra-Hisian block at atrial PCL ≥400 ms
- HPS ERP ≥450 ms
- HPS ERPs inversely related to PCLs
- Abnormal response to procainamide: prolongation of the HV interval by 100% or to >100 ms, or second- or third-degree infra-Hisian AV block

EP Indicators of High Risk for AV Block in Patients With IVCD

- HV interval >100 ms
- Infra-Hisian AV block or HV interval prolongation at atrial PCL >400 ms
- HPS-ERPs inversely related to PCLs
- Infra-Hisian AV block or doubling of the HV interval following procainamide in patients with neurological symptoms compatible with bradyarrhythmia

Possible Indications for Pacing in Patients With IVCD

- LBBB, RBBB, IVCD, RBBB + LAF block, or RBBB + LPF block associated with the following: HV interval >100 ms or HV interval = 60–99 ms in the presence of unexplained syncope or presyncope
- Infra-Hisian block at atrial PCL ≥400 ms (regardless of HV interval or presence of symptoms)
- Alternating BBB (regardless of HV interval or presence of symptoms)

AV, Atrioventricular; BBB, bundle branch block; EP, electrophysiological; ERP, effective refractory period; HPS, His-Purkinje system; HV, His bundle–ventricular; IVCD, intraventricular conduction defect; LAF, left anterior fascicle; LBBB, left bundle branch block; LPF, left posterior fascicle; PCL, pacing cycle length; RBBB, right bundle branch block.

BOX 10.3 ACCF/AHA/HRS Recommendations for Permanent Pacing in Chronic Bifascicular Block

Class I

- Advanced second-degree AV block or intermittent third-degree AV block
- Type 2 second-degree AV block
- Alternating bundle branch block

Class IIa

- Syncope not demonstrated to result from AV block, when other likely causes have been excluded, especially ventricular tachycardia
- Incidental finding at EP study of HV interval ≥ 100 ms in asymptomatic patients
- Incidental finding at EP study of pacing-induced block below the bundle of His that is not physiological

Class IIb

- Neuromuscular diseases, such as myotonic muscular dystrophy, Erb dystrophy (limb-girdle muscular dystrophy), and peroneal muscular atrophy with bifascicular block or any fascicular block, with or without symptoms

Class III

- Fascicular block without AV block or symptoms
- Fascicular block with first-degree AV block without symptoms

ACCF, American College of Cardiology Foundation; AHA, American Heart Association; AV, atrioventricular; EP, electrophysiological; HV, His bundle-ventricular; HRS, Heart Rhythm Society.

Modified from Epstein AE, DiMarco JP, Ellenbogen KA, et al. 2012 ACCF/AHA/HRS focused update incorporated into the ACCF/AHA/HRS 2008 guidelines for device-based therapy of cardiac rhythm abnormalities: a report of the American College of Cardiology Foundation/American Heart Association Task Force on Practice Guidelines and the Heart Rhythm Society. *J Am Coll Cardiol*. 2013;61:e6–75.

REFERENCES

1. Surawicz B, et al. AHA/ACCF/HRS recommendations for the standardization and interpretation of the electrocardiogram: part III: intraventricular conduction disturbances: a scientific statement from the American Heart Association Electrocardiography and Arrhythmias Committee. *Circulation*. 2009;119:e235–e240.
2. El-Sherif N, Jalife J. Paroxysmal atrioventricular block: are phase 3 and phase 4 block mechanisms or misnomers? *Heart Rhythm*. 2009;6:1514–1521.
3. Cabo C. Post-repolarization refractoriness increases vulnerability to block and initiation of reentrant impulses in heterogeneous infarcted myocardium. *Comput Biol Med*. 2015;65:209–219.
4. Brignole M, et al. Syncope due to idiopathic paroxysmal atrioventricular block: long-term follow-up of a distinct form of atrioventricular block. *J Am Coll Cardiol*. 2011;58:167–173.
5. Lee S, Wellens HJJ, Josephson ME. Paroxysmal atrioventricular block. *Heart Rhythm*. 2009;6:1229–1234.
6. Divakara Menon SM, Ribas CS, Ribas Meneclier CA, et al. Intermittent atrioventricular block: what is the mechanism? *Heart Rhythm*. 2012;9:154–155.
7. Carbone V, Carerj S, Calabrò MP. Bundle branch block on alternate beats during atrial fibrillation. *J Electrocardiol*. 2004;37:67–72.
8. Dobrzynski H, et al. Structure, function and clinical relevance of the cardiac conduction system, including the atrioventricular ring and outflow tract tissues. *Pharmacol Ther*. 2013;139:260–288.
9. Syed FF, Hai JJ, Lachman N, et al. The infrahisian conduction system and endocavitary cardiac structures: relevance for the invasive electrophysiologist. *J Interv Card Electrophysiol*. 2014;39:45–56.
10. Kaneko Y, et al. Discrimination between His-bundle and the right bundle branch during electrophysiologic studies. *Pacing Clin Electrophysiol*. 2009;32:72–75.
11. Boyden PA, Hirose M, Dun W. Cardiac Purkinje cells. *Heart Rhythm*. 2010;7:127–135.
12. Severs NJ. The cardiac muscle cell. *Bioessays*. 2000;22:188–199.
13. Gorennek B, et al. Cardiac arrhythmias in acute coronary syndromes: position paper from the joint EHRA, ACCA, and EAPCI task force. *EuroIntervention*. 2015;10:1095–1108.
14. Vijayaraman P, Naperkowski A, Ellenbogen KA, et al. Electrophysiologic insights into site of atrioventricular block lessons from permanent His bundle pacing. *JACC Clin Electrophysiol*. 2015;1:571–581.
15. Dandamudi G, Vijayaraman P. How to perform permanent his bundle pacing in routine clinical practice. *Heart Rhythm*. 2016;13:1–5.
16. Elizari MV, Acunzo RS, Ferreiro M. Hemiblocks revisited. *Circulation*. 2007;115:1154–1163.
17. Eschaliier R, et al. Nonspecific intraventricular conduction delay: definitions, prognosis, and implications for cardiac resynchronization therapy. *Heart Rhythm*. 2015;12:1071–1079.
18. Tzogiias L, et al. Electrocardiographic features and prevalence of bilateral bundle-branch delay. *Circ Arrhythm Electrophysiol*. 2014;7:640–644.
19. Kumar V, et al. Implications of left bundle branch block in patient treatment. *Am J Cardiol*. 2013;111:291–300.
20. Lewinter C, Torp-Pedersen C, Cleland JGF, et al. Right and left bundle branch block as predictors of long-term mortality following myocardial infarction. *Eur J Heart Fail*. 2011;13:1349–1354.
21. Bussink BE, et al. Right bundle branch block: prevalence, risk factors, and outcome in the general population: results from the Copenhagen City Heart Study. *Eur Heart J*. 2013;34:138–146.
22. Fernández-Lozano I, Brugada J. Right bundle branch block: are we looking in the right direction? *Eur Heart J*. 2013;34:86–88.
23. Breithardt G, Breithardt O-A. Left bundle branch block, an old-new entity. *J Cardiovasc Transl Res*. 2012;5:107–116.
24. Josephson ME, Wellens HJJ. The ECG in left bundle branch block and heart failure. *Heart Rhythm*. 2015;12:250–251.
25. Mascioli G, et al. Electrocardiographic criteria of true left bundle branch block: a simple sign to predict a better clinical and instrumental response to CRT. *Pacing Clin Electrophysiol*. 2012;35:927–934.
26. Surawicz B, Knilans TK. *Chou's Electrocardiography in Clinical Practice*. Philadelphia: Saunders Elsevier; 2008.
27. Strauss DG. Understanding ventricular activation. *J Electrocardiol*. 2011;44:282–284.
28. Galeotti L, van Dam PM, Loring Z, et al. Evaluating strict and conventional left bundle branch block criteria using electrocardiographic simulations. *Europace*. 2013;15:1816–1821.
29. Strauss DG, Selvester RH, Wagner GS. Defining left bundle branch block in the era of cardiac resynchronization therapy. *Am J Cardiol*. 2011;107:927–934.
30. Epstein AE, et al. 2012 ACCF/AHA/HRS focused update incorporated into the ACCF/AHA/HRS 2008 guidelines for device-based therapy of cardiac rhythm abnormalities: a report of the American College of Cardiology Foundation/American Heart Association Task Force on Practice Guide. *Circulation*. 2013;127:e283–e352.
31. Padanilam BJ, et al. The surface electrocardiogram predicts risk of heart block during right heart catheterization in patients with preexisting left bundle branch block: implications for the definition of complete left bundle branch block. *J Cardiovasc Electrophysiol*. 2010;21:781–785.

Focal Atrial Tachycardia

OUTLINE

Classification of Atrial Tachycardias, 305

Pathophysiology, 305

- Incessant Atrial Tachycardias, 307
- Anatomical Locations, 307
- Pulmonary Vein Tachycardia, 308
- Multifocal Atrial Tachycardia, 308
- Sinus Node Reentrant Tachycardia, 309

Epidemiology, 309

Clinical Presentation, 309

Initial Evaluation, 309

Principles of Management, 309

- Acute Management, 309
- Chronic Management, 310

Electrocardiographic Features, 311

- P Wave Morphology, 311
- QRS Morphology, 311
- P/QRS Relationship, 311
- Localization of the Tachycardia Site of Origin, 311

Electrophysiological Testing, 318

- Baseline Observations During Sinus Rhythm, 318
- Induction of Tachycardia, 318

Tachycardia Features, 320

Diagnostic Maneuvers During Tachycardia, 321

Diagnostic Maneuvers During Sinus Rhythm After Tachycardia Termination, 323

Exclusion of Other Arrhythmia Mechanisms, 324

Mapping, 324

Conventional Activation Mapping, 324

Pace Mapping, 328

Mapping Postpacing Intervals, 329

Electroanatomic Mapping, 330

Mapping Nonsustained Focal Atrial Tachycardia, 332

Ablation, 333

Target of Ablation, 333

Ablation Technique, 333

Ablation of Para-Hisian Atrial Tachycardias, 333

Endpoints of Ablation, 335

Outcome, 337

CLASSIFICATION OF ATRIAL TACHYCARDIAS

Organized atrial tachycardias (ATs) are broadly categorized as either focal (originating from a small circumscribed area from which it spreads out centrifugally) or macroreentrant (continuous, uninterrupted activation wavefront rotating around a relatively large central obstacle).¹

Focal ATs can be caused by automatic, triggered, or microreentrant mechanisms. The mechanism of macroreentrant atrial tachycardia (MRAT) is reentrant activation around a large central obstacle, generally several centimeters in diameter, at least in one of its dimensions. The central obstacle can consist of normal anatomical structures (venous or valvular orifices) or abnormal structures (scars), and can be fixed, functional (anisotropic conduction block), or a combination of both. There is no single point of origin of activation, and atrial tissues outside the circuit are activated from various parts of the circuit (Table 11.1).^{1,2}

Depending on whether the cavotricuspid isthmus (CTI) is critical to the reentry circuit, MRATs are divided into two groups: “CTI-dependent” or “non-CTI-dependent” MRAT. CTI-dependent MRATs include typical atrial flutter (AFL), lower loop reentry, and intra-isthmus reentry.

The term *atrial flutter* has traditionally been used to refer to a continuously undulating pattern on the ECG, without an isoelectric baseline in at least one lead, whatever the cycle length (CL). *Typical AFL* is reserved for a macroreentrant circuit with the activation wavefront rotating clockwise or counterclockwise around the tricuspid annulus

and using the CTI as an essential part of the reentry circuit. *Atypical AFL* is only a descriptive term for an AT with an ECG pattern of continuous undulation of the atrial complex, different from that in typical AFL. However, the term “atypical AFL” introduces unnecessary confusion, and a mechanistic description of the AT circuit in relation to atrial anatomy is preferred (e.g., perimitral macroreentry, lesional right atrial [RA] macroreentry; see Table 11.1).¹

Importantly, classification of ATs based on the 12-lead electrocardiogram (ECG) has been abandoned. Now it is well recognized that the underlying mechanisms of AT, as defined by conventional and advanced mapping techniques, do not correlate well with ECG patterns. Neither the tachycardia rate nor the lack of isoelectric baseline between atrial deflections on the surface ECG is specific for any arrhythmia mechanism.

This chapter discusses focal AT. Typical AFL and MRAT are discussed in subsequent chapters.

PATHOPHYSIOLOGY

Focal AT is characterized by atrial activation starting at a small area (focus), from which it spreads out centrifugally.¹ “Focal” implies that the site of origin cannot be mapped spatially beyond a single point or a few adjacent points with the resolution of a standard 4-mm-tip catheter. In contrast, MRAT is defined by activation that can be recorded over the entire tachycardia cycle length (TCL) around a large central obstacle, which is generally several centimeters in diameter.¹ Relatively

TABLE 11.1 Classification of Atrial Tachycardias

Focal atrial tachycardia	<ul style="list-style-type: none"> • Automatic atrial tachycardia • Triggered-activity atrial tachycardia • Microreentrant atrial tachycardia
Macroreentrant atrial tachycardia	<ul style="list-style-type: none"> Cavotricuspid isthmus-dependent right atrial macroreentry <ul style="list-style-type: none"> • Clockwise and counterclockwise typical atrial flutter • Double-loop reentry • Lower-loop reentry • Intra-isthmus reentry • Upper-loop reentry Noncavotricuspid isthmus-dependent right atrial macroreentry <ul style="list-style-type: none"> • Lesional or scar-related right atrial macroreentry Left atrial macroreentry <ul style="list-style-type: none"> • Perimitral macroreentry • Pulmonary vein macroreentry • Scar-related macroreentry • Left septal macroreentry • Postsurgical/postablation macroreentry

TABLE 11.2 Electrophysiological Characteristics of Focal Atrial Tachycardia According to Mechanism

	Automaticity	Triggered Activity	Microreentry
Initiation	<ul style="list-style-type: none"> • PES cannot induce AT. • AT initiation frequently requires catecholamines (isoproterenol). • On initiation, TCL tends to shorten progressively (warm up) for several beats until its ultimate rate is achieved. • P wave morphology of initiating beat is identical to other AT beats. 	<ul style="list-style-type: none"> • ATs can be initiated by AES or (more commonly) atrial pacing. • There is usually a direct relationship between the AES coupling interval or PCL initiating the AT and the interval to the onset of the AT and the early CL of the AT. • P wave morphology of initiating beat differs from other AT beats. 	<ul style="list-style-type: none"> • AT can reproducibly be initiated by AES or atrial pacing. • AT initiation is less dependent on catecholamine facilitation. • The initiating AES coupling interval and the interval between the initiating AES and first beat of AT are inversely related. • P wave morphology of initiating beat differs from other AT beats.
Termination	<ul style="list-style-type: none"> • PES cannot terminate AT. • TCL tends to prolong progressively (cool down) for several beats before termination. 	<ul style="list-style-type: none"> • AES and, more effectively, atrial pacing can usually terminate triggered-activity AT. 	<ul style="list-style-type: none"> • AT can reproducibly be terminated by PES.
Response to AES	<ul style="list-style-type: none"> • AES can reset AT (with a flat resetting response). 	<ul style="list-style-type: none"> • AES can reset AT (with a decreasing resetting response). 	<ul style="list-style-type: none"> • AES can reset AT (with an increasing or mixed resetting response).
Response to overdrive atrial pacing	<ul style="list-style-type: none"> • Transient overdrive suppression followed by gradual recovery of prepacing rate. • Automatic AT cannot be entrained by atrial pacing. • The tachycardia return CL following cessation progressively prolongs with increasing the duration or rate of the overdrive pacing train. 	<ul style="list-style-type: none"> • AT cannot be entrained by atrial pacing. • The tachycardia return CL tends to shorten with shortening of the PCL. 	<ul style="list-style-type: none"> • Atrial pacing can entrain AT. • The tachycardia return CL and PPI are fixed regardless of the number of beats in the pacing train.
Response to adenosine	<ul style="list-style-type: none"> • Transient slowing or suppression of tachycardia followed by acceleration to baseline TCL or spontaneous reemergence of AT. 	<ul style="list-style-type: none"> • AT terminates and does not spontaneously reinitiate. 	<ul style="list-style-type: none"> • No effect
Response to vagal maneuvers and adenosine	<ul style="list-style-type: none"> • AT may slow down but does not terminate. 	<ul style="list-style-type: none"> • AT may terminate. 	<ul style="list-style-type: none"> • No effect
Electrogram at site of origin	<ul style="list-style-type: none"> • Discrete electrogram. 	<ul style="list-style-type: none"> • Discrete electrogram. 	<ul style="list-style-type: none"> • Fractionated electrogram that spans at least 35% of the TCL.

AES, Atrial extrastimulus; AT, atrial tachycardia; CL, cycle length; PCL, pacing cycle length; PES, programmed electrical stimulation; PPI, postpacing interval; TCL, tachycardia cycle length.

small reentry circuits can resemble focal AT, especially if limited numbers of endocardial recordings are collected (see Fig. 13.11). The term *localized reentry* has been used to refer to reentry in which the circuit is localized to a small area (covering a surface diameter of less than 3 cm) and does not have an easily identifiable central obstacle.

Available information suggests that a focal activation pattern can be caused by automaticity, triggered activity, or microreentry (Table 11.2). Delineating the mechanism of focal AT, however, can be difficult, and the means of distinguishing focal AT mechanisms through pharmacological testing or electrophysiology (EP) study have limited

sensitivity and specificity. In addition, there is a significant overlap in the EP characteristics of tachycardias with differing mechanisms.³ It is especially difficult to discriminate definitively between triggered activity and microreentry as a mechanism of focal AT; therefore some investigators have classified focal ATs as either automatic or nonautomatic.¹ Furthermore, it is not clear that making such mechanistic distinctions among various types of focal ATs carries clinical significance, especially in the era of catheter ablation, although it is possible that such information could be useful in guiding drug therapy. In contrast, determination of the likely focal versus macroreentrant mechanism is critical for planning the mapping and ablation strategy.⁴

Not infrequently, two or more foci of AT can be found in the same patient. In these patients, the AT appears to have different EP characteristics from focal AT with a single focus, as it tends to involve the LA and has greater cardiovascular comorbidity, shorter CL, longer total activation time, and lower acute and long-term success rates of catheter ablation. The term *multiple focal ATs* needs to be distinguished from *multifocal AT* (MAT), which refers to the continuously shifting site of origin of the atrial impulse (see below).⁵

Incessant Atrial Tachycardias

The term *incessant* is applied to an AT that is present for at least 50% of the time that a patient is monitored. Incessant AT frequently is automatic, but it can also be secondary to reentry or triggered activity. Incessant tachycardias occur in up to 25% of patients with focal AT. Foci arising from the atrial appendages and pulmonary veins (PVs) are frequently incessant (84% and 59%, respectively). Incessant ATs (regardless of the anatomical site of origin) can precipitate cardiomyopathy in approximately one-third of cases. Incessant tachycardias precipitating cardiomyopathy characteristically tend to have long atrial CLs as

compared with ATs not associated with cardiomyopathy and hence may produce negligible symptoms and go unrecognized by the patient until symptoms related to cardiomyopathy develop.⁶

Anatomical Locations

Focal ATs have a predilection for originating from certain anatomical regions of the atria (Fig. 11.1).⁷ The RA is the site of origin for the majority (more than 60%) of focal ATs. Approximately two-thirds of RA ATs are distributed along the so-called ring of fire, extending from the superior aspect of the crista terminalis and down the long axis of the crista ("cristal tachycardias"), to the tricuspid annulus, coronary sinus (CS), and atrioventricular (AV) junction, with an apparent gradation in frequency from superior to inferior. This particular anatomical distribution of ATs may be related to the marked anisotropy characterizing the region of the crista terminalis. Such anisotropy, which is related to poor transverse cell-to-cell coupling, favors the development of microreentry by creating regions of slow conduction. Fractionated electrograms often seen at a successful AT ablation site can be markers of the requisite nonuniform anisotropic substrate. In addition, the normal sinus pacemaker complex is distributed along the long axis of the crista terminalis. The presence of automatic tissue, together with relative cellular uncoupling, may be a requirement for abnormal automaticity such that a normal atrium is prevented from electrotonically inhibiting abnormal phase 4 depolarization. Of note, the presence of structural heart disease increases the probability of RA location of the AT, but from sites outside the crista terminalis.

The PV ostia are the most common sites of origin of focal tachycardias within the LA; they account for approximately 67% of LA ATs and between 3% and 29% of all focal ATs.^{7,8} Other sites of tachycardia clustering include the CS os, mitral and tricuspid annuli, bases of right

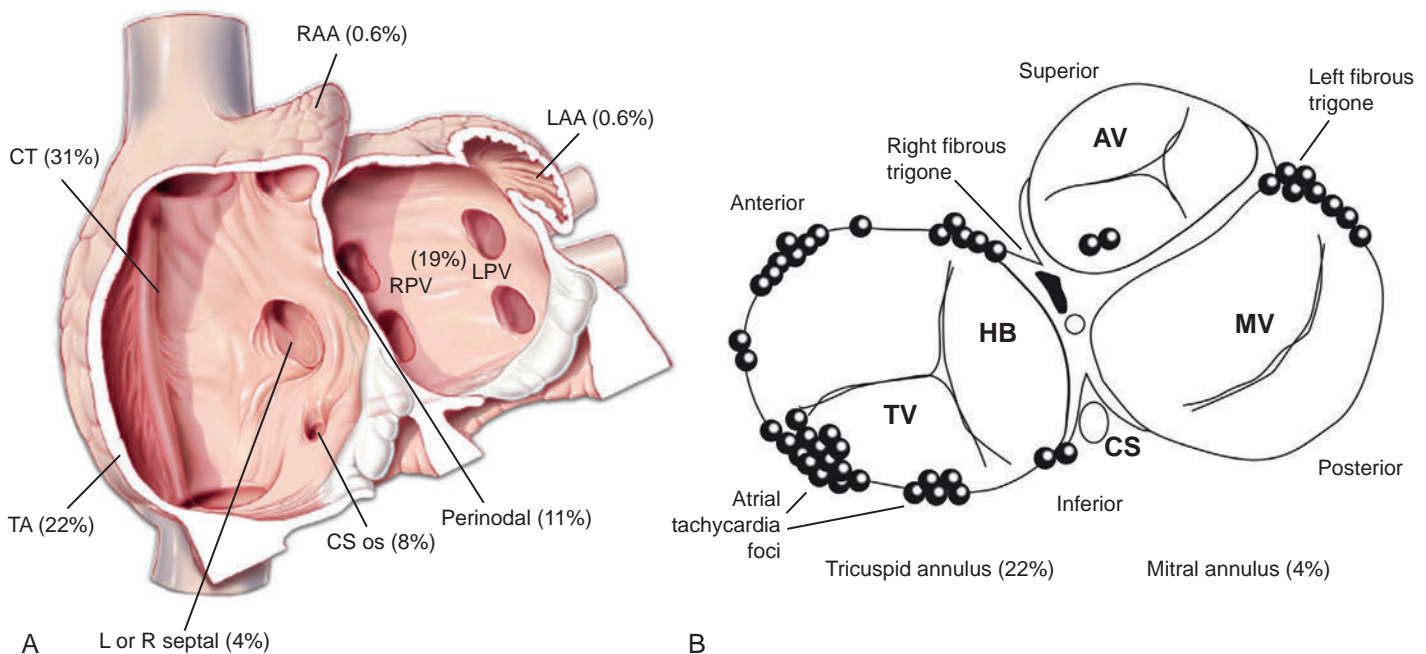


Fig. 11.1 Anatomical Distribution of Atrial Tachycardias. (A) Common anatomical distribution of focal atrial tachycardias showing rough percentage distribution; the atrioventricular annuli have been removed. (B) Common anatomical distribution of mitral and tricuspid annular atrial tachycardias. AV, Aortic valve; CS (os), coronary sinus (ostium); CT, crista terminalis; HB, His bundle; LAA, left atrial appendage; LPV, left pulmonary veins; MV, mitral valve; RAA, right atrial appendage; RPV, right pulmonary veins; TA, tricuspid annulus; TV, tricuspid valve. (From Lee G, Sanders P, Kalman JM. Catheter ablation of atrial arrhythmias: state of the art. *Lancet* (London, England). 2012;380:1509–1519.)

and left atrial appendages, para-Hisian region, and atrial septum. Focal ATs also can arise within the vein of Marshall, superior vena cava (SVC), or inferior vena cava (IVC). ATs have been described originating from the noncoronary aortic sinus of Valsalva. The distribution of AT foci can differ, depending on the patient population.

A recent report found that the majority of triggered-activity focal ATs originate along the crista terminalis and tricuspid and mitral annuli, whereas automatic ATs often originate from the right or left atrial appendage or PVs. Microreentrant ATs are frequently, but not always, related to previous ablation lines performed for AF or MRAT.⁹

Pulmonary Vein Tachycardia

Arrhythmias originating from the PVs can have a critical role in the development of AF in susceptible individuals. Focal ATs arising from the PVs, however, appear to be a distinct clinical entity from the PV arrhythmias associated with AF. Patients with focal PV ATs do not seem to be at risk of AF in the long term; they resemble patients with focal ATs originating elsewhere with a localized isolated substrate that is successfully addressed with a focal ablative approach. Several potential explanations have been suggested for the different behavior. The underlying pathophysiological process in patients with AF is probably fundamentally different. It is a generalized process diffusely affecting the muscular sleeves in all four PVs, often with multiple PV foci originating distally (up to 2 to 4 cm) within the vein, compared with the focal nature of the process in patients with isolated PV tachycardia. In addition, the CLs of the PV ATs are longer (mean CL 340 milliseconds) than the reported CLs of PV tachycardia in AF patients (130 milliseconds). The CL of AT also tends to be irregular in patients with AF, but not in patients with PV AT. It is possible that foci with shorter CL and irregular activity may not conduct in a 1:1 fashion from the PV to the LA, with resulting fibrillatory conduction and AF. Furthermore, patients with AF tend to be older than those with PV AT and consequently more prone to more widespread atrial remodeling associated with age, hypertension, or other pathological processes.^{3,7}

Multifocal Atrial Tachycardia

MAT (also is known as chaotic AT) is usually caused by enhanced automaticity and is characterized by varying morphology of the P waves, suggesting that the pacemaker arises in different atrial locations (Fig. 11.2). The shift in pacemaker focus is usually associated with different PR intervals (depending on its proximity to the atrioventricular node [AVN]) and varying R-R intervals. The ventricular rate is usually 100 to 130 beats/min but may be as low as 90 beats/min or as high as 250 beats/min. Some P waves can be aberrantly conducted, and some can be nonconducted, further contributing to the irregularity of the ventricular rate.

In general, the ECG diagnosis of MAT requires the following observations: (1) discrete P waves (in distinction to AF); (2) at least three distinctly different P wave morphologies in the same ECG lead (in distinction to focal and MRAT); (3) atrial rate faster than 90 to 100 beats/min (in distinction to wandering pacemaker); (4) absence of one dominant atrial pacemaker (in distinction to normal sinus rhythm [NSR] with frequent premature atrial complexes [PACs]); (5) P waves that are separated by isoelectric intervals (in distinction to AFL); and (6) varying PP, PR, and RR intervals.¹⁰

MAT typically is associated with underlying pulmonary, cardiac, or metabolic disease. In particular, MAT is frequently observed in patients with chronic obstructive pulmonary disease (present in approximately 60% of patients with MAT) or congestive heart failure, especially those treated with theophylline, β -adrenergic agonists, or digoxin, or during a period with exacerbation of the underlying disorder, hypoxemia, or electrolyte imbalance (e.g., hypokalemia, hypomagnesemia, acidosis). MAT can also occur in patients following surgical procedures, especially those with postoperative complications such as respiratory compromise, sepsis, acute heart failure, pulmonary embolism, electrolyte abnormalities, or renal insufficiency. These patients also have higher incidence of other atrial arrhythmias, such as frequent PACs, AF, and AFL.¹⁰

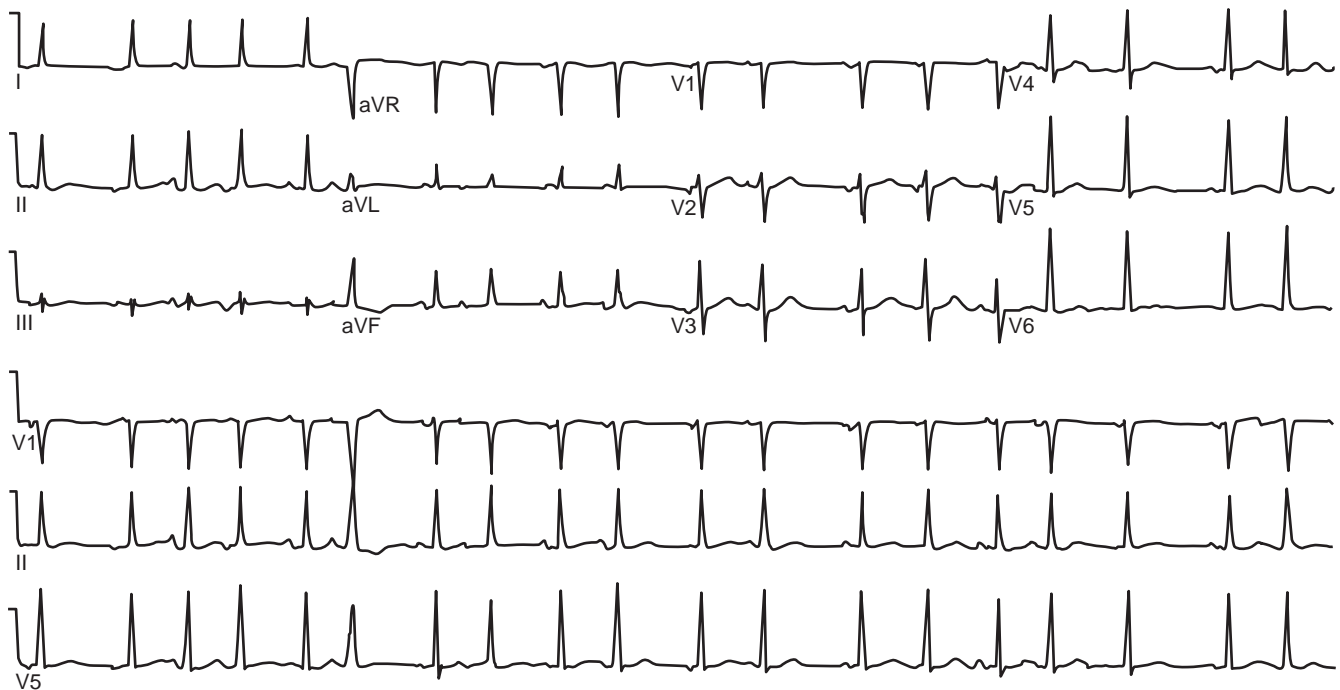


Fig. 11.2 Surface Electrocardiogram of Multifocal Atrial Tachycardia. Note the varying morphology of the P waves and the PR intervals.

MAT does not usually precipitate hemodynamic compromise, and patient's clinical symptoms are primarily related to the underlying illness rather than the tachycardia itself. Hence the management of MAT is mainly directed toward the treatment of the underlying disease, correction of electrolyte abnormalities, and withdrawal of offending drugs (e.g., theophylline, digoxin). IV magnesium can be helpful, even in patients with normal magnesium levels. Pharmacological therapy is associated with limited efficacy in suppressing the arrhythmia and controlling the ventricular rate during MAT. When MAT is symptomatic or leads to decompensation of underlying disease, beta-blockers and verapamil constitute the initial therapy, unless contraindicated because of the presence of bronchospasm or hypotension. Amiodarone can be useful in refractory cases. Electrical cardioversion is not effective and hence not recommended. Catheter ablation is not likely to be effective, given the underlying diffuse atrial abnormalities and severe comorbidities. Ablation of the AVN and pacemaker implantation for rate control is rarely indicated, and should be reserved to patients with severe symptoms related to the tachycardia and failed medical therapy.¹⁰

Sinus Node Reentrant Tachycardia

Sinus node reentrant tachycardia was originally described as a tachycardia that could be induced and terminated by programmed electrical stimulation with a P wave morphology identical or similar to sinus P waves and TCLs of 350 to 550 milliseconds (see Fig. 16.3). There have been some reports of endocardial ablation of sinus node reentrant tachycardias identified by these criteria. However, the precise identification of sinus node reentrant tachycardia remains elusive, and whether the reentry substrate is confined within the sinus node or involves perinodal atrial tissue is unknown, and whether it represents a category distinct from other intraatrial tachycardias is uncertain. More likely, sinus node reentrant tachycardia is a microreentrant focal ATs that happens to be arising along the crista terminalis, very close to the usual location of the sinus node. The arrhythmia typically presents as a paroxysmal tachycardia, and frequently as bursts of nonsustained AT, with P waves that are virtually identical to sinus P waves. Consistent with a reentry mechanism, this tachycardia is usually triggered and terminated abruptly by a PAC. The tachycardia can also be terminated by vagal maneuvers. In contrast to sinus tachycardia, sinus node reentrant tachycardia is characterized by abrupt onset and termination, and often has a longer PR interval than that observed during NSR (since the elevated adrenergic tone that drives the sinus node also accelerates AVN conduction).¹⁰

EPIDEMIOLOGY

Focal atrial ectopy and nonsustained AT are frequently observed on Holter recordings and are seldom associated with symptoms. Sustained focal ATs are relatively infrequent; they are diagnosed in approximately 5% to 15% of patients referred for catheter ablation of supraventricular tachycardia (SVT). However, ATs comprise a progressively greater proportion of paroxysmal SVTs with increasing age, accounting for 23% in patients older than 70 years. Age-related changes in the atrial EP substrate, including cellular coupling and autonomic influences, likely contribute to the increased incidence of AT in older individuals.¹¹ Men and women seem to be equally affected. In adults, focal ATs can occur in the absence of structural heart disease. Nevertheless, the incidence of associated structural heart disease is higher in patients with focal AT than those with other types of paroxysmal SVT. Among focal AT patients, those with multiple tachycardia foci are more likely to have underlying heart disease.¹² The long-term prognosis in patients with focal AT is generally benign, except for those with incessant ATs, which can precipitate tachycardia-induced cardiomyopathy.¹⁰

CLINICAL PRESENTATION

Focal ATs can manifest as paroxysmal or incessant tachycardias. When paroxysmal, AT frequently manifests with episodes of palpitations and heart racing that start and terminate abruptly. Associated symptoms can include lightheadedness, dyspnea, chest discomfort, and weakness. Syncope is rare. Due to the higher prevalence of structural heart disease in this group of patients, symptoms of AT can be more severe than other types of paroxysmal SVTs. Decompensation of underlying heart failure or ischemic heart disease can be precipitated by episodes of AT.

Tachycardia-induced ventricular cardiomyopathy develops in 10% of patients with focal AT, but predominantly in those with incessant or, less commonly, frequently repetitive tachycardia. Incessant AT can precipitate cardiomyopathy in approximately one-third of patients, and frequently manifest with symptoms of congestive heart failure. In contrast to rapid paroxysmal ATs that are more likely to cause significant symptoms of palpitations and be diagnosed earlier in the clinical course, incessant ATs tend to have slower atrial and ventricular rates, and hence patients can remain asymptomatic until they present with decompensated heart failure secondary to tachycardia-induced cardiomyopathy. Elimination of the tachycardia results in normalization of LV function within a few months in the vast majority of patients.⁶

AT can also manifest as a frequently repetitive tachycardia, with frequent episodes of AT interrupted by brief periods of NSR. The repetitive type can be tolerated well for years. It may cause symptoms only in cases of fast heart rates during phases of tachycardia, and it infrequently induces dilated cardiomyopathy.

INITIAL EVALUATION

Clinical symptoms are not usually helpful in distinguishing paroxysmal focal AT from other forms of paroxysmal SVT. Documentation of the arrhythmia during spontaneous symptoms on ECG or ambulatory cardiac monitoring is important to establish the diagnosis. Holter or cardiac event monitoring (depending on the frequency of symptoms) is often adequate. Implantable loop recorders can be helpful in selected cases, with rare episodes associated with severe symptoms of hemodynamic instability (e.g., syncope).

The diagnosis of the incessant and frequently repetitive forms of AT usually can be readily made on ECG recordings based on P wave morphology and the frequent presence of AV block during the tachycardia on ECG recordings. An ECG pattern of AT with discrete P waves and isoelectric intervals is suggestive of a focal mechanism of the AT, but it does not rule out MRAT, especially in patients with complex structural heart disease, prior cardiac surgery for congenital heart disease, or previous AF catheter or surgical ablation. Not infrequently, the diagnosis of focal AT can be established with certainty only by an EP study.

Echocardiography is recommended to exclude or diagnose the presence of structural heart disease. Cardiac stress testing and other diagnostic studies are considered in patients at risk for coronary artery disease.

Invasive EP testing with subsequent catheter ablation can be used for diagnosis and therapy in cases with a clear history of paroxysmal regular palpitations. It can also be considered in patients with preexcitation or disabling symptoms without ECG documentation of an arrhythmia.

PRINCIPLES OF MANAGEMENT

Acute Management

The usual acute therapy for AT consists of IV beta-blockers, diltiazem, or verapamil (Fig. 11.3). However, these drugs have modest efficacy (30% to 50%) in either terminating the focal AT or slowing the

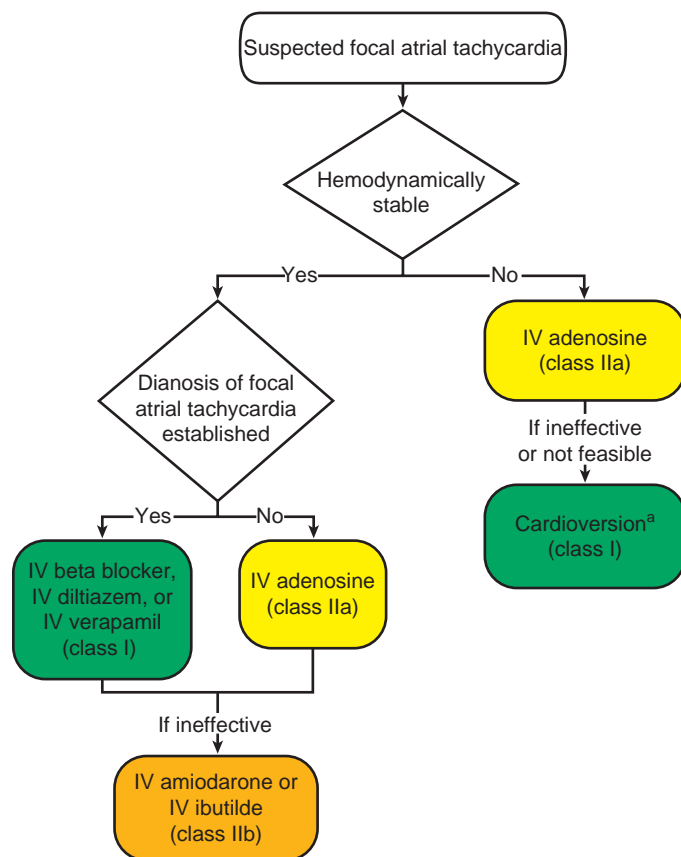


Fig. 11.3 Acute Treatment of Suspected Focal Atrial Tachycardia. Drugs listed alphabetically. ^aFor rhythms that break or recur spontaneously, synchronized cardioversion is not appropriate. IV, Intravenous. (From Page RL, Joglar JA, Caldwell MA, et al. 2015 ACC/AHA/HRS guideline for the management of adult patients with supraventricular tachycardia: a report of the American College of Cardiology/American Heart Association Task Force on Clinical Practice Guidelines and the Heart Rhythm Society. *J Am Coll Cardiol.* 2016;67:e27–e115.)

ventricular rate. Digoxin has not been well studied for focal AT. The response of focal AT to drug therapy is influenced, in part, by the underlying mechanism of the tachycardia. Automatic ATs are more likely to be terminated by beta-blockers, while the response of triggered AT is variable. On the other hand, the response of microreentrant AT can depend on the location of the microreentrant circuit, with those ATs arising from the perinodal region being most sensitive.¹⁰

Vagal maneuvers and adenosine can be used for acute termination of AT. However, ATs can be terminated with vagal maneuvers only on rare occasions, and the response to adenosine is variable. While a significant proportion of triggered ATs will terminate with adenosine, persistence or transient suppression of the tachycardia (with possible transient AV block) is also a common response to adenosine, especially in automatic or microreentrant ATs.¹⁰

For refractory cases, intravenous (IV) ibutilide, class IC drugs (e.g., flecainide, propafenone), or amiodarone can be considered. IV flecainide and propafenone are moderately effective; these agents are not available in the United States. The effectiveness of ibutilide for treatment of focal AT is unclear. IV amiodarone may be reasonable, especially in acute ill patients and those with decompensated heart failure. Electrical cardioversion can be considered for symptomatic patients with drug-resistant arrhythmia. Although electrical cardioversion seldom terminates automatic ATs, it can be successful for triggered and microreentrant ATs.¹⁰

Chronic Management

Long-term therapeutic decisions should consider the severity of symptoms, impact on life style, effectiveness and tolerance of drug therapy, and the presence of concomitant structural heart disease, as well as patient preference (Fig. 11.4).¹⁰

Catheter Ablation

Catheter ablation is recommended in patients with recurrent symptomatic AT, especially when pharmacological therapy is unsuccessful, not tolerated, or not preferred. Catheter ablation is also recommended for incessant AT, even in asymptomatic patients, especially when tachycardia-induced

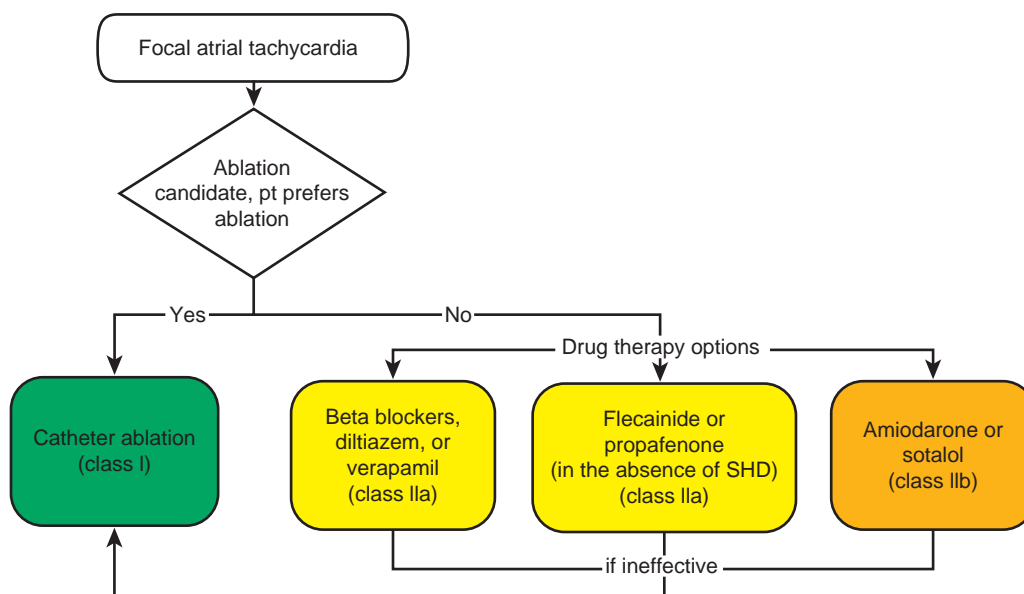


Fig. 11.4 Ongoing Treatment of Suspected Focal Atrial Tachycardia. Drugs listed alphabetically. *pt*, Patient; *SHD*, structural heart disease (including ischemic heart disease). (From Page RL, Joglar JA, Caldwell MA, et al. 2015 ACC/AHA/HRS guideline for the management of adult patients with supraventricular tachycardia: a report of the American College of Cardiology/American Heart Association Task Force on Clinical Practice Guidelines and the Heart Rhythm Society. *J Am Coll Cardiol.* 2016;67:e27–e115.)

cardiomyopathy has developed. In the latter group of patients, complete resolution of LV dysfunction has been observed following successful radiofrequency (RF) catheter ablation of the AT focus.⁶ Regardless of whether the arrhythmia is caused by abnormal automaticity, triggered activity, or microreentry, focal AT can be ablated by targeting the site of origin (focus) of the AT. Catheter ablation for focal AT carries a success rate of more than 90%, with a recurrence rate of 9%. The incidence of significant complications is relatively low (1% to 3%) in experienced centers.¹⁰

Pharmacological Therapy

No large studies have been conducted to assess the effect of pharmacological treatment in patients with focal ATs, but both paroxysmal and especially incessant ATs are reported to be difficult to treat medically. Available data support a recommendation for initial therapy with calcium channel blockers or beta-blockers because these agents may prove to be effective and have low side-effect profiles. If these drugs are unsuccessful, then class IC agents (flecainide and propafenone) in combination with an AVN blocking agent, or class III agents (sotalol and amiodarone), may be considered; however, the potential benefit should be balanced by the potential risks of proarrhythmia and toxicity. Because ATs often occur in older patients and in the context of structural heart disease, class IC agents should be used only after cardiomyopathy and coronary artery disease have been excluded.¹⁰

ELECTROCARDIOGRAPHIC FEATURES

P Wave Morphology

During AT, typically there are discrete P waves at rates of 130 to 240 beats/min, but possibly as slow as 100 beats/min or as fast as 300 beats/min. Antiarrhythmic drugs can slow the atrial rate without abolishing the AT. Classically, there are clearly defined isoelectric intervals between the P waves in all leads (Fig. 11.5). However, in the presence of rapid atrial rates or broad P waves due to intraatrial conduction disturbances, there may be no isoelectric baseline. In these cases, the ECG shows an AFL pattern (continuous undulation without isoelectric baseline; Fig. 11.6).¹ Nevertheless, one report demonstrated a high sensitivity (90%) and specificity (90%) of *quantitative* ECG indexes of shorter atrial activation and longer diastolic intervals in distinguishing focal from MRAT. This approach was effective in cases with and without 1:1 AV conduction and when the P or flutter waves overlay T waves.¹³

P wave morphology depends on the anatomical location of the atrial focus, and it can be used to approximate the site of origin of the AT. However, the P wave can be partially masked by the preceding ST segment or T wave. Vagal maneuvers and adenosine infusion to provide transient AV block can be used to obtain a clear view of the P wave, assuming that the tachycardia does not terminate. The compensatory pause following a premature ventricular complex during the AT can also help delineate P wave morphology (Fig. 11.7).

It has been suggested that the multilead body surface potential recording can be used to help localize the site of origin of the tachycardia. One report described a clinical application of ECG imaging (ECGI) as an adjunctive noninvasive technology to identify the site of origin of a focal AT accurately prior to catheter ablation (eFig. 11.1).^{14,15}

Of note, P wave morphology at the onset of the tachycardia can help determine the mechanism of focal AT. Automatic ATs start with a P wave identical to the P wave during the arrhythmia, and the rate generally increases gradually (warms up) over the first few seconds. In comparison, intraatrial reentry or triggered-activity AT is usually initiated by a P wave from a PAC that generally differs in morphology from the P wave during the established arrhythmia (Fig. 11.8).

QRS Morphology

QRS morphology during AT is usually the same as during NSR. However, functional aberration can occur at rapid atrial rates.

P/QRS Relationship

The AV relationship is usually 1:1 during ATs, but Wenckebach or 2:1 AV block (Fig. 11.9) can occur at rapid rates, in the presence of AVN disease, or in the presence of drugs that slow AVN conduction. The presence of AV block during an SVT strongly suggests AT, excludes atrioventricular reentrant tachycardia (AVRT), and renders atrioventricular nodal reentrant tachycardia (AVNRT) unlikely.

ATs usually have a long RP interval; nonetheless, the RP interval can also be short, depending on the degree of AV conduction delay (i.e., PR interval prolongation) during the tachycardia.

Localization of the Tachycardia Site of Origin

P wave morphology on the 12-lead ECG during ATs is determined not only by the anatomical location of the AT focus but also by the subsequent activation pattern within the atrium of origin as well as the contralateral atrium. The activation sequence of the contralateral atrium is determined by the relative proximity of the source of activation to the insertion site of each of the preferential interatrial connections. These include Bachmann's bundle, which connects the anterosuperior RA and LA, the interatrial connection located in the proximity of the CS os, the rim of the fossa ovalis, as well as small muscular bridges connecting the RA posterior wall with the LA posterior wall near the ostia of the right-sided PVs.^{16,17}

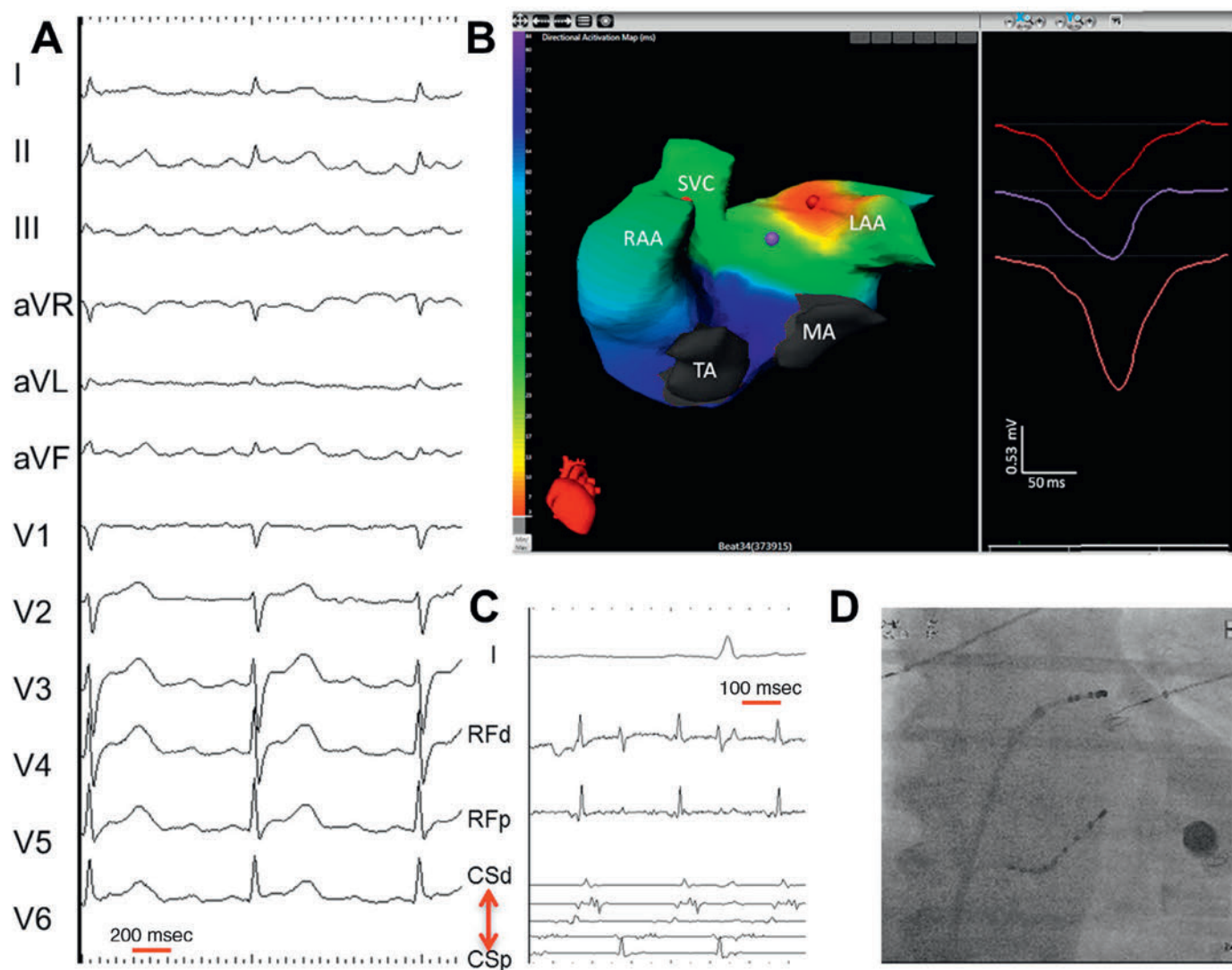
The ECG lead V₁ is the most useful in identifying the likely anatomical site of origin for focal AT. Lead V₁ is located to the right and anteriorly in relation to the atria (which should be considered anatomically as right anterior [RA] and left posterior [LA] structures). Thus, for example, tachycardias originating from the tricuspid annulus have negative P waves in lead V₁ because of the anterior and rightward location of this structure (i.e., activation travels *away* from lead V₁). The P wave in lead V₁ is universally positive for tachycardias originating from the PVs because of the posterior location of these structures (i.e., the impulse travels *toward* lead V₁).

In general, P waves identical to the sinus P wave are suggestive of sinus node reentrant tachycardia or perinodal AT. P wave vector in the inferior leads is indicative of the craniocaudal localization of AT origins. Foci in the superior aspect of the atria (such as superior PVs, atrial appendages, and superior crista terminalis) exhibit positive P waves in the inferior leads, whereas those originating from low atrial locations have negative P waves. ATs originating close to the interatrial septum exhibit P waves that are of shorter duration than the sinus P waves. Anterior RA or LA free wall or annular foci tend to have P waves with late precordial transition to an upright appearance. ATs originating from posterior atrial structures (such as the PVs or crista terminalis) usually have positive P waves in the anterior precordial leads.

Several algorithms (Figs. 11.10 and 11.11) have been proposed for ECG localization of focal AT using P wave morphology.⁷ Importantly, while P wave morphology provides a useful guide to the localization of focal AT in patients without structural heart disease, activation patterns can be altered in patients with prior surgery or extensive atrial ablation or in those with significant structural heart disease, significantly rendering P wave morphology significantly less helpful.¹⁸

Right Versus Left Atrial Tachycardias

Several features of P wave morphology can help distinguish RA from LA foci; leads aVL and V₁ are the most helpful for this purpose. In lead V₁, a negative or biphasic (+/−) P wave predicts RA foci with 100%



eFig. 11.1 Noninvasive Electrocardiogram (ECG) Imaging of Focal Atrial Tachycardia (AT). (A) Surface ECG of clinical AT. (B) Isochronal activation map of a basal LAA source centrifugal AT. The morphology of the virtual unipolar electrogram at the source displays typical QS morphology. (C) Intracardiac electrograms from the lateral left atrium and coronary sinus recorded during the ablation of left atrial source centrifugal AT. (D) Posteroanterior fluoroscopic image showing the location of intracardiac catheters. *CSd*, Distal coronary sinus; *CSp*, proximal coronary sinus; *LAA*, Left atrial appendage; *MA*, mitral annulus; *RAA*, right atrial appendage; *RFd*, distal ablation bipole; *RFp*, proximal ablation bipole; *SVC*, superior vena cava; *TA*, tricuspid annulus. (From Shah AJ, Hocini M, Xhaet O, et al. Validation of novel 3-dimensional electrocardiographic mapping of atrial tachycardias by invasive mapping and ablation: a multicenter study. *J Am Coll Cardiol*. 2013;62:889–897.)

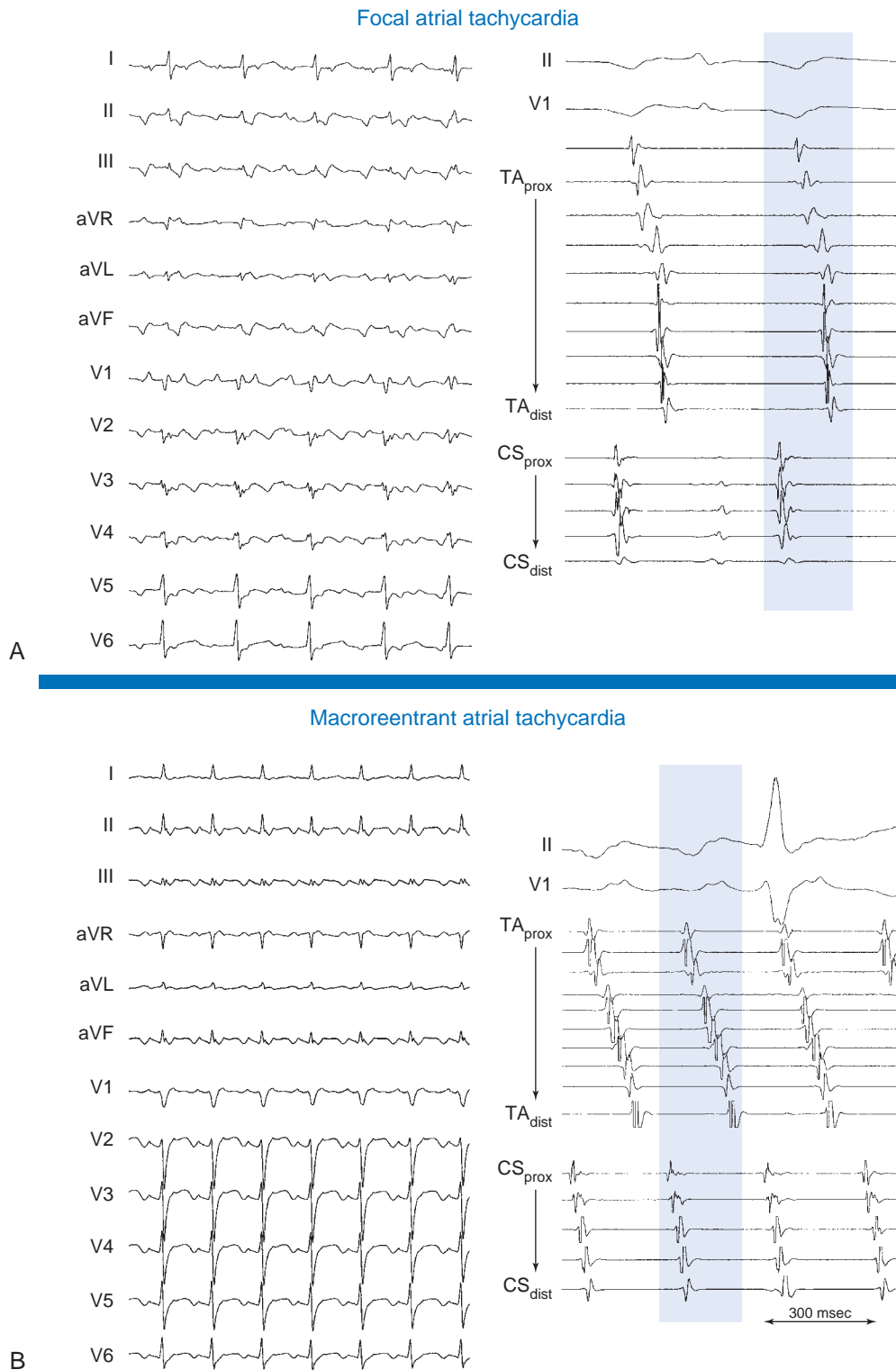


Fig. 11.5 Comparison of Focal and Macroreentrant Atrial Tachycardia (AT). (A) Surface electrocardiogram and endocardial activation sequence of focal AT originating from inferior aspect of the mitral annulus with 2:1 atrioventricular (AV) conduction. (B) Surface electrocardiogram and endocardial activation macroreentrant AT around the tricuspid annulus (counterclockwise typical atrial flutter) with 2:1 AV conduction. As illustrated in this case, discrimination between focal and macroreentry as the mechanism of AT based on the presence of distinct isoelectric intervals between the tachycardia P waves can be challenging, caused by superimposition of the QRS and ST-T waves. Endocardial activation (*shaded area*), however, clearly demonstrates that biatrial activation from all electrodes of the 20-pole ("Halo") catheter (around the tricuspid annulus [TA]) and the coronary sinus (CS) catheter occupies only a small fraction (less than 50%) of the tachycardia cycle length (TCL) during focal AT with over half of the TCL without recorded activity. In contrast, biatrial activation occupies most (~90%) of the tachycardia CL during macroreentrant AT. *dist*, Distal; *prox*, proximal.

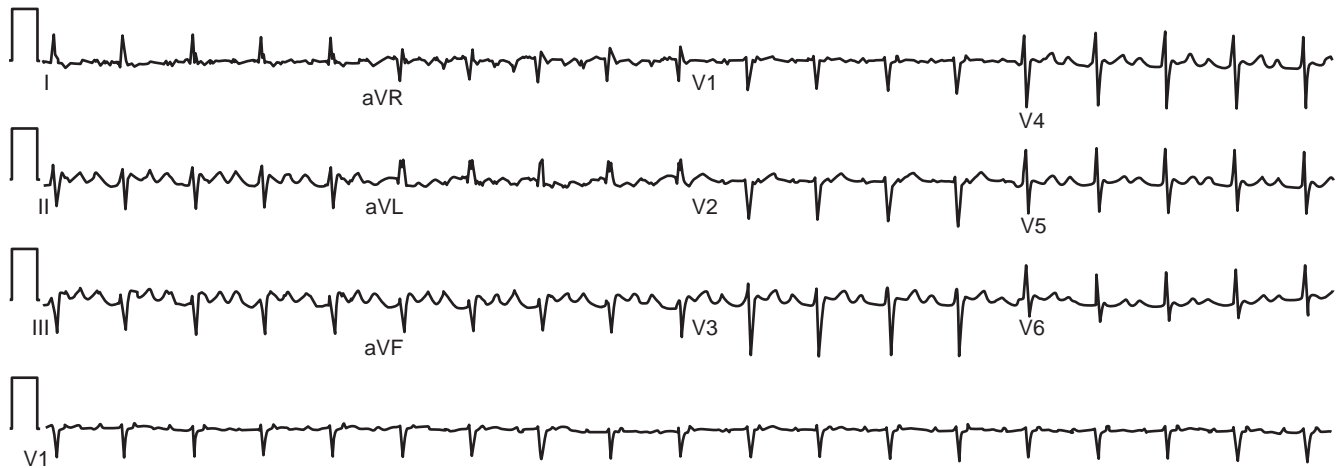


Fig. 11.6 Surface Electrocardiogram of Focal Atrial Tachycardia Originating From the Right Superior Pulmonary Vein. Second-degree 2:1 atrioventricular block is observed during the tachycardia. Note that the tachycardia in the inferior leads mimics atrial flutter as a result of intraatrial conduction abnormalities as well as overlapping T waves.

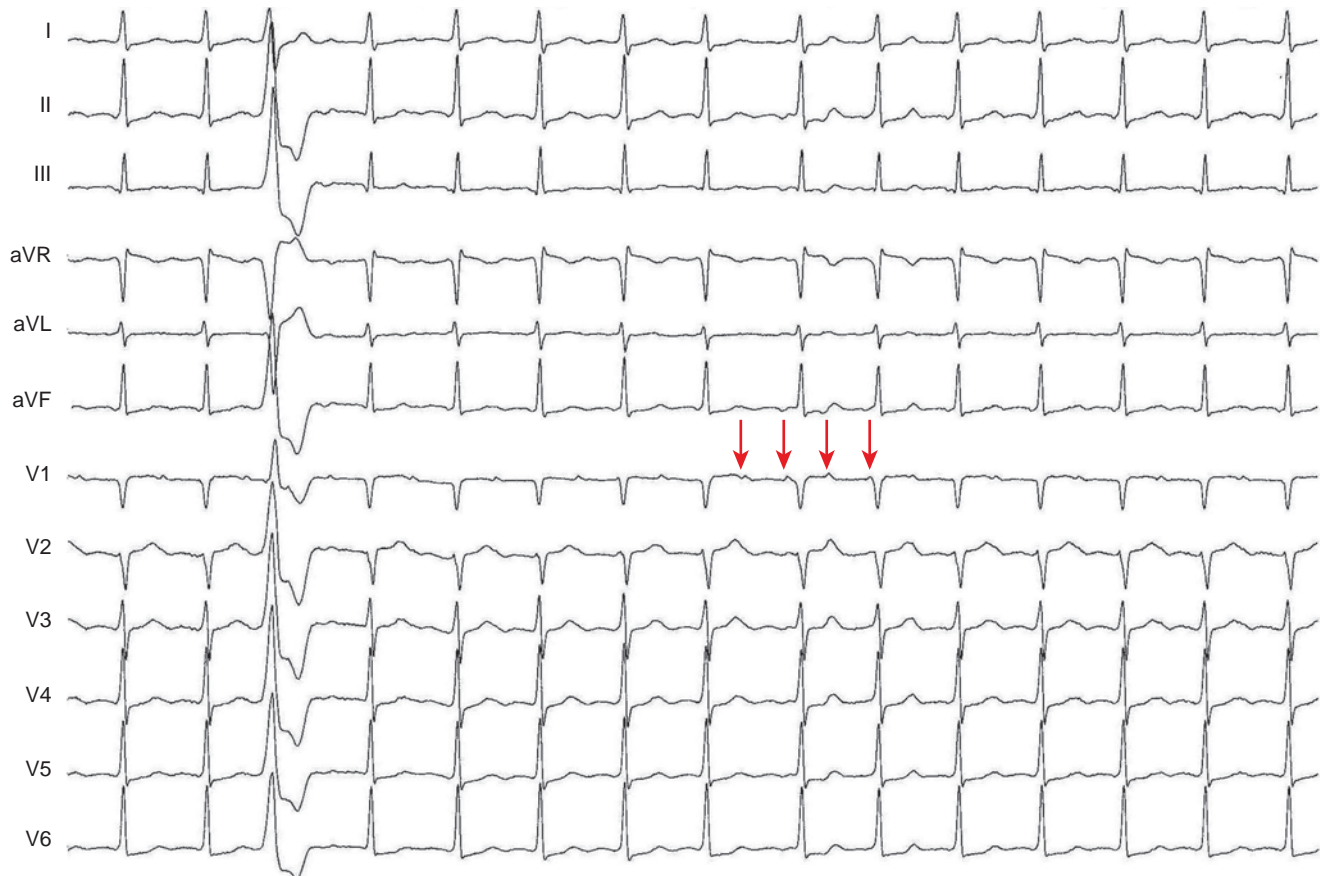


Fig. 11.7 Surface Electrocardiogram of Focal Atrial Tachycardia With 2:1 Atrioventricular (AV) Block. Note that every other P wave lies within the QRS, a pattern mimicking supraventricular tachycardia with 1:1 AV conduction. Careful inspection of the whole recording reveals the hidden P waves sometimes occurring at varying timings within the QRS, as indicated by the arrows.

specificity and positive predictive value (sensitivity and negative predictive value in the range of 60% to 70%). Conversely, positive or biphasic (−/+) P waves in lead V₁ predict LA foci with 100% sensitivity and negative predictive value (specificity of 81% and positive predictive value of 76%).^{7,19}

In lead aVL, a positive or biphasic P wave predicts an RA focus with high accuracy (with the exception of right superior PV foci, whereby lead aVL can also exhibit positive P waves). Also, an isoelectric or negative P wave in lead I was 100% specific for an LA focus, but was only present in 50% of patients with LA foci.⁷



Fig. 11.8 Spontaneous Initiation and Termination of a Midseptal Focal Atrial Tachycardia (AT). The tachycardia is initiated and terminated by premature atrial complexes (arrows) of different morphology from that of the AT, a finding suggesting a nonautomatic mechanism. Note the narrow P wave during AT, consistent with a septal origin. *CS_{dist}*, Distal coronary sinus; *CS_{prox}*, proximal coronary sinus; *HRA*, high right atrium; *RVA*, right ventricular apex.

The predictive value of P wave morphology for localizing the atrium of origin is more limited when the tachycardia foci arise from the interatrial septum. Those ATs are associated with variable P wave morphology and considerable overlap for tachycardias located on the left and right sides of the septum.²⁰ As noted, P waves during ATs arising near the septum are generally narrower than those arising in the RA or LA free wall.

Right Atrial Tachycardias

Crista terminalis. Cristal ATs (i.e., ATs arising from the crista terminalis) are characterized by right-to-left activation sequence, resulting in P waves that are positive and broad in leads I and II, positive in lead aVL, and biphasic in lead V₁ (Fig. 11.12). A negative P wave in lead aVR predicts a cristal origin compared with anterior RA foci with a sensitivity of 100% and specificity of 93%. Biphasic (+/−) P waves in lead V₁ (or positive P waves in lead V₁ during both tachycardia and sinus rhythm), positive P waves in leads I and II, and negative P waves in lead aVR predict a cristal origin with 93% sensitivity, 95% specificity, 84% positive predictive value, and 98% negative predictive value.

High, middle, or low cristal locations can be identified by P wave polarity in the inferior leads.¹⁸ ATs originating from the lower crista terminalis exhibit P waves with isoelectric or biphasic patterns in the inferior leads (II, III, and aVF) and positive (but occasionally biphasic [−/+]) pattern in leads V₃–V₆ (eFig. 11.2).^{16,19}

Although there can be an overlap in tachycardia P wave morphology between superior crista (or SVC) foci and the right superior PV foci, due to the close anatomical proximity of these structures, these foci can be distinguished on the basis of changes to the P wave morphology in lead V₁ during tachycardia as compared with sinus P waves. In right superior PV AT, P waves in lead V₁ are invariably upright during tachycardia but can be either upright or biphasic (+/−) in sinus rhythm. When cristal AT has an upright P wave in lead V₁ (approximately 10%), it is invariably also upright during sinus rhythm. The combination of a biphasic or isoelectric P wave polarity in lead V₁ or a biphasic P wave polarity in lead aVL predicts an SVC focus.¹⁷

Anterior septum. In anterosseptal ATs (originating above the membranous septum), the P wave is biphasic or negative in lead V₁. Because of relatively simultaneous biatrial activation, P wave duration is approximately 20 milliseconds narrower than the sinus P wave. Those ATs can

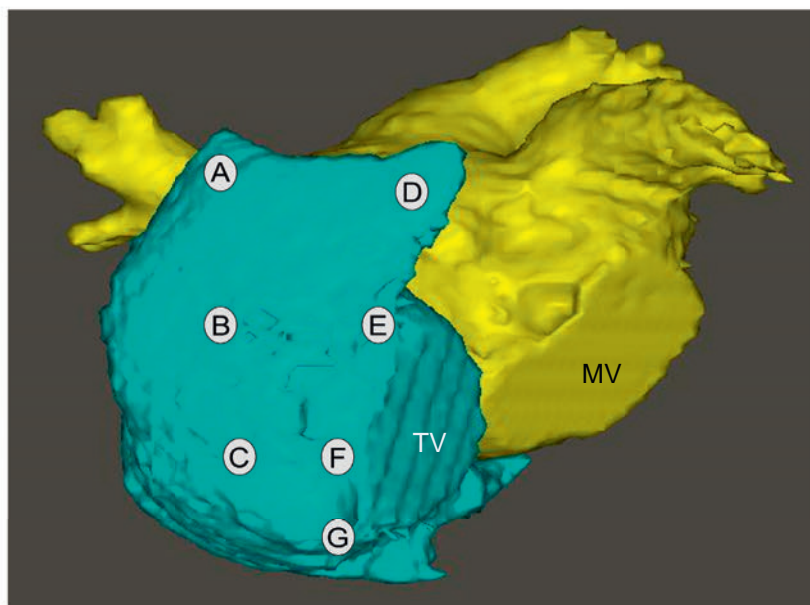
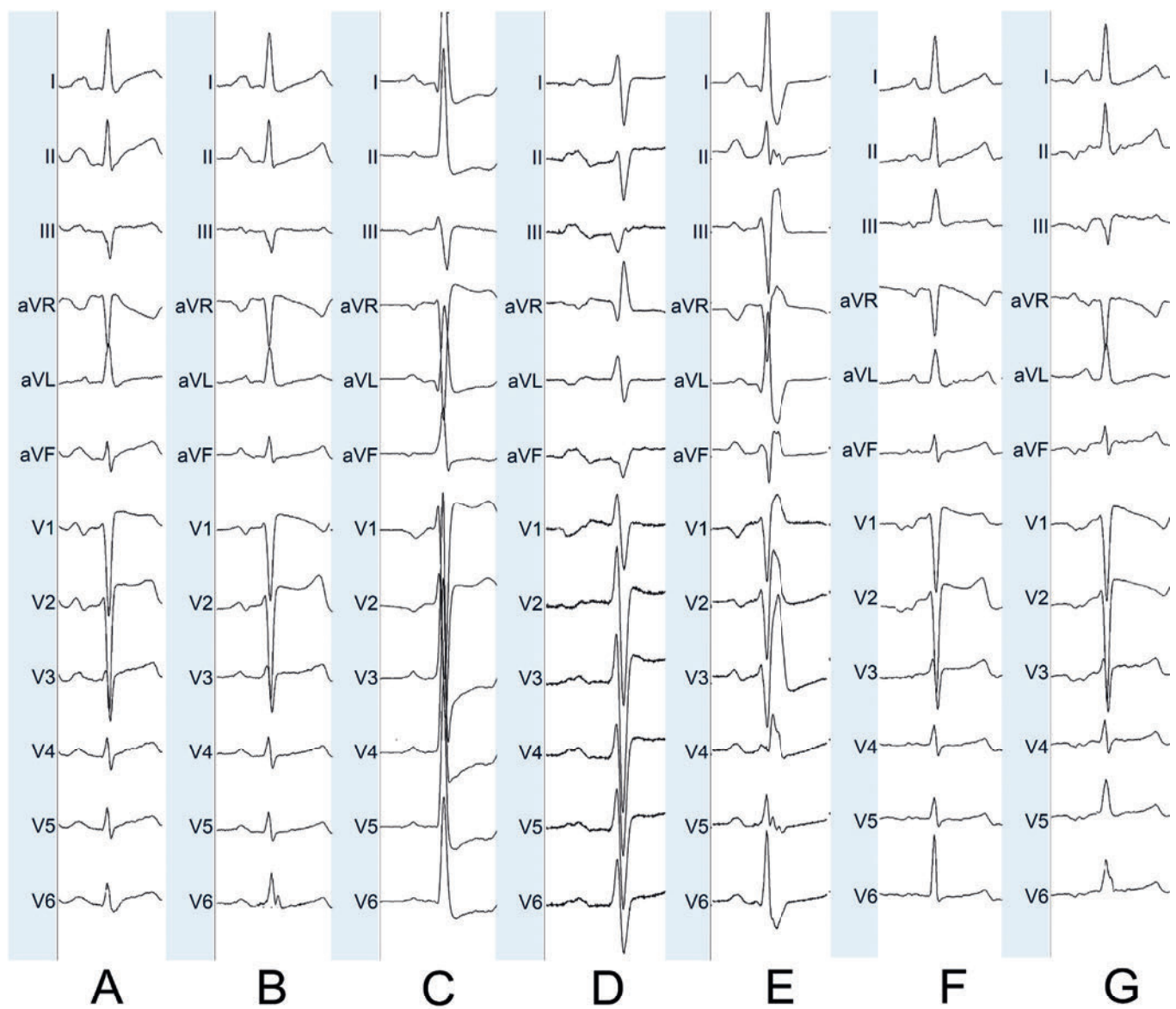
mimic slow-fast AVNRT or orthodromic AVRT utilizing a superoparaseptal bypass tract (BT).

ATs originating in the para-Hisian region (apex of the triangle of Koch) typically exhibit narrow P waves that are consistently positive or isoelectric in leads I and aVL. In the inferior leads, the P wave is negative or biphasic (+/−) in the majority of cases, but can occasionally be positive or biphasic (−/+). In lead V₁, the P wave is typically biphasic, with the dominant positive or negative component opposite to the pattern noted in the inferior leads. The negative inscription of P waves in the inferior leads is likely due to LA activation via CS interatrial connection, while positive P waves suggest activation of the LA via Bachmann's bundle.²¹ In addition, para-Hisian ATs often exhibit a very characteristic narrow and biphasic (−/+) or triphasic (+/−/+) P wave morphology in the precordial leads, especially in V₄ to V₆, and in the inferior leads (eFig. 11.3). Importantly, given the complex anatomical relationship between both sides of the interatrial septum and the aortic root, a P wave morphology consistent with a para-Hisian or anterosseptal location does not accurately predict the successful ablation site (RA, aortomitral continuity, or noncoronary aortic sinus of Valsalva).^{22,23}

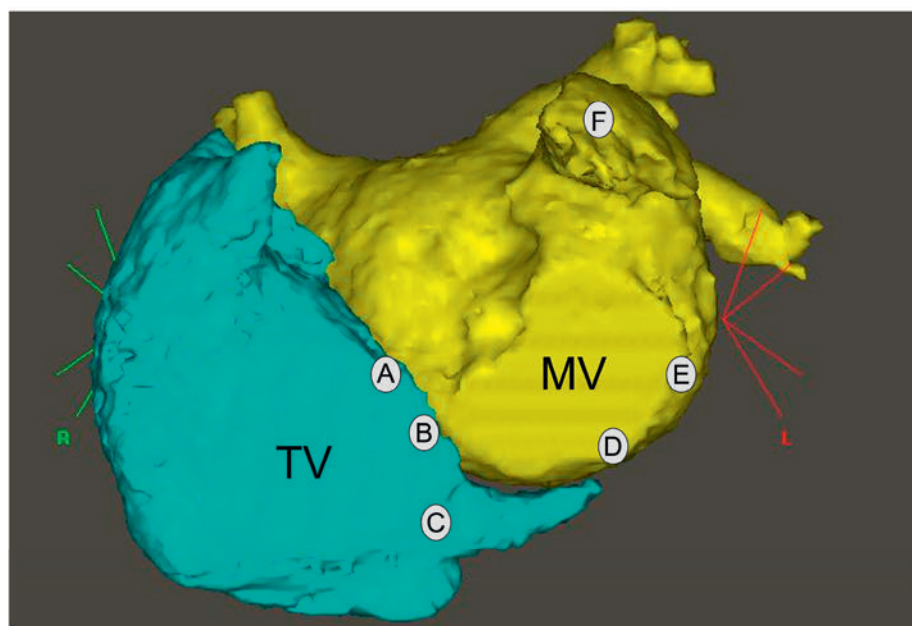
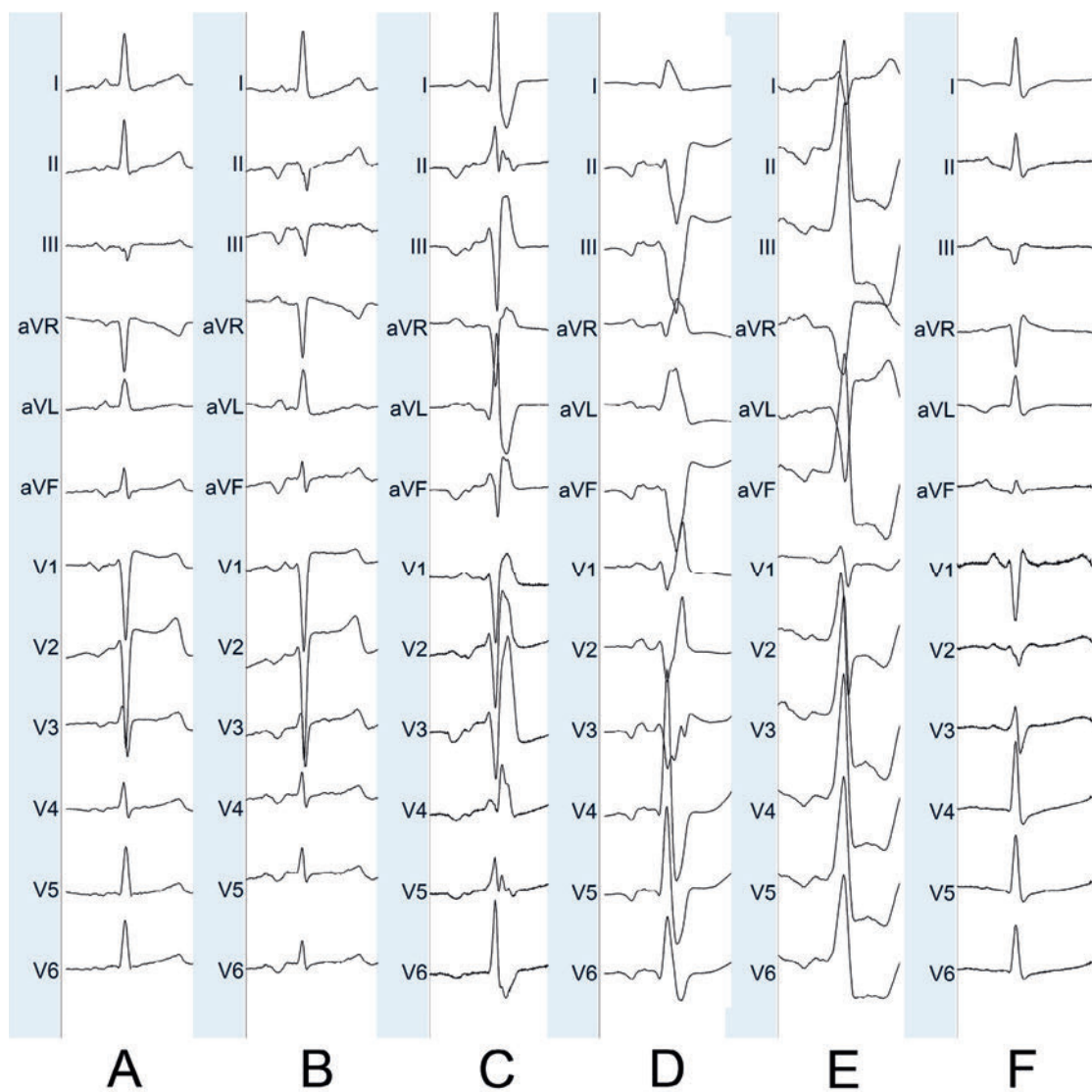
Midseptum. Midseptal ATs (originating below the membranous septum and above the CS os) are associated with P waves that are biphasic or negative in lead V₁ and negative in the inferior leads (see eFig. 11.3). Those ATs can mimic fast-intermediate AVNRT or orthodromic AVRT utilizing a midseptal BT.

Posterior septum. In posteroseptal ATs (originating below and around the CS os), the P wave is positive or isoelectric-positive (but occasionally −/+ biphasic) in lead V₁, exclusively negative in the inferior leads (II, III, and aVF), equally positive in leads aVL and aVR, and exclusively negative (but occasionally −/+ biphasic) in all four precordial leads (V₃–V₆). The precordial transition to negativity is variable (see eFig. 11.3). P wave morphology in those ATs can mimic fast-slow AVNRT or orthodromic AVRT using a posteroseptal BT.¹⁶

Tricuspid annulus. A common feature of tricuspid annular ATs is the presence of an inverted P wave in leads V₁ and V₂, with late precordial transition to an upright appearance (see eFig. 11.2). The nonseptal sites demonstrate negative P waves in lead V₁, whereas inferolateral annular sites tend to have inverted P waves across the precordial leads, and superior sites closer to the septum show transition from negative in lead V₁, through biphasic (−/+), to upright in the lateral precordial

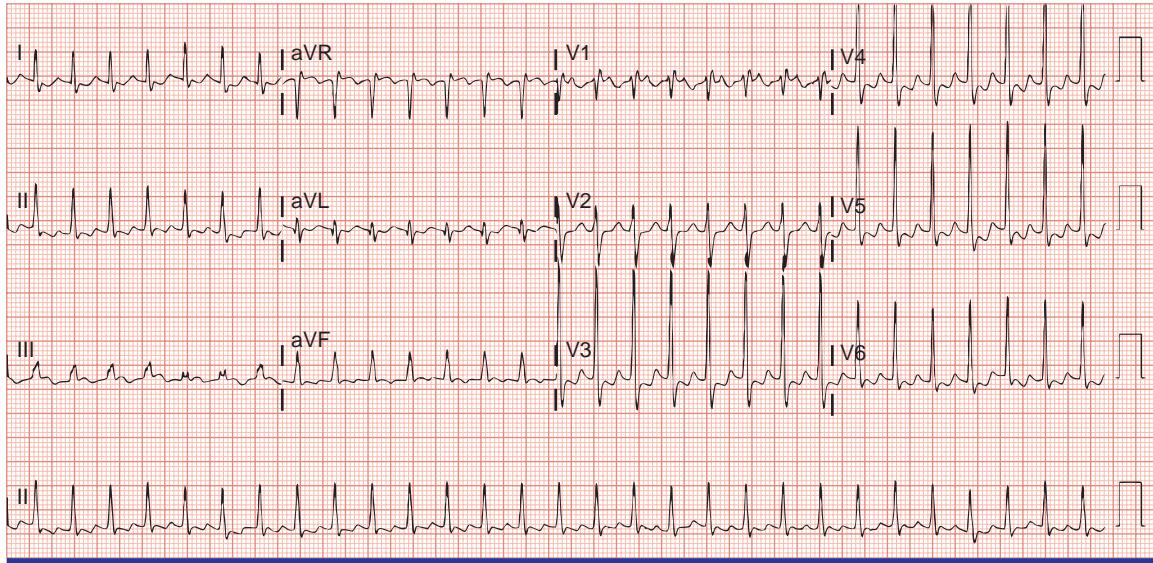


eFig. 11.2 Electrocardiogram (ECG) Morphology of Focal Atrial Tachycardias Originating From Different Sites in the Right Atrium. Three-dimensional cardiac computed tomography of the right and left atria is viewed from the anteroposterior view at the level of the mitral (*MV*) and tricuspid (*TV*) valves. Arrows link the surface ECG P wave morphology during atrial tachycardia with the location of the successful ablation site. (*A*) Superior crista terminalis. (*B*) Mid crista terminalis. (*C*) Low crista terminalis. (*D*) Right atrial appendage. (*E*) Superior tricuspid annulus. (*F*) Lateral tricuspid annulus. (*G*) Inferolateral tricuspid annulus.

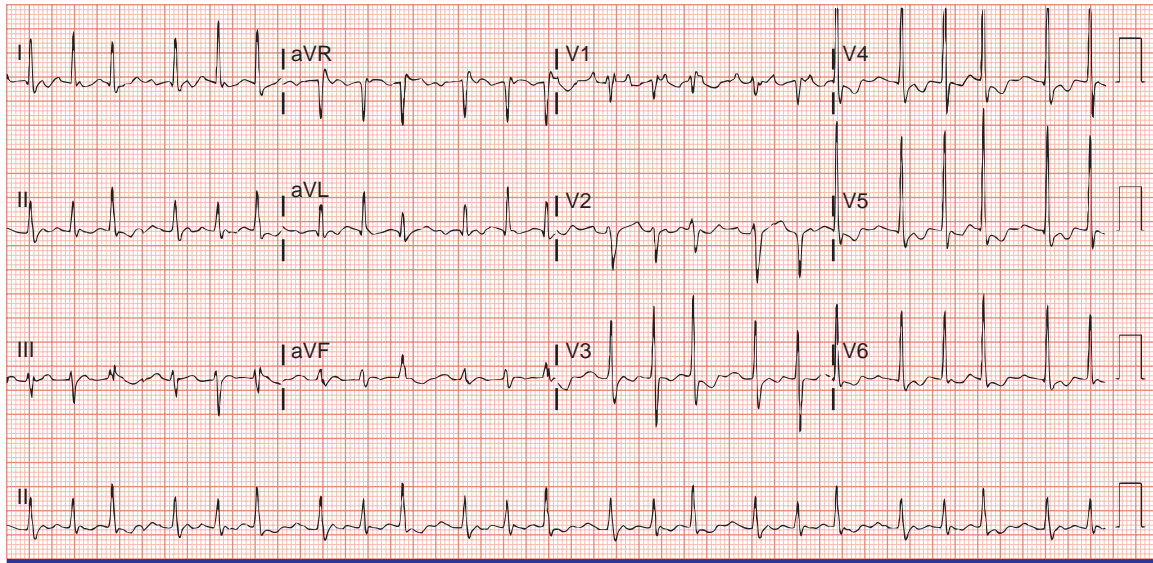


eFig. 11.3 Electrocardiogram (ECG) Morphology of Focal Atrial Tachycardias Originating From Different Sites in the Right and Left Atria. Three-dimensional cardiac computed tomography of the right and left atria is viewed from the left anterior oblique view at the level of the mitral (MV) and tricuspid (TV) valves. Arrows link the surface ECG P wave morphology during atrial tachycardia with the location of the successful ablation site. (A) Para-His. (B) Mid septum. (C) Low septum. (D) Inferior mitral annulus. (E) Inferolateral mitral annulus. (F) Left atrial appendage.

AT with 1:1 AV conduction



AT with Wenchebach AV block



AT with 2:1 AV block

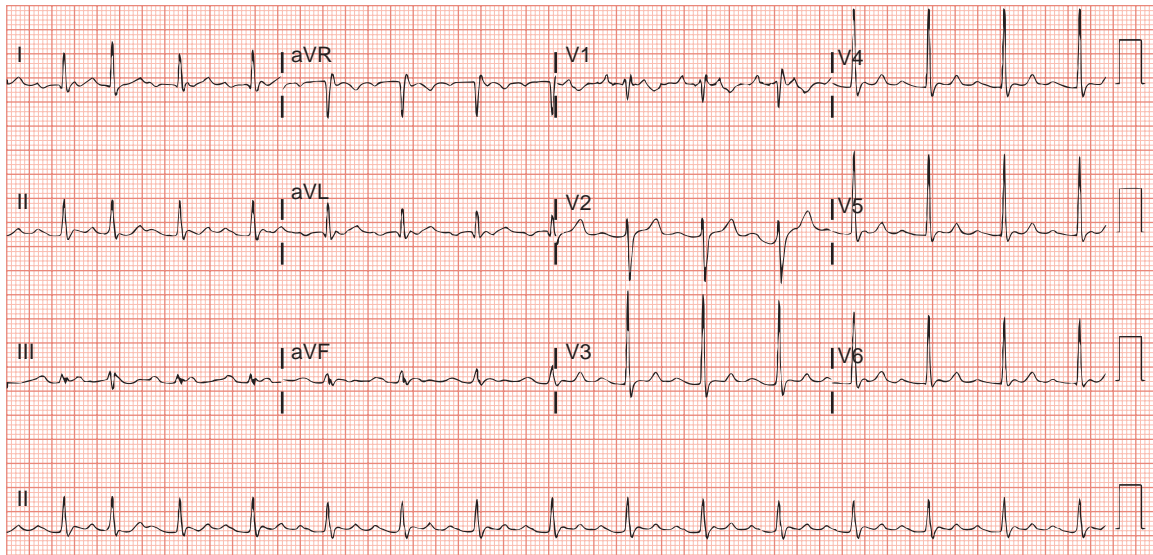


Fig. 11.9 Atrial Tachycardia (AT) With Variable Atrioventricular (AV) Conduction. Surface electrocardiogram of focal AT originating from the superior portion of the antrum of the right superior pulmonary vein. *Top panel*, 1:1 AV conduction during AT results in superimposition of P waves on preceding T waves. *Middle panel*, AT conducts with Wenchebach AV periodicity. *Bottom panel*, AV conduction progresses from Wenchebach to 2:1 second-degree AV block. P waves are now more apparent (especially in lead V1).

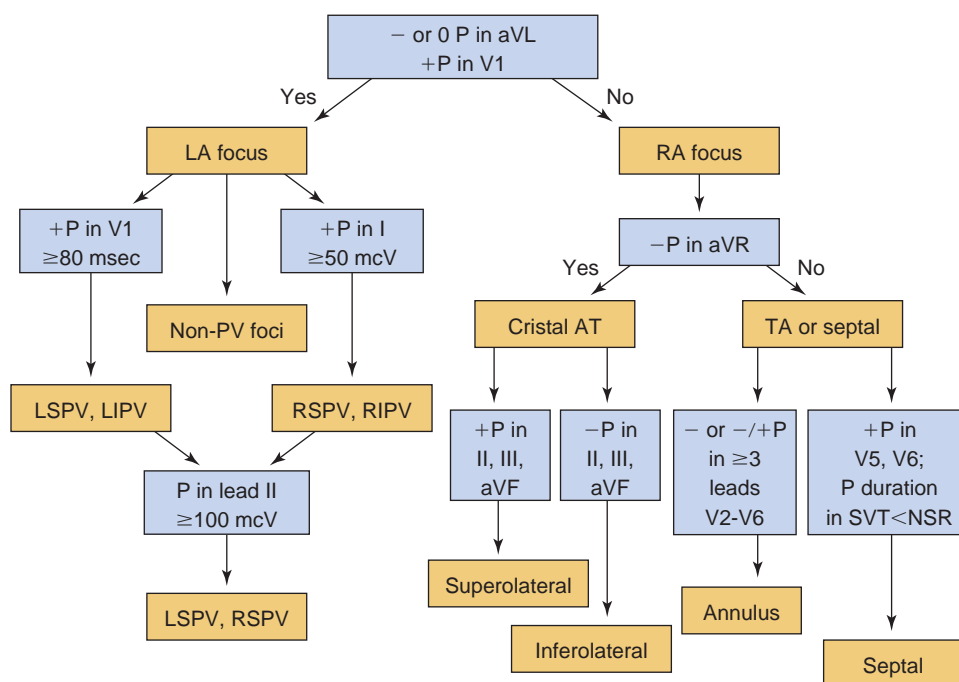


Fig. 11.10 Algorithm for Localization of Atrial Tachycardia (AT) Origin Based on P Wave Morphology on the Surface Electrocardiogram. LA, Left atrial; LIPV, left inferior pulmonary vein; LSPV, left superior pulmonary vein; mcV, microvolt; NSR, normal sinus rhythm; PV, pulmonary vein; RA, right atrial; RIPV, right inferior pulmonary vein; RSPV, right superior pulmonary vein; SVT, supraventricular tachycardia; TA, tricuspid annulus; 0, isoelectric P wave; -/+, biphasic P wave; +P, positive P wave; -P, negative P wave. (From Ellenbogen KA, Wood MA. Atrial tachycardia. In: Zipes DP, Jalife J, eds. *Cardiac Electrophysiology: From Cell to Bedside*. 4th ed. Philadelphia: Saunders; 2002:500–511.)

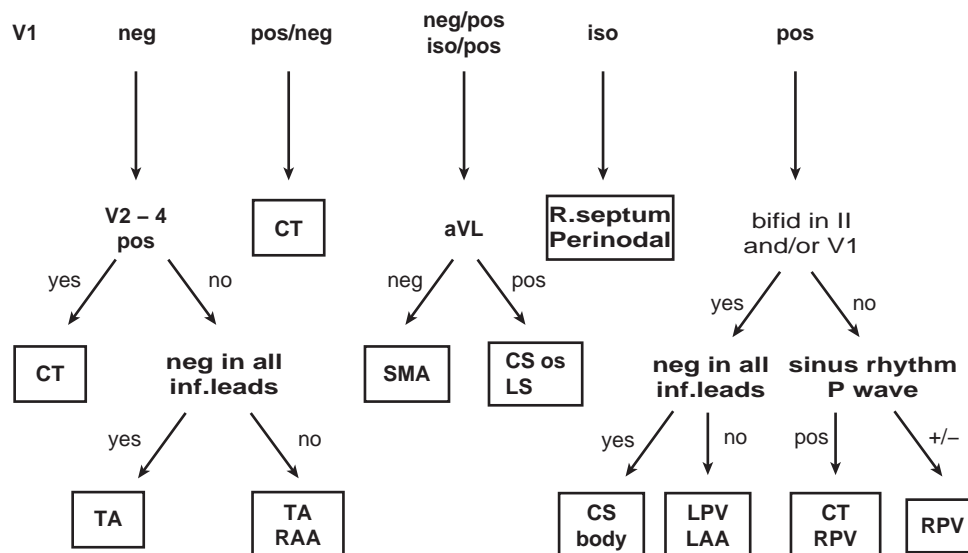


Fig. 11.11 Algorithm for Localizing the Site of Origin of Focal Atrial Tachycardia. The algorithm was constructed on the basis of findings from 130 atrial tachycardias and correctly localized the tachycardia focus in 93%. CS os, Coronary sinus ostium; CT, crista terminalis; LAA, left atrial appendage; LPV, left pulmonary veins; LS, left septum; RAA, right atrial appendage; RPV, right pulmonary vein; SMA, superior mitral annulus; TA, tricuspid annulus. (From Kistler PM, Roberts-Thomson KC, Haqqani HM, et al. P-wave morphology in focal atrial tachycardia: development of an algorithm to predict the anatomic site of origin. *J Am Coll Cardiol*. 2006;48:1010–1017.)

leads. In general, the polarity of leads II and III is deeply negative for an inferolateral annular location and low amplitude, positive, or biphasic for a superior location. In addition, tricuspid annular ATs typically have positive P waves in lead aVL and positive or isoelectric P waves in lead I.¹⁸

In patients with ATs arising from the low RA, P waves that are either exclusively negative or have early negative components in precordial leads V₃–V₆ indicate AT foci at the lower annular aspects of the RA such as the nonseptal tricuspid annulus (6 to 9 o'clock as viewed from the ventricle) and around the CS os, whereas positive P waves in V₃–V₆

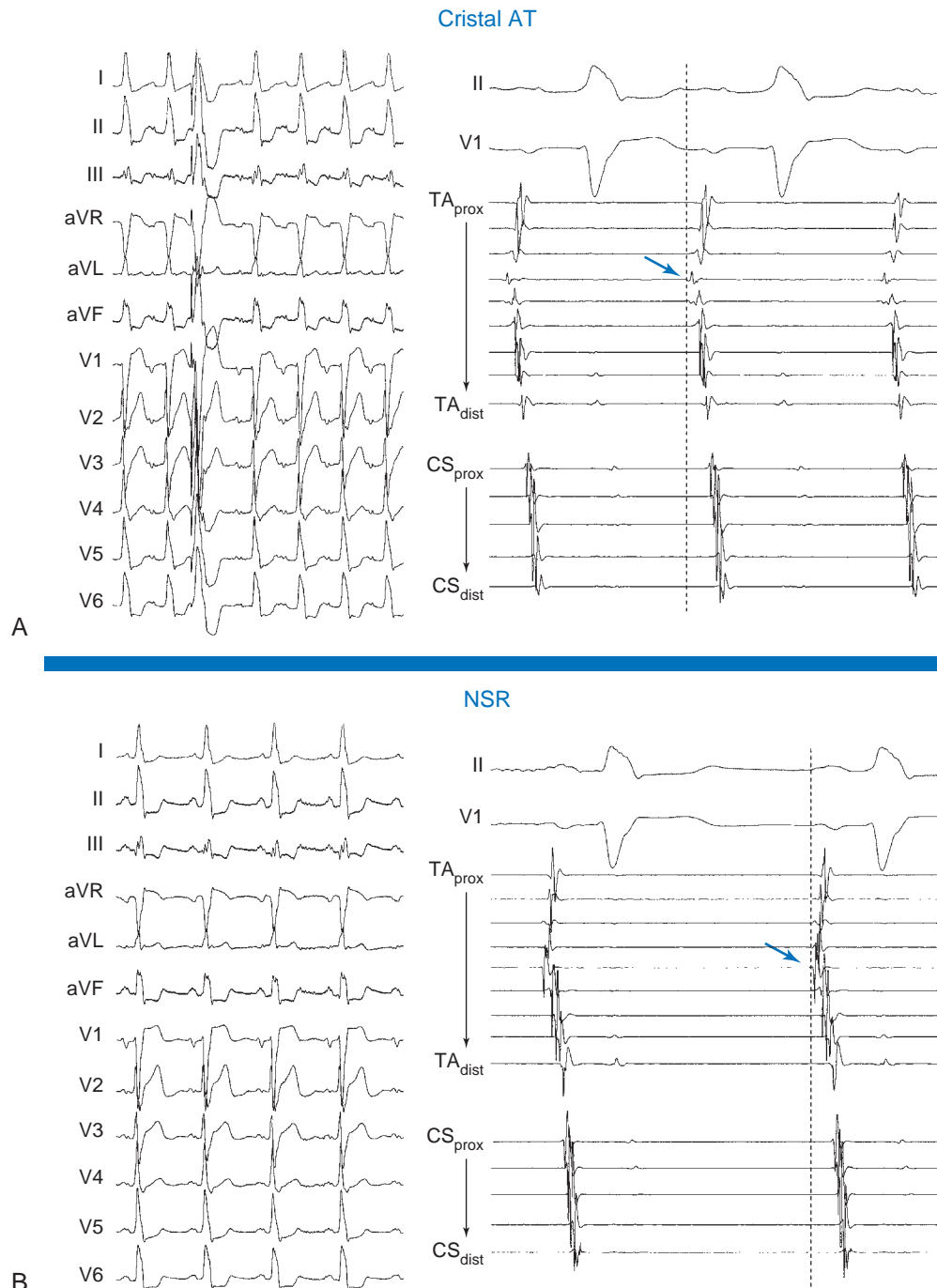


Fig. 11.12 Cristal Atrial Tachycardia (AT). Comparison of P wave morphology and endocardial atrial activation sequence between focal AT originating from the crista terminalis (A) and normal sinus rhythm (NSR) (B) in the same patient. A Halo catheter is positioned around the tricuspid annulus (TA). CS_{dist}, Distal coronary sinus; CS_{prox}, proximal coronary sinus.

predict a low crista terminalis focus. To distinguish ATs of nonseptal tricuspid annular foci from CS os origins, P-wave morphology in leads I and V₁ can be of value. Positive P waves in lead I and negative P waves in lead V₁ suggest nonseptal tricuspid annular foci.¹⁶

RA appendage. Focal ATs originating from the RA appendage typically originate from the lateral base of the appendage but are also well described from an apical location. Because of their close anatomical proximity, these tachycardias are generally indistinguishable from

superior tricuspid annular foci; they exhibit broad, negative, notched P waves in leads V₁ and V₂ and variable precordial transition to positive in lead V₆. P waves in the inferior leads characteristically have low positive amplitudes (see eFig. 11.2).¹⁸

Left Atrial Tachycardias

Pulmonary veins. ATs arising from the PVs are characterized by entirely positive P waves in lead V₁ (in 100% of cases) and across the

precordial leads, isoelectric or negative waves in lead aVL in 86%, and negative waves in lead aVR in 96%. Lead aVL can be biphasic or positive in right-sided PV ATs (eFig. 11.4).⁸

Compared with the right-sided PVs, the left-sided PV foci have several characteristics: positive notching in the P waves in two or more surface leads, an isoelectric or negative P wave in lead I, more positive P waves in lead III than in lead II (P wave amplitude in lead III/II ratio greater than 0.8), and broad P waves in lead V₁ (eFig. 11.5). Right-sided PV foci usually have positive P waves in lead I.

ATs arising from the superior PVs invariably have a positive P wave in the inferior leads. In contrast, ATs arising from the inferior PVs can have inverted, low-amplitude positive, or isoelectric inferior P waves. However, because of the close proximity of the superior and inferior veins and marked anatomical variation, P wave morphology generally is of greater accuracy in distinguishing right-sided from left-sided PVs, in contrast to distinguishing superior from inferior PVs.⁸

ATs arising from the right superior PV are associated with P waves that are narrow and positive in the inferior leads, of equal amplitude in leads II and III, positive in lead V₁, and isoelectric or positive in lead I. The right superior PV is a common site of origin for LA ATs. It is only a few centimeters from the sinus node; hence activation rapidly crosses the septum via Bachmann's bundle to activate the RA in a fashion similar to NSR, a feature explaining the similarities in P wave morphology. However, whereas the P wave is biphasic in lead V₁ during NSR, it is positive in that lead during right superior PV AT (Fig. 11.13).⁸

Despite prior posterior LA ablation, the surface ECG morphology of ATs originating from the PV ostia in patients with prior AF ablation procedures generally is similar to those in patients without prior ablation. However, ATs originating from the bottom of the right or left PVs after prior PV isolation can have a significant negative component or can be completely negative in the inferior leads. This may be related to prior ablation in the superoposterior LA or to a more inferior origin of the tachycardia after prior ablation outside the PV ostium.

LA appendage. In LA appendage ATs, the P wave is positive in the inferior leads (more positive in lead III than in lead II), positive in lead V₁, and deeply negative in leads I and aVL (see eFig. 11.3). The LA appendage closely approximates to the left superior PV, and as such, ATs arising from those locations tend to have similar P wave morphologies. When P wave morphology suggestive of a left superior PV focus (see above), several ECG characteristics suggest an LA appendage origin (reflecting the more anterolateral position of the LA appendage compared with the PVs), including (1) a deeply negative P wave in lead I; (2) negative P waves in leads I and aVL; and (3) upright or biphasic P wave in lead V₁ and isoelectric in leads V₂–V₆. Furthermore, clinical features of the two types of ATs appear to be different; ATs originating from the left superior PV frequently are associated with paroxysmal AF, whereas ATs arising from the LA appendage often present as incessant tachycardias (likely due to an underlying enhanced automaticity mechanism).^{18,17}

Mitral annulus. Mitral annular ATs typically cluster at the superior aspect of the mitral annulus, close to the aortomitral continuity, adjacent to the left fibrous trigone. ATs originating in this circumscribed area are characterized by P waves with an initial narrow negative deflection in lead V₁ followed by a positive deflection. The positivity of the P wave becomes progressively less from lead V₁ through lead V₆. The P wave is negative in leads I and aVL, and isoelectric or slightly positive in the inferior leads (see eFig. 11.3).²⁴

Coronary sinus. ATs arising from the CS musculature typically demonstrate deeply inverted P waves in the inferior leads. P waves are invariably positive in leads aVL and aVR (with greater amplitude in lead aVR). Compared with AT originating from the CS os, ATs

originating from 3 to 4 cm into the body of the CS have broad and positive P waves in lead V₁.¹⁸

Noncoronary aortic sinus of Valsalva. ATs have been described originating from the noncoronary aortic sinus of Valsalva. Because of the close anatomical proximity, the P wave morphology is similar to that of ATs arising from the aortomitral continuity and para-Hisian region (see above). The P waves in leads V₁ and V₂ are usually negative, but biphasic (–/+) P waves in lead V₁ can also be encountered. Unlike aortomitral ATs, those arising from the noncoronary aortic sinus of Valsalva demonstrate positive or isoelectric P waves in leads I and aVL. In the inferior leads, the P waves are low amplitude positive or biphasic (–/+).^{18,21,25}

ELECTROPHYSIOLOGICAL TESTING

Baseline Observations During Sinus Rhythm

The presence of a broad sinus P wave and intraatrial conduction delay suggest atrial disease, which is more prevalent in patients with MRAT, but can still be observed in association with focal AT. Preexcitation, when present, suggests AVRT but does not exclude AT. In addition, the presence of dual AVN physiology suggests AVNRT but does not exclude AT.

Induction of Tachycardia

Frequently, AT foci can become inactive in the EP laboratory environment because of sedative medications, changes in autonomic tone that can be caused by prolonged supine position, patient anxiety, deviation from normal diet, or other changes in daily activities that can have an impact on the circadian variation of AT activity. Thus, in preparation for an AT ablation procedure, several measures should be undertaken. Antiarrhythmic drugs need to be discontinued for at least five half-lives before the EP study. Sedation should be minimized until reproducible inducibility of the arrhythmia is ensured. It may be an appropriate policy to monitor the patient in the EP laboratory initially without sedation. If no spontaneous tachycardia is induced, isoproterenol is administered. If no AT can be induced, a single quadripolar catheter is placed in the RA; and programmed electrical stimulation is performed without and, if no AT is induced, with isoproterenol infusion. If AT remains quiescent, the procedure is aborted and retried at a future date. If AT is inducible at any step, the full EP catheter arrangement and EP study are undertaken (Box 11.1).

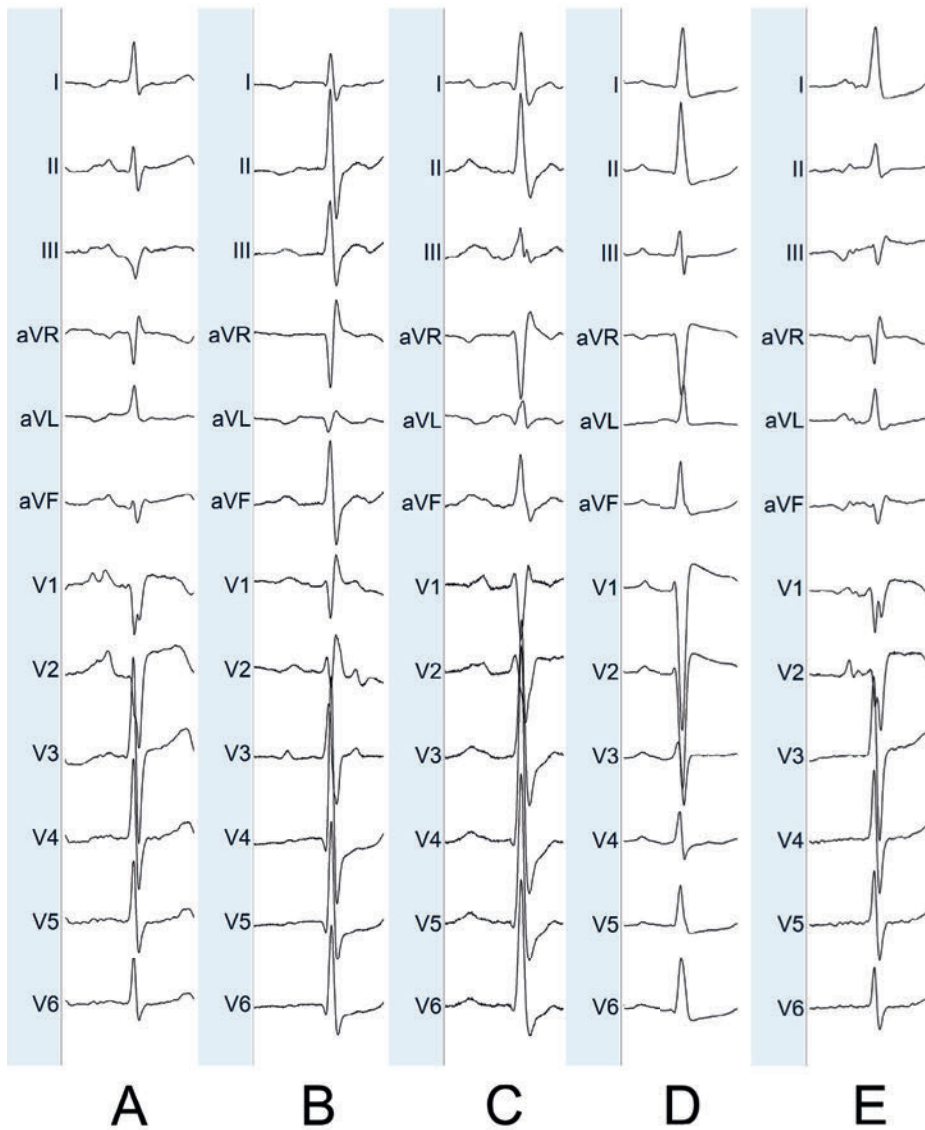
Initiation by Programmed Atrial Stimulation

Microentrant AT is usually easy to initiate with a wide range of atrial extrastimulation (AES) coupling intervals (A₁–A₂ intervals). The

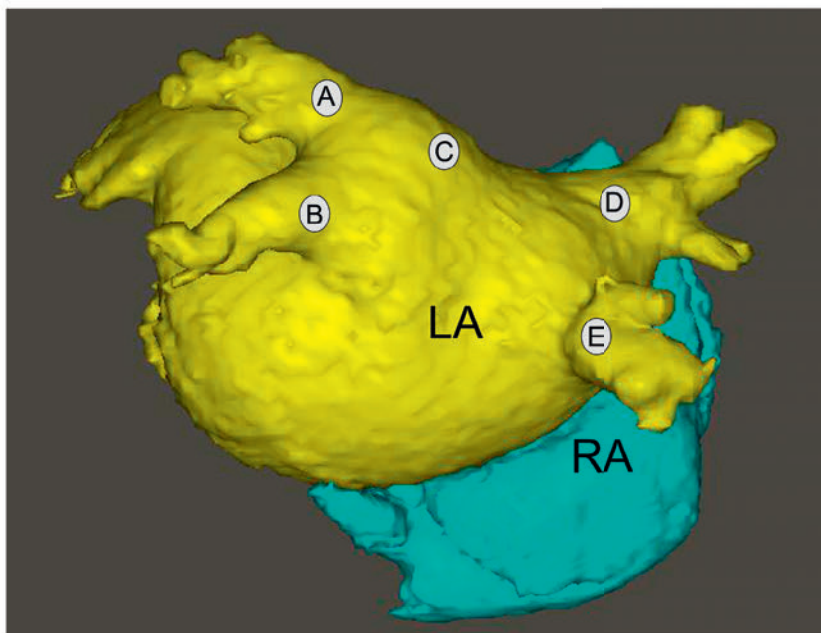
BOX 11.1 Programmed Electrical Stimulation Protocol for Electrophysiological Testing of Atrial Tachycardia

Atrial burst pacing from the RA and CS (down to a PCL at which 2:1 atrial capture occurs)
Single and double AES at multiple pacing drive CLs (600–400 msec) from the RA and CS (down to atrial ERP)
Ventricular burst pacing from the RV apex (down to VA Wenckebach CL)
Single and double VES at multiple pacing drive CLs (600–400 msec) from the RV apex (down to ventricular ERP)

AES, Atrial extrastimulation; CL, cycle length; CS, coronary sinus; ERP, effective refractory period; PCL, pacing cycle length; RA, right atrium; RV, right ventricle; VA, ventricular-atrial; VES, ventricular extrastimulation.



eFig. 11.4 Electrocardiogram (ECG) Morphology of Focal Atrial Tachycardias Originating From Different Sites in the Left Atrium. Three-dimensional cardiac computed tomography of the right (RA) and left atria (LA) is viewed from the posteroanterior view. Arrows link the surface ECG P wave morphology during atrial tachycardia with the location of the successful ablation site. (A) Left superior pulmonary vein (PV). (B) Left inferior PV. (C) LA roof. (D) Right superior PV. (E) Right inferior PV.





eFig. 11.5 Surface Electrocardiogram of Nonsustained Focal Atrial Tachycardia Originating From the Ostium of the Left Superior Pulmonary Vein.

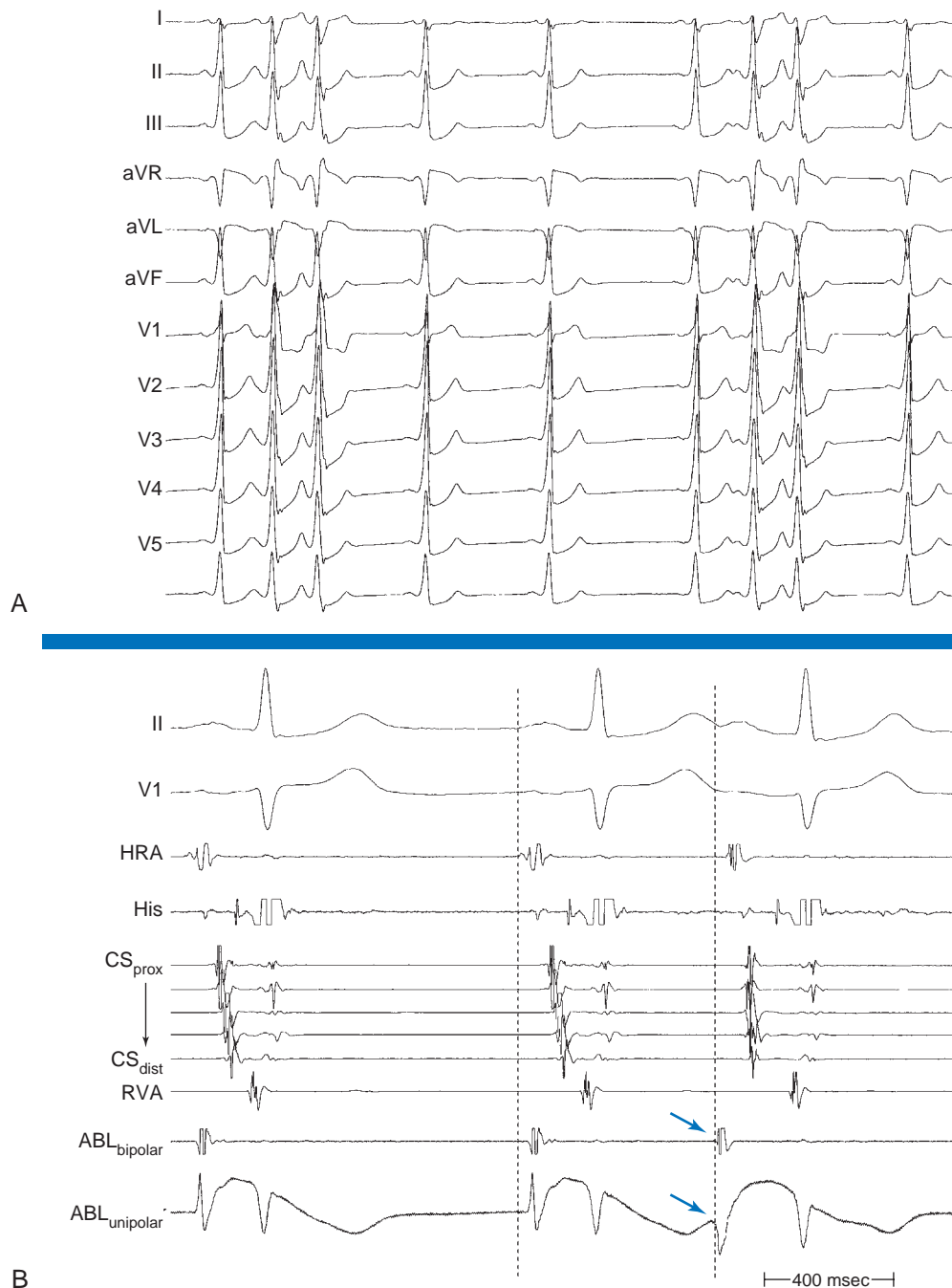


Fig. 11.13 Premature Atrial Complexes (PACs) Originating From the Right Superior Pulmonary Vein (PV). (A) 12-lead surface electrocardiogram illustrating atrial couplets during normal sinus rhythm (NSR). Note the similarities in P wave morphology during PACs versus NSR. (B) Intracardiac recordings from the same patient. Detailed mapping localized the origin of the PACs to the ostium of the right superior PV (as illustrated by bipolar and unipolar recordings from the ablation catheter [ABL]). Note the concordance of timing of the bipolar and unipolar recordings and the QS unipolar electrogram morphology (blue arrows), suggesting the site of origin of activation and a good ablation site. CS_{dist}, Distal coronary sinus; CS_{prox}, proximal coronary sinus; HRA, high right atrium; RVA, right ventricular apex.

initiating AES coupling interval and the interval between the initiating AES and first beat of AT are inversely related. Triggered ATs also can be initiated by AES or (more commonly) atrial pacing. However, initiation frequently requires catecholamines (isoproterenol), and, in contrast to microreentrant AT, there is usually a direct relationship between the coupling interval or pacing cycle length (PCL) initiating the AT and the

interval to the onset of the AT and the early CL of the AT. On the other hand, automatic ATs cannot be reproducibly initiated by AES or atrial pacing and are characteristically sensitive to catecholamine stimulation.⁹

In the setting of microreentry and triggered activity, the first tachycardia P wave is different from subsequent P waves; the first P wave is usually a PAC or an AES that is necessary to start the AT (see Fig. 11.8).

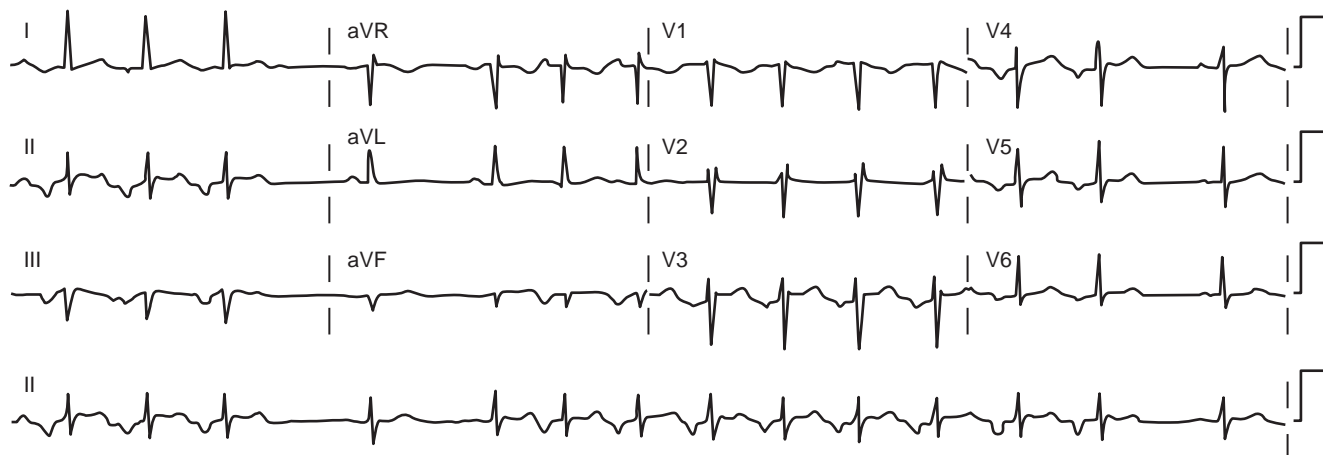


Fig. 11.14 Automatic Atrial Tachycardia. Surface electrocardiogram of repetitive nonsustained atrial tachycardia originating from the inferolateral mitral annular region of the left atrium. Note that the first P wave of the tachycardia is similar in morphology to the subsequent P waves, consistent with abnormal automaticity as the mechanism of the tachycardia.

In contrast, the first tachycardia P wave and subsequent P waves during automatic AT are identical; the AT does not require a PAC to start (Fig. 11.14). Furthermore, the automatic TCL tends to shorten progressively (warm up) for several beats until its ultimate rate is achieved.

No delay in the AH or PR interval is required for initiation of AT, although it can occur. AV block can also occur at initiation.

Initiation by Programmed Ventricular Stimulation

It is uncommon to initiate AT with ventricular extrastimulation (VES) or ventricular pacing because decremental retrograde conduction over the AVN prevents adequate prematurity of atrial activation. However, in the presence of an AV BT, fast retrograde atrial activation mediates adequate prematurity of the conducted ventricular stimulus to the atrium, and AT may be induced.

Tachycardia Features

Atrial Activation Sequence

P wave morphology and atrial activation sequence depend on the site of origin of the AT. Intracardiac activation mapping shows significant portions of the TCL without recorded atrial activity, and atrial activation time is markedly less than the TCL (see Fig. 11.5). However, in the presence of extensive atrial scarring or prior ablation, depolarization from the AT focus can occasionally be followed by very disordered and prolonged conduction so that activation of the entire chamber can extend over (or even exceed) the entire TCL, thus mimicking MRAT.²⁶ Conversely, long isoelectric intervals can occur between the P waves during MRATs and can incorrectly suggest a focal mechanism. This pattern is particularly observed for LA MRATs in the presence of large areas of electrical scar or with the use of antiarrhythmic medications. However, in the latter setting, a *thorough* intracardiac activation map reveals atrial activation spanning the TCL. When mapping is limited to only the atrium contralateral to the origin of the macroreentrant circuit or to only parts of the ipsilateral atrium, a focal mechanism can be falsely implied.

Atrial-Ventricular Relationship

The AH and PR intervals during AT are appropriate for the AT rate and are usually longer than those during NSR. They are inversely related: the faster the AT rate, the longer the AH and PR intervals. Thus the PR interval can be shorter than, longer than, or equal to the RP interval.

The PR interval can also be equal to the RR, and the P wave may fall inside the preceding QRS, thus mimicking typical AVNRT.

AV block can be observed during AT because neither the AVN nor the ventricle is part of the AT circuit. Most incessant SVTs with AV block are probably automatic ATs.

Oscillation of the Tachycardia Cycle Length

Oscillation of the ventricular CL occurs frequently during AT and is the result of changes either in the atrial CL or in AVN conduction. When CL variability results from oscillation of the TCL, changes in the atrial CL are expected to precede and predict similar changes in the ventricular CL. On the other hand, ventricular CL variability can be caused by changes in AV conduction instead of changes in the CL of the AT, in which setting ventricular CL variability is not predicted by a prior change in atrial CL. Because there is no VA conduction during AT, ventricular CL variability by itself is not expected to result in subsequent atrial CL variability.²⁷ In addition, spontaneous changes in the PR and RP intervals with fixed A-A intervals favor AT over other types of SVT (Fig. 11.15).

In contrast to AT, typical AVNRT and orthodromic AVRT generally have CL variability caused by changes in anterograde AVN conduction. Because retrograde conduction through a fast AVN pathway or a BT generally is much less variable than the anterograde conduction through the AVN, the changes in ventricular CL that result from variability in anterograde AVN conduction are expected to precede the subsequent changes in atrial CL.²⁷

Large variation in atrial CLs, when present, help distinguish focal AT from MRAT. Variation in the TCL of more than 15% has been suggested as a reliable marker of a focal AT. In contrast, it is rare for MRATs to display considerable variation in the CL. However, a regular AT can be either focal or macroreentrant.

Effects of Bundle Branch Block

Bundle branch block can occur during AT but does not affect the TCL because the ventricles are not participants in AT.

Termination and Response to Physiological and Pharmacological Maneuvers

In the setting of spontaneous termination, ATs terminate with a QRS complex following the last P wave of the tachycardia. Spontaneous

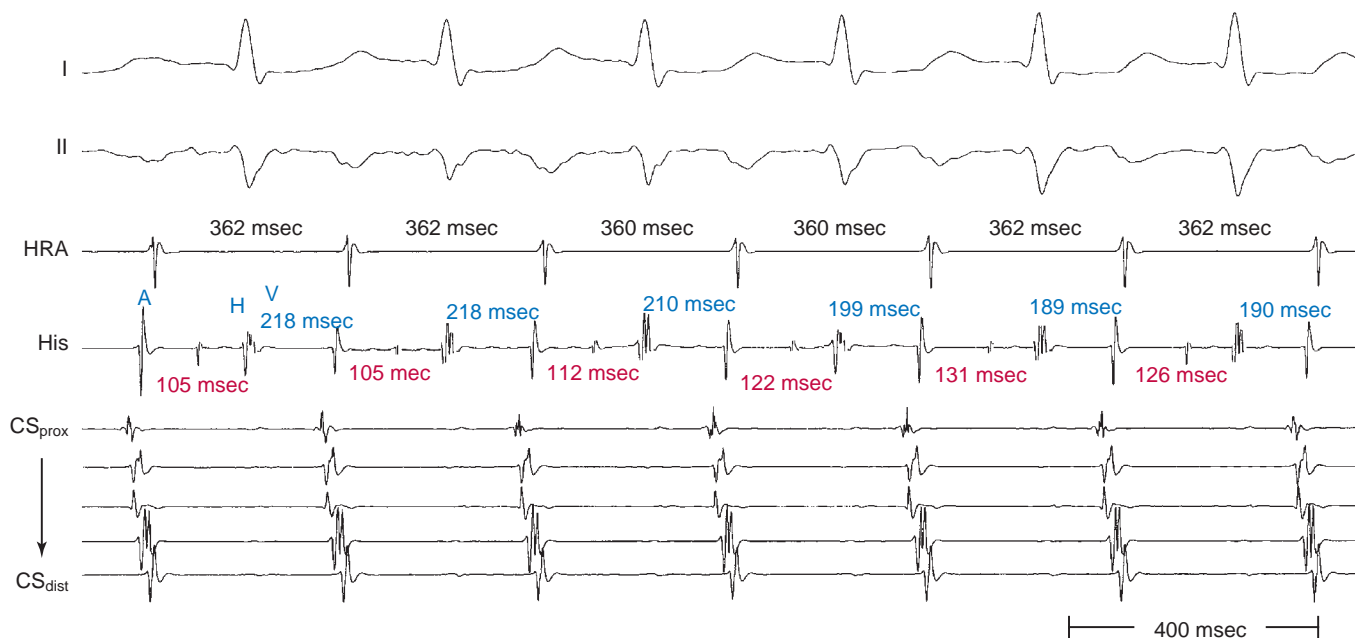


Fig. 11.15 Supraventricular Tachycardia (SVT) With Concentric Atrial Activation Sequence. Note the constant atrial cycle length (*numbers in black*) but variable atrium-to-His bundle interval (*numbers in red*) and ventricular-atrial interval (*numbers in blue*). This observation favors atrial tachycardia (originating from the posteroseptal region) as the mechanism of the tachycardia over other types of SVT. CS_{dist}, Distal coronary sinus; CS_{prox}, proximal coronary sinus; HRA, high right atrium.

termination of AT is usually accompanied by progressive prolongation of the A-A interval, with or without changes in AV conduction.

A large proportion (50% to 80%) of focal ATs can be terminated by adenosine; therefore termination of an SVT in response to adenosine is not helpful in differentiating AT from other SVTs. Usually (in 80% of cases), termination of AT in response to adenosine occurs prior to the onset of AV block (i.e., termination occurs with a tachycardia P wave followed by a QRS). Reproducible termination with a P wave not followed by a QRS indicates other types of SVT because it occurs in AT only if adenosine terminates the AT at the same moment it causes AV block, an unlikely coincidence. In the atrium, adenosine produces antiadrenergic effects (presumably responsible for terminating triggered activity) and increases the acetylcholine- or adenosine-activated potassium (K^+) current (I_{KACH}). The results are shortening of the action potential duration and reduction of the resting membrane potential, which may be responsible for terminating atrial microreentry.⁹

The response of focal AT to adenosine can help identify the mechanism of tachycardia. Adenosine does not slow or terminate microreentrant AT. In contrast, triggered activity ATs typically terminate abruptly in response to adenosine and do not spontaneously reinitiate. An automatic AT either is slowed transiently before gradual resumption of the AT rate or is suppressed transiently before spontaneous reinitiation.⁹

Microreentrant ATs can terminate in response to carotid sinus massage and vagal maneuvers. Triggered activity AT also can terminate in response to carotid sinus massage, vagal maneuvers, verapamil, beta-blockers, and sodium channel blockers. During automatic AT, carotid sinus massage can cause AV block and can slow the atrial rate; however, these interventions generally do not terminate the AT. Only beta-blockers have been useful in termination of paroxysmal (but not incessant) automatic AT. Termination of automatic AT is usually preceded by a cool-down phenomenon of the AT rate.

Diagnostic Maneuvers During Tachycardia

Programmed Atrial Stimulation During Tachycardia

Microreentrant atrial tachycardia. AES can reset microreentrant AT with a resetting response classic for reentry (increasing or mixed response). Atrial pacing can entrain microreentrant AT; however, because the microreentrant circuit is very small, only orthodromic capture is usually observed.

Fusion during resetting or entrainment (a hallmark of macroreentrant tachycardias) cannot be demonstrated in microreentrant AT. For atrial fusion (i.e., fusion of atrial activation from both the tachycardia wavefront and the paced wavefront) to occur during resetting or entrainment, the atrial paced impulse should be able to enter the reentrant circuit, while at the same time the tachycardia wavefront should be able to exit the circuit. This requires spatial separation between the entrance and exit sites to the reentrant circuit, a condition that is lacking in the setting of focal AT. Once the tachycardia wavefront exits the reentry circuit to activate the atrium, any atrial stimulus delivered beyond that time and that results in atrial fusion would not be capable of reaching the reentry circuit because the entry-exit site is already refractory as a result of activation by the exiting tachycardia wavefront, and the atrial stimulus has no alternative way to reach the circuit. Similarly, once an atrial stimulus is capable of reaching the reentry circuit, the shared entry-exit site is rendered refractory and incapable of allowing a simultaneous exit of the tachycardia wavefront. Therefore, during entrainment of microreentrant AT by atrial pacing, the atrial activation sequence and P wave morphology are always that of pure paced morphology.

However, it should be recognized that overdrive pacing of a tachycardia of any mechanism (automatic, triggered activity, or microreentrant) can result in a certain degree of fusion, especially when the PCL is only slightly shorter than the TCL. Such fusion, however, is unstable during the same pacing drive at a constant PCL because pacing stimuli

fall on a progressively earlier portion of the tachycardia cycle, thus producing progressively less fusion and more fully paced morphology. Such phenomena should be distinguished from entrainment, and sometimes this requires pacing for many cycles to demonstrate variable degrees of fusion.

During entrainment of microreentrant AT, the return CL and post-pacing interval (PPI) are fixed regardless of the number of beats in the pacing train. AES and atrial pacing can almost always terminate microreentrant AT (especially sinus node reentrant tachycardia).

Triggered-activity AT. AES can reset triggered-activity AT (with a decreasing resetting response). However, triggered-activity AT cannot be entrained by atrial pacing. Following the delivery of an AES or atrial overdrive pacing during triggered-activity AT, the return CL tends to shorten with shortening of the AES coupling interval or PCL. AES and, more effectively, atrial pacing can usually terminate triggered-activity AT.

Automatic AT. The response of automatic AT to AES is similar to that of the sinus node. A late-coupled AES collides with the tachycardia impulse already exiting the AT focus (zone of collision), resulting in fusion of atrial activation (fusion between the paced and the tachycardia wavefronts) or paced-only atrial activation sequence, and it does not affect the timing of the next AT complex (producing a full compensatory pause). An earlier coupled AES enters the AT focus before the time of the next tachycardia wavefront and therefore resets the AT focus (zone of reset), with a return CL that is not fully compensatory. The return cycle usually remains constant over a range of coupling intervals during the zone of reset. A very early coupled AES encounters a refractory AT focus (following the last tachycardia complex) and would not be able to enter or reset the AT focus. Therefore the next AT complex is on time because the atrium is already fully recovered following that early AES (zone of interpolation).

Automatic AT cannot be entrained by atrial pacing; instead, rapid atrial pacing results in overdrive suppression of the AT rate. The AT resumes after cessation of atrial pacing, but at a slower rate, and gradually speeds up (warms up) to return back to prepacing TCL. The tachycardia return CL following cessation progressively prolongs with increasing the duration or rate of the overdrive pacing train. Occasionally overdrive pacing produces no effect at all on automatic AT.

Ventriculoatrial linking. Following cessation of overdrive atrial pacing (with 1:1 AV conduction) during focal AT, the VA interval (the interval between the last captured QRS complex and the first AT complex) can vary significantly from the VA interval during AT because the timing of the AT return cycle is not related to the preceding QRS. In contrast, in the setting of typical AVNRT and orthodromic AVRT, the postpacing VA interval remains fixed and similar to that during tachycardia (with a less than 10-millisecond variation) after different attempts at atrial entrainment of the SVT. VA linking occurs in the setting of typical AVNRT and orthodromic AVRT because the timing of atrial activation is related to or dependent on ventricular activation and is the result of retrograde VA conduction over the AVN fast pathway (during typical AVNRT) or the BT (during orthodromic AVRT).²⁸

Differential-site atrial pacing. Differential-site atrial pacing can help distinguish AT from other mechanisms of SVT. Overdrive pacing is performed during tachycardia from different atrial sites (high right atrium [HRA] and proximal CS) at the same PCL. Once the presence of 1:1 AV conduction during atrial pacing is verified and the SVT resumes following cessation of pacing, the maximal difference in the postpacing VA intervals (the interval from the last captured ventricular electrogram to the earliest atrial electrogram of the initial tachycardia beat after pacing) among the different pacing sites is calculated (Δ VA interval). In one report, a Δ VA interval of more than 14 milliseconds was diagnostic of AT, whereas a Δ VA interval of less than 14 milliseconds

avored AVNRT or orthodromic AVRT (with the sensitivity, specificity, and positive and negative predictive values all equal to 100%). In orthodromic AVRT and AVNRT, the initial atrial complex following cessation of atrial pacing entraining the SVT is linked to, and cannot be dissociated from, the last captured ventricular complex. In contrast, in the setting of AT, the first atrial return cycle following cessation of pacing is dependent on the distance between the AT origin and pacing site, atrial conduction properties, and mode of the resetting response of the AT, and it is not related to the preceding ventricular activation. Hence the postpacing VA intervals vary among the pacing sites, and the Δ VA interval is relatively large (more than 14 milliseconds).²⁸

Variability in PPIs. The global pattern of activation of an atrial arrhythmia can be rapidly determined by comparing the differences in PPIs obtained with overdrive pacing from a single site (proximal CS) at PCLs 10, 20, and 30 milliseconds shorter than the TCL. Relative stability of the PPI, regardless of its relation to the TCL, number of complexes of overdrive pacing or PCL, is highly suggestive of macroreentrant activation of the atrium. High variability of the PPI, on the other hand, is nearly diagnostic of a non-reentrant process. In one report, low PPI variability (less than 10 milliseconds) identified MRATs with a sensitivity of 94% and a specificity of 100%, whereas high PPI variability (more than 30 milliseconds) identified focal ATs with a sensitivity of 93% and a specificity of 100%.²⁹

In macroreentry, the PPI reflects the time required for the stimulated wavefront to travel to a reentrant circuit, revolve once around the circuit, and travel back to the pacing site. Because this distance remains unchanged when pacing from any given site, pacing at faster rates should theoretically not change the distance traveled, and thus the PPI remains stable (PPI variability should approach zero). Faster pacing rates, however, can decrease conduction velocity because of decremental tissue conduction leading to prolongation of the PPI. Nevertheless, this is less likely to occur when overdrive PCLs are limited to within 30 milliseconds of the TCL. In contrast, variability in the PPI is expected in the setting of automatic ATs; by virtue of the phenomenon of overdrive suppression, automatic foci tend to require more time for recovery as pacing rate or duration increases. Unexpectedly, however, large PPI variability was exhibited by all focal ATs regardless of mechanism (including microreentry). By virtue of their small circuits, the microreentrant ATs have a short excitable gap; it is likely that the paced wavefront will penetrate the circuit during relative refractoriness, with decremental conduction resulting in progressive PPI prolongation.²⁹

Programmed Ventricular Stimulation During Tachycardia

It is uncommon for VES or ventricular pacing to affect an AT unless rapid 1:1 VA conduction is present (especially in the presence of an AV BT or enhanced AVN conduction) and the TCL is relatively long.

If ventricular overdrive pacing does not terminate the tachycardia and the presence of stable 1:1 VA conduction during pacing is verified, the electrogram sequence immediately after the last paced ventricular complex is categorized as either an atrial-ventricular (A-V) or atrial-atrial-ventricular (A-A-V) pattern (Fig. 11.16; see detailed discussion in Chapter 20). Following overdrive ventricular pacing (1:1 VA conduction) during AT, retrograde conduction occurs through the AVN. In this setting, the last retrograde P wave resulting from ventricular pacing is unable to conduct back to the ventricle because the AVN is still refractory to anterograde conduction, and the result is an A-A-V response. Conversely, in the setting of AVNRT or orthodromic AVRT, VA conduction occurs through the retrograde limb of the circuit. Therefore, after the last paced ventricular complex, the anterograde limb of the tachycardia circuit is not refractory, and the last entrained retrograde atrial complex can conduct to the ventricle. This results in an A-V response after the last paced QRS (see Fig. 17.19).²⁸

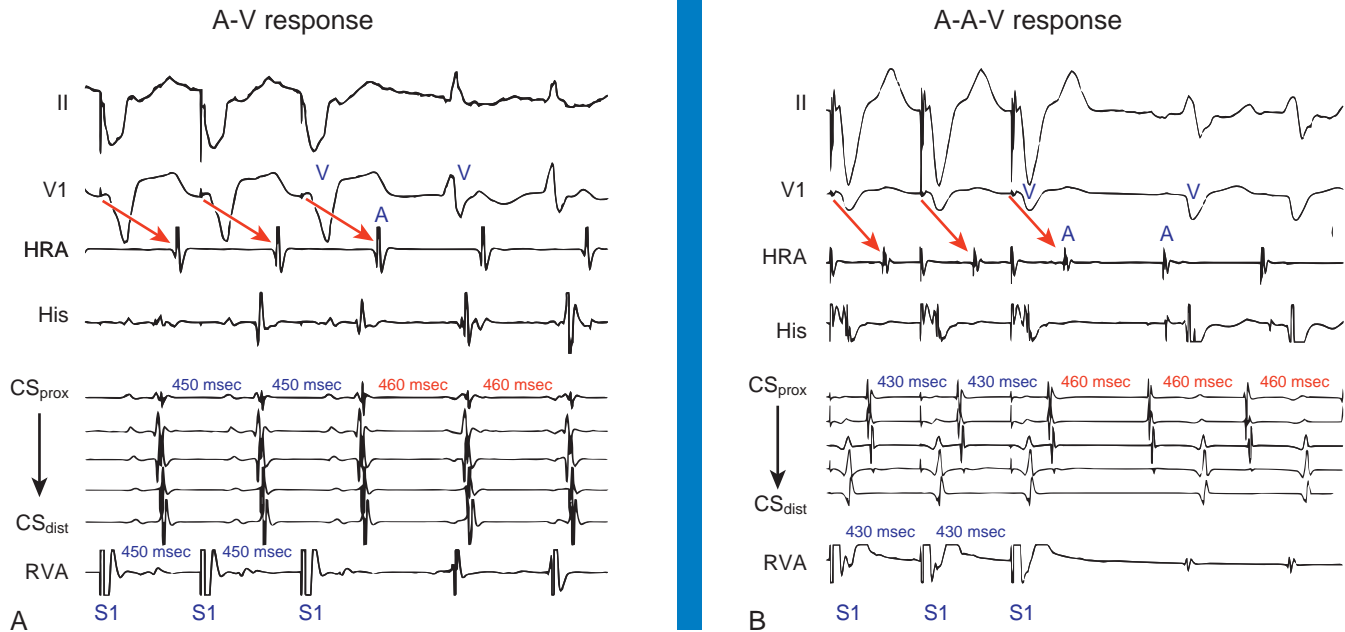


Fig. 11.16 Atrial-Ventricular (A-V) Versus Atrial-Atrial-Ventricular (A-A-V) Response After Ventricular Pacing During Supraventricular Tachycardia (SVT). Overdrive ventricular pacing is performed during five SVTs with concentric atrial activation sequence. Red arrows track ventricular-atrial conduction during ventricular pacing. Numbers indicate ventricular pacing cycle lengths (CLs) and atrial CLs during and after pacing. (A) A-V response is observed following cessation of pacing during typical atrioventricular nodal reentrant tachycardia, which is inconsistent with atrial tachycardia (AT). (B) A-A-V response is observed, consistent with AT originating in the posteroseptal region. CS_{dist}, Distal coronary sinus; CS_{prox}, proximal coronary sinus; HRA, high right atrium; RVA, right ventricular apex.

Importantly, this maneuver is not useful when 1:1 VA conduction during ventricular pacing is absent (Fig. 11.17). In addition, a pseudo-A-A-V response can occur during atypical AVNRT because retrograde conduction during ventricular pacing occurs through the slow pathway (see Fig. 11.17). This can result in a VA interval longer than the PCL; hence the last ventricular paced impulse is followed first by the P wave conducted slowly from the previous paced QRS and then by the P wave resulting from the last paced QRS, thus mimicking an A-A-V response (see Fig. 17.20). Careful identification of the last atrial electrogram that resulted from VA conduction during ventricular pacing avoids this potential pitfall. The last atrial activation resulting from conduction of the last paced ventricular complex follows the preceding P wave with an A-A interval equal to the ventricular PCL.

A pseudo-A-A-V response can also occur during typical AVNRT with long HV intervals or short HA intervals, in which atrial activation precedes ventricular activation. In the latter setting, using His bundle (HB) activation instead of ventricular activation (i.e., characterizing the response as A-A-H or A-H instead of A-A-V or A-V, respectively) can be more accurate and can help eliminate the pseudo-A-A-V response.³⁰

On the other hand, a pseudo-A-V response (Fig. 11.18) can occur with an automatic AT when the maneuver is performed during isoproterenol infusion. Ventricular pacing with 1:1 VA conduction can result in overdrive suppression of the atrial focus, and isoproterenol or epinephrine can cause an increase in junctional automaticity, so that an apparent A-V response occurs. Therefore, when ventricular pacing is performed during catecholamine infusion, it is important to determine that the response after cessation of ventricular pacing is reproducible.²⁸

Diagnostic Maneuvers During Sinus Rhythm After Tachycardia Termination

Atrial Pacing at the Tachycardia Cycle Length

The difference between the AH interval during atrial pacing during NSR at the TCL and that during SVT can help differentiate AT (with long RP interval) from atypical (fast-slow) AVNRT. A ΔAH ($\text{HA}_{\text{pacing}} - \text{AH}_{\text{SVT}}$) greater than 40 milliseconds has been reported to favor fast-slow AVNRT. In contrast, during AT (and orthodromic AVRT utilizing a septal BT), the AH interval during SVT approximates that during atrial pacing. In contrast, a ΔAH of less than 20 milliseconds favors AT and orthodromic AVRT. This criterion has only been tested with RA pacing during RA ATs and should be applied with caution when LA ATs are suspected.³¹

The ΔAH ($\text{AH}_{\text{pacing}} - \text{AH}_{\text{SVT}}$) can also help differentiate typical (slow-fast) AVNRT from AT with a short RP interval. Atrial pacing during NSR at the TCL yields an AH interval that is similar to that during AT but shorter than the AH interval during typical AVNRT. During atrial pacing and AT, AV conduction occurs preferentially over the fast pathway and, hence, is expected to be associated with similar AH and PR intervals (under comparable autonomic tone). In contrast, AV conduction during typical AVNRT occurs over the slow pathway, resulting in a long AH interval.

Ventricular Pacing at the Tachycardia Cycle Length

In the setting of AT (and AVNRT), and under comparable autonomic tone, 1:1 VA conduction over the AVN may or may not be maintained during ventricular pacing at a CL similar to the TCL because of possible retrograde block in the AVN. Anterograde conduction properties of

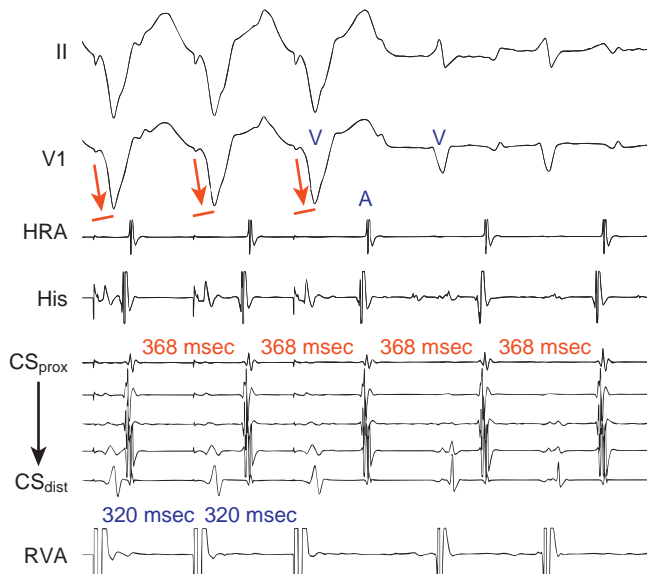


Fig. 11.18 Pseudo-Atrial-Ventricular (A-V) After Ventricular Pacing During Supraventricular Tachycardia (SVT). Overdrive ventricular pacing is performed during five SVTs with concentric atrial activation sequence. Red arrows track ventricular-atrial (VA) conduction during ventricular pacing. Numbers indicate ventricular pacing cycle lengths (CLs) and atrial CLs during and after pacing. Pseudo-A-V response is observed during focal atrial tachycardia secondary to VA dissociation (i.e., absence of VA conduction) during ventricular pacing. *CS_{dist}*, distal coronary sinus; *CS_{prox}*, proximal coronary sinus; *HRA*, high right atrium; *RVA*, right ventricular apex.

TABLE 11.3 Exclusion of Atrioventricular Nodal Reentrant Tachycardia

Parameter	Features
Atrial activation sequence	<ul style="list-style-type: none"> Eccentric atrial activation sequence generally excludes AVNRT (with the exception of left variant of AVNRT).
AV block	<ul style="list-style-type: none"> Spontaneous or induced AV block with continuation of the tachycardia is uncommon in AVNRT.
Oscillations in SVT CL	<ul style="list-style-type: none"> Spontaneous changes in PR and RP intervals with fixed A-A interval excludes AVNRT.
Overdrive ventricular pacing during SVT	<ul style="list-style-type: none"> If overdrive pacing entrains the SVT with an atrial activation sequence different from that during the SVT, AVNRT is unlikely. The presence of an A-A-V electrogram sequence following cessation of overdrive ventricular pacing practically excludes AVNRT.
Overdrive atrial pacing during SVT	<ul style="list-style-type: none"> $\Delta AH (AH_{\text{pacing}} - AH_{\text{SVT}}) < 20 \text{ msec}$ excludes AVNRT. If entrainment cannot be achieved or overdrive suppression is demonstrated, AVNRT is excluded.
Atrial pacing during NSR at the TCL	<ul style="list-style-type: none"> $\Delta AH (AH_{\text{pacing}} - AH_{\text{SVT}}) < 20 \text{ msec}$ excludes AVNRT.

AH, Atrial-His bundle interval; *AV*, atrioventricular; *AVNRT*, atrioventricular nodal reentrant tachycardia; *CL*, cycle length; *NSR*, normal sinus rhythm; *SVT*, supraventricular tachycardia; *TCL*, tachycardia cycle length.

TABLE 11.4 Exclusion of Orthodromic Atrioventricular Reentrant Tachycardia

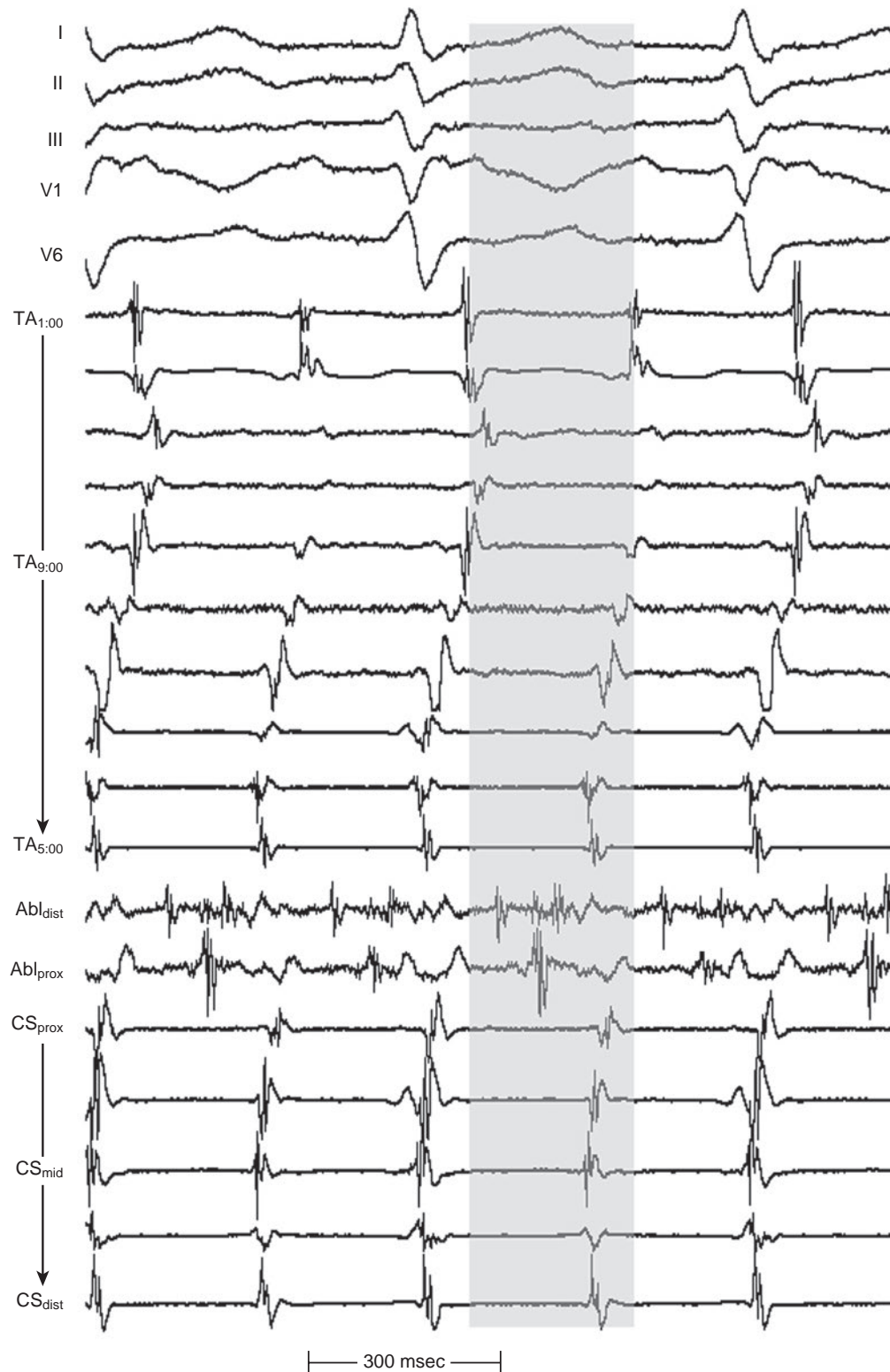
Parameter	Features
Atrial activation sequence	<ul style="list-style-type: none"> Initial atrial activation site away from the AV groove excludes orthodromic AVRT.
VA interval	<ul style="list-style-type: none"> VA interval $< 70 \text{ msec}$ or V-high RA interval $< 95 \text{ msec}$ during SVT excludes orthodromic AVRT.
AV block	<ul style="list-style-type: none"> Spontaneous or induced AV block with continuation of the SVT excludes orthodromic AVRT.
Oscillations in SVT CL	<ul style="list-style-type: none"> Spontaneous changes in PR and RP intervals with a fixed A-A interval excludes orthodromic AVRT.
VES delivered during the SVT	<ul style="list-style-type: none"> With failure to reset (advance or delay) atrial activation with early VES on multiple occasions and at different VES coupling intervals, despite advancement of the local ventricular activation at all sites (including the site of the suspected BT) by $> 30 \text{ msec}$, orthodromic AVRT and presence of AV BT are excluded.
Overdrive ventricular pacing during SVT	<ul style="list-style-type: none"> Ventriculoatrial dissociation during overdrive pacing excludes AVRT. If overdrive pacing entrains the SVT with an atrial activation sequence different from that during the SVT, orthodromic AVRT is unlikely. The presence of an A-A-V electrogram sequence following cessation of overdrive ventricular pacing practically excludes orthodromic AVRT. Lack of VA linking (i.e., the VA interval following the last entrained QRS varies $> 14 \text{ msec}$ depending on site, CL, or duration of pacing) argues against orthodromic AVRT.
Overdrive ventricular pacing during SVT	<ul style="list-style-type: none"> If entrainment cannot be achieved or overdrive suppression is demonstrated, orthodromic AVRT is excluded. If the VA interval of the return cycle after cessation of atrial pacing is variable, orthodromic AVRT is excluded.
Ventricular pacing during NSR at the TCL	<ul style="list-style-type: none"> VA block during pacing excludes orthodromic AVRT.

A-A-V, Atrial-atrial-ventricular; *AV*, atrioventricular; *AVRT*, atrioventricular reentrant tachycardia; *BT*, bypass tract; *CL*, cycle length; *NSR*, normal sinus rhythm; *RA*, right atrium; *SVT*, supraventricular tachycardia; *TCL*, tachycardia cycle length; *VA*, ventriculoatrial; *VES*, ventricular extrastimulation.

As noted, the term *localized reentry* has been used to refer to reentry in which the circuit is localized to a small area and does not have a central obstacle. Thus, if activity accounting for more than 85% of the TCL is present in an area with a diameter of up to 3 cm, localized reentry is considered (eFig. 11.6). Fractionated electrograms spanning more than 35% of the TCL often are observed at the site of origin of microreentrant ATs, whereas foci of automatic and triggered-activity focal ATs typically exhibit discrete electrograms.

Reference Electrogram

Determining the onset of the tachycardia P wave is important in activation mapping. The P wave during AT should be assessed using multiple surface ECG leads and choosing the one with the earliest P onset.



eFig. 11.6 Localized Atrial Reentry. Atrial tachycardia had a pattern of activation consistent with emanation from a focus yet could be entrained from multiple sites without evidence of electrocardiogram or intracardiac fusion. Electrogram at ablation site is very prolonged and fractionated, occupying more than 80 milliseconds of tachycardia cycle length (*shaded*), consistent with localized reentry. *Abl_{dist}*, Distal ablation site; *Abl_{prox}*, proximal ablation site; *CS_{dist}*, distal coronary sinus; *CS_{mid}*, middle coronary sinus; *CS_{prox}*, proximal coronary sinus; *TA*, tricuspid annulus.

TABLE 11.5 Exclusion of Macroreentrant Atrial Tachycardia

Parameter	Features
ECG	<ul style="list-style-type: none"> Focal AT usually has a clearly defined isoelectric baseline between P waves in all leads. MRAT usually lacks an isoelectric baseline between deflections.
Atrial activation sequence	<ul style="list-style-type: none"> Focal AT is characterized by atrial activation starting rhythmically at a small area (focus), and intracardiac mapping shows significant portions of the TCL without recorded atrial activity. MRAT endocardial recordings typically show activation spanning the whole TCL.
Programmed electrical stimulation	<ul style="list-style-type: none"> Focal AT is defined on the basis of dissociation of almost the entire atria from the tachycardia with AES. MRAT circuit usually incorporates large portions of the RA or LA, which would be identified with resetting and entrainment mapping.
TCL variability	<ul style="list-style-type: none"> Variation in the TCL of >15% favors focal AT.
Entrainment mapping	<ul style="list-style-type: none"> Automatic and triggered focal AT cannot be entrained. Microreentrant AT can be entrained but with only orthodromic capture. Constant or progressive fusion, as demonstrated by intermediate P wave morphologies on the ECG, cannot be demonstrated. MRAT is defined by demonstration of concealed or manifest entrainment of the tachycardia with atrial pacing.
PPI variability	<ul style="list-style-type: none"> PPI variability of >30 msec favors focal AT. PPI variability of <10 msec favors MRAT.
Electroanatomic mapping	<ul style="list-style-type: none"> Focal AT is suggested by electroanatomic maps demonstrating radial spreading of activation, from the earliest local activation site in all directions, with total activation time \ll TCL. MRAT is suggested by electroanatomic maps demonstrating continuous progression of colors around the RA with close proximity of earliest and latest local activation, with total activation time approximating TCL.
Response to adenosine	<ul style="list-style-type: none"> Focal AT usually responds to adenosine by slowing or termination. MRAT usually is not influenced by adenosine and may actually accelerate (when the TCL is refractoriness-dependent) secondary to shortening of atrial refractoriness by adenosine.

AES, Atrial extrastimulation; AT, atrial tachycardia; CL, cycle length; ECG, electrocardiogram; LA, left atrium; MRAT, macroreentrant atrial tachycardia; PPI, postpacing interval; RA, right atrium; TCL, tachycardia cycle length.

Increasing surface ECG lead gains can help with this determination. However, the P wave can be buried within the preceding T wave or QRS; in this setting, delivering a VES (or a train of ventricular pacing) to accelerate ventricular activation and repolarization during the tachycardia can facilitate visualization of the buried P wave. After determining P wave onset, a surrogate marker that is easier to track during mapping (such as an HRA or CS electrogram) indexed to the P wave onset where it is clearly seen may be used instead of the P wave onset on the surface ECG (eFig. 11.7).

Local Activation Time

A roving catheter is used to find the site, with the earliest atrial electrogram using unipolar and bipolar recordings. Initially, one should seek the general region of the origin of AT/PACs as indicated by the surface ECG and intracardiac recordings in the CS and Halo catheters. Small movements of the catheter tip in the general target region are undertaken under the guidance of fluoroscopy or electroanatomic mapping until the site with the earliest possible atrial activation relative to the P wave is identified. Activation times are generally measured from the onset or the first rapid deflection of the atrial bipolar electrogram to the onset of the P wave or, preferably, surrogate marker during AT. Using the onset of the local bipolar electrogram is preferable, because it is easier to determine reproducibly when measuring heavily fractionated, low-amplitude atrial electrograms. On the recording system display, displaying the intracardiac channel with the earliest local activation timing adjacent to the mapping catheter channel allows the operator to recognize early activation times immediately at sites sequentially visited by the mapping catheter by visual inspection, rather than having to pause and manually measure local activation times. A triggered sweep mode (constant temporal alignment of the display to a reference electrogram) can also be useful for rapid visual assessment of relative timing of mapped sites. The distal pole of the mapping catheter should be the one used for mapping for the earliest atrial activation site because it is the pole through which RF energy is delivered.

Once the site with the earliest bipolar signal is identified, the unipolar signal from the distal ablation electrode should be used to supplement conventional bipolar mapping. The unfiltered (0.05 to >300 Hz) unipolar signal morphology should show a monophasic QS complex with a rapid negative deflection. Although this electrogram configuration is very sensitive for successful ablation sites, it is not specific. The timing of the unipolar electrograms recorded at those sites distant from the AT focus, however, is later than that at the site of origin of the AT. Thus a QS complex should not be the only mapping finding used to guide ablation. Nonetheless, successful ablation is unusual at sites with an RS complex because these are generally distant from the AT focus.

The timing of the unipolar electrograms is also important. Concordance of the timing of the onset of the bipolar electrogram with that of the filtered or unfiltered unipolar electrogram, with the rapid downslope of the S wave of the unipolar QS complex coinciding with the initial peak of the bipolar signal, helps ensure that the tip electrode, which is the ablation electrode, is responsible for the early component of the bipolar electrogram.

The site of origin of the AT is defined as the site with the earliest presystolic (i.e., preceding the onset of the P wave on the surface ECG) bipolar recording, in which the distal tip shows the earliest intrinsic deflection and QS unipolar electrogram configuration (see Fig. 11.13).

Low-amplitude early signals followed by a sharper discrete signal can represent early components of a fragmented electrogram or far-field signal associated with a second discrete local electrogram. This is most likely to happen in regions where separate structures are in close proximity (e.g., superior crista terminalis and right superior PV; LA appendage and left superior PV; RA appendage and superior tricuspid annulus). Unipolar recordings help distinguish far-field from local electrograms. At endocardial sites where the early signal is far field, the unipolar recording fails to exhibit a QS configuration and the sharp negative deflection coincides with the later, high-frequency potential on the bipolar electrogram rather than the earlier far-field signal.

In some cases, several areas can show equivalently early activation, sometimes even with a central area of early local activation time surrounded with areas having later local activation times. This finding can indicate a deeper focus (e.g., in the crista terminalis) or multiple breakthrough sites from a single focus located in an adjacent structure or



eFig. 11.7 P Wave Onset During Atrial Tachycardia (AT) Revealed by Premature Ventricular Stimulation. During AT, P wave onset is difficult to discern (buried in T wave). Double ventricular extrastimuli (S) during AT pull the QRS complexes earlier and allow the P wave to be seen clearly (dark arrow, dashed line). Thereafter, a stable atrial electrogram (e.g., high right atrium [HRA] or proximal coronary sinus [CS_{prox}]) can be used as a surrogate marker for the P wave onset during mapping. CS_{dist}, Distal coronary sinus; CS_{mid}, middle coronary sinus; His_{dist}, distal His bundle; His_{mid}, middle His bundle; His_{prox}, proximal His bundle; RVA, right ventricular apex.

chamber. This can obviously cause confusion during mapping and ablation attempts, with little apparent effect of ablation at a site with very good electrogram characteristics or successful ablation at a site with less optimal parameters. Special attention should be given to ATs mapped to the midseptum and the right anterosseptal region. For ATs

mapped to the midseptum, especially if presystolic activity is not particularly early (i.e., less than 15 milliseconds pre-P wave onset), the electrogram is not fractionated, and multiple sites have similar activation times, exclusion of LA ATs using transseptal access to the LA is important (Fig. 11.19). For ATs mapped to the right anterosseptal region (HB region),

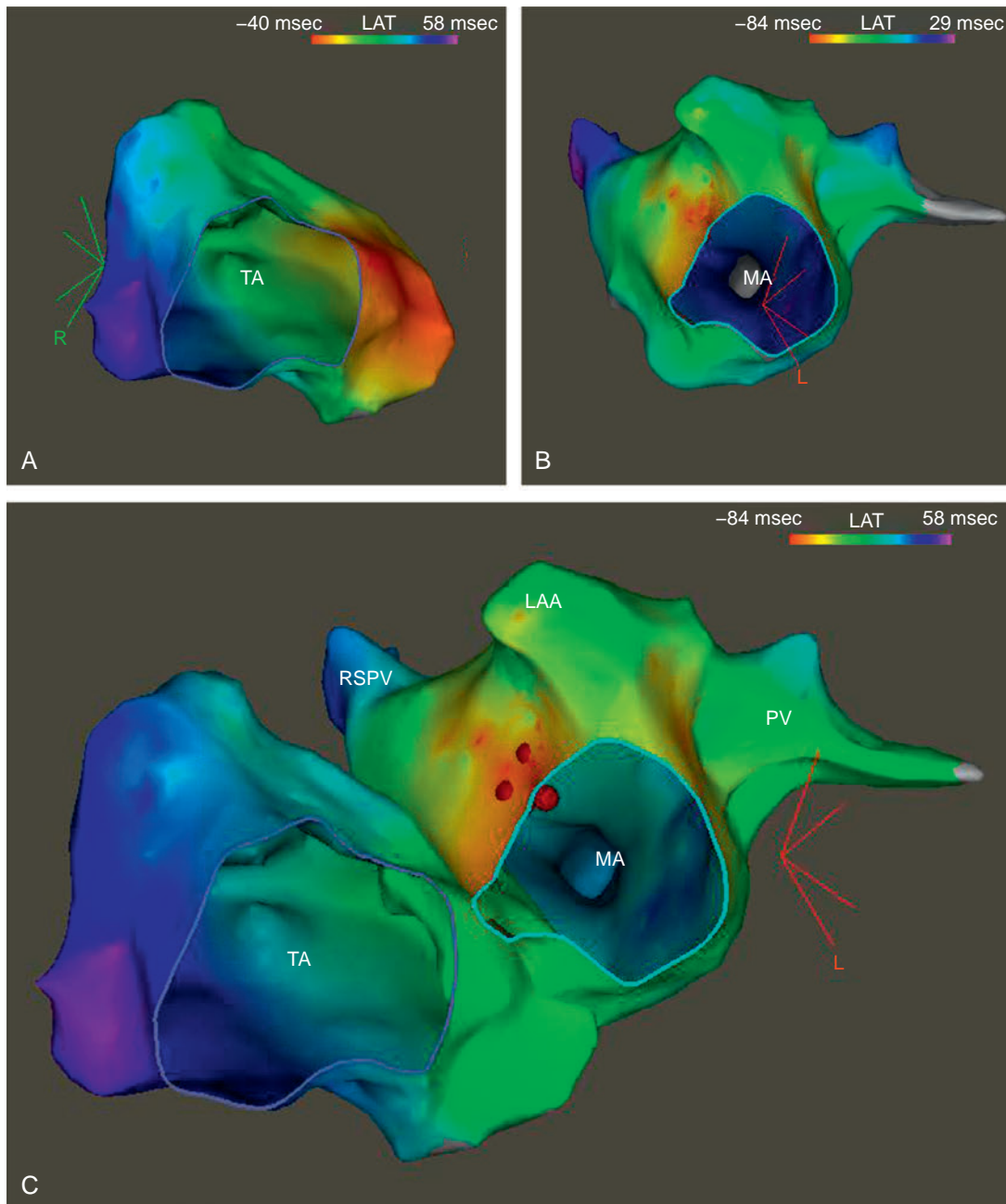


Fig. 11.19 Electroanatomic Activation Map of Focal Atrial Tachycardia Originating From the Anterior Left Atrial (LA) Wall. (A) Left anterior oblique (LAO) view of the CARTO activation map of the right atrium (RA). (B) LAO view of the CARTO activation map of the LA. When mapping is limited to the RA (A), the site of earliest atrial activation was localized to the interatrial septum, with local activation preceding the reference electrogram by 40 milliseconds. When activation mapping is extended to the LA (B), a site with earlier local activation (preceding the reference electrogram by 84 milliseconds) was localized to the anterior LA wall. (C) LAO view of the CARTO activation map of both atria showing that the RA septum activation time is no longer early compared to that of the anterior LA wall. Radiofrequency ablation (*red dots*) at that site eliminated the tachycardia. LAA, Left atrial appendage; LAT, local activation time; MA, mitral annulus; PV, left common pulmonary vein; RSPV, right superior pulmonary vein; TA, tricuspid annulus.

great care must be given to sites in the anteromedial LA septum, right superior PV, aortomitral continuity, noncoronary aortic sinus of Valsalva, and LA free wall, because sites in these regions break through early to the right anterosseptal region, where ablation not only is unsuccessful in eliminating AT but also can result in AV block.

Careful catheter manipulation during mapping should seek to avoid mechanical trauma that can transiently abolish the arrhythmia. Transient catheter-induced interruption of AT by pressure of the catheter can suggest an appropriate site for ablation. This sign is more useful when it is a reproducible phenomenon. Often, however, the tachycardia terminates as the catheter is brushing past the area, and where the catheter comes to rest may not be the same site as where transient AT termination occurred. On the other hand, catheter manipulation frequently induces PACs that can closely mimic target PACs. The findings on the mapping catheter during these catheter-induced complexes are invariably excellent (e.g., substantial presystolic activation time, sharp QS on the unipolar recording). These complexes must be analyzed and carefully compared with prerecorded AT or PAC to avoid delivery of RF energy at sites with no relevance to actual AT.

Tachycardia Transformation

Occasionally, multiple unstable focal ATs or PACs can be encountered during mapping. In this setting, the goal should be to focus mapping on the most frequently encountered AT or PAC. Ablation of the most frequent AT often results in organization of the atria and allows for mapping and ablation of other successive ATs. Importantly, care must be taken to ensure that the correct AT is being mapped and to avoid incorrect sampling of activation times during beats originating from the different foci, which can result in erroneous and confusing activation maps. This can be facilitated by careful attention to changes in P wave morphology or shifting of atrial activation sequences (in the RA or CS), or variations in the TCL during the mapping procedure.

Assessment of simultaneous RA and CS activation sequences by using a multipolar catheter (e.g., duodecapolar or Halo catheters) in the RA around the tricuspid annulus and a decapolar catheter in the CS can facilitate the mapping of ATs. In addition to predicting the anatomic region of interest, it can facilitate recognition of transformation of the index tachycardia to a different morphology induced by catheter manipulation or by pacing maneuvers. This can be especially important when mapping nonsustained AT or PACs.

Right Versus Left Atrial Foci

In addition to P wave morphology on the 12-lead ECG (as noted above), several observations during activation mapping in the RA suggest an LA site of origin the AT, and should prompt consideration for extending the mapping procedure to the LA. First, a distal-to-proximal CS activation sequence is most consistent with LA foci, although ATs originating from the superior RA can result in distal-to-proximal CS activation (especially when the CS catheter is deeply seated into the CS). Importantly, a proximal-to-distal CS activation sequence, although more common during RA AT, can also be observed during ATs originating from the right-sided PVs, LA septum, and aortomitral continuity. Second, when RA mapping localizes the earliest activation site to the superoposterior RA, interatrial septum, or AVN or HB region, an LA site of origin of the AT should be suspected. This is especially true when RA mapping at these sites reveals a relatively large endocardial area with equivalently early local activation times, when the site of earliest local activation is not particularly early, when the unipolar recording at the fails to exhibit a QS configuration, or when the earliest component of the bipolar electrogram is more consistent with far-field recording (i.e., low-amplitude early signal followed by a sharper discrete signal).

Right Atrial Versus Right Superior Pulmonary Vein Foci

AT foci in the region of the right superior PV can quickly propagate to the RA via the closely located Bachmann bundle and posterior-medial interatrial connections. Early activation at the RA breakthrough site(s) usually occurs prior to the P wave onset; as a result, these RA sites can be misdiagnosed during activation mapping as the AT origin.³²

Endocardial atrial activation sequences from the RA, HB, and CS catheters can help predict the location of PAC or AT foci in the SVC or superior RA versus the right superior PV. In one report, the difference in *interatrial* conduction time (between the HRA and distal CS [CS_{dist}] recording electrodes) during NSR versus PAC ($[HRA - CS_{dist}]_{NSR-PAC}$) was significantly longer for right superior PV tachycardias compared with SVC tachycardias. A cutoff value of 20 milliseconds or more of the difference in *interatrial* conduction time could reliably differentiate between both locations. During AT originating from the SVC or superior RA, the tachycardia wavefront activates the RA in a high-low sequence and at the same time propagates through the interatrial connection to the LA, similar to the activation pathway in NSR. As a consequence, there is little change in the interatrial conduction time compared with that during NSR. Conversely, during right superior PV tachycardias, after leaving the vein and entering the LA, the tachycardia wavefront travels to the rest of the LA and simultaneously crosses the interatrial septum to activate the RA. Thus the interatrial conduction time would be much shorter than that during NSR. As a consequence, the difference of interatrial conduction time ($[HRA - CS_{dist}]_{NSR-PAC}$) between the two groups of tachycardias can be a useful prospective method to define the sources of tachycardia before attempting atrial transseptal puncture.³³

Similarly, analyzing *intraatrial* conduction times can facilitate the distinction between PACs or ATs originating from the SVC and high crista terminalis from PV foci. The time interval between HRA and HB atrial activation during PACs originating from the SVC and crista terminalis is significantly longer than that of the sinus beats. A difference in intraatrial conduction time ($[HRA - HB]_{NSR-PAC}$) of less than 0 milliseconds favors SVC or crista terminalis origin. The increased intraatrial conduction delay between HRA and HB recording electrodes is a physiological response to the PACs from the SVC and crista terminalis in the human atrium. In contrast, intraatrial conduction time between the HRA and HB electrodes is shortened in the setting of PV tachycardias because both locations are activated in parallel during PV tachycardias, but in sequence during NSR.³³

Pace Mapping

When atrial activation originates from a point-like source, such as during focal AT or during pacing from an electrode catheter, the resultant P wave recorded on the surface ECG is determined by the sequence of atrial activation, which depends to a large extent on the initial site of myocardial depolarization. In addition, analysis of specific P wave configurations in multiple leads allows estimation of the pacing site location to within several square centimeters. Therefore comparing the paced P wave configuration with that of AT is particularly useful for locating a small arrhythmia focus in a structurally normal heart.

Pace mapping involves pacing from the distal tip of the mapping catheter at sites of interest. Initially, the exact morphology of the tachycardia complex should be determined and used as a template for pace mapping. Pace mapping during the tachycardia (at a PCL 20 to 40 milliseconds shorter than the TCL) is preferable whenever possible because it facilitates rapid comparison of tachycardia and paced complexes at the end of the pacing train. If sustained tachycardia cannot be induced, mapping is performed during spontaneous nonsustained runs or ectopic beats. Although it is preferable to match the PCL and coupling intervals of AESs to those of spontaneous tachycardia or PACs, some reports have suggested that this is not mandatory. Pace mapping is preferably

performed with unipolar stimuli (up to 10 mA, 2 milliseconds) from the distal electrode of the mapping catheter (cathode) and an electrode in the IVC (anode), or with closely spaced bipolar pacing at twice the diastolic threshold, to eliminate far-field stimulation effects.

The greater the degree of concordance between the morphology during pacing and that during tachycardia, the closer the catheter will be to the site of origin of the tachycardia. Pace maps with identical or nearly identical matches of the tachycardia morphology in all 12 surface ECG leads and intracardiac atrial electrograms can be indicative of the site of origin of the tachycardia (Fig. 11.20).

Pace mapping is used as an adjunct to other methods of mapping to corroborate putative ablation sites. It can be of great help, especially when the AT is difficult to induce. However, difficulties in precisely comparing P wave morphologies (low P wave amplitude and superimposition of the P wave on T wave during tachycardia) limit the applicability of pace mapping. Moreover, the spatial resolution of atrial pace mapping is up to 2 cm, which is too imprecise. Utilization of intracardiac activation sequences on multiple catheters (e.g., Halo and CS catheters) can help mitigate those limitations.³⁴ Despite those limitations, many studies have demonstrated efficacy using pace mapping to choose ablation target sites; concordance of P wave morphology during pace mapping and AT has a sensitivity of 86% and a specificity of 37%.

Mapping Postpacing Intervals

Following overdrive atrial pacing from a given site during a relatively regular and stable focal AT, the PPI represents the sum of the conduction time to reach the tissue around the AT focus (perifocal tissue) plus the time required to penetrate the perifocal tissue and reset the focus, plus the TCL, plus the conduction back to the pacing site. Hence if the

pacing site is directly at the AT focus, the PPI should be equivalent to the TCL because of the minimal conduction time between the pacing site and the AT focus. Conversely, pacing at sites distant from the AT focus results in a PPI that is longer than the TCL because of the additional conduction delay between the pacing site and the focus. The difference between the PPI and TCL ($PPI - TCL$) after atrial overdrive pacing of a focal AT was found to have a direct relationship with proximity to the focus, regardless of whether the tachycardia could be entrained. The ($PPI - TCL$) difference approaches zero (and is no more than 20 milliseconds) when pacing directly at the focus of the tachycardia. There appears to be no significant overdrive suppression or acceleration of the AT when pacing at a rate just faster than the AT rate, regardless of the underlying AT mechanism. Therefore the ($PPI - TCL$) difference can be a useful adjunct to localize the AT focus and guide successful ablation sites.³⁵ One must use this technique with caution, since overdrive suppression (that could itself increase the [$PPI - TCL$] difference) is accentuated by pacing for longer durations and/or shorter PCLs. Therefore pacing at a constant PCL, for a similar number of stimuli, from a variety of sites must be used to derive helpful information from this strategy.

In addition, the ($PPI - TCL$) difference can be valuable in distinguishing AT in close proximity to the sinus node from sinus tachycardia. It appears that AT foci, unlike the sinus node, have minimal perifocal conduction delay. Consequently, the ($PPI - TCL$) difference in the setting of focal AT is determined predominantly by the distance from the focus with minimal contribution of the time required to traverse any perifocal tissue, thus explaining the finding that the ($PPI - TCL$) difference approaches zero when pacing is performed directly at the AT focus. In contrast, overdrive pacing during sinus tachycardia is associated with

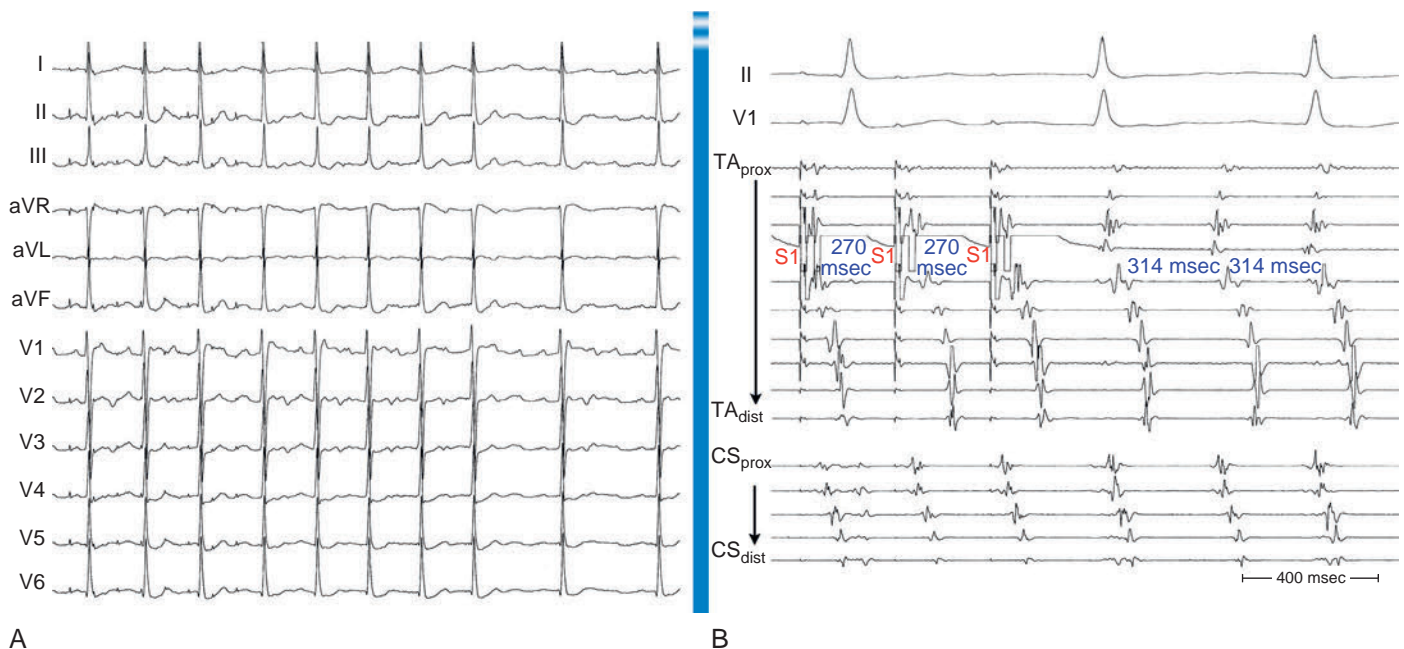


Fig. 11.20 Pace Mapping of Focal Atrial Tachycardia (AT). Surface electrocardiogram (ECG) (A) and intracardiac recordings (B) demonstrating pace mapping performed during sustained focal AT originating from the interatrial septum. Atrial pacing (left aspect of the ECG and intracardiac recordings) is performed during the tachycardia at a cycle length (CL) of 270 milliseconds from the site of earliest activation (recorded by the Halo catheter positioned around the tricuspid annulus [TA]). Concordance between paced (at the left aspect of the ECG and intracardiac recordings) and tachycardia (at the right aspect of the ECG and intracardiac recordings) P wave morphology on the surface ECG, as well as an endocardial atrial activation sequence, suggests proximity of the pacing site to the AT focus. CS_{dist} , Distal coronary sinus; CS_{prox} , proximal coronary sinus.

a PPI that always exceeds (by more than 80 milliseconds) the sinus CL, even when pacing is performed directly at the origin of the sinus impulse. This finding suggests significant perinodal conduction delay. The (PPI – TCL) difference can therefore be used to distinguish perinodal focal AT from sinus tachycardia.³⁵

Electroanatomic Mapping

Mapping Technique

Mapping of focal AT or PACs is typically performed in conjunction of electroanatomic mapping (CARTO, Biosense Webster, Diamond Bar, CA, United States; EnSite NavX, St. Jude Medical, St. Paul, MN, United States; or Rhythmia, Boston Scientific, San Jose, CA, United States). Activation mapping may be performed by point-by-point mapping with a standard mapping/ablation catheter, a high-density multielectrode mapping catheter (e.g., PentaRay, Biosense Webster), or multielectrode arrays.³⁶

Initially, selection of the reference electrogram, positioning of the anatomical reference, and determination of the window of interest are undertaken. This is the fiducial marker on which the entire mapping procedure is based. The reference catheter is usually placed in the CS (because of its stability) by using an electrode recording a prominent atrial electrogram and ensuring that the ventricular electrogram is not the one picked up by the system.³⁷

The mapping-ablation catheter is initially positioned, using fluoroscopy, at known anatomical points that serve as landmarks for the electroanatomic map. Anatomical and EP landmarks (IVC, SVC, CS, HB, and tricuspid annulus for RA mapping and the mitral annulus and PVs for LA mapping) are tagged. The catheter is then advanced slowly around the chamber walls to sample multiple points along the endocardium, thus sequentially acquiring the location of its tip together with the local electrogram (see Fig. 11.19).

Activation mapping is performed to define the atrial activation sequence. The principles used for conventional activation mapping discussed above are also used here to define the site of origin of AT. A reasonable number of points homogeneously distributed in the RA or LA, or both, must be recorded (approximately 80 to 100 points). The local activation time at each site is determined from the intracardiac bipolar electrogram and is measured in relation to the fixed intracardiac electrogram obtained from the reference catheter. Points are added to the map only if stability criteria in space and local activation time requirements are met. The activation map can also be used to catalog sites at which pacing maneuvers are performed during assessment of the tachycardia (e.g., sites with good pace maps).

Activation maps display the local activation time by a color-coded overlay on the acquired 3-D geometry. The electroanatomic maps of focal ATs demonstrate radial spread of activation, from the earliest local activation site in all directions (a well-defined early activation site surrounded by later activation sites; see Fig. 11.19). In these cases, activation time—the total range of activation times, from earliest to latest—is usually markedly shorter than the TCL (see Fig. 6.2). Conversely, a continuous progression of colors, with close proximity of earliest and latest local activation, suggests the presence of a macroreentrant tachycardia. In these cases, total activation time is in a similar range to TCL (see Fig. 12.13).

A stepwise strategy for mapping RA and LA focal tachycardias was described in a study using CARTO to avoid time-consuming whole-chamber map.³⁷ Using this approach, mapping is started with the acquisition of four or five anatomically defined sites at the superior and septal aspects of the tricuspid annulus, and the mapping procedure is strategically continued according to this initial activation sequence. If the initial four-point activation map shows the earliest atrial activation to be at the superior aspect of the tricuspid annulus, mapping is

continued toward the free wall of the RA, including the crista terminalis. When the earliest atrial activation within the four-point area is found at the septal aspect of the tricuspid annulus, mapping is expanded to the triangle of Koch and the paraseptal space. This strategy was found to differentiate reliably between ATs arising from the free wall of the RA, including the crista terminalis and RA appendage, from those arising from the triangle of Koch and paraseptal space, as well as from left-sided ATs. Once the general area of interest is identified, high-density mapping of this area is undertaken to identify the site of the earliest activation within this target area. If the unipolar electrogram at the point of earliest activation at the RA septum or at the high posterior wall still shows a significant R wave, or if RF ablation at that site is unsuccessful, a left-sided AT origin is assumed, and the procedure is extended to the LA.

Advantages

Electroanatomic mapping systems provide a highly accurate geometric rendering of the cardiac chamber with a straightforward geometric display that has the capability to determine the 3-D location and orientation of the ablation catheter accurately.

The capability of the mapping system to associate relevant EP information with the appropriate spatial location in the heart and the ability to study activation patterns (with high spatial resolution [less than 1 mm]) during tachycardia in relation to normal anatomical structures and areas of scar significantly facilitate the mapping and ablation procedure. It can suggest the mechanisms underlying the arrhythmia (distinguishing between a focal origin and macroreentrant tachycardia) and allows rapid visualization of the activation wavefront (propagation maps; Fig. 11.21), thus facilitating the identification of appropriate sites for entrainment mapping and pace mapping. High-resolution activation maps can be obtained in relatively short intervals by using multielectrode catheters (circular catheter or PentaRay) or basket catheter (Orion, Boston Scientific).³⁷

Furthermore, electroanatomic mapping systems provide the capability to create and tag several potential points of interest during the mapping process (e.g., sites with good pace maps) and return to them with great precision. These features provide significant advantages over conventional techniques. The catheter can accurately revisit a critically important recording site identified previously during the study, even if the tachycardia is no longer present or inducible and map-guided catheter navigation is no longer possible. In addition, fluoroscopy time can be reduced during catheter navigation, and the catheter can be accurately guided to positions removed from fluoroscopic markers.

Limitations

The sequential data acquisition required for creation of the electroanatomic map remains time-consuming because the process requires tagging many points, depending on the spatial details needed to analyze a given arrhythmia. Furthermore, because the acquired data are not coherent in time, multiple beats are required, and stable, sustained, or frequently repetitive arrhythmia is usually needed for creation of the activation map. Single PACs or nonsustained AT can be mapped, although at the expense of an appreciable amount of time. This can be facilitated by using multielectrode mapping catheters for data acquisition.

One difficulty with current methods is that incorrect assignment of activation for a small number of electrograms can invalidate the entire activation map; manual adjustment of activation times is often required to achieve the optimal representation. In addition, data interpolation between mapped points is used to improve the quality of the display; however, areas of unmapped myocardium are then assigned simple estimates of timing and voltage information that may not be accurate.

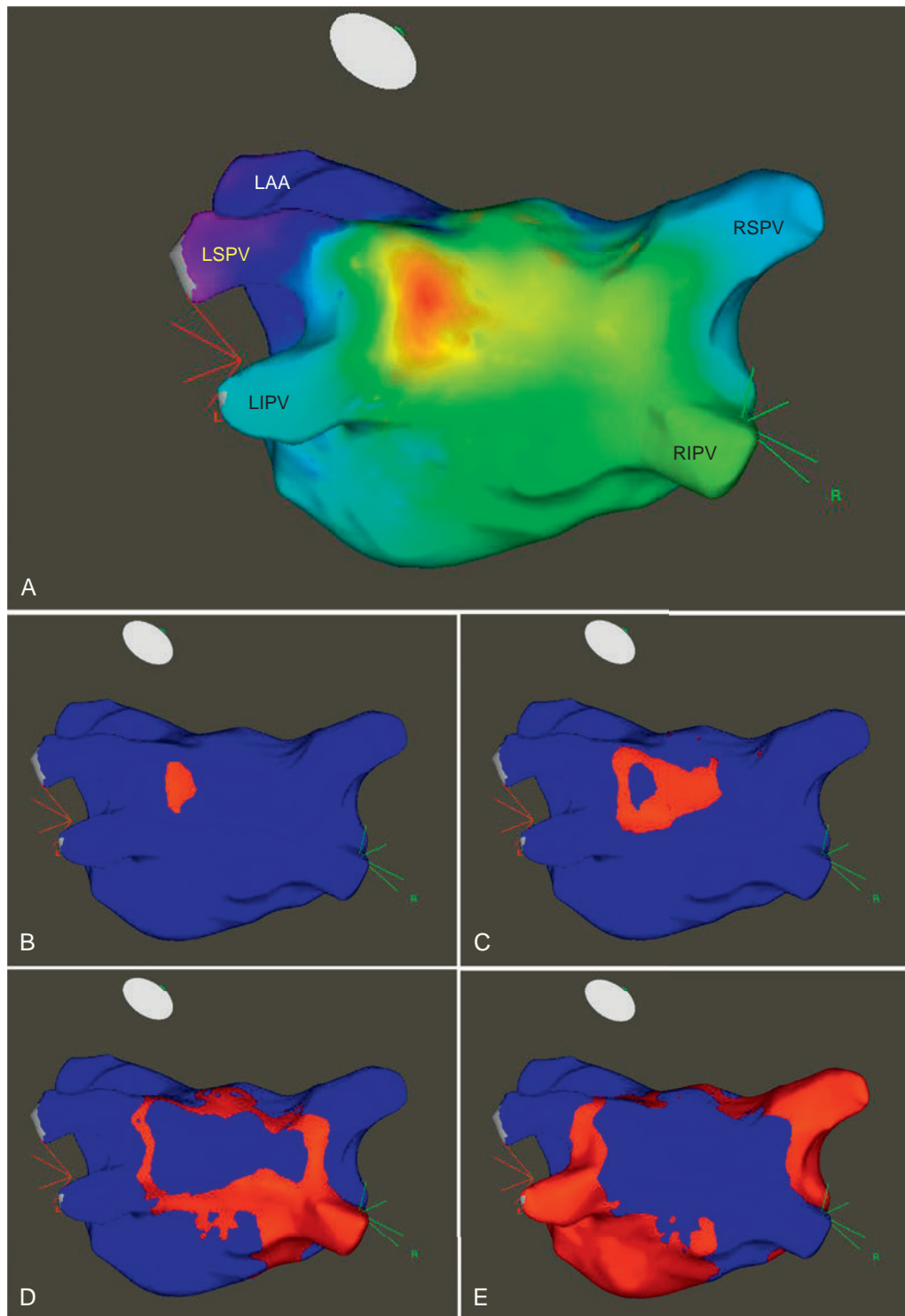


Fig. 11.21 Electroanatomic Mapping of Focal Atrial Tachycardia (AT). (A) Electroanatomic (CARTO) left atrial (LA) activation map in the posteroanterior view constructed during focal AT originating left aspect of the LA roof. During tachycardia, the activation wavefront propagates from the earliest local activation site (red) in all directions. (B–E) LA propagation map during the focal AT. LAA, Left atrial appendage; LIPV, left inferior pulmonary vein; LSPV, left superior pulmonary vein; RIPV, right inferior pulmonary vein; RSPV, right superior pulmonary vein.

In addition, the patient or intracardiac reference catheter can move, thus necessitating remapping. Although a shadow (to record original position) can be placed over this catheter to recognize displacement during the procedure, in which case the catheter can be returned to its original location, this may not always be feasible or accurate. Another limitation specific to the CARTO and Rhythmia systems is the requirement of a proprietary mapping catheter; no other mapping catheter types can be used with these systems. In contrast, the EnSite NavX system can work with most manufacturers' ablation catheters and RF or cryogenerators.

Mapping Nonsustained Focal Atrial Tachycardia

Several mapping modalities can be used when AT is short-lived or cannot be reproducibly initiated or when only infrequent PACs are being targeted by ablation, including simultaneous multisite data acquisition systems (noncontact mapping system, basket catheter, or high-density mapping). These mapping systems can also be used for sustained tachycardias, according to the operator's preference. Moreover, the electroanatomic mapping and pace mapping techniques discussed can be used in these situations.

Ensite Noncontact Mapping System

The EnSite 3000 noncontact mapping system (St. Jude Medical) consists of a noncontact catheter with a multielectrode array surrounding a 7.5-mL balloon mounted at the distal end. Raw data detected by the multielectrode array are transferred to a silicon graphics workstation via a digitalized amplifier system. The multielectrode array is used to construct a 3-D computer model of the virtual endocardium. The system can reconstruct more than 3000 unipolar electrograms simultaneously and superimpose them onto the virtual endocardium, thus producing isopotential maps with a color range representing voltage amplitude. Electrical potentials at the endocardial surface some distance away are calculated. Sites of early endocardial activity, which are likely adjacent to the origin of the AT, are usually identifiable. Noncontact mapping can rapidly identify AT foci and thus delineate starting points for conventional mapping.

The main advantage of noncontact endocardial mapping is its ability to recreate the endocardial activation sequence from simultaneously acquired multiple data points over a few (theoretically one) tachycardia beats, without requiring sequential point-to-point acquisitions. Therefore it can be of great value in mapping nonsustained arrhythmias, PACs, irregular ATs, and rhythms that are not hemodynamically stable.

Technique. The EnSite 3000 system requires placing a 9 Fr multielectrode array and a 7 Fr conventional (roving) mapping-ablation catheter in the cardiac chamber of interest. The balloon catheter is advanced over a 0.035-inch guidewire under fluoroscopy guidance and positioned in the atrium and deployed. The balloon is positioned in the center of the atrium and does not come in contact with the atrial walls being mapped. Aggressive anticoagulation with IV heparin is required to maintain the activated clotting time at 250 to 300 seconds for right-sided and 300 to 400 seconds for left-sided mapping.

The mapping-ablation catheter is positioned in the atrium and used to collect geometry information. The mapping catheter is initially moved to known anatomical locations (IVC, SVC, CS, HB, and tricuspid annulus for RA mapping and mitral annulus and PVs for LA mapping), which are tagged. A detailed geometry of the chamber is then reconstructed by moving the mapping catheter around the atrium. Using this information, the computer creates a model of the atrium.

After the chamber geometry is defined, mapping of the arrhythmia can begin. The data acquisition process is performed automatically by the system, and all data for the entire chamber are acquired simultaneously. The system then reconstructs unipolar electrograms simultaneously

and superimposes them onto the virtual endocardium, thus producing isopotential maps with a color range representing voltage amplitude. A default high-pass filter setting of 2 Hz is used to preserve components of slow conduction on the isopotential map. Color settings are adjusted so that the color range matches 1 to 1 with the millivolt range of the electrogram deflection of interest. The color scale for each isopotential map is set so that white indicates most negative potential and blue indicates least negative potential. Activation can be tracked on the isopotential map throughout the cycle to the onset of the tachycardia beat. Virtual electrograms are then reconstructed at sites of earliest activation on the isopotential maps to look for a unipolar QS pattern. If the atrial electrograms overlap with the T wave, a VES may be delivered to accelerate ventricular depolarization and repolarization and may reveal the following atrial complex without far-field interference.

Isochronal maps can also be created. These maps represent progression of activation throughout the chamber relative to a user-defined electrical reference timing point. Contact mapping using the conventional ablation catheter may also be performed at sites of interest to supplement noncontact mapping findings, and color-coded contact activation maps can be displayed on the same 3-D geometry. Once earliest activation is identified, the site is labeled on the 3-D map, and the locator signal is used to navigate the ablation catheter to it in real time during tachycardia or during normal rhythm when sustained tachycardia is not inducible.

The origin of AT is defined as the earliest site showing a single spot on the isopotential map and a QS pattern on the noncontact unipolar electrogram. Early sites with an rS pattern can represent foci that are epicardial in origin or early activation sites in an adjacent structure. The earliest site that shows an rS pattern with a sudden increase of peak negative potential on the noncontact unipolar electrogram after the AT depolarizes is considered to represent the "break-out point" or "exit" from the tachycardia focus, and the path between the origin and the break-out point likely represents the preferential pathway of conduction from the origin of the AT. As such, the traditionally defined origin of focal AT (by contact mapping techniques), whereby centrifugal activation occurs, potentially represents the breakout point, rather than the real origin of the tachycardia. Ablation at the origin of tachycardia or along the proximal path to the breakout point typically eliminates the arrhythmia.

Limitations. Very-low-amplitude signals may not be detected, particularly if the distance between the center of the balloon catheter and the endocardial surface exceeds 40 mm, thus limiting the accurate identification of diastolic signals. Furthermore, a second catheter is still required for additional mapping and for ablation. Aggressive anticoagulation is required using this mapping modality, and special attention and care are necessary during placement of the large balloon electrode in a nondilated atrium.

Multielectrode Basket Catheter Mapping

The basket catheter consists of an open-lumen catheter shaft with a collapsible, basket-shaped, distal end. The catheter is composed of 64 electrodes mounted on eight flexible, self-expanding, equidistant metallic splines. Each spline carries eight ring electrodes. The electrodes are equally spaced 4 or 5 mm apart, depending on the size of the basket catheter used (with diameters of 48 or 60 mm, respectively). Each spline is identified by a letter (from A to H) and each electrode by a number (from 1 to 8, with electrode 1 having the distal position on the splines). The basket catheter is constructed of a superelastic material to allow passive deployment of the array catheter and optimization of endocardial contact.

Technique. The size of the atrium is initially evaluated (usually with echocardiography) to help select the appropriate size of the basket

catheter. The collapsed basket catheter is advanced under fluoroscopy guidance through an 11 Fr long sheath into the RA or LA; the catheter is then expanded (eFig. 11.8). Electroanatomical relations are determined by fluoroscopically identifiable markers (spline A has one marker and spline B has two markers located near the shaft of the basket catheter). In addition, the electrical signals recorded from certain electrodes (e.g., annular or HB electrograms) can help identify the location of those particular splines.

From the 64 electrodes, 64 unipolar signals and 32 to 56 bipolar signals can be recorded (by combining 1–2, 3–4, 5–6, 7–8, or 1–2, 2–3, until 7–8 electrodes are on each spline). Color-coded activation maps are reconstructed. The concepts of activation mapping discussed earlier are then used to determine the site of origin of the tachycardia. The capacity of pacing from the majority of basket electrodes allows the evaluation of activation patterns, pace mapping, and entrainment mapping. The electrograms recorded from the basket catheter can be used to monitor changes in the activation sequence in real time and thereby indicate the effects of ablation as lesions are created.

After basket catheter deployment, the conventional catheters are introduced and placed in standard positions. The ablation catheter is placed in the region of earliest activity and is used for more detailed mapping of the site of origin of the AT (see eFig. 11.8).

Limitations. The electrode array does not expand to provide adequate contact with the entire atrium. In addition, the system does not permit immediate correlation of activation times to precise anatomical sites. Furthermore, a second catheter is still required for additional mapping and for ablation. The use of basket catheter mapping has largely been replaced by contact and noncontact electroanatomic mapping technologies.

ABLATION

Target of Ablation

The site of origin (or focus) of focal AT is the target of ablation. Bipolar electrograms at the site of successful ablation are typically fractionated and demonstrate moderate to marked presystolic timing. Average presystolic intervals at successful ablation sites are generally longer than 30 milliseconds (but not mid-diastolic, unlike MRAT). However, the key to successful mapping is finding the earliest site because there is great variability in the presystolic interval that will be obtained at successful ablation sites (10 to 40, but rarely as much as 80 milliseconds). QS unipolar electrogram morphology is highly predictive of the successful ablation site and supplements findings of bipolar mapping. Timings of the earliest bipolar and unipolar electrogram should be in agreement (see Fig. 11.13).

Focal ATs arising from the PVs can be targeted by either focal ablation or electrical isolation of the culprit PV. The latter approach can potentially limit the risk of PV stenosis, especially when targeting more distal foci within the PV.

Ablation Technique

For catheter ablation in the focal AT, a nonirrigated 4-mm-tip ablation catheter is usually used. Large-tip or irrigated ablation catheters can be of value for ablation of foci at the crista terminalis. Standard RF power delivery is adjusted to achieve a tip temperature of 55°C to 65°C. The response of the AT focus to a successful RF application should be rapid, typically within a few seconds of RF application. The most common response to successful ablations is abrupt termination. However, in some patients, transient acceleration precedes termination; in others, gradual slowing precedes termination (Fig. 11.22). If the tachycardia is not affected within 10 to 20 seconds, RF energy application is terminated, and the catheter is repositioned slightly for a repeat attempt.

Prolonged RF applications beyond 20 seconds without accompanying changes in AT rate are usually nonproductive.

Extensive ablation in one area that does not terminate AT may cause enough damage to block the spread of activation partially in the region, thus causing a change in P wave morphology (although the actual focus may not have changed), as well as slow propagation of the tachycardia impulse away from the focus of the tachycardia to activate atrial myocardium. The latter effect can result in an increase in the interval between the presystolic electrogram at the focus and P wave onset (Fig. 11.23).

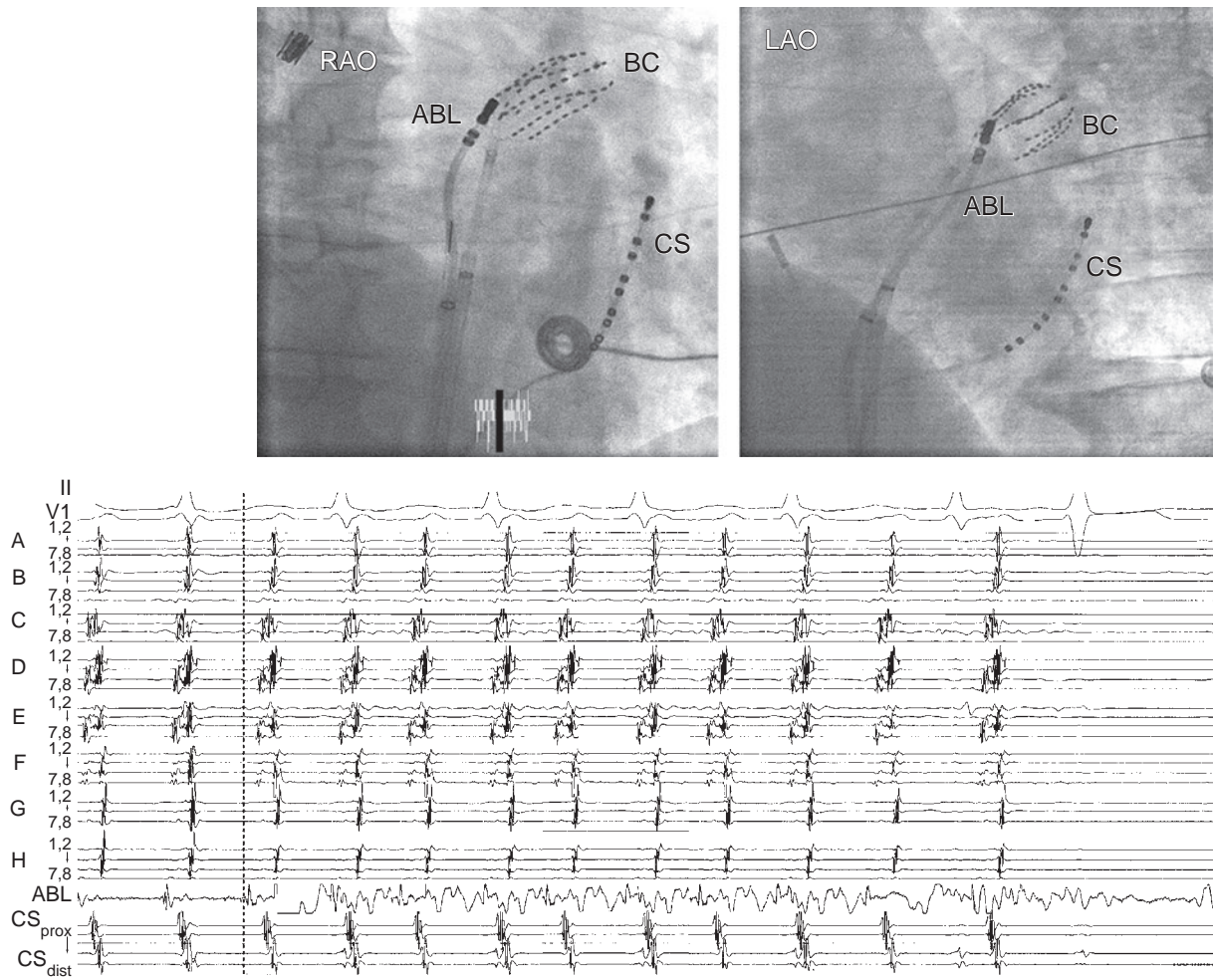
If the AT terminates or changes rate noticeably during the 10-second ablation, the RF application is continued for 30 to 60 seconds. However, in some patients, applications that may be just slightly off-target can cause acceleration of the AT without terminating it. In these cases, the tachycardia rate usually remains accelerated as long as the RF application is in progress, and it returns immediately to the baseline rate when the RF delivery is discontinued. If adequate catheter tip temperature is achieved and good contact is ensured (which can be assessed by observing ST elevation on the unipolar recording), this probably suggests that the catheter is close to, but not exactly at, the proper target area. Continued RF application at a site that produces only acceleration (but not termination) after 15 seconds invites the possibility of transient injury to the AT focus that impedes further ablation and can result in later AT recurrence.

Intracardiac echocardiography (ICE) can be useful to provide focused real-time images of the endocardial surfaces critical for positioning of catheters, establish catheter tip–tissue contact, and monitor energy delivery in the beating heart. In particular, ICE has been used in cristal ATs. In view of the variability in the anatomical course of the crista terminalis, ICE can assist in accurate positioning of the multipolar mapping catheter and guide precise mapping along this structure with the mapping-ablation catheter (eFig. 11.9).

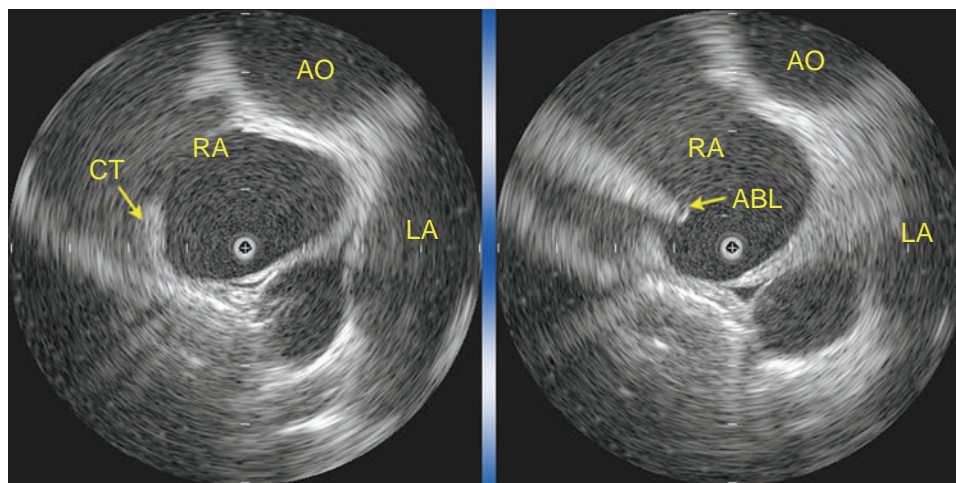
Ablation of Para-Hisian Atrial Tachycardias

Para-Hisian ATs (i.e., ATs with earliest activation in the region of the HB) generally originate from the superior paraseptal area of the atria, in the space delineated between the anterior superoseptal RA, the anterior superoseptal LA, and the noncoronary sinus of Valsalva, likely corresponding to the embryological retroaortic node (remnants of nodal-type AV canal myocardium in the region of the right fibrous trigone).³⁸ Propagation of atrial depolarization from the tachycardia focus occurs almost simultaneously to the para-Hisian RA, the antero-septal LA, and the noncoronary aortic sinus of Valsalva. Therefore, when the site of origin of AT is mapped to the mid or anterior RA septum, mapping should be extended to noncoronary aortic sinus of Valsalva, LA, or both, before starting ablation in the vicinity of the AVN or HB (Figs. 11.24 and 11.25). This is especially important when the presystolic activity is not particularly early (i.e., less than 20 milliseconds pre-P wave onset), the unipolar electrogram does not show an early QS configuration, or when multiple sites with a 15-mm radius have similar activation times.^{21,22,39,40}

Focal ATs arising from the anterior RA septum and para-Hisian regions can be amenable to catheter ablation from multiple approaches including the superoseptal aspect of the RA (posterior to the HB), aortic sinuses of Valsalva (especially noncoronary sinus of Valsalva), or antero-septal part of the LA (aortic-mitral junction). Recent reports have demonstrated that most of those foci can be eliminated by RF ablation within the noncoronary cusp. The aortic root is centrally located with the noncoronary aortic sinus of Valsalva abutting the superior paraseptal region between the RA and the LA, providing an optimal “vantage point” with excellent catheter stability and tissue contact that is relatively removed from the AVN, thus limiting the risk of AV block. Therefore when activation timing at the noncoronary aortic sinus of



eFig. 11.8 Basket Catheter (BC) Mapping of Atrial Tachycardia (AT). *Upper panels*, Fluoroscopic views (right anterior oblique [RAO] and left anterior oblique [LAO]) of the BC positioned at the ostium of the left superior pulmonary vein (PV). *Lower panel*, BC bipolar electrograms (1–2, 3–4, 5–6, 7–8) from the eight splines (A to H) are displayed. The earliest atrial activation during AT is recorded by the proximal electrodes of the E spline of the basket catheter. Detailed mapping obtained by the ablation catheter (ABL) recorded an even earlier activation (*dashed line*) at a site in the left atrial roof just outside the PV ostium. Radiofrequency energy delivery at that site resulted in termination of the tachycardia within a few seconds. CS_{dist} , Distal coronary sinus; CS_{prox} , proximal coronary sinus.



eFig. 11.9 Intracardiac Echocardiographic for Ablation of Cristal Focal Atrial Tachycardia. Intracardiac echocardiographic view (using the mechanical radial imaging system) of the high crista terminalis (*CT*) showing the anatomical structures and location of the ablation catheter (*ABL*) at the site of radiofrequency application (*right panel*). The ablation catheter is located on the high lateral CT. *AO*, Aorta; *LA*, left atrium; *RA*, right atrium.

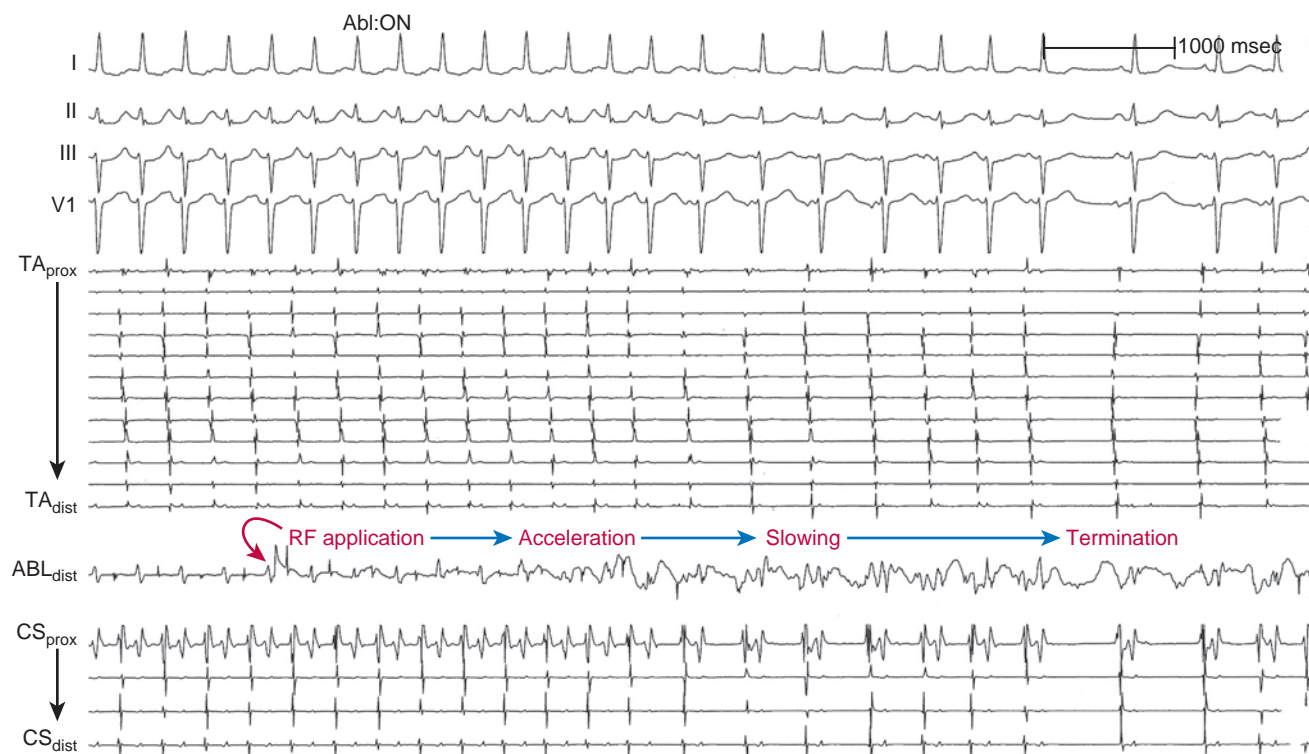


Fig. 11.22 Catheter Ablation of Focal Atrial Tachycardia (AT) Originating From the Superoanterior Aspect of the Mitral Annulus. Four surface electrocardiogram leads and intracardiac recordings from a catheter in the coronary sinus (CS) and a 20-pole Halo catheter positioned around the tricuspid annulus (TA) are shown. Radiofrequency (RF) energy delivery at the successful ablation site resulted within a few seconds in acceleration then slowing of the tachycardia rate followed by termination of the AT and restoration of sinus rhythm. ABL, Ablation site; dist, distal; prox, proximal.

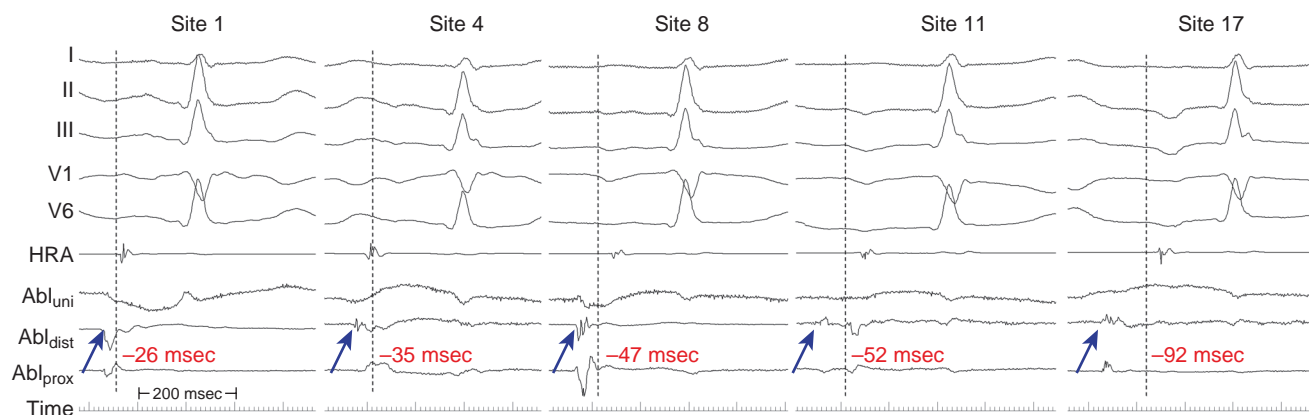


Fig. 11.23 Recordings From Focal Right Atrial Tachycardia During Progressive Ablation. Examples are shown from selected ablation sites. Site 2 shows tachycardia from high right atrium (HRA) with a site 26 milliseconds prior to the P wave onset. Ablation here changed the P wave morphology as shown in subsequent examples, and progressive ablation at sites in the lateral right atrium resulted in lengthening of the interval from electrogram to P wave onset (up to 92 milliseconds). Note also progressive fragmentation of the bipolar ablation recording and degradation of the unipolar recording. Abl_{dist}, Distal ablation site; Abl_{prox}, proximal ablation site; Abl_{uni}, unipolar ablation site.

Valsalva is similar to, or even slightly (less than 10 milliseconds) later than, that at the RA septum, initial ablation at the noncoronary aortic sinus of Valsalva is preferred. Coronary angiography may be considered to delineate aortic sinus of Valsalva anatomy prior to ablation. Alternatively, ablation can be safely and effectively accomplished with ICE guidance.^{22,23,38,41–43}

When the noncoronary aortic sinus of Valsalva approach fails, mapping of the LA may be considered, with attention to the aorto-mitral continuity. If activation is late in the LA (and ablation in the noncoronary aortic sinus of Valsalva is not successful), then ablation in the RA septum may be considered using cryoenergy or careful applications of RF energy.^{38,41,42}

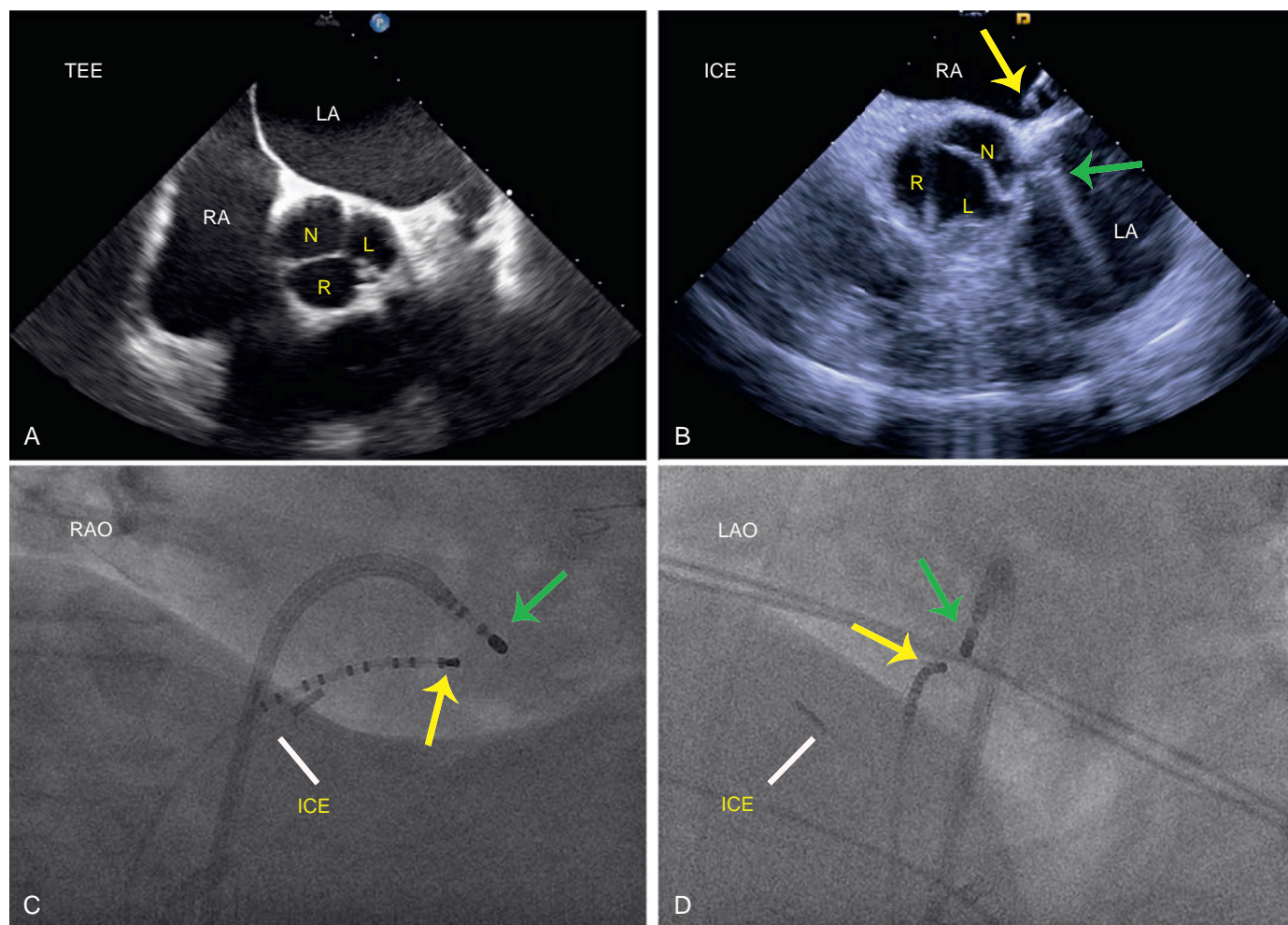


Fig. 11.24 Anatomical Relationship of the Anterior Right Atrial (RA) Septum and Para-Hisian Regions. (A) Transesophageal echocardiography (TEE) showing the interatrial septum in relation to the aortic root and noncoronary aortic sinus of Valsalva (N). (B) Intracardiac echocardiography (ICE) showing mapping catheter positioned in the anterior RA septum (yellow arrow) in the His bundle region, and a second catheter positioned in the immediate left aspect of the septum (green arrow). Notice the close relationship of the noncoronary cusp sinus of Valsalva (N). (C and D) Right (RAO) and left (LAO) anterior oblique fluoroscopy views of mapping catheters positioned at the para-Hisian region (yellow arrows) and anteroseptal part of the left atrium (green arrows). L, Left sinus of Valsalva; R, right sinus of Valsalva.

Ablation of focal ATs near the AVN or HB (in the triangle of Koch) requires special precautions. Titrated RF energy output should be used, starting with 5 W and increasing by 5 W every 10 seconds of energy application, up to a maximum of 40 W. In addition, it is preferable to deliver RF energy during AT; if AT terminates during RF delivery, the RF application is continued at the same power output for 30 seconds and then repeated for 30 seconds or more. If the AT does not terminate with an RF output of 40 W for 30 seconds, then another site should be sought. If accelerated junctional rhythm develops after AT termination, overdrive atrial pacing should be performed to monitor AV conduction, or RF application should be stopped and other sites sought.

To reduce the risk of AV block, RF delivery should be immediately discontinued when (1) impedance rises suddenly (more than 10 Ω), (2) the PR interval (during NSR, atrial pacing, or AT) prolongs, (3) AV block develops, (4) retrograde conduction block is observed during junctional ectopy, or (5) fast junctional tachycardia (CL shorter than 350 milliseconds) occurs because it may herald imminent heart block.

Endpoints of Ablation

Tachycardia Termination

Sudden termination of a sustained AT during RF application suggests a successful ablation. However, reliance on AT termination during RF application as the sole criterion of successful ablation may be misleading because AT may terminate spontaneously or in response to PACs induced by the RF application; hence tachycardia termination may not be a result of ablation of the AT focus. Furthermore, sudden termination of the AT can be associated with catheter dislodgment from the critical site to another site, thus making it difficult to deliver additional lesions at the critical site.

Noninducibility of Tachycardia

To use this criterion as a reliable endpoint, careful assessment of inducibility should be performed prior to ablation; the feasibility and best method of reproducible induction of the AT should be documented at baseline before ablation. In the setting of easy inducibility prior to

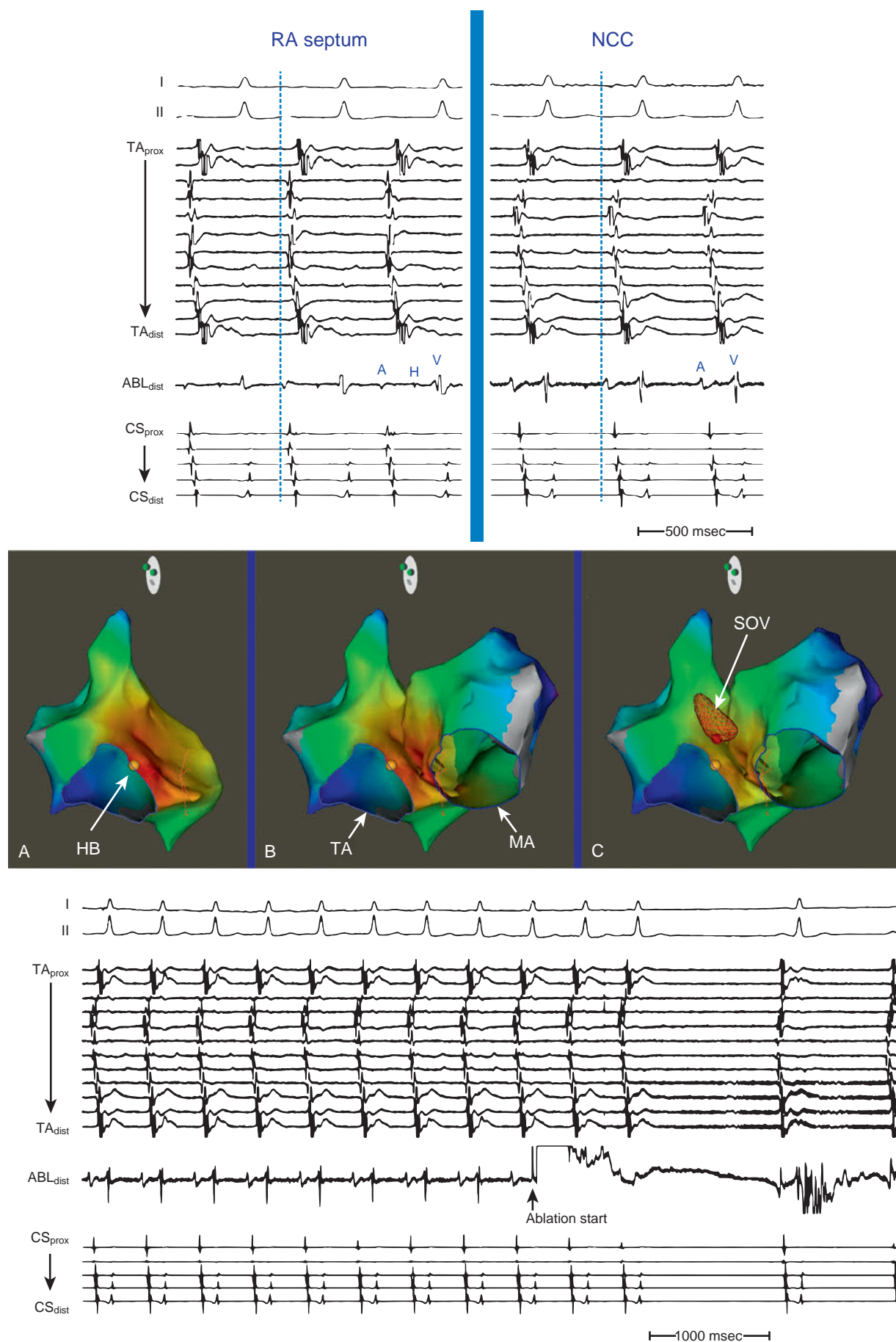


Fig. 11.25 Focal Atrial Tachycardia (AT) Arising From the Noncoronary Aortic Sinus of Valsalva (SOV). *Top panel*, Intracardiac recordings with the ablation catheter positioned at the His bundle (HB) region (*left*) in the anterior right atrial (RA) septum, and then in the noncoronary aortic SOV (*right*). Note that local activation in both regions is presystolic, preceding the onset of the tachycardia P wave, but the timing in the noncoronary SOV is earlier than that at the HB region. *Middle panel*, Electroanatomic activation maps using the CARTO system during sustained AT. (A) Activation mapping was initially performed in the RA, with the earliest local activation in the HB region. (B) Activation mapping is extended to the left atrium (LA) which showed similarly early activation timing at the left side of the atrial septum. (C) Activation mapping is then extended to the noncoronary aortic SOV, where the earliest local activation is seen. *Lower panel*, Radiofrequency catheter ablation at the focus of the AT in the noncoronary aortic SOV instantaneously terminated the tachycardia. AbI_{dist} , Distal ablation; CS_{dist} , distal coronary sinus; CS_{prox} , proximal coronary sinus; MA , mitral annulus; TA_{dist} , distal tricuspid annulus; TA_{prox} , proximal tricuspid annulus.

ablation, one may consider the lack of inducibility as an indicator of successful ablation. Noninducibility of the arrhythmia is inapplicable if the original arrhythmia was not inducible at baseline or was inadvertently terminated mechanically. Tachycardia inducibility should be reassessed 30 minutes after the last successful RF application.

Elevated Pacing Threshold

During pace mapping prior to ablation, if the pacing threshold was assessed and the catheter did not move after successful ablation at that site, pacing can be repeated. Elevation of pacing threshold (at least doubling) can be used as an index of completeness of elimination of viability of the target tissue. If the pacing threshold has not changed, one may consider additional ablation at the site to insure there has been adequate damage to the area. This has not been studied in any systematic way, however.

Outcome

The short-term success rate is variable (range, 69% to 100%; mean, 91%). Complication rates range from 0% to 3% (mean, 3%). Recurrence rates range from 0% to 25% (mean, 9%). The anatomical location of the AT focus influences the outcome.

Atrioventricular Block

AV block can complicate ablation of ATs originating in the vicinity of the AVN or HB. Ablation in the noncoronary aortic sinus of Valsalva or aortomitral continuity can potentially eliminate para-Hisian ATs with lesser risk of AV block. When ablation within the triangle of Koch is attempted, titrated RF energy output and RF application for short duration should be used, coupled with overdrive atrial pacing to monitor AV conduction in case accelerated junctional rhythm occurs. Alternatively, cryoablation may be used with its slightly better safety margin for AV conduction and, moreover, detailed mapping in the right and left anterosseptal regions, because ATs arising along the anterior and anterosseptal LA and even the right superior PV frequently have earliest RA activation at the HB region, with a normal activation pattern along the posterior LA, as recorded by the CS electrodes.

Phrenic Nerve Injury

The right phrenic nerve descends between the parietal pericardium and parietal pleura along the lateral side of the RA between the right superior PV and SVC. When ablation is planned in this region, high-output (10 mA) pacing should be performed prior to RF application.⁴⁴ The ability to pace the phrenic nerve at a candidate ablation site should prompt attempting to find a slightly different site or, if this is not possible, applying RF energy at low power or for a short duration. Even when the phrenic nerve cannot be paced, intermittent fluoroscopic visualization of the ipsilateral diaphragm movement should be performed during









RF application at high-risk sites, and RF delivery should be terminated if diaphragmatic excursion decreases. An alternative approach is to position a catheter in the SVC at a site at which the phrenic nerve can be consistently captured and pace the phrenic nerve during ablation. RF energy delivery should be stopped immediately if diaphragmatic contraction becomes less vigorous or ceases. Early recognition of phrenic nerve injury during RF delivery allows the immediate interruption of the application prior to the onset of permanent injury and is associated with rapid recovery of phrenic nerve function. If phrenic nerve injury prohibits ablation at desired endocardial sites, displacement of the phrenic nerve from the ablation target site via by saline injection or balloon or electrode catheter placement in the pericardial space (through the subxiphoid approach) may be considered.

Sinus Node Dysfunction

Sinus node dysfunction can develop during ablation of ATs originating near the sinus node. The risk is usually low because of the diffuse distribution of the sinus node complex, except in older patients or in those with preexisting sinus node dysfunction.

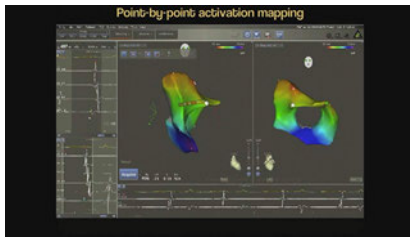
VIDEOS

The following videos accompany this chapter:

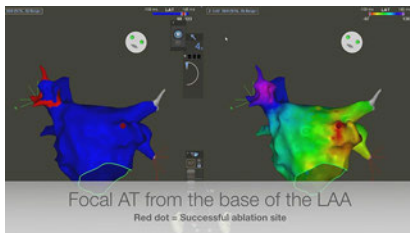
- Video 11.1.** Focal Atrial Tachycardia: CARTO Activation Mapping 
- See **Video 6.2.** Focal Atrial Tachycardia (originating from the infero-lateral tricuspid annulus): EnSite Precision Activation, Propagation, and Voltage Maps 
- See **Video 6.3.** Focal Atrial Tachycardia (originating from the left atrial appendage): EnSite NavX Activation and Propagation Maps 
- Video 11.2.** Focal Atrial Tachycardia (originating from the left atrial posterior wall): CARTO Activation and Propagation Maps 
- Video 11.3.** Focal Atrial Tachycardia (originating from the superior aspect of the mitral annulus): CARTO Activation and Propagation Maps 
- Video 11.4.** Focal Atrial Tachycardia (originating from the lateral aspect of the cavotricuspid isthmus): CARTO Activation and Propagation Maps 
- Video 11.5.** Focal Atrial Tachycardia (originating from the noncoronary aortic sinus of Valsalva): CARTO Activation Maps 
- Video 11.6.** Focal Atrial Tachycardia (originating from the noncoronary aortic sinus of Valsalva): CARTO Activation and Propagation Maps 

REFERENCES

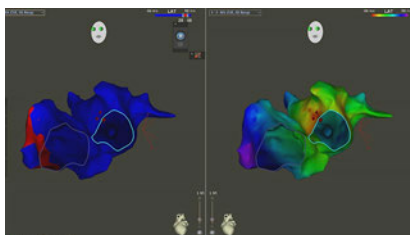
1. Saoudi N, et al. Classification of atrial flutter and regular atrial tachycardia according to electrophysiologic mechanism and anatomic bases: a statement from a joint expert group from the Working Group of



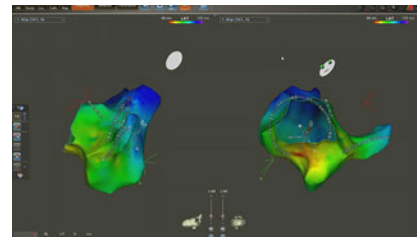
Video 11.1 Focal Atrial Tachycardia: CARTO Activation Mapping. At right, 3-D electroanatomic (CARTO 3) activation map of the right atrium (RA) constructed during focal atrial tachycardia (AT). During tachycardia, point-by-point activation mapping is performed by sampling the location of the catheter together with the local electrogram from a plurality of endocardial sites. Each selected point is tagged on the 3-D map. The local activation time at each site is determined from the intracardiac bipolar electrogram and is measured in relation to the fixed reference electrogram. The acquired local activation times are color-coded and superimposed on the anatomical map with red indicating early-activated sites, blue and purple late-activated areas, and yellow and green intermediate activation times. Known anatomical points, such as the His bundle and tricuspid annulus, are tagged to serve as landmarks for the electroanatomic map. Note that the tachycardia terminates twice during the mapping procedure with catheter manipulation close to the focus of the AT (denoted by red color on the electroanatomic activation map). Burst atrial pacing is utilized to re-induce the tachycardia to continue the mapping procedure.



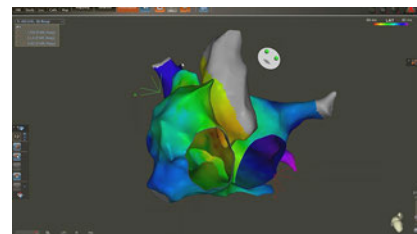
Video 11.2 Focal Atrial Tachycardia (Originating From the Left Atrial Appendage): CARTO Activation and Propagation Maps. Electroanatomic (CARTO 3) activation and propagation maps of a focal atrial tachycardia (AT) originating from the left atrial appendage (LAA). *LSPV*, Left superior PV; *MA*, mitral annulus; *RSPV*, right superior PV.



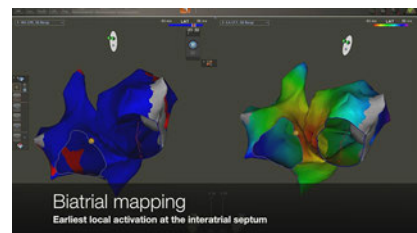
Video 11.3 Focal Atrial Tachycardia (Originating From the Superior Aspect of the Mitral Annulus): CARTO Activation and Propagation Maps. Electroanatomic (CARTO 3) activation and propagation maps of both atria during sustained focal atrial tachycardia (AT) originating from the superior aspect of the mitral annulus (MA). *TA*, Tricuspid annulus.



Video 11.4 Focal Atrial Tachycardia (Originating From the Lateral Aspect of the Cavotricuspid Isthmus): CARTO Activation and Propagation Maps. Electroanatomic (CARTO 3) activation and propagation maps of the right atrium during sustained focal atrial tachycardia (AT) originating from the lateral aspect of the cavotricuspid isthmus. The PentaRay mapping catheter is used to acquire a high-density activation map. *CS*, Coronary sinus; *TA*, tricuspid annulus.



Video 11.5 Focal Atrial Tachycardia (Originating From the Noncoronary Aortic Sinus of Valsalva): CARTO Activation Maps. Electroanatomic (CARTO 3) activation maps of the right and left atria and aortic root during sustained focal atrial tachycardia (AT) originating from the noncoronary aortic sinus of Valsalva. Initially, during right atrial mapping, the interatrial septum exhibited the earliest local activation. During mapping of the left atrium, the earliest activation timing was localized to the interatrial septum. Mapping was then extended to the aortic root, and the focus of the AT was localized to the noncoronary sinus of Valsalva, where radiofrequency ablation successfully eliminated the tachycardia. *CS*, Coronary sinus; *TA*, tricuspid annulus.



Video 11.6 Focal Atrial Tachycardia (Originating From the Noncoronary Aortic Sinus of Valsalva): CARTO Activation and Propagation Maps. Electroanatomic (CARTO 3) activation maps of the right and left atria and aortic root during sustained focal atrial tachycardia (AT) originating from the noncoronary aortic sinus of Valsalva. During right atrial (RA) mapping, the site with the earliest local activation was localized to the His bundle region. During mapping of the left atrium (LA), the earliest activation timing was localized to the interatrial septum. Mapping was then extended to the aortic root, and the focus of the AT was localized to the noncoronary sinus of Valsalva, where radiofrequency ablation successfully eliminated the tachycardia. *CS*, Coronary sinus; *MA*, mitral annulus; *NCC*, noncoronary sinus of Valsalva; *SVC*, superior vena cava; *TA*, tricuspid annulus.

- Arrhythmias of the European Society of Cardiology and the North A. *J Cardiovasc Electrophysiol.* 2001;12:852–866.
2. Scheinman MM, Yang Y, Cheng J. Atrial flutter: part II nomenclature. *Pacing Clin Electrophysiol.* 2004;27:504–506.
3. Roberts-Thomson KC, Kistler PM, Kalman JM. Focal atrial tachycardia I: clinical features, diagnosis, mechanisms, and anatomic location. *Pacing Clin Electrophysiol.* 2006;29:643–652.
4. Chugh A. Adenosine and atrial tachycardia. *Circ Arrhythmia Electrophysiol.* 2016;9:e004449.
5. Hu Y-F, et al. Electrophysiologic characteristics and catheter ablation of focal atrial tachycardia with more than one focus. *Heart Rhythm.* 2009;6:198–203.
6. Medi C, et al. Tachycardia-mediated cardiomyopathy secondary to focal atrial tachycardia: long-term outcome after catheter ablation. *J Am Coll Cardiol.* 2009;53:1791–1797.
7. Kistler PM, et al. P-wave morphology in focal atrial tachycardia: development of an algorithm to predict the anatomic site of origin. *J Am Coll Cardiol.* 2006;48:1010–1017.
8. Kistler PM, et al. Electrophysiological and electrocardiographic characteristics of focal atrial tachycardia originating from the pulmonary veins: acute and long-term outcomes of radiofrequency ablation. *Circulation.* 2003;108:1968–1975.
9. Liu CF, et al. Unifying algorithm for mechanistic diagnosis of atrial tachycardia. *Circ Arrhythm Electrophysiol.* 2016;9:e004028.
10. Page RL, et al. 2015 ACC/AHA/HRS guideline for the management of adult patients with supraventricular tachycardia. *Circulation.* 2016;133:e506–e574.
11. Porter MJ, et al. Influence of age and gender on the mechanism of supraventricular tachycardia. *Heart Rhythm.* 2004;1:393–396.
12. Hillock RJ, Kalman JM, Roberts-Thomson KC, et al. Multiple focal atrial tachycardias in a healthy adult population: characterization and description of successful radiofrequency ablation. *Heart Rhythm.* 2007;4:435–438.
13. Brown JB, Krummen DE, Feld GK, et al. Using electrocardiographic activation time and diastolic intervals to separate focal from macro-re-entrant atrial tachycardias. *J Am Coll Cardiol.* 2007;49:1965–1973.
14. Wang Y, Cuculich PS, Woodard PK, et al. Focal atrial tachycardia after pulmonary vein isolation: noninvasive mapping with electrocardiographic imaging (ECGI). *Heart Rhythm.* 2007;4:1081–1084.
15. Shah AJ, et al. Validation of novel 3-dimensional electrocardiographic mapping of atrial tachycardias by invasive mapping and ablation: a multicenter study. *J Am Coll Cardiol.* 2013;62:889–897.
16. Huo Y, et al. Diagnosis of atrial tachycardias originating from the lower right atrium: importance of P-wave morphology in the precordial leads V3–V6. *Europace.* 2013;15:570–577.
17. Uhm JS, et al. An electrocardiography algorithm combined with clinical features could localize the origins of focal atrial tachycardias in adjacent structures. *Europace.* 2014;16:1061–1068.
18. Teh AW, Kistler PM, Kalman JM. Using the 12-lead ECG to localize the origin of ventricular and atrial tachycardias: part 1. Focal atrial tachycardia. *J Cardiovasc Electrophysiol.* 2009;20:706–709, quiz 705.
19. Wellens HJ, Josephson ME. A regular narrow QRS tachycardia in a young man. *Heart Rhythm.* 2016;13:812–813.
20. Wong MCG, et al. Left septal atrial tachycardias: electrocardiographic and electrophysiologic characterization of a paraseptal focus. *J Cardiovasc Electrophysiol.* 2013;24:413–418.
21. Iwai S, et al. Electrophysiologic properties of para-Hisian atrial tachycardia. *Heart Rhythm.* 2011;8:1245–1253.
22. Madaffari A, et al. Electrocardiographic and electrophysiological characteristics of atrial tachycardia with early activation close to the His-bundle. *J Cardiovasc Electrophysiol.* 2016;27:175–182.
23. Wang Z, et al. Focal atrial tachycardia surrounding the anterior septum: strategy for mapping and catheter ablation. *Circ Arrhythm Electrophysiol.* 2015;8:575–582.
24. Kistler PM, et al. Focal atrial tachycardia arising from the mitral annulus: electrocardiographic and electrophysiologic characterization. *J Am Coll Cardiol.* 2003;41:2212–2219.
25. Das S, et al. Catheter ablation of peri-AV nodal atrial tachycardia from the noncoronary cusp of the aortic valve. *J Cardiovasc Electrophysiol.* 2008;19:231–237.
26. Medi C, Kalman JM. Prediction of the atrial flutter circuit location from the surface electrocardiogram. *Europace.* 2008;10:786–796.
27. Crawford TC, et al. Utility of atrial and ventricular cycle length variability in determining the mechanism of paroxysmal supraventricular tachycardia. *J Cardiovasc Electrophysiol.* 2007;18:698–703.
28. Maruyama M, et al. The VA relationship after differential atrial overdrive pacing: a novel tool for the diagnosis of atrial tachycardia in the electrophysiologic laboratory. *J Cardiovasc Electrophysiol.* 2007;18:1127–1133.
29. Colombowala IK, et al. Variability in post-pacing intervals predicts global atrial activation pattern during tachycardia. *J Cardiovasc Electrophysiol.* 2008;19:142–147.
30. Vijayaraman P, Lee BP, Kalahasty G, et al. Reanalysis of the ‘pseudo A-A-V’ response to ventricular entrainment of supraventricular tachycardia: importance of his-bundle timing. *J Cardiovasc Electrophysiol.* 2006;17:25–28.
31. Katritsis DG, Camm AJ. Atrioventricular nodal reentrant tachycardia. *Circulation.* 2010;122:831–840.
32. Long DY, et al. Electroanatomical mapping of the right atrium during atrial tachycardia originating from right superior pulmonary vein: additional insights on differential diagnosis. *Pacing Clin Electrophysiol.* 2015;38:91–98.
33. Chang K-C, Chen J-Y, Lin Y-C, et al. Usefulness of interatrial conduction time to distinguish between focal atrial tachyarrhythmias originating from the superior vena cava and the right superior pulmonary vein. *J Cardiovasc Electrophysiol.* 2008;19:1231–1235.
34. Hayashi K, et al. Pace mapping for the identification of focal atrial tachycardia origin. *Circ Arrhythm Electrophysiol.* 2016;9:e003930.
35. Mohamed U, et al. A novel pacing maneuver to localize focal atrial tachycardia. *J Cardiovasc Electrophysiol.* 2007;18:1–6.
36. Okubo K, et al. Rapid mapping of right atrial tachycardia using a new multielectrode basket catheter. *J Cardiovasc Electrophysiol.* 2016;27:73–79.
37. Wetzel U, et al. A stepwise mapping approach for localization and ablation of ectopic right, left, and septal atrial foci using electroanatomic mapping. *Eur Heart J.* 2002;23:1387–1393.
38. Pap R, et al. Should the aortic root be the preferred route for ablation of focal atrial tachycardia around the AV node? Support from intracardiac echocardiography. *JACC Clin Electrophysiol.* 2016;2:193–199.
39. Yang J-D, et al. Focal atrial tachycardias from the parahisian region: strategies for mapping and catheter ablation. *Heart Rhythm.* 2017;14:1344–1350.
40. Lyan E, et al. Comparison of strategies for catheter ablation of focal atrial tachycardia originating near the His bundle region. *Heart Rhythm.* 2016;14:998–1005.
41. Tada H. Catheter ablation of tachyarrhythmias from the aortic sinuses of Valsalva. *Circ J.* 2012;76:791–800.
42. Markowitz SM. What is the optimal approach to ablation of para-hisian atrial tachycardias? *JACC Clin Electrophysiol.* 2016;2:200–202.
43. Tovia-brodie O, Rosso R, Belhassen B. Atrial tachycardia originating in the vicinity of the noncoronary sinus of Valsalva: report of a series including the first case of ablation-related complete. *Pacing Clin Electrophysiol.* 2016;39:1165–1173.
44. Johnsrude C. Cryoablation of focal tachycardia originating from the right atrial free wall during upstream phrenic pacing to avoid phrenic nerve injury. *Pacing Clin Electrophysiol.* 2015;38:120–128.

Typical Atrial Flutter

OUTLINE

Pathophysiology, 339

- Right Atrial Anatomy, 339
- Typical Atrial Flutter Circuit, 340
- Interrelationship of Atrial Flutter and Atrial Fibrillation, 341
- Double-Wave Reentry, 342

Epidemiology and Natural History, 343

Clinical Presentation, 343

Initial Evaluation, 343

Principles of Management, 344

- Rate Control, 344
- Restoration of Sinus Rhythm, 345
- Maintenance of Sinus Rhythm, 346
- Prevention of Thromboembolism, 347
- Management of Coexistent Atrial Flutter and Atrial Fibrillation, 347

Electrocardiographic Features, 347

- Flutter Waves, 347
- Atrioventricular Conduction, 348
- QRS Morphology, 348

Electrophysiological Testing, 348

- Induction of Tachycardia, 351
- Tachycardia Features, 351
- Diagnostic Maneuvers During Tachycardia, 353
- Entrainment, 353
- Termination, 355
- Overdrive Suppression, 355
- Acceleration, 355
- Transformation, 356

Mapping, 356

- Activation Mapping, 356
- Entrainment Mapping, 356
- Electroanatomic Mapping, 358
- Noncontact Mapping, 359

Ablation, 359

- Target of Ablation, 359
- Ablation Technique, 359
- Endpoints of Ablation, 364
- Confirmation of Bidirectional Cavotricuspid Isthmus Block, 365
- Outcome, 371

Organized atrial tachycardias (ATs) are broadly categorized as either focal or macroreentrant. Focal ATs exhibit a centrifugal activation pattern originating from a discrete site, and can have automaticity, triggered activity, and microreentrant mechanisms. A macroreentrant AT incorporates a relatively large reentrant circuit around a central obstacle. Depending on whether or not the cavotricuspid isthmus (CTI) is critical to the reentry circuit, macroreentrant ATs are divided into two groups: “CTI-dependent” or “non-CTI-dependent” macroreentrant AT (see **Table 11.1**). CTI-dependent macroreentrant ATs include typical atrial flutter (AFL), lower loop reentry, and intra-isthmus reentry.¹

The term “atrial flutter” has traditionally been used to refer to a continuously waving pattern on the electrocardiogram (ECG), without an isoelectric baseline in at least one lead, whatever the tachycardia cycle length (TCL). “Typical AFL” is reserved for a macroreentrant circuit with the activation wavefront rotating clockwise or counterclockwise around the tricuspid annulus and using the CTI as an essential part of the reentry circuit. “Atypical AFL” is only a descriptive term for an AT with an ECG pattern of continuous undulation of the atrial complex, different from that in typical AFL. However, the term “atypical AFL” introduces unnecessary confusion, and a mechanistic description of the AT circuit in relation to atrial anatomy is preferred.^{1,2}

PATHOPHYSIOLOGY

Right Atrial Anatomy

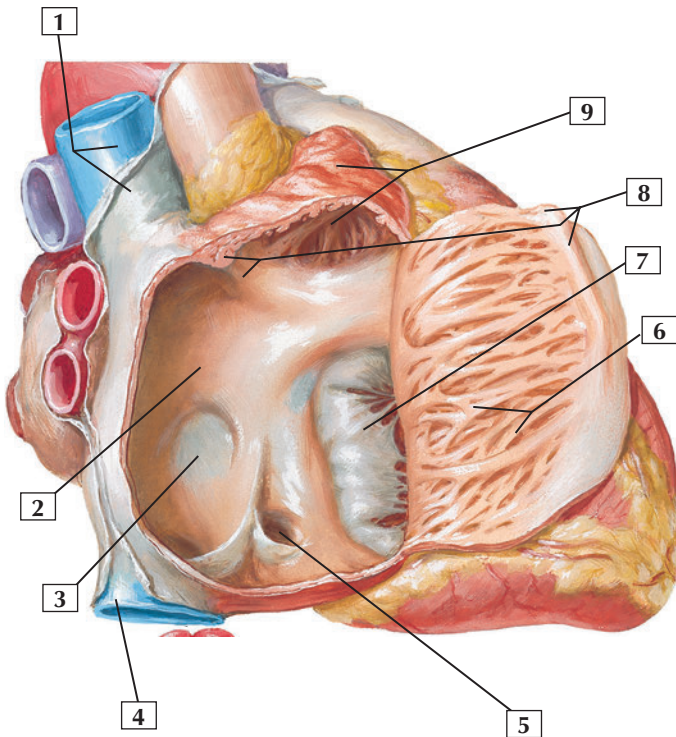
The right atrial (RA) endocardial surface is composed of many orifices and embryonic remnants, accounting for an irregular, complex surface.

The RA endocardium is architecturally divided into three anatomically distinct regions; each is a remnant of embryological development. The posterior smooth-walled RA, derived from the embryonic sinus venosus, receives the superior vena cava (SVC), the inferior vena cava (IVC), and the coronary sinus (CS). It also contains the fossa ovalis, the sinus node, and the atrioventricular node (AVN). The anterolateral trabeculated RA, derived from the “true” embryonic RA, is lined by horizontal, parallel ridges of muscle bundles that resemble the teeth of a comb (the pectinate muscle). It contains the RA appendage and free wall. The atrial septum is primarily derived from the embryonic septum primum and septum secundum.

The SVC enters the roof of the RA between the base of the RA appendage and the superior margin of the interatrial septum. The IVC enters the posterolateral portion of the floor of the RA along the inferior margin of the interatrial septum. The orifice of IVC is guarded by a fibrous or fibrous-muscular semilunar flap, the valve of the IVC (the eustachian valve). The CS enters the inferior aspect of the RA adjacent to the inferior margin of the interatrial septum, slightly more anterior and medial relative to the orifice of the IVC, and closer to the tricuspid annulus. Commonly, the CS orifice is guarded by a semilunar valve, the valve of the CS (valve of Thebesius). On the lower third of the interatrial septum lies the fossa ovalis (**eFig. 12.1**).^{3,4}

The posterior smooth-walled RA and the anterolateral trabeculated RA are separated by the crista terminalis on the lateral wall and the eustachian ridge in the inferior aspect. The sulcus terminalis, where the sinus node is located, is a subtle groove on the epicardial surface of the heart corresponding to the crista terminalis. The crista terminalis

Opened right atrium: right lateral view



1. Superior vena cava
2. Interatrial septum
3. Fossa ovalis
4. Inferior vena cava
5. Opening of coronary sinus
6. Pectinate muscles
7. Septal cusp of tricuspid valve
8. Crista terminalis
9. Right auricle

Comment: The smooth portion of the right atrium is known as the sinus venarum because it develops from the embryonic sinus venosus and receives blood from the superior and inferior venae cavae, and coronary sinus. It is separated from the more muscular portion of the atrium proper by a line, the crista terminalis.

The fossa ovalis is the adult representation of the embryonic foramen ovale.

Although the right atrium is slightly larger than the left atrium, it has thinner walls because the pressure on the right side of the heart is normally lower than that on the left side.

The auricle is a pouch-like appendage of the atrium but is functionally identical to the rest of the atrium.

Clinical: Atrial septal defects make up 10%–15% of congenital cardiac anomalies. In such cases, blood flows from the higher-pressure left atrium into the lower-pressure right atrium.

F. Netter M.D.

eFig. 12.1 Right Atrial Anatomy. (From Netter Images [www.netterimages.com], with permission.)

is a roughly C-shaped, convex, thick muscular band that runs from the high septum, anterior to the orifice of the SVC superiorly, and courses caudally along the posterolateral aspect of the RA. In its inferior extent, it courses anteriorly to the orifice of the IVC. The crista terminalis can vary in size and thickness, most often appearing as distinct ridge, but occasionally can be a broad, a flat, or a thin structure. As the crista reaches the region of the IVC, it is extended by the eustachian valve and eustachian ridge.

The eustachian valve is the remnant of the embryonic sinus venosus valve, which manifests as a flap of variable thickness and mobility along the orifice of the IVC; this valve can continue as a ridge (eustachian ridge) superiorly along the floor of the RA to the CS os, to join the valve of Thebesius, forming the tendon of Todaro, and then continuing onto the interatrial septum as the inferior limbus of the fossa ovalis.^{3,4} The tendon of Todaro is a fine, tendinous cord that runs as an extension of the free-edge of the eustachian ridge toward the central fibrous body. Its insertion into the central fibrous body marks the position of the compact AVN at the apex of the triangle of Koch.⁴

The tricuspid annulus lies anterior to the body of the RA, and its inferior portion lies a short distance (approximately 1 to 4 cm) anterior to the eustachian ridge, although its course varies among individuals. The CTI is the part of the RA between the ostium of the IVC and the eustachian ridge (posteriorly) and the tricuspid annulus (anteriorly). The CTI runs in an anterolateral-to-posteromedial direction, from the low anterior RA to the low septal RA. The CTI belongs to the trabeculated part of the RA, and its surface is very rough. Its width and muscle thickness are variable, from a few millimeters to more than 3 cm in width and more than 1 cm in depth. The CTI becomes wider in a medial-to-lateral direction, and it is thinnest in its central portion. A thick eustachian ridge (greater than 4 mm) is seen in 24% of patients. The eustachian ridge (often composed of partly or largely fibrous tissue) occurs as an elevation on the CTI. The area between the tricuspid annulus and the eustachian ridge is referred to as the sub-eustachian isthmus, whereas the downslope of the eustachian ridge leads to the junction of the RA and IVC. The pectinate muscles fan out from the crista terminalis and encroach upon the CTI for variable distances, but typically spare the myocardium just atrial to the tricuspid valve. This smooth portion of the CTI is referred to as the vestibular portion. The pectinate muscles are more prominent on the lateral side of the CTI, but become progressively thinner as they ramify branches toward the CS os. In the normal heart, CTI anatomy can be flat, “hilly” (from prominent eustachian ridge and pectinate muscles), concave, or have a pouch-like recess.^{5,6} Occasionally there is a depression (sub-eustachian pouch or sinus of Keith) on the CTI just lateral to the CS os, which can be very deep.^{4,7}

Typical Atrial Flutter Circuit

Typical AFL is the most common type of macroreentrant AT. The macroreentrant circuit is defined by anatomical barriers including the tricuspid annulus, crista terminalis, IVC orifice, eustachian ridge, CS os, and probably the fossa ovalis. However, the lines of conduction block necessary to provide adequate path length for the flutter reentry circuit can be functional or anatomical. The anterior boundary of the tachycardia circuit has been well established as being the tricuspid ring. The posterior boundaries, however, are more complex and not as well-defined. The posterior borders occur at a variable distance from the anterior border, narrowest in the region of the eustachian ridge (CTI) and widest in the anterior part of the RA.^{4,7,8}

The CTI provides the protected zone of relatively slow conduction necessary for the flutter reentry circuit. The area of slowest conduction is probably localized in the lateral aspect of the CTI in younger patients and in the medial aspect in older patients.⁹ Conduction velocity in the CTI during pacing in sinus rhythm is slower in patients with typical

AFL compared with those without any history of AFL.⁵ The mechanism of the slower conduction velocity in the CTI, relative to the interatrial septum and RA free wall, is uncertain but can be related to the anisotropic fiber orientation. With aging or atrial dilation, intercellular fibrosis can change the density of gap junctions and produce nonuniform anisotropic conduction through the trabeculations of the CTI.^{7,10}

Key to the development of typical AFL is the formation of a line of block in the region between the SVC and IVC in the RA free wall. This line of block acts as a critical lateral boundary that prevents short-circuiting of the flutter wavefront, whereby the reentrant wave catches the “tail of refractoriness” and hence extinguishes. This line of block is usually functional, but may be fixed. The creation of a line of block between the vena cavae or anterior in the RA free wall permits induction of AFL in otherwise normal atria. This explains the observation that AFL most often does not start immediately after a premature atrial complex (PAC) or burst rapid atrial pacing; rather its onset is usually preceded by a transitional rhythm (atrial fibrillation [AF]) of variable duration, which helps induce the functional line of block between the venae cavae. When a fixed (i.e., anatomic) intercaval line of block exists (e.g., atriotomy scar following surgical repair of congenital heart disease), antecedent AF may not be necessary to produce AFL.¹¹

The crista terminalis plays an important role as a functional barrier during typical AFL. Conduction delay and rate-related transverse block across the crista terminalis has been consistently observed in sinus rhythm and during pacing. During typical AFL, a line of transverse conduction block along the crista terminalis serving as a lateral boundary can be determined by the presence of double and split potentials recorded. Structural characteristics of the crista terminalis influence transverse conduction; steep slope and arborization of the crista terminalis have been implicated as geometric factors in its transverse conduction block. Typical AFL is more likely to occur in the setting of a thicker and continuous crista terminalis, and these patients are more likely to exhibit transverse crista terminalis conduction block at longer pacing cycle lengths (PCLs), as opposed to controls. Similarly, the region posterior to the crista terminalis (the posterior smooth-walled RA) also has been shown to demonstrate functional transverse conduction block during AFL or rapid pacing.^{10,12}

The width of the activation wavefront in typical AFL varies considerably, and is determined by the distance between the anterior and posterior boundaries at any given part of the circuit. It is very narrow inferiorly at the CTI and substantially wider moving upward. Substantial variability in the upper part of the circuit is a result of the large distance between anterior and posterior borders and anatomical barriers superiorly, combined with variability in the completeness of the posterior border. Recent studies suggest that the posterior block line is located along the posteromedial RA wall, posterior to the crista terminalis. Despite a relatively similar activation sequence, the active circuit (as determined by entrainment mapping) is variable. Most commonly, the reentrant wavefront courses not around the tricuspid annulus but obliquely between anterior and posterior borders away from the tricuspid annulus along any available, more rapidly conducting segments. Consequently, significant portions of the RA, including areas around the tricuspid annulus, can often be passively activated. In many subjects, the upper portions of the circuit pass behind the RA appendage and lie near or at the posterior circuit border, or they bifurcate around the SVC or RA appendage. The posterior border can extend completely or partially between the IVC and the SVC.^{8,13,14}

Typical AFL is of two types: counterclockwise and clockwise. In counterclockwise AFL (“counterclockwise” as viewed in the left anterior oblique [LAO] view from the ventricular side of the tricuspid annulus), the activation wavefront propagates caudocephalically up the septal side of the tricuspid annulus toward the crista terminalis and advances

cephalocaudally down the lateral wall of the RA to reach the lateral tricuspid annulus, after which it propagates through the CTI. In clockwise AFL (also known as “reverse typical” AFL), activation propagates in the direction opposite to that in counterclockwise typical AFL (Fig. 12.1). In both types of typical AFL, the flutter circuit is entirely confined within the RA. Left atrium (LA) activation occurs as a bystander and follows transseptal conduction across the inferior CS-LA connection, Bachmann’s bundle, and/or fossa ovalis.

Counterclockwise AFL is the most common form of typical AFL. Clockwise AFL is observed in only 10% of clinical cases, despite the fact that it is easily inducible with programmed electrical stimulation. Clockwise AFL can be induced in the electrophysiology (EP) laboratory in approximately 50% of patients who clinically present with only counterclockwise AFL. The 9:1 clinical predominance of counterclockwise AFL can be related to the localization of an area with a low safety factor for conduction in the CTI, close to the atrial septum. In addition, counterclockwise AFL is more likely to be induced with rapid atrial pacing from the CS os. Conversely, clockwise AFL is more likely to be induced with pacing from the low lateral RA pacing. These observations may be related to the anisotropic properties of the CTI and the devel-

opment of rate-dependent conduction delays and unidirectional block necessary for tachycardia induction, which may be affected by the site of stimulation.

Interrelationship of Atrial Flutter and Atrial Fibrillation

Although AF and typical AFL frequently coexist, the pathophysiological interrelationship between the two arrhythmias is still uncertain. Clinical AFL occurs in more than one-third of patients with AF. AF often precedes the onset of AFL and can also develop after the successful catheter ablation of AFL. Similar predisposing factors are found in both arrhythmias, including age, hypertension, heart failure, sleep apnea, and chronic pulmonary disease. It is likely that the atrial electrical and structural remodeling that underlies or is induced by AF can also promote the occurrence of AFL, or vice versa. Evidence also suggests that AF plays an important role in the genesis of typical AFL. It is also possible that at least some episodes of AFL can degenerate into AF (Fig. 12.2). AFL with sufficiently short cycle lengths (CLs) can result in fibrillatory conduction, which manifests as clinical AF.^{11,15,16}

Multiple studies have shown that, in the vast majority of instances of induced or spontaneous AFL, antecedent AF is necessary for the

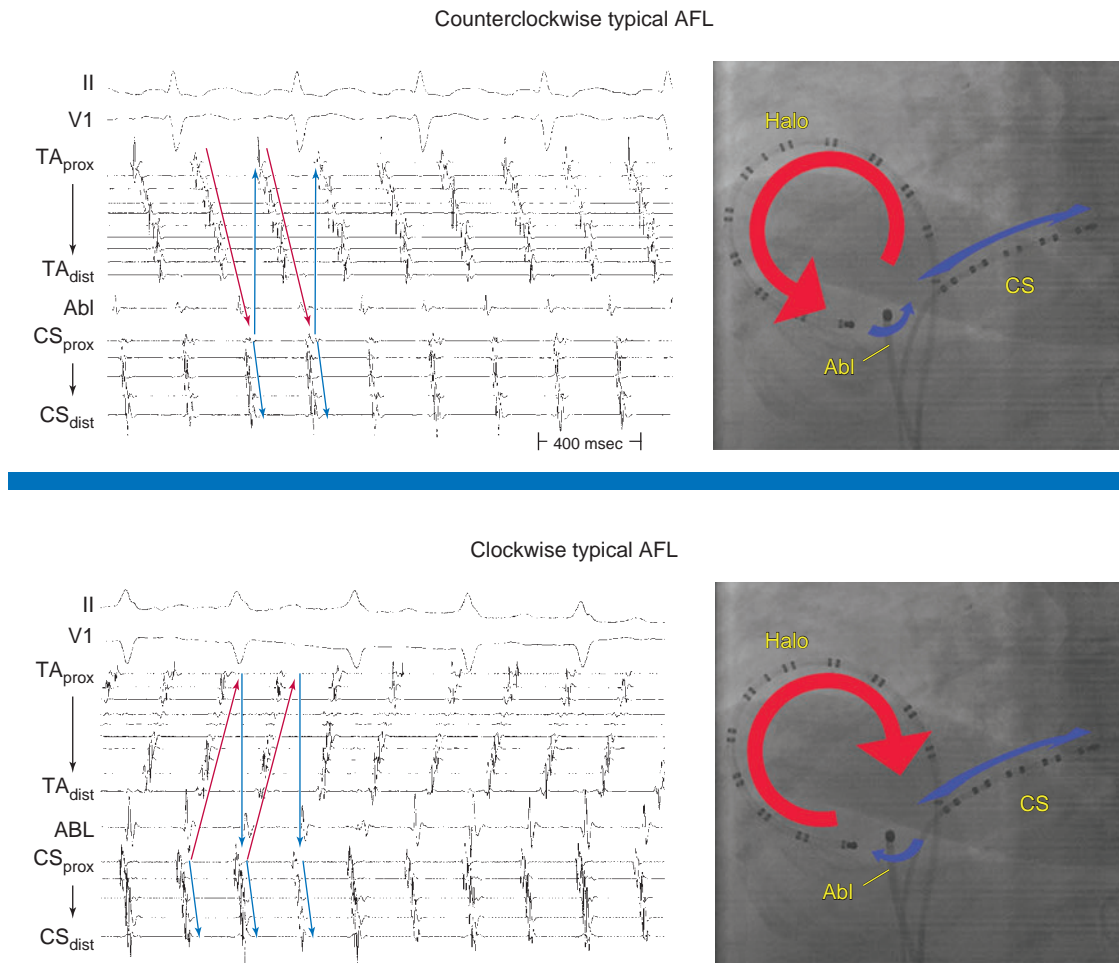


Fig. 12.1 Endocardial Activation During Atrial Flutter (AFL). Counterclockwise (upper panel) and clockwise (lower panel) typical AFL are recorded in the same patient. Catheter position and wavefront activation during the tachycardia are illustrated in a left anterior oblique fluoroscopic view (right side). The ablation catheter (Abl) is positioned at the cavotricuspid isthmus, and the Halo catheter is positioned around the tricuspid annulus, with the distal end at the lateral aspect of the cavotricuspid isthmus. CS, Coronary sinus; CS_{dist}, distal coronary sinus; CS_{prox}, proximal coronary sinus; TA_{dist}, distal tricuspid annulus; TA_{prox}, proximal tricuspid annulus.

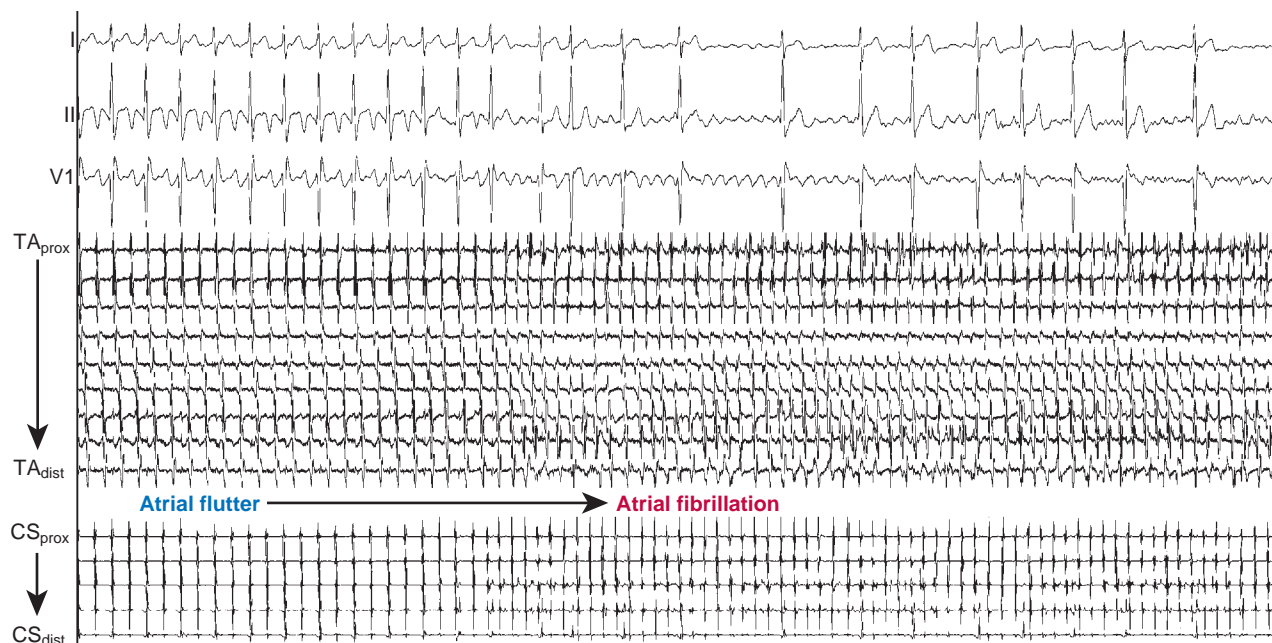


Fig. 12.2 Typical Atrial Flutter (AFL) Degenerating Into Atrial Fibrillation (AF). Surface electrocardiogram and intracardiac recordings are shown during typical counterclockwise AFL that spontaneously converts into AF. Note the faster ventricular response during AFL (with 2:1 atrioventricular conduction) as compared with that during AF because of the slower and more regular atrial rate (as recorded in the coronary sinus and around the tricuspid annulus) during AFL as compared with that during AF. CS_{dist} , Distal coronary sinus; CS_{prox} , proximal coronary sinus; TA_{dist} , distal tricuspid annulus; TA_{prox} , proximal tricuspid annulus.

development of AFL (Fig. 12.3). This is because it is during the AF that a critical lateral boundary (i.e., a functional line of block) necessary for the development of AFL forms between the SVC and IVC. Hence, without preceding AF, it is difficult to initiate AFL.¹⁷ Thus it is not surprising that recent studies have implicated pulmonary vein (PV) triggers in the initiation of typical AFL. The PV triggers induce a transitional period of AF, which then organizes to AFL once the functional line of block critical for the flutter circuit is formed. If this functional boundary does not develop, AF will either persist or spontaneously convert back to sinus rhythm. Not infrequently, the use of antiarrhythmic drug therapy (especially class IC agents) facilitates the conversion of AF to AFL, presumably by changing the atrial substrate to favor development of the intercaval line of block that could not form previously without drug effects.¹⁷

Among patients who initially present with isolated typical AFL, the incidence of AF is very high, around 25 times higher than in the general population, even after the elimination of AFL with catheter ablation. Following AFL ablation, AF can develop in up to 82% of these patients.¹⁸ Hence it appears that AFL is often an early marker of atrial electrical disease that frequently progresses to AF. Eradication of the flutter circuit alone by CTI ablation is not expected to eliminate AF that likely was the underlying trigger for AFL in most patients. After CTI ablation, the atria still are susceptible to PV triggers, which continue to induce AF episodes. After successful ablation of AFL, AF wavefronts can no longer “reorganize” into typical AFL because the CTI (the target for AFL ablation) is no longer available as a critical component of an AFL reentrant circuit, at which time AF either persists or terminates. Frequently, however, AF simply becomes clinically manifest. In fact, it is likely that AF already exists in many patients with supposed “isolated” AFL, but has not been clinically documented because of the preferential organization of AF wavefronts into AFL. Intensified continuous cardiac monitoring fre-

quently confirms the additional existence of AF in many patients with suspected isolated AFL.¹⁹

On the other hand, in patients presenting with both AF and AFL, the successful elimination of AF was found to prevent the recurrence of both AF and AFL. PV isolation alone was equally as effective as the combined ablation strategy (PV isolation plus CTI ablation), and more effective than CTI ablation alone in providing long-term freedom from both arrhythmias.²⁰ Even in patients presenting with isolated AFL and no prior history of AF, PV isolation (without CTI ablation) could prevent the recurrence of AFL.²¹

In summary, data suggest that bursts of AF may serve as the primary electrical disorder in patients with typical AFL. These bursts induce a more stable macroreentrant arrhythmia (typical AFL) in susceptible individuals. After eradication of the flutter substrate by CTI ablation, the same PV triggers manifest as AF. PV isolation can potentially control both arrhythmias in patients with AFL, and those with coexistent AFL and AF.^{15,18,22}

Double-Wave Reentry

A typical AFL circuit with a large excitable gap may allow a second excitation wave to be introduced into the flutter circuit by a critically timed atrial extrastimulus (AES), so that two wavefronts occupy the same circuit simultaneously. This type of AFL is designated “double-wave reentry.”

Double-wave reentry is manifest by acceleration of the tachycardia rate, but with identical surface ECG morphology and intracardiac activation sequence. It can be recognized by the simultaneous activation of the superior and inferior regions of the tricuspid annulus, with all activation being sequential. This rhythm rarely lasts for more than a few beats and can serve as a trigger for AF. Because the CTI is still a necessary part of the circuit, double-wave reentry is amenable to CTI ablation.



Fig. 12.3 Atrial Fibrillation (AF) Degenerating Into Typical Atrial Flutter (AFL). Surface electrocardiogram (ECG) and intracardiac recordings shown normal sinus rhythm (NSR, at left) followed by an early-coupled premature atrial ectopic beat that induces AF (as evident by the disorganized atrial activity on the surface ECG as well as in the coronary sinus and around the tricuspid annulus), which shortly afterwards converts spontaneously into typical counterclockwise AFL. CS_{dist}, Distal coronary sinus; CS_{prox}, proximal coronary sinus; TA_{dist}, distal tricuspid annulus; TA_{prox}, proximal tricuspid annulus.

EPIDEMIOLOGY AND NATURAL HISTORY

It is estimated that the overall incidence of AFL in the United States is 88 per 100,000 person-years. The prevalence of AFL increases with age to almost 600 per 100,000 among those older than 80 years. AFL accounts for approximately 15% of supraventricular arrhythmias. Although in clinical practice AFL appears to be less common than paroxysmal supraventricular tachycardia, population-based data show that in the general population, AFL is diagnosed for the first time more than twice as often. Adjusted for age, the incidence of AFL in men is 2 to 3 times that in women.

Paroxysmal AFL can occur in patients with no apparent structural heart disease, whereas chronic AFL is usually associated with underlying heart disease, such as valvular or ischemic heart disease or cardiomyopathy. At highest risk of developing AFL are men, older adults, and individuals with preexisting heart failure or chronic obstructive lung disease. In approximately 60% of patients, AFL occurs as part of an acute disease process, such as acute pericarditis, acute exacerbation of chronic pulmonary disease, acute pneumonia, thyrotoxicosis, alcoholism, following cardiac or pulmonary surgery, or during acute myocardial infarction (MI).

The natural history of typical AFL is often interlinked with AF. Typical AFL and AF frequently coexist. The majority (75%) of patients with AFL also have documented AF at the time of presentation. Successful CTI ablation to cure AFL does not seem to improve the natural history of progression to AF, even in patients with AFL as the only

clinical arrhythmia. Up to 82% of these patients develop AF; the majority of those develop AF in the first year after ablation of AFL.^{15,18,22}

CLINICAL PRESENTATION

Patients with AFL can be completely asymptomatic, or they may present with a spectrum of symptoms ranging from palpitations, lightheadedness, fatigue, reduced activity tolerance, or dyspnea, to acute pulmonary edema or acute coronary syndrome in susceptible patients.

The clinical manifestations of AFL strongly depend on the ventricular rate during the AFL, the presence of structural heart disease, and the underlying functional status. Fast ventricular rates and the loss of effective atrial contraction have significant hemodynamic consequences, especially in patients with systolic or diastolic heart failure. Furthermore, AFL with a chronically rapid heart rate can lead to tachycardia-mediated cardiomyopathy and heart failure. In fact, some patients remain asymptomatic until they present with a thromboembolic event or with decompensated heart failure secondary to tachycardia-induced cardiomyopathy. AFL occurs in approximately 25% to 35% of patients with AF, in which case AFL may be associated with worsening of the intensity of symptoms because of more rapid ventricular rates.

INITIAL EVALUATION

Clinical symptoms are not usually helpful in distinguishing typical AFL from other atrial tachyarrhythmias. Documentation of the arrhythmia

during spontaneous symptoms on ECG, ambulatory cardiac monitoring, or cardiac implantable electronic devices (loop recorders, pacemakers, defibrillators) is important to establish the diagnosis. The 12-lead ECG diagnosis of typical AFL is frequently accurate, but it can occasionally be misleading (see later).

Initial assessment includes the determination of cardiopulmonary stability, symptom onset and severity, thromboembolic versus hemorrhagic risk, and potential substrates or triggers of AFL. An echocardiogram is necessary to evaluate for structural heart disease. Evaluation for ischemic heart disease is considered in patients with angina, heart failure, or high risk for coronary artery disease. Additional laboratory evaluation typically includes the assessment of serum electrolytes, blood counts, renal and hepatic function, as well as thyroid function.

PRINCIPLES OF MANAGEMENT

Management of AFL should be aimed at identifying and treating underlying causes of the arrhythmia, as well as reducing symptoms, improving quality of life, and preventing cardiovascular morbidity and mortality associated with AFL. In addition, unlike AF, curing AFL is an attainable treatment goal.

There are four main issues that must be addressed in the treatment of AFL: (1) ventricular rate control, (2) restoration of normal sinus rhythm (NSR), (3) maintenance of NSR, and (4) prevention of systemic embolization (Figs. 12.4 and 12.5).²³

Rate Control

Ventricular rate control during AFL is important to prevent hemodynamic instability, improve symptoms and functional capacity, and prevent tachycardia-mediated cardiomyopathy. Oral or intravenous (IV) AVN blockers are utilized for rate control, depending on the severity of symp-

toms and the degree of hemodynamic compromise caused by the tachycardia. Notably, the ventricular rate can be very difficult to control in typical AF, more so than during AFL, because of the slower and more regular atrial rate (see Fig. 12.2). As a consequence, controlling clinical symptoms frequently requires cardioversion.²⁴

Beta-blockers or nondihydropyridine calcium-channel blockers (verapamil and diltiazem) are the drugs of choice for rate control, and appear to have equivalent efficacy. Care should be used in administering these medications in patients with acutely decompensated heart failure. Beta-blockers are preferred in patients with cardiomyopathy, ischemic heart disease, and following surgical procedures. Verapamil and diltiazem are preferred in patients with reactive airway disease.²³

Digoxin is less effective and requires a longer time to achieve rate control, but may be considered if beta-blockers and calcium channel blockers have failed or have intolerable side effects. Digoxin reduces the resting heart rate, but it is seldom effective in ambulatory patients because its effects are mediated by the enhancement of vagal tone, which is offset during exertion. Thus digoxin has traditionally been used as a second-line agent, usually in sedentary patients or those with heart failure or hypotension. Recently, however, several systematic reviews and meta-analyses found that digoxin use was associated with a greater risk for mortality in patients with AF, regardless of concomitant heart failure. Some studies have suggested that AF nullifies the effect of digoxin in reducing hospitalizations for heart failure patients. Hence the long-term use of digoxin has been discouraged.^{24–28}

Amiodarone may be considered for rate control when other AVN blockers are unsuccessful or not tolerated. IV amiodarone is useful for acute control of the ventricular rate, and can be of particular value in acutely ill patients or those with acutely decompensated heart failure or severe hemodynamic compromise. Because of the possibility of termination of AFL by amiodarone, though very small, pericardioversion anticoagulation strategies (as discussed later) should be considered,

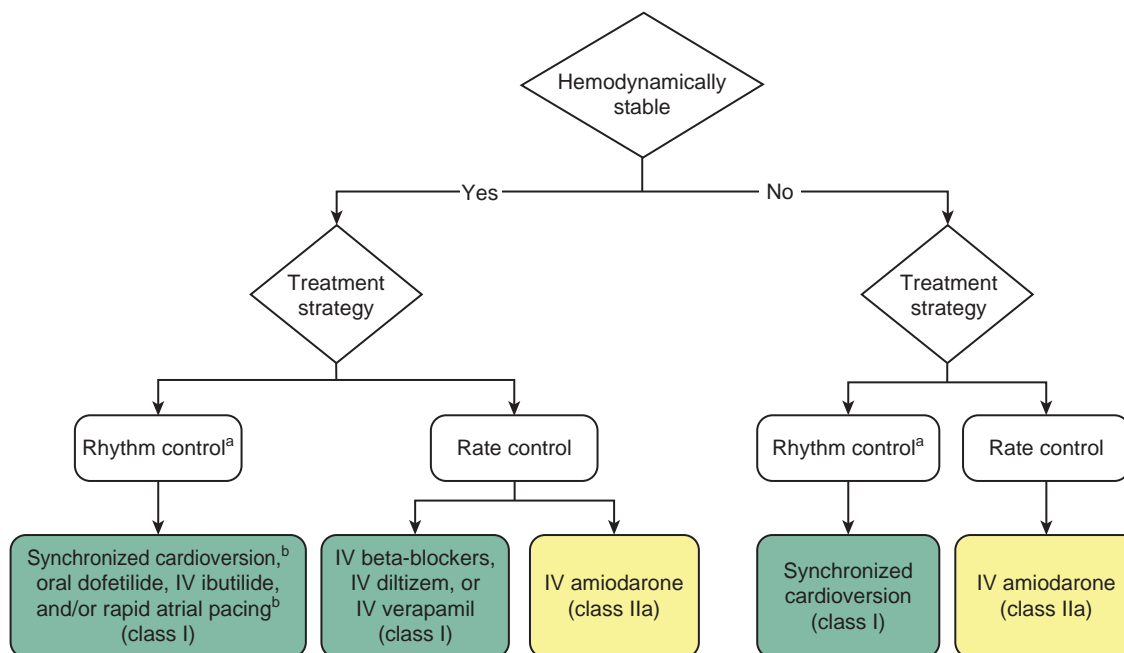


Fig. 12.4 Acute Treatment of Atrial Flutter. Drugs listed alphabetically. ^aAnticoagulation as per guideline is mandatory. ^bFor rhythms that break or recur spontaneously, synchronized cardioversion or rapid atrial pacing is not appropriate. IV, Intravenous. (From Page RL, Joglar JA, Caldwell MA, et al. 2015 ACC/AHA/HRS guideline for the management of adult patients with supraventricular tachycardia: a report of the American College of Cardiology/American Heart Association Task Force on Clinical Practice Guidelines and the Heart Rhythm Society. *J Am Coll Cardiol*. 2016;67:e27–e115.)

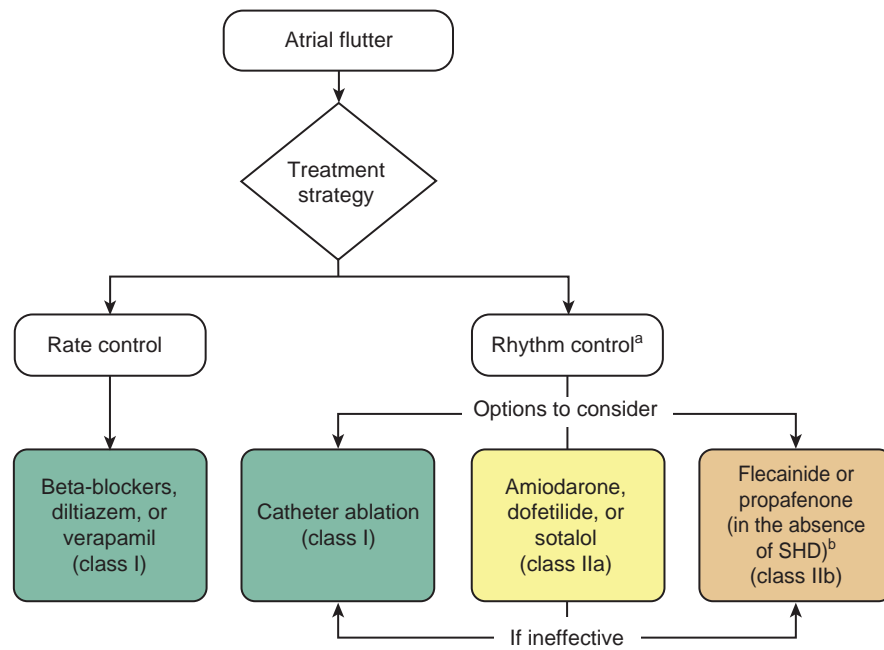


Fig. 12.5 Ongoing Management of Atrial Flutter. Drugs listed alphabetically. ^aAfter assuring adequate anticoagulation or excluding left atrial thrombus by transesophageal echocardiography before conversion. ^bShould be combined with atrioventricular nodal-blocking agents to reduce risk of 1:1 conduction during atrial flutter. SHD, Structural heart disease (including ischemic heart disease). (From Page RL, Joglar JA, Caldwell MA, et al. 2015 ACC/AHA/HRS guideline for the management of adult patients with supraventricular tachycardia: a report of the American College of Cardiology/American Heart Association Task Force on Clinical Practice Guidelines and the Heart Rhythm Society. *Circulation*. 2016;133:e506–e574., with permission.)

depending on the individual patient's risk/benefit profile. Given its potential toxicity, amiodarone is not recommended for long-term rate control.²³

In patients with AFL and ventricular preexcitation causing rapid ventricular response, prompt direct-current cardioversion is recommended, especially when hemodynamic compromise is present. IV procainamide or ibutilide to restore NSR or to slow the ventricular rate may be considered in hemodynamically stable patients. Importantly, drugs that preferentially slow AVN conduction without prolonging bypass tract refractoriness (such as verapamil, diltiazem, adenosine, oral or IV digoxin, and IV amiodarone) can accelerate the ventricular rate and potentially precipitate hemodynamic collapse and ventricular fibrillation (VF) in high-risk patients with Wolff-Parkinson-White syndrome. Unlike the IV route of administration, chronic oral amiodarone therapy can slow or block bypass tract (BT) conduction. Limited data exist regarding the use of beta-blockers; nonetheless, these drugs theoretically pose a similar potential risk in this situation, and they should be used with caution.²⁹

Restoration of Sinus Rhythm

Restoration and maintenance of NSR in patients with AFL is preferred to rate control strategy. The elimination of AFL is associated with relief of symptoms, improved functional status and quality of life, reduced risk of systemic thromboembolism, and prevention of tachycardia-induced cardiomyopathy. In addition, reduction in atrial remodeling can potentially help reduce the future risk of AF. Therefore rate control strategy is reserved to patients with contraindication to anticoagulation, those with intraatrial thrombi, or patients with very poor functional status and multiple comorbidities when the risks associated with rhythm control strategy outweigh the benefits.²³

Several options are available for termination of AFL, including external direct-current therapy, antiarrhythmic drugs, overdrive atrial pacing, and catheter ablation. The timing of attempted cardioversion is influenced by the duration of AFL, the severity of the patient's symptoms, the adequacy of rate control, and the risk of thromboembolism. Prompt cardioversion is recommended for patients with rapid ventricular rates and hemodynamic compromise attributed to AFL (hypotension, acute heart failure, myocardial ischemia) or ventricular preexcitation. Cardioversion is also considered to restore NSR in stable but symptomatic patients with persistent AFL, especially when ventricular rate control remains suboptimal. For stable patients with adequate heart rate control and minimal symptoms, conversion to sinus rhythm may be deferred until catheter ablation, if performed in a timely manner.

Peri-Cardioversion Anticoagulation

In spite of the organized atrial rhythm and apparent preserved atrial contraction during AFL, the thromboembolic risk is practically no different for this rhythm than for AF. In stable patients with AFL of a duration longer than 48 hours or of unknown duration, any mode of cardioversion (electrical, chemical, pacing, or ablation) should be delayed until the patient has been anticoagulated at appropriate levels for 3 to 4 weeks or transesophageal echocardiography (TEE) has excluded atrial thrombi. TEE may also be considered in patients with high thrombotic risk (e.g., severe valvular or congenital heart disease, prior thromboembolic events, severe cardiomyopathy), even when the duration of AFL is less than 48 hours.²³

If urgency of cardioversion (because of severe symptoms or hemodynamic instability) precludes TEE, therapeutic doses of low-molecular-weight heparin or unfractionated heparin should be administered as soon as possible, concurrent with or, preferably, prior to cardioversion.

Electrical Cardioversion

External direct-current cardioversion of AFL is successful in more than 95% and is typically achieved with relatively lower levels of energy (i.e., 5 to 50 joules) as compared with AF. In general, electrical cardioversion is preferred to chemical cardioversion, given the higher efficacy and the lower low risk of proarrhythmia; however, it requires sedation or anesthesia, and is contraindicated in patients with digitalis toxicity or those with hypokalemia.²³

Overdrive Atrial Pacing

Overdrive atrial pacing can terminate AFL in about 82% (range 55% to 100%), and is especially effective in patients receiving antiarrhythmic medications. Overdrive pacing is particularly useful in patients with preexisting atrial pacing wires (as part of a permanent pacemaker or defibrillator, or temporary epicardial pacing wires following cardiac surgery). In these patients, overdrive atrial pacing may be preferred to electrical cardioversion since it obviates the need for sedation. Insertion of a temporary pacing wire for overdrive pace termination of AFL may be considered when electrical cardioversion is contraindicated (e.g., in the setting of digitalis toxicity) or when sedation is not feasible. Trans-esophageal atrial pacing, on the other hand, is rarely utilized, since it requires sedation and esophageal intubation, and is much less effective than electrical cardioversion.²³

Overdrive atrial pacing is started at a rate 5% to 10% faster than the flutter atrial rate and is maintained for 15 or more seconds. Overdrive pacing is repeated at incrementally faster rates until NSR is restored as AF develops. When overdrive atrial pacing alone fails, high-frequency (50-Hz) burst atrial pacing or overdrive pacing with atrial extrastimuli can be effective. One potential drawback to atrial pacing is the potential conversion of AFL to AF; even then, induction of AF can be associated with better ventricular rate control and less symptom, and may subsequently revert spontaneously to NSR.²³

Pharmacological Cardioversion

Pharmacological cardioversion of AFL is generally less effective than electrical cardioversion and carries the potential risk of proarrhythmia, but can be an option when sedation is not available or not well tolerated or when indicated by patient preference.

Ibutilide and dofetilide are the most effective agents for pharmacological conversion of AFL. Other antiarrhythmic agents, including sotalol, amiodarone, class IA (e.g., procainamide), or class IC agents (e.g., flecainide, propafenone), have limited efficacy. AVN blockers (beta-blockers, digoxin, and calcium-channel blockers) are generally not effective for restoration of NSR.²³

IV ibutilide is the drug of choice for chemical cardioversion; it can terminate AFL (usually within 30 minutes) in 38% to 76% of cases, regardless of the duration of the arrhythmia. The efficacy of ibutilide is significantly higher than that of IV procainamide (76% vs. 14%), IV sotalol (70% vs. 19%), and IV amiodarone (87% vs. 29%). However, ibutilide is associated with sustained polymorphic ventricular tachycardia (VT) in 1.2% to 1.7% of cases, and nonsustained VT in 1.8% to 6.7%, which is more likely to occur in patients with reduced left ventricular ejection fraction (LVEF). The risk of VT lingers for 6 or even 8 hours after ibutilide administration, regardless of whether it has terminated AFL; thus patients should not be given this medication in an emergency room setting without observing them on continuous heart rhythm monitoring for this duration. Pretreatment with magnesium can increase the efficacy and reduce the risk of torsades de pointes.²³

Oral dofetilide is also effective for conversion of AFL (70% to 80% conversion rate), more so than in AF. In the majority of patients, conversion to NSR is achieved within 36 hours. However, dofetilide can be associated with proarrhythmia, and its initiation requires continuous

cardiac monitoring for a minimum of 72 hours. IV dofetilide, which is not available in the United States, also appears to be effective for conversion of AFL, and was found to have significantly higher efficacy than IV amiodarone (75% vs. 10%).²³

Because of the limited efficacy and the associated risk of proarrhythmia, chemical cardioversion is generally reserved for selected patients, especially when electrical cardioversion is not feasible because of contraindication to sedation. In addition, when the use of long-term antiarrhythmic medications is planned for the maintenance of NSR, starting drug therapy before electrical cardioversion can be beneficial, as it can help restore NSR in some patients and obviate the need for electrical cardioversion and, in other cases, can potentially enhance the efficacy of electrical cardioversion. In addition, it can help maintain NSR after successful cardioversion and, if a side effect develops that would preclude long term use of the drug, it can be stopped and a different medication tried before the electrical cardioversion is performed.

Importantly, adequate rate control with AVN blockers (beta-blockers, diltiazem, verapamil) should be achieved before instituting class IA (procainamide and disopyramide) or IC drugs (propafenone and flecainide), which can potentially slow the flutter rate and hence facilitate 1:1 AV conduction and paradoxically faster ventricular rates.

Catheter Ablation

Catheter ablation is the definitive treatment for AFL, and it is a reasonable option for restoration of NSR for stable patients who do not require immediate cardioversion and can wait until this procedure is performed. In fact, the presence of the arrhythmia at the time of the procedure helps reliably establish the diagnosis and mechanism of the clinical arrhythmia and differentiate it from other arrhythmias that might be inducible by programmed electrical stimulation but may not be of clinical significance.

Maintenance of Sinus Rhythm

When AFL occurs as part of an acute disease process, such as hyperthyroidism, acute MI, pulmonary embolism, or following cardiac surgery, chronic therapy for the arrhythmia is usually not required after sinus rhythm is restored. In patients with no underlying reversible disorder, the risk of arrhythmia recurrence after initial restoration of NSR is high and hence strategies to maintain NSR should be considered. When long-term rhythm control is required, catheter ablation is superior to antiarrhythmic drugs and is the preferred strategy in most patients.

Catheter Ablation

Catheter ablation is recommended as first-line therapy for most patients with symptomatic or recurrent typical AFL, whether paroxysmal or persistent. The ablation procedure is associated with high long-term success rates (92% after a single procedure and 97% after multiple procedures), and low risk of serious complications (0.4%). In addition to improvement of symptoms and quality of life, successful ablation offers a potential cure of the arrhythmia, reducing the risk of thromboembolism, and potentially eliminating the need for long-term anticoagulation and antiarrhythmic drug therapy.²³

Antiarrhythmic Drug Therapy

Complete maintenance of NSR often is unachievable with current drug therapy. The average 1-year recurrence rate associated with dofetilide is more than 35%, and is even higher for flecainide (approximately 50%). Data are limited regarding the efficacy of other drugs, as most studies combined AFL with AF, with the vast majority of the patients having AF, and without specifying the results for each arrhythmia. Given the significant superiority of catheter ablation and its low complication

rate, long-term antiarrhythmic drug therapy is no longer recommended for most patients with AFL.²³

For patients in whom catheter ablation is not feasible, or when long-term antiarrhythmic drug therapy is preferred, the choice of the antiarrhythmic agent is similar to that used for rhythm control in AF (see Chapter 15). The selection of pharmacological agents (sotalol, dofetilide, amiodarone, flecainide, and propafenone) is largely driven by the safety profile, and should consider coexisting sinus nodal or AVN disease, heart failure, associated therapies, and comorbidities. The presence and extent of concomitant cardiovascular disease have to be carefully considered. A safer, although possibly less efficacious, drug is usually recommended before resorting to more effective but less safe therapies.

Prevention of Thromboembolism

AFL is associated with increased risk of systemic thromboembolism, although likely to a lesser degree than in AF. The risk factors for development of embolic events in AFL are similar to those described for AF. Short-term stroke risk following cardioversion of AFL ranges from 0% to 7%, and the annual thromboembolism rate in patients with sustained AFL is approximately 3%. Therefore the indications for long-term and for peri-cardioversion anticoagulation in patients with AFL are the same as those in patients with AF (see Chapter 15).²³

Management of Coexistent Atrial Flutter and Atrial Fibrillation

AF and AFL frequently coexist in the same patient. Clinical AFL occurs in more than one-third of patients with AF. In these patients, when AF is the predominant arrhythmia, catheter ablation of AFL unlikely would improve clinical outcome. On the other hand, when AFL is the dominant clinical arrhythmia, or when new-onset AFL develops in patients with AF after administering antiarrhythmic drug therapy, hybrid therapy (CTI ablation plus antiarrhythmic medications) can be effective.²³ Ablation of the CTI eliminates the flutter and provides good symptomatic relief, while antiarrhythmic drug therapy is continued to suppress AF. Alternatively, a combined approach of PV antrum isolation plus CTI ablation may be considered. Notably, PV isolation alone (without CTI ablation) was found in small studies to be equally effective in the suppression of both AF and AFL in these patients.

Importantly, the incidence of AF is very high among patients who initially present with isolated AFL, even after ablation of the CTI. Given the fact that up to 82% of patients with “isolated” AFL eventually develop AF, some investigators have proposed additional PV isolation at the time of CTI ablation to improve long-term freedom of AF recurrences. Although small studies suggested some value of this approach, this strategy cannot be recommended for general adoption before confirmation by larger studies because of the increased procedural risk.¹⁹

Anticoagulation therapy is commonly discontinued 1 month after a successful AFL ablation if no other atrial arrhythmias are apparent. However, given the high risk of development of new-onset AF, which is often asymptomatic, patients with typical AFL undergoing successful ablation seem to have an elevated future risk for strokes. Hence intensified cardiac monitoring and anticoagulation therapy may be necessary in this patient population, especially those with significant risk factors (such as obstructive sleep apnea and LA dilation) for developing AF. This is especially important because intermittent and symptom-based surveillance with ambulatory cardiac monitoring is inaccurate and unreliable for identifying patients with AF. However, the current practice guidelines do not provide adequate recommendations regarding the optimal monitoring and anticoagulation strategies for this patient population.^{30,31}

ELECTROCARDIOGRAPHIC FEATURES

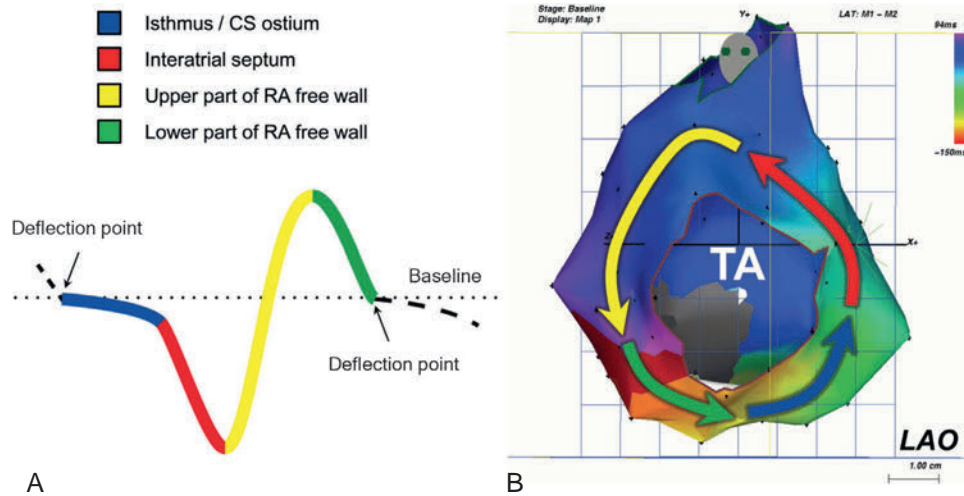
Flutter Waves

Flutter waves appear as atrial complexes of constant morphology, polarity, and CL. Typically, flutter waves are most prominent in the inferior leads (II, III, aVF) and lead V1. In counterclockwise AFL (Fig. 12.6), the flutter waves in the inferior leads resemble a picket fence (sawtooth) because these leads are primarily negative. This pattern consists of a downsloping segment, followed by a sharper negative deflection, and then a sharp positive deflection, with a positive overshoot leading to the next downsloping plateau. The relative size of each component can vary markedly. The flutter waves can exhibit pure negative deflections in the inferior leads, negative and then positive deflections that are equal in size, or a small negative and then a larger positive deflection. Those three varieties coexist with tall positive, small positive, or biphasic P waves in lead V1, respectively. With progression across the precordium, the initial component rapidly becomes inverted and the second component isoelectric usually by lead V2 to V3. This produces the overall impression of an upright flutter wave in lead V1, which becomes inverted by lead V6. A negative deflection always precedes the positive deflection in the inferior leads in counterclockwise AFL, and the degree of positivity in the inferior leads appears to be related to the coexistence of heart disease and LA enlargement. Lead I is low-amplitude isoelectric, and lead aVL is usually upright.³²

The initial part of negative deflections showing gradual voltage decline coincides with activation of the CTI. This short period of relative electrical silence on the surface ECG is related to the small amount of tissue being activated within the isthmus. Then, the sharp negative deflection of flutter wave is caused by caudocranial activation of the interatrial septum and the LA. On the other hand, the upstroke of flutter wave and terminal deflection (from the nadir to terminal deflection point) represent craniocaudal activation in the RA free wall (eFig. 12.2). The absence of positive terminal deflection has been correlated with a greater extent of low voltage area in the RA free wall. In addition, the overall amplitude of the flutter wave, which can be a determinant of the size of positive terminal deflection, depends on the longitudinally directed vector of the RA free wall activation.³³

The surface ECG appearance of clockwise typical AFL is more variable than that of counterclockwise typical AFL, but in many respects, clockwise AFL presents an inversion of the appearance in counterclockwise AFL (see Fig. 12.6). Clockwise AFL generally has broad positive deflections in the inferior leads, with characteristic notching; however, there is an inverted component preceding the upright notched component. Depending on the amplitude of this component, the appearance can be of continuous undulation without an obviously predominant upright or inverted component. On other occasions, it may appear that the inverted component is dominant, thus superficially mimicking counterclockwise AFL. Lead V1 is characterized by a wide negative and usually notched deflection. There is transition across the precordium to an upright deflection in lead V6. Lead I is usually upright, and lead aVL is low-amplitude negative and notched.³²

Typical AFL usually has an atrial rate of 240 to 340 beats/min. However, the flutter rate can be slower in patients with conduction delays in the atrial circuit secondary to prior incomplete CTI ablation (Fig. 12.7), scars from prior cardiac surgery, or antiarrhythmic drugs, whereby flutter CLs as long as 450 milliseconds (i.e., atrial rate less than 150 beats/min) can be observed. If the ventricular response is half the atrial rate, it can be difficult to identify flutter waves “buried” within the QRS or T waves (Fig. 12.8). Close inspection of the QRS and T waves, and comparisons with ECGs obtained in normal sinus rhythm, can help identify buried flutter waves. Furthermore, vagal maneuvers



eFig. 12.2 The Relationship Between Each of F-Wave Components and Activated Site in the Right Atrium (RA). (A) F-wave in the inferior leads including gently downward slope (*blue*), negative deflection (*red*), steep upstroke (*yellow*), and terminal deflection (*green*). (B) The colored curved-arrows correspond to the four portions of F-wave with the same color (in A). CS, Coronary sinus; LAO, left anterior oblique; TA, tricuspid annulus. (From Sasaki K, Sasaki S, Kimura M, et al. Revisit of typical counterclockwise atrial flutter wave in the ECG: electroanatomic studies on the determinants of the morphology. *Pacing Clin Electrophysiol.* 2013;36:978–987, with permission.)

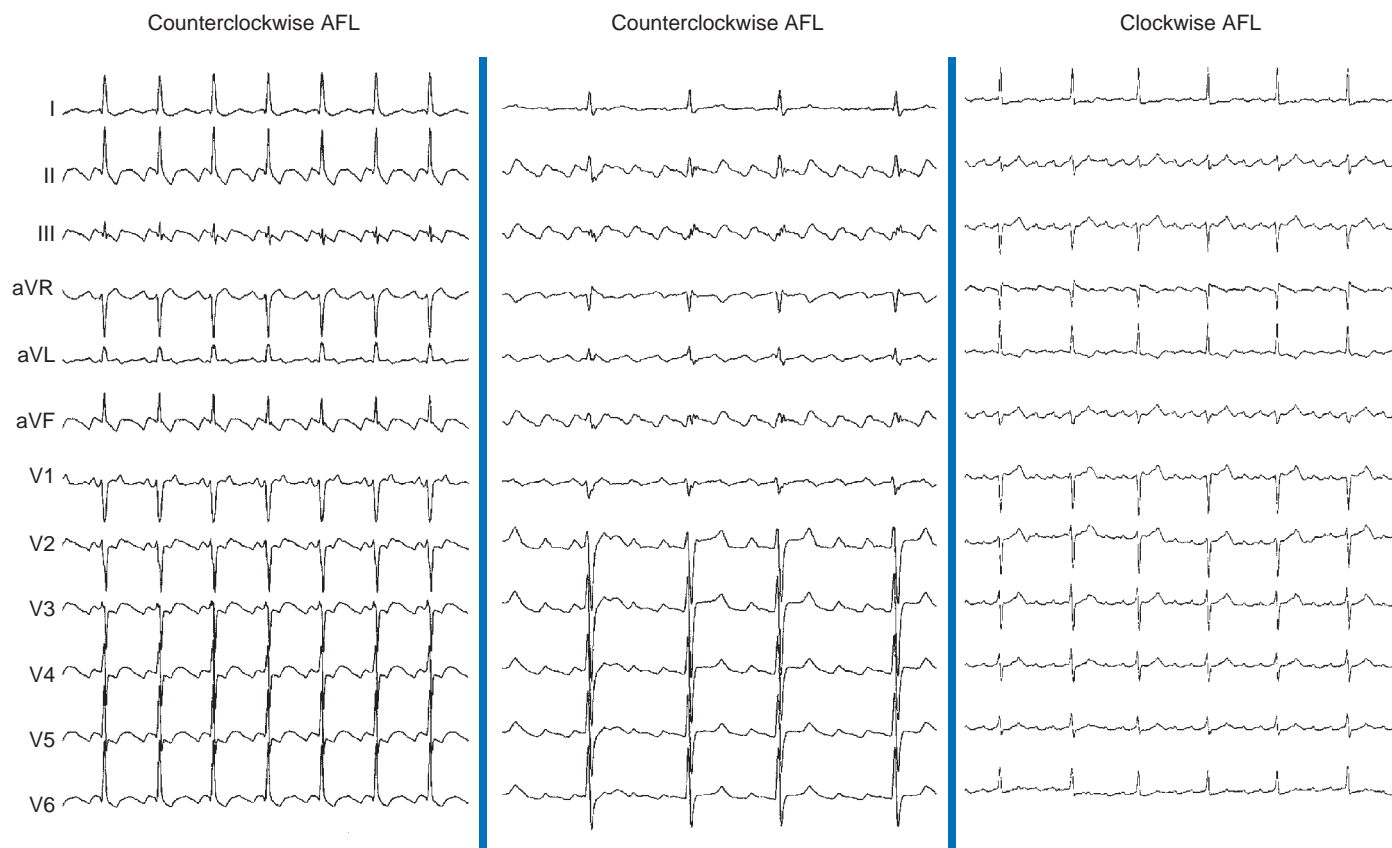


Fig. 12.6 Surface 12-Lead Electrocardiogram of Typical Atrial Flutter (AFL). *Left panel*, counterclockwise AFL with 2:1 atrioventricular (AV) conduction. *Middle panel*, counterclockwise typical AFL with variable AV conduction. *Right panel*, clockwise typical AFL with 4:1 AV conduction.

and AVN blockers can slow AV conduction and unmask the flutter waves (eFig. 12.3).

In patients who have undergone extensive LA ablation for treatment of AF, the P wave morphology during typical CTI-dependent AFL can be very different from the prior description because of alteration of intraatrial and interatrial wavefront propagation. Similarly, non-CTI-dependent macroreentrant ATs can mimic typical CTI-dependent AFL on the surface ECG. Thus arrhythmias that appear to be typical AFL may not be, whereas others that are actually typical AFL may not appear to be.

Atrioventricular Conduction

In general, AV conduction during AFL is characterized by even-integral conduction ratios; for example, with an atrial rate 300/min, the ventricular response is often 150/min or 75/min, not 90 to 100/min, as is often seen in AF. Most commonly, 2:1 AV conduction is present during AFL. Variable AV conduction and larger multiples (e.g., 4:1 or 6:1) are not uncommon. When present, variable AV conduction is the result of multilevel block; for example, proximal 2:1 AV block and more distal 3:2 Wenckebach block result in 5:2 AV Wenckebach block.

Slowing the atrial rate during AFL caused by antiarrhythmic drugs or following a prior incomplete CTI ablation can result in a paradoxical increase in the ventricular rate caused by better AVN conduction of the slower flutter beats (Fig. 12.9). For this reason, it is essential that adequate AVN blockade with beta-blockers or calcium channel blockers is in place before administering antiarrhythmic drugs that can slow the atrial rate during flutter. Rapid 1:1 AV conduction is most commonly

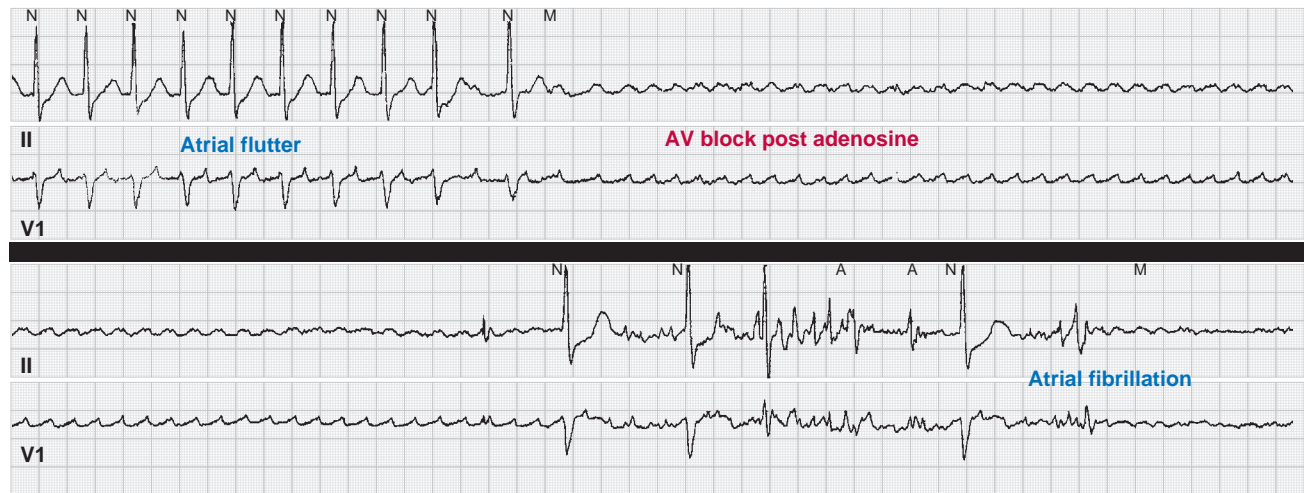
seen in patients with anterogradely conducting AV BTs (Fig. 12.10), but it may also be present in cases of enhanced AVN conduction secondary to high sympathetic tone (e.g., exercise, sympathomimetic drugs).

QRS Morphology

The QRS complex during AFL is often identical to that during sinus rhythm. However, the atrial impulses can be aberrantly conducted because of functional bundle branch block, most frequently right bundle branch block (RBBB) (see Fig. 12.9). Even with normal ventricular conduction, the QRS complex can be slightly distorted by temporal superimposition of flutter waves on the QRS complex. Thus the QRS complex can appear to acquire a new or larger R, S, or Q wave.

ELECTROPHYSIOLOGICAL TESTING

Typically a decapolar catheter (positioned into the CS with the proximal electrodes bracketing the CS os) and a multipolar (20 or 24 pole) Halo catheter (positioned at the tricuspid annulus) are used to map typical AFL. The distal tip of the Halo catheter is positioned at 6 to 7 o'clock in the LAO view, so that the distal electrodes will record the middle and lateral aspects of the CTI, the middle electrodes will record the anterolateral RA, and the proximal electrodes may record the RA septum (depending on the catheter used and RA size). Instead of the Halo and CS catheters, some operators use a single duodecapolar catheter around the tricuspid annulus, thus extending the catheter tip inside the CS. Such a catheter can straddle the CTI and provide recording and pacing from the medial and lateral aspects of the isthmus,



eFig. 12.3 Effects of Adenosine on Atrial Flutter (AFL). Continuous rhythm strip is shown. At left, typical AFL with 2:1 atrioventricular (AV) conduction is observed. The flutter waves are not readily visualized. Administration of intravenous adenosine causing block in the AV node resulting in a long ventricular pause and unmasking of the flutter waves. Also, adenosine results in an increase in the atrial rate and then degeneration into atrial fibrillation.

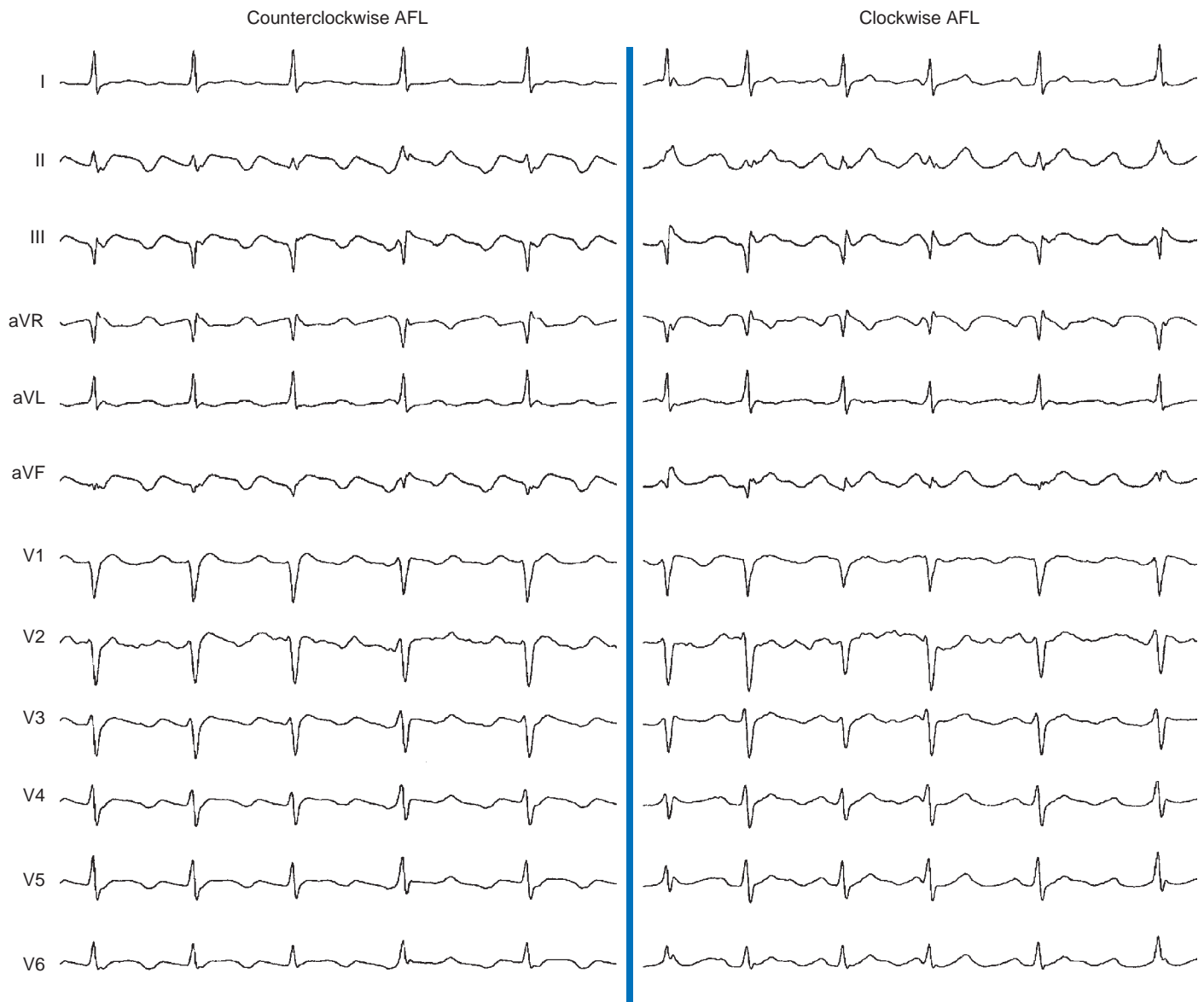


Fig. 12.7 Surface 12-Lead Electrocardiograms During Counterclockwise (*Left*) and Clockwise (*Right*) Typical Atrial Flutter (AFL) in a Patient on Flecainide Therapy. Note the slow flutter cycle length (approximately 350 milliseconds) secondary to the effects of flecainide.

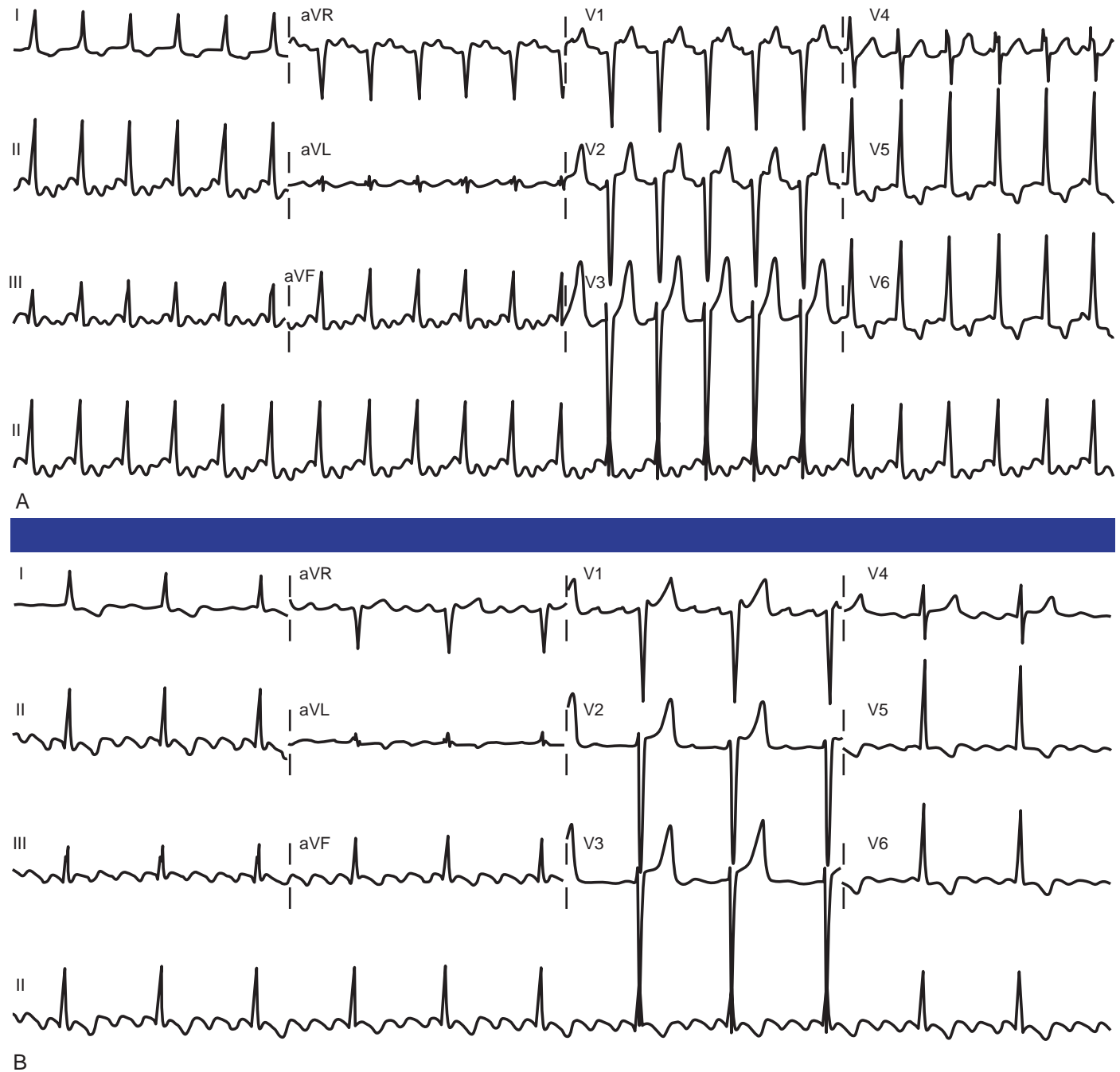


Fig. 12.8 Surface 12-Lead Electrocardiogram of Typical Atrial Flutter (AFL) and Atrial Fibrillation (AF). Counterclockwise typical AFL with 2:1 atrioventricular (AV) conduction (A) and with 4:1 AV conduction (B). Note that when the ventricular response is half the atrial rate, it is difficult to identify flutter waves “buried” within the QRS or T waves (A). However, when the ventricular rate is slowed, flutter wave morphology becomes more easily visualized.

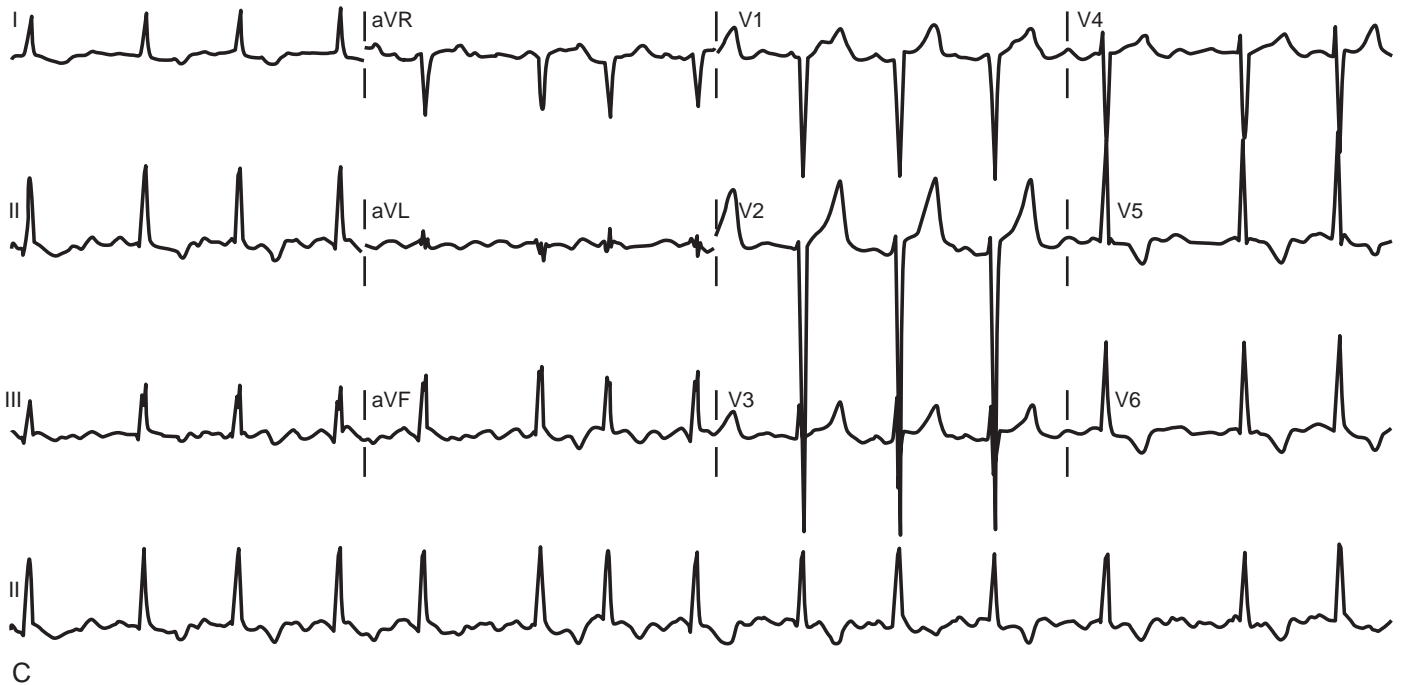


Fig. 12.8, cont'd (C) AF developed in the same patient after ablation of the cavotricuspid isthmus. Note that fibrillation waves are coarse and can mimic Q waves; however, close inspection reveals changes in rate and morphology of atrial activity that are inconsistent with AFL.

assuming good catheter-tissue contact at these locations. In the latter arrangement, however, the body of the duodecapolar catheter crossing over the CTI can potentially hinder manipulation and positioning of the ablation catheter tip to achieve adequate tissue contact for effective ablation.

Induction of Tachycardia

Programmed electrical stimulation protocol typically involves atrial burst pacing from the high RA and CS (down to the PCL, at which 2:1 atrial capture occurs) and single and double AESs (down to the atrial effective refractory period [ERP]) at multiple CLs (600 to 200 milliseconds) from the high RA and CS. Administration of an isoproterenol infusion (1 to 4 $\mu\text{g}/\text{min}$) may be required to facilitate tachycardia induction.

AFL can be induced readily with programmed electrical stimulation in most patients with a clinical history of AFL. Reproducible initiation of counterclockwise AFL is possible in more than 95% of patients. Rapid atrial pacing is more likely to induce AFL than a single AES, but as likely as introducing two AESs. On the other hand, the frequency of single or double AESs initiating AFL is low in patients without a history of AFL (less than 10%). Counterclockwise AFL is more likely to be induced by stimulation from the CS os; conversely, clockwise AFL is more likely to be induced with low lateral RA pacing. Induction of AFL usually occurs once unidirectional CTI block develops during pacing (Fig. 12.11). Not infrequently, a run of AF of variable duration is induced first, which then converts into AFL. The faster the pacing rate and the shorter the AES coupling intervals, the more likely it will be that AF is induced, which is usually self-terminating but can be sustained in less than 10% of patients with no clinical history of AF. The significance of induction of AF in these patients is uncertain.

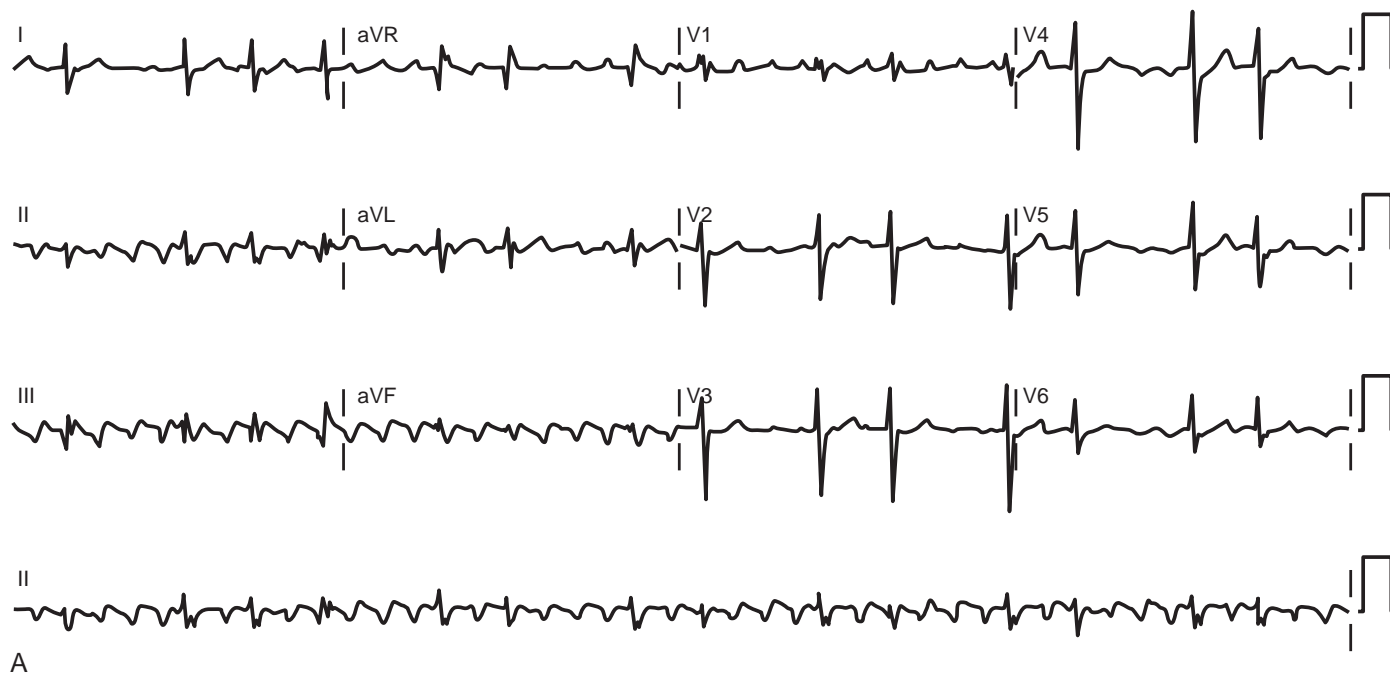
Tachycardia Features

Typical AFL is characterized by a constant atrial CL, polarity, morphology, and amplitude of the recorded bipolar electrograms and by the presence of a single constant macroreentrant circuit with a constant atrial activation sequence. In general, the atrial rate is very regular, with cycle-to-cycle variation of less than 2%. The atrial CL is usually between 190 and 250 milliseconds, but longer TCLs can be observed in patients receiving antiarrhythmic agents or following a prior unsuccessful ablation of the CTI. It is not uncommon for clockwise and counterclockwise AFLs to occur in the same patient, and they often have similar rates, although clockwise AFL can have a slower rate.

As noted, AFL is usually associated with 2:1 AV conduction, but variable AV conduction and larger multiples are not uncommon. Variable AV block is the result of multilevel block; for example, proximal 2:1 AV block and more distal 3:2 Wenckebach block result in 5:2 AV Wenckebach block. It is likely that the proximal 2:1 block occurs in the upper part of the AVN, whereas Wenckebach block occurs in the lower part of the AVN. Distal Wenckebach behavior in the His bundle (HB) would result in a similar AV conduction pattern but is unlikely to occur. In most cases, the nonconducted flutter impulses block in the AVN. However, infranodal AV block can occur, especially in the presence of prolonged His-Purkinje system (HPS) refractoriness caused by antiarrhythmic agents or during Wenckebach cycles in the AVN that leads to long-short cycle activation of the HPS.

The presence of an anterogradely conducting AV BT with a short refractory period can result in preexcited AFL with rapid 1:1 AV conduction. Infusion of isoproterenol can enhance AVN function and occasionally facilitate 1:1 AV conduction, especially when the atrial rate is relatively slow. Adenosine increases the degree of AV block, but

AFL with variable AV conduction



Slow AFL with variable AV conduction



Fig. 12.9 Effects of Antiarrhythmic Drugs on Typical Atrial Flutter (AFL). Baseline surface electrocardiogram in a patient with AFL and variable atrioventricular (AV) conduction (A). Treatment with propafenone results in slowing of the atrial rate during AFL (B) and a paradoxical increase in the ventricular rate caused by better AV nodal conduction of the slower flutter beats (C). Right bundle branch block aberrancy is observed during 1:1 AV conduction.

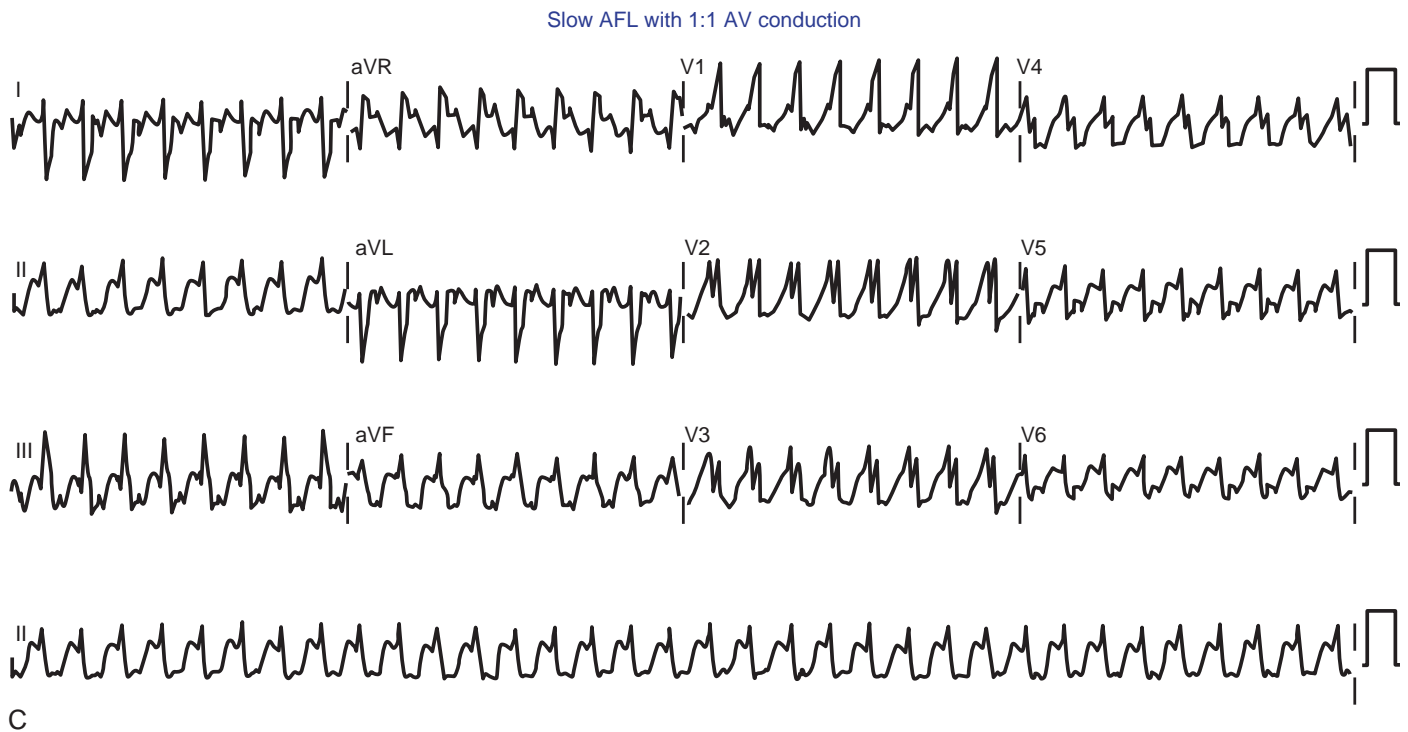


Fig. 12.9, cont'd

it also shortens atrial refractoriness and can result in the degeneration of AFL into AF (see eFig. 12.3).

Diagnostic Maneuvers During Tachycardia

Atrial Extrastimulation During Tachycardia

An AES from the high RA or CS or along the Halo catheter is introduced at a coupling CL 10 milliseconds shorter than the flutter CL, with progressive shortening of the coupling CL by 10 to 30 milliseconds.

An AES commonly results in resetting of the AFL circuit. The closer the site of atrial stimulation is to tissue in the circuit, the easier the resetting of the AFL circuit at longer coupling intervals will be. AFL has a resetting response pattern typical of reentrant circuits with fully excitable gaps: flat (for approximately 15% to 30% of the TCL, equal to approximately 30 to 63 milliseconds in the absence of drugs, and up to 100 milliseconds with class I antiarrhythmic agents) and then an increasing return CL in response to progressively shorter AES coupling intervals, indicating slowing of conduction from the stimulation site or within the circuit. The ability to capture the atrium without affecting (resetting) the AFL circuit timing indicates that the pacing site is outside the AFL circuit (e.g., RA appendage or distal CS).

It is usually difficult for a single AES to terminate AFL because AFL has a sizable fully excitable gap (15% to 30% of the TCL) that makes it difficult for a single AES to penetrate the reentrant circuit with adequate prematurity to terminate the AFL without intervening atrial refractoriness and intraatrial conduction delays. An AES delivered in the region of the CTI has the greatest chance of terminating AFL because it can capture the isthmus tissue with a very short coupling interval (close to the ERP of this critical site), given the lack of intervening tissue between the stimulation site and isthmus. Termination of AFL always occurs because of conduction block in the CTI.

Atrial Pacing During Tachycardia

Burst pacing from the CS or along the Halo catheter is started at a CL 10 to 20 milliseconds shorter than the flutter CL. Intermittent overdrive pacing is repeated at progressively shorter PCLs. The capture of atrial stimuli and acceleration of the atrial rate to the paced rate should be verified before analyzing the flutter response to pacing. The response of AFL to overdrive pacing is evaluated for overdrive suppression, acceleration, transformation into distinct uniform AFL morphologies or AF, entrainment, and the ability and pattern of termination.

Entrainment

Overdrive atrial pacing at long PCLs (i.e., 10 to 30 milliseconds shorter than the TCL) can almost always entrain typical AFL. The slower the pacing rate and the farther the pacing site from the reentrant circuit, the longer the pacing drive will need to be to penetrate and entrain the tachycardia.

Demonstration of entrainment of the AT establishes a reentrant mechanism of the tachycardia and excludes triggered activity and abnormal automaticity as potential mechanisms. However, it is important to understand that the mere acceleration of the tachycardia to the pacing rate and then resumption of the original tachycardia after cessation of pacing do not establish the presence of entrainment. After cessation of each pacing drive, the presence of entrainment should be verified by demonstrating the presence of fixed fusion of the paced complexes at a given PCL, progressive fusion at faster PCLs, and resumption of the same tachycardia morphology following cessation of pacing with a nonfused complex (see Box 5.1).^{34,35}

During entrainment of AFL, fusion of the stimulated impulse can be observed on the surface ECG, but it is easier to recognize on intra-cardiac recordings from the Halo and CS catheters. Entrainment with

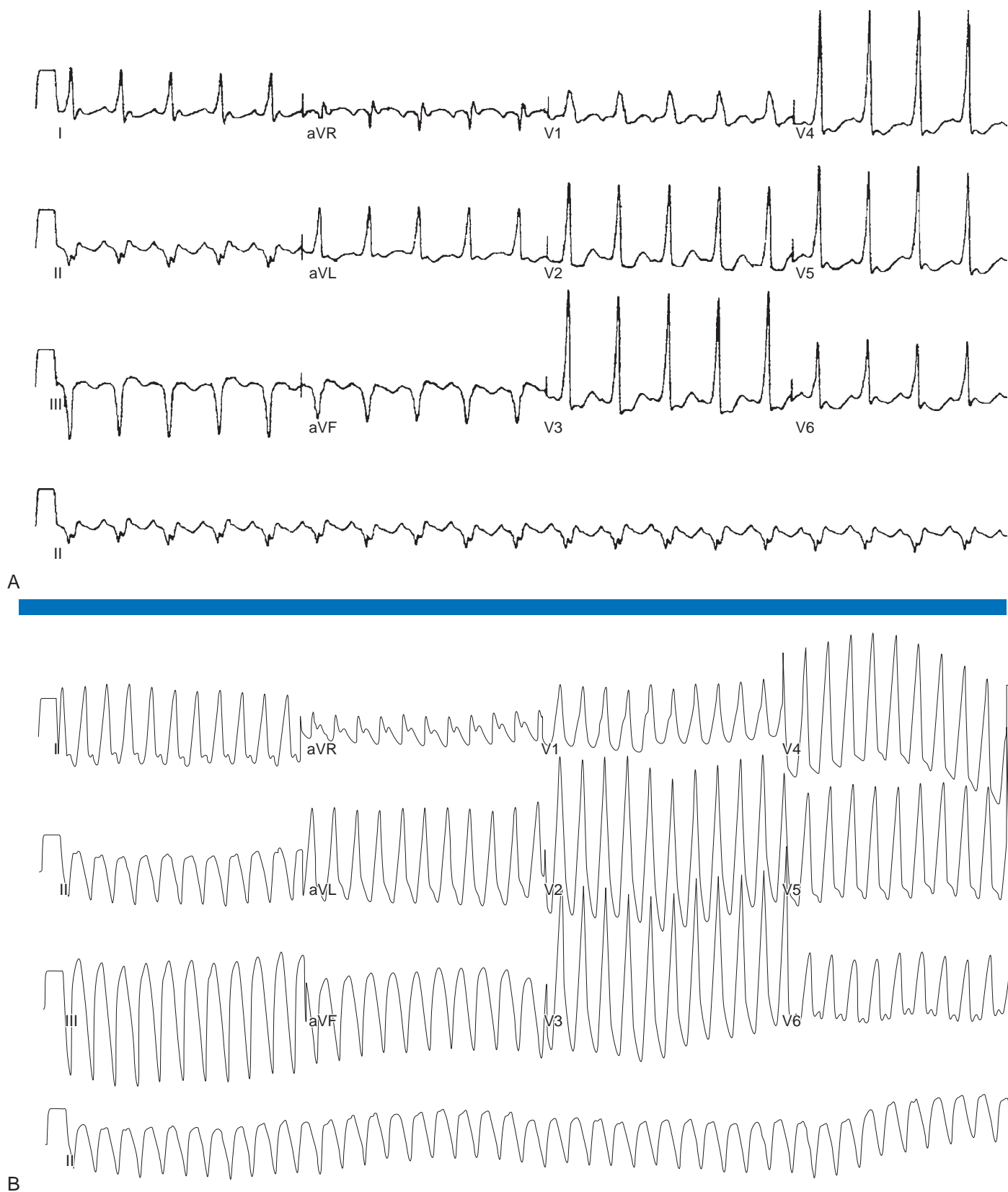


Fig. 12.10 Surface 12-Lead Electrocardiograms During Clockwise Typical Atrial Flutter in a Patient With a Left Posteroseptal Bypass Tract (BT). (A) 2:1 atrioventricular (AV) conduction with QRS fusion (secondary to conduction over both the BT and the AV node). (B) 1:1 AV conduction over the BT with fully preexcited QRS morphology.

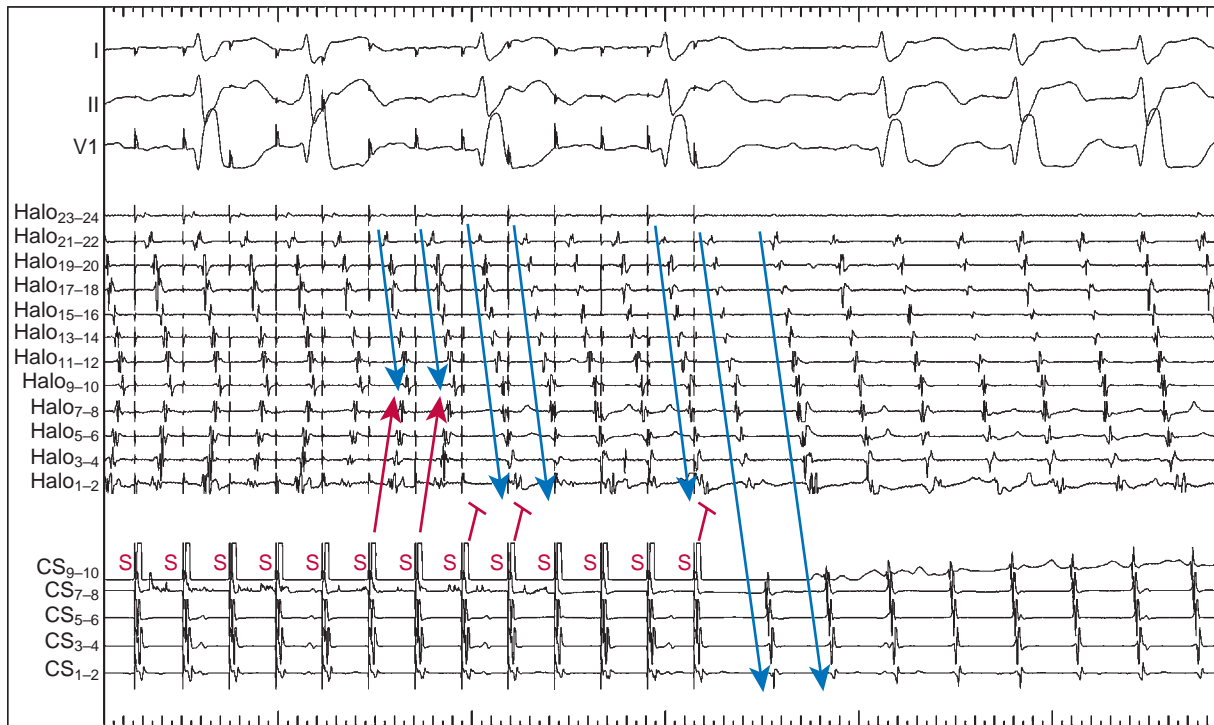


Fig. 12.11 Initiation of Counterclockwise Typical Atrial Flutter (AFL) by Atrial Pacing From the Coronary Sinus (CS). The Halo catheter is positioned around the tricuspid annulus (TA), with the distal bipole (*Halo₁₋₂*) at the lateral aspect of the cavotricuspid isthmus. Burst pacing from the CS ostium (*CS₁₋₂*) results in wavefronts proceeding in both directions around the TA, colliding around *Halo₉₋₁₀* (red and blue arrows). With progressive shortening of the pacing cycle length, the activation wavefront propagates from the pacing site at the CS ostium and blocks before arriving at *Halo₁₋₂* but propagates around the TA in a counterclockwise direction. When pacing stops, this unopposed paced wavefront continues around the TA as counterclockwise AFL, with subsequent proximal-to-distal CS activation by the tachycardia wavefront.

manifest fusion can be demonstrated with pacing from sites outside the CTI, such as lateral RA and CS. Conversely, pacing at the CTI results in entrainment with concealed fusion, whereby flutter waves (on the surface ECG and intracardiac recordings) during pacing are identical to those during the tachycardia.^{34,35}

Termination

More rapid atrial burst pacing (PCL 20 to 50 milliseconds shorter than the TCL) results in termination of AFL in most cases. Termination of AFL during rapid pacing can be indicated by a sudden change of P wave morphology on the surface ECG and by a change of atrial activation sequence in the HB and CS os recordings. This is seen particularly with high RA pacing during counterclockwise AFL, whereby on termination of AFL, the negative flutter waves in the inferior leads change suddenly into upright P waves, thus reflecting a change in the atrial activation sequence to one of high RA pacing (i.e., simultaneous RA lateral and septal activation in a craniocaudal direction). However, if the pacing site is distant from the AFL circuit (e.g., distal CS), a large mass of the atrial tissue can be captured by the pacing stimulus, to produce a marked change in P wave morphology (i.e., manifest fusion) without terminating the AFL.

Failure to terminate AFL with rapid pacing can be caused by any of the following: (1) the pacing rate is not fast enough to impinge on the tail of tissue refractoriness; (2) a short period of pacing (the closer the PCL is to the TCL, the longer the pacing duration will need to be to terminate the tachycardia); (3) a pacing site distant from the AFL circuit, with the intervening atrial tissue preventing penetration of the

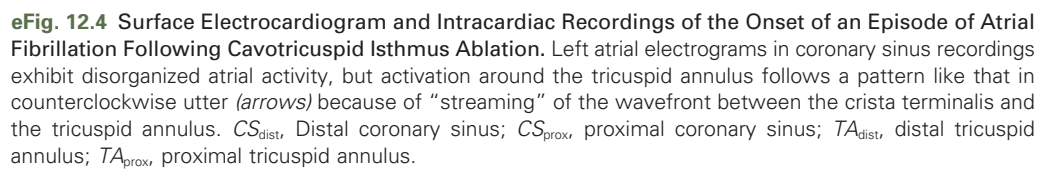
AFL circuit; or (4) the possibility that an apparent AFL on the ECG may actually be AF with “streaming” of the RA activation wavefront or may be a focal nonreentrant AT (eFig. 12.4).

Overdrive Suppression

Overdrive suppression analogous to that seen with automatic AT is not expected in AFL. The postpacing interval (PPI) (measured from the last pacing stimulus that entrained the tachycardia to the next near-field recorded electrogram at the pacing site) remains relatively stable when entrainment of AFL is performed from the same endocardial site, regardless of the length of the pacing drive. This is in contrast to overdrive suppression seen in automatic ATs, which would be associated with progressive delay of the first tachycardia beat return cycle with progressively longer overdrive pacing drives.

Acceleration

Acceleration by overdrive pacing refers to sustained shortening of the TCL following cessation of pacing. Rarely, atrial pacing can accelerate AFL into one of two different tachycardias: double-wave reentry or lower loop reentry. Double-wave reentry is manifest by acceleration of the tachycardia rate but with identical surface and intracardiac electrogram morphology, and it can be recognized by having simultaneous activation of the superior and inferior regions of the tricuspid annulus, with all activation being sequential. This rhythm rarely lasts for more than a few beats and may serve as a trigger for AF. Lower loop reentry is a form of CTI-dependent AFL with a reentrant circuit around the IVC. This arrhythmia is usually transient



and terminates by itself or converts spontaneously into AFL or AF (see Chapter 13).^{36,37}

Transformation

Rapid atrial burst pacing can convert AFL into AF. This is less likely with a slower PCL or pacing from sites within the AFL circuit. Induction of other forms of atrial macroreentry can also be observed, especially with faster pacing rates.

MAPPING

Activation Mapping

The simultaneous recording from endocardial sites around the tricuspid annulus (which encompasses most of the flutter macroreentrant circuit) by the Halo and CS catheters significantly facilitates activation mapping during typical AFL, and sequential point-by-point activation mapping is usually not required.

The RA activation sequence during counterclockwise AFL occurs sequentially down the lateral RA wall and adjacent to the crista terminalis, across the CTI (with some delay because of slow conduction across the CTI), past the CS os, up the atrial septum, over the roof of the RA, and back to the lateral free wall of the RA (in a proximal-to-distal direction along the Halo electrodes; see Fig. 12.1). This sequence is reversed during clockwise AFL (see Fig. 12.1). In both types of typical AFL (counterclockwise and clockwise), activation of the CS propagates in a proximal-to-distal direction. Notably, double potentials are seen on the crista terminalis and along the eustachian ridge and indicate lines of block (fixed or functional) along those structures.¹⁰

The atrial activation sequence in AFL is different from that during sinus rhythm or focal AT originating from the upper RA or LA, in which the activation wavefront propagates from the upper RA (middle or proximal Halo electrodes) down both the RA septum and lateral wall in a craniocaudal direction, toward the distal and proximal-most Halo electrodes.

Occasionally P wave morphology on the surface ECG resembles typical AFL, but intracardiac recordings show parts of the atria (commonly the LA) exhibiting disorganized atrial activity (see eFig. 12.4). Such rhythms behave more like AF than AFL, but they may be converted to true typical AFL with antiarrhythmic drugs.

As noted, double-wave reentry is characterized by an activation sequence identical to that of typical AFL, but at a faster atrial rate and with simultaneous activation of the superior and inferior regions of the tricuspid annulus, with all activation being sequential.

Entrainment Mapping

Entrainment mapping provides information about sites of the RA or LA that are part of the reentrant circuit, those that are outside the circuit, and the critical isthmus in the macroreentrant circuit. Entrainment also qualitatively estimates how far the reentrant circuit is from the pacing site. For entrainment mapping, atrial pacing is typically performed from the CTI, high RA, mid-lateral RA, and proximal and distal CS at PCLs 10 to 30 milliseconds shorter than the TCL.^{38–40}

Before attempting to use entrainment methods for mapping, it is necessary first to demonstrate that the tachycardia can be entrained, thus providing strong evidence that it is caused by reentry rather than by triggered activity or automaticity (see Box 5.2). At sites of entrainment, there should be confirmation of consistent capture of the atrium at the PCL for several beats with minimal or no change in the surface morphology or intracardiac electrograms and continuation of the identical tachycardia after pacing. Evaluation of the PPI or other criteria is meaningless (or even worse, misleading) when the presence of true entrainment has not been established. In addition, it is important to

verify the absence of termination and reinitiation of the tachycardia during the same pacing drive, or transformation of the AFL into a different tachycardia (evident as a change in CL or activation sequence, or both) following cessation of pacing.¹³

Once the presence of entrainment is verified, several criteria can be used to indicate the relation of the pacing site to the reentrant circuit. As discussed in detail in Chapter 13, the first entrainment criterion to be sought is concealed fusion. Entrainment with concealed fusion indicates that the pacing site is in a protected isthmus located within or attached to the reentrant circuit. Whether this protected isthmus is crucial to the reentrant circuit or just a bystander site needs to be verified by other criteria, mainly comparing the PPI with the TCL and the stimulus-exit interval with the electrogram-exit interval (Fig. 12.12). The diagnosis of CTI-dependent AFL is established when pacing from the CTI results in entrainment with concealed fusion and a PPI that is equal (within 20 milliseconds) to the flutter CL and an electrogram-exit interval that is equal (within 20 milliseconds) to the stimulus-exit interval. During counterclockwise AFL, a site medial to the CTI, such as the CS os, may be used to represent the exit of the reentrant wavefront. Conversely, in clockwise AFL, a site lateral to the tricuspid annulus, such as the distal Halo electrode, may be used (Box 12.1).^{34,35}

It is important to recognize that the PPI–TCL value can be misleadingly long despite pacing from sites within the reentrant circuit. In one report in patients with typical AFL, long PPI–TCL values (more than 30 milliseconds) after entrainment from the CTI were observed in 18% of patients despite a PCL within 20 milliseconds of the TCL, and more frequently when the PCL was 30 milliseconds shorter than the TCL and in patients on amiodarone therapy. The long PPI–TCL values are likely

BOX 12.1 Entrainment Mapping of Typical Atrial Flutter

Pacing from sites *outside* the AFL circuit (e.g., from RA appendage or middle or distal CS) results in the following:

- Manifest atrial fusion on the surface ECG or intracardiac recordings (fixed fusion at a single PCL and progressive fusion on progressively shorter PCLs)
- $PPI - TCL > 20$ ms
- The interval between the stimulus artifact to the onset of the flutter wave on the surface ECG is longer than the interval between the local electrogram on the pacing site to the onset of the flutter wave on the surface ECG

Pacing from sites *inside* the AFL circuit (e.g., from the CS os or around the tricuspid annulus) results in the following:

- Manifest atrial fusion on surface ECG or intracardiac recordings (fixed fusion at a single PCL and progressive fusion on progressively shorter PCL)
- $PPI - TCL < 20$ ms
- The interval between the stimulus artifact to the onset of the flutter wave on the surface ECG is equal to the interval between the local electrogram on the pacing site to the onset of the flutter wave on the surface ECG

Pacing from a protected isthmus inside the circuit (cavotricuspid isthmus) results in the following:

- Concealed atrial fusion (i.e., paced atrial waveform on the surface ECG and intracardiac recordings is identical to the AFL waveform)
- $PPI - TCL < 20$ ms
- The interval between the stimulus artifact to the onset of the flutter wave on the surface ECG is equal to the interval between the local electrogram on the pacing site to the onset of the flutter wave on the surface ECG

AFL, Atrial flutter; CL, cycle length; CS, coronary sinus; CS os, coronary sinus ostium; ECG, electrocardiogram; PCL, pacing cycle length; PPI, postpacing interval; RA, right atrium; TCL, tachycardia cycle length.

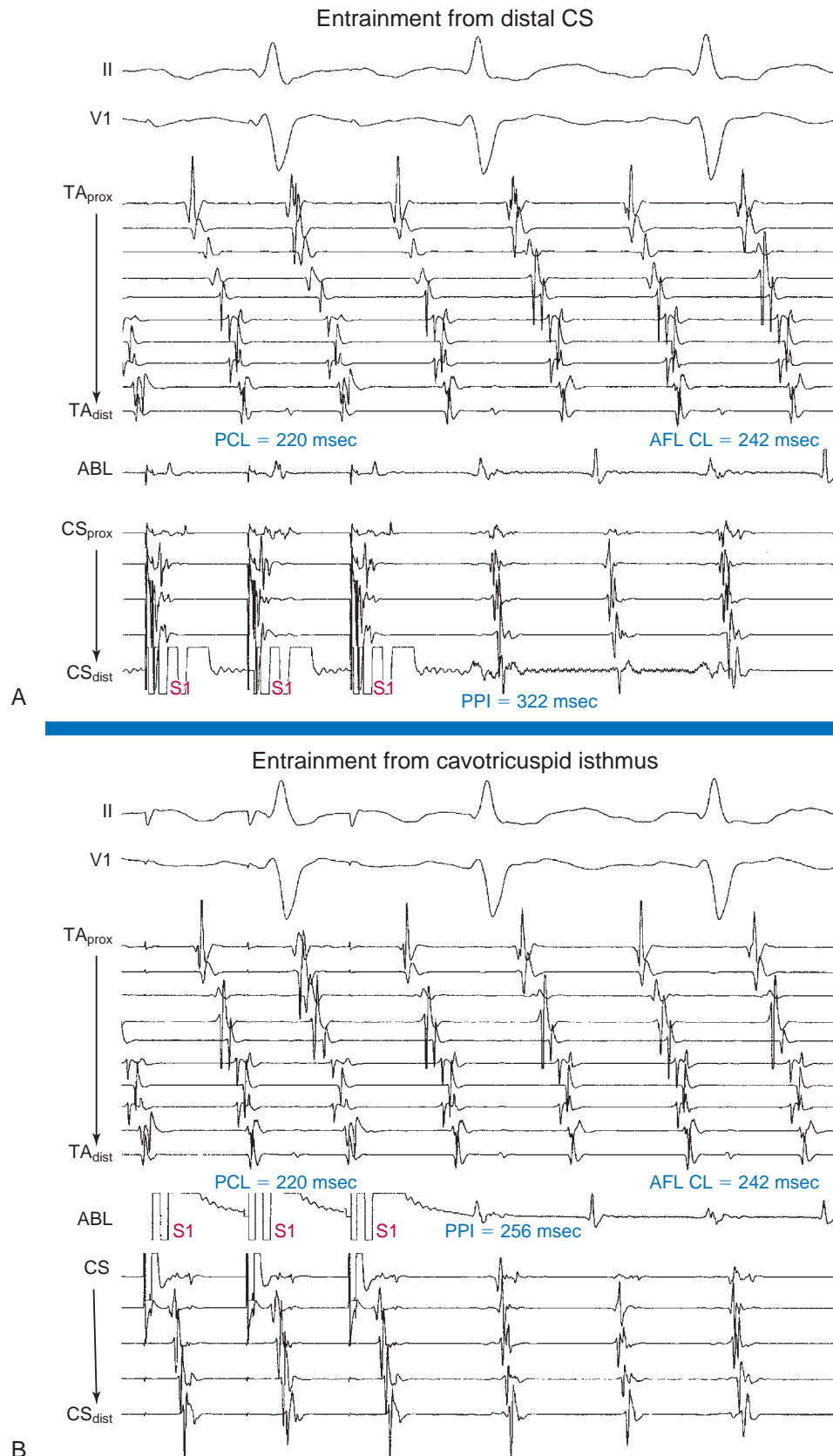


Fig. 12.12 Entrainment of Counterclockwise Typical Atrial Flutter (AFL). (A) Entrainment from the distal coronary sinus (CS) results in manifest atrial fusion and a long postpacing interval (PPI; PPI – AFL cycle length [CL] = 80 milliseconds) because the distal CS is far from the reentrant circuit. (B) Entrainment from ablation catheter positioned at the cavotricuspid isthmus (CTI) results in concealed atrial fusion with a short PPI (PPI – AFL CL = 14 milliseconds), a finding indicating that the CTI is part of the reentrant circuit. *Continued*

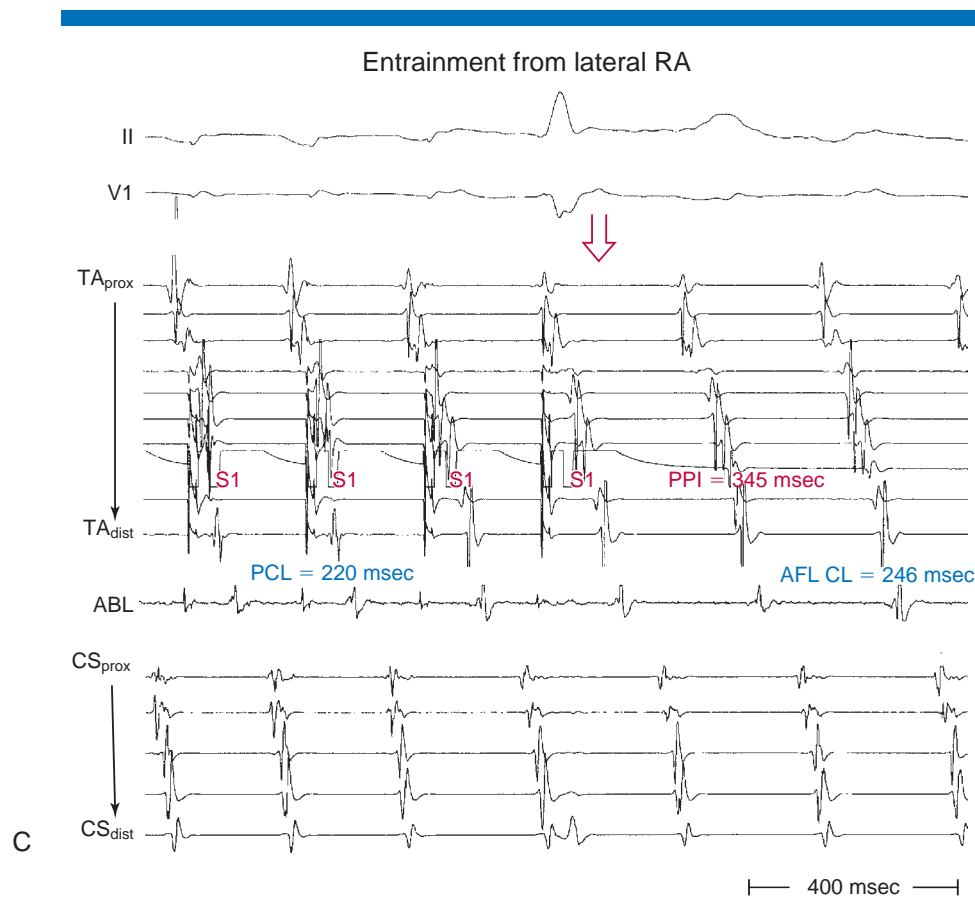


Fig. 12.12, cont'd (C) Entrainment from the lateral right atrial wall is attempted; however, the last paced stimulus fails to capture the 12 atrium (*open arrow*); therefore calculation of the PPI in this case is invalid and produces erroneous results. ABL, Ablation site; CS_{dist}, distal coronary sinus; CS_{prox}, proximal coronary sinus; PCL, pacing cycle length; RA, right atrium; TA_{dist}, distal tricuspid annulus; TA_{prox}, proximal tricuspid annulus.

caused by rate-dependent slowing of conduction or alterations of the activation path. Entrainment from near the IVC in the mid CTI may help minimize the chances of a misleading PPI value. These findings may also apply to other macroreentrant tachycardias.^{41,42}

Using the “number needed to entrain” criterion can overcome these pitfalls. The number needed to entrain assesses the number of captured pacing stimuli required to accelerate tachycardia to the PCL. Recording electrograms from the lateral RA and distal CS and properly timed initiation of the entrainment pacing (the coupling interval of the first paced stimulus is identical to the PCL) are required to measure the number needed to entrain. A small number (1 or 2) of pacing stimuli needed to entrain (with a PCL of 5 to 30 milliseconds shorter than the TCL) is consistent with a PPI–TCL value of less than 20 milliseconds and indicates that the pacing site is within the reentry circuit. A larger number of pacing stimuli needed to entrain (>3 for PCLs of 16 to 50 milliseconds, and >4 for PCLs of 5 to 15 milliseconds shorter than the TCL) indicates that the pacing site is outside the reentry circuit.⁴³ An advantage of this criterion is that it does not require the continuation of tachycardia after pacing for assessment and remains valid even when the tachycardia terminates or changes. The number needed to entrain is also useful when electrograms for assessment of the PPI are difficult to define. In addition, the number needed to entrain does not increase at shorter PCLs, likely because the conduction velocity in the intervening myocardium (between the pacing site and the reentry circuit) is less susceptible to changes in the PCL. This is in contrast to the slow

conduction zone within the reentry circuit, which can display decremental conduction properties at PCLs shorter than the TCL, resulting in misleading long PPIs.⁴³

Electroanatomic Mapping

Although atrial activation sequences in the Halo and CS catheters combined with entrainment mapping techniques are usually adequate to confirm the diagnosis of CTI-dependent typical AFL and facilitate ablation of the CTI, electroanatomic 3-D mapping (CARTO mapping system [Biosense Webster, Diamond Bar, CA], EnSite system [St. Jude Medical, St. Paul, MN], or Rhythmia [Boston Scientific Corp., Marlborough, MA]) can help distinguish between a focal origin and macroreentrant tachycardia by providing a precise description of the macroreentrant circuit and sequence of atrial activation during the tachycardia and rapid visualization of the activation wavefront.

Initially, selection of the reference electrogram, positioning of the anatomical reference, and determination of the window of interest are undertaken. The reference catheter is usually placed in the CS (because of its stability), and an electrode recording a prominent atrial electrogram is selected, thus ensuring that the ventricular electrogram is not the one detected by the system.

The mapping catheter is initially positioned, using fluoroscopy, at known anatomical points that serve as landmarks for the electroanatomic map. Anatomical and EP landmarks (IVC, SVC, CS, HB, and tricuspid annulus) are tagged. A set of six specific points (three at the

tricuspid annulus and three at the mouth of the IVC) is acquired to delineate the individual isthmus anatomy. Activation mapping is performed to define the atrial activation sequence. The catheter is moved slowly around the chamber walls to sample multiple points along the endocardium, thereby sequentially acquiring the location of its tip together with the local electrogram. Reasonable numbers of points are homogeneously distributed in the RA, with careful mapping of endocardial sites around the tricuspid annulus and CTI. The local activation time at each site is determined from the intracardiac bipolar electrogram and is measured in relation to the fixed intracardiac electrogram obtained from the CS (reference) catheter. The activation map may also be used to catalog sites at which pacing maneuvers are performed during assessment of the tachycardia (e.g., sites with good pace maps). Activation maps display the local activation time by a color-coded overlay on the reconstructed 3-D geometry. The selected points of local activation time are color-coded.

The 3-D electroanatomic activation map typically demonstrates a continuous progression of colors around the tricuspid annulus with close proximity of earliest and latest local activation and an activation time in a similar range to TCL, consistent with macroreentry (Fig. 12.13; see Figs. 6.8 and 6.13). During counterclockwise AFL, the activation wavefront exits the CTI as a broad wavefront, spreading anterosuperiorly around the tricuspid annulus, as well as posterosuperiorly in the RA. Lateral spread of the posterior wavefront is blocked along the vertical line in the posterolateral RA, a region marked by double potentials that coincides with the crista terminalis. The posterior wavefront propagates cranially around the SVC to merge with the activation wavefront circulating around the tricuspid annulus. The anterolateral wall of the RA is the last to activate as the wavefront reenters the lateral aspect of the CTI. Importantly, the location where earliest activation and latest local activation meet can be anywhere along the reentry circuit, depending on the timing of the electrical reference (the zero point) chosen for activation mapping (see Fig. 6.11). That location, like in the case of any macroreentrant tachycardia, has no relation to the site of the critical isthmus of the reentry circuit.

Activation mapping of the LA during typical AFL characteristically demonstrates earliest activation of at the interatrial septum or CS os, and activation of the whole LA chamber usually comprises only a portion of the atrial CL (Fig. 12.14).

The 3-D electroanatomic maps can also provide information about the voltage characteristics of the tissues involved in the CTI. The lower the voltage, the easier it is to achieve block in the tissue. Thus 3-D electroanatomic mapping can potentially help select a path in the CTI that is easier to ablate—a path that may not necessarily be the shortest across the isthmus.

Noncontact Mapping

The EnSite 3000 noncontact mapping system (St. Jude Medical) consists of a noncontact catheter with a multielectrode array surrounding a 7.5-mL balloon mounted at the distal end. The 9 Fr balloon catheter is advanced over a 0.035-inch guidewire under fluoroscopy guidance and is positioned in the middle and lower portion of the RA. The balloon is positioned in the center of the RA and does not come in contact with the atrial walls being mapped. IV heparin is administered before balloon deployment to keep the activated clotting time at 250 to 300 seconds. A conventional mapping-ablation catheter is used to collect geometry information. The mapping catheter is initially moved to known anatomical locations (IVC, SVC, CS, HB, and tricuspid annulus), which are tagged. Detailed geometry of the chamber is then reconstructed by moving the mapping catheter around the atrium.

After the chamber geometry is determined, mapping is started during tachycardia. The system simultaneously acquires data for the entire

chamber, and then reconstructs unipolar electrograms and superimposes them onto the virtual endocardium, to produce isopotential maps with a color range representing voltage amplitude (eFig. 12.5; see Fig. 6.21). A default high-pass filter setting of 2 Hz is used to preserve components of slow conduction on the isopotential map. Color settings are adjusted so that the color range matches 1 to 1 with the millivolt range of the electrogram deflection of interest. Activation can be tracked on the isopotential map throughout the tachycardia cycle. Isochronal maps can also be created that represent progression of activation throughout the chamber relative to a user-defined electrical reference timing point.

Although typical AFL is usually readily treated using standard ablation techniques, noncontact mapping can be used to confirm the anatomical location of the flutter circuit, reduce fluoroscopy time, and confirm CTI block after ablation. Noncontact mapping has also been used to identify and guide radiofrequency (RF) ablation of the site of residual conduction following incomplete linear ablation lesions at the isthmus. Because of its ability to record from multiple sites simultaneously, noncontact mapping can rapidly identify gaps in linear lesions. This is accomplished by analysis of one or more paced complexes originating adjacent to the line being assessed. This capability can be particularly helpful in patients who have recurrent AFL following a previous ablation. Because any number of maps can be superimposed on the initial geometry, bidirectional block at the ablation site can be rapidly identified during pacing following ablation. Tagging ablation areas during delivery of each RF impulse and a constantly visible ablation line offer another advantage—they ensure that no area is overlooked or ablated repeatedly.

ABLATION

Target of Ablation

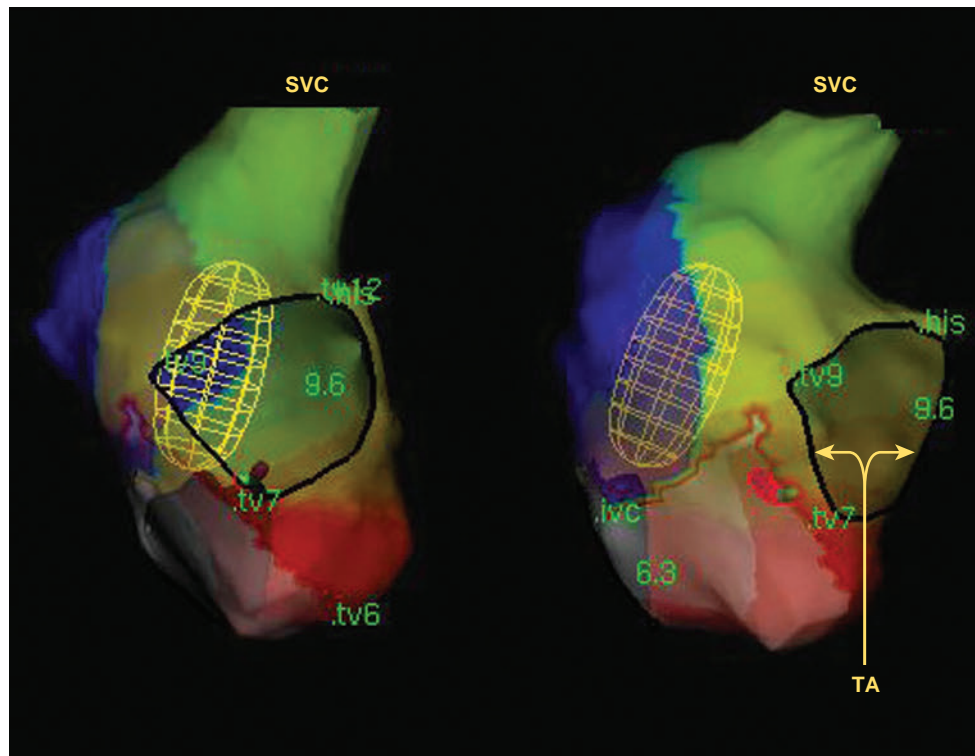
The CTI is the ideal target of AFL ablation because it is accessible, relatively narrow, short, safe to ablate, and essential for the AFL circuit (and not because it is the diseased area or the structure causing the AFL). The central part of the isthmus (the 6 o'clock region in a fluoroscopic LAO view) appears to be the optimal target site because it is the narrowest part of the isthmus (19 ± 4 mm; range, 13 to 26 mm) and relatively thin and therefore is less likely to resist RF ablation. Other advantages of the central isthmus are the increased distance from the paraseptal isthmus, which contains extensions of the AVN or AVN artery in 10% of patients, and the increased distance from the inferolateral isthmus, where the right coronary artery is in close proximity (less than 4 mm) to the endocardium.³

Alternatively, the tricuspid annulus-CS or IVC-CS isthmuses may be targeted (Fig. 12.15). However, for this approach to be successful, ablation within the CS is frequently necessary. Such approaches are less successful in curing AFL. The paraseptal isthmus (tricuspid annulus-CS isthmus) has the thickest wall, compared with other parts of the inferior RA isthmus, although there is significant interindividual variability, and this structure is close to the arterial branch supplying the AVN and, in some cases, can contain the inferior extensions of the AVN. The inferolateral isthmus is the longest portion and is in closest proximity to the right coronary artery.

Ablation Technique

Periprocedural Anticoagulation

In patients with persistent AFL of a duration longer than 48 hours or unknown duration, catheter ablation should be delayed until the patient has been anticoagulated at appropriate levels for 3 to 4 weeks or TEE has excluded atrial thrombi. In these patients, several options exist for periprocedural anticoagulation. Traditionally, a “bridging” strategy of



eFig. 12.5 Noncontact Mapping of Typical Atrial Flutter. Shown are left anterior oblique and posteroanterior views of a color-coded isopotential map of right atrial activation during counter-clockwise typical atrial flutter. SVC, Superior vena cava; TA, tricuspid annulus.

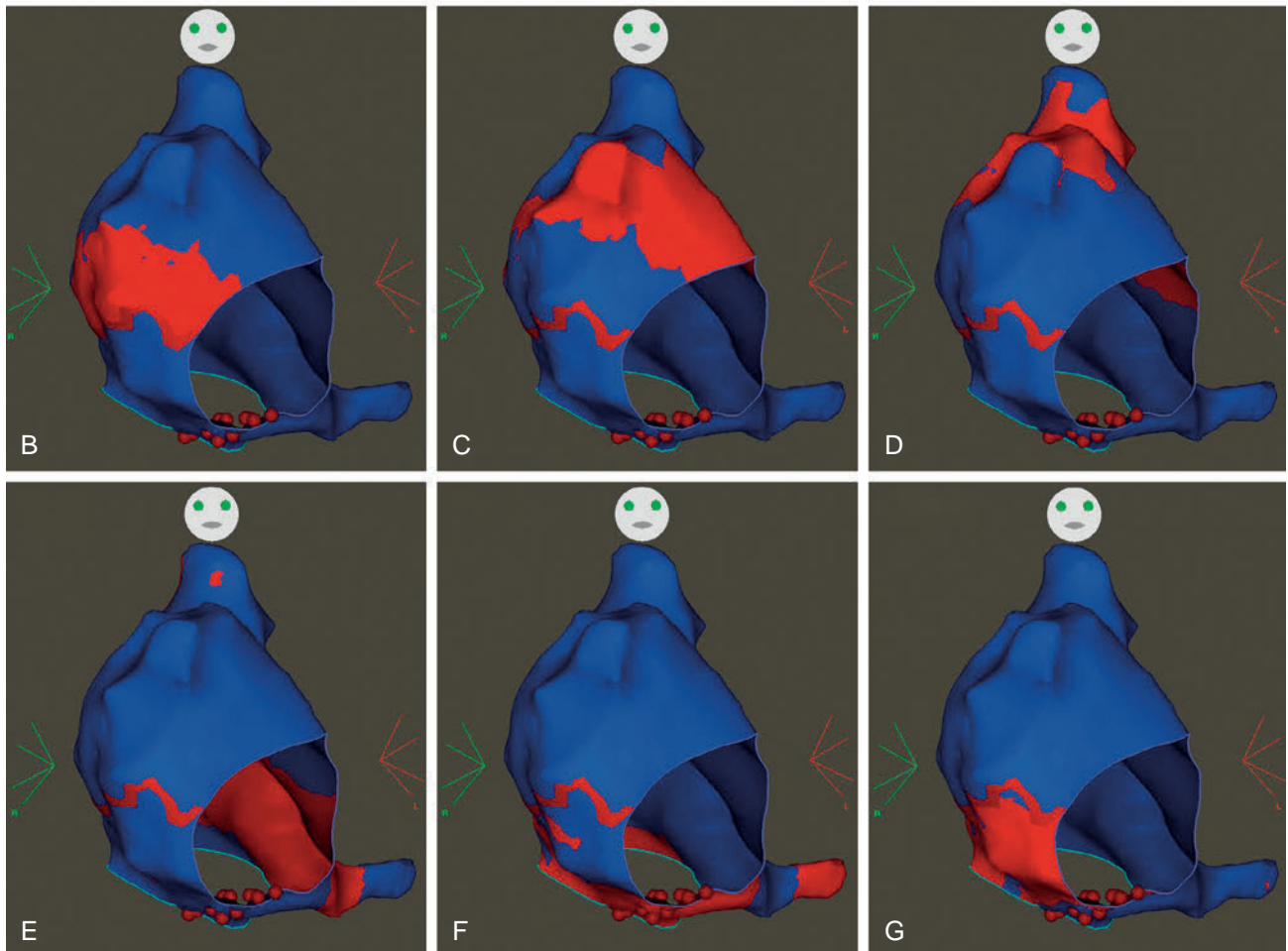
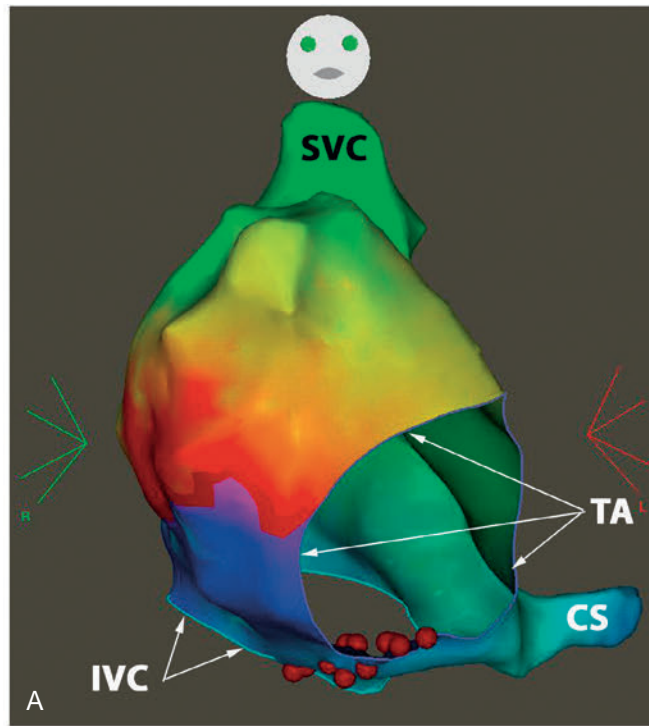


Fig. 12.13 Three-Dimensional Electroanatomic (CARTO) Mapping of Typical Atrial Flutter (AFL). (A) Three-dimensional electroanatomic (CARTO) activation map of the right atrium (RA) in the left anterior oblique view constructed during counterclockwise typical AFL. During tachycardia, the depolarization wavefront travels counterclockwise around the tricuspid annulus (TA), as indicated by a continuous progression of colors (from red to purple) with close proximity of earliest and latest local activation (red meeting purple). Linear ablation (red dots) is performed across the cavotricuspid isthmus. (B to G) Propagation map of the RA during counterclockwise typical AFL (arrows). CS, Coronary sinus; IVC, inferior vena cava; SVC, superior vena cava.

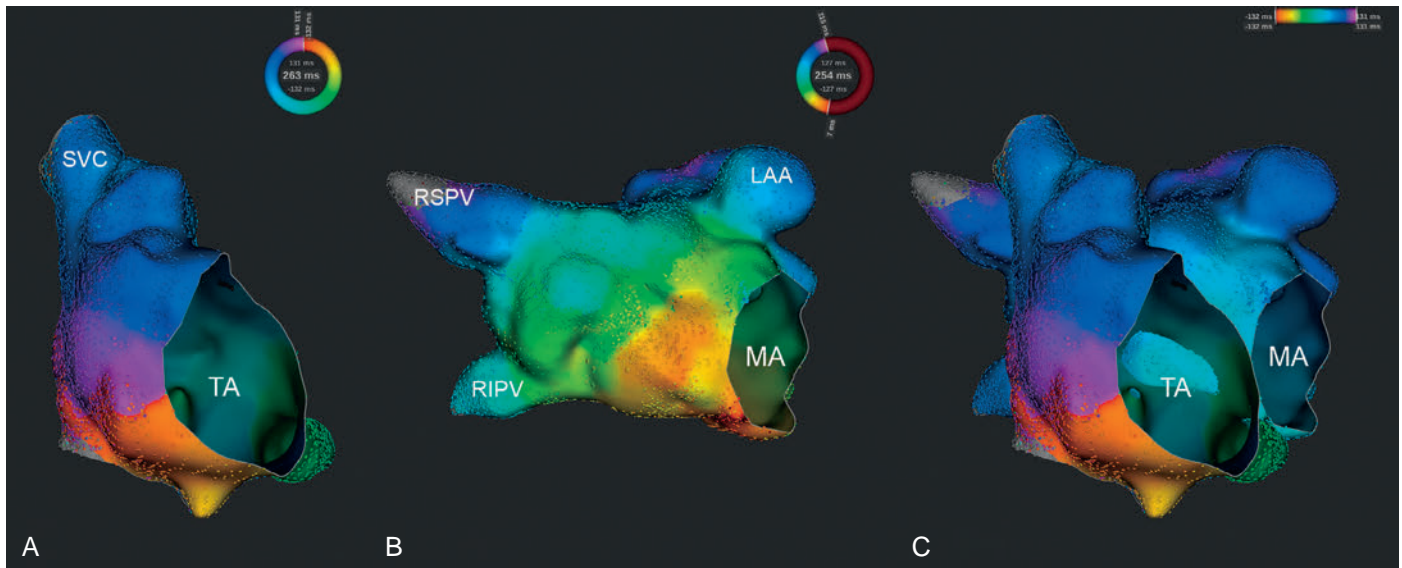


Fig. 12.14 Biatrial Electroanatomic Activation Mapping (Rhythmia) During Typical Counterclockwise Atrial Flutter (AFL). Maps are shown in the right anterior oblique views. (A) Activation map of the right atrium (RA) demonstrates propagation of the depolarization wavefront in a counterclockwise direction around the tricuspid annulus (TA), as indicated by a continuous progression of colors (from red to purple) with close proximity of earliest and latest local activation. Activation of the whole RA chamber extended over the entire atrial cycle length (CL, 263 milliseconds). (B) Activation map of the left atrium (LA) demonstrates focal-like activation pattern with the earliest activation located at the inter-atrial septum and coronary sinus (CS) ostium. Note and activation of the whole LA chamber comprised only half of the atrial CL (127 milliseconds out of 263 milliseconds). (C) Biatrial activation map now reveals that the flutter circuit is entirely confined within the RA, while LA activation occurs as a bystander and follows transseptal conduction across the inferior CS-LA connection, Bachmann's bundle, and/or fossa ovalis. LAA, LA appendage; MA, mitral annulus; RIPV, right inferior pulmonary vein; RSPV, right superior pulmonary vein; SVC, superior vena cava.

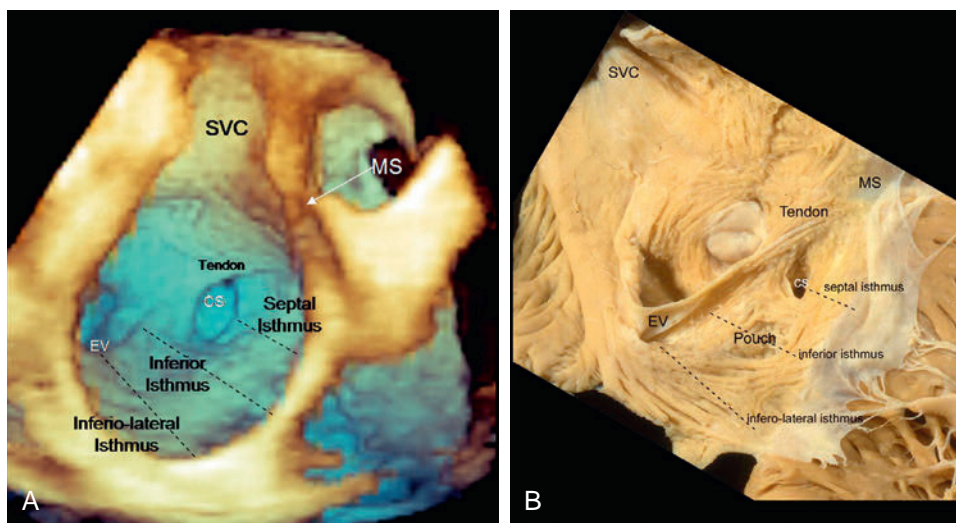


Fig. 12.15 Ablation Target for Typical Atrial Flutter. Three-dimensional transesophageal echocardiography (A) of the cavotricuspid isthmus and a matching anatomical specimen (B) showing the three lines in the cavotricuspid isthmus. The inferior isthmus line is the preferred target for linear ablation of the cavotricuspid isthmus. The endocardial surface has been removed to reveal the musculature of the isthmus. CS, Coronary sinus ostium; CVTI, cavotricuspid isthmus; EV, eustachian valve; MS, membranous septum; SVC, superior vena cava. (From Faletra FF, Ho SY, Auricchio A. Anatomy of right atrial structures by real-time 3D transesophageal echocardiography. *JACC Cardiovasc Imaging*. 2010;3:966-975, with permission.)

conversion of oral anticoagulation therapy to enoxaparin was employed to allow ablation and subsequent hemostasis to be performed during a pause in anticoagulation. Alternatively, catheter ablation may be performed on uninterrupted periprocedural oral anticoagulation (warfarin, dabigatran, factor Xa inhibitors).²⁹

Catheter Positioning

Commonly, a standard large-tip (8-mm) or an irrigated-tip ablation catheter is used. The catheter's curve size and shape can affect the ability to position the catheter on the CTI. Compared to standard 4- or 5-mm-tip ablation catheters, RF ablation catheters with a large distal electrode

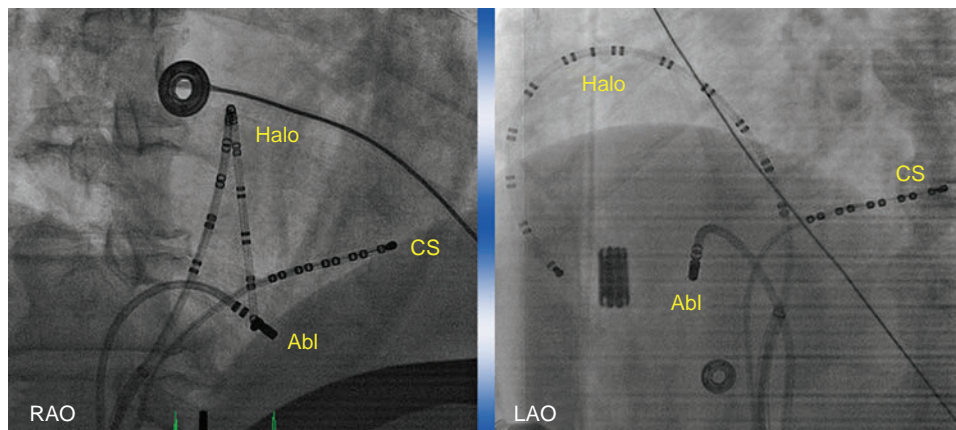


Fig. 12.16 Fluoroscopy of Catheter Ablation of the Cavotricuspid Isthmus. Fluoroscopic views (right anterior oblique [RAO] and left anterior oblique [LAO]) illustrating catheter location during ablation (Abl) of the cavotricuspid isthmus. CS, Coronary sinus.

and irrigated-tip catheters allow the creation of larger lesions in high- and low-flow regions and facilitate ablation of the CTI by achieving a high success rate with a smaller number of RF lesions, shorter procedure times, and less fluoroscopy exposure.

Catheters with larger curves are generally preferred to ensure adequate reach of the ablation electrode to the tricuspid annulus. Also, the use of preshaped guiding sheaths (e.g., SR0, SL1, or ramp sheath; Daig, Minnetonka, MN) can help extend the reach of the catheter tip across the CTI, stabilize the ablation electrode position, and prevent the catheter from sliding off the CTI and in and out of the right ventricle (RV).

The CTI can be localized electroanatomically. The ablation catheter is advanced to the RV under fluoroscopy (right anterior oblique [RAO] view); the tip is deflected to achieve contact with the RV inferior wall and is withdrawn progressively until it records small atrial and large ventricular electrograms. The distal tip of the ablation catheter is then adjusted in the LAO fluoroscopy view until it is midway on the CTI, between the atrial septum and RA lateral wall (pointing toward 6 o'clock in a 45-degree LAO view; Fig. 12.16).

The ratio of the atrial and ventricular electrogram amplitude (A/V ratio) can help localize the position of the ablation catheter across the CTI; the A/V ratio is typically 1:4 or less at the tricuspid annulus, 1:2 to 1:1 at the CTI, and 2:1 to 4:1 near the IVC. The location of the catheter at the CTI can also be confirmed by demonstrating entrainment with concealed fusion during AFL.

Radiofrequency Ablation

The ablation catheter is initially positioned on or near the tricuspid annulus, where ablation is commenced. Then the catheter is gradually withdrawn toward the IVC either during continuous RF energy application or in a sequentially interrupted point-by-point application of RF energy. RF lesions are applied for 30 to 60 seconds at each location, with a power output of 50 to 70 W targeting a temperature of 55°C to 65°C for standard 8-mm-tip ablation, and 40 to 50 W with a temperature limit of 40°C to 45°C for irrigated ablation. With closely spaced RF applications using a nonirrigated electrode (i.e., 4- or 8-mm electrodes), coagulum formation or charring can occur on the electrode and preclude further energy delivery to tissue until the electrode has been cleaned after withdrawing it from the body.

The first RF lesion is initiated from the tricuspid annulus edge with large ventricular and small atrial electrograms, and the last lesion is completed at the IVC edge. It is important that linear lesions span

completely from the tricuspid annulus to the IVC (see Fig. 12.13). After each RF application, the electrogram loses voltage and can become fragmented; the catheter is then withdrawn (2 to 4 mm at a time) toward the IVC until a new area of sharp atrial electrogram is reached, and the next RF application is delivered. This is repeated until the disappearance of atrial electrograms indicates that the catheter has reached the IVC. Before each RF application, the position of the ablation catheter is confirmed fluoroscopically, as described, or by using a 3-D mapping-navigation system.

Ablation is typically performed during AFL or CS pacing (if the patient is in sinus rhythm at the time). When ablation is carried out during AFL, the first endpoint is to terminate AFL during RF energy delivery. During delivery of RF energy, AFL can terminate or its CL can increase transiently or permanently, and a gradual delay in activation between the CS os and the low lateral RA wall can occur. This indicates that the ablation lesions have affected the circuit and should lead to continuation of RF delivery or extension of the lesion to ensure the achievement of complete conduction block across the CTI.

When ablation is performed during sinus rhythm, it is preferable to apply RF energy during continuous CS os pacing (e.g., at PCL of 600 milliseconds). Ablation during CS os pacing allows monitoring the effects of ablation lesions on CTI conduction indicated by progressive delay in activation timing in the low lateral RA (as recorded by the Halo catheter). This helps extending ablation duration at sites where RF lesions result in noticeable delays in CTI conduction. It also helps defining the location of the RF lesion that results in CTI block (indicated by an abrupt change to purely crania-to-caudal sequential lateral RA activation terminating at the lateral side of the ablation line during CS os pacing), so that that site can be revisited if CTI conduction recovers after the initial block. Observing even subtle differences in conduction times during AFL or CS pacing can be facilitated by using a trigger sweep screen, in which two complexes are displayed: the first is aligned on the same electrogram or the stimulus artifact at each occurrence, and the complex that follows the synchronized complex can be seen to occur progressively later as conduction slows.

Not infrequently, ablation of the CTI requires more than one pass of RF delivery across the isthmus. It can be necessary to rotate the ablation catheter away from the initial line of energy application, medially or laterally in the isthmus, to create new or additional lines of ablation eventually resulting in block. At the time of the second pass-over, the ablation line isthmus electrograms will be fragmented, of low voltage, and often double.

Maximum Voltage-Guided Technique

The pectinate muscles fan out from the crista terminalis and encroach upon the CTI for variable distances. Those muscle bundles exhibit significantly heterogeneous trabecular pattern. Although bundle-to-bundle electrical communication can exist, the muscle trabeculae are frequently nonoverlapping and are separated by nonconducting fibrofatty tissue.⁴⁴

The maximum voltage-guided technique is based on the hypothesis that discrete muscle bundles in the CTI (with poor bundle-to-bundle electrical communication, as opposed to a continuous sheet) participate in the flutter circuit. Large atrial electrogram voltages identify the location of these muscle bundles along the isthmus and are selectively targeted for ablation. In effect, bidirectional CTI block is produced by the summation of a series of discrete focal ablations, rather than a continuous ablation line across the CTI. Hence the length of the isthmus that needs to be ablated could be narrower than the “anatomical” isthmus.^{44,45}

Using this technique, the CTI is mapped in the 6 o'clock position, and bipolar atrial electrograms (during AFL or, preferably, during sinus rhythm or CS pacing) are measured from peak to peak during a continuous pull-back along the isthmus. The site of maximum voltage is noted and used as a marker for a presumed muscle bundle. The ablation catheter is positioned at this site, regardless of the location along the line, and RF ablation is performed for 40 to 60 seconds until an amplitude reduction of 50% or more is achieved; complete elimination of all signal is not necessary, since the size of the electrode recording area exceeds the area of extensive damage at the catheter tip. If this ablation lesion does not result in bidirectional CTI block, the line is remapped, and the next largest atrial electrogram is targeted for ablation. This is repeated until bidirectional CTI block is achieved. This method, therefore, targets the signals with highest amplitude along the CTI and does not necessitate a contiguous line of ablation. This technique was found to reduce ablation times significantly compared with a purely anatomical approach; however, this did not translate into a reduction in fluoroscopy or overall procedure time.^{44–46}

Role of Electroanatomic Mapping Systems

Electroanatomic mapping systems (CARTO or NavX) can provide precise spatial localization and tracking of the ablation catheter along the CTI that potentially help shorten fluoroscopy time. In addition, these mapping systems enable visualization of the ablation line as the procedure is carried out so that no area is left out or repeatedly ablated. Therefore it facilitates the creation of ablation lines devoid of gaps across the entire isthmus (see Fig. 12.13).⁴⁷

To help guide ablation, the CTI anatomy needs to be defined on the mapping system. After the usual anatomical landmarks are taken, detailed CTI mapping is performed by withdrawing the catheter at 2- to 3-mm intervals and taking several points along the line. In addition, multiple points at the tricuspid annulus and at the mouth of the IVC are acquired to delineate isthmus anatomy. One specific point is acquired at the most inferior point of the tricuspid annulus, where a small atrial electrogram and a larger ventricular electrogram are recorded. The catheter is then slightly rotated to two additional points at the tricuspid annulus, 1.5 to 2 cm septally and laterally. Three points are then acquired at the mouth of the IVC: one directly opposite to the inferior point of the tricuspid annulus, and the other two points slightly lateral and medial to this point. In this way, the extent of the myocardial isthmus can be clearly defined and depicted in the 3-D space. The isthmus region forms a relatively flat rectangular surface in a caudal projection, and a side-on view is provided by the RAO projection. These views allow visualization of lateral and septal displacement of the catheter tip, as well as the distance from the tricuspid annulus and the IVC. The ablation line can be planned by a trial run across the isthmus. During RF application,

the line is placed to connect the most anterior and posterior points in the CTI; the location of each site of RF application is “tagged” on the system. Each tag is approximately 4 mm in diameter, thus permitting visual estimation of the density of applications needed to produce a linear lesion during the drag. This helps avoid redundant lesion application and can identify potential gaps in the ablation line.⁴⁷ Tags are visual tools and can be displayed as 2 mm or even 1 mm diameters to search for possible gaps in the ablation line.

Electroanatomic mapping also provides information about the voltage characteristics of the tissues within the CTI. This information can be of value in selecting ablation targets and choosing a path across the isthmus that is easier to ablate, which may not necessarily be the shortest path. Voltage mapping of the isthmus is particularly helpful in patients with recurrent AFL following previous ablation attempts; high-voltage and breakthrough sites identified during activation and voltage mapping may then be chosen as ablation targets.⁴⁷

Verification of CTI conduction block following ablation can also be performed using electroanatomic mapping. The activation wavefront during AFL halts at the previously completed line but continues through the breakthrough site (see later).

The benefits of electroanatomic mapping compared with conventional mapping for catheter ablation have been clearly demonstrated in various arrhythmia entities, such as focal and macroreentrant AT, AF, and VT. These benefits include the ability of the technology for exact anatomical reconstruction, renavigation of the catheter accurately to positions removed from fluoroscopic markers, and precise electroanatomic identification of an arrhythmia origin or reentrant circuit. In the setting of typical AFL, however, the reentrant circuit and critical isthmus can be identified in most cases by using conventional mapping and fluoroscopic methods. Therefore it is not surprising that the use of electroanatomic mapping and ablation in one report did not improve on the efficacy and the duration of the procedure as compared with the conventional technique. Nevertheless, fluoroscopy exposure time in that study was significantly reduced in the electroanatomic ablation group by almost 50%; in fact, electroanatomic mapping systems have enabled complete lack of fluoroscopic use during typical AFL ablation. However, this achievement was associated with an increase in the cost of the procedure.⁴⁷

Approach to the Difficult Cavotricuspid Isthmus Ablation

Although ablation of typical AFL is successful in more than 90% of cases, significant difficulties are occasionally encountered when attempting to terminate the flutter or create bidirectional conduction block across the CTI. In these instances, the first step is to reconfirm the diagnosis of CTI-dependent AFL by entrainment mapping on the septal, lateral, and middle portion of the isthmus. Once the diagnosis of typical AFL is verified, other potential contributors to failure of CTI ablation should be considered, including poor catheter contact, inadequate power delivery, thick myocardium, and discontinuous ablation line, typically caused by the presence of pouches, recesses, ridges, and trabeculations within the CTI. These factors can also be responsible for failure to produce bidirectional CTI block or for recovery of CTI conduction and recurrent AFL during follow-up after an acutely successful ablation.^{3,7,48}

Inadequate RF energy delivery. If a standard 4- or 5-mm-tip ablation catheter is used initially, ablation failure may be related to inadequate RF energy delivery. In this setting, RF ablation catheters with a large (8-mm) distal electrode and irrigated-tip catheters allow the creation of larger lesions in high- and low-flow regions. Importantly, local edema caused by a prior ineffective RF application can potentially form a barrier preventing deeper penetration of subsequent RF applications.

Failure to ablate across the entire isthmus. Not infrequently, the curvature of the ablation catheter does not enable the ablation electrode to reach the ventricular aspect of the CTI. In this setting, using preshaped or deflectable guiding sheaths can enable access of the ablation catheter to all locations across the CTI.

In addition, conducting gaps anywhere along the CTI can cause arrhythmia recurrence. Full mapping of the CTI is required to identify those gaps. Quite commonly, conduction recurs at the site at which block was first achieved, but can occur anywhere along the line. Widely separated double potentials indicate local block under the recording catheter bipole. Further ablation of these regions is not necessary. When double potentials separated by an isoelectric interval can be traced in a convergent configuration, with a progressively decreasing interpotential interval, and culminate in a fractionated continuous electrogram, this finding indicates a gap in the line of block, which should be selectively targeted by additional ablation. High-density electroanatomic mapping can be helpful in identifying the gaps in the ablation line.⁴⁹

Sub-eustachian pouches. When present, deep sub-eustachian pouches tend to be most prominent in the vestibular portion close to the septum and are typically associated with a prominent valve of Thebesius (which guards the CS os; see Fig. 12.15). The presence of a prominent sub-eustachian pouch can be suggested by a characteristic inferior dip of the catheter tip when the ablation catheter is dragged back across the isthmus toward the IVC. Catheter stability and power delivery for ablation within these pouches are frequently suboptimal, especially when eustachian ridge act as a fulcrum, preventing the catheter tip from falling into the pouch. Making a tight (180 degrees) curve on the ablation catheter within the RA (or using a preshaped “ramp” guiding sheath or a steerable sheath) and withdrawing the catheter can direct the tip vertically on the CTI (instead of the usual horizontal direction) and help position the ablation electrode deep within the pouch. Then small changes in the angle of catheter curvature enable delivery of contiguous ablation lesions across the floor of the pouch. Alternatively, performing ablation relatively more laterally on the CTI can circumvent the problems of power delivery and potential perforation when ablating within a pouch. If linear ablation more laterally is unsuccessful because of poor catheter stability or thick myocardium, irrigated-tip catheters can be of advantage; however, careful titration of energy delivery is necessary to avoid steam pops. When ablation is still unsuccessful, adequate visualization of the pouch (using RA angiography or phased-array intracardiac echocardiography) can be useful to guide ablation within or around the pouch.^{3,7,48}

Prominent pectinate muscles. Prominent pectinate muscles encroaching on the CTI can be suggested by the presence of sites with unusually high-voltage electrograms (from pectinate muscle ridges) surrounded by areas where abrupt impedance rises and minimal power delivery occurs (likely from poor blood flow in the crevices between pectinate muscles). The thickness of prominent pectinates can prevent transmural ablation lesions and hamper adequate catheter stability. In addition, the catheter tip can become wedged between the pectinate muscles with consequent inadequate power delivery with impedance rise, and coagulum formation may occur because of poor blood circulation. In these situations, performing ablation closer to the septum, where the pectinate muscles are usually less prominent, and using large-tip or irrigated-tip catheters can help achieve successful ablation.^{7,48}

Prominent eustachian ridge. A prominent eustachian ridge can hinder catheter manipulation to the septal aspect of the isthmus because the crest of the ridge can act as a fulcrum, directing the catheter tip laterally when clockwise torque is applied (instead of the expected medial rotation). In addition, when the eustachian ridge is prominent, electrode contact can be difficult to maintain on the upslope of the ridge (the portion between the crest of the eustachian ridge and the tricuspid

annulus). In these situations, the use of preshaped guiding sheaths (e.g., SRO, SL1, or Ramp sheath) often solves the problem.

Cryoablation

Cryothermal ablation utilizes a steerable 9 Fr, 8-mm-tip catheter (Freezor MAX, Medtronic CryoCath, Montreal, Canada). Cryoablation of the CTI is performed using a point-by-point sequential application technique from the TV annulus to the IVC. Each application lasted for 240 seconds, targeting a temperature of -80°C .

Although there is no reason to believe that cryothermal ablation will be more effective than RF ablation of the CTI, cryothermal ablation has the advantage of being less painful. Acute success rates are comparable to those for RF ablation. Data have been mixed, however, regarding long-term outcome after cryoablation. A recent report demonstrated comparable efficacy of cryoablation to RF ablation.⁵⁰ However, other studies found lesion durability from cryoablation to be significantly inferior to that of RF ablation, as evidenced by the higher recurrence rate of symptomatic AFL (11% vs. 0%) and even higher rates of asymptomatic recovery of CTI conduction (34% vs. 15%). In addition, compared with RF ablation, cryoablation is associated with significantly longer procedure times; this is driven mainly by differences in ablation duration, which can be attributed to the longer duration of each cryoablation (4 minutes) compared with RF ablation (up to 60 seconds).⁵¹

Endpoints of Ablation

Tachycardia Elimination

When ablation is performed during AFL, the first endpoint is to terminate the arrhythmia during RF energy delivery. After termination of AFL, programmed atrial stimulation is performed to evaluate inducibility of the arrhythmia. Importantly, the termination or noninducibility of AFL are often not associated with complete isthmus block and hence should not be considered a reliable ablation endpoint without confirmation of the presence of complete bidirectional CTI block. Without achieving CTI block, the substrate for AFL is left intact (even when AFL terminates during ablation) and hence the risk of arrhythmia recurrence is high.

Bidirectional Isthmus Block

Complete bidirectional CTI block is the primary endpoint of ablation of typical AFL. Several methods (Table 12.1) can be used to demonstrate the presence of bidirectional CTI block. However, the distinction between incomplete block with very slow conduction across the CTI versus complete CTI conduction block can be very difficult, even with detailed mapping. Therefore it is important to utilize multiple techniques to confirm the presence of CTI block.

Adenosine Challenge

Recovery of CTI conduction, likely related to nontransmural ablation lesions, is the most common mechanism for long-term recurrence of AFL after ablation. Acute recovery of CTI conduction can occur in more than 15% of patients within minutes to over 1 hour after initially successful ablation. Therefore reconfirmation of CTI block is repeated 30 minutes after the last RF application. Adenosine (12 to 18 mg IV bolus) and, to a lesser degree, isoproterenol infusion (titrated to increase baseline sinus rate by 50%) can help reveal dormant trans-isthmus conduction. In fact, adenosine challenge following AFL ablation was found to provoke transient (for as little as 1 or 2 beats, and usually for less than 1 minute) or persistent resumption of conduction across the CTI in up to 23% of patients. Adenosine-induced second- or third-degree AV block seemed to be a prerequisite for its effects on CTI conduction; therefore the dose of adenosine is increased gradually until second- or third-degree AV block occurs. Adenosine-induced “dormant

TABLE 12.1 Confirmation of Bidirectional Isthmus Block

Method	Technique	Observations Consistent With CTI Block
Atrial activation sequence during atrial pacing	Mapping inferolateral RA activation sequence during pacing from the CS os (at PCL of 600 msec)	Clockwise CTI block is indicated by the observation of a purely descending (craniocaudal) wavefront at the inferolateral wall down to the CTI (proximal-to-distal activation sequence on the Halo catheter positioned around the tricuspid annulus)
Atrial activation sequence during atrial pacing	Mapping septal RA activation sequence during pacing from the low lateral RA (at PCL of 600 msec)	Counterclockwise CTI block is indicated by the observation of a completely descending (craniocaudal) wavefront at the RA septum, with CS os activation occurring after activation of the high RA and the HB region
Transisthmus conduction interval	Measuring transisthmus conduction interval during pacing from CS os, then from low lateral RA pacing (Transisthmus interval equals the interval from the stimulus artifact from one side of the isthmus to the atrial electrogram recorded on the contralateral side)	Prolongation of transisthmus interval post ablation by >50% from baseline (or to an absolute value of ≥ 150 msec)
Double potentials	Mapping of double potentials along the entire CTI ablation line during pacing from either side of the CTI (CS os or low lateral RA, at PCL of 600 msec)	The presence complete corridor of widely spaced double potentials (separated by an interval of ≥ 110 msec) along the entire CTI ablation line
Differential pacing	Mapping of double potentials along the entire CTI ablation line during pacing from low lateral RA, then from midlateral RA (at PCL of 600 msec)	Separation between the double potentials is decreased upon moving the pacing site away from the ablation line (from low lateral to midlateral RA)
Differential pacing	Mapping activation at the CTI ablation line during pacing from low lateral RA, then from midlateral RA, or from CS os then RA septum (at PCL of 600 msec)	Moving the pacing site away from the ablation line (from low lateral to midlateral RA or from CS os to RA septum) shortens the conduction time to the contralateral side of the ablation line
Incremental pacing	Mapping of double potentials along the CTI ablation line during pacing from low lateral RA, then from CS os (at PCLs of 600 msec then 300 msec)	Minimal (<20 msec) variation in the distance between the double potentials in response to progressively faster pacing rates
Incremental pacing	Measuring the interval between atrial electrograms at the HB region and CS os (His-to-CS os interval) during pacing from low lateral RA (at PCLs of 600 msec then 300 msec)	Minimal (<10 msec) variation in the His-to-CS os interval in response to progressively faster pacing rates
Unipolar electrogram morphology	Recording unipolar electrograms at the CTI ablation line during pacing from either side of the CTI (CS os or low lateral RA, at PCL of 600 msec)	Unipolar electrogram recorded at the edge of the ablation line contralateral to the pacing site exhibits monophasic R or Rs wave (large positive deflection followed by a negative deflection with R/s ratio $>3:1$)
Bipolar electrogram morphology	Recording bipolar electrogram just lateral to the CTI ablation line during pacing from the CS os (at PCL of 600 msec)	Bipolar electrogram polarity reverses (as compared to preablation electrogram polarity)
Electroanatomic mapping	Electroanatomic mapping	Pacing from one side of the ablation line results in an activation wavefront propagating in one direction around the tricuspid annulus, with the latest activation in the CTI immediately on the contralateral side of the ablation line

CS os, Coronary sinus ostium; CTI, cavotricuspid isthmus; HB, His bundle; msec, milliseconds; PCL, pacing cycle length; RA, right atrium.

conduction” precedes early relapse of permanent conduction, and hence it can identify a subgroup of patients at higher risk of long-term arrhythmia recurrence. Patients without adenosine-mediated “dormant transisthmus conduction” immediately after CTI block has been demonstrated typically have no recovery of conduction during the postablation waiting period.^{52–54}

Confirmation of Bidirectional Cavotricuspid Isthmus Block

Atrial Activation Sequence During Atrial Pacing

Complete bidirectional CTI block is demonstrated by pacing from the CS os and RA lateral wall and observing that sequential atrial activation terminates at the ablation line, on the contralateral side from the pacing site.

Normally, during atrial pacing at a CL of 600 milliseconds from the CS os, one wavefront propagates from the CS pacing site in a clockwise direction through the CTI to the low lateral RA. The other wavefront

from the CS os ascends up the atrial septum to the high RA in a counterclockwise direction, with resulting collision of wavefronts at the upper part of the lateral RA (the exact location of wavefront collision depends on the relative conduction velocities of the RA and the CTI) and generating an atrial activation sequence with a chevron pattern (Figs. 12.17 and 12.18).

Clockwise CTI block is indicated by the observation of a purely descending wavefront at the lateral wall down to the CTI (proximal-to-distal activation sequence on the Halo catheter positioned around the tricuspid annulus) when pacing from the CS os (i.e., pacing of the septal side of the ablation line). This block is associated with marked prolongation of the CTI conduction duration (i.e., the interval from the CS os to the low lateral RA; see Fig. 12.17). Incomplete clockwise CTI block is said to occur when a descending wavefront at the lateral RA wall still allows the lateral part of the CTI to be activated from the CS os in a clockwise direction across the CTI but at a slower conduction velocity, resulting in displacement of collision of the clockwise and

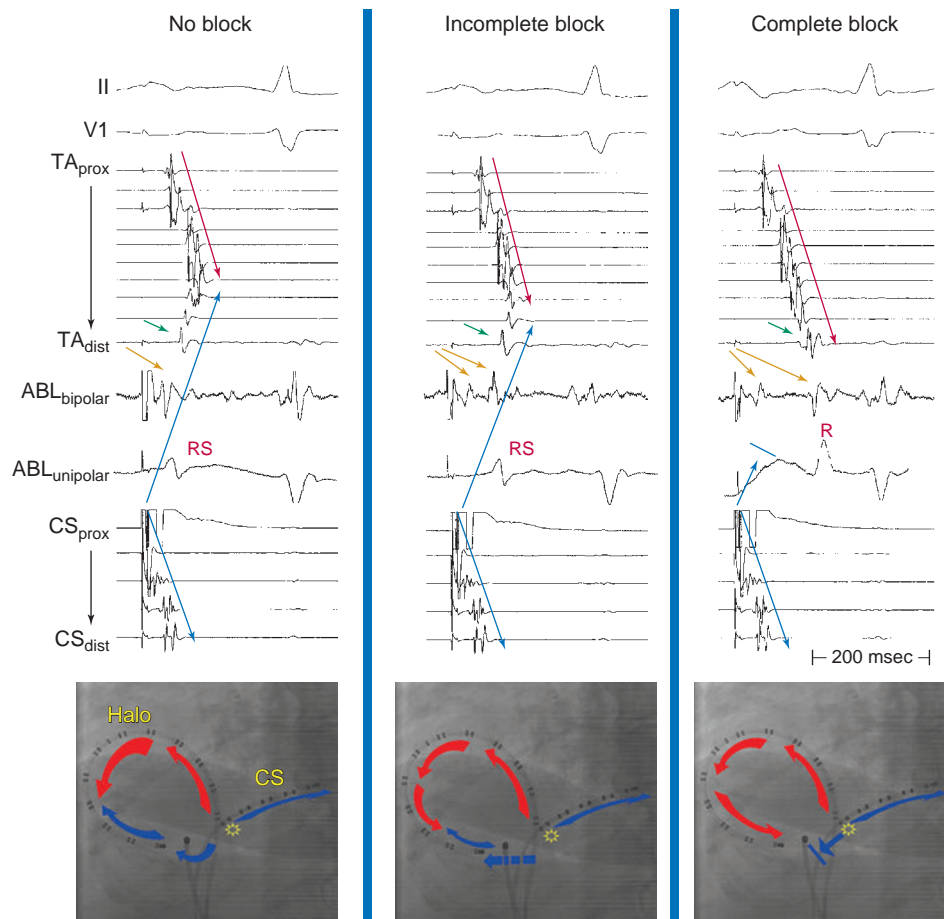


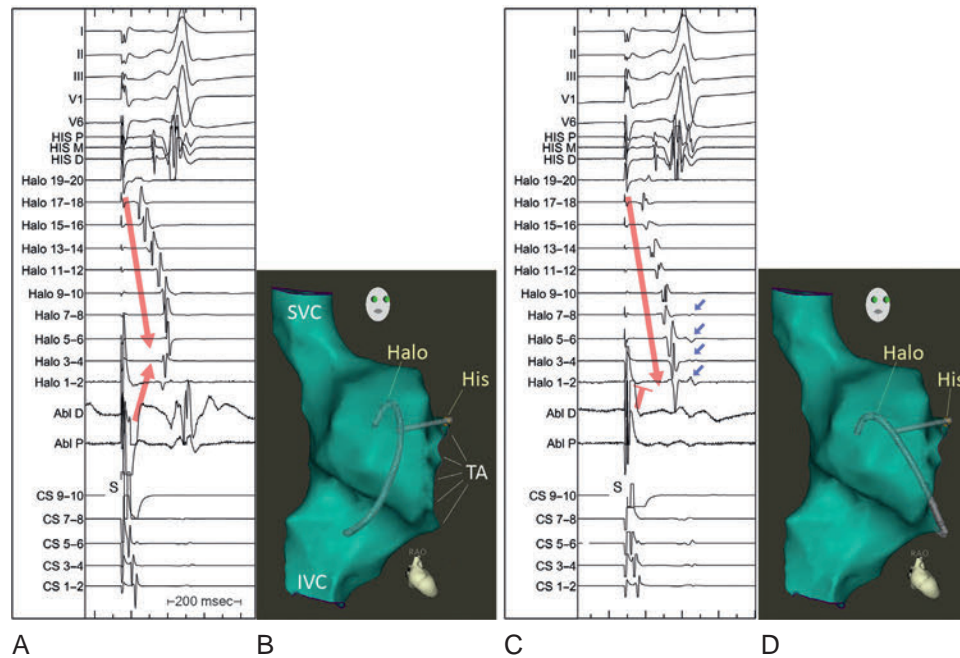
Fig. 12.17 The Use of Coronary Sinus (CS) Pacing to Verify the Presence of Clockwise Cavotricuspid Isthmus (CTI) Block. *Upper panels*, Intracardiac recordings from the right atrium (RA), CS, and CTI. *Lower panels*, Left anterior oblique fluoroscopic view illustrating the position of the ablation catheter at the CTI, and the Halo catheter around the tricuspid annulus (TA), with the distal end at the lateral end of the CTI. When CTI conduction is intact (*left panel*), pacing from the CS ostium results in the collision of activation wavefronts in the lateral RA wall (*red and blue arrows*). *Middle panel*, The collision point moves toward the low lateral RA wall when incomplete block is present. *Right panel*, Complete clockwise CTI block is indicated by the observation of a purely descending wavefront at the lateral wall down to the CTI (proximal-to-distal Halo sequence). The bipolar electrogram recording from the CTI initially shows a single atrial potential (*left panel*, *gold arrow*). With partial CTI ablation, the atrial electrogram splits into two closely adjacent potentials (*middle panel*, *gold arrows*). Complete CTI block is indicated by the observation of double potentials separated by an isoelectric interval (*right panel*, *gold arrows*). In addition, bipolar electrogram polarity reversal (*left panel*) is observed in the distal Halo and the distal ablation electrode recordings when complete block is achieved (as compared with before complete CTI block is achieved in the *right and middle panels*), thus indicating reversal of the direction of the activation wavefront lateral to the line of block (*green and gold arrows*). Positive (R wave) morphology of the unipolar recording lateral to the line of block also indicates complete CTI block (in contrast to biphasic [RS] electrogram morphology when intact conduction or only incomplete block is present). ABL, Ablation site; CS_{dist}, distal coronary sinus; CS_{prox}, proximal coronary sinus; TA_{dist}, distal tricuspid annulus; TA_{prox}, proximal tricuspid annulus.

counterclockwise wavefronts to the lower part of lateral RA. The distal bipole of the Halo catheter (Halo 1-2) at the lateral part of the CTI is activated slightly before or at the same time as bipole Halo 3-4, situated more laterally (see [Figs. 12.17](#) and [12.18](#)).

Importantly, the correct positioning of the Halo catheter at the tricuspid annulus (with the tip of the catheter immediately lateral to the CTI ablation line) is essential for reliable analysis of the activation sequence in the lateral RA and verification of CTI block. Migration of parts of the Halo catheter posterior to the crista terminalis or posterior to the eustachian ridge can suggest incomplete CTI block

(pseudo-conduction) when complete CTI is actually present ([eFig. 12.6](#), [Fig. 12.19](#)). When stable positioning the tip of the Halo catheter in close proximity to the ablation line proves to be difficult, the tip of the ablation catheter can be positioned immediately lateral to the ablation line to complement the recordings obtained by the Halo catheter.

It is also important to recognize that monitoring only the atrial activation sequence of the RA lateral wall recorded by the Halo catheter during CS pacing can lead to diagnostic errors in a significant proportion of patients. This is because of the inability to detect very slow



eFig. 12.6 Effect of Poor Halo Catheter Positioning on Electrograms. In (A), despite extensive ablation (*Abl*) in the cavotricuspid isthmus (CTI), it appears that activation is still proceeding through the CTI to activate Halo electrodes 1–4 directly (*red arrows*). In (B), the electroanatomic map shows that the Halo catheter is incorrectly positioned posteriorly in the right atrium, such that tip electrodes are behind the eustachian ridge and recording the posterior right atrium rather than the CTI position. In (C) and (D), after repositioning the catheter from its prior posterior location to a more tricuspid annular position as indicated by presence of small ventricular electrograms (*blue arrows*, C) and visualized on the electroanatomic map (D), Halo electrode activation now suggests CTI block. CS, Coronary sinus; IVC, inferior vena cava; SVC, superior vena cava; TA, tricuspid annulus.

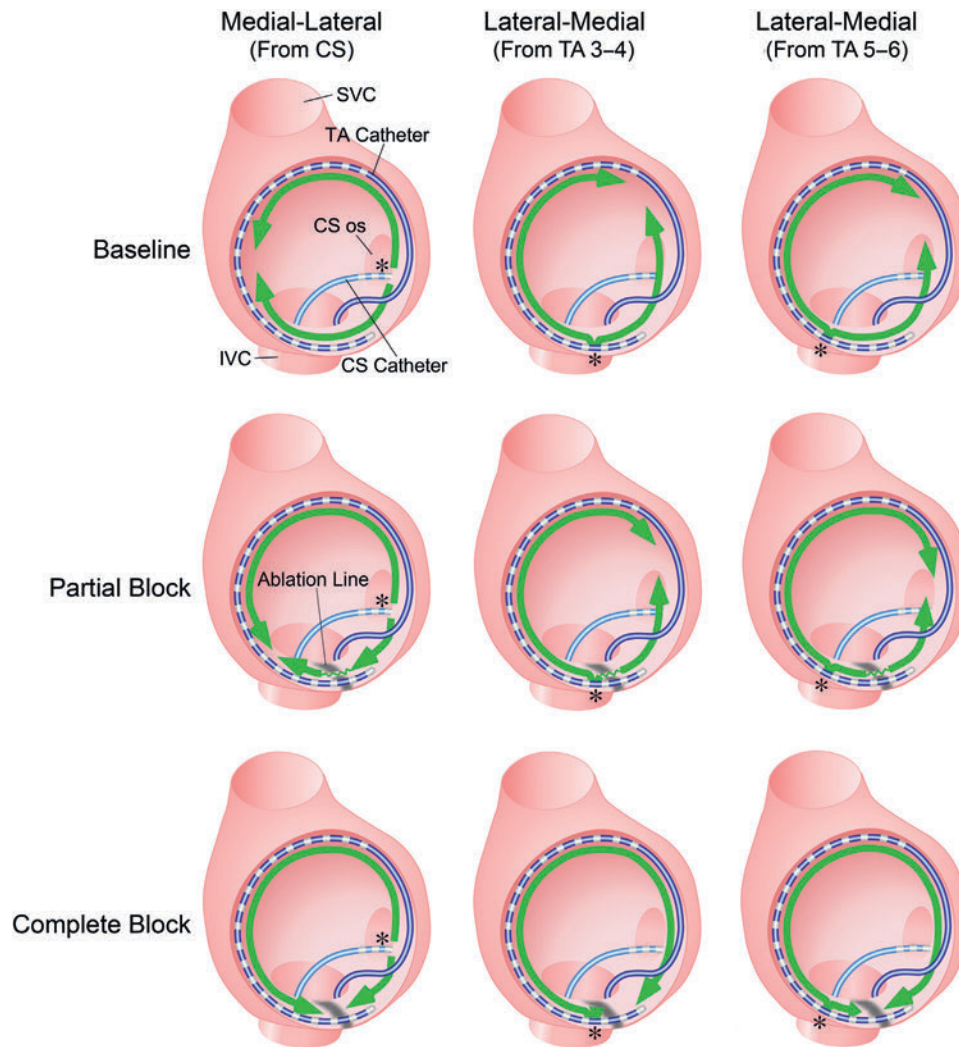


Fig. 12.18 Confirmation of Bidirectional Cavotricuspid Isthmus (CTI) Block Using Differential Pacing. Shown are figures of the right atrium, facing the tricuspid annulus (TA). A 20-pole electrode catheter is arrayed around the TA (dark blue), while another catheter is inside coronary sinus (CS, light blue). An asterisk (*) indicates stimulation site. Nine panels are shown, with pacing from the CS as well as two adjacent pairs of electrode on the TA catheter close to the CTI ablation line, in the baseline state (prior to ablation); in the setting of some ablation but with persistent slow conduction through the CTI; and finally with complete CTI block. Green arrows indicate directions of wavefront propagation from stimulation sites. IVC, Inferior vena cava; SVC, superior vena cava.

residual isthmus conduction that allows the wavefront propagating in an opposite direction to reach the ablation line before conduction through the isthmus is completed. Theoretically, slow but persistent isthmus conduction that can be confined within the ablation line or part of the isthmus distant from an area mapped by the multipolar catheter can therefore be misdiagnosed, no matter how closely the distal tip of the Halo catheter is placed to the ablation line, or even if the Halo catheter is positioned across the ablation line.

During low lateral RA pacing prior to ablation, the RA activation sequence (with intact counterclockwise CTI conduction) exhibits two ascending wavefronts (septal and lateral) leading to impulse collision at the high lateral wall. The caudocranial activation of the RA septum following counterclockwise propagation of the paced wavefront through the CTI results in atrial activation in the CS os preceding that in the HB region (Fig. 12.20, see also Fig. 12.18). Furthermore, intact conduction through the CTI permits the paced wavefront to proceed rapidly

to activate the LA from below (and CS activation propagates in a proximal-to-distal direction), thus giving rise to an inverted P wave in the inferior leads.

In contrast, during low lateral RA pacing, counterclockwise CTI block (or conduction delay) is indicated by the observation of a single ascending wavefront at the lateral wall (distal-to-proximal Halo sequence), followed by a completely descending wavefront at the septum to reach the CS os. Hence, compared with baseline, counterclockwise CTI block is associated with inversion of the direction of the septal activation from ascending to descending. Furthermore, the CS os electrogram is activated after the high RA and the HB region (see Figs. 12.18 and 12.20). In addition, counterclockwise conduction block in the CTI forces the wavefront to activate the LA from above via the Bachmann's bundle—and CS activation propagates in a distal-to-proximal direction—giving rise to a different P wave morphology, with the terminal portion positive in the inferior leads.

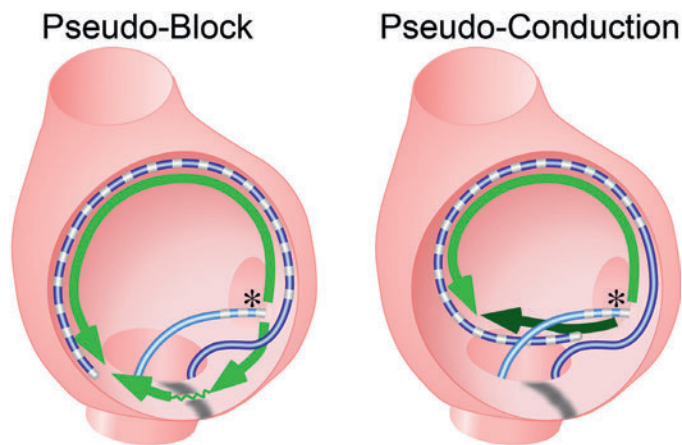


Fig. 12.19 Pseudo-Block and Pseudo-Conduction During Attempted Cavotricuspid Isthmus (CTI) Ablation. Shown are figures of the right atrium, facing the tricuspid annulus (TA) as shown. A 20-pole electrode catheter is arrayed around the TA (dark blue), while another catheter is inside coronary sinus (CS, light blue). An asterisk (*) indicates stimulation site. At left, the 20-pole TA catheter tip is far removed from the ablation line, where slow conduction can remain but not be evident since the wave front from the opposite direction reaches the distal TA electrodes first. This erroneously suggests the presence of CTI block, the solution for which is having recordings closer to the lateral aspect of the ablation line. At right, the TA catheter is positioned too posteriorly (not in CTI); a wave front of activation (dark green) can then proceed posterior to the inferior vena caval orifice to activate the distal TA electrodes first, suggesting persistent CTI conduction (when block is actually present). The solution for this is to position the TA catheter correctly.

Trans-Isthmus Conduction Interval

The trans-isthmus conduction interval is measured during CS os or low lateral RA pacing; it is equal to the interval from the stimulus artifact from one side of the isthmus to the atrial electrogram recorded on the contralateral side. Prolongation of this interval by more than 50% (or to an absolute value of 150 milliseconds or more) suggests CTI block (see Fig. 12.17). This criterion has sensitivity and negative predictive values of 100%. However, the specificity and positive predictive values are less than 90%.

Double Potentials

The demonstration of a continuous corridor of widely split double potentials recorded along the entire length of the ablation line confirms the presence of block. It is important to recognize that double potentials separated by long isoelectric intervals indicate “local block” under the recording catheter bipole, but they can be just adjacent to a conducting gap; therefore meticulous mapping of the entire length of the CTI ablation line is necessary to verify the presence of complete CTI block and to exclude the presence of gaps along the ablation line.⁴⁹

During atrial pacing from either side of the CTI (CS os or low lateral RA), the presence of continuous corridor of widely split double potentials (separated by a peak-to-peak interval of 110 milliseconds or more) along the entire CTI ablation line is the most accurate available indicator of complete CTI block, and generally considered the gold standard for determining complete bidirectional block (see Fig. 12.17). On the other hand, when the interval separating the double potentials is less than 90 milliseconds at any point along the ablation line, complete isthmus block is not confirmed, and the search for persistent conduction through a gap should be carried out. When there is a gap in a line of block, the

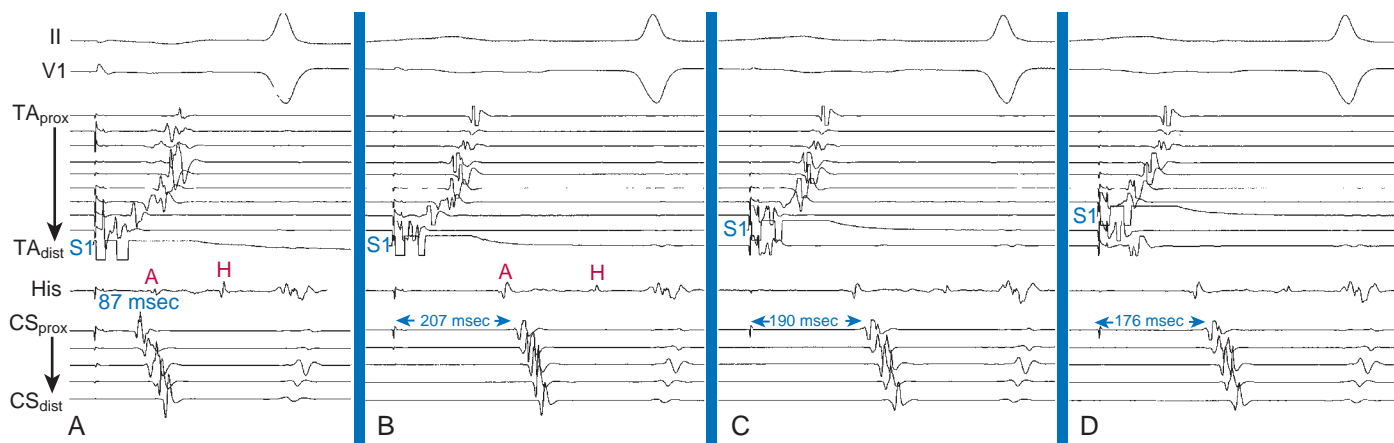


Fig. 12.20 The Use of Differential Pacing From the Lateral Right Atrial (RA) Wall to Verify the Presence of Counterclockwise Cavotricuspid Isthmus (CTI) Block. (A) Pacing from the lateral aspect of the CTI (Halo 1,2) before CTI ablation. (B to D) Pacing from different lateral RA sites along the Halo catheter after CTI ablation (B) pacing from Halo 3,4; (C) pacing from Halo 5,6; (D) pacing from Halo 7,8. When CTI conduction is intact, coronary sinus ostium (CS os) activation occurs via a counterclockwise wavefront across the CTI, and because the CS os is anatomically closer to the pacing site than the His bundle (HB), atrial activation in the CS os electrode precedes that in the HB electrode. In the presence of counterclockwise CTI block, CS os activation occurs via the wavefront propagating in a clockwise direction up the RA lateral wall, over the RA roof, and then down the septum. Consequently, CS os activation (as measured by the stimulus-to-local electrogram interval) occurs progressively earlier during pacing from more cephalic sites along the lateral RA wall (B to D). In addition, activation of the CS os occurs after the high RA and the HB region. CS_{dist}, Distal coronary sinus; CS_{prox}, proximal coronary sinus; TA_{dist}, distal tricuspid annulus; TA_{prox}, proximal tricuspid annulus.

isoelectric interval between the double potentials shortens the closer the electrograms are to the gap. At the gap, in the line of block, double potentials are no longer present, and the electrogram is typically long and fractionated, but can also be discrete. Those gaps are then targeted by additional ablation until complete CTI block is achieved.

This technique requires meticulous mapping of the CTI, and is probably more difficult to perform than the classic activation mapping technique, mainly because of the ambiguity of electrogram interpretation (e.g., multiple, low amplitude, or fragmented potentials) along the ablation line, especially after extensive ablation attempt or broad or nonlinear ablation of the CTI. When double potentials cannot be visualized, the interval between the pair of electrograms immediately on either side of the line of block (the DP + 1 interval), when pacing immediately medial and lateral to the line of block, can be used as an alternative method for verifying complete bidirectional CTI block. This technique requires positioning of a duodecapolar catheter around the tricuspid annulus while extending the catheter tip inside the CS, so that the catheter straddles the CTI and provides recording and pacing from the medial and lateral aspects of the isthmus. The DP + 1 interval cutoff of 140 milliseconds seems to have better or equal sensitivity, specificity, and positive predictive values as compared to other criteria for confirming the presence of CTI block. Nevertheless, it is still very difficult to distinguish incomplete block with very slow conduction from complete isthmus block. In addition, gaps along the ablation line

remote from the duodecapolar catheter would result in a DP + 1 interval that is long in the absence of complete CTI block.⁵²

Differential Pacing

This technique is used to verify whether the double potentials recorded at the ablation line are secondary to complete line of block or the result of slow conduction across the ablation line. Fixed-rate pacing is performed from the low lateral and midlateral RA. With intact CTI conduction, both components of the recorded electrogram (the double potentials) are the result of sequential activation by the same paced wavefront propagating in a counterclockwise direction across the CTI (the two components are linked to the same counterclockwise wavefront). Therefore withdrawal of the pacing site farther away from the ablation line (from low lateral RA to midlateral RA) causes a similar degree of delay of the timing of both components of the electrogram (relative to the pacing stimulus), so that the interval between the double potentials remains constant (Fig. 12.21).

On the other hand, when complete CTI block is present, the first component of the double potentials (at the lateral aspect of the ablation line) reflects activation by the paced wavefront traveling counterclockwise from the nearby pacing site, whereas the second component of the double potential (at the medial aspect of the ablation line) is the result of activation by the wavefront traveling in the opposite direction (clockwise) around the tricuspid annulus. Hence the two components

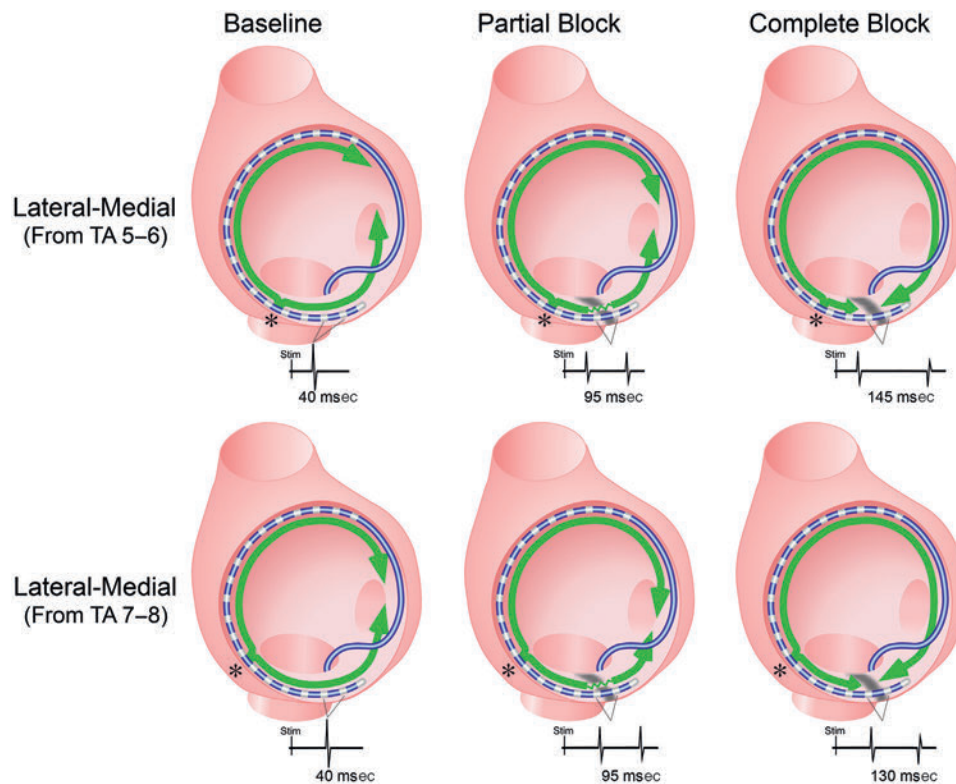


Fig. 12.21 Confirmation of Bidirectional Cavotricuspid Isthmus (CTI) Block Using Distance Between Double Potentials in the Region of the Ablation Line. Shown are figures of the right atrium, facing the tricuspid annulus (TA) as shown. A 20-pole electrode catheter is arrayed around the TA (dark blue). An asterisk (*) indicates stimulation site. At top, wavefronts of activation are shown in three different states (baseline, with partial CTI block, and complete CTI block) when pacing from electrodes 5 and 6; bottom panels show similar findings with pacing from electrodes 7 and 8. As can be seen, split potentials develop during partial ablation, and have the same spacing (95 milliseconds) regardless of which electrodes are paced (although the timing from stimulus to the first of the split potentials occurs later when pacing from a more lateral site). With complete block, the separation of split potentials is widest when pacing closer to the ablation line.

are not linked to a single wavefront; rather they can be dissociated from each other by changing the activation wavefront. As a consequence, withdrawal of the pacing site farther away from the ablation line (from low lateral RA to midlateral RA) results in a delay of the first component of the double potentials, but the second component of the double potentials becomes activated earlier (hence separation of double potentials decreases), since the length of the detour the clockwise wavefront has to travel is shortened by the new (midlateral RA) site of pacing (eFig. 12.7).

Using a similar principle, the local activation time at the CS os electrode during fixed-rate pacing performed from the low lateral and midlateral RA can be used for evaluation of counterclockwise CTI block. Normally (with intact isthmus conduction) CS os activation occurs via propagation of the paced wavefront across the CTI in a counterclockwise direction. Therefore CS os activation occurs earlier during pacing from the low lateral RA compared with the midlateral RA because the low lateral RA is anatomically closer to the CS os. In contrast, when counterclockwise CTI block is present, CS os activation occurs via the wavefront propagating in a clockwise direction around the tricuspid annulus (see Figs. 12.18 and 12.20). Consequently, CS os activation occurs earlier during pacing from the midlateral compared with the low lateral RA, because the length of the detour is shortened by pacing from the midlateral RA.

Incremental Pacing

Incomplete block can be associated with very slow conduction across the CTI, mimicking the activation pattern related to complete block. The incremental pacing maneuver helps distinguish isthmus block from long local conduction delay across the isthmus based on the observation that residual CTI conduction is usually decremental and is worsened at faster pacing rates.

Initially the mapping catheter is used to record double potentials along the CTI ablation line. The catheter is then placed at the site registering the maximum separation between the two potentials (as measured by the “peak-to-peak” distance between them). Then, incremental pacing is performed at either side of the CTI (CS os and the low lateral RA) at PCLs of 600 and 300 milliseconds, and the maximal separation between the double potentials is measured at each PCL.⁵⁵

Minimal (less than 20 milliseconds) variation in the distance between the double potentials in response to progressively faster (from 600 milliseconds to 300 milliseconds) pacing is consistent with complete block across the ablation line. Such observation during CS os pacing indicates complete clockwise isthmus block, and during low lateral RA pacing indicates counterclockwise complete CTI conduction block. On the other hand, prolongation of the interval between separating the double potentials by more than 20 milliseconds at the faster pacing rate suggests persistent residual conduction across the isthmus or CTI functional block.^{55,56}

A variation of this technique evaluates the effect of incremental pacing from the low lateral RA on the interval between atrial activation of the HB region and that at the CS os (His-to-CS os interval). The lack of increase in His-to-CS os atrial interval (variation of less than 10 milliseconds) in response during incremental pacing from the low lateral RA is consistent with complete counterclockwise CTI block, whereas a more than 10 millisecond increase of the His-to-CS os atrial interval with incremental pacing suggests slow conduction and functional block across the CTI. An advantage of the incremental His-to-CS os maneuver is that it does not require the identification of double potentials along the CTI ablation line, which can occasionally be difficult to record.⁵⁷

Another variation employs the effect of incremental pacing from the CS os on atrial activation sequence in the low lateral RA to evaluate

clockwise CTI block. With incomplete CTI block, activation of the low lateral RA during CS os pacing can be delayed, but activation can still occur via the CTI (in a clockwise direction) at the same time or just earlier than the wavefront traveling to the low lateral RA from the counterclockwise direction around the tricuspid annulus. Increasing the pacing rate results in decremental conduction across the now diseased isthmus and causes further delay in activation of the low lateral RA (eFig. 12.8). In contrast, when complete CTI block is present, the lateral RA is activated in a counterclockwise direction across the atrial septum and RA roof. Because these atrial regions conduct nondecrementally, pacing at faster rates should not change the timing of low lateral RA activation significantly, as long as the PCL is longer than atrial refractoriness.

Unipolar Electrogram Morphology

The morphology of the unfiltered unipolar recording indicates the direction of wavefront propagation. Positive deflections (R waves) are generated by propagation toward the recording electrode; negative deflections (QS complexes) are generated by propagation away from the electrode. Conduction along the longitudinal axis of the fibers in cardiac muscle produces a characteristic biphasic (RS or rS) unipolar electrogram. In contrast, positive uniphasic (R) unipolar electrograms are characteristic of the end of propagation of the activation wavefront. Uniphasic (R) unipolar electrograms can also be observed at the point of collision of two wavefronts, and negative waveforms (QS) are recorded in the vicinity of the site of excitation onset.

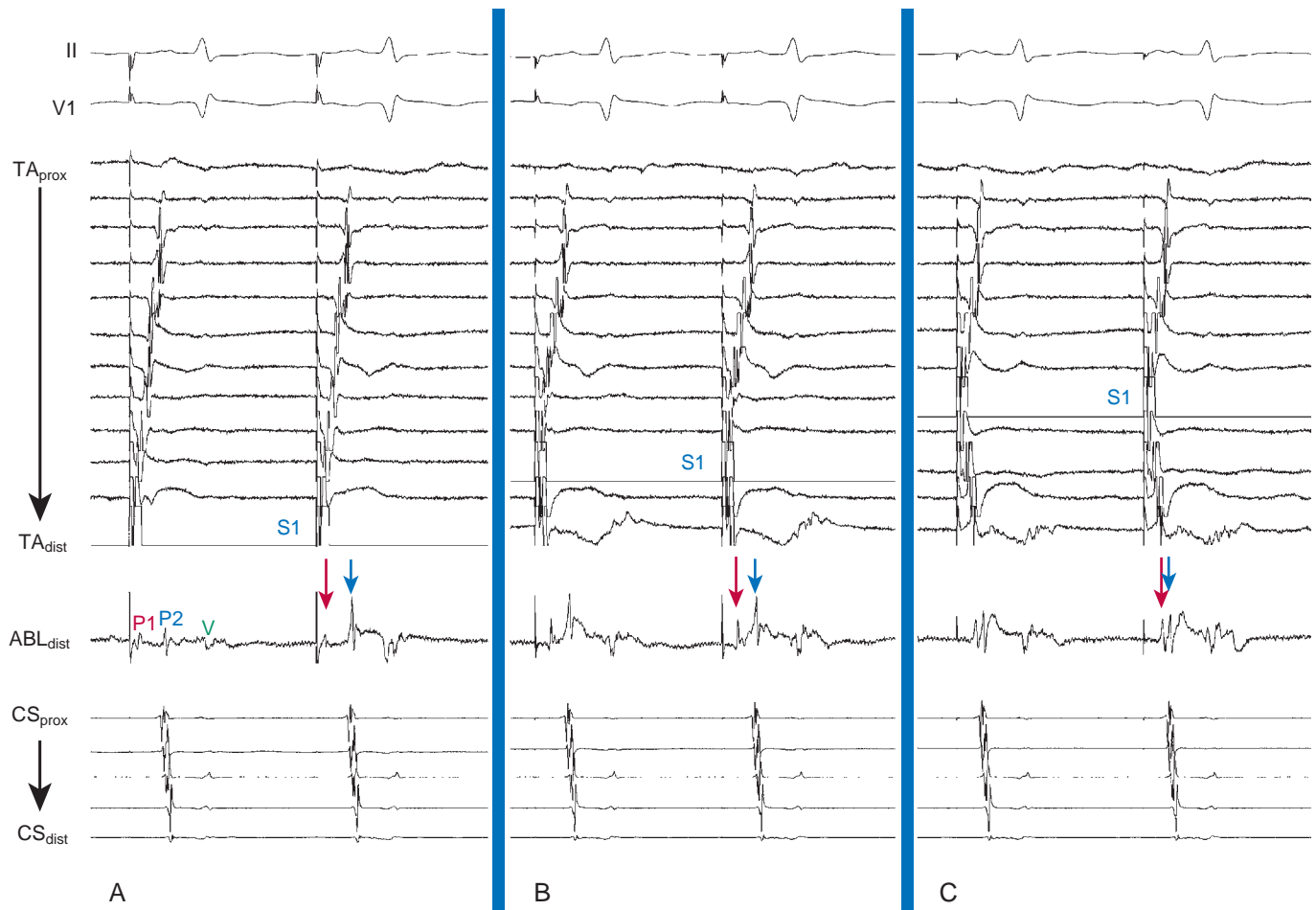
With intact CTI conduction (before ablation), pacing from either side of the CTI results in an RS, rS, or QS pattern on the opposite side of the CTI. A terminal S wave in the unipolar electrogram is expected, because the propagated wavefront propagates through the CTI and moves away from the mapping electrode. In addition, because atrial depolarization along the CTI occurs sequentially in the same direction, the polarity of the initial depolarization is the same from each pair of recording electrodes when using unfiltered unipolar recording on the CTI. A similar pattern is also observed in the presence of incomplete CTI block (after failed CTI ablation). Because unipolar electrograms record relatively distant activity, they are able to detect slow conduction through the CTI independently of the location of the gap, since the wavefront crossing the CTI (sometimes with a prolonged conduction time) has to pass through the mapping electrode, generating a propagation wavefront that moves away from the recording site and hence a terminal S wave.^{58,59}

After CTI block is achieved, the paced wavefront has to travel around the tricuspid annulus before it reaches the mapping electrode, located at the contralateral side of the line of block. Therefore a clear change in the unipolar electrogram is expected (from QS, rS, or RS to R or Rs) because the wavefront now ends at or close to the exploring electrode (see Fig. 12.17). The relative voltage of the R wave is likely to depend on the amount of tissue that depolarizes within the CTI, as well as the distance of the recording electrode from this area.^{58,59}

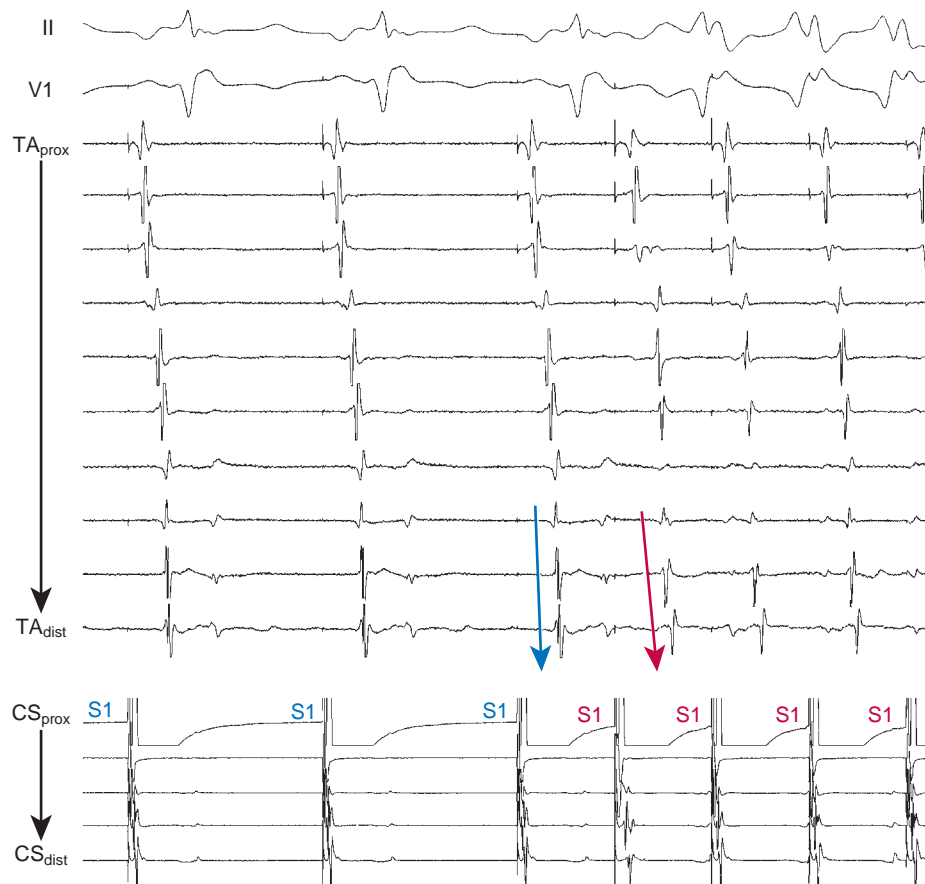
Importantly, to observe the expected change in the morphology of unipolar electrograms, the exploring catheter should be located in close proximity to the line of block. If the exploring catheter is separated from the line of block, activation of the area of tissue between the exploring electrode and the line of block can potentially generate an S wave of sufficient voltage to result in an RS unipolar electrogram.⁵⁸

Bipolar Electrogram Polarity

Bipolar recordings predominantly reflect local activation time; signal subtraction used to create a bipolar signal largely eliminates morphology information at either electrode. Nonetheless, the polarity of the bipolar electrogram is sensitive to the direction of wavefront propagation from



eFig. 12.7 Differential Pacing for Verification of Complete Line of Block. Fixed-rate pacing (S1) is performed from the at lateral aspect of the CT1 (A), low lateral RA (B), and midlateral RA (C) via the Halo catheter placed around the tricuspid annulus with the distal tip (TA_{dist}) positioned just lateral to the CTI. Double potentials (P1 and P2) are recorded on the distal ablation electrode (ABL_{dist}) positioned at the CTI ablation line. Withdrawal of the pacing site farther away from the ablation line (from panel A to B to C) results in a delay of the first component (P1, red arrows) of the double potentials, but the second component (P2, blue arrows) of the double potentials becomes activated earlier (hence separation of double potentials decreases). This is consistent with counterclockwise block across the CTI ablation line, whereby the first component of the double potentials (at the lateral aspect of the ablation line) reflects activation by the paced wavefront traveling counterclockwise from the nearby pacing site; while the second component of the double potential (at the medial aspect of the ablation line) is the result of activation by the wavefront traveling in the opposite direction (clockwise) around the tricuspid annulus. CS_{dist}, Distal coronary sinus; CS_{prox}, proximal coronary sinus; TA_{prox}, proximal tricuspid annulus; V, ventricular electrogram.



eFig. 12.8 Surface Electrocardiogram and Intracardiac Recordings Following Incomplete Ablation of the Cavotricuspid Isthmus (CTI). The activation sequence around the tricuspid annulus during coronary sinus pacing at a cycle length of 600 milliseconds (*blue S1*) suggests block in the CTI (*blue arrow*); however, pacing at a shorter cycle length (300 milliseconds, *red S1*) causes more delay of activation timing (*red arrow*) of the most distal tricuspid annulus electrodes (at the lateral aspect of the CTI) and thus reveals that conduction had been present in the CTI at the slower paced rate. CS_{dist}, Distal coronary sinus; CS_{prox}, proximal coronary sinus; TA_{dist}, distal tricuspid annulus; TA_{prox}, proximal tricuspid annulus.

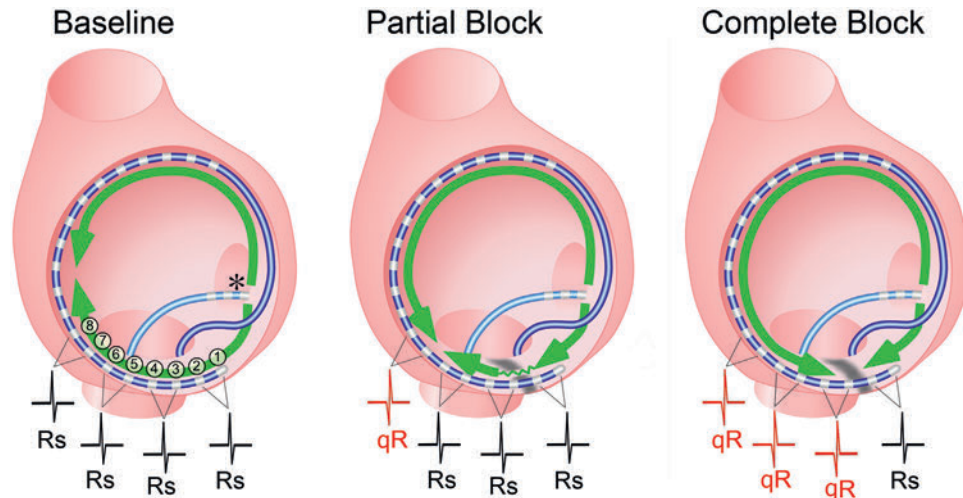


Fig. 12.22 Confirmation of Bidirectional Cavotricuspid Isthmus (CTI) Block Using Change in Bipolar Electrogram Polarity on Opposite Sides of the Ablation Line. Shown are figures of the right atrium, facing the tricuspid annulus (TA) as shown. A 20-pole electrode catheter is arrayed around the TA (dark blue), while another catheter is inside coronary sinus (CS, light blue). An asterisk (*) indicates stimulation site. Individual electrodes on the TA catheter are numbered. The baseline state, pacing from the CS shows the propagation from distal to proximal (electrodes 1–8) on the TA catheter. Each bipolar electrogram has an “Rs” configuration. After some ablation, but with residual conduction through the CTI, electrograms indicating trepidation in the same direction as in the prior panel remain “Rs,” while at electrodes 7–8, trepidation is in the opposite direction, yielding a “qR” configuration. At right, with complete CTI block, propagation has been reversed and electrodes 3–8, each pair of which now shows a qR pattern.

the distal to the proximal poles (cathode to anode). Reversal of the bipolar electrogram polarity can indicate a reversed wavefront direction. This characteristic can be used for verification of the presence of CTI block. A multipolar Halo catheter with short (2 mm) interelectrode spacing is used to map the isthmus. Bipolar electrograms are recorded with the distal electrode serving as the cathode. During CS os pacing, the activation wavefront propagates in a clockwise direction across the CTI, resulting in positive electrogram polarity at the Halo bipole positioned just lateral to an ablation line and parallel to the inferior aspect of the tricuspid annulus. Once complete CTI block is achieved, distal Halo bipole is activated only from the counterclockwise direction, resulting in reversal of electrogram polarity from positive to negative during CS os pacing (Fig. 12.22, see also Fig. 12.17). Importantly, the use of changes in electrogram polarity as an accurate indicator of complete isthmus block requires that the recording electrodes be positioned parallel to the direction of the depolarization wavefronts in the isthmus. If the orientation of the electrodes is somewhat oblique to the direction of the depolarization wavefront, or if the depolarization wavefront progresses across the isthmus in a fashion that is not entirely linear, the initial polarity of an electrogram recorded in the isthmus may not be in the same direction as the predominant polarity of the electrogram.

Electroanatomic Mapping

Electroanatomic 3-D activation mapping can be used to verify CTI block. When clockwise block in the CTI is achieved, proximal CS pacing results in an activation wavefront propagating in a counterclockwise fashion, with the latest activation in the CTI immediately lateral to the ablation line (eFig. 12.9). When conduction across the CTI is still intact, CS pacing produces an activation wavefront that propagates rapidly through the CTI, with the anterolateral RA wall activated last. Similar maps can be generated during low lateral RA pacing to confirm counterclockwise block in the CTI. Activation maps can also be evaluated for the presence of gaps in the ablation lines, as indicated by the early

breakthroughs from the ablation line (Fig. 12.23). However, following CTI ablation, the local electrograms at the ablation line can be complex—with double, triple, or fragmented potentials and unclear local activation time—and electroanatomic activation mapping can be challenging.

Outcome

The inability to create complete CTI block and successfully eliminate typical AFL is unusual in contemporary practice. In a meta-analysis of 158 studies, the overall acute success rate for AFL ablation was 93% for large-tip (8 to 10 mm) or irrigated ablation catheters, and 88% for 4- to 6-mm tip catheters. AFL recurrence rates were significantly reduced by use of large tip or irrigated catheters (7% vs. 14%) and by use of bidirectional CTI block as a procedural endpoint (9% vs. 24%).⁶⁰

For patients in whom typical AFL recurs after ablation, conduction through the CTI is usually responsible. Presumably, such recurrences reflect a failure to achieve bidirectional CTI block during the initial procedure, incorrect initial assessment of bidirectional block, or resumption of conduction across an initially blocked isthmus. The use of the more stringent endpoint of bidirectional CTI block significantly reduces the AFL recurrence rate. The incidence of AFL recurrence does not increase beyond 1 to 6 months of follow-up, a finding suggesting that if recovery of isthmus conduction is going to occur, it will have done so by 6 months.⁶⁰

The overall incidence of complications associated with AFL ablation is 3.2%. The most common are cardiovascular complications. Serious complications are rare (0.4%) and include AV block (most common, 0.2%), cardiac tamponade, transient inferior ST segment elevation or acute occlusion of the right coronary artery, and thromboembolic complications.^{60–62}

Following AFL ablation, AF can develop in approximately 20% to 30% (with short-term follow-up, approximately 1 year) and in up to 82% (with long-term follow-up, approximately 4 years) of patients with or without a prior history of AF. It appears that AFL is often an early

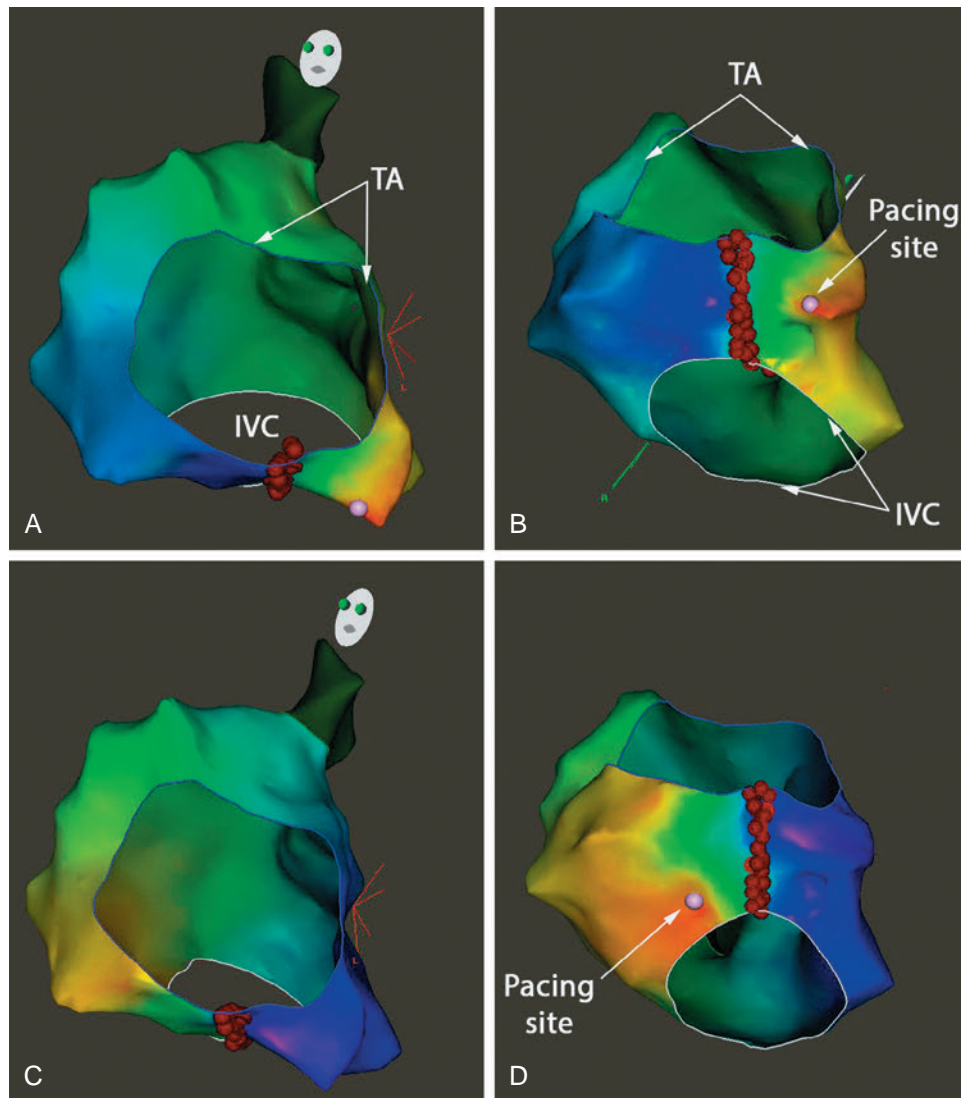


Fig. 12.9 Electroanatomic Mapping for Verification of Cavotricuspid Isthmus (CTI) Block. Left anterior oblique (A and C) and inferior (B and D) views of three-dimensional electroanatomic (CARTO) activation map of the right atrium during atrial pacing. (A and B) During pacing at a site (white dot) medial to the CTI ablation line, complete CTI block in the clockwise direction is indicated by the absence of activation proceeding through the ablation line (red dots); progression of color (from red to purple) indicates that activation of the entire tricuspid annulus (TA) remains counterclockwise, except for the small portion that is situated between the pacing site and the line of block. (C and D) During pacing at a site lateral to the CTI ablation line, complete CTI block in the counterclockwise direction is indicated by the absence of activation proceeding through the ablation line (red dots) and activation of the entire TA in a clockwise direction. IVC, Inferior vena cava.

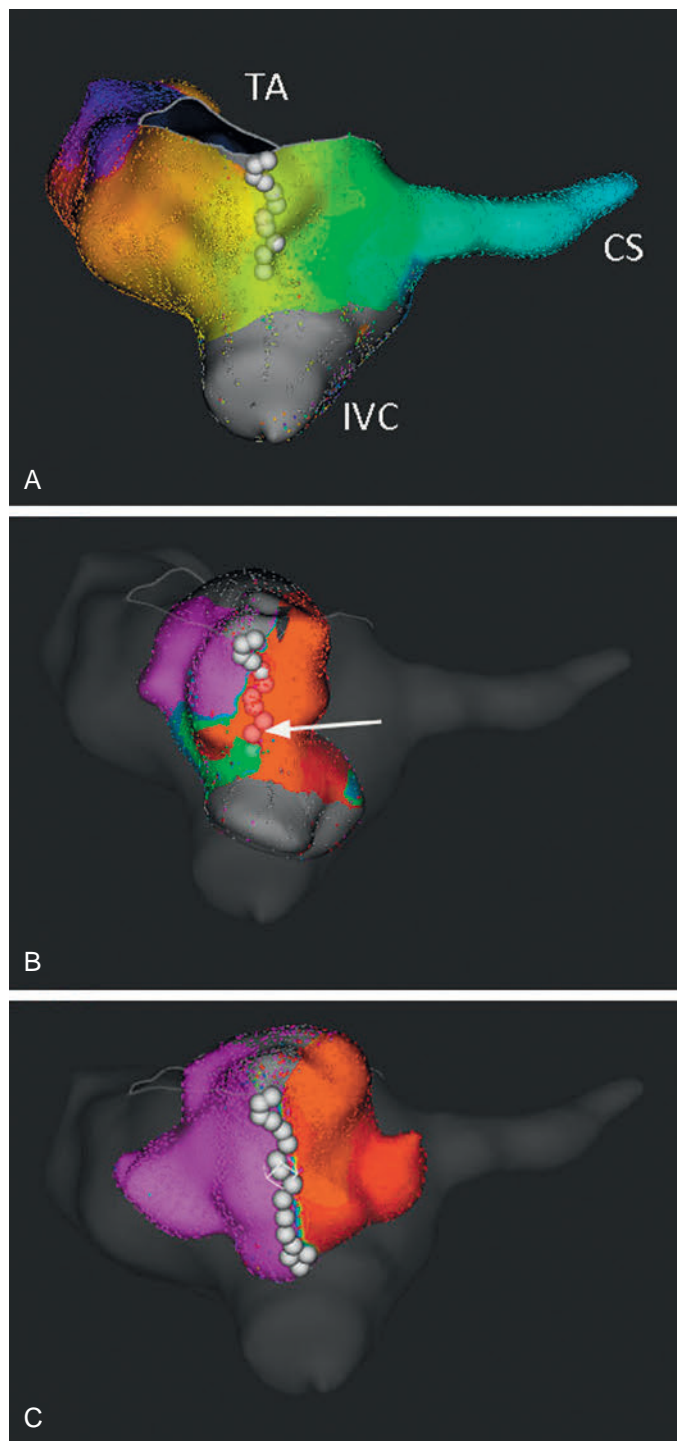


Fig. 12.23 Electroanatomic Mapping of Gaps in the Cavotricuspid Isthmus (CTI) Ablation Line. Inferior views of three-dimension electroanatomic (Rhythmia) activation map of the right atrium and CTI. (A) Activation map is acquired during counterclockwise typical atrial flutter (AFL). Radiofrequency (RF) ablation (*white dots*) across the CTI resulted in termination of AFL. (B) Activation map is acquired during atrial pacing at medial (septal) aspect of the CTI ablation line. An early breakthrough activation (*arrow*) is visualized, indicating a gap in the ablation line. (C) Additional RF ablation is performed at the gap, and activation remapping is performed during pacing at the medial aspect of the CTI ablation line; complete CTI block in the counterclockwise direction is indicated by the absence of activation proceeding through the ablation line. CS, Coronary sinus; IVC, inferior vena cava; TA, tricuspid annulus.

marker of atrial electrical disease that frequently progresses to AF even after curative treatment for AFL. It is well established that CTI is not the cause of typical AFL, and while ablation of the CTI eliminates the AFL, it does not modify atrial remodeling and other pathogenic factors that predisposed to the development of AFL. Hence it should not be surprising that the persistence of those pathogenic factors, which are shared by both AF and AFL, would eventually precipitate AF.

In a meta-analysis, over an average follow-up of 16 months, AF occurred in 23% of patients with no preablation history of AF and in 53% of patients with a history of AF, despite successful AFL ablation. The incidence of AF increased over time in both groups; however, 5 years after ablation, the incidence of AF was similar in those with and without AF before ablation. Antiarrhythmic drug use after ablation was 32%. The long-term use of oral anticoagulation was 66%.⁶⁰ This finding has serious implications for patient selection, long-term arrhythmia-free success rates, postprocedure antiarrhythmic drug use, and long-term anticoagulation. Because AF predating ablation of AFL is very likely to recur, thus limiting the ability to discontinue antiarrhythmic medications or anticoagulation in many patients, the potential benefits of ablation of only AFL should be seriously scrutinized. Nevertheless, since AFL is frequently associated with faster ventricular rates than can be more difficult to control, and hence more severe symptoms than the episodes of AF, catheter ablation of AFL can offer symptomatic relief and improved quality of life in a portion of patients with both AF and AFL, when the AFL is the dominant and more clinically significant arrhythmia. Furthermore, a recent retrospective study found that patients with AFL undergoing CTI ablation (37% also had a history of AF) had a lower risk of systemic thromboembolic events and overall mortality, whether or not a history of AF is present.⁶³

VIDEOS

The following videos accompany this chapter:

See Video 6-6. Typical Atrial Flutter: Rhythmia Batrial Propagation Maps

See Video 6-7. Clockwise and Counterclockwise Typical Atrial Flutter: Rhythmia and CARTO Activation and Propagation Maps

See Video 6-8. Typical Atrial Flutter: EnSite Precision Activation, Voltage, and Propagation Maps

See Video 6-17. Typical Atrial Flutter: Noncontact Mapping

See Video 11-4. Focal Atrial Tachycardia (originating from the lateral aspect of the cavotricuspid isthmus): CARTO Activation and Propagation Maps

Video 12-1. Ablation of the Cavotricuspid Isthmus Guided by Fluoroscopy

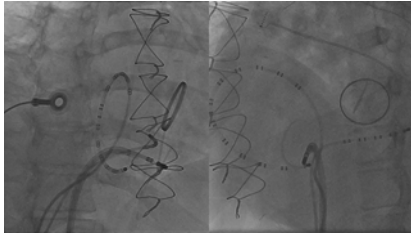
Video 12-2. Confirmation of Conduction Block Across the Cavotricuspid Isthmus: CARTO Mapping During Atrial Pacing

Video 12-3. Catheter Ablation of the Cavotricuspid Isthmus: Guided by Rhythmia Mapping System

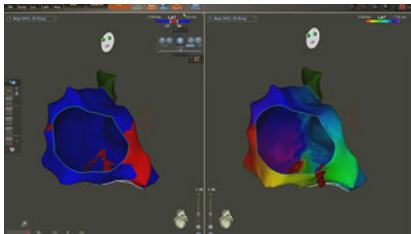
Video 12-4. Catheter Ablation of the Cavotricuspid Isthmus: Mapping Gaps in the Ablation Line

REFERENCES

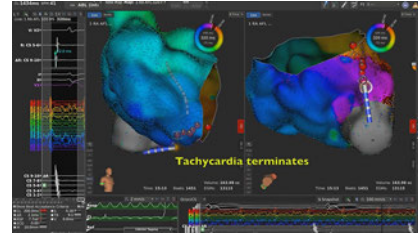
1. Saoudi N, et al. Classification of atrial flutter and regular atrial tachycardia according to electrophysiologic mechanism and anatomic bases: a statement from a joint expert group from the Working Group of Arrhythmias of the European Society of Cardiology and the North American Society of Pacing and Electrophysiology. *J Cardiovasc Electrophysiol.* 2001;12:852–866.
2. Bun SS, Latcu DG, Marchlinski F, et al. Atrial flutter: more than just one of a kind. *Eur Heart J.* 2015;36:2356–2363.



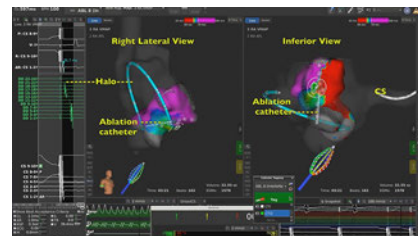
Video 12.1. Ablation of the Cavotricuspid Isthmus Guided by Fluoroscopy. Fluoroscopic images are shown in the RAO and LAO projections during catheter ablation of the CTI in a patient with previous mechanical mitral valve replacement and tricuspid annuloplasty. A multipolar (“halo”) catheter is positioned around the tricuspid annulus and a decapolar catheter in the CS. The ablation catheter is advanced to the right ventricle under fluoroscopy (RAO view); the tip is deflected to achieve contact with the RV inferior wall and withdrawn progressively until the electrogram shows small atrial and large ventricular electrograms. The distal tip of the ablation catheter is then adjusted under fluoroscopy on the CTI in the LAO view until it is midway between the atrial septum and right atrial lateral wall (pointing toward 6 o’clock in a 60-degree LAO view). The catheter is then dragged across the CTI until it reaches the inferior vena cava (as evidenced by drop of the catheter tip at the end of the movie). A preshaped guiding sheath (ramp sheath) is used in this case to help extend the reach of the catheter tip and stabilize its position on the CTI. *AbI*, Ablation catheter; *CS*, coronary sinus; *CTI*, cavotricuspid isthmus; *LAO*, left anterior oblique; *MA*, mitral annulus; *RAO*, right anterior oblique; *TA*, tricuspid annulus.



Video 12.2 Confirmation of Conduction Block Across the Cavotricuspid Isthmus: CARTO Mapping During Atrial Pacing. Electroanatomic (CARTO 3) activation and propagation maps of the right atrium during typical counterclockwise atrial flutter and during atrial pacing after successful ablation of the cavotricuspid isthmus (CTI). Activation mapping is performed during pacing at the medial and then the lateral aspects of the CTI ablation line to confirm presence of complete bidirectional isthmus block. During pacing at a site medial to the CTI ablation line, complete CTI block in the clockwise direction is indicated by the absence of activation proceeding through the ablation line; progression of color (from red to purple) indicates that activation of the entire tricuspid annulus (TA) remains counterclockwise, except for the small portion that is situated between the pacing site and the line of block. During pacing at a site lateral to the CTI ablation line, complete CTI block in the counterclockwise direction is indicated by the absence of activation proceeding through the ablation line and activation of the entire TA in a clockwise direction. *IVC*, Inferior vena cava; *SVC*, superior vena cava.



Video 12.3. Catheter Ablation of the Cavotricuspid Isthmus. Guided by Rhythmia Mapping System. Electroanatomic (Rhythmia) activation and propagation maps of the right atrium is performed during typical counterclockwise atrial flutter. Then, radiofrequency (RF) ablation of the cavotricuspid isthmus (CTI) is performed and results in tachycardia termination. Note that the flutter terminates before complete isthmus ablation. *SVC*, Superior vena cava; *TA*, tricuspid annulus.



Video 12.4. Catheter Ablation of the Cavotricuspid Isthmus. Mapping gaps in the ablation line. Electroanatomic (Rhythmia) activation and propagation maps of the right atrium is performed during typical counterclockwise atrial flutter. Radiofrequency (RF) ablation of the cavotricuspid isthmus (CTI) is performed and successfully terminated the tachycardia. Electroanatomic activation mapping on both sides of the ablation line is performed (using the mini-basket catheter) during atrial pacing to confirm the presence of complete CTI block. Initially, during pacing from the proximal coronary sinus (CS), activation mapping revealed a conduction gap in the CTI ablation line. Additional RF ablation at the gap is performed and repeat activation mapping reveals complete block across the CTI ablation line. *IVC*, Inferior vena cava; *SVC*, superior vena cava; *TA*, tricuspid annulus.

3. Asirvatham SJ. Correlative anatomy and electrophysiology for the interventional electrophysiologist: right atrial flutter. *J Cardiovasc Electrophysiol.* 2009;20:113–122.
4. Faletta FF, Ho SY, Auricchio A. Anatomy of right atrial structures by real-time 3D transesophageal echocardiography. *JACC Cardiovasc Imaging.* 2010;3:966–975.
5. Tai C-T, Chen S-A. Cavotricuspid isthmus: anatomy, electrophysiology, and long-term outcome of radiofrequency ablation. *Pacing Clin Electrophysiol.* 2009;32:1591–1595.
6. Saremi F, et al. Right atrial cavotricuspid isthmus: anatomic characterization with multi-detector row CT. *Radiology.* 2008;247:658–668.
7. Gami AS, et al. Electrophysiological anatomy of typical atrial flutter: the posterior boundary and causes for difficulty with ablation. *J Cardiovasc Electrophysiol.* 2010;21:144–149.
8. Anselme F. Macroreentrant atrial tachycardia: pathophysiological concepts. *Heart Rhythm.* 2008;5:S18–S21.
9. Huang J-L, et al. Right atrial substrate properties associated with age in patients with typical atrial flutter. *Heart Rhythm.* 2008;5:1144–1151.
10. Tai C-T, Chen S-A. Conduction barriers of atrial flutter: relation to the anatomy. *Pacing Clin Electrophysiol.* 2008;31:1335–1342.
11. Bui HM, Khrestian CM, Ryu K, et al. Fixed intercaval block in the setting of atrial fibrillation promotes the development of atrial flutter. *Heart Rhythm.* 2008;5:1745–1752.
12. Morita N, et al. The undetermined geometrical factors contributing to the transverse conduction block of the crista terminalis. *Pacing Clin Electrophysiol.* 2009;32:868–878.
13. Santucci PA, et al. Electroanatomic mapping of postpacing intervals clarifies the complete active circuit and variants in atrial flutter. *Heart Rhythm.* 2009;6:1586–1595.
14. Nakanishi T, et al. Crista terminalis as the anterior pathway of typical atrial flutter: insights from entrainment map with 3D intracardiac ultrasound. *Pacing Clin Electrophysiol.* 2015;38:608–616.
15. Waldo AL, Feld GK. Inter-relationships of atrial fibrillation and atrial flutter mechanisms and clinical implications. *J Am Coll Cardiol.* 2008;51:779–786.
16. Waldo AL. Atrial fibrillation-atrial flutter interactions: clinical implications for ablation. *Circulation.* 2007;116:2774–2775.
17. Waldo AL. More musing about the inter-relationships of atrial fibrillation and atrial flutter and their clinical implications. *Circ Arrhythm Electrophysiol.* 2013;6:453–454.
18. Luria DM, et al. Effect of radiofrequency ablation of atrial flutter on the natural history of subsequent atrial arrhythmias. *J Cardiovasc Electrophysiol.* 19:1145–1150 (2008).
19. Navarrete A, Conte F, Moran M, et al. Ablation of atrial fibrillation at the time of cavotricuspid isthmus ablation in patients with atrial flutter without documented atrial fibrillation derives a better long-term benefit. *J Cardiovasc Electrophysiol.* 2011;22:34–38.
20. Mohanty S, et al. Results from a single-blind, randomized study comparing the impact of different ablation approaches on long-term procedure outcome in coexistent atrial fibrillation and flutter (APPROVAL). *Circulation.* 2013;127:1853–1860.
21. Schneider R, et al. Pulmonary vein triggers play an important role in the initiation of atrial flutter: initial results from the prospective randomized Atrial Fibrillation Ablation in Atrial Flutter (Triple A) trial. *Heart Rhythm.* 2015;12:865–871.
22. Ellis K, et al. Incidence of atrial fibrillation post-cavotricuspid isthmus ablation in patients with typical atrial flutter: left-atrial size as an independent predictor of atrial fibrillation recurrence. *J Cardiovasc Electrophysiol.* 2007;18:799–802.
23. Page RL, et al. 2015 ACC/AHA/HRS guideline for the management of adult patients with supraventricular tachycardia: a report of the American College of Cardiology/American Heart Association Task Force on Clinical Practice Guidelines and the Heart Rhythm Society. *Circulation.* 2016;133:e506–e574.
24. Chao T-F, et al. Rate-control treatment and mortality in atrial fibrillation. *Circulation.* 2015;132:1604–1612.
25. Vamos M, Erath JW, Hohnloser SH. Digoxin-associated mortality: a systematic review and meta-analysis of the literature. *Eur Heart J.* 2015;36:1831–1838.
26. Ouyang A-J, et al. Meta-analysis of digoxin use and risk of mortality in patients with atrial fibrillation. *Am J Cardiol.* 2015;115:901–906.
27. Turakhia MP, et al. Increased mortality associated with digoxin in contemporary patients with atrial fibrillation: findings from the TREAT-AF study. *J Am Coll Cardiol.* 2014;64:660–668.
28. Allen LA, et al. Digoxin use and subsequent outcomes among patients in a contemporary atrial fibrillation cohort. *J Am Coll Cardiol.* 2015;65:2691–2698.
29. January CT, et al. 2014 AHA/ACC/HRS guideline for the management of patients with atrial fibrillation: a report of the American College of Cardiology/American Heart Association Task Force on Practice Guidelines and the Heart Rhythm Society. *J Am Coll Cardiol.* 2014;64:e1–e76.
30. Tomson TT, et al. Risk of stroke and atrial fibrillation after radiofrequency catheter ablation of typical atrial flutter. *Heart Rhythm.* 2012;9:1779–1784.
31. Voight J, et al. Risk of new-onset atrial fibrillation and stroke after radiofrequency ablation of isolated, typical atrial flutter. *Heart Rhythm.* 2014;11:1884–1889.
32. Medi C, Kalman JM. Prediction of the atrial flutter circuit location from the surface electrocardiogram. *Europace.* 2008;10:786–796.
33. Sasaki K, et al. Revisit of typical counterclockwise atrial flutter wave in the ECG: electroanatomic studies on the determinants of the morphology. *Pacing Clin Electrophysiol.* 2013;36:978–987.
34. Deo R, Berger R. The clinical utility of entrainment pacing. *J Cardiovasc Electrophysiol.* 2009;20:466–470.
35. Miyazaki H, Stevenson WG, Stephenson K, et al. Entrainment mapping for rapid distinction of left and right atrial tachycardias. *Heart Rhythm.* 2006;3:516–523.
36. Bochoeyer A, et al. Surface electrocardiographic characteristics of right and left atrial flutter. *Circulation.* 2003;108:60–66.
37. Garan H. Atypical atrial flutter. *Heart Rhythm.* 2008;5:618–621.
38. Almendral J, Caulier-Cisterna R, Rojo-Álvarez JL. Resetting and entrainment of reentrant arrhythmias: Part I: concepts, recognition, and protocol for evaluation: surface ECG versus intracardiac recordings. *Pacing Clin Electrophysiol.* 2013;36:508–532.
39. Josephson ME, Almendral J, Callans DJ. Resetting and entrainment of reentrant ventricular tachycardia associated with myocardial infarction. *Heart Rhythm.* 2014;11:1239–1249.
40. Almendral J. Resetting and entrainment of reentrant arrhythmias: Part II: informative content and practical use of these responses. *Pacing Clin Electrophysiol.* 2013;36:641–661.
41. Vollmann D, et al. Misleading long post-pacing interval after entrainment of typical atrial flutter from the cavotricuspid isthmus. *J Am Coll Cardiol.* 2012;59:819–824.
42. Wong KCK, Rajappan K, Bashir Y, et al. Entrainment with long postpacing intervals from within the flutter circuit: what is the mechanism? *Circ Arrhythm Electrophysiol.* 2012;5:e90–e92.
43. Maruyama M, et al. Number needed to entrain: a new criterion for entrainment mapping in patients with intra-atrial reentrant tachycardia. *Circ Arrhythm Electrophysiol.* 2014;7:490–496.
44. Mechulian A, et al. Further evidence for the ‘muscle bundle’ hypothesis of cavotricuspid isthmus conduction: physiological proof, with clinical implications for ablation. *J Cardiovasc Electrophysiol.* 2013;24:47–52.
45. Gula LJ, et al. Reduction in atrial flutter ablation time by targeting maximum voltage: results of a prospective randomized clinical trial. *J Cardiovasc Electrophysiol.* 2009;20:1108–1112.
46. Subbiah RN, et al. Rapid ablation for atrial flutter by targeting maximum voltage-factors associated with short ablation times. *J Cardiovasc Electrophysiol.* 2007;18:612–616.
47. Hindricks G, et al. Effect of electroanatomically guided versus conventional catheter ablation of typical atrial flutter on the fluoroscopy time and resource use: a prospective randomized multicenter study. *J Cardiovasc Electrophysiol.* 2009;20:734–740.

48. Lo L-W, et al. Characteristics of the cavotricuspid isthmus in predicting recurrent conduction in the long-term follow-up. *J Cardiovasc Electrophysiol.* 2009;20:39–43.
49. Shah D, et al. High-density mapping of activation through an incomplete isthmus ablation line. *Circulation.* 1999;99:211–215.
50. Bastani H, et al. Cryothermal vs. radiofrequency ablation as atrial flutter therapy: a randomized comparison. *Europace.* 2013;15:420–428.
51. Kuniss M, et al. Prospective randomized comparison of durability of bidirectional conduction block in the cavotricuspid isthmus in patients after ablation of common atrial flutter using cryotherapy and radiofrequency energy: the CRYOTIP study. *Heart Rhythm.* 2009;6:1699–1705.
52. Zambito PE, Palma EC. DP+1: another simple endpoint for atrial flutter ablation. *J Cardiovasc Electrophysiol.* 2008;19:10–13.
53. Morales GX, et al. Adenosine testing in atrial flutter ablation: unmasking of dormant conduction across the cavotricuspid isthmus and risk of recurrence. *J Cardiovasc Electrophysiol.* 2013;24:995–1001.
54. Lehrmann H, et al. ‘Dormant transisthmus conduction’ revealed by adenosine after cavotricuspid isthmus ablation. *Heart Rhythm.* 2012;9:1942–1946.
55. Bazan V, et al. Incremental pacing for the diagnosis of complete cavotricuspid isthmus block during radiofrequency ablation of atrial flutter. *J Cardiovasc Electrophysiol.* 2010;21:33–39.
56. Vallès E, et al. Burning the gap: electrical and anatomical basis of the incremental pacing maneuver for cavotricuspid isthmus block assessment. *J Cardiovasc Electrophysiol.* 2016;27:694–698.
57. Valles E, et al. Incremental His-to-coronary sinus maneuver: a nonlocal electrogram-based technique to assess complete cavotricuspid isthmus block during typical flutter ablation. *Circ Arrhythm Electrophysiol.* 2013;6:784–789.
58. Villacastin J, et al. Usefulness of unipolar electrograms to detect isthmus block after radiofrequency ablation of typical atrial flutter. *Circulation.* 2000;102:3080–3085.
59. Lin Y-J, et al. Characteristics of virtual unipolar electrograms for detecting isthmus block during radiofrequency ablation of typical atrial flutter. *J Am Coll Cardiol.* 2004;43:2300–2304.
60. Pérez FJ, et al. Long-term outcomes after catheter ablation of cavo-tricuspid isthmus dependent atrial flutter: a meta-analysis. *Circ Arrhythm Electrophysiol.* 2009;2:393–401.
61. Myktysey A, et al. Right coronary artery occlusion during RF ablation of typical atrial flutter. *J Cardiovasc Electrophysiol.* 2010;21:818–821.
62. Patel NJ, et al. Contemporary utilization and safety outcomes of catheter ablation of atrial flutter in the United States: Analysis of 89,638 procedures. *Heart Rhythm.* 2016;13:1317–1325.
63. Clementy N, et al. Outcomes after ablation for typical atrial flutter (from the Loire Valley Atrial Fibrillation Project). *Am J Cardiol.* 2014;114:1361–1367.

Macroreentrant Atrial Tachycardia

OUTLINE

Pathophysiology, 375

Macroreentry, 375

Dual-Loop Reentry, 375

Localized Reentry, 375

Cavotricuspid Isthmus-Dependent Right Atrial

Macroreentry, 377

Non-CTI-Dependent Right Atrial

Macroreentry, 378

Left Atrial Macroreentry, 378

Epidemiology, 380

Clinical Presentation, 381

Initial Evaluation, 381

Principles of Management, 381

Electrocardiographic Features, 381

Right Atrial Macroreentry, 381

Left Atrial Macroreentry, 382

Electrophysiological Testing, 382

Induction of Tachycardia, 382

Tachycardia Features, 382

Diagnostic Maneuvers During Tachycardia, 383

Mapping, 388

Electroanatomic Mapping, 388

Entrainment Mapping, 392

Noncontact Mapping, 395

Practical Approach to Mapping Macroreentrant Atrial

Tachycardia, 396

Ablation, 397

Target of Ablation, 397

Ablation Technique, 399

Endpoints of Ablation, 400

Ablation of Perimitral Macroreentrant Atrial Tachycardia, 401

Outcome, 404

PATHOPHYSIOLOGY

Organized atrial tachycardias (ATs) are broadly categorized as focal (centrifugal activation originating from a discrete site that incorporates automaticity, triggered activity, and microreentrant mechanisms) or macroreentrant (a relatively large reentrant circuit around a central obstacle).¹ Depending on whether the cavotricuspid isthmus (CTI) is critical to the reentry circuit, macroreentrant atrial tachycardias (MRATs) are divided into two groups: “CTI-dependent” MRAT or “non-CTI-dependent” MRAT (see Table 11.1).

CTI-dependent MRATs include typical atrial flutter (AFL), lower loop reentry, and intra-isthmus reentry. The term “atrial flutter” has traditionally been used to refer to a continuously waving pattern on the electrocardiogram (ECG), without an isoelectric baseline in at least one lead, whatever the cycle length (CL). “Typical AF” is reserved for a macroreentrant circuit with the activation wavefront rotating clockwise or counterclockwise around the tricuspid annulus and using the CTI as an essential part of the reentry circuit. “Atypical AFL” is simply a descriptive term for an AT with an ECG pattern of continuous undulation of the atrial complex, different from that in typical AFL. However, the term “atypical AFL” introduces unnecessary confusion, and a mechanistic description of the AT circuit in relation to atrial anatomy is preferred (e.g., perimitral macroreentry, lesional right atrial [RA] macroreentry).^{1,2}

Macroreentry

The mechanism of MRAT is reentrant activation around a large central obstacle, generally several centimeters in diameter, in at least one of its dimensions. The central obstacle can consist of normal or abnormal structures, and can be fixed, functional, or a combination of both. There is no single point of origin of activation, and atrial tissues outside the

circuit are activated from various parts of the circuit. The CL of MRAT can vary widely and is not a reliable predictor of the mechanism. When the mechanism of MRAT can be further elucidated through different mapping techniques, description of MRAT mechanisms must be made in relation to atrial anatomy, including a detailed description of the obstacles or boundaries of the circuit and the critical isthmuses.¹

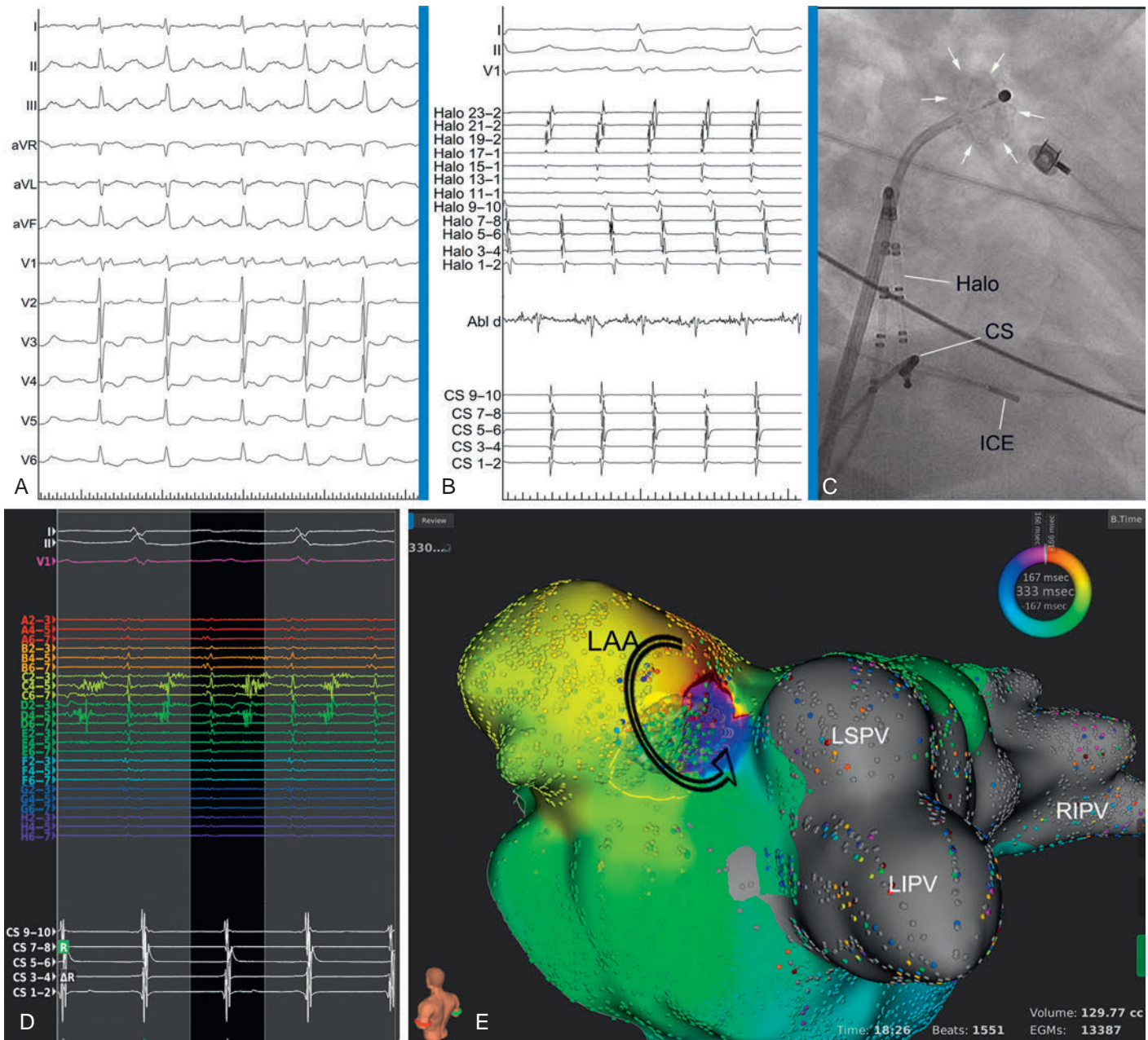
Dual-Loop Reentry

Although MRAT can manifest as an isolated arrhythmia (*single-loop reentry*), it can also occur in conjunction with other reentry circuits (e.g., incisional MRAT and typical AFL). When two atrial macroreentrant circuits coexist and use neighboring anatomical structures, they create the so-called dual-loop reentry. The multiple loops can be engaged simultaneously or encountered sequentially. Not uncommonly, ablation of one tachycardia results in transition to the other; hence, ablation of both circuits is necessary for clinical success.

A figure-eight reentry is a specific type of dual-loop reentry involving two simultaneously coexisting loops with opposite directions of propagation and sharing a common segment of unidirectional activation.

Localized Reentry

The term *localized reentry* has been used to refer to a reentrant circuit that is localized to a small area (covering a surface diameter of <3 cm) and does not have a central obstacle. These circuits typically form in close proximity to scars or prior ablation lines, where severe local conduction abnormalities allow for very slow conduction to support perpetuation of reentry in such a small anatomical path. Typically, low-amplitude, long, fractionated electrograms occupying more than 70% of the tachycardia cycle length (TCL) can be recorded in a small region of the atrium, from which activation spreads out centrifugally to activate the rest of the atrium (Fig. 13.1). Hence, these localized reentry circuits can



mimic focal AT, especially if a limited number of endocardial recordings are collected. Although localized reentry circuits are much smaller than macroreentry circuits, they are still significantly larger than focal “microreentrant” AT, whose site of origin cannot be mapped spatially beyond a single point or a few adjacent points with the resolution of a standard 4-mm-tip catheter.

Cavotricuspid Isthmus-Dependent Right Atrial Macroreentry

Lower loop reentry and intra-isthmus reentry are macroreentrant circuits that are confined to the RA and incorporate the CTI as a critical part of the circuit. However, in contrast to typical AFL, the circuit is not peritricuspid (Fig. 13.2). Nevertheless, because the CTI is still a

necessary part of the circuit, these arrhythmias are amenable to CTI ablation, as is true for patients with typical AFL.^{1,3}

Lower Loop Reentry

Lower loop reentry is a form of CTI-dependent MRAT with a reentrant circuit around the inferior vena cava (IVC); therefore it is confined to the lower part of the RA (see Fig. 13.2). The activation wavefront can rotate around the IVC in a counterclockwise (i.e., the impulse travels within the CTI in a medial-to-lateral direction) or clockwise fashion. A breakdown in the inferoposterior boundaries of the CTI produced by the eustachian ridge and lower crista terminalis causes the circuit to revolve around the IVC (instead of around the tricuspid annulus), across the eustachian ridge, and through the crista terminalis, with slow

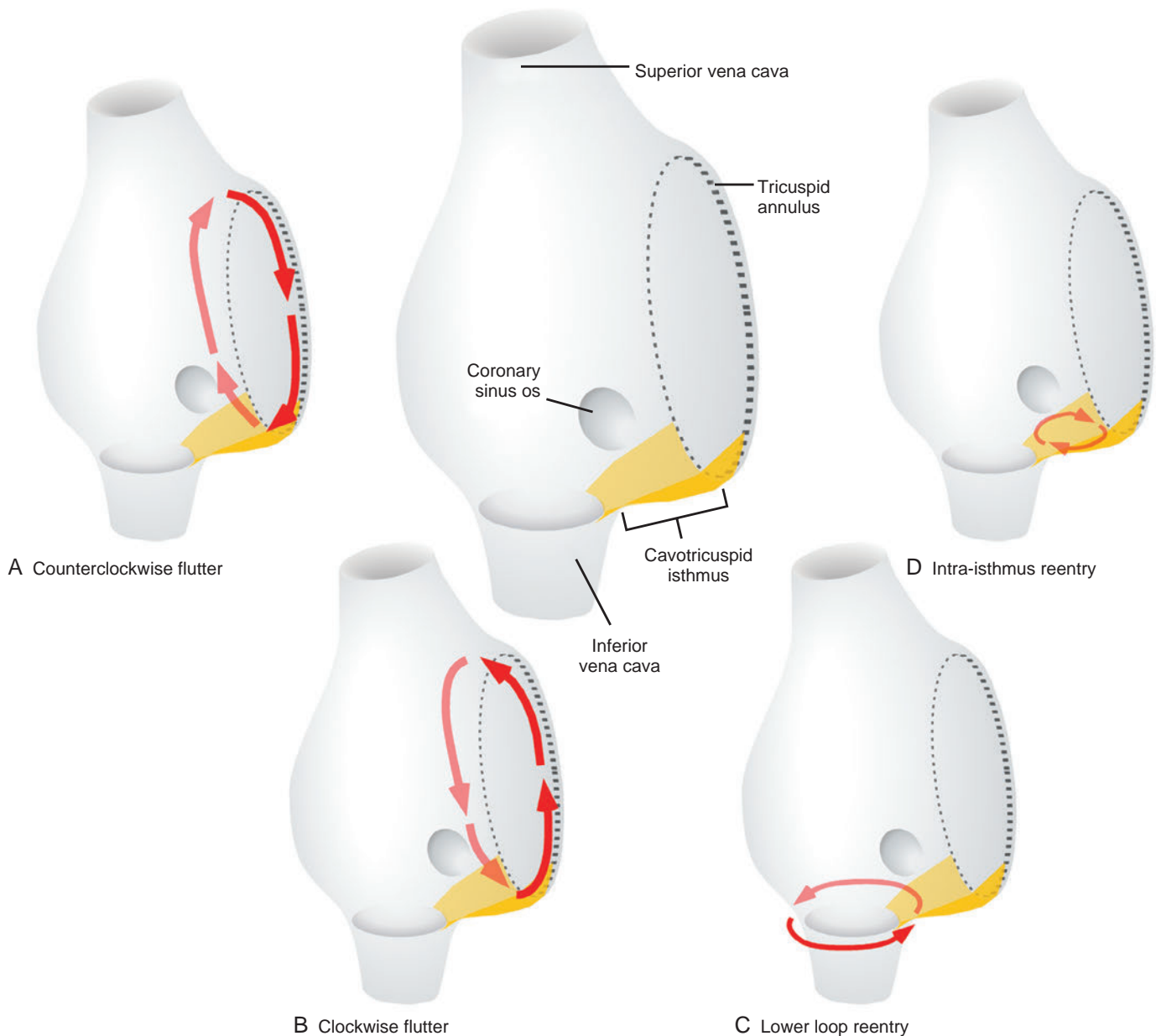


Fig. 13.2 Anatomy of Cavotricuspid-Dependent Atrial Flutter Circuits. *Top, center*, The right atrium is viewed from the right lateral aspect, with the lateral wall semitransparent. The cavotricuspid isthmus is shaded orange. (A) Counterclockwise flutter circuit. (B) Clockwise flutter circuit. (C) Lower loop reentry circuit. (D) Intra-isthmus reentry circuit. See text for discussion. Os, Ostium.

conduction because of transverse activation through that structure. Alternatively, the circuit can exit at the apex of the triangle of Koch and come behind the eustachian ridge to break through across the crista terminalis behind the IVC and then return to the CTI.³

Lower loop reentry often coexists with counterclockwise or clockwise typical AFL and is usually transient and terminates by itself or converts spontaneously into AFL or atrial fibrillation (AF).

Intra-Isthmus Reentry

Intra-isthmus reentry is a reentrant circuit usually occurring within the region bounded by the medial CTI and coronary sinus ostium (CS os) (see Fig. 13.2). Circuits in the mid and lateral portion of the CTI can also occur but are less common.⁴

This arrhythmia can be sustained and usually occurs in patients who have undergone prior, and often extensive, ablation at the CTI. Catheter ablation can result in islands of scarred areas and slowly conducting channels that can potentially provide the substrate for this arrhythmia. In one report, intra-isthmus reentry accounted for 21% of cases of “recurrent” AFL following prior successful CTI ablation. Of note, persistence of bidirectional CTI block following ablation of typical AFL does not exclude the possibility of intra-isthmus reentry, since the reentry circuit can exist medial to the line of CTI block. The reentry circuit can be quite small; fractionated potentials spanning one- to two-thirds of the TCL are typically recorded within the CTI.⁴

The atrial activation sequence around the tricuspid annulus electrograms can exhibit spontaneous or pacing-induced shifts from a counterclockwise to clockwise or fusion patterns. In addition, entrainment mapping from the lateral CTI demonstrates a postpacing interval (PPI) longer than the TCL, a finding indicating that the lateral CTI is not part of the reentrant circuit. On the other hand, pacing from the region of the medial CTI or CS os demonstrates concealed entrainment with a PPI equal to the TCL. Linear ablation across the medial CTI, usually at the site of a very prolonged electrogram, can eliminate the tachycardia.⁴

Non-CTI-Dependent Right Atrial Macroreentry

Incisional Right Atrial Macroreentry

Incisional or scar-mediated RA macroreentry circuits are the most common form of non-CTI-dependent RA MRATs. The incision on the RA free wall is a routine access site for corrective surgery for congenital or acquired heart disease. The atriotomy scar, suture lines, and cannulation sites form fixed obstacles that can potentially promote reentry by providing multiple protected isthmuses along with natural conduction barriers (such as valve annuli and caval ostia) and regions of atrial scarring caused by the underlying heart disease. In its simplest form, incisional RA MRAT uses a circuit that rotates around the atriotomy scar, with the lower turning point located between the end of the scar and the IVC, and the upper turning point located between the upper end of the scar or the superior vena cava (SVC). Other obstacles can also be included in the reentry circuit, such as anatomical structures located in the vicinity of the scar (e.g., SVC or IVC) or functional obstacles (anisotropic conduction delay or block).³

These patients often exhibit multiple clinical or inducible tachycardias, particularly typical AFL, indicating the complexity of the atrial substrate. Importantly, the atriotomy scar in the lateral or posterolateral RA forms a fixed posterior barrier to conduction in the superoinferior direction between the venae cavae, and a lateral boundary necessary for the development of a peritricuspid macroreentry (typical AFL) by preventing short-circuiting of the tricuspid annulus via the posterior atrium. This explains why typical AFL is the most common AT in this

patient population, accounting for more than 70% of all MRATs. Other RA MRATs involving free-wall atriotomy become progressively more common with more extensive atrial incisions.⁵

RA free-wall atriotomy is also widely used to access the left atrium (LA) for surgical replacement of the mitral valve. In fact, RA MRATs are more common than LA macroreentry in this group of patients. Other approaches for mitral valve surgeries involve incisions through the interatrial (Waterston) groove, transeptal incisions, and the superior transeptal approach. The latter surgical approach involves an extensive series of incisions in the lateral and superior RA, the interatrial septum, and the LA roof. Consequently, the superior transeptal approach has been associated with a higher risk of RA MRATs.⁶

Patients with congenital heart disease have a high prevalence of MRAT, particularly after they have undergone reparative or palliative surgical procedures. For MRATs in adults with repaired congenital heart disease, three RA circuits are generally identified: (1) lateral wall circuits with reentry around or related to the lateral atriotomy scar; (2) septal circuits with reentry around an atrial septal prosthetic patch (when present); and (3) typical AFL circuits using the CTI. These arrhythmias are discussed separately in Chapter 14.³

Right Atrial Macroreentry in the Absence of Previous Surgery

Rarely, RA MRATs have been observed in patients without prior surgery in whom the central obstacle is a large area of abnormal atrial myocardium and electrically silent zones, indicating scarring. The mechanism of atrial scarring remains uncertain, but it has been suggested that these low-voltage areas may reflect areas of fibrosis potentially related to inflammatory, infiltrative, or ischemic processes. These patients frequently exhibit multiple clinical or inducible tachycardias. The most common circuit involves macroreentry around the RA free wall, but the vast majority of these patients also have clinical or inducible typical AFL, and many had prior CTI ablation. The electrically silent area forms a fixed posterior conduction barrier, which likely facilitates the development of peritricuspid reentry.⁷

Upper Loop Reentry

This type of MRAT involves the upper portion of the RA, with transverse conduction across the crista terminalis and wavefront collision occurring at a lower part of the RA or within the CTI. The central obstacle of the circuit is composed of the crista terminalis (functional) and the SVC (fixed). The impulse rotating in the circuit can be in a counterclockwise or clockwise direction. The CTI is not an intrinsic part of the reentrant circuit. The lower turnaround point for this circuit is by conduction through a gap in functional block in the crista terminalis. Ablation of this gap can abolish the arrhythmia.⁸ Upper loop reentry can exist as a single loop or as a part of a dual-loop (figure-eight) reentry with lower-loop or with free-wall circuits.

Left Atrial Macroreentry

LA MRATs are frequently related to or coexist with AF. Areas of scar and low-voltage zones, associated with local conduction slowing or block, frequently promote the development of MRAT. Scar areas can be a result of previous atriotomy, surgical or catheter ablation, or can be spontaneous, producing electrically silent areas in the atrium.

Incisional Left Atrial Macroreentry

A variety of incisional LA macroreentry circuits have been described in patients with prior cardiac surgery involving the LA or atrial septum. The atriotomy scar forms a fixed obstacle that, in combination with the often intrinsically diseased atrial myocardium (providing functional obstacles) and normal structural obstacles in the vicinity of atrial incisions, can provide the substrate for macroreentry. Following mitral

valve surgery, low-voltage areas are often detected anterior to the right pulmonary veins (RPsVs), corresponding to LA incisions.⁹

Left Atrial Macroreentry Postablation of Atrial Fibrillation

LA MRAT is a frequent complication of surgical and catheter-based therapies of AF. The incidence and nature of ATs developing post AF ablation are, in large part, determined by the type of ablation performed and by the presence of abnormal LA substrate (see Chapter 15). The incidence seems to be lower following segmental ostial pulmonary vein (PV) isolation than circumferential PV isolation and higher following circumferential or linear LA ablation (more than 30%). The incidence of MRAT is much higher (more than 50%) for approaches of catheter ablation incorporating extensive lesions in the LA to terminate persistent AF. Linear ablation lesions, together with anatomical structures and intrinsically abnormal adjacent atrial myocardium, provide an ideal substrate for reentry. Gaps in the ablation lines further increase the chance for reentry by creating a region of slow conduction (see Fig. 13.1).

The most common form of macroreentry occurring after AF ablation is perimitral MRAT (accounting for approximately 40% of all MRATs). Macroreentrant circuits traversing the LA roof account for approximately 20% (see Fig. 15.60). Less common sites of macroreentry involve the right or left PVs, LA septum, and the base of the LA appendage (Fig. 13.3). Not infrequently, multiple macroreentrant circuits and multiple-loop reentrant circuits are encountered. In addition, localized reentrant circuits are not uncommon, and they usually arise from the vicinity of the isolated PVs or linear lesions.

LA MRATs comprise the majority of arrhythmias developing following surgical ablation of AF. Perimitral macroreentry is the most common, but macroreentry circuits incorporating the LA roof, septum,

and posterior wall, and circuits around the PVs have also been observed. Localized reentrant ATs comprise a sizable minority of the cases.¹⁰

Perimitral Left Atrial Macroreentry

This circuit involves reentry around the mitral annulus in a counter-clockwise or clockwise fashion (Fig. 13.4). The mitral annulus forms the anterior boundary of the reentry circuit, whereas the posterior boundary is formed by a low-voltage zone or scar in the posterior wall of the LA.

Perimitral MRAT is more common in patients with structural heart disease; however, it has been described in patients without obvious structural heart disease. In the latter group, voltage mapping often shows scar or low-voltage areas on the posterior wall of the LA forming the posterior boundary of the reentry circuit. As noted, perimitral macroreentry is the most common MRAT in patients with prior LA ablation procedures for AF, particularly when incomplete linear ablation across the lateral mitral isthmus is performed.¹¹

Circuits Involving the Pulmonary Veins

Various reentrant circuits involve the PVs, especially in patients with AF or mitral valve disease and those with prior catheter ablation of AF (particularly with linear LA ablation lesions), including circuits around one or more PVs (see Fig. 13.3) and posterior scar or low-voltage areas. PV-LA conduction recovery is frequently a critical element in these arrhythmias.

Left Septal Circuits

Left septal circuits occur primarily in patients with previous heart surgery, particularly after mitral valve surgery requiring septal incision, and

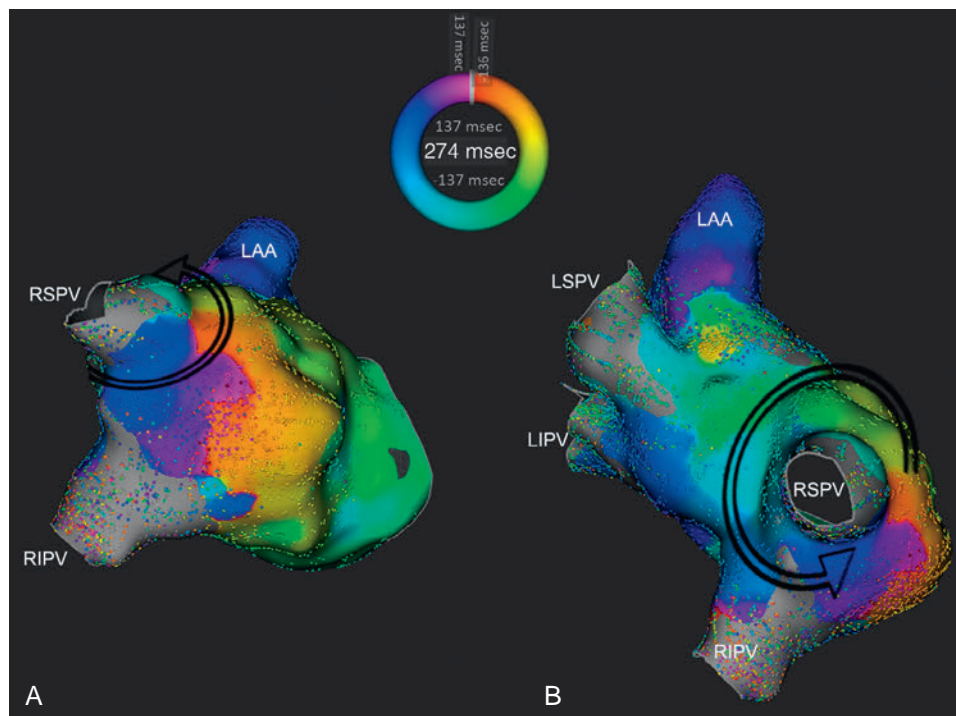


Fig. 13.3 Macroreentrant Atrial Tachycardia (MRAT) Around the Right Superior Pulmonary Vein (PV). Three-dimensional electroanatomic (Rhythmia) activation map of the left atrium (LA) during MRAT (tachycardia cycle length, 274 milliseconds) in a patient with prior wide-area circumferential PV ablation. Right lateral (A) and right posterior oblique (B) views are shown. The path of the reentry circuit, as delineated by the black arrow, uses gaps in the circumferential ablation line around the right-sided PVs. LAA, Left atrial appendage; LIPV, left inferior PV; LSPV, left superior PV; RIPV, right inferior PV; RSPV, right superior PV.

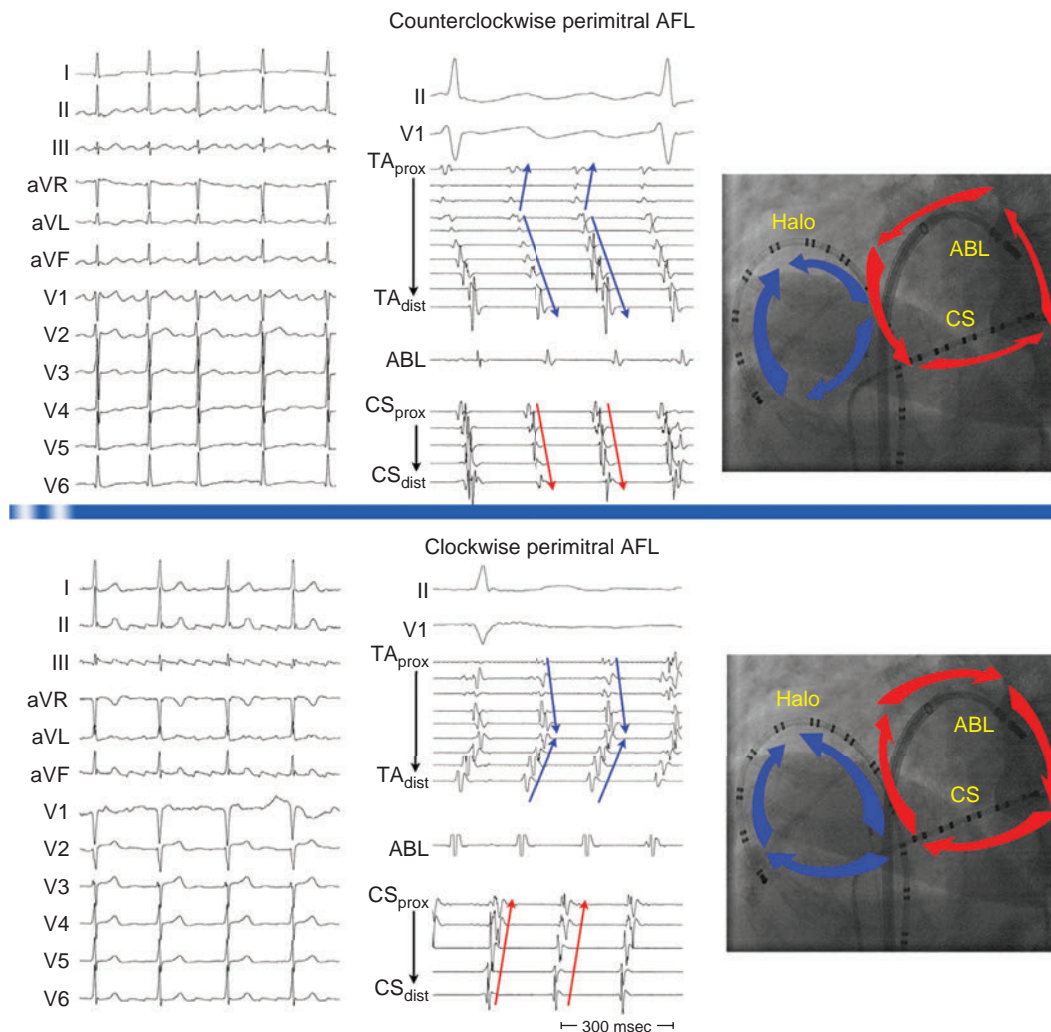


Fig. 13.4 Perimitral Macroreentrant Atrial Tachycardia. Surface electrocardiograms and intracardiac recordings during clockwise (*lower panel*) and counterclockwise (*upper panel*) perimitral macroreentrant atrial tachycardia. Catheter position and wavefront activation during the tachycardia are illustrated in a left anterior oblique fluoroscopic view (*right side*). The ablation catheter (*ABL*) is positioned at the mitral isthmus, and the Halo catheter is positioned around the tricuspid annulus (*TA*), with the distal end at the lateral end of the cavotricuspid isthmus. *AFL*, Atrial flutter; *CS*, coronary sinus; *CS_{dist}*, distal coronary sinus; *CS_{prox}*, proximal coronary sinus; *TA_{dist}*, distal tricuspid annulus; *TA_{prox}*, proximal tricuspid annulus.

those with prior AF ablation. Rarely, MRATs involving the LA septum have been reported in the absence of prior cardiac surgery. These circuits involve the septum primum, which acts as a central obstacle for the reentrant circuit. The right PV ostia serve as its posterior boundary, whereas the mitral annulus serves as the anterior boundary. Atrial dilation and concomitant antiarrhythmic drug therapy also appear to play a role by the prolongation of left intraatrial conduction, which then allows stable macroreentry circuits to persist. In patients with a history of surgery for atrial septal defects, scars or the patch on the septum can serve as the anatomical substrate of left septal circuits.⁹

Left Atrial Macroreentry in the Absence of Previous Surgery or Ablation

LA circuits can be found in patients without a history of atriotomy or prior ablation. Electroanatomic maps in these patients often show electrically silent (low-voltage or scar) areas in the LA, which act as a central obstacle or barrier in the circuit. The pathogenesis of these areas with no electrical signals is not well established. Potential causes include

volume and pressure overload (mitral valve disease, hypertension, heart failure), ischemia (atrial branch occlusion), postinflammation scarring (after myocarditis), atrial amyloidosis, atrial dysplasia, and tachycardia-related structural remodeling. These conditions are frequently associated with diffuse or patchy areas of scarring, which are typically located at the posterior wall (45%), roof (28%), or anteroseptal region (27%) of the LA. The macroreentrant circuits in these patients show considerable anatomical variability and frequently involve multiple simultaneous loops (dual- or triple-loop reentry, or figure-eight reentry).^{12,13}

EPIDEMIOLOGY

MRAT comprises a heterogeneous group of ATs related to different anatomical and electrophysiological (EP) substrates. These arrhythmias are frequently associated with structural heart disease, congenital cardiac defects, previous cardiac surgical procedures, or surgical or catheter ablation procedures for AF. However, MRAT occasionally occurs in a patient with no apparent structural heart disease. Often, these

arrhythmias coexist with AF. Not infrequently, these patients experience sinus node dysfunction (SND), which can be symptomatic or hinder pharmacological therapy of the tachycardia.

Although its exact prevalence among cardiac arrhythmias is difficult to establish clinically, MRAT is not a rare arrhythmia. In fact, the incidence of MRAT has been increasing, likely due to aging of the general population, which implies progressive alteration of the atrial electrical properties with development of an arrhythmogenic substrate, and also due to the rapid growth of surgical and catheter-based ablation procedures for treatment of AF.

CLINICAL PRESENTATION

MRATs are typically persistent. As with AF and typical AFL, patients may present with symptoms related to rapid ventricular response, loss of atrioventricular (AV) synchrony, tachycardia-induced cardiomyopathy, or deterioration of preexisting cardiac disease. In addition, typical AFL and MRAT can contribute to systemic thromboembolic complications and stroke.

The clinical presentation of MRAT can vary widely, from completely asymptomatic to severe hemodynamic compromise. Most patients present with a spectrum of symptoms including palpitations, lightheadedness, fatigue, reduced activity tolerance, and dyspnea. Severe heart failure or acute coronary syndrome can occur in susceptible patients.

INITIAL EVALUATION

Outside typical AFL, the clinician is faced with a wide spectrum of ATs for which therapy and prognosis cannot be defined with routine non-invasive testing, and definitive diagnosis typically requires intracardiac mapping. ECG alone is frequently inadequate to distinguish MRAT from focal AT. Detailed evaluation of cardiac function and anatomy is typically required, especially in patients with congenital heart disease and those with previous cardiac procedures (surgical or catheter based). In addition, detailed knowledge of the congenital anomaly and previous surgical or ablative procedures is very important, such as location of surgical incisions and the presence and location of prosthetic patch material.

PRINCIPLES OF MANAGEMENT

Medical management of MRAT is practically similar to that described for typical AFL (see Chapter 12), including pharmacological rate- and rhythm-control strategies, as well as long-term anticoagulation for stroke. The choice of rate- versus rhythm-control strategies typically considers several factors, including severity of symptoms, response to rate-controlling medications, cardiac function, and associated noncardiac diseases.

With recent advances in the technology to visualize and modify the arrhythmia substrate, ablation of MRAT has become increasingly successful, but can be substantially more difficult than ablation of typical AFL. MRAT can have complex circuits that demand a thorough knowledge of atrial anatomy and a great level of experience to correlate activation patterns with anatomical landmarks. When this type of AT is suspected, such as in patients with congenital heart disease who have had surgery, referral to an experienced center should be considered.

Currently, catheter ablation is recommended in patients with recurrent symptomatic MRAT that is refractory to antiarrhythmic drug therapy, and may also be reasonable as a primary therapy, after carefully weighing potential risks and benefits of treatment options in the individual patient.¹⁴

ELECTROCARDIOGRAPHIC FEATURES

P wave morphology on the surface ECG is usually of limited value for precise anatomical localization of macroreentrant circuits. Analysis of the P wave can be impeded by partial or complete concealment of the P wave within the QRS complexes or T waves when the AT is associated with 1:1 or 2:1 AV conduction. In addition, P wave morphology of a spectrum of RA and LA MRATs is highly variable. The presence of complex anatomy secondary to congenital abnormalities, prior atrial surgery, or a large low-voltage zone (secondary to underlying atrial substrate or extensive catheter or surgical atrial ablation) can modify atrial wavefront propagation in a nonuniform manner, resulting in deviated atrial activation vectors or low-amplitude P waves. Furthermore, P waves produced by different underlying substrates may appear similar if the direction of activation of the atrial septum and LA is similar.

The surface ECG morphology is most characteristic (and hence predictive) for establishing a diagnosis of counterclockwise typical AFL. Nevertheless, atypical ECG patterns have been described for typical AFL after AF ablation. Although clockwise typical AFL also has a characteristic appearance, this is more variable, and it can be mimicked by various other MRATs ("pseudo-typical" morphology). On the other hand, AFL may show distinct isoelectric intervals between P waves, especially in the presence of extensive atrial scarring or a localized macroreentrant circuit, similar to focal AT.⁸

Despite significant limitations, certain ECG features have been demonstrated to help distinguish between the various types of MRAT. To distinguish LA from RA origin of the MRAT, lead V₁ is the most useful. In the absence of previous cardiac surgery or catheter ablation (particularly linear ablation lesions in the LA), P waves that are completely negative in lead V₁ are more frequently associated with RA free-wall circuits. Conversely, in the absence of counterclockwise typical AFL, broad-based upright P waves in lead V₁, especially when accompanied by upright waves in inferior leads or with low-amplitude or isoelectric waves in the other leads, are more frequently associated with LA circuits. LA circuits frequently generate low-amplitude P waves, with some of them having visible waves only in lead V₁.^{2,8} A decreased amplitude of the P waves in the inferior leads is suggestive of LA origin of MRAT. For ATs post AF ablation, negative P waves in any of the precordial leads favors RA MRAT over LA MRAT with a sensitivity and specificity of 83% and 100%, respectively, and an accuracy of 98%. Among LA MRATs, prominent positive flutter waves in lead V₁ favor LA roof or mitral isthmus-dependent MRATs over other LA MRATs, with a sensitivity and specificity of 80% and 83%, respectively, and an accuracy of 81%.¹⁵

In general, a positive P wave in the inferior leads can be observed in clockwise typical AFL, upper loop reentry, and LA macroreentry. P wave polarity in lead I can help distinguish upper loop reentry from clockwise typical AFL. A negative or flat flutter wave polarity in lead I favors upper loop reentry, whereas positive polarity with amplitude of more than 0.07 mV indicates clockwise typical AFL.¹⁶

Right Atrial Macroreentry

Incisional Right Atrial Macroreentry

The surface ECG morphology of free-wall MRAT in a patient with a previous atriotomy is highly variable, depending on factors including the location of the scars and low-voltage areas, the direction of rotation, the presence of coexisting conduction block in the atrium, and the presence of a simultaneous typical AFL. The morphology of the atrial complex on the surface ECG can range from that similar to typical AFL to one characteristic of focal AT (see Fig. 14.3). Often, inverted P waves can be observed in lead V₁. Depending on the predominant direction

of septal activation, RA free-wall MRAT can mimic clockwise or counterclockwise typical AFL.^{8,17}

Upper Loop Reentry

The surface ECG of upper loop reentry closely mimics that of clockwise typical AFL (negative P waves in lead V₁ and positive P waves in the inferior leads) because, in most cases, both arrhythmias share a similar activation sequence of the LA, the septum, and caudocranial activation of the lateral RA. However, negative or isoelectric or flat P waves in lead I favor upper loop reentry over clockwise typical AFL. Conversely, positive P waves in lead I with an amplitude of more than 0.07 mV favor clockwise typical AFL. In addition, the CL of upper loop reentry is usually shorter in comparison with typical AFL.⁸

Lower Loop Reentry

The surface morphology of lower loop reentry is highly variable and can be similar to that of counterclockwise or clockwise typical AFL, but lower loop reentry associated with somewhat higher crista terminalis breaks can produce unusual ECG patterns. Sometimes, the changes are manifested by decreased amplitude of the late positive waves in the inferior leads, probably as a result of wavefront collision over the lateral RA wall.⁸

Intra-Isthmus Reentry

The surface ECG in intra-isthmus reentry commonly exhibits a pattern similar to counterclockwise typical AFL. The same ECG pattern can exist whether the intracardiac atrial activation sequence around the tricuspid annulus exhibits a counterclockwise, clockwise, or fusion pattern. The proximity of the exit site of the reentrant circuit to the CS os promotes more rapid CS and septal activation of the LA, which largely determine inscription of the P wave, regardless of the peritricuspid activation pattern.⁴

Left Atrial Macroreentry

The surface ECG morphology of LA MRAT caused by the different reentrant circuits is variable, and ECG findings are often similar for different underlying substrates, thus making the localization within the LA based on the ECG difficult. LA MRATs are usually associated with prominent positive P waves in lead V₁ and upright (but frequently of low amplitude) deflections in leads II, III, and aVF. However, LA MRAT can result in ECG patterns of focal AT (discrete P waves and isoelectric baseline) because of a high prevalence of generalized atrial disease and slower conduction. Infrequently, LA MRAT can mimic typical AFL on the surface ECG.⁸

Perimitral Left Atrial Macroreentry

Most of these tachycardias show prominent forces in leads V₁ and V₂, with diminished amplitude in the inferior leads (see Fig. 13.4). It has been suggested that a posterior LA scar allows for domination by anterior LA forces. This constellation of findings can mimic counterclockwise or clockwise typical AFL, but the decreased amplitude of frontal plane forces suggests an LA circuit. In patients with prior PV isolation procedures, the surface ECG morphology of counterclockwise perimitral MRAT can be different from that in patients without prior ablation, possibly related to varying degrees of prior LA ablation or scar. In these patients, counterclockwise perimitral MRAT demonstrates positive P waves in the inferior and precordial leads and a significant negative component in leads I and aVL. Furthermore, counterclockwise perimitral MRAT in these patients can have a morphology similar to that of left PV ATs. However, counterclockwise perimitral MRAT is suggested in the presence of a more negative component in lead I, an initial negative component in lead V₂, and a lack of any isoelectric interval between P

waves. Clockwise perimitral MRAT has a limb lead morphology that is the converse of counterclockwise perimitral MRAT and an initial negative component in the lateral precordial leads. Positive P wave in leads I and aVL differentiates clockwise perimitral MRAT from counterclockwise CTI-dependent AFL and left PV AT.¹⁸

Pulmonary Vein Circuits

Because these circuits are related to low-voltage or scar areas, the surface ECG usually shows low-amplitude or flat P waves. These tachycardias have the most variable surface ECG patterns.

Left Septal Circuits

Because the reentry circuit is on the septum, the surface ECG shows prominent, usually positive, P waves only in lead V₁ or V₂ and almost flat waves in most other leads (eFig. 13.1). This pattern can be caused by a septal circuit with anteroposterior forces projecting in lead V₁ and the cancellation of caudocranial forces. This pattern was 100% sensitive for an LA septal circuit, but the specificity of this pattern for any type of LA MRAT was only 64%.

ELECTROPHYSIOLOGICAL TESTING

A decapolar catheter (positioned into the CS with the proximal electrodes bracketing the CS os) and a multipolar (20- or 24-pole) Halo catheter (positioned at the tricuspid annulus) are commonly used to map MRAT. The distal tip of the Halo catheter is positioned at 6 to 7 o'clock in the left anterior oblique (LAO) view, so that the distal electrodes will record the middle and lateral aspects of the CTI, the middle electrodes will record the anterolateral RA, and the proximal electrodes may record the RA septum (depending on the catheter used). Instead of the Halo and CS catheters described, some laboratories use a single duodecapolar catheter around the tricuspid annulus while extending the catheter tip inside the CS. Such a catheter would straddle the CTI and provide recording and pacing from the medial and lateral aspects of the CTI.

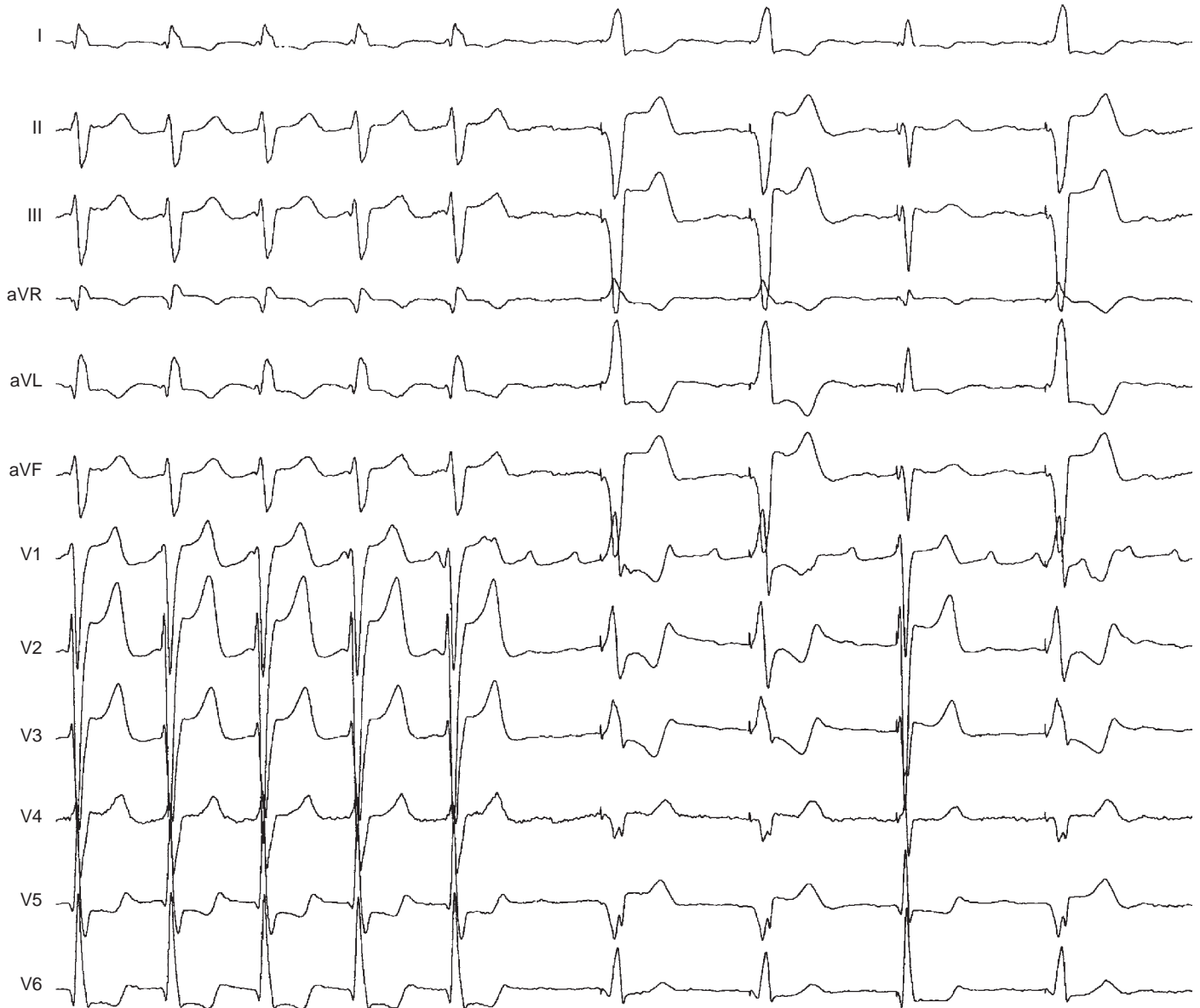
Induction of Tachycardia

Programmed electrical stimulation protocols usually include atrial burst pacing from the high RA and CS—down to a pacing cycle length (PCL) at which 2:1 atrial capture occurs—and single and double atrial extra-stimuli (AES) at multiple PCLs (600 to 300 milliseconds) from the high RA and CS (down to the atrial refractoriness). Isoproterenol infusion (0.5 to 4 µg/min) is administered as needed to facilitate tachycardia induction. The goals of EP testing in patients with MRAT are listed in Box 13.1.

Tachycardia Features

MRAT is characterized by a constant TCL, a constant P wave morphology, and a constant atrial activation sequence. The atrial activation sequence depends on the origin and type of the macroreentrant circuit.

Although the atrial CL during MRAT typically remains constant, considerable variations in the CL can be observed in the atrium contralateral to atrium of origin of the tachycardia (Fig. 13.5). In contrast, focal ATs frequently exhibit alterations in the CL with speeding (warm-up) and slowing (cool-down) at the onset and termination of tachycardia. Variation in the TCL of greater than 15% has been suggested as a reliable marker of a focal AT. However, a regular AT can be focal or macroreentrant. In addition, focal ATs often manifest as bursts of tachycardia with spontaneous onset and termination, although they can be incessant, and they may accelerate in response to sympathetic stimulus. Several criteria can help distinguish focal AT from MRAT (see Table 11.5).⁸



eFig. 13.1 Surface Electrocardiogram of Left Septal Macroreentrant Atrial Tachycardia. The tachycardia developed in a patient with tachycardia-bradycardia syndrome and a permanent pacemaker. The P waves are masked by the QRS and T waves during 2:1 atrioventricular conduction. Administration of adenosine results in atrioventricular block and reveals P wave morphology. Note the prominent positive P waves only in lead V₁ and almost flat waves in most of the other leads.

Atrial activation during MRATs spans the whole TCL. In contrast, intracardiac mapping in the setting of focal ATs shows significant portions of the TCL without recorded atrial activity, and atrial activation time is markedly less than the TCL, even when recording from the entire cardiac chamber of tachycardia origin (see Fig. 11.5). However, in the presence of complex intramyocardial conduction disturbances, activation during focal tachycardias can extend over a large proportion of the TCL, and conduction spread can follow circular patterns suggestive of macroreentrant activation. On the other hand, long isoelectric

intervals can occur between P waves during MRATs; especially when mapping is limited to only the atrium contralateral to the origin of the macroreentrant circuit or to only parts of the ipsilateral atrium, a focal activation can be observed, incorrectly suggesting a focal mechanism. This is particularly observed for LA MRATs in the presence of large areas of electrical silence. Nonetheless, a *thorough* intracardiac activation mapping would reveal atrial activation spanning the TCL.

Occasionally, P wave morphology on the surface ECG resembles AT, but intracardiac recordings show that parts of the atria (commonly the LA) have disorganized atrial activity (Fig. 13.6). Such rhythms behave more like AF than AT, but they may be converted to true typical AFL with antiarrhythmic drugs.

MRAT is usually associated with 2:1 AV conduction, although variable AV conduction and larger multiples are not uncommon. Variable AV conduction is the result of multilevel block; for example, proximal 2:1 AV block and more distal 3:2 Wenckebach block result in 5:2 AV Wenckebach block. Macroreentrant circuits can have long CLs (i.e., 250 to 400 milliseconds) in the presence of extensive atrial disease and antiarrhythmic agents, in which case a relatively rapid ventricular response (with 1:1 AV conduction) can occur.

Diagnostic Maneuvers During Tachycardia

Atrial Extrastimulation During Tachycardia

A focal mechanism is characterized by dissociation of almost the entire atria from the tachycardia with AES. In contrast, the MRAT circuit usually incorporates large portions of the RA or LA, as demonstrated by resetting. In response to AES, MRATs typically demonstrate an increasing or mixed (flat, then increasing) resetting response. AES usually fails to terminate the AT.

Importantly, AES at short coupling intervals can result in transformation of the tachycardia to a different AT or to AF. To minimize the risk of transformation or interruption of the tachycardia, which would hinder tachycardia mapping, atrial stimulation maneuvers during the tachycardia should be used sparingly and only when needed to confirm the diagnosis, or more precisely, to localize the critical portion of the AT circuit as guided by the initial activation mapping.

BOX 13.1 Goals of Programmed Stimulation During Macroreentrant Atrial Tachycardia

1. To confirm that the tachycardia is an AT
2. To confirm that the AT is a macroreentrant circuit
 - Resetting response consistent with reentry
 - Entrainment mapping consistent with reentry
 - Atrial activation spanning the TCL
3. To exclude CTI-dependent atrial flutter
 - Entrainment mapping at the CTI
4. To localize the circuit to the RA versus LA
 - P wave morphology on the surface ECG
 - Atrial activation sequence in the CS and Halo catheters
 - Isolated variation of the RA CL
 - RA activation time <50% of the TCL
 - Entrainment pacing from different RA sites
5. To define the tachycardia circuit
 - Electroanatomic mapping
 - Entrainment mapping
6. To define the critical isthmus in the tachycardia circuit
 - Entrainment mapping

AT, Atrial tachycardia; CL, cycle length; CS, coronary sinus; CTI, cavotricuspid isthmus; ECG, electrocardiogram; LA, left atrium; RA, right atrium; TCL, tachycardia cycle length.

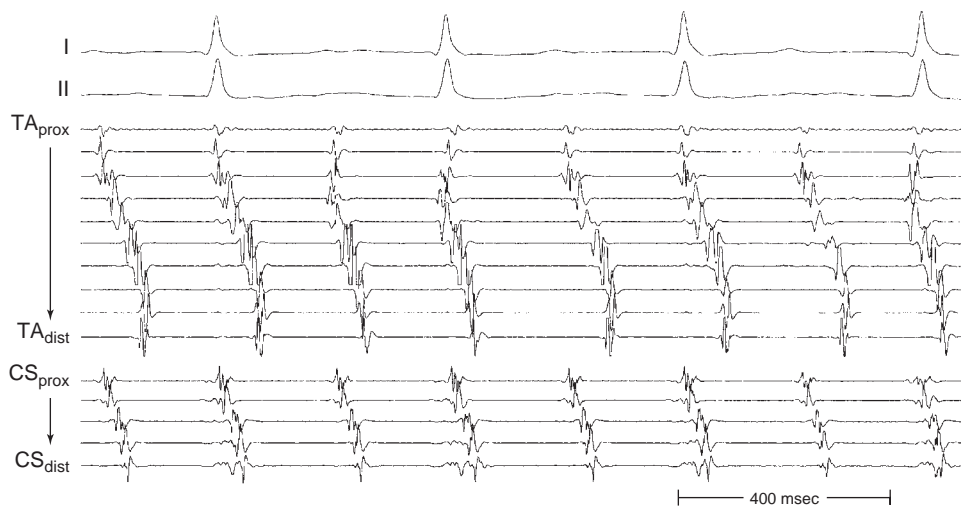


Fig. 13.5 Cycle Length (CL) Variation During Macroreentrant Atrial Tachycardia. Surface electrocardiogram leads I and II and intracardiac recording during left atrial (LA) macroreentry. Note the large spontaneous variations in the right atrial CL and activation sequence (as recorded by a Halo catheter around the tricuspid annulus, TA), with a constant LA CL and activation sequence (as recorded by the coronary sinus catheter). CS_{dist}, Distal coronary sinus; CS_{prox}, Proximal coronary sinus; TA_{dist}, distal tricuspid annulus; TA_{prox}, proximal tricuspid annulus.

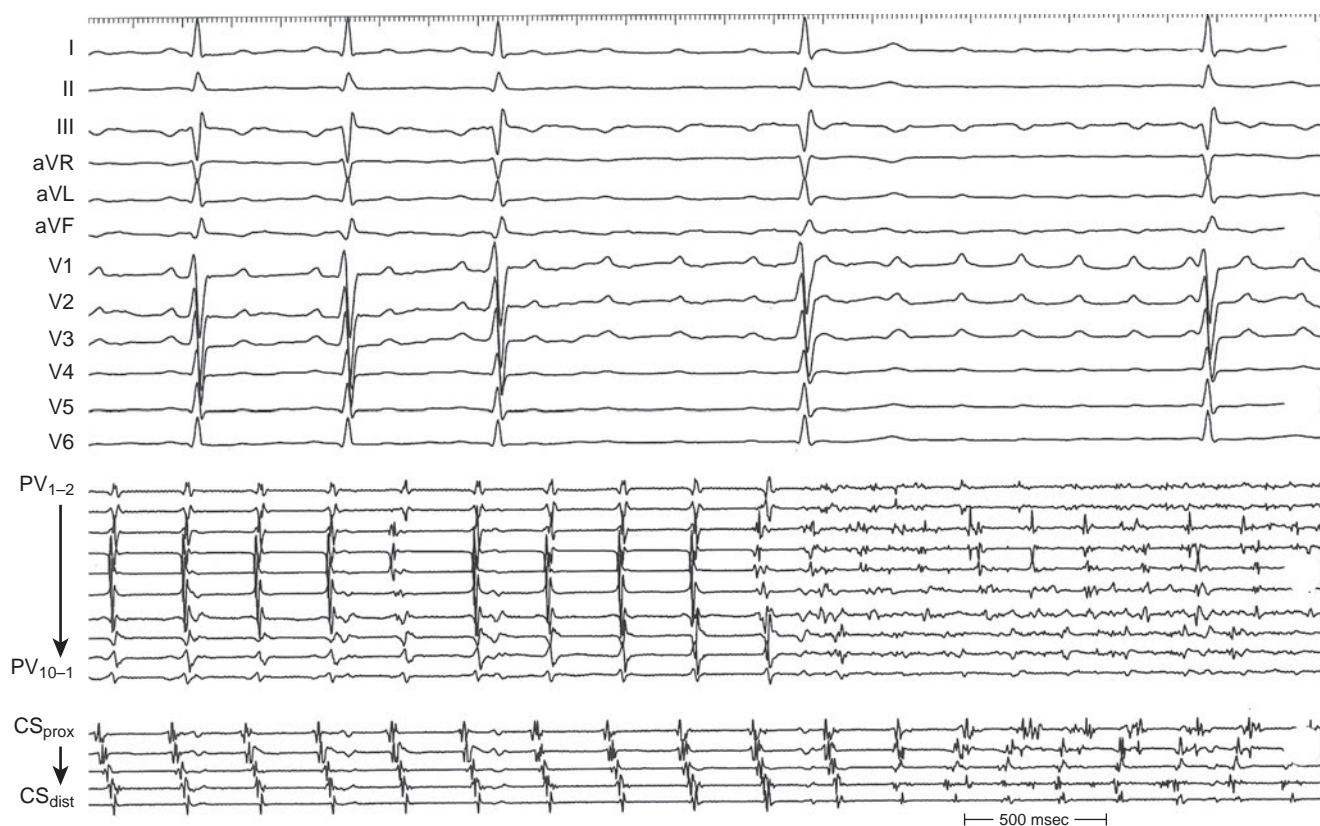


Fig. 13.6 Localized Atrial Macroreentry. Surface 12-lead electrocardiogram (ECG) and intracardiac recordings during left atrial tachycardia (AT) that use a small macroreentrant circuit near the ostium of the right superior pulmonary vein (PV) in a patient with prior extensive wide-area circumferential PV ablation and linear ablation for atrial fibrillation (AF). On the left, P waves are separated by isoelectric intervals, mimicking focal AT, as a result of extensive scarring in the left atrium. In the middle of the recording, the AT converts spontaneously to AF. Note that the intracardiac recordings demonstrate grossly irregular atrial activity during AF as compared with AT; however, on the surface ECG, atrial activity remained relatively organized, and conversion from AT into AF was manifest on the surface ECG by a change in rate and minor changes in morphology of atrial complexes. CS_{dist}, Distal coronary sinus; CS_{prox}, proximal coronary sinus.

Atrial Pacing During Tachycardia

Burst pacing from the CS or along the Halo catheter is started at a CL 10 to 20 milliseconds shorter than the atrial CL, and then the PCL is progressively shortened by 10 to 20 milliseconds. Consistent capture by atrial stimuli and acceleration of all recorded atrial electrograms to the paced rate should be verified before analyzing the tachycardia response to overdrive pacing. The response of AT to overdrive pacing is evaluated for entrainment, overdrive suppression, transformation into distinct AT morphologies or AF, and ability and pattern of termination.

Entrainment. Overdrive atrial pacing at long CLs (i.e., 10 to 30 milliseconds shorter than the TCL) can usually entrain MRAT. The slower the pacing rate and the farther the pacing site from the reentrant circuit, the longer the pacing drive required to penetrate and entrain the tachycardia. Achievement of entrainment of the AT establishes a reentrant mechanism of the tachycardia and excludes triggered activity and abnormal automaticity as potential mechanisms (Fig. 13.7). Entrainment can also be used to estimate qualitatively how far the reentrant circuit is from the pacing site (see later).¹⁹

Entrainment criteria. During constant-rate pacing, entrainment of a reentrant tachycardia results in the activation of all myocardial tissue responsible for maintaining the tachycardia at the PCL, with the resumption of the same tachycardia morphology following cessation

of pacing, with the first postpacing ECG tachycardia complex displaying no fusion but occurring at a return cycle equal to the PCL. Unfortunately, it is almost impossible to document the acceleration of all tissue responsible for maintaining the reentrant circuit to the PCL. Also, it should be recognized that the mere acceleration of the tachycardia to the pacing rate and the subsequent resumption of the original tachycardia after cessation of pacing do not establish the presence of entrainment. Therefore several surface ECG and intracardiac electrogram criteria have been proposed for establishing the presence of entrainment (see Box 5.2). Demonstration of one or more of the four criteria proves the presence of entrainment and supports a reentrant mechanism, but their absence does not exclude entrainment or reentry. Pacing at different endocardial sites and at multiple PCLs and recording activation sequences from multiple intracardiac locations are often required to demonstrate one or more of the entrainment criteria and, hence, establish the diagnosis of macroreentrant tachycardia.^{20,21}

Entrainment with fusion. During entrainment of MRAT, fusion of the stimulated impulse can be observed on the surface ECG, but it is easier to recognize on intracardiac recordings from the Halo and CS catheters. The stimulated impulse has a hybrid morphology between the fully paced atrial impulse and the tachycardia impulse. The ability to demonstrate surface ECG fusion requires a significant mass of atrial myocardium to be depolarized by the paced stimulus and by the

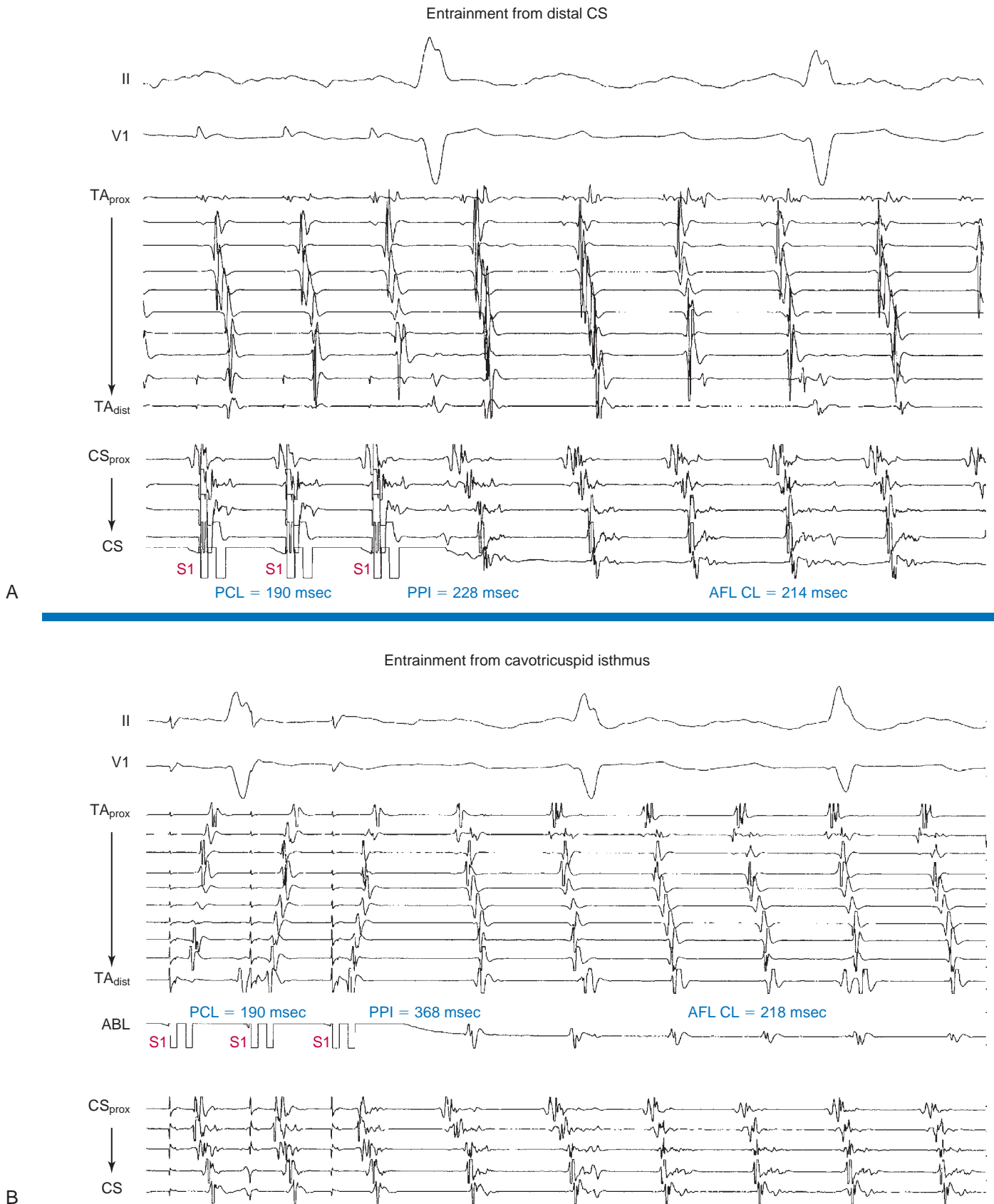
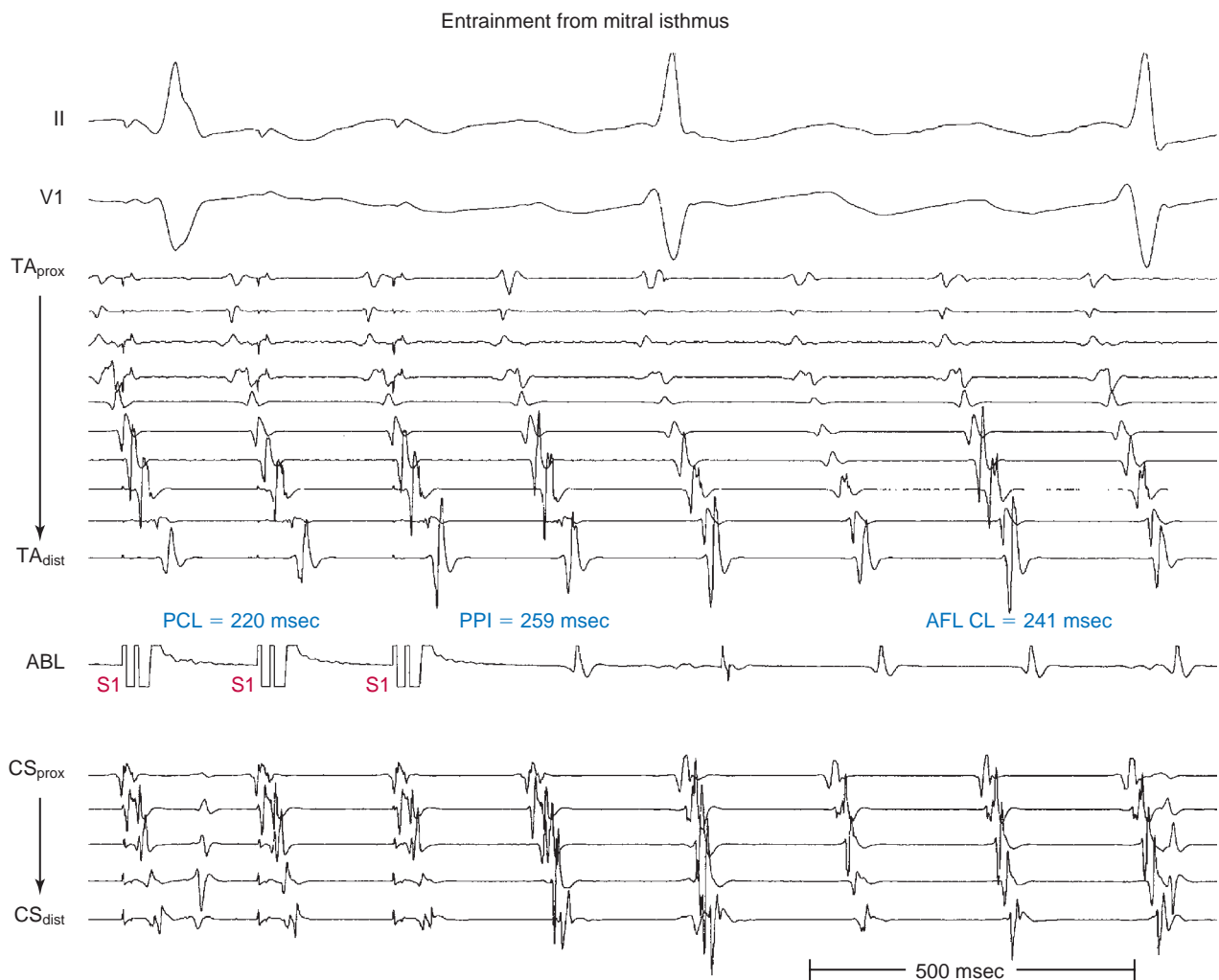


Fig. 13.7 Entrainment of Counterclockwise Perimitral Macroreentrant Atrial Tachycardia. (A) Entrainment from the distal coronary sinus (CS) results in intracardiac atrial fusion (as demonstrated in the CS activation sequence) and a short postpacing interval (PPI) compared to the tachycardia cycle length (TCL) ($PPI - TCL = 14$ milliseconds) because the distal CS is close to the reentrant circuit. (B) Entrainment from the ablation catheter (ABL) positioned at the cavotricuspid isthmus (CTI) results in manifest atrial fusion with a long PPI ($PPI - TCL = 150$ milliseconds), suggesting that the CTI is not part of the reentrant circuit. *Continued*



C

Fig. 13.7, cont'd (C) Entrainment from the ablation catheter positioned at the mitral isthmus, concealed atrial fusion, and a short PPI (PPI – TCL = 18 milliseconds), suggesting that the mitral isthmus is the critical isthmus of the reentrant circuit. CS_{dist}, Distal coronary sinus; CS_{prox}, proximal coronary sinus; TA_{dist}, distal tricuspid annulus; TA_{prox}, proximal tricuspid annulus.

tachycardia. The closer the stimulation site is to the exit of a reentrant circuit, the less likely entrainment will manifest ECG fusion.

It is important to understand that overdrive pacing of a tachycardia of any mechanism can result in a certain degree of fusion, especially when the PCL is only slightly shorter than the TCL. Such fusion, however, is unstable in focal tachycardias during the same pacing drive at a constant PCL because pacing stimuli fall on a progressively earlier portion of the tachycardia cycle, thus producing progressively less fusion and more fully paced morphology. Such phenomena (referred to as “variable fusion”) should be distinguished from “constant fusion” and “progressive fusion” characteristic of entrainment, and sometimes this requires pacing for long intervals to demonstrate variable degrees of fusion. Focal ATs (automatic, triggered activity, or microreentrant) cannot manifest stable fusion during overdrive pacing (i.e., overdrive pacing during focal AT results in a fully paced P morphology and intracardiac activation sequence). Moreover, overdrive pacing frequently results in suppression (automatic) or acceleration (triggered activity) of focal ATs, rather than resumption of the original tachycardia with an unchanged TCL.^{20,21}

Entrainment with manifest fusion. Entrainment of MRATs commonly produces manifest fusion that is stable (fixed) during pacing at a given PCL. Repeated entrainment at PCLs progressively shorter than the TCL results in different degrees of fusion between pacing episodes (while showing fixed fusion within any given episode of pacing), with the resultant P wave configuration looking more like a fully paced configuration as the paced rate increases.

Demonstration of the presence of manifest fusion during entrainment requires knowledge of the tachycardia surface P wave morphology and of pure pacing (at the same site and rate) in the absence of tachycardia. However, in the setting of MRAT, P wave morphology during tachycardia or pure pacing may not be easily visualized in the presence of overlapping QRS complexes and ST-T waves; hence, the intracardiac atrial activation sequence can be utilized as a surrogate to ECG morphology to demonstrate fusion and is preferable due to the ability to have many discrete recordings for comparison of paced versus tachycardia sequences. Manifest fusion is said to be present when the ECG morphology (or intracardiac activation sequence) is a hybrid of the complex morphology of the tachycardia and that observed during pure pacing.

However, fusion can sometimes be difficult to recognize on the surface ECG because the morphology of the purely paced ECG complex may not be readily available. In this setting, the presence of manifest fusion can be inferred by one of the following observations:

1. The surface P wave during entrainment is different from pure tachycardia morphology and the onset of the P wave precedes the pacing stimulus artifact of each paced beat by a fixed interval (see Fig. 13.7; see Fig. 12.12). This observation provides evidence that the tachycardia wavefront has exited from the circuit, and that the initial portion of the P wave (inscribed before the pacing stimulus artifact) is activated orthodromically by the tachycardia wavefront while the latter portion is activated by the paced wavefront.
2. The surface P wave morphology (or intracardiac activation sequence) is different from the pure tachycardia morphology but is inconsistent with the expected morphology during pure pacing at a particular site (for example, AT entrainment from the distal CS producing a proximal-to-distal CS activation sequence).
3. The demonstration of shortening of conduction time (and change in electrogram morphology) at an intracardiac electrode recording site in response to increasing pacing rates during entrainment. Because conduction velocity with an increasing rate is expected to stay the same or decrease, but not increase, a decrease in conduction time (same paced site, same recorded site) in relation to a faster pacing rate demonstrates that there are two routes of activation and that the faster one can only conduct to the recording site at faster pacing

rates. This represents the “fourth” entrainment criterion and is the intracardiac equivalent of the second entrainment criterion (progressive fusion). The amount of tissue antidromically captured is critically dependent on the pacing rate. If the recording site is located in an area activated orthodromically at a slower rate and antidromically at a faster rate, the conduction time will dramatically shorten at the faster pacing rate.²²

4. The demonstration of pacing from electrodes on a multipolar catheter that have late activation times, results in acceleration of electrograms recorded from other electrodes on the same catheter that had earlier activation times during tachycardia (Fig. 13.8). This downstream pacing affecting upstream recordings has been shown to correlate with macroreentry with high specificity.

Entrainment with inapparent fusion. Entrainment with inapparent fusion (also referred to as “local” or “intracardiac” fusion) is said to be present when a fully paced P morphology (with no ECG fusion) results, even when the tachycardia impulse exits the reentrant circuit (orthodromic activation of the presystolic electrogram is present). In this setting, fusion is limited to a small area and does not produce surface ECG fusion, and only intracardiac (local) fusion can be recognized (and even then, only with recording electrodes in the correct location).

Entrainment with concealed fusion. Entrainment with concealed fusion (sometimes also referred to as “concealed entrainment” or “exact entrainment”) is defined as entrainment with orthodromic

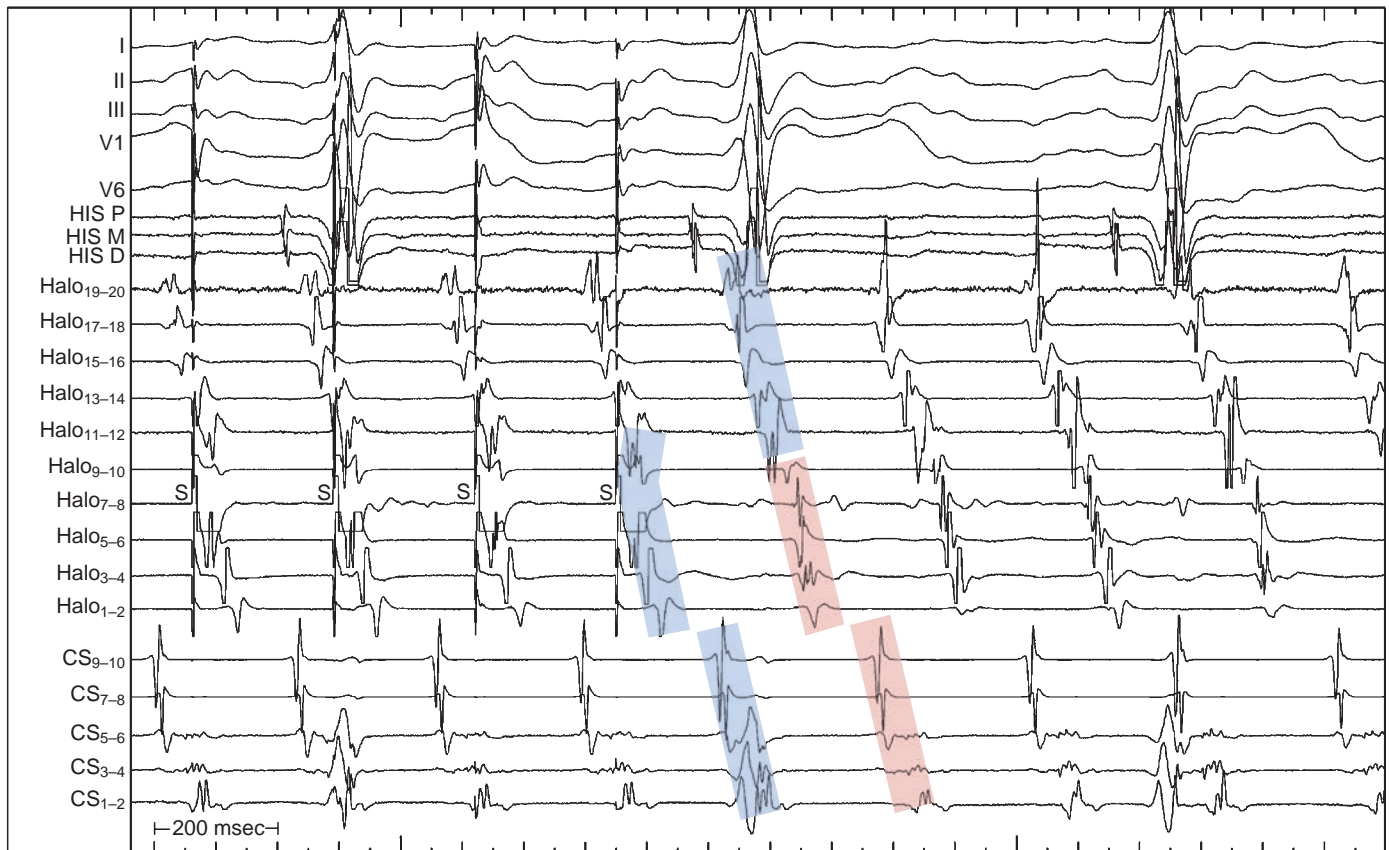


Fig. 13.8 Entrainment of Scar-Related Macroreentrant Right Atrial Tachycardia. Overdrive pacing is performed from the lateral right atrium (Halo 7–8), a site that is “downstream” from other electrodes with earlier activation during tachycardia, but nonetheless controls electrograms that are “upstream” from it on the next cycle. Electrograms shaded in blue are activated at a paced cycle length, indicating they are controlled by the last pacing stimulus, whereas electrograms shaded in red are activated at the tachycardia cycle length. This phenomenon is an indicator of macroreentry.

capture and a surface ECG complex identical to that of the tachycardia. Entrainment with concealed fusion suggests that the pacing site is within a protected isthmus, either inside or outside of, but attached to, the circuit's diastolic corridor.

Pacing in a protected isthmus, either inside or outside or attached to the reentrant circuit isthmus, forces the paced wavefront to travel in one (orthodromic) direction through the same reentrant pathway as the tachycardia wavefront. Propagation of the paced wavefront in the opposite (antidromic) direction is prevented by either a dead end (when one end of the protected isthmus is attached to the circuit and the other end is a dead end) or by colliding with the previous reentrant wavefront propagating orthodromically through the reentrant circuit (when both ends of the protected isthmus are attached to the circuit, whether the isthmus is critical to the circuit or just a bystander). In either situation, the paced wavefront is forced to use the same reentry circuit exit to activate the rest of the atrial myocardium and is prevented from activating the myocardium by propagating in any other direction. Hence, the entrained P wave morphology is identical to that of the tachycardia.^{19,20}

Termination. Rapid atrial burst pacing can usually terminate MRAT. However, termination is less likely when the pacing drive is short or the pacing site is distant from the reentrant circuit. It is important to avoid unintended termination of MRAT because it can be very difficult to reinitiate the clinically relevant AT, particularly in a patient with complex scar and multiple potential circuits.

Overdrive suppression. Overdrive suppression analogous to that seen with automatic AT is not expected in MRAT. As noted, the PPI remains relatively stable when entrainment of MRAT is performed at the same site, regardless of the length of the pacing drive. This is in contrast to overdrive suppression seen in automatic ATs, which would be associated with progressive delay of the first tachycardia beat return cycle with progressively longer pacing drives.

Transformation. Rapid atrial burst pacing can potentially convert MRAT to AF, to typical AFL, or to another type of MRAT. The risk of tachycardia transformation is significant, especially given the frequent prevalence of complex combinations of anatomic and functional obstacles that can support multiple reentrant circuits. Therefore pacing maneuvers during AT should be used sparingly, and only when necessary to confirm the role of critical areas of the circuit (during entrainment mapping, as discussed later). Detection of tachycardia transformation requires careful attention to the atrial activation sequence and the ECG pattern after cessation of pacing. Also, recording multiple simultaneous electrograms on multipolar catheters (e.g., Halo and CS catheters), as continuous endocardial references, facilitates detection of changes in atrial activation sequence.

MAPPING

Detailed knowledge of the congenital anomaly, surgical procedure, and previous ablation strategy, if present, is important in interpreting the results of mapping, in knowing how to access the RA, in assessing the feasibility of the transseptal puncture, and in determining whether fluoroscopy is helpful in localizing the catheters or whether intracardiac echocardiography or transesophageal echocardiography is needed.

The goals of mapping of macroreentrant circuits include localization of the tachycardia circuit (RA vs. LA), identification of circuit boundaries and possible lines of block in relation to atrial anatomy, and identification of the vulnerable segment (critical isthmus) of the reentry circuit in order to guide a specifically tailored ablation strategy. Mapping is best achieved by the combined use of multipolar catheters, a three-dimensional (3-D) electroanatomic mapping system, and entrainment mapping.

The use of a multipolar Halo catheter in the RA (in addition to the CS catheter) is helpful for mapping not only RA MRATs, but also LA MRATs. This catheter allows rapid visualization of an ascending or descending atrial activation sequence and can suggest the location of the reentry circuit (RA vs. LA). In addition, recording in the lateral RA can help identify a scar or line block (by exhibiting low amplitude or double potentials), a common substrate in MRATs. Simultaneous recording of RA activation and CS activation (using a decapolar catheter) can also help rapid identification of tachycardia transformation that may occur during mapping and ablation.

Electroanatomic Mapping

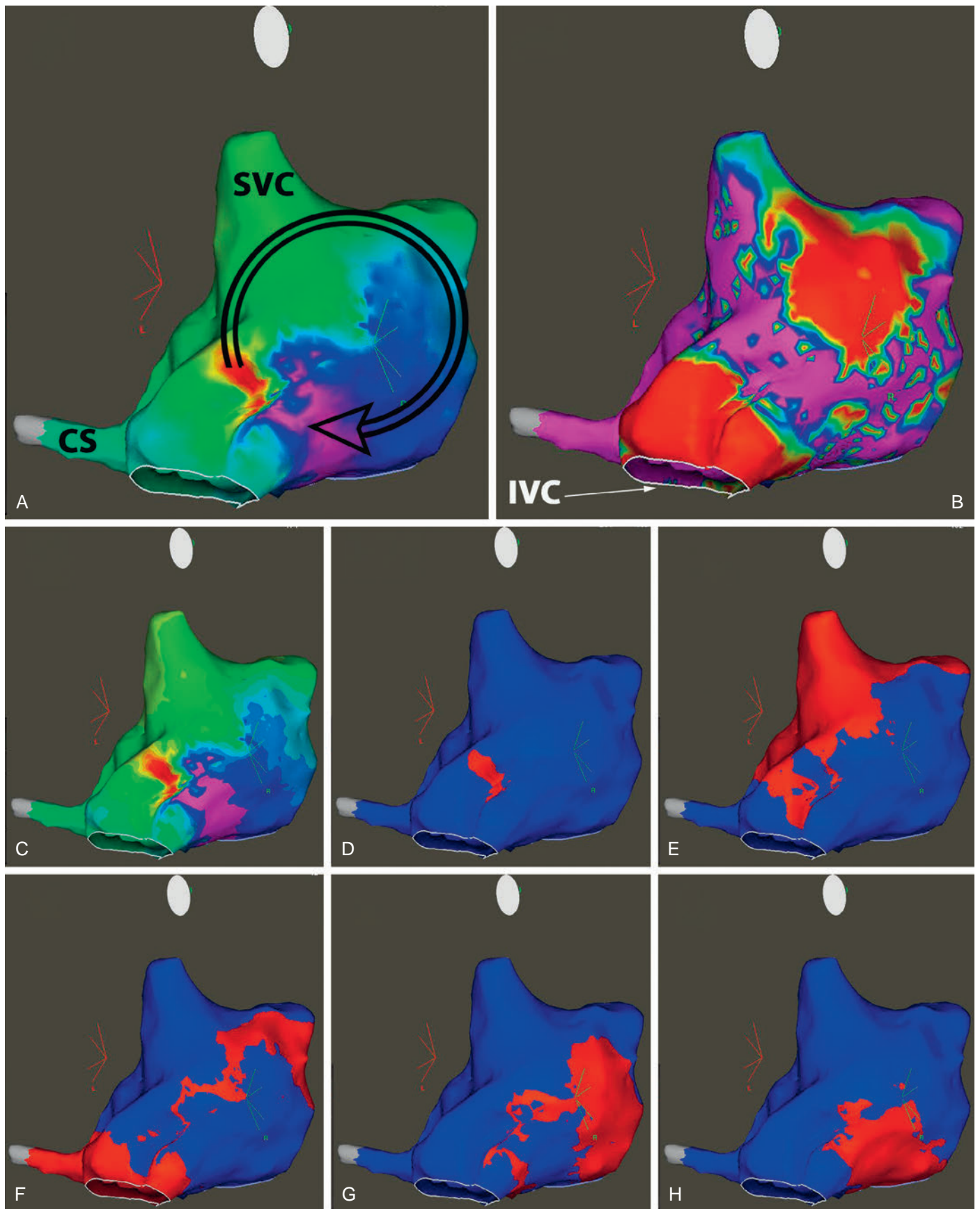
Because the reentrant circuit can involve any of multiple barriers that are frequently removed from fluoroscopic markers, conventional mapping and anatomically guided ablation, as performed for typical CTI-dependent AFL, are not feasible in the majority of MRAT cases. Therefore a 3-D electroanatomic mapping system (CARTO [Biosense Webster, Inc., Diamond Bar, CA] or EnSite NavX [St. Jude Medical, St. Paul, MN]) is typically utilized to help distinguish between a focal origin and macroreentrant tachycardia by providing a precise description of the macroreentrant circuit and sequence of atrial activation during the tachycardia and rapid visualization of the activation wavefront (eFig. 13.2). This can contribute to the understanding of the reentrant circuit in relation to native barriers and surgical scars, identification of all slow-conducting pathways and appropriate sites for entrainment mapping, planning of ablation lines, navigation of the ablation catheter, and verification of conduction block produced by radiofrequency (RF) ablation. Mapping systems also provide the capability to create and tag points of interest during the mapping process (e.g., double potentials and sites with good entrainment findings) and return to them with great precision, as well as denoting sites that should be avoided when ablating (e.g., His bundle [HB] region).

The main goal of activation mapping of MRAT is identification of the complete reentrant circuit and its mid-diastolic critical isthmus. Unlike mapping focal AT, whereby tracking the site with the earliest presystolic local activation timing is the goal of mapping, there is no early or late region for MRAT because the wavefront is continuously propagating around the circuit. Activation can be continuously mapped, and an "earlier" activation time can always be found for any particular point of the circuit. Endocardial recordings often show activation during the isoelectric intervals on the surface ECG. The concept of "early activation" is not applicable to any particular site in the reentrant circuit. Nevertheless, for illustrative purposes, a particular reference point may be designated as the origin of activation (time 0), but it should be understood that this is always arbitrary.

Mapping Technique

Initially, the reference electrogram is selected to compare the timing of sites sampled by the mapping catheter, the anatomical reference is positioned, and the window of interest is defined. The reference catheter is usually placed in the CS (because of its stability); it is important to select a recording with a prominent atrial electrogram and ensure that the ventricular electrogram is not the one detected by the system. The onset of the window of interest is usually set at the mid-diastole between two consecutive P waves with a window duration spanning 90% to 95% of the TCL.

Then, the mapping catheter is used to collect geometry information. Anatomical and EP landmarks (IVC, SVC, CS, HB, and tricuspid annulus for RA mapping, and mitral annulus and PVs for LA mapping) are marked. Identification of those anatomical fixed barriers is very important to help understand propagation of the reentrant activation wavefront in relation to these barriers, identify the tachycardia critical isthmus,



eFig. 13.2 Electroanatomic (CARTO) Mapping of the Macroreentrant Right Atrial (RA) Tachycardia. Mapping was performed during sustained tachycardia in a patient with previous right atriotomy for severe tricuspid valve disease. The right posterolateral view of the RA is presented. (A) Activation map. (B) Bipolar voltage map demonstrates a large area of low bipolar electrogram amplitude (<0.5 mV) in the lateral RA wall at the site of prior surgery. (C) Isochronal map. (D–H) Propagation map demonstrating revolution of the reentrant wave front in a clockwise fashion around the lateral RA low-voltage zone. Visualization of the reentry circuit is facilitated by correlating activation mapping findings with those of voltage mapping. CS, Coronary sinus; IVC, inferior vena cava; SVC, superior vena cava.

and plan an ablation strategy to abolish the tachycardia. Subsequently, the mapping catheter is used to create a virtual model of the endocardial surface of the atrium of interest. This can be performed during normal sinus rhythm (NSR) before induction of tachycardia, or during tachycardia and in conjunction with activation mapping.

Once chamber geometry has been delineated, activation mapping is performed to define the atrial activation sequence. Activation mapping is performed during stable (spontaneous or induced) tachycardia. Importantly, variation of the TCL by more than 10% can potentially prevent complete understanding of the circuit and limit the confidence in the electroanatomic map.

For activation mapping, each point is tagged on the 3-D map as follows: The local activation time at each site is determined from the intracardiac bipolar electrogram and is measured in relation to the fixed intracardiac electrogram obtained from the CS (electrical reference) catheter. Using the onset of the local bipolar electrogram is preferable because it is easier to determine reproducibly when measuring heavily fractionated, low-amplitude atrial electrograms. Points are added to the map only if stability criteria in space and local activation time are met. The end-diastolic location stability criterion is a variation of less than 2 mm, and the local activation time stability criterion is less than 2 milliseconds.

Reasonable numbers of points homogeneously distributed in the RA or LA, or both, must be recorded. Current electroanatomic mapping systems enable rapid activation mapping by the simultaneous acquisition of activation information from multiple electrodes (e.g., circular mapping catheter or PentaRay catheter [Biosense Webster, Diamond Bar, CA, United States]).²³

During the process of activation mapping, acquired conduction barriers encountered by the roving catheter (including surgical incisions, patches, and scars) need to be identified and tagged on the mapping system, otherwise, the mapping system will fill those areas through interpolation of simple estimates of activation timing, resulting in misleading maps. Lines of block (manifest as double or split atrial potentials with two or more discrete electrical activation events per beat separated by a clearly discernible isoelectric period) are tagged for easy identification because they can serve as boundaries for a subsequent ablation strategy design. Silent areas are defined as having an atrial potential amplitude lower than 0.05 mV and the absence of atrial capture at 20 mA (provided that catheter contact is verified). Such areas and surgically related scars, such as atriotomy scars in the lateral RA or atrial septal defect closure patches, are tagged as “scar” (see Figs. 14.1 and 14.2). At sites with double potential, entrainment of the tachycardia can help evaluate which potentials are captured by the pacing stimulus. Local activation times are then reviewed, and the apparent far-field signal is excluded from the activation maps. The activation map can also be used to catalog sites at which pacing maneuvers are performed during assessment of the tachycardia.

Localization of the Reentrant Circuit Chamber (Right Versus Left Atrium)

Analysis of RA and LA activation sequences as recorded by the peritricuspid Halo catheter and CS catheter can sometimes help predict the location of the reentry circuit. CS activation usually propagates in a proximal-to-distal direction in the setting of RA MRATs and in a distal-to-proximal direction in the setting of LA MRATs. However, this is not always true; MRATs localized to the superior RA can result in distal-to-proximal CS activation, and some LA MRATs (e.g., counterclockwise perimitral MRAT) can activate the CS in a proximal-to-distal direction (see Fig. 13.4). *Chevron* and *reverse chevron* activation patterns in the CS suggest roof-dependent LA MRAT, whereby activation propagates down the LA posterior wall to activate the midposterior portion of the

mitral annulus before propagating medially and laterally (*chevron* pattern), or the tachycardia wavefront travels down the medial and lateral walls with later activation of the midposterior mitral annulus (*reverse chevron* pattern; Fig. 13.9).²⁴

In the absence of prior ablation of the CTI, an RA activation occurring sequentially in a proximal-to-distal direction along the Halo electrodes is suggestive of counterclockwise typical AFL. This sequence is reversed during clockwise AFL (see Fig. 12.1). In both types of typical AFL (counterclockwise and clockwise), activation of the CS propagates in a proximal-to-distal direction. A *chevron* activation pattern in the Halo catheter (with earliest activation at the atrial septum near the Bachmann bundle or CS os, and latest activation in the lateral RA free wall) suggests an LA origin.

If an LA origin of the tachycardia remains uncertain, limited entrainment mapping at selected sites may be considered (see below). Otherwise, activation mapping is started in the RA. Activation timing is sampled at selected sites in the RA to quickly define the chamber of origin of the AT (RA vs. LA). During LA MRATs, when mapping is limited to the RA, long segments of the TCL may not be covered by recorded electrograms. When activation timing from 10 roughly evenly distributed sites in the RA (including 3 or 4 points at the tricuspid annulus) spans less than 50% of the TCL (in the absence of extensive RA scarring or prior CTI ablation), an LA origin of the tachycardia is likely. One exception is the presence of a small reentrant RA circuit. Also, during LA macroreentry, RA mapping typically shows nonreentrant activation patterns, clearly different from typical clockwise and counterclockwise AFL. Early RA septal activation relative to other parts of the RA can suggest a focal septal origin in some cases when LA recordings are not obtained (see Fig. 13.4). Local RA conduction disturbances, such as CTI block (from prior isthmus ablation) or transverse block at the crista terminalis, can result in activation of the anterior and septal RA in opposite directions, which mimics reentrant RA activation of typical AFL. In these cases, entrainment mapping clarifies the location of the reentrant circuit (and, perhaps as importantly, which areas are not involved in the arrhythmia).

Activation Map

In atrial macroreentry, the 3-D electroanatomic activation map typically demonstrates a continuous progression of colors around a central obstacle with close proximity of earliest and latest local activation and an activation time in a range similar to the TCL (Fig. 13.10). Conversely, the electroanatomic maps of focal ATs demonstrate radial spread of activation, from the earliest local activation site in all directions. In these cases, total atrial activation time is markedly shorter than the TCL.

It is important to recognize that if an insufficient number of points is obtained, it may be falsely concluded, through the interpolation of activation times, that the wavefront propagates from a focal source (Fig. 13.11).²⁵ This is frequently encountered when the MRAT originates from the chamber contralateral to the one being mapped. In the latter situation, the activation map will localize the site of the earliest local activation to the earliest breakthrough of interatrial conduction. Notably, this breakthrough location, although having the earliest recorded activation timing in that chamber relative to the intracardiac electrical reference, may not be presystolic (as compared to the onset of the P wave on the surface ECG) and, hence, cannot be the site of origin of a focal tachycardia. This provides a further clue to help interpret the activation map and should prompt more detailed mapping.

The initial step is activation mapping to determine whether activation of the entire TCL can be recorded within the LA. In particular, mapping should be carefully carried out around the mitral annulus because this maneuver is easy to perform and identifies a common form of LA MRAT, perimitral MRAT. If comprehensive activation

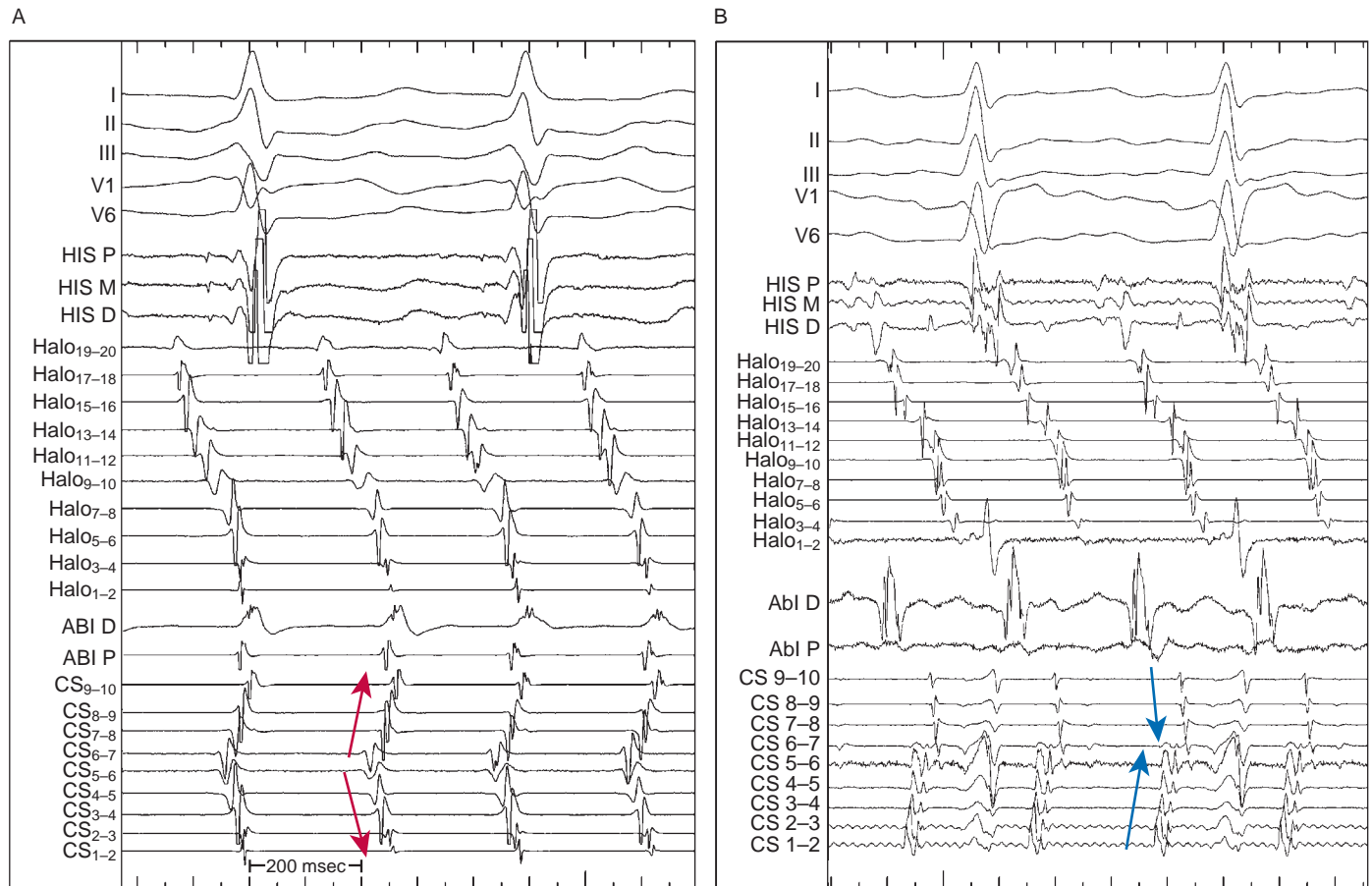


Fig. 13.9 Atrial Activation Patterns in the Coronary Sinus During Roof-Dependent Left Atrial Macroreentry. Two patients with roof-dependent macroreentrant atrial tachycardias showing characteristic “chevron” activation patterns in coronary sinus (CS) recordings. In (A) a standard chevron is seen indicated by red arrows, whereas in (B) a so-called reverse chevron pattern is seen (blue arrows).

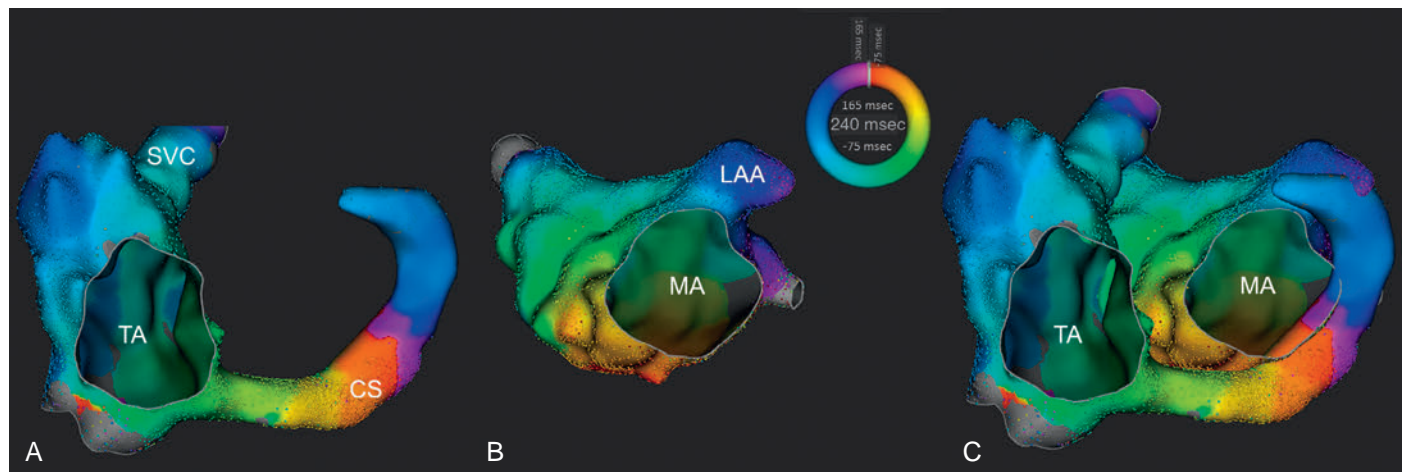


Fig. 13.10 Perimitral Macroreentrant Left Atrial Tachycardia. Three-dimensional electroanatomic (Rhythmia) activation map of the right atrium (A), left atrium (B), and both atria (C) in the left anterior oblique view constructed during counterclockwise perimitral macroreentrant atrial tachycardia. During tachycardia, the activation wavefront travels in a counterclockwise direction around the mitral annulus (MA), as indicated by a continuous progression of colors (from red to purple) with close proximity of earliest and latest local activation (red meeting purple). CS, Coronary sinus; LAA, LA appendage; MA, mitral annulus; SVC, superior vena cava; TA, tricuspid annulus.

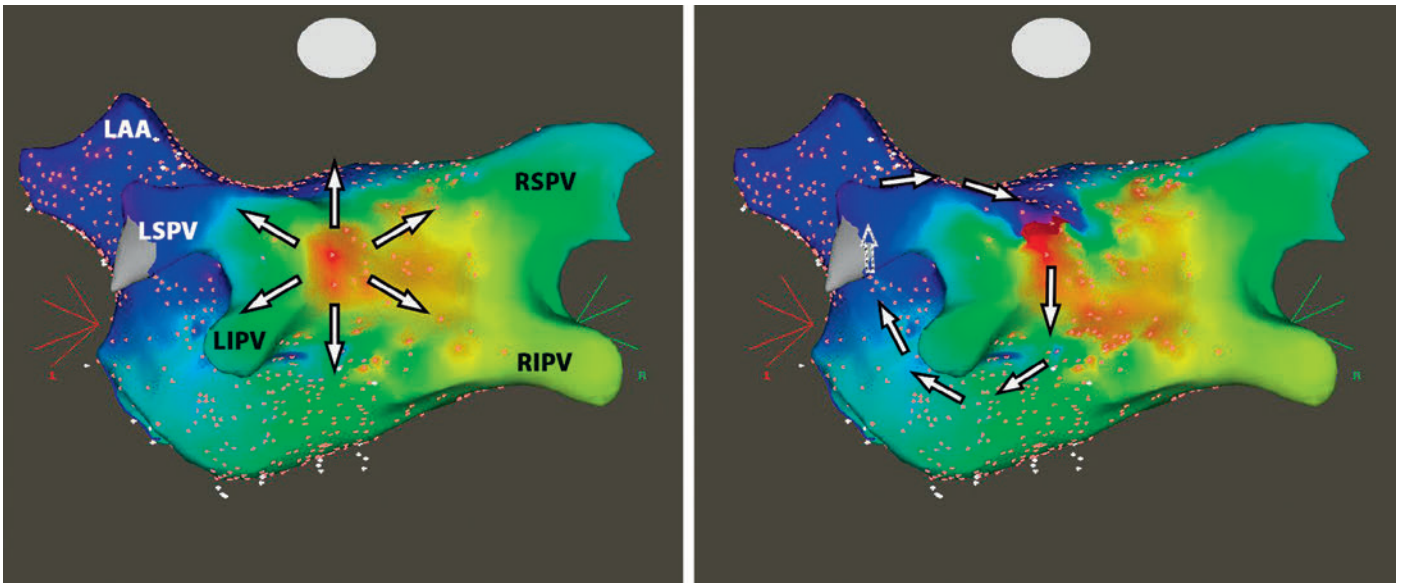


Fig. 13.11 Electroanatomic Mapping During Macroreentrant Atrial Tachycardia. Posteroanterior view of left atrial (LA) electroanatomic (CARTO) activation map in a patient with atrial tachycardia following circumferential pulmonary vein (PV) isolation and LA roof linear ablation for treatment of atrial fibrillation. *Left*, The activation pattern suggests a focal process in the posterosuperior LA with centrifugal spread of activation from the central red area. *Right*, With additional detailed mapping on the LA roof (as reflected by higher density of small white dots; each dot represents a sampled endocardial site), a macroreentrant circuit around the left-sided PVs (and through a gap in the LA roof line) is evident. LIPV, Left inferior PV; LSPV, left superior PV; LAA, LA appendage; RIPV, right inferior PV; RSPV, right superior PV.

mapping in both atria does not cover most of the TCL, two possibilities must be considered: (1) focal AT, or (2) small, localized reentrant circuits, which require much more detailed activation mapping to be identified. Localized reentry should be considered if a local electrogram exhibits low-amplitude, long, fractionated potentials occupying more than 60% of the TCL, and the putative reentry is confined to a small region of one atrium (covering a surface diameter of <3 cm) with a centrifugal activation of the atria from this region. Entrainment with concealed fusion (see later) is only possible with pacing within the small reentry circuit.

Once a reasonable number of points homogeneously distributed in the chamber of interest are obtained, the complete reentrant circuit can be defined as the spatially shortest route of unidirectional activation encompassing the complete CL of the tachycardia in terms of activation timing and returning to the site of earliest activation. Activation wavefronts that do not fulfill these conditions are bystander wavefronts and are not critical to the tachycardia circuit. However, incomplete mapping can lead to confusion about the bystander status of a given activation wavefront or loop, and an incomplete loop can be mistaken for a complete one. High-density mapping or entrainment mapping can clarify this situation by documenting wavefront collision or a long PPI, respectively (see later).

For LA macroreentry, identification of the complete reentrant circuit can be challenging, especially in patients with repaired congenital heart disease, because of the complex suture lines or baffles. Entrainment then becomes an essential tool in these cases to confirm participation of specific areas in the circuit and to try to locate a suitable isthmus area for ablation (see later).

Recently, the Rhythmia mapping system (Boston Scientific Corp., Marlborough, MA, United States) has been used to perform ultrahigh-resolution contact activation mapping on atrial arrhythmias. With this system, a small semispherical basket catheter with eight splines and eight small, printed surface electrodes per spline records unipolar elec-

trograms as it is moved around the atrial chamber (see Fig. 13.1 and Fig. 13.3). Complex automated algorithms are used to analyze and validate very small signals by comparing them to signals from the same electrodes on consecutive complexes, as well as surrounding electrodes. With this, ultrahigh-density maps facilitate accurate delineation of propagation patterns, conduction isthmuses, and lines of preexisting block. Experience with this system in MRAT is limited but promising.^{26–28}

Identification of the Critical Isthmus

Zones of slow conduction, possibly critical to the maintenance of the MRAT circuit, are usually identified by low-amplitude fractionated atrial electrograms. High-density mapping is performed in and around those zones to define their relation to adjacent normal and abnormal conduction barriers. During macroreentry, an isthmus is defined as a corridor of conductive myocardial tissue bounded by nonconductive tissue (barriers) through which the depolarization wavefront must propagate to perpetuate the tachycardia. These barriers can be scar areas or naturally occurring anatomical or functional (present only during tachycardia, but not in sinus rhythm) obstacles. The earliest presystolic electrogram closest to mid-diastole is the most commonly used definition for the center of the isthmus of the reentrant circuit. Isthmuses within low-voltage or scar areas commonly exhibit fragmented or continuous potentials with low voltage and long activation duration.¹⁷

When double potentials separated by an isoelectric interval can be traced in a convergent configuration, with a progressively decreasing interpotential interval, and culminate in a fractionated continuous electrogram, this finding indicates one end of a line of block and activation through the resulting isthmus or around a pivot point at the end of the line of block. These findings should prompt further mapping maneuvers (entrainment mapping) to verify its role in the reentry circuit.

Importantly, electrograms recorded within the critical isthmus frequently exhibit very low amplitudes, likely related to very thin strands of myocardium responsible for diastolic conduction within a large scar

area. The interpretation of these local electrograms can be very difficult in the absence of the full electroanatomic activation maps supported with critical entrainment mapping to confirm participation of adjacent areas in the circuits.

Of note, the location where earliest activation and latest local activation meet (the “early meets late” or “head meets tail” points) can be anywhere along the reentry circuit, depending on the timing of the electrical reference (the zero point) arbitrarily chosen for activation mapping. That location has no inherent relation to the site of the critical isthmus of the reentry circuit. Nonetheless, when the onset of the window of interest is set at the mid-diastole between two consecutive P waves, the region where “early meets late” on the color-coded activation map can potentially correlate with the mid-diastolic isthmus of the reentrant circuit.

Voltage Map

Voltage mapping is performed to define areas of electrical scars, which can be involved in the reentrant circuit or can potentially serve as boundaries for subsequent ablation design strategies (see eFig. 13.2). Atrial bipolar potentials with an amplitude of 0.5 mV or less are typically considered abnormal and termed low-voltage areas. Silent areas (scar) are defined as having an atrial bipolar potential amplitude of less than 0.05 mV and the absence of atrial capture at 20 mA. Superimposition of a bipolar voltage map on the activation map can also help focus auditing of the activation map to areas where low amplitude potentials are recorded. Those electrograms are the ones most prone to inaccurate automatic annotation of the local activation time.

Maps made with multielectrode PentaRay catheters can significantly improve the resolution of substrate scar mapping. Those catheters have smaller electrodes and closer interelectrode spacing (as compared to ablation catheters), which allow for recording bipolar signals from smaller tissue diameters that are less vulnerable to averaging and cancellation effects and, hence, more sensitive in detecting surviving myocardial fibers in low-voltage zones.²³

Propagation Map

Propagation of electrical activation can be superimposed on the 3-D anatomical reconstruction of the RA or LA, thereby allowing visualization of the reentrant circuit of AT in relation to the anatomical and EP landmarks and barriers (see eFig. 13.2). Analysis of the propagation map may allow estimation of the conduction velocity along the reentrant circuit and identification of areas of slow conduction and may thus help locate appropriate sites for entrainment mapping and catheter ablation.

Tachycardia Transformation

It is very important to ensure that the correct AT is being mapped at all points of time, and to remain vigilant to identify any change in the TCL or activation sequence that can result from catheter manipulation, pacing maneuvers, or ablation (eFig. 13.3). Such changes can indicate transition to another tachycardia requiring reassessment. The transition may be obvious, but it is often quite subtle and sometimes imperceptible if only the CS activation is analyzed. Simultaneous recording of RA activation (using a Halo catheter around the tricuspid annulus) and CS activation (using a decapolar catheter) can help in rapid identification of tachycardia transformation. However, it is also necessary to ensure that the change of activation sequence is not secondary to unintentional movement of the recording catheters.

Variations in the CL during MRAT can suggest variations in activation pathways resulting from circuit transformation or simply changes in conduction time; the latter usually manifests as CL alternans. The absence of ECG alterations accompanying changes in activation sequences

can occur because of an insufficient change in electromotive force, because of distance from the recording electrodes, or because of insufficient electrically active tissue. TCL variation can, in some cases, facilitate activation mapping by revealing when electrograms “lead” versus “follow.”

MRATs with multiple loops or those determined by functional lines of block are more prone to transformation. A single-loop tachycardia with a fixed barrier as its core typically remains stable and unchanged during catheter manipulation, and it may even be difficult to pace-terminate, although mechanical “bump” terminations rendering the tachycardia noninducible suggests mechanical stimulation close to a restricted and relatively fragile isthmus.

A change in ECG morphology without a change in the TCL can occur secondary to transformation of a multiple-loop tachycardia by interruption of one loop, a change in bystander activation sufficient to be visible on the surface ECG (typified by the change in CS and LA activation observed during incomplete ablation of the CTI in typical counterclockwise AFL), a change from tachycardia in one atrium to that in the other, or activation of the same circuit in the opposite direction (the last is possible only if the first AT stops at least transiently).

Limitation of the Use of Electroanatomic Mapping

The sequential data acquisition required for creation of the electroanatomic map remains time-consuming because the process requires tagging many points, depending on the spatial details needed to analyze a given arrhythmia. Furthermore, because the acquired data are not coherent in time, multiple beats are required, and stable, sustained, or frequently repetitive arrhythmia is usually needed for creation of the activation map. Also, variation of the TCL by more than 10% can potentially prevent complete understanding of the circuit and limit the confidence in the electroanatomic map.

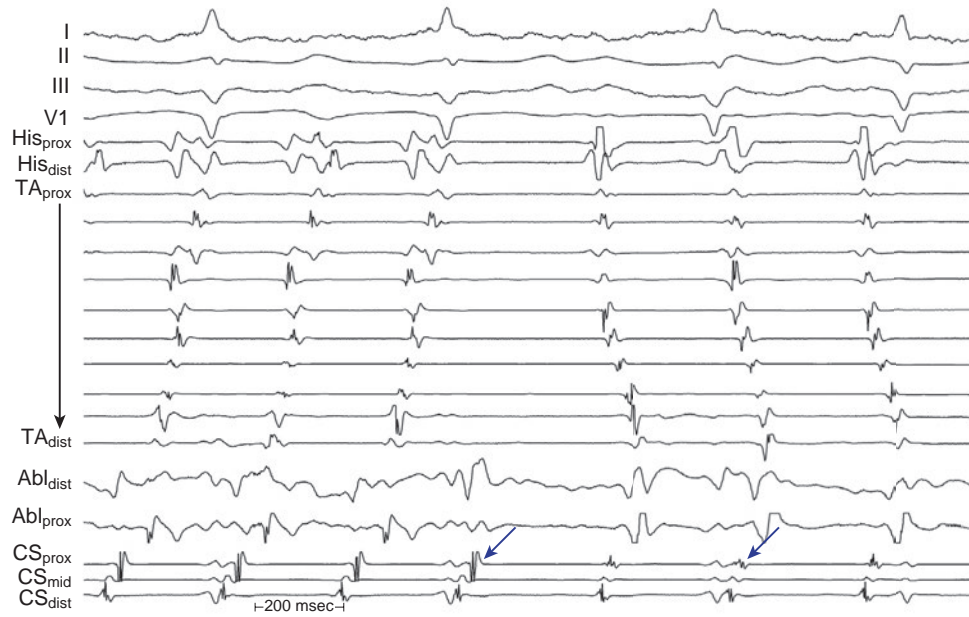
Another difficulty with current technologies is that incorrect assignment of activation for even a small number of electrograms at a few points can invalidate the entire activation map; manual adjustment is often required to achieve the optimal representation. This is especially important when activation timing for the low-amplitude, highly fractionated electrograms, similar to those commonly recorded at the isthmus of macroreentrant circuits, is erroneously assigned, which can potentially result in misleading maps.

Data interpolation between mapped points is also used to improve the quality of the display; however, areas of unmapped myocardium are then assigned simple estimates of timing and voltage information, based on surrounding sampled points, which may not be accurate.

Furthermore, the patient or intracardiac reference catheter can move, thus necessitating remapping. Although a shadow (to record original position) can be placed over this catheter to recognize displacement during the procedure, in which case the catheter can be returned to its original location, this may not always be feasible or accurate.

Entrainment Mapping

Entrainment mapping provides information about sites of the RA or LA that are part of the reentrant circuit, those that are outside the circuit, and the critical isthmus of the circuit. However, before attempting to use entrainment methods for mapping, it is necessary first to demonstrate that the tachycardia can, in fact, be entrained, thus providing strong evidence that it is caused by reentry rather than by triggered activity or automaticity. At sites of entrainment, there should be confirmation of consistent capture of the atrium at the PCL for several beats, with minimal or no change in the surface morphology or intracardiac electrograms, and continuation of the identical tachycardia after cessation of pacing. Evaluation of the PPI or other criteria can be very misleading when the presence of true entrainment has not been established. In addition, it is important to verify the absence of termination and



eFig. 13.3 Tachycardia Transformation. A change in atrial activation sequence is observed during right atrial ablation during macroreentrant atrial tachycardia that interrupts one circuit while another (left atrial) circuit persists (note coronary sinus activation from distal to proximal throughout *[arrows]*). *Abl_{dist}*, Distal ablation site; *Abl_{prox}*, proximal ablation site; *CS*, coronary sinus; *CS_{dist}*, distal coronary sinus; *CS_{prox}*, proximal coronary sinus; *His_{dist}*, distal His bundle; *His_{prox}*, proximal His bundle; *TA_{dist}*, distal tricuspid annulus; *TA_{prox}*, proximal tricuspid annulus.

BOX 13.2 Entrainment Mapping of Macroreentrant Atrial Tachycardia

Pacing From Sites *Outside* the AT Circuit Results in Manifest Entrainment

1. Manifest atrial fusion on surface ECG and intracardiac recordings (fixed fusion at a single PCL and progressive fusion on progressively shorter PCLs). Any change in atrial activation sequence, compared with baseline tachycardia and that of pure pacing, as determined by analysis of all available surface and intracardiac ECG recordings, is considered to represent manifest fusion.
2. PPI–TCL > 20 ms
3. The interval between the stimulus artifact and the onset of the P wave on the surface ECG is longer than the interval between the local electrogram on the pacing site and the onset of the P wave on the surface ECG

Pacing From Sites *Inside* the AT Circuit Results in Manifest Entrainment

1. Manifest atrial fusion on the surface ECG and intracardiac recordings (fixed fusion at a single PCL and progressive fusion on progressively shorter PCLs)
2. PPI–TCL < 20 ms
3. The interval between the stimulus artifact and the onset of the P wave on the surface ECG equals the interval between the local electrogram on the pacing site and the onset of the P wave on the surface ECG

Pacing From a *Protected Isthmus* Inside the Circuit Results in Concealed Entrainment

1. Concealed atrial fusion (i.e., paced atrial waveform on the surface ECG and intracardiac recordings is identical to the tachycardia waveform)
2. PPI–TCL < 20 ms
3. The interval between the stimulus artifact and the onset of the P wave on the surface ECG equals the interval between the local electrogram on the pacing site and the onset of the P wave on the surface ECG

AT, Atrial tachycardia; CL, cycle length; ECG, electrocardiogram; PCL, pacing cycle length; PPI, postpacing interval; TCL, tachycardia cycle length.

reinitiation of the tachycardia during the same pacing drive. Once the presence of entrainment is verified, several criteria can be used to indicate the relation of the pacing site to the reentrant circuit (Box 13.2).¹⁹

Postpacing Interval

The PPI is the interval from the last pacing stimulus that entrained the tachycardia to the next recorded electrogram *at the pacing site*. The PPI should be measured to the *near-field* potential that indicates depolarization of tissue at the pacing site that was actually captured. The PPI represents the time for the wavefront to travel from the pacing site to the reentry circuit, then to revolve around the circuit (following the same path as the tachycardia reentry wavefronts), and finally to return from the circuit to the pacing site. Thus the PPI should equal the TCL (representing one complete revolution through the reentry circuit) plus the time required for the stimulus to propagate from the pacing site to the tachycardia circuit and back to the pacing site. Given that the TCL is stable (which is a prerequisite for entrainment mapping), and that there is no decremental conduction between the pacing site and the reentry circuit, the PPI should remain relatively stable when entrainment of MRAT is performed at the same site, regardless of the length of the pacing drive or CL of pacing over a moderate range.

The greater the difference is between the PPI and the TCL (PPI–TCL), the longer the conduction time will be between the pacing site and the reentry circuit, and the greater the physical (or electrical) distance will be between the pacing site and the circuit (see Fig. 13.7; see Fig. 12.12).

The PPI–TCL value is highly reproducible during repeated entrainment attempts at the same PCL.^{19,29}

Several factors have to be considered when evaluating the PPI. The PPI should be measured to the near-field potential that indicates depolarization of tissue *at the pacing site*. However, assessment of the PPI can be problematic when the electrograms from the pacing site are not discernible, especially in regions of scar, where local near-field potentials are small and often difficult to distinguish or separate from far-field potentials. In addition, recordings of local activation at the pacing site may not be obtainable or interpretable due to electrical noise and signal saturation after the stimulus artifact. In these situations, the PPI can be measured from electrograms recorded by electrodes adjacent to those used for pacing (e.g., the proximal electrodes on the mapping catheter), but this does introduce potential error, particularly in regions of abnormal conduction.²⁰

It is important to recognize that the (PPI–TCL) value can be misleadingly long despite pacing from sites within the reentrant circuit. In one report in patients with typical AFL, long (PPI–TCL) values (more than 30 milliseconds) after entrainment from the CTI were observed in 18% of patients despite a PCL within 20 milliseconds of the TCL, and more frequently when the PCL was more than 30 milliseconds shorter than the TCL and in patients on amiodarone therapy. The long (PPI–TCL) values are likely caused by rate-dependent slowing of conduction or alterations of the activation path. These findings likely also apply to other macroreentrant tachycardias.^{30,31}

In summary, the (PPI–TCL) value serves as an approximate measure of the distance from the pacing site to the reentry circuit. During pacing at a site that is in the circuit, the conduction time between the pacing site and the circuit is 0, and the PPI equals the TCL, provided that three fundamental assumptions are true. First, pacing must capture and entrain the tachycardia. Second, the electrograms used for measurement of the PPI are recorded at the pacing site. Third, conduction through the reentry circuit must not be slowed or altered by pacing.^{31,32}

Number of Pacing Stimuli Needed to Entrain

The number needed to entrain assesses the number of captured pacing stimuli required to accelerate tachycardia to the PCL. Recording electrograms from the lateral RA and distal CS and properly timed initiation of the entrainment pacing (the coupling interval of the first paced stimulus is identical to the PCL) are required to measure the number needed to entrain. A small number (≤ 2) of pacing stimuli needed to entrain the tachycardia (with a PCL of 5 to 30 milliseconds shorter than the TCL) is consistent with a PPI–TCL value of less than 20 milliseconds and indicates that the pacing site is within the reentry circuit. A larger number of pacing stimuli needed to entrain (> 3 for PCLs of 16 to 50 milliseconds, and > 4 for PCLs of 5 to 15 milliseconds shorter than the TCL) indicates that the pacing site is outside the reentry circuit.

An advantage of this criterion is that it does not require continuation of tachycardia after pacing for assessment and remains valid even when the tachycardia terminates or changes. The number needed to entrain is also useful when electrograms for assessment of the PPI are difficult to define. Also, the number needed to entrain does not increase at shorter PCLs, likely because the conduction velocity in the intervening myocardium (between the pacing site and the reentry circuit) is less susceptible to changes in the PCL. This is in contrast to the slow conduction zone within the reentry circuit, which can display decremental conduction properties at PCLs shorter than the TCL, resulting in misleading long PPIs.³³

Conduction Time From the Pacing Site to the Circuit Exit Site

Comparing the stimulus-exit interval with the electrogram-exit interval can help identify the critical isthmus of the reentry circuit. During

entrainment of MRAT, the interval between the pacing stimulus and the onset of the P wave on the surface ECG reflects conduction time from the pacing site to the exit of the reentrant circuit (stimulus-exit interval), regardless of whether the pacing site is inside or outside the reentrant circuit, because activation starts at the pacing site and propagates in sequence to the circuit exit site. On the other hand, during tachycardia, the interval between the local electrogram at a given site and the circuit exit (electrogram-exit interval) can reflect the true conduction time between those two sites if they are activated in sequence (which occurs when that particular site is located within the reentrant pathway), or can be shorter than the true conduction time (i.e., a “pseudo-interval” that does not represent a true conduction time between the two locations) if those two sites are activated in parallel (which occurs when that particular site is located outside the reentrant circuit). Because it is frequently difficult to determine the onset of the P wave on the surface ECG, a reference intracardiac electrogram representing the exit of the circuit is usually used.

Because a diastolic electrogram is not specific for the isthmus and can be recorded from bystander sites, comparing the stimulus-exit interval during entrainment to the electrogram-exit interval (measured at the pacing site) during tachycardia can help distinguish the isthmus sites from attached bystander and inner loop sites. Activation from isthmus sites to the exit of the circuit follows the same pathway during both tachycardia and entrainment. In contrast, attached bystander and inner loop sites are activated in parallel with the exit site during tachycardia but in sequence during entrainment, resulting in a significantly shorter (more than 20 milliseconds) electrogram-exit interval than stimulus-exit interval. On the other hand, at any given pacing site, an electrogram-exit interval that is equal (± 20 milliseconds) to the stimulus-exit interval indicates that the pacing site lies within the reentry circuit and excludes the possibility that the site is a dead-end pathway attached to the circuit (i.e., not a bystander) (see Box 13.2).^{19,34}

This criterion is of value in verifying the relationship of pacing sites demonstrating entrainment with concealed fusion to the reentry circuit. This measurement can produce conflicting results in cases of manifest ECG fusion or when the onset of the surface P wave is not discernable. Therefore this criterion is of little value at pacing sites not exhibiting concealed fusion.²¹ This pitfall can be mitigated by measuring the interval between the last stimulus entraining the tachycardia and a timing reference during the second beat after the stimulus (the N + 1 beat) and then subtracting this interval from a comparable interval between the electrogram (at the pacing site) in any following beat (the so-called N + 1 difference).

Localization of the Reentry Circuit

The difference between the PPI and TCL can qualitatively estimate how far the reentrant circuit is from the pacing site. As noted, the (PPI–TCL) difference represents the conduction time from the pacing site to the reentry circuit and back. Hence, the greater the (PPI–TCL) difference, the longer the conduction time is between the pacing site and reentry circuit, and the greater the physical distance is between the pacing site and circuit. On the other hand, small (PPI–TCL) differences (<20 milliseconds) indicate that the pacing site is within or very close to the reentry circuit.

At the beginning of the mapping procedure, to quickly approximate the region of the MRAT, pacing is initially performed from the CTI, high RA, midlateral RA, and proximal and distal CS. A difference between the PPI and TCL of more than 40 milliseconds at three or more different points in the RA (including the CTI and RA free wall, but excluding the septum and CS) denotes an LA circuit.

Furthermore, during entrainment from the high lateral RA, a PPI–TCL difference of more than 50 milliseconds strongly suggests LA macro-

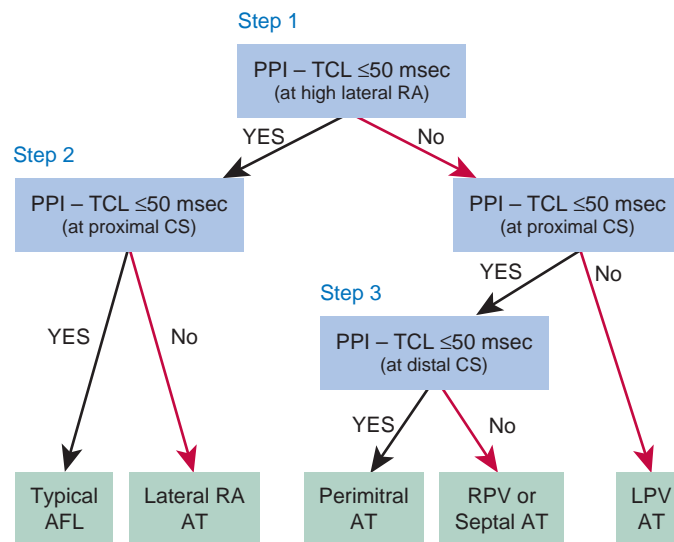


Fig. 13.12 Stepwise Algorithm for Determining the Location of Macroreentrant Atrial Tachycardia (AT) Circuit. See text for discussion. AFL, Atrial flutter; CS, coronary sinus; LPV, left pulmonary vein; PPI, postpacing interval; RA, right atrium; RPV, right pulmonary vein; TCL, tachycardia cycle length. (From Miyazaki H, Stevenson WG, Stephenson K, et al. Entrainment mapping for rapid distinction of left and right atrial tachycardias. *Heart Rhythm*. 2006;3, 516–523, with permission.)

reentry (Fig. 13.12). Exceptions do occur with RA scars, likely due to the potential for a long conduction time between the high RA and a circuit on the other side of a region of conduction block in the low RA. Entrainment from the low RA should identify these circuits. For RA MRATs, a (PPI–TCL) difference of less than 50 milliseconds at the proximal CS distinguishes typical AFL from a lateral RA MRAT. For LA MRATs, a (PPI–TCL) difference of less than 50 milliseconds at the proximal and distal CS distinguished perimitral MRAT from circuits involving the right PVs and septum. When entrainment does not localize the circuit in the LA or RA, a focal or small reentrant arrhythmia should be considered.³⁴ Dual- and multiple-loop reentry should be considered when entrainment mapping (analysis of the PPI) reveals large and disparate regions of the atrium being part of the circuit.

Identification of the Critical Isthmus

For identification of the critical isthmus of the reentrant circuit, entrainment mapping is performed at selected atrial sites identified during activation mapping and propagation mapping in relation to atrial scars, barriers, and lines of block. Entrainment with concealed fusion should be sought first, which indicates that the pacing site is in a protected isthmus located within or attached to the reentrant circuit. Whether this protected isthmus is crucial to the reentrant circuit or is just a bystander site needs to be verified by comparing the PPI with the TCL and the stimulus-exit interval with the electrogram-exit interval, as outlined in Box 13.2.^{19,34}

Color-Coded Mapping of Postpacing Intervals

A graphical representation of entrainment mapping can be constructed by plotting the values of the (PPI–TCL) differences on an electroanatomic mapping system to generate color-coded 3-D entrainment maps. This approach can potentially help accurately determine and visualize the 3-D location of the entire reentrant circuit, even though the area of slow conduction of the tachycardia is not described. Because none of the available electroanatomic mapping systems contains an algorithm for color-coding of entrainment information, the modus for activation

mapping is altered manually. At each 3-D location of the catheter tip stored on the electroanatomic mapping system, entrainment stimulation is performed, and the (PPI–TCL) difference is calculated and entered into the mapping system as if it were an “activation time.” For this purpose, the actual local electrogram stored at the 3-D location is completely disregarded. The annotation marker is manually moved into a position where the numerical timing information equaled the entrainment information (PPI–TCL). That timing information is then displayed in a color-coded fashion as if it were an activation time, but, in fact, it represents information on the length of the entrainment return cycle. With the color range, red (in CARTO) or white (in NavX) represents points closest to the reentrant circuit (i.e., sites with smaller [PPI–TCL] differences, approaching 0, signifying their inclusion in the reentrant circuit), and purple represents points far away from the circuit (i.e., sites with the largest [PPI–TCL] differences).^{35,36}

Color-coded 3-D entrainment mapping allows determination of the full active reentrant circuit (vs. passively activated regions of the chamber) and the obstacle around which the tachycardia is circulating, and it provides very useful information on the location of potential ablation sites. However, ablation will not terminate reentry at all of these sites; the final choice is determined by location of anatomical barriers and width of putative isthmuses, so that strategic ablation lines, mainly connecting to anatomical barriers, can be applied to transect the circuit and eliminate the arrhythmia.^{35,36}

Limitations of Entrainment Mapping

Entrainment techniques can be difficult in patients with incisional AT caused by low-amplitude or absent atrial potentials in the area of surgical incisions. The complexity and low amplitude of the electrograms within circuit isthmuses can make it impossible to reliably measure local PPIs. Furthermore, it can be difficult to consistently capture the atrium during pacing at sites of low-amplitude signals.¹⁷

Fusion during entrainment is difficult to assess on the surface ECG because the pacing artifact and QRS complex frequently obscure the surface P waves, which often have low amplitude in these patients. Furthermore, methodological problems can affect the validity of the PPI. Decremental conduction during pacing increases the PPI and causes false-negative assessment results at some reentry circuit sites. The occasional presence of far-field potentials can also impair the accuracy of entrainment mapping.

Spontaneous variations of the TCL severely compromise use of entrainment mapping, which assumes that the (PPI–TCL) differences result only from the proximity of the pacing site to the circuit and not from variable conduction velocity to, from, or within the circuit. Furthermore, it can be difficult to identify exact catheter positions in relation to anatomical barriers because visualization of these barriers is not possible fluoroscopically. Combining entrainment mapping with electroanatomic mapping can reduce the difficulties created by some of these limitations.

Importantly, overdrive pacing can potentially result in termination or transformation of the clinical tachycardia to another morphology or to AF, especially in the setting of AT with greater CL variability. Therefore it is advisable to begin with electroanatomic mapping, while pacing maneuvers are used sparingly, just to confirm the participation of precise areas in the reentry circuit and to improve understanding of the tachycardia further.^{19,34} The risk of tachycardia alteration or termination can be minimized by synchronized pacing at a PCL slightly (within 20 milliseconds) shorter than the TCL.³⁷

Noncontact Mapping

When AT is short-lived or cannot be reproducibly initiated, simultaneous multisite data acquisition using the noncontact mapping system

(EnSite 3000, St. Jude Medical, Inc., St. Paul, MN) can help map the AT circuit. This system can re-create the endocardial activation sequence from simultaneously acquired multiple data points over a few tachycardia beats without requiring sequential point-to-point acquisitions.

The EnSite 3000 system requires a 9 Fr multielectrode array and a 7 Fr mapping-ablation catheter. To create a map, the balloon catheter is positioned over a 0.035-inch guidewire under fluoroscopic guidance in the cardiac chamber of interest. The balloon is then deployed, and it can be filled with a mixture of contrast and saline to be visualized fluoroscopically. The balloon is positioned in the center of the atrium and does not come into physical contact with the atrial walls being mapped. The position of the array in the chamber must be secured to avoid significant movement that would invalidate the electrical and anatomical information. The array must be positioned as closely as possible (and in direct line of sight through the blood pool) to the endocardial surface being mapped because the accuracy of the map is sensitive to the distance between the center of the balloon and the endocardium being mapped.³⁸

Systemic anticoagulation is critical to avoid thromboembolic complications. Intravenous heparin is usually given to maintain the activated clotting time at 250 to 300 seconds and 300 to 350 seconds for RA and LA mapping, respectively.

A conventional deflectable mapping-ablation catheter is also positioned in the chamber and used to collect geometry information. The mapping catheter is initially moved to known anatomical locations (IVC, SVC, CS, HB, and tricuspid annulus for RA mapping and mitral annulus and PVs for LA mapping), which are tagged. Subsequently, detailed geometry of the chamber is reconstructed by moving the mapping catheter around the atrium. Using this information, the computer creates a model, called a convex hull, of the chamber during diastole.

Once chamber geometry has been delineated, tachycardia is induced, and mapping can begin. The data acquisition process is performed automatically by the system, and all data for the entire chamber are acquired simultaneously. The system then reconstructs more than 3000 unipolar electrograms simultaneously and superimposes them onto the virtual endocardium, to produce color-coded isopotential maps that graphically depict depolarized regions. Activation can be tracked on the isopotential map throughout the tachycardia cycle, and wavefront propagation can be displayed as a user-controlled 3-D “movie.” The color range represents voltage or timing of onset. A default high-pass filter setting of 2 Hz is used to preserve components of slow conduction on the isopotential map. When conduction through gaps in a line of block is suspected of being very slow, the high-pass filter may be set at 1.0 to 0.5 Hz. Color settings are adjusted so that the color range matches 1 to 1 with the millivolt range of the electrogram deflection of interest. Isochronal maps can also be created that represent progression of activation throughout the chamber relative to a user-defined electrical reference timing point. If the atrial electrograms overlap with the T wave, a ventricular extrastimulus may be delivered to accelerate ventricular depolarization and repolarization and reveal the following atrial complex without far-field interference.³⁸

In addition, the system can simultaneously display as many as 32 electrograms as waveforms. Unipolar or bipolar electrograms (virtual electrograms) can be selected (at any given interval of the tachycardia cycle) by using the mouse from any part of the created geometry and displayed as waveforms as if from point, array, or plaque electrodes. The reconstructed electrograms are subject to the same electrical principles as contact catheter electrograms because they contain far-field electrical information from the surrounding endocardium, as well as the underlying myocardial signal vector, and distance from the point where the signal is generated to the array can affect the contribution

to the electrogram. The maps can be particularly useful for identifying slowly conducting pathways, such as the critical slow pathways and rapid breakthrough points of MRAT. The reentry circuit can be fully identified, along with other aspects such as the slowing, narrowing, and splitting of activation wavefronts in the isthmus. The locator technology used to collect the geometry information for the convex hull can then be used to guide an ablation catheter to the proper location in the heart. Ablation lesions can be tagged, thus facilitating the performance of linear ablation devoid of gaps across the tachycardia critical isthmus.³⁸

Substrate mapping based on scar or diseased tissue, which has been introduced into noncontact mapping technology, can be of value in mapping and ablation of MRAT. Dynamic substrate mapping allows the creation of voltage maps from a single cardiac cycle and can identify low-voltage areas, as well as fixed and functional block, on the virtual endocardium through noncontact methodology. High-density voltage mapping of the atrial substrate is performed using the peak negative voltage of the reconstructed unipolar electrograms. An atrial substrate characterized by an abnormally low peak negative voltage (<30% of the maximal peak negative voltage) can potentially predict the slow conduction path within the protected isthmus of the MRAT. When combined with the activation sequence, substrate mapping provides essential information for guiding ablation, even when the arrhythmia is nonsustained.³⁹

Limitations of Noncontact Mapping

Very low-amplitude signals may not be detected, particularly if the distance between the center of the balloon catheter and the endocardial surface exceeds 40 mm or at the regions near the catheter poles, thus limiting the accurate identification of diastolic signals. In addition, the acquired geometry in the current version of the software is somewhat distorted, and multiple set points are required to clearly establish the origin and shape of complicated structures, such as the LA appendage or PVs. Otherwise, these structures may be lost in the interpolation among several neighboring points. A second catheter is still required for more detailed mapping to find the precise site to ablate, and sometimes it is difficult to manipulate an ablation catheter around the outside of the balloon, especially during mapping in the LA. Moreover, aggressive anticoagulation is required when using this system, and special attention and care are necessary during placement of the large balloon electrode in a nondilated atrium.

Practical Approach to Mapping Macroreentrant Atrial Tachycardia

Exclusion of Cavotricuspid Isthmus Dependence

Because CTI-dependent typical AFL is the most common MRAT, even in patients with prior atrial ablation or cardiac surgery, exclusion of the CTI as part of the reentrant circuit is an important initial step. This remains an important step even when the ECG pattern is not classic for counterclockwise or clockwise typical AFL. In fact, typical AFL frequently manifests with an atypical 12-lead ECG appearance (so-called pseudo-atypical flutter) in the setting of markedly abnormal atrial substrate. Typical AFL can be rapidly diagnosed or excluded by mapping of the tricuspid annulus and by entrainment maneuvers at the CTI.

Exclusion of the CTI as part of the reentrant circuit can be established by any of the following: (1) demonstration of bidirectional activation of the CTI during AT, with resulting collision or fusion within the isthmus by activation from opposing directions (the low lateral RA and CS; see Fig. 13.4); (2) recording of double potentials separated by an isoelectric and constant interval throughout the full extent of the CTI during tachycardia (indicating complete CTI conduction block); or (3) entrainment mapping from the CTI that demonstrates manifest atrial fusion with a long PPI (see Fig. 13.7).

Localization of the Reentrant Circuit Chamber (Right Versus Left Atrium)

Patient history. A history of prior surgery or ablation within a particular atrial chamber should focus the intensity of the search for the arrhythmia substrate in that chamber. MRATs can involve anatomical structures to create single- or multiple-loop or circuit reentry. In the setting of previous cardiac surgery, a right-sided location of the arrhythmia is more likely and is often seen years later in patients who had a right lateral atriotomy and who underwent surgical closure of an atrial or ventricular septal defect or valve repair. These arrhythmias can also be seen after more complex surgical correction of congenital heart disease, such as the Mustard or Senning correction of transposition of the great vessels, and also after tricuspid valve surgery. LA macroreentry is more likely in the presence of left heart disease, such as cardiomyopathy or mitral valve disease, and following catheter or surgical ablation of AF. In these patients, spontaneous conduction abnormalities and areas of electrical silence forming the substrate for arrhythmia have been observed.

Electrocardiographic findings. Lead V₁ is the most useful for distinguishing LA from RA origin. In the absence of previous cardiac surgery or catheter ablation (particularly involving linear lesions in the LA), P waves that are completely negative in lead V₁ are more frequently associated with RA free-wall circuits. Conversely, in the absence of counterclockwise typical AFL, broad-based upright P waves in lead V₁ are more frequently associated with LA circuits. A decreased amplitude of the P waves in the inferior leads is suggestive of LA origin of MRAT. LA circuits frequently generate low-amplitude P waves, with some of them having visible waves only in lead V₁.⁸ For ATs post AF ablation, negative P waves in any of the precordial leads favors RA MRAT over LA MRAT with a sensitivity and specificity of 83% and 100%, respectively, and an accuracy of 98%.¹⁵

TCL variations. Large spontaneous variations (30 to 125 milliseconds) or even 2:1 conduction in the RA CL with concomitant variations of less than 20 milliseconds in CS recordings is consistent with an LA origin of the macroreentrant circuit (see Fig. 13.5).

Activation sequence in the CS. CS activation usually propagates in a proximal-to-distal direction in the setting of RA MRATs and in a distal-to-proximal direction in the setting of LA MRATs. However, this is not always true; MRATs localized to the superior RA can result in distal-to-proximal CS activation, and a very distally positioned CS catheter can show a distal-to-proximal activation sequence with almost any RA tachycardia with RA-LA conduction over the Bachmann bundle. Some LA MRATs (e.g., counterclockwise perimitral MRAT) can activate the CS in a proximal-to-distal direction (see Fig. 13.4).⁴⁰

Activation mapping. When activation timing from 10 roughly evenly distributed sites in the RA, including three or four points at the tricuspid annulus, spans less than 50% of the TCL (in the absence of extensive RA scarring or prior CTI ablation), the arrhythmia is probably not located in the RA. In the setting of LA MRATs, RA mapping typically shows a nonreentrant activation pattern with early RA septal activation relative to other parts of the RA when LA recordings are not obtained (see Fig. 13.4).

Entrainment mapping. If macroreentry has been demonstrated, a difference between the PPI and TCL of more than 40 milliseconds at three or more different points in the RA (including the CTI and RA free wall, but excluding the septum and CS) denotes an LA circuit. In the absence of significant conduction delay within the RA, entrainment from the high lateral RA with a PPI–TCL difference of more than 50 milliseconds strongly suggests an LA macroreentry.³⁴

Identification of Barriers and Potential Lines of Block

Identification of the tachycardia circuit barriers is very important in understanding the propagation of the reentrant activation wavefront in relation to these barriers, identifying potential slow-conducting pathways critical to the reentrant circuit, identifying sites to target by entrainment mapping, and planning subsequent ablation strategy to abolish the tachycardia. Electroanatomic 3-D mapping is typically used to facilitate tagging of these anatomical and EP landmarks, rapid visualization of the activation wavefront in the context of the relevant anatomy, and performance of voltage mapping to define areas of electrical scars.

For RA macroreentry, the tricuspid annulus often provides one important barrier. Other naturally fixed barriers include the IVC, SVC, and CS os. For LA macroreentry, the mitral annulus and PVs often provide important barriers. Acquired barriers include surgical incisions or patches, surgical or catheter ablation lines, and atrial regions devoid of electrical activity (electrical scars, defined as having an atrial potential amplitude of <0.05 mV and the absence of atrial capture at 20 mA). A line of block can be identified by the presence of double potentials, thus reflecting conduction up one side of the barrier and down the other side, with the bipolar electrogram recording both waves of activation (see Figs. 14.1 and 14.2).

Identification of the Complete Reentrant Circuit

Electroanatomic activation mapping. Activation mapping is performed to define the atrial activation sequence. Reasonable numbers of points homogeneously distributed in the atrium of origin of the tachycardia must be recorded. Unlike in mapping focal AT, in which tracking the site with the earliest presystolic local activation timing is the goal of mapping, there is no early or late region for MRAT because the wavefront is continuously propagating around the circuit. The complete reentrant circuit is the spatially shortest route of unidirectional activation encompassing the complete CL of the tachycardia in terms of activation timing and returning to the site of earliest activation. Using electroanatomic mapping, this translates into continuous progression of colors (from red to purple in the CARTO system and from white to purple in the NavX system) around the atrium, with close proximity of earliest and latest local activation. In addition, propagation of electrical activation superimposed on the 3-D anatomical reconstruction of the atrium can be visualized as a propagation map in relation to the anatomical and EP landmarks and barriers (see eFig. 13.2). If comprehensive biatrial activation mapping does not cover most of the TCL, two possibilities must be considered: focal AT and small, localized reentrant circuits (i.e., electrical activity accounting for more than 85% of the TCL is present within an area with a diameter of 3 cm or less). Identification of small circuits requires much more detailed activation mapping (see Fig. 13.11).

Entrainment mapping. Entrainment mapping can be used to indicate the relation of pacing sites to the reentrant circuit, and it qualitatively estimates how far the reentrant circuit is from the pacing site (see Fig. 13.7). For RA MRAT, a (PPI–TCL) difference of less than 50 milliseconds at the proximal CS distinguishes typical AFL from a lateral RA MRAT. With LA MRAT, a (PPI–TCL) difference of less than 50 milliseconds at the proximal and distal CS distinguishes perimitral MRAT from macroreentrant circuits involving the right PVs and septum. When entrainment does not localize the circuit in the LA or RA, a focal or small reentrant arrhythmia should be considered. Color-coded 3-D entrainment mapping can facilitate determination of the full active reentrant circuit (vs. passively activated regions of the chamber) and the obstacle around which the tachycardia is circulating, and it provides very useful information on the location of potential ablation sites.³⁴

Identification of the Critical Isthmus

Electroanatomic activation mapping. Once a scar or fixed barrier is localized, its role in supporting reentry is important in determining whether the isthmuses formed around it need ablation. Whether an isthmus is a critical part of the reentrant circuit can be determined by activation mapping during sustained stable reentry and entrainment mapping. The critical isthmus may lie between two anatomical landmarks (e.g., the mitral annulus and the left inferior PV), or it can be a relatively narrow channel bounded by sites of scar or double potentials (marking lines of conduction block). Electrograms recorded within the critical isthmus frequently exhibit long, fractionated, low-amplitude potentials, likely related to very thin strands of myocardium responsible for diastolic conduction within a large scar area. During electroanatomic activation mapping, when the onset of the window of interest is set at mid-diastole between two consecutive P waves, the mid-diastolic isthmus of the reentrant circuit can potentially be identified by the interface of early and late activation (i.e., the region where “early meets late” on the color-coded activation map). High-density mapping is then performed in and around the isthmus to define its limits and width more precisely (see eFig. 13.2).

Of note, stable overdrive pacing of the critical isthmus can be difficult or impossible in RA atriotomy tachycardia because of tachycardia interruption. Isthmus participation in the circuit is often proven by tachycardia interruption with catheter pressure, as well as by tachycardia interruption and noninducibility after RF application in the area. A single, wide, fractionated electrogram can be recorded from the lower pivot point of the circuit in the low lateral RA, close to the IVC, and perhaps also from other isthmuses of the circuit. The line of double potentials or fractionated, low-voltage electrograms can also often be recorded in NSR, to allow tentative localization of the scar and the associated anatomical isthmuses.

Entrainment mapping. For identification of the critical isthmus of the reentrant circuit, entrainment mapping is performed at selected atrial sites identified during activation mapping and propagation mapping in relation to atrial scars, barriers, and lines of block. Entrainment with concealed fusion should be sought, which indicates that the pacing site is in a protected isthmus located within or attached to the reentrant circuit. Whether this protected isthmus is crucial to the reentrant circuit or is just a bystander site needs to be verified by comparing the PPI with the TCL and the stimulus-exit interval with the electrogram-exit interval, as outlined in Box 13.2.

ABLATION

In patients with MRAT, periprocedural anticoagulation management is guided by the same principle used for patients with typical AFL. In patients with persistent MRAT of a duration longer than 48 hours or unknown duration, catheter ablation should be delayed until the patient has been adequately anticoagulated at appropriate levels for 3 to 4 weeks or transesophageal echocardiography has excluded atrial thrombi. In these patients, several options exist for periprocedural anticoagulation. Traditionally, a “bridging” strategy of conversion of oral anticoagulation therapy to enoxaparin, has been employed to allow ablation and subsequent hemostasis to be performed during a pause in anticoagulation. Currently, catheter ablation has been increasingly performed while on uninterrupted periprocedural oral anticoagulation (warfarin, dabigatran, factor Xa inhibitors).

Target of Ablation

The choice of ablation sites should be among those segments of the reentry circuit that offer the most convenient and safest opportunity for creating conduction block. Among other factors are the isthmus

size, anticipated catheter stability, and risk of damage to adjacent structures (e.g., phrenic nerve, sinus node, and atrioventricular node [AVN]).

Ablation is performed by targeting the narrowest identifiable isthmus of conduction accessible within the circuit (allowing the best electrode-tissue contact along the desired line). The ablation line is chosen to transect an area critical for the circuit and, at the same time, to connect two anatomical areas of block—an electrically silent area to an anatomical zone of block (e.g., IVC, SVC, tricuspid annulus, PV, or mitral annulus), or two electrically silent areas. Voltage maps can be used to guide the choice of the ablation site. The likelihood of achieving a complete and transmural ablation line is probably greater in low-voltage zones.^{25,39}

Right Atrial Macroreentry

Lower loop reentry. Lower loop reentry is a form of CTI-dependent MRAT with a reentrant circuit around the IVC. Hence, catheter ablation of the CTI usually eliminates the arrhythmia.

Intra-isthmus reentry. This form of CTI-dependent MRAT is typically confined to the medial aspect of the CTI and the reentry circuit can be quite small. Entrainment pacing from the lateral CTI demonstrates a PPI longer than the TCL, a finding indicating that the lateral CTI is not part of the reentrant circuit. On the other hand, pacing from the region of the medial CTI or CS os demonstrates concealed entrainment with PPI equal to the TCL. Fractionated or double potentials can usually be recorded in this area and can be entrained. Although the anatomical basis of this arrhythmia remains unknown, a linear lesion across the *medial* CTI, usually at the site of a very prolonged electrogram, can cure the tachycardia. Fractionated potentials spanning one- to two-thirds of the TCL are typically recorded within the CTI. The target of ablation is a localized area within the CTI showing the longest duration of fractionated potentials associated with concealed entrainment.

Upper loop reentry. The lower turnaround point for these circuits is by conduction through a gap in functional block in the crista terminalis. Ablation in this conduction gap to complete the line of block is successful in treating this arrhythmia. It is important to exclude proximity of the phrenic nerve and, if possible, the sinus node region

to the chosen ablation site to avoid collateral damage to important structures.

Incisional RA macroreentry. Most frequently, those MRATs incorporate a circuit in the lateral RA wall around the atriotomy scar. In most cases, the lower turning point of the circuit is located between the lower edge of the scar and the orifice of the IVC, which forms the critical isthmus of the circuit. The upper turning point can be located between the end of the scar and the orifice of the SVC or around the SVC. Therefore the usual target of ablation is the isthmus between the lower end of the scar and the IVC (Fig. 13.13; see Fig. 14.2). Alternative ablation strategies include any of the following: (1) targeting the slow conduction area (critical isthmus of the reentrant circuit) as identified by detailed activation and entrainment mapping; (2) extending the scar area to the lateral aspect of the tricuspid annulus; or (3) extending the scar area to the SVC. The last approach can result in injury of the sinus node or phrenic nerve. Therefore when possible, extending the atriotomy to the IVC is preferable. In addition, because most postatriotomy MRATs are often combined with a circuit around the tricuspid annulus in a figure-eight reentry, definitive treatment should include ablation of the CTI. Even when the CTI is not involved in the MRAT circuit, it is recommended to also perform CTI ablation given the high incidence of CTI-dependent AFL in these patients.⁴²

RA macroreentry in the absence of previous surgery. These MRATs are frequently localized to the free wall of the RA and rotate around an obstacle formed by electrically silent areas. In these patients, channels with slow conduction (mid-diastolic isthmus) within the low-voltage zone can represent the mid-diastolic isthmus of the reentry circuit. Once these isthmuses are identified (by activation, entrainment, and voltage mapping), they are selectively targeted by ablation. Alternatively, linear ablation connecting the lower portion of the scar to the IVC can potentially terminate the arrhythmia. Ablation lines connecting the central scar to the SVC or to the tricuspid annulus may also be considered.

Unmappable RA macroreentrant tachycardias. In patients with incomplete maps, a combination of activation, entrainment, and voltage mapping data is used to identify the potential isthmus or zone of slow conduction critical to the reentrant circuit, which is then targeted by

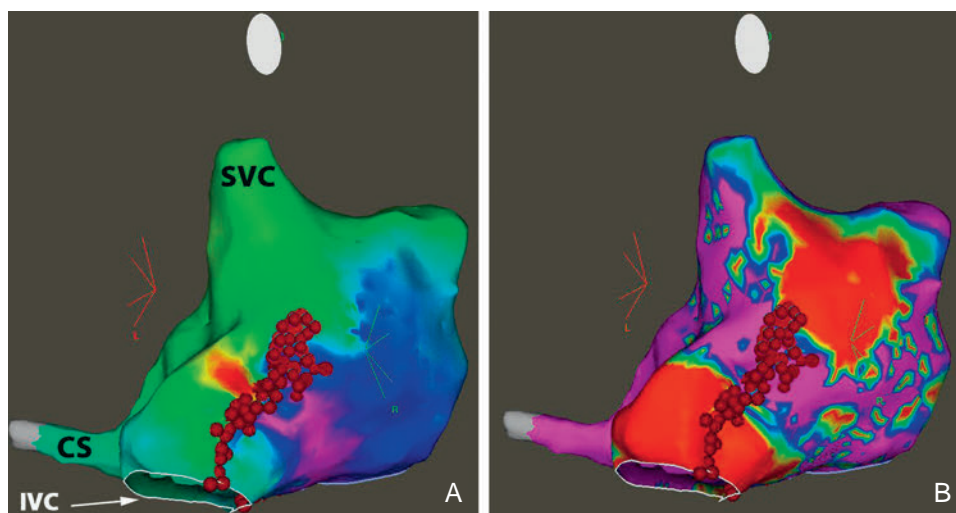


Fig. 13.13 Catheter Ablation of Macroreentrant Right Atrial (RA) Tachycardia. The right posterolateral view of an electroanatomic (CARTO) map of macroreentrant RA tachycardia. (A) Activation map. (B) Bipolar voltage map demonstrates a large area of low bipolar electrogram amplitude (<0.5 mV) in the lateral RA wall at the site of prior surgery. Planning the ablation line is facilitated by correlating activation mapping findings with those of voltage mapping. Linear RF ablation (red dots) is performed to sever the isthmus between the low-voltage zone and the inferior vena cava (IVC). CS, Coronary sinus; SVC, superior vena cava.

catheter ablation. When limitations to this approach still exist (from poor inducibility or frequent change in morphology of the tachycardia), a stepwise ablation strategy may be employed. Because the reentrant circuit in most patients is anchored to the CTI or the atriotomy scar, ablation of the CTI is initially performed. Then, if the tachycardia persists, linear ablation is carried out by targeting the isthmuses related to the lateral atriotomy scar (i.e., connecting the atriotomy to the IVC, to the SVC, or to the tricuspid annulus). Additional ablation lines connecting other areas of conduction block (scar, surgical incision, septal patch, baffle, or natural barriers) may be considered based on substrate mapping findings.^{25,39}

Left Atrial Macroreentry

LA macroreentry following previous surgery. The goal is to localize the area with scar and extend this line of conduction block to an anatomical obstacle, or to transect the circuit by joining anatomical structures. Although this strategy is achievable in most of the atria, it is advisable to avoid attempting to connect the anterior septal region to the mitral annulus in the region of the low left septum because the thickness of the tissue prohibits complete lesions in approximately 40% of patients despite the use of irrigated-tip catheters. The exception to this is the presence of a narrow mid-diastolic isthmus (defined by activation, entrainment, and voltage mapping); this target is then preferable and usually much easier than longer linear lesions.⁹

LA macroreentry following ablation of AF. Knowledge of the type of initial ablation procedure is critical before embarking on AT ablation. ATs following PV isolation procedures can often be focal, typically originating from the vicinity of a reconnected PV. Most of the ATs complicating circumferential and linear LA ablations are macroreentrant, most commonly with circuits around the mitral annulus or involving the LA roof or septum. These circuits are most often related to gaps in ablation lines or to isthmuses created between the ablation lines and other obstacles in the LA. Multiple macroreentrant circuits and multiple-loop reentrant circuits are not infrequently encountered. In addition, localized reentrant circuits are not uncommon, and they usually arise from the vicinity of the isolated PVs or linear lesions.

Mapping and ablation of LA MRATs following circumferential LA ablation or circumferential PV isolation are frequently challenging. Detailed mapping with a high density of points is necessary to elucidate a more complete understanding of the activation pattern during the AT. In addition, mapping of the previously performed ablation lesions is critical to determine whether the ablation lines and PV electrical isolation are complete. When the macroreentrant circuit can be mapped, ablation lesions should be tailored to interrupt the path of the reentrant circuit (see Fig. 15.60). In the absence of complete block across the old ablation lines, the gaps must be reablated. Empirical treatment of unmappable ATs primarily involves electrical isolation of all reconnected PVs and, if needed, empirical linear lesions within the tachycardia circuit, often including a line between the mitral annulus and left inferior PV and a roof line between the superior PVs.⁴³

LA macroreentry in the absence of previous surgery or ablation. Spontaneous LA circuits have been observed. The circuits can propagate around spontaneous scars, frequently located in the posterior LA, but also around the mitral annulus or PVs. The MRAT circuit commonly depends upon a unique slow-conducting isthmus within the scar region. The critical isthmus typically exhibits long-duration fractionated electrograms and coincides with the isoelectric intervals on the 12-lead ECG. The critical isthmus, as confirmed by entrainment mapping, should be selectively targeted by ablation. Frequently, the critical isthmus is relatively narrow; 1 to 3 RF applications at the critical isthmus commonly terminate the tachycardia.¹²

Perimitral LA macroreentry. The standard approach to ablation of perimitral macroreentry involves a linear ablation lesion across the lateral mitral isthmus, connecting the mitral annulus to the ostium of the left inferior PV (eFig. 13.4). Another option is to use an anterior ablation line from the anterior mitral annulus to a region of scar (or to another ablation line in the LA roof connecting both superior PVs) through the anterior LA. Alternatively, linear ablation is performed to connect the anterior-anterolateral mitral annulus to the ostium of the left superior PV (modified anterior line; eFig. 13.5).

Roof-dependent LA macroreentry. The reentry circuit can be interrupted by linear ablation connecting the two superior PVs ("roof line").

Macroreentry around the right PVs. Circuits propagating around the right PVs demonstrate colliding wavefronts along the mitral annulus and a PPI during entrainment that is much longer at the mitral isthmus than at the roof or posterior LA. These MRATs are observed more frequently in the current approach of wide-area atrial ablation to isolate the PVs, because the lesions performed to isolate right and left PVs can potentially create a narrow isthmus in the posterior LA that then forms the substrate for MRAT. A linear lesion connecting both superior PVs through the roof is the best option. This procedure is best performed along the roof, rather than the posterior wall, to avoid the potential risk of atrioesophageal fistulas. Use of a deflectable sheath or ablation catheter with bidirectional deflection capability can facilitate this.

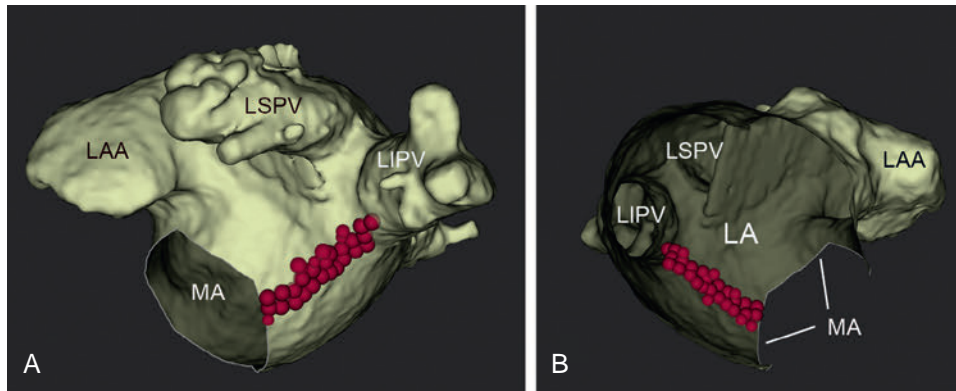
Macroreentry around the left PVs. Circuits around the left PVs seem rare. They can be abolished with a linear lesion joining the left inferior PV to the mitral annulus or with a roofline connecting both superior PVs.

Left septal circuits. The critical isthmus of these circuits is usually located between the septum primum and the right-sided PVs (posterior isthmus) or between the septum primum and the mitral annulus (anterior isthmus). Linear ablation across either isthmus can eliminate the tachycardia, although acute and long-term success rates remain modest. Ablation from the bilateral sides can potentially improve outcome.⁹

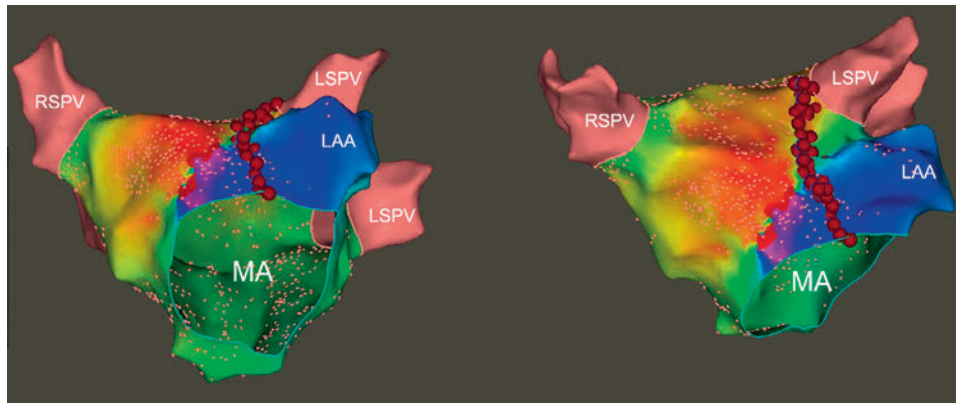
Unmappable LA macroreentrant tachycardias. Some LA MRATs can show some degree of variation in their CL during mapping, in which case conventional and electroanatomic mapping is less useful. Initially, in patients with prior catheter or surgical ablation for AF, all PVs need to be assessed for reconnection via the circular mapping catheter. When PV reconnection is detected, PV reisolation is performed, often requiring only a single ablation lesion. Then, an empirical strategy that commences with ablation at the mitral isthmus and the LA roof is justified because such ablation lines interrupt the most dominant circuits in the LA. Block along each line must be rigorously confirmed, as residual small gaps in the ablation line map facilitate slow reentry.

Ablation Technique

Once the ablation target is identified, ablation involves placing a series of RF lesions to sever the critical isthmus and connect two anatomical or surgical barriers. RF energy can be delivered sequentially point by point to span the targeted isthmus or by dragging the ablation catheter tip during continuous energy administration. The duration and power output of RF application is governed by the location of the ablation target and the risk of injuring neighboring structures (e.g., phrenic nerve, esophagus, AVN). Generally, an effective RF lesion is indicated by reduction of the amplitude of the bipolar electrogram by 80% or breakdown of the local electrogram into double potentials, thus indicating local conduction block. However, the documentation of electrogram breakdown into double potentials depends on the direction of activation relative to the ablation lesion and its size relative to that of the recording bipole and is maximized by activation orthogonal to the



eFig. 13.4 Posterior Mitral Isthmus Ablation Line. Segmented computed tomography (CT) of the left atrium (LA) acquired during catheter ablation of the mitral isthmus. Left lateral (A) and cardioscopic (B) views of the CT scan are shown. Small red dots are tagged sites at which radiofrequency energy was applied across the isthmus between the mitral annulus (MA) and left inferior pulmonary vein (LIPV). LAA, LA appendage; LSPV, left superior pulmonary vein.



eFig. 13.5 Modified Anterior Ablation Line for Perimitral Left Atrial Macroreentry. Three-dimensional electroanatomic (CARTO) activation map of the left atrium in the left anterior oblique (at left) and antero-superior views (at right) constructed during counterclockwise perimitral macroreentrant atrial tachycardia. Linear ablation (purple dots) connecting the anterior-anterolateral mitral annulus to the ostium of the left superior pulmonary vein (LSPV). LIPV, Left inferior pulmonary vein; MA, mitral annulus; RSPV, right superior pulmonary vein.

lesion's largest dimension. Lesion contiguity and continuity depend on ensuring the coalescence of multiple transmural lesions (facilitated by 3-D localization systems).

During delivery of RF energy, the tachycardia can terminate, or its CL can increase transiently or permanently. These findings indicate that the lesions have affected the circuit and should lead to continuation of RF delivery or extension of the lesion to ensure the achievement of complete conduction block across the isthmus. However, it is important to verify that change in the TCL is caused by slowing conduction across the critical isthmus rather than transformation of the index tachycardia into a different circuit, or simply extending a line of conduction block around which it now takes longer for the impulse to propagate.

It is not uncommon for the arrhythmia mechanism to switch rather than terminate following successful ablation. A change in atrial activation sequence or P wave morphology or a sudden change in the atrial CL may indicate that the tachycardia that was being ablated has changed to a different loop or to a different tachycardia. In this setting, it is very important to reevaluate the mechanism and location of the new arrhythmia systematically by using activation and entrainment mapping and to move to the new target if necessary. However, the transition to a different loop of a tachycardia or to a different tachycardia may occur with no discernible change in the activation sequence among the atrial electrograms that are being recorded, P wave morphology, or TCL; this is particularly true if the slower of two tachycardias is targeted and eliminated. It is important to keep this in mind when ablation across an isthmus appears not to affect the tachycardia. The isthmus may have already been blocked and may no longer be participating in the tachycardia. This should be suspected if double potentials are present along the ablation line, and it is easily confirmed by entrainment mapping near the ablation line. If that site was confirmed previously to be part of the reentrant circuit (PPI–TCL difference <20 milliseconds) and now it is outside the tachycardia circuit (PPI–TCL difference >30 milliseconds), this finding indicates that the tachycardia circuit has changed.

Endpoints of Ablation

Tachycardia Termination

Sudden termination of an incessant AT during RF application suggests that the lesion has severed a critical isthmus and that site should be targeted for additional lesions. However, reliance on AT termination during RF application as the sole criterion of a successful ablation is hazardous because such an AT can terminate spontaneously or secondary to mechanical trauma by the ablation catheter, in which case termination can be misleading. RF application itself can induce premature atrial complexes (PACs) that can then terminate AT without eliminating the substrate. In addition, RF application can cause a transient conduction delay or block in the critical isthmus, which can cause acute termination of the tachycardia; then, recovery of conduction can potentially result in later recurrences of the arrhythmia. Moreover, the sudden termination of AT can be accompanied by catheter displacement from the critical site to another site, thus making it difficult to deliver additional energy applications at the critical site.

Noninducibility of Tachycardia

To use the criterion of noninducibility of tachycardia as a reliable endpoint, careful assessment of inducibility should be performed prior to ablation. The feasibility and best method of reproducible induction of the AT should be documented at baseline before ablation, which should then be used for assessment of tachycardia inducibility after an apparently successful ablation. In the setting of easy inducibility prior to ablation, one can consider the lack of inducibility as an indicator of

successful ablation. Tachycardia inducibility should be reassessed 30 minutes after the last successful RF application.

Noninducibility of the arrhythmia is inapplicable if the original arrhythmia was noninducible at baseline, was incessant, or was inadvertently terminated mechanically. Furthermore, noninducibility may reflect conduction delay in the critical isthmus, and not stable block, or it may be secondary to changes in autonomic tone. In these situations, other procedural endpoints need to be employed.

Documentation of a Line of Block

Complete stable conduction block within the reentry path is the most useful and objective endpoint. However, achieving this endpoint can be challenging and may not be as feasible as in CTI ablation for typical AFL. Several techniques can be used to confirm complete conduction block across the ablation line:

Double potentials. The mapping catheter is used to retrace the ablation line during atrial pacing from either side of the ablation line. The demonstration of a continuous corridor of widely split double potentials recorded along the entire length of the ablation line confirms the presence of block. It is important to recognize that double potentials separated by long isoelectric intervals indicate "local block" under the recording catheter bipole, but they can be just adjacent to a conducting gap; therefore meticulous mapping of the entire length of the ablation line is necessary to exclude the presence of gaps in the ablation line and confirm the line of block. When there is a gap in a line of block, the isoelectric interval between the double potentials shortens, the closer the electrograms are to the gap. At the gap in the line of block, double potentials are no longer present, and the electrogram is typically long and fractionated, but can also be discrete. Those gaps are then targeted by additional ablation until complete block is achieved.

Atrial activation sequence. Pacing close to the ablation line and demonstration of marked delay and reversal in the direction of activation on the opposite side of the ablation line is consistent with conduction block across the ablation line, although very slow conduction can be difficult to exclude. Electroanatomic activation mapping during pacing demonstrates earliest activation at side of the ablation line ipsilateral to the pacing site, while the latest activation occurs at the contralateral side, and an early-meets-late zone along the entire length of the ablation line.

Differential pacing. Atrial pacing is performed at two separate sites on the same side of the ablation line, one site very close to the ablation line and the second site 10 to 20 mm farther from the ablation line. Local activation time is recorded on the contralateral side of the ablation line. In the presence of conduction block across the ablation line, moving the pacing site away from the ablation line shortens the conduction time to the contralateral side and shortens the distance between the double potentials straddling the ablation line. Withdrawal of the pacing site farther away from the ablation line results in a delay of the first component of the double potentials (which represents activation on the side of the ablation line ipsilateral to the pacing site). In contrast, the second component of the double potentials (which represent activation on the contralateral side of the ablation line) is activated earlier because the length of the detour around the line block that the paced wavefront must travel is shortened by the new site of pacing. As a consequence, the separation of double potentials decreases. On the other hand, in the setting of incomplete block, both components of the double potentials are the result of sequential activation by the same paced wavefront propagating across the ablation line. Therefore withdrawal of the pacing site farther away from the ablation line causes a similar degree of delay of the timing of both components of the electrogram (relative to the pacing stimulus), so that the interval between the double potentials remains constant.

Ablation of Perimitral Macroreentrant Atrial Tachycardia

The lateral mitral isthmus is short (2 to 4 cm), anatomically bounded by the mitral annulus, left inferior PV ostium, and superiorly by the LA appendage. The average thickness of the atrium along the mitral isthmus is 3.8 mm, with maximum thickness up to 7.7 mm. The CS muscle sleeve, present in up to 75% of patients, inserts into the LA inferior to the mitral isthmus and occasionally extends onto the mitral valve. Mitral isthmus ablation is performed by linear ablation to join the posterolateral mitral isthmus to the left inferior PV (posterior ablation line) (see eFig. 13.4). Alternatively, an ablation line may be deployed extending from the anterior-anterolateral mitral annulus to the left superior PV (anterior ablation line) (see eFig. 13.5).¹¹

Posterior Mitral Isthmus Ablation Line

The CS catheter is positioned to bracket the planned linear lesion between its proximal and distal bipoles. The ablation catheter is introduced into the LA through a long sheath and flexed with a 90- to 180-degree curve to achieve good contact and stability. Initially, the catheter tip is positioned at the ventricular edge of the lateral mitral annulus, where the A:V electrogram shows a 1:1 to 2:1 ratio, to begin ablation. Of note, a true annular site can be deceptively far away (toward the ventricle) from the CS catheter location (often considered to be an indicator of annular location). The sheath and catheter are then rotated clockwise and dragged gradually to extend the ablation line posteriorly, ending at the left inferior PV ostium (Fig. 13.14). In general, ablation is commenced at about the 3- or 4-o'clock position on the mitral isthmus and reaches the 2- to 3-o'clock position at the upper end of the line.⁴⁴ Because myocardial sleeves extend into the left inferior PV, electrical

isolation of this PV is frequently required to serve as a reliable anchor for the mitral isthmus ablation line.⁴⁵

RF energy is delivered with an 8-mm-tip catheter with a target temperature of 50°C to 55°C and a power of 50 to 70 W. Externally irrigated catheters are preferably used with a power of 25 to 40 W and a maximum temperature limit of 40°C to 45°C. Each RF application is extended for 90 to 120 seconds at each site. The stability of the catheter is monitored during RF applications by using electrogram recordings and intermittent fluoroscopy to exclude inadvertent displacement, which could result in high-energy delivery in the left inferior PV ostium or LA appendage.⁴⁴

When ablation is performed during NSR, the effect of each RF application is assessed on the local electrogram during pacing from the proximal bipole of the CS catheter located immediately posteromedial of the line, to maximize conduction delay. Splitting of the local potentials, with a resulting increase in the delay from the pacing artifact, is considered evidence of an effective local lesion. After the initial attempt to create this line, mapping is performed along the line to identify and ablate endocardial gaps, defined as sites showing the shortest delay between the pacing artifact and the local atrial potential, which can be single, narrow double, or fractionated.⁴⁴

Persisting epicardial conduction is suspected when the linear lesion results in adequate voltage abatement on the endocardial aspect while a large atrial potential is still recorded in the CS catheter, or when endocardial conduction delay is recorded on the ablation catheter but not on the adjacent distal bipole of the CS catheter (anterolateral to the ablation line).

Epicardial ablation within the CS is required to achieve block in more than 70% of cases (probably less with use of contact force

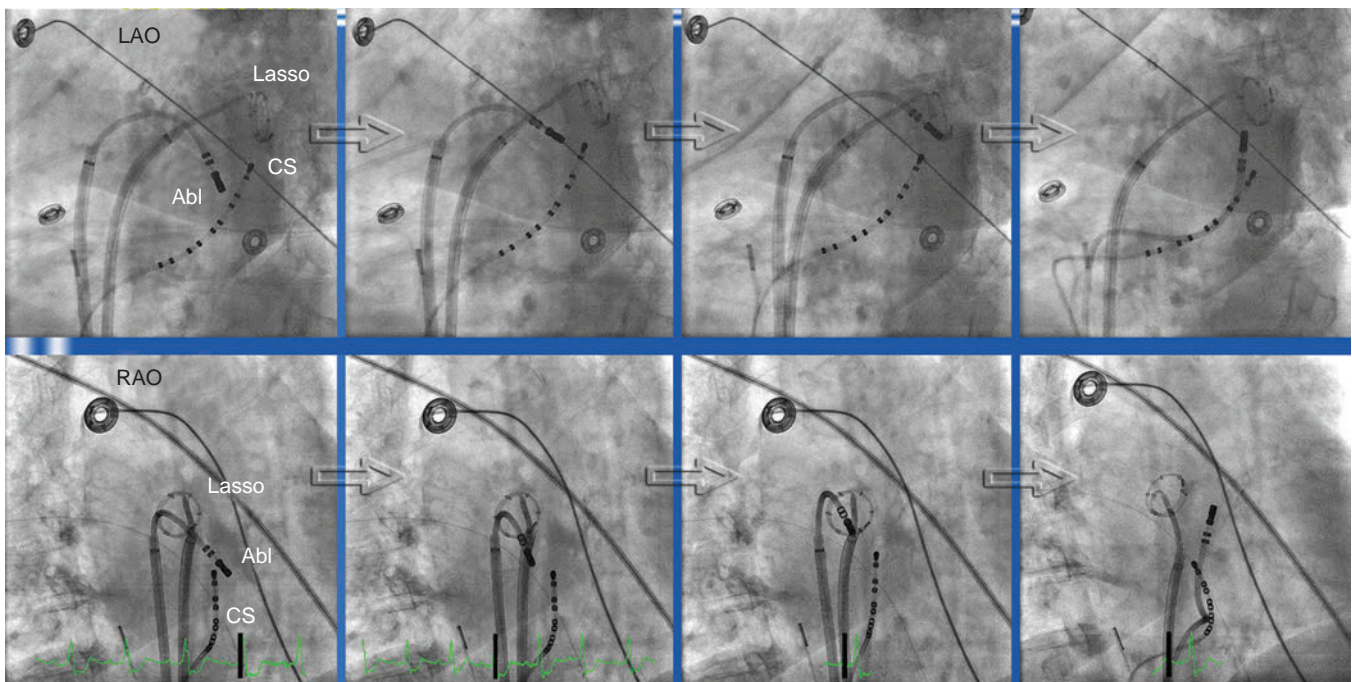


Fig. 13.14 Catheter Ablation of the Lateral Mitral Isthmus. Right anterior oblique (RAO; upper panels) and left anterior oblique (LAO; lower panels) fluoroscopy views of catheter placement during mitral isthmus ablation. A ring catheter (Lasso) is positioned at the ostium of the left inferior pulmonary vein. Ablation is started with the ablation catheter (Abl) at the ventricular aspect of the mitral annulus (left panel). The catheter is then moved gradually to the mid-isthmus and subsequently to the junction with the ostium of the left inferior pulmonary vein (middle panels). When the endocardial approach fails, epicardial ablation of the mitral isthmus is attempted through the coronary sinus (CS; right panel).

measurements and irrigated RF). The relatively low success rate of mitral isthmus block can be explained by several mechanisms. The shape and depth of the atrial myocardium vary greatly around the mitral isthmus, and the depth of the tissue (resulting from the double muscular layers of LA and CS) may be the limiting factor in achieving a transmural lesion by endocardial ablation alone. In addition, local cooling effects of blood flow in the circumflex coronary artery and the great cardiac vein (both pass in close proximity to the mitral isthmus) may act as a heat sink, preventing adequate tissue heating by RF delivery and making isthmus block difficult. Some investigators suggested that temporary displacement of the venous blood pool by using an air-filled CS balloon could potentially facilitate transmural mitral isthmus lesions during endocardial catheter ablation. However, studies evaluating the efficacy of this approach arrived to conflicting results, suggesting that arterial blood flow through an interposed circumflex artery may be more efficient in dissipating heat and pose a bigger challenge to ablation than the coronary venous flow.⁴⁶

When epicardial ablation is required, the ablation catheter is withdrawn from the LA and is introduced into the CS to map the epicardial side of the isthmus and identify fractionated or early potentials suggestive of an epicardial gap. The catheter is torqued toward the atrial side of the AV groove, to avoid ablation within a ventricular branch (which carries higher risk of coronary artery injury). Ablation within the CS is performed using an externally irrigated-tip catheter with a power limit of 20 to 25 W, and usually maximal flow (60 mL/min) is necessary (see Fig. 13.14). RF application should be discontinued if there is a rapid rise or fall in impedance or a rapid rise in temperature. Sometimes a power setting of 30 to 35 W is required for successful ablation. A higher power setting should be considered when a tachycardia fails to respond to ablation with 20 to 25 W and when entrainment mapping or activation mapping indicates that the CS is still an appropriate target site. A recent report described the feasibility of epicardial ablation of the mitral isthmus via the percutaneous subxiphoid approach in patients with severely symptomatic perimitral MRAT and failed endocardial and CS ablation.⁴⁷ If it appears that all electrograms in the target area have been eliminated, repeating pacing from opposite sides of the ablation line should be performed to ascertain if perimitral reentry persists, or if the ablation line is complete and the arrhythmia has changed to another form.

Anterior Mitral Isthmus Ablation Line

The ablation catheter is advanced through the transseptal sheath to the anterior-anterolateral mitral annulus, and delivery of RF lesions is started when the A/V ratio is 1:2. Linear ablation is then performed with counterclockwise rotation of the transseptal sheath and progressive release of the ablation catheter curve. The ablation line is extended just in front of (anteromedial to) the orifice of the LA appendage, and then the catheter is advanced to extend the linear lesion to the ostium of the left superior PV (see eFig. 13.5).^{47,48}

In one report, the anterior ablation line was found to be safe, feasible, and very effective, achieving tachycardia termination in 97% of cases and bidirectional block across the line in 86% of patients, without the need for RF ablation within the CS. Therefore this type of linear lesion can serve as a first-line approach for perimitral MRAT or as an alternative approach when an epicardial ablation deep within the CS is not feasible for completion of the lateral mitral isthmus ablation line.⁴⁸ Delay of activation of the LA appendage often results, with potential deleterious hemodynamic effects. In addition, if a posterior ablation line is attempted without apparent success, and the strategy is changed to an anterior ablation line, it is possible that both lines will be complete and could then effectively isolate the LA appendage electrically.

Confirmation of Mitral Isthmus Block

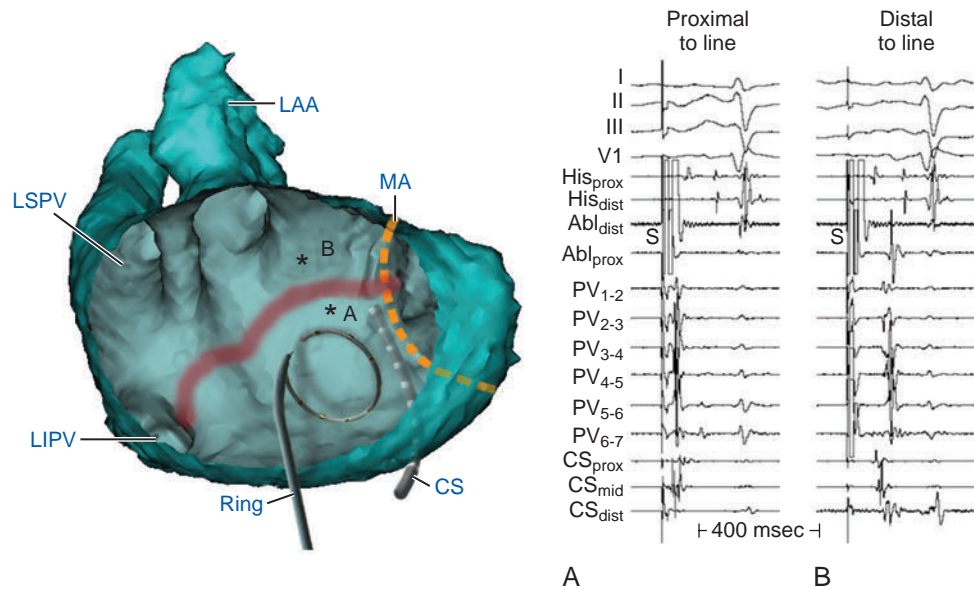
For perimitral MRAT, the lateral mitral isthmus is the traditional target of ablation. Mitral isthmus ablation has a well-defined demonstrable procedural endpoint of bidirectional conduction block analogous to CTI ablation. Validation of mitral isthmus conduction block is greatly facilitated by its proximity to the CS, which allows pacing and recording on either side of the ablation line to confirm bidirectional block. Several criteria are used to confirm the presence of bidirectional mitral isthmus block. The CS catheter is placed within the CS so that the distal bipole is positioned just posteromedial to the ablation line, while the mapping catheter is positioned endocardially in the LA just anterolateral to the ablation line. Alternatively, the CS catheter can be positioned to straddle the ablation line.

Double potentials. The presence of widely separated (by 150- to 300-millisecond intervals) local double potentials along the length of the ablation line during pacing from either side of the ablation line confirms the presence of block.

Atrial activation sequence. Mapping the activation detour during pacing from the posteromedial side of the line through the CS catheter demonstrates marked delay and reversal in the direction of activation at the anterolateral side of the isthmus. Pacing anterolateral to the ablation line via the ablation catheter placed endocardially demonstrates a proximal-to-distal activation sequence along the CS posteromedial side of the line, thus confirming bidirectional conduction block (Fig. 13.15). It is important to ensure that the distal bipole of the CS catheter is positioned very close to the ablation line; otherwise, a proximal-to-distal activation sequence along the CS can be interpreted as evidence of block when only conduction delay across the ablation line is present. The activation detour during complete isthmus block can also be determined using 3-D electroanatomic mapping (Fig. 13.16).⁴⁴

Differential pacing. With the distal bipole of the CS catheter placed just posteromedial to the ablation line, the pacing site is changed from the distal to the proximal bipole of the CS catheter without moving any of the catheters. The stimulus-to-electrogram timing at an LA site close to the opposite side of the ablation line is measured before and after changing the pacing site. With complete block, the stimulus-to-electrogram interval is shortened after shifting the pacing site from the distal to proximal CS bipole (Fig. 13.15; eFig. 13.6).⁴⁴

It is important to recognize that pacing and recording maneuvers for assessing mitral isthmus block are usually carried out from two different compartments (LA and CS). The venous wall of the CS is surrounded by a sleeve of atrial myocardium that extends for 25 to 51 mm from the CS os, which is continuous with the RA myocardium proximally, but it is usually separated from the LA by adipose tissue. This separation is variably bridged by muscular strands producing electrical continuity between the CS musculature and the LA. Therefore pacing within the CS can potentially capture local CS musculature but not the LA myocardium. This can result in a delay in LA activation during CS pacing given that the paced impulse has to travel via an LA-CS muscular connection that can be at a distance from the pacing site. As a consequence, delayed activation of the LA (as recorded by the mapping or ablation catheter positioned within the LA) can be misinterpreted as evidence of conduction block across the mitral isthmus ("pseudoblock") when actually no such block is present. This is also true during pacing endocardially within the LA without capturing the CS muscular sleeve. Therefore it is critical to verify that both the CS and LA are captured by the paced stimulus to avoid erroneous diagnosis. These pitfalls can be avoided by pacing (in the LA or CS) at an output high enough to ensure capture of endocardial LA, as well as the epicardial CS tissue. However, pacing at output higher than necessary can cause wide-area capture such that the site across the ablation line is stimulated simultaneously with the pacing site,



eFig. 13.6 Bidirectional Block Across the Mitral Isthmus Ablation Line. Endoscopic view of a computed tomography scan of the left side of the left atrium (LA). The orifices of the left superior pulmonary vein (LSPV) and left inferior PV (LIPV) and LA appendage (LAA) are shown. An ablation line (red shading) has been made between mitral annulus (MA, orange dashes) and the LIPV orifice to transect the mitral isthmus. A multipolar ring catheter is situated on the LA endocardium as shown; the tip of the coronary sinus (CS) catheter (situated epicardial to the LA) is proximal to the ablation line. During pacing from A (asterisk), proximal to the ablation line, the ring catheter recordings appear soon after the stimulus artifact and CS electrodes are activated from distal to proximal. Pacing from B (asterisk), distal to the ablation line, shows the ring electrodes are activated much later than before, and the CS is now activated from proximal to distal, thus indicating bidirectional block at the mitral isthmus. *Abl_{dist}*, Distal ablation site; *Abl_{prox}*, proximal ablation site; *CS_{dist}*, distal coronary sinus; *CS_{mid}*, middle coronary sinus; *CS_{prox}*, proximal coronary sinus; *His_{dist}*, distal His bundle; *His_{prox}*, proximal His bundle; *PV*, pulmonary vein.

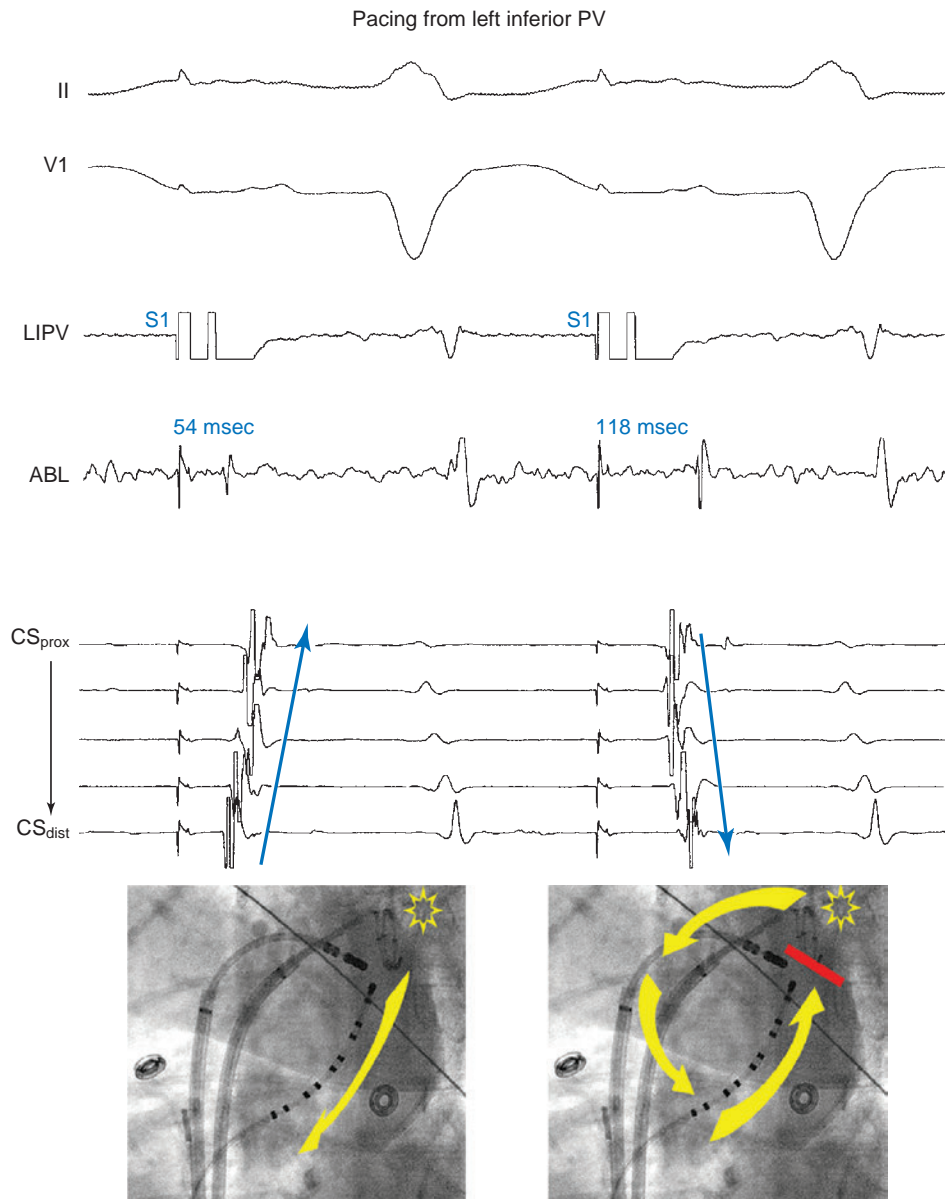


Fig. 13.15 Verification of Bidirectional Mitral Isthmus Block. *Upper panel*, Ablation of the mitral isthmus is performed during pacing anterolateral to the ablation line (a Lasso catheter positioned at the ostium of the left inferior pulmonary vein [LIPV] is used in this case). With intact isthmus conduction, coronary sinus (CS) activation occurs through the wavefront propagating in the counterclockwise direction; thus a distal-to-proximal CS activation sequence is observed. When clockwise isthmus block is achieved, CS activation occurs through the wavefront propagating in the clockwise direction; thus reversal of the CS activation sequence is observed. The ablation catheter (ABL) is positioned at the septal aspect of the line of block. The stimulus-to-electrogram interval recorded by the ablation catheter prolongs suddenly on development of clockwise isthmus block. *Lower panels*, Differential pacing is performed from the proximal and distal CS (CS_{prox} , CS_{dist}) bipoles (both positioned at the posteromedial aspect of the ablation line) to verify the presence of counterclockwise isthmus block. In the presence of counterclockwise block, activation lateral to the ablation line (as recorded by the Lasso catheter in the LIPV) occurs through the wavefront propagating in a clockwise direction up the left atrial (LA) septal wall and over the LA roof. Consequently, LIPV activation occurs earlier during pacing from the proximal CS (*left panel*) compared with the distal CS (*right panel*). A yellow star marks the pacing site. *Continued*

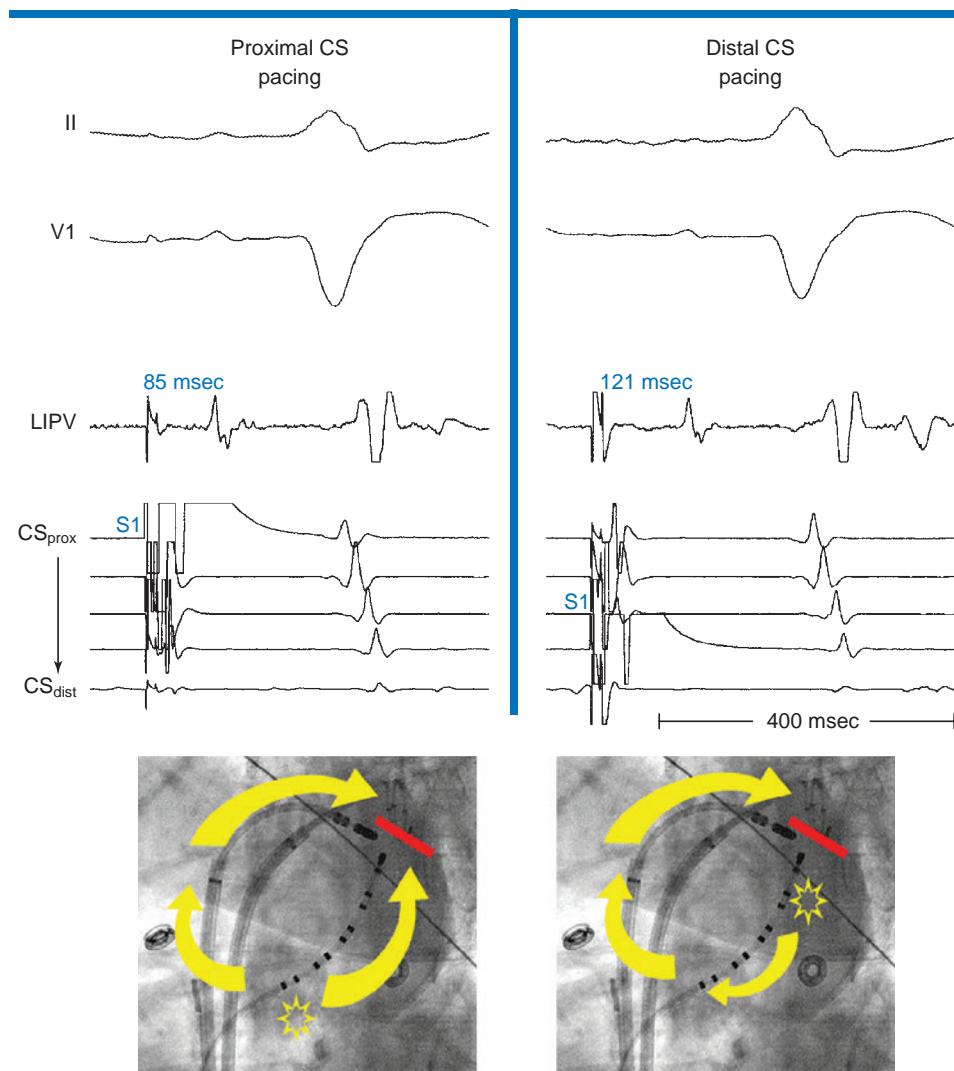


Fig. 13.15, cont'd

especially when the pacing bipole is very close to or straddles the ablation line.⁴⁴

The LA appendage is frequently selected as a pacing and recording site during verification of the presence of mitral isthmus block. In the setting of the anterior ablation line, the LA appendage is located lateral to the line of ablation. However, in the setting of the posterior ablation line, the LA appendage is located anteromedial to the ablation line. In the latter setting, however, one should understand that the LA appendage is not always a reliable site for pacing anteromedial to the ablation line, because epicardial connections between the appendage and the vein of Marshall can potentially mediate conduction to the distal CS even in the presence of isthmus block.^{45,49}

Outcome

Short-term success rates are reasonably good (approximately 90% in experienced centers). However, recurrence rates of the same or other tachycardias are high; up to 59% of cases required repeat ablation in some studies. Long-term freedom from arrhythmias can be achieved in 73% to 90% of patients after multiple procedures. The best outcomes have been observed for MRATs related to surgical incisions. Acute and long-term success seem to be lower for septal circuits (likely due to the structural complexity and thickness of the interatrial septum), macroreentry related to idiopathic scar (likely related to the presence of diffuse

atrial myopathy), and in patients with multiple tachycardias.⁵⁰ Some patients undergo ablation while taking antiarrhythmic drugs such as amiodarone; when the drug is stopped after an apparently successful ablation procedure, resurgence of the same or other tachycardias can occur if the drug had been suppressing a circuit or initiators of reentry.

In patients with perimitral MRAT, bidirectional block at the lateral mitral isthmus can be acutely achieved in 65% to 92% of patients, with ablation within the CS being required in about two-thirds of patients (less than this now with more routine use of irrigated RF and contact force sensing catheters). In one report, the modified anterior line (extending from the anterior/anterolateral mitral annulus to the ostium of the left superior PV) resulted in bidirectional block across the ablation line in 86% of patients. On the other hand, a complete line of block could be achieved in only 58% when combining a roof line with an anterior line connecting the mitral annulus and the right superior PV or the septal part of the roof line.

Catheter ablation of MRATs can potentially cause significant complications, due to the extended periods of mapping and catheter manipulation, frequent need for LA access, and relatively large areas of linear ablation required in many patients. Ablation of LA MRATs can be associated with complications similar to those observed in AF ablation (see Chapter 15). For RA MRATs, complications are similar to those reported for focal ATs (see Chapter 11).⁵⁰

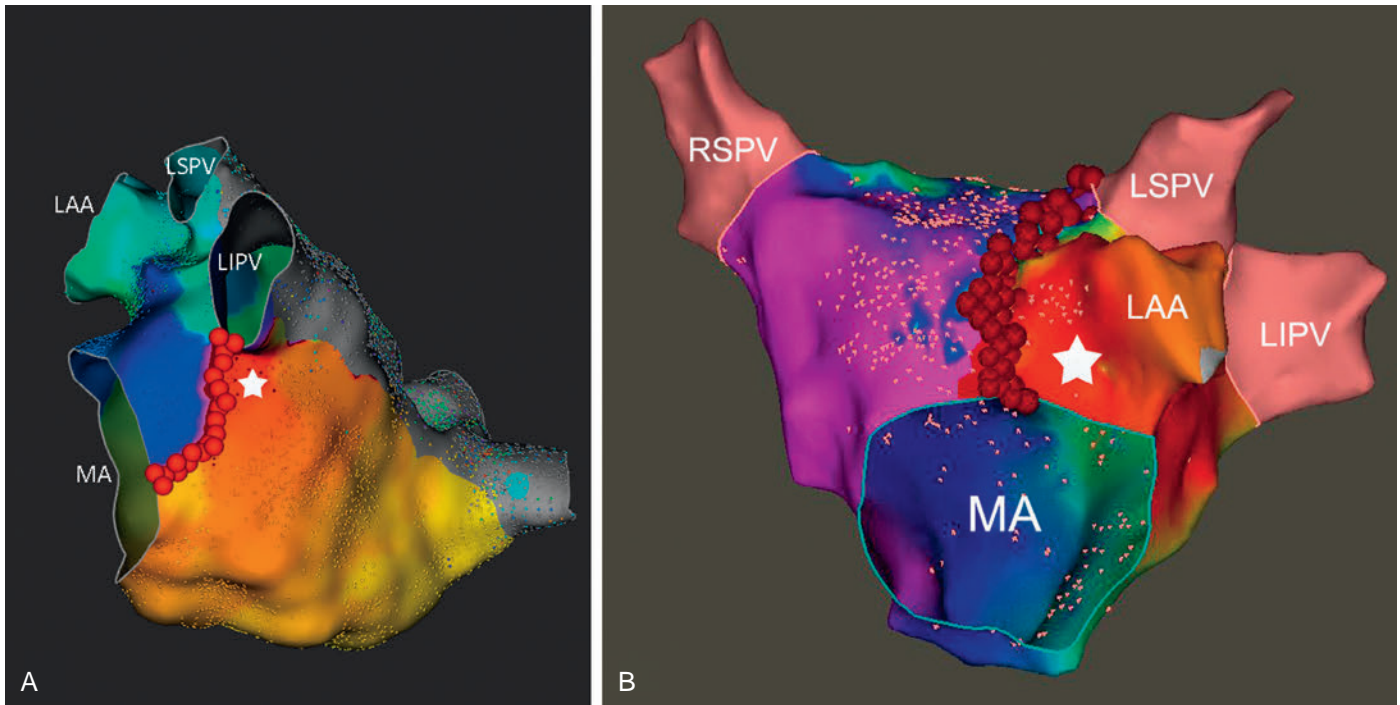


Fig. 13.16 Confirmation of Block Across the Ablation Line. (A) Left lateral view of three-dimensional electroanatomic (Rhythmia) activation map of the left atrium (LA). Linear ablation (posterior mitral isthmus ablation line, *purple dots*) successfully terminated perimitral LA macroreentry. The activation color map displays the activation pattern following restoration of sinus rhythm and during atrial pacing (*asterisk*) just posterior to the ablation line. Note the formation of an early-meets-late zone (*violet to red*) along the entire length of the ablation line demonstrating the achievement of a continuous conduction block. (B) Left anterior oblique view of three-dimensional (CARTO-3) activation map of the LA. Linear ablation (modified anterior mitral isthmus ablation line, *purple dots*) successfully terminated perimitral LA macroreentry. The activation color map displays the activation pattern during atrial pacing (*asterisk*) at the root of the LA appendage (LAA), just lateral to the ablation line. Note the formation of an early-meets-late zone (*violet to red*) along the entire length of the ablation line demonstrating the achievement of a continuous conduction block. LIPV, Left inferior pulmonary vein; LSPV, left superior pulmonary vein; MA, mitral annulus; RSPV, right superior pulmonary vein.

VIDEOS

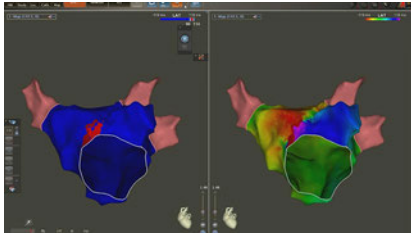
The following videos accompany this chapter:

- ▶ **Video 13.1.** Clockwise and Counterclockwise Perimitral Left Atrial Macroreentry: CARTO Activation and Propagation Maps
- ▶ **Video 13.2.** Macroreentrant Atrial Tachycardia (involving the pulmonary veins): Rhythmia Propagation, Activation, and Voltage Maps
- ▶ **Video 13.3.** Incisional Right Atrial Macroreentry: CARTO Activation, Voltage, Propagation, and Ripple Maps

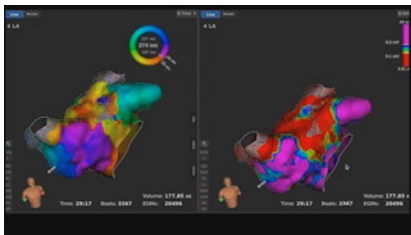
See **Video 6.13.** Small Atrial Macroreentry: Rhythmia Activation and Propagation Maps

REFERENCES

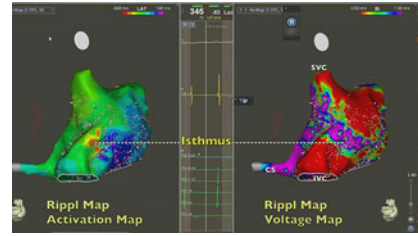
- Saoudi N, et al. Classification of atrial flutter and regular atrial tachycardia according to electrophysiologic mechanism and anatomic bases: a statement from a joint expert group from the Working Group of Arrhythmias of the European Society of Cardiology and the North American Society of Pacing and Electrophysiology. *J Cardiovasc Electrophysiol.* 2001;12:852–866.
- Bun SS, Latcu DG, Marchlinski F, et al. Atrial flutter: more than just one of a kind. *Eur Heart J.* 2015;36:2356–2363.
- Garan H. Atypical atrial flutter. *Heart Rhythm.* 2008;5:618–621.
- Hoffmayer KS, Scheinman MM. Intraisthmus reentry. *Card Electrophysiol Clin.* 2012;4:539–543.
- Anguera I, et al. Long-term outcome after ablation of right atrial tachyarrhythmias after the surgical repair of congenital and acquired heart disease. *Am J Cardiol.* 2015;115:1705–1713.
- Kanagasundram AN, et al. A novel criterion for conduction block after catheter ablation of right atrial tachycardia after mitral valve surgery. *Circ Arrhythm Electrophysiol.* 2013;6:39–47.
- Wieczorek M, Hoeltgen R. Right atrial tachycardias related to regions of low-voltage myocardium in patients without prior cardiac surgery: catheter ablation and follow-up results. *Europace.* 2013;15:1642–1650.
- Medi C, Kalman JM. Prediction of the atrial flutter circuit location from the surface electrocardiogram. *Europace.* 2008;10:786–796.
- Adachi T, et al. Left septal atrial tachycardia after open-heart surgery: relevance to surgical approach, anatomical and electrophysiological characteristics associated with catheter ablation, and procedural outcomes. *Circ Arrhythm Electrophysiol.* 2015;8:59–67.
- Huo Y, et al. Atrial arrhythmias following surgical AF ablation: electrophysiological findings, ablation strategies, and clinical outcome. *J Cardiovasc Electrophysiol.* 2014;25:725–738.
- Miyazaki S, Shah AJ, Hocini M, et al. Recurrent spontaneous clinical perimitral atrial tachycardia in the context of atrial fibrillation ablation. *Heart Rhythm.* 2015;12:104–110.
- Zhang J, et al. Electroanatomic characterization and ablation outcome of nonlesion related left atrial macroreentrant tachycardia in patients



Video 13.1 Clockwise and Counterclockwise Perimitral Left Atrial Macroreentry: CARTO Activation and Propagation Maps. Shown are electroanatomic (CARTO) activation and propagation maps of the left atrium during clockwise and counterclockwise perimitral macroreentrant atrial tachycardias in two different patients. *LAA*, Left atrial appendage; *LIPV*, left inferior pulmonary vein; *LSPV*, left superior pulmonary vein; *RIPV*, right inferior pulmonary vein; *RSPV*, right superior pulmonary vein.



Video 13.2 Macroreentrant Atrial Tachycardia (involving the pulmonary veins): Rhythmia Propagation, Activation, and Voltage Maps. Electroanatomic (Rhythmia) activation and propagation maps of the left atrium (LA) acquired during sustained atrial tachycardia in a patient with prior history of catheter ablation of atrial fibrillation (circumferential antral pulmonary vein [PV] isolation) and electrical isolation of the LA posterior wall (with linear ablation across the LA roof and floor). Propagation and activation maps demonstrate atrial macroreentry around the right superior PV. Local electrograms recorded at different parts of the reentry circuit are also shown. *LAA*, Left atrial appendage; *LSPV*, left superior pulmonary vein; *MA*, mitral annulus; *RIPV*, right inferior pulmonary vein; *RSPV*, right superior pulmonary vein.



Video 13.3 Incisional Right Atrial Macroreentry: CARTO Activation, Voltage, Propagation, and Ripple Maps. Electroanatomic (CARTO 3) activation, voltage, propagation, and ripple maps of the right atrium acquired during a macroreentrant right atrial tachycardia in a patient with prior atriotomy. Note large low-voltage (scar) areas in the right atrial free wall with a channel of myocardium with preserved voltage that serves as the isthmus of the macroreentrant circuit. This case demonstrates how ripple mapping better correlates the activation sequence with underlying substrate than does activation and propagation mapping. Linear ablation across the isthmus successfully eliminated the tachycardia. *CS*, Coronary sinus; *IVC*, inferior vena cava; *SVC*, superior vena cava; *TA*, tricuspid annulus.

- without obvious structural heart disease. *J Cardiovasc Electrophysiol.* 2013;24:53–90.
13. Fukamizu S, et al. Macroreentrant atrial tachycardia in patients without previous atrial surgery or catheter ablation: clinical and electrophysiological characteristics of scar-related left atrial anterior wall reentry. *J Cardiovasc Electrophysiol.* 2013;24:404–412.
 14. Page RL, et al. 2015 ACC/AHA/HRS guideline for the management of adult patients with supraventricular tachycardia: a report of the American College of Cardiology/American Heart Association Task Force on Clinical Practice Guidelines and the Heart Rhythm Society. *Circulation.* 2016;133:e506–e574.
 15. Chang S-L, et al. Differentiating macroreentrant from focal atrial tachycardias occurred after circumferential pulmonary vein isolation. *J Cardiovasc Electrophysiol.* 2011;22:748–755.
 16. Yuniadi Y, et al. A new electrocardiographic algorithm to differentiate upper loop re-entry from reverse typical atrial flutter. *J Am Coll Cardiol.* 2005;46:524–528.
 17. Wo H, et al. Successful treatment of macroreentrant atrial tachycardia by radiofrequency ablation targeting channels with continuous activation. *Pacing Clin Electrophysiol.* 2014;37:927–938.
 18. Gerstenfeld EP, et al. Surface electrocardiogram characteristics of atrial tachycardias occurring after pulmonary vein isolation. *Heart Rhythm.* 2007;4:1136–1143.
 19. Deo R, Berger R. The clinical utility of entrainment pacing. *J Cardiovasc Electrophysiol.* 2009;20:466–470.
 20. Josephson ME, Almendral J, Callans DJ. Resetting and entrainment of reentrant ventricular tachycardia associated with myocardial infarction. *Heart Rhythm.* 2014;11:1239–1249.
 21. Almendral J. Resetting and entrainment of reentrant arrhythmias: part II: informative content and practical use of these responses. *Pacing Clin Electrophysiol.* 2013;36:641–661.
 22. Almendral J, Caulier-Cisterna R, Rojo-Álvarez JL. Resetting and entrainment of reentrant arrhythmias: part I: concepts, recognition, and protocol for evaluation: surface ECG versus intracardiac recordings. *Pacing Clin Electrophysiol.* 2013;36:508–532.
 23. Anter E, Tschabrunn CM, Josephson ME. High-resolution mapping of scar-related atrial arrhythmias using smaller electrodes with closer interelectrode spacing. *Circ Arrhythm Electrophysiol.* 2015;8:537–545.
 24. Pascale P, et al. Pattern and timing of the coronary sinus activation to guide rapid diagnosis of atrial tachycardia after atrial fibrillation ablation. *Circ Arrhythm Electrophysiol.* 2013;6:481–490.
 25. De Ponti R, et al. Electroanatomic mapping and ablation of macroreentrant atrial tachycardia: comparison between successfully and unsuccessfully treated cases. *J Cardiovasc Electrophysiol.* 2010;21:155–162.
 26. Lațcu DG, et al. Selection of critical isthmus in scar-related atrial tachycardia using a new automated ultrahigh resolution mapping system. *Circ Arrhythm Electrophysiol.* 2017;10:e004510.
 27. Anter E, et al. Evaluation of a novel high-resolution mapping technology for ablation of recurrent scar-related atrial tachycardias. *Heart Rhythm.* 2016;13:2048–2055.
 28. Schaeffer B, et al. Characterization, mapping, and ablation of complex atrial tachycardia: initial experience with a novel method of ultra high-density 3D mapping. *J Cardiovasc Electrophysiol.* 2016;27:1139–1150.
 29. Derejko P, Podziemski P, Zebrowski JJ, et al. Effect of the restitution properties of cardiac tissue on the repeatability of entrainment mapping response. *Circ Arrhythm Electrophysiol.* 2014;7:497–504.
 30. Vollmann D, et al. Misleading long post-pacing interval after entrainment of typical atrial flutter from the cavotricuspid isthmus. *J Am Coll Cardiol.* 2012;59:819–824.
 31. Wong KCK, Rajappan K, Bashir Y, et al. Entrainment with long postpacing intervals from within the flutter circuit: what is the mechanism? *Circ Arrhythm Electrophysiol.* 2012;5:e90–e92.
 32. Asirvatham SJ, Stevenson WG. Mapping reentry. *Circ Arrhythm Electrophysiol.* 2016;9:e003609.
 33. Maruyama M, et al. Number needed to entrain: a new criterion for entrainment mapping in patients with intra-atrial reentrant tachycardia. *Circ Arrhythm Electrophysiol.* 2014;7:490–496.
 34. Miyazaki H, Stevenson WG, Stephenson K, et al. Entrainment mapping for rapid distinction of left and right atrial tachycardias. *Heart Rhythm.* 2006;3:516–523.
 35. Santucci PA, et al. Electroanatomic mapping of postpacing intervals clarifies the complete active circuit and variants in atrial flutter. *Heart Rhythm.* 2009;6:1586–1595.
 36. Esato M, et al. Color-coded three-dimensional entrainment mapping for analysis and treatment of atrial macroreentrant tachycardia. *Heart Rhythm.* 2009;6:349–358.
 37. Barbhuiya CR, et al. Avoiding tachycardia alteration or termination during attempted entrainment mapping of atrial tachycardia related to atrial fibrillation ablation. *Heart Rhythm.* 2015;12:32–35.
 38. Tai C-T, Chen S-A. Noncontact mapping of the heart: how and when to use. *J Cardiovasc Electrophysiol.* 2009;20:123–126.
 39. Huang JL, et al. Substrate mapping to detect abnormal atrial endocardium with slow conduction in patients with atypical right atrial flutter. *J Am Coll Cardiol.* 2006;48:492–498.
 40. Steven D, Seiler J, Roberts-Thomson KC, et al. Mapping of atrial tachycardias after catheter ablation for atrial fibrillation: use of bi-atrial activation patterns to facilitate recognition of origin. *Heart Rhythm.* 2010;7:664–672.
 41. Deleted in review.
 42. Enriquez A, et al. Postoperative atrial tachycardias following mitral valve surgery: mechanisms and outcomes of catheter ablation. *Heart Rhythm.* 2016;14:520–526.
 43. Gopinathannair R, et al. Atrial tachycardias after surgical atrial fibrillation ablation. clinical characteristics, electrophysiological mechanisms, and ablation outcomes from a large, multicenter study. *J Am Coll Cardiol EP.* 2017;3:865–874.
 44. Shah AJ, et al. Prevalence and types of pitfall in the assessment of mitral isthmus linear conduction block. *Circ Arrhythm Electrophysiol.* 2012;5:957–967.
 45. Asirvatham SJ, Stevenson WG. Inequalities for left atrial ablation. *Circ Arrhythm Electrophysiol.* 2016;9:1–3.
 46. Yokokawa M, Sundaram B, Garg A, et al. Impact of mitral isthmus anatomy on the likelihood of achieving linear block in patients undergoing catheter ablation of persistent atrial fibrillation. *Heart Rhythm.* 2011;8:1404–1410.
 47. Berruezo A, Bisbal F, Fernández-Armenta J. Transthoracic epicardial ablation of mitral isthmus for treatment of recurrent perimitral flutter. *Heart Rhythm.* 2014;11:26–33.
 48. Tzeis S, et al. The modified anterior line: an alternative linear lesion in perimitral flutter. *J Cardiovasc Electrophysiol.* 2010;21:665–670.
 49. Jiang C-X, et al. Ridge-related reentry despite apparent bidirectional mitral isthmus block. *Heart Rhythm.* 2016;13:1845–1851.
 50. Coffey JO, et al. Catheter ablation of scar-related atypical atrial flutter. *Europace.* 2013;15:414–419.

Atrial Tachyarrhythmias in Adults With Congenital Heart Disease

OUTLINE

Pathophysiology, 407

- Macroreentrant Atrial Tachycardia, 407
- Focal Atrial Tachycardia, 408
- Atrial Fibrillation, 408
- Early Postoperative Atrial Tachycardia, 408
- Atrial Septal Defect, 409
- Tetralogy of Fallot, 409
- Dextro-Transposition of the Great Arteries, 410
- Univentricular Hearts With Fontan Palliation, 410

Epidemiology and Natural History, 410

Clinical Presentation, 411

Initial Evaluation, 411

Principles of Management, 411

- Rate Control, 411
- Restoration of Sinus Rhythm, 411

Maintenance of Sinus Rhythm, 412

Prevention of Systemic Embolization, 412

Electrocardiographic Features, 412

Mapping, 412

- Vascular and Cardiac Access, 413
- Mapping Approach, 415
- Exclusion of Cavotricuspid Isthmus Dependence, 415
- Identification of Barriers and Potential Lines of Block, 416
- Identification of the Complete Reentrant Circuit, 416
- Identification of the Critical Isthmus, 417

Ablation, 417

- Target of Ablation, 417
- Ablation Technique, 418
- Endpoints of Ablation, 419
- Outcome, 420

PATHOPHYSIOLOGY

Cardiac arrhythmias are a common problem in patients with congenital heart disease (CHD), particularly after they have undergone reparative or palliative surgical procedures. Atrial tachyarrhythmias are the most prevalent, with a lifetime risk of approximately 50%, regardless of the severity of the congenital defects. Macroreentry localized to the right atrium (RA) is the most common mechanism, followed by atrial fibrillation (AF). Focal ATs are also observed, but less frequently.¹

Macroreentrant Atrial Tachycardia

For macroreentrant atrial tachycardias (MRATs) in adults with repaired CHD, three RA circuits are generally identified: (1) lateral wall circuits with reentry around or related to the lateral atriotomy scar; (2) septal circuits with reentry around an atrial septal patch; and (3) typical atrial flutter (AFL) circuits using the cavotricuspid isthmus (CTI). Peritricuspid reentry (typical clockwise or counterclockwise CTI-dependent AFL) is the most common single mechanism and usually coexists with other forms. Atrial macroreentry in the RA free wall is the most common form of non-CTI-dependent RA macroreentry. Left atrial (LA) macroreentrant circuits are infrequent in this patient population.

The complexity of the MRAT circuits depends on the underlying congenital anomaly and the complexity of the surgical repair. Very complex or multiple reentry circuits can be seen after placement of an intraatrial baffle (Mustard or Senning correction for transposition of the great vessels) in an extremely dilated RA, after a Fontan procedure, and in patients with a univentricular heart.²

Anatomical factors promoting macroreentry in patients with CHD include abnormalities of the underlying cardiac anatomy, surgically created anastomoses, and atriotomy scars, resulting in barriers to impulse propagation and protected isthmuses with adjacent anatomical structures. Conduction abnormalities can be further aggravated by atrial

dilatation and scarring secondary to persisting pressure or volume overload after cardiac surgery or because of residual septal defects, valvular abnormalities, or ventricular dysfunction. At greatest risk are patients with single ventricular physiology and Fontan circulation, atrial baffles created by Mustard and Senning procedures for treatment of D-transposition of the great arteries, and repaired tetralogy of Fallot; but patients with simple atrial septal defect repair are also vulnerable years after surgical repair.

The best characterization of MRAT caused by atriotomy is activation around an incision scar in the lateral RA wall, with a main superoinferior axis (Fig. 14.1). This is a common problem in patients who have undergone surgery for congenital or valvular heart disease. The length, location, and orientation of the atriotomy incisions, as well as potential electrical conduction gaps across the atriotomy, are important determinants of arrhythmogenicity. Not only does the central obstacle include the scar, but also functional block can magnify this obstacle to include the superior vena cava (SVC). The anterior RA wall is commonly activated superoinferiorly (descending activation pattern), as in counterclockwise typical AFL. However, the septal wall frequently lacks a clear-cut inferosuperior (ascending) activation pattern. A line of double potentials can be recorded in the lateral RA, extending superoinferiorly. Double potential separation can be more marked and demonstrate a voltage lower than in typical AFL. Narrow passages (isthmuses) in the circuit can be found between the SVC and the superior end of the atriotomy scar, between the inferior vena cava (IVC) and the inferior end of the atriotomy, between the atriotomy scar and the tricuspid annulus, between the atriotomy and the crista terminalis, or even within the scar itself (Fig. 14.2).

Typical AFL is also often associated with RA atriotomy. In fact, the single most common form of AT among patients with CHD appears to be CTI-dependent AFL, accounting for more than 70% of all MRATs, particularly in patients with simpler anatomical lesions (e.g., tetralogy

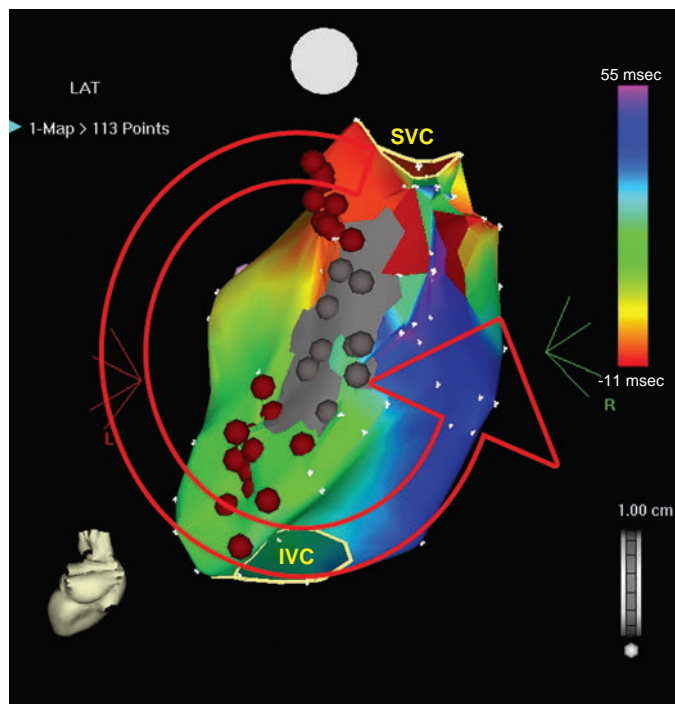


Fig. 14.1 Incisional Right Atrial Macroreentry. Electroanatomic (CARTO) activation map of macroreentrant atrial tachycardia in a patient with previous surgical repair of an atrial septal defect. Gray areas in the posterolateral right atrium represent areas of unexcitable scar related to previous atriotomy, characterized by very low-voltage electrograms. During tachycardia, the activation wavefront travels in a macroreentrant circuit around the atriotomy scar. Ablation lines (red dots) connecting the atriotomy scar to the inferior vena cava (IVC) and superior vena cava (SVC) successfully eliminated the tachycardia.

of Fallot, atrial and ventricular septal defects) (Fig. 14.3). The atriotomy scar in the lateral or posterolateral RA forms a fixed posterior barrier to conduction in the superoinferior direction between the vena cavae, a lateral boundary necessary for the development of a peritricuspid reentry (typical AFL) by preventing short-circuiting of the tricuspid annulus via the posterior atrium. Other RA MRATs involving free wall atriotomy become progressively more common with more extensive atrial incisions.³

Reentry circuits can also occur in the sinus node region, possibly as a result of injury related to the superior atrial cannulation site for the bypass pump. These circuits can be quite small, often manifesting as focal tachycardia in the sinus node region, and they frequently can be ablated in a single location without establishing a particular line of block.

More recently, ATs arising from the morphological LA (i.e., the pulmonary venous atrium) have been described after surgical repair of CHD. The incidence of those ATs is higher in patients with univentricular hearts and those with prior ipsilateral atrial surgery. The mechanism of those ATs is more heterogeneous than that arising from the morphologic RA (i.e., the systemic venous atrium). Macroreentry is a less predominant mechanism, accounting for less than 50% of cases.⁴

Focal Atrial Tachycardia

Focal mechanisms underlying postoperative AT have been rarely reported in this patient population. Nonautomatic focal ATs are predominantly found in adults, with most foci in the RA. The mechanism underlying focal AT is unknown. Both triggered and microreentrant mechanisms have been suggested. Viable myocardial fibers embedded within areas of

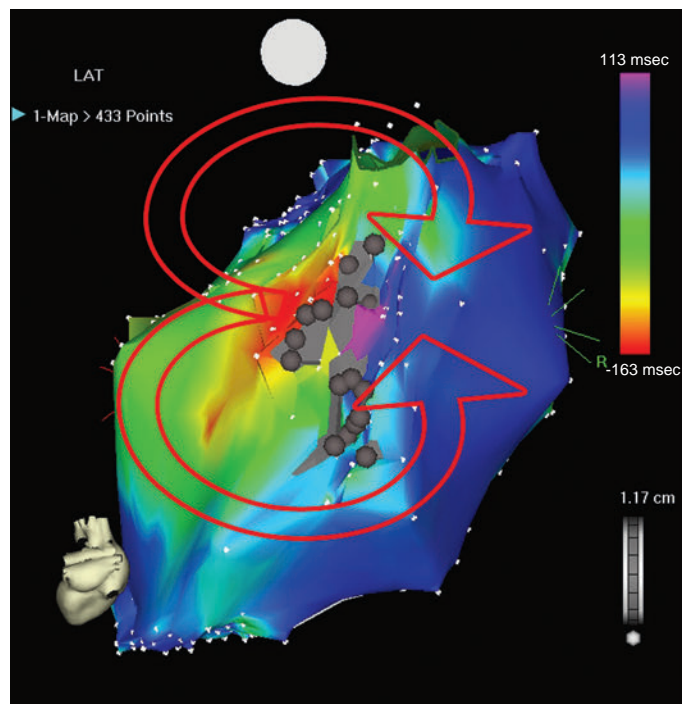


Fig. 14.2 Right Atrial (RA) Figure-of-8 Macroreentry. Electroanatomic (CARTO) activation map of macroreentrant atrial tachycardia in a patient with previous surgical repair of an atrial septal defect. Gray areas in the posterolateral RA represent areas of unexcitable scar related to previous atriotomy, characterized by very low-voltage electrograms. During tachycardia, the activation wavefront travels from the midposterior RA superiorly and inferiorly, and both counterclockwise and clockwise wavefronts return to the region proximal to the exit site (purple) to complete the circuit by propagating through a narrow isthmus bounded by two areas of unexcitable scar (figure-of-8 reentry). Radiofrequency ablation targeting the gap in the atriotomy scar successfully eliminated the tachycardia. IVC, Inferior vena cava; SVC, superior vena cava.

scar tissue, which play a pivotal role in the initiation and perpetuation of macroreentrant tachycardias, can also be the site of origin of a focal AT and thus play an important role in the pathogenesis of these ATs.

Atrial Fibrillation

During long-term follow-up, AF develops in more than one-third of patients with CHD. Compared with MRAT patients, those with AF tend to be older and the arrhythmia develops later after surgery. AF is frequently associated with markers of left-sided heart disease (i.e., left ventricular [LV] systolic dysfunction and LA dilation) and is most commonly seen in patients with congenital aortic stenosis, mitral valve disease, palliated single ventricles, unrepaired heart defects, or end-stage heart disease.² Compared to patients without congenital heart defects or with simple congenital heart defects, AF develops at a younger age in patients with complex congenital heart defects. Coexistence of episodes of AF and regular AT has been reported in a considerable number of patients (33%). Regular AT preceded development of AF in approximately two-thirds of patients. Approximately 30% of patients who have previously undergone successful catheter ablation for MRAT develop AF during long-term follow-up.^{5,6}

Early Postoperative Atrial Tachycardia

Arrhythmias are also frequently observed in the early postoperative period after corrective surgery in children, occurring in 14% to 48% in the first few days after surgery. The most common arrhythmia in

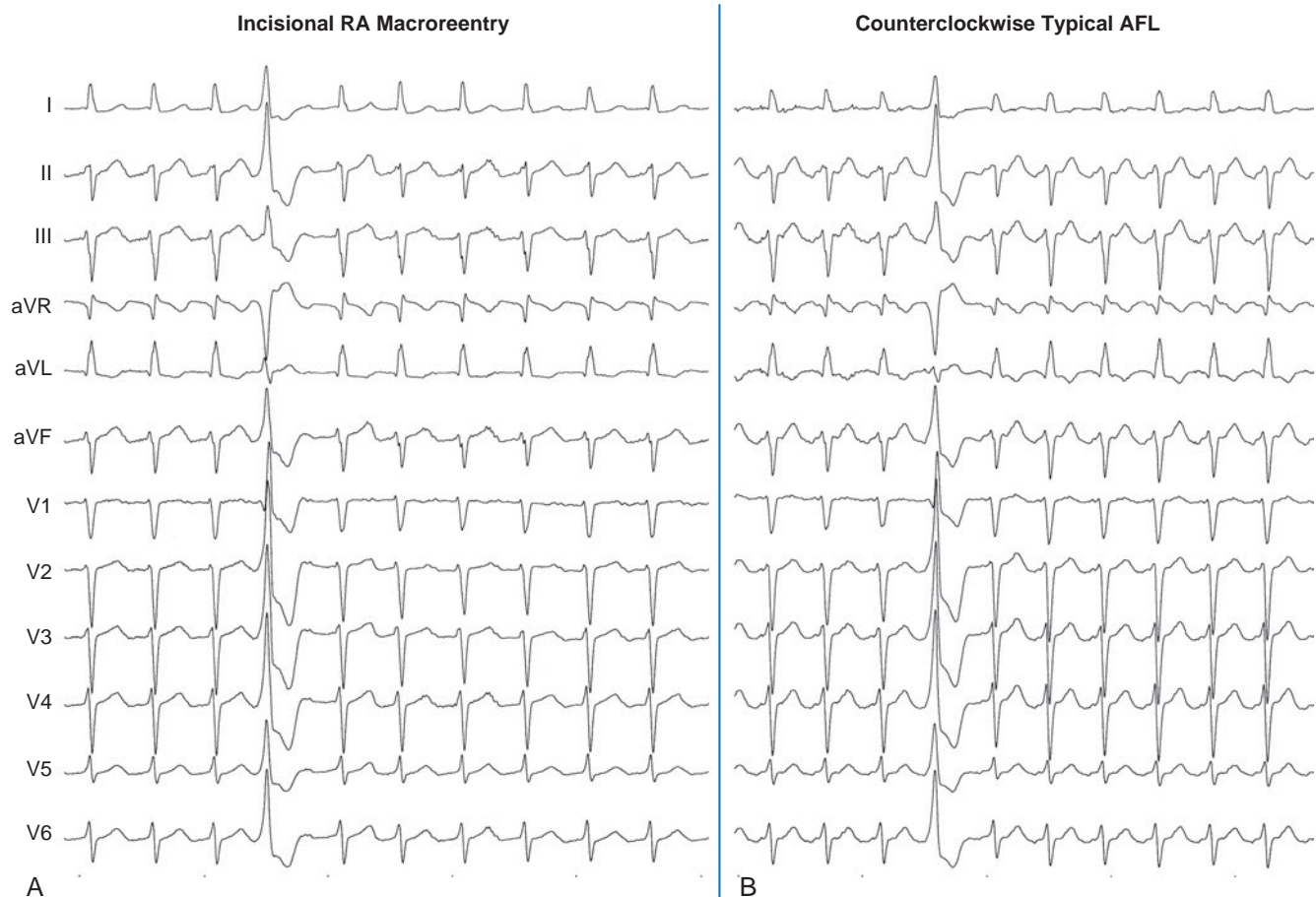


Fig. 14.3 Surface Electrocardiograms of Two Types of Atrial Macroreentrant Atrial Tachycardia in a Patient With Previous Surgical Repair of Atrial Septal Defect. (A) Macroreentrant circuit around the atriotomy scar. (B) Counterclockwise typical atrial flutter (AFL) that developed following successful ablation of the scar-related macroreentry. Spontaneous premature ventricular complexes allow better visualization of the P wave (flutter wave) morphology. RA, Right atrial.

this period is junctional tachycardia, occurring in 5% to 10% of the operated children and usually self-limiting. Other supraventricular arrhythmias are also seen in 4%. The occurrence of early postoperative arrhythmias seems to be related to procedural factors of cardiac surgery, which are, in turn, related to the complexity of the congenital malformation. Local inflammation, metabolic and hemodynamic stress, as well as inotropic drug therapy can potentially promote automatic and triggered activity focal atrial and junctional tachycardias. Early postoperative arrhythmias influence the long-term outcome of patients with CHD and have been found to be a predictor of late complications, such as ventricular dysfunction, late arrhythmias, and late mortality. However, whether preventing these arrhythmias will influence the long-term survival of patients with CHD is unknown.

Atrial Septal Defect

Atrial septal defects are among the most common congenital heart lesions in adults. In the absence of surgical repair, the prevalence of supraventricular arrhythmias increases with age, with typical AFL being the most common. In the presence of atriotomy incisions, sutures, or patches, non-CTI-dependent MRATs can occur or coexist with typical AFL. Common substrates include macroreentry along the lateral RA wall and double-loop or figure-of-8 circuits. The septal patch itself is rarely a critical conduction obstacle.⁷

The timing of surgical closure of the atrial septal defect appears to affect the incidence of atrial arrhythmias. Approximately 60% of patients who have undergone surgical closure at adult age (older than 40 years) continue to have atrial tachyarrhythmias (AT and AF) during follow-up after surgery. In contrast, surgical closure performed during childhood provides a substantially lower incidence of arrhythmias. The impact of transcatheter atrial septal defect closure on atrial arrhythmias is less clear. In one series, all patients with persistent arrhythmias remained in AF or AFL after closure.^{6,8}

Tetralogy of Fallot

Tetralogy of Fallot is the most common cyanotic congenital heart condition, and it accounts for approximately 10% of the adult CHD patient group. ATs occur commonly (12% to 34%) during extended follow-up after tetralogy of Fallot repair. The observed prevalence of atrial arrhythmias is modestly higher than that of ventricular arrhythmias (15%). The most common atrial circuit is typical AFL. Other circuits often involve the lateral RA wall and may be multiple, often with a double-loop type of reentry. Nonautomatic focal ATs are infrequent and most commonly arise adjacent to suture points, with radial spread of activation. The prevalence of AF increases with advancing age. In the first few decades of life, AF is far less common than MRAT, but it becomes more common (more than 30%) than MRAT after 55 years of age.⁹

Dextro-Transposition of the Great Arteries

Dextro-transposition (D-transposition) of the great arteries accounts for 5% to 7% of congenital heart defects. The Mustard and Senning procedures utilize an intraatrial baffle constructed from prosthetic material or pericardium (Mustard) or from the atrial septum and RA free wall (Senning) to redirect the venous blood from the IVC, and the IVC to the LV via the mitral valve, and the pulmonary venous blood to the RV via the tricuspid valve ("atrial switch procedure"). The "new RA" is called the systemic venous atrium and the "new LA" becomes the pulmonary venous atrium.¹⁰ Both procedures were performed from the early 1960s until approximately 1985 as the major long-term surgical palliation procedures for young children having D-transposition of the great arteries. Hence, there is a population of patients in their early 30s to late 50s who have undergone these operations and who are at an increased risk (15% to 48%) of having supraventricular arrhythmias, with similar rates in patients with Mustard and Senning baffles. Since the mid-1980s, with development of coronary artery reimplantation techniques, arterial switch surgery has supplanted atrial redirection as the procedure of choice for D-transposition of the great arteries, and it has been associated with a significantly lower risk of arrhythmias, with a reported arrhythmia-free survival rate of 97% after 25 years of follow-up.^{4,8,10,11}

The most common arrhythmia in patients after Mustard or Senning operations for transposition is atrial macroreentry, occurring in up to 30% of these patients. Typical AFL accounts for up to 75% of all MRATs, but non-CTI-dependent MRATs with critical zones of slow conduction between a suture line and the SVC orifice, mitral valve annulus, and pulmonary vein orifice have all been described. Focal ATs adjacent to suture lines are not uncommon. Importantly, the tricuspid valve is on the pulmonary venous side while the IVC is on the systemic venous side of the circulation; as a consequence, the CTI is necessarily divided between the two sides. Therefore access to the pulmonary venous atrium is almost always necessary for ablation of MRAT and typical AFL, which can be accomplished via a retrograde aortic approach through the tricuspid valve or by transbaffle puncture.^{1,11}

Univentricular Hearts With Fontan Palliation

Among patients with CHD, the incidence of MRAT is highest (up to 50% within a decade of surgery) in older patients who have had older-style palliative surgeries for univentricular hearts, typically varieties of the Fontan procedure. In the older-style Fontan (atriopulmonary [RA appendage-to-pulmonary artery] anastomosis) operations, extensive suture lines, and long-term hemodynamic stress result in marked RA dilation, hypertrophy, and fibrosis. Overall, the most common arrhythmia in these patients is typical AFL, but other MRATs as well as focal ATs are also observed. MRAT circuits in Fontan patients can be complex and multiple, and they represent the most challenging arrhythmias for mapping and ablation.^{1,12} Pericaval circuits have been identified specifically in Fontan patients. In all CTI-dependent circuits, successful ablation requires access to the pulmonary venous atrium (via a fenestration in the intracardiac baffle or a transbaffle puncture) to create the line between the tricuspid annulus and IVC.^{13,14}

The incidence of atrial tachyarrhythmias appears to be reduced by 50% to 70% in patients with total cavopulmonary connections in comparison with classical atriopulmonary connections. Newer Fontan designs (total cavopulmonary connections) bypass the RA to a large extent, using either a lateral tunnel or an extracardiac conduit, thereby avoiding RA dilation and resulting in significant reduction in MRAT incidence to 2% to 7%. In the latter group, however, the macroreentry circuits are typically located on the pulmonary venous side of the tunnel or conduit, requiring complex techniques for accessing the arrhythmia substrate (tunnel/conduit puncture). In patients who have already

developed arrhythmias and then undergo lateral caval tunnel conversion to decompress the right atrium, arrhythmias often subside after this procedure (during which various forms of maze surgery can also be performed), but in many cases, atrial arrhythmias remain problematic.^{1,7,12}

EPIDEMIOLOGY AND NATURAL HISTORY

Congenital heart defects complicate approximately 0.5% to 1% of all live births. Currently, more than 1 million adults are living with CHD in the United States and 1.8 million in Europe. This group now outnumbers children with CHD, reflecting the marked improvements in the early diagnosis and surgical and medical management of congenital heart surgery. The prevalence of atrial arrhythmias is 15% in adults with CHD; for patients with complex congenital defects, the lifetime risk of atrial arrhythmias is more than 50%.⁶

Atrial tachyarrhythmias are an important source of morbidity and mortality in this patient population. Atrial arrhythmias are associated with a 50% increase in mortality and a two-fold increased risk of heart failure or stroke.¹⁵ Approximately 50% of 20-year-olds with CHD will develop an atrial tachyarrhythmia during their lifetime. The incidence of atrial arrhythmias is highest among patients with single ventricle with a Fontan circulation (29% to 60%) and those with transposition of the great arteries after Mustard or Senning operations (14% to 48%), but atrial tachyarrhythmias remain prevalent even in patients with simple congenital defects.^{6,7}

MRAT is the most common mechanism for symptomatic tachyarrhythmias in the adult population with CHD. Surgical incisions in the RA for repair of atrial septal defects are probably the most common causes of lesion-related reentry in adults. Usually, MRAT appears many years after operations that involved an atriotomy or other surgical manipulation. This arrhythmia can infrequently follow simple procedures, such as closure of an atrial septal defect, but the incidence is highest among patients with advanced dilation, thickening, and scarring of their RA. Other risk factors for MRAT include severe myocardial dysfunction, poor hemodynamic status, concomitant sinus node dysfunction (SND), and older age at the time of cardiac surgery. It should be recognized, however, that typical AFL is more common than non-CTI-dependent MRAT, even in this population, and both macroreentry circuits often coexist in a single patient. Importantly, the development of new-onset atrial arrhythmias can be a consequence, rather than a cause, of hemodynamic deterioration.

As noted, AF develops in more than one-third of patients with CHD during long-term follow-up, and is more common in patients with severe congenital defects, residual left-sided lesions, or unrepaired heart disease. AF can coexist with MRAT, and can persist after successful ablation of MRAT.⁵ AF is rarely seen in atrial septal defect patients, before the age of 40 years, but the incidence can approach 50% in unrepaired patients beyond 60 years of age.^{6,7}

The overall prevalence of thromboembolic complications in the relatively young CHD population, with and without atrial arrhythmias, has been estimated to be 10-fold to 100-fold higher than in age-matched controls. During a follow-up period of 5 (0 to 24) years, cerebrovascular accidents occurred in 13% of patient with CHD. A higher rate was associated with the absence of sinus rhythm and in patients with cyanotic heart disease. Notably, a considerable number of cerebrovascular events occurred before the initial documented AF episodes, likely due to dilated cardiac chambers with sluggish flow, intracardiac prosthetic material, intracardiac shunts, and associated hypercoagulable states. Nevertheless, it remains unclear whether subclinical episodes of AF play a role in these events.^{5,15}

SND is not infrequent in this patient population, and can potentially hinder pharmacological therapy in patients with atrial tachyarrhythmias.

CHD, such as sinus venosus atrial septal defects and heterotaxy syndromes (particularly left atrial isomerism), can be associated with SND, even though no surgery has been performed. A more common cause of SND in patients with CHD is injury to the sinus node caused by corrective cardiac surgery. Most commonly associated with this complication is the Mustard, Senning, Glenn, and Fontan operations, as well as repair of atrial septal defects, especially of the sinus venosus type. Surgical incisions, suture lines, and cannulation of the SVC can result in direct damage to the sinus node, its blood supply, or neural inputs.¹⁵ In addition, SND may develop as a consequence of longstanding hemodynamic perturbations or the atrial arrhythmias frequently observed in this patient population.

CLINICAL PRESENTATION

MRATs are typically chronic or long-lasting, but can also be paroxysmal. As with AF and typical AFL, patients can present with symptoms related to rapid ventricular response, loss of atrial contribution to ventricular filling, tachycardia-induced cardiomyopathy, or deterioration of pre-existing cardiac disease. Although MRATs can be asymptomatic, patients typically present with a spectrum of symptoms including palpitations, dizziness, reduced activity tolerance, and dyspnea. Severe decompensation of heart failure can develop. Importantly, the onset of AT often coincides with the presence of significant hemodynamic abnormalities (e.g., worsening ventricular function, baffle obstruction or leak, or progression of valvular or conduit stenosis, or regurgitation) that precipitate or contribute to the development of arrhythmia.

Generally, in the adult population with CHD, MRATs tend to be slower than typical AFL, with atrial rates in the range of 150 to 250 per minute. In the setting of a normal atrioventricular node (AVN) function, such rates frequently conduct in a rapid 1:1 atrioventricular (AV) pattern and can potentially result in hypotension, syncope, or possibly circulatory collapse in patients with limited myocardial reserve. This phenomenon can potentially be compounded by ineffective atrial transport and ventricular dysfunction. Even if the ventricular response rate is well controlled, sustained MRAT can cause debilitating symptoms in some patients because of the loss of AV synchrony and can contribute to thromboembolic complications.

Late-onset supraventricular arrhythmias in patients with CHD can potentially have a major impact not only on morbidity but also on mortality. Rapidly conducting atrial tachyarrhythmias can potentially cause rapid hemodynamic deterioration and trigger ventricular arrhythmias (tachycardia-induced tachycardia) and sudden cardiac death in patients with systemic right ventricles and univentricular hearts.

INITIAL EVALUATION

In patients with CHD, arrhythmia onset can herald a changing hemodynamic profile and can be the first sign of deterioration. Therefore, if arrhythmias occur, a thorough evaluation of the hemodynamic status is warranted. In addition, detailed evaluation of cardiac function, and anatomy and knowledge of the congenital anomaly and previous surgical procedures, are very important. This evaluation can require trans-thoracic or transesophageal echocardiography, right or left heart catheterization, angiography of the desired cardiac chamber, and cardiovascular magnetic resonance (CMR).¹⁵

PRINCIPLES OF MANAGEMENT

AT in CHD patients can result in significant hemodynamic consequences, and prompt management is important. Management of AT should address four main issues: (1) ventricular rate control; (2) restoration

of normal sinus rhythm (NSR); (3) maintenance of NSR; and (4) prevention of systemic embolization.

Rate Control

Ventricular rate control during AT is important to prevent hemodynamic instability and improve symptoms in patients with CHD. Oral or IV AVN blockers are utilized for rate control, depending on the severity of symptoms and the degree of hemodynamic compromise caused by the tachycardia. Beta-blockers or nondihydropyridine calcium-channel blockers (verapamil and diltiazem) are the drugs of choice for rate control. Ventricular rate control, however, is often challenging and, for patients with rapid ventricular rates and hemodynamic compromise, hypotension, or acute heart failure, prompt electrical cardioversion is recommended.¹⁵

Restoration of Sinus Rhythm

Ventricular rate control during AT is usually difficult to achieve, and even with adequate rate control, a subset of patients (e.g., those with a univentricular hearts or systemic right ventricles with decreased contractility) may not tolerate prolonged periods with loss of AV synchrony. Hence, unless contraindicated, restoration and maintenance of NSR is preferred in most patients, particularly in the setting of moderate or complex CHD. Rate control strategy generally is reserved to patients with contraindication to anticoagulation and those with intraatrial thrombi, or those in whom rhythm control strategies have failed.¹⁵

The timing of attempted cardioversion is influenced by the duration of AT, the severity of the patient's symptoms, the adequacy of rate control, and the risk of thromboembolism. In stable patients with AT of a duration longer than 48 hours or of unknown duration, any mode of cardioversion (electrical, chemical, pacing, or ablation) should be delayed until the patient has been anticoagulated at appropriate levels for 3 to 4 weeks or transesophageal echocardiography (TEE) has excluded atrial thrombi. Even when the duration of AT is less than 48 hours, TEE also should be considered prior to cardioversion in patients with high thrombotic risk, including those with transposition of the great arteries, tetralogy of Fallot, Eisenmenger syndrome, Ebstein anomaly, intracardiac baffles, Fontan operation, mechanical valve prosthesis, prior thromboembolism, or severe ventricular dysfunction. Patients with Fontan palliation are at a particularly high risk for thromboembolic complications, such that TEE may be considered prior to cardioversion regardless of the anticoagulation status.

If urgency of cardioversion (because of severe symptoms or hemodynamic instability) precludes TEE, therapeutic doses of low-molecular-weight heparin or unfractionated heparin should be administered as soon as possible concurrent with, or preferably prior to, cardioversion.

Several options are available for termination of MRAT, including external direct-current cardioversion, antiarrhythmic drugs, and overdrive atrial pacing. Generally, direct-current cardioversion is preferred to chemical cardioversion given the higher efficacy and the lower risk of proarrhythmia, especially when the arrhythmia is poorly tolerated and prompt cardioversion is necessary. Intravenous ibutilide is a reasonable option for pharmacological cardioversion. Sotalol is less effective than ibutilide. Data are limited regarding the efficacy of other antiarrhythmic agents. Overdrive pacing is particularly useful in patients with preexisting atrial pacing wires in place (as part of a permanent pacemaker or defibrillator, or temporary epicardial pacing wires following cardiac surgery). For stable patients with adequate heart rate control and minimal symptoms, conversion to sinus rhythm may be deferred until catheter ablation, if this can be performed in a timely manner.¹⁷

Maintenance of Sinus Rhythm

Catheter Ablation

In adults with CHD and frequent recurrent symptomatic MRAT, catheter ablation is superior to antiarrhythmic drugs and is the preferred strategy in most patients. Referral to a center with expertise in adult CHD is strongly recommended. At experienced centers, catheter ablation carries short-term success rates of nearly 90%, but late recurrences of tachycardia, or development of new ones, are common. Nonetheless, ablation results are far superior to the extent of control obtained with medications alone.^{7,15,17}

Antiarrhythmic Drug Therapy

Chronic pharmacological therapy for MRAT in adults with CHD has limited long-term efficacy. Furthermore, most antiarrhythmic agents carry the risk of proarrhythmia, and many agents aggravate SND and compromise ventricular function, thus diminishing their utility in these patients, particularly in the absence of pacemaker therapy. Therefore long-term antiarrhythmic drug therapy is reserved for patients in whom catheter ablation is not feasible or is unsuccessful.¹⁷

Class IC agents (flecainide or propafenone) are an acceptable first-line therapy in patients with simple congenital defects and no other structural heart disease. However, those drugs should be avoided in patients with pathological hypertrophy of the systemic ventricle, systemic or subpulmonary ventricular dysfunction, or coronary artery disease. In those patients, both amiodarone and dofetilide may be considered. The use of sotalol is discouraged given the data linking it to increased mortality.¹⁷

Although amiodarone is likely the most effective antiarrhythmic agent for long-term rhythm control, its use should be reserved for patients in whom other antiarrhythmic agents have failed or are not tolerated. Even then, nonpharmacological options should be thoughtfully considered prior to committing a young patient to long-term amiodarone therapy, given the high risk of side effects.¹⁵ The drug may be used on a temporary basis to effect rhythm control for relief of symptoms prior to definitive ablation therapy (if this cannot be performed within a few days). However, amiodarone must be discontinued at least 1 to 2 weeks prior to the procedure to ensure that target tachycardias can be initiated and characterized for optimal ablation outcomes.

Surgical Ablation

Surgical ablation (RA maze procedure) may be considered in patients with AT refractory to medical therapy and catheter ablation, or in those requiring reoperation for hemodynamic reasons. This procedure is used most commonly for patients with failing Fontan procedures and the most refractory variety of MRAT and is usually combined with a revision of the Fontan connection or conversion from an older atriopulmonary anastomosis to a cavopulmonary connection. This typically includes debulking the RA, removing the thrombus, excising RA scar tissue, implanting an epicardial pacemaker, performing a modified RA maze procedure, and, in patients with prior documented AF, performing a left-sided maze procedure as well. Case series with short-term follow-up report promising results, with arrhythmia recurrence rates of 13% to 30%.

Pacemaker Implantation

Pacemaker implantation can be useful for those patients who have concomitant SND as a prominent component of their clinical picture. In these patients, prevention of severe sinus bradycardia not only allows for the use of drugs necessary for rate and rhythm control but also can potentially improve the hemodynamic status and often result in marked reduction in AT frequency. Pacemakers with advanced programming

features that incorporate AT detection and automatic burst pacing also can be beneficial in select cases, but they carry the risk of accelerating the atrial rate and must thus be used cautiously in patients with rapid AV conduction.

Prevention of Systemic Embolization

Long-term anticoagulation is recommended in patients with atrial arrhythmias and moderate or complex forms of CHD, regardless of the CHA₂DS₂-VASC score, since these patients exhibit a particularly high thrombotic risk. On the other hand, for patients with simple non-valvular forms of CHD, indications for long-term anticoagulation are similar to those in patients with AF (see Chapter 15).

New oral anticoagulants may be considered as an alternative to warfarin in patients with simple forms of CHD and no prosthetic heart valve or hemodynamically significant valve disease. On the other hand, the efficacy and safety of these agents have not been established to allow their utilization in patients with moderate or complex forms of CHD, especially those with Fontan surgery.¹⁵

Of note, clot formation in the RA is common in this patient population, especially in patients with old-style Fontan procedures, unlike patients without CHD in whom LA thrombus is the major concern.¹⁷

ELECTROCARDIOGRAPHIC FEATURES

As noted, MRATs in the adult population with CHD tend to have relatively slow atrial rates (in the range of 150 to 250 per minute) and can be associated with 1:1 AV conduction.

The surface electrocardiogram (ECG) morphology of RA free wall macroentry in a patient with a previous atriotomy is highly variable. The presence of complex anatomy secondary to congenital abnormalities, prior atrial surgery, or large low-voltage zones can modify atrial wavefront propagation in a nonuniform manner, with resulting altered atrial activation vectors or low-amplitude P waves.

P wave morphology on the surface ECG is usually of limited value for precise anatomical localization of macroreentrant circuits. Even typical AFL frequently manifests with an atypical 12-lead ECG appearance (so-called pseudo-atypical flutter) in the setting of markedly complex congenital malformation or surgical correction. Variation in the direction of wavefront rotation, the presence of coexisting conduction block in the atrium, and the presence of simultaneous typical AFL can add to the variability of P wave morphology. In addition, analysis of the flutter wave can be impeded by partial or complete concealment of the P wave within the QRS complexes or T waves when the AT is associated with 1:1 or 2:1 AV conduction (see Fig. 14.3).

The morphology of the atrial complex on the surface ECG can range from that similar to typical AFL to that characteristic of focal AT. Often, inverted flutter waves can be observed in lead V₁. Depending on the predominant direction of septal activation, RA free wall macroreentrant AT can mimic either clockwise or counterclockwise typical AFL.

MAPPING

Detailed knowledge of the patient's congenital and operative anatomy is essential for planning the ablation procedure, predicting the anatomical substrates for the tachycardia, interpreting the results of mapping techniques, and ascertaining how to access the systemic and pulmonary venous atria. Details of previous cardiac surgeries regarding surgical incisions, shunts, anastomoses, baffles, patches, or surgical ablation lesions need to be obtained from prior operative notes, hemodynamic catheterization reports, angiography, and other imaging studies. Preprocedural CMR or computed tomography (CT) can provide invaluable anatomical information on cardiac, vascular, and other intrathoracic

structures, and allow image integration with the electroanatomic map. Furthermore, intracardiac or transesophageal echocardiography can facilitate intracardiac catheter navigation and, when required, guide transseptal or transbaffle access.^{6,7}

Vascular and Cardiac Access

Feasibility and adequacy of vascular access must be confirmed in advance. Table 14.1 includes those conditions that are expected to pose vascular or cardiac chamber access challenges and methods that have been reported to allow catheter access. There is often limited opportunity to place the standard number of diagnostic electrode catheters due to access issues; alternative approaches to obtain endocardial access may include hepatic veins (via transhepatic puncture) and a retrograde approach to the atria from the ventricles.^{4,8,13}

Access to the Systemic Venous Atrium

The femoral veins may not provide access to the systemic venous atrium because of iliofemoral vein occlusion (resulting from multiple prior transvenous diagnostic and therapeutic cardiac procedures for the congenital anatomy) or interruption of the IVC. In these patients, access to the heart via the SVC (through the internal jugular and subclavian veins) or transhepatic venous access can be an alternative approach.^{6,7,18}

Access to the Arrhythmia Substrate and Cavotricuspid Isthmus

Knowledge of the location of the CTI (in the systemic versus pulmonary venous atrium), which is the most common target for catheter ablation, can help anticipate the need for transseptal/baffle access. Also, transseptal/baffle access can be required when non-CTI-dependent MRATs are mapped to the anatomical LA or to the portion of the native RA baffled to the pulmonary venous side of the circulation.

In patients with tetralogy of Fallot, atrial and ventricular septal defects, or anomalous pulmonary veins, postoperative cardiac anatomy approximates normal. In those patients, most MRAT circuits are located

in the RA, and cardiac access techniques, to a large extent, are similar to those in patients with MRAT and typical AFL in the absence of CHD. On the other hand, in patients who have undergone a Mustard or Senning procedure for D-transposition of the great arteries, postoperative anatomy of the atria presents unique challenges. The Mustard and Senning procedures direct the venous blood from the IVC, and IVC to the LV via the mitral valve, and the pulmonary venous blood to the RV via the tricuspid valve (“atrial switch procedure”). Thus the tricuspid valve is on the pulmonary venous side while the IVC is on the systemic venous side of the circulation; hence, the CTI is necessarily divided between the two sides (Fig. 14.4). Therefore access to the pulmonary venous atrium is almost always necessary for the ablation of MRAT including typical AFL, and can be accomplished via a retrograde aortic approach through the tricuspid valve or by transbaffle puncture.¹⁰

The most complex anatomy is confronted post Fontan procedures for univentricular hearts. Among patients who have had atriopulmonary (RA-to-pulmonary artery) anastomosis, ablation of the CTI requires access to the pulmonary venous atrium (via a fenestration in the baffle or a transbaffle puncture).¹³ Even in newer Fontan designs (total cavopulmonary connections), whereby the RA is bypassed to a large extent, using either a lateral tunnel or an extracardiac conduit, MRAT circuits are typically located on the pulmonary venous side of the tunnel or conduit, necessitating transbaffle access.^{1,12,14}

Access to the Coronary Sinus and Atrioventricular Node

It is important to recognize that the coronary sinus (CS) may not be easily accessible in patients with complex CHD. After a Mustard procedure for D-transposition of the great arteries, the location of the intraatrial baffle with respect to the CS and triangle of Koch is variable. The Mustard baffle can include or exclude the CS os, resulting in positioning the CS os in the pulmonary or systemic venous atrium, respectively (Fig. 14.5).^{4,7,8,11} During the Mustard and the Senning procedure, the intraatrial baffle is routinely sutured posterior to the AVN. As a result, the AVN is always located in the pulmonary venous atrium.¹⁰

TABLE 14.1 Conditions Associated With Challenges for Vascular and Cardiac Chamber Access

Occlusion or Access Challenge	Associated Conditions	Alternate Strategies
Iliofemoral venous occlusion	<ul style="list-style-type: none"> D-TGA undergoing BAS as newborn prior to 1985 Any complex patient with history of multiple catheterizations 	<ul style="list-style-type: none"> Internal jugular, subclavian veins Transhepatic venous (especially for transseptal access)
Interrupted inferior vena cava (above renal veins)	<ul style="list-style-type: none"> Heterotaxy (left atrial isomerism) 	<ul style="list-style-type: none"> Internal jugular, subclavian veins Transhepatic venous (especially for transseptal access) Femoral vein to azygous vein
Access to pulmonary venous atrium	<ul style="list-style-type: none"> “Lateral tunnel,” TCPC types of Fontan procedures 	<ul style="list-style-type: none"> Transbaffle puncture Through baffle fenestration, if present Hybrid procedure (cardiothoracic surgeon performs limited thoracotomy, atrial purse string) Retrograde from aorta
Access to supra-annular rim of systemic venous atrium	<ul style="list-style-type: none"> Fontan procedure-treated patients with supra-annular patch (especially in double inlet ventricle) 	
Access to pulmonary venous atrium	<ul style="list-style-type: none"> D-TGA after Mustard or Senning procedure 	<ul style="list-style-type: none"> Transbaffle puncture Retrograde from aorta
Access to any atrial tissue	<ul style="list-style-type: none"> Fontan procedure-treated patients with extracardiac conduit 	<ul style="list-style-type: none"> Transconduit puncture Transthoracic puncture (consult cardiothoracic surgeon) Hybrid procedure (cardiothoracic surgeon performs limited thoracotomy, atrial purse string) Retrograde from aorta

BAS, Balloon atrial septostomy; D-TGA, D-transposition of the great arteries; TCPC, total cavopulmonary connection.

Modified with permission from Kanter RJ. Pearls for ablation in congenital heart disease. *J Cardiovasc Electrophysiol.* 2010;21:223–230.

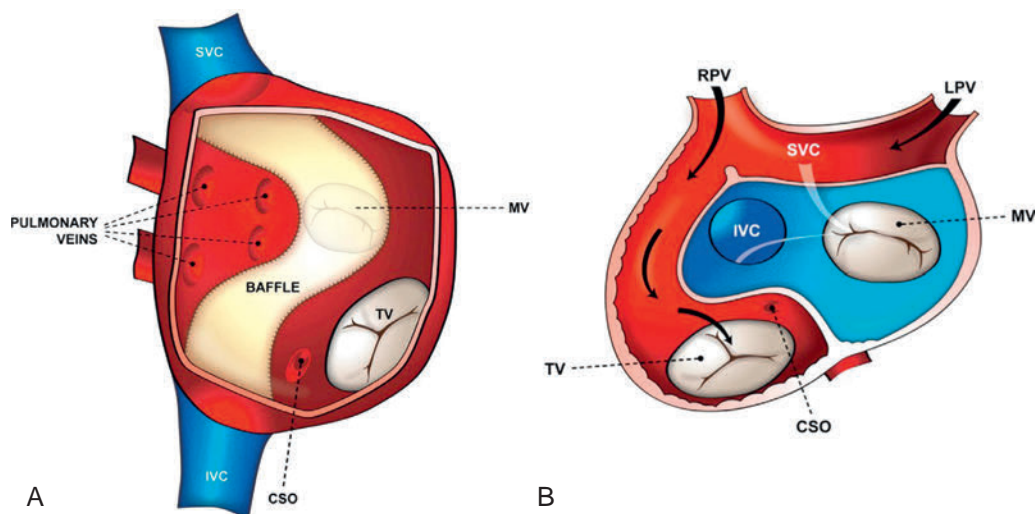


Fig. 14.4 Cavotricuspid Isthmus in D-transposition of the Great Arteries With Mustard and Senning Baffles. (A) Right anterior oblique view of a Mustard baffle is schematically depicted. (B) Axial view of a Senning baffle. Systemic venous return via the superior vena cava (SVC) and inferior vena cava (IVC) is directed toward the mitral valve (MV), whereas pulmonary venous return is directed toward the tricuspid valve (TV). Note that the cavotricuspid isthmus is divided in two, with the IVC portion on the systemic and TV portion on the pulmonary venous side of the circulation. CSO, Coronary sinus ostium; LPV, left pulmonary vein; RPV, right pulmonary vein. (From Khairy P, Van Hare GF. Catheter ablation in transposition of the great arteries with Mustard or Senning baffles. *Heart Rhythm*. 2009;6:283–289.)

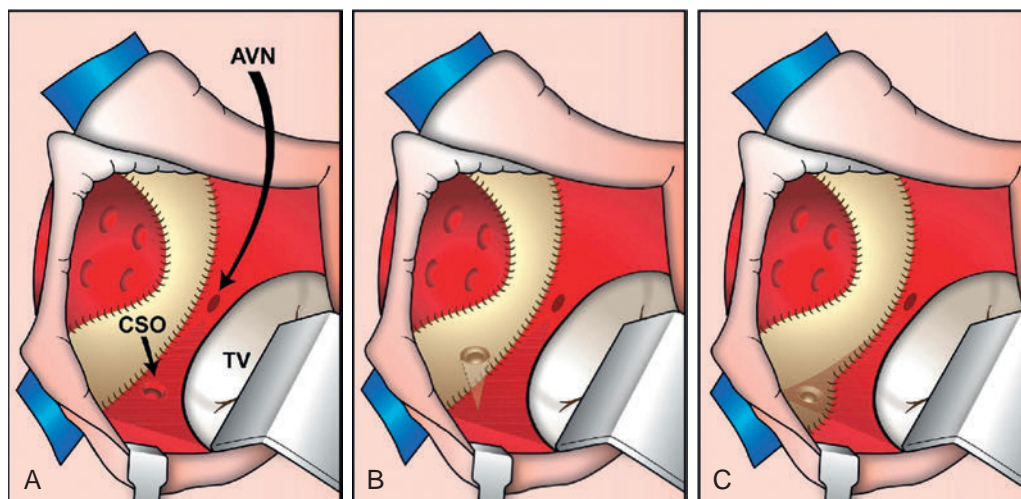


Fig. 14.5 Triangle of Koch in D-transposition of the Great Arteries With Mustard Baffle. Three surgical variants for Mustard procedures are portrayed. (A) The coronary sinus is excluded from a baffle that is sutured posterior to its ostium (CSO), such that Koch's triangle is entirely in the pulmonary venous atrium. (B) The coronary sinus is surgically incised to redirect coronary venous flow into the Mustard baffle, with the Koch's triangle in the pulmonary venous atrium. (C) The anterior portion of the Mustard baffle is sutured anterior to the CSO to include coronary venous egress, such that the inferoposterior section of the Koch triangle is within the systemic venous atrium. AVN, Atrioventricular node; TV, tricuspid valve. (From Khairy P, Van Hare GF. Catheter ablation in transposition of the great arteries with Mustard or Senning baffles. *Heart Rhythm*. 2009;6:283–289, with permission.)

Access to the Pulmonary Venous Atrium

As noted, the arrhythmogenic substrate can be located partially or completely in the pulmonary venous atrium in patients with complex CHD, including those who have undergone a Mustard or Senning procedure for D-transposition of the great arteries, or a Fontan operation with an intraatrial baffle or extracardiac conduit. Ablating the tachycardia

substrate in these patients usually requires access to the pulmonary venous atrium.^{4,8,11}

Access to the pulmonary venous atrium can be technically challenging in patients with complex congenital defects and surgical baffles or septal patches. An understanding of the atrial septal anatomy, type of septal patches, extracardiac conduits, and any surgically created baffles,

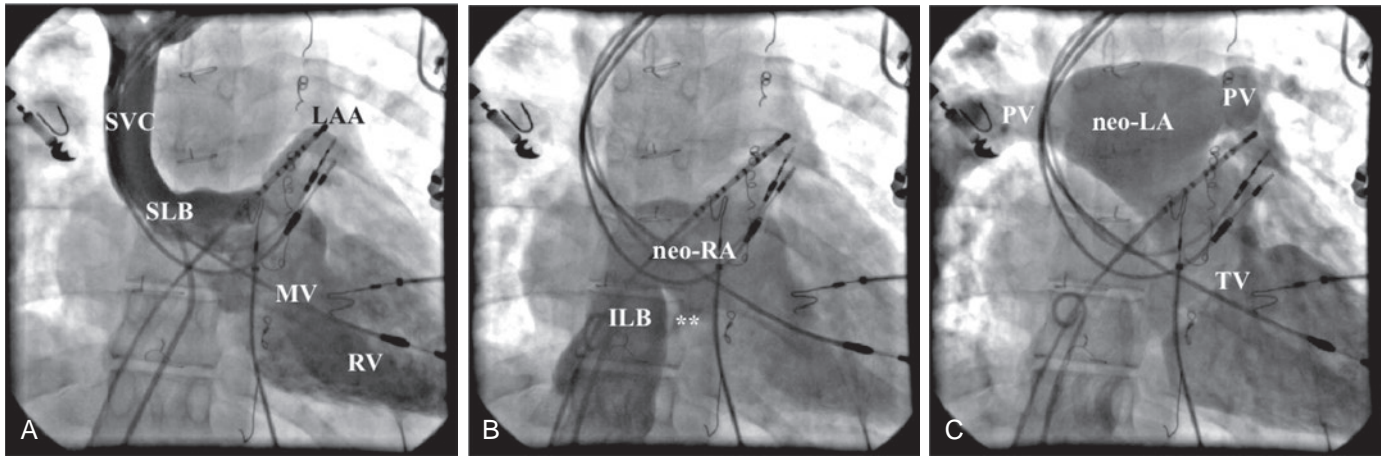


Fig. 14.6 Angiography of a Senning Baffle. (A) Power contrast injection in the superior limb of the Senning baffle (SLB) shows unobstructed flow from the superior vena cava (SVC) with no intraatrial shunting. The reference catheter is positioned in the left atrial appendage (LAA), next to atrial pacing leads. (B) Power contrast injection of the inferior limb of the baffle (ILB) reveals a baffle leak, marked by the asterisks. This shunt was used to access the neo-left atrium (neo-LA). Flow into the neo-right atrium (neo-RA) is unimpeded. (C) Delayed imaging shows unobstructed pulmonary venous (PV) return into the neo-LA and toward the tricuspid valve (TV). MV, Mitral valve; RV, right ventricle. (From Khairy P, Van Hare GF. Catheter ablation in transposition of the great arteries with Mustard or Senning baffles. *Heart Rhythm*. 2009;6:283–289, with permission.)

as well the presence of baffle leaks or obstructions, is essential to plan access strategies to the pulmonary venous atrium. In addition, preprocedure CT or CMR or angiography of the systemic venous atrium during the procedure can help to investigate the presence of residual interatrial communications (e.g., baffle leak or septal patch defect), which might be used for transseptal access (Fig. 14.6). If a fenestration is not present, access to that chamber can require needle puncture of the native atrial septum, septal patch, or baffle. Although the retrograde aortic approach can provide access to the pulmonary venous atrium, it may not always permit adequate catheter reach or stability for successful ablation. These difficulties can be mitigated by using remote-controlled magnetic navigation (Stereotaxis; St. Louis, MO), which eliminates many of the limitations related to curve radius or reach.^{6,7,10}

Transseptal catheterization is feasible in most patients with prior surgical repair of an atrial septal defect. However, an understanding of the method of repair and utilization of intracardiac echocardiography (ICE) guidance are essential.¹⁹ In patients with a septal stitch or pericardial or Dacron patch, puncture can be achieved through the thickened septum or the patch. Transseptal access is typically not achievable through a Gore-Tex patch because of its resistant texture; instead, puncture can be performed directly through neighboring native interatrial tissue. When the patch is wide, sufficient free septal tissue for transseptal puncture may not be available, in which setting transseptal access to the LA may not be feasible. In patients with atrial septal defect closure devices, puncture is preferably performed at the portion of the septum located inferior and posterior to the closure device and not through the device itself. When areas of native septum are not available for transseptal access, recent reports described successful LA access through a direct puncture of the closure device.^{20,21} Radiofrequency (RF)-powered transseptal needles can facilitate access across the often thickened septum or synthetic baffles or patches.^{7,10}

Mapping Approach

Mapping may proceed using one of several strategies: if the patient presents during ongoing tachycardia, activation mapping can be used to characterize the arrhythmia's propagation, location of barriers and

potential isthmuses, and voltage. Alternatively, overdrive pacing may be used first, to determine tachycardia mechanism; although the vast majority of tachycardias in this population are due to macroreentry, an important minority are due to focal discharge for which linear ablation strategies (see below) have little benefit. Overdrive pacing may result in transient suppression followed by resurgence of these arrhythmias, rather than entrainment. If activation mapping is performed first, it may indicate a likely focal source with roughly centrifugal propagation, but this should not be taken as diagnostic of a focal process. Regardless of which strategy is used first (activation mapping or overdrive pacing), each should be performed if possible, since each provides important information regarding the tachycardia.

If the patient presents to the procedure in sinus rhythm, pacing can be performed at a number of sites from stationary catheters (CS, halo, etc.) for comparison of pure pacing activation sequences to those obtained while pacing from these sites during tachycardia that is subsequently initiated, in order to diagnose macroreentry. Voltage mapping can then be performed, determining low voltage or scar areas, likely atriotomy or baffle/patch regions, other barriers to propagation, such as valve annuli and caval orifices, and potential tachycardia isthmuses. The location of the normal conduction system and phrenic nerve can be determined, after which tachycardia can be initiated.

Exclusion of Cavotricuspid Isthmus Dependence

Exclusion of the CTI as part of the AT circuit is an important initial step because typical clockwise or counterclockwise AFL is the most common MRAT in patients with CHD (particularly in patients with simpler anatomical lesions such as the tetralogy of Fallot and atrial and ventricular septal defects), even if the P wave morphology is not characteristic for these arrhythmias. Exclusion of the CTI as part of the reentrant circuit can be established by any of the following: (1) demonstration of bidirectional activation of the CTI during AT, with resulting collision or fusion within the isthmus by activation from opposing directions (the low lateral RA and CS); (2) recording of double potentials separated by an isoelectric and constant interval throughout the full extent of the CTI during tachycardia; or (3) entrainment mapping from

the CTI demonstrating manifest atrial fusion with a long post-pacing interval.^{22,23}

If typical AFL is excluded, attention should be directed to potential reentrant circuits anchored by a right lateral atriotomy scar or a surgical patch. Subsequently, more complex or dual- or multiple-loop reentrant circuits (especially in patients with complex congenital malformations) should be considered; these require a more comprehensive and detailed mapping approach.

Identification of Barriers and Potential Lines of Block

Electroanatomic mapping (CARTO mapping system [Biosense Webster, Inc., Diamond Bar, CA, United States] or EnSite NavX system [St. Jude Medical, St. Paul, MN, United States]) is typically used to help facilitate identification of the macroreentrant circuit and the sequence of atrial activation during tachycardia and rapid visualization of the activation wavefront in the context of the relevant anatomy. These mapping systems allow for good reconstruction of 3-D anatomical shell of the often distorted cardiac chamber and integration of the created chamber geometry with preacquired cardiac CT or CMR images or with intra-procedural ICE or rotational angiography images (Fig. 14.7).¹

Mapping of MRATs in patients with CHD follows the same principles discussed for mapping of other types of MRATs (see Chapter 13 for detailed discussion). Initially, potential tachycardia circuit barriers are identified (during sinus rhythm or tachycardia) and marked on the electroanatomic map to help understand propagation of the reentrant

activation wavefront in relation to these barriers, identify potential slow-conducting pathways critical to the reentrant circuit, identify sites to target by entrainment mapping, and plan subsequent ablation strategy to abolish the tachycardia. The tricuspid annulus often provides one important barrier. Other naturally fixed barriers (i.e., independent of the precise form of activation and present also in sinus rhythm) include the IVC, SVC, and CS os. Acquired barriers include surgical incisions or patches, lines of block, and electrical scars. Confluent areas of low voltage (less than 0.05 mV) can localize areas of scar tissue. Such areas and surgically related scars, such as atriotomy scars in the lateral RA or atrial septal defect closure patches, are tagged as “scar” (see Figs. 14.1 and 14.2). Ensuring adequate catheter-tissue contact is essential, as low voltage due to lack of contact simulates scar. Fortunately, use of contact force-sensing catheters largely obviates this problem.

Identification of the Complete Reentrant Circuit

Electroanatomic activation mapping during AT is performed to define the atrial activation sequence and identify the complete reentrant circuit and its mid-diastolic critical isthmus. Reasonable numbers of points homogeneously distributed in the atrium must be recorded; it is important to record from all areas of the atrium (lateral RA can be difficult to reach and it can appear that the entire chamber has been sampled when, in fact, significant portions remain unmapped). The local activation time at each site is determined from the intracardiac bipolar electrogram and is measured in relation to the fixed intracardiac electric

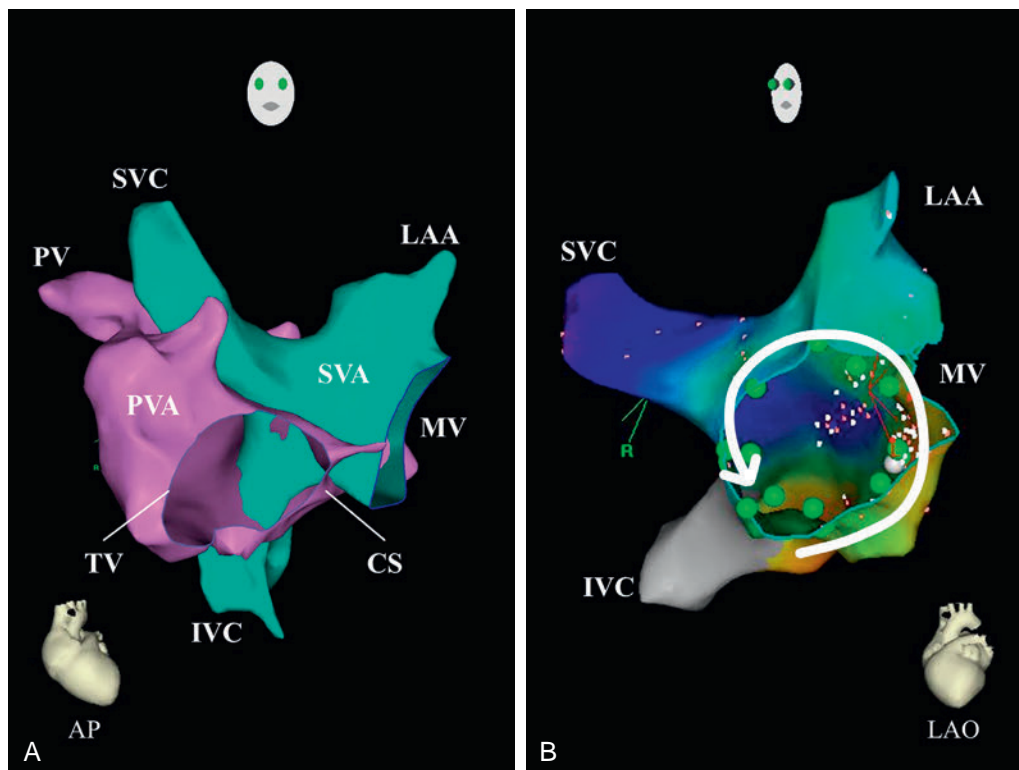


Fig. 14.7 Atrial Macroreentry After the Mustard Procedure. (A) Anatomical reconstruction illustrating the anatomy of the pulmonary venous atrium (PVA) and systemic venous atrium (SVA) in a patient after the Mustard procedure. (B) An electroanatomic activation map of a macroreentry tachycardia in another patient with transposition of the great arteries corrected by the Mustard procedure. This map shows an activation map of the SVA from the left anterior oblique (LAO) view, with a reentry wavefront circulating around the mitral valve. AP, Anterior posterior; CS, coronary sinus; IVC, inferior vena cava; LAA, left atrial appendage; MV, mitral valve; PV, pulmonary vein; SVC, superior vena cava; TV, tricuspid valve. (From Houck CA, Teuwen CP, Bogers AJ, de Groot NM. Atrial tachyarrhythmias after atrial switch operation for transposition of the great arteries: treating old surgery with new catheters. *Heart Rhythm*. 2016;13:1731–1738, with permission.)

reference. Usually a catheter in the CS (if accessible) provides a stable reference electrogram. Using the onset of the local bipolar electrogram is preferable because it is easier to determine reproducibly when measuring heavily fractionated, low-amplitude atrial electrograms.

The complete reentrant circuit is the spatially shortest route of unidirectional activation encompassing the complete cycle length (CL) of the tachycardia in terms of activation timing and returning to the site of earliest activation. Using electroanatomic mapping, this translates into continuous progression of colors around the atrium, with close proximity of earliest and latest local activation. In addition, propagation of electrical activation superimposed on the 3-D anatomical reconstruction of the atrium can be visualized as a propagation map in relation to the anatomical and electrophysiological (EP) landmarks and barriers.

Unlike in mapping focal AT, in which tracking the site with the earliest presystolic local activation timing is the goal of mapping, there is no early or late region for MRAT because the wavefront is continuously propagating around the circuit. Entrainment pacing is performed at multiple atrial sites, especially around the tricuspid annulus and other atrial sites suspected to be critical to the reentry circuit, as identified by activation mapping. Entrainment mapping can be used to indicate the relation of pacing sites to the reentrant circuit (see Fig. 13.12). A (postpacing interval [PPI]–tachycardia cycle length [TCL]) difference of less than 50 milliseconds at the proximal CS distinguishes typical AFL from a lateral RA MRAT.²⁴

It is very important to remain vigilant during the mapping process and identify any change in the TCL or activation sequence, which can result from catheter manipulation, pacing maneuvers, or ablation. Such changes can indicate transformation of a multiple loop tachycardia by the interruption of one loop, a change in bystander activation, or a transition to another tachycardia, which requires reassessment. The transition may be obvious but is often quite subtle and sometimes imperceptible if only the CS activation is analyzed. Simultaneous recordings of RA activation (using a Halo catheter around the tricuspid annulus) and CS activation (using a decapolar catheter) can help rapid identification of tachycardia transformation; a change in tachycardia may be indicated by either a change in activation pattern (often subtle), a change in TCL, or both.

Sometimes, it can be impossible to map the entire circuit, especially in patients with complex CHD, because of the complex anomalies, suture lines, and baffles. In this setting, a combination of activation, entrainment, and voltage mapping data is used to identify the potential isthmus or zone of slow conduction critical to the reentrant circuit, which is then targeted by catheter ablation.

Identification of the Critical Isthmus

Once a scar or fixed barrier is localized, determining its role in supporting reentry is important in determining whether the isthmuses formed around it need ablation. Whether an isthmus is a critical part of the reentrant circuit can be determined by activation mapping during sustained stable reentry and entrainment mapping. The critical isthmus can lie between two anatomical barriers (e.g., the atriotomy scar and IVC orifice), or it can be a relatively narrow channel bounded by sites of scar or double potentials (marking anatomical or functional lines of conduction block). Electrograms recorded within the critical isthmus frequently exhibit wide, fractionated, low amplitude potentials (eFig. 14.1). The line of double potentials or fractionated, low-voltage electrograms also can often be recorded in NSR, to allow tentative localization of the scar and the associated anatomical isthmuses.

During electroanatomic activation mapping, when the onset of the window of interest is set at mid-diastole between two consecutive P waves, the mid-diastolic isthmus of the reentrant circuit can potentially be identified by the interface of early and late activation (i.e., the region

where “early meets late” on the color-coded activation map). High-density mapping is then performed in and around the isthmus to more precisely define its limits and width.

Once one or more potential isthmuses are identified during activation mapping and propagation mapping in relation to atrial scars, barriers, and lines of block, entrainment is performed to determine their role for supporting the reentrant circuit. Entrainment with concealed fusion should be sought; this indicates that the pacing site is in a protected isthmus located within or attached to the reentrant circuit. It should be recognized, however, that in patients with complex anatomy and surgical repairs, critical corridors of slow conduction can exist anywhere in the RA, and multiple circuits are the rule. As a consequence, entrainment with concealed fusion is highly nonspecific for most circuits in these patients. Therefore whether the protected isthmus is crucial to the reentrant circuit or just a bystander site needs to be verified by comparing the PPI with the TCL and the stimulus-exit interval with the electrogram-exit interval. Features of entrainment when pacing from different sites are listed in Table 13.2.^{22,23}

The critical isthmus of the reentry circuit often is an area of very slow conduction. As a result, stable overdrive pacing of the critical isthmus during MRAT can be difficult or impossible in these patients because of tachycardia interruption; in some cases, this occurs without propagation of the impulse and indicates that the pacing site is in a critical isthmus, despite being unable to show standard entrainment. Isthmus participation in the circuit is often proven by tachycardia interruption with catheter pressure (eFig. 14.2), as well as by tachycardia interruption and noninducibility after RF application in the area. Mechanical interruption of tachycardia can potentially render it non-inducible for extended periods of time thereafter; moving the catheter away from the site at which this occurred, the use of epinephrine, isoproterenol, or adenosine, or simply waiting up to 30 minutes may allow reinitiation of tachycardia. If the catheter tip electrode was being moved slowly and methodically when mechanical termination occurred, logging that site on the electroanatomic mapping system can facilitate subsequent ablation even if tachycardia cannot be reinitiated; however, if the catheter movements around the time of mechanical interruption were more coarse, caution should be exercised in determining what site may have been affected by the catheter trauma.

In some cases, the best ablation target is a systolic, rather than diastolic, electrogram; this occurs especially in very large and scarred atria, where very slow propagation occurs from a reentrant corridor to the rest of the atrium. Such sites are uninteresting from an activation mapping perspective and only can be discovered by overdrive pacing at sites that have very delayed conduction during sinus rhythm, or are in regions that are suspected to contain a diastolic corridor from voltage or activation mapping during other tachycardias. Such overdrive pacing at these sites produces a perfect intracardiac pace match with tachycardia, with a very long stimulus-P interval and PPI approximating TCL.

ABLATION

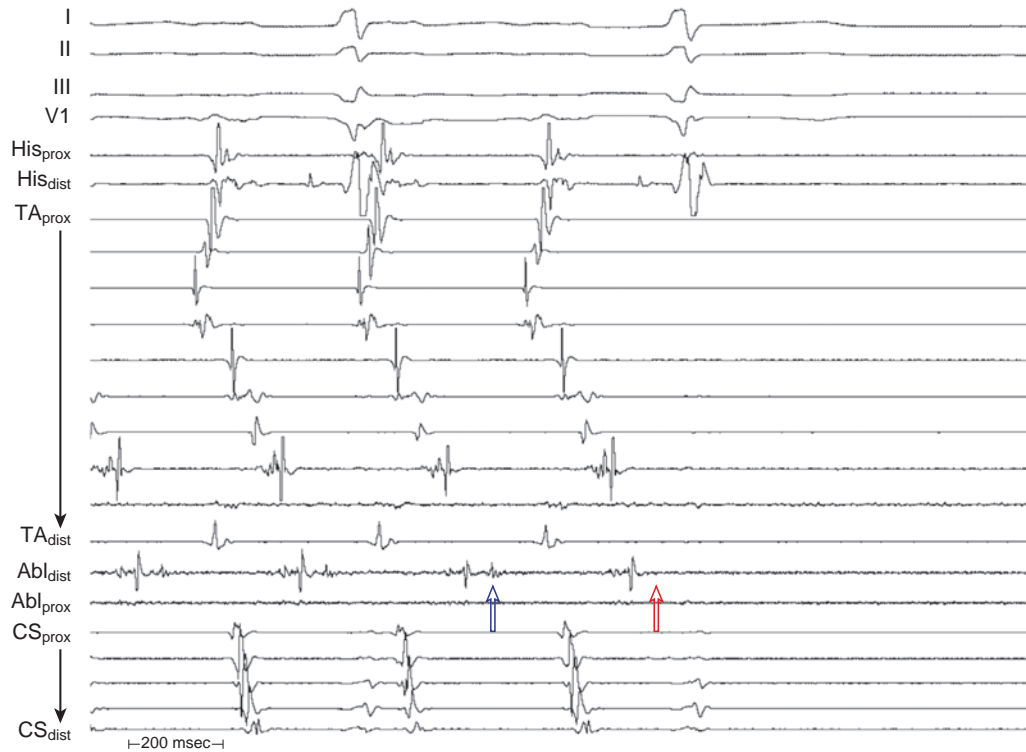
Target of Ablation

The choice of ablation sites should be among those segments of the reentry circuit that offer the most convenient and safest opportunity for creating a conduction block. Among other factors are the isthmus size, the anticipated catheter stability, and the risk of damage to adjacent structures (e.g., phrenic nerve, sinus node, and AVN).

Ablation is performed by targeting the narrowest identifiable isthmus of conduction accessible within the circuit (allowing the best electrode-tissue contact along the desired line). The ablation line is chosen to transect an area critical for the circuit and, at the same time, connect two anatomical areas of block, an electrically silent area to an anatomical



eFig. 14.1 Postatriotomy Right Atrial Macroreentry. Electrocardiogram leads and intracardiac recordings are shown during non-isthmus-dependent macroreentrant atrial tachycardia (AT) in a patient with a repaired atrial septal defect. A prolonged, fractionated diastolic electrogram is observed at the ablation site. Note the repetitive recording (*arrow*) that nearly spans the cardiac cycle. The patient had a right atriotomy as the basis of atrial tachycardia and incurred complete heart block during surgery (hence the ventricular pacemaker). Abl_{dist}, Distal ablation site; CS_{dist}, distal coronary sinus; CS_{mid}, middle coronary sinus; CS_{prox}, proximal coronary sinus; His_{prox}, proximal His bundle; TA_{dist}, distal tricuspid annulus; TA_{prox}, proximal tricuspid annulus.



eFig. 14.2 Catheter-induced Termination of Macroreentrant Atrial Tachycardia (AT). Electrocardiogram leads and intracardiac recordings are shown during an episode of non-isthmus-dependent atrial macroreentrant AT in a patient with prior atriotomy. The episode had lasted 3 months at the time of the study, yet catheter pressure at the site from which the distal ablation site (*Abl_{dist}*) recording was made terminated AT twice. Note the multicompartment electrogram (*blue arrow*), the last portion of which is missing when AT terminates (*red arrow*). *Abl_{prox}*, Proximal ablation site; *CS_{dist}*, distal coronary sinus; *CS_{prox}*, proximal coronary sinus; *His_{dist}*, distal His bundle; *His_{prox}*, proximal His bundle; *TA_{dist}*, distal tricuspid annulus; *TA_{prox}*, proximal tricuspid annulus.

zone of block (e.g., IVC, SVC, or tricuspid annulus), or two electrically silent areas.

Although successful ablation is most frequently achieved by targeting the “slow zone” of atrial conduction presumed necessary for maintenance of reentry, some investigators have emphasized the need for considering both the anatomy and EP simultaneously to identify a susceptible bridge of tissue, which connects two areas of electrical block (see Fig. 13.13). Such an approach requires careful review of the details of the atrial surgery, in addition to detailed mapping of the atria in its “usual” rhythm (i.e., sinus or atrial pacing) and during reentry.

Because typical AFL is the most common mechanism underlying MRAT in the patient population with CHD, determination of the role of the CTI in supporting reentry is evaluated first, and the CTI should be targeted by ablation if it is proved to be critical to the AT circuit (Fig. 14.8). Ablation of the CTI may also be reasonable in all CHD patients with MRAT, even those presenting with non-CTI-dependent RA macroreentry, because the CTI can support reentry in most patients with prior right atriotomy. Importantly, in some congenital heart malformations (e.g., AV canal defects), the AVN and His bundle can have unusual locations, and can be displaced just anterior to the ostium of the CS. Consequently, ablating in the right inferior paraseptal region can cause AV block. Therefore for patients with CTI-dependent macroreentry, the location of the conduction system should be carefully characterized and more lateral ablation lines are generally preferred, to prevent AV block.

If participation of the CTI in the reentrant circuit is excluded, or if the tachycardia persists or transforms into a different tachycardia after ablation of the CTI, participation of the lateral RA wall in the AT circuit should be assessed. Non-CTI-dependent RA macroreentry is frequently localized to the free wall of the RA, anchored by the atriotomy scar, in which setting the ablation strategy includes any of the following: (1) to target the slow conduction area (critical isthmus of the reentrant circuit) as identified by detailed activation and entrainment mapping (see Fig. 14.2); (2) to extend the atriotomy (double potential or scar) to the IVC (see Fig. 14.1); or (3) to extend the scar area to the SVC (see

Fig. 14.1). The last approach can result in injury of the sinus node or phrenic nerve. Therefore, when possible, extending the atriotomy to the IVC is preferable (and is generally technically easier). As noted, additional ablation of the CTI may be considered in these patients because these circuits are often combined with a circuit around the tricuspid annulus in a figure-of-8 reentry, such that ablation of both the CTI and one of the lateral wall options must be performed to eliminate and prevent reentrant AT (see Fig. 14.8).

Rarely, more complex circuits, such as around the right septal patch, as seen in patients with Mustard or Senning repairs, are observed. However, the approach to ablation is the same: the area with slow conduction or scar is extended to an anatomical obstacle.

Another focus for reentry circuits is the region of the sinus node. These circuits may be quite small, often manifesting as focal tachycardia in the sinus node region, and they can often be ablated in a single location without establishing a particular line of block.

In patients with incomplete maps, a combination of activation, entrainment, and voltage mapping data is used to identify the potential isthmus or zone of slow conduction critical to the reentrant circuit, which is then targeted by catheter ablation. When limitations to this approach still exist (from poor inducibility or frequent change in morphology of the tachycardia), a stepwise ablation strategy may be employed. Because the reentrant circuit in most patients is anchored to the CTI or the atriotomy scar, ablation of the CTI is initially performed. Then, if the tachycardia persists, linear ablation is carried out by targeting the isthmuses related to the lateral atriotomy scar (i.e., connecting the atriotomy to either the IVC or SVC). Additional ablation lines connecting other areas of conduction block (scar, surgical incision, septal patch, baffle, or natural barriers) may be considered based on substrate mapping findings.

Ablation Technique

Once the ablation target is identified, ablation involves placing a series of RF lesions to sever the critical isthmus and connect two anatomical or surgical barriers. Because some congenital malformations and

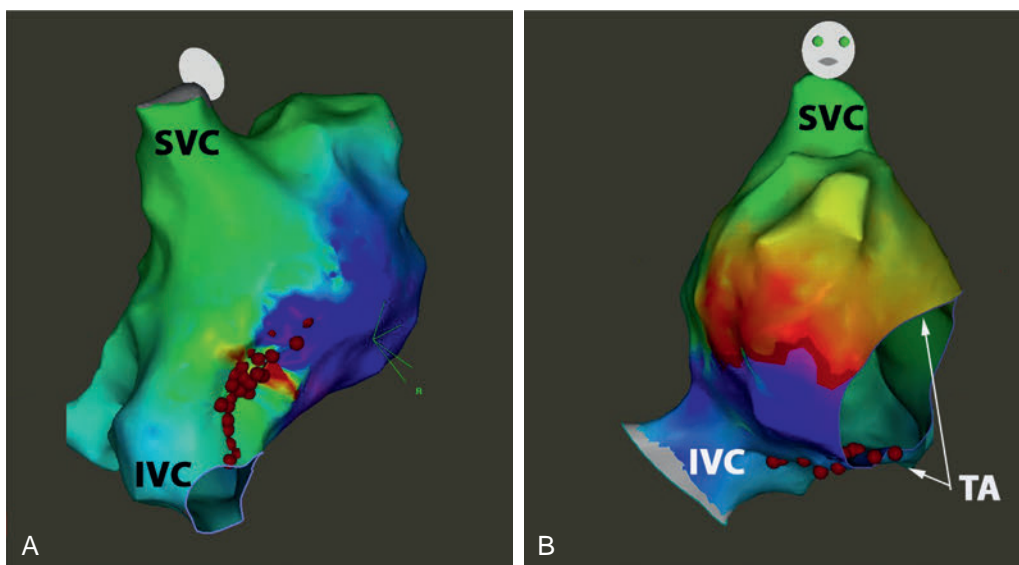


Fig. 14.8 Dual Right Atrial (RA) Macroreentry Circuits. (A) Right posterolateral view of electroanatomic (CARTO) activation map of incisional macroreentrant RA tachycardia. (B) Right anterolateral view of electroanatomic (CARTO) activation map of typical atrial flutter in the same patient. Linear radiofrequency ablation (red dots) is performed to sever the isthmus between the atriotomy scar and the inferior vena cava (IVC) as well as linear ablation across the cavotricuspid isthmus. Ablation is facilitated by correlating activation mapping findings with those of voltage mapping. SVC, Superior vena cava; TA, tricuspid annulus.

surgical repairs are associated with myocardial hypertrophy and extensive fibrotic regions, creation of confluent and transmural lesions can be difficult, especially in the presence of low intracavitary blood flow that often impairs convective cooling and limits RF energy. Therefore irrigated (25 to 50 W) or 8-mm (target temperature, 60°C to 70°C; 50 to 60 W) tip RF catheter is usually necessary. RF application is maintained for up to 60 seconds until the bipolar atrial potential recorded from the ablation electrode is decreased by 80% or split into double potentials, indicating local conduction block. The coalescence of multiple RF lesions can be facilitated by the use of an electroanatomic mapping system.

In view of the often dilated and distorted atrial chambers, the use of long, preformed or deflectable vascular sheaths is helpful to augment the reach of the ablation catheter and ensure adequate and stable catheter-tissue contact. ICE and contact-force catheter contact technology can be used to ensure good contact.^{1,11}

During delivery of RF energy, the tachycardia can terminate, or its CL can increase transiently or permanently. These findings usually indicate that the lesions have affected the circuit and should prompt continuation of RF delivery or extension of the lesion to ensure the achievement of complete conduction block across the isthmus. Alternatively, the tachycardia can transform to a different loop or to a different tachycardia (rather than terminate), as indicated by a change in activation sequence or CL, or both, in which setting the reassessment of the new tachycardia mechanism and location is necessary before continued RF ablation. Importantly, persistence of the tachycardia with little discernible change in CL or activation sequence despite extensive ablation across an isthmus, which was initially found to be critical to the tachycardia circuit (by entrainment mapping techniques), usually indicates multiple circuits, often with a double-loop type of reentry. In this setting, it is imperative to verify whether the isthmus is still critical to the reentrant circuit by repeating the entrainment mapping. Sometimes, complete isthmus block is already achieved (as suggested by the presence of double potentials along the ablation line), and the isthmus is no longer participating in the tachycardia circuit (as suggested by entrainment mapping findings), as a result of a change in the tachycardia circuit that occurred during ablation. This can be observed during ablation of the CTI in the setting of double-loop reentry that uses the lateral wall as well as the CTI. Achieving complete block across the CTI does not eliminate the tachycardia that is now dependent on a different isthmus (e.g., the lateral RA around or within the atriotomy scar).

Ablation near the region of the superior crista terminalis and SVC can result in right phrenic nerve injury and diaphragmatic paralysis. Pacing with a high output (10 mA at 2 milliseconds) from the ablation catheter at the target site can help identify the location of the right phrenic nerve. In addition, suspicion of phrenic nerve injury should be considered in the case of hiccup, cough, or decrease in diaphragmatic excursion during energy delivery. Early recognition of phrenic nerve injury during RF delivery allows the immediate interruption of the application prior to the onset of permanent injury and is associated with the rapid recovery of phrenic nerve function. A good practice is to delineate the course of the phrenic nerve during the baseline rhythm by pacing at high current strength and logging the sites of phrenic capture (as indicated by diaphragmatic contraction) on the electroanatomic mapping system. Ablation in these areas should be avoided if possible. In some cases, the phrenic nerve can have major branches; therefore simply avoiding ablation at sites of known phrenic capture may be insufficient to avoid damage to a portion of the nerve, and one should consider high output pacing at candidate ablation sites prior to ablation. This of course risks termination or transformation of tachycardia so should be used with care.

Endpoints of Ablation

Tachycardia Termination

Sudden termination of AT during RF application suggests that the lesion has affected a critical isthmus, and that site should be targeted for additional lesions. However, AT termination during RF application is not adequate as the sole criterion of a successful ablation because such an AT can also terminate spontaneously, secondary to premature atrial complexes induced by RF energy delivery, and by partial, rather than complete, isthmus block.

Noninducibility of Tachycardia

To use this criterion as a reliable endpoint, careful assessment of inducibility should be performed prior to ablation, and the feasibility and best method of reproducible induction of the AT should be documented at baseline before ablation. In the setting of easy inducibility prior to ablation, one can consider the lack of inducibility as an indicator of successful ablation. Noninducibility of the arrhythmia is inapplicable if the original arrhythmia is incessant, noninducible at baseline, or was inadvertently terminated mechanically. Noninducibility may also reflect conduction delay in the critical isthmus, and not stable block, or it may be secondary to changes in autonomic tone.

Documentation of a Line of Block

Complete stable conduction block within the reentry path is the most useful and objective endpoint. For a vertically oriented RA free wall atriotomy, assessment of conduction block can be facilitated by the use of a multielectrode Halo catheter. Several techniques can be used to confirm complete conduction block across the ablation line:

Double potentials. The mapping catheter is used to retrace the ablation line during atrial pacing from either side of the ablation line. The demonstration of a continuous corridor of widely split double potentials recorded along the entire length of the ablation line confirms the presence of block. When there is a gap in a line of block, the isoelectric interval between the double potentials shortens the closer the electrograms are to the gap. At the gap, in the line of block, double potentials are no longer present, and the electrogram is typically long and fractionated, but also can be discrete.

Atrial activation sequence. Pacing close to the ablation line and demonstration of marked delay and reversal in the direction of activation on the opposite side of the ablation line is consistent with conduction block across the ablation line, although very slow conduction can be difficult to exclude. Electroanatomic activation mapping during pacing demonstrates the earliest activation at the side of the ablation line ipsilateral to the pacing site, while the latest activation occurs at the contralateral side, and an early-meets-late zone along the entire length of the ablation line. In the setting of incisional RA macroreentry treated with linear ablation connecting the scar to the IVC, the presence of conduction block across the ablation line can be confirmed by demonstrating a high-to-low activation of the RA on one side of the ablation line during pacing at the low RA on the contralateral side of the ablation line.⁶

Differential pacing. Atrial pacing is performed at two separate sites on the same side of the ablation line: one site is very close to the ablation line and the second site is 10 to 20 mm further away. Local activation time is recorded on the contralateral side of the ablation line. In the presence of conduction block across the ablation line, moving the pacing site away from the ablation line shortens the conduction time to the contralateral side, and shortens the distance between the double potentials straddling the ablation line. Withdrawal of the pacing site further away from the ablation line results in a delay of the first component of the double potentials (which represents activation on

the side of the ablation line ipsilateral to the pacing site). In contrast, the second component of the double potentials (which represent activation on the contralateral side of the ablation line) becomes activated earlier since the length of the detour the wavefront has to travel around the line of block is shortened by the new site of pacing. As a consequence, the separation of double potentials decreases. On the other hand, in the setting of incomplete block, both components of the double potentials are the result of sequential activation by the same paced wavefront propagating across the ablation line. Therefore withdrawal of the pacing site further away from the ablation line causes a similar degree of delay of the timing of both components of the electrogram (relative to the pacing stimulus), so that the interval between the double potentials remains constant.

Outcome

Acute and long-term success rates of catheter ablation of MRATs in CHD patients are influenced by the complexity of underlying congenital defect and surgical repair, and the complexity of the reentry circuits. In addition, atrial enlargement and myocardial hypertrophy and extensive scarring in this patient population can interfere with RF energy delivery, and limit RF lesion depth. Nevertheless, the combined use of 3-D mapping and irrigated ablation has improved the acute procedural success rate to the range of 66% to 97% in experienced centers. However, recurrence rates after acutely successful catheter ablation still remain relatively high (10% to 59%), particularly in the Fontan group. These can be the same tachycardias or new tachycardias, as the substrate continues to change with time. Nonetheless, the overall results are far superior to pharmacological therapy.^{1,7,11}

VIDEOS



The following video accompanies this chapter:

See Video 13-1. Incisional Right Atrial Macroreentry: CARTO Activation, Voltage, Propagation, and Ripple Maps

REFERENCES

1. Sherwin ED, Triedman JK, Walsh EP. Update on interventional electrophysiology in congenital heart disease: evolving solutions for complex hearts. *Circ Arrhythm Electrophysiol*. 2013;6:1032–1040.
2. Triedman JK. Atypical atrial tachycardias in patients with congenital heart disease. *Heart Rhythm*. 2008;5:315–317.
3. Anguera I, et al. Long-term outcome after ablation of right atrial tachyarrhythmias after the surgical repair of congenital and acquired heart disease. *Am J Cardiol*. 2015;115:1705–1713.
4. Moore JP, Russell M, Mandapati R, et al. Catheter ablation of tachycardia arising from the pulmonary venous atrium after surgical repair of congenital heart disease. *Heart Rhythm*. 2015;12:297–304.
5. Teuwen CP, et al. Time course of atrial fibrillation in patients with congenital heart defects. *Circ Arrhythm Electrophysiol*. 2015;8:1065–1072.
6. Arujuna A, de Bono J. Maximizing the effectiveness of ablation for arrhythmias in the congenital heart patients. *Curr Cardiol Rep*. 2016;18:69.
7. Philip Saul J, et al. PACES/HRS expert consensus statement on the use of catheter ablation in children and patients with congenital heart disease. *Heart Rhythm*. 2016;13:e251–e289.
8. Kanter RJ. Pearls for ablation in congenital heart disease. *J Cardiovasc Electrophysiol*. 2010;21:223–230.
9. Wu M-H, et al. Arrhythmic burdens in patients with tetralogy of Fallot: a national database study. *Heart Rhythm*. 2015;12:604–609.
10. Houck CA, Teuwen CP, Bogers AJ, et al. Atrial tachyarrhythmias after atrial switch operation for transposition of the great arteries: treating old surgery with new catheters. *Heart Rhythm*. 2016;13:1731–1738.
11. Wu J, et al. Acute and long-term outcome after catheter ablation of supraventricular tachycardia in patients after the Mustard or Senning operation for D-transposition of the great arteries. *Europace*. 2013;15:886–891.
12. Lasa JJ, Glatz AC, Daga A, et al. Prevalence of arrhythmias late after the fontan operation. *Am J Cardiol*. 2014;113:1184–1188.
13. Correa R, et al. Mechanism and ablation of arrhythmia following total cavopulmonary connection. *Circ Arrhythm Electrophysiol*. 2015;8:318–325.
14. Moore JP, et al. Catheter ablation of supraventricular tachyarrhythmia after extracardiac Fontan surgery. *Heart Rhythm*. 2016;13:1891–1897.
15. Khairy P, et al. PACES/HRS expert consensus statement on the recognition and management of arrhythmias in adult congenital heart disease. *Heart Rhythm*. 2014;11:e102–e165.
16. Deleted in review.
17. McLeod CJ, Warnes C. Recognition and management of arrhythmias in adult congenital heart disease. *Curr Opin Cardiol*. 2016;31:117–123.
18. Patients ASE, Marchese P, Ho SY, et al. Contemporary outcomes of supraventricular tachycardia ablation in congenital heart disease. *Circ Arrhythm Electrophysiol*. 2013;6:606–613.
19. Tzeis S, Andrikopoulos G, Deisenhofer I, et al. Transseptal catheterization: considerations and caveats. *Pacing Clin Electrophysiol*. 2010;33:231–242.
20. Santangeli P, et al. Transseptal access and atrial fibrillation ablation guided by intracardiac echocardiography in patients with atrial septal closure devices. *Heart Rhythm*. 2011;8:1669–1675.
21. Li X, et al. Safety and feasibility of transseptal puncture for atrial fibrillation ablation in patients with atrial septal defect closure devices. *Heart Rhythm*. 2014;11:330–335.
22. Josephson ME, Almendral J, Callans DJ. Resetting and entrainment of reentrant ventricular tachycardia associated with myocardial infarction. *Heart Rhythm*. 2014;11:1239–1249.
23. Almendral J. Resetting and entrainment of reentrant arrhythmias: part II: informative content and practical use of these responses. *Pacing Clin Electrophysiol*. 2013;36:641–661.
24. Miyazaki H, Stevenson WG, Stephenson K, et al. Entrainment mapping for rapid distinction of left and right atrial tachycardias. *Heart Rhythm*. 2006;3:516–523.

Atrial Fibrillation

OUTLINE**Pathophysiology, 422**

- Classification of Atrial Fibrillation, 422
- Mechanism of Atrial Fibrillation, 423
- Substrate for Atrial Fibrillation, 427
- Atrial Remodeling in Atrial Fibrillation, 429
- Role of Autonomic Nervous System in Atrial Fibrillation, 430
- Role of the Pulmonary Veins in Atrial Fibrillation, 430
- Genetics in Atrial Fibrillation, 433

Epidemiology, 433

- Atrial Fibrillation Risk Prediction, 434
- Clinical Risk Factors Predisposing to Atrial Fibrillation, 434
- Drug-Induced Atrial Fibrillation, 438
- Postoperative Atrial Fibrillation, 439

Clinical Presentation, 439

- Symptomatic Atrial Fibrillation, 439
- Atrial Fibrillation Symptom Scales, 440
- Silent Atrial Fibrillation, 440
- Device-Detected Atrial Fibrillation, 440

Risk of Thromboembolism, 441

- Stroke Risk Stratification, 442
- Bleeding Risk Stratification, 443

Initial Evaluation, 444

- Diagnostic Cardiac Testing, 444
- Laboratory Testing, 445
- Electrophysiological Testing, 445
- Other Diagnostic Tests, 445
- Screening for Atrial Fibrillation, 445

Principles of Management, 445

- Prevention of Systemic Embolization, 445
- Rate Control, 448
- Rhythm Control, 449
- Upstream Therapy, 455
- Risk Factor Management, 456
- Management of Postoperative Atrial Fibrillation, 457

Electrocardiographic Features, 457

- Atrial Activity, 457
- Atrioventricular Conduction During Atrial Fibrillation, 458
- QRS Morphology, 461

Catheter Ablation of Atrial Fibrillation, 462

- Evolution of Catheter Ablation Approaches for Atrial Fibrillation, 462
- Periprocedural Management, 463
- Technical Aspects Common to Different Methods of Ablation, 465

Focal Ablation of Pulmonary Vein Triggers, 467

- Rationale, 467
- Identification of Arrhythmogenic Pulmonary Veins, 467
- Mapping Pulmonary Vein Ectopy, 467
- Target of Ablation, 470

Ablation Technique, 470

Endpoints of Ablation, 470

Outcome, 470

Segmental Ostial Pulmonary Vein Isolation, 471

Rationale, 471

Circumferential Mapping of Pulmonary Vein Potentials, 471

Target of Ablation, 480

Ablation Technique, 480

Endpoints of Ablation, 480

Outcome, 483

Circumferential Antral Pulmonary Vein Isolation, 483

Rationale, 483

Identification of Pulmonary Vein Antra, 483

Target of Ablation, 485

Ablation Technique, 487

Endpoints of Ablation, 493

Outcome, 493

Circumferential Left Atrial Ablation, 494

Rationale, 494

Electroanatomic Mapping, 494

Target of Ablation, 495

Ablation Technique, 495

Endpoints of Ablation, 496

Outcome, 497

Linear Atrial Ablation, 497

Left Atrial Roof Line, 497

Left Atrial Posterior Wall Isolation, 498

Lateral Mitral Isthmus Line, 498

Cavotricuspid Isthmus Line, 500

Focal Impulse and Rotor Mapping, 501

Rationale, 501

Focal Impulse and Rotor Modulation Mapping, 501

Target of Ablation, 501

Ablation Technique, 501

Endpoints of Ablation, 502

Outcome, 503

Ablation of Complex Fractionated Atrial Electrograms, 504

Rationale, 504

Mapping Complex Fractionated Atrial Electrograms, 504

Target of Ablation, 506

Ablation Technique, 506

Endpoints of Ablation, 506

Outcome, 507

Pulmonary Vein Denervation, 507

Rationale, 507

Localization of Ganglionated Plexuses, 507

Target of Ablation, 508

Ablation Technique, 508

Endpoints of Ablation, 509

Outcome, 509

Ablation of Non–Pulmonary Vein Triggers, 509

- Rationale, 509
- Mapping of Non–Pulmonary Vein Triggers, 509
- Mapping and Ablation of the Ligament of Marshall, 510
- Electrical Isolation of the Superior Vena Cava, 512
- Electrical Isolation of the Coronary Sinus, 513
- Electrical Isolation of the Left Atrial Appendage, 515
- Outcome, 515

Voltage-Guided Substrate Modification, 515

- Rationale, 515
- Target of Ablation, 515
- Ablation Technique, 515
- Endpoint of Ablation, 516
- Outcome, 516

Outcome and Efficacy of Catheter Ablation of Atrial Fibrillation, 516

- Success Rates, 517
- Recurrence of Atrial Tachyarrhythmias, 519
- Atrial Tachycardia and Flutter Following Ablation of Atrial Fibrillation, 520
- Complications of Catheter Ablation of Atrial Fibrillation, 522

Recommendations and Controversies, 525

- Determination of the Necessity of Pulmonary Vein Electrical Isolation, 525
- Determination of the Necessity of Adjunctive Substrate Modification, 525

Atrioventricular Junction Ablation, 526

- Rationale, 526
- Target of Ablation, 527

- Ablation Technique, 527
- Endpoints of Ablation, 528
- Outcome, 528

Atrioventricular Nodal Modification, 530

- Rationale, 530
- Target of Ablation, 530
- Ablation Technique, 531
- Endpoints of Ablation, 531
- Outcome, 531

Percutaneous Left Atrial Appendage Device Closure, 531

- Left Atrial Appendage Anatomy, 532
- Left Atrial Appendage Imaging, 532
- Left Atrial Appendage Catheterization, 534
- Watchman Device, 534
- Amplatzer Cardiac Plug, 535

Percutaneous Left Atrial Appendage Ligation, 537

- Left Atrial Appendage Imaging, 537
- Device Specification, 537
- Epicardial Access, 537
- Endocardial Access, 537
- Connecting the Epicardial and Endocardial Magnet-Tipped Guidewires, 538
- Snaring the Left Atrial Appendage, 538
- Postoperative Management, 538
- Outcome, 538

Surgical Left Atrial Appendage Exclusion, 540**PATHOPHYSIOLOGY****Classification of Atrial Fibrillation**

Atrial fibrillation (AF) has been described as lone, idiopathic, nonvalvular, valvular, paroxysmal, persistent, or permanent. Each of these classifications has implications regarding mechanisms as well as response to therapy. At the initial detection of AF, it is impossible to know the subsequent pattern of duration and frequency of recurrences. Thus a designation of first-detected episode of AF is made on the initial diagnosis, irrespective of the duration of the arrhythmia. When the patient has experienced two or more episodes, AF is classified as recurrent.

After termination of an episode of AF, the rhythm can be classified as paroxysmal or persistent (Table 15.1). *Paroxysmal AF* is characterized by self-terminating episodes that generally last less than 7 days. *Persistent AF* lasts longer than 7 days and often requires electrical or pharmacological cardioversion. Subcategories of persistent AF (according to arrhythmia duration) include *early persistent AF* (defined as AF that is sustained beyond 7 days but is less than 3 months in duration) and *longstanding persistent AF* (defined as AF that is sustained longer than 1 year but is being considered for ablation). *Permanent AF* refers to AF in which cardioversion has failed or AF that has been sustained for more than 1 year and further attempts to restore normal sinus rhythm (NSR) were unsuccessful or have been abandoned.¹

Although useful, this arbitrary classification does not account for all presentations of AF and overlap occurs. Paroxysmal AF often progresses to longer, non-self-terminating episodes. In addition, the pattern of AF can change in response to treatment. AF that has been persistent can become paroxysmal with antiarrhythmic drug therapy, and AF that had been permanent can potentially be cured or made paroxysmal by surgical or catheter-based ablation. Furthermore, the distinction between

TABLE 15.1 Classifications of Atrial Fibrillation

AF Pattern	Definition
First diagnosed AF	AF that has not been diagnosed before, irrespective of the duration of the arrhythmia or the presence and severity of AF-related symptoms.
Paroxysmal AF	Self-terminating, in most cases within 48 hours. Some AF paroxysms may continue for up to 7 days. ^a
Persistent AF	AF that lasts longer than 7 days, including episodes that are terminated by cardioversion, either with drugs or by direct current cardioversion, after 7 days or more.
Longstanding persistent AF	Continuous AF lasting for ≥1 year when it is decided to adopt a rhythm control strategy.
Permanent AF	AF that is accepted by the patient (and physician). Hence, rhythm control interventions are, by definition, not pursued in patients with permanent AF. Should a rhythm control strategy be adopted, the arrhythmia would be re-classified as “longstanding persistent AF.”

^aThe distinction between paroxysmal and persistent AF is often not made correctly without access to long-term monitoring. Hence, this classification alone is often insufficient to select specific therapies. If both persistent and paroxysmal episode are present, the predominant pattern should guide the classification.

AF, Atrial fibrillation.

From Kirchhof P, Benussi S, Kotecha D, et al. 2016 ESC guidelines for the management of atrial fibrillation developed in collaboration with EACTS. *Eur Heart J*. 2016;37:2893–2962.

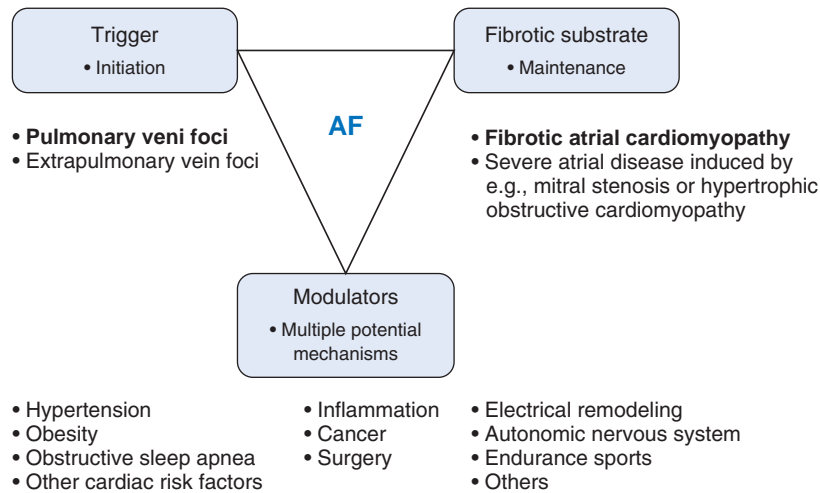


Fig. 15.1 The Pathophysiological Triangle in Atrial Fibrillation (AF). (From Kottkamp H, Schreiber D. The substrate in “early persistent” atrial fibrillation. *JACC Clin Electrophysiol.* 2016;2:140–142.)

persistent and permanent AF is not only a function of the underlying arrhythmia but also a reflection of the clinical pragmatism of the patient and physician. The severity of symptoms associated with AF, anticoagulation status, and patient preference all affect the decision of whether and when cardioversion will be attempted. This decision would then affect the duration of sustained AF and could lead to a diagnosis of persistent or permanent AF. Furthermore, significant discrepancies exist between the clinical AF classification and the objective cardiac device-derived assessments of AF temporal persistence (in AF patients with pacemakers or defibrillators) (eFig. 15.1). Patients within the same clinical class (“paroxysmal” or “persistent” AF) are highly heterogeneous with regard to AF temporal persistence, arrhythmia burden, and stages of disease.²

AF can be classified as valvular or nonvalvular. The 2012 focused update of the European Society of Cardiology (ESC) guidelines defined valvular AF as rheumatic valvular disease (predominantly mitral stenosis) or prosthetic heart valves. Similarly, the 2014 American Heart Association/American College of Cardiology/Heart Rhythm Society (AHA/ACC/HRS) guidelines for the management of patients with AF defined nonvalvular AF as AF in the absence of rheumatic mitral stenosis or a mechanical heart valve, but explicitly added bioprosthetic heart valves or mitral valve repair within the “valvular heart disease” group.^{3,4}

The terms “lone” and “idiopathic” AF have been variably defined in the literature, but they generally refer to younger AF patients who have no clinical or echocardiographic evidence of cardiopulmonary disease, hypertension, or diabetes mellitus. However, this categorization is being abandoned since the category of lone AF no longer has mechanistic or clinical utility. Similarly, the term “chronic AF” has variable definitions and should not be used to describe populations of patients with AF.^{5,4}

Mechanism of Atrial Fibrillation

The pathogenesis of AF remains incompletely understood and is believed to be complex, multifactorial, and variable in different individuals. Two concepts of the underlying mechanism of AF have received considerable attention: factors that trigger AF and factors that perpetuate the arrhythmia. In general, patients with frequent, self-terminating episodes of AF are likely to have a predominance of factors that trigger AF, whereas patients with AF that does not terminate spontaneously are more likely to have a predominance of perpetuating factors. Although such gross generalization has clinical usefulness, often there is considerable overlap

of these mechanisms. The typical patient with paroxysmal AF has identifiable ectopic foci initiating the arrhythmia, but these triggers cannot be recorded in all patients. Conversely, occasional patients with persistent or permanent AF can be cured of their arrhythmia by ablation of a single triggering focus, a finding suggesting that perpetual firing of the focus can potentially be the mechanism sustaining this arrhythmia in some cases.^{6,7}

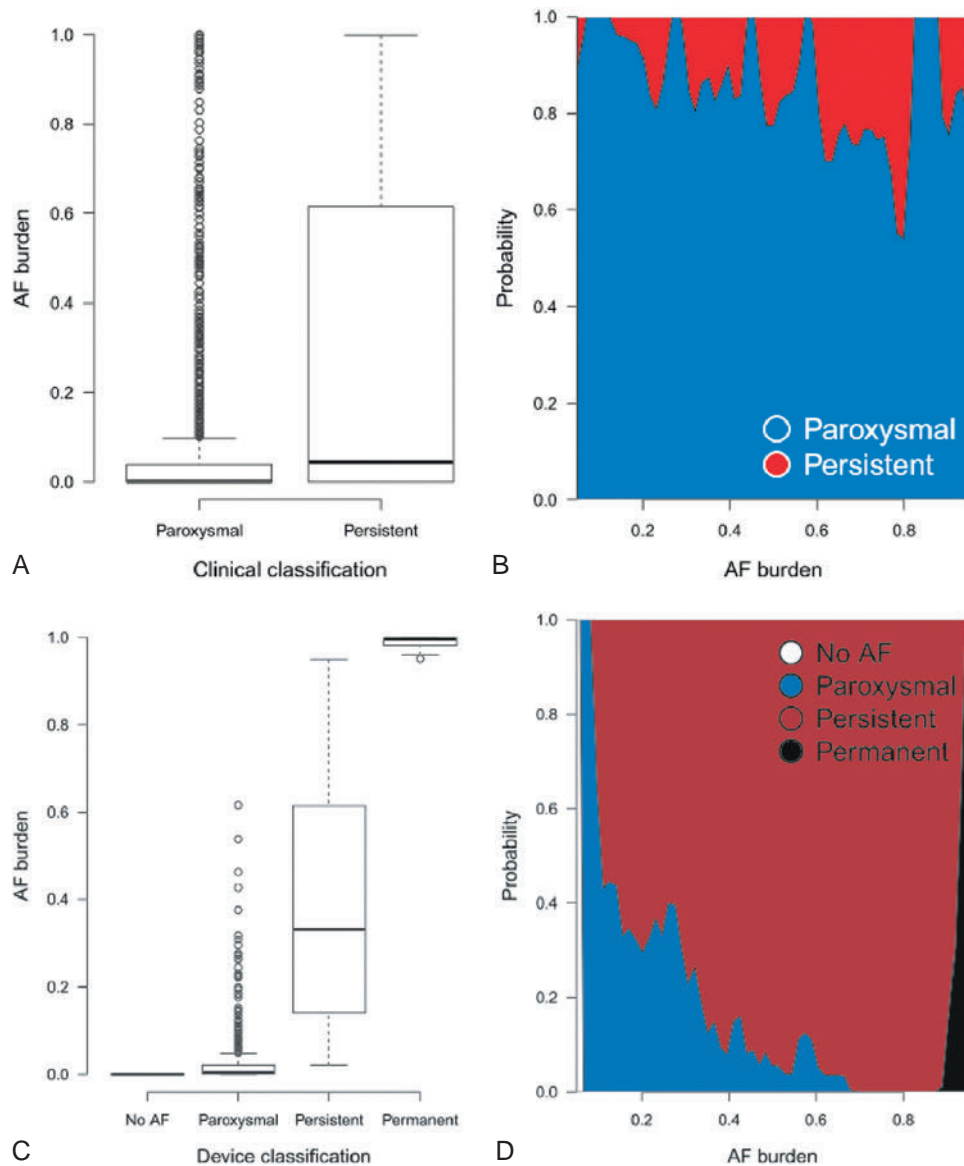
Advanced mapping technologies, along with studies in animal models, have suggested the potential for complex pathophysiological substrates and modifiers responsible for AF (Fig. 15.1), including the following: (1) continuous aging or degeneration of atrial tissue and the cardiac conduction system; (2) progression of structural heart disease (e.g., valvular heart disease and cardiomyopathy); (3) myocardial ischemia, local hypoxia, electrolyte derangement, and metabolic disorders (e.g., atherosclerotic heart disease, chronic lung disease, hypokalemia, and hyperthyroidism); (4) inflammation related to pericarditis or myocarditis, with or without cardiac surgery; (5) genetic predisposition; (6) drugs; and (7) autonomic influences.^{1,8}

Mechanism of Initiation of Atrial Fibrillation

The factors responsible for the onset of AF include triggers that induce the arrhythmia and a receptive substrate that sustains it. The triggers are diverse yet may not cause AF in the absence of other contributors. There are two different types of arrhythmias that can potentially play a role in generating AF: premature atrial complexes (PACs) that initiate AF (focal triggers) and focal tachycardia that either induces fibrillation in the atria or mimics AF by creating a pattern of rapid and irregular depolarization wavefronts in the atria for as long as the focus continues to discharge.⁹

The mechanism of initiation of AF is not certain in most cases and likely is multifactorial. Triggers propagating into the atrial myocardium can potentially initiate multiple reentrant wavelets and AF. In some patients with paroxysmal AF, impulses initiated by ectopic focal activity propagate into the left atrium (LA) and encounter heterogeneously recovered tissue. If reentry were assumed to be the mechanism of AF, initiation would require an area of conduction block and a wavelength of activation short enough to allow the reentrant circuits to persist in the myocardium.

Once triggered, AF can be self-sustained, in which case the continued firing of the focus may not be required for maintenance of the arrhythmia, and ablation of the focus may not terminate AF, but can potentially



eFig. 15.1 Clinical Versus Cardiac Device-Derived Classification of Atrial Fibrillation (AF). (A) Distribution of the AF burden in the clinical classification groups (paroxysmal, persistent). (B) The probability of being in either of the clinical classification groups at any given AF burden level (conditional density plot). For example, at an AF burden of 0.2, the probability of being classified as “paroxysmal” or “persistent” was approximately 0.8 and 0.2, respectively. As the AF burden increases, intuitively one would expect that the probability of being classified as “paroxysmal” AF decreases and the probability of being classified as “persistent” increases. Unexpectedly, at AF burdens of 0.9, the probability of being classified as “paroxysmal” or “persistent” was also approximately 0.8 and 0.2, respectively, showing the disconnection between clinical classification and temporal persistence. Even at very high burdens the vast majority of patients were classified as having “paroxysmal” AF. (C) Distribution of the atrial fibrillation (AF) burden in the device-derived classification groups (no AF, paroxysmal, persistent, permanent). (D) The probability of being in any of the device classification groups at any given AF burden level (conditional density plot). As AF burden increases, the probability of being classified in a progressively more severe classification (no AF, paroxysmal, persistent, permanent) increases. This is in contrast to the clinical AF classification (B). (From Charitos EI, Pürerfellner H, Glotzer TV, et al. Clinical classifications of atrial fibrillation poorly reflect its temporal persistence: insights from 1,195 patients continuously monitored with implantable devices. *J Am Coll Cardiol.* 2014;63:2840–2848.)

prevent the reinitiation of AF. Conversely, initiation and maintenance of AF can depend on uninterrupted periodic activity of a few discrete reentrant or triggered sources localized to the LA (i.e., focal drivers), emanating from such sources to propagate through both atria and interact with anatomic or functional obstacles, thus leading to fragmentation and multiple wavelet formation. Factors such as wavefront curvature, sink-source relationships, and spatial and temporal organization all are relevant to the understanding of the initiation of AF by the interaction of the propagating wavefronts with such anatomic or functional obstacles. Indeed, all these factors, which differ from triggers, importantly affect the initiators of AF.

AF triggering factors include sympathetic or parasympathetic stimulation, bradycardia, PACs (which may be the most common cause; Fig. 15.2), atrial flutter (AFL; see Fig. 12.2), supraventricular tachycardias (SVTs; especially those mediated by atrioventricular [AV] bypass tracts [BTs]; Fig. 15.3), and acute atrial stretch. Identification of these triggers has clinical importance because treatment approaches directed at elimination of the triggers (e.g., catheter ablation of the initiating PACs or SVT) can be curative in selected patients.

PV triggers. Triggering foci of rapidly firing cells within the sleeves of atrial myocytes extending into the pulmonary veins (PVs) have been shown to be the underlying mechanism in most cases of paroxysmal AF. Supporting this idea are clinical studies of impulses generated by single foci propagating from individual PVs or other atrial regions to

the remainder of the atria as fibrillatory waves and abolition of AF by radiofrequency (RF) ablation to eliminate or isolate the PV foci. The PVs also represent the main trigger site for AF initiation in patients with recurrent persistent AF, with an overall prevalence similar to that found in patients with paroxysmal AF.¹⁰

Based on several features, the thoracic veins are highly arrhythmogenic. The PV-LA junction has discontinuous myocardial fibers separated by fibrotic tissues and hence is highly anisotropic. Insulated muscle fibers can promote reentrant excitation, automaticity, and triggered activity. These regions likely resemble the juxtaposed islets of atrial myocardium and vascular smooth muscle in the coronary sinus (CS) and AV valves that, under normal circumstances, manifest synchronous electrical activity but develop delayed after-depolarizations and triggered activity in response to catecholamine stimulation, rapid atrial pacing, or acute stretch.

Furthermore, the PVs of patients with paroxysmal AF demonstrate abnormal properties of conduction so that there can be markedly reduced refractoriness within the PVs, progressive conduction delay within the PV in response to rapid pacing or programmed stimulation, and often conduction block between the PV and the LA. Such findings are much more common in patients with paroxysmal AF than in normal subjects. Rapidly firing foci can often be recorded within the PVs with conduction block to the LA. Administration of catecholamines such as isoproterenol can lead to shortening of the LA refractory period, thereby



Fig. 15.2 Atrial Fibrillation (AF) Induction by Premature Atrial Complexes (PACs) Originating From the Right Superior Pulmonary Vein (PV). Two monomorphic PACs (arrows) occur at short coupling intervals and are inscribed within the T wave. The second PAC (red arrows) triggers AF.

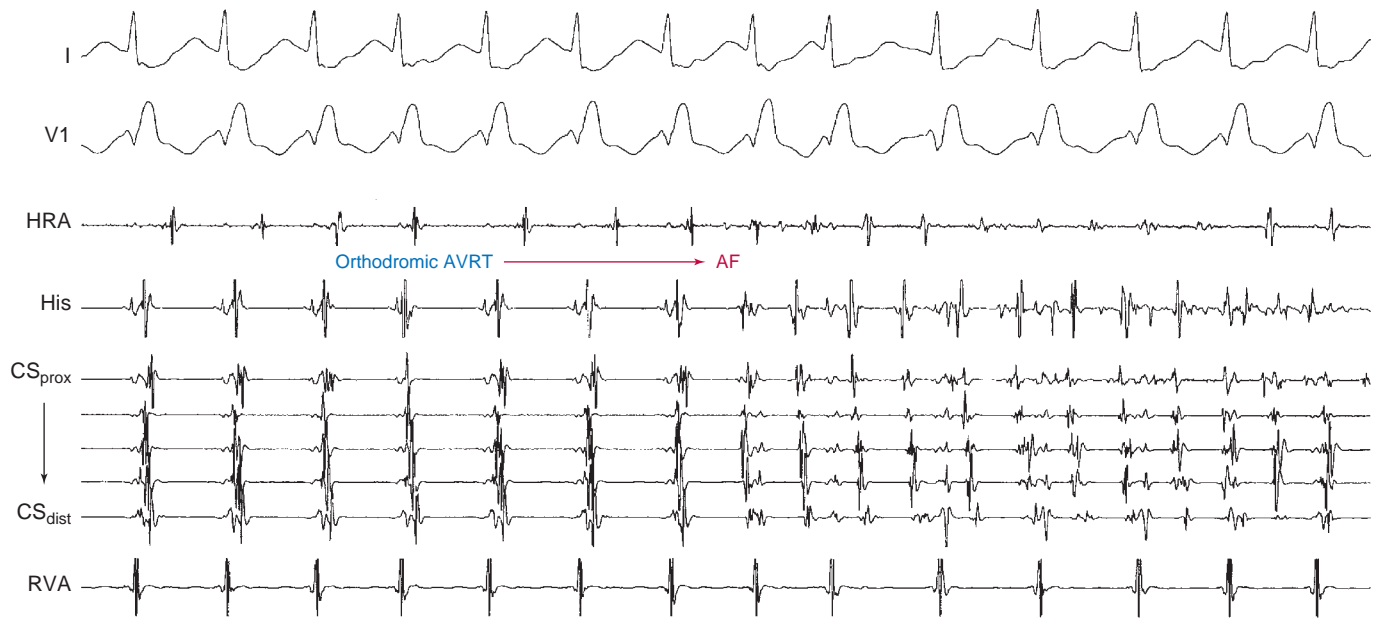


Fig. 15.3 Atrial Fibrillation (AF) Induction by Orthodromic Atrioventricular Reentrant Tachycardia (AVRT). *CS_{dist}*, Distal coronary sinus; *CS_{prox}*, proximal coronary sinus; *HRA*, high right atrium; *RVA*, right ventricular apex.

allowing these foci to propagate to the LA and induce AF. These discontinuous properties of conduction within the PV can also provide a substrate for reentry within the PV itself, although this remains to be proven.

Non-PV triggers. Although more than 90% of AF triggering foci that are mapped during electrophysiological (EP) studies in patients with paroxysmal AF occur in the PVs, foci within the superior vena cava (SVC), small muscle bundles in the ligament of Marshall, and the musculature of the CS have been identified. Although these latter locations of triggering foci are uncommon in patients with paroxysmal AF, the common factor is that the site of origin is often within a venous structure that connects to the atrium. Other sites of initiating foci can be recorded in the LA wall or along the crista terminalis in the right atrium (RA).

Mechanism of Maintenance of Atrial Fibrillation

Having been initiated, AF can be brief; however, various factors can act as perpetuators, thus ensuring the maintenance of AF. One factor is the persistence of the triggers and initiators that induced the AF, which then act as an engine driving the continuation of AF. In this setting, maintenance of AF is dependent on the continued firing of the focus (the so-called “focal driver”). Alternatively, AF can persist even in the absence of the focal drivers. Without focal drivers, persistence of AF results from a combination of electrical and structural remodeling processes characterized by atrial dilation and shortening of atrial refractoriness (see later). These factors can be present at baseline but can also be induced by the AF itself.

The mechanisms responsible human AF remain controversial. Several theories have been proposed to explain the EP mechanisms underlying AF, including the multiple wavelet theory and the localized source hypothesis.¹¹

Multiple wave reentry hypothesis. For many years, the “multiple wave reentry” hypothesis was the most widely held theory on the maintenance of AF, and was a key development in our understanding of the

mechanism of AF. On the basis of a computer model of AF, Moe and associates hypothesized that AF is sustained by multiple randomly wandering wavelets in both atria that collide with each other and extinguish themselves or create new, daughter wavelets that continually reexcite the atria and perpetuate the arrhythmia.¹² Those functional reentrant circuits are therefore unstable; some disappear, whereas others reform. These circuits have variable, but short, cycle lengths (CLs) to which atrial tissue cannot respond in a 1:1 fashion. As a result, functional block, slow conduction, and multiple wavefronts develop. It has been suggested that at least four to six independent wavelets are required to maintain AF. These wavelets rarely reenter themselves but can reexcite portions of the myocardium recently activated by another wavefront, a process called random reentry. In simulated cardiac tissue, multiple wavelet fibrillation is equivalent to spiral/scroll waves that are inherently unstable and spontaneously develop wavebreaks along the arm of the rotor which then form daughter wavelets.¹¹ Because multiple wave reentry fibrillation is purely reentrant, its initiation requires a trigger to create the original unstable spiral/scroll wave that subsequently breaks up to create daughter wavelets; however, once initiated, additional triggers are no longer required to maintain fibrillation.¹¹

The persistence of multiple-circuit reentry depends on the ability of a tissue to maintain enough simultaneously reentering wavefronts so that electrical activity is unlikely to extinguish simultaneously in all parts of the atria. Therefore the larger the number of wavelets present, the more likely the arrhythmia will be sustained. The number of wavelets coexisting at any moment depends on the atrial mass, excitation wavelength, refractory period, conduction velocity, and anatomic obstacles in different portions of the atria. In essence, a large atrial mass with short refractory periods and prominent conduction delay would yield increased wavelets and would present the most favorable situation for AF to be sustained.

Clinical support for this hypothesis seemed to come from the surgical maze and some substrate-based catheter ablation procedures, which were proposed to result in dividing the atrial into small electrical

compartments and, thus, disallowing maintenance of the randomly propagating wavelets.¹³ The reentrant circuits that comprise multiple wave reentry are functional, multiple, and dynamic; thus ablation of multiple wave reentry is not aimed at eliminating the possibility of its existence but at maximizing the probability of its spontaneous termination through collisions between circuit cores and unexcitable tissue boundaries via atrial debulking and compartmentalization.¹⁴

Localized source hypothesis. In contrast to the nonhierarchical, self-sustaining disorganized electrical activity implicated in the multiple wavelet theory, recent evidence suggests the presence of hierarchical electrical organization in which localized sources drive disorganized activity. This hypothesis suggests that AF is intermittently maintained by a small number of localized (spatially stable) high-frequency sources with periods of self-sustaining disorganization. Rotors and focal sources exhibit 1:1 activation within their spatial domain, with peripheral disorganization. This concept was supported by experimental studies using high-resolution optical mapping, which demonstrated spatial and temporal organization during AF. Localized sources can be either discrete foci with centrifugal spread of activation or small anatomic reentry circuits or functional rotors.¹³

When cardiac impulses are continuously generated at a rapid rate from any source or any mechanism, they activate the tissue of that cardiac chamber in a 1:1 manner, up to a critical rate. Once this critical rate is exceeded, not all the tissue of that cardiac chamber can respond in a 1:1 fashion (e.g., because the CL of the driver is shorter than the refractory periods of those tissues), and “fibrillatory conduction” develops. Fibrillatory conduction can be caused by spatially varying refractory periods or by the structural properties of atrial tissue, with source-sink mismatches providing spatial gradients in the response. Fibrillatory conduction is characterized by activation of tissues at variable CLs, all longer than the CL of the driver, because of variable conduction block; in that manner, activation is fragmented. This is the mechanism of AF in several animal models in which the driver consists of a stable, abnormal automatic focus of a very short CL, a stable reentrant circuit with a very short CL, or an unstable reentrant circuit with a very short CL. It also appears to be the mechanism of AF in patients in whom activation of the atria at very short CLs originates in one or more PVs. The impulses from the PVs seem to precipitate and maintain AF.¹³

The concept of fibrillatory conduction is relevant to the “mother rotor fibrillation” hypothesis, in which a fast stationary or meandering spiral/scroll wave in one region of the tissue develops peripheral wavebreaks as the spiral/scroll arm propagates into surrounding tissue with longer refractory periods. Though some investigators suggest that these mother rotors are likely fixed, others have suggested that they may precess (i.e., wobble), albeit in small fairly well-defined areas. In atria with extensive fibrosis, multiple stable rotors can possibly coexist in different regions, insulated by intervening tissue that cannot maintain 1:1 conduction. This variant is equivalent to mother rotor fibrillation with multiple stable mother rotors. Unlike multiple wavelet fibrillation in which the functional reentry is inherently unstable and nonlocalized and the spontaneous peripheral wavebreaks play a causal role in both initiating and maintaining fibrillation, “mother rotor fibrillation” is driven by a localized source and the peripheral wave breaks are non-causal epiphenomena. However, similar to multiple wave reentry fibrillation, mother rotor fibrillation is purely reentrant and requires a trigger to initiate the original rotor; once initiated, no further triggers are necessary to perpetuate fibrillation.^{11,15}

Recently, several mapping studies have provided clinical evidence of the localized source hypothesis by demonstrating that rotational or focal drivers in localized regions maintain AF, and that AF could be eliminated by directly ablating sites of rotors and focal sources that

exhibit high-frequency, periodic activity, based on either electrogram visual analysis, dominant frequency analysis, or panoramic endocardial mapping using phase analysis (see below).^{16–22}

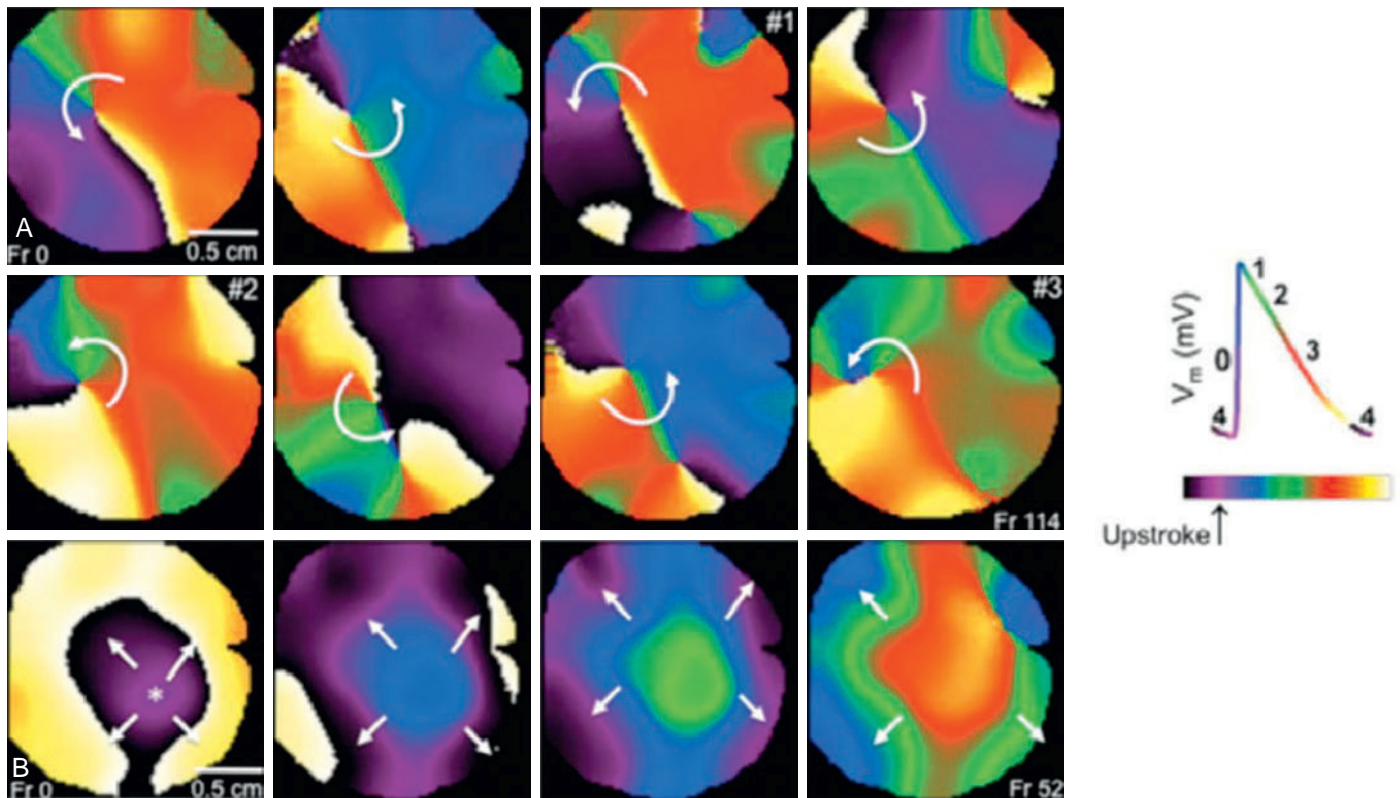
Mapping human AF. The complexity of AF electrograms, with varying amplitude and morphology as well as spatiotemporal CL variations, poses significant challenges to mapping human AF. Recent clinical studies have demonstrated conflicting mechanisms underlying sustained AF; one source of the discrepancies likely arises from differences in scale (global vs. regional) and spatial resolution of the mapping techniques. A second possible factor is the approach employed to analyze fibrillatory wavefront dynamics, using either phase mapping or activation time.²³

Conventional activation mapping techniques used in the EP lab, which assign a specific time point on the unipolar electrogram as the marker of local activation, cannot be employed during AF; fibrillation electrograms typically are fractionated and low amplitude, and are prone to artifacts.²⁴ Spectral analysis and phase mapping of cardiac potentials have been used by researchers to overcome some of those challenges. Both algorithms derive originally from optical mapping experiments conducted in ex vivo hearts. Although optical mapping provides much higher spatiotemporal resolution and accuracy when tracking rotor formation and maintenance, current optical mapping strategies do not allow panoramic endocardial mapping and require the use of potentially toxic voltage-sensitive dyes that preclude their use for human in vivo studies.^{11,13,25}

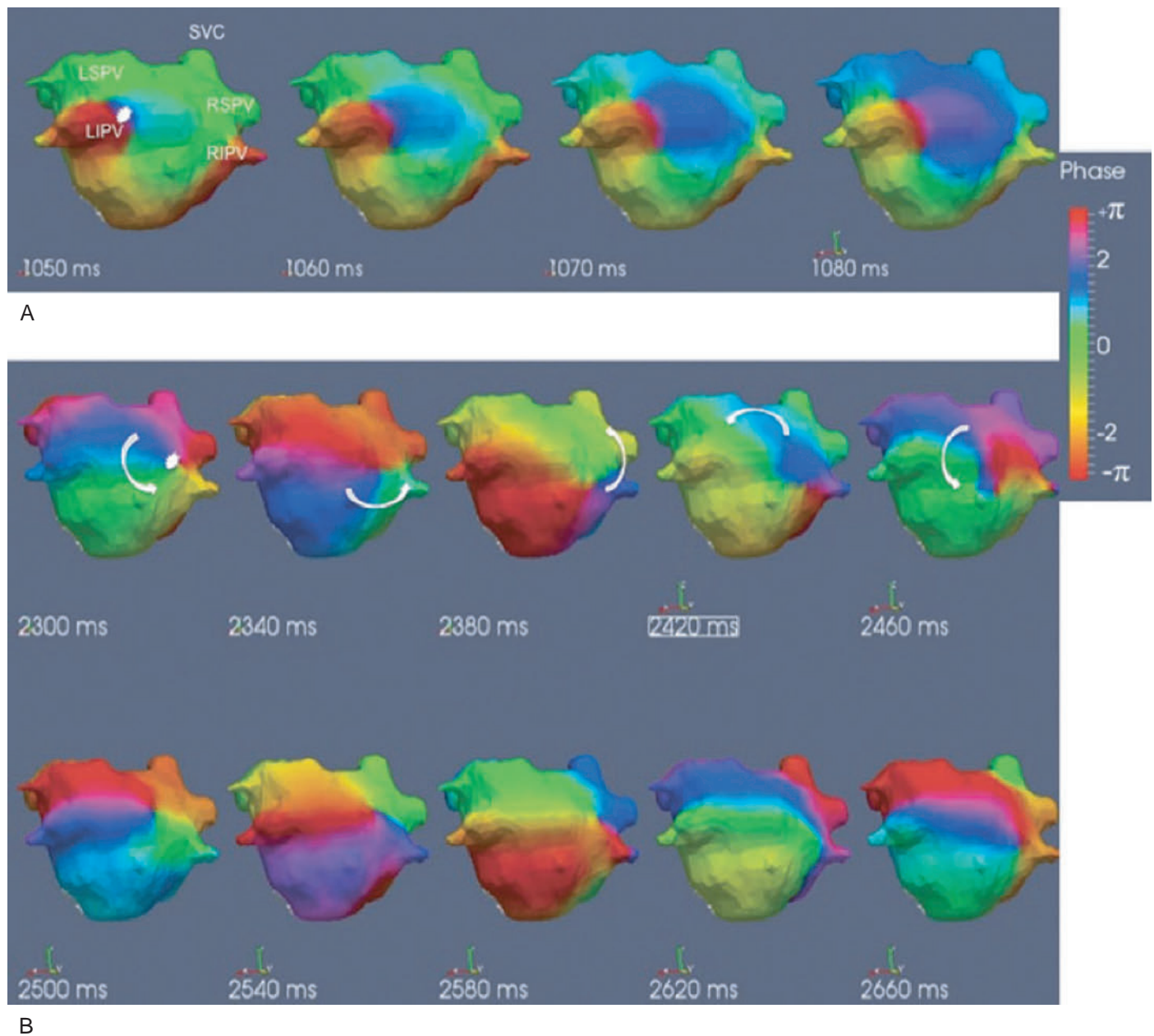
The “spectrum” of a signal displays its energy distribution in the frequency domain. Frequency domain analysis can identify the frequency of the highest peak in the spectrum (i.e., “dominant frequency”), which is often used as a surrogate for the average activation rate at a specific location. Hence, spectral analysis can map the distribution of AF frequencies and localize the areas with the highest activation frequencies (i.e., the shortest CLs, dominant frequency), which usually coincide with the location of AF sources (foci or rotors) that maintain AF. Those techniques have demonstrated that AF has significant periodic elements with varying degrees of regularity, and that certain regions of the atria can have higher activation frequencies than other regions, suggesting that these areas can potentially be the drivers that maintain AF and can provide targets of ablation therapy. A limitation of spectral analysis is that frequency domain mapping produces time-averaged frequency information over space, thereby losing the ability to track temporal variations of the signal.^{11,13,24,25}

“Phase” is a measure of where a signal is in its cycle of oscillation at a given point in time. Phase mapping computes oscillations in the signal over its entire duration, independent of its amplitude, and characterizes a temporal signal in its instantaneous phase of the activation/recovery cycle at each time point. Computation of phase involves the transformation of the signal to the phase domain by selecting a specific CL from the temporal signal. Analysis of phase changes over space provides information on the patterns of organization (repetitive activity) and enables visualization of the spatiotemporally distributed patterns of propagation during cardiac fibrillation. Importantly, phase mapping makes it possible to detect rotational wavefronts (rotors) and determines their center of rotation (singularity point) (eFig. 15.2). However, phase mapping has the propensity to introduce false rotors during complex activation patterns, such as wavefront propagation about a line of block.²⁴

In the clinical setting, recent studies employing panoramic atrial mapping during AF have used phase analysis of contact atrial endocardial electrograms from basket electrode catheters (focal impulse and rotor modulation [FIRM], Fig. 15.4) or reconstructed atrial electrograms from body surface recordings (electrocardiogram [ECG] imaging, eFig. 15.3). Those studies demonstrated the presence of atrial driver regions



eFig. 15.2 Varying Activation Patterns Identified in Phase Movies From the Left Atrium of the Sheep Heart. (A) Sequential snapshots show a rotor pivoting around a phase singularity (point where all phases converge). (B) Breakthrough activation pattern. The wave seems on the center of the field of view and propagates outward. *Right*, Key for the different phases of the action potential is color-coded. (From Quintanilla JG, Pérez-Villacastín J, Pérez-Castellano N, et al. Mechanistic approaches to detect, target, and ablate the drivers of atrial fibrillation. *Circ Arrhythmia Electrophysiol.* 2016;9:1–12.)



eFig. 15.3 Phase Mapping of Electrocardiogram Imaging Data Showing Posterior View of Left Atrium During Paroxysmal Atrial Fibrillation. Panel A shows serial snapshots of a single wave emerging out of the left inferior pulmonary vein (PV, white star) and reaching right PVs in 30 milliseconds while it expands radially to the roof and inferior walls. Panel B shows serial snapshots of two successive rotations (white arrows) of a rotor located near the ostia of right PVs. The core of the rotor (white star at the center of rainbow-colored phases of rotor) is seen meandering in a small region in this example. The blue wave indicates the depolarizing front, which makes one full rotation in 160 milliseconds. The phases of wave propagation are color coded using rainbow scale. The blue color represents depolarizing wave and the green represents the end of repolarization. The wavefront can be read by following the blue color. The time (milliseconds) at the bottom of each snapshot represents the moment in the time window when the snapshot was taken. LIPV, Left inferior PV; LSPV, left superior pulmonary vein; RIPV, right inferior PV; RSPV, right superior PV; SVC, superior vena cava. (From Haissaguerre M, Hocini M, Shah AJ, et al. Noninvasive panoramic mapping of human atrial fibrillation mechanisms: a feasibility report. *J Cardiovasc Electrophysiol*. 2013;24:711–717.)

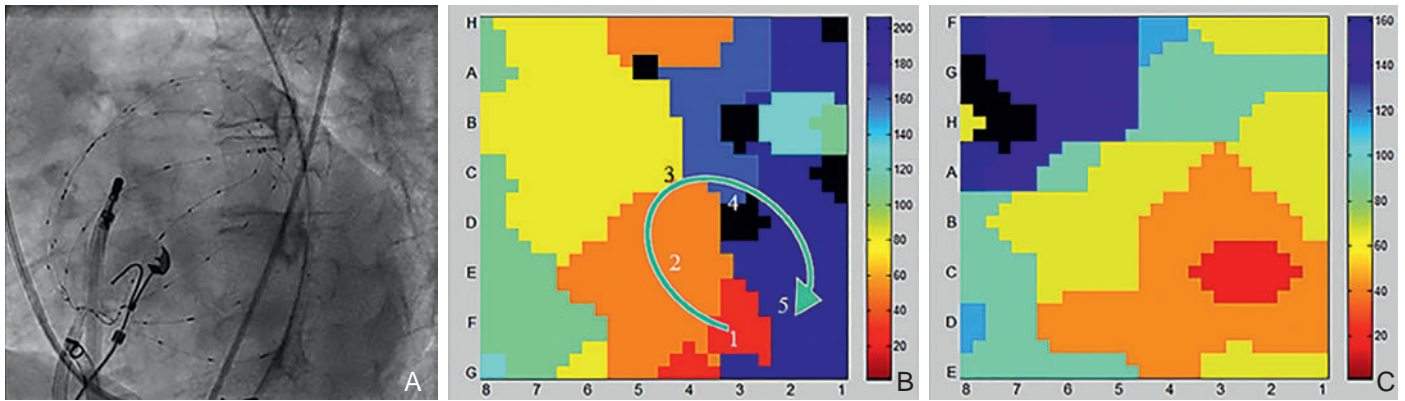


Fig. 15.4 Focal Sources of Atrial Fibrillation Identified by Focal Impulse and Rotor Modulation (FIRM) Mapping. (A) Fluoroscopic view (left anterior oblique) of the multielectrode basket catheter deployed in the left atrium. (B) FIRM mapping shows a left atrial rotor with counterclockwise rotation (from red to blue on the activation time scale with red representing early activation). (C) FIRM mapping shows a left atrial focal impulse originating from electrodes 2 and 3 spline C and D of the basket catheter (red represents early activation with a centrifugal pattern). (From Sommer P, Kircher S, Rolf S, et al. Successful repeat catheter ablation of recurrent longstanding persistent atrial fibrillation with rotor elimination as the procedural endpoint: a case series. *J Cardiovasc Electrophysiol*. 2016;27:274–280.)

with a high prevalence of transient rotors, and suggested that AF is sustained by spiral waves (rotors) or focal sources, or both, which are sufficiently stable in space to be targeted by ablation. Both approaches identified phase singularity points (core of a rotor) as a target for ablation. Elimination of those rotors and focal source could acutely modify or terminate AF and substantially improve ablation outcome. Localized sources can potentially explain modulation of AF by ablation insufficient to limit critical mass and AF termination by localized intervention.^{16–22}

It is important to note that while both ECG imaging and FIRM mapping use phase analysis to determine rotational conduction behavior during AF, detection of rotors using those techniques provides fundamentally different results regarding the spatial behavior of rotors. FIRM mapping demonstrates spatially stable rotors in both atria; many of these rotors are detectable for many seconds up to minutes at the same location. In contrast, ECG imaging techniques show that the reentrant circuits are not spatially stable but meandered substantially throughout the atrium; nevertheless, they recurred repetitively at specific sites that can potentially provide a target for ablation. The reason for the significant discrepancy between the spatial behavior of rotors identified by these different techniques is currently unclear. In a recent study comparing resolution requirements for detection of stationary and meandering rotors found that rotor trajectories can be lost at resolutions for which stable rotors are still identifiable, which may explain differences in findings on rotor stability with basket catheters identifying stable rotors and noninvasive ECG imaging identifying transient meandering rotors.²³

However, despite these data, the rotor paradigm is neither confirmed nor universally accepted, with recent studies raising questions about the efficacy of rotor-targeted ablation. Sufficient spatial resolution is essential for the accurate detection of rotors and focal sources. Although stationary rotors may be identified at coarse resolutions, meandering rotors are lost. While most clinically used catheters offer sufficient spatial resolution to identify and track rotor core location for the range of wavelengths occurring in human AF, mapping catheters with localized coverage (e.g., quadripolar or ring catheters) are not capable of tracking rotors unless the catheter is fortuitously placed over a rotor that does not meander outside the margins of the catheter poles. In contrast, basket catheters provide global coverage. However, the low resolution

of the basket catheters renders them prone to false detections; interpolation of phases is inherently biased toward detection of rotors as the algorithm is devised to demonstrate rotational activity, and focal activation might be displayed as rotational activity if the wavefront reaches the surrounding electrodes sequentially. This can potentially explain, in part, the large incidence of rotors using FIRM mapping, the low AF termination rate with ablation, and poor long-term success for ablating rotors detected by basket catheters. On the other hand, ECG imaging lacks the ability to discern among epicardial breakthroughs, spontaneous depolarizations, and (subcentimeter) microreentry, which are seen as focal activity.^{13,23}

Substrate for Atrial Fibrillation

As noted, AF results from the interplay between a trigger for initiation and a vulnerable EP substrate for maintenance. The fact that most potential triggers do not initiate AF suggests some role for functional and structural substrates in most patients. However, the relative contribution of triggers versus substrate can vary with the clinical context, and the exact nature of the interaction between triggers and substrate remains to be elucidated.

AF commonly occurs in the context of other cardiac or noncardiac pathological conditions, such as valvular disease, hypertension, ischemic heart disease, heart failure, or hyperthyroidism. Depending on the type, extent, and duration of such external stressors, a cascade of time-dependent adaptive, as well as maladaptive, atrial responses develops to maintain homeostasis (so-called “atrial remodeling”), including changes at the ionic channel level, cellular level, extracellular matrix level, or a combination of these, which result in electrical, functional, and structural consequences.

A hallmark of atrial structural remodeling is atrial dilation, often accompanied by a progressive increase in interstitial fibrosis. Atrial arrhythmias, especially AF, are the most common manifestations of electrical remodeling. Increased dispersion in atrial refractoriness and inhomogeneous dispersion of conduction abnormalities, including block, slow conduction, and dissociation of neighboring atrial muscle bundles, are key elements in the development of the substrate of AF. Importantly, different pathological conditions can be associated with a different set of remodeling responses in the atria.

Even in the setting of the AF occurring in the absence of apparent structural heart disease, there is accumulating evidence that occult abnormalities (e.g., patchy fibrosis, inflammatory infiltrates, loss of myocardial voltage, conduction slowing, altered sinus node function, and vascular dysfunction) can be observed and likely represent an early stage of atrial remodeling contributing to the substrate of AF.

Atrial Electrophysiological Properties

In normal atrial cardiomyocytes, phase 0 of the action potential is mediated by the rapidly activating sodium (Na^+) current (I_{Na}). These potentials are called *fast response* potentials (see Chapter 1). As a result, the atrium has several properties that permit the development of very complex patterns of conduction and an extremely rapid atrial rate, as seen in AF. The action potential duration is relatively short, and reactivation can occur partially during phase 3 and usually completely within 10 to 50 milliseconds after return to the diastolic potential. The refractory period shortens with increasing rate, and very rapid conduction can occur.

Patients with AF and no apparent structural heart disease appear to have increased dispersion of atrial refractoriness, which correlates with enhanced inducibility of AF and spontaneous episodes. Some patients have site-specific dispersion of atrial refractoriness and intraatrial conduction delays resulting from nonuniform atrial anisotropy.

Atrial Fibrosis

Atrial fibrosis plays an important role in the pathophysiology of AF. Atrial fibrosis results from various cardiac insults that share common fibro-proliferative signaling pathways. Fibrotic myocardium exhibits slow and inhomogeneous conduction, with spatial “nonuniform anisotropic” impulse propagation, likely secondary to reduced intercellular coupling, discontinuous branching architecture, and zigzagging circuits. When combined with inhomogeneous dispersion of refractoriness within the atria, conduction block provides milieu necessary for the development of reentry. The greater the slowing of conduction velocity in fibrotic myocardium, the shorter the anatomic circuit needed to sustain a reentrant wavelet. In fact, reentrant circuits need be only a few millimeters in length in discontinuously conducting tissue. Thus atrial regions with advanced fibrosis can harbor local sources for AF. Such a hypothesis would not preclude the remainder of the atria from showing fibrillatory conduction or functional reentrant waves.^{7,26–29}

Increased atrial fibrosis is a manifestation of the normal aging process as well as various pathological conditions such as hypertension, coronary artery disease, heart failure, and sleep apnea. Increased atrial fibrosis has been demonstrated even in patients with so-called “lone” or “idiopathic” AF, suggesting that AF in these patients potentially represents an arrhythmic manifestation of “fibrotic atrial myopathy.” The strong association of sinus node dysfunction (SND) and AF (the bradycardia-tachycardia syndrome) also suggests that replacement of atrial myocytes by fibrosis likely plays an important part in the pathogenesis of AF, although in some instances the bradycardia component is a functional response to the tachycardia. Recent studies using delayed-enhancement cardiovascular magnetic resonance (CMR) imaging and electroanatomic voltage mapping demonstrated that the extent and distribution of the fibrotic atrial changes can vary widely among patients with AF. Nonetheless, a higher degree of fibrosis often is observed in patients with persistent AF versus paroxysmal AF. In addition, atrial fibrosis defined by delayed-enhancement CMR was found to be independently associated with AF recurrence in patients undergoing catheter ablation procedures.^{7,27,30}

Importantly, AF itself seems to produce various alterations of atrial architecture that further contribute to atrial remodeling, mechanical dysfunction, and perpetuation of fibrillation. Longstanding AF results

in loss of myofibrils, accumulation of glycogen granules, disruption in cell-to-cell coupling at gap junctions, and organelle aggregates.²⁶

Changes in AF characteristics during evolving fibrosis also have a direct impact on why electrical or drug treatment ultimately fails to achieve conversion to NSR. In the markedly fibrotic and discontinuous atrial tissue, characterized by discontinuous anisotropy, marked degree of gap junctional uncoupling, and fiber branching, the safety factor for propagation is higher than in normal tissue. Hence, blocking of the Na^+ current to the same degree as is necessary for the termination of functional reentry may not terminate reentry caused by slow and fractionated conduction in fibrotic scars of remodeled atria. Conduction in discontinuous tissue is mostly structurally determined and leads to excitable gaps behind the wavefronts. If a gap is of critical size, the effectiveness of drugs that prolong atrial refractoriness will be limited. Furthermore, scar tissue is likely to exhibit multiple entry and exit points and multiple sites at which unidirectional block occurs. This can potentially lead to activity whose appearance in local extracellular electrograms changes from beat to beat, as well as beat-to-beat CL variability. Although such regions can be expected to respond to defibrillation, AF can resume after extrasystoles or normal sinus beats immediately after conversion, with unidirectional block recurring because of scar.

Atrial Stretch

Atrial stretch and dilation can play a role in the development and persistence of AF. Clinically, AF episodes occur more frequently in association with conditions known to cause elevated LA pressure and atrial stretch, such as acutely decompensated systolic or diastolic heart failure. In addition, the echocardiographic LA volume index and restrictive transmitral Doppler flow patterns are strong predictors of the development of AF.

The structure of the dilated atria can potentially have important EP effects related to stretch of the atrial myocardium (so-called “electromechanical feedback”). Acute atrial stretch reduces the atrial refractory period and action potential duration and depresses atrial conduction velocity, potentially through a reduction of cellular excitability by the opening of stretch-activated channels or changes in cable properties (membrane resistance, capacitance, core resistance). Regional stretch for less than 30 minutes activates the immediate early gene program, thus initiating hypertrophy and altering action potential duration in affected areas. Moreover, acutely altered stress and strain patterns augment the synthesis of angiotensin II, which induces myocyte hypertrophy. Angiotensin II can contribute to arrhythmogenic electrical dispersion by regionally increasing L-type calcium (Ca^{2+}) current (I_{CaL}) and decreasing the transient outward potassium (K^+) current (I_{to}). Altered stretch of atrial myocytes also results in opening of stretch-activated channels, increasing G protein-coupled pathways. This leads to increased protein kinase A and C activity, and enhanced I_{CaL} through the cell membrane, and increased release of Ca^{2+} from the sarcoplasmic reticulum, thus promoting afterdepolarizations and triggered activity. Furthermore, acute stretch can promote an increase in dispersion of refractoriness and spatial heterogeneity by causing conduction block and potentially contributing to the development of AF. These alterations occur nonuniformly because stretch is greater in areas of thin versus thick atrial myocardium.

In addition, chronic atrial stretch, as a result of AF and several conditions associated with AF, can promote atrial fibrosis via the activation of multiple profibrotic and hypertrophic signaling pathways.

Inflammation

There is increasing evidence that implicates inflammation (and its downstream effects, including atrial fibrosis) in the pathogenesis of

AF. Clinically, AF occurs frequently in the setting of inflammatory states such as cardiac surgery and acute pericarditis. In addition, the levels of inflammatory biomarkers (C-reactive protein [CRP] and interleukin-6 [IL-6]) are significantly increased in patients with AF, findings suggesting the presence of systemic inflammation in these patients. Elevation of the levels of CRP and IL-6 has been shown to predict future development, recurrence, and burden of AF. There is also evidence suggesting that inflammation is involved in electrical and structural atrial remodeling. Furthermore, inflammation appears to increase the inhomogeneity of atrial conduction directly, potentially via disruption of expression of connexin proteins, leading to impaired intercellular coupling.³¹

It is also likely that inflammation can be a consequence of AF. CRP levels decrease following restoration of NSR. Rapid atrial activation in AF results in Ca^{2+} overload in atrial myocytes that can potentially result in cell death, which induces a low-grade inflammatory response. The inflammation, in turn, can induce healing and reparative fibrosis that likely enhance remodeling and promote perpetuation of the arrhythmia.

Currently, the exact role of inflammation in AF is poorly defined, and it remains unclear whether inflammation is actually involved in the mechanisms underlying AF or whether it is simply an epiphenomenon. Although therapies directed at attenuating the inflammatory burden (e.g., glucocorticoids, statins, and angiotensin II inhibitors) appear promising, early clinical trials do not support a significant benefit.³²

Atrial Remodeling in Atrial Fibrillation

AF is a progressive arrhythmia. In 14% to 24% of patients with paroxysmal AF, persistent AF develops, even in the absence of progressive underlying heart disease. Furthermore, conversion of AF to NSR, electrically or pharmacologically, becomes more difficult when the arrhythmia has been present for a longer period. In fact, the arrhythmia itself results in a cascade of electrical and structural changes in the atria that are themselves conducive to the perpetuation of the arrhythmia ("AF begets AF"), a process known as remodeling. Recurrent AF can potentially lead to irreversible atrial remodeling and eventually permanent structural changes that account for the progression of paroxysmal to persistent and finally to permanent AF, characterized by the failure of electrical cardioversion and pharmacological therapy to restore and maintain NSR. Even after cessation of AF, these abnormalities persist for periods that vary in proportion to the duration of the arrhythmia.³³

Changes in atrial EP features induced by AF can occur through alterations in ion channel activities that cause partial depolarization and abbreviation of atrial refractoriness. These changes promote the initiation and perpetuation of AF (electrical remodeling) and the modification of cellular Ca^{2+} handling, which causes contractile dysfunction (contractile remodeling), as well as atrial dilation with associated structural changes (structural remodeling). Experimentally, electrical and contractile remodeling begins shortly after the onset of AF, with a parallel decrease in both atrial refractory period and contractility over the first minutes of AF. This is followed by further abbreviation in atrial refractoriness and increase in atrial dimensions over the following days. Structural changes follow a much slower time course, likely starting after several weeks.^{34,35}

Electrical Remodeling

Electrical remodeling results from the high rate of electrical activation. The EP changes typical of atrial myocytes during AF include shortening of the action potential duration and atrial refractory period, and reduction in the amplitude of the action potential plateau. Furthermore, AF results in deficiency in the ability of the repolarization time course (action potential duration) to adapt to changes in rate

("abnormal restitution"); consequently, the atrial refractory period fails to lengthen appropriately at slow rates (e.g., with return to NSR). These changes can contribute to the stability of a longer lasting form of AF because, according to the multiple wavelet theory, a short wavelength results in smaller wavelets, which increase the maximum number of wavelets, given a certain atrial mass. Tachycardia-induced changes in refractoriness are spatially heterogeneous, and there is increased variability both within and among various atrial regions, which can promote atrial vulnerability and AF maintenance and provide a substrate for reentry.

The mechanisms for electrical remodeling and shortening of the atrial refractory period are not entirely clear. Several potential explanations exist, including ion channel remodeling, angiotensin II, and atrial ischemia. The principal components of electrical remodeling include reduction in the L-type Ca^{2+} current (ICaL), rectifier background K^{+} current (IK1), and constitutive acetylcholine-regulated K^{+} current (IKACH), and abnormal expression and distribution of the gap junctions.³³

Downregulation of ICaL seems to be responsible for shortening of the atrial action potential, whereas a decrease in Ito is considered to result in loss of physiological rate adaptation of the action potential. The fast atrial rate during AF causes accumulation of intracellular Ca^{2+} . The reduction in ICaL can be explained by a decreased expression of the L-type Ca^{2+} channel $\alpha 1\text{C}$ subunit, likely as a compensatory mechanism to minimize the potential for cytosolic Ca^{2+} overload secondary to increased Ca^{2+} influx during the rapidly repetitive action potentials during AF. Verapamil, an L-type Ca^{2+} channel blocker, was shown to attenuate electrical remodeling and hasten complete recovery without affecting inducibility of AF, whereas intracellular Ca^{2+} overload, induced by hypercalcemia or digoxin, enhances electrical remodeling. Electrical remodeling can be attenuated by the sarcoplasmic reticulum's release of the Ca^{2+} antagonist ryanodine, a finding suggesting the importance of increased intracellular Ca^{2+} to the maladaptation of the atrial myocardium during AF.³³

Angiotensin II may also be involved in electrical remodeling, and angiotensin II inhibitors may prevent the remodeling process. Angiotensin-converting enzyme inhibitors reduce the incidence of AF in patients with left ventricle (LV) dysfunction after myocardial infarction (MI) and in patients with chronic ischemic cardiomyopathy. Atrial ischemia is another possible contributor to electrical remodeling and shortening of the atrial refractory period via activation of the $\text{Na}^{+}\text{-H}^{+}$ exchanger.

More recently, microRNAs (miRNAs or miRs), a group of small noncoding RNA molecules that negatively regulate gene expression, were found to have an important role in a wide range of electrical and structural atrial remodeling processes.^{34,36} Furthermore, experimental studies showed that the rapid rates of AF can lead to autonomic atrial remodeling, with heterogeneous increase in atrial sympathetic innervation, which can potentially promote enhanced automaticity, triggered activity, and spatially heterogeneous abbreviation of refractoriness.⁷

Furthermore, persistent AF can result in other changes within the atria, including gap junctional remodeling, manifest as an increase in the expression and distribution of connexin 43 and heterogeneity in the distribution of connexin 40, both of which are intercellular gap junction proteins.

Contractile and Structural Remodeling

Sustained AF has also been associated with structural changes such as myocyte hypertrophy, myocyte death, tissue fibrosis, impaired atrial contractility, and atrial stretch and dilation. Atrial dilation increases electrical instability by shortening the effective refractory period and slowing atrial conduction. These structural changes, many of which

probably are irreversible, appear to occur over periods of weeks to months.³³

Cellular remodeling is caused by the apoptotic death of myocytes with myolysis. AF results in marked changes in atrial cellular substructures, including loss of myofibrils, accumulation of glycogen, changes in mitochondrial shape and size, fragmentation of sarcoplasmic reticulum, and dispersion of nuclear chromatin.

Contractile remodeling is likely caused by downregulation of ICaL (resulting in reduced release of Ca^{2+} during systole), as well as myolysis (loss of sarcomeres). Contractile remodeling can potentially cause thrombus formation and atrial dilation. Contractile remodeling starts early after onset of AF, and its recovery generally takes longer than reversal of electrical remodeling, likely because of the time it takes for the atria to replace lost sarcomeres.³⁵

In addition to remodeling of the atria, the sinus node can undergo remodeling, resulting in SND and bradyarrhythmias caused by reduced sinus node automaticity or prolonged sinoatrial conduction. The phenomenon of sinus node remodeling likely contributes to the episodes of bradycardia seen in the tachycardia-bradycardia syndrome and may reduce sinus rhythm stability and increase the stability of AF. As mentioned earlier, elements of the sinus bradycardia appear to be functionally reversible if the tachycardia is prevented.

Studies suggest that the PVs are more susceptible to electrical alterations resulting from AF than the atria. Although the PVs display significantly longer refractory periods at baseline than the atria, they exhibit more prominent shortening of refractoriness after a brief episode of pacing-induced AF. Moreover, the short-term presence of AF does influence PV EP properties by slowing the conduction velocity without affecting the conduction times of the atria. Structural changes in the atria after remodeling, such as stretch, can also lead to increased PV activity. Atrial stretch can lead to increased intraatrial pressure, causing a rise in the rate and spatiotemporal organization of electrical waves originating in the PVs. These changes imply that electrical and structural remodeling increases the likelihood of ectopic PV automaticity and AF maintenance.

Tachycardia-induced atrial remodeling can potentially underlie various clinically important phenomena, such as the tendency of patients with other forms of supraventricular arrhythmias to develop AF, the tendency of AF to recur early after electrical cardioversion, the resistance of longer duration AF to antiarrhythmic medications, and the tendency of paroxysmal AF to become persistent.

If NSR is restored within a reasonable time period, EP changes and atrial electrical remodeling appear to normalize gradually, atrial size decreases, and atrial mechanical function is restored. These observations lend support to the idea that the negative downhill spiral in which AF begets AF can be arrested with NSR that perpetuates NSR, and restoration of NSR may forestall progressive remodeling and the increase in duration and frequency of arrhythmic episodes by reverse remodeling.

Role of Autonomic Nervous System in Atrial Fibrillation

Cardiac function is modulated by both the extrinsic and the intrinsic cardiac autonomic nervous systems. The extrinsic (central) system is composed of sympathetic and parasympathetic components, and includes neurons in the brain and spinal cord and nerves directed to the heart. The intrinsic system is composed of a large network of autonomic cardiac ganglia buried throughout the epicardial fat within the pericardial space and in the ligament of Marshall. Groups of several cardiac ganglia comprise plexuses that coalesce in specific locations, and different groups of ganglia have different sites of innervation throughout the heart. Atrial ganglia contain afferent neurons from the atrial myocardium and from the central autonomic nervous system, and

efferent cholinergic and adrenergic neurons, with heavy innervation of the PV myocardium and the atrial myocardium surrounding the ganglionic plexuses. In addition, an extensive array of interconnecting neurons creates a communication network among the different ganglionic plexuses, as well as between the ganglionic plexuses and the atrium and PV myocardium. The intrinsic system receives input from the extrinsic system and but acts independently to modulate numerous cardiac functions, including automaticity, contractility, and conduction.³⁷

Several studies have demonstrated that both divisions of the autonomic nervous system are involved in the initiation, maintenance, and termination of AF, with a predominant role of the parasympathetic system. Enhanced sympathetic activity shortens the atrial refractory period and also increases sarcoplasmic reticulum calcium release in the atrium and PV myocardium, promoting after-depolarization-related PACs and atrial tachycardia (AT), which in turn can initiate AF.^{38,39} On the other hand, increased vagal tone is frequently involved in the onset of AF in patients with structurally normal hearts. Parasympathetic stimulation results in nonuniform shortening of the atrial effective refractory periods, thereby setting up substrate for reentry, promoting the initiation and perpetuation of AF. Vagal stimulation can also lead to the emergence of focal triggers in the atrium. It is important to note that imbalances in the intrinsic cardiac nervous system (rather than an enhanced tone per se) are thought to be involved in the pathogenesis of AF. A shift toward an increase in sympathetic tone or toward a loss of vagal tone has been observed before postoperative paroxysmal AF, whereas a shift toward vagal predominance was observed in young patients with nocturnal episodes of paroxysmal AF.^{40,41}

The electrical properties of the PVs also are modulated by changes in autonomic tone. Anatomic studies revealed that the PVs and the adjoining posterior LA have a unique autonomic profile that differs from the rest of the atria, which likely contributes to the genesis of both focal triggers and sustained microreentry in this region. Ganglionated plexuses cluster within fat pads at the PV entrances and heavily innervate each of the myocardial sleeves of the four PVs. Activation of the ganglionic plexuses at the PV-LA junction promotes AF by a combined parasympathetic and sympathetic action.^{41,42}

Studies suggest that the extrinsic autonomic input to the heart (i.e., from the brain and spinal cord) exerts inhibitory control over the ganglionated plexuses and that attenuation or loss of this control would allow the ganglionated plexuses to become hyperactive. The ganglionic plexuses function as “integration centers” that modulate autonomic innervation. Hyperactivity of ganglionic plexuses can be proarrhythmic while low-level activity may be antiarrhythmic. Recent evidence suggests that noninvasive cardiac autonomic neuromodulation therapies (such as transcutaneous electrical stimulation of the vagus nerve) suppress ganglionated plexus activity, with consequent increased effective refractory period of the atrial and PV myocardium and suppressed AF inducibility. Other approaches to modulation of the extrinsic cardiac autonomic nervous system (e.g., renal sympathetic denervation and ganglion stellatum ablation) are being investigated for antiarrhythmic treatment. Furthermore, ablation of ganglionated plexuses located at the atrial entrances or antra of the PVs can potentially abolish or reduce AF inducibility.⁴³

Role of the Pulmonary Veins in Atrial Fibrillation

There is little controversy now that the PVs play a major role in triggering and maintaining AF, as established by animal and human models, especially in the setting of paroxysmal AF. Fibrillatory conduction is likely initiated by rapid discharges from one or several focal sources within the atria; in most patients with AF (94%), the focus is in one of the PVs (see Fig. 15.2). Extra-PV sites can also trigger AF, but this

occurs in a minority of cases, likely no more than 10% of patients. AF is also perpetuated by microreentrant circuits, or rotors, that exhibit high-frequency periodic activity from which spiral wavefronts of activation radiate into surrounding atrial tissue. Conduction becomes slower and less organized with increasing distance from the rotors, likely because of atrial structural remodeling, resulting in fibrillatory conduction. Interestingly, the dominant rotors in AF appear to cluster primarily in the junction between the LA and PVs. One study also demonstrated that the PV-LA region has heterogeneous EP properties capable of sustaining reentry. As noted earlier, autonomic inputs can be important in triggering and maintaining AF, and many of these inputs are clustered close to the PV-LA junction.

The role of PVs in the initiation and perpetuation of persistent AF seems less prominent than in the setting of paroxysmal AF, likely secondary to the electrical and structural remodeling associated with persistent AF. Non-PV triggers occur more commonly, and the reentry sites required for AF perpetuation are more often found outside the PV-LA junction in persistent AF than in paroxysmal AF.

Pulmonary Vein Anatomy

PVs can have variable anatomy. Most hearts examined are found to have four PVs with distinct ostia. The PV ostia are ellipsoid with a longer superoinferior dimension, and funnel-shaped ostia are frequently noted in patients with AF. The right superior PV lies just behind the SVC or RA, and the right inferior PV projects horizontally. The left superior PV lies between the LA appendage (LAA) and the descending aorta, and the left inferior PV courses near the descending aorta (Fig. 15.5). The superior PVs project forward and upward, whereas the inferior PVs project backward and downward. PVs are larger in patients with AF than in normal subjects, in men than in women, and in persistent versus paroxysmal AF.

Significant variability of PV morphologies can be observed in 40% of patients undergoing AF ablation, including: (1) common ostium (in approximately 25% of patients; Fig. 15.6) of left-sided or, less frequently, right-sided PV; (2) supernumerary right PVs (right middle PV is observed in 8% to 29% of patients; see Fig. 15.6); (3) anomalous PVs arising from the LA roof; and (4) multiple ramification and early branching (especially of the right inferior PV).

The PVs are covered by myocardial sleeves formed by one or more layers of myocardial fibers oriented in a circular, longitudinal, oblique, or spiral direction. These sleeves, continuing from the LA into the PV, vary from 2 to 25 mm in length (mean, 13 mm). The length of the myocardial sleeves usually has a distinctive distribution; superior PVs have longer and better developed myocardial sleeves than inferior PVs, which can potentially explain why arrhythmogenic foci are found more often in the superior PVs than in the inferior PVs. It should be noted that all PVs in all individuals have such myocardial sleeves, regardless of the presence or absence of AF.

The walls of the PVs are composed of a thin endothelium, a media of smooth muscle, and a thick outer fibrous adventitia. The transition from atrial to venous walls is gradual because the myocardial sleeves from the LA overlap with the smooth muscle of the venous wall. The myocardial sleeves are thickest at the venoatrial junction (mean, 1.1 mm) and then gradually taper distally. Furthermore, the thickness of the sleeves is not uniform, with the inferior walls of the superior veins and the superior walls of the inferior veins having the thicker sleeves. Throughout the PV, and even at the venoatrial junction, there are gaps in the myocardial sleeves mainly composed of fibrous tissue. The arrangement of the myocyte bundles within the sleeves is rather complex. There appears to be a mesh-like arrangement of muscle fascicles made up of circularly oriented bundles (spiraling around the long axis of the vein) that interconnect with bundles that run in a longitudinal orientation

(along the long axis of the vein). Such an arrangement, together with the patchy areas of fibrosis seen, can be relevant to the role of the PVs in the initiation of AF.

Electrophysiology of Pulmonary Vein Musculature

As noted, the PVs play a crucial role in the initiation and, in some cases, maintenance of AF. However, it is not clear what makes this region so susceptible to the arrhythmia. There are, at present, limited data available on the ionic mechanisms that underlie the arrhythmogenicity of PVs. Detailed mapping studies have suggested that reentry within the PVs is most likely responsible for their arrhythmogenicity, although abnormal automaticity and triggered activity have also been observed. However, the rarity with which AF continues within the PV after electrical isolation (see later) calls into question whether the PVs are adequate in themselves to maintain AF.

The EP features of the PV, with its distinct area of slow conduction, decremental conduction, nonuniform anisotropy, and heterogeneous repolarization, create potential substrates for reentry. The heterogeneous fiber orientation in the transition from the LA to the PV sleeve results in unique conduction properties in this area. It is possible that the complex arrangement of muscle fibers within the myocardial sleeves and the uneven distribution of interspersed connective and adipose tissue account for the greater degree of decremental conduction observed in the myocardial sleeves than in the LA and for the heterogeneity in conduction properties and refractory periods among the fascicles in the myocardial sleeves. Therefore the fractionation of PV potentials commonly observed during premature stimulation (which usually indicates local slowing of conduction) is consistent with anisotropic properties that can be attributable to the complex arrangement of muscle fascicles within the myocardial sleeves.

Several studies suggested that abnormal automaticity or triggered activity, either alone or in combination with the reentrant mechanisms described previously, can play a role in the initiation of AF. These studies suggested that the propensity of PVs to exhibit abnormal automaticity or triggered activity is enhanced by pathological conditions. Further work also implicated LA posterior wall in the genesis of AF. Studies suggested that the PVs, together with the posterior LA, have an important role in the persistent form of AF. However, the nature of the relationship between this arrhythmogenic region and the pathological conditions that provide a substrate for AF has not been elucidated. Whether the critical region is the posterior LA, the PVs, or both, has been the source of ongoing debate.

Pulmonary Vein Tachycardia Versus Pulmonary Vein Fibrillation

In patients with paroxysmal AF originating from the PVs, a wide spectrum of atrial arrhythmias can coexist. Extensive monitoring frequently documents coexisting paroxysms of AT and AF. Furthermore, patients with paroxysmal AF usually have multiple foci in multiple PVs, and many of these foci originate distally in those veins.

In patients whose only clinical arrhythmia is PV AT, the clinical course is more comparable to that in patients with AT from other anatomic locations than to patients with PV AF. Those patients demonstrate a largely focal process, without evidence of a more progressive and diffuse disease as observed in the population with paroxysmal AF, and they have no tendency to develop further atrial arrhythmias during long-term follow-up. Notably, when patients with PV AT present with recurrence, in almost all cases this is from the original focus. In contrast, patients with paroxysmal AF have recurrences from foci in other PVs and from within the body of the LA. Importantly, in most patients with PV AT, the focus is located at the ostium of the vein (or within 1 cm of the ostium), rather than from further distally

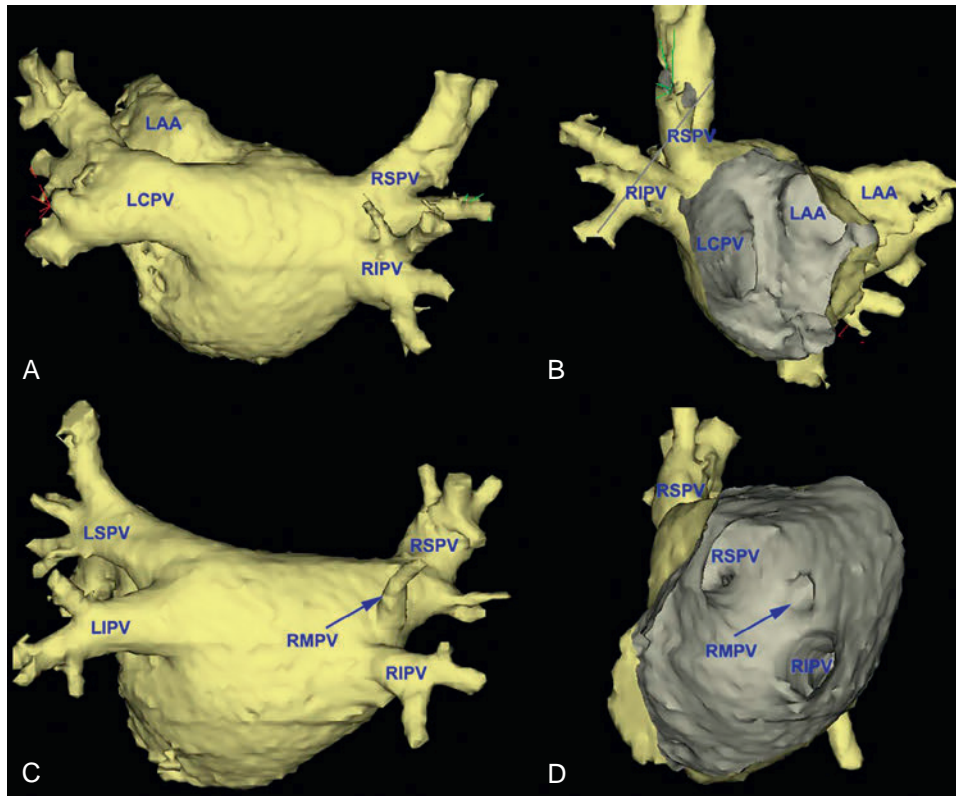


Fig. 15.6 Cardiac Computed Tomography Angiogram (Posteroanterior and Cardioscopic Views) of the Left Atrium and Pulmonary Veins (PVs). (A and B) The left-sided PVs share a common ostium. (C and D) Three PVs are observed on the right side. LAA, Left atrial appendage; LCPV, left common PV; LSPV, left superior PV; RIPV, right inferior PV; RMPV, right middle PV; RSPV, right superior pulmonary vein.

because of the significant overlap in the arrhythmia characteristics (initiation, response to drugs).

Genetics in Atrial Fibrillation

It is increasingly recognized that a widespread heritable component underlies AF, especially in patients without apparent risk factors. Studies have shown that at least 5% of all patients with AF and 15% to 20% of those with AF and structurally normal hearts had a positive family history. Family history of AF is associated with a 40% increased risk of first-degree relatives developing AF. The association between family history and risk of AF development is stronger with increased numbers of affected first-degree relatives and younger age.⁹

Several genes and genomic regions linked to AF and its substrate have been identified in families, individuals, and different populations. Genetic factors play a critical role in modulating the risk of the arrhythmia both in rare families with mendelian patterns of AF inheritance and in the general population. Although familial AF may be a monogenetic disorder, nonfamilial AF may be a multigenetic disease in which genetic factors interact with environmental variables.⁹

Classic mendelian genetics and candidate gene approaches have identified AF-causing mutations in genes encoding cardiac ion channels, cardiac gap junctions, signaling molecules, as well as transcription factors. Those channelopathies are commonly associated with other phenotypic manifestations, such as the long QT, short QT, or Brugada syndromes, as well as inherited cardiomyopathies.⁴⁴ AF is prevalent in cardiac channelopathies and can be the presenting feature in some patients. Studies demonstrated AF prevalence of 2% to 29% in long QT syndrome, 6%

to 53% in Brugada syndrome, 18% to 70% in short QT syndrome, and 11% to 37% in patients with catecholaminergic polymorphic ventricular tachycardia (VT).⁴⁵ These genetic variants promote AF by either abbreviating atrial refractoriness (facilitating reentry), prolonging atrial action potential duration (facilitating triggered activity), or impairing intercellular coupling (resulting in conduction heterogeneity).^{30,46}

It is noteworthy that a recent study described a rare autosomal recessive atrial cardiomyopathy characterized by progressive fibrosis of the atrial myocardium and clinically manifesting with atrial arrhythmias (including AF), atrial dilation, and potential atrial electrical standstill.³⁰

Furthermore, whole-exome sequencing (WES) and genome-wide association studies (GWASs) have identified multiple single-nucleotide polymorphisms (SNPs), a type of common genetic variant, as genetic risks associated with AF in the population. The precise molecular mechanisms underlying these variants remain unclear, owing partly to their presence in noncoding areas of the genome with no known effect on protein expression or function. SNPs presumably act as promoters or enhancers of proximate genes. The closest genes identified with various SNPs are involved in diverse functions, such as in encoding of transcription factors, cytoskeletal and scaffolding proteins, and ion channels.^{44,47–49}

EPIDEMIOLOGY

AF is the most common sustained arrhythmia encountered in clinical practice, accounting for approximately one-third of hospitalizations for cardiac rhythm disturbances. The worldwide age-adjusted prevalence of AF is estimated at 0.596% in men and 0.373% in women,

approximately 33 million people. Each year more than 5 million people develop AF worldwide. The prevalence of AF in the general population in the Western world has been estimated at 0.5% to 2%, although the true prevalence of AF is probably higher given the common occurrence of asymptomatic (subclinical) AF. Furthermore, the frequency of AF is progressively increasing in the general population, likely due to increased longevity and the success in reducing overall cardiovascular mortality, as well as increased prevalence of risk factors for AF (such as hypertension and obesity). In 2010, the prevalence of AF in the United States was estimated to be between 2.7 and 6.1 million. This is expected to rise to about 5.6 to 12 million in 2050. In Europe, AF affects about 8 million people and this number is expected to rise to 18 million by 2060.⁵⁰

AF is a progressive disease. More than half of individuals who experience an initial episode of AF will eventually develop recurrent AF, typically within the first 2 years of follow-up. AF progresses from paroxysmal to persistent (despite antiarrhythmic therapy) in approximately 10% at 1 year, in 25% to 30% at 5 years, and in more than 50% beyond 10 years. Furthermore, progression from paroxysmal and persistent AF to permanent AF occurs in up to 34% of patients at 4 years after the initial diagnosis. Maintenance of NSR becomes progressively more difficult as the duration of persistent AF increases. Only 40% to 60% of patients with persistent AF of less than 1 year's duration remain in NSR 1 year after initiation of antiarrhythmic drug therapy, despite multiple cardioversions; whereas patients with persistent AF of more than 3 year's duration have only a 15% likelihood of long-term sinus rhythm. Increased age, diabetes, heart failure, chronic pulmonary disease, and hypertension are among potential predictors of progression to permanent AF. AF occurring in otherwise healthy patients is less likely to progress.⁵¹ Also, AF patients treated with catheter ablation exhibit a substantially lower risk of progression of the arrhythmia.^{9,52}

AF is independently associated with significantly increased morbidity and mortality, including a fivefold increased risk for stroke, a twofold increased risk for dementia, a threefold risk for heart failure, and a twofold increased risk for MI. The mortality rate of patients with AF is approximately double that of patients in NSR and is linked to the severity of underlying heart disease and associated comorbidities.⁵³ Cardiac causes (sudden cardiac death [SCD], heart failure, and MI) account for almost one-half of deaths in anticoagulated patients with AF, whereas stroke and bleeding only account for approximately 6% of all deaths each as the principal cause. The risk of death appears higher in the presence of heart failure, renal insufficiency, diabetes, advanced age, and male gender.^{9,44,54,55}

Atrial Fibrillation Risk Prediction

Several prediction models for new-onset AF have been proposed to help identify high-risk individuals and serve as a benchmark to test potential novel risk factors. The Framingham Heart Study (FHS) and the Atherosclerosis Risk in Communities (ARIC) Study each developed a risk for the prediction of AF. More recently, the Cohorts for Heart and Aging Research in Genomic Epidemiology–Atrial Fibrillation (CHARGE-AF) consortium developed and validated a simple risk model for prediction of incident AF using pooled data (greater than 26,000 individuals) from prospective cohort studies, including the Cardiovascular Health Study, FHS, and ARIC. The variables used in the CHARGE-AF risk prediction score include: age, race, height, weight, systolic blood pressure, diastolic blood pressure, current smoking, use of antihypertensive medication, diabetes, history of MI, and history of heart failure. In addition to these variables, the “augmented” CHARGE-AF prediction score also incorporates the PR interval and ECG-derived LV hypertrophy.^{1,56,57}

Clinical Risk Factors Predisposing to Atrial Fibrillation

AF can be related to a transient reversible cause, such as thyrotoxicosis, acute MI, acute pericarditis, recent cardiac surgery, acute pulmonary disease, alcohol intake, or electrocution. In these cases, AF generally disappears after treatment of the underlying precipitating condition.

AF is thought to be secondary to underlying structural heart disease in more than 70% of patients and is the final arrhythmic expression of a diverse family of diseases. AF derives from a complex continuum of predisposing factors that appear to involve disease processes that contribute to the triggering of AF (e.g., sympathetic and parasympathetic nervous systems [neurogenic AF], predisposing arrhythmias, or ectopic foci in PVs), increase atrial distention (e.g., valvular heart disease, hypertension, and heart failure), decrease the ratio of atrial myocyte to fibrotic tissue, possibly including an increased rate of apoptotic cell death (e.g., hypertension and ischemic heart disease), disrupt intercellular communications (e.g., pericarditis and edema), increase inflammatory mediators (e.g., pericarditis and myocarditis), or alter energy and redox states that modulate the function of ion channels and gap junctions. Table 15.2 lists cardiovascular and other conditions independently associated with AF.

The most frequent causes of acute AF are MI and cardiothoracic surgery. The most common clinical risk factors for chronic AF are hypertension and ischemic heart disease, with the subset of patients having congestive heart failure most likely to experience the arrhythmia. In the developing world, hypertension and rheumatic valvular (usually mitral) and congenital heart diseases are the most commonly related conditions.^{55,58,59}

The presence of SND also predicts an increased risk for AF. Atrial high-rate episodes (usually indicative of AF or AFL) lasting longer than 5 minutes were noted in 29% of the patients receiving pacemakers for SND but with no prior history of AF.

In younger patients, approximately 30% to 45% of paroxysmal cases and 20% to 25% of persistent cases of AF occur in the absence of any chronic or acute risk factors for the arrhythmia, a condition historically referred to as lone AF. However, given the ambiguous definition in the literature and lack of mechanistic or clinical utility, categorizing AF as “lone” or “idiopathic” is potentially confusing and should not be used to guide therapeutic decisions.⁵

Unmodifiable Risk Factors

Age. The prevalence of AF increases with advancing age. AF is uncommon in childhood except after cardiac surgery. AF occurs in less than 1% of individuals younger than 60 years, but in approximately 6% of those older than 65 years, and in more than 10% of those older than 80 years. The median age of patients with AF is approximately 75 years. About 75% of patients with AF are 65 years of age or older, and 45% of patients with AF are 75 years of age or older.⁵⁹ In adults 55 years of age and older, the lifetime risk of the development of AF is approximately 24% in men and 22% in women.⁹

Gender. The age-adjusted annual incidence of AF is higher in men compared with women (3.8 vs. 1.6 per 1000 person-years). Similarly, the age-adjusted prevalence of AF is higher in men than in women (10.3% vs. 7.4% in adults aged greater than or equal to 65 years). However, gender-related differences in AF incidence and prevalence appear to be related to other risk factors. One report found that, after adjusting for AF-related risk factors, male gender was no longer an independent risk factor for AF. Of note, the lifetime risk for AF is similar between men and women despite higher AF incidence in men, likely related to the shorter life expectancy in men.⁹

Race. The age-adjusted risk of developing AF is higher in whites as compared to blacks, Asians, and Hispanics.⁹

TABLE 15.2 Cardiovascular and Other Conditions Independently Associated With Atrial Fibrillation

Characteristic/Comorbidity	Association With AF
Genetic predisposition (based on multiple common gene variants associated with AF) ⁶⁴	HR range 0.4–3.2
Older age ¹⁹	HR:
50–59 years	1.00 (reference)
60–69 years	4.98 (95% CI 3.49–7.10)
70–79 years	7.35 (95% CI 5.28–10.2)
80–89 years	9.33 (95% CI 6.68–13.0)
Hypertension (treated) vs. none ¹⁹	HR 1.32 (95% CI 1.08–1.60)
Heart failure vs. none ¹⁹	HR 1.43 (95% CI 0.85–2.40)
Valvular heart disease vs. none ²⁰⁵	RR 2.42 (95% CI 1.62–3.60)
Myocardial infarction vs. none ¹⁹	HR 1.46 (95% CI 1.07–1.98)
Thyroid dysfunction ^{206,207}	(reference: euthyroid)
Hypothyroidism	HR 1.23 (95% CI 0.77–1.97)
Subclinical hyperthyroidism	RR 1.31 (95% CI 1.19–1.44)
Overt hyperthyroidism	RR 1.42 (95% CI 1.22–1.63)
Obesity ^{19,208}	HR:
None (BMI <25 kg/m ²)	1.00 (reference)
Overweight (BMI 25–30 kg/m ²)	1.13 (95% CI 0.87–1.46)
Obese (BMI >31 kg/m ²)	1.37 (95% CI 1.05–1.78)
Diabetes mellitus vs. none ¹⁹	HR 1.25 (95% CI 0.98–1.60)
Chronic obstructive pulmonary disease ²⁰⁹	RR:
FEV1 ≥80%	1.00 (reference)
FEV1 60%–80%	1.28 (95% CI 0.79–2.06)
FEV1 <60%	2.53 (95% CI 1.45–4.42)
Obstructive sleep apnea vs. none ²¹⁰	HR 2.18 (95% CI 1.34–3.54)
Chronic kidney disease ²¹¹	OR:
None	1.00 (reference)
Stage 1 or 2	2.67 (95% CI 2.04–3.48)
Stage 3	1.68 (95% CI 1.26–2.24)
Stage 4 or 5	3.52 (95% CI 1.73–7.15)
Smoking ²¹²	HR:
Never	1.00 (reference)
Former	1.32 (95% CI 1.10–1.57)
Current	2.05 (95% CI 1.71–2.47)
Alcohol consumption ²¹³	RR:
None	1.00 (reference)
1–6 drinks/wk	1.01 (95% CI 0.94–1.09)
7–14 drinks/wk	1.07 (95% CI 0.98–1.17)
15–21 drinks/wk	1.14 (95% CI 1.01–1.28)
>21 drinks/wk	1.39 (95% CI 1.22–1.58)
Habitual vigorous exercise ²¹	RR:
Nonexercisers	1.00 (reference)
<1 day/wk	0.90 (95% CI 0.68–1.20)
1–2 days/wk	1.09 (95% CI 0.95–1.26)
3–4 days/wk	1.04 (95% CI 0.91–1.19)
5–7 days/wk	1.20 (95% CI 1.02–1.41)

AF, Atrial fibrillation; BMI, body mass index; CI, confidence interval; FEV1, forced expiratory volume in 1 second; HR, hazard ratio; OR, odds ratio; RR, risk ratio.

From Kirchhof P, Benussi S, Kotecha D, et al. 2016 ESC guidelines for the management of atrial fibrillation developed in collaboration with EACTS. *Eur Heart J*. 2016;37:2893–2962.

Genetics. More than 5% of all patients with AF and 15% to 20% of those with AF in the absence of known causal conditions had a positive family history. Offspring of parents with AF (especially those with early-onset AF with no conventional risk factors) have a two- to threefold greater risk of developing AF. Several genes and genomic regions linked to AF and its substrate have been identified in families, individuals, and different populations. However, whether genetic profiles can be constructed to identify at-risk populations and whether intervention on modifiable risk factors can reduce the risk of AF in populations with genetic predisposition remain to be investigated.^{9,44,60}

Modifiable Risk Factors

Hypertension. Hypertensive heart disease is the most common underlying chronic disorder in patients with AF in developed countries. In fact, hypertension has been found to affect 49% to 90% of the participants in major AF clinical trials. Hypertension per se increases the risk of incident AF by about twofold. Furthermore, the coexistence of hypertension and AF increase the risk of stroke, heart failure, hospitalization, and overall mortality by twofold as compared to AF patients without hypertension. Longstanding hypertension, especially if suboptimally controlled, is associated with sympathetic activation, activation of the renin–angiotensin–aldosterone system, LV hypertrophy, diastolic dysfunction, LA stretch, and structural atrial remodeling, all of which can contribute to development and progression of AF. In addition, hypertension commonly coexists with multiple morbidities that also increase the risk of AF, such as heart failure, coronary artery disease, diabetes, and obesity.⁶¹

Of note, longitudinal patterns or long-term trajectories of systolic blood pressure, pulse pressure, and hypertension treatment were associated with higher 15-year risk of AF development, and performed better than single time-point measurements, especially where prolonged hypertension is present and antihypertensive treatment is used. Interestingly, distinct trajectories for diastolic blood pressure were not associated with increased 15-year risk of AF.⁵⁸

Heart failure. Heart failure and AF share several risk factors and common pathophysiologic processes. In a global AF registry, heart failure was prevalent in 33% of paroxysmal, 44% of persistent, and 56% of permanent AF patients. In the Framingham study, 41% of patients with AF and heart failure developed heart failure first, 38% developed AF first, and in the remaining 21% AF and heart failure occurred at the same time. On the other hand, AF develops in up to 42% of heart failure patients. The prevalence of AF increases with heart failure severity, ranging from 5% in functional class I patients compared with approximately 50% in class IV patients. Among a cohort of heart failure patients with preserved left ventricular ejection fraction (LVEF), 29% had a history of AF, and AF or AFL was documented in 65% of those presenting with acute diastolic heart failure.^{62,63}

Patients with concomitant heart failure and AF exhibit a grim prognosis, with a 1-year mortality of 9.5% and worsening of heart failure in almost 25%. In heart failure patients undergoing implantable cardioverter-defibrillator (ICD) implantation, a history of AF at time of procedure identifies additional risk of heart failure and death, and the new detection of AF afterward is associated with even higher rates of death.^{63,64}

In addition to their shared underlying risk factors, AF and heart failure also are independent risk factors for one another. AF can be both a cause and a consequence of heart failure. Heart failure is a potent risk factor for incident AF, with a sixfold increase in the risk of developing AF, while AF is associated with a threefold increased risk of incident heart failure. AF can cause impairment of systolic and diastolic ventricular function not present in sinus rhythm. The loss of atrial systole as well as AF-induced impaired atrial function and atrial fibrosis result

in reduced LV filling and cardiac output and can be a direct cause of diastolic heart failure. In addition, irregular and rapid ventricular rates in AF can lead to LV systolic dysfunction (tachycardia-induced cardiomyopathy). AF is also associated with LV myocardial fibrosis, which contributes to diastolic dysfunction. On the other hand, increased ventricular filling pressures and afterload, functional valvular regurgitation, and activation of the renin–angiotensin–aldosterone system in heart failure can lead to atrial stretch, fibrosis, and dilation. In addition, altered calcium handling and calcium overload in heart failure can promote initiation and perpetuation of AF.^{63–65}

Valvular heart disease. AF has been conventionally classified into “valvular” or “nonvalvular” AF. While the 2012 ESC Guidelines defined valvular AF as rheumatic valvular disease (predominantly mitral stenosis) or prosthetic heart valves, the 2014 AHA/ACC/HRS guidelines defined nonvalvular AF as AF in the absence of rheumatic mitral stenosis, or a mechanical heart valve, but explicitly added bioprosthetic heart valves or mitral valve repair.³

A wide spectrum of valvular lesions can lead to the development of AF. The major independent risk factor is LA enlargement, which is more likely to result from mitral valve disease. Elevated LA pressure causes myocardial stretch and atrial remodeling, which promote AF.

Rheumatic heart disease, now uncommon in developed countries, remains an important underlying substrate for AF in the developing world. The prevalence of AF in these patients varies with the type of valve disease, occurring in only 1% of patients with aortic valvular disease, 16% of those with isolated mitral regurgitation, 29% of patients with isolated mitral stenosis, and 52% of those with combined mitral stenosis and regurgitation. In addition, the risk of AF is known to correlate with LA size; the incidence of AF rises from 3% when the LA diameter is less than 40 mm to 54% if the LA diameter exceeds 40 mm. Patients with mitral stenosis and AF are at a particularly high risk for thromboembolic events and have been excluded from any further trials studying anticoagulation regimens for AF. The risk of thromboembolism is higher for AF patients with mitral than those with aortic valve disease.

Nonrheumatic valvular heart disease is common in patients with “nonvalvular” AF (i.e., valve disease with neither rheumatic mitral stenosis nor valve prosthesis), with reported prevalence of up to 25%, especially those with permanent AF. The majority of these patients have mitral regurgitation (61%), aortic regurgitation (24%), and aortic stenosis (32%). Of note, an increased thromboembolic risk has been observed in nonvalvular AF patients who have nonrheumatic native valve disease compared with those without valve disease; however, neither the valve disease per se nor its severity was clearly associated with this risk. Those patients were older and had a higher CHA₂DS₂-VASc score, which was likely to explain the higher embolic risk.³

Coronary artery disease. Coronary artery disease is present in more than 20% of patients with AF. In contrast, the prevalence of AF in the total population with chronic stable coronary artery disease is relatively low. Nonetheless, AF occurs transiently in 6% to 22% of patients with acute coronary syndromes, and its occurrence in this setting is associated with increased short- and long-term morbidity and mortality. Ischemic heart disease can predispose to the development of AF by atrial stretch and dilation secondary to ischemia-related diastolic and systolic ventricular dysfunction as well as atrial ischemia.

Recent evidence suggests that AF patients are at substantially increased risk (by 47%) of incident MI compared with those without AF. The relative risk is particularly higher in patients free of coronary artery disease at baseline (by 71%), in those younger than 60 years, and in women. Several mechanisms have been proposed to account for the increased risk of MI in AF patients: (1) AF-induced prothrombotic

state caused by increased systemic platelet activation, thrombin generation, and endothelial dysfunction; (2) AF-mediated inflammation that can potentially promote plaque rupture and MI; (3) direct coronary thromboembolism from LAA clots; (4) demand ischemia related to fast ventricular rates during AF; and (5) presence of common risk factors that predispose to the development of both AF and coronary artery disease (e.g., diabetes, hypertension, advanced age).^{66–68}

Congenital heart disease. During long-term follow-up, AF develops in more than one-third of patients with congenital heart disease. AF is more common in patients with severe congenital defects, residual left-sided lesions, or unrepaired heart disease. AF is frequently associated with markers of left-sided heart disease (i.e., LV systolic dysfunction and LA dilation) and is most commonly seen in patients with congenital aortic stenosis, mitral valve disease, palliated single ventricles, unrepaired heart defects, or end-stage heart disease.⁶⁹ Compared to patients without congenital heart defects or with simple congenital heart defects, AF develops at a younger age in patients with complex congenital heart defects. AF is rarely seen in patients with atrial septal defects before the age of 40 years, but the incidence can approach 50% in unrepaired patients beyond 60 years of age.^{70–72}

Coexistence of episodes of AF and macroreentrant atrial tachycardia (MRAT) has been reported in a considerable number of patients (33%) with congenital heart disease. Regular ATs preceded development of AF in about two-thirds of patients. Approximately 30% of patients who have previously undergone successful catheter ablation for MRAT develop AF during long-term follow-up.^{70,73}

Obstructive sleep apnea. Accumulating evidence demonstrates an independent association between AF and obstructive sleep apnea. AF occurs in 5% of individuals with severe sleep apnea and only 1% of those without sleep apnea. The prevalence of at least moderate sleep apnea was reported in up to 32% of patients with AF and structurally normal hearts. Furthermore, cross-sectional studies demonstrated that patients with AF had a significantly higher risk of obstructive sleep apnea than matched controls (49% vs. 33%), and multivariate analysis demonstrated a strong independent association between sleep apnea and AF (odds ratio, 2.2). In addition, several prospective studies showed that obstructive sleep apnea predicts the occurrence of future AF. Untreated obstructive sleep apnea was associated with a remarkably high rate of AF recurrence at 1 year compared with patients with unknown sleep apnea status (83% vs. 53%). The risk of AF in patients with obstructive sleep apnea appears to increase linearly along with the severity of obstructive sleep apnea. In some patients with obstructive sleep apnea and paroxysmal AF, paroxysms of AF were found to be nocturnal and, at least in part, temporally related to respiratory obstructive events.^{61,74}

Obstructive sleep apnea can affect AF response to medical and catheter ablation therapies. Patients with obstructive sleep apnea can have 25% to 31% increased risk for AF recurrence after catheter ablation in comparison with patients with no sleep apnea. On the other hand, the use of continuous positive airway pressure (CPAP) therapy is associated with more than 40% relative risk reduction in AF recurrence in patients with obstructive sleep apnea, regardless of the AF treatment strategy (medical therapy or catheter ablation).^{75,76}

Several mechanisms are proposed by which obstructive sleep apnea increases the risk of AF. Repetitive forced inspiration against a collapsed upper airway during apneic episodes generates substantial shifts in intrathoracic pressure, with consequent increase of venous return, leading to increased RV preload and LV afterload. Pressure and volume overload causes stretch of the atria and PV ostia. Acute atrial stretch can shorten atrial refractoriness (possibly by opening of stretch-activated ion channels) and impair atrial conduction. Repeated atrial stretch can lead to structural atrial remodeling with dilation and fibrosis. In addition,

repetitive apneas and hypopneas are accompanied by intermittent hypoxemia and hypercapnia, which cause chemoreceptor-induced sympathetic activation and parasympathetic withdrawal. Sympathetic hyperactivity (which is further enhanced by recurrent arousal) results in peripheral vasoconstriction and systemic hypertension, as well as increased heart rate, and reduced heart rate variability. Also, intermittent hypoxia and postapneic reoxygenation induce oxidative stress and inflammatory processes contributing to LA remodeling and fibrosis. These mechanisms can act as both triggers and perpetrators of AF, and can predispose to arrhythmia recurrence and affect response to different pharmacologic and nonpharmacologic therapies for AF. CPAP therapy is likely to effectively reverse these mechanisms and thereby decrease AF occurrence. Finally, obstructive sleep apnea often coexists with multiple morbidities that also increase the risk of AF, such as heart failure, diabetes, obesity, and systemic hypertension.^{74–76}

Obesity. Obesity (body mass index [BMI] greater than 30 kg/m²) is associated with a significantly higher risk of AF. Overweight populations have higher incidence, prevalence, severity, and progression of AF compared with their normal weight counterparts. A recent meta-analysis found that for every 5 kg/m² increase in BMI, there were 10% to 29% greater risks of incident, postoperative, and postablation AF.^{77,78} In overweight and obese individuals with symptomatic AF, progressive long-term sustained weight loss has a dose-dependent effect on long-term freedom from AF. Notably, weight fluctuation of greater than 5% had an adverse effect on overall freedom from AF, with a twofold greater likelihood of recurrent arrhythmia.^{44,61,79} A recent meta-analysis found a 3.1% greater risk of recurrent AF postablation for every one unit increase in BMI.

Obesity is often associated with cardiometabolic comorbidities, such as hypertension, diabetes mellitus, autonomic dysfunction, and sleep apnea, all of which can generate a susceptible AF substrate. However, obesity also appears to be a distinct risk factor for AF, independent of the coincidental accumulation of other comorbidities. Obesity was linked to higher risk of AF even among young and seemingly healthy individuals. Several mechanisms have been proposed to explain the association between obesity and AF. Progressive weight gain results in electrical and structural atrial remodeling, atrial interstitial fibrosis, increased LA pressure and volume, ventricular hypertrophy and impaired diastolic function, low-grade systemic inflammation, and myocardial lipidosis. Obesity has also been associated with increased epicardial fat thickness, which has been associated with AF, likely due to altered atrial electrophysiology and autonomic imbalance. On the other hand, weight loss is associated with reversal of atrial dilation and LV hypertrophy.^{79–81}

Diabetes. Diabetes appears to confer an increased risk for the development of AF. In the FHS, diabetes was associated with 40% higher risk of AF in men and 60% higher risk in women after 38 years of follow-up. Other studies found that AF was more prevalent in subjects with pre-diabetes compared to controls and correlated positively with hemoglobin A1c. Notably, intensive glycemic control does not affect the rate of new-onset AF.^{44,82,83}

Several mechanisms can potentially underlie the association of diabetes and AF. Diabetes-related cardiomyopathy leads to ventricular systolic or diastolic dysfunction, increased filling pressures, and atrial remodeling. In addition, cardiac autonomic neuropathy has been implicated by leading to sympathetic overactivity and neural remodeling. Furthermore, insulin resistance can be associated with a proinflammatory environment within the myocardium.^{82,83}

Hyperthyroidism. The prevalence of AF in patients with overt hyperthyroidism ranges between 10% and 15%, and the risk is approximately sixfold that of the euthyroid population. Also, subclinical hyperthyroidism is a risk factor associated with a threefold increase in

development of AF. The risk of AF is higher in men, in the elderly, and in patients with triiodothyronine (T3) toxicosis.^{44,84}

About two-thirds of the patients with AF due to hyperthyroidism revert spontaneously to NSR after treatment of the thyrotoxic state, typically within 3 to 6 months of becoming euthyroid. Even though hyperthyroidism is considered a reversible cause of AF, the arrhythmia persists or recurs in up to 30% to 40% of patients after restoring a euthyroid status. Older age (greater than 55 years), long duration of hyperthyroidism (greater than 5 years), long duration of pretreatment AF, severe LV dysfunction, and LA enlargement are independent predictors for continued AF following the successful treatment of hyperthyroidism.^{44,84}

Among all patients with new-onset AF, less than 1% of AF incidence is caused by overt hyperthyroidism. Although the yield of abnormal thyroid function testing in these patients is low, the benefit associated with the ability to restore patients with thyrotoxicosis to a euthyroid state and NSR justifies thyroid-stimulating hormone (TSH) testing in most patients with recent onset of otherwise unexplained AF.

The mechanisms by which hyperthyroidism enhances vulnerability to AF likely include abbreviation of the atrial action potential duration and refractory period, increased atrial ectopic activity, elevation of LA pressure secondary to increased LV mass and impaired ventricular relaxation, and myocardial ischemia resulting from increased resting heart rate.^{44,84}

Pulmonary embolism. AF can occur in the setting of acute pulmonary embolism, likely secondary to acute RV pressure overload and subsequent RA dilation. AF can be seen as a presenting sign, during the early phase, or later in the course of recovery from pulmonary embolism.⁸⁵ Furthermore, patients with prior pulmonary embolism exhibit a substantially increased (ninefold) incidence of late onset AF.⁸⁶

Of note, some studies have suggested that AF can potentially be a cause, rather than a consequence, of pulmonary embolism. The prothrombotic state associated with AF can potentially promote RA thrombus formation with subsequent embolization to the lungs. However, this hypothesis has yet to be confirmed.⁸⁶

Chronic kidney disease. Chronic kidney disease (CKD) increases the risk of the development of AF. Among patients with chronic kidney disease, the prevalence of AF is two- to threefold higher than reported in the general population. Moreover, AF prevalence increases in a dose-dependent fashion as renal function worsens. In one report, the prevalence of AF was 1.0% among adults without CKD, and 2.8%, 2.7%, and 4.2% among adults with stage 1 to 2, stage 3, and stage 4 t–5 CKD, respectively. Other measures of kidney dysfunction, such as albuminuria, are also associated with higher AF risk. Importantly, incident AF is independently associated with increased risk of progression to end-stage renal disease requiring dialysis in adults with chronic kidney disease (likely due to the proinflammatory, profibrotic, and prothrombotic state as well as altered hemodynamics associated with AF).

Several possible mechanisms can potentially explain the high rate of identified AF among patients with chronic kidney disease, including a high prevalence of shared risk factors between chronic kidney disease and AF (e.g., advanced age, LV hypertrophy, hypertension, diabetes), increased systemic inflammation, sympathetic activation, myocardial fibrosis, and activation of the renin–angiotensin–aldosterone system.

Exercise and fitness. Recent data describing the intensity, duration, and frequency of exercise suggest a U-shaped relationship with AF and mortality. Sedentary lifestyle significantly increases the risk of AF, while moderate-intensity exercise is protective against future AF in both men and women. However, vigorous long-term exercise training has a gender-specific association with AF risk. Compared with sedentary counterparts, men who exercised at a vigorous intensity had a threefold

risk of incident AF. In contrast, women exercising at vigorous intensities actually had a lower incidence of AF.^{61,87,88}

The mechanisms of AF promotion by endurance exercise remain speculative. Proposed contributors include atrial stretch and dilatation, LV hypertrophy, chronic systemic inflammation, increased vagal tone, sinus node remodeling, anatomic adaptation, and illicit drugs. However, it remains unclear why intense physical activity increases the AF risk only in men and not in women. Of note, AF in athletes is less likely to be associated with the common risk factors for AF identified in the general population.^{87,88} On the other hand, physical inactivity predisposes to AF risk factors (e.g., hypertension, obesity, and diabetes), and is associated with systemic inflammation and sympathetic activation.⁹

Alcohol. AF is the most common arrhythmia associated with alcohol consumption. Importantly, the total amount and pattern of alcohol drinking as well as the type of alcoholic beverage appear to impact AF risk. Habitual moderate (7 to 21 standard drinks/wk) and heavy (greater than 21 standard drinks/wk) alcohol consumption, even after correcting for binge drinking, increases the incidence of AF in a dose-dependent manner, with an 8% increase in AF risk for each 1 standard drink per day (or 12 g pure alcohol per day) increase of alcohol consumption.

In addition, an association exists between binge-pattern drinking (greater than 5 drinks on a single occasion) and increased AF risk, independent of the number of drinks consumed per week. AF in the setting of acute consumption is well recognized, occurring in up to 60% of binge drinkers. In fact, the “holiday heart syndrome” describes AF occurring following weekends or holidays when alcohol intake is increased. Furthermore, the risk for AF was found to be most pronounced with liquor, modest for wine, and no excess risk was detected with beer.^{44,89}

Among patients with a history of AF, alcohol consumption is associated with an increased risk of progression from paroxysmal to persistent AF as well as increased risk of AF recurrence following catheter ablation. A safe level of daily alcohol consumption in AF patients has not been identified.⁹⁰

Several mechanisms have been implicated in mediating the adverse effects of alcohol. Ethanol can lead to electrical atrial remodeling, resulting in slowing of intraatrial conduction and abbreviation of atrial refractoriness. Other potential mechanisms include sympathetic stimulation, modulation of vagal tone, alterations in oxidative stress, electrolyte imbalances (hypokalemia, hypomagnesemia), and alcohol-induced cardiomyopathy. Furthermore, ethanol and its metabolite, acetaldehyde, have direct cardiotoxic effects, including direct effects on atrial excitation-contraction coupling, inhibition of calcium release from the sarcoplasmic reticulum, generation of oxidative stress, accelerated protein catabolism, and derangements in fatty acid metabolism and transport.^{44,89,91,92}

Smoking. Several, but not all, studies demonstrated an association between past and current cigarette smoking and an increased risk of AF. In one report, current smokers exhibited almost twice the risk of AF as compared to never smokers. Past smokers also had an increased risk of AF, albeit lower than those who continued to smoke. Furthermore, the cumulative amount of smoking in cigarette-years was correlated with an increased risk of developing AF. In addition, second-hand smoking, particularly when present during development and early childhood, was statistically significantly associated with the presence of AF. This relationship was particularly strong in the absence of known AF risk factors. Of note, smoking has also been reported to predict worse outcome (i.e., increased risk of intracranial bleeding, mortality, and the combined outcome of stroke or death) in patients with AF.^{44,93}

Several mechanisms can be involved in the associations of smoking with AF. Nicotine itself has been linked to cardiac arrhythmias, including AF, likely secondary to sympathetic activation, atrial electrical alterations, atrial fibrosis, and atrial structural remodeling. Furthermore, carbon monoxide can influence cardiac automaticity. In addition, oxidant substances and polycyclic aromatic hydrocarbons can potentially play a role.⁹³

Caffeine. Caffeine, a methylxanthine compound that is chemically similar to theophylline, increases neurohormonal and sympathetic stimulation. Therefore caffeine has been addressed as a potential trigger for AF. However, studies failed to demonstrate any significant relationship between habitual or heavy caffeine consumption and incident AF.⁴⁴

Recreational drugs. Data on recreational (illicit) drugs as risk factors for AF per se are sparse. AF has not been reported to be associated with amphetamine, heroin, or LSD abuse. Limited reports suggest a potential effect of the abuse of cannabis, cocaine, ecstasy, and anabolic androgenic steroids on AF.⁴⁴

Cannabis, the most commonly used recreational drug, has been associated with several cases of AF (starting within minutes to 3 hours of cannabis use) in young people without comorbidities. The underlying mechanism probably is related to sympathetic activation and reduced coronary microcirculation.⁹⁴

Drug-Induced Atrial Fibrillation

Several cardiovascular and noncardiovascular drugs can induce AF. The overall incidence of drug-induced AF is relatively low; however, since drug-induced AF in most cases is paroxysmal, spontaneously terminating in a few minutes or hours, the true incidence of drug-induced AF is probably underestimated.

Transient AF is observed in approximately 3% of patients receiving adenosine for treating SVT and up to 17% of those receiving adenosine during EP studies. Also, AF can be induced by positive inotropic agents such as dobutamine for stress echocardiography (0.4% to 2%) and milrinone (5%). Furthermore, the use of dopamine, or dobutamine following cardiac surgery is associated with a higher incidence of postoperative AF. Paroxysmal AF is a relatively common complication (17%) following intracoronary injection of acetylcholine for the provocation of coronary spastic angina.

Several antineoplastic agents can induce AF, including intrapericardial cisplatin (12% to 32%), cyclophosphamide (2%), anthracyclines (1% to 10%), IL-2 (4% to 8%), melphalan (6% to 12%), 5-fluorouracil (1%), and paclitaxel (1% to 1.7%). Other drugs reportedly implicated in precipitating AF include nonsteroidal antiinflammatory agents, high-dose corticosteroids, ondansetron (an antiemetic agent), aminophylline, theophylline, antipsychotic agents (e.g., clozapine, olanzapine), antidepressants (e.g., fluoxetine, trazodone), bisphosphonates (e.g., alendronate), and ivabradine.

Several classes of drugs can induce AF through very different mechanisms, including: (1) alteration of atrial EP properties, with increased focal activity, shortened action potential duration and refractoriness, or reduced conduction velocity (e.g., adenosine, parasympathomimetics, sympathomimetics, and theophylline); (2) adrenergic or vagal stimulation (e.g., acetylcholine, adenosine, sympathomimetics); (3) direct cardiotoxicity causing myocardial fibrosis, cardiomyopathy, myocarditis, or pericarditis (e.g., cancer chemotherapy); (4) myocardial ischemia secondary to coronary vasospasm, thrombosis, or arteritis (e.g., acetylcholine, chemotherapy agents, ondansetron, and sumatriptan); (5) electrolyte disturbances (e.g., diuretics, glucocorticoids); (6) abnormalities in calcium handling (e.g., inotropic agents); (7) release of proinflammatory cytokines (e.g., IL-2); and (8) increased oxidative stress (e.g., cancer chemotherapy).^{44,94}

Postoperative Atrial Fibrillation

Epidemiology

Postoperative AF complicates cardiac surgery in 15% to 63% of patients. The risk of AF is highest among patients undergoing combined coronary artery bypass grafting and mitral valve replacement (63%) and the lowest among patients undergoing isolated coronary revascularization surgery (15% to 40%) and cardiac transplantation (11% to 24%). Postoperative AF has also been known to complicate noncardiac surgery (incidence, 0.3% to 13.7%), especially thoracic and large colorectal surgeries.⁹⁵

Clinical risk factors for the development of postoperative AF include advanced age (greater than 65 years), male gender, Caucasian race, hypertension, prior AF, mitral valve disease, heart failure, LV hypertrophy, diastolic dysfunction, increased LA size, history of MI, withdrawal of beta-blocker therapy, obesity, low BMI, chronic obstructive pulmonary disease, anemia, prolonged PR interval, diabetes, renal dysfunction, tobacco use, and high baseline CRP levels. The CHADS2 and CHA2DS2-VASc scores were also found to be predictive of AF after cardiac surgery.⁹⁶

Several factors related to the surgical procedure also potentially contribute to the development of AF. These include operative trauma from surgical dissection and manipulation, pericardial lesions, atrial dilation (caused by LV dysfunction and intraoperative volume overload), perioperative use of catecholamines, parasympathetic activation, and electrolyte imbalances.⁹⁷

The onset of postoperative AF peaks at 24 to 72 hours after surgery, and declines to 2% at discharge. Among patients with no prior history of AF, postoperative is usually self-limited, terminating within 24 hours in the majority of patients, with a mean duration of about 11 to 12 hours. However, despite its usually transient nature, the arrhythmia is not limited to the early postoperative phase, and can recur between day 6 and day 30 after the operation in about 25% of patients.^{96,97}

Prognosis

The occurrence of postoperative AF is associated with a twofold increase in cardiovascular mortality and morbidity. Postoperative AF is associated with a two- to fourfold increase in stroke risk at 30 days, and is an important predictor of in-hospital and long-term mortality. Numerous postoperative complications have been correlated with postoperative AF, including congestive heart failure, stroke, bleeding complications (from anticoagulation), renal insufficiency, infection, ventricular arrhythmias, prolonged ventilation, reintubation, readmission to the intensive care unit, and prolongation of hospital stay (by about 4 to 5 days). However, it is important to note that a causal relationship between postoperative AF and its associated adverse outcomes is still not well defined.⁹⁷⁻⁹⁹

Mechanism

Although the exact pathophysiology of postoperative AF remains incompletely understood, both acute perioperative and chronic factors appear to play an important role in the initiation and maintenance of the arrhythmia. Acute perioperative factors that have been implicated in the creation of atrial susceptibility to AF include pericardial inflammation, heightened sympathetic tone, use of inotropes, acute atrial injury, ischemia, and oxidative stress, as well as acute atrial dilation secondary to pressure or volume overload. Also, it is likely that a preexisting atrial electrical and structural arrhythmogenic substrate increases the vulnerability to the development of AF when subjected to the acute perioperative stress. In fact, the majority of patients with postoperative AF have underlying atrial disease. Further, the presence of preexistent atrial

substrate likely explains the increased risk for developing future AF among patients with new-onset postoperative AF, suggesting that the development of postoperative AF can be a surrogate for an underlying cardiac substrate.^{95,97}

CLINICAL PRESENTATION

Symptomatic Atrial Fibrillation

AF can be symptomatic or asymptomatic, even in the same patient. Symptoms associated with AF vary, depending on the ventricular rate, the underlying functional status, the duration of AF, the presence and severity of structural heart disease, and the individual patient's perception.

The hemodynamic consequences of AF are related to loss of coordinated atrial contraction, rapid ventricular rate, and irregularity of ventricular rhythm (independent of rate), as well as long-term consequences such as atrial and ventricular cardiomyopathy. Loss of effective atrial contraction can potentially reduce cardiac output by 15% to 25%. These consequences are magnified in the presence of impaired diastolic ventricular filling, hypertension, mitral stenosis, LV hypertrophy, and restrictive cardiomyopathy. Irregularity of the cardiac cycle, especially when accompanied by short coupling intervals, and rapid heart rates in AF can lead to reduction in diastolic filling, stroke volume, and cardiac output.^{100,101}

Most patients with AF complain of palpitations, chest discomfort, dyspnea, generalized fatigue, or dizziness, although significant interindividual and intraindividual variability exists. Although palpitation, or awareness of the irregularity of the heartbeat, is prominent in more than half of patients with AF (more common in those with paroxysmal AF), its correlation with documented arrhythmia is unimpressive. Dyspnea and fatigue can result in significant activity intolerance.

Chest pain can be related to demand ischemia secondary to reduced cardiac output during AF in patients with coronary artery disease; however, chest pain can occur in AF patients despite the absence of coronary artery disease, potentially related to impaired microvascular flow. Furthermore, AF with a chronically rapid heart rate (more than 120 to 130 beats/min) can lead to tachycardia-mediated cardiomyopathy and heart failure.

Syncope is an uncommon complication of AF that can occur on termination of the arrhythmia in patients with SND or (especially at the onset of an episode) because of rapid ventricular rates in patients with hypertrophic cardiomyopathy, aortic stenosis, or ventricular pre-excitation over a BT. The first presentation of asymptomatic AF can be catastrophic—an embolic complication or acute decompensation of heart failure.¹⁰²

AF is associated with two- to three-times higher risk of cognitive decline and all forms of dementia, including Alzheimer's disease, senile dementia, and vascular dementia. Potential mechanisms of dementia in AF patients include embolic or hemorrhagic strokes, altered cerebral blood flow in AF, and cerebral micro-bleeds from anticoagulation, oxidative stress, and proinflammatory or prothrombotic status.⁵⁵

In some patients, paroxysmal AF can be classified as either *vagal* or *adrenergic*, depending on the types of triggers and the temporal distribution of the arrhythmic episodes. Vagal AF typically occurs in young male patients without structural heart disease and characteristically develops during sleep or postprandial. In contrast, patients with adrenergic AF are usually older, often with evidence of underlying heart disease, and AF episodes usually occur during the day and are associated with physical or emotional stress. In patients with paroxysmal AF, the prevalence of vagal AF probably ranges between 6% and 25%, whereas that of adrenergic AF ranges between 7% and 16%. Pure adrenergic

and vagotonic forms of paroxysmal AF are uncommon. Approximately 12% of patients with paroxysmal AF exhibit features of mixed vagal and adrenergic patterns.

It is important to note that many patients with AF do not complain of palpitations and present primarily with occult cardiac symptoms, such as fatigue and effort intolerance. Such complaints should not be dismissed as “unrelated,” and those patients should not be labeled “asymptomatic.” On the other hand, many patients with persistent or permanent AF have one or more comorbid conditions (such as sleep apnea, heart failure, pulmonary disease) that can considerably contribute to specific complaints and to overall quality of life. Therefore it is imperative to establish a correlation between any symptoms and AF, as well as ventricular response rates. The effect of regulation of ventricular rate during persistent AF or conversion to NSR on a patient’s symptoms and quality of life can help assess the relative contribution of AF to the patient’s complaints. This is particularly important when the impact of AF on patient’s symptoms and quality of life is being considered as the indication for therapeutic interventions (such as ablation).

Atrial Fibrillation Symptom Scales

The Canadian Cardiovascular Society Severity in Atrial Fibrillation (CCS-SAF) scale (Table 15.3) and the modified European Heart Rhythm Association (EHRA) symptom scale (Table 15.4) have been developed to describe symptom severity and assess the functional consequences of symptoms in AF patients (analogous to the New York Heart Association [NYHA] congestive heart failure functional class and the CCS angina severity class). These scales can provide objective assessment of the patient’s subjective state, help guide symptom-orientated treatment decisions, and facilitate longitudinal patient profiling.

Silent Atrial Fibrillation

Asymptomatic, or silent, AF occurs frequently; approximately one-third of patients with AF and up to 65% of AF episodes have been shown to be asymptomatic. Furthermore, a poor correlation between symptoms and AF has been demonstrated, and perception of AF patients of their prevailing rhythm is often inaccurate. Continuous monitoring with a pacemaker with dedicated functions for AF detection showed that as many as 40% of patients experienced AF-like symptoms in the absence of AF, whereas 38% of patients with a history of AF had episodes of AF lasting more than 48 hours noted at the time of interrogation even though these patients were asymptomatic. Therefore the lack of symptoms should not be equated with the absence of AF, even in patients previously presented with symptomatic episodes of AF.^{100,101}

In individuals with no prior history of AF, silent AF can be noticed incidentally on routine physical examination or preoperative assessment, during active electrocardiographic screening in at-risk populations (e.g., patients with ischemic strokes), or in patients with cardiac implantable electronic devices (pacemakers, defibrillators, loop recorders). Furthermore, AF can be detected by new technologies, such as smartphone cases with ECG electrodes, smart watches, and blood pressure machines with AF detection algorithms. Occasionally, AF is discovered only after a complication attributable to AF (e.g., stroke or congestive heart failure). Up to 30% of patients presenting with cryptogenic strokes are found to have AF that was not previously recognized.^{55,103,104}

Asymptomatic AF, especially when paroxysmal, is often missed. It is estimated that 10% to 27% of all patients with AF remain undiagnosed due to the lack of symptoms. In the United States, the prevalence of undiagnosed AF is about 1% to 2% in the general population. Importantly, clinically silent AF is similar to symptomatic AF in terms of overall risks of death, cardiovascular death, or thromboembolic events.

TABLE 15.3 Canadian Cardiovascular Society Severity of Atrial Fibrillation Scale

Step 1: Symptoms

- Identify the presence of the following symptoms:
- Palpitation
- Dyspnea
- Dizziness, presyncope, or syncope
- Chest pain
- Weakness or fatigue

Step 2: Association

Is AF, when present, associated with the foregoing symptoms? For example: Ascertain whether any of the foregoing symptoms are present during AF and are likely caused by AF (as opposed to some other cause).

Step 3: Functionality

Determine whether the symptoms associated with AF (or the treatment of AF) affect the patient’s functionality (subjective QOL).

CCS-SAF Class Definitions

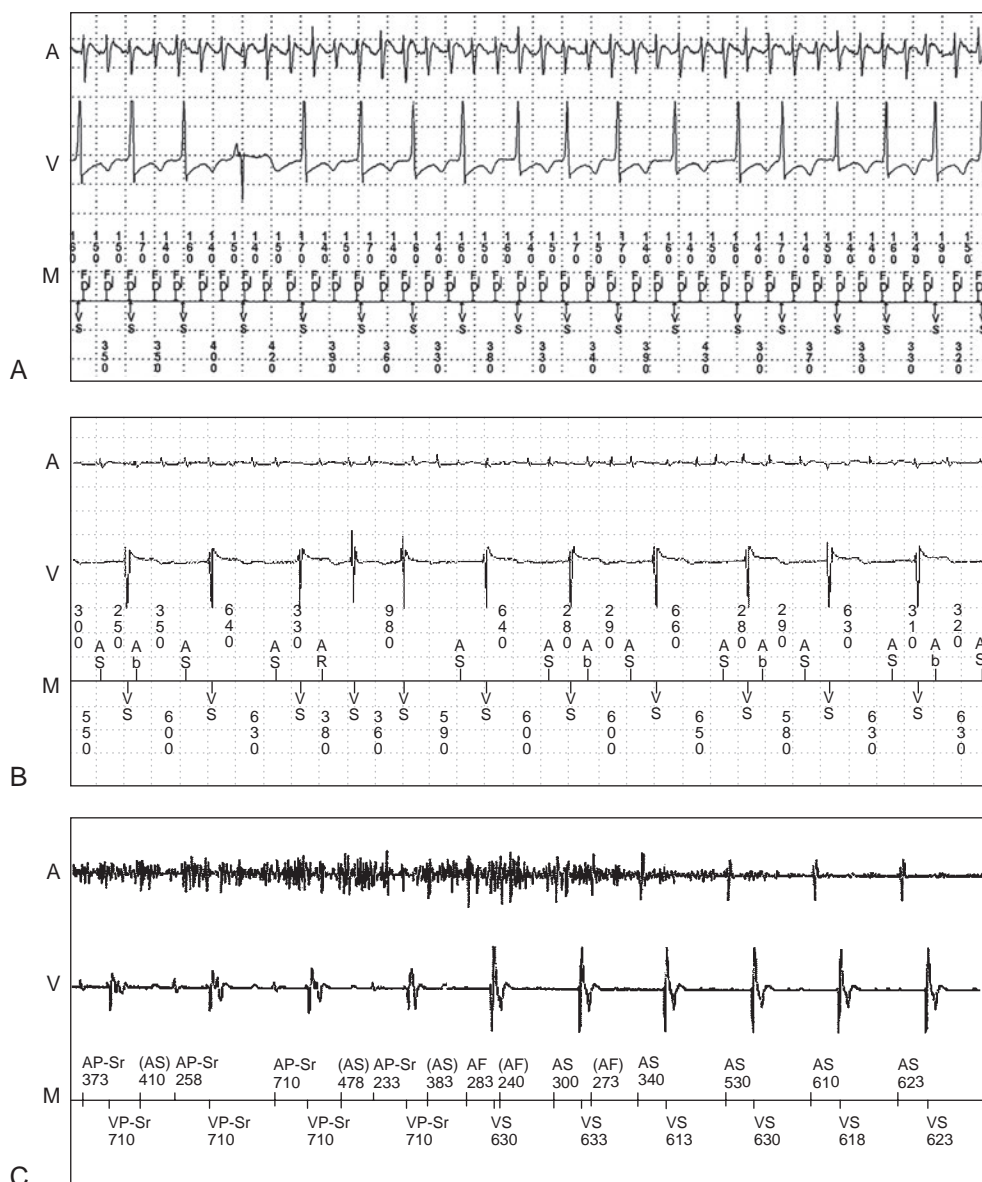
- | | |
|---------|--|
| Class 0 | Asymptomatic with respect to AF |
| Class 1 | Symptoms attributable to AF have minimal effect on patient’s general QOL <ul style="list-style-type: none"> • Minimal and/or infrequent symptoms, or • Single episode of AF without syncope or heart failure |
| Class 2 | Symptoms attributable to AF have minor effect on patient’s general QOL <ul style="list-style-type: none"> • Mild awareness of symptoms in patients with persistent or permanent AF, or • Rare episodes (e.g., less than a few per year) in patients with paroxysmal or intermittent AF |
| Class 3 | Symptoms attributable to AF have a moderate effect on patient’s general QOL <ul style="list-style-type: none"> • Moderate awareness of symptoms on most days in patient with persistent or permanent AF, or • More common episodes (e.g., more than every few months) or more severe symptoms, or both, in patients with paroxysmal or intermittent AF |
| Class 4 | Symptoms attributable to AF have a severe effect on patient’s general QOL <ul style="list-style-type: none"> • Very unpleasant symptoms in patients with persistent or paroxysmal AF and/or • Frequent and highly symptomatic episodes in patients with paroxysmal or intermittent AF, and/or • Syncope thought to result from AF, and/or • Congestive heart failure secondary to AF |

AF, Atrial fibrillation; CCS, Canadian Cardiovascular Society; QOL, quality of life; SAF, severity of atrial fibrillation.

From Dorian P, Guerra PG, Kerr CR, et al. Validation of a new simple scale to measure symptoms in atrial fibrillation: the Canadian Cardiovascular Society Severity in Atrial Fibrillation (CCS-SAF) scale. *Circ Arrhythm Electrophysiol*. 2009;2:268–275.

Device-Detected Atrial Fibrillation

Implanted pacemakers or defibrillators with atrial leads are capable of continuously monitoring the heart rhythm and detection of high atrial rates, providing a unique opportunity to identify the occurrence and burden of AF and correlating those episodes to patient’s symptoms (eFig. 15.4). The incidence of device-detected atrial high rate episodes varies depending on patient population, programmed device parameters



eFig. 15.4 Cardiac Device-Detected Atrial High Rate Episodes. Pacemaker interrogation strips from three different patients with dual-chamber pacemakers. (A) AF is present on the atrial (A) channel and correctly annotated on the marker (M) channel, with an atrial cycle length ranging between 140 and 190 milliseconds. Rapid and irregular ventricular response is observed on the ventricular (V) channel. (B) AF is present on the atrial channel, and the ventricular channel shows a well-controlled, irregular rhythm. On the marker channel, many of the low-amplitude atrial signals are under-sensed, leading to failure to detect atrial arrhythmias. (C) Sinus rhythm is present, but intermittent noise (high-frequency signals observed in the initial two-thirds of the recording) on the atrial channel is erroneously annotated on the marker channel as atrial activity, leading to inappropriate detection of atrial arrhythmias. AP, Atrial paced; AR, atrial-sensed event in the refractory period; AS, atrial sensed; FD, fibrillation detection; VP, ventricular paced; VS, ventricular sensed.

TABLE 15.4 The Modified European Heart Rhythm Association Symptom Scale

Modified EHRA Score	Symptoms	Description
1	None	AF does not cause any symptoms
2a	Mild	Normal daily activity not affected by symptoms related to AF
2b	Moderate	Normal daily activity not affected by symptoms related to AF, but patient troubled by symptoms ^a
3	Severe	Normal daily activity affected by symptoms related to AF
4	Disabling	Normal daily activity discontinued

^aEHRA class 2a and 2b can be differentiated by evaluating whether patients are functionally affected by their AF symptoms. AF-related symptoms are most commonly fatigue/tiredness and exertional shortness of breath, or less frequently palpitations and chest pain. AF, Atrial fibrillation; EHRA, European Heart Rhythm Association. From Kirchhof P, Benussi S, Kotecha D, et al. 2016 ESC guidelines for the management of atrial fibrillation developed in collaboration with EACTS. *Eur Heart J*. 2016;37:2893–2962.

(atrial rate and duration detection thresholds), and length of follow-up duration. In patients without prior history of AF, silent AF (as indicated by device-detected atrial high-rate episodes) is observed in nearly 30% of dual-chamber pacemaker recipients and 25% of cardiac resynchronization device recipients.^{103,105–107}

Accuracy of Device-Detected Atrial Fibrillation

Atrial high-rate episodes have been used as a surrogate for AF, and several studies have documented positive correlation between device-identified atrial high-rate episodes and ECG-documented episodes of AF or AFL with a high degree of sensitivity and specificity. However, different trials used different definitions of an atrial high-rate event (i.e., different programmed detection parameters of atrial rate and duration), and a clear consensus definition is still lacking. Nonetheless, employing an atrial rate cut-off of at least 220 beats/min (or greater than 250 beats/min for better specificity) sustained for durations exceeding 5 minutes provides good sensitivity and specificity for clinically confirmed AF (approaching 98% sensitivity and 100% specificity). Shorter cutoffs can lead to over-detection, commonly due to far-field R- and T-wave oversensing.¹⁰³

It is important to interpret device-stored data with caution. False-positive AF detection can result from oversensing (e.g., far-field R- and T-wave oversensing by the atrial lead, electrical interference, myopotentials, or repetitive nonreentrant ventriculoatrial synchrony) (see eFig. 15.4). On the other hand, under-detection of atrial activity is not uncommon due to the small amplitude of atrial electrograms during AF. In addition, atrial high-rate episodes are not specific for AF and can be triggered by AT and AFL. Inspection of device-stored electrograms (and not only marker channels) is important to verify the accuracy of the device diagnostics. However, because of the limited memory allocated for intracardiac electrograms, pacing devices may store only limited electrogram data to corroborate that the events labeled as atrial high-rate episodes or automatic mode switch events are indeed AF or AFL.^{106,107}

False-positive AF detection is also frequently encountered with implantable loop recorders with AF detection algorithms. False-positive detections are often caused by noise oversensing, frequent atrial or ventricular premature beats, T-wave oversensing, or sinus arrhythmia.

In one report, the accuracy of implantable loop recorders to detect true AF on a per patient basis was 96%; however, when the same analysis was performed on a per episode basis, then the overall accuracy of AF detection was only 48%.¹⁰⁷

Clinical Implications of Device-Detected Atrial Fibrillation

Several studies have clearly demonstrated that device-detected silent AFs are associated with increased risk of ischemic stroke and systemic embolism. The risk of thromboembolism appears to be related to the duration of AF episodes (or atrial high-rate episodes) as well as the patients' risk factor profile (CHA2DS2-VASc score).^{103,107}

The critical burden of atrial high-rate episodes beyond which thromboembolic risk is increased and that warrants therapeutic intervention remains to be defined. Several studies attempted to assess the burden of AF that is associated with adverse clinical outcomes, and AF burden thresholds ranging from 5 minutes to 24 hours were found in different reports to have clinical relevance. However, data are sparse on whether treatment with anticoagulation for subclinical device-detected atrial high-rate episodes reduces the risk of stroke to a similar degree as it does in clinical AF. In addition, current clinical practice guidelines for the treatment of device-detected atrial high-rate episodes are lacking. Based on current evidence, it seems appropriate to consider long-term oral anticoagulation for stroke prevention in high-risk patients with atrial high-rate episodes lasting longer than 5 to 6 minutes, when false-positive AF detections are excluded.^{103,106,107}

Of note, while device-detected silent AF is known to increase stroke risk, there does not seem to be a proximate temporal relationship between device-detected atrial high-rate episodes and the occurrence of strokes. In fact, in the majority of patients of a study population, no AF was detected on device recordings in the 30 days preceding the thromboembolic events. Although these data imply that the mechanism of stroke may not be related solely to the AF episodes, the association between the observation of atrial high-rate episodes and increased risk of stroke has been consistent, and silent AF is viewed as the culprit in cryptogenic stroke in these patients.¹⁰⁸ However, the value of continuous device-detected atrial arrhythmia information to guide therapeutic intervention for stroke prevention remains to be determined. A recent study suggested that a strategy of urgent initiation of anticoagulation based on device-detected AF did not improve outcomes, likely because of temporal dissociation between AF and stroke. Furthermore, withdrawal of anticoagulation in AF patients after arrhythmia-free periods on device interrogation was associated with worse outcome, implying that the decision on long-term anticoagulation in patients with AF should be based on more comprehensive, individualized assessment of risk and benefit rather than temporal incidence of arrhythmias detected by cardiac devices.¹⁰⁹

RISK OF THROMBOEMBOLISM

AF is a major risk factor for thromboembolism, causing approximately 15% of the ischemic strokes in the United States, 36% of strokes in patients older than 80 years, and up to 20% of cryptogenic strokes. Moreover, cardioembolic strokes caused by AF are large and multiple, often involve bilateral infarcts, and are associated with the highest rates of mortality and permanent disability. Specifically, patients with AF-related stroke show a 50% likelihood of death within 1 year, compared with 27% for strokes not related to AF.^{1,59}

In the FHS, patients with rheumatic heart disease and AF had a 17-fold increased risk of stroke compared with age-matched controls. For nonvalvular AF, the risk of stroke is estimated to be two to seven times that of subjects without arrhythmia, thus resulting in an average incidence of stroke of 5% per year. This rate may increase to 7% per

year when silent cerebral ischemic events and transient ischemic attacks are taken into account.

Although patients with AF in the setting of rheumatic valvular disease are expected to be at high risk of stroke, the stroke risk in nonvalvular AF is not homogeneous across the various subgroups of patients. The risk ranges from less than 1.5% per year in otherwise healthy AF patients who are less than 59 years old to more than 10% per year in older patients, especially when AF is associated with specific conditions or comorbidities. Prior history of stroke, transient ischemic attack, or thromboembolism, age, gender, ethnicity, hypertension, diabetes, coronary artery disease, peripheral artery disease, cardiomyopathy, and heart failure are important risk factors.¹¹⁰

Previous systematic reviews have not identified AF pattern (paroxysmal, persistent, or permanent) as an important prognostic risk factor for thromboembolism. In fact, AF stroke risk prediction models have in general not included AF type, and current clinical guidelines recommend that decisions regarding oral anticoagulation be made independently of AF pattern. However, recent data suggest that persistent and permanent AF is associated with an almost twofold higher rate of stroke or systemic embolism than paroxysmal AF after adjustment for other independent predictors.^{1,111–113}

In addition, a range of biomarkers have been identified as potential predictors of thromboembolic events in AF patients. These include markers of thrombosis (von Willebrand factor, D-dimer), myocardial necrosis (troponin), renal function (creatinine clearance, proteinuria), and the natriuretic peptides (N-terminal pro-B-type natriuretic peptide [NT-proBNP], BNP).

Severe findings on transesophageal echocardiography (TEE) have been identified as independent predictors of stroke and thromboembolism, including the presence of an LA thrombus (relative risk, 2.5), complex aortic plaques (relative risk, 2.1), spontaneous echo contrast (relative risk, 3.7), and low LAA velocities (up to 20 cm/s; relative risk, 1.7). Limited data suggest that large LAA dimensions on CMR may predict a higher risk of thromboembolism.

Stroke Risk Stratification

Several prominent risk stratification schemes have been developed to help distinguish patients with AF who are at high risk of ischemic stroke and other systemic thromboembolism from those with a risk sufficiently low that anticoagulation may not be beneficial when considering the associated bleeding risks.

The CHADS₂ index, named for a combination of clinical risk factors (Table 15.5), was the first risk stratification scheme to gain widespread acceptance due to its relative ease of use. The CHADS₂ system stratifies patients into low- (CHADS₂ score of 0), moderate- (score of 1 to 2), and high-risk (score of 3 to 6) categories. The stroke rate per 100 patient-years without antithrombotic therapy increases by a factor of approximately 1.5 for each one-point increase in the CHADS₂ score: from

1.9% for a score of 0 to 18.2% for a score of 6. A major limitation of the CHADS₂ scheme is the inadequate discrimination of risk. In fact, a large proportion (more than 60%) of patients are classified as having intermediate risk. Furthermore, this risk scheme is not adequately sensitive in identifying AF patients who are truly at low risk; many patients with AF categorized as low-risk by the CHADS₂ score still have stroke rates exceeding 1% per year.

Some of the limitations of the CHADS₂ scheme have been addressed by the newer CHA₂DS₂-VASc scoring system, which incorporates all components of the CHADS₂ system but with greater emphasis on age and includes two additional factors: female sex and vascular disease (Table 15.6). The CHA₂DS₂-VASc score has the major advantage of discriminating risk probability in lower risk patients and has been shown in multiple cohorts to be the best for identifying truly low-risk patients, even in those with a CHADS₂ score of 0 (Table 15.7). A low-risk score is defined as a CHA₂DS₂-VASc score of 0, an intermediate risk is defined as a score of 1, whereas a high-risk CHA₂DS₂-VASc score is defined by a score of 2 or greater.^{1,114}

The R2CHADS₂ risk model has emerged from an analysis of the ROCKET-AF (Rivaroxaban Once Daily Oral Direct Factor Xa Inhibition Compared with Vitamin K Antagonism for Prevention of Stroke and Embolism Trial in Atrial Fibrillation) population and was validated in an ATRIA (Anticoagulation and Risk Factors in Atrial Fibrillation) population. In addition to incorporating the same components of the CHADS₂ score, the R2CHADS₂ scheme awards 2 points for renal dysfunction.¹¹⁵

The ATRIA score contains elements of R2CHADS₂ but importantly gives different scores for age ranges that vary according to whether the patient had also suffered a stroke or transient ischemic attack (Table 15.8). In one report, the ATRIA score outperformed CHADS₂ and CHA₂DS₂-VASc risk scores largely because its use resulted in an appropriate downward classification (toward no risk).¹¹⁶

The ABC (age, biomarkers, clinical history) stroke risk score incorporates two biomarkers (NT-proBNP and high sensitivity cardiac troponin) and two clinical risk predictors (age and prior stroke) (Fig. 15.7).¹¹⁷

It is important to note that all current risk scores for the prediction of ischemic stroke in AF perform modestly. The ACC/AHA/HRS and ESC guidelines recommend the CHA₂DS₂-VASc score for stroke risk stratification in AF.¹¹⁶

Importantly, stroke risk assessment schemes have been established for patients with “nonvalvular” AF. Patients with mechanical valves require anticoagulation with vitamin K antagonists irrespective of the presence of AF. Also, AF patients with mitral stenosis are at a particularly

TABLE 15.5 CHADS₂ Scoring System for Predicting Stroke and Thromboembolism in Atrial Fibrillation

Letter	Clinical Characteristic	Points
C	Congestive heart failure	1
H	Hypertension	1
A	Age ≥75 years	1
D	Diabetes mellitus	1
S2	Stroke, transient ischemic attack, or thromboembolism	2
Maximum points		6

TABLE 15.6 CHA₂DS₂-VASc Scoring System for Predicting Stroke and Thromboembolism in Atrial Fibrillation

Letter	Clinical Characteristic	Points
C	Congestive heart failure or left ventricular dysfunction	1
H	Hypertension	1
A2	Age ≥75 years	2
D	Diabetes mellitus	1
S2	Stroke, transient ischemic attack, or thromboembolism	2
V	Vascular disease (prior myocardial infarction, peripheral artery disease, or aortic plaque)	1
A	Age 65–74 years	1
S	Sex category (i.e., female gender)	1
Maximum points		9

TABLE 15.7 Stroke or Other Thromboembolism Events Based on the CHA2DS2-VASc Scoring System

CHA2DS2-VASc Score	COHORT OF PATIENTS ON ANTICOAGULATION		COHORT OF PATIENTS OFF ANTICOAGULATION	
	Patients (n = 7239)	Adjusted Stroke Rate ^a (%/year)	Patients (n = 1084)	Adjusted Stroke Rate ^b (%/year)
0	1	0	103	0
1	422	1.3	162	0.7
2	1230	2.2	184	1.9
3	1730	3.2	203	4.7
4	1718	4.0	208	2.3
5	1159	6.7	95	3.9
6	679	9.8	57	4.5
7	294	9.6	25	10.1
8	82	6.7	9	14.2
9	14	15.2	1	100

^aTheoretical thromboembolism rates without anticoagulation therapy: assuming that warfarin provides a 64% reduction in thromboembolic risk. Data from Lip GY, Frison L, Halperin JL, Lane DA. Identifying patients at risk of stroke despite anticoagulation. *Stroke*. 2010;41:2731–2738.

^bTheoretical thromboembolism rates without antiplatelet therapy: assuming that aspirin provides a 22% reduction in thromboembolic risk.

CHA2DS2-VASc, updated version of the CHADS2 (congestive heart failure, hypertension, age, diabetes, and stroke [doubled]) system, with additional risk factors.

Data from Lip GY, Nieuwlaet R, Pisters R, et al. Refining clinical risk stratification for predicting stroke and thromboembolism in atrial fibrillation using a novel risk factor-based approach. *Chest*. 2010;137:263–272.

TABLE 15.8 Anticoagulation and Risk Factors in Atrial Fibrillation Stroke Risk Score

Risk Factor	Points Without Prior Stroke	Points With Prior Stroke
Age, years		
≥85	6	9
75–84	5	7
65–74	3	7
<65	0	8
Female	1	1
Diabetes mellitus	1	1
CHF	1	1
Hypertension	1	1
Proteinuria	1	1
eGFR <45 or ESRD	1	1

CHF, Congestive heart failure; eGFR, estimated glomerular filtration rate; ESRD, end-stage renal disease.

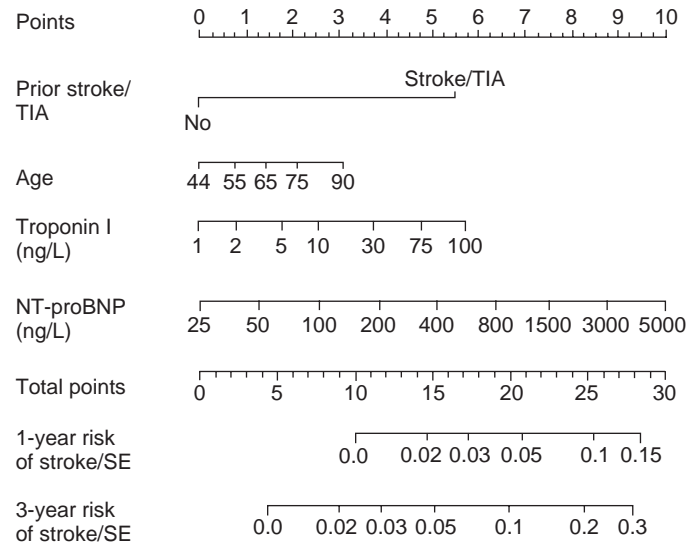


Fig. 15.7 The ABC (Age, Biomarkers, Clinical History) Stroke Risk Score. Nomogram for the ABC risk score. For each predictor, read the points assigned on the 0–10 scale at the top and then sum these points. Find the number on the “Total Points” scale and then read the corresponding predictions of 1- and 3-year risk of stroke or systemic embolism below it. Continuous variables are represented from the 1st to the 99th percentiles. The prediction model is preferably used as a web-based calculator or app. NT-proBNP, N-terminal pro-B-type natriuretic peptide; SE, systemic embolism; TIA, transient ischemic attack. (From Hijazi Z, Lindbäck J, Alexander JH, et al. The ABC (age, biomarkers, clinical history) stroke risk score: a biomarker-based risk score for predicting stroke in atrial fibrillation. *Eur Heart J*. 2016;37(20):1582–1590.)

high risk for systemic thromboembolism and have been excluded from any further trials studying anticoagulation regimens for AF. The 2014 AHA/ACC/HRS guidelines also include patients bioprosthetic heart valves or mitral valve repair in the definition of “valvular” AF.

On the other hand, stroke risk stratification using the above risk schemes appears to be adequate to guide treatment decisions regarding prophylactic anticoagulation therapy in patients with “nonvalvular” AF who have left valvular disease not included in the definition of “valvular” AF (e.g., nonrheumatic mitral regurgitation or aortic valve disease).^{3,4} In a recent report, left valvular disease was present in 22% of all non-valvular AF patients, and although the embolic risk is higher in these patients compared with those without valve disease, neither the valve disease per se nor its severity was clearly associated with this risk, and a higher CHA2DS2-VASc score in these patients was likely to explain these results.

Bleeding Risk Stratification

Oral anticoagulation is associated with increased risk of bleeding. It is estimated that up to 44% of patients with AF have one or more absolute or relative contraindications for long-term oral anticoagulation therapy, most commonly related to increased risk of bleeding. Therefore an assessment of bleeding risk should be part of the patient assessment before starting anticoagulation. The risk of bleeding should be weighed against the potential benefit of stroke prevention in individual patients considered for anticoagulation therapy.

Several risk models have been proposed to predict bleeding risk on antithrombotic therapy. Only the HAS-BLED (Table 15.9), HEMORR2HAGES (Table 15.10), ATRIA (Table 15.11), and ORBIT scores (Table 15.12) have been derived or validated in AF populations.¹¹⁸

TABLE 15.9 Clinical Characteristics Comprising the HAS-BLED Bleeding Risk Score

Letter	Clinical Characteristic	Points
H	Hypertension ^a	1
A	Abnormal liver or renal function	1 or 2
S	Stroke	1
B	Bleeding	1
L	Labile INR	1
E	Elderly (age >65)	1
D	Drugs or alcohol	1 or 2
Maximum score		9

^aHypertension is defined as systolic blood pressure >160 mm Hg. Abnormal kidney function is defined as the presence of long-term dialysis or renal transplantation or serum creatinine concentration of at least 200 μ mol/L. Abnormal liver function is defined as chronic hepatic disease (e.g., cirrhosis) or biochemical evidence of significant hepatic derangement (e.g., bilirubin more than twice the upper limit of normal, in association with aspartate aminotransferase, alanine aminotransferase, and alkaline phosphatase more than three times the upper limit of normal). Bleeding refers to previous bleeding history or predisposition to bleeding, or both (e.g., bleeding diathesis, anemia). Labile INRs refers to unstable or high INRs or poor time in therapeutic range (e.g., <60%). Drugs or alcohol use refers to concomitant use of drugs (e.g., antiplatelet agents, nonsteroidal antiinflammatory drugs, or alcohol abuse). INR, International normalized ratio.

TABLE 15.10 HEMORR2HAGES Bleeding Risk Score

Letter	Clinical Characteristic	Points
H	Hepatic or renal disease	1
E	Ethanol abuse	1
M	Malignancy	1
O	Older age	1
R	Reduced platelet count or function	1
R	Rebleeding risk	2
H	Hypertension	1
A	Anemia	1
G	Genetic factors	1
E	Excessive fall risk	1
S	Stroke	1
Maximum score		12

TABLE 15.11 Anticoagulation and Risk Factors in Atrial Fibrillation Bleeding Risk Score

Clinical Characteristic	Points
Anemia	3
Severe renal disease	3
Age \geq 75 years	2
Prior bleeding	1
Hypertension	1
Maximum score	10

TABLE 15.12 ORBIT Bleeding Risk Score

Letter	Clinical Characteristic	Points
O	Older age (\geq 75 years old)	1
R	Reduced hemoglobin, reduced hematocrit, or anemia	2
B	Bleeding history	2
I	Insufficient kidney function (eGFR <60 mg/dL per 1.73 m ²)	1
T	Treatment with antiplatelets	1
Maximum score		7

eGFR, Estimated glomerular filtration rate.

In a study evaluating three bleeding risk scores (HAS-BLED, HEMORR2HAGES, and ATRIA), all three tested risk schemes demonstrated only modest performance in predicting the outcome of any clinically relevant bleeding, although the HAS-BLED score performed better than the HEMORR2HAGES and ATRIA scores; only HAS-BLED demonstrated a significant predictive performance for intracranial hemorrhage. Given its simplicity, the HAS-BLED score may be an attractive method for the estimation of oral anticoagulant-related bleeding risk for use in clinical practice, as recommended by the ESC guidelines. Patients are categorized as low, intermediate, and high bleeding risk according to HAS-BLED scores 0 to 1, 2, and 3 or higher, respectively. A score higher than 2 suggests a risk of major bleeding of 1.9% per year, whereas a score of 5 is associated with a risk of major bleeding of up to 12.5% per year.

It is important to understand that bleeding risk assessment is not a static phenomenon, and many common clinical factors that increase bleeding risk are potentially reversible. Further, a high bleeding risk score is not a reason to withhold anticoagulation therapy as such patients can potentially derive even greater net clinical benefit while on oral anticoagulation therapy. Instead, a high score should prompt careful review and follow-up as well as aggressive efforts at amelioration of potentially reversible bleeding risk factors (e.g., uncontrolled hypertension, labile international normalized ratios [INRs], balance problems, concomitant use of antiplatelet agents, alcohol excess, anemia, and renal or hepatic insufficiency).

INITIAL EVALUATION

The initial evaluation of a patient with suspected or documented AF includes characterizing the pattern of the arrhythmia (e.g., paroxysmal or persistent), determining underlying causes (e.g., heart failure, pulmonary problems, hypertension, hyperthyroidism), defining associated cardiac and extracardiac conditions, and identifying potential complications of AF. In addition, a thorough history should be obtained to estimate of the risk of stroke (using the CHA2DS2-VASc scheme), bleeding risk, and quantify AF-related symptoms (e.g., CCS-SAF and modified EHRA scores). A careful history results in a well-planned focused work-up that serves as an effective guide to therapy.

The physical examination can suggest AF based on irregular pulse, irregular jugular venous pulsations, and variation in the intensity of the first heart sound. Examination can also disclose associated valvular heart disease, myocardial abnormalities, or heart failure.

Diagnostic Cardiac Testing

Ambulatory cardiac monitoring can be required for documentation of AF, its relation to symptoms, and evaluation of the adequacy of heart rate control. Transthoracic echocardiography is performed to evaluate

for structural heart disease, assess cardiac function, and evaluate atrial size. Exercise testing is often used to assess the adequacy of rate control with exercise in permanent AF, to reproduce exercise-induced AF, and to evaluate for associated ischemic heart disease. Although ischemia per se does not appear to be a common cause of AF, identifying underlying coronary artery disease (in patients with risk factors) is particularly important if the use of a class IC antiarrhythmic drug is being considered.^{1,4,102}

Laboratory Testing

Laboratory evaluation includes assessment of serum electrolytes, renal, and hepatic function, and a blood count. Assessment for thyrotoxicosis is indicated for all patients with a first episode of AF, when the ventricular response to AF is difficult to control, or when AF recurs unexpectedly after cardioversion. Serum should be obtained for measurement of TSH and free thyroxine (T₄), even if there are no other symptoms suggestive of hyperthyroidism, because the risk of AF is increased even in patients with subclinical hyperthyroidism.⁴

Of note, plasma levels of B-type natriuretic peptide or N-terminal pro-B-type natriuretic peptide can be elevated in patients with paroxysmal and persistent AF in the absence of clinical heart failure, and levels decrease rapidly after restoration of sinus rhythm.⁴

Electrophysiological Testing

Rarely, EP testing can be required, especially in patients with wide QRS complex tachycardia or a possible predisposing arrhythmia, such as AFL or paroxysmal SVT. Clues to the presence of paroxysmal SVT include a history of episodes of regular rapid palpitations dating from teenage or early adult years (unusual for AF to occur de novo in this age group) and termination of episodes of palpitations with vagal maneuvers or adenosine (which should not occur with AF).

Other Diagnostic Tests

Other diagnostics as guided by clinical presentation may include chest radiography, pulmonary function tests, and sleep study.

Screening for Atrial Fibrillation

AF is an important cause of embolic stroke, and subclinical (silent) AF should be considered in all survivors of an ischemic stroke, especially those of undetermined source (i.e., cryptogenic stroke). Studies have demonstrated that AF can be detected on ambulatory cardiac monitoring in more than 6% of unselected stroke patients and in up to 30% of those with cryptogenic stroke, with the latter accounting for approximately one-third of all ischemic strokes. In a recent meta-analysis, the overall proportion of newly detected AF was 7.4%, but varied widely depending on the timing, duration, and method of cardiac monitoring. Extending continuous electrocardiographic monitoring from 24 hours to 30 and 180 days increased the detection of AF from 4.2% to 15.2% and 29.2%, respectively. Hence, long-term (greater than or equal to 30 days) continuous ECG monitoring (noninvasive or using an implantable loop recorder) is recommended after cryptogenic stroke, and probably is also reasonable in all survivors of an ischemic stroke, even when another competing cause for stroke has been identified clinically (e.g., hypertension or carotid artery stenosis).^{55,59,119}

Opportunistic screening for silent AF (pulse palpation during a general practitioner consultation for any reason, followed by an ECG if the pulse was irregular) may also be considered in at-risk populations (e.g., individuals older than 65 years and patients with heart failure).^{55,120}

Furthermore, patients with pacemakers or defibrillators should be followed periodically and their devices interrogated on a regular basis for any evidence of AF, as suggested by automatic mode switch or atrial high-rate episodes. Wireless remote monitoring with predefined auto-

matic alerts helps reduce the time to a clinical decision in response to the alert, compared with standard in-office follow-up.¹⁰⁶

PRINCIPLES OF MANAGEMENT

Management of AF should be aimed at identifying and treating underlying causes of the arrhythmia, as well as reducing symptoms, improving quality of life, and preventing cardiovascular morbidity and mortality associated with AF. There are four main issues that must be addressed in the treatment of AF: (1) prevention of systemic embolization; (2) ventricular rate control; (3) restoration and maintenance of NSR; and (4) risk factor modification.¹

The choice of therapy is influenced by patient preference, associated structural heart disease, severity of symptoms, and whether the AF is recurrent paroxysmal, recurrent persistent, or permanent. In addition, patient education is critical, given the potential morbidity associated with AF and its treatment. For control of symptoms, a safety-driven approach is of paramount importance because most treatments (drug, surgery, ablation) have the capacity to produce significant morbidity and even mortality.

Prevention of Systemic Embolization

Antithrombotic Drug Therapy

Antiplatelet therapy. Aspirin is associated with only modest (22%) reduction in the incidence of stroke, corresponding to an absolute stroke risk reduction of 1.5% per year as compared with placebo. Thus except in the lowest risk patients, aspirin alone is not a viable treatment option for stroke prevention. The combination of aspirin plus clopidogrel is superior to aspirin therapy alone (28% relative risk reduction), but it is associated with a significantly increased risk of major bleeding (2.0% vs. 1.3% per year) to levels generally similar to those associated with warfarin therapy.

Vitamin K antagonists. Vitamin K antagonists (warfarin) reduce stroke risk by approximately 64%, corresponding to an absolute annual strokes risk reduction of 2.7% as compared with placebo. Warfarin is superior to aspirin, with relative risk reduction of 39% for stroke and 29% for cardiovascular events. However, warfarin increases the risk of major bleeding by approximately 70% compared with aspirin. Although the risk of intracranial hemorrhage is doubled with adjusted-dose warfarin compared with aspirin, the absolute risk increase appears to be small (0.2% per year). In addition, randomized clinical trials have shown that warfarin is superior to the combination of aspirin plus clopidogrel for prevention of vascular events in patients with AF at high risk of stroke (relative risk reduction of 40%), with similar risks for major bleeding events. Combinations of warfarin (INR, 2.0 to 3.0) with antiplatelet therapy offer no incremental benefit in stroke risk reduction while they increase the risk of bleeding.

The reduction in ischemic stroke with warfarin in patients with paroxysmal AF is probably similar to that in patients with persistent or permanent AF. The benefit of warfarin is greatest for patients at higher risk of stroke, and there appears to be little benefit for those with no risk factors. The true efficacy of warfarin is likely to be even higher than suggested by trial results because many of the strokes in the warfarin-treated groups occurred in patients who were noncompliant at the time of the stroke.

The estimated annual incidence of bleeding associated with warfarin therapy is 0.6% for fatal bleeding, 3.0% for major bleeding, and 9.6% for major or minor bleeding. The risk of bleeding appears to be especially high during the first year of treatment. The addition of aspirin to warfarin further increases the rate of bleeding with a threefold increase in the rates of intracranial hemorrhage. Notably, the risk of major bleeding in older patients (greater than 80 years) receiving warfarin

therapy, although higher than younger patients, is acceptably low (2.5% per year), and these patients can still benefit from warfarin prophylaxis when a good quality of anticoagulation is obtained. The risk of falling and intracranial bleeding should be considered but not overstated.

An INR between 2.0 and 3.0 is recommended for most patients with AF who receive warfarin therapy. The risk of stroke doubles when the INR falls to 1.7, and values up to 3.5 do not confer an increased risk of bleeding complications. A higher goal (INR between 2.5 and 3.5) is reasonable for patients at particularly high risk for embolization (e.g., prior thromboembolism, rheumatic heart disease, prosthetic heart valves). Similarly, in patients who sustain ischemic stroke or systemic embolism during treatment with therapeutic doses of warfarin (INR, 2.0 to 3.0), raising the intensity of anticoagulation to a higher INR range of 3.0 to 3.5 should be considered. This approach is probably preferable to adding an antiplatelet agent because an appreciable risk in major bleeding is seen with warfarin only when the INR is greater than 3.5 and is likely to be less than that associated with combination therapy.

Warfarin therapy is associated with several limitations that have dampened the enthusiasm of both patients and clinicians: a narrow therapeutic window that requires periodic INR monitoring and frequent dose adjustments, multiple drug and dietary interactions, genetic variability in response (accounting for 39% to 56% of the variability in the warfarin dose), long half-life (36 to 42 hours), and slow onset of action. In several trials, more than one-third of the patients refused warfarin therapy, largely because of the lifestyle changes required, the inconvenience of INR monitoring, and concern about bleeding risk. These issues have contributed to the underutilization of anticoagulation therapy in patients who can stand to derive benefit from it. In fact, it is estimated that less than 50% of eligible patients were treated with warfarin. Of those patients prescribed warfarin, there is ongoing attrition of its use to approximately 40% by 4 years.

Several series have highlighted the difficulties of maintaining the INR in the therapeutic range. More than one-third of patients taking warfarin are not maintained in the therapeutic range, thus exposing them to increased risk of either stroke (with subtherapeutic INRs) or bleeding (with supratherapeutic INRs). It has been found that if a patient's INR is not maintained in the therapeutic range at least 65% of the time, the advantage of taking warfarin over aspirin is nullified.

Non-vitamin K antagonist oral anticoagulants. There are two classes of non-vitamin K antagonist oral anticoagulants (NOACs): factor Xa inhibitors (such as rivaroxaban, apixaban, and edoxaban), and direct thrombin inhibitors (dabigatran). In general, NOACs are at least as effective as warfarin for the prevention of stroke and systemic thromboembolism in patients with nonvalvular AF and are much safer regarding the risk of intracranial hemorrhage compared to warfarin, with the annual rate ranging from 0.23% to 0.50%. However, limited data exist concerning the potential advantage of using NOACs in patients taking warfarin with optimal INR control (time in therapeutic range more than 75%).

NOACs have several potential advantages over warfarin, including their rapid onset of action, predictable therapeutic effect, less complex pharmacodynamics, limited dietary and drug interactions, and stable dose-related coagulation profile allowing for fixed dosing and obviating the need for routine monitoring. These advantages will likely promote greater use of anticoagulants, enhance patients' compliance, allow for routine therapy without monitoring, and possibly eliminate the need for anticoagulation with parenteral agents such as heparin ("bridge therapy"). However, warfarin will remain the mainstay of treatment for patients with "valvular" AF and those with mechanical heart valves.

In a meta-analysis of trials randomizing NOACs to warfarin, NOACs were associated with: (1) significantly reduced composite stroke or

systemic embolic events (19%), primarily driven by a reduction in hemorrhagic stroke; (2) a nonsignificant (14%) reduction in major bleeding, a reflection of decreased intracranial hemorrhage; and (3) a significant reduction in all-cause mortality. Major bleeding rates with these agents exceeded 2% to 3% per year, and minor bleeding rates were over 10% per year. In addition, by 2 years, 21% to 33% of patients discontinued the NOAC.

There are no direct head-to-head trials comparing the NOACs. In a meta-analysis using adjusted indirect comparisons, there was significant heterogeneity in results. Dabigatran lowered the composite of systemic emboli or stroke (vs. rivaroxaban), and apixaban lowered the risk of major gastrointestinal bleeding (vs. both rivaroxaban and dabigatran). Currently, there is no clear evidence to support a possible class-effect of a direct thrombin inhibitor or factor Xa inhibitors.¹²¹

Nonpharmacological Interventions

The LAA has been implicated as the source of emboli in approximately 90% of patients with nonvalvular AF. Therefore several approaches have targeted exclusion of the LAA from the systemic circulation to prevent systemic thromboembolism and obviate the need for long-term oral anticoagulation therapy in patients with nonvalvular AF. These approaches can be of value in many AF patients, given the fact that up to 44% of patients with AF have one or more absolute or relative contraindications for chronic oral anticoagulation therapy, most commonly related to increased risk of bleeding. Furthermore, the safety and efficacy of chronic anticoagulation therapy can be limited by medication compliance, costs, and interactions with food and other medications.¹²²

Three main techniques are being utilized to accomplish LAA exclusion: percutaneous endocardial, percutaneous epicardial, and surgical approaches. Device-based endocardial LAA exclusion, such as Watchman (Boston Scientific, Natick, MA, United States) and Amplatzer Cardiac Plug (St. Jude Medical, Minneapolis, MN, United States), result in mechanical occlusion of the LAA. LAA exclusion with the endo-epicardial system (Lariat, SentreHEART, Redwood City, CA, United States) and surgical epicardial ligation result in both mechanical and electrical isolation of the LAA as a result of LAA infarction. Currently, these techniques are in different stages of evaluation and clinical development.

The ESC recommends percutaneous LAA closure device (Watchman and Amplatzer) use in nonvalvular AF patients with high stroke risk and contraindications to long-term oral anticoagulation. The 2014 AHA/ACC/HRS currently only recommends surgical excision of the LAA in patients undergoing cardiac surgery.

Potential candidates for percutaneous LAA closure include AF patients at high stroke risk with high risk of bleeding under oral anticoagulation, those with ischemic stroke despite well-controlled oral anticoagulation therapy, high probability of therapeutic noncompliance to oral anticoagulation, and intolerance to oral anticoagulation therapy due to severe hepatic or renal dysfunction or drug interactions (Box 15.1). The procedure is contraindicated in patients at low stroke risk, those with valvular AF (e.g., mitral stenosis, mechanical cardiac valves), in the presence of other indications for long-term or lifelong oral anticoagulation therapy (e.g., venous thromboembolism, intracardiac clots), LAA thrombus, and contraindications for transseptal catheterization (Box 15.2).

It is important to note that, although LAA exclusion procedures have been increasingly used for patients with nonvalvular AF, these procedures should not be considered universally as a substitute for oral anticoagulation therapy. Many of the disadvantages of warfarin therapy can be addressed by using NOACs rather than LAA exclusion, especially given the paucity of data supporting such procedures as compared to the large, prospective, randomized studies indicating the efficacy and safety of NOACs.

BOX 15.1 Possible Indications for Percutaneous Left Atrial Appendage Closure in Patients With Nonvalvular Atrial Fibrillation

- High stroke risk in conjunction to high bleeding risk under oral anticoagulation
- Ischemic stroke despite well-controlled oral anticoagulation therapy
- High probability of therapeutic noncompliance to oral anticoagulation
- Intolerance to oral anticoagulation therapy due to severe hepatic or renal dysfunction or drug interactions

BOX 15.2 Contraindications for Percutaneous LAA Closure in Patients With Nonvalvular AF

- Low stroke risk
- Valvular AF
- Presence of other indications for long-term oral anticoagulation
- LAA thrombus
- Contraindications for transseptal catheterization

AF, Atrial fibrillation; LAA, left atrial appendage.

Recommendations for Long-Term Stroke Prevention

The cornerstone of management of patients with AF is adequate thromboprophylaxis. Essential to this is appropriate risk stratification and the need to balance the benefit of stroke prevention and the risk of bleeding with anticoagulant therapies (see above). Decision making for thromboprophylaxis by antithrombotic therapy must balance the risk of stroke against the risk of major bleeding, especially intracranial hemorrhage, which is associated with a high risk of death and disability.

Patients with valvular AF (those with mitral stenosis or valvular prosthesis) should be managed with oral anticoagulation. For nonvalvular AF, the CHA₂DS₂-VASc scoring system (see Tables 15.6 and 15.7) is currently the best validated and most clinically useful for risk stratification and is advocated by both European and United States guidelines. The initial decision step is to identify patients who are truly at low risk for ischemic stroke, in whom no antithrombotic therapy is recommended. These include patients without clinical stroke risk factors (i.e., CHA₂DS₂-VASc score of 0 in men or 1 in women); female gender does not appear to increase stroke risk in the absence of other stroke risk factors. On the other hand, oral anticoagulation therapy is recommended for patients of both sexes with CHA₂DS₂-VASc stroke risk score greater than or equal to 2. Those recommendations apply to all patients with AF irrespective of the type of AF (paroxysmal or nonparoxysmal).

There is uncertainty regarding the optimal antithrombotic therapy in low thromboembolic risk patients (i.e., CHA₂DS₂-VASc score of 1 in men or 2 in women). According to the 2014 AHA/ACC/HRS guidelines, no antithrombotic therapy or treatment with an oral anticoagulant or aspirin can be considered in these patients. On the other hand, recent studies, as well as ESC guidelines, support a positive advantage for stroke prevention with oral anticoagulation compared with no therapy or with aspirin in these patients. Furthermore, the use of NOACs may lower the threshold for initiating anticoagulation for AF patients, given the positive net clinical benefit of NOACs, even in patients with a CHA₂DS₂-VASc score of 1.

Importantly, treatment decisions should be individualized. Careful assessment of the risk of bleeding and patient preference is crucial. The

TABLE 15.13 SAME-TT2R2 score

Letter	Clinical Characteristic	Points
S	Sex (female)	1
A	Age (<60 years)	1
Me	Medical history ^a	1
T	Treatment strategy (rhythm control) ^b	1
T	Tobacco use (within 2 years)	2
R	Race (nonwhite)	2
Maximum points		8

^aTwo of the following: hypertension, diabetes mellitus, coronary disease or prior myocardial infarction, peripheral vascular disease, congestive heart disease, previous stroke, pulmonary disease and hepatic or renal disease.

^bInteracting drugs, e.g., amiodarone for rhythm control.

expected clinical benefit of anticoagulation therapy should be balanced against the bleeding risk and should be thoroughly discussed with the informed patient. For equivocal cases, considering other possible risk predictors and risk models beyond the CHA₂DS₂-VASc scheme (e.g., renal function, biomarkers, findings on TEE) can potentially provide additional prognostic information and help identify those patients at a truly low thromboembolic risk.¹²³

The choice of anticoagulation therapy (warfarin vs. NOACs) is usually influenced by patient's preference, comorbidities, renal function, cost, and drug interactions. The use of SAME-TT2R2 score (Table 15.13) can potentially identify those patients in whom warfarin therapy is more likely to be associated with labile INRs and, consequently, serious bleeding and thromboembolism (SAME-TT2R2 score greater than 2). In those patients, NOACs are expected to offer a particular advantage.

In high-risk patients who cannot be treated with oral anticoagulation because of poor tolerance or noncompliance issues or because of strong patient preference, dual antiplatelet therapy (aspirin plus clopidogrel) can be considered. However, dual antiplatelet therapy is not an alternative to oral anticoagulation in patients at high bleeding risk because the risk of major bleeding associated with dual antiplatelet therapy is generally similar to that with oral anticoagulation. In the latter group, aspirin monotherapy is associated with lesser bleeding risk, although at the expense of less protection from systemic thromboembolism. Percutaneous LAA exclusion procedures have become an important therapeutic alternative to long-term antithrombotic therapy in these patients.

Anticoagulation in the Pericardioversion Period

Patients without a contraindication to oral anticoagulation who have been in AF for more than 48 hours should receive 3 to 4 weeks of oral anticoagulation with warfarin or NOACs (with documented therapeutic INRs for those on warfarin) prior to and after cardioversion. This approach is also recommended for patients with AF who have valvular disease, evidence of LV dysfunction, recent thromboembolism, or AF of unknown duration.

The rationale for anticoagulation prior to cardioversion is based on observational studies showing that more than 85% of LA thrombi resolve after 4 weeks of anticoagulation therapy. Cardioversion-related clinical thromboembolic events have been reported in 5% to 7% of patients who did not receive anticoagulation before cardioversion (this risk appears to be much lower [less than 1%] for AF of less than 48-hour duration).

An alternative approach that eliminates the need for prolonged anticoagulation prior to cardioversion, particularly in low-risk patients

who would benefit from earlier cardioversion, is the use of TEE-guided cardioversion. Cardioversion is performed if TEE excludes the presence of intracardiac clots. Anticoagulation after cardioversion, however, is still necessary.

After cardioversion, it is recommended to continue oral anticoagulation therapy for at least 4 weeks. This recommendation deals only with protection from embolic events related to the cardioversion period. Subsequently, the long-term recommendations for patients who have been cardioverted to NSR but are at high risk for thromboembolism are similar to those for patients with chronic AF, even though the patients are in NSR.

A different approach with respect to anticoagulation can be used in low-risk patients (with no mitral valve disease, severe LV dysfunction, or history of recent thromboembolism) in whom there is reasonable certainty that AF has been present for less than 48 hours. Such patients have a low risk of clinical thromboembolism (0.8% in one study) if converted early, even without surveillance TEE. The ACC/AHA guidelines do not recommend long-term anticoagulation prior to cardioversion in such patients, but they do recommend heparin use at presentation and during the pericardioversion period. The optimal therapy after cardioversion in this group is uncertain. A common practice is to administer aspirin for a first episode of AF that converts spontaneously and anticoagulation for at least 4 weeks in all other patients. Aspirin should not be considered for patients with AF of less than 48 hours' duration if there is associated rheumatic mitral valve disease, severe LV dysfunction, or recent thromboembolism. Such patients should be treated the same as patients with AF of longer duration: 3 to 4 weeks of oral anticoagulation or shorter term anticoagulation with screening TEE prior to elective electrical or pharmacological cardioversion, followed by prolonged anticoagulation therapy after cardioversion.

Rate Control

Pharmacologic Therapy

Ventricular rate control during AF is important to prevent hemodynamic instability, improve symptoms and functional capacity, improve quality of life, and, over the long-term, prevent tachycardia-mediated cardiomyopathy. Oral or intravenous (IV) atrioventricular node (AVN) blockers are used for rate control, depending on the severity of symptoms and the degree of hemodynamic compromise caused by the tachycardia. In addition, correction of secondary causes of fast ventricular rates during AF (e.g., infection, hyperthyroidism, anemia, pain, and pulmonary embolism) is essential to achieve adequate rate control.⁵⁵

Beta-blockers or nondihydropyridine calcium channel blockers (verapamil and diltiazem) are the drugs of choice for rate control, and appear to have equivalent efficacy. Care should be used in administering those medications in patients with acutely decompensated heart failure. Beta-blockers are preferred in patients with cardiomyopathy, ischemic heart disease, and following surgical procedures. Verapamil and diltiazem are preferred in patients with reactive airway disease.^{4,55}

Digoxin is less effective and requires a longer time to achieve rate control, but may be considered if beta-blockers and calcium channel blockers have failed or have intolerable side effects. While digoxin reduces the resting heart rate, it is seldom effective in ambulatory patients because its effects are mediated by enhancement of vagal tone, which is offset during exertion. Thus digoxin has traditionally been used as a second-line agent, usually in sedentary patients or those with heart failure or hypotension. Recently, however, several systematic reviews and meta-analyses found that digoxin use was independently associated with a greater risk for mortality in patients with AF, regardless of concomitant heart failure. Some studies have suggested that AF nullifies the effect of digoxin in reducing hospitalizations for heart failure patients. Hence, the long-term use of digoxin is discouraged.^{124–128}

Amiodarone can be considered for rate control when other AVN blockers are unsuccessful or not tolerated. IV amiodarone is useful for acute control of the ventricular rate, and can be of particular value in acutely ill patients or those with acutely decompensated heart failure or severe hemodynamic compromise. Because of the probability of termination of AF by amiodarone, though very small, pericardioversion anticoagulation strategies should be considered, depending on the individual patient's risk/benefit profile. Oral amiodarone can be useful for ventricular rate control when other measures are unsuccessful or contraindicated; however, long-term potential toxicity should be carefully considered.¹²⁹

In patients with AF and ventricular preexcitation causing rapid ventricular response, prompt direct-current cardioversion is recommended, especially when hemodynamic compromise is present. IV procainamide or ibutilide to restore NSR or slow the ventricular rate can be considered in hemodynamically stable patients. Importantly, drugs that preferentially slow AVN conduction without prolonging BT refractoriness (such as verapamil, diltiazem, adenosine, oral or IV digoxin, and IV amiodarone) can accelerate the ventricular rate and potentially precipitate hemodynamic collapse and VF in high-risk patients. Unlike the IV route of administration, chronic oral amiodarone therapy can slow or block BT conduction. Limited data exist regarding the use of beta-blockers; nonetheless, these drugs theoretically pose a similar potential risk and they should be used with caution.¹³⁰

Adequacy of rate control should be assessed at rest and with exertion. However, parameters for optimal rate control in AF remain controversial. It appears reasonable to target a resting heart rate of 60 to 80 beats/min and 90 to 115 beats/min during moderate exercise. Ambulatory monitoring can help assess adequacy of rate control; goals of therapy include a 24-hour average heart rate lower than 100 beats/min and no heart rate higher than 100% of the maximum age-adjusted predicted exercise heart rate. Also, a maximum heart rate of 110 beats/min during a 6-minute walk test is a commonly used target. Nonetheless, one study found that a more lenient rate control (resting heart rate less than 110 beats/min) is not inferior to strict rate control (heart rate less than 80 beats/min at rest and less than 110 beats/min during moderate exercise). Such an approach can be more convenient in clinical practice and can be considered especially in asymptomatic patients with permanent AF and no significant structural heart disease, but periodic monitoring of LV function is necessary to evaluate for the potential risk of tachycardia-mediated cardiomyopathy. Of note, lenient rate control does not seem to increase the risk of adverse atrial or ventricular remodeling.⁴

In some patients with SND or tachycardia-bradycardia syndrome, pacemaker implantation can be required to protect from severe bradycardia while allowing the use of AVN blockers for adequate control of fast ventricular rates during AF or the use of antiarrhythmic drug therapy for maintenance of NSR (see Fig. 8.6). In one report, nearly 20% of patients with AF required pacemaker placement for symptomatic bradycardia, most within 5 years of their AF diagnosis, which was especially common in those with a history of heart failure. In patients with SND, atrial or dual-chamber pacing significantly decreases the incidence of subsequent AF compared with ventricular pacing.¹³⁰

Atrioventricular Junction Ablation

Ablation of the AV junction combined with permanent pacemaker implantation (the “ablate and pace” approach), provides robust control of ventricular rate as well as regularization of the R-R interval. However, because it is permanent and mandates lifelong pacing, AV junction ablation usually is considered as a last resort approach in AF patients when rhythm control strategies fail and pharmacological rate control therapy is poorly tolerated or unsuccessful. AV junction ablation is

especially useful when excessive ventricular rates induce a tachycardia-mediated decline in LV systolic function, despite appropriate medical therapy.

Furthermore, among patients with LV systolic dysfunction and AF, AV junction ablation has emerged as an important adjunctive therapy for cardiac resynchronization recipients. It has been estimated that 20% to 25% of those eligible for cardiac resynchronization have AF, and the cumulative incidence of new-onset AF/ATs ranges between 20% and 40% according to device interrogations. In patients with permanent AF or frequent persistent or paroxysmal arrhythmia episodes despite attempts to maintain NSR, intrinsic ventricular rate during AF (even though within the normal range) can override the biventricular pacing rate and reduce the percentage of effectively biventricular paced QRS complexes, thus precluding optimal ventricular resynchronization. Ablation of the AV junction in this setting has been associated with a reduction in all-cause mortality, a reduction in cardiovascular mortality, and an improvement in LVEF compared with those patients who were managed medically. It is important to note that the percentage of biventricular pacing determined by device counters often is artificially high because of invalid counting of fusion (hybrid between paced and intrinsic QRS morphologies) and pseudo-fusion complexes (pacing artifacts delivered but intrinsic QRS morphology not altered). In these patients, exercise ECG testing can help detect loss of effective ventricular synchronization and determine the percentage of pure biventricular pacing. AV junction ablation can also be required in ICD patients experiencing inappropriate therapies triggered by fast ventricular rates during AF.⁴

Rhythm Control

Restoration and maintenance of NSR in patients with AF can have several potential benefits, including relief of symptoms, improved functional status and quality of life, and prevention of tachycardia-induced cardiomyopathy. Attenuation of electrical and structural atrial remodeling associated with AF (and hence retarding the progression of AF), and improvement in LV function also have been described. The impact of rhythm control on mortality, however, remains to be determined.

Unfortunately, complete maintenance of NSR (i.e., 100% freedom from AF recurrence) often is unachievable with current drug therapies and remains an impractical treatment goal. It has been estimated that the average 1-year recurrence rate associated with amiodarone approximates 35%, and the recurrence rates for other currently available antiarrhythmic drug therapies are even higher (more than 50%). However, it is likely that individuals with AF can derive benefit from even partial restoration of NSR.

Reversion to Normal Sinus Rhythm

When rhythm control strategy is chosen, both electrical and pharmacological cardioversion methods are appropriate options. The timing of attempted cardioversion is influenced by the duration of AF, severity of patient's symptoms, adequacy of rate control, and risk of thromboembolism. Prompt cardioversion is recommended for patients with rapid ventricular rates and hemodynamic compromise attributed to AF (hypotension, acute heart failure, myocardial ischemia) or ventricular preexcitation, when rate-control drug therapy is unsuccessful or not tolerated. Cardioversion is also considered to restore NSR in stable but symptomatic patients with persistent AF, especially when ventricular rate control remains suboptimal.

Timing of cardioversion. In stable patients with AF of a duration longer than 48 hours or of unknown duration, any mode of cardioversion (electrical, pharmacological, or ablation) should be delayed until the patient has been anticoagulated at appropriate levels for 3 to 4 weeks or TEE has excluded atrial thrombi, regardless of the CHA₂DS₂-

VASc score. TEE can also be considered in patients with high thrombotic risk (e.g., severe valvular or congenital heart disease, prior thromboembolic events, severe cardiomyopathy), even when the duration of AF is less than 48 hours.¹²⁹

If urgency of cardioversion (because of severe symptoms or hemodynamic instability) precludes TEE, therapeutic doses of low-molecular-weight heparin, unfractionated heparin, or a non-vitamin K oral anticoagulant should be administered as soon as possible concurrent with or, preferably prior to, cardioversion, followed by long-term anticoagulation therapy.⁴

Electrical cardioversion. The overall success rate of electrical cardioversion for AF is about 90% and is inversely related to the duration of AF and LA size. The initial use of maximum-energy shocks, biphasic waveform, and anterior-posterior (as opposed to anterior-left lateral) electrode placement can help improve the efficacy of cardioversion and minimize the number of shocks required and, hence, the duration of sedation. In AF patients with ICDs, the electrodes should ideally be placed at least 8 cm away from the device in an anterior-posterior arrangement. The ICD can be used for internal cardioversion; however, the success rate is far lower than with external cardioversion, and each shock uses about 2 weeks of battery capacity.

Occasionally, electrical cardioversion fails to terminate AF, or AF recurs shortly after transient restoration of NSR. It is important to distinguish failure to terminate AF with a certain shock energy from successful termination of AF with nearly immediate recurrence. When AF fails to terminate, using higher energy levels, delivering a biphasic rather than monophasic waveform, applying external pressure on the cardioversion patches, changing the shock vector by altering the electrode pad position, and performing cardioversion during exhalation can improve effectiveness in some patients.

When AF recurs early after a successful cardioversion, repeated shocks at any energy are unlikely to have greater benefit. On the other hand, pretreatment with amiodarone, dofetilide, flecainide, ibutilide, propafenone, or sotalol can enhance success of electrical cardioversion and prevent early AF recurrence. In addition, pretreatment with a drug such as ibutilide can help lower the defibrillation threshold. The administration of IV magnesium sulfate alone before electric cardioversion does not appear to increase the rate of successful cardioversion of AF.^{4,131}

When the long-term use of antiarrhythmic drug therapy is planned for maintenance of NSR, initiation of drug therapy 1 to 3 days before electrical cardioversion (or a few weeks in the setting of amiodarone) to achieve effective drug levels at the time of cardioversion can help maintain NSR and prevent immediate recurrences of AF following cardioversion. This also confirms that the patient can tolerate the medication from a side effect perspective prior to cardioversion.⁵⁵

Of note, for AF of recent onset (less than 48 hours), newly started (less than 12 hours) AF episodes can be more difficult to terminate with electrical cardioversion than AF episodes lasting 12 to 48 hours, and failure of electrical cardioversion in the acute phase does not predict later successful cardioversion or spontaneous conversion to NSR in these patients.¹³²

Electrical cardioversion is usually preferred to pharmacological cardioversion because of greater efficacy and a low risk of proarrhythmia; however, it requires conscious sedation or anesthesia. Importantly, electrical cardioversion is contraindicated in patients with ongoing toxic reactions from digitalis or patients with hypokalemia.

The incidence of acute arrhythmic complications related to electrical cardioversion is very low. Ventricular arrhythmias needing intervention are extremely rare, irrespective of shock energy output or the concurrent use of antiarrhythmic drugs, although may be more common in patients receiving digitalis. Significant bradyarrhythmias (asystole greater than 5 seconds or heart rate less than 40 beats/min) resulting from

SND and the effect of sedation are observed in about 1% of patients. Almost all external defibrillators have the capability of back-up bradycardia pacing through the defibrillation patches, which can be used transiently if needed. In addition, IV atropine or isoproterenol should be available. Of note, a large proportion (more than 40% in one report) of patients exhibiting severe bradyarrhythmias following successful cardioversion require pacemaker implantation during short-term follow-up.

Pharmacological cardioversion. The efficacy of pharmacological cardioversion of AF is modest (30% to 70%), and is highest when initiated within 7 days of the onset of an episode of AF. While several antiarrhythmic drugs can be used for chemical cardioversion of AF, ibutilide and dofetilide are the most effective agents. Other antiarrhythmic drugs, including sotalol, amiodarone, and class IC agents (e.g., flecainide, propafenone) have limited efficacy. AVN blockers (beta-blockers, digoxin, and calcium-channel blockers) are generally not effective for restoration of NSR.¹²⁹

The risk of proarrhythmia is higher for chemical than electrical cardioversion. Therefore pharmacological cardioversion necessitates continuous cardiac monitoring (to detect SND, AV block, ventricular arrhythmias, and conversion into AF) for an interval that is dependent on the agent used (usually approximately half the drug elimination half-life).

Despite its limited efficacy, pharmacological cardioversion remains an option when sedation (which is required for electrical cardioversion) is not available or not well tolerated or when indicated by patient preference. In addition, as noted previously, when the use of long-term antiarrhythmic medications is planned for maintenance of NSR, starting drug therapy before electrical cardioversion can be beneficial, as it can help restore NSR in some patients and obviate the need for electrical cardioversion and, in other cases, can potentially enhance the efficacy of electrical cardioversion and prevent early recurrence of AF. Importantly, termination of AF may result in unanticipated sinus pauses/asystole with resultant presyncope or syncope, especially when using agents that can suppress sinus node function.

Ibutilide. IV ibutilide can restore NSR in 28% to 51% of AF patients, with an average conversion time of less than 33 minutes. Pretreatment with ibutilide also improves the efficacy of electrical cardioversion. Importantly, ibutilide is associated with sustained polymorphic VT (torsades de pointes) in 1.2% to 2.4% of cases, and nonsustained VT in 1.8% to 6.7%, which is more likely to occur in patients with QT prolongation, marked hypokalemia, or a very low LVEF. Pretreatment with IV magnesium can increase the efficacy and reduce the risk of torsades de pointes.

Dofetilide. Dofetilide can convert persistent AF to NSR in up to 60% of patients, typically within 36 hours of drug initiation. Dofetilide is rarely used solely for the purpose of cardioversion; rather, it is typically initiated for long-term rhythm control. When initiated in patients with persistent AF, electrical cardioversion is usually delayed for 24 to 48 hours to allow for potential pharmacological cardioversion. Of note, AF termination during dofetilide loading appears to be a predictor of durable response, even in longstanding persistent patients. Dofetilide is not available in Europe.

Amiodarone. Amiodarone has very limited efficacy (approximately 25%) in terminating persistent AF, and is not a preferred agent solely for the purpose of cardioversion. When successful, conversion to NSR occurs several hours or days after initiation of IV amiodarone, and after days to weeks of long-term loading of oral amiodarone.

Flecainide and propafenone. The class IC agents flecainide and propafenone can be used for pharmacologic cardioversion of AF; successful conversion to NSR typically occurs within 8 hours. The efficacy of flecainide for pharmacological cardioversion of recent-onset (less

than 24 hours) AF is significantly higher than that of amiodarone, sotalol, procainamide, and propafenone, with conversion rates ranging between 52% and 92% in different reports. In comparison with oral flecainide, IV flecainide is no more effective for pharmacological cardioversion of recent-onset AF, although IV flecainide has a more rapid onset of action (mean time to cardioversion 55 vs. 110 minutes). Propafenone (IV or oral) can be used for the acute termination of AF (rate of conversion to NSR ranges from 56% to 83%). IV preparations of flecainide and propafenone are not available in the United States. Importantly, the use of class IC agents is contraindicated in patients with significant structural heart disease, particularly those with LV systolic dysfunction or coronary artery disease. In addition, class IC drugs can potentially convert AF into AFL with relatively slow atrial rate and, hence, facilitate 1:1 AV conduction and paradoxically faster ventricular rates. Therefore adequate rate control with AVN blockers (beta-blockers, diltiazem, verapamil) should be achieved before instituting antiarrhythmic therapy. Once the safety of pharmacological conversion with propafenone or flecainide has been established in the hospital setting, repeat patient-administered cardioversion using oral propafenone (450 to 600 mg) or flecainide (200 to 300 mg), in addition to a beta-blocker or nondihydropyridine calcium channel blocker, can be appropriate on an outpatient basis (the “pill-in-the-pocket” approach). This approach is usually employed in selected patients with infrequent symptomatic episodes of AF lasting at least several hours at a time and recurring less than once a month.

Vernakalant. Vernakalant has been approved in Europe for the cardioversion of recent-onset AF (duration less than or equal to 7 days for patients not undergoing surgery, and less than or equal to 3 days for postcardiac surgery patients). IV vernakalant offers an AF conversion rate of about 62% within 90 minutes and appears to be much more effective than IV amiodarone. Some studies have also suggested its superiority to flecainide and propafenone. Vernakalant is not available in the United States.¹³³

Other antiarrhythmic agents. Sotalol, dronedarone, quinidine, and procainamide offer very low efficacy for acute termination of AF, and are not recommended for pharmacological cardioversion.

Maintenance of Normal Sinus Rhythm

Only 20% to 30% of patients who are successfully cardioverted maintain NSR for more than 1 year without chronic antiarrhythmic therapy. This is more likely to occur in patients with AF for less than 1 year, no enlargement of the LA (less than 4.0 cm), and a reversible cause of AF (such as hyperthyroidism, pericarditis, pulmonary embolism, or cardiac surgery). It has been thought that the drugs most likely to maintain NSR suppress triggering ectopic beats and arrhythmias and affect atrial EP properties to diminish the likelihood of AF. There is therefore a strong rationale for antiarrhythmic drug therapy in patients who have a moderate to high risk of recurrence, provided that the therapy is effective and that toxic and proarrhythmic effects are low. Prophylactic drug treatment is seldom indicated in patients with a first-detected episode of AF and can also be avoided in patients with infrequent and well-tolerated paroxysmal AF.

Amiodarone has been directly compared to dronedarone, sotalol, and propafenone and found to be substantially more effective, with a 1-year rate of maintaining NSR of 65%. Dofetilide offers 50% to 65% efficacy in maintaining NSR at 1 year. Other antiarrhythmic agents have only modest efficacy (30% to 50% at 1 year). Drug selection is largely driven by the safety profile, the presence and extent of concomitant cardiovascular disease, hepatic and renal dysfunction, and drug-drug interactions. A safer, although possibly less efficacious, drug is usually recommended before resorting to more effective but less safe therapies (Fig. 15.8; Table 15.14).¹³⁴

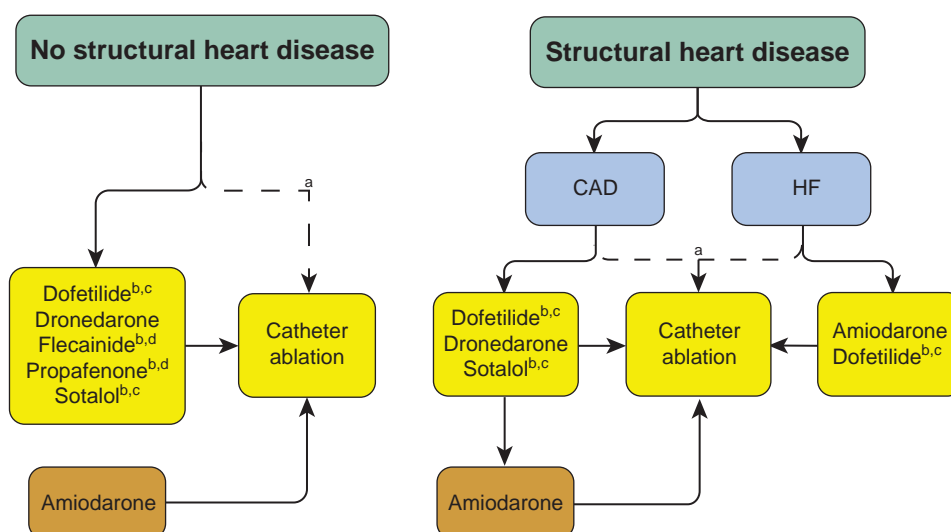


Fig. 15.8 Strategies for Rhythm Control in Patients With Paroxysmal and Persistent Atrial Fibrillation. Drugs are listed alphabetically. ^aCatheter ablation is only recommended as first-line therapy for patients with paroxysmal AF (class IIa recommendation), depending on patient preference when performed in experienced centers. ^bNot recommended with severe LVH (wall thickness greater than 1.5 cm). ^cShould be used with caution in patients at risk for torsades de pointes ventricular tachycardia. ^dShould be combined with AV nodal blocking agents. AF, Atrial fibrillation; AV, atrioventricular; CAD, coronary artery disease; HF, heart failure; LVH, left ventricular hypertrophy. (From January CT, Wann LS, Alpert JS, et al. 2014 AHA/ACC/HRS guideline for the management of patients with atrial fibrillation: a report of the American College of Cardiology/American Heart Association Task Force on Practice Guidelines and the Heart Rhythm Society. *J Am Coll Cardiol.* 2014; 64:e1–e76.)

TABLE 15.14 Most Commonly Used Antiarrhythmic Drugs for the Treatment of Atrial Fibrillation

Antiarrhythmic Drug	Year of Approval	Channels Blocked	Noncardiovascular Toxicity	Cardiovascular Toxicity
Flecainide	1975	INa	Dizziness, headache, visual blurring	AFL with 1:1 conduction; VT; may unmask Brugada-type ST elevation
Propafenone	1976	INa, β -AR	Metallic taste, dizziness, visual blurring	AFL with 1:1 conduction; VT; may unmask Brugada-type ST elevation
Sotalol	1992	IKr, β -AR	Bronchospasm	Bradycardia, torsades de pointes
Amiodarone	1967	IKr, INa, ICaL, IKur, Ito, IKACH If, β -AR, α -AR	Pulmonary (acute hypersensitivity pneumonitis, chronic interstitial infiltrates); hepatitis; thyroid (hypothyroidism or hyperthyroidism); photosensitivity; blue-gray skin discoloration; nausea; ataxia; tremor; alopecia	Sinus bradycardia
Dronedaron	2009	IKr, INa, ICa, IKur, Ito, IKACH If, β -AR, α -AR	Anorexia; nausea; hepatotoxicity	Bradycardia
Dofetilide	2000 (US only)	IKr	None	Torsades de pointes
Disopyramide	1962	INa, IKr, Acetylcholine	Anticholinergic: dry mouth, urinary retention, constipation, blurry vision	CHF exacerbation, torsades de pointes

AFL, Atrial flutter; AR, adrenoceptor; CHF, congestive heart failure; ICaL, L-type Ca^{2+} current; If, funny current; IKACH, acetylcholine-activated inward rectifier K^{+} current; IKr, rapidly activating delayed rectifier K^{+} current; IKur, ultra-rapidly activating delayed rectifier K^{+} current; Ito, transient outward K^{+} current; INa, Na^{+} current; VT, ventricular tachycardia.

In patients with AF and minimal or no heart disease, flecainide, propafenone, sotalol, and dronedaron are preferred; amiodarone should be chosen later in the sequence of drug therapy because of its potential toxicity. In patients with adrenergically mediated AF, beta-blockers represent first-line treatment, followed by sotalol. The anticholinergic activity of long-acting disopyramide makes it a relatively attractive

choice for patients with vagally mediated AF. In contrast, propafenone is not recommended in vagally mediated AF because its (weak) intrinsic beta-blocking activity may aggravate this type of paroxysmal AF.

In patients with substantial LV hypertrophy (LV wall thickness greater than 1.4 cm), it is recommended to avoid sotalol, flecainide, and propafenone because of concern of increased proarrhythmic risk. Dronedaron,

although not specifically tested in this population, is likely to be safe. Amiodarone is usually considered when symptomatic AF recurrences continue to affect the quality of life in these patients.

In patients with coronary artery disease, sotalol, dofetilide, or dronedarone are recommended as first-line therapy, while flecainide and propafenone are contraindicated. Amiodarone is considered the drug of last resort in this population because of its potential toxicity.

Dofetilide and amiodarone are the only agents available for patients with AF with concomitant heart failure; other antiarrhythmic agents can be associated with substantial toxicity and proarrhythmia.

Quinidine is associated with increased mortality, likely the result of ventricular proarrhythmia secondary to QT interval prolongation. Hence, this drug has largely been abandoned for AF therapy.

Given the suboptimal efficacy of antiarrhythmic drug therapy, expectations and treatment goals have to be pragmatic. Reduction of the burden of AF and its impact on quality of life can be a reasonable outcome. Occasional AF recurrences may not require a change in antiarrhythmic drug therapy. When treatment with a single drug fails, combinations of antiarrhythmic drugs can be tried. Useful combinations include sotalol or amiodarone in addition to a class IC agent. However, when drug therapy is deemed unsuccessful and a rhythm control strategy is abandoned, antiarrhythmic drug should not be continued.

Amiodarone. Amiodarone, although not approved by the US Food and Drug Administration for AF, is the most commonly prescribed and the most effective antiarrhythmic agent for the treatment of AF. However, the use of amiodarone is associated with significant adverse effects (including pulmonary, hepatic, thyroid, neurologic, and ophthalmic toxicity). QT prolongation is common but very rarely associated with torsades de pointes (0.5%). Although suppression of sinus and AV nodal function can occur early within the first few days of oral amiodarone therapy, the antiarrhythmic effect and QT prolongation can be delayed for days or weeks. A loading phase accelerates the onset of its antiarrhythmic activity. Amiodarone increases concentrations of warfarin, statins, and digoxin, and warfarin dose adjustment is often necessary. Appropriate periodic surveillance for lung, liver, and thyroid toxicity is required. Because of its potential toxicities, amiodarone should only be used after consideration of risks and when other agents have failed or are contraindicated.

Dofetilide. Dofetilide offers up to 65% efficacy in maintaining NSR at 1 year. Dofetilide has been demonstrated to be reasonably safe in heart failure and post-MI populations. However, because of the risk of QT prolongation and VT, initiation of dofetilide requires a 3-day mandatory in-hospital loading period under continuous telemetry and ECG monitoring. Excessive QT prolongation or VT prompting drug discontinuation during the loading period has been reported in almost 20% of the patients. Concomitant usage of other QT-prolonging drugs increases the risk of these adverse events by almost twofold. Overall, the risk of torsades de pointes in patients receiving dofetilide ranges from 0.7% to 3.3%. In a retrospective cohort study of 1404 AF patients treated with dofetilide for a 5-year period, the incidence of torsades de pointes was 1.2%. Risk predictors included female gender, low LVEF, and greater QTc prolongation. Dofetilide is not approved in Europe.

Flecainide and propafenone. Class IC agents are preferred first-line agents for rhythm control in patients with AF without structural heart disease, in whom both drugs are well tolerated and have a low risk of toxicity. On the other hand, these agents are contraindicated in patients with marked LV hypertrophy, coronary artery disease, or heart failure because of the risk of ventricular arrhythmias. Further, both flecainide and propafenone exhibit negative inotropic effects and should be avoided in patients with LV dysfunction. As noted previously, propafenone and flecainide are associated with a significant incidence of AFL

with relatively slow atrial rate, which can be associated with 1:1 AV conduction and very fast ventricular rates; therefore adequate rate control with AVN blockers is recommended before instituting class IC drug therapy. In addition, class IC agents can delay His-Purkinje system (HPS) conduction and prolongation of the QRS duration, which when excessive (more than 25% compared with baseline) can be a marker for proarrhythmia risk.

Sotalol. Sotalol has only modest efficacy in maintaining NSR (30% to 50% at 1 year). Sotalol causes drug-induced QT prolongation and torsades de pointes, especially in the setting of renal failure, hypokalemia, or the concomitant use of other QT-prolonging drugs. Therefore sotalol is often initiated in an inpatient setting with ECG monitoring to observe for excessive QT prolongation and proarrhythmia, especially when the drug is initiated during AF. However, drug initiation in an outpatient setting is also common, especially in low-risk patients with no underlying structural heart disease, QTc less than 450 milliseconds, normal electrolytes and renal function, and are in NSR at the time of drug initiation. Sotalol can be used in patients with ischemic heart disease, but should be avoided in patients with marked LV hypertrophy and those with renal insufficiency.

Dronedarone. Dronedarone is a structural analogue of amiodarone that lacks the iodine moieties. Although dronedarone is associated with a lower incidence of noncardiovascular side effects than amiodarone, it is significantly less efficacious. The major cardiac adverse effects of dronedarone are bradycardia and QT prolongation. Torsades de pointes is rare but has been reported. Dronedarone can be used for AF in patients without structural heart disease, but is contraindicated (because of increased mortality) in patients with NYHA class III or IV heart failure and in patients who have had a recent (in the past 4 weeks) episode of decompensated heart failure, especially in the presence of LV systolic dysfunction. In patients with permanent AF, dronedarone increases the combined endpoint of stroke, cardiovascular death, and hospitalization. Therefore dronedarone is contraindicated in patients whose sinus rhythm is not restored.

Disopyramide. Disopyramide is a sodium channel-blocking drug with potent anticholinergic and negative inotropic effects that can be considered for rhythm control in patients with AF. Because of its prominent vagolytic effects, disopyramide can be useful in “vagally mediated” AF (e.g., AF occurring in athletes or during sleep). Also, its negative inotropic effects make disopyramide beneficial in treating AF in patients with hypertrophic cardiomyopathy (HCM) associated with dynamic left ventricular outflow tract (LVOT) obstruction; however, these effects preclude its use in patients with underlying LV systolic dysfunction.

Rhythm Control Versus Rate Control

In the past, many physicians preferred rhythm control to rate control. Reversion of AF and maintenance of NSR restores normal hemodynamics and had been thought to reduce the frequency of embolism. However, two major randomized clinical trials—AFFIRM (Atrial Fibrillation Follow-Up Investigation of Rhythm Management) and RACE (Rate Control versus Electrical Cardioversion for Persistent Atrial Fibrillation)—compared rhythm and rate control in a select population at moderate stroke risk and found that embolic events occurred with equal frequency, regardless of whether a rate control or rhythm control strategy was pursued, and this occurred most often after warfarin had been stopped or when the INR was subtherapeutic. Both studies also showed an almost significant trend toward a lower incidence of the primary endpoint with rate control strategy. There was no difference in the functional status or quality of life. Hence, those trials provided evidence that both rhythm control and rate control are reasonable approaches (both strategies requiring long-term anticoagulation for stroke prevention), and suggested that rate control is an acceptable

approach in most patients. The AF-Congestive Heart Failure (AF-CHF) study demonstrated similar results among patients with AF with concomitant heart failure. The results of those randomized controlled comparisons of rhythm and rate control therapies were confirmed by more recent observation studies, registries, and meta-analyses.^{135,136}

However, it would be incorrect to extrapolate that NSR offers no benefit over AF and that effective treatments to maintain NSR need not be pursued. First, these trials were not comparisons of NSR and AF; they compared a rate control strategy to a rhythm control strategy that attempted to maintain NSR but fell short, and crossover between treatment arms occurred at a high rate. The failure of AFFIRM and RACE trials in showing any difference between rate and rhythm control is not so much a positive statement for rate control but rather a testimony to the ineffectiveness of antiarrhythmic drug therapy in maintaining NSR over the long term. When the data from these trials were analyzed according to the patient's actual rhythm (as opposed to his or her treatment strategy), the benefit of NSR over AF became apparent: the presence of NSR was found to be one of the most powerful independent predictors of survival, along with the use of warfarin, even after adjustment for all other relevant clinical variables. Patients in NSR are almost half as likely to die compared with those with AF. This benefit, however, is offset by the use of antiarrhythmic drug therapy, which increases the risk of death.¹³⁶

Therefore achieving and maintaining NSR remain viable and important treatment goals. However, because currently available antiarrhythmic agents commonly fail to suppress AF completely and have safety profiles that are less than ideal, it is reasonable to reserve it to the populations of patients likely to derive the greatest benefit from rhythm control. The selection of rhythm control or rate control strategies should be individualized and take into consideration the nature, intensity, and frequency of symptoms, patient preferences, comorbid conditions, and the risk of recurrent AF. According to analyses of available data, rhythm control can be an appropriate approach in young AF patients and those with newly diagnosed AF, significant symptoms, poorly controlled ventricular response, or tachycardia-mediated cardiomyopathy. On the other hand, asymptomatic or mildly symptomatic patients, especially those older than 65 years, and women with persistent AF who have hypertension or other underlying heart diseases can be better suited for rate control therapy.¹³⁷

It is important to note that current guidelines do not routinely recommend a rhythm control strategy for reducing the risk of mortality, stroke, or heart failure; rather, the primary indication for rhythm control therapy is for the reduction of symptoms and improvement in quality of life.¹³⁵

Catheter Ablation of Atrial Fibrillation

Catheter ablation of AF provides higher efficacy with comparable safety as antiarrhythmic drug therapy. AF ablation has been shown to significantly improve symptoms, exercise capacity, quality of life, and LV function, even in the presence of concurrent heart disease and when ventricular rate control has been adequate before ablation. Catheter ablation was also found to be associated with better quality of life, higher rates of freedom from both AF and antiarrhythmic medications, and lower rates of AF progression when compared with AVN ablation and biventricular pacing in symptomatic patients with AF and cardiomyopathy (LVEF less than or equal to 40%). Further, a recent study found that catheter ablation of AF superior to medical rate control strategy in patients with idiopathic cardiomyopathy, with significant improvement in the LVEF; restoration of NSR with catheter ablation resulted in significant improvements in LV systolic function, particularly in the absence of ventricular fibrosis on CMR. However, evidence is insufficient to determine whether AF ablation reduces all-cause mortality or stroke. Therefore the primary

justification for an AF ablation procedure at this time is the presence of symptomatic AF.^{1,55,130,138,139}

At the current time, patient selection criteria for AF ablation should include weighing risks and potential benefits associated with the procedure, as well as consideration of other factors such as severity of symptoms, quality of life, presence and severity of structural heart disease and other comorbidities, and availability of other reasonable treatment options. In addition, the projected ablation success rate with the operator's own experience and the tools available to him or her should be taken into consideration.

The ideal candidate for catheter ablation of AF has symptomatic episodes of paroxysmal or persistent AF, has not responded to one or more class I or III antiarrhythmic drugs, does not have severe comorbid conditions or severe structural heart disease, has an LA diameter smaller than 50 to 55 mm and, for those with longstanding AF, has had AF for less than 5 years. Catheter ablation of AF is likely to be of little or no benefit in patients with end-stage cardiomyopathy or massive enlargement of the LA (more than 60 mm), or in patients who have severe mitral regurgitation or stenosis and are deemed inappropriate candidates for valvular intervention. With improvements in the efficacy and safety of the procedure, the inclusion criteria for catheter ablation of AF continue to evolve; expanded indications at many centers now include patients with longstanding persistent AF and those with cardiomyopathy.^{130,138}

Current guidelines recommend catheter ablation in patients with symptomatic paroxysmal or nonparoxysmal AF as a second-line treatment after failure of or intolerance to class I or III antiarrhythmic drug therapy (Fig. 15.9). It is reasonable to use similar indications for AF ablation in selected patients not well represented in clinical trials, including those with heart failure, cardiomyopathy, younger patients (less than 45 years) and older patients (greater than 75 years). However, the risks and benefits of catheter ablation must be carefully assessed in these patients. A lower success rate or a higher complication rate can be expected in AF patients with concomitant heart disease, obesity, sleep apnea, severe LA dilation, longstanding persistent AF, as well as frail, elderly patients.^{1,55,130,140}

Indication for catheter ablation of symptomatic atrial fibrillation

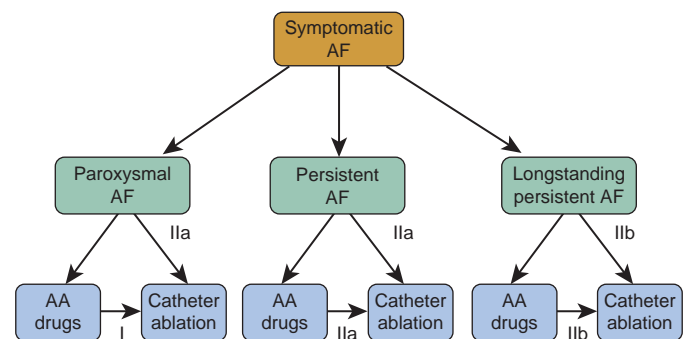


Fig. 15.9 The 2017 HRS/EHRA/ECAS/APHS/SOLAECE Indications for Catheter Ablation of Symptomatic Atrial Fibrillation (AF). Shown in this figure are the indications for catheter ablation of symptomatic paroxysmal, persistent, and longstanding persistent AF. The class for each indication based on whether ablation is performed after failure of antiarrhythmic drug therapy or as first-line therapy is shown. (From Calkins H, Hindricks G, Cappato R, et al. 2017 HRS/EHRA/ECAS/APHS/SOLAECE expert consensus statement on catheter and surgical ablation of atrial fibrillation. *Heart Rhythm*. 2017;14:e275–e444.)

It is important to recognize that there are still no randomized controlled data demonstrating that a patient's stroke risk is reduced by ablation. Therefore AF catheter ablation should not be performed with the sole intent of obviating the need for anticoagulation.^{1,130}

Complications of catheter ablation can have catastrophic outcomes in certain patients, including those with severe obstructive carotid artery disease, cardiomyopathy, aortic stenosis, nonrevascularized left main or three-vessel coronary artery disease, severe pulmonary arterial hypertension, or hypertrophic cardiomyopathy with severe LV outflow obstruction. Another relative contraindication is a history of major lung resection because of the severe impact of potential PV stenosis. Furthermore, because of the risk of thromboembolic events during the procedure and in the early postoperative period, patients who cannot be anticoagulated during and for at least 2 months after the ablation procedure should not be considered for catheter ablation of AF. Also, catheter ablation should not be performed in patients with an LAA thrombus or a recently implanted LAA closure device.

Catheter ablation as first-line therapy. Recent studies have demonstrated superior efficacy of catheter ablation as a first-line therapy as compared to pharmacological therapy, though most patients enrolled in those studies were generally healthy with predominantly paroxysmal AF. According to the 2017 HRS/EHRA/ECAS/APHRS/SOLAECE expert consensus statement, it is reasonable to consider catheter ablation as a first-line rhythm-control treatment (before therapeutic trials of class I or III antiarrhythmic drug therapy) for AF in select patients with symptomatic paroxysmal or persistent AF who prefer interventional therapy (see Fig. 15.9). This approach can be of particular value when poor tolerance to antiarrhythmic drugs is anticipated, such as in patients with tachycardia-bradycardia syndrome in whom pharmacological rhythm control strategies would necessitate pacemaker implantation. Similarly, catheter ablation is often recommended as an initial approach in high-level competitive athletes with paroxysmal or persistent AF in whom pharmacologic therapy can negatively affect athletic performance. The efficacy of this approach in unselected patient populations, however, still awaits confirmation by randomized studies, and the risk-benefit ratio of this approach in the individual patient should be carefully considered.^{1,140}

Catheter ablation for asymptomatic AF. Symptoms of persistent AF can be quite subtle and nonspecific (e.g., lack of energy, effort intolerance) and may not be recognized by the patients or can be attributed to other comorbidities (such as sleep apnea or heart failure). Before labeling AF patients as “asymptomatic,” it is important to obtain a careful history to elicit symptoms. Also it is appropriate to attempt restoration of NSR (with electrical or pharmacological cardioversion, with or without long-term antiarrhythmic drug therapy) and then assess the patient's symptom status while in NSR as compared to AF. Despite the lack of overt symptoms, AF ablation can still be a feasible way to improve well-being in these patients.¹

In addition, catheter ablation of AF may still be considered (class IIB) in select patients with truly asymptomatic paroxysmal or persistent AF (those who did not experience any improvement during a “trial of NSR”) when performed by an experienced operator and following a detailed discussion of the risks and benefits. The patient should be informed that AF, whether symptomatic or asymptomatic, is associated with an increased risk of stroke, heart failure, dementia, and mortality, and while it is possible that maintenance of NSR with AF ablation can potentially reduce these risks, these potential benefits remain unproven. Deferring ablation while awaiting the results of clinical trials can potentially allow progression of AF to a stage when the efficacy of AF ablation is significantly reduced. Importantly, while this approach can be acceptable in select asymptomatic patients, it is not recommended for patients with longstanding persistent AF and those with clinical whose clinical profile would be associated with a low procedural efficacy and safety.¹

Surgical Ablation of Atrial Fibrillation

The classic Cox-maze procedure involves creating a series of incisions in the left and right atria designed to direct the propagation of the sinus impulse through both atria while interrupting the multiple macroreentrant circuits thought to be responsible for AF. This procedure is the most effective means of curing AF, eliminating the arrhythmia in 75% to 95% up to 15 years after surgery. Improvements and simplifications of the surgical technique culminated in the Cox-maze III procedure, which became the gold standard for the surgical treatment of AF. Nonetheless, because of its complexity, technical difficulty, and risk of mortality and other complications, the maze procedure did not gain widespread acceptance.¹

To simplify the procedure, the standard cut-and-sew surgical technique has been replaced with linear epicardial ablation using unipolar or bipolar RF ablation, cryoablation, laser, high-frequency ultrasound, or microwave energy. Most surgical epicardial ablation procedures have been performed in conjunction with mitral valve surgery; the combination of mitral valve repair and cure of AF can enable selected patients to avoid life-long anticoagulation.

Current surgical instrumentation now enables minimally invasive approaches to be performed epicardially on the beating heart through mini-thoracotomies with video assistance. Bipolar RF is the predominant energy source used, and bilateral PV isolation is the most common lesion set, with some approaches adding ganglionic plexus ablation, as well as exclusion of the LAA. However, despite elimination of the need for median sternotomy and cardiopulmonary bypass, these procedures are still relatively invasive. To minimize the invasiveness of the procedure further, a totally thoracoscopic approach has been developed. Although multiple series described high success rates for paroxysmal AF (89% at 12 months of follow-up), success has been limited in patients with persistent and longstanding persistent AF (25% to 87%). In one report, the overall complication rate was 10%, with a perioperative mortality rate of 1.8%.¹

More extensive ablation lines, in addition to PV antral isolation and ganglionic plexus ablation, as well as documentation of complete PV isolation by demonstration of EP entrance or exit block, conduction block across ablation lines, and the detection and confirmation of ablation of the parasympathetic component of the ganglionic plexuses, are being evaluated to improve outcome. Some series reported a single procedure success rate of 86% at 1 year without the use of antiarrhythmic drugs.

Surgical ablation of AF is recommended in patients undergoing concomitant open heart surgery (whether ablation is performed after failure of antiarrhythmic drug therapy or as first-line therapy and regardless of the duration of the arrhythmia). Such an approach is also reasonable in patients undergoing closed cardiac surgery (e.g., coronary bypass or surgery) (Fig. 15.10).

Currently, stand-alone and hybrid surgical AF ablation can be considered for symptomatic patients with AF who were refractory to one or more attempts at catheter ablation or who are not candidates for catheter ablation (e.g., patients not candidates for long-term anticoagulation and those with an LA thrombus). Although surgical ablation was found in one report to have superior efficacy to catheter ablation, the complication rate after surgical ablation was higher. Hence, the decision to recommend surgical AF ablation before considering catheter ablation for patients with symptomatic AF refractory to drug therapy and no other indication for cardiac surgery remains controversial, and it should be based on institutional experience with both techniques, the relative outcomes and risks of each in the individual patient, as well as patient preference (see Fig. 15.10). Given the degree of patient discomfort, longer hospitalizations and recovery times, and the risk of bleeding following surgery, most patients prefer catheter to surgical ablation.^{1,130}

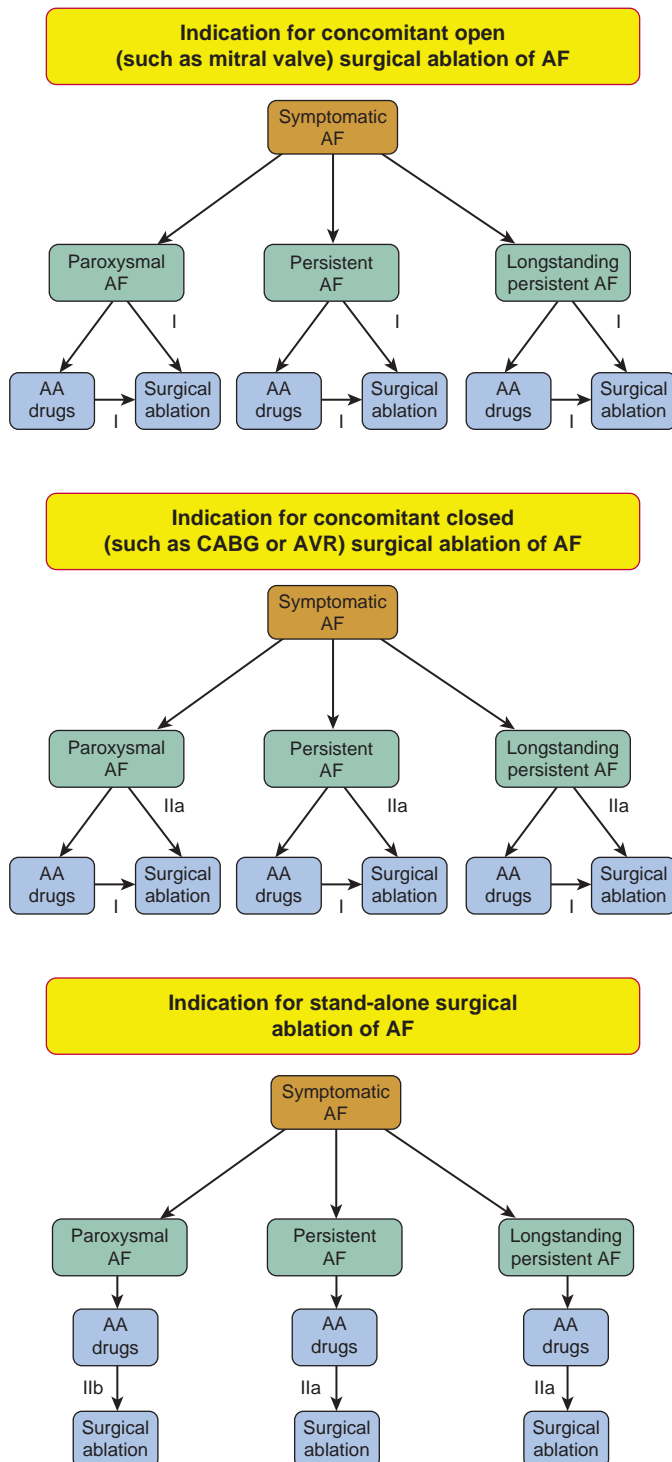


Fig. 15.10 The 2017 HRS/EHRA/ECAS/APHS/SOLAECE Indications for Surgical Ablation of Atrial Fibrillation (AF). Shown in this figure are the indications for surgical ablation of paroxysmal, persistent, and longstanding persistent AF. The class for each indication based on whether ablation is performed after failure of antiarrhythmic drug therapy or as first-line therapy is shown. The indications for surgical AF ablation are divided into whether the AF ablation procedure is performed concomitantly with an open surgical procedure (such as mitral valve replacement), a closed surgical procedure (such as coronary artery bypass graft [CABG] surgery), or as a stand-alone surgical AF ablation procedure performed solely for treatment of AF. AVR, Aortic valve replacement. (From Calkins H, Hindricks G, Cappato R, et al. 2017 HRS/EHRA/ECAS/APHS/SOLAECE expert consensus statement on catheter and surgical ablation of atrial fibrillation. *Heart Rhythm*. 2017;14:e275–e444.)

Other Nonpharmacological Approaches for Rhythm Control

Atrial antitachycardia pacing. Several pacing algorithms have been developed to inhibit the initiation of AF episodes. These include continuous atrial pacing just faster than the intrinsic sinus rate, overdrive atrial pacing after a PAC, algorithms for preventing pauses after PACs, and overdrive atrial pacing after the termination of an episode of AF to suppress an early arrhythmia recurrence. A multitude of studies tested the efficacy of those algorithms and showed no consistent reduction in AF burden or improvement in AF symptoms. Similarly, dual-site atrial pacing and atrial septal pacing site did not show benefits.

Modern pacemakers are equipped with a variety of atrial antitachycardia pacing (ATP) algorithms designed to terminate atrial tachyarrhythmias. ATP is delivered at an atrial CL shorter than the detected arrhythmia with the administration of a number of pulses of fixed duration (burst pacing), or sequences at progressively shorter intervals (ramp pacing) to abort episodes of AFL or AT. Prior generations of ATP algorithms demonstrated a modest efficacy (30% to 60%) in terminating slow regular ATs, less effective with rapid ATs, and ineffective at treating established AF. Further, the clinical impact of these algorithms on the burden of the arrhythmia is small. It is important to note that, besides the need for organized atrial tachyarrhythmias, the efficacy of ATP is crucially reliant on early detection of AT and correct rhythm classification by the device.¹³⁰

More recently, a new-generation atrial ATP (“reactive ATP”) was developed to target atrial tachyarrhythmias at onset (when the atrial CL is relatively long) and after any change in rate or regularity when the episode may be most amenable to termination by pacing. Transitions toward more regular or slower rhythms are not infrequent (reportedly occurring in 64% of atrial tachyarrhythmia episodes), even after hours following the onset of the arrhythmia. Unlike standard ATP algorithms, reactive ATP continues to monitor atrial rhythm and watches for any change in rate or regularity, and then opportunistically applies ATP when the episode is most amenable to termination by pacing (eFig. 15.5). In a recent study, reactive ATP reduced the risk of progression of AF to permanent or persistent AF.¹⁴¹

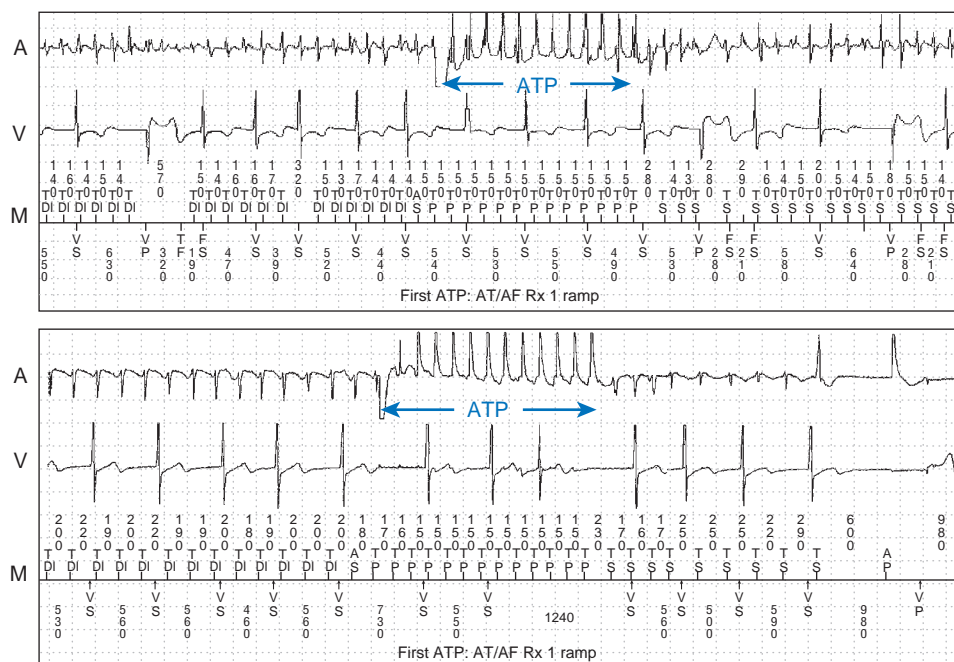
Currently, pacemaker implantation is not indicated for the sole purpose of prevention or treatment of AF in patients without other indications for pacemaker implantation. Nonetheless, ATP offers a therapeutic option for rhythm control in patients with permanent dual-chamber pacemakers or defibrillators that have this feature.

Atrial defibrillators. Atrial defibrillators can terminate AF with high acute success rates, but the need for repeated shocks and the resulting patient discomfort often render this option intolerable. Therefore implanted defibrillators are no longer recommended for rhythm control in AF patients.¹³⁰

Upstream Therapy

Upstream therapy refers to the use of non-ion-channel drug therapy that modifies the atrial substrate upstream of AF to reduce susceptibility to, or progression of, AF. The goal of this approach is attenuation and reversal of atrial structural remodeling to prevent new-onset AF (i.e., primary prevention) or recurrent AF (i.e., secondary prevention). Although some studies demonstrated a potential value of upstream therapy for primary prevention of AF in selected patients, data regarding its value for secondary prevention have been disappointing.⁴⁴

Given the role of fibrosis and inflammation in the pathogenesis of AF, drugs that suppress fibrosis, as well as antiinflammatory and antioxidative drugs, are being investigated both alone and in combination with traditional antiarrhythmic drug therapy. Among these drugs are several angiotensin-converting enzyme inhibitors, angiotensin II type 1 receptor blockers, antialdosterone agents, statins (3-hydroxy-3-methylglutaryl-coenzyme A reductase inhibitors), and omega-3 polyunsaturated fatty acids. These agents seem to reduce atrial fibrosis and



eFig. 15.5 Examples of Atrial Antitachycardia Pacing (ATP). *Upper panel*, Ramp ATP therapy delivered during atrial fibrillation fails at terminating the arrhythmia. *Lower panel*, In the same patient, ramp ATP therapy delivered when the tachycardia transitions into a more organized and slower arrhythmia successfully terminates the tachycardia and restores atrial-paced rhythm within 2 seconds of ATP delivery. AF, Atrial fibrillation; AP, atrial-paced event; AT, atrial tachycardia; TD, tachycardia detection; TP, tachycardia pacing; TS, tachycardia-sensed; VP, ventricular-paced event; VS, ventricular-sensed event.

were found to potentially reduce atrial structural remodeling and AF susceptibility in various AF experimental models. However, clinical trials produced inconclusive results, both for the primary and secondary prevention of AF.⁶¹

Although several studies have suggested a beneficial effect of renin–angiotensin–aldosterone system inhibitors for primary prevention of AF in patients with heart failure and LV systolic dysfunction or hypertrophy, no convincing benefit has been observed in patients without underlying heart disease or for secondary AF prevention. Therefore inhibitors of the angiotensin axis can be considered for AF management when the arrhythmia is associated with other underlying conditions that are themselves associated with myocardial fibrotic remodeling (e.g., LV systolic dysfunction and possibly hypertension with LV hypertrophy), but are not recommended in patients with no apparent cardiovascular disease.^{26,61,137}

No convincing evidence currently exists to support the use of polyunsaturated fatty acids or fish oil for either primary or secondary AF prevention. While some studies demonstrated a protective effect of statins against new-onset AF in patients undergoing coronary artery bypass graft surgery, other studies arrived at conflicting results. On the other hand, short-term colchicine has been associated with lower rates of postoperative AF and reduced early AF recurrence after catheter ablation.^{26,61,137}

Risk Factor Management

There is growing evidence supporting aggressive risk factor modification for primary prevention of AF, management of symptomatic AF, reducing the risk of AF recurrence postablation, and reducing thromboembolic complications of AF (Fig. 15.11). Pursuing and managing hypertension, diabetes, sleep apnea, obesity, and alcohol consumption need to be adopted as a systematic routine in the management of AF patients.^{7,61,44}

Hypertension

Hypertension is an independent risk factor for AF and stroke. Although treatment of hypertension has not been consistently shown to decrease AF risk, it is an important component of reducing cardiovascular complications and thromboembolic risk.⁶¹

Diabetes

Although diabetes is an independent risk factor for the development of AF and thromboembolic complications, there are limited data on diabetes management and AF risk. Intense glycemic control does not appear to directly impact the incidence or course of AF. Nonetheless, optimization of diabetes management and prevention of cardiovascular complications may indirectly reduce risk of AF.^{61,82,83}

Sleep Disordered Breathing

An independent association exists between AF and obstructive sleep apnea. Therefore AF patients should be actively screened for undiagnosed obstructive sleep apnea and evaluated when clinically suspected. Treatment of sleep apnea, when diagnosed, is an important component of AF management. CPAP therapy is associated with more than 40% relative risk reduction in AF recurrence in patients with obstructive sleep apnea, regardless of the AF treatment strategy (pharmacological or invasive).^{61,75}

Lifestyle Modifications

Lifestyle interventions aimed at maintaining a healthy body weight and cardiorespiratory fitness, in the context of a comprehensive risk factor modification, are recommend for both prevention and management of AF. Weight reduction in overweight and obese AF patients, especially those with type II diabetes and hypertension, can improve management of concomitant cardiometabolic risk factors, and was shown to improve symptoms and reduce AF burden.

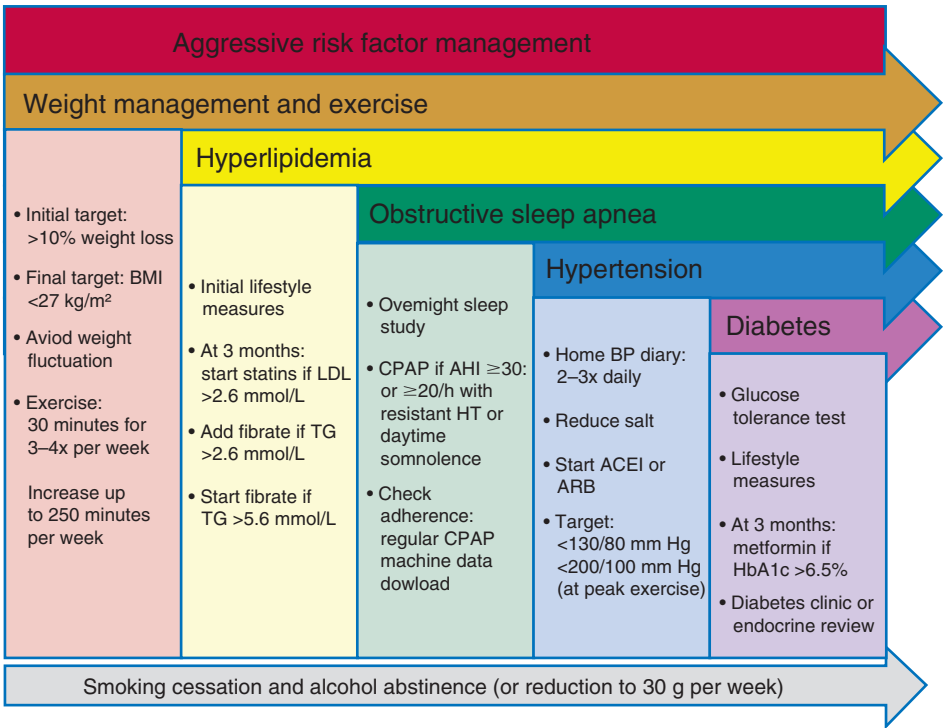


Fig. 15.11 Risk Factor Management for Prevention of Atrial Fibrillation. ACEI, Angiotensin converting enzyme inhibitor; AHI, apnea–hypopnea index; ARB, angiotensin receptor blocker; BMI, Body mass index; BP, blood pressure; CPAP, continuous positive airway pressure; LDL, low-density lipoprotein; TG, triglyceride. (From Lau DH, Schotten U, Mahajan R, et al. Novel mechanisms in the pathogenesis of atrial fibrillation: practical applications. *Eur Heart J.* 2016;37:1573–1581.)

In addition, regular, moderate exercise appears to benefit overweight and obese patients with symptomatic paroxysmal or persistent AF. One study found a significant dose-response relationship between baseline cardiorespiratory fitness with a 20% reduction in the risk of AF recurrence for each metabolic equivalent (MET) increase in baseline cardiorespiratory fitness. The benefits gained from cardiorespiratory fitness are additive to the effect of weight loss. Increased cardiorespiratory fitness is associated with beneficial effects on blood pressure, diabetic control, lipid profile, and inflammation, all of which can potentially contribute to reduced AF burden. However, guidelines on appropriate weight loss and fitness targets are still lacking.^{61,137,142}

Habitual and binge alcohol drinking increases the risk of new-onset AF as well as the risk of arrhythmia progression in patients with AF. Therefore reducing alcohol consumption can potentially be an effective strategy for primary and secondary AF prevention. In this context, however, a safe level of daily alcohol consumption in AF patients has not been established. In addition, appropriate counseling should be provided for smoking cessation and recreational drug abuse.^{44,89,90}

Management of Postoperative Atrial Fibrillation

Primary Prevention

Multiple strategies for preventing postoperative AF have been studied. Prophylaxis of AF using perioperative beta-blockers, amiodarone, and sotalol has shown promising results. However, no strategy completely eliminates the occurrence of postoperative AF.⁹⁹

Beta-blockers. Oral beta-blockers have been consistently shown to reduce the development of postoperative AF (from 39% to 31%, in one report) and, in the absence of contraindications, are strongly recommended for virtually all patients undergoing cardiac surgery. Generally, oral beta-blocker therapy is started at least 2 to 3 days before surgery, or within 24 hours after surgery if not given preoperatively. The dose is up-titrated as tolerated. In patients already receiving chronic beta-blocker therapy, the drug should be continued without interruption perioperatively.

Amiodarone. Amiodarone reduces the incidence of postoperative AF by more than 50% (compared with placebo); however, its incremental value is less well defined when compared with beta-blocker therapy. Preoperative use of amiodarone to prevent postoperative AF is a class IIa recommendation in the 2014 ACC/AHA/HRS guidelines.⁹⁹

Different regimens of amiodarone have been evaluated. Oral regimens were started at 1, 5, or 7 days before nonemergent surgery and continued for several days postoperatively. IV regimens involve starting amiodarone infusion immediately before or immediately after surgery, which is continued for 48 hours followed by oral therapy for 3 to 4 days. In a recent study, the efficacy of amiodarone in prevention of postoperative AF was maintained irrespective of route (oral vs. IV) and timing of administration (preoperative vs. immediate postoperative), and regardless of the duration of therapy, when at least 300 mg of IV amiodarone was loaded, and a total dose of 1 g was administered.¹⁴³

Sotalol. Sotalol was found to be more effective than beta-blockers for postoperative AF prophylaxis. There was no significant difference in the rates between sotalol and amiodarone. Sotalol therapy is usually started 24 to 48 hours before surgery or four hours after surgery.¹⁴⁴ However, the risk of bradycardia and torsade de pointes, especially in those with electrolyte disturbances, has limited the widespread use of sotalol for the prevention of postoperative AF.⁴⁴

Other therapies. Despite some suggestion of beneficial effects, current evidence does not support the routine prophylactic use of corticosteroids, atrial pacing, posterior pericardiotomy, antioxidant vitamins C and E, n-3 polyunsaturated fatty acids, statins, magnesium, or colchicine to prevent postoperative AF in the cardiac surgical popula-

tion. Studies using verapamil, digoxin, or procainamide showed no significant benefits compared to a placebo.

Perioperative infusion of human natriuretic peptide (carperitide), which inhibits the renin-angiotensin-aldosterone system, was recently shown to reduce the occurrence of postoperative AF in patients undergoing coronary bypass grafting.¹⁴⁵

Of note, prophylactic PV epicardial isolation in patients undergoing coronary bypass grafting does not decrease the incidence of postoperative AF or its clinical impact.⁹⁸

Rate Versus Rhythm Control

Beta-blockers are the drugs of choice for rate control in patients with postoperative AF. The indications for cardioversion of AF and recommendations for rhythm- versus rate-control strategies are similar to those discussed for nonsurgical patients. When antiarrhythmic drug therapy is required for rhythm control, amiodarone is the drug of choice. Sotalol can be considered if amiodarone is contraindicated. Class IC agents, such as flecainide and propafenone, generally are avoided in these patients given the presence of structural heart disease.⁹⁹

Prevention of Systemic Embolization

Guidelines for stroke prevention in nonsurgical AF patients apply to those with postoperative AF. Most of these patients have multiple stroke risk factors but also increased risk of bleeding in the postoperative phase. Therefore the decision to initiate anticoagulation therapy should be guided by the individual patient's bleeding risk and CHA2DS2-VASc score. Data are lacking regarding the threshold burden or duration of postoperative AF at which anticoagulation is favored, but AF lasting for longer than 48 hours should prompt strong consideration of anticoagulation therapy. The optimal duration for which anticoagulation must be continued after cessation of postoperative AF is uncertain.⁹⁹

Follow-Up of Patients With Postoperative Atrial Fibrillation

Follow-up is recommended at 6 to 12 weeks after surgery to evaluate the presence of persistent or paroxysmal AF and reassess management strategy. Ambulatory cardiac monitoring should be considered to screen for asymptomatic paroxysmal arrhythmias. The optimal frequency and intensity of cardiac rhythm monitoring beyond the 3-month period are not known. If AF is documented, long-term anticoagulation should be considered based on the CHA2DS2-VASc score, and the need for rate versus rhythm control should be reassessed. If there is no evidence of symptomatic or asymptomatic AF beyond the immediate postoperative period, discontinuation of antiarrhythmic drug therapy, if initiated after cardiac surgery, is recommended.

ELECTROCARDIOGRAPHIC FEATURES

Atrial Activity

AF is characterized by rapid and irregular atrial fibrillatory waves (f waves) and a lack of clearly defined P waves, with an undulating baseline that can alternate between recognizable atrial activity and a nearly flat line (Fig. 15.12). Atrial fibrillatory activity is generally best seen in lead V₁ and in the inferior leads. Less often, the f waves are most prominent in leads I and aVL.

The rate of the fibrillatory waves is generally between 350 and 600 beats/min. With up to 600 impulses generated every minute, syncytial contraction of the atria is replaced by irregular atrial twitches. Therefore the fibrillating atria look like a bag of worms in that the contractions are very rapid and irregular. The f waves vary in amplitude, morphology, and intervals, thus reflecting the multiple potential types of atrial activation that may be present at the same time at different locations throughout the atria. The f waves can be fine (amplitude less than

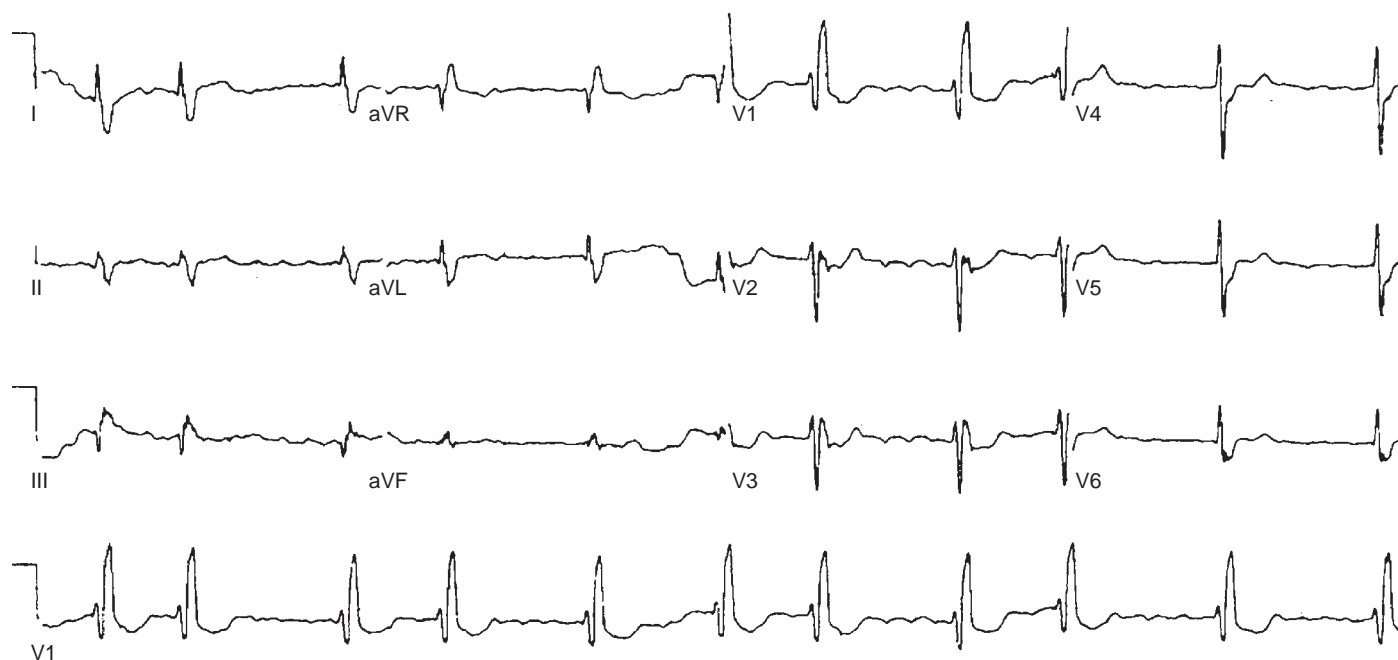


Fig. 15.12 Surface Electrocardiogram of Atrial Fibrillation With Chronic Right Bundle Branch Block.

0.5 mm on ECG) or coarse (amplitude more than 0.5 mm). On occasion, the f waves can be inapparent on the standard and precordial leads, which is most likely to occur in permanent AF. It was initially thought that the amplitude of the f waves correlated with increasing atrial size; however, echocardiographic studies have failed to show a correlation among the amplitude of the f waves, the size of the atria, and the type of heart disease. The amplitude, however, may correlate with the duration of AF.

AF should be distinguished from other rhythms in which the R-R intervals are irregularly irregular. These include multifocal AT (see Fig. 15.2), wandering atrial pacemaker, multifocal PACs, and AT or AFL with varying AV block. In general, distinct (although often abnormal and possibly variable) P (or flutter) waves are present during these arrhythmias, in contrast to AF. Patients with rheumatic mitral stenosis often demonstrate large-amplitude fibrillatory waves in the anterior precordial leads (V_1 and V_2), which can be confused with AFL. However, careful examination of the fibrillatory waves reveals them to have a varying CL and morphology. The distinction between AF and AFL can also be confusing in patients who demonstrate a transition between these arrhythmias. Thus AF may organize to AFL or AFL may degenerate to AF (eFig. 15.6). Occasionally, extracardiac artifacts (e.g., 60 cycle/min muscle tremors, as in parkinsonism) can mimic f waves.

Atrioventricular Conduction During Atrial Fibrillation

The ventricular response in AF is typically irregularly irregular, and the ventricular rate depends on multiple factors, including the EP properties of the AVN, the rate and organization of atrial inputs to the AVN, the level of autonomic tone, the effects of medications that act on the AV conduction system, and the presence of preexcitation over an AV BT.

The ventricular rate in untreated patients usually ranges from 90 up to 170 beats/min. Ventricular rates that are clearly outside this range suggest some concurrent influence. Ventricular rates slower than 60 beats/min are seen with AVN disease and can be associated with the

sick sinus syndrome, drugs that affect conduction, and high vagal tone, as can occur in a well-conditioned athlete. The ventricular rate in AF can become rapid (more than 200 beats/min) during exercise, with catecholamine excess (Fig. 15.13), parasympathetic withdrawal, thyrotoxicosis, or preexcitation (Fig. 15.14). The ventricular rate can be very rapid (more than 300 beats/min) in patients with the Wolff-Parkinson-White syndrome, with conduction over AV BTs having short anterograde refractory periods.

The compact AVN is located anteriorly in the triangle of Koch. There are two distinct atrial inputs to the AVN, anteriorly via the interatrial septum and posteriorly via the crista terminalis (see Chapter 9). Experiments in a rabbit AVN preparation demonstrated that propagation of impulses during AF through the AVN to the His bundle (HB) is critically dependent on the relative timing of activation of septal inputs to the AVN at the crista terminalis and interatrial septum. Other investigators showed that the ventricular response also depends on atrial input frequency.

Concealed conduction likely plays the predominant role in determining the ventricular response during AF. The constant bombardment of atrial impulses into the AVN creates substantial and varying degrees of concealed conduction, with atrial impulses that enter the AVN but do not conduct to the ventricle, thus leaving a wake of refractoriness encountered by subsequent impulses. This also accounts for the irregular ventricular response during AF. Although the AVN would be expected to conduct whenever it recovers excitability after the last conducted atrial impulse, which would then be at regular intervals, the ventricular response is irregularly irregular because of the varying depth of penetration of the numerous fibrillatory impulses approaching the AVN, leaving it refractory in the face of subsequent atrial impulses.

Alterations of autonomic tone can have profound effects on AVN conduction. Enhanced parasympathetic and sympathetic tone have negative and positive dromotropic effects, respectively, on AVN conduction and refractoriness. An additional factor is the use of AVN blocking agents such as digoxin, calcium channel blockers, or beta-blockers. There also



eFig. 15.6 Surface Electrocardiogram and Intracardiac Recordings Demonstrating Spontaneous Conversion of Atrial Fibrillation (*At Left*) Into Typical Atrial Flutter (*Right*). *CS_{dist}*, Distal coronary sinus; *CS_{prox}*, proximal coronary sinus; *HB*, His bundle; *HRA*, high right atrium.

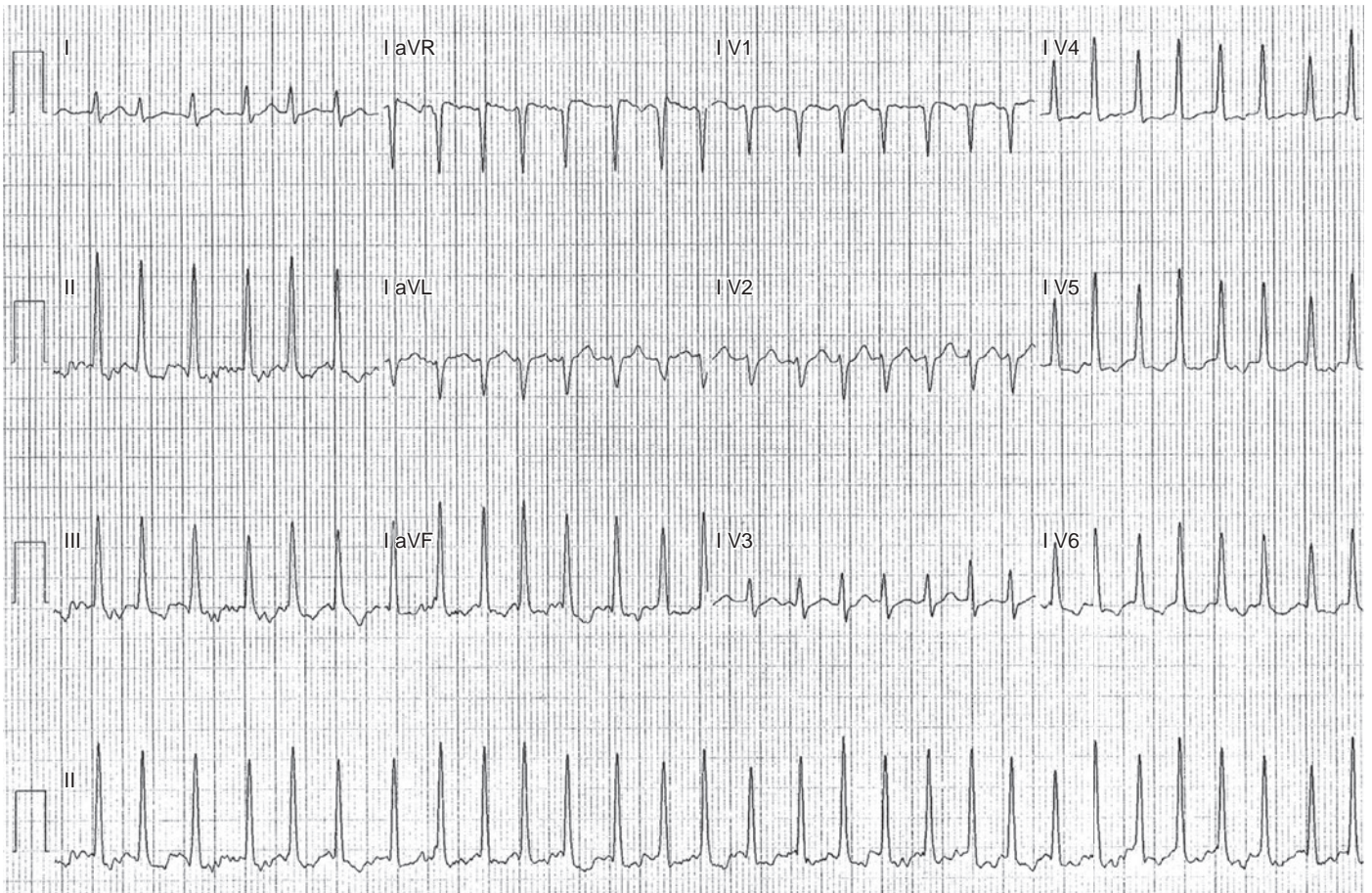


Fig. 15.13 Surface Electrocardiogram of Atrial Fibrillation With Rapid Ventricular Response in a Patient With Septic Shock on Dopamine Infusion.

may be a circadian rhythm for both AVN refractoriness and concealed conduction that accounts for the circadian variation in ventricular rate.

Ventricular Preexcitation During Atrial Fibrillation

The presence of a grossly irregular, very rapid ventricular response (more than 250 beats/min) with QRS duration longer than 120 milliseconds during AF rarely results from conduction over the AVN and strongly implies conduction over an AV BT (see Fig. 15.14). At very fast heart rates, there is usually a tendency toward regularization of the R-R intervals; therefore distinguishing preexcited AF from VT or pre-excited SVT can be difficult. However, careful measurement always discloses definite irregularities. Moreover, very rapid and irregular VTs are usually unstable and quickly degenerate into VF. Thus, when a rapid, irregular wide QRS complex tachycardia is noted in a patient who has a reasonably stable hemodynamic state, preexcited AF is the most likely diagnosis.

The ability to conduct rapidly over an AV BT is determined primarily by the intrinsic conduction and refractoriness properties of the AV BT. However, as with AVN conduction, factors such as spatial and temporal characteristics of atrial wavefronts during AF, autonomic tone, and concealed conduction influence activation over the AV BT. Very rapid AV conduction during AF can occur in the presence of AV BTs with very short refractoriness, especially when normal conduction through the AVN and HPS is blocked (as occurs with AVN blocking drugs) and ventricular activation occurs only via the rapidly conducting BT, which would then eliminate retrograde concealment into the BT. This would

result in extremely rapid ventricular rates, possibly more than 300 beats/min, which can occasionally degenerate into VF.

Regular Ventricular Rate During Atrial Fibrillation

Regular ventricular rate during AF indicates associated abnormalities. A regular, slow ventricular rhythm during AF suggests a junctional or ventricular rhythm, either as an escape mechanism with complete AV block or as an accelerated pacemaker activity with AV dissociation (see Fig. 9.27). Rarely, the R-R interval can be regularly irregular and show group beating with the combination of complete heart block and a lower nodal pacemaker with a Wenckebach type of exit block. Patients with severe underlying heart disease may develop the combination of AF and VT, leading to a rapid, regular, wide QRS complex tachycardia.

Effect of Digitalis Toxicity on the Ventricular Response

With increasing degrees of digitalis toxicity, high-grade but not complete AV block during AF initially leads to single junctional or ventricular escape beats. Higher degrees of AV block result in such a small number of atrial impulses being conducted that the lower pacemaker takes over, thus leading to an escape junctional or ventricular rhythm with a regular R-R interval for two or more cycles. On occasion, the junctional rate can increase, possibly because of digitalis-induced triggered activity, and it is called nonparoxysmal junctional tachycardia. Increasing digitalis toxicity can result in a Wenckebach exit block and give the appearance of an irregular ventricular rhythm with restoration of AF conduction,

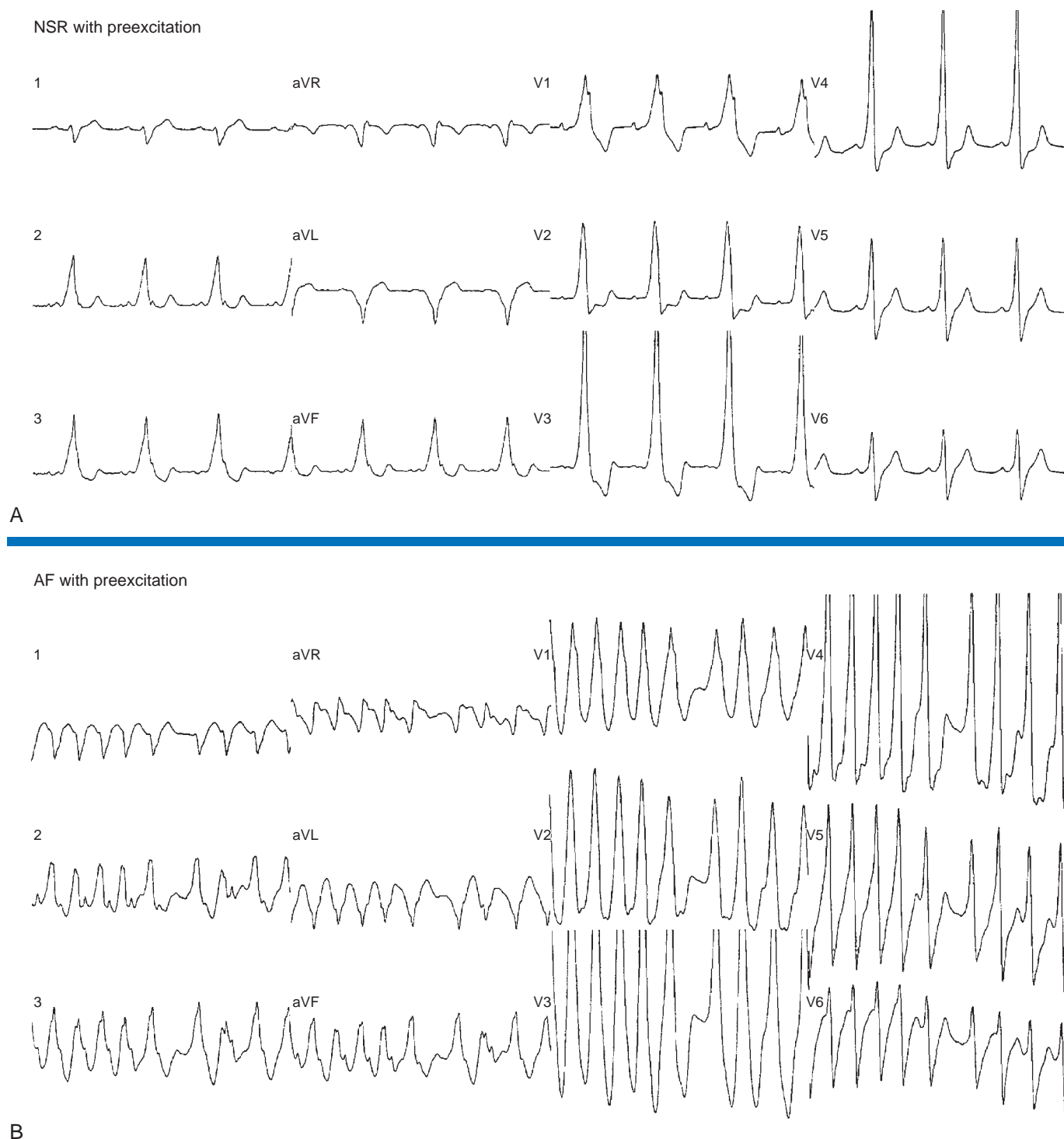


Fig. 15.14 Preexcited Atrial Fibrillation (AF). (A) Electrocardiogram (ECG) showing normal sinus rhythm (NSR) with a Wolff-Parkinson-White pattern and preexcitation using a left lateral bypass tract (BT). (B) ECG showing preexcited AF (i.e., AF with conduction over the BT).

but the rhythm shows repetitive group beating because of the exit block. Complete AV block is marked by a regular escape rhythm with no conducted beats, a finding that may lead to the erroneous assumption that the patient has converted to NSR. Infrequently, impulses from the lower pacemaker travel alternately down the right and left bundle branches or alternate fascicles of the left bundle branch, resulting in a

bidirectional tachycardia. This arrhythmia, which is also frequently a reflection of marked digitalis toxicity, may appear to be ventricular bigeminy. In true bigeminy, however, the ventricular beat in the bigeminal pattern is premature. In comparison, the R-R interval is regular with a bidirectional tachycardia because all the beats arise from a single pacemaker.

QRS Morphology

The QRS complexes during AF are narrow and normal unless AV conduction is abnormal because of functional (rate-related) aberration, preexisting bundle branch block (BBB) (see Fig. 15.12), or preexcitation over an AV BT (see Fig. 15.14).

Aberrant conduction commonly occurs during AF. Aberrancy is caused by the physiological changes of the conduction system refractory periods that are associated with sudden changes in heart rate. The refractoriness of the HPS tissue is directly related to the preceding R-R interval. Thus there can be aberrant conduction from a long R-R interval followed by a short cycle. In this scenario, the refractory period of the bundles increases during the long R-R interval (long cycle). The QRS complex that ends the long pause will be conducted normally but is followed by a prolonged refractory period of the bundle branches. If the next QRS complex occurs after a short coupling interval, it can be conducted aberrantly because one of the bundle branches is still refractory due to a lengthening of the refractory period (the Ashman phenomenon). The gross irregularity of the ventricular response during AF yields an abundance of different R-R intervals; therefore the long-short cycle sequence occurs commonly, and the Ashman phenomenon is seen frequently during AF; right bundle branch block (RBBB) aberrancy is more common than left bundle branch block (LBBB) aberrancy, because the right bundle branch has a longer refractory period at slower heart rates. The left anterior fascicle is also frequently involved, often in combination with RBBB. In contrast, functional aberration is uncommon in the HB, the left posterior fascicle, or the main left bundle. Moreover, CLs preceding the pause may also affect the chance for aberrancy after the pause.

The aberrancy caused by the Ashman phenomenon can be present for one beat and have a morphology that resembles a PVC, or it can

involve several sequential complexes, suggesting VT. The persistence of aberrancy may reflect a time-dependent adjustment of refractoriness of the bundle branch to an abrupt change in CL, or it can potentially be the result of concealed transseptal activation.

Although functional BBB is common in AF, PVCs are even more frequent, and it is important to differentiate between aberrant ventricular conduction and VT when repetitive wide QRS complexes occur during AF. The presence or absence of a long-short cycle sequence may not be helpful in differentiating aberration from ectopy for two reasons. Although a long cycle (pause) sets the stage for the Ashman phenomenon, it also tends to precipitate ventricular ectopy. Moreover, concealed conduction occurs frequently during AF, and therefore it is never possible to determine exactly when a bundle branch is activated from the surface ECG.

The proper diagnosis of aberrant conduction is a continuing challenge, but it can usually be accomplished by careful analysis of the rhythm strip and application of certain criteria. An aberrantly conducted beat caused by functional BBB generally has the pattern of a classic bundle branch or fascicular block. A PVC is usually followed by a longer R-R cycle, indicating the occurrence of a compensatory pause, the result of retrograde conduction into the AVN and anterograde block of the impulse originating in the atrium. The presence of long R-R cycles after the wide QRS complex that have identical CLs also suggests a ventricular origin (see eFig. 10.2). Furthermore, the absence of a long-short cycle sequence associated with the wide or aberrant QRS complex suggests that it is of ventricular origin. Aberrancy is likely not present if, with inspection of a long ECG rhythm strip, there are R-R interval combinations that are longer and shorter than those associated with the wide QRS complex. Also, a ventricular origin is likely if there is a fixed coupling interval between the normal and wide QRS complexes (Fig. 15.15).

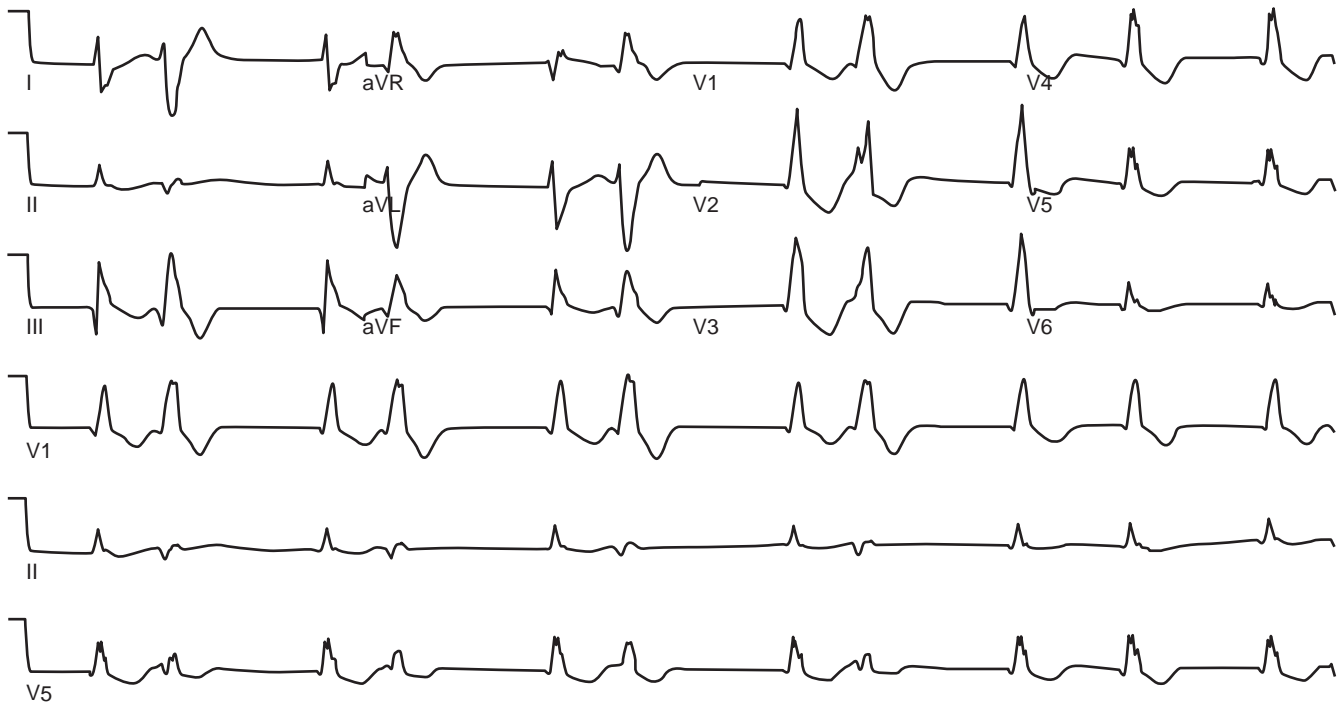


Fig. 15.15 Surface Electrocardiogram of Atrial Fibrillation (AF) With Right Bundle Branch Block and Premature Ventricular Complexes (PVCs). Ventricular bigeminy is present. Note the fixed coupling interval of the PVCs. Also, QRS morphology during PVCs is different from that during conducted AF complexes and is inconsistent with aberration.

CATHETER ABLATION OF ATRIAL FIBRILLATION

Evolution of Catheter Ablation Approaches for Atrial Fibrillation

Catheter Ablation of Atrial Fibrillation: Elimination of Triggers

Focal ablation of triggers. The landmark publication of Haïssaguerre and colleagues in 1998 demonstrated that paroxysmal episodes of AF are consistently initiated by spontaneous triggers or atrial extrasystoles. Remarkably, 94% of those triggers originated from the sleeves of LA muscle investing the PVs. Spontaneous reinitiation of AF could be eliminated by focal ablation at the site of origin of the trigger. The initial technique was to identify and ablate the culprit focus within the PV, but this approach was limited by the complication of PV stenosis and the recognition that multiple PVs were involved in most patients, which led to frequent recurrences after a “successful” procedure. Moreover, it is frequently difficult to elicit PV arrhythmia in the EP laboratory to allow adequate mapping and ablation.

PV isolation. Recognition of major limitations of focal ablation has led to the development of the PV electrical isolation technique. Recognizing that PV musculature conducts to LA musculature by discrete connections has allowed investigators to target those connections using multipolar catheters shaped into rings or baskets. Ablation is performed with a separate roving catheter at the site of earliest activation sequentially until PV electrical activity disappears or becomes dissociated from the LA activity (Fig. 15.16). Using this strategy, between 20% and 60% of the PV circumference is targeted by ablation. PV isolation has the additional advantage of simultaneously treating all triggering foci within the vein, thereby obviating the need to elicit and map those foci individually. For the same reason, investigators were soon led to attempt to isolate as many PVs as possible at the initial ablation session. Comparative case series ultimately demonstrated that empirical isolation of the four PVs led to superior outcomes over isolating fewer veins.

It was subsequently found that the incidence of PV stenosis could be reduced significantly by ablating just outside the PV ostia (i.e., on the atrial aspect). Using this approach, ablation is performed circumferentially around the antrum of each of the four PVs (see Fig. 15.16). In addition to elimination of PV triggers, circumferential antral PV isolation was found to modify potentially important elements of the AF substrate, which commonly localize to the antral regions of the PV (e.g., rotors and ganglionated plexuses). Furthermore, the circumferential ablation lines incorporate a large area of the posterior LA, contributing to atrial debulking.

With further research, it was also observed that non-PV foci were an important source of AF in some patients, although percentages varied among different groups. Among the sources identified are the vein of Marshall, the CS, and the SVC, all of which are, like the PVs, thoracic veins. Targeting those triggers by either focal ablation or electrical isolation of the involved thoracic veins has been attempted in selected patients.

Catheter Ablation of Atrial Fibrillation: Substrate Modification

Cox and colleagues developed a series of techniques for the surgical disruption of AF. The final iteration, the maze III procedure, was based on a model of AF in which maintenance of the arrhythmia requires persistence of a critical number of circulating wavelets of reentry, each of which requires a critical mass of atrial tissue to sustain it. The concept behind the maze III, in which a series of complete, transmural incisions are made in the left and right atria, was that by dividing the atria into small enough electrically isolated compartments, reentrant activity was

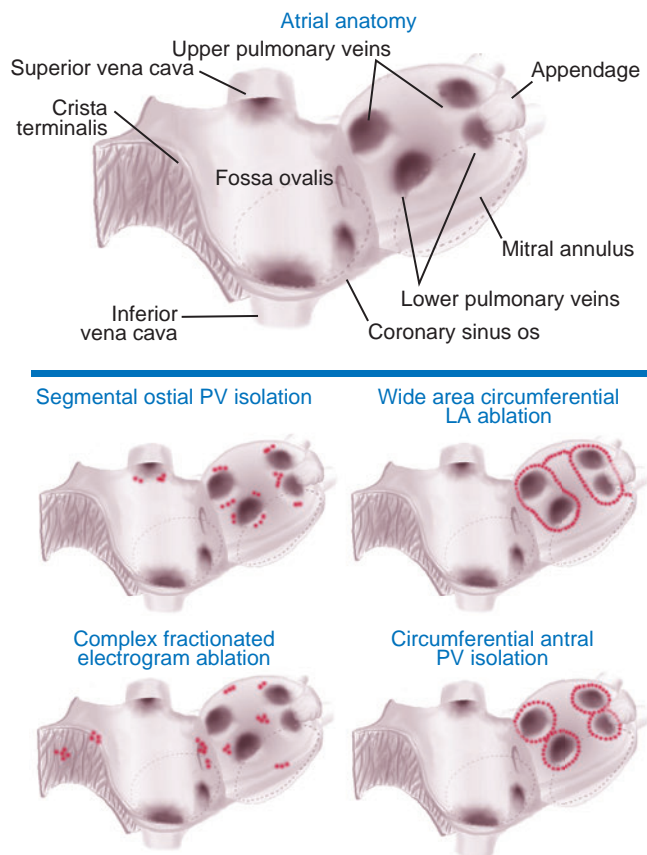


Fig. 15.16 Catheter Ablation of Atrial Fibrillation (AF). Atrial anatomy is shown at top; both atria are opened and viewed from the front. Various procedures for catheter ablation of AF are shown (red dots are ablation lesions). See text for further discussion. LA, Left atrium; PV, pulmonary vein.

no longer possible and maintenance of AF could be prevented, regardless of the mode of initiation. However, application of the maze III operation has been limited by the morbidity and risk associated with sternotomy-thoracotomy and cardiopulmonary bypass, as well as by the limited adoption by cardiothoracic surgeons. With the success of the Cox-maze procedure, multiple variations of the procedure have been performed, most of which have involved the use of a smaller lesion set. The LA lesion set was found to be fairly adequate to prevent AF, whereas RA lesions were required to prevent the development of AFL. Isolation of the PVs and posterior LA was a feature common to all successful iterations of the maze procedure. Therefore this and other similar compartmentalization procedures have evolved over time and now predominantly involve the LA. In general, all these approaches have lower success rates than the maze III procedure.

The success of surgical linear lesions led to the development of the catheter-based approach to perform linear ablation. Initial attempts at delivering long lines of RF ablation aimed at mimicking the lines of the surgical maze. Schwartz and associates reported recreation of the maze III lesion set in a small series of patients by using specially designed sheaths and standard RF catheters. Although the efficacy was modest, complication rates were high, and procedure and fluoroscopy times were exceedingly long, this report demonstrated a proof of concept that led others to try to improve the catheter-based approach. Further refinement of the linear catheter ablation technique involved creating a series of ablation lesions using RF catheters to create specific lesion

sets in the RA (two lines) and LA (three or four lines). The RA lesion sets consisted of an intercaval line along the interatrial septum and a cavotricuspid isthmus (CTI) line to prevent AFL. LA lesions were designed to connect the four PVs to each other and to the mitral annulus. As increasing evidence emerged regarding the importance of the LA in the maintenance of AF, ablation targets became limited to the LA.

In the late 1990s, Pappone and coworkers developed the wide-area circumferential ablation approach using three-dimensional (3-D) electroanatomic mapping. RF ablation was performed circumferentially around ipsilateral PVs, with the endpoint of ablation being the absence or marked reduction in the amplitude of electrical signals within the encircling lesions (see Fig. 15.16). Despite lack of evidence showing that PVs treated in this way are electrically isolated from the LA, this group began reporting results for paroxysmal AF which were just as good as or better than those working with the ostial segmental PV isolation approach. Furthermore, patients with persistent or permanent AF treated with the Pappone approach achieved freedom from AF almost as good as in patients with paroxysmal AF and far better than reports of patients treated with segmental PV isolation. Further iterations have required a strategy closer to the surgical maze—that is, lines to connect the ipsilateral pairs of the PVs and a line to link the left PV encircling lesion to the mitral annulus, which can be described as the *catheter maze*. Such lines further improved the outcomes of paroxysmal AF and have produced good results for ablation of longstanding persistent AF as well. It became clear that producing lines with proven transmural conduction block leads to a lower rate of recurrence of AF. However, achieving this is technically challenging and requires long, arduous procedures. Also, gaps in these lines could promote macroreentrant AT.

Later on, several other ablation strategies were developed aiming to modify potential substrates that underlie the sustenance of AF. These include ablation of atrial sites exhibiting complex fractionated electrograms reflecting regions with slow conduction, which were thought to be critical for maintaining AF. In addition, neuromodulation has been attempted by selective ablation of LA ganglionated plexuses (see Fig. 15.16). More recently, the localized source hypothesis as the underlying mechanism for AF has received close attention (see above). Studies employing panoramic atrial mapping during AF have used phase analysis of contact atrial endocardial electrograms from basket electrode catheters (FIRM) or reconstructed atrial electrograms from body surface recordings (ECG imaging) to identify regions of recurrent organized rotational activity (rotors) and focal sources (focal drivers) within the atria, which can potentially have a mechanistic role in sustaining AF, and design tailored ablation strategies that selectively targeted those sources. In addition, new, patient-tailored substrate modification strategies have been used targeting fibrotic atrial regions identified by voltage mapping or CMR.

At this time circumferential PV isolation remains the “gold standard” and the recommended approach for catheter ablation of AF. However, its success rate remains suboptimal especially in patients with persistent AF in whom a variety of additional ablation techniques have been proposed to improve procedural outcome. In general, substrate-based ablation techniques are used in conjunction with circumferential antral PV isolation; their use as a stand-alone procedure for either paroxysmal or persistent AF without any attempt to isolate the PVs electrically has been associated with high rates of arrhythmia recurrence, and this approach has been largely abandoned.¹⁴⁶

Periprocedural Management

Antiarrhythmic Drug Therapy

Antiarrhythmic medications are frequently stopped more than five half-lives before the ablation procedure because they can suppress spontaneous firing and fractionation of the electrograms that can be used to

guide ablation. However, a longer period (approximately 6 months) is required for amiodarone, which may not be practical. Hence, amiodarone may be continued or discontinued before or after ablation.

In patients with persistent AF, it may be reasonable to attempt electrical cardioversion and maintenance of NSR using antiarrhythmic medications as a prelude to ablation. Restoration of NSR, even for a relatively short time, can potentially result in reverse electrical atrial remodeling and improve the outcome of the ablation procedure.

Continuing antiarrhythmic drug therapy after ablation can potentially reduce the incidence of early recurrences of symptomatic atrial arrhythmias and the need for cardioversion or hospitalization for arrhythmia management. However, this strategy does not seem to improve long-term freedom from AF. Also, antiarrhythmic treatment can be initiated in select patients, such as those with incomplete or unsuccessful ablation procedures and patients with early recurrences of AF or AFL after ablation.^{147,148}

In patients discharged with antiarrhythmic drug therapy, such therapy is usually discontinued after 1 to 3 months if no recurrence of AF is observed. In patients discharged without antiarrhythmic drug therapy who develop recurrent AF, antiarrhythmic drug therapy is initiated unless the patient is satisfied with the extent of symptomatic improvement or elects to undergo a repeat ablation procedure.¹⁴⁸

Of note, a recent study found that, in patients free of AF at the end of 3 months following catheter ablation, continued use of previously ineffective antiarrhythmic drug therapy was associated with a lower rate of recurrences of atrial tachyarrhythmias and repeat ablation, without compromising the quality of life. This hybrid rhythm control approach can be a reasonable strategy in select AF patients.

Periprocedural Anticoagulation

Catheter ablation of AF is associated with significant risk of thromboembolism during and for several weeks following the procedure. The transiently heightened prothrombotic state associated with AF ablation is observed even in patients who were identified as low-risk before ablation. Ablation-related thromboembolism can be attributed to thrombus formation on the LA catheters and sheaths, char formation at the tip of the ablation catheter or at the site of ablation, development of LA thrombi due to stunned atrial tissue after conversion of AF to NSR, or thrombus formation over the disrupted endothelium from the ablation lesions. On the other hand, anticoagulation can increase the risk of hemorrhagic complications, including hemopericardium, pericardial tamponade, and vascular complications. Therefore rigorous periprocedural anticoagulation is of paramount importance to prevent thromboembolic events while minimizing hemorrhagic complications.

Preprocedural anticoagulation. Patients undergoing catheter ablation of AF are anticoagulated with warfarin (INR 2.0 to 3.0) or a NOAC for more than 3 to 4 weeks before the procedure. Two strategies of periprocedural anticoagulation have been used. The first strategy involves interruption of oral anticoagulation before the procedure and bridging with enoxaparin or IV heparin. With this strategy, oral anticoagulation is usually stopped (2 to 5 days for warfarin, and 1 to 2 days for NOACs) before the procedure, and replaced with enoxaparin or IV heparin once oral anticoagulation levels become subtherapeutic (i.e., when INR becomes less than 2.0 or when the next NOAC dose is due). Enoxaparin is stopped 12 to 24 hours and heparin is stopped 4 to 6 hours before ablation, and then restarted after ablation 4 to 6 hours after vascular hemostasis is successfully achieved, and continued until therapeutic levels of oral anticoagulation (INR 2.0 to 3.0) are reached. This approach, however, not only is impractical and cumbersome, but also exposes the patient to inadequate anticoagulation in the immediate postablation period, when anticoagulation is especially important given the heightened risk of cardiac thromboembolism due to tissue inflammation and

endothelial damage inherently associated with ablation. In addition, the use of enoxaparin or IV heparin is associated with high risk of vascular access complications.

An alternative strategy that is being used more frequently is the continuation of periprocedural oral anticoagulation without the use of heparin or enoxaparin for bridging. With this strategy, oral anticoagulation (with warfarin at a therapeutic INR) is continued at the time of ablation. This approach was found superior to the interrupted warfarin strategy and heparin bridging in terms of both the efficacy (lower risk of periprocedural thromboembolism) and safety (lower risk of bleeding) and, hence, has become the preferred anticoagulation approach in AF patients undergoing catheter ablation. Uninterrupted anticoagulation strategies eliminate a period of inadequate anticoagulation immediately following the ablation procedure, and it potentially reduces the risk of acute bleeding complications by obviating the need for heparin or enoxaparin therapy after ablation.¹⁴⁹ Similar data are emerging for NOACs; several recent studies found that uninterrupted administration of NOACs (with or without holding one or two doses of the NOAC in the day prior to the procedure) did not differ significantly from interrupted or continuous warfarin treatment with regard to the incidence of periprocedural thromboembolism, and may be associated with a lower risk of bleeding complications during the periprocedural period.^{150,151}

Intraprocedural anticoagulation. Intraprocedural anticoagulation with IV heparin is administered to all patients, even those with therapeutic levels of oral anticoagulation at the time of the procedure. During the initial experience with AF ablation, anticoagulation with heparin was delayed until after the LA access had been achieved because of fear of complications with the transseptal puncture. Later, it became evident that such a strategy can allow thrombus formation on sheaths, catheters, and high-profile wires in the RA before transseptal puncture, and these thrombi could potentially travel to the LA. In addition, recent evidence suggests that unfractionated heparin displays unexpected slow anticoagulation kinetics in a significant proportion of patients for up to 20 minutes after infusion. Hence, many operators now favor complete heparinization after vascular access, and clearly before transseptal puncture.^{152,153}

Initially, a loading dose of IV heparin is administered, followed by intermittent boluses or continuous infusion; heparin infusion can potentially prevent wide fluctuation of activated clotting time (ACT) levels, especially during long procedures. The ACT should be checked at 10- to 15-minute intervals until therapeutic anticoagulation is achieved, and then at 15- to 30-minute intervals for the duration of the procedure. Heparin dose is adjusted to achieve a target ACT of 300 to 350 seconds, even when using an uninterrupted oral anticoagulation strategy. Studies have shown that an ACT below 300 seconds during the procedure, and failure to administer IV heparin bolus before transseptal catheterization, are related to major thromboembolic complications.

Of note, patients receiving uninterrupted periprocedural warfarin therapy appear to require lower doses of heparin and reach the target ACT (greater than or equal to 300 seconds) faster as compared to patients with subtherapeutic INRs. In contrast, in patients on uninterrupted NOAC therapy, achieving the target ACT often is more delayed and requires larger doses of IV heparin. Therefore more frequent ACT monitoring and higher heparin doses should be used in the latter group of patients. A recent report proposed an individualized heparin dosing regimen: an initial heparin bolus of 50 units/kg in patients who are therapeutically anticoagulated with warfarin, 75 units/kg in patients who are not anticoagulated prior to ablation, and 120 units/kg for patients who are anticoagulated on a NOAC and have held one to two doses.¹⁵⁴

At the conclusion of the ablation procedure, sheath removal requires interruption of anticoagulation to achieve adequate hemostasis. Heparin

infusion can be discontinued and the sheaths removed when the ACT is less than 200 seconds. Alternatively, protamine can be administered to reverse heparin effects (1 mg of protamine for every 100 units of heparin received in the previous 2 hours). Hemostasis can be achieved by either direct pressure or the use of a figure-of-8 suture.

Postprocedural anticoagulation. Oral anticoagulation is restarted as soon as possible after the procedure, provided there is no evidence of ongoing bleeding or a significant pericardial effusion. In patients treated with NOACs, the NOAC is restarted 3 to 5 hours after completion of the procedure and removal of the vascular sheaths. For patients on uninterrupted warfarin therapy with therapeutic INR, warfarin daily regimen is resumed postablation. In patients with subtherapeutic INR the day of the procedure, bridging with enoxaparin or IV heparin is recommended until a therapeutic INR is achieved; however, substituting warfarin with a NOAC postablation is a preferred strategy and can potentially reduce the risk of bleeding associated with heparin or enoxaparin bridging.

Oral anticoagulation is continued for a minimum of 2 to 3 months after ablation in all patients, regardless of the CHA2DS2-VASc score or rhythm status. Decisions regarding the use of oral anticoagulation for more extended periods should be based on the patient's stroke risk profile (CHA2DS2-VASc score) and according to the guidelines for other patients with AF, and not on the perceived success or failure of the ablation procedure. Anticoagulation can be discontinued in patients with low stroke risk (CHA2DS2-VASc 0 in men or 1 in women), unless cardioversion is anticipated or has recently been performed. On the other hand, long-term anticoagulation is recommended for patients with a CHA2DS2-VASc score of 2 in men or 3 in women. Although some reports showed that discontinuation of anticoagulation therapy 3 months after successful catheter ablation can be safe over medium-term follow-up in some subsets of patients, this has not been confirmed by a large prospective randomized trial and therefore remains unproven. There is far greater flexibility as to how anticoagulation is managed in patients at an intermediate risk of stroke (CHA2DS2-VASc of 1 in men or 2 in women).

When discontinuation of oral anticoagulation therapy is being considered (based on the preference of a well-informed patient) following an apparently successful ablation procedure in a patient with a high risk of stroke, recurrences of AF should be excluded with confidence, which requires extended periods of continuous cardiac monitoring (see below). Reliance only on symptoms as an indicator for AF recurrence or event-triggered ambulatory monitoring can be misleading and can underestimate the incidence of recurrence. In addition, these patients should consider undergoing continuous or frequent ECG monitoring at regular intervals to screen for silent AF as long as they remain untreated with systemic anticoagulation.

Of note, some data have shown a temporal dissociation of actual AF episodes and thromboembolic events, suggesting presence of an underlying atrioopathy that results independently in both AF and thromboembolic risk. In such cases, elimination of AF may not impact thromboembolic risk.

Transesophageal Echocardiography

TEE is performed in most patients undergoing AF ablation to screen for LA thrombus. Although it is optional in patients with paroxysmal AF and no structural heart disease, preablation TEE is often performed in patients who are in AF at the time of the procedure, regardless of the anticoagulation status prior to ablation. The presence of intracardiac thrombus should prompt cancellation of the procedure and mandate 4 to 8 more weeks of anticoagulation, followed by another TEE.

Some reports suggested that a TEE may not be necessary in patients receiving uninterrupted oral anticoagulation therapy for 4 weeks

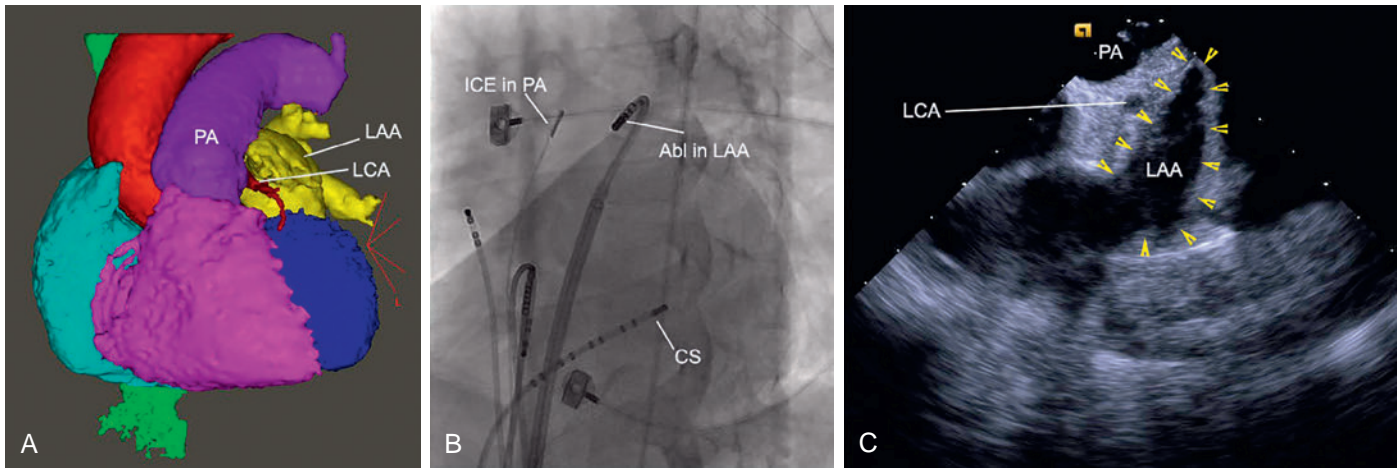


Fig. 15.17 Intracardiac Echocardiography (ICE) of the Left Atrial Appendage (LAA). (A) Segmented three-dimensional cardiac computed tomography (in the left anterior oblique [LAO] projection) showing the anatomic relationship between the LAA and pulmonary artery (PA). (B) Fluoroscopic view (LAO) of the ICE transducer positioned in the PA for imaging of the LAA. The ablation catheter (*Abl*) is positioned in the LAA. (C) ICE image of the LAA (*arrowheads*) acquired with the ICE transducer position in the PA. CS, Coronary sinus; LCA, left coronary artery.

preceding the ablation and through the day of the procedure. However, other studies reported a substantial prevalence of LAA clots among patients with full anticoagulation and in those with paroxysmal AF (up to 6.4% in those with high CHA2DS2-VASc score), and suggested that TEE should be performed in all patients prior to ablation. Therefore until more data are available, the risk of a thromboembolic event must be weighed against relatively low risk of moderate sedation and TEE, by taking into consideration the type of AF (paroxysmal vs. persistent), anticoagulation status, CHA2DS2-VASc score, LA diameter, and LV function. At this time, it may be reasonable to perform TEE in all patients, with the possible exception of those with paroxysmal AF and a CHA2DS2-VASc score of 0.^{1,155,156}

The technique of 64-slice computed tomography (CT) scanning has been used to screen for atrial thrombi with reportedly high diagnostic accuracy, but TEE remains the gold standard and the preferred imaging modality. In addition, the use of intraprocedural intracardiac echocardiography (ICE) may be considered for screening of LAA thrombi (imaging from the pulmonary artery is preferred, Fig. 15.17) in patients who cannot undergo TEE; however, the data are currently insufficient to recommend widespread use of ICE imaging as an alternative to TEE (eFig. 15.7).

Postprocedural Electrocardiogram Monitoring

Patients are generally hospitalized the night after the procedure, with cardiac monitoring, and discharged home the following day. After hospital discharge, the method and frequency of cardiac monitoring depends on individual needs and the consequences of arrhythmia detection.

Patients who report symptoms compatible with an arrhythmia should undergo ambulatory cardiac monitoring, which (depending on the frequency of symptoms) may include 12-lead ECGs, Holter monitors, patient-activated event recorders, and automatically activated external loop recorders.

On the other hand, arrhythmia monitoring to assess the efficacy of the ablation procedure is typically delayed for at least 3 months following ablation because early recurrences of atrial arrhythmias are common during the first 1 to 3 months after ablation and many of them resolve spontaneously. Importantly, the disappearance of arrhythmia symptoms postablation should not be equated with absence of AF.

In fact, the proportion of asymptomatic compared with symptomatic arrhythmia events in AF patients often increases after ablation. Therefore long-term cardiac ambulatory monitors to screen for asymptomatic occurrences of atrial arrhythmias need to be considered. Mobile cardiac telemetry devices are often used, and they provide continuous monitoring for a period of 2 to 4 weeks with real-time AF detection. Since the rate of detection of AF on cardiac monitoring is directly related to the duration and frequency of monitoring, continuous monitoring over extended periods is recommended when detection of asymptomatic AF would influence decision making regarding anticoagulant therapy after ablation. While periodic monitoring with mobile cardiac telemetry devices if often employed, implanted loop recorders (for continuous long-term surveillance) and smartphone-based ECG monitors (for intermittent long-term surveillance) can be considered to improve patient's compliance.¹

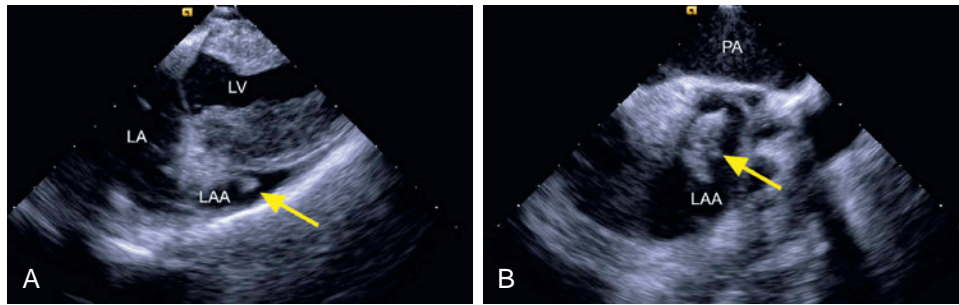
Pulmonary Vein Imaging

CMR or contrast-enhanced, multislice CT scanning of the LA with 3-D reconstruction is performed to define the anatomy of the PVs before the procedure (see Fig. 15.6). After ablation, CT or CMR is important to evaluate for evidence of PV stenosis in patients in whom there is a clinical suspicion. Although some investigators recommend routine follow-up imaging for detection of asymptomatic PV stenosis 3 to 4 months after ablation of AF, it is unknown whether early diagnosis and treatment of asymptomatic PV stenosis provide any long-term advantage to the patient. Nevertheless, follow-up PV imaging should be considered during the initial experience of a new AF ablation procedure for quality assurance.

Technical Aspects Common to Different Methods of Ablation

Sedation During Ablation

In most patients, deep sedation or general anesthesia is used to prevent patient movements during long and potentially painful procedures and improve catheter and mapping system stability. Conscious sedation is used less frequently; the choice often is determined by the institutional preference and also by assessment of the patient's suitability for conscious sedation. Advantages of general anesthesia include optimal airway



eFig. 15.7 Intracardiac Echocardiography (ICE) of Left Atrial Appendage (LAA) Thrombus (*Arrow*). In A, the ICE transducer is positioned at the tricuspid annulus. In B, the ICE transducer is positioned in the pulmonary artery (PA). LA, Left atrium; LV, left ventricle.

management, pain control, patient immobilization, as well as enhanced tolerance of esophageal temperature probes. Furthermore, phrenic nerve stimulation, if performed, can cause significant movement in nonanesthetized patients.

Left Atrial Access

Mapping and ablation in the LA are performed through a transseptal approach (see detailed discussion in **Chapter 4**). Even if a patent foramen ovale exists, some operators prefer septal puncture to access the LA since the foramen ovale is typically higher on the septum than might afford optimal reach to all LA locations. Generally, one or two transseptal punctures are performed, and one or two long vascular sheaths are introduced into the LA. The long sheaths are flushed with heparinized saline at a low infusion rate during the entire procedure, whether or not they are withdrawn into the RA during the LA mapping and ablation portion of the procedure.

For ablation strategies utilizing a multielectrode catheter for LA-PV mapping (in addition to the ablation catheter) using two transseptal accesses, one for each catheter is preferred to using a single transseptal access and exchanging diagnostic and ablation catheters over the transseptal sheath. The latter technique can potentially increase the risk for embolic events due to manipulation of the sheath introducing air or thrombi.

Identification of the Pulmonary Veins

Initial approaches of focal ablation targeting arrhythmic foci within the PVs were associated with high incidences of PV stenosis. To avoid this serious complication, the ablation procedure has evolved over time to an increasingly proximal ablation, first at the venous ostium or venoatrial junction and most recently proximal to the PV to encompass the antral region. However, the more proximal ablation approaches require correct identification of the ostia and PV-LA junction, and given the marked variation in PV anatomy, assessment of the number of PVs and anatomy of the ostia is essential when planning an ablation strategy. Various imaging techniques have been developed in an attempt to identify the PV ostium more accurately, but exact localization of this structure remains difficult, and the exact definition of the PV ostium varies, depending on the imaging modality used. Ultimately, however, the choice of imaging modality is dictated by local availability.

Fluoroscopy. Entry into the PV is clearly identified as the catheter leaves the cardiac shadow on fluoroscopy and electrical activity disappears; however, the ostium is located more proximally. The inferior portion of the PV ostia can be localized by advancing the catheter into the PV with downward deflection of the tip and then dragging back while fluoroscopically monitoring the drop off the ostial edge of the catheter.

Intracardiac echocardiography. Phased-array ICE can be used to visualize the antrum and ostium of the PVs (see detailed discussion in **Chapter 6**). ICE has the advantage of providing real-time imaging of the PVs. In contrast to angiography, ICE can define the proximal edge of the PV antrum (see **Fig. 6.32**).

Electroanatomic mapping. Electroanatomic mapping systems (CARTO, Biosense Webster, Diamond Bar, CA, United States; EnSite NavX, St. Jude Medical, St. Paul, MN, United States; or Rhythmia, Boston Scientific, San Jose, CA, United States) have been used to construct a 3-D shell of the LA and identify the PVs.

Combining electroanatomic mapping systems with cardiac imaging. Cardiac CT and CMR provide critical information regarding the number, location, and size of the PVs, which is needed in planning the ablation and selecting appropriately sized mapping and ablation devices. In addition, preacquired CMR and CT scans have the advantage of allowing full integration with 3-D mapping systems and real-time

catheter navigation on a 3-D CT or CMR image, which can facilitate identification of PV ostia and ablation targets (see detailed discussion in **Chapter 6**).

PV angiography. PV angiography can be used at the time of catheter ablation to detail PV anatomy. Selective PV angiography is performed using a 5- to 10-mL hand injection of contrast medium through a long sheath (for angiography of right superior, left superior, and left inferior PVs) or NIH catheter (for angiography of right inferior PV; **eFig. 15.8**). A limitation of the selective PV venography approach is that noncatheterized PVs can be missed if a preacquired CT or CMR is not available to ensure that all the PVs are identified. Alternatively, PV angiography is performed by injecting contrast in the left and right pulmonary arteries or the pulmonary trunk; PVs are then assessed during the venous phase of pulmonary arteriography. A third technique used for PV angiography involves contrast injection in the body of the LA or at the roof of the right or left superior PV ostium immediately after administration of an adenosine IV bolus to induce AV block; the contrast medium will fill the LA body, PV antrum, and proximal part of the PV during the phase of ventricular asystole.

An important limitation of PV angiography is that it images only the tubular portion and does not adequately define the full posterior extension of the PV. Studies of PV anatomy from pathological specimens and 3-D CT scans have shown that the PV is funnel-shaped, with a tube that fans out into a proximal cup that blends into the posterior atrial wall, referred to as the antrum. Furthermore, the PV antrum connects to the LA wall at an oblique angle. The posterior aspect of each PV is more proximal, whereas the anterior segments of the PVs are more distal.

Catheterization of the Pulmonary Veins

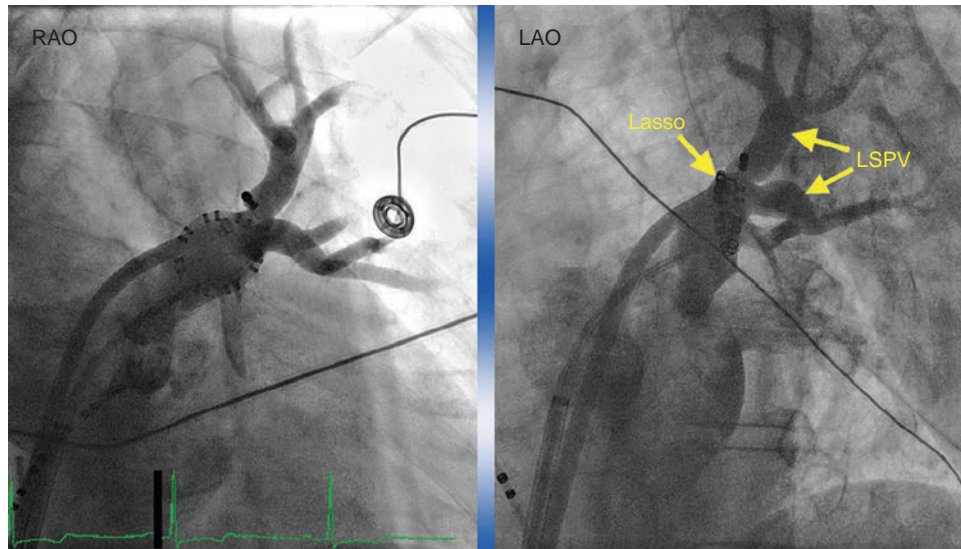
In the anteroposterior fluoroscopic view, the PV ostia are situated on both sides of the spine. Clockwise rotation of the catheter inside the LA directs its tip posteriorly and toward the PVs. It is frequently necessary to apply clockwise torque to both the catheter and its long sheath.

For catheterization of the left PVs, the catheter should be directed anteroposteriorly in the right anterior oblique (RAO) fluoroscopic view and to the left in the left anterior oblique (LAO) view. Care must be taken to avoid advancing the catheter into the LAA, in which case the catheter is directed anteriorly (to the right in the RAO view) and not anteroposteriorly. Advancing a catheter into the LAA results in an increase in electrogram amplitude, rather than decreasing amplitude, when advancing into a PV.

For catheterization of the right PVs, the catheter is rotated further clockwise and is directed to the right in the RAO view and anteroposteriorly in the LAO view. An alternative method for reaching the ostia of the right PVs is to loop the catheter around the lateral, inferior, and then septal LA walls, laying the catheter down along the wall, and dragging the catheter by withdrawing it along the posterior right ostia. Forming a tight loop with maximal deflection of the catheter and using rotational movements can provide greater stability during ablation, particularly at the anterior aspect of the PVs.

Counterclockwise rotation of the catheter inside the LA would lead the catheter into the LV. Care must be taken not to allow the circular (Lasso) catheter to cross the mitral annulus because it can then become trapped with the mitral valve apparatus. Usually, reversal of the catheter movement (clockwise torque) that resulted in this situation helps correct it. Also, advancing the sheath over the shaft of the catheter (into the LV) and pushing forward, to free the catheter tip from entanglement, is usually successful.

The use of transseptal steerable sheaths can improve catheter stability and tissue contact and facilitate access to more distant parts of the LA, especially in patients with severe LA dilatation.



eFig. 15.8 Pulmonary Vein (PV) Angiography. Fluoroscopic (right anterior oblique [RAO] and left anterior oblique [LAO]) views of the left superior PV (LSPV). The ring catheter is positioned at the PV ostium.

FOCAL ABLATION OF PULMONARY VEIN TRIGGERS

Rationale

There are two different types of arrhythmias that can play a role in generating AF, and both can be addressed by focal ablation. One type is a PAC (or runs of PACs) that triggers self-sustained AF (focal triggers). Ablation of a focal trigger does not terminate AF but prevents its reinitiation (see Fig. 15.2). A second type is a focal tachycardia that either induces fibrillation in the atria or mimics AF by creating a pattern of rapid and irregular depolarization wavefronts in the atria. Such a tachycardia acts as a focal driver and is necessary for the continuation and maintenance of AF. Ablation of a focal driver results in the termination of AF and prevention of its reinitiation. Focal tachycardias that initiate or mimic AF can be recognized in the EP laboratory because they are frequently associated with exit block between the site of origin of the tachycardia and the rest of the atria (Fig. 15.18).

Several observations have provided evidence that the electrical activity that arises in the PVs plays a role in the maintenance of AF. By analyzing surface ECG and 24-hour Holter recordings, studies have shown that most paroxysmal AF episodes are initiated by a single PAC. Although focal sources of AF can be found in the RA, LA, CS, SVC, or vein of Marshall, most foci are located within a PV. It is possible that intermittent bursts of PV tachycardia serve to perpetuate AF in the same fashion as bursts of rapid atrial pacing (see Fig. 15.18).

There can be a subset of patients with focally induced AF in whom ablation of a single dominant focus can result in cure, without the need for empirical isolation of all PVs. A more limited ablation approach requires shorter procedure and fluoroscopy times and can be safer. These are important considerations in a relatively young patient population. However, if other PVs or sources are dormant at the time of the procedure but become active subsequently, the patient may experience more AF episodes.

Identification of Arrhythmogenic Pulmonary Veins

Definition of an Arrhythmogenic Pulmonary Vein

An arrhythmogenic PV is defined by single or multiple ectopic discharges originating from the vein, with or without conduction to the LA. During ectopy from an arrhythmogenic PV, there is a reversal in activation sequence, from the distal PV trunk (source) to the ostium and LA (exit), with the PV potential preceding the LA potential (eFig. 15.9; Fig. 15.19). Conversely, if the explored PV is not the origin of ectopy, it is passively activated, as in NSR, with a proximal-to-distal sequence and a PV potential after or fusing with the LA potential.

Ectopic discharges with a short coupling interval may not be conducted to the LA, thus producing isolated PV potentials confined within the PV. These can be recognized as a PV potential coincident with or just after the ventricular electrogram and can be distinguished from a potential of ventricular origin by their spontaneous disappearance (intermittent PV potential) or suppression during atrial pacing (Fig. 15.20).

During an episode of AF, rapid rhythms arising in the PVs (variably referred to as rapid focal activity, repetitive rapid activity, intermittent PV tachycardia, or paroxysmal CL shortening) are common and can play an important role in the maintenance of AF or can be markers of an arrhythmogenic PV that triggers AF during NSR. The CL of local activity within the arrhythmogenic PV is shorter than that of the atrium. In contrast, the local CL in passively activated PVs is similar to or longer than that of the atrium (see Fig. 15.18).

Provocation of Pulmonary Vein Ectopy

If PV ectopy does not spontaneously develop during EP monitoring or is not sufficiently sustained, one or a combination of several provocative

maneuvers can be tried to induce the arrhythmia, including physiological procedures (e.g., Valsalva maneuvers, carotid sinus massage, or deep breathing), pharmacological agents (isoproterenol, IV infusion at 1 to 8 µg/min; and adenosine, rapid IV injection, 12 mg and then 18 mg, up to 20 to 60 mg), and slow-rate atrial pacing (bursts of 3 to 10 stimuli at 100 to 200 beats/min looking for post-pause ectopy). In addition, in patients who present with AF at the time of ablation, electrical cardioversion of AF often reproducibly induces PACs from the same location as spontaneous PACs, and those PACs that follow cardioversion can potentially reinitiate AF. If AF is not present at baseline, rapid burst atrial pacing to induce AF, followed by electrical cardioversion, can be attempted to identify early postcardioversion PV triggers.

Mapping Pulmonary Vein Ectopy

Electrocardiogram Localization of Pulmonary Vein Ectopy

ATs arising from the PVs are characterized by entirely positive P waves in lead V₁ (in 100% of cases) and across the precordial leads, isoelectric or negative waves in lead aVL in 86%, and negative waves in lead aVR in 96%. Lead aVL can be biphasic or positive in right-sided PV ATs (Fig. 15.21; see eFig. 11.4).¹⁵⁷

Left PV ATs have several characteristics (as compared with right PV ATs), including positive notching in the P waves in two or more surface leads, an isoelectric or negative P wave in lead I, more positive P waves in lead III than in lead II (P wave amplitude in lead III/II ratio greater than 0.8), and broad P waves in lead V₁. Right-sided PV foci usually have positive P waves in lead I (see Fig. 15.21).

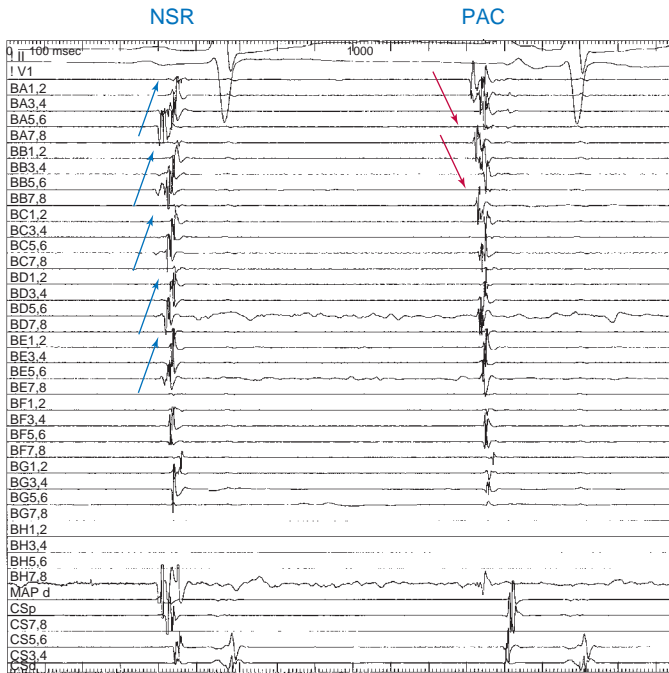
ATs arising from the superior PVs invariably have a positive P wave in the inferior leads. In contrast, ATs arising from the inferior PVs can have inverted, low-amplitude positive or isoelectric inferior P waves. However, because of the close proximity of the superior and inferior veins and marked anatomic variation, P wave morphology generally is of greater accuracy in distinguishing right-sided from left-sided PVs, in contrast to distinguishing superior from inferior PVs.¹⁵⁷

ATs arising from the right superior PV are associated with P waves that are narrow and positive in the inferior leads, of equal amplitude in leads II and III, positive in lead V₁, and isoelectric or positive in lead I. The right superior PV is a common site of origin for LA ATs. It is only a few centimeters from the sinus node; hence, activation rapidly crosses the septum via Bachmann's bundle to activate the RA in a fashion similar to NSR, a feature explaining the similarities in P wave morphology. However, whereas the P wave is biphasic in lead V₁ during NSR, it is positive in that lead during right superior PV AT (see Fig. 15.21; see Fig. 11.13).¹⁵⁷

Endocardial Activation Mapping

Initially, the PV of interest is identified based on earliest activation of triggers in the CS and RA catheters. If no sharp bipolar activity is recorded in the RA at least 10 milliseconds before the onset of the ectopic P wave, the ectopic beats are considered to have originated in the LA. Following initial identification, the ablation catheter is placed and maneuvered to the appropriate PV.

Activation mapping within the PV is performed during ectopy. It is important to have adequate frequency of PACs from each focus, to be able to acquire enough points and identify the earliest activation sequence. Electroanatomic mapping or multielectrode mapping catheters, such as the circular catheter (a 10- or 20-pole catheter with a distal ring configuration) or PentaRay catheter (Biosense Webster) or multielectrode arrays (see Fig. 4.3) positioned in the PV, can be of value in mapping the source of ectopy. The ectopic focus is localized inside the selected PV according to the earliest atrial activity relative to the reference electrogram or the onset of the ectopic P wave. PV depolarization during ectopy is marked by a spike (an electrogram of sharp



eFig. 15.9 Mapping of Pulmonary Vein (PV) Ectopy Using a Basket Catheter. The basket catheter is positioned in the left superior PV. Bipolar recordings are obtained from the eight electrodes (1-2, 3-4, 5-6, 7-8) on each of the eight splines (BA through BH) of the basket catheter. *Left*, During normal sinus rhythm (NSR), PV activation propagates from proximal (ostial) to distal, as reflected by earlier activation timing on the proximal basket electrodes than the distal ones (*blue arrows*). *Right*, In contrast, during a premature atrial complex (PAC) originating from this PV, activation occurs earliest deep in the vein and progressively later toward the ostium and the left atrial (LA) exit, resulting in distal to proximal venous activation on the basket catheter recordings (*red arrows*). Note that the PV potentials precede the onset of the P wave on the surface electrocardiogram during PV ectopy, but they occur late after P wave onset during NSR.

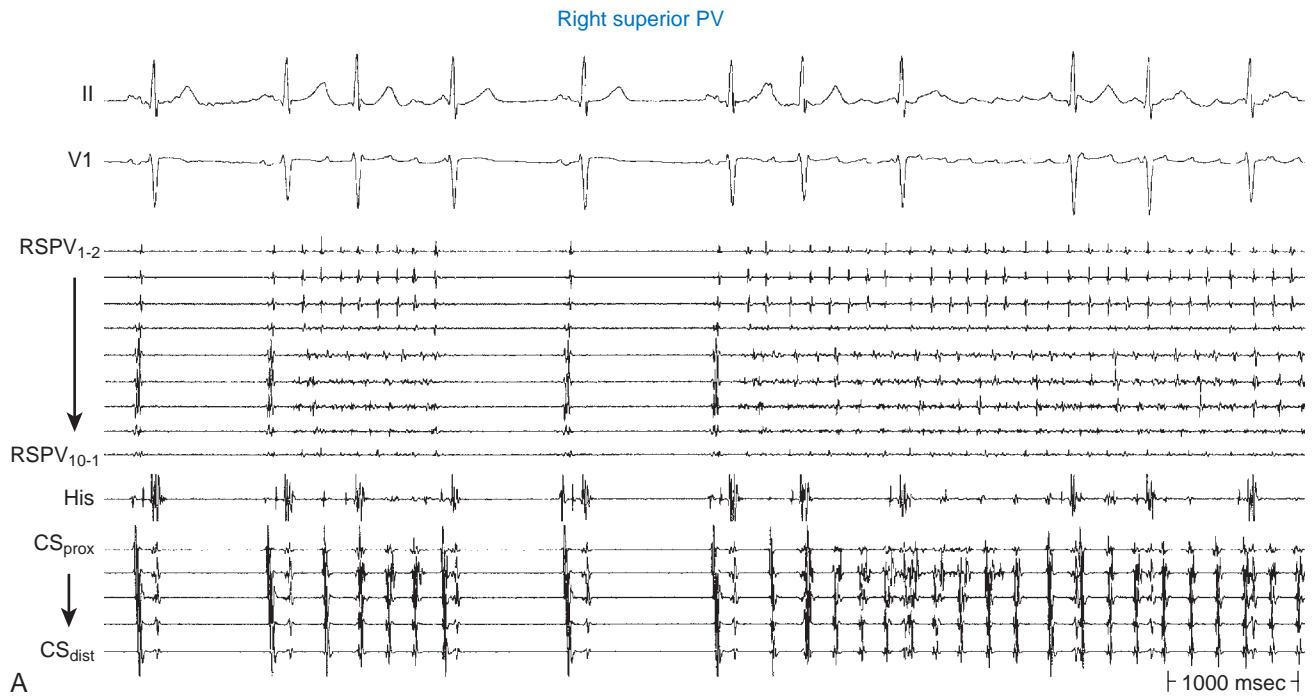


Fig. 15.18 Atrial Fibrillation (AF) Initiation From the Right Superior Pulmonary Vein (RSPV). (A) A burst of nonsustained PV tachycardia followed by a second sustained episode. Note that the local cycle length (CL) in the ring catheter recordings from the RSPV is significantly shorter than atrial CL recorded in the coronary sinus (CS) during AF, indicating that this PV is most probably the source and driver of AF. (B) Recordings from the left superior PV (LSPV) in the same patient during spontaneous initiation of AF showing LSPV activity with a CL similar to the atrial CL, a finding suggesting that this PV is activated passively. CS_{dist}, Distal coronary sinus; CS_{prox}, proximal coronary sinus.

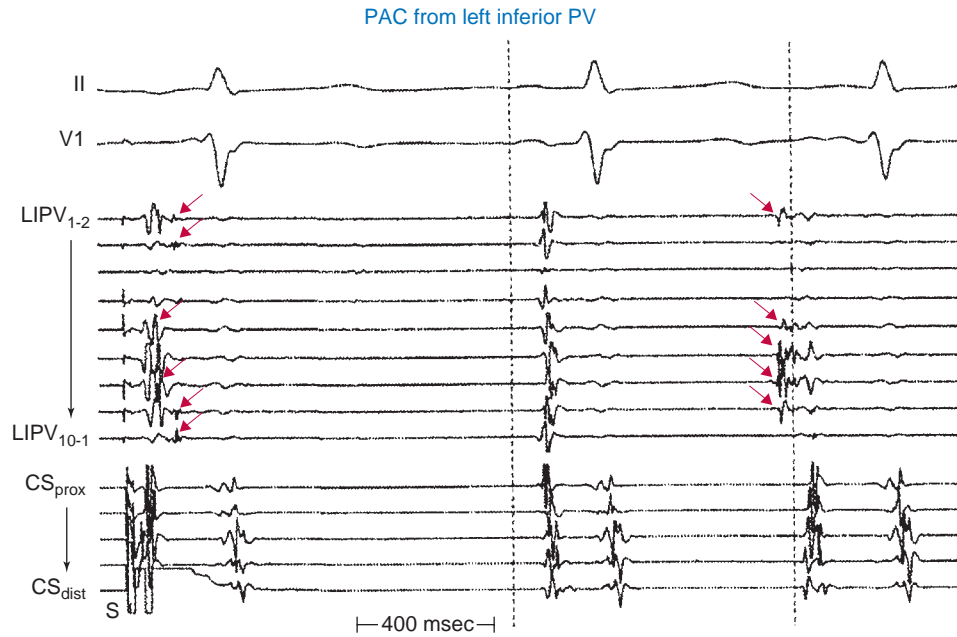


Fig. 15.19 Mapping Pulmonary Vein (PV) Ectopy Using a Ring Catheter. The ring catheter is positioned at the ostium of the left inferior PV (LIPV). *Left*, During pacing from the distal coronary sinus (CS) (at left), PV potentials (red arrows) follow the left atrium (LA) potentials. During normal sinus rhythm (middle complex), LA and PV potentials overlap, and they occur in the second half of the P wave. *Right*, During a premature atrial complex (PAC) originating from the LIPV, reversal of the electrogram sequence in the ring catheter recording is observed, with the PV potentials (red arrows) preceding the LA potentials and occurring well before the onset of the P wave on the surface electrocardiogram (dashed line). CS_{dist}, Distal coronary sinus; CS_{prox}, proximal coronary sinus.



Fig. 15.20 Concealed and Manifest Premature Pulmonary Vein (PV) Complexes. During pacing (S) from the proximal coronary sinus (CS_{prox}), a sharp potential (green arrow) is seen in several PV recording electrodes, followed by a second spike (red arrow) after the QRS complex. This is not a ventricular electrogram, since after the second paced complex, the delayed spike results in a propagated atrial premature complex (blue arrow). After the third stimulus, the main atrial electrogram is seen (green arrow) but the delayed PV spike is absent (open red arrow) due to its being refractory from the prior complex. The last paced complex is similar to the first. CS_{dist}, Distal coronary sinus; CS_{mid}, middle coronary sinus; RIPV, right inferior PV.

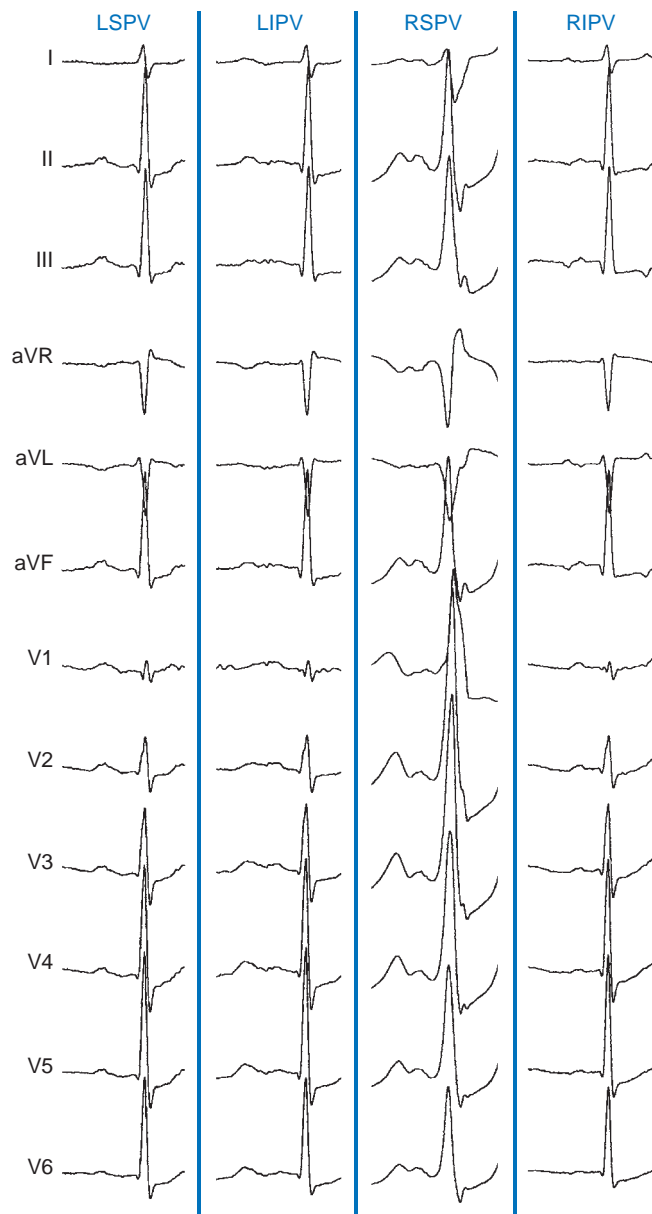


Fig. 15.21 Surface Electrocardiogram of Spontaneous Premature Atrial Complexes Originating From the Pulmonary Veins. *LIPV*, left inferior pulmonary vein; *LSPV*, left superior pulmonary vein; *RIPV*, right inferior pulmonary vein; *RSPV*, right superior pulmonary vein.

onset and short duration) preceding the onset of the ectopic P wave by 106 ± 24 milliseconds (range, 40 to 160 milliseconds) (see [eFig. 15.9](#); see [Fig. 15.19](#)). The spike is typically localized, and its amplitude rapidly decreases when the catheter tip is turned or moved a few millimeters. Bystander or far-field activity from contiguous branches can be distinguished by temporal delay or lower amplitude. The spike occurs earliest deep in the vein and progressively later toward the ostium and LA exit, thus resulting in distal-to-proximal venous activation during multipolar recordings (see [eFig. 15.9](#)). A second electrogram component with a slow deflection (depolarization rate [dV/dt] of less than 0.5 mV/ms), reflecting later LA activation, is temporally distinct from the spike inside the vein and then approaches and becomes continuous with the spike at the ostium.

Mechanically induced beats can be prevented by avoiding manipulation of the catheters during the recordings. These beats are excluded

by comparing the ECG pattern and intracardiac activation sequence with the confirmed spontaneous ectopic beats.

If the frequency of spontaneous or induced ectopy remains insufficient, focal mapping and ablation of AF can become difficult. In these cases, the use of a multielectrode basket catheter mapping (see [eFig. 15.9](#)) or noncontact mapping (EnSite) system can map a single beat and help identify the origin of spontaneously occurring PACs and PACs induced following cardioversion of spontaneous or induced AF.

Following successful ablation of the initially targeted PV triggers, a second PV is usually targeted if there are either significant spontaneous isolated PACs (at least 5 per minute), at least two separate PACs inducing AF, or PACs originating from the same PV inducing AF following cardioversion on at least two occasions.

Target of Ablation

The site showing the earliest atrial activity relative to the reference electrogram or onset of the ectopic P wave is targeted by ablation. If more than one PV is arrhythmogenic, the PV producing the most repetitive ectopy or AF-triggering ectopy is targeted first. If ablation of the ectopic focus fails, or the source is more than 1 cm within the PV, electrical isolation of the arrhythmogenic PV should be considered (see later). In addition, ablation can be performed at sites with catheter-induced repetitive ectopy, manifesting as a burst of rapid PACs starting on touching the wall, sustained irritability while at the site, and acute termination of rapid activity on release of the catheter.

Ablation Technique

RF energy is delivered using a 4-mm-tip catheter with a target temperature of 45°C to 50°C and a maximal power output of 25 to 30 W. When an irrigated-tip ablation catheter is used, RF power output is further reduced to minimize the risk of PV stenosis. At successful ablation sites, a rapid burst of PACs originating from that site often develops during RF energy delivery, or an abrupt disappearance of triggering PACs is observed. Cryoablation has also been used to target these sites although the precision of mapping is less (6-mm catheter tip).

Endpoints of Ablation

The endpoint of ablation is elimination of ectopy, spontaneous or induced by provocative maneuvers (using both the same provocative maneuvers and defibrillation protocols as before the ablation). Elimination or dissociation of PV potentials from atrial activity is also a satisfactory endpoint.

Outcome

Early experience with the focal ablation of PV arrhythmias has indicated that the recurrence rate is high and the success rate is only modest, even in experienced laboratories. The suboptimal results can be attributed to the limitations of the technique. Many patients have multiple foci in the same PV or in multiple PVs. Multiple arrhythmogenic PVs are usually associated with older age, longer AF duration, and larger atrial dimensions. In addition, there may be a paucity of spontaneous or inducible arrhythmias during the procedure. The spontaneous occurrence of ectopic beats and paroxysms of AF is unpredictable, and provocative procedures are not consistently effective. Mapping can also be made difficult by frequent recurrences of persistent AF requiring multiple cardioversions. Furthermore, after a successful procedure, new foci may emerge. Remapping usually shows new foci in the ablated vein or in other veins, rather than recurrence of the original focus.

It is also important to recognize that RF ablation inside the PVs carries a significant risk of PV stenosis, which limits the amount of RF energy that can be safely delivered within a PV. Some degree of PV stenosis was detected by increased PV flow velocity on TEE in 42% of

cases in one report. An increased risk of PV stenosis has been associated with the use of RF power more than 45 W.

Focal ablation has been successful only in highly selected patients with frequently recurring paroxysmal AF. Reported rates of a positive outcome using a focal ablation approach to eliminate AF triggers have varied from 38% to 80%. AF recurrences appear to be related to recovery of initially targeted foci or emergence of new nontargeted ones in the same or in a different PV. Because of these safety and efficacy limitations, this method is generally not used currently.

SEGMENTAL OSTIAL PULMONARY VEIN ISOLATION

Rationale

Electrical Isolation of Pulmonary Veins

On the basis of the knowledge of the AF initiation mechanism by focal discharges in the PVs, electrical disconnection at the PV ostium seemed to be a better ablative technique than focal ablation to inactivate focal triggers of AF. Ablation guided by mapping focal ectopy has a high recurrence rate and low long-term success and is limited by unpredictability, inconsistent inducibility, and the risk of inducing AF requiring cardioversion multiple times during the procedure. Moreover, the appearance of multiple sources of AF triggers and the high recurrence rate argue for more extensive ablation strategy. PV isolation has been introduced to address these issues.

PV potentials identify muscular sleeves that extend from the LA into the PVs. These muscular bands are responsible for transmitting triggering impulses from the vein to the LA. The myocardial fibers that envelop the PVs may not be present along the entire circumference of the PV ostia. Therefore to eliminate conduction in and out of a PV, ablation along the entire circumference of the ostium may not be necessary. Instead, ablation can be targeted to the segments of the ostium at which muscle fibers are present, which typically involves RF application to 30% to 80% of the circumference of the PVs. These sites are identified by the presence of high-frequency depolarizations, which represent PV muscle potentials.

The major advantages of this technique are that it eliminates the need for detailed mapping of all PV foci and that there is a clear-cut endpoint of ablation, even when spontaneous arrhythmias are absent, and PV stenosis is far less likely to occur (although it is still possible).

Which Pulmonary Veins to Isolate

Only arrhythmogenic PVs. Focal ablation deep in a PV carries a risk of PV stenosis. Restricting RF delivery to the ostium of the arrhythmogenic PV, as in segmental ostial PV isolation, can help reduce this risk. Furthermore, a more limited ablation approach (as compared with isolation of all PVs) requires shorter procedure and fluoroscopy times and can potentially be safer.

All four PVs. Electrical isolation of only the arrhythmogenic PV was shown to have a limited success rate. Furthermore, identification of the arrhythmogenic PV can be difficult and time consuming, because focal activity can be difficult to observe or induce during the ablation procedure. In addition, the prevalence of multiple arrhythmogenic PVs is high (greater than 70%). Therefore isolation of only the “culprit” PV identified during the procedure may allow the emergence of focal ectopy from other PVs, which can potentially cause AF recurrence after the procedure. Moreover, electrical disconnection may not be achieved by ostial ablation to only the targeted PV in patients with electrical connections between the PVs (i.e., across the carina between left PVs).

Evidence has suggested that almost all PVs are capable of generating the premature depolarizations that trigger AF, and the upper PVs are

responsible for most AF triggers (the left superior PV is the vein with the longest muscular sleeve). Only a few (0% to 30%) foci have been identified in the inferior PVs (the right inferior PV is the least important source of triggers). Therefore unless no PV potentials are present at its ostium (a rare finding), all four PVs should be targeted, whenever feasible.

Circumferential Mapping of Pulmonary Vein Potentials

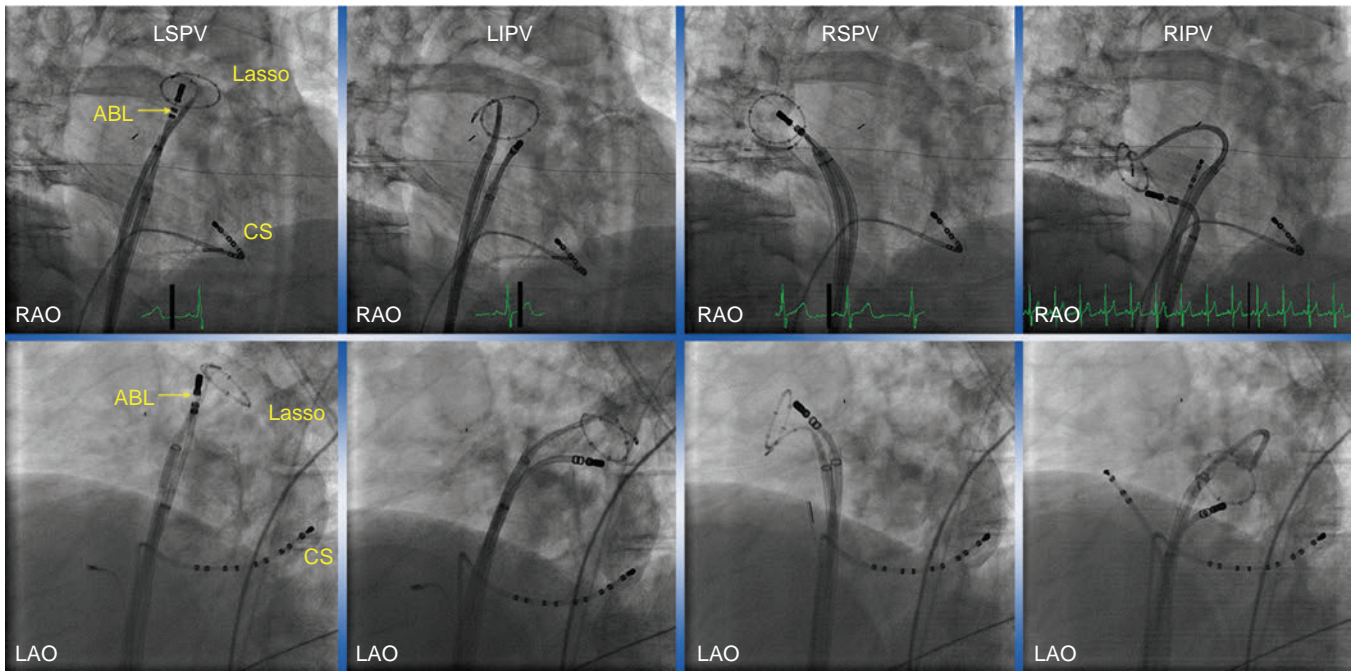
Ring Catheter Mapping

A deflectable decapolar catheter with a distal ring configuration is advanced sequentially into each PV and is used for ostial mapping (eFig. 15.10). The ring catheter enables circumferential mapping of the PV ostia perpendicular to the axis of the vein. Lasso catheters are of different sizes. The selection of a 15-, 20-, or 25-mm-diameter Lasso catheter can be guided by the estimated size of the PVs on preprocedural imaging (CT or CRM). PV angiographically also can be performed, but is rarely needed (see eFig. 15.8). Because of the highly variable sizes of PV ostia, fixed-diameter catheters may not always achieve catheter stability and optimal electrogram recordings. In some cases, suboptimal positioning, poor wall contact, and poor stability of an inappropriately sized circumferential catheter underestimate the number of PV potentials and can result in failure to isolate the PV completely because of undetected residual PV-atrial electrical connections. Some of those issues can be addressed by using an expandable 15- to 25-mm-diameter ring catheter. The expandable ring catheter is introduced into each PV and withdrawn to the most proximal stable position, with optimal wall contact ensured by progressive loop expansion. These catheters enable more proximal and stable placement and optimal wall contact at the PV ostia. This is important because the ablation target is not within the ostia, but in the atrial tissue proximal to the LA-PV junction.

The ring catheter is positioned within a PV and gradually withdrawn to within 5 mm of the ostium. It is important to position the ring catheter at the ostium of the PV; when it is positioned too deeply in the PV, PV potentials can be missed (Fig. 15.22). Subsequently, circumferential mapping of the PV is performed by obtaining 10 bipolar electrograms (1-2, 2-3, up to 10-1 electrode pairs) with the circular arranged electrodes of the ring catheter. The band-pass settings for the bipolar recordings are 30 to 500 Hz. Pacing from each pair of electrodes from the ring catheter has been used by some to ensure appropriate ring catheter sizing (80% of electrode pairs resulting in capture) and to demonstrate conduction from the veins to the atrium before ablation. Alternatively, the ablation catheter may be used to pace locations in the PV that capture and conduct to the atrium; these sites are tagged on the electroanatomic mapping system for subsequent use after PV isolation; pacing at these sites without conduction to atrium signifies PV exit block (see below).

Ring catheters with 20 poles are also available and can offer higher resolution circumferential mapping and improve the differentiation of PV from LA potentials. The conventional wide bipolar electrograms record the PV potentials, as well as the larger LA potentials, which can obscure or mimic the PV potentials. In contrast, the high-resolution electrograms minimize the extent of far-field electrogram detection and display very small or completely absent LA potentials. In the context of PV isolation during sustained AF, improved discrimination between atrial and PV potentials can facilitate the recognition of complete PV disconnection and possibly limit the number of unnecessary RF applications. On the other hand, when a ring catheter and closely spaced electrodes make poor contact with the PV wall or are placed deep within the PV, near-field potentials may not be seen, which leads to under-detection of PV potentials.

The use of a navigational system (CARTO-3, EnSite NavX, or Rhythmia) in ostial segmental PV isolation provides accurate nonfluoroscopic



eFig. 15.10 Fluoroscopy Views (Right Anterior Oblique [RAO] and Left Anterior Oblique [LAO]) of the Ring Catheter Positioned at the Ostium of the Four Pulmonary Veins (PVs). Panels from left to right: Left superior PV (LSPV), left inferior PV (LIPV), right superior PV (RSPV), and right inferior PV (RIPV). Note that during ablation, the ablation catheter (ABL) is always positioned at the atrial side of the ring catheter. CS, Coronary sinus.

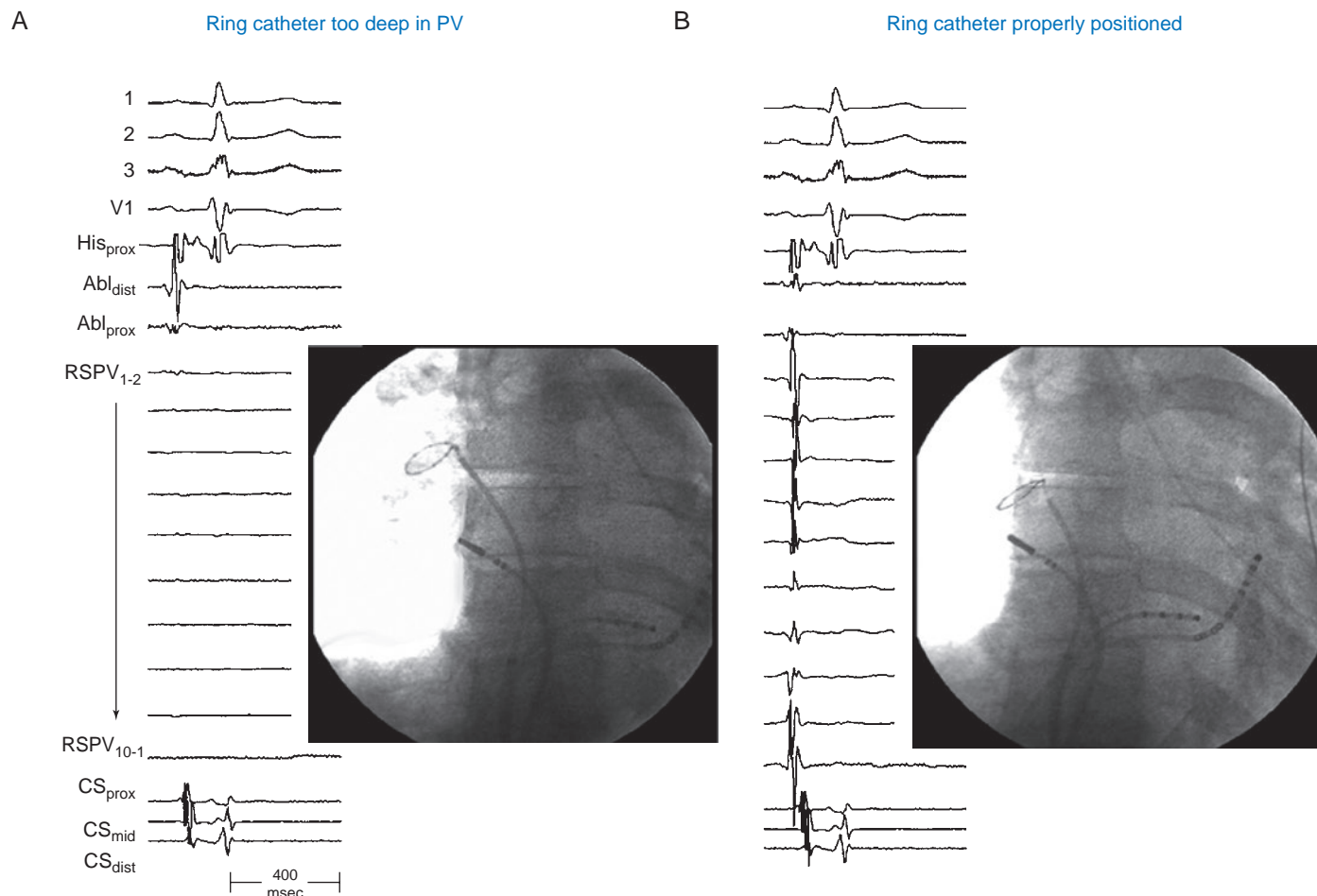


Fig. 15.22 Recordings From a Ring Catheter in the Right Superior Pulmonary Vein (RSPV). (A) The ring catheter is situated too deep in the vein; recordings suggest no pulmonary vein (PV) potentials. (B) The ring catheter pulled back 1.5 cm, showing abundant PV potentials. *Abl_{dist}*, Distal ablation site; *Abl_{prox}*, proximal ablation site; *CS_{dist}*, distal coronary sinus; *CS_{mid}*, middle coronary sinus; *CS_{prox}*, proximal coronary sinus; *His_{prox}*, proximal His bundle.

visualization of multiple catheter tips and curves (including the ring catheter) and allows a real-time assessment of wall contact and catheter stability, as well as assessment of the spatial relationship between ablation and ring catheters. Furthermore, these systems can take a shadow or snapshot of the position of the ring catheter and, hence, facilitate accurate repositioning of the catheter in the case of displacement from its original location. Also, the system enables labeling the electrodes on the ring catheters, thus allowing precise navigation of the ablation catheter to the labeled pole of the ring catheter without the assistance of fluoroscopy.

Mapping During Normal Sinus Rhythm

It is preferable to perform PV mapping during NSR or atrial pacing whenever possible because AF reduces PV potential amplitude and makes them more difficult to identify. Therefore if the patient is in AF, electrical cardioversion is usually performed to restore NSR. Ibutilide or amiodarone can also be administered intravenously to prevent immediate recurrences of AF after cardioversion. Isolation can still be achieved if AF persists, however (see below).

PV mapping during NSR typically shows double or multiple potentials that are usually recorded in a progressively later temporal sequence, synchronous with the first (right PVs) or second (left PVs) half of the

sinus P wave (Fig. 15.23). The first low-frequency potential reflects activation of the adjacent LA. The latest high-frequency electrograms indicate PV potentials.

Identification of PV potentials using pacing maneuvers. PV potentials often are fused with the far-field LA electrograms but can be identified by their high-frequency appearance. Not uncommonly, an isoelectric interval separates the far-field LA electrogram and the near-field PV potential. The basis for this separation is unclear; however, evidence has suggested that there is an area of slow conduction at the proximal PV. The interval between the far-field electrogram and the PV potential can differ based on the site of pacing, likely related to fiber orientation (anisotropy), which can make it easier to enter the vein from certain wavefront directions or because the far-field electrogram is not actually coming from the LA but is arising from a neighboring structure. Therefore pacing from different atrial sites (most commonly high RA or distal CS) can help separate PV potentials from far-field atrial signals (see Figs. 15.23 and 15.24). Furthermore, incremental rate atrial pacing and premature atrial stimulation from the same atrial site can sometimes result in conduction delay between the LA and PV at the PV ostium, which often exhibits decremental conduction properties (Fig. 15.25). Thus if a complex electrogram is seen on a PV mapping catheter and, with faster or premature pacing, one of

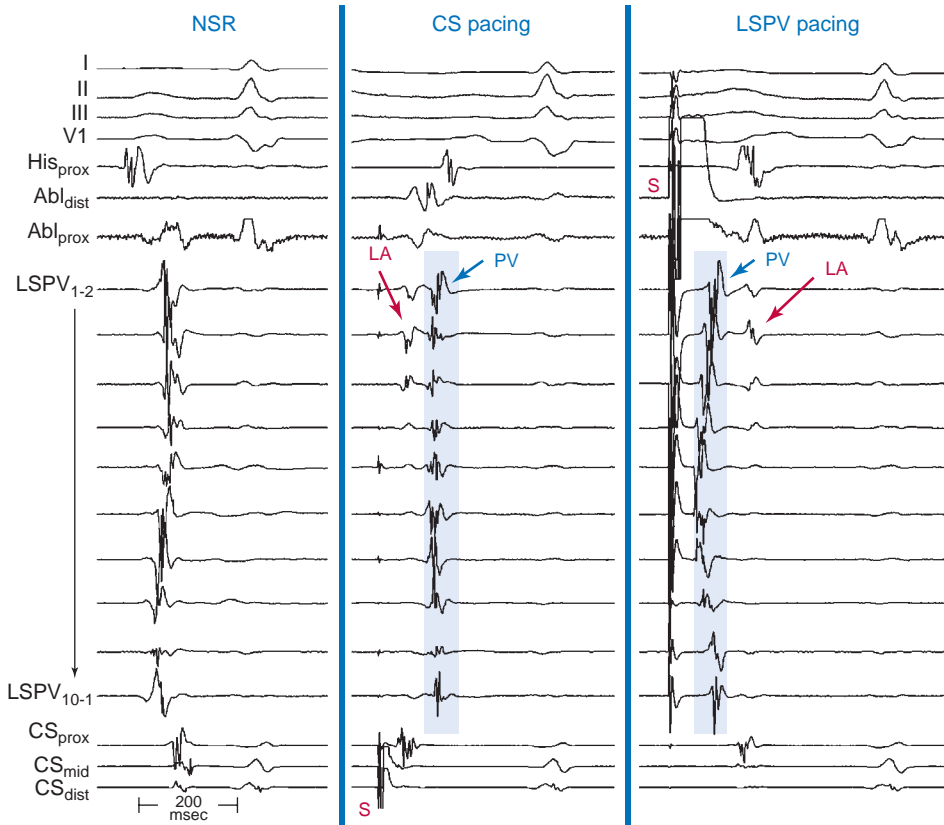


Fig. 15.23 Differential Atrial Pacing to Identify Pulmonary Vein (PV) Potentials. *Left panel*, During normal sinus rhythm (NSR), the atrial and left superior PV (LSPV) potentials are superimposed and distinction of PV potentials from left atrial (LA) electrograms is difficult, if not impossible. *Middle panel*, During coronary sinus (CS) pacing, PV potentials (shaded area) are delayed relative to LA potentials and are thus readily discerned. *Right panel*, Pacing from within the LSPV also shows a clear delineation of PV versus LA potentials; in this case, PV potentials precede LA potentials. *Abl_{dist}*, Distal ablation site; *Abl_{prox}*, proximal ablation site; *CS_{dist}*, distal coronary sinus; *CS_{mid}*, middle coronary sinus; *CS_{prox}*, proximal coronary sinus; *His_{prox}*, proximal His bundle.

the potentials is seen to occur later after the far-field atrial electrogram, the delayed signal likely is a PV potential.

Right-sided PVs are typically mapped during NSR or RA pacing. For left PVs, the ostial PV potentials are sometimes not obvious during NSR because of the superimposed LA potential; therefore pacing from the distal CS (at a pacing cycle length [PCL] of 600 milliseconds) allows their separation and easy recognition of PV potentials (see Fig. 15.23). However, even during CS pacing, the atrial and PV potentials still can overlap in approximately 50% to 60% of left PVs (see Fig. 15.25). The separation can be less evident in the posterior PV antrum, which is closer to the CS. Pacing from the LAA can help in this situation.

Because of the anatomic proximity of the PVs to several other structures that are electrically active, complex signals can be recorded by a catheter placed in the PV. For example, a catheter placed in the left superior PV can potentially record electrical activity in the LA, LAA, left inferior PV, and ligament of Marshall. Similarly, a mapping catheter placed in the right superior PV may record electrical activity in the right middle PV, right inferior PV (particularly a superior branch), RA, LA, and SVC (Fig. 15.26). When a typical PV potential is recorded in a left PV, the far-field electrogram usually is coming from the LA. When mapping catheters are placed in the right-sided PV, often the main far-field electrogram is the RA electrogram, and the second far-field electrogram, if seen, is the LA electrogram. In general, only the PV potential itself is near-field; all other structures picked up by the antenna

of the mapping catheter are blunted and far-field. However, this criterion alone is insufficient for identifying the true PV potential. For example, if a catheter is deep within the left superior PV, where no PV musculature is present, the LAA electrograms will appear relatively near-field. Similarly, when RF ablation has already been performed, edema near the PV ostium and inadvertent ablation within the PV (more frequent than generally realized) will cause PV potentials to be less sharp and less near-field in character. Various pacing maneuvers can differentiate from among these possibilities and can help exclude or prove a relationship of various components of the electrogram recorded from a PV to anatomic structures surrounding that particular PV. An important feature of far-field potentials is that they should be seen only on electrodes that “face” the structure in question; for instance, with a catheter in the left superior PV, signals that are recorded on electrodes adjacent to the LAA can represent far-field recordings from that structure, whereas signals visible only on electrodes at the posterior aspect of the left superior PV cannot be far-field LAA potentials (Fig. 15.27).

One pacing maneuver commonly used when complex electrograms are recorded on a mapping catheter placed in a PV is pacing at specific sites likely to be responsible for the components of the electrogram. The premise of such a maneuver is that pacing from a particular site causes the electrogram originating from that site to occur earlier, close to the pacing stimulus. For example, because of the proximity of the LAA to the left PVs (especially the left superior PV), far-field LAA

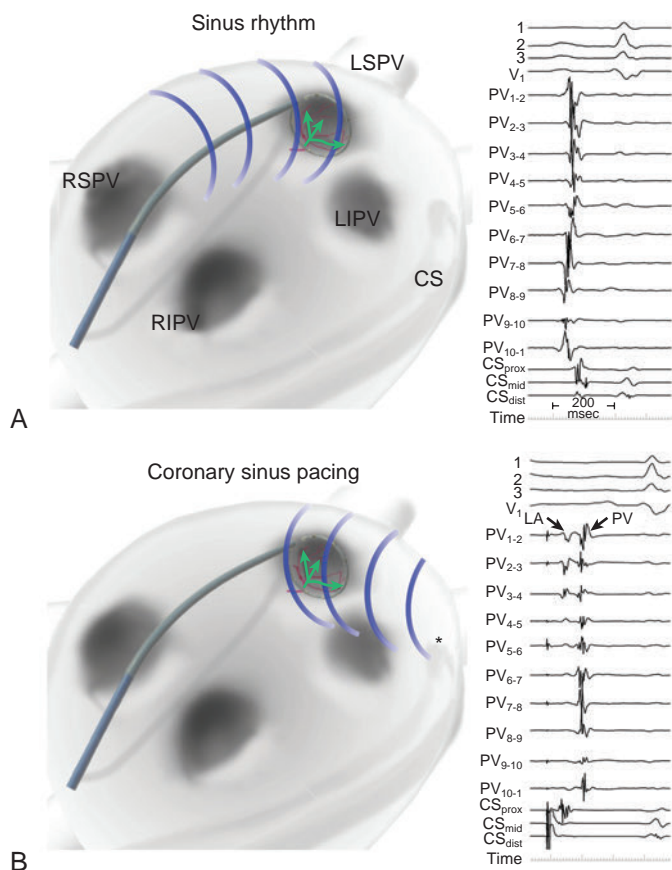


Fig. 15.24 Depiction of Differential Activation of Left Atrial (LA) and Pulmonary Vein (PV) Potentials. The LA is opened from the front, showing orifices of PVs; a ring catheter is in the left superior PV (LSPV). Red strands indicate a muscular PV fascicle extending into the LSPV; green arrows indicate propagation into the PV over the fascicle. (A) During sinus rhythm, the wavefront propagates as indicated by blue curved lines and activates LA tissue around the PV and the PV fascicle at almost the same time, yielding a summated electrogram at right. (B) During pacing from the coronary sinus (CS, at asterisk), the wavefront approaches from a different direction and activates LA muscle well before the PV fascicle is entered, accounting for the delay in PV potential inscription at right. CS_{dist}, Distal coronary sinus; CS_{mid}, middle coronary sinus; CS_{prox}, proximal coronary sinus; LIPV, left inferior pulmonary vein; RIPV, right inferior pulmonary vein; RSPV, right superior pulmonary vein.

potentials can be recorded in these PVs, and PV potentials can be confused with LAA potentials. These potentials are distinguished from PV potentials by differential pacing from the distal CS and LAA. If a pacing catheter is placed in the LAA and LAA capture is documented, the LAA component of the complex electrogram will occur early and will be drawn toward the pacing artifact (Fig. 15.28). Thus the electrogram that moves the closest to the pacing stimulus can be diagnosed as originating from the LAA. Similar reasoning can be applied when pacing in an ipsilateral PV—if a component of the electrogram recorded in the left superior PV is, in fact, a left inferior PV potential.

LA electrograms, particularly when fragmented secondary to partial ablation, can also be mistaken for a PV potential, and pacing from a site in the LA close to, but not within, the PV (perivenous pacing) can help define the LA electrogram component of a complex PV recording. When pacing from a perivenous location, the LA signal will occur very close to, and often will merge with, the saturation artifact related to

the pacing spike. However, because pacing is being performed proximal to the site of ostial delay, the PV potential remains unchanged or may occur with slightly more delay. The shift of the LA signal, which now is being captured by perivenous pacing, toward the pacing spike indicates the origin of that component of a complex signal. Differentiation of RA, LA, and PV potentials recorded within right-sided PVs can also be achieved using similar maneuvers (Fig. 15.29).

Multisite simultaneous pacing is an extension of the basic concept that pacing from a particular site will cause earlier occurrence of the electrogram arising from that site. For example, pacing from the CS alone is compared with simultaneous pacing from both the CS and LAA, with specific attention paid to the transition in the recorded electrogram between single-site (e.g., CS only) and dual-site (e.g., CS and LAA) pacing, which can help immediate distinction of the various components of a complex signal recorded within the PV.

Ablation target sites. Target sites for ablation are selected by identifying the earliest bipolar PV potentials or the unipolar electrograms with the most rapid (sharpest) intrinsic deflection on high-speed recordings (150 to 200 mm/s) that have equivalent or earlier activation relative to the earliest PV potential recorded on the adjacent ring catheter recording sites (Fig. 15.30).

Electrogram polarity reversal can also be used as an additional indicator of breakthroughs from the LA to the PVs and identify potential ablation targets. *Polarity reversal* is defined as a sudden change in the main deflection of the PV potential. The reversal occurs as the wavefront of activation propagates radially in the PV from its connection with the LA, thus reaching contiguous bipolar recording electrodes in opposing directions (see Figs. 15.30 and 15.31).

Mapping During Atrial Fibrillation

Although segmental ostial PV isolation is accomplished most efficiently during NSR, maintaining NSR during an ablation procedure may not be readily achievable, particularly in patients with longstanding persistent AF. During an ongoing episode of AF, PV potentials can be obscured during the chaotic electrical activity of AF. Nevertheless, segmental ostial PV isolation was found to be as feasible and successful during AF as during NSR. An advantage of mapping during AF is that it obviates the need for the administration of antiarrhythmic drugs and for multiple electrical cardioversions in patients with frequent AF recurrences during the procedure. Two approaches have been described for PV isolation during AF: the first uses intermittent bursts of PV tachycardia to guide PV isolation, and the second uses organized PV potentials during AF to guide PV isolation.

Intermittent PV tachycardia. Prior studies demonstrated that rapid rhythms arising in the PVs (intermittent PV tachycardia) are common during AF and can play an important role in the maintenance of AF, or they can be a marker of an arrhythmogenic PV that triggers AF. Those intermittent bursts of PV tachycardia indicate the presence of an underlying arrhythmogenic muscle fascicle near the ostial recording sites and therefore can be used to guide segmental ostial ablation to isolate the PVs during AF.

During AF, the PVs are sequentially mapped with the ring catheter to assess the presence of intermittent PV tachycardia, defined as a PV rhythm that intermittently has a CL shorter than the AF CL recorded in the adjacent LA. When intermittent PV tachycardia is recorded on several electrodes, the ostial site corresponding to the most rapid intrinsic deflection of the unipolar electrogram should be targeted by RF applications. If PV tachycardia is not observed, ostial sites that display a high-frequency bipolar PV potential or rapid unipolar intrinsic deflection during AF can alternatively be targeted for ablation.

If AF terminates during ablation, PV potentials are then assessed during NSR and atrial pacing. If there is evidence of residual conduction

Decremental conduction at the PV ostium

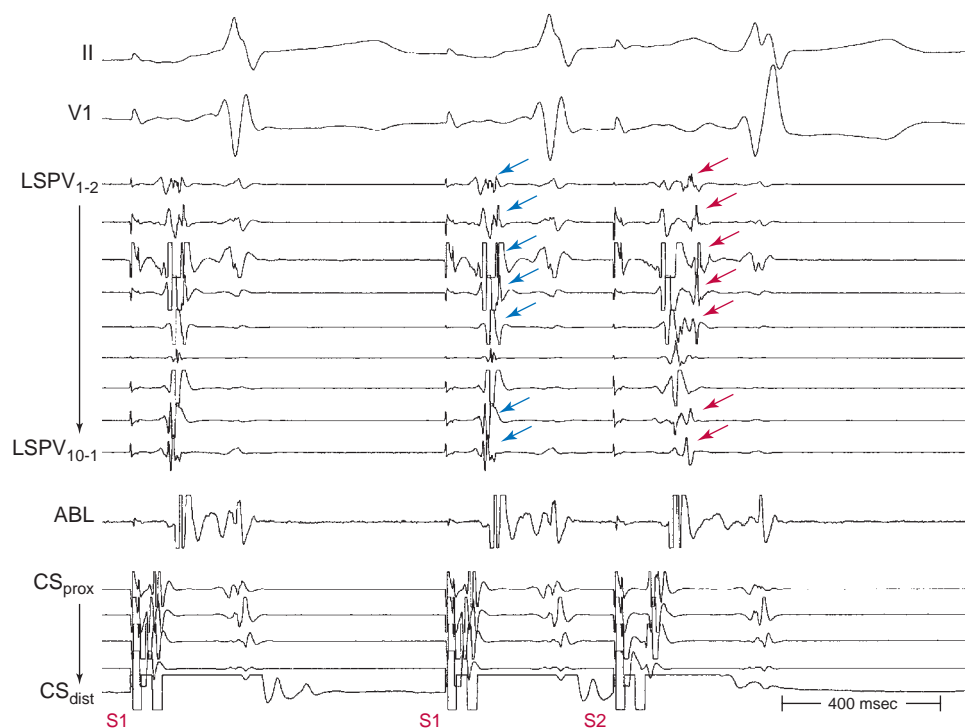


Fig. 15.25 Decremental Conduction at the Pulmonary Vein (PV) Ostium. During coronary sinus (CS) drive pacing, complex electrograms (blue arrows) are recorded by the ring catheter positioned at the ostium of the left superior PV (LSPV). An atrial extra-stimulus from the distal CS results in conduction delay between the left atrium (LA) and the PV at the PV ostium. Therefore PV potentials (red arrows) become delayed and separated from atrial electrograms. ABL, Ablation catheter; CS_{dist}, distal coronary sinus; CS_{prox}, proximal coronary sinus.

Right superior PV

SVC



Fig. 15.26 Superior Vena Cava (SVC) Activity Recorded in the Right Superior Pulmonary Vein (PV). *Left panel*, Recordings from a ring catheter positioned at the ostium of the right superior PV showing high-amplitude PV potentials that disappear midway through the recording because of isolation of the vein with radiofrequency ablation. Another set of lower amplitude signals (arrows) remains and was present prior to PV isolation. *Right panel*, These potentials represent far-field SVC recordings, shown as sharp near-field recordings after the ring catheter is positioned in the SVC. Abl_{dist}, Distal ablation site; Abl_{prox}, proximal ablation site; CS_{dist}, distal coronary sinus; CS_{mid}, middle coronary sinus; CS_{prox}, proximal coronary sinus; His_{prox}, proximal His bundle.

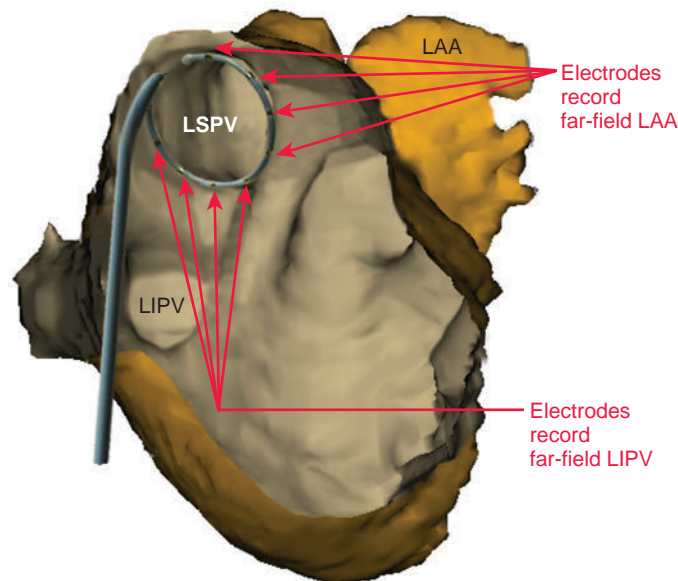


Fig. 15.27 Left Pulmonary Veins Versus Left Atrial Appendage (LAA). Cutaway view of the left atrium showing the inside of the lateral aspect. A ring catheter is depicted in the left superior pulmonary vein (LSPV). Far-field recordings can be made from adjacent structures on certain electrodes of the ring catheter as indicated, such as LAA or left inferior pulmonary vein (LIPV).

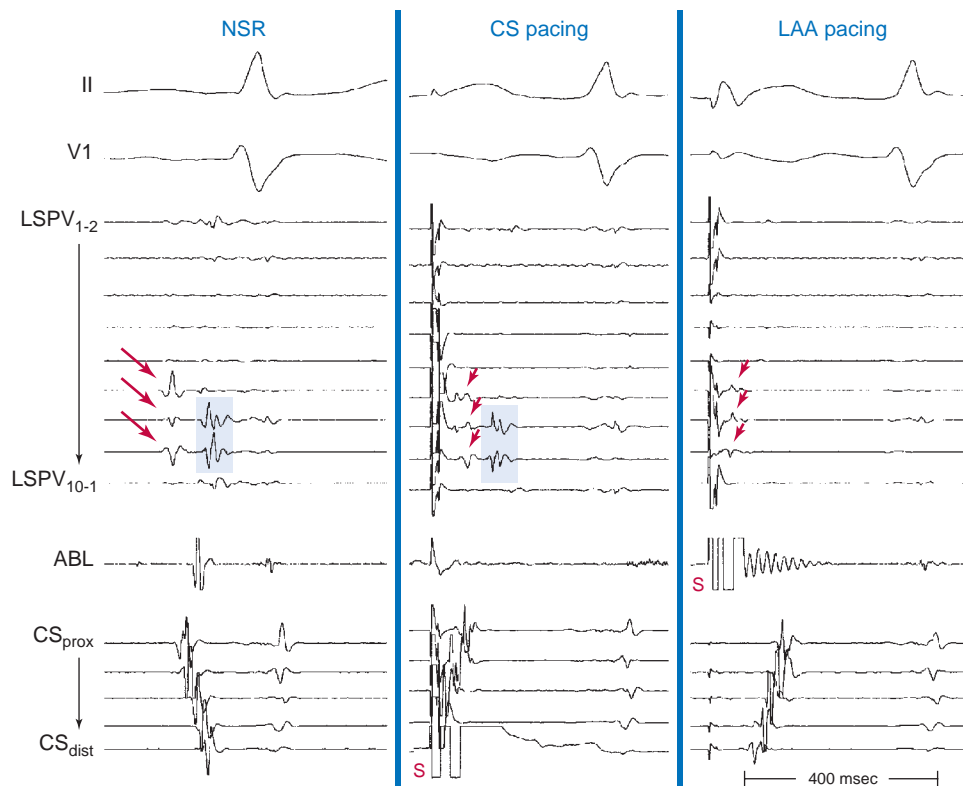


Fig. 15.28 Differential Pacing for Identification of Pulmonary Vein (PV) Potentials. During electrical isolation of the left superior PV (LSPV) in normal sinus rhythm (NSR), residual electrograms were persistent despite multiple radiofrequency (RF) applications. The initial electrograms (red arrows) were consistent with left atrial (LA) far-field activity. However, the late electrograms (shaded area) were suggestive of PV activity. Pacing from the distal coronary sinus (CS) resulted in anticipation of both early and late electrograms. Pacing via the ablation catheter (ABL) positioned in the LA appendage (LAA) resulted in disappearance of the late electrograms (i.e., those electrograms merged with the saturation artifact related to the pacing spike), a finding suggesting that those electrograms in fact represented LAA activity. Therefore the presence of PV potentials was excluded, and no further RF ablation was necessary. CS_{dist}, Distal coronary sinus; CS_{prox}, proximal coronary sinus.

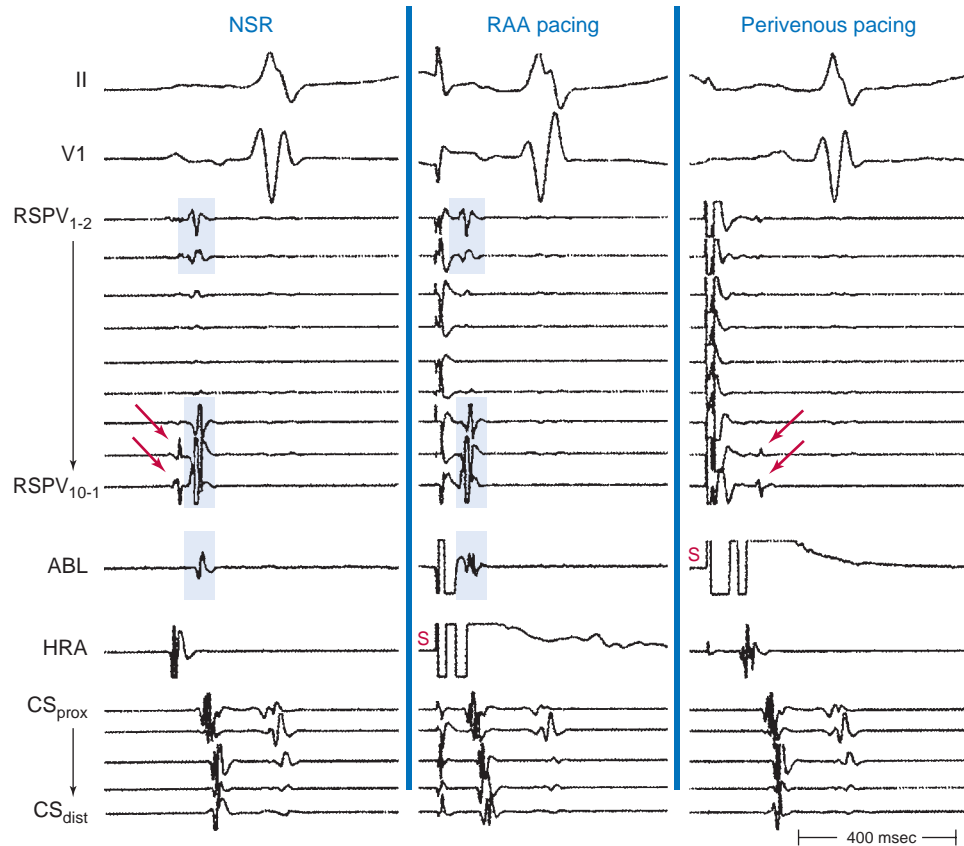


Fig. 15.29 Differential Pacing to Distinguish Pulmonary Vein (PV) Potentials From Right and Left Atrial Potentials. During electrical isolation of the right superior PV (RSPV) in normal sinus rhythm (NSR), residual electrograms (blue shaded area and red arrows) were persistent despite multiple radiofrequency (RF) applications. Pacing from the right atrial (RA) appendage (RAA) resulted in disappearance of the earlier electrograms (red arrows; i.e., those electrograms merged with the saturation artifact related to the pacing spike), a finding suggesting that those electrograms in fact represented RA activity. During pacing just outside the ostium of the RSPV (using the ablation catheter), the second set of electrograms (shaded area) disappeared, whereas the RA electrograms (red arrows) persisted in the ring catheter recordings, indicating that the second set of electrograms in fact represented left atrial activity. Therefore the presence of PV potentials was excluded, and no further RF ablation was necessary. ABL, Ablation catheter; CS_{dist}, distal coronary sinus; CS_{prox}, proximal coronary sinus; HRA, high right atrium.

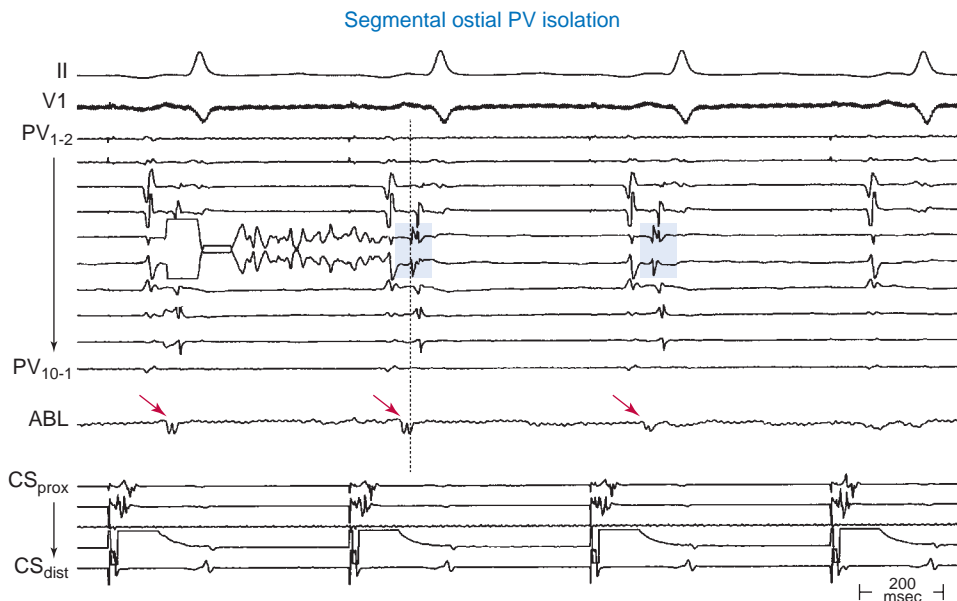


Fig. 15.30 Segmental Ostial Pulmonary Vein (PV) Isolation. During circumferential ostial PV mapping using a ring catheter, electrical connections between the left atrium (LA) and the PV (target sites for ablation) are identified by recording the earliest bipolar PV potentials with electrogram polarity reversal on adjacent poles (shaded electrograms). Note that the distal bipoles of the ablation catheter record even an earlier sharp PV potential (arrows). The presence of ablation artifact on the recording from a specific ring catheter pole confirms the pole the catheter is on and that the catheter is in the same plane as the ring catheter. Catheter ablation at that site results in complete elimination of PV potentials and LA-PV block (last complex). ABL, Ablation catheter; CS_{dist}, distal coronary sinus; CS_{prox}, proximal coronary sinus.

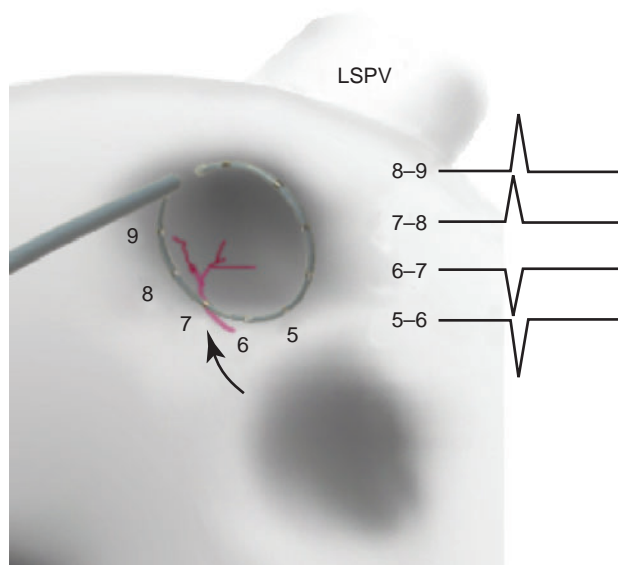


Fig. 15.31 Bipolar Electrogram Polarity Reversal. The ring electrode catheter (electrodes numbered) is situated in the ostium of the left superior pulmonary vein (LSPV); a strand of atrial muscle crosses from the left atrium (LA) to the pulmonary vein (PV) (red) and branches within the vein. The arrow indicates propagation of the wavefront of activation from the LA to the PV. The strand crosses at electrode 7; recordings from surrounding bipoles indicate the direction of propagation away from (negative deflection) or toward (positive deflection) the bipole. The point at which the polarity reverses from positive to negative is where the strand crosses into the PV.

over a PV fascicle, RF energy is delivered at these ostial sites during NSR or atrial pacing. On the other hand, if AF is still present after isolation of a PV, electrical cardioversion is performed. If AF recurs, other PVs are isolated during AF and, if NSR is maintained, the remaining PVs are isolated during NSR or atrial pacing.

Organization of PV potentials. PV potentials can be classified at baseline as organized (have a consistent activation sequence for more than 10 seconds) or disorganized (activation sequence on the ring catheter varies from beat to beat). Approximately 37% of PVs have organized PV potentials (more for inferior than superior PVs—53% vs. 26%; Fig. 15.32). When the PV activation pattern is organized (from the beginning or after some anatomically guided RF applications), the area showing the earliest activation or demonstrating polarity reversal on the ring catheter is targeted.

For disorganized PV potentials, ablation is performed circumferentially around the ring catheter on the ostial side of the PV. The top and bottom segments of the PV are targeted first because of the high prevalence of LA-PV breakthroughs at these sites. In most cases, initial RF applications result in organization of PV activity. This activity is probably secondary to progressive reduction of LA-PV breakthroughs that diminishes the mass of fibrillatory conduction within the PV and channels the electrical activity through the last remaining fascicles connecting the LA to the PV, thereby activating the PV in an organized fashion. This consequently enables EP-guided PV isolation.

Organized PV activity can represent fewer LA-PV connections and therefore may require fewer RF applications than PVs with disorganized activity. This may explain the greater frequency of organized activity in the inferior PVs, presumably because of the presence of less extensive muscular sleeves in these veins as demonstrated by pathological studies.

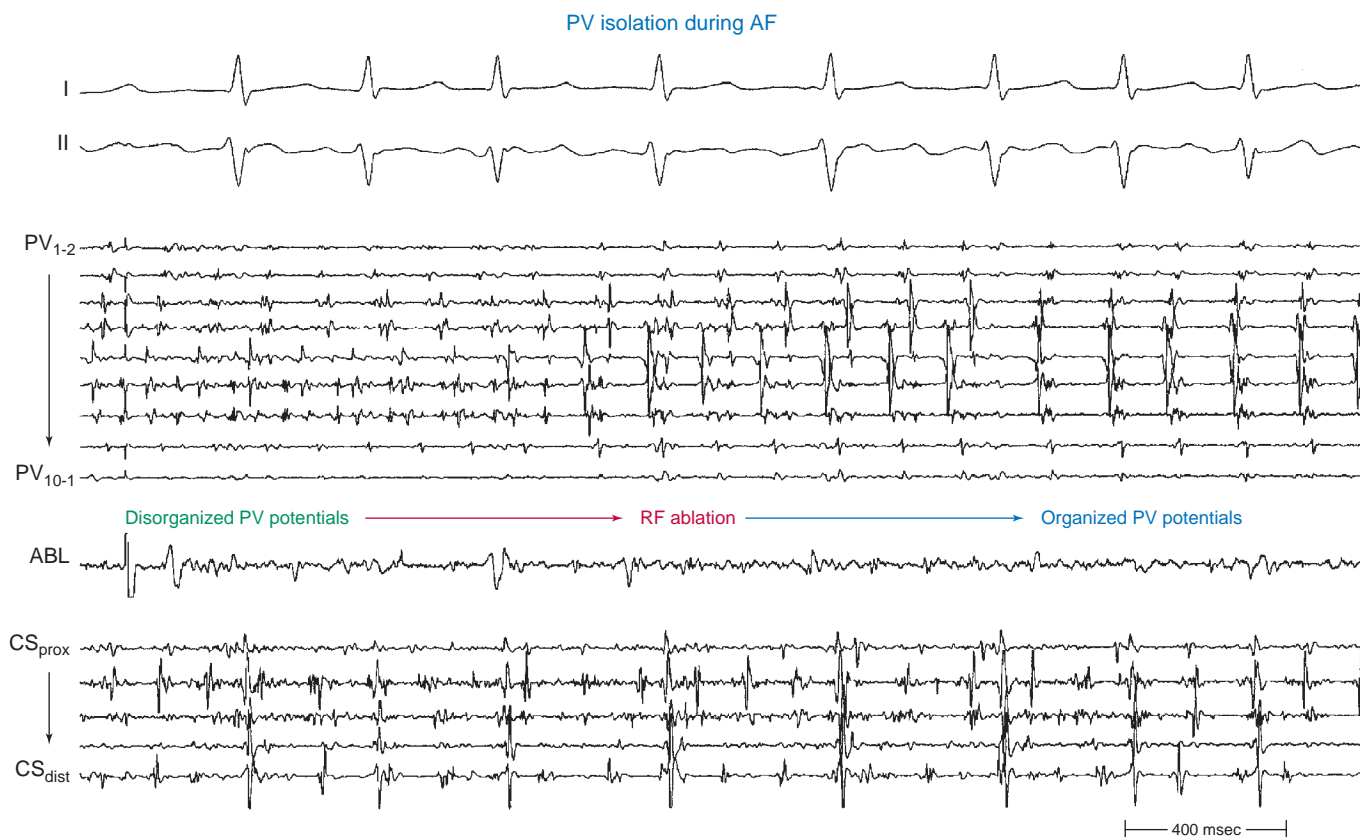


Fig. 15.32 Pulmonary Vein (PV) Isolation During Atrial Fibrillation (AF). Initially (at left), PV potentials are disorganized. During radiofrequency (RF) application at the PV ostium, the PV potentials become organized. See text for discussion. ABL, Ablation catheter; CS_{dist}, distal coronary sinus; CS_{prox}, proximal coronary sinus.

Basket Catheter Mapping

The basket catheter (Constellation, Boston Scientific) is composed of 64 electrodes mounted on 8 flexible, self-expanding splines (see Fig. 4.3). Each spline is identified by a letter (from A to H) and each electrode by a number (distal 1 to proximal 8). The 32 bipolar electrograms provide 3-D mapping of PV activation.

Basket catheter positioning. After transseptal access is gained, an 8.5 Fr soft-tipped guiding sheath with a 90- or 120-degree curve or, preferably, a deflectable sheath, is introduced into the PVs. A steerable ablation catheter can help introduce the sheath into the PVs (especially the inferior PVs). The ablation catheter is introduced through the sheath, and once it is engaged in the PV, the sheath is advanced over the ablation catheter. Once the sheath is in place in the PV, the steerable catheter is removed and is replaced by the basket catheter. The basket catheter is introduced into the sheath so that the tip of the basket catheter reaches the tip of the sheath; the sheath is then pulled back to allow expansion of the basket catheter (eFig. 15.11). Alternatively, the basket catheter is inserted into the PVs with the sheath positioned in the LA. However, although this technique was found to be safe because of the very flexible splines of the basket catheter, extreme caution is required to avoid venous perforation by the stiff catheter tip.

A basket catheter with a diameter of 31 mm is chosen when the diameter of the main PV trunk is 26 mm or smaller, and a basket catheter with a diameter of 38 mm is used when the PV diameter is greater than 26 mm or when there is a common ostium. The PV diameter is determined by preacquired CMR, CT scanning, or PV angiography. The position of the basket catheter in relation to the PV ostium can be determined by PV angiography (Fig. 15.33) or ICE. If necessary, the basket catheter is retracted to obtain optimal contact to the main trunk and ostium of the PV.

Basket catheter mapping. The basket catheter is deployed within the target PV with its most proximal electrodes positioned at the PV ostium, as determined by selective PV angiography. PV activation can be followed during NSR or CS pacing propagating through the four levels of bipolar electrograms from proximal ostial (¼) to distal (½) inside the PV. During ectopic beats or initiation of AF, the activation can be followed from the source of ectopy to its exit to the LA (see eFig. 15.9).

Ablation is performed at the junction between the PV and the LA targeting the site of earliest PV potential recording or shortest atrial-PV potential delay. The location of the ostium is determined by electrogram morphology and by noting the shape of the basket catheter

because it conforms to the PV, and ostial anatomy can be confirmed by angiography.

Advantages of the basket catheter. The basket catheter offers higher resolution as compared to the ring catheter for mapping of the LA-PV junction. In addition, the basket catheter provides information about the anatomy of the PV, such as exact ostium localization, because the basket catheter takes the shape of the PV (see Fig. 15.33) and allows 3-D reconstruction of the PV activation from the ostium to deep inside the PV.

Furthermore, the distal poles of the basket catheter can be used to monitor changes in the activation sequence in real time and to demonstrate the effects of ablation at the ostium as lesions are created. They also provide an immediate indication of successful PV isolation by the disappearance of the distal PV potentials. The system also helps identify areas near the PV ostium with fragmented potentials and with discharging ostial foci, which can be localized in a single beat.

Basket catheter–guided PV isolation can potentially minimize the risk of PV stenosis, first by reducing the number of RF applications and second by avoiding ablation inside the PV, because the basket catheter allows localization of the PV ostium during the entire procedure. Thus the use of complementary navigation systems or ICE appears to be nonessential when using the basket catheter for PV isolation.

Disadvantages of the basket catheter. Carbonizations, which appear as dark material attached to the basket catheter electrodes or splines, can form after ablation on the splines of the basket catheter, which can potentially cause embolism. Carbonizations are thought to be caused by the concentration of RF energy on the thin splines that results in very high local temperatures that induce denaturation of serum proteins. However, the risk of carbonization can be diminished with the use of an irrigated-tip catheter as opposed to conventional ablation catheters.

Another disadvantage is that the basket catheter is nondeflectable and has limited maneuverability, and it requires a special sheath with a limited number of preshaped curves. Sometimes, it can be challenging to introduce a basket catheter into the inferior PVs. The use of a deflectable transseptal sheath can facilitate catheterization of the PVs.

In addition, the splines may contact one another when the basket catheter is positioned within a relatively small PV, thereby inducing electrical artifact (see Fig. 15.33). Similarly, the splines may not always be equally spaced relative to the circumference of the PV. As a result, areas in which several splines are clustered may be densely mapped, whereas other regions are less densely recorded.

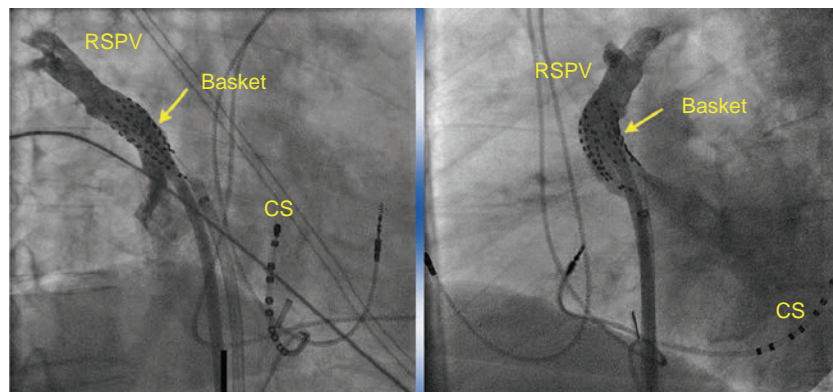
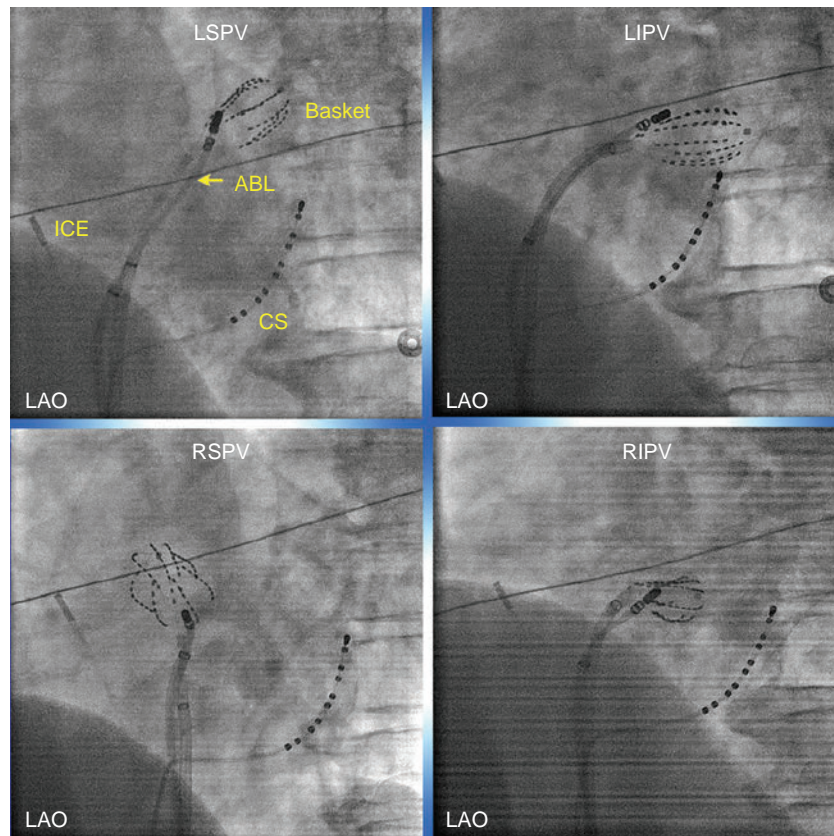


Fig. 15.33 Pulmonary Vein (PV) Angiography to Define Basket Catheter Positioning. Fluoroscopic right anterior oblique and left anterior oblique views of angiography of the right superior PV (RSPV) with a basket catheter positioned in the vein. Note that the basket catheter takes the shape of the PV and provides anatomic information about the location of the ostium and size of the PV. CS, Coronary sinus.



eFig. 15.11 Left Anterior Oblique (LAO) Fluoroscopic Views of Basket Catheter Positioned in the Four Pulmonary Veins (PVs). A long deflectable sheath is used to help position the basket catheter in the different PVs. *ABL*, Ablation catheter; *CS*, coronary sinus; *ICE*, intracardiac echocardiography; *LIPV*, left inferior pulmonary vein; *LSPV*, left superior pulmonary vein; *RIPV*, right inferior pulmonary vein; *RSPV*, right superior pulmonary vein.

Target of Ablation

The objective of the mapping and ablation procedure is to identify PV potentials along the circumference of the PV ostium and ablate to completely eliminate these potentials. Electrical isolation of all PVs is performed without attempting to identify the PVs demonstrating arrhythmogenicity. RF ablation is targeted to the ostial portion of the breakthrough segments (electrical connections) connecting the LA to the PV, which are identified as the earliest PV potentials recorded from the ring catheter. The PV potential reflects the activation of muscular LA bands extending into the PV with longitudinal, oblique, or complex courses and ending in a cul-de-sac or even looping back in the LA. The source, its course within the PV, and its exit into the LA may all be considered appropriate individual targets for ablation. The PV potential is recorded over a broader area proximally, but with great variability. Therefore a few seconds of energy application can be sufficient at some proximal sites to eliminate downstream PV muscle activity, whereas wide or repeated RF applications may have been required in others.

Once the presence of the PV potentials along the PV circumference is defined on the ring catheter, target sites for ablation are selected by identifying the earliest bipolar PV potentials or the unipolar electrograms with the most rapid (sharpest) intrinsic deflection on high-speed recordings (150 to 200 mm/s) that had equivalent or earlier activation relative to the earliest PV potential recorded on the adjacent ring catheter recording sites (see Fig. 15.30). The ablation catheter then is maneuvered to a position adjacent to the target electrode pair of the ring catheter and withdrawn to the edge of the ostium (at the atrial side of the ring catheter). RF ablation is performed within 5 to 15 mm of the PV ostium; the exact location usually depends on catheter stability. This is safer (regarding the risk of PV stenosis) than more distal applications, especially in smaller veins.

Several PV potential electrogram characteristics predict a successful ablation site: (1) timing of the (unipolar and bipolar) PV potential electrogram recorded by the ablation catheter equal to or earlier than the earliest PV potential recorded by the ring catheter (see Fig. 15.30); (2) larger (unipolar and bipolar) electrogram amplitude; (3) steeper intrinsic deflection of the unipolar electrogram; and (4) identical morphologies of the unipolar electrograms recorded by the ablation catheter and by the contiguous electrode of the ring catheter.

Ablation Technique

A temperature-controlled, 4- or 8-mm-tip deflectable catheter or an irrigated-tip ablation catheter can be used. For 8-mm-tip catheters, RF ablation is performed with the maximum temperature set at 45°C to 55°C, the power set at 70 W or lower, and for a duration of 20 to 60 seconds. Power limit is usually reduced to 25 W for the case of a left inferior PV and to 20 W if the PV diameter is less than 15 mm. For irrigated-tip catheters, power is set at 25 to 35 W or lower and temperature at 40°C or lower. RF applications are delivered for a maximum of 60 seconds to achieve an impedance drop of 5 to 10 Ω at the ablation site. RF application can be repeated or prolonged when a change occurs in activation or morphology of the PV potentials, as determined by circumferential mapping recorded downstream. The presence of high-amplitude electrical artifact on the recording from a specific ring catheter pole confirms the pole with which the ablation catheter is in contact and that the catheter is in the same plane as the ring catheter (see Fig. 15.30); ablation should not be performed at such locations, since (1) if the ring catheter is inside the PV, so is the ablation catheter tip, and (2) carbonization may occur on the ring catheter electrode in contact with the ablation electrode.

A successful ablation site is defined as a site at which an application of RF energy results in elimination of a PV potential at more than one

ring catheter recording sites or delay (shift) of a PV potential by at least 10 milliseconds at more than two ring catheter recording sites (Fig. 15.34). Once a shift or elimination of PV potentials at some ring catheter poles is achieved, the ablation catheter is adjusted to target the new ring catheter pole recording the now earliest PV potential. This maneuver is repeated until the whole PV is electrically isolated. Complete electrical isolation of the PV is defined as complete entrance block into the PV during AF and elimination or dissociation of all ostial PV potentials during NSR and atrial pacing (see Fig. 15.34), as well as exit block from the vein (see later).

The extent of the circumference ablated is variable among PVs. When ablation is performed proximal to the PV ostium or during AF, more circumferential ablation is often required to achieve PV isolation. Occasionally, electrical connections exist between ipsilateral PVs, and elimination of these connections is important only when isolation of only one of the two PVs is the goal of the ablation procedure. The electrical connections between PVs are identified by mapping the earliest activation at the ostium of an untargeted PV during pacing inside the targeted PV; then, ablation is performed at this untargeted PV ostium to achieve electrical disconnection.

When the basket catheter is used for PV mapping, it is recommended to use an irrigated-tip catheter at a maximum temperature of 45°C, maximum power of 25 to 30 W, and flow rate during ablation of 17 mL/min.

Endpoints of Ablation

Electrical Disconnection of the Pulmonary Vein

Complete PV electrical disconnection is confirmed by the demonstration of bidirectional block at the LA-PV junction, that is, the absence of conduction from the LA to PV (entry block) and in the opposite direction from PV to LA (exit block).

In general, the presence of entrance block appears to be effective in predicting bidirectional block across the PV-LA junction, and is commonly used as the primary endpoint in AF ablation. However, permanent PV exit conduction block is the ultimate goal of PV electrical isolation for prevention of PV-induced AF and, hence, demonstration of the presence of exit block is a reasonable endpoint for PV isolation.

Entrance block. Entrance block into the PV (i.e., LA-PV conduction block) can be recognized by the complete elimination of all ostial PV potentials recorded by the ring catheter (during NSR, atrial pacing, or AF) or the appearance of dissociated PV potentials (see Figs. 15.34 and 15.35).

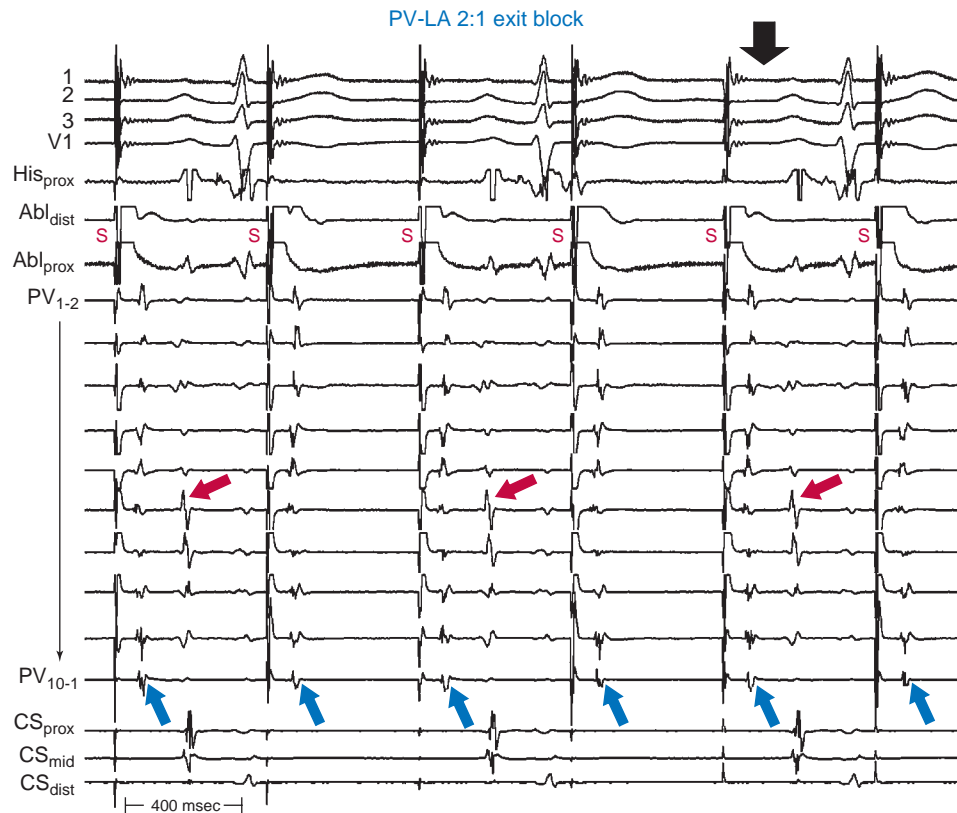
Exit block. Exit block is verified by the absence of conduction from the PV to the LA during intra-PV pacing or during spontaneous PV ectopy or PV tachycardia (eFig. 15.12). The observation of spontaneous dissociated potentials from the PVs following their isolation confirms exit block. The presence of exit block also can be verified by PV pacing performed from multiple sites in a circumferential manner as possible by using the bipoles of the ring catheter or mapping-ablation catheter positioned distal to the PV and LA junction. When local PV capture is difficult to demonstrate because of the pacing stimulus masking the PV electrogram, decremental pacing can be used to unmask local PV potentials.

Prior reports suggested that demonstration of entry block into the PV is not a sufficient condition to conclude exit block. In one report, residual PV-LA exit conduction after achieving entrance block (i.e., unidirectional LA-PV block) was demonstrated by pacing maneuvers in more than 40% of the PVs, suggesting that the demonstration of only entrance block is an insufficient endpoint (eFig. 15.13). The fact that tachycardias can be induced in isolated PV segments emphasize the importance of achieving PV exit block. However, more recent reports found that the true incidence of unidirectional block had been overestimated (the

Electrical isolation of the left superior PV



eFig. 15.12 Electrical Isolation of the Left Superior Pulmonary Vein (LSPV). Complete electrical isolation of the LSPV resulted in termination of atrial fibrillation (AF) and conversion to normal sinus rhythm on the surface electrocardiogram and coronary sinus (CS) recordings, whereas AF continued in the LSPV (PV-left atrial exit block). ABL, Ablation catheter; CS_{dist}, distal coronary sinus; CS_{mid}, middle coronary sinus; CS_{prox}, proximal coronary sinus.



eFig. 15.13 Pulmonary Vein (PV)–Left Atrium (LA) 2:1 Exit Block. The ring catheter is positioned at the ostium of the left superior PV. During pacing using the ablation catheter positioned more distally in the vein, consistent capture of PV potentials is shown (*blue arrows*) but only every other PV potential conducts to LA (*red arrows*). Note very long delay between the stimulus and the P wave of the conducted complex (*black arrow*). *Abl_{dist}*, Distal ablation site; *Abl_{prox}*, proximal ablation site; *CS_{dist}*, distal coronary sinus; *CS_{mid}*, middle coronary sinus; *CS_{prox}*, proximal coronary sinus; *His_{prox}*, proximal His bundle.

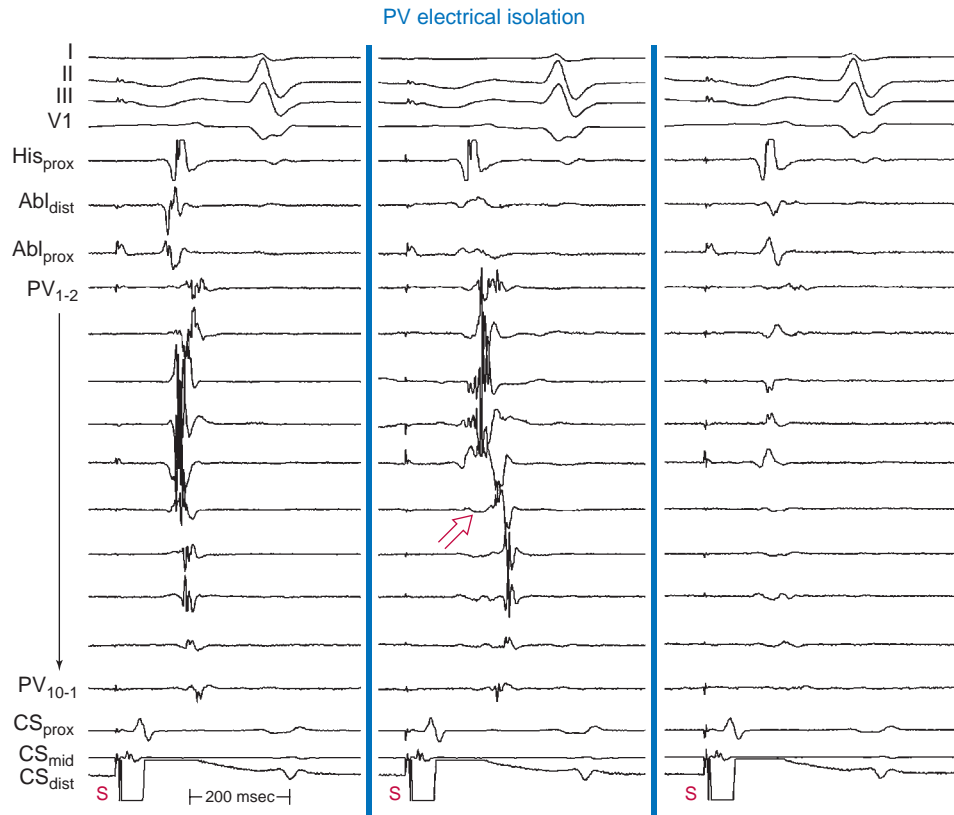


Fig. 15.34 Electrical Isolation of the Right Superior Pulmonary Vein (PV). *Left panel*, Baseline recordings from a ring catheter situated at the PV ostium. During coronary sinus (CS) pacing, left atrial (LA) and PV potentials overlap. *Middle panel*, After some encircling ablation, some of the PV potentials are shifted to a later time (arrow) and become separated from far-field LA electrograms. *Right panel*, On completion of isolation, no PV potentials are visible (entrance block into the PV). *Abl_{dist}*, Distal ablation site; *Abl_{prox}*, proximal ablation site; *His_{prox}*, proximal His bundle; *CS_{dist}*, distal coronary sinus; *CS_{mid}*, middle coronary sinus; *CS_{prox}*, proximal coronary sinus.

incidence in the latter studies was 1.5% to 16%), and that exit pacing maneuvers can erroneously indicate PV-LA exit conduction due to capture of far-field structures neighboring the PV ostium or due to the presence of electrical connections between ipsilateral PVs. Therefore it is critical to recognize these phenomena during intra-PV pacing to avoid unnecessary ablation.

LAA capture during pacing from the left superior PV, and SVC capture during pacing from the right superior PV can masquerade as persistent conduction from the PV to the LA. True exit conduction is considered to be present if PV-LA conduction occurs during pacing from the posterior aspect of those veins (i.e., away from the anteriorly positioned LAA and SVC). Two additional maneuvers can be employed to distinguish the presence or absence of exit block. If LA capture is observed with pacing from the anterior aspect of the PV, the pacing output is gradually decreased to lose capture of the far-field structure while maintaining PV capture. The observation of local PV capture with exit block during this maneuver is consistent with a diagnosis of pseudo-exit conduction during high output pacing caused by far-field capture. In addition, the presence of early activation within the far-field structure (recorded by a catheter positioned in the LAA or SVC), closely coupled to the pacing stimulus and preceding local PV activation during pacing from the anterior aspect of the PV, is also diagnostic of pseudo-exit conduction.

Intra-PV pacing maneuvers can unmask electrical connections between ipsilateral PVs (present in up to 18% of patients), which

manifest as intact LA conduction during intra-PV pacing after elimination of all potentials in that PV, thus indicating unidirectional block. This is relevant when only one (and not all) PV is targeted for isolation. Exit block can be inferred if sites of PV capture (during NSR) were located on the electroanatomic mapping system prior to isolation, and pacing at such sites after isolation show no propagation to the LA.¹⁵⁸

Waiting Period and Pharmacological Provocation

Early recovery of PV conduction can be observed in up to 93% of patients and 50% of PVs, with about one-third of the PVs demonstrating a first recurrence at 30 minutes and one-sixth showing a first recurrence at 60 minutes. Notably, recovery of PV conduction is more frequently observed in the left superior PV as compared with the other PVs. Therefore reconfirmation of PV isolation after a 30- or even 60-minute waiting period after initial PV isolation or pharmacological provocation with adenosine (up to 30 mg rapid IV bolus) or isoproterenol (up to 20 µg/min IV infusion) has been suggested to improve outcome. Incorporation of shorter waiting time (20 to 30 minutes) in conjunction of adenosine administration can also be reasonable. Of note, each of those methods seems to have unique features in uncovering PV reconnection, and the results of the different methods may not be in agreement. In other words, PV reconnection can potentially be unmasked only after a waiting period but not by administration of adenosine, and vice versa. Even the sites of PV reconnection uncovered

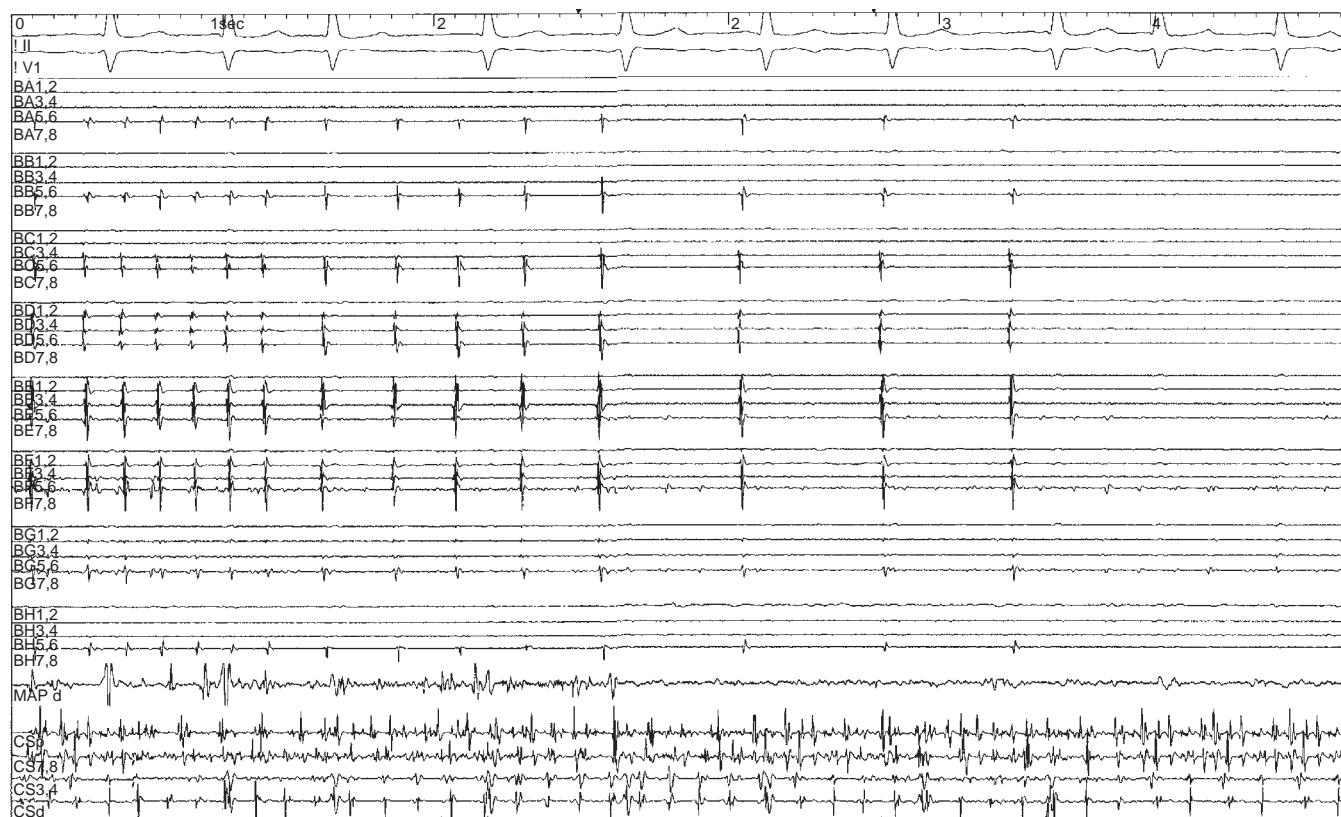


Fig. 15.35 Pulmonary Vein (PV) Isolation During Atrial Fibrillation (AF) Using a Basket Catheter. Bipolar recordings from the eight electrodes (1-2, 3-4, 5-6, 7-8) on each of the eight splines (BA through BH) of the basket catheter positioned in the left superior PV initially show sharp PV potentials. Radiofrequency ablation during AF results in gradual slowing and then disappearance of all PV potentials and persistence of residual low-amplitude, far-field, left atrial (LA) electrograms, consistent with LA-PV entrance block. AF continues in the coronary sinus (CS) recordings.

by one method can be different from those uncovered by the other methods.

The administration of adenosine has been shown to transiently unmask dormant conduction between the PVs and the LA. Activation of adenosine-sensitive potassium channels hyperpolarizes the resting membrane potential of atrial myocytes injured by RF energy and, hence, can potentially restore excitability by removing voltage-dependent sodium current inactivation, facilitating electrical conduction and resulting in transient PV-LA reconnection. Adenosine-mediated dormant conduction can be revealed in up to 53% of patients, and PVs that demonstrated dormant conduction with adenosine are more likely to recover conduction spontaneously after initial isolation. However, studies investigating the implications of adenosine-induced PV reconnection have yielded conflicting results regarding whether adenosine-mediated PV conduction recovery is an independent predictor of AF recurrence, and whether targeting dormant PV conduction provoked by adenosine with additional ablation lesions improves long-term arrhythmia-free outcomes. It is important to note that there is a dose-dependent effect when assessing for dormant PV conduction. Adenosine doses sufficient to induce AV block with at least 1 nonconducted atrial paced beat are likely required to unmask dormant PV conduction (eFig. 15.14). The dose can be gradually escalated until AV block is observed. Alternatively, administering higher doses (e.g., 30 mg IV) from the start can be appropriate.

It is important to note that adenosine testing has several limitations. Because adenosine only reveals PV reconnection transiently, targeting

the precise area of reconnection can be difficult, and evaluating the efficacy of additional ablation lesions is not feasible without repeating adenosine administration. Also, it remains uncertain whether adenosine testing should be repeated to assess separately for both persistent entrance and exit block.^{159,160}

Data suggest that adenosine is superior to isoproterenol for unmasking dormant PV conduction after PV isolation, with no significant additional value of combining the two. Therefore the role of isoproterenol infusion (alone or in conjunction with adenosine) appears limited.

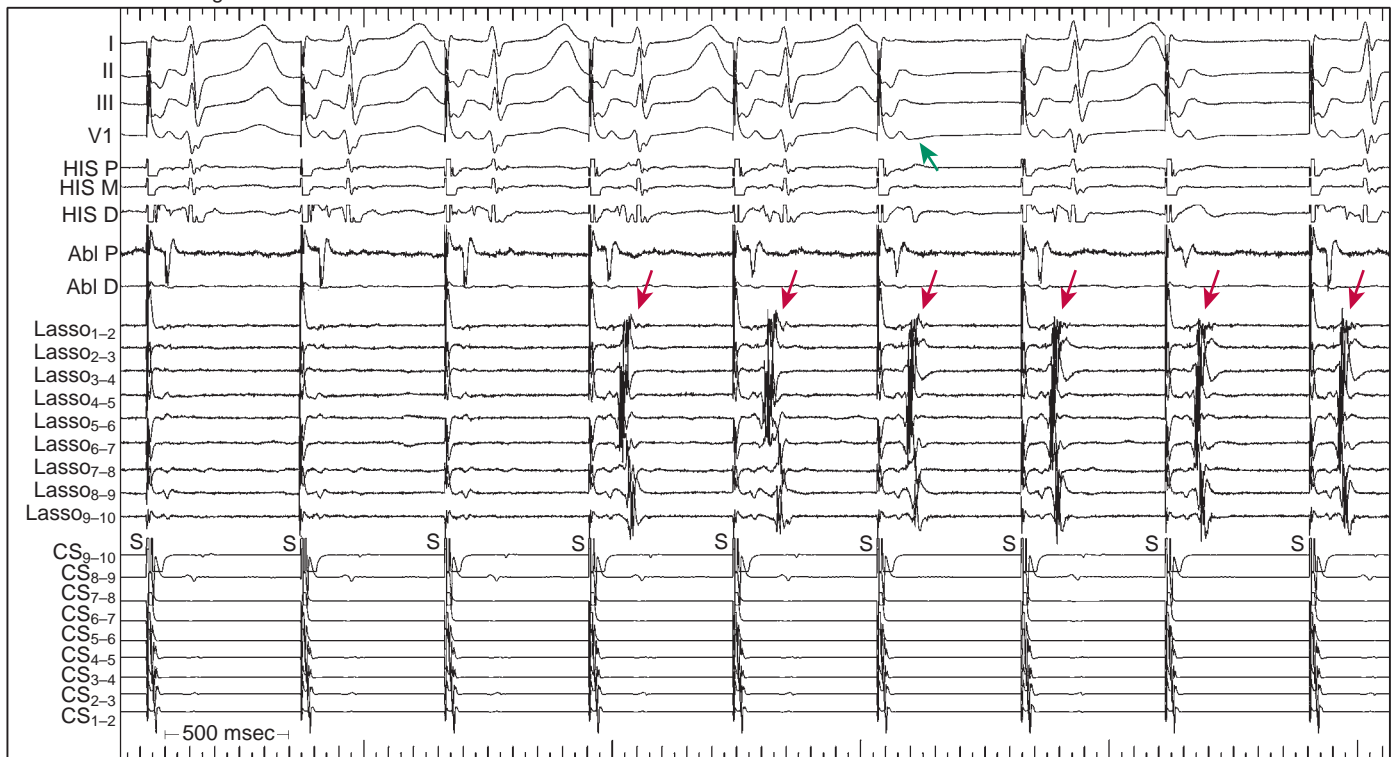
A recent expert consensus statement considered a 20- to 30-minute waiting phase reasonable to incorporate into an AF ablation procedure (class IIa), and that administration of adenosine 20 minutes after initial PV isolation phase may be considered (class IIb).

Inability to Isolate a Pulmonary Vein

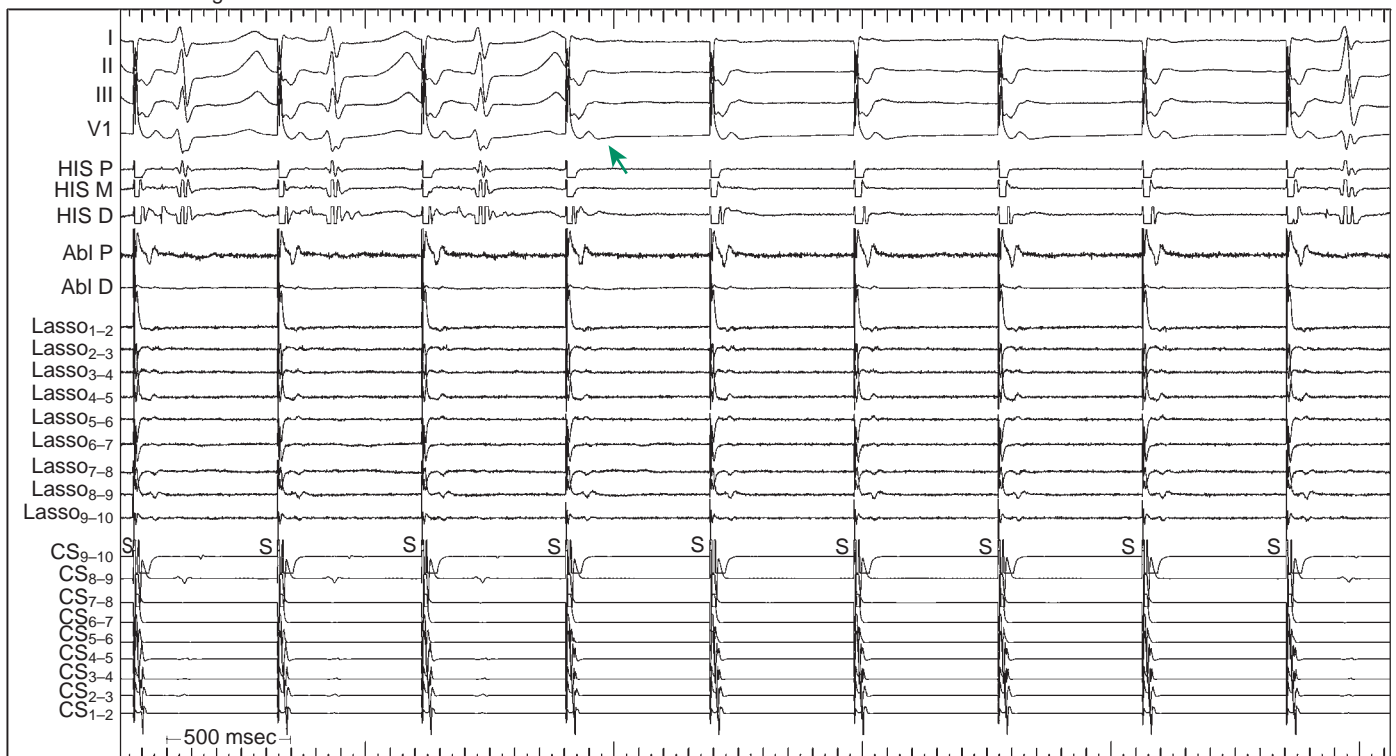
More than 90% of PVs can be electrically isolated from the LA by conventional applications of RF energy along segments of the ostia, guided by PV potentials. The inability to abolish the arrhythmogenic PV potential or its recovery (even in a very discrete area and with a prolonged conduction time) is associated with a higher AF recurrence rate.

The inability to disconnect the PV has been demonstrated in 3% to 24% of targeted PVs in previous studies and can be attributable to anatomic variations in the geometry of the ostia that could limit optimal recording of PV potentials with the ring catheter. Using an expandable

A. Adenosine following initial PV isolation



B. Adenosine following additional PV isolation



eFig. 15.14 Adenosine Administration Revealing Dormant Pulmonary Vein (PV) Conduction. Surface electrocardiogram and intracardiac recordings from ring catheter (*Lasso*) in left superior PV following PV isolation. (A) The first three stimulated complexes (*S*) show atrial capture with atrioventricular (AV) conduction but no conduction into the PV; commencing with the 4th stimulus, PV conduction is seen (*red arrow*) and continues for another six complexes. A dazzling effect on AV induction is not manifest until two complexes later (*green arrow*). (B) Repeat ablation has been performed and at this time adenosine results in AV block (*green arrow*) but no restoration of PV conduction. *Abl D*, Distal ablation site; *Abl P*, proximal ablation site; *CS*, coronary sinus; *His D*, distal His bundle; *His M*, middle His bundle; *His P*, proximal His bundle.

ring catheter or using ICE to guide positioning of the ring catheter aids in stabilizing the mapping catheter. In addition, some fascicles can be too thick to be ablated with conventional RF energy, and the use of high-power output or an irrigated-tip ablation catheter can be required to isolate those PVs. The inability to isolate a PV also can be caused by the presence of electrical connections between ipsilateral veins (which are observed in approximately 18% of the patients). In these patients, ostial ablation of an untargeted PV is required for successful disconnection of the targeted PV. Occasionally, the proximity of a targeted PV to an important extracardiac structure (esophagus, phrenic nerve) limits the ability to isolate the vein fully.¹⁵⁸

Outcome

Segmental ostial PV isolation represented an important advance in catheter treatment of AF and was found more efficacious than focal ablation for the control of paroxysmal AF. As compared with focal ablation, PV isolation eliminates the need for detailed mapping of spontaneous ectopy, and there is a clear-cut endpoint of ablation, even when spontaneous arrhythmias are absent. Importantly, the risk of PV stenosis is less than that with focal PV ablation.

On the other hand, the benefit of empiric isolation of all PVs over the identification and selective isolation of arrhythmogenic veins is less clear. Previous comparative case series demonstrated that empirical isolation of all PVs led to superior outcomes over isolating fewer veins, which is expected given that most (up to 71%) patients prove to have three or more arrhythmogenic PVs. Nevertheless, in patients with predominantly paroxysmal AF, isolation of arrhythmogenic veins identified using a comprehensive stimulation protocol was found as effective as empiric isolation of all PVs in achieving long-term arrhythmia control after a single ablation procedure, and potentially is associated with shorter fluoroscopy times and fewer adverse events. However, identification of the arrhythmogenic PVs during an EP study remains challenging, laborious, and time consuming.¹⁶¹

Reconnection of previously isolated PVs (caused by recovery of conduction through inadequately ablated fascicles in the muscle sleeves surrounding the PV) is probably the most common reason for recurrent AF after PV isolation, at least among patients with paroxysmal AF. Other causes include ectopy from PVs not targeted or could not be isolated at the initial procedure, and the presence of non-PV triggers. In one study on the recurrence of AF following PV electrical isolation, most triggers were found to originate from previously targeted PVs (54%), whereas one-third of recurrent triggers (32%) originated from PVs that were not ablated during the initial session. Notably, 61% of previously isolated PVs in that series had evidence of recovered PV potentials. Therefore acutely successful PV isolation does not confer permanent disconnection of the PV musculature from the LA, and in most isolated PVs residual conduction remains or recurs with time.

Predictors of early recurrence of AF include older age (65 years or more), the presence of associated cardiovascular disease, the presence of multiple AF foci, the presence of AF foci from LA free wall, LA enlargement, and longstanding persistent AF. Predictors of late recurrence of AF include the presence of early recurrence of AF and the presence of multiple AF foci.

In most reports, a successful outcome was defined as the absence of any symptomatic atrial arrhythmias beyond the first 2 to 3 months after ablation without the use of antiarrhythmic drugs. Medium-term success has reportedly been achieved in up to 70% of patients with paroxysmal AF but in only 30% of patients with persistent AF. This finding suggests that intervention with PV isolation in patients with drug-refractory paroxysmal AF should not be postponed until the AF becomes persistent. Once AF has become persistent, it is likely that PV

isolation will have to be supplemented by some other type of ablation procedure directed at the atrial myocardium. The less satisfactory outcome of PV isolation in persistent AF suggests that the PVs play a less critical role in generating AF once the AF has become persistent. It is possible that the EP and anatomic remodeling that occurs during persistent AF often allows the atria to continue fibrillating independently of the PVs. The overall major complication rate is 6.3%, including stroke (0.7%), cardiac tamponade (1.2%), and significant PV stenosis (4.3%).

CIRCUMFERENTIAL ANTRAL PULMONARY VEIN ISOLATION

Rationale

The muscular sleeves of the PVs extend proximally to the antral-LA junction and are not restricted to the tubular portion of the PV. This finding is not surprising because embryologically the PVs originate from the posterior LA wall, so that a continuum exists between the atrial wall and PVs. Therefore it is likely that the PV antrum also has an arrhythmogenic potential similar to that of the tubular portion of the PVs. Furthermore, the PV antrum can potentially harbor ganglionated plexuses that have been implicated in the genesis of AF, as well as high-frequency activity or rotors that are thought to have anchor points necessary for perpetuation of AF. Hence, ablation at the antrum not only is effective to isolate PVs electrically, but also it can eliminate other potential mechanisms of AF. In addition, a large area of the posterior LA is included inside the ablation lines and a considerable amount of atrial debulking (approximately 25% to 30%) may occur after antral PV isolation.

Circumferential antral PV isolation has several additional advantages over segmental ostial PV isolation. This technique does not rely on localizing the sites of electrical breakthroughs into the PV, and thus it is easier to perform during AF. Furthermore, this approach reduces the risk of PV stenosis because ablation is performed in the LA, away from the PV ostia (Fig. 15.36). In addition, in some patients with PV anatomic variations, this approach can be more favorable. One such variation is the presence of a common ostium of the left PVs, occurring in up to 32% of patients undergoing PV isolation. Such common ostia typically are too large to allow a stable position of the ring catheter. Another anatomic variation is the presence of a right middle PV, present in up to 21% of patients, which typically is separated from the right superior PV and right inferior PV by a narrow rim of atrial tissue. This would predispose to sliding of the ablation catheter into the PV during ablation. Another anatomic finding that renders extraostial PV isolation more favorable is a PV ostial diameter of less than 10 mm. RF application at a small ostium carries a higher risk of PV stenosis.

Circumferential antral PV isolation has been shown to be more effective in preventing AF recurrence than segmental ostial PV isolation, and this procedure has become a preferred ablation strategy in patients with paroxysmal and persistent AF. The preferred ablation target is the outmost atrial side of the PV ostium.¹⁰

Identification of Pulmonary Vein Antra

The objective of the mapping and ablation procedure is to identify PV potentials along the perimeter of the PV antrum and ablate to eliminate these potentials completely. Reliable definition of the anatomy of PV antra is crucial to provide an effective set of lesions. A navigation system is used to provide 3-D anatomic images that allow safe maneuvering of the ablation catheter to complete the lesions at the antrum and eliminate conduction to PVs. However, the use of these systems does not replace circumferential PV mapping and an EP endpoint to the procedure.

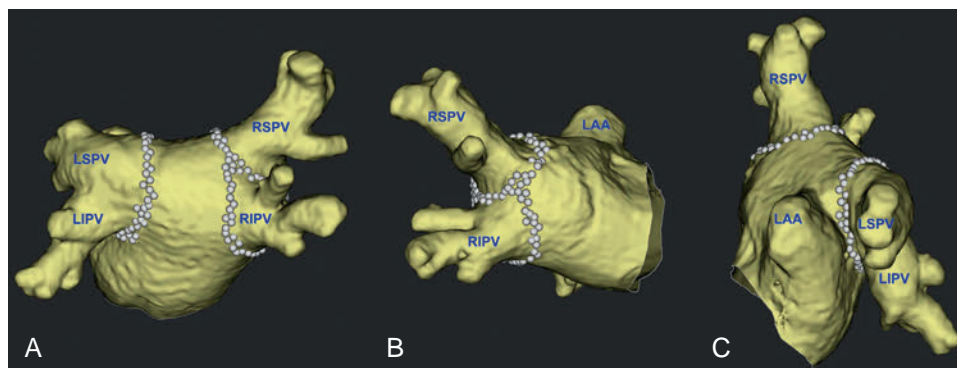


Fig. 15.36 Circumferential Antral Electrical Isolation of the Pulmonary Veins (PVs). Segmented three-dimensional computed tomography scan of the left atrium (LA) and PVs shown in posteroanterior (A), right lateral (B), and left lateral (C) views. Contiguous radiofrequency lesions are deployed (*white dots*) in the LA proximal to the ostia of the PVs, creating a circumferential line around each of the right-sided PV ostia. The left-sided PVs share a large common ostium, and en bloc encirclement of those ostia is performed. LAA, LA appendage; LIPV, left inferior PV; LSPV, left superior PV; RIPV, right inferior PV; RSPV, right superior PV.

Ring Catheter Mapping

The ring catheter is used for circumferential ostial mapping of PV potentials, as described for segmental ostial PV isolation. However, the breakthrough segments (electrical connections) connecting the LA to the PV, identified as the earliest PV potentials recorded from the ring catheter, are not specifically mapped or targeted. Instead, the entire perimeter of the PV ostium is the target for the ablation procedure. Using the ring catheter enables circumferential mapping of the PV ostia perpendicular to the axis of the vein and serves as a landmark for the PV ostium around which RF lesions are delivered. In addition, the ring catheter is vital for confirming complete electrical isolation of the PV, an important endpoint of this ablation strategy.

Basket Catheter Mapping

The technique of positioning the basket catheter into the PVs was described earlier in this chapter (see [eFig. 15.11](#)). For antral PV isolation, the basket catheter is introduced toward the distal PV under fluoroscopy guidance and then is pulled back as proximally as possible without dislodgment until its most proximal electrodes are positioned at the PV antrum, which is identified by selective angiography. The basket catheter can help identify the true junction between the PVs and LA anatomically and electrically. Because the basket catheter conforms to the shape of the PV, it provides information about the anatomy of the PV.

Furthermore, longitudinal mapping with a basket catheter can help identify the transition zone between the PV and LA potentials. Far-field LA potentials are normally recorded almost simultaneously all over the PV, whereas the activation sequence of the PV potentials is from proximal to distal when the activation propagates from the LA to the distal PV. Consequently, the interval between the LA potentials and PV potentials is shorter at the proximal PV than at the distal PV. At the transition zone, total fusion of the PV and LA potentials occurs ([eFig. 15.15](#)). Therefore the potential recorded at the transition zone may reflect the activation of the PV antrum. A transverse activation pattern, indicated by simultaneous activation recorded by some neighboring electrode pairs along the spline, sometimes occurs around the LA-PV junction before the longitudinal activation pattern within the PVs. This pattern may reflect the activation of the circle of myocardium at the PV antrum.

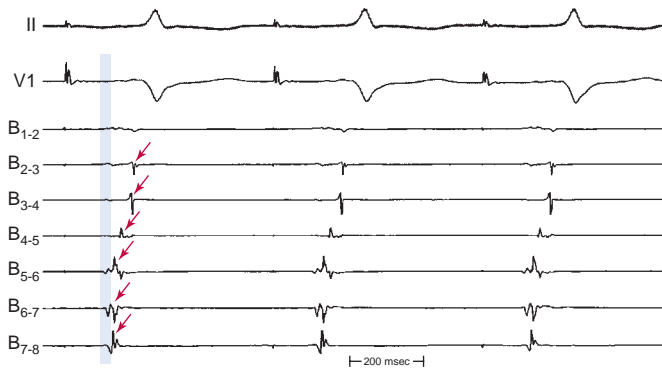
On the basis of these findings, PV antrum potentials are defined as single sharp potentials formed by the total fusion of the PV and LA

potentials around the PV ostium or single sharp potentials with a transverse activation pattern around the PV ostium (see [eFig. 15.15](#)). Targeting those potentials by RF ablation would target the transition zone between the PV ostium and LA. When potentials conforming to the definition of PV antrum potentials are observed from some electrode pairs on the same spline, the antrum potential recorded from the most proximal electrode pair is targeted. RF applications are also delivered to the gap between the targeted electrode pairs on the neighboring splines to produce a continuous RF lesion at the PV antrum.

Electroanatomic Mapping

Different navigation tools, including the EnSite NavX, CARTO, and Rhythmia systems, have been used to facilitate circumferential PV isolation. These systems can provide a high-resolution reconstruction of the LA and defining PV ostia and antra and allow real-time visualization of the ablation catheter within the reconstructed 3-D geometry (see [Fig. 6.3](#)). In addition, ablation lesions can be tagged, thus facilitating creation of lines of block with considerable accuracy by serial RF lesion placement and allowing verification of the continuity of ablation line.

Using either the CARTO or NavX system, the 3-D shell representing the LA and PVs is constructed using the ablation or ring catheter, or both. With the Rhythmia system, the mini-basket array catheter (Orion, Boston Scientific) is used to construct the anatomic shell. To acquire the PVs, entry into the vein is clearly identified as the catheter leaves the cardiac shadow on fluoroscopy, the impedance usually rises to more than 140 to 150 Ω , and electrical activity disappears. Because of the orientation of some veins and the limitations of catheter shape, it can be difficult to enter deeply into some veins, but the impedance still rises when the catheter is in the mouth of the vein. To differentiate between PVs and LA more clearly, voltage criteria (fractionation of local bipolar electrogram) and impedance (rise more than 4 Ω higher than the mean LA impedance) can be used to define the PV ostium. Mapping of each PV is performed by placing the mapping catheter 2 to 4 cm inside the PV and slowly pulling it back to the LA under fluoroscopic or electroanatomic mapping guidance. Care should be taken to reconstruct each PV ostium and the transition toward the LA (antrum), posterior free wall, mitral isthmus, and left interatrial septum. Subsequently, the system is allowed to create the geometry automatically while the ablation (or ring) catheter is moved throughout the LA. Sequential positioning of a catheter at multiple sites along the endocardial surface of the LA establishes that chamber's geometry.



eFig. 15.15 Identification of the Pulmonary Vein (PV) Antrum Using the Basket Catheter. The basket catheter is positioned in the left superior PV. Shown are seven bipolar recordings obtained from the eight electrodes (1-2, 2-3, to 7-8) on one of the eight splines (B₁₋₂ through B₇₋₈) of the basket catheter. During coronary sinus pacing, far-field left atrial (LA) potentials are normally recorded almost simultaneously all over the PV (*shaded area*). In contrast, PV activation propagates from proximal (ostial) to distal, and the interval between the LA potentials and the PV potentials is shorter at the proximal PV than at the distal PV. At the transition zone (PV antrum), a total fusion of the PV and LA potentials occurs (B₇₋₈).

The ring catheter is used for mapping PV potentials in conjunction with EnSite or CARTO electroanatomic mapping systems; the mini-basket catheter (Orion) is used for form mapping in conjunction with Rhythmia (Fig. 15.37).

Computed Tomography and Magnetic Resonance Imaging

CMR and CT provide critical information regarding the number, location, and size of PVs, as needed for planning the ablation and selecting appropriately sized ablation devices. Resulting images also identify branching patterns of potentially arrhythmogenic PVs, disclose the presence of fused superior and inferior veins into antral structures, and clarify the potentially confounding origins of far-field electrograms that masquerade as PV potentials.

Furthermore, the segmented CT/CMR volumes can be downloaded on the electroanatomic mapping system platforms. The 3-D electroanatomic maps can be simultaneously displayed side-by-side with CT/CMR segmented cardiac scans to confirm cardiac structures and guide ablation. These systems also enable registration of the preacquired 3-D CT/CMR images of LA reconstructions on the real-time 3-D electroanatomic maps reconstructed from multiple endocardial locations. This allows real-time visualization of the location and orientation of the catheter tip within the registered CT/CMR anatomic framework (see Fig. 6.3). The process of image integration—preprocedural CT and CMR image acquisition, image segmentation and extraction, and image registration—is discussed in Chapter 6.

Intracardiac Echocardiography

Phased-array ICE has been used in AF ablation procedures for several purposes: to assist with transseptal puncture, to identify the number and position of PVs, to identify the true border of the PV antrum, to determine the branching patterns of the right PVs needed for total PV isolation, to guide the positioning of the ring and ablation catheters at the antrum of the PV, to verify ablation catheter tip to tissue contact, to assess the degree of PV occlusion during balloon-based ablative interventions, and to detect procedural complications (e.g., pericardial effusion, LA thrombus, and PV stenosis).

For ICE imaging, a 10 or 8 Fr 64-element phased-array ultrasound catheter is positioned in the middle of the RA via an 11 or 9 Fr left femoral venous access. The ICE catheter remains in the RA for the entire procedure to guide transseptal puncture, define PV anatomy, and monitor for microbubble formation during RF ablation. A 7.5- or 8.5-MHz imaging frequency optimizes visualization of LA structures and PVs beyond the interatrial septum. PV imaging is uniformly possible by first visualizing the membranous fossa from a middle to low RA catheter tip position. From this view, clockwise catheter rotation allows visualization of the LAA, followed by long-axis views of the left superior and inferior PVs (see Figs. 4.11 and 6.32). Further clockwise rotation of the catheter brings the orifice of the right superior and inferior PVs into view. The LA ostia of these veins are typically viewed en face, to yield an owl's eye appearance at the vein's orifice.

As the operator images each vein, the ring and ablation catheters can be positioned at the antral-LA interface for ablation. Because the PV antrum is a large-diameter structure, its circumference cannot be mapped using a stationary ring catheter fixed in one position. Instead, the ring catheter must be sequentially positioned along each segment of the antral circumference to look for PV potentials. ICE can identify the true border of the PV antrum and guide positioning of the ring and ablation catheters. Therefore the ring catheter is a roving catheter in this procedure. An operator's assistant often must hold the ring catheter in position around the antrum for stability. When mapping the anterior segments of the left PVs or septal segments of the right

PVs, the ring catheter must be advanced slightly because of the oblique nature of the antral-LA interface.

In addition, ICE can help with the registration process of the CT/CMR image with the electroanatomic mapping system. Furthermore, the CARTOSound Image Integration Module (Biosense Webster) allows incorporating a real-time ICE volume map of the LA and PVs with the electroanatomic map, either as a stand-alone tool to guide navigation and ablation or as a facilitator of CT/CMR image integration (see Chapter 6). Overall accuracy in the LA and PV anatomic reconstruction using the CARTO fast anatomic mapping (FAM) module was found to be superior to the ICE-guided approach. ICE-derived anatomic reconstruction often yields a significant underestimate of true dimensions of both LA and PV when ultrasound exploration is performed by placing the ICE catheter in the RA only. Hence, ablation points fall beyond the 3-D ICE-derived surface contour more often than when guided by FAM or merged 3-D ICE-CT volume rendering. This limitation can potentially be overcome by placing the ICE catheter in the CS, in the RV, or directly in the LA, but a more extensive approach is time consuming and can increase complications. Nevertheless, ICE-derived mapping techniques reduce both fluoroscopy time and the time spent in the LA. Furthermore, the ICE direct visualization of distinct anatomic structures allows a good alignment with CT/CMR and makes this technique suitable for integration processes. On the other hand, FAM allows a more accurate rendering of both LA and PV, which can potentially replace the need for preacquired CT/CMR.^{162,163}

Target of Ablation

The ablation procedure is based on electrical isolation of all PVs. The objective is to identify PV potentials along the circumference of the PV antrum and ablate to eliminate these potentials completely. However, unlike segmental ostial PV isolation, the ostial portions of the breakthrough segments (electrical connections) connecting the LA to the PV (identified as the earliest PV potentials recorded from the ring catheter) are not the sole target of ablation. Complete encirclement of each PV antrum with ablation lesions is the goal of the ablation procedure, which would consequently result in PV isolation (see Fig. 15.36). All PVs are targeted.

Ablation lines consist of contiguous focal lesions deployed in the LA at a distance exceeding 5 mm proximal to the ostia of the PVs, to create a circumferential line of conduction block around each PV.¹⁶⁴ PV isolation is performed 10 mm or more from the ostium of the right PVs, as well as for the posterior and superior aspects of the left PVs, to enhance efficacy and prevent PV stenosis. However, ablation at the anterior portions of the left PVs usually requires energy be delivered less than 5 mm from the ostium of the PV to achieve catheter stability. Wider ablation lines encircling the entire PV antrum and encompassing a larger size of the LA isolated surface area can potentially improve long-term ablation outcome.

When two or three ipsilateral PV ostia are coalescent, en bloc encirclement of those ostia is performed (i.e., one encirclement for the right-sided PVs or one encirclement for the left-sided PVs), and no ablation line between the ipsilateral PVs is deployed (see Fig. 15.36). Importantly, single encirclement of ipsilateral PVs predisposes to breakthrough conduction of both ipsilateral PVs in case of a single gap in the en bloc circle. Furthermore, one report found that AF triggers originate frequently from the carina region of the PVs; hence, ablation in this area between ipsilateral PVs can be effective for targeting the source of the PV triggers. Of note, ablation along the ridge between ipsilateral PVs is frequently necessary to achieve complete electrical isolation of the PVs despite an apparently complete circumferential antral ablation ring.

Acute PV electrical isolation often can be achieved before anatomic completion of the RF ablation line encircling the PV antrum. However,

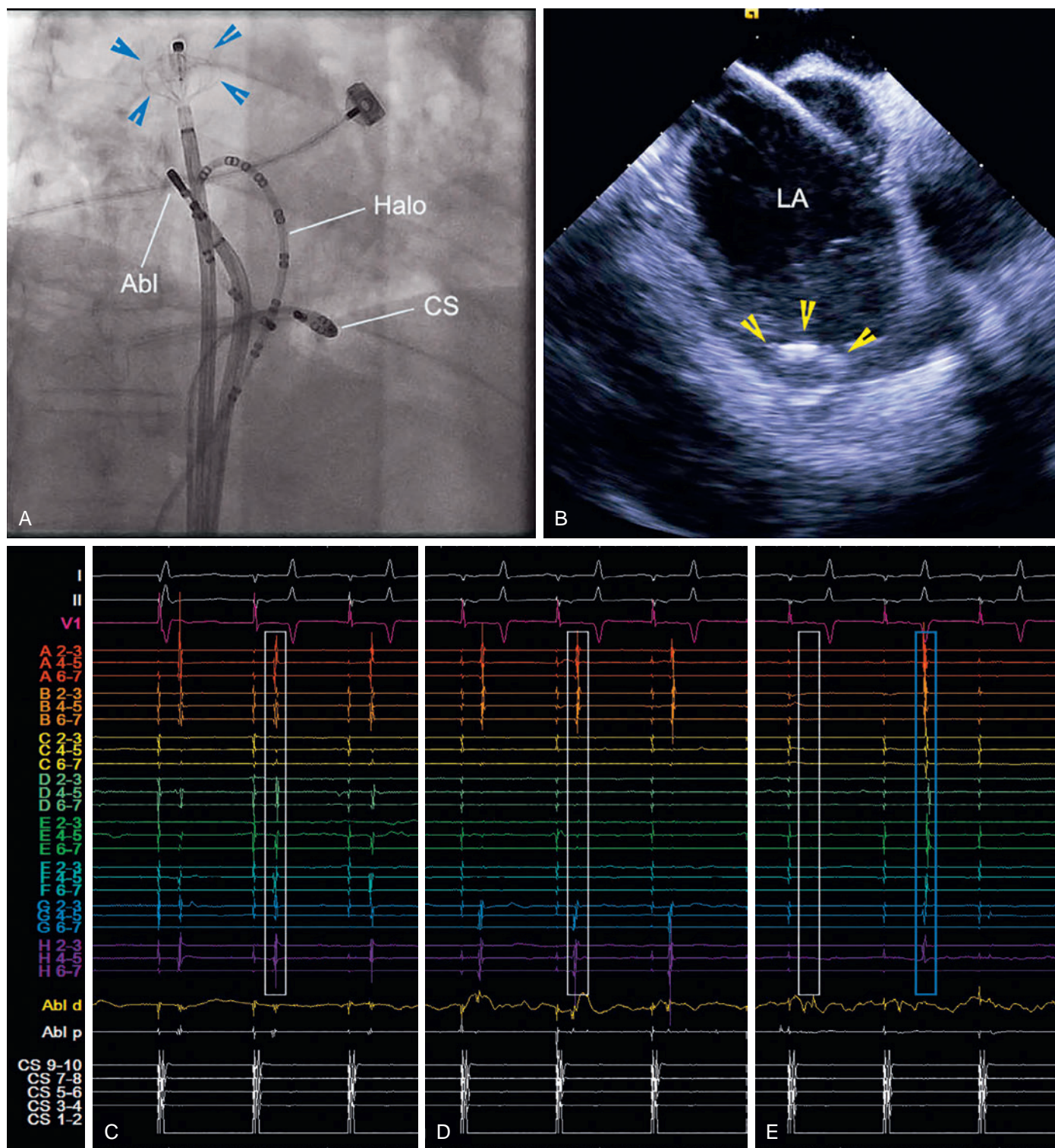


Fig. 15.37 Pulmonary Vein (PV) Isolation Using the Mini-Basket Catheter (Orion). (A) Fluoroscopy (right anterior oblique view) of the Orion catheter (*arrowheads*) positioned at the ostium of the left superior PV. Also shown are the Halo catheter (positioned in the right atrium around the tricuspid annulus), the ablation (*Abl*) catheter, and the coronary sinus (*CS*) catheter. (B) Intracardiac echocardiography (ICE) showing the Orion catheter (*arrowheads*) positioned at the ostium of the left superior PV. (C–E) Surface electrocardiogram and intracardiac bipolar recordings obtained from the electrodes 2-3, 4-5, and 6-7, on each of the eight splines (A through H) of the mini-basket catheter. Circumferential antral PV isolation was performed during CS pacing using radiofrequency energy. At baseline (C), PV potentials recorded by the mini-basket catheter are prominent (encased in the *white rectangle*). After ablation of part of the PV circumference (D), PV potentials are eliminated. Ablation around the entire circumference of the PV antrum (E) results in complete elimination of PV potentials on all splines of the mini-basket catheter. In addition, spontaneous PV ectopy (*blue rectangle*) is observed, and is dissociated from the left atrium (LA).

it is likely that reversible tissue injury caused by tissue stunning, edema, ischemia affecting the unablated tissue within the gaps in the incomplete ablation line. It is important to recognize that unlike segmental ostial PV isolation, whereby complete electrical isolation of the PV can be achieved with noncontiguous ablation line along the PV ostium targeting individual PV muscular sleeves, a noncontiguous ablation line during circumferential antral ablation is unlikely to produce durable PV isolation; electrical reconnection can occur once the unablated PV muscular sleeves recover from the transient injury. As such, initial development of PV entrance and exit block is not a sufficient endpoint for ablation when it occurs with incomplete circumferential antral PV ablation line. Anatomic completion of the circumferential ablation line by contiguous, high-quality RF ablation lesions is required to improve long-term durability of PV isolation.¹⁶⁵

Ablation Technique

Several ablation technologies have been used for circumferential PV isolation. Most commonly, RF ablation is performed with an irrigated-tip ablation catheter. Alternatively, an 8-mm-tip standard ablation catheter can be used. Technological evolution is now aimed at developing new catheter designs for circumferential ablation of the PVs as an alternative for the conventional point-by-point RF ablation. Currently, two multielectrode circumferential catheter systems are undergoing clinical evaluation: The PV ablation catheter (PVAC, Medtronic, Minneapolis, MN, United States) and the nMARC system (Biosense Webster) (see **Chapter 7; Figs. 7.11 and 7.12**).

Furthermore, balloon-based ablation devices using different energy sources (e.g., cryothermal energy, laser energy, RF, and high-intensity focused ultrasound [HIFU]) have been evaluated. The cryoballoon (Arctic Front, Medtronic) and laser balloon (Heartlight, CardioFocus, Marlborough, MA, United States) catheters have proven feasibility, safety, and efficacy in the treatment of AF. Because of severe complications in the form of atrioesophageal fistula, the HIFU balloon is no longer in clinical use (see **Chapter 7**). The clinical evaluation of the RF balloon catheter (Hot Balloon Catheter, Hayama Arrhythmia Institute, Kanagawa, Japan) is still in its initial stages.

Conventional Radiofrequency Ablation

Ablation is started at the posterior wall of each PV, usually fluoroscopically facing the border of the spine in the anteroposterior projection, and continued around the venous perimeter. With the catheter tip at the PV ostium, the posterior wall of the right PV is reached by counterclockwise torque of the catheter and the left PV by clockwise torque. For ablation at the anterior portions of the left PVs, energy must usually be delivered within a few millimeters of the vein (because of a relatively narrow border between the left PVs and the LAA, and the difficulty to balance the catheter tip on the narrow rim of tissue separating these structures) to achieve effective disconnection. Ablation on the venous aspect of the ridge is commonly performed for simplicity; ablation on the LAA side is feasible, but the RF energy must ablate tissue on the posterior wall of the appendage as well as the anterior wall of the PV, so it is more difficult. Sites of RF energy delivery are tagged on the reconstructed 3-D map. This tagging helps ensure coalescence of the ablation lesions to ensure continuity of the ablation line, assuming ablation at each site has been effective (see **Fig. 15.36**).¹⁶⁴

Open irrigation RF catheters are preferred for AF ablation. RF power output has a significant impact on the efficacy and safety of catheter ablation for AF. The optimal power output associated with the best balance between safety and efficacy outcomes appears generically to range between 25 and 45 W. Higher power output at shorter duration (15 to 20 seconds) also appears safe and efficacious. Titration of power output with real-time visualization of microbubbles by ICE (down

titrating by 5 W upon appearance of microbubbles) rather than fixed or limited empirical settings of power output during RF ablation appears to be beneficial.¹⁶⁶

Using an irrigated-tip catheter, power output is limited to 25 to 30 W (or even less) on the LA posterior wall (where the atrial wall is thin and esophageal proximity presents potential danger), and to 30 to 50 W on the left PV-LAA ridge and anterior LA wall, and a target temperature of less than 43°C and irrigation rates of 5 to 20 mL/min (0.9% heparinized saline). Some evidence indicates that ablation over the thin posterior wall, especially near the esophagus, can be performed with lower power as well as low irrigation rates (since irrigation fundamentally allows greater power delivery to deeper tissue, which is not desirable on the posterior wall). Less often, ablation is performed using an 8-mm-tip conventional ablation catheter, with a maximum power of up to 70 W and a target temperature of 50°C to 55°C.

RF energy is delivered for 30 to 60 seconds at each point, until the maximal local electrogram amplitude is decreased by 50% to 90% or double potentials are observed or to achieve an impedance drop of 5 to 10 Ω at the ablation site. RF application can be prolonged for 1 to 2 minutes when a change occurs in the activation or morphology of the PV potentials, as determined by circumferential mapping recorded downstream on the ring catheter. Typically, PV potentials become progressively delayed until disappearing entirely (or showing dissociated firing). If PV potentials remain after completion of ipsilateral circumferential ablation, additional RF applications targeting earliest residual potentials can be performed.

Alternatively, short RF applications (for 2 to 5 seconds) at a higher power (50 W, irrigation rate 30 mL/min, maximum temperature 43°C) can be employed. The latter approach results in momentarily higher LA tissue temperatures and allows the tip to be set at a high power to injure the superficial tissue while minimizing time-dependent deep heating through excessive heat transfer. Typically, the ablation catheter is dragged continuously in small increments every 2 to 5 seconds during continuous RF delivery, and ablation is repeated at each site, if required, for many times throughout the procedure until the local atrial electrogram is completely eliminated. It is probably reasonable to allow at least 2-minute time intervals before returning to ablate a previously ablated site to allow for heat dissipation, especially when ablating at the LA posterior wall, to avoid excessive esophageal heating.

Adequate and stable catheter tip-tissue contact is critical to ensure effective and permanent ablation lesions. The use of steerable transseptal sheaths facilitates more stable catheter positioning and access to all desired ablation targets for PV isolation. In addition, ICE can provide detailed anatomic information and real-time information of the location of the tip electrode of the ablation catheter and can help confirm catheter stability. Real-time measurements of the contact force of the ablation tip have been introduced using different technologies (see **Chapter 7; see Fig. 7.8**). Using a force-sensing RF catheter (with a minimum targeted contact force of 5 to 10 g) is recommended.

Cryoballoon Ablation

The cryothermal balloon ablation system (Arctic Front, Medtronic) consists of a nondeflectable, 10.5 Fr catheter with distally mounted coaxial double inner-outer cooling balloons ("balloon within a balloon," outer balloon maximum diameter, 23 or 28 mm) (see **Fig. 7.15**). The refrigerant nitrous oxide (N_2O) is delivered under pressure from the console into the inner balloon chamber via a lumen within 2 mm of the catheter tip, where it absorbs heat energy as it undergoes liquid-to-gas phase change, resulting in inner balloon cooling to temperatures of -80°C or lower. During cryotherapy, temperature is monitored via a thermocouple located at the inner balloon. The balloon catheter is delivered to the LA via a 15 Fr deflectable sheath with a 12 Fr inner

lumen (FlexCath; Medtronic). A small-caliber octapolar circular mapping catheter (Achieve, Medtronic) passes through the central lumen of the cryoballoon, allowing real-time PV mapping during cryoablation and also providing central luminal support (instead of a guidewire).

Positioning the cryoballoon. Transseptal LA access is obtained using a standard transseptal sheath. A low anterior transseptal puncture site (at the lower third of the septum and anterior reach at the plane of ICE where the mitral valve is in view) is recommended to allow more space for the balloon to be rotated posteriorly to the right inferior PV. The delivery sheath (FlexCath) for cryoballoon catheter is then exchanged over a long stiff guidewire extended into the left superior PV.

Selection of cryoballoon size (23 vs. 28 mm) is based on PV size using preacquired CT/CMR, PV angiography, or TEE. However, whenever possible, the larger diameter cryoballoon is preferred since it is associated more proximal (antral) location of the circumferential ablation lesions as well as lesser risk of phrenic nerve injury during applications to the right PVs.

The deflated cryoballoon is inserted into the steerable delivery sheath and advanced over either an extra-stiff 0.032-mm guidewire or the Achieve catheter. The mapping catheter should always lead the cryoballoon catheter to prevent trauma from the stiffer cryoballoon catheter tip. Also, when maneuvering the sheath to the desired PV, the balloon with the soft-tipped mapping catheter should always lead the sheath to avoid sheath trauma in the LA or PV.¹⁶⁷

The mapping catheter is navigated into each of the PVs under fluoroscopy of ICE guidance and is advanced deep into the target PV. The deflated cryoballoon catheter is then advanced outside the sheath toward the PV ostium over the mapping catheter. Once in position at the PV antrum, the cryoballoon is inflated (outside of the PV, to avoid any mechanical damage) and then is advanced into the PV to occlude the vein.

Assessment of PV occlusion. Once the cryoballoon is inflated at the PV antrum, complete occlusion of the PV with the cryoballoon should be verified. Efficient cryoablation and PV electrical isolation requires adequate contact and seal of the cryoballoon over the PV ostium. Adequate contact is important in creating a complete circumferential PV lesion without gaps. Adequate seal prevents blood flow around the balloon during freezing, which otherwise can limit tissue cooling and impair lesion formation because of convective warming.

PV occlusion can be assessed by selective PV angiography, analysis of the PV pressure waveform, as well as ICE. Complete PV occlusion is confirmed by contrast injection into the distal lumen of the cryoballoon showing total contrast retention with no backflow to the LA (eFig. 15.16). Also, the disappearance of flow on color Doppler obtained by ICE or TEE can help confirm complete PV occlusion (Fig. 15.38). In addition, PV occlusion can be assessed by analysis of the PV pressure waveform (recorded through the central lumen of the balloon catheter), although the accuracy of this method is still debated. Normally, intra-PV pressure tracing is similar to that of the LA. During NSR, the LA pressure waveform displays a small A (atrial) wave and a large V (ventricular) wave. In AF, the A wave is absent. Upon PV antral occlusion by the cryoballoon, intra-PV pressure tracing measured via the inner lumen of the balloon catheter changes to a wedged PV tracing with loss of the A wave (during NSR) and an increase in the slope and amplitude of the V wave (Fig. 15.39).¹⁶⁸

If PV occlusion is not achieved, the device can be turned clockwise and counterclockwise or even slightly withdrawn until PV flow disappears. Also, the guidewire (or mapping catheter) can be positioned in a different PV branch to change the orientation of the balloon at the PV ostium (see eFig. 15.16). Also, applying forward pressure and advancing the sheath against the proximal hemisphere of the balloon can

provide support for better PV occlusion. Among the other maneuvers used to facilitate PV occlusion by the cryoballoon is the “hockey stick technique,” which helps optimize tissue contact at the inferior circumference of the inferior PVs. This technique involves advancing the sheath (with the mapping catheter or guidewire placed in the PV with a maximal bend to the superoposterior LA) and pushing the balloon into the inferior part of the PV ostium. The “pull-down technique” is used if angiography indicates perfect contact of the balloon only at the superior circumference of the PV but not at the lower PV circumference. The pull-down involves waiting for the balloon to adhere to the superior aspect of the targeted vein (generally after 60 seconds), followed by catheter and shaft deflection to pull the frozen balloon downward to achieve contact with the inferior portion of the vein and thereby eliminate the inferior gap. If complete occlusion cannot be achieved, separate energy applications can be delivered after adjustment of the balloon angle of engagement to ensure complete encirclement of the PV antrum.¹⁶⁷

If no leak around the balloon is visible on venogram, the cryoballoon is slightly withdrawn to allow a leak around the PV–balloon interface to better define the PV ostium and ensure that the balloon is not seated inside the PV (the “proximal-seal” technique). The balloon is then gently pushed to regain PV occlusion.¹⁶⁷

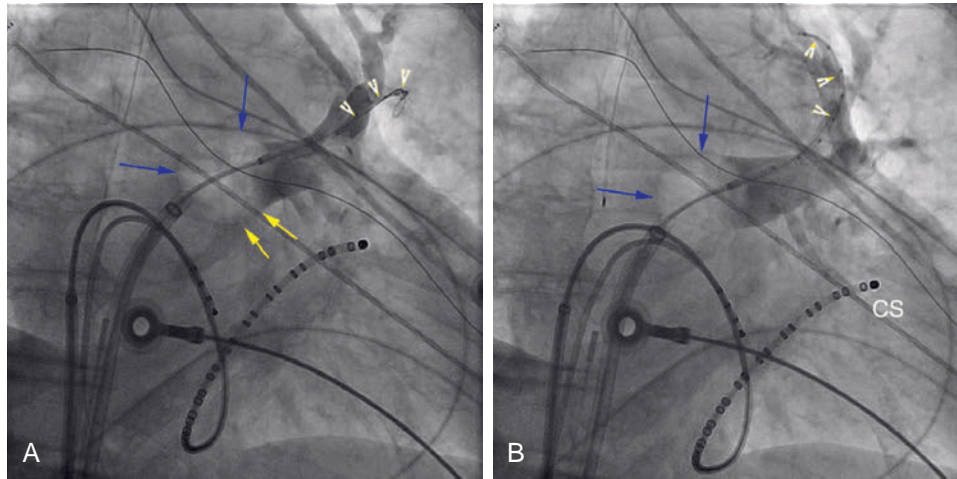
If antral occlusion of a left common PV could not be obtained, a sequential ablation approach is employed, targeting the superior branch of the left common PV followed by ablation of the inferior branch, thus accepting rather distal ablation without treatment of the antral aspect of the left common PV.^{169,170}

Mapping PV potentials. Once PV occlusion is optimized, the Achieve mapping catheter is repositioned as proximal to the PV ostium as possible (without compromising the degree of pulmonary venous occlusion) to record PV potentials. However, due to its small caliber, the Achieve catheter rarely achieves true circumferential contact with the PV ostium (leading to PV potentials being recorded on only a portion of the bipoles) and it often lacks the mechanical support needed for adequate mapping of the PV ostia. Furthermore, distal positioning of the mapping catheter within the PV can be necessary to optimize cryoballoon-PV antrum contact (eFig. 15.16). In the latter setting, repositioning of the mapping catheter can be attempted immediately (within 10 seconds) after initiation of a freezing cycle. After about 15 seconds into the freezing cycle, the central lumen is frozen, and the wire cannot be moved.^{167,171}

Not infrequently, adequate PV potential recording using the Achieve mapping catheter is not feasible when the cryoballoon is in position. Therefore the PV ostia must be carefully mapped before and after the cryoablation lesion has been delivered in order to verify electrical PV isolation. This can be performed using the Achieve catheter or using a separate conventional circular mapping catheter (e.g., Lasso catheter) introduced into the LA through the same transseptal sheath as the cryoballoon (before and after cryotherapy) or through a second transseptal sheath.^{167,171}

Cryoenergy application. After confirmation of adequate PV antral seal, cryoenergy is applied. Each cryoenergy application is extended for 180 seconds, with a maximum of 1 bonus application after the attainment of PV isolation. During freezing, maneuvering the cryoballoon should be avoided as it can cause mechanical tissue damage due to cryo-adhesion of the balloon to the endocardial wall. Once the freeze application stops, the balloon and tissue interface should be allowed to thaw and temperature reach 35°C before moving the cryoballoon.¹⁶⁷

Several parameters are monitored during cryoapplication, including the time-temperature curve (Fig. 15.40), the nadir balloon temperature achieved, ablation effects on PV potentials recorded by the Achieve mapping catheter, as well as esophageal luminal temperature (with the



eFig. 15.16 Pulmonary Vein (PV) Angiography to Assess Venous Occlusion by the Cryoballoon. The cryoballoon catheter (*blue arrows*) is inflated and positioned at the ostium of the left superior PV. (A) Angiography of the PV (right oblique view) is performed by injection of contrast into the distal lumen of the cryoballoon shows small leak at the inferior aspect of the PV ostium (*yellow arrows*). (B) The Achieve mapping catheter (*arrowheads*) is advanced into a different branch of the PV to change the orientation of the balloon at the PV ostium, and now no leak around the balloon is visible on venogram. CS, Coronary sinus.

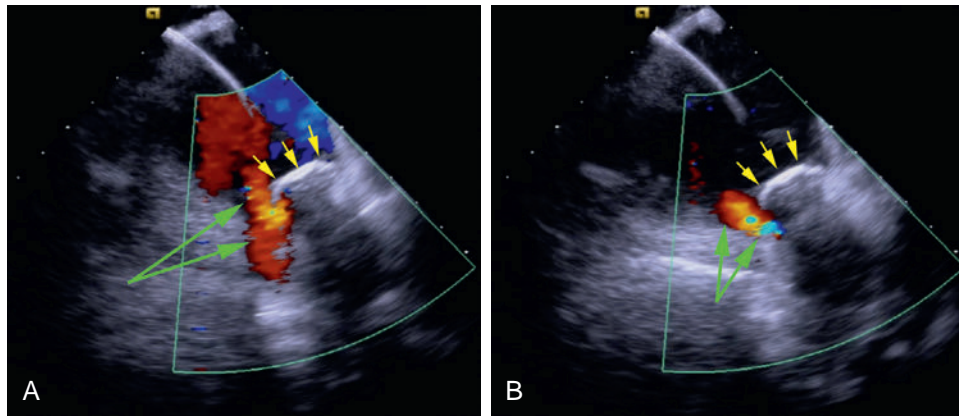


Fig. 15.38 Intracardiac Echocardiography to Assess Pulmonary Vein (PV) Occlusion by the Cryoballoon. The cryoballoon (yellow arrows) is positioned at the antrum of the left superior PV. (A) Color Doppler reveals flow (green arrows) at the inferior aspect of the balloon consistent with flow from the nearby left inferior PV. (B) Color Doppler reveals flow (green arrows) at the inferior aspect of the balloon consistent with leak from the left superior PV itself, indicating incomplete PV occlusion.

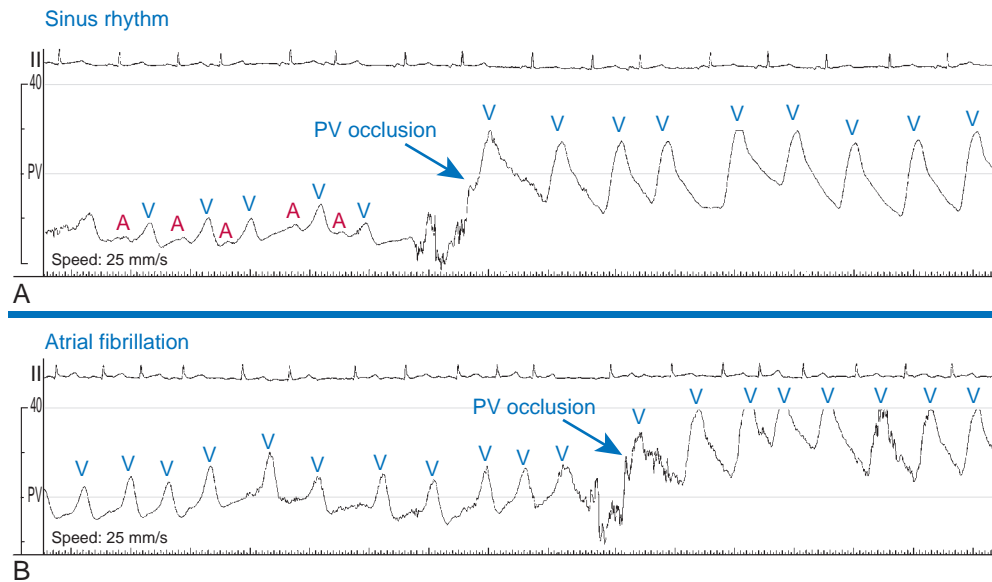


Fig. 15.39 Assessment of Pulmonary Vein (PV) Occlusion by Analysis of PV Pressure Waveform. The cryoballoon is positioned at the antrum of the left superior PV. The intra-PV pressure waveform is recorded through the inner lumen of the cryoballoon catheter. (A) Cryoballoon PV isolation is performed during sinus rhythm. Before complete PV occlusion (at left), the intra-PV pressure tracing is similar to that of the left atrium, with a small A (atrial) wave and a large V (ventricular) wave. Upon PV antral occlusion by the cryoballoon (at right), the intra-PV pressure tracing changes to a wedged PV tracing with a large V wave and disappearance of the A wave. (B) Cryoballoon PV isolation is performed during atrial fibrillation. At baseline, before PV occlusion (at left), no A waves can be visualized during atrial fibrillation. Upon PV antral occlusion by the cryoballoon (at right), the intra-PV pressure tracing displays an increase in the slope and amplitude of the V wave.

esophageal temperature probe positioned as close as possible to the inflated cryoballoon).

Several intraprocedural cryoablation data can serve as indirect indicators of satisfactory PV occlusion, efficient cryoablation lesion, and durable of PV isolation. These include: (1) fast cooling rate during cryoablation (the achievement of -40°C within 60 seconds); (2) the achievement of nadir temperature of -51°C or colder; and (3) time-to-PV isolation during freezing of 60 seconds or less (and preferably less than 43 seconds). A bonus freeze often is delivered when the cooling

rate is relatively slow (i.e., does not attain -40°C within 60 seconds) or the time-to-PV isolation during freezing exceeds 60 seconds.¹⁷²

The delivery of cryotherapy is aborted if (1) the PV is not isolated within 90 seconds; (2) the temperature fails to descend to -40°C ; (3) any warning signs of phrenic nerve injury are observed; or (4) luminal esophageal temperature lower than 12°C to 15°C . The balloon is then repositioned before another application. In addition, a steep and rapid descent in temperature (colder than -40°C at 30 seconds) and nadir temperatures of -55 to -60°C are potential indicators of a distal (rather

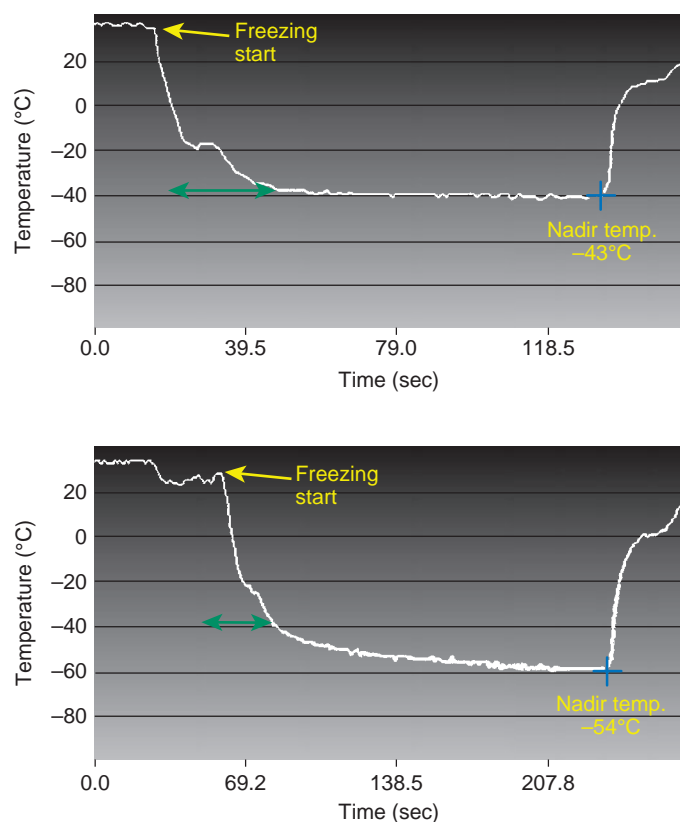


Fig. 15.40 Time-Temperature Curve During Cryoballoon Ablation. During the first cryoapplication (*top*), the cooling rate is relatively slow (as indicated by the slow descent of the balloon temperature and the longer time interval to achieve a balloon temperature of -40°C [double head green arrow]) and the nadir temperature achieved is only -41°C . In contrast, the cooling rate is faster and nadir temperature achieved (-54°C) is colder during the second cryoapplication (*bottom*).

than antral) cryoballoon location within the PV (with consequent reduced exposure of the balloon surface area to circulating blood in the atria and, hence, limited convective warming effects of blood flow), and should prompt cessation of cryoenergy delivery. Placement of the balloon deep inside the PV should be avoided because it can lead to increased freezing area and greater ice formation, which can potentially increase the risk of PV stenosis as well as injury to adjacent extracardiac structures (such as the esophagus and phrenic nerve).^{167,173}

After one or two freezing cycles, the balloon is deflated, and the circular mapping catheter is inserted into the PV to assess for isolation. If PV isolation is not achieved, the cryoballoon is repositioned, and additional freezes are applied. If remnant ostial potentials are still recorded, electrical isolation is segmentally completed by focal cryoablation using an 8-mm cryoablation catheter or by RF ablation.¹⁷⁴

Prevention of phrenic nerve injury. Before engagement of right-sided PVs with the cryoballoon, continuous phrenic nerve pacing is performed (at a PCL of 1000 to 1200 milliseconds, at twice capture threshold) using a diagnostic catheter positioned in the SVC, above level of the cryoballoon. When the procedure is performed under general anesthesia, it is important to avoid paralytic agents or use short-acting paralytic agents only at the time intubation and allow sufficient time for the paralytic effect to fade away before ablation or use a reversal agent (e.g., neostigmine).^{175,176}

Successful capture of the phrenic nerve is confirmed when contraction of the right hemidiaphragm can be observed both under

fluoroscopy or ICE and with manual palpation of the right subcostal region. Phrenic nerve capture can also be monitored by diaphragmatic electromyography (see Chapter 32).^{175,176}

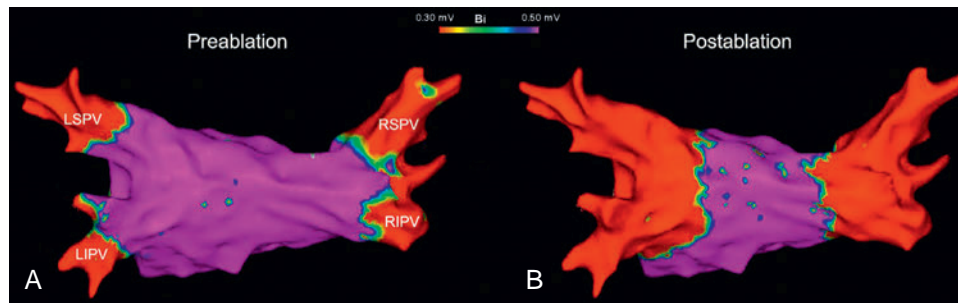
Once the cryoballoon is inflated and just before starting cryoenergy application, optimal phrenic nerve capture and compound motor activation potential (CMAP) amplitude are determined again because the PV ostial geometry and relationship with the phrenic nerve can be altered by balloon inflation. Then, phrenic nerve pacing is started when the freezing temperature reaches -20°C (to avoid balloon dislodgment due to diaphragmatic contraction in the first phase of cryoenergy application). Pacing is continued throughout the whole duration of the cryoenergy application.

The freeze should be immediately aborted if diaphragmatic excursion (on palpation, fluoroscopy, or ICE) becomes less vigorous or ceases or if the maximal diaphragmatic CMAP amplitude is reduced by more than 30% from baseline (see Fig. 32.6). A decrease in diaphragmatic CMAP amplitude is the earliest sign of detectable injury to the phrenic nerve; studies showed that a 30% reduction in diaphragmatic CMAP amplitude presaged impending hemidiaphragmatic paralysis by approximately 30 seconds, making it a valuable method for monitoring phrenic nerve function.

An immediate balloon deflation technique can also be used to help reduce the extent of phrenic nerve injury. While stopping the flow of refrigerant to the balloon allows passive balloon rewarming, balloon deflation and subsequent warming can be delayed. Because the balloon temperature must reach $+20^{\circ}\text{C}$ to allow balloon deflation, continued venous occlusion can slow the passive rewarming process, further prolonging the period of cold-induced injury. An alternate procedure involves forced deflation of the balloon without waiting for rewarming to occur. For this, the stop button on the console is pressed, which halts the refrigerant flow, and 2 seconds later the button is pressed a second time, which causes the pump to apply a vacuum to the balloon, causing immediate deflation. Immediate balloon deflation removes obstruction to blood flow, accelerating tissue rewarming, and helps retract the PV wall away from the phrenic nerve. Although the cryoballoon adheres strongly to tissue during freezing, this adherence is indirect; the balloon adheres to the ice shell, which in turn adheres to the tissue. During immediate balloon deflation, the balloon separates cleanly from the ice shell but the ice shell-tissue interface remains intact.^{177,178}

Advantages. Cryoablation offers several potential advantages over RF ablation, including elimination of the risk of coagulum formation (which should reduce stroke risk), and absence of coagulative necrosis of the ablated tissue (which can potentially reduce the risk of tamponade, PV stenosis, and pericarditis). Although the highly variable anatomy of the PVs provides a significant challenge for any balloon-based technology (it requires the shaft of the catheter to be directed coaxially to the PV), the cryothermal balloon overcomes this problem because the entire balloon can freeze and adhere to the adjacent tissue. As such, the perimeter of the balloon in closest apposition to the vein becomes the source of ablation, irrespective of the orientation in the vein. Also, compared with other balloon-based ablation technologies (HIFU and endoscopic laser), the cryoballoon is less direction-dependent because the refrigerant jet inside the balloon is directed to produce the lowest ablation temperatures in a large circular zone on the anterior third of the balloon. As such, cryoballoon ablation may be expected to isolate the muscular PV sleeves, as well as the PV antrum (eFig. 15.17).

A series of technical modifications have been implemented to the second-generation cryoballoon system, which improved the simplicity, safety, and efficacy of the procedure. The new design improves cooling properties, including reengineering of the cryogen ports to ensure formation of a larger and homogeneous hemispheric cooling zone (involving the entire leading hemisphere of the balloon surface) compared to



eFig. 15.17 Voltage Map of the LA and Pulmonary Veins (PVs) (Posteroanterior View) Is Performed Before (A) and After (B) PV Isolation Using the Second-Generation Cryoballoon. Endocardial atrial bipolar electrogram with amplitudes of greater than or equal to 0.5 mV are purple, and those with amplitudes of less than 0.3 mV are shown in red, with interpolation of color for intermediate amplitudes. Note the voltage abatement at the level of the antrum of each of the PVs, indicating the level of ablation achieved using the second-generation 28-mm cryoballoon. *LIPV*, Left inferior PV; *LSPV*, left superior PV; *RIPV*, right inferior PV; *RSPV*, right superior PV.

equatorial cooling zone in the previous iteration. In addition, the new system allows insertion of a stiffened circumferential mapping catheter through the distal lumen of cryoballoon for the recording of PV potentials during ablation. Unfortunately, the long distal tip of the second-generation cryoballoon often precludes real-time recording of PV potentials. Currently under evaluation, the third-generation cryoballoon has its tip shortened by 40% to allow positioning of the circumferential mapping catheter at the PV ostium and enhance the ability to monitor real-time PV electrograms and utilize the time-to-PV isolation to guide cryoapplications.¹⁷⁹

Of note, pain reactions occur significantly less often in patients treated with cryoablation compared to RF ablation. This can allow for cryoballoon ablation procedures to be performed under conscious or deep sedation, without general anesthesia.¹⁸⁰

Disadvantages. Unlike point-by-point RF ablation, cryoenergy cannot be modified selectively in different regions around the PVs. Because uniform cooling is obtained circumferentially with the cryoballoon, structures posterior to the thinner LA wall remain susceptible to collateral damage with cooling. Furthermore, the cryoballoon is not designed for the creation of linear or focal lesions.

Also, variations in PV anatomy can influence the effectiveness of cryoballoon ablation, likely due to the difference in the venous seal obtained being dependent on the PV ostial shape and cryoballoon alignment. Also, cryoablation of the right inferior PV, in particular, remains challenging. A low anterior transseptal puncture allows more space for the balloon to be rotated posteriorly to the right inferior PV.^{167,181}

Laser Ablation

The laser ablation catheter technology (HeartLight, CardioFocus) consists of a nonsteerable, compliant balloon catheter with an adjustable diameter (maximal diameter, 35 mm) that allows treatment of PVs of 9 to 32 mm in diameter. Within the central shaft of the balloon catheter is a 2 Fr endoscope that permits real-time visualization of the target tissue. The central shaft also contains lumens for circulating deuterium dioxide (D_2O) to cool the balloon and a maneuverable optical fiber that generates a 30-degree arc/spot of both nonablative visible light and near-infrared ablative light energy (Fig. 15.41).^{182–184}

Ablation technique. The laser balloon is inserted at the PV antrum through a 16 Fr steerable transseptal sheath. Selective PV angiography or ICE can be used to verify appropriate position of the balloon (see Fig. 15.41). Varying balloon inflation pressure allows for adjustment to the individual PV anatomy to optimize PV occlusion and maximize balloon-tissue contact. The balloon is filled with a mixture of contrast and D_2O and irrigated internally at 20 mL/min to minimize absorption of laser energy. Once the balloon is deployed, the endoscope enables real-time visualization through the face of the balloon (both the tissue and blood in contact with the balloon) at the targeted PV antrum and monitoring for the intrusion of blood into the space between the balloon and the tissue.¹⁸³

The arc generator consists of an optical fiber located within the central shaft that projects a 30-degree arc of light onto regions of balloon-tissue contact guided by an endoscopic view of the PV antrum (areas of balloon-tissue contact are visualized as blanched white, whereas

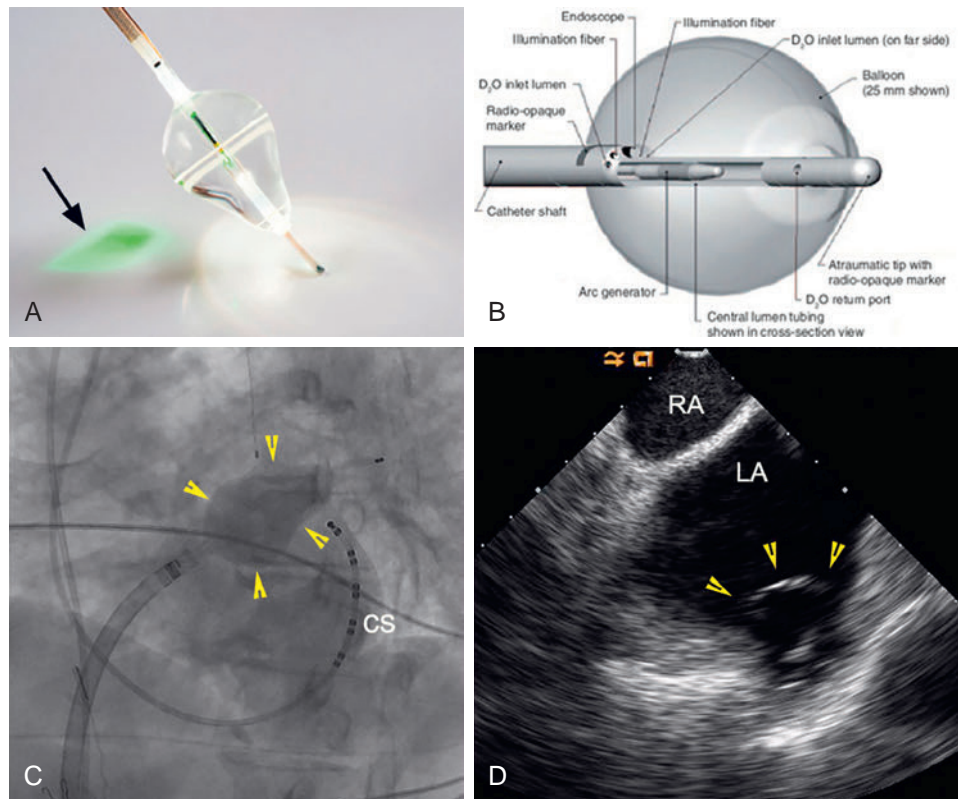


Fig. 15.41 The Laser Ablation Balloon Catheter Technology. (A) The visually guided laser balloon is shown with the aiming and ablation spot of light (arrow). (B) The catheter structure and the inflated balloon. (C) Fluoroscopic image (left anterior oblique projection) of the laser balloon (arrowheads) deployed at the antrum of the left superior pulmonary vein (LSPV). (D) Intracardiac echocardiographic image of the inflated balloon (arrowheads) at the antrum of the LSPV. CS, Coronary sinus; LA, left atrium; RA, right atrium. (A, Modified from CardioFocus, Inc., Marlborough, MA; B, modified from Bordonjon S, Chun KR, Gunawardene M, et al. Endoscopic ablation systems. *Expert Rev Med Devices*. 2013;10:177–183.)

contact with blood is visualized as red). This arc serves as an aiming beam for laser delivery and can be maneuvered along the balloon face with endoscopic visualization to facilitate individual lesion application in an anatomically flexible lesion design that adapts to the highly variable PV anatomy (Fig. 15.42). Once the proper location is identified, a diode laser is used to deliver laser energy at 980 nm. The laser fiber can be advanced or withdrawn to shift the site of lasing along the longitudinal axis of the catheter, and can be rotated to any location on the face of the balloon.^{184,183}

Laser energy is delivered at power output of 5.5 to 12 W for 20 to 30 seconds, depending on the thickness of tissue, proximity of the esophagus or phrenic nerve, and presence of blood in the field of view. To minimize the risk of thrombus formation, a 5.5-W energy is applied for 30 seconds when ablation is required in regions of overlapping moving blood along the periphery of the endoscopic view. Stagnant blood at the center of the endoscopic image represents blood from the target PV that is completely occluded by the balloon; ablation is avoided in this region due to a high risk of thrombus formation at any laser energy dose.¹⁸⁴

Under visual guidance, ablation lesions are deployed in a point-by-point fashion in a circumferential, contiguous, and overlapping manner around the PV. Each individual ablation lesion covers 30 degrees of a circle, and lesions are overlapped by 30% to 50% to minimize gaps between adjacent lesions (lesions can be tracked visually using special software, see Fig. 15.42). Because the catheter shaft obscures one-fifth of the circumference, the endoscope has a 115-degree field of view; thus catheter rotation is required to complete the ablation around the circumference of the PV antrum. Esophageal temperature is continuously monitored and energy delivery is terminated if the esophageal temperature exceeds 38.5°C. During ablation of the right superior PV, phrenic nerve pacing is performed from the SVC to monitor for phrenic nerve injury (using similar technique to that previously described for cryoballoon PV isolation).

Importantly, the laser balloon does not have the capability of simultaneous mapping and ablation. Mapping of PV potential is performed using a ring catheter before and after ablation. The ring catheter should not be left in the same PV while the laser balloon is deployed and during circumferential ablation because its shaft can impede balloon-tissue

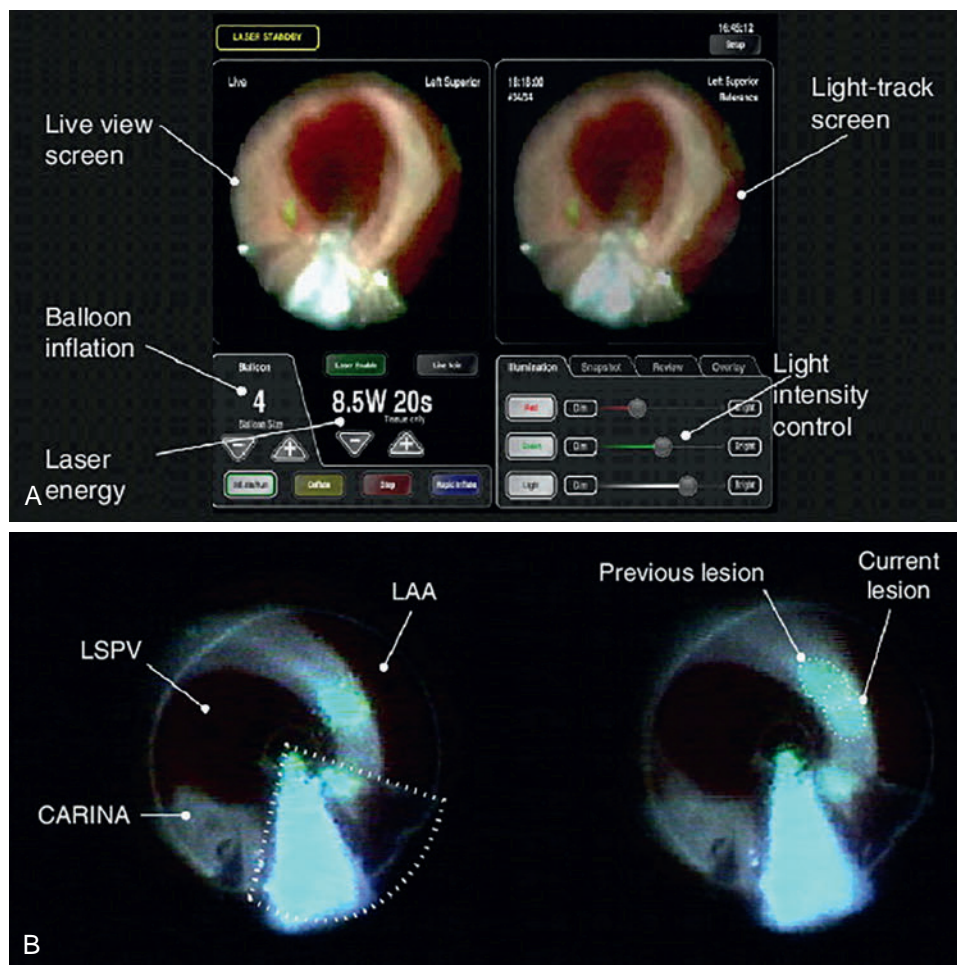


Fig. 15.42 Endoscopic Visual Guidance for Laser Ablation. (A) Touchscreen snapshot of the endoscopic ablation system console. (B) An endoscopic view is shown with the balloon positioned in the left superior pulmonary vein (LSPV). At left, The maneuverable aiming and ablation spot is shown. The carina between the two left-sided veins and the left atrial appendage (LAA) can be visualized. The blind spot created by the shaft on the eccentric endoscope is highlighted by the dotted line. At right, Visualization of lesion overlapping (LightTrac software). The lesions are highlighted by dotted lines. (From Bordignon S, Chun KR, Gunawardene M, et al. Endoscopic ablation systems. *Expert Rev Med Devices*. 2013;10:177–183.)

contact. After completion of the ablation circle, the balloon is deflated, and the ring catheter is inserted into the PV to assess for electrical isolation. However, if PV isolation is incomplete after a single ablation, the ring catheter may be placed distally to the inflated laser balloon to visualize PV electric activity online during laser energy application. In this case, the shaft of the ring catheter is positioned opposite to the presumed electrical gap to avoid incomplete PV sealing at the targeted ablation site.

The laser ablation catheter technology offers distinct advantages over both RF ablation and the cryoballoon catheter. Unlike point-by-point RF ablation, the laser balloon offers stable catheter position with limited navigation efforts and without the use of an electroanatomic mapping system. Unlike the cryoballoon catheter, the visually guided laser balloon is unique in that it uses a compliant, variable diameter balloon, thus allowing a single balloon catheter to accommodate multiple PV sizes and shapes. In addition, the endoscope provides real-time direct visualization of the target tissue. Another important feature is the ability to customize the ablation lesion and selectively titrate energy to each part of the circumferential lesion set, similar to point-by-point RF ablation. With other balloon catheters, the operator cannot choose which part of the balloon would deliver ablative energy or adjust the intensity of tissue destruction around the balloon; as a result, the portion of the LA adjacent to the esophagus or phrenic nerve receives the same energy as those areas where deeper lesions are desired.¹⁸⁵

Endpoints of Ablation

Common intraprocedural endpoints of circumferential antral PV isolation include electrical isolation of all PVs, noninducibility of AF, and elimination of residual potentials inside the circumferential ablation lines. Importantly, these endpoints, even when successfully achieved during the procedure, often do not persist over time, both in patients with and in those without AF recurrences. Nevertheless, there is a consensus on the importance of the complete bidirectional electrical isolation of all PVs as a procedural endpoint. On the other hand, less agreement exists on the value of the other endpoints.¹

Electrical Disconnection of All Pulmonary Veins

The endpoint of ablation is complete bidirectional electrical isolation of all four PVs, as described earlier for segmental ostial PV isolation. According to the 2017 HRS/EHRA/ECAS/APHRS/SOLAECE expert consensus statement, achievement of electrical isolation requires, at a minimum, assessment and demonstration of entrance block into the PV. Monitoring for PV reconnection for 20 minutes following initial PV isolation is reasonable. In addition, pharmacological provocation with adenosine and demonstration of exit block may be considered.¹

When en bloc encirclement of ipsilateral PVs (with no ablation line between the PVs) is performed, assessment of PV entrance and exit block is simplified by placing the ring catheter in one PV and the ablation catheter in the ipsilateral PV, and pacing from the ablation catheter. If there are no PV potentials recorded on the ring catheter during NSR and ipsilateral PV capture occurs (indicated by appearance of PV potentials on the ring catheter) but does not conduct to the LA (that must no longer be in AF to assess), this demonstrates both entrance and exit block into and out of both PVs (eFig. 15.18).

Elimination of Residual Potentials Inside the Circumferential Ablation Lines

The value of complete voltage abatement (i.e., reduction of the atrial electrogram amplitude by greater than 80% or a decrease to less than 0.1 mV as determined by local electrogram analysis and voltage mapping) inside the circumferential ablation lines in preventing the recurrence

of AF remains controversial and requires further investigation (see eFig. 15.17). Some studies suggested that the elimination of residual potentials inside the LA-PV junctions or carina after PV isolation offer an incremental benefit on the recurrence of AF. In contrast, other studies showed no additional benefit of this approach.

Noninducibility of Atrial Fibrillation

Induction of sustained AF is thought to indicate the presence of a potential atrial substrate capable of maintaining AF; however, its value as a predictor for clinical outcome remains controversial. Elimination of PV potentials correlates with clinical success better than the acute suppression of AF inducibility. However, a successful outcome is sometimes observed without complete PV potential elimination, and some supposedly unsuccessfully treated patients experience remarkable improvement with a previously ineffective drug.

Different pacing protocols and multiple definitions of inducibility of AF have been employed in different studies. Aggressive pacing protocols can decrease the specificity, yet more conservative pacing protocols can potentially decrease the predictive value. In fact, aggressive atrial pacing (at PCLs shorter than 180 milliseconds) can induce AF in up to 26% of patients without a history of AF. Further investigation is needed to optimize the specificity of using AF induction as an endpoint for AF ablation.

Commonly, induction of AF is attempted by burst pacing at a PCL of 250 milliseconds with sequential decrement down to 200 milliseconds (as long as 1:1 capture is maintained) for 5 to 10 seconds at least three times from the CS and then repeated from the RA. If AF is not inducible, isoproterenol (10 to 20 µg/min IV infusion) is then administered, and atrial pacing is repeated. Also, AF induction by a 30-joule external biphasic shock delivered during the vulnerable period of atrial refractoriness (i.e., synchronized to the R wave) may predict recurrent AF after PV isolation. This predictor of AF recurrence can provide additive information over inducibility with burst atrial pacing alone.

Many (up to 57%) patients with paroxysmal AF have no inducible AF after PV isolation. This subset can represent a group that can potentially benefit from PV isolation alone and do not require additional substrate modification. Induction of AF should prompt reconfirmation of complete electrical isolation in all PVs. If AF remains inducible despite complete PV isolation, additional substrate-based atrial ablation may be considered (see later discussion).¹⁸⁶

Outcome

Circumferential antral PV isolation (with an endpoint of electrical isolation of all PVs) has become the most widely used AF ablation strategy, and is currently recommended during all AF ablation procedures.

Radiofrequency Pulmonary Vein Isolation

In patients with paroxysmal AF, the rates arrhythmia-free survival at 12 months following RF circumferential antral PV isolation ranges between 59% and 89%. Circumferential antral PV isolation offers a better outcome compared with ostial segmental PV isolation for paroxysmal AF (approximately 71% vs. 64%). The incremental clinical benefit of adjuvant linear LA ablation or complex fractionated atrial electrogram (CFAE) ablation, or both, in patients with paroxysmal AF has been controversial and is likely to be small or negligible. For patients with persistent AF, the success rates of circumferential antral PV isolation (approximately 50% to 70%) are less than for paroxysmal AF but are still better than those achieved by ostial segmental PV isolation, and adjunctive substrate modification seems to offer additional benefit in AF control, although this remains controversial.¹⁸⁷



eFig. 15.18 Demonstration of Entrance and Exit Block From Both Right-Sided Pulmonary Veins (PVs). The PV catheter is situated in the right superior PV (RSPV), and the ablation catheter in the right inferior PV (RIPV), after antral isolation of both right PVs as a unit. *At left*, pacing is performed from the RIPV ablation catheter, showing capture of potentials (inferred by conduction to the RSPV), but no conduction to the left atrium that remains in consistent sinus rhythm. No PV potentials are seen in either the ablation (RIPV) or RSPV catheter during the two sinus rhythm complexes at right (entrance block into both PVs). *Abl D*, Distal ablation site; *Abl P*, proximal ablation site; *CS*, coronary sinus; *HIS D*, distal His bundle; *HIS P*, proximal His bundle.

Cryoballoon Pulmonary Vein Isolation

Studies comparing cryoablation with open-irrigated RF ablation in the setting of paroxysmal AF ablation demonstrated statistical equivalence between the two technologies in terms of safety and efficacy, with arrhythmia-free survival over the first 1 to 2 years of follow-up ranging from 54% to 85%. Limited data also suggest comparable outcomes in patients with persistent AF, and comparable rate of freedom from AF at 1 year after a single RF procedure (42% to 67%).^{188–192}

Major procedure-related adverse events with the second-generation cryoballoon have been reported in approximately 5% of patients, with phrenic nerve injury being the most important complication. Phrenic nerve injury is significantly more common following second-generation cryoballoon ablation (approximately 3% to 5%) as compared to RF ablation. Nonetheless, this rate is much less than that observed with the first-generation cryoballoon system (up to 13%). Phrenic nerve palsy generally is transient, with complete resolution observed within 1 year in most cases. In a recent report, the incidence of right phrenic nerve injury during the procedure and persistent phrenic nerve injury was 9.0% and 3.0%, respectively; however, all patients recovered spontaneously during follow-up.¹⁹³ The risk for persistent phrenic nerve injury can be minimized by ensuring the cryoballoon position is as antral as possible, by using the bigger (28 mm) cryoballoon, and by close monitoring of phrenic nerve function (including CMAP monitoring) during ablation.^{188–192}

The rate of esophageal thermal lesions detected by endoscopy following ablation using the second-generation cryoballoon ranges between 3% and 19%. Compared to esophageal lesions after RF-based ablation, lesions after cryoballoon ablation tend to be more superficial, asymptomatic, and frequently heal in a few weeks. Importantly, the incidence of atrioesophageal fistula is very rare. The risk of esophageal injury can potentially be avoided by avoiding freezing durations exceeding 4 minutes, avoiding application of more than 2 freezes to a PV, and avoiding balloon nadir temperatures colder than -60°C . Also, monitoring of luminal esophageal temperature during cryoablation and using a cutoff of 12°C to 15°C for interrupting freezing can help minimize the risk of esophageal damage.

It has become evident that cryoballoon ablation can be associated with PV stenosis (the rate of symptomatic PV stenosis or PV stenosis requiring intervention was 0.17%). A distal position of the cryoballoon with respect to the PV ostium, especially when using the smaller 23-mm balloon, can potentially increase the risk of these complications. It is possible that using the big (28-mm) cryoballoon for all veins can help direct cryothermal lesions proximal to the PV ostium at the antral level and thereby reduce the risk of phrenic nerve injury and PV stenosis.

Late PV electrical reconnection occurs mostly at the superior aspects in superior PVs and at the inferior quadrants of inferior PVs, and is most common in the right inferior PV. Notably, the incidence and characteristics of PV reconnections after a second-generation cryoballoon ablation were similar between patients with and those without clinical AF recurrences.

Laser Balloon Pulmonary Vein Isolation

The laser ablation catheter technology appears to be equivalent to RF ablation with respect to efficacy and safety in patients with paroxysmal AF, with arrhythmia-free survival over the first year of follow-up ranging from 60% to 88%. In several studies, the rate of acute PV electrical isolation achieved using the laser balloon ranged from 98% to 100%, with a highly durable rate of isolation of the PVs demonstrated on remapping studies. Laser balloon ablation is associated with higher incidence of diaphragmatic paralysis as compared to RF ablation (3.5% vs. 0.6%), but lower risk of severe PV stenosis (0% vs. 2.9%). In a single-center randomized study, AF recurrence after ablation was similar

using the laser balloon compared with the first-generation cryoballoon. The initial clinical experience with this technology suggests the ability to achieve reliable and lasting PV electrical isolation in patients with highly variable PV shapes and sizes.^{183,184}

CIRCUMFERENTIAL LEFT ATRIAL ABLATION

Rationale

Attempts to replicate the results of the maze procedure in the EP laboratory have consisted of the creation of linear lesions in the LA or RA, or both. In the past, multiple catheters with coil electrodes positioned against the atrial wall were used to create the linear lesions without having to reposition the catheter repeatedly. Currently, linear ablation lesions are created with individual contiguous applications of RF energy on a point-by-point basis. RF ablation is performed circumferentially around the ipsilateral PVs, with the endpoint of ablation being the absence or marked reduction (80%) in the amplitude of electrical signals within the encircling lesions.

Whereas the efficacy of PV isolation depends on complete and lasting PV disconnection from the LA, the efficacy of circumferential LA ablation does not. This finding highlights the fact that circumferential LA ablation (also referred to as wide-area LA ablation or circumferential PV ablation) eliminates AF by mechanisms other than complete PV isolation. Several mechanisms of action can be involved. First, there is substrate modification by LA compartmentalization. Approximately 25% to 30% of the LA myocardium is excluded by the encircling lesions, thereby limiting the area available for circulating wavelets needed to perpetuate AF. The ablation lines can also eliminate anchor points for rotors or mother waves that drive AF and make reentry pathways unsuitable. Autonomic denervation by ablation of vagal inputs to the posterior LA wall is another potential mechanism. Furthermore, the ligament of Marshall, which inserts in close proximity to the left superior PV and can be a source of triggers for AF, can potentially be eliminated by the ablation line that encircles the left-sided PVs. Modification of PV arrhythmogenic activity can also be operative. By encircling the PVs, LA ablation can potentially eliminate the triggers and driving mechanisms of paroxysmal AF that arise in the PVs. Although complete conduction block across the encircling lesions may not be achieved, decremental conduction can occur, particularly at shorter CLs, and it can impede the conduction of PV tachycardias to the LA.

There are several differences between circumferential LA ablation and PV isolation strategies. From a mechanistic standpoint, segmental ostial ablation electrically isolates the PVs, thereby eliminating the arrhythmogenic activity in the PVs that triggers or perpetuates episodes of paroxysmal AF. However, sources of AF that do not originate in the PVs and the substrate that supports the maintenance of AF are not addressed by PV isolation. From a technical aspect, segmental ostial and circumferential antral PV isolation techniques require the insertion of two catheters into the LA, whereas linear LA ablation requires only a single catheter in the LA. Also, while PV isolation requires the identification of PV potentials, circumferential LA ablation is primarily an anatomic approach to ablation. Furthermore, the risk of PV stenosis, which is a major concern during ostial PV isolation, is minimized during circumferential LA ablation because most ablation sites are more than 1 cm away from PV ostia.

Electroanatomic Mapping

The ablation catheter is advanced into the LA through a transseptal puncture. A nonfluoroscopic 3-D electroanatomic navigation system is used for generating and validating the continuity of the circular ablation lines (see Fig. 6.36). Integration of CT or CMR scans into the electroanatomic mapping system improves visualization of complex

LA geometries and can potentially improve the safety and success of catheter ablation for AF.

If validation of the circumferential lesions around PVs and the completeness of conduction block across the ablation lines are to be used as endpoints for the ablation procedure, propagation maps have to be created before and after RF ablation. In addition, the collected data can be displayed as voltage maps, which can be useful to define scar areas and electrically diseased tissues. In patients in NSR at the beginning of the procedure, maps are acquired during pacing from the CS or RA at a CL of 600 milliseconds. In patients in AF at the end of the mapping procedure, electrical cardioversion to restore NSR is performed to allow stimulation maneuvers.

Target of Ablation

The ablation lines are typically created with encircling lesions around the left- and right-sided PVs, 1 to 2 cm from the PV ostia. The circumferential ablation lines may surround each of the PVs, or, instead of encircling each PV, one big circle is placed around the PVs of each side. An ablation line is also created across the LA roof to connect the two circumferential ablation lines and often another ablation line across the mitral isthmus between the inferior portion of the left-sided encircling lesion and the lateral mitral annulus (see later discussion) (Fig. 15.43). In some patients, additional ablation lines are created in the septum and anterior wall that extend from the roof line to the mitral isthmus. At present, the number and location of LA linear lesions should be tailored to the individual patient. The ideal configuration would combine technical ease and safety with long-term control of AF.

Ablation Technique

Once an electroanatomic map of the main PVs and LA has been adequately reconstructed, RF ablation is performed 1 to 2 cm from the PV

ostia to encircle the left- and right-sided PVs. However, because there is a narrow rim of atrial tissue between the anterior aspect of the left superior PV and the LAA in approximately 50% of patients, ablation within 1 cm of the ostium of this vein sometimes is required.

Circumferential ablation lines are usually created starting at the lateral mitral isthmus and withdrawing the ablation catheter tip posteriorly and then anteriorly to the left-sided PVs, passing between the left superior PV and the LAA before completing the circumferential line on the posterior wall of the LA. The ridge between the left superior PV and the LAA can be identified by fragmented electrograms caused by collision of activity from the LAA and left superior PV-LA. The LAA is identifiable by a significantly higher impedance (more than 4 Ω higher than the LA mean), a high-voltage local bipolar electrogram, with characteristically organized activity in fibrillating patients. The right PVs are ablated in a similar fashion. Ablation sites are tagged on the model of the LA created with the electroanatomic mapping system, and that system is used for generating and validating the continuity of circular lines.

An irrigated-tip ablation catheter is typically used with power settings of 20 to 30 W on the posterior wall, 35 to 50 W elsewhere, with a temperature limit of less than 43°C. Alternatively, a solid 8-mm-tip ablation catheter may be used, with RF energy set to a target temperature of 55°C to 65°C and a power limit of 70 to 100 W. The power and temperature limits are reduced in the posterior LA wall to 50 W and 55°C to minimize the risk of injury to the surrounding structures. A series of RF applications is delivered until the maximum local bipolar electrogram amplitude decreases by 80% to 90% or to less than 0.05 to 0.1 mV, or to a maximum RF duration of 40 milliseconds, whichever comes first. Alternatively, RF energy is applied continuously on the planned circumferential ablation lines as the catheter is gradually dragged along the line, with repositioning of the catheter tip every 10 to 20

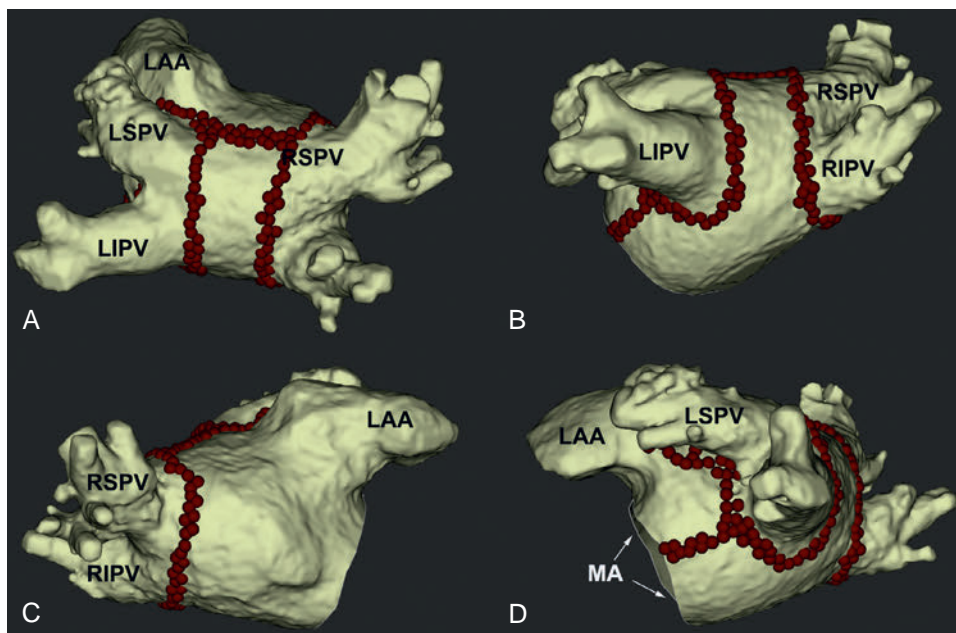


Fig. 15.43 Circumferential Left Atrial Ablation. Segmented three-dimensional computed tomography scan of the left atrium (LA) and pulmonary veins (PVs) shown in posteroanterior (A), modified posteroanterior (B), right anterior oblique (C), and left lateral (D) views. Contiguous radiofrequency lesions (red dots) are deployed in the LA, creating circumferential lines around ipsilateral PVs. An ablation line is also created across the LA roof to connect the two circumferential ablation lines and another ablation line across the lateral mitral isthmus between the inferior portion of the left-sided encircling lesion and the lateral mitral annulus. LAA, LA appendage; LIPV, left inferior PV; LSPV, left superior PV; MA, mitral annulus; RIPV, right inferior PV; RSPV, right superior PV.

seconds. Continuous catheter movement, often in a to-and-fro fashion over a point, helps keep the catheter tip temperature down as a result of passive cooling.

Power, impedance, and electrical activity are monitored continuously during navigation and ablation. Impedance can increase suddenly if a thrombus forms on the catheter tip. A much more useful indicator is a 40% to 50% reduction in the power delivered to reach target temperature. If thrombus formation is suspected, catheter withdrawal from the LA without advancing the transeptal sheath can be necessary to avoid stripping any thrombus present on the catheter tip as the catheter is withdrawn into the sheath, which can result in systemic embolization.

RF application should be immediately terminated when the catheter position deviates significantly from the planned line or falls into a PV, when impedance rises suddenly, or when the patient develops cough, burning pain, or severe bradycardia.

After completion of the circular lesions around the left- and the right-sided PVs, the area within the ablation lines is explored with the ablation catheter. RF energy is applied at sites that have a local electrogram amplitude greater than 0.1 mV. In addition, when AF is still present, sites inside the encircling ablation lines where the CL is shorter than the atrial CL in the CS also are ablated.

Endpoints of Ablation

To date, circumferential LA ablation for AF has stood apart from most other types of ablation procedures in that a clear-cut EP endpoint has not been defined. The only endpoint of ablation used in most studies has been voltage abatement. Although one study suggested that complete block across the ablation lines is a useful EP endpoint, this was not confirmed in two other studies.

Voltage Mapping

The primary endpoint for circumferential ablation is the reduction in voltage within the isolated regions by more than 80% to 90% or the recording of low (less than 0.05 to 0.1 mV) peak-to-peak bipolar potentials inside the lesion, as determined by local electrogram analysis and voltage mapping.

Postablation voltage mapping is performed using the preablation map for the acquisition of new points (on the existing LA geometry) to permit accurate comparison of preablation and postablation bipolar voltage maps. After completion of the circular lesions around the left- and right-sided PVs, the area within the ablation lines is explored with the ablation catheter, and RF energy is applied at sites that have a local electrogram amplitude greater than 0.1 mV. As an anatomy-based ablation strategy, this can be the only required endpoint.

Activation Mapping

Another endpoint used for lesion validation requires the acquisition of two activation-propagation maps during CS and RA pacing for left- and right-sided PVs, respectively. The rationale behind this setting is to pace from a site close to the lesions and shorten conduction time to the ablation site, thereby allowing detection of delayed activation inside the circular line.

Several criteria are used to define line continuity: (1) low peak-to-peak bipolar potentials (less than 0.1 mV) inside the lesion, as determined by local electrogram analysis and voltage mapping; (2) local activation time delay of more than 30 milliseconds between contiguous points lying in the same axial plane on the external and internal sides of the line, as assessed by activation mapping; and (3) gaps in the ablation lines, defined as breakthroughs in an ablated area and identified by sites with single potentials and by early local activation. Changes in activation spread are also evaluated with propagation mapping. Incomplete block

is revealed by impulse propagation across the line; in this case, further RF applications are given to complete the line of block.

Importantly, the only predictive criterion for a successful ablation seems to be the amount of postablation low-voltage encircled area. Therefore validation of the circumferential lesions around PVs by pacing maneuvers, the completeness of conduction block across the ablation lines, and the search for gaps in the ablation lines are not routinely performed.

Pulmonary Vein Isolation

Controversial data have been published regarding the influence of PV disconnection during circumferential LA ablation. Several reports suggested that complete electrical isolation of the PVs is not necessary for a successful outcome. Hence, complete PV isolation is not required as an endpoint for circumferential LA ablation. In fact, this ablation strategy typically is associated with incomplete PV isolation. Nonetheless, although PV potentials were still present in one or more PVs in 80% of patients, there usually is a conduction delay between the LA and PVs, and the prevalence of PV tachycardias is markedly reduced after circumferential LA ablation.

Of interest, conduction gaps in the ablation lines and LA-PV connection sites can be characterized by multicomponent electrograms without isoelectric lines during sinus rhythm and by multicomponent electrograms or continuous activity during AF. In one report, targeting those sites with ablation was shown to increase the PV disconnection rate during circumferential LA ablation to more than 85% of PVs, which can potentially improve clinical outcome.

Termination of Persistent Atrial Fibrillation

Termination of AF during the procedure occurs in approximately one-third of patients (more commonly in paroxysmal than persistent AF). If AF does not terminate during RF, transthoracic cardioversion is performed at the conclusion of ablation. If AF recurs immediately after the cardioversion, the completeness of the lines is reassessed, and additional ablation lines should be considered. Additional ablation consists of ablation lines created along the LA septum, roof, posterior mitral isthmus, or anterior wall, on the basis of the presence of fractionated or rapid atrial activity (see later discussion).

Organized Atrial Arrhythmias

When LA ablation is performed during an ongoing episode of AF, the AF converts to NSR or to a more organized type of atrial tachyarrhythmia in approximately 20% to 30% of patients. LA ablation can create macroreentrant circuits, thus mediating conversion of AF into AT. The most common type of macroreentry is mitral isthmus-dependent macroreentry. In addition, macroreentrant circuits (single or multiple-loop reentry as well as small-loop reentry) can be created by gaps in the ablation lines that encircle the PVs, mostly located on the ridge between the LAA and the left superior PV. Entrainment and activation mapping should be performed during organized ATs, and detailed online mapping to search for gaps in the ablation lines should be performed. RF applications at the gaps in the circumferential ablation lines or linear ablation across the lateral mitral isthmus or LA roof can be required for elimination of those ATs.

Noninducibility of Atrial Fibrillation

Whether noninducibility of AF can be used as a clinical endpoint of ablation in patients with AF who have undergone circumferential LA ablation is still controversial. Some reports found that inducibility of AF after ablation was an independent predictor of recurrent AF. One study suggested performing additional ablation when AF is still inducible after the initial procedure. Circumferential LA ablation renders AF

noninducible by rapid atrial pacing in approximately 40% of patients with paroxysmal AF. With additional LA ablation lines, the percentage of patients in whom AF was rendered noninducible increases to approximately 90%, and such an endpoint is associated with a better clinical efficacy than when AF was still inducible. Conversely, other reports showed a rather low predictive accuracy of the postablation stimulation test that prohibited its use as a reliable procedural endpoint for individual patients; these reports suggested that continuation of ablation caused by a positive stimulation test or AF persistence may lead to overtreatment in a substantial proportion of patients.

Outcome

In multiple reports, long-term success was achieved in approximately 74% of patients with paroxysmal AF and in 49% of patients with persistent or permanent AF.

One study suggested that circumferential LA ablation to encircle the PVs is preferable to segmental ostial PV isolation as the first approach in patients with symptomatic paroxysmal AF. In contrast, another prospective randomized study comparing the two strategies showed the opposite results. Not unexpectedly, the opposite results in the two studies were obtained because of the large variability in the success rate observed in patients undergoing circumferential LA ablation (88% vs. 47%), whereas the success rates in patients undergoing segmental ostial PV isolation were similar (67% vs. 71%).

Although some studies reported that PV electrical isolation was not related to the success of the procedure, more recent studies found that rigorously achieving complete PV electrical isolation improved the success of circumferential LA ablation as compared with the purely anatomic endpoint of abatement of electrical activity by the ablation catheter recording within the encircled regions. Currently, the Heart Rhythm Society's consensus statement on AF ablation strongly urges demonstration of PV isolation with whatever ablation strategy used. Because PV isolation is not necessarily achieved (or even intended) with circumferential LA ablation, this procedure has not been commonly used.

LINEAR ATRIAL ABLATION

Linear ablation lesions in the LA and RA in conjunction with circumferential LA ablation or circumferential antral PV isolation were proposed to improve the clinical outcome of AF ablation by modifying the atrial substrate that maintains AF. Ablation strategies can involve the LA roof line connecting the left and right superior PVs, lateral mitral isthmus line connecting the mitral annulus to the left inferior PV, electrical isolation of the entire posterior LA wall, and ablation of the CTI in the RA.

Left Atrial Roof Line

Rationale

Although the exact mechanism by which the LA roof supports the fibrillatory process is unclear, evidence has implicated this region in the substrate for AF. In addition, the LA roof represents a region demonstrating highly fragmented electrograms, perhaps indicating the presence of substrate capable of sustaining localized reentry or focal activity that may maintain fibrillation, and it also has the potential for supporting macroreentry around the PVs using the LA roof.

Some reports suggested that ablation at the LA roof has a direct effect on the fibrillation process, by prolonging the fibrillatory CL and terminating the arrhythmia in some patients and rendering AF noninducible in patients with inducible or sustained arrhythmia after PV isolation. This finding implicated the LA roof in the substrate maintaining AF after PV isolation.

Linear ablation was previously performed posteriorly or anteriorly across the LA. However, a posterior ablation line between the two superior PVs carries a higher risk of atriopharyngeal fistula. Transection of the anterior LA results in significantly delayed activation of the lateral LA during NSR, which has potentially deleterious hemodynamic consequences. Therefore these lines are currently substituted with the LA roof line (see Fig. 6.36).

Ablation Technique

LA roof ablation is performed after circumferential LA ablation or circumferential antral PV isolation. Commencing at the encircling lesion at the left superior PV, the sheath and catheter assembly are rotated clockwise posteriorly and are dragged toward the right superior PV. To achieve stability along the cranial LA roof, the catheter may be directed toward the left superior PV and the sheath rotated to face the right PVs, or vice versa. Two alternative methods can also be used to reach the LA roof for ablation. First, the catheter can be looped around the lateral, inferior, septal, and then cranial walls, then lay the catheter down along the cranial wall of the LA to allow dragging of the catheter by withdrawal from the left to the right superior PV ostia. Second, the catheter can be maximally deflected to form a tight loop near the left superior PV, with the tip facing the right PVs. Releasing the curve positions the catheter tip adjacent to the right superior PV ostia and allows dragging back to the left PV. Using a catheter with bidirectional deflection capability, or a unidirectional catheter in a deflectable sheath, can facilitate ablation on the LA roof.

The stability of the catheter is monitored during RF applications with the use of the proximal electrograms, intermittent fluoroscopy, or a navigation system to recognize inadvertent displacement of the catheter. Electroanatomic mapping is used for real-time monitoring and to tag the ablation sequence. RF energy is delivered for 60 to 120 seconds at each point while the local atrial electrograms are monitored. Local potential elimination or formation of double potentials during pacing or AF signifies the effectiveness of ablation locally.

Endpoints of Ablation

The EP endpoint of ablation is the demonstration of a complete line of block joining the two superior PVs. Following the restoration of NSR, complete linear block is defined by point-by-point mapping of an online corridor of double potentials along the entire length of the LA roof during pacing from the anterior LA (from the LAA or the distal CS) or during NSR and by demonstration of an activation detour circumventing the right and left PVs to activate the posterior wall caudocranially (instead of the craniocaudal activation typically observed during NSR and LAA pacing), with no conduction through the LA roof. When residual conduction is demonstrated, detailed mapping is performed to identify and ablate gaps in the linear lesion.¹

Outcome

Previous studies have shown that the addition of linear ablation to PV isolation has improved outcomes. On the contrary, more recent randomized studies and meta-analyses found no incremental benefit of additional LA linear ablation over PV isolation alone in both persistent and paroxysmal AF.¹⁹⁴

A successful linear ablation strategy depends on achieving durable complete conduction block across the ablation lines. However, although acute success rates are high, reconduction rates via gaps in the ablation line late after the procedure remain high, likely explaining the lack of benefit associated with additional linear ablation. Importantly, conduction gaps in the ablation lines may not only result in recurrence of AF, but may also be proarrhythmic, promoting the development of gap-related macro- or microreentrant ATs. Further, the efficacy of linear

ablation in modifying the substrate that maintains AF has been questioned, since several studies showed that the addition of linear ablation lesions did not reduce the rate of recurrent AF.^{30,146,194–196}

Of note, the sinus node artery courses over the LA roof from its source in the circumflex coronary artery to the sinus node region, and can be injured or destroyed with a roof line, resulting in SND.

Left Atrial Posterior Wall Isolation

Rationale

The role of the LA posterior wall in initiation and perpetuation of AF has been suggested by both human and animal studies. The LA posterior wall embryologically originates from the same cells of the primordial PV, suggesting that both of these structures potentially contribute to the development of AF. Focal discharges initiating AF not infrequently originate from the posterior LA. Furthermore, the LA posterior wall can harbor rotors that can participate in maintaining AF. Therefore targeting the LA posterior wall ablation can potentially modify the substrate responsible for both initiation and maintenance of AF. Several studies have suggested that deployment of linear lesions along the LA to exclude the posterior wall in addition to PV ablation can potentially improve long-term outcome, at least in cases with nonparoxysmal AF.^{197,198}

Ablation Technique

Following circumferential PV ablation, isolation of the LA posterior wall is achieved by an ablation line joining the two superior PVs (LA roof line) and a second ablation line joining the two inferior PVs (LA floor line). The lateral boundaries of the box isolation are formed by the contiguous lesions previously created by circumferential PV ablation, forming the so-called “box lesion” (Fig. 15.44).¹⁹⁹

Ablation of the LA roof is performed as described earlier. Following the roof line, a contiguous line of ablation lesions joins the inferior PVs to isolate the LA posterior wall. Commencing at the lesion at the left inferior PV, the sheath and catheter are rotated clockwise posteriorly and dragged toward the right inferior PV. RF power output is limited to 20 to 30 W to minimize the risk of atrioesophageal fistula.

During ablation, the slowing of LA posterior wall activity with progressive completion of the posterior LA rectangle and termination of AF can be observed in some patients. Complete linear block can be verified by the demonstration of no conduction through the LA roof and inferior lines by point-by-point sequential mapping either conventionally or by electroanatomic mapping (eFig. 15.19), or by recording and pacing from a catheter on the posterior wall showing lack of conduction from LA to these electrodes and capture of potentials without conduction to LA in a manner analogous to showing entrance and exit block after PV isolation. Persistent conduction across to the posterior wall should prompt meticulous online mapping to identify and ablate gaps in the linear lesions.

Importantly, the path of the esophagus is invariably crossed perpendicularly while creating the floor line of the box lesion, which can hinder the ability to create a complete line of block.¹⁹⁹

An alternative strategy is to target the entire LA posterior wall by extensive nonlinear ablation lesions until complete isolation is achieved (Fig. 15.45). Also, some investigators suggested a more individualized approach guided by scar (voltage) mapping. The latter approach employs ablation of the LA posterior wall only in patients with low voltage areas in that region, with scar homogenization as the goal of the ablation.²⁰⁰

Endpoints of Ablation

The endpoints of box isolation are the demonstration of the absence or dissociation of electrical activity within the ablated zone (i.e., entrance block), as well as failure to capture the LA outside the isolated region

(i.e., exit block) during pacing from the posterior LA and all PVs (after the restoration of NSR) (Fig. 15.46).^{197,199}

Outcome

Studies the value of LA posterior wall isolation as an adjunctive strategy in combination with circumferential PV isolation have arrived at conflicting results. In a study in patients with paroxysmal AF, exclusion of the LA posterior wall did not improve the outcome of circumferential PV isolation for AF. On the other hand, a recent meta-analysis demonstrated that PV isolation with posterior wall isolation provided additional benefits over PV isolation alone, with a significant reduction in AF recurrence, but no significant difference in AT recurrence.^{197,201}

Lateral Mitral Isthmus Line

Rationale

Emerging evidence has implicated regions of conduction slowing and block associated with atrial remodeling in the substrate predisposing to AF. In the LA, studies demonstrated preferential propagation that is closely correlated with muscle fiber orientation along the posterior LA and circumferentially around the mitral annulus. Such preferential propagation occurring in response to functional or anatomic conduction block (perhaps exacerbated by AF or conditions predisposing to AF) is capable of facilitating reentry using the mitral isthmus, as recognized with common forms of LA macroreentry, and thus can have a role in the milieu that maintains AF.

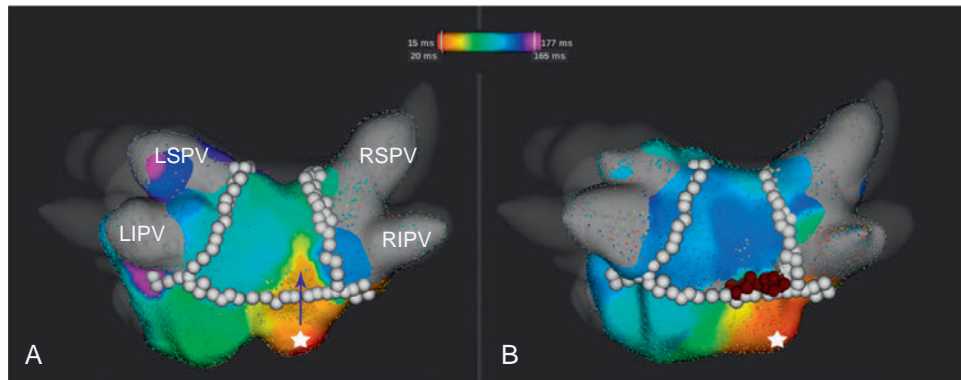
Because of the contiguity with the left PVs and LAA, ablation of the mitral isthmus results in a long (functional) line of conduction block that transects the lateral LA from the mitral isthmus to the roof. Its EP consequences can be considered analogous to those produced by CTI ablation, in which a short line is amplified by the crista terminalis to result in a long line of functional conduction block. It is thus possible that ablation of the mitral isthmus, as an adjunct to other ablation strategies for AF, helps modify a large region of the LA substrate for AF by eliminating anatomic or functional reentry involving the mitral isthmus or PVs. In addition, it can eliminate arrhythmogenic triggers arising from the ligament of Marshall.

LA macroreentrant ATs can develop following catheter ablation of AF in up to 50% of cases. The most common type of LA macroreentry is mitral isthmus-dependent AT, and it seems more likely that this type of AT is a direct result of LA ablation. The potential of this complication underscores the importance of an ablation line across the mitral isthmus. Ablation of the mitral isthmus is discussed in detail in Chapter 13.

Outcome

Most studies have failed in demonstrating an incremental benefit of ablation of the lateral mitral isthmus over PV isolation alone, even when combined to linear ablation across the LA roof. It is important to recognize that continuous linear lesions are difficult to achieve, even under direct visualization during intraoperative ablation. It has been shown that creating transmural permanent lines of block across the mitral isthmus line in particular is technically challenging and sometimes requires ablation deep within the CS.

Gaps within the ablation lines, whether secondary to areas of recovery or areas missed initially, can produce areas of slow conduction and a substrate for macroreentry. Therefore when linear LA ablation is applied, complete bidirectional conduction block across the ablation lines should be verified to reduce the risk of development of macroreentrant ATs related to gaps in the ablation lines (refer to Chapter 13 for detailed discussion). Bidirectional block at the lateral mitral isthmus can be acutely achieved in 65% to 92% of patients, with ablation within CS being required in about two-thirds of patients.²⁰²



eFig. 15.19 Confirmation of Block Across the Ablation Line. Posterior views of three-dimensional electroanatomic (Rhythmia) activation map of the left atrium (LA). Circumferential radiofrequency (RF) ablation is performed around ipsilateral pulmonary veins (PVs), and an ablation line (*white dots*) is performed connecting the inferior PVs. (A) The activation color map obtained during atrial pacing (*asterisk*) just inferior to the ablation line shows incomplete line of block, with wavefront propagation through a gap in the medial aspect of the ablation line (*arrow*). (B) Additional RF applications (*purple dots*) were delivered at the region of gaps in the ablation line. Then, activation mapping during pacing from the same atrial site was repeated; note the formation of an early-meets-late zone (*violet to red*) along the entire length of the ablation line demonstrating the achievement of a continuous conduction block. *LIPV*, Left inferior PV; *LSPV*, left superior PV; *RIPV*, right inferior PV; *RSPV*, right superior PV.

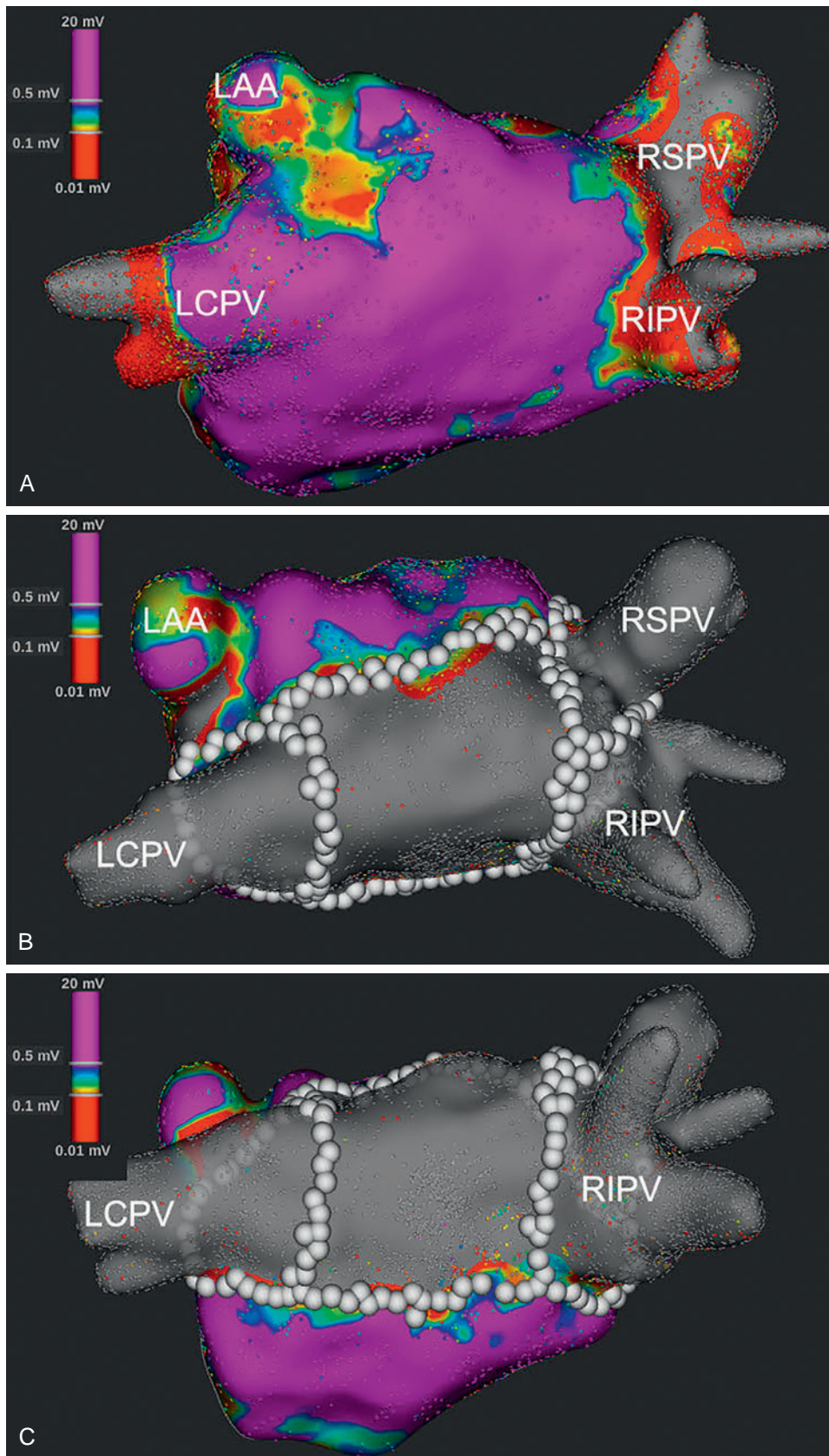


Fig. 15.44 Left Atrial Posterior Wall Isolation (Box Lesion). Three-dimensional reconstruction of the left atrium (LA, posterior view) using the Rhythmia electroanatomic system before (A) and after (B and C) catheter ablation of atrial fibrillation. Small white circles are tagged sites at which RF energy was applied to isolate the pulmonary veins (PVs). Electrical isolation of the LA posterior wall (box isolation) is performed by an ablation line joining the two superior PVs (*roofline*) and a second ablation line joining the two inferior PVs (*inferior line*). Sites with voltage lower than 0.1 mV are red on the map, and those with voltage higher than 0.5 mV are purple, with interpolation of color for intermediate amplitudes. The gray area denotes no detectable signal (scar). Note the voltage abatement encompassing all PVs and the whole LA posterior wall within the box lesion. LAA, LA appendage; LCPV, left common PV; RIPV, right inferior PV; RSPV, right superior PV.

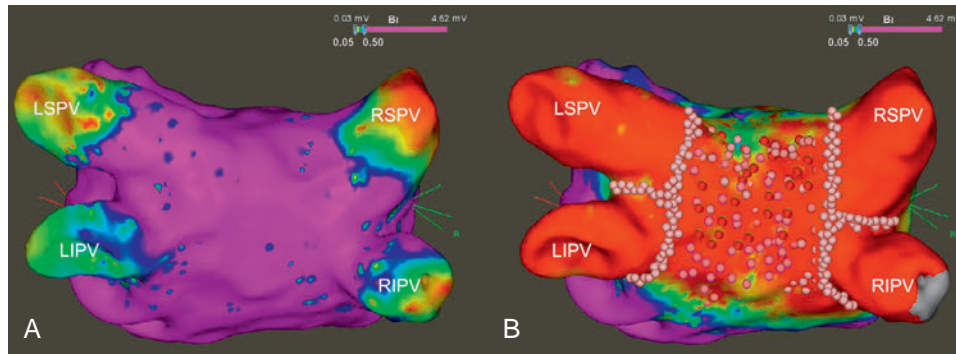


Fig. 15.45 Left Atrial Posterior Wall Isolation. Three-dimensional reconstruction of the left atrium (LA, posterior view) using the CARTO electroanatomic system before (A) and after (B) catheter ablation of atrial fibrillation. Small white and red circles are tagged sites at which RF energy was applied. After circumferential antral isolation of the pulmonary veins (PVs), nonlinear ablation lesions are applied to the LA posterior wall. Note the voltage abatement encompassing all PVs and the whole LA posterior wall within the box lesion. Sites with voltage lower than 0.05 mV are red on the map, and those with voltage higher than 0.5 mV are purple, with interpolation of color for intermediate amplitudes. *LIPV*, Left inferior PV; *LSPV*, left superior PV; *RIPV*, right inferior PV; *RSPV*, right superior PV.

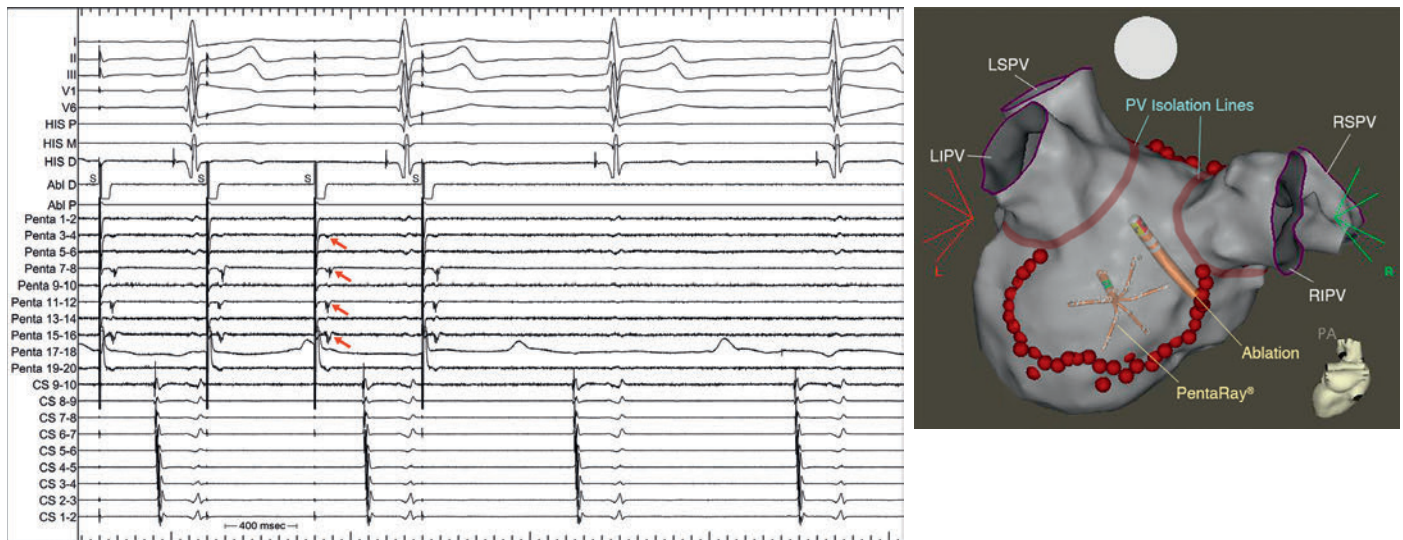


Fig. 15.46 Left Atrial (LA) Posterior Wall Isolation. At left, intracardiac recordings from a multipolar catheter (Penta) on the LA posterior wall after ablation encompassing the area with radiofrequency applications (see figure at right; the patient had previous pulmonary vein [PV] isolation). Stimulation (S) is performed from the ablation catheter, also on the posterior wall; stimuli are followed by electrograms on Penta recordings (red arrows), while the atrium (surface electrocardiogram, coronary sinus [CS] recordings) remains in sinus rhythm. After cessation of pacing, there are no electrograms from the Penta electrodes, indicating entrance and exit block into and out of the posterior wall. *Abl D*, Distal ablation site; *Abl P*, proximal ablation site; *His D*, distal His bundle; *His M*, middle His bundle; *His P*, proximal His bundle; *LIPV*, left inferior PV; *LSPV*, left superior PV; *PA*, pulmonary artery; *RIPV*, right inferior PV; *RSPV*, right superior PV.

Due to the prospect of facilitating macroreentry with incomplete ablation as well as risk of injury to the circumflex coronary artery, routine mitral isthmus ablation (in the absence of documented perimitral macroreentry) is not currently recommended.

Cavotricuspid Isthmus Line

AF and AFL frequently coexist in the same patient. Clinical AFL occurs in more than one-third of patients with AF. AF often precedes the onset of AFL and can also develop after the successful catheter ablation of AFL. Typical AFL, usually induced either by atrial pacing or by

AF, can be observed in approximately half of patients undergoing PV isolation for AF.

Although typical AFL and AF frequently coexist, their precise interrelationship is unclear. It is possible that the same premature depolarizations that trigger AF also trigger AFL, or that the EP and structural remodeling that accompany AF also promote the occurrence of AFL, or vice versa. Evidence suggests that AF plays an important role in the genesis of typical AFL; spontaneous or induced typical AFL does not start immediately after a premature beat or burst rapid atrial pacing; rather, its onset is generally preceded by a transitional rhythm (AF) of

variable duration. AF can promote the formation of an intercaval functional line of block in the RA, which can be critical for the initiation of AFL. Also, class IC and IA antiarrhythmic drugs and amiodarone used to suppress AF commonly promote AFL.

On the other hand, it is also possible that at least some episodes of AFL can degenerate into AF. AFL with a short CL can result in fibrillatory conduction. In addition, AFL can induce atrial electrical remodeling that predisposes to development of AF.

In patients with AF and no known history of AFL, the potential benefit of adjunctive CTI ablation on the risk of recurrence of AF after PV isolation has not been confirmed by large studies. Therefore routinely performing typical AFL ablation in all patients undergoing AF ablation may not provide added clinical benefit but can potentially add time, cost, and risk.²⁰³

On the other hand, CTI ablation is recommended in patients undergoing AF ablation whenever typical AFL is observed clinically. In addition, the occurrence of typical AFL in the course of a catheter ablation procedure aimed at elimination of AF was shown to be predictive of symptomatic AFL during follow-up after PV isolation, even in patients who had no prior clinical history of AFL, a risk that was lowered by combining AF and AFL ablation in those patients. Thus supplementary CTI ablation in conjunction with AF ablation is recommended in these patients.²⁰⁴

Of note, in patients with paroxysmal AF who had periods of typical AFL, PV isolation alone, although not interrupting the reentrant circuit in typical AFL, can potentially control both arrhythmias, a finding suggesting that AF initiated by PV triggers can be the precursor rather than the consequence of AFL. This is consistent with the observation that AFL commonly starts after a transitional rhythm of variable duration, usually AF. However, these findings were not confirmed by other studies that showed no benefit of PV isolation on the risk of recurrence of typical AFL.

FOCAL IMPULSE AND ROTOR MAPPING

Rationale

FIRM is a novel mapping system (RhythmView, Abbott, Chicago, IL, United States) that uses a 64-electrode basket catheter for panoramic simultaneous recording of atrial activation and computational spatiotemporal mapping of AF.

FIRM mapping has been used to identify patient-specific AF drivers, that is, regions in the atrium that can potentially be responsible for maintaining AF, to design tailored ablation strategies. FIRM mapping records AF unipolar electrograms in a wide field-of-view across the majority of both atria and then employs physiologically directed computational methods to create activation trails, which can identify putative regions of recurrent organized rotational activity (rotors) and focal sources (focal drivers) within the atria, which appear to have a mechanistic role in sustaining AF.^{205,206}

Focal Impulse and Rotor Modulation Mapping

Initially, atrial geometry is constructed using an electroanatomic mapping system (EnSite NavX or CARTO). Typically, PV isolation is performed first; if AF persists thereafter, rotor/focal source mapping is then performed.

The technique involves use of a multipolar basket catheter (Constellation, Boston Scientific; or FIRMap, Abbott) with 8 splines, each having 8 equally spaced electrodes (total, 64 electrodes). The basket catheter is introduced via an 8.5-Fr long sheath from the femoral vein sequentially into the RA and then (transseptally) into the LA. The basket size, either 48 or 60 mm (Constellation) or 50, 60, or 70 mm (FIRMap), is selected on the basis of atrial size determined from preprocedure CT

angiography or intraprocedural ICE. Generally, the RA is mapped first and the LA second. The basket catheter is manipulated to achieve good contact with as much of the atrium as possible on the basis of fluoroscopic and ICE imaging and unipolar and bipolar electrogram quality (Fig. 15.47). Upsizing the basket catheter needs to be considered when optimal endocardial coverage (greater than 75% of atrial chamber surface) by basket catheter electrodes cannot be achieved. Downsizing the basket size should be considered when excessive basket distortion or insufficient basket expansion occurs. IV heparin is infused to achieve an ACT of more than 300 seconds.^{198,207}

Wide-area contact mapping uses monophasic action potentials to separate potentially reproducible elements (principal components) of activation in AF from bystander disorganized activation in a clinically meaningful fashion. FIRM mapping is performed during spontaneous or induced sustained AF. Unipolar atrial electrograms from the basket catheter are filtered at 0.05 to 500 Hz and recorded at 1-kHz sampling frequency (eFig. 15.20). Unipolar electrograms are recorded during AF for 1 minute and exported to a dedicated proprietary mapping system (RhythmView). Multiple 1-minute recordings are typically analyzed over a period of 5 to 10 minutes. The system filters out QRS complexes and T waves and analyzes the unipolar atrial electrograms, taking into account rate-dependent refractoriness ("restitution") and conduction slowing to determine physiologically plausible activation paths. Using phase-based algorithms, RhythmView software provides maps of putative propagation of electric activity during AF (isopotential movies and isochronal activation maps) projected onto a 2-D grid representing the endocardial surface of the atrium studied. AF (FIRM) maps are analyzed intraprocedurally to guide ablation.^{198,205,208}

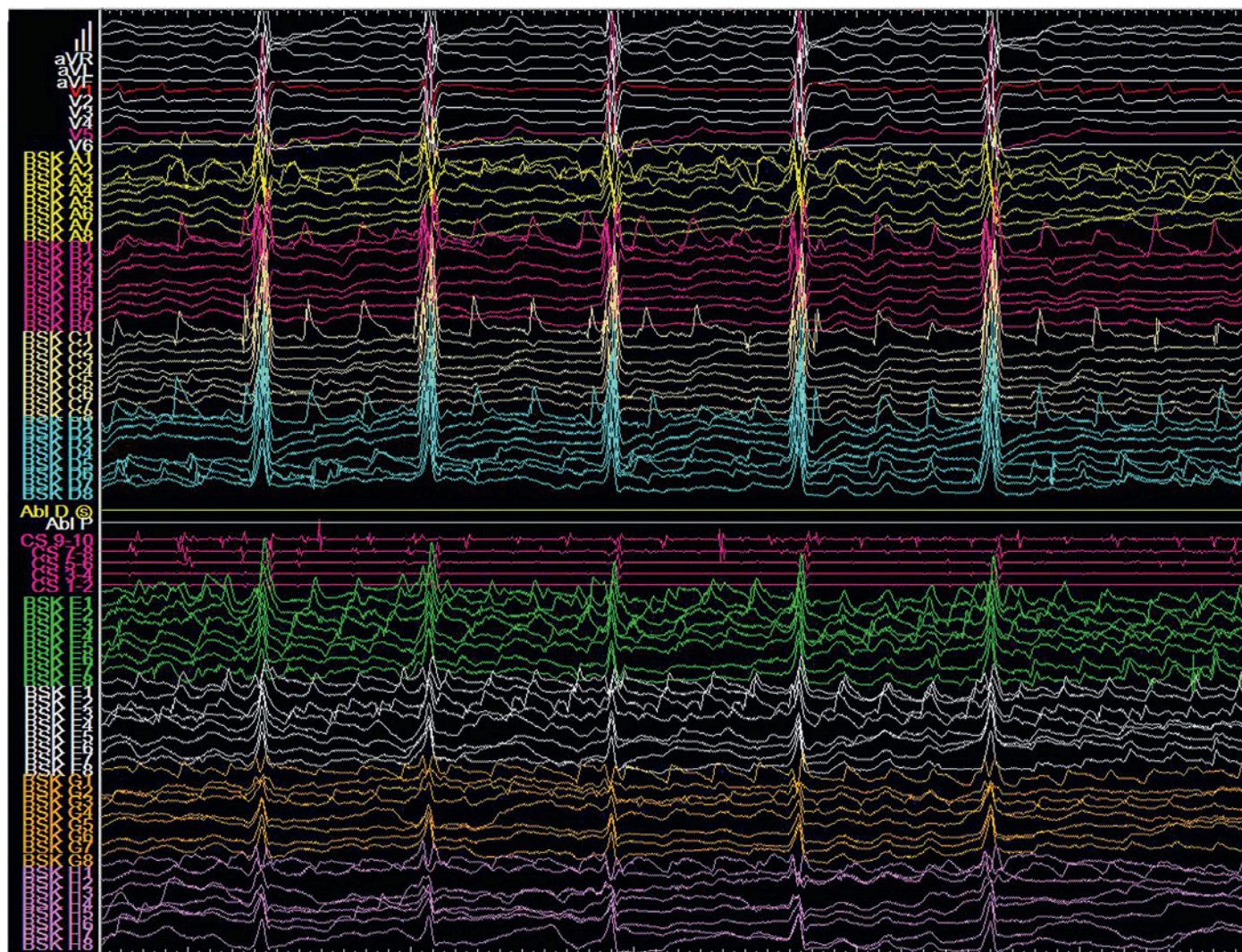
Rotors are defined as phase singularities with emanating spiral waves that disorganize in surrounding tissue. Repetitive focal drivers are defined as activation emanating centrifugally from a source region. Clinically, rotors or focal drivers observed in FIRM maps are diagnosed as AF sources only if they lie in spatially reproducible regions (i.e., showing spatial stability) for minutes (i.e., showing temporal stability). This definition excludes transient or migratory activity that would be difficult to target for ablation.^{21,209}

Target of Ablation

RF ablation targets electrical rotors and focal impulses that lie in reproducible regions, with precession, on repeated analysis for thousands of cycles. Sources often cluster around the PV antra, the base of the LA and RA appendages, the LA roof, and the lateral mitral isthmus. However, sources have been found in almost all locations but are not typically within 1 cm of a valve annulus (possibly similar to the property of experimental rotors that extinguish when a nonconducting barrier is encountered).^{198,205,208,210}

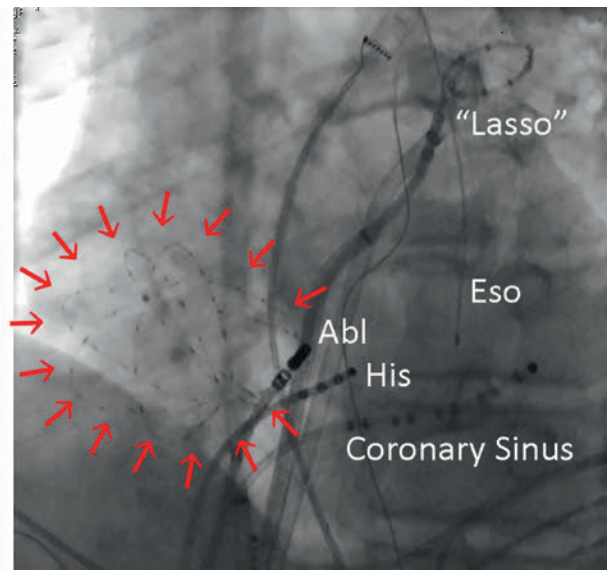
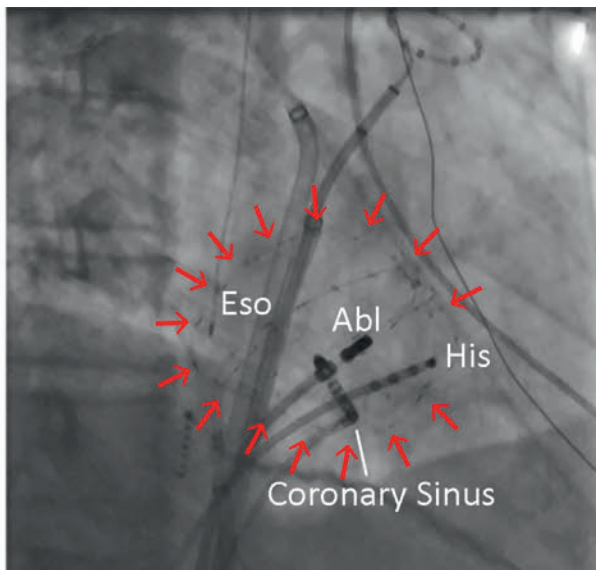
Ablation Technique

Based on basket grid coordinates, referenced to electrode positions on electroanatomic shells, the ablation catheter is manipulated within the area corresponding to the center of rotation (for rotors) or focal impulse origin, as indicated by the FIRM map. Generally, the splines and electrodes at this source and surrounding region of about 2 cm² are identified and targeted by ablation (Fig. 15.48). RF ablation is performed using an irrigated-tip ablation catheter (power output, 25 to 35 W; maximum temperature, 42°C). Energy is applied with the aim of eliminating or drastically reducing amplitude of electrograms in the area (20 to 40 seconds per lesion). A lesion set is created, targeting the region within a radius of 1 to 2 cm of the rotor coordinate, until AF terminates, organizes to another tachycardia, or the entire rotor region has been ablated (which usually requires about 5 to 10 minutes of RF energy application) (see Fig. 15.48). Usual care is taken

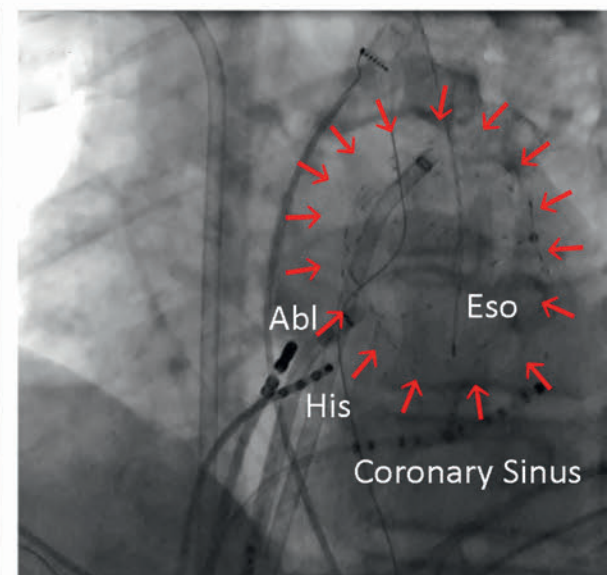
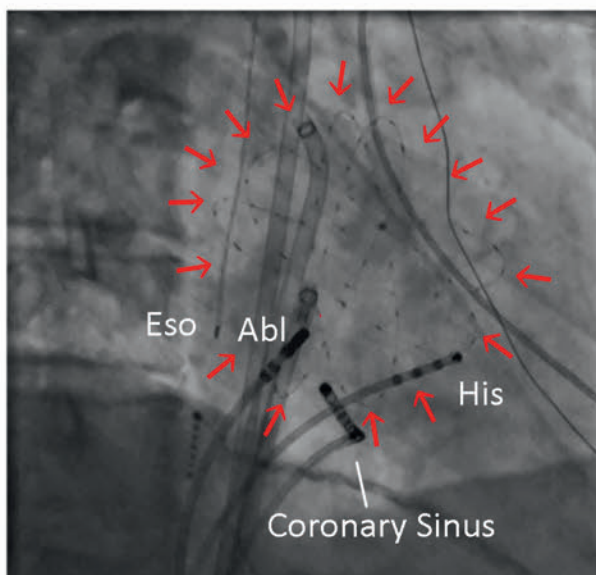


eFig. 15.20 Basket Catheter Electrograms for Rotor Mapping. Unipolar atrial fibrillation (AF) recordings from basket catheter (*BSK*) in left atrium; 12 electrocardiogram leads (*top*) and red signals (*center*, from coronary sinus [*CS*]) show clear AF. Recordings from each basket spline are grouped by color (8 recordings from each of 8 splines). *Abl D*, Distal ablation site; *Abl P*, proximal ablation site.

Right Atrium



Left Atrium



Right Anterior Oblique

Left Anterior Oblique

Fig. 15.47 Basket Catheter Positions for Rotor Mapping. A 50-mm basket catheter is placed in the right atrium (RA) via a long sheath, then transseptally into the left atrium (LA). Red arrows indicate extent of basket splines. Note that in the LA, the basket is posterior to the coronary sinus (right anterior oblique), and covers most of the LA (left anterior oblique). *Abl*, Ablation catheter; *Eso*, esophageal temperature probe.

to avoid damage to nearby structures such as phrenic nerve, esophagus, and AVN.

Once a lesion set is completed in a target zone, a repeat FIRM map is created. If the rotor is still present, additional RF is delivered and the map recreated. If the target rotor or source is no longer evident, other rotors or focal sources are sought. If no further sources are evident on remapping, the basket position in the atrium can be adjusted to cover additional areas not well seen before. When AF terminates during ablation, reinduction is attempted with pacing; if sustained AF is reinduced, and a new FIRM map is created.

Once no further sources can be identified, the other atrial chamber is mapped, targeted, and ablated in an identical manner. Iterative cycles of mapping of sources, ablation, remapping, and catheter repositioning

are repeated until there are no further sources (at which time cardioversion is performed) or AF cannot be reinitiated (if it has previously terminated with ablation). Basket catheters currently are available in 50-, 60-, and 70-mm diameter to accommodate most atria. In the majority of cases, baskets chosen to fit the LA work well in the RA.^{198,205,208}

Usually, an average of 3 to 5 sources is found and targeted for ablation; 80% to 90% are rotors. More are found in LA than RA, in persistent than paroxysmal AF. Mapping and ablation of rotors and focal sources adds approximately 1 hour to the procedure.

Endpoints of Ablation

RF ablation is performed to achieve local potential abatement at the ablation target area with the acute endpoint of AF source (rotor or

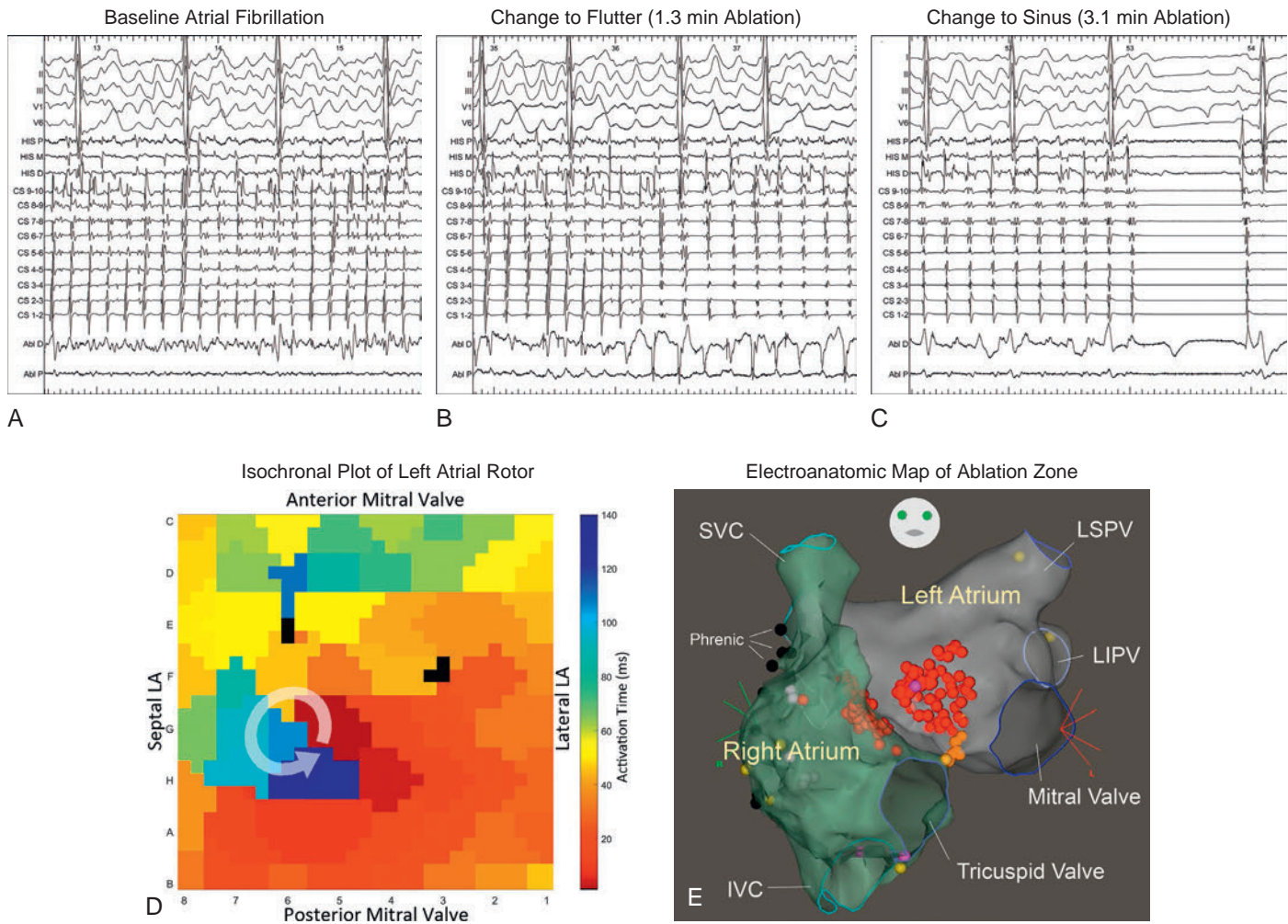


Fig. 15.48 Focal Impulse and Rotor Modulation (FIRM). A left atrial (LA) rotor is identified by FIRM mapping in a patient with persistent atrial fibrillation (AF) for more than 8 months. (A) AF at baseline. (B) After 1.3 min of ablation at rotor site, AF organizes to an atypical flutter. (C) After 3.1 min of ablation, the rhythm terminates to sinus rhythm. (D) Anteroseptal LA rotor on mapping diagram. (E) Anterior view of electroanatomic shells (right atrium—green, LA—gray); successful septal LA rotor ablation site (red dots; total ablated area approximately 20 cm²). *Abl D*, Distal ablation site; *Abl P*, proximal ablation site; *CS*, coronary sinus; *His D*, distal His bundle; *His M*, middle His bundle; *His P*, proximal His bundle; *IVC*, inferior vena cava; *LIPV*, left inferior PV; *LSPV*, left superior PV; *SVC*, superior vena cava.

focal impulse) elimination, as confirmed with FIRM remapping. FIRM mapping is repeated until all AF sources in both atria are identified and ablated, AF organizes into focal or macroreentrant AT, or converts to NSR.^{198,205,208}

When AF organizes into a regular AT, this is mapped and ablated with conventional approaches. Electrical cardioversion is performed if AF persists after elimination of all FIRM-identified sources and no new sources are identified on FIRM remapping.²¹¹

Outcome

Initial studies using FIRM showed that rotors and focal sources are present in the vast majority of patients with AF. Ablation of AF drivers as guided by FIRM, in the form of small numbers of stable rotors or focal sources distributed in both atria and frequently located outside the PV ostia, resulted in high rates of acute termination and long-term freedom from recurrent AF. Those studies reported superiority of FIRM in AF suppression as compared with conventional ablation techniques.

In particular, termination of persistent AT when ablating at areas indicated by mapping provided a strong validation for the technique.²⁰⁶

However, subsequent relatively small studies failed to replicate the findings of initial reports. Some of the most recent studies reported a low acute procedural success in paroxysmal and nonparoxysmal AF population after targeting the FIRM-identified rotors and very high long-term arrhythmia recurrence as compared to conventional approaches to AF ablation. Therefore an ablation strategy targeting FIRM-identified rotors, alone or in conjunction with PV isolation, remains controversial, given the lack of randomized data supporting its efficacy. Such studies are underway.^{198,210–212}

Several factors have been proposed to explain the disparate results of FIRM-guided ablation. One possible explanation is that the fundamental premise that rotors are the driving mechanism of AF may not be accurate. FIRM is based on the premise that AF is sustained by spiral waves or rotors or focal sources, or both, which were sufficiently stable in space to be eliminated by targeted ablation. It is still controversial

whether stable rotors exist in human AF and whether they are responsible for maintenance of AF, rather than a passive epiphenomenon of disorganized fibrillatory activation. The ability to determine the true mechanism of apparently focal activation can be limited by inadequate spatiotemporal resolution, insufficient sampling duration, low fidelity of interpolation, and poor differentiation of true local activation from far-field contamination. In fact, studies showed that FIRM-identified rotor sites did not exhibit quantitative atrial electrogram characteristics expected from rotors (i.e., greater electrical periodicity, unique spectral characteristics, such as higher dominant frequency and higher Shannon entropy) and did not differ quantitatively from surrounding tissue.²⁰⁹ Furthermore, one report demonstrated the lack of relationship between sites of FIRM-identified rotors and low voltage areas identified on atrial substrate maps.²¹³ Therefore the area targeted for ablation by the software may not be related to the pathophysiologic mechanisms underlying the arrhythmia. Moreover, it remains unclear whether functional rotors can be effectively ablated.²⁰⁹

Another possibility is the dependence of FIRM on a basket catheter that may not adequately adapt to individual variation in atrial geometry to provide optimal atrial coverage. It is inevitable that the basket catheter will bridge endocardial valleys and fail to fill out all the endocardial geometry. Also, panoramic mapping with the basket catheter provides insufficient spatial resolution due to poor tissue contact by the basket catheter electrodes, basket distortion, and interspline bunching, as well as inadequate electrode density to accurately detect rotors near the equatorial electrodes. This results in incomplete sampling of the atrial surface, potentially leaving mechanistically critical regions unmapped. To account for the missing electrograms (up to 50%) and limited spatial resolution of a basket catheter, extensive interpolation is required. Even within regions with adequate physical sampling, the signal quality is often too poor or the atrial coverage insufficient to perform phase analysis. The resulting activation maps are of such low resolution that it is difficult to precisely identify the site of any localized sources for ablation. This shortcoming would be expected to miss sources that may be present rather than falsely show sources. In addition, there are limitations, though minor, inherent in the representation of a complex 3-D structure as a 2-D rectangular grid of regularly spaced electrodes that assumes an ideal spherical fit of the basket catheter.^{16,209,210,214}

While significant questions remain regarding existence, methods of detection and meaning of rotors/focal sources detected by FIRM, the relatively high rate of AF termination to either AT/AFL or NSR and apparent improvement in mid-term freedom from recurrent AF in larger observational studies suggest the technique has validity.

ABLATION OF COMPLEX FRACTIONATED ATRIAL ELECTROGRAMS

Rationale

Evaluation of the complexity and frequency of intracardiac electrograms can help in understanding the pathophysiology of AF. Atrial electrograms during sustained AF have three distinct patterns: single potentials, double potentials, and complex fractionated potentials. Continuous propagation of multiple wavelets in the atria and wavelets as offspring of atrial reentry circuits has been suggested as the mechanism by which AF can be perpetuated without continuous focal discharge. Fractionated and continuous electrical activity has been assumed to indicate the presence of wave collision, slow conduction, or pivot points where the wavelets turn around at the end of the arcs of functional blocks. Thus areas of CFAEs during AF can potentially represent continuous reentry of the fibrillation waves into the same area or overlap of different wavelets entering the same area at different times, although the mapping

resolution to discern whether such rotors even exist in human AF is still limited.

Such complex electrical activity has a relatively short CL and heterogeneous temporal and spatial distribution. A relatively short CL may indicate the presence of a driver, analogous to the frequency gradient from the drivers or rotors to the rest of the atria observed in experimental models of AF, in which the central core of these rotors can have high-frequency electrical activity, whereas the periphery of the rotors displays complex electrograms because of wave break and fibrillatory conduction. Importantly, regions of CFAEs have been shown to remain spatially and temporally stable in individual patients, particularly when these regions were measured over several seconds, a surprising finding considering the earlier observation that a proposed underlying mechanism for AF is random reentry and that the reentrant wavelets are expected to meander.

Several studies suggested that areas of CFAEs are critical sites for AF perpetuation and can serve as target sites for AF ablation. It has been proposed that once CFAEs are eliminated by ablation, AF can no longer be sustained because the random reentry paths are altered or eliminated so that the fibrillation wavelets can no longer reenter the ablated areas. Whereas PV isolation targets the triggering foci, ablation of CFAEs targets the substrate for AF. However, some connections between both approaches probably exist. Data suggest that PVs and their antra are the key areas where CFAEs are located; these areas need to be ablated to achieve conversion of AF to NSR. It is thus very likely that many patients may respond to ablation in the PV regions because of both trigger elimination and substrate modification.

Mapping Complex Fractionated Atrial Electrograms

Mapping of CFAEs is performed during AF. In patients in NSR at the time of study, AF is induced by rapid atrial pacing, with or without isoproterenol infusion. During sustained AF, biatrial electroanatomic mapping is performed. The CS or RA appendage recording is used for electrical reference during mapping. Atrial CLs are monitored and recorded from the reference and mapping catheters. Sites with CFAEs can be tagged and associated with the atrial geometry created by the electroanatomic mapping system and thereby serve as target sites for ablation. During AF, the local activation time of the arrhythmia is of no value in guiding activation sequence mapping.

The definition of CFAEs has not been consistent. Initially, CFAEs were defined as: (1) fractionated atrial electrograms composed of at least two deflections or have a perturbation of the baseline with continuous deflection of a prolonged activation complex over a 10-second recording period; or (2) atrial electrograms with a very short CL (less than 120 milliseconds) averaged over a 10-second recording period (Fig. 15.49). More recently, CFAEs have been defined as having any of the following: (1) a magnitude of less than 0.25 mV; (2) a duration longer than 50 milliseconds with multiple (greater than 3) deflections from the isoelectric line; or (3) continuous electrical activity without an isoelectric line, verified visually. Some investigators, using unipolar mapping, defined fragmented potentials as electrograms exhibiting two or more negative deflections within 50 milliseconds. The limit of 50 milliseconds was based on the assumption that the atrial refractory period during AF and the interval between two successive fibrillation waves were 50 milliseconds or more.^{30,215}

An important limitation of this approach is that the visual appearance of CFAEs is variable, and they often are of very low amplitude (less than 0.25 mV); therefore their identification by visual inspection can be challenging and is highly subjective and investigator-dependent (Fig. 15.50). To improve the accuracy of CFAE mapping, custom software has been developed with algorithms that enable automated detection and tagging of areas of CFAEs and incorporated into either the CARTO

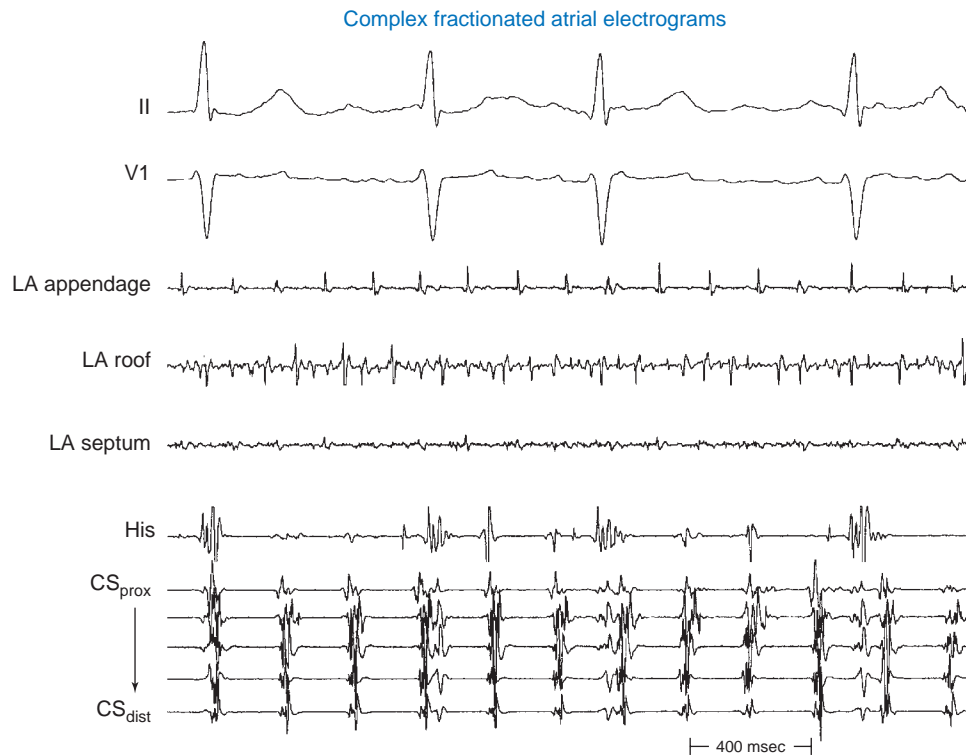


Fig. 15.49 Examples of Complex Fractionated Atrial Electrograms. Fractionated atrial electrograms with a very short cycle length, compared with the rest of the atria, were recorded in the left atrial (LA) roof. In the LA septum, fractionated electrograms with continuous prolonged activation complex were observed. See text for discussion. CS_{dist} , Distal coronary sinus; CS_{prox} , proximal coronary sinus.



Fig. 15.50 Fractionated Atrial Electrograms. Recordings from near ligament of Marshall (*Abl*) showing complex fragmented atrial electrograms (high-frequency, somewhat repetitive spikes [arrows]); these are not consistently present over the duration of the recording, whereas similar activity is intermittently seen in the His recordings (right atrial). Abl_{dist} , Distal ablation site; Abl_{prox} , proximal ablation site; CS_{dist} , distal coronary sinus; CS_{prox} , proximal coronary sinus; His_{dist} , distal His bundle; His_{prox} , proximal His bundle.

or NavX EnSite electroanatomic mapping systems. This software offers valuable advantages in the detection, quantification, and regionalization of CFAEs.

Currently, the automatic algorithms are variable and are dependent on the recording technology (NavX and CARTO). In the CARTO system, fractionation is generally determined by the shortest complex interval between two consecutive deflections over a measuring period. The low-voltage window is usually programmed at 0.05 to 0.15 mV (to exclude

both noise and high-voltage signal from the analysis). The intervals between successive peaks falling within this window are measured. Intervals falling within a programmable duration (usually 60 to 120 milliseconds) are identified and the number of such intervals during the entire 2.5-second sampling window calculated; this is designated the “interval confidence level” (ICL). The assumption is that a greater number of short intervals between low-amplitude multi-deflection complexes in a given time duration (2.5 seconds) reflects more frequent

and repetitive CFAE and, hence, higher ICL. The CARTO software can also measure CFAE by either the “shortest complex interval” (which is the shortest interval found in milliseconds out of all the intervals identified between consecutive CFAE complexes) or the “average complex interval” (which is the average of all the intervals identified between consecutive CFAE complexes for each 2.5-second electrogram). CFAE areas are displayed on the whole-chamber map in a color-coded manner according to the degree of fractionated signals and their CLs for easier identification (eFig. 15.21).^{215–217}

The algorithm embedded in the EnSite mapping system uses a different principle, the “CFAE mean.” The CFAE mean is defined as the average time interval between consecutive deflections ($-dV/dt$) in a local AF intracardiac bipolar electrogram recorded over a specified length of time (5 to 8 seconds). The mean interdeflection time interval (i.e., the mean CL) is then projected onto the LA anatomic shell as a color-coded display. The shorter the mean CL, the more rapid and fractionated the local electrogram. Regions with mean CLs shorter than 120 milliseconds are considered to correspond to CFAE. To optimize algorithm accuracy, bipolar recordings are filtered at 30 to 500 Hz (to avoid sensing noise), electrogram width is set at less than 10 to 20 milliseconds (to avoid detecting far-field signals), and electrogram “refractory” period is set at 30 to 50 milliseconds (less than 30 milliseconds is regarded as nonphysiological). In addition, the baseline signal noise level is determined, and the peak-to-peak electrogram amplitude detection limit is set just higher than the noise level (typically, 0.03 to 0.05 mV) to minimize noise detection while allowing detection of CFAEs, which are typically of very low amplitude (less than 0.5 mV). This algorithm is probably most analogous to the “average complex interval” map from the CARTO software. Advantages of the EnSite system include an adjustable duration of recording from 1 to 8 seconds and the ability to record electrograms from multiple poles of several catheters simultaneously, which can potentially occupy a significant proportion of local AF CL.^{196,215–217}

Importantly, assessment of fractionated electrograms during AF requires a recording duration of at least 5 seconds at each site to obtain a consistent fractionation and accurate analysis. A small mapping catheter tip (4 mm), good atrial contact, and stable mapping catheter position for several seconds while mapping at each location are important to obtain high-quality recordings.

In general, CFAEs can be identified in most (80%) areas of the LA, but they appear to be predominantly located in the interatrial septum, LA roof, posterior wall, mitral annulus, and PV ostia. Less commonly, CFAEs are located in the RA, involving the septal region, crista terminalis, and CTI, as well as the CS os. Notably, patients with paroxysmal AF appear to have more CFAE sites identified around the PV ostia, whereas CFAEs detected in patients with persistent AF appear to be more evenly distributed over all areas of the LA. However, these findings have not been consistent across studies using different CFAE detection methods.

Target of Ablation

Atrial ablation is performed at atrial sites that harbor CFAEs characterized by the following: (1) low-voltage (range 0.04 to 0.25 mV) signals that have multiple potentials with continuous deflection of a prolonged activation complex; (2) stationary CFAEs that have temporal and spatial stability; and (3) short CL (less than 120 milliseconds) electrograms that occur repeatedly with a relatively stable frequency with or without multiple potentials as CFAEs. CFAE sites that are fleeting, have high amplitude, or have a relatively long CL (greater than 150 milliseconds) are not targeted by ablation.²¹⁸

The atrial septum, followed by the regions of the PVs, is the most common site for CFAEs. The most common localizations for termina-

tion and regularization of AF during CFAE ablation are the regions of the PV ostia, the interatrial septum, and the LA anterior wall close to the roof of the LAA.

After ablation of CFAEs in the LA, those in the CS and RA are targeted. RA ablation aimed at termination of AF can potentially offer a clinical benefit in patients with longstanding persistent AF, but it does not seem to improve outcome in patients with persistent AF of shorter durations.²¹⁸

Ablation Technique

The ablation typically begins at sites at which CFAEs have the shortest interval and preferably also have a high ICL. RF energy is applied using an 8-mm-tip or, preferably, an irrigated-tip catheter. Lower power output is applied in the CS and along the LA posterior wall. RF application is typically continued for 30 to 60 seconds at each site, aiming to eliminate or organize local electrograms.¹⁹⁶

The typical response of CFAE ablation procedures for persistent AF is a progressive increase in CL, and AF organizes into AFL or AT. It is rare for persistent AF to convert to NSR without changing to AT or AFL first.²¹⁸

Once AF organizes into AFL or AT, residual CFAEs around the tagged or previously ablated areas are sought and ablated. When the areas with CFAEs are completely eliminated, the focus or reentry circuit underlying the AT is mapped and specifically targeted by ablation. Administration of IV ibutilide can help lengthen the tachycardia cycle length (TCL), reduce residual fibrillatory conduction, and unmask the primary arrhythmia. If the arrhythmias are not successfully terminated by ablation or ibutilide, external cardioversion is performed.²¹⁸

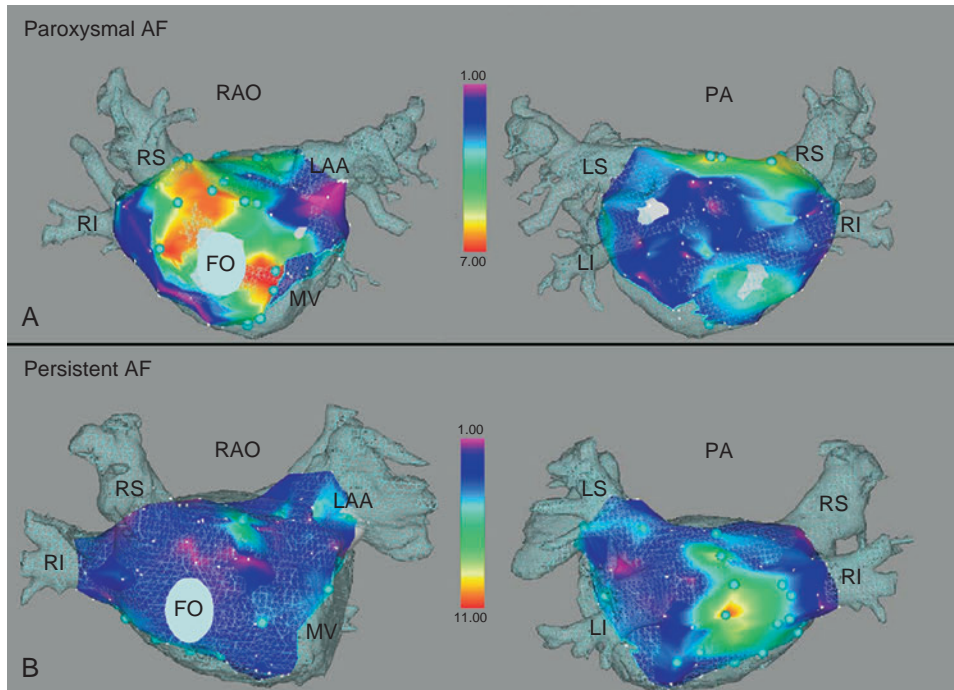
When CFAE ablation is combined with PV isolation, some investigators recommend that CFAE ablation be performed before PV isolation, since the PV antra commonly harbor target CFAE. Others, however, recommend targeting CFAEs after, rather than before, PV isolation because that latter strategy can itself reduce the burden of CFAEs and minimize the consequent need for extensive LA ablation.^{196,218}

Endpoints of Ablation

The ablation endpoints when targeting CFAEs are uncertain. In most studies, the primary endpoints were complete elimination of the areas with CFAEs or organization and slowing of local electrograms, conversion of AF to NSR (either directly or first to an AT) for patients with persistent AF, or noninducibility of AF (with isoproterenol and atrial pacing) for patients with paroxysmal AF. When areas with CFAEs are completely eliminated, but arrhythmias continue as organized AFL or AT, those arrhythmias are mapped and ablated.³⁰

AF termination (conversion to AT or NSR) in patients with persistent AF can potentially be a challenging endpoint to achieve and generally requires very long procedure times. Reports demonstrated the limited ability of CFAE ablation to terminate persistent AF. Furthermore, although AF termination during ablation can potentially predict the mode of recurrence (AT vs. AF), its correlation with long-term success is still controversial. AF recurrence rates of more than 50% were observed even in patients in whom AF was terminated during CFAE ablation. Thus ablation of all areas displaying the electrogram of interest in the LA and CS can be a reasonable alternative endpoint when ablation fails to terminate AF.

Preliminary reports suggested the clinical utility of monitoring dominant frequency in real time to guide catheter ablation of AF. A critical decrease (11% or higher, measured in lead V₁ and the CS) of dominant frequency following CFAE ablation can potentially indicate adequate elimination of drivers of AF and is associated with clinical efficacy that is as high as when AF is terminated by ablation. However, these findings require validation in prospective studies.



eFig. 15.21 CARTO Maps of Complex Fractionated Atrial Electrograms (CFAEs). CFAE maps with registered left atrial (LA) CT surface reconstruction (shown as wire frame), shown in right anterior oblique (RAO) view (left-sided images) and posteroanterior (PA) view (right-sided images), in patients with paroxysmal atrial fibrillation (AF) (A) and persistent AF (B). The CFAE maps are color-coded, with red representing the highest interval confidence level (ICL) and purple representing the lowest ICL. Highly repetitive CFAE sites (ICL greater than or equal to 5) are tagged with light blue dots on the CFAE maps. As shown in this example, the highly repetitive CFAE sites are more likely located at the pulmonary vein (PV) ostia, interatrial septum, and mitral annulus area in patients with paroxysmal AF, whereas patients with persistent AF have highly repetitive CFAE sites predominantly identified on the LA posterior wall. FO, Fossa ovalis; LAA, left atrial appendage; LI, left inferior PV; LS, left superior PV; MV, mitral valve; RI, right inferior PV; RS, right superior PV. (From Scherr D, Dalal D, Cheema A, et al. Automated detection and characterization of complex fractionated atrial electrograms in human left atrium during atrial fibrillation. *Heart Rhythm*. 2007;4:1013.)

Outcome

Initial single-center studies using CFAE ablation as a stand-alone strategy for ablation of AF showed high success rates (up to 92% freedom from AF at 1-year follow-up after one or two ablation procedures). However, these results were not universally reproducible by other investigators, and several recent trials demonstrated that CFAE ablation alone is not a sufficient strategy for successful treatment of AF.

On the other hand, CFAE ablation can be of potential value as an adjunct strategy in combination with PV isolation, particularly in patients with persistent AF whose response to other ablation strategies is sub-optimal, as well as patients undergoing redo ablation for recurrent AF. However, even this approach has come under considerable scrutiny with the publication of randomized studies and meta-analyses showing no additional benefit conferred by CFAE ablation in conjunction to PV isolation as compared to PV isolation alone in patients with persistent or longstanding AF. Furthermore, in patients undergoing PV isolation plus CFAE ablation, there was no significant difference in outcome between those who had complete CFAE elimination and those who did not.^{146,196,219,220}

Notably, the mode of recurrence after CFAE ablation was predominantly organized AT or AFL, usually related to gaps within the ablation regions. Commonly, extensive CFAE ablation creates islands of noncontiguous lesions, leading to areas of slow conduction and predisposing to atrial macroreentry, thereby increasing the proarrhythmic potential.³⁰

The conflicting results of different studies can be partly the result of variability of mapping techniques, the inconsistencies in CFAE electrogram interpretations, differences in the type and size of the mapping electrode, and differences in the accompanying lesion set.²¹⁹ Furthermore, multiple algorithms and visual methods were used in different studies to guide CFAE ablation, which likely resulted in targeting different “substrate” sites, resulting in variable outcomes. In fact, in a recent study evaluating the diagnostic accuracy of several automated algorithms against manual determinations, CFAEs determined by automated bipolar algorithms were highly variable and correlated poorly with established AF substrate complexity measures and the agreement among them was poor. Furthermore, results of those algorithms were sensitive to inter-electrode spacing with an increase in CFAE detected with increased interelectrode distance.²¹⁶

Importantly, the benefits of AF substrate ablation have to be balanced against the potential risks in individual patients, especially given that CFAE ablation involves additional ablation lesions that can encompass extensive amounts of the atrial surface area, which can potentially compromise long-term atrial contractile function, produce arrhythmogenic atrial scarring, prolong procedure and radiation times, and increase risks of acute procedural complications.

In its current iteration, the CFAE ablation approach is limited by uncertainties regarding the mechanistic significance, efficacy, and the endpoint of the ablation strategy. The lack of standardization in CFAE definition and differences in mapping technologies and electrogram measurements, especially given the lack of comparative information for the current technologies, adds to the challenge. Furthermore, although multiple studies have found that ablation at sites of CFAEs could prolong the CL or terminate AF, their true significance in the pathophysiology of AF remains to be determined, and the sensitivity and specificity of CFAEs in identifying sites critical to perpetuation of AF are uncertain. The mechanistic relevance of all sites of CFAEs in specific clinical contexts and in individual patients can potentially differ. Some CFAE sites can simply result from passive atrial activation and reflect shortening in the AF CL, random collision of fibrillatory waves, wave disruption adjacent to rapidly firing foci or rotors, or nonuniform anisotropic conduction. In fact, significant spatiotemporal variability of CFAEs

exists across studies for uncertain reasons. Whether all CFAE sites need to be targeted for catheter ablation is still not known, and reliable criteria to distinguish active from passive electrogram patterns and define optimal ablation targets are lacking.²²¹

PULMONARY VEIN DENERVATION

Rationale

Experimental and clinical data suggest that the autonomic nervous system plays a critical role in the initiation and maintenance of AF. High-frequency stimulation of epicardial autonomic plexuses can induce triggered activity from the PVs and potentially shorten the atrial refractory periods, providing a substrate for the conversion of PV firing into sustained AF. Clinical studies found that ablation of the ganglionated plexuses located at the antra of the PVs (by specifically targeting the ganglionated plexuses or inadvertently during standard PV ablation procedures) can potentially reduce the risk of recurrence of AF.⁴¹

Localization of Ganglionated Plexuses

Autonomic inputs to the heart converge at several locations; these convergence points are typically embedded in the epicardial fat pads and form ganglionated plexuses that contain autonomic ganglia and nerves. There are seven major ganglionated plexuses, including four located in the LA around the PVs and one located within the ligament of Marshall. In the LA, the ganglionated plexuses are located around the antral regions of the PVs and in the crux (Fig. 15.51). The superior left ganglionated plexus is located on the roof of the LA, medial to the left superior PV, and often extends to the medial aspect of the LAA. The

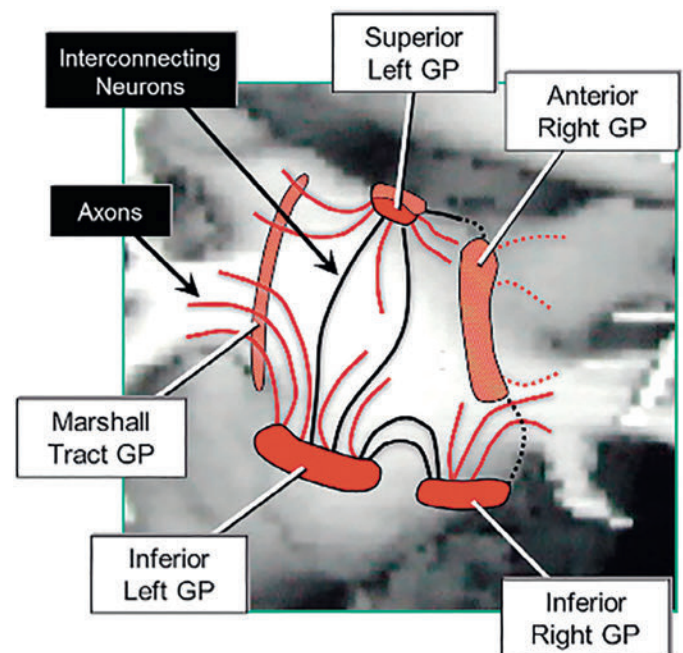


Fig. 15.51 Left Atrial (LA) Ganglionated Plexuses (GPs). Schematic posterior view of the LA. The five major left atrial autonomic GPs and axons (superior left GP, inferior left GP, anterior right GP, inferior right GP, and ligament of Marshall) are shown. Hatched areas represent the anterior LA surface, and solid areas represent the posterior LA surface. The GPs innervate the adjacent pulmonary veins and surrounding atrium. Interconnecting neurons connect within and between GP. (From Stavrakis S, Nakagawa H, Po SS, et al. The role of the autonomic ganglia in atrial fibrillation. *JACC Clin Electrophysiol*. 2015;1:1–13.)

anterior right ganglionated plexus is located just anterior to the right superior PV and adjacent to the caudal end of the sinus node, and often extends inferiorly, to the region anterior to the right inferior PV. The inferior left ganglionated plexus is located at the inferior aspect of the posterior wall of the LA, 1 to 3 cm below the left inferior PV. The inferior right ganglionated plexus is also located at the inferior aspect of the posterior wall of the LA below the right inferior PV and may extend toward the area adjacent to the crux of the heart, where another atrial ganglionated plexus (the crux ganglionated plexus) is located.²²²

High-frequency electrical nerve stimulation allows for precise determination of the location, threshold, and predominance of the parasympathetic or sympathetic response of the ganglionated plexuses. The distal electrode of the mapping-ablation catheter is used to deliver high-frequency stimulation (1200 beats/min [20 Hz], at 12 to 24 V and pulse width 1 to 10 milliseconds) using a Grass stimulator (S88X dual output square pulse stimulator, Grass Instruments Division, Astro Med, Warwick, RI, United States). Tolerance of the conscious patient to the stimulation still must be determined because most reports have described use of this approach in deeply sedated patients.

High-frequency stimulation of a ganglionated plexus can elicit both parasympathetic and sympathetic responses. A parasympathetic response is typically elicited immediately (within 4 seconds) following stimulation, with return to baseline values on cessation of stimulation. A sympathetic response requires longer stimulation durations (8 to 10 seconds). A predominant efferent parasympathetic response to a 5-second high-frequency stimulation is defined as: (1) induction of sinus bradycardia (slower than 40 beats/min); (2) AV block (second- or third-degree AV block during sinus rhythm or a 50% or higher increase in mean R-R interval during AF); or (3) sudden decrease in blood pressure (20 mm Hg or greater reduction of systolic blood pressure). The sites of positive parasympathetic responses to high-frequency stimulation are marked on the electroanatomic map. If no response occurs, the catheter is moved to adjacent sites. It is important to limit high-frequency stimulation to only 2 to 5 seconds, to avoid eliciting a sympathetic response that would otherwise mask or attenuate the parasympathetic response (e.g., by facilitating AV conduction and increasing blood pressure).²²³

Before applying high-frequency stimulation to inferior ganglionated plexuses, it is important to ensure that the catheter tip is not close to the ventricle to avoid induction of VF. When high-frequency stimula-

tion is applied during NSR, AF generally occurs and usually terminates within seconds or minutes. Repeated stimulation usually results in sustained AF, at least in patients with a clinical history of AF.

Alternatively, ganglia identification and ablation can be accomplished by a purely anatomic technique without the need for specific localization with high-frequency stimulation. The suboptimal sensitivity of high-frequency stimulation in identifying *all* LA ganglionated plexuses can result in partial and nonhomogeneous atrial denervation. In addition, high-frequency stimulation commonly requires general anesthesia and carries the risk of repeated induction of AF. The anatomic approach is based on studies in humans demonstrating that the largest accumulation of PV-related cardiac neural structures is localized to the inferior and posterior surface of the roots of both left and right inferior PVs, as well as on the anterior surface of the root of the right superior PV.

Target of Ablation

During ablation of AF, the LA ganglionated plexuses are specifically targeted by ablation, as identified by high-frequency stimulation (rectangular electrical stimuli delivered at a frequency of 20 to 50 Hz for 5 seconds). Alternatively, ablation of ganglionated plexuses can be performed according to their anatomic locations instead of relying on the parasympathetic response to high-frequency stimulation, since the anatomic locations of the four major atrial ganglionated plexuses vary minimally among patients (Fig. 15.52).²²²

Ablation Technique

High-frequency stimulation is performed in the LA adjacent to the antral region of the PVs and the region of the LA crux. Once identified, the location of a ganglionated plexus is tagged on the electroanatomic map. Generally, the four major LA ganglionated plexuses can be identified and localized using high-frequency stimulation in the majority of patients; though it is not uncommon that one or more ganglionated plexuses cannot be identified, especially in patients with persistent AF. RF is delivered after all ganglionated plexus sites have been identified.

RF ablation is usually performed using an irrigated-tip catheter (25 to 35 W for 40 to 60 seconds). RF power and duration are reduced at sites close to the esophagus (15 to 20 W for 20 to 30 seconds). After each RF application, high-frequency stimulation is repeated immediately at the same site. If a positive parasympathetic response is still elicited,

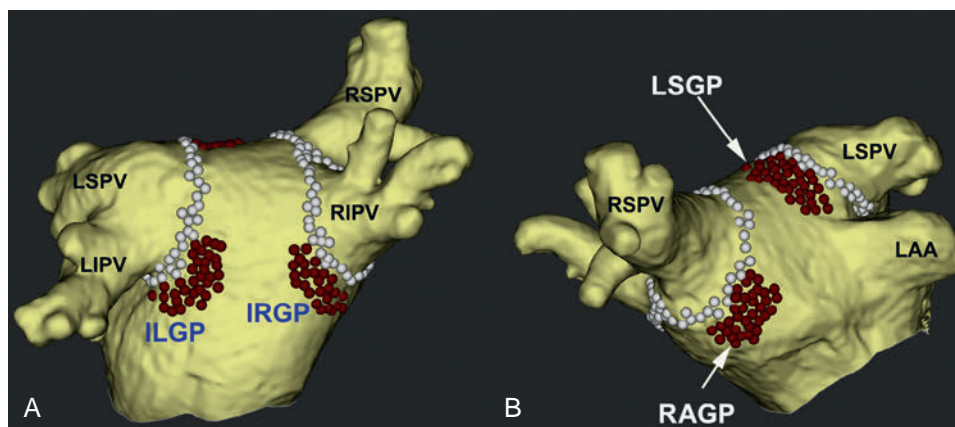


Fig. 15.52 Anatomic Ablation of Left Atrial Ganglionated Plexuses (GPs). Segmented three-dimensional computed tomography of the left atrium is shown in a posteroanterior (A) and cranial right anterior oblique (B) views. Initially, circumferential antral pulmonary vein (PV) isolation is performed (*white dots*). Then, the ablation lesions were expanded (*red dots*) to cover the anatomic site of presumed GP clusters. *ILGP*, Inferior left GP; *IRGP*, inferior right GP; *LAA*, left atrial appendage; *LIPV*, left inferior PV; *LSPV*, left superior PV; *LSGP*, left superior GP; *RAGP*, right anterior GP; *RIPV*, right inferior PV; *RSPV*, right superior PV.

RF applications are repeated until such a response is no longer elicited. Notably, RF energy delivery does not usually elicit a parasympathetic response, even at sites with positive response to high-frequency stimulation. Thus the absence of an autonomic response should not prompt termination of RF application. Because there is experimental evidence that ablation of the inferior right ganglionated plexus can potentially attenuate the parasympathetic response of other ganglionated plexuses to high-frequency stimulation and hence render subsequent localization of other ganglionated plexuses challenging, it is preferred to stimulate and ablate the inferior right ganglionated plexus last.

When using an anatomic approach for localization of the ganglionated plexuses, the presumed ganglionated plexus clusters near the PV antra are targeted by RF ablation. Because the exact anatomic borders of ganglionated plexus clusters are unknown and their location can vary slightly in different patients, a relatively extensive regional ablation is performed by delivering RF energy at multiple sites in and around the presumed anatomic location of each ganglionated plexus. Using this approach, vagal reflexes can be observed in at least one-third of patients, typically within a few seconds of the onset of RF application (eFig. 15.22). When a vagal reflex is observed during RF application, RF energy should be delivered until these reflexes are abolished, or for up to 30 seconds. It is important to note that the specificity and sensitivity of eliciting such vagal responses during RF application are not known; similar responses can be triggered by pericardial pain during RF energy delivery. In addition, as noted previously, vagal responses are not usually observed during RF ablation directly over the location of the ganglionated plexuses identified by high-frequency stimulation or even while applying RF energy to the plexuses during epicardial surgical ablation.

Endpoints of Ablation

The endpoint of ablation is the abolition of all vagal reflexes evoked by high-frequency stimulation over the ganglionated plexus sites marked on the electroanatomic map. For anatomically guided atrial autonomic denervation, the endpoint of the ablation procedure is elimination of electrical activity (peak-to-peak bipolar electrogram less than 0.1 mV) in the specified areas and abolition of any vagal effects during RF energy delivery.

Outcome

At present, no reports have suggested that targeting of ganglionated plexuses as a stand-alone procedure will consistently terminate AF or prevent its reinitiation. On the other hand, several studies incorporating ganglionated plexus mapping and ablation with PV-based ablation procedures for the treatment of AF have produced promising, though variable, results. It is important to note that data suggest that the outcome of ganglionated plexus ablation guided by the vagal responses elicited by high-frequency stimulation is inferior to that guided by the anatomic locations of the ganglionated plexuses. It is likely that high-frequency stimulation underestimates the extent of the major atrial ganglionated plexuses and thus translates into significantly less autonomic denervation and subsequently a lower success rate. Currently, an anatomic approach to ganglionated plexus ablation is preferred.^{41,222}

Because the ganglionated plexuses are predominantly located near the PV antra, regions that are typically targeted by the different AF ablation strategies, whether the clinical benefits of ablation in these regions are related to selective ganglionated plexus modification and parasympathetic denervation, as opposed to interference with other AF-related mechanisms, is not known. On the other hand, some type of atrial denervation is likely to be inadvertently achieved after PV-based ablation procedures, which can potentially underlie, at least in part, the efficacy of these procedures. The conventional wide-area PV isolation

transects three of the four major atrial ganglionated plexuses (the superior left, anterior right, and part of the inferior right ganglionated plexuses), the ligament of Marshall, as well as many small clusters of autonomic ganglia and nerves. Nevertheless, ganglionated plexus responses still are commonly observed after extensive PV isolation (especially around the right inferior and left inferior ganglionated plexuses), and positive ganglionated plexus responses appear to predict an increased risk for AF recurrence after extensive PV isolation, especially in patients with paroxysmal AF.^{41,222,224}

It is important to note that the ganglionated plexuses reside in epicardial fat pads and can be difficult to ablate endocardially. Epicardial ablation during thoracoscopic surgery for AF can allow more selective ganglionated plexus ablation without ablating the underlying atrial myocardium. However, in a recent report, epicardial ganglionated plexus ablation during thoracoscopic minimally invasive AF surgery did not reduce AF recurrence. Also, parasympathetic denervation has been shown to recover after ganglionated plexus ablation, likely secondary to atrial neural resprouting and reinnervation, with the potential for future heightened sensitivity to remaining neural stimulation. This can potentially limit the long-term benefit of ganglionated plexus ablation.⁴²

ABLATION OF NON-PULMONARY VEIN TRIGGERS

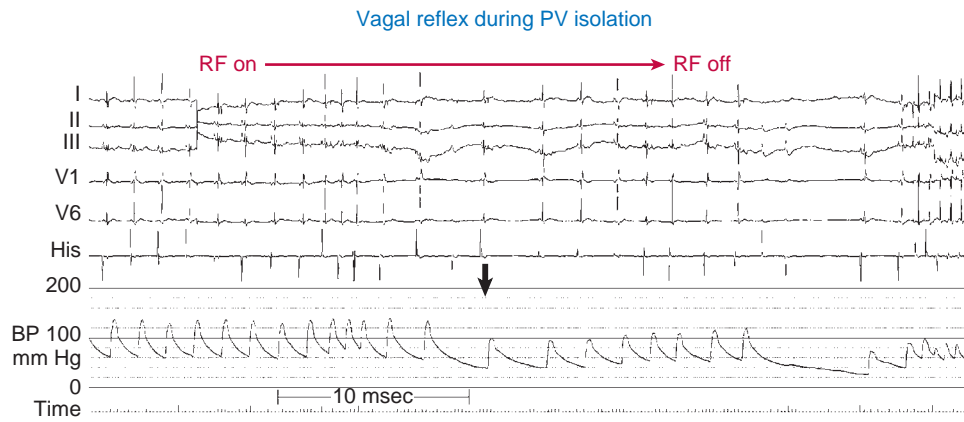
Rationale

Although the PVs are the major site of ectopic foci initiating AF, non-PV ectopic beats can initiate AF. Several reports have identified non-PV triggers initiating AF in about 20% to 30% of unselected patients with paroxysmal and nonparoxysmal AF (range, 3% to 61% of patients undergoing AF ablation). The proportion of patients manifesting non-PV triggers is higher in those with previously failed PV isolation procedure. The non-PV ectopic beats can arise from the SVC (most common, especially in female patients), LA posterior wall (especially in patients with LA enlargement), crista terminalis, CS, ligament of Marshall, interatrial septum, or LAA. In addition, SVTs, such as atrioventricular nodal reentrant tachycardia (AVNRT) and atrioventricular reentrant tachycardia (AVRT), can be identified in up to 4% in unselected patients referred for AF ablation and can serve as a triggering mechanism for AF (see Fig. 15.3). Also, the presence of non-PV ectopic beats can play an important role in the recurrence of AF after PV isolation. Therefore targeting these foci can potentially decrease arrhythmia recurrence and improve procedural outcome.^{225–228}

Mapping of Non-Pulmonary Vein Triggers

Spontaneous activation of AF-initiating triggers is infrequently observed during EP procedures, especially given the heavy sedation or general anesthesia used in these procedures. Therefore provocative maneuvers are necessary in the vast majority of patients. Two different strategies are used to evaluate the potential existence of non-PV sources of AF: (1) pharmacological provocation to induce ectopic arrhythmogenic atrial activity; and (2) electrical cardioversion of spontaneous or induced AF.^{226,227}

The initial step is to locate the spontaneous onset of ectopic beats initiating AF in the baseline state or after high-dose isoproterenol infusion. A bolus of high-dose adenosine (12 to 24 mg) may also be used to provoke the spontaneous onset of AF. If spontaneous AF does not develop, intermittent atrial pacing (8 to 12 beats) at a PCL of 200 to 300 milliseconds from the high RA or CS is used to facilitate spontaneous initiation of AF after a pause in the atrial pacing. If spontaneous AF does not occur, burst pacing from the high RA or CS is used to induce sustained AF. After an episode of pacing-induced AF is sustained for 5 to 10 minutes, external cardioversion is attempted to convert the AF to NSR and observe the spontaneous reinitiation of AF.^{226,227}



eFig. 15.22 Vagal Reflex During Pulmonary Vein (PV) Isolation. Sinus rhythm is present at the beginning of the tracing; when radiofrequency (RF) energy is applied ("RF on"), blood pressure (BP) and heart rate decrease markedly (sinus bradycardia and nonconducted P wave). After energy is stopped ("RF off"), a short episode of atrial fibrillation ensues.

The onset pattern of spontaneous AF is analyzed, and the earliest ectopic site is considered to be the initiating focus of AF. The method used to provoke spontaneous AF is repeated at least twice to ensure reproducibility. P wave morphology on the surface ECG and atrial activation sequences from the high RA, HB, and CS catheters can predict the site of origin of the PACs. Mapping techniques are discussed in detail in **Chapter 11**.

Mapping and Ablation of the Ligament of Marshall

Rationale

The ligament of Marshall is an epicardial vestigial fold that results from the embryonic obliteration of the left anterior cardinal vein extending from the left subclavian/innominate vein to the CS. Occasionally, the left anterior cardinal vein remains open as the normal variant of persistent left SVC, but most commonly only its intracardiac portion remains patent as the vein of Marshall.^{229–231}

The ligament of Marshall contains the vein of Marshall, autonomic nerves, and muscle tracts (the Marshall bundle). The vein of Marshall originates at its junction with CS (at the level of the valve of Vieussens), courses along the epicardial surface of the lateral mitral isthmus, and extends to the epicardial surface of LA ridge that separates the LAA from the left-sided PVs. The transition from the extracardiac ligamentous structure to the intracardiac vein of Marshall occurs in the region between the left superior PV and base of the LAA.

The proximal portions of the Marshall bundles connect directly to the CS myocardial sleeves, while the distal portions of the myocardial sleeve extend upward into the PV and LA free wall, and insert into the epicardial region of the LA ridge between the LAA and left-sided PVs. The Marshall bundle provides a direct epicardial electrical bridge between the left lateral ridge and the CS muscle sleeve which bypasses the lateral atrial free wall. The ligament of Marshall also provides a conduit for parasympathetic and sympathetic nerves, connecting the extrinsic cardiac nervous system to the intrinsic cardiac ganglia, specifically the inferior left ganglion plexus.^{229–231}

The ligament of Marshall has been implicated in the initiation and perpetuation of AF and, thus, has been targeted by catheter ablation. Several attributes of the ligament of Marshall have been proposed to explain its mechanistic role in AF. The ligament of Marshall was shown to have electrically active myocardial tissue capable of generating focal automatic activity that can potentially contribute to the development of AF. Furthermore, multiple connections among the Marshall bundle, LA, and CS can potentially create paths for reentrant excitation, leading to more complex and rapid activations. In fact, electrograms recorded from the ligament of Marshall during AF often exhibit short CLs, high dominant frequency, and CFAEs. Furthermore, rich innervation of the ligament of Marshall, predominantly by sympathetic fibers at its PV junction and parasympathetic ganglia at its CS junction, has been observed. The ligament of Marshall serves as a vehicle of parasympathetic and sympathetic innervations that modulate electrical properties of atrial tissue and contribute to AF maintenance. High-frequency stimulation of the ligament of Marshall can induce AF, presumably by direct activation of such extrinsic nerves. Ablation of the ligament of Marshall can contribute to LA parasympathetic denervation strategies.^{229,232}

The ligament of Marshall should be considered as a source of paroxysmal AF, especially in young patients with a history compatible with adrenergic AF. In addition, whenever an ectopic beat is mapped to the region around the posterolateral mitral annulus or a left-sided PV ostium, an origin from the ligament of Marshall should be considered. The P wave morphology associated with vein of Marshall ectopic activity is characterized by an isoelectric P wave in leads I and aVL, positive in leads III, aVF, and V₂ to V₅, and it is similar to that seen with ectopic

beats arising from the left PVs. The P waves can be biphasic or negative in lead II.²²⁷

It is also important to recognize that the Marshall bundle can provide a direct electrical connection (epicardial bridge) between the LA ridge or left PVs and the muscle sleeves of the CS. This bridge can bypass the endocardial ablation lines across the lateral mitral isthmus or surrounding the left-sided PVs, rendering those lesion sets ineffective in achieving PV electrical isolation or bidirectional mitral isthmus block. In these situations, successful ablation necessitates ablation of the Marshall bundle.^{229,230,231}

Mapping the Ligament of Marshall

The ligament of Marshall can be mapped epicardially or endocardially. The endocardial approach involves cannulation of the CS (preferably via the SVC approach) with a 7 Fr luminal decapolar CS catheter. A venogram of the CS is obtained in the RAO 30-degree view to visualize the vein of Marshall and its ostium inside the CS. A 7 Fr luminal CS catheter is then directly engaged into the ostium of the vein of Marshall, and a 1.4 Fr mapping catheter is inserted into the inner lumen of the CS catheter and advanced toward the vein of Marshall.

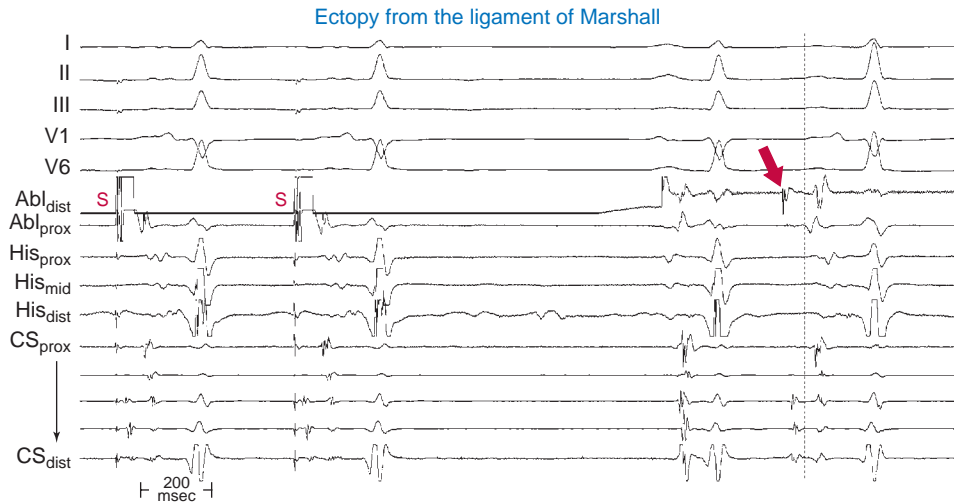
However, cannulation of the vein of Marshall is not always successful because of various anatomic and technical reasons. In patients whose vein of Marshall either is not visible on a CS venogram or is visible but cannot be cannulated, the percutaneous (subxiphoid) epicardial approach may result in successful mapping and ablation (**Fig. 15.53**). This latter approach has the advantage of free catheter movement and is not limited by the size of the vein of Marshall. However, the endocardial approach is the best method for differentiating ligament of Marshall ectopy from other sources.

Because the ligament of Marshall can have multiple insertion sites in the LA free wall or near the PV ostium, it can be difficult to differentiate ligament of Marshall ectopy from PV or LA posterior free wall ectopy. Ectopy or rapid tachycardias arising from the PV typically demonstrate an early near-field potential on catheters placed within the PV and a late far-field electrogram consistent with LA activation. Often, the exit delay (interval between the early near-field and the late far-field potentials) exceeds the entrance delay seen in sinus rhythm with activation from the LA to the PV. Despite this exit delay, however, the earliest atrial activation should be in the perivenous area. In addition, if the earliest activation of ectopic beats is in the mid or distal CS and double potentials are present at those sites, the ligament of Marshall as the source of ectopy should be considered (**eFig. 15.23**).

In addition, the possibility of ligament of Marshall ectopy should be considered when the so-called triple potentials (a discrete sharp potential preceding the LA and PV potentials) are recorded around the PV ostium. Furthermore, in patients with ectopic beats from the ligament of Marshall, double potentials are present at the orifice of or inside the left PVs, and distal CS pacing can help differentiate the ligament of Marshall potential from the PV musculature potential. If the second deflection of double potentials is attributable to the activation of the ligament of Marshall, the interval between the CS os and the second deflection will be shorter during distal CS pacing compared with NSR. In contrast, if the second deflection is attributable to activation of the PV musculature, the interval between the CS os and the second deflection will be longer during distal CS pacing compared with NSR.²³⁰

Certain observations and pacing maneuvers can indicate electrical conduction occurring via the Marshall bundle, including (1) unexpected PV activation sequence during NSR, (2) unexpectedly early exit from PV ectopy, and (3) unexpected PV activation sequence during low-output CS pacing.²³⁰

During NSR, PV activation spreads from proximal (PV ostium) to distal. If earlier activation is seen deep within the PV than near the



eFig. 15.23 Ectopy From the Ligament of Marshall (LOM). The recordings are from a patient with atrial fibrillation caused by ectopy from the region of the LOM. *Right*, Sinus complex and premature atrial complex from the LOM with a very early potential recorded by the ablation catheter in this area. Note the same potential occurring in coronary sinus (CS) recordings. *Left*, Pace mapping replicates the atrial activation sequence during the ectopy complex. *Abl_{dist}*, Distal ablation site; *Abl_{prox}*, proximal ablation site; *CS_{dist}*, distal coronary sinus; *CS_{prox}*, proximal coronary sinus; *His_{dist}*, distal His bundle; *His_{prox}*, proximal His bundle.

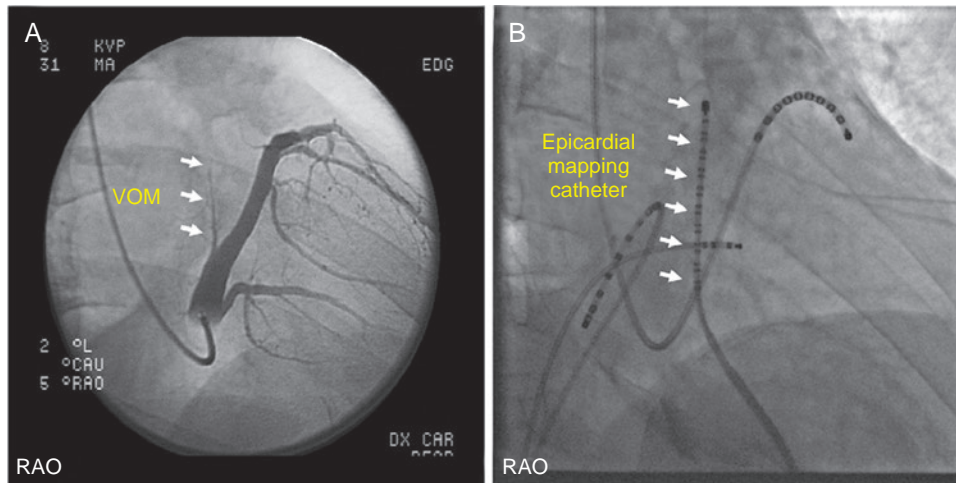


Fig. 15.53 Two Different Approaches to Mapping of the Ligament of Marshall. (A) Vein of Marshall (VOM) visualized by balloon occlusion coronary sinus (CS) angiogram. A 1.5 Fr mapping catheter can be inserted via the CS into this VOM for endocardial mapping. (B) Epicardial mapping catheter inserted via a subxiphoid pericardial puncture. RAO, Right anterior oblique. (From Hwang C, Fishbein MC, Chen P. How and when to ablate the ligament of Marshall. *Heart Rhythm*. 2006;3:1505.)

ostium, a bypass of the ostium with direct activation of the middle or distal PV via the vein of Marshall is likely. Similarly, when ectopy from within the left-sided PVs results in unexpectedly early activation of the LA, whereby the PV potential at the focus of ectopy precedes the earliest LA activation site by less than 45 milliseconds, mapping of the ligament of Marshall should be considered.²²⁹

Pacing from the CS can help unmask conduction over the Marshall bundle. With high-output pacing in the mid-CS, there is capture of both the myocardium of the CS itself and the adjacent LA. With lower-output pacing, in most cases there will be capture of the myocardium of the CS only, with the LA activated from the CS through a CS-to-LA connection. In some patients, the CS-to-LA connection is small and discrete and, if the connection is not close to the site of pacing within the CS, there can be considerable delay between the CS myocardial electrograms and adjacent LA tissue electrograms (Fig. 15.54). This observation can be used to determine whether PV activation is occurring via the vein of Marshall. During low-output CS pacing, the LA is not directly activated. Because PV activation depends on LA activation, in most cases, when the LA electrogram is delayed, PV potentials also are delayed. When the time from stimulus to PV potential remains fixed regardless of whether direct capture of the LA occurs, PV activation is dependent only on CS muscular activation and a connection via the Marshall bundle very likely is present (see Fig. 15.54).

Importantly, electrical connections from left-sided PVs to the CS via the ligament of Marshall need to be suspected when electrical isolation of those veins fails despite complete circumferential antral ablation lines. This is often the case when PV potentials are recorded in distal left-sided PVs, while the antrum remains electrically silent. Similarly, when bidirectional block across the lateral mitral isthmus ablation line cannot be achieved despite extensive ablation, an epicardial electrical connection via the Marshall bundle bridging the endocardial linear lesion set in the mitral isthmus should be considered.

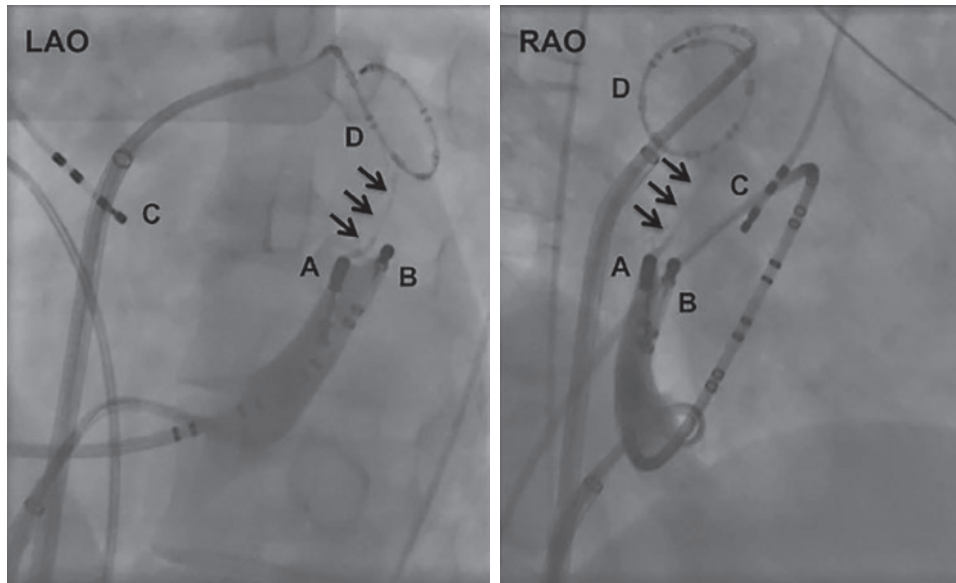
Ablation of the Ligament of Marshall

Ablation of the ligament of Marshall can be performed endocardially (via the LA), epicardially (via the CS or subxiphoid approach), or by ethanol infusion in the vein of Marshall.

Cannulation of the vein of Marshall with a mapping catheter and direct recording of the ligament of Marshall potentials from the vein of Marshall can be used as the anatomic targets for endocardial ablation and to confirm successful elimination of the ligament of Marshall potentials. Also, placing a ring catheter at the antrum of the left inferior PV can help guide and then confirm simultaneous isolation of the PV antrum and ligament of Marshall.

Even when cannulation of the vein of Marshall is not feasible, obtaining a CS venogram to visualize the vein of Marshall can be used as an indirect method to trace the possible route of the ligament of Marshall to help guide ablation (see Fig. 15.53). Traditionally, CS venography is performed utilizing a balloon catheter. The vein of Marshall is identified as a branch of the CS directed posteriorly (best shown in the RAO fluoroscopic projection) and superiorly. Recent reports described the feasibility of nonocclusive CS venography using open-irrigated ablation catheters (eFig. 15.24). The ablation catheter is initially positioned at the mitral annulus in the 4 o'clock position in the CS in the LAO view, and then gently pulled back to the proximal CS during manual contrast injection through the external irrigation lumen with a 5.0-mL syringe and without balloon occlusion. When the vein of Marshall is visualized, selective venography can be performed in the same manner after introducing the irrigation catheter into the ostium of the vein. The location of the ostium of the vein of Marshall can be marked in the 3-D electroanatomic map, and if the diameter is large enough, the ablation catheter is advanced into the vein to mark its anatomic course.²³¹

Ablation of the ligament of Marshall is performed at the LA endocardial aspect facing the epicardial vein of Marshall as tagged on the electroanatomic map or by the mapping catheter inside the vein. The site having the shortest distance from the LA endocardium to the ligament of Marshall is located along the inferoanterior aspect of the left lateral ridge, just below the left inferior PV ostium. RF energy application from the endocardium to this region eliminates ligament of Marshall potentials in more than 90% of the cases. Occasionally, ablation at more superior aspects of the left lateral ridge near the orifice of the left PV or in the LAA is required to eliminate all ligament of Marshall connections. Also, ablation targeting the vein of Marshall can be performed from inside the CS, typically around the ostium of the vein of Marshall.²³¹



eFig. 15.24 A Modified Technique of Selective Vein of Marshall Venography Using an Open-Irrigated Ablation Catheter. The left panel shows the left anterior oblique (LAO) projection, and the right panel shows the right anterior oblique (RAO) projection. Contrast dye injection through the ablation catheter (A) visualizing the oblique course of the vein of Marshall (arrows). A duodecapolar deflectable catheter (B) placed in the coronary sinus. A reference catheter (C) placed in the aortic valve cusp. A Lasso catheter placed in the left inferior pulmonary vein (D). (From Lee JH, Nam GB, Kim M, et al. Radiofrequency catheter ablation targeting the vein of Marshall in difficult mitral isthmus ablation or pulmonary vein isolation. *J Cardiovasc Electrophysiol.* 2017;28:386–393.)

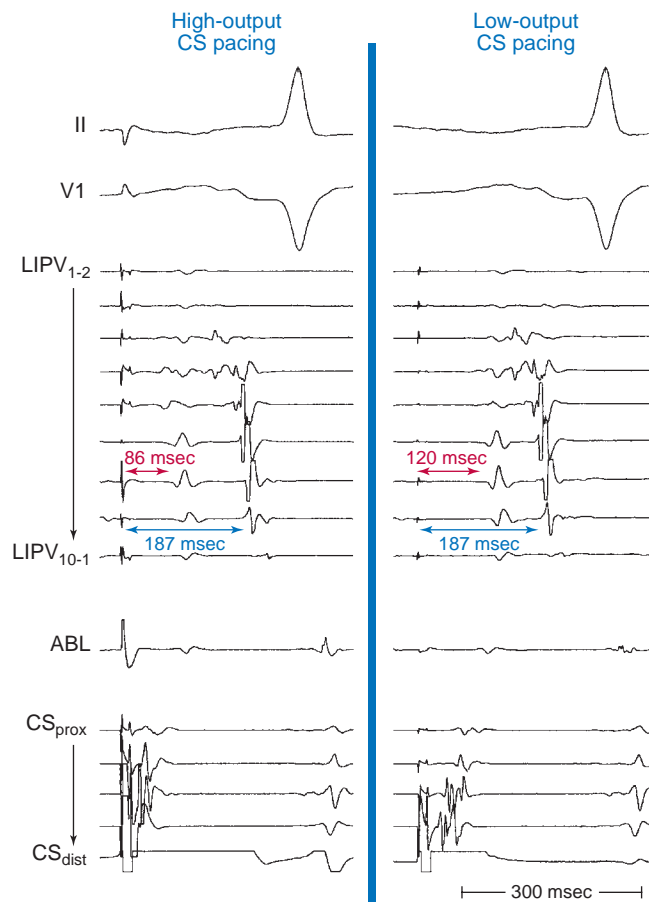


Fig. 15.54 Identification of Vein of Marshall Activation Using Differential-Output Coronary Sinus (CS) Pacing. *Left panel*, During high-output CS pacing, both the left atrium (LA) and CS musculature are captured directly. *Right panel*, During low-output CS pacing, only the CS musculature is captured directly; the LA is activated from the CS through a CS to LA connection. In this case, the CS-LA connection is not close to the site of pacing within the CS; therefore considerable delay is observed between the CS myocardial electrograms and the adjacent LA tissue electrograms. Despite the delay in LA activation (as reflected by the interval between the pacing artifact and the LA electrograms) during low-output versus high-output CS pacing, the timing of left inferior pulmonary vein (LIPV) activation remains constant (as reflected by the fixed interval between the pacing artifact and the PV potentials in both cases), thus indicating that PV activation is occurring via the vein of Marshall and is independent of LA activation. ABL, Ablation catheter; CS_{dist}, distal coronary sinus; CS_{prox}, proximal coronary sinus.

Successful ablation is confirmed by the elimination of ligament of Marshall potentials along the entire length of the ligament (as recorded by the mapping catheter inside the vein of Marshall) and the presence of exit block between the ligament of Marshall and the LA during pacing from multiple sites within the vein of Marshall. Also, complete bidirectional electrical isolation (with entrance and exit block) of the entire left PV antrum confirms elimination of all connections to the LA, including the left PVs and ligament of Marshall.

Infrequently, endocardial ablation alone cannot eliminate all connecting fibers, as evidenced by the ability to still record ligament of Marshall potentials. In these situations, most of the remaining connections are located in the ridge between the anterior border of the left PVs and the posterior wall of the appendage. In some patients, the ridge can be as thick as 10 mm, and complete isolation still may not

be possible, even when using an irrigated-tip catheter and a high-power setting. In these difficult cases, a combined endocardial and epicardial approach can be used to ablate ligament of Marshall ectopy initiating AF and is associated with a higher success rate.

An alternative approach uses ethanol infusion to ablate the Marshall bundle. After the vein of Marshall is cannulated with a coronary vein sub-selection catheter, an angioplasty balloon is advanced over a guide-wire into the proximal vein of Marshall. A selective venogram is performed during balloon inflation. Then, two to four serial injections of ethanol are administered through the balloon lumen (1 mL 98% ethanol over 2 minutes). With each injection, the balloon is retracted slightly until the final injection is delivered at the most proximal junction of the vein of Marshall with the CS.²³²

Electrical Isolation of the Superior Vena Cava

Rationale

Histologically, atrial myocardial sleeves extend into the SVC for up to 2 to 5 cm. Those sleeves can harbor ectopic pacing cells that can spontaneously depolarize triggering atrial arrhythmias (eFig. 15.25). The SVC has been described as one of the most common non-PV AF sources (accounting for up to 55% of non-PV triggers of AF). The incidence of SVC triggers has been reported to be 2% to 12% of patients undergoing AF ablation. A recent study demonstrated that, in a subset of patients, the SVC plays a role in AF not only as a trigger but also as a driver. Of interest, long SVC sleeves (greater than 30 mm), large SVC potentials (greater than 1.0 mV), smaller LA size, and the coexistence of spontaneous typical AFL have been proposed as predictors of an arrhythmogenic SVC in patients undergoing ablation of paroxysmal AF.^{233–235}

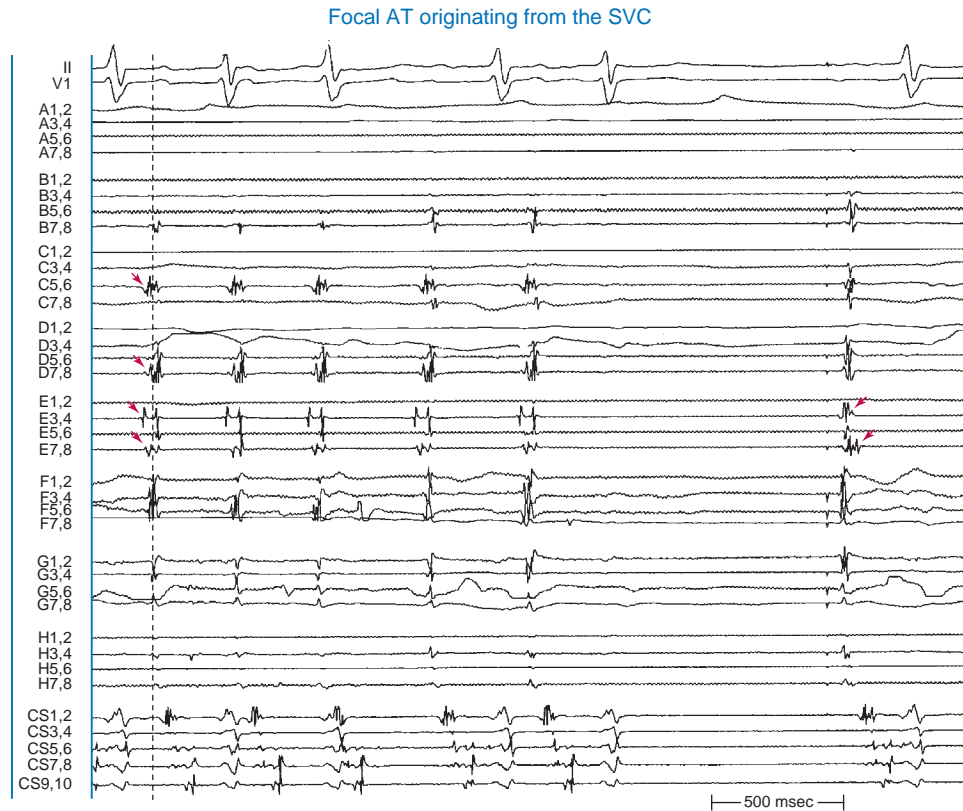
Electrical isolation of SVC from the RA is likely a better strategy than focal ablation of ectopy inside the SVC; it obviates the need for detailed mapping of the exact origin of the ectopic focus, as well as the need for RF ablation inside the SVC, which may carry the risk of SVC stenosis. Nevertheless, injury to the sinus node and phrenic nerve remains a concern.

SVC isolation is recommended when SVC triggers are recognized after pacing maneuvers or isoproterenol infusion, and elimination of SVC triggers is associated with improved long-term maintenance of sinus rhythm after AF ablation. The value of empirical isolation of the SVC as an adjunctive strategy for AF ablation needs further evaluation. A limited number of randomized trials have been conducted to assess the role of prophylactic SVC isolation in addition to PV isolation in AF and arrived at conflicting results. A recent meta-analysis suggests that this approach does not provide any incremental benefit in AF recurrence compared to PV isolation alone. However, such an approach can potentially be beneficial in selected patients with paroxysmal AF and prevalent non-PV triggers.^{233,236,237}

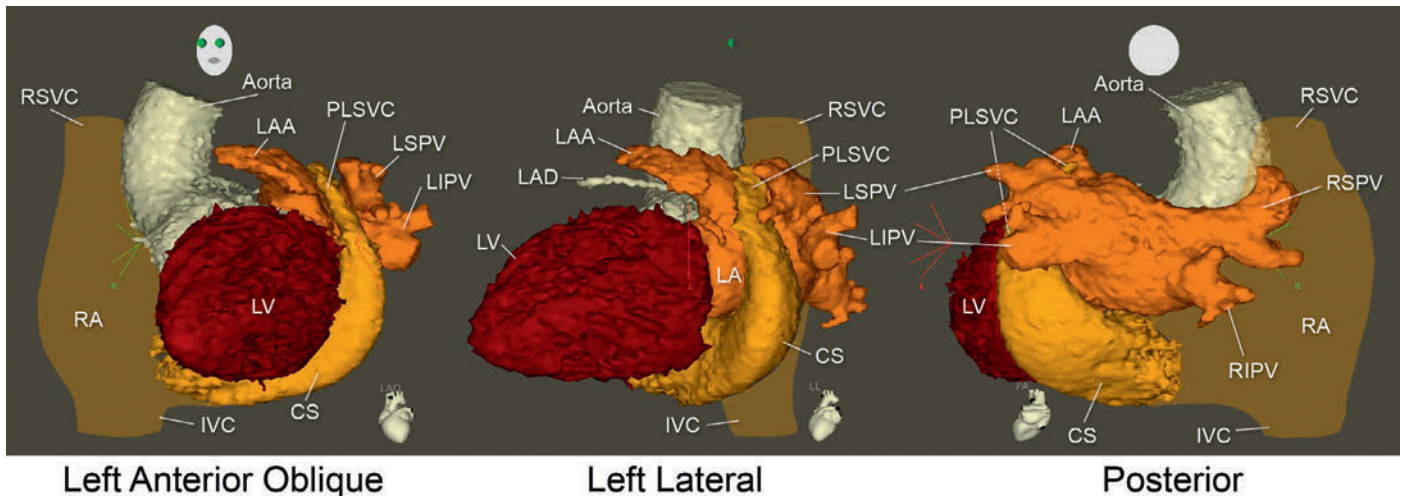
Occasionally, a patient has a persistent left SVC; when present, this is often a source of AF and should be considered for electrical isolation, especially if AF continues after PV isolation or recurs after cardioversion. As noted, in most patients, the left SVC atrophies and becomes the vein or ligament of Marshall, coursing between the left PVs and LAA. A persistent left SVC may be suspected on preprocedure imaging (echocardiogram showing a very large CS; CT scan or magnetic resonance imaging [MRI] showing the persistent left SVC [eFig. 15.26]). Isolation of this structure can be performed much like right SVC isolation, using a multielectrode ring catheter in the left SVC at the level of the LAA. Care must be taken to avoid injury to the left phrenic nerve that may be adjacent to the left SVC more cephalad than the LAA.

Mapping of Superior Vena Cava Ectopy

Mapping of SVC ectopy is generally performed using a ring catheter, basket catheter, or 3-D electroanatomic mapping system (Fig. 15.55).



eFig. 15.25 Focal Atrial Tachycardia (AT) Originating From the Superior Vena Cava (SVC). The basket catheter is positioned in the SVC–right atrial (RA) junction. Bipolar recordings are obtained from the eight electrodes (1-2, 3-4, 5-6, 7-8) on each of the eight splines (A through H) of the basket catheter. During AT (*at left*), SVC potentials (*arrowheads*) precede RA potentials and also precede P wave onset on the surface electrocardiogram (*dashed line*). During RA pacing (*at right*), SVC potentials overlap with or follow RA potentials. CS, Coronary sinus.



eFig. 15.26 Persistent Left Superior Vena Cava (PLSVC). CT scan showing relationships of structures; note that the PLSVC is situated between the left superior (LSPV) and left inferior pulmonary veins (LIPV), and left atrial appendage (LAA); note also how the increased drainage results in marked enlargement of the coronary sinus (CS). The shape of the right atrium (RA) is drawn in due to poor opacification on the scan. IVC, Inferior vena cava; LAD, left anterior descending coronary artery; LV, left ventricle; RIPV, right inferior PV; RSPV, right superior PV; RSVC, right superior vena cava.

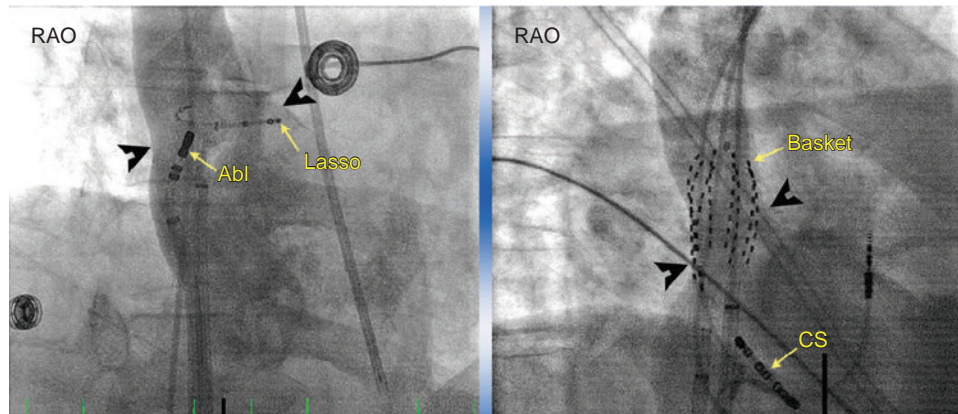


Fig. 15.55 Superior Vena Cava (SVC) Angiogram. Fluoroscopic right anterior oblique (RAO) views of SVC angiography with the ring (Lasso) catheter (at left) and basket catheter (at right) positioned at the SVC–right atrial junction (black arrowheads). Note that the size of the ring catheter is usually smaller than the circumference of the SVC, and repositioning of the ring catheter is typically required for circumferential mapping and electrical isolation of the SVC. Abl, Ablation catheter; CS, coronary sinus.

During NSR or atrial pacing, the intracardiac recordings from inside the lower level of the SVC (near the SVC-RA junction) frequently exhibit a blunted far-field atrial electrogram followed by a sharp and discrete SVC potential. At a more cranial level of the SVC, the SVC potential precedes the atrial electrogram during the SVC ectopic beat (Fig. 15.56). Furthermore, the intracardiac recordings in the higher SVC frequently exhibit double potentials. The first potential represents the SVC potential, and the second potential represents the far-field right superior PV potential. Simultaneous recordings from the right superior PV also exhibit a double potential during SVC ectopy. The recording from the right superior PV shows that the first potential is a far-field potential from the SVC, and the second potential is true activation of the right superior PV.

Electrical Isolation of the Superior Vena Cava

The SVC is isolated using the same technique and endpoint as used for segmental ostial PV isolation. Ablation targets the ostial portion of the breakthrough segments (electrical connections) connecting the RA to the SVC, identified as the earliest SVC potentials recorded from the ring catheter. Compared with PV isolation, it is easier to interrupt the conduction between the RA and the SVC. Most patients exhibit only two breakthrough sites. A ring or basket catheter can be used for mapping SVC potentials (see Fig. 15.56).

RF energy is applied at the level approximately 5 mm above the circumference of the SVC-RA junction (defined as the point below which the cylindrical SVC flares into the RA). Therefore the SVC-RA junction should be determined carefully before ablation. The SVC-RA junction can be confirmed by SVC venography (see Fig. 15.55), by ICE (eFig. 15.27), or by the electrical signals. SVC venography can be performed by placing a pigtail catheter at the top of the SVC and using a contrast injector (a total of 40 mL of contrast medium over 2 seconds) and biplane fluoroscopic views (RAO, 30 degrees; LAO 60 degrees). The overlapping of the anterior wall of the SVC and RA appendage is near the level of the SVC-RA junction.

The ring catheter is placed just above the RA-SVC junction at the level of the lower border of the pulmonary artery, as seen by ICE (see eFig. 15.27). The size of the ring catheter is usually smaller than the circumference of the SVC, and repositioning of the ring catheter is typically required for circumferential mapping and electrical isolation of the SVC (see Fig. 15.55). The SVC-RA junction exhibits an eccentric,

not a round, shape; thus the basket or ring catheter may not contact the wall well. Therefore one needs to manipulate the catheter to contact the whole SVC-RA circumference to confirm the presence or disappearance of SVC potentials.

The circumference of the SVC-RA junction is mapped (during NSR or atrial pacing) to determine the region of earliest SVC potentials recorded from the ring catheter. An isoelectric interval often separates the far-field RA electrogram and the near-field SVC potential. Not uncommonly, SVC potentials are fused with the far-field RA electrograms but can be identified by their high-frequency appearance. In addition, pacing maneuvers from the RA appendage and SVC can help discriminate SVC potentials from far-field RA electrograms by unmasking a decremental conduction property of the SVC-RA junction and separating those potentials from each other.

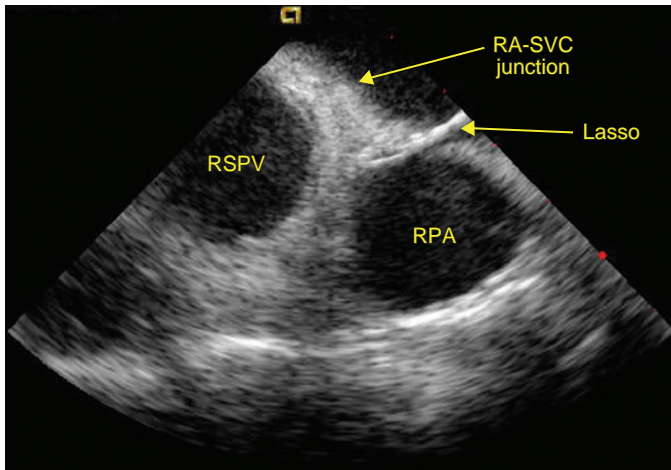
RF application in the SVC has potential risks of developing several complications, including SVC stenosis, sinus node injury and right phrenic nerve injury. Acceleration of the sinus rate during RF delivery is a sign that heat injury to the sinus node is occurring and should prompt discontinuation of RF application.

The SVC is located much closer to the course of the right phrenic nerve than are the right PVs, which explains the higher incidence of phrenic nerve injury during SVC isolation than during PV isolation. The right phrenic nerve courses immediately adjacent to the anterolateral wall of the SVC, but it veers posterolaterally at the level of the SVC-RA junction, where it is most vulnerable to injury during SVC isolation procedures. More inferiorly, it passes close to the junction of the LA to the right superior PV. Techniques to monitor right phrenic nerve function (as discussed previously) should be employed during SVC isolation. Early detection of nerve injury is essential to prevent permanent phrenic nerve injury since transient nerve injury occurs early and before permanent injury.²³⁸

Electrical Isolation of the Coronary Sinus

Rationale

The venous wall of the CS is surrounded by a continuous sleeve of atrial myocardium that extends for 25 to 51 mm from the CS os. This muscle is continuous with the RA myocardium proximally, but it is usually separated from the LA by adipose tissue. This separation can be bridged by muscular strands producing electrical continuity between the CS musculature and the LA. The muscular tissue in the wall of the



eFig. 15.27 Intracardiac Echocardiography for Electrical Isolation of the Superior Vena Cava (SVC). The intracardiac echocardiography catheter positioned in the high right atrium (RA) is used to guide positioning of the ring catheter at the RA-SVC junction (at the level of the lower border of the right pulmonary artery [RPA]). RSPV, Right superior pulmonary vein.

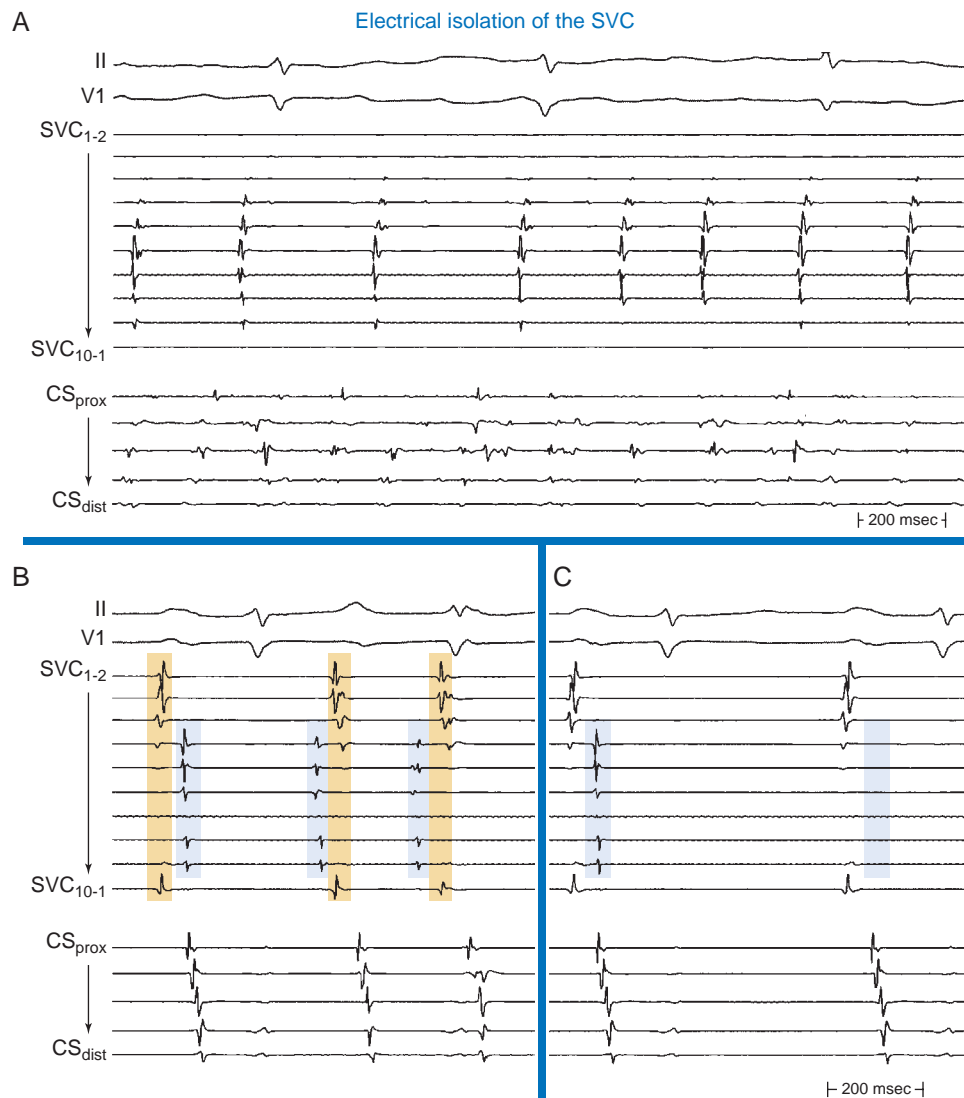


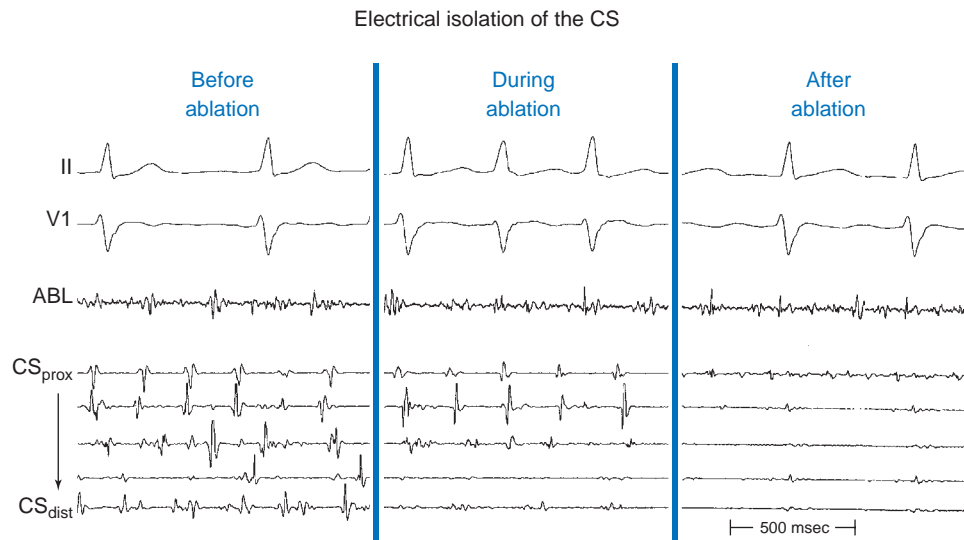
Fig. 15.56 Electrical Isolation of the Superior Vena Cava (SVC). This recording was obtained from a ring catheter positioned at the SVC–right atrium (RA) junction during electrical isolation of the SVC. (A) During atrial fibrillation, SVC potentials are observed at a cycle length (CL) longer than the atrial CL observed in the coronary sinus (CS) recordings. (B) The first complex is normal sinus, during which SVC potentials (blue shading) are observed following RA potentials (orange shading). The second and third complexes are premature atrial complexes originating from the SVC, during which SVC potentials precede RA potentials. (C) Radiofrequency energy application at a single site results in the disappearance of SVC potentials (at right) and complete SVC entrance block. CS_{dist}, Distal coronary sinus; CS_{prox}, proximal coronary sinus.

CS appears to be electrophysiologically active, capable of spontaneous depolarization and mediating slow conduction, which can potentially contribute to initiation or perpetuation of AF.²³⁹

Ablation Technique

The muscular strands connecting the CS musculature to the LA connections are targeted by RF ablation for electrical isolation of the CS from the LA. Isolation of the CS is commenced along the endocardial aspect and completed from within the CS, as required. The ablation catheter is dragged along the endocardium of the inferior LA after looping the catheter to position it parallel to the CS catheter. After achieving a 360-degree loop in the LA, the catheter is gradually withdrawn initially along the septal area anterior to the right PVs and ablation commenced at the inferior LA along the posterior mitral annulus

from a site adjacent to the CS as progressing to the lateral LA (at the 4-o'clock position in the LAO projection). The endpoint is elimination of local endocardial electrograms bordering the mitral isthmus in an attempt to eliminate or prolong the CL of sharp potentials present within the CS (eFig. 15.28). Ablation within the CS is started distally (at the 4-o'clock position in the LAO projection) and pursued along the CS up to the ostium by targeting local sharp potentials at individual sites or as a continuous drag. During AF, ablation within the CS is performed at all sites showing persistent or intermittent rapid activity, either continuous electrograms or discrete electrograms displaying CLs shorter than the CL measured in the LAA. Finally, additional RF applications are continued around the CS orifice from the RA. CS disconnection is confirmed by the dissociation or abolition of sharp potentials in its first 3 cm.



eFig. 15.28 Electrical Isolation of the Coronary Sinus (CS). Intracardiac recordings illustrating CS electrograms during atrial fibrillation before, during, and after successful electrical isolation of the CS. Following complete electrical isolation, the local sharp potentials within the CS are eliminated. *ABL*, Ablation catheter; *CS_{dist}*, distal coronary sinus; *CS_{prox}*, proximal coronary sinus.

Electrical Isolation of the Left Atrial Appendage

Rationale

The role of the LAA in initiating and maintaining AF and atrial arrhythmias has increasingly been recognized. In some studies, approximately one quarter of patients presenting for repeat AF catheter ablation have inducible focal electrical activity that localizes to the LAA. Drivers of AF appear to originate from the LAA up to one-third of patients with longstanding persistent AF. Excision of the LAA is often proposed as a contributing factor to the high success rates for surgical AF ablation incorporating this approach. These findings have prompted some investigators to advocate empirical isolation of the LAA in this group of patients. However, electrical isolation of the LAA remains controversial as many investigators have found substantially lower prevalence of LAA sources of AF/AT, and until more evidence arises, LAA isolation needs to be considered only in selected cases.

Ablation Technique

The best strategy to achieve LAA electrical isolation remains to be determined. Segmental or circumferential isolation involves ablation at the ostial aspect of the LAA (similar to ostial isolation of the PVs). In contrast, wide-area isolation of the LAA incorporates linear ablation across the LA roof and lateral mitral isthmus in addition to an ablation line extending from the anterior mitral annulus to the left superior PV. The latter approach can potentially capture additional arrhythmogenic substrate, although it has been associated with a significantly higher risk of LAA thrombus formation.²⁴⁰

The endpoint of the ablation procedure is bidirectional electrical isolation of the LAA, defined as: (1) demonstration of entrance block—disappearance of all LAA potentials documented with a circular catheter placed within the LAA, regardless of the underlying cardiac rhythm; and (2) demonstration of exit block—LAA electric activity dissociated from the LA during LAA ectopy or pacing from within the LAA.

Recent studies suggest that electrical isolation of the LAA can improve long-term outcomes when combined to PV isolation in patients with longstanding persistent AF. However, achieving durable appendage isolation appears challenging and technically demanding. Importantly, LAA isolation (wide area isolation in particular) appears to be associated with an increased incidence of LA thrombus formation and stroke despite oral anticoagulation therapy, likely secondary to the lack of proper mechanical function in the LAA as a result of ablation. Therefore life-long anticoagulation or, preferably, percutaneous LAA closure (e.g., Watchman device) is recommended in these patients.^{241,242}

In addition, two epicardially based LAA exclusion devices have been demonstrated to produce electrical isolation of the LAA: the Lariat (SentreHEART); and the Atriclip (Atricure, Minneapolis, MN, United States). These devices result in progressive atrophy and fibrosis of the excluded appendage and also provide an effective mechanical barrier to thromboembolism. Whether such a procedure is a useful adjunct to PV isolation in patients with persistent AF is currently being investigated. In addition, isolation of the LAA with resultant loss of its mechanical activity deprives the patient of one of the benefits of NSR, LA transport function mediated to a significant degree by the LAA. Under these circumstances, a combination of trigger detection/elimination and modification of substrate (on which triggers act) can be reasonable.

Outcome

Several studies showed that non-PV ectopic beats play an important role in the recurrence of AF after PV isolation, and that AF ablation outcome can be improved if non-PV foci are detected and eliminated. Nonetheless, it is frequently difficult to map all non-PV triggers in a

single procedure. However, it is currently unclear whether an attempt should be made before and after PV isolation to observe the spontaneous or provoked ectopic beats initiating AF to evaluate for non-PV sources of this ectopy during initial and repeat ablation procedures. Also, given the fact that inducing those triggers is usually challenging and time consuming, it is uncertain whether prophylactic isolation of frequent anatomic sources of non-PV triggers (e.g., SVC, LA posterior wall, LAA, ligament of Marshall) is warranted, even without demonstration of the presence of such triggers.^{226,243}

Of note, the mere presence of non-PV triggers of AF appears to predict a higher risk of AF recurrence after catheter ablation. This is likely related to the difficulty in mapping and elimination of all triggers in the index procedure, particularly with the presence of multiple foci and the poor inducibility during EP testing.²²⁶

VOLTAGE-GUIDED SUBSTRATE MODIFICATION

Rationale

Atrial fibrosis plays an important role in the genesis and maintenance of AF. Myocardial fibrosis is associated with reduced intercellular coupling, slow and inhomogeneous conduction, dispersion of atrial refractory periods, and nonuniform anisotropic impulse propagation, which can promote reentry and perpetuate AF. The regional localization and the extent of LA scarring can be detected by late-enhancement CMR and correlates with reduced electrogram amplitudes on electroanatomic voltage mapping. Atrial scar burden predicts recurrence of AF following catheter ablation.^{200,244}

Recent studies have suggested a new, patient-tailored substrate modification strategy targeting fibrotic regions. Atrial scar (voltage) mapping can identify patients with more advanced disease and serve to guide more extensive ablation beyond PV isolation. This is in contrast to other substrate-based ablation strategies (such as linear ablation and posterior wall isolation) that applies ablation lesions empirically in all patients.

Target of Ablation

Voltage-guided substrate modification targets the potentially arrhythmogenic LA low-voltage zones identified on endocardial electroanatomic voltage mapping (atrial electrogram amplitude less than 0.5 mV) with ablation lesions aiming for complete box isolation of those areas or scar homogenization.^{200,244,245}

Ablation Technique

Initially, circumferential PV isolation is performed. Endocardial electroanatomic voltage mapping then is performed, preferably during NSR. In patients with persistent AF following PV isolation, electrical cardioversion is carried out to restore NSR before voltage mapping. In patients with refractory AF, voltage mapping may be performed during AF. Multielectrode catheters (e.g., PentaRay, Lasso, or mini-basket catheter) are often used to acquire high-density voltage maps.^{30,244,246,247}

Low-voltage areas are identified by the presence of three adjacent points exhibiting bipolar peak-to-peak voltage amplitudes less than 0.5 mV. Once identified, smaller low-voltage areas are ablated to achieve electric silence (bipolar electrogram less than 0.1 mV) and homogenize the fibrotic zone (Fig. 15.57). For the larger low-voltage areas, linear ablation along their borders is performed circumferentially (box isolation of fibrotic areas, BIFAs) to achieve complete electrical isolation of the fibrotic areas, an approach similar to that used for circumferential PV isolation (Fig. 15.58).^{30,244,246,247}

In addition, to prevent the formation of narrow, potentially proarrhythmic residual isthmuses, linear ablation is performed to connect the BIFA ablation lines or scar areas to the closest ablation line or to

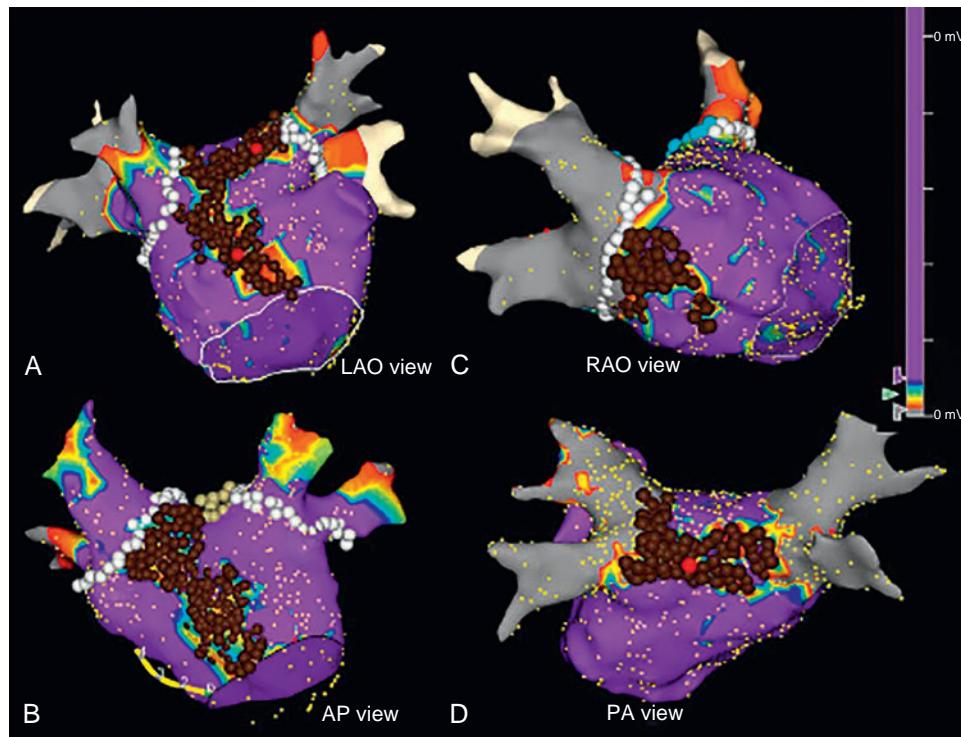


Fig. 15.57 Voltage-Guided Substrate Modification for Atrial Fibrillation. Left atrial (LA) voltage maps in four different patients (A–D) showing variable severity and localization of LA fibrosis. (A) Regional low voltage zone ablation on the LA anterior wall and roof, creating anterior and roof lines. (B) Low voltage zone ablation of the anterior wall; a strategic roof line was added to prevent a secondary atrial tachycardia. The gold tags show the lesions creating the roof line. (C and D) Low voltage zone ablation on the septal wall and posterior wall, respectively. The white and blue tags show the ablated regions in the pulmonary vein isolation, and the brown tags show the ablated regions in the low voltage zones. The red tags indicate the termination sites of the reinduced atrial fibrillation. AP, Anterior-posterior; LAO, left anterior oblique; PA, posterior-anterior; RAO, right anterior oblique. (From Yamaguchi T, Tsuchiya T, Nakahara S, et al. Efficacy of left atrial voltage-based catheter ablation of persistent atrial fibrillation. *J Cardiovasc Electrophysiol.* 2016;27:1055–1063.)

the mitral annulus. When an ablation line is created, the achievement of bidirectional block across the line should be verified.^{30,244,246,247}

Endpoint of Ablation

The endpoint of the box isolation (BIFA) is complete electrical isolation of the low-voltage areas, as confirmed by entrance and exit block. Scar homogenization aims at elimination of all electrograms and achieving electric silence (bipolar electrogram less than 0.1 mV) within the low-voltage zone, as confirmed by voltage remapping. Whenever linear ablation is performed across narrow isthmuses, bidirectional block across the ablation line should be sought, as confirmed by double potentials along the line and activation sequence mapping during atrial pacing from both sides of the line.^{30,244,246,247}

Outcome

Substrate ablation targeting low-voltage areas in the atrium has been emerging as a potential approach to enhance the efficacy of AF ablation, particularly for persistent AF. Recently, several small studies demonstrated a potential benefit for regional voltage-guided LA substrate modification in conjunction with PV isolation in patients with persistent AF and those undergoing redo ablation for paroxysmal AF. In a recent meta-analysis, this approach was found significantly more effective than PV isolation alone or PV isolation plus conventional empirical linear ablation in patients undergoing catheter ablation of nonparoxysmal AF. Notably,

voltage-guided substrate modification appears to have lower proarrhythmic potential (as demonstrated by the lower incidence of postablation AT rate) as compared to empirical LA linear ablation strategies.²⁴⁴

However, the best methods of defining scar (CMR vs. voltage mapping) and techniques for modifying scar regions (box isolation vs. scar homogenization) are yet to be determined. In addition, voltage-guided ablation strategies share the same limitations as those encountered during voltage mapping. The optimal voltage cutoffs for definition of abnormal LA substrate remain uncertain. Further, the measured voltage also depends on the rhythm (NSR vs. AF), and the electrode contact with tissue, among other variables. Also, far-field potentials can potentially obscure voltage maps.²⁴⁸

OUTCOME AND EFFICACY OF CATHETER ABLATION OF ATRIAL FIBRILLATION

There are several hypothetical benefits of ablation of AF and restoration of sinus rhythm: improvement in quality of life, reduction of stroke risk, reduction in heart failure risk, and improved survival. Cumulative evidence suggests that catheter ablation is superior to antiarrhythmic drug therapy in the management of paroxysmal and persistent AF in terms of improved AF-free survival, AF burden, and quality of life. However, evidence is insufficient to determine whether AF catheter ablation reduces all-cause mortality or stroke. Therefore the primary

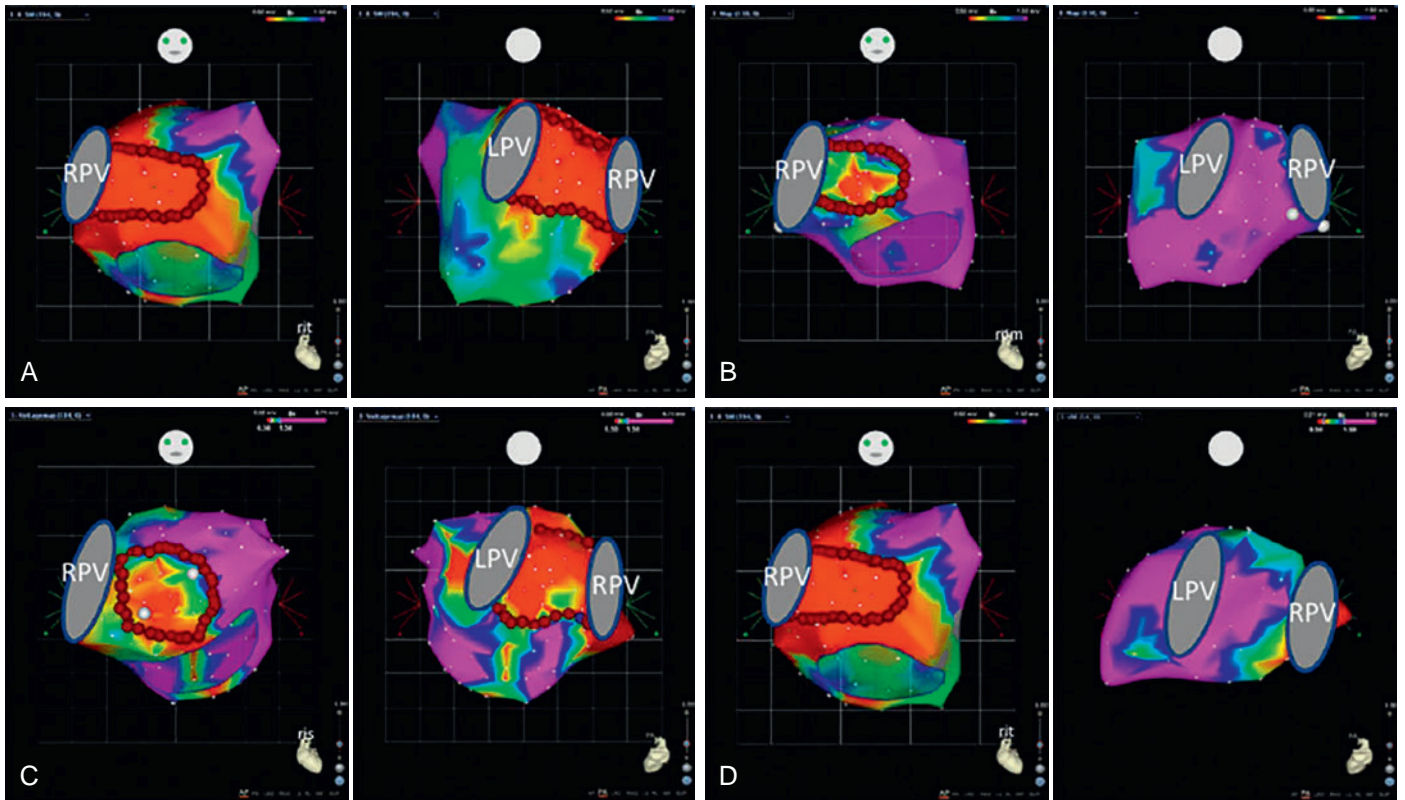


Fig. 15.58 Voltage-Guided Ablation of Atrial Fibrillation. Left atrial voltage maps in four different patients (A–D) showing variable severity and localization of left atrial fibrosis. Box isolation of the fibrotic areas is performed in all cases with connection to the preexisting PV isolation lines. Color coding: red for substantially reduced voltages less than 0.5 mV and purple greater than 1.5 mV. LPV, Left pulmonary veins; RPV, right pulmonary veins. (From Kottkamp H, Berg J, Bender R, et al. Box isolation of fibrotic areas (BIFA): a patient-tailored substrate modification approach for ablation of atrial fibrillation. *J Cardiovasc Electrophysiol.* 2016;27: 22–30.)

justification for an AF ablation procedure at this time is the presence of symptomatic AF.¹

Success Rates

With operator experience, greater consistency in the technique, and the advent of more advanced mapping and ablation technologies, AF ablation has proved to be very effective treatment for symptomatic AF. Reportedly, current techniques of RF catheter ablation can achieve a 60% to 90% improvement in selected patients with medically refractory AF, with similar success rates being reported by several different groups. Although success rates are not perfect, they are two- to threefold better than anything achievable by antiarrhythmic medications. Furthermore, successful control of AF by ablation seems to be durable, given the long follow-up reported by some groups and the observation that most recurrences tend to occur early in the follow-up period, and they only infrequently occur late after ablation.²⁴⁹

It is important to note that significant discrepancies in success rates have been reported for similar procedural techniques for catheter ablation of AF by different centers. These discrepancies can potentially arise from several factors, including variation in study design, different patient population characteristics (age, cardiac disease, LA size), different types of AF (paroxysmal vs. persistent vs. longstanding), differences in follow-up duration and strategy, and differences in definition of success (complete freedom from all atrial arrhythmias vs. AF vs. symptomatic arrhythmias, with or without antiarrhythmic agents). Also, the efficacy

of AF ablation can be largely influenced by the operator's experience and the volume of ablations.

Furthermore, consideration needs to be given to the adoption of a subclassification of AF based on clinical criteria if the magnitude of the therapeutic impact of catheter ablation on patients' quality of life is to be meaningfully assessed. For a patient whose condition is transformed from a predominant pattern of highly symptomatic persistent AF before ablation, to a pattern of asymptomatic or symptomatic short-lived episodes of transient AF (lasting a few minutes) after ablation, the procedure could be deemed clinically successful. In contrast, a binary outcome analysis limited to whether a patient has any recurrence of AF at any time or is free of AF recurrence would classify the ablation as a failed procedure, and any clinical benefit to the patient would not be recognized.

Ongoing clinical trials (CABANA [Catheter Ablation Versus Antiarrhythmic Drug Therapy for Atrial Fibrillation] and EAST [Early Therapy of Atrial Fibrillation for Stroke Prevention Trial]) should provide new information regarding the efficacy of catheter ablation as compared to antiarrhythmic drug therapy as a primary strategy for control of AF for reducing total mortality and other secondary outcome measures, and regarding the value of early application of a rhythm-control therapy (with ablation, antiarrhythmic drug therapy, or both) in reducing the risk of stroke, cardiovascular death, or heart failure.

Several clinical variables can potentially predict lower success rates of AF ablation, including larger LA size, persistent versus paroxysmal

AF, longer AF duration, older patient's age, female gender, number of antiarrhythmic drugs failed before ablation, higher CHADS₂ and CHA₂DS₂-VASc scores, and the presence of hypertension, untreated obstructive sleep apnea, coronary artery disease, and metabolic syndrome. In addition, several reports attempted to identify preprocedural markers of the extent of pathological atrial tissue remodeling and predictors of success (e.g., quantification of atrial fibrosis and scar burden on CMR and severity of LA enlargement) that may help improve selection criteria. Although the LA size and duration of longstanding AF, among other markers, can potentially predict lower procedure success rates, most of these markers do not adequately distinguish subjects in whom ablation should categorically be avoided. The question of how to identify patients in whom structural remodeling and scarring have become irreversible and it is too late to intervene remains unanswered, although preliminary data from cardiac CMR, assessing the degree of LA scarring, hold promise. Nonetheless, it is now well recognized that intervention relatively early in the course of persistent AF helps achieve a better outcome.¹

Ablation of Paroxysmal Atrial Fibrillation

In the setting of paroxysmal AF, RF ablation of AF (generally circumferential antral PV isolation with little to no adjuvant ablation) was found superior to antiarrhythmic drug therapy in several studies, with success rates (freedom from arrhythmias at 12 months) ranging from 59% to 89% (compared to 5% to 23% with antiarrhythmic drug therapy). In many of these studies, a single repeat ablation procedure was required in 10% to 25% of patients. Circumferential antral PV isolation is more effective than segmental ostial PV isolation. The role of adjunctive substrate-based ablation techniques (linear ablation, CFAE ablation, voltage-guided substrate modification, and vagal denervation) is controversial, but these approaches appear to have little value, if any, over antral PV isolation alone in patients with paroxysmal AF.¹

Ablation of Nonparoxysmal Atrial Fibrillation

In patients with persistent AF, circumferential antral PV isolation offers success rates of 32% to 67% after a single procedure and 59% to 88% after multiple procedures. In a meta-analysis of recently published studies using the latest technology, PV isolation alone resulted in a 67% freedom from recurrent AF in the 12 months after ablation in patients with persistent AF and minimal structural heart disease.^{1,249}

Purely anatomic techniques of PV ablation have been found to be inferior to techniques that rigorously confirm complete PV electrical isolation (single procedure success rate of 27% vs. 57% at 2 years of follow-up). CFAE ablation as a stand-alone strategy appears inadequate for successful treatment of AF (pooled success rate of only 26%). Similarly, evidence for rotor ablation efficacy is observational and has not been widely reproduced. Segmental ostial PV isolation is inadequate for arrhythmia control, with single-procedure, drug-free success rates of approximately 22%, and multiple-procedure success rates lower than 55%.

Importantly, regardless of the ablation strategy, multiple procedures appear to be required in nearly half of patients with nonparoxysmal AF. Nonetheless, maintenance of NSR is significantly higher with ablation as compared to antiarrhythmic drug therapy.

Impact on Quality of Life

Patients with AF have substantially impaired quality of life, comparable to patients with coronary artery disease and congestive heart failure; hence, symptomatic improvement is the main objective in the treatment of AF patients. Several studies have demonstrated greater improvement in symptoms and quality of life scores with catheter ablation compared with drug therapy. Those improvements were observed whether abla-

tion was used as a first-line or second-line therapy in patients with symptomatic AF.

It is important to note that, although improvements in quality of life scores are often related to reduction of arrhythmia burden, the quality of life improvement after AF ablation is not entirely dependent on efficacy of the ablation procedure. In fact, up to 65% of patients with documented recurrences of AF after ablation exhibit improvement of symptoms during the AF episodes and report significant improvement of the physical component of the quality of life. Reduction of symptomatic episodes after ablation can potentially arise from a placebo effect or autonomic denervation. It is worth noting that the improvement of quality of life observed postablation appears to fade with time.²⁵⁰

Impact on Cardiac Structure and Function

Restoration of sinus rhythm is expected to improve atrial mechanical function as compared with AF; however, the impact of catheter ablation of AF on LA transport function is still under investigation. Several studies demonstrated an increase in the LA voltage and a decrease in the LA volume following AF ablation. Reversal of atrial electrical remodeling following restoration of NSR can happen within 1 week, and reverse structural remodeling has been demonstrated by imaging studies during long-term follow-up after successful AF ablation.

On the other hand, extensive ablation of atrial tissue replaces myocardium with scar and prolongs intraatrial conduction, which can potentially result in asynchronized contraction of the LA, possibly attenuating atrial contractile performances. The decline in LA systolic function appears to be strongly correlated with the volume of RF ablation scar. Furthermore, extensive septal ablation can potentially damage the Bachmann bundle and delay LA activation, attenuating LA contribution to LV filling, especially when the latest activity in the LA occurs after the QRS, because of closure of the mitral valve before completion of LA contraction. It is likely that the smaller the surface area occupied by scar tissue, the greater the probable benefit for atrial contractile function.

In addition, pulmonary hypertension with LA diastolic dysfunction and preserved atrial systolic function (so-called "stiff LA syndrome") has been observed in 1.4% of patients following AF ablation. Patients with extensive atrial scarring, small LA (45 mm or less), diabetes mellitus, obstructive sleep apnea, and high LA pressure seem to be more prone to develop this syndrome. Symptomatic patients manifest with dyspnea and congestive heart failure. Further refinement of techniques to identify sites crucial for maintenance of AF or subsequent AT on an individual basis is therefore necessary to minimize the extent of LA injury and to maximize the mechanical benefit of catheter ablation therapy for AF.

In patients with heart failure and LV systolic dysfunction, AF ablation was shown to produce significant improvement in LV function, LV dimensions, symptoms, exercise capacity, and quality of life compared with a medical rate control strategy. In one report, catheter ablation strategy resulted in an early improvement in LV function, which was evident at 1 month and was sustained at 1 year compared with the rate control group. Of note, restoration of NSR by AF ablation was found to improve LV function even in patients with preserved LV systolic function. Therefore prior to accepting a rate control strategy, catheter ablation should be considered in patients with heart failure and drug-refractory AF, whether or not the cardiomyopathy is suspected to be related to rapid ventricular rates during AF. In fact, data have also demonstrated that adequate rate control alone is insufficient to prevent AF-mediated cardiomyopathy in a subset of AF patients.¹³⁹

Impact on Stroke Risk

Several observation studies have investigated the long-term risk of stroke after ablation and suggested that successful ablation of AF can lower

the risk of stroke via maintenance of NSR. These studies, however, mainly included patients with a low to intermediate risk of stroke, and incorporated relatively short follow-up intervals with variable utilization of oral anticoagulation. The potential benefits of AF ablation on stroke risk reduction have not been confirmed by large prospective randomized trials and therefore remain unproven.

Recurrence of Atrial Tachyarrhythmias

Recurrences of atrial tachyarrhythmias (AF, AFL, or AT) are common, observed in more than 50% of patients following catheter ablation, regardless of the ablation technique. The incidence of recurrent AF seems to be higher in patients with persistent AF (47%) as compared with paroxysmal AF (33%), in patients older than 65 years (48%) versus patients younger than 65 years (28%), and in patients with structural heart disease (47% to 74%) versus patients without structural heart disease (29% to 50%). Less consistent predictors of AF recurrence include the presence of comorbidities such as hypertension, sleep apnea, and diabetes.

The incidence of AF recurrences increases with increasing follow-up duration and intensity of cardiac monitoring. Considering the intermittent nature of the arrhythmia and the inconsistency of symptoms, the exclusive reliance on patient reporting of symptomatic recurrences results in an underestimation of the rate of arrhythmia recurrence. To obtain reliable information about the success of AF ablation, repeated ambulatory monitoring with automatic detection of arrhythmias is necessary.

Recurrences of atrial arrhythmias after ablation are generally classified according to the timing of first occurrence following the index ablation procedure: (1) early recurrence (within 3 months); (2) late recurrence (from 3 months to 1 year); and (3) very late recurrence (more than 1 year). Most arrhythmia recurrences occur within the first 12 months, and most patients who remain free of AF at 1 year after ablation are likely to remain in NSR at long-term follow-up. Among patients who develop recurrent AF, approximately 76% do so within the first 6 months after ablation, 86% by 12 months, and 92% by 24 months. Although there continues to be an ongoing risk of recurrent AF, new recurrences of AF are infrequent beyond 12 to 24 months following ablation.

Early Recurrences

Early recurrences of atrial arrhythmias have been reported in up to 50% of patients; usually, they peak within the first few weeks and then gradually decrease to lower levels in the period of 3 months after ablation.

The mechanism of early postablation AF is unclear but seems to be different from that of the patient's preablation arrhythmia. Several mechanisms have been implicated, including local inflammation in response to RF thermal injury or pericarditis, systemic inflammation, heightened adrenergic tone, changes in medicines, fluid and electrolyte imbalances, and a delayed therapeutic effect of RF ablation likely attributable to lesion growth or maturation.¹

In addition, failure to identify and modify AF triggers (e.g., incomplete isolation of the PVs, recovery of conduction in a previously isolated PV, or untreated non-PV foci triggers) can manifest with early AF recurrences. In fact, early recurrences of atrial arrhythmias following AF ablation have been reproducibly associated with long-term arrhythmia recurrence. The rates of late recurrences are significantly higher in patients with early arrhythmia recurrences than in those without (54% vs. 7%).

Nevertheless, it is important to recognize that early recurrences of atrial arrhythmias do not necessarily imply long-term procedural failure. In many patients, early atrial arrhythmias resolve completely upon

resolution of the transient factors promoting early arrhythmia recurrences; up to half of patients who experience such early recurrences remain free of atrial arrhythmias during long-term follow-up. Therefore current guidelines recommend a "blanking period" of 3 months after the initial ablation, during which re-ablation in response to arrhythmia recurrence is not recommended.^{1,148,251}

Although early arrhythmia recurrences are an independent predictor of long-term arrhythmia recurrence, the strength of this association differs depending on timing of the arrhythmic events within the blanking period, with later onset (in the second and third months after ablation) being more predictive. In a report of patients with early recurrences of atrial arrhythmias, the incidence of arrhythmia recurrences beyond the blanking period was 44% when the first episode of atrial arrhythmias was in the first month, 69% if in the second month, and 98% if in the third month. Therefore some investigators have suggested limiting the blanking period to the first 1 to 2 months and postponing redo procedures until after this time.²⁵² Patients experiencing recurrences of atrial arrhythmias only in the first 2 weeks following ablation are as likely to achieve long-term ablation success as patients who did not experience any arrhythmic events. This is consistent with the studies demonstrating that transient proarrhythmic factors following the ablation procedure (including inflammation and autonomic dysfunction) typically resolve by one month. Arrhythmias occurring after the resolution of inflammatory changes likely reflect reestablishment of the original AF substrate.²⁵¹

Late Recurrences

Late recurrences of atrial arrhythmias can be observed in 25% to 40% of patients. Beyond the early postablation period, recurrent AF following PV isolation is predominantly caused by PV triggers originating from previously isolated PVs rather than non-PV foci. Recurrence of PV-LA conduction in one or more PV is almost universal (more than 80%).¹

Very Late Recurrences

Very late AF recurrences, developing after an initial freedom from AF during the first year following ablation, are observed in approximately 4% to 10%. These recurrences appear still to be triggered by foci from reconnected PVs in most cases; however, non-PV triggers can also play an important role. The insidious and progressive arrhythmogenic substrate formation during a period of apparent AF elimination is also a likely cause.

Management of Recurrent Atrial Fibrillation

As noted previously, administration of antiarrhythmic drug therapy to patients who undergo catheter ablation for AF can decrease early recurrence of atrial arrhythmias. However, the long-term risk of AF recurrence does not seem to be affected by early, prophylactic, short-term use of antiarrhythmic drugs. Nonetheless, because early recurrences of AF are common and do not necessarily predict long-term recurrences, some operators choose to treat all patients with suppressive antiarrhythmic drugs during the first 1 to 3 months following ablation, a strategy that can potentially help decrease morbidity related to symptomatic arrhythmia episodes and the need for cardioversion or hospitalization. In patients discharged with antiarrhythmic drug therapy, such therapy is discontinued if no recurrence of AF is observed after 1 to 3 months.¹

For early AF recurrences (occurring within the blanking period), a pharmacological rhythm control strategy can be considered. In patients discharged without antiarrhythmic drug therapy who develop paroxysmal episodes of AF, antiarrhythmic drug therapy often is initiated unless the patient is satisfied with the extent of symptomatic improvement. For persistent AF, the early restoration of NSR can improve the

likelihood of long-term maintenance of NSR, regardless of when the arrhythmia first recurs after the ablation procedure. As noted above, it is recommended to avoid redo ablation within the blanking period (especially within the first 1 to 2 months postablation) until ensuring that the arrhythmias are not related to the transient postablation proarrhythmic milieu. Nonetheless, re-ablation can be considered for highly symptomatic atrial arrhythmias that prove to be refractory to medical therapy.

Management decisions for AF recurring beyond the blanking periods should consider the arrhythmia burden and impact on patient's quality of life. A rhythm control strategy is recommended for persistent or symptomatic paroxysmal AF. If AF recurs following discontinuation of antiarrhythmic medications, it is common practice to reinstitute the antiarrhythmic drug. The index ablation procedure for AF can be partially effective and allow a patient with AF that was previously refractory to antiarrhythmic drug therapy to become responsive to drugs.

Redo ablation can also be considered for late AF recurrences, especially when antiarrhythmic drug therapy is not effective, not tolerated, or not preferred. However, it is important to recognize that recurrence of AF after the initial ablation procedure should not prompt automatic redo ablation. Because improvement in quality of life and reduction of symptoms are the main goals of ablation, the mere recurrence of AF after the initial ablation procedure should not be the only basis for recommending re-ablation. Reassessment of the degree of improvement the patient experienced following the initial procedure, the severity of symptoms during AF recurrences, the burden of AF, and the potential response to antiarrhythmic drugs should all be taken into consideration before recommending re-ablation. Some patients experience a substantial palliative effect of ablation whereby AF recurrences cause minor or no symptoms, whereas others achieve satisfactory control with antiarrhythmic drugs that previously failed in the treatment of AF. Many of those patients may prefer to continue pharmacological therapy rather than undergo a repeat ablation procedure. However, in other patients it can be desirable to eliminate all arrhythmias and possibly eliminate antiarrhythmic drug therapy; hence, repeat ablation may be considered in the setting of AF recurrence following the initial procedure. In general,

recurrences of AF or AT after an initial AF ablation procedure lead to a repeat ablation procedure in 15% to 50% of patients.¹

When a repeat ablation procedure is performed for recurrent AF, the initial approach is to assess each PV for reconnection. In most patients, recovery of PV-LA conduction is observed in one or more PV, and PV reisolation is recommended and is frequently sufficient. This can be accomplished by selective ablation targeting only the segment of the PV circumference in which the PV reconnection is detected (Fig. 15.59). Alternatively, ablation can be performed circumferentially around the antrum of the reconnected PV or around all PVs, whether reconnected or isolated at baseline (especially when the original AF ablation strategy did not incorporate circumferential antral PV isolation).²⁵³

In the minority of patients with recurrent AF despite chronically isolated PVs, several ablation strategies have been proposed, including (1) ablation of provoked non-PV triggers; (2) empirical electrical isolation of common sources of non-PV triggers (e.g., SVC, CS, LA posterior wall, ligament of Marshall, LAA); (3) ablation of autonomic ganglia; (4) empirical linear ablation (LA roof line, mitral isthmus line, CTI line, posterior wall box lesion); or (5) substrate modification guided by FIRM mapping, CFAE mapping, or voltage mapping. However, definitive evidence of the benefit or superiority of any of these techniques over the others is lacking. Patients with AF despite PV isolation likely represent a population with more complex underlying mechanisms of arrhythmia, and the success of repeat ablation in these patients is modest, regardless of the ablation strategy employed.^{1,253,254}

Atrial Tachycardia and Flutter Following Ablation of Atrial Fibrillation

LA tachycardia or flutter is a known complication of catheter-based therapies of AF, accounting for about half of all atrial tachyarrhythmias observed following ablation. Originally reported in association with LA scar following mitral valve or maze surgical procedures, several reports demonstrated focal and macroreentrant ATs occurring after linear LA ablation and circumferential and segmental PV isolation, with an incidence ranging between 2% and 50%. The incidence seems to be lower following segmental ostial PV isolation than circumferential

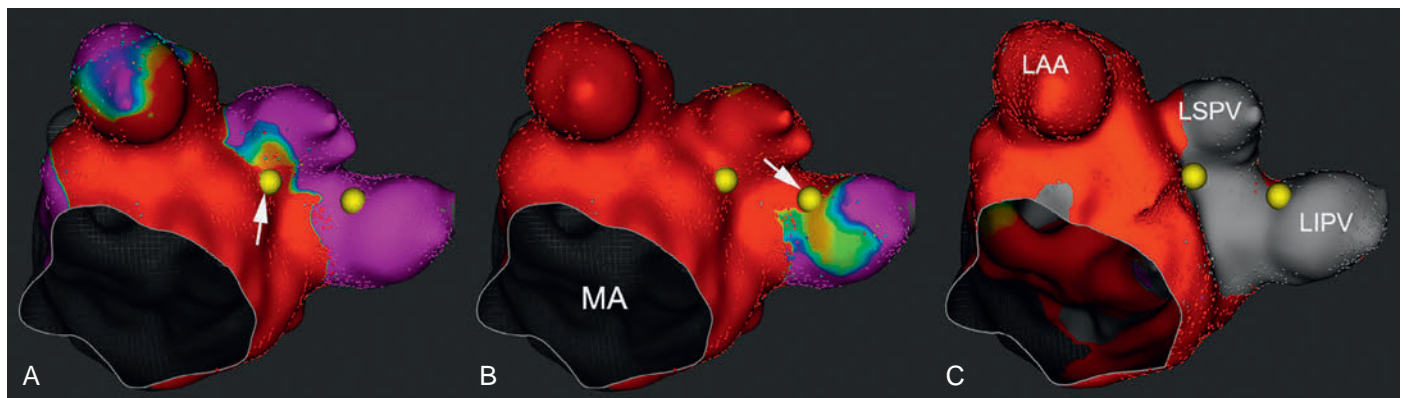


Fig. 15.59 Reconnection of Previously Isolated Pulmonary Veins (PVs). Electroanatomic (Rhythmia) activation map of the left atrium and PVs (left anterior oblique view) is performed during pacing from the distal coronary sinus. Red color indicates already activated sites; purple color indicates sites activated late; and color spectrum in between shows the location of the propagating activation wavefront. (A) Conduction into the left superior PV (LSPV) occurs through a conducting gap (yellow dot, arrow) at the inferomedial aspect of the previous circumferential antral ablation line. (B) Conduction of the left inferior PV (LIPV) is also intact, by more delayed than that into the LSPV. Reconnection of the LIPV occurs through a gap at the carina between the left-sided PVs (yellow dot, arrow). (C) After selective ablation targeting the gaps in the previous ablation lines, activation mapping reveals electrically silent left sided PVs (gray color) and complete electrical isolation. LAA, Left atrial appendage; MA, mitral annulus.

PV isolation and much higher following circumferential or linear LA ablation (more than 30%). Targeting CFAEs without linear lesions or PV isolation is associated with a moderate risk (8.3%) of postablation ATs. Following stepwise approaches of catheter ablation incorporating extensive lesions in the LA and RA to terminate persistent AF, ATs can be observed in more than 50% of patients. Although typical AFL should be considered in the differential diagnosis of regular tachycardias (even in the presence of atypical ECG patterns) observed following AF ablation, most of these arrhythmias arise from the LA and can be focal or macroreentrant.¹

LA tachycardias tend to occur at variable time intervals after AF ablation procedures. AT (macroreentrant or focal) can develop during the course of the ablation procedure or up to 1 year after the procedure, but the most common timing appears to be 1 to 2 months after ablation. This time course suggests that healing of ablation lines likely contributes to the substrate for atrial reentry. The occurrence of ATs early after ablation is common and potentially, but not necessarily, predicts later recurrences of both AT and AF. Nevertheless, these tachycardias can be problematic because they frequently are incessant and are associated with rapid ventricular rates, and they are more likely to require electrical cardioversion when compared with the episodes of AF prior to ablation.

Most organized ATs after AF ablation have been shown to be reentrant, and the vast majority are related to gaps in prior ablation lines. Sometimes, confined PV tachycardia in a previously isolated PV can regain ability to propagate into the LA via a gap in the circumferential PV lesion set, resulting in recurrent atrial tachyarrhythmias conducting.²⁵⁴

The three predominant catheter-based techniques for AF ablation appear to be associated with different rates and types of postprocedure ATs. Segmental ostial PV isolation is associated with a lower incidence of atrial tachyarrhythmias (less than 5%). When they do occur, these arrhythmias tend to be focal ATs, often originating from ostial segments of reconnected PVs. Reisolation of the PV and ablation of non-PV foci are usually sufficient to treat this proarrhythmia. LA macroreentry has been reported after segmental PV isolation, but this situation appears to be significantly less common. Most reentrant circuits use the ablated zone as a central obstacle, resulting in perimitral or peri-PV reentry, with the latter more prevalent in patients with larger atria.

Circumferential antral PV isolation has also been complicated by LA tachyarrhythmias, both focal and macroreentrant, and PV-LA conduction recovery is frequently a critical element in these arrhythmias. The area of recovery within an ablated region of the antrum can potentially create a region of slow conduction and the substrate for micro- or macroreentry. When this area is a critical limb of the reentry circuit, reisolation of the PVs by ablation within the antrum terminates the tachycardia. In some cases, it is also possible that the recovered PV conduction allows PV triggers to induce a tachycardia that does not involve the PV antra. These patients also benefit from PV reisolation and elimination of PV triggers. Macroreentrant ATs involving a PV typically involve two gaps in the isolation line; while ablation of one gap can eliminate AT, it is advisable to eliminate the second gap and thereby reisolate the PV. These ATs are less common after PV isolation with cryoballoon compared with RF-based PV isolation.

Wide-area circumferential LA ablation is frequently complicated by LA macroreentrant ATs. Most of those ATs are related to gaps in prior ablation lines, a finding that implies that most postablation ATs are avoidable, either by limiting the amount of linear ablation and/or by confirming complete conduction block across linear lesions. Not infrequently, multiple different tachycardias occur in individual patients. The long linear lesions required in this approach to prevent AF also create new fixed obstacles to propagation, adjacent areas of block, and slow conduction, and eventual discontinuities represent ideal substrates

for large reentrant circuits. Perimitral macroreentrant AT traversing the mitral isthmus is the most common, accounting for approximately 40% of macroreentrant ATs, and macroreentrant circuits traversing the LA roof account for approximately 20%. Less common sites of macroreentry involve the right or left PVs, LA septum, the CTI, and the base of the LAA. Focal ATs also have been reported following circumferential LA ablation, but macroreentrant ATs are much more common. Not infrequently, multiple macroreentrant circuits and multiple-loop reentrant circuits are encountered. In addition, localized reentrant circuits are not uncommon, and they usually arise from the vicinity of the isolated PVs or linear lesions.

Modification of the original circumferential LA ablation technique has involved the addition of linear ablation connecting the superior PVs (roof line) and connecting the left inferior ablation line to the mitral annulus (mitral isthmus line). Whereas some studies demonstrated a reduction in the incidence of postprocedure LA tachycardias, others actually raised concern that the addition of linear lesions, if incomplete, could lead to an increased rather than decreased incidence of this problem. As noted, even when complete conduction block across the linear lesions is achieved, the ablation lines can potentially promote reentry by providing conduction obstacles and protected isthmuses with adjacent anatomic structures in the LA. Therefore these additional ablation lines can actually contribute to, rather than prevent, macroreentry, and further studies are needed to define their role in the ablation strategy.

Importantly, LA macroreentry can be induced in a large percentage (38%) of patients immediately after circumferential LA ablation for AF; however, such inducibility does not seem to predict those patients who subsequently develop clinical episodes of LA tachycardias. Also, the lack of inducibility of such arrhythmias after ablation is not a good predictor of long-term clinical success. Therefore mapping and ablation of LA macroreentry induced during catheter ablation for AF do not seem necessary.

Management of Atrial Tachycardias Following Ablation of Atrial Fibrillation

There is currently no well-defined standard treatment strategy for ATs following AF ablation procedures, and treatment should be tailored to the potential arrhythmia mechanism. It is important to recognize that many of these arrhythmias are self-limited and resolve spontaneously in up to half of patients within the first 3 to 6 months of follow-up. Therefore efforts should be focused at suppressing these arrhythmias with electrical cardioversion and antiarrhythmic medications or controlling the ventricular response with AVN blocking drugs; ablation for LA macroreentrant ATs should be postponed for approximately 3 to 4 months after diagnosis, unless symptoms cannot be controlled. Class III antiarrhythmic agents (dofetilide, sotalol, or amiodarone), together with AVN blockers, are generally preferred for treatment of organized ATs following AF ablation. Class IC antiarrhythmic agents promote slow conduction that can potentially facilitate macroreentrant tachycardias.¹

Understanding the initial lesion set is critical before embarking on AT ablation. For focal ATs following PV isolation procedures, most of the foci are located in a PV or in the antrum of a PV, and reisolation of all reconnected PVs appears to be sufficient in most cases. The septal aspect of ablation lines encircling the right PVs and the area anterior to the left superior PV are particularly vulnerable to recovery of conduction after circumferential PV isolation, thus predisposing patients to the development of LA tachycardia. Particular attention should be paid at these sites to ensure continuous transmural lesions. If the PVs are excluded as the site of origin of a focal AT, mapping then should focus on the other most likely sites of origin, including the posterior LA, mitral annulus, CS, SVC, and crista terminalis. Nonetheless, PV

isolation is still appropriate if there is evidence of PV conduction, even if the focal AT is not arising in the PV, to minimize the possibility of recurrent AF.

Mapping and ablation of LA macroreentry following circumferential LA ablation or circumferential antral PV isolation are frequently challenging. Detailed mapping with a high density of points is necessary to elucidate the mechanism of the arrhythmias, and is discussed in detail in **Chapter 13**. When the macroreentrant circuit can be mapped, ablation lesions should be tailored to interrupt the path of the reentrant circuit. The mitral isthmus, LA roof, and septum account for 75% of the ablation target sites for macroreentrant ATs from the LA. Successful catheter ablation has been reported in approximately 85% of macroreentrant ATs arising in the LA in highly experienced laboratories; however, ablation of macroreentrant ATs occurring in the septal wall is challenging and less successful. Electrical isolation of all reconnected PVs is also appropriate.

Multiple macroreentrant circuits and multiple-loop reentrant circuits are not infrequently encountered after catheter ablation of AF, especially following extensive ablation strategies (**Fig. 15.60**). Transition from one tachycardia to another tachycardia incorporating a different loop of the same circuit or using a different circuit can be encountered during mapping or after successful ablation of the initial tachycardia. In addition, localized reentrant circuits are not uncommon, especially following ablation of longstanding AF. These small circuits usually arise from the vicinity of the isolated PVs or linear ablation lesions.²⁵⁴

Complications of Catheter Ablation of Atrial Fibrillation

Catheter ablation of AF is one of the most complex interventional EP procedures, and the risk associated with such a procedure is higher than for the ablation of most other arrhythmias. Complications include local vascular complications, cardiac perforation, systemic embolism, esophageal injury, PV stenosis, phrenic nerve injury, valvular injury, and proarrhythmia resulting from reentrant tachycardias arising from incomplete ablative lesions.²⁵⁵

Numerous studies have reported major complication rates following catheter ablation for AF ranging from 3.9% to 6.3% and an overall mortality rate of approximately 0.1% to 0.2%. The most frequent causes of mortality were tamponade (25%), atrioesophageal fistula, and (16%)

stroke (16%). There appears a significant association between operator and hospital volume and adverse outcomes.⁵⁵

It is also important to realize that surgical intervention can be life-saving should a severe mechanical complication, such as rupture or massive cardiac perforation or catheter entrapment, occur. Therefore catheter ablation of AF should not be performed, particularly in higher risk patients, if surgical back-up is not readily available.

Pulmonary Vein Stenosis

PV stenosis after AF ablation has been reported with a wide range of incidence, depending on the ablation technique, the operator's experience, and the method for detection of PV stenosis (**see Figs. 32.7 and 32.8**). From 1999 to 2004, reported incidence ranged from 0% to 44% (median 5.4%), whereas later studies reported incidence from 0% to 19% (median 3.1%). Focal ablation and then ostial PV ablation carry the highest risk for PV stenosis. Circumferential antral LA ablation, with ablation limited to atrial tissue outside the PV orifice, seems to have the lowest rates of PV stenosis, whereas the use of an individual encircling lesion set that requires RF ablation between the ipsilateral PVs carries a relatively higher risk. Stenosis seems to be more common in the left-sided PVs. Delivery of energy inside the PV during ablation, although undesirable, is more likely in the left PVs because the ablation catheter moves easily into them when patients breathe.

The prevalence of this complication has decreased because of various factors, including abandonment of in-vein ablation at the site of the AF focus, limiting ablation to the extraostial portion of the PV or PV antrum, use of advanced imaging techniques to define the PV antrum and guide catheter placement, reduction in target ablation temperature and energy output, and increased operator experience. Nonetheless, severe PV stenosis remains an important complication, affecting approximately 1.0% of patients (**see Chapter 32**).

In a recent study of 976 patients who underwent antral PV isolation (from 2005 to 2016) with routine pre- and postablation screening by CMR or CT, mild, moderate, and severe PV stenosis was observed in 31%, 4%, and 1% of patients, respectively. Symptomatic PV stenosis necessitating intervention occurred in only 1 patient (0.1%).²⁵⁶

Although experimental studies have suggested that cryoablation is associated with little or no risk of PV stenosis in humans, PV stenosis has been increasingly reported in clinical studies. In one report of patients undergoing PV isolation using second-generation cryoballoon, mild, moderate, and severe PV stenosis was observed in 31%, 5%, and 1% of the PVs, respectively. The mean reduction of the PV dimension was 18%. A baseline PV ostium, using the smaller 23-mm balloon, and a lower minimum freezing temperature (below -53.5°C) during cryoballoon ablation were associated with a higher risk of PV narrowing. Cryoenergy application sites may be located in a more distal portion of PVs when using the smaller cryoballoon or when the baseline PV ostial size is larger than the largest available cryoballoon. Similarly, significantly low balloon temperatures are potential indicators of a distal cryoballoon location. In addition, supplementation of cryoballoon ablation of the PV with focal ostial RF ablation can be associated with a higher risk of PV stenosis.^{257,258}

Significant PV stenosis (greater than 50% diameter decrease) appears to be exceedingly rare following laser balloon PV isolation, but experience using this technology is limited.^{184,259}

Although PV angiography, electroanatomic mapping, and impedance monitoring have been used to avoid delivery of RF energy to the PV ostia or within the PVs, these techniques are still imperfect. Electroanatomic mapping, for example, relies on the patient's position remaining unchanged throughout the procedure. With patient movement, the 3-D electroanatomic reconstruction of the LA and PVs may not accurately reflect true, contemporaneous anatomy. Similarly, PV

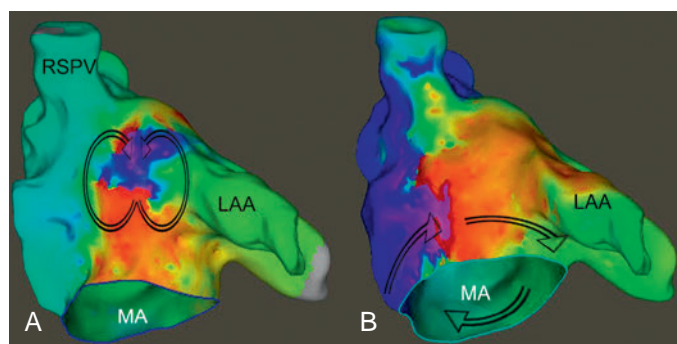


Fig. 15.60 Electroanatomic (CARTO) Mapping of the Macroreentrant Left Atrial (LA) Tachycardias Postablation of Atrial Fibrillation (AF). Activation mapping was performed during two different sustained tachycardias in the same patient with previous wide-area circumferential LA ablation for AF (including LA roof line and mitral isthmus line). The right posterolateral view of the RA is presented. (A) The activation map reveals a figure-of-8 macroreentry circuit at the LA roof that is related to a conduction gap in the previous LA roof ablation line. (B) The activation map demonstrates clockwise perimitral LA macroreentry. LAA, LA appendage; MA, mitral annulus; RSPV, right superior PV.

angiography is typically performed immediately prior to the start of PV ablation. Not only does this provide a crude two-dimensional representation of true PV anatomy, but patient movement later in the procedure can also result in misalignment of the true PV anatomy with that reflected by the PV angiograms. Although impedance monitoring provides online feedback to the location of the ablation catheter relative to the PV, one study found no significant difference in impedance between PV ostial and LA sites. Therefore it is possible for movement of the ablation catheter into the PV ostia to be missed.¹

Atrioesophageal Fistula

Ablation-related esophageal injury is common following AF ablation using RF or cryoenergy. Esophageal mucosal changes consistent with thermal injury are reported in up to 48% of the patients following AF ablation, and clinically silent esophageal ulcerations confirmed by esophagogastroscope or capsule endoscopy can be observed in 10% to 20%. Rarely, esophageal perforation can occur, with or without fistula formation. Fistulas can develop connecting the esophageal lumen to either the LA or pericardium (see Fig. 32.9).^{260–262}

The true incidence of atrioesophageal fistula after RF catheter ablation is unknown, but has been estimated to be between 0.01% and 0.25% post RF ablation and 0.009% to 0.014% following cryoballoon PV isolation, although underreporting is likely. Despite its rarity, atrioesophageal fistula remains a devastating complication associated with high mortality (more than 60%), and accounts for 15.6% of cases with fatal outcome (the second leading cause of death post AF ablation, following cardiac tamponade).^{1,260}

During RF ablation, the risk of esophageal injury likely is enhanced by increasing magnitude and duration of local tissue heating, which is related to catheter tip size, contact pressure, catheter orientation, and energy power output and duration. In addition, ablation strategies incorporating extensive ablation in the LA posterior wall, the type of AF, the use of nasogastric tubes or esophageal temperature probes, and general anesthesia have been associated with an increased rate of esophageal ulcerations. However, the lack of clarity regarding the exact pathophysiology of esophageal injury has hampered efforts to avoid it.

Current approaches to mitigate esophageal injury include the following: (1) assessment of esophageal position before and during ablation (see Fig. 32.11); (2) avoiding ablation in the vicinity of the esophagus; (3) mechanical displacement of the esophagus; (4) monitoring of the esophageal temperature during energy delivery; and (5) reduction of ablation energy power output and duration at sites close to the esophagus. However, no single technique or ablation strategy has been shown so far to unequivocally eliminate or minimize the risk of. Therefore it appears prudent to apply a combination of these preventive techniques during AF ablation. These strategies are discussed in detail in Chapter 32.^{263,264}

Cardiac Tamponade

The risk of intrapericardial bleeding with cardiac tamponade during AF ablation (averaging 1.3%) is higher than that associated with other EP procedures, likely secondary to the common need for two or more transseptal punctures, extensive intracardiac catheter manipulation and ablation, and prolonged high-dose heparinization during the procedure. Cardiac tamponade is the most dramatic complication observed during AF ablation and the leading cause of procedure-related mortality, responsible for 25% of fatalities.²⁶⁵

Several factors can affect the risk of developing cardiac tamponade. High RF power output can increase the risk of cardiac perforation. An audible pop associated with an abrupt rise in impedance is heard in many patients who develop tamponade. Popping occurs because of tissue boiling causing endocardial tissue rupture, and it is increased by

irrigated-tip ablation, high tissue-catheter interface flow, poor or unstable tissue contact, and high catheter tip temperature. Notably, the atrial dome is susceptible to perforation injury during transitioning the catheter tip between the left and right superior PVs. Mechanical perforation can also occur from inadvertent movement of the catheter inside the LAA while it is being positioned during left superior PV or mitral isthmus ablation. Although the use of ICE can potentially limit the risk of cardiac perforation by guiding transseptal puncture and visualizing microbubbles in the LA during RF ablation, it has not eliminated the risk of perforations.

Most perforations occur in the LA. Percutaneous pericardiocentesis effectively restores hemodynamic function in the majority of cases, and up to 16% of cases require surgical closure. Continuation of warfarin through the ablation procedure does not appear to increase the risk of cardiac tamponade. However, patients with therapeutic INR levels who develop cardiac perforation are likely to have a larger amount of blood removed from their pericardium for stabilization and require more blood transfusion units, but the need to undergo emergency surgical exploration is not increased as compared with patients with normal INR levels.²⁶⁶

The occurrence of cardiac perforation is associated with short-term recurrent AF in most patients, in part because the ablation procedure is interrupted by the complication prior to achieving electrical endpoints. Other patients probably have a higher rate of arrhythmia recurrence because of pericardial inflammation, but in most patients this appears to be transient. Most patients with completed ablations have favorable long-term rates of AF elimination, although still lower than expected with uncomplicated cases.

Recent data suggest that the risk of cardiac perforation appears higher in RF catheter ablation as compared to balloon-based PV isolation (cryoballoon and laser balloon). This might be related to the more extensive catheter manipulation required for RF ablation, the safety of which tends to be more dependent on operator and institutional experience.²⁶⁷

Thromboembolism

Systemic thromboembolism is a serious complication of AF ablation, with a reported incidence of 0.1% to 2.8%. In a recent meta-analysis, the rate of stroke was approximately 0.3% and that of transient ischemic attacks was 0.2%. Prior history of stroke or transient ischemic attack is the most potent individual risk factor for cerebrovascular accidents complicating AF ablation; patients with a history of cerebrovascular accidents had a ninefold increased risk of periprocedural stroke. In addition, the incidence of periprocedural stroke increases in a stepwise fashion with an increasing CHA₂DS₂-VASc score.

Thromboembolic events typically occur within 24 hours of the ablation procedure, with the high-risk period extending for the first 2 weeks following ablation. Cerebral thromboembolism is most common, but emboli can also involve the coronary, abdominal, or peripheral vascular circulations.

Importantly, recent studies using diffusion-weighted MRI of the brain have demonstrated a high incidence of acute, asymptomatic cerebral emboli, detected on MRI in up to 50% of patients in the first 24 to 48 hours following AF ablation. The pathogenesis of those lesions remains uncertain, and a majority of the new lesions regress on follow-up MRI. In general, the risk of asymptomatic cerebral emboli associated with AF ablation has been similar between irrigated RF and cryoballoon technologies, but is consistently higher following phased RF multielectrode catheters (PVAC). The long-term prognostic implications of asymptomatic cerebral emboli following AF ablation remain unknown; to date, no clear link has been established between postablation asymptomatic cerebral emboli and long-term cognitive decline.

Therefore, currently, the routine use of brain MRI postablation is not recommended.¹

Potential sources of emboli include thrombus formation on the LA catheters and sheaths, char formation at the tip of the ablation catheter or at the site of ablation, endocardial disruption from the ablation lesions, embolization of air, dislodgment of a preexisting LA thrombus by catheter manipulation, development of thrombi in the LAA after conversion of AF to sinus rhythm, or thrombus formation over the disrupted endothelium. One study correlated new brain MRI lesions with the number of catheter exchanges in and out of LA sheaths.

Careful attention to anticoagulation before, during, and after the ablation procedure is critical to minimize the risk of stroke. TEE should be considered in most patients undergoing AF ablation to screen for LA thrombus. Aggressive intraprocedural anticoagulation is critical, including early heparin administration (preferably before the transseptal puncture), followed by continuous infusion to maintain the ACT above 300 seconds. Also, an uninterrupted perioperative oral anticoagulation strategy (as discussed previously) eliminates a period of inadequate anticoagulation immediately following the ablation procedure and can potentially reduce the risk of thromboembolism.

In addition, meticulous attention to sheath management is paramount to prevent thrombus formation and air embolization, with visualized aspiration and flushing whenever catheters are inserted into the sheaths and continuous flushing of transseptal sheaths with heparinized saline. Open irrigated-tip RF ablation catheters or cryoablation can potentially decrease the formation of char and thrombus at the tip of the ablation catheter. Also, the use of ICE can enable detection of intracardiac thrombi and accelerated bubble formation consistent with endocardial tissue disruption with RF application.

Air Embolism

The most common cause of air embolism is introduction of air into the transseptal sheath. Although air can be introduced through the infusion line, air embolism can also occur with suction when catheters are removed. Careful sheath management, including constant infusion of heparinized saline and air filters, should be observed. Whenever catheters are removed, they need to be withdrawn slowly to minimize suction effects and the fluid column within the sheath should be aspirated simultaneously. The sheath should then be aspirated and irrigated to ascertain that neither air nor blood has collected in the sheath. Particular care is advised when inserting and removing balloon catheters through large sheaths.

Arterial air emboli can distribute to almost any organ, but they have devastating clinical sequelae when they enter the end arteries (see Chapter 32). This situation can lead to the hypoxic manifestations of myocardial injury and cerebrovascular accidents. A common presentation of air embolism during AF ablation is acute inferior ischemia or heart block. This reflects preferential downstream migration of air emboli into the right coronary artery (see eFig. 32.2). Air embolism to the cerebral vasculature can be associated with altered mental status, seizures, and focal neurological signs. The central nervous system dysfunction is attributable to both mechanical obstruction of the arterioles and thrombotic-inflammatory responses of air-injured endothelium (see eFig. 32.3).

Catheter Entrapment in the Mitral Valve Apparatus

There are several reports of the ring catheter becoming entrapped in the mitral valve apparatus during AF ablation, resulting in valve injury that required thoracic surgery and valve replacement. The risk of this complication can be minimized by preventing anterior displacement of the ring catheter during the ablation. Catheter position can be monitored by using a combination of orthogonal fluoroscopy (ensuring that

the ring catheter remains behind the CS on the RAO view) and ICE, as well as by paying close attention to the characteristics of the electrograms recorded on the catheter.

Catheters entangled in the valve apparatus can be difficult to free by clockwise and counterclockwise rotation of the shaft, especially after significant tugging has occurred. To prevent this, prior to pulling on the catheter, one may consider advancing the catheter toward the LV apex. Advancing the sheath over the catheter may facilitate the effort further and is also recommended so that the catheter can be withdrawn into the sheath and the whole assembly withdrawn to the LA.

Forcible traction of the catheter can potentially damage the valve and ultimately necessitate mitral valve replacement. Therefore when gentle manipulation and moderate traction are unsuccessful, removing the catheter by thoracic surgery should be considered.

Phrenic Nerve Injury

Phrenic nerve injury has been reported following AF ablation using RF, cryotherapy, laser, and ultrasound energy. In addition, phrenic nerve injury occurs independently of the strategy of AF ablation used (PV isolation vs. wide-area circumferential LA ablation). Complete or partial recovery of diaphragmatic function is observed in most patients (more than 80%), but can take several months.

Right phrenic nerve injury can be observed after RF electrical isolation of the right-sided (mostly superior) PV (up to 0.48%) or isolation of the SVC (2.1%). The incidence of right phrenic nerve injury is significantly higher in the setting of cryoballoon PV isolation, occurring in more than 11% with the first-generation cryoballoon. Using the second-generation cryoballoon, transient (intraprocedural only) and persistent right phrenic nerve injury has been observed in 9.0% and 3.0% of patients, respectively. Rarely, left phrenic nerve injury can occur during endocardial ablation AF or AT in the region of the proximal roof of the LAA and ablation within the distal CS.^{175,176}

Studies indicated that transient phrenic nerve injury occurs early and uniformly before permanent injury. Therefore when ablation is performed in areas at high risk of phrenic nerve injury (inferoanterior part of right PV ostium, posteroseptal part of the SVC, and proximal LAA roof), monitoring of phrenic nerve function is necessary to prevent permanent damage. This approach entails continuous pacing of the phrenic nerve (using a catheter positioned in the SVC at a site superior to the ablation target site) during energy application, with simultaneous monitoring ipsilateral diaphragmatic contractility (by palpation, fluoroscopy, ICE, or diaphragmatic electromyography) (see Fig. 32.6). Early recognition of impending phrenic nerve injury during energy delivery allows immediate interruption of the energy delivery prior to the onset of permanent injury, which is associated with the rapid recovery of phrenic nerve function.^{1,177}

When the procedure is performed under general anesthesia, it is important to avoid paralytic agents or use short-acting paralytic agents only at the time intubation and allow sufficient time for the paralytic effect to fade away before ablation or use a reversal agent (e.g., neostigmine).^{175,176,268}

Peri-Esophageal Vagal Nerve Injury

The right and left vagal nerves descend alongside the esophagus into the abdomen and innervate most of the upper gastrointestinal system and control esophageal peristalsis, the esophageal and pyloric sphincters, and gastric motility. In the posterior mediastinum, the right and left vagal trunks form a plexus anteriorly (34%), posteriorly (19%), or both anteriorly and posteriorly (44%) around the lower portion of the esophagus. Anterior esophageal plexus lies in close proximity to the LA posterior wall, rendering it susceptible to thermal injury during RF and cryoballoon LA ablation.

Clinically manifest gastroparesis appears to occur more commonly with cryoballoon ablation as compared with RF ablation of AF (10% vs. 6% in one report), but is more likely to be reversible. During cryoablation, lower temperatures during ablation of the inferior PVs and small LA size are associated with increased risk of gastroparesis.

Silent upper gastrointestinal functional abnormalities after AF ablation, as detected by functional studies (esophageal manometry and gastric emptying studies), are common, occurring in up to 74% of the patients. Typically, these abnormalities are transient and resolve within 3 to 6 months.^{269,270}

Peri-esophageal vagal nerve injury typically manifests with symptoms related to gastroparesis and delayed gastric emptying, including epigastric discomfort, abdominal pain, nausea, vomiting, and bloating. Symptoms often develop within a few hours to a few days after the ablation procedure. The duration and severity of symptoms can vary widely, but the vast majority of patients eventually recover almost completely with conservative treatment.^{271,272}

Patients are diagnosed with peri-esophageal vagal nerve injury if they exhibit symptoms of delayed gastric emptying and if the findings of gastrointestinal fluoroscopy, endoscopy, or CT reveal the presence of a medium to large amount of food residue even after overnight fasting, indicating gastric hypomotility. Other methods to evaluate gastric motility include scintigraphy using isotope-labeled solid food or real-time MRI.²⁷³

Significantly symptomatic patients are managed with fasting and then gradual introduction of small, low-fat, and low-fiber meals. Erythromycin, mosapride, and metoclopramide can be of value in stimulating gastric motility.

Stiff Left Atrial Syndrome

The stiff LA syndrome refers to extensive atrial scarring secondary to RF ablation, which can lead to reduced LA compliance. The impaired LA diastolic dysfunction can cause increased LA pressure and pulmonary hypertension, and precipitate right heart failure. Preoperative risk factors include LA scar, small LA diameter (less than 45 mm), elevated mean LA pressure, diabetes, and sleep apnea syndrome.²⁷⁴

The incidence of stiff LA syndrome after RF ablation is estimated at 1.4% to 8%. However, it is possible that this complication remains under-recognized because of mild or nonspecific symptoms that could be attributed to other comorbidities (e.g., recurrent atrial arrhythmias or sleep apnea).²⁷⁴

Stiff LA syndrome typically presents with symptoms of right heart failure associated with pulmonary hypertension and elevated LA pressure (with large V waves recorded on pulmonary capillary wedge pressure or LA pressure tracings), in the absence of significant LV dysfunction, mitral regurgitation, or PV stenosis. The diagnosis requires a high index of suspicion and relies on clinical symptoms, measurement of LA pressure, and the determination of pulmonary arterial pressure. Diuretics are the main therapeutic intervention. Sildenafil may be considered in refractory cases.^{274–276}

Sinus Bradycardia Due to Sinoatrial Artery Damage

The sinus node artery arises from the circumflex coronary artery in about 40% of patients and courses over the roof of the LA. In this location, it is vulnerable to damage by roof line ablation (connecting contralateral PV antral isolation lines). Damage is suspected when extreme sinus bradycardia, that had not been present prior to ablation, is observed immediately after ablation and in the absence of ablation in the high lateral RA that could affect sinus node function. Despite the frequency of extensive ablation on the LA roof, this complication is quite rare (less than 1% of patients); permanent pacing is necessary in a significant proportion due to persistence of unacceptably slow sinus rates.

Pericarditis

Mild, self-limited pericarditis, manifesting as pleuritic chest pain, is very common in the early postoperative period, and is likely related to epicardial inflammation resulting from transmural ablation lesions. However, a more severe form of ablation-induced pericarditis can develop in 0.1% and 0.6% of patients, which can manifest several days or weeks postablation, and can result in delayed pericardial effusion and cardiac tamponade. In addition, acute pericarditis likely underlies some of the early recurrences of atrial tachyarrhythmias postablation. There is currently no evidence to support the use of nonsteroidal antiinflammatory drugs or steroids to prevent AF recurrences.¹

RECOMMENDATIONS AND CONTROVERSIES

Determination of the Necessity of Pulmonary Vein Electrical Isolation

Although durable PV electrical isolation increases the likelihood of procedural success, several studies have found that the relationship between durable PV isolation and freedom from AF was modest, and was a significant overlap between AF recurrence and status of PV electrical conduction; electrical reconnection in at least one PV occurred in 86% of patients with AF recurrence and in 59% patients who were AF-free during follow-up.

In addition, strategies without complete PV isolation or non-PV foci-targeted, such as ablation of atrial ganglionated plexuses, focal impulse and rotor ablation, CFAE ablation, and linear catheter ablation without PV isolation, have also been reported to be effective in AF treatment, suggesting multiple mechanisms involved.²⁷⁷

Nonetheless, PV electrical isolation is widely accepted as an objective, standard, and generalizable endpoint and is currently considered central to any AF catheter ablation strategy, and most centers performing AF ablation are empirically isolating all four PVs, without mapping or specific targeting of the trigger of the focus causing the arrhythmia. Furthermore, ablation is preferably performed outside the tubular portion of the PV (i.e., antral ablation as opposed to ostial ablation) to avoid the risk of PV stenosis and improve the efficacy of the procedure. The antrum blends into the posterior wall of the LA, and, on the posterior wall, there is little space between adjacent antra. Therefore to encompass as much of the PV structure as possible, ablation needs to be performed around the entire antrum, along the posterior LA wall. Although different groups may refer to ablation in this region by different names, such as wide-area LA ablation, circumferential antral PV ablation, or extraostial isolation, the lesion sets produced by the procedures are all similar. There is less consensus, however, on the distance from the PV ostia at which the optimal circumferential lesions should be placed. The greater the distance is, the greater the number of applications and density of lesions will be required to achieve isolation, but the lower the likelihood of PV stenosis. Furthermore, the greater the distance is from the ostia, the larger will be the area encircled and the greater the potential impact of the lesion set on atrial rotors and sites within the posterior LA, which can potentially contribute to the maintenance of AF. However, it is clear that wide-area circumferential LA ablation minimizes the risk of PV stenosis, but at the cost of a higher incidence of macroreentrant ATs and more extensive LA ablation with possible deleterious hemodynamic effects.^{1,10}

Determination of the Necessity of Adjunctive Substrate Modification

While elimination of PV triggers appears to be an adequate initial ablation strategy for patients with paroxysmal AF, atrial substrate modification takes on a more important role in the setting of persistent AF. However, current techniques of substrate modification are technically

challenging and lack adequate procedural endpoints to determine when enough ablation has been performed to modify the atrial substrate sufficiently. In addition, these approaches involve more extensive ablation that can potentially increase the risk of complications, impair LA mechanical function, and predispose to the development of LA macroreentry. Therefore to balance efficacy and safety, it is not recommended to use such an approach for all patients. A rational approach that targets a particular patient profile, rather than a unified strategy used for all patients, may be advisable.

For paroxysmal AF, circumferential antral electrical isolation of all PVs is the procedure of choice. If a focal trigger is identified outside the PVs, it should be targeted if possible. The clinical value of adjunctive substrate-based techniques has not been definitively proven, and these approaches are likely unnecessary, especially during the initial ablation procedure.

The optimal ablation strategy in patients with persistent and longstanding persistent AF remains controversial. Currently, circumferential antral isolation of all PVs is recommended as the cornerstone of most ablation procedures in patients with nonparoxysmal AF. In addition to elimination of the most common AF triggers, this technique incorporates substrate modification by considerable debulking of the atrium as well as elimination of CFAEs, rotors, and ganglionated plexuses commonly located within the circumferential ablation lesions around the PV antra.

However, an ablation strategy limited primarily to antral PV isolation is associated with lower long-term AF-free survival rates in patients with nonparoxysmal AF than those with paroxysmal AF, suggesting that modification of AF substrate outside the PVs appears to be necessary in selected patients. In fact, many observational studies demonstrated that adjunctive substrate-based ablation techniques could improve ablation efficacy. Some substrate-based strategies involve empirical ablation of presumably arrhythmogenic atrial substrate, including linear LA ablation (LA roof and mitral isthmus lines, and LA posterior wall isolation), CFAE ablation, PV denervation, and empiric isolation of extra-PV structures without demonstration of their role as triggering foci in an individual patient. More recently, individualized ablation strategies have been proposed, whereby patient-specific arrhythmogenic atrial substrate is identified and targeted for ablation. Those strategies include voltage-guided substrate modification and focal impulse and rotor ablation.

Accordingly, supplementary linear LA ablation, CFAE ablation, or rotor ablation was recommended by many investigators, especially in patients with longstanding persistent AF or during redo ablation after failure of an initial PV-based ablation procedure.²⁷⁸

Other investigators recommended stepwise or tailored approaches of increasing ablation lesions until persistent AF is terminated by ablation or until AF is rendered noninducible by rapid atrial pacing or infusion of isoproterenol or adenosine. A common approach involved starting with circumferential antral PV isolation, which is then followed by linear ablation across the LA roof, CS isolation, ablation of CFAEs, mitral isthmus ablation, and SVC isolation in a stepwise fashion whereby each step is started if AF still persists after completion of earlier steps. It should be noted, however, that despite the best efforts with various combinations of several ablation strategies, converting chronic AF to NSR solely by ablation may not occur in most patients. Hence, an endpoint of acute termination of chronic AF may not be practical. Moreover, whether acute termination of chronic AF by RF ablation is a predictor of long-term clinical efficacy remains to be proven.^{219,220}

Of note, substrate-based ablation techniques are typically used in conjunction with PV isolation. Their use as a stand-alone procedure for either paroxysmal or persistent AF without any attempt to isolate the PVs electrically has been associated with high rates of recurrence, and this approach has been abandoned by many centers.¹⁴⁶

Importantly, at present, no strategy is proven to improve outcomes for AF ablation beyond antral PV isolation. Recent randomized trials and meta-analyses have suggested that the commonly applied ablation sets beyond PV isolation provide inconsistent benefit. The Substrate and Trigger Ablation for Reduction of Atrial Fibrillation Part II (STAR-AF II) and the Catheter Ablation of Persistent Atrial Fibrillation (CHASE AF) randomized studies demonstrated that the success of PV isolation was not improved by the empirical uniform or stepwise (aimed at AF termination) application of extensive adjuvant ablation (LA linear lesions or CFAE ablation) after either a single or multiple ablation procedures.^{146,219,220,249,279}

Therefore until better evidence of the benefit of extra-PV ablation is available, circumferential antral PV isolation alone appears reasonable, though often inadequate in itself, at least in an initial ablation procedure for patients with paroxysmal and nonparoxysmal AF. Even for patients undergoing redo ablation for AF, an initial strategy of PV reisolation appears reasonable.

Nonetheless, it is important to recognize that while it is true that current substrate-based ablation strategies have not improved that outcome, the efficacy of PV isolation alone remains suboptimal, especially in nonparoxysmal AF. Therefore improved understanding of the underlying mechanisms of AF is necessary to enable the identification and targeting the arrhythmogenic substrate.²⁸⁰

It remains unclear why adjunctive ablation strategies have not improved overall arrhythmia-free outcome. It may be that they are helpful in some patients but not all, or helpful in some but harmful in others, negating any signal of benefit in large trials. It is also possible that, just as in the case of PV isolation, where the strategy seems to be of benefit but its execution is imperfect (with recurrent PV-LA conduction associated with AF recurrence), the theory behind adjunctive ablation strategies is sound, but they are imperfectly performed leading to no net benefit.

According to the 2017 HRS/EHRA/ECAS/APHRS/SOLAECE expert consensus statement, electrical isolation of all PVs is recommended during all AF ablation procedures, as is concomitant ablation of the CTI in patients with clinical or inducible typical AFL. Also, if a reproducible focal trigger that initiates AF is identified outside the PV ostia at the time of an AF ablation procedure, ablation of the focal trigger should be considered. Posterior wall isolation might be considered for initial or repeat ablation of persistent or longstanding persistent AF. If linear ablation lesions are applied, completeness of conduction block across the ablation line should be verified. The usefulness of other substrate-based mapping and ablation approaches (including linear ablation of various sites, ablation of ganglionated plexuses, CFAE ablation, FIRM, and voltage-guided ablation) as an initial or repeat ablation strategy for persistent or longstanding persistent AF is not well established.¹

ATRIOVENTRICULAR JUNCTION ABLATION

Rationale

AV junction ablation and permanent pacemaker implantation (the “ablate and pace” strategy) are often considered as a last resort treatment, reserved mainly for patients with highly symptomatic AF with rapid ventricular rates when both rhythm control and medical rate control strategies have failed or were poorly tolerated, especially those with tachycardia-induced cardiomyopathy.

In addition, in patients with advanced heart failure requiring cardiac resynchronization therapy that continue to have a high burden of AF despite a rhythm control approach, AV junction ablation can potentially improve long-term survival, NYHA class, and LV systolic function. In order to achieve the benefit of cardiac resynchronization therapy, it must

be operating at or near 100% of the time. This level can be difficult to achieve in AF patients; even though the ventricular rate during AF can be “well controlled” with medical therapy, ventricular rates often exceed the lower rate limit of the pacemaker. In these patients, AV junction ablation ensures a high percentage of biventricular pacing without fusion from AF impulses conducted through the AVN and attenuates cardiac output impairment resulting from R-R interval variability. AV junction ablation also can be of value in ICD recipients in whom rapid ventricular rates during AF trigger inappropriate ICD shocks.⁴

The pacemaker can be single-chamber (VVI) for permanent AF, dual-chamber (DDD) for paroxysmal or recurrent persistent AF, or biventricular for patients with LV systolic dysfunction. Also, direct HB pacing (with the pacing electrode positioned in the membranous septum) or para-Hisian pacing can enable physiological pacing in patients without distal conduction disease by recruiting the native HPS, thus avoiding electrical dyssynchrony and potentially preventing pacing-induced cardiomyopathy and heart failure (see Chapter 9).

Ablation of the AV junction is successful in almost 100% of cases, and late recovery of AV conduction is rare. However, this procedure still mandates anticoagulation, possibly requires antiarrhythmic therapy to control nonpermanent AF, and commits the patient to life-long pacing therapy.^{281,282}

The timing of AV junction ablation in relation to pacing is debatable, mainly in the setting of paroxysmal AF. In most EP laboratories, permanent pacemaker implantation is performed prior to the ablation procedure. Long-term pacemaker function does not seem to be affected by RF ablation; however, the pacemaker may develop a transient unpredictable response during RF application in up to 50% of patients, including inhibition, switching to back-up mode, oversensing, undersensing, loss of capture, exit block, and electromechanical interference. These responses argue for the use of an external pacemaker during the ablation procedure. In patients with paroxysmal AF, a dual-chamber pacemaker may be implanted first, and the need for AV junction ablation is reassessed after 1 to 3 months of intensification of medical therapy (i.e., AVN blocking drugs).

Target of Ablation

The ablation target site of this approach is located closer to the compact AVN than the HB in the anterosuperior region of the triangle of Koch. This approach selectively ablates the AVN, and not the HB. This ensures ablation of the proximal part of the AV junction to preserve underlying automatism and to avoid complete pacemaker dependency. Occasionally, when ablation of the AVN is unsuccessful, RF ablation of the HB may be performed using a right- or left-sided approach.

Ablation Technique

A 4- or 8-mm-tip ablation catheter is initially positioned at the AV junction to obtain the maximal amplitude of the bipolar His potential recorded from the distal pair of the electrodes. The catheter is then withdrawn while using consistent clockwise torque on the catheter to maintain septal contact until the His potential becomes small or barely visible, or disappears while recording a relatively large atrial electrogram (A/V ratio greater than 1) or, in patients with AF, until the His potential disappears under the fibrillatory waves (Fig. 15.61). The presence of His and atrial signal on the distal bipole of the ablation catheter, together with an absence of ventricular signal on the proximal bipole, significantly improves the odds of successful AVN ablation without new-onset RBBB.²⁸³

An alternative approach is to position a quadripolar catheter at the HB position. The tip of the ablation catheter is then withdrawn to approximately 2 cm below and to the left of the tip of the HB catheter in the RAO view (Fig. 15.62). Occasionally, in 5% to 15% of patients,

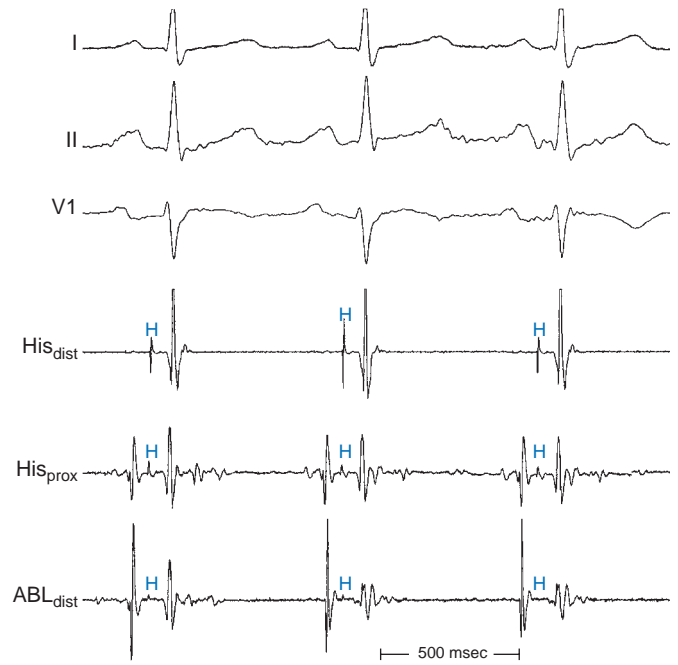


Fig. 15.61 Optimal Ablation Site for Atrioventricular Junction Ablation During Normal Sinus Rhythm. The distal ablation electrodes (ABL_{dist}) record a small His potential and a large atrial electrogram (atrial-ventricular ratio greater than 1). More prominent His potentials, such as recorded by the proximal or distal His bundle catheter bipoles, suggest inappropriate site for ablation. His_{dist} , Distal His bundle; His_{prox} , proximal His bundle.

when the right-sided approach is undesirable or unsuccessful, a left-sided approach to ablate the HB may be used. The ablation catheter is advanced retrogradely through the aorta into the LV, withdrawn so that the catheter tip lies against the membranous septum just below the aortic valve, and records a large HB electrogram and small atrial electrogram (Fig. 15.63). Often, no atrial electrogram is seen. A large atrial electrogram suggests that the catheter tip is close to the LA above the aortic valve; ablation should not be attempted at this site. The left-sided approach typically requires fewer RF applications than the right-sided approach.

Several reports described the feasibility of catheter ablation of the AV junction performed via the SVC during concurrent implantation of a pacemaker or defibrillator. Implantation of the RV lead is performed first, followed by ablation of the AV junction. In patients undergoing device upgrade, in whom the old RV lead is to be utilized for the new device system, AV junction ablation is performed before implantation of the other (atrial and/or CS) leads. Once satisfactory pacing and sensing function of the RV lead is verified, this lead is connected to a temporary pacemaker programmed to the VVI mode at a pacing rate of 30 per minute to provide back-up pacing during and after ablation of the AV junction. Subsequently, the ablation catheter is introduced through the subclavian vein into the RV and is positioned near the HB region by deflection of the tip superiorly to form a J shape; the catheter is then withdrawn so that it lies across the superior margin of the tricuspid annulus (Fig. 15.64). Alternatively, the catheter can be looped in the RA (figure-of-6) and the body of the loop advanced in the RV so that the tip of the catheter is pointing toward the RA and lying on the septal aspect of the RA. Gentle withdrawal of the catheter can increase the size of the loop and allow the catheter tip to rest on the HB location (see Fig. 15.64). From that location, fine manipulation of

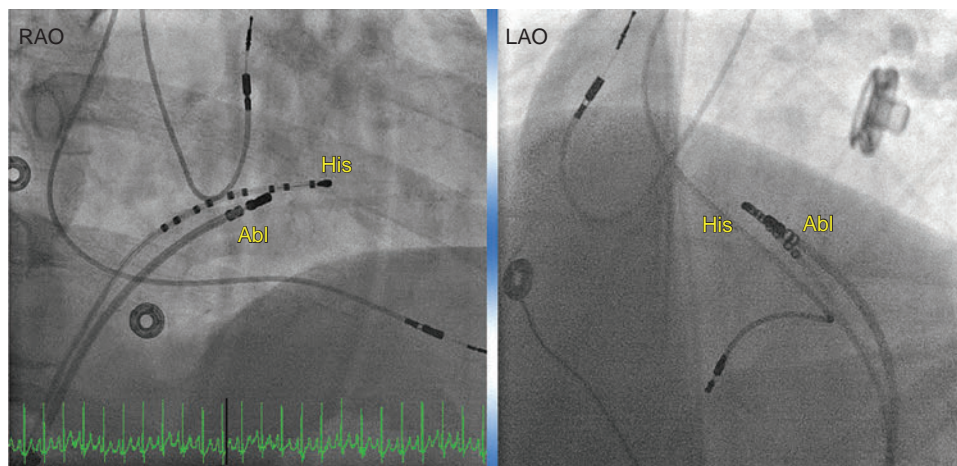


Fig. 15.62 Right-Sided Approach to Ablation of the Atrioventricular Junction. Fluoroscopic (right anterior oblique [RAO] and left anterior oblique [LAO]) views of the ablation catheter position (Abl) in relation to the His bundle (HB) catheter at the optimal site of atrioventricular junction ablation. The distal ablation electrode is positioned just proximal and inferior to the proximal HB electrodes.

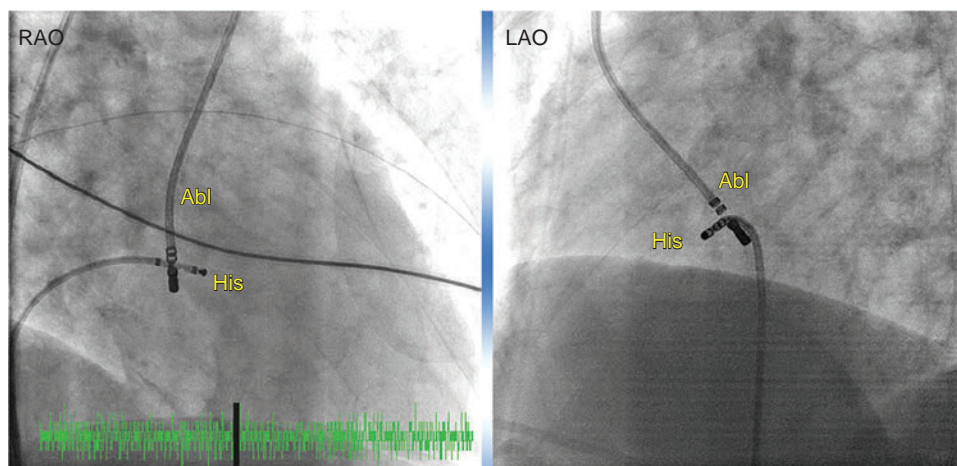


Fig. 15.63 Left-Sided Approach to Ablation of the Atrioventricular Junction. Fluoroscopic (right anterior oblique [RAO] and left anterior oblique [LAO]) views of the ablation catheter introduced via a transaortic approach in relation to the His bundle (HB) catheter at the optimal site for atrioventricular junction ablation (Abl). The distal ablation electrode is positioned just below the aortic cusp in the left ventricular outflow region, opposite the HB catheter in the right ventricle.

the tip of the catheter is performed to bring to the region of the compact AVN in the anterosuperior aspect of the triangle of Koch (a location proximal and inferior to the HB region). Clockwise rotation of the catheter is essential to maintain adequate contact with the septal aspect of the RA. Once successful ablation AV junction is achieved, the ablation catheter is withdrawn, and the atrial lead (or CS lead in patients undergoing biventricular device implantation) is implanted via the same introducer sheath used for ablation.²⁸⁴

RF energy is delivered with a power output of 50 W, targeting a temperature of 60°C to 70°C, and for a duration of 30 to 120 seconds. AV block may appear immediately or after several RF applications. Typically, at good ablation sites, an accelerated junctional rhythm is induced during RF application (Fig. 15.65).

Endpoints of Ablation

The endpoint of ablation is achieving complete AV block. It is preferable to achieve AVN block with a slow, stable junctional escape rhythm

to avoid total pacemaker dependency; however, sometimes this is difficult to achieve, and HB ablation with fascicular or no escape rhythm is the end result (see Fig. 15.65).

Outcome

Complete AV block is successfully achieved by a right-sided ablation approach in 93% to 97% of patients. Achieving complete AVN block specifically, however, is less successful (80% to 90%). Ablation of the AV junction can be difficult to achieve in patients with atrial enlargement or hypertrophy, and in the presence of moderate-to-severe tricuspid regurgitation. Overall, the recurrence of AV conduction after an acutely successful AV junction ablation is approximately 4% to 5%.^{285,286}

Most patients who undergo RF ablation of the AV junction are pacemaker dependent after the procedure, as defined by lack of an escape rhythm that is faster than 40 beats/min. Following AV junction ablation, an escape rhythm develops in 70% to 100% of cases, and the absence of escape rhythm immediately after ablation seems to be the

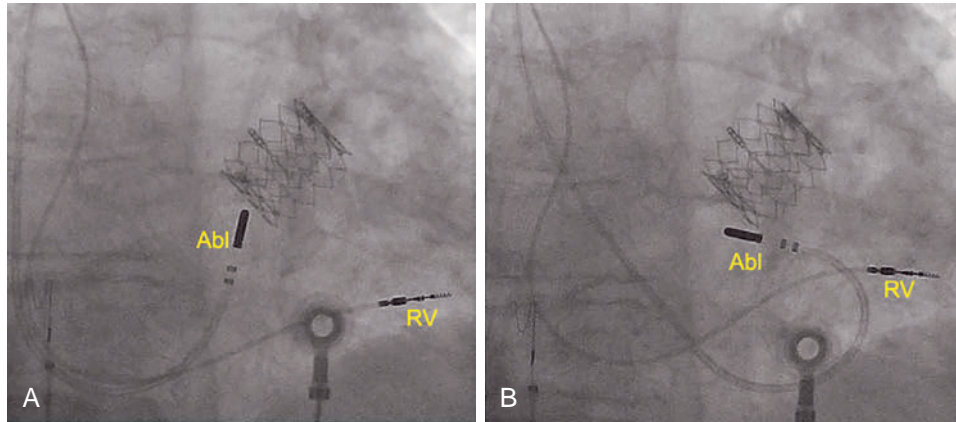


Fig. 15.64 Ablation of the Atrioventricular Junction via the Superior Vena Caval Approach. Fluoroscopic (right anterior oblique) views of the ablation (*Abl*) catheter introduced via the left axillary vein. Implantation of the pacemaker ventricular lead is initially performed. A transcatheter aortic valve prosthesis is also seen. The ablation catheter is positioned near the His bundle region by deflection of the tip superiorly to form a J shape and then withdrawing the catheter so that it lies across the superior margin of the tricuspid annulus (A), or by looping the catheter in the right atrium (RA; figure-of-6) and then advancing the body of the loop into the right ventricle (RV) so that the tip of the catheter is pointing toward the RA and lying on the septal aspect of the RA (B).

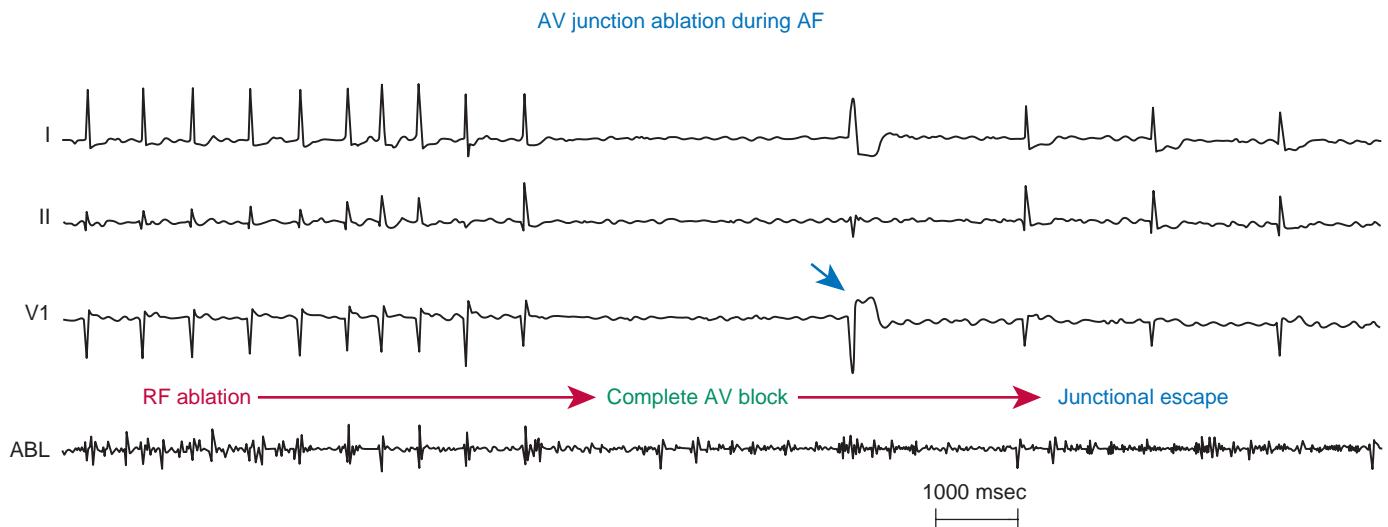


Fig. 15.65 Atrioventricular (AV) Junction Ablation (*ABL*) During Atrial Fibrillation (*AF*). A ventricular pacemaker was implanted prior to ablation and programmed to VVI pacing mode at 30 beats/min. Radiofrequency (*RF*) application results in complete AV block with an escape ventricular paced complex (*blue arrow*) followed by the emergence of a junctional escape rhythm at 35 beats/min.

only predictor for long-term pacemaker dependency. Although the appearance of an escape rhythm does not obviate the need for pacing, it may provide reassurance in case of pacemaker failure.

Malignant ventricular arrhythmias and SCD have been observed in the early phase following AV junction ablation. Polymorphic VTs are related to electrical instability caused by an initial prolongation and then slow adaptation of repolarization caused by changes in the heart rate and ventricular activation sequence. Most polymorphic VTs, torsades de pointes, and VF that have been reported seem to be consistent with a pause- or bradycardia-dependent mechanism. Anomalous dynamics of the paced QT intervals have been observed until the second day after AV junction ablation in patients with chronically rapid ventricular rates during persistent AF, resulting in prolongation of the QT interval when the (paced) heart rate is less than 75 beats/min. This finding may explain the ventricular arrhythmias occurring after AV junction ablation and

may also explain the beneficial effects of temporary pacing at relatively fast rates. On the other hand, bradycardia may not be the sole factor. Sympathetic tone augmentation following AV junction ablation has been described in patients paced at 60 beats/min, thus causing prolongation of the action potential duration and RV refractoriness, whereas sympathetic tone was reduced in patients paced at 90 beats/min. Such an increase in sympathetic activity and prolongation in action potential duration can potentially promote early after-depolarization and triggered activity, which can mediate torsades de pointes and polymorphic VT. To reduce the risk of these arrhythmias, routine pacing at 80 beats/min has been recommended following AV junction ablation. Patients with high-risk factors for arrhythmias, such as congestive heart failure or impaired LV function, may require pacing at higher rates (e.g., at 90 beats/min for 1 to 3 months) as well as in-hospital monitoring for at least 48 hours. Adjustment of the pacing rate, although rarely to less

than 70 beats/min, is usually undertaken after 1 week in most patients, preferably after an ECG evaluation for repolarization abnormalities at the lower rate.²⁸⁶

Another adverse effect of the ablate and pace approach is ventricular dyssynchrony induced by RV pacing, which can lead to impairment of LV systolic function. Positioning the ventricular pacing electrode in the RV septum, HB pacing, and biventricular pacing are being evaluated to reduce the impact of this potential problem.

ATRIOVENTRICULAR NODAL MODIFICATION

Rationale

AVN modification is performed to injure the AVN to reduce the ventricular rate during AF without producing complete heart block. AVN slow pathway ablation has been observed to increase the refractory period of the fast pathway, rendering it incapable of as rapid AV conduction as had been present before slow pathway ablation. As compared with ablation of the AV junction, AVN modification has the advantage in that it results in adequate control of the ventricular rate in most

patients while obviating the need for a permanent pacemaker. Therefore it may be appropriate to attempt first to modify AV conduction in patients with AF and rapid ventricular rates who are appropriate candidates for ablation of the AV junction. Because the risk of inadvertent complete AV block is approximately 20%, the use of the procedure should be limited at present to patients with AF who are symptomatic enough for ablation of the AV junction and implantation of a permanent pacemaker to be justified.

Target of Ablation

The right posteroseptal area along the tricuspid annulus extending from the CS os to the recording site of the HB can be divided into three regions: posterior, medial, and anterior. The conventional technique for ablation of the AV junction uses sites located anteriorly and superiorly on the tricuspid annulus. In contrast, with the technique used to modify AV conduction, the target sites are located inferiorly and posteriorly near the tricuspid annulus close to the CS os (i.e., in the posterior or midatrial septum) (Fig. 15.66). In the presence of dual AVN physiology, the slow AVN pathway is targeted, as described for ablation of AVNRT.

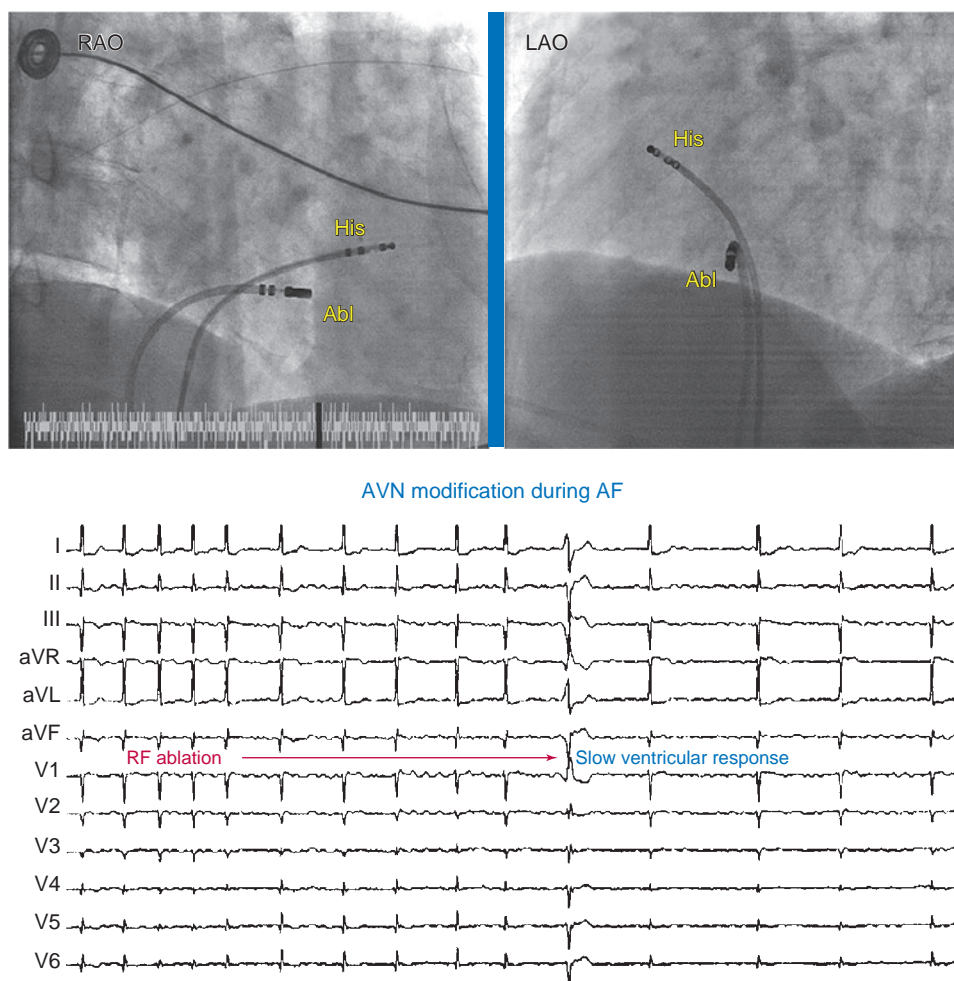


Fig. 15.66 Atrioventricular Node (AVN) Modification During Atrial Fibrillation (AF). *Upper panel*, Fluoroscopic (right anterior oblique [RAO] and left anterior oblique [LAO]) views of the ablation catheter position (Abl) in relation to the His bundle catheter at the optimal site of AVN modification. The distal ablation electrode is positioned in the posteroatrial or midatrial septum near the tricuspid annulus, close to the coronary sinus ostium. *Lower panel*, AF with rapid ventricular response is initially observed (*at left*). Radiofrequency (RF) application results in slowing of the ventricular rate (*at right*) but not complete AV block, as indicated by irregularity of the rhythm.

Ablation Technique

Two quadripolar-electrode catheters are inserted into a femoral vein and positioned at the HB and in the RV. An ablation catheter with a 4-mm tip is used. In patients with no demonstrable dual AVN physiology, RF energy is delivered during AF with continuous infusion of isoproterenol (4 µg/min) to permit immediate assessment of the effect of each RF application. The ventricular rate during AF, obtained after administration of isoproterenol, is presumed to simulate the maximal rate of clinical AF. If NSR is present, AF is induced by rapid atrial pacing before the delivery of RF energy. The ablation catheter is initially positioned against the posterior RA septum, at the level of or lower than the CS os, to record a stable electrogram for at least 10 seconds, with a maximal A/V electrogram amplitude ratio of 0.5 or lower.

RF energy is delivered for 20 seconds at 30 W. If there is no change in the ventricular rate or no accelerating junctional rhythm within 20 seconds, higher energy (an increment of 5 W every 20 seconds, up to 40 W) is delivered to the same site. Whenever there is an abrupt lengthening of the R-R interval or appearance of an accelerated junctional rhythm, the application of energy is immediately discontinued (see Fig. 15.66). If the ventricular rate is still higher than the endpoint ventricular rate (i.e., more than 130 beats/min), higher energy output is delivered to the effective site, or the ablation site is changed and the catheter is repositioned in progressively upward (more superior and anterior) positions along the tricuspid annulus until the endpoint is achieved. RF energy should not be delivered at the upper third of the atrial septum, where an HB potential is visible.

If the endpoint ventricular rate could not be achieved after RF application to the posterior and mid-atrial septum, a decision should be made about whether to attempt complete ablation of AVN. In the presence of dual AVN physiology, RF energy is delivered during NSR to eliminate a slow AVN pathway. The ablation technique is similar to that described for ablation of AVNRT.

Endpoints of Ablation

The endpoint of the procedure is an average ventricular rate of 120 to 130 beats/min or 70% to 75% of the maximum preablation ventricular rate during infusion of isoproterenol (4 µg/min).

Outcome

Short-Term Results

The immediate success of AVN modification to control the ventricular rate without inducing pathological AV block is approximately 75% to 92%.

Long-Term Results

In one report, 92% of patients with paroxysmal AF and uncontrolled ventricular rates refractory to antiarrhythmic drugs achieved adequate slowing of the ventricular rate and were free of symptoms without any antiarrhythmic drug or the need for a permanent pacemaker. The mean resting, ambulatory, and minimal ventricular rates during AF usually remained stable during an interval from 2 days to 3 months after the modification procedure. However, the mean maximal ventricular rate tended to increase (by up to 25%) during this period, which may reflect partial recovery of AV conduction from the immediate effects of RF energy. Nevertheless, the mean maximal ventricular rate during exercise or isoproterenol infusion at 3 months of follow-up remained approximately 25% lower than at baseline, a degree of attenuation adequate to result in the persistent resolution of symptoms.

Atrioventricular Block

Inadvertent complete AV block that necessitates implantation of a permanent pacemaker occurs in approximately 20% to 25% of patients. Of those patients who develop transient AV block during RF application, approximately two-thirds develop persistent AV block within the first 36 to 72 hours after the procedure. It may be that transient thermal injury to the AV conduction system results in an inflammatory reaction responsible for the delayed occurrence of permanent injury. Regardless of the mechanism, if transient AV block occurs during an attempt to modify AV conduction, continuous ECG monitoring on an inpatient basis is appropriate for 3 to 4 days to watch for a recurrence of AV block.

Limitations

The AVN modification approach has several disadvantages, including subsequent development of inadvertent complete AV block, as well as failure to maintain adequate long-term rate control. Also, AVN modification is applicable only to patients who do not have symptoms caused by irregular heart rhythm. An irregular, conducted rhythm can be hemodynamically less efficient than a regular paced rhythm. Therefore AVN modification without pacemaker implantation has fallen out of favor and is now rarely performed.

PERCUTANEOUS LEFT ATRIAL APPENDAGE DEVICE CLOSURE

Percutaneous device closure of the LAA has emerged as a promising alternative therapeutic approach for stroke reduction in selected patients with nonvalvular AF. The Watchman LAA occlusion device has the largest body of clinical randomized and nonrandomized data that has shown the safety and efficacy of this device as an alternative to warfarin for thromboembolic prophylaxis in patients with nonvalvular AF. Other devices such as the Amplatzer Cardiac Plug (St. Jude Medical), WaveCrest LAA occluder (Coherex Medical, Salt Lake City, UT, United States), and the LAmbré LAA occluder (Lifetech Scientific Corp, Shenzhen, China), have not been tested in randomized controlled trials, and the data regarding the safety and efficacy of these devices are limited. The Amplatzer Cardiac Plug is approved in Europe but not the United States.

The Watchman device is approved as an alternative to warfarin for stroke prevention in the United States and Europe. In the United States, the Watchman device is approved as an alternative to warfarin for stroke prevention in patients with nonvalvular AF who: (1) are at increased risk of stroke and systemic embolism on the basis of CHADS₂ or CHA₂DS₂-VASc scores; (2) deemed by their physicians to be suitable for warfarin therapy; and (3) have an appropriate rationale to seek a nonpharmacological alternative to warfarin, taking into account the safety and efficacy of the device compared with warfarin. Exclusion criteria include contraindications to warfarin, any comorbidity requiring ongoing warfarin, or preexisting LA thrombus.¹²²

The safety of the Watchman in patients who are poor candidates for even short-term anticoagulant or antiplatelet therapy is currently unknown. In the United States, patients with an absolute contraindication to oral anticoagulation therapy are presently not considered candidates for the Watchman device. However, recent studies suggest that a history of spontaneous major bleeding might not be an absolute contraindication for short-term oral anticoagulation therapy that is required after Watchman device implantation. Nonetheless, it is important to note that inadequate LAA closure by the Watchman device can potentially be thrombogenic; even with continued anticoagulation, the risk for thromboembolism in these patients can be higher than without

the Watchman device. This risk should be carefully considered given the fact that the majority of patients referred for LAA occlusion have poor tolerance to long-term oral anticoagulation.

Left Atrial Appendage Anatomy

The LAA is the only cardiac structure in the LA derived from the primitive atrium; the main LA is formed from the outgrowth of the PVs. The LAA interior surface is formed by a smooth endocardial surface and pectinate muscles that form ridges (trabeculations) and cavities. Despite the heavily trabeculated endocardium, the LAA wall is remarkably thin (approximately 1 mm). The LAA lies anteriorly in the AV sulcus in close proximity to the left circumflex artery, the great cardiac vein, the left phrenic nerve, and the left PVs. The tip of the LAA can be in a variety of positions, lying over the pulmonary trunk and the left anterior descending coronary artery, pointing posteriorly, or directed medially towards the back of the aorta.²⁸⁷

The anatomy of the LAA is highly variable in terms of its size, shape, and number of lobes. In approximately 54% of the population, the LAA is composed of two lobes, and in one-third of the population is composed of three lobes, with the lobes often lying in different planes. The shape of the LAA orifice can also vary and can be classified into five types, including oval (most common, 69%); foot-like (10%), triangular (8%); water drop-like (8%); and round (6%). The LAA ostium typically lies horizontal to the left superior PV but can also be superior or inferior to it.

Most often, the LAAs are classified into four morphological groups (Fig. 15.67): (1) chicken wing (most common, 48%): an LAA with an obvious bend in the proximal part of the dominant lobe or folding back of the LAA anatomy on itself at some distance from the perceived LAA ostium; (2) cactus (30%): an LAA with a dominant central lobe with secondary lobes extending from the central lobe in both superior and inferior directions; (3) windsock (19%): an LAA with a dominant lobe of sufficient length (greater than 4 cm) as the primary structure; and (4) cauliflower (3%): an LAA with limited overall length (less than the LAA ostium) and with more complex internal characteristics. These various LAA configurations can influence device/size selection and implantation success.

The LAA has long been recognized as the site of thrombus formation in most patients with nonvalvular AF. The LAA, with its trabeculations, provides the appropriate setting during fibrillation for blood stasis and thrombus formation. LAA morphology appears to be associated with different degrees of thromboembolic risk, with chicken wing morphology exhibiting the least stroke risk (4% vs. 10% to 18%). In addition, an increased number of lobes is associated with a higher risk of

LAA thrombus. Of note, the degree of pectinate trabeculations appears to be mild in LAAs with chicken wing morphology, moderate in cases with a cactus morphology, and extensive in LAAs with a cauliflower morphology.

The specific varying shapes of the LAA and its orifice have important implications for device closure of the appendage. All current closure devices of which all are circular in shape, and may not always conform to the LAA ostium. Furthermore, a horn-shaped configuration of the LAA (with a wide ostium and narrow “landing zone” [i.e., the area within the LAA where the device will be positioned]) can pose higher risk of device dislodgement. In these patients, choosing a device large enough to cover the ostium and yet maintain the optimal degree of oversizing in the landing zone (i.e., the area within the LAA where the device will be positioned) to secure anchorage can be a challenge. Also, LAA configuration can impact device design selection. Amplatzer devices are implanted in a relatively proximal position in the LAA (as compared to the Watchman device), which can be of advantage in relatively shallow LAAs and those with complex anatomy.

Left Atrial Appendage Imaging

Preprocedural imaging of the LAA is used to screen suitable candidates and to define LAA morphology and dimensions as well as exclude the presence of intracardiac clots.

TEE is the gold standard for thrombus detection within the LAA, and is also used to assess the shape and size of the LAA ostium, the width of the landing zone, the length of the LAA and—if possible—the number, shape, and location of the lobes.

Although TEE alone is commonly utilized for LAA morphology and measurements, it may not be sufficient for challenging LAA morphology. Cardiac CT angiography provides superior spatial resolution for assessment of LAA configuration, which has additional advantages for procedural preplanning (e.g., selecting device type, decision on device implant position and angles) aside from sizing measurements.²⁸⁸

Intraprocedurally, TEE and contrast angiography are commonly utilized to assess device sizing, guide device delivery and deployment, and assess adequacy of LAA closure. The utility of ICE has not been well established, but ICE is likely inferior to TEE for these purposes. Reliance on any particular imaging modality will depend on the expertise of the operator and institution. TEE images are recorded at set angles according to recommendations by the product manufacturers. For instance, for the Watchman device, diameters and depths were measured at 0 degree, 45 degrees, 90 degrees, and 135 degrees (Fig. 15.68). For Amplatzer devices, landing zones are measured at short-axis and long-axis views. Angiography of the LAA is performed in several views (RAO

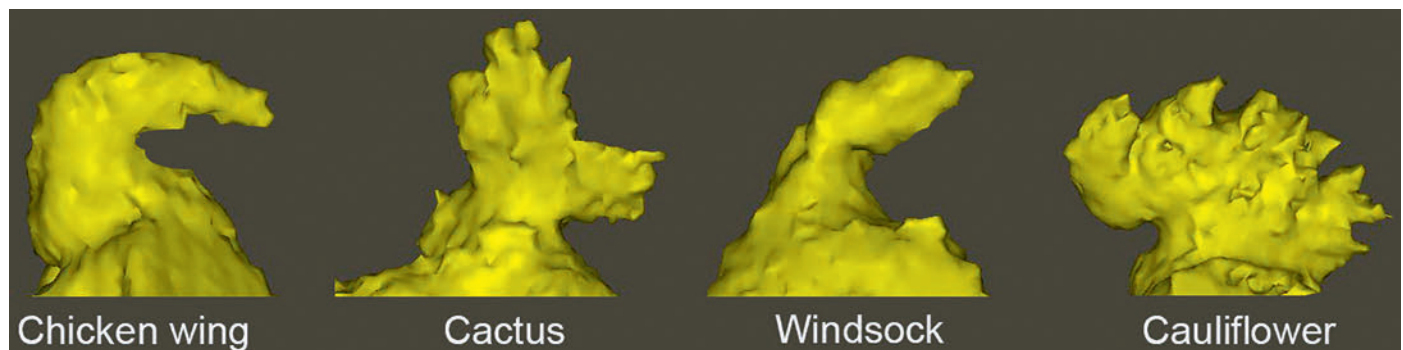


Fig. 15.67 Morphological Types of the Left Atrial Appendage (LAA). Segmented computed tomographic images of the LAA in four different patients.

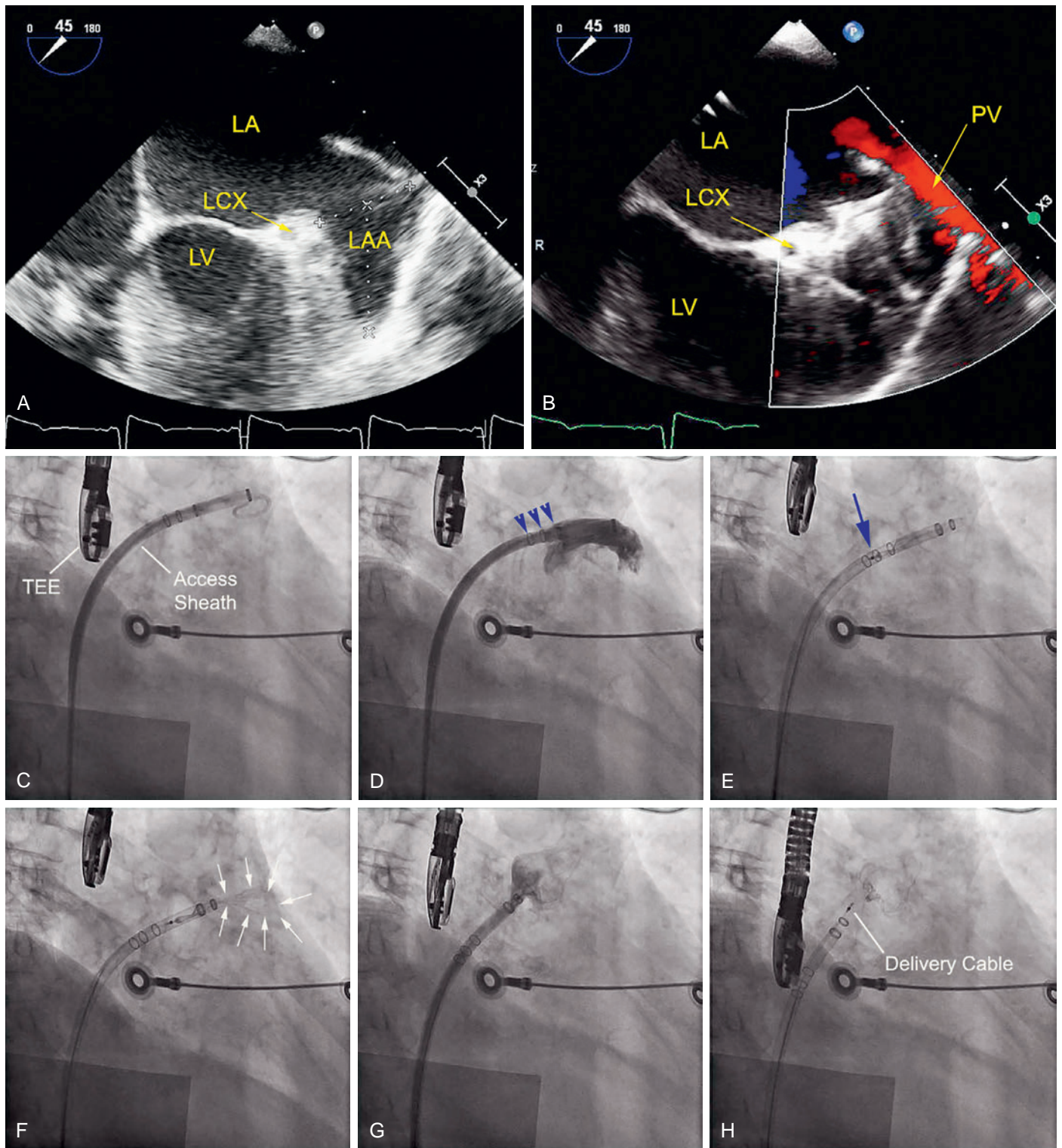


Fig. 15.68 Left Atrial Appendage (LAA) Closure With the Watchman Device. Transesophageal echocardiography (TEE, A and B) and fluoroscopic images (C–H, caudal right anterior oblique projections) during implantation of the Watchman device. (A) TEE measurements of the LAA diameter and depth at 45-degree angle. (B) TEE Doppler image at the same angle showing the Watchman device fully deployed in the LAA, with no flow jet in the LAA around the device. Flow can be seen in the left superior pulmonary vein (PV) adjacent to the LAA. (C) The access sheath and a pigtail catheter are positioned within the LAA. (D) Contrast angiography (via the pigtail catheter) is performed to delineate LAA anatomy. Note the three radiopaque marker bands (blue arrowheads) on the access sheath used for device sizing. (E) The Watchman device is positioned within the access sheath. The length of the device (blue arrow) corresponds to the marker band indicating the LAA ostium. (F) The Watchman device is partially unsheathed. (G) The Watchman device is fully deployed in the LAA, but still connected to the delivery catheter. Contrast angiography (via the access sheath) reveals no peri-device leak. (H) The Watchman device is released. LA, Left atrium; LCX, left circumflex coronary artery; LV, left ventricle.

caudal and cranial projections typically outline the LAA best), delineating shape and size (see Fig. 15.68).²⁸⁸

Importantly, the LAA size is dependent on the loading status as well as on the presence of sinus rhythm or AF. Therefore to avoid undersizing the LAA, it is recommended to assess LAA dimensions during the procedure after establishing a mean filling pressure in the LA in the high normal range (greater than 10 mm Hg). Infusion of normal saline can be required to optimize volume status.

Left Atrial Appendage Catheterization

Percutaneous LAA occlusion is usually performed under general anesthesia and with TEE and fluoroscopic guidance. LA access is achieved via a transseptal puncture. A puncture site at inferoposterior aspect of the septum is recommended to enhance access to the LAA. Anterior septal puncture (or through a patent foramen ovale) should be avoided due to difficulty to turn the guide catheter adequately to the anteriorly located axis of the LAA. TEE (or ICE) is used to guide atrial septal puncture. IV heparin is administered immediately after or, preferably, before LA access, and the ACT is maintained above 250 seconds.

After the transseptal puncture, an extra-stiff 0.035-inch guidewire is positioned into the left superior PV and the transseptal sheath is exchanged over the wire for the access catheter. To position the access catheter into the LAA, an angiographic catheter is advanced through the access sheath over a soft J-tipped 0.035-inch wire. The sheath and pigtail catheter are withdrawn slightly from the left superior PV and turned counterclockwise to fall into the ostium of the LAA. Then, the pigtail catheter is positioned into the distal portion of the LAA, and the access sheath is subsequently advanced over the pigtail catheter until the proximal marker band corresponding to the maximum device diameter is at or just distal to the LAA ostium. Great care needs to be taken to avoid damage to the fragile and thin-walled LAA during catheter placement; manipulating the access sheath in the LAA without an adjunctive device (pigtail catheter) and advancing past pigtail loop should be avoided. Once the access sheath is in proper position, pigtail catheter can be removed.

Watchman Device Device Specifications

The Watchman device is a self-expanding, nickel titanium (nitinol)-framed structure. The device has fixation barbs facing the circumference of the appendage (to minimize dislodgement and embolization) and a permeable polyethylene terephthalate membrane that covers the surface of the device facing the LA. Watchman devices come in 5 sizes (21, 24, 27, 30, and 33 mm) to accommodate varying LAA anatomy and size.

The Watchman device is attached to a delivery cable and is delivered through a dedicated 14 Fr sheath with 12 Fr inner diameter and 75-cm working length. The access sheaths come in a double- or single-curve configuration to accommodate varying appendage orientation. There are 3 radiopaque marker bands (33, 27, and 21 mm) on the distal sheath, which should be aligned to the LAA ostium according to the selected device size (see Fig. 15.68).

Device Sizing

The device size is typically chosen 10% to 20% larger than the diameter of the landing zone within the LAA body (measured on TEE from the area of the left circumflex coronary artery across the LAA to 1 cm inward from the tip of the ridge separating LAA and left superior PV). The oversizing allows for sufficient device compression and stable positioning. The device is not recommended for LAAs with diameters less than 17 mm or more than 30 mm, or when the LAA length is less than the diameter of the landing zone.

Device Deployment

The access sheath has three markers corresponding to device size and is advanced into the LAA until the marker aligns with the ostial plane of the appendage (see Fig. 15.68). After purging, the device is advanced via a delivery catheter in the access sheath until the marker of the device catheter matches the most distal marker on the access sheath. Then, the access sheath is pulled back over the device until the device catheter and access sheath are connected. At this point, no further advancement of the device is permitted (to avoid LAA injury). Once the proper position of the sheathed device within the LAA is confirmed by biplane fluoroscopy and TEE, the device is deployed (unsheathed) by retracting the access sheath and delivery catheter simultaneously while maintaining device position (see Fig. 15.68). Once deployed, angiography and TEE are used to verify proper positioning and stability.

To avoid device embolization, several criteria must be confirmed via fluoroscopy and TEE before device release, including: (1) Position: the plane of maximum diameter of the device should be at or just distal to the orifice of the LAA, and should not protrude greater than 4 to 7 mm beyond the LAA ostium (depending on device size outlined in the manufacturer's instructions for use manual); (2) Anchor: a tug test is performed under fluoroscopy or TEE monitoring to confirm proper anchoring; the access sheath is withdrawn 1 to 2 cm from the face of the device and the deployment knob is gently retracted and released, demonstrating simultaneous movement of the device and appendage; (3) Size: the plane of the maximum device diameter is measured using TEE in the 4 standard views: 0, 45, 90, and 135 and ensure the thread is visible. When properly sized, the maximum diameter of the device is 80% to 92% of its original size (i.e., device compression of 8% to 20%). Device compression ensures the device exerts enough radial force to keep it stable against opposing LAA walls; and (4) Seal: the device should cover the entire LAA ostium, with all LAA lobes being distal to the device, and with no or minimal (less than 5 mm by color Doppler) residual flow around the margins of the device. If the device release criteria are satisfactory, the device is released by counterclockwise rotation of the delivery catheter (see Fig. 15.68).²⁸⁹

If one or more of those criteria appears suboptimal, the device can be retrieved and exchanged or repositioned. The recaptured device can be withdrawn but cannot be advanced within the LAA. Therefore if the device is too deep in the LAA, it has to be recaptured and repositioned more proximally. If the device is too proximal, a complete recapture and exchange of the device are necessary.

Postoperative Management

All Watchman-implanted patients in the United States are required to take warfarin for at least 45 days postimplantation. TEE is performed at 45 days, 6 months, and 12 months to evaluate for residual peridevice flow. Warfarin is discontinued if the LAA closure is complete or the width of the flow jet is less than 5 mm on color Doppler. Once warfarin is stopped, dual antiplatelet therapy with aspirin and clopidogrel are prescribed until completion of 6-month follow-up. Following 6-month follow-up, aspirin alone is prescribed indefinitely. Long-term warfarin is continued in patients without adequate LAA closure.¹²² NOACs or dual-antiplatelet therapy instead of warfarin early after LAA closure with the Watchman device were found safe in recent reports, but these treatment strategies have not yet been confirmed in large studies.^{290,291}

If surveillance TEE at 45 days shows incomplete LAA seal, with a peridevice flow jet greater than 5-mm, warfarin must be continued, and follow-up TEE in another 3 months should be performed. If the leak remains greater than 5 mm, the implant is considered a failure and the patient needs to remain on oral anticoagulation.

Outcome

A recent meta-analysis of two randomized clinical trials and two non-randomized registries demonstrated high procedural success rates of LAA occlusion with the Watchman device; more than 93% of device patients discontinued warfarin by 1 year. LAA closure was noninferior to long-term warfarin therapy for the composite outcome of stroke, systemic embolism, and cardiovascular/unexplained death. All-cause stroke rates were similar between groups, but the pathophysiology of stroke was significantly different; more warfarin patients experiencing hemorrhagic strokes and more Watchman patients experiencing ischemic strokes. In addition, all-cause bleeding was similar between groups; however, when periprocedural bleeding was excluded, bleeding rates were significantly lower in the Watchman group (likely related to withdrawal of chronic anticoagulation therapy in device patients). However, this reduction in hemorrhagic stroke was balanced by a relative increase in ischemic stroke. In fact, ischemic strokes continue to occur after 1 year following LAA closure. Of particular concern, these late ischemic strokes may be related to late thrombus formation on the Watchman device in the absence of anticoagulation. The increased risk of ischemic stroke may relate to possible technical failures of the device: failure to completely obliterate LAA flow, anatomic remodeling of the LAA ostium over time resulting in more leaks, or the development of thrombus on the device.²⁹²

Device-related thrombosis remains a concern even after successful percutaneous endovascular Watchman device implantation. The risk is thought to be highest early after the implant, when endothelialization on the device is still incomplete. For this reason, the standard medical treatment after Watchman implantation, as studied in prospective trials, includes warfarin for 45 days. In the PROTECT-AF (Watchman Left Atrial Appendage System for Embolic Protection in Patients With Atrial Fibrillation) trial, device-related thrombosis was observed in 5.7% of patients, with thrombosis occurring less frequently at 45 days (with patients still taking warfarin) compared to 6 or 12 months (device-related thrombus rates 1.4%, 3.9%, and 2.5%, respectively), suggesting that anticoagulation therapy early after Watchman implant is protective. Interestingly, the rate of device-associated thrombosis was comparable in observational studies investigating a dual antiplatelet regimen after endocardial LAA closure device implantation (Watchman and Amplatzer Cardiac Plug).^{290,293}

Other procedural complications include device migration, device embolization, cardiac perforation with tamponade, as well as systemic air or thrombus embolism.

Amplatzer Cardiac Plug

Device Specifications

The Amplatzer Cardiac Plug is a self-expanding nitinol platform with a distal lobe (which secures the device within the LAA) and a proximal disc (which seals the LA side of the LAA ostium). The lobe and disc are connected by a short flexible central waist, with two polyester patches sewn onto the two components. The lobe of the device is designed to conform to the inner wall of the LAA with a depth of 10 mm or more and is surrounded by fixation barbs to secure device placement and minimize the risk of embolization (Fig. 15.69). The flexible waist allows the disc to self-orient to the cardiac wall and facilitates conformation to variable appendage shapes. Unlike the Watchman device, the length of the Amplatzer Cardiac Plug is shorter than its diameter and, thus, it can be implanted in appendages that are shorter than wide. The lobe size ranges between 16 and 30 mm (with a step size of 2 mm). The diameter of the disc is 4 or 6 mm larger than the lobe for the 16 to 22 mm or 24 to 30 mm devices, respectively.

The Amulet, a second-generation Amplatzer Cardiac Plug, has been designed with strategic modifications at improving device stability and

sealing performance as well as reducing thrombus formation on the atrial side of the device, without changing the main design of the original Amplatzer Cardiac Plug (see Fig. 15.69). These modifications include a longer distal lobe, larger diameter of the proximal disc, longer waist between the distal lobe and the proximal disc, recessed end-screw on the proximal disc, and more fixation barbs. The Amulet comes in eight sizes to seal LAAs with landing zones from 11 to 31 mm in diameter. Also, the more proximal device positioning within the LAA allows for placement regardless of distal anatomy or existence of multiple distal lobes. The longer waist allows for more flexible placement within the LAA and better conformation to angles between the LAA body and ostium.^{294,295}

Device Sizing

In general, the Amplatzer Cardiac Plug lobe size is typically chosen 1.5 to 3 mm larger than the widest diameter of the landing zone within the LAA body (measured in both short-axis and long-axis views on TEE at 10 mm within the LAA orifice perpendicular to the neck axis). With the new Amulet, a larger oversize is recommended: 3 to 5 mm for 16- to 22-mm devices and 3 to 6 mm for 25- to 34-mm devices. The oversizing improves stability of the device and proper anchoring of the lobe. The Amplatzer Cardiac Plug is not recommended for LAAs with diameters more than 29 mm (more than 31 mm for the Amulet) or with length less than 10 mm (less than 7.5 mm for the Amulet).²⁹⁴

Device Deployment

With the delivery sheath at least 15 mm inside the LAA, the first half of the device (lobe) is deployed by withdrawing the delivery sheath, and after confirming the optimal position by TEE and fluoroscopy, the remainder of the lobe is deployed by pushing it out. Once the optimal angle and position of the lobe at the landing zone are confirmed, the disc is deployed by further retracting the sheath while still gently pushing on the device (eFig. 15.29).²⁹⁴

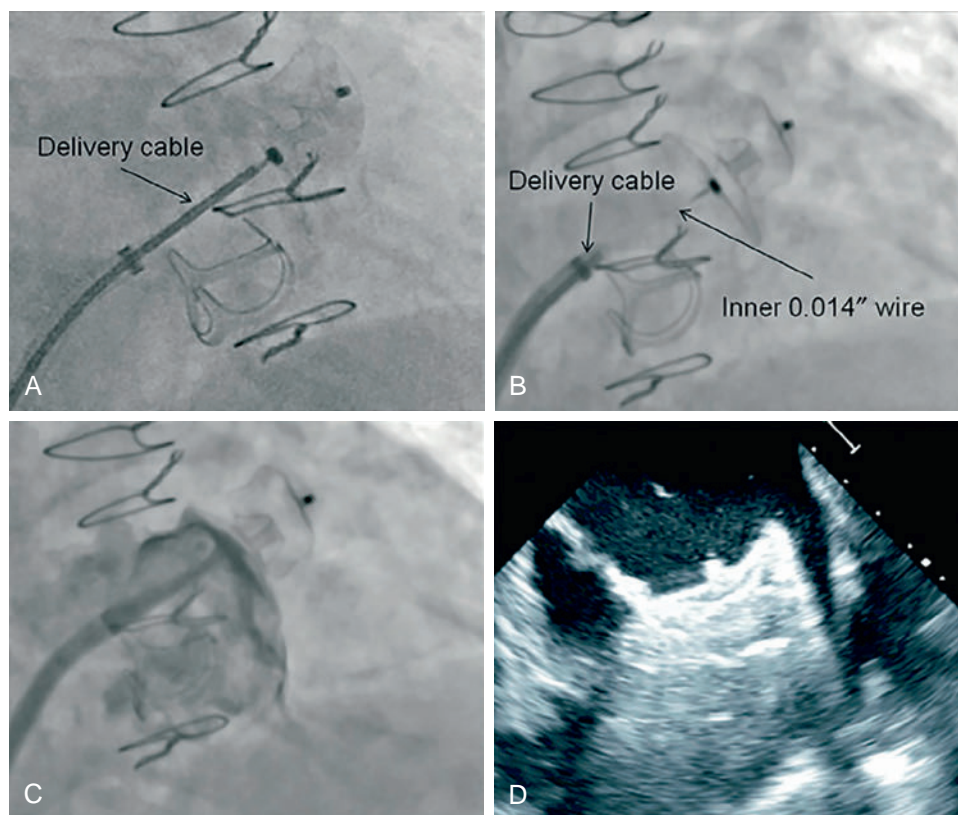
Device release criteria include: (1) Position: the lobe should not protrude more than one-third beyond the left circumflex artery on TEE; (2) Anchor: a tug test is performed under fluoroscopy or TEE monitoring to confirm proper anchoring; (3) Size: the lobe should be visibly compressed (tire shape) with an appreciable separation of lobe and the disc; and (4) Seal: the disc should assume a slightly concave shape and cover the entire LAA orifice and provide apposition against the chamber wall under gentle tension, with no or minimal residual flow around the margins of the device. If the device release criteria are satisfactory, the device is released by counterclockwise rotation of the delivery cable. If one or more of those criteria appears suboptimal, the device can be retrieved and exchanged or repositioned.²⁸⁹

Postoperative Management

Currently, directions for use of the Amplatzer Cardiac Plug and the Amulet recommend dual antiplatelet therapy for 3 months followed by aspirin alone. In the absence of randomized trials and rigorous follow-up, the significance of device-related thrombosis is not entirely known, but this risk remains a concern. Some investigators have advocated more individualized anticoagulation regimens after LAA occlusion with the Amplatzer devices. A short course of anticoagulation therapy (similar to that used following Watchman) can potentially reduce the risk of early thrombus formation, especially in patients with markers of increased risk of thrombus formation.²⁹⁶

Outcome

The initial Amplatzer device used for LAA occlusion was the Amplatzer septal occluder. The Amplatzer Cardiac Plug is the first dedicated Amplatzer device specifically designed for LAA closure. The Amplatzer



eFig. 15.29 Amulet Device Implantation. Sequence of the Amulet implantation showing the initial position of the delivery cable (A), the inner 0.014" wire attached to the system after pulling back the delivery cable (B) and the final result after releasing the device without angiographic leak (C) and optimal echocardiographic positioning (D). (From Freixa X, Chan JL, Tzikas A, et al. The Amplatzer™ Cardiac Plug 2 for left atrial appendage occlusion: novel features and first-in-man experience. *EuroIntervention*. 2013;8:1094–1098.)

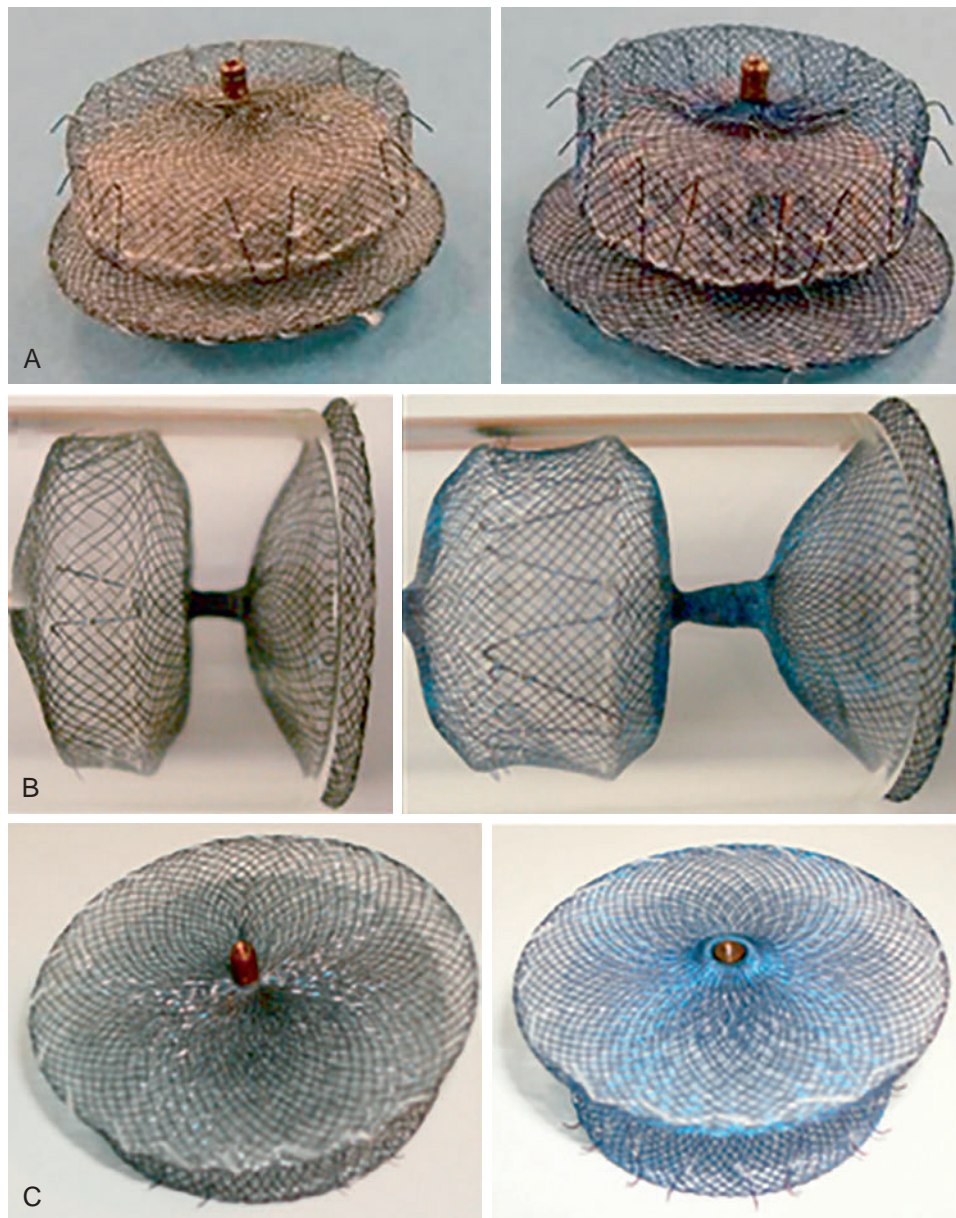


Fig. 15.69 Comparison Between the Amplatzer Cardiac Plug (ACP) and the Amulet. Comparison between the ACP 1 (left) and the ACP 2 (right) highlighting the greater diameter of the Amulet distal lobe (A and B) and waist (B), the increased number of stabilizing barbs (A) and the inversion of the disc end-screw (C). (From Freixa X, Chan JL, Tzikas A, et al. The Amplatzer™ Cardiac Plug 2 for left atrial appendage occlusion: novel features and first-in-man experience. *EuroIntervention*. 2013;8:1094–1098.)

Amulet device is a second-generation Amplatzer LAA closure device that is an evolution of the Amplatzer Cardiac Plug.

To date, the published reports of the Amplatzer Cardiac Plug and the Amulet are not as robust as those of the Watchman device. These devices are available outside of the United States, and they have been marketed for use with antiplatelet therapy only, albeit with little supportive evidence.

Several nonrandomized studies in AF patients with contraindications to systemic anticoagulation showed favorable efficacy and safety outcomes. The incidence of device-associated thrombosis has varied among different studies from 3% to 17%.¹²²

In the largest report of the Amplatzer Cardiac Plug data from 1047 consecutive patients treated in 22 centers, procedural success was 97%,

with a 5% rate of major adverse events. Follow-up TEE (performed in only 63% of patients) revealed device-related thrombosis in 4.4%. The annual rate of systemic thromboembolism was 2.3%, and that of major bleeding was 2.1%. However, in other reports, device-related thrombosis was observed on routine TEE follow-up in up to 17% of patients during treatment with dual antiplatelet therapy. The risk of thrombosis increases with incomplete LAA closure. Notably, thrombosis appeared to originate from the central end-screw of the device in a significant proportion of cases. In addition, placing the disc deeper within the LAA results in cul-de-sac formation that may exhibit low flow and the potential for thrombus formation.^{296,297}

Design modifications in the second-generation Amplatzer device (Amulet) were aimed to reduce thrombogenicity and improve LAA

seal. Nonetheless, a recent report found a high incidence of device-related thrombosis (17%) despite continued antiplatelet therapy.

PERCUTANEOUS LEFT ATRIAL APPENDAGE LIGATION

Currently the Lariat procedure is being performed in patients with AF who have a high risk of stroke and have relative or absolute contraindications to oral anticoagulation (e.g., such as recurrent bleeding, intracranial bleeding) and those in whom oral anticoagulation had been ineffective in preventing stroke.

Contraindications to the Lariat procedure include unamenable LAA size, morphology, or orientation (as evaluated on preprocedural cardiac CT angiography), intraatrial thrombi, and a history of conditions that would result in pericardial adhesions (e.g., pericarditis, open-heart surgery, thoracic radiation, and prior epicardial ablation).

A particular benefit of the Lariat device when compared with other endovascular devices, particularly the Watchman device, is that anticoagulation is not required preoperatively. Unlike other endocardial LAA occlusion devices, the Lariat leaves no foreign body in the endocardial surface of the LA. Hence, the Lariat procedure can be performed in patients with contraindications to anticoagulation. Nevertheless, early (1 month) and late (2 to 4 months) partial reopenings with bidirectional flow between the LAA and the LA have been reported following the Lariat procedure. Therefore some investigators have recommended short-term oral anticoagulation therapy (similar to the regimen used following the Watchman procedure) in patients with no absolute contraindications until complete LAA exclusion have been confirmed on follow-up TEE.²⁹⁸

A potential added benefit of the Lariat procedure, which is not shared by LAA plug devices, is that it results in electrical isolation of the LAA. Also, the Lariat procedure may be considered when the LAA is too large for either the Watchman or the Amplatzer Cardiac Plug devices, as long as the maximal ostial diameter is less than 40 mm.²⁹⁹

Left Atrial Appendage Imaging

Preprocedural imaging of the LAA with cardiac CT angiography and TEE is critical to assess the LAA anatomy, exclude LAA thrombus, and guide the placement of the endocardial and epicardial magnet-tipped guidewires.

Preprocedural CT angiography with 3-D reconstruction is important to identify LAA morphology and dimensions that are not compatible with the Lariat suture delivery device, including: (1) LAA diameter greater than 40 mm; (2) superiorly oriented LAA with the LAA apex directed behind the pulmonary artery; (3) multilobed LAA with different orientation in different planes exceeding 40 mm; and (4) a posteriorly rotated heart.^{299,300}

TEE can be used to confirm LAA morphology and rule out LAA thrombus, especially when there is incomplete filling of the LAA using CT angiography. Intraprocedurally, TEE and angiography are commonly used to guide delivery and deployment of the device, and assess adequacy of LAA closure.³⁰⁰

Device Specification

The Lariat system consists of the following components: (1) the Lariat suture delivery device; (2) two (0.025-inch endocardial and 0.035-inch epicardial) magnet-tipped guidewires (FindrWIRZ); (3) a large (15-mm) compliant occlusion balloon catheter; and (4) an epicardial sheath (13 Fr epicardial cannula) with compliant atraumatic tip.

The Lariat procedure is a percutaneous adaptation of the surgical exclusion of LAA with a suture. The suture material delivered by the Lariat snare is identical to the suture material used during open-heart

surgery to exclude LAA. The Lariat device is deployed by means of a trans-pericardial approach using an epicardial snare with a pretied suture to lasso and occlude the LAA.

To isolate the LAA, this system requires both endocardial and epicardial approaches. Initially, pericardial access is obtained (before administration of IV heparin) and an epicardial soft-tipped access cannula is inserted into the pericardial space. Then, transseptal puncture is performed and the endocardial magnet-tipped guidewire is advanced transseptally to the apex of the LAA. Via the percutaneous epicardial access sheath, the epicardial magnet-tipped guidewire is advanced towards the LAA to connect coaxially with the endocardially positioned magnet-tipped guidewire. The two guidewires form a rail at the LAA tip to facilitate advancing the Lariat device to snare and ligate the LAA. The lasso-like suture (snare) is advanced via the epicardial sheath over the epicardial magnet-tipped guidewire to the base of the LAA. The suture is then deployed to strangulate the LAA.²⁸⁹

Epicardial Access

The pericardial access is achieved via the subxiphoid approach, as described in **Chapter 4**. Preprocedural CT angiogram is used to identify anatomic landmarks and guide the trajectory of the pericardial needle that would provide the most direct access to the LAA. The needle-in-needle technique is preferred to minimize the risk of RV injury. An anterior pericardial approach is required to facilitate maneuvering the Lariat suture delivery device over the anterior surface of the RV and posteriorly toward the tip of the LAA in its most anterior aspect. A posterior pericardial access results in the Lariat device approaching the LAA toward its lateral aspect, thus precluding the snare from going over the anteriorly directed apex of the LAA. Also, a pericardial access that is too medial makes it difficult to direct the Lariat suture delivery device posteriorly toward the apex of the LAA.

The combined use of the anteroposterior and left-lateral fluoroscopic views is recommended to assure anterolateral pericardial access. In the anteroposterior fluoroscopic view, the needle is directed toward the left shoulder, just lateral to the pulmonary artery and the hilum of the pulmonary vasculature. In the left lateral fluoroscopic view, the needle is directed to the anterior surface of the RV, 1 to 2 cm above the apex of the heart.³⁰⁰

Once pericardial access is obtained, serial dilators are used to dilate the epicardial access route and a 13 Fr soft-tipped guide cannula and its dilator are advanced over the guidewire into the pericardial space. There is a curve at the end of the epicardial sheath (marked by the black colored flat surface of the proximal end of the sheath) that should be directed away from the surface of the heart (i.e., the black-colored flat surface is oriented at 12 o'clock) when advancing the sheath. The dilator and the sheath are advanced over the superior aspect of the RV until the tip of the dilator approaches the edge of the cardiac silhouette in the anteroposterior view. The black flat surface of the sheath is then slowly rotated to 9 o'clock and the sheath is then advanced over the dilator until it nears the tip of the dilator, and the dilator is then removed. The dilator and the sheath should never be advanced into the pericardial space without the guidewire. Similarly, the sheath should never be advanced without the dilator or the Lariat device.

Endocardial Access

An inferoposterior septal puncture site is recommended to facilitate access to the LAA. A higher transseptal puncture or transseptal access through a patent foramen ovale tends to direct the transseptal sheath toward the left PVs and make it difficult to engage the anterior part of the LAA with the endocardial magnet wire.³⁰⁰

A pigtail catheter is advanced over the guidewire into the LAA and contrast angiography is performed to assess the LAA size and

orientation. Then, the pigtail catheter is removed and the occlusion balloon catheter and the endovascular magnet-tipped guidewire are advanced (as a unit) into the LAA. The endovascular magnet-tipped guidewire is then carefully navigated to the distal end of the LAA and is stabilized (Fig. 15.70). The endocardial magnet-tipped guidewire should be placed in the most anterosuperior aspect of the LAA (in the 30-degree LAO or 90-degree left-lateral fluoroscopic views). An angiogram (through the occlusion balloon catheter) is performed to confirm guidewire placement. Subsequently, the balloon is inflated and positioned just distal to the ostium of the LAA. Once proper position is confirmed on TEE and angiography, the balloon is deflated.

Connecting the Epicardial and Endocardial Magnet-Tipped Guidewires

The epicardial magnet-tipped guidewire is then introduced into the pericardial space through the epicardial sheath and carefully navigated toward the endocardial magnet-tipped guidewire until both magnets connect end to end (see Fig. 15.70). Coaxial alignment of the two guidewires (as confirmed on RAO and LAO fluoroscopic views) is necessary to provide a monorail for the Lariat device, and is facilitated by proper positioning of the endocardial magnet in the anterior aspect of the LAA and correct orientation of the epicardial sheath.

Snaring the Left Atrial Appendage

The Lariat is back-loaded over the epicardial magnet-tipped guidewire and, with the snare closed, advanced over the guidewire into the pericardial sheath. The curve at the end of the Lariat device should be aligned to that of the epicardial sheath to facilitate the anterior-to-posterior direction the snare must travel within the pericardial space to advance over the apex of the LAA. The correct orientation of the snare within the pericardial space is confirmed when the radio-opaque marker on the distal end of the Lariat device is on the left side in the 30-degree LAO fluoroscopic view and the legs of the snare are parallel.³⁰⁰

While maintaining the orientation of the flat surface of the Lariat handle and the flat/black end of the pericardial sheath together, the Lariat device is carefully advanced over the epicardial magnet-tipped guidewire. Once past the pericardial sheath, the snare is opened fully in the pericardial space.

The Lariat suture system is guided along the epicardial guidewire (under fluoroscopic monitoring) and looped over the LAA, while maintaining the magnets in the same position and avoiding excessive slack or tension on the epicardial guidewire. Occasionally, gentle rocking of the device and manipulation (rotating as well as advancement or retraction) of the sheath can help facilitate the advancement of the snare over the LAA. If the magnets detach anytime during this process, then the Lariat suture system is retracted and the magnets are reengaged.

Subsequently, the occlusion balloon is inflated at the LAA ostium. The fluoroscopic markers on the balloon can be used to ensure that the Lariat has been fully advanced over the LAA ostium. Multiple fluoroscopic views and TEE are used to confirm the position of the Lariat snare and verify that all the lobes of the LAA are beyond the Lariat suture. At that point, the snare is tightened to approximate the tissue (see Fig. 15.70). LA angiography and Doppler TEE are used to ensure complete closure of the LAA (less than 1 mm flow on cross-section). If the position of the snare is not satisfactory, the snare can be released and repositioned to capture the intended closure site.

Once satisfactory exclusion of the LAA by the closed snare is confirmed, the occlusion balloon is deflated and the magnet-tipped guidewires are disconnected by pulling the endocardial guidewire while holding the epicardial guidewire. The deflated balloon and endocardial guidewire are then removed from the LAA. The preloaded, pretied suture is then released from the snare and tightened. LAA closure is verified again

with angiography and TEE (see Fig. 15.70). The Lariat device is then pulled back off the LAA and, after a few minutes, complete LAA closure is confirmed one more time with angiography and TEE. If closure is incomplete, the Lariat can be readvanced over the LAA and tightened again. Once complete LAA closure is verified, the suture is cut. All the wires and sheaths are then retracted and a pericardial drain is placed and will be left in place.³⁰⁰

Postoperative Management

A pericardial drain is left in place for the next 24 to 48 hours to allow for prompt management of potential pericardial effusion. The drain may be removed once the absence of reaccumulating effusion is verified on echocardiographic examinations over a 24-hour period. Antibiotic therapy is administered as long as the pericardial drain is in place.

Colchicine is frequently used to reduce pain associated with pericarditis and the prevention of Dressler syndrome. Colchicine is usually initiated on the day of the procedure and maintained for 3 to 4 weeks. Nonsteroidal antiinflammatory drugs can be added to colchicine. Oral corticosteroids can be considered for severe or persistent pericarditis.³⁰⁰

Surveillance TEE is recommended at 4 to 6 weeks after the procedure to assess thrombus and leaks. If there is a leak, a repeat TEE at 3 to 6 months is recommended. In patients with no absolute contraindications, it may be prudent to continue oral anticoagulation postoperatively until surveillance TEE excludes the presence of persistent LAA leak and thrombus formation. Dual antiplatelet therapy (aspirin and clopidogrel) or aspirin alone can be considered in patients who cannot tolerate short-term oral anticoagulation.³⁰⁰

Outcome

The Lariat suture delivery device is a suture snare catheter that is FDA approved for tissue approximation. Although the FDA approval does not specify the use of the device as a tool to ligate the LAA to decrease the risk of stroke, and despite the lack of evidence for device effectiveness and safety for that purpose, the Lariat procedure has been performed in a substantial number of patients in the United States as well as internationally, primarily to reduce the risk of stroke in AF patients with contraindications to oral anticoagulation therapy.¹²²

There have been no randomized controlled trials investigating the Lariat device to date. Recent studies evaluating the safety and efficacy of the Lariat device have reported acute procedural success rates exceeding 90%. Although several thousand Lariat procedures have been performed so far in the United States, the true safety profile of the Lariat device is yet to be fully characterized.

In a retrospective, multicenter study of 154 consecutive patients, device success (defined as Lariat suture deployment with less than 5 mm leak) was 94%, and major complications occurred in 10%, including 1 death due to respiratory failure and 14 major bleeds, 3 of which required emergent surgery. Complete LAA closure on follow-up TEE was maintained in 79% of patients, while leaks of less than 5 mm were observed in 14%, and leaks of greater than or equal to 5 mm in 6%. The true incidence and clinical significance of post-Lariat leaks have not been well defined and will require further investigation.¹²²

A recent review of the FDA MAUDE (Manufacturer and User Facility Device Experience) database revealed high rates of procedure-related mortality and morbidity, prompting the FDA to issue a safety alert to health care providers and patients about these issues. More recently, in a large study of 712 patients undergoing the Lariat procedure, the overall acute success rate with Lariat deployment is 95.5%. Follow-up TEE showed a leak of 2 to 5 mm in 6.5% and a thrombus in 2.5%. One patient had a leak of greater than 5 mm. Cardiac perforation occurred in 3.5%, with less than half of cases requiring surgical repair. Delayed complications (pericarditis requiring protracted treatment, and pericardial

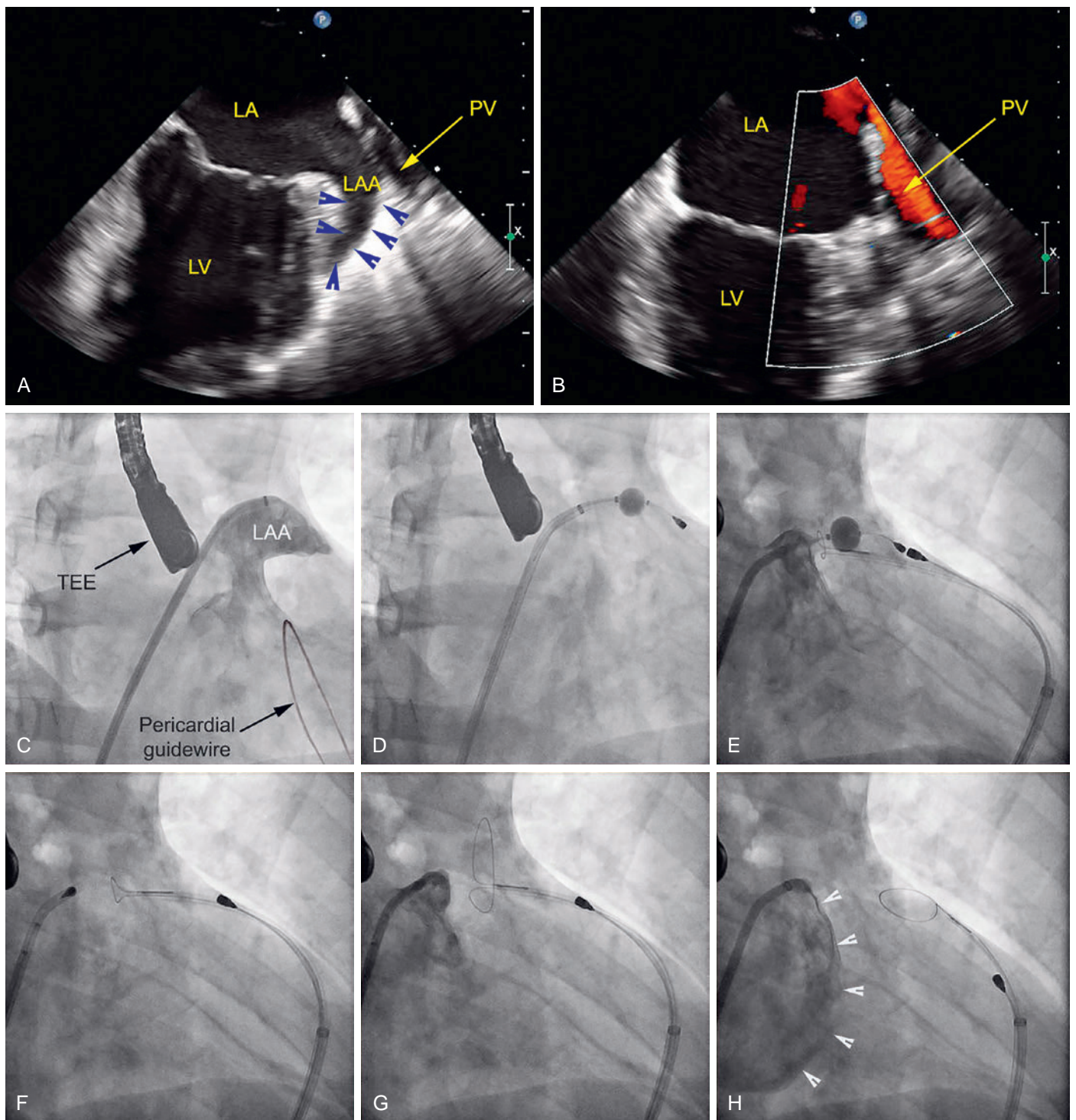


Fig. 15.70 Percutaneous Left Atrial Appendage (LAA) Ligation Using the Lariat Device. Transesophageal echocardiography (TEE, A and B) and fluoroscopic images (C–H, caudal right anterior oblique projections) during Lariat ligation of the LAA. (A) TEE at baseline showing the LAA. (B) TEE Doppler image after LAA ligation showing obliteration of the LAA, with no flow jet in the LAA. Flow can be seen in the left superior pulmonary vein (PV) adjacent to the LAA. (C) After obtaining pericardial access (pericardial guidewire is visualized), left atrial (LA) access is obtained via a transseptal atrial puncture. The transseptal sheath and a pigtail catheter are positioned within the LAA. Contrast angiography of the LAA is performed to delineate LAA anatomy. (D) The endocardial magnet-tipped guidewire is placed in the most anterosuperior aspect of the LAA. The balloon is inflated and positioned just distal to the ostium of the LAA. (E) The epicardial magnet-tipped guide wire is advanced via the pericardial sheath and navigated toward the endocardial magnet-tipped guidewire until both magnets connect end to end. Then, the Lariat is guided along the epicardial guidewire, and the snare is tightened around the base of LAA. Exclusion of the LAA by the closed snare is confirmed by angiography (via the transseptal sheath). (F) The occlusion balloon is deflated and the magnet-tipped guidewires are disconnected. The preloaded, pretied suture is then released from the snare and tightened. (G) LAA closure is verified again with angiography. (H) The Lariat device is then pulled back off the LAA. Contrast angiography (via the transseptal sheath) of the LA (arrowhead delineate the LA border outlined by the contrast dye) confirms complete exclusion of the LAA. LV, Left ventricle.

and pleural effusion after discharge) occurred in 4.8%. Some technical modifications appear to have improved procedure safety in this study as compared to previous studies, including the use of micropuncture needle to access the pericardial space (which reduced the incidence of pericardial perforation), and the periprocedural use of colchicine (which reduced the incidence and severity of pericarditis).³⁰¹

It is important to note the Lariat procedure can potentially fill a void of therapeutic options for patients who cannot take oral anticoagulation. However, appropriate patient selection is critical for procedure success and safety. LAA size and anatomy should be carefully evaluated prior to the procedure. In a recent large study, almost 25% of patients who were initially thought to be Lariat eligible were excluded because of anatomic issues.³⁰¹

The role of LAA ligation seems to extend to arrhythmia reduction as well. The LAA can potentially play an important role in initiation and perpetuation of AF, which can be responsible for arrhythmia recurrence following PV isolation procedures. Hence, electrical isolation of the LAA is being increasingly considered in selected patients. Endocardial RF ablation has been traditionally used to achieve electrical isolation of the LAA. In patients undergoing cardiac surgery and epicardial ablation for AF, LAA ligation or excision has been shown in some (but not all) studies to enhance arrhythmia-free survival. Recently, percutaneous ligation of the LAA using the Lariat procedure was found to result in both mechanical and electrical exclusion of LAA, likely secondary to ischemic necrosis of the LAA distal to the ligation site. Initial reports have demonstrated a potential value this procedure as adjunct to catheter ablation of nonparoxysmal AF. The value of sequential Lariat ligation of the LAA with AF ablation is being evaluated in patients with persistent AF is currently being investigated.^{301–304}

Pericardial Bleeding

Intrapericardial bleeding can complicate the pericardial access as well as the atrial septal puncture (see Chapter 4). Further, bleeding can result from perforation of the LAA during placement of the magnet-tipped guidewire or snaring the LAA, and LAA laceration or avulsion during tightening of the suture.³⁰⁰

Pericardial bleeding related to the epicardial access procedure is most commonly a result of RV puncture. Laceration of the myocardium or epicardial vessels can occur during manipulation of the pericardial sheath. The use of the “needle-in-needle” technique can help reduce the risk of significant bleeding in the setting of inadvertent RV puncture. Also, careful sheath manipulation and leading with a guidewire before advancing or moving the curl of the pericardial sheath are imperative to reduce the risk of abrasion or laceration of pericardial structures.

RV puncture is usually benign if only the needle or guidewire has entered the chamber in a patient who is not anticoagulated. It is not uncommon to aspirate 10 to 30 mL of bloody drainage from the pericardial sheath early in the procedure. At this point, anticoagulation should not have been administered; therefore any bleeding should be self-limited and is generally considered a minor complication because it is not necessary to interrupt the procedure. Systemic anticoagulation with IV heparin is started when subsequent atrial transseptal puncture is performed, but only after verifying the absence of continued pericardial bleeding. However, persistent or severe pericardial bleeding can occur, occasionally requiring surgical intervention. Therefore precautions must be in place for managing severe bleeding, including availability of appropriate surgical expertise.³⁰⁰

The risk of LAA laceration or avulsion can be increased by overprolapsing or twisting the Lariat device during tightening of the suture. In addition, ligating the LAA distal to its ostium or releasing the suture on only one lobe of a multilobed LAA can increase the likelihood of tearing the LAA due to the friability and thinness of the LAA tissue.³⁰⁰

Pericarditis

Pericarditis is a common complication of the Lariat procedure, and likely the result of the profound inflammatory response to LAA ligation. Postprocedural pericarditis typically manifests as precordial discomfort and friction rub, and often is mild and self-limiting, resolving within a few days with oral nonsteroidal antiinflammatory agents. It is important to note that inflammatory pericarditis can render the epicardial space percutaneously inaccessible for repeat procedures.²⁹⁸

Prophylaxis with colchicine or nonsteroidal antiinflammatory drugs is often used to prevent Dressler syndrome. Oral steroids may be considered for the treatment of refractory cases. Although injection of steroids into the pericardial space has been used following epicardial ablation procedures to help reduce postprocedural pericarditis, this approach has not been recommended following LAA ligation due to the concern of potential interference with the healing process necessary for the complete chronic closure of the LAA. A transthoracic echocardiogram is recommended 7 days after the procedure if the patient has persistent pericarditis to assess for a pericardial effusion (Dressler syndrome). Late pericardial effusion can be transudative or exudative and may represent volume retention from reduced ANP release after LAA ligation.²⁹⁸

Incomplete Appendage Closure and Thrombus Formation

Percutaneous suture ligation of LAA results in extensive inflammation of LAA leading to fibrosis, scarring, and permanent closure of LAA, with complete endothelialization of the endocardial surface at suture site. The inflammatory reaction can also involve the LA, which can potentially promote thrombus formation.

A 2.2% incidence of LAA orifice thrombus has been reported during follow-up surveillance. Thrombus formation can result from an inflammatory reaction at the ligation site, epithelial denuding at the LAA orifice during balloon catheter retrieval, and suboptimal suture deployment. Loosening of the knot and tissue necrosis at the suture site are potential mechanisms of thromboembolic complications.

Incomplete LAA ligation after Lariat is not uncommon. In a significant proportion of patients undergoing the Lariat procedure, a partial LAA opening with a residual LAA cavity develops. In one report, intraprocedural residual flow into the LAA (leak) were observed in 10% of patients, while 32% had recanalized residual LAA cavities, which were morphologically similar to the original LAA, albeit significantly smaller in volume. Nonetheless, the Lariat device appears to be associated with a lower rate of leaks at 1 year as compared with the Watchman device. Further, the leaks following the Lariat procedure tend to be smaller and concentric (gunny sack effect), as compared to the eccentric leak (edge effect) following the Watchman procedure. The implications of a small leak (less than 5 mm) are unknown. If the leak is greater than 5 mm, alternate stroke prevention measures should be considered.^{305,306}

SURGICAL LEFT ATRIAL APPENDAGE EXCLUSION

Open surgical LAA amputation, suture ligation, or stapling is commonly performed in patients with AF who are undergoing valvular or coronary artery bypass surgery or as an adjunct to the maze procedure. In addition, various minimally invasive thorascopic LAA exclusion techniques (LAA excision, stapling, and clipping) have emerged as isolated surgical procedures or in conjunction with minimally invasive maze procedures for ablation of AF. Recently, thorascopic stand-alone LAA exclusion has been reported in a small group of patients with contraindications to anticoagulation. However, data are still limited regarding its efficacy and safety of these approaches. Also, dedicated LAA exclusion devices have been developed, including the AtriClip Device System (AtriCure, West Chester, OH, United States) and the Tiger Paw System (Maquet

Cardiovascular, Wayne, NJ, United States). Initial studies using the AtriClip demonstrated significant improvement in procedure success and safety.¹²²

An important limitation to surgical exclusion of the LAA is the high rate of incomplete exclusion of the LAA, which is said to range from 10% to 80%, depending on the surgical technique. Most clinical trials reported rates of successful LAA occlusion of only 55% to 66%. The highest success of complete LAA occlusion was with surgical excision and the lowest with LAA suture ligation or stapling. Dehiscence of the sutures can result in reopening of the LAA orifice or persistent flow between the appendage and the LA (eFig. 15.30).

The presence of incomplete LAA occlusion can promote thrombus formation secondary to blood stagnation, and is associated with a significantly higher risk of ischemic stroke/systemic embolization than complete LAA closure or LAA stump. In one report, 41% of patients with unsuccessful exclusion had LAA thrombus whereas there was none with excision. Furthermore, the rate of systemic thromboembolism in patients with incomplete LAA closure and not receiving oral anticoagulation therapy is three to five times greater than that predicted by CHADS₂ CHA₂DS₂-VASc score risk-stratification schemes. As such, routine postoperative screening for incomplete appendage ligation (by TEE or CT angiography) is recommended before discontinuation of anticoagulation therapy.³⁰⁷

Currently, no strong evidence exists to support the benefit of surgical LAA exclusion during routine cardiac surgery as a potential strategy to decrease the incidence of stroke in AF patients. In a meta-analysis of five clinical trials involving 1400 patients undergoing LAA exclusion or excision there appeared to be no clear benefit for LAA surgical exclusion, primarily due to the high rates of incomplete occlusion of the LAA as demonstrated by TEE. On the other hand, findings of a more recent meta-analysis suggested a potential benefit of surgical LAA resection in reducing the incidence of stroke in short- and long-term follow-up, although the statistical power was limited. Future prospective, randomized trials are necessary to definitively assess the long-term benefits and risks of LAA exclusion during cardiac surgery.³⁰⁸

VIDEOS

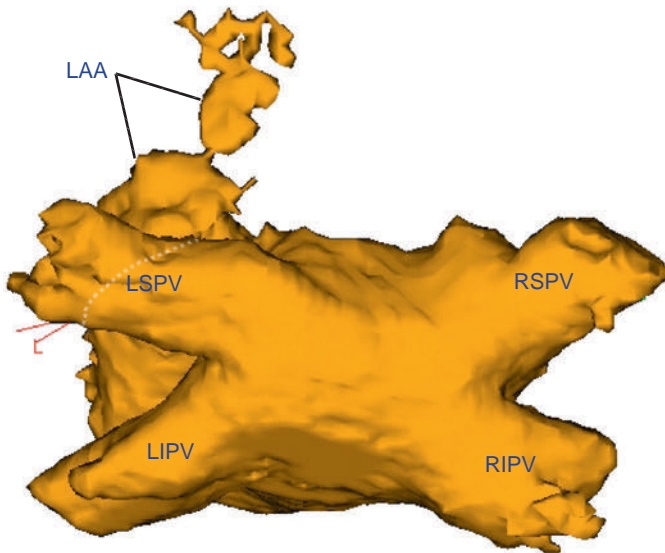
The following videos accompany this chapter:

- ▶ See **Video 6.22.** Cardiac Anatomy (Segmented computed tomography)
- ▶ See **Video 6.23.** Segmented Computed Tomography of the Left Atrium and Pulmonary Veins
- ▶ **Video 15.1.** Left Atrial Appendage Imaging: Intracardiac Echocardiography (ICE)
- ▶ See **Video 6.4.** Fast Anatomic Mapping (FAM): CARTO-3
- ▶ **Video 15.2.** Circumferential Antral Pulmonary Vein Isolation: CARTO Merge
- ▶ See **Video 6.21.** CARTO Sound: Ablation of Atrial Fibrillation
- ▶ See **Video 6.15.** Electrical Isolation of the Pulmonary Veins and Left Atrial Posterior Wall: Rhythmia Voltage Mapping
- ▶ **Video 15.3.** Mapping Gaps in Circumferential Pulmonary Vein Ablation Lines: Rhythmia Activation and Propagation Maps
- ▶ See **Video 7.2.** Cryoballoon Pulmonary Vein Isolation: Contrast Angiography for Assessment of Vein Occlusion
- ▶ See **Video 7.1.** Cryoballoon Positioning for Pulmonary Vein Isolation: Contrast Pulmonary Vein Angiography
- ▶ See **Video 7.3.** Cryoballoon Positioning for Pulmonary Vein Isolation: Intracardiac Echocardiography
- ▶ See **Video 7.4.** Laser Balloon Pulmonary Vein Isolation
- ▶ **Video 15.4.** Phrenic Nerve Function Monitoring Using Intracardiac Echocardiography (ICE)

- Video 15.5.** Right Superior Pulmonary Vein Occlusion: Transesophageal Echocardiography (TEE) Before and After Stenting
- Video 15.6.** Right Superior Pulmonary Vein Occlusion: Computed Tomography (CT) Before and After Stenting
- Video 15.7.** Pulmonary Vein Stenting
- Video 15.8.** Atrioesophageal Fistula: Computed Tomography (CT)
- Video 15.9.** Pneumopericardium: Computed Tomography Scan of the Chest
- See **Video 13.1.** Clockwise and Counterclockwise Perimitral Left Atrial Macroreentry: CARTO Activation and Propagation Maps
- See **Video 13.2.** Macroreentrant Atrial Tachycardia (involving the pulmonary veins): Rhythmia Propagation, Activation, and Voltage Maps
- See **Video 6.11.** Macroreentrant Atrial Tachycardia (Related to Gaps in LA Roof Ablation Line): CARTO Activation and Propagation Maps
- See **Video 6.12.** Macroreentrant Atrial Tachycardia (Involving the LA Posterior Wall): Rhythmia Activation and Propagation Maps
- See **Video 6.13.** Small Atrial Macroreentry: Rhythmia Activation and Propagation Maps
- See **Video 6.14.** Ripple Mapping: Mapping Gaps in Ablation Line
- Video 15.10.** Left Atrial Appendage Device Closure (Watchman Device)
- Video 15.11.** Transesophageal Echocardiography (TEE) Imaging of the Left Atrial Appendage During Watchman Device Placement
- Video 15.12.** Left Atrial Appendage (LAA) Device Closure: Watchman Device Partial Retrieval
- Video 15.13.** Watchman Device Implantation: Complete Device Retrieval
- Video 15.14.** Watchman Device Embolization
- Video 15.15.** Percutaneous Left Atrial Appendage (LAA) Ligation (Lariat): TEE Imaging
- Video 15.16.** Percutaneous Left Atrial Appendage (LAA) Ligation (Lariat)

REFERENCES

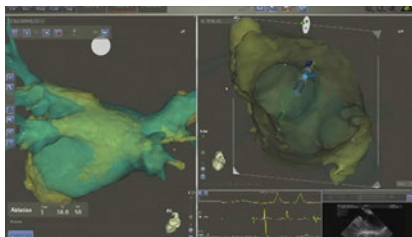
1. Calkins H, et al. 2017 HRS/EHRA/ECAS/APHRS/SOLAECE expert consensus statement on catheter and surgical ablation of atrial fibrillation. *Heart Rhythm*. 2017;14:e275–e444.
2. Charitos EI, Pürerfellner H, Glotzer TV, et al. Clinical classifications of atrial fibrillation poorly reflect its temporal persistence: insights from 1,195 patients continuously monitored with implantable devices. *J Am Coll Cardiol*. 2014;63:2840–2848.
3. Breithardt G, et al. Valvular heart disease among non-valvular atrial fibrillation: a misnomer, in search of a new term. *Eur Heart J*. 2015;36:1794–1797.
4. January CT, et al. 2014 AHA/ACC/HRS guideline for the management of patients with atrial fibrillation: a report of the American College of Cardiology/American Heart Association Task Force on practice guidelines and the Heart Rhythm Society. *J Am Coll Cardiol*. 2014;64:e1–e76.
5. Wyse DG, et al. Lone atrial fibrillation: does it exist? *J Am Coll Cardiol*. 2014;63:1715–1723.
6. Page SE. The substrate in “early persistent” atrial fibrillation. *JACC Clin Electrophysiol*. 2016;2:140–142.
7. Lau DH, et al. Novel mechanisms in the pathogenesis of atrial fibrillation: practical applications. *Eur Heart J*. 2016;37:1573–1581.
8. Nattel S, Dobrev D. Controversies about atrial fibrillation mechanisms: aiming for order in chaos and whether it matters. *Circ Res*. 2017;120:1396–1398.
9. Staerk L, et al. Atrial fibrillation: epidemiology, pathophysiology, and clinical outcomes. *Circ Res*. 2017;120:1501–1517.
10. Santangeli P, et al. Prevalence and distribution of focal triggers in persistent and long-standing persistent atrial fibrillation. *Heart Rhythm*. 2016;13:374–382.
11. Weiss JN, Qu Z, Shivkumar K. Ablating atrial fibrillation: a translational science perspective for clinicians. *Heart Rhythm*. 2016;13:1868–1877.
12. Moe GK, et al. A computer model of atrial fibrillation. *Am Heart J*. 1964;67:200–220.



eFig. 15.30 Incomplete Surgical Occlusion of the Left Atrial Appendage (LAA). Three-dimensional cardiac computed tomography scan of the left atrium and pulmonary veins (PVs) (cranial posteroanterior view) of a patient who had undergone a thoracoscopic maze procedure with LAA ligation, and had recurrent atrial fibrillation. The LAA has a narrow stalk in the middle, at the presumed ligation point. Dotted (behind left superior pulmonary vein [LSPV])/dashed white lines indicate the actual orifice of the LAA, where ligation should have occurred. LIPV, Left inferior PV; RSPV, right superior PV; RIPV, right inferior PV.



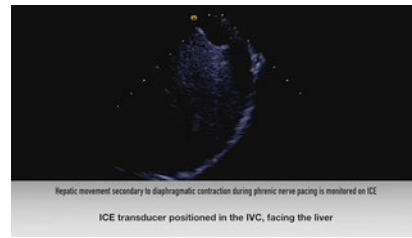
Video 15.1 Left Atrial Appendage Imaging: Intracardiac Echocardiography (ICE). ICE imaging of the LAA showing a thrombus in the LAA. Images are obtained with the ICE transducer positioned in the PA and then at the tricuspid annulus. LA, Left atrium; LAA, left atrial appendage; LV, left ventricle; PA, pulmonary artery.



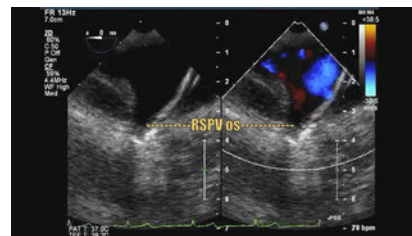
Video 15.2 Circumferential Antral Pulmonary Vein Isolation: CARTO Merge. The CARTO-Merge Module allows for images from a preacquired computed tomography angiogram of the left atrium (LA) and pulmonary veins (PVs) to be integrated on the electroanatomic image of the cardiac chamber created with the CARTO system. Shown are posteroanterior (PA) view of the LA and a cardioscopic view of the antrum of the left inferior PV (LIPV). CARTO-3 allows visualization of both the ablation and ring catheters. A surface electrocardiogram lead and ablation catheter recording are continuously monitored. Real-time intracardiac echocardiography (ICE) of the LA, LIPV, and left ventricle (LV) is also obtained to monitor catheter positioning as well as to monitor for the potential development of pericardial effusion. The ring catheter is positioned at the ostium of the LIPV. Ablation is commenced at the posterior aspect of the LIPV antrum. Radiofrequency (RF) energy is delivered in short applications (for 2 to 5 seconds) at a higher power (50 W, irrigation rate 30 mL/min, maximum temperature 43°C). The ablation catheter is dragged continuously in small increments every 2 to 5 seconds during continuous RF delivery, and ablation is repeated at each site, if required, for many times throughout the procedure until the local atrial electrogram is completely eliminated.



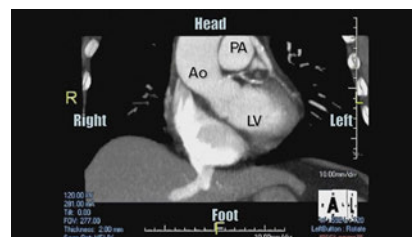
Video 15.3 Mapping Gaps in Circumferential Pulmonary Vein Ablation Lines: Rhythmia Activation and Propagation Maps. Electroanatomic (Rhythmia) activation and propagation maps of the left atrium (LA) acquired during atrial pacing in a patient with prior history of catheter ablation of atrial fibrillation (circumferential pulmonary vein [PV] isolation and LA roof linear ablation). Propagation and activation maps demonstrate two conduction gaps in the previous circumferential ablation lines around the left-sided PVs. After radiofrequency (RF) ablation targeting the gaps, repeat activation map demonstrated complete PV isolation. LAA, Left atrial appendage; LIPV, left inferior PV; LSPV, left superior PV; MA, mitral annulus.



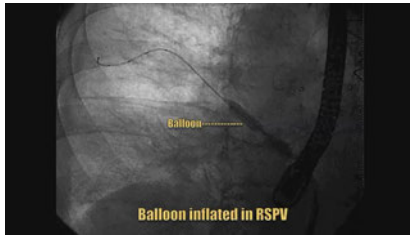
Video 15.4 Phrenic Nerve Function Monitoring Using Intracardiac Echocardiography (ICE). For monitoring right phrenic nerve function (during laser or cryoballoon isolation of the right superior pulmonary vein), a diagnostic catheter is positioned at the anterolateral aspect of the superior vena cava at a site above the level of ablation where the phrenic nerve can be consistently captured. ICE (with the transducer positioned in the inferior vena cava [IVC] at the level of the diaphragm and pointed at the liver) is used to continuously visualize hepatic movement from the diaphragmatic excursion, indicative of successful phrenic nerve capture during continuous pacing. Initially, hepatic movement is observed at the pacing rate. Later, hepatic movement decreases, indicating reduction of the strength of the diaphragmatic contraction and phrenic nerve injury.



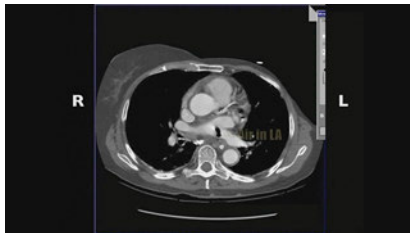
Video 15.5 Right Superior Pulmonary Vein Occlusion: Transesophageal Echocardiography (TEE) Before and After Stenting. TEE in a patient with total occlusion of the right superior pulmonary vein (RSPV) postablation of atrial fibrillation. At baseline, the RSPV is completely occluded with no flow on color Doppler. After intervention, the stent is visualized at the ostium of the RSPV, and blood flow is now restored.



Video 15.6 Right Superior Pulmonary Vein Occlusion: Computed Tomography (CT) Before and After Stenting. Cardiac CT in a patient with total occlusion of the right superior pulmonary vein (RSPV) postablation of atrial fibrillation. Horizontal sections of the CT scan are arranged serially from cephalic to caudal direction demonstrating complete absence of the RSPV. Parasagittal sections of the CT scan are arranged serially from anterior to posterior direction demonstrating complete absence of the RSPV. Parasagittal sections of the CT scan are arranged serially from anterior to posterior direction following stenting of the RSPV demonstrate patent stent. A, Anterior; Ao, aorta; F, foot; H, head; L, left; LA, left atrium; LIPV, left inferior pulmonary vein; LV, left ventricle; LSPV, left superior pulmonary vein; P, posterior; PA, pulmonary artery; R, right; RA, right atrium; RIPV, right inferior pulmonary vein; RV, right ventricle.



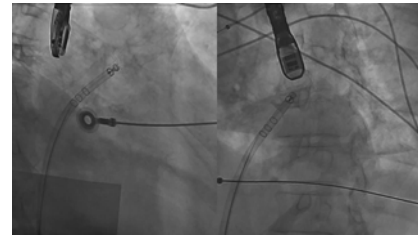
Video 15.7 Pulmonary Vein Stenting. A series of angiograms in a patient with total occlusion of the right superior pulmonary vein (RSPV) postablation of atrial fibrillation. Angiography of the right pulmonary artery is performed. The levophase of the angiogram reveals filling of the left atrium mainly via the right inferior pulmonary vein (RIPV, which has mild ostial stenosis). However, the RSPV is absent due to complete occlusion. Note the severely reduced perfusion of the upper and middle lobes of the right lung compared to the lower lobe. Contrast injection in the antrum of the RSPV confirms complete occlusion of the vein. An angioplasty wire is advanced through the occluded vein. An angioplasty balloon is inflated in the RSPV. After stenting, venous flow is restored, and contrast injection at the antrum of the RIPV reveals patent RIPV and RIPV. Severe ostial stenosis of the right middle pulmonary vein (RMPV) is also observed.



Video 15.8 Atrioesophageal Fistula: Computed Tomography (CT). Cardiac CT in a patient with an atrioesophageal fistula postablation of atrial fibrillation (AF). Horizontal sections of the CT scan are arranged serially from cephalic to caudal direction demonstrating normal cardiac anatomy. Shown are CT scan prior to ablation and repeat CT scan performed 6 days postablation. Horizontal sections of the CT scan demonstrating air embolus into the left atrium (LA) and at the level of the MV. LV, Left ventricle; MV, mitral valve; NGT, nasogastric tube positioned in the esophagus.



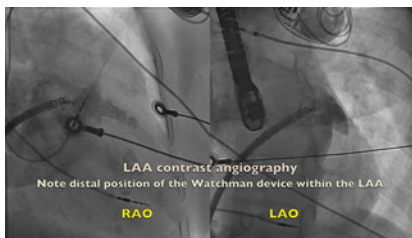
Video 15.9 Pneumopericardium: Computed Tomography Scan of the Chest. Computed tomography scan of the chest was obtained in a patient presenting with chest pain 2 weeks after undergoing catheter ablation of atrial fibrillation. Air accumulation within the pericardial space is observed. No intracardiac air is observed.



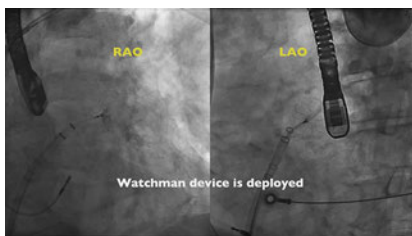
Video 15.10 Left Atrial Appendage (LAA) Device Closure (Watchman Device). Fluoroscopic images are shown in the right anterior oblique (RAO) and left anterior oblique (LAO) views during LAA closure with the Watchman device. After transseptal atrial puncture, a pigtail catheter is advanced through the access sheath and used to facilitate catheterization of the LAA. Then, contrast angiography of the LAA is performed to assess LAA anatomy. Subsequently, the Watchman device is advanced via a delivery catheter in the access sheath until the marker of the device catheter matches the most distal marker on the access sheath. Contrast angiography is repeated to assess device sizing and guide device delivery and deployment. Once the proper position of the sheathed device within the LAA is confirmed by biplane fluoroscopy and TEE, the device is deployed (unsheathed) by retracting the access sheath and delivery catheter simultaneously while maintaining device position. Left atrium (LA) angiography is used to verify proper positioning and stability. A tug test is performed to confirm proper anchoring of the device; the access sheath is withdrawn 1 to 2 cm from the face of the device and the deployment knob is gently retracted and released. Then, the device is released by counterclockwise rotation of the delivery catheter.



Video 15.11 Transesophageal Echocardiography (TEE) Imaging of the Left Atrial Appendage During Watchman Device Placement. TEE imaging is performed at baseline to evaluate the size of the left atrial appendage (LAA) and exclude the presence of LAA thrombus. The dimensions of the LAA are measured in multiple angles. After deployment of the Watchman device, TEE is used to assess appropriate landing zone of the device, adequate device compression, and adequate seal of the LAA.



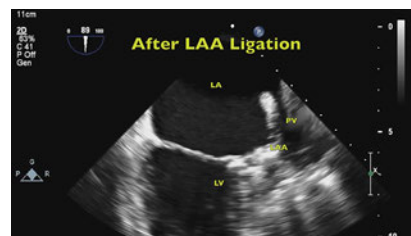
Video 15.12 Left Atrial Appendage (LAA) Device Closure: Watchman Device Partial Retrieval. Fluoroscopic images are shown in the right anterior oblique (RAO) and left anterior oblique (LAO) views during LAA closure with the Watchman device. After transseptal atrial puncture, a pigtail catheter is advanced through the access sheath and used to facilitate catheterization of the LAA. Then, contrast angiography of the LAA is performed to assess LAA anatomy. Subsequently, the Watchman device is advanced via a delivery catheter in the access sheath. Note proximal marker is more distal to the plane of the LAA ostium. The device is deployed (unsheathed) by retracting the access sheath and delivery catheter simultaneously while maintaining device position. Left atrium (LA) angiography and transesophageal echocardiography (TEE) images showed an inappropriately distal position of the Watchman device within the LAA, failing to seal the entire LAA ostium. Partial retrieval of the device was performed and the device was redeployed more proximally, with LA angiography and TEE images confirming appropriate device position.



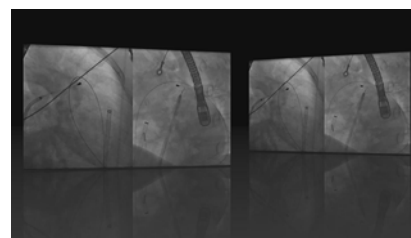
Video 15.13 Watchman Device Implantation: Complete Device Retrieval. Fluoroscopic images are shown in the right anterior oblique (RAO) and left anterior oblique (LAO) views during left atrial appendage (LAA) closure with the Watchman device. After transseptal atrial puncture, a pigtail catheter is advanced through the access sheath and used to facilitate catheterization of the LAA. Then, contrast angiography of the LAA is performed to assess LAA anatomy. Note the noncoaxial engagement of the access sheath to the LAA. Subsequently, the Watchman device is advanced via a delivery catheter in the access sheath. The device is deployed (unsheathed) by retracting the access sheath and delivery catheter simultaneously while maintaining device position. LAA angiography and transesophageal echocardiography (TEE) reveals proximal and noncoaxial position of the Watchman device. Complete retrieval of the device was performed.



Video 15.14 Watchman Device Embolization. Fluoroscopic images are shown in the right anterior oblique (RAO) projection during left atrial appendage (LAA) closure with the Watchman device. After transseptal atrial puncture, a pigtail catheter is advanced through the access sheath and used to facilitate catheterization of the LAA. Then, contrast angiography of the LAA is performed to assess LAA anatomy. Note the shallow depth of the LAA compared to the width of the ostium. Subsequently, the Watchman device is advanced via a delivery catheter in the access sheath. The device is deployed (unsheathed) by retracting the access sheath and delivery catheter simultaneously while maintaining device position. LAA angiography and TEE reveals a proximal position of the Watchman device. The Watchman device could not be visualized on the chest x-ray performed on the day following the procedure. Therefore a CT scan of the chest was performed to look for the Watchman device. The device was found to have embolized into the abdominal aorta. The device could be retrieved via a trans-femoral arterial approach.



Video 15.15 Percutaneous Left Atrial Appendage (LAA) Ligation (Lariat): Transesophageal Echocardiography (TEE) Imaging. TEE imaging is performed at baseline to evaluate the size of the LAA and exclude the presence of LAA thrombus. After LAA ligation, TEE is used to assess adequate seal of the LAA. LA, Left atrium; LV, left ventricle; PV, pulmonary vein.



Video 15.16 Percutaneous Left Atrial Appendage (LAA) Ligation (Lariat). Fluoroscopic images are shown in the right anterior oblique (RAO) and left anterior oblique (LAO) views during percutaneous LAA ligation (the Lariat procedure). After transseptal atrial puncture, a pigtail catheter is advanced through the access sheath and used to facilitate catheterization of the LAA. Then, contrast angiography of the LAA is performed to assess A pigtail catheter is advanced over the guidewire into the LAA and contrast angiography is performed to assess the LAA size and orientation. Then, the pigtail catheter is removed and the endovascular magnet-tipped guidewire is advanced and carefully navigated to in the most anterosuperior aspect of the LAA. The epicardial magnet-tipped guide wire is then introduced into the pericardial space through the epicardial sheath and carefully navigated towards the endocardial magnet-tipped guidewire until both magnets connect end to end. The Lariat is back-loaded over the epicardial magnet-tipped guidewire and advanced to snare and ligate the LAA. Left atrium (LA) angiography is performed to confirm complete closure of the LAA.

13. Quintanilla JG, et al. Mechanistic approaches to detect, target, and ablate the drivers of atrial fibrillation. *Circ Arrhythmia Electrophysiol.* 2016;9:1–12.
14. Carrick RT, Benson BE, Bates JHT, et al. Prospective, tissue-specific optimization of ablation for multiwavelet reentry: predicting the required amount, location, and configuration of lesions. *Circ Arrhythmia Electrophysiol.* 2016;9:e003555.
15. Hansen BJ, et al. Atrial fibrillation driven by micro-anatomic intramural re-entry revealed by simultaneous sub-epicardial and sub-endocardial optical mapping in explanted human hearts. *Eur Heart J.* 2015;36:2390–2401.
16. Laughner J, et al. Practical considerations of mapping persistent atrial fibrillation with whole-chamber basket catheters. *JACC Clin Electrophysiol.* 2016;2:55–65.
17. Lalani GG, et al. Organized sources are spatially conserved in recurrent compared to pre-ablation atrial fibrillation: further evidence for non-random electrical substrates. *J Cardiovasc Electrophysiol.* 2016;661–669.
18. Walters TE, et al. Temporal stability of rotors and atrial activation patterns in persistent human atrial fibrillation: a high-density epicardial mapping study of prolonged recordings. *JACC Clin Electrophysiol.* 2015;1:14–24.
19. Haissaguerre M, et al. Noninvasive panoramic mapping of human atrial fibrillation mechanisms: a feasibility report. *J Cardiovasc Electrophysiol.* 2013;24:711–717.
20. Lim HS, et al. Noninvasive mapping to guide atrial fibrillation ablation. *Card Electrophysiol Clin.* 2015;7:89–98.
21. Schricker AA, Lalani GG, Krummen DE, et al. Rotors as drivers of atrial fibrillation and targets for ablation. *Curr Cardiol Rep.* 2014;16:509.
22. Hansen BJ, et al. Advances in arrhythmia and electrophysiology maintenance of atrial fibrillation are reentrant drivers with spatial stability the key? *Circ Arrhythmia Electrophysiol.* 2016;9:e004398.
23. Roney CH, et al. Spatial resolution requirements for accurate identification of drivers of atrial fibrillation. *Circ Arrhythmia Electrophysiol.* 2017;10:e004899.
24. Vijayakumar R, Vasireddi SK, Cuculich PS, et al. Methodology considerations in phase mapping of human cardiac arrhythmias. *Circ Arrhythmia Electrophysiol.* 2016;9:e004409.
25. Ng J, Goldberger JJ. Understanding and interpreting dominant frequency analysis of AF electrograms. *J Cardiovasc Electrophysiol.* 2007;18:680–685.
26. Dzeshka MS, Lip GYH, Snezhitskiy V, et al. Cardiac fibrosis in patients with atrial fibrillation: mechanisms and clinical implications. *J Am Coll Cardiol.* 2015;66:943–959.
27. Kottkamp H. Human atrial fibrillation substrate: towards a specific fibrotic atrial cardiomyopathy. *Eur Heart J.* 2013;34:2731–2738.
28. Nattel S. Molecular and cellular mechanisms of atrial fibrosis in atrial fibrillation. *JACC Clin Electrophysiol.* 2017;3:425–435.
29. Hansen BJ, Zhao J, Fedorov VV. Fibrosis and atrial fibrillation: computerized and optical mapping. *JACC Clin Electrophysiol.* 2017;3:531–546.
30. Kottkamp H, Bender R, Berg J. Catheter ablation of atrial fibrillation how to modify the substrate? *J Am Coll Cardiol.* 2015;65:196–206.
31. Dewland TA, et al. Inflammation as a mediator of the association between race and atrial fibrillation results from the health ABC study (Health, Aging, and Body Composition). *JACC Clin Electrophysiol.* 2015;1:248–255.
32. Sirish P, et al. Molecular mechanisms and new treatment paradigm for atrial fibrillation. *Circ Arrhythm Electrophysiol.* 2016;9:e003721.
33. Nattel S, Harada M. Atrial remodeling and atrial fibrillation: recent advances and translational perspectives. *J Am Coll Cardiol.* 2014;63:2335–2345.
34. Jalife J, Kaur K. Atrial remodeling, fibrosis, and atrial fibrillation. *Trends Cardiovasc Med.* 2015;25:475–484.
35. Maury P, et al. Lack of correlations between electrophysiological and anatomical-mechanical atrial remodeling in patients with atrial fibrillation. *Pacing Clin Electrophysiol.* 2015;38:617–624.
36. McManus DD, et al. Plasma microRNAs are associated with atrial fibrillation and change after catheter ablation (the miRhythm study). *Heart Rhythm.* 2015;12:3–10.
37. Rivarola EW, et al. Targets and end points in cardiac autonomic denervation procedures. *Circ Arrhythmia Electrophysiol.* 2017;10:e004638.
38. Stavarakis S, et al. Low-level transcutaneous electrical vagus nerve stimulation suppresses atrial fibrillation. *J Am Coll Cardiol.* 2015;65:867–875.
39. Wang X, et al. Long-term effects of ganglionated plexi ablation on electrophysiological characteristics and neuron remodeling in target atrial tissues in a canine model. *Circ Arrhythmia Electrophysiol.* 2015;8:1276–1283.
40. Huang J-H, et al. Modulation of autonomic nervous activity in the termination of paroxysmal atrial fibrillation. *Pacing Clin Electrophysiol.* 2017;40:401–408.
41. Stavarakis S, et al. The role of the autonomic ganglia in atrial fibrillation. *JACC Clin Electrophysiol.* 2015;1:1–13.
42. Driessen AHG, et al. Ganglion plexus ablation in advanced atrial fibrillation: the AFACT study. *J Am Coll Cardiol.* 2016;68:1155–1165.
43. Linz D, Ukena C, Mahfoud F, et al. Atrial autonomic innervation: a target for interventional antiarrhythmic therapy? *J Am Coll Cardiol.* 2014;63:215–224.
44. Gorenek B, et al. European Heart Rhythm Association (EHRA)/European Association of Cardiovascular Prevention and Rehabilitation (EACPR) position paper on how to prevent atrial fibrillation endorsed by the Heart Rhythm Society (HRS) and Asia Pacific Heart Rhythm Society (APHRS). *Europace.* 2017;19:190–225.
45. Enriquez A, Antzelevitch C, Bismah V, et al. Atrial fibrillation in inherited cardiac channelopathies: from mechanisms to management. *Heart Rhythm.* 2016;13:1878–1884.
46. Hayashi K, et al. Functional characterization of rare variants implicated in susceptibility to lone atrial fibrillation. *Circ Arrhythmia Electrophysiol.* 2015;8:1095–1104.
47. Anumonwo JMB, Kalifa J. Risk factors and genetics of atrial fibrillation. *Cardiol Clin.* 2014;32:485–494.
48. Lubitz SA, et al. Novel genetic markers associate with atrial fibrillation risk in Europeans and Japanese. *J Am Coll Cardiol.* 2014;63:1200–1210.
49. Shoemaker MB, et al. Common genetic variants and response to atrial fibrillation ablation. *Circ Arrhythmia Electrophysiol.* 2015;8:296–302.
50. Krijthe BP, et al. Projections on the number of individuals with atrial fibrillation in the European Union, from 2000 to 2060. *Eur Heart J.* 2013;34:2746–2751.
51. De Sisti A, et al. Evaluation of time course and predicting factors of progression of paroxysmal or persistent atrial fibrillation to permanent atrial fibrillation. *Pacing Clin Electrophysiol.* 2014;37:345–355.
52. Proietti R, et al. A systematic review on the progression of paroxysmal to persistent atrial fibrillation: shedding new light on the effects of catheter ablation. *JACC Clin Electrophysiol.* 2015;1:105–115.
53. Kotecha D, Chudasama R, Lane DA, et al. Atrial fibrillation and heart failure due to reduced versus preserved ejection fraction: a systematic review and meta-analysis of death and adverse outcomes. *Int J Cardiol.* 2016;203:660–666.
54. Gomez-Outes A, et al. Causes of death in anticoagulated patients with atrial fibrillation. *J Am Coll Cardiol.* 2016;68:2508–2521.
55. Kirchhof P, et al. 2016 ESC Guidelines for the management of atrial fibrillation developed in collaboration with EACTS. *Eur Heart J.* 2016;37:2893–2962.
56. Alonso A, et al. Simple risk model predicts incidence of atrial fibrillation in a racially and geographically diverse population: the CHARGE-AF consortium. *J Am Heart Assoc.* 2013;2:e000102.
57. Kolek MJ, et al. Evaluation of a prediction model for the development of atrial fibrillation in a repository of electronic medical records. *JAMA Cardiol.* 2016;1:1007–1013.
58. Rahman F, et al. Trajectories of risk factors and risk of new-onset atrial fibrillation in the Framingham Heart Study. *Hypertens (Dallas, Tex. 1979).* 2016;68:597–605.
59. Pistoia F, et al. The epidemiology of atrial fibrillation and stroke. *Cardiol Clin.* 2016;34:255–268.

60. Jurkko R, et al. Characteristics of atrial fibrillation and comorbidities in familial atrial fibrillation. *J Cardiovasc Electrophysiol.* 2013;24:768–774.
61. Miller JD, et al. Obesity, exercise, obstructive sleep apnea, and modifiable atherosclerotic cardiovascular disease risk factors in atrial fibrillation. *J Am Coll Cardiol.* 2015;66:2899–2906.
62. Leong-Sit P, Tang ASL. Atrial fibrillation and heart failure. *Curr Opin Cardiol.* 2015;30:161–167.
63. Kotecha D. Heart failure with preserved ejection fraction and atrial fibrillation: vicious twins. *J Am Coll Cardiol.* 2016;68:2217–2228.
64. Kotecha D, Piccini JP. Atrial fibrillation in heart failure: what should we do? *Eur Heart J.* 2015;36:3250–3257.
65. Trulock KM, Narayan SM, Piccini JP. Rhythm control in heart failure patients with atrial fibrillation: contemporary challenges including the role of ablation. *J Am Coll Cardiol.* 2014;64:710–721.
66. Violi F, Soliman EZ, Pignatelli P, et al. Atrial fibrillation and myocardial infarction: a systematic review and appraisal of pathophysiologic mechanisms. *J Am Heart Assoc.* 2016;5:e003347.
67. Guo X-Y, et al. Atrial fibrillation is associated with an increased risk of myocardial infarction: insights from a meta-analysis. *Atherosclerosis.* 2016;254:1–7.
68. Soliman EZ, et al. Atrial fibrillation and risk of ST-segment-elevation versus non-ST-segment-elevation myocardial infarction: the Atherosclerosis Risk in Communities (ARIC) Study. *Circulation.* 2015;131:1843–1850.
69. Friedman JK. Atypical atrial tachycardias in patients with congenital heart disease. *Heart Rhythm.* 2008;5:315–317.
70. Arujuna A, de Bono J. Maximizing the effectiveness of ablation for arrhythmias in the congenital heart patients. *Curr Cardiol Rep.* 2016;18:69.
71. Philip Saul J, et al. PACES/HRS expert consensus statement on the use of catheter ablation in children and patients with congenital heart disease. *Heart Rhythm.* 2016;13:e251–e289.
72. Manuguerra R, Callegari S, Corradi D. Inherited structural heart diseases with potential atrial fibrillation occurrence. *J Cardiovasc Electrophysiol.* 2016;27:242–252.
73. Teuwen CP, et al. Time course of atrial fibrillation in patients with congenital heart defects. *Circ Arrhythmia Electrophysiol.* 2015;8:1065–1072.
74. Caples SM, Somers VK. Sleep-disordered breathing and atrial fibrillation. *Prog Cardiovasc Dis.* 2009;51:411–415.
75. Shukla A, et al. Effect of obstructive sleep apnea treatment on atrial fibrillation recurrence: a meta-analysis. *JACC Clin Electrophysiol.* 2015;1:41–51.
76. Qureshi WT, et al. Meta-analysis of continuous positive airway pressure as a therapy of atrial fibrillation in obstructive sleep apnea. *Am J Cardiol.* 2015;116:1767–1773.
77. Wong CX, et al. Obesity and the risk of incident, post-operative, and post-ablation atrial fibrillation: a meta-analysis of 626,603 individuals in 51 studies. *JACC Clin Electrophysiol.* 2015;1:139–152.
78. Nalliah CJ, Sanders P, Kottkamp H, et al. The role of obesity in atrial fibrillation. *Eur Heart J.* 2015;37:1565–1572.
79. Pathak RK, et al. Long-term effect of goal-directed weight management in an atrial fibrillation cohort: a long-term follow-up study (LEGACY). *J Am Coll Cardiol.* 2015;65:2159–2169.
80. Hatem SN. Atrial fibrillation and obesity not just a coincidence. *J Am Coll Cardiol.* 2015;66:12–13.
81. van Rosendaal AR, et al. Association between posterior left atrial adipose tissue mass and atrial fibrillation. *Circ Arrhythmia Electrophysiol.* 2017;10:e004614.
82. Hajhosseiny R, Matthews GK, Lip GYH. Metabolic syndrome, atrial fibrillation, and stroke: tackling an emerging epidemic. *Heart Rhythm.* 2015;12:2332–2343.
83. Pallisgaard JL, et al. Risk of atrial fibrillation in diabetes mellitus: a nationwide cohort study. *Eur J Prev Cardiol.* 2016;23:621–627.
84. Klein I, Danzi S. Thyroid disease and the heart. *Curr Probl Cardiol.* 2016;41:65–92.
85. Bikdeli B, Ziki M, Lip G. Pulmonary embolism and atrial fibrillation: two sides of the same coin? A systematic review. *Semin Thromb Hemost.* 2017;43:849–863.
86. Ng ACC, et al. The prevalence and incidence of atrial fibrillation in patients with acute pulmonary embolism. *PLoS ONE.* 2016;11:e0150448.
87. Mohanty S, et al. Differential association of exercise intensity with risk of atrial fibrillation in men and women: evidence from a meta-analysis. *J Cardiovasc Electrophysiol.* 2016;27:1021–1029.
88. Redpath CJ, Backx PH. Atrial fibrillation and the athletic heart. *Curr Opin Cardiol.* 2015;30:17–23.
89. Larsson SC, Drca N, Wolk A. Alcohol consumption and risk of atrial fibrillation: a prospective study and dose-response meta-analysis. *J Am Coll Cardiol.* 2014;64:281–289.
90. Voskoboinik A, et al. Alcohol and atrial fibrillation: a sobering review. *J Am Coll Cardiol.* 2016;68:2567–2576.
91. McManus DD, et al. Alcohol consumption, left atrial diameter, and atrial fibrillation. *J Am Heart Assoc.* 2016;5:e004060.
92. Qiao Y, et al. Impact of alcohol consumption on substrate remodeling and ablation outcome of paroxysmal atrial fibrillation. *J Am Heart Assoc.* 2015;4:e002349.
93. Dixit S, et al. Secondhand smoke and atrial fibrillation: data from the Health eHeart Study. *Heart Rhythm.* 2016;13:3–9.
94. Tamargo J, Caballero R, Delpón E. Drug-induced atrial fibrillation. *Expert Opin Drug Saf.* 2012;11:615–634.
95. Turagam MK, et al. Circulating biomarkers predictive of postoperative atrial fibrillation. *Cardiol Rev.* 2016;24:76–87.
96. Bidar E, et al. A prospective randomized controlled trial on the incidence and predictors of late-phase postoperative atrial fibrillation up to 30 days and the preventive value of biatrial pacing. *Heart Rhythm.* 2014;11:1156–1162.
97. Yadava M, Hughey AB, Crawford TC. Postoperative atrial fibrillation: incidence, mechanisms, and clinical correlates. *Cardiol Clin.* 2014;32:627–636.
98. Kiaii B, et al. Postoperative atrial fibrillation is not pulmonary vein dependent: results from a randomized trial. *Heart Rhythm.* 2015;12:699–705.
99. Ha ACT, Mazer CD, Verma S, et al. Management of postoperative atrial fibrillation after cardiac surgery. *Curr Opin Cardiol.* 2016;31:183–190.
100. Garimella RS, et al. Accuracy of patient perception of their prevailing rhythm: a comparative analysis of monitor data and questionnaire responses in patients with atrial fibrillation. *Heart Rhythm.* 2015;12:658–665.
101. Xiong Q, Proietti M, Senoo K, et al. Asymptomatic versus symptomatic atrial fibrillation: a systematic review of age/gender differences and cardiovascular outcomes. *Int J Cardiol.* 2015;191:172–177.
102. Dillon P, Ghanbari H. Diagnostic evaluation and follow-up of patients with atrial fibrillation. *Cardiol Clin.* 2014;32:507–519.
103. Benezet-Mazuecos J, Rubio JM, Farr J. Atrial high rate episodes in patients with dual-chamber cardiac implantable electronic devices: unmasking silent atrial fibrillation. *Pacing Clin Electrophysiol.* 2014;37:1080–1086.
104. Chen-Scarabelli C, Scarabelli TM, Ellenbogen KA, et al. Device-detected atrial fibrillation: what to do with asymptomatic patients? *J Am Coll Cardiol.* 2015;65:281–294.
105. Witt CT, et al. Early detection of atrial high rate episodes predicts atrial fibrillation and thromboembolic events in patients with cardiac resynchronization therapy. *Heart Rhythm.* 2015;12:2368–2375.
106. Surapaneni P, Safadi A, Contractor T, et al. Device-detected atrial fibrillation—perils and pitfalls. An update. *Cardiol Clin.* 2016;34:299–306.
107. Tomson TT, Passman R. Management of device-detected atrial high-rate episodes. *Card Electrophysiol Clin.* 2015;7:515–525.
108. Goltzer TV, Ziegler PD. Cryptogenic stroke: is silent atrial fibrillation the culprit? *Heart Rhythm.* 2015;12:234–241.
109. Martin DT, et al. Randomized trial of atrial arrhythmia monitoring to guide anticoagulation in patients with implanted defibrillator and cardiac resynchronization devices. *Eur Heart J.* 2015;36:1660–1668.
110. Kabra R, Girotra S, Vaughan Sarrazin M. Refining stroke prediction in atrial fibrillation patients by addition of African-American ethnicity to CHA2DS2-VASc score. *J Am Coll Cardiol.* 2016;68:461–470.

111. Vanassche T, et al. Risk of ischaemic stroke according to pattern of atrial fibrillation: analysis of 6563 aspirin-treated patients in ACTIVE-A and AVERROES. *Eur Heart J*. 2015;36:281–287.
112. Steinberg BA, et al. Higher risk of death and stroke in patients with persistent vs. paroxysmal atrial fibrillation: results from the ROCKET-AF trial. *Eur Heart J*. 2015;36:288–296.
113. Ganesan AN, et al. The impact of atrial fibrillation type on the risk of thromboembolism, mortality, and bleeding: a systematic review and meta-analysis. *Eur Heart J*. 2016;37:1591–1602.
114. Chao TF, et al. Comparisons of CHADS2 and CHA2DS2-VASc scores for stroke risk stratification in atrial fibrillation: which scoring system should be used for Asians? *Heart Rhythm*. 2016;13:46–53.
115. Chao T-F, et al. Can oral anticoagulants be stopped safely after a successful atrial fibrillation ablation? *J Thorac Dis*. 2015;7:172–177.
116. Van Den Ham HA, Klungel OH, Singer DE, et al. Comparative performance of ATRIA, CHADS2, and CHA2DS2-VASc risk scores predicting stroke in patients with atrial fibrillation: results from a national primary care database. *J Am Coll Cardiol*. 2015;66:1851–1859.
117. Hijazi Z, et al. The ABC (age, biomarkers, clinical history) stroke risk score: a biomarker-based risk score for predicting stroke in atrial fibrillation. *Eur Heart J*. 2016;37:1582–1590.
118. O'Brien EC, et al. The ORBIT bleeding score: a simple bedside score to assess bleeding risk in atrial fibrillation. *Eur Heart J*. 2015;36:3258–3264.
119. Ringwala SM, Tomson TT, Passman RS. Cardiac monitoring for atrial fibrillation in cryptogenic stroke. *Cardiol Clin*. 2016;34:287–297.
120. Moran PS, Teljeur C, Ryan M, et al. Systematic screening for the detection of atrial fibrillation. *Cochrane Database Syst Rev*. 2016;(6): CD009586.
121. Dong Y, Dong Q. New oral anticoagulants: how do we use them wisely? *Curr Cardiol Rep*. 2015;17:1–8.
122. Masoudi FA, et al. 2015 ACC/HRS/SCAI left atrial appendage occlusion device societal overview. *Heart Rhythm*. 2015;12:e122–e136.
123. Lau YC, Lip GYH. Which drug should we use for stroke prevention in atrial fibrillation? *Curr Opin Cardiol*. 2014;29:293–300.
124. Chao T-F, et al. Rate-control treatment and mortality in atrial fibrillation. *Circulation*. 2015;132:1604–1612.
125. Vamos M, Erath JW, Hohnloser SH. Digoxin-associated mortality: a systematic review and meta-analysis of the literature. *Eur Heart J*. 2015;36:1831–1838.
126. Ouyang A-J, et al. Meta-analysis of digoxin use and risk of mortality in patients with atrial fibrillation. *Am J Cardiol*. 2015;115:901–906.
127. Turakhia MP, et al. Increased mortality associated with digoxin in contemporary patients with atrial fibrillation: findings from the TREAT-AF study. *J Am Coll Cardiol*. 2014;64:660–668.
128. Allen LA, et al. Digoxin use and subsequent outcomes among patients in a contemporary atrial fibrillation cohort. *J Am Coll Cardiol*. 2015;65:2691–2698.
129. Page RL, et al. 2015 ACC/AHA/HRS guideline for the management of adult patients with supraventricular tachycardia: a report of the American College of Cardiology/American Heart Association Task Force on clinical practice guidelines and the Heart Rhythm Society. *Circulation*. 2016;133:e506–e574.
130. January CT, et al. 2014 AHA/ACC/HRS guideline for the management of patients with atrial fibrillation: a report of the American College of Cardiology/American Heart Association Task Force on practice guidelines and the Heart Rhythm Society. *J Am Coll Cardiol*. 2014;64:e1–e76.
131. Rajagopalan B, et al. Efficacy of intravenous magnesium in facilitating cardioversion of atrial fibrillation. *Circ Arrhythmia Electrophysiol*. 2016;9:e003968.
132. Grönberg T, et al. Can we predict the failure of electrical cardioversion of acute atrial fibrillation? the FinCV study. *Pacing Clin Electrophysiol*. 2015;38:368–375.
133. Hanley CM, Robinson VM, Kowey PR. Status of antiarrhythmic drug development for atrial fibrillation: new drugs and new molecular mechanisms. *Circ Arrhythmia Electrophysiol*. 2016;9:1–9.
134. Zimetbaum P. Antiarrhythmic drug therapy for atrial fibrillation. *Cardiol Clin*. 2014;32:533–549.
135. Noheria A, et al. Rhythm control versus rate control and clinical outcomes in patients with atrial fibrillation. *JACC Clin Electrophysiol*. 2015;2:221–229.
136. Chatterjee S, Sardar P, Lichstein E, et al. Aikat, S. Pharmacologic rate versus rhythm-control strategies in atrial fibrillation: an updated comprehensive review and meta-analysis. *Pacing Clin Electrophysiol*. 2013;36:122–133.
137. Zakeri R, et al. The burden of proof: the current state of atrial fibrillation prevention and treatment trials. *Heart Rhythm*. 2017;14:763–782.
138. Wu L, et al. Comparison of radiofrequency catheter ablation between asymptomatic and symptomatic persistent atrial fibrillation: a propensity score matched analysis. *J Cardiovasc Electrophysiol*. 2016;27:531–535.
139. Prabhu S, et al. Catheter ablation versus medical rate control in atrial fibrillation and systolic dysfunction. *J Am Coll Cardiol*. 2017;70:1949–1961.
140. Carrizo AG, Morillo CA. Catheter ablation as first-line therapy for atrial fibrillation: ready for prime-time? *Curr Cardiol Rep*. 2016;18:71.
141. Padeletti L, et al. New-generation atrial antitachycardia pacing (reactive ATP) is associated with reduced risk of persistent or permanent atrial fibrillation in patients with bradycardia: Results from the MINERVA randomized multicenter international trial. *Heart Rhythm*. 2015;12:1717–1725.
142. Pathak RK, et al. Impact of CARDIOrespiratory FITness on arrhythmia recurrence in obese individuals with atrial fibrillation: the CARDIO-FIT study. *J Am Coll Cardiol*. 2015;66:985–996.
143. Chatterjee S, Sardar P, Mukherjee D, et al. Timing and route of amiodarone for prevention of postoperative atrial fibrillation after cardiac surgery: a network regression meta-analysis. *Pacing Clin Electrophysiol*. 2013;36:1017–1023.
144. Kolek MJ, et al. Genetic and clinical risk prediction model for postoperative atrial fibrillation. *Circ Arrhythmia Electrophysiol*. 2015;8:25–31.
145. Sezai A, et al. Carperitide and atrial fibrillation after coronary bypass grafting: the Nihon University Working Group Study of Low-Dose HANP Infusion Therapy during Cardiac Surgery Trial for Postoperative Atrial Fibrillation. *Circ Arrhythmia Electrophysiol*. 2015;8:546–553.
146. Verma A, et al. Approaches to catheter ablation for persistent atrial fibrillation. *N Engl J Med*. 2015;372:1812–1822.
147. Goldenberg GR, et al. Antiarrhythmic therapy as an adjuvant to promote post pulmonary vein isolation success: a meta-analysis. *J Interv Card Electrophysiol*. 2016;47:171–176.
148. Kaitani K, et al. Efficacy of Antiarrhythmic Drugs Short-Term Use after Catheter Ablation for Atrial Fibrillation (EAST-AF) trial. *Eur Heart J*. 2016;37:610–618.
149. Wu S, et al. Meta-analysis of efficacy and safety of new oral anticoagulants compared with uninterrupted vitamin K antagonists in patients undergoing catheter ablation for atrial fibrillation. *Am J Cardiol*. 2016;117:926–934.
150. Zhao Y, et al. New oral anticoagulants compared to warfarin for perioperative anticoagulation in patients undergoing atrial fibrillation catheter ablation: a meta-analysis of continuous or interrupted new oral anticoagulants during ablation. *J Interv Card Electrophysiol*. 2017;48:267–282.
151. Calkins H, et al. Uninterrupted dabigatran versus warfarin for ablation in atrial fibrillation. *N Engl J Med*. 2017;376:1627–1636.
152. Gabus V, et al. Short-term heparin kinetics during catheter ablation of atrial fibrillation. *Pacing Clin Electrophysiol*. 2015;38:1142–1150.
153. Briceno DF, Natale A, Di Biase L. Heparin kinetics: The 'holy grail' of periprocedural anticoagulation for ablation of atrial fibrillation. *Pacing Clin Electrophysiol*. 2015;38:1137–1141.
154. Briceno DF, et al. Clinical impact of heparin kinetics during catheter ablation of atrial fibrillation: meta-analysis and meta-regression. *J Cardiovasc Electrophysiol*. 2016;27:683–693.
155. Nishikii-Tachibana M, et al. Prevalence and clinical determinants of left atrial appendage thrombus in patients with atrial fibrillation before pulmonary vein isolation. *Am J Cardiol*. 2015;116:1368–1373.

156. Di Biase L, et al. Is transesophageal echocardiogram mandatory in patients undergoing ablation of atrial fibrillation with uninterrupted novel oral anticoagulants? Results from a prospective multicenter registry. *Heart Rhythm*. 2016;13:1197–1202.
157. Kistler PM, et al. Electrophysiological and electrocardiographic characteristics of focal atrial tachycardia originating from the pulmonary veins: acute and long-term outcomes of radiofrequency ablation. *Circulation*. 2003;108:1968–1975.
158. Squara F, et al. Electrical connection between ipsilateral pulmonary veins: prevalence and implications for ablation and adenosine testing. *Heart Rhythm*. 2015;12:275–282.
159. Ghanbari H, et al. Role of adenosine after antral pulmonary vein isolation of paroxysmal atrial fibrillation: a randomized controlled trial. *Heart Rhythm*. 2016;13:407–415.
160. Prabhu S, et al. Determining the optimal dose of adenosine for unmasking dormant pulmonary vein conduction following atrial fibrillation ablation: electrophysiological and hemodynamic assessment. DORMANT-AF study. *J Cardiovasc Electrophysiol*. 2016;28:13–22.
161. Zhang B, Zhen Y, Tao A, et al. Efficacy of selective arrhythmogenic pulmonary veins isolation versus empirical all pulmonary veins isolation for atrial fibrillation: a meta-analysis of randomized and observational studies. *J Interv Card Electrophysiol*. 2014;39:233–240.
162. Rordorf R, et al. Anatomical mapping for atrial fibrillation ablation: a head-to-head comparison of ultrasound-assisted reconstruction versus fast anatomical mapping. *Pacing Clin Electrophysiol*. 2015;38:187–195.
163. Okumura Y, et al. Effect of catheter tip-tissue surface contact on three-dimensional left atrial and pulmonary vein geometries: potential anatomic distortion of 3D ultrasound, fast anatomical mapping, and merged 3D CT-derived images. *J Cardiovasc Electrophysiol*. 2013;24:259–266.
164. El Haddad M, et al. Determinants of acute and late pulmonary vein reconnection in contact force-guided pulmonary vein isolation. *Circ Arrhythmia Electrophysiol*. 2017;10:e004867.
165. Baldinger SH, et al. The timing and frequency of pulmonary veins unexcitability relative to completion of a wide area circumferential ablation line for pulmonary vein isolation. *JACC Clin Electrophysiol*. 2016;2:14–23.
166. Yuyun MF, Stafford PJ, Sandilands AJ, et al. The impact of power output during percutaneous catheter radiofrequency ablation for atrial fibrillation on efficacy and safety outcomes: a systematic review. *J Cardiovasc Electrophysiol*. 2013;24:1216–1223.
167. Su W, et al. Best practice guide for cryoballoon ablation in atrial fibrillation: the compilation experience of more than 3000 procedures. *Heart Rhythm*. 2015;12:1658–1666.
168. Sharma A, et al. Outcomes following cryoballoon ablation for atrial fibrillation guided by pressure waveform monitoring without the routine use of pulmonary venography. *J Interv Card Electrophysiol*. 2017;49:75–82.
169. Ströcker E, et al. Second-generation cryoballoon ablation in the setting of left common pulmonary veins: procedural findings and clinical outcome. *Heart Rhythm*. 2017;14:1311–1318.
170. Heeger C-H, et al. Acute efficacy, safety, and long-term clinical outcomes using the second-generation cryoballoon for pulmonary vein isolation in patients with a left common pulmonary vein: a multicenter study. *Heart Rhythm*. 2017;14:1111–1118.
171. Andrade JG, Dubuc M, Collet D, et al. Pulmonary vein signal interpretation during cryoballoon ablation for atrial fibrillation. *Heart Rhythm*. 2015;12:1387–1394.
172. Aryana A, et al. Verification of a novel atrial fibrillation cryoablation dosing algorithm guided by time-to-pulmonary vein isolation: results from the Cryo-DOSING Study (Cryoballoon-ablation DOSING Based on the Assessment of Time-to-Effect and Pulmonary Vein Isolation Guidance). *Heart Rhythm*. 2017;14:1319–1325.
173. Iacopino S, et al. Second generation cryoballoon ablation without the use of real-time recordings: a novel strategy based on a temperature guided approach to ablation. *Heart Rhythm*. 2016;14:322–328.
174. Chun KRJ, et al. Individualized cryoballoon energy pulmonary vein isolation guided by real time pulmonary vein recordings, the randomized ‘ICE-T’ Trial. *Heart Rhythm*. 2016;14:495–500.
175. Mondésert B, et al. Clinical experience with a novel electromyographic approach to preventing phrenic nerve injury during cryoballoon ablation in atrial fibrillation. *Circ Arrhythm Electrophysiol*. 2014;7:605–611.
176. Franceschi F, et al. Electromyographic monitoring for prevention of phrenic nerve palsy in second-generation cryoballoon procedures. *Circ Arrhythmia Electrophysiol*. 2015;8:303–307.
177. Kowalski M, Ellenbogen KA, Koneru JN. Prevention of phrenic nerve injury during interventional electrophysiologic procedures. *Heart Rhythm*. 2014;11:1839–1844.
178. Ghosh J, Sepahpour A, Chan KH, et al. Immediate balloon deflation for prevention of persistent phrenic nerve palsy during pulmonary vein isolation by balloon cryoablation. *Heart Rhythm*. 2013;10:646–652.
179. Aryana A, et al. Catheter ablation using the third-generation cryoballoon provides an enhanced ability to assess time to pulmonary vein isolation facilitating the ablation strategy : short- and long-term results of a multicenter study. *Heart Rhythm*. 2016;13:2306–2313.
180. Attanasio P, et al. Pain reactions during pulmonary vein isolation under deep sedation: cryothermal versus radiofrequency ablation. *Pacing Clin Electrophysiol*. 2016;39:452–457.
181. Kajiyama T, et al. Anatomic parameters predicting procedural difficulty and balloon temperature predicting successful applications in individual pulmonary veins during 28-mm second-generation cryoballoon ablation. *JACC Clin Electrophysiol*. 2016;3:580–588.
182. Bordignon S, et al. Energy titration strategies with the endoscopic ablation system: lessons from the high-dose vs. low-dose laser ablation study. *Europace*. 2013;15:685–689.
183. Dukkipati SR, et al. Pulmonary vein isolation using a visually guided laser balloon catheter: the first 200-patient multicenter clinical experience. *Circ Arrhythm Electrophysiol*. 2013;6:467–472.
184. Dukkipati SR, et al. Pulmonary vein isolation using the visually guided laser balloon a prospective, multicenter, and randomized comparison to standard radiofrequency ablation. *J Am Coll Cardiol*. 2015;66:1350–1360.
185. Buch E, Shivkumar K. Catheter ablation of atrial fibrillation advent of second-generation technologies. *J Am Coll Cardiol*. 2015;66:1361–1363.
186. Leong-Sit P, et al. Inducibility of atrial fibrillation and flutter following pulmonary vein ablation. *J Cardiovasc Electrophysiol*. 2013;24:617–623.
187. Gula LJ, et al. Pulmonary vein isolation with incomplete antral ablation lines: is more ablation necessary? Results of a randomized trial. *J Cardiovasc Electrophysiol*. 2016;27:298–302.
188. Cardoso R, et al. Cryoballoon versus radiofrequency catheter ablation in atrial fibrillation : a meta-analysis. *J Cardiovasc Electrophysiol*. 2016;27:1151–1159.
189. Liu X-H, Chen C-F, Gao X-F, et al. Safety and efficacy of different catheter ablations for atrial fibrillation: a systematic review and meta-analysis. *Pacing Clin Electrophysiol*. 2016;39:883–899.
190. Koektuerk B, et al. Cryoballoon ablation for pulmonary vein isolation in patients with persistent atrial fibrillation: one-year outcome using second generation cryoballoon. *Circ Arrhythm Electrophysiol*. 2015;8:1073–1079.
191. Guhl EN, et al. Efficacy of cryoballoon pulmonary vein isolation in patients with persistent atrial fibrillation. *J Cardiovasc Electrophysiol*. 2016;27:423–427.
192. Boveda S, et al. Outcomes after cryoballoon or radiofrequency ablation for persistent atrial fibrillation : a multicentric propensity-score matched study. *J Interv Card Electrophysiol*. 2016;47:133–142.
193. Ichihara N, et al. Prevalence and pre-procedural predictors associated with right phrenic nerve injury in electromyography-guided, second-generation cryoballoon ablation. *JACC Clin Electrophysiol*. 2016;2:508–514.
194. Zhang Z, et al. Linear ablation following pulmonary vein isolation in patients with atrial fibrillation: a meta-analysis. *Pacing Clin Electrophysiol*. 2016;39:623–630.
195. Wynn GJ, et al. Batrial linear ablation in sustained nonpermanent AF: results of the substrate modification with ablation and antiarrhythmic

- drugs in nonpermanent atrial fibrillation (SMAN-PAF) trial. *Heart Rhythm*. 2016;13:399–406.
196. Wong KCK, et al. No benefit of complex fractionated atrial electrogram ablation in addition to circumferential pulmonary vein ablation and linear ablation: benefit of complex ablation study. *Circ Arrhythmia Electrophysiol*. 2015;8:1316–1324.
 197. Bai R, et al. Proven isolation of the pulmonary vein antrum with or without left atrial posterior wall isolation in patients with persistent atrial fibrillation. *Heart Rhythm*. 2016;13:132–140.
 198. Mohanty S, et al. Impact of rotor ablation in non-paroxysmal AF patients: results from a randomized trial (OASIS). *J Am Coll Cardiol*. 2016;68:274–282.
 199. Higuchi S, et al. Is it necessary to achieve a complete box isolation in the case of frequent esophageal temperature rises? Feasibility of shifting to a partial box isolation strategy for patients with non-paroxysmal atrial fibrillation. *J Cardiovasc Electrophysiol*. 2016;27:897–904.
 200. Cutler MJ, et al. Impact of voltage mapping to guide whether to perform ablation of the posterior wall in patients with persistent atrial fibrillation. *J Cardiovasc Electrophysiol*. 2016;27:13–21.
 201. He X, et al. Left atrial posterior wall isolation reduces the recurrence of atrial fibrillation: a meta-analysis. *J Interv Card Electrophysiol*. 2016;46:267–274.
 202. Coffey JO, et al. Catheter ablation of scar-related atypical atrial flutter. *Europace*. 2013;15:414–419.
 203. Navarrete A, Conte F, Moran M, et al. Ablation of atrial fibrillation at the time of cavotricuspid isthmus ablation in patients with atrial flutter without documented atrial fibrillation derives a better long-term benefit. *J Cardiovasc Electrophysiol*. 2011;22:34–38.
 204. Mohanty S, et al. Results from a single-blind, randomized study comparing the impact of different ablation approaches on long-term procedure outcome in coexistent atrial fibrillation and flutter (approval). *Circulation*. 2013;127:1853–1860.
 205. Sommer P, et al. Successful repeat catheter ablation of recurrent longstanding persistent atrial fibrillation with rotor elimination as the procedural endpoint: a case series. *J Cardiovasc Electrophysiol*. 2016;27:274–280.
 206. Zaman JAB, Peters NS, Narayan SM. Rotor mapping and ablation to treat atrial fibrillation. *Curr Opin Cardiol*. 2015;30:24–32.
 207. Narayan SM, Krummen DE, Clopton P, et al. Direct or coincidental elimination of stable rotors or focal sources may explain successful atrial fibrillation ablation: on-treatment analysis of the CONFIRM trial (conventional ablation for AF with or without focal impulse and rotor modulation). *J Am Coll Cardiol*. 2013;62:138–147.
 208. Narayan SM, et al. Ablation of rotor and focal sources reduces late recurrence of atrial fibrillation compared with trigger ablation alone: extended follow-up of the CONFIRM trial (conventional ablation for atrial fibrillation with or without focal impulse and rotor modulation). *J Am Coll Cardiol*. 2014;63:1761–1768.
 209. Benharash P, et al. Quantitative analysis of localized sources identified by focal impulse and rotor modulation mapping in atrial fibrillation. *Circ Arrhythmia Electrophysiol*. 2015;8:554–561.
 210. Berntsen RF, Håland TF, Skårdal R, et al. Focal impulse and rotor modulation as a stand-alone procedure for the treatment of paroxysmal atrial fibrillation: a within-patient controlled study with implanted cardiac monitoring. *Heart Rhythm*. 2016;13:1768–1774.
 211. Gianni C, et al. Acute and early outcomes of focal impulse and rotor modulation (FIRM)-guided rotors-only ablation in patients with nonparoxysmal atrial fibrillation. *Heart Rhythm*. 2016;13:830–835.
 212. Buch E, et al. Long-term clinical outcomes of focal impulse and rotor modulation for treatment of atrial fibrillation: a multicenter experience. *Heart Rhythm*. 2016;13:636–641.
 213. Schade A, et al. Spatial relationship of focal impulses, rotors and low voltage zones in patients with persistent atrial fibrillation. *J Cardiovasc Electrophysiol*. 2016;27:507–514.
 214. Steinberg JS, et al. Focal impulse and rotor modulation: acute procedural observations and extended clinical follow-up. *Heart Rhythm*. 2017;14:192–197.
 215. Aksu T, Umer T, Guler E, et al. Unanswered questions in complex fractionated atrial. *Pacing Clin Electrophysiol*. 2016;39:1269–1278.
 216. Lau DH, et al. Indices of bipolar complex fractionated atrial electrograms correlate poorly with each other and atrial fibrillation substrate complexity. *Heart Rhythm*. 2015;12:1415–1423.
 217. Sohal M, et al. Is mapping of complex fractionated electrograms obsolete? *Arrhythmia Electrophysiol Rev*. 2015;4:109–115.
 218. Oketani N, et al. Ablation of complex fractionated electrograms is useful for catheter ablation of persistent atrial fibrillation: protagonist point of view. *Heart Rhythm*. 2016;13:2098–2100.
 219. Conti S, Verma A. Ablation of complex fractionated electrograms may not be useful for catheter ablation of persistent atrial fibrillation. *Heart Rhythm*. 2016;13:2098–2100.
 220. Vogler J, et al. Pulmonary vein isolation versus defragmentation the CHASE-AF Clinical Trial. *J Am Coll Cardiol*. 2015;66:2743–2752.
 221. Providência R, et al. Is there still a role for complex fractionated atrial electrogram ablation in addition to pulmonary vein isolation in patients with paroxysmal and persistent atrial fibrillation? *Circ Arrhythmia Electrophysiol*. 2015;8:1017–1029.
 222. Katritsis DG, et al. Autonomic denervation added to pulmonary vein isolation for paroxysmal atrial fibrillation: a randomized clinical trial. *J Am Coll Cardiol*. 2013;62:2318–2325.
 223. Pokushalov E, et al. Ganglionated plexus ablation vs linear ablation in patients undergoing pulmonary vein isolation for persistent/long-standing persistent atrial fibrillation: a randomized comparison. *Heart Rhythm*. 2013;10:1280–1286.
 224. Kurotobi T, et al. Features of intrinsic ganglionated plexi in both atria after extensive pulmonary isolation and their clinical significance after catheter ablation in patients with atrial fibrillation. *Heart Rhythm*. 2015;12:470–476.
 225. Zhao Y, et al. Importance of non-pulmonary vein triggers ablation to achieve long-term freedom from paroxysmal atrial fibrillation in patients with low ejection fraction. *Heart Rhythm*. 2016;13:141–149.
 226. Theis C, et al. Arrhythmia termination versus elimination of dormant pulmonary vein conduction as a procedural end point of catheter ablation for paroxysmal atrial fibrillation. *Circ Arrhythm Electrophysiol*. 2015;8:1080–1087.
 227. Santangeli P, Marchlinski FE. Techniques for provocation, localization and ablation of nonpulmonary vein triggers for atrial fibrillation. *Heart Rhythm*. 2017;14:1087–1096.
 228. Hojo R, et al. Development of nonpulmonary vein foci increases risk of atrial fibrillation recurrence after pulmonary vein isolation. *JACC Clin Electrophysiol*. 2017;3:547–555.
 229. Rodríguez-Mañero M, Schurmann P, Valderrábano M. Ligament and vein of Marshall: a therapeutic opportunity in atrial fibrillation. *Heart Rhythm*. 2016;13:593–601.
 230. Lerman BB. Ablating the obscure: the curious case of the vein of Marshall. *J Cardiovasc Electrophysiol*. 2017;28:394–395.
 231. Lee JH, et al. Radiofrequency catheter ablation targeting the vein of Marshall in difficult mitral isthmus ablation or pulmonary vein isolation. *J Cardiovasc Electrophysiol*. 2017;28:386–393.
 232. Báez-Escudero JL, Keida T, Dave AS, et al. Ethanol infusion in the vein of Marshall leads to parasympathetic denervation of the human left atrium: implications for atrial fibrillation. *J Am Coll Cardiol*. 2014;63:1892–1901.
 233. Miyazaki S, et al. Role of arrhythmogenic superior vena cava on atrial fibrillation. *J Cardiovasc Electrophysiol*. 2014;25:380–386.
 234. Ejima K, et al. Impact of an empiric isolation of the superior vena cava in addition to circumferential pulmonary vein isolation on the outcome of paroxysmal atrial fibrillation ablation. *Am J Cardiol*. 2015;116:1711–1716.
 235. Miyazaki S, et al. Factors predicting an arrhythmogenic superior vena cava in atrial fibrillation ablation: insight into the mechanism. *Heart Rhythm*. 2014;11:1560–1566.
 236. Sharma SP, Sangha RS, Dahal K, et al. The role of empiric superior vena cava isolation in atrial fibrillation: a systematic review and meta-analysis of randomized controlled trials. *J Interv Card Electrophysiol*. 2016;48:61–67.

237. Higuchi K, Yamauchi Y, Hirao K, et al. The importance of superior vena cava isolation in ablation strategy for atrial fibrillation. *Curr Opin Cardiol*. 2013;28:2–6.
238. Miyazaki S, et al. Electrical superior vena cava isolation using a novel pace-and-ablate technique under diaphragmatic electromyography monitoring. *Heart Rhythm*. 2017;14:678–684.
239. Morita H, Zipes DP, Morita ST, et al. The role of coronary sinus musculature in the induction of atrial fibrillation. *Heart Rhythm*. 2012;9:581–589.
240. Reissmann B, et al. Durability of wide-area left atrial appendage isolation: results from extensive catheter ablation for treatment of persistent atrial fibrillation. *Heart Rhythm*. 2017;14:314–319.
241. Di Biase L, et al. Left atrial appendage isolation in patients with longstanding persistent AF undergoing catheter ablation. *J Am Coll Cardiol*. 2016;68:1929–1940.
242. Rillig A, et al. Unexpectedly high incidence of stroke and left atrial appendage thrombus formation after electrical isolation of the left atrial appendage for the treatment of atrial tachyarrhythmias. *Circ Arrhythm Electrophysiol*. 2016;9:e003461.
243. Hayashi K, et al. Importance of nonpulmonary vein foci in catheter ablation for paroxysmal atrial fibrillation. *Heart Rhythm*. 2015;12:1918–1924.
244. Blandino A, et al. Left atrial substrate modification targeting low-voltage areas for catheter ablation of atrial fibrillation: a systematic review and meta-analysis. *Pacing Clin Electrophysiol*. 2017;40:199–212.
245. Yang G, et al. Catheter ablation of nonparoxysmal atrial fibrillation using electrophysiologically guided substrate modification during sinus rhythm after pulmonary vein isolation. *Circ Arrhythmia Electrophysiol*. 2016;9:e003382.
246. Kottkamp H, Berg J, Bender R, et al. Box isolation of fibrotic areas (BIFA): a patient-tailored substrate modification approach for ablation of atrial fibrillation. *J Cardiovasc Electrophysiol*. 2016;27:22–30.
247. Yamaguchi T, et al. Efficacy of left atrial voltage-based catheter ablation of persistent atrial fibrillation. *J Cardiovasc Electrophysiol*. 2015;2015:1055–1063.
248. Rolf S, Dagues N, Hindricks G. Voltage-based ablation: the growing evidence for the role of individually tailored substrate modification for atrial fibrillation. *J Cardiovasc Electrophysiol*. 2016;27:31–33.
249. Voskoboinik A, et al. Revisiting pulmonary vein isolation alone for persistent atrial fibrillation: a systematic review and meta-analysis. *Heart Rhythm*. 2017;14:661–667.
250. Siontis KC, et al. Radiofrequency ablation versus antiarrhythmic drug therapy for atrial fibrillation: meta-analysis of quality of life. *Morb Mortal*. 2016;2:170–180.
251. Liang JJ, et al. Early recurrence of atrial arrhythmias following pulmonary vein antral isolation: timing and frequency of early recurrences predicts long-term ablation success. *Heart Rhythm*. 2015;12:2461–2468.
252. Alipour P, et al. Defining blanking period post pulmonary vein antrum isolation. *JACC Clin Electrophysiol*. 2016;3:568–576.
253. Sadek MM, et al. Recurrent atrial arrhythmias in the setting of chronic pulmonary vein isolation. *Heart Rhythm*. 2016;13:2174–2180.
254. Barbhuiya CR, et al. Recurrence of atrial arrhythmias despite persistent pulmonary vein isolation after catheter ablation for atrial fibrillation. *JACC Clin Electrophysiol*. 2016;2:723–731.
255. Moser J, et al. Complication rates of catheter ablation of atrial fibrillation in patients aged ≥ 75 years versus <75 years—results from the German Ablation Registry. *J Cardiovasc Electrophysiol*. 2016;28:258–265.
256. Teunissen C, et al. Incidence of pulmonary vein stenosis after radiofrequency catheter ablation of atrial fibrillation. *JACC Clin Electrophysiol*. 2016;3:589–598.
257. Narui R, et al. Incidence and factors associated with the occurrence of pulmonary vein narrowing after cryoballoon ablation. *Circ Arrhythmia Electrophysiol*. 2017;10:e004588.
258. Matsuda J, et al. Pulmonary vein stenosis after second-generation cryoballoon ablation. *J Cardiovasc Electrophysiol*. 2017;28:298–303.
259. Kumar N, et al. Pulmonary vein stenosis after laser balloon ablation for atrial fibrillation. *JACC Clin Electrophysiol*. 2015;1:220–221.
260. Barbhuiya CR, et al. Global survey of esophageal injury in atrial fibrillation ablation. *JACC Clin Electrophysiol*. 2016;2:143–150.
261. Müller P, et al. Higher incidence of esophageal lesions after ablation of atrial fibrillation related to the use of esophageal temperature probes. *Heart Rhythm*. 2015;12:1464–1469.
262. Fürnkranz A, et al. Reduced incidence of esophageal lesions by luminal esophageal temperature-guided second-generation cryoballoon ablation. *Heart Rhythm*. 2015;12:268–274.
263. Eitel C, et al. Successful nonsurgical treatment of esophagopericardial fistulas after atrial fibrillation catheter ablation: a case series. *Circ Arrhythmia Electrophysiol*. 2013;6:675–681.
264. Black-Maier E, et al. Risk of atrioesophageal fistula formation with contact force-sensing catheters. *Heart Rhythm*. 2017;14:1328–1333.
265. Pedersen MEF, et al. Management of tamponade complicating catheter ablation for atrial fibrillation. *JACC Clin Electrophysiol*. 2016;3:367–373.
266. Michowitz Y, et al. Effects of sex on the incidence of cardiac tamponade after catheter ablation of atrial fibrillation results from a worldwide survey in 34943 atrial fibrillation ablation procedures. *Circ Arrhythmia Electrophysiol*. 2014;7:274–280.
267. Chun KRJ, et al. Complications in catheter ablation of atrial fibrillation in 3,000 consecutive procedures. *JACC Clin Electrophysiol*. 2017;3:154–161.
268. Yamada T, Kay GN. Recognition and prevention of complications during epicardial ablation. *Card Electrophysiol Clin*. 2010;2:127–134.
269. Aksu T, Golcuk S, Guler TE, et al. Gastroparesis as a complication of atrial fibrillation ablation. *Am J Cardiol*. 2015;116:92–97.
270. Miyazaki S, et al. Esophagus-related complications during second-generation cryoballoon ablation—insight from simultaneous esophageal temperature monitoring from 2 esophageal probes. *J Cardiovasc Electrophysiol*. 2016;27:1038–1044.
271. Kuwahara T, et al. Clinical characteristics and management of periesophageal vagal nerve injury complicating left atrial ablation of atrial fibrillation: lessons from eleven cases. *J Cardiovasc Electrophysiol*. 2013;24:847–851.
272. Lakkireddy D, et al. Effect of atrial fibrillation ablation on gastric motility: the Atrial Fibrillation Gut Study. *Circ Arrhythmia Electrophysiol*. 2015;8:531–536.
273. Knopp H, et al. Incidental and ablation-induced findings during upper gastrointestinal endoscopy in patients after ablation of atrial fibrillation: a retrospective study of 425 patients. *Heart Rhythm*. 2014;11:574–578.
274. Yang Y, et al. Stiff left atrial syndrome: a complication undergoing radiofrequency catheter ablation for atrial fibrillation. *J Cardiovasc Electrophysiol*. 2016;27:884–889.
275. Khurram IM, et al. Association between left atrial stiffness index and atrial fibrillation recurrence in patients undergoing left atrial ablation. *Circ Arrhythmia Electrophysiol*. 2016;9:1–10.
276. Verma I, Tripathi H, Sikachi RR, et al. Pulmonary hypertension due to radiofrequency catheter ablation (RFCA) for atrial fibrillation: the lungs, the atrium or the ventricle? *Heart Lung Circ*. 2016;25:1177–1183.
277. Nery PB, et al. Relationship between pulmonary vein reconnection and atrial fibrillation recurrence. *JACC Clin Electrophysiol*. 2016;2:474–483.
278. Liang JJ, et al. Pulmonary vein antral isolation and nonpulmonary vein trigger ablation are sufficient to achieve favorable long-term outcomes including transformation to paroxysmal arrhythmias in patients with persistent and long-standing persistent atrial fibrillation. *Circ Arrhythmia Electrophysiol*. 2016;9:e004239.
279. Buch E, Shivkumar K. Could less be more in catheter ablation for persistent atrial fibrillation? Pulmonary vein isolation reconsidered. *Heart Rhythm*. 2017;14:668–669.
280. Goldenberg GR, et al. The incremental benefit of non-pulmonary vein left atrial ablation in patients undergoing a repeat persistent atrial fibrillation ablation procedure. *J Interv Card Electrophysiol*. 2017;48:185–191.
281. Vijayaraman P, Naperkowski A, Ellenbogen KA, et al. Electrophysiologic insights into site of atrioventricular block lessons from permanent His bundle pacing. *JACC Clin Electrophysiol*. 2015;1:571–581.
282. Vijayaraman P, Dandamudi G, Bauch T, et al. Imaging evaluation of implantation site of permanent direct His bundle pacing lead. *Heart Rhythm*. 2014;11:529–530.

283. Kulkarni N, et al. His bundle pacing for identifying optimal ablation sites in patients undergoing atrioventricular junction ablation. *Pacing Clin Electrophysiol.* 2017;40:242–246.
284. Issa ZF, Amr BS, Laham H. Long-term follow-up in AV junction ablation via the SVC in patients undergoing concurrent device implantation: a single center experience. *Pacing Clin Electrophysiol.* 2015;38:254–258.
285. Reddy YM, et al. Impact of tricuspid regurgitation on the success of atrioventricular node ablation for rate control in patients with atrial fibrillation: the Node Blast Study. *Am J Cardiol.* 2015;116:900–903.
286. Chatterjee NA, et al. Atrioventricular nodal ablation in atrial fibrillation a meta-analysis and systematic review. *Circ Arrhythmia Electrophysiol.* 2012;5:68–76.
287. Naksuk N, Padmanabhan D, Yogeswaran V, et al. Left atrial appendage. *JACC Clin Electrophysiol.* 2016;2:403–412.
288. Saw J, et al. Comparing measurements of CT angiography, TEE, and fluoroscopy of the left atrial appendage for percutaneous closure. *J Cardiovasc Electrophysiol.* 2016;27:414–422.
289. Meier B, et al. EHRA/EAPCI expert consensus statement on catheter-based left atrial appendage occlusion. *EuroIntervention.* 2015;10:1109–1125.
290. Enomoto Y, et al. Use of non-warfarin oral anticoagulants instead of warfarin during left atrial appendage closure with the Watchman device. *Heart Rhythm.* 2016;14:19–24.
291. Boersma LV, et al. Efficacy and safety of left atrial appendage closure with WATCHMAN in patients with or without contraindication to oral anticoagulation: 1-year follow-up outcome data of the EWOLUTION trial. *Heart Rhythm.* 2017;14:1302–1308.
292. Holmes DR, et al. Left atrial appendage closure as an alternative to warfarin for stroke prevention in atrial fibrillation: a patient-level meta-analysis. *J Am Coll Cardiol.* 2015;65:2614–2623.
293. Main ML, et al. Assessment of device-related thrombus and associated clinical outcomes with the WATCHMAN left atrial appendage closure device for embolic protection in patients with atrial fibrillation (from the PROTECT-AF trial). *Am J Cardiol.* 2016;117:1127–1134.
294. Freixa X, et al. The Amplatzer™ Cardiac Plug 2 for left atrial appendage occlusion: novel features and first-in-man experience. *EuroIntervention.* 2013;8:1094–1098.
295. Lam SCC, et al. Left atrial appendage closure using the Amulet device: an initial experience with the second generation Amplatzer cardiac plug. *Catheter Cardiovasc Interv.* 2015;85:297–303.
296. Sedaghat A, et al. Thrombus formation after left atrial appendage occlusion with the Amplatzer Amulet device. *JACC Clin Electrophysiol.* 2017;3:71–75.
297. Tzikas A, et al. Left atrial appendage occlusion for stroke prevention in atrial fibrillation: multicentre experience with the AMPLATZER cardiac plug. *EuroIntervention.* 2016;11:1170–1179.
298. Bartus K, et al. Anatomic analysis of the left atrial appendage after closure with the LARIAT device. *Circ Arrhythmia Electrophysiol.* 2014;7:764–767.
299. Syed FF, Friedman PA. Left atrial appendage closure for stroke prevention emerging technologies. *Card Electrophysiol Clin.* 2014;6:141–160.
300. Koneru JN, Badhwar N, Ellenbogen KA, et al. LAA ligation using the LARIAT suture delivery device: tips and tricks for a successful procedure. *Heart Rhythm.* 2014;11:911–921.
301. Lakkireddy D, et al. Short and long-term outcomes of percutaneous left atrial appendage suture ligation: results from a US multicenter evaluation. *Heart Rhythm.* 2016;13:1030–1036.
302. Romanov A, et al. Effect of left atrial appendage excision on procedure outcome in patients with persistent atrial fibrillation undergoing surgical ablation. *Heart Rhythm.* 2016;13:1803–1809.
303. Lakkireddy D, et al. Left atrial appendage ligation and ablation for persistent atrial fibrillation: the LAALA-AF registry. *JACC Clin Electrophysiol.* 2015;1:153–160.
304. Afzal MR, et al. Impact of left atrial appendage exclusion using an epicardial ligation system (LARIAT) on atrial fibrillation burden in patients with cardiac implantable electronic devices. *Heart Rhythm.* 2015;12:52–59.
305. Kreidieh B, et al. Left atrial appendage remodeling after lariat left atrial appendage ligation. *Circ Arrhythmia Electrophysiol.* 2015;8:1351–1358.
306. Pillarisetti J, et al. Endocardial (Watchman) vs epicardial (Lariat) left atrial appendage exclusion devices: understanding the differences in the location and type of leaks and their clinical implications. *Heart Rhythm.* 2015;12:1501–1507.
307. Aryana A, et al. Association between incomplete surgical ligation of left atrial appendage and stroke and systemic embolization. *Heart Rhythm.* 2015;12:1431–1437.
308. Tsai Y-C, et al. Surgical left atrial appendage occlusion during cardiac surgery for patients with atrial fibrillation: a meta-analysis. *Eur J Cardiothoracic Surg.* 2015;47:847–854.

Inappropriate Sinus Tachycardia

OUTLINE

Anatomy and Physiology of the Sinus Node, 549

Pathophysiology, 549

Epidemiology and Natural History, 550

Clinical Presentation, 550

Initial Evaluation, 550

Holter Monitoring, 550

Exercise Testing, 551

Isoproterenol Provocation, 551

Autonomic Evaluation, 551

Electrophysiological Testing, 551

Differential Diagnosis, 551

Postural Orthostatic Tachycardia Syndrome, 551

Supraventricular Tachycardia, 552

Principles of Management, 552

Pharmacological Therapy, 552

Catheter Ablation, 553

Surgical Ablation, 553

Electrophysiological Testing, 553

Induction of Tachycardia, 553

Tachycardia Features, 553

Exclusion of Other Arrhythmia Mechanisms, 554

Ablation, 554

Target of Ablation, 554

Ablation Technique, 554

Endpoints of Ablation, 555

Outcome, 558

ANATOMY AND PHYSIOLOGY OF THE SINUS NODE

The sinus node is a subepicardial, “crescent-” or “tadpole”-shaped structure located laterally within the epicardial groove of the sulcus terminalis of the right atrium (RA) at the junction of the anterior trabeculated appendage with the posterior smooth-walled venous component. The endocardial aspect of the sulcus terminalis is marked by the crista terminalis. Starting epicardially at the junction of the superior vena cava (SVC) and the right atrial appendage, the sinus node courses downward and to the left along the sulcus terminalis, to end subendocardially almost to the inferior vena cava (IVC). In adults, the sinus node measures 8 to 22 mm long and 2 to 3 mm wide and thick. The right phrenic nerve often runs in close proximity to the sinus node, where it lies on the fibrous pericardium immediately overlying the lateral and anterolateral quadrants of the SVC–right atrial junction (see Fig. 8.1).^{1–4}

The sinus node normally is the dominant pacemaker of the heart. Its pacemaker function is determined by its low maximum diastolic membrane potential and steep phase 4 spontaneous depolarization. Importantly, the pacemaker activity is not confined to a single cell in the sinus node; rather, sinus node cells function as electrically coupled oscillators that discharge synchronously because of mutual entrainment. Current evidence suggests a “pacemaker hierarchy” within the sinus node. At faster rates, the sinus impulse originates in the superior portion (head) of the sinus node, whereas at slower rates, the impulse arises from a more inferior part (toward the tail). The hierarchy mediates heart rate changes (in response to physiological stimuli) via a dynamic craniocaudal shift in the “leading pacemaker” site.

Notably, the sinus node is functionally insulated from the surrounding atrial myocytes, except at a limited number of different conduction pathways (exit sites) that allow transmission of sinus impulses to atrial myocardium, likely responsible for the variations in P wave morphology and polarity commonly observed at different sinus rates.^{3,5–7} Neural and hormonal factors influence both the site of pacemaker activation,

likely via shifting points of initial activity, and the point of exit from the sinus node complex.^{2,8–10}

PATHOPHYSIOLOGY

Sinus tachycardia is a physiological response to sympathetic activation and/or parasympathetic withdrawal. Inappropriate sinus tachycardia (IST) is a nonparoxysmal tachyarrhythmia characterized by a persistent increase in resting sinus rate unrelated to, or out of proportion of, the level of physical, emotional, pathological, or pharmacological stress, or an exaggerated heart rate response to minimal exertion or a change in body posture. IST is neither a response to a pathological process (e.g., heart failure, hyperthyroidism, or drug effects) nor a result of physical deconditioning. Crucial to this definition is the presence of associated symptoms.^{10–13}

The underlying mechanism(s) of IST is poorly understood and remains controversial. Potential mechanisms include enhanced automaticity, disorder of autonomic responsiveness of the sinus node, altered sinus nodal intrinsic regulation, and sympathovagal imbalance, with excessive sympathetic drive and/or reduced vagal influence on the sinus node. A primary abnormality of sinus node function has been suggested, as evidenced by a higher intrinsic heart rate (after muscarinic and beta-receptor blockade) than that found in normal controls or a blunted response to adenosine with less sinus CL prolongation than in control subjects (with and without autonomic blockade). In addition, β -adrenergic receptor hypersensitivity, α -adrenergic receptor hyposensitivity, M_2 muscarinic receptor hyposensitivity, brain stem dysregulation, depressed efferent cardiovascular reflex, central and peripheral nociceptive effects, hypothalamic paraventricular nucleus stimulation, and impaired baroreflex control have been offered as likely explanations. Chronic beta-receptor stimulation by autoantibodies and autonomic neuritis or autonomic neuropathy can play a role in some cases. The extent to which each of these mechanisms contributes to tachycardia

and associated symptoms is unknown, but the underlying mechanisms are likely multifactorial and complex.^{12,14,15}

Recently, IST has been linked to sinus node channelopathy. A gain-of-function mutation in the *HCN4* gene (which encodes the protein that contributes to formation of *I_f* channels) has been identified in a cohort of patients with IST. HCN mutations can be associated with IST through increased sensitivity to cyclic adenosine monophosphate-dependent activation.^{10,16}

In some patients, there can be an overlap between IST and disorders, such as chronic fatigue syndrome and neurocardiogenic syncope, and other patients can have a psychological component of hypersensitivity to somatic input. Other groups with similar or overlapping laboratory findings and clinical course include patients with hyperadrenergic syndrome, idiopathic hypovolemia, orthostatic hypotension, and mitral valve prolapse syndrome. It is possible that the phenotype of IST is the result of a number of unrelated disorders (much like ventricular tachycardia is the phenotype of many unrelated causes).

EPIDEMIOLOGY AND NATURAL HISTORY

The vast majority of patients afflicted with IST are young women (mean age, 38 ± 12 years), although IST has also been identified in older individuals. IST affects people working in health care in disproportionate numbers, for unknown reasons. The prevalence of IST (symptomatic or asymptomatic) in a middle-aged population (up to 1.2% in one report) appears to be higher than previously assumed.¹⁷

Despite the chronic nature of the disorder and long-lasting symptoms, the natural course and prognosis of IST are generally benign. IST rarely is associated with tachycardia-induced cardiomyopathy, perhaps due to the frequently observed nocturnal slowing of the heart rate.¹²

CLINICAL PRESENTATION

The clinical presentation of the arrhythmia is highly variable, ranging from totally asymptomatic patients identified during routine medical examination to those with short, paroxysmal episodes of palpitations to individuals with chronic, incessant, and incapacitating symptoms. The most prominent symptoms are palpitations, fatigue, and exercise intolerance. IST can also be associated with a host of other symptoms, including chest discomfort, dyspnea, orthostatic intolerance, lightheadedness, dizziness, presyncope, and syncope. Symptoms can start abruptly or insidiously, but typically persist for months or years. Importantly, symptoms may not consistently correlate with periods of tachycardia or can be disproportionate to the severity of the tachycardia. In fact, successful treatment of the tachycardia may not lead to improvement of symptoms. Associated psychiatric conditions are not infrequent, but their relationship to IST is uncertain.^{11,12,18}

INITIAL EVALUATION

IST is an ill-defined clinical syndrome with diverse clinical manifestations. There is no gold standard to make a definitive diagnosis of IST, and the diagnosis remains a clinical one, after exclusion of other causes of symptomatic tachycardia. Clinical examination and routine investigations allow the elimination of secondary causes for the tachycardia but are generally not helpful in establishing the diagnosis of IST.

A thorough history and physical examination is essential to exclude specific physiological, psychological, and pathological causes of appropriate sinus tachycardia (Box 16.1). Blood pressure and heart rate need to be taken in the supine, sitting, immediate standing, and at 2- and 5-minute intervals. Depending on the clinical context, additional work-up can include echocardiography, complete blood count, thyroid function

BOX 16.1 Causes of Appropriate Sinus Tachycardia	
Physiological	Medical Conditions
Exercise	Pain
Emotion	Anemia
Pregnancy	Infection
	Volume depletion
Drugs/Substances	Hypotension
Anticholinergics	Anxiety
Sympathomimetics	Fever
Beta-blocker withdrawal	Pericarditis
Vasodilators	Hypoglycemia
Thyroid hormones	Hyperthyroidism
Decongestants	Cushing disease
Albuterol	Pheochromocytoma
Salmeterol	Cardiomyopathy
Theophylline	Heart failure
Caffeine	Myocardial infarction
Alcohol	Pericarditis
Tobacco	Pulmonary embolism
Cocaine	Chronic pulmonary disease
Amphetamine	Neuropathies
	SVT ablation
	AF ablation

AF, Atrial fibrillation; SVT, supraventricular tachycardia.

BOX 16.2 Characteristics of Inappropriate Sinus Tachycardia	
Daytime resting sinus rate ≥100 beats/min	
Mean 24-h sinus rate ≥90 to 95 beats/min	
Exaggerated heart rate response to minimal physical or emotional stress	
P wave morphology similar to normal sinus rhythm	
Markedly distressing symptoms	
Lack of secondary causes of sinus tachycardia	

tests, fasting blood sugar, urinary metanephrines, or 24-hour urinary sodium excretion. Evaluation for occult drug abuse (urine and blood drug screening) and psychiatric conditions also need to be considered.

The syndrome of IST is characterized by the following: (1) a relative or absolute increase in sinus rate out of proportion to the physiological demand (a daytime resting sinus rate of more than 100 beats/min, with a mean heart rate more than 90 to 95 beats/min on 24-hour Holter monitor, or an exaggerated heart rate response to minimal physical or emotional stress); (2) P wave axis and morphology during tachycardia that are similar to those noted during normal sinus rhythm; (3) lack of secondary causes of sinus tachycardia; and (4) markedly distressing symptoms of palpitations, fatigue, dyspnea, and anxiety during tachycardia, with an absence of symptoms during normal sinus rates (Box 16.2).

Holter Monitoring

Ambulatory Holter recordings characteristically demonstrate a mean heart rate of more than 90 to 95 beats/min (Fig. 16.1). However, some patients have either a physiological or normal sinus rate at rest (less than 85 beats/min) with an inappropriate tachycardia response to a minimal physiological challenge or a moderately elevated resting heart rate (more than 85 beats/min) with an accentuated (inappropriate)



Fig. 16.1 A 24-Hour Trend of the Long-Term Electrocardiogram Showing Inappropriate Sinus Tachycardia Throughout Usual Activity and on Awakening.

heart rate response to minimal exertion. Importantly, this quantitative definition of ‘inappropriate’ is arbitrary, and validation of the reproducibility of the heart rate and activity correlation can be challenging.^{12,17,18}

Exercise Testing

Exercise electrocardiogram testing typically shows an early and excessive increase of heart rate in response to minimal exercise (heart rate greater than 130 beats/min within 90 seconds of exercise; Bruce protocol), with a maximal heart rate achieved rapidly. This heart rate response is differentiated from physical deconditioning by chronicity and the presence of associated symptoms.

Isoproterenol Provocation

Isoproterenol provocation helps demonstrate sinus node hypersensitivity to β -adrenergic stimulation. Isoproterenol is administered as escalating IV boluses at 1-minute intervals, starting at 0.25 μ g, with doubling of the dose every minute, until a target heart rate increase of 35 beats/min higher than baseline or a maximum heart rate of 150 beats/min is reached. In patients with IST, the target heart rate is reached with an isoproterenol dose of $0.29 \pm 0.1 \mu$ g (vs. $1.27 \pm 0.4 \mu$ g in normal controls).

Autonomic Evaluation

Evaluation of autonomic cardiovascular reflexes can include assessment of intrinsic heart rates, heart rate variation in response to deep breathing, standing and Valsalva maneuver, baroreflex sensitivity, the cardiovagal response (measured by the cold-face test), as well as blood pressure responses to standing and sustained handgrip. Frequently, IST is associated with marked impairment of baroreflex sensitivity (a measure of vagal reflex activity) at rest and during orthostatic stress, suggesting abnormal function of the efferent parasympathetic pathway. IST patients are less responsive to the cold face test (a modification of the diving reflex), demonstrating a substantial incapacity of the heart rate to decrease. However, the clinical value of such tests is questionable and, hence, their routine use is not recommended.^{11,19–21}

Electrophysiological Testing

Invasive electrophysiological (EP) testing can be considered when other arrhythmias are suspected or when a decision to proceed with catheter ablation is undertaken. It is important to recognize that sinus node modification to target IST is a clinical decision, and it must be

made prior to the invasive EP study itself. The diagnosis of IST and the treatment approach should be established before the patient is brought to the EP laboratory.

DIFFERENTIAL DIAGNOSIS

Postural Orthostatic Tachycardia Syndrome

Postural orthostatic tachycardia syndrome (POTS) is a multisystem disorder of the autonomic nervous system, associated with an abnormal response to standing. POTS is characterized by the presence of symptoms of orthostatic intolerance (i.e., the provocation of symptoms on standing that are relieved by recumbence) associated with an exaggerated heart rate increase (30 beats/min or more, or an absolute sinus rate exceeding 120 beats/min) when moving from a recumbent to a standing position held for more than 30 seconds in the absence of orthostatic hypotension (defined as greater than 20 mm Hg drop in systolic blood pressure). For teenagers (12 to 19 years), the required rate increment is at least 40 beats/min.^{11,12}

POTS typically manifests with symptoms of cerebral hypoperfusion (e.g., lightheadedness, presyncope, visual disturbances, cognitive impairment, mental clouding) and excessive sympathetic hyperactivity (e.g., palpitations, chest pain, anxiety, tremulousness), which can cause substantial functional disability. Only a minority of patients with POTS report frank syncope. Importantly, chronic debilitating conditions (e.g., prolonged bed rest), the use of medications known to diminish vascular or autonomic tone, and disorders that might cause tachycardia (e.g., dehydration, anemia) need to be excluded before the diagnosis of POTS is made.²²

The pathophysiological mechanisms of orthostatic intolerance in POTS are heterogeneous and include impaired regulation of peripheral vascular resistance, hyperadrenergic responses, chronic hypovolemia, and deconditioning. Patients with POTS often have high levels of upright plasma norepinephrine, and many patients have a low blood volume.²³

POTS has been classified into several subtypes, including neuropathic and hyperadrenergic POTS. ‘Neuropathic POTS’ is likely caused by primary partial dysautonomia (likely related to an autoimmune process) or peripheral autonomic denervation secondary to other diseases (e.g., diabetes, multiple sclerosis, amyloidosis, sarcoidosis, systemic lupus, alcohol, chemotherapy). In this form, peripheral vasoconstriction in response to orthostatic stress is impaired due to peripheral autonomic neuropathy, resulting in excessive peripheral venous pooling in the lower extremities and mesenteric vasculature and a state of

TABLE 16.1 Inappropriate Sinus Tachycardia Versus Postural Orthostatic Tachycardia Syndrome

	IST	POTS
Definition	HR >100 beats/min at rest (with a mean 24-h HR >90 beats/min not due to primary causes) associated with distressing symptoms	HR increase of >30 beats/min (or an absolute HR >120 beats/min) that occurs within the first 10 min of standing or upright tilt in the absence of orthostatic hypotension, associated with distressing symptoms
HR response to postural change	Increase, but less pronounced than that in POTS. Also, the increase in HR in IST occurs immediately upon standing, unlike POTS.	Profound HR increase (≥ 30 beats/min)
Trigger of tachycardia	Tachycardia is induced by both physiological and emotional stresses without regard to body position	Tachycardia is generally induced only by orthostatic stress
Resting HR in the supine position	Frequently higher than 100 beats/min	Usually within normal range, and rarely exceed 100 beats/min
Response of norepinephrine plasma levels to postural change	Generally, no exaggerated change in norepinephrine levels	Norepinephrine levels increase to ≥ 600 pg/mL is suggestive of hyperadrenergic POTS

HR, Heart rate; IST, inappropriate sinus tachycardia; POTS, postural orthostatic tachycardia syndrome.

“functional” hypovolemia (i.e., low central blood volume) and cerebral hypoperfusion. This, in turn, triggers a sympathetic reflex causing a compensatory increase in both heart rate and myocardial contractility. “Hyperadrenergic POTS” is associated with excessive sympathetic discharge, which can be primary (e.g., norepinephrine reuptake transporter deficiency secondary to genetic mutations), or secondary (precipitated by hypovolemia or drugs). Most patient with hyperadrenergic POTS display exaggerated response to isoproterenol infusion and extremely high plasma levels of norepinephrine (greater than 600 ng/mL) during upright posture.^{11,20,24}

IST shares several characteristics with POTS. Both IST and POTS appear to have abnormal autonomic modulation, associated with exaggerated sinus rate response to orthostatic stress and a multitude of cardiac and noncardiac symptoms that can be debilitating. In addition, both syndromes occur predominantly in young women. Nonetheless, important differences exist between the two conditions (Table 16.1), and the distinction between IST and POTS is important since IST treatments (including catheter ablation of the sinus node) rarely improve, and can even worsen, symptoms in patients with POTS. On the other hand, treatments for POTS can be useless for IST.^{11,12} If orthostatic vital signs are normal and the clinical suspicion of POTS is high, a tilt-table test might be helpful because it can provide vital signs over more prolonged periods than a simple stand test.²⁰

Supraventricular Tachycardia

Supraventricular tachycardias (SVTs), especially sinus nodal reentry or ectopic atrial tachycardias arising at the vicinity of the sinus node, can potentially mimic IST. In addition, IST has been observed following catheter ablation of SVT, in particular following ablation in the Koch’s triangle area (slow and fast pathways of atrioventricular node [AVN], or bypass tracts), which is suspected to result from autonomic dysfunction after ablation and loss of parasympathetic regulation. Therefore careful evaluation is warranted to distinguish the cause of palpitations following an ablation procedure (IST vs. recurrent SVT).²⁵ Fortunately, the post-ablation form of the disorder tends to be transient, with symptoms dissipating within 3 to 4 months post-ablation in the majority of patients.

SVTs typically present with paroxysmal episodes of tachycardia characterized by sudden onset and termination. Warm up and cool down over a few beats also can be observed, especially during automatic atrial tachycardias (ATs). In contrast, IST is nonparoxysmal and is

characterized by more gradual increase and gradual decrease in heart rate with changes in autonomic tone or at the initiation and termination of the tachycardia, respectively.

Adenosine and vagal maneuvers result in either no effect or abrupt termination of SVT, as opposed to gradual slowing of IST. However, automatic ATs can respond to these interventions with transient slowing of the tachycardia rate followed gradual resumption of the AT rate.

Incessant AT can present a diagnostic challenge. Those ATs can be sustained for hours or days, and the tachycardia rate can vary with variations in the level of autonomic tone. Nonetheless, the tachycardia rate typically remains elevated, even during sleep. IST, in contrast, displays more pronounced nocturnal rate variability. Also, incessant ATs usually arise from foci away from the sinus node (most commonly form the atrial appendages and pulmonary veins); therefore the tachycardia P wave usually has a markedly different morphology from the sinus P wave, which facilitates the diagnosis. Furthermore, while SVTs can be associated with long or short RP intervals, IST is invariably associated with long RP intervals (i.e., RP interval longer than PR interval). If SVTs are suspected, an EP study may be considered.

PRINCIPLES OF MANAGEMENT

Conservative medical management with a multidisciplinary approach is the mainstay of therapy for patients with IST. Significant care and attention, effective communication, and patient education are fundamental aspects in management. It is also important to remain empathetic to patients’ complaints and avoid dismissal and minimization of the impact IST can have on the patient’s quality of life.¹¹

Patients will likely benefit by understanding of the basic pathophysiology, natural history, and prognosis of IST. Also, patients should be informed about the expected success and the potential side effects of the various treatment strategies currently available. Patients should be encouraged and empowered to participate in the decision-making process.

Lifestyle changes are beneficial, including avoiding stimulants (drugs, alcohol, and caffeine) and preserving consistent sleep patterns. Exercise training, especially coupled with beta-blocker therapy, can potentially improve quality of life, although the benefit remains unproven.^{11,13}

Pharmacological Therapy

Currently, treatment of IST is generally palliative and directed at controlling symptoms. Heart rate reduction is a goal for most treatment

strategies; however, controlling the heart rate may not alleviate symptoms. Beta-blockers are prescribed as first-line therapy for most patients. Nondihydropyridine calcium channel blockers (verapamil and diltiazem) are acceptable alternatives when beta-blockers are ineffective or not tolerated. Small dosages of benzodiazepines and beta-blocker combinations may also be considered. However, all these regimens have been limited by poor long-term tolerance to the drugs, disappointing long-term clinical response, and lack of strong evidence for benefit.^{11–13}

Ivabradine is a novel selective inhibitor of cardiac pacemaker ion current (I_f), which is highly expressed in the sinus node and contributes to sinus node automaticity. Ivabradine selectivity induces heart rate reduction without any modification in cardiac contractility, or atrioventricular and intraventricular conduction times. Blockade of the I_f current induced by ivabradine is dose and heart rate dependent, resulting in greater effects during fast heart rates and limiting the risk of symptomatic bradycardia. Clinical trials have demonstrated ivabradine to be an effective anti-anginal agent in patients with ischemic heart disease and to offer significant hemodynamic benefits in patients with systolic heart failure and higher baseline heart rates. Several smaller studies also suggest that ivabradine lowers the mean daily and maximal heart rates in patients with IST, improves symptoms, enhances exercise-stress tolerance, and markedly improves quality of life. Ivabradine may be considered a second-line therapy in patients refractory to or intolerant of beta-blockers and nondihydropyridine calcium channel blockers. Ivabradine can also provide benefits when added to beta-blocker therapy. However, large-cohort studies are needed to confirm these results, and long-term safety and efficacy of ivabradine are still to be evaluated.^{13,25–27}

Treatments targeting volume expansion (e.g., generous salt and fluid intake, fludrocortisone, erythropoietin), sympatholytic agents (clonidine, reserpine), cholinesterase inhibitors (pyridostigmine), and phenobarbital have been suggested, but clinical experience is very limited.^{11,12,28} Inconsistent responses to various therapies may suggest that different root causes produce a common apparent phenotype (IST).

Catheter Ablation

Sinus node modification by catheter ablation remains a potentially important therapeutic option in the most refractory cases of IST. Despite high acute procedural success rates (76% to 100%) in reducing sinus rates, the long-term clinical success of catheter ablation for IST remains low (recurrence of symptoms in 27% to 45%, in many cases despite successful reduction of rate), and the risk of complications is significant. Therefore the procedure should be considered as a last resort treatment and only for highly selected patients with debilitating symptoms that are directly related to sinus tachycardia, who have failed lifestyle modifications and all pharmacological treatments, and who have no evidence of other autonomic abnormalities (e.g., POTS).^{11,12,13}

Importantly, if symptoms (especially palpitations) persist despite adequate rate control achieved with medications, sinus node modification would not be expected to offer additional benefit. Furthermore, catheter ablation of the sinus node can result in devastating hemodynamic effects in patients with POTS. Sinus node modification can eliminate the “appropriate” reflex sinus tachycardia needed to overcome the abnormal orthostatic changes (inappropriate vasodilation or inadequate vasoconstriction) in these patients, which can lead to significant hypotension. Therefore the accurate distinction between IST and POTS is extremely important before considering sinus node modification procedures.

Because of the possibility of unsatisfactory results of ablation, it is important to have an understanding with the patient and family about likely outcomes and implications (needing a pacemaker or repeat ablation procedure, persistence of symptoms despite good heart rate control) prior to an ablation procedure.¹³

Surgical Ablation

Multiple surgical techniques have been described for the treatment of IST. Traditionally, surgical ablation of the sinus node is performed through a median sternotomy and cardiopulmonary bypass approach. The procedure is also performed using a thoracoscopic approach or through a mini thoracotomy. Both the traditional and minimally invasive techniques have been associated with limited clinical efficacy and high risk of symptomatic bradycardia requiring permanent pacing therapy. Hence, these treatment approaches are not considered except for the extreme cases and only after all other therapeutic options have been exhausted.^{29,30}

ELECTROPHYSIOLOGICAL TESTING

The goals of EP testing in patients with IST are to exclude other tachycardias that can mimic sinus tachycardia, such as AT originating near the superior aspect of the crista terminalis or right superior pulmonary vein, and to ensure that the tachycardia occurring spontaneously or with isoproterenol infusion acts in a manner consistent with an exaggeration of normal sinus node physiology.

Sedation during procedures is problematic; excessive sedation can potentially impede the ability to initiate other SVTs that mimic IST, as well as creating uncertainty as to what the endpoint heart rate should be after sinus node modification (see later); on the other hand, these procedures can last several hours during which significant patient movement (if not sedated) can potentially invalidate extensive and detailed mapping. Most operators use some form of sedation during these procedures.

For activation mapping, a multipolar (20-pole) crista catheter is placed along the crista terminalis in addition to the catheters used for a routine EP evaluation (coronary sinus, His bundle, and right ventricle [RV]). The crista catheter is positioned on the crista terminalis from the superomedial aspect originating at the junction of the SVC and RA appendage, with continuation along the crista toward the junction of the IVC and RA inferolaterally. Catheter contact with the crista terminalis can be enhanced by using a long sheath (Fig. 16.2). Intracardiac echocardiography (ICE) also may be used to identify the crista terminalis and guide mapping catheter positioning as well as radiofrequency (RF) ablation (see later).

Induction of Tachycardia

Programmed electrical stimulation is performed before and after isoproterenol infusion. Isoproterenol infusion is started at 0.5 to 1.0 $\mu\text{g}/\text{min}$ and titrated every 3 to 5 minutes to a maximum of 6 $\mu\text{g}/\text{min}$. Atropine (1 mg) can also be administered to assess the maximum sinus rate.

It is important to document failure to induce AT and other SVTs during programmed stimulation. IST cannot be initiated with atrial rapid pacing or extrastimulation, but it can be induced by adrenergic stimulation. Initiation of IST is associated with a gradual increase of the sinus rate, with a gradual shift of the earliest atrial activation site up the crista terminalis.

The relevance of EP phenomena, such as dual AVN physiology or AVN echo beats, should be cautiously evaluated in patients in whom the only documented symptomatic tachycardia appears to have a sinus mechanism. Targeting these bystander substrates by catheter ablation can be associated with significant risks and no clinical benefit.

Tachycardia Features

The atrial activation sequence during IST is characterized by a cranio-caudal activation sequence along the crista, with the site of earliest atrial

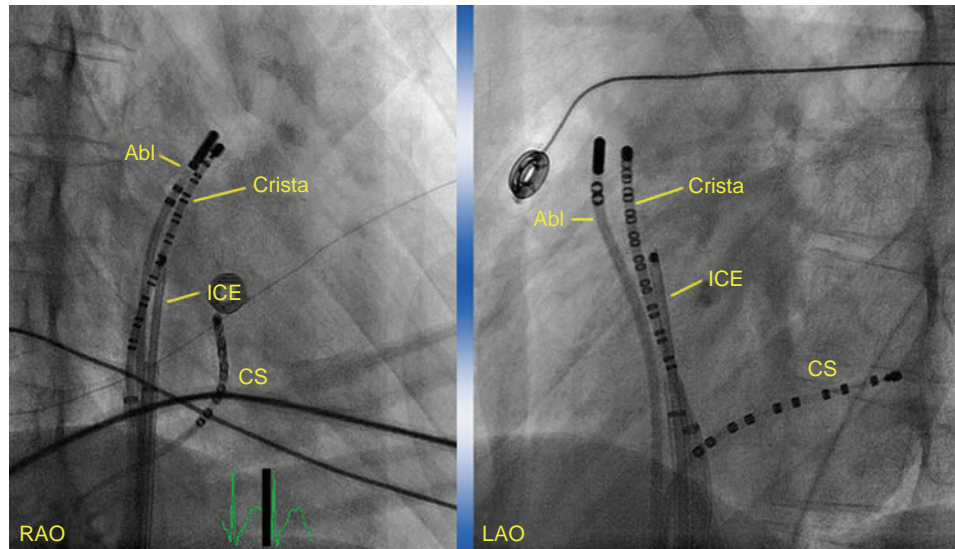


Fig. 16.2 Catheter Ablation of Inappropriate Sinus Tachycardia. Right anterior oblique (RAO) and left anterior oblique (LAO) fluoroscopic view during sinus node modification. Multipolar (crista) catheter is placed along the crista terminalis with intracardiac echocardiography (ICE) guidance. Abl, Ablation catheter; CS, coronary sinus.

activation shifting up the crista at faster rates and down the crista at slower rates. The earliest atrial activation site always occurs along the crista terminalis (as confirmed by the multipolar catheter placed on the crista) despite a changing tachycardia rate or autonomic modulation (isoproterenol and atropine).

In contrast to focal AT, IST is characterized by a gradual increase and decrease in heart rate with changes in autonomic tone or at the initiation and termination of the tachycardia. In addition, adrenergic stimulation reproducibly causes an increase in IST rate and a cranial shift in atrial activation along the crista terminalis, whereas vagal stimulation causes slowing of the IST rate with caudal shift.

Exclusion of Other Arrhythmia Mechanisms

Several clues can help distinguish sinus tachycardia from sinus node reentrant tachycardia and focal AT. Sinus node reentry is easily and reproducibly initiated with atrial extrastimulation (AES), and AT can be initiated with AES, burst pacing, or adrenergic stimulation. In contrast, IST cannot be initiated with programmed electrical stimulation. In addition, initiation of AT and sinus node reentrant tachycardia is accompanied by a sudden change in atrial rate (although AT can then warm up over a few beats), as opposed to the gradual increase of the IST rate over seconds to minutes. Furthermore, the atrial activation sequence shifts suddenly at the onset of AT or sinus node reentrant tachycardia, as opposed to a gradual cranial shift of the earliest atrial activation up the crista terminalis with adrenergic stimulation as the sinus rate increases during IST. Although the rate of focal AT can continue to increase with continued adrenergic stimulation, this is not associated with a further shift in the atrial activation sequence.

Sinus node reentry is easily and reproducibly terminated with programmed stimulation, whereas IST cannot be terminated with programmed stimulation. The termination of focal AT and sinus node reentry is sudden, as opposed to gradual slowing (cool-down) of the IST rate (Fig. 16.3). Vagal maneuvers result in abrupt termination of sinus node reentry and in either no effect or abrupt termination of AT, while a gradual slowing and inferior shift down the crista terminalis of the site of origin characterizes IST. Abrupt termination of the tachycardia

with a single RF application suggests AT because IST originates from a widespread area involving the superior crista terminalis.

ABLATION

Target of Ablation

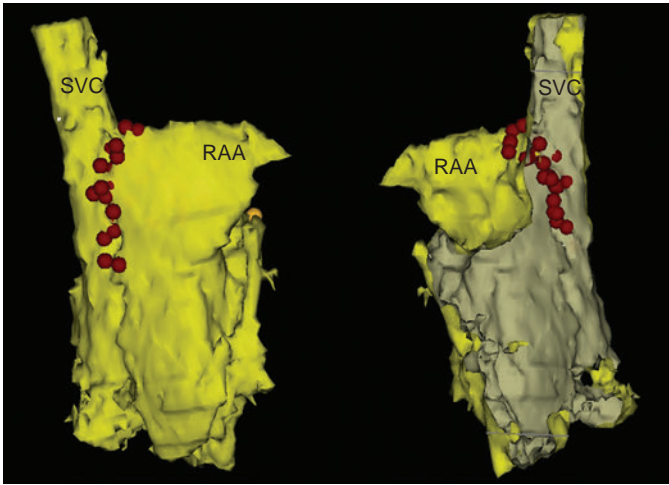
Understanding the anatomy and physiology of the sinus node (see Chapter 8) is critical for identifying the target of ablation for sinus node modification. The sinus node region is a distributed complex characterized by rate-dependent site differentiation (i.e., there is anatomical distribution of impulse generation with changes in sinus rate), which allows for targeted ablation to eliminate the fastest sinus rates while maintaining some degree of sinus node function.

Sinus node modification targets the site of most rapid discharge, generally at the superior aspect of the crista terminalis. One must recognize, however, that sinus node modification is not a focal ablation, but requires complete abolition of the cranial portion of the sinus node complex (eFig. 16.1). Ideally, this procedure eliminates the areas of the sinus node responsible for rapid rates while preserving some chronotropic competence.

Of note, while the head and proximal body portion of the sinus node usually are located subepicardially, lying 0.1 to 1.0 mm beneath the fatty tissue of the sulcus terminalis on the epicardial surface, the remaining nodal body and tail portions penetrate inferiorly and obliquely into the musculature of crista terminalis to end subendocardially almost to the IVC. This is relevant to the ablation procedure, since the superior portion of the sinus node (which constitutes the target of ablation) can be more difficult to ablate with endocardial catheter techniques. On the other hand, the inferior portion of the sinus node, which is to be preserved, is likely to be more vulnerable to endocardial ablation.³

Ablation Technique

The crista terminalis is not visible on fluoroscopy and has a varied course among patients. Therefore some operators prefer using ICE to help identify the crista, position the tip of the ablation catheter with firm contact on the crista, and assess the RF lesion (see eFig. 11.9). A



eFig. 16.1 Integrated computed tomography (CT) and electroanatomic (CARTO) map of the right atrium acquired during sinus node modification. Right anterior oblique and cardioscopic views of the CT scan are shown. Note the area targeted by radiofrequency ablation (*red dots*) starting cranially at the medial portion of the crista as it courses in front of the superior vena cava (SVC). RAA, Right atrial appendage.

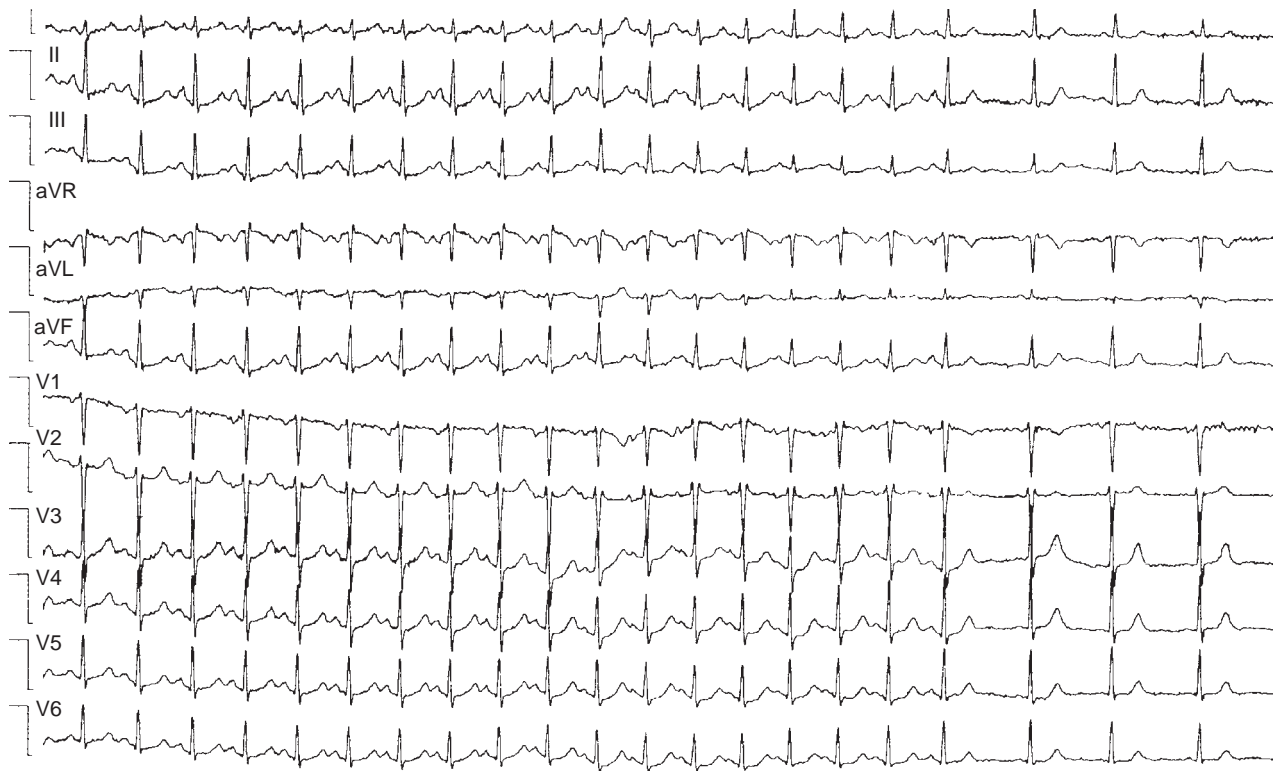


Fig. 16.3 Focal Atrial Tachycardia. A 12-lead electrocardiogram showing perinodal focal atrial tachycardia (or sinus node reentrant tachycardia) with abrupt termination and restoration of normal sinus rhythm. Note the similarities between the tachycardia and sinus P wave morphology.

3-D contact mapping system (CARTO, NavX, Rhythmia) or noncontact mapping can also help delineate relevant anatomical structures (SVC, boundaries of atrium), define the extent of the earliest site of activation during IST, delineate the course of the phrenic nerve (sites at which pacing stimulates the diaphragm), and catalog the sites of ablation (Fig. 16.4).^{31,32} Some operators define the site of earliest activation during the resting baseline rhythm and tag this region as one to hopefully avoid during subsequent ablation (eFig. 16.2).

A multipolar catheter is placed along the crista terminalis (with or without ICE guidance). A standard ablation catheter with a 4- or 8-mm-tip or an irrigated-tip catheter is used for RF application. For nonirrigated ablation, RF power is adjusted to achieve a tip temperature of 50°C to 60°C or an impedance drop of 5 to 10 Ω , or both. For irrigated ablation, RF power up to 40 to 50 W may be considered, keeping the tip temperature less than 43°C.³³

RF lesions are applied as guided by the earliest atrial activation time, usually along superior regions of the crista terminalis using the guidance of the crista catheter. The local endocardial activation time recorded by the ablation catheter at successful sites typically precedes the onset of the surface P wave during the tachycardia by 25 to 45 milliseconds (Fig. 16.5).

RF ablation is performed under maximal adrenergic stimulation with isoproterenol (with or without parasympathetic blockade with atropine) to reveal the superior portions of the crista terminalis as the earliest sites of atrial activation. The medial portion of the crista as it courses in front of the SVC is usually the site of earliest activation for the fastest sinus rates; this portion of the crista should be targeted by RF ablation first. Progressively inferior portions of the crista are then ablated until the target heart rate reduction is achieved. Whenever a sustained change in sinus rate or P wave axis is observed, activation mapping is repeated to identify the new sites with the earliest atrial

activation to target with ablation (see Fig. 16.4). This technique often requires ablating an estimated area of $12 \pm 4 \times 19 \pm 5$ mm.

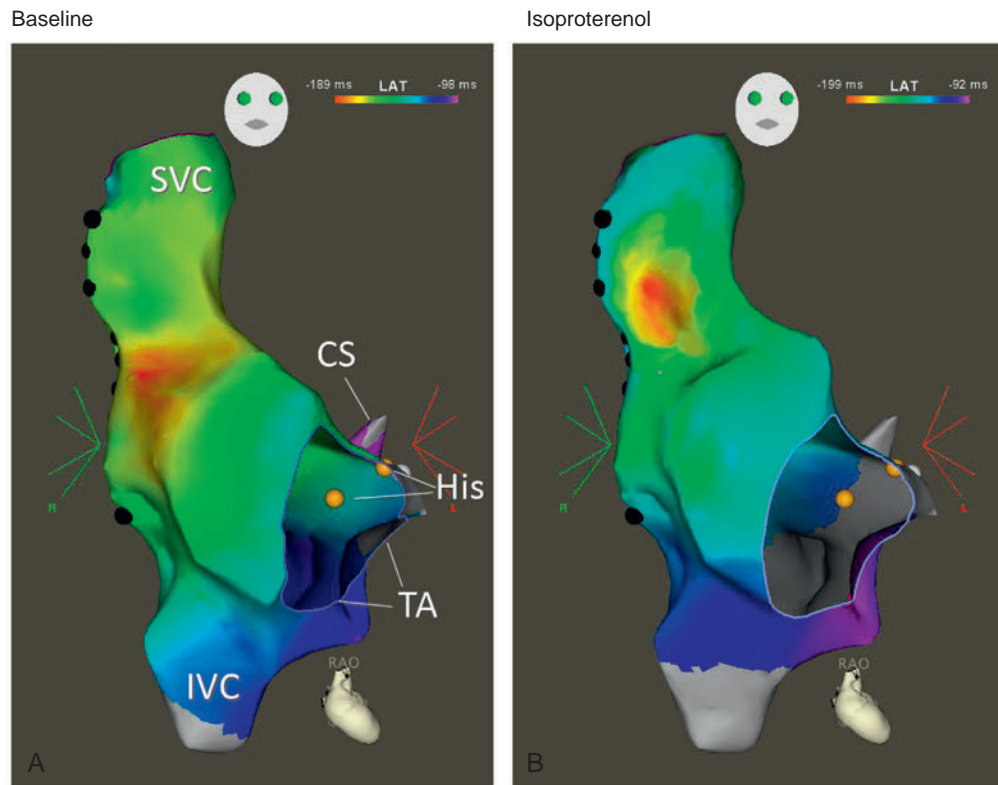
RF energy delivery at any one site should probably be limited to 30 seconds because these are usually closely spaced applications, which carry the risk of char formation with longer applications. Pacing from the ablation catheter tip at high output (5 to 10 mA) is necessary before each RF application to verify the absence of diaphragmatic stimulation to avoid phrenic nerve injury.

Acceleration of the sinus rate followed by a marked subsequent rate reduction or the appearance of a junctional rhythm during ablation is an indicator of a successful ablation site. Most patients demonstrate a stepwise reduction in sinus rate during the course of ablation, which is associated with migration of the site of earliest atrial activation in a craniocaudal direction along the crista terminalis (see Fig. 16.5). However, it is not uncommon to observe an abrupt reduction in the sinus rate in response to RF ablation at a focal site of earliest atrial activation (Fig. 16.6). Echocardiographic lesion characteristics using ICE can also provide a guide for directing additional RF lesions. The effective RF lesion has an increased or changed echodensity completely extending to the epicardium with the development of a trivial linear low-echodensity or echo-free interstitial space, which suggests a transmural RF lesion.³³

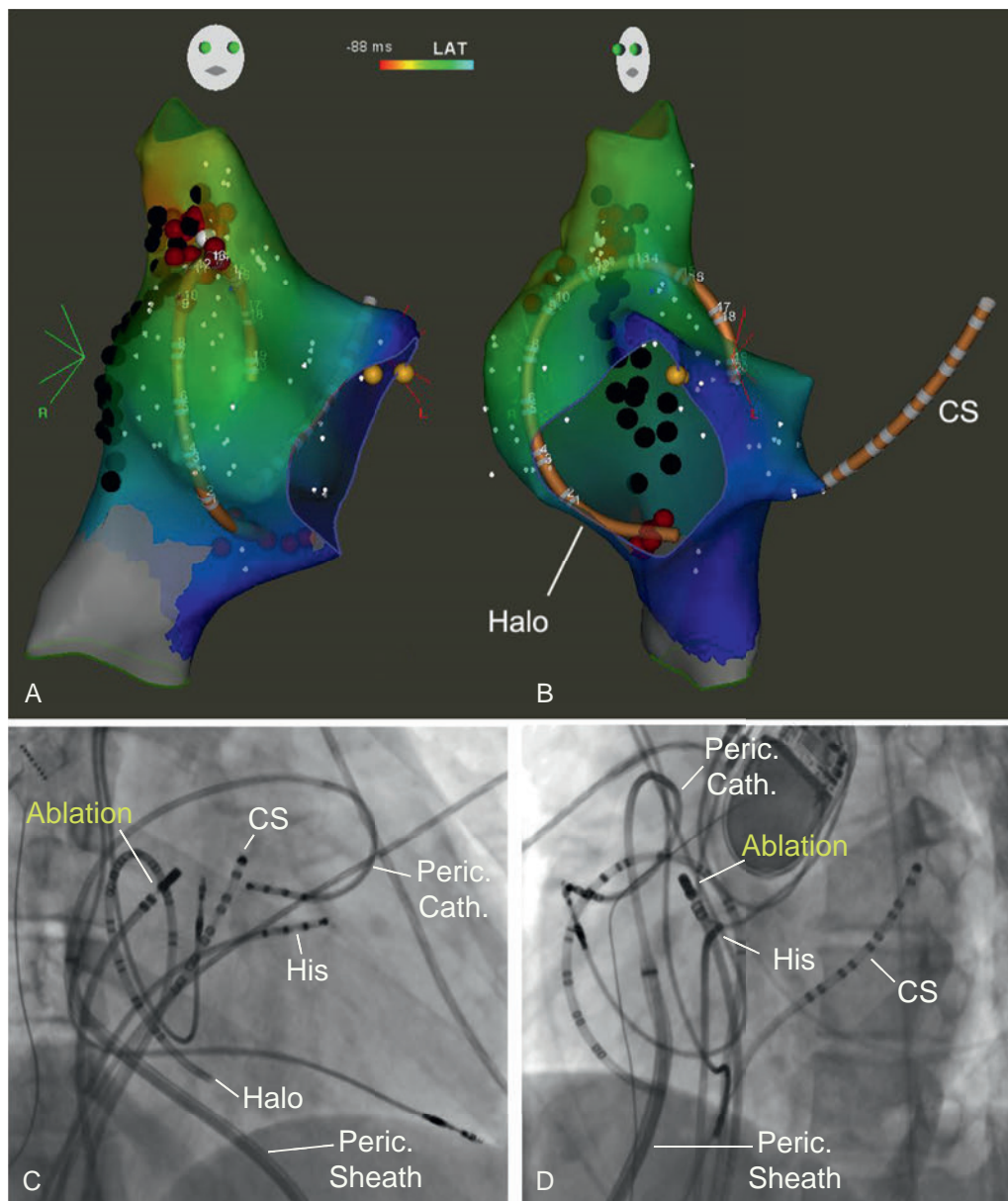
Feasibility of the epicardial ablation (via the subxiphoid pericardial approach) for sinus node modification has been recently demonstrated in a small series. Epicardial access can also help reduce the risk of phrenic nerve injury during endocardial ablation. Instilling saline or placing a deflectable electrode catheter in the pericardial space can help physically displace the phrenic nerve from the ablation zone (eFig. 16.3).^{34,35}

Endpoints of Ablation

Acute procedural success is defined as: (1) abrupt reduction of the sinus rate by 30 beats/min or more during RF delivery or a 20% to 25%



eFig. 16.2 Use of isoproterenol to “force” site of impulse formation to more cephalad portion of sinus node. (A) Baseline electroanatomic activation map of sinus rhythm showing a site (*red*) at the junction of the superior vena cava (SVC) and right atrial body. (B) After isoproterenol administration, the site of earliest activation has moved closer to the SVC. Black dots are sites of phrenic nerve capture. CS, Coronary sinus; IVC, inferior vena cava; TA, tricuspid annulus.



eFig. 16.3 Phrenic nerve displacement during sinus node modification. (A and B) Electroanatomic maps in a patient with inappropriate sinus tachycardia showing ablation sites (*red dots*) very close to sites of phrenic nerve capture (*black dots*). (C and D) Fluoroscopic views of catheters during sinus node modification. A deflectable quadripolar electrode catheter (*Peric. Cath.*) has been introduced through a sheath in the pericardium (*Peric. Sheath*) to physically displace the right phrenic nerve and enable safe ablation of the sinus node region from an endocardial approach. A and C are shown in right anterior oblique projection. B and D are shown in left anterior oblique projection. CS, Coronary sinus catheter.

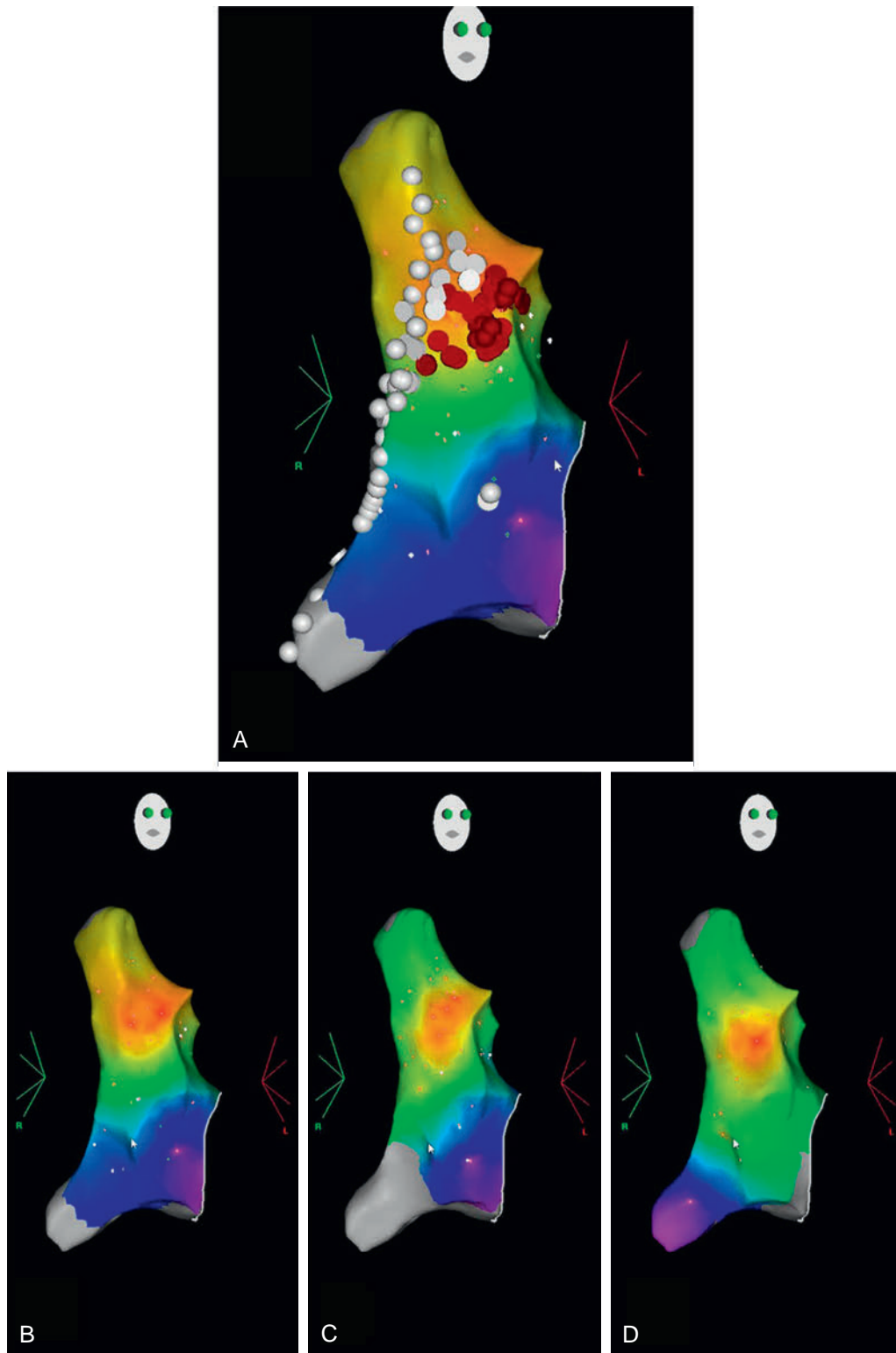


Fig. 16.4 Electroanatomic Map of Inappropriate Sinus Tachycardia. (A) Right anterior oblique view of the right atrium showing electroanatomic (CARTO) activation map of inappropriate sinus tachycardia. White dots indicate course of phrenic nerve capture during high-output pacing; red dots indicate ablation lesions. (B to D) Successful ablation with repeat activation mapping showing shifts of the site of origin of the sinus P wave from the superior aspect of the crista terminalis (B) at baseline to progressive more caudal sites (C and D) along the crista as a result of ablation of sinus node modification. (Modified from Peyrol M, Lévy S. Clinical presentation of inappropriate sinus tachycardia and differential diagnosis. *J Interv Card Electrophysiol.* 2015;46:33–41.)

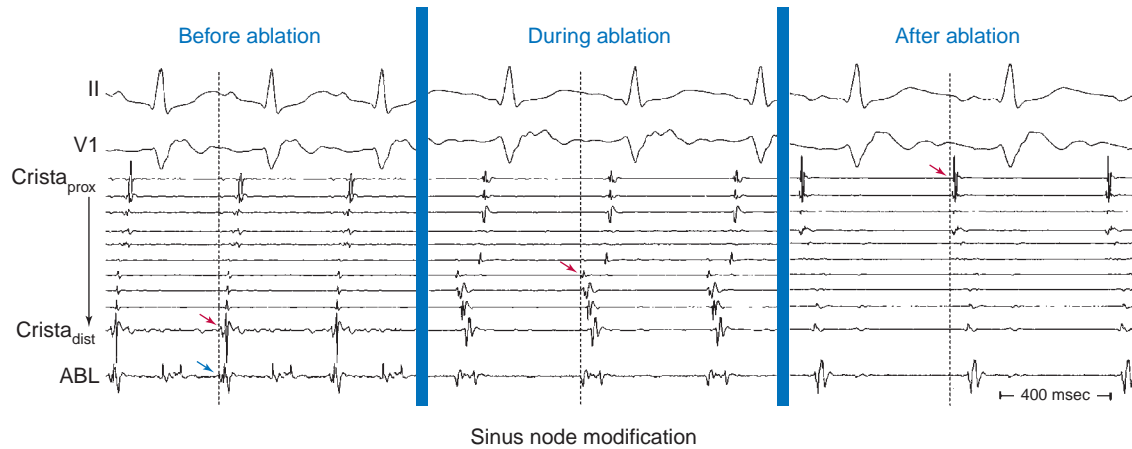


Fig. 16.5 Intracardiac Recordings During Sinus Node Modification. *Left panel*, Before ablation (ABL) and under adrenergic stimulation, sinus tachycardia is observed, with the earliest local activation (red arrows) recorded by the most distal (cranial) electrodes of the crista catheter, just anterior to the superior vena cava-right atrial junction. Note that local activation recorded by the ablation catheter (blue arrow) precedes the onset of the P wave (indicated by the vertical dashed line) by 20 to 30 milliseconds. *Middle panel*, Following ablation of the most cranial part of the sinus node, the sinus rate becomes slower, and the activation sequence shifts toward more proximal (caudal) electrodes 7 to 8 on the crista catheter. *Right panel*, Following successful sinus node modification, the sinus rate (under constant adrenergic stimulation) is reduced by more than 30%, and the atrial activation sequence shifts to the most proximal (caudal) crista catheter electrodes. Note the P wave is now inverted in lead II. *dist*, Distal; *prox*, proximal.

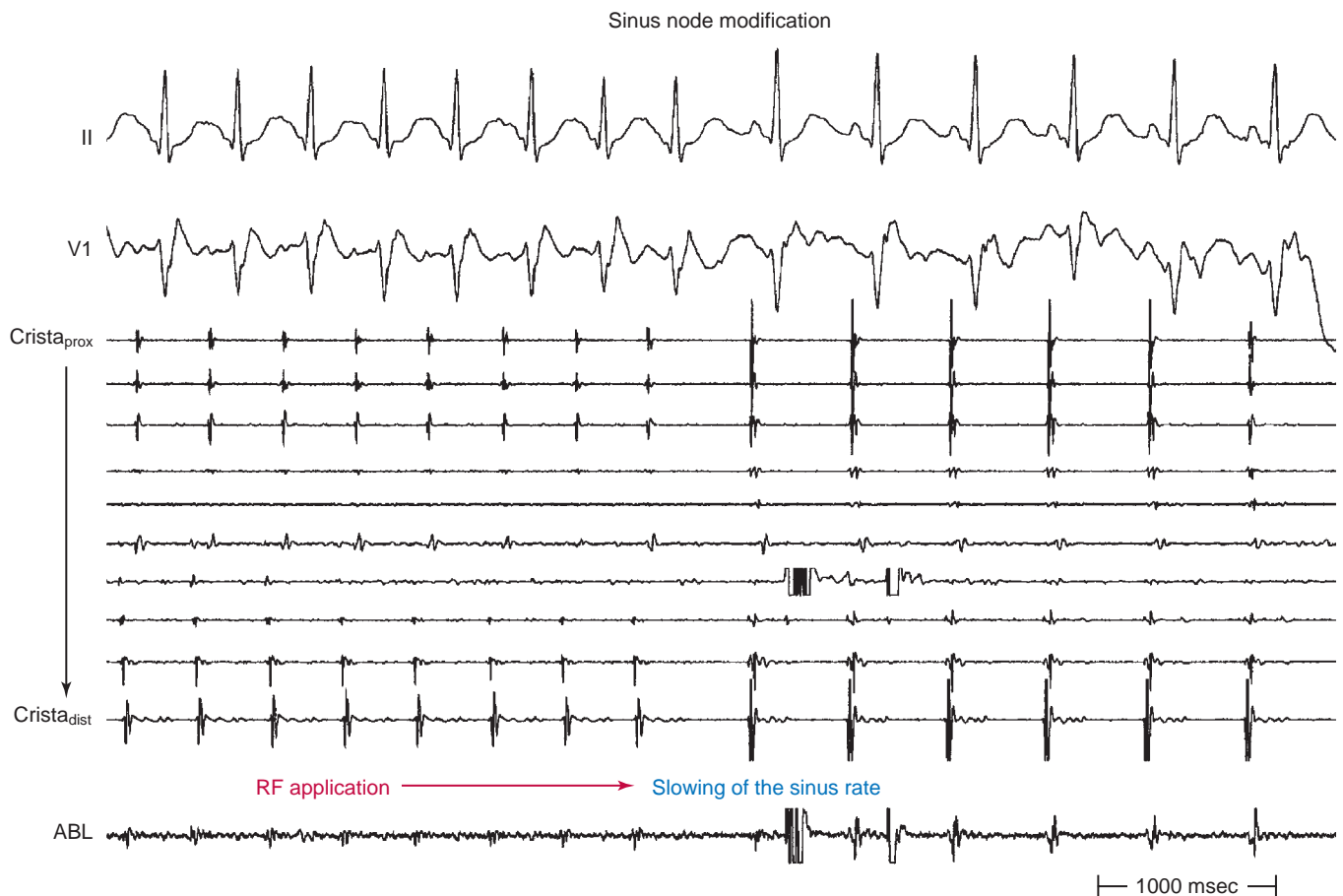


Fig. 16.6 Sinus Node Modification. An abrupt reduction in the sinus rate is observed in response to radio-frequency (RF) ablation (ABL) at a focal site of earliest atrial activation. *dist*, Distal; *prox*, proximal.

decline in maximum heart rate (or an absolute sinus rate of less than 120 beats/min) during infused isoproterenol and atropine; (2) persistent reduction of the resting sinus rate by 10% or more (or an absolute resting sinus rate of less than 90 beats/min); (3) maintenance of a superiorly directed P wave (negative P wave in lead III); and (4) inferior shift of the site of earliest atrial activation down the crista terminalis, even with maximal adrenergic stimulation.³³

RF ablation of IST often is difficult and requires multiple RF applications; a mean of 12 RF applications (range, 6 to 92) was required in one study. The resilience of the sinus node to endocardial catheter ablation can be explained, in part, by the architectural features of the node—the dense matrix of connective tissue in which the specialized sinus node cells are packed; the cooling effect of the nodal artery; the subepicardial nodal location; and the thick terminal crest, particularly in relation to the nodal portion caudal to the sinus node artery. In addition, the length of the sinus node, the absence of an insulating sheath, the presence of nodal radiations, and caudal fragments offer a potential for multiple breakthroughs of the nodal wavefront.³³

Outcome

Prior to undertaking ablation of the sinus node for IST, both the physician and the patient should have realistic expectations and understanding of the goals of ablation and potential outcomes. Relatively few patients will achieve the desired combination of relief of symptoms and normal resting heart rate and chronotropic response without the need for implantation of a permanent pacemaker. In some patients, symptoms persist despite successful EP endpoints of the ablation procedure. In others, IST is replaced by an equally (or even more) bothersome accelerated junctional rhythm at 80 to 90 beats/min with retrograde conduction. In these patients, a generalized dysautonomia can potentially be the underlying cause.

RF ablation is, at best, only modestly effective for managing patients with IST. Although short-term success rates can be favorable (76% to 100%), long-term outcomes are disappointing, with clinical success rates ranging between 23% and 83%. Complete ablation of the sinus node (targeting the entire crista terminalis) resulting in junctional rhythm has better long-term success (72%) but requires pacemaker insertion.^{33,36}

Most recurrences occur 1 to 6 months after the procedure and are typically related to tachycardia recurrence after an initially successful procedure. A repeat procedure may be necessary in patients with intolerable symptoms. Symptomatic recurrence or persistence of symptoms in the absence of documented IST and despite persisting evidence of a successful EP outcome has been observed in some cases. Persistent symptoms, despite heart rate reduction, may be suggestive of a more global dysautonomia that also happens to affect the sinus node.^{33,12}


Complications of sinus node modification include cardiac tamponade, SVC syndrome, diaphragmatic paralysis, and sinus node dysfunction. Cardiac tamponade is rare and usually is caused by penetration of an unattended RV catheter in a thin female patient with rapid and vigorous heart action because of high-dose isoproterenol infusion. Transient SVC syndrome can develop because of extensive lesion creation and edema at the SVC-RA junction. This can rarely cause permanent SVC stenosis. More targeted ablation using ICE may help avoid this complication.

Diaphragmatic paralysis secondary to damage to the right phrenic nerve should be minimized if ablative lesions are confined to the crista itself or placed just anterior to it. Using ICE to guide ablation makes this complication unlikely because the phrenic nerve is a posterior structure. Pacing with a high output (greater than 10 mA at 2 milliseconds) from the ablation catheter at the target site without capture of the phrenic nerve and continuous pacing higher in the SVC to capture the phrenic nerve during RF ablation are reassuring, but their efficacy

has never been assessed; in fact, there have been cases in which phrenic palsy developed several days after ablation despite taking all the above precautions. In addition, suspicion of phrenic nerve injury should be considered in the case of hiccup, cough, or a decrease in diaphragmatic excursion during energy delivery. Early recognition of phrenic nerve injury during RF delivery allows the immediate interruption of the energy application prior to the onset of permanent injury and is associated with rapid recovery of phrenic nerve function. If phrenic nerve injury prohibits ablation at desired endocardial sites, displacement of the phrenic nerve from the ablation target site via saline injection or balloon catheter placement in the pericardial space (through the sub-xiphoid approach) can be considered.^{34,35,37} Persistent slow junctional rhythm requiring pacemaker insertion is rare. Such junctional rhythm usually disappears with the return of sinus rhythm within several days.³⁸

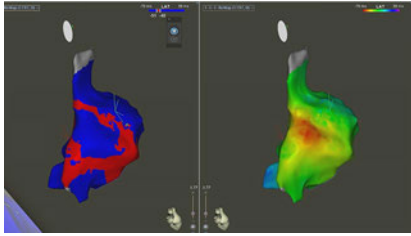
VIDEOS

The following video accompanies this chapter:

Video 16.1. Sinus Node Modification: CARTO Activation and Propagation Maps 

REFERENCES

1. Sánchez-Quintana D, et al. Sinus node revisited in the era of electroanatomical mapping and catheter ablation. *Heart*. 2005;91:189–194.
2. Anderson RH, Yanni J, Boyett MR, et al. The anatomy of the cardiac conduction system. *Clin Anat*. 2009;22:99–113.
3. Murphy C, Lazzara R. Current concepts of anatomy and electrophysiology of the sinus node. *J Interv Card Electrophysiol*. 2016;46:9–18.
4. Ho SY, Sánchez-Quintana D. Anatomy and pathology of the sinus node. *J Interv Card Electrophysiol*. 2016;46:3–8.
5. Fedorov VV, Glukhov AV, Chang R. Conduction barriers and pathways of the sinoatrial pacemaker complex: their role in normal rhythm and atrial arrhythmias. *Am J Physiol Heart Circ Physiol*. 2012;302:H1773–H1783.
6. Unudurthi SD, Wolf RM, Hund TJ. Role of sinoatrial node architecture in maintaining a balanced source-sink relationship and synchronous cardiac pacemaking. *Front Physiol*. 2014;5:446.
7. Nikolaidou T, Aslanidi OV, Zhang H, et al. Structure-function relationship in the sinus and atrioventricular nodes. *Pediatr Cardiol*. 2012;33:890–899.
8. Lau DH, Roberts-Thomson KC, Sanders P. Sinus node revisited. *Curr Opin Cardiol*. 2011;26:55–59.
9. Stiles MK, et al. High-density mapping of the sinus node in humans: role of preferential pathways and the effect of remodeling. *J Cardiovasc Electrophysiol*. 2010;21:532–539.
10. Baruscotti M, Bianco E, Bucchi A, et al. Current understanding of the pathophysiological mechanisms responsible for inappropriate sinus tachycardia: role of the If ‘funny’ current. *J Interv Card Electrophysiol*. 2016;46:19–28.
11. Sheldon RS, et al. 2015 heart rhythm society expert consensus statement on the diagnosis and treatment of postural tachycardia syndrome, inappropriate sinus tachycardia, and vasovagal syncope. *Heart Rhythm*. 2015;12:e41–e63.
12. Olshansky B, Sullivan RM. Inappropriate sinus tachycardia. *J Am Coll Cardiol*. 2013;61:793–801.
13. Page RL, et al. 2015 ACC/AHA/HRS guideline for the management of adult patients with supraventricular tachycardia: a report of the American College of Cardiology/American Heart Association Task Force on Clinical Practice Guidelines and the Heart Rhythm Society. *Circulation*. 2016;133:e506–e574.
14. Chiale PA, et al. Inappropriate sinus tachycardia may be related to an immunologic disorder involving cardiac beta adrenergic receptors. *Heart Rhythm*. 2006;3:1182–1186.



Video 16.1 Sinus Node Modification: CARTO Activation and Propagation Maps. Electroanatomic (CARTO 3) activation maps of the right atrium during sinus rhythm before and after sinus node modification for the treatment of inappropriate sinus tachycardia. The site of origin of the sinus P wave (during maximal isoproterenol stimulation) shifts from the superior aspect of the crista terminalis at baseline to a more caudal site along the crista. *IVC*, Inferior vena cava; *SVC*, superior vena cava.

15. Hildreth CM, Padley JR, Pilowsky PM, et al. Impaired serotonergic regulation of heart rate may underlie reduced baroreflex sensitivity in an animal model of depression. *Am J Physiol Heart Circ Physiol*. 2008;294: H474–H480.
16. Baruscotti M, et al. A gain-of-function mutation in the cardiac pacemaker HCN4 channel increasing cAMP sensitivity is associated with familial inappropriate sinus tachycardia. *Eur Heart J*. 2017;38:280–288.
17. Still A-M, et al. Prevalence, characteristics and natural course of inappropriate sinus tachycardia. *Europace*. 2005;7:104–112.
18. Peyrol M, Lévy S. Clinical presentation of inappropriate sinus tachycardia and differential diagnosis. *J Interv Card Electrophysiol*. 2016;46:33–41.
19. Palamarchuk IS, Baker JR, Kimpinski K. The utility of Valsalva maneuver in the diagnoses of orthostatic disorders. *Am J Physiol Regul Integr Comp Physiol*. 2016;310:R243–R252.
20. Nwazue VC, et al. Postural tachycardia syndrome and inappropriate sinus tachycardia: role of autonomic modulation and sinus node automaticity. *J Am Heart Assoc*. 2014;3:e000700.
21. Ptaszynski P, et al. Noninvasive assessment of autonomic cardiovascular activity in patients with inappropriate sinus tachycardia. *Am J Cardiol*. 2013;112:811–815.
22. Ricci F, De Caterina R, Fedorowski A. Orthostatic hypotension: epidemiology, prognosis, and treatment. *J Am Coll Cardiol*. 2015;66: 848–860.
23. Gamboa A, et al. Inspiratory resistance improves postural tachycardia: a randomized study. *Circ Arrhythm Electrophysiol*. 2015;8:651–658.
24. George SA, et al. The international POTS registry: evaluating the efficacy of an exercise training intervention in a community setting. *Heart Rhythm*. 2016;13:943–950.
25. Ptaszynski P, et al. Ivabradine in combination with metoprolol succinate in the treatment of inappropriate sinus tachycardia. *J Cardiovasc Pharmacol Ther*. 2013;18:338–344.
26. Kumar Goyal V, Godara S, Chandra Sadasukhi T, et al. Management of inappropriate sinus tachycardia with ivabradine in a renal transplant recipient. *Drug Discov Ther*. 2014;8:132–133.
27. Ptaszynski P, Kaczmarek K, Ruta J, et al. Ivabradine in the treatment of inappropriate sinus tachycardia in patients after successful radiofrequency catheter ablation of atrioventricular node slow pathway. *Pacing Clin Electrophysiol*. 2013;36:42–49.
28. Annamaria M, et al. Treatment of inappropriate sinus tachycardia with ivabradine. *J Interv Card Electrophysiol*. 2016;46:47–53.
29. Kreisel D, Bailey M, Lindsay BD, et al. A minimally invasive surgical treatment for inappropriate sinus tachycardia. *J Thorac Cardiovasc Surg*. 2005;130:598–599.
30. Selten K, Van Brakel TJ, Van Swieten HA, et al. Mapping-guided total excision of the sinoatrial node for inappropriate sinus tachycardia. *J Thorac Cardiovasc Surg*. 2014;147:e56–e58.
31. Lin D, et al. Use of noncontact mapping and saline-cooled ablation catheter for sinus node modification in medically refractory inappropriate sinus tachycardia. *Pacing Clin Electrophysiol*. 2007;30: 236–242.
32. Nagarakanti R, Saksena S. Three-dimensional mapping and intracardiac echocardiography in the treatment of sinoatrial nodal tachycardias. *J Interv Card Electrophysiol*. 2016;46:55–61.
33. Gianni C, et al. Catheter ablation of inappropriate sinus tachycardia. *J Interv Card Electrophysiol*. 2016;46:63–69.
34. Jacobson JT, Kraus A, Lee R, et al. Epicardial/endocardial sinus node ablation after failed endocardial ablation for the treatment of inappropriate sinus tachycardia. *J Cardiovasc Electrophysiol*. 2014;25: 236–241.
35. Rubenstein JC, Kim MH, Jacobson JT. A novel method for sinus node modification and phrenic nerve protection in resistant cases. *J Cardiovasc Electrophysiol*. 2009;20:689–691.
36. Rodríguez-Mañero M, et al. Ablation of inappropriate sinus tachycardia: a systematic review of the literature. *JACC Clin Electrophysiol*. 2017;3: 253–265.
37. Ibarra-Cortez SH, et al. Strategies for phrenic nerve preservation during ablation of inappropriate sinus tachycardia. *Heart Rhythm*. 2016;13: 1238–1245.
38. Cuculich PS, Cooper JA, Faddis MN. Superior vena cava obstruction caused by repeated radiofrequency sinus node modification procedures. *Heart Rhythm*. 2009;6:865–866.

Atrioventricular Nodal Reentrant Tachycardia

OUTLINE

Anatomy and Physiology of the Atrioventricular Node, 560

Triangle of Koch, 560

Atrioventricular Node, 560

Pathophysiology, 562

Tachycardia Circuit, 562

Types of Atrioventricular Nodal Reentry, 563

Epidemiology, 566

Clinical Presentation, 567

Initial Evaluation, 567

Principles of Management, 567

Acute Management, 567

Chronic Management, 567

Electrocardiographic Features, 569

Electrocardiographic Manifestations of Dual Atrioventricular Nodal Physiology, 569

Electrocardiographic Manifestations of Atrioventricular Nodal Reentrant Tachycardia, 569

Electrophysiological Testing, 570

Baseline Observations During Sinus Rhythm, 570

Induction of Tachycardia, 575

Tachycardia Features, 578

Diagnostic Maneuvers During Tachycardia, 580

Diagnostic Maneuvers During Sinus Rhythm After Tachycardia Termination, 586

Exclusion of Other Arrhythmia Mechanisms, 587

Ablation, 591

Target of Ablation, 591

Ablation Technique, 591

Endpoints of Ablation, 595

Outcome, 595

Cryoablation of the Slow Pathway, 596

ANATOMY AND PHYSIOLOGY OF THE ATRIOVENTRICULAR NODE

The atrioventricular node (AVN) is the only normal electrical connection between the atria and the ventricles; the fibrous skeleton acts as an insulator to prevent electrical impulses from entering the ventricles by any other route. The main function of the AVN is modulation of atrial impulse transmission to the ventricles; it introduces a delay between atrial and ventricular systole, thereby allowing atrial systole and ventricular filling to complete prior to the initiation of ventricular systole.¹ Another primary function of the AVN is to limit the number of impulses conducted from the atria to the ventricles. This function is particularly important during fast atrial rates (e.g., during atrial fibrillation [AF] or atrial flutter [AFL]), in which only a few impulses are conducted to the ventricles, and the remaining impulses are blocked in the AVN (facilitated by the relatively long refractory period of the AVN). In addition, fibers in the lower part of the AVN can exhibit automatic impulse formation, serving as a subsidiary pacemaker.^{2,3}

Triangle of Koch

The triangle of Koch constitutes the endocardial surface of the region of the lower right atrium (RA) septum. It is bordered anteriorly by the insertion of the septal leaflet of the tricuspid valve and posteriorly by the fibrous tendon of Todaro. The apex of the triangle is formed by the junction of these two boundaries. The base of the triangle is formed by the anteromedial edge of the coronary sinus ostium (CS os) and is continuous with the sub-eustachian pouch (Fig. 17.1; see Fig. 9.2, eFig. 12.1).^{2,3}

The tendon of Todaro is a fibrous band that connects to the central fibrous body as a fibrous extension of the membranous septum. It courses obliquely between the fossa ovalis and the CS os, crossing the eustachian ridge in the floor of the RA, and connecting to the valve of the inferior vena cava (IVC) (eustachian valve).⁴

Of note, the interatrial sulcus is displaced to the far left of the inter-ventricular sulcus; the atrioventricular (AV) valves are not isoplanar; and the attachment of the septal leaflet of the tricuspid valve into the most anterior part of the central fibrous body is displaced a few millimeters apically relative to the attachment of the septal leaflet of the mitral valve. Thus the true septal part of the AV junction (the RA–left ventricle [LV] sulcus) actually separates the inferomedial RA from the posterior superior process of the LV (the right side above the tricuspid valve while the left side is below the mitral valve). Hence, the triangle of Koch can be considered the RA side of the AV muscular septum.

The mean distances from the His bundle (HB) electrogram recording site (at the apex of the triangle of Koch) to the upper and lower lips of the CS os are 10 mm (range, 0 to 23 mm), and 20 to 25 mm (range, 9 to 46 mm), respectively. However, it is important to note that electroanatomic mapping studies revealed individual variations in the locations of the HB and slow pathway recording sites as well as anatomic variations in the sizes of the Koch triangle and the CS os. A downward deviation of the HB to the midseptum is not uncommon, especially in older patients. Such a downward deviation of the HB may account for unexpected AV block during slow pathway ablation.⁵

Atrioventricular Node

The AVN is an intraatrial structure, measuring approximately 5 mm long, 5 mm wide, and 0.8 mm thick in adults. The compact node is

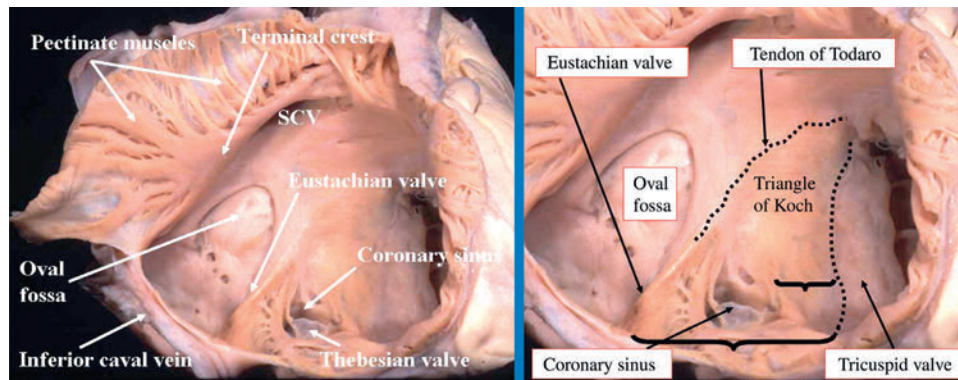


Fig. 17.1 Anatomy of the Triangle of Koch. *Left*, The interior of the morphologically right atrium has been revealed by making a cut in the appendage parallel to the atrioventricular groove, and reflecting the wall of the appendage upwards. Note that the pectinate muscles forming the wall of the appendage take their origin from the terminal crest, and sweep round to insert on the posterior septal wall, having passed beneath the mouth of the coronary sinus, this being guarded by the Thebesian valve. *Right*, The important posterior wall of the right atrium has been enlarged. Note the location of the triangle of Koch, delimited by the site of the tendon of Todaro, the attachment of the septal leaflet of the tricuspid valve, and the mouth of the coronary sinus. The small bracket shows the site of the septal isthmus, whereas the large bracket shows the inferior, or cavotricuspid, isthmus. SCV, Superior caval vein. (From Anderson RH, Cook AC. The structure and components of the atrial chambers. *Europace*. 2007;9[Suppl 6]:3–9.)

adjacent to the central fibrous body on one side but is uninsulated by fibrous tissue on its other sides, thus allowing contiguity with the atrial myocardium. The AVN is located beneath the RA endocardium at the apex of the triangle of Koch, anterior to the CS os and directly above the insertion of the septal leaflet of the tricuspid valve, where the tendon of Todaro merges with the central fibrous body. Slightly more anteriorly and superiorly is where the HB penetrates the AV junction through the central fibrous body and the posterior aspect of the membranous AV septum.

When traced inferiorly, toward the base of the triangle of Koch, the compact AVN area separates into two extensions, usually with the artery supplying the AVN running between them. The prongs bifurcate toward the CS os along the tricuspid annulus (right posterior [inferior] extension) and toward the mitral annulus (left posterior [inferior] extension). The right posterior nodal extension and its corresponding atrionodal (AN) approaches have been implicated as the anatomic substrate for the so-called “slow pathway” in the atrioventricular nodal reentrant tachycardia (AVNRT) circuit. The tachycardia circuit also can involve the left posterior nodal extension (see later). The “fast pathway” is less well defined from an anatomic and structural standpoint. The probable anatomic substrate of this pathway consists of the transitional cell layers located around the compact AVN (in the anterior portion of the triangle of Koch) at the interface between the compact node and the transitional cells.^{2,3,6}

Functionally, based on activation times during anterograde and retrograde propagation, and on the action potential characteristics from microelectrode recordings in the rabbit AV junction, the cells of the AVN and perinodal region are frequently described as AN, N (nodal), and NH (nodal-His), with the AN and NH regions more sodium dependent for depolarization, and the N region being calcium dependent, and the likely region where calcium channel blockers act. The transition from one cell area to the other is gradual, with intermediate cells exhibiting intermediate action potentials with great changes related to the autonomic tone.

Atrionodal Region

The AN region corresponds to the cells in the transitional region that are activated shortly after the adjacent atrial cells. Transitional cells are

histologically distinct from both the cells of the compact AVN and the working atrial myocytes, and they are not insulated from the surrounding myocardium, but tend to be separated from one another by thin fibrous strands. Transitional cells do not represent conducting tracts but a bridge funneling atrial depolarization into the compact AVN via discrete AN inputs (approaches). AN approaches connect the working atrial myocardium from the left and right sides of the atrial septum to the left and right margins of the compact node, with wider extensions inferiorly and posteriorly between the compact node and the CS os and into the eustachian ridge. In humans and animals, two such AN inputs are commonly recognized in the right septal region: the anterior (superior) approaches, which travel from the anterior limbus of the fossa ovalis and merge with the AVN closer to the apex of the triangle of Koch; and the posterior (inferior) approaches, which are located in the inferoseptal RA and serve as a bridge with the atrial myocardium at the CS os. Although both inputs have traditionally been assumed to be RA structures, growing evidence supports the AV conduction apparatus as a transeptal structure that reaches both atria. A third, middle group of transitional cells has also been identified to account for the nodal connections with the septum and left atrium (LA).^{2,3}

Nodal Region

The N region corresponds to the region where the transitional cells merge with midnodal cells. The N cells represent the most typical of the nodal cells, which are smaller than atrial myocytes, are closely grouped, and frequently are arranged in an interweaving fashion. Sodium channel density is lower in the midnodal zone of the AVN than in the AN and NH cell zones. The inward L-type calcium current is the basis of the upstroke of the N cell action potential. The N cells are characterized by a less negative resting membrane potential and low action potential amplitude, slow rates of depolarization and repolarization, few intercellular connections (e.g., gap junctions), and reduced excitability compared with surrounding cells. Therefore conduction is slower through the compact AVN than the AN and NH cell zones. In fact, the N cells in the compact AVN appear to be responsible for the major part of AV conduction delay and exhibit decremental properties in response to premature stimulation because of their slow rising and longer action potentials. Fast pathway conduction through the AVN apparently bypasses

many of the N cells by transitional cells, whereas slow pathway conduction traverses the entire compact AVN. Importantly, the recovery of excitability after conduction of an impulse is faster for the slow pathway than for the fast pathway, for reasons that are unclear.¹

Nodal-His Region

The NH region corresponds to the lower nodal cells, typically distal to the site of Wenckebach block, connecting to the insulated penetrating portion of the HB. The action potentials of the NH cells are closer in appearance to the fast-rising and long-action potentials of the HB.

PATHOPHYSIOLOGY

Tachycardia Circuit

The exact electroanatomic circuit responsible for AVNRT remains elusive. Current evidence suggests that dual AVN pathway physiology constitutes the substrate for AVN reentry. The different atrial inputs to the AVN, rather than functional longitudinal dissociation within the compact AVN, represent the fast and slow pathways involved in the reentrant circuit. The right and left inferior extensions of the AVN and their corresponding AN inputs have been implicated as the anatomic substrate for the slow pathway(s) in the AVNRT circuit. However, the fast pathway is less well defined from an anatomic and structural standpoint. The probable anatomic substrate of this pathway consists of the transitional cell layers located around the compact AVN (in the anterior portion of the triangle of Koch) at the interface between the compact node and transitional cells.^{2,3,6-8}

It is important to recognize that dual AVN physiology characterizes the normal AVN electrophysiology, and the presence of dual (or multiple) AVN pathways can be demonstrated in most individuals with or without AVNRT, and is not necessarily indicative of the existence of functional reentry.^{2,3} However, although the potential substrate for AVNRT (dual pathways) is normally available, only a minority of normal individuals develop AVN reentry. This is likely related to the fact that reentry requires several other conditions to be met at the same time, including appropriately timed conduction times and refractoriness over the two pathways as well as the prevalence of perfectly timed triggers (premature atrial complex [PACs] or premature ventricular complex [PVCs]).

The understanding of the AVN as having superior (anterior) and inferior (posterior) right and left inputs that form the fast and slow pathways, respectively, is a simple conceptual framework that seems to enable the clinician to confront most cases. Reentry occurring along these pathways is the basic mechanism for the various subtypes of AVNRT. The proximal atrial insertions of the fast and slow pathways are anatomically distinct during retrograde conduction, and several important functional differences exist between the two pathways.^{2,3,6-8}

Differences Between the Fast and Slow Pathways

The fast and slow pathways exhibit different electrophysiological (EP) properties. In general, the fast pathway demonstrates faster conduction velocity but longer refractory periods than the slow pathway. However, many exceptions exist.⁶

The fast pathway forms the normal physiological conduction axis, and the atrial-His bundle (AH) interval during conduction over the fast pathway is usually no longer than 220 milliseconds. Longer AH intervals can be caused by conduction over the slow pathway.

Furthermore, the AVN dual pathways are greatly influenced by changes in the sympathovagal balance. Sympathetic stimulation shortens conduction time and refractoriness, whereas vagal stimulation provides the opposite effect. However, the relative extent of these effects on the two pathways can be different, which can potentially cause conduction to shift from one pathway to the other. An increase in vagal tone

preferentially prolongs the effective refractory period (ERP) of the fast pathway compared to the slow pathway. Adrenergic stimulation tends to shorten the anterograde and retrograde ERP of the fast pathway to a greater extent than that of the slow pathway. Conversely, beta-blockers tend to prolong ERP of the fast pathway more than that of the slow pathway. Notably, adenosine produces differential effect on anterograde and retrograde conduction over the different AVN pathways. The effect of adenosine seems to be far less potent on retrograde fast pathway conduction than on the retrograde slow pathway and anterograde fast and slow pathway conduction. The mechanism of adenosine resistance of retrograde fast pathway conduction (both in patients with slow-fast AVNRT and in normal subjects) remains unclear.⁹

Investigators used several approaches to identify the location of the atrial input of AVN pathways involved in the AVNRT circuit. The pathway serving as the retrograde limb of an AVNRT circuit can be identified by mapping the site of earliest retrograde atrial activation during AVNRT. The anterograde limb of the AVNRT circuit can be identified by using the resetting response to late-coupled atrial extra-stimulation (AES); the site where the AES (with the longest coupling interval) *resets the tachycardia* identifies the anterograde limb. Atrial entrainment of AVNRT can also identify the anterograde limb of the reentry circuit; the site of the shortest stimulus-to-His interval with a postpacing interval (PPI) equal to the tachycardia cycle length (TCL) identifies the location of the atrial input to the anterograde pathway. Several studies demonstrated that slow pathways with longer conduction times frequently have a more inferior location in the triangle of Koch when compared with locations producing shorter AH intervals. However, atypical locations of those pathways are not infrequent.

Fast Pathway

Typically, a single fast pathway is identified in normal subjects and in patients with AVNRT. During retrograde fast pathway conduction, the earliest retrograde atrial activation is typically recorded at the apex of the triangle of Koch (superior to the compact AVN, at the same site recording the proximal His potential). However, detailed mapping localized the earliest site of atrial activation to the anterior interatrial septum posterior to the tendon of Todaro and eustachian ridge (outside the triangle of Koch, at a level approximately 10 mm inferior to the level recording the proximal HB potential).⁸

Slow Pathways

Data suggest the presence of several slow pathways that can potentially participate in various forms of AVNRT, either as the anterograde or retrograde limbs of the reentry circuit. The slow pathway most commonly incorporated in the AVNRT circuit is formed by the rightward inferior AVN extension (and its corresponding AN approaches), which travels in the triangle of Koch between the tricuspid annulus and the CS os and connects selectively to the floor of the CS os. The earliest atrial activation during retrograde conduction over this pathway is typically located at the inferior aspect of the triangle of Koch, close to the CS os.^{2,3,6} The second most commonly used slow pathway is formed by the leftward inferior AN extension, which travels within the myocardial coat of the proximal CS leftward (transseptally) toward the left inferoseptal region and mitral annulus. An eccentric activation sequence in the CS is observed during retrograde conduction over this pathway, with the earliest activation site at the roof of the proximal CS (1 to 3 cm from the CS os). Two other slow pathways (inferolateral left atrial pathway and anterosseptal pathway) have been described but are less frequently observed. The earliest retrograde atrial activation is located close to the inferolateral mitral annulus in the LA (for the inferolateral left atrial slow pathway) or the anterior atrial septum, close to the proximal HB (for the anterosseptal slow pathway).

Multiple slow pathways (as demonstrated by multiple discontinuities in the AVN function curves; see later) are present in up to 14% of patients with AVNRT, although not all these pathways are involved in the initiation and maintenance of AVNRT. For example, an eccentric CS activation pattern has been reported frequently (14% to 80%) among patients with atypical forms of AVNRT. Whether the retrograde left-sided AN connection constitutes the critical component of the reentrant circuit or is only an innocent bystander in atypical AVNRT with the eccentric CS activation pattern remains controversial. It may be possible for both the leftward and rightward extensions, either together or separately, to participate in AVN reentry. Right-sided ablation is probably sufficient for most of these patients. However, in some patients, the slow pathway participating in the reentrant circuit cannot be ablated from the posteroseptal RA or the CS os, and requires ablation along the roof of the CS, as much as 5 to 6 cm from the CS os, or mitral annulus.

Upper Turnaround Point

Based on rare cases of dissociation of atrial activation from the tachycardia (e.g., persistence of AVNRT during different patterns of ventriculoatrial [VA] block or during AF) and on similarities between fast-slow AV conduction and longitudinal-transverse conduction in nonuniform anisotropy, early studies proposed that AVNRT results from reentry within the compact AVN (i.e., subatrial) secondary to functional longitudinal dissociation within the AVN into fast and slow pathways. Those studies suggested the presence of an upper common pathway, at least in a subset of patients.

However, current evidence, derived from histological studies, computer modeling, multielectrode recordings, and optical mapping, supports the role of perinodal atrial myocardium and suggests that the fast and slow pathways involved in the reentrant circuit of AVNRT represent conduction over different AN connections, thus making at least a small amount of atrial tissue a necessary part of the reentrant circuit (see [Video 17.1](#)). The common presence of multiple atrial breakthroughs, and the frequent changes in timing and location of retrograde activation without significant alteration in AVNRT cycle, argues against the existence of an “upper common pathway” or a focal atrial exit site from the AVNRT circuit in the majority of patients.

Lower Turnaround Point

The AVNRT circuit does not involve the ventricles; however, the location of the lower turnaround point of AVN reentry relative to the HB has been controversial. There is good evidence that the distal junction of the slow and fast pathways is located in the AVN, with the existence of a region of AVN tissue extending between the distal junction of the two pathways and the HB (called the “lower common pathway”), at least in a subset of patients.

The existence of a lower common pathway was proposed to explain several observations, including (1) AV block occurring without interruption of AVNRT and without recording of a His electrogram; (2) ventricular extrastimulation (VES) during AVNRT prematurely depolarizing the HB without affecting the tachycardia; (3) AES during AVNRT resulting in changes in the relative activation of HB and atrium (i.e., varying His bundle-atrial [HA] intervals); and (4) the HA interval during ventricular pacing at the TCL is longer than that during AVNRT.^{10,11}

The HA interval (measured from the end of the His potential to the earliest atrial activation in the HB recording, assuming stable activation sequence) during ventricular pacing represents a true conduction time between the HB and atrium. In the presence of a lower common pathway, the HA interval during AVNRT represents the relative activation times between the HB and junctional atrium, since the reentrant wavefront travels retrogradely up an AVN pathway to activate the atrium,

while at the same time propagating down the lower common pathway to activate the HB (i.e., the HA is a “pseudo-interval”). Consequently, in the presence of a lower common pathway between the AVNRT circuit and HB recording site, the HA during AVNRT is expected to be shorter than that during ventricular pacing. The difference between the two HA intervals (Δ HA interval) is proportional to the length of the lower common pathway.

However, these phenomena can be interpreted in ways that do not involve the presence of a common pathway. For example, the first two phenomena assume that the recorded “proximal HB” potential corresponds to the actual “proximal end of the HB,” which is probably inaccurate in many cases. Hence, those phenomena also can be explained by intra-Hisian block occurring beyond the site of HB recording rather than in a “lower common pathway.”¹⁰ Furthermore, the last two phenomena assume that retrograde conduction follows the same pathway during pacing and tachycardia, and the difference between the HA interval during tachycardia and that during ventricular pacing at the TCL was assumed to reflect the conduction time over the lower common pathway. On the contrary, mapping studies have demonstrated that the breakthrough of atrial activation during AVNRT is frequently slightly discordant from that observed during ventricular pacing. Hence, relying on the measuring the HA interval from the same recording sites, rather than detailed mapping for the true site of “earliest” atrial activation, may not be accurate.¹⁰

Types of Atrioventricular Nodal Reentry

AVNRT can manifest in different forms depending on the anatomic substrate forming the anterograde and retrograde pathways incorporated in the reentry circuit. Traditionally, AVNRT has been classified into “typical” or “atypical” forms. Typical AVNRT (anterograde slow-retrograde fast) accounts for 90% of AVNRTs. Atypical AVNRT variants are traditionally subclassified as either fast-slow or slow-slow types. The distinction between these various forms of AVNRT has been based on: (1) the absolute values of the AH and HA intervals; (2) the AH/HA ratios; (3) the pattern of earliest retrograde atrial activation; and (4) the identification of a lower common pathway ([Table 17.1](#)).

However, this classification approach has several limitations. As noted previously, the methodology for determining the presence or absence of a lower common pathway is not reliable (as discussed above). In addition, retrograde atrial activation over both fast and slow conduction patterns exhibit significant heterogeneity in all forms of AVNRT. Both typical and atypical AVNRT are compatible with varying retrograde atrial activation patterns. Furthermore, the conduction properties of the fast and slow AVN pathways (and thus the absolute and relative values of the AH and HA intervals) depend on the autonomic status, and can change in the same patient during the same EP study in response to changes in the sympathovagal balance.¹⁰

A more simplified and clinically practical scheme was recently proposed, which classifies the different types of AVNRT into only two categories, typical versus atypical, based only on the AH/HA ratio and absolute HA (or VA) intervals, while disregarding the retrograde atrial activation sequence and the demonstration of a lower common pathway ([Table 17.2](#)). Also, both fast-slow and slow-slow atypical AVNRTs were combined together since the distinction between the two types is often arbitrary in view of the lack of a unanimously accepted definition.¹⁰

The HA interval is measured from earliest deflection of the HB activation to the earliest rapid deflection of the atrial activation in the HB electrogram. The VA interval (measured from the onset of ventricular activation on surface electrocardiogram [ECG] to the earliest rapid deflection of the atrial activation on the HB electrogram) is also a practical and easily obtainable criterion, when the His potential cannot be reproducibly and reliably recorded during tachycardia.

TABLE 17.1 Traditional Classification of Atrioventricular Nodal Reentrant Tachycardia Types

	Typical (Slow-Fast)	Atypical (Fast-Slow)	Atypical (Slow-Slow)
AH interval	>200 ms	<200 ms	>200 ms
HA interval	<70 ms	≥70 ms	≥70 ms
AH/HA ratio	>1	<1	≥1
Site of earliest retrograde atrial activation	Apex of the triangle of Koch	CS os or within 1–2 cm of the proximal CS	CS os or within 1–2 cm of the proximal CS
Lower common pathway	Short or absent	Long	Long

AH, Atrial–His bundle; CS os, coronary sinus ostium; HA, His bundle–atrial.

TABLE 17.2 Simplified Classification of Atrioventricular Nodal Reentrant Tachycardia Types

	Typical (Slow-Fast)	Atypical (Fast-Slow or Slow-Slow)
HA interval	≤70 msec	>70 msec
VA interval	≤60 msec	>60 msec
AH/HA ratio	>1	Variable

AH, Atrial–His bundle; HA, His bundle–atrial; VA, ventriculoatrial.

Typical (Slow-Fast) Atrioventricular Nodal Reentrant Tachycardia

Anterograde conduction. The anterograde limb of the reentry circuit is formed by a slow pathway. Mapping studies localized the input to the anterograde slow pathway to the midseptum (in 50%) or inferior septum (33%), and infrequently to the superior septum (13%) or CS (3%).^{8,10,12} Some investigators subdivided typical slow-fast AVNRT according to the putative slow pathway used anterogradely, based on the site of successful ablation. At least three subtypes were described: (1) rightward inferior extension slow-fast AVNRT (most common), which is typically eliminated by ablation at the inferior aspect of the triangle of Koch; (2) leftward inferior extension slow-fast AVNRT (uncommon, 5%), which requires ablation within the triangle of Koch superior to the level of CS os and closer to the compact AVN or at the roof of the proximal CS (1 to 3 cm from the CS os); and (3) inferolateral left atrial slow-fast AVNRT (rare), which requires ablation close to the inferolateral mitral annulus in the LA.

Retrograde conduction. Typical AVNRT uses the fast pathway for retrograde conduction. During slow-fast AVNRT, the earliest retrograde atrial activation is usually recorded at the anterior interatrial septum posterior to the tendon of Todaro, close to the apex of the triangle of Koch (Fig. 17.2).⁸

Importantly, retrograde atrial activation has been mapped to the inferior triangle of Koch, the roof of the CS (1 to 3 cm from the CS os), or the left side of the septum in up to 9% of patients (Fig. 17.3). These forms of AVNRT were considered variants of slow-fast AVNRT with an inferior exit for the retrograde fast pathway. More recently, however, those AVNRTs with earliest retrograde atrial activation outside the traditional location of the fast pathway (formerly described as “posterior” or “leftward inferior extension” or “left variant” slow-fast AVNRT) have been considered as a variant “slow-slow AVNRT.” In the latter setting, two slow pathways (the right and left inferior AVN extensions) are used in the AVNRT circuit. The very short (and occasionally nega-

tive) HA interval observed during tachycardia, despite retrograde conduction over a slow pathway, could be explained by the presence of a relatively long lower common pathway. Retrograde conduction over the slow pathway with simultaneous bystander conduction over the lower common pathway (from the distal junction of the two slow pathways to the HB) results in simultaneous atrial and ventricular activation and shortening of the recorded HA interval, which mimics slow-fast AVNRT.^{8,10} Older patients (>60 years) often have longer conduction times over the retrograde fast pathway, resulting in HA intervals similar to those in slow-slow AVNRT, but still with the earliest atrial activation at the tendon of Todaro.

Lower common pathway. The presence of a lower common pathway in typical AVNRT remains controversial. Nevertheless, it is recognized that the lower common pathway in typical AVNRT, if present, is very short (as assessed by the degree of HB prematurity required for a VES to reset the tachycardia, and by comparing the HA interval during AVNRT with that during ventricular pacing at the TCL).^{8,10,11}

AH/HA ratio. The AH interval is long (>200 milliseconds), due to anterograde conduction over the slow pathway. The HA interval is relatively short (<70 milliseconds) given the fast retrograde conduction. This produces an AH/HA ratio of greater than 1 and simultaneous atrial and ventricular activations (the onset of atrial activation appears before, at the onset, or just after the QRS complex).

Atypical (Fast-Slow) Atrioventricular Nodal Reentrant Tachycardia

Anterograde conduction. The nature of anterograde pathway conduction during fast-slow AVNRT remains poorly understood.⁷ Although this variant was initially thought of as using the same circuit as typical slow-fast AVNRT but in the reverse direction, recent data suggest that anterograde “fast pathway” during atypical AVNRT is distinct from the retrograde “fast pathway” during typical AVNRT. Some investigators have suggested that anterograde conduction during fast-slow AVNRT is mediated by a slow pathway, and that the fast pathway is a bystander that mediates conduction to the HB (and results in a short AH interval) but without contributing to the reentry circuit (analogous to AVNRT with ventricular preexcitation over a bystander bypass tract [BT]).^{7,8,10} Of note, patients with fast-slow AVNRT often exhibit multiple AH interval jumps during AES testing, which is consistent with the presence of multiple slow pathways, and supporting reentry between two “slow pathways.”

Retrograde conduction. A slow pathway forms the retrograde limb of the reentry circuit. The earliest retrograde atrial activation (over the slow pathway) during fast-slow AVNRT is traditionally reported at the base of the triangle of Koch, near the CS os (see Fig. 17.2). However, other locations are also frequent, including mid or superior septum, distal CS, or left side of the septum (see Fig. 17.2). Thus fast-slow

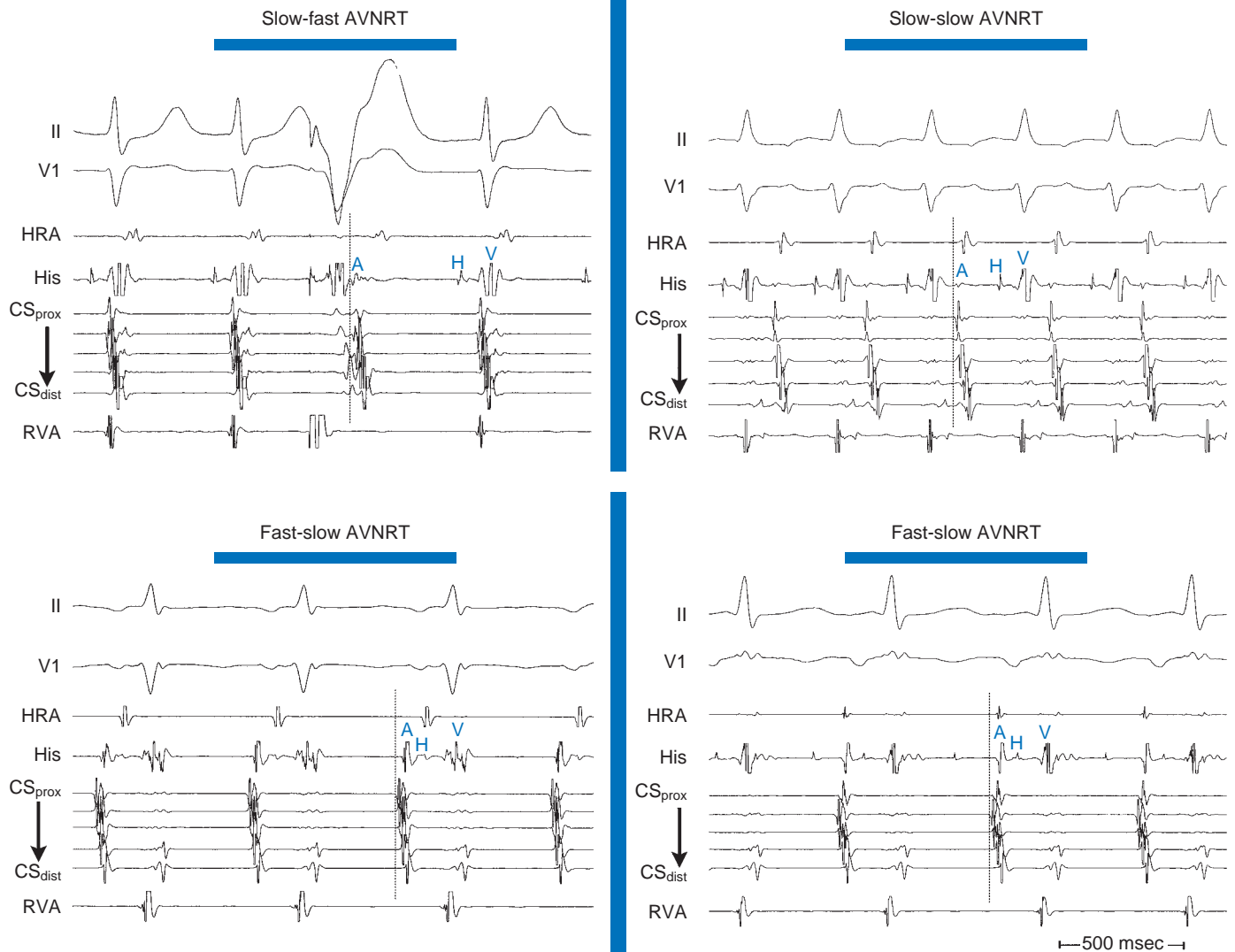


Fig. 17.2 Surface Electrocardiogram and Endocardial Recordings of the Different Types of Atrioventricular Nodal Reentrant Tachycardia (AVNRT). The dashed line marks the site with the earliest atrial activation. In slow-fast (typical) AVNRT, the initial site of atrial activation is usually recorded in the His bundle (HB) catheter. In slow-slow AVNRT, the P wave lies outside the QRS in the ST-T wave, and the RP interval is longer than that in slow-fast AVNRT. The earliest retrograde atrial activation is usually in the inferoposterior part of the triangle of Koch. Slow pathways with longer conduction times have a more inferior location in the triangle of Koch. In fast-slow AVNRT, the earliest site of retrograde atrial activation is usually recorded at the base of the triangle of Koch or coronary sinus ostium. An eccentric retrograde atrial activation sequence with the earliest retrograde activation site inside the CS can be observed in atypical fast-slow AVNRT. CS_{dist}, Distal coronary sinus; CS_{prox}, proximal coronary sinus; HRA, high right atrium; RVA, right ventricular apex.

AVNRT can be of posterior, anterior, or middle type according to the mapped location of the retrograde slow pathway.^{8,10}

Lower common pathway. A relatively long lower common pathway has been observed in fast-slow AVNRT, in contrast to slow-fast AVNRT.

AH/HA ratio. The AH interval is shorter than the HA interval (30 to 185 milliseconds vs. 135 to 435 milliseconds), resulting in long RP tachycardia and an AH/HA ratio less than 1.^{8,10} The long HA interval is a result of slow retrograde conduction over the slow pathway. The short AH interval represents anterograde conduction over the fast pathway; however, whether this pathway serves as the anterograde limb of the reentry circuit, or as just a bystander, is being debated.

Atypical (Slow-Slow) Atrioventricular Nodal Reentrant Tachycardia

As the name implies, the reentrant circuit in slow-slow AVNRT uses two slow pathways (the right and left inferior AVN extensions). These patients often exhibit multiple AH interval jumps during AES testing, which is consistent with multiple slow pathways.

Anterograde conduction. A slow pathway forms the anterograde limb of the reentry circuit. Data suggest the slow pathway used for anterograde conduction in slow-slow AVNRT is similar to the one used for retrograde conduction during fast-slow AVNRT.¹³

Retrograde conduction. A second slow (or “intermediate”) pathway serves as the retrograde limb of the reentry circuit. The earliest retrograde

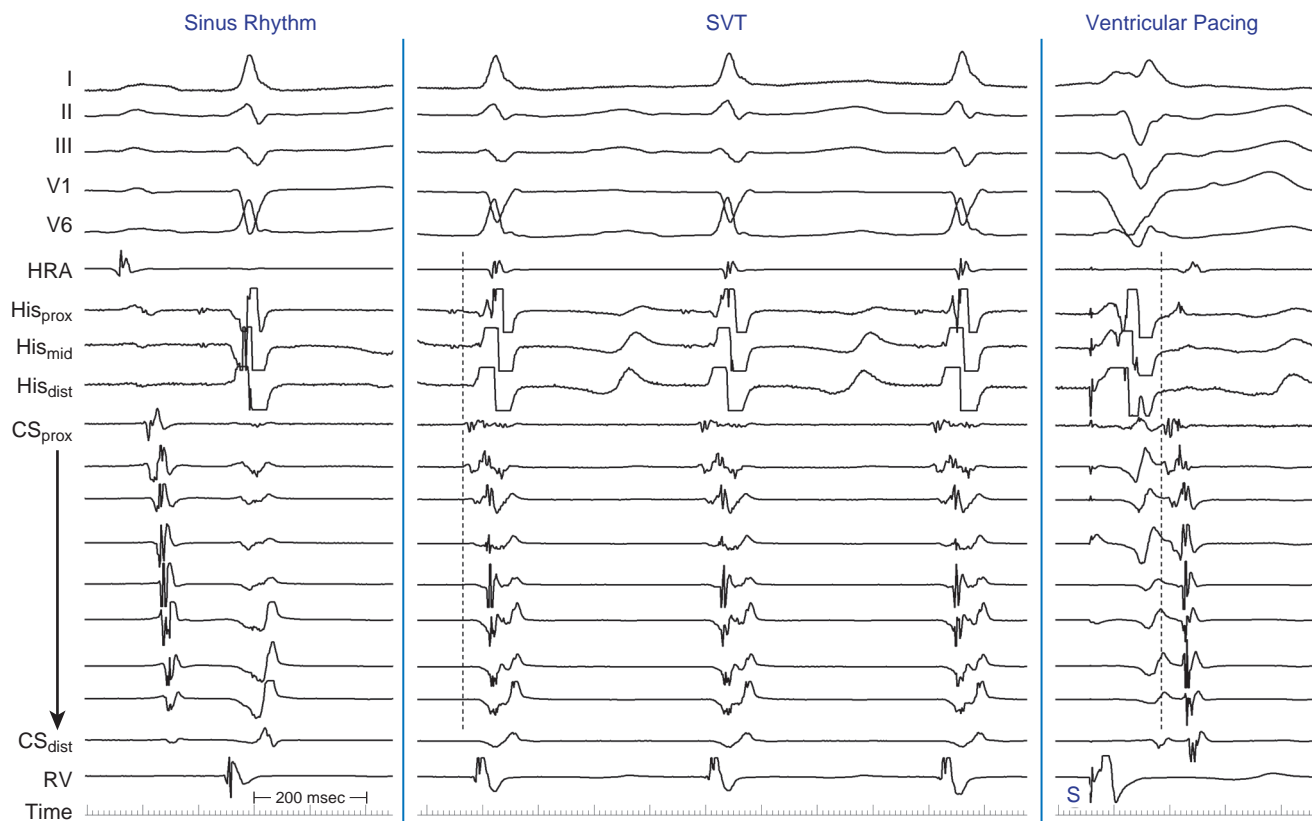


Fig. 17.3 Retrograde Atrial Activation During Typical Atrioventricular Nodal Reentrant Tachycardia. Sinus rhythm is shown on the left, slow-fast atrioventricular nodal reentrant tachycardia is shown in the center, and ventricular pacing during sinus rhythm appears on the right. The dashed line denotes earliest atrial activation (proximal CS, near ostium), significantly before the His bundle atrial activation (most visible during ventricular pacing). *CS_{dist}*, Distal coronary sinus; *CS_{prox}*, proximal coronary sinus; *His_{dist}*, distal His bundle; *His_{mid}*, middle His bundle; *His_{prox}*, proximal His bundle; *HRA*, high right atrium; *RV*, right ventricle; *SVT*, supra-ventricular tachycardia.

atrial activation occurs along the roof of the proximal CS (1 to 3 cm from the CS os) or, less commonly, at the inferoposterior aspect of the triangle of Koch (see Fig. 17.2). Of note, patients with this form of AVNRT can also have retrograde conduction over the fast pathway, which can be demonstrated during ventricular pacing, which is not part of the reentrant circuit.¹³

Lower common pathway. Slow-slow AVNRT exhibits a relatively long lower common pathway, significantly longer than that in typical AVNRT.

AH/HA ratio. The AH interval is long (>200 milliseconds) due to the slow retrograde conduction over the slow pathway. The HA interval is often shorter than the AH interval, but is usually greater than 70 milliseconds, and the AH/HA ratio remains greater than 1. The short HA interval observed during slow-slow AVNRT (despite retrograde conduction over a slow pathway) could be explained by the presence of a relatively long lower common pathway. Retrograde conduction over the slow pathway with simultaneous bystander conduction over the lower common pathway (from the distal junction of the two slow pathways to the HB) results in simultaneous atrial and ventricular activation, and shortening of the recorded HA interval, which mimics slow-fast AVNRT.

Although the HA interval during slow-slow AVNRT is usually longer than that during slow-fast AVNRT, a significant overlap exists. Slow-slow AVNRT can exhibit very short AH intervals, mimicking slow-fast AVNRT. In fact, this form of AVNRT was considered a variant of slow-

fast AVNRT, formerly described as “posterior” or “type B” AVNRT (which accounted for approximately 2% of patients with slow-fast AVNRT). Nonetheless, several features of slow-slow AVNRT can help distinguish it from slow-fast AVNRT, including: (1) the earliest retrograde atrial activation is recorded at the roof of the CS or at the inferior triangle of Koch, rather than the fast pathway area; (2) there is a much wider range of HA intervals; (3) there is a much more common cycle length (CL) changes and especially changes in HA interval during tachycardia; and (4) there is a relatively long lower common pathway (HA interval during ventricular pacing at the TCL exceeding the HA interval during tachycardia [Δ HA] by ≥ 15 milliseconds).

Epidemiology

AVNRT is the most common form of paroxysmal supraventricular tachycardia (SVT). The absolute number of patients with AVNRT and its proportion of paroxysmal SVT increase with age. The reason may be related to the normal evolution of AVN physiology over the first two decades of life, as well as to age-related changes in atrial and AVN physiology observed in later decades. AVNRT is unusual in children younger than 5 years, and it typically initially manifests in early adult life (e.g., in the teens). Conversely, atrioventricular reentrant tachycardia (AVRT) manifests earlier, with an average of more than 10 years separating the time of clinical presentation of AVRT and that of AVNRT. AVNRT onset has been reported after the age of 50 years in 16% and before the age of 20 years in 18%.¹⁴ There is also a striking 2:1

predominance of AVNRT in women, in whom symptoms start at a significantly younger age. As such, female sex and older age (i.e., teens vs. newborns or young children) favor the diagnosis of AVNRT over AVRT. Gender differences in the anterograde and retrograde AVN EP properties have been observed and may contribute to the pathogenesis of AVNRT.¹⁵ There is no significant association of AVNRT with other types of structural heart disease; patients with ventricular tachycardia (VT) in the absence of structural heart disease have a higher prevalence of AVNRT.

Clinical Presentation

Patients with AVNRT typically present with the clinical syndrome of paroxysmal SVT. This is characterized as regular rapid tachycardia of abrupt onset and termination. Patients commonly describe palpitations and dizziness. Rapid ventricular rates can be associated with complaints of dyspnea, weakness, chest pain, or presyncope, and can at times be disabling. True syncope is uncommon but can occur, especially in elderly patients. Episodes can last from seconds to several hours. AVNRT can occur spontaneously or on provocation with exertion, caffeine, or alcohol. Patients often learn to use certain maneuvers, such as the carotid sinus massage or the Valsalva maneuver, to terminate the arrhythmia, although many require pharmacological treatment.¹⁴

About half of patients with typical AVNRT report experiencing a pounding sensation in the neck during tachycardia, which likely is related to pulsatile reversed flow when the RA contracts against a closed tricuspid valve due to simultaneous contraction of atria and ventricles. The physical examination correlate of this phenomenon is continuous pulsing cannon A waves in the jugular venous waveform (described as the “frog” sign). This clinical feature has been reported to distinguish paroxysmal SVT resulting from AVNRT from that caused by orthodromic AVRT. Although atrial contraction during AVRT occurs against closed AV valves, the longer VA interval results in separate ventricular and then atrial contraction and a relatively lower RA and venous pressure. Therefore the presence of palpitations in the neck is experienced less commonly (about 17%) in patients with AVRT.¹⁵ Polyuria is particularly common with AVNRT and is related to higher right atrial pressures and elevated levels of atrial natriuretic protein in patients with AVNRT compared with patients who have AVRT or AFL.¹⁴

INITIAL EVALUATION

History, physical examination, and 12-lead ECG constitute an appropriate initial evaluation. In patients with brief, self-terminating episodes, an event recorder is the most effective way to obtain ECG documentation. An echocardiographic examination should be considered in patients with documented sustained SVT to exclude the possibility of structural heart disease. Further diagnostic studies (e.g., cardiac stress testing) are indicated only if there are signs or symptoms that suggest structural heart disease.

The diagnosis of AVNRT as the mechanism of SVT can be strongly suspected based on the surface ECG but can be difficult to confirm, especially when only single-lead rhythm strips are available during the SVT. However, EP testing is not indicated unless a decision to proceed with catheter ablation is undertaken.

PRINCIPLES OF MANAGEMENT

Acute Management

Because maintenance of AVNRT is dependent on AVN conduction, maneuvers or drugs that slow AVN conduction and prolong AVN refractoriness can be used to terminate the tachycardia. Initially, maneuvers that increase vagal tone (e.g., Valsalva maneuvers, gagging, carotid sinus

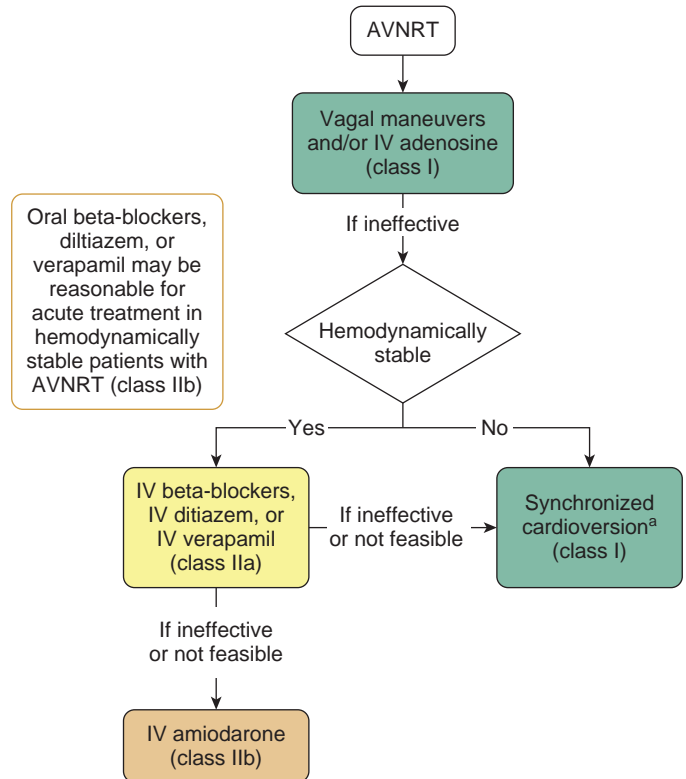


Fig. 17.4 Acute Treatment of Atrioventricular Nodal Reentrant Tachycardia (AVNRT). ^aFor rhythms that break or recur spontaneously, synchronized cardioversion is not appropriate. IV, Intravenous. (From Page RL, Joglar JA, Caldwell MA, et al. 2015 ACC/AHA/HRS guideline for the management of adult patients with supraventricular tachycardia: a report of the American College of Cardiology/American Heart Association Task Force on Clinical Practice Guidelines and the Heart Rhythm Society. *J Am Coll Cardiol*. 2016;67:e27–e115.)

massage) are used. When vagal maneuvers are unsuccessful, tachycardia termination can be achieved with antiarrhythmic drugs whose primary effects increase refractoriness or decrease conduction (negative dromotropic effect) over the AVN (Fig. 17.4). Adenosine is the drug of choice and is successful in more than 95% of cases. In addition, intravenous (IV) diltiazem and verapamil are particularly effective in terminating AVNRT and can be used in hemodynamically stable patients. Beta-blockers are also a reasonable option. Digoxin, which has a slower onset of action than the other AVN blockers, is not favored for the acute termination of AVNRT, except if there are relative contraindications to the other agents.¹⁴

Class IA and IC sodium channel blockers can also be used in treating an acute event of AVNRT when other regimens have failed, a strategy that is rarely needed. Electrical cardioversion is recommended for hemodynamically unstable patients and those with persistent arrhythmia refractory to pharmacological therapy. Energies in the range of 10 to 50 J are usually adequate.¹⁴

Chronic Management

Because AVNRT is generally a benign arrhythmia that does not influence survival, the primary indication for its treatment relates to its impact on a patient's quality of life (Fig. 17.5). Factors that contribute to the therapeutic decision include the frequency and duration of tachycardia, tolerance of symptoms, the effectiveness and tolerance of antiarrhythmic drugs, the need for lifelong drug therapy, and the presence

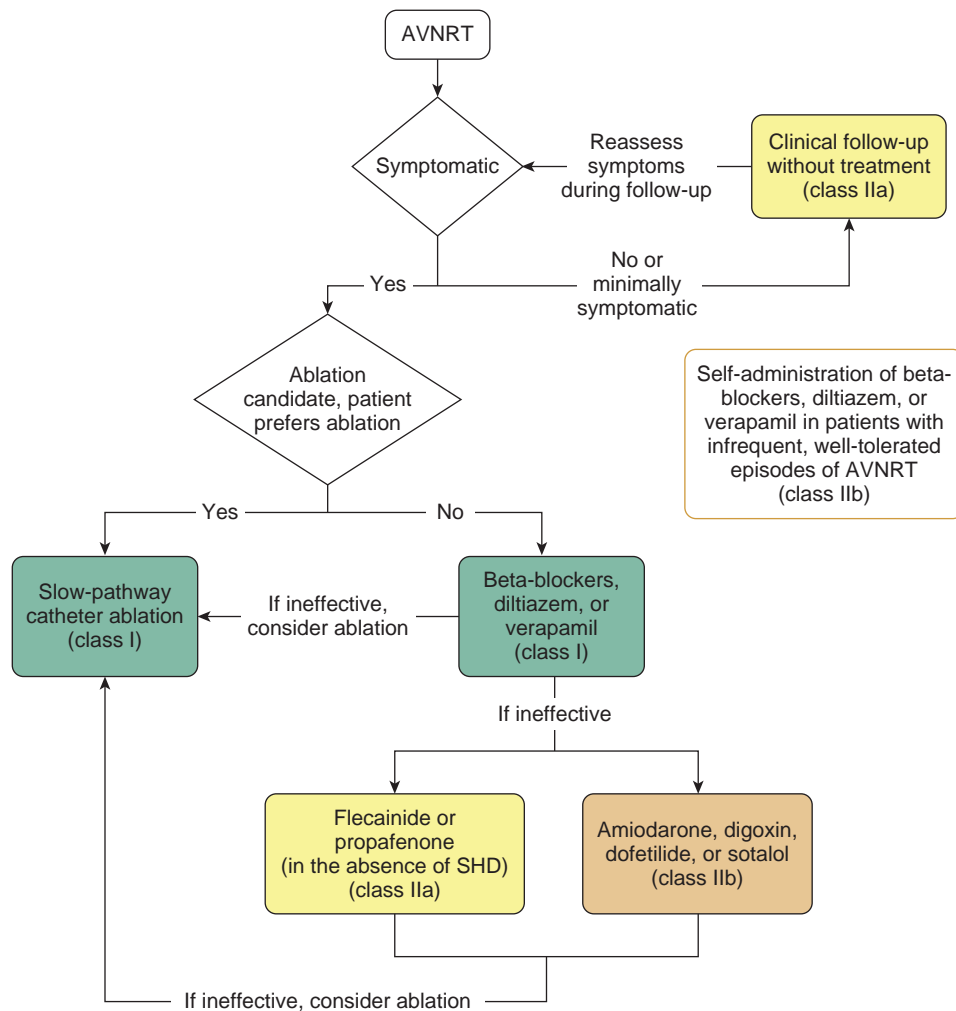


Fig. 17.5 Ongoing Management of Atrioventricular Nodal Reentrant Tachycardia (AVNRT). Drugs listed alphabetically. SHD, Structural heart disease (including ischemic heart disease). (From Page RL, Joglar JA, Caldwell MA, et al. 2015 ACC/AHA/HRS guideline for the management of adult patients with supraventricular tachycardia: a report of the American College of Cardiology/American Heart Association Task Force on Clinical Practice Guidelines and the Heart Rhythm Society. *Circulation*. 2016; 133:e506–e574.)

of concomitant structural heart disease. Patients who develop a highly symptomatic episode of paroxysmal SVT, particularly if it requires an emergency room visit for termination, may elect to initiate therapy after a single episode. In contrast, a patient who presents with minimally symptomatic episodes of paroxysmal SVT that terminate spontaneously or in response to Valsalva maneuvers may elect to be followed clinically without specific therapy. These patients should be taught how to correctly perform vagal maneuvers and be educated about when to seek medical attention.¹⁴

Catheter Ablation

Once it is decided to initiate treatment for AVNRT, the question arises whether to initiate pharmacological therapy or to use catheter ablation. Because of its high efficacy (>95%) and low incidence of complications, catheter ablation has become the preferred therapy over long-term pharmacological therapy and can be offered as an initial therapeutic option. It is reasonable to discuss catheter ablation with all patients suspected of having AVNRT. However, patients considering radiofrequency (RF) ablation must be willing to accept the risk, albeit low, of AV block and pacemaker implantation.^{14,16}

Pharmacological Therapy

For patients with AVNRT who are not candidates for, or prefer not to undergo, catheter ablation, long-term pharmacological therapy can be effective in 30% to 60% of patients. Most pharmacological agents that depress AVN conduction (including beta-blockers and calcium channel blockers) can reduce the frequency of recurrences of AVNRT. If those agents are ineffective, class IC (flecainide or propafenone in patients without structural or ischemic heart disease) or class III antiarrhythmic agents (sotalol or dofetilide) may be considered. Given the potential adverse effects of digoxin and amiodarone, these agents are generally reserved as last-resort therapy.^{14,16}

Outpatients may use a single dose of verapamil, diltiazem, or propranolol to acutely terminate an episode of AVNRT. This so-called pill-in-the-pocket approach (i.e., administration of a drug only during an episode of tachycardia for the purpose of termination of the arrhythmia when vagal maneuvers alone are not effective) is appropriate to consider for patients with infrequent episodes of AVNRT that are prolonged but well tolerated, and it obviates exposure of patients to long-term and unnecessary therapy between rare arrhythmic events. This approach necessitates the use of a drug that has a short onset of action

(i.e., immediate-release preparations). Candidate patients should be free of significant LV dysfunction, sinus bradycardia, and preexcitation. Single-dose oral therapy with diltiazem (120 mg) plus propranolol (80 mg) has been shown to be superior to both placebo and flecainide in terminating AVNRT.¹⁴

ELECTROCARDIOGRAPHIC FEATURES

Electrocardiographic Manifestations of Dual Atrioventricular Nodal Physiology

As noted, dual pathway physiology characterizes the normal AVN electrophysiology, which is prevalent in most normal individuals. However, the ECG normally reveals only the conduction of the fast pathway, while slow pathway conduction generally remains concealed. The most common ECG manifestation of dual AVN physiology is AVNRT. In addition, several ECG manifestations can be explained by dual pathways physiology.^{3,2,6}

Two Families of PR Intervals

A shift of anterograde conduction from the fast pathway to the slow pathway can manifest as sudden prolongation of the PR interval, and vice versa (Fig. 17.6). This shift can occur spontaneously and result in alternans of the PR interval (i.e., long and short PR intervals alternate with each other) or manifest as two families of PR intervals (short and long), with sudden and sustained prolongation or shortening of the PR interval that can be observed on different occasions. The shift also can be precipitated by a change in autonomic tone or by a PAC or a PVC that causes conduction block or concealment in one pathway and allows conduction over the other (Fig. 17.7).^{6,17}

Dual Ventricular Response to a Single Supraventricular Beat

Rarely, a single atrial impulse (e.g., PAC) can conduct simultaneously along the slow and fast pathways, producing two QRS complexes (“double fire”). The reverse can also occur, with two atrial impulses from one ventricular complex.

Rapid Ventricular Rates During Atrial Fibrillation

Ventricular rates during AF can exhibit a bimodal distribution of R-R intervals on Holter recordings. The shorter R-R intervals (the faster ventricular rates) are believed to be a result of conduction over the slow pathway (because of its shorter refractory periods), while the fast pathway mediates relatively slower ventricular rates. Ablation of the slow AVN pathways in these patients can potentially eliminate the fast ventricular rates and produce a unimodal R-R interval distribution.⁶

Electrocardiographic Manifestations of Atrioventricular Nodal Reentrant Tachycardia

P Wave Morphology

In typical (slow-fast) AVNRT, the P wave is usually not visible because of the simultaneous atrial and ventricular activation. The P wave can distort the initial portion of the QRS (mimicking a q wave in the inferior leads), lie just within the QRS (inapparent), or distort the terminal portion of the QRS (mimicking an s wave in the inferior leads or a terminal r wave in lead V1) (Fig. 17.8). When apparent, the P wave is significantly narrower than the sinus P wave, and is negative in the inferior leads, findings that are consistent with concentric retrograde atrial activation over the fast AVN pathway. In atypical AVNRT, the P wave is relatively narrow, negative in the inferior leads, and positive in lead V1 (see Fig. 17.8).⁸ Compared to orthodromic AVRT using a

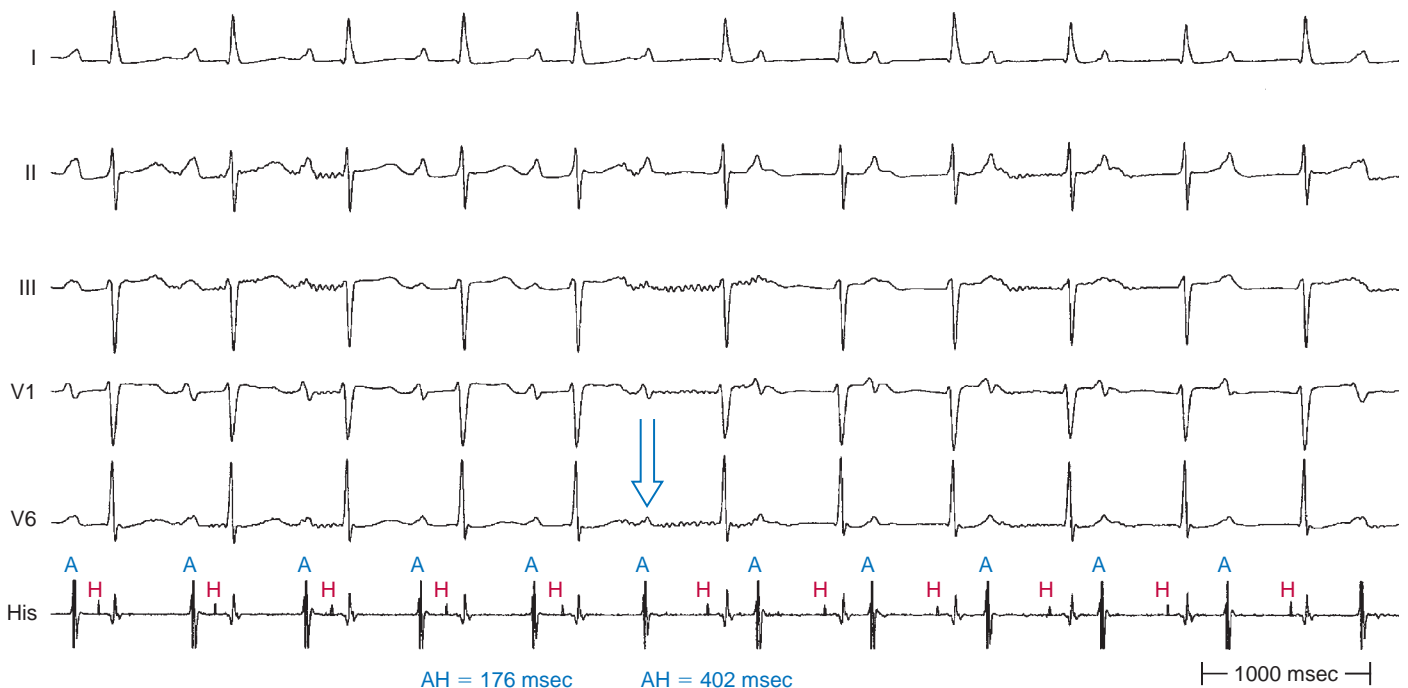


Fig. 17.6 Dual Atrioventricular Node Physiology Manifesting as Two Different PR Intervals During Normal Sinus Rhythm. Note that the shift in atrioventricular conduction from the fast to the slow atrioventricular node pathway (arrow) occurs without any changes in the sinus cycle length (680 milliseconds). This phenomenon indicates that the fast pathway anterograde effective refractory period is long relative to the sinus cycle length. AH, Atrial-His bundle.

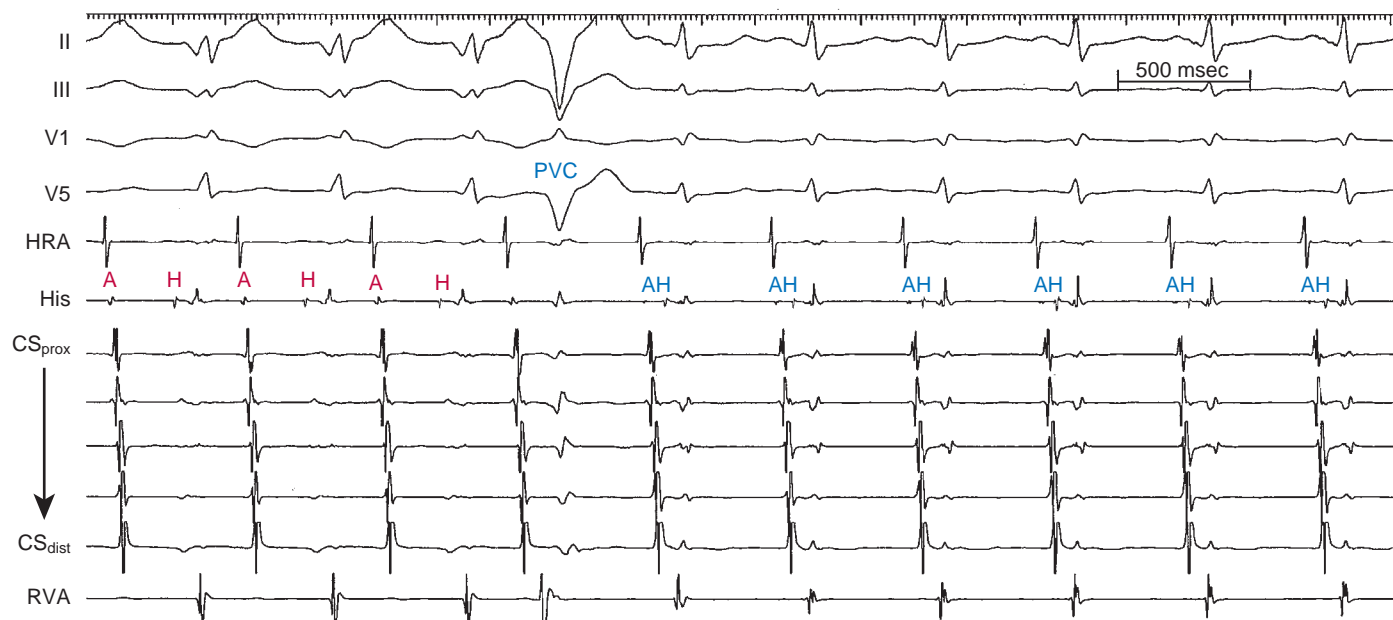


Fig. 17.7 Dual Atrioventricular Node Physiology. Sinus rhythm with atrioventricular conduction over the slow pathway and long PR and AH intervals (*to the left*). After a premature ventricular complex (PVC) that results in concealed retrograde conduction into the slow pathway, anterograde atrioventricular conduction shifts from the slow pathway to the fast pathway with sudden shortening of the PR interval. AH, Atrial-His bundle; CS_{dist}, distal coronary sinus; CS_{prox}, proximal coronary sinus; HRA, high right atrium; RVA, right ventricular apex.

posteroseptal BT; the retrograde P waves in slow-slow AVNRT are more negative in lead aVF (>0.16 mV negative amplitude).¹⁸

QRS Morphology

The QRS morphology during AVNRT is usually the same as in normal sinus rhythm (NSR). The development of prolonged functional aberration during AVNRT is uncommon, and it usually occurs following the induction of AVNRT by ventricular stimulation more frequently than by atrial stimulation, or following the resumption of 1:1 conduction to the ventricles after a period of block below the tachycardia circuit. At times, alternans of QRS amplitude can occur when the tachycardia rates are rapid. Occasionally, AVNRT can coexist with ventricular preexcitation over an AV BT, whereby the BT is an innocent bystander.

P-QRS Relationship

In typical (slow-fast) AVNRT, the RP interval is very short (−40 to 75 milliseconds). Variation of the P-QRS relationship with or without block can occur during AVNRT, especially in atypical variants of the tachycardia. This phenomenon usually occurs when the conduction system and the reentry circuit are unstable during initiation or termination of the tachycardia, which is likely secondary to decremental conduction in the lower common pathway. The ECG manifestation of P-QRS variations with or without AV block during tachycardia, especially at the initiation of tachycardias or in cases of nonsustained tachycardias, can be misdiagnosed as atrial tachycardias (ATs). Moreover, the variations can be of such magnitude that long RP tachycardia can masquerade for brief periods of time as short RP tachycardia.

Usually, the A/V ratio during AVNRT is equal to 1; however, 2:1 AV block can be present because of a block below the reentry circuit (usually below the HB and, infrequently, in the lower common pathway). In such cases, narrow, inverted P wave morphology in the inferior leads inscribed exactly between QRS complexes strongly suggests AVNRT (Fig. 17.9). The incidence of reproducible sustained 2:1 AV block during

induced episodes of AVNRT is approximately 10%. Rarely, VA block can occur because of a block in an upper common pathway; however, some of these cases may represent reentry using a retrogradely conducting nodofascicular or nodoventricular pathway with intranodal block above the level of the circuit (see Chapter 19).

In atypical (fast-slow) AVNRT, the RP interval is longer than the PR interval. In slow-slow AVNRT, the RP interval is usually shorter than, and sometimes equal to, the PR interval. Occasionally, the P wave is inscribed in the middle of the cardiac cycle, thus mimicking AT with 2:1 AV conduction (see Fig. 17.2). Slow-slow AVNRT can be associated with RP intervals and P wave morphology similar to that during orthodromic AVRT using a posteroseptal AV BT. However, although both SVTs have the earliest atrial activation in the posteroseptal region, conduction time from that site to the HB region is significantly longer in AVNRT than in orthodromic AVRT. The results are a significantly longer RP interval in lead V1 and a significantly larger difference in the RP interval between lead V1 and inferior leads during AVNRT. Therefore Δ RP interval (V1 − III) of more than 20 milliseconds suggests slow-slow AVNRT (sensitivity, 71%; specificity, 87%).⁸

ELECTROPHYSIOLOGICAL TESTING

EP testing is used to study the inducibility and mechanism of the SVT and to guide catheter ablation. Typically, three quadripolar catheters are positioned in the high RA, the right ventricular (RV) apex, and the HB region, and a decapolar catheter is positioned in the CS (see Fig. 4.4). A typical programmed electrical stimulation protocol used for EP testing in patients with AVNRT is outlined in Box 17.1.

Baseline Observations During Sinus Rhythm

Programmed Atrial Stimulation During Sinus Rhythm

Anterograde dual AVN physiology. Demonstration of anterograde dual AVN pathway conduction curves requires a longer ERP of the fast

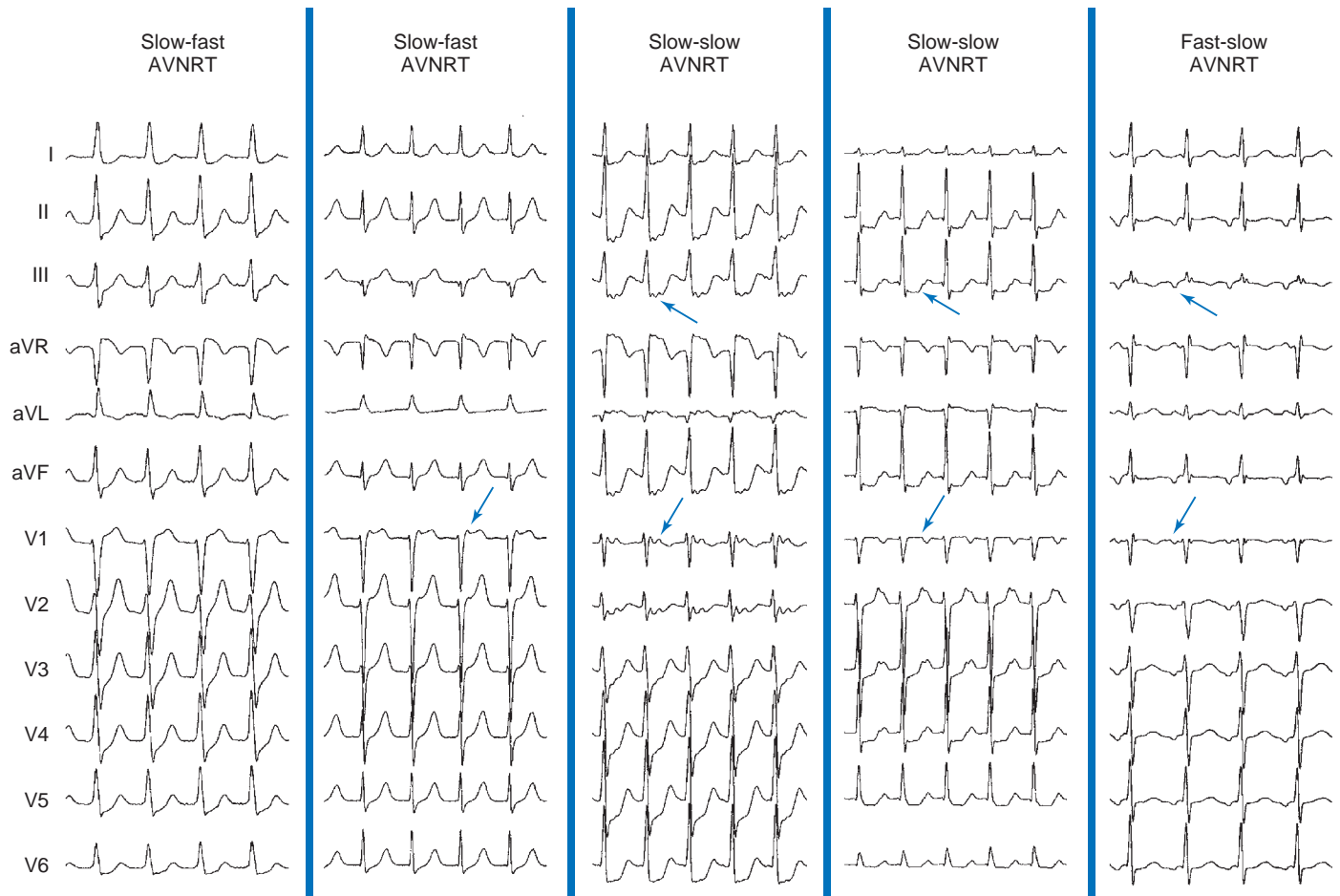


Fig. 17.8 Electrocardiogram Morphology of the Different Types of Atrioventricular Nodal Reentrant Tachycardia (AVNRT). Arrows mark the P waves. In slow-fast (typical) AVNRT, the P wave may lie within the QRS (invisible, *first panel*) or distort the terminal portion of the QRS (mimicking an r wave in lead V1, *second panel*). In slow-slow AVNRT, the P wave lies outside the QRS in the ST-T wave, and the RP interval is longer than that in slow-fast AVNRT. In fast-slow AVNRT, the P wave lies before the QRS with a long RP interval. In all varieties of AVNRT, the P wave is relatively narrow, negative in the inferior leads, and positive in lead V1.

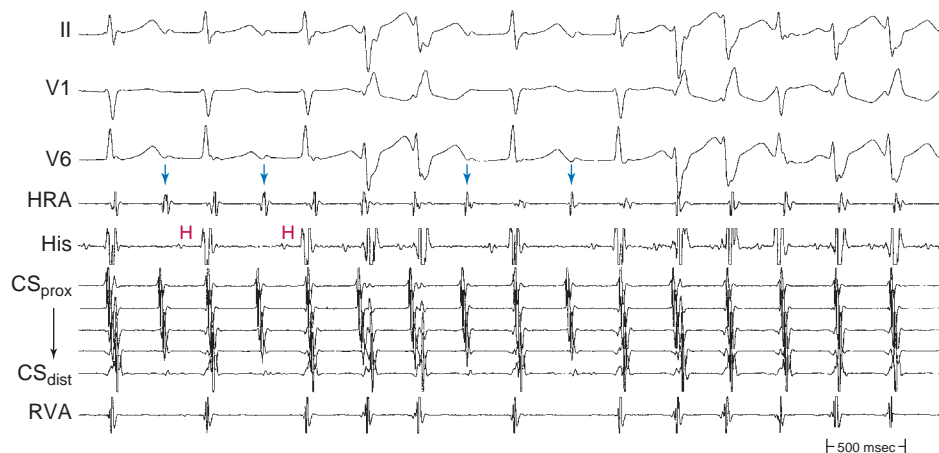


Fig. 17.9 Typical Atrioventricular Nodal Reentrant Tachycardia With Intermittent 2:1 Atrioventricular (AV) Block. His potential (*H*) is observed following conducted atrial impulses, but not after blocked atrial impulses, thus indicating AV block in the lower common pathway or in the portion of the His bundle proximal to the recording site. Note that intermittent AV block results in long-short cycle sequences associated with a right bundle branch block (RBBB) pattern during complexes conducted following a short cycle. RBBB is also observed intermittently during supraventricular tachycardia with 1:1 AV conduction. Note the lack of effect of RBBB on the tachycardia cycle length (A-A interval) or ventricular-atrial interval. *CS_{dist}*, Distal coronary sinus; *CS_{prox}*, proximal coronary sinus; *HRA*, high right atrium; *RVA*, right ventricular apex.

BOX 17.1 Programmed Stimulation Protocol for Electrophysiological Testing of Atrioventricular Nodal Reentrant Tachycardia

Atrial burst pacing from the RA and CS (down to AV Wenckebach CL)
 Single and double AESs at multiple CLs (600–400 ms) from the high RA and CS (down to atrial ERP)
 Ventricular burst pacing from the RV apex (down to VA Wenckebach CL)
 Single and double VESs at multiple CLs (600–400 ms) from the RV apex (down to ventricular ERP)
 Administration of isoproterenol infusion as needed to facilitate tachycardia induction (0.5–4 µg/min)

AES, Atrial extrastimulus; AV, atrioventricular; CL, cycle length; CS, coronary sinus; ERP, effective refractory period; RA, right atrium; RV, right ventricle; VA, ventriculoatrial; VES, ventricular extrastimulus.

BOX 17.2 Dual Atrioventricular Node Physiology

Manifestations of Anterograde Dual Atrioventricular Node Physiology

- A “jump” in the AH interval of ≥ 50 ms in response to a 10-ms decrement of the AES coupling interval or atrial PCL
- Dual ventricular response to a single atrial beat (“double fire”)
- PR interval exceeding the R-R interval during rapid atrial pacing
- Two distinct PR or AH intervals during NSR or fixed-rate atrial pacing

Manifestations of Retrograde Dual Atrioventricular Node Physiology

- A “jump” in HA interval of ≥ 50 ms in response to a 10-ms decrement of the VES coupling interval or ventricular PCL
- Two atrial responses to a single ventricular impulse

AES, Atrial extrastimulation; AH, atrial-His; CL, cycle length; NSR, normal sinus rhythm; PCL, pacing cycle length; VES, ventricular extrastimulation.

pathway than the slow pathway ERP and the atrial functional refractory period (FRP), as well as a sufficient difference in conduction times between the two pathways. Dual AVN physiology can be diagnosed by demonstrating one of the following: (1) a “jump” in the AH interval in response to progressively more premature AES; (2) two ventricular responses to a single atrial impulse; (3) a PR interval exceeding the R-R interval during rapid atrial pacing; or (4) different PR or AH intervals during NSR or fixed-rate atrial pacing (Box 17.2).⁶

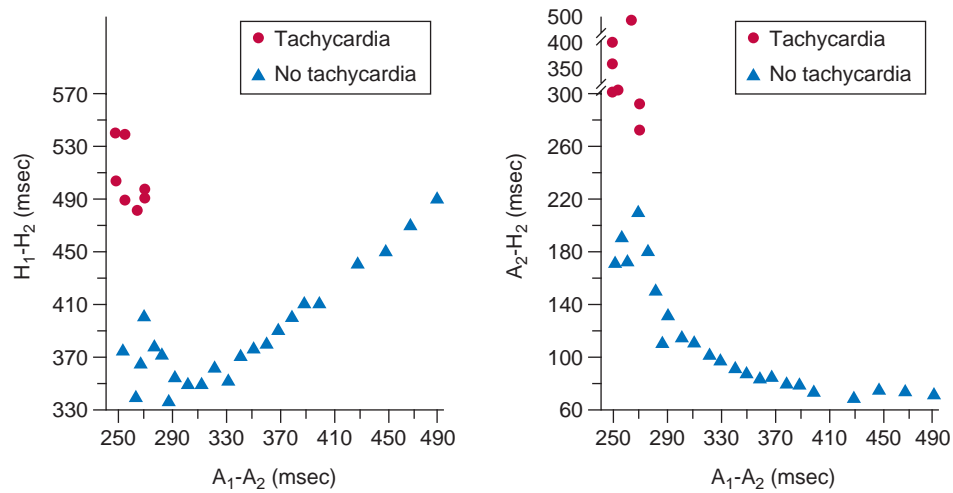
AH interval jump. In contrast to the normal pattern of AVN conduction, in which the AH interval gradually lengthens in response to progressively shorter AES (i.e., shorter coupling intervals), patients with dual AVN physiology usually demonstrate a sudden increase (“jump”) in the AH interval at a critical AES (A1-A2) coupling interval (eFig. 17.1). Conduction with a short PR or AH interval reflects fast pathway conduction, whereas conduction with a long PR or AH interval reflects slow pathway conduction. The AH interval jump signals block of anterograde conduction of the progressively premature AES over the fast pathway (once the AES coupling interval becomes shorter than the fast pathway ERP) and anterograde conduction over the slow pathway (which has an ERP shorter than the AES coupling interval), with a longer conduction time (i.e., longer A2-H2 interval). A jump in the A2-H2 (or H1-H2) interval of ≥ 50 milliseconds in response to a 10

millisecond shortening of either the A1-A2 interval (i.e., AES coupling interval) or the A1-A1 interval (i.e., pacing cycle length [PCL]) is defined as a discontinuous AVN function curve and is considered evidence of dual anterograde AVN pathways (see Fig. 4.23).

Two ventricular responses to a single atrial impulse. Rapid atrial pacing or AES can result in two ventricular complexes to a single paced atrial impulse (referred to as “1:2 response”).¹⁹ The first ventricular complex is caused by conduction of the atrial impulse over the fast AVN pathway, and the second complex is caused by conduction over the slow AVN pathway (Fig. 17.10). This response requires a unidirectional retrograde block in the slow AVN pathway. Typically, in the presence of dual AVN pathways, conduction propagates simultaneously over both fast and slow AVN pathways. However, the wavefront conducting down the fast pathway reaches the distal junction of the two pathways before the impulse conducting down the slow pathway; hence, it conducts retrogradely up the slow pathway to collide with the impulse conducting anterogradely down that pathway. Thus the anterograde impulse conducting down the slow pathway does not have the opportunity to reach the HB and the ventricle. Rarely, however, the slow pathway conducts only anterogradely or has a very long retrograde ERP. In this setting, the wavefront traveling anterogradely down the fast pathway blocks (but does not conceal) in the slow pathway retrogradely and fails to retard the impulse traveling anterogradely down that pathway. Consequently, the wavefront traveling down the slow pathway can reach the HB and ventricle to produce a second His potential and QRS in response to a single atrial impulse. Because retrograde block in the slow pathway is a prerequisite to a 1:2 response, when such a phenomenon is present, it indicates that the slow pathway cannot support reentrant tachycardia using the slow pathway as the retrograde limb. The 1:2 response should be differentiated from pseudo-simultaneous fast and slow pathway conduction, which is a much more common phenomenon during rapid atrial pacing. In the latter case, all paced atrial impulses block anterogradely in the fast pathway and conduct exclusively down the slow pathway with prolonged AH intervals (with PR intervals longer than atrial PCL), so that the last paced atrial impulse falls before the His potential caused by conduction of the preceding paced atrial impulse. Thus the last paced atrial impulse is followed by two His potentials and two ventricular complexes. The last response may then be followed by induction of AVN echo beats or AVNRT, mimicking simultaneous fast and slow pathway conduction (Fig. 17.11).

PR interval longer than RR interval. The PR interval gradually prolongs as the atrial pacing rate increases. When a critical pacing rate is reached, the PR interval typically exceeds the R-R interval, with all AVN conduction over the slow AVN pathway (see Fig. 17.11). This manifests as *crossing over* of the pacing stimulus artifacts and QRSs; that is, the paced atrial complex is conducting not to the QRS immediately following it, but rather to the next QRS, because of a very long PR interval. There should be consistent 1:1 AV conduction that remains stable over the span of several cycles for this observation to be interpreted (i.e., without Wenckebach block). Such slow AVN conduction, sometimes called “skipped P waves,” is seen only when conduction propagates over a slow AVN pathway, and it is not seen in the absence of dual AVN physiology. This phenomenon is diagnostic of the presence of dual AVN physiology, even in the absence of an AH interval jump and therefore is very helpful in patients with smooth AVN function curves. In fact, 96% of patients with AVNRT and smooth AVN function curves have a PR/RR interval ratio greater than 1 (i.e., PR interval longer than PCL) during atrial pacing at the maximal rate with consistent 1:1 AV conduction (vs. 11% in controls).

Two distinct AH intervals during NSR or at identical atrial PCLs. This phenomenon can occur when the fast pathway anterograde ERP is long relative to the sinus or paced CL (see Fig. 17.6). Such a



eFig. 17.1 Dual Atrioventricular Node Physiology. H_1-H_2 intervals (*left*) and A_2-H_2 intervals (*right*) are at various A_1-A_2 intervals, with a discontinuous atrioventricular nodal curve. At a critical A_1-A_2 interval, the H_1-H_2 and A_1-H_2 intervals increase markedly. At the break in the curves, atrioventricular nodal reentrant tachycardia is initiated. (From Olgin JE, Zipes DP. Specific arrhythmias: diagnosis and treatment. In: Libby P, Bonow RO, Mann DL, Zipes DP, eds. *Braunwald's Heart Disease: A Textbook of Cardiovascular Medicine*. 7th ed. Philadelphia: Saunders; 2008:880.)

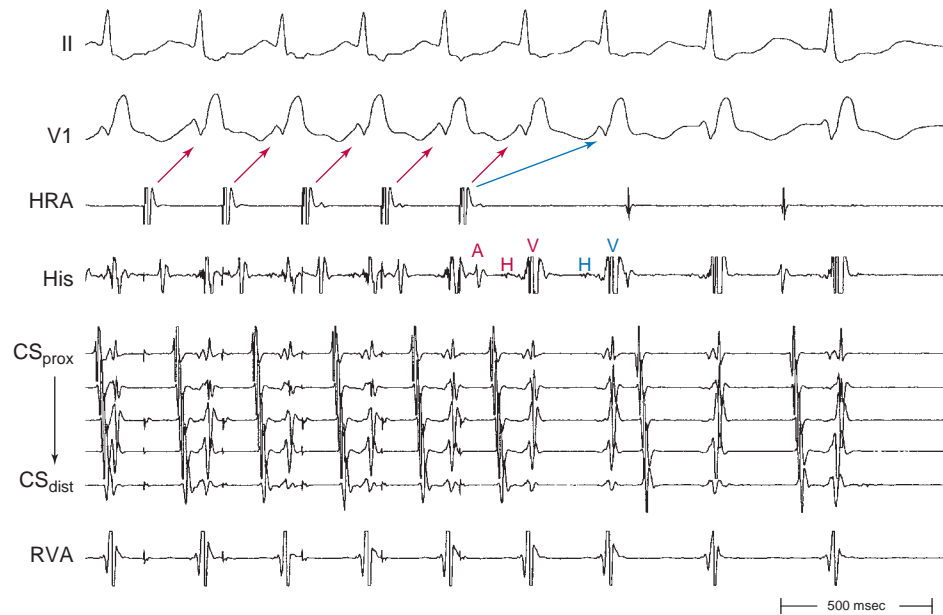


Fig. 17.10 Dual Atrioventricular Node (AVN) Physiology: Two Ventricular Complexes to a Single Paced Atrial Impulse. Rapid atrial pacing during normal sinus rhythm. Each paced atrial impulse conducts anterogradely over the fast AVN pathway (red arrows). However, the last paced impulse conducts anterogradely over both the fast (red arrow) and slow (blue arrow) pathways, resulting in two His bundle and ventricular responses. *CS_{dist}*, Distal coronary sinus; *CS_{prox}*, proximal coronary sinus; *HRA*, high right atrium; *RVA*, right ventricular apex.

phenomenon also requires a long retrograde ERP of the fast pathway. Otherwise, AVN echo beats or AVNRT would result, because once the impulse blocks anterogradely in the fast pathway and is conducted down the slow pathway, it would subsequently conduct retrogradely up the fast pathway if the ERP of the fast pathway were shorter than the conduction time (i.e., shorter than the AH interval) over the slow pathway.

Determinants for the occurrence of sustained slow pathway conduction include markedly abnormal, anterograde and retrograde conduction properties of the fast pathway and, possibly, differential sensitivity to vagal activity of the fast pathway, compared with the slow pathway.¹⁷

Multiple AVN pathways. Multiple AH interval “jumps” in response to AES, a finding suggesting the presence of multiple AVN pathways, can be observed in up to 14% of patients with AVNRT, especially in those with atypical variants of AVNRT. These phenomena are characterized by multiple AH interval jumps of 50 milliseconds or more in response to an increasingly premature AES. In these patients, a single AES can initiate multiple jumps in only 68%, whereas double AESs or atrial pacing is required in 32%. Such patients can have AVNRT with longer TCLs and longer ERP and FRP of the AVN. It is uncommon for multiple AVNRTs with different TCLs and P-QRS relationships to be present in the same patient.

Prevalence of dual AVN physiology. The presence of dual AVN pathways can usually be demonstrated by using a single AES or atrial pacing in 85% of patients with clinical AVNRT. In 95% of patients, the presence of dual AVN pathways can be revealed by using multiple AESs, multiple-drive CLs (typically 600 and 400 milliseconds), and multiple pacing sites (typically high RA and CS).

Occasionally, the AH interval continuously prolongs (without a discrete “jump”) in response to more premature AES, with “smooth transition” of anterograde conduction from the fast pathway to the slow pathway, until retrograde conduction starts over the “fast pathway”

and AVNRT is induced. Failure to demonstrate dual AVN physiology in patients with AVNRT can be caused by minimal differences in the anterograde refractory periods of the fast and slow AVN pathways. In this setting, dissociation of refractoriness of the fast and slow AVN pathways is required and can be achieved by any of the following: (1) introduction of an AES at a shorter pacing drive CL; (2) introduction of multiple AESs; (3) burst atrial pacing; or (4) pharmacological modulation of AVN dual pathway conduction and refractoriness.⁶

In general, if fast pathway conduction is suppressed at baseline (as evidenced by a long AH interval at all atrial pacing rates or VA block during ventricular pacing), isoproterenol infusion (and occasionally atropine) usually facilitates fast pathway conduction. In contrast, if the baseline ERP of the fast pathway is very short, conduction over the slow pathway can be difficult to document. Increasing the degree of sedation or infusion of esmolol can prolong the fast pathway ERP and allow recognition of slow pathway conduction.

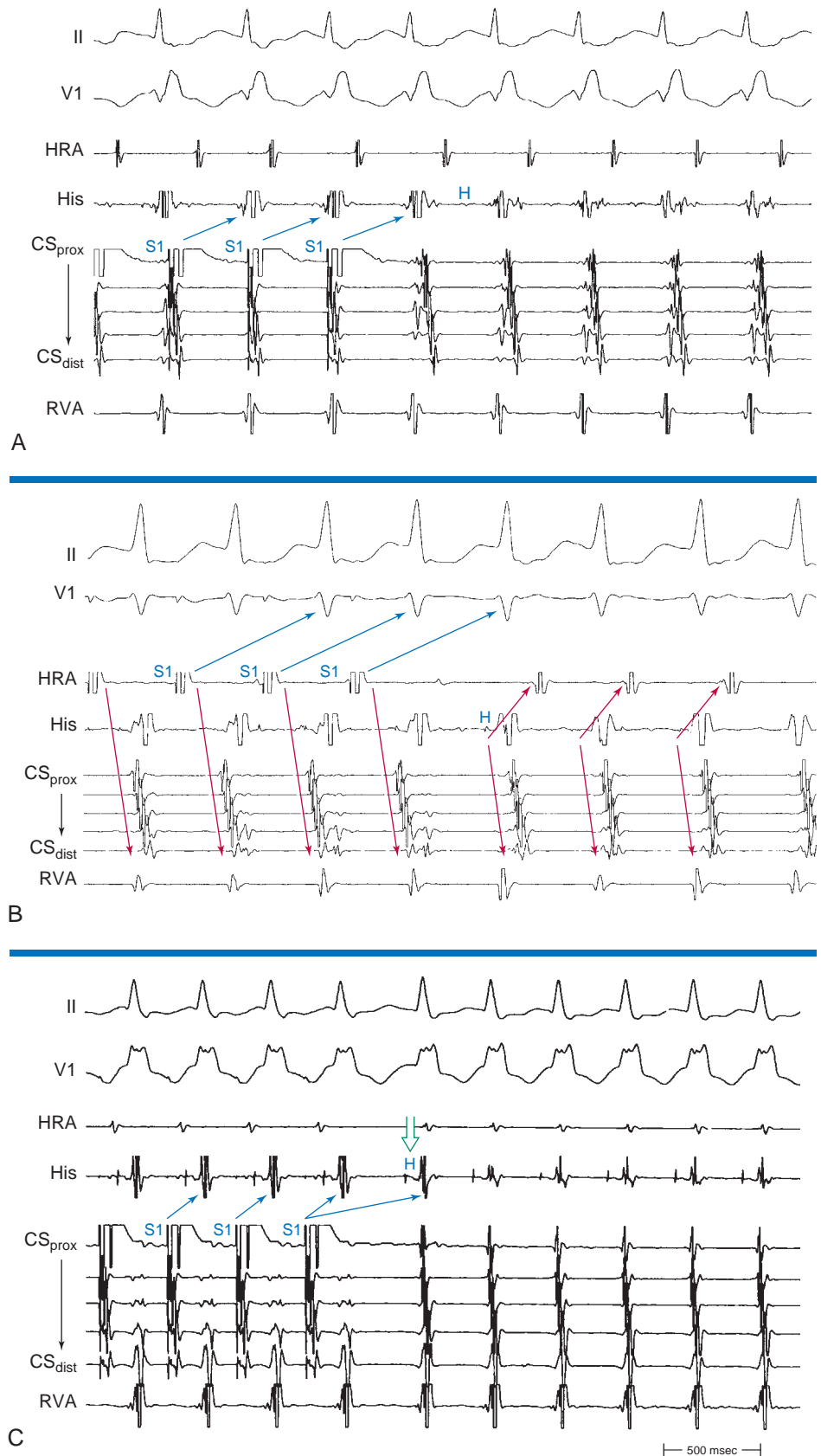
Another potential reason for the inability to demonstrate dual AVN physiology is a block in the fast AVN pathway at the pacing drive CL (i.e., fast pathway ERP is longer than pacing drive CL). In addition, atrial FRP can limit the prematurity of the AES. Consequently, AVN activation cannot be adequately advanced to produce block in the fast pathway because a more premature AES would result in more intraatrial conduction delay and less premature stimulation of the AVN. This obstacle can be overcome by the introduction of an AES following a shorter pacing drive CL, introduction of multiple AESs, burst atrial pacing, or stimulation from multiple atrial sites.

Programmed Ventricular Stimulation During Sinus Rhythm

Retrograde dual AVN physiology. Demonstration of retrograde dual AVN pathway conduction curves requires a longer retrograde ERP of the fast pathway than slow pathway ERP and ventricular and His-Purkinje system (HPS) FRP, as well as a sufficient difference in

Fig. 17.11 Induction of Typical Atrioventricular Nodal Reentrant Tachycardia (AVNRT) With Atrial Pacing.

(A) Each of the atrial paced impulses (*S1*) conducts anterogradely over the slow atrioventricular node (AVN) pathway. The last paced impulse, following anterograde conduction down the slow pathway, also conducts retrogradely up the fast AVN pathway to initiate typical AVNRT with right bundle branch block (RBBB). (B) Each of the atrial paced impulses conducts anterogradely over the slow AVN pathway with a long PR interval (*blue arrows*); this is longer than the pacing cycle length, resulting in crossing over, which can mimic a 1:2 atrioventricular response caused by anterograde conduction over both the fast and slow AVN pathways. Following anterograde conduction down the slow pathway, the last paced impulse also conducts retrogradely over the fast pathway, initiating typical AVNRT. Red arrows illustrate atrial activation sequence during atrial pacing versus AVNRT. (C) Atrial pacing from the coronary sinus ostium induces typical AVNRT. Each of the atrial paced impulses (*S1*) conducts over the fast AVN pathway except for the last paced impulse, which conducts over both the fast and slow AVN pathways (*blue arrows*), resulting in a 1:2 response (i.e., 2 ventricular responses to a single atrial impulse); this is followed by induction of typical AVNRT with RBBB. The possibility of conduction of the paced atrial beats over the slow AVN pathway with a long atrial–His bundle (AH) interval (longer than the paced cycle length) is unlikely because the His potential preceding the first tachycardia complex (indicated by the *green arrow*) occurs later (i.e., at a longer AH interval) than what would be expected if that His potential was actually a result of conduction of the last atrial stimulus (as compared with the previous AH intervals). *CS_{dist}*, Distal coronary sinus; *CS_{prox}*, proximal coronary sinus; *HRA*, high right atrium; *RVA*, right ventricular apex.



conduction times between the two pathways. In a pattern analogous to that of anterograde dual AVN physiology, ventricular stimulation can result in discontinuous retrograde AVN function curves, manifesting as a jump in the H2-A2 (or A1-A2) interval of 50 milliseconds or more in response to a 10 millisecond decrement of the VES coupling interval (V1-V2) or ventricular PCL (V1-V1). This finding must be distinguished from sudden VA prolongation caused by VH interval (but not HA interval) prolongation related to retrograde functional block in the right bundle branch (RB) and transseptal activation of HB through the left bundle branch (LB) (see eFig. 4.9). A 1:2 response (i.e., two atrial responses to a single ventricular stimulus) can also be observed (see Box 17.2).

Failure to demonstrate retrograde dual AVN physiology in patients with atypical AVNRT can be caused by similar fast and slow AVN pathway retrograde refractory periods. Dissociation of refractoriness of the fast and slow AVN pathways may be required and usually can be achieved by any of the following: (1) introduction of VESs at a shorter pacing drive CL; (2) introduction of multiple VESs; (3) burst ventricular pacing; or (4) administration of drugs such as beta-blockers, verapamil, or digoxin. In addition, retrograde block in the fast AVN pathway at the pacing drive CL (i.e., the PCL is shorter than the fast pathway ERP) and ventricular or HPS FRP interval limiting the prematurity of the VES can also account for such failure.

Differential-site RV pacing. Differential-site RV pacing can help exclude the presence of a retrogradely conducting septal AV BT. The response to differential RV pacing can be evaluated by comparing two variables between RV basal and RV apical (or midseptal) pacing: the VA interval (i.e., the stimulus-to-atrial [SA] interval) and atrial activation sequence (see Fig. 18.28). This maneuver is discussed in detail in Chapter 20.²⁰

The RV apical septum, although anatomically more distant from the atrium than the RV base, is nonetheless electrically closer because of the proximity of the distal RB to the pacing site. As a result, in the absence of a retrogradely conducting septal AV BT, pacing at the RV apex allows entry into the rapidly conducting HPS and results in a shorter VA interval during pacing from the apex than from the base. In addition, retrograde atrial activation sequence remains constant during pacing both at the RV apex and at the RV base because the atrium is activated over a single route (the AVN) in both settings.

A shorter VA interval during RV basal pacing than during RV apical pacing or a change in retrograde atrial activation sequence in response to differential RV pacing (RV base vs. RV apex) indicates the presence of an AV BT. However, differential-site RV pacing does not exclude the presence of a distant right or left free-wall BT or slowly conducting BT, whereby retrograde conduction occurs preferentially over the AVN.²⁰ Also, the occurrence of right bundle branch block (RBBB) (but not left bundle branch block [LBBB]) also can alter the significance of the VA interval criterion (see Fig. 20.6).

Para-Hisian Pacing During Sinus Rhythm

Para-Hisian pacing helps exclude the presence of a septal AV BT, which can mediate orthodromic AVRT with a retrograde atrial activation sequence similar to that during AVNRT. In the absence of a BT, para-Hisian pacing results in a shorter SA (or VA) interval when the HB-RB is captured ($S - H = 0$ and $SA = HA$) than the SA interval when only the ventricle is captured ($SA = S - H + HA$) with no change in the atrial activation sequence or HA interval. This response to para-Hisian pacing is termed *pattern 1* or *AVN/AVN pattern*.

A change in the retrograde atrial activation sequence with loss of HB-RB capture indicates the presence of a retrogradely conducting BT. Similarly, an SA (VA) interval that is constant regardless of whether the HB RB is being captured indicates the presence of a BT, whereas

prolongation of the SA (or VA) interval on loss of HB capture, compared with that during HB capture, excludes the presence of a retrogradely conducting BT, except for slowly conducting and far free-wall BTs. Please refer to Chapter 20 for a more detailed discussion of para-Hisian pacing.

Induction of Tachycardia

Initiation by Programmed Atrial Stimulation

Typical (slow-fast) AVNRT. Clinical AVNRT almost always can be initiated with an AES that blocks anterogradely in the fast pathway, conducts down the slow pathway, and then conducts retrogradely up the fast pathway. Only when anterograde conduction down the slow pathway is slow enough ("critical AH interval") to allow for recovery of the fast pathway to conduct retrogradely does reentry occur (see eFig. 17.1). This critical AH interval is not a fixed interval. It can change with changes in pacing drive CL, changes in autonomic tone, or after drug administration, thus reflecting changes in the fast pathway retrograde ERP.

There is a zone of AES coupling intervals (A1-A2) associated with AVNRT induction called the tachycardia zone. This zone usually begins at coupling intervals associated with marked prolongation of the AH intervals. This AVN conduction delay (AH interval prolongation), and not the AES coupling interval, is of prime importance for the genesis of AVNRT.

Atrial pacing can initiate AVNRT at PCLs associated with sufficient AVN conduction delay (see Fig. 17.11), especially during atypical Wenckebach periodicity, when anterograde block occurs in the fast pathway and conduction shifts to the slow pathway.

Rarely, AES or atrial pacing can produce a "1:2 response" with anterograde conduction over both the fast and slow pathways, as explained earlier (see Fig. 17.11). Such a response predicts easy induction of slow-fast AVNRT by ventricular stimulation because poor slow pathway retrograde conduction would increase the opportunity for the ventricular stimulus to block in the slow pathway and conduct up the fast pathway to return down the slow pathway and initiate AVNRT.

The site of atrial stimulation can affect the ease of inducibility of AVNRT, probably because of different atrial inputs to the AVN or different atrial FRPs. Therefore it is important to perform atrial stimulation from both the RA and CS.

AVN echo beats and AVNRT usually occur at the same time that dual pathways are revealed (see Fig. 4.23). In 20% of patients, the dual AVN pathway AH interval jump occurs without concurrent occurrence of echo beats or AVNRT because of failure of retrograde conduction up the fast pathway. This failure can be caused by the absence of a distal connection between the two AVN pathways, a long retrograde ERP of the fast AVN pathway, or concealment of the AES anterogradely into the fast AVN pathway (i.e., the AES propagates some distance into the fast pathway before being blocked). The last event results in anterograde postdepolarization refractoriness, which would consequently make the fast pathway refractory to the wavefront invading it in the retrograde direction. The latter phenomenon can be diagnosed by demonstrating that the AH interval following the AES that fails to produce an echo beat is longer than the shortest ventricular PCL with 1:1 retrograde conduction. Such a PCL is a marker of the fast pathway retrograde ERP. This finding implies that an AES blocking in the fast pathway and conducting over the slow pathway, with an AH interval exceeding fast pathway ERP and still not conducting retrogradely over the fast pathway, is caused by anterograde concealment (and not just block) into the fast pathway.

Markers of poor retrograde conduction over the fast AVN pathway predict difficulty inducing AVNRT. These markers include the absence of VA conduction, poor VA conduction (manifest as retrograde AVN

Wenckebach CL longer than 500 milliseconds), and retrograde dual pathways (indicative of long retrograde ERP of the fast pathway, which must exceed the refractoriness of the slow pathway for retrograde dual pathways to be demonstrable). In fact, retrograde fast AVN pathway characteristics (i.e., ERP) are the major determinant of *whether* reentry (AVN echoes or AVNRT) occurs, whereas conduction delay anterogradely over the slow pathway (i.e., “critical AH interval”) determines *when* reentry is to occur.

Although isolated AVN echoes can occur as long as VA conduction is present, the ability to initiate sustained AVNRT also requires the capability of the slow pathway to sustain repetitive anterograde conduction. In other words, sustenance of AVNRT requires that the TCL be longer than the ERP of all components of the circuit. Typically, for AVN reentry to occur, the fast pathway should be able to support 1:1 VA conduction at a ventricular PCL shorter than 400 milliseconds (i.e., retrograde Wenckebach CL shorter than 400 milliseconds), and the slow pathway should be able to support 1:1 AV conduction at an atrial PCL shorter than 350 milliseconds (i.e., anterograde Wenckebach CL shorter than 350 milliseconds). The shorter the AH interval during anterograde conduction over the fast pathway, the better the retrograde conduction over the same pathway (i.e., the shorter the HA interval), and the better the inducibility of AVNRT. Nevertheless, it is important to recognize that during EP testing, these criteria are dependent on the cardiac autonomic tone at that moment, and they can change dramatically by changing the level of patient sedation or the use of isoproterenol

or by prolonged periods of rapid pacing (particularly ventricular) that cause hypotension and a reflex increase in adrenergic tone, which then affect inducibility of AVNRT.

Atypical AVNRT. Anterograde dual AVN physiology is usually not demonstrable in patients with atypical AVNRT. In addition, as noted, the presence of a “1:2 response” to AES predicts noninducibility of atypical AVNRT because it indicates failure of the slow pathway to support retrograde conduction, a prerequisite for the atypical AVNRT circuit.

When atypical AVNRT is initiated with atrial stimulation, it is usually with modest prolongation of the AH interval over the fast pathway and anterograde block in the slow pathway, followed by retrograde slow conduction over the slow pathway (Fig. 17.12). Therefore a critical AH interval delay is not obvious.

Initiation by Programmed Ventricular Stimulation

Typical (slow-fast) AVNRT. Ventricular stimulation induces typical AVNRT by different mechanisms. The most common mechanism involves retrograde block of the ventricular stimulus in the slow pathway and retrograde conduction up the fast pathway, followed by anterograde conduction down the slow pathway. This occurs when the retrograde ERP of the slow pathway exceeds that of the fast pathway. This means that induction occurs without the demonstration of retrograde dual AVN physiology, and no critical VA or HA interval is required for induction. Occasionally, an interpolated

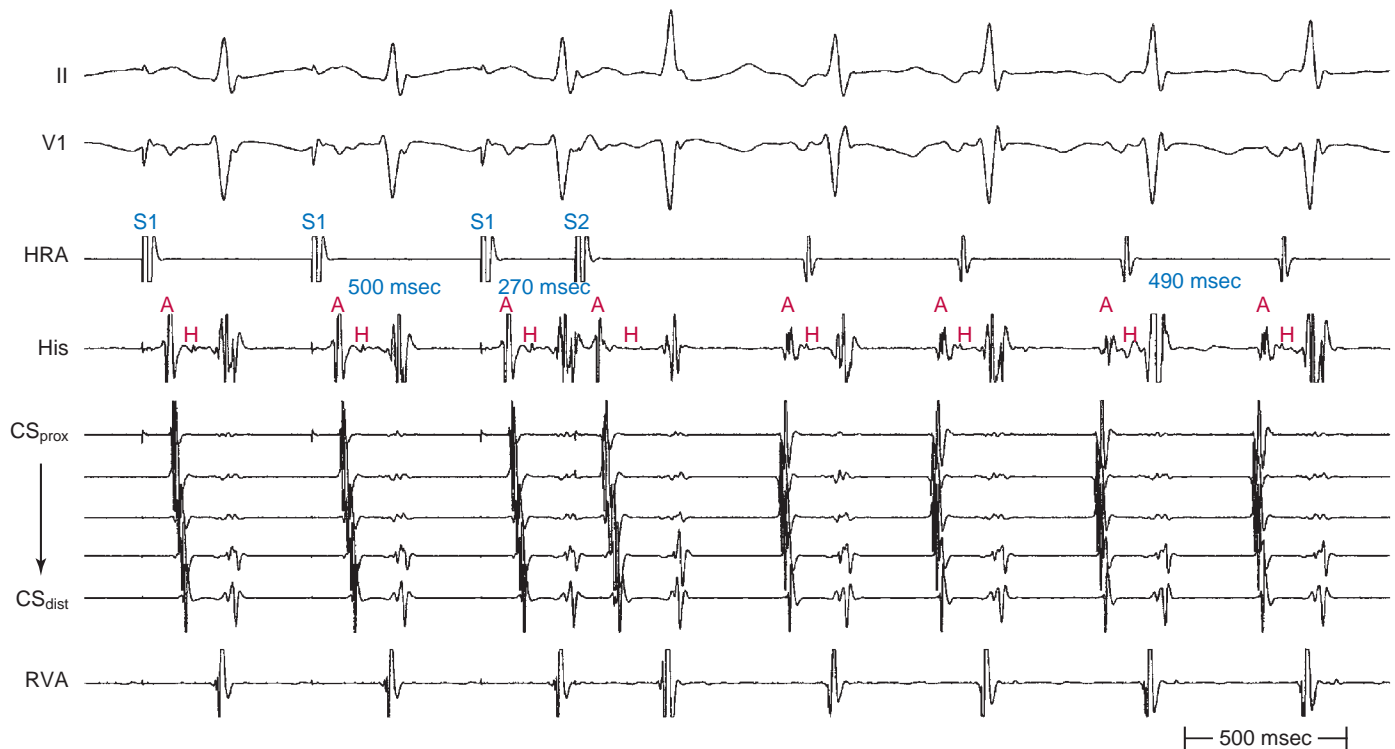


Fig. 17.12 Induction of Fast-Slow Atrioventricular Nodal Reentrant Tachycardia (AVNRT) With Atrial Extrastimulation (AES). AES delivered from the high right atrium (HRA) at a coupling interval of 270 milliseconds after a drive cycle length (CL) of 500 milliseconds initiated atypical AVNRT with a CL of 490 milliseconds. Note that the AES conducted with only a modest prolongation of the atrial–His bundle (AH) interval. In addition, comparing the AH interval between atrial drive pacing and that during the SVT (because the tachycardia CL approximates the pacing CL) reveals that ΔAH ($AH_{\text{pacing}} - AH_{\text{SVT}}$) is more than 40 milliseconds, thus favoring AVNRT over atrial tachycardia and orthodromic atrioventricular reentrant tachycardia. CS_{dist} , Distal coronary sinus; CS_{prox} , proximal coronary sinus; HRA, high right atrium; RVA, right ventricular apex.

PVC can block in the slow pathway retrogradely and penetrate the fast pathway and cause concealment, so that the fast pathway will be refractory when the next sinus beat occurs. The sinus beat would then block in the fast pathway and conduct down the slow pathway and initiate typical AVNRT. This mechanism is uncommon. Retrograde VA conduction over the fast AVN pathway is usually good, and VA block rarely occurs in patients with typical AVNRT initiated by ventricular stimulation.

Ventricular stimulation is less effective than atrial stimulation in inducing typical AVNRT (success rate is approximately 10% with VES and 40% with ventricular pacing), whereas atypical AVNRT can be induced almost as frequently by ventricular stimulation as by atrial stimulation. It is difficult for VES to induce typical AVNRT because the prematurity with which the VES arrives at the AVN can be limited by conduction delay in the HPS or in the lower common pathway. The ERP of the HPS may exceed that of the slow AVN pathway. This limitation can usually be overcome by the introduction of multiple VESs, use of a shorter drive CL, or ventricular pacing, which results in the adaptation and shortening of the HPS ERP. In addition, the anterograde ERP of the slow pathway may exceed the ventricular PCL so that the slow pathway is incapable of anterograde conduction of the ventricular impulse conducting retrogradely over the fast pathway. Similar retrograde ERPs of the slow and fast pathways also can limit the successful initiation of AVNRT by ventricular stimulation. As noted, manipulation of the autonomic tone with vagal maneuvers or drugs can facilitate dissociation of those ERPs. Another explanation for the lower success rate of AVNRT induction by ventricular stimulation is that the ventricular stimulus can penetrate (and not just block) in the slow pathway retrogradely, thus causing concealment that renders that pathway refractory and incapable of anterograde conduction of the ventricular impulse traveling retrogradely over the fast pathway.

Burst ventricular pacing can overcome many of the problems imposed by HPS refractoriness in the induction of typical AVNRT (Fig. 17.13). During ventricular pacing, the AVN is the primary site of conduction delay. However, block in the lower common pathway and repetitive

concealment (not just block) in the slow AVN pathway can still limit the success of ventricular pacing in inducing typical AVNRT.

When induction of the SVT is achieved by ventricular pacing at a CL similar to the subsequent TCL or by a VES that activates the HB at a coupling interval (i.e., H1-H2 interval) similar to the H-H interval during the SVT (i.e., similar to the TCL), the HA interval following the initiating ventricular stimulus then is compared with that during the SVT. During AVNRT, the HA interval of the ventricular stimulus initiating the SVT is longer than the HA interval during the SVT because both the HB and atrium are activated in sequence during ventricular stimulation but in parallel during AVNRT (Fig. 17.14). This is even exaggerated by the fact that the AVN usually exhibits greater decremental conduction with repetitive engagement of impulses than in response to a single impulse at a similar coupling interval. Therefore the more prolonged the HA interval with the initiating ventricular stimulus, the more likely the SVT is AVNRT. On the other hand, if the SVT uses an AV BT for retrograde conduction, the HA interval during the initiating ventricular stimulus (at a coupling interval comparable to the TCL) is shorter than that during orthodromic AVRT because the HB and atrium are activated in parallel during ventricular pacing (when atrial activation is mediated by retrograde BT conduction), but in sequence during SVT.

The intervals immediately following tachycardia initiation with a VES (delivered from the RV apex) provide data that are essentially equivalent to those observed with ventricular entrainment (see below). The interval from the VES to atrial activation (surface VA or "SA" interval) is compared to the surface VA interval during SVT, and the post VES return cycle (i.e., the interval from the VES to the subsequent RV apical depolarization) is compared to the TCL. An SA interval that exceeds the surface VA interval during SVT by less than 85 milliseconds is consistent with orthodromic AVRT. Similarly, a post VES return cycle exceeding the TCL by less than 115 milliseconds indicates orthodromic AVRT. The small differences between those intervals are related to the proximity of the RV apical pacing site to the SVT reentry circuit. Larger differences in these intervals are observed in the setting of AVNRT or

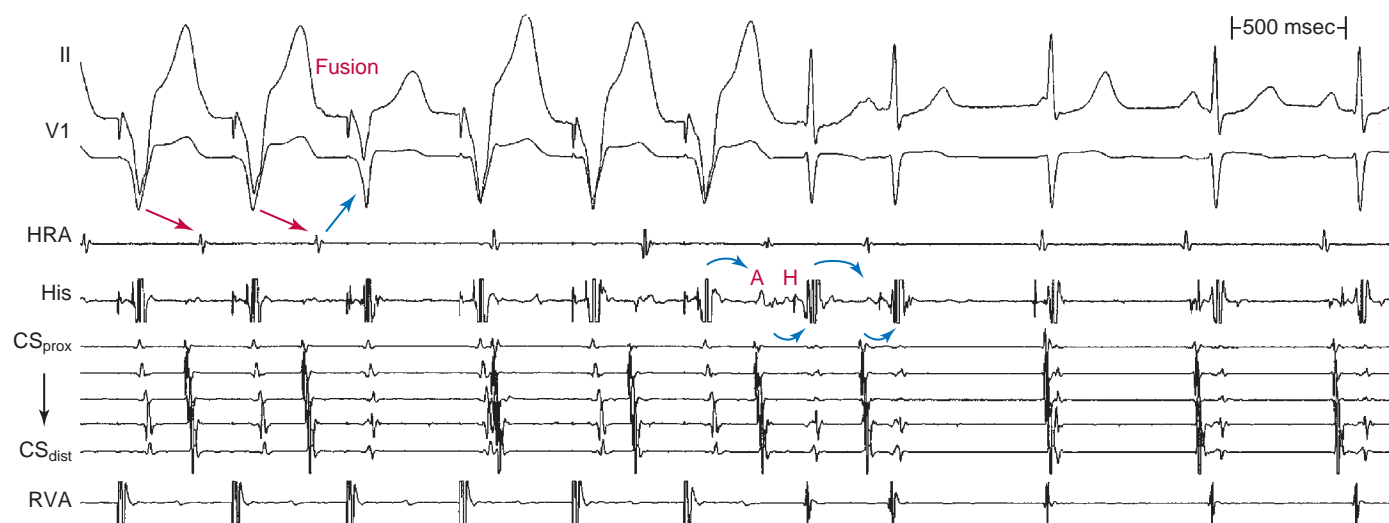


Fig. 17.13 Induction of Atrioventricular Node (AVN) Echo Beats by Ventricular Pacing. Note that ventriculoatrial conduction during ventricular pacing is occurring up the slow AVN pathway (red arrows). This results in AVN echo beats caused by anterograde conduction over the fast pathway, which results in occasional QRS fusion (i.e., fusion between the echo beat and the paced impulse) during the pacing drive. Cessation of ventricular pacing is followed by double AVN echo beats (blue arrows). CS_{dist}, Distal coronary sinus; CS_{prox}, proximal coronary sinus; HRA, high right atrium; RVA, right ventricular apex.

administration of atropine, a finding suggesting that the site of block is not in the AVN. In addition, a VES introduced during the 2:1 AV block consistently results in 1:1 conduction, indicating that the AV block is functional and that the level of block is infranodal. Therefore what was previously thought to be 2:1 AVN block in the lower common pathway of the AVN (because of the absence of visible His potentials) is more likely to be intra-Hisian block. VA block during AVNRT rarely has been reported (see Fig. 17.13).

As noted, variations A/V relationship, with or without AV block during tachycardia, should not be misdiagnosed as AT; they can be atypical or, rarely, typical forms of AVNRT. Moreover, the variations could be of such magnitude that a long RP tachycardia can masquerade for brief periods of time as a short RP tachycardia.

Oscillation in the tachycardia cycle length. When CL variability is observed during typical AVNRT, it is generally caused by changes in anterograde conduction over the slow AVN pathway. Because retrograde conduction through the fast pathway generally is much less variable, the changes in the ventricular CL that result from variability in anterograde AVN conduction precede and predict the subsequent changes in the atrial CL (eFig. 17.2), as is the case in orthodromic AVRT.

Effect of bundle branch block. The development of prolonged functional aberration during AVNRT is uncommon, and it usually occurs at initiation of the tachycardia or after resumption of 1:1 AV conduction after a period of block in the HB or lower common pathway (see Fig. 17.9). When bundle branch block (BBB) does occur during AVNRT, it does not influence the TCL (A-A or H-H intervals) because the ventricles are not required for the tachycardia circuit.

Termination and response to physiological and pharmacological maneuvers. The TCL is correlated best with the conduction time down the slow pathway. Spontaneous or pharmacologically mediated changes in the TCL are also more closely associated with changes in slow pathway conduction. Spontaneous termination of typical AVNRT occurs because of a block in the fast or the slow pathway. However, the better the retrograde fast pathway conduction, the less likely it will be the site of the block. Carotid sinus massage and vagal maneuvers can terminate typical AVNRT with gradual anterograde slowing and then block in

the slow pathway, whereas block in the fast pathway in this setting is uncommon.

AVN blockers (digoxin, calcium channel blockers, and beta-blockers) prolong the refractoriness of the fast and slow pathways to similar or different degrees. Such effects mediate termination of AVNRT. However, they can also potentially help dissociate the ERP of the fast and slow pathways and unmask dual AVN physiology and, thus, facilitate inducibility of AVNRT. Adrenergic stimulation tends to shorten the anterograde and retrograde ERP of the fast pathway to a greater extent than that of the slow pathway. Conversely, beta-blockers tend to prolong ERP of the fast pathway more than that of the slow pathway.⁶

Adenosine produces differential effects on anterograde and retrograde conduction over the different AVN pathways. The effect of adenosine is far less potent on retrograde fast pathway conduction than on the retrograde slow pathway and anterograde fast and slow pathway conduction. During slow-fast AVNRT, adenosine can increase the TCL by prolonging the AH interval (i.e., anterograde slow pathway conduction), with little or no change of conduction time and conduction sequence of the retrograde fast pathway. The mechanism of adenosine resistance of retrograde fast pathway conduction (both in patients with slow-fast AVNRT and in normal subjects) remains unclear.⁹

Atypical Atrioventricular Nodal Reentrant Tachycardia

The earliest site of retrograde atrial activation during atypical AVNRT is usually recorded at the base of the triangle of Koch or CS os, and CS breakthrough is observed in most patients. The CS breakthrough is likely part of or very close to the reentry circuit, as demonstrated by entrainment mapping.

The RP interval during atypical fast-slow AVNRT is longer than the PR interval. In addition, the PR and AH intervals are shorter during AVNRT than during NSR (Fig. 17.15).

Usually, the A/V ratio equals 1, as is the case for typical AVNRT. BBB can occur but does not influence the TCL. In contrast to typical AVNRT, CL variability during atypical AVNRT is usually caused by changes in retrograde conduction over the slow AVN pathway. Anterograde conduction occurs over the more stable fast AVN pathway and

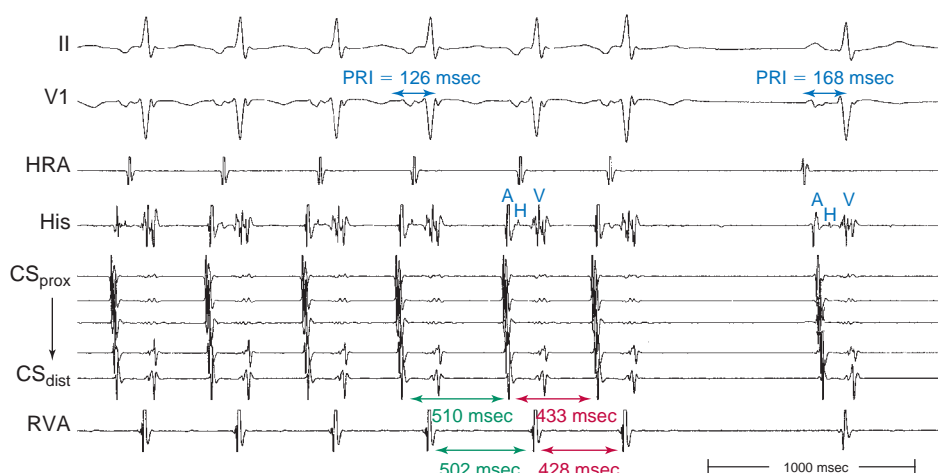
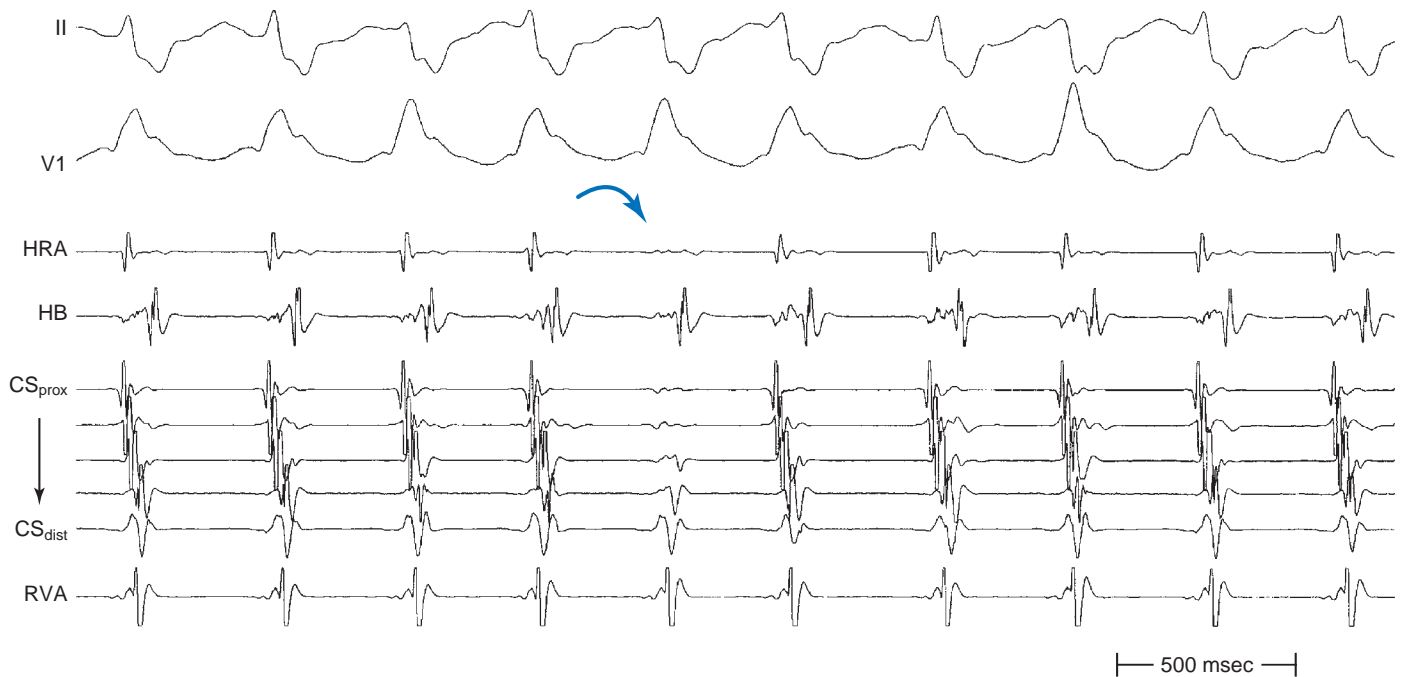


Fig. 17.15 Spontaneous Termination of Atypical (Fast-Slow) Atrioventricular Nodal Reentrant Tachycardia (AVNRT). Oscillation of the tachycardia cycle length (CL) is observed just before termination. Note that changes in the atrial CL predict changes in the subsequent ventricular CL because CL variability during atypical AVNRT is usually caused by changes in retrograde conduction over the slow atrioventricular node (AVN) pathway, whereas anterograde conduction occurs over the more stable fast AVN pathway and is less subject to variability. In addition, the PR interval (PRI) and atrial-His bundle interval are shorter during AVNRT than those during sinus rhythm. CS_{dist}, Distal coronary sinus; CS_{prox}, proximal coronary sinus; HRA, high right atrium; RVA, right ventricular apex.



eFig. 17.2 Typical Atrioventricular Nodal Reentrant Tachycardia With Right Bundle Branch Block. Intermittent ventriculoatrial block is observed (*arrow*) secondary to block in an upper common pathway. Oscillation of the tachycardia cycle length is observed before the block. Note the changes in the H-H and V-V intervals preceding similar changes in the A-A interval. Both atrial tachycardia and orthodromic atrioventricular reentrant tachycardia are excluded by the fact that the atrium is not necessary for continuation of the tachycardia. *CS_{dist}*, Distal coronary sinus; *CS_{prox}*, proximal coronary sinus; *HRA*, high right atrium; *RVA*, right ventricular apex.

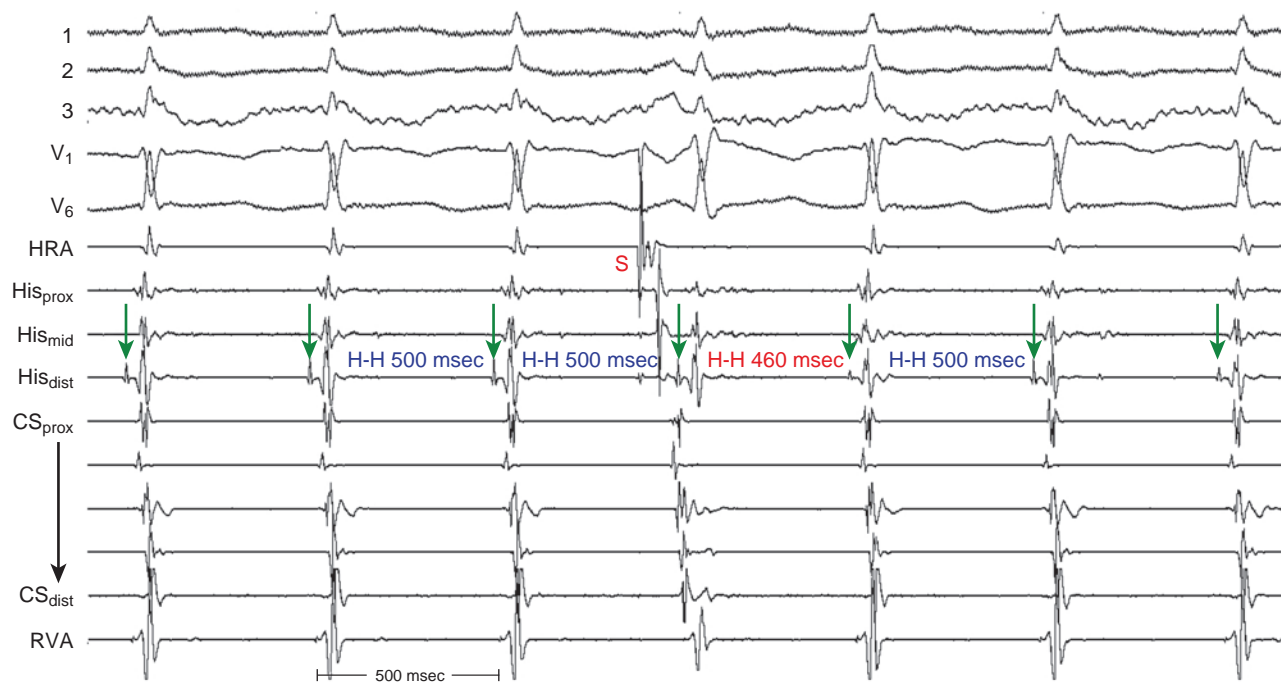


Fig. 17.16 Atrial Extrastimulation During Atrioventricular Nodal Reentrant Tachycardia (AVNRT). An atrial extrastimulation delivered during AVNRT has no effect on the timing of the immediately following His potential ($H-H$ interval = 500 milliseconds) but advances the timing of the next His potential ($H-H$ interval = 460 milliseconds). Arrows mark His potentials. CS_{dist} , Distal coronary sinus; CS_{prox} , proximal coronary sinus; His_{dist} , distal His bundle; His_{mid} , middle His bundle; His_{prox} , proximal His bundle; HRA , high right atrium; RVA , right ventricular apex.

is less subject to variability (see Fig. 17.15). Therefore, during atypical AVNRT, changes in the atrial CL predict changes in the subsequent ventricular CL (as is the case in AT). Carotid sinus massage, vagal maneuvers, adenosine, and AVN blockers (e.g., digoxin, calcium channel blockers, and beta-blockers) generally terminate atypical AVNRT by gradual slowing and then block in the retrograde slow pathway (see Fig. 17.15). Termination of atypical AVNRT with adenosine can also result from block in the fast AVN pathway; however, the value of this observation in distinguishing between atypical AVNRT and orthodromic AVRT using a slow retrograde BT is questionable.

Diagnostic Maneuvers During Tachycardia

Programmed Atrial Stimulation During Tachycardia

Resetting. A late-coupled AES usually fails to reach the AVN with adequate prematurity and thus fails to affect the tachycardia, and a full compensatory pause results. However, the AES can result in concealment in perinodal tissue and, consequently, retard conduction of the impulse traveling retrogradely up the fast pathway and, hence, result in a delay in the timing of the next atrial activation. This is usually manifested by an AES that delays the subsequent atrial activation but without affecting the timing of HB and ventricular activation.

During typical AVNRT, an early-coupled AES frequently penetrates the AVN and resets the reentry circuit, with a resulting compensatory pause that is less than, equal to, or greater than a full compensatory pause, depending on the degree of anterograde conduction delay that the AES encounters down the slow pathway (because of the decremental conduction properties of the AVN). The AES orthodromically propagates through the anterograde slow pathway, with a resulting alteration of the subsequent $H-H'$ interval, whereas it antidromically collides with

the preceding tachycardia wavefront traveling retrogradely up the fast pathway (Fig. 17.16). Progressively more premature AESs encounter progressive anterograde conduction delay in the slow pathway, and an increasing resetting response pattern occurs. In atypical AVNRT, an early-coupled AES can reset the SVT in a fashion similar to that seen in typical AVNRT; however, the delay in conduction that the AES will engender is mainly in the retrograde limb of the circuit (i.e., the slow pathway). Of note, an AES that accelerates the next His potential and resets tachycardia is indicative of focal junctional tachycardia (Fig. 17.17).

Resetting with manifest fusion (a hallmark of macroreentrant tachycardias) cannot be demonstrated in AVNRT. For atrial fusion (i.e., fusion of atrial activation from both the tachycardia wavefront and the AES) to occur, the AES should be able to enter the reentrant circuit, while at the same time the tachycardia wavefront should be able to exit the circuit. This requires spatial separation between the entry and exit sites to the reentrant circuit, a condition that seems to be lacking in the setting of AVNRT. Once the tachycardia wavefront exits the reentry circuit to activate the atrium, any AES delivered beyond that time and resulting in atrial fusion is not capable of reaching the reentry circuit because the entry-exit site is already refractory in response to activation by the exiting wavefront, and the AES has no alternative way of reaching the circuit. Similarly, once an AES is capable of reaching the reentry circuit, the entry and exit site region is made refractory and incapable of allowing a simultaneous exit of the tachycardia wavefront.

During typical AVNRT, a very early-coupled AES can block anterogradely in the slow pathway, and it usually collides with the retrograde wavefront traveling up the fast pathway to terminate the SVT. However, if the TCL is sufficiently long, with a wide fully excitable gap, and the AES is appropriately timed, the AES can block anterogradely in the

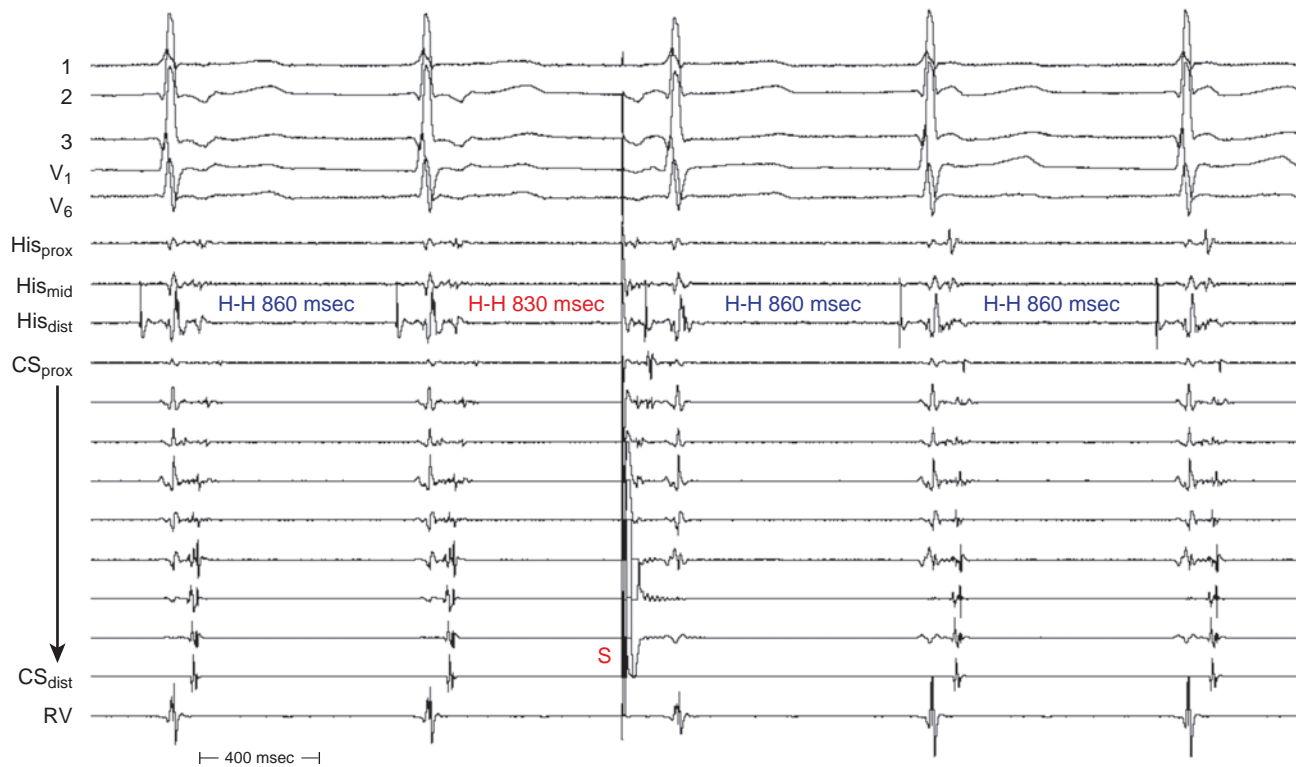


Fig. 17.17 Atrial Extrastimulation During Focal Junctional Rhythm. An atrial extrastimulation delivered during focal junctional rhythm advances the timing of the immediately following His potential ($H-H$ interval = 830 milliseconds) and resets the timing of the following His potential ($H-H$ interval = 860 milliseconds). CS_{dist} , distal coronary sinus; CS_{prox} , proximal coronary sinus; His_{dist} , distal His bundle; His_{mid} , middle His bundle; His_{prox} , proximal His bundle; RV , right ventricular.

slow pathway and still conduct down the fast pathway to capture the HB and ventricle and terminate the SVT before the SVT wavefront traveling down the slow pathway reaches the lower turnaround point. Therefore the last HB and ventricular electrograms before termination are advanced and premature, in contrast to termination secondary to an AES blocking anterogradely in the slow and fast pathways, whereby the last HB and ventricular electrograms of the SVT occur on time. This phenomenon occurs more commonly in atypical AVNRT.

During atypical AVNRT, a very early-coupled AES can conduct down the fast pathway during retrograde slow pathway activation and block retrogradely in the slow pathway. In this setting, the AES results in a premature HB and ventricular activation, and the AVNRT is terminated before the expected atrial activation.

Termination. The ability of an AES to terminate AVNRT depends on the following: (1) the TCL (AVNRT with a TCL shorter than 350 milliseconds is rarely terminated by a single AES, unless atrial stimulation is performed close to the AVN); (2) the distance of the site of atrial stimulation from the AVN (which would influence the ability of the AES to arrive to the AVN with adequate prematurity); (3) the refractoriness of the intervening atrial tissue (which can be overcome by delivery of multiple AESs); (4) atrial conduction velocity resulting from the AES; and (5) the size of the excitable gap in the reentrant circuit.

Atrial entrainment. Atrial pacing at a CL approximately 10 to 30 milliseconds shorter than the TCL is usually able to entrain AVNRT. In contrast to orthodromic AVRT, entrainment with atrial fusion cannot be demonstrated during AVNRT, a finding suggesting that the reentrant circuit in AVNRT does not have widely separate atrial entry and exit sites. Therefore, during entrainment of AVNRT by atrial pacing, the

atrial activation sequence and P wave morphology are always similar to those of the pure paced morphology. However, one study showed orthodromic capture of the atrial electrogram at the HB recording site (i.e., the bipolar HB electrogram morphology is identical to that during the tachycardia and is unaffected by pacing, and the first PPI is identical to the PCL) during entrainment from the CS or CS_{prox} region, a finding consistent with intracardiac atrial fusion. This suggests the absence of an upper common pathway between a reentrant circuit and atrial tissue surrounding the AVN and supports the concept that the reentrant circuit in AVNRT incorporates the atrial tissue surrounding the AVN. The AH interval during entrainment is usually longer than that during AVNRT because the atrial and the His electrograms are activated in parallel during AVNRT, and in sequence during atrial pacing entraining the AVNRT (in response to the presence of intervening atrial tissue separating the site of atrial stimulation from the reentry circuit).^{22,23}

Ventriculoatrial linking. The initial atrial complex following cessation of atrial pacing entraining typical AVNRT is *linked* to, and cannot be dissociated from, the last captured ventricular complex (and the last HB activation). As a consequence, postpacing VA intervals are fixed and similar to those during tachycardia (with less than 10 milliseconds variation) after different attempts at atrial entrainment, regardless of the site, duration, or CL of the entraining atrial pacing drive. VA linking is also observed after the introduction of an AES with a wide range of coupling intervals during tachycardia. VA linking occurs in the setting of typical AVNRT because the timing of atrial activation is dependent on activation of the lower turnaround point (and, hence, the HB and ventricular activation) by the last paced atrial impulse before traveling retrogradely up the fast pathway to activate the atrium. VA linking can

also be observed in orthodromic AVRT, whereby atrial activation is always dependent on the preceding ventricular activation. In contrast, in the setting of AT, the first atrial return cycle following cessation of pacing is dependent on the distance between the AT origin and pacing site, the atrial conduction properties, and the mode of the resetting response of the AT, and it is not related to the preceding ventricular activation. Hence, the postpacing VA intervals following different attempts at entrainment can vary especially when pacing at different rates or durations, or from different atrial sites.⁸

Programmed Ventricular Stimulation During Tachycardia

Resetting. For a VES to reset the AVNRT circuit, it needs to advance (prematurely activate) the HB timing by a degree that is dependent on the following: (1) the TCL, (2) the local ventricular ERP, (3) the time needed for the VES to reach the HB, and (4) the length of the lower common pathway. The longer the lower common pathway is, the more the timing of HB activation must be advanced so that the VES will be able to activate the AVNRT circuit prematurely. Therefore, in atypical (fast-slow and slow-slow) AVNRT, which typically has a long lower common pathway, the HB activation must be advanced by more than 30 to 60 milliseconds. Conversely, in typical (slow-fast) AVNRT, the lower common pathway is short or absent, and the tachycardia is typically reset by the VES as soon as the HB activation is advanced.⁸

A late-coupled VES may block in the HPS or lower common pathway and may not affect the SVT (Fig. 17.18A). A late-coupled VES that resets the SVT without first retrogradely activating the HB (i.e., VES delivered before or within 50 milliseconds after the expected inscription of the anterograde His potential) excludes AVNRT (except when a bystander AV BT is present).

An early-coupled VES can reset AVNRT, especially when the TCL is relatively long (>350 milliseconds). The resetting VES antidromically collides with the preceding tachycardia wavefront traveling anterogradely and is conducted through the retrograde pathway to reset the tachycardia (see Fig. 17.18). The resetting of AVNRT with fusion of the QRS cannot be demonstrated because of the shared entry-exit site (i.e., the HB) from the ventricle to the circuit.

Termination. Termination of AVNRT with VES is difficult (more so than termination with AES) and is rare when the TCL is shorter than 350 milliseconds. Such termination favors the diagnosis of orthodromic AVRT. In typical AVNRT, when termination occurs, it is usually caused by block of the VES in the anterograde or retrograde limb of the AVNRT circuit. The slower the SVT is, the more likely the block will be to occur in the anterograde slow pathway. Ventricular pacing can terminate AVNRT more easily than VES because rapid ventricular pacing can modulate and overcome the refractoriness of the intervening HPS. VES always terminates atypical AVNRT by blocking retrogradely in the slow pathway.

Ventricular entrainment. Ventricular pacing at a CL approximately 10 to 30 milliseconds shorter than the TCL is usually able to entrain AVNRT. Visualization of the His potential before atrial activation during entrainment helps differentiate AVNRT from orthodromic AVRT. If the His potential cannot be visualized during ventricular pacing, two other parameters can be helpful to distinguish AVNRT from orthodromic AVRT: the VA interval during ventricular pacing and the PPI.^{22,23}

Δ VA interval. Entrainment of the SVT by RV pacing can help differentiate orthodromic AVRT from AVNRT by evaluating the VA interval during SVT (measured from the onset of surface QRS to the high RA electrogram) versus the VA interval during pacing (i.e., the SA interval, measured from the ventricular pacing stimulus to the high RA electrogram). The ventricle and atrium are activated in sequence during orthodromic AVRT and during ventricular pacing, but in parallel during AVNRT. Therefore the VA interval during orthodromic AVRT

approximates that during ventricular pacing (see Fig. 18.43). In contrast, the VA interval during AVNRT is much shorter than that during ventricular pacing (Figs. 17.19 and 17.20). In general, a difference in the VA interval (Δ VA [$VA_{\text{pacing}} - VA_{\text{SVT}}$]) greater than 85 milliseconds is consistent with AVNRT, whereas a Δ VA of less than 85 milliseconds is consistent with orthodromic AVRT (see Fig. 20.14).^{24,25}

Postpacing interval. The PPI after entrainment of AVNRT from the RV apex is significantly longer than the TCL (the [PPI – TCL] difference is usually >115 milliseconds) because the reentrant circuit in AVNRT (confined above the HB and not involving the ventricle) is far from the ventricular pacing site. In AVNRT, the PPI reflects the conduction time from the pacing site through the RV muscle and HPS, once around the reentry circuit and back to the pacing site. Therefore the difference between the PPI and TCL reflects twice the sum of the conduction time through the RV muscle, the HPS, and the lower common pathway. In orthodromic AVRT using a septal BT, the PPI reflects the conduction time through the RV to the septum, once around the reentry circuit and back to the pacing site. In other words, the difference between the PPI and TCL reflects twice the conduction time from the pacing site through the ventricular myocardium to the reentry circuit. Because the ventricle is an essential component of the AVRT circuit, the RV apex is closer to the tachycardia circuit. Therefore the PPI more closely approximates the TCL in orthodromic AVRT using a septal BT ([PPI – TCL] difference is usually <115 milliseconds) compared with AVNRT. This maneuver was studied specifically for differentiation between atypical AVNRT and orthodromic AVRT using a septal BT, but the principle also applies to typical AVNRT (see Figs. 17.19 and 17.20). For borderline values, ventricular pacing at the RV base can help exaggerate the difference between the PPI and TCL in the setting of AVNRT, but without significant changes in the setting of orthodromic AVRT (see differential-site RV entrainment below).⁸

Importantly, overdrive ventricular pacing during entrainment can induce decremental anterograde AVN conduction. Subtracting the increment in AVN conduction time in the first PPI (postpacing AH interval – prepacing AH interval) from the (PPI – TCL) difference (the so-called “corrected” [PPI – TCL]) has been found to improve the accuracy of this criterion. The difference between the AV intervals (postpacing AV interval – prepacing AV interval) can be taken for the latter adjustment when a clear His deflection is not visible. A corrected (PPI – TCL) of less than 110 milliseconds was found to be highly accurate in identifying orthodromic AVRT as distinct from AVNRT.^{26,27}

Of note, determinations of the corrected (PPI – TCL) and Δ VA ($VA_{\text{pacing}} - VA_{\text{SVT}}$) after resetting with single or double VESs from the RV apex, is of similar value for discrimination between AVNRT and orthodromic AVRT, even when the SVT is interrupted by ventricular pacing. Corrected (PPI – TCL) of more than 110 milliseconds and Δ VA of more than 110 milliseconds after resetting identify AVNRT.²⁸

However, there are several potential pitfalls to those criteria. The TCL and VA interval are often perturbed for a few cycles after entrainment. For this reason, care should be taken not to measure unstable intervals immediately after ventricular pacing. In addition, spontaneous oscillations in the TCL and VA intervals can be seen. The discriminant points chosen may not apply when the spontaneous variability is more than 30 milliseconds. Furthermore, it is possible to mistake isorhythmic VA dissociation for entrainment if the pacing train is not sufficiently long or the PCL is too close to the TCL. Finally, those criteria may not apply to BTs with significant decremental properties, although small decremental intervals are unlikely to provide a false result.²⁹

Manifest ventricular fusion. No QRS fusion is manifest during ventricular entrainment of AVNRT, and QRS morphology is that of pure paced morphology. Fusion during resetting or entrainment of AVNRT with ventricular stimulation would require the paced ventricular

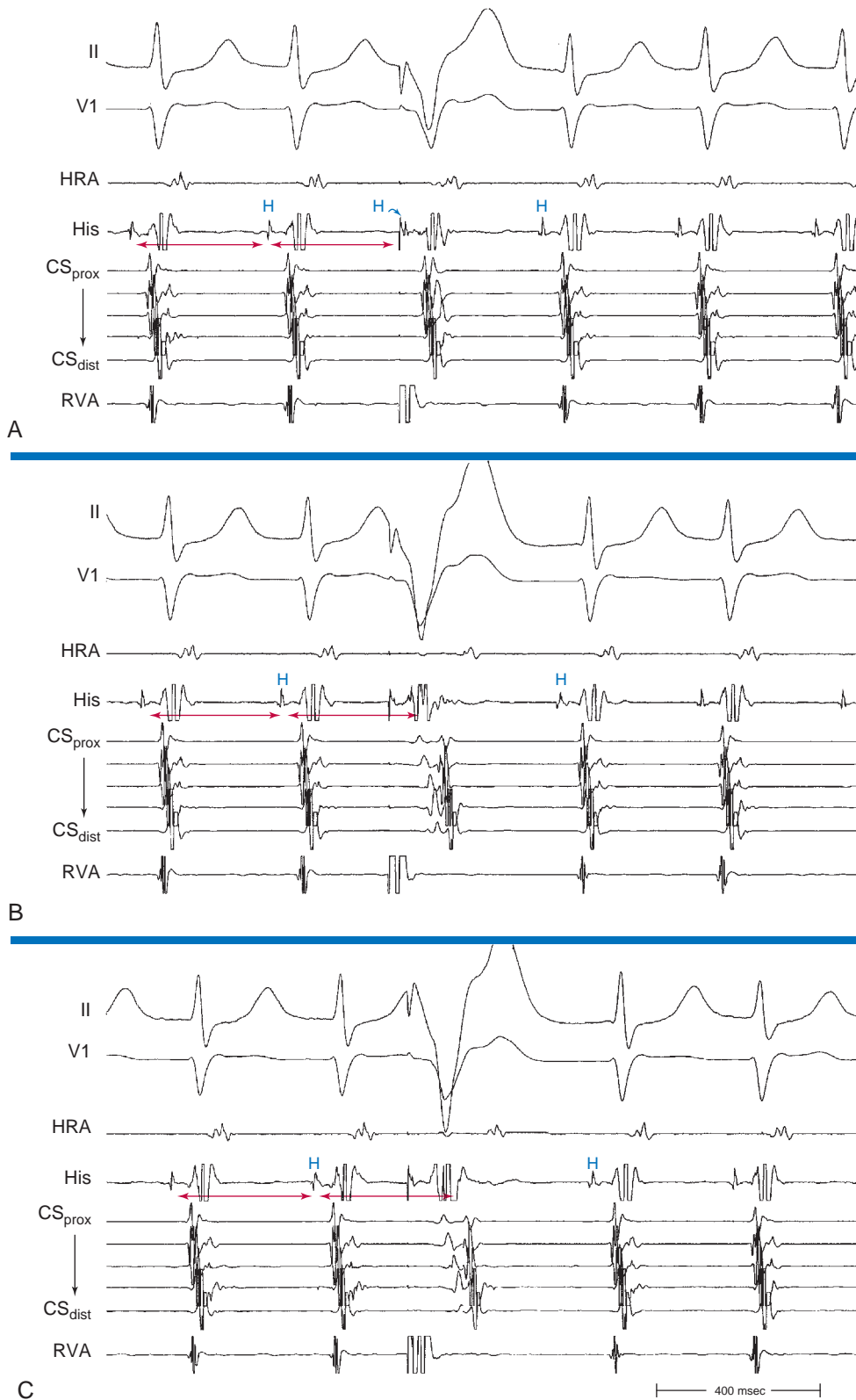


Fig. 17.18 Resetting of Atrioventricular Nodal Reentrant Tachycardia (AVNRT) With Ventricular Extrastimulation (VES) at Different Coupling Intervals. (A) Late-coupled VES delivered when the His bundle is refractory fails to reset the AVNRT. In fact, the anterograde His potential (*H*) is visualized shortly after the pacing artifact (*arrows*), occurring at the expected timing (the tachycardia cycle length is indicated by the *red lines*). (B) An early VES delivered well before the expected time of the anterograde His potential fails to reset the tachycardia. The fact that this VES advances ventricular activation at all recorded sites by approximately 70 milliseconds and still fails to reset the tachycardia excludes orthodromic atrioventricular reentrant tachycardia. (C) Earlier VES results in resetting of the supraventricular tachycardia, as indicated by earlier timing of the following atrial activation. Double arrows indicate the H-H interval during tachycardia. CS_{dist}, Distal coronary sinus; CS_{prox}, proximal coronary sinus; HRA, high right atrium; RVA, right ventricular apex.

wavefronts to enter the circuit propagating through the HB at the time that impulses are exiting through this structure. The HB is also the site of exit of the tachycardia circuit to the ventricular tissue. Therefore collision of the antidromic wavefront and the orthodromic wavefront from the preceding beat occurs in AVN tissue and not in the ventricle. Under

such circumstances, constant fusion during entrainment is impossible (unless a second connection exists between the atria and ventricles; i.e., an innocent bystander BT). Manifest ventricular fusion during entrainment of SVT indicates that the reentrant circuit includes ventricular tissue (diagnostic of AVRT), thus excluding both AVNRT and AT.^{22,23}

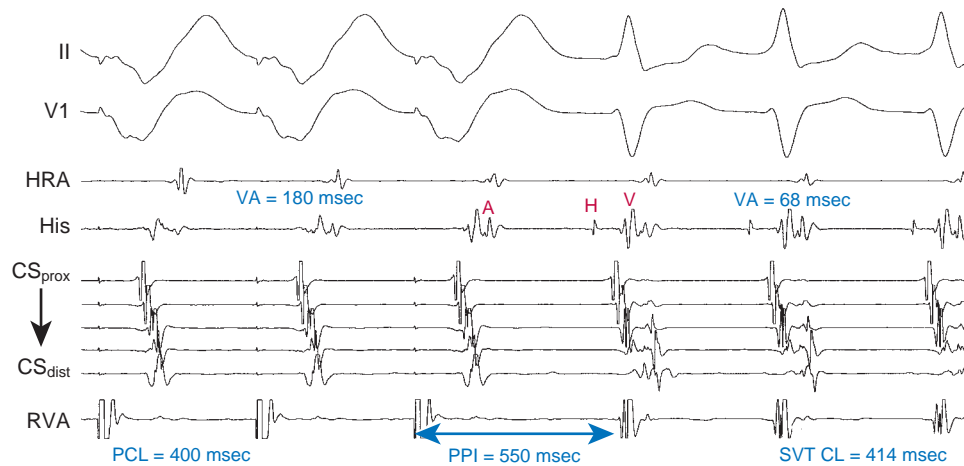


Fig. 17.19 Entrainment of Typical Atrioventricular Nodal Reentrant Tachycardia (AVNRT) With Ventricular Pacing. Pacing is performed from the right ventricular apex (RVA). The postpacing interval minus tachycardia cycle length (PPI – TCL) is more than 115 milliseconds, and the Δ VA interval ($VA_{\text{pacing}} - VA_{\text{SVT}}$) is more than 85 milliseconds. The atrial activation sequence during ventricular pacing is identical to that during AVNRT. No QRS fusion is observed. Cessation of ventricular pacing is followed by an A-V electrogram sequence. CS_{dist} , distal coronary sinus; CS_{prox} , proximal coronary sinus; HRA, high right atrium; PCL, pacing cycle length; SVT, supraventricular tachycardia; VA, ventriculoatrial.

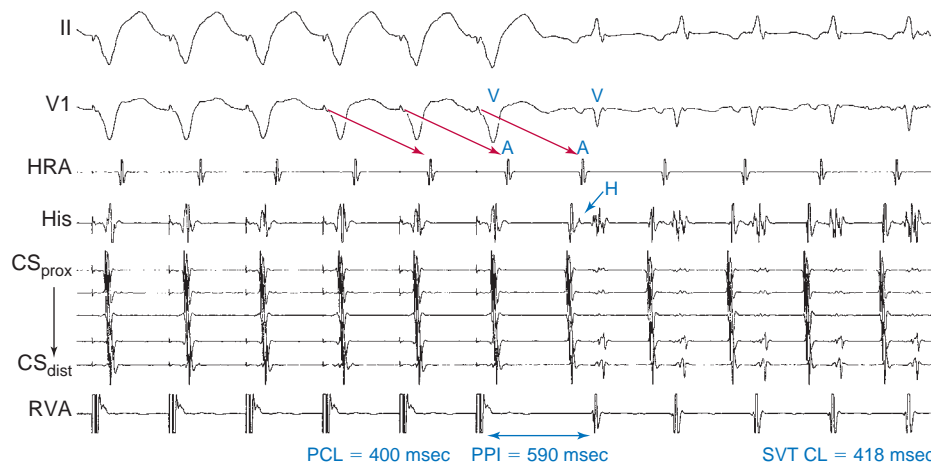


Fig. 17.20 Entrainment of Atypical Atrioventricular Nodal Reentrant Tachycardia (AVNRT) With Ventricular Pacing. Pacing is performed from the right ventricular apex (RVA). The postpacing interval minus tachycardia cycle length (PPI – TCL = 172 milliseconds) is long, and the Δ VA interval ($VA_{\text{pacing}} - VA_{\text{SVT}} = 188$ milliseconds) is also long; both criteria favor AVNRT over orthodromic atrioventricular reentrant tachycardia. Note that the atrial activation sequence during RV pacing is similar to that during the SVT, again favoring AVNRT over other types of SVT. In addition, a pseudo-A-A-V electrogram sequence is observed following cessation of ventricular pacing because retrograde conduction occurs through the slow pathway during ventricular pacing with a long VA interval (red arrows), longer than the pacing cycle length (PCL); hence, the last ventricular paced impulse is followed first by the P wave conducted slowly from the previous paced QRS and then by the P wave resulting from the last paced QRS, thus mimicking an A-A-V electrogram sequence. This is confirmed by the observation that the last atrial activation resulting from conduction of the last paced ventricular complex follows the preceding P wave with an A-A interval equal to the ventricular PCL. CL, Cycle length; CS_{dist} , distal coronary sinus; CS_{prox} , proximal coronary sinus; HRA, high right atrium; SVT, supraventricular tachycardia; VA, ventriculoatrial.

Differential-site RV entrainment. Differential-site RV entrainment (from RV apex vs. RV base) can help distinguish AVNRT from orthodromic AVRT. Because the reentrant circuit in AVNRT is confined above the HB and does not involve the ventricle, the base of the RV is electrically more distant (although anatomically closer) to the tachycardia circuit than the RV apex, given that the His-Purkinje network directly inserts in the RV apex. Consequently, the PPI after entrainment

of AVNRT from the RV base is longer than that following entrainment from the RV apex. The difference in PPI from the RV base versus the RV apex is largely composed of the extra time required to reach the circuit from the base versus the apex (approximately 30 milliseconds). Conversely, in orthodromic AVRT, in which the ventricles are an obligatory part of the circuit, the basal pacing site relative to the RV apex is variably related to the circuit, closer than the RV apex with septal BTs

and equidistant with free wall BTs, but the paced wavefront from either the RV apex or the RV base tends to have, on average, approximately equal access and proximity to the reentrant circuit involved in orthodromic AVRT. Therefore the time taken to reach the circuit (and hence the PPI) tends to be similar, irrespective of the location of the BT.

As noted, decremental conduction can occur during entrainment of either AVNRT or orthodromic AVRT, and most commonly it occurs during conduction through the AVN, especially the AVN slow pathway. The degree of decrement is dependent on both the pacing rate and the functional refractory properties of the AVN. Therefore the PPI will prolong if decrement occurs, but the degree of decrement is not expected to be materially different from basal rather than apical pacing, as long as the pacing rates are the same or similar. To avoid potential error introduced by decremental conduction within the AVN, correction of the PPI is preferred, and it is obtained by subtracting any increase in the AV interval of the return cycle beat (compared with the AV interval during SVT). In one study, a differential corrected (PPI – TCL) of more than 30 milliseconds after transient entrainment was observed in all cases of AVNRT (i.e., corrected PPI following pacing from the RV base was consistently at least 30 milliseconds longer than that following pacing from the RV apex), and corrected (PPI – TCL) of less than 30 milliseconds was observed in all cases of orthodromic AVRT. In addition, differential VA interval (SA interval during entrainment from RV base vs. RV septum) of more than 20 milliseconds was consistent with AVNRT, whereas a differential VA interval of less than 20 milliseconds was consistent with orthodromic AVRT.³⁰

Length of pacing drive required for entrainment. Careful analysis of the beginning of RV pacing during the SVT can help differentiate orthodromic AVRT from AVNRT. In the setting of orthodromic AVRT, ventricular tissue is the only intervening tissue between the pacing wavefront and the ventricular insertion site of the BT. Therefore, once ventricular capture is achieved during RV pacing, the paced wavefront propagates to the ventricular insertion site of the BT quickly and resets the tachycardia. Consequently, RV pacing results in a faster response of resetting the tachycardia. On the other hand, during AVNRT, the paced wavefront has to penetrate the HPS and AVN tissue prior to resetting the tachycardia. This results in delayed resetting of the tachycardia compared with orthodromic AVRT. After initiation of synchronized RV pacing during SVT at a PCL 10 to 40 milliseconds shorter than the TCL, once constant-appearing paced RV complexes (either pure capture or fixed fusion) are observed (as evidenced by fixed pacing morphology of the surface ECG), the number of RV paced beats required to accelerate the atrial CL to the PCL is determined. The first controlled atrial beat (accelerated to the PCL) is identified by demonstrating a fixed SA interval. One report demonstrated that using a cutoff of one beat to accelerate the atria to the PCL could identify all orthodromic AVRT cases and essentially exclude all cases of AVNRT with high accuracy. When two or more beats are required to accelerate the atria to the PCL, AVNRT is favored over orthodromic AVRT (see Fig. 20.13).³¹

Atrial resetting during the transition zone. On initiation of RV pacing trains during SVT at a rate slightly faster than the TCL, there is a transition zone during which the pacing train fuses with anterograde ventricular activation (i.e., the zone in which the paced QRS complexes show progressive fusion with the SVT complexes) until a stable QRS morphology is observed (either completely paced or constantly fused). In patients with AVNRT or AT, acceleration of the timing of atrial activation cannot occur through the AVN during the transition zone. The reason is that the HB is expected to be refractory, as indicated by at least some ventricular activation still occurring by anterograde conduction over the HPS, similar to the concept of entrainment with manifest fusion discussed previously. If perturbation of atrial timing occurs during

the transition zone, it indicates the presence of a retrogradely conducting BT, which can be an integral part of the SVT circuit (i.e., orthodromic AVRT) or a bystander. In one report, these criteria showed excellent diagnostic accuracy and could be applied regardless of whether entrainment was achieved or whether the SVT terminated during pacing. Perturbation of atrial timing for 15 milliseconds or longer or a fixed SA interval measured from the last beat of the transition zone was seen in all the patients with orthodromic AVRT and in none of the patients with AVNRT or AT (unless a bystander retrogradely conducting BT is present).³²

Atrial and ventricular electrogram sequence following cessation of ventricular pacing. Following ventricular entrainment of typical AVNRT, an “A-V” electrogram sequence is observed after the last paced QRS (see Fig. 17.19). In contrast, following overdrive ventricular pacing (1:1 VA conduction) during AT, retrograde conduction occurs through the AVN. In this setting, the last retrograde P wave resulting from ventricular pacing is unable to conduct back to the ventricle because the AVN is still refractory to anterograde conduction, and the result is an A-A-V response (as discussed in detail in Chapter 20). Importantly, this maneuver is not useful when 1:1 VA conduction during ventricular pacing is absent (see Fig. 11.17). In addition, a pseudo-A-A-V response can occur during atypical AVNRT because retrograde conduction during ventricular pacing occurs through the slow pathway. This can result in a VA interval that is longer than the PCL; hence, the last ventricular paced impulse is followed first by the P wave conducted slowly from the previous paced QRS and then by the P wave resulting from the last paced QRS, thus mimicking an A-A-V response (see Fig. 17.20). Careful identification of the last atrial electrogram that resulted from VA conduction during ventricular pacing avoids this potential pitfall. The last atrial activation resulting from conduction of the last paced ventricular complex follows the preceding P wave with an A-A interval equal to the ventricular PCL. A pseudo-A-A-V response can also occur during typical AVNRT with long HV intervals or short HA intervals, or both, in which atrial activation precedes ventricular activation. In the latter setting, using HB activation instead of ventricular activation (i.e., characterizing the response as A-A-H or A-H instead of A-A-V or A-V, respectively) can be more accurate and can help eliminate misinterpretation of the pseudo-A-A-V response.³³

Para-Hisian Pacing During Tachycardia

Overdrive para-Hisian pacing during the SVT helps exclude the presence of a septal AV BT, which can mediate an orthodromic AVRT with a retrograde atrial activation sequence similar to that during AVNRT (discussed in detail in Chapter 20).

During SVT, para-Hisian pacing is performed at a PCL 10 to 30 milliseconds shorter than the TCL. Responses to this maneuver are then classified as (1) entrainment: when the atrial CL is accelerated to the PCL, without a change in the atrial activation sequence, and the tachycardia resumes after pacing is discontinued; (2) termination: when pacing results in termination of the tachycardia; and (3) AV dissociation: when HB capture is confirmed and no change in the atrial CL is observed.

Because the HB is a necessary component for the circuit in AVRT, overdrive capture of the HB during AVRT should result in immediate entry into the tachycardia (manifesting as either entrainment or termination of the SVT). In contrast, HB overdrive pacing during AVNRT may not immediately enter the circuit because the HB is not an obligate component. Therefore entry into the tachycardia circuit within one beat indicates AVRT, whereas entry into the circuit occurring only after three or more beats is consistent with AVNRT.³⁴

Furthermore, para-Hisian entrainment of the SVT is performed by alternately pacing at high-energy output for HB-RB capture or lower

energy output for HB-RB noncapture. Entrainment with HB-RB capture is recorded separately from that without HB-RB capture. The SA and local VA intervals during HB-RB capture and noncapture are then examined. If para-Hisian entrainment cannot be performed because of repetitive termination of the tachycardia during pacing attempts, single or double VESs can be given to reset the tachycardia (para-Hisian resetting). These VESs are delivered at progressively shorter coupling intervals until the first VES that reliably advances or resets the tachycardia. This is performed alternately with high- or low-energy outputs to achieve HB-RB capture and noncapture, respectively. As with para-Hisian entrainment, the retrograde atrial activation sequence and timing are compared during para-Hisian resetting to characterize the response.³⁵

In AVNRT (typical or atypical), the AVN-AVN pattern is observed in response to para-Hisian entrainment or resetting; that is, both the SA and the local VA intervals increase during HB-RB noncapture compared with HB-RB capture. Conversely, in orthodromic AVRT, the BT-BT pattern or BT-BT_L pattern is observed (see Chapter 20 for detailed discussion).

A Δ SA interval of less than 40 milliseconds was found to be a reasonable guide for separating the AVN-AVN from the BT-BT response. Patients with AVNRT uniformly have a Δ SA interval of greater than 40 milliseconds, whereas those with AVRT have a Δ SA interval of less than 40 milliseconds (except for rare patients with a left lateral BT). Using the Δ local VA interval (instead of Δ SA interval) provides a more accurate parameter for discrimination between AVNRT and AVRT.

Diagnostic Maneuvers During Sinus Rhythm After Tachycardia Termination

When pacing the atrium or ventricle at the TCL, it is important that the autonomic tone be similar to its state during the tachycardia because alterations of autonomic tone can independently influence AV or VA conduction.

Atrial Pacing at the Tachycardia Cycle Length

The difference in the AH interval between atrial pacing (at the TCL) and SVT can allow differentiation of fast-slow AVNRT from other types of long RP tachycardias. A Δ AH ($AH_{\text{pacing}} - AH_{\text{SVT}}$) greater than 40 milliseconds has been reported to favor AVNRT. In contrast, during AT and orthodromic AVRT using a septal BT, the AH interval during SVT approximates that during atrial pacing and, thus, a Δ AH of less than 20 milliseconds favors AT and orthodromic AVRT. This has only been tested with RA pacing during right ATs and should be applied with caution when a left AT is suspected.⁸

The Δ AH ($AH_{\text{pacing}} - AH_{\text{SVT}}$) can also help differentiate typical (slow-fast) AVNRT from AT with a long PR interval. Atrial pacing during NSR at the TCL yields an AH interval that is similar to that during AT but shorter than the AH interval during typical AVNRT. During atrial pacing in patients with AT, AV conduction occurs preferentially conduction over the fast pathway and, hence, is expected to be associated with similar AH and PR intervals (under equivalent autonomic tone). In contrast, AV conduction during typical AVNRT occurs over the slow pathway, resulting in a long AH interval.

Ventricular Pacing at the Tachycardia Cycle Length

Δ HA interval. Ventricular pacing at the TCL results in HA and VA intervals that are longer during pacing than those during AVNRT when assessed with standard 5 mm spacing quadripolar catheters in the HB position. With more closely spaced HB recording electrodes, the HA interval during pacing (HA_{pacing}) can be less than that during tachycardia (HA_{SVT}), a finding implying that part of the proximal HB is part of the AVNRT circuit (i.e., absence of a lower common pathway). Whether or not the HA interval during pacing is longer than that during tachy-

cardia thus depends in large part on how proximal an HB recording is made. The Δ HA interval ($HA_{\text{pacing}} - HA_{\text{SVT}}$) is typically more than -10 milliseconds because the HA interval during AVNRT is shortened by parallel activation of both the HB and the atrium during the tachycardia (i.e., the HA interval is a “pseudo-interval” that represents activation times of the HB and atrium), whereas the HB and atrium are activated sequentially during ventricular pacing (i.e., the HA interval represents a true conduction time interval from the HB to the atrium; Fig. 17.21). The Δ HA interval is even more pronounced in atypical AVNRT, which has a lower common pathway that is longer than that in typical AVNRT. This is in contrast to orthodromic AVRT, in which HA_{pacing} is shorter than HA_{SVT} because the HB and atrium are activated sequentially during orthodromic AVRT but in parallel during ventricular pacing (the atrium is activated via the BT). As a result, the Δ HA interval in the setting of orthodromic AVRT is typically less than -10 milliseconds.¹¹ The Δ HA criterion can only be used when (1) retrograde conduction during ventricular pacing occurs over the same pathway as during SVT and (2) one can discern a retrograde HB potential during ventricular pacing.

Ventriculoatrial block. Under comparable autonomic tone, 1:1 VA conduction over the AVN may or may not be maintained during ventricular pacing at the TCL because of possible retrograde block in

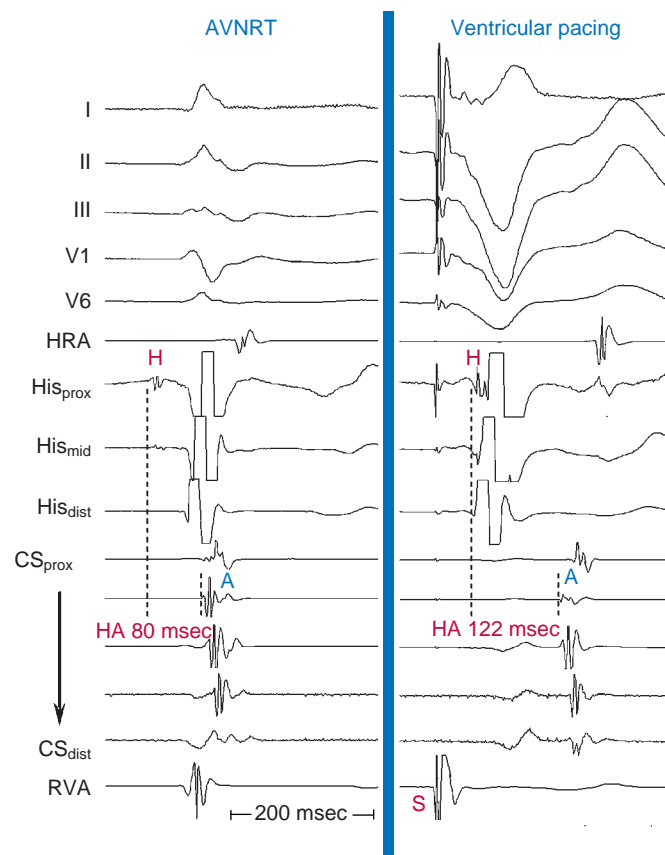


Fig. 17.21 His Bundle-Atrial (HA) Interval During Tachycardia Versus Ventricular Pacing. HA intervals (marked by dashed lines) during atrioventricular nodal reentrant tachycardia (AVNRT; left) and ventricular pacing at tachycardia cycle length in the same patient (right), measured from His potential onset to onset of atrial activation (near CS_{prox}). Notice that the HA interval is shorter during AVNRT than that during pacing because the atrium and His bundle are activated in parallel during AVNRT but in sequence during ventricular pacing. CS_{dist}, Distal coronary sinus; CS_{prox}, proximal coronary sinus; His_{dist}, distal His bundle; His_{mid}, middle His bundle; His_{prox}, proximal His bundle; HRA, high right atrium; RVA, right ventricular apex.

the lower common pathway. Anterograde conduction properties of the lower common pathway may allow 1:1 conduction from the AVNRT circuit down to the ventricle, but its retrograde conduction properties may not allow 1:1 VA conduction during ventricular pacing at a PCL similar to the TCL. Thus the presence of VA block during ventricular pacing favors AT and AVNRT with lower common pathway physiology over orthodromic AVRT.

Atrial activation sequence. The atrial activation sequence during ventricular pacing is usually (but not necessarily) similar to that during AVNRT. A different atrial activation sequence suggests the presence of a retrogradely conducting BT (which may or may not be related to the SVT), but also can be observed in AVNRT when the retrogradely conducting AVN pathway during AVNRT is different from that used during ventricular pacing.

Exclusion of Other Arrhythmia Mechanisms

Other tachycardia mechanisms (orthodromic AVRT, AT, and focal junctional tachycardia) can mimic AVNRT, and should be excluded. Several maneuvers can help with the differential diagnosis. However, it is important to note that limitations exist to all diagnostic maneuvers, and assessment of the response to multiple different pacing maneuvers in determining the mechanism of SVT should be considered, rather than relying upon a single maneuver.

Atrial Tachycardia

Focal ATs arising from the anterosseptal region can mimic typical AVNRT, and those originating from the right or left posteroseptal region can mimic atypical AVNRT. The various EP testing maneuvers used to exclude these tachycardias are outlined in [Box 17.3](#).

Atrioventricular Reentrant Tachycardia

Orthodromic AVRT using superoparaseptal BTs or posteroseptal BTs can mimic typical or atypical AVNRT, respectively. Several maneuvers can help distinguish between the two arrhythmias ([Box 17.4](#)).

Focal Junctional Tachycardia

Focal junctional tachycardia (also known as “nonparoxysmal,” “non-reentrant,” or “ectopic” junctional tachycardia) originates from the AV junction (encompassing the AVN and HB). Junctional tachycardia is rare in adults, and is encountered more frequently in children. It occurs mainly as a transient arrhythmia following cardiac surgery, most likely a result of ischemic injury to the cardiac conduction system during cardiopulmonary bypass, which is exacerbated by the use of sympathomimetic agents in the early postoperative period. In addition, junctional tachycardia can be associated with digoxin toxicity and myocardial ischemia. Rarely, paroxysmal or incessant junctional tachycardia can be observed, with a presentation similar to that of focal AT. The mechanism of junctional tachycardia is likely related to enhanced automaticity, but abnormal automaticity and triggered activity also can play a role in some patients.

ECG features of junctional tachycardia. Junctional tachycardia can manifest as a regular narrow QRS tachycardia with a short RP interval and retrograde P waves, mimicking typical AVNRT. Junctional tachycardia can also present as an irregular narrow QRS tachycardia with retrograde conduction block and intermittent AV dissociation (often isorhythmic), mimicking multifocal AT or AF. On the other hand, VA block is often observed, resulting in SVT with intermittent AV dissociation (often isorhythmic). When associated with aberrant conduction and wide QRS complex, junctional tachycardia can mimic VT, particularly if VA conduction is absent.

The differentiation of AVNRT from junctional tachycardia is of clinical importance because ablation of the latter is associated with an

BOX 17.3 Exclusion of Atrial Tachycardia

Oscillations in TCL

- Changes in atrial CL that are predicted by changes in the preceding ventricular CL argue against AT.
- Spontaneous changes in TCL accompanied by constant VA interval (VA linking) exclude AT.

SVT Induction by AES

- “Critical AH” required for SVT induction favors AVNRT over AT.
- If the VA interval of the first tachycardia beat is reproducibly identical to that during the rest of the SVT (“VA linking”), AT is very unlikely.

VES During SVT

- VES that terminates the SVT without atrial activation excludes AT.
- VES that delays the next atrial activation excludes AT.

Overdrive Ventricular Pacing During SVT

- The presence of A-V electrogram sequence following cessation of pacing is consistent with AVNRT and generally excludes AT.
- Atrial activation sequence during pacing similar to that during the SVT favors AVNRT over AT.

Overdrive Atrial Pacing During SVT

- ΔAH interval ($AH_{\text{pacing}} - AH_{\text{SVT}} > 40$ ms favors AVNRT over AT.
- If the VA interval following the last entrained QRS is reproducibly constant (with <10 ms variation), despite pacing at different CLs or for different durations (VA linking) and similar to that during TCL, AT is unlikely.
- If the VA interval following the last entrained QRS is reproducibly constant (with <14 ms variation), despite pacing at different atrial sites (VA linking), AT is unlikely.

SVT Termination

- Reproducible termination of the SVT (spontaneous or in response to adenosine or vagal maneuvers) with a P wave not followed by a QRS excludes AT, except in the case of a nonconducted PAC terminating the AT.

Atrial Pacing During NSR at TCL

- ΔAH interval ($AH_{\text{pacing}} - AH_{\text{SVT}} > 40$ ms excludes AT.
- AV block during atrial pacing (under similar autonomic tone) argues against AT.

AES, Atrial extrastimulation; AH, atrial–His bundle; AT, atrial tachycardia; AV, atrioventricular; A-V, atrium–ventricle; AVNRT, atrioventricular nodal reentrant tachycardia; CL, cycle length; NSR, normal sinus rhythm; PAC, premature atrial complex; SVT, supraventricular tachycardia; TCL, tachycardia cycle length; VA, ventriculoatrial; VES, ventricular extrastimulus.

increased risk of AV block.⁸ AV dissociation, when present, excludes the AVRT and makes AVNRT highly unlikely. Bursts of short RP tachycardia without initiation by PACs or PR prolongation are more consistent with junctional tachycardia rather than AVNRT.

EP features of junctional tachycardia. The EP hallmark of junctional tachycardia is the presence of a His potential preceding the QRS complex. The HV interval is typically normal, but can be prolonged in the setting of distal HPS disease.

Unlike AVNRT, junctional tachycardia is nonreentrant, and cannot be induced or terminated by programmed stimulation. Initiation of the tachycardia is usually spontaneous (and often requires isoproterenol administration), with the absence of a critical AH delay ([Box 17.5](#)). In addition, junctional tachycardia is characterized by a gradual increase in tachycardia rate (warm-up) following initiation, marked CL variation,

BOX 17.4 Exclusion of Orthodromic Atrioventricular Reentrant Tachycardia**VA Interval During SVT**

- VA interval <70 ms or a V–high RA interval <95 ms during SVT excludes orthodromic AVRT.

AV Block During SVT

- Spontaneous or induced AV block with continuation of the SVT excludes orthodromic AVRT.

VES During the SVT

- Failure to reset (advance or delay) atrial activation with early-coupled VES on multiple occasions and at different VES coupling intervals, despite advancement of the local ventricular activation at all sites (including the site of the suspected BT) by >30 ms, excludes orthodromic AVRT and the presence of AV BT.
- Δ VA interval ($VA_{\text{pacing}} - VA_{\text{SVT}}$) >110 ms (after resetting with single or double VESs from the RV apex) argues against AVRT.
- Corrected (PPI – TCL) >110 ms (after resetting with single or double VESs from the RV apex) argues against AVRT.
- When a VES resets the SVT without atrial activation (i.e., the VES advances the subsequent His potential and QRS), orthodromic AVRT is excluded.

Entrainment of SVT by Ventricular Pacing

- Δ VA ($VA_{\text{pacing}} - VA_{\text{SVT}}$) >85 ms argues against orthodromic AVRT.
- PPI – TCL >115 ms (or corrected [PPI – TCL] >110 ms) argues against orthodromic AVRT.
- Acceleration of the SVT to the PCL occurring only after ≥ 2 beats with stable paced QRS morphology is consistent with AVNRT and argues against orthodromic AVRT.
- Differential corrected PPI – TCL of >30 ms after transient entrainment from the RV apex versus the RV base is consistent with AVNRT and argues against orthodromic AVRT.
- Differential VA interval (SA interval during entrainment from RV base versus RV septum) of >20 ms is consistent with AVNRT and argues against orthodromic AVRT.

Entrainment of SVT by Atrial Pacing

- Δ AH interval ($AH_{\text{pacing}} - AH_{\text{SVT}}$) of >40 ms favors AVNRT over orthodromic AVRT.

Para-Hisian Entrainment or Resetting

- Prolongation of the SA and the local VA intervals on loss of HB capture, compared with that during HB capture is consistent with AVNRT and argues against orthodromic AVRT.
- The change in the stimulus to earliest atrial activation time (Δ SA interval) with loss of HB–RB capture >40 ms is consistent with AVNRT and argues against orthodromic AVRT.
- Entry into the tachycardia circuit (manifesting as resetting, entrainment, or termination of the SVT) occurring only after three or more beats is consistent with AVNRT and argues against orthodromic AVRT.

Ventricular Pacing During NSR at the TCL

- Δ HA ($HA_{\text{pacing}} - HA_{\text{SVT}}$) >–10 ms is consistent with AVNRT and argues against orthodromic AVRT.

Atrial Pacing During NSR at the TCL

- Δ AH ($AH_{\text{pacing}} - AH_{\text{SVT}}$) >40 ms is consistent with AVNRT and argues against orthodromic AVRT.

Differential RV Pacing During NSR

- Pacing at the RV base producing a longer VA (SA) interval and identical atrial activation sequence compared with that during pacing at the RV apex excludes the presence of a septal AV BT mediating an orthodromic AVRT.

Para-Hisian Pacing During NSR

- Loss of HB RB capture resulting in an increase in the SA interval in all electrograms (equal to the increase in the S–H interval), with no change in the atrial activation sequence or HA interval, excludes the presence of a septal AV BT mediating an orthodromic AVRT.

AH, Atrial–His bundle interval; AV, atrioventricular; AVNRT, atrioventricular nodal reentrant tachycardia; AVRT, atrioventricular reentrant tachycardia; BT, bypass tract; CL, cycle length; HA, His bundle–atrial; HB, His bundle; NSR, normal sinus rhythm; PPI, postpacing interval; RA, right atrium; RB, right bundle branch; RV, right ventricle; SA, stimulus-to-atrial; S–H, stimulus-to-His bundle; SVT, supraventricular tachycardia; TCL, tachycardia cycle length; VA, ventriculoatrial; VES, ventricular extrastimulation.

BOX 17.5 Exclusion of Focal Junctional Tachycardia**Tachycardia Induction**

- Spontaneous initiation of the tachycardia (with or without isoproterenol) with absence of a critical AH delay is consistent with junctional tachycardia.
- Failure of tachycardia inducibility with programmed electrical stimulation favors junctional tachycardia.

Tachycardia Features

- Incessant tachycardia is consistent with junctional tachycardia and practically excludes AVNRT.
- AV dissociation favors junctional tachycardia over AVNRT.

AES During SVT

- An early AES (delivered prior to HB depolarization) that advances the His potential immediately after it without terminating the tachycardia is consistent with junctional tachycardia.
- An AES (delivered from the proximal CS) timed to HB refractoriness that either terminates or resets the tachycardia the His potential of the subsequent cycle effectively excludes junctional tachycardia and confirms a diagnosis of AVNRT.

Overdrive Atrial Pacing During SVT

- An “H–H–A” response following cessation of overdrive atrial pacing (with 1:1 AV conduction) during SVT is consistent with junctional tachycardia, whereas an “H–A” response favors AVNRT.
- An AH interval during atrial pacing that is significantly shorter than AH interval during SVT is consistent with junctional tachycardia.
- Dissociation of atrial activation from HB activation during atrial pacing is consistent with junctional tachycardia.

Overdrive Ventricular Pacing During SVT

- Zero or positive Δ HA interval ($HA_{\text{pacing}} - HA_{\text{SVT}}$) is consistent with junctional tachycardia.
- Negative Δ HA interval is consistent with AVNRT.

AES, Atrial extrastimulation; AH, atrial–His bundle; AV, atrioventricular; AVNRT, atrioventricular nodal reentrant tachycardia; CS, coronary sinus; HA, His bundle–atrial; HB, His bundle; SVT, supraventricular tachycardia.

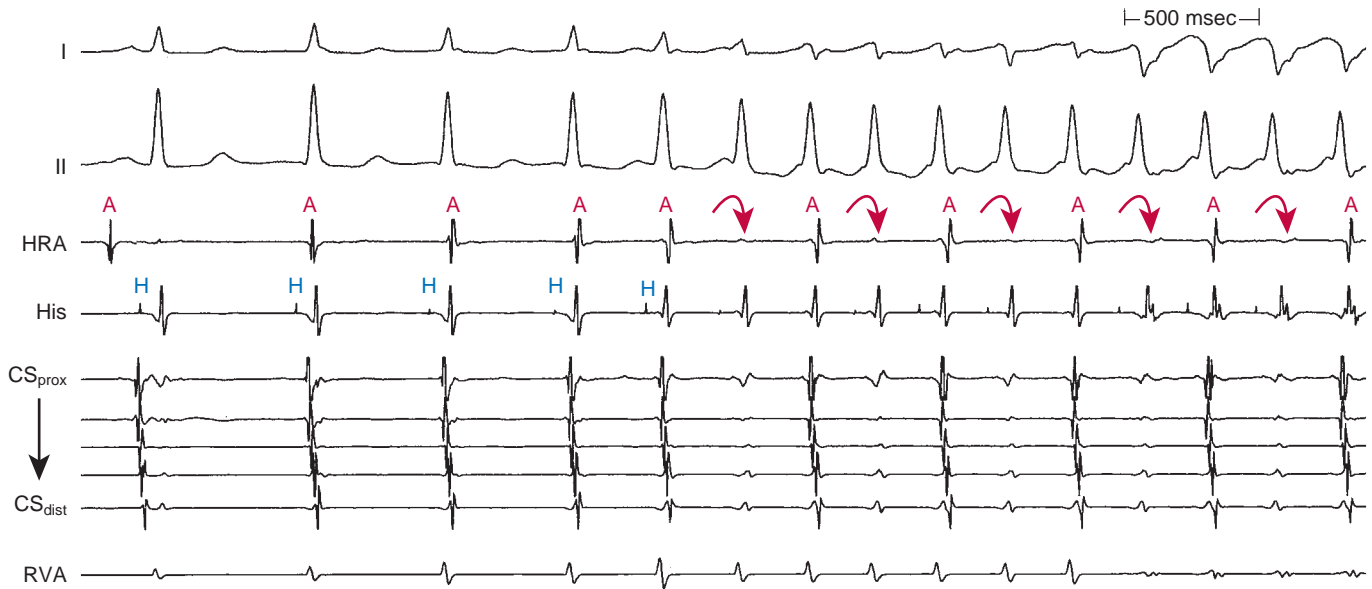


Fig. 17.22 Automatic Junctional Tachycardia. First beat to the left is sinus, followed by spontaneous, unprovoked onset of junctional tachycardia. Notice the first beat of the tachycardia starts with a His potential (*H*) and is not preceded by any trigger. The tachycardia rate accelerates (warms up). Conduction to the ventricle is maintained, but 2:1 ventriculoatrial block develops at faster tachycardia rate (*arrows*), as well as right bundle branch block aberrancy. *A*, Atrial electrogram; *CS_{dist}*, distal coronary sinus; *CS_{prox}*, proximal coronary sinus; *HRA*, high right atrium; *RVA*, right ventricular apex.

and slow decrease in tachycardia rate (cool-down), rather than an abrupt termination (Fig. 17.22).⁸

When junctional tachycardia is associated with aberrant conduction and AV dissociation, it becomes important to differentiate the tachycardia from VT. The His potential with anterograde propagation (i.e., proximal to distal His) preceding the QRS by a normal or prolonged HV interval largely excludes myocardial and fascicular VT.

Atrial extrastimulation. An early AES (delivered prior to HB depolarization) that advances the His potential immediately after it without terminating the tachycardia indicates that the retrograde fast pathway is not essential for the circuit and is consistent with junctional tachycardia (see Fig. 17.17). For such an AES to advance the immediately following His potential (with a short AH interval), it has to be conducted over the AVN fast pathway. In the setting of AVNRT, conduction of the AES over the fast pathway (which constitutes the retrograde limb of the typical slow-fast AVNRT circuit) would render that pathway refractory to further participation in AVNRT and, hence, AVNRT would be terminated (Fig. 17.23). In typical AVNRT, an early AES can conduct anterogradely only over the slow pathway and, hence, it can do so only with a long AH interval and can affect not the immediate His potential but only the subsequent one (see Fig. 17.16).^{8,36}

An AES (delivered from the proximal CS) timed to HB refractoriness that either terminates or resets the tachycardia (i.e., delays or advances the His potential of the subsequent cycle) effectively excludes junctional tachycardia and confirms a diagnosis of AVNRT (see Fig. 17.23). In this maneuver, the timing of HB activation is a surrogate marker for the time when the retrograde AVN fast pathway is refractory; hence, for an AES to be able to influence the subsequent His timing, the presence of an AVN slow pathway is required to mediate anterograde conduction of the AES.^{8,37–39} Rarely, a patient with junctional tachycardia has an anterograde slow AVN pathway that can be used to advance the timing of the subsequent HB activation, falsely suggesting AVNRT. However, the next HB activation cannot be delayed in this situation.

Atrial pacing during tachycardia. Following overdrive atrial pacing (with 1:1 AV conduction) during tachycardia, HB and atrial electrogram sequence can help distinguish AVNRT from junctional tachycardia. Atrial overdrive pacing is performed from the high RA or CS at a PCL 20 to 30 milliseconds shorter than TCL until the His potential is advanced to the PCL, at which point pacing is terminated. Upon resumption of the tachycardia, the first return electrogram after the last advanced His potential is examined.

Atrial overdrive pacing during junctional tachycardia transiently suppresses the arrhythmia focus, with immediate resumption of the tachycardia following the cessation of pacing. As a result, the first return electrogram will be a junctional beat preceded by a His potential that travels retrogradely over the AVN to activate the atrium, resulting in an “H-H-A” response. In contrast, an “H-A” electrogram sequence after the last paced atrial complex is consistent with typical AVNRT, whereby the last paced will conduct anterogradely over the slow pathway and exit the AVN into the HB while echoing retrogradely up the fast pathway, to activate the atrium.^{11,38,40,41}

Importantly, a pseudo-H-H-A response is commonly observed during typical AVNRT. Because anterograde conduction during atrial pacing occurs through the slow pathway, the AH interval is long and can be longer than the PCL (A-A interval), so that the last paced atrial beat is followed first by the HB electrogram resulting from slow AV conduction of the preceding paced atrial beat and then by the HB electrogram resulting from the last paced atrial beat. In other words, the atrial pacing spike typically precedes the His potential and QRS that were advanced from the previous atrial paced beat. Hence, after cessation of pacing, the immediate His potential is the result of the one before the last atrial paced beat, with the subsequent His potential being the one advanced from the last atrial paced beat, resulting in a pseudo H-H-A response. To avoid this potential pitfall, the H-H intervals should be measured during and after atrial overdrive pacing and the last His potential resulting from AV conduction during atrial pacing is carefully examined.

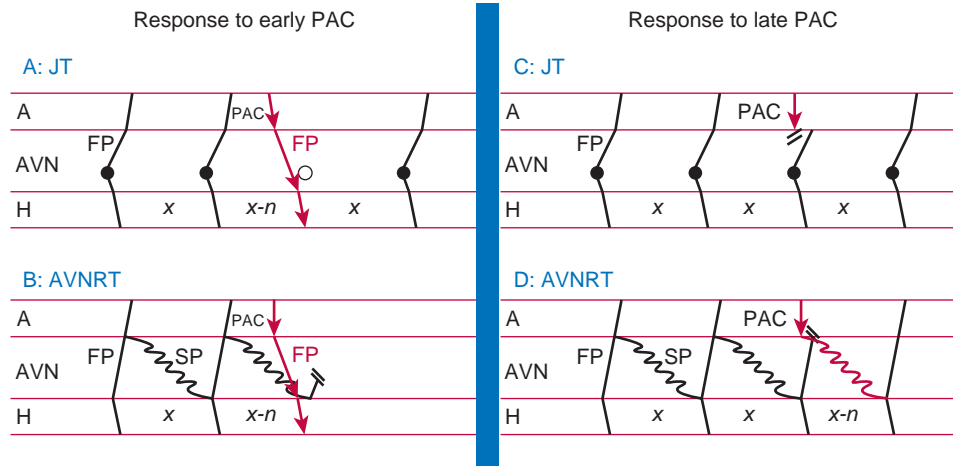


Fig. 17.23 Tachycardia Response to Early- and Late-Premature Atrial Complex (PAC). *Left panel*, Tachycardia response to early-coupled PACs. (A) Response in junctional tachycardia (JT): Solid circles represent junctional focus. Black lines show conduction through atrioventricular node (AVN), His (H), and atrium (A). Red arrow indicates PAC. Open circle represents the anticipated JT beat timing if no PAC were delivered. An early PAC advances the immediate JT beat and His timing by AVN fast pathway (FP) activation and JT continues. (B) Response in atrioventricular nodal reentrant tachycardia (AVNRT): an early PAC may advance the immediate His by activation of the AVN FP. However, that makes the FP refractory and unavailable for retrograde conduction, terminating the AVNRT circuit. Red arrow indicates PAC and its response. *Right panel*, Tachycardia response to late-coupled PACs. The PAC is delivered when AV junction is refractory (local atrial activation from PAC occurs at or after His activation). (C) Response in JT: a PAC delivered at a time the AV junction focus has already depolarized blocks at the AVN and is unable to influence the immediate or the next junction beat. (D) Response in AVNRT: a similarly timed PAC can influence the next beat of AVNRT by early engagement of the slow pathway (SP). Although this figure shows advancement of the next beat ($x-n$), delay of the next beat or termination of tachycardia are also specific to AVNRT. X and $x-n$ = H-H intervals. (From Padanilam BJ, Manfredi JA, Steinberg LA, Olson JA, Fogel RI, Prystowsky EN. Differentiating junctional tachycardia and atrioventricular node re-entry tachycardia based on response to atrial extrastimulus pacing. *J Am Coll Cardiol*. 2008;52:1711–1717.)

The last advanced His potential characteristically occurs at an H-H interval equal to the atrial PCL, whereas the first tachycardia His potential usually occurs at a longer return CL. The atrial and HB electrogram sequence following this last advanced His potential should be noted. If an atrial electrogram follows, an H-A response is diagnosed; if a His potential follows, an H-H-A response is diagnosed.⁴¹

Of note, the paced AH interval can be helpful in differentiating junctional tachycardia from typical AVNRT. The paced AH interval during atrial overdrive pacing of AVNRT is longer than the paced AH interval during atrial overdrive pacing of junctional tachycardia. During atrial overdrive pacing of AVNRT, anterograde AV conduction uses only the slow pathway because the fast pathway (which is used as the retrograde limb of the reentry circuit) is refractory from retrograde conduction. In contrast, during atrial overdrive pacing of junctional tachycardia, anterograde AV conduction is mediated by the fast pathway.

In addition, dissociation of atrial activation from HB activation can frequently be demonstrated with atrial pacing during junctional tachycardia. Such an observation is inconsistent with AVNRT.

Ventricular pacing during tachycardia. Zero or positive Δ HA interval (i.e., HA interval during RV pacing minus HA interval during tachycardia, $HA_{\text{pacing}} - HA_{\text{SVT}}$) has been reported to indicate junctional tachycardia. During both junctional tachycardia and RV pacing, the HA interval represents the true time interval of impulse conduction from the HA to the atrium. In contrast, the HA interval during AVNRT is a “pseudo-interval,” representing the relative activation timing of the HB and atrium, and the value of the HA interval depends on the presence and length of the lower common pathway. Hence, the Δ HA interval in AVNRT is negative (averaging about -10 milliseconds). However,

difficulty in obtaining a clear His signal with RV pacing limits the utility of this maneuver.³⁸

Management of junctional tachycardia. In general, data regarding the management of junctional tachycardia is limited, and mostly has been reported in pediatric literature. Pharmacologic therapy offers modest efficacy. While about two-thirds of patients experience partial improvement, complete suppression of the arrhythmia is achieved in only a minority of patients. Beta-blockers are often used as first-line chronic therapy for junctional tachycardia. Alternative medications include verapamil, diltiazem, flecainide, propafenone, and procainamide. The efficacy of amiodarone has been reported only in pediatric patients. The value of digoxin has not been well established.¹⁴

Catheter ablation may be reasonable in patients with junctional tachycardia and offers success rates of more than 80%. However, in view of the reported 5% to 10% risk of AV block, catheter ablation is generally reserved for highly symptomatic patients in whom drug therapy has been ineffective or not tolerated. Cryoablation has a significant safety advantage in these patients.¹⁴ Catheter ablation typically targets the focus of the tachycardia. When VA conduction is intact during junctional tachycardia, the site of earliest atrial activation serves as the initial target for ablation. If this fails, or if VA conduction is absent, then sequential empiric lesions can be applied in the posterior septum (the slow AV nodal pathway region), the mid-septum, and the anterior septum, incurring higher risks of permanent AV block. Occasional patients have isolated junctional premature complexes (that must be distinguished from PACs); these may be highly symptomatic and may warrant ablation therapy if medical treatment is unsuccessful.

ABLATION

Ablation of the slow AVN pathway is indicated in patients with SVT and documented AVNRT during EP testing, but it also can be performed in patients with documented SVT that is morphologically consistent with AVNRT on a preprocedure ECG or rhythm strip but in whom only dual AVN physiology (but not tachycardia) is demonstrated during an EP study. Slow pathway ablation also may be considered at the discretion of the physician when sustained (>30 seconds) AVNRT is induced incidentally during an ablation procedure directed at a different clinical tachycardia.

Target of Ablation

The slow pathway is the target of ablation for all variants of AVNRT. Initially, the rightward inferior AVN extension is targeted. Then, the leftward inferior AVN extension is targeted if needed. Rarely, ablation of the inferolateral left atrial pathway can be necessary.

Historically, the initial approach of RF ablation of AVNRT was modification of AVN conduction by the energy application near the anterosuperior aspect of the triangle of Koch (fast pathway ablation or the “anterior approach”). However, because the fast pathway constitutes the physiological anterograde conduction axis and is located in close proximity to the compact AVN and HB, this procedure was associated with an unacceptable risk of AV block or unphysiologically long PR intervals (which can cause symptoms similar to those of the pacemaker syndrome), and was consequently abandoned. In addition, in patients with multiple slow pathways, ablation of the fast pathway can be associated with persistently inducible AVNRT with anterograde conduction over a second slowly conducting pathway. Since the early 1990s, selective ablation of the AVN slow pathway by lesions created near the postero-inferior base of the triangle of Koch between the CS os and tricuspid annulus (the “posterior approach”) has proved to be a more successful and safer procedure. Unlike fast pathway ablation, successful ablation of the slow pathway can eliminate all variants of AVNRT.

However, selective slow pathway ablation can be particularly challenging in certain clinical situations. For example, in patients with evidence of impaired fast pathway conduction (usually older patients with TCL >400 milliseconds), ablation of the slow pathway can result in mandatory conduction through the impaired fast pathway, and Wenckebach block during rest can develop. Whether the fast pathway should be targeted for ablation instead of the slow pathway in these patients is controversial. Similarly, some patients with AVNRT have a markedly prolonged PR interval during NSR, a finding that suggests the possibility of absent anterograde fast pathway conduction and a high risk of complete AV block if the slow pathway is ablated. On the other hand, the fast pathway in such patients can be affected by an electrotonic interaction with the slow pathway, and elimination of this effect by slow pathway ablation often shortens the ERP of the fast pathway. In fact, in many of these patients, the AH interval remains stable or even shortens after slow pathway ablation.¹⁷

The site of the slow pathway to be targeted by ablation can be defined by one of two approaches: a purely anatomic approach and an electroanatomic approach. Despite the lack of precise knowledge of the pathophysiological substrate for AVNRT, ablation procedures have fortunately been very successful.

Anatomic Approach

The sequence of ablation sites chosen for RF delivery is related to the probability of successful slow pathway ablation at each site and the risk of impairing AV conduction. The most common site for effective and safe ablation is the location of the rightward inferior AVN extension at the isthmus of tissue between the tricuspid annulus and the CS os

(Fig. 17.24); ablation at this site has a success rate of 95%. Occasionally, successful ablation can require the catheter positioned along the tricuspid annulus inferior to the CS os or at the floor of the CS os. If those sites are unsuccessful, RF delivery is attempted at the roof of the proximal CS (1 to 3 cm from the CS os), the site of leftward inferior AVN extension. Rarely, successful slow pathway ablation can require ablation on the left side of the posterior atrial septum, along the mitral annulus (the site of inferolateral left atrial pathway). Successful ablation sites in this region typically exhibit an A/V ratio of 1:10 to 1:2. If ablation at all of these sites is unsuccessful, RF delivery may be considered at more cephalad sites along the tricuspid annulus superior to the upper edge of the CS os (presumably near the junction of the leftward and rightward inferior extensions), closer to the compact AVN, but only if the risk of complete AV block can be justified by the severity of clinical symptoms.

Electroanatomic Approach

The electroanatomic approach is guided by the identification of slow pathway potentials in conjunction with anatomic landmarks. These potentials have been used by some investigators to define the site of the slow pathway within the triangle of Koch, and they can be used as a guide to target ablation.

It has been suggested that activation of the slow pathway is associated with inscription of discrete electrical potentials, often referred to as slow pathway potentials. The origin of these potentials is uncertain. Whether they represent nodal tissue activation, anisotropic conduction through muscle bundles in various sites in the triangle of Koch, or a combination of both, remains unclear. The electrogram morphology of the slow potentials has been variously described as sharp and rapid (representing the atrial connection to the slow pathway; see Fig. 17.24), or slow and broad with low amplitude (representing slow potentials; see Fig. 17.24). The timing of slow potentials during NSR was reported to follow closely (within 10 to 40 milliseconds) local atrial activation near the CS os, or span the AH interval (it can occur as late as the His potential). This activation sequence is reversed during AVNRT (i.e., slow pathway potential precedes the atrial electrogram). However, such potentials are not specific to the triangle of Koch or to patients with AVNRT, and they can be recorded near the tricuspid annulus at sites distant from the slow pathway. Despite these observations, the probability of recording putative slow potentials at the site of effective slow ablation is more than 90%.

For ablation of atypical (slow-slow and fast-slow) AVNRT, the slow pathway used by the reentry circuit for retrograde conduction is targeted by ablation, and this target can be different from the AVN slow pathway used for anterograde conduction. Therefore ablation can be guided by the site of earliest retrograde atrial activation during atypical AVNRT, which is usually localized to the isthmus of tissue between the tricuspid annulus and the CS os in fast-slow AVNRT and along the anterior aspect of the CS in slow-slow AVNRT (Fig. 17.25).

Importantly, in the setting of typical (slow-fast) AVNRT, the site with the earliest atrial activation during tachycardia should not be targeted by mapping and ablation, since this location is often at the fast pathway exit site and ablation can cause AV block.^{11,42} It is also important to know that in some cases of typical slow-fast AVNRT, the fast pathway can have a more posterior location, and the earliest atrial activation site during the tachycardia is near the CS os. In such cases, ablation should be performed with caution because RF application at the usual slow pathway anatomic site can result in PR interval prolongation or heart block. Cryoablation can be an advantage in these situations.

Ablation Technique

For slow pathway ablation, a quadripolar, 4-mm-tip, deflectable ablation catheter is advanced through a femoral vein. Rarely, an SVC approach

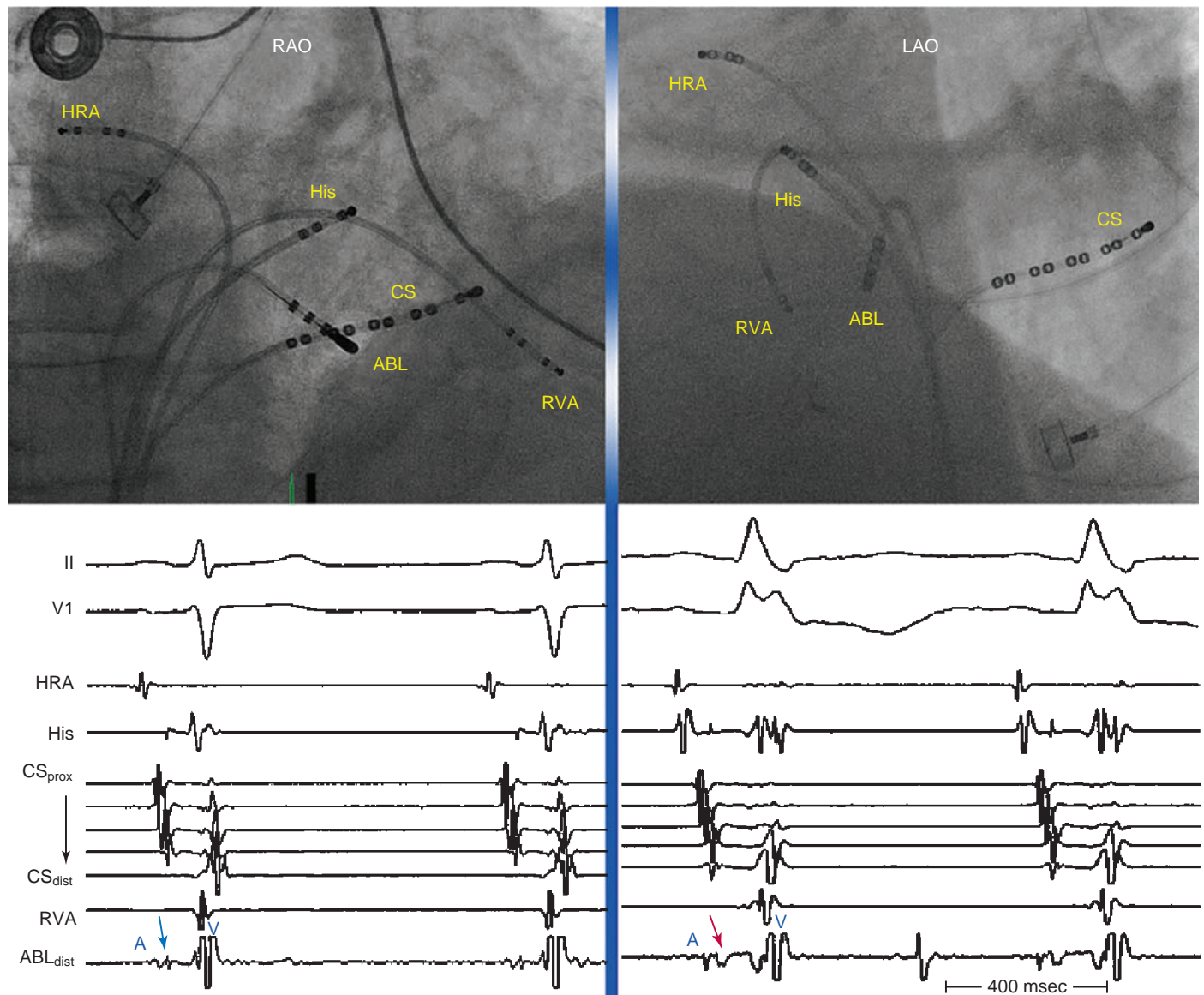


Fig. 17.24 Ablation of Atrioventricular Nodal Reentrant Tachycardia (AVNRT). *Upper panel*, Right anterior oblique (RAO) and left anterior oblique (LAO) fluoroscopic views of a typical catheter setup during AVNRT ablation. The ablation catheter (ABL) is positioned at the slow pathway location in the lower portion of the triangle of Koch, away from the His bundle (His) and anterior to the coronary sinus (CS) (those landmarks are defined by the His bundle and CS catheters, respectively). *Lower panel*, Intracardiac recordings during ablation of the slow pathway. Note the sharp (blue arrow, left lower panel) and broad (red arrow, right lower panel) potentials recorded between the atrial and ventricular electrograms at the ablation sites. Those potentials were suggested to reflect activation of the slow pathway (slow pathway potentials). ABL_{dist}, Distal ablation bipole; CS_{dist}, distal coronary sinus; CS_{prox}, proximal coronary sinus; His_{dist}, distal His bundle; His_{mid}, middle His bundle; His_{prox}, proximal His bundle; HRA, high right atrium; RVA, right ventricular apex.

(through the internal jugular or subclavian vein) is required because of IVC obstruction or barriers, and one report demonstrated the feasibility of this approach. Large-tip and irrigated-tip catheters have no role in catheter ablation of the slow pathway because the larger lesions they create can increase the risk of AV block, and the superficial location of AVN tissue does not require large or deep lesions.⁴²

Anatomic Approach

The anatomic approach is based on targeting the anatomic landmarks of the slow pathway. As noted, the target of slow pathway ablation is

the isthmus of tissue between the tricuspid annulus and the CS os. Using the right anterior oblique (RAO) fluoroscopy view, which best displays the triangle of Koch in profile, the ablation catheter is advanced into the RV, moved inferiorly so that it lies anterior to the CS os, and then withdrawn until the distal pair of electrodes records small atrial and large ventricular electrograms (with an A/V electrogram amplitude ratio during NSR of 1:10 to 1:2). Gentle clockwise torque is maintained to keep the catheter in contact with the low atrial septum. This positions the catheter along the tricuspid annulus immediately anterior to the CS os (see Fig. 17.24). Positioning is best performed during NSR,



Fig. 17.25 Ablation Target in Atypical (Fast-Slow) Atrioventricular Nodal Reentrant Tachycardia (AVNRT). Ablation is guided by the site of earliest retrograde atrial activation during atypical fast-slow AVNRT, which is usually localized to the isthmus of tissue between the tricuspid annulus and the CS os. A small spike (arrows) precedes the earliest atrial electrogram. *ABL_{dist}*, Distal ablation bipole; *ABL_{prox}*, proximal ablation bipole; *CS os*, coronary sinus ostium; *CS_{dist}*, distal coronary sinus; *CS_{prox}*, proximal coronary sinus; *His_{dist}*, distal His bundle; *His_{mid}*, middle His bundle; *His_{prox}*, proximal His bundle; *HRA*, high right atrium; *RVA*, right ventricular apex.

rather than AVNRT, because the atrial and ventricular electrograms at the tricuspid annulus are more easily discerned. The catheter often slips into the CS when one applies even a small amount of torque because the CS is large in many of these patients. If the catheter does not easily reach far enough into the ventricle, yielding an A/V ratio of only 1:1, or if catheter stability is inadequate or falls into the CS repeatedly, a long sheath with a slight septal angulation can be helpful. Moreover, some ablation catheters have asymmetrical bidirectional deflection curves, an option that can prove to be of value for catheter reach and stability in some cases.⁴²

Electroanatomic Approach

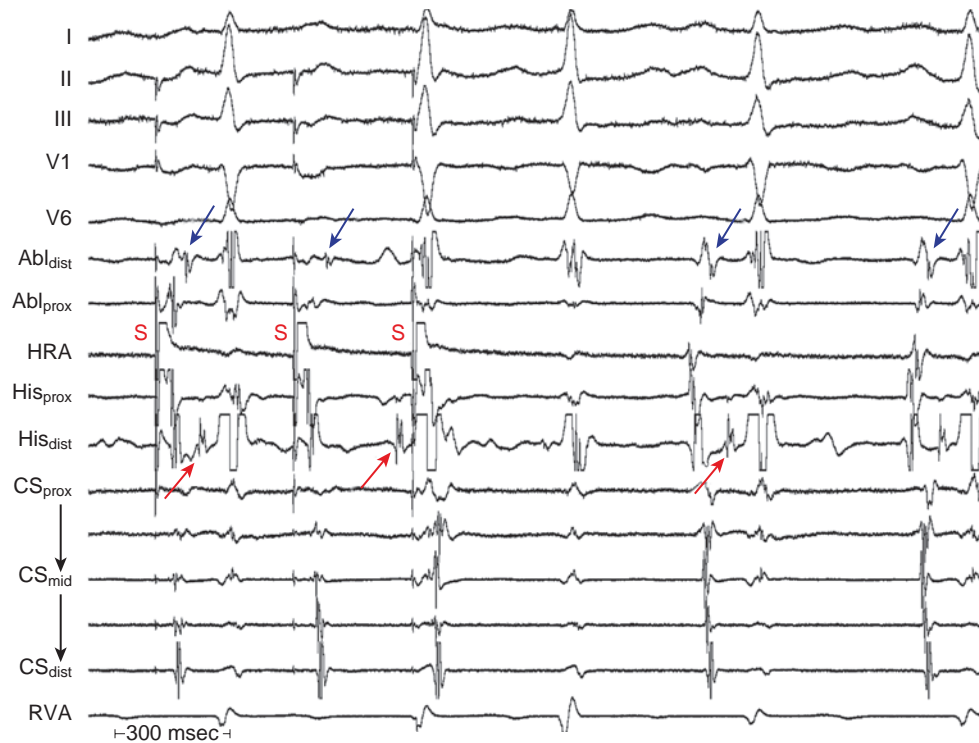
The target site is identified by slow pathway potentials (see Fig. 17.24). Initially, the triangle of Koch is mapped from the apex (where the HB is recorded) and then moved toward the CS os. This approach also helps evaluate the extension of the zone recording a His potential. Slow pathway potentials are usually recorded at the mid-anterosseptal position, where they are located in the middle of the isoelectric line connecting the atrial and ventricular electrograms. Moving the mapping catheter inferiorly, the slow pathway potential moves toward the atrial electrogram, and when the optimal site for slow pathway ablation is reached, it merges with the atrial electrogram. Because electrograms with these characteristics can be recorded near the tricuspid annulus at sites distant from the slow pathway, the region explored with the ablation catheter should be limited to the posterior septum, near the

CS os. In the left anterior oblique (LAO) fluoroscopy view, using the HB and CS os positions (as defined by the HB and CS catheters) as landmarks, the most common area where the slow potentials are recorded is in the posterior third of the line connecting those two landmarks.

Validation of slow pathway potentials can be useful and can be achieved by demonstrating that they represent slow and decremental conduction properties. Typically, brief runs of incremental atrial pacing or AES produce a decline in the amplitude and slope, an increase in the duration, and a separation of the slow potential from the preceding atrial electrogram until disappearance of any consistent activity. This is especially helpful in the presence of a sharp slow pathway potential, to distinguish it from a proximal HB recording (eFig. 17.3). Catheter-induced junctional ectopy, when resulting from catheter pressure in this area, as opposed to the HB, indicates that the catheter tip is at a good ablation site. In patients with slow-slow and slow-fast AVNRT, mapping during AVNRT often shows a discrete potential 20 to 40 milliseconds prior to the earliest atrial electrogram; this may indicate the slow pathway and signify a good target site.

Radiofrequency Energy Delivery

Catheter stability should be optimized before starting RF energy application to help avoid inadvertent AV block. This can require the use of long, preshaped sheaths and the cessation of isoproterenol infusion if hyperdynamic contractility is present. In addition, good positioning of the other EP catheters defining the anatomic landmarks demarcating



eFig. 17.3 Slow Pathway Potential. A putative slow pathway potential (*blue arrows*) is validated as being distinct from the His bundle potential (*red arrows*) by a burst of atrial stimulation. *ABL_{dist}*, Distal ablation bipole; *ABL_{prox}*, proximal ablation bipole; *CS_{dist}*, distal coronary sinus; *CS_{prox}*, proximal coronary sinus; *His_{dist}*, distal His bundle; *His_{mid}*, middle His bundle; *His_{prox}*, proximal His bundle; *HRA*, high right atrium; *RVA*, right ventricular apex; *S*, stimulus.

the triangle of Koch and the location of HB is mandatory. During RF application, catheter position should be continuously monitored with fluoroscopy or a real-time 3-D mapping system.

Ablation should be performed during NSR, when it is easier to maintain a stable catheter position. When ablation is carried out during AVNRT, sudden termination of the tachycardia during RF delivery can potentially result in dislodgment of the ablation catheter, inadvertent AV block, or an incomplete RF lesion.

Typical RF settings consist of a maximum power of 50 W and a maximum temperature of 55°C to 60°C, continued for 30 to 60 seconds, or until the junctional rhythm extinguishes (see later). Impedance and ECG should be carefully monitored throughout RF application. However, in the case of slow pathway ablation, the decrement in impedance associated with successful energy applications is usually small (approximately 2.5 Ω); such a small change precludes the clinical usefulness of impedance monitoring as an indicator of a successful RF application.

Junctional Rhythm

An accelerated junctional rhythm typically develops within a few seconds of RF delivery at the effective ablation site (Fig. 17.26). The mechanism of this rhythm is unclear but is likely secondary to enhanced automaticity in AVN tissue because of thermal injury. Accelerated junctional rhythm during RF ablation is usually associated with subtle differences in the retrograde atrial activation sequence (compared to that during AVNRT). Occurrence of this rhythm is strongly correlated with successful ablation sites; it occurs more frequently (94% vs. 64%) and for a longer duration (7 vs. 5 seconds) during successful compared with unsuccessful RF applications. However, junctional rhythm is not specific for slow pathway ablation and is routinely observed during intentional fast pathway and AVN ablation. More rapid junctional tachycardia, on the other hand, is probably caused by thermal injury of the HB and heralds impending AV block (Fig. 17.27).^{42,43}

When an accelerated junctional rhythm occurs, careful monitoring of VA conduction during this rhythm is essential, and overdrive atrial pacing may be performed to ensure the maintenance of 1:1 anterograde AV conduction (see Fig. 17.26). Occasionally, atrial pacing at a rate sufficiently fast to override the junctional rhythm results in AV Wencke-

bach block at baseline, even before the onset of RF energy delivery. In this case, isoproterenol may be used to shorten the AV block CL and maintain 1:1 AV conduction during pacing.⁴⁴

The absence of junctional rhythm during RF application usually corresponds to an unsuccessful ablation site. When an accelerated junctional rhythm does not develop within 10 to 20 seconds of RF delivery, RF application should be stopped, and the catheter tip should be repositioned to a slightly different site or until better contact is verified, and a new RF application is attempted. Nevertheless, a junctional rhythm may not occur in several situations, including atypical forms of AVNRT (fast-slow and slow-slow) and some cases of typical (slow-fast) AVNRT undergoing repeat ablation.

After an RF application that results in an accelerated junctional rhythm, programmed electrical stimulation (atrial and ventricular stimulation) is performed to determine the presence or absence of slow pathway conduction, AVN echoes, and tachycardia inducibility. If the result is unsatisfactory, the ablation catheter is moved to a slightly different site, and RF energy is reapplied. After several RF applications that do not elicit junctional rhythm, testing for inducibility of AVNRT or dual pathways should be performed; in rare cases, the slow pathway has been eliminated despite the lack of junctional rhythm, and additional RF applications are not only unnecessary but also potentially hazardous.

Several observations should prompt immediate discontinuation of RF application, including: (1) a sudden impedance rise (more than 10 Ω); (2) prolongation of the PR interval (during NSR or atrial pacing); (3) the development of AV block; (4) a fast junctional tachycardia (CL shorter than 350 milliseconds); and (5) a retrograde conduction block during junctional ectopy (see Fig. 17.27). Although the last observation can herald anterograde AV block in the case of typical AVNRT and necessitates immediate discontinuation of RF delivery, the absence of retrograde conduction over the fast pathway is a common occurrence in patients with atypical AVNRT, even before ablation. In this setting, the occurrence of junctional rhythm with no VA conduction may not be such an ominous sign; in fact, such an occurrence can indicate successful ablation of the slow pathway and thus should prompt ongoing RF delivery. As noted earlier, atrial pacing at a rate sufficient to overdrive



Fig. 17.26 Catheter Ablation of the Atrioventricular Node Slow Pathway. Radiofrequency (RF) energy delivery during normal sinus rhythm results in accelerated junctional rhythm with intact ventriculoatrial conduction. Overdrive atrial pacing at a rate faster than the junctional rhythm rate was started and confirmed intact atrioventricular conduction. This observation can indicate a good ablation site, with no injury to the fast pathway. ABL_{dist}, distal ablation bipole; CS_{dist}, distal coronary sinus; CS_{prox}, proximal coronary sinus; HRA, high right atrium; RVA, right ventricular apex.

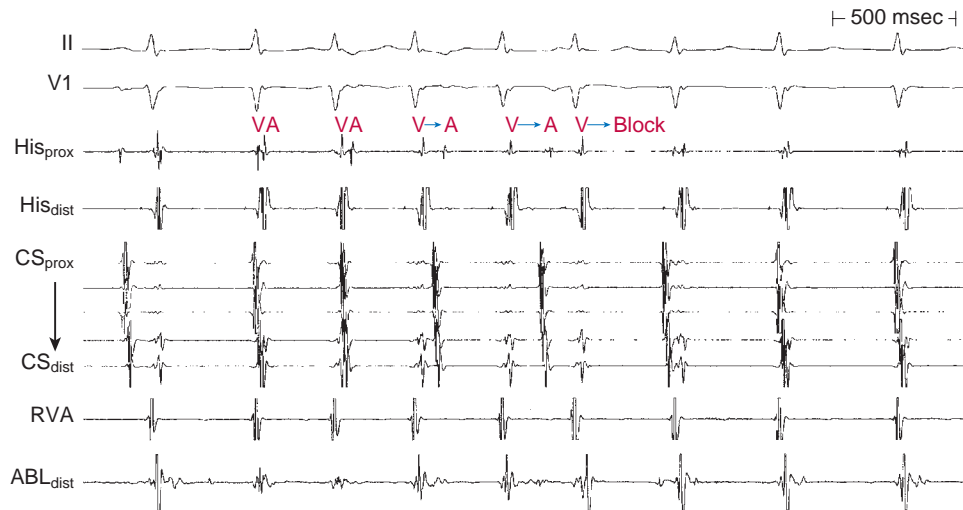


Fig. 17.27 Junctional Rhythm During Atrioventricular Node Slow Pathway Ablation. Radiofrequency energy delivery during normal sinus rhythm results in junctional tachycardia. Wenckebach ventriculoatrial (VA) block is observed during the junctional rhythm, a sign that heralds injury to the His bundle and should prompt immediate termination of RF application. *ABL_{dist}*, Distal ablation bipole; *CS_{dist}*, distal coronary sinus; *CS_{prox}*, proximal coronary sinus; *His_{dist}*, distal His bundle; *His_{prox}*, proximal His bundle; *RVA*, right ventricular apex.

junctional rhythm allows the monitoring of anterograde fast pathway conduction and helps to ensure safe RF application.⁴⁴

Endpoints of Ablation

Elimination of Slow Pathway Conduction

The optimal endpoint for slow pathway ablation is the complete elimination of slow pathway conduction and dual AVN physiology without impairing the fast pathway. This is evidenced by loss of conduction over the slow pathway (i.e., disappearance of discontinuous AV conduction curves), alteration of Wenckebach CL (shorter or longer), an increase in the ERP of the AVN, and preservation of intact anterograde and retrograde AVN (fast pathway) conduction. In many cases, the ERP of the fast pathway can actually shorten, which is likely secondary to the withdrawal of electrotonic inhibition imposed on the fast pathway by the slow pathway.¹⁷

Noninducibility of Tachycardia

Elimination of all evidence of slow pathway conduction is not a necessary requirement for a successful slow pathway ablation procedure. It suffices to eliminate the inducibility of AVNRT and 1:1 anterograde conduction over the slow pathway, with and without isoproterenol infusion. Complete elimination of all anterograde slow conduction is not essential for clinical success and is actually associated with a slightly higher risk of AV block. In patients with a successful slow pathway ablation procedure, 40% to 50% will still have dual AVN physiology, and 75% of those patients will have single AVN echoes, but AVNRT is not inducible (these patients are said to have undergone slow pathway modification). In most patients who no longer have inducible AVNRT after ablation in the slow pathway region, residual discontinuous AVN function curves and single AVN echoes do not predict an increased risk of AVNRT recurrence.⁴⁵

Therefore noninducibility of AVNRT (with and without isoproterenol infusion), with residual evidence of dual AVN pathways (AH interval jump) and single AVN echoes with an echo zone shorter than 30 milliseconds, is an acceptable endpoint. However, double AVN echoes or single echoes produced over a wide range of coupling intervals usually predict inducibility of AVNRT with the addition of isoproterenol or atropine, as well as late clinical recurrence of SVT.

When AVNRT or dual AVN physiology is poorly inducible at baseline, it may not be possible to confirm the efficacy of RF ablation. In this setting, other parameters can be indicative of a successful ablation, including the disappearance of a PR/RR ratio greater than 1 during rapid atrial pacing with 1:1 AV conduction, prolongation of the Wenckebach CL, and a decrease in fast pathway ERP.

If isoproterenol was required for initiation of SVT prior to ablation, isoproterenol should be discontinued during ablation and readministered afterward to assess the efficacy of ablation adequately. If isoproterenol was not necessary for SVT initiation prior to ablation, it need not be used for postablation testing. However, if the presence of single AVN echoes is accepted as an endpoint, isoproterenol infusion is then required during postablation testing to verify noninducibility of double echoes or AVNRT.

Reassessment of tachycardia inducibility is typically repeated 30 minutes after the last successful RF application. However, there are no data supporting the hypothesis that such a waiting period leads to reduced recurrence rates following acutely successful ablation. In fact, one report demonstrated that a procedure-prolonging waiting period may be omitted without compromising the patient's long-term outcome results.

Ventriculoatrial Block

Unlike patients with slow-fast AVNRT, those with atypical (slow-slow or fast-slow) AVNRT frequently lack retrograde conduction over the fast pathway even before ablation. In these patients, achievement of complete VA block during ablation indicates the elimination of retrograde conduction over all slow pathways. This endpoint is associated with less arrhythmia recurrence.

Outcome

Acute success rates of AVNRT ablation are approximately 97% to 99%, and they are similar whether the ablation is guided anatomically or electroanatomically. The recurrence rate after apparently successful ablation is approximately 2% to 5%. In 40% of patients with AVNRT recurrences, slow pathway conduction recovers after initial evidence of its abolition. Most AVNRT recurrences take place within the first days to months after ablation.

Atrioventricular Block

The most important complication of AVNRT ablation is AV block, which occurs in approximately 0.2% to 0.8% of patients. AV block generally develops during RF delivery or within the first 24 hours after ablation, and is almost always preceded by junctional ectopy with VA block. The level of AV block is usually in the AVN. Predictors of AV block include proximity of the anatomic ablation site to the compact AVN, the occurrence of fast junctional tachycardia (CL <350 milliseconds) during RF application, the occurrence of junctional rhythm with VA block, the number of RF applications (related to the amount of tissue damage), and significant worsening of anterograde AV conduction during the ablation procedure.

Of note, AV block occasionally develops unexpectedly, even when selective slow pathway ablation is performed at the inferior aspect of the triangle of Koch. This may be related to direct damage to the compact AVN, injury to the right coronary artery or AVN artery, or direct damage to a posteriorly located fast pathway.¹² Sometimes, transient AVN block develops as a result of mechanical trauma during manipulation of the ablation catheter. This may indicate the presence of a relatively small compact AVN that may be more susceptible to heart block during ablation. Catheter-induced AV block typically resolves after seconds to minutes. Careful catheter positioning to avoid sites at which catheter-induced block occurs generally results in successful ablation without AV block.^{5,44}

The development of AV block requiring pacemaker implantation late after the procedure is relatively low (0.4% over 10 years), but remains greater than that observed in patients with other SVTs and in the general population. Late development of AV block can potentially be related to subclinical AVN injury during the procedure that contributes to the accelerated degeneration of AVN function over time, or to the continuing healing process of the RF lesion leading to fibrosis and extension of the lesion size. Of note, the occurrence of even transient AV block during the ablation procedure, especially in older patients, was found to be a marker for the development of AV block requiring pacemaker implantation late after the procedure.⁴⁶

Palpitations

Palpitations occur in 20% to 30% of patients following ablation of AVNRT. These are generally transient and usually are not caused by recurrent AVNRT. Most are caused by PACs or PVCs, which subside spontaneously and require no treatment other than reassurance. Inappropriate sinus tachycardia can develop in some patients after AVNRT ablation, a finding that suggests disruption of the parasympathetic or sympathetic inputs into the sinus node and AVN.

Other Complications

Other procedural complications include cardiac tamponade (in 0.2% of patients), hematoma (0.2%), and femoral artery pseudoaneurysm (0.1%). In addition, subclinical activation of the coagulation system (e.g., elevated plasma levels of the D-dimer) is common during RF ablation. Nevertheless, clinically detectable embolic events are uncommon (0.7%). Treatment with aspirin may be considered for 6 to 8 weeks following ablation, to minimize the risk of thrombus formation in the RA or vena cavae.

Cryoablation of the Slow Pathway

Target of Cryoablation

The target of ablation is the region of the slow pathway, identified anatomically or electroanatomically, as described for standard RF ablation. The target site should be identified during NSR whether cryoablation is to be performed during NSR or AVNRT because the A/V ratio and electrogram morphology usually are obscured during AVNRT.

Cryoablation Technique

Cryomapping. Cryomapping (ice mapping) is designed to verify that ablation at the chosen site will have the desired effect (i.e., block in the slow pathway) and to reassure the absence of complications (i.e., AV block). Cryomapping is performed at a temperature of -30°C . At this temperature, the “test cryolesion” is reversible (for up to 60 seconds), and the catheter is stuck to the atrial endocardium within an ice ball that includes the tip of the catheter (cryoadherence). Formation of an ice ball at the catheter tip and adherence to the underlying myocardium are signaled by the appearance of electrical noise recorded from the ablation catheter’s distal bipole. In the cryomapping mode, the temperature is not allowed to drop to less than -30°C , and the duration of energy application is limited to 60 seconds. Once an ice ball is formed, various pacing protocols are performed to test the modification or disappearance of slow pathway conduction.⁴⁷

Cryomapping is usually performed during NSR in patients with discontinuous anterograde dual AVN conduction curve. For patients without a clear discontinuity in the AVN conduction curve, cryomapping may be performed during AVNRT, which is feasible without the risk of catheter dislodgment on termination of the tachycardia (because of cryoadherence).

During cryoablation of the slow pathway, junctional rhythm is not observed. Thus other parameters must be used to validate the potential effectiveness of the ablation site. In fact, the absence of junctional rhythm can be advantageous because it allows the maintenance of NSR during ablation and enables monitoring of the PR interval throughout the procedure. In addition, the maintenance of NSR during cryoablation allows various pacing maneuvers to be performed during ongoing cryoenergy application, to evaluate the effect of the ablation on slow pathway conduction. The disappearance of dual AVN physiology, the noninducibility of AVNRT, and the modification of the fast pathway ERP predict a successful ablation site. When cryoablation is performed during AVNRT, progressive AH interval lengthening followed by termination of AVNRT indicates slow pathway block.^{47,48}

Slow pathway block usually occurs quickly (within 10 to 20 seconds) at the optimal target site. If cryomapping does not yield the desired result within 20 to 30 seconds or causes unintended AV conduction delay or block, the cryomapping procedure is interrupted. After a few seconds, to allow the catheter to thaw and become dislodged from the tissue, the catheter is moved to a different site, and cryomapping is repeated.

Cryoablation. When sites of successful cryomapping are identified by demonstrating satisfactory slow pathway block or modification with no impairment of the basal anterograde AV conduction, the cryoablation mode is activated, whereby a target temperature lower than -75°C is sought (a temperature of approximately -75°C to -80°C is generally achieved). The application is then continued for 4 minutes, to create an irreversible lesion. If the catheter tip is in close contact with the endocardium, a prompt drop in catheter tip temperature should be seen as soon as the cryoablation mode is activated. A slow decline in temperature or a very high flow rate of refrigerant during ablation suggests poor catheter tip tissue contact; in such cases, cryoablation should be interrupted and the catheter repositioned.^{47,48}

Once a successful cryolesion is achieved, applying one or two additional (“bonus”) cryolesions at the same site can potentially further increase the lesion size and help reduce the risk of tachycardia recurrence. At the successful ablation site, ablation is typically continued for two or three consecutive freeze-thaw cycles of 4 minutes each (total of 12 minutes cryoablation). After rewarming the catheter tip to the body temperature, the next freezing cycle is started immediately without moving the catheter tip away from the successful ablation site. Bonus lesions are not recommended if transient PR interval prolongation or AV block was observed during the first application.^{47,48}

The successful site for cryomapping and cryoablation of the slow pathway frequently is found in the midseptal region of the Koch triangle, more superiorly than the usual site of successful RF ablation. On rare occasions, AV block does not appear during cryomapping at a particular site but develops during cryoablation at the same site. Fortunately, this resolves quickly if the cryoablation is interrupted promptly.

Endpoints of Cryoablation

The goal of cryoablation is the complete elimination of slow pathway function. This usually requires delivery of several cryoapplications at closely adjacent sites. If a discontinuity in the anterograde AVN conduction curve and single AVN echoes persist despite multiple cryoapplications, this is still a reasonable endpoint, provided that multiple AVN echoes or AVNRT are not inducible, even during isoproterenol infusion. If acute procedural success cannot be achieved with a standard 4-mm-tip catheter, a 6-mm-tip catheter can be used, which can help yield larger and deeper cryolesions.^{47,48}

Outcome of Cryoablation

Previously published reports with cryoablation of AVNRT in pediatric patients demonstrated acute procedural success rates of 83% to 100% and recurrence rates ranging from 3% to 20%. Recurrences seem to be less common in the younger patient population. Although the use of bonus cryoapplications to consolidate the acutely successful cryoablation and the choice of larger-tip cryocatheters (8 mm and 6 mm vs. 4 mm tips) to create larger lesions have been associated with fewer long-term recurrences without compromising safety, the overall procedural success rate has remained consistently lower than that of RF ablation. In a meta-analysis of cryoablation versus RF ablation for AVNRT, cryoablation was associated with a lower risk of permanent AV block (0% vs. 0.75%) but a higher risk of long-term AVNRT recurrence (9.7% vs. 3.8%) and longer total procedure time (111.7 minutes vs. 81.2 minutes).^{47–50}

The safety of cryoablation is indisputable. Not a single case of persistent AV block has been reported, even when using large-tip cryocatheters, and despite the fact that transient AV block occurs in up to 2% to 23% of patients during cryomapping at -30°C or during cryoablation at -75°C .

Rarely, transient AV block is observed shortly following the ablation procedure (within the first 24 hours), despite normal AV conduction during cryoablation and at the end of the procedure. The mechanism of late AV block is unclear, especially given the fact that, in contrast to RF ablation, cryoenergy leads to a more limited and well-circumscribed fibrosis, without any signs of chronic inflammation.⁵¹

Advantages of Cryoablation

One of the distinct advantages of cryothermal technology is the ability to demonstrate loss of function of tissue with cooling reversibly (ice mapping or cryomapping), thereby demonstrating the functionality of prospective ablation sites without inducing permanent injury. Furthermore, once the catheter tip temperature is reduced to less than 0°C , progressive ice formation at the catheter tip causes adherence to the adjacent tissue (cryoadherence), which maintains stable catheter contact at the site of ablation and minimizes the risk of catheter dislodgment during changing cardiac rhythm.^{47,48}

Cryoablation can be of particular advantage in patients with AVNRT with posterior displacement of the fast pathway or AVN, and those with a small space in the triangle of Koch between the HB and the CS os, when ablation must be performed in the midseptum. However, given the high success rate and low risk of RF slow pathway ablation, it may be difficult to demonstrate a clinical advantage of cryoablation over RF ablation of unselected AVNRT cases. Therefore the use of cryo-

ablation may be recommended in specific circumstances in which the use of RF can be more likely to cause AVN damage. These circumstances include patients with unusual cardiac anatomy that makes safe RF delivery difficult, those with evidence of impaired AV conduction at baseline, those who need ablation in the close vicinity of the compact AVN following unsuccessful RF ablation at more posterior sites, pediatric patients, and patients in whom even the small risk of AV block associated with RF ablation is considered unacceptable.

VIDEOS

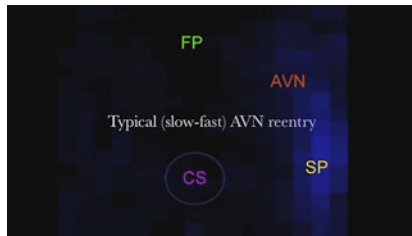
The following video accompanies this chapter:

Video 17.1. Atrioventricular Nodal Reentry: Optical Mapping



REFERENCES

1. Dobrzynski H, et al. Structure, function and clinical relevance of the cardiac conduction system, including the atrioventricular ring and outflow tract tissues. *Pharmacol Ther.* 2013;139:260–288.
2. Lee P-C, Chen S-A, Hwang B. Atrioventricular node anatomy and physiology: implications for ablation of atrioventricular nodal reentrant tachycardia. *Curr Opin Cardiol.* 2009;24:105–112.
3. Kurian T, Ambrosi C, Hucker W, et al. Anatomy and electrophysiology of the human AV node. *Pacing Clin Electrophysiol.* 2010;33:754–762.
4. Faletra FF, Ho SY, Auricchio A. Anatomy of right atrial structures by real-time 3D transesophageal echocardiography. *JACC Cardiovasc Imaging.* 2010;3:966–975.
5. Yamaguchi T, et al. Anatomical and electrophysiological variations of Koch's triangle and the impact on the slow pathway ablation in patients with atrioventricular nodal reentrant tachycardia: a study using 3D mapping. *J Interv Card Electrophysiol.* 2013;37:111–120.
6. Mani BC, Pavri BB. Dual atrioventricular nodal pathways physiology: a review of relevant anatomy, electrophysiology, and electrocardiographic manifestations. *Indian Pacing Electrophysiol J.* 2014;14:12–25.
7. Katritsis DG, et al. Coexistent types of atrioventricular nodal re-entrant tachycardia. *Circ Arrhythm Electrophysiol.* 2015;8:1189–1193.
8. Katritsis DG, Camm AJ. Atrioventricular nodal reentrant tachycardia. *Circulation.* 2010;122:831–840.
9. Efimova E, et al. Adenosine sensitivity of retrograde fast pathway conduction in patients with slow-fast atrioventricular nodal reentrant tachycardia: a prospective study. *Heart Rhythm.* 2014;11:871–876.
10. Katritsis DG, Josephson ME. Classification of electrophysiological types of atrioventricular nodal re-entrant tachycardia: a reappraisal. *Europace.* 2013;15:1231–1240.
11. Asirvatham SJ, Stevenson WG. Atrioventricular nodal reentry tachycardia chameleon in disguise. *Circ Arrhythm Electrophysiol.* 2014;7:355–357.
12. Suzuki A, et al. Visualization of the antegrade fast and slow pathway inputs in patients with slow-fast atrioventricular nodal reentrant tachycardia. *Pacing Clin Electrophysiol.* 2014;37:874–883.
13. Nakatani Y, et al. Electrophysiological and anatomical differences of the slow pathway between the fast-slow form and slow-slow form of atrioventricular nodal reentrant tachycardia. *Europace.* 2014;16:551–557.
14. Page RL, et al. 2015 ACC/AHA/HRS guideline for the management of adult patients with supraventricular tachycardia: a report of the American College of Cardiology/American Heart Association Task Force on Clinical Practice Guidelines and the Heart Rhythm Society. *Circulation.* 2016;133:e506–e574.
15. González-Torrecilla E, et al. Combined evaluation of bedside clinical variables and the electrocardiogram for the differential diagnosis of paroxysmal atrioventricular reciprocating tachycardias in patients without pre-excitation. *J Am Coll Cardiol.* 2009;53:2353–2358.
16. Hoffmann BA, et al. Ablation of atrioventricular nodal reentrant tachycardia in the elderly: results from the German Ablation Registry. *Heart Rhythm.* 2011;8:981–987.
17. Park JS, Hwang H, Joung B, et al. Clinical and electrophysiologic characteristics before and after radiofrequency ablation of sustained slow



Video 17.1 Atrioventricular Nodal Reentry: Optical Mapping. Optical mapping in an isolated canine atrioventricular node (AVN) preparation. The first stimulus (*S1*) conducts anterogradely over both the slow and fast AVN pathways (*SP* and *FP*, respectively). A premature stimulus (*S2*) blocks anterogradely in the *FP*, travels down the *SP* and then retrogradely up the *FP* to initiate typical (slow-fast) AVN reentry.

- atrioventricular nodal pathway conduction. *JACC Clin Electrophysiol.* 2016;2:367–374.
18. Nakatani Y, et al. Differentiation of slow-slow form of AVNRT from AVRT through a posteroseptal accessory pathway by retrograde P-wave amplitude. *Pacing Clin Electrophysiol.* 2016;39:241–249.
19. Mendenhall GS, Voigt A, Saba S. Insights into atrioventricular nodal function from patients displaying dual conduction properties: interactive and orthogonal pathways. *Circ Arrhythm Electrophysiol.* 2013;6:364–370.
20. Derval N, et al. Differential sequential septal pacing: a simple maneuver to differentiate nodal versus extranodal ventriculoatrial conduction. *Heart Rhythm.* 2013;10:1785–1791.
21. Obeyesekere M, et al. Tachycardia induction with ventricular extrastimuli differentiates atypical atrioventricular nodal reentrant tachycardia from orthodromic reciprocating tachycardia. *Heart Rhythm.* 2012;9:335–341.
22. Josephson ME, Almendral J, Callans DJ. Resetting and entrainment of reentrant ventricular tachycardia associated with myocardial infarction. *Heart Rhythm.* 2014;11:1239–1249.
23. Deo R, Berger R. The clinical utility of entrainment pacing. *J Cardiovasc Electrophysiol.* 2009;20:466–470.
24. Akerström F, et al. Performance of the SA-VA difference to differentiate atrioventricular nodal reentrant tachycardia from orthodromic reentrant tachycardia in a large cohort of consecutive patients. *Pacing Clin Electrophysiol.* 2015;38:1066–1072.
25. González-Torrecilla E, et al. Differences in ventriculoatrial intervals during entrainment and tachycardia: a simpler method for distinguishing paroxysmal supraventricular tachycardia with long ventriculoatrial intervals. *J Cardiovasc Electrophysiol.* 2011;22:915–921.
26. González-Torrecilla E, et al. First postpacing interval after tachycardia entrainment with correction for atrioventricular node delay: a simple maneuver for differential diagnosis of atrioventricular nodal reentrant tachycardias versus orthodromic reciprocating tachycardias. *Heart Rhythm.* 2006;3:674–679.
27. Kannankeril PJ, Bonney WJ, Dzurik MV, et al. Entrainment to distinguish orthodromic reciprocating tachycardia from atrioventricular nodal reentry tachycardia in children. *Pacing Clin Electrophysiol.* 2010;33:469–474.
28. Javier García-Fernández F, et al. Differentiation of atrioventricular nodal reentrant tachycardia from orthodromic reciprocating tachycardia by the resetting response to ventricular extrastimuli: comparison to response to continuous ventricular pacing. *J Cardiovasc Electrophysiol.* 2013;24:534–541.
29. Nagashima K, et al. Anterograde conduction to the His bundle during right ventricular overdrive pacing distinguishes septal pathway atrioventricular reentry from atypical atrioventricular nodal reentrant tachycardia. *Heart Rhythm.* 2015;12:735–743.
30. Segal OR, et al. Differential ventricular entrainment: a maneuver to differentiate AV node reentrant tachycardia from orthodromic reciprocating tachycardia. *Heart Rhythm.* 2009;6:493–500.
31. Dandamudi G, et al. A novel approach to differentiating orthodromic reciprocating tachycardia from atrioventricular nodal reentrant tachycardia. *Heart Rhythm.* 2010;7:1326–1329.
32. AlMahameed ST, Buxton AE, Michaud GF. New criteria during right ventricular pacing to determine the mechanism of supraventricular tachycardia. *Circ Arrhythm Electrophysiol.* 2010;3:578–584.
33. Vijayaraman P, Lee BP, Kalahasty G, et al. Reanalysis of the ‘pseudo A-A-V’ response to ventricular entrainment of supraventricular tachycardia: importance of his-bundle timing. *J Cardiovasc Electrophysiol.* 2006;17:25–28.
34. Singh DK, et al. His overdrive pacing during supraventricular tachycardia: a novel maneuver for distinguishing atrioventricular nodal reentrant tachycardia from atrioventricular reciprocating tachycardia. *Heart Rhythm.* 2014;11:1327–1335.
35. Pérez-Rodon J, et al. Entrainment from the para-Hisian region for differentiating atrioventricular node reentrant tachycardia from orthodromic atrioventricular reentrant tachycardia. *Europace.* 2008;10:1205–1211.
36. Asirvatham SJ, Stevenson WG. Taking the slower pathway. *Circ Arrhythm Electrophysiol.* 2015;8:236–238.
37. Lane C, Veenhuyzen GD, Quinn FR. A conflict of evidence: AVNRT or junctional tachycardia? *Heart Rhythm.* 2013;10:767–769.
38. Katritsis DG, Josephson ME. Differential diagnosis of regular, narrow-QRS tachycardias. *Heart Rhythm.* 2015;12:1667–1676.
39. Padanilam BJ, et al. Differentiating junctional tachycardia and atrioventricular node re-entry tachycardia based on response to atrial extrastimulus pacing. *J Am Coll Cardiol.* 2008;52:1711–1717.
40. Ho RT, Pietrasik G, Greenspon AJ. A narrow complex tachycardia with intermittent atrioventricular dissociation: What is the mechanism? *Heart Rhythm.* 2014;11:2116–2119.
41. Fan R, et al. Novel use of atrial overdrive pacing to rapidly differentiate junctional tachycardia from atrioventricular nodal reentrant tachycardia. *Heart Rhythm.* 2011;8:840–844.
42. Asirvatham SJ, Stevenson WG. Atrioventricular nodal block with atrioventricular nodal reentrant tachycardia ablation. *Circ Arrhythm Electrophysiol.* 2015;8:745–747.
43. Bagherzadeh A, Keshavarzi T, Farahani MM, et al. Determinants of immediate success for catheter ablation of atrioventricular nodal reentry tachycardia in patients without junctional rhythm. *J Interv Card Electrophysiol.* 2014;39:19–23.
44. Chen H, et al. Atrioventricular block during slow pathway ablation: entirely preventable? *Circ Arrhythm Electrophysiol.* 2015;8:739–744.
45. Reddy CD, Silka MJ, Bar-Cohen Y. A comparison of AV nodal reentrant tachycardia in young children and adolescents: electrophysiology, ablation, and outcomes. *Pacing Clin Electrophysiol.* 2015;38:1325–1332.
46. Liao J-N, et al. Permanent pacemaker implantation for late atrioventricular block in patients receiving catheter ablation for atrioventricular nodal reentrant tachycardia. *Am J Cardiol.* 2013;111:569–573.
47. Pieragnoli P, et al. Cryoablation of typical AVNRT: younger age and administration of bonus ablation favor long-term success. *Heart Rhythm.* 2015;12:2125–2131.
48. Qureshi MY, Ratnasamy C, Sokoloski M, et al. Low recurrence rate in treating atrioventricular nodal reentrant tachycardia with triple freeze-thaw cycles. *Pacing Clin Electrophysiol.* 2013;36:279–285.
49. Hanninen M, et al. Cryoablation versus RF ablation for AVNRT: a meta-analysis and systematic review. *J Cardiovasc Electrophysiol.* 2013;24:1354–1360.
50. Drago F, et al. Cryoablation of AVNRT in children and adolescents: early intervention leads to a better outcome. *J Cardiovasc Electrophysiol.* 2014;25:398–403.
51. Kiplapinar N, et al. Assessment of atrioventricular conduction following cryoablation of atrioventricular nodal reentrant tachycardia in children. *Pacing Clin Electrophysiol.* 2014;37:712–716.

Typical Atrioventricular Bypass Tracts

OUTLINE

Types of Bypass Tracts, 599

- Atrioventricular Bypass Tracts, 599
- Atrionodal Bypass Tracts, 599
- Atrio-Hisian Bypass Tracts, 599
- Atypical Bypass Tracts, 600

Types of Preexcitation Syndromes, 600

- Wolff-Parkinson-White Syndrome, 600
- Concealed Bypass Tracts, 600
- Lown-Ganong-Levine Syndrome, 600
- Mahaim Variant of Preexcitation, 600

Pathophysiology, 600

- Wolff-Parkinson-White Syndrome, 600
- Atrioventricular Bypass Tracts, 601
- Atrioventricular Reentry, 602
- Other Arrhythmias Associated With Wolff-Parkinson-White Syndrome, 603

Epidemiology and Natural History, 606

- Wolff-Parkinson-White Pattern, 606
- Wolff-Parkinson-White Syndrome, 606
- Sudden Death, 606
- Associated Cardiac Abnormalities, 606
- Familial Wolff-Parkinson-White Syndrome, 606
- Concealed Bypass Tracts, 607

Clinical Presentation, 607

Initial Evaluation, 607

- Methods for Evaluation of Bypass Tract Refractory Period, 607

Principles of Management, 608

- Acute Management, 608
- Chronic Management, 609

Electrocardiographic Features, 612

- Electrocardiography of Preexcitation, 612
- Supraventricular Tachyarrhythmias Associated With Wolff-Parkinson-White Syndrome, 614
- Electrocardiographic Localization of the Bypass Tract, 614

Electrophysiological Testing, 623

- Baseline Observations During Sinus Rhythm, 623
- Induction of Tachycardia, 633
- Tachycardia Features, 637
- Diagnostic Maneuvers During Tachycardia, 641
- Diagnostic Maneuvers During Sinus Rhythm After Tachycardia Termination, 648
- Exclusion of Other Arrhythmia Mechanisms, 649

Localization of the Bypass Tract, 649

- Pacing From Multiple Atrial Sites, 649
- Preexcitation Index, 649
- Effects of Bundle Branch Block During Orthodromic Atrioventricular Reentrant Tachycardia, 652
- Ventricular Entrainment During Orthodromic Atrioventricular Reentrant Tachycardia, 652
- Earliest Ventricular Activation Site During Anterograde Bypass Tract Conduction, 655
- Earliest Atrial Activation Site During Retrograde Bypass Tract Conduction, 655
- Atrial Electrogram Polarity Reversal During Retrograde Bypass Tract Conduction, 656
- Direct Recording of Bypass Tract Potential, 657
- Local Atrioventricular (or Ventriculoatrial) Interval, 658

Ablation, 660

- Target of Ablation, 660
- Ablation Technique: General Considerations, 661
- Endpoints of Ablation, 662
- Ablation of Left Free-Wall Bypass Tracts, 663
- Ablation of Right Free-Wall Bypass Tracts, 666
- Ablation of Anteroseptal (Superoparaseptal) and Midseptal Bypass Tracts, 667
- Ablation of Posteroseptal (Inferoparaseptal) Bypass Tracts, 670
- Ablation of Epicardial Bypass Tracts, 672
- Causes of Failed Bypass Tract Ablation, 673
- Outcome, 674

TYPES OF BYPASS TRACTS

Bypass tracts (BTs) are remnants of the atrioventricular (AV) connections caused by incomplete embryological development of the AV annuli and failure of the fibrous separation between the atria and ventricles. There are several types of BTs, according to the structures they connect, including AV, atrionodal, atrio-Hisian, atriofascicular, fasciculoventricular, and nodofascicular BTs.¹

Atrioventricular Bypass Tracts

AV BTs are strands of working myocardial cells connecting atrial and ventricular myocardium across the electrically insulating fibrofatty tissues of the AV junction bypassing the atrioventricular node (AVN)-His-Purkinje

system (HPS). In the older literature, these BTs were called Kent bundles, although incorrectly (Kent described AVN-like tissue in the right atrial [RA] free wall that did not connect to the ventricle). Thus the use of the term *bundle of Kent* should be discouraged.

Atrionodal Bypass Tracts

Atrionodal BTs connect the atrium to the distal or compact AVN. They have been called James fibers and are of uncertain physiological significance.

Atrio-Hisian Bypass Tracts

Atrio-Hisian BTs connect the atrium to the His bundle (HB); these BTs are rare.

Atypical Bypass Tracts

The term “atypical BTs” is used here to describe variants of BTs that connect the atrium (atriofascicular BTs), AVN (nodofascicular and nodoventricular BTs), or HB (fasciculoventricular BTs) to distal Purkinje fibers or ventricular myocardium. In addition, this term encompasses slowly conducting short AV BTs and long AV BTs. Although many of those variants of BTs are sometimes referred to as “Mahaim fibers,” it is more appropriate to describe them based on their anatomic connections.

TYPES OF PREEXCITATION SYNDROMES

Several patterns of preexcitation can occur, depending on the anatomy of the BT and the direction in which impulses are conducted. Conduction from the atria to the ventricles normally occurs via the AVN-HPS. Patients with preexcitation have an additional or alternative pathway, the BT, which directly connects the atria and ventricles and bypasses the AVN. The term *syndrome* is used when the anatomical variant is responsible for tachycardia.

Wolff-Parkinson-White Syndrome

In the Wolff-Parkinson-White (WPW) syndrome, AV conduction occurs, partially or entirely, through an AV BT, which results in earlier activation (preexcitation) of the ventricles than if the impulse had traveled through the AVN.

Concealed Bypass Tracts

Concealed AV BTs refer to AV BTs that do not manifest anterograde conduction and therefore do not result in ventricular preexcitation. Because they do not result in alteration of the QRS complex in the electrocardiogram (ECG), they cannot be detected by inspection of the surface ECG; they are called *concealed*. However, the concealed BT can conduct in a retrograde fashion, thereby creating a reentrant circuit with impulses traveling from the atrium to the AVN, HPS, ventricle, and then back to the atrium via the BT.

Lown-Ganong-Levine Syndrome

In the setting of Lown-Ganong-Levine (LGL) syndrome, preexcitation purportedly occurs via atrio-Hisian BTs or, alternatively, no BT is present and enhanced AVN conduction accounts for the ECG findings. The net effect is a short PR interval without delta wave or QRS prolongation. It is important to stress, however, that LGL is not a recognized syndrome with an anatomical basis, but only an ECG description, and the use of the term should be discouraged.

Mahaim Variant of Preexcitation

The so-called Mahaim variant of preexcitation does not typically result in a delta wave because these pathways, which usually terminate in the

conducting system or in the ventricular myocardium close to the conducting system, conduct slowly, and the AVN-HPS has adequate time to activate most of the ventricular muscle mass.

It is worth noting that some of the older literature refers to eponymous pathways that were originally anatomically described with subsequent attempts made to correlate these structures with physiologic findings. With more recent data from intracardiac recordings, many of these correlations have been shown to be incorrect and thus the use of the eponyms adds confusion to discussions about them. For instance, the pathways described by Kent (AV nodal–like tissue at the free-wall AV valve annulus) more resemble atriofascicular fibers than they do typical AV fibers, and atriofascicular fibers in turn possess the physiology initially (incorrectly) attributed to Mahaim fibers. Table 18.1 displays some of the terminology; it is evident why use of eponymous terms is discouraged.

PATHOPHYSIOLOGY

Wolff-Parkinson-White Syndrome

WPW *pattern* refers to the constellation of ECG abnormalities related to the presence of a manifest AV BT (i.e., ventricular preexcitation: short PR interval, delta wave, wide QRS complex) in asymptomatic patients (Fig. 18.1). WPW *syndrome* refers to the combination of ventricular preexcitation and either a documented tachyarrhythmia or symptoms of a tachyarrhythmia.¹

Because the AV BT typically conducts faster than the AVN, the onset of ventricular activation is earlier than if depolarization occurred only via the AVN, resulting in a shortened PR (P-delta) interval. Furthermore, because the BT exhibits practically nondecremental conduction, the early ventricular activation (i.e., P-delta interval) remains almost constant at all atrial rates (Fig. 18.2).

Preexcited intraventricular conduction in WPW propagates from the insertion point of the AV BT in the ventricular myocardium via direct muscle-to-muscle conduction. This process is inherently slower than ventricular depolarization resulting from rapid HPS conduction. Thus, although the initial excitation of the ventricles (via the BT) occurs earlier, it is followed by slower activation of the ventricular myocardium than occurs normally. The net effect is that the QRS complex consists of fusion between the early ventricular activation caused by preexcitation with the later ventricular activation resulting from impulse propagation through the AVN-HPS to the ventricles. The initial part of ventricular activation resulting in the upstroke of the QRS complex is slurred because of slow muscle-to-muscle conduction; this is termed a *delta wave*.

Depending on the relative contribution from ventricular activation by the normal AVN-HPS versus the manifest BT, a variable degree of preexcitation occurs. The more rapid the conduction along the BT in relation to the AVN, the greater the amount of myocardium depolarized

TABLE 18.1 Historical Description of Different Bypass Tracts

Eponymous Pathway	Anatomical Description	Proposed Physiological Role/Syndrome	Actual Physiologic Role
Kent bundle	Clusters of nodal cells at nonseptal AV junction	Anomalous AV connection/WPW syndrome	None (possibly atriofascicular pathways)
James fiber	Atriocompact nodal connection	LGL syndrome	Enhanced AVN conduction
Brechenmacher fiber	Atrio-Hisian connection	LGL syndrome	Enhanced AVN conduction
Mahaim fiber	Connection from compact AVN to ventricle	Septal WPW pathways with decremental conduction	Probably none
Paladino fiber	Connection from proximal AVN to ventricle	Septal WPW pathways with decremental conduction	Probably none

AV, Atrioventricular; AVN, atrioventricular nodal; LGL, Lown-Ganong-Levine; WPW, Wolff-Parkinson-White.

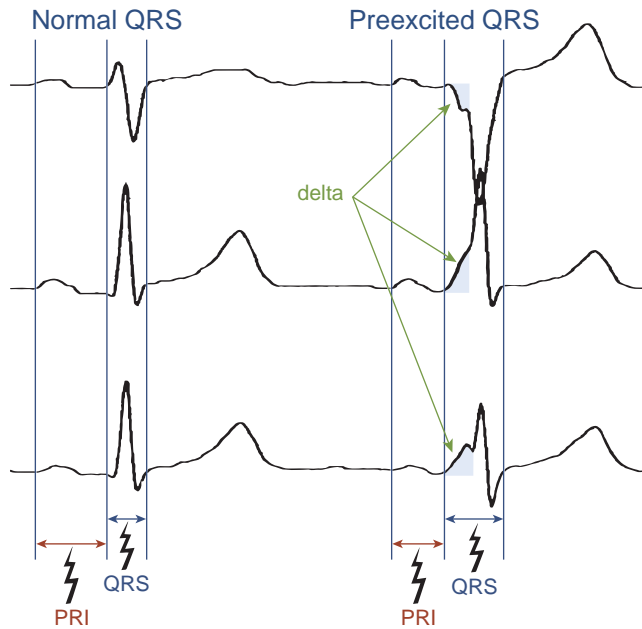


Fig. 18.1 Ventricular Preexcitation. Three surface electrocardiogram leads during normal sinus rhythm. The first sinus P wave is conducted over the normal atrioventricular node-His Purkinje system (AVN-HPS), resulting in a normal PR interval (PRI) and a normal QRS complex. The second P wave is conducted over the AVN and a bypass tract (BT). AV conduction over the BT is faster than over the AVN, resulting in pre-excitation of the ventricle and shortening of the PRI. Then, preexcited intraventricular conduction propagates from the insertion point of the BT in the ventricular myocardium via direct muscle-to-muscle (slow) conduction, producing an initial slurred “delta” wave (shaded area of the QRS complex). The rest of the QRS complex is produced by the rapidly conducting HPS. Therefore the preexcited QRS results from fusion between activation over the BT (which accounts for the initial delta wave) and activation over the AVN-HPS (which accounts for the rest of the QRS complex).

via the BT, resulting in a more prominent or wider delta wave and increasing prolongation of the QRS complex duration.¹

Atrioventricular Bypass Tracts

The cardiac skeleton consists of four rings of dense connective tissue that surround the AV canals (mitral and tricuspid) and extend to the origins of the aorta and the pulmonary trunk, providing structure and support for the heart as well as electrical isolation between the atria and the ventricles. The aortic valve occupies the central position with the other valve rings attached to it. The right fibrous trigone includes the triangular formation between the aortic valve and the medial parts of the tricuspid and mitral valves, and it represents the largest thickening and strongest portion of the cardiac skeleton. Together with the membranous septum, the right fibrous trigone constitutes the central fibrous body (see Fig. 9.1).

The AV junctions are the areas of the heart where the atrial musculature connects to the annuli of the mitral and tricuspid valves. The AVN-HPS, which lies in the septal component of the AV junction, is the only normal electrical connection between the atria and the ventricles. The fibrous skeleton and AV valvular annuli (annulus fibrosus) act as insulators to prevent electrical impulses from conducting to the ventricles by any other route. The main function of the AVN is modulation of atrial impulse transmission to the ventricles, thereby coordinating atrial and ventricular contractions; it receives, delays, and conveys atrial impulses to the ventricles.

AV BTs are aberrant muscle bundles that connect the atria to the ventricles outside of the normal AV conduction system. AV BTs are found most often in the parietal AV junctional areas, including the paraseptal areas. They breach the insulation provided by the fibrofatty tissues of the AV groove (sulcus tissue) and the hinge lines (fibrous annulus) of the valves. They are rarely found in the area of fibrous continuity between the aortic and mitral valves because in this area there is usually a wide gap between the atrial myocardium and ventricular myocardium to accommodate the aortic outflow tract. The remainder of the AV groove may be divided into quadrants consisting of the left free wall, right free wall, and posteroseptal and anteroseptal spaces. The distribution of BTs within these regions is not homogeneous—46% to 60% of BTs are found within the left free-wall space; 25% are within the posteroseptal space; 13% to 21% of BTs are within the right free-wall space; up to 7% are within the right superoparaseptal (formerly called anteroseptal) space; and less than 5% are located in the midseptum (Fig. 18.3).

AV BTs are usually short and very thin muscular strands (typically 5 to 10 mm in length, with a maximal diameter of 0.1 to 7 mm) but can occasionally exist as broad bands of tissue. They can course through the AV groove at variable depths ranging from subepicardial to subendocardial locations. The AV BT can run in an oblique course rather than perpendicular to the transverse plane of the AV groove. As a result, the fibers can have an atrial insertion point that is transversely from less than one to several centimeters removed from the point of ventricular attachment. Some posteroseptal pathways insert into coronary sinus (CS) musculature rather than atrial myocardium and can be associated with the coronary venous system or diverticula from a CS branch vein.

Multiple AV BTs occur in 5% to 10% of patients. BTs are defined as multiple when they are separated by more than 1 to 3 cm at the AV junction. The most common combination of widely spaced multiple BTs is posteroseptal and right free-wall BTs. The incidence of multiple BTs is particularly high in patients with antidromic atrioventricular reentrant tachycardia (AVRT) (50% to 75%), patients in whom atrial fibrillation (AF) resulted in ventricular fibrillation (VF), and patients with Ebstein anomaly.

Although the majority (approximately 60%) of AV BTs conduct both anterogradely and retrogradely (i.e., bidirectionally), some AV BTs are capable of propagating impulses in only one direction. BTs that conduct only in the anterograde direction are uncommon (less than 5%), often cross the right AV groove, and frequently possess decremental conduction properties. On the other hand, BTs that conduct only in the retrograde direction occur more frequently, accounting for 17% to 37% of all BTs. When the BT is capable of anterograde conduction, ventricular preexcitation is usually evident during normal sinus rhythm (NSR), and the BT is referred to as *manifest*. BTs capable of retrograde-only conduction are referred to as *concealed*.

Because working myocardial cells make up the vast majority of AV BTs, conduction over those BTs is mediated by the rapid inward sodium current, similar to normal His-Purkinje tissue and atrial and ventricular myocardium. Therefore AV BTs have rather constant anterograde and retrograde conduction at all rates until the refractory period is reached, at which time conduction is completely blocked. Thus conduction over AV BTs usually behaves in an all-or-none fashion (i.e., nondecremental conduction), although with careful measurement, there is often a small amount of prolongation of conduction intervals (10 to 15 milliseconds) over the BT when the pacing rate is just below that at which block occurs. In contrast, the AVN, which depends on the slow inward calcium current for generation and propagation of its action potential, exhibits what has been called *decremental conduction*, whereby conduction time of the impulse propagating through the AVN prolongs as the atrial

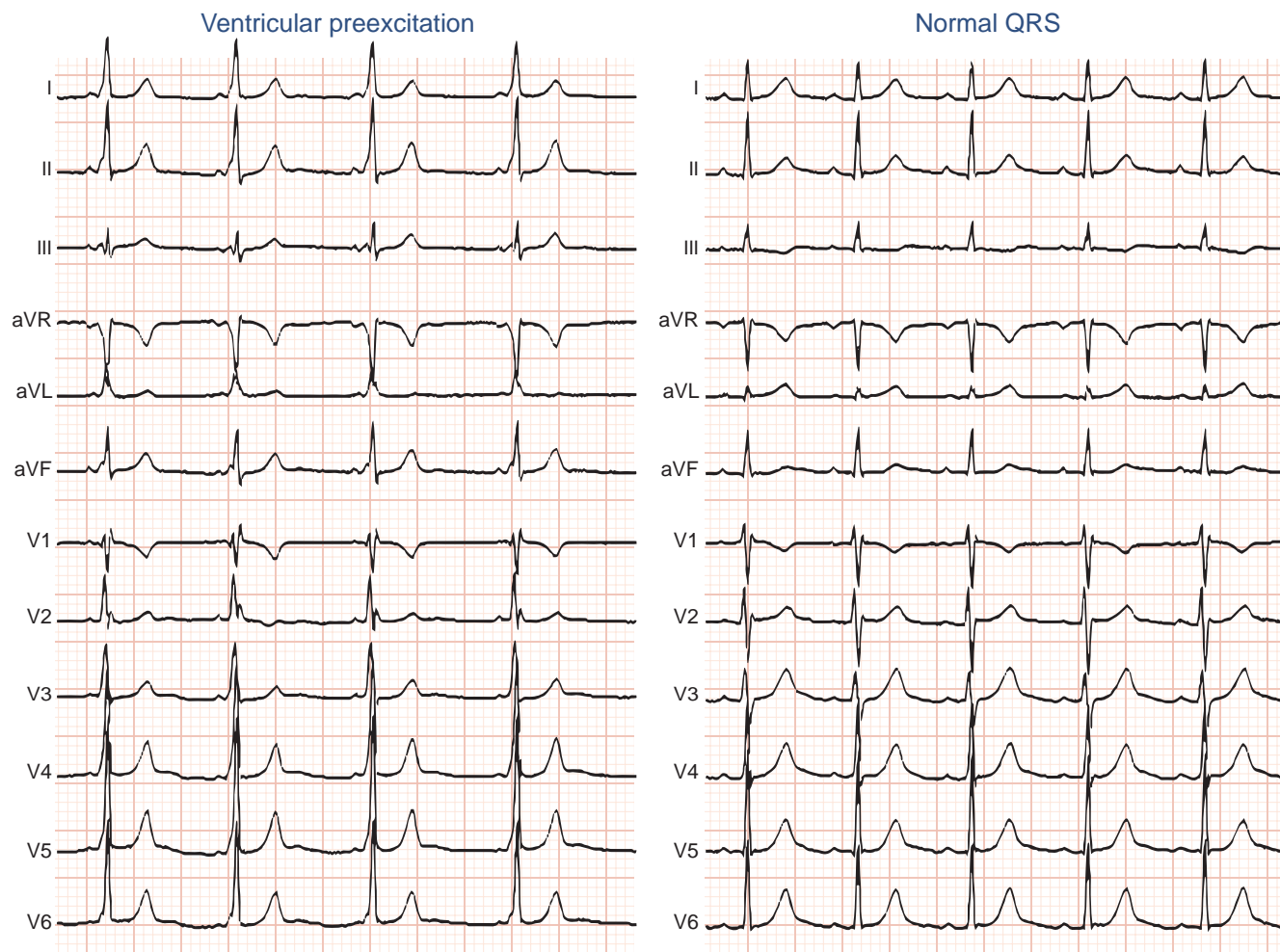


Fig. 18.2 Wolf-Parkinson-White Electrocardiogram (ECG) Pattern. Surface ECG of normal sinus rhythm with ventricular preexcitation (*left*) and without preexcitation (*right*) in the same patient.

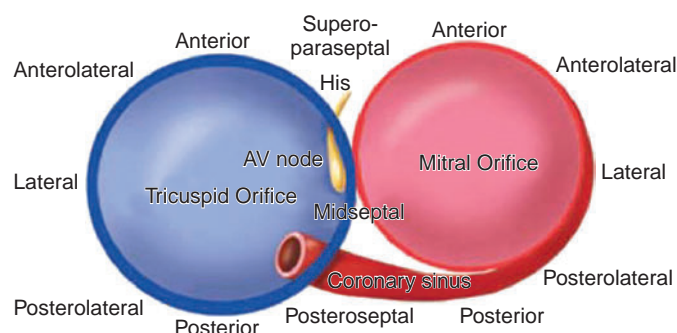


Fig. 18.3 Locations of Atrioventricular (AV) Bypass Tracts by Anatomical Region. Tricuspid and mitral valve annuli are depicted in a left anterior oblique view. Locations of the coronary sinus, AV node, and His bundle are shown. AV bypass tracts may connect atrial to ventricular myocardium in any of the regions shown. (From Miller JM, Zipes DP. Therapy for cardiac arrhythmias. In: Libby P, Bonow R, Mann DL, et al., eds. *Braunwald's Heart Disease: A Textbook of Cardiovascular Medicine*. 8th ed. Philadelphia: WB Saunders; 2007:779–830.)

cycle length (CL) shortens. Thus AV conduction is more rapid through the AV BT than through the AVN, a difference that is exaggerated at faster heart rates. This difference has potentially great clinical importance. A primary function of the AVN is to limit the number of impulses conducted from the atria to the ventricles, which is particularly important during fast atrial rates (e.g., AF or atrial flutter [AFL]) when only a fraction of impulses are conducted to the ventricles, whereas the remainder are blocked in the AVN. However, in the presence of nondecrementally conducting AV BTs with short refractory periods, these arrhythmias can lead to very fast ventricular rates that can degenerate into VF.

Atrioventricular Reentry

AVRT is a macroreentrant tachycardia with an anatomically defined circuit that consists of two distinct pathways, the normal AV conduction system and an AV BT, linked by common proximal (atrial) and distal (ventricular) tissues. If sufficient differences in conduction time and refractoriness exist between the normal conduction system and the BT, a properly timed premature impulse of atrial or ventricular origin can initiate reentry. AVRTs are the most common (80%) tachycardias associated with the WPW syndrome. AVRT is divided into orthodromic and antidromic according to the direction of conduction in the AVN-HPS (Fig. 18.4). Orthodromic indicates normal direction (anterograde) of conduction over AVN-HPS during AVRT.

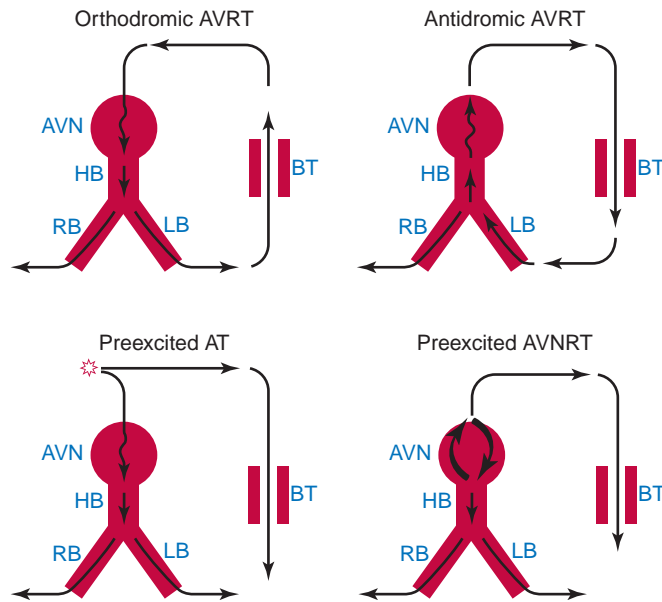


Fig. 18.4 Bypass Tract–Related Tachycardias. Schematic representation of the reentrant circuit during orthodromic atrioventricular reentrant tachycardia (AVRT), antidromic AVRT, preexcited atrial tachycardia (AT), and preexcited atrioventricular nodal reentrant tachycardia (AVNRT) using a left-sided bypass tract (BT). HB, His bundle; LB, left bundle branch; RB, right bundle branch.

Orthodromic Atrioventricular Reentrant Tachycardia

In orthodromic AVRT, the AVN-HPS serves as the anterograde limb of the reentrant circuit (i.e., the pathway that conducts the impulse from the atria to the ventricles), whereas an AV BT serves as the retrograde limb (see Figs. 18.4 and 18.5). Approximately 50% of BTs participating in orthodromic AVRT are manifest (able to conduct bidirectionally) and 50% are concealed (able to conduct retrogradely only). Therefore a WPW pattern may or may not be present on the surface ECG during NSR. When preexcitation is present, the delta wave seen during NSR is lost during orthodromic AVRT because anterograde conduction during the tachycardia occurs over the normal AV conduction system, and not via the BT (i.e., the ventricle is not preexcited). Orthodromic AVRT accounts for approximately 90% to 95% of AVRT episodes in patients with a manifest BT and 35% of all paroxysmal supraventricular tachycardias (SVTs).¹

Antidromic Atrioventricular Reentrant Tachycardia

Antidromic AVRT is a preexcited AVRT whereby an AV BT serves as the anterograde limb and the AVN-HPS serves as the retrograde limb of the reentrant circuit (see Figs. 18.4 and 18.5). Consequently, the QRS complex during antidromic AVRT is fully preexcited (i.e., the ventricles are activated totally by the BT with no contribution from the normal conduction system). The BT involved in the antidromic AVRT circuit must be capable of anterograde conduction and, therefore, preexcitation is typically observed during NSR. Other, less frequent, forms of preexcited AVRT utilize one AV BT as the anterograde conduction and a second BT for retrograde conduction or a combination of one BT plus the AVN-HPS in either direction (eFig. 18.1).¹

Clinically, antidromic AVRT is much less frequent than orthodromic AVRT, occurring in less than 5% of patients with WPW syndrome, and can be induced in the electrophysiology (EP) laboratory in less than 10%. The low prevalence of antidromic AVRT is related to the EP properties of the AVN, because good retrograde ventriculoatrial (VA)

conduction is required to sustain tachycardia. Clinical presentation, sex, age, and orthodromic AVRT induction appear similar in patients with and without inducible antidromic AVRT. Patients with antidromic AVRT induction more frequently have BTs with more rapid conduction properties than other WPW patients.²

Susceptibility to antidromic AVRT appears to be facilitated by a distance of at least 4 cm between the BT and the normal AV conduction system. Consequently, most antidromic AVRTs use a lateral (right or left) BT as the anterograde route for conduction. Because posteroseptal BTs are in close proximity to the AVN, those BTs are rarely part of antidromic AVRT if the other limb is the AVN and not a second free-wall BT. Up to 50% to 75% of patients with spontaneous antidromic AVRT have multiple BTs (manifest or concealed), which may or may not be utilized as the retrograde limb during the tachycardia.²

Permanent Junctional Reciprocating Tachycardia

Permanent junctional reciprocating tachycardia (PJRT) is a rare form of nearly incessant orthodromic AVRT mediated by a concealed, retrogradely conducting AV BT that has slow and decremental conduction properties. Conduction properties of this retrograde BT are slower than the anterograde conduction properties of the AVN and those of typical fast BTs found in patients with AVRT. The BT in PJRT is most often located in the posteroseptal region, although other portions of the AV groove can also harbor this unusual pathway. Because these BTs are almost always concealed and have slow conduction, all elements necessary for reentry are present at all times, and thus PJRT can be present much of the time (i.e., incessant), with only short interludes of sinus rhythm. The incessant nature of PJRT can result in tachycardia-induced cardiomyopathy.^{1,3}

Other Arrhythmias Associated With Wolff-Parkinson-White Syndrome

Atrial tachycardia (AT), AFL, AF, and atrioventricular nodal reentrant tachycardia (AVNRT) can all coexist with a BT. In these preexcited tachycardias, the BT serves as a bystander route for ventricular or atrial activation, and is not required for the initiation or maintenance of the arrhythmia.

Atrioventricular Nodal Reentrant Tachycardia and Atrial Tachycardia

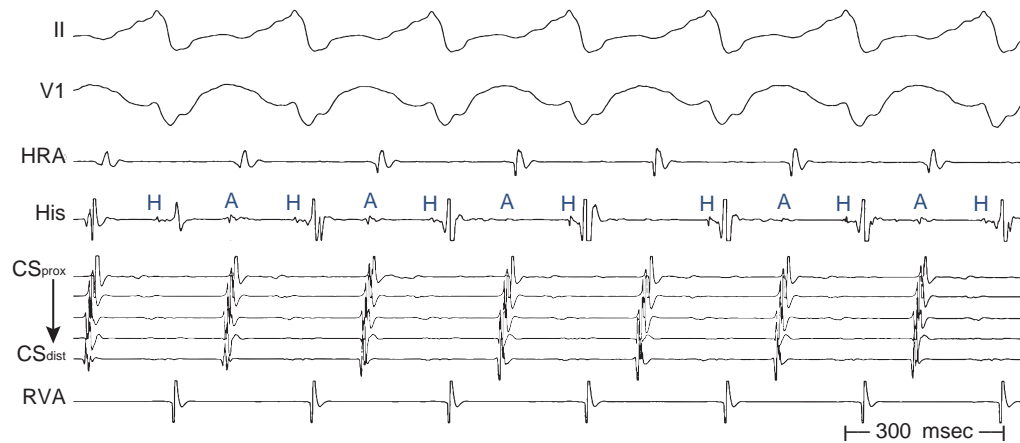
Both AVNRT and AT can use the bystander BT to transmit impulses to the ventricle (see Fig. 18.4). When AVNRT occurs in the WPW syndrome, the arrhythmia can be difficult to distinguish from AVRT without EP testing.

Atrial Fibrillation

The overall incidence of AF in patients with WPW syndrome varies from 12% to 39%. AF is typically paroxysmal. Persistent AF is rare in these patients. AF is most common in patients with anterogradely conducting BTs. Patients with antidromic AVRT, multiple BTs, and BTs that have a short anterograde effective refractory period (ERP) are more prone to develop AF. In individuals with WPW, AF is often preceded by AVRT that degenerates into AF (Fig. 18.6).

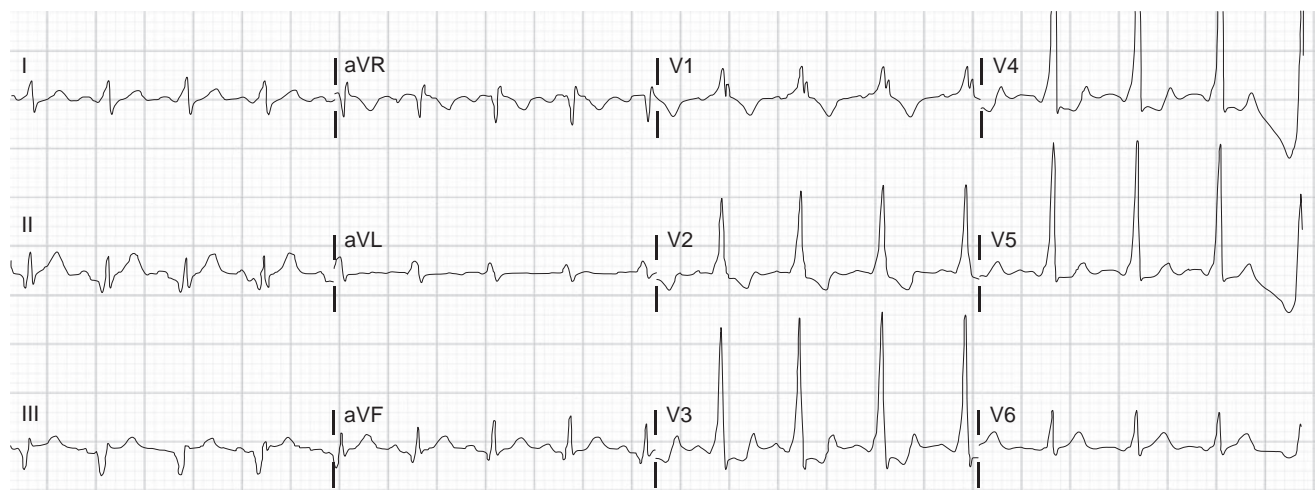
The frequency with which intermittent AF occurs in patients with the WPW syndrome is striking because of the low prevalence of coexisting structural heart disease or other predisposing factors for AF. This observation suggests that the AV BT itself can be related to the genesis of AF, supported by the fact that when the BT is ablated, AF may not recur.

The mechanisms by which AVRT precipitates AF are not well understood. The rapid atrial rate can cause disruption in atrial activation and reactivation, creating an EP substrate conducive to AF. The observation

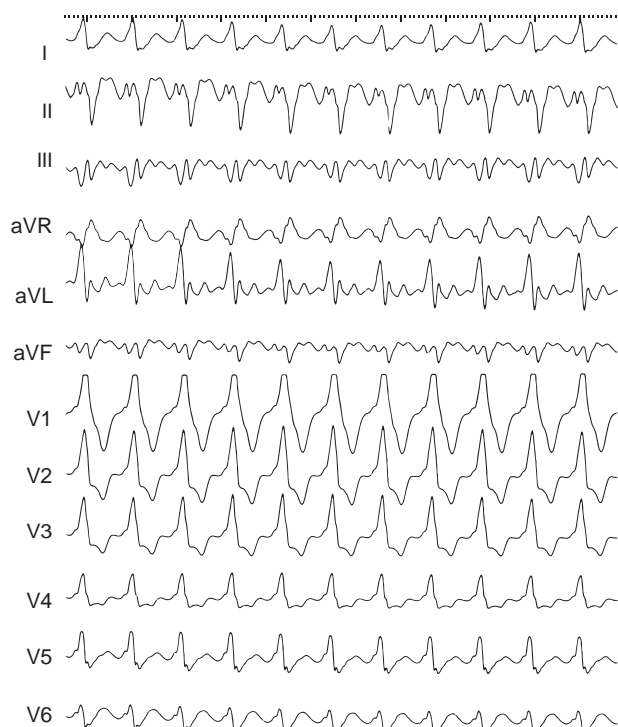


eFig. 18.1 Preexcited Atrioventricular Reentrant Tachycardia. The anterograde limb of the reentry circuit is mediated by a right lateral bypass tract (BT), as indicated by the preexcited QRS morphology. The retrograde limb of the circuit is mediated by a left lateral BT, as indicated by the eccentric atrial activation sequence. A, Atrial electrogram; CS_{dist}, distal coronary sinus; CS_{prox}, proximal coronary sinus; H, His bundle potential; HRA, high right atrium; RVA, right ventricular apex.

NSR



Antidromic AVRT



Orthodromic AVRT

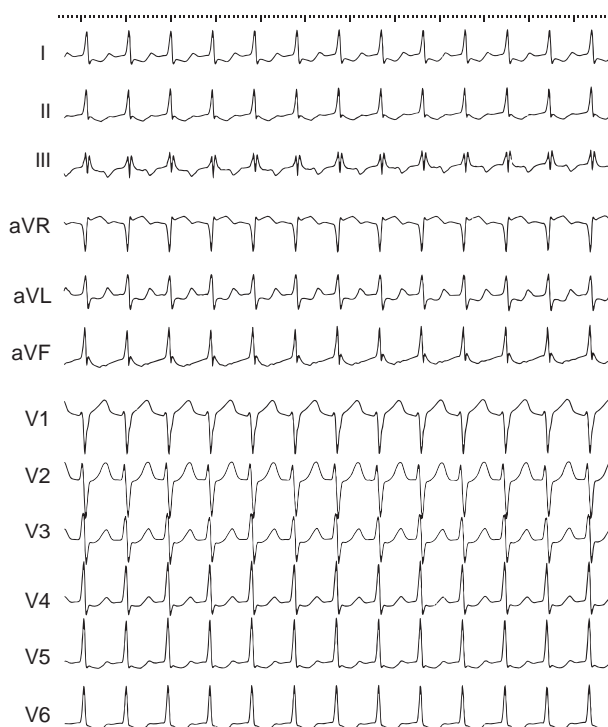


Fig. 18.5 Orthodromic and Antidromic Atrioventricular Reentrant Tachycardias (AVRTs) in a Patient With a Bidirectional Left Posteroseptal Bypass Tract (BT). Ventricular preexcitation is evident during normal sinus rhythm (NSR). The narrow complex tachycardia represents orthodromic AVRT using the BT as the retrograde limb of the reentrant circuit. Antidromic AVRT utilizes the BT for anterograde atrioventricular conduction, resulting in wide complex tachycardia.

that most patients with BT and AF who undergo BT ablation are cured of both AVRT and AF is compatible with this hypothesis. Another possibility is that the complex geometry of networks of BTs predisposes to AF by fractionation of the activation wavefronts. Localized reentry has been recorded in some patients, using direct recordings of the activation of the BTs. Hemodynamic changes, atrial stretch caused by atrial contraction against closed AV valves during ventricular systole, can also play a role. Ablation of the BT can cure AF in more than 90% of

patients; however, vulnerability to AF persists in up to 56%, and the response to atrial extrastimulation (AES) is also unaltered by ablation.

AF in younger WPW patients is usually associated with the BT and is unlikely to occur after ablation; in contrast, older patients may have recurrence of AF from causes unrelated to the BT. Nonetheless, recent studies have challenged the role of BT ablation in modulating the risk of AF particularly in adult patients, and show persistently higher rates of AF in WPW patients (hazard ratio, 4.77) compared with the general



Fig. 18.6 Antidromic Atrioventricular Reentrant Tachycardia (AVRT) Converting Into Nonsustained Preexcited Atrial Fibrillation (AF). Normal sinus rhythm (NSR) follows. Preexcitation is mediated via a left anterior bypass tract.

population despite catheter ablation of the BT.⁴ Trends of increased risk of AF in ablated WPW patients suggest that mechanisms other than those directly related to the presence of a BT, such as underlying atrial myopathy, may play a role in AF genesis.

Atrial Flutter

About 4% of WPW patients present with AFL. AFL is the most common (60%) regular preexcited tachycardia in patients with WPW syndrome. AFL is caused by a macroreentrant circuit within the RA and therefore exists independently of the BT, and AFL does not have the same causal association to AV BTs as AF. In some patients with WPW syndrome who develop AFL, AVRT is often the initiating event. This relationship can be mediated by contraction-excitation feedback into the atria during the AVRT.

AFL, like AF, can conduct anterogradely via a BT causing a preexcited tachycardia. Depending on the various refractory periods of the normal and pathological AV conduction pathways, AFL can potentially conduct 1:1 to the ventricles during a preexcited tachycardia, making the arrhythmia difficult to distinguish from VT (see Fig. 12.10).

Ventricular Fibrillation and Sudden Cardiac Death

The mechanism of sudden cardiac death (SCD) in patients with WPW is likely the occurrence of AF or AFL with a very rapid ventricular rate, which provokes VF. Although the frequency with which AF with rapid AV conduction via a BT degenerates into VF is unknown, the incidence of SCD in patients with WPW syndrome is rather low, ranging from 0% to 0.39% annually in several large case series. The trigger for AF in this population of patients is generally an episode of AVRT. In fact, most patients who have been resuscitated from VF secondary to pre-excitation have a previous history of AVRT, AF, or both. Nonetheless, SCD can be the first manifestation of WPW syndrome.⁵

Several factors can help identify the patient with WPW who is at increased risk for VF, including symptomatic AVRT, septal location of the BT, presence of multiple BTs, and male gender. In addition, the risk of SCD associated with WPW appears highest in the first two decades of life.¹ Nonetheless, it is clear that the most important factor for the occurrence of VF in these patients is the ability of the BT to conduct rapidly to the ventricles. This is best measured by determining the shortest and average preexcited R-R intervals during AF or, alternatively,

by measuring the anterograde ERP of the BT. If the BT has a very short anterograde ERP (less than 250 milliseconds), a rapid ventricular response can occur with degeneration of the rhythm to VF. A short preexcited R-R interval during AF (≤ 220 milliseconds) appears to be a sensitive clinical marker for identifying children at risk for SCD, although its positive predictive value in adults is only 19% to 38%.⁵

Drug therapy can be an additional determinant of the risk of VF in patients with preexcitation. Several pharmacological agents can potentially enhance BT conduction and increase the ventricular rate during AF and, hence, increase the risk of VF (see later).

Ventricular Tachycardia

Coexisting VT is uncommon in patients with WPW syndrome because structural heart disease is very infrequent in this young patient population. Naturally, older patients are subject to coronary artery and other diseases that can cause VT.

EPIDEMIOLOGY AND NATURAL HISTORY

Wolff-Parkinson-White Pattern

The prevalence of WPW pattern on the surface ECG is 0.1% to 0.3% in the general population.¹ The prevalence is increased to 0.55% among first-degree relatives of affected patients, suggesting a familial component. The annual incidence of newly diagnosed cases of preexcitation in the general population was substantially lower (0.004%) in a diverse population of residents from Olmsted County, Minnesota, 50% of whom were asymptomatic. The incidence in men is twice that in women, and is highest in the first year of life, with a secondary peak in young adulthood.⁵

The WPW pattern on the surface ECG can be intermittent and can even permanently disappear with loss of anterograde but preserved retrograde conduction. Loss of preexcitation has been observed in up to 31% of adults and in 0% to 33% of children and adolescents over a 5-year time period. Intermittent and persistent loss of preexcitation may indicate that the BT has a relatively longer baseline ERP, which makes it more susceptible to age-related degenerative changes and variations in autonomic tone.⁶

Wolff-Parkinson-White Syndrome

The prevalence of the WPW syndrome is substantially lower than that of the WPW ECG pattern. At present, it is estimated that approximately 65% of adolescents and 40% of adults over 30 years of age with a WPW pattern on a resting ECG are asymptomatic.⁵

The occurrence of arrhythmias is related to the age at the time preexcitation is discovered and can vary with location and EP properties of the BT. AVRT manifests early in life, with an average of more than 10 years separating the time of clinical presentation of AVRT versus that of AVNRT.¹ Up to 70% of children (8 to 12 years of age) who are asymptomatic at the time of diagnosis of WPW ECG pattern remain asymptomatic over median follow-up of 57 months. About 30% eventually develop an arrhythmic event, which can be potentially life-threatening in approximately 10% of patients. In contrast, only a minority (10%) of adults who are asymptomatic at the time of diagnosis of ventricular preexcitation develop cardiac arrhythmias over median follow-up of 67 months, which can be potentially life-threatening in approximately 5% of patients. The vast majority of patients in whom preexcitation is first uncovered after the age of 40 remain asymptomatic.⁵ In a large meta-analysis, the annual risk of developing SVT was 0.25% of WPW patients.⁷

A male predominance among WPW patients has been observed. Furthermore, men tend to have a higher incidence of antidromic AVRT, more prevalent left-sided BTs, and shorter anterograde BT ERP. Also,

men usually present with AVRT at an older age than women. In contrast, women were found to have a higher prevalence of multiple BTs, orthodromic AVRT, and right-sided BTs. In addition, Asians appear to have right free-wall BTs substantially more frequently than other races.^{8,9}

Sudden Death

The incidence of SCD among patients with asymptomatic preexcitation is difficult to ascertain. A large meta-analysis (including 1869 patients with asymptomatic ventricular preexcitation from 20 studies with 11,722 patient-years of follow-up) found a total of 10 cases of SCD, with SCD rates between 0 and 4.5 events per 1000 person-years of follow-up, and an overall risk of SCD in adults and children of 2.5 per 1000 person-years (or 3% to 4% over a lifetime). Italian studies reported all but one SCD event.^{6,7}

In general, children seem to have a numerically higher event rate than adults. The majority of victims were between the ages of 10 and 40 years. Patients with WPW who are most susceptible to SCD are symptomatic; however, SCD can be the first event in patients with asymptomatic preexcitation.⁷ Several characteristics have been reported among patients who experienced potentially life-threatening events, including younger age (less than 30 years), male gender, history of AF, prior syncope, associated congenital or other heart disease, and familial WPW. Low-risk WPW patients also showed a characteristic EP profile (older age, lower tachyarrhythmia inducibility, longer anterograde refractory ERP of BTs, and low likelihood of baseline retrograde BT conduction or multiple BTs).⁷

Associated Cardiac Abnormalities

Most patients with AV BTs do not have coexisting structural cardiac abnormalities, except for those that are age related. The association of ventricular preexcitation with structural congenital heart defects is well recognized. Up to 20% of children with WPW also have congenital heart disease. Associated congenital abnormalities, when present, are more likely to be right sided than left sided. Ebstein anomaly is the congenital lesion most strongly associated with the WPW syndrome. As many as 10% of such patients have one or more BTs; most of these are located in the right free-wall or the right posteroseptal space. Ventricular preexcitation has also been described in patients with transposition of great arteries, pulmonary atresia, patent ductus arteriosus, tetralogy of Fallot, total anomalous pulmonary venous return, and ventricular septal defects.^{5,6}

Familial Wolff-Parkinson-White Syndrome

Typically, WPW syndrome occurs sporadically; however, in a minority of cases it is inherited. A familial form of WPW has infrequently been reported and is usually inherited as an autosomal dominant trait. Among patients with the WPW syndrome, 3.4% have first-degree relatives with a preexcitation syndrome. The genetic cause of a rare form of familial WPW syndrome has been described. The clinical phenotype is characterized by the presence of preexcitation on the ECG, frequent SVTs (including AF), progressive conduction system disease, and left ventricular (LV) hypertrophy (distinct from sarcomeric hypertrophic cardiomyopathy). Patients typically present in late adolescence or the third decade with syncope or palpitations. Premature SCD occurred in 10% of patients. Paradoxically, by the fourth decade of life, progression to advanced SND or AV block (with the loss of preexcitation) requiring pacemaker implantation was common. Approximately 80% of the patients older than 50 years had chronic AF. Causative mutations in the *PRKAG2* gene were identified in these families. The *PRKAG2* gene encodes the gamma-2 regulatory subunit of the adenosine monophosphate (AMP)-activated protein kinase, which is a key regulator of metabolic pathways, including glucose metabolism. The penetrance

of the disease for WPW syndrome was complete, but the expression was variable. The described phenotype of this syndrome is similar to the autosomal recessive glycogen storage disease, Pompe disease. Given the function of the AMP-activated protein kinase and this similarity, the PRKAG2 syndrome is likely a cardiac-specific glycogenosis syndrome. This syndrome thus belongs to the group of genetic metabolic cardiomyopathies, rather than to the congenital primary arrhythmia syndromes. The annulus fibrosus, which normally insulates the ventricles from the atria, is thinned and disrupted by glycogen-filled myocytes, and these anomalous microscopic AV connections, rather than morphologically distinct BTs, appear to provide the anatomic substrate for ventricular preexcitation. Of note, certain mutations in PRKAG2 have been associated with nodoventricular BTs.¹⁰

Another genetic form of WPW syndrome is associated with mutations in the bone morphogenetic protein-2 (BMP2) gene, which belongs to the class of transforming growth factor, The TGF- β -superfamily of proteins, and is involved in the development of the annulus fibrosus. This syndrome is characterized by variable cognitive deficits and dysmorphic features in addition to ventricular preexcitation.¹¹

Concealed Bypass Tracts

The true prevalence of concealed BTs is unknown because, unlike the situation with the WPW ECG pattern, these BTs are concealed on the surface ECG and are only expressed during AVRT; only symptomatic patients undergo EP testing. As noted, orthodromic AVRT accounts for approximately 95% of AVRTs and 35% of all paroxysmal SVTs, and 50% of the BTs that participate in orthodromic AVRT are concealed. SVTs using a concealed BT have no gender predilection and tend to occur more frequently in younger patients than in those with AVNRT; however, significant overlap exists. PJRT most often occurs in early childhood, although clinically asymptomatic patients presenting later in life are not uncommon.

CLINICAL PRESENTATION

The majority of patients with preexcitation are asymptomatic and are discovered incidentally on an ECG obtained for unrelated reasons. When symptomatic arrhythmias occur in the WPW patient, the disorder is called the WPW syndrome. The two most common types of arrhythmias in the WPW syndrome are AVRT and AF. Patients with AVRT experience symptoms characteristic of paroxysmal SVT with abrupt onset and termination, including rapid and regular palpitations, chest pain, dyspnea, presyncope, and rarely, syncope. Episodes can last from seconds to several hours. Symptoms are usually mild and short-lived and terminate spontaneously or with vagal maneuvers. However, occasionally patients present with disabling symptoms, especially in the presence of structural heart disease.^{1,12}

AVRT, which in general is well tolerated by the patient when additional heart disease is absent, can deteriorate into AF; the latter can be a life-threatening arrhythmia if the BT has a short anterograde refractory period, resulting in very fast ventricular rates, with possible degeneration into VF and SCD. The incidence of SCD in patients with the WPW syndrome has been estimated to range from 0.15% to 0.39% over a 3- to 10-year follow-up. It is unusual for cardiac arrest to be the first symptomatic manifestation of WPW syndrome. Conversely, in about 50% of cardiac arrest cases in WPW patients, it is the first manifestation of WPW syndrome.

PJRT commonly presents as a frequently recurring or incessant tachycardia that is refractory to drug therapy and can lead to tachycardia-induced cardiomyopathy and heart failure symptoms.

Rarely, significant ventricular preexcitation during NSR can result in ventricular dysfunction secondary to dyssynchronous ventricular

contraction. Improvement of left ventricular ejection fraction has been described after ablation of septal BTs in pediatric patients.⁵

INITIAL EVALUATION

History, physical examination, and 12-lead ECG constitute an appropriate initial evaluation. In patients with brief, self-terminating episodes of palpitations, an event recorder is the most effective way to obtain ECG documentation. Also, echocardiographic examination is recommended to exclude structural heart disease.

Several other noninvasive tests have been proposed as useful for evaluating symptomatic patients and risk-stratifying patients for SCD risk. However, the sensitivity and specificity of noninvasive testing have been shown to be limited. Invasive EP testing may be considered in patients with arrhythmias and those with a WPW ECG pattern when noninvasive testing does not lead to the conclusion that the anterograde ERP of the BT is relatively long. However, a strategy to perform an EP study for all asymptomatic patients with the WPW ECG pattern for the purpose of risk stratification is still controversial and not widely accepted.

Methods for Evaluation of Bypass Tract Refractory Period

Demonstration of Intermittent Preexcitation

Intermittent preexcitation has historically been thought to confer a lower risk of SCD than persistent preexcitation. Observation of intermittent loss of the preexcitation pattern on ambulatory monitoring or serial ECGs is generally correlated with a long BT anterograde ERP. The longer refractory period of the BT decreases the frequency of manifest preexcitation during NSR and is expected to lower the risk of mediating rapid preexcited ventricular activation during AF. Nevertheless, EP studies in symptomatic patients with intermittent preexcitation found that 10% to 24% can have BTs capable of conducting at rapid rates during AF (with anterograde ERP or shortest preexcited R-R interval less than 250 milliseconds), perhaps related to autonomic influences. However, similar findings have not yet been demonstrated in asymptomatic patients with intermittent preexcitation.^{13,14}

Intermittent preexcitation can be observed on ambulatory monitoring in up to 67% of patients. It is important, however, to distinguish intermittent preexcitation from inapparent preexcitation (see later) and from a bigeminal ventricular rhythm with a long coupling interval.^{1,5} Although intermittent preexcitation is a predictor of poor anterograde conduction through the BT, it has rarely been observed in some patients with cardiac arrest. Furthermore, the presence of intermittent preexcitation does not predict retrograde conduction properties of the BT nor preclude the development of AVRT.⁵

Loss of Preexcitation During Exercise

Demonstration of a sudden loss of preexcitation (indicated by abrupt loss of the delta wave associated with prolongation of the PR interval and normalization of the QRS) during exercise is consistent with block in the BT and is consistent with a long BT ERP (greater than 300 milliseconds). Importantly, rapid AVN conduction during exercise can potentially mask persistent preexcitation. Therefore only *abrupt* and *complete* loss of preexcitation during exercise should be sought as a surrogate of a long anterograde ERP of the BT.⁵

Loss of preexcitation during exercise is a good predictor that the patient is not at risk for VF even during sympathetic stimulation. However, the frequency of block in the BT during exercise is low (approximately 10% to 20%), and thus sensitivity of this test is poor. On the other hand, persistence of preexcitation during exercise stress has a sensitivity of 96% but a specificity of only 17% in predicting either a

shortest preexcited R-R less than 250 milliseconds during AF or a BT ERP of less than 250 milliseconds (positive predictive value of 40% and negative predictive value of 88%).⁵

Bypass Tract Conduction Block in Response to Antiarrhythmic Agents

When the administration of ajmaline (1 mg/kg IV over 3 minutes) or procainamide (10 mg/kg IV over 5 minutes) results in complete block of the BT during NSR, a long anterograde ERP (greater than 270 milliseconds) of the BT is likely. The shorter the BT ERP, the less likely it would be blocked by these drugs. Also, the amount of ajmaline required to block conduction over the BT correlates with the duration of the anterograde ERP of the BT. However, the incidence of BT block in response to these drugs is low and, although the occurrence of block predicts a long ERP of the BT, failure to produce block does not necessarily suggest a short ERP. Moreover, pharmacological testing is carried out at rest and therefore does not indicate what effect the drug will have on the BT ERP during sympathetic stimulation, such as exercise, emotion, anxiety, and recreational drug use. Importantly, the specificity of loss of preexcitation after administration of sodium blockers is poor compared to the shortest preexcited R-R intervals during inducible AF. Given these limitations, pharmacologic challenge is no longer routinely utilized.⁵

Evaluation of Ventricular Response During Atrial Fibrillation

During spontaneous or induced AF, the propensity for rapid AV conduction can be judged by the interval between consecutively preexcited QRS complexes. A mean preexcited R-R interval greater than 250 milliseconds and a shortest preexcited R-R greater than 220 milliseconds predict low risk for SCD, with a negative predictive value of more than 95%; however, the positive predictive value is low (20%).⁵

Response of Preexcitation to Transesophageal Atrial Stimulation

There is good correlation between the value of the anterograde ERP of the BT obtained during single-test programmed atrial stimulation and atrial pacing at increasing rates and the ventricular rate during AF. Programmed electrical stimulation of the atrium can be performed by the transesophageal route and the value of the anterograde ERP of the BT can be determined.

Electrophysiological Testing

Programmed atrial stimulation is used to evaluate the anterograde ERP of the BT. Because BT refractoriness shortens with decreasing pacing cycle length (PCL), the ERP should be determined at multiple PCLs (preferably ≤ 400 milliseconds). In addition, atrial stimulation should be performed close to the BT atrial insertion site to obviate the effect of intraatrial conduction delay. Incremental-rate atrial pacing is performed to determine the maximal rate at which 1:1 conduction over the BT occurs. Induction of AF should be performed to determine the average and the shortest R-R interval during preexcited AF. Atrial and ventricular stimulation is also performed to evaluate inducibility of AVRT as well as the number and location of BTs.⁵

A shortest preexcited R-R interval less than 220 to 250 milliseconds during AF has been shown to be the best discriminator of those at risk of VF, with a high sensitivity (88% to 100%) and a high negative predictive value for identifying children and young adults with WPW syndrome at risk for VF. However, the positive predictive value is low (19% to 38%), largely due to the very low incidence of SCD in these patients. Also, a shortest preexcited R-R interval less than 250 milliseconds during AF has been noted in 20% to 26% of asymptomatic adults with a WPW pattern, and in up to 67% when isoproterenol is

administered. Thus, although isoproterenol raises the sensitivity of invasive EP testing, it markedly reduces the specificity.⁵

On the other hand, BT ERP less than 240 milliseconds appears to significantly correlate with only AVRT inducibility, but as an isolated variable, it is less predictive of life-threatening events and exhibits significant overlap between WPW patients with VF and those without VF. The presence of multiple BTs and the ability to induce sustained AVRT, especially when AVRT spontaneously degenerates into AF, have been proposed to predict risk of malignant ventricular arrhythmias. The lack of retrograde conduction over the BT appears to be at lower risk for SCD. However, the predictive value of these criteria remains limited and significant overlap exists.^{1,5}

PRINCIPLES OF MANAGEMENT

Acute Management

Symptomatic Patients With Concealed Bypass Tracts

Patients with orthodromic AVRT utilizing a concealed BT are treated in a similar fashion as those with paroxysmal SVT. Vagal maneuvers (including Valsalva and carotid sinus massage) are the first-line intervention for acute conversion of the tachycardia; though the overall success rate is limited (approximately 28%). If SVT persists, adenosine is recommended, and it offers a success rate of 90% to 95%. For refractory tachycardia, IV diltiazem, verapamil, or beta-blockers can terminate orthodromic AVRT in the majority of patients. Synchronized cardioversion is recommended for hemodynamically unstable patients and for those refractory or intolerant to drug therapy (Fig. 18.7).¹

Symptomatic Patients With Manifest Bypass Tracts

In patients with manifest preexcitation during NSR presenting with AVRT (orthodromic or antidromic), vagal maneuvers are the first-line intervention for tachycardia termination (see Fig. 18.7). For persistent SVT, adenosine is recommended. Importantly, adenosine should be used with caution because it can induce AF with a rapid ventricular rate in the presence of an anterogradely conducting BT. This is unusual and should not be viewed as a contraindication to adenosine use, but one should be prepared for emergency cardioversion before administering adenosine to SVT patients.¹

For refractory AVRT, IV diltiazem, verapamil, or beta-blockers can be considered to block conduction in the AVN, which represents either the retrograde or anterograde limb in the AVRT circuit. AVN blocking drugs, however, are ineffective in patients with preexcited AVRT that utilizes two separate BTs for anterograde and retrograde conduction. Drug treatment directed at the BT (ibutilide, procainamide, flecainide) may also be considered. When drug therapy fails or hemodynamic instability is present, electrical cardioversion should be considered. It is important to note that IV diltiazem and verapamil can result in hemodynamic collapse if the AVRT does not terminate or AF is induced with rapid conduction over the BT degenerating to VF, and one must be prepared for immediate electrical cardioversion if that occurs (see later).

Preexcited Atrial Fibrillation

In patients with AF or AFL, ventricular preexcitation, and rapid ventricular response, prompt direct-current cardioversion is recommended, especially when hemodynamic compromise is present. IV procainamide or ibutilide to restore NSR or slow the ventricular rate may be considered in hemodynamically stable patients. Both drugs slow BT conduction.

Importantly, drugs that preferentially slow AVN conduction without prolonging BT refractoriness (such as verapamil, diltiazem, beta-blockers, adenosine, oral or IV digoxin, and IV amiodarone) can accelerate the ventricular rate and potentially precipitate hemodynamic collapse and

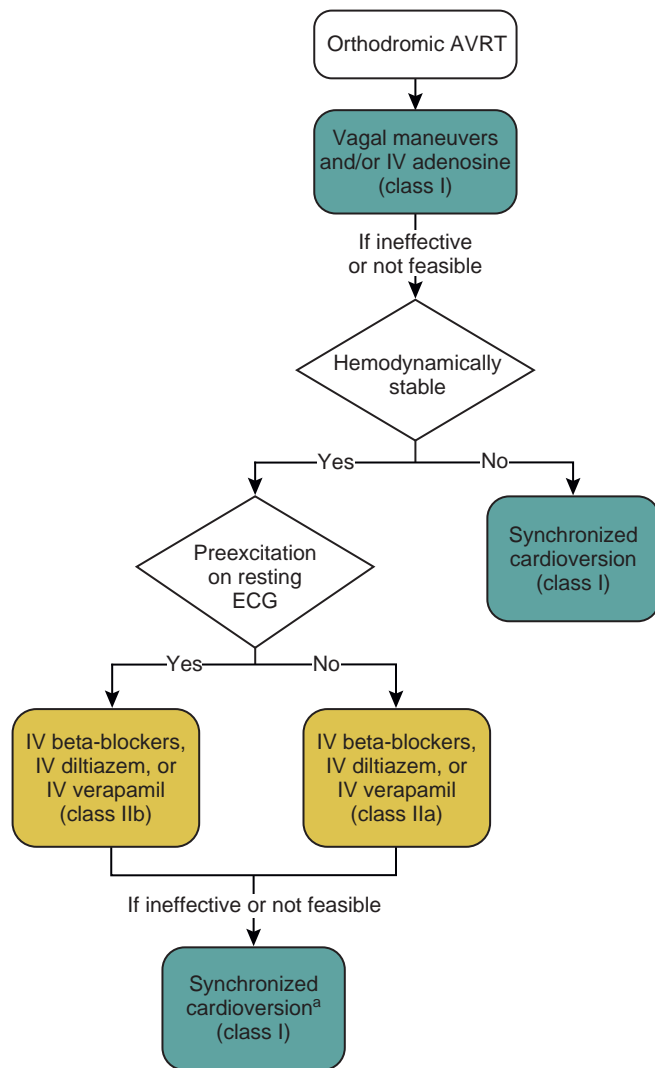


Fig. 18.7 Acute Treatment of Orthodromic Atrioventricular Reentrant Tachycardia (AVRT). ^aFor rhythms that break or recur spontaneously, synchronized cardioversion is not appropriate. IV, Intravenous. (From Page RL, Joglar JA, Caldwell MA, et al. 2015 ACC/AHA/HRS guideline for the management of adult patients with supraventricular tachycardia: a report of the American College of Cardiology/American Heart Association Task Force on Clinical Practice Guidelines and the Heart Rhythm Society. *J Am Coll Cardiol*. 2016;67:e27–e115.)

VF in high-risk patients. Several mechanisms are probably involved; hypotension produced by some of those medications is followed by a sympathetic discharge that enhances BT conduction. Furthermore, slowing or blocking conduction through the AVN prevents competitive concealed retrograde conduction into the BT by normally conducted beats and, as a result, can potentially enhance conduction over the BT. In addition, the rapid and irregular ventricular rate, hypotension, and sympathetic discharge probably result in fractionation of the ventricular wavefront and VF. Also, digoxin increases the ventricular rate by shortening BT refractoriness. Lidocaine, for reasons that are unclear, has also been associated with degeneration of AF into VF. It is occasionally used in patients with WPW who have a wide QRS complex tachycardia that might be misinterpreted as VT. Unlike the IV route of administration, chronic oral amiodarone therapy can slow or block BT conduction.¹

Chronic Management

Symptomatic Patients With Concealed Bypass Tracts

Catheter ablation is considered first-line therapy (class I) for patients with paroxysmal SVT involving a concealed BT (i.e., orthodromic AVRT). However, because concealed BTs are not associated with an increased risk of SCD in these patients, catheter ablation can be presented as one of a number of potential therapeutic approaches, including pharmacological therapy and clinical follow-up alone. When pharmacological therapy is selected for patients with concealed BTs, it is reasonable to consider a trial of beta-blocker therapy, diltiazem, or verapamil (Fig. 18.8). These agents are effective for preventing recurrent tachycardia in approximately 50% of patients. Antiarrhythmic agents may be considered for patients with refractory tachycardia; however, the risk and benefits of these drugs should be carefully considered.¹

Symptomatic Patients With Manifest Bypass Tracts

Catheter ablation is considered the treatment of choice for patients with WPW syndrome—that is, patients with manifest preexcitation along with documented arrhythmias (antidromic or orthodromic AVRT or preexcited AF) or symptoms consistent with cardiac arrhythmias. Catheter ablation is curative in more than 95% of patients with a relatively low complication rate (about 3%), and it also obviates the unwanted side effects of pharmacological therapy.¹

For patients with WPW syndrome who are not candidates for, or prefer not to undergo catheter ablation, antiarrhythmic drugs to block BT conduction are considered (see Fig. 18.8). Class IC agents such as flecainide and propafenone (in patients without structural heart disease or ischemic heart disease), and class III drugs, such as sotalol and dofetilide, may be considered. Oral amiodarone is a last resort therapy, given the associated risks of long-term therapy. In general, antiarrhythmic drug therapy can offer symptomatic improvement in up to 90% of patients, although complete disappearance of symptoms is observed in only 30%.¹

Chronic oral beta-blocker, verapamil, and diltiazem may be used for the treatment of patients with WPW syndrome, particularly if their BT has been demonstrated to be incapable of rapid anterograde conduction. However, these agents must be used with caution and after a discussion with the patient concerning the potential risk of rapid conduction over the BT if AF develops. Digoxin, on the other hand, should be avoided because it can shorten the refractory period of the BT and, hence, is potentially harmful in patients with manifest BTs.¹

Asymptomatic Patients With Manifest Bypass Tracts

Asymptomatic young WPW patients have about 30% risk of becoming symptomatic, and a very small, but definite risk of life-threatening arrhythmias and SCD. Therefore, in the recent Pediatric and Congenital Electrophysiology Society (PACES) and the Heart Rhythm Society (HRS) expert consensus document on treatment of asymptomatic young WPW subjects, risk stratification is recommended to identify a potential subgroup of patients with BTs with “high-risk” properties that may confer an increased risk for lethal cardiac arrhythmias and in whom the risk-to-benefit ratio favors prophylactic ablation (Fig. 18.9).⁵

Initial risk stratification utilizes noninvasive testing (e.g., Holter monitoring, exercise stress testing) to ascertain true loss of preexcitation at physiological heart rates. Complete and abrupt loss of preexcitation during exercise testing or intermittent loss of preexcitation during ECG or ambulatory monitoring, indicate long anterograde ERP of the BT and help identify patients at low risk of rapid conduction over the BT and SCD (Box 18.1).^{5,15}

Inability to clearly demonstrate absolute loss of ventricular preexcitation on noninvasive testing warrants consideration for transesophageal

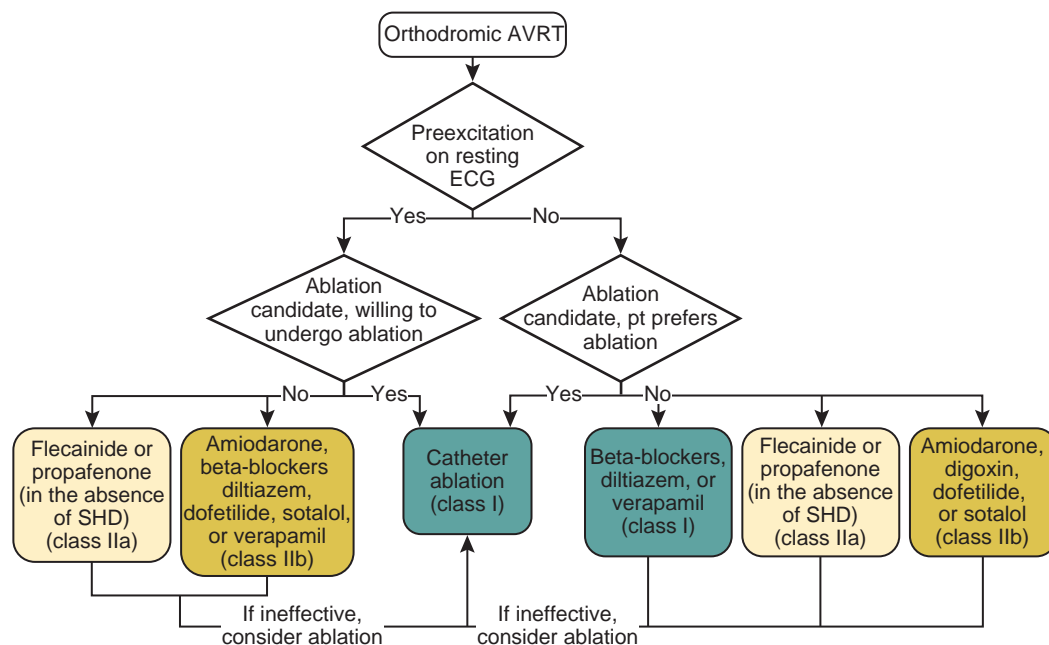
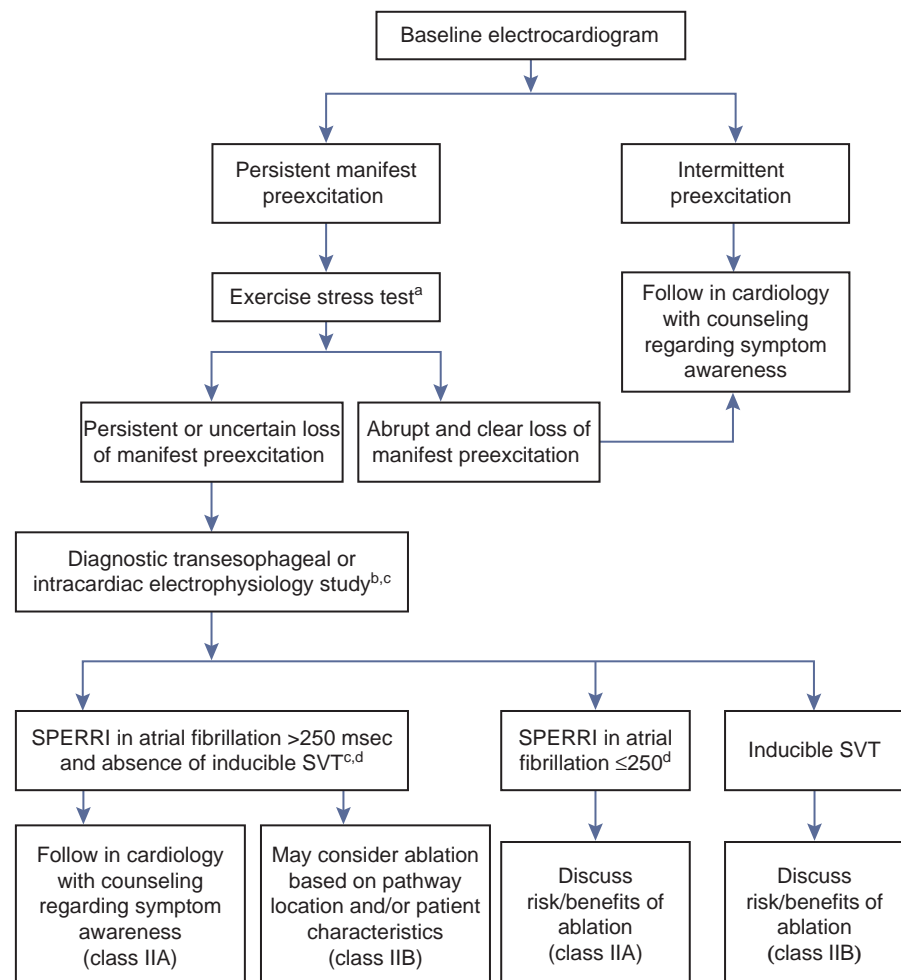


Fig. 18.8 Ongoing Management of Orthodromic Atrioventricular Reentrant Tachycardia (AVRT). Drugs listed alphabetically. *pt*, Patient; *SHD*, structural heart disease (including ischemic heart disease). (From Page RL, Joglar JA, Caldwell MA, et al. 2015 ACC/AHA/HRS guideline for the management of adult patients with supraventricular tachycardia: a report of the American College of Cardiology/American Heart Association Task Force on Clinical Practice Guidelines and the Heart Rhythm Society. *J Am Coll Cardiol*. 2016;67:e27–e115.)

Fig. 18.9 Management Algorithm for Young Asymptomatic Patients With Wolff-Parkinson-White Electrocardiogram Pattern. ^aPatients unable to perform an exercise stress test should undergo risk stratification with an electrophysiological study. ^bPrior to invasive testing, patients and their parents/guardians should be counseled on the risks and benefits of proceeding with invasive studies, risks of observation only, and risks of medication strategy. ^cPatients participating at moderate- to high-level competitive sports should be counseled concerning the risk-benefit of ablation. ^dIn the absence of inducible atrial fibrillation, the shortest preexcited R-R interval determined by rapid atrial pacing is a reasonable surrogate. *SPERRI*, Shortest pre-excited R-R interval *SVT*, supraventricular tachycardia. (From Cohen MI, Triedman JK, Cannon BC, et al. PACES/HRS expert consensus statement on the management of the asymptomatic young patient with a Wolff-Parkinson-White [WPW, ventricular preexcitation] electrocardiographic pattern. *Heart Rhythm*. 2012;9:1006–1024.)



BOX 18.1 Findings Suggestive of Lower Risk of Life-Threatening Events in Wolff-Parkinson-White Patients

- Intermittent loss of the preexcitation pattern on ambulatory monitoring or serial electrocardiograms
- Abrupt and complete loss of preexcitation during exercise
- Loss of preexcitation after administration of sodium blockers
- Mean preexcited R-R interval >250 msec and shortest preexcited R-R >220 msec during atrial fibrillation
- Anterograde effective refractory period of the bypass tract <240 msec

or intracardiac EP testing. However, the benefits and risk of invasive risk stratification should be based on individual considerations such as age, gender, occupation, and athletic involvement, and should be thoroughly discussed with the patient or, in the case of a child, with the parents. Given the low risk associated with invasive EP testing (0.1% to 1%), it is reasonable to consider this approach for risk stratification in asymptomatic WPW patients. Several EP findings help identify high-risk patients who may benefit from catheter ablation, including: (1) shortest preexcited R-R interval less than 250 milliseconds during induced AF; (2) the presence of multiple BTs; (3) spontaneous degeneration of induced AVRT into preexcited AF; and (4) BT anterograde ERP less than 240 milliseconds.¹ The critical obligatory condition for VF is the presence of a short anterograde functional refractory period of the BT, which is best reflected in the shortest R-R interval between preexcited beats in AF.^{5,16} Although the ability to induce sustained AVRT has been considered by some as a potential risk factor, this has not been supported by recent studies.²

The role of isoproterenol challenge during EP testing has not yet been clearly defined. Isoproterenol administration can significantly shorten the shortest preexcited R-R interval and, as a result, increase the proportion of asymptomatic patients in the “high-risk” category. Thus some investigators suggested the use of a more stringent threshold for the shortest preexcited R-R interval (≤ 220 milliseconds) instead of the threshold adopted by the 2012 PACES/HRS Guidelines (≤ 250 milliseconds) for definition of “high-risk” BTs when EP testing is performed under the influence of isoproterenol.¹⁷

In low-risk patients, as determined by noninvasive or invasive testing, it is appropriate to pursue a strategy of follow-up with ECGs and reevaluation at selected intervals with a high degree of suspicion for new arrhythmia symptoms. This strategy should incorporate patient education about the potential risks associated with preexcitation and the symptoms of arrhythmias that should prompt them to seek medical attention. It is also advisable to give the patient a copy of his or her ECG and a short note about the fact that the WPW pattern is present to help prevent the misdiagnosis of MI and to explain the basis of cardiac arrhythmias in case they develop later. Importantly, WPW patients most susceptible to SCD are symptomatic. Thus the evolution of the clinical status from an asymptomatic state to symptoms (e.g., syncope or palpitations) likely portends a higher risk for SCD. Once WPW patients become symptomatic, catheter ablation may be considered, regardless of the prior risk assessment.⁵

In patients with high-risk BT characteristics, prophylactic catheter ablation is reasonable. A combination of inducible AVRT and short R-R interval during preexcited AF provides the best indication for ablation. Catheter ablation of the BT, regardless of BT characteristics, is also reasonable in asymptomatic patients with high-risk occupations (e.g., school bus drivers, police, and pilots), and is probably reasonable in: (1) patients involved in moderate- to high-intensity competitive

sports; (2) patients with structural heart disease; (3) patients with ventricular dysfunction secondary to dyssynchronous contractions; and (4) patients with BT locations associated with lower risk of procedural complications (such as AV block or coronary artery injury), which can counterbalance the potential benefit of ablation. However, because knowledge about the success and complication rates plays a major role in decision-making, the physician must consider his or her own success and complication rates for ablation of the specific location of the BT identified, and that information should be made available to the patient.⁵

It is important to recognize that the majority of adult patients with asymptomatic preexcitation have a benign course with few clinically significant arrhythmic events occurring over time; the risk of SCD is low, is seen mainly in children, and is rarely the initial clinical manifestation. Hence, observation without further evaluation or treatment remains a reasonable option in these patients, even when noninvasive low-risk markers are not evident. The key is a clear understanding by the patient of the relative merits of each strategy. The well-informed patient needs to choose between a very small risk of potentially life-threatening arrhythmia over a long period of time and a one-time small procedural risk associated with EP testing and catheter ablation. Certain patients such as athletes and those in higher risk occupations will generally choose ablation. Others, especially patients older than 30 years, may prefer the small risk of a conservative strategy.^{5,18}

It is important to note that both invasive and noninvasive EP markers, despite their high sensitivity and negative predictive value, lack specificity for identifying patients at risk of life-threatening ventricular arrhythmias, largely due to the very low incidence of SCD.⁷ The great majority of individuals with WPW, even with a shortest preexcited R-R interval less than 250 milliseconds during AF, will not experience SCD; thus the positive value of predicting SCD remains very low. Therefore the management of asymptomatic patients with a WPW pattern remains controversial.⁷

The ability of noninvasive risk stratification to identify low-risk patients is low (less than 20%). Hence, according to the 2012 PACES/HRS Guidelines, invasive EP evaluation would be recommended for the majority of young asymptomatic WPW patients, and the majority of those would undergo catheter ablation. A recent report retrospectively examined the consequences of following the published guidelines in 85 asymptomatic patients (less than 18 years old) with ventricular preexcitation ECG pattern persisting at peak exercise, to assess the outcomes of invasive risk stratification applying current guidelines. Approximately 38% of the patients exhibited adverse BT properties at EP study, fulfilling either the class IIA indication (shortest preexcited R-R interval less than 250 milliseconds during AF) or class IIB indication (AVRT inducibility) for catheter ablation. The use of isoproterenol infusion during EP testing shifted an additional 36% of those tested into one of these two indication classes. About 69% of young patients subjected to risk stratification underwent BT ablation as a result of the evaluated BT properties or patient/parental decision.^{17,19}

Although complications of a diagnostic EP study are generally minor and not life-threatening, the risks associated with an ablation procedure are likely at least similar to the risk of SCD in asymptomatic WPW patients. In three large series, procedure-related complications occurred in 1.8% to 8.2% of cases, and death as a consequence of ablation occurred in 0.07% to 0.19%.⁷ If routine EP testing were to be performed in the majority of asymptomatic WPW patients, many patients would proceed immediately to catheter ablation and, in others, there would be a strong temptation to ablate when catheters are in place (regardless of predicted SCD risk), especially given the fact that the criteria for ablation usually will not be black or white. This greatly increases the risk to the patient, which can potentially nullify the benefit of elimination of SCD risk achieved by BT ablation. A recent study using decision analysis software

to construct a risk-benefit decision tree for a target population of 20- to 40-year-old asymptomatic patients with WPW, found the decision to ablate resulted in a reduction of 10-year mortality risk of 8.8 patients for 1000 patients. The study suggested that it is necessary to treat 112 asymptomatic patients with WPW to save one life over 10 years.¹⁸

Finally, the physician and the patient must have a shared understanding of the value of invasive EP study for risk stratification, rather than as a therapeutic tool. These issues have to be resolved before proceeding with invasive measures, and the risks and benefits of proceeding with ablation of BT found not to have high-risk characteristics should be discussed thoroughly with patients in advance of the EP procedure.⁵

Wolff-Parkinson-White Patients and Sports Participation

WPW syndrome accounts for approximately 1% of deaths in athletes. Although many of the cases of SCD with WPW are associated with exercise, training does not alter the EP properties in WPW.

Catheter ablation is the treatment of choice for symptomatic WPW patients (whether or not engaged in athletics). For asymptomatic WPW patients engaged in moderate- to high-level competitive sports, non-invasive and, if needed, invasive risk stratification is advisable. For those with high-risk BT characteristics, ablation of the BT is recommended before clearance for competitive sports because of risk for life-threatening arrhythmias.^{5,20} In low-risk patients, as determined by noninvasive or invasive testing, BT ablation may still be appropriate, but competitive sports may be allowed without ablation, especially when BT ablation confers an unacceptable potential risk (e.g., AV block in the setting of midseptal or superoparaseptal BTs).^{5,20}

ELECTROCARDIOGRAPHIC FEATURES

Electrocardiography of Preexcitation

Anterogradely conducting AV BTs produce the classic WPW ECG pattern characterized by a fusion between conduction via the BT and the normal AVN-HPS: (1) short PR (P-delta) interval (less than 120 milliseconds); (2) slurred upstroke of the QRS (delta wave); and (3) wide QRS (>120 milliseconds) (see Figs. 18.1 and 18.2).^{13,14}

The degree of preexcitation depends on several factors, including conduction time over the AVN-HPS, conduction time from the sinus node to the atrial insertion site of the BT (which depends on the distance, conduction, and refractoriness of the intervening atrial tissue), and conduction time through the BT (which depends on the length, thickness, and conduction properties of the BT).

Pharmacological and/or physiological maneuvers that alter AVN conduction (e.g., carotid sinus massage, Valsalva maneuvers, adenosine, beta-blockers) can be used to alter the degree of preexcitation, thereby confirming the diagnosis of the presence of an anterogradely conducting AV BT.

The ECG pattern displayed by some patients with WPW syndrome can simulate the pattern found in other cardiac conditions and can alter the pattern seen in the presence of other cardiac disease. A negative delta wave (presenting as a Q wave) can mimic a myocardial infarction (MI) pattern. Conversely, a positive delta wave can mask the presence of a previous MI. Intermittent WPW can also be mistaken for frequent premature ventricular complexes (PVCs) (Fig. 18.10). If the WPW pattern persists for several beats, the rhythm can be misdiagnosed as an accelerated idioventricular rhythm or, if sufficiently rapid, VT. The

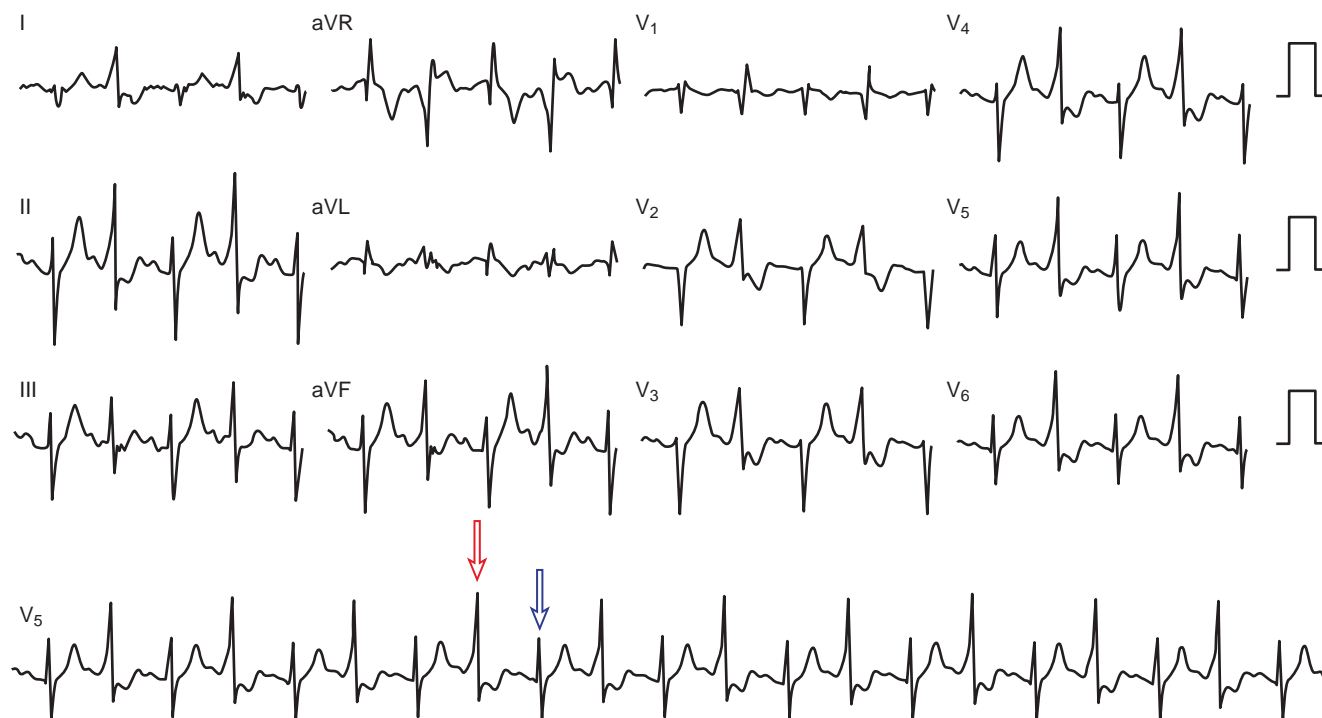


Fig. 18.10 Preexcitation Alternans. Surface electrocardiogram during sinus tachycardia demonstrating intermittent preexcitation in which a QRS complex manifesting a delta wave (red arrow) alternates with a normal QRS complex (blue arrow) (i.e., preexcitation alternans). Note the intermittent abrupt loss of delta wave associated with prolongation of the PR interval and the presence of a stable sinus rate, indicating that loss of preexcitation is secondary to anterograde block in the bypass tract (i.e., intermittent preexcitation) rather than enhanced atrioventricular nodal conduction.

WPW pattern is occasionally seen on alternate beats and may suggest ventricular bigeminy. An alternating WPW and normal pattern can occasionally suggest electrical alternans. On the other hand, late-coupled PVCs (eFig. 18.2) and ventricular pacing (eFig. 18.3) with inapparent pacing artifacts can occasionally mimic ventricular preexcitation.

Inapparent Versus Intermittent Preexcitation

Inapparent preexcitation. With inapparent preexcitation, preexcitation is absent on the surface ECG despite the presence of an anterogradely conducting AV BT because conduction over the AVN-HPS reaches the ventricle faster than that over the BT. In this setting, the PR interval is shorter than the P-delta interval would be if preexcitation were present. Therefore the transition from manifest to inapparent preexcitation is characterized by normalization of the QRS in conjunction with *shortening* of the PR interval, reflecting the now better AVN-HPS conduction.

Inapparent preexcitation is usually caused by: (1) enhanced AVN conduction, so that it is faster than conduction over the BT; (2) prolonged intraatrial conduction from the site of atrial stimulation to the atrial insertion site of the BT (most often left lateral), favoring antero-grade conduction and depolarization of the ventricle over the AVN-HPS; or (3) prolonged conduction over the BT, so that it is slower than AVN-HPS conduction.

Intermittent preexcitation. Intermittent preexcitation is defined as the presence and absence of preexcitation on serial ECGs or ambulatory cardiac monitoring (Fig. 18.11). True intermittent preexcitation is characterized by an abrupt loss of the delta wave (regardless of how fast or slow AVN conduction is), with *prolongation* (normalization) of the PR interval (reflecting the loss of the faster BT conduction, and the

subsequent conduction over the slower AVN), and normalization of the QRS in the absence of any significant change in heart rate.^{13,14}

The mechanism of intermittent preexcitation is poorly understood, but is likely related to the BT refractory period and cellular connectivity within the BT. Potential mechanisms include (1) phase 3 (i.e., tachycardia-dependent) or phase 4 (i.e., bradycardia-dependent) block in the BT (see Chapter 10); (2) anterograde or retrograde concealed conduction produced by PVCs, premature atrial complexes (PACs), or atrial arrhythmias; (3) BTs with a long ERP and the gap phenomenon in response to PACs; and (4) BTs with a long ERP and supernormal conduction.

Preexcitation alternans is a form of intermittent preexcitation in which a QRS complex manifesting a delta wave alternates with a normal QRS complex (see Fig. 18.10). **Concertina preexcitation** is another form of intermittent preexcitation in which the PR intervals and QRS complex durations show a cyclic pattern; that is, preexcitation becomes progressively more prominent over a number of QRS complex cycles followed by a gradual diminution in the degree of preexcitation over several QRS cycles, despite a fairly constant heart rate.

Differentiation between intermittent preexcitation and inapparent preexcitation on an ECG showing QRS complexes with and without preexcitation can be achieved by comparing the P-delta interval during preexcitation and the PR interval when preexcitation is absent. Loss of preexcitation associated with a PR interval longer than the P-delta interval is consistent with intermittent preexcitation (see Fig. 18.11), whereas loss of preexcitation associated with a PR interval shorter than the P-delta interval is consistent with inapparent preexcitation. Furthermore, maneuvers that slow AVN conduction (e.g., carotid sinus massage, AVN blockers) would unmask inapparent preexcitation but would not affect intermittent preexcitation.

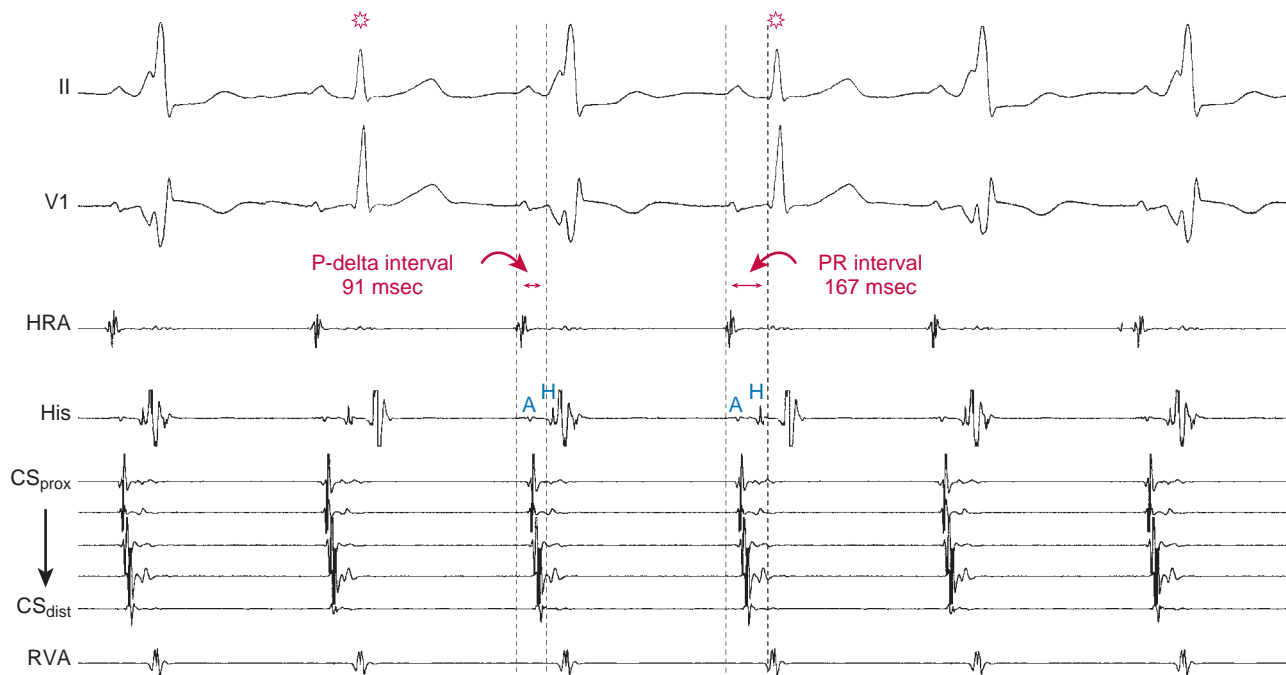
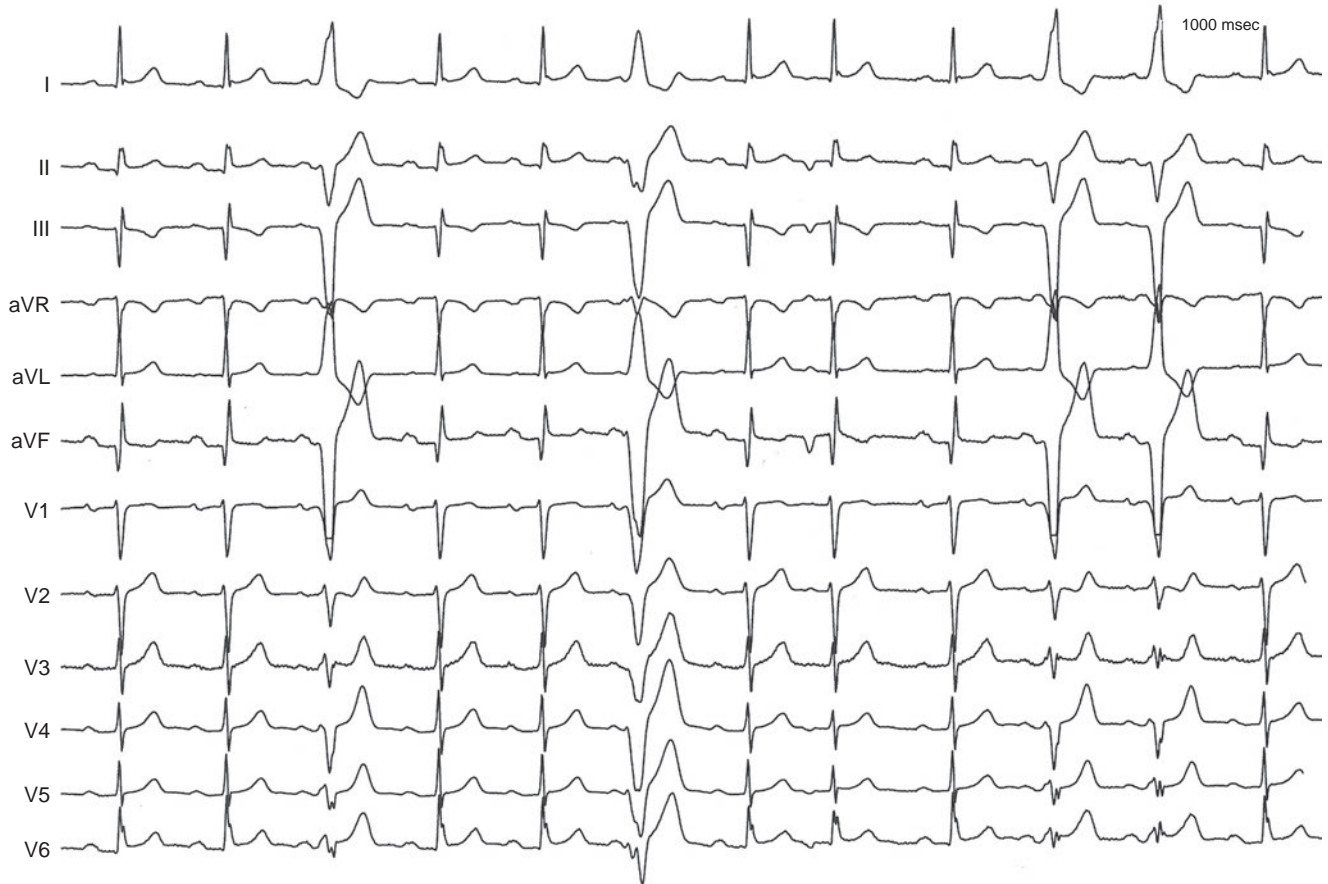


Fig. 18.11 Intermittent Preexcitation. Surface electrocardiogram leads II and V1 and intracardiac recordings in a patient with Wolf-Parkinson-White syndrome and a right anterior bypass tract (BT). Note the intermittent abrupt loss of delta wave (stars) associated with prolongation of the PR interval and normalization of the His bundle–ventricular interval, despite the presence of a constant atrial–His bundle (AH) interval (atrioventricular node [AVN] conduction) and a stable sinus rate, indicating that loss of preexcitation is secondary to antero-grade block in the BT (i.e., intermittent preexcitation) rather than enhanced AVN conduction. A, Atrial electrogram; CS_{dist}, distal coronary sinus; CS_{prox}, proximal coronary sinus; H, His bundle potential; HRA, high right atrium; RVA, right ventricular apex.



eFig. 18.2 Late-Coupled Premature Ventricular Complexes (PVCs) Mimicking Intermittent Ventricular Preexcitation. Surface electrocardiogram of normal sinus rhythm with late-coupled PVCs, which are inscribed shortly after the sinus P waves, resulting in a short PR interval and wide QRS complexes mimicking intermittent ventricular preexcitation. Note that the degree of widening of the QRS and the variability of the QRS morphology and the varying relationship to the preceding P waves all argue against ventricular preexcitation.



eFig. 18.3 Ventricular Pacing Mimicking Ventricular Preexcitation. Surface electrocardiogram (ECG) of normal sinus rhythm with atrial-tracking ventricular pacing. The QRS complexes are the result of fusion from ventricular pacing and conduction over the normal atrioventricular conduction axis, resulting in a pseudo-delta wave, mimicking a Wolf-Parkinson-White ECG pattern. The pacing artifacts are very small, but careful inspection reveals those artifacts most clearly in lead III.

Supraventricular Tachyarrhythmias Associated With Wolff-Parkinson-White Syndrome

Orthodromic Atrioventricular Reentrant Tachycardia

The ECG during orthodromic AVRT shows retrograde P waves inscribed within the ST-T wave segment with an RP interval that is usually less than half of the tachycardia R-R interval (i.e., RP interval < PR interval) (Fig. 18.12). The RP interval remains constant, regardless of the tachycardia cycle length (TCL), because it reflects nondecremental retrograde conduction over the BT. QRS morphology during orthodromic AVRT is generally normal and not preexcited, even when preexcitation is present during NSR (see Fig. 18.5). Functional bundle branch block (BBB) can be observed frequently during orthodromic AVRT at fast rates (see Fig. 18.12). The presence of BBB during SVT in a young person (less than 40 years) should raise the suspicion of orthodromic AVRT incorporating a BT ipsilateral to the blocked bundle, because the longer conduction time through the involved ventricle engendered by the BBB facilitates orthodromic reentry by enabling all portions of the circuit enough time to recover excitability from the prior cycle. This is particularly true with left bundle branch block (LBBB), which is very uncommon in younger patients.

Orthodromic AVRT tends to be a rapid tachycardia, with rates ranging from 150 to more than 250 beats/min, generally faster in younger people. A beat-to-beat oscillation in QRS amplitude (QRS alternans) is present in up to 38% of cases and is most commonly seen when the rate is very rapid (Fig. 18.13). The mechanism for QRS alternans is not clear but may partly result from oscillations in the relative refractory period of the distal portions of the HPS.

Ischemic-appearing ST segment depression also can occur during orthodromic AVRT, even in young individuals who are unlikely to have coronary artery disease. An association has been observed between repolarization changes (ST segment depression or T wave inversion) and the underlying mechanism of the tachycardia because such changes are more common in orthodromic AVRT than AVNRT (57% vs. 25%). Several factors can contribute to ST segment depression in these arrhythmias, including changes in autonomic tone, intraventricular conduction disturbances, a longer VA interval, and a retrograde P wave of longer duration that overlaps into the ST segment.²¹ The location of the ST segment changes can vary with the location of the BT; ST segment depression in leads V3 to V6 is almost invariably seen with a left lateral BT, whereas ST segment depression and a negative T wave in the inferior leads is associated with a posteroseptal or posterior BT. A negative or notched T wave in leads V2 or V3 with a positive retrograde P wave in at least two inferior leads suggests an anteroseptal BT. However, ST segment depression occurring during orthodromic AVRT in an older patient mandates consideration of possible coexisting ischemic heart disease.

Antidromic Atrioventricular Reentrant Tachycardia

Antidromic AVRT is characterized by a wide (fully preexcited) QRS complex, usually regular R-R intervals, and ventricular rates of up to 250 beats/min (see Fig. 18.5). The width of the preexcited QRS complex and the amplitude of the ST-T wave segment usually obscure the retrograde P wave on the surface ECG. When the P waves can be identified, they are inscribed within the ST-T wave segment with an RP interval that may be more than half of the tachycardia R-R interval because retrograde conduction occurs slowly via the AVN-HPS. The PR (P-delta) interval remains constant, regardless of the TCL, because it represents nondecremental anterograde conduction over the BT.

Permanent Junctional Reciprocating Tachycardia

PJRT tends to be incessant, stopping and starting spontaneously every few beats without initiating PACs or PVCs. The heart rate is usually

between 120 and 200 beats/min and the QRS duration is generally normal. Slow retrograde conduction over the BT causes the RP interval during PJRT to be long, usually more than half of the tachycardia R-R interval (Fig. 18.14). The P waves resulting from retrograde conduction are easily seen on the ECG and are inverted in leads II, III, aVF, and V3 to V6.

Atrioventricular Nodal Reentrant Tachycardia and Atrial Tachycardia

Both AVNRT and AT can be associated with partially or fully preexcited QRS complex secondary to anterograde conduction to the ventricles over the bystander BT. When AVNRT occurs in the WPW syndrome, the arrhythmia can be difficult to distinguish from orthodromic AVRT without EP testing.

Atrial Fibrillation

There are several characteristic findings on the ECG in patients with AF conducting over a BT, so-called preexcited AF. The rhythm is irregularly irregular, and can be associated with very rapid ventricular response caused by the nondecremental anterograde AV conduction over the BT (Fig. 18.15). However, a sustained rapid ventricular rate of more than 180 to 200 beats/min will often create R-R intervals that appear to be regular when the ECG is recorded at 25 mm/s. Although the QRS complexes are conducted aberrantly, resembling those during preexcited NSR, their duration can be variable and they can become normalized. This is not related to the R-R interval (i.e., it is not a rate-related phenomenon), but rather is related to the variable relationship between conduction over the BT and AVN-HPS. Preexcited and normal QRS complexes often appear “clumped.” This can result from concealed retrograde conduction into the BT or the AVN (Fig. 18.16).

The QRS complex during preexcitation is a fusion between the impulse that preexcites the ventricles caused by rapid conduction through a BT and the impulse that takes the usual route through the AVN. The number of impulses that can be transmitted through the BT and the amount of preexcitation depend on the refractoriness of the BT and AVN. The shorter the anterograde ERP of the BT, the more rapid is the anterograde impulse conduction over the BT and, because of more preexcitation, the wider the QRS complexes. Patients who have a BT with a very short ERP and rapid ventricular rates represent the group at greatest risk for development of VF.

Anterograde block in the BT during AF abolishes retrograde concealment into the AVN, which in turn allows the AVN to recover its excitability and conduct anterogradely. In turn, these conducted impulses through the AVN can result in retrograde concealment into the BT, causing anterograde block of the BT and, thereby, slowing the ventricular rate.

Atrial Flutter

AFL, like AF, can conduct anterogradely via a BT resulting in a preexcited tachycardia. Depending on the various refractory periods of the normal and pathological AV conduction pathways, AFL can potentially conduct 1:1 to the ventricles during a preexcited tachycardia, making the arrhythmia difficult to distinguish from VT (see Fig. 12.10).

Electrocardiographic Localization of the Bypass Tract

Careful analysis of the preexcitation pattern during NSR can potentially allow an accurate approximation of the location of the BT. This provides the electrophysiologist with important information that can guide patient counseling regarding the risks and benefits of ablation. In particular, it provides some guidance about the proximity of the BT to the normal conduction system and the subsequent risk of AV block associated with an ablation attempt, as well as the need for left heart catheterization

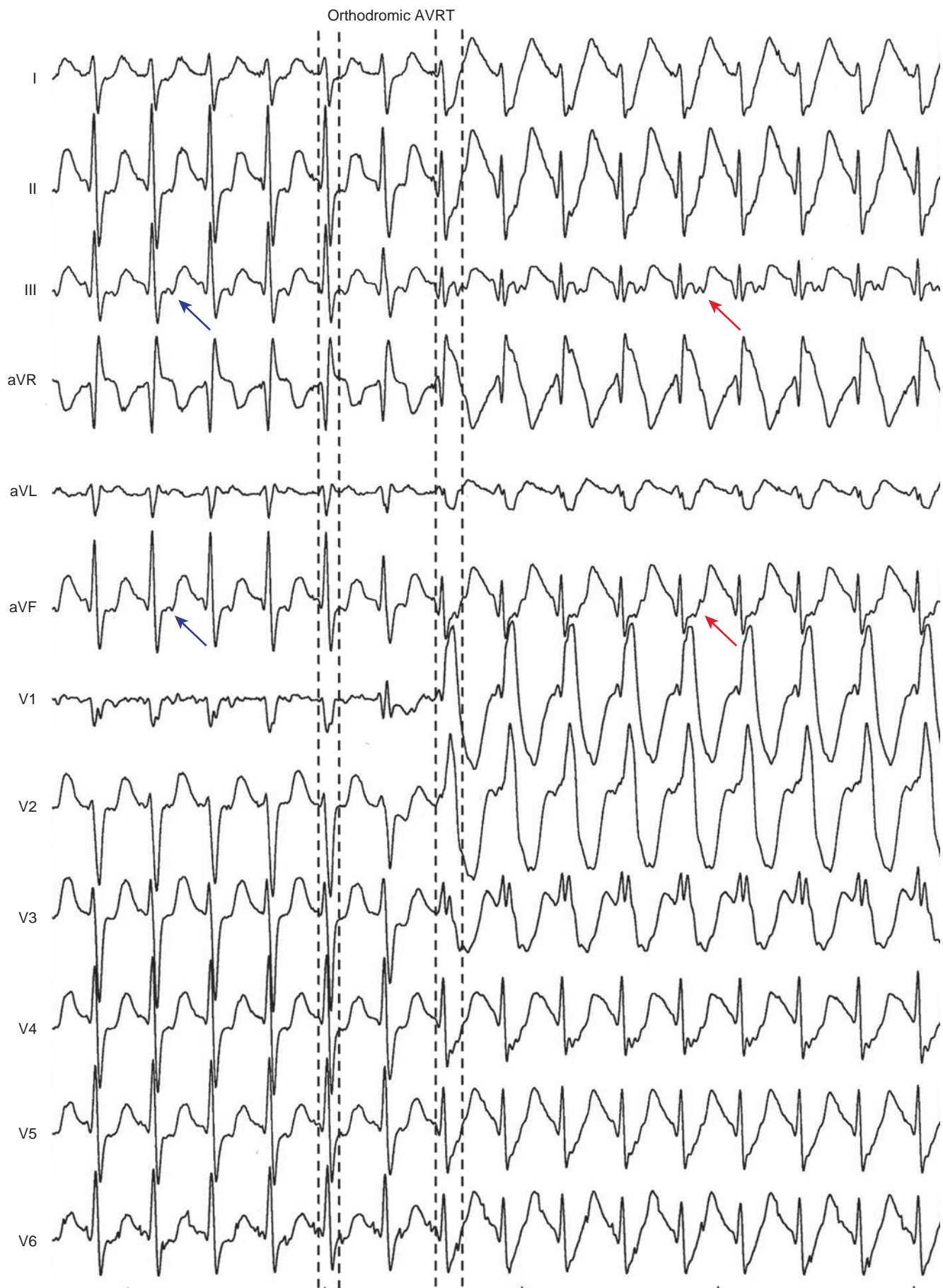


Fig. 18.12 Orthodromic Atrioventricular Reentrant Tachycardia (AVRT) Using a Concealed Superoparaseptal Bypass Tract (BT). Note the P waves (arrows) inscribed within the ST-T wave segment (short RP interval). Ischemic-appearing ST segment depression is also observed. Functional right bundle branch block occurs in the right side of the tracing, with prolongation of the RP (ventriculoatrial [VA]) interval, suggesting that retrograde VA conduction during the supraventricular tachycardia is mediated by a right-sided BT. The dashed lines denote the QRS onset and P wave onset.

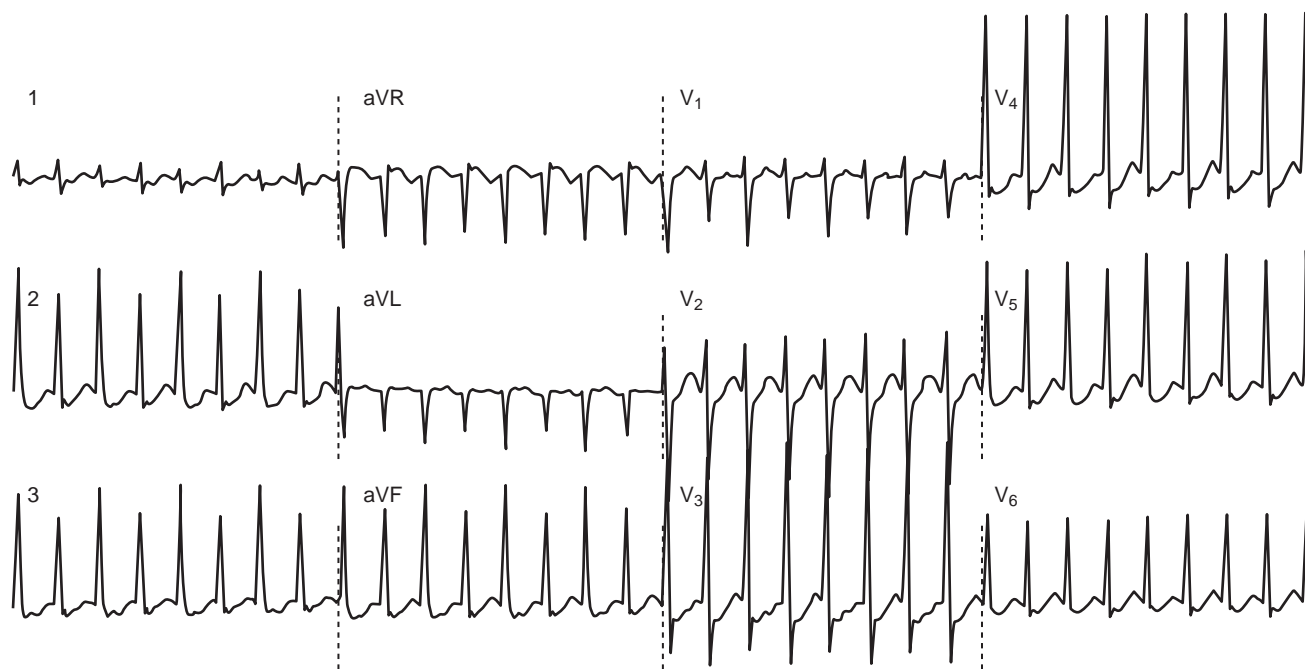


Fig. 18.13 Electrocardiogram (ECG) of Orthodromic Atrioventricular Reentrant Tachycardia Showing QRS Alternans in Multiple ECG Leads.

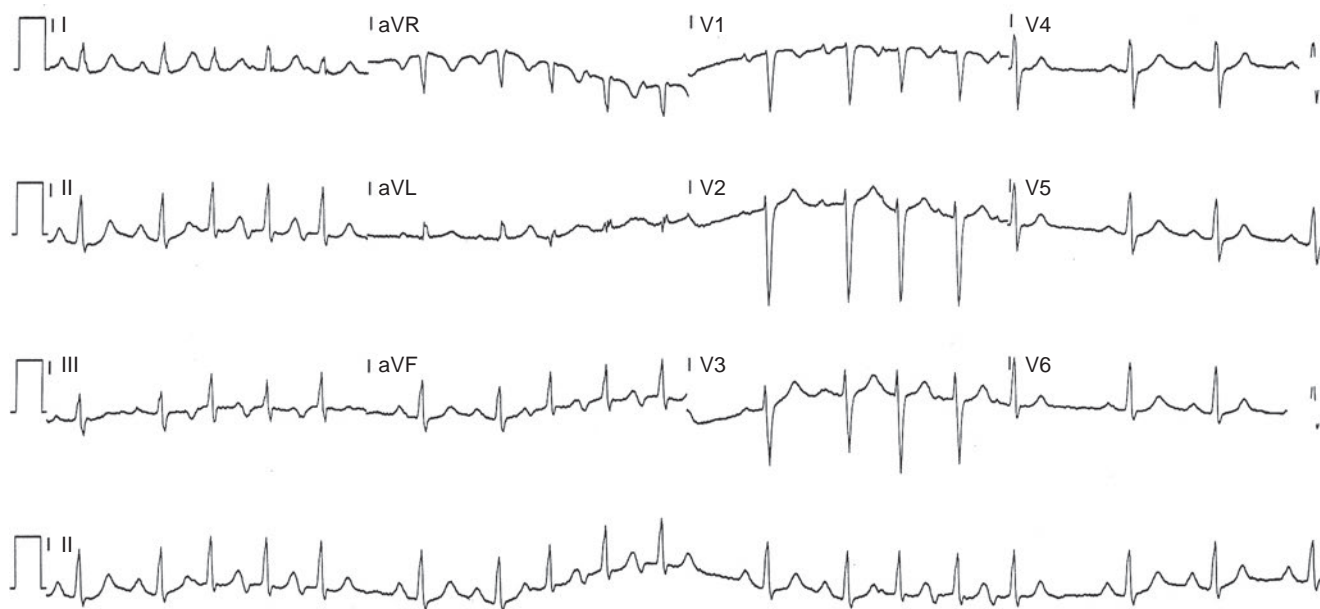


Fig. 18.14 Surface Electrocardiogram (ECG) of Permanent Junctional Reciprocating Tachycardia (PJRT). Note the incessant nature of the arrhythmia, stopping and starting spontaneously every few beats without initiating atrial or ventricular ectopic beats. Slow retrograde conduction over the bypass tract causes the RP interval during PJRT to be long (long RP tachycardia). The P waves resulting from retrograde conduction are easily seen on the ECG and are inverted in the inferior leads.

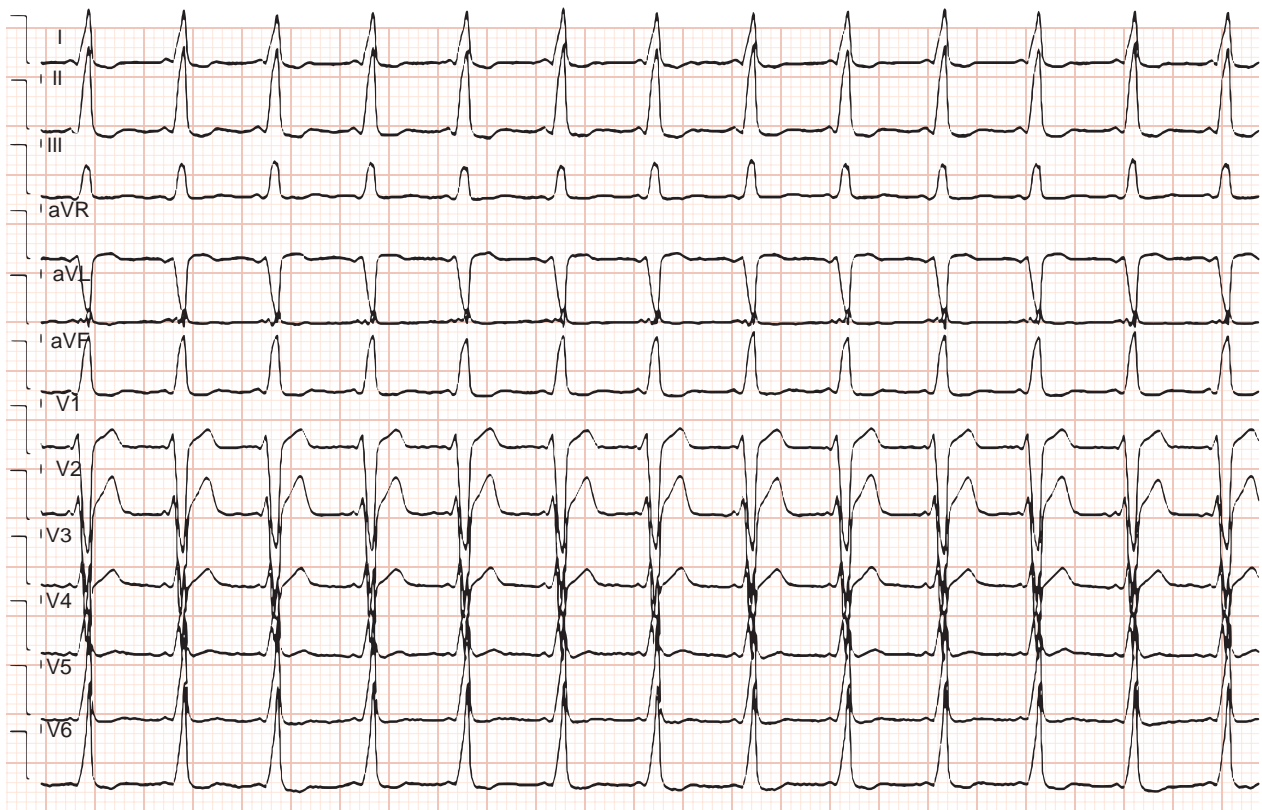
and atrial septal puncture and their potential complications. In addition, it can help in planning the ablation procedure, such as the use of cryoablation for septal BTs or the need for special equipment for atrial septal puncture for left-sided BTs.

Localization Using the Delta Wave

Delta wave morphology reflects the ventricular insertion site of the BT and, hence, is helpful in approximating the BT location, especially when

maximal preexcitation is present. However, during NSR, only partial ventricular preexcitation is usually observed, which limits the accuracy of BT localization based on the surface ECG. In addition, the degree of preexcitation can vary in an individual, depending on heart rate, autonomic tone, and AVN function, as well as the location and EP characteristics of the BT. Therefore it is important first to assess the degree of preexcitation visible throughout the entire ECG and then use only delta wave polarity for localization (the first 20 to 60 milliseconds

Sinus rhythm with ventricular preexcitation



Preexcitation atrial fibrillation



Fig. 18.15 Electrocardiogram of Sinus Rhythm Atrial Fibrillation With Ventricular Preexcitation. Ventricular preexcitation by the same right superoparaseptal bypass tract. Note the fast ventricular rate during preexcited atrial fibrillation (exceeding 100 beats/min).



Fig. 18.16 Preexcited Atrial Fibrillation. Note the “clumping” of preexcited and normal QRS complexes, likely due to concealed retrograde conduction into the bypass tract or the atrioventricular node.

of the QRS in most cases, unless fully preexcited) rather than the overall QRS polarity, which may vary from each other.

Several algorithms have been developed to predict the anatomic location of manifest BTs based on delta wave polarity on the surface ECG (Box 18.2; Figs. 18.17–18.20). Although these algorithms facilitate prediction of the location of a BT, they are inherently limited by biological variability in anatomy (e.g., rotation of the heart within the thorax), variable degree of preexcitation and QRS fusion, the presence of more than one manifest BT, intrinsic ECG abnormalities (such as prior MI and ventricular hypertrophy), patient body habitus, and technical variability in ECG acquisition and electrode positioning. The accuracy of these algorithms in more recent studies has not reached the accuracy previously reported by their designers.²² Therefore these algorithms should be regarded as an orientation rather than a precise localization tool. No single published algorithm offers extremely high sensitivity and specificity for all BT locations. The algorithms appear most accurate in predicting left free-wall BT locations and least accurate in predicting midseptal or right anteroseptal BT locations. Hence, it may be more realistic to initially identify a general area in which the BT is located, and then to apply more subtle criteria from one or more of the algorithms to attempt a more precise localization. This can be achieved by applying some basic rules while maintaining a mental 3-D representation of the mitral and tricuspid annuli and their anatomical relationships to adjacent structures as they lie within the chest (i.e., “attitudinally correct orientation”) while analyzing the ECG and predicting morphology of the preexcited QRS.

Of note, the mere presence and the degree of preexcitation can sometimes help in predicting the location of the BT. Posteroseptal and right-sided BTs tend to be associated with a prominent degree of preexcitation because of the proximity to the sinus node, whereas left lateral BTs are often associated with subtle preexcitation. Nevertheless, when preexcitation is prominent, the accuracy of surface ECG localization of manifest BTs tends to be higher for the diagnosis of left free-wall BTs than for BTs in other locations.

On the surface ECG, analysis of delta wave polarity and amplitude progression in precordial leads, and frontal plane horizontal and vertical axes, are valuable for predicting the site of origin of manifest BTs (Fig. 18.21).

Precordial transition. Lead V1 is a unipolar lead positioned at the right anterior chest wall. Therefore, as the BT location shifts progressively more to the left or posteriorly, the precordial transition (i.e., the first precordial lead where the R wave amplitude exceeds the S wave amplitude) becomes sequentially earlier, thereby transforming the precordial preexcited QRS morphology from a late transition LBBB pattern of the preexcited QRS to a positively concordant right bundle branch block (RBBB) pattern. Hence, left-sided BTs exhibit positive delta waves in lead V1, while right-sided BTs exhibit negative delta waves. The farther the BT is to the left or posteriorly on the mitral annulus, the larger the positive delta wave, and the farther the BT is to the right along the tricuspid annulus, the deeper the negative delta wave is in lead V1.

Frontal plane horizontal axis. Lead I primarily reflects the horizontal axis. BTs closer to the left axilla will produce a deeply negative

BOX 18.2 Delta Wave Characteristics During Preexcitation According to Bypass Tract Location^a**Left Lateral/Left Anterolateral BTs**

- A. R/S ≥ 1 in V2 and positive delta in III, or R/S < 1 in V2 and positive delta in III and V1
- B. RS transition $\leq V1$ and > 2 positive delta in the inferior leads or S $>$ R in aVL
- C. QS or QR morphology in aVL and no negative QRS in III and V1

Left Posterior/Left Posterolateral BTs

- A. R/S ≥ 1 in V1 and V2, no positive delta in III and positive delta in V1
- B. R/S transition $\leq V1$, no ≥ 2 positive delta in the inferior leads, no S $>$ R in aVL, in lead I R $<$ (S 0.8 mV), and the sum of the inferior delta is not negative
- C. Positive QRS in aVL and an equiphasic QRS or positive in V1 and no negative QRS in III

Left Posteroseptal BTs

- A. R/S ≥ 1 in V2, no positive delta in III, and positive delta and R/S < 1 in V1
- B. R/S transition $\leq V1$, no ≥ 2 positive delta in the inferior leads, no S $>$ R in aVL, in lead I R $<$ (S 0.8 mV), and the sum of the inferior delta is negative
- C. Negative QRS in III, V1, and aVF, tallest precordial R wave in V2–V4 and R wave width in V1 > 0.06 msec

Midseptal BTs

- A. R/S < 1 in V2, no positive delta in III, and negative delta in V1
- B. R/S transition between V2 and V3 or between V3 and V4 but the delta amplitude in lead II ≥ 1.0 mV (septal location), and the sum of delta polarities in inferior leads is -1 , 0 , or $+1$ mV
- C. Negative QRS in leads III, V1, and aVF, tallest precordial R in leads V2–V4 and R wave width in V1 < 0.06 msec

Right Posteroseptal BTs

- A. R/S ≥ 1 in V2 and no positive delta in III and V1
- B. The sum of delta polarities in inferior leads is less than or equal to -2 mV
- C. Negative QRS in leads III, V1, and aVF and tallest precordial R in V5 or V6

Right Posterior/Right Posterolateral BTs

- A. R/S < 1 in V2, no positive delta in III and no negative delta in V1, and negative delta polarity in aVF
- B. R/S transition between V3 and V4 with delta amplitude in lead II < 1.0 mV or $\geq V4$ and the delta axis is < 0 degrees and the R in lead III is ≤ 0 mV
- C. Positive QRS in III, negative in V1, and RS morphology in aVL

Right Lateral/Right Anterolateral BTs

- A. R/S < 1 in V2, no positive delta in III and no negative delta in V1 and negative or biphasic delta in aVF
- B. R/S transition between leads V3 and V4 with delta amplitude in lead II < 1.0 mV or $> V4$ and the delta axis is < 0 degrees and the R amplitude in lead III is < 0 mV
- C. Positive QRS in leads aVL and III and negative in V1

Right Anterior/Right Superoparaseptal BTs

- A. R/S < 1 in V2, positive delta in III and no positive delta in V1
- B. The sum of delta polarities in inferior leads is ≥ 2
- C. Positive QRS in aVF and negative in leads III and V1

^aA, algorithm of Chiang and colleagues; B, algorithm of Fitzpatrick and colleagues; C, algorithm of Xie and colleagues.

BT, Bypass tract; R/S, R-S wave ratio.

From Katsouras CS, Greakas GF, Goudevenos JA, et al. Localization of accessory pathways by the electrogram. *Pacing Clin Electrophysiol.* 2004;27:189.

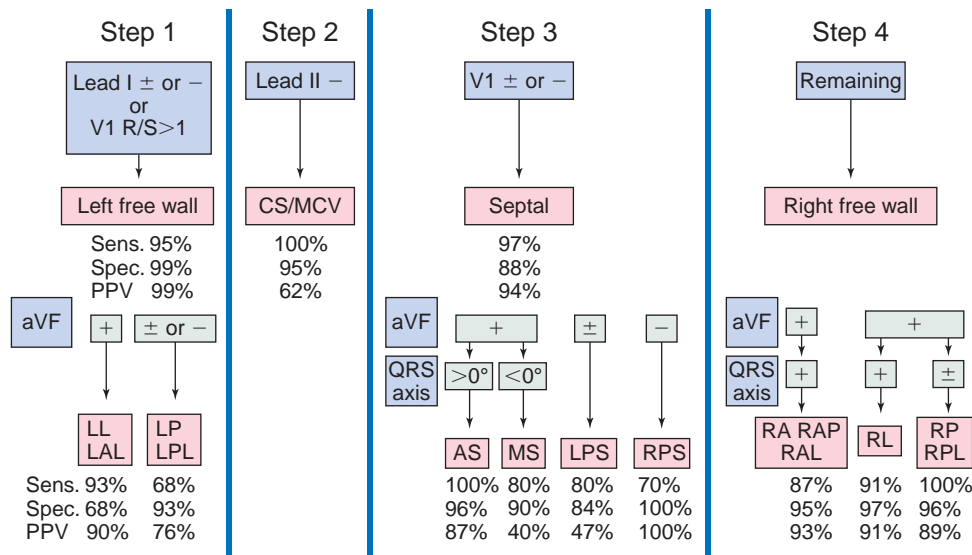


Fig. 18.17 Algorithm for Localization of Bypass Tract Using Delta Wave Morphology on the Surface Electrocardiogram. +, Positive delta wave; ±, isoelectric delta wave; −, negative delta wave; AS, right anteroseptal; CS/MCV, coronary sinus/middle cardiac vein; LAL, left anterolateral; LL, left lateral; LP, left posterior; LPL, left posterolateral; LPS, left posteroseptal; MS, midseptal; PPV, positive predictive value; RA, right anterior; RAL, right anterolateral; RAP, right anterior paraseptal; RL, right lateral; RP, right posterior; RPL, right posterolateral; RPS, right posteroseptal; R/S, R-S wave ratio; Sens., sensitivity; Spec., specificity. (From Arruda M, Wang X, McClelland J. ECG algorithm for predicting sites of successful radiofrequency ablation of accessory pathways [abstract]. *Pacing Clin Electrophysiol.* 1993;16:865.)

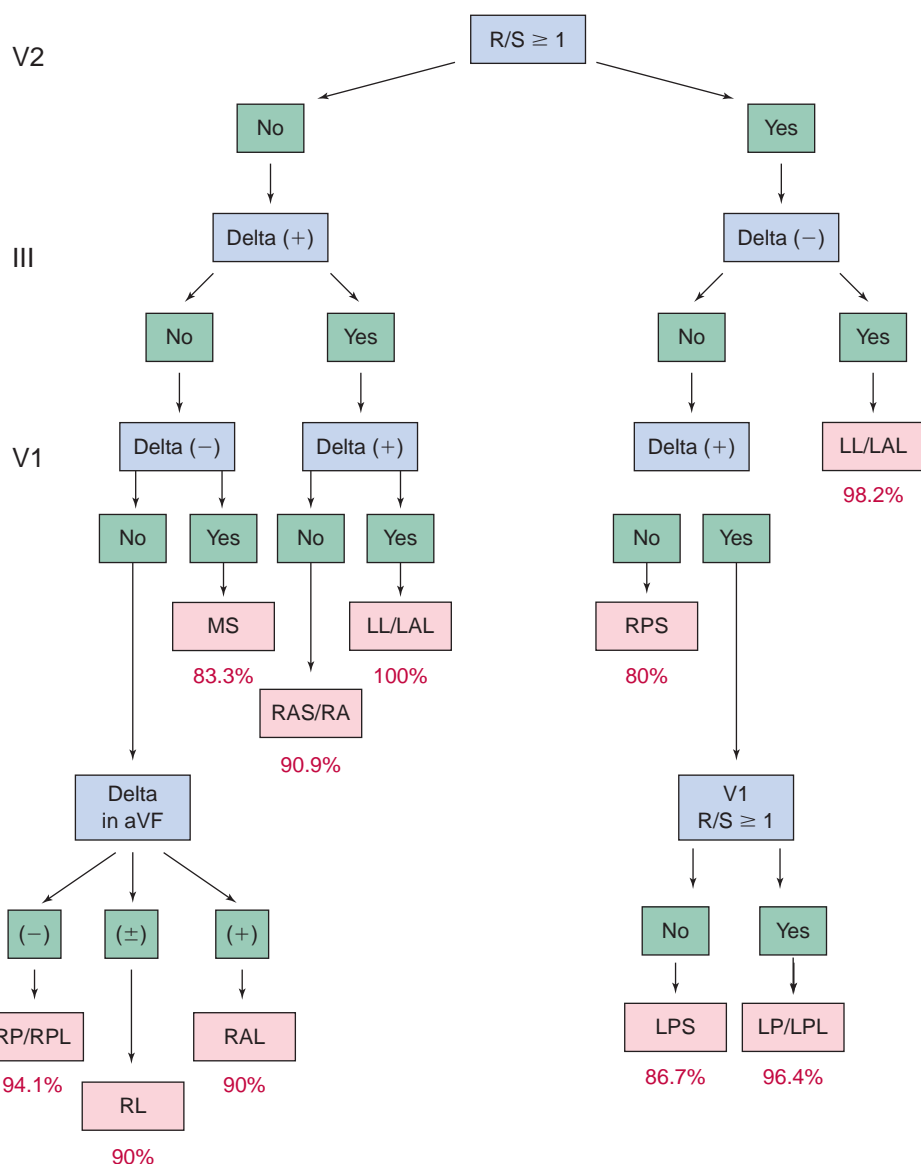


Fig. 18.18 Stepwise Algorithm for Localization of the Bypass Tract (BT) by Delta Wave Polarity. Numbers indicate the accuracy of the algorithm for each BT location. LAL, Left anterolateral; LL, left lateral; LP, left posterior; LPL, left posterolateral; LPS, left posteroseptal; MS, midseptal; RA, right anterior; RAL, right anterolateral; RAS, right anteroseptal; RL, right lateral; RP, right posterior; RPL, right posterolateral; RPS, right posteroseptal; R/S, R-S wave ratio. (From Chiang CE, Chen SA, Teo WS, et al. An accurate stepwise electrocardiographic algorithm for localization of accessory pathways in patients with Wolf-Parkinson-White syndrome from a comprehensive analysis of delta waves and R/S ratio during sinus rhythm. *Am J Cardiol.* 1995;6:40.)

complex in lead I (i.e., rightward axis). Conversely, BTs closer to the right axilla are strongly positive in lead I (i.e., leftward axis). Leads II/aVL and III/aVR also have net leftward and rightward vectors, respectively. Hence, as the BT location moves progressively to the left (e.g., from anterior to lateral mitral annulus), the delta wave assumes progressively less positive/more negative deflection in lead I, a taller R wave in lead III than in lead II, and a larger S wave in lead aVL compared to lead aVR. Opposite changes are expected as the BT location moves progressively to the right (from anteromedial to lateral tricuspid annulus).

Frontal plane vertical axis. The inferior leads (II, III, and aVF) reflect the vertical axis. Therefore BTs located at the superior aspect of the tricuspid or mitral annulus exhibit positive deflections in the inferior

leads (i.e., vertical axis). The magnitude of the inferiorly directed vector diminishes as the site of origin shifts from superior to inferior regions of either annulus.

Left vs. right free-wall BTs. Delta wave polarity in right precordial leads is most helpful in distinguishing between right- and left-sided free-wall BTs. Ventricular activation originating from the right ventricle (RV) (as mediated by right-sided BTs) is expected to produce a predominantly negative deflection in right precordial leads, whereas more posterior or left-sided sites of origin produce more positive deflections. Hence, an R/S ratio greater than 1 or a dominant R wave in lead V1 is consistent with left-sided BTs, whereas R/S transition after lead V2 suggests right-sided BTs. When the R/S transition is at lead V2 or between

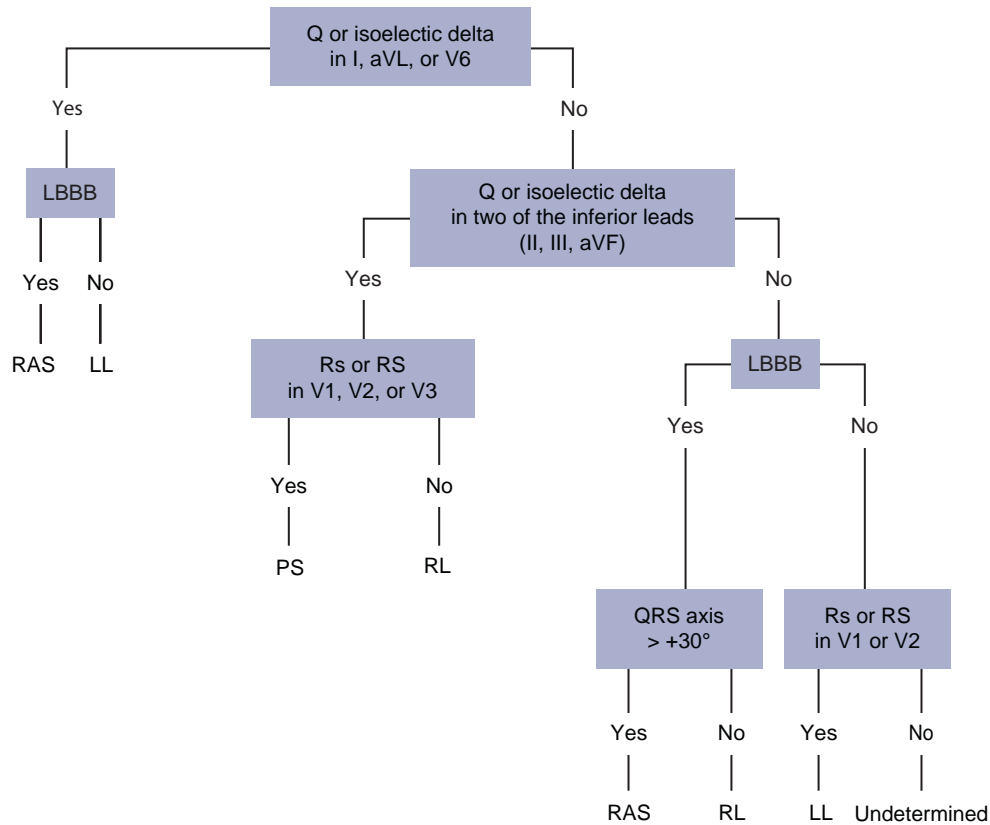


Fig. 18.19 Algorithm of Bypass Tract Localization Based on Delta Wave Morphology on the Surface Electrocardiogram. *LBBB*, Left bundle branch block-type pattern (QRS ≥ 90 milliseconds in lead I with an rS pattern in leads V1 or V2); *LL*, left lateral; *PS*, posteroseptal; *RL*, right lateral; *RAS*, right anteroseptal; *QRS* $> 30^\circ$, QRS axis $> +30^\circ$. (From Fox DJ, Klein GJ, Skanes AC, Gula LJ, Yee R, Krahn AD. How to identify the location of an accessory pathway by the 12-lead ECG. *Heart Rhythm*. 2008;5:1763–1766.)

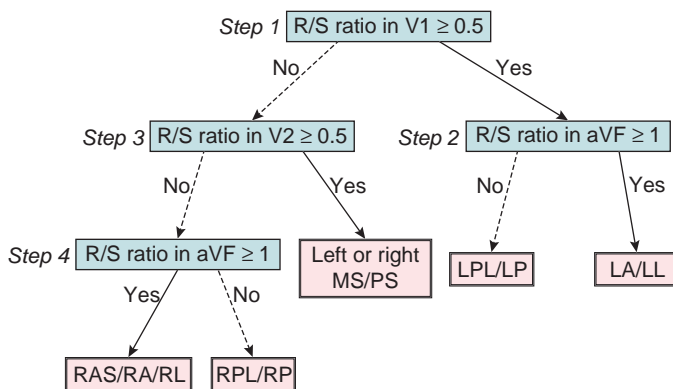


Fig. 18.20 Stepwise Electrocardiogram Algorithm for the Determination of Bypass Tract Location. *LA*, Left anterior; *LL*, left lateral; *LP*, left posterior; *LPL*, left posterolateral; *MS*, midseptal; *PS*, posteroseptal; *RA*, right anterior; *RAS*, right anteroseptal; *RL*, right lateral; *RP*, right posterior; *RPL*, right posterolateral. (From Taguchi N, Yoshida N, Inden Y, et al. A simple algorithm for localizing accessory pathways in patients with Wolff-Parkinson-White syndrome using only the R/S ratio. *J Arrhythmia*. 2014;30:439–443.)

leads V1 and V2, the R/S wave in the left lateral limb leads (I and aVL) favors right-sided BTs, otherwise left-sided BTs are likely.

Left-sided BTs. All left free-wall BTs exhibit positive delta wave polarity in the right precordial leads, an R/S ratio greater than 1, or a dominant R wave in lead V1. Because of its superior location in the

IV, BTs originating from the anterior mitral annulus exhibit larger R wave amplitudes in the inferior leads. As the BT location shifts progressively more laterally, R wave amplitude becomes progressively larger in lead III and smaller in lead II. The delta wave amplitude ratio in leads III/II is greater than 1 for posterolateral BTs and less than 1 for anterolateral BTs. BTs located at the inferior aspects of the mitral annulus exhibit negative delta waves in the inferior leads. Furthermore, BT locations at the lateral aspect of the mitral annulus produce a more negative delta wave in the left lateral limb leads (aVL and I) than anterior or posterior annular locations. In fact, a negative delta wave in the left lateral leads (aVL, I, and V6) is pathognomonic of a left lateral BT.

Right-sided BTs. BTs arising from the tricuspid annulus demonstrate negative delta wave polarity in the right precordial leads and positive polarity in leads V5 and V6. As the BT location moves from medial/septal to lateral locations along the tricuspid annulus, the precordial transition becomes later (at lead V3 in septal locations, and after lead V3 in free-wall locations) and the negative delta wave becomes deeper in anterior precordial leads (V1 to V3). Right-sided BTs typically display a large positive delta wave in the left lateral limb leads (aVL and I), but a predominantly negative delta wave in lead aVR. Delta wave polarity in the inferior leads is positive in anterior annular BTs. As the BT location moves laterally and inferiorly, the delta wave becomes more negative in the inferior leads. Positive delta waves in leads II and aVF are consistent with anteroseptal locations, whereas negative delta waves in the inferior leads suggest posteroseptal locations. Flat or biphasic delta waves suggest midseptal locations.

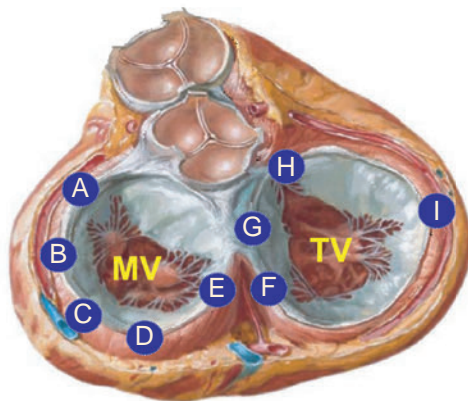
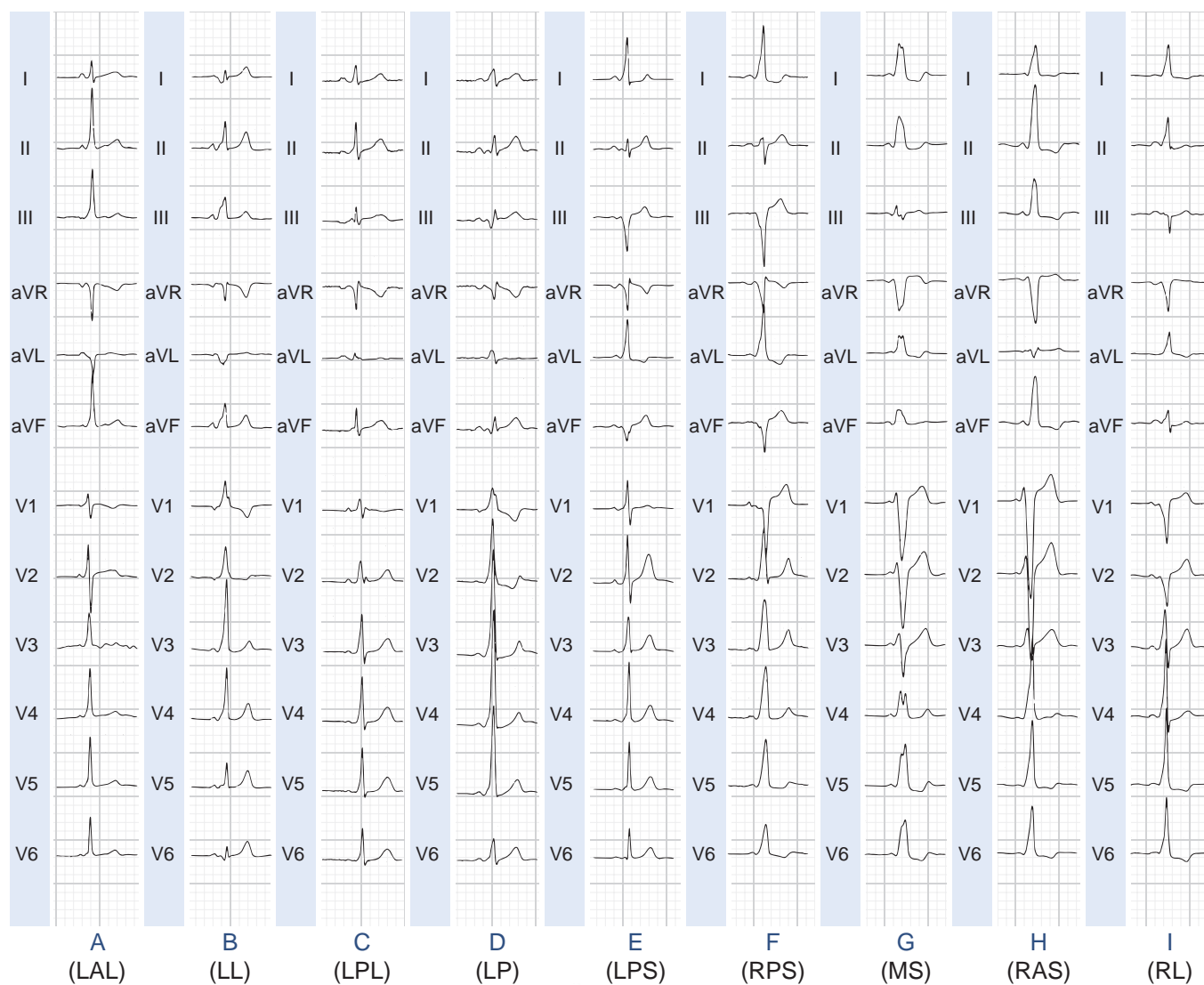


Fig. 18.21 Delta Wave Morphology on the Surface Electrocardiogram (ECG) During Ventricular Preexcitation. Representative surface 12-lead ECG of delta wave morphology (*top panels*) with the corresponding location of the successful ablation site around the valvular annulus on an anatomic illustration (*bottom*). (A) left anterolateral (LAL); (B) left lateral (LL); (C) left posterolateral (LPL); (D) left posterior (LP); (E) left posteroseptal (LPS); (F) right posteroseptal (RPS); (G) midseptal (MS); (H) right anteroseptal (superoparaseptal, RAS); (I) right lateral (RL). MV, Mitral valve; TV, tricuspid valve. (Anatomic illustration of mitral and tricuspid annuli is shown at the bottom [from Netter Images {www.netterimages.com} with permission].)

Anteroseptal BTs. Right superoparaseptal (anteroseptal) BTs connect the RA and RV free walls at the anteromedial aspect of the tricuspid annulus. Because of its relatively superior and anterior ventricular insertion compared to the rest of the ventricular mass, these BTs exhibit positive delta waves in the inferior leads (II, III, and aVF). In addition, delta waves are often negative in leads V1 and V2, but slightly positive ($R/S < 1$) delta waves also are observed. Similar to right free-wall BTs, delta waves are typically positive in leads I and aVL and negative in lead aVR.

Midseptal BTs. The delta wave is positive in lead II, predominantly negative in lead III, and negative or isoelectric in lead aVF. The delta wave in lead V1 is usually negative and R/S transition occurs after lead V2 (usually between leads V2 and V3). However, variations are not infrequent, especially in the inferior leads and in V2. Midseptal BTs can be differentiated from superoparaseptal and para-Hisian BTs by a negative delta wave in lead III, a biphasic delta wave in lead aVF, and a larger R/S ratio in lead V2, likely due to the posterior location of the AV septum compared to the anterior tricuspid annulus.²³

Posteroseptal BTs. Posteroseptal BTs are characterized by a deeply negative delta wave in lead III. The delta wave is often negative in lead aVF, especially for right posteroseptal BT locations. A negative delta wave in lead II predicts an epicardial location of the posteroseptal BT. The delta wave in lead V1 can be negative, isoelectric, or positive. Lead V2 typically displays a positive delta wave, with the R wave larger than the S wave. A negative delta wave polarity in lead V1 with abrupt transition to positive polarity (with R/S ratio greater than 1) in lead V2 favors a right-sided location of the posteroseptal BT, whereas left posteroseptal BTs are often associated with biphasic or positive delta wave polarity in leads V1 and V2. An R/S ratio greater than 1 in lead V1 is a more accurate marker of left posteroseptal BTs. The tallest precordial R wave is typically recorded in the midprecordial leads (V2 to V4) in left posteroseptal BTs, and in the lateral precordial leads (V5 or V6) in right posteroseptal BTs.

Localization Using Polarity of the Retrograde P Wave Morphology

The polarity of the retrograde P waves during orthodromic AVRT is dependent on the location of the atrial insertion of the BT, and is helpful in localizing the BT. However, the P wave is usually inscribed within the ST segment and its morphology may not be easily determined.^{24,25}

In general, P wave morphology in leads I and V1 and in the inferior leads is most helpful (Fig. 18.22). A negative P wave vector in lead I is highly suggestive of left free-wall BTs, whereas a positive vector is suggestive of right free-wall BTs. On the other hand, a negative P wave in lead V1 predicts right-sided BTs. P wave polarity in the inferior leads, positive or negative, suggests superior or inferior location of the BT, respectively.^{24,25}

Left free-wall BTs have positive P waves in lead V1 and negative P waves in leads I and aVL. If the retrograde P wave is negative in all three inferior leads, the BT is located at the inferoposterior mitral annulus. As the BT location moves to the lateral mitral annulus, the P wave becomes isoelectric or biphasic in one of the three inferior leads. The P wave becomes positive in all inferior leads for left anterior/anterolateral BTs. Thus, as the BT moves from posterior to anterior locations along the mitral annulus, the positive P wave is seen initially in lead III, followed by lead aVF and lead II.^{24,25}

For right free-wall BTs, the P wave is negative in lead V1 and positive or isoelectric in lead I. If the P wave is positive in all inferior leads, the BT is located in the anterior wall. If the P wave is negative in all inferior leads, the BT is located in the posterior wall. However, moving from the posterior to the anterior location, the positive P wave is seen initially in lead II, followed by lead aVF and lead III.²⁴

Posteroseptal BTs display positive P waves in leads V1, aVR, and aVL, and isoelectric or biphasic P waves in lead I. P waves are negative in all inferior leads (II, III, aVF). Left posterior BTs also have negative P waves in the inferior leads, but the P waves are more negative in lead II than in lead III and are more positive in lead aVR than in lead aVL. Discrimination between left and right posteroseptal BTs based on P wave morphology is limited. In contrast, anteroseptal BTs display positive P waves in inferior leads and biphasic P waves in lead V1.²⁴

ELECTROPHYSIOLOGICAL TESTING

EP testing is used to study the features, location, and number of BTs and the tachycardias, if any, associated with them (Box 18.3). Typically, three quadripolar catheters are positioned in the high RA, RV apex or septum, and HB region, and a decapolar catheter is positioned in the CS (see Fig. 4.4). If a right-sided BT is suspected, a duo-decapolar (Halo) catheter along the tricuspid annulus can be helpful.

Some investigators have advocated a simplified approach to ablation using only one or two catheters. Although often successful, 10% of patients with preexcitation have multiple arrhythmias, and 10% to 20% of such patients have multiple BTs that can result in a very complex procedure. Because it is difficult to know beforehand in any given patient whether the procedure will be straightforward or complex, the single-catheter approach to ablation of arrhythmias should be discouraged.²⁶

Baseline Observations During Sinus Rhythm

Ventricular preexcitation is associated with a short His bundle–ventricular (HV) or H-delta interval during NSR. The HV interval can even be negative or the His potential can be buried in the local ventricular electrogram. The QRS is a fusion between conduction over the BT and that over the AVN-HPS. The site of earliest ventricular activation is near the ventricular insertion site of the BT (i.e., near the tricuspid annulus or mitral annulus at the base of the heart). Slowing of conduction in the AVN by carotid sinus massage, AVN blockers, or rapid atrial pacing unmasks and increases the degree of preexcitation, because these maneuvers do not affect the conduction over the BT. Dual AVN pathways are present in 8% to 40% of patients.

Programmed Atrial Stimulation During Sinus Rhythm

In the presence of a manifest AV BT, atrial stimulation from any atrial site can help unmask preexcitation if it is not manifest during NSR because of fast AVN conduction. Incremental rate atrial pacing and progressively premature AES produce decremental conduction over the AVN (but not over the BT), increasing the degree of preexcitation and shortening the HV interval, until the His potential is inscribed within

BOX 18.3 Goals of Electrophysiological Evaluation in Patients With Wolff-Parkinson-White Syndrome

- Confirming the presence of an atrioventricular BT
- Evaluation for the presence of multiple BTs
- Localization of the BT(s)
- Evaluation of the refractoriness of the BT and its implications for life-threatening arrhythmias
- Induction and evaluation of tachycardias
- Demonstration of the BT role in the tachycardia
- Evaluation of other tachycardias not dependent on the presence of the BT
- Termination of the tachycardias

BT, Bypass tract.

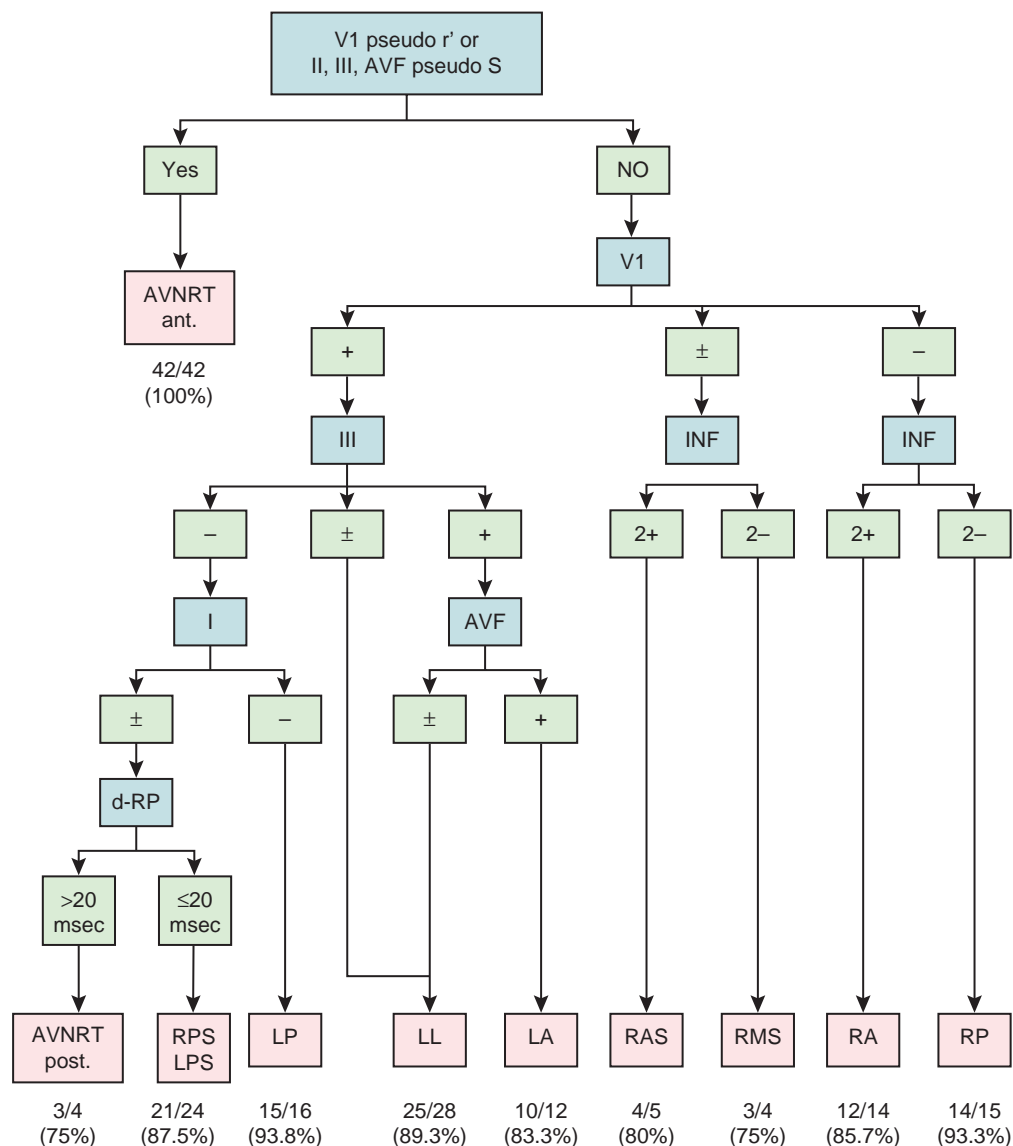


Fig. 18.22 Stepwise Algorithm for Predicting Bypass Tract Location Based on Retrograde P Wave Morphology During Orthodromic Atrioventricular Reentrant Tachycardia. The accuracy of the algorithm is indicated based on results of a prospective study in 164 patients. The denominator is the total number of patients in that group; the numerator is the number of patients with correct predictions. AVNRT, Atrioventricular nodal reentrant tachycardia; INF, inferior leads (II, III, aVF); LA, left anterior; LL, left lateral; LP, left posterior; LPS, left posteroseptal; RA, right anterior; RAS, right anteroseptal; RMS, right midseptal; RP, right posterior; RPS, right posteroseptal. (From Tai CT, Chen SA, Chiang CE, et al. A new electrocardiographic algorithm using retrograde P waves for differentiating atrioventricular node reentrant tachycardia from atrioventricular reciprocating tachycardia mediated by concealed accessory pathway. *J Am Coll Cardiol.* 1997;29:394–402.)

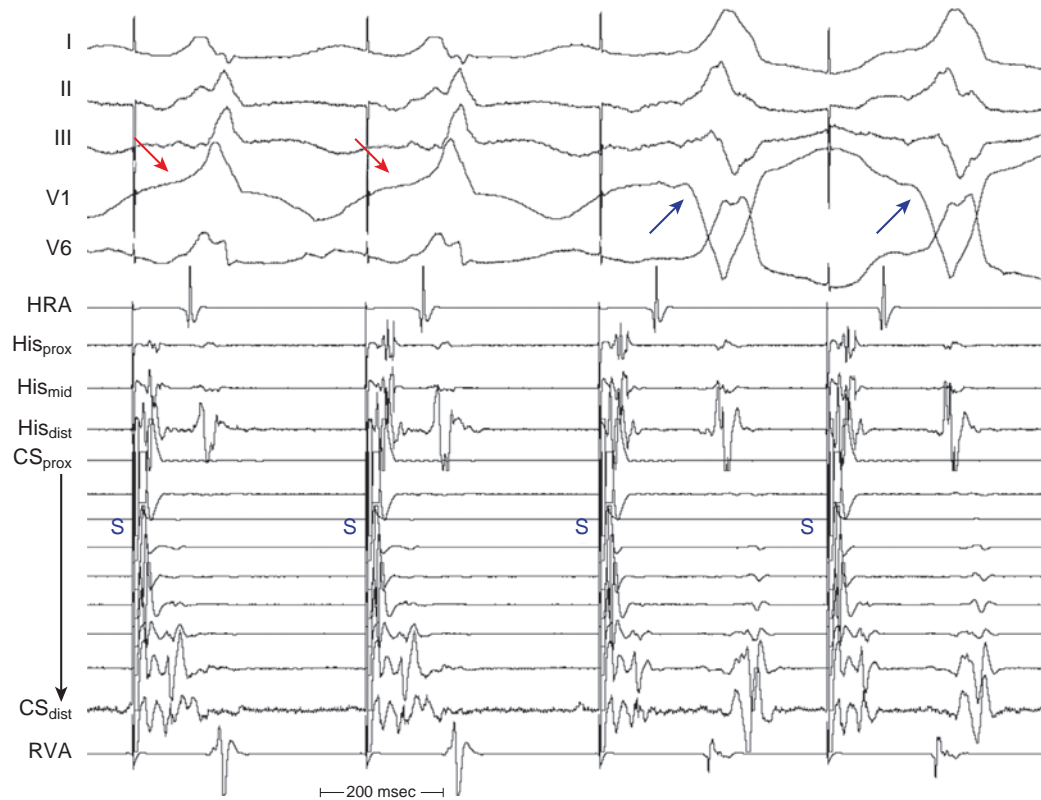
the QRS. The His potential remains activated anterogradely over the AVN until anterograde block in the AVN occurs; the QRS then becomes fully preexcited, and the His potential becomes retrogradely activated (Fig. 18.23).

Atrial stimulation close to or at the AV BT insertion site results in maximal preexcitation and the shortest P-delta interval because of the lack of intervening atrial tissue whose refractoriness may otherwise limit the ability of atrial stimulation to activate the AV BT as early (Fig. 18.24). Atrial pacing can reveal the presence of multiple BTs (eFig. 18.4). Rare cases of catecholamine-dependent BTs have been reported that require isoproterenol infusion to manifest preexcitation that is absent at baseline.

The failure of atrial stimulation to increase the amount of preexcitation can be caused by: (1) markedly enhanced AVN conduction; (2) the presence of another AV BT; (3) pacing-induced block in the AV BT because of a long ERP of the BT (longer than that of the AVN); (4) total preexcitation already present at the basal state caused by prolonged or absent AVN-HPS conduction; (5) decremental conduction in the BT; or (6) the presence of a fasciculoventricular BT rather than an AV BT.

Programmed Ventricular Stimulation During Sinus Rhythm

Retrograde ventriculoatrial conduction. The normal AVN response to rate-incremental ventricular pacing or progressively premature single



eFig. 18.4 Atrial Pacing in the Presence of Two Bypass Tracts (BTs). Surface electrocardiogram and intracardiac recordings during coronary sinus pacing (S) in a patient with both right and left lateral BTs. The first two complexes show a left lateral preexcitation pattern (*red arrows*), whereas this pathway fails to conduct on the last two complexes, which show a right lateral preexcitation pattern (*blue arrows*). *CS_{dist}*, Distal coronary sinus; *CS_{prox}*, proximal coronary sinus; *His_{dist}*, distal His bundle; *His_{mid}*, middle His bundle; *His_{prox}*, proximal His bundle; *HRA*, high right atrium; *RVA*, right ventricular apex.

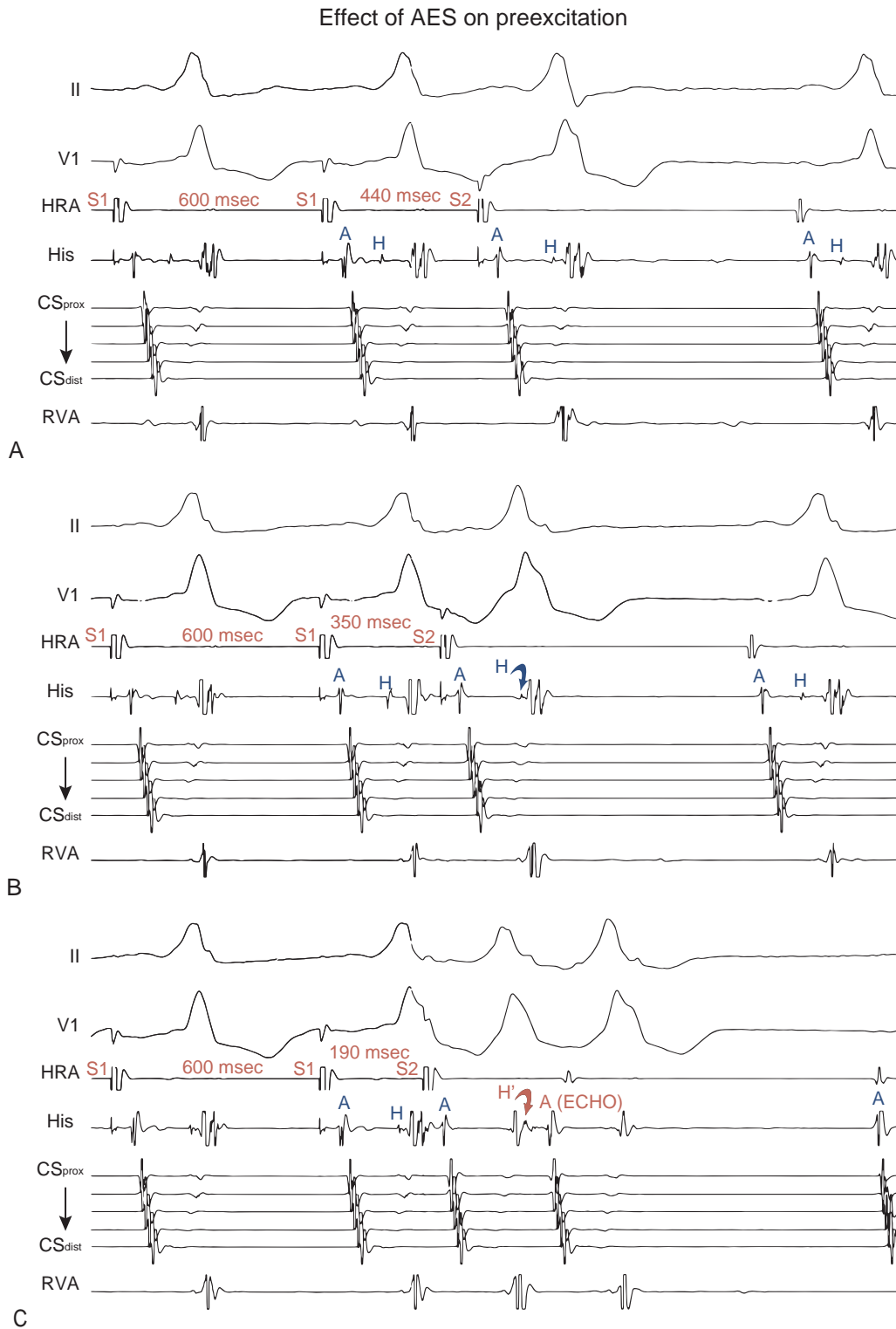


Fig. 18.23 Effect of Atrial Extrastimulation (AES) on Preexcitation. (A) Preexcitation is manifest during normal sinus rhythm and atrial pacing associated with a short His bundle–ventricular (HV) interval (–11 milliseconds). AES produces decremental conduction over the atrioventricular node (AVN) (with prolonged atrial–His bundle interval) but not over the bypass tract (constant P–delta interval), increasing the degree of preexcitation with the His potential inscribed within the QRS (HV interval of –64 milliseconds). (B) An earlier coupled AES produces more pronounced preexcitation and an HV interval of –93 milliseconds. (C) A more premature AES produces full preexcitation with the His bundle activated retrogradely (*H'*), followed by ventriculoatrial conduction over the AVN and an echo beat (atrioventricular reentry). *A*, Atrial electrogram; *CS_{dist}*, distal coronary sinus; *CS_{prox}*, proximal coronary sinus; *H*, His bundle potential; *HRA*, high right atrium; *RVA*, right ventricular apex.

Effect of site of pacing on preexcitation

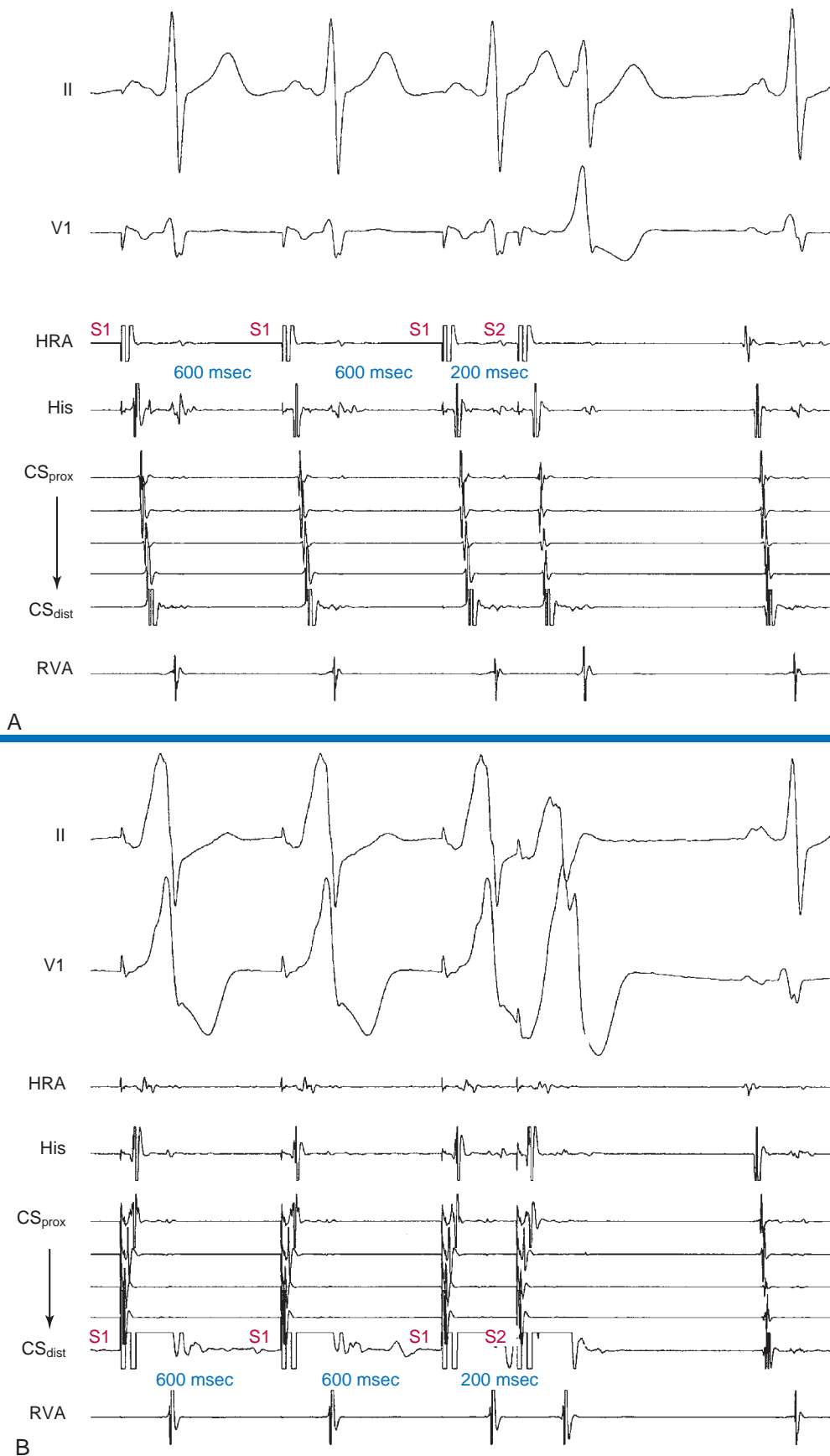


Fig. 18.24 Effect of Site of Pacing on Preexcitation. (A) In the presence of a manifest left lateral bypass tract (BT), pacing from the high right atrium at a cycle length (CL) of 600 milliseconds produces minimal preexcitation. The degree of preexcitation increases with premature stimulation because of delay in atrio-ventricular nodal conduction. (B) In the same patient, pacing at the same CLs from the distal coronary sinus, close to or at the BT insertion site, results in a larger degree of preexcitation and shorter P-delta interval because of the lack of intervening atrial tissue whose refractoriness might otherwise limit the ability of atrial stimulation to activate the BT as early. *CS_{dist}*, Distal coronary sinus; *CS_{prox}*, proximal coronary sinus; *HRA*, high right atrium; *RVA*, right ventricular apex.

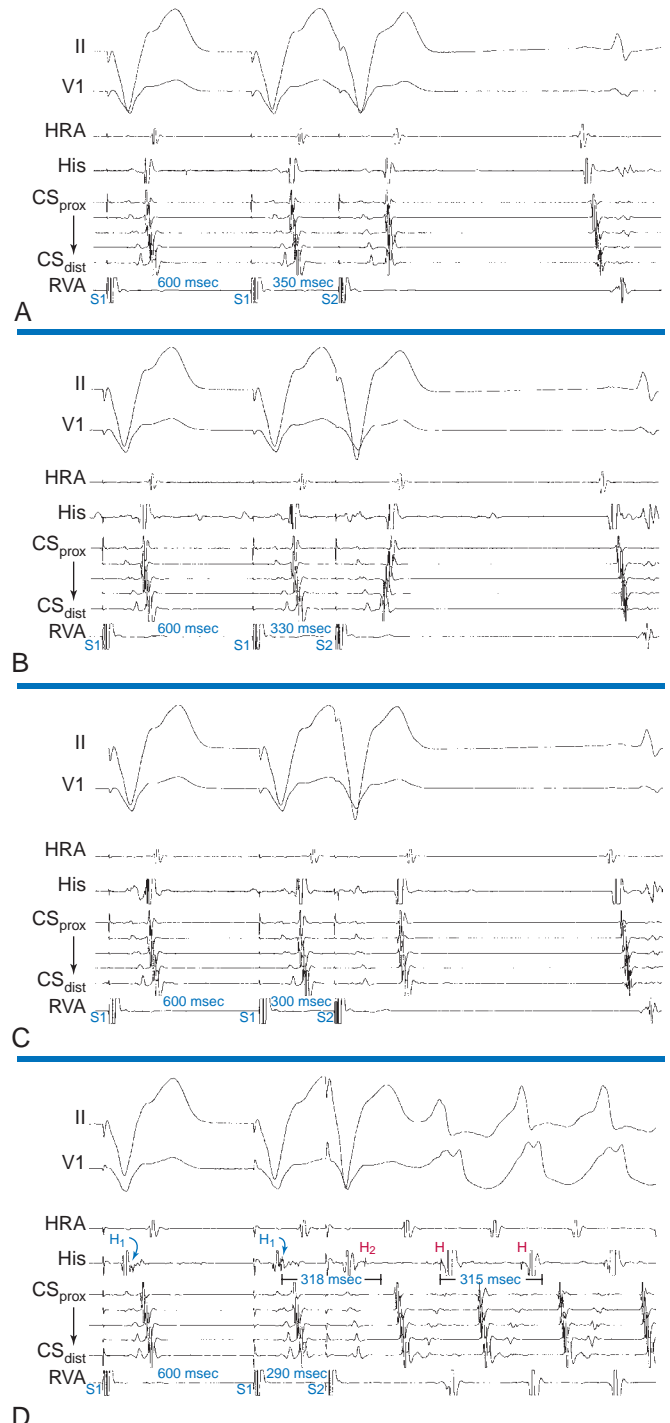
ventricular extrastimulation (VES) is a gradual delay of VA conduction (manifest as gradual prolongation of the VA and His bundle–atrial [HA] intervals) as the PCL or VES coupling interval decreases. Conversely, nondecremental VA conduction characterizes BT conduction. Nonetheless, some BTs with retrograde decremental conduction properties can also exhibit prolongation of conduction time and VA interval with ventricular pacing or VES. In addition, at short ventricular PCLs or VES coupling intervals, intramyocardial conduction delay can occur, resulting in prolongation in the VA interval; however, the local VA interval at the BT location remains unchanged. Furthermore, short ventricular PCLs or VES coupling intervals can encroach on the BT refractoriness, causing some decremental conduction, with a consequent increase in the surface VA interval and the local VA interval.

The absence of VA conduction (at long ventricular PCLs) or the presence of decremental VA conduction makes the presence of a retrogradely conducting BT unlikely, except for the rare catecholamine-dependent BTs that require isoproterenol infusion for demonstration.

Retrograde atrial activation sequence. In the presence of a retrogradely conducting AV BT (whether manifest or concealed), VES during NSR can result in VA conduction over the BT, AVN, both, or neither (Fig. 18.25). Conduction over the BT alone is the most common pattern at short PCLs or short VES coupling intervals. In this setting, the VA conduction time is fairly constant over a wide range of PCLs and VES coupling intervals (given the absence of intraventricular conduction abnormalities or additional BTs). On the other hand, retrograde conduction over both the BT and HPS-AVN is especially common when RV pacing is performed at long PCLs or long VES coupling intervals and in the presence of a left-sided BT. This occurs because it is easier to engage the RB and conduct retrogradely through the AVN than it is to reach a distant left-sided BT. In this setting, the atrial activation pattern depends on the refractoriness and conduction times over both pathways and usually exhibits a variable degree of fusion. In addition, VA conduction can proceed over the HPS-AVN alone, resulting in a normal pattern of VA conduction, or can be absent because of block in both the HPS-AVN and BT, which is especially common with short PCLs and very early VES.

Ventricular stimulation resulting in eccentric retrograde atrial activation sequence not consistent with normal conduction over the AVN is consistent with VA conduction over an AV BT (see Fig. 18.25). Ventricular pacing can also reveal the presence of multiple BTs (Fig. 18.26). However, a concentric retrograde atrial activation sequence does not exclude the presence of a septal or paraseptal BT or a free-wall BT when VA conduction is mediated by the AVN. In addition, AVN slow pathway conduction can be associated with an eccentric atrial activation sequence in the CS. Accurate analysis of an atrial activation sequence frequently

Fig. 18.25 Retrograde Conduction During Ventricular Extrastimulation (VES) in a Patient With a Bidirectional Left Lateral Bypass Tract (BT). (A) The ventricular pacing drive is conducted retrogradely over the atrioventricular node (AVN) with a concentric atrial activation sequence. The VES is conducted over both the AVN and BT (atrial fusion). (B) An earlier VES encounters delay in the His-Purkinje system (HPS)–AVN and conducts solely over the BT with an eccentric atrial activation sequence. (C) An early-coupled VES blocks retrogradely in the BT and conducts solely over the AVN. (D) The VES conducts only over the HPS-AVN with more pronounced ventriculoatrial (VA) delay, which allows recovery of the BT and anterograde conduction, initiating antidromic atrioventricular reentrant tachycardia (AVRT). The VA delay is provided by conduction delay, not only within the AVN but also within the HPS. Note that the VES encounters retrograde block in the right bundle branch, and His bundle activation is mediated by retrograde conduction over the left bundle branch. Consequently, the His potential is visible after the ventricular electrogram. Note that despite the fact that the H1-H2 interval following VES approximates the H-H interval during supraventricular tachycardia (SVT), the His bundle–atrial interval following the initiating VES is shorter than that during the SVT, which favors antidromic AVRT over preexcited atrioventricular nodal reentrant tachycardia as the mechanism of the SVT. CS_{dist}, Distal coronary sinus; CS_{prox}, proximal coronary sinus; HRA, high right atrium; RVA, right ventricular apex.



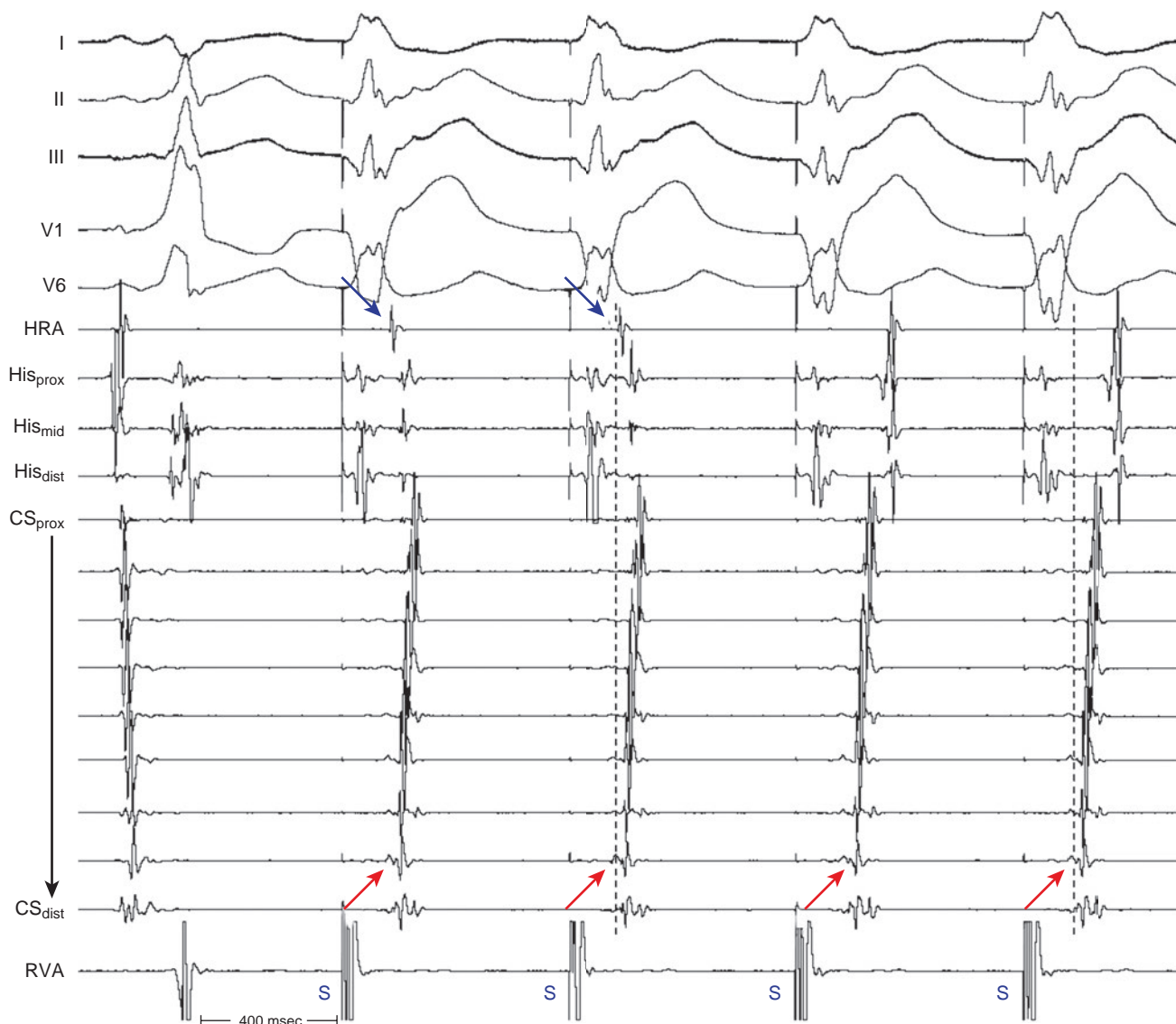


Fig. 18.26 Ventricular Pacing Revealing the Presence of Multiple Bypass Tracts (BTs). The first complex shows sinus rhythm with preexcitation, showing a left free-wall pattern. Four complexes of right ventricular apical (RVA) pacing follow, the first two paced complexes (S) show fusion of retrograde activation over both a left lateral BT (red arrows), which is present in each complex, and a right lateral BT (blue arrows). The last two paced complexes conduct over the left lateral BT. Dashed lines aid in comparing activation sequences. CS_{dist}, Distal coronary sinus; CS_{prox}, proximal coronary sinus; His_{dist}, distal His bundle; His_{mid}, middle His bundle; His_{prox}, proximal His bundle; HRA, high right atrium.

requires the use of multielectrode catheters around the tricuspid annulus and deep in the CS.²⁷

VES during HB refractoriness. A VES delivered when the HB is refractory (i.e., when the His potential is already manifest or within 35 to 55 milliseconds before the time of the expected His potential) that results in atrial activation is diagnostic of the presence of a retrogradely conducting BT. Because the HPS-AVN is already refractory and cannot mediate VA conduction, retrograde atrial activation from ventricular stimulation has to be mediated by a BT.

Furthermore, an early coupled VES that results in an atrial activation that either precedes HB activation (Fig. 18.27) or is associated with an apparent HA interval shorter than that during drive complexes indicates “atrial preexcitation” via an AV BT.

Importantly, if a VES delivered when the HB is refractory does not result in atrial activation, this does not necessarily exclude the presence of a retrogradely conducting AV BT, because such a VES can be associated with retrograde block in the BT itself (see Fig. 18.25). In addition, the lack of such a response does not exclude the presence of unidirectional (anterograde-only) AV BTs.

Retrograde RBBB during VES. During the delivery of progressively premature single VESs, an abrupt increase in the VA conduction interval is often observed. This can be due to a variety of reasons including: (1) retrograde block in the AVN fast pathway and subsequent VA conduction over the slow pathway; (2) retrograde block in the RB and subsequent retrograde conduction over the left bundle branch (LB); or (3) retrograde block in the BT and subsequent VA conduction only over the AVN.

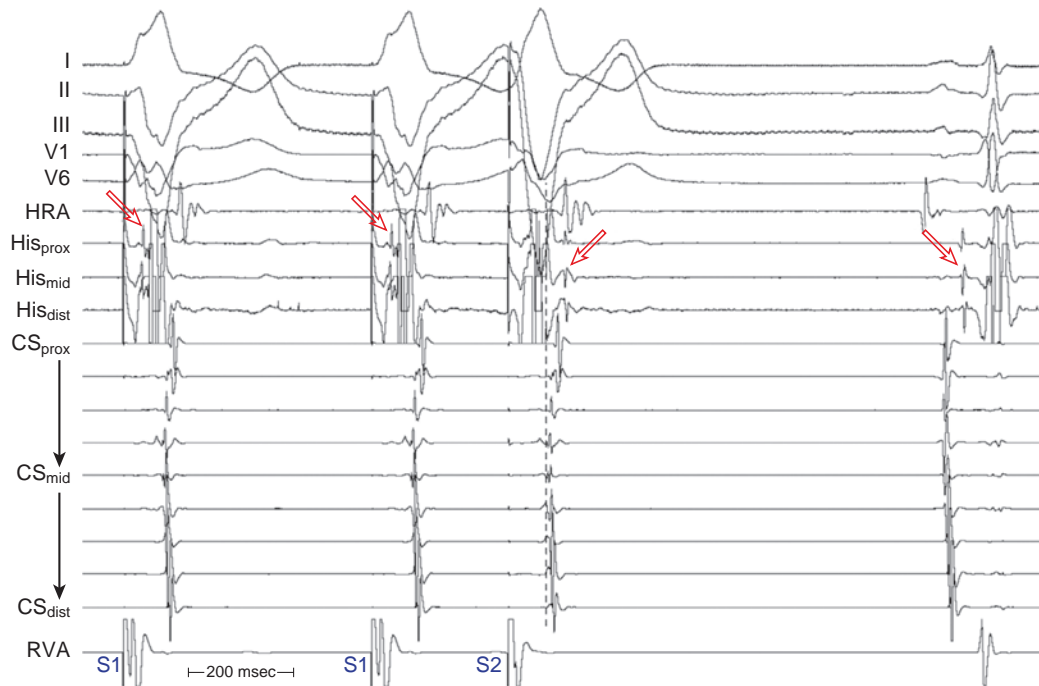


Fig. 18.27 Ventricular Extrastimulation Revealing the Presence of a Bypass Tract (BT). A retrograde His potential is present on both drive complexes (*S1*) and following the extrastimulus (*arrows*). Although atrial activation also follows each stimulus, it occurs (*dashed line*) before the inscription of the His potential on the ventricular extrastimulus (*S2*). Thus a BT is present because atrial activation is not dependent on His bundle–atrioventricular activation. *CS_{dist}*, Distal coronary sinus; *CS_{mid}*, middle coronary sinus; *CS_{prox}*, proximal coronary sinus; *His_{dist}*, distal His bundle; *His_{mid}*, middle His bundle; *His_{prox}*, proximal His bundle; *HRA*, high right atrium; *RVA*, right ventricular apex.

Retrograde RBBB occurs frequently during VES testing, and can be diagnosed by observing the retrograde His potential during the drive train and its abrupt delay following the VES. Often, however, it is difficult to visualize the retrograde His potential during the pacing train; nevertheless, the sudden appearance of an easily distinguished retrograde His potential, separate from the ventricular electrogram following the VES, can be sufficient to recognize retrograde RBBB.

Prolongation of the ventriculo-His (VH) interval is observed on development of retrograde RBBB because conduction must traverse the interventricular septum (which requires approximately 60 to 70 milliseconds in normal hearts), enter retrograde via the LB, and ascend to reach the HB. Although an increase in the VH interval necessarily occurs with retrograde RBBB, whether a similar increase occurs in the VA interval depends on the nature of VA conduction (over the AVN vs. BT).

Measurement of the effect of the development of retrograde RBBB during VES on the retrograde VH and VA intervals can help distinguish between retrograde AVN and BT conduction. In the absence of a BT, the AVN can be activated in a retrograde fashion only after retrograde activation of the HB; as a consequence, VA activation will necessarily be delayed with retrograde RBBB, and the increase in the VA interval will be similar to the increase in the VH interval. On the other hand, when retrograde conduction is via a BT, there will be no expected increase in the VA interval when retrograde RBBB is induced. Thus the increase in the VA interval is minimal and always less than the increase in the VH interval.²⁸

Differential-site RV pacing. The response of the VA interval (i.e., the stimulus-to-atrial [SA] interval) and atrial activation sequence to differential-site RV pacing (i.e., RV basal versus RV apical pacing) can

help demonstrate or exclude the presence of a retrogradely conducting septal AV BT (Fig. 18.28).

The RV apex, although anatomically more distant from the atrium than the RV base, is nonetheless electrically closer because of the proximity of the distal RB to the pacing site. Consequently, in the absence of a retrogradely conducting septal AV BT, pacing at the RV apex allows entry into the rapidly conducting HPS and results in a shorter VA interval during pacing from the apex than from the base. Pacing from the RV base requires the paced wavefront to travel a longer distance by muscle-to-muscle conduction to reach the RV apex and then propagate retrogradely through the RB and HB. In other words, the VH interval is shorter with pacing at the RV apex versus the RV base. In the presence of a retrogradely conducting septal BT, pacing at the RV base allows the wavefront to access the BT rapidly and activate the atrium with a shorter VA interval than during RV apical pacing, which is distant from the ventricular insertion site of the BT (i.e., because the V-BT interval is shorter with pacing at the RV base versus the RV apex).

In the absence of a retrogradely conducting BT, the atrial activation sequence will be similar during pacing at the RV apex and at the RV base because the atrium is activated exclusively over the AVN in both settings. On the other hand, if a septal AV BT is present, atrial activation results from VA conduction over the septal BT during pacing at the RV base, and over the AVN, the BT, or a fusion of both during pacing at the RV apex. Therefore a change in the retrograde atrial activation sequence in response to RV base versus RV apex pacing indicates the presence of an AV BT, but a constant atrial activation sequence is not helpful in excluding the presence of a BT.

Of note, the exact entrance to the HPS (i.e., the terminus of the RB) is difficult to identify; the entrance site can be located in the

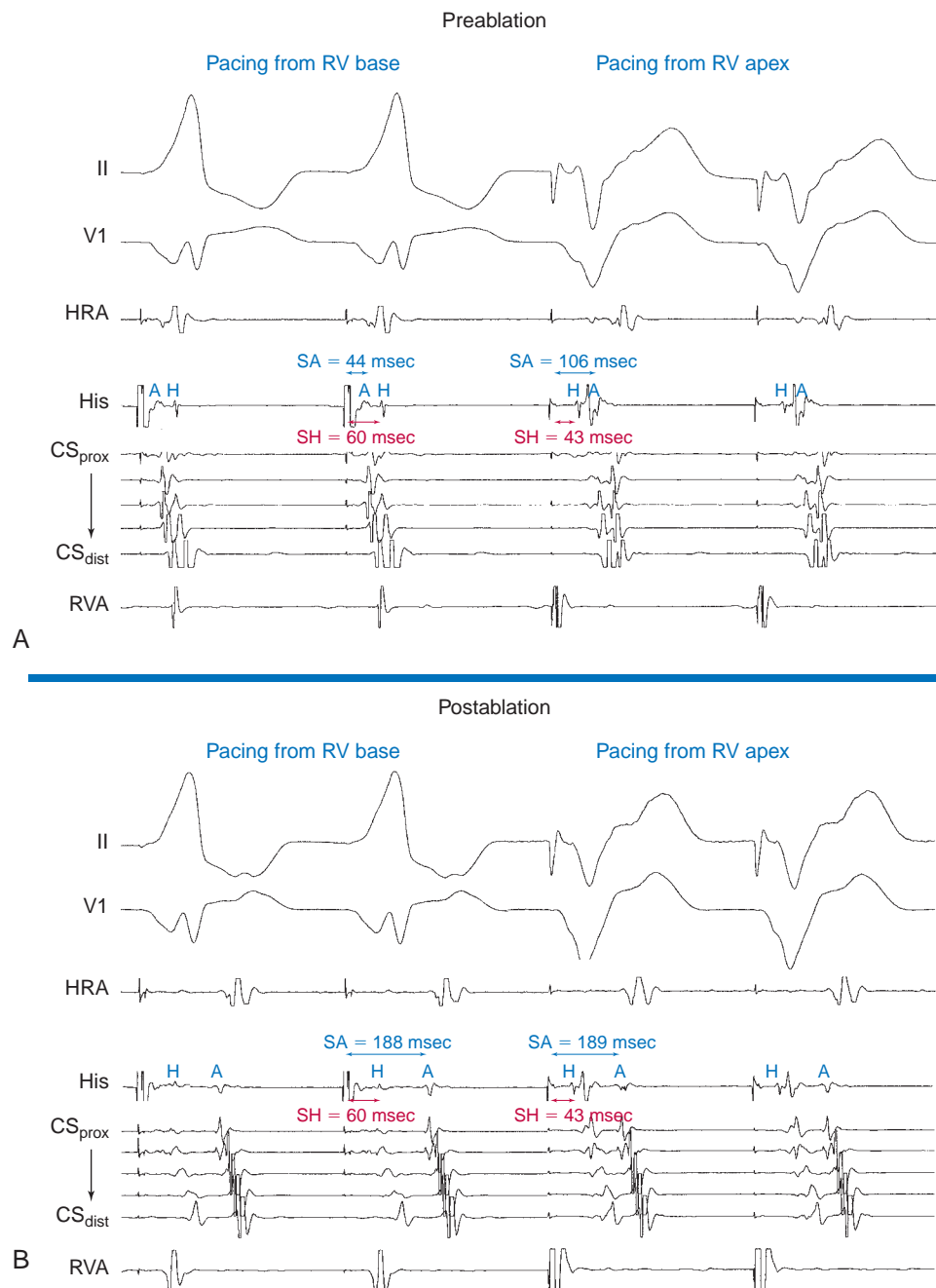


Fig. 18.28 Differential-Site Right Ventricular (RV) Pacing in a Patient With Concealed Superoparaseptal Bypass Tract (BT). In each panel, the first two complexes show RV basal-septal pacing, and the last two complexes show RV apical pacing. (A) RV pacing is performed before ablation of the BT. The stimulus-to-atrial (SA) (ventriculoatrial [VA]) interval is shorter during pacing at the RV base than during pacing at the RV apex, suggesting VA conduction occurring over a BT. Note that atrial activation occurs even before His bundle (HB) activation during pacing from the RV base, suggesting that VA conduction is independent of the atrioventricular node (AVN). (B) RV pacing is performed after successful ablation of the BT. During pacing from the RV apex, the SA interval is longer than before ablation, and it prolongs further by pacing at the RV base, consistent with the occurrence of VA conduction exclusively over the AVN. Note that in both panels the stimulus–His bundle (SH) (ventriculo-His) interval during RV apical pacing is shorter than that during RV basilar pacing because of the faster access of the paced wavefront to the right bundle branch–His bundle (RB–HB) during pacing at the RV apex. However, when VA conduction occurs over a BT (A), the SA interval remains constant; in contrast, in the absence of a BT (B), the SA interval shortens, coinciding with shortening of the S–H interval during pacing at the RV apex compared with pacing at the RV base. *CS_{dist}*, Distal coronary sinus; *CS_{prox}*, proximal coronary sinus; *HRA*, high right atrium; *RVA*, right ventricular apex.

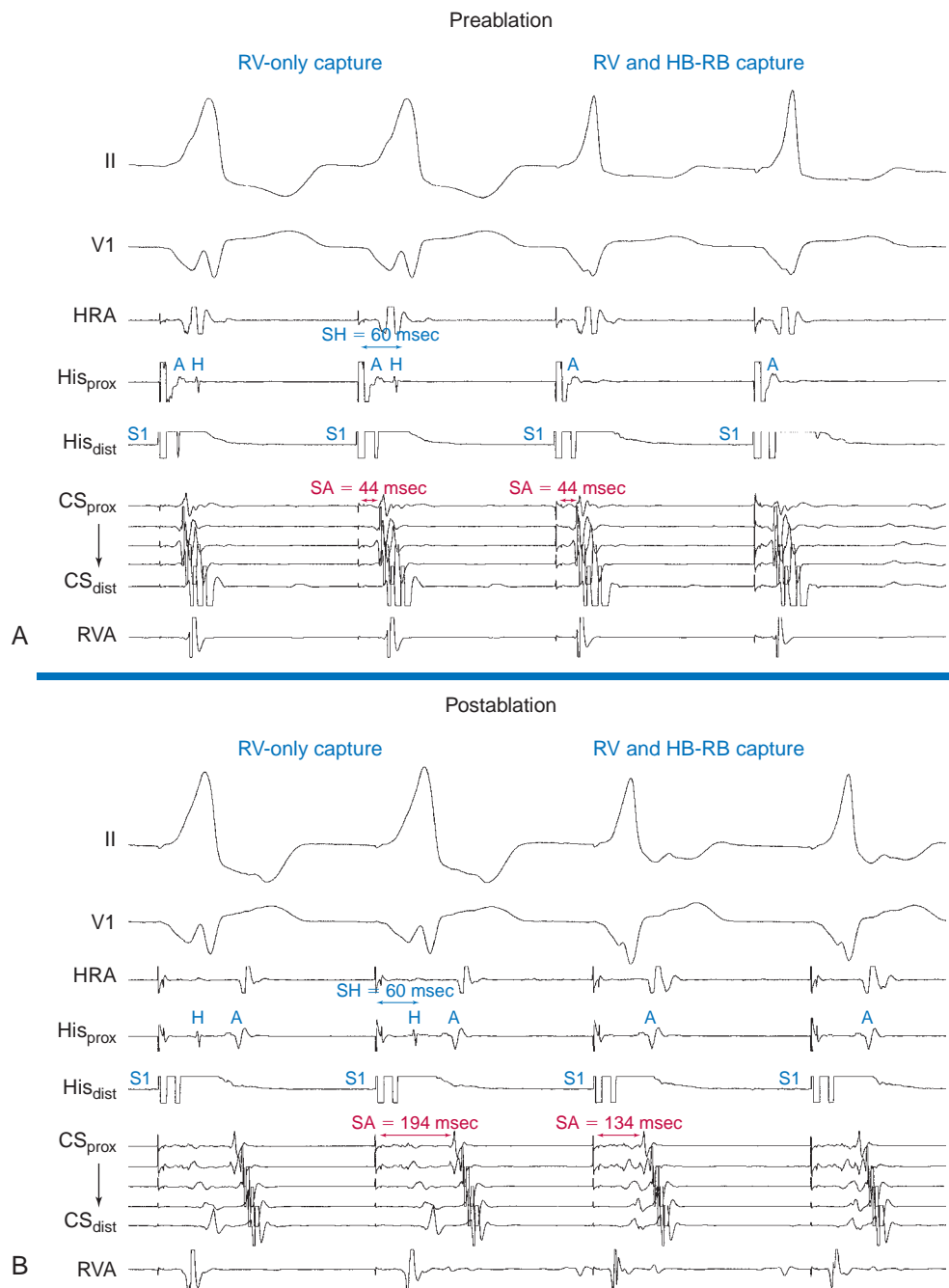


Fig. 18.30 Para-Hisian Pacing in a Patient With a Concealed Superoparaseptal Bypass Tract (BT). In each panel, the first two complexes show right ventricle (RV)-only capture, and the last two complexes show RV and His bundle–right bundle branch (HB-RB) capture. The loss of HB-RB capture is identified by delay in the HB activation (stimulus–His bundle [SH] interval = 60 milliseconds) and widening of the QRS. The His potential is not visible during HB-RB capture. (A) Para-Hisian pacing is performed before ablation of the BT; the stimulus-atrial (SA) interval remains unchanged regardless of whether HB-RB capture occurs, because retrograde ventriculoatrial (VA) conduction occurs over the BT in either setting. In fact, during RV-only capture, the SA interval is shorter than the SH interval, indicating that VA conduction is independent of the atrioventricular node (AVN). (B) Para-Hisian pacing is performed after successful ablation of the BT; the SA interval is longer than before ablation, and it prolongs further on loss of HB-RB capture, concomitant with delay in HB activation (i.e., prolongation in the SH interval) and a constant HA interval, indicating that VA conduction is mediated only by the AVN. Note that the activation sequence before ablation (VA conduction occurring over the BT) is slightly different from after ablation (VA conduction occurring over the AVN). However, in each case (preablation and postablation), the atrial activation sequence occurs over the same pathway and remains constant, regardless of whether HB-RB occurs. *CS_{dist}*, Distal coronary sinus; *CS_{prox}*, proximal coronary sinus; *His_{dist}*, distal His bundle; *His_{prox}*, proximal His bundle; *HRA*, high right atrium; *RVA*, right ventricular apex.

whereas prolongation of the VA (SA) interval on loss of HB capture, compared with that during HB capture, excludes the presence of a retrogradely conducting septal BT, except for slowly conducting and far free-wall BTs.³¹

Dual-Chamber Sequential Extrastimulation During Sinus Rhythm

Although the various ventricular pacing maneuvers described previously can expose an eccentric or nondecremental atrial activation pattern that suggests retrograde conduction over a BT rather than the AVN, in certain circumstances, these maneuvers may not be adequate to confirm the presence or absence of BT conduction, especially when the BT has an ERP, retrograde atrial activation pattern, and conduction time similar to the AVN. In particular, identification, mapping, and verification of success of ablation of BT function can be challenging in the setting of septal BTs with a retrograde activation pattern similar to retrograde AVN conduction, slowly conducting BTs, as well as BTs with decremental properties.³²

Dual-chamber sequential extrastimulation is a useful maneuver for identifying concealed slowly conducting BTs not revealed with standard pacing maneuvers. This maneuver relies on concealed AVN conduction during a critically timed AES to cause transient retrograde AVN blockade at the time a VES is delivered, thereby allowing the BT to become manifest with the VES (analogous to delivering a VES during SVT while the HB is refractory).³²

The dual-chamber sequential extrastimulation maneuver consists of an eight-beat drive train of simultaneous atrial and RV pacing at 600 milliseconds, followed by an AES (A2) delivered at a coupling interval equal to the AVN ERP, followed by a VES (V2) delivered at a coupling interval equal to the drive train CL (600 milliseconds). Repeat drives are then performed with decrements of 10 milliseconds for V2 until VA block is observed.³²

The critically timed A2 prolongs the AVN refractory period via concealed anterograde conduction, causing V2 to block in the AVN when it would have conducted had A2 not been delivered. If a BT is

present, V2 conducts back to the atrium while the AVN remains refractory, resulting in a retrograde atrial activation pattern consistent with exclusive BT conduction. Although there can also be some degree of concealed anterograde conduction into the BT during A2 stimulation, the more pronounced decremental properties of AVN tissue should prolong AVN refractoriness to a greater degree than that of the BT, allowing exclusive retrograde conduction over the BT to remain intact during V2 stimulation.³²

This maneuver has several potential limitations. First, atrial ERP may exceed anterograde AVN ERP. In addition, local atrial ERP at the site of BT insertion can render the atrium refractory to the wavefront traveling retrogradely over the BT. Therefore atrial pacing during this maneuver should ideally be performed at a site in close proximity to the atrial insertion of the BT if possible. Furthermore, the AES may cause anterograde concealed conduction in the BT, potentially resulting in BT conduction block during delivery of V2. The success of this pacing maneuver relies on the differential effects of concealed conduction into the AVN and BT, with greater extension of refractoriness in the former than the latter.³²

Induction of Tachycardia

Initiation by Programmed Atrial Stimulation

Orthodromic AVRT: bidirectional AVT BT. In the presence of a manifest AV BT, initiation of orthodromic AVRT with an AES requires the following: (1) anterograde block in the AV BT; (2) anterograde conduction over the AVN-HPS; and (3) slow conduction over the AVN-HPS, with adequate delay to allow for the recovery of the atrium and AV BT and subsequent retrograde conduction over the BT (Fig. 18.31; see Fig. 3.9). The first two requirements are facilitated by the fact that, while the BT conducts more rapidly than the AVN, it has a longer ERP, so the early atrial impulse blocks anterogradely in the BT but conducts over the AVN. For the third condition, the site of AV delay is not important; it is most commonly in the AVN, but it can also occur in the HB, bundle branches, or ventricular myocardium. Because the coupling intervals of the AES required to achieve anterograde block in

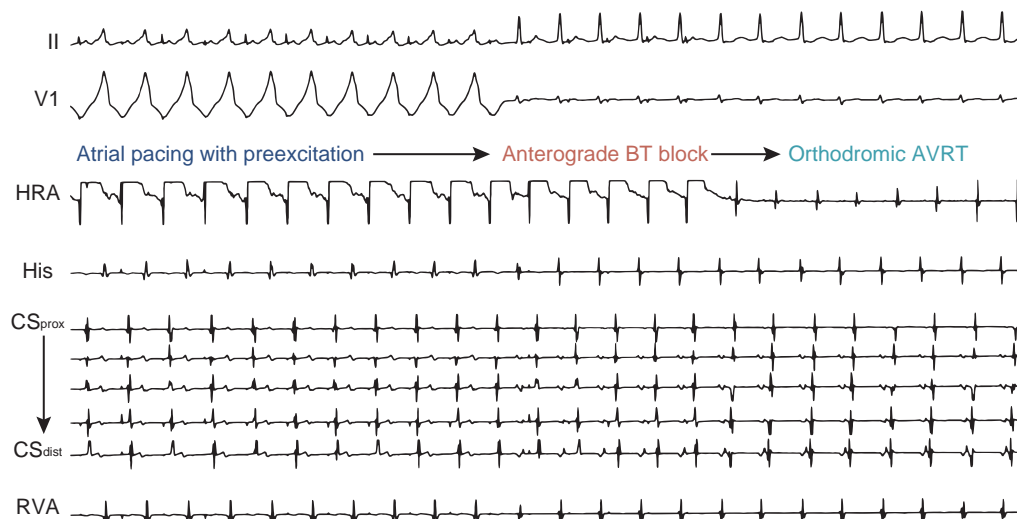


Fig. 18.31 Induction of an Orthodromic Atrioventricular Reentrant Tachycardia (AVRT) Using a Bidirectional Bypass Tract (BT) With Atrial Pacing. Rapid atrial pacing is initially associated with ventricular preexcitation via a left lateral BT. With pacing at a progressively shorter cycle length, anterograde block in the BT develops, as evident with loss ventricular preexcitation concurrent with prolongation of the PR interval. Cessation of pacing is followed by initiation of orthodromic AVRT utilizing the same BT as the retrograde limb of the reentry circuit. CS_{dist}, distal coronary sinus; CS_{prox}, proximal coronary sinus; HRA, high right atrium; RVA, right ventricular apex.

the BT are usually short, sufficient AVN delay is usually present so that orthodromic AVRT is initiated once anterograde BT block occurs. The presence of dual AVN physiology can facilitate the initiation of orthodromic AVRT by providing adequate AV delay by mediating anterograde conduction over the slow AVN pathway. BBB ipsilateral to the AV BT provides an additional AV delay that can facilitate tachycardia initiation.

Induction of orthodromic AVRT is easier with atrial stimulation at a site in close proximity to the AV BT insertion site; the closer the stimulation site is to the BT, the easier it is to encroach on the refractory period of the BT and achieve block, because it is not limited by the refractoriness or conduction time of intervening atrial tissue. Furthermore, the earlier the atrial insertion of the BT is activated, the more likely it will recover before arrival of the retrograde wavefront to the BT atrial insertion site, thereby facilitating reentry. Thus one may actually require less anterograde AV delay if recovery of excitability is shifted earlier in time. In addition, different sites of atrial stimulation can produce different AVN conduction velocities and refractoriness (even at the same AES coupling intervals).

If SVT induction fails, the use of multiple AESs, rapid atrial pacing, and pacing closer to the BT would achieve block in the BT and produce adequate AV delay.

AES can also result in a 1:2 response caused by conduction over both the BT and the AVN-HPS (i.e., a single AES resulting in two ventricular complexes; the first is fully preexcited and the second is normal). For this response to occur, significant delay in AVN-HPS conduction should be present (usually anterograde conduction is mediated by the slow AVN pathway) to allow for recovery of the ventricle after its activation via the BT. AES can also produce sinus nodal or AVN echo beats that in turn may block in the BT and achieve adequate AV delay to initiate orthodromic AVRT.

Orthodromic AVRT: concealed AV BT. Orthodromic AVRT in patients with concealed BTs is identical to that in patients with manifest BTs (Figs. 18.32 and 18.33). The only difference is that in patients with concealed BTs, anterograde block in the BT is already present. Consequently, the only condition needed to induce orthodromic AVRT is adequate AV delay (in the AVN or HPS) to allow for recovery of the atrium and atrial insertion site of the AV BT. Therefore orthodromic AVRT initiation requires less premature coupling intervals of the AESs in patients with concealed BTs than in patients with WPW.

Permanent junctional reciprocating tachycardia. PJRT is usually incessant and is initiated by spontaneous shortening of the sinus CL, without a triggering PAC or PVC. The tachycardia can be transiently terminated by PACs or PVCs but usually resumes after a few sinus beats (eFig. 18.5). This phenomenon has three potential mechanisms: a rate-related decrease in the retrograde ERP of the BT, a rate-related decrease in atrial refractoriness that allows the impulse to reactivate the atrium retrogradely over the BT, or a concealed Wenckebach block with block at the atrial-BT junction terminating the Wenckebach cycle, relieving any anterograde concealed conduction that may have prevented retrograde conduction up the BT. The latter is the most likely mechanism, because such slow BTs actually demonstrate decremental conduction at rapid rates and, in most cases, the atrial ERP at the atrial-BT junction is shorter than the RP (VA) interval. Thus some sort of anterograde concealment during NSR in the BT must be operative, preventing tachycardia from always occurring. Late-coupled AESs can also readily initiate PJRT.

Antidromic AVRT. The initiation of antidromic AVRT by an AES requires the following: (1) intact anterograde conduction over the BT; (2) anterograde block in the AVN or HPS; and (3) intact retrograde conduction over the HPS-AVN once the AVN resumes excitability

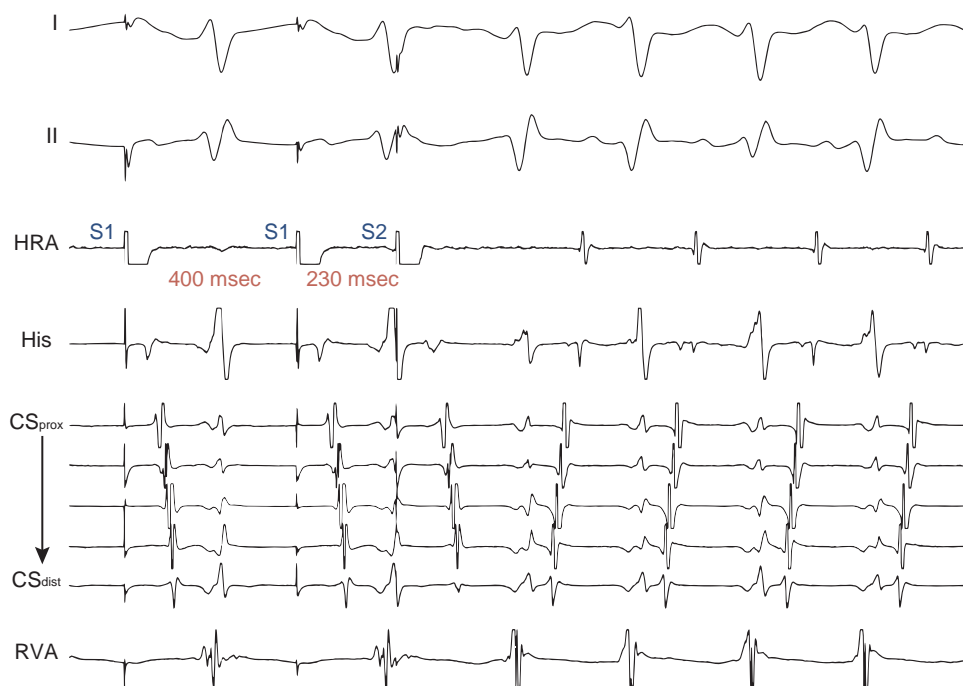
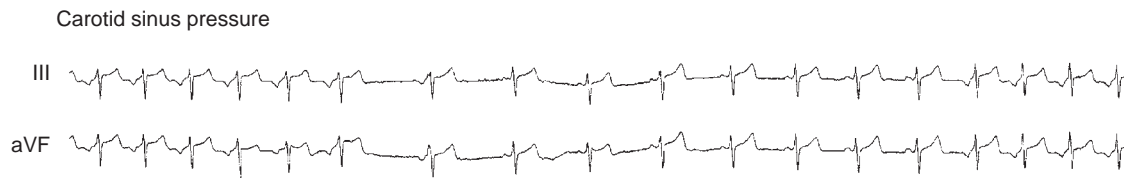


Fig. 18.32 Induction of an Orthodromic Atrioventricular Reentrant Tachycardia Using a Concealed Bypass Tract (BT) With Atrial Extrastimulation (AES). Note that the AES (S2) conducts with atrioventricular (AV) delay, which allows for recovery of the atrium and atrial insertion site of the AV BT. The atrial activation sequence during the tachycardia is eccentric in the coronary sinus recording, consistent with left free lateral BT. CS_{dist}, Distal coronary sinus; CS_{prox}, proximal coronary sinus; HRA, high right atrium; RVA, right ventricular apex.



eFig. 18.5 Permanent Junctional Reciprocating Tachycardia (PJRT). Two surface electrocardiogram leads are shown during PJRT. Carotid sinus pressure is applied (*at left*), resulting in termination of the tachycardia caused by block in the bypass tract (the tachycardia terminates with a QRS). Several escape and sinus complexes follow, and then the SVT resumes. This phenomenon gives rise to the use of the term *permanent* or *incessant*.

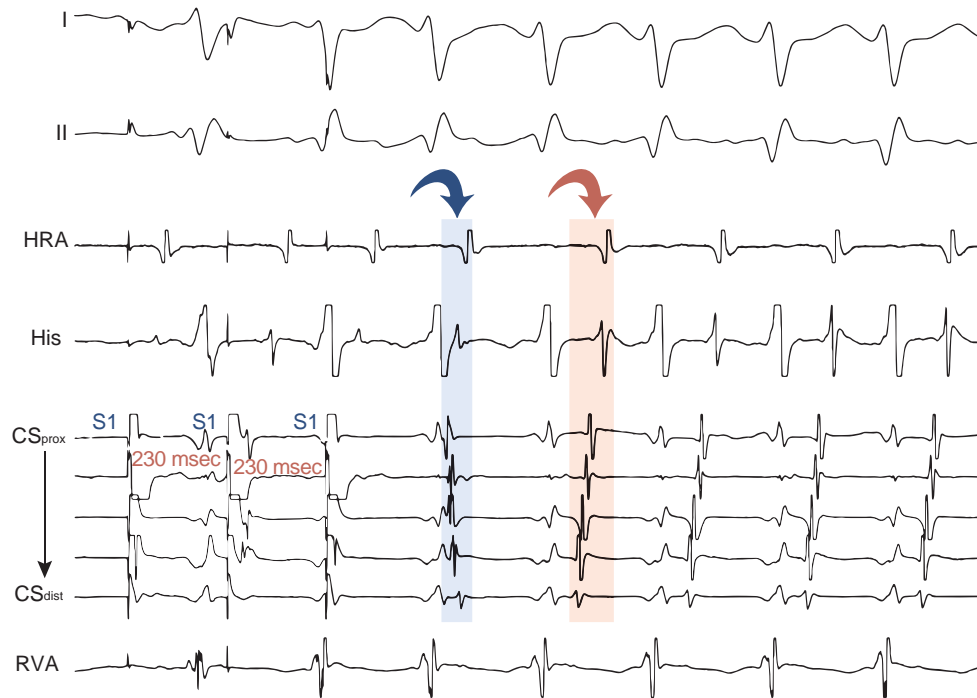


Fig. 18.33 Induction of an Orthodromic Atrioventricular Reentrant Tachycardia (AVRT) Using a Concealed Bypass Tract (BT) With Atrial Pacing. The last atrial paced complex conducts anterogradely over the slow atrioventricular nodal (AVN) pathway and results in an AVN echo beat (blue arrow and shade) and simultaneous atrial and ventricular activation. The echo beat induces orthodromic AVRT with an eccentric atrial activation sequence (red arrow and shade), consistent with left free lateral BT. Note that the VA interval during the AVN echo beat is significantly shorter than that during orthodromic atrioventricular nodal reentrant tachycardia. CS_{dist} , Distal coronary sinus; CS_{prox} , proximal coronary sinus; HRA, high right atrium; RVA, right ventricular apex.

following partial anterograde penetration (see Fig. 18.23). The latter is usually the limiting factor for the initiation of antidromic AVRT. A delay of more than 150 milliseconds between atrial insertion of the BT and HB is probably required for the initiation of antidromic AVRT.

Several mechanisms of antidromic AVRT initiation can be operative. The AES can block in the AVN with anterograde conduction down the BT and subsequent retrograde conduction over the HPS-AVN. In this setting, VH interval prolongation is required to allow recovery of the AVN. Because antidromic AVRTs have relatively short VA intervals, this mechanism of initiation is probably uncommon, except with left-sided BTs, which would potentially provide sufficient VH delay to allow retrograde conduction. Tachycardia initiation can be facilitated by a short retrograde AVN ERP, a common finding in patients with these SVTs. Alternatively, the AES may block in the AVN, with anterograde conduction down the BT and subsequent retrograde conduction over a different BT. Subsequent complexes can conduct retrogradely over the AVN-HPS or the second BT. Changing TCL (and VA interval) may relate to whether retrograde conduction proceeds over the AVN-HPS or the second BT. A third potential mechanism for the initiation of antidromic AVRT involves AES conduction over the BT and simultaneously over the slow pathway of a dual AVN pathway situation, with anterograde block in the fast AVN pathway. Conduction beyond the HB to the ventricle is not possible because of ventricular refractoriness, yet an AVN echo to the atrium may occur, which in turn may conduct anterogradely over the BT, when the ventricle would have recovered excitability, and subsequently back up the now-recovered AVN, initiating antidromic AVRT. AVN reentry may not persist or may be preempted by retrograde con-

duction up the fast AVN pathway because of the premature ventricular activation over the BT. In this scenario, the location of the His potential will depend on whether it was anterograde or retrograde.

In general, if atrial stimulation induces antidromic AVRT, multiple BTs are often operative. Whether they are operative throughout the SVT depends on the relative retrograde activation times over the additional BTs and HPS-AVN and the varying degree of anterograde and retrograde concealment into the additional BTs and HPS-AVN during the SVT.

The site of atrial stimulation plays an important role in inducibility of AVRT, and can also determine the type of AVRT initiated in patients with bidirectional BTs. The closer the stimulation site to the BT, the more likely anterograde block in the BT will occur and orthodromic AVRT will result. Conversely, antidromic AVRT is more likely to occur with atrial stimulation close to the AVN.

Initiation by Programmed Ventricular Stimulation

Orthodromic AVRT. Ventricular stimulation can induce orthodromic AVRT in the majority of patients (inducibility rate of 60% with VES and 80% with ventricular pacing), regardless of whether the BT is manifest or concealed (Fig. 18.34). Initiation of orthodromic AVRT by ventricular stimulation requires the following: (1) retrograde block of the ventricular impulse in the HPS-AVN; (2) retrograde conduction only over the BT; and (3) adequate VA conduction delay to allow for recovery of the AVN-HPS from any concealment produced by ventricular stimulation, so it can support anterograde conduction of the reentrant impulse. Because the BT retrograde ERP is usually very short, the prime

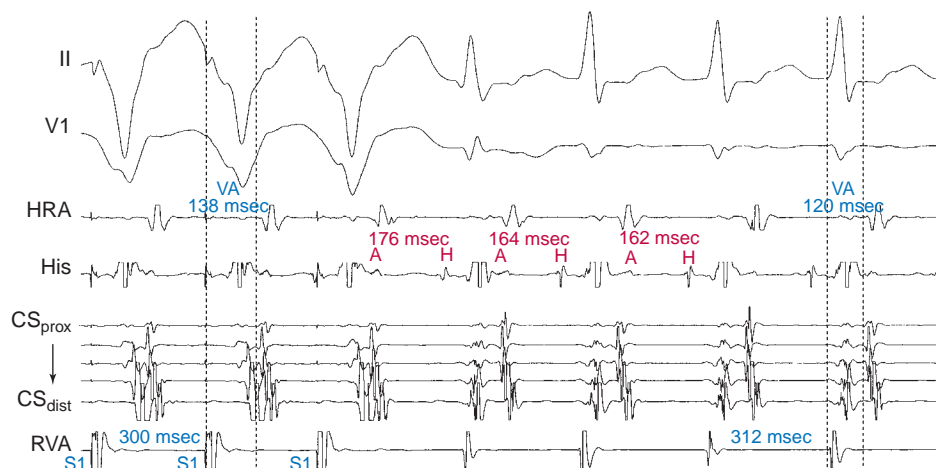


Fig. 18.34 Induction of an Orthodromic Atrioventricular Reentrant Tachycardia (AVRT) Using a Concealed Posteroseptal Bypass Tract With Ventricular Pacing. Note that although the ventricular pacing cycle length (CL) approximates the tachycardia CL, the ventriculoatrial (VA) interval (*dashed lines*) during ventricular pacing is only slightly longer than that during supraventricular tachycardia (SVT), which favors orthodromic AVRT over atrioventricular nodal reentrant tachycardia as the mechanism of the SVT. In addition, the atrial–His bundle interval of the first SVT complex is longer than that of subsequent beats, indicating retrograde concealment in the AVN produced by the last ventricular stimulus. CS_{dist}, Distal coronary sinus; CS_{prox}, proximal coronary sinus; HRA, high right atrium; RVA, right ventricular apex.

determinant of orthodromic AVRT initiation is the extent of retrograde conduction and/or concealment in the HPS-AVN.

Multiple modes of initiation of orthodromic AVRT can be present, depending on the PCL or VES coupling interval, conduction velocities, and refractoriness of the HPS-AVN and BT, as well as the site of ventricular stimulation. Ventricular pacing at a CL or a VES with a coupling interval that is shorter than the ERP of the AVN but longer than that of the HPS and BT would block retrogradely in the AVN and conduct over the BT to initiate orthodromic AVRT. Block in the AVN, which is more likely to occur with rapid ventricular pacing or VES delivered after a short pacing drive CL, can cause concealment and subsequent delay in anterograde conduction of the first SVT impulse over the AVN, resulting in longer AH and PR intervals of the first SVT beat compared with subsequent beats (see Fig. 18.34). On the other hand, ventricular pacing at a CL or a VES with a coupling interval shorter than the ERP of the HPS, but longer than that of the BT, would block retrogradely in the HPS and conduct over the AV BT to initiate orthodromic AVRT. When block occurs in the HPS, which is more likely to occur with a VES delivered during NSR or after a long pacing drive CL, the first SVT beat will approach a fully recovered AVN and conduct with short AH and PR intervals equal to subsequent SVT beats. In this setting, adequate prolongation of the HV interval may be required to allow for the recovery of ventricular refractoriness for the ventricle to be activated and support reentry, because AVN delay may have not been sufficient. When HV interval prolongation is required to initiate orthodromic AVRT, it is almost invariably associated with LBBB. A short-coupled VES, especially following a pacing drive with a long CL, that blocks retrogradely in both the BT and RB and conducts transseptally and then retrogradely over the LB, can result in a bundle branch reentrant (BBR) beat that conducts to the ventricle down the RB, and then retrogradely to the atrium over the AV BT, mediating the initiation of orthodromic AVRT. The long HV interval often associated with BBR beats, plus the LBBB pattern, facilitate the induction of orthodromic AVRT using a left-sided BT (Fig. 18.35).

When induction of the SVT is achieved by ventricular pacing at a PCL similar to the subsequent TCL or by a VES that activates the HB

at a coupling interval (i.e., H1-H2 interval) similar to the H-H interval during the SVT (i.e., similar to the TCL), the HA interval following the initiating ventricular stimulus is then compared with that during the SVT. During AVNRT, the HA interval of the ventricular stimulus initiating the SVT is longer than the HA interval during the SVT because both the HB and atrium are activated in sequence during ventricular stimulation but in parallel during AVNRT (see Fig. 17.14). This is even exaggerated by the fact that the AVN usually exhibits greater decremental conduction with repetitive engagement of impulses than to a single impulse at a similar coupling interval. Therefore the more prolonged the HA interval with the initiating ventricular stimulus, the more likely the SVT is AVNRT. On the other hand, if the SVT uses an AV BT for retrograde conduction, the HA interval during the initiating ventricular stimulus (at a coupling interval comparable to the TCL) is shorter than that during orthodromic AVRT because the HB and atrium are activated in parallel during ventricular pacing (when atrial activation is mediated by retrograde BT conduction), but in sequence during SVT.

The intervals immediately following tachycardia initiation with a VES (delivered from the RV apex) provide data that are essentially equivalent to those observed with ventricular entrainment (see later). The interval from the VES to atrial activation (surface VA or “SA” interval) is compared to the surface VA interval during SVT, and the post-VES return cycle (i.e., the interval from the VES to the subsequent RV apical depolarization) is compared to the TCL. An SA interval that exceeds the surface VA interval during SVT by less than 85 milliseconds is consistent with orthodromic AVRT. Similarly, when the post-VES return cycle exceeds the TCL by less than 115 milliseconds, orthodromic AVRT is suggested. The small differences between those intervals are related to the proximity of the RV apical pacing site to the SVT reentry circuit. Larger differences in these intervals are observed in the setting of AVNRT or orthodromic AVRT utilizing a left lateral BT or a septal BT with decremental conduction. The unique advantage of this technique is that it does not require a sustained tachycardia that can be successfully entrained.³³

Permanent junctional reciprocating tachycardia. Ventricular stimulation is less effective in initiating PJRT because of the already

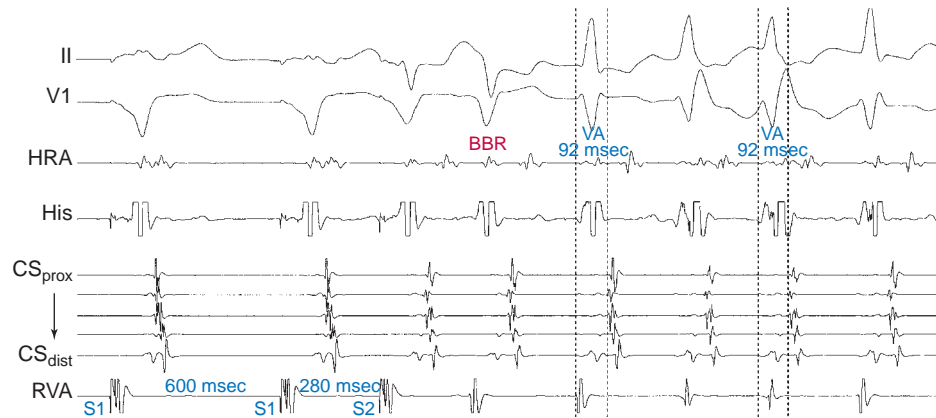


Fig. 18.35 Induction of an Orthodromic Atrioventricular Reentrant Tachycardia (AVRT) Using a Concealed Left Posteroseptal Bypass Tract (BT) With Ventricular Extrastimulation (VES). The VES conducts retrogradely over the BT, but also results in a bundle branch reentrant (BBR) beat, which in turn conducts to the atrium over the BT and initiates orthodromic AVRT. Note that right bundle branch block (RBBB) develops shortly after initiation of the tachycardia; however, the ventriculoatrial (VA) interval (dashed lines) remains constant, regardless of the presence or absence of RBBB, because the BT is in the contralateral ventricle. *CS_{dist}*, Distal coronary sinus; *CS_{prox}*, proximal coronary sinus; *HRA*, high right atrium; *RVA*, right ventricular apex.

impaired conduction in the BT, such that an early VES produces block in the BT. A late-coupled VES (when the HB is refractory) can initiate SVT in some cases.

Antidromic AVRT. Initiation of classic antidromic AVRT by ventricular pacing and VES requires the following: (1) retrograde block in the BT; (2) retrograde conduction over the AVN or HPS; and (3) adequate VA delay to allow for recovery of the atrium and BT so it can support subsequent anterograde conduction (see Fig. 18.25).

When induction of the SVT is achieved by ventricular pacing at a CL similar to the TCL or by a VES that activates the HB at a coupling interval (i.e., H1-H2 interval) similar to the H-H interval during the SVT, the HA interval following the initiating ventricular stimulus is always equal to or shorter than that during the antidromic AVRT. This is because the HB and atrium are activated in sequence during antidromic AVRT and in parallel during ventricular stimulation (in the presence of a retrogradely conducting BT). Therefore an HA interval of the initiating ventricular stimulus longer than the HA interval during SVT favors preexcited AVNRT and excludes antidromic AVRT (see Fig. 18.25). Moreover, because the AVN usually exhibits greater decremental conduction with repetitive engagement of impulses than to a single impulse at a similar coupling interval, the more prolonged the HA interval with the initiating ventricular stimulus, the more likely that the SVT is preexcited AVNRT.

Tachycardia Features

Orthodromic Atrioventricular Reentrant Tachycardia

Atrial activation sequence. The initial site of atrial activation during orthodromic AVRT depends on the atrial insertion site of the BT, but is always near the AV groove and without multiple breakthrough points. The atrial activation sequence during orthodromic AVRT should be identical to that during ventricular pacing at comparable CLs when VA conduction occurs exclusively over the BT. However, retrograde conduction during ventricular pacing can proceed over the AVN or over both the BT and AVN, resulting in fusion of atrial activation, depending on the site of ventricular stimulation relative to the BT and HPS, and on retrograde conduction and refractoriness of the HPS-AVN.

Atrial-ventricular relationship. The conduction time over the typical (fast) AV BT is approximately 30 to 120 milliseconds. Therefore the RP interval during orthodromic AVRT is short, but longer than that during typical AVNRT, because in the setting of orthodromic AVRT the wavefront has to activate the ventricle before it reaches the ventricular insertion site of the BT at the AV groove and subsequently conduct to the atrium. Consequently, a very short VA interval (less than 70 milliseconds) or short V–high RA interval (less than 95 milliseconds) largely excludes orthodromic AVRT, and favors typical AVNRT (see Fig. 18.33).³⁴ However, VA intervals shorter than 70 milliseconds have occasionally been observed in patients with orthodromic AVRT utilizing left lateral or left posteroseptal BTs.³⁵ Importantly, the RP and VA intervals during orthodromic AVRT remain constant regardless of oscillations in the TCL from whatever cause and regardless of changes in the PR interval (AH interval); as a consequence, the TCL is most closely associated with the PR interval (i.e., anterograde AVN conduction) and the RP/PR ratio may vary (Fig. 18.36).

A 1:1 A-V relationship is a prerequisite for maintenance of AVRT because parts of both the atrium and the ventricle are essential components of the reentrant circuit. If an SVT persists despite the presence of AV or VA block, orthodromic AVRT is excluded.

When dual AVN pathways are present, the slow AVN pathway functions in most cases as the anterograde limb during orthodromic AVRT. An AH interval of more than 180 milliseconds during orthodromic AVRT suggests a slow AVN pathway mediating the anterograde limb of the reentrant circuit, whereas an AH interval of less than 160 milliseconds suggests anterograde conduction over the fast AVN pathway. Obviously, orthodromic AVRT using the slow pathway will have a longer TCL.

Slow-slow AVNRT is associated with an RP interval and P wave morphology similar to that during orthodromic AVRT using a posteroseptal AV BT. However, although both SVTs have the earliest atrial activation in the posteroseptal region, conduction time from that site to the HB region is significantly longer in AVNRT than in orthodromic AVRT, resulting in a significantly longer RP interval in lead V1 and a larger difference in the RP interval between lead V1 and the inferior leads. Therefore a Δ RP interval (V1 to III) longer than 20 milliseconds

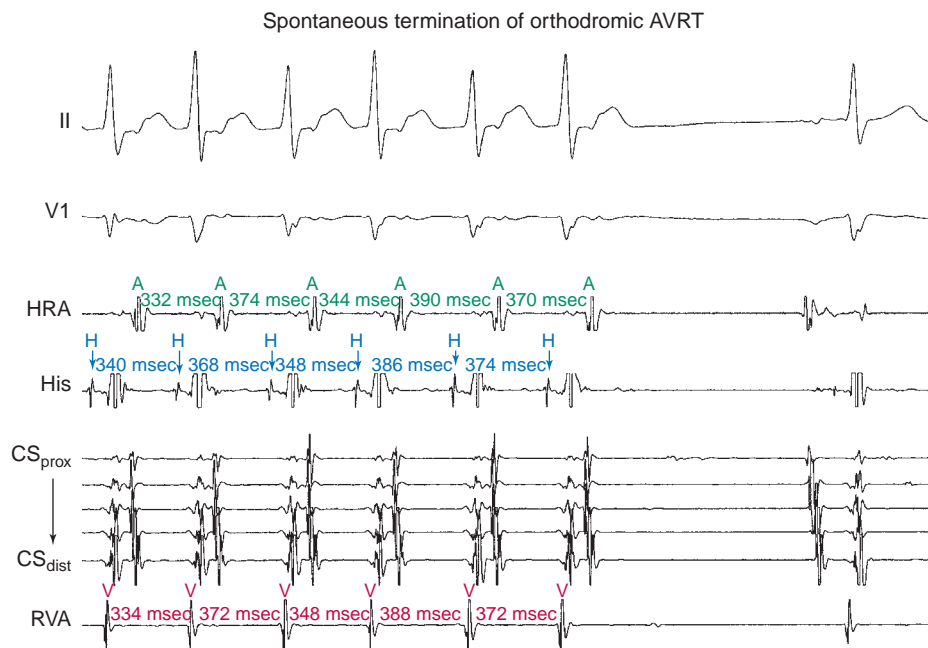


Fig. 18.36 Spontaneous Termination of Orthodromic Atrioventricular Reentrant Tachycardia (AVRT) Using a Concealed Superoparaseptal Bypass Tract. Note that the tachycardia terminates with an atrial complex not followed by a QRS, consistent with anterograde block in the atrioventricular node (AVN). Also, note the oscillation in the tachycardia cycle length (CL) preceding termination. Changes in H-H and V-V intervals precede the subsequent changes in A-A intervals, and the ventriculoatrial (VA) interval remains constant despite oscillation of the CL. This indicates that the variability in the tachycardia CL is secondary to changes in the anterograde conduction over the AVN, whereas VA conduction over the retrograde limb of the reentrant circuit (the bypass tract) remains constant. CS_{dist} , Distal coronary sinus; CS_{prox} , proximal coronary sinus; HRA, high right atrium; RVA, right ventricular apex.

suggests slow-slow AVNRT with a sensitivity of 71%, specificity of 87%, and positive predictive value of 75%.

Effects of BBB. The presence of BBB during SVT is much more common in orthodromic AVRT than AVNRT or AT; in fact, the majority of SVTs with sustained LBBB are orthodromic AVRTs. Two reasons have been proposed to explain why prolonged aberration occurs less commonly during AVNRT than orthodromic AVRT. First, the induction of AVNRT requires significant AVN delay, which makes the H1-H2 interval longer and makes aberration unlikely. Conversely, in orthodromic AVRT, AVN conduction need not be slow, resulting in a shorter AH interval and an impulse encroaching on HPS refractoriness, in turn resulting in BBB. Second, LBBB facilitates the induction of orthodromic AVRT when a left-sided AV BT is present by providing the necessary AV delay required to maintain the reentry circuit.³⁶

BBB is more common when AVRT is initiated by an AES that is delivered during NSR or after long pacing drive CLs, during which HPS refractoriness is longest and AVN conduction and refractoriness are shortest. When AVRT is induced by atrial stimulation, RBBB is twice as common as LBBB. In contrast, when AVRT is induced by ventricular stimulation, LBBB is much more common than RBBB (because of retrograde concealment of the paced wavefront in the LB). In addition, the incidence of BBB is more common in AVRTs induced by ventricular stimulation than those induced by atrial stimulation (75% vs. 50%).

BBB ipsilateral to the BT results in prolongation of the “surface VA interval.” Block in the ipsilateral bundle branch forces the reentrant circuit to follow a longer path. Hence, more time is needed for the tachycardia wavefront to travel from the AVN down the HB and contralateral bundle branch, and then transseptally to the ventricle ipsilateral to the BBB in order to reach the BT and then activate the atrium

(Fig. 18.37). However, the “local VA interval” (measured at the site of BT insertion) remains constant. On the other hand, the TCL usually increases in concordance with the increase in the surface VA interval as a result of ipsilateral BBB because of the now larger tachycardia circuit. However, because the time the wavefront spends outside the AVN is now longer because of the larger circuit, AVN conduction may improve to a small degree, resulting in shortening of the AH interval (PR interval), which can potentially counterbalance, at least in part, the effects of prolongation of the VA interval on the total TCL. Thus the surface VA interval and not the TCL should be used to assess the effects of BBB on the SVT (see Figs. 18.37 and 18.38).

Prolongation of the surface VA interval during SVT in response to BBB by more than 35 milliseconds compared to that with normal QRS or contralateral BBB indicates that an ipsilateral free-wall BT is present and is participating in the SVT (i.e., diagnostic of orthodromic AVRT) (see Fig. 18.38). On the other hand, prolongation of the surface VA by 25 to 35 milliseconds suggests a septal or paraseptal BT (posteroseptal AV BT in association with LBBB, and superoparaseptal AV BT in association with RBBB). In contrast, BBB contralateral to the BT does not influence the VA interval or TCL because the contralateral ventricle is not part of the reentrant circuit (see Figs. 18.35 and 18.37). Of note, prolongation of the VA interval by more than 45 milliseconds in response to RV pacing entraining the orthodromic AVRT is also diagnostic of a left-sided BT, whereby RV pacing results in effects analogous to those created by LBBB and, as a consequence, VA interval prolongation.

Oscillations in the tachycardia cycle length. Oscillation of the TCL during orthodromic AVRT can occur and generally is caused by changes in the anterograde conduction over the AVN (see Fig. 18.36). Because retrograde conduction through the BT is much less variable,

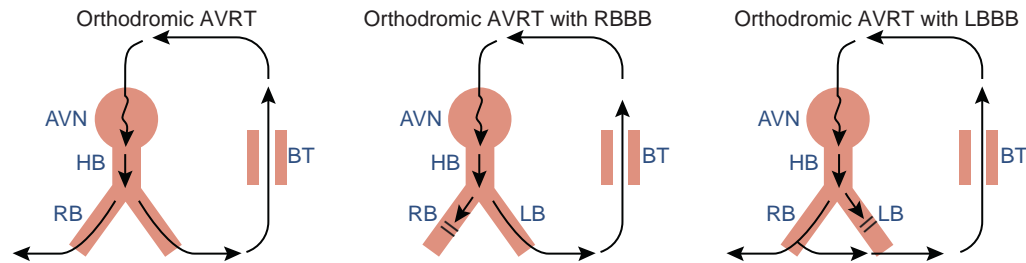


Fig. 18.37 Schematic Illustration of the Effect of Bundle Branch Block on the Reentrant Circuit During Orthodromic Atrioventricular Reentrant Tachycardia (AVRT) Using a Left-Sided Bypass Tract (BT). Block in the left bundle branch (LB) (ipsilateral to the BT) results in prolongation of the reentrant pathway and, therefore, prolongation of the ventriculoatrial interval. In contrast, block in the right bundle branch (RB) (contralateral to the BT) has no effect on the reentrant circuit. AVN, Atrioventricular node; HB, His bundle; LBBB, left bundle branch block; RBBB, right bundle branch block.

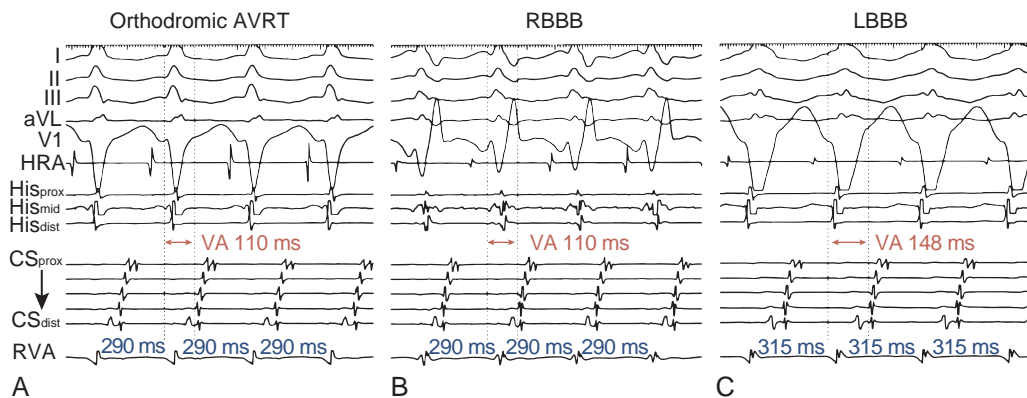


Fig. 18.38 Effect of Bundle Branch Block on Orthodromic Atrioventricular Reentrant Tachycardia (AVRT). Orthodromic AVRT is recorded in the same patient. (A) Orthodromic AVRT with normal intraventricular conduction. (B) Orthodromic AVRT with right bundle branch block (RBBB). (C) Orthodromic AVRT with left bundle branch block (LBBB). Note that the tachycardia cycle length (TCL) and ventriculoatrial (VA) interval are not affected by the development of RBBB. In contrast, the development of LBBB during tachycardia is associated with prolongation of the VA interval (by 38 milliseconds) and a lesser degree of prolongation of the TCL (by 25 milliseconds), indicating the presence and participation of a left lateral bypass tract in the reentrant circuit. CS_{dist}, Distal coronary sinus; CS_{prox}, proximal coronary sinus; His_{dist}, distal His bundle; His_{mid}, middle His bundle; His_{prox}, proximal His bundle; HRA, high right atrium; RVA, right ventricular apex.

the changes in ventricular CL that result from variability in the antero-grade AVN conduction precede the subsequent changes in atrial CL, and changes in atrial CL do not predict changes in subsequent ventricular CL (similar to observations during typical AVNRT). In contrast, changes in atrial CL predict the changes in subsequent ventricular CL during atypical AVNRT and AT.³⁷

In addition, orthodromic AVRT in the presence of dual AVN physiology can be associated with antegrade conduction alternating over the slow and fast AVN pathways, resulting in a regular irregularity of the TCL (alternating long and short cycles). Alternatively, the presence of dual AVN pathways can lead to two separate stable TCLs. In either setting, the RP interval during the SVT remains constant.

QRS alternans. Alternans of the QRS complex amplitude during a relatively slow SVT is almost always indicative of orthodromic AVRT (see Fig. 18.13). On the other hand, although QRS alternans during fast SVTs is most commonly seen in orthodromic AVRT, it can also be seen with other types of SVT.

Termination and response to physiological and pharmacological maneuvers. Spontaneous termination of orthodromic AVRT is usually caused by gradual slowing and then block in the AVN (see Fig. 18.36), sometimes causing initial oscillation in the TCL, with alternate com-

plexes demonstrating a Wenckebach periodicity before block. However, termination with block in the BT without any perturbations of the TCL can occur during very rapid AVRT or following a sudden shortening of the TCL (e.g., after resolution of ipsilateral BBB or shift of antero-grade conduction from the slow to the fast AVN pathway).

Carotid sinus massage can terminate orthodromic AVRT by gradual slowing and then block in the AVN. Adenosine, digoxin, verapamil, diltiazem, and beta-blockers terminate orthodromic AVRT by block in the AVN; therefore the SVT terminates with a P wave that is not followed by a QRS. Verapamil rarely produces block in the BT and, when it does, block is usually preceded by oscillation in the TCL produced by changes in AVN conduction, leading to long-short sequences. Class IA and IC antiarrhythmic agents can produce block in the BT with variable effect on the AVN-HPS. Amiodarone can terminate AVRT by block in the AVN, HPS, or AV BT. Sotalol affects the AVN with little or no effect on the AV BT.

Permanent junctional reciprocating tachycardia

Atrial activation sequence. The initial site of atrial activation is most often in the posteroseptal part of the triangle of Koch near the coronary sinus ostium (CS os), similar to that in atypical AVNRT (Fig. 18.39).³

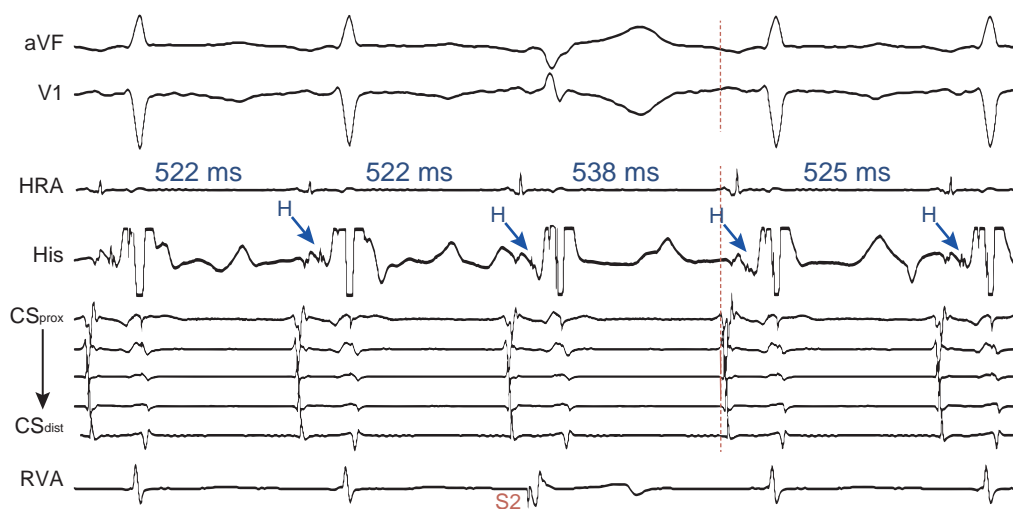


Fig. 18.39 Ventricular Extrastimulation (VES) During Permanent Junctional Reciprocating Tachycardia. The supraventricular tachycardia has a stable baseline cycle length (522 milliseconds). A single VES (*S2*) introduced during His bundle refractoriness retards the timing of the next atrial complex (538 milliseconds). The anticipated timing of the high right atrium electrogram is indicated by the dashed line. *CS_{dist}*, Distal coronary sinus; *CS_{prox}*, proximal coronary sinus; *HRA*, high right atrium; *RVA*, right ventricular apex.

Atrial-ventricular relationship. Because the retrograde limb of the reentry circuit is the slow BT (which conducts more slowly than the AVN), the RP interval is longer than the PR interval, similar to fast-slow AVNRT (see Figs. 18.14 and 18.39). In contrast to the typical (fast) AV BTs, the RP interval during PJRT is not fixed because the BT serving as the retrograde limb of the reentrant circuit has decremental properties. Similar to all types of AVRTs, a 1:1 A-V relationship is a prerequisite to sustenance of the tachycardia.

Oscillations in the TCL. The tachycardia rate typically fluctuates (100 to 220 beats/min) in response to autonomic tone and physical activity, and the rate changes result from modulation of the PR and RP intervals. Typically, the TCL is often just longer than the shortest CL at which the BT can conduct retrogradely.

Effects of BBB. BBB affects PJRT in a manner analogous to that described for orthodromic AVRT.

Termination and response to physiological and pharmacological maneuvers. Carotid sinus massage and AVN blockers (adenosine, digoxin, calcium channel blockers, and beta-blockers) usually terminate PJRT by block in the AVN (two-thirds) or in the BT (one-third) (see eFig. 18.5). Although the mode of tachycardia termination by adenosine has been suggested to distinguish between PJRT and atypical AVNRT, one report has shown that termination of atypical AVNRT with adenosine can also result from block in the fast AVN pathway and, therefore, its value in distinguishing between atypical AVNRT and PJRT is questionable.

Antidromic AVRT

Atrial activation sequence. The initial site of atrial activation in classic antidromic AVRT is consistent with retrograde conduction over the AVN. If the preexcited AVRT is using a second BT for retrograde conduction, then the atrial activation sequence will depend on the location of that BT (see eFig. 18.1). In addition, ventricular activation precedes HB activation by more than 10 milliseconds during classic antidromic AVRT because the ventricle and HB are activated sequentially by the same reentrant wavefront. On the other hand, during preexcited AVNRT, the ventricle and HB can be activated in parallel (the ventricle is activated via the bystander BT and the HB activated via the AVN). Therefore, during a preexcited SVT, a positive HV interval (i.e., HB activation preceding ventricular activation) or

a VH interval not more than 10 milliseconds, especially when the HA interval is not more than 50 milliseconds, favors preexcited AVNRT over antidromic AVRT.

Atrial-ventricular relationship. The conduction time over classic (fast) AV BTs is approximately 30 to 120 milliseconds. Therefore the PR is short and fixed, regardless of oscillations in the TCL from whatever cause. Similar to all types of AVRT, the A/V ratio is always equal to 1. If the SVT persists in the presence of AV or VA block, antidromic AVRT is excluded.

Oscillations in the TCL. Antidromic AVRT can be irregular. Tachycardia CL changes are usually caused by changes in retrograde conduction over different fascicles of the HPS with different VA intervals (regardless of the type and degree of changes in the VH or HA intervals), retrograde conduction over dual AVN pathways (with different HA intervals), different routes of anterograde conduction (with different AV intervals), and/or retrograde conduction over different BTs (with different VA intervals). When the change in the TCL can be ascribed to a change in the VH interval or the subsequent HA interval, it suggests that retrograde conduction occurs over the HPS and AVN and not over a second BT.

The TCL tends to be shorter during classic antidromic AVRT than orthodromic AVRT when these arrhythmias occur in the same patient. This may be explained by the fact that antidromic AVRT uses the fast AVN pathway (of a dual AVN physiology) retrogradely, whereas orthodromic AVRT uses the slow pathway anterogradely or, in the absence of dual AVN physiology, this may be merely supportive evidence that retrograde conduction during antidromic AVRT uses another fast BT instead of the slower AVN. On the other hand, antidromic AVRTs using two or more BTs may have longer TCLs than orthodromic AVRT or classic antidromic AVRT because the two BTs are typically in opposite chambers and are incorporated in a larger reentrant circuit than one involving a midline AVN.

Effects of BBB. Retrograde BBB affects antidromic AVRT in a manner analogous to that described for orthodromic AVRT. Abrupt prolongation of the VH and VA intervals and TCL when retrograde BBB occurs is consistent with retrograde HB activation via the ipsilateral bundle branch, which is typical for antidromic AVRT using an ipsilateral AV BT, but can also occur in preexcited AVNRT. However, if VH

prolongation is accompanied by prolongation of the VA interval (without a change in the activation sequence) and the TCL, true antidromic tachycardia (using the AV conduction system as the retrograde limb) can be diagnosed and preexcited AVNRT is excluded. Lack of effects on the VH interval can occur in: (1) preexcited AVRT (utilizing a second BT as the retrograde limb); (2) antidromic AVRT utilizing a left-sided BT; (3) antidromic AVNRT utilizing an atriofascicular BT inserting into the RB proximal to the site of RBBB; and (4) preexcited AVNRT.

Termination and response to physiological and pharmacological maneuvers. Various physiological and pharmacological maneuvers affect the BT and AVN during antidromic AVRT in a fashion similar to that described for orthodromic AVRT. Carotid sinus massage and adenosine terminate classic antidromic AVRT after ventricular activation, secondary to retrograde block up the AVN. In contrast, pre-excited typical AVNRT terminates after atrial activation, secondary to anterograde block down the slow AVN pathway.

Tachycardia termination or prolongation of the VA (and VH) interval and TCL with transient RBBB, caused by mechanical trauma or introduction of VES, is diagnostic of antidromic AVRT using a right-sided or septal BT and excludes preexcited AVNRT. Continuation of an SVT at the same TCL, despite anterograde block in the BT (by drugs, mechanical trauma caused by catheter manipulation, or ablation), excludes antidromic AVRT.

Diagnostic Maneuvers During Tachycardia

Programmed Atrial Stimulation During Tachycardia

Orthodromic AVRT

Resetting. AES can easily reset orthodromic AVRT. In fact, it is usual for AES not to affect the SVT because of the large size and large excitable gap of the reentrant circuit. However, this can be influenced by the distance between the site of atrial stimulation and the atrial region incorporated in the AVRT circuit (i.e., atrial myocardium between the BT and the AVN). Because only parts of the atrium ipsilateral to the BT are requisite components of the orthodromic AVRT circuit, AES delivered in the contralateral atrium may not affect the circuit, whereas

AESs delivered at sites in close proximity to the BT or the AVN have the highest success at resetting the reentrant circuit.

AES over a wide range of coupling intervals can reset orthodromic AVRT via conduction down the AVN-HPS. In this setting, atrial activation is a fusion of the AES and the SVT impulse traveling retrogradely up the BT. The next QRS can be early or late, depending on the degree of slowing of conduction of the AES anterogradely down the AVN (i.e., the degree of prolongation of the A2-H2 interval).

Termination. An early-coupled AES can terminate the SVT, usually by block in the AVN-HPS. In this setting, the SVT terminates with an AES not followed by a QRS (i.e., AV block). Alternatively, the AES can render the atrium refractory to the SVT impulse traveling retrogradely up the BT, in which case the SVT terminates with an AES followed by a QRS (i.e., VA block). The AES can also anterogradely penetrate the BT and collide with the retrogradely traveling SVT wavefront (VA block). Lastly, the AES can conduct down the AVN-HPS and advance the next QRS, which then blocks in the still-refractory BT or atrium (VA block).

Atrial entrainment. Atrial pacing at a CL approximately 10 to 30 milliseconds shorter than the TCL can generally entrain orthodromic AVRT (Fig. 18.40).

Resetting and entrainment with manifest atrial fusion. Resetting and entrainment with manifest atrial fusion can be demonstrated in AVRT. The morphology of the fusion P wave is hybrid between the tachycardia P wave morphology and the fully paced P wave morphology. This can be difficult to demonstrate if the P waves cannot be visualized on the surface ECG (due to overlapping ST-T wave), which is usually the case; however, manifest fusion can be demonstrable on intracardiac recordings (see Fig. 18.40). Atrial fusion results from intraatrial collision of the impulse propagating from the paced site with the tachycardia impulse emerging from the BT. In contrast, manifest fusion cannot be demonstrated during resetting or entrainment of AVNRT. For atrial fusion (i.e., fusion of atrial activation from both the tachycardia wavefront and the AES) to occur, the AES should be able to enter the reentrant circuit, while at the same time the tachycardia wavefront should be able to exit the circuit. This requires spatial

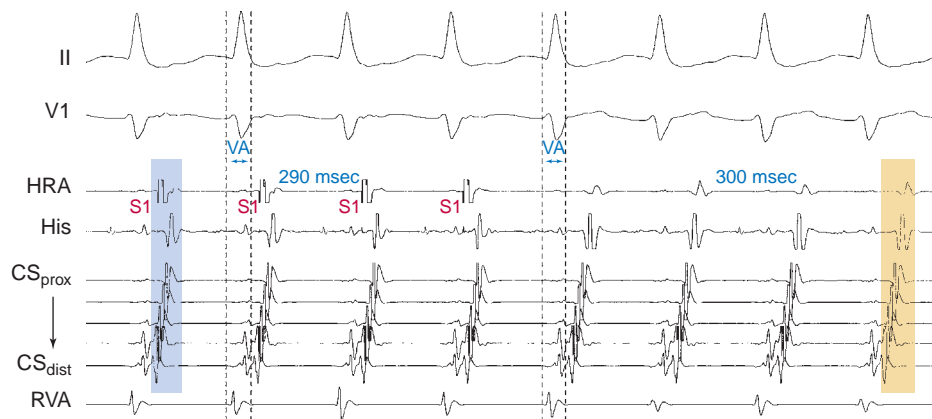


Fig. 18.40 Atrial Entrainment of Orthodromic Atrioventricular Reentrant Tachycardia (AVRT). Overdrive atrial pacing is from the high right atrium (HRA) during an AVRT using a left lateral bypass tract (BT). Note that the atrial activation sequence during entrainment (blue shade) is different from the tachycardia atrial activation sequence (yellow shade), and is also different from the expected purely paced atrial activation sequence as evidenced by a distal-to-proximal activation sequence in the coronary sinus. This indicates the presence of atrial fusion (between the paced and tachycardia wavefronts) during entrainment, which is consistent with AVRT and excludes both focal atrial tachycardia and atrioventricular nodal reentrant tachycardia. Note that the ventriculoatrial (VA) interval (dashed lines) of the return cycle after cessation of atrial pacing is similar to that of the supraventricular tachycardia (VA linking), because retrograde VA conduction of the last entrained QRS is mediated by the BT. CS_{dist}, Distal coronary sinus; CS_{prox}, proximal coronary sinus; RVA, right ventricular apex.

separation between the entry and exit sites to the reentrant circuit, a condition that seems to be lacking in the setting of AVNRT.^{38,39}

Ventriculoatrial linking. The initial atrial complex following cessation of atrial pacing entraining orthodromic AVRT is *linked* to, and cannot be dissociated from, the last captured ventricular complex. As a consequence, the VA intervals of the return cycle after cessation of atrial pacing are fixed and similar to those during tachycardia (with less than 10 milliseconds of variation) after different attempts at SVT entrainment (see Fig. 18.40). The postpacing VA intervals typically remain constant regardless of the site, duration, or CL of the entraining atrial pacing drive because the timing of atrial activation is dependent on retrograde VA conduction of the last entrained QRS mediated by the BT, which is fixed and constant. VA linking is also observed after introduction of an AES with a wide range of coupling intervals during tachycardia. VA linking can also be observed in typical AVNRT but not AT.^{34,40}

Antidromic AVRT. AES is of value in distinguishing antidromic AVRT from preexcited AVNRT. A late-coupled AES, delivered close to the BT atrial insertion site during SVT when the AV junctional atrium is refractory (i.e., when the atrial electrogram is already manifest in the HB recording at the time of AES delivery) that advances (accelerates) the timing of both the next ventricular activation and the subsequent atrial activation, proves that the SVT is an antidromic AVRT using an AV BT anterogradely, and excludes preexcited AVNRT (Fig. 18.41A). Because the AV junctional atrium is refractory at the time of the AES, the AES cannot penetrate the AVN; hence, resetting of the SVT by such an AES is therefore incompatible with AVNRT.

Also, an AES delivered during the SVT that advances ventricular activation and does not influence the VA interval excludes preexcited AVNRT and is diagnostic of antidromic AVRT (see Fig. 18.41A). The VA interval should change in the setting of preexcited AVNRT because the AES penetrates the AVN, producing slower conduction down the AVN slow pathway before the reentrant wavefront conducts retrogradely over the fast pathway and activates the atrium. As a consequence, the delay in atrial activation is expected to produce a longer VA interval, given the presence of a fixed AV interval in response to the AES (mediated by anterograde conduction down the bystander BT in the setting of preexcited AVNRT). In addition, the advanced ventricular activation (resulting from anterograde conduction of the AES over the bystander BT) can potentially invade and capture the HB retrogradely and conduct up the fast AVN pathway and reset the AVNRT circuit. Then the VH interval of the advanced QRS plus the HA interval in response to this QRS should add up to the same VA interval on an undisturbed AVNRT, which is clearly unlikely.

Exact atrial and ventricular capture by an AES delivered when the AV junction is depolarized excludes AVNRT (see Fig. 18.41A). An AES that captures the ventricle at the same coupling interval as that of the AES indicates that the atrial stimulation site is inside the reentrant circuit, because if there were intervening atrial tissue between the stimulation site and the tachycardia circuit (as is the case during AVNRT), the AV interval would prolong, and consequently, the V-V interval would exceed the AES coupling interval.

The presence of a fixed and short VH interval during entrainment of the SVT with atrial pacing suggests antidromic AVRT, and makes AVNRT unlikely (but does not exclude AVNRT). Moreover, failure of entrainment by atrial pacing to influence the VA interval during SVT excludes preexcited AVNRT.

An early-coupled AES can terminate antidromic AVRT by retrograde block in the AVN-HPS (the SVT terminates with an AES followed by a QRS; i.e., VA block; see Fig. 18.41B) or by anterograde block in the BT (the SVT terminates with an AES not followed by a QRS; i.e., AV block; see Fig. 18.41C).

Programmed Ventricular Stimulation During Tachycardia

Orthodromic AVRT

Resetting. VES can easily reset orthodromic AVRT, and is frequently capable of terminating the tachycardia (Fig. 18.42).³⁴ However, the ability of the VES to affect the SVT depends on the distance between the site of ventricular stimulation to the ventricular insertion site of the BT and on the VES coupling interval. Because only parts of the ventricle ipsilateral to the BT are requisite components of the orthodromic AVRT circuit, a VES delivered in the contralateral ventricle may not affect the circuit. However, failure to reset (advance or delay) atrial activation with an early-coupled VES and at different VES coupling intervals, despite advancement of the local ventricular activation at all sites (including the site of the suspected BT) by more than 30 milliseconds, excludes orthodromic AVRT and the presence of a retrogradely conducting BT.⁴¹

Preexcitation index. The preexcitation index analyzes the degree of prematurity (coupling interval) of the latest coupled VES (delivered from the RV apex) that is capable of resetting the tachycardia. Later coupled VESs with a relative preexcitation index (the ratio of the VES coupling interval to the TCL) of more than 90% suggests that the BT is close to the site of ventricular stimulation (i.e., right-sided or septal BT). An absolute preexcitation index (TCL minus VES coupling interval) of at least 75 milliseconds suggests a left free-wall BT; an index of less than 45 milliseconds suggests a septal BT; and an index of 45 to 75 milliseconds is indeterminate. AVNRT would require even earlier coupled VESs and could be distinguished from AVRT if the absolute preexcitation index was greater than 100 milliseconds.⁴²

VES during HB refractoriness. A VES delivered when the HB is refractory (i.e., when the His potential is already manifest or within 35 to 55 milliseconds before the time of the expected His potential) that advances (accelerates, i.e., makes it activate earlier than expected) the next atrial activation is diagnostic of the presence of a retrogradely conducting BT. Such a VES has to conduct and advance atrial activation via a BT because the HPS-AVN is already refractory and cannot mediate retrograde conduction of the VES to the atrium (see Fig. 18.42). Although such an observation excludes AVNRT, it does not exclude AT or prove orthodromic AVRT, and the preexcited atrial activation can reset or even terminate an AT, whereby the BT is an innocent bystander. However, if this VES advances atrial activation with an activation sequence identical to that during the SVT, this suggests that the SVT is orthodromic AVRT and the BT is participating in the SVT, although it does not exclude the rare case of an AT originating at a site close to the atrial insertion site of a bystander AV BT. Furthermore, a VES delivered when the HB is refractory may not affect the next atrial activation if the ventricular stimulation site is far from the BT. Conduction from the ventricular stimulation site to the BT, local ventricular refractoriness, and the TCL all determine the ability of a VES to reach the reentrant circuit before ventricular activation over the normal AVN-HPS.

Although such a VES can advance atrial activation during AT through fast retrograde conduction over a bystander BT, it should not be able to delay an AT beat by conduction over the AV BT. Thus a VES delivered when the HB is refractory that delays the next atrial activation indicates that the VES was conducted with some delay over the BT and that the next atrial activation was dependent on this slower conduction; hence, the BT is participating in the SVT, proving orthodromic AVRT as the mechanism of the SVT. Similarly, a VES delivered when the HB is refractory that terminates the SVT without atrial activation is diagnostic of AVRT.

Exact and paradoxical capture. Exact and paradoxical capture phenomena are diagnostic of AVRT. A VES that captures the atrium at the same coupling interval as that of the VES (exact capture phenomenon) indicates that the ventricular stimulation site is inside the

AES during antidromic AVRT

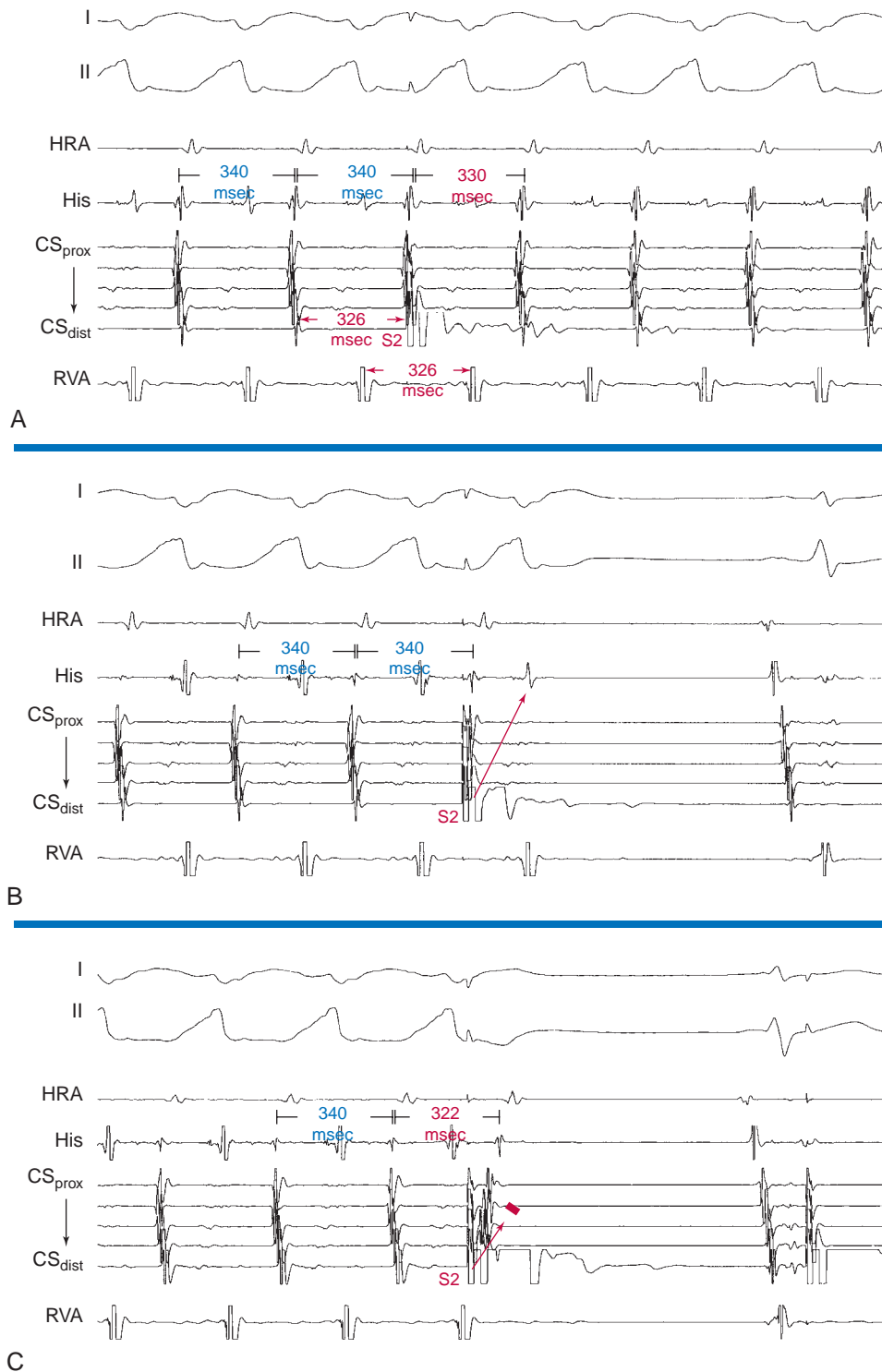


Fig. 18.41 Atrial Extrastimulation (AES) During Antidromic Atrioventricular Reentrant Tachycardia (AVRT) Using a Left Lateral Bypass Tract (BT). (A) A late-coupled AES delivered when the atrioventricular (AV) junction is refractory (as indicated by lack of advancement of the timing of the local atrial electrogram recording by the His bundle catheter) resets both the next ventricular activation and the subsequent atrial activation. This proves that the supraventricular tachycardia (SVT) is an antidromic AVRT using an AV BT anterogradely, and excludes preexcited atrioventricular nodal reentrant tachycardia (AVNRT). In addition, the reset ventricular activation occurs at a coupling interval identical to the AES coupling interval (i.e., exact coupling phenomenon), and the ventriculoatrial (VA) interval following the AES remains similar to that during SVT, which is consistent with antidromic AVNRT. (B) Late-coupled AES delivered when the AV junction is refractory advances the subsequent QRS and terminates the SVT by retrograde block in the His-Purkinje system–atrioventricular node. (C) An earlier AES terminates the SVT without conduction to the ventricle (i.e., anterograde block in the BT). The AES advances the timing of AV junctional atrial activation. CS_{dist}, Distal coronary sinus; CS_{prox}, proximal coronary sinus; HRA, high right atrium; RVA, right ventricular apex.

reentrant circuit, because if there were intervening tissue involved, the VA interval would increase and, subsequently, the A-A interval would exceed the VES coupling interval. Similarly, a VES that captures the atrium at a shorter coupling interval than that of the VES (paradoxical capture phenomenon) indicates that the ventricular stimulation site is not only inside the reentrant circuit but also closer to the ventricular insertion site of the BT than the initial site of ventricular activation

over the AVN-HPS during the SVT, so that the VA interval following the VES is shorter than that during the SVT. This is easier to demonstrate with RV apical pacing during orthodromic AVRT mediated by a right-sided BT.

Termination. Termination of orthodromic AVRT by VES can occur secondary to block of the VES retrogradely in the BT, conduction of the VES retrogradely over the AVN-HPS with or without conduction

VES during orthodromic AVRT

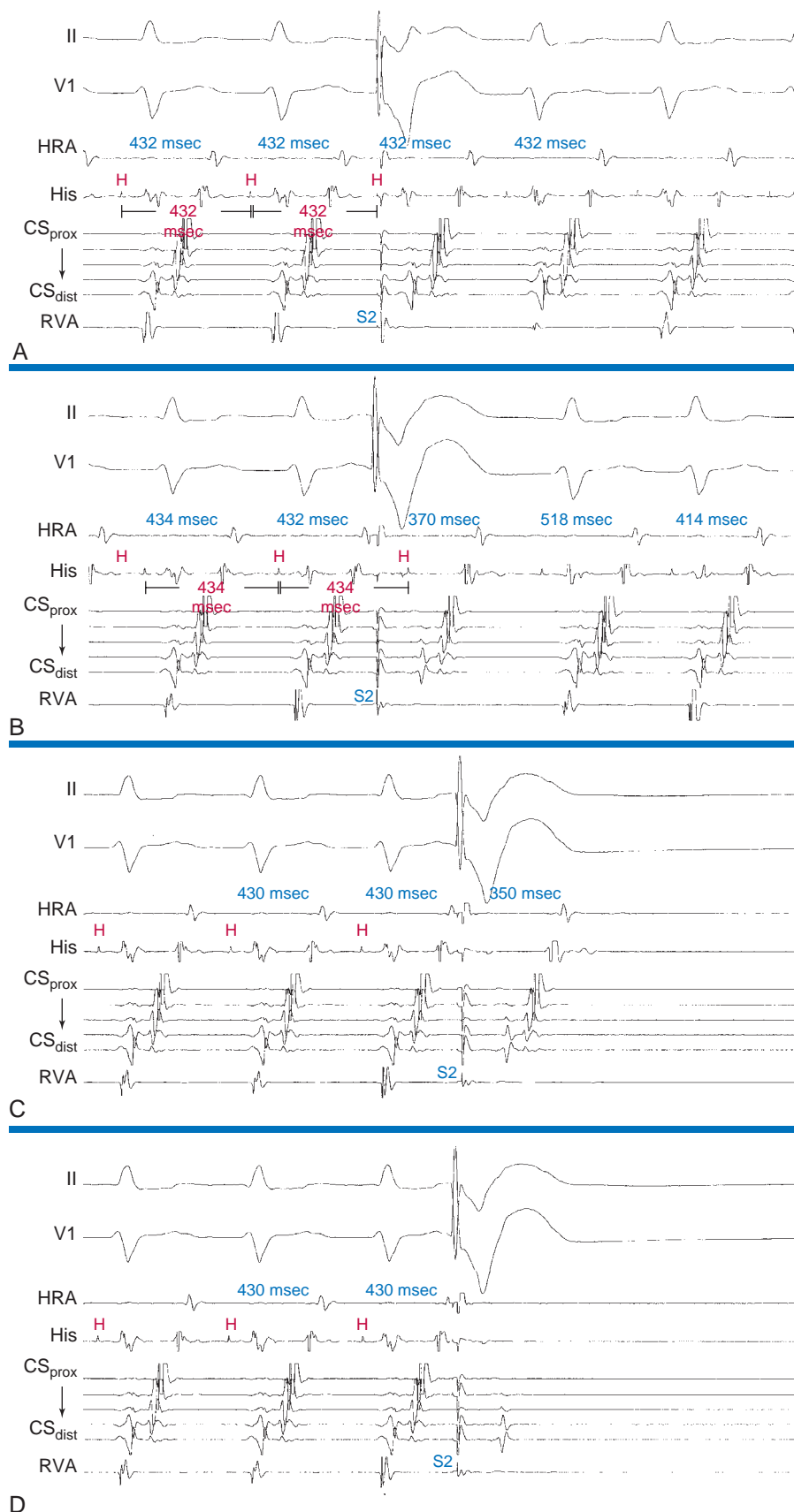


Fig. 18.42 Ventricular Extrastimulation (VES) During Orthodromic Atrioventricular Reentrant Tachycardia (AVRT) Using a Left Lateral Bypass Tract (BT). (A) A late-coupled VES delivered when the His bundle (HB) is refractory (as indicated by lack of advancement of the timing of the His potential) fails to reset the supraventricular tachycardia (SVT). (B) An earlier VES fails to advance the timing of the HB but advances the subsequent atrial activation, indicating the presence of a retrogradely conducting BT, and suggests orthodromic AVRT. Note that the reset atrial impulse is followed by a prolonged atrial–His bundle (AH) interval caused by decremental anterograde conduction in the atrioventricular node (AVN). However, the local ventriculoatrial (VA) interval (retrograde BT conduction) remains constant. (C) An earlier VES delivered before the HB is refractory resets the subsequent atrial activation and terminates the SVT by anterograde atrioventricular block in the AVN. (D) A more premature VES terminates the SVT by retrograde VA block in the BT, excluding atrial tachycardia, but can still occur in atrioventricular nodal reentrant tachycardia because the VES is delivered before anterograde activation of the HB and could potentially penetrate the AVN. CS_{dist}, Distal coronary sinus; CS_{prox}, proximal coronary sinus; HRA, high right atrium; RVA, right ventricular apex.

up the BT, or retrograde conduction of the VES up the BT and preexcitation of the atrium and subsequent anterograde block in the AVN-HPS (the most common mechanism) (see Fig. 18.42). Termination of SVT with a single VES strongly suggests orthodromic AVRT as the mechanism of SVT in three settings: (1) when the VES is late-coupled (greater than 80% of TCL); (2) when the TCL is less than 300 milliseconds; and (3) when the VES is delivered during HB refractoriness and is associated with no atrial activation.

Ventricular entrainment. Ventricular pacing at a CL approximately 10 to 30 milliseconds shorter than the TCL can easily entrain AVRT. Although the mere demonstration of the tachycardia does not help discrimination between the different SVT mechanisms, several parameters during ventricular entrainment can help establish the lower portion of the tachycardia circuit as macroreentrant involving the HPS/ventricle (AVRT) or not (AVNRT), including the presence of manifest fusion, VA interval during ventricular pacing as compared with that during SVT, the postpacing interval (PPI), and differential-site ventricular entrainment.⁴³

Manifest ventricular fusion. A requirement for the presence of fusion is spatial separation between the sites of entrance to and exit from the reentrant circuit. In orthodromic AVRT, the entrance and exit of the reentrant circuit (to and from ventricular tissue) are separated from each other, the entrance being from the HPS and the exit being at the BT ventricular insertion site. In this setting, the paced wavefront can activate a portion of the ventricles and enter the AVRT circuit and at the same time the tachycardia wavefront emerge from the reentry circuit at a distant exit site and activate another part of the ventricles. Also, the relative proximity of the pacing site to the entry and exit sites

of the reentry circuit, is a critical determinant for the occurrence of fusion during resetting and entrainment. Pacing at a site closer to the BT ventricular insertion site (e.g., LV pacing in the setting of left free-wall BTs, and RV basal pacing in the setting of right-sided or septal BTs) than the entrance of the reentrant circuit to ventricular tissue (i.e., the HPS) would result in a larger degree of fusion of QRS morphology between baseline morphology during orthodromic AVRT and that of fully paced QRS (Fig. 18.43).⁴⁴

Manifest ventricular fusion during SVT entrainment is proof that the ventricle is part of the SVT circuit (i.e., diagnostic of AVRT). On the other hand, such phenomena cannot occur during AVNRT and AT because of the lack of spatial separation of the entrance and exit of the AVNRT or AT circuit to the ventricles and because the ventricles are not an obligatory part of that circuit.

Δ VA interval. Entrainment of the SVT by RV pacing can help differentiate orthodromic AVRT from AVNRT by evaluating the VA interval during SVT (measured from the onset of surface QRS to high RA electrogram) versus the VA interval during pacing (i.e., the SA interval, measured from the ventricular pacing stimulus to the high RA electrogram). The ventricle and atrium are activated in sequence during orthodromic AVRT and during ventricular pacing, but in parallel during AVNRT. Therefore the VA interval during orthodromic AVRT approximates that during ventricular pacing (see Fig. 18.43). In contrast, the VA interval during AVNRT would be much shorter than that during ventricular pacing (see Fig. 17.19). In general, a difference in the VA interval (Δ VA [$VA_{\text{pacing}} - VA_{\text{SVT}}$]) greater than 85 milliseconds is consistent with AVNRT, whereas a Δ VA of less than 85 milliseconds is consistent with orthodromic AVRT (see Fig. 20.14).^{45,46}

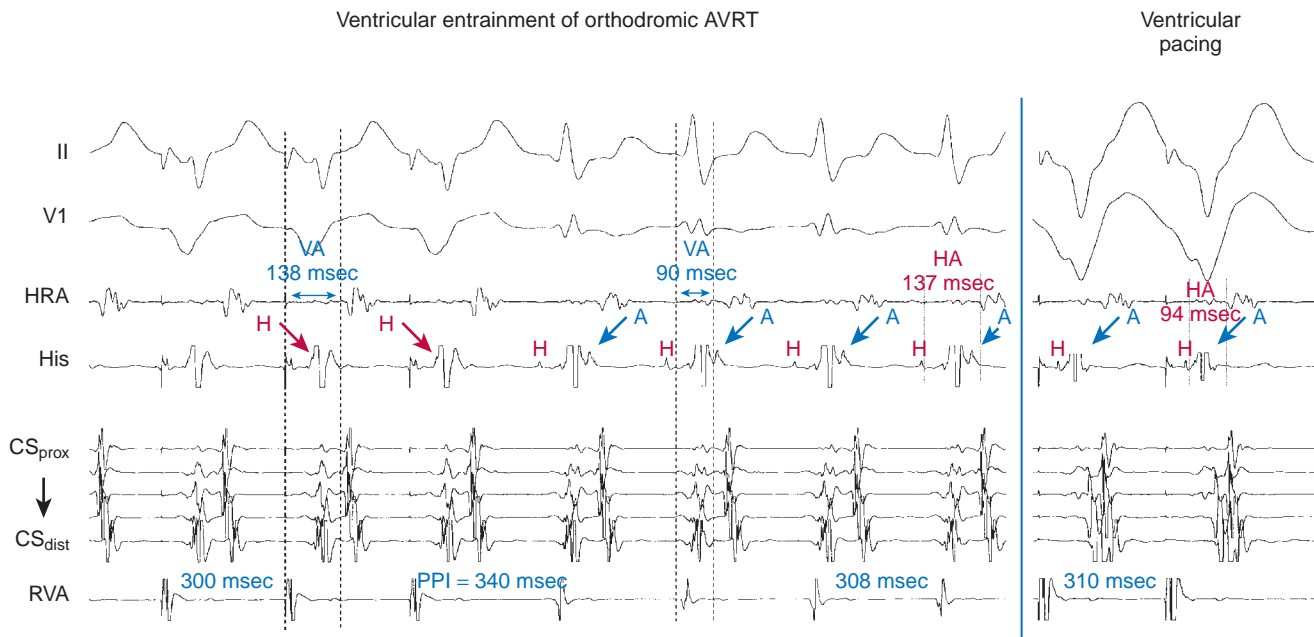


Fig. 18.43 Ventricular Entrainment of Orthodromic Atrioventricular Reentrant Tachycardia (AVRT) Using a Concealed Superoparaseptal Bypass Tract. Note that the Δ VA interval ($VA_{\text{pacing}} - VA_{\text{SVT}}$) is less than 85 milliseconds and the (PPI - TCL) is less than 115 milliseconds, both of which favor orthodromic AVRT over atrioventricular nodal reentrant tachycardia (AVNRT). In addition, ventricular fusion (between the paced and tachycardia wavefronts) is observed during entrainment (right, pure paced QRS morphology), which is consistent with AVRT and excludes AVNRT. Comparing the HA interval during the tachycardia (left) with that during ventricular pacing during normal sinus rhythm at the TCL (right) demonstrates that the Δ HA interval ($HA_{\text{pacing}} - HA_{\text{SVT}}$) is -43 milliseconds, which favors orthodromic AVRT over AVNRT; the HA interval is measured from the end of the His potential to the atrial electrogram in the high right atrium (HRA). CS_{dist} , Distal coronary sinus; CS_{prox} , proximal coronary sinus; HA, His bundle-atrial; PPI, postpacing interval; RVA, right ventricular apex; SVT, supraventricular tachycardia; TCL, tachycardia cycle length; VA, ventriculoatrial.

Postpacing interval. The PPI reflects conduction time from the ventricular pacing site to the SVT circuit, once around the reentry circuit, and then back to the pacing site. The difference between the PPI and TCL ($PPI - TCL$) represents the conduction time from the pacing site to the reentry circuit and back. Thus the ($PPI - TCL$) difference can qualitatively estimate how far the reentrant circuit is from the pacing site; the greater the ($PPI - TCL$) difference, the longer the conduction time between the pacing site and reentry circuit, and the greater the “electrical” distance is between the pacing site and the circuit.

The reentry circuit in AVRT involves the BT, ipsilateral atrium, AVN-HB, and ipsilateral bundle branch and ventricle. On the other hand, the circuit of AVNRT (typical or atypical) is confined above the HB. Because the RV is closer to the AVRT circuit as compared to the AVNRT circuit, the ($PPI - TCL$) difference following entrainment from the RV apex is smaller in the setting of AVRT than during AVNRT (see Fig. 18.43). In fact, a ($PPI - TCL$) difference of more than 115 milliseconds was found to identify AVNRT, whereas a ($PPI - TCL$) difference of less than 115 milliseconds was consistent with orthodromic AVRT. For borderline values, ventricular pacing at the RV base can help exaggerate the ($PPI - TCL$) difference in the setting of AVNRT, but without significant changes in the setting of orthodromic AVRT (see differential-site RV entrainment later).^{47,48}

A relatively common phenomenon encountered during entrainment of orthodromic AVRT by ventricular pacing is the prolongation of the AH interval because of either decremental conduction properties of the AVN or (in the presence of dual AVN physiology) a jump of antero-grade conduction from the fast pathway to the slow pathway. The prolonged AH interval on the last entrained beat will contribute to prolongation of the PPI that is not reflective of the distance of the pacing site from the circuit. Thus the ($PPI - TCL$) differences obtained after entrainment of orthodromic AVRT employing a septal BT can actually overlap with those observed after entrainment of AVNRT. “Correction” of the PPI by subtracting the increment in AVN conduction time in the first PPI (postpacing AH interval minus prepacing AH interval) from the ($PPI - TCL$) difference (“corrected” [$PPI - TCL$]) has been found to improve the accuracy of this criterion. The difference between AV intervals (postpacing AV interval minus prepacing AV interval) can be taken for the latter adjustment when a His deflection is not clearly visible (assuming the HV interval remains constant). A corrected ($PPI - TCL$) difference of less than 110 milliseconds was found to be more accurate in distinguishing orthodromic AVRT from AVNRT than the uncorrected ($PPI - TCL$) difference.^{49,50}

Furthermore, during orthodromic AVRT, the corrected ($PPI - TCL$) difference can help localize the BT used for retrograde conduction. The RV apical pacing site is closer to the reentrant circuit of orthodromic AVRT utilizing a right-sided BT than orthodromic AVRT utilizing a left-sided BT. Hence, as expected, the corrected ($PPI - TCL$) difference is shorter (less than 55 milliseconds) in patients with orthodromic AVRT with a right-sided BT when pacing the RV apex. Patients with left-sided BTs typically have a corrected ($PPI - TCL$) difference of more than 55 milliseconds.⁵¹

Of note, determinations of the corrected ($PPI - TCL$) and ΔVA ($VA_{\text{pacing}} - VA_{\text{SVT}}$) after resetting with single or double VESs from the RV apex, is of similar value for discrimination between AVNRT and orthodromic AVRT, even when the SVT is interrupted by ventricular pacing. Corrected ($PPI - TCL$) of more than 110 milliseconds and ΔVA of more than 110 milliseconds after resetting identify AVNRT.⁵²

Importantly, there are several potential pitfalls of the ΔVA interval and the PPI criteria discussed previously. The TCL and VA interval are often perturbed for a few cycles after entrainment. For this reason, care should be taken not to measure unstable intervals immediately after ventricular pacing. In addition, oscillations in the TCL and VA intervals

can occur spontaneously during the SVT. The discriminant points chosen may not apply when the spontaneous variability is greater than 30 milliseconds. Also, it is possible to mistake isorhythmic VA dissociation for entrainment if the pacing train is not long enough or the PCL is too close to the TCL. Furthermore, this test is less reliable and should be used with caution in patients with left lateral BTs.

In addition, these criteria may not apply to BTs with significant decremental properties, although small decremental intervals are unlikely to provide a false result. A higher cutoff value of 125 milliseconds was found to increase the sensitivity for orthodromic AVNRT while maintaining high specificity. Slow, decremental BT conduction can also affect the sensitivity of the ΔVA criteria for orthodromic AVRT, but the specificity remains high. Therefore, if any standard criteria positive for orthodromic AVRT ($PPI - TCL < 115$ milliseconds, corrected [$PPI - TCL$] < 110 milliseconds, and $\Delta VA < 85$ milliseconds) is diagnostic of orthodromic AVRT, despite discordance among each other (which can occur about 50% of the time).⁴³

Differential-site RV entrainment. Differential-site RV entrainment (from RV apex vs. RV base) can help distinguish AVNRT from orthodromic AVRT. Because the reentrant circuit in AVNRT is confined above the HB and does not involve the ventricle, the base of the RV is electrically more distant (although anatomically closer) to the tachycardia circuit than the RV apex, given that the His-Purkinje network directly inserts near the RV apex. Consequently, the PPI after entrainment of AVNRT from the RV base is longer than that following entrainment from the RV apex. The difference in PPI from the RV base versus the RV apex is largely composed of the extra time required to reach the circuit from the base versus the apex (approximately 30 milliseconds). Conversely, in orthodromic AVRT, in which the ventricles are an obligatory part of the circuit, the basal pacing site relative to the RV apex is variably related to the circuit, closer than the RV apex with septal BTs and equidistant with free-wall BTs, but the paced wavefront from either the RV apex or RV base tends to have, on average, approximately equal access and proximity to the reentrant circuit involved in orthodromic AVRT. Therefore the time taken to reach the circuit (and hence the PPI) tends to be similar, irrespective of the location of the BT.

Correction of the PPI (to avoid potential error introduced by decremental conduction within the AVN during ventricular pacing) increases the accuracy of this method, although the degree of decrement is not expected to be materially different from basal rather than apical pacing as long as the pacing rates are the same or similar. The “corrected PPI” is obtained by subtracting any increase in the AV interval of the return cycle beat (as compared with the AV interval during SVT). A differential corrected ($PPI - TCL$) difference of more than 30 milliseconds after transient entrainment was found to be consistent with AVNRT (i.e., corrected [$PPI - TCL$] difference following pacing from the RV base was consistently at least 30 milliseconds longer than that following pacing from the RV apex). In contrast, a corrected ($PPI - TCL$) difference of less than 30 milliseconds was observed in all cases of orthodromic AVRT. In addition, a differential VA interval (VA interval during entrainment from RV base versus RV septum) of more than 20 milliseconds was consistent with AVNRT, whereas a differential VA interval of less than 20 milliseconds was consistent with orthodromic AVRT.^{53,54}

The main advantage of this technique is that the differential VA interval can be calculated from the last paced beat if the tachycardia is terminated after transient entrainment.

Length of pacing drive required for entrainment. Assessing timing and type of response of SVT to RV pacing can also help differentiate orthodromic AVRT from AVNRT. In the setting of orthodromic AVRT, ventricular tissue is the only intervening tissue between the pacing wavefront and the ventricular insertion site of the BT. Therefore once ventricular capture is achieved during RV pacing, the paced wavefront

propagates to the ventricular insertion site of the BT quickly and resets the tachycardia. Consequently, RV pacing results in a faster response of resetting the tachycardia. In the setting of AVNRT, the pacing site is distant from the SVT circuit, and the paced wavefront has to propagate through ventricular tissue, then through the HPS followed by AVN tissue prior to resetting the tachycardia. As a consequence, resetting of AVNRT is delayed for several captured paced beats as compared with orthodromic AVRT.

After initiation of synchronized RV pacing during SVT at a CL that is 10 to 40 milliseconds shorter than the TCL, once constant-appearing QRS complexes (as evidenced by fixed pacing morphology of the surface ECG, either pure paced morphology or fixed QRS fusion) are observed, the number of RV paced beats required to accelerate the SVT to the PCL is determined. The first atrial capture beat accelerated to the PCL is identified by demonstrating a fixed ventricular SA capture interval. One report demonstrated that using a cutoff of one beat to accelerate the SVT to the PCL could identify all orthodromic AVRT cases and essentially exclude all cases of AVNRT with high accuracy. On the contrary, if two or more beats are required to accelerate SVT to the PCL, this can distinguish AVNRT from orthodromic AVRT with very high confidence as well (see Fig. 20.13).

The major advantage of this method is its independence of tachycardia continuation after cessation of pacing. However, it is likely that these criteria may not be applicable at PCLs more than 40 milliseconds shorter than the TCL or prematurity of more than 80% of the TCL because resetting of the tachycardia can occur earlier in AVNRT in response to a greater degree of penetration into the tachycardia circuit. In addition, these findings may not apply in cases in which AVNRT occurs in the setting of a bystander BT because SVT may be reset using the bystander BT. In addition, although this technique is effective for differentiating septal pathways from atypical AVNRT, it may be less useful in patients with BTs remote from the pacing stimulus (e.g., left free-wall BTs) (see Fig. 20.15).⁵⁵

Atrial resetting during the transition zone. On initiation of RV pacing trains during SVT at a rate slightly faster than the TCL, there is a transition zone during which the pacing train fuses with anterograde ventricular activation (i.e., the zone in which the paced QRS complexes show progressive fusion with the SVT complexes) until stable QRS morphology is observed (either completely paced or constantly fused). The transitional zone begins with progressive fusion beats between the paced and tachycardia wavefronts and ends with the first beat of stable QRS morphology, the latter representing constant fusion in the case of orthodromic AVRT and a fully paced QRS morphology in patients with AVNRT. In patients with AVNRT or AT, acceleration of the timing of atrial activation cannot occur through the AVN during the transition zone. The reason is that the HB is expected to be refractory, as indicated by at least some ventricular activation still occurring by anterograde conduction over the HPS. If perturbation of atrial timing occurs during the transition zone, it indicates the presence of a retrogradely conducting BT, which can be an integral part of the SVT circuit (i.e., orthodromic AVRT) or a bystander (Fig. 18.44). In one report, these criteria showed excellent diagnostic accuracy and could be applied regardless of whether entrainment was achieved or whether the SVT terminated during pacing. Perturbation of atrial timing of at least 15 milliseconds or a fixed SA interval measured from the last beat of the transition zone was seen in all the patients with orthodromic AVRT and in none of the patients with AVNRT or AT (unless a bystander retrogradely conducting BT is present).^{54,56}

Of note, the number of reset beats (defined as fixed SA interval) in the transitional zone (during ventricular overdrive pacing from the RV apex during orthodromic AVRT) depends on the proximity of the BT to the pacing site; hence, it can predict BT location. Right-sided BTs produce reset earlier than left-sided BTs, and a cut-off of more than two beats with a fixed SA interval within the transitional zone was found to successfully discriminate between left-sided and right-sided BTs.⁵⁷

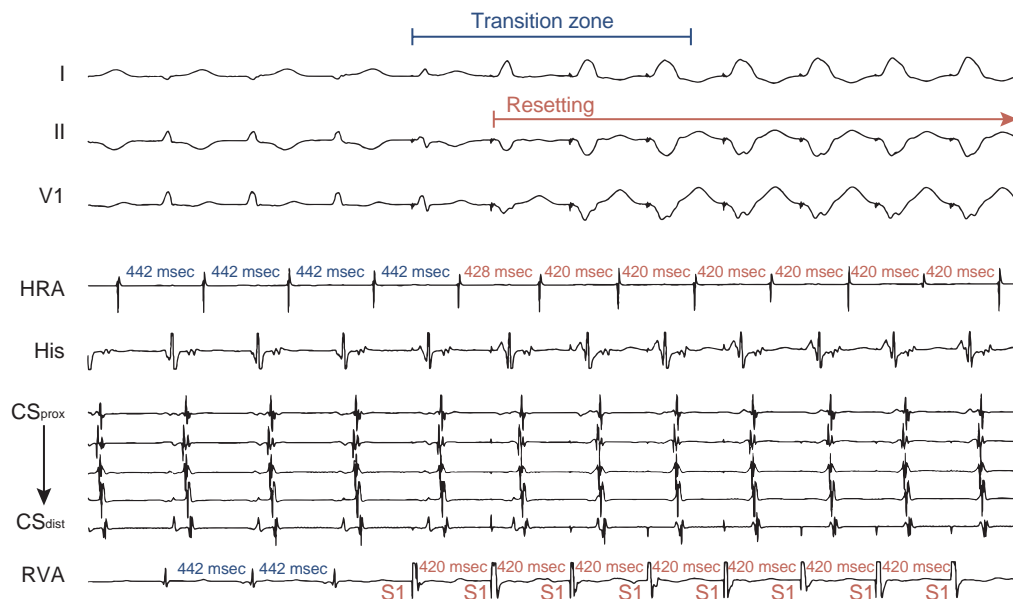


Fig. 18.44 Resetting of Supraventricular Tachycardia (SVT) During the Transition Zone. Overdrive ventricular pacing is started from the RVA at a cycle length (CL) of 420 milliseconds, slightly shorter than the SVT CL (442 milliseconds). On initiation of right ventricular pacing, there is a transition zone during which the paced wavefronts fuse with anterograde ventricular activation, before stable QRS morphology ensues. Note that advancement of atrial activation (resetting) initially occurred during the transition zone, indicating orthodromic atrioventricular reentrant tachycardia as the mechanism of the SVT. CS_{dist}, Distal coronary sinus; CS_{prox}, proximal coronary sinus; HRA, high right atrium; RVA, right ventricular apex.

Permanent junctional reciprocating tachycardia. A VES delivered during PJRT can produce decremental conduction in the BT and prolongation of the VA interval, resulting in possible delay of the next atrial activation (i.e., post excitation or delay of excitation; see Fig. 18.39). Such a response excludes AT, and when this occurs in response to a VES delivered when the HB is refractory, it is diagnostic of orthodromic AVRT, and excludes both AT and AVNRT. In addition, a late-coupled VES introduced when the HB is refractory frequently blocks retrogradely in the BT and reproducibly terminates the tachycardia without reaching the atrium, again excluding both AT and AVNRT.⁴³

The ability to preexcite the atrium with a VES introduced when the HB is refractory is difficult to demonstrate in PJRT because of the long conduction time over the BT, the decremental conduction properties of the BT, and the fact that the TCL is just longer than the shortest length at which the BT is capable of retrograde conduction. This can be facilitated by introduction of the PVC at a site closer to the BT ventricular insertion.

Antidromic AVRT. Similar to orthodromic AVRT, ventricular pacing and VES can easily entrain or reset antidromic AVRT because the ventricle is part of the reentrant circuit. Because both orthodromic and antidromic AVRTs use similar reentry circuits, the concepts of resetting and entrainment discussed for orthodromic AVRT also apply, to a large degree, to antidromic AVRT.

Of note, the development of retrograde RBBB following a VES introduced during the SVT can help distinguish antidromic AVRT from AVNRT. When the VES results in retrograde RBBB (i.e., blocks retrogradely in the RB), such RBBB will not change the timing of the next atrial activation in the setting of AVNRT. In contrast, in antidromic AVRT using a right-sided BT, such RBBB will increase the size of the reentrant circuit, because the impulse cannot reach the HB through the RB and has to travel transeptally and then retrogradely over the LB. This results in prolongation in the VA interval and delay in the timing of the next atrial activation. The increment in the VA interval is caused by prolongation of the VH interval and, if RBBB persists, the SVT will have a long VH interval.

Antidromic AVRT can usually be terminated by ventricular pacing. Termination occurs by retrograde invasion and concealment in the BT, resulting in anterograde block over the BT following conduction to the atrium through the AVN.

Para-Hisian Pacing During Tachycardia

Para-Hisian pacing during tachycardia can help discriminate between AVRT and AVNRT. This pacing maneuver is discussed in detail in **Chapter 20**. Briefly, entrainment of the SVT is performed by pacing at the para-Hisian region using the HB catheter at a PCL that is 10 to 30 milliseconds shorter than the TCL. Entrainment is confirmed when the atrial CL accelerates to the PCL, without a change in the atrial activation sequence, and the tachycardia continues after pacing is discontinued.⁵⁸

Para-Hisian entrainment is performed by alternately pacing at high-energy output for HB-RB capture or lower energy output for HB-RB noncapture. Entrainment with HB-RB capture is recorded separately from that without HB-RB capture. The SA and local VA intervals during HB-RB capture and noncapture are then examined.

If para-Hisian entrainment cannot be performed because of repetitive termination of the tachycardia during entrainment attempts, isoproterenol infusion may be used to help sustain the rhythm. Alternatively, single or double VESs can be given to reset the tachycardia (para-Hisian resetting). These VESs are delivered at progressively shorter coupling intervals until the first VES that reliably advances or resets the tachycardia. This is performed alternately with high- or low-energy outputs to achieve HB-RB capture and noncapture, respectively. As with para-Hisian

entrainment, the retrograde atrial activation sequence and timing are compared during para-Hisian resetting to characterize the response.

In AVNRT (typical or atypical), the AVN-AVN pattern is observed in response to para-Hisian entrainment or resetting; that is, both the SA and the local VA intervals increase during HB-RB noncapture compared with HB-RB capture.

In orthodromic AVRT, the BT-BT pattern or BT-BT_L pattern is observed. In the setting of a BT-BT pattern, the SA and local VA intervals are usually not significantly different between HB-RB capture and noncapture. Conversely, in the case of a BT-BT_L pattern, the SA interval increases on HB-RB noncapture, but without significant change in the local VA interval.

A ΔSA interval of less than 40 milliseconds was found to be a reasonable guide to separating the AVN-AVN from the BT-BT response. Patients with AVNRT uniformly have a ΔSA interval of greater than 40 milliseconds, whereas those with AVRT have a ΔSA interval of less than 40 milliseconds (except for rare patients with a left lateral BT). Using the Δ local VA interval (instead of the ΔSA interval) provide a more accurate parameter for discrimination between AVNRT and AVRT.

An AVN-AVN or fusion pattern during para-Hisian entrainment or resetting has not been observed in patients with AVNRT. This is a potential advantage over para-Hisian pacing during NSR in identifying the presence of a BT. Because retrograde VA conduction can only proceed over a single route during entrainment of the SVT (assuming that a complex scenario such as multiple BTs is not present), the various forms of retrograde fusion that might be seen during para-Hisian pacing during NSR cannot occur during para-Hisian entrainment or resetting.

Diagnostic Maneuvers During Sinus Rhythm After Tachycardia Termination

Atrial Pacing at the Tachycardia Cycle Length

Under comparable autonomic tone, the PR and AH intervals during atrial pacing at a CL similar to the TCL should be comparable to those during orthodromic AVRT. These findings are also observed in the setting of AT. In contrast, the AH and PR intervals during atrial pacing would be longer than those during tachycardia in the setting of AVNRT, assuming the slow pathway has been engaged. A ΔAH (AH_{pacing} – AH_{SVT}) of more than 40 milliseconds has been reported to favor AVNRT.⁴⁸

A major limitation of ΔAH criteria, however, is the sensitivity of the AVN to rapid fluctuations in autonomic tone so that comparison of AH intervals between tachycardia and pacing should be done close in time, allowing for minimal change in the autonomic state of the patient.⁴³

Ventricular Pacing at the Tachycardia Cycle Length

Under comparable autonomic tone status, 1:1 VA conduction over the AVN should be maintained during ventricular pacing at a CL similar to the TCL. If VA block develops during ventricular pacing, orthodromic AVRT is unlikely, and AT and AVNRT are favored.

In addition, ventricular pacing during NSR at a PCL similar to the TCL results in HA and VA intervals that are shorter than those during orthodromic AVRT because the HB and atrium are activated sequentially during orthodromic AVRT but in parallel during ventricular pacing whereby the atrium is activated via the BT (see Fig. 18.43). To help distinguish between orthodromic AVRT and AVNRT, the HA interval is measured from the *end* of the His potential (where the impulse leaves the HB to enter the AVN) to the atrial electrogram in the high RA recording and the ΔHA interval (HA_{pacing} – HA_{SVT}) is calculated. In the setting of orthodromic AVRT the ΔHA interval is typically less than –10 milliseconds. In contrast, in the setting of AVNRT the ΔHA interval is typically more than –10 milliseconds because the HA interval during

AVNRT is shortened by parallel activation of both the HB and the atrium during the tachycardia (i.e., the HA interval is a “pseudo-interval” that represents activation times of the HB and atrium), whereas the HB and atrium are activated sequentially during ventricular pacing in the absence of a BT (i.e., the HA interval represents a true conduction time interval from the HB to the atrium). The Δ HA interval is even more pronounced in atypical AVNRT, which has a lower common pathway that is longer than that in typical AVNRT. In focal junctional tachycardia, the Δ HA interval is typically close to 0.³⁰

The Δ HA interval criterion has high specificity, sensitivity, and positive predictive accuracy for differentiation between AVNRT and orthodromic AVRT, but it has certain limitations. The main limitation of the Δ HA interval criterion is the ability to record the retrograde His potential during ventricular pacing. The retrograde His potential generally appears before the local ventricular electrogram in the HB tracing, and can be verified by the introduction of a VES that causes the His potential to occur after the local ventricular electrogram. Moreover, pacing from different sites (e.g., midseptum) may allow earlier penetration into the HPS and facilitate observation of a retrograde His potential. When the retrograde His potential is not visualized, using the Δ VA interval instead of the Δ HA interval is not as accurate in discriminating orthodromic AVRT from AVNRT. Another limitation is that VA conduction during ventricular pacing may not occur over the BT but propagates preferentially over the HPS-AVN, leading to earlier atrial activation over this pathway than over the BT. If this were the case, the HA interval during ventricular pacing would be shorter than that observed if the atrium were activated via the BT. This would yield a more negative Δ HA interval.

It is important to recognize that the atrial activation sequence during ventricular pacing can be mediated by retrograde conduction over the BT, over the AVN, or a fusion of both, and consequently it can be similar to or different from that during orthodromic AVRT.

Exclusion of Other Arrhythmia Mechanisms

AVNRT and AT arising near the AV groove can mimic orthodromic AVRT and, in the presence of a manifest BT, those tachycardias can be associated with ventricular preexcitation mimicking antidromic AVRT, whereby the BT is functioning as an innocent bystander. Therefore EP testing is required, not just to identify the presence of a BT, but also to define its role in any clinical or inducible arrhythmia. Boxes 18.4 and 18.5 summarize the EP findings indicative of the presence of a BT and its potential participation in an inducible SVT. Exclusion of other SVT mechanisms is necessary because the mere presence of a BT is not adequate to make a diagnosis and a treatment strategy (Boxes 18.6–18.8).

Furthermore, the presence of multiple BTs is not infrequent, and careful EP testing is required to evaluate this possibility. Several clinical

and EP findings are indicative of the presence of multiple BTs (Box 18.9; Figs. 18.45 and 18.46; see eFig. 18.1). However, despite these various methods, many BTs are not identified until after catheter ablation of the first BT. Failure to detect the presence of multiple BTs during EP testing has been reported in as many as 5% to 15% of patients. This may be explained by the fact that changes in the preexcitation pattern can be subtle in shifting from one BT to another. Furthermore, one BT can preferentially conduct during atrial pacing or participate in preexcited tachycardias while another BT can be responsible for the retrograde limb during orthodromic AVRT or ventricular pacing. In addition, there may be fusion of BT conduction, anterograde or retrograde. Repetitive concealed conduction into the BT during AVRT may also preclude identification of that BT before ablation of the first BT.

LOCALIZATION OF THE BYPASS TRACT

Several EP techniques can help map the location of the AV BT and guide catheter ablation (Box 18.10). Those techniques are best used in combination to improve mapping accuracy and ablation outcome.

Pacing From Multiple Atrial Sites

The closer the pacing site to the BT atrial insertion, the more rapidly the impulse reaches the BT relative to the AVN and, thus, the greater the degree of preexcitation and the shorter the P-delta interval. This method is especially helpful when the BT cannot conduct retrogradely, prohibiting localization with atrial mapping during SVT or ventricular pacing.

Preexcitation Index

The preexcitation index analyzes the coupling interval of the VES (delivered from the RV) that resets orthodromic AVRT as a percentage of the TCL. A relative preexcitation index (the ratio of the coupling interval to the TCL) of more than 90% of a VES that advances atrial activation during orthodromic AVRT suggests that the BT is close to the site of ventricular stimulation (i.e., RV or septal BT). An absolute preexcitation index (TCL minus VES coupling interval) of at least 75 milliseconds suggests a left free-wall BT, an index of less than 45 milliseconds suggests a septal BT, and an index of 45 to 75 milliseconds is indeterminate.

BOX 18.4 Electrophysiological Findings Indicating Presence of Retrograde Atrioventricular Bypass Tract Function

- Eccentric atrial activation sequence during ventricular pacing
- RV apical pacing producing longer VA interval and/or different atrial activation sequence compared with that during RV basilar pacing
- Para-Hisian pacing producing similar VA interval with and without HB capture or producing different atrial activation sequence depending on whether the HB is captured
- VES delivered when the HB is refractory advances the next atrial activation during SVT

HB, His bundle; RV, right ventricular; SVT, supraventricular tachycardia; VA, ventriculoatrial; VES, ventricular extrastimulus.

BOX 18.5 Electrophysiological Findings Indicating Presence and Participation of Atrioventricular Bypass Tract in Supraventricular Tachycardia

- VES delivered during SVT when the HB is refractory terminates the SVT without atrial activation.
- VES delivered during SVT when the HB is refractory delays the next atrial activation.
- VES during SVT captures the atrium at the same coupling interval as that of the VES (exact capture phenomenon).
- VES delivered during SVT captures the atrium at a shorter coupling interval than that of the VES (paradoxical capture phenomenon).
- VA interval (with or without concomitant prolongation in TCL) prolonged during the SVT secondary to the development of BBB.
- Entrainment of the SVT by ventricular pacing results in prolongation of the VA interval ($VA_{\text{pacing}} > VA_{\text{SVT}}$).

BBB, Bundle branch block; HB, His bundle; SVT, supraventricular tachycardia; TCL, tachycardia cycle length; VA, ventriculoatrial; VES, ventricular extrastimulus.

BOX 18.6 Exclusion of Atrial Tachycardia**Effects of BBB**

- Prolongation of surface VA interval during SVT (with or without TCL prolongation) on development of BBB excludes AT.

Oscillations in TCL

- Spontaneous changes in TCL accompanied by constant VA interval (VA linking) exclude AT.
- Changes in atrial CL that are predicted by the change in the preceding ventricular CL argue against AT.

VES During SVT

- VES that terminates the SVT without atrial activation excludes AT.
- VES that delays the next atrial activation excludes AT.
- VES during SVT that captures the atrium at the same coupling interval as that of the VES (exact capture phenomenon) excludes AT.
- VES delivered during SVT that captures the atrium at a shorter coupling interval than that of the VES (paradoxical capture phenomenon) excludes AT.
- When a VES delivered during HB refractoriness advances the next atrial activation with an atrial activation sequence similar to that during SVT, AT is unlikely.
- Manifest ventricular fusion during resetting excludes AT.

Overdrive Ventricular Pacing During SVT

- If atrial activation sequence during ventricular entrainment is similar to that during the SVT, AT is less likely.

- Presence of A-V electrogram sequence at cessation of ventricular pacing generally excludes AT.
- Manifest ventricular fusion during entrainment indicates AVRT and excludes AT.

Overdrive Atrial Pacing During SVT

- If the VA interval following the last entrained QRS is reproducibly constant (with <10 msec variation), despite pacing at different CLs or for different durations (VA linking) and similar to that during TCL, AT is unlikely.
- If the VA interval following the last entrained QRS is reproducibly constant (with <14-msec variation), despite pacing at different atrial sites (VA linking), AT is unlikely.
- Demonstration of entrainment with manifest atrial fusion excludes focal AT.

Atrial Pacing During NSR at Tachycardia CL

- If the VA interval following the last entrained QRS is reproducibly constant (with <10-msec variation), despite pacing at different CLs or for different durations (VA linking) and similar to that during TCL, AT is unlikely.
- If the VA interval following the last entrained QRS is reproducibly constant (with <14-msec variation), despite pacing at different atrial sites (VA linking), AT is unlikely.

Ventricular Pacing During NSR at Tachycardia CL

- If retrograde atrial activation sequence during ventricular pacing is similar to that during SVT, AT is less likely.

AT, Atrial tachycardia; AVRT, atrioventricular reentrant tachycardia; BBB, bundle branch block; CL, cycle length; HB, His bundle; NSR, normal sinus rhythm; SVT, supraventricular tachycardia; TCL, tachycardia cycle length; VA, ventriculoatrial; VES, ventricular extrastimulus.

BOX 18.7 Exclusion of Atrioventricular Nodal Reentrant Tachycardia**SVT Induction by VES**

- $\Delta VA (VA_{VES} - VA_{SVT}) < 85$ msec favors orthodromic AVRT over AVNRT.
- $(PPI_{VES} - TCL) < 115$ msec favors orthodromic AVRT over AVNRT.

Atrial Activation Sequence

- Eccentric atrial activation sequence during the SVT excludes AVNRT (with the exception of left variant AVNRT).

Effects of BBB

- Prolongation of VA interval or TCL on development of BBB excludes AVNRT.

Oscillations in TCL

- Spontaneous changes in TCL accompanied by constant VA interval (VA linking) make AVNRT unlikely.

Differential RV Pacing

- If the atrial activation sequence changes during pacing at the RV apex versus pacing at the RV base, AVNRT is less likely.
- If the SA interval is shorter with pacing from the base than from the apex at the same PCL, AVNRT is less likely.

VES During SVT

- VES delivered during SVT when the HB is refractory that resets (advances or delays) or terminates the SVT excludes AVNRT.
- VES during SVT that conducts to the atrium at the same coupling interval as that of the VES (exact capture phenomenon) excludes AVNRT.
- VES delivered during SVT that conducts to the atrium at a shorter coupling interval than that of the VES (paradoxical capture phenomenon) excludes AVNRT.

- Manifest ventricular fusion during resetting excludes AVNRT.
- Preexcitation index (the difference between the TCL and the longest VES coupling interval at which atrial capture occurs during tachycardia) ≥ 100 msec characterizes AVNRT, whereas an index <45 msec is consistent with AVRT with a septal BT.
- Corrected $(PPI - TCL) < 110$ msec (after resetting with single or double VESs from the RV apex) argues against AVNRT.

Overdrive Ventricular Pacing During SVT

- ΔVA interval ($VA_{pacing} - VA_{SVT}$) <85 msec argues against AVNRT.
- $PPI - TCL < 115$ msec argues against AVNRT.
- Corrected $PPI - TCL < 110$ msec argues against AVNRT.
- Manifest ventricular fusion during entrainment indicates AVRT and excludes AVNRT.
- Acceleration of the SVT to the PCL occurring after a single captured paced RV complex is consistent with orthodromic AVRT and essentially excludes AVNRT.
- Differential corrected $PPI - TCL$ of <30 msec after transient entrainment from the RV apex versus the RV base is consistent with orthodromic AVRT and excludes AVNRT.
- Differential VA interval (ventricular stimulus-to-atrial interval during entrainment from RV base vs. RV septum) of <20 msec is consistent with orthodromic AVRT and excludes AVNRT.
- Atrial resetting (perturbation of atrial timing by >15 msec) during the transition zone is consistent with orthodromic AVRT and excludes AVNRT or AT (unless a bystander retrogradely conducting BT is present).
- Acceleration of the SVT to the PCL occurring by the first beat with stable paced QRS morphology is consistent with orthodromic AVRT and essentially excludes AVNRT.

BOX 18.7 Exclusion of Atrioventricular Nodal Reentrant Tachycardia—cont'd**AES During SVT**

- Demonstration of resetting with manifest atrial fusion excludes AVNRT.

Overdrive Atrial Pacing During SVT

- ΔAH interval ($AH_{\text{pacing}} - AH_{\text{SVT}}$) < 20 msec excludes AVNRT.
- Demonstration of entrainment with manifest atrial fusion excludes AVNRT.

Para-Hisian Pacing During SVT

- SA and the local VA intervals that remain constant regardless of whether the HB-RB is being captured indicate orthodromic AVRT and exclude AVNRT.
- SA interval prolongation on HB-RB noncapture, but without significant change in the local VA interval, indicates orthodromic AVRT and excludes AVNRT.
- ΔSA interval < 40 msec indicates AVRT (except for rare patients with a left lateral BT) and argue against AVNRT.

- Entry into the tachycardia circuit within 1 beat indicates AVRT, whereas entry into the circuit occurring only after 3 or more beats is consistent with AVNRT.

Atrial Pacing During NSR at Tachycardia CL

- ΔAH interval ($AH_{\text{pacing}} - AH_{\text{SVT}}$) < 20 msec excludes AVNRT.

Ventricular Pacing During NSR at Tachycardia CL

- ΔHA interval of less than -10 msec makes AVNRT unlikely.

Para-Hisian Pacing During NSR

- Para-Hisian pacing producing similar VA interval, regardless of whether HB capture occurs, and/or different atrial activation sequence, depending on whether HB capture occurs, makes AVNRT unlikely.

AES, Atrial extrastimulation; AH, atrial–His bundle; AVNRT, atrioventricular nodal reentrant tachycardia; AVRT, atrioventricular reentrant tachycardia; BBB, bundle branch block; BT, bypass tract; CL, cycle length; HA, His bundle–atrial interval; HB, His bundle; NSR, normal sinus rhythm; PCL, pacing cycle length; PPI, postpacing interval; RB, right bundle branch; RV, right ventricle; SA, stimulus-to-atrial; SVT, supraventricular tachycardia; TCL, tachycardia cycle length; VA, ventriculoatrial; VES, ventricular extrastimulus.

BOX 18.8 Differentiation Between Antidromic Atrioventricular Reentrant Tachycardia and Preexcited Atrioventricular Nodal Reentrant Tachycardia**SVT Features**

- $HA_{\text{SVT}} < 70$ msec excludes antidromic AVRT.
- Positive HV or VH interval ≤ 10 msec (especially when HA interval is ≤ 50 msec) suggests AVNRT.

Termination of SVT

- Continuation of the SVT at the same TCL, despite anterograde block in the BT (by drugs, mechanical trauma, or ablation), is diagnostic of AVNRT and excludes antidromic AVRT.
- Block of the BT by drugs and subsequent induction of narrow-complex SVT with the same TCL, HA interval, and retrograde atrial activation sequence as that of the preexcited SVT induced before the BT block is diagnostic of preexcited AVNRT and excludes antidromic AVRT.
- Termination of SVT in response to carotid sinus massage or adenosine:
 - AVNRT terminates after atrial activation (secondary to anterograde block down the slow pathway).
 - Classic antidromic AVRT terminates after ventricular activation (secondary to retrograde block up the AVN).

Effects of BBB

- Prolongation of surface ECG VA interval (often with prolonged TCL) on development of BBB excludes AVNRT.

SVT Induction With Ventricular Stimulation

- Induction of the SVT by ventricular pacing at a PCL similar to the TCL or by a VES that advances the timing of the His potential by a coupling interval (i.e., H1-H2 interval) similar to the H-H during the SVT, the HA interval following such a VES is compared with that during the SVT:
 - HA_{VES} or $HA_{\text{pacing}} > HA_{\text{SVT}}$ is diagnostic of AVNRT and excludes antidromic AVRT.
 - HA_{VES} or $HA_{\text{pacing}} \leq HA_{\text{SVT}}$ is diagnostic of antidromic AVRT and excludes AVNRT.

AES Delivered During SVT

- Late-coupled AES is delivered close to the BT atrial insertion site during SVT when the AV junctional atrium is refractory. If it advances the timing of both the next ventricular activation and the subsequent atrial activation, it proves that the SVT is antidromic AVRT using an AV BT anterogradely, and excludes preexcited AVNRT.
- AES during the SVT that advances ventricular activation and does not affect VA interval excludes AVNRT and is diagnostic of antidromic AVRT.
- Exact atrial and ventricular capture by AES delivered when the AV junction is depolarized excludes AVNRT.

Entrainment of SVT by Atrial Pacing

- Failure of entrainment by atrial pacing to influence the VA interval during SVT excludes AVNRT.
- The presence of a fixed short VH interval during entrainment of the SVT with atrial pacing suggests antidromic AVRT, and makes AVNRT unlikely (but does not exclude AVNRT).

Entrainment of SVT by Ventricular Pacing

- Failure of entrainment by ventricular pacing to influence the VA interval during SVT excludes AVNRT.

Ventricular Pacing During NSR at the Tachycardia CL

- Pacing at the RV apex at TCL is performed, and the HA interval during RV pacing is compared with the HA interval during SVT. (It is important to verify that VA conduction occurred only over the same pathway as during SVT for this analysis to be valid.)
 - $HA_{\text{pacing}} > HA_{\text{SVT}}$ is diagnostic of AVNRT and excludes AVRT.
 - $HA_{\text{pacing}} \leq HA_{\text{SVT}}$ is diagnostic of AVRT and excludes AVNRT.
- VA block during RV apical pacing excludes AVRT.

AES, Atrial extrastimulus; AV, atrioventricular; AVNRT, atrioventricular nodal reentrant tachycardia; AVRT, atrioventricular reentrant tachycardia; BBB, bundle branch block; BT, bypass tract; CL, cycle length; HA, His bundle–atrial; ECG, electrocardiogram; HV, His bundle–ventricular; NSR, normal sinus rhythm; PCL, pacing cycle length; RV, right ventricle; SVT, supraventricular tachycardia; TCL, tachycardia cycle length; VA, ventriculoatrial; VES, ventricular extrastimulus; VH, ventricular–His bundle.

BOX 18.9 Electrophysiological Findings Indicating Presence of Multiple Atrioventricular Bypass Tracts

During Preexcited Rhythms (NSR, PACs, Spontaneous or Induced AF, RA, and LA Pacing)

- Changing anterograde delta wave (i.e., variations in preexcited QRS morphology). Atrial pacing from different sites (high RA and CS) may accentuate preexcitation over one BT and not the other, and help unmask the changes in the delta wave.
- Atypical pattern of preexcitation (i.e., does not conform to an expected QRS morphology for a given location)
- Changing anterograde delta wave following antiarrhythmic agents (e.g., amiodarone or class I agents) that may block one BT and not the other or following ablation of one BT

During Ventricular Pacing at Different CLs and From Multiple Pacing Sites

- Evidence of multiple routes of retrograde atrial activation:
- Changing P wave morphology or atrial activation sequence
- Multiple atrial breakthrough sites
- Changing VA interval
- Evidence of mismatch of site of anterograde preexcitation and site of retrograde atrial activation observed during ventricular pacing

During Orthodromic AVRT

- Evidence of multiple routes of retrograde atrial activation:
- Changing P wave morphology or atrial activation sequence
- Multiple atrial breakthrough sites
- Changing VA interval
- Failure to delay atrial activation at all sites with the development of BBB ipsilateral to the BT
- Evidence of multiple routes of anterograde ventricular activation:
- Intermittent anterograde fusion (preexcited) complexes
- Evidence of mismatch of site of anterograde preexcitation and site of retrograde atrial activation observed during orthodromic AVRT

During Antidromic AVRT

- Eccentric atrial activation sequence
- Varying degrees of anterograde fusion
- Changing VH interval without any change in the TCL or atrial activation sequence (suggesting that the HPS is not part of the reentrant circuit)
- Tachycardia CL during antidromic AVRT slower than orthodromic AVRT in the same patient (in absence of dual AVN pathways)
- Anterograde ventricular activation over posteroseptal BT
- The mere presence of antidromic AVRT

AF, Atrial fibrillation; AVN, atrioventricular node; AVRT, atrioventricular reentrant tachycardia; BBB, bundle branch block; BT, bypass tract; CL, cycle length; CS, coronary sinus; HPS, His-Purkinje system; LA, left atrium; NSR, normal sinus rhythm; PAC, premature atrial complex; RA, right atrium; TCL, tachycardia cycle length; VA, ventriculoatrial; VH, ventriculo-His.

Effects of Bundle Branch Block During Orthodromic Atrioventricular Reentrant Tachycardia

Prolongation of the TCL and, more importantly, the surface VA interval by more than 35 milliseconds following the development of BBB is diagnostic of AVRT using a free-wall BT ipsilateral to the BBB (LBBB with left-sided BT, and RBBB with right-sided BT). Superoparaseptal and posteroseptal BTs are associated with a lesser degree of prolongation of the VA interval (approximately 5 to 25 milliseconds) on the

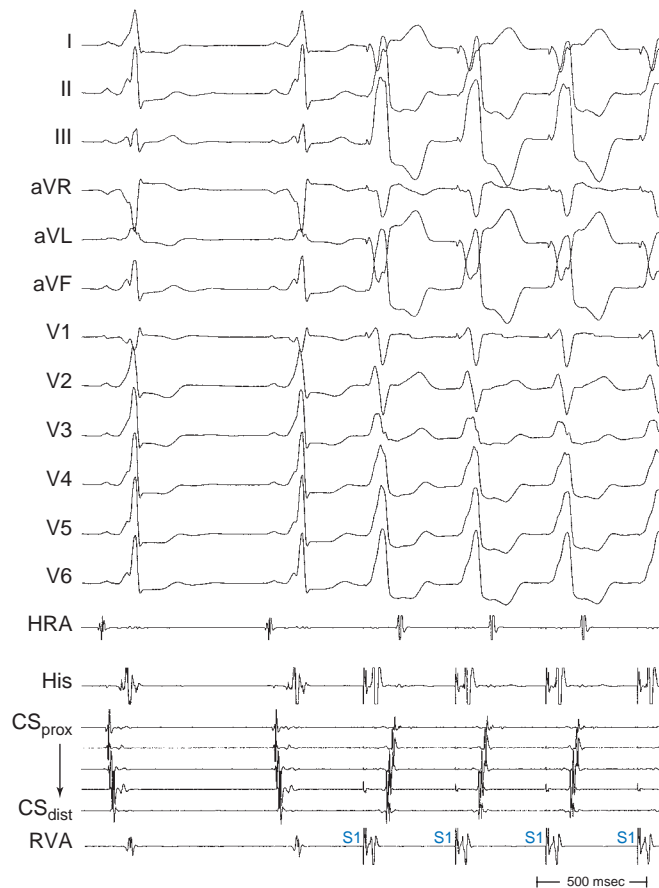


Fig. 18.45 Identifying Multiple Bypass Tracts (BTs) in the Same Patient. The presence of multiple BTs is indicated by the mismatch of sites of anterograde preexcitation during normal sinus rhythm (the delta wave morphology is consistent with anterograde conduction over a right anterior BT) and site of retrograde atrial activation observed during ventricular pacing (the atrial activation sequence is consistent with ventriculoatrial conduction over a left lateral BT). CS_{dist}, Distal coronary sinus; CS_{prox}, proximal coronary sinus; HRA, high right atrium; RVA, right ventricular apex.

development of BBB (RBBB with superoparaseptal BT, and LBBB with posteroseptal BT). In an analogous fashion, entrainment of the SVT by ventricular pacing that results in prolongation of the VA interval ($VA_{\text{pacing}} > VA_{\text{SVT}}$) suggests that the SVT is orthodromic AVRT mediated by an AV BT in the ventricle contralateral to the site of ventricular pacing.

Ventricular Entrainment During Orthodromic Atrioventricular Reentrant Tachycardia

During orthodromic AVRT, the corrected (PPI – TCL) difference following entrainment from the RV apex can help localize the BT used for retrograde conduction. The RV apical pacing site is closer to the reentrant circuit of orthodromic AVRT utilizing a right-sided BT than orthodromic AVRT utilizing a left-sided BT. Hence, as expected, the corrected (PPI – TCL) difference is shorter (less than 55 milliseconds) in patients with orthodromic AVRT with a right-sided BT when pacing the RV apex. Patients with left-sided BTs typically have a corrected (PPI – TCL) difference of more than 55 milliseconds.⁵¹

Furthermore, upon initiation of ventricular overdrive pacing from the RV apex during orthodromic AVRT, there is a “transitional zone” during which the paced QRS complexes show progressive fusion with

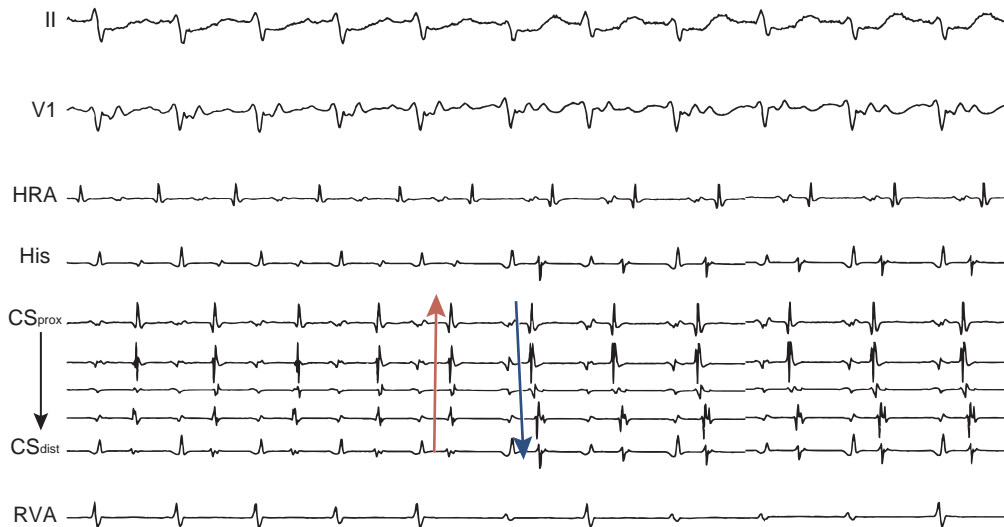


Fig. 18.46 Orthodromic Atrioventricular Reentrant Tachycardia With Multiple Routes of Retrograde Atrial Activation. The presence of multiple bypass tracts is indicated by the shift in retrograde atrial activation sequence (indicated by the *red and blue arrows*) during tachycardia. *CS_{dist}*, Distal coronary sinus; *CS_{prox}*, proximal coronary sinus; *HRA*, high right atrium; *RVA*, right ventricular apex.

BOX 18.10 Electrophysiological Maneuvers for Localization of the Bypass Tract

Pacing From Multiple Atrial Sites

- Proximity to the BT atrial insertion is indicated by shortening of the P-delta interval during atrial pacing.

Preexcitation Index of VES From the RV

- A relative preexcitation index >90% suggests right-sided or septal BT.
- An absolute preexcitation index ≥ 75 msec suggests a left free-wall BT.
- An absolute preexcitation index <45 msec suggests a septal BT.
- An absolute preexcitation index of 45–75 msec is indeterminate.

Effects of BBB During Orthodromic AVRT

- Prolongation of the TCL and, more importantly, the surface VA interval by >35 msec following the development of BBB is diagnostic of AVRT using a free-wall BT ipsilateral to the BBB (LBBB with left-sided BT, and RBBB with right-sided BT).
- Superoparaseptal and posteroseptal BTs are associated with a lesser degree of prolongation of the VA interval (approximately 5–25 ms) on the development of BBB (RBBB with superoparaseptal BT, and LBBB with posteroseptal BT).

Ventricular Entrainment During Orthodromic AVRT From the RV Apex

- Corrected (PPI – TCL) difference <55 msec is consistent with a right-sided BT.
- Corrected (PPI – TCL) difference >55 msec is consistent with a left-sided BT.
- Resetting of ≥ 3 atrial beats (with fixed SA intervals) within the transitional zone suggests a right-sided BT.
- Resetting of only 1 or 2 atrial beats during the transitional zone suggests a left-sided BT.

Mapping Ventricular Activation During Preexcited Rhythm

- The site of earliest local ventricular activation (preceding the onset of the delta wave) along the tricuspid and mitral annuli identifies the BT ventricular insertion site.

Mapping Atrial Activation During Retrograde Bypass Tract Conduction

- The site of earliest local atrial activation along the tricuspid and mitral annuli during orthodromic AVRT or during ventricular pacing with retrograde conduction over the BT, identifies the BT atrial insertion site.
- The site of polarity reversal of the atrial unfiltered bipolar electrogram (with the electrodes oriented parallel to the axis of the annulus) during orthodromic AVRT or during ventricular pacing with retrograde conduction over the BT, identifies the BT atrial insertion site.

Mapping Bypass Tract Potential

- Recording a BT potential 10–30 ms before the onset of the delta wave (during anterograde preexcitation) or between the ventricular and atrial electrograms at the earliest site of retrograde atrial activation (during orthodromic AVRT or ventricular pacing) identifies the BT location.

Local AV or VA Interval

- When the BT crosses the AV groove perpendicularly, the site of the shortest local VA interval (during retrograde BT conduction) and the site of the shortest local AV interval (during anterograde BT conduction) can indicate the BT location and is often considered the optimal target for BT ablation.

AV, Atrioventricular; AVRT, atrioventricular reentrant tachycardia; BBB, bundle branch block; BT, bypass tract; LBBB, left bundle branch block; PPI, postpacing interval; RBBB, right bundle branch block; RV, right ventricle; SA, stimulus-to-atrial; TCL, tachycardia cycle length; VA, ventriculoatrial; VES, ventricular extrastimulus.

the SVT complexes, until stable QRS morphology is observed (either completely paced or constantly fused). The closer the BT location is to the RV apical pacing site, the earlier atrial resetting will occur during the transitional zone, and the greater the number of complexes that show advancement of atrial activation (as defined by acceleration of atrial

activation to the ventricular pacing rate with fixed SA intervals) during the transitional zone (Fig. 18.47). Right-sided BTs produce reset earlier than left-sided BTs, and resetting of at least three atrial beats (with fixed SA intervals) within the transitional zone was found to successfully identify right-sided BTs. Left-sided BTs allow atrial resetting later after

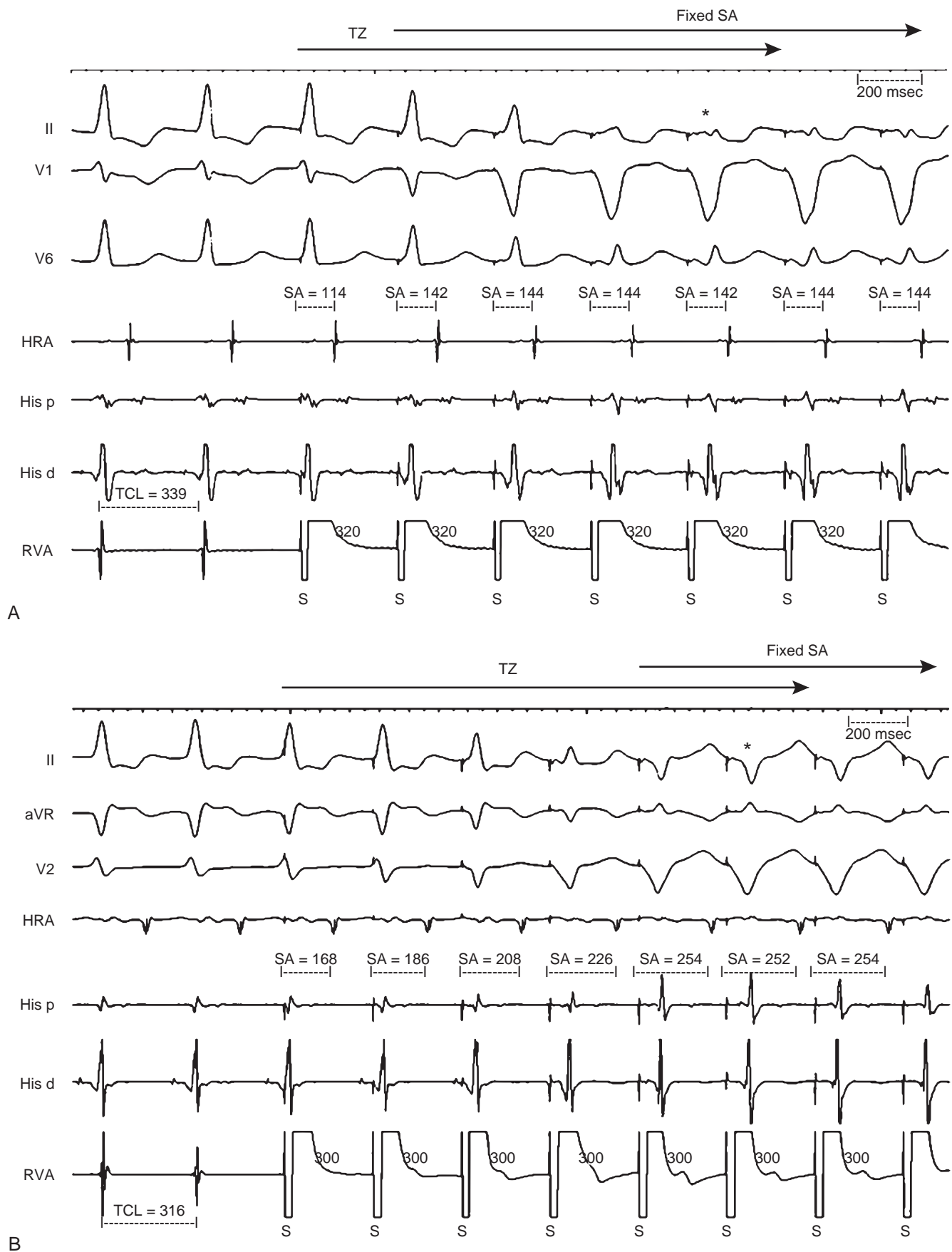


Fig. 18.47 Ventricular Entrainment During Orthodromic Atrioventricular Reentrant Tachycardia (AVRT) for Bypass Tract (BT) Localization. (A) Orthodromic AVRT over a right lateral BT with a tachycardia cycle length (TCL) of 339 milliseconds. Right ventricular apical (RVA) overdrive pacing is delivered at 320 milliseconds and the number of beats with a fixed stimulus-atrial (SA) interval within the transition zone (TZ) is 4 (the 4 last beats of the TZ). (B) Orthodromic AVRT using a right posteroseptal BT with a TCL of 316 milliseconds. RVA overdrive pacing is delivered at 300 milliseconds and the number of beats with a fixed SA interval within the TZ is two (the last two beats of the TZ). The star indicates the first paced beat with a fixed QRS-morphology, representing the last beat of the TZ. His d, Distal His bundle; His p, proximal His bundle; HRA, high right atrium. (From Akerström F, Pachón M, García-Fernández FJ, et al. Number of beats in the transition zone with fixed SA interval during right ventricular overdrive pacing determines accessory pathway location in orthodromic reentrant tachycardia. *Pacing Clin Electrophysiol.* 2015;39:21–27.)

starting ventricular overdrive pacing (due to the larger distance between the BT and the pacing site) and, hence, only one or two reset beats during the transitional zone would reveal atrial resetting. Septal BTs had numbers of reset complexes that overlapped with right- and left-sided BTs.⁵⁷

Earliest Ventricular Activation Site During Anterograde Bypass Tract Conduction

During ventricular preexcitation (preexcited sinus or atrial paced rhythm, or antidromic AVRT), the surface ECG lead with the earliest onset of the delta wave, preferably with a relatively sharp delineation of its onset, should be selected and used as the timing reference during mapping (eFig. 18.6). The site of earliest local ventricular activation (preceding the onset of the delta wave) along the tricuspid and mitral annuli identifies the BT ventricular insertion site.

Both bipolar and unipolar recordings on the ablation catheter should be used for mapping (Fig. 18.48). Bipolar electrograms display electrogram components and timing and may demonstrate a BT potential. The unfiltered (0.05 to 300 Hz) unipolar signal morphology should show a monophasic QS complex with a rapid negative deflection if the site was at the origin of impulse formation in the ventricle (i.e., BT

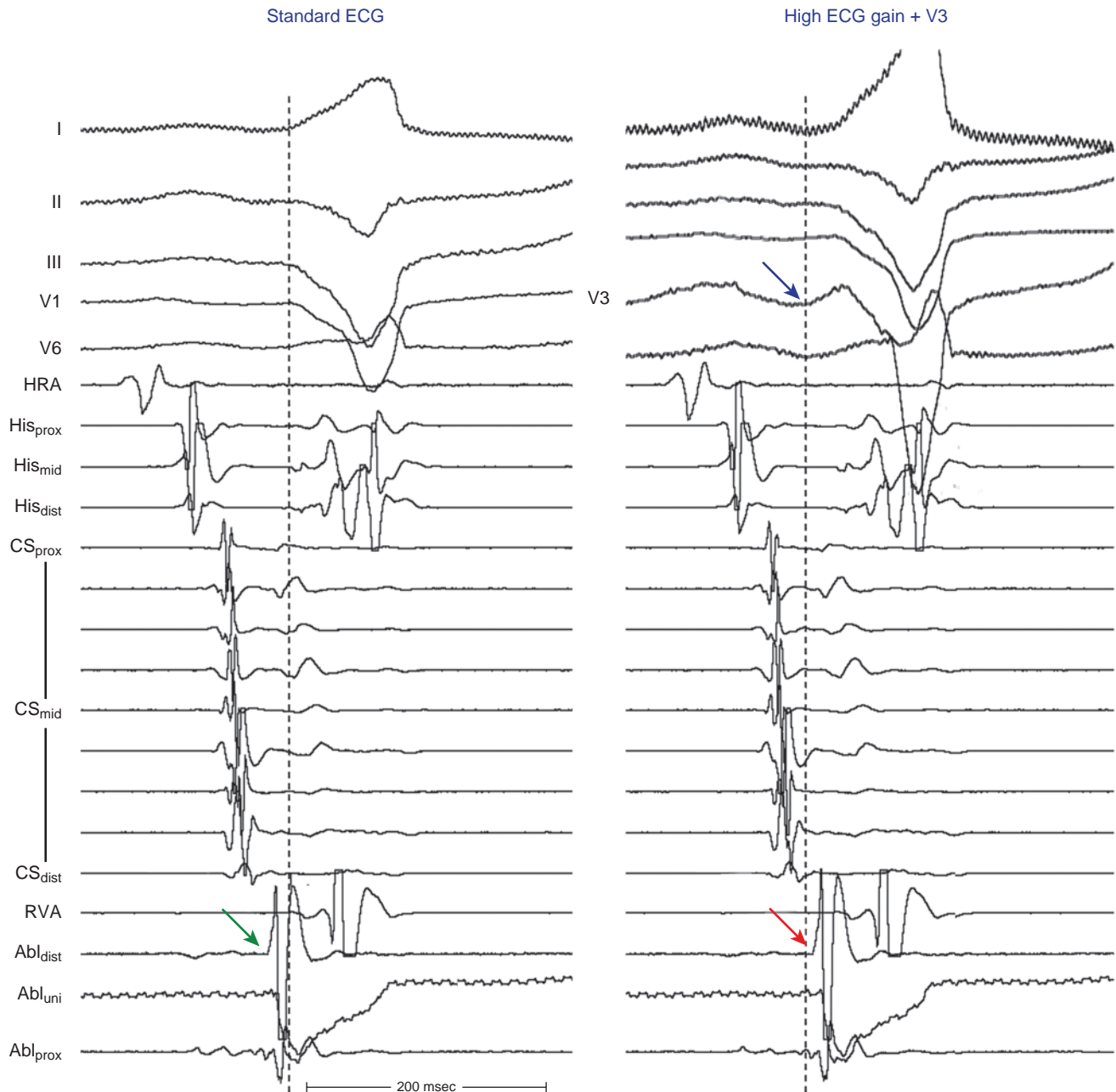
insertion site). Concordance of the timing of the onset of the bipolar electrogram with that of the unipolar electrogram (with the rapid downslope of the S wave of the unipolar QS complex coinciding with the initial peak of the bipolar signal) helps ensure that the tip electrode, which is the ablation electrode, is responsible for the early component of the bipolar electrogram. If only bipolar recordings are used, one does not know which of the two poles is responsible for the earliest component of the bipolar electrogram.

Earliest Atrial Activation Site During Retrograde Bypass Tract Conduction

During orthodromic AVRT or during ventricular pacing with retrograde conduction over the BT, the site of earliest atrial activation along the tricuspid and mitral annuli identifies the BT atrial insertion site. When mapping is performed during ventricular pacing, fusion of atrial activation, caused by simultaneous retrograde conduction over both the AVN and the BT, has to be considered because it can affect the accuracy of mapping. This can be an issue in the setting of septal BTs whereby the retrograde atrial activation sequence over the BT may not be very different from that over the AVN. Dissociation of retrograde conduction over the BT from that over the AVN is required in these situations, and



Fig. 18.48 Catheter Ablation (ABL) of a Left Anterolateral Bypass Tract (BT) During Anterograde Conduction. ABL is performed during preexcited atrial pacing. Preexcitation is observed during the first three complexes. The dashed line indicates the onset of the delta wave. Note the sharp negative deflection (QS morphology) in the unipolar recording. Also, note the concordance of the timing of the unipolar and bipolar electrograms (blue arrows), which precedes the onset of the delta wave by 10 to 15 milliseconds. A sharp potential (possible BT potential, red arrow) is recorded between the atrial and ventricular electrograms. RF application at this site successfully eliminated preexcitation (last two complexes). CS_{dist}, Distal coronary sinus; CS_{prox}, proximal coronary sinus; HRA, high right atrium; RVA, right ventricular apex.



eFig. 18.6 Surface Electrocardiogram (ECG) and Intracardiac Recordings of Possible Ablation Site. On the left, with standard ECG recordings, the features of the ablation site electrograms suggest this would be a good ablation site (*green arrow*) because they occur well before the onset of the delta wave (*dashed line*). However, on the right, the very same complex is shown, but with increased gain on surface ECG leads as well as an addition of lead of V3 (showing sharp delineation of delta wave onset, *blue arrow*). Now, the dashed line that denotes the true onset of surface preexcitation reveals that the putative ablation site is not attractive (*red arrow*). *Abl_{dist}*, Ablation distal bipolar electrodes; *Abl_{prox}*, ablation proximal bipolar electrodes; *Abl_{uni}*, ablation distal unipolar electrode; *CS_{dist}*, distal coronary sinus; *CS_{mid}*, middle coronary sinus; *CS_{prox}*, proximal coronary sinus; *His_{dist}*, distal His bundle; *His_{mid}*, middle His bundle; *His_{prox}*, proximal His bundle; *HRA*, high right atrium; *RVA*, right ventricular apex.

can usually be achieved with ventricular stimulation from sites closer to the BT and with the use of AVN blockers (e.g., adenosine) to ensure preferential retrograde conduction over the BT.

As with ventricular mapping, both bipolar and unipolar recordings on the distal ablation electrode should be used for atrial mapping (Fig. 18.49). Determining what components of a complex ablation electrode recording is atrial versus ventricular can be facilitated by rapid burst ventricular pacing that does not conduct 1:1 retrogradely (Fig. 18.50) or by introduction of a VES that does not conduct retrogradely during fixed-rate ventricular pacing (Fig. 18.51). In either case, the principle is to compare the electrogram that is known to have no atrial component with the electrogram in question (with some atrial component), any difference being due to the contribution of the atrial electrogram.

Atrial Electrogram Polarity Reversal During Retrograde Bypass Tract Conduction

The morphology and amplitude of the bipolar electrograms are influenced by the orientation of the bipolar recording axis to the direction of propagation of the activation wavefront. Although the direction of wavefront propagation cannot be reliably inferred from the morphology of the bipolar signal, a change in morphology can be a useful finding,

and the unfiltered bipolar electrogram with the electrodes oriented parallel to the axis of the annulus can be used to localize the atrial insertion site of the BT.

During retrograde BT conduction (orthodromic AVRT or ventricular pacing), BT atrial insertion is identified as the site where the polarity of the atrial potential reverses. Because the site of BT atrial insertion is usually discrete, atrial activation propagates in two opposite directions along the annulus from the insertion site. As a result, an RS configuration electrogram will be present on one side of the BT, where the wavefront is propagating from the distal electrode toward the proximal electrode, and a QR morphology electrogram on the other side, where the wavefront is propagating from the proximal electrode toward the distal electrode.

This technique is typically used for localization of left free-wall BTs via the transeptal approach, which allows an electrode orientation parallel with atrial activation along the mitral annulus. As the ablation catheter is moved along the mitral annulus during retrograde BT conduction, the amplitude and polarity of the atrial electrogram are examined. With the tip electrode negative, and the catheter lying on the mitral annulus from anterior to posterior, an upright atrial electrogram indicates a catheter position anterior to the insertion site,

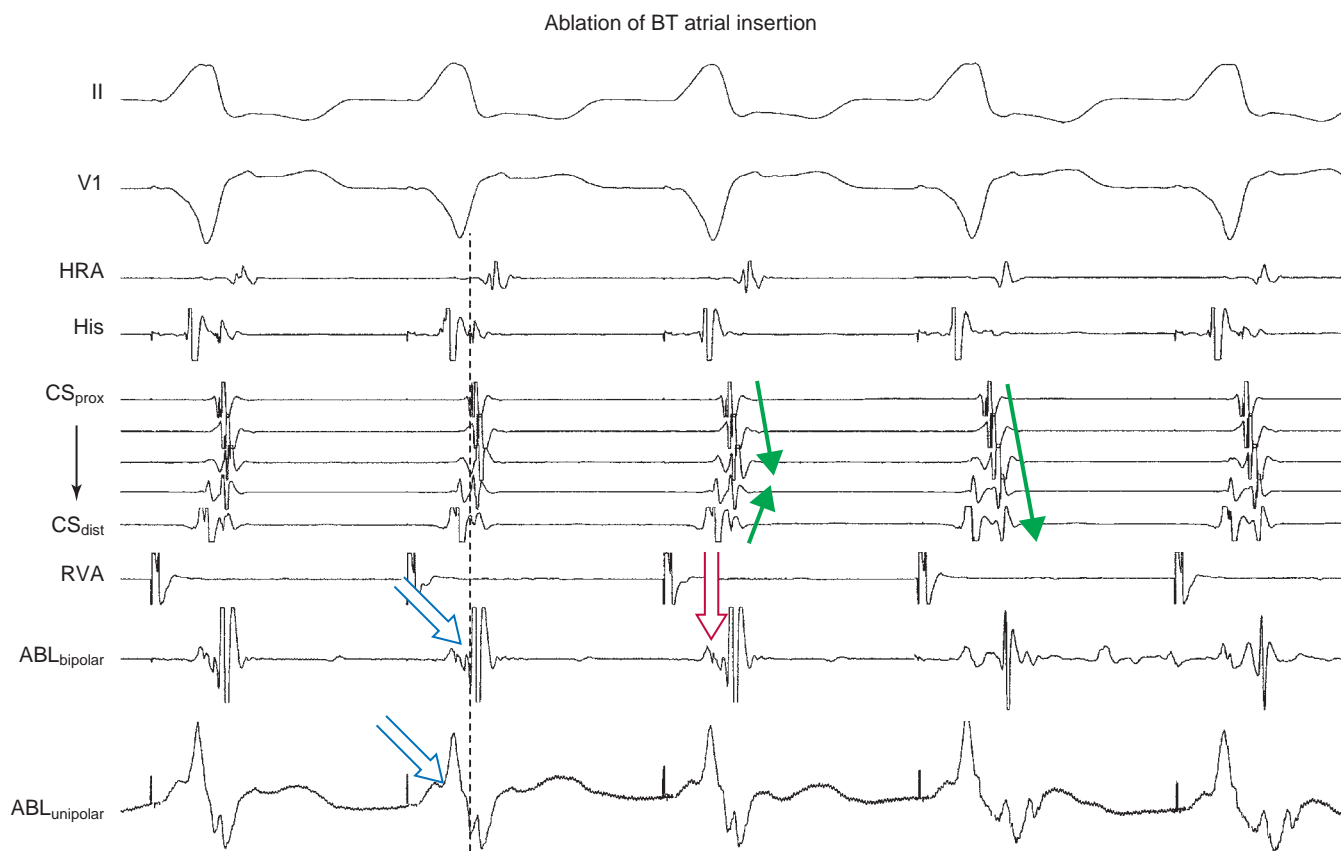


Fig. 18.49 Catheter Ablation (ABL) of a Left Lateral Bypass Tract (BT) During Retrograde Conduction. ABL is performed during ventricular pacing with atrial fusion (ventriculoatrial conduction occurring over both the BT and atrioventricular node [AVN]). The dashed line indicates the onset of the earliest atrial activation. Note the sharp negative deflection (QS morphology) in the unipolar recording. The timing of the unipolar electrogram coincides with the bipolar electrogram (blue arrows) and precedes the delta wave by 5 to 10 milliseconds. The atrial and ventricular electrograms merge, and the true morphology of the ventricular electrogram is unmasked after successful ablation (last two complexes). A sharp potential (possible BT potential, red arrow) is recorded between the two electrograms. After successful elimination of the BT function, atrial activation occurs exclusively over the AVN (last two complexes, green arrows). *CS_{dist}*, Distal coronary sinus; *CS_{prox}*, proximal coronary sinus; *HRA*, high right atrium; *RVA*, right ventricular apex.

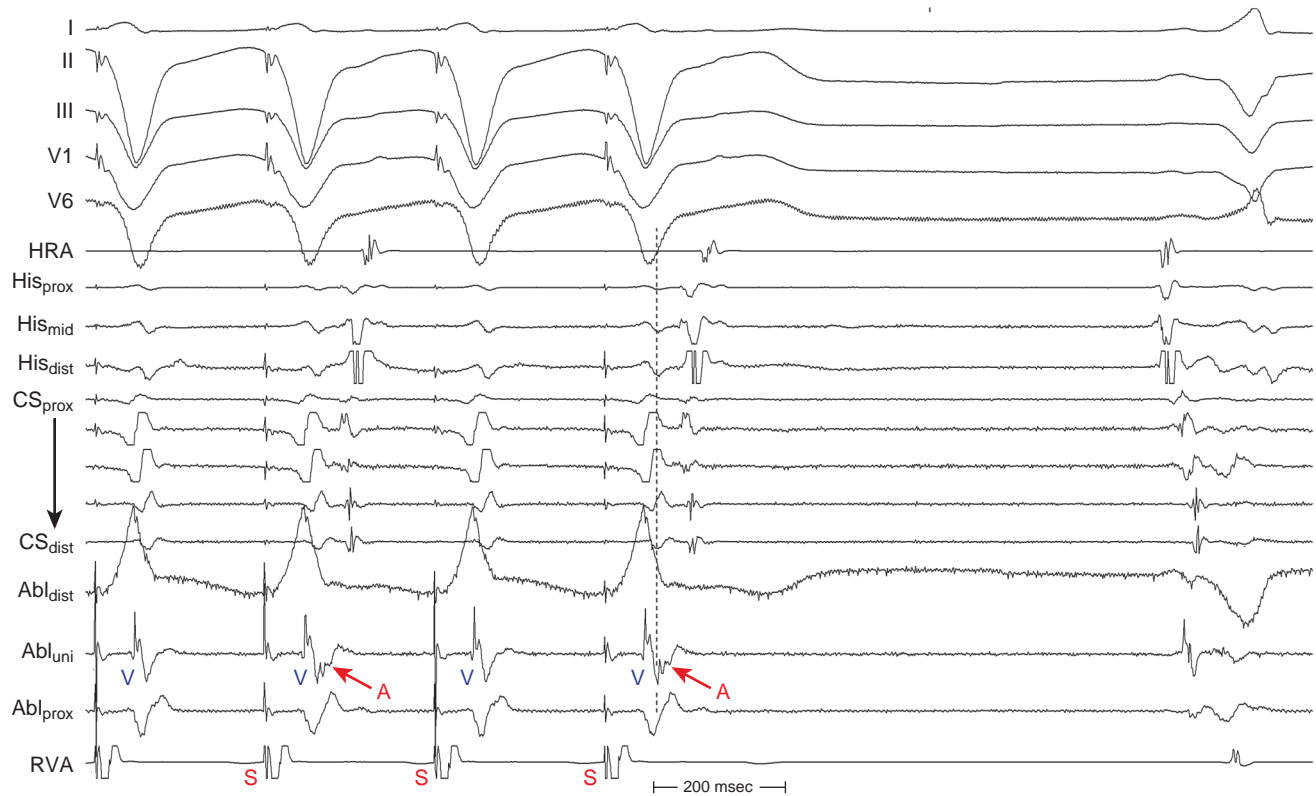


Fig. 18.50 Using Ventricular Pacing to Evaluate Ablation Site Electrogram Components. Burst ventricular pacing is shown at a rate that produces 2:1 retrograde conduction over the bypass tract (BT). This facilitates determination of what portion of the ablation site recording is atrial versus ventricular, because whatever is present in recordings on cycles during which retrograde conduction is present, but absent when retrograde conduction fails, is the atrial (or BT plus atrial) recording (red arrows). *Abl_{dist}*, Ablation distal bipolar electrodes; *Abl_{prox}*, ablation proximal bipolar electrodes; *Abl_{uni}*, ablation distal unipolar electrode; *CS_{dist}*, distal coronary sinus; *CS_{prox}*, proximal coronary sinus; *His_{dist}*, distal His bundle; *His_{mid}*, middle His bundle; *His_{prox}*, proximal His bundle; *HRA*, high right atrium; *RVA*, right ventricular apex.

whereas a negative electrogram indicates positions posterior to the insertion site. When the bipole approaches and then passes directly over the atrial insertion site, the atrial electrogram becomes diminished in amplitude, isoelectric, and fractionated. As the catheter moves from one side of the insertion site to the other side, reversal of the atrial electrogram polarity is observed. This maneuver has a sensitivity of 97%, specificity of 46%, and positive predictive value of 75%. For BTs at other locations, mapping can be facilitated by using a multipolar catheter positioned in the CS or around the tricuspid annulus (e.g., Halo catheter); the site of the BT atrial insertion is enclosed between the two adjacent bipoles, demonstrating atrial electrogram polarity reversal.

Direct Recording of Bypass Tract Potential

The BT potential manifests as a sharp narrow spike on both unipolar and bipolar recordings 10 to 30 milliseconds before the onset of the delta wave during anterograde preexcitation or between the ventricular and atrial electrograms at the earliest site of retrograde atrial activation during orthodromic AVRT or ventricular pacing. The BT potential amplitude averages 0.5 to 1 mV at successful ablation sites (see Figs. 18.48 and 18.49). Similar electrical signals, however, can be a component of the atrial or ventricular electrogram, and proof that an electrical signal is actually a BT potential can be difficult, because it needs to be dissociated from the local atrial and ventricular electrograms.

During anterograde BT conduction (NSR or atrial pacing), dissociation of the anterograde BT potential from the ventricular potentials can be achieved by introduction of VES with progressively shorter coupling intervals. Dissociation of the BT potential from the local ventricular potential is confirmed when a late-coupled VES (occurring at the time of the anterograde BT potential) advances the ventricular electrogram without affecting the timing or morphology of the BT potential. Furthermore, dissociation of the BT potential from the local atrial potential is confirmed when an earlier VES advances the BT potential without affecting the timing or morphology of the atrial electrogram (Fig. 18.52).

A retrograde BT potential (during ventricular pacing or orthodromic AVRT) can be validated by introduction of progressively premature AES. A late-coupled AES can advance the timing of the local atrial potential without affecting the retrograde BT potential, providing evidence that the BT potential is not related to atrial activation. In addition, dissociation of the BT potential from the local ventricular potential is confirmed when an earlier AES advances the BT potential (i.e., anterogradely activate the BT) without affecting the timing or morphology of the local ventricular electrogram (Fig. 18.53).

However, these criteria for validation of BT potentials are often difficult to achieve. Therefore validation of BT potentials by programmed electrical stimulation is often not practical in clinical settings; instead, such a potential is called *possible* or *probable* BT potential.

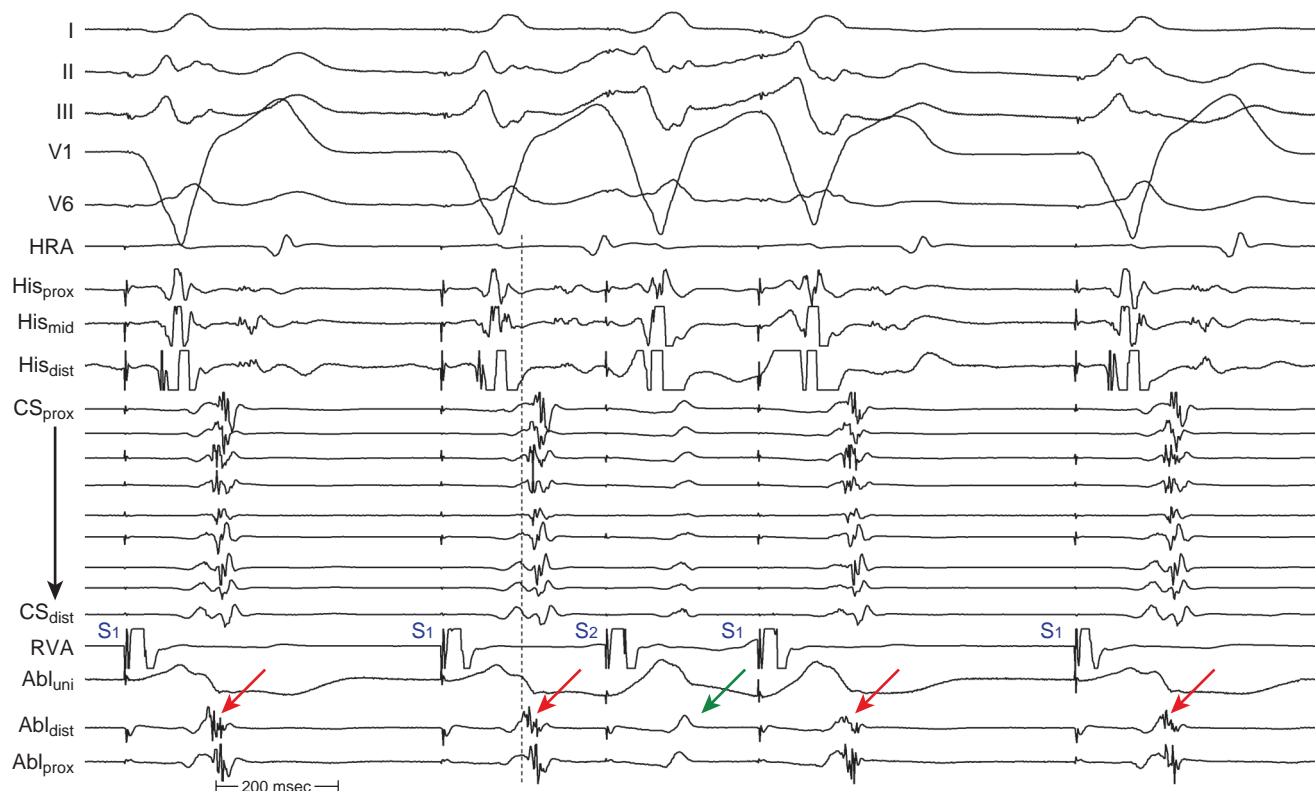


Fig. 18.51 Using Ventricular Extrastimuli to Evaluate Ablation Site Electrogram Components. Determining what part of a complex ablation site recording is atrial or bypass tract (BT) is aided by introducing an extrastimulus (*S2*) during a fixed-rate drive, which fails to conduct retrogradely while drive complexes do conduct. The portion of the electrogram that is absent on this complex (*green arrow*), but present on others (*red arrows*), is the atrial (\pm BT) component. *Abl_{dist}*, Ablation distal bipolar electrodes; *Abl_{prox}*, ablation proximal bipolar electrodes; *Abl_{uni}*, ablation distal unipolar electrode; *CS_{dist}*, distal coronary sinus; *CS_{prox}*, proximal coronary sinus; *His_{dist}*, distal His bundle; *His_{mid}*, middle His bundle; *His_{prox}*, proximal His bundle; *HRA*, high right atrium; *RVA*, right ventricular apex.

Targeting an isolated BT potential has been associated with the highest rate of ablation success. The usefulness of this criterion, however, has been limited by difficulty in locating or validating a BT potential in clinical practice. The difficulty in identifying the BT potential is often related to the oblique course of the BT. A ventricular or atrial wavefront propagating concurrently with the BT can overlap and mask the BT potential. Pacing from the site producing the shorter local VA or local AV intervals helps identify the BT potential in most of these cases.

Local Atrioventricular (or Ventriculoatrial) Interval

When the BT crosses the AV groove perpendicularly, the site of the shortest local VA interval (during retrograde BT conduction) and the site of the shortest local AV interval (during anterograde BT conduction) can indicate the BT location and is often considered the optimal target for BT ablation. However, the reliability of this criterion has been debated and can be misleading in the setting of oblique BTs. Short local VA intervals can occur at sites along the valve annulus distant from the BT because atrial and ventricular activation wavefronts can propagate circumferentially along the annulus, and the timing of local atrial and ventricular activation can be close to one another at multiple sites along the annulus (Fig. 18.54). Furthermore, with oblique BTs, the shortest local VA interval can be shifted away from the BT in the direction of the ventricular wavefront if the velocity of the ventricular wavefront along the annulus is less than the velocity of the atrial wavefront.

Similarly, the site of the shortest local AV interval can be shifted away from the BT in the direction of the atrial wavefront if the atrial wavefront is slower than the ventricular wavefront.

With an oblique course, the local VA and AV intervals vary by reversing the direction of the paced ventricular and atrial wavefronts, respectively. During ventricular pacing, a ventricular wavefront propagating from the direction of the ventricular end (concurrently with BT activation) produces an artificially short local VA interval (measured at the site of earliest retrograde atrial activation), because activation along the BT proceeds to the earliest atrial activation site simultaneously and in the same direction as the ventricular wavefront at the ventricular aspect of the AV groove. Contrariwise, a ventricular wavefront propagating in the opposite (countercurrent) direction produces a longer local VA interval because the ventricular wavefront must pass the site of earliest atrial activation before reaching the ventricular end of the BT (Fig. 18.55). This has important implications for localizing oblique AV BTs. With a concurrent wavefront, the ventricular potential can overlap the BT potential and atrial electrogram, masking the site of earliest atrial activation and BT potential. If the velocity of the ventricular wavefront along the annulus were slower than the BT and atrial wavefronts, the shortest local VA interval would be shifted away from the BT. A countercurrent wavefront should expose the atrial activation sequence and BT potential, but would result in a longer VA interval measured at the site of earliest retrograde atrial activation.

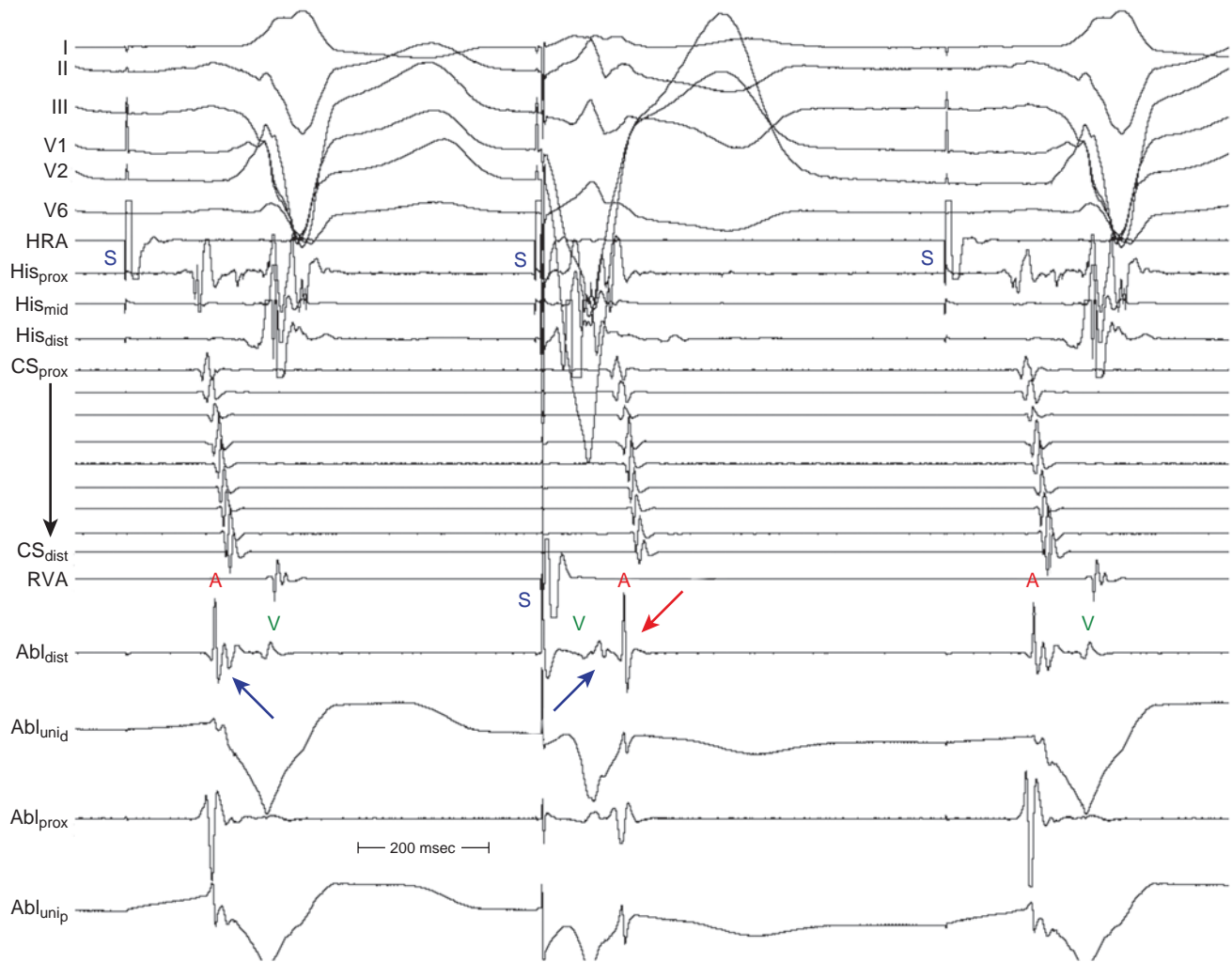


Fig. 18.52 Dissociation of Bypass Tract (BT) Potential From Local Atrial Potential. Surface electrocardiogram and intracardiac recordings evaluate possible BT potential. Fixed-rate atrial pacing is present on all three complexes shown. On the first complex, a blue arrow points to a possible BT potential following the sharp atrial potential (A). This same sharp atrial potential is seen at the same rate as atrial pacing on all three complexes. On the middle complex, a single ventricular extrastimulus is delivered almost simultaneously with the atrial drive stimulus (S). Here, the blue arrow shows that the putative BT potential does not follow the sharp atrial recording (red arrow indicates its absence), and thus is not part of the atrial electrogram. *Abl_{dist}*, Ablation distal bipolar electrodes; *Abl_{prox}*, ablation proximal bipolar electrodes; *Abl_{uni_d}*, ablation distal unipolar electrode; *CS_{dist}*, distal coronary sinus; *CS_{prox}*, proximal coronary sinus; *His_{dist}*, distal His bundle; *His_{mid}*, middle His bundle; *His_{prox}*, proximal His bundle; *HRA*, high right atrium; *RVA*, right ventricular apex.

Similarly, during atrial pacing, a concurrent atrial wavefront would shorten the local AV interval (measured at the site of earliest ventricular activation) and could mask the BT potential and site of earliest ventricular activation. A countercurrent atrial wavefront should lengthen the local AV and expose the BT potential and ventricular activation sequence (see Fig. 18.55).

Reversing the paced ventricular or atrial wavefronts can increase the local VA or local AV interval, respectively, by at least 15 milliseconds in more than 85% of patients, which suggests that most BTs have an oblique course. The increase in the local VA or local AV intervals can facilitate identification of the BT potential. An anterograde or retrograde BT potential can be recorded in more than 85% of patients with oblique BTs, which is much more frequent than that with nonoblique BTs,

because fusion of the atrial, BT, and ventricular potentials may be expected with nonoblique BTs.

During retrograde BT conduction, the earliest atrial activation can be recorded 3 to 5 mm (or possibly more) from the actual BT insertion. Ablation is likely to be successful if the electrode is located 3 to 5 mm from the atrial insertion in the direction of the ventricular insertion and unsuccessful if located in the opposite direction. During anterograde BT conduction, ablation at a site recording earliest ventricular activation is likely to be successful, even if the electrode is located 3 to 5 mm from the ventricular end but in the direction of the atrial insertion and unsuccessful if located in the opposite direction. This explains the 40% ablation success for the criterion of local ventricular activation preceding the onset of the delta wave by less than

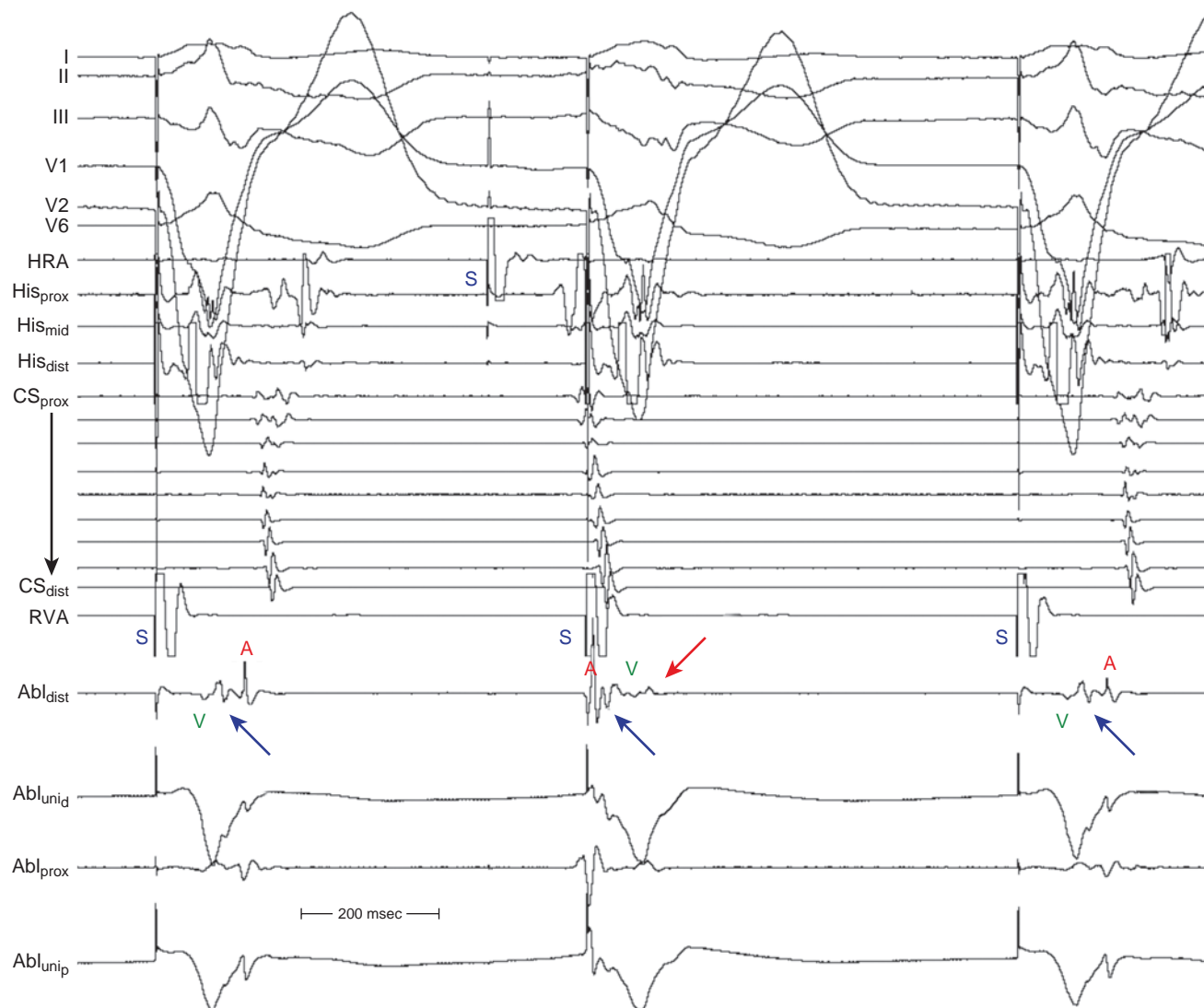


Fig. 18.53 Dissociation of Bypass Tract (BT) Potential From Local Ventricular Potential. Surface electrocardiogram and intracardiac recordings evaluate possible BT potential in the same patient as in Fig. 18.35. Fixed-rate ventricular pacing is shown in all three complexes, with a single atrial extrastimulus (AES) introduced during the middle complex. The blue arrow in the first complex points to a putative BT potential between ventricular (V) and atrial (A) electrograms. In the middle complex, the AES is timed such that the BT potential follows the atrial electrogram (blue arrow), and not the ventricular recording (red arrow). Thus it is not part of the ventricular electrogram. *Abl_{dist}*, Ablation distal bipolar electrodes; *Abl_{prox}*, ablation proximal bipolar electrodes; *Abl_{unip}*, ablation distal unipolar electrode; *CS_{dist}*, distal coronary sinus; *CS_{prox}*, proximal coronary sinus; *His_{dist}*, distal His bundle; *His_{mid}*, middle His bundle; *His_{prox}*, proximal His bundle; *HRA*, high right atrium; *RVA*, right ventricular apex.

0 milliseconds during anterograde BT conduction, even though ventricular activation can usually be recorded as much as 30 milliseconds before the delta wave in right-sided BTs and 15 to 20 milliseconds in left-sided BTs.

ABLATION

Target of Ablation

The BT is the target of ablation. Although BT conduction can be eliminated by ablation anywhere between the atrial and ventricular ends, radiofrequency (RF) applications targeted to the atrial end (site of earliest atrial activation during retrograde BT conduction) or ventricular end

(site of earliest ventricular activation during anterograde BT conduction) occasionally fail, likely because of the broader dimension of BT at the insertion site compared to the annular aspect.

The best site of ablation of an AV BT is where it crosses the mitral or tricuspid annulus. Localization of the BT can be achieved with different mapping methods, as described earlier. Ablation should be performed at the same side of the annulus to the one being mapped (i.e., ablation on the atrial side during mapping of the atrial insertion site during retrograde BT conduction, and ablation on the ventricular side during mapping of the earliest ventricular activation during anterograde BT conduction). This is especially important for oblique BTs, whereby the earliest ventricular activation site during anterograde BT conduction

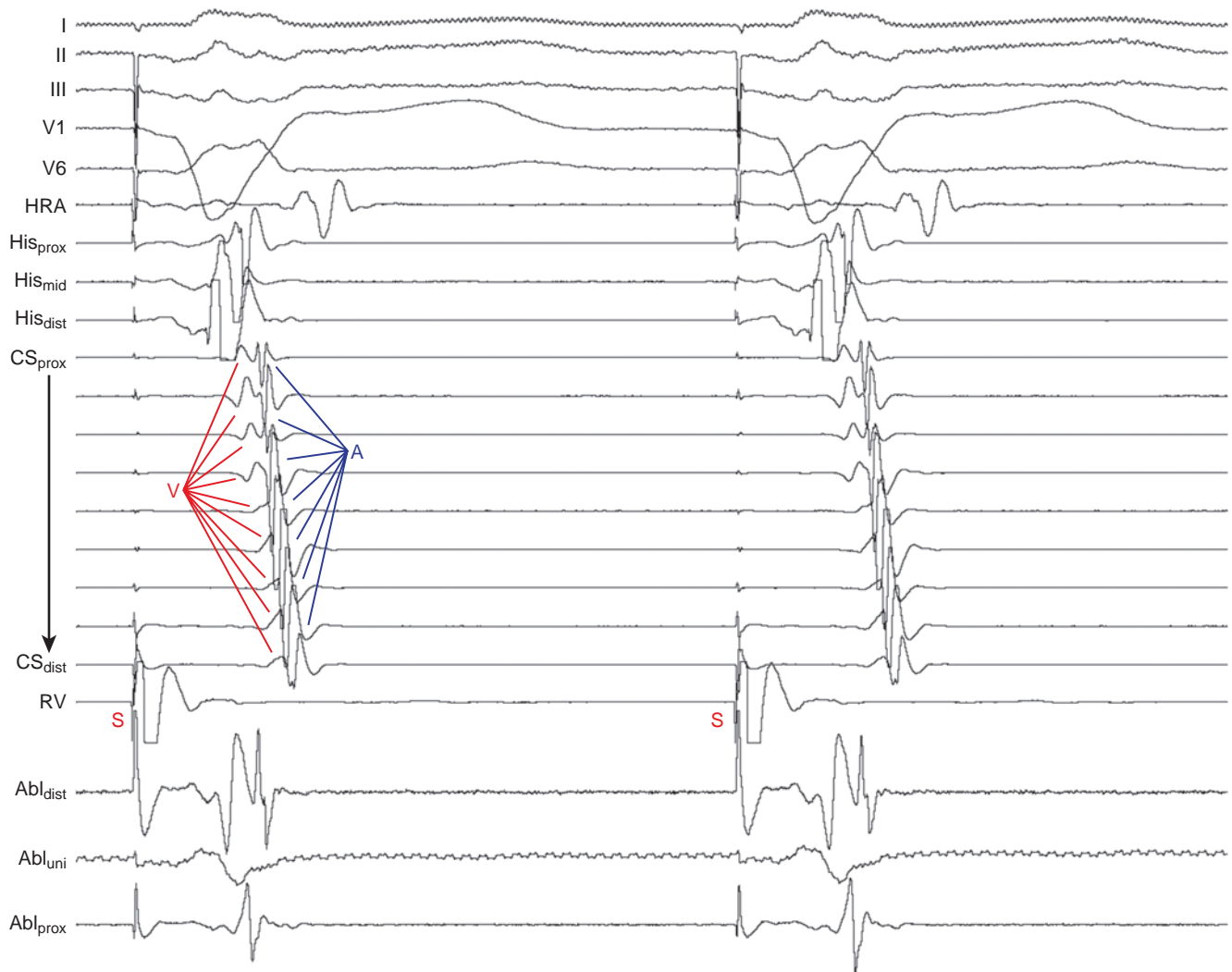


Fig. 18.54 Local Ventriculoatrial Interval for Bypass Tract Localization. Two ventricular paced complexes with retrograde conduction are shown. Ventricular (V) and atrial (A) recordings are as designated by lines. Of the recordings indicated, the earliest atrial electrogram is at the proximal coronary sinus (CS_{prox}), whereas the shortest local ventriculoatrial (VA) interval is far more distal in the coronary sinus recordings; in fact, in the distal coronary sinus (CS_{dist}), the VA interval is negative. Abl_{dist} , Ablation distal bipolar electrodes; Abl_{prox} , ablation proximal bipolar electrodes; Abl_{uni} , ablation distal unipolar electrode; His_{dist} , distal His bundle; His_{mid} , middle His bundle; His_{prox} , proximal His bundle; HRA , high right atrium; RVA , right ventricular apex.

from the atrial aspect of the annulus can be distant from the atrial insertion site of the BT; hence, ablation at the atrial aspect would not be successful.

Criteria of successful ablation sites during anterograde or retrograde activation mapping of BTs are presented in [Box 18.11](#) (see [Figs. 18.48](#) and [18.49](#)). The predictive accuracy of any single criterion is limited. Therefore selection of the optimal ablation target site should be guided by multiple criteria.

Ablation Technique: General Considerations

When preexcitation is present, ablation can be performed during NSR or, preferably, atrial pacing. For concealed BTs, RF energy is delivered during ventricular pacing, which usually allows for detection of an altered retrograde atrial activation sequence. RF energy delivery during AVRT is avoided if possible because of potential catheter dislodgment from its critical position upon interruption of BT conduction (and

thus abrupt tachycardia termination). This event can be associated with transient loss of conduction over the BT for a variable period of time without resulting in permanent damage to the BT due to premature interruption of the RF application. Occasionally, BT conduction can resume hours to days after the procedure; therefore one may not find a suitable target to complete the RF lesion if not addressed adequately during the initial attempt. Ablation during continuous pacing prevents this problem. For incessant orthodromic AVRT (e.g., PJRT), or when retrograde mapping during orthodromic AVRT is used to determine the optimal atrial ablation site, it is preferable to entrain the AVRT with ventricular pacing at a slightly shorter PCL so that block in the BT and termination of the SVT during RF energy delivery will be followed by ventricular pacing at a rate similar to that of the SVT, minimizing catheter movement. Also, the use of an electroanatomic mapping system can obviate this problem by tagging the initial site of ablation, allowing precise return to that site.

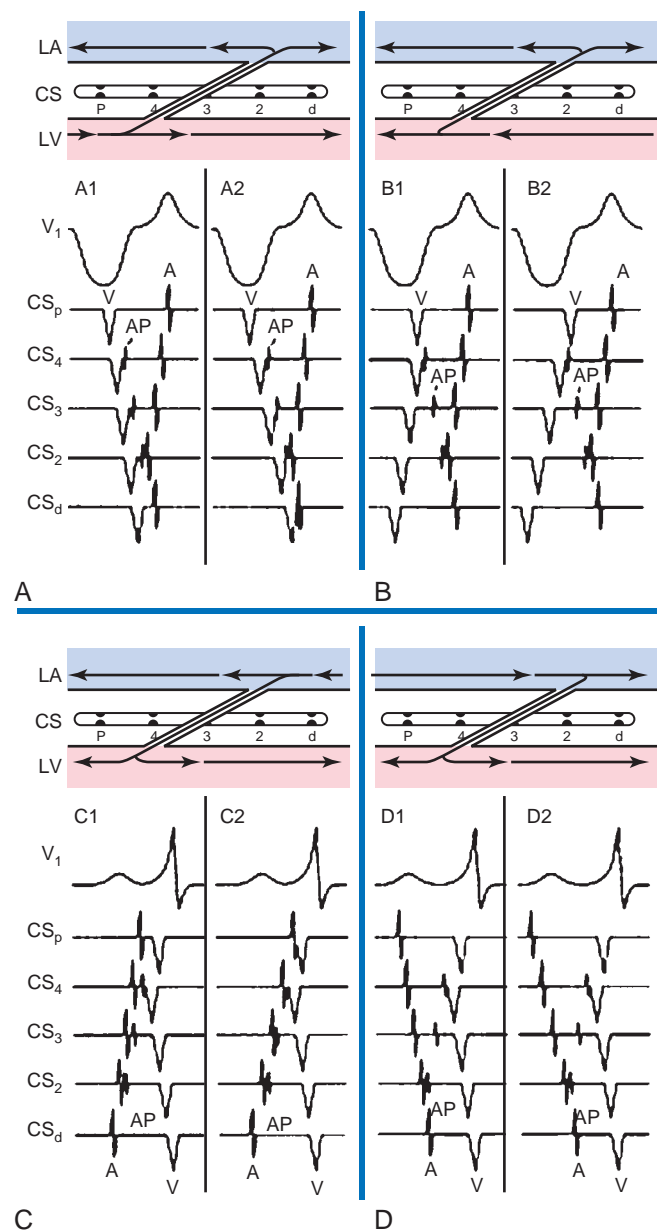


Fig. 18.55 Schematic Representation of Anterograde and Retrograde Activation of a Left Free-Wall Bypass Tract. The oblique course illustrates a change in electrogram timing with the reversal of the paced ventricular wavefront (A and B) and reversal of the paced atrial wavefront (C and D). AP, Accessory pathway potential; CS, coronary sinus; d, distal; LA, left atrium; LV, left ventricular; p, proximal. (From Otomo K, Gonzalez MD, Beckman KJ, et al. Reversing the direction of paced ventricular and atrial wavefronts reveals an oblique course in accessory AV pathways and improves localization for catheter ablation. *Circulation*. 2001;104:550.)

For most free-wall BTs, complete bidirectional block can be achieved with a conventional 4-mm-tip ablation catheter, using a power setting of 50 W and targeting a temperature of 60°C. If BT conduction block is transient, permanent BT block can usually be obtained with better and more consistent contact at the same site. It is rare that an 8-mm or irrigated-tip ablation catheter is necessary; failure of BT ablation is almost always a result of inadequate mapping or poor tissue contact and not inadequacy of the lesion size created by a 4-mm-tip standard ablation catheter. Nevertheless, irrigated-tip catheters can be helpful

when ablating in small branches of the CS because power delivery with a standard 4-mm electrode is limited because of less passive cooling in small vessels.

An electrode temperature of 55°C to 60°C should be sought. Transient loss of BT function is seen at roughly 50°C, and permanent loss of function occurs at 60°C. Therefore sites with favorable electrogram characteristics should not be abandoned until a temperature higher than 50°C to 55°C is reached. Conversely, repeated energy applications at the same location after achieving a temperature of 55°C or higher are unlikely to succeed.

Loss of BT conduction is expected within 1 to 6 seconds of RF application (once the target temperature and power delivery have been reached) for most successful lesions. If no effect is seen after 15 seconds of RF delivery, energy delivery should be discontinued because it is unlikely to be beneficial, and mapping criteria and catheter contact should be reexamined. If BT conduction is eliminated during the application, RF delivery should be continued for up to 60 seconds. Occasionally, BT conduction can be eliminated in one direction only (most typically loss of anterograde conduction with persistence of retrograde conduction). Thus testing for conduction in each direction is mandatory after what appears to be a successful RF application.

Transient interruption of BT conduction during RF delivery, with subsequent reappearance of conduction within seconds or minutes after energy delivery is completed, may be observed, and is more common with right than left free-wall BTs. In this setting, the use of multisite “insurance lesions” is discouraged, and the use of one or two ablation sites should be the goal, which requires careful mapping to achieve.

If BT function is not eliminated at a site with apparent favorable electrographic features, catheter contact with the tissue may be inadequate. Adequacy of catheter contact can be verified by evaluating the electrode temperature, catheter stability on fluoroscopy, electrogram stability, and ST elevation on the unipolar electrogram (Fig. 18.56). If the electrode temperature is consistently higher than 50°C with more than 25 W of energy delivered to the tissue during the RF application, good catheter contact is likely; however, if electrode temperature reaches more than 50°C but with very low power (less than 10 W), coagulum may have formed at the catheter tip. Also, catheter “shimmering” on fluoroscopy suggests poor contact. Similarly, changing electrographic amplitudes before or during ablation suggest inadequate catheter contact. Furthermore, ablation-related injury usually yields ST elevation on the unipolar electrogram; if absent, inadequate tissue heating is likely.

Endpoints of Ablation

Bypass Tract Bidirection Conduction Block

Confirmation of complete loss of BT function, and not just noninducibility of tachycardias, is essential. Confirmation of loss of anterograde BT function using AES and atrial pacing is achieved by demonstrating lack of preexcitation and marked prolongation of the local AV interval at the ablation site. Atrial stimulation should be performed at sites and rates that were associated with preexcitation before ablation. As noted, it is possible to have loss of anterograde conduction with persistence of retrograde conduction (less commonly the opposite). Therefore care must be taken to ensure bidirectional conduction block.

Confirmation of complete loss of retrograde BT function using VES and ventricular pacing is achieved by demonstrating concentric and decremental retrograde atrial activation, consistent with VA conduction over the AVN, VA dissociation, and/or marked prolongation of the local VA interval at the ablation site. Ventricular stimulation should be performed at sites and rates that were associated with retrograde VA conduction over the BT before ablation. Para-Hisian pacing and RV apical versus RV basilar pacing can also help confirm the absence of septal and paraseptal BTs (Figs. 18.28 and 18.30). Occasionally, AVN

BOX 18.11 Electrophysiological Criteria of Successful Bypass Tract Ablation Sites**Criteria of Successful Ablation Sites During Anterograde Activation Mapping**

- Stable catheter position, as confirmed fluoroscopically and by observing a stable electrogram (<10% change in amplitude in atrial and ventricular electrograms over 5–10 beats).
- Atrial electrogram amplitude >0.4 mV, or A/V ratio >0. Both atrial and ventricular electrogram components should be recorded from the ablation (tip) electrode. When ablating from the atrial aspect of the annulus, the atrial electrogram is usually equal to or larger than the ventricular electrogram. Sometimes, the two can merge and it may be difficult to determine whether both components are present. Rapid atrial or ventricular pacing resulting in block in the BT can help eliminate ventricular or atrial electrogram (respectively) so that the exact morphology of the other component can be visualized.
- Local AV interval on the ablation catheter is usually short (25–50 msec, except for previously damaged, slowly conducting, oblique, or epicardial BTs).
- The local ventricular electrogram on the ablation catheter should precede the onset of the delta wave on the ECG by a mean of 0–10 msec for left-sided BTs and 10–30 msec for right-sided BTs (the local ventricular electrogram is measured from the peak of the bipolar electrogram or the maximal dV/dt in the unipolar electrogram).
- QS (or, less preferably, rS) morphology of the unipolar electrogram. Right-sided BTs usually have unipolar recordings that show more pronounced (rapid and deeper) QS configuration than left-sided BTs.
- Continuous electrical activity (defined as isoelectric interval of <5 msec between ventricular and atrial electrograms).
- Presence of BT potential.

Criteria of Successful Ablation Sites During Retrograde Activation Mapping

- Stable catheter position, as confirmed fluoroscopically and by observing a stable electrogram (<10% change in amplitude in atrial and ventricular electrograms over 5–10 beats).
- Earliest local atrial activation timing.
- Local VA interval during retrograde activation of the BT is short (25–50 msec, except for previously damaged, slowly conducting, oblique, or epicardial BTs), usually resulting in inscription of the atrial electrogram on the ascending portion of the terminal ventricular electrogram. The “pseudo-disappearance” of the atrial electrogram within the terminal portion of the ventricular electrogram (forming a W sign) during orthodromic AVRT is a manifestation of an extremely short local VA interval, which correlates with successful ablation sites.
- Surface QRS to local atrial electrogram interval ≤70 msec (during orthodromic AVRT).
- The local VA interval remains constant regardless of the direction in which the ventricular wavefront engaging the BT is traveling (i.e., despite pacing from different ventricular sites). If one uses the ventricular approach to ablate a concealed BT, the ventricular insertion site can be identified as one that maintains a constant local VA interval, despite differences in direction of activation to the ventricular site.
- Continuous electrical activity (defined as isoelectric interval <5 msec between ventricular and atrial electrograms).
- Presence of BT potential.

AV, Atrium to ventricle; AVRT, atrioventricular reentrant tachycardia; BT, bypass tract; ECG, electrocardiogram; VA, ventriculoatrial.

conduction is so brisk that it is difficult to determine if a left-sided BT has been eliminated; in this case, pacing from the LV (either passing the ablation catheter through the mitral orifice and pacing LV endocardium, or advancing the CS catheter into a ventricular branch to pace) gives an advantage to conduction over a left-sided BT compared to the AVN.

Adenosine Testing

Administration of adenosine (starting dose 12 mg, 15 to 30 minutes after successful BT ablation) has been proposed to help unmask dormant BT conduction. Doses of adenosine are increased (in 6- to 12-mg increments) as needed to ensure adequate response in the form of AV block or sinus slowing. Then, atrial and ventricular programmed stimulation is performed to evaluate the presence of BT conduction. In a recent study, adenosine could induce transient anterograde and retrograde BT conduction (dormant conduction) after apparently successful BT ablation in 12% of patients. The mechanism of this phenomenon is thought to be secondary to membrane hyperpolarization of partially depolarized cardiac tissue after ablation. Dormant conduction was manifest during the bradycardia phase of adenosine effect. The presence of dormant BT conduction was associated with higher rates of repeat BT ablation, particularly in patients in whom dormant BT conduction was not successfully abolished during the initial procedure.⁵⁹

Ablation of Left Free-Wall Bypass Tracts**Anatomical Considerations**

The mitral annulus is an anatomically ill-defined structure that demarcates the hinge line of the mitral leaflets at the junctional zone that separates the LA and LV. The mitral annulus is not a rigid fibrous ring but pliable and dynamic, changing shape during the cardiac cycle. En

face, the mitral annulus resembles a kidney bean. When viewed in a 3-D perspective, the annulus has a nonplanar saddle shape, with elevated septal and lateral segments. The anterior flatter portion of the mitral annulus is continuous with the noncoronary and left coronary aortic cusps (the aortomitral continuity). Both annuli are anchored at two junctions: the left fibrous trigone (anchoring the anteromedial aspect of the mitral annulus to the base of the left coronary cusp) and the right fibrous trigone (formed by the triangular formation between the aortic valve and the medial parts of the tricuspid and mitral valves). Between the two trigones, a rigid and broad fibrous curtain (often referred to as the aortic curtain) extends across the anterior leaflet of the mitral valve and supports the aortic valve leaflets. The posterior part of the mitral annulus runs distal to the left and right fibrous trigones and includes the low points of the saddle close to the lateral and medial commissures and the posterior saddle horn. Compared to the anterior portion, the posterior mitral annulus is more loosely anchored to the surrounding tissue, allowing it to move freely with myocardial contraction and relaxation. The commissural diameter being larger than the anteroposterior diameter.⁶⁰

The aortic and mitral valvular orifices are fitted alongside each other (at the aortomitral continuity) within the elliptical ostium of the LV, with no ventricular muscle between. As a result, BTs are rarely found in the region of the aortomitral continuity. Left-sided BTs predominantly cross the free-wall portion of the mitral annulus.

Although the atrial insertion of the BT is typically discrete in size (1 to 3 mm) and close to the mitral annulus, the ventricular insertion site tends to ramify over the region of tissue and can be displaced a small distance away from the mitral annulus, toward the ventricular apex. The BT crosses the annulus on its epicardial aspect and may cross

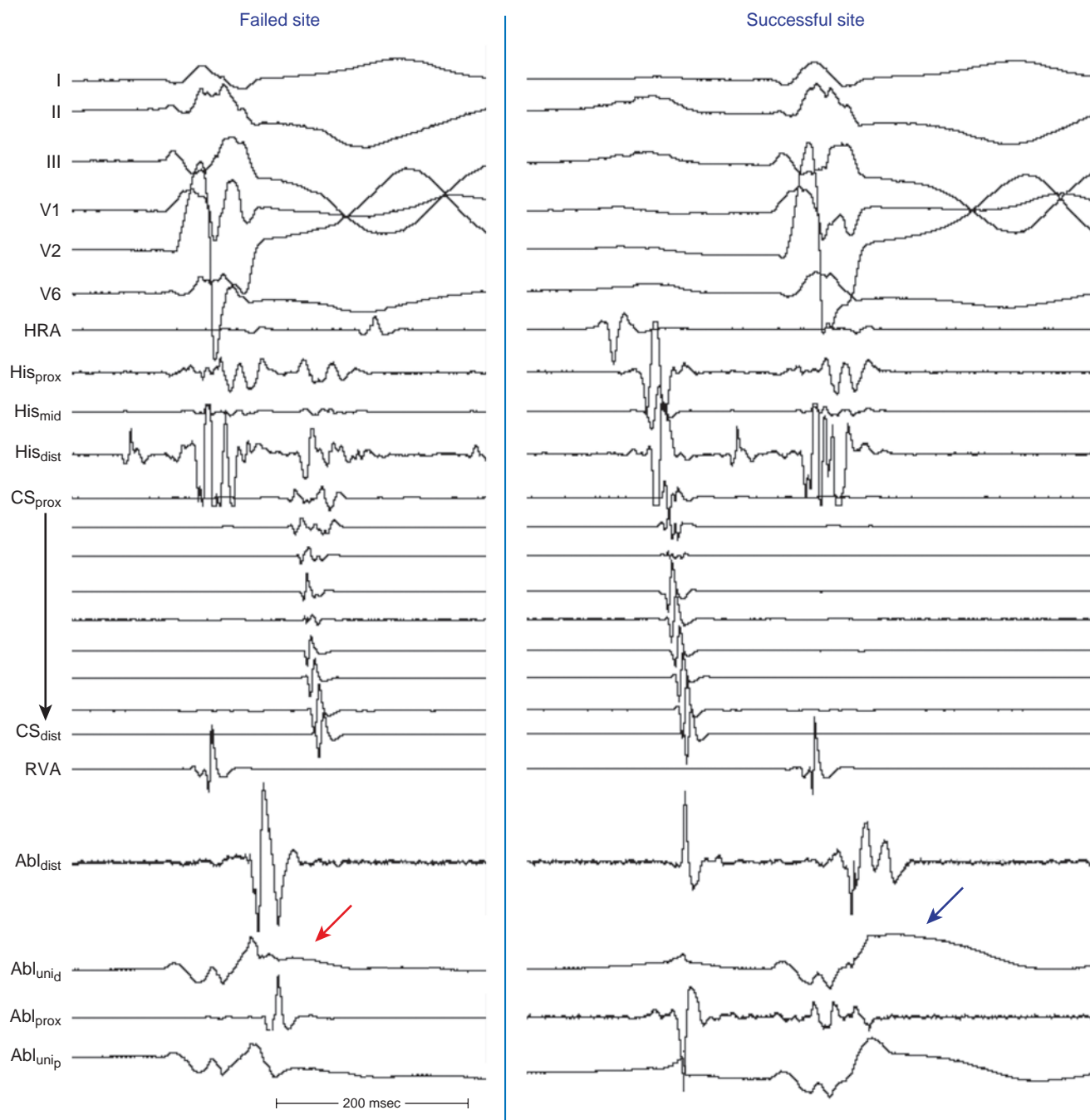


Fig. 18.56 Effect of Ablation on Unipolar ST Segment. On the left ("Failed Site"), recordings during orthodromic atrioventricular reentrant tachycardia are shown following an unsuccessful ablation attempt. The distal ablation unipolar (Abl_{unip}) recording shows minimal, if any, ST segment shift in the ventricular recording (red arrow). On the right ("Successful Site"), a single complex of sinus rhythm is shown with significant ST elevation (blue arrow), indicating injury has occurred at that site. Abl_{dist} , Ablation distal bipolar electrodes; Abl_{prox} , ablation proximal bipolar electrodes; Abl_{unip} , ablation proximal unipolar electrode; CS_{dist} , distal coronary sinus; CS_{prox} , proximal coronary sinus; His_{dist} , distal His bundle; His_{mid} , middle His bundle; His_{prox} , proximal His bundle; HRA , high right atrium; RVA , right ventricular apex.

at variable depths within the epicardial fat pad. Most left free-wall BTs cross the mitral annulus obliquely, with the atrial insertion typically 4 to 30 mm proximal (posterior) to the more distal (anterior) ventricular insertion site (as mapped from within the CS).

Conduction at the insertion sites of the BT is markedly anisotropic because of almost horizontal orientation of the atrial and ventricular

fibers as they insert into the mitral annulus. In addition, the atrial fibers run parallel to the annulus, giving rise to rapid conduction away from the insertion site, parallel to the annulus, and slow conduction to the free-wall of the atrium, perpendicular to the annulus.

Importantly, while the CS is useful as a guide for mapping the mitral annulus in the left anterior oblique (LAO) fluoroscopy view, it has a

variable relationship to the mitral annulus (eFig. 18.7). The CS lies 2 cm superior to the mitral annulus as it empties into the RA. Anterolaterally, the CS frequently overrides the LV. Thus, depending on the distance from the ostium, the CS can lie above the mitral annulus and be associated with the LA, or can cross over the LV side of the mitral annulus. Furthermore, the CS is located more inferior to the mitral annulus on fluoroscopy in most patients. Therefore electrograms recorded from the CS can only provide gross estimates of the true atrial and ventricular insertion sites of the BT and can only be used to guide the ablation catheter to areas in which more detailed mapping needs to be performed.⁶¹

Technical Considerations

Transaortic (retrograde) approach. The right femoral artery is the most commonly used access for the transaortic approach. A long vascular sheath can provide added catheter stability, although with a possibly increased risk of thromboembolism. Anticoagulation is started before the LV is accessed to maintain the activated clotting time (ACT) between 250 and 300 seconds. The ablation catheter is advanced to the descending aorta and, in this position, a tight J curve is formed with the catheter tip before passage to the aortic root to minimize catheter manipulation in the arch. In the right anterior oblique (RAO) fluoroscopy view, the curved catheter is advanced through the aortic valve with the J curve opening to the right, so the catheter passes into the LV, oriented anterolaterally. The straight catheter tip must never be used to cross the aortic valve because of the risk of leaflet perforation. Once in the LV, and while maintaining a tight curve, the catheter is rotated counterclockwise and withdrawn in the LA as the tip turns posteriorly. By opening the J curve slightly, the tip can easily map the mitral annulus; clockwise torque moves the tip anteriorly (distally along the CS), and counterclockwise torque returns the tip posteriorly (proximally along the CS). Alternatively, after crossing the aortic valve, the catheter can be straightened and steered directly under the mitral annulus to the BT location or withdrawn in the LV outflow tract, rotated posteriorly with a slight curve, and then advanced under the posterior mitral annulus for left paraseptal or posterior BTs. When the ablation catheter is approximated along the mitral annulus, the catheter tip is simultaneously withdrawn and straightened slightly to slip under the annulus for fine manipulation. For left lateral and anterior BTs, extended-reach catheters may be required.

Catheter positions beneath the annulus between the ventricular myocardium and mitral leaflet are most stable for ablation of the BT ventricular insertion, but manipulation can be constrained by the chordae. Catheter positions above or along the annulus provide more freedom to map along the mitral annulus but are sometimes too unstable for successful energy delivery. Initial mapping is performed with the ablation electrode on the annulus. From this general area, the catheter is then positioned beneath the mitral annulus for more precise mapping. Catheter tip positions beneath the mitral annulus are suggested by proximity to the CS catheter, motion concomitant with the CS catheter, and an A/V electrogram ratio of less than 1.

Because the transaortic approach targets the ventricular insertion site of the BT, it is best suited for mapping anterograde BT activation (i.e., preexcitation). Mapping retrograde activation from the subannular position is more difficult than for anterograde mapping because of obscuration of the low-amplitude atrial electrogram following the large ventricular electrogram.

Although BT locations are commonly defined by mapping along the CS catheter, this only approximates localization of the subannular ablation site because of the oblique course of left free-wall BTs, displacement of the CS above the mitral annulus, variable basilar-apical ventricular insertion of the BT, and BT location beyond the distal CS electrode.

Transseptal approach. Transseptal and transaortic approaches are equally effective for ablation of left free-wall BTs. The transseptal approach is primarily used for mapping of the BT atrial insertion site during retrograde BT conduction (orthodromic AVRT or ventricular pacing), while ventricular mapping of manifest BTs (during preexcitation) using the transseptal approach is limited.

The transseptal approach has several advantages over the transaortic approach. The transseptal approach provides better access to far lateral and anterolateral BT locations, easier catheter maneuverability in the LA, and less risk of coronary injury. In addition, no arterial access is required with the transseptal approach, and vascular recovery is therefore shorter. However, the transseptal approach provides less catheter stability and is associated with a higher risk of cardiac perforation and air embolism. Furthermore, the transseptal approach entails higher cost if intracardiac echocardiography is used.

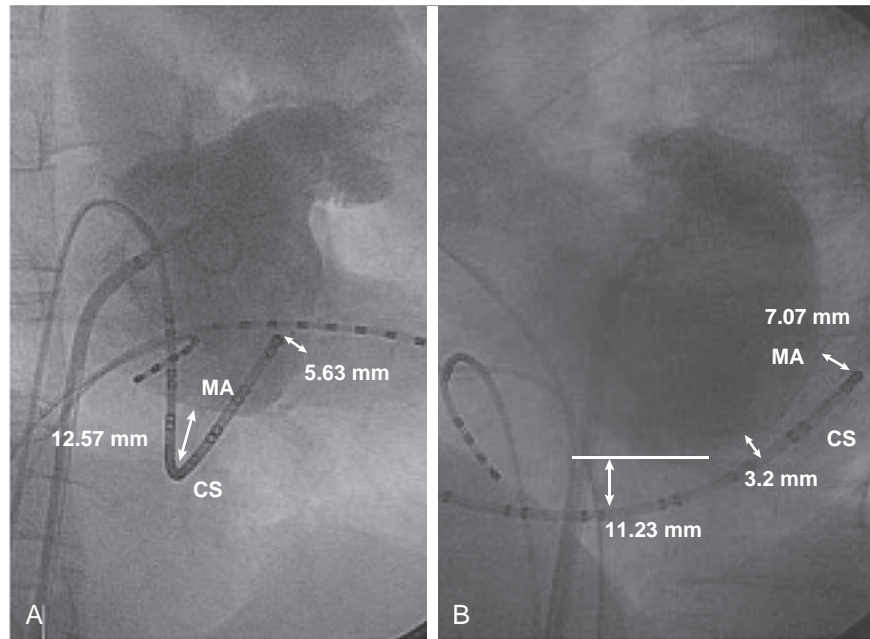
While mapping using the standard transseptal sheath, the ablation catheter's curvature can be modified according to BT location. For left posterior BTs, the catheter typically reaches the annulus without modifying the sheath position. The sheath is progressively withdrawn toward the RA for optimal catheter apposition at lateral BT locations, and it is almost entirely withdrawn toward the RA for anterior BTs. Alternatively, preformed or deflectable sheaths may be used. Ablation catheters with bidirectional asymmetric deflections can also be of value in some cases.

Once the ablation catheter is positioned on the mitral annulus in a 30-degree RAO view, mapping is performed in the LAO view. In the absence of preformed septal sheaths, gentle clockwise torque is needed to maintain the catheter on the posterior mitral annulus. No torque is needed for lateral positions. As the catheter is moved anteriorly, counterclockwise torque is necessary to keep the catheter tip on the annulus. In the anterior positions, the catheter tip can dislodge into the LA appendage or LV, and attention to intracardiac electrograms is necessary when mapping anterior regions, because the CS catheter rarely provides an accurate fluoroscopic reference in this setting. The goal is to maintain the catheter tip on the atrial aspect of the mitral annulus, so that the mitral annulus can be easily mapped by advancing and withdrawing the catheter, causing it to slide along the mitral annulus freely in parallel to the CS catheter. Advancing the catheter moves the tip posteriorly; withdrawing it moves the tip anteriorly. The ventricular aspect of the mitral annulus can be mapped by passing the catheter tip across the mitral valve and deflecting the tip toward the annulus.

The transseptal approach facilitates mapping of the atrial aspect of the mitral annulus. Catheter position on the atrial aspect of the annulus can be verified by recording a bipolar A/V electrogram amplitude ratio greater than 1, and a unipolar electrogram PR segment displacement from baseline without ST segment displacement. The stability of the catheter can be assessed by PR segment elevation (confirming good atrial tissue contact), consistent local electrographic amplitudes, and concordant motion of the CS and ablation catheters.

Because of the mobility of the ablation catheter and the electrode orientation parallel with atrial activation along the mitral annulus, a unique vectorial mapping technique is possible with the transseptal approach. As noted, using the unfiltered bipolar electrogram with the electrodes oriented parallel to the axis of the mitral annulus, the BT atrial insertion can be identified as the site at which the polarity of the atrial potential reverses.

Occasionally, ablation of far-left lateral BTs can result in apparent successful elimination of BT conduction, but shift to another, more septal pathway. Although the latter can happen, this finding is commonly due to ablation of tissue proximal to the BT insertion, such that CS activation must proceed from the (unablated) BT more distally and then activate the rest of the CS in a proximal-distal direction. Clues



eFig. 18.7 Anatomical Relationship Between the Coronary Sinus (CS) and Mitral Annulus. The distances between the CS and mitral annulus (MA) in the right anterior oblique projection (A) are 12.57 and 5.63 mm during systole at the proximal and distal CS, respectively. The distances between the CS and MA in the left anterior oblique projection (B) are 11.23 and 7.07 mm during systole at the proximal, middle, and distal CS, respectively. (From Kim J, Hwang G, Seo K, et al. Anatomical discrepancy between the coronary sinus and the mitral annulus by fluoroscopy. *Int J Arrhythm*. 2016;17:14–19.)

that this is the case include: (1) no change in the SVT CL (if ablation has been attempted in SVT); (2) no change in the ablation electrogram (because the BT has not been ablated); and (3) the earliest atrial activation was at the distal CS recordings, where ablation was attempted (eFig. 18.8). This can be prevented by mapping more distally than the site of earliest activation in CS recordings, and making certain the “earliest” site is surrounded by later ones.

Ablation of Right Free-Wall Bypass Tracts

Anatomical Considerations

Unique features of the tricuspid annulus and important anatomic differences as compared with the mitral annulus have often rendered ablation of right-sided BTs more challenging than that of left free-wall BTs. In addition, transient interruption of BT conduction during RF delivery, with subsequent resumption of conduction within seconds or minutes, and recurrence rates over the first few weeks after initially successful BT ablation, are more common with right-sided BTs compared with left-sided BTs.

A significantly larger endocardial area is present along the tricuspid ring because of the larger circumference compared with the mitral ring (approximately 12 vs. 10 cm). In addition, BTs can exist anywhere around the tricuspid annulus, whereas the mitral ring has an area of fibrous continuity with the noncoronary and left coronary aortic cusps (the aortomitral continuity) where BTs are rarely found. Despite these facts, right-sided BTs are much less common than left-sided BTs (12% vs. 59%).

In contrast to the mitral annulus, the tricuspid valve annulus is less well developed and frequently discontinuous. The tricuspid fibrous ring is often incomplete and has several gaps at which atrial and ventricular muscle fibers nearly abut. Right free-wall BTs can consist of thin strands crossing the epicardial aspect of the annulus (similar to left free-wall BTs) or pass subendocardially as relatively broad bands of tissue through the fibrous discontinuities. Furthermore, right free-wall BTs can insert into the myocardium (typically on the atrial side) several millimeters away from the fibrous annulus and have been associated with a higher prevalence of branching pathways.⁶²

Unlike the mitral valve, which attaches to its fibrous annulus at a right angle, the tricuspid valve attaches to its annulus at an acute angle oriented toward the RV, making it more difficult to wedge an ablation catheter underneath the tricuspid valve. In addition, unlike left free-wall AV BTs, which tend to pass close to the hinge line of the mitral valve, the AV groove between the RA and RV is much deeper than on the left side. The deep groove can allow the RA wall to fold over onto the RV wall, and the BT muscle bundles can cross at any depth. Hence, the right-sided BTs can be somewhat removed from the tricuspid annulus. In fact, atrial insertion of the BT can be as far as 1 cm away from the annulus in the folded-over atrial sac. The folded-over atrium and the bizarre angle required for mapping of the inferior and posterolateral aspect of the RA by a catheter passed through the RA from the inferior vena cava (IVC) can make it difficult to achieve a stable catheter position at the tricuspid annulus because of a tendency of the catheter to fall into the folded-over sac. Thus sometimes the superior vena cava (SVC) approach is required to allow full exploration of the folded-over atrial sac and the inferior-inferolateral positions around the tricuspid annulus. The standard IVC approach, however, is usually adequate to map the superior aspects of the tricuspid annulus. If the IVC approach is used, a guiding sheath can be especially helpful for better catheter stability and tissue contact. The use of a multipolar (Halo) catheter positioned around the tricuspid annulus can provide good regional localization to guide the ablation catheter.⁶³

Furthermore, closely adjacent but anatomically discrete sites of catheter ablation can be necessary to eliminate anterograde and retro-

grade BT conduction in up to 10% of patients—the incidence is highest (18.6%) with right free-wall BTs. The explanation for this phenomenon is not clear but probably relates to the complexity of fiber orientation, possibly branching over 1 to 2 cm along the annulus. This factor emphasizes the importance of identifying and targeting both the atrial and the ventricular BT insertion sites.

Right-sided AV BTs are associated with higher incidences of anatomic variations and congenital abnormalities along the tricuspid annulus. Ebstein anomaly is an abnormality of the tricuspid valve in which the septal and often the posterior leaflets are displaced a variable distance into the RV and the anterior leaflet is usually malformed, excessively large, and abnormally attached or adherent to the RV free wall. The true tricuspid annulus, on the other hand, is not anatomically displaced, but can be poorly developed, with extensive discontinuities of the fibrous architecture. Thus a portion of the RV is “atrialized” in that it is located on the atrial side of the tricuspid valve, and the remaining functional RV is small. The atrialized portion of the RV is morphologically and electrically ventricular but functionally atrial. Ebstein anomaly can be associated with other cardiac anomalies, including a patent foramen ovale, atrial and ventricular septal defects, and RV outflow tract obstruction.

Right-sided BTs have been reported in 10% to 30% of patients with Ebstein anomaly, and they are multiple in up to 50% of patients. The BTs bridge the true anatomical tricuspid annulus, regardless of where the valve is located. Ablation of these BTs can be challenging because the electrical signals recorded from the atrialized portion of the RV can be complex and fractionated. Furthermore, identification of the true AV groove, along which BTs are targeted, can be difficult. Coronary angiography or insertion of a thin multielectrode catheter in the right coronary artery can be necessary to help identify the true AV groove and guide ablation catheter positioning. In addition, electroanatomic activation mapping during NSR can help define the *electrical* AV junction (true tricuspid annulus), where annular atrial and ventricular electrograms are recorded. Ablation is usually accomplished at the true tricuspid annulus, above the displaced valve leaflet, although some patients may undergo successful ablation from the ventricular side of the tricuspid annulus (but still above the valve leaflet).

Technical Considerations

Characteristically, successful ablation sites for right-sided BTs display local AV intervals that are shorter than those for BTs elsewhere, local ventricular electrograms preceding the onset of the delta wave by an interval longer than that for BTs elsewhere (18 ± 10 milliseconds for right-sided BTs versus 0 ± 5 milliseconds for left-sided BTs), and the unipolar recording showing more pronounced (rapid and deeper) QS configurations (Fig. 18.57).

Most commonly, ablation of right-sided BTs is approached from the atrial aspect. The optimal site of ablation is the earliest atrial activation site during retrograde BT conduction (during orthodromic AVRT or ventricular pacing), preferably with a BT potential present. The earliest site of atrial activation is identified using a roving catheter or a multipolar (Halo) catheter along the tricuspid annulus. If mapping is performed during ventricular pacing, conduction over both the BT and AVN can occur, resulting in atrial fusion, which can interfere with localization of the BT. Ventricular pacing performed close to the BT ventricular insertion site can accentuate atrial activation over the BT.

Occasionally, the BT can be better approached from the ventricular side. Ventricular activation mapping is performed during preexcited NSR, atrial pacing, preexcited SVT, or antidromic AVRT. The site of the earliest ventricular activation during preexcitation, preferably with a BT potential present, would be the optimal site. The earliest onset of ventricular activation recorded on the ablation catheter (using unipolar or bipolar electrograms) should precede the onset of the delta wave by



eFig. 18.8 Apparent Shift of Atrial Activation During Ablation for Orthodromic Atrioventricular Reentrant Tachycardia (AVRT) Using a Left Lateral Bypass Tract (BT). On the first three cycles, the atrial activation sequence is distal-to-proximal in the coronary sinus (CS). In the middle, atrial activation sequence suddenly shifts to proximal-to-distal in the CS due to ablation near the distal CS recording, but proximal to the actual BT insertion site. Left atrial/CS conduction is interrupted along the CS. AVRT does not terminate and is in fact the same arrhythmia (tachycardia cycle length remains unchanged, and the interval from QRS onset [dashed line] to ablation recording [arrow] also remains unchanged). CS propagation continues distally from the ablation site to the septum (not illustrated), activating the CS between the ostium and BT location in the proximal-distal direction. *Abl_{dist}*, Ablation distal bipolar electrodes; *CS_{dist}*, distal coronary sinus; *CS_{mid}*, middle coronary sinus; *CS_{prox}*, proximal coronary sinus; *His_{dist}*, distal His bundle; *His_{mid}*, middle His bundle; *His_{prox}*, proximal His bundle; *HRA*, high right atrium; *RVA*, right ventricular apex.

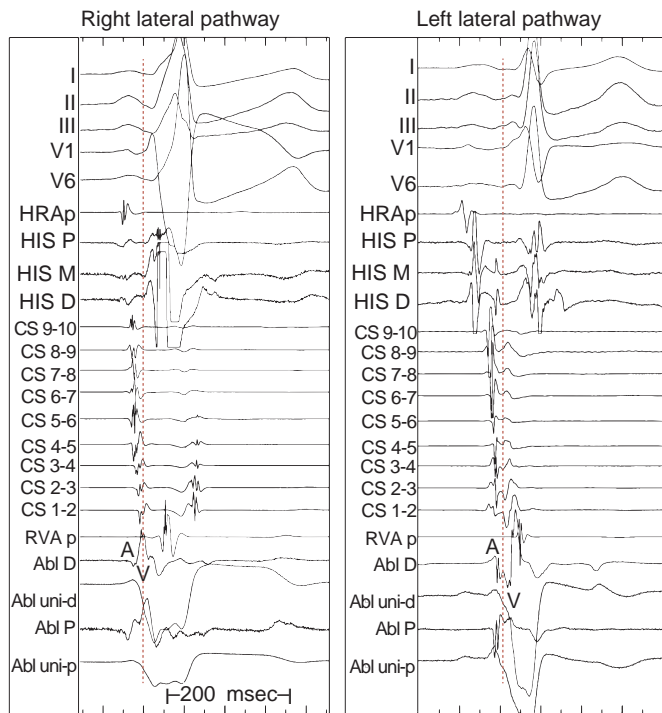


Fig. 18.57 Differences in Mapping Site Electrogram Characteristics With Right Versus Left Lateral Anterogradely Conducting Bypass Tracts (BTs). Dotted lines denote delta wave onset in each panel; A and V are atrial and ventricular components of the ablation recording. At left is a right lateral BT; note the ventricular electrogram precedes the delta wave onset and the unipolar recording has a deep negative deflection, also before the delta wave. In contrast, with a left lateral BT (*right panel*), the ventricular recording in the distal bipole begins coincident with the delta wave onset and the unipolar recording is not as sharp and occurs after the delta wave onset. *Abl D*, Ablation distal bipolar electrodes; *Abl P*, ablation proximal bipolar electrodes; *Abl uni-d*, ablation distal unipolar electrode; *Abl uni-p*, ablation proximal unipolar electrode; *CS*, coronary sinus; *HIS D*, distal His bundle; *HIS M*, middle His bundle; *HIS P*, proximal His bundle; *HRA*, high right atrium; *RVA*, right ventricular apex.

at least 10 to 25 milliseconds. For concealed BTs, the ventricular insertion site cannot be determined by ventricular activation mapping because of the lack of preexcitation. In this setting, recording of a BT potential can be especially useful in guiding ablation.

The tricuspid annulus is usually mapped in the LAO fluoroscopy view. The right posterior, posterolateral, and lateral regions are usually best mapped from the IVC approach. The right anterior and anterolateral regions can also often be ablated using the IVC approach, but the SVC approach can offer more stable and better catheter-tissue contact in these areas. The catheter can be prolapsed across the tricuspid valve to help stabilize the tip on the tricuspid annulus. In the LAO view, the HB is located at about 1 o'clock and the CS at 5 o'clock; right free-wall BTs span from approximately 6 to 12 o'clock. Right anterior BTs are at the most superior aspect of the tricuspid annulus, right superoparaseptal BTs are located near the HB catheter, and right posterior free-wall BTs are located at the most posterior aspect of the tricuspid annulus, whereas right posteroseptal BTs are located near the CS.

Although the location of the mitral annulus is reasonably indicated by the CS catheter, the location of the tricuspid annulus is not as easily discerned because there is no analogous venous structure to mark with a catheter. Furthermore, because the mitral and tricuspid annuli are

not always in the same plane, the CS catheter is only a rough guide to the location of the tricuspid annulus in the RAO view. Attempts at providing an endocardial reference catheter along the tricuspid annulus have been made using a 20-pole Halo catheter. This approach has had limited success because the catheter often does not position directly on the AV groove. Introducing the Halo catheter through a preformed sheath can provide better catheter stability along the tricuspid annulus. Occasionally, a fine angioplasty wire can be passed into the right coronary artery to delineate the location of the tricuspid annulus. The latter approach, however, has not been widely adopted, possibly in part because of concerns of prolonged instrumentation of the right coronary artery during the procedure. Another approach is to create a three-dimensional electroanatomic map (EnSite-NavX; St. Jude Medical, St. Paul, MN, United States) of the right coronary artery. After right coronary artery angiography, a 2.3-Fr octapolar microcatheter (Cardima Inc., Fresno, CA, United States) is inserted in the right coronary artery. Mapping and acquisition of the bipolar electrograms recorded by the microcatheter are performed during anterograde or retrograde BT conduction. This map allows for early removal of the catheter from the coronary artery while continuously displaying electroanatomic information to assist with mapping of the BT.⁶⁴

To target the ventricular aspect of the tricuspid annulus, the catheter is introduced across the tricuspid valve and looped back on itself in the RV underneath the valve until a small atrial electrogram and a larger ventricular electrogram are recorded, confirming adequate proximity to the tricuspid annulus. A long sheath may be used to stabilize the body of the catheter and direct the catheter to several different locations along the tricuspid annulus.

Three-dimensional electroanatomic mapping can help ablation of right-sided BTs, and is especially useful in the presence of multiple BTs or complicated anatomy. An electroanatomic color-coded activation map along the tricuspid annulus can be constructed, either along the atrial side, during orthodromic AVRT or ventricular pacing, or along the ventricular side, during anterograde preexcitation. Sites of interest can be tagged for further reference, so that the ablation catheter can be returned to any of them with precision. Information with regard to catheter stability and movement can also be provided.⁶²

Ablation of Anteroseptal (Superoparaseptal) and Midseptal Bypass Tracts

Anatomical Considerations

The midseptum is the only true muscular septal area between the offset attachments of the mitral and tricuspid valves, and it corresponds roughly to the location of the triangle of Koch. The triangle of Koch constitutes the endocardial surface of the region of the lower RA septum. It is bordered anteriorly by the insertion of the septal leaflet of the tricuspid valve and posteriorly by the fibrous tendon of Todaro. The apex of the triangle is formed by the junction of these two boundaries. The base of the triangle is formed by the anteromedial edge of the CS os and is continuous with the sub-eustachian pouch (*see Figs. 17.1 and 9.2*).^{65,66} Of note, the interatrial sulcus is displaced to the far left of the inter-ventricular sulcus, and because the AV valves are not isoplanar (the attachment of the septal leaflet of the tricuspid valve into the most anterior part of the central fibrous body is displaced a few millimeters apically relative to the attachment of the septal leaflet of the mitral valve), the true septal part of the AV junction (the RA-LV sulcus) actually separates the inferomedial RA from the posterior superior process of the LV (the right side above the tricuspid valve while the left side is below the mitral valve). Hence, the triangle of Koch can be considered the RA side of the AV muscular septum.

The compact AVN is located beneath the RA endocardium at the apex of the triangle of Koch, anterior to the CS os and directly above

the insertion of the septal leaflet of the tricuspid valve, where the tendon of Todaro merges with the central fibrous body. Slightly more anteriorly and superiorly is where the HB penetrates the AV junction through the central fibrous body and the posterior aspect of the membranous AV septum.^{65,66}

BTs with an atrial insertion in the floor of the triangle of Koch, posteroinferior to the compact AVN and HB and above the anterior portion of the CS os, have been labeled as midseptal; these BTs are the only truly septal BTs; hence, they can be referred to simply as septal BTs.

The previously named anterosseptal and posteroseptal areas are not truly “septal” but are parts of the parietal AV junction that are anterior and posterior to the true septum, respectively. Anterosuperior to the AV septum and compact AVN and HB, the tricuspid annulus diverges laterally away from the membranous part of the septum to course along the supraventricular crest of the RV (crista supraventricularis). This muscular structure interposes between the attachments of the leaflets of the tricuspid and pulmonic valves in the roof of the RV. BTs in this area (at the apex of the triangle of Koch) are labeled anterosseptal, but they must be considered “superoparaseptal” right free-wall BTs because anatomically they do not belong to the septum. There is no atrial septum in the region anterior to the HB recording site; the aortic root separates the right and left atrial walls here.

BTs are classified as “superoparaseptal” if the BT potential and His potential are simultaneously recorded from the mapping catheter placed at the HB region. A “para-Hisian” BT (which accounts for only 1% to 2% of all BTs) is a superoparaseptal BT with intimate proximity to the HB and is defined when the location of its successful catheter ablation coincided with either the largest recordable His potential or a His potential greater than 0.1 mV.⁶⁷

Electrocardiographic Considerations

The surface ECG can be valuable in anticipating septal or paraseptal locations of the BT and planning the catheter ablation procedure. Right superoparaseptal (anterosseptal) and midseptal BTs typically exhibit positive delta waves in leads I, aVL, and V3 through V6. Delta wave polarity in leads V1 and V2 can vary. Because of their superior location, right superoparaseptal BTs are associated with positive delta waves in all inferior leads (II, III, and aVF). In contrast, the delta wave in midseptal BTs is positive in lead II, predominantly negative in lead III, and negative or isoelectric in lead aVF. The combination of a negative delta wave in lead V1 and R/S transition in leads V3 to V4 suggests right-sided midseptal BT, whereas a biphasic delta wave in lead V1 and earlier QRS transition (in leads V1 to V2) suggest a left-sided location of the midseptal BT.

The surface ECG can also help distinguish para-Hisian locations of the BT (which is associated with the highest risk of AV block during ablation) from other superoparaseptal or septal locations. The presence of a negative delta wave in leads V1 and V2 was found to carry high specificity (92%) but poor sensitivity (25%) to detect the ventricular insertion of BTs with a strict invasive definition of para-Hisian location. In addition, the sum of initial r-wave amplitudes in those precordial ECG leads of less than 0.5 mV could be a useful, adjunctive marker in the noninvasive identification of these BTs (sensitivity 85%; specificity 75.5%).⁶⁷

Technical Considerations

A superoparaseptal location of the BT is initially suggested when the BT potential and His potential are simultaneously recorded from the diagnostic EP catheter placed at the HB region.⁶⁷ AES or short bursts of atrial pacing can help distinguish BT potential from the His potential. Atrial impulses that block in the AVN but conduct over the BT results in fully preexcited QRS morphology preceded by the BT potential but

with concomitant loss of the His potential. On the other hand, atrial impulses that block in the BT result in loss of preexcitation and BT potential recording but preserve His potential recording.

The precise location of the BT is verified by mapping this space in a 30-degree LAO fluoroscopy view using the ablation catheter advanced via the IVC. The use of a long vascular sheath can help stabilize the catheter tip during mapping and ablation in the superoparaseptal region. Also, mapping via the SVC approach is sometimes necessary to optimize catheter position and contact. Not infrequently, catheter-induced mechanical trauma can cause conduction block in the BT, which can hinder BT mapping and ablation. Therefore careful catheter manipulation is warranted during mapping in the region of the BT.

The optimal site of ablation is one from which the atrial and ventricular electrograms are recorded in conjunction with a BT potential, but with no or only a tiny His potential (less than 0.1 mV). Preferably, the ventricular insertion site (with V/A electrogram amplitude ratio greater than 2) of the BT is targeted with ablation to minimize the risk of damage to the AVN (the HB is more resistant to ablation on the ventricular aspect, generally within a fibrous sheath at that location). Occasionally, ablation is required in the presence of a marked (greater than 0.1 mV) His potential recorded through the ablation catheter (i.e., true “para-Hisian” BTs). Ablation of these BTs from the aortic root has been described and can be an important option to consider in these challenging cases.^{68,69}

For midseptal BTs, successful ablation is achieved in an area bounded superiorly by the electrode recording the His potential, and posteroinferiorly by the CS os, as marked by the apex of curvature in the CS catheter. The optimal site of ablation for a right midseptal BT is one from which atrial and ventricular electrograms are recorded simultaneously with a BT potential in between. Ablation is first attempted from the right side. If it is ineffective or early recurrence occurs after termination of RF application, then the left-sided approach is attempted.

For manifest BTs, RF application is performed during NSR or atrial pacing, which helps monitor both BT and AVN-HB conduction during RF energy delivery. In the setting of concealed para-Hisian BTs, it is challenging to assess the success of RF application and monitor AV conduction simultaneously. When RF delivery is performed during ventricular pacing, monitoring the success of RF application is not possible because the retrograde atrial activation sequence during ventricular pacing can be similar with either BT or AVN conduction. Atrial pacing during RF delivery is preferable because it helps monitor AV conduction and override junctional rhythms that may occur during RF delivery; however, it is not helpful for assessing the efficacy of RF application because the BT conducts retrogradely only. RF delivery during orthodromic AVRT is another option; however, this will certainly have the potential for catheter dislodgment on SVT termination, and such dislodgment can endanger the AVN-HB. Moreover, application of RF energy during orthodromic AVRT will not allow monitoring of AV conduction. In this setting, monitoring of the mode of termination of orthodromic AVRT during RF delivery is essential. Termination of orthodromic AVRT with an atrial electrogram signifies potential damage to the anterograde limb of the SVT circuit (i.e., the AVN), and therefore RF delivery should be immediately stopped. On the other hand, termination of orthodromic AVRT with a ventricular electrogram suggests successful block in the retrograde limb of the SVT circuit (i.e., the BT), and therefore RF delivery should be continued, with careful monitoring of AV conduction during NSR following termination of the SVT. Another valuable option is RF delivery during atrial-entrained orthodromic AVRT with manifest atrial fusion. This technique enables continuous monitoring of effects of RF application on BT function and also obviates a sudden change in ventricular rate on termination of the SVT. In addition, this technique allows monitoring of AV conduction during

RF application once the orthodromic AVRT is terminated, and therefore reduces the risk of damage to the AVN-HB. During successful RF application, termination of orthodromic AVRT will be indicated by transformation from the tachycardia P wave morphology and atrial activation sequence into a fully paced atrial activation sequence at the same rate.

Ablation in the region of the triangle of Koch is associated with 2% to 10% incidence of AV block and, to reduce this risk, such BTs should be ablated with the catheter placed on the tricuspid annulus or on the ventricular side of the tricuspid annulus, preferably with the use of lower RF power. Titrated RF energy output can be used for true para-Hisian BTs, starting with 5 W, and increasing by 5 W every 10 seconds of energy application, up to a maximum of 40 W. For other superoparaseptal BTs, ablation can be started at 30 W, targeting a temperature of 50°C to 60°C.

During RF ablation within the triangle of Koch, the occurrence of junctional tachycardia is not uncommon and is associated with loss of preexcitation; this should not be misinterpreted as successful ablation leading to continuing RF energy delivery. Instead, overdrive atrial pacing should be performed to monitor AV conduction or RF application should be stopped and other sites sought (Fig. 18.58). RF application should be stopped after 10 to 15 seconds if no block in the BT is achieved to minimize potential damage to the AVN-HB.

To reduce the risk of AV block, RF delivery should be immediately discontinued when the following occur: (1) the impedance rises suddenly (greater than 10 Ω); (2) the PR interval (during NSR or atrial pacing) prolongs; (3) AV block develops; (4) retrograde conduction block is observed during junctional ectopy; or (5) fast junctional tachycardia (TCL less than 350 milliseconds) occurs, which may herald imminent heart block.

Cryoablation of Superoparaseptal and Midseptal Bypass Tracts

Cryothermal ablation of BTs in the superoparaseptal and midseptal areas, both at high risk of permanent AV block with RF ablation, is successful and extremely safe. Cryoablation may also be used to ablate selected cases of epicardial left-sided BTs within the CS, well beyond the middle cardiac vein, once attempts using the transseptal and

transaortic approaches have failed. The experience with cryoablation in unselected BTs, however, is more limited and less satisfactory; this is likely related to multiple factors, including the learning curve and the smaller size of the lesion produced by cryoablation. In addition, many of the features of cryothermal energy that distinguish it from RF energy, and which are optimal for septal ablation, are less important or even useless for ablation of BTs located elsewhere.⁷⁰

A 6-mm-tip or 8-mm-tip cryocatheter is usually used. Not infrequently, because of the limited maneuverability and the wide distal electrode spacing of the cryocatheter (which can displace the geometric center point of the measuring bipole and greatly decreases precision), mapping of the target BT ablation site may need to be performed using a steerable quadripolar EP catheter with 2–5–2-mm distal electrode spacing prior to cryoablation.⁷¹

Cryomapping. Cryomapping, or ice mapping, is designed to verify that ablation at the chosen site will have the desired effect (i.e., block in the BT) and to ensure the absence of complications (i.e., AV block). Cryomapping is performed at -30°C in the selected site. At this temperature, the lesion is reversible (for up to 60 seconds) and the catheter is “stuck” to the endocardium in an ice ball that includes the tip of the catheter (cryoadherence). This permits programmed electrical stimulation to test the disappearance of BT conduction during ongoing ablation and also allows ablation to be performed during AVRT without the risk of catheter dislodgment on tachycardia termination. In the cryomapping mode, the temperature is not allowed to drop below -30°C , and the time of application is limited to 60 seconds. Formation of an ice ball at the catheter tip and adherence to the underlying myocardium are signaled by the appearance of electrical noise recorded from the ablation catheter’s distal bipole.

In patients with manifest preexcitation, cryomapping may be performed during NSR or atrial pacing (to monitor for loss of delta waves), during ventricular pacing (to monitor retrograde BT block), or during AVRT (to monitor tachycardia termination). For concealed BTs, cryomapping is preferably performed either during orthodromic AVRT or during ventricular pacing. Once an ice ball is formed, programmed electrical stimulation is repeated to verify that the BT has been blocked.

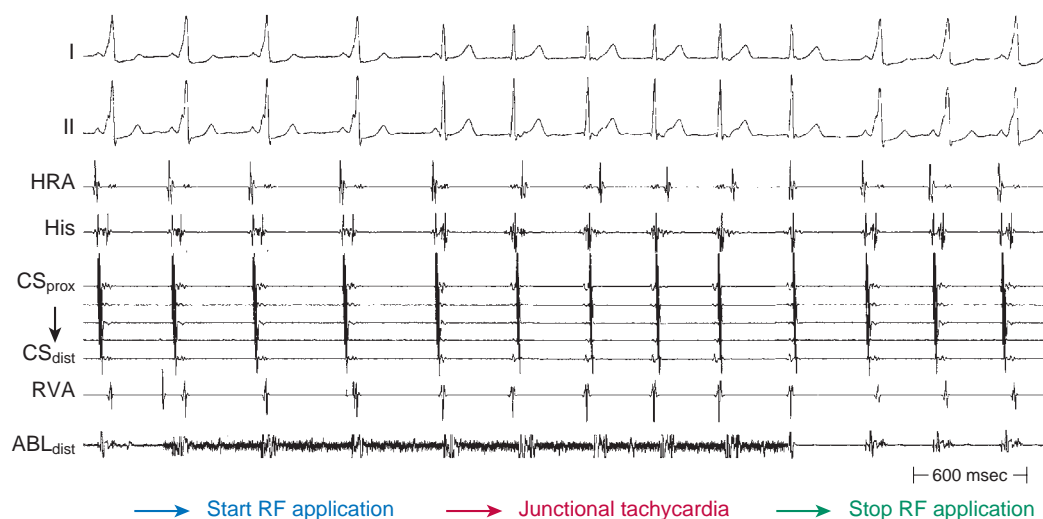


Fig. 18.58 Junctional Tachycardia During Radiofrequency (RF) Ablation of a Superoparaseptal Bypass Tract. The first few complexes demonstrate normal sinus rhythm with preexcitation. A few seconds after starting RF energy delivery, junctional tachycardia develops, with loss of preexcitation. This prompted immediate termination of RF application, after which preexcitation resumed. *ABL_{dist}*, Ablation distal bipolar electrodes; *CS_{dist}*, distal coronary sinus; *CS_{prox}*, proximal coronary sinus; *HRA*, high right atrium; *RVA*, right ventricular apex.

If cryomapping does not produce BT conduction block after 10 to 30 seconds of freezing or results in detrimental effects on AV conduction, cryomapping is interrupted and, after a few seconds, allowing the catheter to thaw and become dislodged from the tissue, the catheter can be moved to a different site and cryomapping repeated. Alternatively, if the test application is unsuccessful but mapping findings are very favorable, after rewarming, further 30-second applications are tested, decreasing the temperature by 10°C for every step of the application, up to the last application at -70°C. This is because the amount of cryothermal energy required for permanent ablation is individualized, ranging from an application of -40°C for 40 seconds to one of -75°C for 480 seconds; limiting test applications to only -30°C can limit the applicability of cryoablation for these patients. In addition, the use of cryothermal energy at temperatures lower than -30°C should be considered safer than RF energy at these critical sites.

Cryoablation. When sites of successful cryomapping are identified by demonstrating BT conduction block with no modification of the normal AVN-HB conduction, the cryoablation mode is activated, in which a target temperature below about -75°C is sought (a temperature of -75°C to -80°C is generally achieved). The application is then continued for up to 480 seconds, creating an irreversible lesion. If the catheter tip is in close contact with the endocardium, a prompt drop in catheter tip temperature should be seen as soon as the cryoablation mode is activated. A slow decline in temperature or very high flow rates of refrigerant during ablation suggests poor catheter tip-tissue contact and, in such a case, cryoablation is interrupted and the catheter is repositioned. Additional cryoablation “bonus” applications (usually two to three freeze-thaw-freeze cycles) may be applied to consolidate the lesion formation and improve long-term success rates.

Advantages of cryoablation. Cryoablation has several distinct advantages. First, “cryomapping” allows creation of “test lesions,” in which ablation target sites are cooled to a temperature that reversibly and temporarily halts local electrical activity. This enables valuation of the success and safety of the cryotherapy, and untoward effects caused by cryotherapy can be detected and reversed by interruption of cryotherapy before inducing permanent tissue damage. This is of particular value when ablation is performed in the close vicinity of the compact AVN or HB. Second, cryoadherence enhances catheter stability during ablation. This facilitates creating small, discrete cryolesions, which helps avoid damage to adjacent structures. Also, cryoablation may be performed during SVT without the concern of catheter dislodgement upon tachycardia termination.

On the other hand, the cryocatheter is not yet as steerable as the conventional RF catheter. Catheter stiffness and limited maneuverability can limit proper positioning of the catheter tip and potentially result in tissue trauma and transient mechanical AV or BT block. Furthermore, the large electrode spacing decreases the specificity of mapping of the BT. These limitations can potentially be overcome by the use of an electroanatomic mapping system and a conventional EP catheter with 2-mm spacing for mapping of the precise BT location before targeting that site with cryoablation.⁷¹

Outcome of cryoablation. In recent series, the acute success rate of cryoablation of BTs in the superoparaseptal and midseptal regions exceeded 90% (range, 60% to 100%). However, recurrence rates after initially successful cryoablation remain high (occurring in up to 20% of patients), and overall success rates have been lower than those with RF ablation of BTs. Nevertheless, whereas RF ablation of some superoparaseptal and midseptal BTs may otherwise be abandoned (in up to 17% of patients) because of a prohibitive risk of AV block, cryoablation is a viable, and often successful, option to eliminate those BTs. Many patients often prefer a strategy to minimize the risk of procedural AV block even when associated with a lower rate of procedural success.

Although transient modifications of the normal AV conduction can be observed during cooling, no permanent modifications have been observed. RBBB has occurred on occasion, but inadvertent permanent AV block has yet to be reported. In fact, immediate discontinuation of cryothermal energy application at any temperature on observation of modification of AVN conduction results in return to baseline conditions shortly afterward.⁷¹⁻⁷³

Ablation of Posteroseptal (Inferoparaseptal) Bypass Tracts

Anatomical Considerations

The posteroseptal region corresponds to a complex anatomic region where the four cardiac chambers reach their maximal proximity posteriorly (i.e., the crux), and incorporates the converging segments of the AV rings as well as the CS with its proximal branches. The posteroseptal region spans the area between the central fibrous body (superiorly), the interventricular septum (anteriorly), the right posterior paraseptal region (right lateral border), and the left posterior paraseptal region (left lateral border). Posteroseptal BTs can be located in a relatively wide area either at an epicardial site around the proximal CS or the middle cardiac vein or at an endocardial site along the tricuspid annulus in the immediate vicinity of the CS os, or along the posteromedial ventricular aspect of the mitral annulus. Because the posteroseptal region is actually posterior to the septum and not a septal structure, posteroseptal BTs are more appropriately referred to as right- or left-sided “inferoparaseptal” or “posterior paraseptal” BTs.

Because the interatrial sulcus is displaced to the far left of the interventricular sulcus, and because the AV valves are not isoplanar (the tricuspid annulus is displaced apically 5 to 10 mm in relation to the mitral annulus), the true septal part of the AV junction (the RA to LV sulcus) actually separates the inferomedial RA from the posterior superior process of the LV. The undersurface of the CS is about 1 cm above the mitral annulus. The CS os abuts the superior margin of the RA-to-LV sulcus and the paraseptal mitral annulus in the pyramidal space, providing an access for BT ablation. The right margin of the posteroseptal space includes the area surrounding the CS os and the inferior portion of the triangle of Koch. The left margin (the junction of the posterior septum and left free wall) lies as far as 2 to 3 cm from the CS os. The epicardial dimension of the posteroseptal space at the level of the valve annuli extends a mean of 3.4 ± 0.5 cm. BTs can be located anywhere within this relatively large space or in the adjacent right or left free walls. BTs located close to the edges of the septum can be ablated from the adjacent atrial or ventricular cavity, but BTs located deep within the posteroseptal space or near the epicardial aspect require ablation from within the CS or cardiac veins. BTs located in the proximal 1.5 cm of the CS are almost always in the posterior septal region. Those located between 1.5 and 3 cm from the CS os can be in the left free-wall or posterior septal region, and those located more than 3 cm from the CS os are almost invariably in the left free wall.

Most posteroseptal BTs are believed to be RA-to-LV BTs, with the ventricular insertion attaching onto the posterior superior process of the LV, but some posteroseptal BTs are considered to be left paraseptal (connecting the LA to the LV) or right paraseptal (connecting the RA to the RV). Up to 20% of posteroseptal BTs connect the myocardial coat of the CS (which is connected anatomically and electrically to both the RA and LA) to the LV.⁷⁴⁻⁷⁶

Electrocardiographic Considerations

Prediction of the site of successful ablation of posteroseptal BTs into either the right or the left heart has been attempted by analysis of the preexcitation pattern on the surface ECG. In addition to the obvious limitation of the surface ECG in the case of concealed BTs (47.5% in

a recent report), reports on the accuracy of surface ECG features to differentiate BTs associated with the three compartments of the inferior paraseptal space have been conflicting. Furthermore, although ECG characteristics of ventricular preexcitation can potentially predict the ventricular insertion site of the BT, the ability to predict the successful approach to BT ablation remains limited.

Previous reports found that, in patients with preexcitation, a negative delta wave polarity in lead V1 and positive polarity in lead V2 favors right-sided localization of a posteroseptal BT, whereas left posteroseptal BTs were associated with biphasic or positive delta wave polarity in leads V1 and V2. Recent reports, however, have questioned the predictive value of such a criterion. The vast majority of posteroseptal BTs can be successfully ablated at the tricuspid annulus or within the proximal CS, although the delta wave polarity on the ECG suggests a left ventricular origin. This phenomenon can be explained by the fact that many posteroseptal BTs are “RA-to-LV” fibers and an RA approach for ablation would suffice even though the delta wave polarity in lead V1 is suggestive of left posteroseptal BTs.^{74–76}

On the other hand, the R/S ratio in lead V1 was found to be an accurate ECG parameter to predict the site of successful ablation of posteroseptal BTs. This finding might be related to the observation that the ventricular insertion of “RA-to-LV” posteroseptal BTs attaches onto the posterosuperior process of the LV, resulting in earlier activation of the posterobasal LV with positive delta wave and predominantly negative QRS morphology (R/S ratio less than 1) in lead V1. In contrast, the ventricular insertion of “LA-to-LV” BTs attaches to the posteromedial aspect of the mitral annulus, resulting in a positive delta wave and a predominantly positive QRS morphology (R/S ratio greater than 1) in lead V1.⁷⁵

Posteroseptal BTs typically display deeply negative delta waves in lead III. Lead aVF is also negative in right posteroseptal BTs, but less commonly negative in left posteroseptal BTs. A steeply negative delta wave in lead II is a specific indicator for epicardial posteroseptal BTs (typically requiring ablation from within the coronary venous system).

Technical Considerations

Ablation of posteroseptal BTs is usually more difficult than other BT locations because of the complexity of the anatomical structures involved. Mapping and ablation can be required at either the mitral or the tricuspid annulus, or inside the CS or its proximal branches. Therefore the ability to discriminate BTs amenable to ablation from the right side (on the tricuspid ring or inside the coronary venous system) from those

requiring ablation on the mitral annulus can potentially have great impact on procedure outcome and safety by reducing procedural and fluoroscopy times, reducing the number of unsuccessful RF applications, and avoiding unnecessary LA access and its potential complications.^{74,75}

In addition to the ECG criteria discussed above, invasive EP findings have been used to predict the successful ablation site of manifest or concealed posteroseptal BTs (Table 18.2; Fig. 18.59). The response of the VA interval during orthodromic AVRT to the development of BBB has been suggested to help distinguish between right and left posteroseptal BTs. Prolongation of the surface VA interval in response to BBB by 10 to 30 milliseconds compared to that with normal QRS predicts the ventricular insertion of the posteroseptal BT in the ventricle ipsilateral to the side of BBB. However, the utility of this observation in predicting the successful approach to ablation is limited.⁷⁴

Measurement of the Δ VA interval during orthodromic AVRT (the difference in VA intervals measured at the HB catheter and at the site of earliest atrial activation in the CS) was found to be useful for predicting the successful approach. A Δ VA interval of 25 milliseconds or more suggests a left endocardial BT, whereas a Δ VA interval less than 25 milliseconds favors a right endocardial BT. This suggests that atrial activation is relatively early in the HB region during retrograde conduction through both right endocardial and CS-associated BTs, compared with left endocardial BTs.⁷⁴

Furthermore, a previous report found that a VA interval less than 50 milliseconds recorded at the left posteroseptal region during RV pacing identified 71% of patients with left posteroseptal BTs, with 100% specificity. In patients with a VA interval greater than 50 milliseconds, a difference in the VA intervals of less than 20 milliseconds recorded at the HB region and at the left posteroseptal region during RV pacing predicted right posteroseptal BT with a sensitivity of 97%, a specificity of 85%, and a positive predictive value of 91%.

PJRT is usually caused by a slowly conducting BT, commonly located in the posteroseptal region. Although the mere presence of a long-RP orthodromic AVRT has been suggested to favor a right endocardial BT, in 50% of cases, such BTs can be located in the left posterior or free wall (greater than 4 cm inside the CS). In the remaining 50%, the BT is located between the base of the pyramidal space formed by the points of pericardial deflection that contact the posterior RA and LA. None have been reported in the anteroseptal region.⁷⁴

An earliest atrial activation during orthodromic AVRT in the middle CS favors a left endocardial ablation site. However, recent studies found that a large proportion (more than one-third) of patients with an

TABLE 18.2 Electrocardiographic and Electrophysiological Criteria for Discrimination Between Right and Left Posteroseptal Bypass Tracts

	Favors Right Posteroseptal Bypass Tract	Favors Left Posteroseptal Bypass Tract
Electrocardiogram	<ul style="list-style-type: none"> • Delta wave negative in lead V1 and positive in lead V2 • R/S ratio in lead V1 <1 • Prolongation of VA interval • <25 ms 	<ul style="list-style-type: none"> • Biphasic or positive delta wave polarity in leads V1 and V2 • R/S ratio in lead V1 >1 • No change in VA interval • ≥25 ms
Response of orthodromic AVRT to left bundle branch block		
Δ VA interval during orthodromic AVRT (the difference in VA intervals measured at the HB catheter and the site of earliest atrial activation in the CS)		
Δ VA interval during RV pacing (the difference in VA intervals measured at the HB catheter and the left posteroseptal region)	<ul style="list-style-type: none"> • VA >50 ms and ΔVA <20 ms 	<ul style="list-style-type: none"> • <50 ms
Site of earliest retrograde atrial activation	<ul style="list-style-type: none"> • CS ostium 	<ul style="list-style-type: none"> • Mid CS
CS electrogram characteristics at earliest retrograde site	<ul style="list-style-type: none"> • Sharp/blunt CS atrial electrogram sequence 	<ul style="list-style-type: none"> • Blunt/sharp CS atrial electrogram sequence

AVRT, Atrioventricular reentrant tachycardia; CS, coronary sinus; HB, His bundle; RV, right ventricular; VA, ventricular-to-atrial.

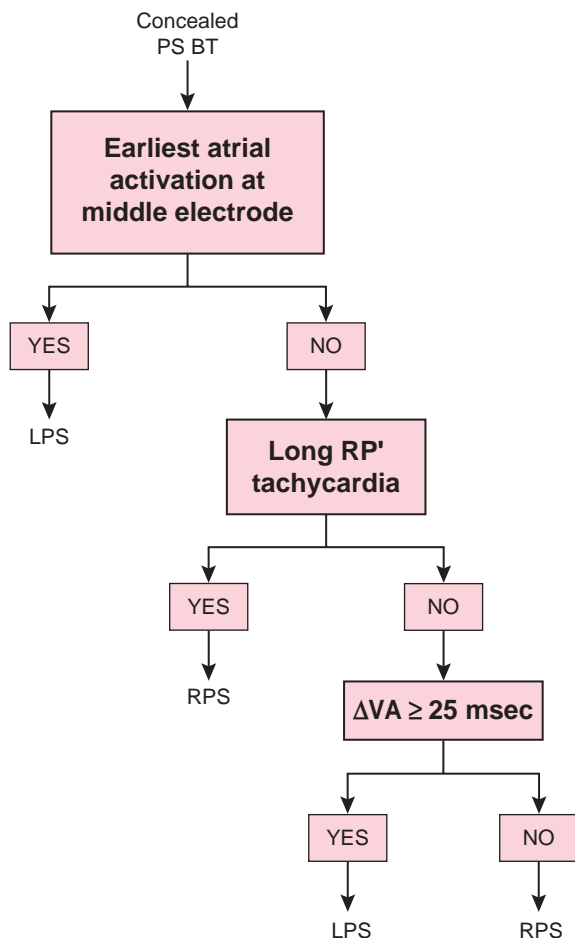


Fig. 18.59 Algorithm for Identifying the Need for Left Endocardial Ablation of Concealed Posteroseptal (PS) Bypass Tracts (BTs). ΔVA , difference in ventricular-to-atrial conduction time between the His bundle recording and the earliest site in the coronary sinus. LPS, Left posteroseptal; RPS, right posteroseptal; VA, ventriculoatrial. (From Chiang CE, Chen S, Tai C, et al. Prediction of successful ablation on concealed posteroseptal accessory pathways by a novel algorithm using baseline electrophysiological parameters. *Circulation*. 1996;93:982–991.)

earliest activation site at or distal to the mid-CS required ablation inside the CS after a failed left endocardial approach, and 35% of all BTs ablated from the right side produced such an eccentric retrograde atrial activation. Therefore the ability of the site of earliest atrial activation during AVRT to predict the successful ablation approach seems very limited, mainly because CS-associated BTs can produce a very much eccentric retrograde atrial activation sequence.⁷⁴

Careful analysis of CS electrograms recorded by a catheter placed inside the CS can help distinguish between left and right posteroseptal BTs. “Atrial” electrograms recorded from inside the proximal CS originate not only from LA myocardium, but also from activation of the CS myocardial coat. This results in “fragmented” or double potentials, with a low-amplitude, blunt “far-field” LA component and a larger, sharp “near-field” signal from the CS musculature. The sequence of LA and CS myocardial coat activation at the earliest “atrial” electrograms in the CS recorded during retrograde BT conduction can guide mapping of these BTs into right- or left-sided compartments of the posteroseptal space. An activation wavefront traveling from the posteroseptal RA toward the left (e.g., by pacing posterior to the CS os) will first activate the muscle coat covering the proximal CS, producing a large, sharp

signal recorded by the electrodes inside the CS. Discrete connections of the CS musculature with the LA will activate the LA myocardium, producing a lower-amplitude, blunt, “far-field” signal on the CS electrodes. Thus two-component “fragmented” or double potentials will be recorded in the proximal CS, with the sharp component preceding the blunt signal (sharp/blunt sequence). The same sequence (sharp/blunt) of potentials is expected to happen when a retrogradely conducting right-sided “endocardial” BT first activates RA myocardium and when a BT inserts directly into the CS musculature (as is the case with epicardial CS-associated BTs). In contrast, when pacing is performed from the lateral LA, the sequence is the opposite (blunt/sharp), with CS musculature activation following activation of LA myocardium. This sequence should be produced if a BT connects to LA myocardium (i.e., left-sided “endocardial” AV BTs), the first signal recorded in the CS being a “far-field” potential followed by later activation of the CS musculature resulting in a blunt/sharp sequence of potentials. Different conduction velocities of LA myocardium and CS musculature can cause the sequence of potentials to change farther away from the insertion site of the BT, explaining the importance of analyzing the electrograms recorded at the earliest site. The recording of double potentials inside the CS has been found to be especially common during retrograde conduction through posteroseptal BTs.⁷⁴

Generally, a right-sided endocardial approach is initially adopted for mapping and ablation of BTs in the posteroseptal region. The posteroseptal tricuspid annulus, including the CS os and its most proximal part, and inferomedial RA are carefully mapped. If the ablation site fails or no appropriate ablation site can be obtained, the left posteroseptal area is mapped (with a transaortic or transeptal approach, as described for left-sided BTs). A primary left-sided approach may also be considered if multiple ECG and EP features suggest a left-sided location of the BT. If endocardial mapping fails, an epicardial approach via the CS is then considered (see later discussion).

Ablation of Epicardial Bypass Tracts

Anatomical Considerations

Epicardial BTs can be found at any location, but are most common in the posteroseptal and left posterior regions. Epicardial BTs account for 4% of left-sided BT ablation cases and 10% of those in patients referred after a failed ablation attempt.⁷⁷

Embryologically, the CS develops from the sinus venosus, together with the smooth part of the RA. As a remnant of sinus venosus musculature, a cuff of striated muscle covers the proximal CS, continuous with RA myocardium at the CS os. The CS muscle coat extends for 25 to 51 mm from the CS os and may extend for several millimeters over the necks of the middle cardiac vein and posterior coronary vein. Although this muscle coat is usually separated from the LA by adipose tissue, broad and extensive muscular strands frequently bridge this separation, producing electrical continuity between the CS musculature and the LA. These myocardial sleeves or cords, however, do not usually extend into the ventricular myocardium. In variations, an AV BT (referred to as an “epicardial” BT) is formed by a connection between a sleeve-like extension of the CS myocardial coat (along the middle cardiac vein, posterior cardiac vein, or another coronary vein) and the epicardial surface of the LV myocardium (CS-ventricular BT).⁷⁸ In some cases, the muscle creating this connection is found in the neck of a CS diverticulum, usually arising within the proximal 1.5 cm of the CS and before the middle cardiac vein. The prevalence of CS-associated epicardial BTs is approximately 22% to 36% among patients with posteroseptal or left posterior BTs, and is up to 47% among patients with a previous failed ablation attempt. This highlights the difficulty of localizing these BTs.⁷⁴

Other types of unusual BTs that cannot be ablated with a standard endocardial approach at the annulus have been described. These include

BTs that connect an atrial appendage to its respective ventricle, which can be successfully ablated using a transcutaneous pericardial approach or endocardial ablation over a large area; ablation at the valve annulus is uniformly unsuccessful in these cases. Another example is BTs closely associated with the ligament of Marshall, which can be ablated by targeting this ligament.⁷⁹

Electrocardiographic Considerations

ECG predictors of epicardial posteroseptal BTs include the following: (1) steep negative delta wave in lead II; (2) steep positive delta wave in lead aVR; and (3) deep S wave in lead V6. A negative delta wave in lead II has the highest sensitivity and a positive delta in lead aVR has the highest specificity for prediction of the presence of epicardial (i.e., requiring ablation within the CS and its branches) versus endocardial posteroseptal BTs.⁷⁵

Technical Considerations

An epicardial location of the BT is suggested when the earliest site of endocardial ventricular activation does not precede the onset of the delta wave, and when a very large BT potential can be easily recorded on the CS electrodes. During anterograde conduction over a CS-ventricular BT, endocardial mapping of the RV and LV identifies far-field activation (unipolar potential has a wide initial R wave), with the earliest far-field ventricular potential recorded 1 to 3 cm apical to the tricuspid and mitral annuli. At those sites, the local endocardial ventricular activation (as indicated by a rapid downstroke on the unfiltered unipolar electrogram) is recorded late (greater than 15 milliseconds after the onset of the far-field ventricular potential), reflecting ventricular activation from epicardium to endocardium.

On the other hand, mapping within the CS during anterograde conduction over a CS-ventricular BT reveals the earliest ventricular activation, usually recorded from the branch of the CS containing the myocardial extension. At this location, the local ventricular activation is preceded by a high-frequency potential (similar to an anterograde BT potential) generated by activation of the CS myocardium extending along the venous branch (CS myocardial extension potential).

During retrograde conduction over a CS-ventricular BT, the CS muscular coat is activated prior to the LA myocardium, and the high-frequency component generated by the CS myocardial extension (similar to a retrograde BT potential) precedes the low-frequency component generated by activation of the LA. In contrast, with left-sided “endocardial” BTs, the impulse activates the LA before the CS and the low-frequency, far-field signal from the LA will precede the sharp CS component.⁷⁴

Elimination of CS-ventricular BT requires ablation within the coronary venous system. Ablation of these BTs from the endocardial aspect at the mitral annulus often fails because of the extensive connections between the CS myocardial coat and the LA and the absence of a clear endocardial location for the ventricular insertion of the CS-ventricular BT. Generally, ablation is ineffective when attempted endocardially targeting the site of earliest anterograde ventricular activation or targeting the site of earliest retrograde atrial activation. Of note, endocardial ablation at the site of earliest retrograde atrial activation often produces only a shift in the site of earliest atrial activation (mimicking multiple BTs) because ablation usually results in interruption of one of the multiple connections of the CS myocardial coat to the atria.⁷⁴

The CS provides a useful route for mapping and ablation of epicardial BTs. CS-ventricular BTs are generally ablatable on the floor of the CS at the orifice of a venous branch or within a CS diverticulum. The middle (or “posterior interventricular”) cardiac vein is a well-established site for posterior epicardial BTs, and is useful for approaching AV BTs located in the inferior pyramidal space. This vein courses with the posterior descending coronary artery in the posterior interventricular groove

and enters the CS close to the RA orifice or, rarely, enters directly into the RA. At its junction with the CS, the venous entrance is occasionally much dilated, forming a venous diverticulum. CS venography is typically required to help delineate its anatomy and guide ablation.^{77,78}

The ideal ablation site is located within the branch of the CS containing the CS myocardial extension (coronary vein or neck of a CS diverticulum), at the site recording the largest, sharpest CS myocardial extension potential (similar to a BT activation potential) on the unipolar electrogram recorded from the ablation electrode. Typically, an irrigated-tip ablation catheter is used to allow more consistent delivery of RF energy, with less heating at the electrode-tissue interface. Standard RF energy delivery is often limited because of impedance or temperature rise (due to limited cooling from surrounding blood flow). Irrigated RF energy output of 10 to 20 W is initially delivered at sites within the CS, with the ablation catheter tip directed toward the ventricle within the CS (by maintaining a gentle counterclockwise torque on the ablation catheter).

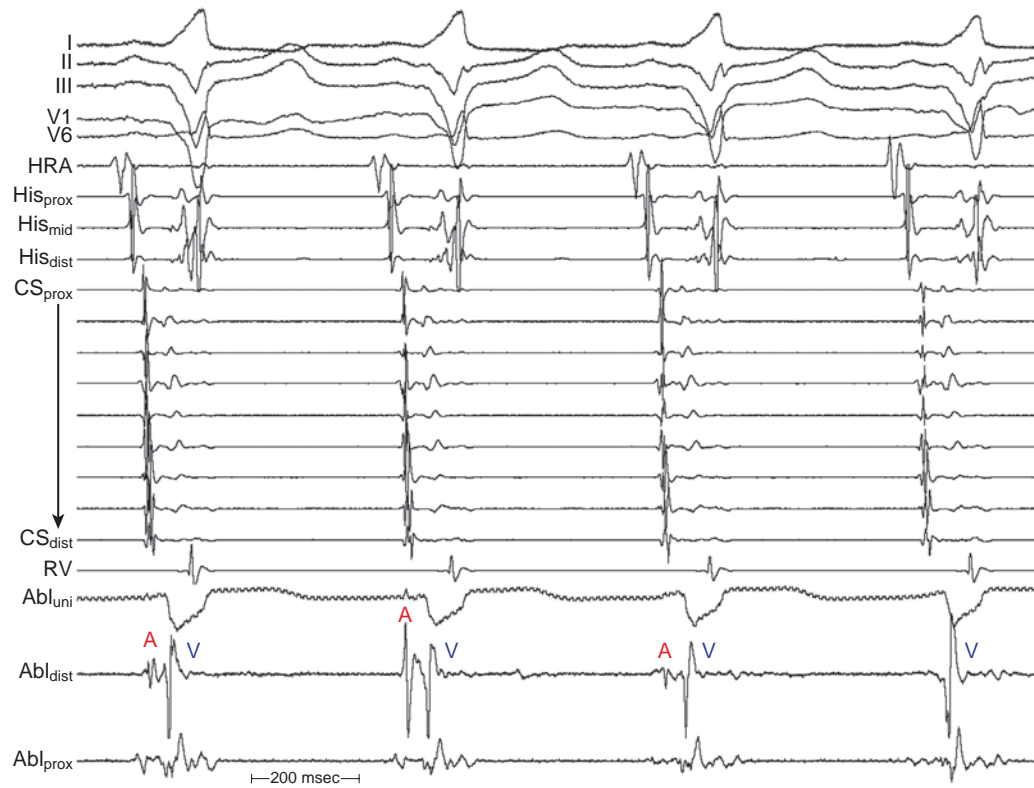
Importantly, in some patients, branches of the distal right coronary artery (posterolateral branch) or left circumflex artery (posterior descending artery) course between the vein and the ventricle, just below the CS, adjacent to the ideal ablation site. RF ablation in close proximity to a coronary artery is associated with a high risk of arterial injury and should be avoided. Therefore once the ablation catheter is positioned at the target site, and before RF energy delivery, coronary arteriography is performed to outline the spatial relationship between the target vein and the adjacent coronary artery. Although the minimal safe distance between ablation sites and coronary arteries is not clear, the risk is highest for distances less than 2 mm and is negligible for distances more than 5 mm. Coronary arteriography is also performed after ablation to rule out damage to coronary arteries.⁸⁰

When close proximity of a coronary artery (within 2 to 4 mm) prohibits RF ablation, cryoablation offers a safe and reasonably effective alternative (albeit less effective than RF ablation).⁸¹ Freezing seems less likely to damage adjacent coronary arteries. Cryoablation may also be considered because it is not limited by high impedance and is likely facilitated by low blood flow. However, the cryocatheter can be difficult to maneuver in the coronary venous system.⁸⁰

The coronary venous approach can also be useful for mapping and ablation of left-sided AV BTs around the mitral valve and those traversing the inferior pyramidal space, the inferior BTs. Nevertheless, BTs located very close to the hinge of the mitral valve can be difficult to ablate because the CS is some distance away. Rarely, a transcutaneous pericardial approach is required to ablate epicardial BTs that are posteroseptal or right-sided. The success of this approach, however, remains limited, likely due to the anatomy of the AV groove, the thick epicardial fat layer covering the region where BTs are located, as well as the close proximity to the epicardial coronary arteries.^{77,78}

Causes of Failed Bypass Tract Ablation

Technical difficulties are the most common cause of failed BT ablation. These difficulties are typically related to catheter manipulation and stability (eFig. 18.9) or inability to access the target site. Catheter instability can lead to poor tissue contact and insufficient tissue heating at the optimal target site. These challenges are more common with right-sided BTs because of the smooth atrial aspect of the tricuspid annulus. Such difficulties can be overcome by using preformed guiding sheaths to help stabilize the catheter, using different catheter curvatures and shaft stiffness, changing the approach for ablation (e.g., from transseptal to transaortic, or from IVC to SVC), or changing the ablation modality. Also, cryoablation can help achieve better catheter stability and target sites that might otherwise be avoided because of the risk of damage to neighboring structures. Large (8-mm) ablation electrodes and cooled



eFig. 18.9 Poor Choice of Ablation Sites Because of Unstable Recordings. In the distal ablation bipolar (Abl_{dist}) recording, the atrial and ventricular electrograms have constantly changing amplitudes, signifying unstable electrode contact with tissue. Ablation should not be performed until the recordings are stable. Abl_{prox} , Ablation proximal bipolar electrodes; Abl_{uni} , ablation distal unipolar electrode; CS_{dist} , distal coronary sinus; CS_{prox} , proximal coronary sinus; His_{dist} , distal His bundle; His_{mid} , middle His bundle; His_{prox} , proximal His bundle; HRA , high right atrium; RVA , right ventricular apex.

RF ablation can also help generate large RF lesions; however, other causes of ablation failure should be considered first before shifting to those approaches, which are only rarely required for BT ablation because the target tissue (BT) is generally a thin strand, ablation of which should not require a large amount of tissue damage.

Mapping errors are the second most common cause of ablation failure. Mapping pitfalls are largely related to inaccurate localization of a BT that has an oblique course. This is more likely to occur when retrograde atrial activation mapping is performed with the ablation catheter positioned at the ventricular side of the annulus; because of the oblique course of the BT, the site of earliest atrial activation recorded from the ventricular aspect of the annulus does not correspond to the ventricular insertion site. Similar situations can occur when the ablation catheter is positioned on the atrial aspect of the annulus and RF applications are delivered where the earliest ventricular activation is recorded. In these situations, mapping for the earliest atrial activation site with the catheter on the atrial side of the annulus, or mapping for the earliest ventricular activation site with the catheter on the ventricular side of the annulus, should be undertaken.

Failure to recognize that a posteroseptal BT is left-sided rather than right-sided, and epicardial location of a left-sided or a posteroseptal BT, are other potential causes of failed ablation of those BTs. Detailed mapping in the CS should be considered in such situations. Furthermore, some BTs insert in the ventricle at a distance from the annulus, in which case a search for a presumed BT potential within the ventricle adjacent to the region of the earliest ventricular activation recorded at the annulus can be helpful. Unusual BTs (e.g., atriofascicular BTs) and anatomical abnormality (e.g., congenital heart disease) also account for some failures in BT ablation.

Failure to recognize the existence of multiple pathways can result in apparent failure of ablation of the target BT or recurrent tachycardia. Subtle changes in delta wave morphology during ablation of the target BT can help recognize the presence of more than one manifest BT. Furthermore, the use of a multielectrode EP catheter around the mitral annulus (via the CS) or tricuspid annulus (Halo catheter) can help recognize changes in retrograde atrial activation sequence or local VA timing during ablation of the target BT, which can be indicative of the presence of a second BT. In addition, concealed septal or para-septal BTs can be missed after ablation of a free-wall BT. Programmed ventricular and HB stimulation is important to avoid tachycardia recurrence.

Catheter-induced trauma to the BT also can lead to ablation failure (eFig. 18.10). Mechanical injury to the BT often persists for some time, leading to discontinuation of the mapping and ablation procedure in many cases, and the long-term risk for recovery of BT function is high. Superoparaseptal and atriofascicular BTs exhibit the highest susceptibility to mechanical trauma, followed by left free-wall BTs. The outcome can still be improved in these situations by close observation of the ECG recordings to recognize catheter-induced trauma of a BT promptly and, whenever conduction block in the BT does not resolve within 1 minute, by immediate application of RF energy, provided that the catheter has not moved from the site of presumed trauma. The location of the catheter tip when mechanical trauma occurred can be logged on electroanatomic mapping systems; some of these allow the user to “play back” where the catheter was seconds before the trauma occurred (if there is a question as to whether it has moved from that location). In addition, adenosine (likely due to its hyperpolarizing effects on atrial and BT tissues) can potentially transiently revive conduction through the injured BT secondary to mechanical trauma or partially successful ablation. This can help facilitate intermittent mapping during the transient adenosine effect.⁸² Finally, pace mapping the annulus to replicate the delta wave morphology can help guide ablation.

Outcome

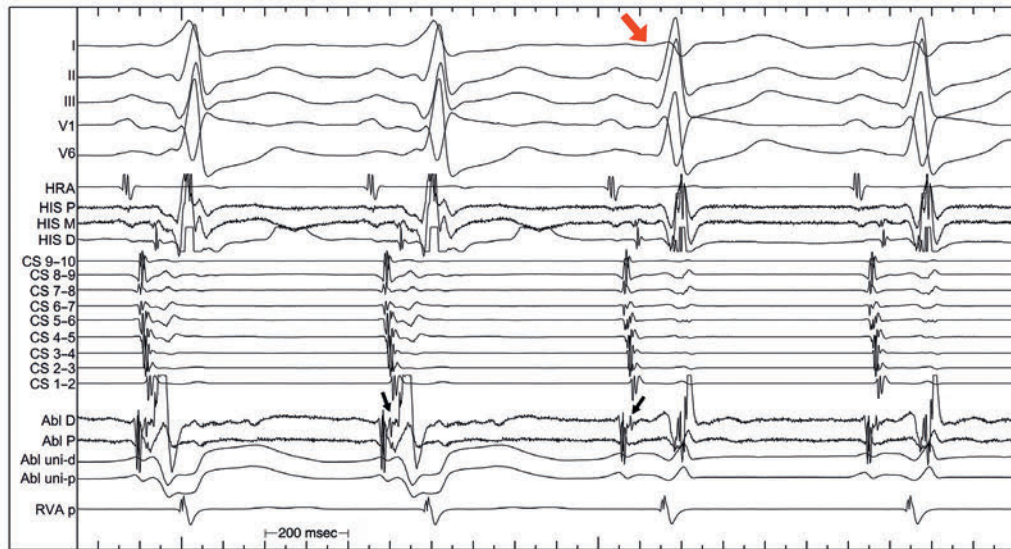
RF ablation is a highly effective and curative treatment for AVRT, with acute success rates greater than 95%. Acutely successful RF ablation is usually persistent and late recurrence of BT conduction after ablation is rare (4%). Short runs of palpitations after ablation are frequent, are usually caused by isolated or short runs of PACs or PVCs and not by recurrence of BT conduction, and can be easily managed with symptomatic treatment. When BT-mediated tachycardia does recur, symptoms are usually observed during the first month after ablation; on the other hand, later onset of symptoms (more than 3 months after the ablation) are highly suggestive of SVTs not related to the ablated BT and justify a thorough evaluation (e.g., event monitoring, long-term ECG monitoring, new EP study).

In a survey of 6065 patients, the long-term success rate was 98% and a repeat procedure was necessary in 2.2% of cases. Serious complications (e.g., cardiac tamponade, AV block, coronary artery injury, retroperitoneal hemorrhage, stroke) occurred in 0.6% of patients, with one fatality (0.02%). Thus the one-time risk of catheter ablation appears to be considerably lower than the cumulative annual risk associated with the WPW syndrome. Hence, catheter ablation remains the treatment of choice for patients with the WPW syndrome who may be at risk for life-threatening arrhythmias. In addition, the highly favorable risk-benefit ratio justifies the use of catheter ablation as first-line therapy for any patient with BT-dependent tachycardia requiring treatment.

Success rates and risk of complications vary with different BT locations. Acute and long-term success rates are highest for left free-wall BTs. The immediate success rate of transaortic ablation of left free-wall BTs is 86% to 100% (highest with anterograde BT activation), and the recurrence rate is 2% to 5%, less frequent than for BTs at other locations. Complications of this approach include vascular complications (50% of all complications: groin hematoma, aortic dissection, and thrombosis), cardiac tamponade, stroke, coronary dissection (from direct catheter trauma), injury to the left circumflex coronary artery (from subannular RF application), valvular damage, and systemic embolism (from aortic atherosclerosis, catheter tip coagulum, or ablation site thrombosis). The transseptal approach, on the other hand, is associated with a success rate of 85% to 100%, a recurrence rate of 3% to 6.6%, and a complication rate of 0% to 6%. Such complications include coronary spasm, cardiac tamponade, systemic embolization (0.08%), and death (0.08%).

As compared with other BT locations, ablation of right free-wall BT is associated with the lowest acute success rate (88%), and highest recurrence rate (21%), but a low complication rate. On the other hand, ablation of posteroseptal BTs is associated with higher success rates (up to 98%) and a recurrence rate of 12%. For superoparaseptal BT ablation, the reported success rate is up to 97%, with a risk of RBBB in 5% to 10% of cases. Similarly, ablation of midseptal BTs is associated with a success rate of 98%, with an incidence of first-degree AV block in 2% and second-degree AV block in 2%. Although with superoparaseptal BT ablation RF energy is frequently applied at locations with visible His potential, the risk of high-grade AV block is higher for ablation of midseptal BTs because the compact AVN is located in the midseptum. In contrast to the well-insulated HB, the compact AVN is fragile and more vulnerable to damage during ablation.^{62,76}

The ablation of epicardial BTs (within the CS) is associated with a success rate of 62% to 100% and a complication rate of 0% to 6%. Complications associated with this approach include CS spasm, cardiac tamponade, pericarditis, and right coronary artery spasm or occlusion. The overall incidence of coronary artery injury is low (0.1%) and it can present immediately or several weeks after ablation.⁸³



eFig. 18.10 Catheter Trauma Leading to Loss of Preexcitation. Red arrow shows sudden absence of preexcitation with no change in cycle length or premature complexes. The black arrows in the distal ablation (*Abl D*) bipolar recording point to a possible bypass tract potential, with conduction interrupted distal to the bypass tract potential. *CS*, Coronary sinus; *HRA*, high right atrium; *RVA*, right ventricular apex

REFERENCES

- Page RL, et al. 2015 ACC/AHA/HRS guideline for the management of adult patients with supraventricular tachycardia: a report of the American College of Cardiology/American Heart Association Task Force on Clinical Practice Guidelines and the Heart Rhythm Society. *Circulation*. 2016;133:e506–e574.
- Brembilla-Perrot B, et al. Incidence and prognostic significance of spontaneous and inducible antidromic tachycardia. *Europace*. 2013;15:871–876.
- Kang KT, et al. Permanent junctional reciprocating tachycardia in children: a multicenter experience. *Heart Rhythm*. 2014;11:1426–1432.
- Bunch TJ, et al. Long-term natural history of adult Wolff-Parkinson-White syndrome patients treated with and without catheter ablation. *Circ Arrhythmia Electrophysiol*. 2015;8:1465–1471.
- Cohen MI, et al. PACES/HRS expert consensus statement on the management of the asymptomatic young patient with a Wolff-Parkinson-White (WPW, ventricular preexcitation) electrocardiographic pattern. *Heart Rhythm*. 2012;9:1006–1024.
- Cain N, Irving C, Webber S, et al. Natural history of Wolff-Parkinson-White syndrome diagnosed in childhood. *Am J Cardiol*. 2013;112:961–965.
- Obeyesekere MN, et al. Risk of arrhythmia and sudden death in patients with asymptomatic preexcitation: a meta-analysis. *Circulation*. 2012;125:2308–2315.
- Huang SY, et al. Gender differences of electrophysiologic characteristics in patients with accessory atrioventricular pathways. *Heart Rhythm*. 2011;8:571–574.
- Kim SS, Knight BP. Long term risk of Wolff-Parkinson-White pattern and syndrome. *Trends Cardiovasc Med*. 2017;27:260–268.
- Katritsis DG. Wolff-Parkinson-White syndrome and antidromic atrioventricular reentrant tachycardia. *Europace*. 2013;15:779–780.
- Lalani SR, et al. 20p12.3 microdeletion predisposes to Wolff-Parkinson-White syndrome with variable neurocognitive deficits. *J Med Genet*. 2009;46:168–175.
- Brembilla-Perrot B, et al. Age-related prognosis of syncope associated with a preexcitation syndrome. *Pacing Clin Electrophysiol*. 2013;36:803–810.
- Mah DY, et al. The electrophysiological characteristics of accessory pathways in pediatric patients with intermittent preexcitation. *Pacing Clin Electrophysiol*. 2013;36:1117–1123.
- Kiger ME, et al. Intermittent versus persistent Wolff-Parkinson-White Syndrome in children: electrophysiologic properties and clinical outcomes. *Pacing Clin Electrophysiol*. 2015;39:14–20.
- Czosek RJ, Anderson J, Cassidy A, et al. Cost-effectiveness of various risk stratification methods for asymptomatic ventricular pre-excitation. *Am J Cardiol*. 2013;112:245–250.
- Al-Khatib SM, et al. Risk stratification for arrhythmic events in patients with asymptomatic pre-excitation: a systematic review for the 2015 ACC/AHA/HRS guideline for the management of adult patients with supraventricular tachycardia. *Circulation*. 2016;133:e575–e586.
- Cohen M, Triedman J. Guidelines for management of asymptomatic ventricular pre-excitation brave new world or Pandora's box? *Circ Arrhythmia Electrophysiol*. 2014;7:187–189.
- Chevalier P, et al. Prophylactic radiofrequency ablation in asymptomatic patients with Wolff-Parkinson-White is not yet a good strategy: a decision analysis. *Circ Arrhythmia Electrophysiol*. 2013;6:185–190.
- Kubuš P, Vít P, Gebauer RA, et al. Electrophysiologic profile and results of invasive risk stratification in asymptomatic children and adolescents with the Wolff-Parkinson-White electrocardiographic pattern. *Circ Arrhythmia Electrophysiol*. 2014;7:218–223.
- Zipes DP, et al. Eligibility and disqualification recommendations for competitive athletes with cardiovascular abnormalities: Task Force 9: arrhythmias and conduction defects: a scientific statement from the American Heart Association and American College of Cardiology. *Circulation*. 2015;132:e315–e325.
- Rivera S, et al. The retrograde P-wave theory: explaining ST segment depression in supraventricular tachycardia by retrograde AV node conduction. *Pacing Clin Electrophysiol*. 2014;37:1100–1105.
- Maden O, et al. Comparison of the accuracy of three algorithms in predicting accessory pathways among adult Wolff-Parkinson-White syndrome patients. *J Interv Card Electrophysiol*. 2015;44:213–219.
- Taguchi N, et al. A simple algorithm for localizing accessory pathways in patients with Wolff-Parkinson-White syndrome using only the R/S ratio. *J Arrhythmia*. 2014;30:439–443.
- Tai C-T, et al. A new electrocardiographic algorithm using retrograde P waves for differentiating atrioventricular node reentrant tachycardia from atrioventricular reciprocating tachycardia mediated by concealed accessory pathway. *J Am Coll Cardiol*. 1997;29:394–402.
- Fitzgerald DM, Hawthorne HR, Crossley GH, et al. P wave morphology during atrial pacing along the atrioventricular ring. ECG localization of the site of origin of retrograde atrial activation. *J Electrocardiol*. 1996;29:1–10.
- Capone CA, et al. Three-catheter technique for ablation of left-sided accessory pathways in Wolff-Parkinson-White is less expensive and equally successful when compared to a five-catheter technique. *Pacing Clin Electrophysiol*. 2015;38:1405–1411.
- Wright JM, Singh D, Price A, et al. Two cases of supraventricular tachycardia after accessory pathway ablation. *Circ Arrhythm Electrophysiol*. 2013;6:26–31.
- Kapa S, et al. Utilization of retrograde right bundle branch block to differentiate atrioventricular nodal from accessory pathway conduction. *J Cardiovasc Electrophysiol*. 2009;20:751–758.
- Derval N, et al. Differential sequential septal pacing: a simple maneuver to differentiate nodal versus extranodal ventriculoatrial conduction. *Heart Rhythm*. 2013;10:1785–1791.
- Asirvatham SJ, Stevenson WG. Atrioventricular nodal reentry tachycardia chameleon in disguise. *Circ Arrhythm Electrophysiol*. 2014;7:355–357.
- Nakagawa H, Jackman WM. Para-Hisian pacing: useful clinical technique to differentiate retrograde conduction between accessory atrioventricular pathways and atrioventricular nodal pathways. *Heart Rhythm*. 2005;2:667–672.
- Sauer WH, Lowery CM, Cooper JM, et al. Sequential dual chamber extrastimulation: a novel pacing maneuver to identify the presence of a slowly conducting concealed accessory pathway. *Heart Rhythm*. 2008;5:248–252.
- Obeyesekere M, et al. Tachycardia induction with ventricular extrastimuli differentiates atypical atrioventricular nodal reentrant tachycardia from orthodromic reciprocating tachycardia. *Heart Rhythm*. 2012;9:335–341.
- Knight BP, et al. Diagnostic value of tachycardia features and pacing maneuvers during paroxysmal supraventricular tachycardia. *J Am Coll Cardiol*. 2000;36:574–582.
- Nagashima K, et al. Ventriculoatrial intervals ≤ 70 ms in orthodromic atrioventricular reciprocating tachycardia. *Pacing Clin Electrophysiol*. 2016;39:1108–1115.
- Yang Y, et al. Quantitative effects of functional bundle branch block in patients with atrioventricular reentrant tachycardia. *Am J Cardiol*. 2000;85:826–831.
- Crawford TC, et al. Utility of atrial and ventricular cycle length variability in determining the mechanism of paroxysmal supraventricular tachycardia. *J Cardiovasc Electrophysiol*. 2007;18:698–703.
- Josephson ME, Almendral J, Callans DJ. Resetting and entrainment of reentrant ventricular tachycardia associated with myocardial infarction. *Heart Rhythm*. 2014;11:1239–1249.
- Deo R, Berger R. The clinical utility of entrainment pacing. *J Cardiovasc Electrophysiol*. 2009;20:466–470.
- Maruyama M, et al. The VA relationship after differential atrial overdrive pacing: a novel tool for the diagnosis of atrial tachycardia in the electrophysiology laboratory. *J Cardiovasc Electrophysiol*. 2007;18:1127–1133.
- Calvo D, et al. Differential responses of the septal ventricle and the atrial signals during ongoing entrainment. *Circ Arrhythm Electrophysiol*. 2015;8:1201–1209.
- Verma N, Knight BP. Ventricular overdrive pacing: beyond V-A-V and V-A-A-V. *Pacing Clin Electrophysiol*. 2015;39:2015–2016.
- Ho RT, Frisch DR, Pavri BB, et al. Electrophysiological features differentiating the atypical atrioventricular node-dependent long RP

- supraventricular tachycardias. *Circ Arrhythm Electrophysiol.* 2013;6: 597–605.
44. Boyle PM, Veenhuijzen GD, Vigmond EJ. Fusion during entrainment of orthodromic reciprocating tachycardia is enhanced for basal pacing sites but diminished when pacing near Purkinje system end points. *Heart Rhythm.* 2013;10:444–451.
45. Akerström F, et al. Performance of the SA-VA difference to differentiate atrioventricular nodal reentrant tachycardia from orthodromic reentrant tachycardia in a large cohort of consecutive patients. *Pacing Clin Electrophysiol.* 2015;38:1066–1072.
46. González-Torrecilla E, et al. Differences in ventriculoatrial intervals during entrainment and tachycardia: a simpler method for distinguishing paroxysmal supraventricular tachycardia with long ventriculoatrial intervals. *J Cardiovasc Electrophysiol.* 2011;22:915–921.
47. Platonov M, Schroeder K, Veenhuijzen GD. Differential entrainment: beware from where you pace. *Heart Rhythm.* 2007;4:1097–1099.
48. Katriotis DG, Camm AJ. Atrioventricular nodal reentrant tachycardia. *Circulation.* 2010;122:831–840.
49. Kannankeril PJ, Bonney WJ, Dzurik MV, et al. Entrainment to distinguish orthodromic reciprocating tachycardia from atrioventricular nodal reentry tachycardia in children. *Pacing Clin Electrophysiol.* 2010;33: 469–474.
50. González-Torrecilla E, et al. First postpacing interval after tachycardia entrainment with correction for atrioventricular node delay: a simple maneuver for differential diagnosis of atrioventricular nodal reentrant tachycardias versus orthodromic reciprocating tachycardias. *Heart Rhythm.* 2006;3:674–679.
51. Boonyapisit W, et al. Determining the site of accessory pathways in orthodromic reciprocating tachycardia by using the response to right ventricular pacing. *Pacing Clin Electrophysiol.* 2015;39:115–121.
52. Javier García-Fernandez F, et al. Differentiation of atrioventricular nodal reentrant tachycardia from orthodromic reciprocating tachycardia by the resetting response to ventricular extrastimuli: comparison to response to continuous ventricular pacing. *J Cardiovasc Electrophysiol.* 2013;24: 534–541.
53. Segal OR, et al. Differential ventricular entrainment: a maneuver to differentiate AV node reentrant tachycardia from orthodromic reciprocating tachycardia. *Heart Rhythm.* 2009;6:493–500.
54. Nagashima K, et al. Anterograde conduction to the His bundle during right ventricular overdrive pacing distinguishes septal pathway atrioventricular reentry from atypical atrioventricular nodal reentrant tachycardia. *Heart Rhythm.* 2015;12:735–743.
55. Dandamudi G, et al. A novel approach to differentiating orthodromic reciprocating tachycardia from atrioventricular nodal reentrant tachycardia. *Heart Rhythm.* 2010;7:1326–1329.
56. AlMahameed ST, Buxton AE, Michaud GF. New criteria during right ventricular pacing to determine the mechanism of supraventricular tachycardia. *Circ Arrhythm Electrophysiol.* 2010;3:578–584.
57. Akerström F, et al. Number of beats in the transition zone with fixed SA interval during right ventricular overdrive pacing determines accessory pathway location in orthodromic reentrant tachycardia. *Pacing Clin Electrophysiol.* 2015;39:21–27.
58. Pérez-Rodon J, et al. Entrainment from the para-Hisian region for differentiating atrioventricular node reentrant tachycardia from orthodromic atrioventricular reentrant tachycardia. *Europace.* 2008;10: 1205–1211.
59. Spotnitz MD, et al. Mechanisms and clinical significance of adenosine-induced dormant accessory pathway conduction after catheter ablation. *Circ Arrhythm Electrophysiol.* 2014;7:1136–1143.
60. Dal-Bianco JP, Levine RA. Anatomy of the mitral valve apparatus. Role of 2D and 3D echocardiography. *Cardiol Clin.* 2013;31:151–164.
61. Kim J. Anatomical discrepancy between the coronary sinus and the mitral annulus by fluoroscopy. 2016;17:14–19.
62. Chen M, et al. Right-sided free wall accessory pathway refractory to conventional catheter ablation: lessons from 3-dimensional electroanatomic mapping. *J Cardiovasc Electrophysiol.* 2010;21:1317–1324.
63. Ho SY. Accessory atrioventricular pathways: getting to the origins. *Circulation.* 2008;117:1502–1504.
64. Fishberger SB, Hernandez A, Zahn EM. Electroanatomic mapping of the right coronary artery: a novel approach to ablation of right free-wall accessory pathways. *J Cardiovasc Electrophysiol.* 2009;20:526–529.
65. Lee P-C, Chen S-A, Hwang B. Atrioventricular node anatomy and physiology: implications for ablation of atrioventricular nodal reentrant tachycardia. *Curr Opin Cardiol.* 2009;24:105–112.
66. Kurian T, Ambrosi C, Hucker W, et al. Anatomy and electrophysiology of the human AV node. *Pacing Clin Electrophysiol.* 2010;33:754–762.
67. González-Torrecilla E, et al. Reappraisal of classical electrocardiographic criteria in detecting accessory pathways with a strict para-Hisian location. *Heart Rhythm.* 2013;10:16–21.
68. DeMazumder D, Barcelon B, Cockrell J, et al. Ablation of an anterosseptal accessory pathway from the aortic root using electroanatomic mapping. *Heart Rhythm.* 2014;11:2122–2123.
69. Wilsmore BR, Tchou PJ, Kanj M, et al. Catheter ablation of an unusual decremental accessory pathway in the left coronary cusp of the aortic valve mimicking outflow tract ventricular tachycardia. *Circ Arrhythm Electrophysiol.* 2012;5:104–108.
70. Tanidir IC, et al. Cryoablation with an 8-mm-tip catheter for right-sided accessory pathways in children. *Pacing Clin Electrophysiol.* 2016;39: 797–804.
71. Karadeniz C, Akdeniz C, Turan O, et al. Cryoablation of septal accessory pathways in children: midterm results. *Pacing Clin Electrophysiol.* 2014;37: 1095–1099.
72. Collins KK. Cryoablation, limited fluoroscopy, and more. *Pacing Clin Electrophysiol.* 2014;37:1093–1094.
73. Swissa M, et al. Cryotherapy ablation of parahisian accessory pathways in children. *Heart Rhythm.* 2015;12:917–925.
74. Pap R, et al. Ablation of posteroseptal and left posterior accessory pathways guided by left atrium-coronary sinus musculature activation sequence. *J Cardiovasc Electrophysiol.* 2008;19:653–658.
75. Haghjoo M, et al. Electrocardiographic and electrophysiologic predictors of successful ablation site in patients with manifest posteroseptal accessory pathway. *Pacing Clin Electrophysiol.* 2008;31:103–111.
76. Macedo PG, Patel SM, Bisco SE, et al. Septal accessory pathway: anatomy, causes for difficulty, and an approach to ablation. *Indian Pacing Electrophysiol J.* 2010;10:292–309.
77. Scanavacca MI, et al. Accessory atrioventricular pathways refractory to catheter ablation: role of percutaneous epicardial approach. *Circ Arrhythm Electrophysiol.* 2015;8:128–136.
78. Habib A, Lachman N, Christensen KN, et al. The anatomy of the coronary sinus venous system for the cardiac electrophysiologist. *Europace.* 2009;11(suppl 5):v15–v21.
79. Mah D, et al. Epicardial left atrial appendage and biatrial appendage accessory pathways. *Heart Rhythm.* 2010;7:1740–1745.
80. Stavrakis S, et al. Risk of coronary artery injury with radiofrequency ablation and cryoablation of epicardial posteroseptal accessory pathways within the coronary venous system. *Circ Arrhythm Electrophysiol.* 2014;7: 113–119.
81. Mao J, et al. Catheter ablation of accessory pathways near the coronary sinus: value of defining coronary arterial anatomy. *Heart Rhythm.* 2015; 12:508–514.
82. Lapage MJ, Walsh MJ, Reed JH, et al. Adenosine mapping for adenosine-dependent accessory pathway ablation. *Pacing Clin Electrophysiol.* 2014;37:610–615.
83. Roberts-Thomson KC, et al. Coronary artery injury due to catheter ablation in adults: presentations and outcomes. *Circulation.* 2009;120: 1465–1473.

Atypical Bypass Tracts

OUTLINE

“Mahaim Fibers,” 677

“Mahaim Tachycardia,” 677

Atypical Atrioventricular and Atriofascicular Bypass Tracts, 677

Long Decrementally Conducting Atrioventricular and Atriofascicular Bypass Tracts, 677

Short Decrementally Conducting Atrioventricular Bypass Tracts, 678

Arrhythmias Associated With Atypical Atrioventricular and Atriofascicular Bypass Tracts, 678

Electrocardiographic Features, 678

Electrophysiological Testing, 679

Differential Diagnosis, 684

Mapping, 684

Ablation, 688

Nodofascicular and Nodovertricular Bypass Tracts, 688

Arrhythmias Associated With Nodofascicular and

Nodovertricular Bypass Tracts, 688

Electrocardiographic Features, 689

Electrophysiological Testing, 689

Mapping, 690

Ablation, 690

Fasciculoventricular Bypass Tracts, 690

General Considerations, 690

Electrocardiographic Features, 690

Electrophysiological Testing, 690

Atrio-Hisian Bypass Tracts, 692

General Considerations, 692

Supraventricular Tachycardias in Patients With Short PR

Intervals, 695

Electrophysiological Testing, 695

A working definition of an atypical bypass tract (BT) is a conduction pathway that bypasses all or part of the normal conduction system but is not a rapidly conducting pathway connecting atrium and ventricle near the mitral or tricuspid annulus. Thus pathways that connect the atrium to the His bundle (HB) (atrio-Hisian BT), the atrioventricular node (AVN) to the His-Purkinje system (HPS) (nodofascicular BT), or the ventricle (nodovertricular BT), or the HPS to the ventricle (fasciculoventricular BT) fit into this designation (Fig. 19.1).

“MAHAIM FIBERS”

In 1937, during pathological examination of the heart, Mahaim and Benatt identified islands of conducting tissue extending from the HB into the ventricular myocardium. These fibers were called *Mahaim fibers* or *fasciculoventricular fibers*. This description was subsequently expanded to include connections between the AVN and the ventricular myocardium (nodovertricular fibers). Later, it was recognized that BTs could arise from the AVN and insert into the right bundle branch (RB) (nodofascicular fibers). This classification for Mahaim fibers persisted until evidence suggested that the anatomical substrate of tachycardias with characteristics previously attributed to nodovertricular and nodofascicular fibers is actually atrioventricular (AV) and atriofascicular BTs with decremental conduction properties (i.e., conduction slows at faster heart rates) (Fig. 19.1). Although these BTs are sometimes collectively referred to as “Mahaim fibers,” the use of this term is discouraged because it is more illuminating to name the precise BT according to its connections. In this chapter, these BTs are collectively referred to as *atypical* BTs to differentiate them from the more common (*typical*) rapidly conducting AV BTs, which insert into ventricular myocardium near the AV annulus and result in the Wolff-Parkinson-White (WPW) syndrome, or concealed BTs.¹

“MAHAIM TACHYCARDIA”

The term *Mahaim tachycardia* is used to describe the typical constellation of electrophysiological (EP) features that characterize the unusual form of reentrant tachycardia using an atypical BT without implying the underlying anatomical cause. It should be noted that, because the term was originally applied to an anatomical finding and subsequently (incorrectly) applied to physiology that matched what would be expected from this anatomy, it has given rise to more confusion than understanding. Hence use of the term *Mahaim tachycardia* should generally be discouraged; instead, one should simply describe the physiological characteristics of the tachyarrhythmia.

ATYPICAL ATRIOVENTRICULAR AND ATRIOFASCICULAR BYPASS TRACTS

Long Decrementally Conducting Atrioventricular and Atriofascicular Bypass Tracts

Atriofascicular and long AV BTs constitute the majority (80%) of atypical BTs. These BTs predominantly arise from the right atrium (RA) free wall; cross the tricuspid annulus in the lateral, anterolateral, or anterior region; extend along the right ventricular (RV) free wall to the region where the moderator band usually inserts at the apical third of the RV free wall; and insert into the distal part of the RB (atriofascicular BT) or into the ventricular myocardium close to the RB (long decrementally conducting AV BT). These BTs are functionally similar to the normal AV junction, with an AVN-like structure leading to an HB-like structure. In essence, these BTs function as an auxiliary conduction system parallel to the normal conduction system (AVN-HPS). Similar to the normal AVN, these BTs demonstrate decremental conduction (related to the

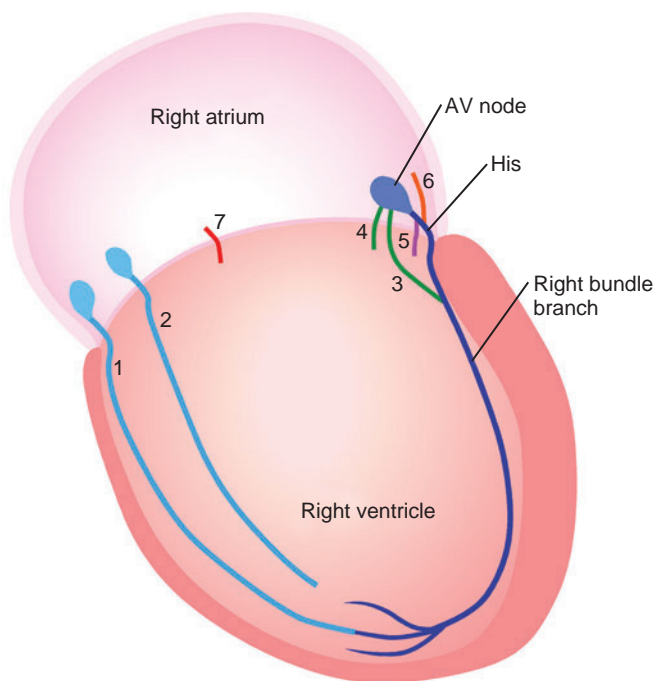


Fig. 19.1 Types of Bypass Tracts (BTs). The right atrium and ventricle are depicted. 1, Atriofascicular BT; 2, long atrioventricular BT; 3, nodo-fascicular BT; 4, nodovenous BT; 5, fasciculoventricular BT; 6, atrio-Hisian BT; 7, typical short atrioventricular BT. AV node, Atrioventricular node.

slow rate of recovery of excitability) and Wenckebach-type block in response to rapid atrial pacing and are sensitive to adenosine. The conduction delay in these BTs has been localized to the intraatrial portion of the BT (the AVN-like portion), whereas the interval from the inscription of the BT potential at the tricuspid annulus and the onset of ventricular activation (BT-V interval) remains constant.²⁻⁴ These BTs are typically unidirectional, conducting only in the anterograde direction; retrograde conduction block in the BT occurs near the atrial insertion.

Short Decrementally Conducting Atrioventricular Bypass Tracts

These BTs are analogous to the decrementally conducting concealed BTs responsible for permanent junctional reciprocating tachycardia (PJRT) (see Chapter 18) in that they bridge the AV rings and insert proximally into ventricular myocardium in close proximity to the AV annulus. These BTs primarily arise from the RA free wall but can also arise from the posterior or septal region. Left-sided BTs with decremental conduction characteristics have rarely been described. These BTs demonstrate prolonged conduction time over their length (more than 30 milliseconds) and decremental conduction and Wenckebach-type block in response to rapid atrial pacing. However, they do not consistently appear to be responsive to adenosine, which suggests that their structure is not composed of AVN-like tissue. Similar to atriofascicular BTs, short AV BTs conduct only anterogradely.⁵

An acquired form of short AV decrementally conducting BTs has been reported to be caused by incomplete radiofrequency (RF) ablation of typical rapidly conducting AV BTs. These BTs are capable of being part of an arrhythmia circuit. The decrease in conduction velocity may potentially be related to a decrease in cell-to-cell coupling caused by RF ablation-mediated injury.⁶

Arrhythmias Associated With Atypical Atrioventricular and Atriofascicular Bypass Tracts

Atypical AV and atriofascicular BTs in patients with clinical arrhythmias have the following characteristics: (1) unidirectional (anterograde-only) conduction (with rare exceptions); (2) long conduction times; and (3) decremental conduction (i.e., cycle length [CL]-dependent slowing of conduction).

Atypical BTs constitute 3% to 5% of all BTs. The incidence is slightly higher (6%) in patients presenting with supraventricular tachycardia (SVT) with left bundle branch block (LBBB) morphology. Multiple BTs occur in 10% of patients with atypical BTs. In some cases, ventricular preexcitation over a rapidly conducting AV BT can mask the presence of an atypical BT, which becomes apparent only after ablation of the typical BT. Dual AVN pathways or multiple BTs occur in 40% of patients with atypical BTs. Atypical BTs can also be associated with Ebstein anomaly.

Supraventricular Tachycardias Requiring a Bypass Tract for Initiation and Maintenance

Antidromic atrioventricular reentrant tachycardia (AVRT) can use the atypical AV and atriofascicular BT anterogradely and the HPS-AVN retrogradely. Preexcited AVRT can also use the atypical BT anterogradely and a second AV BT retrogradely. In the latter case, the AVN can participate as an innocent bystander mediating anterograde or retrograde fusion.

Because these atypical BTs almost always conduct anterogradely only, they cannot mediate orthodromic AVRT but can mediate antidromic AVRT or can be innocent bystanders during other SVTs (e.g., atrioventricular nodal reentrant tachycardia [AVNRT]). However, they can coexist with typical rapidly conducting AV BTs. Right-free-wall atriofascicular BTs capable of both anterograde and retrograde conduction that participate in both antidromic and orthodromic AVRT have rarely been reported.

Supraventricular Tachycardias Not Requiring a Bypass Tract for Initiation and Maintenance

AVNRT, atrial tachycardia (AT), atrial flutter (AFL), or atrial fibrillation (AF) can coexist with atypical BTs, in which case the atypical AV and atriofascicular BTs function as bystanders, wholly or partly responsible for ventricular activation during the tachycardia. Of note, the overall incidence of AF in patients with atypical BTs is low (less than 2%); it is much lower than in those with the classic WPW syndrome. AVNRT is observed in less than 10% of patients with atypical BT-related tachycardia.¹

Electrocardiographic Features

Normal Sinus Rhythm

During normal sinus rhythm (NSR), the electrocardiogram (ECG) shows a normal QRS or minimal preexcitation in most patients with atypical BTs. Subtle preexcitation can be suspected by the absence of the normal septal forces (small q waves) in leads I, aVL, V₅, and V₆ and the presence of an rS complex in lead III in the setting of a narrow QRS. The degree of preexcitation depends on the relative conduction time over the AVN and BT. Maneuvers that prolong conduction over the AVN (e.g., atrial pacing, vagal maneuvers, or drugs) to a greater degree than prolongation of BT conduction will increase the degree of preexcitation.

Because atypical AV and atriofascicular BTs exhibit decremental conduction, increasing the atrial pacing rate results in prolongation of the P-delta interval. This is in contrast to the setting with typical rapidly conducting AV BTs, during which progressively faster atrial pacing rates result in increasing delay in AVN conduction, an increasing degree of

ventricular preexcitation, and a relatively fixed P-delta interval. The P-delta interval remains constant regardless of the degree of preexcitation because conduction over the typical BT displays less decrement than does the AVN.

Preexcited QRS Morphology

For atriofascicular BTs, the preexcited QRS is relatively narrow (133 ± 10 milliseconds); its morphology is classic for typical LBBB with a QRS axis between 0 and -75 degrees and a late precordial R/S transition zone (at lead V_4 or V_5 and sometimes V_6). A monophasic R wave, in lead I and rS pattern in lead V_1 are typically observed. The delta wave, classically seen with BTs inserting into the myocardium near the annuli, is characteristically absent. However, for long decrementally conducting AV BTs, the QRS is relatively wider (166 ± 26 milliseconds) and the LBBB pattern is less typical (with broad initial R in lead V_1). The QRS is even wider and the LBBB pattern is less typical with decrementally conducting short AV BTs than that with atriofascicular or long decrementally conducting AV BTs.⁷

Supraventricular Tachycardias

Arrhythmias associated with atypical BTs exhibit LBBB morphology and, most often in the setting of long decrementally conducting AV and atriofascicular BTs, left axis deviation on the surface ECG (Fig. 19.2). Several ECG features suggest (although are not diagnostic of) atypical BTs as the cause of an SVT with LBBB pattern, including (1) QRS axis between 0 and -75 degrees, (2) QRS duration of 150 milliseconds or less, (3) R wave in lead I, (4) rS complex in lead V_1 , and (5) precordial R wave transition in lead V_4 or later.

Electrophysiological Testing

Baseline Observations During Sinus Rhythm

In the baseline state, minimal or no preexcitation is present; thus the His bundle–ventricular (HV) interval is normal or slightly short.

Programmed atrial stimulation during sinus rhythm. Progressively shorter atrial pacing cycle lengths (PCLs) or atrial extrastimulation (AES) coupling intervals produce decremental conduction in both the atypical BT and, to a greater degree, the AVN (Fig. 19.3). Consequently, the atrial–His bundle (AH) interval increases, the QRS morphology gradually shifts to a more preexcited LBBB morphology, and the AV (A-delta) interval increases. However, the AV (A-delta) interval increases to a lesser degree than the AH interval. This is in contrast to the setting of typical rapidly conducting AV BTs whereby the AV (A-delta) interval remains constant despite prolongation of the AH interval and exaggeration of the degree of preexcitation, because the A-delta interval represents the constant, nondecremental conduction time over the typical AV BT.

With progressively shorter atrial PCLs or AES coupling intervals, the HV interval decreases as the His potential becomes progressively inscribed into the preexcited QRS (usually within the first 5 to 25 milliseconds after the onset of the QRS). The His potential eventually becomes activated retrogradely as the wavefront travels anterogradely down the BT and then retrogradely up the RB to the HB (Fig. 19.3). When the His potential is lost within the QRS, it is unclear whether anterograde AV conduction continues to propagate over the HB or block has occurred.

At the point of maximal preexcitation, the AV (A-delta) interval continues to prolong with more rapid pacing because of the decremental conduction properties of the BT, but the His-QRS relationship remains unaltered because the HB is activated retrogradely until block in the BT occurs. The fixed VH interval, despite shorter PCLs or AES coupling intervals, suggests that the BT inserts into or near the distal RB at the anterior free wall of the RV with retrograde conduction to the HB.

Whenever the VH interval is less than 20 milliseconds, insertion into the RB (i.e., atriofascicular or nodofascicular BT) is likely. On the other hand, with long decrementally conducting AV BTs, which insert into the ventricular myocardium close to the RB, the VH interval approximates the HV interval minus the duration of the His potential (because the His potential is activated retrogradely).

For short decrementally conducting BTs, the HB is activated anterogradely, and retrograde conduction to the HB is only seen following AV block or during antidromic AVRT. Decremental conduction (progressive prolongation of the AV interval) and Wenckebach-type block can develop in the BT. The conduction delay in these BTs is localized to the intraatrial portion of the BT; the interval from the inscription of the BT potential at the tricuspid annulus to the onset of ventricular activation (BT-V interval) remains constant.

Dual AVN physiology is common in patients with atypical BTs. Sometimes during AES, a jump from the fast to the slow AVN pathway prolongs the AH interval to a degree sufficient to unmask preexcitation over the BT, at which time the His potential becomes inscribed within the QRS.

The site of the earliest ventricular activation during preexcitation is at the RV apex for long, decrementally conducting AV BTs and atriofascicular BTs, but it is adjacent to the annulus near the base of the RV for short, decrementally conducting AV BTs (Fig. 19.4).

The site of atrial stimulation does not influence the degree of preexcitation in the setting of nodofascicular and nodoventricular BTs. Contrariwise, preexcitation becomes more prominent when atrial stimulation is performed closer to the atrial insertion site of AV or atriofascicular BTs.

Programmed ventricular stimulation during sinus rhythm. Because these BTs rarely have retrograde conduction, ventriculoatrial (VA) conduction during ventricular pacing is mediated solely by the HPS-AVN with a concentric atrial activation sequence and decremental properties in response to progressively shorter ventricular PCLs or ventricular extrastimulation (VES) coupling intervals. If rapid and fixed VA conduction is present, a separate retrogradely and rapidly conducting AV BT should be excluded.

Response to physiological and pharmacological maneuvers. Atriofascicular and long AV BTs are usually sensitive to autonomic changes and to adenosine, similar to the AVN. Adenosine produces conduction delay or block in most atypical BTs except for short decrementally conducting AV BTs (eFigs. 19.1 and 19.2). The conduction delay is localized to the intraatrial portion of the BT (i.e., between atrial and BT electrograms); the interval from the inscription of the BT potential at the tricuspid annulus and the onset of ventricular activation remains constant (analogous to adenosine effects of the AH and HV intervals of the normal AVN-HPS). When adenosine administration slows AVN conduction, an increase in the degree of preexcitation is noted in all types of BTs (as long as adenosine does not block the BT).

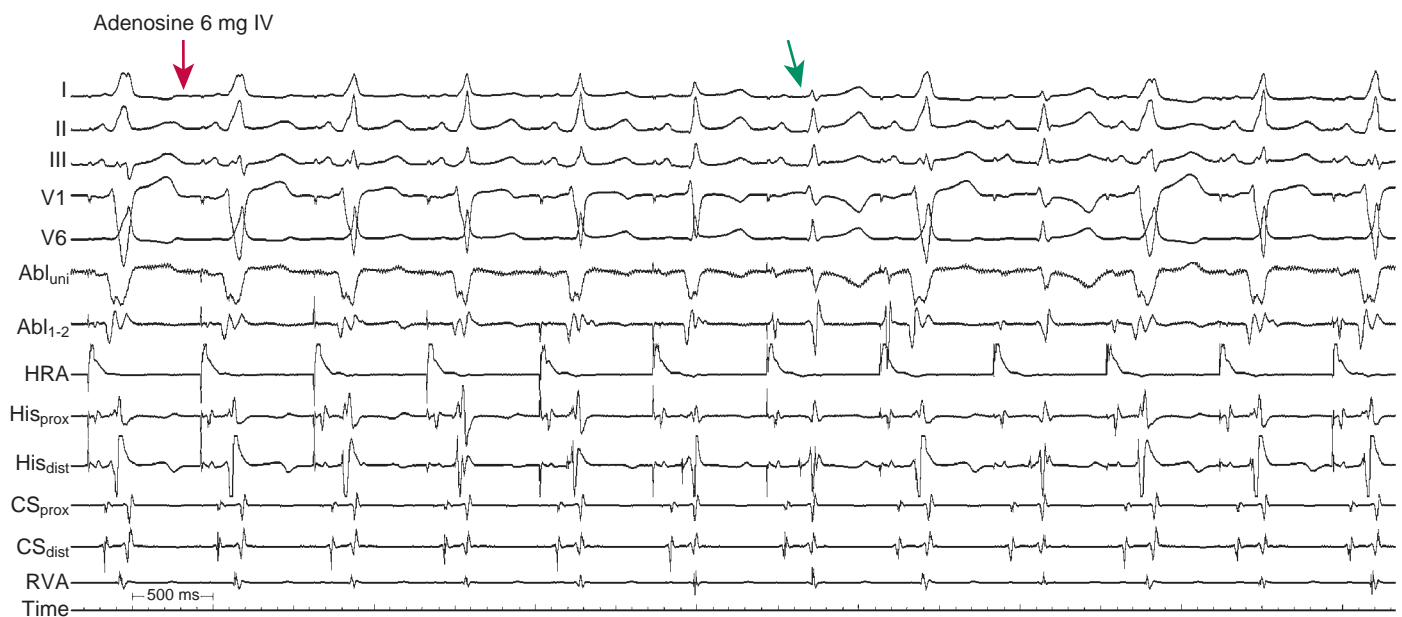
Induction of Tachycardia

Initiation by programmed atrial stimulation. Initiation of antidromic AVRT by an AES requires the following: (1) intact anterograde conduction over the BT, (2) anterograde block in the AVN or HPS, and (3) intact retrograde conduction over the HPS-AVN once the AVN resumes excitability following partial anterograde penetration. Whereas the latter is usually the limiting factor for the initiation of antidromic AVRT using typical rapidly conducting AV BTs, it is readily available in the setting of atypical BTs. This is because of the slow decremental conduction anterogradely over the atypical BT, providing adequate delay for full recovery of the HPS-AVN.

As noted, progressively shorter atrial PCLs (especially from the RA) result in progressive AV (A-delta) interval prolongation and a greater

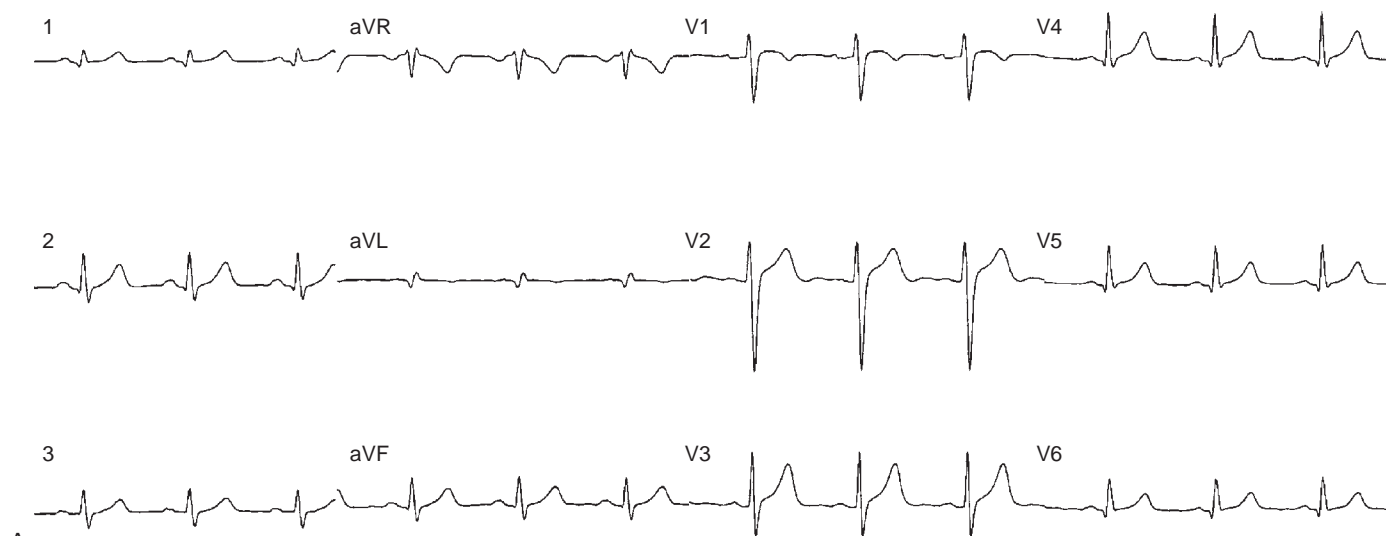


eFig. 19.1 Adenosine-Sensitive Posterior Septal Atrioventricular (AV) Bypass Tract. Adenosine was administered by rapid injection 5 seconds before the beginning of the recording, made during ventricular pacing (S). Dashed red lines denote onset of retrograde atrial activation. After the first two stimuli, activation appears earliest in the His recordings (AV nodal, *green arrow*), but on the third and fourth complexes, the AV node is blocked and conduction is over a septal pathway (*blue arrow*). However, after this, there is complete retrograde block with high-to-low sinus atrial complexes. CS, Coronary sinus catheter; HRA, high right atrial catheter.



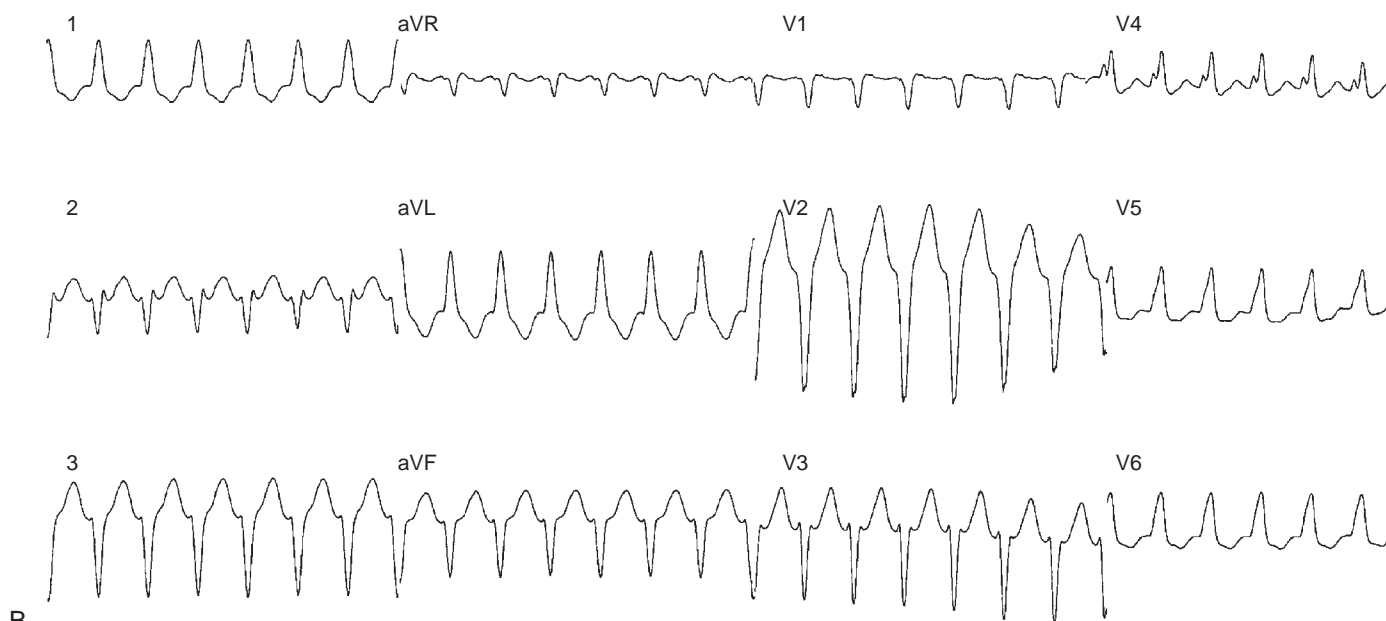
eFig. 19.2 Adenosine Transiently Blocks a Slowly Conducting Right Lateral Atrioventricular Bypass Tract. Adenosine is administered as shown during atrial pacing; preexcitation gradually decreases then transiently disappears (*green arrow*), returning consistently toward the end of the recording. Abl, Ablation catheter; CS, coronary sinus catheter; CS_{dist}, distal coronary sinus catheter; CS_{prox}, proximal coronary sinus catheter; His_{dist}, distal His bundle; His_{prox}, proximal His bundle; HRA, high right atrial catheter; IV, intravenously; RVA, right ventricular apical.

NSR



A

Antidromic AVRT



B

Fig. 19.2 Atriofascicular Bypass Tracts (BTs). (A) Normal sinus rhythm (NSR) with no evidence of preexcitation. (B) Antidromic atrioventricular reentrant tachycardia (AVRT) using an atriofascicular BT. QRS morphology during tachycardia resembles left bundle branch block aberration because of anterograde activation over the atriofascicular BT. Retrograde P waves can be seen after the end of the QRS.

degree of preexcitation until it is maximal. Often, once maximal preexcitation has been achieved, cessation of pacing is followed by preexcited SVT. Progressively shorter AES coupling intervals similarly result in progressive AV (A-delta) interval prolongation and a greater degree of preexcitation until it is maximal. When anterograde AVN conduction fails but conduction persists over the BT, the HPS-AVN can be activated retrogradely to initiate antidromic AVRT.

The sudden appearance of preexcitation associated with a “jump” from the fast to the slow AVN pathway with a His potential inscribed

before ventricular activation or with a VH interval of less than 10 milliseconds strongly favors AVNRT. Although a slowly conducting atriofascicular BT that becomes manifest with a jump to the slow AVN pathway cannot be excluded, a consistent pattern of dual pathway dependence and an HV relationship too short to be retrograde from the distal RB would be unlikely. Induction of AVNRT with AES is almost always associated with a dual pathway response, which may not be seen if the impulse conducts anterogradely over the BT and captures the HB before it is activated by the impulse traversing the slow AVN pathway

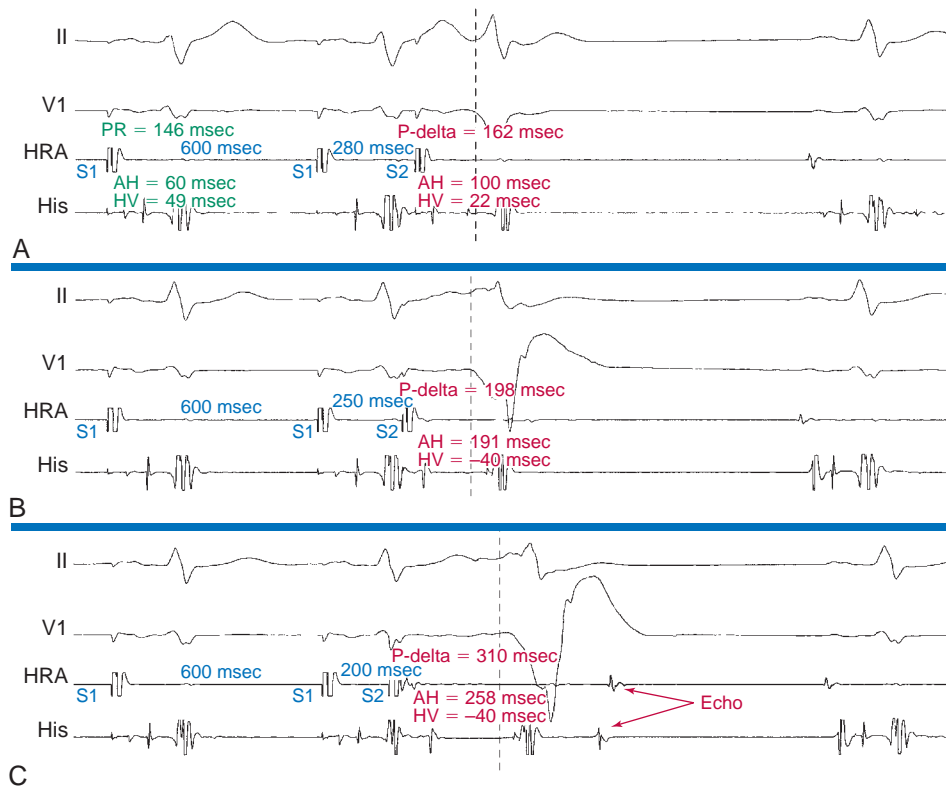


Fig. 19.3 Effect of Atrial Extrastimulation (AES) on Preexcitation Via a Long Atrioventricular (AV) Bypass Tract (BT). No preexcitation is observed during normal sinus rhythm and during the pacing drive at a cycle length of 600 milliseconds (normal PR and His bundle–ventricular [HV] intervals). (A) AES produces decremental conduction in the atrioventricular node (AVN) with prolongation of the atrial–His bundle (AH) interval (from 60 to 100 milliseconds), associated with manifest preexcitation and shortening of the HV interval (from 49 to 22 milliseconds). (B and C) Progressively shorter AES coupling intervals produce decremental conduction in the BT and, to a greater degree, in the AVN. Consequently, the AH interval prolongs, the QRS morphology gradually shifts to a more preexcited left bundle branch block morphology, and the AV (P-delta) interval prolongs. However, the P-delta interval prolongs to a lesser degree than the AH interval. The HV interval decreases (becomes negative) but remains fixed (B and C), although the P-delta interval continues to prolong with more premature AES because of decremental conduction over the BT. The fixed ventricular–His bundle (VH) interval, despite shorter AES coupling intervals, suggests that the BT inserts into or near the distal right bundle branch (RB) at the anterior free wall of the right ventricle, with retrograde conduction to the His bundle (HB). However, because the VH interval is modestly long (40 milliseconds), a long decrementally conducting AV BT inserting into the ventricle close to the RB is more likely than an atriofascicular BT. (C) AV reentrant echo complex (red arrows) secondary to anterograde conduction over the BT and retrograde conduction over the AVN. HRA, High right atrial catheter.

anterogradely. In other cases, a jump can be seen, so that the anterograde His potential follows the QRS with a typical AVN echo to initiate SVT, analogous to 1:2 conduction initiating antidromic AVRT.

Initiation by programmed ventricular stimulation. Initiation of antidromic AVRT by ventricular pacing or VES requires the following: (1) retrograde block in the BT, which is almost always available, because the atypical BTs are usually unidirectional (anterograde only); (2) retrograde conduction over the HPS–AVN; and (3) adequate VA delay to allow for recovery of the atrium and BT so it can support subsequent anterograde conduction.

Ventricular pacing can initiate SVT in 85% of cases. Initiation is almost always associated with retrograde conduction up a relatively fast AVN pathway, followed by anterograde conduction down a slow pathway, which is associated with preexcitation. The anterograde slow pathway can be a BT (i.e., antidromic AVRT) or a slow AVN pathway (i.e., AVNRT with an innocent bystander BT). During induction of the SVT by ventricular pacing at a CL similar to the tachycardia cycle

length (TCL) or by a VES that advances the His potential by a coupling interval similar to the H–H interval during the SVT, the His bundle–atrial (HA) interval following the ventricular stimulus is compared with that during the SVT. An HA interval that is longer with ventricular pacing or VES initiating the SVT than that during the SVT suggests AVNRT. This occurs despite the fact that the H1–H2 interval of the VES (i.e., the interval between the His potential activated anterogradely by the last sinus beat to the His potential activated retrogradely by the VES initiating the SVT) exceeds the H–H interval during the SVT. Because the AVN usually exhibits greater decremental conduction with repetitive engagement of impulses than in response to a single impulse at a similar coupling interval, the more prolonged the HA with the initiating ventricular stimulus, the more likely the SVT is AVNRT. If the SVT uses the BT for anterograde conduction, the HA interval during ventricular pacing or the VES initiating the SVT, at a comparable coupling interval as the TCL, should have the same HA interval as during the SVT.

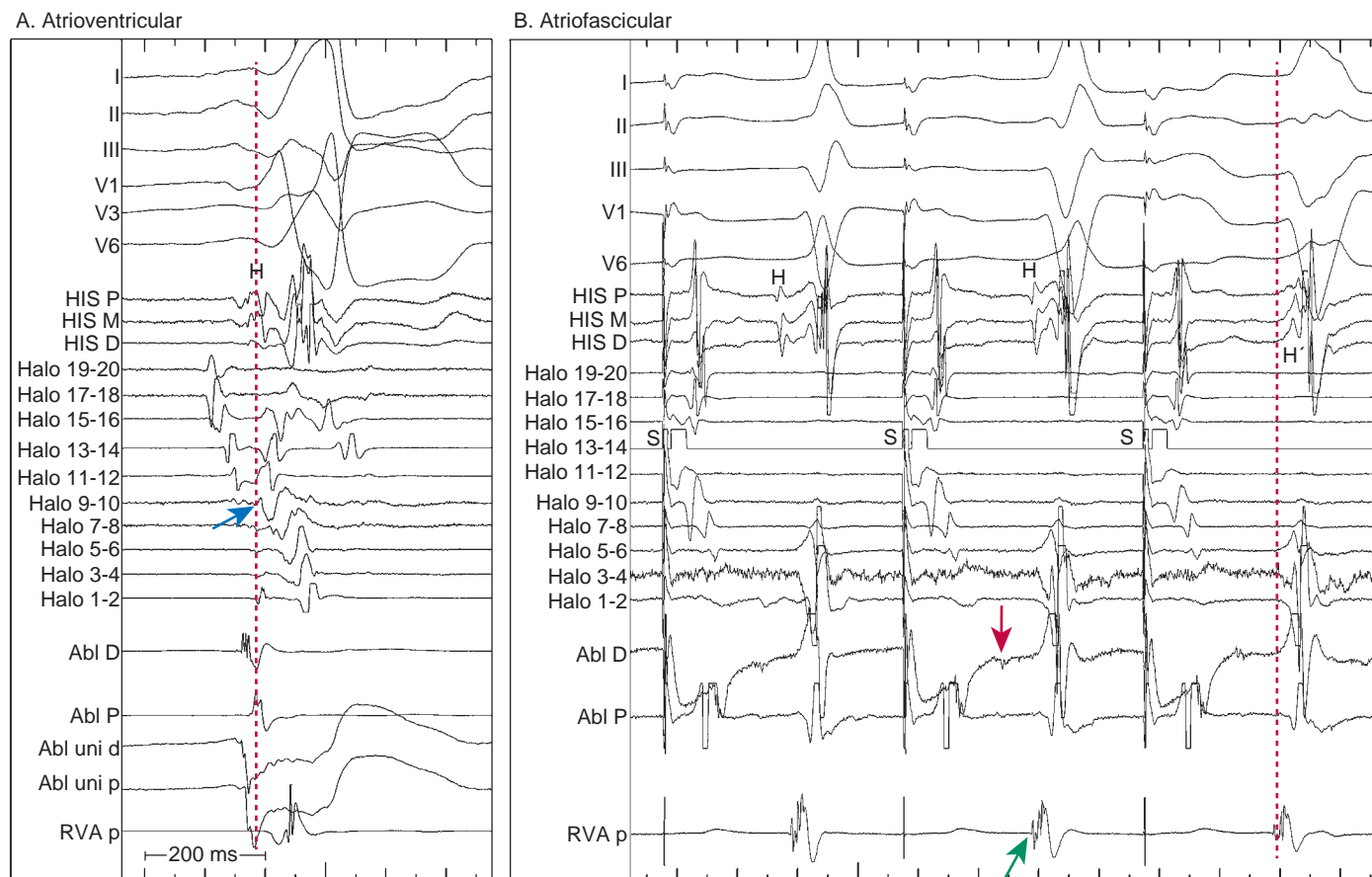


Fig. 19.4 Comparison of Atrioventricular and Atriofascicular Pathway Characteristics. Dashed red lines denote onset of preexcited QRS complexes. (A) Right anterolateral atrioventricular pathway. Note earliest ventricular activation during preexcitation at the lateral tricuspid annulus ("Halo 9-10," blue arrow, also noted on ablation [Abl] recordings), whereas the right ventricular apical (RVA) recording is much later. (B) Atriofascicular pathway; three complexes of atrial pacing (S) from the lateral tricuspid annulus are shown, with anterograde His potentials (H) on the first two (which show increasing degrees of preexcitation), then retrograde on the third (H'), since this complex is fully preexcited. Note that the earliest ventricular activation is now at the RVA, where a right bundle potential is seen (green arrow); ventricular activation at the annulus is later. An atriofascicular pathway potential is noted in the ablation recording (red arrow) from the annulus, but the local ventricular recording there follows the RVA recording.

Features of Tachycardia

Antidromic AVRT

Site of earliest ventricular activation. In the setting of atriofascicular, nodofascicular, and long decrementally conducting AV BTs, the earliest ventricular activation occurs at or near the RV apex. In contrast, for nodoventricular and short decrementally conducting AV BTs, the earliest ventricular activation occurs adjacent to the tricuspid annulus.

VH interval. For atriofascicular and nodofascicular BTs, the VH interval is short (16 ± 5 milliseconds), much shorter than the nonpreexcited HV interval and also shorter than the VH interval during ventricular pacing, because the BT inserts into the RB; hence the HB and ventricle are activated in parallel during antidromic AVRT but in sequence during ventricular pacing. Conduction time to the distal RB is short ($V\text{-RB} = 3 \pm 5$ milliseconds). For long decrementally conducting AV BTs, the VH interval is short (37 ± 9 milliseconds) but longer than that of atriofascicular BTs because the ventricle and HB are activated in sequence, not in parallel. In this setting, the VH interval approximates the HV interval minus the duration of the His potential because the BT inserts close to the RB and the His potential is activated retrogradely.

In the presence of long decrementally conducting AV BTs, conduction time to the distal RB ($V\text{-RB} = 25 \pm 6$ milliseconds) is longer than that for atriofascicular BTs. During antidromic AVRT using a nodoventricular or a short decrementally conducting AV BT, intermediate VH intervals are observed whereby the His potential is inscribed within the QRS. The VH interval during the AVRT is longer than the nonpreexcited HV interval as well as the VH interval during RV apical pacing, exceeding it by the time it takes the impulse to travel from the ventricular insertion site of the BT at the RV base to the distal RB (i.e., because of the long V-RB interval). When antidromic AVRT occurs in the presence of retrograde right bundle branch block (RBBB), the VH interval is long (the His potential is inscribed after the QRS and the VH interval is longer than the nonpreexcited HV interval). Retrograde block over the RB results in anterograde conduction over the distal RB (in the setting of atriofascicular BTs) or RV and transeptal impulse propagation with subsequent retrograde conduction over the left bundle branch (LB) into the HB and AVN. This results in an antidromic AVRT with a macroreentrant circuit incorporating the LB retrogradely and either an atriofascicular, a long decrementally conducting, or a short decrementally conducting AV BT anterogradely.

Atrioventricular relationship. For atriofascicular BTs, long decrementally conducting AV BTs, and short decrementally conducting AV BTs, a 1:1 A-V relationship is a prerequisite for the maintenance of antidromic AVRT, because parts of both the RA and the RV are critical components of the reentrant circuit. The AV interval is often more than 150 milliseconds due to the decremental conduction properties of the BT. However, in the setting of nodofascicular and nodoventricular BTs, the atrium is neither part of nor required for the reentrant circuit, and VA block or AV dissociation can (although rarely) be present without disrupting the SVT.

Response to drugs. These SVTs are very responsive to and are terminated easily with adenosine, calcium channel blockers, and beta-blockers.

Changes in TCL. Changes in the rate of antidromic AVRT using an atriofascicular or a long AV BT as the anterograde limb of the circuit can occur secondary to changes in the VA conduction time due to either retrograde RBBB or shift of retrograde conduction over a fast AVN pathway to conduction over a slow AVN pathway. Prolongation of the TCL reflects prolongation of the VH interval in the former setting but prolongation of the HA interval in the latter setting. In addition, VA conduction over the HB-AVN axis changing into VA conduction over a second BT can alter the TCL. When this occurs the change in the TCL will depend on the location of the ventricular insertion site of the second BT and the conduction properties of that BT. Therefore there can be a shortening or a prolongation of the TCL. The behavior of the V-RB and VH intervals in that situation will depend on where the block is located in the RB-HB-AVN axis.⁸

Response to RBBB. The development of RBBB (e.g., secondary to catheter-induced mechanical trauma or VES) during antidromic

AVRT increases the size of the reentrant circuit because the impulse cannot reach the HB through the RB, and it has to travel transeptally and then retrogradely over the LB. This results in prolongation in the VA interval and delay in the timing of the next atrial activation and, as a result, prolongation of the TCL. The increment in the VA interval occurs because of prolongation of the VH interval, while the HA interval remains constant.⁹

Diagnostic Maneuvers During Tachycardia

Programmed atrial stimulation during tachycardia

Resetting. To prove the presence of a BT and its participation in the SVT, a late-coupled AES is delivered from the lateral RA (close to the BT) when the AV junctional portion of the atrium is refractory (as indicated by the lack of advancement of local atrial activation in the HB or coronary sinus ostium [CS os] recording), so that the AES does not penetrate the AVN. This maneuver is analogous to the introduction of VES when the HB is refractory during orthodromic AVRT. If this AES resets (advances or delays) the timing of the next ventricular activation, it indicates that an anterogradely conducting AV or atriofascicular BT is present, and excludes nodoventricular and nodofascicular BTs. If the AES advances (or delays) the timing of the next ventricular activation and the advanced (or delayed) QRS morphology is identical to that during the SVT, this proves that the AV or atriofascicular BT also mediates preexcitation during the SVT, either as an integral part of the SVT circuit or as an innocent bystander (i.e., preexcited AVNRT). On the other hand, if the AES advances the timing of both the next ventricular activation and subsequent atrial activation, it proves that the SVT is an antidromic AVRT using an AV or atriofascicular BT anterogradely and excludes preexcited AVNRT (Fig. 19.5). Advancement of

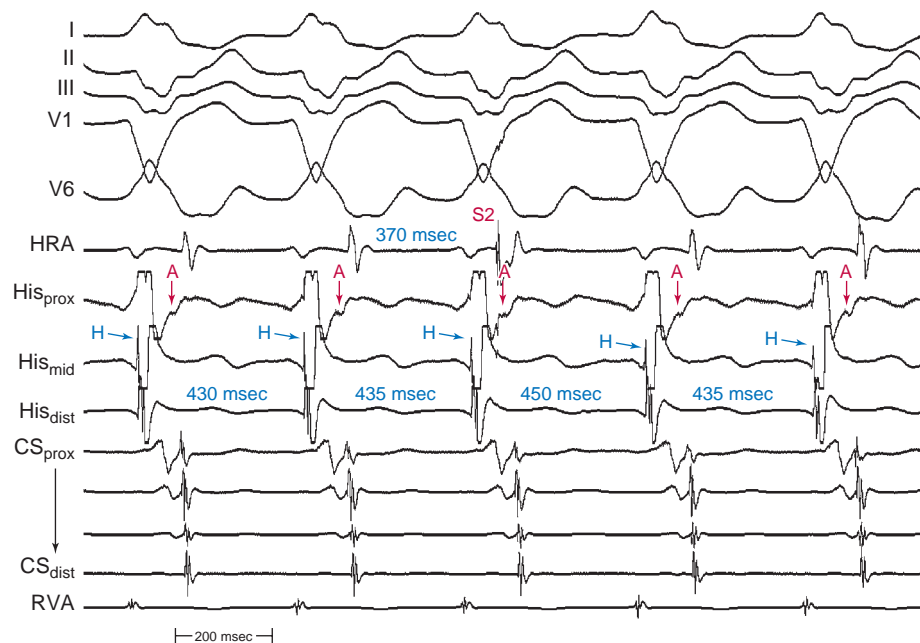


Fig. 19.5 Atrial Extrastimulation (AES) During Antidromic Atrioventricular Reentrant Tachycardia (AVRT) Using an Atriofascicular Bypass Tract. A late-coupled AES (S2) delivered from the right atrium (RA) when the AV junctional atrium is refractory (as evidenced by the failure of the AES to affect the timing of atrial activation recorded by the proximal His bundle and proximal coronary sinus electrodes) results in a delay in the timing of the next QRS ("postexcitation") as well as a delay in the timing of the following atrial activation. This confirms the diagnosis of antidromic AVRT and excludes preexcited atrioventricular nodal reentrant tachycardia and ventricular tachycardia as potential mechanisms of this wide QRS complex tachycardia. CS_{dist}, Distal coronary sinus catheter; CS_{prox}, proximal coronary sinus catheter; His_{dist}, distal His bundle; His_{prox}, proximal His bundle; HRA, high right atrial catheter; RVA, right ventricular apical.

both ventricular and atrial activation by such an AES requires anterograde conduction over the BT followed by retrograde conduction over the AVN. This can occur during antidromic AVRT but not in AVNRT because, in the setting of AVNRT, the HB would be refractory owing to anterograde activation by the time the advanced ventricular impulse invades the HPS retrogradely, with subsequent failure of the advanced ventricular activation to penetrate the HPS-AVN and affect the timing of subsequent atrial activation.⁹

Entrainment. During entrainment of the SVT by atrial pacing at a PCL slightly shorter than the TCL, the presence of a fixed short VH interval suggests antidromic AVRT but does not exclude AVNRT. Atrial pacing can usually terminate the SVT, whereby anterograde block is always produced in the AVN with or without block in the BT. A short-coupled AES can block in the BT, terminating the SVT (in the setting of antidromic AVRT) or changing the SVT to a narrow QRS complex SVT at the same CL and same HA interval (in the setting of preexcited AVNRT).

Programmed ventricular stimulation during tachycardia. Introduction of a VES during the SVT that results in RBBB can be of diagnostic value. During AVNRT, such RBBB will not change the time of the next atrial activation because the ventricle and HPS are not parts of the AVNRT circuit. Conversely, during antidromic AVRT, retrograde block in the RB increases the size of the reentrant circuit and, as a result, prolongs the VH and VA intervals as well as the TCL.

Ventricular pacing can usually terminate the SVT. Termination occurs by retrograde invasion and concealment in the BT, resulting in anterograde block over the BT following conduction to the atrium through the AVN.

Differential Diagnosis

The goal of programmed electrical stimulation during SVT is evaluation of the relationships between the His potential, the QRS, and the VH interval during atrial pacing and during SVT and differentiation between the different types of atypical BTs (Box 19.1 and Fig. 19.6). In addition, exclusion of a separate BT is necessary, especially if a rapid and fixed VA interval exists during incremental rate ventricular pacing. Furthermore, it is important to differentiate between antidromic AVRT using the BT anterogradely and preexcited AVNRT, in which the BT is a bystander (Box 19.2).¹⁰

Mapping

Mapping principles for typical AV BTs—searching for sites with the earliest atrial activation during retrograde BT conduction and earliest ventricular activation during anterograde BT conduction—are largely inapplicable in the case of atypical BTs because of their unusual course and conduction properties. Therefore different approaches are employed.

Mapping of the ventricular insertion site of atriofascicular and long decrementally conducting AV BTs is difficult because of the long intra-cardiac course and distal insertion of these BTs, which shows extensive arborization over a wide area of ventricular muscle with a diameter of up to 0.5 to 2 cm. A propensity to temporary loss of conduction of the atypical BT because of catheter trauma further complicates ventricular mapping.

Since the majority of atypical BTs conduct anterogradely only, mapping of the atrial insertion site can be challenging but can be performed by (1) P-delta interval mapping by stimulation at different atrial

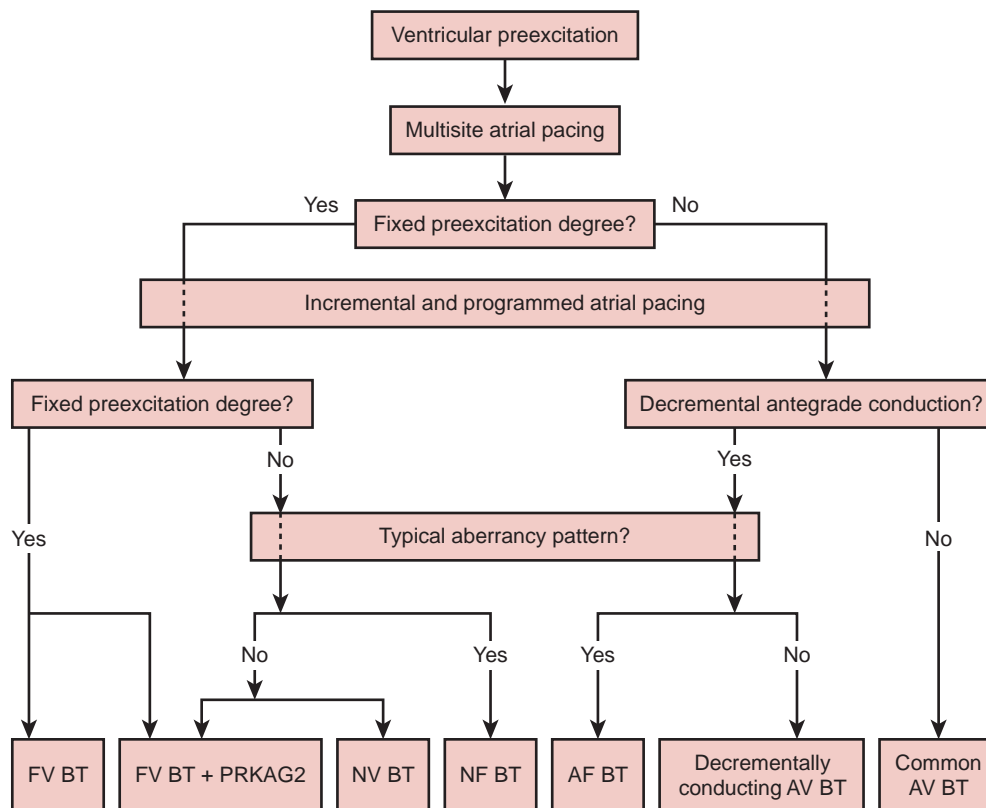


Fig. 19.6 Diagnostic Algorithm for Various Patterns of Preexcitation. AF, Atriofascicular; AV, atrioventricular; BT, bypass tract; FV, fasciculoventricular; NF, nodofascicular; NV, nodoventricular. (From Ali H, Sorgente A, Lupo P, et al. Nodo- and fasciculoventricular pathways: electrophysiological features and a proposed diagnostic algorithm for preexcitation variants. *Heart Rhythm*. 2015;12:1677–1682.)

BOX 19.1 Differentiation Among Different Types of Atypical BTs**Preexcited QRS Morphology**

- Atriofascicular BTs: The QRS is relatively narrow (133 ± 10 msec) and is classic for typical LBBB morphology.
- Long decrementally conducting AV BTs: The QRS is wider (166 ± 26 msec) and the LBBB pattern is less typical (with broad initial R in V1) than that with atriofascicular BTs.
- Nodofascicular BTs: Same as for atriofascicular BTs.
- Nodoverricular BTs: The QRS is significantly wider and the LBBB pattern is less typical than that with atriofascicular or long decrementally conducting AV BTs.
- Short decrementally conducting AV BTs: The QRS is significantly wider and the LBBB pattern is less typical than that with atriofascicular or long decrementally conducting AV BTs.

Site of Earliest Ventricular Activation

- Atriofascicular BTs: The earliest ventricular activation occurs at or near the RV apex.
- Long decrementally conducting AV BTs: The earliest ventricular activation occurs at or near the RV apex.
- Nodofascicular BTs: The earliest ventricular activation occurs at or near the RV apex.
- Nodoverricular BTs: The earliest ventricular activation occurs adjacent to the tricuspid annulus.
- Short decrementally conducting AV BTs: The earliest ventricular activation occurs adjacent to the tricuspid annulus.

Influence of Site of Atrial Stimulation

- Atriofascicular BTs: Preexcitation increases when atrial stimulation is performed closer to the atrial insertion site.
- Long decrementally conducting AV BTs: Preexcitation increases when atrial stimulation is performed closer to the atrial insertion site.
- Nodofascicular BTs: The degree of preexcitation is not influenced by the site of atrial stimulation.
- Nodoverricular BTs: The degree of preexcitation is not influenced by the site of atrial stimulation.
- Short decrementally conducting AV BTs: Preexcitation increases when atrial stimulation is performed closer to the atrial insertion site.

AES Delivered From Lateral RA During Antidromic AVRT When AV Junctional Atrium Is Refractory

- Atriofascicular BTs: The AES can advance or delay the next ventricular activation.

- Long decrementally conducting AV BTs: The AES can advance or delay the next ventricular activation.
- Nodofascicular BTs: The AES cannot advance the next ventricular activation.
- Nodoverricular BTs: The AES cannot advance the next ventricular activation.
- Short decrementally conducting AV BTs: The AES can advance or delay the next ventricular activation.

VH Interval During Maximal Preexcitation or Antidromic AVRT

- Atriofascicular BTs: The VH interval is short (VH interval = 16 ± 5 msec and V-RB interval = 3 ± 5 msec; VH interval < HV interval and < VH interval during RV pacing).
- Long decrementally conducting AV BTs: The VH interval is short but longer than that with atriofascicular BTs (VH interval = 37 ± 9 msec and V-RB interval = 25 ± 6 msec).
- Nodofascicular BTs: The VH interval is short, as for atriofascicular BTs.
- Nodoverricular BTs: The VH interval is intermediate (His potential is inscribed in the QRS, VH interval \geq HV interval; VH interval > HV interval and > VH interval during RV pacing).
- Short decrementally conducting AV BTs: The VH interval is intermediate, as for nodoverricular BTs.
- Antidromic AVRT in presence of retrograde RBBB: The VH interval is long (His potential is inscribed after the QRS, VH interval > HV interval).

Presence of VA Block or AV Dissociation

- VA block or AV dissociation during the SVT excludes atriofascicular, short decrementally conducting AV BTs, and long decrementally conducting AV BTs but does not exclude nodofascicular and nodoverricular BTs.

Effects of Adenosine

- Adenosine produces conduction delay in most atypical BTs (except for short decrementally conducting BTs).
- When adenosine administration slows AVN conduction but not the BT, an increase in the degree of preexcitation is noted in all types of BTs except for fasciculoventricular BTs, whereby the degrees of preexcitation and HV interval remain fixed.

AES, Atrial extrastimulation; AV, atrioventricular; AVN, atrioventricular node; AVRT, atrioventricular reentrant tachycardia; BT, bypass tract; HV, His bundle–ventricular; LBBB, left bundle branch block; RA, right atrium; RBBB, right bundle branch block; RV, right ventricle; SVT, supraventricular tachycardia; VA, ventriculoatrial; VH, ventricular–His bundle; V-RB, ventricular–right bundle branch.

sites, (2) recording of the BT potential at the tricuspid annulus, and (3) AES from the RA during antidromic AVRT.⁴

Careful mapping of the tricuspid annulus and the anterior free wall of the RV typically demonstrates discrete potentials with complexes comparable to those recorded at the AV junction. The BT potential is analogous to the His potential. Atrial pacing, AES, and adenosine produce delays proximal to the BT potential with a constant BT potential to the QRS (BT–V) interval. Faster atrial pacing produces Wenckebach block proximal to the BT potential.

Mapping the Atrial Insertion Site

Mapping the shortest atrial stimulus to the delta (S–V) interval. The mapping catheter is advanced from site to site along the atrial

aspect of the tricuspid annulus while pacing from its distal tip. The resulting interval between the stimulus and the onset of the delta wave (S–V interval) should decrease progressively as the BT atrial insertion site is approached and increase as it is passed. Thus the atrial pacing site associated with the shortest S–V interval is the site closest to the BT atrial insertion site. It is essential that pacing at different sites be performed at a constant PCL to avoid rate-dependent conduction slowing in the BT as a reason for changing the S–V interval.

This method is rarely used because of several limitations: (1) a constant distance of the mapping-pacing catheter from the tricuspid annulus must be maintained to reduce the influence of the time spent traversing intervening atrial tissue; (2) catheter manipulation during pacing can result in initiation of tachycardia, which must then be

BOX 19.2 Differentiation Between Antidromic AVRT and Preexcited AVNRT Using an Atypical BT

SVT Induction

- Induction of the SVT by ventricular pacing at a CL similar to the TCL, or by a VES that advances the His potential by a coupling interval similar to the H-H interval during the SVT; the HA interval following such a ventricular stimulus is compared with that during the SVT:
- $HA_{VES} > HA_{SVT}$ is diagnostic of AVNRT and excludes antidromic AVRT.
- $HA_{VES} \leq HA_{SVT}$ is diagnostic of antidromic AVRT and excludes AVNRT.

Features of the SVT

- Positive HV interval or VH interval ≤ 10 msec (especially when HA interval is ≤ 50 msec) suggests AVNRT.
- Continuation of the SVT at the same TCL despite anterograde block in the BT (by extrastimuli, drugs, mechanical trauma caused by catheter manipulation, or ablation) is consistent with AVNRT and excludes antidromic AVRT.
- Termination of the SVT or prolongation of the VA (and VH) interval and TCL with transient RBBB (caused by mechanical trauma or introduction of VES) is consistent with antidromic AVRT and excludes AVNRT.

AES Delivered From Lateral RA When AV Junction Is Refractory

- If the AES advances the timing of both the following ventricular activation and the subsequent atrial activation, it proves that the SVT is an antidromic AVRT using an AV or atriofascicular BT anterogradely and excludes preexcited AVNRT.

Entrainment of the SVT With Atrial Pacing

- The presence of a fixed short VH interval during entrainment of the SVT with atrial pacing favors antidromic AVRT over AVNRT (but does not exclude AVNRT).

RV Apical Pacing During NSR

- RV apical pacing at the TCL is performed and the HA interval during RV apical pacing versus the HA interval during SVT are compared:
- $HA_{SVT} < HA_{\text{pacing}}$ is diagnostic of AVNRT and excludes antidromic AVRT.
- $HA_{SVT} \geq HA_{\text{pacing}}$ is diagnostic of antidromic AVRT and excludes AVNRT.

AES, Atrial extrastimulation; AV, atrioventricular; AVNRT, atrioventricular nodal reentrant tachycardia; AVRT, atrioventricular reentrant tachycardia; BT, bypass tract; CL, cycle length; HA, His bundle–atrial; HV, His bundle–ventricular; NSR, normal sinus rhythm; RA, right atrium; RBBB, right bundle branch block; RV, right ventricle; SVT, supraventricular tachycardia; VA, ventriculoatrial; VES, ventricular extrastimulation; VH, ventricular–His bundle.

terminated to continue mapping; (3) optimal sites can be overlooked if they cannot be consistently paced because of unstable catheter contact; and (4) this method cannot be applied in the setting of incessant tachycardia or when AF is present.

AES mapping during supraventricular tachycardias. The BT atrial insertion site is close to the site from which the longest coupled AES delivered during preexcited tachycardia advances the timing of the next ventricular activation. Alternatively, the BT atrial insertion site is close to the site from which the greatest amount of advancement of the next ventricular activation occurs when using a fixed AES coupling interval.

This method is rarely used because of several limitations: (1) it is time-consuming; (2) it cannot be used if the SVT is difficult to initiate,

is nonsustained, or is irregular (such that spontaneous changes in AV intervals confuse the assessment); (3) a constant distance of the mapping-pacing catheter from the tricuspid annulus must be maintained to reduce the influence of the time spent traversing intervening atrial tissue; and (4) optimal sites can be overlooked if they cannot be consistently paced because of unstable catheter contact.

Mapping the Ventricular Insertion Site

Mapping the distal fascicular insertion site (for atriofascicular BTs). The distal insertion site of atriofascicular BTs can be localized by careful mapping along the lateral RV wall toward the apex, seeking the earliest site of ventricular activation during anterograde BT conduction (Fig. 19.7). A distal RB recording is usually present at this site. This method can be used to map any rhythm during which consistent preexcitation is present (atrial pacing, AF, and preexcited SVT). However, seeking the distal insertion is less precise because a distal RB recording may be localized, but not the portion into which the atriofascicular fiber inserts. It is most useful if the course of the atriofascicular BT can be traced from the tricuspid annulus to its insertion into the RB. In addition, ablation at the distal site offers no advantage unless catheter stability is better at that location as opposed to the tricuspid annulus. If the RB is ablated rather than the BT, RBBB will result. This will not only fail to eliminate the BT function but can also facilitate induction and maintenance of the SVT by increasing the size of the reentry circuit. This may be the only usable method in the presence of intractable AF, in which annular BT potentials are not readily distinguished from fibrillatory atrial signals.⁴

Mapping the distal ventricular insertion site (for slowly conducting AV BTs). Mapping is performed in the same fashion as for typical rapidly conducting AV BTs—seeking the ventricular site with the earliest unipolar or bipolar ventricular electrogram recording. However, there is evidence that a variable degree of arborization of the distal insertion site occurs in some patients. This feature makes the ventricular insertion site a less attractive ablation target because of the potential of requiring ablation of a relatively large amount of ventricular myocardium to be effective.

Mapping the Bypass Tract Potential

Direct recording of the BT potential at the tricuspid annulus is the most precise and preferred method of localizing the atypical BT. Mapping is performed during preexcited rhythm (typically during RA pacing or preexcited SVT). The BT potential is usually a low-amplitude, high-frequency recording made at the tricuspid annulus (*Mahaim* or *M potential*), which resembles a His potential (Figs. 19.4 and 19.8). Only the annular and subannular portions of the BT have been successfully recorded; attempts to record potentials from the atrial portion (corresponding to nodal-like tissue) have been unsuccessful. Distinct atrial, BT, and ventricular potentials can be found near the BT atrial insertion along the tricuspid annulus. Local ventricular activation at this location is delayed, occurring after the QRS onset, since ventricular activation starts close to the RV apex.

However, recording of a BT potential along the tricuspid annulus may not be successful in up to 48% of cases. Furthermore, because of its low amplitude, the BT potential can be difficult to visualize during AF. In addition, this technique presents the risk of producing mechanical block in the BT. Nevertheless, this method is less time-consuming and more precise than the previous ones.

Mapping Sites of Mechanically Induced Loss of Preexcitation

Atypical BTs are particularly sensitive to mechanical trauma, and catheter manipulation along the tricuspid annulus during mapping of the BT

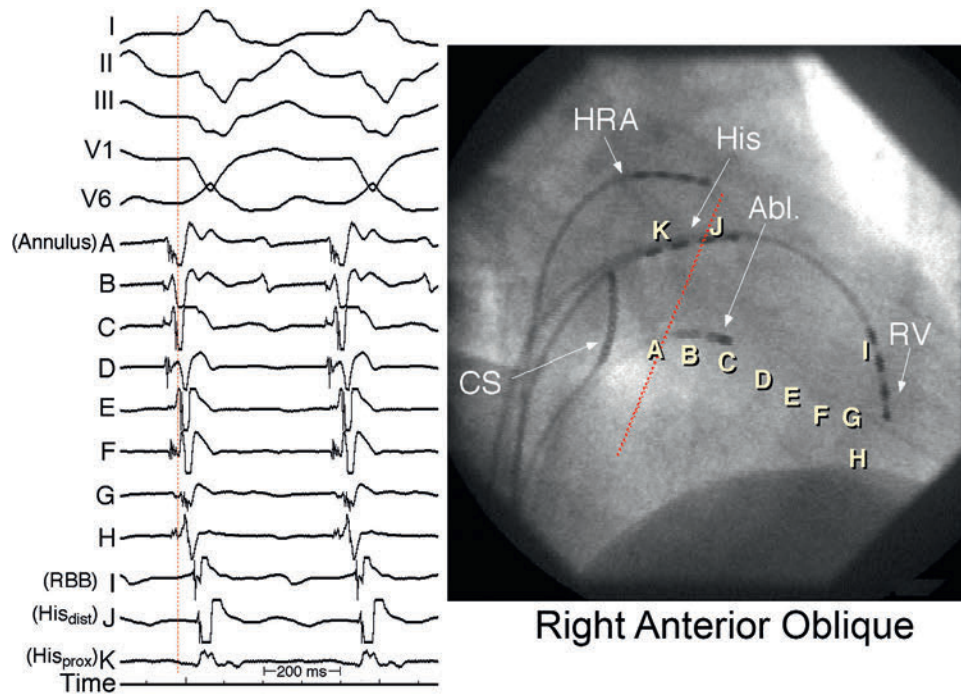


Fig. 19.7 Anatomical Course of the Atriofascicular Pathway. Two complexes of antidromic tachycardia using an atriofascicular pathway are shown (red dashed line denotes onset of QRS complex). Letters on electrogram lines correspond to locations shown in the fluoroscopic image at right. *Abl.*, Ablation catheter; *CS*, coronary sinus catheter; *His_{dist}*, distal His bundle; *His_{prox}*, proximal His bundle; *HRA*, high right atrial catheter; *RBB*, right bundle branch; *RV*, right ventricular catheter.

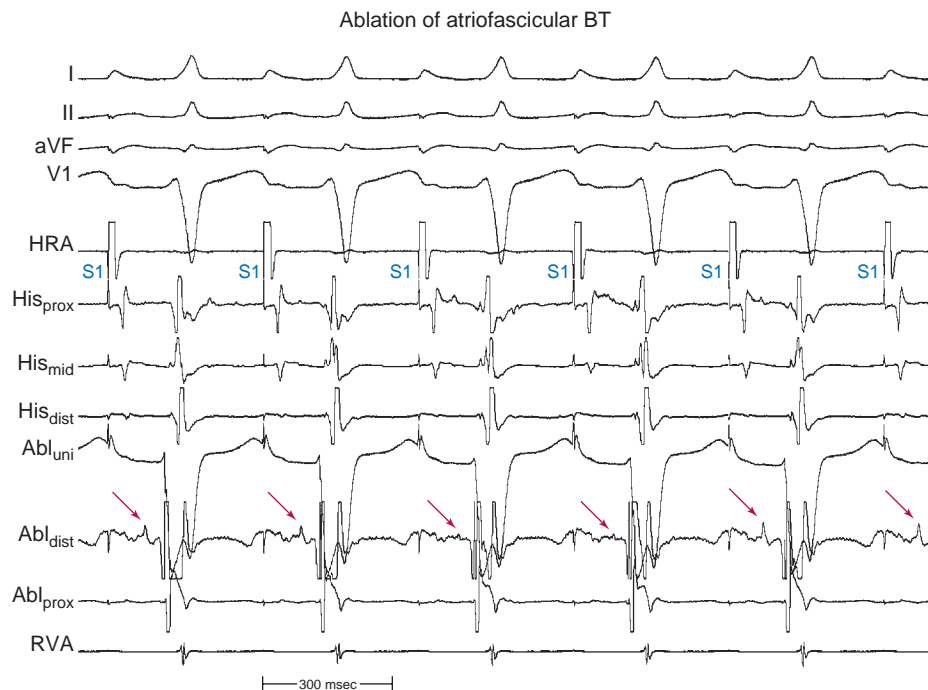


Fig. 19.8 Ablation of an Atriofascicular Bypass Tract (BT). A discrete potential (arrows) is shown in the ablation recording during atrial pacing, with a small His potential occurring just after the onset of the pre-excited QRS. Ablation at this site eliminated this BT in 2 seconds. *Abl_{dist}*, Distal ablation catheter; *Abl_{prox}*, proximal ablation catheter; *His_{dist}*, distal His bundle; *His_{prox}*, proximal His bundle; *HRA*, high right atrial catheter; *RVA*, right ventricular apical.

can result in loss of BT function, even as a result of gentle pressure from the catheter tip. Atriofascicular BTs are more susceptible to mechanically induced block, probably suggesting that these BTs are composed of thinner strands or are located closer to the endocardium. When mapping is performed during preexcited atrial pacing or SVT, damage to the BT is indicated by a sudden loss of preexcitation or SVT termination. This phenomenon can be used to localize the BT precisely (“bump mapping”). Conduction block typically occurs while a BT potential is still recorded; thus conduction is interrupted within the ventricular course of the BT. Block usually lasts from a few beats to a few minutes but can last for hours, after which preexcitation resumes. This method can be used during any consistently preexcited rhythm (atrial pacing, AF, and antidromic AVRT). However, if it occurs during antidromic AVRT, termination of the tachycardia can result in catheter displacement and loss of the exact location of the BT. In addition, interruption of BT conduction can occur as the catheter is moving past the area, and where the catheter comes to rest may not be the same site as where loss of BT function occurred; in this situation, the target cannot be relocated until BT conduction resumes.

Delivery of RF energy at a site at which catheter pressure caused loss of preexcitation may successfully eliminate conduction in the BT; however, it is best to wait to deliver energy until preexcitation resumes because of the possibility that the catheter position may have changed. Electroanatomic mapping systems can help tag sites of interest, facilitating precise relocation of the ablation catheter to these sites if it has been determined that these are good ablation targets.

Adenosine (likely due its hyperpolarizing effects on atrial and BT tissues) can transiently restore conduction through the injured BT secondary to mechanical trauma or partially successful ablation. This can facilitate intermittent mapping during the transient adenosine effect but can require repeated drug administration.¹¹

Ablation

Target of Ablation

For atriofascicular and long AV BTs, direct recording of the BT potential at the tricuspid annulus is the most precise and preferred method of localizing the BT and serves as the target of ablation (Fig. 19.8). A three-component electrogram, including an atrial component, a BT (M) potential and a ventricular component, can frequently be identified near the BT atrial insertion along the tricuspid annulus. The local AV interval is usually longer than the surface VA interval because ventricular activation starts close to the RV apex, so that the local ventricular activation at the annular portion of the BT occurs after QRS onset. A specific BT potential can be recorded in about two-thirds of cases, typically along the right lateral, posterolateral, and anterolateral tricuspid annulus.

When a BT potential along the tricuspid annulus cannot be recorded, ablation of the proximal (atrial) or distal (ventricular) insertion sites of atriofascicular BTs becomes an alternative. Those approaches, however, are complex and less successful; they also often require time-consuming mapping (as discussed previously) and a larger number of RF lesions. Ablation at the ventricular insertion site of the BT offers no advantage over targeting the atrial insertion site because there is evidence that a variable degree of arborization of the distal insertion site occurs in some patients, with the potential of requiring ablation of a relatively large amount of ventricular myocardium to be effective. In addition, ablation of the ventricular insertion site is commonly (57%) associated with the development of RBBB. Ablation of the RB can carry a proarrhythmic effect and facilitate induction of the SVT or cause incessant tachycardia; however, this is not a concern as long as the BT itself is also successfully ablated.⁴

Catheter ablation of the AVN fast pathway, serving as the retrograde route of antidromic AVRT, had been reported as a therapeutic alternative. This, however, is associated with a significant risk of complete AV block and is not recommended.¹²

Ablation Technique

Once an appropriate target site for ablation has been identified, RF energy may be applied during NSR, atrial pacing, or antidromic AVRT. Atrial pacing is preferred to ensure that adequate preexcitation is evident (unlike NSR) to be able to assess the efficacy of ablation, and that the rhythm remains the same after elimination of preexcitation (unlike antidromic AVRT) to prevent catheter dislodgment.⁴

The use of long preshaped or steerable sheaths can help achieve good catheter positioning and stability along the tricuspid annulus. Typical RF settings consist of a maximal power of 50 W and a maximal temperature of 55°C to 60°C, continued for 30 to 60 seconds after elimination of the BT function (i.e., after disappearance of preexcitation). During RF energy delivery, an accelerated preexcited rhythm is often observed. This so-called *Mahaim automatic tachycardia* is analogous to the accelerated junctional rhythm observed during AVN modification and is presumably secondary to heating-related automaticity of nodal-like tissue of the BT. Accelerated automatic beats during RF ablation have been considered a marker of a successful result and should not be misinterpreted as an inaccurate location but rather should prompt continuation of RF energy delivery for a sufficient duration after termination of this rhythm. Heat-induced automaticity during RF ablation is observed less commonly in short, decrementally conducting AV BTs as compared with atriofascicular BTs (50% vs. 91%).

A recent report found cryoablation to be a reliable and effective alternative to RF ablation in the treatment of atriofascicular BTs in children.¹³

Endpoints of Ablation

Complete loss of BT function, not just noninducibility of tachycardias, is an essential endpoint. BT block is confirmed by demonstrating loss of preexcitation with atrial pacing and AES and noninducibility of AVRT. Atrial stimulation should be performed at sites and rates that were associated with preexcitation before ablation.

Outcome

The acute success rates for ablation of atriofascicular BTs range between 68% and 90%, with long-term recurrence rates of about 10% and 15%.¹²

NODOFASCICULAR AND NODOVENTRICULAR BYPASS TRACTS

Nodoventricular/nodofascicular BTs arise in the normal AVN and insert into ventricular myocardium near the para-Hisian region (nodoventricular) or into the RB (nodofascicular). The hallmark of nodofascicular/nodoventricular BTs is their infra-atrial nature. Unlike other atypical BTs, nodofascicular/nodoventricular BTs can exhibit anterograde-only, bidirectional, or retrograde-only (concealed) conduction (Box 19.1 and Fig. 19.6).¹⁴

Arrhythmias Associated With Nodofascicular and Nodoventricular Bypass Tracts

Nodoventricular or nodofascicular BTs can participate as the retrograde limb of orthodromic AVRT (“nodofascicular reentrant tachycardia”). However, only rare reports have implicated these BTs as the anterograde limb of antidromic AVRT unless another AV BT (rather than the HB) serves as the retrograde limb.¹⁵

Electrocardiographic Features

Nodofascicular/nodoventricular BTs commonly present with minimal preexcitation. During ventricular preexcitation mediated via manifest nodofascicular BTs, the QRS is relatively narrow (133 ± 10 milliseconds), and its morphology is classic for typical LBBB with a QRS axis between 0 and -75 degrees and a late precordial R/S transition zone at lead V_4 or beyond (similar to atriofascicular BTs). A monophasic R wave, in lead I and rS pattern in lead V_1 are typically observed. The QRS is wider and the LBBB pattern is less typical with nodoventricular BTs than that with nodofascicular BTs.⁷

Electrophysiological Testing

Baseline Observations During Sinus Rhythm

Nodofascicular/nodoventricular BTs are not totally infranodal, but they bypass only a portion of the AVN with decremental conduction properties. Consequently, the atrial impulse has to propagate through the proximal portion of the AVN, which underlies the “decremental” conduction properties of these BTs and their exquisite “AVN-like” sensitivity to isoproterenol and adenosine. Therefore only minimal preexcitation is usually apparent during NSR. In addition, atrial stimulation with progressively shorter PCL or AES coupling intervals causes progressive prolongation of the atrial stimulus-delta (S-delta) interval. As a result, the degree of preexcitation can change and the HV interval can decrease even to negative values. This phenomenon usually necessitates a significant AH prolongation to dissociate the anterograde conduction over the nodofascicular/nodoventricular BT and the distal portion of the AVN and consequently to change the degree fusion and preexcitation. The more proximal the emergence level of the BT from the AVN, the more evident this feature, and vice versa.¹⁶

Characteristically, the site of atrial stimulation does not influence the degree of preexcitation in the setting of nodofascicular and nodoventricular BTs (similar to fasciculoventricular BTs). In contrast, preexcitation becomes more prominent when atrial stimulation is performed closer to the atrial insertion site of AV or atriofascicular BTs.

The presence of preexcited junctional beats (originating proximally, such as those during ablation of the slow AVN pathway) excludes AV and atriofascicular BTs and favors the diagnosis of an fasciculoventricular or nodofascicular/nodoventricular BT. Conversely, junctional beats originating from the proximal HB cause normalization of the HV interval and QRS morphology in the setting of nodofascicular/nodoventricular BTs but maintain an identical degree of preexcitation in the presence of a fasciculoventricular BT.¹⁶

Tachycardia Features

In the setting of orthodromic AVRT utilizing a nodofascicular or nodoventricular BT, both atrial and ventricular activation is mediated by the normal AVN-HPS. The QRS complex is narrow since the AVN-HPS forms the anterograde limb of the tachycardia circuit. Furthermore, retrograde activation is mediated initially by the BT, which then inserts within the AVN, and the upper turnaround point of the reentry circuit is subatrial. For atrial activation to occur, the tachycardia wavefront has to travel retrogradely over the upper portion of the AVN. Hence the earliest atrial activation occurs at the insertion of the AVN fast (or slow) pathway.

For nodofascicular and nodoventricular BTs, the atrium is neither part of nor required for the reentrant circuit, and VA block or AV dissociation can be present without disrupting the SVT. This is in contrast to AVRT utilizing AV or atriofascicular BTs, whereby a 1:1 AV relationship is critical for continuation of the tachycardia.

Diagnostic Maneuvers During Tachycardia

Nodofascicular reentrant tachycardia shares many features with orthodromic AVRT using an AV BT as the retrograde limb of the circuit, and

BOX 19.3 Differentiation Between Nodofascicular Reentrant Tachycardia and Orthodromic AVRT Using an AV BT

Diagnostic Maneuvers During NSR

- Progressive prolongation of the atrial stimulus-delta (S-delta) interval during atrial stimulation with progressively shorter PCL or AES coupling intervals is consistent with nodofascicular/nodoventricular BTs.
- The degree of ventricular preexcitation in the setting of nodofascicular and nodoventricular BTs is not influenced by the site of atrial stimulation. In contrast, preexcitation becomes more prominent when atrial stimulation is performed closer to the atrial insertion site of AV BTs.
- The presence of preexcited junctional beats excludes AV BTs and favors the diagnosis of an fasciculoventricular or nodofascicular/nodoventricular BT.

Diagnostic Maneuvers During SVT

- VA block or AV dissociation during the SVT suggests that nodofascicular and nodoventricular BTs exclude AV BTs.
- Dissociation of the atrium from the tachycardia during atrial pacing maneuvers suggests that nodofascicular and nodoventricular BTs exclude AV BTs.
- ΔAH interval ($AH_{\text{pacing}} - AH_{\text{SVT}}$) > 40 msec favors nodofascicular reentrant tachycardia.
- AVN/AVN response pattern during para-Hisian pacing favors a nodofascicular BT.
- Manifest ventricular fusion during RV apical pacing argues against a nodofascicular BT and favors nodoventricular and AV BTs.

AES, Atrial extrastimulation; AH, atrial–His bundle; AV, atrioventricular; AVN, atrioventricular node; AVRT, atrioventricular reentrant tachycardia; BT, bypass tract; HA, His bundle–atrial; NSR, normal sinus rhythm; PCL, pacing cycle length; RV, right ventricular; SVT, supraventricular tachycardia.

similar maneuvers are utilized to identify the presence of a retrogradely conducting BT and its participation in the reentrant circuit (see Boxes 18.3 and 18.4). However, a few differences exist, which are helpful in identifying the presence of a nodofascicular/nodoventricular BT (Box 19.3). Most importantly, the nodofascicular reentrant tachycardia circuit is completely subatrial; therefore the atrium can be dissociated from the tachycardia circuit by pacing maneuvers. In addition, because of the parallel activation of the atrium and HB during nodofascicular reentrant tachycardia (since the tachycardia circuit is subatrial), the AH interval during tachycardia is shorter than the AH interval during atrial pacing. In contrast, the AH interval during orthodromic AVRT utilizing an AV BT approximates that during atrial pacing, given similar sequential activation of the atrium and HB in both settings. As a result, the ΔAH interval ($AH_{\text{pacing}} - AH_{\text{SVT}}$) during nodofascicular reentrant tachycardia can be longer than 40 milliseconds, as occurs with AVNRT, but it is less than 40 milliseconds in orthodromic AVRT utilizing an AV BT. The ΔAH interval criterion is especially helpful to distinguish nodofascicular reentrant tachycardia from PJRT. Moreover, a nodofascicular BT can show an AVN/AVN response pattern with para-Hisian pacing, especially if it originates from the proximal branch of the RB. In such a case, the SA interval with direct HB-RB capture would be shorter than during pure myocardial capture where the RB is retrogradely activated.¹⁷

Of note, slow, decremental BT conduction can affect the sensitivity of the postpacing interval (PPI)–TCL, ΔVA and ΔHA criteria for orthodromic AVRT, although the specificity of these criteria remains high. Long PPIs are common and a [PPI–TCL] less than 125 milliseconds

seems better than a cutoff of 115 milliseconds for differentiating orthodromic AVRT (PJRT and nodofascicular reentrant tachycardia) from atypical AVNRT. In a recent report, any standard criterion positive for orthodromic AVRT ([PPI–TCL] < 115 milliseconds, corrected [PPI–TCL] < 110 ms, Δ VA < 85 milliseconds, and Δ HA < 0 milliseconds) was found to be diagnostic of orthodromic AVRT despite discordance between them, which occurred 50% of the time.¹⁷

Resetting of the SVT with a VES delivered when the HB is refractory can help to identify the presence of nodofascicular/nodoventricular BTs. Not infrequently, such a VES causes a delay in the next atrial activation in the setting of slow or decremental BT mediating retrograde conduction during SVT, which confirms the diagnosis of orthodromic AVRT (similar to PJRT). The degree of the delay depends on the relative prematurity of the VES compared with the degree of BT conduction delay.^{17,18}

Manifest ventricular fusion can be demonstrated during RV entrainment of orthodromic AVRT using a nodoventricular BT. However, in the setting of a nodofascicular BT, the tachycardia circuit is contained within the specialized conduction system; hence manifest ventricular fusion may not be demonstrable.¹⁷

Mapping

Mapping the BT potential at the midseptum has been reported, but a distinct BT potential is usually difficult to differentiate from the RB potential. Alternatively, the BT distal insertion can be mapped using VES or ventricular entrainment. The distal insertion site of the BT is identified as the site where maximum advancement of the His potential can be achieved with a single VES (with a fixed coupling interval) during orthodromic tachycardia or at the site where the shortest PPI (during concealed entrainment) occurs with the shortest stimulus-to-His (VH) interval can be demonstrated.

Ablation

For nodofascicular and nodoventricular BTs, ablation targets the site where the BT potential is recorded or, alternatively, the BT distal insertion site. The initial ablation target is typically located in the AVN slow pathway region (between the CS os and tricuspid annulus). Ablation in the midseptum or floor of the CS may be required.¹⁴ Importantly, RF ablation of nodofascicular/nodoventricular pathways is associated with an increased risk of AV block. Cryoablation offers significant safety advantage in these cases.

FASCICULOVENTRICULAR BYPASS TRACTS

General Considerations

Fasciculoventricular BTs are among the rarest forms of preexcitation (1.2% to 5.1% of atypical BTs). They connect the HB to ventricular myocardium in the anterosseptal location; this is likely due to a gap in, or absence of, the usually present fibrous sheath that insulates the HB from adjacent myocardium. These fibers do not give rise to any reentrant tachycardia and appear to be only an ECG and EP curiosity. Even during AF and AFL, a rapid ventricular response is not expected in the presence of a normal AVN proximal to the BT (Box 19.1 and Fig. 19.6). However, it is important to distinguish fasciculoventricular BTs from superoparaseptal AV BTs to avoid unnecessary invasive EP procedures and potential harm to the AVN–HB if such a BT is mistakenly targeted by ablation because this form of preexcitation does not require treatment.¹⁶

Of note, a rare form of familial fasciculoventricular BTs has been reported in association with mutations in the *PRKAG2* gene (which encodes the gamma-2 regulatory subunit of the adenosine monophosphate [AMP]–activated protein kinase). These patients have a high

incidence of syncope, cardiac arrest, ventricular hypertrophy, atrial arrhythmias, sinus bradycardia, and complete AV block; therefore they should be distinguished from those without structural heart disease.^{16,19}

Electrocardiographic Features

In patients with fasciculoventricular BTs, preexcitation is always present during NSR. The ECG preexcitation pattern can mimic that of manifest WPW pattern, especially that of superoparaseptal AV BTs, with a normal frontal plane axis between 0 and 75 degrees and precordial RS transitional zone in leads V₂–V₃. With fasciculoventricular BTs, the PR interval is normal despite the presence of preexcitation (Fig. 19.9). This is in contrast to superoparaseptal AV BTs, which result in the WPW pattern with significant shortening of the PR interval because of the relative proximity of the BT location to the sinus node.

Several ECG findings in lead V₁ favor fasciculoventricular BTs as the cause of preexcitation, including (1) a PR interval longer than 110 milliseconds, (2) R wave width less than 35 milliseconds, (3) S wave amplitude less than 20 mm, (4) a flat or negative delta wave, and (5) notching in the descending limb of the S wave (Fig. 19.9).

Electrophysiological Testing

Baseline Observations During Sinus Rhythm

With fasciculoventricular BTs, preexcitation is present during NSR with a normal AH interval and fixed and short but positive HV interval (usually greater than 10 milliseconds). The earliest ventricular activation occurs at the HB region (Box 19.4).

The presence of preexcited junctional beats excludes AV and atriofascicular BTs and favors the diagnosis of a fasciculoventricular BT. These junctional beats may occur spontaneously or be provoked by isoproterenol infusion, RF ablation of the slow pathway, or the pause induced after burst atrial pacing or adenosine administration. These beats are associated with the same degree of preexcitation and the same HV interval as during NSR (Fig. 19.10), even when these beats are associated with retrograde VA block and no atrial depolarization. However, junctional beats emerging proximally in the AV junction (e.g., during RF ablation of the AVN slow pathway) may produce preexcitation over fasciculoventricular BTs as well as nodofascicular/nodoventricular BTs. Conversely, junctional beats originating from the HB distal to the origin of the fasciculoventricular BT can cause normalization of the HV interval and QRS morphology.¹⁶

BOX 19.4 Features of Fasciculoventricular Bypass Tracts

- Preexcitation is present in NSR with a normal PR interval with a transitional zone in V₂–V₃.
- The earliest ventricular activation occurs at the HB region.
- The degree of preexcitation is not influenced by the site of atrial stimulation.
- Incremental rate atrial pacing results in progressive prolongation in the P-delta interval, but the degree of preexcitation is not influenced by the pacing rate.
- HB pacing does not change the degree of preexcitation or the HV interval.
- Junctional beats (even when associated with retrograde VA block) are associated with the same degree of preexcitation and the same HV interval as during NSR.

HB, His bundle; HV, His bundle–ventricular; NSR, normal sinus rhythm.

Programmed Atrial Stimulation

Progressively shorter atrial PCLs or AES coupling intervals produce progressive, physiological prolongation of the PR and AH intervals but with a fixed degree of preexcitation, a constant and positive (usually greater than 10 milliseconds) HV interval, and a fixed relationship between the HB and RB potentials (Fig. 19.11). AVN Wenckebach block can develop, which is then associated with a fixed degree of preexcitation and a constant, short HV interval. The loss of AV conduction is associated with loss of preexcitation.

AES can result in block in the fasciculoventricular BT, producing a sudden loss of preexcitation and prolongation of the HV interval to normal values (Fig. 19.11). Multisite atrial pacing has no effect on the preexcitation degree in fasciculoventricular BTs (similar to nodofascicular/nodoventricular BTs). This maneuver is helpful to differentiate these BTs from AV and atriofascicular BTs.

Programmed His Bundle Stimulation

HB pacing normalizes the HV interval and eliminates preexcitation in all types of BTs except for fasciculoventricular BTs, in which a fixed

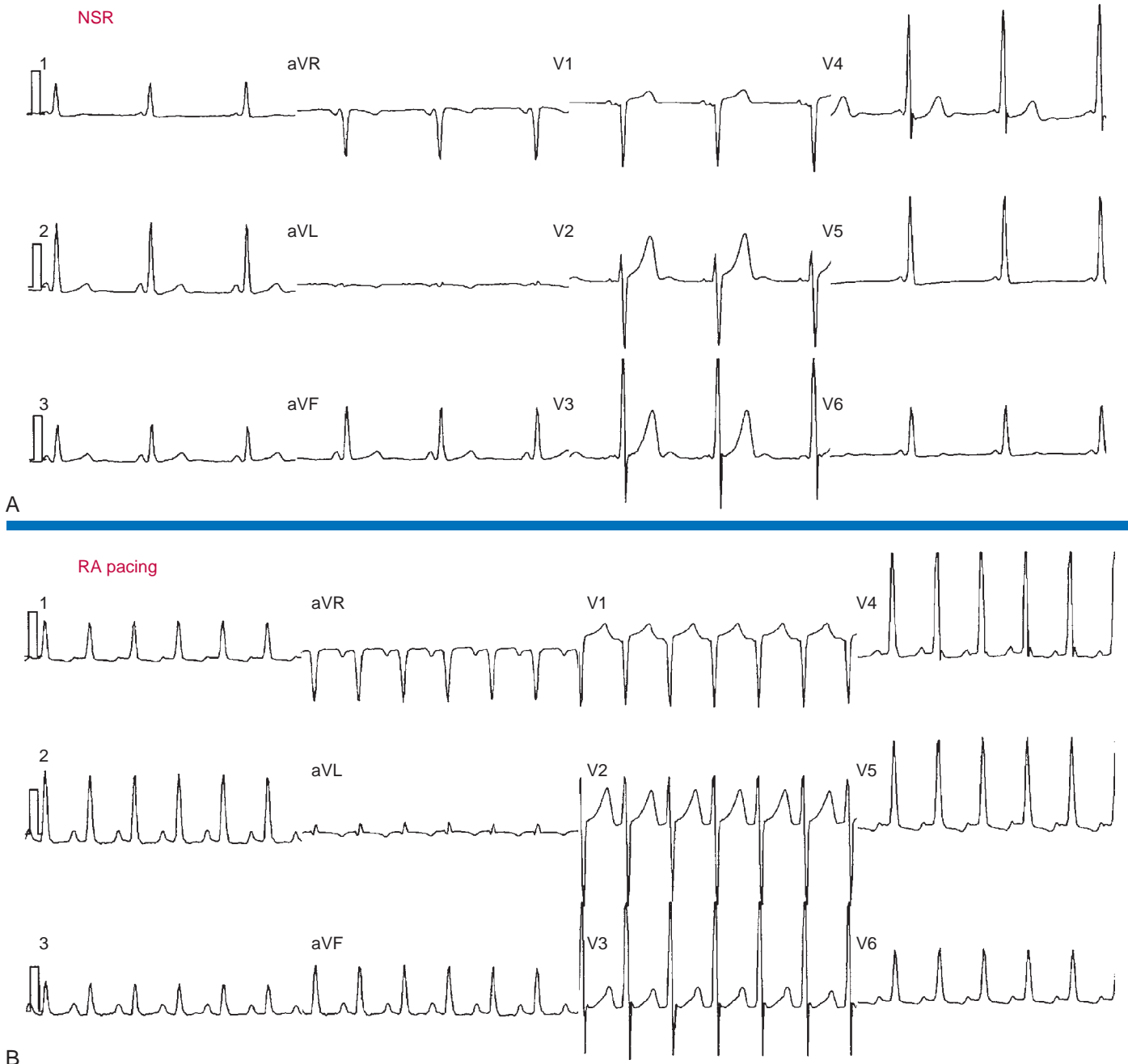


Fig. 19.9 Electrocardiogram (ECG) of Fasciculoventricular Bypass Tracts. (A) Surface ECG of normal sinus rhythm (NSR) with preexcitation over a fasciculoventricular pathway. Note the short PR and slight slurring of the QRS upstroke in several leads. (B) Pacing from the right atrium (RA) at the shortest cycle length associated with 1:1 atrioventricular (AV) conduction results in no change in the mild degree of preexcitation compared with NSR despite atrioventricular nodal conduction delay (longer PR interval).

Continued



Fig. 19.9, cont'd (C) Atrial fibrillation (AF) is present, with no change in the mild degree of preexcitation compared with NSR regardless of the R-R interval. (D) Surface ECG during His bundle (HB) pacing in the same patient. The same degree of preexcitation persists as in NSR. Retrograde P waves are visible (arrows), deforming the end of QRS complexes.

degree of preexcitation and a constant short HV interval remain unchanged during HB pacing (Fig. 19.10).¹⁶

Response to Pharmacological Maneuvers

When adenosine administration slows AVN conduction, an increase in the degree of preexcitation is noted in all types of BTs as long as adenosine does not block the BT except for fasciculoventricular BTs, in which the degree of preexcitation and HV interval remain fixed.

ATRIO-HISIAN BYPASS TRACTS

General Considerations

Patients with palpitations who had a short PR interval but normal QRS complex in the resting ECG were first described in 1938 and then further evaluated by Lown and colleagues in 1952. The latter report consisted of a retrospective examination of 13,500 ECGs and identified short PR intervals in a mixed group of 200 subjects, most of whom had a normal

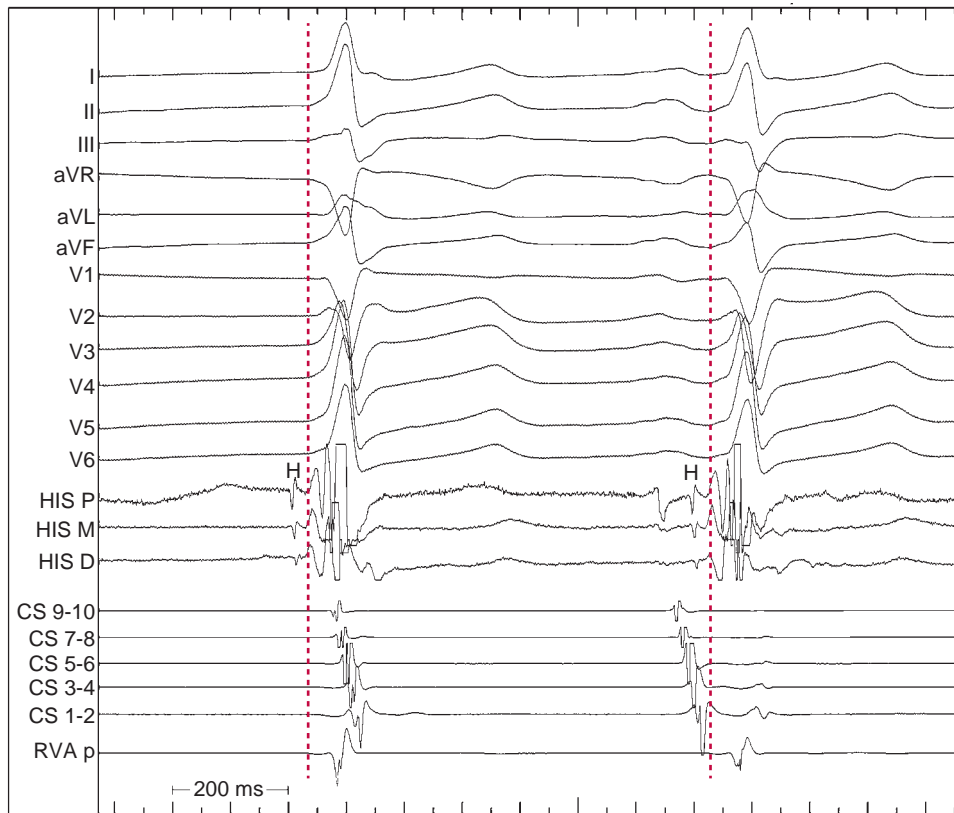


Fig. 19.10 Fasciculoventricular Bypass Tract. Full 12 leads of electrocardiogram are shown with intracardiac recordings during a junctional complex at left and a sinus complex with atrioventricular conduction at right. A dotted red line denotes QRS onset. Preexcitation is present in both QRS complexes to the same degree, indicative of a fasciculoventricular pathway. The His (*H*)-ventricular interval is short (28 milliseconds). CS, Coronary sinus catheter; *RVA*, right ventricular apical.

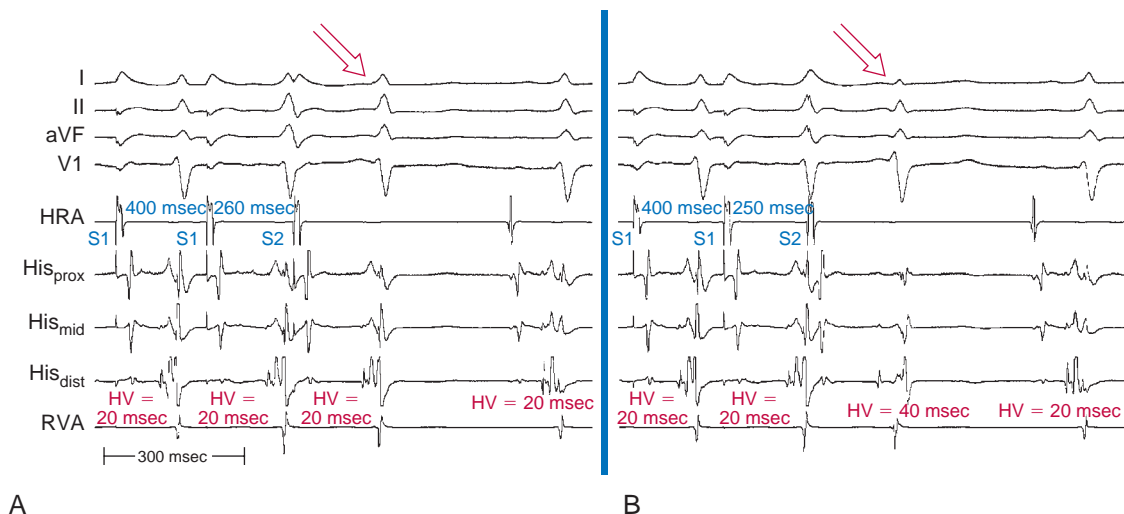


Fig. 19.11 Effect of Atrial Stimulation of Fasciculoventricular Bypass Tracts (BTs). (A) Minimal preexcitation is present during normal sinus rhythm, with the same during atrial pacing and following an atrial extra-stimulus (AES) that lengthens the atrial-His bundle interval, but the His bundle-ventricular (HV) interval remains fixed at only 20 milliseconds. These features are consistent with a fasciculoventricular pathway. (B) A more premature AES results in block in the fasciculoventricular pathway, resulting in a narrow QRS complex and normal HV interval (40 milliseconds). Note the difference in QRS complex morphology following the AESs (arrows). *His_{dist}*, Distal His bundle; *His_{prox}*, proximal His bundle; *HRA*, high right atrial catheter; *RVA*, right ventricular apical.

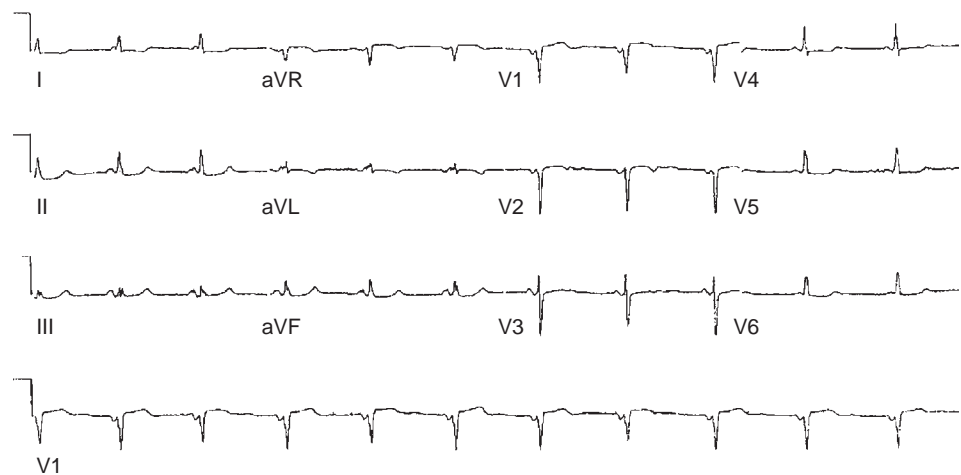


Fig. 19.12 Surface Electrocardiogram of an Asymptomatic Patient With a Short PR Interval and No Preexcitation.

TABLE 19.1 Electrophysiological Characteristics of Enhanced AVN Conduction Versus Atrio-Hisian BTs		
	Enhanced AVN Conduction	Atrio-Hisian BTs
Sinus rhythm	<ul style="list-style-type: none">• AH interval is short (<60 msec).• HV interval is normal.	<ul style="list-style-type: none">• AH interval is short (<60 msec).• HV interval is short.
Programmed atrial stimulation	<ul style="list-style-type: none">• AH interval prolongs with progressively shorter atrial PCLs and AES coupling intervals.• AH interval prolongation is smooth, continuous, and blunted.• Maximal increase in the AH interval of ≤100 msec during pacing at a PCL of 300 msec compared with the value measured during NSR.• The maximal AH interval (at any PCL) is ≤200 msec.• 1:1 AV conduction is maintained at atrial PCLs <300 msec.	<ul style="list-style-type: none">• AH interval remains short with no or minimal prolongation in response to progressively shorter atrial PCLs and AES coupling intervals.• Block in the BT is associated with a simultaneous increase in the PR and AH intervals and normalization of the HV interval.
Programmed ventricular stimulation	<ul style="list-style-type: none">• HA interval is usually short, and shorter than the AH interval at comparable PCLs.• HA interval typically remains relatively short with little prolongation in response to progressively shorter ventricular PCLs and VES coupling intervals.	<ul style="list-style-type: none">• VA conduction is unpredictable in these patients. VA conduction can be absent and, when present, it is not as good as AV conduction.
Response to pharmacological and physiological maneuvers	<ul style="list-style-type: none">• AH interval prolongs in response to beta-blockers, verapamil, digoxin, carotid sinus massage, and vagal maneuvers.	<ul style="list-style-type: none">• AV conduction over the atrio-Hisian BT is not affected by autonomic modulation.• Conduction block in the BT requires class IA or IC agents or amiodarone.

AES, Atrial extrastimulation; AH, atrial–His bundle; AV, atrioventricular; AVN, atrioventricular node; BT, bypass tract; CL, cycle length; HA, His bundle–atrial; NSR, normal sinus rhythm; PCLs, pacing cycle lengths; VA, ventriculoatrial; VES, ventricular extrastimulation.

QRS complex (Fig. 19.12). The authors described a “syndrome” (“Lown-Ganong-Levine [LGL] syndrome”) characterized by short PR interval, narrow QRS complex, and recurrent paroxysmal SVTs. They initially ascribed this syndrome to the presence of an atrioventricular nodal BT. However, a variety of explanations were later offered to account for the short PR interval.

Although the incidence of palpitations was significantly higher in those patients with short PR intervals when compared with a control group with normal PR intervals (17% vs. 0.5%), most contemporary electrophysiologists do not consider the “LGL syndrome” to be a recognized syndrome consisting of a single entity but rather an electrocardiographic description. It probably represents one end of the normal spectrum of AVN conduction properties. Therefore use of the term

“LGL syndrome” is inappropriate and should be discouraged and the mechanism responsible for the short PR interval should be used instead. The persistence of the term probably relates to the appealing parallel with the initials of the WPW syndrome.²⁰

The short PR interval can have different mechanisms: (1) enhanced AVN conduction (perhaps using specialized intranodal fibers), which is believed responsible for most cases of short PR interval and is secondary to an anatomically small AVN, enhanced sympathetic tone, or a variant of normal; (2) atrio-Hisian BT (rare), in which case AF or AFL with a rapid ventricular response is the presenting arrhythmia (Table 19.1); (3) ectopic atrial rhythm with differential input into the AVN; and (4) isorhythmic AV dissociation, whereby the short PR interval is not caused by a conducted P wave.

An “enhanced AVN conduction” has been arbitrarily defined as (1) AVN conduction time (AH interval) less than 60 milliseconds during NSR, (2) 1:1 AV conduction at atrial PCLs less than 300 milliseconds, and (3) maximal increment in the AH interval of 100 milliseconds or less during pacing at a PCL of 300 milliseconds compared with the value measured during NSR.

Supraventricular Tachycardias in Patients With Short PR Intervals

Patients With Enhanced Atrioventricular Node Conduction

The mechanism(s) of SVTs in patients with enhanced AVN conduction does not appear to differ significantly from those in patients with normal PR intervals (AVNRT being the most common, followed by orthodromic AVRT). The TCL of AVNRT occurring in patients with short PR intervals is not different from that in patients with normal PR intervals. This is expected because the TCL of AVNRT is determined by conduction over the slow AVN pathway, which is similar in these patients and those with normal PR intervals. In contrast, the TCL of orthodromic AVRT tends to be much shorter in these patients than in patients with normal PR intervals, which is expected because the circuit of orthodromic AVRT uses the fast AVN pathway for anterograde conduction. In fact, in any SVT with a TCL shorter than 250 milliseconds, enhanced AVN conduction and orthodromic AVRT should be suspected. In such patients, bundle branch block (BBB) is common during SVT (to provide sufficient AV delay necessary to maintain reentry), resulting in wide complex tachycardia.²⁰

Patients With Atrio-Hisian Bypass Tracts

These patients primarily present with AF and AFL with a rapid ventricular response and do not develop reentrant SVTs using the AV junction as one limb. Rapid ventricular rates during AF depend on refractoriness of the tissue responsible for AV conduction (i.e., AVN or BT) and not on the site of insertion for that tissue.

Electrophysiological Testing

Baseline Observations During Sinus Rhythm

Enhanced AVN conduction is characterized by a short AH interval (less than 60 milliseconds) and normal HV interval. In rare cases in which the AVN is completely bypassed by an atrio-Hisian BT, the HV interval is short. The HV interval in these cases is artifactually short because the proximal HB and the ventricle are activated in parallel, since the atrio-Hisian BT inserts into the distal HB (i.e., the proximal HB is activated retrogradely).²⁰

Programmed Atrial Stimulation

Patients with enhanced AVN conduction. The AH interval prolongs with progressively shorter atrial PCLs and AES coupling intervals. The prolongation in the AH interval is smooth, continuous, and blunted, with a maximal increase in the AH interval of 100 milliseconds or less during pacing at a CL of 300 milliseconds compared with the value measured during NSR. The maximal AH interval (at any PCL) is rarely longer than 200 milliseconds and 1:1 conduction typically is maintained at PCLs shorter than 300 milliseconds.

The AH interval response can be characteristic of dual AVN physiology, with an initial blunted small prolongation in the AH interval followed by a significant jump at a critical PCL or AES coupling interval while maintaining 1:1 conduction at PCLs shorter than 300 milliseconds. In such patients, the maximal AH interval can be longer than 200 milliseconds, and the maximal prolongation in the AH interval can be greater than 100 milliseconds. Atrial pacing from the CS is associated with shorter AH intervals, shorter Wenckebach CLs, and shorter AVN effective refractory periods, suggesting a preferential input into the AVN.²⁰

Patients with atrio-Hisian BTs. The AH interval remains short with no or minimal prolongation in response to progressively shorter atrial PCLs and AES coupling intervals. Block in the BT, which can usually be achieved by antiarrhythmic agents or occasionally by the induction of AF, is associated with a simultaneous increase in the PR and AH intervals and normalization of the HV interval.²¹

Programmed Ventricular Stimulation

Patients with enhanced AVN conduction. Retrograde AVN conduction is extremely rapid in these patients. In general the HA interval is shorter than the AH interval at comparable PCLs. The HA interval typically remains relatively short with little prolongation in response to progressively shorter ventricular PCLs and VES coupling intervals. A concealed AV BT mediating retrograde VA conduction should be excluded, which can be achieved by a variety of pacing maneuvers (see Chapter 18).

Patients with atrio-Hisian BTs. VA conduction is unpredictable in these patients. In many cases VA conduction is absent and, even when present, is not as good as AV conduction.

Response to Pharmacological and Physiological Maneuvers

Patients with enhanced AVN conduction. The AH interval prolongs in response to beta-blockers, verapamil, digoxin, carotid sinus massage, and vagal maneuvers. Complete autonomic blockade results in increases in the AH interval and AVN functional refractory period but a minimal change in the AVN effective refractory period (suggesting sympathetic tone predominance in these patients, in contrast to individuals with normal AVN conduction in whom vagal tone predominates).

Patients with atrio-Hisian BTs. AV conduction over the atrio-Hisian BT is not affected by autonomic modulation. Conduction block in the BT requires class IA or IC agents or amiodarone. Conduction block is associated with an immediate, sudden, and marked prolongation of the AH and HV intervals to normal values.

REFERENCES

1. Bhatia A, Sra J, Akhtar M. Preexcitation syndromes. *Curr Probl Cardiol.* 2016;41:99–137.
2. Benditt DG, Lü F. Atriofascicular pathways: fuzzy nomenclature or merely wishful thinking? *J Cardiovasc Electrophysiol.* 2006;17:261–265.
3. Sternick EB, et al. The atrioventricular interval during pre-excited tachycardia: a simple way to distinguish between decrementally or rapidly conducting accessory pathways. *Heart Rhythm.* 2009;6:1351–1358.
4. Kothari S, et al. Atriofascicular pathways: where to ablate? *Pacing Clin Electrophysiol.* 2006;29:1226–1233.
5. Sternick EB, et al. Short atrioventricular Mahaim fibers: observations on their clinical, electrocardiographic, and electrophysiologic profile. *J Cardiovasc Electrophysiol.* 2005;16:127–134.
6. Sternick EB, et al. Postablation-acquired short atrioventricular Mahaim-type fibers: observations on their clinical, electrocardiographic, and electrophysiologic profile. *Heart Rhythm.* 2012;9:850–858.
7. Sternick EB, et al. Electrocardiogram during tachycardia in patients with anterograde conduction over a Mahaim fiber: old criteria revisited. *Heart Rhythm.* 2004;1:406–413.
8. Sternick EB, et al. Effects of right bundle branch block on the antidromic circus movement tachycardia in patients with presumed atriofascicular pathways. *J Cardiovasc Electrophysiol.* 2006;17:256–260.
9. Asirvatham SJ, Stevenson WG. Wobble. *Circ Arrhythm Electrophysiol.* 2015;8:985–987.
10. Stevenson WG, Asirvatham SJ. Teaching rounds in cardiac electrophysiology. *Circ Arrhythm Electrophysiol.* 2010;3:563.

11. Lapage MJ, Walsh MJ, Reed JH, et al. Adenosine mapping for adenosine-dependent accessory pathway ablation. *Pacing Clin Electrophysiol.* 2014;37:610–615.
12. Mönning G, et al. Predictors of long-term success after catheter ablation of atriofascicular accessory pathways. *Heart Rhythm.* 2012;9:704–708.
13. Ozturk E, et al. Electroanatomic mapping guided cryoablation of mahaim pathways in children with limited fluoroscopy exposure. *Pacing Clin Electrophysiol.* 2015;38:362–367.
14. Hoffmayer KS, et al. Variable clinical features and ablation of manifest nodofascicular/ventricular pathways. *Circ Arrhythm Electrophysiol.* 2015; 8:117–127.
15. Modi S, Foster W, Todd DM, et al. Postoperative wide complex tachycardia: an alternative hypothesis. *Heart Rhythm.* 2012;10: 305–307.
16. Ali H, et al. Nodo- and fasciculoventricular pathways: electrophysiological features and a proposed diagnostic algorithm for preexcitation variants. *Heart Rhythm.* 2015;12:1677–1682.
17. Ho RT, et al. Electrophysiological features differentiating the atypical atrioventricular node-dependent long RP supraventricular tachycardias. *Circ Arrhythm Electrophysiol.* 2013;6:597–605.
18. Katritsis DG, Josephson ME. Differential diagnosis of regular, narrow-QRS tachycardias. *Heart Rhythm.* 2015;12:1667–1676.
19. Katritsis DG. Wolff-Parkinson-White syndrome and antidromic atrioventricular reentrant tachycardia. *Europace.* 2013;15:779–780.
20. Scheinman M. Enhanced AV nodal conduction and Brechenmacher tracts. *Pacing Clin Electrophysiol.* 2013;36:135–136.
21. Brechenmacher CJ. Atrio-hisian fibers anatomy and electrophysiology. *Pacing Clin Electrophysiol.* 2013;36:137–141.

Paroxysmal Supraventricular Tachycardias

OUTLINE

Epidemiology and Natural History, 697

Clinical Presentation, 698

Initial Evaluation, 699

Principles of Management, 699

Acute Management, 699

Chronic Management, 701

Electrocardiographic Features, 702

Regularity of the Tachycardia, 702

Atrial Activity, 702

Characterization of P/QRS Relationship, 703

QRS Morphology, 703

Effects of Interventions, 703

Electrophysiological Testing, 703

Baseline Observations During Sinus Rhythm, 704

Programmed Electrical Stimulation During Sinus Rhythm, 704

Induction of Tachycardia, 710

Tachycardia Features, 710

Diagnostic Maneuvers During Tachycardia, 714

Diagnostic Maneuvers During Sinus Rhythm After Tachycardia Termination, 722

Practical Approach to Electrophysiological Diagnosis of Supraventricular Tachycardia, 723

Step 1, 723

Step 2, 727

Step 3, 727

Step 4, 727

Step 5, 728

A “supraventricular” origin of a tachycardia implies the obligatory involvement of one or more cardiac structures above the bifurcation of the His bundle (HB), including the atrial myocardium, atrioventricular node (AVN), proximal HB, coronary sinus (CS), pulmonary veins, venae cavae, or abnormal atrioventricular (AV) connections other than the HB (i.e., bypass tracts [BTs]).¹

Narrow QRS complex supraventricular tachycardia (SVT) is a tachyarrhythmia with a rate greater than 100 beats/min and a QRS duration of less than 120 milliseconds. Narrow complex SVTs include sinus tachycardia, inappropriate sinus tachycardia, sinoatrial nodal reentrant tachycardia, focal atrial tachycardia (AT), multifocal AT, atrial fibrillation (AF), atrial flutter (AFL), junctional tachycardia, atrioventricular nodal reentrant tachycardia (AVNRT), and atrioventricular reentrant tachycardia (AVRT). These tachycardias can be divided into those that require only atrial tissue for their initiation and maintenance (sinus tachycardia, AT, AF, and AFL), and those that require the AV junction (junctional tachycardia, AVNRT, and AVRT).

Paroxysmal SVT is the term generally applied to intermittent SVT other than AF, AFL, and multifocal AT, and describes a clinical syndrome characterized by the presence of a regular and rapid tachycardia of abrupt onset and termination (Fig. 20.1). The major causes are AVNRT (approximately 50% to 60% of cases), AVRT (approximately 30% of cases), and focal AT (approximately 10% of cases).

years. The risk of developing paroxysmal SVT is twofold greater in women than men.¹

In a large cohort of patients with symptomatic paroxysmal SVT referred for ablation, AVNRT was the most common mechanism (56%), followed by AVRT (27%) and AT (17%). However, the mechanism of paroxysmal SVT was significantly influenced by both age and gender. The majority of patients with AVRT are men (55%), whereas the majority of patients with AVNRT and AT are women (70% and 62%, respectively). As patients grew older, there was a significant and progressive decline in the number of patients presenting with AVRT, which was the predominant mechanism in the first decade, and a striking increase in AVNRT and AT (Fig. 20.2). These trends were similar in both genders, although AVNRT replaced AVRT as the predominant mechanism much earlier in women.²

AVNRT is the predominant mechanism overall in patients undergoing ablation, and after the age of 20 years it accounts for the largest number of ablations in each age group. AVNRT is unusual in children under 5 years of age, and typically initially manifests in early life, often in the teens. There is a striking 2:1 predominance of women in the AVNRT group, which remains without clear physiological or anatomical explanation. Female sex and older age (teens vs. early childhood years) favor the diagnosis of AVNRT over AVRT.³

AVRT presents earlier in life than AVNRT (most commonly in the first two decades of life), with an average of more than 10 years separating the time of clinical presentation of AVRT versus AVNRT. The early predominance of AVRT is consistent with the congenital nature of the substrate. However, a minority of patients have relatively late onset of symptoms associated with AVRT and thus continue to account for a small proportion of ablations in older patients. Men account for a higher proportion of AVRT at all ages.⁴

Focal ATs comprise a progressively greater proportion of paroxysmal SVT with increasing age, accounting for 23% of paroxysmal SVTs in

EPIDEMIOLOGY AND NATURAL HISTORY

Paroxysmal SVT with sudden onset and termination is relatively common. In the United States, the estimated prevalence in the general population is 2.29 per 1000, with an incidence of 36 per 100,000 person-years. Paroxysmal SVT in the absence of structural heart disease can present at any age but most commonly first presents between ages 12 and 30

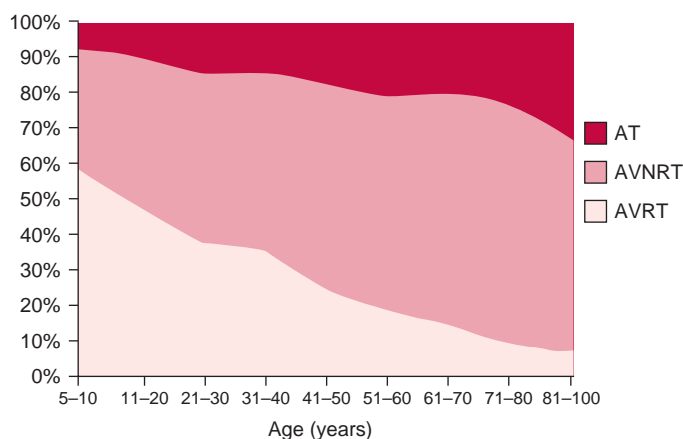


Fig. 20.1 Proportion of Paroxysmal Supraventricular Tachycardia Mechanisms by Age. AT, Atrial tachycardia; AVNRT, atrioventricular nodal reentrant tachycardia; AVRT, atrioventricular reentrant tachycardia. (From Porter MJ, Morton JB, Denman R, et al. Influence of age and gender on the mechanism of supraventricular tachycardia. *Heart Rhythm*. 2004;1:393.)

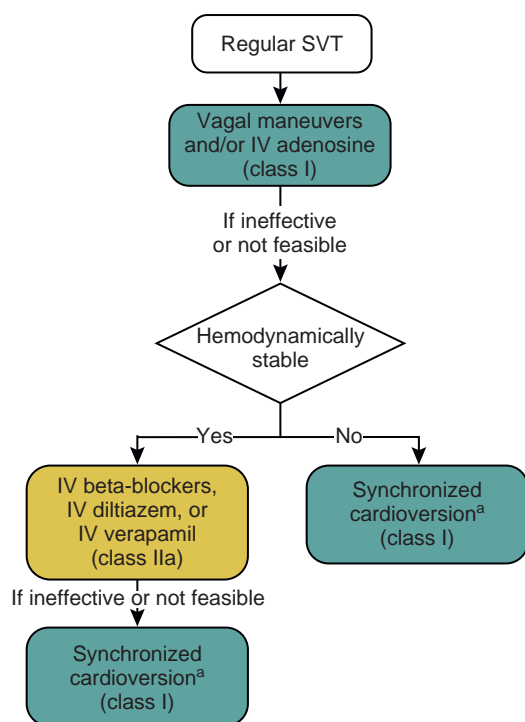


Fig. 20.2 Acute Treatment of Regular Supraventricular Tachycardia (SVT) of Unknown Mechanism. Drugs listed alphabetically. ^aFor rhythms that break or recur spontaneously, synchronized cardioversion is not appropriate. IV, Intravenous. (From Page RL, Joglar JA, Caldwell MA, et al. 2015 ACC/AHA/HRS guideline for the management of adult patients with supraventricular tachycardia: a report of the American College of Cardiology/American Heart Association Task Force on Clinical Practice Guidelines and the Heart Rhythm Society. *J Am Coll Cardiol*. 2016;67:e27–e115.)

patients older than 70 years. Although there is a greater absolute number of women with AT, the proportion of AT in both genders is similar. Age-related changes in the atrial electrophysiology (EP) substrate (including cellular coupling and autonomic influences) likely contribute to the increased incidence of AT in older individuals.² In adults, focal ATs can occur in the absence of structural heart disease; nonetheless, the

incidence of associated structural heart disease is higher in AT than other types of paroxysmal SVT.⁵ The long-term prognosis in patients with focal AT is generally benign, except for those with incessant ATs, which can precipitate tachycardia-induced cardiomyopathy.¹

Unlike AF and AFL, paroxysmal SVT does not appear to be a risk marker for stroke. In fact, unexplained stroke is rare in patients with SVT. Nonetheless, a strong link exists between SVT and atrial arrhythmias, particularly paroxysmal AF, even in patients with no ventricular preexcitation. The prevalence of a history of AF in the SVT patient population is approximately 2.6% compared to 0.4% to 2% in the general population. In addition, AVRT and, less frequently, AVNRT can serve as triggers for AF.⁶

CLINICAL PRESENTATION

The clinical syndrome of paroxysmal SVT is characterized as a regular rapid tachycardia of abrupt onset and termination. Episodes can last from seconds to several hours. Patients commonly describe palpitations and heart racing, frequently associated with complaints of dyspnea, weakness, chest pain, dizziness, or even frank syncope. The impact of SVT on quality of life varies according to the frequency and duration of episodes, and the severity of symptoms.¹ Patients often learn to use certain maneuvers such as carotid sinus massage or the Valsalva maneuver to terminate the arrhythmia, although many require pharmacological treatment to achieve this.

Neck pounding can occur during tachycardia, which is related to pulsatile reversed flow when the right atrium (RA) contracts against a closed tricuspid valve. The physical examination correlate of this phenomenon is continuous pulsing cannon A waves in the jugular venous waveform (described as the “frog” sign). This clinical feature has been reported to distinguish typical AVNRT from orthodromic AVRT. Although the atrial contraction during orthodromic AVRT does occur against closed AV valves, the longer ventriculoatrial (VA) interval during the tachycardia results in separate ventricular and then atrial contractions and, hence, relatively lower RA and venous pressures. Therefore symptoms of “shirt flapping” or “neck pounding” are experienced less commonly in patients with AVRT than those with AVNRT (17% vs. 50%). In addition, polyuria, which related to higher RA pressures and elevated levels of atrial natriuretic protein, is more common in patients with AVNRT compared with patients who have AVRT.¹

Dizziness can occur initially because of hypotension, but it then disappears when the sympathetic response to the SVT stabilizes the blood pressure (typically within 30 to 60 seconds). Reductions of blood pressure and cardiac output (and the associated reflex sympathetic activity) are likely to be most prominent in SVTs with simultaneous atrial and ventricular activation (e.g., typical AVNRT) than those with short VA intervals (e.g., slow-slow AVNRT or orthodromic AVRT), and least prominent in long RP tachycardias (e.g., atypical AVNRT, permanent junctional reciprocating tachycardia [PJRT], and AT).¹

True syncope is rare but can occur, especially in elderly patients. Syncope at the initiation of SVT is commonly vagally mediated, especially in young patients, and is benign in nature. However, malignant ventricular arrhythmias as a cause of syncope should be considered in patients with manifest preexcitation. In these patients, AVRT can deteriorate into AF, which can be associated with very fast ventricular rates, with possible degeneration into ventricular fibrillation (VF).

In patients with underlying structural heart disease, symptoms can be more severe. Decompensation of underlying heart failure or ischemic heart disease can be precipitated by episodes of SVT. Truly paroxysmal SVT rarely leads to a tachycardia-induced cardiomyopathy. However, PJRT and focal AT can manifest as a frequently recurring or incessant tachycardia that can precipitate cardiomyopathy and heart failure. Elimination of the tachycardia results in normalization of left ventricular (LV) function within a few months in the vast majority of patients.⁷

INITIAL EVALUATION

History, physical examination, and an electrocardiogram (ECG) constitute an appropriate initial evaluation of patients presenting with symptoms suggestive of paroxysmal SVT. However, clinical symptoms are not usually helpful in distinguishing different forms of paroxysmal SVT. A 12-lead ECG during tachycardia can be helpful for defining the mechanism of paroxysmal SVT. Ambulatory 24- or 48-hour Holter recording can be used for documentation of the arrhythmia in patients with frequent (i.e., several episodes per week) but self-terminating tachycardias. A cardiac event monitor is often more useful than a 24-hour recording in patients with less frequent arrhythmias. Implantable loop recorders can be helpful in selected cases with rare episodes associated with severe symptoms of hemodynamic instability (e.g., syncope).

An echocardiographic examination should be considered in patients with documented sustained SVT to exclude the possibility of structural heart disease. Exercise testing is rarely useful for diagnosis unless the arrhythmia is clearly triggered by exertion. Further diagnostic studies are indicated only if there are signs or symptoms that suggest structural heart disease. Of note, troponin I and T levels (especially high-sensitivity Troponin T) are elevated in a significant proportion (more than 50%)

of patients presenting with SVT, but this elevation does not constitute a clear biomarker of clinically significant coronary artery disease.⁸ Similarly, striking ST segment depression during SVT, that resolves quickly on cessation of tachycardia, is not uncommon but does not signify obstructive coronary artery disease.

Invasive EP testing is not indicated unless a decision to proceed with catheter ablation is undertaken. EP testing with subsequent catheter ablation may also be used for diagnosis and therapy in cases with a clear history of paroxysmal regular palpitations. It may also be considered in patients with preexcitation or disabling symptoms without ECG documentation of an arrhythmia.

PRINCIPLES OF MANAGEMENT

Acute Management

Most episodes of paroxysmal SVT require intact 1:1 AVN conduction for continuation and are therefore classified as AVN-dependent. AVN conduction and refractoriness can be modified by vagal maneuvers and by many pharmacological agents and thus are the weak links targeted by most acute therapies. Termination of a sustained episode of SVT is usually accomplished by producing a transient block in the AVN (Fig. 20.3).

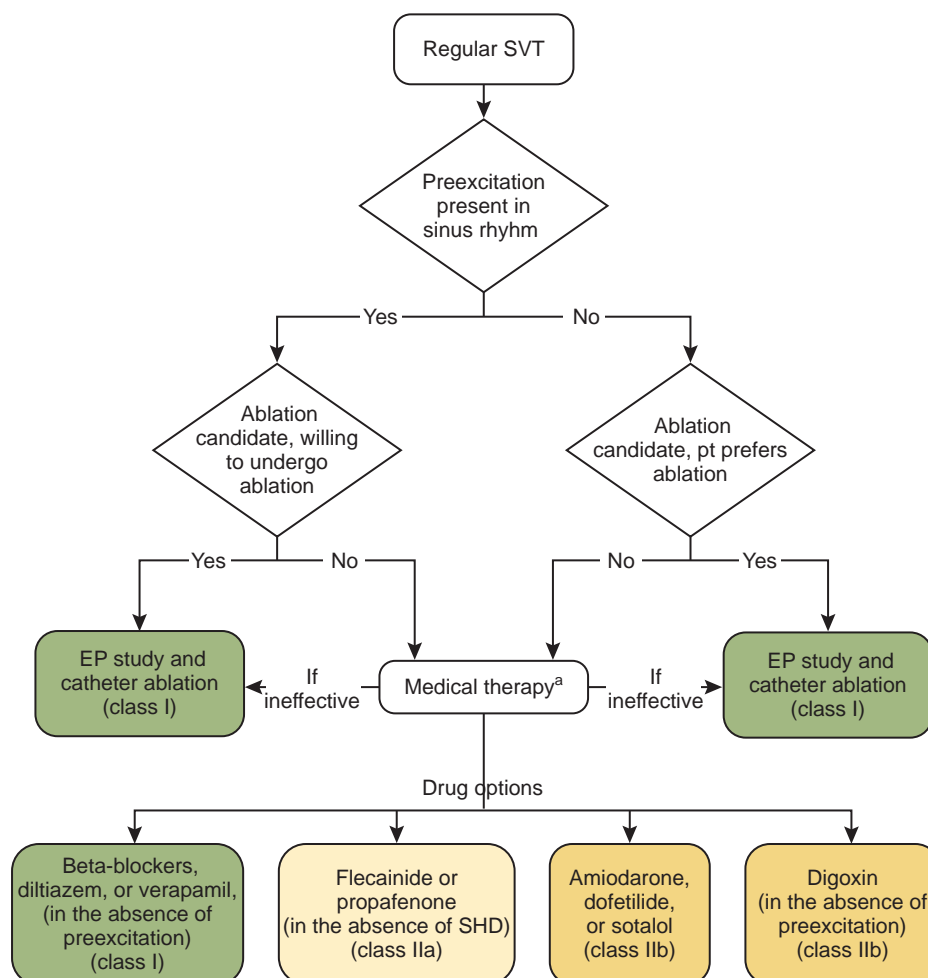


Fig. 20.3 Ongoing Management of Supraventricular Tachycardia (SVT) of Unknown Mechanism. Drugs listed alphabetically. ^aClinical follow-up without treatment is also an option. EP, Electrophysiology; pt, patient; SHD, structural heart disease (including ischemic heart disease); SVT, supraventricular tachycardia. (From Page RL, Joglar JA, Caldwell MA, et al. 2015 ACC/AHA/HRS guideline for the management of adult patients with supraventricular tachycardia: a report of the American College of Cardiology/American Heart Association Task Force on Clinical Practice Guidelines and the Heart Rhythm Society. *J Am Coll Cardiol*. 2016;67:e27–e115.)

For acute conversion of SVT, vagal maneuvers (including Valsalva and carotid sinus massage) are the first-line intervention, although their success rate remains limited (less than 30%). Valsalva is the most effective technique in adults, but carotid sinus massage can also be effective. The so-called modified Valsalva (patient supine, with legs slightly elevated to increase venous return and decrease reflex sympathetic tone) has also been useful. Facial immersion in water is the most reliable method in infants. Vagal maneuvers are less effective once a sympathetic response to paroxysmal SVT has become established, so patients should be advised to try them soon after onset of symptoms.¹

When vagal maneuvers are unsuccessful, termination can be achieved with antiarrhythmic drugs whose primary effects increase AVN refractoriness or decrease AVN conduction. In most patients, the drug of choice is intravenous (IV) adenosine. In hemodynamically stable patients, IV diltiazem, verapamil, or beta-blockers are appropriate therapy for SVT that is refractory to adenosine or recurs after initial termination, and are successful in 64% to 98% of cases. Electrical cardioversion is recommended for acute treatment in patients with hemodynamically unstable SVT when vagal maneuvers or adenosine are ineffective or not feasible.¹

The advantages of adenosine include its rapid onset of action (usually within 10 to 25 seconds via a peripheral vein), short half-life (less than 10 seconds), and high degree of efficacy. The effective dose of adenosine is usually 6 to 12 mg, given as a rapid bolus over 1 to 2 seconds at a peripheral site, followed by a vigorous flush of normal saline. If a central IV access site is used, the initial dose should not exceed 3 mg and may be as little as 1 mg. Doses up to 12 mg terminate over 90% of paroxysmal SVT episodes (predominantly AVRT and AVNRT). Sequential dosing can be given at 60-second intervals because of adenosine's rapid metabolism. In AVNRT, termination is usually caused by block in the slow pathway. In AVRT, termination occurs secondary to block in the AVN. Termination can also occur indirectly, that is, because of adenosine-induced premature atrial complexes (PACs) or premature ventricular complexes (PVCs). Adenosine also can terminate a significant proportion of focal ATs; therefore termination of an SVT in response to adenosine is not helpful in differentiating AT from other SVTs. Even when AT persists, adenosine can be useful diagnostically by producing transient AV block and unmasking the independent atrial activity during AT. Of note, adenosine is cleared rapidly; hence, reinitiation of paroxysmal SVT after initial termination can occur. Either repeated administration of the same dose of adenosine or substitution of a calcium channel blocker or beta-blocker typically is effective.

Importantly, adenosine shortens the atrial refractory period, and atrial ectopy can induce AF. This can be dangerous if the patient has a BT capable of rapid anterograde conduction, which can result in a rapid ventricular response that can degenerate into VF. In patients with Wolff-Parkinson-White (WPW) syndrome and AF, adenosine can result in a rapid ventricular response that can degenerate into VF. However, this problem has not been observed frequently, and the use of adenosine for diagnosis and termination of regular SVTs, including AVRT, is appropriate as long as close patient observation and preparedness to treat potential complications, such as with immediate electrical cardioversion/defibrillation, are maintained.

The AVN action potential is calcium channel-dependent, and the non-dihydropyridine calcium channel blockers verapamil and diltiazem are effective for terminating AVN-dependent paroxysmal SVT. The recommended dosage of verapamil is 5 mg IV over 2 minutes, followed in 5 to 10 minutes by a second 5- to 7.5-mg dose. The recommended dose of diltiazem is 20 mg IV followed, if necessary, by a second dose of 25 to 35 mg. Paroxysmal SVT termination should occur within 5 minutes of the end of the infusion, and more than 90% of patients with AVN-dependent paroxysmal SVT respond. As with adenosine,

transient arrhythmias, including PACs, PVCs, AF, and bradycardia, can be seen after paroxysmal SVT termination with calcium channel blockers. Hypotension can also develop, particularly if the paroxysmal SVT does not terminate. Adenosine and verapamil have been reported to have a similar high efficacy in terminating paroxysmal SVT, with a rate of success ranging from 59% to 100% for adenosine and from 73% to 98.8% for verapamil, according to the dose and mode of administration. However, data also suggest that the efficacy of adenosine and verapamil is influenced by the arrhythmia rate. Adenosine appears to be more effective at terminating SVT with faster rates. In contrast, the efficacy of verapamil in restoring sinus rhythm was inversely related to the rate of paroxysmal SVT.

IV beta-blockers including propranolol (1 to 3 mg), metoprolol (5 mg), and esmolol (500 µg/kg over 1 minute and a 50-µg/kg per minute infusion) are also useful for acute termination. Digoxin (0.5 to 1.0 mg) is considered the least effective of the four categories of drugs available, but is a useful alternative when there is a contraindication to the other agents.

AVN-dependent paroxysmal SVT can present with a wide QRS complex in patients with fixed or functional aberration, or if a BT is used for anterograde conduction. Most wide complex tachycardias, however, are caused by mechanisms that can worsen after IV administration of beta-blockers and calcium channel blockers. Unless there is strong evidence that a wide QRS tachycardia is AVN-dependent, verapamil, diltiazem, and beta-blockers should not be used.

Limited data are available on the acute pharmacological therapy of ATs. Vagal maneuvers only rarely terminate AT, and the response to adenosine is variable. IV beta-blockers, diltiazem, or verapamil have modest efficacy (30% to 50%) in terminating the focal AT or slowing the ventricular rate. Class I or III antiarrhythmic drugs given orally or parenterally may be considered for refractory ATs. Adenosine does not slow or terminate microreentrant AT. In contrast, triggered activity ATs typically terminate abruptly in response to adenosine and do not spontaneously reinitiate. Automatic ATs are either slowed transiently by adenosine before gradual resumption of the AT rate or suppressed transiently before spontaneous reinitiation.⁹ Microreentrant ATs can terminate in response to carotid sinus massage and vagal maneuvers. Triggered activity ATs can also terminate in response to carotid sinus massage, vagal maneuvers, verapamil, beta-blockers, and sodium channel blockers. During automatic AT, carotid sinus massage can cause AV block and can slow the atrial rate; however, these interventions generally do not terminate the AT. Only beta-blockers have been useful in termination of paroxysmal (but not incessant) automatic AT. Termination of automatic AT is usually preceded by a cool-down phenomenon of the AT rate.^{1,9}

In general, most stable patients with SVT respond to pharmacological therapy, with conversion success rates of 80% to 98%. Electrical cardioversion is also recommended for patients with hemodynamically stable SVT when pharmacological therapy is ineffective or contraindicated. However, electrical cardioversion is inappropriate if the SVT is terminating and reinitiating spontaneously.¹

In patients with manifest preexcitation during normal sinus rhythm (NSR) presenting with AVRT (orthodromic or antidromic), vagal maneuvers are the first-line intervention for tachycardia termination. For persistent SVT, adenosine is recommended. Importantly, adenosine should be used with caution because it can induce AF with a rapid ventricular rate in the presence of an anterogradely conducting BT. This is unusual and should not be viewed as a contraindication to adenosine use, but one should be prepared for emergency cardioversion before administering adenosine to SVT patients. For refractory AVRT, IV diltiazem, verapamil, or beta-blockers may be considered to block conduction in the AVN, which represents the retrograde or anterograde limb in the AVRT circuit. AVN blocking drugs, however, are ineffective

in patients with an antidromic AVRT that utilizes two separate BTs for anterograde and retrograde conduction. Drug treatment directed at the BT (ibutilide, procainamide, flecainide) may be considered. When drug therapy fails or hemodynamic instability is present, electrical cardioversion should be considered.¹

Chronic Management

Most paroxysmal SVTs are generally benign and do not influence survival; therefore the primary indication for treatment is to alleviate symptoms and improve quality of life. The threshold for initiation of therapy and the decision to treat SVT with oral pharmacological therapy or catheter ablation depends on the frequency and duration of the arrhythmia, severity of symptoms, presence of concomitant structural heart disease, and patient preference (Fig. 20.4). The threshold for

treatment is also influenced by whether the patient is a competitive athlete, a woman considering pregnancy, or someone with a high-risk occupation (e.g., pilots, bus drivers).¹

Catheter Ablation

Given the high success rates and the low complication rate, catheter ablation is the treatment of choice in patients who desire to avoid or are unresponsive or intolerant to drug therapy.¹ Catheter ablation is also recommended for incessant SVT, even in asymptomatic patients, especially when tachycardia-induced cardiomyopathy has developed.

Pharmacological Therapy

For patients requiring therapy who are reluctant to undergo catheter ablation, drug therapy remains a viable alternative. Calcium channel blockers and beta-blockers may be considered in patients without ventricular preexcitation during NSR. Verapamil, propranolol, and digoxin likely have equivalent efficacy, and can improve symptoms in 60% to 80% of patients. However, verapamil, diltiazem, and beta-blockers are generally preferred to digoxin. The effective dose of digoxin is usually higher than that commonly used in clinical practice today. Given the risk of toxicity, digoxin should be reserved for patients who cannot take beta-blockers, diltiazem, or verapamil or a class IC agent (flecainide or propafenone) and must be used with caution in the presence of renal dysfunction.¹

In patients who do not respond, classes IC and III drugs may be considered. Flecainide and propafenone affect the AVN and BTs, reduce SVT frequency in 86% to 93% of patients, and may be considered in patients without ischemic or structural heart disease. Sotalol, dofetilide, and amiodarone are second-line agents. The probability of remaining free of SVT after 6 months of treatment is about 50% for dofetilide and 54% for propafenone, compared to 6% for placebo. However, the potential benefit should be balanced by the potential risks of proarrhythmia and toxicity. Because sympathetic stimulation can antagonize the effects of many antiarrhythmic agents, concomitant therapy with a beta-blocker can improve efficacy.¹

Pharmacological management of ATs has not been well evaluated in controlled clinical trials. Depending on the mechanism responsible for the arrhythmia, beta-blockers or calcium channel blockers may be considered as first-line drug therapy. Class IC agents in combination with an AVN blocking agent, or class III agents (sotalol and amiodarone) are second-line therapy (see Chapter 11).

Patients with SVT should be educated on how to perform vagal maneuvers. Those with well-tolerated episodes of paroxysmal SVT that always terminate spontaneously or with vagal maneuvers do not require chronic prophylactic therapy. Selected patients may be treated only for acute episodes. Outpatients may use a single oral dose of verapamil, diltiazem, or propranolol to acutely terminate an episode of SVT. This so-called pill in the pocket is a reasonable treatment option for patients who have SVT episodes that are sustained but infrequent enough that daily preventive therapy is not desired. This approach necessitates the use of a drug that has a short onset of action (i.e., immediate-release preparations); crushing the drug tablet can potentially facilitate absorption. Candidate patients should be free of significant LV dysfunction, sinus bradycardia, and preexcitation.¹

For patients with ventricular preexcitation, antiarrhythmic drugs to block BT conduction are considered. Class IC agents (in patients without structural heart disease or ischemic heart disease), and class III drugs, such as sotalol and dofetilide, may be considered. Oral amiodarone is a last resort therapy, given the associated risks of long-term therapy. In general, antiarrhythmic drug therapy can offer symptomatic improvement in up to 90% of patients, although complete disappearance of symptoms is observed in only 30%. Chronic oral beta-blockers,

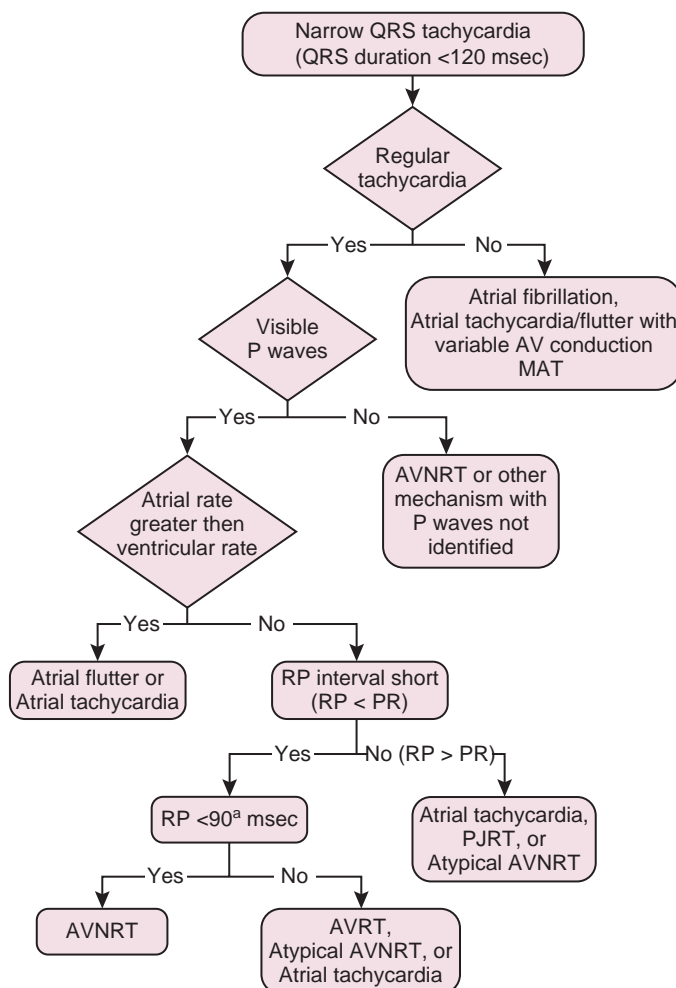


Fig. 20.4 Differential Diagnosis of Narrow QRS Tachycardia. Patients with junctional tachycardia may mimic the pattern of slow-fast atrioventricular nodal reentrant tachycardia (AVNRT) and may show atrioventricular (AV) dissociation and/or marked irregularity in the junctional rate. ^aRP refers to the interval from the onset of surface QRS to the onset of visible P wave (note that the 90-millisecond interval is defined from the surface electrocardiogram, as opposed to the 70-millisecond ventriculoatrial interval that is used for intracardiac diagnosis). AVRT, Atrioventricular reentrant tachycardia; MAT, multifocal atrial tachycardia; PJRT, permanent junctional reciprocating tachycardia. (From Page RL, Joglar JA, Caldwell MA, et al. 2015 ACC/AHA/HRS guideline for the management of adult patients with supraventricular tachycardia: a report of the American College of Cardiology/American Heart Association Task Force on Clinical Practice Guidelines and the Heart Rhythm Society. *J Am Coll Cardiol*. 2016;67:e27–e115.)

verapamil, and diltiazem may be used for the treatment of patients with WPW syndrome, particularly if their BT has been demonstrated to be incapable of rapid anterograde conduction. However, these agents must be used with caution and after a discussion with the patient concerning the potential risk of rapid conduction over the BT if AF develops. Digoxin, on the other hand, should be avoided because it can shorten the refractory period of the BT and, hence, is potentially harmful in patients with manifest BTs.¹

ELECTROCARDIOGRAPHIC FEATURES

Regularity of the Tachycardia

Most SVTs are associated with a regular ventricular rate. If the rhythm is irregular, the ECG should be scrutinized for discrete atrial activity and for any evidence of a pattern in the irregularity (e.g., grouped beating typical of Wenckebach periodicity). If the rhythm is irregularly irregular (i.e., no pattern can be detected), the mechanism of the arrhythmia is multifocal AT, AFL with variable AV conduction, or AF (Fig. 20.5). Multifocal AT is an irregularly irregular atrial rhythm characterized by more than three different P wave morphologies, with the P waves separated by isoelectric intervals and associated with varying P-P, R-R, and PR intervals (see Fig. 11.2). On the other hand, AF is characterized by rapid and irregular atrial fibrillatory activity and, in the presence of normal AVN conduction, by an irregularly irregular ventricular response. P waves cannot be detected in AF, although coarse fibrillatory waves and prominent U waves can sometimes give the appearance of P waves. At times, the fibrillatory activity is so fine as to

be undetectable. If the patient's rhythm is regular or has a clearly discernible pattern, the ECG should next be assessed for P waves (atrial activity).¹

Atrial Activity

The P waves may be easily discernible; however, frequently, comparison with a normal baseline ECG is needed and can reveal a slight alteration in the QRS, ST segment, or T waves, suggesting the presence of the P wave. If the P waves cannot be clearly identified, carotid sinus massage or the administration of IV adenosine may help clarify the diagnosis. These maneuvers may also terminate the SVT.¹

Atrial Rate

An atrial rate greater than 250 beats/min is usually caused by AFL. However, overlap exists, and AT and AVRT can occasionally be faster than 250 beats/min, especially in youngsters. Although AVRT tends to be faster than AVNRT and AT, significant overlap exists and this criterion does not usually help in distinguishing among different SVTs.¹⁰

P Wave Morphology

P waves indicate the result of atrial activation and may be broadly classified as concentric or eccentric. A P wave morphology identical to a sinus P wave suggests sinus tachycardia, inappropriate sinus tachycardia, sinoatrial nodal reentrant tachycardia, or AT arising close to the region of the sinus node. A nonsinus P wave morphology can be observed during AVNRT (P wave is concentric due to midline retrograde activation; see Fig. 17.8), AVRT (P wave can be eccentric or concentric due

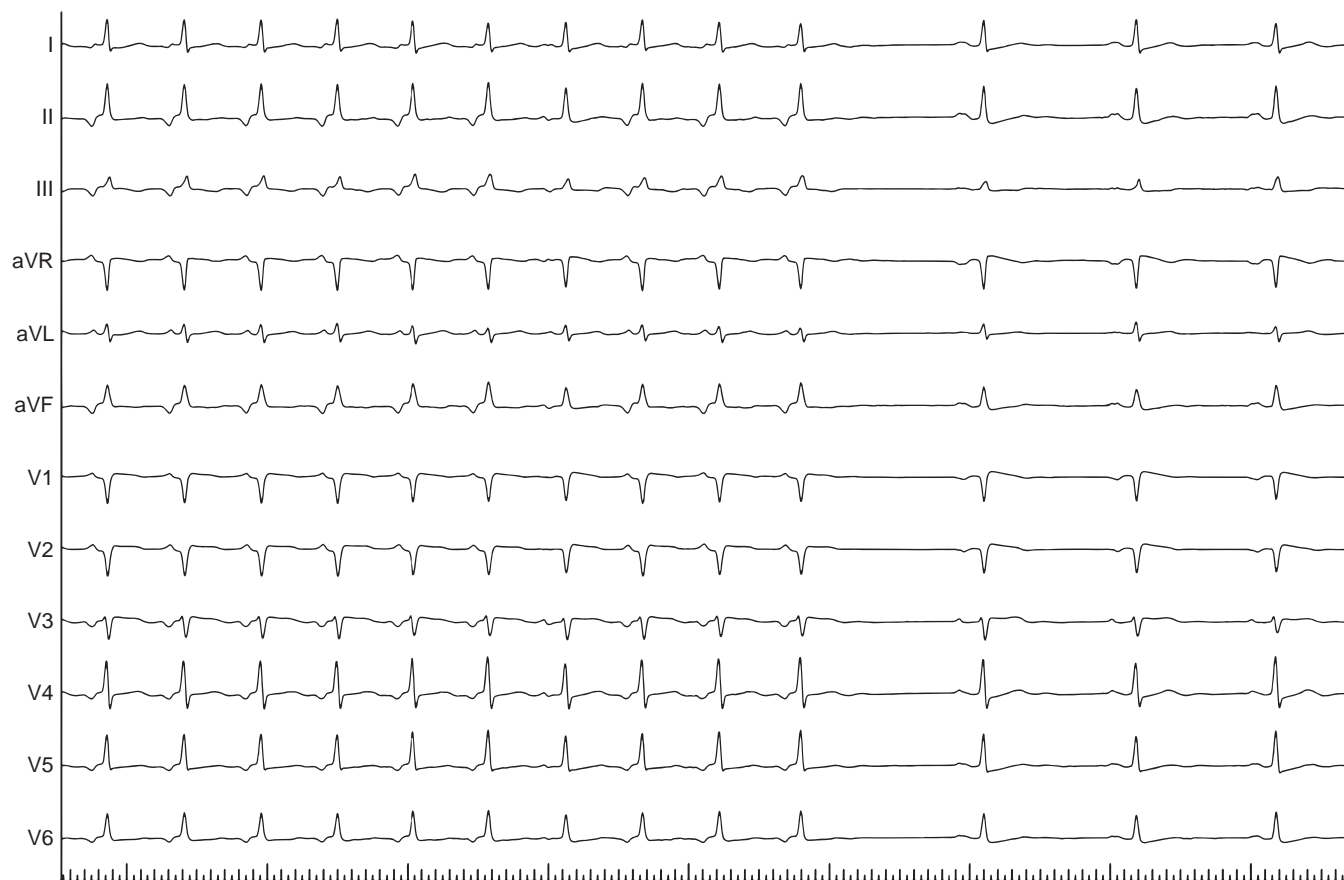


Fig. 20.5 Supraventricular Tachycardia. Surface electrocardiogram of a narrow complex supraventricular tachycardia with a long RP interval. The tachycardia terminates spontaneously and sinus rhythm ensues (at left).

to retrograde conduction over the BT; **see Fig. 18.12**), AT (P wave can be eccentric or concentric), and AFL (lack of distinct isoelectric baselines between atrial deflections is suggestive of AFL, but can also be seen occasionally in AT; **see Fig. 12.6**). The P waves may not be discernible on the ECG, which suggests typical AVNRT or, less commonly, AVRT (especially in the presence of bundle branch block [BBB] contralateral to the BT).¹ It is best to characterize P waves during SVT morphologically at the outset (concentric, eccentric) rather than attaching a mode of activation (i.e., retrogradely activated); for example, upright P waves in the inferior leads, though usually due to AT, may nonetheless be retrogradely conducted over an anterior BT, and although inverted P waves in inferior leads are often retrogradely conducted, focal AT from the coronary sinus ostium (CS os) can have an identical appearance. Thus not all retrograde P waves are inverted in the inferior leads, and not all inverted P waves in inferior leads are retrogradely conducted.

Characterization of P/QRS Relationship

RP-PR Interval Ratio

In general, SVTs are classified according to the RP interval as “short RP” (RP < PR) or “long RP” (RP > PR) tachycardias (**see Fig. 20.5**). The RP-to-PR ratio is not diagnostic of any tachycardia type but does help in creating a differential diagnosis of the possible tachycardia types. During short RP SVTs, the ECG will show P waves inscribed within the ST-T wave with an RP interval that is less than half the tachycardia R-R interval. Such SVTs include typical AVNRT (most common), orthodromic AVRT, AT with prolonged AV conduction, and slow-slow AVNRT. A very short RP interval (less than 90 milliseconds) is consistent with typical AVNRT and excludes AVRT. In typical AVNRT, the P wave is not usually visible because of the simultaneous atrial and ventricular activation. The P wave may distort the initial portion of the QRS (mimicking a q wave in inferior leads) or lie just within the QRS (inapparent) or distort the terminal portion of the QRS (mimicking an s wave in inferior leads or r' in lead V₁; **see Fig. 17.8**).

Long RP SVTs (**see Fig. 20.1**) include AT (most common), atypical (fast-slow) AVNRT, and AVRT using a slowly conducting AV BT (e.g., PJRT). If the PR interval during the SVT is shorter than that during NSR, AT and AVRT are very unlikely, and atypical AVNRT, which is associated with an apparent shortening of the PR interval, is the likely diagnosis. ATs originating close to the AV junction are also a possibility.

The PR intervals during AT are appropriate for the AT rate and are usually longer than those during NSR. The faster the AT rate, the longer the PR interval. Thus the PR interval can be shorter than, longer than, or equal to the RP interval. The PR interval may also be equal to the RR, and the P wave may fall inside the preceding QRS, thus mimicking typical AVNRT.

Slow-slow AVNRT can be associated with RP intervals and P wave morphology similar to that during orthodromic AVRT using a posteroseptal AV BT. However, although both SVTs have the earliest atrial activation in the posteroseptal region, conduction time from that site to the HB region is significantly longer in AVNRT than in orthodromic AVRT. The results are a significantly longer RP interval in lead V₁ and a significantly larger difference in the RP interval between lead V₁ and inferior leads during AVNRT. Therefore Δ RP interval (V₁–III) of more than 20 milliseconds suggests slow-slow AVNRT (sensitivity, 71%; specificity, 87%).¹¹

When the P wave is not visible, typical AVNRT is the most likely diagnosis, but AT with a long PR interval (P wave is obscured within the QRS) and junctional tachycardia are also possible.

Atrial-Ventricular Relationship

SVTs with an A/V ratio of 1 (i.e., equal number of atrial and ventricular events) include AVNRT, AVRT, and AT. On the other hand, an A/V ratio

during the SVT of greater than 1 indicates the presence of AV block and that the ventricles are not required for the SVT circuit, thereby excluding AVRT and suggesting either AT (most common; **see Fig. 11.7**) or AVNRT (rare; **see Fig. 17.9**). AV dissociation (even complete AV block) can be observed during AT (most common) or AVNRT (rare).¹ VA block during SVT is rare, but can occur in automatic junctional tachycardia with retrograde VA block and orthodromic AVRT using a nodofascicular or nodoventricular BT for retrograde conduction. Intra-Hisian reentry is another potential mechanism, but it is a theoretical entity whose clinical occurrence has not convincingly been demonstrated.^{12–14}

QRS Morphology

The QRS morphology during SVT is usually the same as in NSR. However, SVT can present as a wide complex tachycardia (QRS duration greater than 120 milliseconds) due to rate-related aberrant conduction, pre-existing intraventricular conduction disturbance (IVCD), or ventricular preexcitation over an anterogradely conducting BT.¹

Functional aberration during SVT is much more common in orthodromic AVRT than AVNRT or AT (90% of SVTs with sustained left bundle branch block [LBBB] are orthodromic AVRTs). Thus the mere presence of LBBB aberrancy during SVT is suggestive of orthodromic AVRT, but can still occur in other types of SVTs.¹⁵

Preexcited SVTs include antidromic AVRT, whereby the BT is an essential part of the tachycardia circuit, and AVNRT and AT with ventricular preexcitation over a bystander BT.

QRS alternans during fast SVTs is most commonly seen in orthodromic AVRT but can also be seen with other types of SVTs as well. However, when QRS alternans occurs during a relatively slow SVT, the diagnosis is almost always orthodromic AVRT.

Effects of Interventions

Carotid sinus massage or adenosine can result in one of four possible effects: (1) temporary decrease in the atrial rate in patients with sinus tachycardia or automatic AT; (2) slowing of AVN conduction and AVN block, which can unmask atrial electrical activity—that is, reveal P waves or flutter waves in patients with AT or AFL by decreasing the number of QRS complexes that obscure the electrical baseline; (3) terminating the SVT; or (4) no effect is observed.

Carotid sinus massage or adenosine can terminate the SVT, especially if the rhythm is AVNRT or AVRT by transient slowing and block of AVN conduction and interrupting the reentry circuit; termination of focal AT can occur but is much less common. A continuous ECG tracing should be recorded during these maneuvers because the response can aid in the diagnosis and changes can be subtle (rate slowing or transient AV block). Termination of the tachycardia with a P wave after the last QRS complex is most common in AVRT and typical AVNRT and is rarely seen with AT (**see Fig. 18.36**), whereas termination of the tachycardia with a QRS complex is more common with AT, atypical AVNRT, and PJRT (**see eFig. 18.5**). If the tachycardia continues despite development of AV block, the rhythm is almost certainly AT or AFL; AVRT is excluded and AVNRT is very unlikely.¹

ELECTROPHYSIOLOGICAL TESTING

Discussion in this section will focus on differential diagnosis of narrow QRS complex paroxysmal SVTs, including focal AT, orthodromic AVRT, and AVNRT. The goals of EP testing in these patients include the following: (1) evaluation of baseline cardiac electrophysiology; (2) induction of SVT; (3) evaluation of the mode of initiation of the SVT; (4) definition of atrial activation sequence during the SVT; (5) definition of the A/V relationship at the onset and during the SVT; (6) evaluation of the effect of BBB on the tachycardia cycle length (TCL) and VA

interval; (7) evaluation of the SVT circuit and requirement for the atria, HB, or ventricles in the initiation and maintenance of the SVT; (8) evaluation of the SVT response to programmed atrial and ventricular stimulation; and (9) evaluation of the effects of drugs and physiological maneuvers on the SVT.

Baseline Observations During Sinus Rhythm

The presence of preexcitation during NSR suggests AVRT as the likely diagnosis; however, it does not exclude other causes of SVT during which the BT is an innocent bystander. Furthermore, the absence of preexcitation during NSR does not exclude the presence of an AV BT or the diagnosis of AVRT.

Programmed Electrical Stimulation During Sinus Rhythm

The programmed stimulation protocol typically includes: (1) ventricular burst pacing from the right ventricular (RV) apex (down to the pacing cycle length [PCL] at which VA block develops); (2) single and double ventricular extrastimulus (VES; down to the ventricular effective refractory period [ERP]) at multiple PCLs (600 to 400 milliseconds) from the RV apex; (3) atrial burst pacing from the high RA and CS (down to the PCL at which 2:1 atrial capture occurs); (4) single and double atrial extrastimulations (AESs) (down to the atrial ERP) at multiple PCLs (600 to 400 milliseconds) from the high RA and CS; and (5) administration of isoproterenol infusion (0.5 to 4 $\mu\text{g}/\text{min}$) or epinephrine (0.05 to 0.2 $\mu\text{g}/\text{kg}$ per minute) infusion as needed to facilitate tachycardia induction or sustenance.

Programmed Atrial Stimulation During Sinus Rhythm

Dual AVN physiology. Although the demonstration of dual AVN physiology during programmed atrial stimulation favors AVNRT as the mechanism of SVT (positive predictive value greater than 80%), it is not an uncommon finding in patients with other types of SVTs. Furthermore, failure to demonstrate dual AVN physiology does not exclude the possibility of AVNRT, and might be related to similar fast and slow AVN pathway ERPs. Then, dissociation of refractoriness of the fast and slow AVN pathways can be necessary (see Chapter 17).

Ventricular preexcitation. Atrial stimulation can help unmask preexcitation if it is not manifest during NSR because of fast AVN conduction, slow BT conduction, or distant (left lateral) BT location. AES and atrial pacing from any atrial site result in slowing of AVN conduction and, consequently, unmask or increase the degree of preexcitation over the AV BT (see Fig. 18.23). Moreover, atrial stimulation close to the BT insertion site results in maximal preexcitation and the shortest P-delta interval because of the ability to advance the activation of the AV BT down to its ERP from pacing at this site caused by the lack of intervening atrial tissue, whose conduction time and refractoriness can otherwise limit the ability of the AES to stimulate the BT prematurely (see Fig. 18.24).

The failure of atrial stimulation to increase the amount of preexcitation can be caused by: (1) markedly enhanced AVN conduction; (2) the presence of another AV BT; (3) pacing-induced block in the AV BT because of a long ERP of the BT (longer than that of the AVN); (4) total preexcitation already present at the basal state caused by prolonged or absent AVN-His-Purkinje system (HPS) conduction; (5) decremental conduction in the BT; or (6) the presence of a fasciculoventricular BT rather than an AV BT.

Extra atrial beats. AES and atrial pacing can trigger extra atrial beats or echo beats. Those beats can be caused by different mechanisms.

Intraatrial reentrant beats. These beats usually occur at short coupling intervals, and can originate anywhere in the atrium. Therefore

the atrial activation sequence depends on the site of origin of the beat. The more premature the AES, the more likely it will induce nonspecific intraatrial reentrant beats and short runs of irregular AT or AF.

Catheter-induced atrial beats. These beats usually have the earliest activation site recorded at that particular catheter tip and have the same atrial activation sequence as the atrial impulse produced by pacing from that catheter. Portions of the catheter proximal to the tip usually do not elicit mechanically induced ectopic impulses.

AVN echo beats. AVN echoes occur in the presence of anterograde dual AVN physiology (see Fig. 4.23). Such beats require anterograde block of the atrial stimulus in the fast AVN pathway, anterograde conduction down the slow pathway, and then retrograde conduction up the fast pathway. AVN echo beats have several features: they appear reproducibly after a critical A_2 - H_2 interval; the atrial activation sequence is consistent with retrograde conduction over the fast pathway, with the earliest atrial activation site in the HB; and the VA interval is very short, but it can be longer if the atrial stimulus causes anterograde concealment (and not just block) in the fast pathway.

AV echo beats. AV echo beats occur secondary to anterograde conduction of the atrial stimulus over the AVN-HPS and retrograde conduction over a BT (concealed or bidirectional BT). If preexcitation is manifest during atrial stimulation, the last atrial impulse inducing the echo beat will demonstrate loss of preexcitation because of anterograde block in the BT, and the atrial activation sequence and P wave morphology of the echo beat will depend on the location of the BT mediating VA conduction (see Fig. 3.9). These beats have a relatively short VA interval (QRS onset to earliest atrial activation) but always longer than 70 milliseconds. Moreover, the VA interval of the AV echo beat remains constant, regardless of the varying coupling interval of the AES triggering the echo beat ("VA linking"). Of note, AV echo beats also can occur secondary to anterograde conduction of the atrial stimulus over a manifest BT and retrograde conduction over the AVN, in which setting the last paced beat is associated with anterograde block in the AVN and fully preexcited QRS complex.

Programmed Ventricular Stimulation During Sinus Rhythm

Retrograde VA conduction. The absence of VA conduction (at ventricular PCLs greater than 600 milliseconds and despite isoproterenol administration) or the presence of decremental VA conduction makes the presence of a retrogradely conducting BT unlikely.

The normal AVN response to rate-incremental ventricular pacing or progressively premature single VESs is a gradual delay of VA conduction (manifest as gradual prolongation of the VA and His bundle-atrial [HA] intervals) as the PCL or VES coupling interval decreases. Non-decremental VA conduction suggests BT conduction, although fast pathway conduction in patients with AVNRT often shows minimal decrement. Nonetheless, some BTs with retrograde decremental conduction properties can also exhibit prolongation of conduction time and VA interval with ventricular pacing or VES. In addition, at short ventricular PCLs or VES coupling intervals, intramyocardial conduction delay can occur, resulting in prolongation in the VA interval; however, the local VA interval at the BT location remains unchanged. Furthermore, short ventricular PCLs or VES coupling intervals can encroach on the BT refractoriness, causing some decremental conduction, with a consequent increase in the surface VA interval and the local VA interval.

During the delivery of progressively premature single VESs, an abrupt increase in the VA conduction interval is often observed. This may be due to a variety of reasons including: (1) retrograde block in the AVN fast pathway and subsequent VA conduction over the slow pathway; (2) retrograde block in the right bundle branch (RB) and subsequent retrograde conduction over the left bundle branch (LB);

or (3) retrograde block in the BT and subsequent VA conduction only over the AVN.

Retrograde atrial activation sequence. VA conduction over the AVN produces a classic concentric atrial activation sequence starting in the anterosseptal or posteroseptal region of the RA because of retrograde conduction over either the fast or the slow AVN pathways, respectively. The duration of atrial activation is short because both atria are roughly simultaneously activated. Thus, if a normal P wave lasts 80 milliseconds (about 40 milliseconds for each atrium), a concentrically activated P wave (and total atrial activation time) approximates 40 milliseconds.

Eccentric retrograde atrial activation (i.e., lateral left atrium or RA earlier than AV junction and opposite chamber) can also occur. In the presence of a retrogradely conducting AV BT (whether manifest or concealed), atrial activation can result from conduction over the BT, over the AVN, or a fusion of both (see Fig. 18.25). Conduction over the BT alone is the most common pattern at short PCLs or short VES coupling intervals. In this setting, the VA conduction time is fairly constant over a wide range of PCLs and VES coupling intervals (given the absence of intraventricular conduction abnormalities or additional BTs). On the other hand, retrograde conduction over both the BT and HPS-AVN is especially common when RV pacing is performed in the presence of a left-sided BT at long PCLs or long VES coupling intervals. This occurs because it is easier to engage the RB and conduct retrogradely through the AVN than it is to reach a distant left-sided BT. In this setting, the atrial activation pattern depends on the refractoriness and conduction times over both pathways and usually exhibits a variable degree of fusion. In addition, VA conduction can proceed over the HPS-AVN alone, resulting in a normal pattern of VA conduction, or can be absent because of block in both the HPS-AVN and BT, which is especially common with short PCLs and very early VES.

An eccentric atrial activation sequence in response to ventricular stimulation suggests the presence of an AV BT mediating VA conduction (see Fig. 18.25). However, a concentric retrograde atrial activation sequence does not exclude the presence of a septal or paraseptal BT, or a free-wall BT located far from the pacing site, allowing for preferential VA conduction over the AVN. In addition, AVN slow pathway conduction can be associated with an eccentric atrial activation sequence in the CS. Accurate analysis of the atrial activation sequence frequently requires the use of multielectrode catheters around the tricuspid annulus and deep in the CS.¹⁶

Retrograde dual AVN physiology. Demonstration of retrograde dual AVN physiology during programmed ventricular stimulation suggests AVNRT (occurring most commonly during atypical AVNRT), but it can also be observed with other SVTs. Importantly, failure to demonstrate retrograde dual AVN physiology in patients with AVNRT can be the result of similar fast and slow AVN pathway ERPs, in which setting dissociation of refractoriness of the fast and slow AVN pathways is required (see Chapter 17).

VA block at a ventricular PCL greater than 600 milliseconds or decremental VA conduction during ventricular pacing makes the presence of a retrogradely conducting BT unlikely, except for decrementally conducting BTs and the rare catecholamine-dependent BTs. In addition, development of VA block during ventricular pacing in response to adenosine suggests the absence of a BT.

VES during His bundle refractoriness. A VES delivered when the HB is refractory (i.e., when the His potential is already manifest or within 35 to 55 milliseconds before the time of the expected His potential) that results in atrial activation is diagnostic of the presence of a retrogradely conducting BT. Because the HPS-AVN is already refractory and cannot mediate VA conduction, retrograde atrial

activation from ventricular stimulation will necessarily be mediated by a BT.

Furthermore, an earlier VES that does conduct to the HB and results in an atrial activation that either precedes HB activation (see Fig. 18.27) or is associated with an apparent HA interval shorter than that during drive complexes indicates “atrial preexcitation” via an AV BT.

Importantly, if a VES delivered when the HB is refractory does not result in atrial activation, this does not necessarily exclude the presence of a retrogradely conducting AV BT, because such a VES can be associated with retrograde block in the BT itself (see Fig. 18.25). In addition, the lack of such a response does not exclude the presence of unidirectional (anterograde-only) AV BTs.

Differential-site RV pacing. Differential-site RV pacing can help exclude the presence of a retrogradely conducting septal AV BT. The response to differential-site RV pacing can be evaluated by comparing two variables between RV basal and RV apical pacing: the VA interval (i.e., the stimulus-to-atrial [S-A] interval) and atrial activation sequence (see Fig. 18.28).

VA interval. In the absence of a septal BT, the RV apex, although anatomically more distant from the atrium than the RV base, is nonetheless electrically closer because of its proximity to the entrance to the HPS (i.e., RB terminus). Therefore the VA interval is shorter during pacing from the RV apex than that during RV basal pacing. In contrast, in the presence of a septal BT, the RV base is closer than the RV apex to the BT ventricular insertion site. As a result, the VA interval is shorter during RV basal pacing compared to apical pacing. Therefore, when the VA interval during RV apical pacing is longer than that during RV basal pacing, a retrogradely conducting AV BT is diagnosed (see Fig. 18.28), and when the VA interval during RV apical pacing is shorter than that during RV basal pacing, a retrogradely conducting septal BT is excluded. Importantly, while this maneuver suggests AVN conduction, it may not exclude the presence of a free wall or a slowly conducting BT. It is important to ensure that the basal pacing site captures neither the HB or the RB, nor the atrium, which would yield spurious results.

Atrial activation sequence. In the absence of a retrogradely conducting BT, the atrial activation sequence remains identical regardless of the RV pacing site because retrograde VA conduction propagates only over the AVN in both settings. In contrast, in the presence of a septal BT, atrial activation results from VA conduction over the BT during pacing at the RV base (because of its immediate proximity to the BT), and over the AVN, the BT, or a fusion of both during pacing at the RV apex. Therefore a change in retrograde atrial activation sequence in response to differential RV pacing (RV base vs. RV apex) indicates the presence of an AV BT, but a constant atrial activation sequence is not helpful in excluding the presence of a BT, because AVN-HPS conduction delay can allow retrograde VA conduction to occur over the BT during RV pacing from both the apex and the base.

Limitations. This maneuver does not exclude the presence of a distant right or left free-wall BT because the site of pacing is far from the BT; as a consequence, pacing from the RV apex or RV base may result in preferential VA conduction exclusively over the AVN and a constant atrial activation sequence. This can be avoided by moving the basal pacing site closer to the putative BT location along the tricuspid or mitral annulus.¹⁷

In addition, this maneuver does not exclude the presence of a slowly conducting BT. The VA interval criterion identifies the actual route of VA conduction and therefore the fastest path of this conduction; hence, a slowly conducting BT would be missed in the presence of fast VA conduction over the HPS-AVN.

The occurrence of right bundle branch block (RBBB) (but not LBBB) also can alter the significance of the VA interval criterion, especially

when VA conduction propagates over the HPS-AVN. In the presence of retrograde RBBB, VA conduction occurs over the LB-HB; therefore the VA interval depends on the distance between the pacing site and the LB rather than the RB, and access of the paced wavefront to the LB can be faster for RV basilar or septal pacing compared with pacing from the RV apex (Fig. 20.6).

Of note, the exact entrance to the HPS (i.e., the terminus of the RB) is difficult to identify; the entrance site can be located in the mid-septum and not at the RV apex. In such situations, both the RV base and apex can be equidistant from the entrance to the HPS so that pacing at either location will produce a constant VA interval during retrograde conduction over the AVN. Therefore patient-to-patient variability with regard to the distance of the pacing catheter to the RB terminus can potentially introduce conflicting results. This problem is largely resolved by first pacing from the HB region (while avoiding HB capture) and then moving the pacing catheter in a stepwise fashion along the septum toward the RV apex. Pacing from sequential sites in this path brings the catheter closer to the RB terminus (entrance of the

HPS), as reflected by shortening of the VA interval for AVN conduction, but not for BT conduction. As the pacing catheter is moved farther apically, the pacing sites become less useful diagnostically because the relative distance from the RB terminus to the insertion of the BT becomes less clear.¹⁷

Retrograde RBBB during VES. Retrograde RBBB occurs frequently during VES testing, and it can be diagnosed by observing the retrograde His potential during the drive train and its abrupt delay following the VES. Often, however, it is difficult to visualize the retrograde His potential during the pacing train; nevertheless, the sudden appearance of an easily distinguished retrograde His potential, separate from the ventricular electrogram following the VES, can be sufficient to recognize retrograde RBBB.

Prolongation of the VH interval is observed on development of retrograde RBBB because conduction must traverse the interventricular septum (which requires approximately 60 to 70 milliseconds in normal hearts), conduct retrogradely via the LB, and ascend to reach the HB. Although an increase in the VH interval necessarily occurs with retrograde

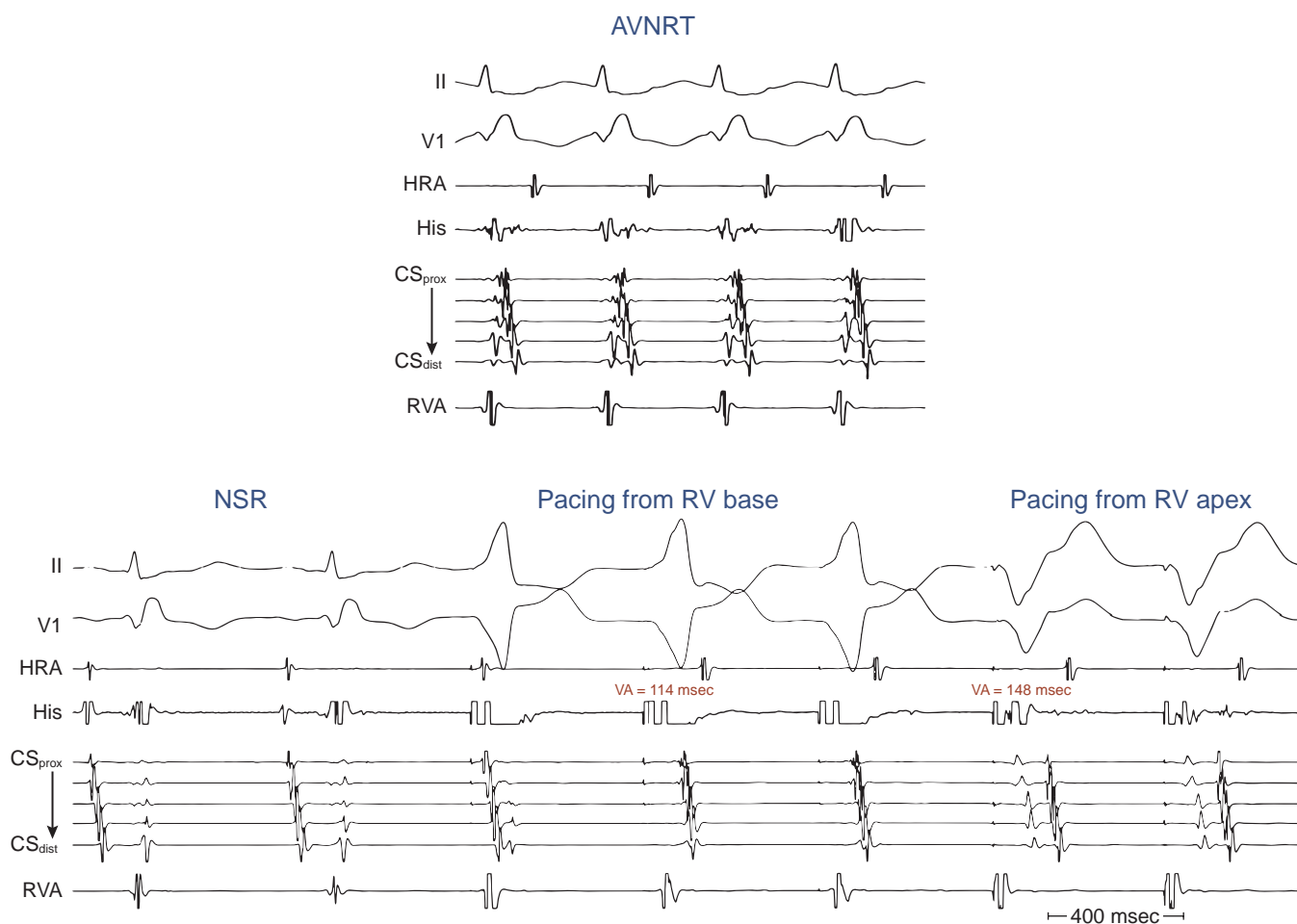


Fig. 20.6 Differential-Site Right Ventricular (RV) Pacing During Sinus Rhythm in the Presence of Right Bundle Branch Block (RBBB). Comparison between RV basal versus apical pacing during normal sinus rhythm (NSR, bottom panel) in a patient with typical atrioventricular nodal reentrant tachycardia (AVNRT) and RBBB (top panel) but no bypass tracts (BTs). RBBB is also observed during NSR (beginning of bottom panel). In the absence of a retrogradely conducting BT, pacing from the RV apex is expected to result in a shorter ventriculoatrial (VA) interval than pacing from the RV base. However, in this case, the presence of RBBB produces misleading results because retrograde VA conduction occurs over the left bundle branch–His bundle, and the VA interval depends on the distance between the pacing site to the left bundle branch, as opposed to the right bundle branch. CS_{dist}, Distal coronary sinus; CS_{prox}, proximal coronary sinus; HRA, high right atrium; RVA, right ventricular apex.

RBBB, whether a similar increase occurs in the VA interval depends on the nature of VA conduction (over the AVN vs. BT).

Measurement of the effect of the development of retrograde RBBB during VES on the retrograde VH and VA intervals can help in distinguishing between retrograde AVN and BT conduction. In the absence of a BT, the AVN can be activated in a retrograde fashion only after retrograde activation of the HB; as a consequence, VA activation will necessarily be delayed with retrograde RBBB, and the increase in the VA interval will be similar to the increase in the VH interval. On the other hand, when retrograde conduction is via a BT, there will be no expected increase in the VA interval when retrograde RBBB is induced. Thus the increase in the VA interval is minimal and always less than the increase in the VH interval.¹⁸

Extra ventricular beats. Ventricular stimulation can trigger extra ventricular beats or echo beats. These beats can be caused by different mechanisms.

Bundle branch reentrant beats. During RV stimulation at close coupling intervals, progressive retrograde conduction delay and block occur in the RB, so that retrograde HB activation occurs via the LB. At this point, the His potential usually follows the local ventricular electrogram. Further decrease in the VES coupling interval produces an increase in retrograde HPS conduction delay. When a critical degree of HPS delay (S_2 - H_2 interval) is attained, the impulse can return down the initially blocked RB and result in a QRS of similar morphology to the paced QRS at the RV apex—specifically, it will look like a typical LBBB pattern with left axis deviation because ventricular activation originates from conduction over the RB. The HV interval of the bundle branch reentry beat is usually longer than or equal to the HV interval during NSR. Retrograde atrial activation over the AVN, if present, follows the His potential (see Fig. 4.26); if over a left-sided BT, atrial activation follows the QRS.

AVN echo beats. AVN echoes are caused by reentry in the AVN in patients with retrograde dual AVN physiology (see Fig. 17.13). The last paced beat conducts retrogradely up the slow AVN pathway and then anterogradely down the fast pathway to produce the echo beat. AVN echoes appear reproducibly after a critical H_2 - A_2 interval (or V_2 - A_2 interval, when the His potential cannot be seen), and manifest as extra beats with a normal anterograde QRS morphology and atrial activity preceding the His potential before the echo beat. This phenomenon can occur at long or short coupling intervals and depends only on the degree of retrograde AVN conduction delay. In most cases, this delay is achieved before the appearance of a retrograde His potential beyond the local ventricular electrogram (i.e., before retrograde block in the RB).

AV echo beats. These beats occur secondary to retrograde block in the HPS-AVN and retrograde VA conduction over an AV BT, followed by anterograde conduction over the AVN. Alternatively, echo beats can result from retrograde block in the BT and retrograde VA conduction over the AVN-HPS, followed by anterograde conduction over the AV-BT. In the first setting, the echo beat displays a narrow QRS; in the latter setting, the echo beat is fully preexcited (see Fig. 18.25).

Intraventricular reentrant beats. This response occurs most commonly in the setting of a cardiac pathological condition, especially coronary artery disease, and usually occurs at short coupling intervals. It can have any QRS morphology, but more often RBBB than LBBB in patients with prior myocardial infarction. These responses are usually nonsustained (1 to 30 complexes) and typically polymorphic. In patients without prior clinical ventricular arrhythmias, such responses are of no clinical significance.

Catheter-induced ventricular beats. Such beats usually have the earliest ventricular activation site recorded at that particular catheter

tip and have the same QRS morphology as the QRS produced by pacing from that catheter.

Para-Hisian Pacing During Sinus Rhythm

Concept of para-Hisian pacing. The para-Hisian pacing site is unique because it is anatomically close but electrically distant from the HB. Para-Hisian pacing at high output simultaneously captures the HB or proximal RB, as well as the adjacent ventricular myocardium. At lower output, direct HB-RB capture is lost and retrograde activation of the HB is delayed because the HB and RB are insulated from the adjacent myocardium and the peripheral inputs to the Purkinje system are located far from the para-Hisian pacing site. By maintaining local ventricular capture while intermittently losing HB-RB capture, retrograde VA conduction can be classified as dependent on the timing of local ventricular activation (BT), HB activation (AVN), or both (fusion).

Para-Hisian pacing can result in capture of the ventricle (indicated by a wide paced QRS), the atrium (indicated by atrial activation in the HB region immediately following the pacing artifact), the HB (indicated by narrow paced QRS), or any combination of these (see Fig. 18.29). Careful attention must be given to minimize the atrial signal seen on the recording from the pacing electrode pair to ensure that local atrial capture does not occur during pacing.

Technique of para-Hisian pacing. Ideally, two quadripolar catheters (one for pacing and another for recording) or a single octapolar catheter (for both pacing and recording) is placed at the distal HB-RB region. Alternatively, a single quadripolar HB catheter (which is typically used during a diagnostic EP study) is used, taking into account that such an approach would limit the ability to record the retrograde His potential and HA interval.¹⁹

Overdrive ventricular pacing is performed (from the pair of electrodes on the HB catheter that records activation of the distal HB-RB) at a long PCL (greater than 500 milliseconds) and high output. During pacing, direct HB-RB capture is indicated by narrowing of the paced QRS width. The pacing output and pulse width are then decreased until the paced QRS widens, which is associated with a delay in the timing of the retrograde HB potential, indicating loss of HB-RB capture. The pacing output is increased and decreased to gain and lose HB-RB capture, respectively, while local ventricular capture is maintained. Occasionally, the HB can be captured uniquely (without myocardial capture), resulting in a QRS identical to the patient's normally conducted QRS.¹⁹

Response to para-Hisian pacing. When the ventricle and HB are captured simultaneously, the wavefront activates the ventricles over the HPS and results in a relatively narrow QRS. The wavefront can also travel retrogradely over the AVN to activate the atrium with an SA interval (i.e., the interval from the pacing stimulus to the atrial electrogram) that represents conduction time over the proximal part of the HB and AVN (i.e., SA interval = HA interval) because the onset of ventricular activation and HB activation occur simultaneously (i.e., stimulus-His bundle [SH] interval = 0).¹⁹

When the ventricle is captured but not the atrium or HB, the wavefront activates the ventricles by muscle-to-muscle conduction, resulting in a wide QRS with LBBB morphology caused by pacing in the RV. Once the wavefront reaches the RV apex, it conducts retrogradely up the RB and then over the HB and AVN to activate the atrium. In this setting, the SA interval represents the conduction time from the RV base to the HB (SH interval) plus the conduction time over the HB and AVN (HA interval). Thus, normally (in the absence of a retrogradely conducting BT), para-Hisian pacing results in a shorter SA interval when the HB (or HB plus RV) is captured than the SA interval when only the ventricle is captured.¹⁹

In the presence of a septal AV BT, the SA interval usually remains fixed regardless of whether the HB is being captured, because in both situations the paced impulse travels retrogradely over the BT, with constant conduction time to the atrium as long as local ventricular myocardium is being captured. Atrial activation in this setting can be secondary to activation over the BT, especially when only the ventricle is captured, or a result of fusion of conduction over both the BT and AVN, especially when both the ventricle and the HB are captured. Nevertheless, because VA conduction time over the BT is faster than that over the AVN, the timing of the earliest atrial activation (i.e., the SA and local VA intervals) remains constant, regardless of whether HB-RB capture occurs and regardless of whether atrial activation occurs exclusively over the AV BT or as a fusion of conduction over both the AV BT and AVN.¹⁹

Seven patterns of response to para-Hisian pacing can be observed (Box 20.1; see Figs. 18.29 and 18.30). In patients with retrogradely conducting BTs, in whom retrograde conduction occurs over both the

AVN and BT during para-Hisian pacing, the amount of atrial myocardium activated by each of the two pathways (atrial fusion) is dependent on four variables: (1) the magnitude of delay in retrograde activation of the HB (i.e., SH interval); (2) retrograde conduction time over the AVN (HA interval); (3) intraventricular conduction time from the para-Hisian pacing site to the ventricular end of the BT (SV_{BT}); and (4) retrograde conduction time over the BT (VA_{BT}). The first two variables (SH plus HA) form the SA interval resulting from retrograde VA conduction over the AVN, and the latter two variables (SV_{BT} plus VA_{BT}) form the SA interval resulting from retrograde VA conduction over the BT. The amount of the atria activated by the AVN is greater during HB-RB capture, secondary to a minimal SH interval (i.e., SA interval = HA interval). Loss of HB-RB capture results in prolongation of the SH interval and, therefore, an increase in the amount of atria activated by the BT, resulting in a change in the retrograde atrial activation sequence. Consequently, a change in the retrograde atrial activation sequence with loss of HB-RB capture always indicates the presence of

BOX 20.1 Response Patterns to Para-Hisian Pacing

Pattern 1 (AVN/AVN Pattern)

- Retrograde conduction occurs exclusively over the AVN regardless of whether the HB-RB is captured.
- Loss of HB-RB capture results in an increase in the SA interval in all electrograms equal to the increase in the SH interval, with no change in the atrial activation sequence. The HA interval remains essentially the same.
- This response indicates that retrograde conduction is dependent on HB activation and not on local ventricular activation.
- This pattern is observed in all patients with AVNRT and is not observed in any patient with a septal or right free-wall BT. However, this pattern can be observed in some patients with a left free-wall BT or PJRT, in which case retrograde AVN conduction masks the presence of retrograde BT conduction.

Pattern 2 (BT-BT Pattern)

- Retrograde conduction occurs exclusively over a single BT.
- The SA interval is identical during HB-RB capture and noncapture, indicating that retrograde conduction is dependent on local ventricular activation and not on HB activation.
- This pattern does not exclude the presence of retrograde conduction over the AVN with longer conduction time or a second BT with longer conduction time or located far from the pacing site.

Pattern 3 (BT-BT_L Pattern)

- Retrograde conduction occurs exclusively over a BT.
- Loss of HB-RB capture is associated with a delay in the timing of ventricular activation close to the BT. This results in an increase in the SA interval in all electrograms, with no change in the atrial activation sequence. The local VA interval, recorded close to the BT, remains approximately the same. The increase in the SA interval is less than the increase in the SH interval. Therefore the HA interval is shortened with loss of HB-RB capture, indicating that retrograde conduction cannot be occurring over the AVN. Two mechanisms have been identified accounting for the delay in timing of ventricular activation close to the BT.
- Activation of the HPS results in earlier ventricular activation near some BTs located far from the para-Hisian pacing site, such as left lateral or anterolateral BTs.
- Decreasing the pacing output to lose HB-RB capture occasionally results in a small delay in ventricular activation close to the pacing site.

- Pattern 3 is referred to as the BT-BT_L pattern, where BT_L refers to a lengthening of the SA interval with loss of HB-RB capture.

Pattern 4 (AVN-BT Pattern)

- Loss of HB-RB capture is associated with atrial activation exclusively over the BT.
- Loss of HB-RB capture results in an increase in SA and local VA intervals in all electrograms, with the least increase occurring in the electrogram closest to the BT.
- The HA interval shortens, indicating that the atrium near the AVN is activated by the BT before retrograde conduction over the AVN is complete.

Pattern 5 (AVN-Fusion Pattern)

- Loss of HB-RB capture results in activation of part of the atria by the AVN and part by the BT.
- Loss of HB-RB capture is associated with an increase in SA and local VA intervals in all electrograms.
- The HA interval remains constant, indicating that part of the atria was still activated by the AVN.

Pattern 6 (Fusion-BT Pattern)

- Loss of HB-RB capture results in atrial activation exclusively over the BT.
- Loss of HB-RB capture is associated with no change in the SA or local VA intervals recorded near the BT.
- In the HB electrogram, the SA interval increases, but not as much as the SH interval, leading to a decrease in the HA interval. This indicates that the atrial myocardium in that region is no longer activated by the AVN.

Pattern 7 (Fusion-Fusion Pattern)

- The atria continue to be activated by both the AVN and the BT during loss of HB-RB capture, with more of the atria activated by the BT than during HB-RB capture.
- Like pattern 6, loss of HB-RB capture is associated with minimal change in the SA or local VA intervals recorded close to the BT; however, the HA interval remains essentially the same, indicating that part of the atria is still activated by the AVN.

AVN, Atrioventricular node; AVNRT, atrioventricular nodal reentrant tachycardia; BT, bypass tract; HA, His bundle–atrial; HB-RB, His bundle–right bundle branch; HPS, His-Purkinje system; PJRT, permanent junctional reciprocating tachycardia; SA, stimulus-atrial; SH, stimulus–His bundle; VA, ventriculoatrial.

retrograde conduction over both the BT and AVN. There are four such patterns (patterns 4 through 7). In patterns 4 and 5, HB-RB capture is associated with activation of the atria exclusively by retrograde conduction over the AVN. In patterns 6 and 7, HB-RB capture results in atrial activation over both the AVN and the BT.¹⁹

Interpretation of results of para-Hisian pacing. The response to para-Hisian pacing can be determined by comparing the following four variables between HB-RB capture and noncapture while maintaining local ventricular capture and no atrial capture: (1) atrial activation sequence, (2) SA interval, (3) local VA interval, and (4) HA interval (see Figs. 18.29 and 18.30).

The SA interval is defined as the interval between the pacing stimulus and atrial electrogram. It should be recorded at multiple sites, including those close to the site of earliest atrial activation during SVT.

The local VA interval is defined as the local ventricular-to-atrial electrogram interval in the electrode position with the earliest retrograde atrial activation time. For the local VA to be relied on, it actually has to be measured at the site of earliest atrial activation (this requires positioning a catheter at the site of earliest atrial activation recorded during SVT). The high RA catheter, for example, may not be satisfactory for evaluation of the local VA interval in the presence of a septal BT.

The HA interval is recorded in the HB electrogram; however, this measurement can be obtained only if two catheters are placed in the HB position (one catheter for pacing and a second catheter for recording) or if an octapolar catheter is used for pacing and sensing around the HB. The use of a single quadripolar HB catheter, which is typically used during a diagnostic EP study, negates the ability to record the retrograde His potential and HA interval during pacing. However, the combination of the SA and local VA intervals is sufficient to identify the presence of a retrograde BT.

If the SA (and local VA) interval at any site remains fixed, regardless of whether HB-RB capture occurs, while the HA interval shortens, retrograde conduction is occurring only over an AV BT. In this setting, the HA interval shortens on loss of HB-RB capture because the HB and atrium are activated in parallel and HB activation is delayed because of prolongation of the SH interval, while atrial activation timing remains unchanged because it results from retrograde conduction over the AV BT and is independent of the timing of HB activation. On the other hand, if the SA (and local VA) interval increases in all electrograms (including the electrode recording the earliest atrial activation) coincident with loss of HB-RB capture, while the HA interval remains essentially the same, retrograde conduction is occurring only over the AVN.

An identical retrograde atrial activation sequence during HB-RB capture and noncapture indicates that retrograde conduction is occurring over the same system (either the BT or AVN) and does not help prove or exclude the presence of a BT (especially a septal BT; see Fig. 18.30). A change in the retrograde atrial activation sequence with loss of HB-RB capture, however, indicates the presence of retrograde conduction over both a BT and the AVN. Morphological change in the atrial electrogram recorded at the AV junction without overlapping the ventricular electrogram also seems to have diagnostic significance, indicating the presence of both BT and AVN conduction.

Limitations of para-Hisian pacing. The location of the BT and the retrograde conduction time over the BT must be taken into account when interpreting the results of para-Hisian pacing. For superoparaseptal BTs, the SV_{BT} interval is short. For BTs located progressively farther from the para-Hisian pacing site, the SV_{BT} increases progressively. This is not a significant factor for midseptal, posteroseptal, or most right free-wall BTs. However, for left free-wall BTs, which are located far from the pacing site, the SV_{BT} interval can be sufficiently long to have the

entire atria activated by the AVN, even during loss of HB-RB capture. In this setting, para-Hisian pacing can produce an AVN retrograde conduction pattern, regardless of whether the HB-RB is captured (pattern 1: AVN-AVN), and fail to identify the presence of retrograde BT conduction (because of the long SV_{BT}). However, a left lateral BT should not be a diagnostic challenge because of the obvious eccentric retrograde atrial activation sequence during orthodromic AVRT, and para-Hisian pacing is performed mainly to investigate the presence of a septal BT. In addition, for BTs located far from the para-Hisian pacing site, it is important to record atrial activation close to the suspected site of the BT. Otherwise, the change in the atrial activation sequence may not be identified, incorrectly suggesting that retrograde conduction is occurring over just the AVN. This is most likely to occur in patients with short retrograde AVN conduction (short HA interval) and a BT located far from the pacing site.

Para-Hisian pacing may fail to identify retrograde conduction over a slowly conducting BT (e.g., PJRT) because of the long VA_{BT} interval. Performing para-Hisian entrainment or resetting during SVT can help in these situations (see later). In addition, although para-Hisian pacing during NSR can help prove the presence of an AV BT, it does not show whether that BT is operative during the SVT.

In patients with very proximal retrograde RBBB, RB capture may fail to produce early retrograde activation of the HB, limiting the use of para-Hisian pacing in these patients. This observation suggests that HB-RB capture actually represents capture of the proximal RB and not HB capture. This is supported by the observation that, during HB-RB capture, the HB potential is often recorded 10 to 20 milliseconds after the pacing stimulus. Importantly, para-Hisian pacing has been performed successfully in many patients with more distal RBBB (see Fig. 18.29).

Assurance of lack of atrial capture by the pacing stimulus is important for correct interpretation of the results of para-Hisian pacing. Atrial capture is indicated by a very short SA interval in the electrodes just proximal to the pacing electrodes. It is sometimes helpful to withdraw the para-Hisian pacing catheter until atrial capture alone is seen; if the SA interval in the presence of ventricular capture is not longer than this, atrial capture was also present and the test should be repeated at a more distal pacing site.

Dual-Chamber Sequential Extrastimulation During Sinus Rhythm

Dual-chamber sequential extrastimulation is a useful maneuver for identifying retrogradely conducting AV BTs, even slowly conducting BTs and BTs with decremental properties. This maneuver relies on concealed AVN conduction during a critically timed AES to cause transient retrograde AVN blockade at the time a VES is delivered, thereby allowing the BT to become manifest with the VES (analogous to delivering a VES during HB refractoriness).²⁰

The dual-chamber sequential extrastimulation maneuver consists of an eight-beat drive train of simultaneous atrial and RV pacing at 600 milliseconds, followed by an AES (A_2) delivered at a coupling interval equal to the AVN ERP, followed by a VES (V_2) delivered at a coupling interval equal to the drive train cycle length (CL) (600 milliseconds). Repeat drives are then performed with decrements of 10 milliseconds for V_2 until VA block is observed.²⁰

The critically timed A_2 prolongs the AVN refractory period via concealed anterograde conduction, causing V_2 to block in the AVN when it would have conducted had A_2 not been delivered. If a BT is present, V_2 conducts back to the atrium while the AVN remains refractory, resulting in a retrograde atrial activation pattern consistent with exclusive BT conduction. Although there can also be some degree of concealed anterograde conduction into the BT during A_2 stimulation, the more pronounced decremental properties of AVN tissue should

prolong AVN refractoriness to a greater degree than that of the BT, allowing exclusive retrograde conduction over the BT to remain intact during V_2 stimulation.²⁰

This maneuver has several potential limitations. First, atrial ERP may exceed anterograde AVN ERP. In addition, local atrial ERP at the site of BT insertion can render the atrium refractory to the wavefront traveling retrogradely over the BT. Therefore atrial pacing during this maneuver ideally should be performed at a site in close proximity to the atrial insertion of the BT if possible. Furthermore, the AES may cause anterograde concealed conduction in the BT, potentially resulting in BT conduction block during delivery of V_2 . The success of this pacing maneuver relies on the differential effects of concealed conduction into the AVN and BT, with greater extension of refractoriness in the former than the latter.²⁰

Induction of Tachycardia

Initiation by Programmed Atrial Stimulation

Inducibility. All types of paroxysmal SVTs can be inducible with atrial stimulation (except automatic AT). Initiation can require catecholamines (isoproterenol) with any type of SVT, and this observation does not help for differential diagnosis. However, automatic AT can start spontaneously (without atrial stimulation) during isoproterenol or epinephrine infusion.

SVT initiation that is reproducibly dependent on a critical atrial–His bundle (AH) interval is classic for typical AVNRT (see Fig. 17.11). This is because anterograde block in the fast pathway in conjunction with sufficient delay in anterograde conduction over the slow pathway (“critical AH interval”) are necessary to allow for recovery of the fast pathway to conduct retrogradely and initiate AVN reentry. Atypical AVNRT is usually initiated with modest prolongation of the AH interval along the fast pathway with anterograde block in the slow pathway, followed by retrograde slow conduction over the slow pathway. Therefore a critical AH interval delay is not obvious (see Fig. 17.12).

Orthodromic AVRT usually requires some AV delay for initiation; however, the delay can occur anywhere along the AVN–HPS axis. In patients with baseline manifest preexcitation, initiation of orthodromic AVRT is usually associated with anterograde block in the AV BT and loss of preexcitation following the initiating atrial stimulus, which would then allow that BT to conduct retrogradely during the SVT.

No delay in the AH or PR interval is required for initiation of AT, although it can occur. AV block can also occur at initiation. Automatic ATs cannot be reproducibly initiated by AES or atrial pacing.

Warm-up. Progressive shortening of the TCL for several beats (warm-up) before its ultimate rate is achieved is characteristic of automatic AT, but may occur in other SVTs as well.

VA interval. If the VA interval of the first tachycardia beat is reproducibly identical to that during the rest of the SVT, AT is very unlikely, and such “VA linking” is suggestive of typical AVNRT and orthodromic AVRT.

Initiation by Programmed Ventricular Stimulation

Inducibility. Ventricular stimulation commonly induces AVRT and AVNRT. On the other hand, it is uncommon to initiate AT with VES or ventricular pacing because decremental retrograde conduction over the AVN prevents adequate prematurity of atrial activation.

Postpacing intervals. If SVT is induced during VES, the interval between the VES (delivered from the RV apex) that initiates SVT and the first cycle of tachycardia can provide information about the circuit that are essentially equivalent to those observed with ventricular entrainment (see later). The interval from the VES to atrial activation (surface VA or “S–A” interval) is compared to the surface VA interval during SVT, and the post-VES return cycle (i.e., the interval from the VES to

the subsequent RV apical depolarization) is compared to the TCL. An SA interval that exceeds the surface VA interval during SVT by less than 85 milliseconds is consistent with orthodromic AVRT. Similarly, when the post-VES return cycle exceeds the TCL by less than 115 milliseconds, orthodromic AVRT is indicated. The small differences between those intervals are related to the proximity of the RV apical pacing site to the AVRT reentry circuit. Larger differences in these intervals are observed in the setting of AVNRT or orthodromic AVRT utilizing a left lateral BT or a septal BT with decremental conduction. The unique advantage of this technique is that they do not have a requirement for sustained tachycardia that can be successfully entrained.²¹

Furthermore, when induction of the SVT is achieved by ventricular pacing at a CL similar to the subsequent TCL or by a VES that activates the HB at a coupling interval (i.e., H_1 – H_2 interval) similar to the H–H interval during the SVT (i.e., similar to the TCL), the HA interval following the initiating ventricular stimulus is then compared with that during the SVT. During AVNRT, the HA interval of the ventricular stimulus initiating the SVT is longer than the HA interval during the SVT, because both the HB and atrium are activated in sequence during ventricular stimulation but in parallel during AVNRT (see Fig. 17.14). This is even exaggerated by the fact that the AVN usually exhibits greater decremental conduction with repetitive engagement of impulses than to a single impulse at a similar coupling interval. Therefore the more prolonged the HA interval with the initiating ventricular stimulus, the more likely the SVT is AVNRT. On the other hand, if the SVT uses an AV BT for retrograde conduction, the HA interval during the initiating ventricular stimulus (at a coupling interval comparable to the TCL) is shorter than that during orthodromic AVRT because the HB and atrium are activated in parallel during ventricular pacing (when atrial activation is mediated by retrograde BT conduction), but in sequence during SVT.

Tachycardia Features

Atrial Activation Sequence

During typical AVNRT, the initial site of atrial activation is usually recorded in the HB catheter at the apex of the triangle of Koch. In contrast, the initial site of atrial activation during atypical AVNRT is usually recorded at the base of the triangle of Koch or CS os (see Fig. 17.2). On the other hand, in orthodromic AVRT, the initial site of atrial activation depends on the location of the AV BT, but is always near the AV groove, without multiple breakthrough points. It is comparable to that during ventricular pacing when VA conduction occurs exclusively over the AV BT. The atrial activation sequence during AT depends on the origin of the AT, and can simulate that of other types of SVTs.

In summary, eccentric atrial activation during SVT excludes typical and atypical AVNRT, except for the left variant of AVNRT, during which the earliest atrial activation occurs in the proximal or mid-CS. Furthermore, an eccentric atrial activation sequence that originates away from the AV rings is diagnostic of AT and excludes both AVNRT and AVRT.

Atrial-Ventricular Relationship

PR–RP intervals. During AT, the PR interval is appropriate for the AT rate and is usually longer than that during NSR. The faster the AT rate, the longer the PR interval. Thus the PR interval can be shorter, longer, or equal to the RP interval. The PR interval can also be equal to the R–R and the P wave can then fall within the preceding QRS, mimicking typical AVNRT.

During typical AVNRT, the RP interval is very short (–40 to 75 milliseconds); in contrast, during atypical fast-slow AVNRT, the RP interval is longer than the PR interval. On the other hand, during orthodromic AVRT, the RP interval is short but longer than that in typical AVNRT because the wavefront has to activate the ventricle before it

reaches the AV BT and subsequently conduct retrogradely to the atrium. Thus the ventricle and atrium are activated in sequence, in contrast to AVNRT, during which the ventricle and atrium are activated in parallel, resulting in abbreviation of the VA interval. Consequently, a very short VA interval (less than 70 milliseconds) or short V–high RA interval (less than 95 milliseconds) largely excludes orthodromic AVRT, and favors typical AVNRT. However, VA intervals shorter than 70 milliseconds have occasionally been observed in adult patients with orthodromic AVRT utilizing left lateral or left posteroseptal BTs.^{22,23}

Because the retrograde limb of the reentry circuit in PJRT is the slow BT (which conducts more slowly than the AVN), the RP interval is longer than the PR interval, similar to fast-slow AVNRT (see Figs. 18.14 and 18.39).

AV block. The presence of AV block during SVT excludes AVRT, is uncommon during AVNRT, and strongly favors AT (Fig. 20.7). AV block occurs commonly during AT, with either Wenckebach periodicity or fixed-ratio block. AV block may also occur during AVNRT because of block below the reentry circuit (usually below the HB and infrequently in the lower common pathway), which can occur especially at the onset of the SVT, during acceleration of the SVT, and following a PVC or a VES (see Fig. 17.9).

VA block. VA block during SVT is a rare phenomenon, and may occasionally be observed in infraatrial SVTs, including junctional ectopic tachycardia and orthodromic AVRT using a nodofascicular or nodoventricular BT for retrograde conduction. VA block during AVNRT has been reported (see eFig. 17.2). Intra-Hisian reentry is another potential mechanism, but it is a theoretical entity whose clinical occurrence has not been convincingly demonstrated.^{12–14}

Variation of the P/QRS relationship. Spontaneous changes in the PR and RP intervals with fixed atrial-atrial (A-A) interval favor AT and exclude orthodromic AVRT (Fig. 20.8). On the other hand, spontaneous changes in TCL accompanied by a constant VA interval (“VA linking”) suggest orthodromic AVRT (see Fig. 18.36). During orthodromic AVRT, the RP interval remains fixed, regardless of oscillations in TCL from whatever cause or changes in the PR (AH) interval. Thus the RP/PR ratio may vary, and the TCL is most closely associated with the PR interval (i.e., anterograde slow conduction). In contrast to the classic fast AV BTs, the RP interval during PJRT is not fixed because the BT serving as the retrograde limb of the reentrant circuit has decremental properties.

Variation of the P/QRS relationship (with changes in the AH interval, HA interval, and AH/HA ratio), with or without block, can occur during AVNRT, especially in atypical or slow-slow AVNRT. This phenomenon usually occurs during initiation or termination of the tachycardia or in cases of nonsustained tachycardias, likely because of decremental conduction in the lower common pathway.

The ECG manifestation of P/QRS variations, with or without AV block during tachycardia, should not be misdiagnosed as AT; they can be atypical or, rarely, typical forms of AVNRT. Moreover, the variations could be of such magnitude that a long RP tachycardia can masquerade for brief periods of time as short RP tachycardia.

Oscillation in Tachycardia Cycle Length

Analysis of TCL variability can provide useful diagnostic information that is available even when episodes of SVT are nonsustained. TCL variability of at least 15 milliseconds in magnitude was found to occur

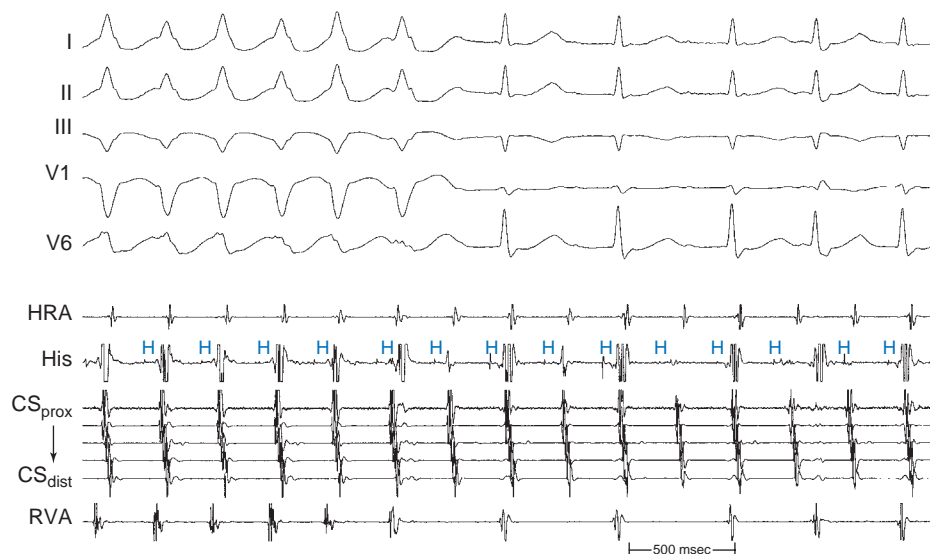


Fig. 20.7 Supraventricular Tachycardia (SVT) With Concentric Atrial Activation Sequence and Intermittent Atrioventricular (AV) Block. *At left*, A wide complex tachycardia with left bundle branch block (LBBB) pattern and 1:1 AV ratio is shown. Simultaneous atrial and ventricular activation is observed, excluding atrioventricular reentrant tachycardia (AVRT) as the mechanism of the tachycardia, and favoring typical atrioventricular nodal reentrant tachycardia (AVNRT) or atrial tachycardia (AT) with a long PR interval. *At right*, 2:1 AV block is observed without disruption of the tachycardia. Normalization of QRS morphology is observed during the period of 2:1 AV block, suggesting that wide QRS morphology during 1:1 AV conduction was a result of functional LBBB. The development of AV block with continuation of the tachycardia confirms that the ventricle is not part of the tachycardia circuit and, thus, excludes AVRT. The presence of His potentials, even during the blocked beats, suggests that the block is infra-Hisian. The observation of AV block favors AT, but does not exclude AVNRT. The ventriculoatrial (VA) interval remains constant following both the narrow and wide QRS complexes, which suggests AVNRT. Other pacing maneuvers confirmed that this SVT was in fact typical AVNRT. CS_{dist}, Distal coronary sinus; CS_{prox}, proximal coronary sinus; HRA, high right atrium; RVA, right ventricular apex.

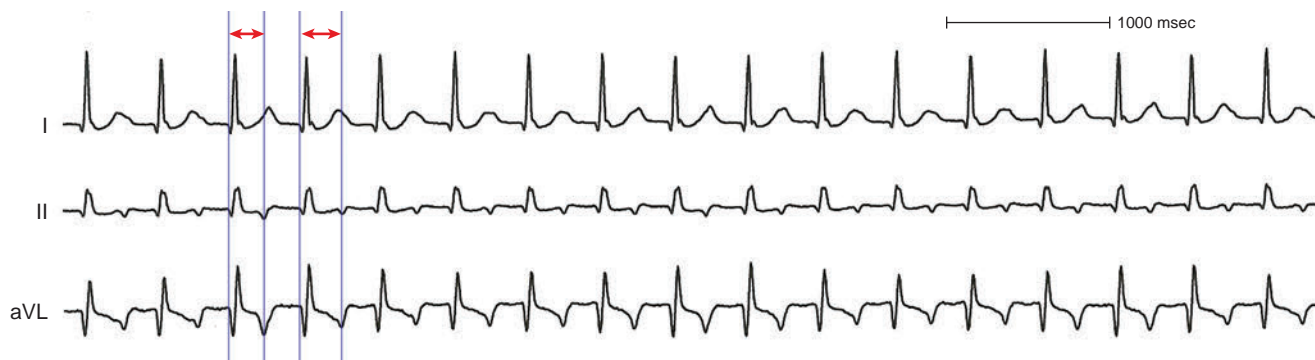


Fig. 20.8 Supraventricular Tachycardia (SVT) With Variable RP Intervals. Three surface electrocardiogram leads are shown. The P waves are inscribed within the T waves, and are more discernible with negative polarity in lead aVL. Note that the RP interval varies during the SVT (arrows) with constant atrial-atrial intervals, consistent with atrial tachycardia as the mechanism of the SVT and excludes orthodromic atrioventricular reentrant tachycardia.

in up to 73% of paroxysmal SVTs and was equally prevalent in AT, AVNRT, and orthodromic AVRT.

Changes in atrial CL preceding similar changes in subsequent ventricular CL strongly favor AT or atypical AVNRT (see Fig. 17.15). In contrast, when the change in atrial CL is predicted by the change in preceding ventricular CL, typical AVNRT (see eFig. 17.2) or orthodromic AVRT is the most likely mechanism (see Fig. 18.36).

The AVN participates either actively or passively in all types of narrow complex SVTs and the AV interval can vary depending on the preceding atrial CL and autonomic tone. A change in anterograde or retrograde AVN conduction can result in TCL variability in AVNRT or orthodromic AVRT. However, during AT, changes in anterograde AVN conduction produce only changes in ventricular CL, whereas the atrial CL remains unaffected. Therefore spontaneous changes in the ventricular CL in conjunction with fixed A-A interval (typically manifesting as variations in the PR and RP intervals) favor AT.²⁴

Changes in atrial CL during AT result from changes in the CL of the atrial focus itself, and this causes similar variability in the conducted ventricular CL. Therefore, when there is CL variability in both the atrium and ventricle, changes in atrial CL during AT would be expected to precede and predict the changes in ventricular CL. However, ventricular CL variability can be caused by changes in AV conduction instead of changes in the CL of an AT, in which case ventricular CL variability may not be predicted by a prior change in atrial CL during AT. Nevertheless, because there is no VA conduction during AT, ventricular CL variability alone would not be expected to result in atrial CL variability during AT.²⁴

In contrast to AT, typical AVNRT and orthodromic AVRT generally have CL variability because of changes in anterograde AVN conduction. Because retrograde conduction through a fast AVN pathway or a BT is generally much less variable than anterograde conduction through the AVN, the changes in ventricular CL that result from variability in anterograde AVN conduction would be expected to precede the subsequent changes in atrial CL. This explains why the change in atrial CL does not predict the change in subsequent ventricular CL in typical AVNRT and orthodromic AVRT. On the other hand, in atypical AVNRT, anterograde conduction occurs over the more stable fast AVN pathway and retrograde conduction is more subject to variability. This explains the finding that changes in atrial CL predict the changes in subsequent ventricular CL in atypical AVNRT (as is the case in AT).²⁴

In addition, orthodromic AVRT in the presence of dual AVN physiology can be associated with anterograde conduction alternating over

the slow and fast AVN pathways, resulting in a regular irregularity of the TCL (alternating long and short cycles). Importantly, the RP interval during the SVT remains constant, regardless of the PR interval.

Effects of Bundle Branch Block

The development of BBB during SVT that does not influence the TCL (A-A or H-H interval) or the VA interval is consistent with AT, AVNRT (see Fig. 17.9), and orthodromic AVRT using a BT in the ventricle contralateral to the BBB, because the ventricle affected by conduction delay is not part of the SVT circuit (see Fig. 18.35), but excludes orthodromic AVRT using a BT ipsilateral to the BBB.

BBB ipsilateral to the AV BT mediating orthodromic AVRT results in prolongation of the “surface VA interval” (QRS onset to atrial electrogram) compared to that during narrow QRS tachycardia because of the extra time required for the impulse to travel from the AVN down the HB and contralateral bundle branch, and transeptally to the ipsilateral ventricle to reach the AV BT and then activate the atrium (see Fig. 18.37). However, the “local VA interval” (measured at the site of BT insertion) remains constant. In addition, the TCL usually increases in concordance with the increase in the surface VA interval as a result of ipsilateral BBB because of the now-larger tachycardia circuit; however, because the time the wavefront spends outside the AVN is now longer, AVN conduction may improve, resulting in shortening in the AH interval (and PR interval), which can potentially counterbalance, at least in part, the effects of prolongation of the VA interval on the total TCL. Thus the surface VA interval and not the TCL should be used to assess the effects of BBB on the SVT (see Fig. 18.12).

Prolongation of the surface VA interval during SVT in response to BBB by more than 35 milliseconds suggests that an ipsilateral free-wall AV BT is present and is participating in the SVT (i.e., diagnostic of orthodromic AVRT). On the other hand, prolongation of the surface VA by 25 to 35 milliseconds suggests a septal AV BT (posteroseptal AV BT in association with LBBB, and superoparaseptal AV BT in association with RBBB) (Fig. 20.9). In contrast, BBB contralateral to the AV BT does not influence the VA interval or TCL because the contralateral ventricle is not part of the reentrant circuit (see Figs. 18.35 and 18.37).

Because the occurrence of BBB during SVT is much more common in orthodromic AVRT than AVNRT or AT (90% of SVTs with sustained LBBB are orthodromic AVRTs), the mere presence of LBBB aberrancy during SVT is suggestive of orthodromic AVRT, but can still occur in other types of SVTs.



Fig. 20.9 Effect of Right Bundle Branch Block (RBBB) on Supraventricular Tachycardia (SVT). RBBB is initially present during an SVT with short RP interval and concentric atrial activation. Introduction of a ventricular extrastimulus (S2) from the right ventricular apex (RVA) during the tachycardia is followed by resolution of RBBB ("peeling back" refractoriness). Note that the loss of RBBB is associated with shortening of the ventriculoatrial (VA) interval (by 21 milliseconds) and a milder degree of shortening of the tachycardia cycle length (by 8 milliseconds), indicating the presence and participation of a septal BT in the reentrant circuit, which establishes the diagnosis of orthodromic atrioventricular reentrant tachycardia. CS_{dist}, Distal coronary sinus; CS_{prox}, proximal coronary sinus; HRA, high right atrium.

Tachycardia Termination and Response to Physiological and Pharmacological Maneuvers

Spontaneous termination. Spontaneous termination of orthodromic AVRT usually occurs because of anterograde gradual slowing and then block in the AVN, sometimes causing initial oscillation in the TCL, with alternate complexes demonstrating a Wenckebach periodicity before block. However, termination with retrograde block in the AV BT can occur without any perturbations of the TCL during very rapid orthodromic AVRT or following a sudden shortening of the TCL (e.g., after resolution of ipsilateral BBB or shift of anterograde conduction from the slow to the fast AVN pathway).

Spontaneous termination of AVNRT occurs because of block in the fast or slow pathway. However, the better the retrograde fast pathway conduction, the less likely that it is the site of block.

Spontaneous termination of AT is usually accompanied by progressive prolongation of the A-A interval, with or without changes in AV conduction. During AT with 1:1 AV conduction, the last beat of AT is conducted to the ventricle. Spontaneous termination of SVT with a P wave not followed by a QRS practically excludes AT, except coincidentally or in the case of a nonconducted PAC terminating the AT (neither of which will be reproducible).

Termination with adenosine. Adenosine terminates the vast majority of orthodromic AVRTs (by blocking AVN conduction) and AVNRTs (by blocking slow pathway conduction). Also, a significant proportion of focal ATs can be terminated by adenosine, typically (80%) prior to the onset of AV block (i.e., termination occurs with a tachycardia P wave that is followed by a conducted QRS). Although adenosine may not terminate ATs, it can help confirm the diagnosis of AT when it causes transient AV block without terminating the tachycardia. In addition, adenosine can help identify automatic ATs, which are generally transiently slowed but not terminated, with gradual resumption of the AT rate.

Adenosine generally terminates atypical AVNRT by gradual slowing and then block in the retrograde slow pathway. Adenosine usually terminates PJRT by block in the AVN (two-thirds) or in the BT (one-third) (see eFig. 18.5). Although the mode of tachycardia termination by adenosine has been suggested to distinguish between PJRT and atypical AVNRT, one report has shown that termination of atypical AVNRT with adenosine can also result from block in the fast AVN pathway and, therefore, its value in distinguishing between atypical AVNRT and PJRT is questionable.

In summary, the mere termination of SVT in response to adenosine is usually not helpful in differentiating SVTs. However, the pattern of SVT termination can be helpful in two situations: First, reproducible termination of the SVT with a QRS not followed by a P wave excludes orthodromic AVRT using a rapidly conducting AV BT as the retrograde limb (adenosine blocks the AVN and not the BT), is unusual in typical AVNRT (adenosine blocks the slow pathway with little or no effect on fast pathway conduction), and is consistent with AT, PJRT, or atypical AVNRT. Second, reproducible termination of the SVT with a P wave not followed by a QRS excludes AT, because it occurs in AT only if adenosine terminates the AT at the same moment it causes AV block, which is an unlikely coincidence (Fig. 20.10).²⁵

Termination with vagal maneuvers. Carotid sinus massage and vagal maneuvers can slow or terminate sinus node reentrant tachycardia and 25% of microreentrant ATs (especially those with long TCLs and those arising in the RA), and, to a lesser degree, triggered-activity ATs. However, these interventions may slow but do not generally terminate automatic AT.

Orthodromic AVRT usually terminates with gradual slowing and then block in the AVN. Typical AVNRT usually terminates with gradual anterograde slowing and then block in the slow pathway; block in the fast pathway is uncommon. In addition, carotid sinus massage and vagal maneuvers terminate atypical AVNRT by gradual slowing and

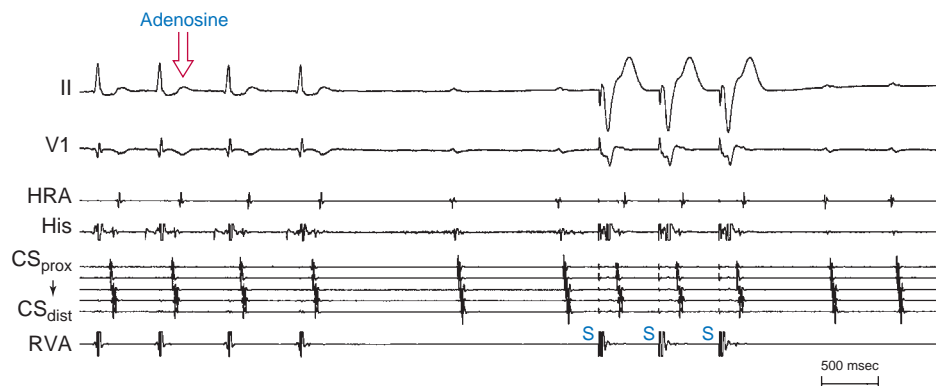


Fig. 20.10 Termination of Supraventricular Tachycardia (SVT) With Adenosine. Administration of adenosine during an SVT with concentric atrial activation sequence and short RP interval results in termination of the SVT with an atrial complex not followed by a QRS, which is inconsistent with atrial tachycardia. Following termination of the SVT, complete atrioventricular (AV) block during sinus rhythm is observed; however, ventricular pacing is associated with intact ventriculoatrial (VA) conduction and a retrograde atrial activation sequence identical to that during the SVT, which suggests that VA conduction is not mediated by the atrioventricular node (AVN) but by an AV bypass tract (BT). The SVT is in fact an orthodromic atrioventricular reentrant tachycardia using a concealed septal BT, and termination with adenosine was the result of block in the AVN. Retrograde conduction over the BT was not affected by adenosine. *CS_{dist}*, Distal coronary sinus; *CS_{prox}*, proximal coronary sinus; *HRA*, high right atrium; *RVA*, right ventricular apex.

then block in the retrograde slow pathway (see Fig. 17.15). Carotid sinus massage usually terminates PJRT by block in either the AVN or the BT.

Diagnostic Maneuvers During Tachycardia

Atrial Extrastimulation During Tachycardia

Resetting. An AES can reset AT, AVNRT, and orthodromic AVRT, and demonstration of resetting by itself is not helpful in distinguishing among the different types of SVTs. However, several characteristics of tachycardia resetting can help in the differential diagnosis.

Manifest atrial fusion. Resetting with manifest atrial fusion (as demonstrated by intermediate P wave morphologies on the surface ECG, or partial activation change recorded by multiple endocardial electrodes) can be demonstrated only in orthodromic AVRT and macroreentrant atrial tachycardia (MRAT), but not with AVNRT or focal AT. For atrial fusion (i.e., fusion of atrial activation from both the tachycardia wavefront and the AES) to occur, the AES should be able to enter the reentrant circuit while at the same time the tachycardia wavefront should be able to exit the circuit. This requires spatial separation between the entry and exit sites to the reentrant circuit, a condition that seems to be lacking in the setting of AVNRT and focal AT.

Resetting response curve. AES can reset microreentrant AT, AVNRT, and orthodromic AVRT with a resetting response classic for reentry (increasing or mixed response). In contrast, triggered activity AT exhibits a decreasing resetting response curve, and automatic AT exhibits an increasing response curve.

Termination. Termination of SVT with an AES is not usually helpful for the differential diagnosis. An AES can reproducibly terminate reentrant AT, AVNRT, and orthodromic AVRT. Termination of triggered activity AT is less reproducible. AES generally does not terminate automatic AT.

Atrial Overdrive Pacing During Tachycardia

Entrainment. Overdrive pacing at a CL approximately 10 to 30 milliseconds shorter than the TCL is usually able to entrain reentrant AT, AVNRT, and orthodromic AVRT but not triggered activity or automatic ATs.

Manifest atrial fusion. As discussed earlier, entrainment with manifest atrial fusion can be demonstrated only in AVRT and MRAT, but not with AVNRT or focal AT (see Fig. 18.40). Therefore, during entrainment of AVNRT and focal AT by atrial pacing, the atrial activation sequence and P wave morphology are always similar to those of pure paced morphology. Importantly, variable degrees of surface P wave or intracardiac electrogram fusion can be observed at the beginning of overdrive pacing, and should not be mistaken for constant fusion during entrainment.^{26,27}

ΔAH interval. During entrainment at a PCL close to the TCL, the AH interval during entrainment is longer than that during AVNRT. In contrast, in the setting of AT and orthodromic AVRT, the AH interval is comparable during SVT and entrainment with atrial pacing.

Acceleration. Overdrive pacing during triggered activity-related AT generally produces acceleration of the atrial CL. Following atrial overdrive pacing during AT due to triggered activity, the return atrial CL tends to shorten with shortening of the PCL.

Overdrive suppression. Automatic AT cannot be entrained by atrial pacing; however, rapid atrial pacing results in overdrive suppression of the AT rate. The AT resumes after cessation of atrial pacing but at a slower rate and gradually speeds up (warms up) to return to prepacing TCL. The atrial return CL following cessation is progressively prolonged with an increase in the duration or rate of the overdrive pacing train. This is in contrast to the return cycles and postpacing intervals (PPIs) that remain fixed following entrainment of reentrant circuits (microreentrant AT, AVNRT, and orthodromic AVNRT), regardless of the length of the pacing drive.

Termination. Termination of SVT with atrial pacing is not usually helpful for differential diagnosis. Atrial pacing can reproducibly terminate reentrant AT, AVNRT, and orthodromic AVRT, but not automatic AT. Termination of triggered activity AT is less reproducible.

VA linking. Following cessation of overdrive atrial pacing during SVT, the VA interval (the interval between the last captured QRS complex and the first tachycardia atrial complex) can help distinguish between the different mechanisms of SVT.

VA linking following different pacing rates and durations. Overdrive atrial pacing is performed from the same atrial site

(e.g., proximal CS) at different PCLs (10, 20, and 30 milliseconds shorter than the TCL), and for different durations (e.g., 10 and 20 seconds). If “VA linking” is present (i.e., the VA interval is reproducibly constant despite pacing at different CLs or for different durations and is similar to that during SVT), AT is unlikely. If no VA linking is demonstrable, AT is more likely than other types of SVTs (see Fig. 18.40). VA linking occurs in the setting of typical AVNRT and orthodromic AVRT because the timing of atrial activation is dependent on the preceding ventricular activation and is the result of retrograde VA conduction over the AVN fast pathway (during typical AVNRT) or the BT (during orthodromic AVRT), which is relatively fixed and constant. As a consequence, postpacing VA intervals are fixed and similar to those during tachycardia (with less than 10 milliseconds variation) after different attempts at atrial entrainment, regardless of the site, duration, or CL of the entraining atrial pacing drive. Conversely, following cessation of overdrive pacing (with 1:1 AV conduction) during focal AT, the postpacing VA interval can vary significantly from the VA interval during AT (especially when pacing at different rates or durations), because the timing of the tachycardia atrial return cycle is not related to the preceding ventricular activation.^{11,22,28}

VA linking following different pacing sites. Overdrive atrial pacing is performed from the high RA and proximal CS, at the same PCL (10 to 30 milliseconds shorter than the TCL), and for the same duration. When comparing the postpacing VA intervals following overdrive pacing from the high RA versus from the proximal CS, a maximal difference in the postpacing VA intervals (Δ VA interval) of more than 14 milliseconds is diagnostic with AT, whereas a Δ VA interval of less than 14 milliseconds favors AVNRT or orthodromic AVRT. This is because, in the setting of AT, the first atrial return cycle following cessation of pacing is dependent on the distance between the AT origin and pacing site, atrial conduction properties, and mode of the resetting response of the AT, and it is not related to the preceding ventricular activation. Hence, the postpacing VA intervals vary among the pacing sites, and the Δ VA interval is relatively large (more than 14 milliseconds).²⁸

Ventricular Extrastimulation During Tachycardia

Resetting. Single VESs are delivered during tachycardia to scan diastole, initially at long coupling intervals (10 to 20 milliseconds shorter than the TCL), then with progressively shorter coupling intervals (10-millisecond decrements) until loss of ventricular capture.

VES can reset any SVT, and resetting by itself is not diagnostic of a specific type of SVT. Orthodromic AVRT is the easiest SVT to be reset and even terminated by VES (see Fig. 18.42).²² Significant portions of the ipsilateral ventricle or ventricular septum are requisite components of the orthodromic AVRT circuit, making it vulnerable to penetration and resetting even by a late-coupled VES. However, a VES delivered in the contralateral ventricle may not affect the circuit, and resetting is facilitated by delivery of the VES closer to the potential BT location.

For AVNRT, the ability of a VES to affect the SVT depends on its ability to activate the HB prematurely and penetrate the AVN. Even when HB activation is advanced by the VES, the ability of the paced impulse to invade the AVN will depend on the length of the lower common pathway; the longer the lower common pathway, the more the timing of HB activation must be advanced. In fast-slow or slow-slow AVNRT, which typically has a long lower common pathway, the HB activation must be advanced by more than 30 to 60 milliseconds. In contrast, in slow-fast AVNRT, the lower common pathway (if present) is shorter and the tachycardia is typically reset by the VES as soon as the HB activation is advanced.

During AT, a VES can advance the next atrial activation when given the chance to conduct retrogradely and prematurely to the atrium, which requires significantly shorter VES coupling intervals.¹¹

Certain situations during resetting can help discriminate between the different SVT mechanisms, including the following:

Preexcitation index. The preexcitation index (defined as the difference between the TCL and the longest VES coupling interval at which atrial capture occurs during tachycardia) of 100 milliseconds or more characterizes AVNRT, whereas an index less than 45 milliseconds is consistent with AVRT with a septal BT.⁴

Resetting with different atrial activation sequence. The retrograde atrial activation sequence following a VES that resets the tachycardia is usually similar to that during SVT in the setting of AVNRT and orthodromic AVRT, because it should conduct over the tachycardia retrograde limb (except in the presence of a bystander retrogradely conducting AV BT). In contrast, a retrograde atrial activation sequence following the VES is usually different from that during AT, except for ATs originating close to the AV junction.

Manifest ventricular fusion. Resetting with manifest QRS fusion can be observed during orthodromic AVRT, especially during pacing at a site closer to the BT ventricular insertion site than the entrance of the reentrant circuit to ventricular tissue (i.e., the HPS). Such a phenomenon, on the other hand, cannot occur during AVNRT or focal AT because of the lack of spatial separation of the entrance and exit to the tachycardia circuit.

Failure of resetting. Late-coupled VESs may fail to reset the SVT, even orthodromic AVRT, especially when delivered from a site far from the BT location. However, failure of early single or double VESs to reset the SVT, despite advancement of ventricular electrograms in the electrode recording the earliest atrial activation during the SVT (which would be close to the potential BT ventricular insertion site) by more than 30 milliseconds, excludes orthodromic AVRT.²⁹

Resetting without atrial activation. The ability of a VES to reset the SVT without atrial activation (i.e., the VES advances the subsequent His potential and QRS) excludes AT and orthodromic AVRT, because it proves that the atrium is not part of the SVT circuit.

Resetting with delay of atrial activation. The ability of a VES to delay the next atrial activation excludes AT. This can be observed more often during PJRT (see Fig. 18.39) and less commonly during AVNRT, and is caused by decremental conduction in the retrograde limb of the tachycardia circuit (the decrementally conducting concealed BT in the setting of PJRT).

Resetting during His bundle refractoriness. A VES delivered when the HB is refractory (i.e., when the His potential is already manifest or within 35 to 55 milliseconds before the time of the expected His potential) that advances (accelerates) the next atrial activation is diagnostic of the presence of a retrogradely conducting BT. Such a VES has to conduct and advance atrial activation via a BT because the HPS-AVN is already refractory and cannot mediate retrograde conduction of the VES to the atrium (Fig. 20.11; see Fig. 18.42). Although such an observation proves the presence of a retrogradely conducting AV BT, it does not prove its participation in the SVT (i.e., does not prove the diagnosis of orthodromic AVRT), because both AT and AVNRT can coexist with a bystander AV BT. However, if this VES advances atrial activation with an activation sequence identical to that during the SVT, this suggests that the SVT is orthodromic AVRT and the BT is participating in the SVT, although it does not exclude the rare case of an AT originating at a site close to the atrial insertion site of a bystander AV BT. Although such a VES can advance atrial activation during AT through fast retrograde conduction over a bystander BT, it should not be able to delay an AT beat by conduction over the AV BT. Thus a VES delivered when the HB is refractory that delays the next atrial activation indicates that the VES was conducted with some delay over the BT (due to decremental BT conduction) and that the next atrial activation was dependent on this slower conduction; hence, the BT is participating in the SVT, proving

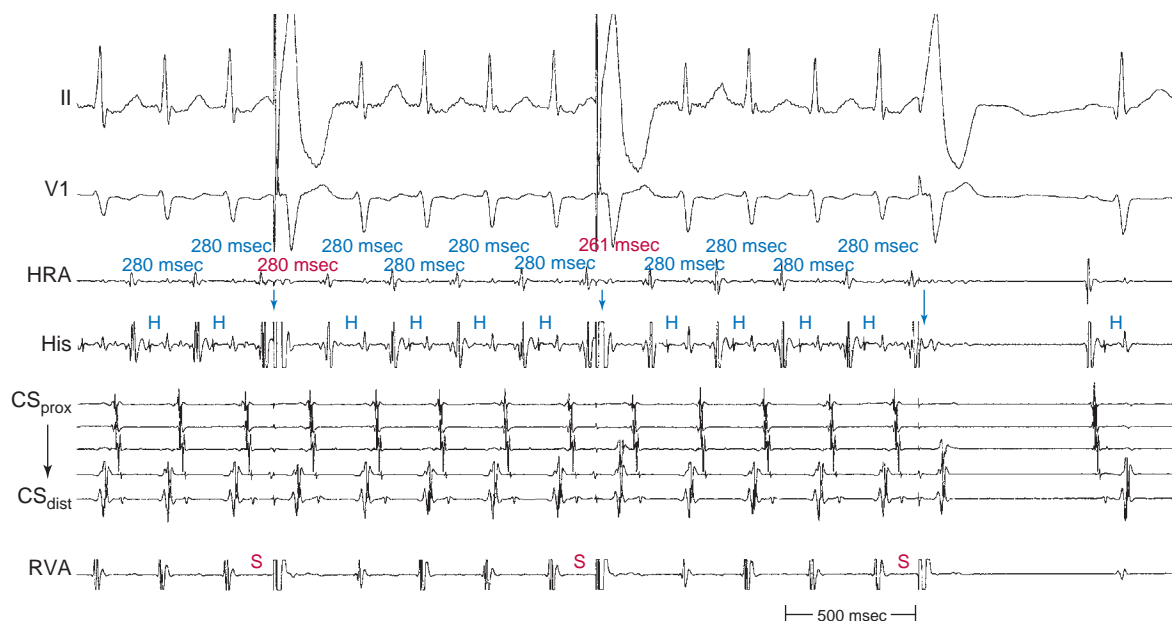


Fig. 20.11 Ventricular Extrastimulation (VES) During Supraventricular Tachycardia (SVT). VESs were delivered at progressively shorter coupling intervals during a narrow complex SVT with concentric atrial activation sequence. Timing of the anticipated anterograde His bundle (HB) activation is indicated by the blue arrows. The first VES is delivered during HB refractoriness and fails to reset the tachycardia, a phenomenon that does not help in the differential diagnosis. The second VES is delivered slightly earlier but still during HB refractoriness, and it does accelerate the following atrial activation. Atrial activation sequence during the reset atrial complex is identical to that during SVT. This observation excludes atrioventricular nodal reentrant tachycardia (AVNRT), and favors orthodromic atrioventricular reentrant tachycardia (AVRT), but does not exclude the rare example of atrial tachycardia (AT) with a bystander bypass tract with atrial insertion close to the AT focus. The third VES is delivered during HB refractoriness (within 40 milliseconds before the anticipated anterograde HB activation) and it terminates the tachycardia without conducting to the atrium. This observation, when reproducible, excludes both AVNRT and AT, and proves that the tachycardia is an orthodromic AVRT. *CS_{dist}*, Distal coronary sinus; *CS_{prox}*, proximal coronary sinus; *HRA*, high right atrium; *RVA*, right ventricular apex.

orthodromic AVRT (e.g., PJRT or nodofascicular reentrant tachycardia) as the mechanism of the SVT. Similarly, a VES delivered when the HB is refractory that terminates the SVT without atrial activation is diagnostic of AVRT.^{4,30}

Termination. Termination of AVNRT with a single VES is difficult and occurs rarely when the TCL is less than 350 milliseconds; such termination favors the diagnosis of orthodromic AVRT, which can usually be readily terminated by single or double VESs. Termination of the SVT with a VES delivered when the HB is refractory excludes AVNRT and AT (see Fig. 20.11), except in the presence of an innocent bystander BT mediating VA conduction. Reproducible termination of the SVT with a VES not followed by atrial activation excludes AT (see Fig. 18.42) and, if this occurs with a VES delivered while the HB is refractory, it excludes both AT and AVNRT (see Fig. 20.11).

Ventricular Overdrive Pacing During Tachycardia

Ventricular pacing is performed at a CL 10 to 30 milliseconds shorter than the TCL; the PCL is then progressively reduced by 10 to 20 milliseconds in a stepwise fashion with cessation of ventricular pacing after each PCL to verify continuation versus termination of the SVT. The presence of ventricular capture during ventricular pacing should be verified. In addition, the presence of 1:1 VA conduction and acceleration of the atrial rate to the PCL should be carefully examined (Fig. 20.12). It is also important to verify the continuation of the SVT following cessation of ventricular pacing and whether SVT termination,

with or without reinduction of the SVT, has occurred during ventricular pacing (Fig. 20.13).

VA dissociation. When overdrive ventricular pacing during SVT fails to accelerate the atrial CL to the PCL (i.e., the ventricles are dissociated from the tachycardia), AVRT is excluded, AT is the most likely diagnosis, but AVNRT is still possible.

Atrial activation sequence. As noted, the retrograde atrial activation sequence during ventricular pacing is usually similar to that during the SVT in the setting of AVNRT and orthodromic AVRT because it should conduct over the tachycardia retrograde limb. On the other hand, the retrograde atrial activation sequence during ventricular pacing is usually different from that during AT, except for ATs originating close to the AV junction. A pitfall of this criterion is the presence of a bystander AV BT, which can provide another retrograde route capable of mediating retrograde conduction during ventricular pacing without being part of the SVT circuit. In this setting, ventricular pacing can result in a retrograde atrial activation sequence different from that of AVNRT or orthodromic AVRT. The presence of such an AV BT, however, is generally easy to verify with ventricular stimulation during NSR.

Entrainment. Ventricular pacing is almost always able to entrain AVNRT and orthodromic AVRT and, if 1:1 VA conduction is maintained, reentrant AT. Although the mere demonstration of tachycardia entrainment does not help discrimination between the different SVT mechanisms, several parameters during ventricular entrainment can help establish the lower portion of the tachycardia circuit as macroreentry

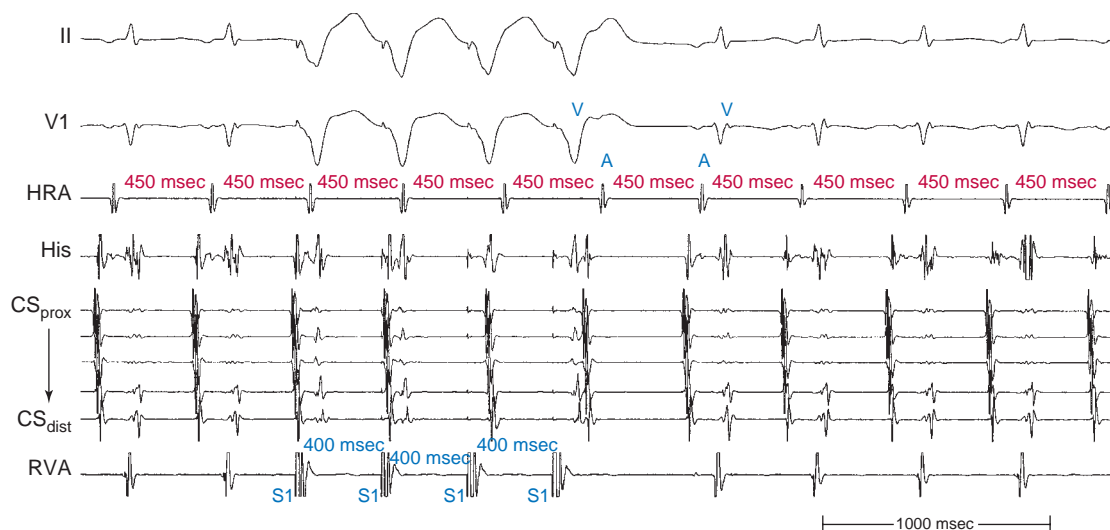


Fig. 20.12 Overdrive Ventricular Pacing During Supraventricular Tachycardia (SVT). The SVT has a long RP interval and concentric atrial activation sequence, which favors atypical atrioventricular nodal reentrant tachycardia (AVNRT), atrial tachycardia (AT) originating close to the atrioventricular junction, or orthodromic atrioventricular reentrant tachycardia (AVRT) using a slowly conducting septal bypass tract. Overdrive ventricular pacing during the tachycardia fails to entrain the tachycardia or capture the atrium (no ventriculoatrial [VA] conduction) because the tachycardia atrial cycle length (CL; 450 milliseconds) remains stable and unaltered by the faster ventricular pacing CL (400 milliseconds). Therefore analysis of the postpacing interval or VA interval during pacing versus SVT is invalid. Analysis of the response sequence following cessation of pacing (atrial-ventricular vs. atrial-atrial-ventricular [A-A-V] response) is also invalid in view of the lack of 1:1 VA conduction during ventricular pacing (resulting in a pseudo-A-A-V response). Nonetheless, the fact that ventricular pacing has dissociated the atrium from the ventricle excludes AVRT. However, other pacing maneuvers are required for differentiation between atypical AVNRT and AT. CS_{prox}, proximal coronary sinus; HRA, high right atrium; RVA, right ventricular apex.

involving the HPS/ventricle (AVRT) or not (AVNRT, AT).³⁰ These parameters include the presence of manifest ventricular fusion, VA interval during ventricular pacing as compared with that during SVT, the PPI, and differential-site ventricular entrainment.^{26,27}

Manifest ventricular fusion. As discussed previously, manifest ventricular fusion during SVT entrainment is proof that the ventricle is part of the SVT circuit (i.e., diagnostic of AVRT), excluding AVNRT, AT, and junctional tachycardia (see Fig. 18.43). During ventricular entrainment of AVNRT, AT, or junctional tachycardia, the QRS morphology is that of pure ventricular pacing. A requirement for the presence of fusion is spatial separation between the sites of entrance to and exit from the reentrant circuit, which is absent in the setting of AVNRT, AT, and junctional tachycardia, each of which has a single “gate” to the ventricles (the HB). In orthodromic AVRT, the entrance (HPS) and exit (BT ventricular insertion site) of the reentrant circuit to and from ventricular tissue are separated from each other. In this setting, the paced wavefront can activate a portion of the ventricles and enter the AVRT circuit and at the same time the tachycardia wavefront emerge from the reentry circuit at a distant exit site and activate another part of the ventricles. Also, the relative proximity of the pacing site to the entry and exit sites of the reentry circuit is a critical determinant for the occurrence of fusion during resetting and entrainment. Pacing at a site closer to the BT ventricular insertion site (e.g., LV pacing in the setting of left free-wall BTs, and RV basal pacing in the setting of right-sided or septal BTs) than the entrance of the reentrant circuit to ventricular tissue (i.e., the HPS) results in a larger degree of fusion of QRS morphology between baseline morphology during orthodromic AVRT and that of fully paced QRS (see Fig. 18.43).^{31,32}

It is important to understand, however, that overdrive pacing of a tachycardia of any mechanism (including focal AT, junctional tachycardia, and AVNRT) can result in a certain degree of fusion, especially when the PCL is only slightly shorter than the TCL. Such fusion, however, is unstable during the same pacing drive at a constant CL because the pacing stimuli fall on a progressively earlier portion of the tachycardia cycle, producing progressively less fusion and more fully paced morphology. Such phenomena should be distinguished from entrainment, and sometimes this requires pacing for long periods to demonstrate variable degrees of fusion.

ΔVA interval. Entrainment of the SVT by RV pacing can help differentiate orthodromic AVRT from AVNRT by evaluating the VA interval during SVT (measured from the onset of surface QRS to high RA electrogram) versus the VA interval during pacing (i.e., SA interval measured from the ventricular pacing stimulus to the high RA electrogram). The ventricle and atrium are activated in sequence during orthodromic AVRT and during ventricular pacing, but in parallel during AVNRT. Therefore the VA interval during orthodromic AVRT approximates that during ventricular pacing (see Fig. 18.43). In contrast, the VA interval during AVNRT would be much shorter than that during ventricular pacing (see Fig. 17.19). In general, a difference in the VA interval ($\Delta VA [VA_{\text{pacing}} - VA_{\text{SVT}}]$) greater than 85 milliseconds is consistent with AVNRT, whereas a ΔVA of less than 85 milliseconds is consistent with orthodromic AVRT (Fig. 20.14).^{33,34}

This measurement resembles the “stimulus-exit” interval versus “electrogram-exit” interval criterion used in entrainment mapping of macroreentrant AT and VT. In the setting of AVNRT and AVRT, the “electrogram” is represented by the QRS onset, and the “exit” is

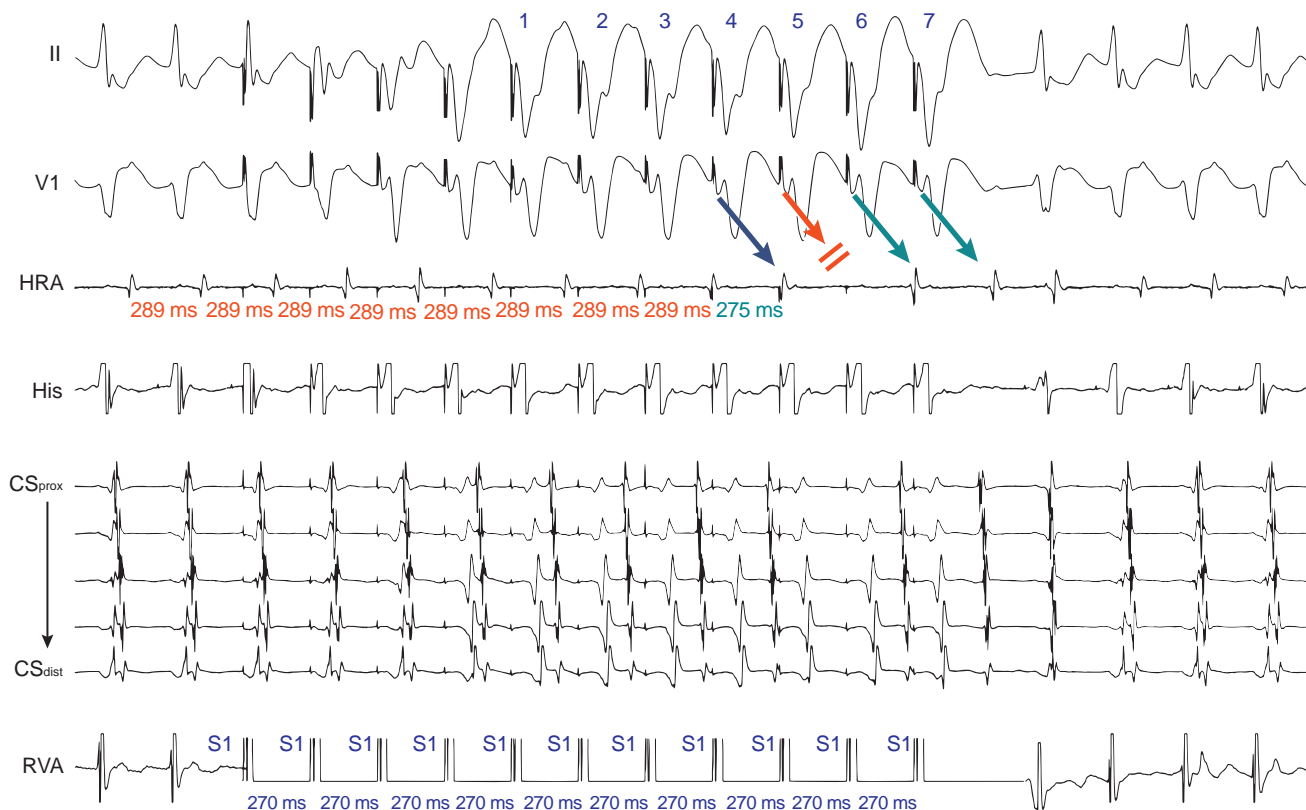


Fig. 20.13 Overdrive Ventricular Pacing During Atrioventricular Nodal Reentrant Tachycardia (AVNRT).

The tachycardia has a short RP interval and concentric atrial activation sequence and simultaneous atrial and ventricular activation, consistent with typical AVNRT. Overdrive ventricular pacing (*S1*) started from the right ventricular apex (*RVA*) at a cycle length (*CL*) 18 milliseconds shorter than the tachycardia *CL*. The numbers 1 to 7 indicate the paced QRS complexes with stable (purely paced) morphology. Note that the first constant-appearing QRS complex to reset atrial activation is QRS #4 (as indicated by the *blue arrow*), which excludes atrioventricular reentrant tachycardia, and is consistent with AVNRT. Also note that the tachycardia terminates after that, and QRS #5 is not followed by atrial activation (*red arrow*). QRS #6 and #7 conduct retrogradely to the atrium (*green arrows*) and reinitiate typical AVNRT. Since the tachycardia was terminated and then reinitiated during the same pacing drive, entrainment is not present, and analysis of the postpacing interval is not valid. *CS_{dist}*, Distal coronary sinus; *CS_{prox}*, proximal coronary sinus; *HRA*, high right atrium.

represented by the subsequent atrial electrogram, which is orthodromically captured during ventricular entrainment and represents the exit site from the reentry circuit to the atrium. Hence, the stimulus to the subsequent atrial-entrained electrogram interval (SA interval) is compared to the electrogram (QRS onset) to the subsequent atrial electrogram during tachycardia (VA interval). As a consequence, the shorter the difference between the two intervals, the closer the pacing site to the reentry circuit.³²

Postpacing interval. The PPI reflects conduction time from the ventricular pacing site to the SVT circuit, once around the reentry circuit, and then back to the pacing site. The difference between the PPI and TCL ($PPI - TCL$) represents the conduction time from the pacing site to the reentry circuit and back. Thus the ($PPI - TCL$) difference can qualitatively estimate how far (in terms of conduction time) the reentrant circuit is from the pacing site; the greater the ($PPI - TCL$) difference, the longer the conduction time between the pacing site and reentry circuit, and the greater the “electrical” distance is between the pacing site and the circuit.³²

Because the RV is closer to the AVRT circuit as compared to the AVNRT circuit, the ($PPI - TCL$) difference following entrainment from the RV apex is smaller in the setting of AVRT than during AVNRT. In

fact, a ($PPI - TCL$) difference of more than 115 milliseconds was found to identify AVNRT (see Figs. 17.19 and Fig. 20.14), whereas a ($PPI - TCL$) difference of less than 115 milliseconds was consistent with orthodromic AVRT (see Fig. 18.43). For borderline values, ventricular pacing at the RV base can help exaggerate the ($PPI - TCL$) difference in the setting of AVNRT, but without significant changes in the setting of orthodromic AVRT (see differential-site RV entrainment later).^{11,35}

A relatively common phenomenon encountered during entrainment of orthodromic AVRT by ventricular pacing is the prolongation of the AH interval because of decremental conduction properties of the AVN or (in the presence of dual AVN physiology) a jump of anterograde conduction from the fast pathway to the slow pathway. The prolonged AH interval on the last entrained beat will contribute to prolongation of the PPI that is not reflective of the distance of the pacing site from the circuit. Thus the ($PPI - TCL$) differences obtained after entrainment of orthodromic AVRT employing a septal BT can actually overlap with those observed after entrainment of AVNRT. “Correction” of the PPI by subtracting the increment in AVN conduction time in the first PPI (postpacing AH interval minus prepacing AH interval) from the ($PPI - TCL$) difference (“corrected” [$PPI - TCL$]) has been found to improve the accuracy of this criterion. The difference between AV intervals

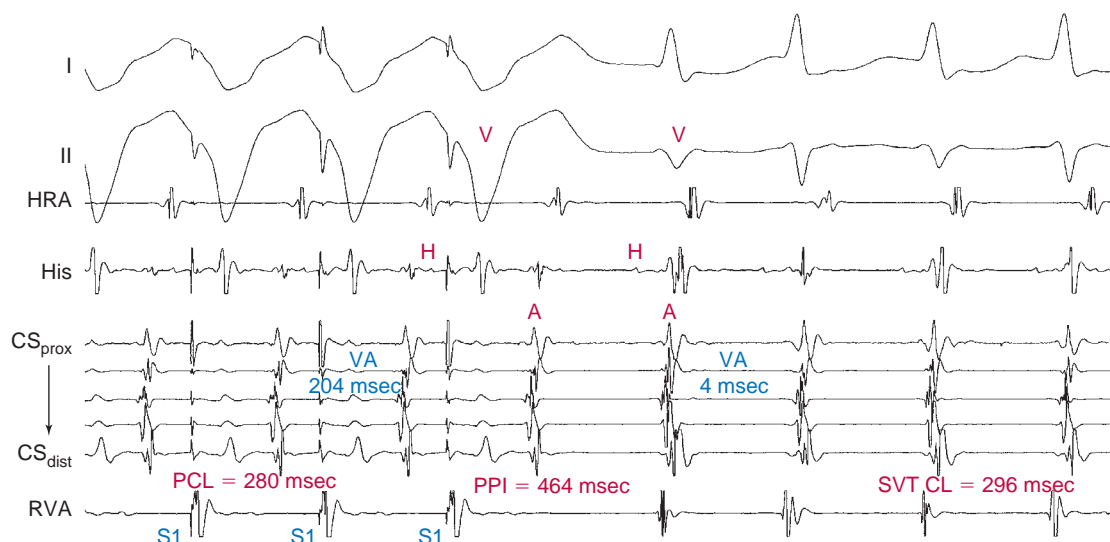


Fig. 20.14 Ventricular Entrainment of Supraventricular Tachycardia (SVT). Ventricular entrainment if achieved with pacing from the RVA. Several features in this tracing can help in the differential diagnosis of the SVT. First, atrial and ventricular activation occur simultaneously during the SVT, which excludes atrioventricular reentrant tachycardia (AVRT). Second, atrial activation during the SVT is eccentric, with earliest activation in the mid-coronary sinus (CS), which favors atrial tachycardia (AT) over atrioventricular nodal reentrant tachycardia (AVNRT). Third, the atrial activation sequence during ventricular pacing is identical to that during SVT, which favors AVNRT and AVRT over AT. Fourth, following cessation over ventricular pacing, the post-pacing interval (PPI) minus SVT cycle length (CL), ($PPI - SVT\ CL$), is more than 115 milliseconds, and the Atriculoatrial (VA) interval ($VA_{\text{pacing}} - VA_{\text{SVT}}$) is more than 85 milliseconds, which favors AVNRT over AVRT. Fifth, although characterization of the activation sequence following cessation of ventricular pacing (atrial-atrial-ventricular [A-A-V] vs. atrial-ventricular [A-V] response) is unclear (because of the simultaneous occurrence of atrial and ventricular activation in the first tachycardia complex, replacing ventricular activation with HB activation [i.e., characterizing the response as A-A-H or A-H instead of A-A-V or A-V, respectively]) reveals an A-H response, which favors AVRT and AVNRT over AT. In summary, AVRT can be reliably excluded by the simultaneous atrial and ventricular activation. AT is excluded by the A-H response following cessation of ventricular pacing and by the identical atrial activation sequence during the SVT and ventricular pacing. The left variant of typical AVRT (with an eccentric atrial activation sequence) is the mechanism of the SVT. CS_{dist}, Distal coronary sinus; CS_{prox}, proximal coronary sinus; HRA, high right atrium; PCL, pacing cycle length; RVA, right ventricular apex.

(postpacing AV interval minus prepacing AV interval) can be taken for the latter adjustment when a His deflection is not clearly visible (assuming the HV interval remains constant). In a study of patients with both typical and atypical forms of AVNRT, as well as orthodromic AVRT using septal and free-wall BTs, a corrected ($PPI - TCL$) difference of less than 110 milliseconds was found more accurate in identifying orthodromic AVRT from AVNRT than the uncorrected ($PPI - TCL$) difference.^{36–38}

Of note, determinations of the corrected ($PPI - TCL$) and ΔVA ($VA_{\text{pacing}} - VA_{\text{SVT}}$) after resetting with single or double VESs from the RV apex, are of similar value for discrimination between AVNRT and orthodromic AVRT even when the SVT is interrupted by ventricular pacing. Corrected ($PPI - TCL$) of more than 110 milliseconds and ΔVA of more than 110 milliseconds after resetting are consistent with AVNRT.³⁹

Importantly, there are several potential pitfalls to the ΔVA interval and PPI criteria discussed previously. The TCL and VA interval are often perturbed for a few cycles after entrainment. For this reason, care should be taken not to measure unstable intervals immediately after ventricular pacing. In addition, oscillations in the TCL and VA intervals can occur spontaneously during the SVT. The discriminant points chosen may not apply when the spontaneous variability is greater than 30 milliseconds. Also, it is possible to mistake isorhythmic VA dissociation for entrainment if the pacing train is not long enough or the PCL is

too close to the TCL. Furthermore, this test is less reliable and should be used with caution in patients with left lateral BTs. In addition, these criteria may not apply to BTs with significant decremental properties, although small decremental intervals are unlikely to provide a false result.

Conventional SVT criteria during entrainment from the ventricle establish the lower portion of the tachycardia circuit as macroreentrant involving the HPS/ventricle (AVRT) or not. Importantly, slow, decremental BT conduction (e.g., during PJRT or nodofascicular reentrant tachycardia) can affect the sensitivity of the ΔVA and ΔHA criteria for orthodromic AVRT, although the specificity of these criteria remains high. Therefore any standard criteria that is positive for orthodromic AVRT ($[PPI - TCL] < 115$ milliseconds, corrected $[PPI - TCL] < 110$ milliseconds, $\Delta VA < 85$ milliseconds, and $\Delta HA < 0$ milliseconds) is considered diagnostic for orthodromic AVRT, despite discordance among them, which can occur up to 50% of the time. In addition, a higher cutoff value of 125 milliseconds was found to increase the sensitivity for orthodromic AVRT while maintaining a high specificity.³⁰

Differential-site RV entrainment. Differential-site RV entrainment (from RV apex vs. RV base) can help distinguish AVNRT from orthodromic AVRT. Because the reentrant circuit in AVNRT is confined above the HB and does not involve the ventricle, the base of the RV is electrically more distant (although anatomically closer) from the tachycardia

circuit than the RV apex, given that the His-Purkinje network directly inserts near the RV apex. Consequently, the PPI after entrainment of AVNRT from the RV base is longer than that following entrainment from the RV apex. The difference in PPI from the RV base versus the RV apex is largely composed of the extra time required to reach the circuit from the base versus the apex (approximately 30 milliseconds). Conversely, in orthodromic AVRT, in which the ventricles are an obligatory part of the circuit, the basal pacing site relative to the RV apex is variably related to the circuit, closer than the RV apex with septal BTs and equidistant with free-wall BTs, but the paced wavefront from the RV apex or RV base tends to have, on average, approximately equal access and proximity to the reentrant circuit involved in orthodromic AVRT. Therefore the time taken to reach the circuit (and hence the PPI) tends to be similar, irrespective of the location of the BT.

Correction of the PPI (to avoid potential error introduced by decremental conduction within the AVN during ventricular pacing) increases the accuracy of this method, although the degree of decrement is not expected to be materially different from basal rather than apical pacing as long as the pacing rates are the same or similar. The “corrected PPI” is obtained by subtracting any increase in the AV interval of the return cycle beat (as compared with the AV interval during SVT). A differential corrected (PPI – TCL) difference of more than 30 milliseconds after transient entrainment was found to be consistent with AVNRT (i.e., corrected [PPI – TCL] difference following pacing from the RV base was consistently at least 30 milliseconds longer than that following pacing from the RV apex). In contrast, a corrected (PPI – TCL) difference of less than 30 milliseconds was observed in all cases of orthodromic AVRT. In addition, a differential VA interval (VA interval during entrainment from RV base vs. RV septum) of more than 20 milliseconds was consistent with AVNRT, whereas a differential VA interval of less than 20 milliseconds was consistent with orthodromic AVRT.^{40,41}

The main advantage of this technique is that the differential VA interval can be calculated from the last paced beat if the tachycardia is terminated after transient entrainment.

Length of pacing drive required for entrainment. Assessing timing and type of response of SVT to RV pacing can help differentiate orthodromic AVRT from AVNRT. In the setting of orthodromic AVRT, ventricular myocardium is the only intervening tissue between the pacing wavefront and the ventricular insertion site of the BT. Therefore once ventricular capture is achieved during RV pacing, the paced wavefront propagates to the ventricular insertion site of the BT quickly and resets the tachycardia (i.e., advances or delays atrial activation time). Consequently, RV pacing results in resetting of AVRT with septal or right-sided BT immediately once the RV is fully captured by the paced wavefront. During AVNRT, on the other hand, the pacing site is distant from the SVT circuit, and the paced wavefront has to propagate through ventricular tissue, then through the HPS, followed by AVN tissue prior to resetting the tachycardia. As a consequence, resetting of AVNRT is delayed for several captured paced beats as compared with orthodromic AVRT (eFig. 20.1). This observation is consistent with the concept that overdrive pacing begins to advance a reentrant tachycardia precisely when the total pacing prematurity exceeds the (PPI – TCL) after correcting for conduction velocity changes associated with the shorter CL.⁴²

After initiation of synchronized RV pacing during SVT at a CL 10 to 40 milliseconds shorter than the TCL, once constant-appearing paced QRS complexes (either pure capture or fixed fusion) are observed, the number of constant-appearing paced QRS complexes required to accelerate atrial activation timing to the PCL is determined. The first atrial beat accelerated to the PCL is identified by demonstrating a fixed ventricular stimulus-to-atrial capture interval (SA interval). One report demonstrated that resetting of the SVT occurring by the first beat with stable paced QRS morphology identifies all orthodromic AVRT and

essentially excludes AVNRT with high accuracy. On the other hand, resetting of the SVT occurring only after two or more beats with stable (fully paced) QRS morphology is consistent with AVNRT (see Fig. 20.13).

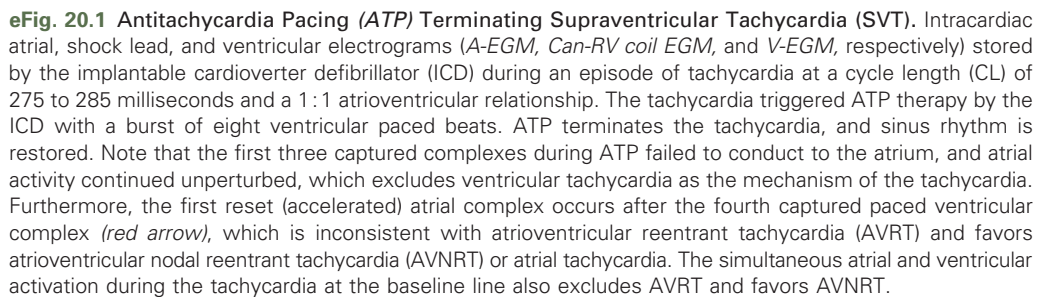
The major advantage of this method is its independence of tachycardia continuation after cessation of pacing. However, it is likely that these criteria may not be applicable at PCLs more than 40 milliseconds shorter than the TCL or with prematurity of more than 80% of the TCL (which can occur with poorly synchronized stimulation), because resetting of the tachycardia can occur earlier in AVNRT in response to a greater degree of penetration into the tachycardia circuit. In addition, these findings may not apply in cases in which AVNRT occurs in the setting of a bystander BT because SVT may be reset using the bystander BT. In addition, although this technique is effective for differentiating septal pathways from atypical AVNRT, it may be less useful in patients with BTs remote from the pacing stimulus (e.g., left free-wall BTs) (Fig. 20.15).^{43,44}

Atrial resetting during the transition zone. On initiation of synchronized RV pacing trains during SVT at a rate slightly faster than the TCL, there is a transition zone during which the pacing train fuses with anterograde ventricular activation (i.e., the zone in which the paced QRS complexes show progressive fusion with the SVT complexes) until a stable QRS morphology is observed (either completely paced or constantly fused). The transitional zone begins with progressive fusion beats between the paced and tachycardia wavefronts and ends with the first beat of stable QRS morphology, the latter representing constant fusion in the setting of orthodromic AVRT and a fully paced QRS morphology in patients with AVNRT or AT. In patients with AVNRT or AT, acceleration of the timing of atrial activation cannot occur through the AVN during the transition zone. The reason is that the HB is expected to be refractory, as indicated by at least some ventricular activation still occurring by anterograde conduction over the HPS. If perturbation of atrial timing occurs during the transition zone, it indicates the presence of a retrogradely conducting BT, which can be an integral part of the SVT circuit (i.e., orthodromic AVRT) or a bystander. In one report, these criteria showed excellent diagnostic accuracy and could be applied regardless of whether entrainment was achieved or whether the SVT terminated during pacing. Perturbation of atrial timing of at least 15 milliseconds or a fixed SA interval measured from the last beat of the transition zone was seen in all the patients with orthodromic AVRT and in none of the patients with AVNRT or AT (unless a bystander retrogradely conducting BT is present).^{41,45}

Atrial and ventricular electrogram sequence following cessation of ventricular pacing

Technique. During SVT, synchronized ventricular overdrive pacing is initiated at a PCL 10 to 30 milliseconds shorter than the TCL until 1:1 VA conduction occurs, at which point pacing is stopped. If pacing results in termination of the tachycardia, SVT is reinduced, and the maneuver is repeated. If ventricular pacing does not terminate the tachycardia and the presence of stable 1:1 VA conduction is verified, the electrogram sequence immediately after the last paced ventricular complex is categorized as an atrial-ventricular (A-V) or atrial-atrial-ventricular (A-A-V) pattern (see Fig. 11.16).

Interpretation. During AVNRT or orthodromic AVRT, when the ventricle is paced at a CL shorter than the TCL and all electrograms are accelerated to the pacing rate without terminating the tachycardia, VA conduction occurs through the retrograde limb of the circuit. Therefore, after the last paced ventricular complex, the anterograde limb of the tachycardia circuit is not refractory, and the last entrained retrograde atrial complex can conduct to the ventricle. This results in an A-V response following cessation of pacing. However, when the ventricle is paced during AT and 1:1 VA conduction is produced, retrograde conduction occurs through the AVN. In this setting, the last retrograde



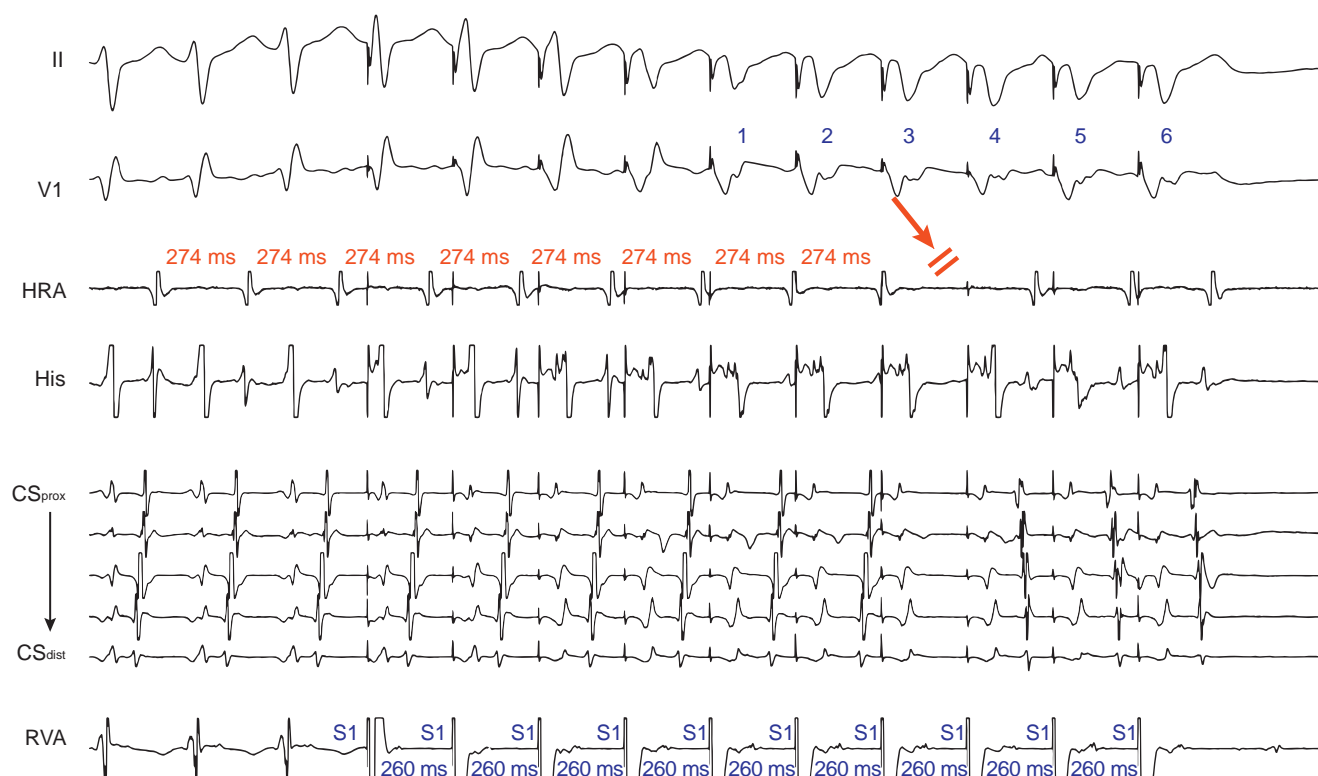


Fig. 20.15 Overdrive Ventricular Pacing During Atrioventricular Reentrant Tachycardia (AVRT). The tachycardia has a short RP interval and an eccentric atrial activation sequence consistent with orthodromic AVRT utilizing a left lateral bypass tract as the retrograde limb. Overdrive ventricular pacing (S1) started from the right ventricular apex (RVA) at a cycle length (CL) 14 milliseconds shorter than the tachycardia CL. The numbers 1 to 6 indicate the paced QRS complexes with stable morphology. Note that the first constant-appearing QRS complex to affect atrial activation is QRS #3 (as indicated by the red arrow). Although this finding typically indicates atrioventricular nodal reentrant tachycardia, and excludes orthodromic AVRT utilizing a septal bypass tract (BT), it can also be observed in orthodromic AVRT when the BT is remote from the ventricular pacing site, like in this case. CS_{dist}, Distal coronary sinus; CS_{prox}, proximal coronary sinus; HRA, high right atrium.

atrial complex resulting from ventricular pacing is unable to conduct back to the ventricle because the AVN is refractory to anterograde conduction and there is no alternate route for anterograde conduction to the ventricle available (unlike AVNRT and AVRT), and the result is an A-A-V response.

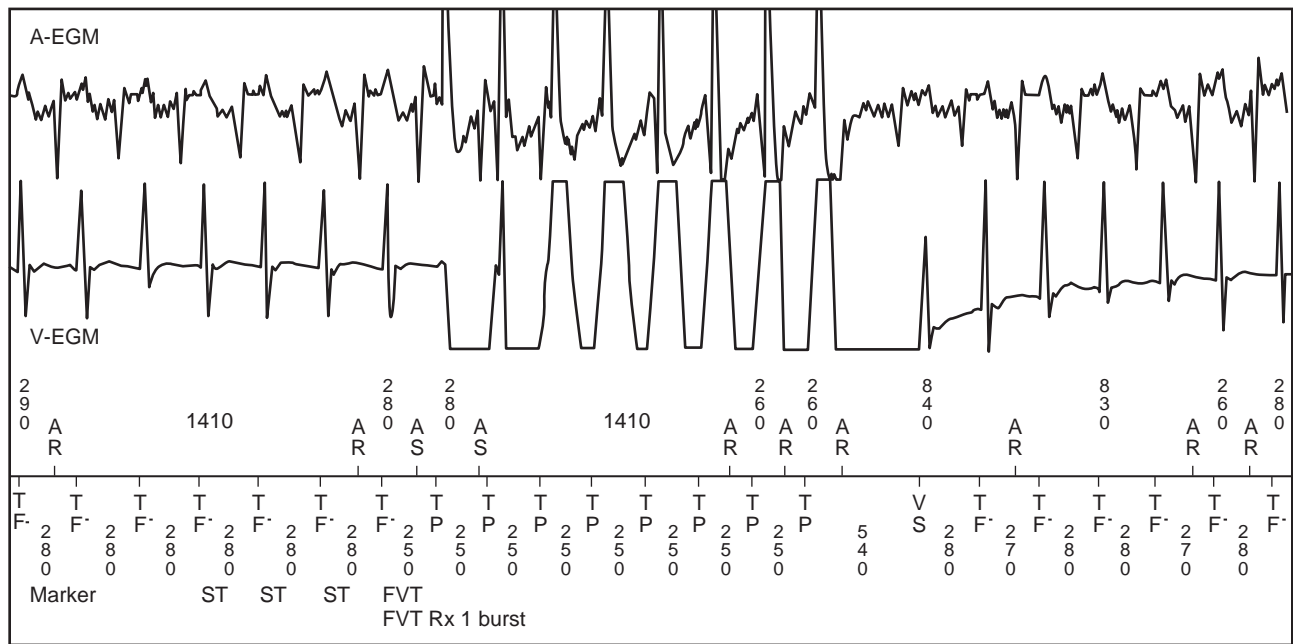
Pitfalls. This pacing maneuver is not useful when 1:1 VA conduction during ventricular pacing is absent. Thus, when determining the response after ventricular pacing during SVT, the presence of 1:1 VA conduction must be confirmed. Isorhythmic VA dissociation can mimic 1:1 VA conduction, especially when the pacing train is not long enough or the PCL is too slow (see Fig. 11.17).

Pseudo-A-A-V response. A pseudo-A-A-V response can occur during atypical AVNRT (eFig. 20.2). Because retrograde conduction during ventricular pacing occurs through the slow pathway, the VA interval is long and can be longer than the PCL (V-V interval), so that the last paced QRS is followed first by the atrial complex resulting from slow VA conduction of the preceding paced QRS and then by the atrial complex resulting from the last paced QRS. To avoid this potential pitfall, the A-A intervals are measured during and after ventricular overdrive pacing, and the last atrial electrogram resulting from VA conduction during ventricular pacing is carefully examined. The last retrograde atrial complex characteristically occurs at an A-A interval equal to the ventricular PCL, whereas the first tachycardia atrial complex usually occurs at a longer return CL.

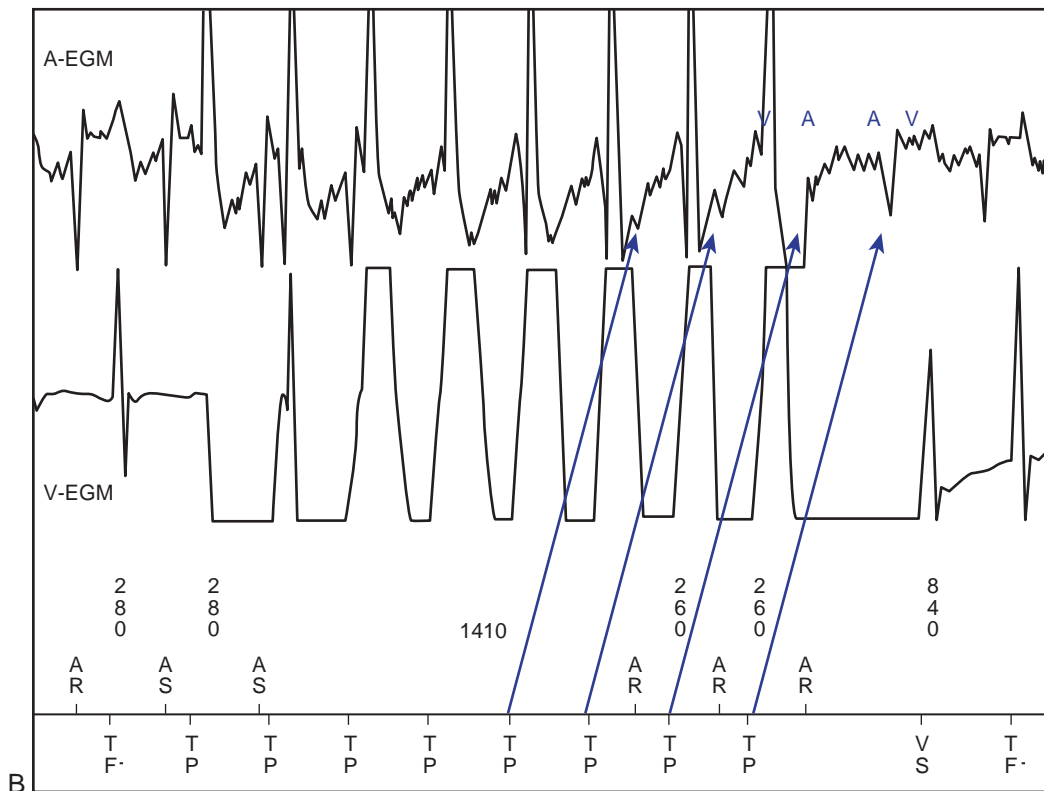
A pseudo-A-A-V response can also occur when 1:1 VA conduction is absent during overdrive ventricular pacing (see Fig. 20.12), during typical AVNRT with long HV intervals or short HA intervals (whereby atrial activation may precede ventricular activation), and in patients with a bystander BT. Replacing ventricular activation with His activation (i.e., characterizing the response as A-A-H or A-H instead of A-A-V or A-V, respectively) can be more accurate and can help eliminate the pseudo-A-A-V response in patients with AVNRT and long HV intervals, short HA intervals, or both.⁴⁶

Pseudo-A-V response. A pseudo-A-V response can occur with an automatic AT when the maneuver is performed during isoproterenol infusion. Ventricular pacing with 1:1 VA conduction can result in overdrive suppression of the atrial focus, and isoproterenol can enhance junctional automaticity, so that an apparent A-V response occurs. Therefore, when ventricular pacing is performed during an isoproterenol infusion, it is important to determine that the response after cessation of ventricular pacing is reproducible.²⁸

A pseudo-A-V response can theoretically occur when AT coexists with retrograde dual AVN pathways or a bystander BT. In such cases, the last retrograde atrial complex would have an alternative route for anterograde conduction to the ventricle, other than the one used for retrograde VA conduction during ventricular pacing, thus resulting in an A-V response. However, clinical occurrence of these theoretical scenarios has not been observed, probably because of retrograde penetration



A



B

Fig. 20.2 Antitachycardia Pacing (ATP) During Supraventricular Tachycardia (SVT). (A) Intracardiac atrial and ventricular electrograms (A-EGM and V-EGM, respectively) stored by the implantable cardioverter defibrillator (ICD) during an episode of SVT at a cycle length (CL) of 280 to 290 milliseconds and a 1:1 atrioventricular relationship. The SVT inappropriately triggered ATP therapy by the ICD with a burst of eight ventricular paced beats at a CL of 250 milliseconds. ATP fails to terminate the tachycardia, which resumes at the baseline CL. (B) Magnification of a portion of the upper panel showing atrial and ventricular intracardiac electrograms during ATP. Arrows track ventriculoatrial (VA) conduction following the last four paced ventricular complexes. VA conduction during ATP is present and can be verified by demonstrating acceleration of the atrial rate to that of the paced ventricular rate. After cessation of ATP, the tachycardia resumes with an atrial-atrial-ventricular (A-A-V) electrogram sequence, which is evident on interrogation of the atrial and ventricular channel electrograms (lower panel). However, careful analysis to identify the last reset atrial complex (occurring at a CL similar to the pacing CL) indicates a pseudo-A-A-V response rather than an A-A-V electrogram sequence, which is consistent with atypical AV nodal reentrant tachycardia as the mechanism of the SVT. See text for discussion.

of both AVN pathways or of the AVN and the BT during ventricular pacing, so that both pathways are refractory to anterograde conduction on cessation of pacing.²⁸

Termination. Ventricular pacing can easily terminate orthodromic AVRT, and failure to terminate the SVT with ventricular pacing argues against orthodromic AVRT. Termination of AVNRT is also common, but AT is less likely to be terminated by ventricular pacing.

Para-Hisian Pacing During Tachycardia

Para-Hisian entrainment or resetting

Technique. Entrainment of the tachycardia is performed by pacing at the para-Hisian region using the HB catheter at a PCL 10 to 30 milliseconds shorter than the TCL. Entrainment is confirmed when the atrial CL accelerates to the PCL, without a change in the atrial activation sequence, and the tachycardia continues after pacing is discontinued.⁴⁷

Para-Hisian entrainment is performed by alternately pacing at high-energy output for HB-RB capture or lower energy output for HB-RB noncapture. Entrainment with HB-RB capture is recorded separately from that without HB-RB capture. The SA (stimulus-to-earliest atrial activation) and local VA intervals during HB-RB capture and noncapture are then examined.

One must be cautious about performing the para-Hisian entrainment maneuver by simply decreasing the pacing energy output during the same run to achieve HB-RB noncapture. That is, even though the SVT may have been entrained during HB-RB capture, on loss of HB-RB capture, the initial paced complexes typically do not entrain the SVT. This initial failure of entrainment occurs because of the sudden increase in the distance from the pacing site to the actual reentrant circuit. During HB-RB capture of AVNRT, the pacing site is near the circuit (the HB-RB); however, during HB-RB noncapture, the pacing site (the basal RV myocardium) is well outside the circuit. This limitation would not apply if HB-RB noncapture is performed *prior* to HB-RB capture. That is, if the pacing output is increased while the SVT is being entrained during HB-RB noncapture, the circuit almost certainly will be entrained on HB-RB capture (unless the SVT terminates).

If para-Hisian entrainment cannot be performed because of repetitive termination of the tachycardia during entrainment attempts, isoproterenol or epinephrine infusion may be used to help sustain the rhythm. Alternatively, single or double VESs can be given to reset the tachycardia (para-Hisian resetting). These VESs are delivered at progressively shorter coupling intervals until the first VES that reliably advances or resets the tachycardia. This is performed alternately with high- or low-energy outputs to achieve HB-RB capture and noncapture, respectively. As with para-Hisian entrainment, the retrograde atrial activation sequence and timing are compared during para-Hisian resetting to characterize the response.

Interpretation. In AVNRT (typical or atypical), the AVN-AVN pattern is observed in response to para-Hisian entrainment or resetting. Both the SA and the local VA intervals increase during HB-RB noncapture compared with HB-RB capture.

In orthodromic AVRT, the BT-BT pattern or BT-BT_L pattern is observed. In the setting of a BT-BT pattern, the SA and local VA intervals are usually not significantly different between HB-RB capture and noncapture. Conversely, in the case of a BT-BT_L pattern, the SA interval increases on HB-RB noncapture, but without significant change in the local VA interval.

A Δ SA interval of less than 40 milliseconds was found to be a reasonable guide to separating the AVN-AVN from the BT-BT response. Patients with AVNRT uniformly have a Δ SA interval of greater than 40 milliseconds, whereas those with AVRT have a Δ SA interval of less than 40 milliseconds (except for rare patients with a left lateral BT). Using the Δ local VA interval (instead of the Δ SA interval) pro-

vides a more accurate parameter for discrimination between AVNRT and AVRT.

Fusion patterns during para-Hisian entrainment or resetting have not been observed in patients with AVNRT. This is a potential advantage over para-Hisian pacing during NSR in identifying the presence of a BT. Because retrograde VA conduction can only proceed over a single route during entrainment of the SVT (assuming that a complex scenario such as multiple BTs is not present), the various forms of retrograde fusion that might be seen with para-Hisian pacing during NSR cannot occur with para-Hisian entrainment or resetting.

Para-Hisian overdrive pacing

Technique. During SVT, para-Hisian pacing is performed at a PCL 10 to 30 milliseconds shorter than the TCL. Responses to this maneuver are then classified as follows: (1) entrainment occurs when the atrial CL is accelerated to the PCL, without a change in the atrial activation sequence, and the tachycardia resumed after pacing was discontinued; (2) termination occurs when pacing results in termination of the tachycardia; and (3) AV dissociation occurs when HB capture is confirmed and no change in the atrial CL is observed.

When response 1 or 2 is observed, the number of beats required to enter the tachycardia circuit is determined. Any change in atrial timing (advance or delay of at least 10 milliseconds) or termination of the SVT is considered to represent entry into the tachycardia circuit. The surface ECG is examined to determine the first beat where a consistent nonfused paced QRS morphology is observed. This beat is taken as beat 1 for the purposes of analysis. The number of beats required to enter the tachycardia circuit is determined by counting from beat 1 each time the maneuver is performed.

Interpretation. Because the HB is a necessary component for the circuit in AVRT, overdrive capture of the HB during AVRT should result in immediate entry into the tachycardia. In contrast, HB overdrive pacing during AVNRT may not immediately enter the circuit because the HB is not an obligate component. Therefore entry into the tachycardia circuit within 1 beat indicates AVRT, whereas entry into the circuit occurring only after 3 or more beats is consistent with AVNRT.⁴⁸

This technique does not require confirmation of both HB capture and noncapture. In addition, unlike para-Hisian entrainment whereby termination of the SVT occurs frequently and precludes analysis of Δ SA interval, termination of SVT during para-Hisian overdrive pacing serves as confirmation that the pacing stimulus has entered and perturbed the tachycardia circuit.⁴⁸

Of note, this principle should apply to any tachycardia using a BT and the HB, including atriofascicular, concealed nodofascicular, decremental, and left lateral BTs. Moreover, it should be useful in distinguishing AVNRT with bystander pathway participation from antidromic AVRT.⁴⁸

Diagnostic Maneuvers During Sinus Rhythm After Tachycardia Termination

When pacing the atrium or ventricle at the TCL, it is important that the autonomic tone be similar to its state during the tachycardia because alterations of autonomic tone can independently influence AV or VA conduction.

Atrial Pacing at the Tachycardia Cycle Length

Δ AH interval. The difference in the AH interval between atrial pacing (at the TCL) and SVT can allow differentiation of fast-slow AVNRT from other types of long RP tachycardias. A Δ AH ($HA_{\text{pacing}} - AH_{\text{SVT}}$) greater than 40 milliseconds favors AVNRT. In contrast, during AT and orthodromic AVRT utilizing a septal BT, the AH interval during SVT approximates that during atrial pacing. In contrast, a Δ AH of less than 20 milliseconds favors AT and orthodromic AVRT. This has only

been tested with RA pacing during right ATs and should be applied with caution when a left AT is suspected.¹¹

The ΔAH ($\text{AH}_{\text{pacing}} - \text{AH}_{\text{SVT}}$) can also help differentiate typical (slow-fast) AVNRT from AT with a long PR interval. Atrial pacing during NSR at the TCL yields an AH interval that is similar to that during AT but shorter than the AH interval during typical AVNRT. During atrial pacing and AT, AV conduction occurs preferentially over the fast pathway and, hence, is expected to be associated with similar AH and PR intervals (under comparable autonomic tone). In contrast, AV conduction during typical AVNRT occurs over the slow pathway, resulting in a long AH interval.

Ventricular Pacing at the Tachycardia Cycle Length

ΔHA interval. To help distinguish between orthodromic AVRT and AVNRT, ventricular pacing is performed during NSR (with PCL equal to the TCL), and the HA interval during SVT is compared to that during ventricular pacing. The HA interval is measured from the *end* of the His potential (where the impulse leaves the HB to enter the AVN) to the atrial electrogram in the high RA recording and the ΔHA interval ($\text{HA}_{\text{pacing}} - \text{HA}_{\text{SVT}}$) is calculated.

In the setting of orthodromic AVRT, the ΔHA interval is typically less than -10 milliseconds. Ventricular pacing results in HA and VA intervals that are shorter than those during orthodromic AVRT, because the HB and atrium are activated sequentially during orthodromic AVRT but in parallel during ventricular pacing whereby the atrium is activated via the BT (see Fig. 18.43).

In contrast, in the setting of AVNRT the ΔHA interval is typically more than -10 milliseconds because the HA interval during AVNRT is shortened by parallel activation of both the HB and the atrium during the tachycardia (i.e., the HA interval is a “pseudo-interval” that represents activation times of the HB and atrium), whereas the HB and atrium are activated sequentially during ventricular pacing in the absence of a BT (i.e., the HA interval represents a true conduction time interval from the HB to the atrium). The ΔHA interval is even more pronounced in atypical AVNRT, which has a lower common pathway that is longer than that in typical AVNRT. In focal junctional tachycardia, the ΔHA interval is typically close to 0.⁴⁹

The main limitation of the ΔHA interval criterion is the ability to record the retrograde His potential during ventricular pacing. Retrograde His potential generally appears before the local ventricular electrogram in the HB tracing, and can be verified by the introduction of a VES that causes the His potential to occur after the local ventricular electrogram. Moreover, pacing from different sites (e.g., midseptum) may allow earlier penetration into the HPS and facilitate observation of a retrograde His potential. When the retrograde His potential is not visualized, using the ΔVA interval instead of the ΔHA interval is not as accurate in discriminating orthodromic AVRT from AVNRT.⁴

Another limitation is that VA conduction during ventricular pacing may not occur over the BT but propagates preferentially over the HPS-AVN, leading to earlier atrial activation over this pathway than over the BT. If this were the case, the HA interval during ventricular pacing would be shorter than that observed if the atrium were activated via the BT. This would yield a more negative ΔHA interval.

VA block. In the setting of AT and AVNRT, and under comparable autonomic tone, 1:1 VA conduction over the AVN may or may not be maintained during ventricular pacing at a PCL similar to the TCL because of possible retrograde block in the AVN or the lower common pathway. Anterograde conduction properties of the AVN or the lower common pathway may allow 1:1 conduction from the AT or AVNRT circuit down to the ventricle, but its retrograde conduction properties may not allow 1:1 retrograde conduction from the ventricle up to the atrium during ventricular pacing at a CL similar

to the TCL. On the contrary, in the setting of orthodromic AVRT, 1:1 VA conduction is expected to be maintained because of the presence of an AV BT that is capable of mediating VA conduction at rate at least as fast as that during the AVRT. Therefore, if VA block is observed during ventricular pacing at the TCL, orthodromic AVRT is excluded (with the exception of orthodromic AVRT using a slowly conducting AV BT), and AT or AVNRT with lower common pathway physiology is more likely.

Atrial activation sequence. The retrograde atrial activation sequence during ventricular pacing is usually similar to that during SVT in the setting of AVNRT, but slight differences of activation sequence can also be observed when the retrogradely conducting AVN pathway during AVNRT is different from that utilized during ventricular pacing. In the setting of orthodromic AVRT, a retrograde atrial activation sequence during ventricular pacing can be similar to or different from that during tachycardia, depending on whether retrograde VA conduction during ventricular pacing propagates over the AVN, the BT, or both. For AT, the retrograde atrial activation sequence during ventricular pacing is usually different from that during AT, except for ATs originating close to the AV junction.

PRACTICAL APPROACH TO ELECTROPHYSIOLOGICAL DIAGNOSIS OF SUPRAVENTRICULAR TACHYCARDIA

It is important to understand that there is no single diagnostic maneuver or algorithm that is adequate in distinguishing among the different types of SVTs in all cases. Each maneuver has its own applications and limitations, and almost all described diagnostic maneuvers have exceptions to their primary interpretation.⁴ Although several diagnostic criteria were found to have high specificity, sensitivity is frequently limited. Therefore the investigator will often need to use a combination of SVT features and pacing maneuvers to establish an accurate diagnosis. Systematic evaluation of all possibilities and adherence to fundamental EP principles will help establish the correct diagnosis. Each step during the EP study in these patients can offer valuable information to the vigilant investigator that, if recognized, can potentially reduce procedure time and improve outcome.

It is important for the electrophysiologist to be fully conversant with the maneuvers used for the differential diagnosis of the different arrhythmias. Exercising the application of these techniques on a routine basis, even when the diagnosis of the underlying arrhythmia mechanism has been established, helps the operator to correctly apply those diagnostic maneuvers in the more challenging cases and become familiar with the pitfalls, exceptions, and the spectrum of behavior of each technique.

Tables 20.1 to 20.3 and Fig. 20.16 outline some of the proposed strategies for the EP diagnosis of narrow complex SVTs. Baseline tachycardia features, atrial and ventricular programmed stimulation during the tachycardia and then during sinus rhythm after tachycardia termination, provide a diagnosis of the mechanism of SVT in the vast majority of cases.

Step 1

Characterize the A/V relationship, RP-PR ratio, and atrial activation sequence during tachycardia (see Table 20.1). The differential diagnosis is most challenging in the setting of SVTs with a concentric atrial activation sequence and a 1:1 A/V relationship. SVTs with very short RP intervals (simultaneous atrial and ventricular activation) and a concentric atrial activation sequence include: (1) typical AVNRT; (2) AT with a focus close to the AV junction with a long PR interval; (3) and junctional tachycardia. The differential diagnosis of a short

TABLE 20.1 Diagnostic Strategy for Narrow QRS Supraventricular Tachycardia: Tachycardia Features

Atrial activation sequence	<ul style="list-style-type: none"> Eccentric atrial activation sequence excludes AVNRT (except for the left variant of AVNRT). An initial atrial activation site away from the AV groove and AV junction is diagnostic of AT and excludes both AVNRT and orthodromic AVRT.
RP-PR interval ratio	<ul style="list-style-type: none"> Short RP with VA interval of <70 msec or a ventricular-to-high RA interval of <95 msec during SVT excludes orthodromic AVRT, and is consistent with AVNRT (most common), but can occur during AT with a long PR interval or junctional tachycardia (rare). Short RP with VA interval of >70 msec suggests orthodromic AVRT (most common), slow-slow AVNRT, and AT with a long PR interval. Long RP suggests fast-slow AVNRT, PJRT, and AT.
AV block	<ul style="list-style-type: none"> Spontaneous or induced AV block with continuation of the tachycardia is consistent with AT, excludes AVRT, and is uncommon in AVNRT.
VA block	<ul style="list-style-type: none"> VA block excludes orthodromic AVRT, and rarely occurs during AVNRT. Other potential mechanisms of SVT with VA block include junctional tachycardia with retrograde VA block and nodofascicular or nodoventricular reentrant tachycardia.
Effects of BBB	<ul style="list-style-type: none"> BBB does not affect the TCL or VA interval in AT, AVNRT, or orthodromic AVRT using a BT contralateral to the BBB. BBB that prolongs the VA interval, with or without affecting the TCL, is diagnostic of orthodromic AVRT using an AV BT ipsilateral to the BBB and excludes AT and AVNRT.
Tachycardia CL variations	<ul style="list-style-type: none"> Spontaneous changes in PR and RP intervals with a fixed A-A interval is consistent with AT, and excludes orthodromic AVRT. Spontaneous changes in the TCL accompanied by a constant VA interval ("VA linking") favor orthodromic AVRT. Changes in atrial CL preceding similar changes in subsequent ventricular CL strongly favor AT or atypical AVNRT. Changes in ventricular CL preceded by similar changes in the atrial CL favor typical AVNRT or orthodromic AVRT.
Tachycardia termination	<ul style="list-style-type: none"> Termination of SVT (spontaneous or in response to adenosine or vagal maneuvers) with a P wave not followed by a QRS practically excludes AT, except in the case of a nonconducted PAC terminating the AT. Reproducible SVT termination in response to adenosine with a QRS not followed by a P wave excludes orthodromic AVRT using a rapidly conducting AV BT as the retrograde limb, is unusual in typical AVNRT, and is consistent with AT, PJRT, or atypical AVNRT.

A-A, Atrial-atrial; AT, atrial tachycardia; AV, atrioventricular; AVNRT, atrioventricular nodal reentrant tachycardia; AVRT, atrioventricular reentrant tachycardia; BBB, bundle branch block; BT, bypass tract; CL, cycle length; PAC, premature atrial complex; PJRT, permanent junctional reciprocating tachycardia; RA, right atrium; SVT, supraventricular tachycardia; TCL, tachycardia cycle length; VA, ventriculoatrial.

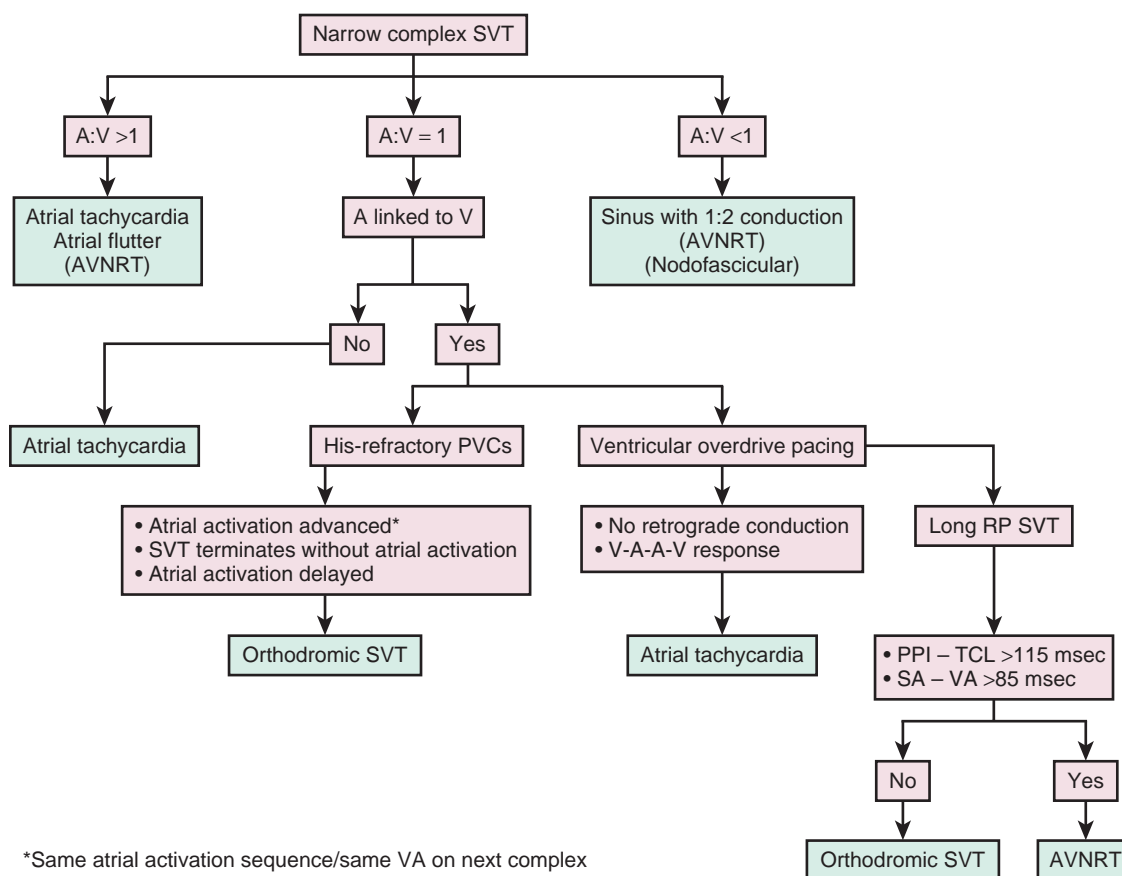


Fig. 20.16 Algorithm for Diagnosis of Narrow Complex Supraventricular Tachycardia (SVT). Items in parentheses are rarely seen. AVNRT, Atrioventricular nodal reentry; CL, cycle length; PPI, postpacing interval; PVC, premature ventricular complex; SA, stimulus-to-atrial interval; TCL, tachycardia cycle length; VA, ventriculoatrial interval.

TABLE 20.2 Diagnostic Strategy for Narrow QRS Supraventricular Tachycardia: Programmed Electrical Stimulation During Tachycardia**Ventricular Extrastimulation**

Resetting with ventricular fusion	<ul style="list-style-type: none"> Resetting with manifest QRS fusion is consistent with orthodromic AVRT and excludes both AVNRT and focal AT.
Preexcitation index	<ul style="list-style-type: none"> Preexcitation index (the difference between the TCL and the longest VES coupling interval at which atrial capture occurs during tachycardia) ≥ 100 msec characterizes AVNRT, whereas an index < 45 msec is consistent with AVRT with a septal BT.
VA interval	<ul style="list-style-type: none"> ΔVA interval ($VA_{\text{pacing}} - VA_{\text{SVT}}$) > 110 msec (after resetting with single or double VESs from the RV apex) is consistent with AVNRT.
Postpacing interval	<ul style="list-style-type: none"> Corrected (PPI – TCL) > 110 msec (after resetting with single or double VESs from the RV apex) is consistent with AVNRT.
When the VES advances the next atrial activation	<ul style="list-style-type: none"> Advancement of the next atrial impulse occurring with a VES delivered when the HB is not refractory usually does not help differentiate among the different types of SVTs. If advancement occurs when the HB is refractory, AVNRT is excluded. If advancement occurs with an atrial activation sequence similar to that during SVT, regardless of the timing of the VES, AT is less likely than AVNRT or orthodromic AVRT.
When the VES delays the next atrial activation	<ul style="list-style-type: none"> When advancement occurs when the HB is refractory, with an atrial activation sequence similar to that during SVT, AVNRT is excluded, AT is unlikely, and orthodromic AVRT is the most likely diagnosis.
When the VES resets the next QRS without atrial activation	<ul style="list-style-type: none"> When the VES causes delay in the next atrial activation, regardless of the timing of the VES, AT is excluded, and when such delay occurs with a VES delivered when the HB is refractory, both AVNRT and AT are excluded.
When the VES terminates the SVT	<ul style="list-style-type: none"> When a VES resets the SVT without atrial activation (i.e., the VES advances the subsequent His potential and QRS), both AT and orthodromic AVRT are excluded. When termination occurs reproducibly with a VES delivered when the HB is refractory, AVNRT is excluded, and the presence of a retrogradely conducting AV BT is diagnosed. If the atrial activation sequence following the VES is similar to that during the SVT, orthodromic AVRT is indicated and AT is practically excluded, except for the rare case in which AT originates close to the atrial insertion site of an innocent bystander AV BT. When termination occurs reproducibly with a VES that does not activate the atrium, regardless of the timing of the VES in relation to the HB, AT is excluded; when this phenomenon is observed with a VES delivered when the HB is refractory, both AT and AVNRT are excluded and orthodromic AVRT is diagnosed.
When the VES fails to affect the next atrial activation	<ul style="list-style-type: none"> If resetting does not occur with a relatively late VES, this usually does not help in the differential diagnosis of SVT. If resetting does not occur with an early VES, despite advancement (by > 30 msec) of the local ventricular activation at ventricular sites near the site of earliest atrial activation, orthodromic AVRT and the presence of a retrogradely conducting AV BT are excluded.

Ventricular Pacing

VA dissociation	<ul style="list-style-type: none"> When overdrive ventricular pacing during SVT fails to accelerate atrial CL to the PCL (i.e., the ventricles are dissociated from the tachycardia), AVRT is excluded, AT is the most likely diagnosis, but AVNRT is still possible.
VA interval	<ul style="list-style-type: none"> ΔVA interval ($VA_{\text{pacing}} - VA_{\text{SVT}}$) > 85 msec is consistent with AVNRT. ΔVA of < 85 msec is consistent with orthodromic AVRT.
Postpacing interval	<ul style="list-style-type: none"> (PPI – TCL) > 115 msec (or corrected [PPI – TCL] > 110 msec) is consistent with AVNRT. (PPI – TCL) < 115 msec (or corrected [PPI – TCL] < 110 msec) is consistent with orthodromic AVRT.
Entrainment with ventricular fusion	<ul style="list-style-type: none"> Manifest ventricular fusion during entrainment indicates AVRT and excludes both AVNRT and AT.
Differential-site right ventricular entrainment	<ul style="list-style-type: none"> Differential corrected (PPI – TCL) of > 30 msec after transient entrainment from the RV apex vs. the RV base is consistent with AVNRT. Differential corrected (PPI – TCL) of < 30 msec is consistent with orthodromic AVRT. Differential VA interval (ventricular stimulus-to-atrial interval during entrainment from RV base vs. RV septum) of > 20 msec is consistent with AVNRT. Differential VA interval of < 20 msec is consistent with orthodromic AVRT.
Atrial resetting during the transition zone	<ul style="list-style-type: none"> Atrial resetting (perturbation of atrial timing by > 15 msec) during the transition zone is consistent with orthodromic AVRT and excludes AVNRT or AT (unless a bystander retrogradely conducting BT is present).
Length of pacing drive required for entrainment	<ul style="list-style-type: none"> Acceleration of the SVT to the PCL occurring by the first beat with stable paced QRS morphology is consistent with orthodromic AVRT and essentially excludes AVNRT. Acceleration of the SVT to the PCL occurring only after ≥ 2 beats with stable paced QRS morphology is consistent with AVNRT and excludes orthodromic AVRT.
Atrial activation sequence during ventricular pacing	<ul style="list-style-type: none"> Atrial activation sequence during pacing different from that during the SVT is consistent with AT and practically excludes both orthodromic AVRT and AVNRT. Atrial activation sequence during pacing similar to that during the SVT favors orthodromic AVRT or AVNRT over AT.
Atrial and ventricular electrogram sequence following cessation of ventricular pacing	<ul style="list-style-type: none"> A-A-V response is consistent with AT (as long as pseudo-A-A-V response is excluded). A-V response is consistent with AVNRT and orthodromic AVRT.

Continued

TABLE 20.2 Diagnostic Strategy for Narrow QRS Supraventricular Tachycardia: Programmed Electrical Stimulation During Tachycardia—cont'd**Atrial Extrastimulation**

Resetting with atrial fusion

- Demonstration of resetting with manifest atrial fusion excludes AVNRT and focal AT.

Atrial Pacing

Entrainment during atrial pacing

- Demonstration of entrainment excludes automatic and triggered activity ATs.

Entrainment with atrial fusion

- Demonstration of entrainment with manifest atrial fusion excludes AVNRT and focal AT.

Overdrive suppression

- Overdrive suppression of the SVT favors automatic AT and excludes AVNRT and orthodromic AVRT.

AH interval

- ΔAH interval ($AH_{\text{pacing}} - AH_{\text{SVT}}$) of >40 msec favors AVNRT over AT and orthodromic AVRT.

- ΔAH interval of <20 msec favors AT and orthodromic AVRT over AVNRT.

VA linking

- On cessation of overdrive atrial pacing (with 1:1 AV conduction), if the VA interval following the last entrained QRS is reproducibly constant (<10 msec variation), despite pacing at different CLs or for different durations (VA linking) and similar to that during SVT, AT is unlikely.

- If no VA linking is demonstrable, AT is more likely than other types of SVT.

Differential-site atrial pacing

- On cessation of overdrive atrial pacing (with 1:1 AV conduction) from different atrial sites (high RA and proximal CS) at the same PCL, a maximal difference in the postpacing VA intervals (the interval from last captured ventricular electrogram to the earliest atrial electrogram of the initial tachycardia beat after pacing) among the different atrial pacing sites (ΔVA interval) of >14 msec is consistent with AT.

- ΔVA interval of <14 msec favors AVNRT or orthodromic AVRT over AT.

Para-Hisian Entrainment or Resetting

SA and local VA intervals

- Prolongation of the SA and the local VA intervals on loss of HB capture, compared with that during HB capture is consistent with AVNRT.

- SA and the local VA intervals that remain constant regardless of whether the HB-RB is being captured indicate orthodromic AVRT.

- SA interval prolongation on HB-RB noncapture, but without significant change in the local VA interval, indicates orthodromic AVRT.

- The change in the stimulus to earliest atrial activation time (ΔSA interval) with loss of HB-RB capture >40 msec is consistent with AVNRT.

- ΔSA interval <40 msec indicates AVRT (except for rare patients with a left lateral BT).

The number of beats required to capture the atrium with para-Hisian pacing during SVT

- Entry into the tachycardia circuit within 1 beat indicates AVRT, whereas entry into the circuit occurring only after 3 or more beats is consistent with AVNRT.

A-A-V, Atrial-atrial-ventricular; A-V, atrial-ventricular; AH, atrial-His bundle interval; AT, atrial tachycardia; AV, atrioventricular; AVNRT, atrioventricular nodal reentrant tachycardia; AVRT, atrioventricular reentrant tachycardia; BT, bypass tract; CL, cycle length; CS, coronary sinus; HB, His bundle; PCL, pacing cycle length; PPI, postpacing interval; RA, right atrium; RB, right bundle branch; RV, right ventricle; SA, stimulus-atrial; SVT, supraventricular tachycardia; TCL, tachycardia cycle length; VA, ventriculoatrial; VES, ventricular extrastimulus.

TABLE 20.3 Diagnostic Strategy for Narrow QRS Supraventricular Tachycardia: Programmed Electrical Stimulation During Sinus Rhythm**Tachycardia Induction**

Catecholamine administration

- Spontaneous SVT initiation during isoproterenol administration is consistent with automatic AT or junctional tachycardia.

AES

- "Critical AH" required for SVT induction is consistent with typical AVNRT.

- If the VA interval of the first tachycardia beat is reproducibly identical to that during the rest of the SVT ("VA linking"), AT is very unlikely, and is suggestive of typical AVNRT and orthodromic AVRT.

VES

- ΔVA ($VA_{\text{VES}} - VA_{\text{SVT}}$) <85 msec is consistent with orthodromic AVRT.

- ΔVA interval >85 msec favors AVNRT.

- $(PPI_{\text{VES}} - TCL) <115$ msec is consistent with orthodromic AVRT.

- $(PPI_{\text{VES}} - TCL) >115$ msec favors AVNRT.

Atrial Pacing From High Right Atrium at Tachycardia Cycle Length

AH interval

- ΔAH interval ($AH_{\text{pacing}} - AH_{\text{SVT}}$) of >40 msec favors AVNRT over AT and orthodromic AVRT.

- ΔAH interval of <20 msec favors AT and orthodromic AVRT over AVNRT.

Ventricular Pacing From Right Ventricular Apex at Tachycardia Cycle Length

HA interval

- ΔHA interval ($HA_{\text{pacing}} - HA_{\text{SVT}}$) of more than -10 msec favors AVNRT.

- ΔHA interval of less than -10 msec favors orthodromic AVRT.

TABLE 20.3 Diagnostic Strategy for Narrow QRS Supraventricular Tachycardia: Programmed Electrical Stimulation During Sinus Rhythm—cont'd

Retrograde atrial activation sequence	• Retrograde atrial activation sequence during ventricular pacing similar to that during SVT favors orthodromic AVRT and AVNRT over AT.
VA block	• The presence of VA block or decremental VA conduction during ventricular pacing at a CL similar to the TCL and under comparable autonomic tone argues against orthodromic AVRT and favors AT and AVNRT.
Differential-Site Right Ventricular Pacing	
VA interval	<ul style="list-style-type: none"> • When the VA (S-A) interval during RV apical pacing is shorter than that during RV basal pacing, a retrogradely conducting septal BT is excluded. • When the VA (S-A) interval during RV apical pacing is longer than that during RV basal pacing, a retrogradely conducting AV BT is diagnosed.
Atrial activation sequence	<ul style="list-style-type: none"> • Retrograde atrial activation sequence that is different depending on the site of ventricular pacing indicates the presence of a BT. • Constant atrial activation sequence does not help exclude or prove the presence of an AV BT.
Para-Hisian Pacing	
Atrial activation sequence	<ul style="list-style-type: none"> • Identical retrograde atrial activation sequence, with and without HB capture, indicates that retrograde conduction is occurring over the same system during HB-RB capture and noncapture (either the BT or AVN) and does not help prove or exclude the presence of BT. • Retrograde atrial activation sequence that is different depending on whether HB is captured indicates the presence of a BT.
HA and VA intervals	<ul style="list-style-type: none"> • VA (S-A) interval (recorded at multiple sites, including close to the site of earliest atrial activation during SVT) that is constant regardless of whether the HB-RB is being captured indicates the presence of a BT. • Prolongation of the VA (S-A) interval on loss of HB capture, compared with that during HB capture, excludes the presence of a retrogradely conducting BT, except for slowly conducting and far free-wall BTs.
Dual-Chamber Sequential Extrastimulation	
VA conduction	• VA conduction of V_2 indicates the presence of a retrogradely conducting BT.

AES, Atrial extrastimulation; AH, atrial-His bundle interval; AT, atrial tachycardia; AV, atrioventricular; AVN, atrioventricular node; AVNRT, atrioventricular nodal reentrant tachycardia; AVRT, atrioventricular reentrant tachycardia; BT, bypass tract; CL, cycle length; HA, His bundle–atrial; HB, His bundle; PPI, postpacing interval; RB, right bundle branch; RV, right ventricle; S-A, stimulus-atrial; SVT, supraventricular tachycardia; TCL, tachycardia cycle length; VA, ventriculoatrial; VES, ventricular extrastimulus.

RP SVT with a concentric atrial activation sequence includes (1) AT with a focus close to the AV junction; (2) orthodromic AVRT using a septal or paraseptal BT; and (3) slow-slow AVNRT. Long RP SVTs with a concentric atrial activation sequence include: (1) atypical (fast-slow) AVNRT; (2) PJRT; and (3) nodofascicular reentrant tachycardia (orthodromic AVRT using a concealed nodofascicular/nodoventricular BT). Narrow-complex tachycardia with VA block is rare; the differential diagnosis includes (1) typical AVNRT; (2) junctional tachycardia; and (3) nodofascicular reentrant tachycardia (orthodromic AVRT using a concealed nodofascicular/nodoventricular BT).

Step 2

Overdrive Ventricular Pacing During the Supraventricular Tachycardia

Ventricular pacing during the SVT represents the single most important diagnostic maneuver and can provide several clues to the diagnosis of most SVTs. Therefore it is preferable to employ this maneuver as an initial step in the diagnostic approach. When sustained SVT is inducible, overdrive pacing from the RV apex and RV base is performed at a PCL 10 to 30 milliseconds shorter than the TCL; the PCL is then progressively reduced by 10 to 20 milliseconds in a stepwise fashion with cessation of ventricular pacing after each PCL to verify continuation versus termination of the SVT. Several diagnostic criteria can be applied including the VA interval during pacing versus tachycardia, PPI, atrial activation sequence, presence of manifest ventricular fusion, and the length of pacing drive required to enter the tachycardia circuit, and

the atrial and ventricular electrogram sequence following cessation of pacing (see Table 20.2).³⁰

Step 3

Ventricular Extrastimulation During Supraventricular Tachycardia

Subsequently, a VES is delivered when the HB is refractory and then at progressively shorter VES coupling intervals (approximately 10-millisecond stepwise shortening of the VES coupling interval) so as to scan all of diastole. First, ventricular capture of the VES should be verified, and then the effect of the VES on the following atrial activation (advancement, delay, termination, or no effect) should be evaluated, as well as the timing of the VES in relation to the expected His potential during the SVT. Furthermore, conduction of the VES to the atrium and sequence of atrial activation following the VES should be carefully examined (see Fig. 20.11).³⁰

Step 4

Overdrive Atrial Pacing During the Supraventricular Tachycardia

Atrial pacing is performed at a PCL 10 to 20 milliseconds shorter than the TCL. The PCL is then progressively reduced by 10 to 20 milliseconds in a stepwise fashion, with discontinuation of atrial pacing after each PCL to ensure continuation versus termination of the SVT. The AH interval, and presence of entrainment, atrial fusion, and VA linking should be evaluated (see Table 20.2).³⁰

Step 5

After tachycardia termination, ventricular and atrial pacing at the TCL, differential site RV pacing (RV apex vs. base), and para-Hisian pacing maneuvers are performed (see Table 20.3).

REFERENCES

- Page RL, et al. 2015 ACC/AHA/HRS guideline for the management of adult patients with supraventricular tachycardia: a report of the American College of Cardiology/American Heart Association Task Force on Clinical Practice Guidelines and the Heart Rhythm Society. *Circulation*. 2016;133:e506–e574.
- Porter MJ, et al. Influence of age and gender on the mechanism of supraventricular tachycardia. *Heart Rhythm*. 2004;1:393–396.
- González-Torrecilla E, et al. Combined evaluation of bedside clinical variables and the electrocardiogram for the differential diagnosis of paroxysmal atrioventricular reciprocating tachycardias in patients without pre-excitation. *J Am Coll Cardiol*. 2009;53:2353–2358.
- Katrtsis DG, Josephson ME. Differential diagnosis of regular, narrow-QRS tachycardias. *Heart Rhythm*. 2015;12:1667–1676.
- Hillock RJ, Kalman JM, Roberts-Thomson KC, et al. Multiple focal atrial tachycardias in a healthy adult population: characterization and description of successful radiofrequency ablation. *Heart Rhythm*. 2007;4:435–438.
- Brembilla-Perrot B, Delobelle J. Prevalence of stroke among patients with paroxysmal supraventricular tachycardia. *Pacing Clin Electrophysiol*. 2013;36:180–186.
- Medi C, et al. Tachycardia-mediated cardiomyopathy secondary to focal atrial tachycardia: long-term outcome after catheter ablation. *J Am Coll Cardiol*. 2009;53:1791–1797.
- Pablo Costabel J, et al. High-sensitivity cardiac troponin levels in supraventricular tachyarrhythmias. *Pacing Clin Electrophysiol*. 2016;39:588–591.
- Liu CF, et al. Unifying algorithm for mechanistic diagnosis of atrial tachycardia. *Circ Arrhythm Electrophysiol*. 2016;9:e004028.
- Mills MF, et al. Is there a difference in tachycardia cycle length during SVT in children with AVRT and AVNRT? *Pacing Clin Electrophysiol*. 2016;39:1206–1212.
- Katrtsis DG, Camm AJ. Atrioventricular nodal reentrant tachycardia. *Circulation*. 2010;122:831–840.
- Castillo Castillo J, Peñafiel Verdú P, Martínez Sánchez J, et al. Narrow irregular QRS tachycardia with AV dissociation: what is the mechanism? *J Cardiovasc Electrophysiol*. 2013;24:364–366.
- Issa ZF. Mechanism of paroxysmal supraventricular tachycardia with ventriculoatrial conduction block. *Europace*. 2009;11:1235–1237.
- Lim PCY, et al. Paroxysmal supraventricular tachycardia with ventriculoatrial block and qrs duration shortening: what is the mechanism? *J Cardiovasc Electrophysiol*. 2016;27:616–617.
- Yang Y, et al. Quantitative effects of functional bundle branch block in patients with atrioventricular reentrant tachycardia. *Am J Cardiol*. 2000;85:826–831.
- Wright JM, Singh D, Price A, et al. Two cases of supraventricular tachycardia after accessory pathway ablation. *Circ Arrhythm Electrophysiol*. 2013;6:26–31.
- Derval N, et al. Differential sequential septal pacing: a simple maneuver to differentiate nodal versus extranodal ventriculoatrial conduction. *Heart Rhythm*. 2013;10:1785–1791.
- Kapa S, et al. Utilization of retrograde right bundle branch block to differentiate atrioventricular nodal from accessory pathway conduction. *J Cardiovasc Electrophysiol*. 2009;20:751–758.
- Nakagawa H, Jackman WM. Para-Hisian pacing: useful clinical technique to differentiate retrograde conduction between accessory atrioventricular pathways and atrioventricular nodal pathways. *Heart Rhythm*. 2005;2:667–672.
- Sauer WH, Lowery CM, Cooper JM, et al. Sequential dual chamber extrastimulation: a novel pacing maneuver to identify the presence of a slowly conducting concealed accessory pathway. *Heart Rhythm*. 2008;5:248–252.
- Obeyesekere M, et al. Tachycardia induction with ventricular extrastimuli differentiates atypical atrioventricular nodal reentrant tachycardia from orthodromic reciprocating tachycardia. *Heart Rhythm*. 2012;9:335–341.
- Knight BP, et al. Diagnostic value of tachycardia features and pacing maneuvers during paroxysmal supraventricular tachycardia. *J Am Coll Cardiol*. 2000;36:574–582.
- Nagashima K, et al. Ventriculoatrial intervals ≤ 70 ms in orthodromic atrioventricular reciprocating tachycardia. *Pacing Clin Electrophysiol*. 2016;39:1108–1115.
- Crawford TC, et al. Utility of atrial and ventricular cycle length variability in determining the mechanism of paroxysmal supraventricular tachycardia. *J Cardiovasc Electrophysiol*. 2007;18:698–703.
- Efimova E, et al. Adenosine sensitivity of retrograde fast pathway conduction in patients with slow-fast atrioventricular nodal reentrant tachycardia: a prospective study. *Heart Rhythm*. 2014;11:871–876.
- Josephson ME, Almendral J, Callans DJ. Resetting and entrainment of reentrant ventricular tachycardia associated with myocardial infarction. *Heart Rhythm*. 2014;11:1239–1249.
- Deo R, Berger R. The clinical utility of entrainment pacing. *J Cardiovasc Electrophysiol*. 2009;20:466–470.
- Maruyama M, et al. The VA relationship after differential atrial overdrive pacing: a novel tool for the diagnosis of atrial tachycardia in the electrophysiologic laboratory. *J Cardiovasc Electrophysiol*. 2007;18:1127–1133.
- Calvo D, et al. Differential responses of the septal ventricle and the atrial signals during ongoing entrainment. *Circ Arrhythm Electrophysiol*. 2015;8:1201–1209.
- Ho RT, Frisch DR, Pavri BB, et al. Electrophysiological features differentiating the atypical atrioventricular node-dependent long RP supraventricular tachycardias. *Circ Arrhythm Electrophysiol*. 2013;6:597–605.
- Boyle PM, Veenhuyzen GD, Vigmond EJ. Fusion during entrainment of orthodromic reciprocating tachycardia is enhanced for basal pacing sites but diminished when pacing near Purkinje system end points. *Heart Rhythm*. 2013;10:444–451.
- Almendral J. Resetting and entrainment of reentrant arrhythmias: part II: informative content and practical use of these responses. *Pacing Clin Electrophysiol*. 2013;36:641–661.
- Akerström F, et al. Performance of the SA-VA difference to differentiate atrioventricular nodal reentrant tachycardia from orthodromic reentrant tachycardia in a large cohort of consecutive patients. *Pacing Clin Electrophysiol*. 2015;38:1066–1072.
- González-Torrecilla E, et al. Differences in ventriculoatrial intervals during entrainment and tachycardia: a simpler method for distinguishing paroxysmal supraventricular tachycardia with long ventriculoatrial intervals. *J Cardiovasc Electrophysiol*. 2011;22:915–921.
- Platonov M, Schroeder K, Veenhuyzen GD. Differential entrainment: beware from where you pace. *Heart Rhythm*. 2007;4:1097–1099.
- Kannankeril PJ, Bonney WJ, Dzurik MV, et al. Entrainment to distinguish orthodromic reciprocating tachycardia from atrioventricular nodal reentry tachycardia in children. *Pacing Clin Electrophysiol*. 2010;33:469–474.
- González-Torrecilla E, et al. First postpacing interval after tachycardia entrainment with correction for atrioventricular node delay: a simple maneuver for differential diagnosis of atrioventricular nodal reentrant tachycardias versus orthodromic reciprocating tachycardias. *Heart Rhythm*. 2006;3:674–679.
- Boonyapisit W, et al. Determining the site of accessory pathways in orthodromic reciprocating tachycardia by using the response to right ventricular pacing. *Pacing Clin Electrophysiol*. 2015;39:115–121.
- Javier García-Fernández F, et al. Differentiation of atrioventricular nodal reentrant tachycardia from orthodromic reciprocating tachycardia by the resetting response to ventricular extrastimuli: comparison to response to continuous ventricular pacing. *J Cardiovasc Electrophysiol*. 2013;24:534–541.

40. Segal OR, et al. Differential ventricular entrainment: a maneuver to differentiate AV node reentrant tachycardia from orthodromic reciprocating tachycardia. *Heart Rhythm*. 2009;6:493–500.
41. Nagashima K, et al. Anterograde conduction to the His bundle during right ventricular overdrive pacing distinguishes septal pathway atrioventricular reentry from atypical atrioventricular nodal reentrant tachycardia. *Heart Rhythm*. 2015;12:735–743.
42. Kaiser DW, et al. The precise timing of tachycardia entrainment is determined by the postpacing interval, the tachycardia cycle length, and the pacing rate: theoretical insights and practical applications. *Heart Rhythm*. 2016;13:695–703.
43. Dandamudi G, et al. A novel approach to differentiating orthodromic reciprocating tachycardia from atrioventricular nodal reentrant tachycardia. *Heart Rhythm*. 2010;7:1326–1329.
44. Rosman JZ, et al. Resetting criteria during ventricular overdrive pacing successfully differentiate orthodromic reentrant tachycardia from atrioventricular nodal reentrant tachycardia despite interobserver disagreement concerning QRS fusion. *Heart Rhythm*. 2011;8:2–7.
45. AlMahameed ST, Buxton AE, Michaud GF. New criteria during right ventricular pacing to determine the mechanism of supraventricular tachycardia. *Circ Arrhythm Electrophysiol*. 2010;3:578–584.
46. Vijayaraman P, Lee BP, Kalahasty G, et al. Reanalysis of the ‘pseudo A-A-V’ response to ventricular entrainment of supraventricular tachycardia: importance of His-bundle timing. *J Cardiovasc Electrophysiol*. 2006;17:25–28.
47. Pérez-Rodon J, et al. Entrainment from the para-Hisian region for differentiating atrioventricular node reentrant tachycardia from orthodromic atrioventricular reentrant tachycardia. *Europace*. 2008;10:1205–1211.
48. Singh DK, et al. His overdrive pacing during supraventricular tachycardia: a novel maneuver for distinguishing atrioventricular nodal reentrant tachycardia from atrioventricular reciprocating tachycardia. *Heart Rhythm*. 2014;11:1327–1335.
49. Asirvatham SJ, Stevenson WG. Atrioventricular nodal reentry tachycardia chameleon in disguise. *Circ Arrhythm Electrophysiol*. 2014;7:355–357.

Wide Complex Tachycardias

OUTLINE

Clinical Considerations, 730

Causes of Wide Complex Tachycardias, 730

Clinical History, 730

Physical Examination, 731

Laboratory Testing, 732

Pharmacological Intervention, 732

Electrocardiographic Features, 732

Ventricular Tachycardia Versus Aberrantly Conducted

Supraventricular Tachycardia, 732

Algorithms for the Electrocardiographic Diagnosis of Wide Complex Tachycardia, 738

Ventricular Tachycardia Versus Preexcited Supraventricular Tachycardia, 742

Limitations of Electrocardiographic Criteria for Diagnosis of Wide Complex Tachycardia, 742

Electrophysiological Testing, 742

Baseline Observations During Normal Sinus Rhythm, 742

Induction of Tachycardia, 743

Tachycardia Features, 743

Diagnostic Maneuvers During Tachycardia, 744

CLINICAL CONSIDERATIONS

Causes of Wide Complex Tachycardias

A narrow QRS complex (120 milliseconds or less) requires rapid, highly synchronous electrical activation of the right ventricle (RV) and left ventricle (LV), which can only be achieved through the specialized, rapidly conducting His-Purkinje system (HPS). A wide QRS complex implies less synchronous ventricular activation of longer duration, which can be due to intraventricular conduction disturbances (IVCDs), or ventricular activation not mediated by the His bundle (HB) but by a bypass tract (BT) (preexcitation) or from a site within a ventricle (ventricular arrhythmias). IVCDs can be fixed and present at all heart rates, and they can be intermittent and related to either tachycardia or bradycardia. IVCDs can be caused by structural abnormalities in the HPS or ventricular myocardium or by functional refractoriness in a portion of the conduction system (i.e., aberrant ventricular conduction).¹

Wide complex tachycardia (WCT) is a rhythm with a rate of more than 100 beats/min and a QRS duration of more than 120 milliseconds (Fig. 21.1). Several arrhythmias can manifest as WCTs (Table 21.1); the most common is ventricular tachycardia (VT), which accounts for 80% of all cases of WCT. Supraventricular tachycardia (SVT) with aberrancy accounts for 15% to 20% of WCTs. SVTs with bystander preexcitation and atrioventricular reentrant tachycardia (AVRT) account for 1% to 6% of WCTs.

In the stable patient who will undergo a more detailed assessment, the goal of evaluation should include determination of the cause of the WCT (particularly distinguishing between VT and SVT). Accurate diagnosis of the WCT requires information obtained from the history, physical examination, response to certain maneuvers, and careful inspection of the electrocardiogram (ECG), including rhythm strips and 12-lead tracings. Comparison of the ECG during the tachycardia with that recorded during sinus rhythm, if available, can also provide valuable information.

Clinical History

Age

WCT in a patient older than 35 years is likely to be VT (positive predictive value of up to 85%). SVT is more likely in the younger patient (positive predictive value of 70%).

Symptoms

Some patients with WCT present with few or no symptoms (e.g., palpitations, lightheadedness, diaphoresis), whereas others can have severe manifestations, including chest pain, dyspnea, syncope, seizures, and cardiac arrest. The severity of symptoms during a WCT is not useful in determining the tachycardia mechanism because symptoms are primarily related to the fast heart rate, associated heart disease, and the presence and extent of LV dysfunction, rather than to the mechanism of the tachycardia. It is important to recognize that VT does not necessarily result in hemodynamic compromise or collapse; on the other hand, rapid SVT can cause decompensation in susceptible patients. Misdiagnosis of VT as SVT on the basis of hemodynamic stability is a common error that can lead to inappropriate and potentially dangerous therapy.

Duration of the Arrhythmia

SVT is more likely if the tachycardia has recurred over a period of more than 3 years. The first occurrence of a WCT after myocardial infarction (MI) strongly implies VT.

Presence of Underlying Heart Disease

The presence of structural heart disease, especially coronary heart disease and a previous MI, strongly suggests VT as the cause of WCT. In one report, more than 98% of patients with a previous MI had VT as the cause of WCT, whereas only 7% of those with SVT had an MI. It should be realized, however, that VT can occur in patients with no apparent heart disease, and SVT can occur in those with structural heart disease.

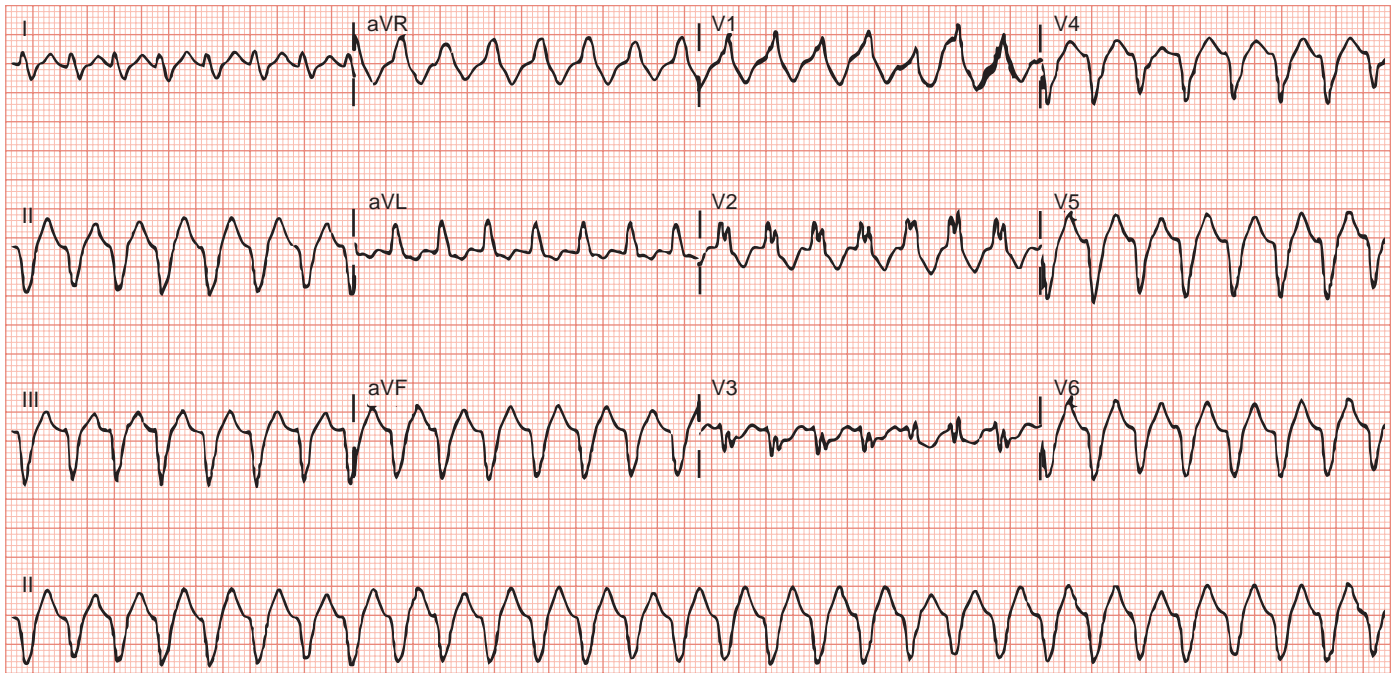


Fig. 21.1 Wide Complex Tachycardia. Electrocardiogram obtained in a patient with prior inferior wall infarction. The underlying mechanism is ventricular tachycardia related to the left ventricular inferior wall scar.

TABLE 21.1 Causes of Wide QRS Complex Tachycardia

Cause	Description, Examples
VT	Macroreentrant VT Focal VT
SVT with aberrancy	Functional BBB Preexisting BBB
Preexcited SVT	Antidromic AVRT AT or AVNRT with bystander BT
SVT with preexisting nonaberrant QRS	Bizarre QRS patterns in repaired congenital heart disease, cardiac malpositions, unusual hypertrophy patterns
SVT with antiarrhythmic drugs	Class IA and IC agents
Electrolyte abnormalities	Hyperkalemia
Ventricular pacing	

AT, Atrial tachycardia; AVNRT, atrioventricular nodal reentrant tachycardia; AVRT, atrioventricular reentrant tachycardia; BBB, bundle branch block; BT, bypass tract; SVT, supraventricular tachycardia; VT, ventricular tachycardia.

Pacemaker or Implantable Cardioverter-Defibrillator Implantation

A history of pacemaker or implantable cardioverter-defibrillator (ICD) implantation should raise the possibility of a device-associated tachycardia. Ventricular pacing can be associated with a small and almost imperceptible stimulus artifact on the ECG. The presence of an ICD is also of importance because such a device should identify and treat a sustained tachyarrhythmia, depending on device programming, and because the presence of an ICD implies that the patient is known to have an increased risk of ventricular tachyarrhythmias.

Medications

Many different medications have proarrhythmic effects. The most common drug-induced tachyarrhythmia is torsades de pointes. Frequently implicated agents include antiarrhythmic drugs (such as sotalol, dofetilide, and quinidine) and certain antimicrobial drugs (such as erythromycin). Diuretics are a common cause of hypokalemia and hypomagnesemia, which can predispose to ventricular tachyarrhythmias, particularly torsades de pointes in patients taking antiarrhythmic drugs. Furthermore, class I antiarrhythmic drugs, especially class IC agents, can decrease conduction velocity at faster heart rates (use dependency). As a result, these drugs can cause aberration and widening of the QRS complex during any tachyarrhythmia.

Digoxin can cause almost any cardiac arrhythmia, especially with increasing plasma digoxin concentrations above 2.0 ng/mL (2.6 mmol/L). Digoxin-induced arrhythmias are more frequent at any given plasma concentration if hypokalemia is also present. The most common digoxin-induced arrhythmias include monomorphic VT (often with a relatively narrow QRS complex), bidirectional VT (a regular alternation of two wide QRS morphologies, each with a different axis), and nonparoxysmal junctional tachycardia.

Physical Examination

Most of the elements of the physical examination, including the blood pressure and heart rate, are of importance primarily in determining the presence and severity of hemodynamic instability and, thus, how urgently a therapeutic intervention is required. In patients with significant hemodynamic compromise, a thorough diagnostic evaluation should be postponed until acute management has been addressed. In this setting, emergency cardioversion is the treatment of choice and does not require knowledge of the mechanism of the arrhythmia.

Evidence of underlying cardiovascular disease should be sought, including the sequelae of peripheral vascular disease or stroke. A healed sternal incision is obvious evidence of previous cardiothoracic surgery. A pacemaker or defibrillator, if present, can typically be palpated in the

left or, less commonly, right pectoral area below the clavicle, although some older devices are found in the anterior abdominal wall or subaxillary region.

An important objective of the physical examination in the stable patient is to attempt to document the presence of AV dissociation. The presence of AV dissociation strongly suggests VT, although its absence is less helpful. AV dissociation, when present, is typically diagnosed on ECG; however, it can produce a number of characteristic findings on physical examination. Intermittent cannon A waves may be observed on examination of the jugular pulsation in the neck, and they reflect intermittent simultaneous atrial and ventricular contraction. Cannon A waves must be distinguished from the continuous and regular prominent A waves seen during some SVTs. Such prominent waves result from simultaneous atrial and ventricular contraction occurring with every beat. In addition, highly inconsistent fluctuations in the blood pressure can occur because of the variability in the degree of LA contribution to LV filling, stroke volume, and cardiac output. Moreover, variability in the occurrence and intensity of heart sounds (especially S_1) can also be observed and is heard more frequently when the rate of the tachycardia is slower.

The response to carotid sinus massage can suggest the cause of the WCT. The heart rate during sinus tachycardia and automatic AT will gradually slow with carotid sinus massage and then accelerate on release. The ventricular rate during AT and AFL can transiently slow with carotid sinus massage because of slowing and block of atrioventricular node (AVN) conduction. The arrhythmia itself, however, is unaffected. Atrioventricular nodal reentrant tachycardia (AVNRT) and AVRT will either terminate or remain unaltered with carotid sinus massage. VTs are generally unaffected by carotid sinus massage, although this maneuver can potentially slow the atrial rate and, in some cases, expose AV dissociation. Some VTs, such as idiopathic VT from the RV outflow tract, can infrequently terminate in response to carotid sinus massage.

Laboratory Testing

The plasma potassium and magnesium concentrations should be measured as part of the laboratory evaluation. Hypokalemia and hypomagnesemia can predispose to the development of ventricular tachyarrhythmias; however, correction of abnormalities of electrolytes is never sufficient for therapy. Hyperkalemia can cause a wide QRS complex rhythm, usually with a slow rate, with loss of a detectable P wave (the putative sinoventricular rhythm; eFig. 21.1) or abnormalities of AVN conduction. In patients taking digoxin, quinidine, or procainamide, plasma concentrations of these drugs should be measured to assist in evaluating possible drug toxicity.

Pharmacological Intervention

The administration of certain drugs can be useful for diagnostic, as opposed to therapeutic, purposes. Termination of the arrhythmia with lidocaine suggests, but does not prove, that VT is the mechanism. Infrequently an SVT, especially AVRT, can terminate with lidocaine. On the other hand, termination of the tachycardia with procainamide or amiodarone does not distinguish between VT and SVT. Termination of the arrhythmia with digoxin, verapamil, diltiazem, or adenosine strongly implies SVT. However, VT can also occasionally terminate after the administration of these drugs.

Unless the cause for the WCT is definitely established, however, verapamil and diltiazem should not be administered because they have been reported to cause severe hemodynamic deterioration in patients with VT and can even provoke VF and cardiac arrest. Adenosine is suggested in the 2010 Adult Advanced Cardiac Life Support (ACLS) guidelines if a WCT is monomorphic, regular, and hemodynamically tolerated, because adenosine may help convert the rhythm to sinus and

may help in the diagnosis. When doubt exists, it is safest to assume any WCT is VT, particularly in patients with known cardiovascular disease.² Direct current cardioversion in unstable patients and IV procainamide or amiodarone in hemodynamically stable patients are the appropriate management approach.

ELECTROCARDIOGRAPHIC FEATURES

Ventricular Tachycardia Versus Aberrantly Conducted Supraventricular Tachycardia

Because the diagnosis of a WCT cannot always be made with complete certainty, the unknown rhythm should be presumed to be VT in the absence of contrary evidence. This conclusion is appropriate both because VT accounts for up to 80% of cases of WCT and because making this assumption guards against inappropriate and potentially dangerous therapy. As noted, the IV administration of drugs used for the treatment of SVT (verapamil, diltiazem, or beta-blockers) can cause severe hemodynamic deterioration in patients with VT and can even provoke VF and cardiac arrest. Therefore these drugs should not be used when the diagnosis is uncertain.

In general, most WCTs can be classified as having one of two patterns: right bundle branch block (RBBB)-like pattern (QRS polarity is predominantly positive in leads V_1 and V_2), or left bundle branch block (LBBB)-like pattern (QRS polarity is predominantly negative in leads V_1 and V_2). The determination that the WCT has an RBBB-like pattern or an LBBB-like pattern does not, by itself, assist in making a diagnosis; however, this assessment should be made initially because it has further implications for evaluating several other features on the ECG, including the QRS axis, the QRS duration, and the QRS morphology (Box 21.1; Fig. 21.2).³

Rate

The rate of the WCT is of limited value in distinguishing VT from SVT because there is wide overlap in the distribution of heart rates for SVT and VT. When the rate is around 150 beats/min, AFL with 2:1 AV conduction and aberrancy should be considered.

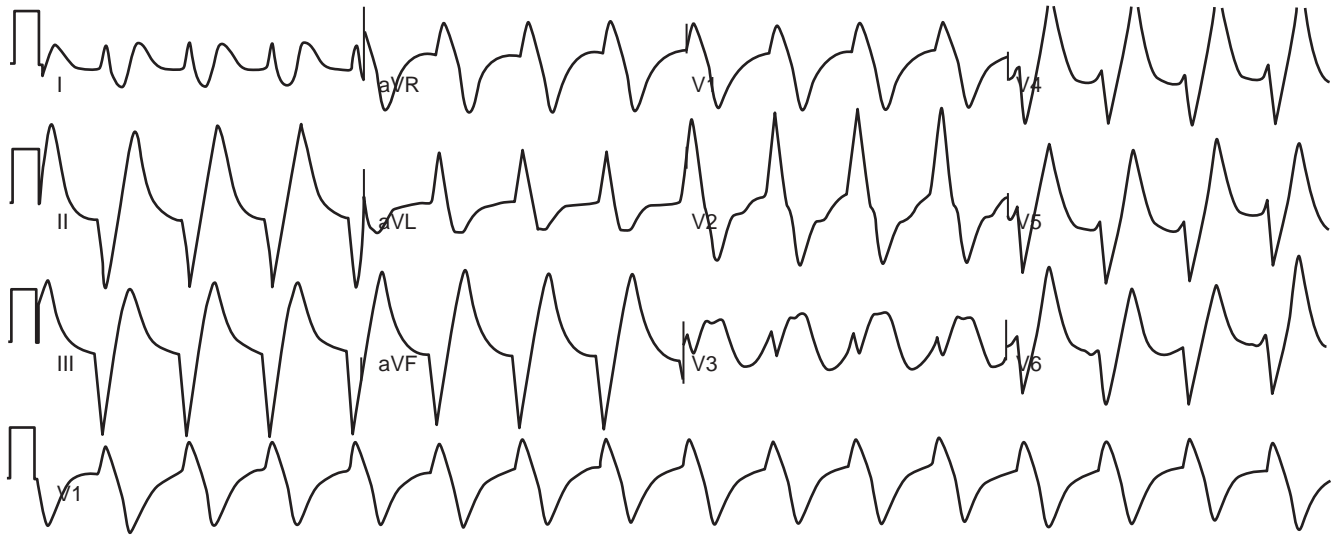
Regularity

Regularity of the WCT is not helpful in distinguishing VT from SVT because, in general, both are regular. However, VT is often associated with slight irregularity of the RR intervals, QRS morphology, and ST-T waves. Although marked irregularity strongly suggests AF, VTs can be particularly irregular within the first 30 seconds of onset and in patients treated with antiarrhythmic drugs.

Atrioventricular Dissociation

AV dissociation is characterized by atrial activity (P waves) that is completely independent of ventricular activity (QRS complexes). The atrial rate is usually slower than the ventricular rate (Fig. 21.3). A regular R-R interval in the presence of AF would most likely be AV dissociated.

AV dissociation is the hallmark of VT (specificity is almost 100%). However, although the presence of AV dissociation establishes VT as the cause, its absence (because of retrograde atrial capture) is not as helpful (sensitivity is 20% to 50%). AV dissociation can be present but not obvious on the surface ECG because of rapid ventricular rates. In addition, AV dissociation is absent in a large subset of VTs (especially those at a slower rate); in fact, approximately 30% of VTs have 1:1 retrograde VA conduction (see Fig. 21.2) and an additional 15% to 20% have second-degree (2:1 or Wenckebach) VA block (Fig. 21.4). Furthermore, AV dissociation can be observed during subatrial SVT, such as junctional ectopic tachycardia and nodofascicular reentrant tachycardia.



eFig. 21.1 Wide QRS Complex Rhythm Caused by Hyperkalemia.

BOX 21.1 Electrocardiographic Criteria Favoring Ventricular Tachycardia**AV Relationship**

- Dissociated P waves
- Fusion beats
- Capture beats
- A/V ratio <1

QRS Duration

- >160 ms with LBBB pattern
- >140 ms with RBBB pattern
- QRS during WCT is narrower than in NSR

QRS Axis

- Shift of >40 degrees between NSR and WCT
- Right superior (northwest) axis (−90 degrees to ±180 degrees)
- Left axis deviation with RBBB morphology
- Right axis deviation with LBBB morphology

Precordial QRS Concordance

- Positive concordance
- Negative concordance

QRS Morphology

- Contralateral BBB in WCT and NSR
- Absence of RS patterns in all precordial leads
- RS interval >100 ms in precordial leads with an RS morphology
- Lead II R wave peak time ≥50 ms

• Criteria in lead aVR:

- Presence of an initial R wave
- Presence of an initial r or q wave with width >40 ms
- Notching on the descending limb of a negative onset of a predominantly negative QRS complex
- $V_i/V_t \leq 1$

QRS Morphology in RBBB-Like WCT Pattern

- Lead V_1 :
 - Monophasic R, biphasic qR, Rs, or Rr' complex
 - Broad initial R wave (≥40 msec)
 - Rabbit ear sign: Double-peaked R wave with the left peak taller than the right peak
- Lead V_6 :
 - rS, QS, QR, or R complex
 - R/S ratio <1

QRS Morphology in LBBB-Like WCT Pattern

- Lead V_1/V_2 :
 - Broad initial R wave (≥30 msec)
 - RS interval >70 msec
 - R wave during WCT taller than the R wave during NSR
 - Slow descent to the nadir of the S (notching in the downstroke of the S wave)
- Lead V_6 :
 - Any Q wave or QS complex

AV, Atrioventricular; BBB, bundle branch block; LBBB, left bundle branch block; NSR, normal sinus rhythm; RBBB, right bundle branch block; WCT, wide complex tachycardia.

Several ECG findings are helpful in establishing the presence of AV dissociation, including the presence of dissociated P waves, fusion beats, or capture beats.

Dissociated P waves. When the P waves can be clearly seen and the atrial rate is unrelated to and slower than the ventricular rate, AV dissociation consistent with VT is present (Fig. 21.5). An atrial rate faster than the ventricular rate is more often seen with SVTs having AV conduction block. However, during a WCT, the P waves are often difficult to identify; they can be superimposed on the ST segment or T wave (resulting in altered morphology). Sometimes the T waves and initial or terminal portions of the QRS complex can resemble atrial activity and be mistaken for P waves. If the P waves are not obvious on the ECG, several alternative leads or modalities can help in their identification, including a modified chest lead placement (Lewis leads), an esophageal lead (using an electrode wire or nasogastric tube), RA recording (obtained by an electrode catheter in the RA), carotid sinus pressure (to slow VA conduction and therefore change the atrial rate in the case of VT), or invasive EP testing.

Fusion beats. Ventricular fusion occurs when a ventricular ectopic beat and a supraventricular beat (conducted via the AVN and HPS) simultaneously activate the ventricular myocardium. The resulting QRS complex has a morphology intermediate between the appearance of a sinus QRS complex and that of a purely ventricular complex. Intermittent fusion beats during a WCT are diagnostic of AV dissociation and therefore of VT (see Fig. 21.5). However, it is also possible for PVCs during SVT with aberration to produce fusion beats, which would erroneously be interpreted as evidence of AV dissociation and VT.

Capture beats. A capture beat (once called “Dressler beat”) is a normal QRS complex, identical to the sinus QRS complex, occurring

during the VT at a rate *faster* than the VT. The term *capture beat* indicates that the normal conduction system has momentarily captured control of ventricular activation from the VT focus (see Fig. 21.5). Fusion and capture beats are more commonly seen when the tachycardia rate is slower. These beats do not alter the rate of the VT, although a change in the preceding and subsequent RR intervals is frequently observed.

QRS Duration

In general, a wider QRS duration favors VT. In the setting of RBBB-like WCT, a QRS duration more than 140 milliseconds suggests VT, whereas for LBBB-like WCT, a QRS duration more than 160 milliseconds suggests VT. In an analysis of several studies, a QRS duration more than 160 milliseconds overall was a strong indicator of VT (likelihood ratio greater than 20:1). On the other hand, a QRS duration less than 140 milliseconds is not helpful for excluding VT because VT can sometimes be associated with a relatively narrow QRS complex, especially if it originates from the septum.

A QRS duration more than 160 milliseconds is not helpful in identifying VT in several settings including: (1) preexisting BBB, although it is uncommon for the QRS to be wider than 160 milliseconds in this situation; (2) preexcited SVT (see Chapter 18); and (3) the presence of drugs capable of slowing intraventricular conduction (e.g., class IA and IC drugs). Of note, a QRS complex that is narrower during WCT than during normal sinus rhythm (NSR) suggests VT. However, this is rare, occurring in less than 1% of VTs.

Rarely (4% in one series), VT can have a relatively narrow QRS duration (less than 120 to 140 milliseconds). This can be observed in VTs of septal origin or those with early penetration into the HPS, as occurs with fascicular (verapamil-sensitive) VT.

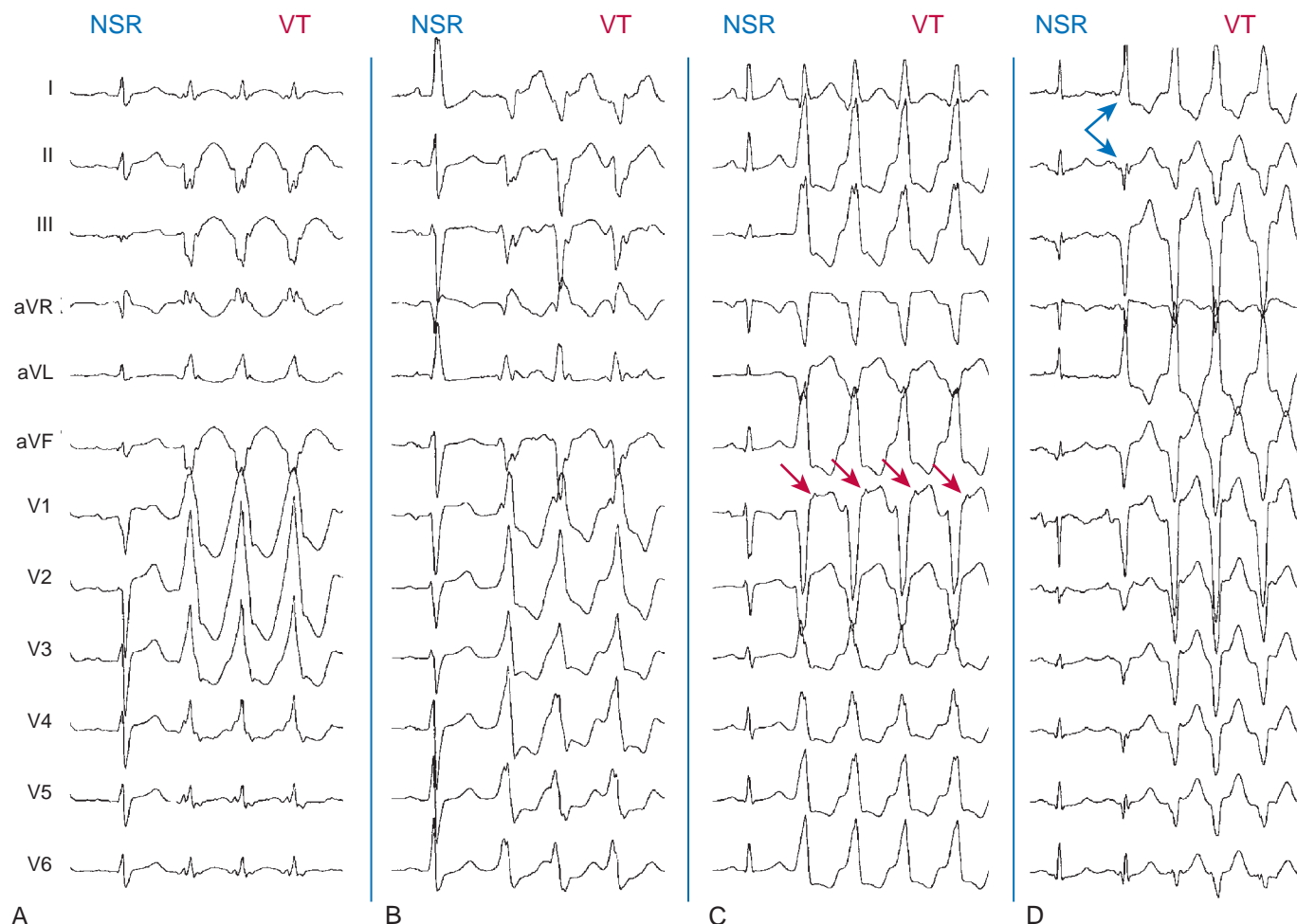


Fig. 21.2 Electrocardiogram Morphology During Normal Sinus Rhythm (NSR) Versus Ventricular Tachycardia (VT). (A) VT with right bundle branch block (RBBB) pattern, positive concordance, and long RS interval. Note the monophasic R in lead V₁ during VT and the significant shift in the frontal plane axis in VT versus NSR. (B) VT with an RBBB pattern and long RS interval. Note the superior (“northwest”) frontal plane axis during VT. (C) VT with a left bundle branch block (LBBB) pattern, long RS interval, and 1:1 ventriculoatrial conduction. Retrograde P waves (red arrows) are visible following the QRSs during VT. (D) VT with LBBB pattern and negative concordance. Note that the second QRS (blue arrows) is a fusion between the sinus beat and the VT beat.

QRS Axis

In general, the more leftward the axis, the greater the likelihood of VT. In addition, a significant axis shift (more than 40 degrees) between the baseline NSR and WCT is suggestive of VT (see Fig. 21.2A). Also, a right superior (“northwest”) axis (axis from -90 degrees to ± 180 degrees) is rare in SVT and strongly suggests VT (sensitivity 20%, specificity 96%; see Fig. 21.2B).

In a patient with an RBBB-like WCT, a QRS axis to the left of -30 degrees suggests VT (see Fig. 21.2A), and in a patient with an LBBB-like WCT, a QRS axis to the right of $+90$ degrees suggests VT. Furthermore, RBBB with a normal axis is uncommon in VT (less than 3%) and is suggestive of SVT.

Precordial QRS Concordance

Concordance is present when the QRS complexes in the six precordial leads (V₁ through V₆) are either all positive in polarity (tall R waves) or all negative in polarity (deep QS complexes). Negative concordance is strongly suggestive of VT (see Fig. 21.2D). Rarely, SVT with LBBB aberrancy will demonstrate negative concordance, but there is almost

always some evidence of an R wave in the lateral precordial leads. Positive concordance is most often caused by VT (see Fig. 21.2A); however, this pattern may also be caused by preexcited SVT using a left posterior BT. Although the presence of precordial QRS concordance strongly suggests VT (greater than 90% specificity), its absence is not helpful diagnostically (approximately 20% sensitivity).

QRS Morphology

As a general rule, if the WCT is caused by SVT with aberration, then the QRS complex during the WCT must be compatible with some form of BBB that could result in that QRS configuration. If there is no combination of bundle branch or fascicular blocks that could result in such a QRS configuration, then the diagnosis, by default, is VT or preexcited SVT.⁴ As noted, WCTs can be classified as having RBBB-like pattern or LBBB-like pattern. Certain features of the QRS complex have been described that favor VT in RBBB-like or LBBB-like WCTs (Fig. 21.6).⁵

RBBB pattern. Development of RBBB alters the activation sequence of the RV, whereas the LV is activated normally. Because the LB is not

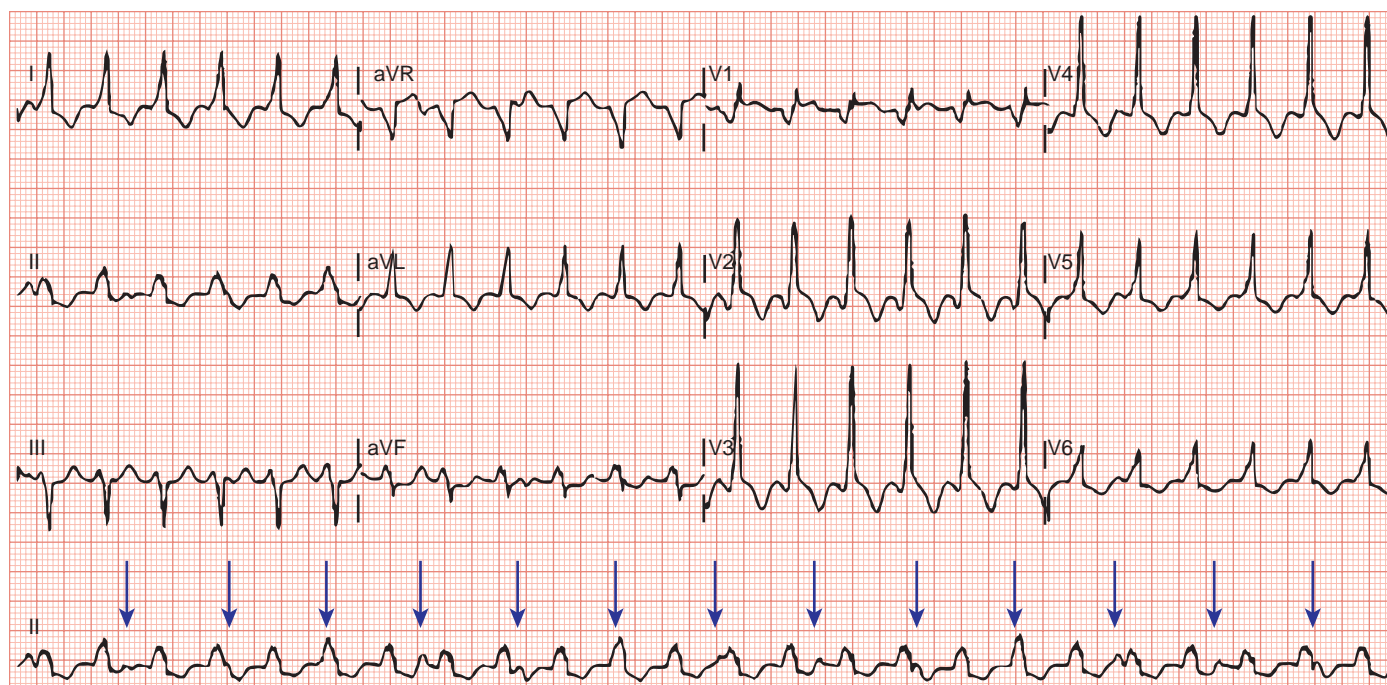


Fig. 21.3 Atrioventricular Dissociation During Ventricular Tachycardia. Note that the P waves (arrows) are completely independent of QRS complexes. The atrial rate is slower than the ventricular rate.

affected, the initial septal activation (the initial 30 milliseconds of the QRS complex), which depends on the LB, remains normal, occurring from left to right, and results in septal q waves in leads I, aVL, and V₆ and r waves in leads V₁, V₂, and aVR.

Septal activation is followed by activation of the LV (within the subsequent 40 to 60 milliseconds), occurring over the LB in a leftward and posterior vector and resulting in R waves in the leftward leads (I, aVL, and V₆), as well as s (or S) waves in the anterior precordial leads (V₁ and V₂). This appearance is usually similar to that in normal subjects because the LV is normally electrically predominant during this phase of the QRS.¹

The asynchronous depolarization caused by RBBB is primarily manifested in the later portion of the QRS, beyond the first 80 milliseconds of the QRS. During this time, RV activation spreads slowly by conduction through working muscle fibers rather than the specialized Purkinje system, and it occurs predominantly after activation of the LV has completed. The forces generated by the late, unopposed RV free wall activation result in a terminal rightward and anterior positivity, manifesting as a second positive deflection that can be small (r') or large (R') in the anterior precordial leads (V₁ and V₂) and S waves in the leftward leads (I, aVL, and V₆; see Fig. 10.10). The QRS axis is unaffected by RBBB; left or right axis deviation can indicate concurrent LAF or LPF block, respectively (see Fig. 10.10).⁶

Lead V₁. In the patient with a WCT and positive QRS polarity in lead V₁ (RBBB pattern), a triphasic RSR', rSr', rR', or rSR' complex in lead V₁ favors SVT (where the capital letter indicates large-wave amplitude or duration, and the lowercase letter indicates small-wave amplitude and duration; see Fig. 21.6). In contrast, a monophasic R, biphasic qR complex, or broad R (greater than 30 milliseconds) in lead V₁ favors VT (sensitivity of these patterns for recognizing VT is 97%, specificity is 88%; Fig. 21.7). In addition, a double-peaked R wave in lead V₁ favors VT if the left peak is taller than the right peak (the so-called rabbit ear sign; likelihood ratio greater than 50:1). A taller right rabbit ear does not help in distinguishing SVT from VT.⁵

Lead V₆. An Rs complex in lead V₆ favors SVT, whereas a qRS, qrS, rS, QS pattern, or an R/S ratio less than 1 in lead V₆ is a strong indicator of VT (likelihood ratio greater than 50:1; see Fig. 21.7).⁵

LBBB pattern. The normal sequence of ventricular activation is altered dramatically in LBBB. Complete LBBB results in delayed and abnormal activation and diffuse slowing of conduction throughout the LV. During LBBB, activation of the LV originates from the right bundle (RB) in a right to left direction, in contrast to the normal situation in which the first part of the LV myocardium to be activated is the septum in a left to right direction via a small septal branch of the LB. Thus LBBB results in reversal of the direction of the initial septal activation sequence (within the initial 30 milliseconds of the QRS complex), with the activation traveling from right to left and from apex to base and to the RV apex and free wall. RV activation is typically completed within the first 45 milliseconds of the onset of the QRS, before the onset of LV activation. However, because the septum is a larger structure than the RV free wall, septal activation predominates, eliciting a leftward and usually anterior vector and resulting in loss of the normal small q waves and initiation of a wide, slurred R wave in leads I, aVL, and V₆ and an rS or QS pattern in lead V₁ (see Fig. 10.11). As a consequence, Q waves of a prior MI can disappear, and new Q waves can emerge.¹

Following septal activation, LV activation (starting as late as 44 to 58 milliseconds into the QRS) spreads slowly by conduction through working muscle fibers rather than the HPS, with spatial vectors oriented to the left and posteriorly because the LV is a leftward and posterior structure. As a consequence, the delayed LV activation (unopposed by the now completed RV activation) produces large, broad, and notched or slurred R waves (without q or s waves) in the leftward leads (I, aVL, and V₆), with delayed R wave peak time in the left precordial leads (more than 60 milliseconds). The slowing and notching of the mid-QRS portion are caused by slow transseptal conduction. The terminal activation vector results from depolarization of the anterolateral LV wall that produces a small vector that is also directed to the left and posteriorly.¹



Fig. 21.4 Ventricular Tachycardia (VT) With Type 1 Second-Degree (Wenckebach) Ventriculoatrial (VA) Block. The first beat is sinus with normal atrioventricular (AV) conduction. VT develops with an initially short VA interval (blue arrows), which then slightly prolongs (red arrows), and then VA block occurs (green arrows). Note that the VT has a right bundle branch block with long RS interval (in lead V₂).

LBBB may cause no shift or variable degrees of left and superior shift of the frontal plane QRS axis. Pronounced left axis deviation can be associated with additional delay in activation in the LV secondary to myocardial disease. Right axis deviation in the setting of LBBB is rare and can be caused by RV hypertrophy or MI. A superior axis may also be observed in patients with RV enlargement.⁷

Importantly, recent evidence proposed more “strict” ECG criteria for identification of LBBB, including a terminal negative deflection in

V₁, mid-QRS notching/slurring in at least two of the leads V₁, V₂, V₅, V₆, I, and/or aVL, and a higher cutoff for QRS duration (140 milliseconds or longer for men and 130 milliseconds or longer for women). During true complete LBBB, mid-QRS notching/slurring (beginning after the first 40 milliseconds and ending at approximately two-thirds through the QRS duration) likely corresponds to the time of breakthrough of activation to the LV endocardium (first notch) and then to the LV posterolateral wall epicardium (second notch).⁸ In a simulation

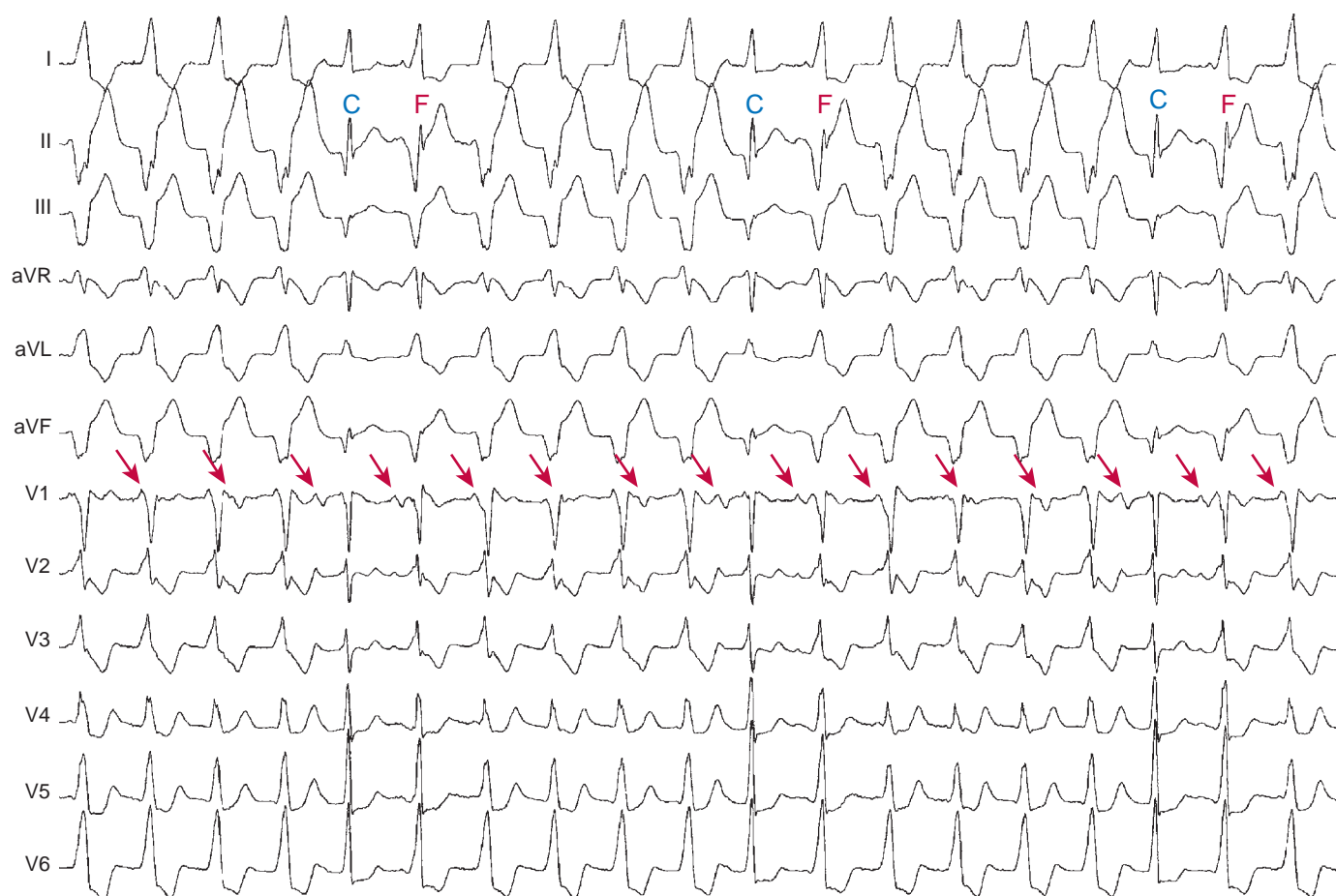


Fig. 21.5 Ventricular Tachycardia (VT) With Atrioventricular (AV) Dissociation. Sustained monomorphic VT with a cycle length (CL) of 488 milliseconds with AV dissociation coexists with sinus rhythm with a CL of 616 milliseconds. The sinus P waves can be clearly seen (arrows) marching throughout the different phases of the VT QRS complexes, and the atrial rate is unrelated to and slower than the ventricular rate. Because of the relatively slow VT rate, capture (C) and fusion (F) beats are observed frequently.

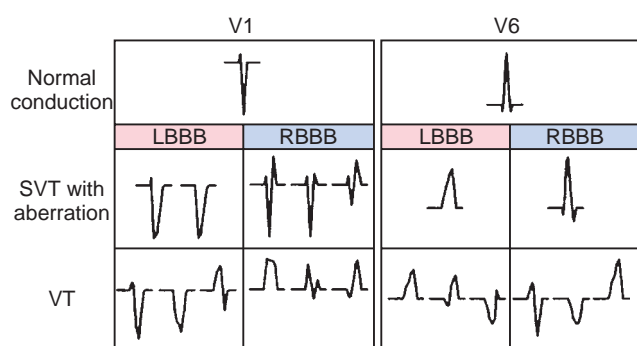


Fig. 21.6 QRS Morphologies in Wide Complex Tachycardias. Diagrammatic representation of common QRS morphologies encountered in ventricular tachycardia (VT) and supraventricular tachycardia (SVT) with aberration in leads V₁ and V₆ for both left bundle branch block (LBBB) and right bundle branch block (RBBB) patterns. Note the initial portions of the QRS complex in normal and aberrant QRS complexes, contrasted with the initial QRS forces in VT complexes. The RS configurations can be designated as an RBBB or LBBB type (grouped with LBBB-type morphologies).

study, these “strict” ECG criteria for LBBB were found to be have greater specificity (100% vs. 48%) and equivalent sensitivity (100%) in diagnosing complete LBBB as compared with the conventional LBBB criteria.⁹

Lead V₁. In the patient with a WCT and a negative QRS polarity in lead V₁ (LBBB pattern), the absence of an initial R wave (or a small initial R wave of less than 30 milliseconds) in lead V₁ or V₂ favors SVT, whereas a broad initial R wave of 30 milliseconds or more in lead V₁ or V₂ favors VT (see Fig. 21.7). In addition, an R wave in lead V₁ during a WCT taller than that during NSR favors VT. Furthermore, a slow descent to the nadir of the S wave, notching in the downstroke of the S wave, or an RS interval (from the onset of the QRS complex to the nadir of the S wave) of more than 70 milliseconds in lead V₁ or V₂ favors VT. In contrast, a swift, smooth downstroke of the S wave in lead V₁ or V₂ with an RS interval of less than 70 milliseconds favors SVT. In an analysis of several studies, the presence of any of these three criteria in lead V₁ (broad R wave, slurred or notched downstroke of the S wave, and delayed nadir of S wave) was a strong indicator of VT (likelihood ratio greater than 50:1). In addition, an Rs, or “W” complex in lead V₁ and fragmentation of QRS (notching, which usually represents myocardial scar) strongly favor VT.⁵

Lead V₆. The QRS morphology in lead V₆ is also of value; the presence of any Q or QS wave in lead V₆ favors VT (likelihood ratio

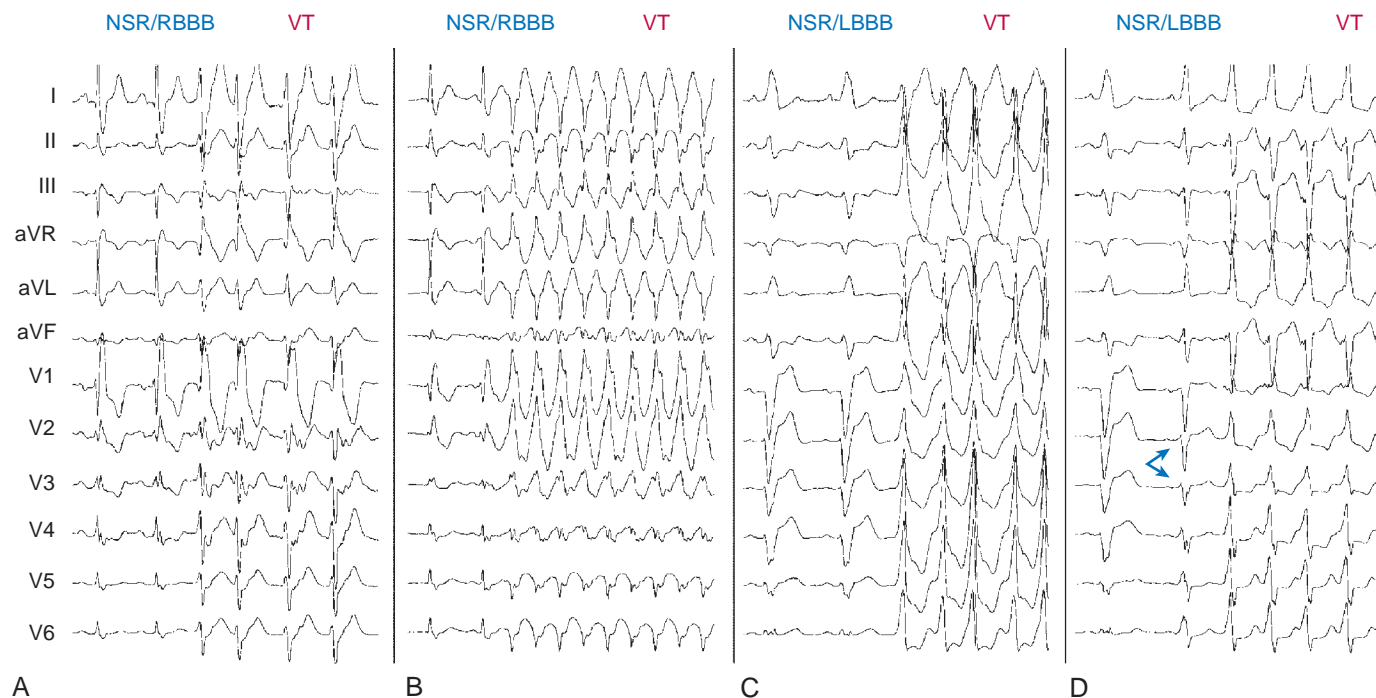


Fig. 21.7 Electrocardiogram Morphology During Normal Sinus Rhythm (NSR) With Bundle Branch Block (BBB) Versus Ventricular Tachycardia (VT). (A) NSR with right bundle branch block (RBBB) and VT with RBBB pattern. Note the loss of the initial r wave in V_1 and the larger S wave in V_6 during VT compared with NSR with RBBB. In addition, note the shift in the frontal plane QRS axis from $+90$ degrees during NSR with RBBB to the northwest quadrant during VT. (B) NSR with RBBB and VT with RBBB pattern. Note the change in QRS morphology in lead V_1 (from rsR during NSR with RBBB to monophasic R during VT) and lead V_6 (from RS during NSR with RBBB to QS during VT). In addition, no RS complexes are observed in the precordial leads during VT. (C) NSR with left bundle branch block (LBBB) and VT with RBBB pattern. Note the positive precordial concordance during VT. (D) NSR with LBBB and VT with RBBB pattern. Note the positive precordial concordance during VT. The second QRS (blue arrows) is a fusion between the sinus beat and the VT beat, and the fusion QRS is narrower than both the sinus and VT complexes.

greater than 50:1; see Fig. 21.2D), whereas the absence of a Q wave in lead V_6 favors SVT.⁵

BBB during sinus rhythm. When a previous 12-lead surface ECG is available, comparison of the QRS morphology during NSR and WCT is helpful. In general, if the QRS complexes during tachycardia are identical to those during NSR, the tachycardia is supraventricular (since all beats of supraventricular origin should conduct exclusively over the contralateral bundle and the QRS morphological pattern is expected to remain unaltered); otherwise, the arrhythmia is more likely to be ventricular in origin. Contralateral BBB in WCT and NSR (i.e., LBBB during WCT and RBBB during NSR, or vice versa) strongly favors VT (see Fig. 21.7C and D).

It is important to note, however, that identical QRS morphology during NSR and WCT, although strongly suggestive of SVT, can also occur in BBR and interfascicular reentrant VTs.

In addition, in patients with fixed BBB during NSR (especially those with chronic RBBB), rapid tachycardia rates can potentially provoke changes in QRS morphology, which can erroneously suggest VT as the mechanism. This can potentially be caused by more slowing in the blocked bundle branch (due to the presence of conduction delay, rather than complete BBB during NSR), appearance or disappearance of fascicular hemiblock in cases of RBBB (whether complete or incomplete), or appearance or disappearance of distal blocks in the Purkinje network. Thus, in patients with preexisting BBB and QRS morphology during WCT different from that during NSR, but with the same BBB pattern,

it does not necessarily imply that the tachycardia is VT. In these cases, superior accuracy to diagnose VT was observed with “R wave peak time of 50 milliseconds or more at lead II” and for an algorithm with the combination of two criteria “R wave peak time of 50 milliseconds or more at lead II” and “absence of RS patterns in precordial leads.”^{4,10}

Variation in QRS and ST-T Morphology

Subtle, non-rate-related fluctuations or variations in the QRS and ST-T wave configuration among complexes during the same or different episodes suggest VT and reflect variations in the VT reentrant circuit within the myocardium. In contrast, because most SVTs follow fixed conduction pathways, they are generally characterized by complete uniformity of QRS and ST-T shape, unless the tachycardia rate changes.

Algorithms for the Electrocardiographic Diagnosis of Wide Complex Tachycardia

The various criteria for the diagnosis of WCT listed are difficult to apply in isolation because most patients will have some, but not all, of the features described.³ Several algorithms have been proposed to guide integrating ECG findings into a diagnostic strategy. Fig. 21.8 illustrates an example of one approach.¹¹ The effect of history of prior MI, preexcited tachycardias, antiarrhythmic medication usage, precordial lead placement, heart transplantation status, and the presence of congenital heart disease on QRS morphology criteria should be taken into account while applying these elements. Preexcited tachycardias

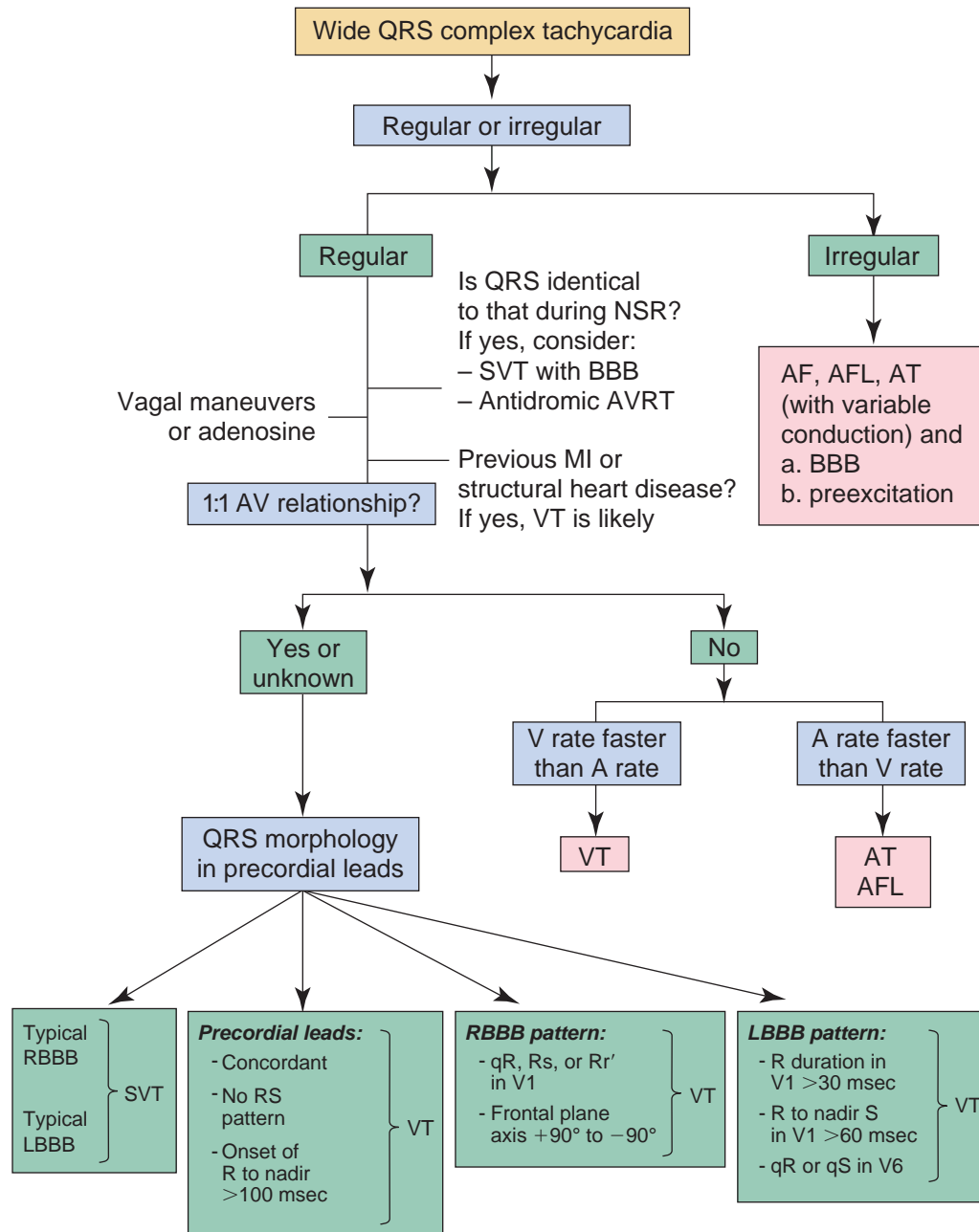


Fig. 21.8 Differential Diagnosis for Wide QRS Complex Tachycardia. A, Atrial; AF, atrial fibrillation; AFL, atrial flutter; AT, atrial tachycardia; AV, atrioventricular; AVRT, atrioventricular reentrant tachycardia; BBB, bundle branch block; LBBB, left bundle branch block; MI, myocardial infarction; NSR, normal sinus rhythm; RBBB, right bundle branch block; SVT, supraventricular tachycardia; V, ventricular; VT, ventricular tachycardia. (From Blomström-Lundqvist C, Scheinman MM, Aliot EM, et al. ACC/AHA/ESC guidelines for the management of patients with supraventricular arrhythmias—executive summary: a report of the American College of Cardiology/American Heart Association Task Force on Practice Guidelines and the European Society of Cardiology. *Circulation*. 2003;108:1871–909.)

may not be differentiated consistently with the proposed criteria, especially those using epicardial left-sided paraseptal or left-sided inferoposterior BTs.

Brugada Criteria

The most commonly used algorithm is the so-called Brugada algorithm or Brugada criteria. This is a stepwise, decision tree–like algorithm in which four criteria for VT are sequentially considered (Fig. 21.9).¹²

Step 1. All precordial leads are inspected to detect the presence or absence of an RS complex (i.e., complexes with both R and S waves of any amplitude, but QR, QRS, QS, monophasic R, or rSR complexes are not considered RS complexes). If an RS complex cannot be identified in any precordial lead, the diagnosis of VT can be made with 100% specificity.

Step 2. If an RS complex is clearly identified in one or more precordial leads, the interval between the onset of the R wave and the nadir

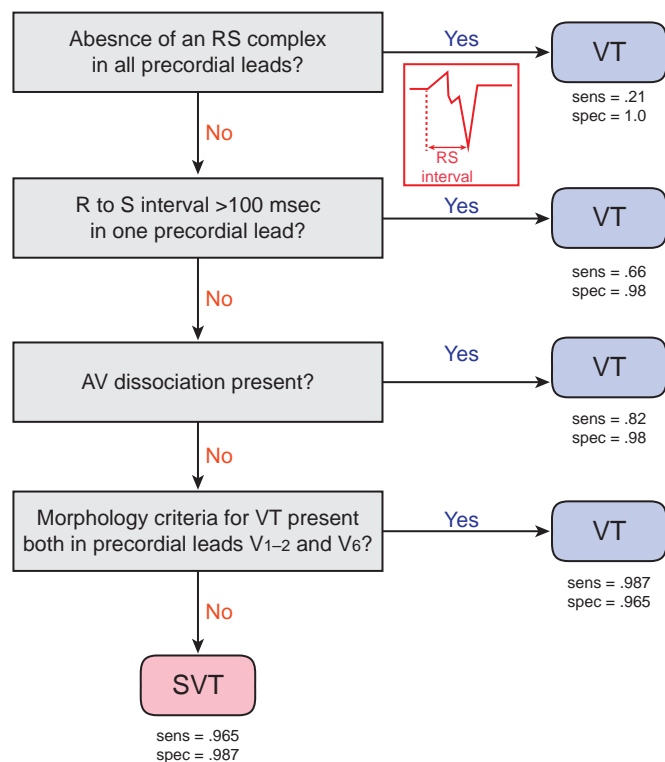


Fig. 21.9 Brugada Algorithm for Distinguishing Ventricular Tachycardia (VT) From Supraventricular Tachycardia (SVT). As indicated in the inset, the RS interval is between the onset of the R wave and the nadir of the S wave. AV, Atrioventricular; *sens*, sensitivity; *spec*, specificity. (From Brugada P, Brugada J, Mont L, et al. A new approach to the differential diagnosis of a regular tachycardia with a wide QRS complex. *Circulation*. 1991;83:1649–1659.)

of the S wave (the RS interval) is measured. The longest RS interval is considered if RS complexes are present in multiple precordial leads. If the longest RS interval is more than 100 milliseconds, the diagnosis of VT can be made with a specificity of 98% (see Fig. 21.9).

Step 3. If the longest RS interval is less than 100 milliseconds, either VT or SVT still is possible and the presence or absence of AV dissociation must therefore be determined. Evidence of AV dissociation is 100% specific for the diagnosis of VT, but this finding has a low sensitivity. The rationale proposed for the RS interval criterion is that during myocardial VTs, initial ventricular activation is slow because of muscle-to-muscle conduction close to the site of origin of the tachycardia. This results in prolongation of the initial portion of the QRS (time to the intrinsicoid deflection), as reflected by the RS interval utilized in this algorithm. This is in contrast to SVT with aberrancy, whereby initial ventricular activation is fast since it is mediated by the conducting bundle branch and HPS.

Step 4. If the RS interval is less than 100 milliseconds and AV dissociation cannot clearly be demonstrated, the QRS morphology criteria for V_1 -positive and V_1 -negative WCTs are considered. The QRS morphology criteria consistent with VT must be present in lead V_1 or V_2 and in lead V_6 to diagnose VT. A supraventricular origin of the tachycardia is assumed if either the V_1 and V_2 or V_6 criteria are not consistent with VT.

The Brugada algorithm was originally prospectively applied to 554 patients with electrophysiologically diagnosed WCTs. The reported sensitivity and specificity were 98.7% and 96.5%, respectively. Other authors also found the Brugada criteria useful, although they reported

a lower sensitivity (79% to 92%) and specificity (43% to 70%). The presence of preexisting BBB and the use of antiarrhythmic drugs result in a low specificity (63%) of the second Brugada criterion.

Griffith Algorithm

According to the Griffith algorithm, SVT is diagnosed only if the QRS morphology matches typical BBB. Typical LBBB manifests an rS or QS wave in leads V_1 and V_2 , delay to S wave nadir less than 70 milliseconds, and R wave and no Q wave in lead V_6 . Typical RBBB manifests an rSR' wave in lead V_1 and an RS wave in lead V_6 , with R wave height greater than S wave depth. When morphology criteria for the diagnosis of SVT are satisfied, inspecting the ECG for the presence of AV dissociation (which establishes the diagnosis of VT) further improves the overall accuracy. The Griffith algorithm had a sensitivity for VT of 95% and a specificity 64%.¹³

Bayesian Algorithm

The Bayesian algorithm is based on the likelihood ratio. It uses a list of 19 ECG features effective in discriminating VT from SVT with corresponding likelihood ratios. The Bayesian algorithm correctly diagnosed 52% of SVTs, 95% of VTs, and 97% of fascicular VTs. This algorithm, however, is cumbersome and impractical to use in most clinical settings.¹³

Vereckei Algorithm

A newer algorithm for differential diagnosis of WCT was analyzed in 453 monomorphic WCTs recorded from 287 patients, based on the following: (1) the presence of AV dissociation; (2) the presence of an initial R wave in lead aVR; (3) QRS morphology; and (4) estimation of the initial (V_i) and terminal (V_t) ventricular activation velocity ratio (V_i/V_t), determined by measuring the voltage change (i.e., the vertical excursion in millivolts) on the ECG tracing during the initial 40 milliseconds (V_i) and the terminal 40 milliseconds (V_t) of the same biphasic or multiphasic QRS complex (Fig. 21.10).^{14,15}

This algorithm had superior overall total accuracy than that of the Brugada algorithm (90.3% vs. 84.8%). The total accuracy of the fourth Brugada criterion was significantly lower (68% vs. 82.2%) than that of the V_i/V_t criterion in the fourth step, accounting for most of the difference in outcome between the two methods.^{14,15}

The rationale proposed for the V_i/V_t criterion is that during WCT caused by SVT the initial activation of the septum should be invariably rapid (mediated by the HPS) and the intraventricular conduction delay causing the wide QRS complex occurs in the mid to terminal part of the QRS. In contrast, in WCT caused by VT, there is initial slower muscle-to-muscle spread of activation until the impulse reaches the HPS, after which the rest of the ventricular muscle is more rapidly activated, resulting in a V_i/V_t ratio less than 1 during VT.^{14,15}

The vector of initial ventricular activation during SVT and NSR is directed away from lead aVR, yielding a negative QRS (QS) complex. Thus an initial dominant R or Rs complex in lead aVR suggests VT. However, an rS complex in lead aVR (but with an R/S ratio less than 1) can occur as a normal variant or in patients with inferior MI due to loss of initial inferiorly directed forces.

Antiarrhythmic drugs that impair conduction in the HPS or ventricular myocardium (e.g., class I drugs and amiodarone) would be expected to decrease the V_i and V_t approximately to the same degree; therefore the V_i/V_t ratio should not change significantly. Although the V_i/V_t ratio reflects the electrophysiology of many VTs, there are a number of exceptions to these criteria. First, disorders involving the myocardium locally can alter the V_i or V_t . For example, a decreased V_i with unchanged V_t can be present in the case of an SVT occurring in the presence of an anteroseptal MI, leading to the misdiagnosis of VT. Similarly, a scar situated at a late activated ventricular site can result in a decreased V_t

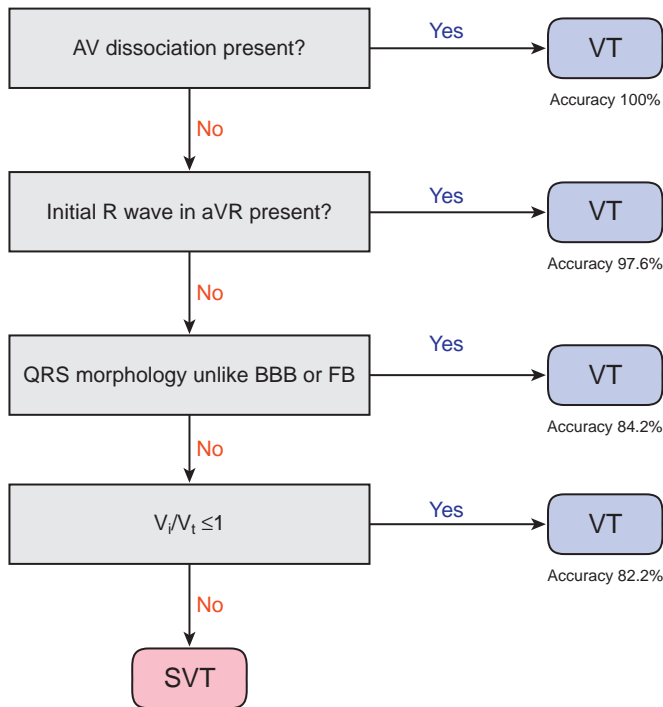


Fig. 21.10 Verecke Algorithm for Distinguishing Ventricular Tachycardia (VT) From Supraventricular Tachycardia (SVT). AV, Atrioventricular; BBB, bundle branch block; FB, fascicular block; V_i/V_t , ratio of initial (V_i) to terminal (V_t) ventricular activation velocity. (From Verecke A, Duray G, Szénási G, et al. Application of a new algorithm in the differential diagnosis of wide QRS complex tachycardia. *Eur. Heart J.* 2007; 28:589–600.)

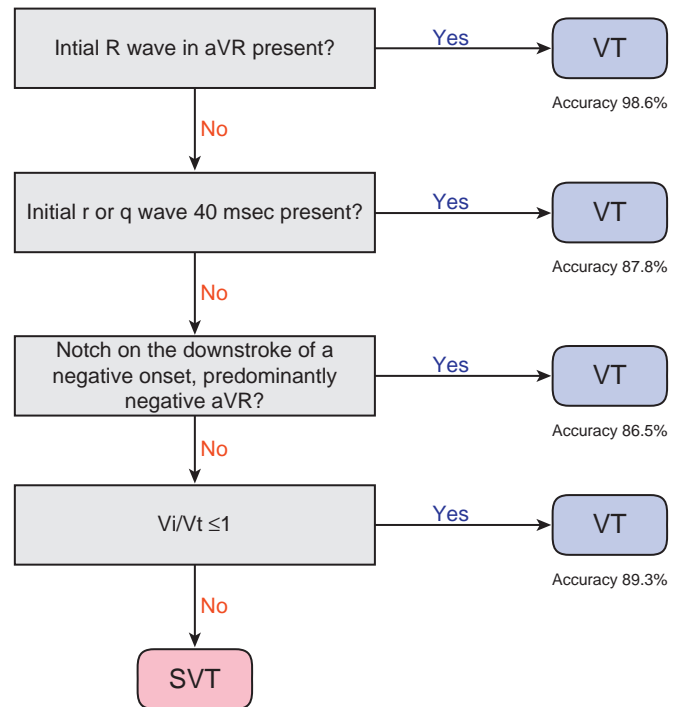


Fig. 21.11 The aVR Algorithm for Differential Diagnosis of Wide QRS Complex Tachycardia. SVT, Supraventricular tachycardia; V_i/V_t , ratio of initial (V_i) to terminal (V_t) ventricular activation velocity; VT, ventricular tachycardia. (From Verecke A, Duray G, Szénási G, et al. New algorithm using only lead aVR for differential diagnosis of wide QRS complex tachycardia. *Heart Rhythm.* 2008;5:89–98.)

in the presence of VT, leading to the misdiagnosis of SVT. Second, in the case of a fascicular VT, the V_i is not slower than the V_t . Third, if the exit site of the VT reentry circuit is very close to the HPS, it might result in a relatively narrow QRS complex, and the slowing of the V_i can last for such a short time that it cannot be detected by the surface ECG.^{14,15} A limitation of the initial R wave in lead aVR criterion can rarely be observed in patients with chronic cor pulmonale or severe emphysema associated with RV hypertrophy.¹⁶

The aVR Algorithm

The positive aVR criterion in the Verecke algorithm suggesting VT was further tested in 483 WCTs in 313 patients, and another algorithm based solely on QRS morphology in lead aVR was developed for distinguishing VT from SVT (Fig. 21.11).¹⁷ This algorithm classifies VTs into two main groups: (1) VTs arising from the inferior or apical region of the ventricles yielding an initial R wave in lead aVR, and (2) VTs arising from other regions and lacking an initial R wave in aVR.¹⁶ VTs originating from sites other than the inferior or apical wall of the ventricles, but not showing an initial R wave in aVR, should yield a slow, initially upward vector component of variable size pointing toward lead aVR (absent in SVT), even if the main vector in these VTs points downward, yielding a totally or predominantly negative QRS in lead aVR.

Thus, in VT without an initial R wave in lead aVR, the initial part of the QRS in lead aVR should be less steep (“slow”), which may be manifested as (1) an initial r or q wave with a width of more than 40 milliseconds, (2) notching on the descending limb (downstroke) of a negative onset, predominantly negative QRS complex, or (3) a slower ventricular activation during the initial 40 milliseconds than during the terminal 40 milliseconds of the QRS (i.e., $V_i/V_t \leq 1$) in lead aVR.

In contrast, in SVT with BBB, the initial part of the QRS in lead aVR is steeper (fast) because of the invariably rapid septal activation going away from lead aVR, resulting in a narrow (≤ 40 milliseconds) initial r or q wave and V_i/V_t ratio of more than 1.¹⁷

The overall accuracy of the aVR algorithm was 91.5%, which is similar to the Verecke algorithm and superior to the Brugada algorithm (90.3% and 84.8%, respectively). The aVR algorithm can be difficult to apply when the QRS in lead aVR is low amplitude and multiphasic. In addition, assessment of the V_i/V_t ratio in the lead aVR can be challenging using printed ECGs without a magnifying glass.¹⁷

Lead II R Wave Peak Time

The time interval necessary for full depolarization of the ventricular free wall (from the endocardium to the epicardium) beneath any given ECG electrode corresponds to the interval from the beginning of the QRS complex to the time of initial downstroke of the R wave after it has peaked (or to the time of initial upstroke of the S wave after it has reached its nadir). This interval is termed *R wave peak time* (in preference to the term *intrinsicoid deflection*). Normally the upper limit of normal for R wave peak time is 35 milliseconds in the right precordial leads, and 45 milliseconds in the left precordial leads. During NSR or SVT with RBBB, the R wave peak time is delayed in the right precordial leads (greater than 50 milliseconds), whereas in LBBB the R wave peak time is delayed in the left precordial leads (greater than 60 milliseconds).

A recent report found that the R wave peak time in lead II was significantly longer in VT compared with SVT with aberrancy, and a cutoff value of 50 milliseconds or greater identified VT with high sensitivity, specificity, and positive predictive values (93%, 99%, and 98%, respectively). However, this criterion has not been tested prospectively

or validated in patients with preexisting conduction system disease, antiarrhythmic drug therapy, electrolyte imbalance, prior MI, or pre-excited tachycardias. In addition, certain types of VTs such as fascicular VT, BBR VT, and septal myocardial VTs can have a shorter QRS onset-to-peak time because of their origin within or in close proximity to the His-Purkinje network.¹⁸

Ventricular Tachycardia Versus Preexcited Supraventricular Tachycardia

Differentiation between VT and preexcited SVT is particularly difficult because ventricular activation begins outside the normal intraventricular conduction system in both tachycardias (see Fig. 12.10). Thus ventricular activation mediated by a typical AV BT will mimic a VT originating from the base of the ventricles at the site of BT insertion. As a result, the algorithms for WCT, and most of the traditional QRS morphology criteria discussed above, tend to misclassify SVTs with preexcitation as VT. However, preexcitation is an uncommon cause of WCT, particularly if other factors, such as age and past medical history, suggest another diagnosis.

For cases in which preexcitation is thought to be likely, such as a young patient without structural heart disease or a patient with a known BT, a separate algorithm has been developed by Brugada and colleagues (Fig. 21.12). This algorithm consists of three steps.

Step 1

The predominant polarity of the QRS complex in leads V_4 through V_6 is defined as positive or negative. If predominantly negative, the diagnosis of VT can be made with 100% specificity. This is because the vast majority of BTs insert at the base of the RV or LV, ventricular preexcitation should yield a predominantly positive QRS complex in the apical precordial leads.

Step 2

If the polarity of the QRS complex is predominantly positive in V_4 through V_6 , the ECG should be examined for the presence of a qR

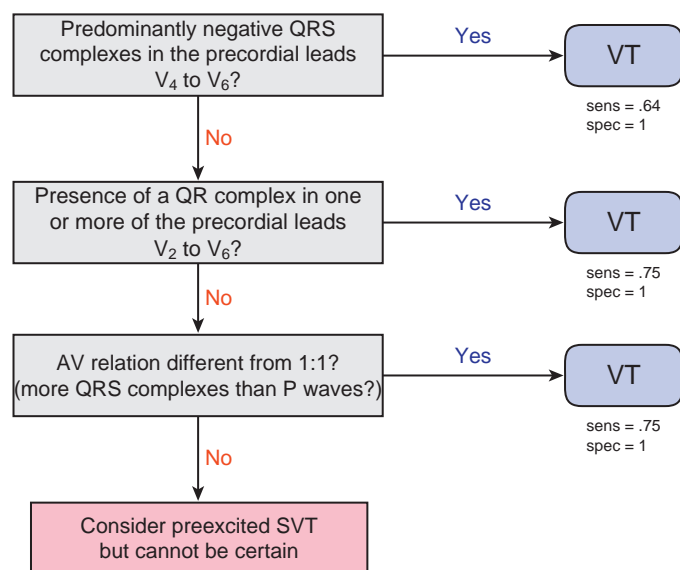


Fig. 21.12 Brugada Algorithm for Distinguishing Ventricular Tachycardia (VT) From Preexcited Supraventricular Tachycardia (SVT). AV, Atrioventricular; EP, electrophysiology; sens, sensitivity; spec, specificity. (From Antunes E, Brugada J, Steurer G, Andries E, Brugada P. The differential diagnosis of a regular tachycardia with a wide QRS complex on the 12-lead ECG. *Pacing Clin Electrophysiol.* 1994;17:1515–1524.)

complex in one or more of precordial leads V_2 through V_6 . If a qR complex can be identified, VT can be diagnosed with a specificity of 100%. QR or qR complexes should not be observed in those leads during ventricular preexcitation in the absence of structural heart disease.

Step 3

If a qR wave in leads V_2 through V_6 is absent, the AV relationship is then evaluated. If a 1:1 AV relationship is not present and there are more QRS complexes present than P waves, VT can be diagnosed with a specificity of 100%.

If the ECG of the WCT does not display any morphological characteristics diagnostic of VT after using this algorithm, the diagnosis of preexcited SVT must be considered. Although this algorithm has a specificity of 100% for VT, it has a sensitivity of only 75% for the diagnosis of preexcited SVT when all three steps are answered negatively (i.e., 25% of such cases are actually VT).

Limitations of Electrocardiographic Criteria for Diagnosis of Wide Complex Tachycardia

Unfortunately, the value of QRS morphological criteria in the diagnosis of a WCT is subject to several limitations. Most of the associations between the QRS morphology and tachycardia origin are based on statistical correlations, with substantial overlap. Moreover, most of the morphological criteria favoring VT are also present in a substantial number of patients with intraventricular conduction delay present during sinus rhythm, limiting their applicability in these cases. In addition, morphological criteria tend to misclassify SVTs with preexcitation as VT. However, preexcitation is an uncommon cause of WCT (1% to 6% in most series), particularly if other factors (e.g., age, history) suggest another diagnosis. Finally, in patients with VT in the absence of structural heart disease, many of the criteria are unreliable due to rapid muscle-muscle conduction.

In addition, independent studies utilizing the algorithms discussed above could not reproduce the high sensitivity, specificity, and predictive values initially reported by the original authors. In a study comparing five ECG methods (including the R wave peak time criterion, Brugada criteria, Griffith algorithm, Bayesian algorithm, and the aVR algorithm) for WCT differential diagnosis, the diagnostic accuracy was only modest (69% to 78%), and was equivalent between the various ECG methods (Table 21.2). Nonetheless, these methods differed in terms of sensitivity, specificity, and likelihood ratios. Therefore a diagnosis of VT or SVT by one test does not have the same diagnostic value as the same diagnosis made using another algorithm.¹³ The R wave peak time criterion was very specific for VT (i.e., unlikely to misclassify SVT as VT), but lacked sensitivity. Although the Griffith algorithm had high sensitivity (i.e., unlikely to miss a diagnosis of VT), its major limitation was low specificity for VT (it misclassified 60% of SVTs as VT). Hence the Griffith algorithm may be considered when a highly sensitive method for VT diagnosis is desired, and the R wave peak time criterion may be preferred when a high degree of specificity for VT diagnosis is required.¹³

In a pediatric population, the overall test accuracy was found to be lower for both Brugada and aVR algorithms (69% and 66%, respectively). When compared to the R wave peak time criterion, the aVR algorithms had superior accuracy (84% vs. 79%) and sensitivity (92% vs. 79%) but lower specificity (65% vs. 81%).¹⁶

ELECTROPHYSIOLOGICAL TESTING

Baseline Observations During Normal Sinus Rhythm

The presence of preexcitation during NSR or atrial pacing suggests SVT, and the absence of preexcitation during NSR and atrial pacing excludes preexcited SVT.

TABLE 21.2 Sensitivity, Specificity, Positive and Negative Likelihood Ratios for Ventricular Tachycardia Diagnosis, and Overall Diagnostic Accuracy (Percentage of Correct Diagnoses) for Five Methods of Wide QRS-Complex Tachycardia Differentiation

	Brugada	Griffith	Bayesian	Lead aVR	Lead II RWPT	P
Accuracy (%)	77.5 (71.8–82.5)	73.1 (67.2–78.5)	74.7 (68.9–79.9)	71.9 (66.0–77.4)	68.8 (62.7–74.4)	.04 ^a
Specificity (%)	59.2 (48.8–69.0)	39.8 (30.0–50.2)	52.0 (41.7–62.2)	48.0 (37.8–58.3)	82.7 (73.7–89.6)	<.001 ^{b,c}
Sensitivity (%)	89.0 (83.0–93.5)	94.2 (89.3–97.3)	89.0 (83.0–93.5)	87.1 (80.8–91.9)	0.60 (0.52–0.68)	<.001 ^{b,d}
LR(+)	2.18 (1.71–2.78)	1.56 (1.33–1.85)	1.86 (1.50–2.30)	1.67 (1.37–2.04)	3.46 (2.20–5.43)	—
LR(–)	0.18 (0.11–0.30)	0.15 (0.07–0.29)	0.21 (0.13–0.34)	0.27 (0.17–0.42)	0.48 (0.39–0.60)	—

Numbers in parentheses are the 95% confidence intervals.

^aBrugada vs. lead II RWPT.

^bLead II RWPT vs. any other algorithm.

^cP = .01 for Griffith vs. Brugada or vs. Bayesian.

^dP = .05 for Griffith vs. aVR.

RWPT, R-wave peak time.

From Jastrzebski M, Kukla P, Czarnecka D, Kawecka-Jaszcz K. Comparison of five electrocardiographic methods for differentiation of wide QRS-complex tachycardias. *Europace*. 2012;14:1165–1171.

Induction of Tachycardia

The mode of induction cannot distinguish between SVT and VT. Both atrial and ventricular stimulation may induce SVT or VT. VTs that can be induced with atrial pacing include verapamil-sensitive VT, adenosine-sensitive VT, and BBR VT.

Tachycardia Features

Atrioventricular Relationship

A 1:1 AV relationship can occur in VT and SVT. When the atrial rate is faster than the ventricular rate, VT is unlikely, except in the rare case of coexistent atrial and VTs (Fig. 21.13). In contrast, when the ventricular rate is faster than the atrial rate, VT is more likely, except for the rare case of junctional tachycardia, or AVNRT or orthodromic nodofascicular or nodoventricular reentry with VA block.

Oscillation in the Tachycardia Cycle Length

Variations in the tachycardia cycle length (TCL; the V-V intervals) that are dictated and preceded by similar variations in the A-A intervals (in WCTs with 1:1 AV relationship) or by similar variations in the H-H intervals (in WCTs with positive HV intervals) are consistent with SVT with aberrancy or BBR VT (Fig. 21.14). In contrast, variations in the V-V intervals that predict the subsequent H-H or A-A interval changes are consistent with myocardial VT or preexcited SVT.¹⁹

Atrial Activation Sequence

A concentric atrial activation sequence can occur in SVT and VT, whereas an eccentric atrial activation sequence practically excludes VT.

QRS Morphology

As noted, when the QRS configuration of the WCT is not compatible with any known form of aberration, the rhythm is likely to be VT or preexcited SVT. QRS morphology during WCT that is identical to that during NSR may occur in SVT with BBB, preexcited SVT (when NSR is also fully preexcited), BBR VT, and interfascicular VT.

His Bundle–Ventricular Interval

When the HV interval is positive (i.e., the His potential precedes the QRS onset), an HV interval during the WCT shorter than that during NSR ($HV_{WCT} < HV_{NSR}$) indicates VT or preexcited SVT. In contrast, an HV_{WCT} equal to or longer than HV_{NSR} indicates SVT with aberrancy or BBR VT (see Figs. 18.41 and 26.3).

When the HV interval is negative (i.e., the His potential follows the onset of the QRS), BBR VT and SVT with aberrancy are excluded. However, myocardial VTs and preexcited SVT generally have negative HV intervals (see eFig. 22.5).

Response to Right Bundle Branch Block

Abrupt prolongation of the VH interval when retrograde RBBB occurs (caused by catheter-induced trauma or introduction of ventricular extrastimuli [VESs]) is consistent with retrograde HB activation via the RB, which is typical for antidromic AVRT using a right-sided BT, but can also occur in preexcited AVNRT and in VTs originating in the RV.

However, if VH prolongation is accompanied by prolongation of the VA interval (without a change in the activation sequence) and the TCL, true antidromic tachycardia (using the AV conduction system as the retrograde limb) can be diagnosed and preexcited AVNRT is excluded.

On the other hand, continuation of the WCT after development of RBBB excludes BBR VT, except for the rare case of intrafascicular reentry. Lack of effects on the VH interval excludes antidromic AVRT using a right-sided BT, but can occur in (1) preexcited AVRT (utilizing a second BT as the retrograde limb) or (2) antidromic AVRT utilizing a left-sided BT, (3) antidromic AVNRT utilizing an atriofascicular BT inserting into the RB proximal to the site of RBBB, (4) preexcited AVNRT, and (5) VTs originating in the LV.²⁰

His Bundle–Right Bundle Electrogram Sequence

When both the HB and RB potentials are recorded, an HB–RB–V activation sequence occurs in SVT with aberrancy and in BBR VT with an LBBB pattern. In either case, the HB–RB interval during WCT is equal to or longer than that in NSR. On the other hand, an RB–HB–V activation sequence occurs in antidromic AVRT using an atriofascicular or right-sided BT, the uncommon type of BBR VT with RBBB pattern, or myocardial VT originating in the RV. An RB–V–HB activation sequence occurs in antidromic AVRT using atriofascicular BT, and a V–RB–HB or a V–HB–RB activation sequence can occur in VT.

Effects of Adenosine

Termination of WCT with adenosine can occur in SVT and adenosine-sensitive VT. Adenosine can cause transient AV block and unmask atrial activity in the setting of aberrantly conducted AFL, AF, or AT. On the other hand, adenosine can have no effect on the WCT, whether it is a VT or SVT.

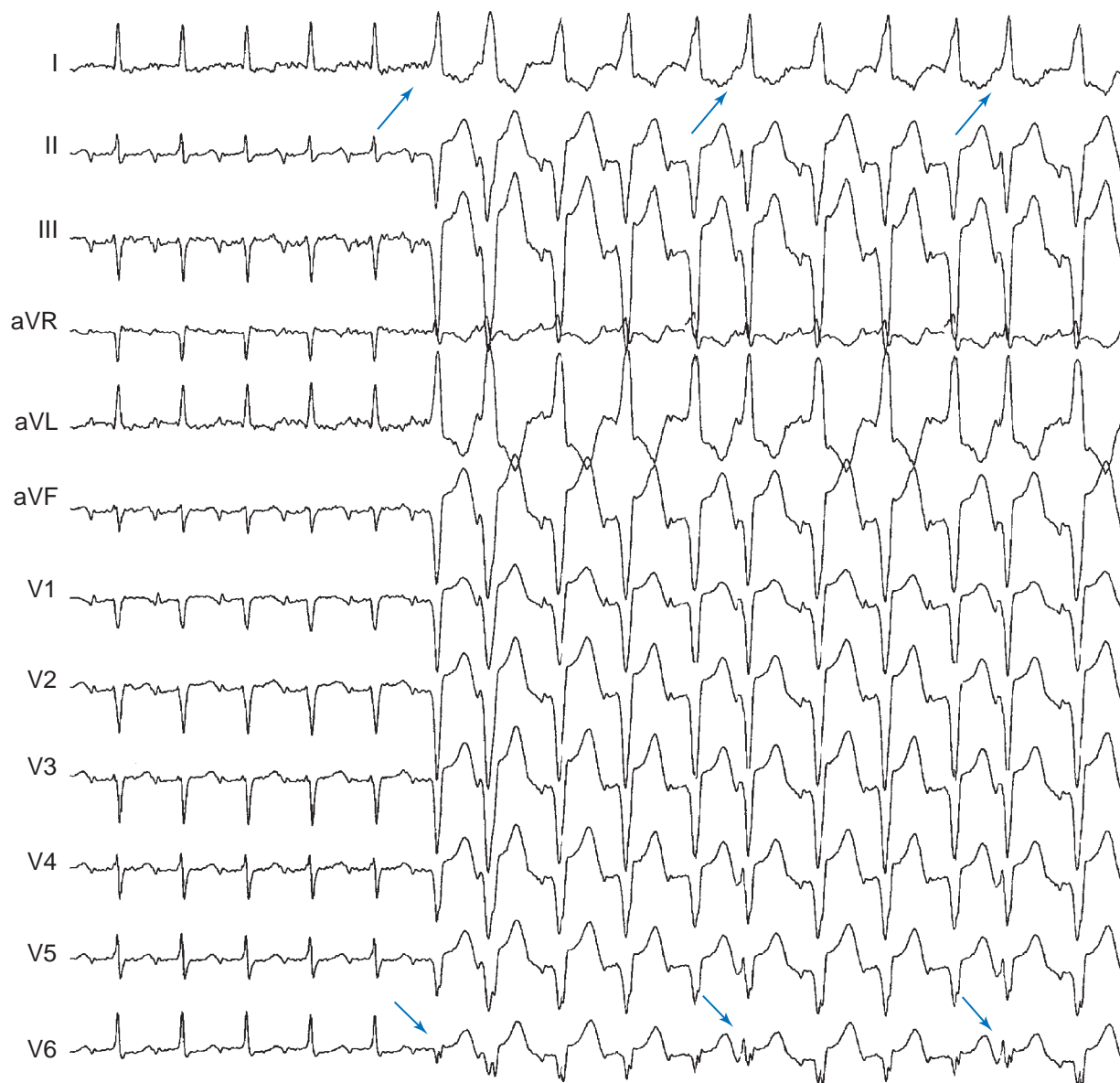


Fig. 21.13 Coexistent Atrial and Ventricular Tachycardias. Surface electrocardiogram of atrial tachycardia (AT) with a narrow QRS complex with the development of ventricular tachycardia (VT) with a left bundle branch block (LBBB)-like pattern. Although the atrial rate is faster than the ventricular rate, aberrant conduction during AT as the mechanism of the widening of the QRS can be excluded by observation of QRS morphology in lead V₆ (QS) inconsistent with LBBB aberrancy, a significant shift in the frontal plane QRS axis between AT and VT, and the presence of fusion beats (*arrows*). In addition, the atrial rate continues unperturbed, whereas the ventricular rate is slightly irregular.

Diagnostic Maneuvers During Tachycardia

Atrial Extrastimulation

An atrial extrastimulation (AES), regardless of its timing, that advances the next ventricular activation with similar QRS morphology to that of the WCT excludes VT (see Fig. 18.41). Also, an AES (regardless of its timing) that delays the next ventricular activation excludes VT (see Fig. 19.3).

With a late-coupled AES delivered when the AV junctional portion of the atrium is refractory (as indicated by the lack of advancement of local atrial activation in the HB or coronary sinus [CS] os recording), if the AES advances the next ventricular activation, it proves the presence of an anterogradely conducting AV BT and excludes any arrhythmia

mechanism that involves anterograde conduction over the AVN in the absence of a bystander BT. Moreover, if the AES advances the next ventricular activation with similar QRS morphology as that of the WCT, it proves that the BT is mediating ventricular activation during the WCT (as an integral part of the SVT circuit or as a bystander) and that the WCT is a preexcited SVT, and VT is excluded. In addition, if the AES advances the timing of both the next ventricular activation and the subsequent atrial activation, it proves that the SVT is an antidromic AVRT using an AV or atriofascicular BT anterogradely, and excludes preexcited AVNRT and VT (see Fig. 18.41). Also, if the AES delays the next ventricular activation, it proves that the SVT is an antidromic AVRT using an atrioventricular or atriofascicular BT anterogradely, and excludes preexcited AVNRT and VT (see Fig. 19.3).^{21,22}

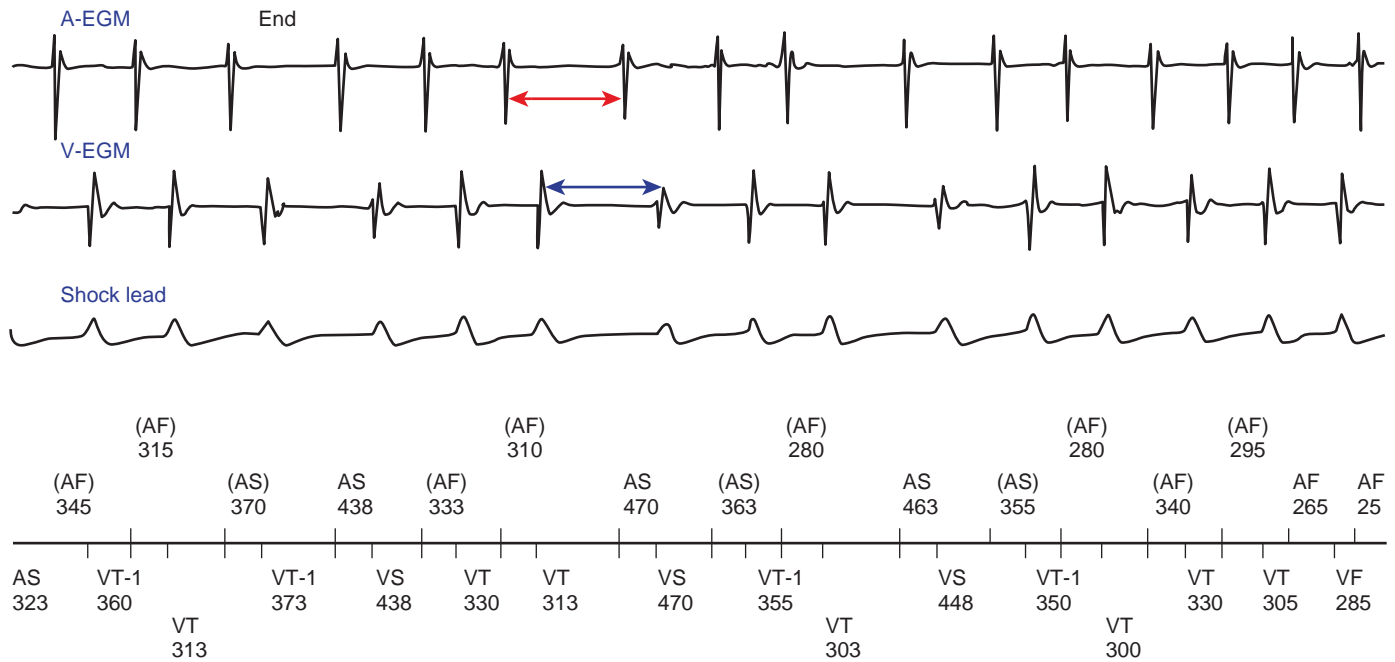


Fig. 21.14 Oscillation in the Tachycardia Cycle Length. Intracardiac atrial electrogram (A-EGM) and ventricular electrogram (V-EGM) and shock lead electrograms stored by the implantable cardioverter-defibrillator during an episode of tachycardia with a 1 : 1 atrioventricular relationship. Note that variations in the tachycardia cycle length (the V-V intervals; blue double-headed arrow) are dictated and preceded by similar variations in the A-A intervals (red double-headed arrow), which is consistent with supraventricular tachycardia rather than ventricular tachycardia sensed marker event (VT). AF, Atrial fibrillation sensed marker event; AS, atrial sensed marker event; VS, ventricular sensed marker event.

Atrial Pacing

The ability to entrain the WCT with atrial pacing can occur in VT and SVT. However, the ability to entrain the WCT with similar QRS morphology to that of the WCT (i.e., entrainment with concealed QRS fusion) excludes myocardial VT and is consistent with SVT, but can also occur in BBR VT. On the other hand, atrial entrainment of WCT with manifest QRS fusion can occur in VT in the presence of a bystander BT, or in AVRT with multiple BTs, but not in antidromic AVRT without another BT, nor in SVT with aberrancy.²¹

The ability to dissociate the atrium with rapid atrial pacing without influencing the TCL (V-V interval) or QRS morphology suggests VT and excludes preexcited SVTs, AT with aberrancy, and orthodromic AVRT with aberrancy. However, it does not exclude junctional ectopic tachycardia, nodofascicular reentrant tachycardia, or the rare case of AVNRT with aberrancy associated with anterograde block in an upper common pathway during rapid atrial pacing.

The response to atrial overdrive pacing during WCTs with a 1 : 1 AV relationship can help distinguish VT from SVT. The concept is analogous to examination of the response to ventricular overdrive pacing during narrow complex tachycardia. During VT, atrial overdrive pacing at a pacing cycle length (PCL) 20 to 60 milliseconds shorter than the TCL with 1 : 1 AV conduction results in anterograde capture with changing or narrowing of the tachycardia QRS morphology. When the tachycardia resumes after cessation of pacing, the earliest event (after the last reset ventricular complex) occurs in the ventricle because the atrium is being passively driven by the ventricle during the tachycardia. This results in a “V-V-A response.” On the contrary, during antidromic AVRT or aberrantly conducted SVT, anterograde conduction occurs over a BT or AVN; and on cessation of atrial pacing, the last reset ventricular activation conducts to the atrium over the retrograde limb of the circuit, resulting in a “V-A response” and continuation of the tachycardia

(Fig. 21.15). This pacing maneuver is not useful when 1 : 1 AV conduction during atrial pacing is absent. Thus, when determining the response after atrial pacing during WCT, the presence of 1 : 1 VA conduction must be confirmed. Isorhythmic AV dissociation can mimic 1 : 1 AV conduction, especially when the pacing train is not long enough or the PCL is too slow. It is also important to ensure that atrial pacing does not terminate the tachycardia.^{21,22}

A “pseudo-V-V-A response” can occur during SVTs associated with a long AV interval during atrial pacing (Fig. 21.16). Because anterograde conduction during atrial pacing occurs through the slow AVN pathway, the AV interval can be longer than the PCL (A-A interval), so that the last paced P wave is followed first by the QRS complex resulting from slow AV conduction of the preceding paced atrial beat, and then by the QRS complex resulting from the last paced P wave. Careful examination of the last QRS complex that resulted from AV conduction during atrial pacing helps avoid this potential pitfall; the last controlled QRS complex characteristically occurs at an R-R interval equal to the atrial PCL, whereas the first tachycardia QRS complex usually occurs at a different return cycle length (CL). Furthermore, a “pseudo-V-A response” can theoretically occur in the setting BBR VT or in those with intra- or interfascicular reentrant VT, whereby the return atrial impulse may precede the first non-reset QRS complex.^{21,22}

Ventricular Extrastimulation

In WCTs with 1 : 1 AV relationship, a VES that resets (advances or delays) the next QRS without affecting the A-A interval is consistent with VT and practically excludes SVT. In addition, a VES delivered when the HB is refractory and that terminates the WCT without atrial activation is consistent with VT, but can also occur in orthodromic AVRT with aberrant conduction or in antidromic AVRT using a second BT as the retrograde limb of the circuit.

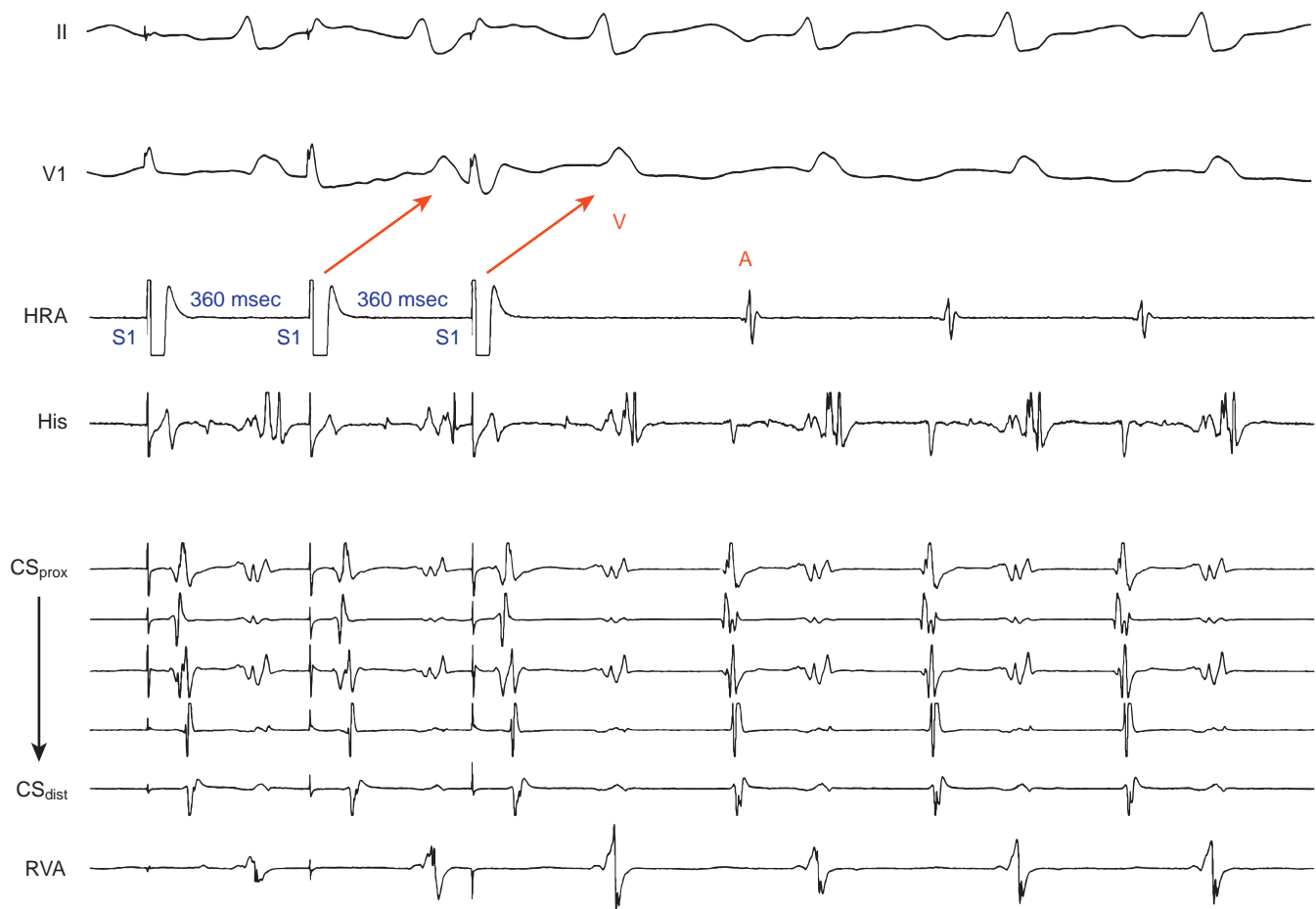


Fig. 21.15 V-A Response to Atrial Overdrive Pacing During Wide QRS Complex Tachycardia. The QRS morphology and His bundle–ventricular interval (45 milliseconds) during atrial pacing (*arrows*) are similar to those during tachycardia. On cessation of pacing, the last atrial-paced beat is followed by a “V-A response” consistent with supraventricular tachycardia as the mechanism. This tachycardia was an atypical atrioventricular nodal tachycardia with right bundle branch block aberrancy. *CS_{dist}*, Distal coronary sinus; *CS_{prox}*, proximal coronary sinus; *HRA*, high right atrium; *RVA*, right ventricular apex.

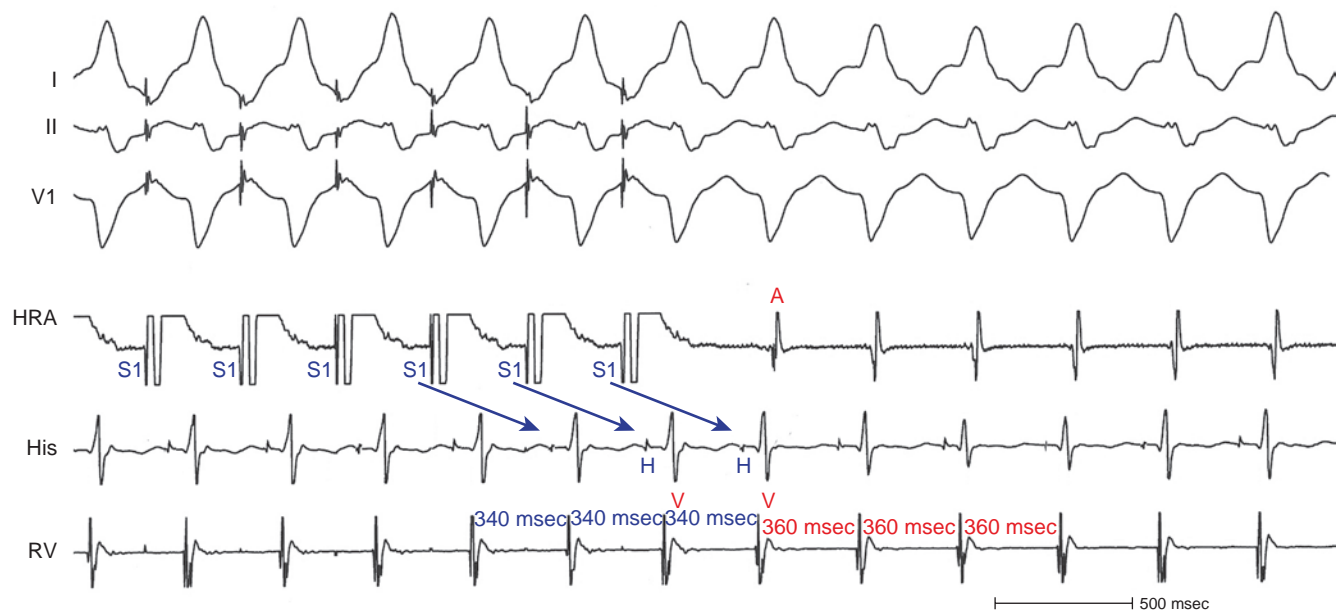


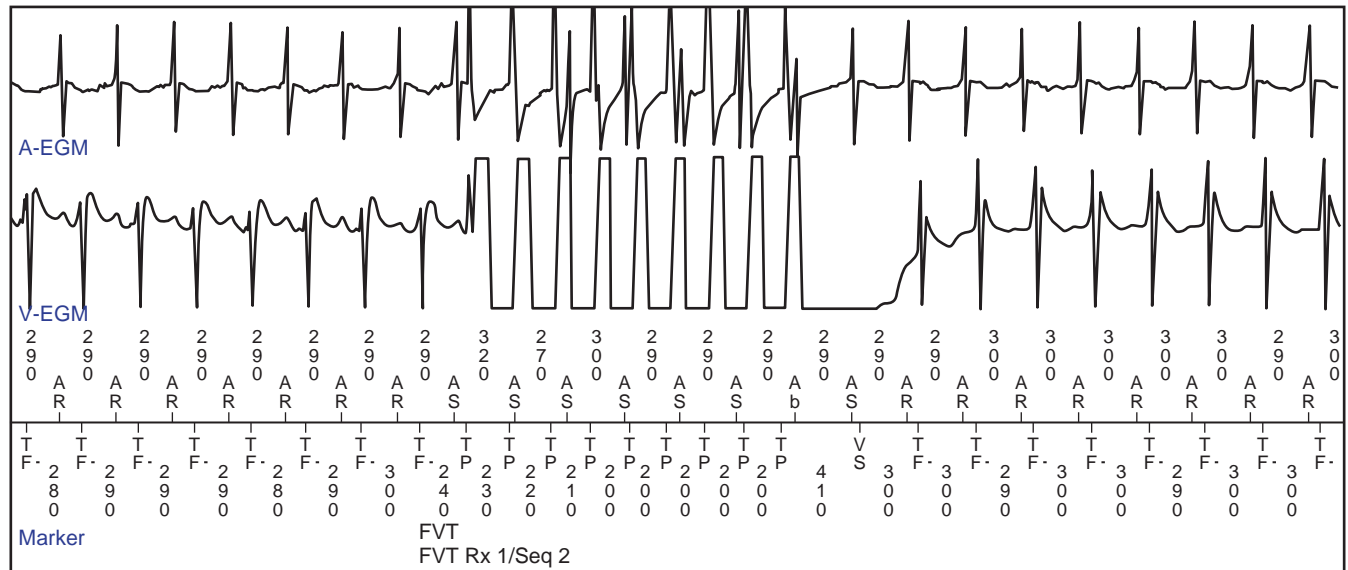
Fig. 21.16 Pseudo-V-V-A Response to Atrial Overdrive Pacing During Wide QRS Complex Tachycardia. The QRS morphology and His bundle–ventricular interval (45 milliseconds) during atrial pacing are similar to those during tachycardia. On cessation of pacing, the last atrial-paced beat is followed by a “V-V-A response” suggestive of ventricular tachycardia as the mechanism. However, although the last atrial-paced beat is followed by two QRS complexes, the last captured QRS complex (which characteristically occurs at an R-R interval equal to the atrial pacing cycle length [CL]) is actually the second one (as indicated by *blue arrows*), due to anterograde conduction over the slow atrioventricular (AV) nodal pathway, resulting in an AV interval longer than the pacing CL. Therefore the actual response is a “V-A response” consistent with supraventricular tachycardia. This supraventricular tachycardia was atrioventricular nodal tachycardia with left bundle branch aberrancy. *HRA*, High right atrium; *RV*, right ventricle.

Ventricular Pacing

When overdrive ventricular pacing during the WCT fails to accelerate the atrial CL to the PCL (i.e., the ventricles are dissociated from the tachycardia), VT and AVRT are excluded, AT is the most likely diagnosis, but AVNRT is still possible (eFig. 21.2). In addition, entrainment with manifest QRS fusion can occur in VT or AVRT but excludes AT and AVNRT, whereas entrainment with concealed fusion excludes SVT with aberrancy. Furthermore, entrainment from the RV apex followed by a postpacing interval that is equal (within 30 milliseconds) to the TCL excludes AVNRT, AT, and myocardial VT, but can occur with BBR VT and AVRT using a right-sided BT.

REFERENCES

1. Surawicz B, et al. AHA/ACCF/HRS recommendations for the standardization and interpretation of the electrocardiogram: part III: intraventricular conduction disturbances: a scientific statement from the American Heart Association Electrocardiography and Arrhythmias Committee. *Circulation*. 2009;119:e235–e240.
2. Page RL, et al. 2015 ACC/AHA/HRS guideline for the management of adult patients with supraventricular tachycardia: a report of the American College of Cardiology/American Heart Association Task Force on Clinical Practice Guidelines and the Heart Rhythm Society. *Circulation*. 2016;133:e506–e574.
3. Yadav AV, et al. Utility of conventional electrocardiographic criteria in patients with idiopathic ventricular tachycardia. *JACC Clin Electrophysiol*. 2017;3:669–677.
4. Datino Romaniega T, et al. Specificity of electrocardiographic criteria for the differential diagnosis of wide QRS complex tachycardia in patients with intraventricular conduction defect. *Heart Rhythm*. 2013;10:1393–1401.
5. Das MK, Rajdev A, Kalra V. Wide complex tachycardia. *Card Electrophysiol Clin*. 2014;6:511–523.
6. Tzogias L, et al. Electrocardiographic features and prevalence of bilateral bundle-branch delay. *Circ Arrhythm Electrophysiol*. 2014;7:640–644.
7. Josephson ME, Wellens HJJ. The ECG in left bundle branch block and heart failure. *Heart Rhythm*. 2015;12:250–251.
8. Strauss DG. Understanding ventricular activation. *J Electrocardiol*. 2011;44:282–284.
9. Galeotti L, van Dam PM, Loring Z, et al. Evaluating strict and conventional left bundle branch block criteria using electrocardiographic simulations. *Europace*. 2013;15:1816–1821.
10. Datino T, et al. Rate-related changes in QRS morphology in patients with fixed bundle branch block: implications for differential diagnosis of wide QRS complex tachycardia. *Eur Heart J*. 2008;29:2351–2358.
11. Blomström-Lundqvist C, et al. ACC/AHA/ESC guidelines for the management of patients with supraventricular arrhythmias—executive summary: a report of the American College of Cardiology/American Heart Association Task Force on Practice Guidelines and the European Society of Cardiology. *Circulation*. 2003;108:1871–1909.
12. Brugada P, Brugada J, Mont L, et al. A new approach to the differential diagnosis of a regular tachycardia with a wide QRS complex. *Circulation*. 1991;83:1649–1659.
13. Jastrzebski M, Kukla P, Czarnecka D, et al. Comparison of five electrocardiographic methods for differentiation of wide QRS-complex tachycardias. *Europace*. 2012;14:1165–1171.
14. Verecke A, Duray G, Szénási G, et al. Application of a new algorithm in the differential diagnosis of wide QRS complex tachycardia. *Eur Heart J*. 2007;28:589–600.
15. Dendi R, Josephson ME. A new algorithm in the differential diagnosis of wide complex tachycardia. *Eur Heart J*. 2007;28:525–526.
16. Verecke A. Current algorithms for the diagnosis of wide QRS complex tachycardias. *Curr Cardiol Rev*. 2014;10:262–276.
17. Verecke A, Duray G, Szénási G, et al. New algorithm using only lead aVR for differential diagnosis of wide QRS complex tachycardia. *Heart Rhythm*. 2008;5:89–98.
18. Pava LF, et al. R-wave peak time at DII: a new criterion for differentiating between wide complex QRS tachycardias. *Heart Rhythm*. 2010;7:922–926.
19. Foreman JR, Steinberg LA, Prystowsky EN, et al. Mechanism of a wide QRS complex tachycardia with variable atrial, His, and ventricular relationships. *Circ Arrhythmia Electrophysiol*. 2015;8:981–984.
20. Asirvatham SJ, Stevenson WG. Wobble. *Circ Arrhythmia Electrophysiol*. 2015;8:985–987.
21. Abdelwahab A, et al. A technique for the rapid diagnosis of wide complex tachycardia with 1:1 AV relationship in the electrophysiology laboratory. *Pacing Clin Electrophysiol*. 2009;32:475–483.
22. Badhwar N, Scheinman MM. Electrophysiological diagnosis of wide complex tachycardia: Editorial. *Pacing Clin Electrophysiol*. 2009;32:473–474.



A • V-V □ A-A VF = 330 msec FVT = 280 msec

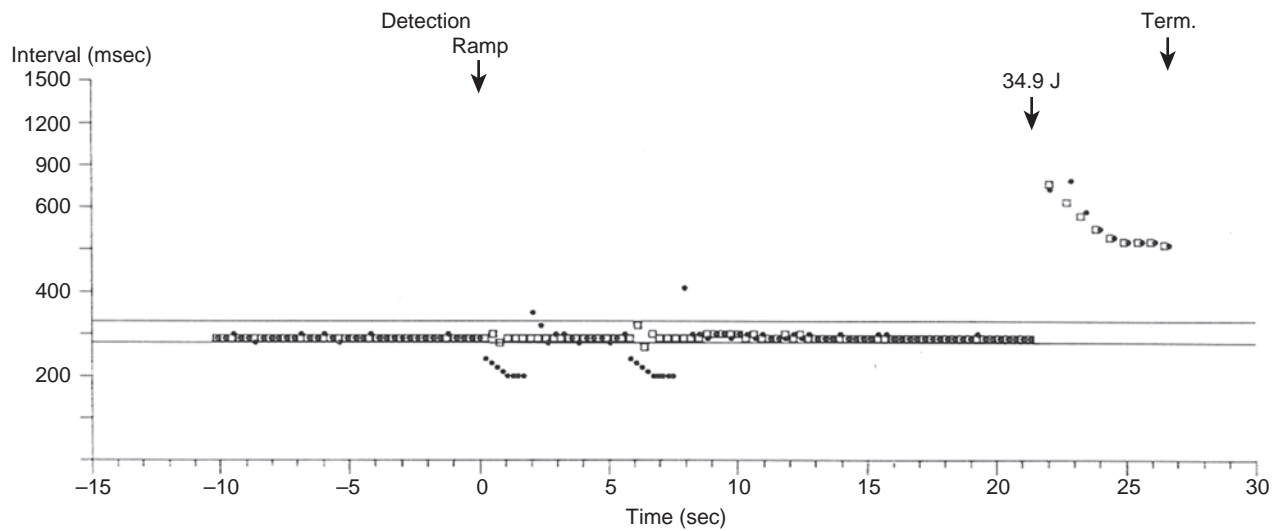


Fig. 21.2 Response to Overdrive Ventricular Pacing During Tachycardia. (A) Intracardiac atrial and ventricular electrograms (A-EGM and V-EGM, respectively) stored by the implantable cardioverter-defibrillator (ICD) during an episode of tachycardia at a cycle length (CL) of 290 milliseconds and a 1 : 1 AV relationship. The tachycardia triggered antitachycardia pacing (ATP) therapy by the ICD with a ramp of nine ventricular paced beats. ATP fails to terminate the tachycardia, which resumes at the baseline CL. (B) A plot of atrial versus ventricular CLs during the tachycardia and two sequences of ramp ATP. Note that the atrial rate continues unperturbed during ventricular pacing (i.e., ventriculoatrial dissociation was evident during ATP), which excludes ventricular tachycardia and orthodromic atrioventricular reentrant tachycardia and is consistent with either atrial tachycardia or atrioventricular nodal reentrant tachycardia.

Ventricular Arrhythmias in Ischemic Heart Disease

OUTLINE

Classification of Ventricular Tachyarrhythmias, 748

- Classification According to Tachycardia Morphology, 748
- Classification According to Tachycardia Duration, 749
- Classification According to QRS Morphology in Lead V₁, 749
- Classification According to Tachycardia Mechanism, 749

Pathophysiology, 749

- Mechanisms of Ventricular Arrhythmias Associated With Acute Ischemia, 749
- Mechanisms of Ventricular Arrhythmias Associated With Healed Infarction, 750

Epidemiology and Natural History, 751

- Premature Ventricular Complexes, 752
- Accelerated Idioventricular Rhythm, 752
- Reperfusion Arrhythmias, 752
- Nonsustained Ventricular Tachycardia, 752
- Polymorphic Ventricular Tachycardia, 752
- Ventricular Fibrillation, 752
- Sudden Cardiac Death, 752
- Sustained Monomorphic Ventricular Tachycardia, 752

Clinical Presentation, 753

Initial Evaluation, 753

- Evaluation of Type and Burden of Ventricular Arrhythmias, 753
- Evaluation of the Triggers of Ventricular Arrhythmias, 753
- Evaluation of Myocardial Ischemia, 753
- Role of Electrophysiological Testing, 753

Risk Stratification, 754

- Ventricular Arrhythmias, 754
- Syncope, 754
- Left Ventricular Ejection Fraction, 754
- Invasive Electrophysiological Testing, 756
- Measures of Cardiac Repolarization, 756
- Measures of Autonomic Imbalance, 756
- Measures of Myocardial Conduction Disorders, 757
- Genetic Testing, 757
- Cardiac Magnetic Resonance Imaging, 757

Risk Stratification Early Postinfarction, 757

Principles of Management, 757

- Pharmacological Therapy, 757
- Implantable Cardioverter-Defibrillator, 758
- Catheter Ablation, 760
- Alternative Interventional Treatment, 762

Electrocardiographic Features, 762

- Electrocardiographic Clues to the Underlying Substrate, 762
- Electrocardiographic Localization of Postinfarction Ventricular Tachycardia, 763
- Epicardial Ventricular Tachycardias, 767

Electrophysiological Testing, 768

- Induction of Tachycardia, 768
- Tachycardia Features, 770
- Diagnostic Maneuvers During Tachycardia, 771
- Exclusion of Other Arrhythmia Mechanisms, 779

Mapping, 780

- Preprocedural Evaluation, 780
- Left Ventricular Access, 781
- Hemodynamic Support, 781
- Electroanatomic Mapping, 782
- Activation Mapping, 784
- Entrainment Mapping, 786
- Pace Mapping, 792
- Substrate Mapping During Baseline Rhythm, 795
- Noncontact Mapping, 800
- Mapping Postinfarction Premature Ventricular Complexes, 801
- Mapping of Epicardial Circuits, 801
- Practical Approach to Ventricular Tachycardia Mapping, 802

Ablation, 805

- Target of Ablation, 805
- Ablation Technique, 808
- Endpoints of Ablation, 810
- Outcome, 811

CLASSIFICATION OF VENTRICULAR TACHYARRHYTHMIAS

Ventricular tachycardia (VT) is defined as a tachycardia (rate greater than 100 beats/min) with three or more consecutive beats that originates below the bifurcation of the His bundle (HB), in the specialized conduction system, the ventricular muscle, or in a combination of both tissues, independent of atrial and atrioventricular node (AVN) conduction.^{1,2}

Classification According to Tachycardia Morphology

Monomorphic VT has a single stable QRS morphology from beat to beat, indicating repetitive ventricular depolarization with the same activation sequence (Fig. 22.1).

Multiple monomorphic VTs refers to more than one morphologically distinct monomorphic VT, occurring as different episodes or induced at different times.

Polymorphic VT has clearly defined QRS complexes with a continuously changing morphology or multiform QRS morphology (i.e., no constant morphology for more than five complexes, no clear isoelectric baseline between QRS complexes, or QRS complexes that have different morphologies in multiple simultaneously recorded leads), indicating a variable sequence of ventricular activation and no single site of origin.¹

Torsades de pointes is a polymorphic VT associated with a long QT interval, and is electrocardiographically characterized by twisting of the peaks of the QRS complexes around the isoelectric line during the arrhythmia.

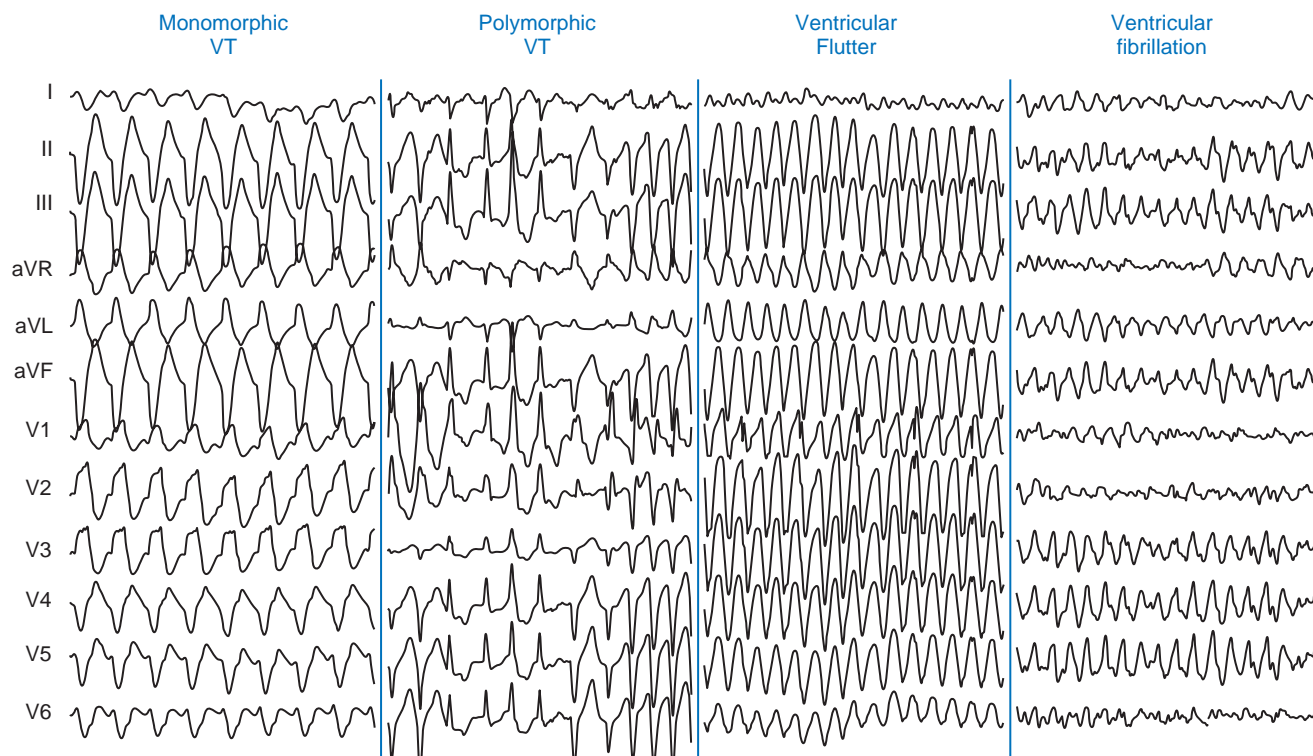


Fig. 22.1 Surface Electrocardiogram of Different Types of Ventricular Tachycardia (VT).

Pleomorphic VT has more than one morphologically distinct QRS complex occurring during the same episode of VT, but the QRS morphology is not continuously changing.

Bidirectional VT is a VT associated with a beat-to-beat alternans in the QRS frontal plane axis, often associated with digitalis toxicity or catecholaminergic VT.

Ventricular flutter is a term that has been applied to a rapid (250 to 350 complexes/min) VT that has a sinusoidal QRS configuration that prevents clear identification of the QRS morphology.

Ventricular fibrillation (VF) is a rapid (usually greater than 300 complexes/min), chaotic tachycardia without consistently identifiable QRS complexes.¹

Classification According to Tachycardia Duration

Sustained VT lasts for more than 30 seconds or requires termination (e.g., cardioversion) in less than 30 seconds because of hemodynamic compromise, whereas *nonsustained VT* is a tachycardia at more than 100 beats/min lasting for three or more complexes but for less than 30 seconds and not requiring termination.

During electrophysiological (EP) testing, nonsustained VT is defined as more than five or six complexes of non–bundle branch reentrant (BBR) VT, regardless of morphology. BBR complexes are frequent (50%) in normal individuals in response to ventricular extrastimulus (VES) and have no relevance to clinical nonsustained VT.

Repetitive polymorphic responses are also common (up to 50%) during programmed ventricular stimulation, especially in response to multiple (three or more) VESs with very short coupling intervals (less than 180 milliseconds). The clinical significance of induced polymorphic nonsustained VT is questionable.

Incessant VT is a continuous sustained VT that recurs promptly over several hours despite repeated interventions (e.g., electrical cardioversion) for termination. Less commonly, incessant VT manifests as repeated bursts of VT that spontaneously terminate for a few intervening sinus

beats, followed by the next tachycardia burst. The latter form is more common with the idiopathic VTs (see Fig. 23.1).

Classification According to QRS Morphology in Lead V₁

Monomorphic VT can be classified as having one of two patterns: a right bundle branch block (RBBB)–like pattern or a left bundle branch block (LBBB)–like pattern. VTs with an LBBB-like pattern have a predominantly negative QRS polarity in lead V₁ (QS, rS, qrS), whereas VTs with a RBBB-like pattern have a predominantly positive QRS polarity in lead V₁ (rsR', qR, RR, R, RS). Importantly, this classification pertains to QRS morphology only in lead V₁; the VT may not show features consistent with the same BBB configuration in other leads. Also, the determination that the VT has an RBBB-like pattern or an LBBB-like pattern does not, by itself, assist in making a diagnosis; however, this assessment should be made initially because it has further implications for evaluating several other features on the ECG, including the QRS axis, the QRS duration, and the QRS morphology.

Classification According to Tachycardia Mechanism

Focal VT has a point source of earliest ventricular activation with a centrifugal spread of activation from that site. The mechanism can be abnormal automaticity, triggered activity, or microreentry. *Scar-related reentrant VT* describes arrhythmias that have characteristics of reentry and originate from an area of myocardial scar identified from electrogram characteristics or myocardial imaging. Large reentry circuits that can be defined over several centimeters are commonly referred to as “macroreentry” circuits.

PATHOPHYSIOLOGY

Mechanisms of Ventricular Arrhythmias Associated With Acute Ischemia

Acute myocardial ischemia leads to local tissue hypoxia, depletion of adenosine triphosphate (ATP), and anaerobic glycolysis causing intracellular

acidosis. ATP depletion impairs the function of the ATP-dependent $\text{Na}^+\text{-K}^+$ pump, causing net K^+ leakage from the myocyte and elevation of extracellular K^+ concentration. This results in depolarization of the resting membrane potential of the surviving Purkinje fibers and, as a consequence, abnormal automaticity.^{3,4}

In addition, intracellular acidification and accumulation of H^+ ions activate the $\text{Na}^+\text{-H}^+$ exchanger, which extrudes H^+ in exchange for Na^+ entry, causing increased intracellular Na^+ concentration. The latter activates the $\text{Na}^+\text{-Ca}^{2+}$ exchanger in the reverse mode, which extrudes Na^+ in exchange for Ca^{2+} entry, causing intracellular Ca^{2+} overload in the ischemic myocardium which, in turn, leads to delayed afterdepolarizations (DADs) and triggered arrhythmias.⁵

Furthermore, membrane depolarization causes Na^+ channel inactivation and, as a result, reduced fast Na^+ current and reduced action potential upstroke, leading to slowed conduction and altered refractoriness.

Although an initial prolongation of the action potential duration can be observed (likely caused by an increase in the late Na^+ current), abbreviation of the action potential duration develops shortly afterward secondary to reduced Na^+ entry (due to Na^+ channel inactivation), reduced Ca^{2+} entry (due to inhibition of Ca^{2+} channels by acidosis), and enhanced K^+ efflux (due to activation of ATP-sensitive potassium current, IK-ATP , caused by reduced intracellular ATP).^{3,4}

Importantly, the effects of ischemia on the EP properties of myocardial cells are heterogeneous. Shortening of the action potential duration and reduction of upstroke velocity and amplitude are more pronounced within the central zone of ischemia and subepicardium than within the border zone and subendocardium. On the other hand, the surrounding normal myocardium can have an increase in conduction velocity (secondary to increased catecholamines) and decrease in refractoriness. This heterogeneity of action potential duration and dispersion of refractoriness provide a substrate for an injury current to flow between the ischemic and the nonischemic cells located at the border zone. In addition, myocardial ischemia causes disruption of gap junctions, leading to cellular uncoupling, with consequent slow and anisotropic conduction, and unidirectional conduction block, providing a substrate for reentry.^{3,4,6}

High levels of catecholamines, endothelin-1 activation, increased lysophosphatidylcholine (a phospholipid that accumulates in ischemic myocardium), mechanical stretch (induced by the viable myocardium surrounding the infarct zone), electrolyte abnormalities (particularly hypokalemia and hypomagnesemia), preexisting myocardial abnormalities (e.g., prior myocardial infarction [MI], hypertrophy, depressed ejection fraction), and genetic predisposition (likely mediated by mutations or polymorphism in genes encoding ion channels), can all significantly modify the EP properties of the substrate and contribute to arrhythmogenesis. Prolonged and severe acute ischemia and delayed or unsuccessful revascularization increase the risk of ventricular arrhythmias during an acute ischemic event.⁴

Experimental studies demonstrated that arrhythmia mechanisms undergo dynamic changes in the early minutes and hours after onset of myocardial ischemia. Two temporally distinct phases of ventricular arrhythmia develop in response to ischemic injury: phase 1 is the reversible phase of acute MI, whereas phase 2 is the infarct evolution phase (eFigs. 22.1 and 22.2).⁴

Phase 1: Acute Phase of Myocardial Ischemia

Phase 1, occurring during the first 2 to 30 minutes, is reversible if perfusion is restored within 15 minutes of coronary occlusion. It is estimated that 30% to 50% of sudden cardiac deaths (SCDs) during acute MI occur during phase 1 of ischemic injury, with VF occurring without or with a short interval of preceding symptoms.^{3,4}

Phase 1 is divided in 2 subphases: phase 1A (2 to 10 minutes) and phase 1B (10 to 30 minutes). Ventricular arrhythmias occurring within

the first 10 minutes following the onset of myocardial ischemia (phase 1A) are predominantly related to reentry within the ischemic myocardium caused by heterogeneity of conduction and refractoriness in normal and ischemic tissue. Phase 1A arrhythmias typically manifest as bursts of VT that rarely degenerate into VF.

On the other hand, ventricular arrhythmias occurring between 10 and 30 minutes following the onset of ischemia (phase 1B) seem to be mediated by abnormal automaticity, and possibly reentry, though the exact mechanism(s) remains uncertain. Phase 1B appears more arrhythmogenic than phase 1A, and arrhythmias in this phase more frequently evolve into VF.^{3,4}

Phase 2: Subacute Phase of Myocardial Ischemia

Persistent myocardial ischemia beyond the first 30 minutes leads to irreversible myocardial necrosis (Phase 2, infarct evolution phase), which extends between 1.5 and 48 hours after the onset of ischemia. Nonetheless, subendocardial Purkinje fibers are more resistant to ischemia and may survive, but with altered EP properties predisposing to arrhythmia generation. Reduced resting membrane potentials, Ca^{2+} overload, and heterogeneity of conduction and refractoriness at the infarct border zone, all can lead to focal (abnormal automaticity and triggered activity) and reentrant arrhythmias.^{3,4}

Of note, there is a period of low arrhythmogenesis lasting for 30 to 60 minutes between phases 1 and 2. There is no explanation for this phenomenon.

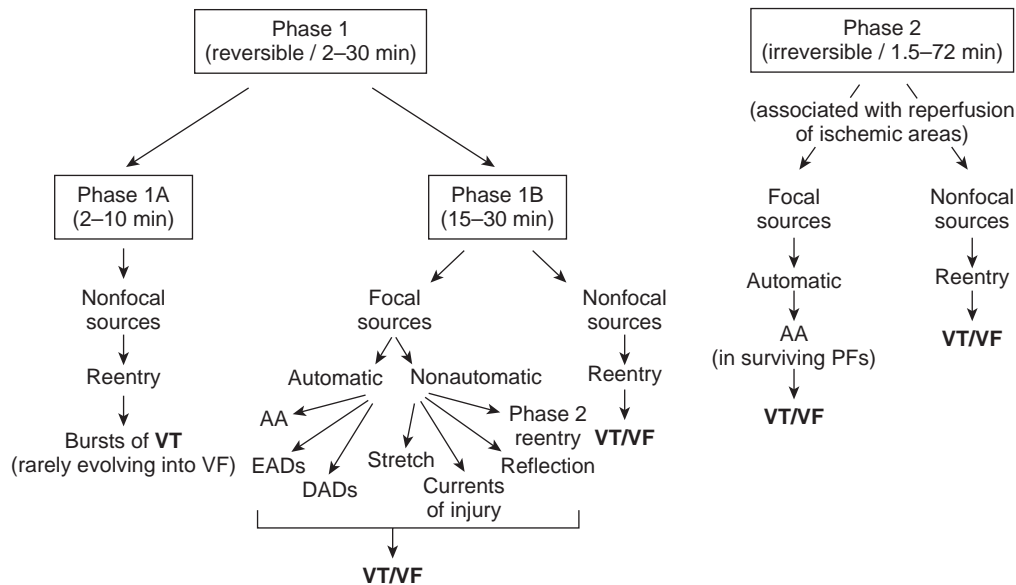
Mechanisms of Ventricular Arrhythmias Associated With Healed Infarction

Most post-MI sustained monomorphic ventricular tachycardias (SMVTs) are caused by macroreentry involving the region of the ventricular scar. Left ventricular (LV) remodeling begins almost immediately after acute MI. Experimental studies suggest that the EP substrate for monomorphic VT gradually forms in the subacute phase (in the first week) following acute MI and once established, appears to remain stable into the chronic phase. EP and electroanatomical characteristics demonstrated no difference between induced VT during the subacute and chronic phases, with comparable sites of earliest presystolic activation. These sites are located predominantly in the border zone adjacent to dense injury areas in both phases.^{3,4,7}

Persistent coronary occlusion typically leads to a central core of dense transmural scar in the territory supplied by the occluded artery, surrounded by a thin rim (border zone) where fibrotic tissue and viable myocardial fibers are intermixed. Conversely, early reperfusion (achieved by thrombolytics or coronary intervention) can lead to a more complex substrate, with nontransmural myocardial necrosis (primary subendocardial necrosis and variable epicardial sparing depending on the duration of coronary occlusion) and heterogeneous (and even patchy) scarring with multiple channels of viable myocardium embedded within the scar region, and complex border zones. The scar and fibrosis resulting from MI are distinctly different from nonischemic etiologies. Compared with post-MI VT, the scar in dilated cardiomyopathy (DCM) tends to be smaller and less confluent, with less endocardial involvement and less transmural involvement. Whereas ischemia produces a predictable wedge-shaped wavefront of necrosis progressing from subendocardium to epicardium (and scar areas larger endocardially than epicardially), usually confined to a specific coronary vascular territory, scars in nonischemic DCM have been shown to have a predilection for the midmyocardium and epicardium. In contrast to the dense post-MI scar with isolated surviving myocardial bundles, scarring in nonischemic DCM is patchy with fewer fixed boundaries and protected channels or isthmuses, which can alter the extent of local conduction slowing.^{8,9}

Phase 1 (reversible / 2–30 min)	Phase 2 (irreversible / 1.5–72 min)	
<ul style="list-style-type: none"> ↓ ATP ↑ Lactic acid ↑ $[Na^+]_i$ (Na^+ overload) Cell swelling ↑ $[Ca^{2+}]_i$ (Ca^{2+} overload) ↑ $[K^+]_e$ (K^+ efflux) ↑ Catecholamines ↑ Amphiphiles Membrane depolarization I_{Na} inactivation ↓ V_{max} Slow conduction Altered excitability ↑ Late I_{Na} Initial prolongation of APD ↓ I_{Ca} ↑ I_{K-ATP} Final abbreviation of APD 	<ul style="list-style-type: none"> ↓ ATP to < 10% ↓ Glycogen ↓ Anaerobic glycolysis ↑ Lactic acid ↑ $[Na^+]_i$ (Na^+ overload) ↑ $[Ca^{2+}]_i$ (Ca^{2+} overload) ↑ $[K^+]_e$ to = 20 mM Membrane depolarization I_{Na} inactivation ↓ V_{max} Slow conduction Abbreviation of APD 	During the healing process of ventricular muscle and in surviving PFs

eFig. 22.1 Biochemical and Electrophysiological Characteristics of Phase 1 and Phase 2 Ischemia-Mediated Ventricular Arrhythmias. APD, Action potential duration; I_{Na} , sodium channel current; I_{Ca} , inward calcium current; I_{K-ATP} , ATP-sensitive potassium current. (From Di Diego JM, Antzelevitch C. Ischemic ventricular arrhythmias experimental models and their clinical relevance. *Heart Rhythm*. 2011;8:1963–1968.)



eFig. 22.2 Temporal Distribution and Genesis of Ischemic Ventricular Arrhythmias. AA, Abnormal automaticity; EADs, early afterdepolarizations; DADs, delay afterdepolarizations; PFs, Purkinje fibers; VF, ventricular fibrillation; VT, ventricular tachycardia. (From Di Diego JM, Antzelevitch C. Ischemic ventricular arrhythmias experimental models and their clinical relevance. *Heart Rhythm*. 2011;8:1963–1968.)

Generally, the reentrant circuit arises in areas of a dense fibrotic scar interspersed with bundles of viable myocytes with poor intercellular coupling (due to altered gap junctions), producing a zigzag course of activation along a pathway lengthened by branching and merging bundles of surviving myocytes, leading to nonuniform anisotropic conduction (see Fig. 3.18). Heterogeneity in tissue composition and autonomic innervation in these regions can create areas of slow conduction and block, which promote reentry.

Buried in the arrhythmogenic substrate is the common central pathway (critical isthmus), which is a narrow path of tissue with abnormal conduction properties, causing slowing of impulse propagation and allowing reentry to occur. The isthmus itself can be surrounded by dead ends or branches that do not participate in the common pathway of the main reentrant circuit (i.e., bystander channels). The critical isthmus is typically protected by boundaries formed of both fixed and functional conduction block. Fixed conduction barriers are anatomically determined by the heterogeneous scar geometry or a valvular annulus. Development of functional conduction block is a prerequisite for initiation of VT in most cases, forming at least one border of the diastolic pathway. Evidence indicates that formation of functional block leading to reentry is associated with a large dispersion in refractory periods over short anatomical distances.¹⁰

Depolarization of the small mass of tissue within the isthmus is usually not detectable on the surface ECG and constitutes the electrical diastole between QRS complexes during VT. The wavefront leaves the isthmus at the exit site and propagates out to depolarize the remainder of the ventricles, producing the QRS complex. After leaving the exit of the isthmus, the reentrant wavefront can return to the entrance of the isthmus through an outer loop or an inner loop (see Fig. 5.16). An outer loop is a broad sheet of myocardium along the outer border of the infarct. The reentrant wavefront propagates through the outer loop while at the same time activating the rest of the myocardium, corresponding to electrical systole (QRS complex) on the surface ECG. Reentrant circuits can have one or more outer loops. An inner loop is a conduction pathway within scars, communicating with the common central pathway (critical isthmus) forming a circuit. The inner loop can serve as an integral part of the reentrant circuit or function as a bystander pathway. The dominant loop is the circuit loop outside the common central pathway with the shortest conduction time. If conduction through the inner loop is slower than conduction from the exit to entrance sites (through the outer loop), the inner loop will serve as a bystander, and the outer loop will be the dominant loop. If conduction through the inner loop is faster than conduction through the outer loop, it will form an integral component of the reentrant circuit and is designated as the dominant inner loop. Bystander loops can serve as a potential component of a new reentrant circuit if the dominant loop is ablated.^{5,10} This may manifest as sudden slowing of the VT rate without changing QRS morphology during ablation of the dominant nonisthmus loop.

Studies using electroanatomic substrate mapping found that ischemic cardiomyopathy patients without clinical SMVT had markedly smaller endocardial low-voltage areas, fewer scar-related electrograms (i.e., fractionated, isolated, and very late potentials, which represent electrically viable sites within the scar), and fewer putative conducting channels compared with patients with spontaneous SMVT, despite equally severe LV dysfunction as well as similar infarct age and distribution. These differences in the myocardial EP substrate can play an important role in VT arrhythmogenesis in the chronic post-MI context. Both the extent of the scar areas (electrogram voltage less than 0.5 mV) and the presence of numerous channels within this zone seem to be critical to the development of VT. Although the border zone region of the scar (electrogram voltage, 0.5 to 1.5 mV) did not differ in area

between the two groups, this zone also had a significantly higher prevalence of putative conducting channels in the SMVT patients. This suggests a fundamentally different scar composition (more “arrhythmogenic”) in the SMVT patients. As noted, inhomogeneous scarring with varying degrees of subendocardial myocardial fiber preservation within dense zones of fibrosis leads to slowed conduction, nonuniform anisotropy, and the potential for channels within the scar zone—conditions necessary for the development of reentry.¹¹

It is common for patients with post-MI VT to have more than one VT morphology. Even in patients presenting with a single SMVT, multiple distinct uniform VTs can be induced in the EP laboratory, especially in patients receiving antiarrhythmic therapy. The induction of multiple VT morphologies during an ablation procedure suggests that the arrhythmogenic substrate can support multiple reentrant circuits or different exit sites from a single circuit. Distinct VT morphologies (as defined by the 12-lead ECG and tachycardia cycle length [TCL]) often share a common isthmus but differ in propagation direction or location across the isthmus perimeter during reentry, but can also arise from distinct, usually adjacent, circuits.

A focal mechanism of VT (abnormal automaticity or triggered activity) has been implicated in the setting of acute ischemia. Focal VT can also occur in the absence of an acute ischemic event in patients with chronic ischemic heart disease. In one study, a focal mechanism was present in up to 9% of VTs that were induced in patients with ischemic heart disease during EP study for radiofrequency (RF) ablation.¹²

Infrequently, SMVT in the setting of chronic coronary artery disease (CAD) is related to a nonischemic arrhythmogenic substrate rather than a healed infarct. CAD can coexist with nonischemic cardiomyopathy, in which setting, arrhythmogenic substrate is inconsistent with the distribution of CAD, with VT morphologies originating in the periannular basal ventricular segments and frequent epicardial VT exits.¹³

EPIDEMIOLOGY AND NATURAL HISTORY

Coronary heart disease is the most frequent cause of clinically documented VT and VF (76% to 82% of patients). The incidence of ventricular arrhythmias in the periinfarct period and long-term post MI seems to have decreased over the past decades, likely due to the contemporary coronary revascularization strategies and pharmacological therapy, which have reduced 1-year mortality rates to less than 5%. Sustained VT and VF continue to occur in almost 6% of patients in the very early phase of acute MI, and they remain a major cause of death in the first 30 days after MI, particularly in those with LV dysfunction or heart failure.^{3,4,14,15}

Among almost 41,000 patients with ST-elevation MI treated with thrombolysis in the GUSTO-1 trial, 3.5% developed VT alone and 2.7% developed both VT and VF. In general, the incidence of sustained VT/VF complicating non-ST-elevation acute coronary syndrome (non-ST-elevation MI and unstable angina) has been lower; a pooled analysis of four major trials of more than 26,000 patients with non-ST-elevation acute coronary syndrome, 2.1% developed sustained ventricular arrhythmias. More contemporary estimates suggest a lower incidence (1.5%) of sustained VT/VF in this patient population. In a study examining all patients undergoing percutaneous intervention for acute coronary syndromes (ranging from unstable angina to ST-elevation MI) in the New York State registry, just over 5% of patients experienced sustained VT/VF.^{3,4,16}

In general, in the setting of acute ST-elevation MI, sustained ventricular arrhythmias are most frequent within 24 to 48 hours after the onset of ischemia. In contrast, these events do not appear to be confined predominantly to the first 48 hours after non-ST-elevation acute coronary events.¹⁶

Premature Ventricular Complexes

Premature ventricular complexes (PVCs) are seen in most cases of acute MI. Early PVCs (within the first 48 hours) do not appear to affect the prognosis. In contrast, repetitive complex PVCs (ventricular bigeminy, couplets, or multiform PVCs) occurring beyond 48 hours after acute MI can be associated with increased arrhythmic risk, particularly in patients with larger infarctions and impaired LV function.

Accelerated Idioventricular Rhythm

Accelerated idioventricular rhythm occurs in up to 50% of patients with acute MI, predominantly occurring in the first 12 hours after admission for acute MI. Although more common in patients with successful reperfusion therapy, accelerated idioventricular rhythm is neither a sensitive nor a very specific marker for successful reperfusion.

Reperfusion Arrhythmias

Ventricular arrhythmias upon reperfusion typically manifest as bursts of PVCs with long coupling intervals and accelerated idioventricular rhythms occurring at the moment of reperfusion, and are hemodynamically well tolerated. These arrhythmias originate within the reperfusion zone and likely reflect myocellular reperfusion injury. Reperfusion injury produces a second peak of myocardial necrosis, which depends on the duration of the preceding ischemia. Alteration of the EP substrate and, in particular, intracellular Ca^{2+} overload combined with increased catecholamines, likely play a central role in reperfusion arrhythmias. Abnormal automaticity is the likely mechanism.

In conjunction with thrombolytic therapy, reperfusion ventricular arrhythmias were considered as a noninvasive marker of successful infarct artery recanalization; however, current evidence suggests that those arrhythmias are neither specific nor sensitive. In the more contemporary era of primary percutaneous coronary intervention (PCI), the presence of ventricular arrhythmia bursts timed closely to reperfusion appears to predict larger infarct size in patients presenting with ST-segment elevation MI and treated with primary PCI resulting in brisk epicardial flow restoration (TIMI 3 flow) and rapid and complete ST-segment resolution.^{17,18}

Nonsustained Ventricular Tachycardia

Nonsustained VT is observed in 1% to 7% of acute MI patients. Nonsustained VT occurring early (within the first 2 to 3 hours) following acute MI does not appear to predict poor prognosis. Arrhythmic episodes occurring later (after the first 24 hours, and particularly after the first week), in the course of acute MI portend a worse prognosis. Beyond the periinfarct period, nonsustained VT is common in ischemic heart disease, recorded in 30% to 80% of patients during long-term ambulatory monitoring, or detected by cardiac implanted devices.^{1,19}

Polymorphic Ventricular Tachycardia

Polymorphic VT, which occurs in 0.3% to 2% of patients, is usually due to abnormal automaticity or triggered activity associated with ischemia or reperfusion. In the setting of coronary disease, polymorphic VT is generally considered a marker of ongoing ischemia and is often suppressed by antiischemic interventions. Unlike monomorphic VT, polymorphic VT is rarely seen in patients with healed MI in the absence of acute myocardial ischemia.

Ventricular Fibrillation

VF occurs in 3.7% of all acute ST-elevation MIs in the first 48 hours, and this is likely an underestimation because prehospital events are not included. When all VF events, before and after 48 hours, were included, VF was found to occur in 6.7% of ST-elevation MI patients and in

1.3% of non-ST-elevation MI patients. The majority of arrhythmic episodes occur early (within the first 48 hours) in the course of acute MI.

Primary VF (i.e., VF that occurs during the first 48 hours of an uncomplicated MI, without recurrent ischemia or heart failure), is associated with an up to fivefold increase in hospital mortality (greater than 50% due to LV failure or cardiogenic shock) but appears to have little effect on long-term mortality in patients who survived to hospital discharge.²⁰ Conversely, *nonprimary VF* (i.e., VF that occurs beyond the first 48 hours following MI or in the setting of recurrent ischemia or heart failure) is associated with marked increases in both 30-day mortality and 6-month mortality. The temporal cutoff between “early” and “late” arrhythmias at 48 hours following MI, however, is arbitrary to some extent; data to suggest that this should be at 24 hours or even earlier exist.¹⁴

Several factors appear to be associated with an increased risk of early VF during the periinfarction period, including ST-elevation MI, larger infarct size, inferoposterior MI, periinfarction angina, incomplete revascularization, hypokalemia, hypotension, male gender, younger age, and history of smoking.¹⁴

Sudden Cardiac Death

SCD accounts for up to 15% of total mortality in industrialized countries and claims the lives of more than 200,000 to 400,000 people per year in the United States (precise number not known and impacted by how estimates are obtained). Approximately 50% of deaths in patients with prior MI occur suddenly and unexpectedly. Ventricular arrhythmias are responsible for most of these deaths in stable ambulatory populations. Most SCD victims have known heart disease—most frequently CAD or prior MI.

Cardiac arrest is the initial manifestation of heart disease in approximately 50% of cases. Such patients are more likely to have single-vessel coronary disease and normal or mildly abnormal LV systolic function than cardiac arrest victims with prior MI. Although heart failure increases risk for both sudden and nonsudden death, a history of heart failure is present in only approximately 10% of cardiac arrest victims.

Acute MI is a common precipitant of out-of-hospital cardiac arrest, especially in older patients. About 40% of out-of-hospital cardiac arrest survivors develop overt signs of an MI (e.g., ST-segment elevation, Q waves, or elevated cardiac enzymes), and 50% are found to have an acutely occluded coronary vessel on coronary angiography.²⁰

The risk for arrhythmic and total mortality is highest in the first month after an acute MI and stays high during the first 6 months after acute MI. After the first year post MI, there appears to be a relatively quiescent period of relatively low rates of SCD, followed by a second peak 4 to 10 years after acute MI. The later occurrence of SCD likely results from delayed ventricular remodeling resulting in the creation or activation of reentrant VT circuits on the infarct border and from heart failure developing late after MI.

Although cardiac arrest and SCD in post-MI patients are predominantly caused by VT or VF, several studies in patients with cardiac arrest have shown that VF as the causative rhythm appears to be decreasing, being replaced by pulseless electrical activity and asystole. The cause of this change is unknown, but it may reflect patients with sicker hearts who are living longer due to better therapy. Hearts with advanced disease may be more likely to develop pulseless electrical activity and asystole than VF.

Sustained Monomorphic Ventricular Tachycardia

“Early” SMVT within the first 24 to 48 hours of acute MI is uncommon, and occurs in about 2% to 3% of ST-elevation MI patients and in less than 1% of non-ST-elevation MI patients. Although early SMVT is

associated with an increase in in-hospital mortality, studies showed that mortality at 1 year (among 21- to 30-day survivors) is not increased, suggesting that the arrhythmogenic mechanisms can be transient in early post-MI SMVT. Nevertheless, it is important to understand that data are limited regarding the long-term prognostic significance of SMVT in the early post-MI setting because most studies combined VT and VF or sustained and nonsustained VT without specifying the results for each arrhythmia. Many investigators consider SMVT, even when occurring in the early hours following MI, to be an indicator of the presence of an already established permanent substrate (developing necrosis or preexisting scar) and, hence, an indicator of high long-term risk for arrhythmic events.

On the other hand, the typical patient with SMVT occurring during the subacute and healing phases, beginning more than 48 hours after an acute MI, has had a large, often complicated infarct with a reduced left ventricular ejection fraction (LVEF), and such VT is a predictor of a worse prognosis. SMVT within 3 months of an MI is associated with a 2-year mortality rate of 40% to 50%, with most deaths being sudden. Predictors of increased mortality in these patients include anterior wall MI, frequent episodes of sustained or nonsustained VT, heart failure, and multivessel coronary disease, particularly in individuals with residual ischemia.

Early reperfusion of infarct-related arteries results in less aneurysm formation, smaller scars, and less extensive EP abnormalities, although a significant risk of late VT (often with rapid TCLs) persists. In patients with ST-elevation MI treated with primary PCI, delayed reperfusion (greater than 5 hours after MI) was associated with a sixfold increase in the odds of inducible SMVT by programmed electrical stimulation (performed 6 to 10 days post MI) as well as an increased risk of spontaneous ventricular arrhythmias and SCD (after a mean follow-up of 28 ± 13 months) compared with early reperfusion (≤ 3 hours), independent of LVEF. It was estimated that each 1-hour delay in reperfusion conferred a 10.4% increase in the odds of inducible VT.

Most episodes of post-MI SMVT occur during the chronic phase. Among all patients presenting with SMVT in the setting of significant structural heart disease, ischemic heart disease is the most frequent etiology, comprising 54% to 59% of patients who receive an implantable cardioverter-defibrillator (ICD) or who are referred for catheter ablation.¹

VT occurs in 1% to 2% of patients late after MI, but the time interval from MI to first episode of VT is highly variable. The first episode can be seen within the first year post MI, but the median time of occurrence is about 3 years, and SMVT can occur as late as 10 to 15 years after an MI. Late SMVT often reflects significant LV dysfunction and the presence of a ventricular aneurysm or scarring. Late arrhythmias can also result from new cardiac events. The annual mortality rate for SMVT that occurs after the first 3 months following acute MI is approximately 5% to 15%. Predictors of life-threatening ventricular arrhythmias include residual ischemia in the setting of damaged myocardium, LVEF less than 40%, and electrical instability, including inducible or spontaneous VT, particularly in those who present with cardiac arrest.

Recent evidence suggests that coronary revascularization before or shortly after ICD placement in high-risk post-MI patients with LV dysfunction and wide QRS duration can potentially reduce the risk for life-threatening ventricular arrhythmias and appropriate ICD shocks.

The relationship between SMVT and VF is uncertain, and it is not clear how often VF is triggered by SMVT rather than occurring *de novo*. SMVT can simply be the company kept by VF in a number of patients or, in the appropriate setting such as recurrent ischemia, a rapid VT can develop a wavefront that becomes fractionated, leading to VF.

CLINICAL PRESENTATION

Clinical presentation of ventricular arrhythmias in patients with CAD is variable. In the setting of acute ischemia, sustained ventricular arrhythmias can manifest as palpitations or worsening angina, but more often present with syncope and cardiac arrest. In chronic ischemic heart disease, VT results in a wide spectrum of clinical presentations, ranging from mild symptoms (palpitations) to symptoms of hypoperfusion (lightheadedness, altered mental status, presyncope, and syncope), exacerbation of heart failure and angina, and cardiovascular collapse. Patients with ICDs may experience ICD shocks triggered by the arrhythmia. Incessant VT, even at relatively slow rates, can lead to hemodynamic deterioration and heart failure. Hemodynamic consequences associated with VT are related to ventricular rate, duration of VT, presence and extent of LV dysfunction, ventricular activation sequence (i.e., ventricular dyssynchrony), and loss of atrioventricular (AV) synchrony.

INITIAL EVALUATION

Evaluation of Type and Burden of Ventricular Arrhythmias

Identifying and quantifying the types and burden of sustained and nonsustained VT and PVCs are necessary. In addition to 12-lead ECG, ambulatory cardiac monitoring (Holter or event monitoring) or implantable loop recorders may be required to document the type, burden, and clinical impact of the arrhythmia. In patients with ICDs, stored device data such as electrogram morphology and TCL can be used to identify the clinical VT.

Evaluation of the Triggers of Ventricular Arrhythmias

Initial testing in patients with post-MI VT should evaluate for reversible causes of the arrhythmia. These include electrolyte imbalances, acute ischemia, heart failure, hypoxia, hypotension, drug effects, and anemia.

Evaluation of Myocardial Ischemia

Although recurrent SMVT is rarely due to acute myocardial ischemia in patients with known CAD, diagnostic evaluation for acute or persistent ischemia is warranted to improve patient outcome, especially if the severity of CAD has not been previously established or prior episodes of VT caused hemodynamic compromise. This may include echocardiographic examination, exercise testing, and cardiac catheterization. In patients with reversible myocardial ischemia, coronary revascularization may be warranted, and can potentially reduce the risk of life-threatening ventricular arrhythmias. However, if the severity of coronary disease has been recently defined and symptoms and hemodynamic tolerance of VT do not suggest significant ischemia, further evaluation may not be required.

Role of Electrophysiological Testing

Invasive EP testing should be considered in post-MI patients presenting with unexplained syncope or sustained palpitations, and those with wide complex tachycardia of uncertain mechanism. In addition, EP testing can be used for risk stratification late after MI in patients with ischemic cardiomyopathy and nonsustained VT (see later). However, EP testing is not recommended in patients with documented sustained VT unless catheter ablation is planned.¹

Programmed stimulation induces VT in over 90% of patients with a history of VT. Although the rate and QRS morphology of the induced VT can differ from that observed during spontaneous tachycardia, the induction of VT signifies the presence of a fixed anatomical substrate associated with an increased likelihood of future spontaneous events.

RISK STRATIFICATION

There are more than 50 million North American adults with CAD and more than 7 million have had an MI. However, only a fraction of these patients will suffer a cardiac arrest. Therefore noninvasive risk assessment after MI is required to identify patients at risk of SCD.

Various tests assessing the extent of myocardial damage and scarring, myocardial conduction disorders, dispersion of repolarization, and autonomic imbalance have been proposed to identify patients at high risk of SCD who are likely to benefit from prophylactic ICD therapy. Some of these techniques potentially identify the underlying substrate (e.g., myocardial scar, intramyocardial conduction abnormalities) or triggers (e.g., autonomic imbalance, nonsustained VT) of malignant ventricular arrhythmias. However, most of these techniques have not been validated in independent populations and, although they can predict higher risk of total mortality, their ability to predict arrhythmic death is uncertain (i.e., limited specificity). In addition, most conventional risk stratifiers of SCD have a relatively low positive predictive value that would preclude their wide application as guidelines for ICD implantation in patients known to be at risk for SCD.²¹

To date, only two approaches have been proven useful in guiding prophylactic ICD therapy in post-MI patients: the presence of significant LV dysfunction alone or in combination with the inducibility of sustained VT/VF during programmed electrical stimulation beyond the early phase after MI. It should be recognized, however, that the development of SCD in post-MI patients is multifactorial, and multiple events need to coincide for a cardiac arrest to ensue; therefore no one risk stratification test alone will be sufficient for all patients. Rather, combining multiple tests in screening for the different potential mechanisms of SCD may be necessary. Furthermore, because progression of ischemic heart disease can result in the evolution of new mechanisms of SCD in individual patients, repetition of risk stratification tests at certain intervals may be required. It would seem reasonable (in the absence of data) to retest every 2 years in apparently stable patients to detect potential changes in substrate, regardless of which tests appear to have the highest yield.

Ventricular Arrhythmias

In general, on the basis of large thrombolytic trials, the occurrence of ventricular arrhythmias and cardiac arrest in the early course (within the first 24 to 48 hours) of an uncomplicated acute MI is associated with increased in-hospital and 30-day mortality, but has not been considered a marker of long-term mortality beyond hospital discharge. Early ventricular arrhythmias likely represent a transient, reversible arrhythmogenic event caused by acute ischemia and reperfusion rather than a permanent arrhythmogenic substrate; hence, they do not predict an increased risk for recurrent arrhythmic events in patients who are successfully revascularized. Nonetheless, the long-term prognostic significance of SMVT in the early hours post MI remains uncertain, as most studies combined VT and VF or sustained and nonsustained VT without specifying the results for each arrhythmia. Many investigators consider SMVT, even when occurring in the early hours following MI, to be an indicator of the presence of an already established permanent substrate (developing necrosis or preexisting scar) and, hence, an indicator of high long-term risk for arrhythmic events.¹⁵

On the other hand, multiple studies confirm that the occurrence of sustained ventricular arrhythmias (VT and VF) late (greater than 48 hours following MI) or in the context of complicated MI is associated with significantly worse long-term prognosis and high risk of SCD, even after successful revascularization. The temporal cutoff between “early” and “late,” however, remains uncertain. Many investigators prefer a 24-hour (rather than 48-hour) cutoff. Furthermore, some more con-

temporary studies found that both early and late sustained VT/VF were associated with a markedly increased risk of all-cause death at 30 days and 1 year after discharge despite revascularization.^{3,4,14–16}

Repetitive complex PVCs (ventricular bigeminy, couplets, or multiform PVCs) occurring beyond 48 hours after acute MI can be associated with increased arrhythmic risk, particularly in patients with larger MIs and impaired LV function. In a recent report evaluating ventricular ectopy on Holter recordings obtained 6 weeks after acute MI in patients with LVEF of 40% or less, frequent PVCs (≥ 10 per hour), prevalence of repeating forms of PVCs, and low coupling interval variability were potentially useful risk markers of fatal or near-fatal arrhythmias after MI.²² However, the utility of these risk markers in guiding ICD implantation is limited.

The occurrence of nonsustained VT in the subacute and chronic phases post MI has been found to predict an increased risk of cardiovascular death. Nonsustained VT has been used for risk stratification but only in conjunction with moderate to severe LV dysfunction (LVEF $\leq 40\%$) and inducible VT at EP study. Nonetheless, the current guidelines do not recommend surveillance cardiac monitoring beyond 24 to 48 hours of hospitalization after an acute coronary event.¹⁹

Syncope

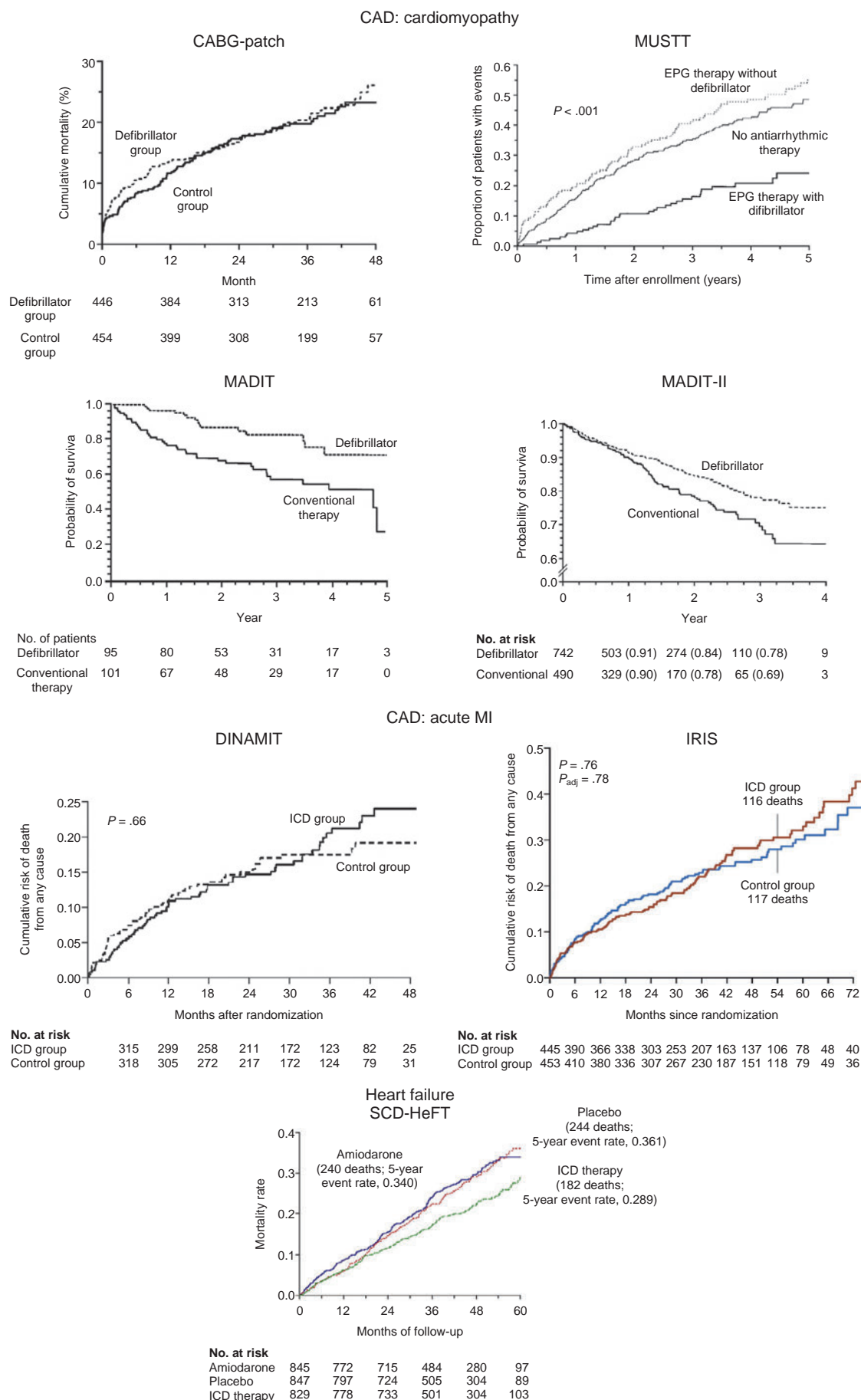
Patients with syncope (that is thought to be due to ventricular tachyarrhythmia) in the setting of structural heart disease (including LV systolic dysfunction or prior MI) have an increased incidence of SCD and overall mortality. It is recommended that these patients undergo ambulatory cardiac monitoring or invasive EP testing. If sustained VT is detected on cardiac monitoring or is inducible at EP study, an arrhythmic cause of syncope should be considered, and ICD implantation is recommended.¹⁵

Left Ventricular Ejection Fraction

Multiple studies evaluating survival of patients with prior MI established a clear relationship between reduced LVEF and increased mortality (Table 22.1; eFig. 22.3).¹⁵ However, these trials were designed to evaluate the usefulness of ICD in high-risk groups, defined mainly by reduced LVEF, and not to evaluate different variables, including LVEF, as risk stratifiers. In essence, these studies show that a reduced LVEF is associated with an increased SCD risk and that ICD therapy improves survival, but they do not establish LVEF as the optimal risk stratification variable for arrhythmic mortality.²¹

LVEF behaves as a continuous variable, with gradually increasing mortality risk until the LVEF declines to 40% and then markedly increasing risk for values less than 40%. Nevertheless, the exact mechanisms involved in the strong correlation between decreased LV systolic function and increased incidence of SCD are not clearly defined. LVEF is a global measure of heart function and is only loosely correlated with the amount of myocardial scar.²³

Although low LVEF identifies one patient population at relatively increased risk for SCD, there are clear limitations to LVEF as the ideal risk stratification test for deciding whether to implant an ICD for primary prevention of SCD. LV systolic dysfunction lacks specificity. There is no evidence of any direct mechanistic link between low LVEF and mechanisms responsible for ventricular tachyarrhythmias and no study has demonstrated that reduced LVEF is specifically related to SCD. In fact, in studies that enrolled all patients after MI, patients with LVEF less than 30% to 35% account for no more than 50% of sudden cardiac arrest victims. Thus, although LVEF is a good marker of risk for *total* mortality, it does not provide insight into how patients are likely to die (sudden vs. nonsudden). Furthermore, patients with low LVEF are not uniform with regard to other prognostic markers, and not all are at high risk for SCD.²¹



eFig. 22.3 Survival Curves for the Implantable Cardioverter-Defibrillator (ICD)-Only Primary Prevention Trials in Patients With Cardiomyopathy Due to Coronary Artery Disease (CAD) or Acute Myocardial Infarction (MI). All curves represent mortality/survival. CABG-Patch, Coronary artery bypass graft-patch; DINAMIT, defibrillator in acute myocardial infarction trial; EPG, electrophysiologically guided; IRIS, immediate risk stratification improves survival study; MADIT, multicenter automatic defibrillator trial; MUSTT, multicenter unsustained tachycardia trial; SCD-HeFT, sudden cardiac death in heart failure trial. (From Kusumoto FM, Calkins H, Boehmer J, et al. HRS/ACC/AHA expert consensus statement on the use of implantable cardioverter-defibrillator therapy in patients who are not included or not well represented in clinical trials. *J Am Coll Cardiol.* 2014;64:1143–1177.)

Another limitation of LVEF is its poor sensitivity. Although most studies have focused on patients with markedly reduced LVEF, this group currently accounts for only 10% to 15% of MI survivors, and most contemporarily managed post-MI patients who suffer a cardiac arrest have better-preserved LV systolic function (i.e., LVEF $\geq 35\%$).

It is also recognized that methods of LVEF determination lack precision. Different imaging modalities can produce significantly different LVEF values, and the accuracy of techniques varies among laboratories and institutions, and there is evidence that prognosis, and hence risk, depends on the method by which the LVEF is measured. It is therefore

TABLE 22.1 Randomized Primary Prevention Trials of Implantable Cardioverter-Defibrillator Therapy in Coronary Artery Disease

Study	Inclusion Criteria	Enrolled Patients	Findings
Ischemic Cardiomyopathy Multicenter Automatic Defibrillator Implantation Trial (MADIT) (11)	<ul style="list-style-type: none"> • Prior MI, LVEF <0.35; NSVT • Inducible nonsuppressible sustained VT/VF at EPS • >3 weeks post MI • >2 months post-CABG • >3 months post-PTCA 	<ul style="list-style-type: none"> • 196 patients enrolled, 95 in ICD arm • Mean age: 63 years • 92% male • Mean LVEF: 0.26 • 90 with prior CABG, 44 with prior PTCA, 53 with ≥ 2 prior MIs • 100% NSVT 	<ul style="list-style-type: none"> • Reduced mortality with ICD (HR: 0.46; $P = .009$)
Coronary Artery Bypass Graft (CABG) Patch Trial (12)	<ul style="list-style-type: none"> • LVEF ≤ 0.35, abnormal SAEKG, undergoing CABG 	<ul style="list-style-type: none"> • 900 patients enrolled, 446 randomized to epicardial ICD implantation at time of CABG • Mean age: 64 years • 84% male • Mean LVEF: 0.27 • 100% CABG 	<ul style="list-style-type: none"> • No difference in survival with ICD (HR: 1.07; 95% CI: 0.81–1.42; $P = .64$) • Arrhythmic mortality at 42 months: control 6.9%, ICD 4.0% ($P = .057$)—45% reduction in arrhythmic death • 71% of deaths were nonarrhythmic: non-arrhythmic cardiac mortality at 42 months: control 12.4%, ICD 13.0% ($P = .275$)
Multicenter Unsustained Tachycardia Trial (MUSTT) (10)	<ul style="list-style-type: none"> • EF ≤ 0.40 • NSVT within the last 6 months • ≥ 4 days post MI or revascularization 	<ul style="list-style-type: none"> • 2202 patients enrolled, 704 patients with inducible VT, 161 received ICDs • Median age: 67 years • 90% male • Median EF: 0.30 • 56% prior CABG • 16% within 30 days of an MI • 100% NSVT • NYHA class (I/II/III/IV): 37/39/24/0 	<ul style="list-style-type: none"> • Risk of sudden death reduced in patients with ICDs (HR: 0.24; 95% CI: 0.13–0.45; $P < .001$)
Multicenter Automatic Defibrillator Implantation Trial II (MADIT-II) (2)	<ul style="list-style-type: none"> • >21 years old • EF ≤ 0.30 • >1 month after MI • >3 months after revascularization 	<ul style="list-style-type: none"> • 1232 patients enrolled, 742 in ICD arm • Median age: 64 years • 84% male • EF: 0.23 • 57% prior CABG • NYHA class (I/II/III/IV): 35/35/25/5 	<ul style="list-style-type: none"> • After average f/u of 20 months, ICD group had Lower mortality (HR: 0.69; 95% CI: 0.51–0.93; $P = .016$) • ICD associated with an absolute 5.6% decrease in mortality
Both Ischemic and Nonischemic Cardiomyopathy Sudden Cardiac Death in Heart Failure Trial (SCD-HeFT) (1)	<ul style="list-style-type: none"> • 18 years old • EF $<35\%$ • NYHA class II or III 	<ul style="list-style-type: none"> • 2521 patients enrolled, 829 received ICDs • Median age: 60 years • 76% male • EF: 0.25 • 33 patients within 30 days of an MI • 23% NSVT • NYHA class (I/II/III/IV): 0/70/30/0 	<ul style="list-style-type: none"> • After median f/u of 46 months, ICD group had Lower mortality (HR: 0.77; 95% CI: 0.62–0.96; $P = .007$) compared with placebo or amiodarone groups • ICD associated with an absolute 7.2% decrease in mortality
Acute Coronary Artery Disease Defibrillator in Acute Myocardial Infarction Trial (DINAMIT) (14)	<ul style="list-style-type: none"> • 18–80 years old • MI past 6–40 days • EF <0.35 • Abnormal HRV 	<ul style="list-style-type: none"> • 674 patients enrolled, 332 received ICDs • Average age: 61 years • 76% male • EF: 0.28 • Index MI: • 72% Anterior • 72% new Q wave • Peak CK: 2300 U/L • Reperfusion: 63% • 26% PCI • 27% thrombolysis • 10% both 	<ul style="list-style-type: none"> • After mean f/u of 30 months, no difference in mortality between ICD and no ICD groups (HR: 1.08; 95% CI: 0.76–1.55; $P = .66$) • ICD group had a significant decrease in risk of death due to arrhythmia (HR: 0.42; 95% CI: 0.22–0.83; $P = .009$) but a significant increase in risk of nonarrhythmic death (HR: 1.75; 95% CI: 1.11–2.76; $P = .02$)

Continued

TABLE 22.1 Randomized Primary Prevention Trials of Implantable Cardioverter-Defibrillator Therapy in Coronary Artery Disease—cont'd

Study	Inclusion Criteria	Enrolled Patients	Findings
Immediate Risk Stratification Improves Survival Study (IRIS) (15)	<ul style="list-style-type: none"> MI in the past 5–31 days and either: <ul style="list-style-type: none"> EF \leq40% and initial HR $>$90 beats/min NSVT $>$150 beats/min 	<ul style="list-style-type: none"> 898 enrolled, 445 received ICDs Average age: 63 years 77% male EF: 0.35 Index MI: <ul style="list-style-type: none"> 64% anterior 77% STEMI Reperfusion: 77% 72% PCI 16% thrombolysis (+/- PCI) 	<ul style="list-style-type: none"> After mean f/u of 37 months, no difference in mortality between the ICD and no ICD groups (HR: 1.04; 95% CI: 0.81–1.35; $P = .78$) ICD group had a significant decrease in sudden cardiac death (HR: 0.55; 95% CI: 0.31–1.00; $P = .049$) but a significant increase in risk of nonsudden cardiac death (HR: 1.92; 95% CI: 1.29–2.84; $P = .001$)

CABG, Coronary artery bypass grafting; CI, confidence interval; CK, creatine kinase; EF, ejection fraction; EPS, electrophysiological study; HR, hazard ratio; HRV, heart rate variability; ICD, implantable cardioverter-defibrillator; LVEF, left ventricular ejection fraction; MI, myocardial infarction; SAECC, signal-averaged electrocardiogram, STEMI, ST segment elevation myocardial infarction; NSVT, nonsustained ventricular tachycardia; NYHA, New York Heart Association; PCI, percutaneous coronary intervention; PTCA, percutaneous transluminal coronary angioplasty; VF, ventricular fibrillation; VT, ventricular tachycardia.

From Kusumoto FM, Calkins H, Boehmer J, et al. HRS/ACC/AHA expert consensus statement on the use of implantable cardioverter-defibrillator therapy in patients who are not included or not well represented in clinical trials. *J Am Coll Cardiol*. 2014;64:1143–1177.

recommended to use the LVEF determination that clinicians believe is the most clinically accurate and appropriate in their institution.²⁴

Invasive Electrophysiological Testing

Inducibility of VT/VF during invasive EP testing identifies patients at risk of spontaneous ventricular tachyarrhythmia and, hence, can enhance the predictive accuracy of reduced LVEF for post-MI patients with high mortality risk. Programmed ventricular stimulation is probably the most effective stratification technique for identification of post-MI patients at high risk for development of monomorphic VT, but the sensitivity is inadequate to predict SCD, especially in patients with severe LV systolic dysfunction.²¹

The first MADIT study demonstrated that those patients with inducible VT/VF and LVEF of 35% or less late after MI are likely to benefit from prophylactic ICD therapy. Moreover, the absolute mortality reduction in MADIT I (26.2% over 27 months) was substantially greater than what was found in either MADIT II or SCD-HeFT. Similar results were found in MUSTT. However, secondary analysis from MUSTT revealed that despite the significant difference in outcome between inducible patients enrolled in the trial and noninducible patients enrolled in a registry, EP inducibility was of limited value because the 5-year mortality rate in inducible patients was 48% compared with 44% in noninducible patients. Later, data from MADIT II showed that there is no need for additional risk stratifiers (including EP testing) when LVEF is so low. In more than 80% of patients randomized to the ICD arm of MADIT II, invasive EP testing with an attempt to induce tachyarrhythmias was performed at the time of ICD placement. VT inducibility, observed in 40% of studied patients, was not effective in identifying patients with cardiac events defined as VT, VF, or death. These observations from both MUSTT and MADIT II subanalyses suggest that in patients with substantially depressed LV function, EP inducibility should not be considered a useful predictor of outcome. It is possible, however, that inducibility might have much better predictive value in post-MI patients with LVEF greater than 30% or greater than 35%.

Furthermore, using inducible VT/VF to guide prophylactic ICD therapy is limited by low sensitivity. Post-MI patients with LVEF of 35% or less and no inducible VT/VF still appear to have a substantial (greater than 25%) risk of serious events over the near term. Furthermore, there are no data to support the use of invasive EP testing in

post-MI patients with LVEF values greater than 40% or in the early post-MI period. In fact, the BEST-ICD trial found that inducible VT/VF early after MI does not predict benefit from ICD therapy. In contrast, the CARISMA study found that inducible VT identified 6 weeks following an acute MI was a strong predictor of future life-threatening arrhythmias. In addition, EP testing is invasive and not practical for broad application as a screening tool.

Nonetheless, EP testing can be valuable when used in patients in whom the risk of sustained arrhythmias and SCD is intermediate, and the potential benefit of ICD therapy uncertain. Current guidelines recommend prophylactic ICD therapy in post-MI patients with nonsustained VT and LVEF less than 40% if sustained VT/VF is inducible at EP study.

Measures of Cardiac Repolarization

Microvolt-level T wave alternans (TWA) has emerged as a promising noninvasive marker of risk for SCD. TWA, measured on the surface ECG, detects subtle beat-to-beat oscillations in cardiac repolarization and has been linked to cellular mechanisms of arrhythmogenesis. Initial clinical studies of TWA demonstrated a high negative predictive value ($\geq 95\%$). In addition, an abnormal TWA was associated with significantly increased mortality risk as well as risk of arrhythmic events, although the positive predictive values were far more variable, depending on the characteristics of the study populations and pretest probability. Although those studies suggested that TWA could potentially provide prognostically useful information beyond the LVEF and help guide selection of appropriate patients for prophylactic ICD therapy, more recently, several large multicenter studies of TWA failed to support these findings. In fact, the latter studies strongly suggested that a negative TWA result should not be used to withhold ICD therapy among patients who meet other standard criteria.²⁵

Other noninvasive measures of dispersion of repolarization, including QT dispersion, QT variability, and QT dynamics, have had similar mixed predictive results in studies with limited clinical applicability.²³

Measures of Autonomic Imbalance

Methods to assess the autonomic nervous system, which has been thought to be a modulator between triggers of ventricular tachyarrhythmias and the underlying substrate (including heart rate variability, baroreflex sensitivity, heart rate turbulence, and deceleration capacity) have been

evaluated for SCD risk stratification. Multiple studies have correlated relative excess of sympathetic tone (or deficient parasympathetic tone) with increased mortality in post-MI patients as well as increased propensity for VF during acute ischemia. Although the majority of studies showed no significant difference in relative risk for SCD versus total mortality, a recent meta-analysis found that heart rate turbulence was a powerful predictor of both cardiac death and arrhythmic events in post-acute-MI patients with LVEF greater than 30%, and its performance was improved in combination with TWA. Nevertheless, these measures need further validation to support their use in guiding prophylactic ICD therapy.^{23,26,27}

Measures of Myocardial Conduction Disorders

Increased QRS duration on a surface ECG has been associated with a higher risk of death after MI and appears to reflect greater LV dysfunction, but association with SCD has not been proven. Similarly, the presence of late potentials on signal-averaged ECG failed to identify patients likely to benefit from ICD therapy. Because of the lack of discrimination in the mode of death, these noninvasive markers of risk have not had widespread adoption.

More recently, fragmentation of the QRS complex on the 12-lead surface ECG (filter range, 0.15 to 100 Hz; AC filter, 60 Hz, 25 mm/s, 10 mm/mV), which likely signifies inhomogeneous ventricular activation due to myocardial scar or ischemia in patients with CAD, has been found to potentially predict increased risk of appropriate ICD therapies in patients who received an ICD for primary and secondary prevention.²³ In a recent meta-analysis, fragmented QRS was found to be an indicator of all-cause mortality and SCD risk. The risk was greater in patients with LVEF of 35% or less and in those with QRS duration exceeding 120 milliseconds. However, in the absence of a prospective study of ICD implantation, randomized on the basis of fragmented QRS, it is not clear how the tool should be applied in clinical practice.^{28,29}

Genetic Testing

There is compelling evidence that a genetic mechanism may increase patient susceptibility to SCD following MI, and genetic assessment may play a role in the future. However, there is presently no evidence for using genetic testing to identify post-MI patients at risk.

Cardiac Magnetic Resonance Imaging

Characteristics of myocardial scar architecture and tissue heterogeneity in the periinfarct zone, as defined by contrast-enhanced cardiovascular magnetic resonance (CMR), can potentially identify a proarrhythmic substrate, and appear to be strong predictors of ventricular arrhythmias and appropriate ICD therapies. In patients with ischemic cardiomyopathy, nontransmural (rather than transmural) hyperenhanced areas were found to predict a higher risk of sustained VT. Current evidence, however, does not support the use of CMR for SCD prognostication. Large prospective trials are still required to evaluate the reliability of these techniques for risk stratification.^{23,30–32}

Risk Stratification Early Postinfarction

The risk of SCD is greatest in the first month after MI and appears to decline in the first year after MI. Nevertheless, both prospective and retrospective studies of prophylactic ICD therapy have failed to show a reduction in all-cause mortality in early post-MI patients. The reasons for the lack of benefit of early ICD implantation after MI are unclear. The reduction in the rate of death due to arrhythmia associated with ICD therapy was offset by an increase in the rate of death from nonarrhythmic cardiac causes (e.g., LV rupture, acute mitral regurgitation) in the ICD groups (see Table 22.1; see eFig. 22.3). This discrepancy not only highlights the limitations of current risk stratification techniques,

but also reflects relative differences in the risk factors for SCD at different time points after MI and the fact that nonarrhythmic death accounts for an appreciable percentage of deaths during that time period. In addition, some portion of the post-MI population will eventually recover LV function, rendering them at lower risk of SCD.

Heart rate and creatinine clearance measured at baseline are strongly associated with SCD during the in-hospital period, whereas recurrent cardiovascular events (including heart failure, MI, and rehospitalization) and a baseline LVEF of 40% or less are more strongly associated with the occurrence of SCD after discharge.

Although the cumulative incidence of SCD is greatest in post-MI patients with an LVEF of 30% or less, the incidence of SCD is higher in patients with an LVEF greater than 40% in the first 30 days after MI when compared with patients with an LVEF of 30% or less after 90 days. The strength of the association between LVEF and survival free from SCD appears to be greatest in long-term follow-up (greater than 6 months). Currently, there is no strategy (invasive or noninvasive) that can reliably predict the risk for SCD or guide empiric ICD implantation soon after an MI. Data suggest it is best to wait 2 to 3 months after acute MI before performing risk stratification.

Some evidence suggests a potential benefit of EP testing in risk stratification in patients with ST-elevation MI and LVEF less than 40% treated with primary PCI. Inducible SMVT by programmed electrical stimulation performed 6 to 10 days post MI was associated with an increased risk of spontaneous VT/VF and SCD (after a mean follow-up of 28 ± 13 months). However, further evaluation in randomized clinical trials is required before adoption of this approach.

PRINCIPLES OF MANAGEMENT

Pharmacological Therapy

Acute Therapy

When ventricular arrhythmias are precipitated by acute ischemia, immediate reperfusion is critical. In addition, beta-blockers should be started, electrolyte abnormalities (hypomagnesemia and hypokalemia) should be corrected, treatment of decompensated heart failure should be optimized, and proarrhythmic medications should be discontinued.^{4,14}

For PVCs and nonsustained VT, antiarrhythmic drugs, aside from beta-blockers, are *not* recommended because this strategy does not improve either short- or long-term outcomes, and, with some drugs, may actually increase mortality. However, when the burden of PVCs or nonsustained VT is large despite beta-blocker therapy and significantly impact the clinical condition (worsening angina or heart failure), treatment with antiarrhythmic medications (amiodarone) may be useful. Most episodes of accelerated idioventricular rhythm are transient and benign, and do not require specific treatment.^{4,14}

For sustained ventricular arrhythmias, the degree of hemodynamic tolerance should dictate the initial therapeutic strategy. Treatment of VF and pulseless VT and should follow the Advanced Cardiac Life Support (ACLS) protocol. Electrical cardioversion is recommended for VTs causing severe symptoms of angina, heart failure decompensation, or hemodynamic deterioration. Whenever possible, a 12-lead ECG should be recorded before cardioversion. Recurrent polymorphic VT or VF can be an indicator of incomplete reperfusion or recurrence of acute ischemia, especially in the presence of ST segment or T wave changes during normal sinus rhythm (NSR). Therefore immediate coronary angiography and revascularization should be considered.^{1,4}

In patients with hemodynamically stable sustained VT, IV amiodarone is the drug of choice. IV procainamide and sotalol are alternatives. Lidocaine is less effective in the absence of acute ischemia; however, it can be considered in combination with procainamide or amiodarone if the latter drugs are ineffective alone.¹

In patients with drug-refractory electrical storm, neuraxial modulation (thoracic epidural anesthesia, left or bilateral cardiac sympathetic denervation) may significantly reduce arrhythmia burden. Deep sedation and mechanical ventilation can be useful in the management of these patients. Mechanical hemodynamic support (LV assist devices or extracorporeal life support) should be considered for hemodynamic stabilization.^{1,14,33–35} Once reversible factors are rectified and hemodynamic status is optimized as possible, catheter ablation should be considered early in the course of treatment for refractory patients. New approaches, such as renal artery denervation, are being studied.^{14,36}

Importantly, in patients with acute ischemia and no ventricular arrhythmias, prophylactic treatment with antiarrhythmic drugs has not proven beneficial and may even be harmful and is not therefore recommended.¹⁴

Chronic Therapy

In patients with ventricular arrhythmias, antiarrhythmic medication may be considered as adjunctive therapy in ICD recipients who experience frequent symptoms or device discharges triggered by ventricular arrhythmias. Antiarrhythmic drug therapy can also be considered for patients with high burden of PVCs or nonsustained VT that are refractory to beta-blockers and are causing significant symptoms, worsening cardiomyopathy, or interfering with cardiac resynchronization therapy.¹

It is important to understand that, with the exception of beta-blocker therapy, no antiarrhythmic medication has been demonstrated to reduce the mortality of patients with SMVT. The significant reduction of VT episodes with antiarrhythmic drug therapy does not appear to translate into a mortality benefit. These observations suggest that recurrent VT in ICD patients might be only a marker of advanced disease that cannot be modified by prevention of recurrent VT. In addition, antiarrhythmic drugs are of modest efficacy and have important side effects, with a potential for increase in all-cause mortality with amiodarone. Therefore the goal of antiarrhythmic drugs in VT patients is to improve quality of life in symptomatic patients or those with frequent VT leading to ICD shocks.³⁷

There are three main indications for antiarrhythmic drug therapy along with an ICD: (1) to reduce the frequency of ventricular arrhythmias in patients with unacceptably frequent ICD therapies; (2) to reduce the rate of VT so that it is better tolerated hemodynamically and more amenable to pace termination or low-energy cardioversion; and (3) to suppress other arrhythmias (e.g., sinus tachycardia, atrial fibrillation [AF], nonsustained VT) that cause symptoms or interfere with ICD function or cause inappropriate discharges.¹

When ICD patients need drugs because of frequent shocks, the weight of evidence supports optimizing beta-blocker therapy. When long-term antiarrhythmic therapy is required, amiodarone and sotalol are the most commonly used drugs. Sotalol is less effective than amiodarone, but given its more favorable adverse effect profile than amiodarone, it may be a better first-line antiarrhythmic medication in appropriate patients. However, sotalol is generally avoided in patients with a severely reduced LVEF due to its negative inotropic effects and the risk of torsades de pointes.

For refractory VT, escalating doses of amiodarone (300 or 400 mg/day) or adding a class I (mexiletine) or class III (dofetilide) agent to amiodarone therapy may be considered. It may be appropriate to attempt gradual withdrawal of antiarrhythmic medications in patients who remain free of arrhythmic events over a reasonable period of follow-up (12 to 18 months).^{38,39} For patients who cannot tolerate amiodarone or sotalol, dofetilide has been suggested as an alternative. Azimilide can be effective with fewer side effects (except torsades de pointes), but is not approved by the US Food and Drug Administration

or European authorities, and experience is limited. No comparative data for amiodarone and azimilide are available. Class IC medications (flecainide and propafenone) are not recommended in patients with prior MI.³⁷

Although some reports suggested the early use of antiarrhythmic drugs (after the first episode of VT or after a single ICD shock), this approach is likely to overtreat a large group of patients who will never have an ICD intervention but are exposed to drug side effects; or the drug may elicit an ICD intervention due to proarrhythmia. At this point, the decision as to when to start adjuvant antiarrhythmic drug therapy in patients who receive an ICD for secondary prevention should be individualized, with the expectation that well-designed therapy can reduce ICD shocks and improve quality of life.

The influence of ischemia in the genesis of SMVT in patients with chronic stable CAD remains controversial. Data suggest that coronary revascularization alone is unlikely to significantly reduce the risk of recurrence of VT in post-MI patients with SMVT in the absence of an acute coronary syndrome. On the contrary, revascularization might be beneficial in patients presenting with VF, polymorphic VT, or exercise-induced arrhythmias associated with ischemia.^{39,40}

Prophylactic antiarrhythmic drug therapy has no proven beneficial effects, and can be harmful in CAD patients, even those deemed to be at high risk of SCD.¹⁴ Similarly, antiarrhythmic drugs are not recommended in patients with asymptomatic PVCs or nonsustained VT for the purpose of arrhythmia suppression.

Implantable Cardioverter-Defibrillator Secondary Prevention

ICD therapy has a proven mortality benefit among patients with structural heart disease and a history of VT or VF, with a 7% absolute reduction and a 25% relative reduction in all-cause mortality (as compared with amiodarone therapy), due entirely to a 50% reduction in arrhythmic death.^{24,39,41}

Implantation of an ICD is recommended for secondary prevention in patients with prior cardiac arrest or sustained VT, even when systolic function is normal, and even in patients undergoing successful catheter ablation of the VT or responding to antiarrhythmic therapy, because the latter two approaches do not sufficiently reduce residual risk of SCD (Table 22.2; Fig. 22.2). Also, ICD implantation is recommended in patients with syncope and inducible SMVT even if they do not otherwise meet criteria for primary prevention. Importantly, in patients with incessant VT or VF, an ICD should not be implanted until sufficient arrhythmia is achieved to prevent repeated ICD shocks.^{1,39}

Although one report has questioned the benefit from an ICD compared with pharmacological therapy in patients with VT and LVEF exceeding 40%, the guidelines did not stratify recommendations based on the LVEF. This seems appropriate for two reasons: the prognostic importance of the LVEF was based on subset analysis and, given the current ease of ICD implantation, the potential adverse consequences of choosing a possibly less effective therapy are too great.

Sustained VT or VF occurring within the first 24 to 48 hours of an uncomplicated acute MI are usually considered to be a result of a transient, reversible arrhythmogenic event caused by acute ischemia rather than a permanent arrhythmogenic substrate; hence, they are thought to be relatively benign and do not predict an increased risk for recurrent arrhythmic events in patients who are successfully revascularized. Early ICD implantation is not recommended in those patients unless coronary revascularization is not possible and there is evidence of significant preexisting LV dysfunction.¹⁴ On the other hand, ICD implantation is recommended for all patients who develop sustained VT or VF beyond the first 48 hours following acute MI or in the context of a complicated MI, which are considered indicators of

TABLE 22.2 AHA/ACC/HRS Recommendations for Prevention of Sudden Cardiac Death in Patients With Ischemic Heart Disease

Secondary Prevention	
• In patients with ischemic heart disease, who either survive SCA due to VT/VF or experience hemodynamically unstable VT or stable VT not due to reversible causes, an ICD is recommended if meaningful survival greater than 1 year is expected.	Class I
• In patients with ischemic heart disease and unexplained syncope who have inducible sustained monomorphic VT on EP study, an ICD is recommended if meaningful survival of greater than 1 year is expected.	Class I
Primary Prevention	
• In patients with LVEF of 35% or less that is due to ischemic heart disease who are at least 40 days post MI and at least 90 days postrevascularization, and with NYHA class II or III HF despite GDMT, an ICD is recommended if meaningful survival of greater than 1 year is expected.	Class I
• In patients with LVEF of 30% or less that is due to ischemic heart disease who are at least 40 days post MI and at least 90 days postrevascularization, and with NYHA class I HF despite GDMT, an ICD is recommended if meaningful survival of greater than 1 year is expected.	Class I
• In patients with NSVT due to prior MI, LVEF of 40% or less and inducible sustained VT or VF at EP study, an ICD is recommended if meaningful survival of greater than 1 year is expected.	Class I
• In nonhospitalized patients with NYHA class IV symptoms who are candidates for cardiac transplantation or an LVAD, an ICD is reasonable if meaningful survival of greater than 1 year is expected.	Class IIa
• An ICD is not indicated for NYHA class IV patients with medication-refractory HF who are not also candidates for cardiac transplantation, an LVAD, or a CRT defibrillator that incorporates both pacing and defibrillation capabilities.	Class III

AHA, American Heart Association; ACC, American College of Cardiology; CRT, cardiac resynchronization therapy; EP, electrophysiological; GDMT, guideline-directed management and therapy; HF, heart failure; HRS, Heart Rhythm Society; ICD, implantable cardioverter-defibrillator; LVAD, left ventricular assist device; LVEF, left ventricular ejection fraction; MI, myocardial infarction; NSVT, nonsustained ventricular tachycardia; NYHA, New York Heart Association; SCA, sudden cardiac arrest; VF, ventricular fibrillation; VT, ventricular tachycardia.

From Al-Khatib SM, Stevenson WG, Ackerman MJ, et al. 2017 AHA/ACC/HRS guideline for management of patients with ventricular arrhythmias and the prevention of sudden cardiac death: a report of the American College of Cardiology/American Heart Association Task Force on Clinical Practice Guidelines and the Heart Rhythm Society. *Heart Rhythm*. 2017 Oct 26. [Epub ahead of print]

worse long-term prognosis and high risk of SCD, even after successful revascularization. Early ICD implantation (or the temporary use of a wearable cardioverter-defibrillator) is usually recommended in those patients. However, it is worth noting that the temporal cutoff between “early” and “late” is not clear. Many investigators prefer a 24-hour (rather than 48-hour) cutoff.^{24,42}

Importantly, prolonged episodes of sustained monomorphic VT or VF may be associated with a rise of cardiac enzymes related to myocardial supply-demand mismatch rather than a primary coronary event. Therefore, in patients with CAD who present with sustained VT or VF and modest elevations of cardiac enzymes, it should not be assumed that a new MI was the cause of the VT or VF. If clinical evaluation for ischemia does not support the occurrence of a new MI, these patients should be treated similarly to patients who have sustained VT and no documented rise in cardiac enzymes, including ICD implantation for secondary prevention.²⁴

Although ICDs improve overall survival, they do not eliminate the substrate responsible for sustained arrhythmias and therefore do not prevent arrhythmias. Furthermore, ICD shocks, both appropriate and inappropriate, are associated with increased mortality and reduced quality of life. To reduce the risk of these events, ICD detection criteria and therapies should be programmed to minimize inappropriate shocks, prevent shocks for potentially self-terminating VTs, and favor anti-tachycardia pacing therapies when feasible.⁴³ Long VT detection intervals prior to the delivery of ICD therapies and rapid VF detection rates reduce shocks and improve mortality in patients receiving an ICD for primary prophylaxis. The value of programming a long VT detection time in patients with a history of sustained VT or VF is less certain.¹ Furthermore, although device programming can reduce the frequency of ICD shocks, it does not reduce the risk of VT recurrence or eliminate the symptoms associated with the arrhythmia, such as palpitations, dizziness, and syncope.³⁷

Primary Prevention

Current guidelines recommend prophylactic ICD implantation in patients with prior MI and reduced LVEF (less than 35%) who are on optimal medical management (see Table 22.2; Fig. 22.3). These recommendations are based on the fundamental relationship that exists between reduced LVEF and cardiovascular mortality and the findings of MADIT II and SCD-HeFT. Both MADIT II and SCD-HeFT clearly demonstrated a mortality benefit from prophylactic ICD therapy in patients with a history of MI and severely reduced LVEF ($\leq 30\%$ and $\leq 35\%$, respectively). However, the absolute mortality reduction in these trials was modest: 5.6% over 27 months in MADIT II and 7.3% over 60 months in SCD-HeFT. Fewer than one in five ICD recipients in MADIT II and SCD-HeFT received appropriate ICD therapies over average follow-up periods of 20 and 60 months, respectively. Because appropriate ICD therapies overestimate the mortality benefit of ICD therapy by at least twofold, fewer than 1 in 10 patients who receive a prophylactic ICD for an LVEF of 35% or less post MI are likely to receive a survival benefit in the near term. In two meta-analyses of these trials, ICD therapy in high-risk CAD patients resulted in a net risk reduction for total mortality of 20% to 30%.^{24,39,41,44}

EP testing appears most useful as an adjunct study in patients having equivocal results after noninvasive testing and in whom the potential benefit of ICD therapy is uncertain. Examples include patients with remote MI, nonsustained VT, and an LVEF between 30% and 40%, as suggested by the most recent guidelines, or in combination with other clinical risk factors or symptoms suggestive of VTs including palpitations, presyncope, and syncope. Patients with CAD who are found to have inducible monomorphic VT during programmed stimulation should be treated for the prevention of SCD. The mode of stimulation (burst pacing, single, or double VESs vs. triple VESs) of sustained VT does not influence prognosis and should not influence treatment decisions.

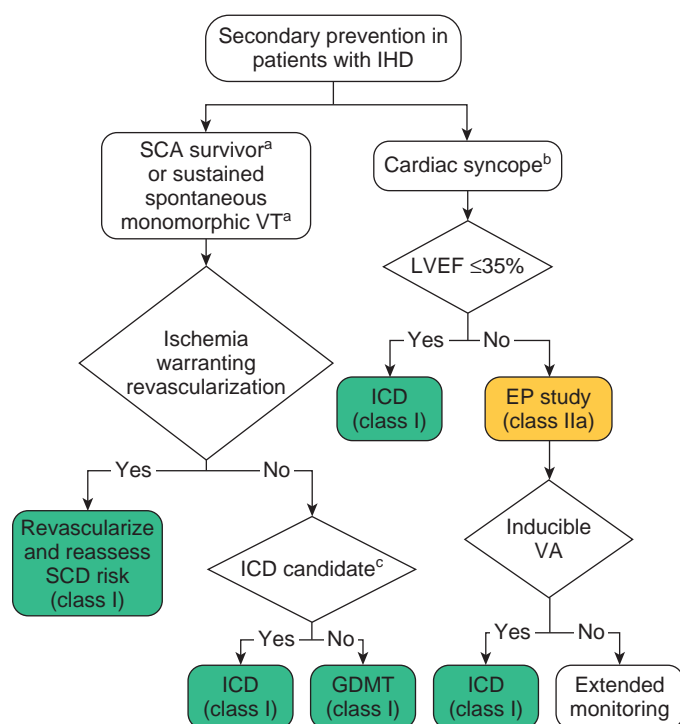


Fig. 22.2 AHA/ACC/HRS Recommendations for Secondary Prevention of Sudden Cardiac Death (SCD) in Patients With Ischemic Heart Disease (IHD). ^aExclude reversible causes. ^bHistory consistent with an arrhythmic etiology for syncope. ^cICD candidacy as determined by functional status, life expectancy, or patient preference. EP, Electrophysiological; GDMT, guideline-directed management and therapy; ICD, implantable cardioverter-defibrillator; LVEF, left ventricular ejection fraction; SCA, sudden cardiac arrest; VA, ventriculoatrial; VT, ventricular tachycardia. (From Al-Khatib, SM, Stevenson WG, Ackerman MJ, et al. 2017 AHA/ACC/HRS guideline for management of patients with ventricular arrhythmias and the prevention of sudden cardiac death: a report of the American College of Cardiology/American Heart Association Task Force on Clinical Practice Guidelines and the Heart Rhythm Society. *Heart Rhythm*. 2017 Oct 26. [Epub ahead of print])

In the acute to subacute period after MI, the arrhythmia substrate is dynamic. LV function can improve in up to 70% of patients. Although the risk of SCD is highest in the first month after MI, there is currently no reliable risk stratification strategy that can guide early prophylactic ICD implantation. In fact, primary prevention trials with ICD have failed to show a reduction in all-cause mortality (despite a decrease in arrhythmic mortality) in early post-MI patients identified on the basis of the current risk stratifiers. SCD in this period may occur from not only arrhythmic, but also nonarrhythmic (mechanical) causes, limiting ICD benefits. Accordingly, the current published guidelines recommend avoiding ICD implantations in the early post-MI phase. Therefore, in the early post-MI period, medical therapy and coronary revascularization, when feasible, should be optimized. The LVEF should then be measured at least 40 days after the MI and, if the LVEF remains at 35% or less, the patient should be considered for ICD implantation. Whether the 40-day waiting period still applies in patients with acute MI who have known LV dysfunction and who have previously satisfied criteria for implantation of a primary prevention ICD is still controversial. Because those patients have an increased rate of nonarrhythmic mortality that is unlikely to be significantly impacted by early ICD implantation, some investigators recommend implementing the 40-day waiting period in these patients.^{15,24,42}

It is important to understand, however, that the mere presence of elevated cardiac enzymes does not establish a diagnosis of acute MI. If

clinical evaluation for ischemia does not support the occurrence of a new MI, early implantation of an ICD is recommended in patients who otherwise would be candidates for implantation on the basis of primary prevention or secondary prevention criteria. The requirement to delay ICD implantation for 40 days after presentation is not applicable if a clear diagnosis of acute MI is not established. This mandatory waiting period should not be imposed on patients who would otherwise qualify for an ICD for either primary or secondary prevention.^{15,24}

Similarly, the waiting period may not be mandated in patients who, within 40 days of an MI, require a nonelective permanent pacemaker implantation or present with syncope that is thought to be due to ventricular tachyarrhythmia (by clinical history, documented nonsustained ventricular tachycardia [NSVT], or EP study), who would also meet primary prevention criteria for implantation of an ICD, and recovery of LV function is uncertain or not expected. Early ICD implantation with appropriately selected pacing capabilities is recommended in these patients.¹⁵

In addition, improvement of LVEF of 5% to 6% or more can be observed in 15% to 65% of patients following coronary revascularization. Therefore LVEF should be reevaluated 6 to 12 weeks after coronary revascularization to assess potential indications for primary prevention ICD implantation. As noted previously, the waiting period may not be mandatory for patients in whom recovery of LV function is uncertain or not expected and either require a nonelective permanent pacemaker implantation or present with syncope that is thought to be due to ventricular tachyarrhythmia (by clinical history, documented NSVT, or EP study).^{14,15}

Wearable cardioverter-defibrillators effectively terminate VT and VF and are a potential therapeutic option to bridge patients from hospital discharge until follow-up evaluation of LV function to assess the value of ICD for primary prevention of SCD. The wearable external defibrillator vest can provide protection from SCD during the early period after MI until arrhythmic risk may be reduced after improvement in LVEF or until ICD implantation can be performed for those with persistently reduced LVEF.³ In one report, the risk of VT/VF was highest in the first month of wearable cardioverter-defibrillator use, with a median time until first treatment of 9 days, and 1.4% of patients were resuscitated by the external defibrillator in the early weeks post MI. Of treated patients, 75% received therapy in the first month of use, and 96% in the first 3 months of use.^{45,46} However, whether wearable external defibrillators improve total mortality is uncertain. No randomized study has validated the role of wearable cardioverter-defibrillators in preventing early SCD compared to optimal medical therapy alone. A wearable cardioverter-defibrillator would not be expected to offer a mortality benefit where an ICD does not except by avoiding early deaths related to ICD implantation (estimated at only 0.2%). Total mortality rate is expected to remain high (based on the previous ICD trial results) because both ICDs and wearable external defibrillators will favorably impact arrhythmic causes of death, but will not treat nonarrhythmic causes of mortality.^{47,48}

Catheter Ablation

Catheter ablation of post-MI VT is generally indicated as a *palliative* and *adjunctive* therapy in post-MI patients with ICD who experience frequent recurrences of VT or ICD therapies. Recurrences of VT/VF causing frequent ICD therapies (including ICD shocks) are relatively common; approximately 20% to 35% of ICD recipients for primary prevention and up to 45% of those who receive an ICD for secondary prevention will receive an appropriate shock within 3 years of implantation.

Although ICD shocks for rapid VT or VF reduces the risk of SCD by approximately 60%, the occurrence of shocks can have deleterious consequences. ICD shocks are associated with progressive heart failure

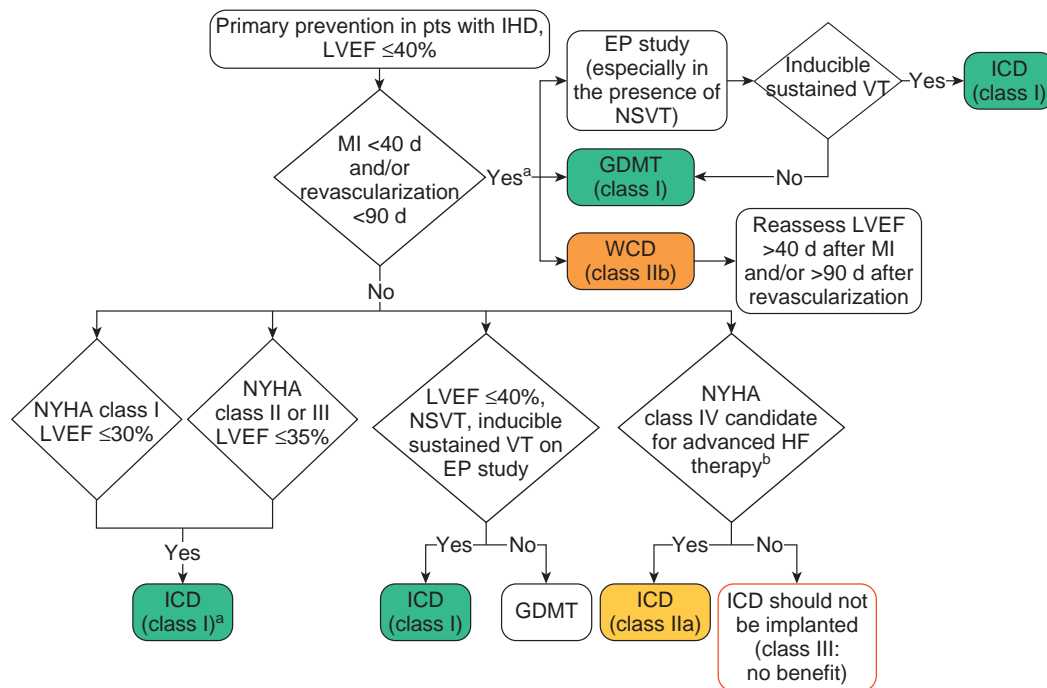


Fig. 22.3 AHA/ACC/HRS Recommendations for Primary Prevention of SCD in Patients With Ischemic Heart Disease. ^aScenarios exist for early ICD placement in select circumstances such as patients with a pacing indication or syncope. ^bAdvanced HF therapy includes CRT, cardiac transplant, and left ventricular assist device. CRT, Cardiac resynchronization therapy; EP, electrophysiological; GDMT, guideline-directed management and therapy; HF, heart failure; ICD, implantable cardioverter-defibrillator; IHD, ischemic heart disease; LVEF, left ventricular ejection fraction; MI, myocardial infarction; NSVT, nonsustained ventricular tachycardia; NYHA, New York Heart Association; pts, patients; SCD, sudden cardiac death; VT, ventricular tachycardia; WCD, wearable cardioverter-defibrillator. (From Al-Khatib, SM, Stevenson WG, Ackerman MJ, et al. 2017 AHA/ACC/HRS guideline for management of patients with ventricular arrhythmias and the prevention of sudden cardiac death: a report of the American College of Cardiology/American Heart Association Task Force on Clinical Practice Guidelines and the Heart Rhythm Society. *Heart Rhythm*. 2017 Oct 26. [Epub ahead of print])

symptoms, a significant decline in psychosocial quality of life, and a two- to fivefold increase in nonarrhythmic mortality, despite termination of the acute arrhythmic event. The incidence of appropriate shocks can be reduced by using antitachycardia pacing in the VT or VF detection zones, or with up-titration of effective medical therapies. If optimization of pharmacological therapies and device programming fails to suppress appropriate ICD shocks for VT, or when ventricular arrhythmias precipitate significant symptoms, such as angina, presyncope, syncope, or worsening heart failure, catheter ablation is recommended.^{14,49,50}

Compared to antiarrhythmic drug therapy, catheter ablation is significantly more effective in reducing the risk of VT recurrences in patients with ischemic cardiomyopathy, and has emerged to become a standard of care to prevent medically refractory ICD shocks. Successful VT ablation can minimize long-term exposure to antiarrhythmic drugs or substantially reduce their dose requirement, which can potentially improve long-term outcomes.^{50,51} However, a reduction in overall mortality has yet to be demonstrated.^{1,37}

Catheter ablation reduces VT recurrences and thereby ICD interventions by more than 75% in patients after multiple ICD shocks.⁵² However, most patients with post-MI VT have multiple types of monomorphic VTs, and elimination of all VTs often is not feasible, and because the recurrence of an ablated VT or the onset of a new VT can be fatal, RF ablation is rarely used as the sole therapy for VT. Instead, VT ablation is typically used for patients with CAD as an adjunct to an ICD. In this patient population, the incidence of ablation procedure-related death ranges from 0% to 3%, and the incidence of major complications ranges from 3.6% to 10%.¹

Catheter ablation is necessary and can be life saving in patients with electrical storm and incessant VT without any apparent correctable cause and despite adequate medical treatment. Repeated ICD shocks within a short time interval, known as an ICD “storm,” occur in 10% to 25% of patients. Accumulated evidence suggests that acute suppression of VT in an electrical storm can be achieved in up to 90% of patients. However, arrhythmic recurrences are frequent during follow-up. In the setting of incessant VT, catheter ablation is preferred over antiarrhythmic drug therapy. Catheter ablation may also be considered for patients with recurrent polymorphic VT or VF when those arrhythmias are triggered by PVCs of consistent QRS morphology. In this setting, ablation targets the arrhythmia trigger rather than the substrate.^{1,4,14}

The optimal time of catheter ablation in ICD patients (after multiple ICD interventions or before any ICD intervention) remains unclear. Current guidelines recommend considering catheter ablation for VT that recurs despite antiarrhythmic drug therapy or when antiarrhythmic drugs are not tolerated or desired (Box 22.1). In clinical practice, VT ablation is often not considered until pharmacological options have been exhausted, often after the patient has suffered substantial morbidity from recurrent episodes of VT and ICD shocks. However, recent studies suggest that catheter ablation should generally be considered early in the course treatment of post-MI VT, before escalating medication therapy, or even before initiating antiarrhythmic drug therapy in select patients. In fact, small randomized studies of treatment after the first VT episode in post-MI patients have demonstrated significantly reduced VT recurrences following ablation compared with conventional medical therapy. Interestingly, in this patient population the ablation-related mortality

BOX 22.1 Expert Consensus Recommendations on Catheter Ablation of Ventricular Tachycardia in Patients With Structural Heart Disease

Catheter Ablation Is Recommended for:

- Symptomatic SMVT, including VT terminated by an ICD, that recurs despite antiarrhythmic drug therapy or when antiarrhythmic drugs are not tolerated or not desired.
- Incessant SMVT or VT storm not due to a transient reversible cause.
- Frequent PVCs, nonsustained or sustained VT that is presumed to cause ventricular dysfunction.
- Bundle branch reentrant or interfascicular VTs.
- Recurrent sustained polymorphic VT and VF that is refractory to antiarrhythmic therapy when there is a suspected trigger that can be targeted for ablation.

Catheter Ablation Is Reasonable for:

- One or more episodes of SMVT despite therapy with one or more class I or III antiarrhythmic drugs.
- Patients with ischemic heart disease and ICD shocks for SMVT or symptomatic SMVT that is recurrent, or hemodynamically tolerated, even if they have not failed antiarrhythmic drug therapy.

Ventricular Tachycardia Catheter Ablation Is Contraindicated for:

- Patients with a mobile ventricular thrombus (epicardial ablation may be considered).
- Asymptomatic PVCs and/or nonsustained VT that are not suspected of causing or contributing to ventricular dysfunction.
- VT due to transient, reversible causes, such as acute ischemia, hyperkalemia, or drug-induced torsade de pointes.

ICD, Implantable cardioverter-defibrillator; PVCs, premature ventricular complexes; SMVT, sustained monomorphic ventricular tachycardia; VT, ventricular tachycardia; VF, ventricular fibrillation.

Modified from Al-Khatib SM, Stevenson WG, Ackerman MJ, et al. 2017 AHA/ACC/HRS guideline for management of patients with ventricular arrhythmias and the prevention of sudden cardiac death. *Heart Rhythm*. 2017 Oct 26. [Epub ahead of print]; Aliot EM, Stevenson WG, Almendral-Garrote JM, et al. EHRA/HRS expert consensus on catheter ablation of ventricular arrhythmias: developed in a partnership with the European Heart Rhythm Association (EHRA), a Registered Branch of the European Society of Cardiology (ESC), and the Heart Rhythm Society (HRS); in collaboration with the American College of Cardiology (ACC) and the American Heart Association (AHA). *Heart Rhythm*. 2009;6:886–933.

rate was 0%, and major complications occurred in 3.8% to 4.7%.^{53,54} In contrast, acute and long-term ablation success is more limited when VT ablation is performed in patients with previous MI selected after failure of prior antiarrhythmic drug therapy. Whether earlier ablation can alter the prognosis of post-MI VT and improve survival compared with comprehensive medical therapy over extended follow-up remains uncertain.^{39,55–57}

Catheter ablation also should be considered for patients with frequent PVCs or nonsustained or sustained VT that is presumed to cause ventricular dysfunction.^{14,49}

Alternative Interventional Treatment

Several interventional approaches, such as transcatheter ethanol ablation, surgical cryoablation, or percutaneous catheter ablation facilitated

by a surgically created epicardial window, can be considered for selected patients with recurrent or incessant VT in whom antiarrhythmic drug therapy and percutaneous endocardial and epicardial catheter ablation have failed or are not feasible (e.g., due to presence of pericardial adhesion or mechanical aortic and mitral valves, or proximity to coronary arteries). However, experience with these approaches is limited, and they are considered last-resort options.^{58,59}

Transcatheter ethanol ablation can be of value for intramural circuits that are refractory to endocardial-epicardial ablation techniques. This technique requires subselective cannulation of the coronary arterial branches supplying the target region. Before ethanol injection, the appropriate target can be confirmed by infusion of iced saline through the arterial lumen. Alcohol injection is performed only if iced saline successfully terminates the VT or renders it noninducible by programmed electrical stimulation.⁵⁸

An epicardial window can allow access to epicardial substrates when percutaneous epicardial access is not feasible. Surgical creation of a subxiphoid pericardial window and manual dissection with lysis of pericardial adhesions can allow catheter mapping and ablation. Surgical treatment of ventricular arrhythmias is rarely required today, but remains a viable therapeutic option for VT refractory to conventional therapies, especially patients requiring surgical coronary revascularization or aneurysm resection and LV reconstruction for refractory heart failure, or known LV thrombus.⁵⁸

ELECTROCARDIOGRAPHIC FEATURES

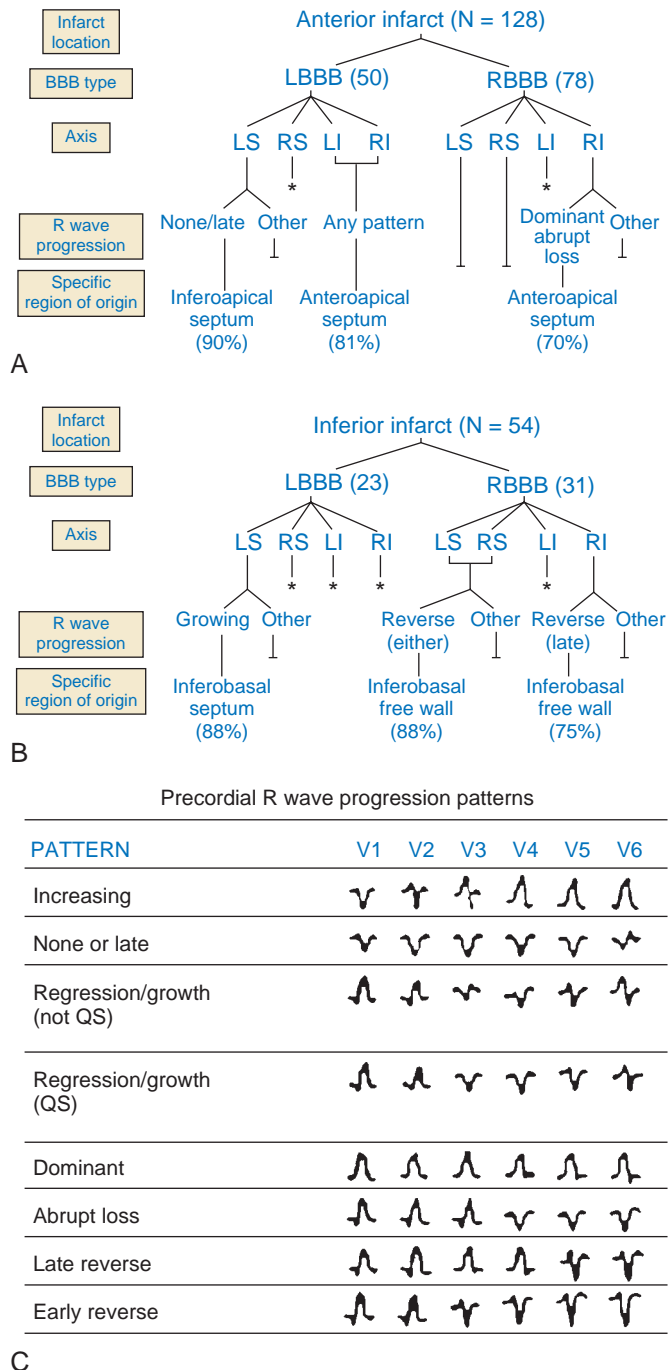
In general, QRS patterns are less accurate in localizing the “site of origin” of reentrant VTs in patients with prior MI and wall motion abnormalities than they are for focal VTs in patients with normal hearts. Nonetheless, the ECG is capable of regionalizing the VT to areas smaller than 15 to 20 cm², even in the most abnormal hearts.

The site of origin of VT is the source of electrical activity producing the VT QRS. Although this is a discrete site of impulse formation in automatic and triggered (i.e., focal) rhythms, during reentrant VT it represents the exit site from the diastolic pathway (isthmus) to the myocardium giving rise to the QRS. The pattern of ventricular activation, and hence the resultant QRS morphology, depends on how the wavefront propagates from the site of origin to the remainder of the heart; this can be totally different during VT than during pacing from the same site in NSR. It is also important to recognize that the 12-lead ECG provides information about the VT exit site from the scar border and not about the site to be targeted by ablation. Ablation of post-MI reentrant VTs targets the critical isthmus of the reentrant circuit, which can be some distance (1 to 3 cm) removed from the exit site indicated by the surface ECG. Ablation of the exit site typically fails in eliminating the tachycardia.⁶⁰

A sophisticated algorithm has been developed using eight different patterns of R wave progression in the precordium in addition to the relationship with prior anterior or inferior MI, axis deviation, and BBB pattern. This algorithm has a predictive accuracy of more than 70% for a specific QRS morphology to identify a particular endocardial region of 10 cm² or less (Fig. 22.4).⁶¹ A second algorithm that utilizes the BBB pattern on the 12-lead surface ECG and polarity in the limb leads for VT localization was found to predict the LV VT exit site region in 71% of clinical VTs without prior knowledge of infarct location (Figs. 22.5 and 22.6).⁶² More recently, an automated computerized algorithm was shown to improve the utility of the 12-lead ECG for localizing the VT exit site.^{60,63}

Electrocardiographic Clues to the Underlying Substrate

VTs arising from normal myocardium typically have rapid initial forces, whereas slurring of the initial forces is frequently seen when the VT



C

Fig. 22.4 Algorithm Correlating Region of Origin to 12-Lead Electrocardiogram of Ventricular Tachycardia (VT), Derived from the Retrospective Analysis. (A) Anterior infarct-associated VTs. (B) Inferior infarct-associated VTs. The first branch point is bundle branch block (BBB) configuration, followed by QRS axis and R wave progression. When possible, a specific region of origin is indicated. The number of VTs in each group is indicated in parentheses. A vertical line ending in an asterisk indicates inadequate numbers of VTs for analysis; a vertical line terminating in a horizontal bar indicates adequate numbers for analysis, but no specific patterns. (C) Precordial R wave progression patterns. Eight different patterns are listed, with the number of examples in parentheses. Typical R wave patterns for V₁ through V₆ are shown. I, Inferior; L, left; LBBB, left bundle branch block; R, right; RBBB, right bundle branch block; S, superior. (From Miller JM, Marchlinski FE, Buxton AE, Josephson ME. Relationship between the 12-lead electrocardiogram during ventricular tachycardia and endocardial site of origin in patients with coronary artery disease. *Circulation*. 1988;77:759–766.)

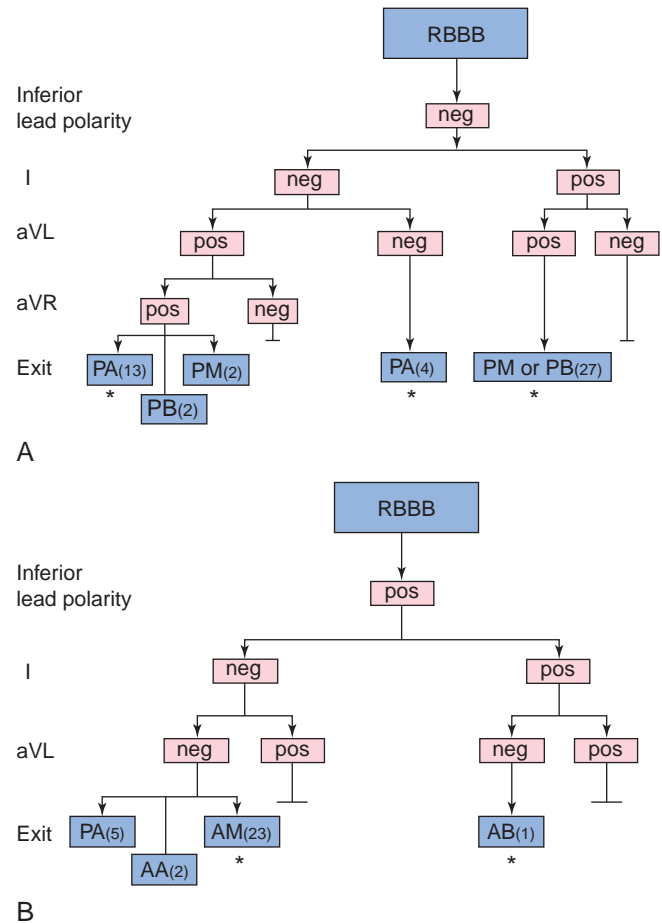


Fig. 22.5 Algorithm Correlating 12-Lead Electrocardiogram (ECG) Morphology of Right Bundle Branch Block (RBBB) Ventricular Tachycardia (VT) With Exit Site Region, Derived From Retrospective Analysis. (A) VT with negative (neg) polarity in the inferior leads. (B) VT with positive (pos) polarity in the inferior leads. A vertical line ending a horizontal bar indicates that no VT with this ECG pattern was identified. Exit sites with a positive predictive value of at least 70% are marked by asterisks. The numbers of VTs for each ECG pattern and exit site region identified in retrospective analysis are shown in parentheses. AA, Anteroapical; AB, anteroapical; AM, midanterior; PA, posteroapical; PB, posterobasal; PM, midposterior. (From Segal OR, Chow AWW, Wong T, et al. A novel algorithm for determining endocardial VT exit site from 12-lead surface ECG characteristics in human, infarct-related ventricular tachycardia. *J Cardiovasc Electrophysiol*. 2007;18:161–168.)

arises from an area of scar or from the epicardium. In addition, VTs originating from very diseased hearts usually have lower amplitude complexes than those arising in normal hearts, and the presence of notching and fractionation of the QRS can be a sign of scar tissue with resultant disrupted wavefront propagation.

Although QS complexes can be seen in a variety of disorders, the presence of qR, QR, or Qr complexes in related leads is highly suggestive of the presence of an infarct. Sometimes it is easier to recognize the presence of MI during VT than during NSR (i.e., LBBB in NSR masking an infarct).

Electrocardiographic Localization of Postinfarction Ventricular Tachycardia

QRS Duration

QRS duration is affected by the proximity of the VT origin to the septum. Post-MI VTs almost always arise in the LV or interventricular

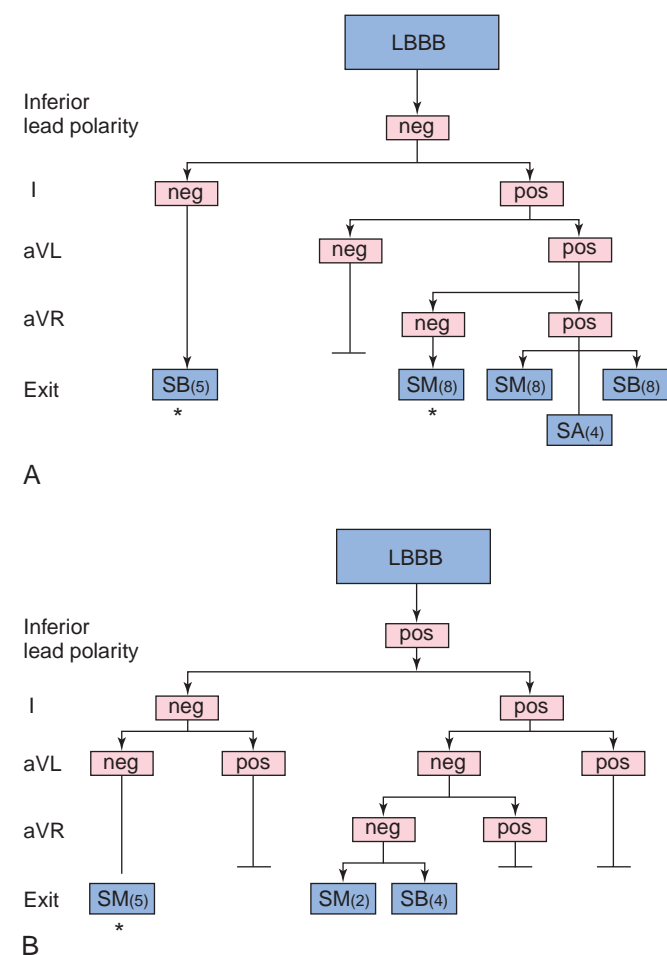


Fig. 22.6 Algorithm Correlating 12-Lead Electrocardiogram (ECG) Morphology of Left Bundle Branch Block (LBBB) Ventricular Tachycardia (VT) With Exit Site Region, Derived From Retrospective Analysis. (A) VT with negative (*neg*) polarity in the inferior leads. (B) VT with positive (*pos*) polarity in the inferior leads. A vertical line ending with a horizontal bar indicates that no VTs with this ECG pattern were identified. SA, Anteroseptal; SB, basal septum; SM, midseptum. Exit sites with a positive predictive value of at least 70% are marked by asterisks. Numbers of VTs for each ECG pattern and exit site region identified in retrospective analysis are shown in parentheses. (From Segal OR, Chow AW, Wong T, et al. A novel algorithm for determining endocardial VT exit site from 12-lead surface ECG characteristics in human, infarct-related ventricular tachycardia. *J Cardiovasc Electrophysiol*. 2007;18:161–168.)

septum. Septal VTs generally have QRS durations that are narrower than free-wall VTs because of more nearly simultaneous activation of RV and LV from a septal source, and because of earlier entry into the His-Purkinje system (HPS), which more rapidly activates the latter portion of the QRS complex. In addition, QRS width during VT is affected by the amount of myocardial disease, and is wider with poor overall ventricular conduction.⁵

QRS Axis

A right superior QRS axis suggests apical septal or apical lateral sites of origin, often demonstrating QS in leads I, II, and III and QS or rS in leads V₅ and V₆. A right inferior axis suggests a high basal origin (high LV septum, or high lateral LV). A left inferior axis is occasionally associated with VTs arising from the top of the LV septum. Sometimes, the QRS axis is inappropriate for the exit site. This almost always occurs with large apical infarcts. Typically, discrepan-

cies occur in VTs with LBBB or RBBB with a right or left superior axis. Such discrepancies can be related to abnormalities of conduction out of the area of the reentrant circuit toward the rest of the myocardium.

Bundle Branch Block Pattern

Post-MI VTs with RBBB patterns always arise in the LV, and VTs with LBBB patterns almost always arise in or adjacent to the LV septum. Therefore LBBB patterns, which all cluster on or adjacent to the septum, have a higher predictive accuracy (regardless of the presence of anterior vs. inferior MI) than RBBB patterns, which could be septal or located on the free wall. Most VTs with RBBB patterns associated with inferior MI are clustered in a small region, but are more widely disparate with anterior MI (Figs. 22.7–22.9).⁵

Precordial Concordance

VTs with positive concordance in all precordial leads arise only at the base of the heart (left ventricular outflow tract, along the mitral or aortic valves, or in the basal septum), whereas a negative concordance is observed only in VTs originating near the apical septum, most commonly seen with anteroseptal MI.

Presence of QS Complexes

The presence of a QS complex in any lead suggests that the wavefront is propagating away from that site. Therefore QS complexes in the inferior leads suggest that the activation is originating in the inferior wall, QS complexes in leads V₂ to V₄ suggest anterior wall origin, QS complexes in leads V₃ to V₅ suggest an apical location, and QS complexes in leads V₅ and V₆ suggest a lateral wall exit. The presence of Q waves in leads I, V₁, V₂, and V₆ is seen in VTs with an RBBB pattern originating near the apex, but not those originating in the inferobasal parts of the LV. R waves in leads I, V₁, V₂, and V₆ are specific for VTs with an RBBB or LBBB pattern of posterior origin. In addition, the presence of Q waves in leads I and V₆ in VTs with an LBBB pattern is seen with apical septal locations, whereas the presence of R waves in leads I and V₆ is associated with inferobasal septal locations.⁵

Inferior Myocardial Infarction Ventricular Tachycardias

With inferior MI, most VTs have basal exit sites and thus have relatively preserved precordial R waves (that usually are present in leads V₂ to V₄ with the persistence of an r or R wave through lead V₆). However, more extensive inferior MIs can result in apical exits (Fig. 22.10).⁵

VT with LBBB morphology. VTs with LBBB (especially when left axis deviation is present) have a characteristic location at the inferobasal septum (see Fig. 22.8). As the VT axis shifts to a more normal axis, the exit site moves higher up along the septum. Rarely, inferior MI VTs can have exit sites as high as the aortic valve along the septum. Very rarely, the VT can only be ablated from the RV.⁵

VT with RBBB morphology. In VTs with RBBB, the R waves can persist across the precordium (positive concordance). When the VT originates near the posterior basal septum and when it arises more laterally (or posteriorly), there can be a decrease in the R wave amplitude across the precordium because the infarct can extend to the posterolateral areas (see Fig. 22.7). Left axis deviation is seen in inferior MI VTs when the exit site is near the septum. As the VT exit moves from the midline toward the lateral (i.e., posterior) wall, the QRS axis becomes directed more rightward or superior.⁵

The mitral isthmus (between the mitral annulus and inferior infarct scar) contains a critical region of slow conduction in some patients with VT following inferior MI, providing a vulnerable and anatomically localized target for catheter ablation. This critical zone of slow conduction is activated parallel to the mitral annulus in either direction, resulting in two distinct QRS configurations not seen in VTs arising from other

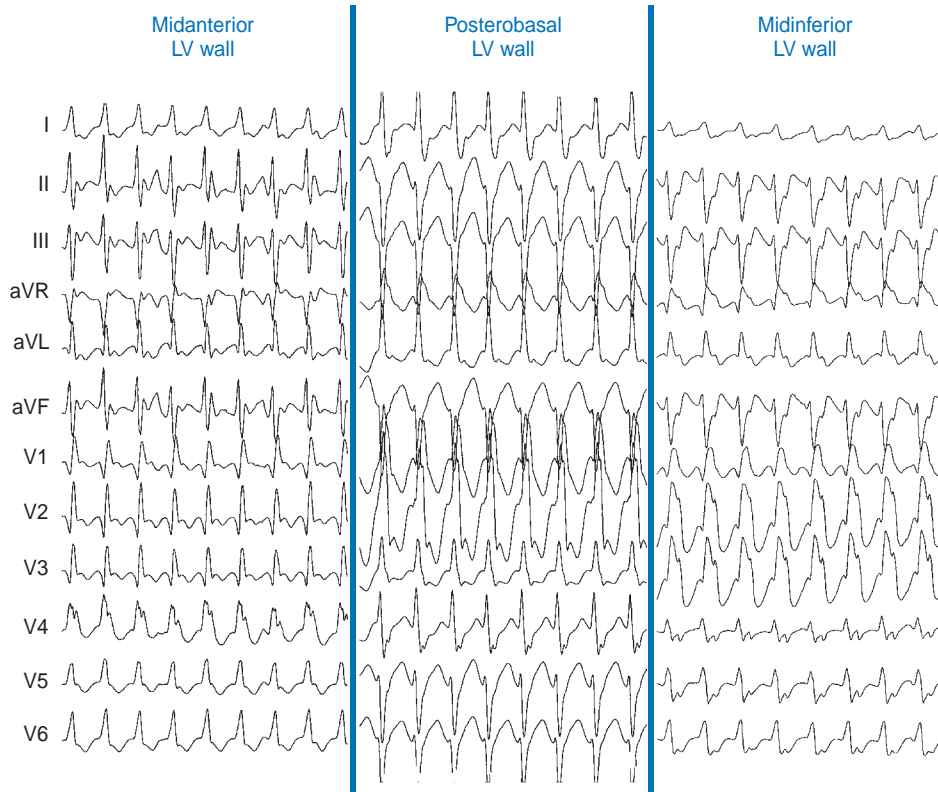


Fig. 22.7 Surface Electrocardiogram of Sustained Monomorphic Ventricular Tachycardia With Right Bundle Branch Block (RBBB) Pattern. *Left panel*, Ventricular tachycardia (VT) with RBBB pattern and normal axis in a patient with prior anterior myocardial infarction (MI). The site of origin was mapped to the midanterior left ventricular (LV) wall. Note the qR pattern in leads V₁ to V₃, consistent with anterior infarct. *Middle panel*, VT with RBBB pattern and left superior axis in a patient with prior inferior MI. The site of origin was mapped to the posterobasal LV free wall. *Right panel*, VT with RBBB pattern and left superior axis in a patient with prior inferior MI. The site of origin was mapped to the midinferior LV wall.

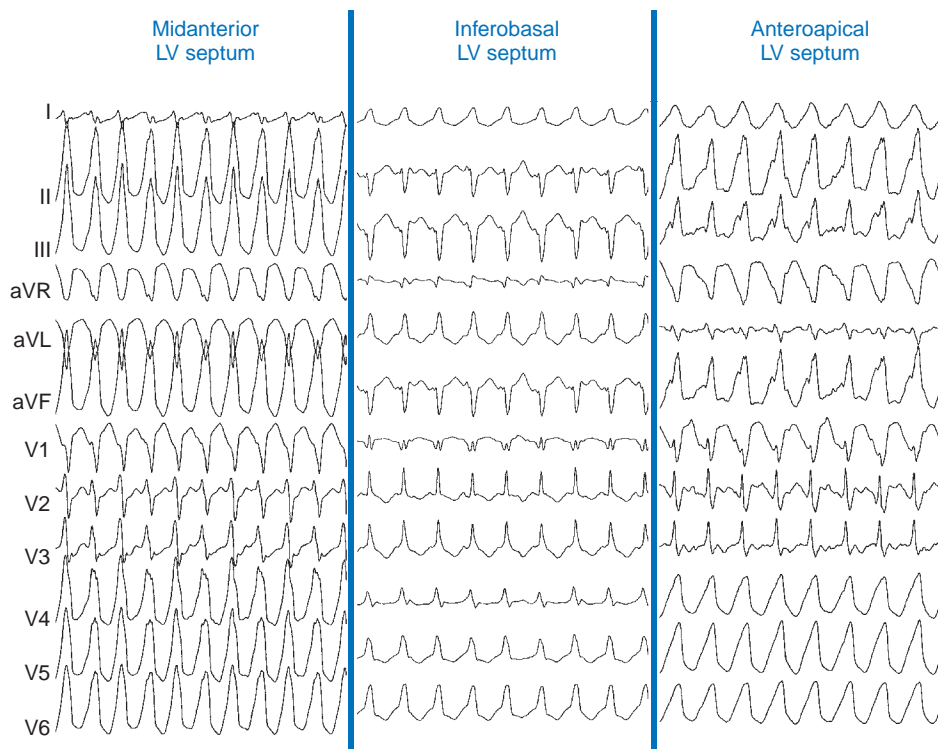


Fig. 22.8 Surface Electrocardiogram of Sustained Monomorphic Ventricular Tachycardia With Left Bundle Branch Block (LBBB) Pattern. *Left panel*, Ventricular tachycardia (VT) with LBBB pattern and right inferior axis in a patient with prior anterior myocardial infarction (MI). The site of origin was mapped to the midanterior left ventricular (LV) septum. *Middle panel*, VT with LBBB pattern and left superior axis in a patient with prior inferior MI. The site of origin was mapped to the inferobasal LV septum. *Right panel*, VT with LBBB pattern and left inferior axis in a patient with prior anterior MI. The site of origin was mapped to the anteroapical LV septum.

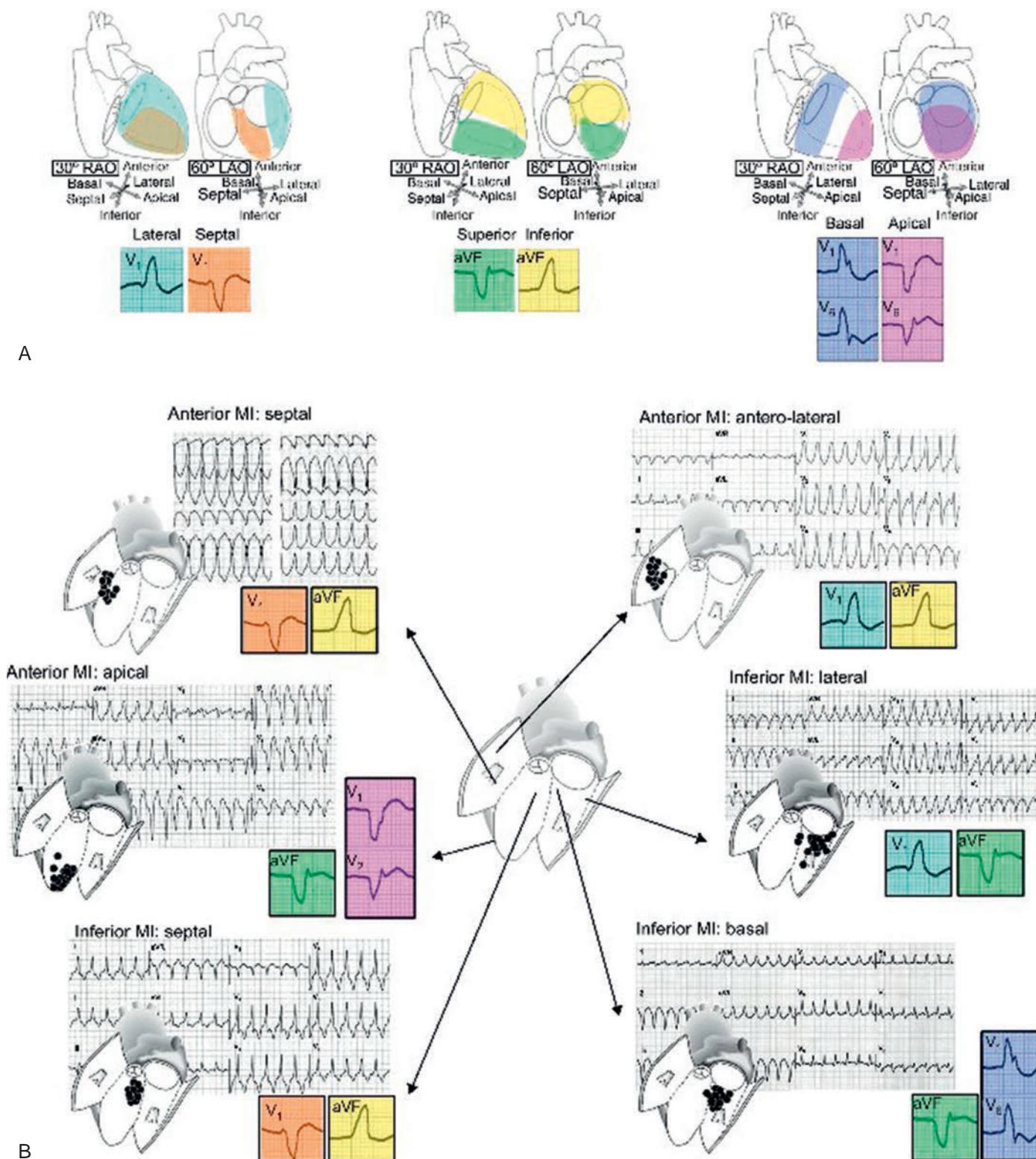


Fig. 22.9 Electrocardiographic Location of Ventricular Tachycardia (VT) Origin. (A) Location should be assessed based on three axes: septal/lateral, superior/inferior, and basal/apical. (B) Examples of VTs from different locations arising from scars of anterior or inferior myocardial infarction (MI). Although complete electrocardiographic assessment requires analysis of all three axes, only some representative leads essential for the diagnosis in each case are shown in the colored squares. LAO, Left anterior oblique; RAO, right anterior oblique. (From Benito B, Josephson ME. Ventricular tachycardia in coronary artery disease. *Rev Española Cardiol. [English ed.]*. 2012;65:939–955.)

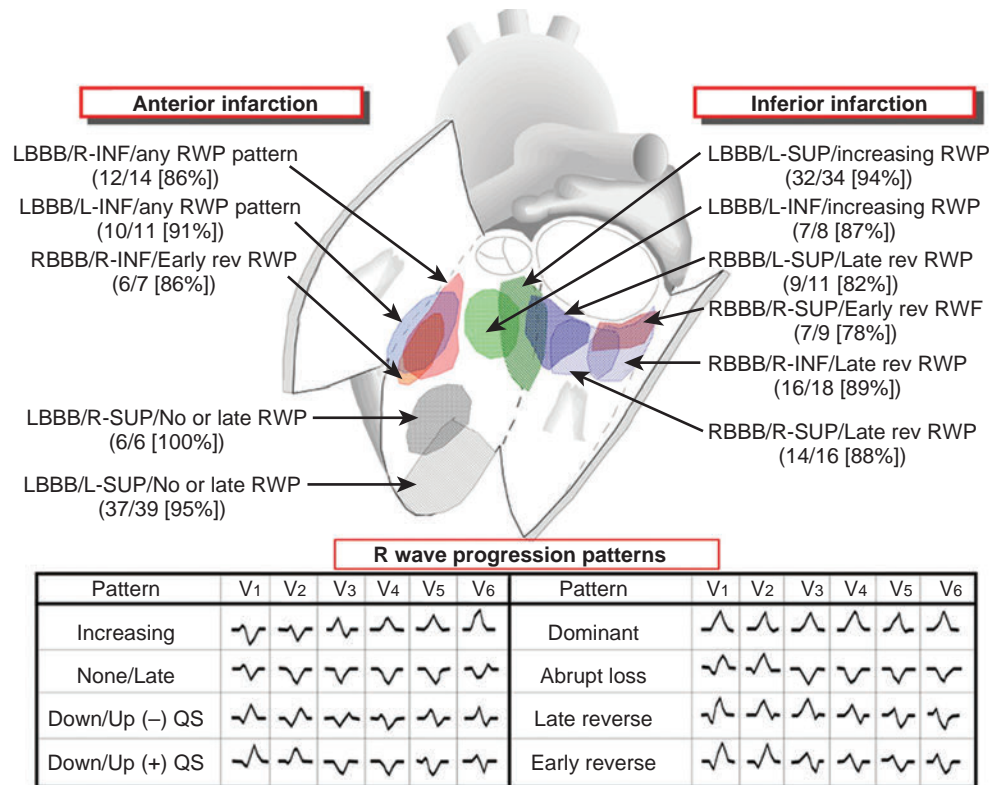


Fig. 22.10 Scheme of Regions of Ventricular Tachycardia Exit Sites in Postinfarction Patients. *INF*, inferior axis; *L*, left; *LBBB*, left bundle branch block; *R*, right; *RBBB*, right bundle branch block; *RWP*, precordial R-wave progression pattern (diagrammed in table at bottom); *SUP*, superior axis. (From Miller JM, Scherschel JA. Catheter ablation of ventricular tachycardia: skill versus technology. *Heart Rhythm*. 2009;6:S86–S90, with permission.)

sites: LBBB pattern (rS in lead V₁, R in lead V₆) with left superior axis, and RBBB pattern (R in lead V₁, QS in lead V₆) and right superior axis.⁵

Anterior Myocardial Infarction Ventricular Tachycardias

Anterior MIs are usually associated with more extensive myocardial damage. Therefore the accuracy of the ECG in localizing the origin of VTs associated with anterior MI is less than in those with inferior MI.⁵

VT with LBBB morphology. VTs with an LBBB pattern and left axis deviation usually originate from the inferoapical septum, but occasionally there is a discrepancy, with the exit site being more superior than expected for the QRS axis. LBBB morphology VTs with left superior axis usually exit from the apical septum. However, LBBB VTs associated with large anteroseptal MIs can present with QS complexes across the precordium (i.e., negative precordial concordance), and they are always associated with a Q wave in leads I and aVL. If an R wave is seen in lead V₁ along with the Q wave in lead aVL, the location of the exit site is more posterior on the septum, closer to the middle third (see Fig. 22.8). VTs with LBBB and right inferior axis generally exit from the superior midseptal aspect of the anterior scar, but occasionally can exit just off the septum (see Fig. 22.10).⁵

VT with RBBB morphology. RBBB VTs originating from the LV apex usually have a right and superior axis. Lead V₁ usually has a qR or, occasionally, a monophasic R wave, but there is almost always a QS or QR complex in leads V₂, V₃, and/or V₄. More commonly, when there are QS complexes in leads I, II, and III, there are also QS complexes across the precordium from lead V₂ through V₆.

VTs with RBBB and right inferior axis can exit superiorly on the septum but also can exit from the superolateral regions of the scar

across the apex on the free wall. In both cases, there is a negative deflection in leads aVR and aVL, and the QS ratio in aVR and aVL can help distinguish these entities. Generally, VTs with LBBB or RBBB patterns and a marked inferior right axis arise superiorly on what is usually the edge of an anterior aneurysm.⁵

The most difficult VTs to localize are VTs with RBBB and right superior axis associated with anterior MI. QS complexes in the lateral leads (V₄ to V₆) reflect an origin near the apex, regardless of whether it is septal or lateral. It is almost impossible to distinguish VTs arising from the apical septum and the apical free wall based on the ECG alone. It is only when the VT location moves more posterolaterally that a difference can be appreciated as the R wave in lead aVR becomes dominant over the R wave in lead aVL. This is usually associated with a large apical aneurysm, but occasionally can also be seen with a posterolateral MI.⁵

High Posterolateral Myocardial Infarction Ventricular Tachycardias

VTs associated with high posterior MI (left circumflex artery territory) are characterized by a prominent R wave in leads V₁ to V₄ and right inferior axis.

Epicardial Ventricular Tachycardias

Epicardial VT exits are uncommon in post-MI VT because of the subendocardial nature of the underlying substrate. With all other factors being equal, an epicardial origin of ventricular activation widens the initial part of the QRS complex (pseudo-delta wave). When the initial activation starts in the endocardium, rapid depolarization of the ventricles occurs along the specialized conducting system, resulting in a

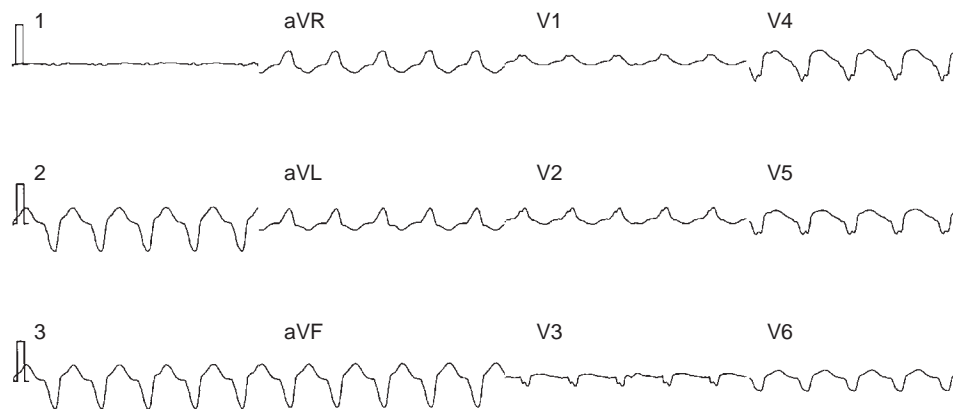


Fig. 22.11 Electrocardiogram of Post-Myocardial Infarction Ventricular Tachycardia That Required Epicardial Ablation. Note delayed QRS upstroke in V_2 and delayed S wave downstroke (pseudo-delta wave) and long RS interval in V_3 and V_4 .

relatively narrower QRS on the surface ECG and the absence of a pseudo-delta wave. In contrast, when the initial ventricular activation occurs in the epicardium, the intramyocardial conduction delay produces a slurred initial part of the QRS complex.⁵

Several ECG findings suggest an epicardial origin of the LV VT with an RBBB pattern, and all generally rely on the late engagement of rapidly conducting His-Purkinje fibers by tachycardia circuit exits on the epicardium, including the presence of a pseudo-delta wave, very wide QRS complex (duration ≥ 200 milliseconds), long R wave peak time in lead V_2 , and shortest RS complex duration in any precordial lead longer than 120 milliseconds (Fig. 22.11). However, the proposed 12-lead ECG features for differentiation of epicardial versus endocardial VT exit sites were assessed in patients without MI, and their utility for localization of post-MI VTs has not been validated. ECG criteria for identifying an epicardial origin of VT appear to be region and substrate specific. In fact, in a more recent study, these ECG characteristics failed to reliably identify post-MI VTs requiring epicardial ablation. Slow initial forces can be present during tachycardia at the MI scar region and, hence, not specific for epicardial origins. Furthermore, the presence of typical Q waves in the VT ECGs of patients with previous MI precludes the use of morphological ECG criteria, and when present in the precordial leads, Q waves can interfere with the measurement of all interval criteria. It is also important to note that the VT 12-lead ECG provides information about the VT exit site from the scar border, which is generally not the ablation target. In post-MI VT, the critical isthmus constitutes the target for ablation; this isthmus can be complex, and can have an endocardial and epicardial trajectory permitting successful ablation from the endocardium (especially in the presence of wall thinning) even in a VT with an epicardial exit. Therefore endocardial mapping should be the first approach to catheter ablation for VTs in patients with ischemic heart disease, even when the surface ECG suggests an epicardial origin of the tachycardia.^{5,60,64,65}

ELECTROPHYSIOLOGICAL TESTING

Induction of Tachycardia

Recommended Stimulation Protocols

For evaluation of ventricular arrhythmias, multipolar catheters are typically positioned in the high RA, the HB position, and the RV apex. Recording the His potential during VT is important to differentiate BBR VT from myocardial VT. The most commonly used stimulation protocol applies pacing output at twice the diastolic threshold current

and a pulse width of 1 to 2 milliseconds. Single VESs during NSR and at pacing drive cycle lengths (CLs) of 600 and 400 milliseconds are delivered, first from the RV apex and then from the right ventricular outflow tract (RVOT). The prematurity of extrastimuli is increased until refractoriness or induction of sustained VT is achieved. Long-short cycle sequences may be tested. If these measures fail to induce VT, double and then triple VESs are used in the same manner. Because a VES with a very short coupling interval is more likely to induce VF as opposed to monomorphic VT, it may be reasonable to limit the prematurity of the VESs to a minimum of 180 milliseconds when studying patients for whom only inducible SMVT would be considered a positive endpoint. If VT still cannot be induced, rapid ventricular pacing is started at a CL of 400 milliseconds, gradually decreasing the pacing cycle length (PCL) until 1:1 ventricular capture is lost or a PCL of 220 milliseconds is reached. Repeating the protocol at other pacing drive CLs, at other RV or LV stimulation sites, or after administration of isoproterenol or procainamide is then attempted.⁶⁶

An alternative stimulation protocol uses a shorter pacing drive CL (350 milliseconds) and a reverse order of the pacing drive CL (i.e., starting the stimulation protocol at 350, then 400, and then 600 milliseconds). This *accelerated protocol* has been shown in one report to reduce the number of protocol steps and duration of time required to induce monomorphic VT by an average of more than 50% and improves the specificity of programmed electrical stimulation without impairing the yield of monomorphic VT.⁶⁷

Another proposed stimulation protocol exclusively uses four VESs; at no point are one, two, or three VESs used. At each basic drive train PCL, programmed electrical stimulation is initiated with coupling intervals of 290, 280, 270, and 260 milliseconds for the first through fourth VES. The coupling intervals of the VESs are then shortened simultaneously in 10-millisecond steps until S_2 (the first VES) falls during the refractory period or a 200-millisecond coupling interval is reached. If S_2 is refractory at 290 milliseconds, all extrastimuli are lengthened by 30 milliseconds, and programmed electrical stimulation is then initiated. This *six-step protocol* was tested in a single report and was shown to improve the specificity and efficiency of programmed electrical stimulation without compromising the yield of inducibility of monomorphic VT in patients with CAD.⁶⁸

Number of VESs. The sensitivity of programmed electrical stimulation to initiate SMVT increases with increasing the number of VESs used, but at the expense of decreasing specificity. The use of three VESs seems optimal because it offers the highest sensitivity associated with

an acceptable specificity. More aggressive stimulation is likely to produce nonspecific responses, usually polymorphic VT or VF.

In the majority of patients with CAD undergoing EP testing for risk stratification for SCD, triple VESs are typically required for VT induction. Sustained VT induced with triple VESs is usually faster and more likely to result in hemodynamic compromise. Despite these differences, long-term prognosis does not appear to be affected by the mode of induction. In a recent report, there was no difference in the incidence of arrhythmic death or all-cause mortality at 2 years between patients induced with burst pacing, one or two VESs, and those induced with three VESs.

When SMVT is studied, the use of four VESs may be considered. However, when a patient resuscitated from cardiac arrest is studied, four VESs should not be used because the likelihood of inducing a nonspecific response (polymorphic VT/VF) is far higher than that of inducing SMVT (10:1). Of note, triple VESs are required to induce SMVT in 20% to 40% of patients presenting with SMVT and in 40% to 60% of patients presenting with cardiac arrest.

Pacing drive CL. The use of at least two pacing drive CLs (typically 600 and 400 milliseconds) can enhance the sensitivity of induction of SMVT in patients presenting with sustained VT of any morphology or those with cardiac arrest. VES at shorter or longer drive CLs or even in NSR can be necessary to initiate VT in some patients. Abrupt changes in CL can also facilitate VT induction. The CL used can also influence the number and prematurity of VESs required to initiate VT. Rapid ventricular pacing has a low yield in VT initiation.

In a minority of patients with prior SMVT or cardiac arrest, VT can be initiated only with VES during NSR. On the other hand, most VTs that can be induced during NSR can also be induced during ventricular pacing or VESs delivered after a pacing drive.

Site of ventricular stimulation. In contrast to automatic or triggered-activity VT, in which the stimulation site has no effect on VT inducibility, reentrant VT can demonstrate absolute or relative site specificity for initiation. In most cases, development of functional unidirectional block is a prerequisite for initiation of macroreentrant VT; however, during VES, functional block may not always develop despite short coupling intervals, suggesting that formation of functional block is dependent on the direction of activation following stimulation. Therefore the use of at least two sites of stimulation enhances the ability to induce VT.

If triple VESs are delivered only from the RV apex, 10% to 20% of patients will require the use of a second RV or LV pacing site for initiation of SMVT (less than 5% require an LV site). If double VESs are used, 20% to 30% will require a second pacing site (10% require an LV site). Because the number of VESs required for initiation can differ depending on the site of stimulation, which occurs in approximately 20% of patients with SMVT, the site that allows the use of the fewest number of VESs is preferred to avoid nonspecific responses. Thus it is preferable to stimulate from both the RV apex and the RVOT at each drive CL and with the number of VESs before proceeding to more aggressive stimulation.

If stimulation from the RV apex and RVOT fails to initiate VT, stimulation from the LV may be used. However, the yield is low (2% to 5%) for patients with SMVT and somewhat higher in patients with cardiac arrest.

Atrial extrastimulation (AES) can initiate VT in approximately 5% of patients with SMVT. Usually, those VTs can also be initiated by VES, are usually slower, and are reproducibly initiated over a broad zone of VES coupling intervals. Initiation with AES is more common in patients without CAD.

Pacing current output. Increasing the current (more than twice the diastolic threshold current or pulse width more than 2 milliseconds)

produces only a small increase in sensitivity of initiating SMVT, but this is outweighed by a significant decrease in specificity and increase in the incidence of VF. The use of currents more than 5 mA is not recommended.

Isoproterenol administration. Isoproterenol has a low yield in facilitating induction in patients with CAD and SMVT and is more useful in initiation of exercise-related VTs or triggered-activity OT VTs.

Reproducibility of Ventricular Tachycardia Initiation

More than 90% of patients with clinical SMVT will have inducible VT, regardless of the underlying pathology, with the exception of exercise-induced VT. Patients with cardiac arrest or nonsustained VT have a lower incidence of inducibility; inducibility is higher in patients with CAD.

SMVT can be reproducibly initiated from day to day and year to year, especially in patients with CAD. However, the exact mode of initiation is not necessarily reproducible. Once SMVT is initiated, it is easier to reinstate by repeating the same stimulation protocol that was initially successful, either longitudinally (by repeating the entire protocol) or horizontally (by repeating each coupling interval).

Although reproducibility of sustained VT can be variable when comparing induction during the initial month post MI with subsequent months, induction of any sustained VT in the more chronic phase of MI is highly reproducible over both short-term and extended time intervals. However, a change in the number of extrastimuli required for VT reinduction is reported in 30% to 70% of patients, and is more common as the time interval between studies increases. Similar inconsistencies are reported in the exact QRS morphology and TCL of induced VTs during repeated testing. These data confirm that the substrate for chronic post-MI inducible VT per se can be highly stable for up to several years in the absence of major changes in clinical status. However, the mode of induction and VT characteristics demonstrate substantial variability; therefore it is improbable that such features would predict long-term outcome.

Endpoints of Programmed Electrical Stimulation

Induction of clinical SMVT. Induction of SMVT is very specific (especially with a VES coupling interval of more than 240 milliseconds), and only occurs in patients with spontaneous VT, cardiac arrest, or an arrhythmogenic substrate. In patients who had spontaneous VT prior to the EP study, the endpoint of programmed electrical stimulation should be induction of the clinical arrhythmia or the presumed arrhythmia. Clinical VT is defined as an inducible SMVT that matches the 12-lead ECG QRS morphology and approximate CL of the patient's documented, spontaneously occurring SMVT. Nonclinical VTs are defined as inducible SMVTs that were not previously known to have occurred spontaneously.

Induction of multiple SMVTs. The majority (85%) of patients with post-MI VT have more than one inducible VT morphology. Even in patients presenting with a single clinical SMVT, multiple distinct uniform VTs may be induced in the EP laboratory, especially during antiarrhythmic therapy. Multiple VT morphologies are defined as two or more inducible VTs having at least one of the following: (1) contralateral BBB patterns; (2) a frontal plane axis of 30 degrees or more divergent; (3) marked differences in individual ECG leads recorded from the same electrode locations; (4) a precordial transition zone in one or more leads or a different dominant deflection in more than one precordial lead; and (5) a different TCL (more than 100 milliseconds for VTs with a similar morphology). A change in VT morphology need not reflect a change in a reentrant circuit or site of impulse formation but may merely reflect a change in the overall pattern of ventricular activation. In some cases, pacing can reverse the direction of wavefront

propagation within the same reentrant loop. The majority of multiple morphologically distinct SMVTs arise from the same region of the heart (i.e., have closely located exit sites or shared components of an isthmus or diastolic pathway).

Multiple uniform VTs inducible in the EP laboratory are of clinical significance because the distinction between clinical and nonclinical is often uncertain. Clinically, the ECG of spontaneous VTs terminated by an ICD or emergency medical technician is often not available. Even when available, differences in ECG lead placement, patient position, and antiarrhythmic drugs can influence the similarity between two episodes of VT that arise from the same circuit. In addition, the presence of multiple VT morphologies might have been overlooked because of the lack of 12-lead ECGs obtained during multiple spontaneous episodes on a variety of different antiarrhythmic agents. The use of single-lead rhythm strips to record VT has been a major misleading factor suggesting that there is only one VT. The minimum number of ECG leads required to discern differences between different VT origins or circuits is not clear. The TCL alone is influenced by antiarrhythmic drugs and can be similar for different VTs or may be different for VTs originating from the same region and, therefore, is unreliable as a sole indicator of clinical VT. Of note, inducible VTs never seen spontaneously in the preablation state can occur spontaneously following ablation of the clinical VT.

Therefore the term *clinical VT* should be reserved for induced VTs that are known to have the same 12-lead ECG QRS morphology and approximate TCL as a spontaneous VT. Other VTs should be designated as either *presumptive clinical* or *previously undocumented* VT morphology.

Induction of polymorphic VT or VF. When EP testing is performed in patients presenting with SMVT, polymorphic VT and VF must be considered as nonspecific responses. Both sustained and nonsustained polymorphic VT and VF can be induced, even in normal subjects. In general, induction of VF requires multiple VESs delivered at shorter coupling intervals (usually less than 180 milliseconds) than induction of SMVT.

On the other hand, induction of polymorphic VT or VF in a patient who presents with cardiac arrest can have a different implication. Because cardiac arrest can be initiated by a polymorphic VT, the induction of polymorphic VT in this patient population can be significant. Therefore, although doubt will always exist, reproducible polymorphic VT induction is treated as a possible indicator of the clinical arrhythmia. Features that suggest that a polymorphic VT can be mechanistically meaningful are reproducible initiation of the same polymorphic VT template, especially from different stimulation sites; inducibility with relatively mild stimulation (single or double VESs); and transformation of the polymorphic VT to SMVT by procainamide.

Of note, the induction of any arrhythmia (SMVT, polymorphic VT, or VF) in the setting of a recent MI (less than 1 month) may not have clinical significance.

Induction of very fast VT. The induction of VT with a TCL longer than 230 milliseconds is predictive of recurrent ventricular arrhythmia in high-risk patients, such as those with prior MI and reduced LVEF ($\leq 40\%$), ischemic cardiomyopathy presenting with syncope, resuscitated cardiac arrest, or asymptomatic nonsustained VT. In up to 20% of patients undergoing EP testing, VT with a TCL ranging from 200 to 250 milliseconds can be inducible. Although a limited number of studies have closely and specifically examined long-term outcomes of this group of patients, and although previous large ICD trials, such as MADIT and MUSTT, excluded such patients if this arrhythmia was induced by more than two VESs, there is a growing body of evidence that an inducible fast VT is of sufficient clinical importance that it should no longer be considered a nonspecific finding of EP testing because it poses a

significant risk of spontaneous ventricular arrhythmia or SCD over long-term follow-up. This risk appears equivalent to that of patients with inducible VT with a TCL between 250 and 320 milliseconds, and markedly worse than that of patients who are noninducible or have inducible VF. These findings seem to be consistent regardless of the mode of induction of VT (with 2, 3, or 4 VESs), or measured LVEF ($\leq 30\%$ or between 31% and 40%).⁶⁸

Tachycardia Features

His Bundle Activation

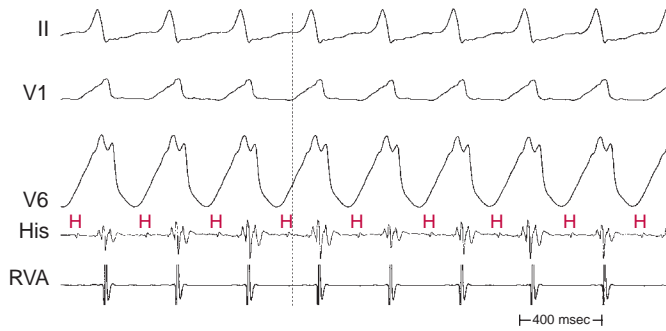
No visible His potential during VT. The His potential may not be observed during VT in many patients, likely because the retrograde His potential is masked by ventricular activation or because of suboptimal catheter position. A proper HB catheter position can be verified by observation of the immediate appearance of the His potential on termination of the VT, the disappearance of the His potential on initiation of VT, or the sudden appearance of the His potential when spontaneous or induced supraventricular beats capture the HB (with or without ventricular capture) during VT. In addition, when complete ventricular–His bundle (VH) block is present, dissociated His potentials will be observed (an extremely rare phenomenon).

Visible His potential during VT. His potentials can be recorded during VT in approximately 80% of patients. When the His potential is visible during VT, it is often difficult to determine whether the recorded His potential is anterograde or retrograde, and whether an apparent His potential is actually a right bundle branch (RB) potential. Recording the RB or left bundle branch (LB) potentials to demonstrate that their activation precedes HB activation during VT, and HB pacing producing a longer His bundle–ventricular (HV) interval than the one noted during VT, usually helps clarify the situation.

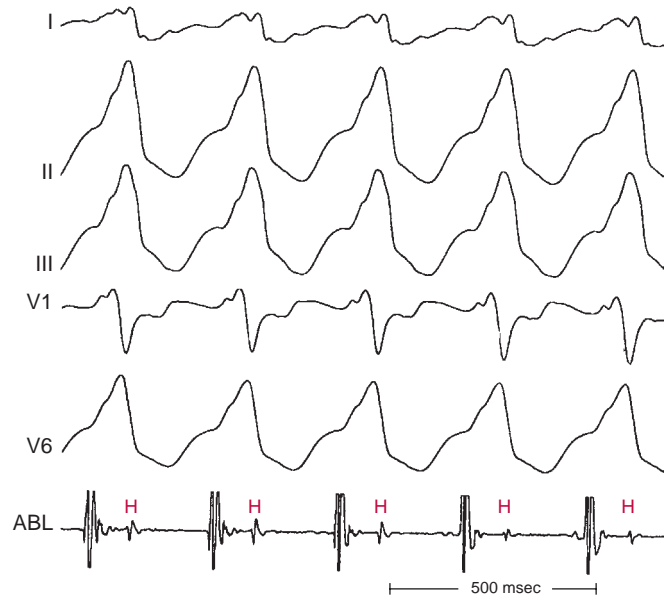
In post-MI VT, the relative timing of the retrograde His potential in the QRS depends on how quickly the HPS is engaged and how slowly the impulse reaches the ventricle to produce the QRS. Thus depending on the relative conduction time up the HPS versus through the slowly conducting muscle to give rise to the QRS, the His potential can occur before, during, or after the QRS. The His potential can occasionally occur before ventricular activation (with an HV interval during VT shorter than that during NSR; eFig. 22.4) and can also occur just after the onset of ventricular activation (eFig. 22.5). The occurrence of an HV interval (i.e., with the His potential preceding the QRS onset) shorter than that during NSR (in the absence of preexcitation) or a VH interval (i.e., with the His potential following the QRS onset) implies the presence of retrograde HB activation.

Engagement of the HPS, when present, can allow for more rapid activation of the myocardium, which in turn results in a narrower QRS. Some have suggested that the site of origin of such VTs is within the HPS (i.e., fascicular VTs), although proof that such VTs originate from the fascicles and differ from other forms of VT is often lacking. The retrograde His potential appears to reflect passive activation of the HPS, rather than involvement of the HPS in the reentrant circuit. This concept is supported by several observations. HB deflections can appear intermittently (typically in a 2:1 or 3:2 fashion, and occasionally in a Wenckebach periodicity), and changes in the VH interval can occur without changes in the TCL (eFig. 22.6). In fact, marked changes in the TCL can be present with no changes in the VH interval. Furthermore, AES or atrial pacing can result in anterograde capture of the HB in the presence or absence of ventricular capture or fusion beats. Such an event, linking atrial activation to the HB deflection, proves that HB deflections are caused by anterograde activation and are unrelated to maintenance of the VT in the vast majority of cases.

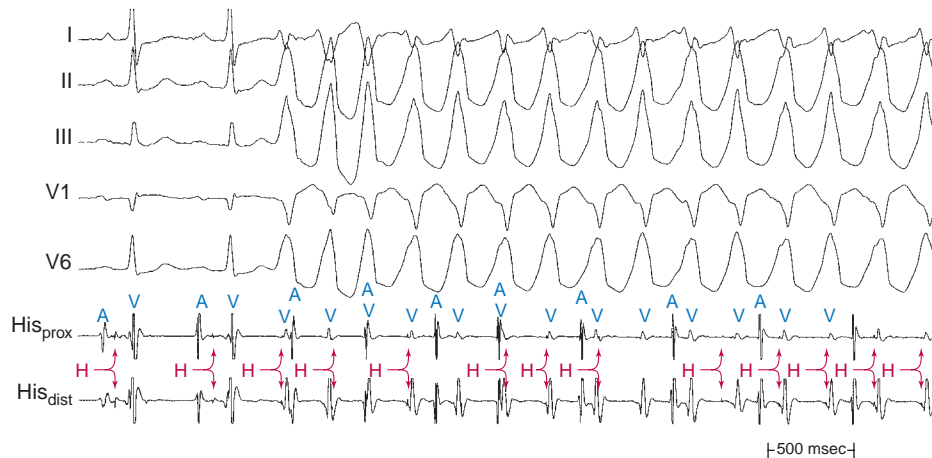
For wide complex tachycardias with the His potential preceding the QRS, an HV interval that is shorter during tachycardia than during



eFig. 22.4 Ventricular Tachycardia With Short Constant His Bundle (HB)–Ventricular Interval, Consistent With Early Retrograde Activation of the HB. *RVA*, Right ventricular apex.



eFig. 22.5 Ventricular Tachycardia With a Constant Ventricular–His bundle Interval, Consistent With Retrograde Activation of the His Bundle (HB). HB activation is recorded by the ablation catheter (*ABL*) positioned in the left ventricular outflow tract.



eFig. 22.6 Ventricular Tachycardia (VT) With Variable Relationship Between Ventricular and His Bundle (HB) Activation. HB catheter position is verified by observation of His potentials during normal sinus rhythm at left. His potentials are observed intermittently during VT, with variable relationship to the QRS complexes, suggesting that the His–Purkinje system is not an essential part of the VT circuit. *His_{dist}*, Distal His bundle; *His_{prox}*, proximal His bundle.

NSR suggests VT or preexcited supraventricular tachycardia (SVT), whereas an HV interval during tachycardia that is equal to or longer than that during NSR suggests SVT with aberrancy (see Fig. 20.9) or BBR VT (see Fig. 26.3). A changing AH interval or failure to observe anterograde His potential during VT with AV dissociation suggests the presence of retrograde conduction with concealment in the AVN.

The mere presence of a His potential before the QRS with a normal HV interval is not absolutely reliable evidence that the tachycardia is an SVT. The HV interval during VT is usually less than that during NSR; hence, if infranodal conduction delay is present during NSR, the VT can exist in the presence of an apparently normal HV interval (i.e., 35 to 55 milliseconds), but will be less than that during NSR. In post-MI VT, because ventricular activation is occurring in diastole (albeit slow enough not to be apparent on the surface ECG), the HPS could be activated during this time, giving rise to a short or possibly normal HV interval during the VT. The time to conduct retrogradely to the HB can theoretically be less than the time required to exit from the VT circuit and produce the onset of the QRS, thereby producing an HV interval. Such VTs, which are rare, have a relatively narrow QRS. BBR VT can also give rise to an HV interval that is longer than that during NSR.

Right Ventricular Apical Local Activation Time

In the setting of apical MI, VT with an RBBB pattern is common, but QRS morphologies of lateral versus septal apical locations significantly overlap, with variable early R wave progression and a similar frontal plane axis. Assessing the activation time to a fixed reference endocardial recording at the RV apex can help regionalize a septal versus lateral origin for such VTs. For RBBB-type VT in the setting of an apical infarct, the QRS-to-RV apical activation time is consistently less than 100 milliseconds for an LV septal apical origin and more than 125 milliseconds for a lateral apical origin. The same values for the QRS-to-RV apical activation time will also help identify a septal versus lateral wall origin in the setting of prior nonapical infarcts.

Relationship of Ventricular Stimulus to the Onset of Ventricular Tachycardia

Conduction delay is required for the initiation of reentrant rhythms; thus an inverse relationship between the coupling interval of the VES initiating the VT or the pacing train CL and the interval from the VES to the first VT complex favors reentry. In contrast, a linear relationship of the PCL or VES coupling interval to the interval to the first VT complex and initial CL of the VT favors triggered activity. In reentrant VT, the initial CL reflects conduction through the VT circuit, which in the absence of exit block should demonstrate the same or longer CL as the remaining VT cycles, depending on whether any conduction delay is produced in the circuit on initiation.

Diagnostic Maneuvers During Tachycardia

The response of VT to programmed stimulation can be studied only for SMVT. Nonsustained VT is too short and unpredictable in duration to allow reliable evaluation. Polymorphic VT is invariably associated with rapid hemodynamic collapse. Also, SMVT must be well tolerated and must have a stable TCL to evaluate the response to stimulation. Fast, unstable SMVT can usually be slowed by antiarrhythmic drugs (e.g., procainamide) to permit evaluation by programmed stimulation.

Ventricular Extrastimulation During Tachycardia

Initially, a single VES is delivered at a coupling interval 10 to 20 milliseconds shorter than the TCL. The coupling interval is then gradually decreased by 5- to 10-millisecond decrements, until the local effective refractory period (ERP) is reached. The RV apex is used as the initial site of stimulation. Stimulation from other sites (RVOT and LV) can

also be used to gain information regarding the site specificity of a given response. The return CL is analyzed to evaluate whether the VES has influenced the VT in terms of resetting, ability and pattern of termination, and site specificity for stimulation affecting the VT.

If resetting or termination of VT is not observed with single VESs, stimulation is repeated using double VESs. The first VES is delivered at a coupling interval 20 milliseconds greater than the longest coupling interval at which a single VES resets the VT, or 20 milliseconds above the local ERP if a single VES fails to interact with the VT. The second VES is delivered at a coupling interval equal to the TCL, and then this coupling interval is progressively decreased in 5- to 10-millisecond decrements until the local ERP is reached. The use of double VESs allows comparable coupling intervals to reach the circuit at a greater relative degree of prematurity and ability to influence the VT than if the same coupling interval were used for a single VES. By this methodology, only a single VES interacts with the circuit; if the two VESs are delivered such that each VES interacts with the site of impulse formation, interpretation of the response would then be difficult. Thus the first VES is delivered so that it will not interact with the circuit but will help the second VES to do so.

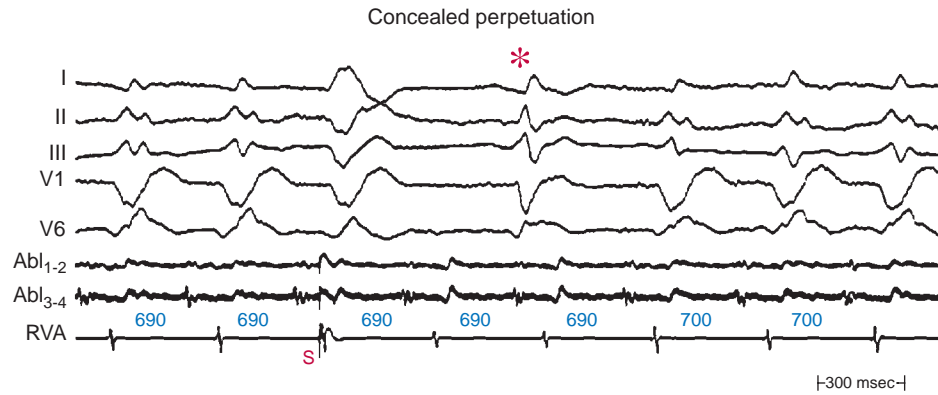
The response of VT to VES is evaluated for manifest or concealed perpetuation, resetting with or without fusion, and termination.

Manifest perpetuation. Manifest perpetuation is said to be present when the VES fails to influence the VT, resulting in a full compensatory pause surrounding the VES. Factors influencing the ability of the VES to interact with the VT include the TCL, local ventricular ERP at the stimulation site, and distance between the stimulation site and VT circuit. The TCL and duration of the excitable gap are the most important factors; the faster the VT (especially with TCLs less than 300 milliseconds) and the shorter the duration of the reentrant circuit excitable gap, the more difficult it is for the VES to enter the VT circuit. Local ERP at the stimulation site and at the site of impulse formation can also limit the prematurity with which the VES can be introduced. Furthermore, the farther the stimulation site is from the VT circuit, the more difficult it is for the VES to reach the circuit with adequate prematurity.

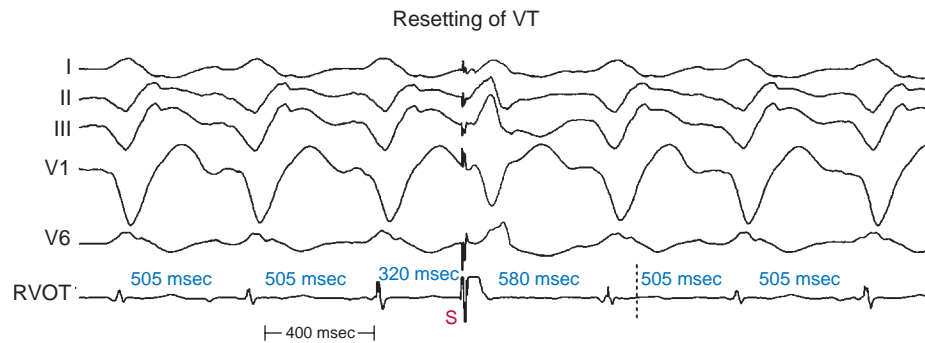
Failure of a VES to affect the VT circuit helps demonstrate the extent of the ventricular myocardium that is *not* required for the VT. Thus the ability to capture significant portions of the ventricle by the VES without affecting the VT suggests that those captured areas are not required for the VT circuit. Similarly, intermittent capture of the HPS during VT suggests that it also is not necessary to maintain the VT, regardless of where the His potential is located relative to the QRS during the VT. In an analogous fashion, atrial captures (occurring spontaneously or in response to atrial stimulation) may occur without influencing the VT. The demonstration that neither the proximal HPS nor the majority of the ventricles are required to sustain the VT suggests that the VT circuit must occupy a relatively small and electrocardiographically silent area of the heart.

Concealed perpetuation. Concealed perpetuation implies that the VES not only fails to influence the VT circuit, but is also followed by a pause that exceeds the TCL or that is occasionally interrupted by a sinus capture before the next VT beat. Such pauses are a form of functional exit block because the VT impulse is unable to exit the circuit and depolarize the ventricles that have just been activated by the VES (eFig. 22.7).

Resetting. Resetting is the interaction of a premature wavefront with a tachycardia, resulting in either advancement (acceleration) or delay of the subsequent tachycardia beat (eFig. 22.8). The first return VT complexes should have the same morphology and CL as the VT before the VES, regardless of whether a single or multiple extrastimuli are used.



eFig. 22.7 Concealed Perpetuation in Ventricular Tachycardia (VT). For reentrant slow VT (cycle length, 690 msec), a single ventricular extrastimulus (VES) is introduced (S) that seems to terminate the VT; a conducted sinus complex (*) follows and then VT recurs. However, inspection of the distal ablation (Abl1-2) electrogram shows that VT never actually terminated because the mid-diastolic electrogram continues unperturbed by the VES. RVA, Right ventricular apex.



eFig. 22.8 Resetting of Ventricular Tachycardia (VT). A single ventricular extrastimulus from the right ventricular outflow tract (RVOT) captures the ventricle during VT and causes the subsequent QRS to occur earlier than anticipated (dashed line), indicating resetting.

The introduction of a single VES (S_2) during VT yields a return cycle (S_2V_3) if the VT is not terminated. If S_2 does not affect the VT circuit, the coupling interval (V_1-S_2) plus the return cycle (S_2V_3) will be equal to twice the VT cycle ($2 \times V_1V_1$); that is, a fully compensatory pause will occur (see Fig. 3.13). Resetting of VT occurs when a less than fully compensatory pause occurs (by at least 20 milliseconds). In this situation, $[V_1S_2 + S_2V_3]$ will be less than $[2 \times V_1V_1]$, as measured from the surface ECG. TCL oscillation should be taken into account when the return cycle is evaluated. To account for any TCL oscillation, at least a 20-millisecond shortening of the return cycle is required to demonstrate resetting. When more than a single VES is used, the relative prematurity should be corrected by subtracting the coupling interval(s) from the spontaneous tachycardia cycles when the VESs are delivered.^{69,70}

To reset a reentrant VT, the stimulated wavefront must reach the reentrant circuit, encounter excitable tissue within the circuit (i.e., enter the excitable gap of the reentrant circuit), collide in the antidromic (retrograde) direction with the previous tachycardia beat, and continue in the orthodromic (anterograde) direction to exit at an earlier than expected time and perpetuate the tachycardia (see Fig. 3.14). If the VES encounters a fully excitable tissue, which commonly occurs in reentrant tachycardias with large excitable gaps, the tachycardia is advanced (i.e., made to occur earlier) by the extent to which the stimulated wavefront arrives at the entrance site prematurely. If the tissue is partially excitable, which can occur in reentrant tachycardias with small or partially excitable gaps, or even in circuits with large excitable gaps when the VES is very premature, the stimulated wavefront will encounter some conduction delay in the orthodromic direction within the circuit. As a consequence, the degree of advancement of the next tachycardia beat will depend on both the degree of prematurity of the VES and the degree of slowing of its conduction within the circuit. Therefore the reset tachycardia beat can be early, on time, or later than expected.^{69,70}

Effect of number of VESs. When refractoriness of the intervening tissue between the pacing site and the reentrant circuit limits the ability of an extrastimulus to reach the reentrant circuit with adequate prematurity, the use of double extrastimuli can be helpful. The first extrastimulus, although not resetting the tachycardia, does shorten the local refractory period at the pacing site and reverse the activation sequence in part of the intervening tissue, allowing the second extrastimulus to access and interact with the reentrant circuit with a greater degree of prematurity at comparable coupling intervals. Approximately 60% of VTs can be reset with a single VES and 85% with double VESs using RV pacing. All VTs reset by a single VES can also be reset by double VESs. Double VESs produce resetting over a longer range of coupling intervals and should therefore be used to characterize the excitable gap of the VT more fully. The resetting zone is approximately 70 milliseconds for most VTs, but is usually longer in those VTs reset by both single and double VESs than those requiring double VESs. Resetting zones in response to single VESs usually occupy 10% to 20% of the VT cycle. This is increased to approximately 25% in response to double VESs, but occasionally can exceed 30%, even in response to a single VES. VTs with LBBB morphology are less likely to require double VESs for resetting than VTs with RBBB morphology, regardless of the frontal plane axis, because VTs with LBBB arise in or adjacent to the septum, closer to the RV stimulation site.^{69,71}

Effect of site of stimulation. Resetting does not require that the pacing site be located within the reentrant circuit. The closer the pacing site is to the circuit, however, the less premature a single VES can be and reach the circuit without being extinguished by collision with a wave emerging from the circuit. The longest coupling interval for a VES to be able to reset a reentrant tachycardia depends on (1) the TCL; (2) the duration of the excitable gap of the tachycardia; (3) refractori-

ness at the pacing site; and (4) the conduction time from the pacing site to the reentrant circuit. Neither local ventricular ERP nor local activation time influences the number of VESs required for resetting. Approximately 10% to 20% of VTs demonstrate site specificity in response to VES. Using double VESs reduces this site specificity. Approximately 70% of VTs can be reset with a single VES delivered to the RV apex or RVOT. Resetting of VT by a single VES can always be achieved from some site in the LV, even when resetting cannot be achieved from RV sites.

Return cycle. The return cycle is the time interval from the resetting VES to the next excitation of the pacing site by the new orthodromic VT wavefront. This corresponds to the time required for the stimulated impulse to reach the circuit, conduct through the circuit, exit the circuit, and travel back to the pacing site. The noncompensatory pause following the VES and the return cycle are typically measured at the pacing site; however, they can also be measured to the onset of the QRS complex on the surface ECG. Conduction time between the pacing site and the VT circuit may or may not be equal to that from the VT circuit to the pacing site. Differences in the VT circuit entrance and exit can result in differences in conduction time to and from the pacing site. These differences depend on the site of stimulation and VT site of origin. In VTs reset by both single and double VESs, the shortest return cycle seen by both methods is usually the same. If the return cycle is measured from the VES producing resetting to the onset of the first return VT QRS complex on the surface ECG, the shortest return cycle will be less than the TCL in more than 40% of VTs. Because stimulation is usually performed from the RV, conduction time into the VT circuit is incorporated into that measurement. If one considers conduction time between the pacing site and the circuit to be equal to that from the circuit to the pacing site (i.e., local activation time) and subtracts this value from the return cycle as measured to the surface ECG QRS, the resultant value for the return cycle is less than the TCL in 80% of VTs.

Resetting response curves. Flat or mixed (i.e., flat, and then increasing) response curves characterize reentrant VTs. A flat curve is noted in approximately two-thirds of VTs, suggesting that a fully excitable gap is present. It also signifies anatomically separate entrance and exit sites of the circuit (see Fig. 3.15). In approximately 40% of VTs, the types of resetting curves can vary, depending on the site of ventricular stimulation. VESs from different pacing sites likely engage different sites in the VT circuit that are in different states of excitability or refractoriness and, therefore, result in different conduction velocities and resetting patterns.

Resetting with fusion. The ability to reset a tachycardia after it has begun activating the myocardium (i.e., resetting with fusion) excludes focal mechanisms (automatic, triggered activity, and microreentry) and is diagnostic of macroreentry. Resetting with ECG fusion requires wide separation (in time and/or distance) of entry and exit sites of the VT circuit, with the stimulus wavefront preferentially engaging the entrance. For resetting with fusion to occur, the VES wavefront has to reach the entrance of the reentrant circuit before it reaches the exit, and, at the same time, allow for the VT wavefront to exit the reentrant circuit, while the VT wavefront is unable to reach the entrance of the circuit before the paced wavefront (Fig. 22.12).

Fusion of the stimulated impulse can be observed on the surface ECG and/or intracardiac recordings if the stimulated impulse is intermediate in morphology between a fully paced complex and the tachycardia complex. The ability to recognize surface ECG fusion requires a significant mass of myocardium to be depolarized by both the VES and VT. If presystolic activity in the reentrant circuit is present before delivery of the VES that resets the VT, this must be considered to represent local fusion. Thus a VES delivered after the onset of the tachycardia QRS on the surface ECG that enters and resets the VT circuit will always

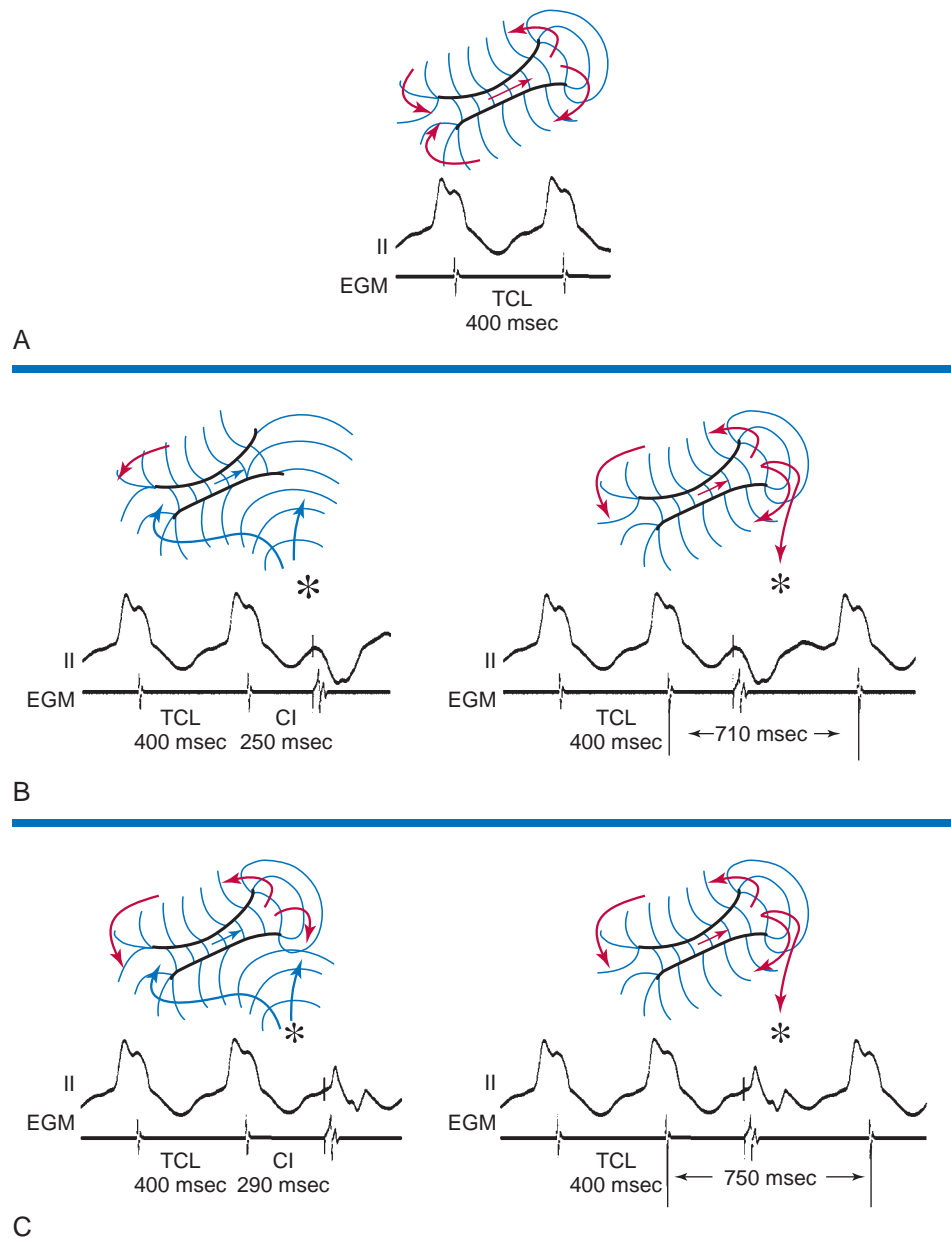


Fig. 22.12 Schematic Representation of the Relationship of the Return Cycle During Resetting of Ventricular Tachycardia (VT) to the Absence or Presence of Surface Electrocardiogram (ECG) Fusion. (A) Stylized VT circuit, with direction of propagation as shown; electrogram is from a remote site. (B) Single ventricular extrastimulus (VES) is introduced during VT at a coupling interval of 250 milliseconds. *Left panel*, The VES occurs early enough that the circuit's exit site is captured; thus there is no fusion. Meanwhile, the paced wavefront (*blue arrows*) enters the entrance of the diastolic corridor before the approaching wavefront of the prior VT cycle (*red arrow*), allowing resetting. *Right panel*, Resetting is demonstrated in that the first VT cycle after the VES occurs at less than twice the tachycardia cycle length (TCL). (C) A slightly later VES is introduced, with a paced wavefront (*blue arrows*) approaching the diastolic pathway's exit after the VT wavefront (*red arrows*) has already left; this results in ECG fusion. Meanwhile, as before, the paced wavefront arrives at the entrance site before the VT wavefront, allowing resetting. The right panel again shows fusion. *Asterisks*, Pacing site; *CI*, coupling interval; *EGM*, intracardiac electrogram.

demonstrate local fusion. Resetting with local fusion and a totally paced surface QRS complex suggests that the reentrant circuit is physically small.

The farther the stimulation site is from the reentrant circuit, the less likely that resetting with ECG fusion will occur. In this setting, the VES should be delivered at a shorter coupling interval to enable

the paced wavefront to reach the VT circuit with sufficient prematurity; hence, the stimulated impulse is more likely to capture both the exit and entrance sites and therefore have a purely paced QRS morphology without fusion.⁶⁹

Resetting with surface ECG QRS fusion during RV stimulation is observed in 60% of VTs, 40% of which are usually reset with a VES

delivered after the onset of the VT QRS. VTs reset with fusion have a higher incidence of flat resetting curves, longer resetting zones, and significantly shorter return cycles (measured from the stimulus to the onset of the VT QRS) than VTs not reset with fusion. The return cycle corrected to the TCL is shorter with VTs reset with fusion (0.89 vs. 1.12). In 80% of VTs reset with fusion, the return cycle is shorter than the TCL measured at the onset of the QRS (vs. only 4% of VTs reset without fusion). The return cycle minus local activation time is equal to the time for the wavefront to traverse the distance from the entrance to the exit of the circuit. This interval is less than the TCL in 100% of VTs reset with fusion. These findings are consistent with widely separate entrance and exit sites of the VT circuit.

Tachycardia termination. Termination of VT by a VES occurs when the VES collides with the preceding tachycardia impulse antidromically and blocks in the reentrant circuit orthodromically (see Fig. 3.14). This occurs when the VES enters the reentrant circuit early enough in the relative refractory period because it fails to propagate in the anterograde direction and encounters absolutely refractory tissue. In the retrograde direction, it confronts increasingly recovered tissue and is able to propagate until it collides with the circulating wavefront and terminates the arrhythmia.

Termination of VT by a single VES is uncommon. The closer the stimulation site to the circuit, the more prematurely a VES can engage the VT circuit because the refractoriness and conduction delay in intervening myocardial tissue are avoided. The success of termination, however, is directly related to the number of VESs used. Occasionally, when stimulation is performed at the critical isthmus of the VT circuit, termination can occur with a nonpropagated VES that fails to depolarize the bulk of the myocardium but is adequate to depolarize the isthmus and make it refractory to the incoming VT wavefront, resulting in termination of the VT (Fig. 22.13).

Ventricular Pacing During Tachycardia

Rapid ventricular pacing is performed during VT at a PCL 10 to 20 milliseconds shorter than the TCL. The PCL is then decreased in 10-millisecond decrements in a stepwise fashion until the VT is terminated. Pacing is stopped after each PCL and the response of VT to pacing is assessed. It is important to ensure that termination and reinitiation of the VT have not occurred during the pacing train, which would then affect the interpretation of the VT response.

It is critical to synchronize the initiation of pacing to the electrogram at the pacing site because absence of synchronization will lead

to a variable coupling interval of the first paced impulse to the VT. It is also important to perform overdrive ventricular pacing at each PCL for sufficiently long duration to allow the pacing drive to penetrate and affect the VT circuit. Pacing for a short period is a common mistake; it results in erroneous evaluation of the VT response. For VTs that are not stable enough to allow completion of an entire stimulation protocol, synchronized bursts of pacing at variable PCLs for a specified but variable number of beats, can usually be performed and can provide information about resetting or entrainment, overdrive suppression, and termination.

The response of VT to overdrive pacing is evaluated for overdrive suppression, acceleration, transformation into distinct uniform VT morphologies, entrainment, ability and pattern of termination, and site specificity for stimulation affecting the VT.

Overdrive suppression. Overdrive suppression analogous to that seen with automatic rhythms has not been observed in post-MI VTs, although prolonged return cycles can be seen at rapid pacing rates.

Tachycardia acceleration. Acceleration by overdrive pacing refers to sustained shortening of the TCL following cessation of pacing. Acceleration occurs in about 25% of VTs, and is more common with ventricular pacing than with VES (35% vs. 5%). However, overdrive acceleration of VT analogous to that seen in triggered rhythms (i.e., linear relation of PCL to early acceleration of the TCL) is uncommon in post-MI VT. Because rapid ventricular pacing is usually required to terminate faster VTs, these VTs have a higher incidence of acceleration (40% of VTs with TCL less than 300 milliseconds with rapid ventricular pacing). Approximately 50% of the accelerated VTs can be terminated with even faster ventricular pacing; the other 50% (which can be polymorphic VT or ventricular flutter) require electrical cardioversion.

Acceleration is classified according to the morphology of the accelerated tachycardia: VT morphology identical to or different from the original VT, or polymorphic VT. An accelerated VT with a QRS morphology identical to the original VT suggests that the accelerated VT is using the same exit of the original VT circuit. The most likely mechanism underlying this form of VT acceleration is an area of block that determines the size of the reentrant circuit, which is determined to some extent by refractoriness. Rapid pacing can shorten the refractoriness in a proximal region of the arc of block, which would in turn shorten the length of the reentrant pathway. If the distal component of the arc of block remains unchanged, acceleration of the VT will occur with the same exit site and hence the same QRS morphology.

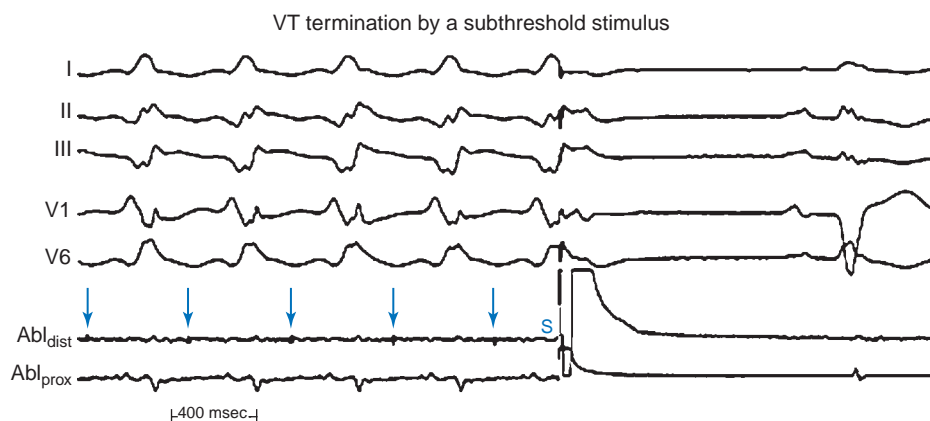


Fig. 22.13 Ventricular Tachycardia (VT) Termination by a Nonpropagated Ventricular Extrastimulus (VES). VT is shown with the ablation electrode recording a small mid-diastolic potential (arrows). A single VES (S) is delivered during VT that does not appear to capture myocardium, yet terminates the tachycardia. *Abl_{dist}*, Distal ablation site; *Abl_{prox}*, proximal ablation site.

Alternatively, rapid pacing can remove block in a shorter potential pathway, creating a smaller circuit.

On the other hand, a VT morphology different from the original VT can be secondary to a change in the exit site from the same circuit, a reversal of the reentrant circuit, or the termination of the initial VT and initiation of a different VT. Polymorphic VT with or without degeneration to VF can occur because of the inability of the myocardium to respond to the short PCL with the development of changing activation wavefronts, leading to multiple reentrant wavelets that can degenerate into VF. There is no way to predict which type of acceleration will occur. However, in the presence of antiarrhythmic drugs, acceleration to different morphologically distinct VTs is common.

Tachycardia transformation. Transformation of the index VT into a second uniform VT with distinct morphology can occur in response to overdrive pacing. It is not uncommon for stimulation during one VT to induce another VT of different morphology and TCL, only to be changed to a third or fourth one by continued stimulation. The significance of all these multiple morphologically distinct VTs induced during overdrive pacing of the index VT is uncertain if they were never seen before spontaneously or induced by programmed stimulation during NSR. Usually, however, these VTs can also be induced by programmed electrical stimulation. Nevertheless, any VT (even if not seen before) that is uniform and has a TCL longer than 250 milliseconds should be regarded as clinically important. Those VTs may not have been observed previously because the original VT dominates because it is more readily inducible. Induction of rapid unstable VTs (TCL < 250 milliseconds) in patients who presented with only stable VT does not have prognostic value.

The ability to change from one VT to another with a different TCL using single or double VESs is infrequent during triggered rhythms (other than those because of digitalis), and is another observation that is most compatible with a reentrant mechanism.

Entrainment. Overdrive ventricular pacing at long PCLs (i.e., 10 to 30 milliseconds shorter than the TCL) can almost always entrain reentrant VTs. The slower the pacing rate and the farther the pacing site from the reentrant circuit, the longer the pacing drive required to penetrate and entrain the tachycardia.

Following the first beat of the pacing train that penetrates and resets the reentrant circuit, the subsequent stimuli will interact with the reset circuit, which has an abbreviated excitable gap. Depending on the degree that the excitable gap is preexcited by that first resetting stimulus, subsequent stimuli fall on fully or partially excitable tissue. Entrainment is said to be present when two consecutive extrastimuli conduct orthodromically through the circuit with the same conduction time while colliding antidromically with the preceding paced wavefront. During entrainment, the paced stimuli enter the reentrant circuit, block with the existing tachycardia wavefront in the antidromic direction, and conduct through the circuit in the orthodromic direction to produce the return cycle beat.

Entrainment criteria. The traditional definition of entrainment states that, during constant-rate pacing, entrainment of a reentrant tachycardia results in the activation of all myocardial tissue responsible for maintaining the tachycardia at the PCL, with the resumption of the same tachycardia morphology following cessation of pacing, with the first postpacing ECG tachycardia complex displaying no fusion but occurring at a return cycle equal to the PCL. Importantly, the mere acceleration of the tachycardia to the pacing rate and the subsequent resumption of the original tachycardia after cessation of pacing do not establish the presence of entrainment. Therefore several surface ECG and intracardiac electrogram criteria have been proposed for establishing the presence of entrainment (see Fig. 5.17 and Box 5.1).⁶⁹⁻⁷¹ These criteria are discussed in more detail in Chapter 5.

Entrainment with fusion. A stimulated impulse is said to be fused when its morphology is a hybrid between that of a fully paced QRS morphology (when pacing is performed at the identical site and rate but in the absence of tachycardia) and a tachycardia QRS morphology (in the absence of pacing) (Fig. 22.14; and see Figs. 5.17 and 5.19). The ability to demonstrate QRS fusion on the surface ECG requires a significant mass of myocardium to be depolarized by both the extrastimulus and the tachycardia. The farther the stimulation site is from the reentrant circuit, the less likely entrainment with ECG fusion will occur.⁷⁰

During entrainment of reentrant VT, varying degrees of QRS fusion at different pacing rates are caused by a progressive increase in the amount of myocardium activated by the antidromic paced wavefront at progressively shorter PCLs. Importantly, fusion remains fixed at each of the PCLs, but a different degree of fixed fusion is manifest at different PCLs (see Figs. 5.17 and 5.19).

Focal tachycardias (automatic, triggered activity, or microreentrant) cannot manifest fixed fusion during overdrive pacing (Fig. 22.15). It is important to note that overdrive pacing of tachycardia of any mechanism can result in a certain degree of fusion, especially when the PCL is only slightly shorter than the TCL. Such fusion, however, is unstable during the same pacing drive at a constant PCL because pacing stimuli fall on a progressively earlier portion of the tachycardia cycle and produce progressively less fusion and more fully paced morphology. Such a phenomenon (referred to as “variable fusion”) should be distinguished from the “constant fusion” and “progressive fusion” characteristics of entrainment, and sometimes this distinction requires pacing for long intervals to demonstrate variable degrees of fusion. Moreover, overdrive pacing frequently results in suppression (automatic) or acceleration (triggered activity) of focal tachycardias, rather than resumption of the original tachycardia with an unchanged TCL.^{69,71}

Entrainment with manifest fusion. Demonstration of the presence of manifest fusion during entrainment requires knowledge of the surface ECG morphology of the tachycardia and of pure pacing (at the same site and rate) in the absence of tachycardia. Manifest fusion is said to be present when the QRS morphology is a hybrid of the QRS morphology of the tachycardia and that observed during pure pacing (see Figs. 5.17 and 5.19).

Entrainment of reentrant VT commonly produces manifest fusion that is stable (fixed) during the pacing drive at a given PCL; repeated entrainment at PCLs progressively shorter than the TCL results in different degrees of QRS fusion, with the resultant QRS configuration looking more like a fully paced configuration (see Figs. 5.17 and 5.19). When entrainment is manifest, the last captured wave is entrained (occurring at the PCL) but does not demonstrate fusion.⁶⁹

Entrainment with inapparent fusion. Entrainment with inapparent fusion (also referred to as “local” or “intracardiac fusion”) is said to be present when a fully paced QRS morphology (with no surface ECG fusion) is observed during entrainment, even though the tachycardia wavefront does exit the reentrant circuit (i.e., orthodromic activation of the presystolic electrogram is present). In this setting, fusion is limited to a small area and does not produce surface ECG fusion, and only intracardiac (local) fusion can be recognized (see Fig. 5.20).

Local fusion can only occur when the presystolic electrogram is activated orthodromically. Collision with the last paced impulse must occur distal to the presystolic electrogram, either at the exit from the circuit or just outside the circuit. In such cases, the return cycle measured at this local electrogram will equal the PCL. Therefore a stimulus delivered after the onset of the surface ECG QRS during entrainment will always demonstrate local fusion. This is to be distinguished from entrainment with antidromic capture, whereby the return cycle, even when

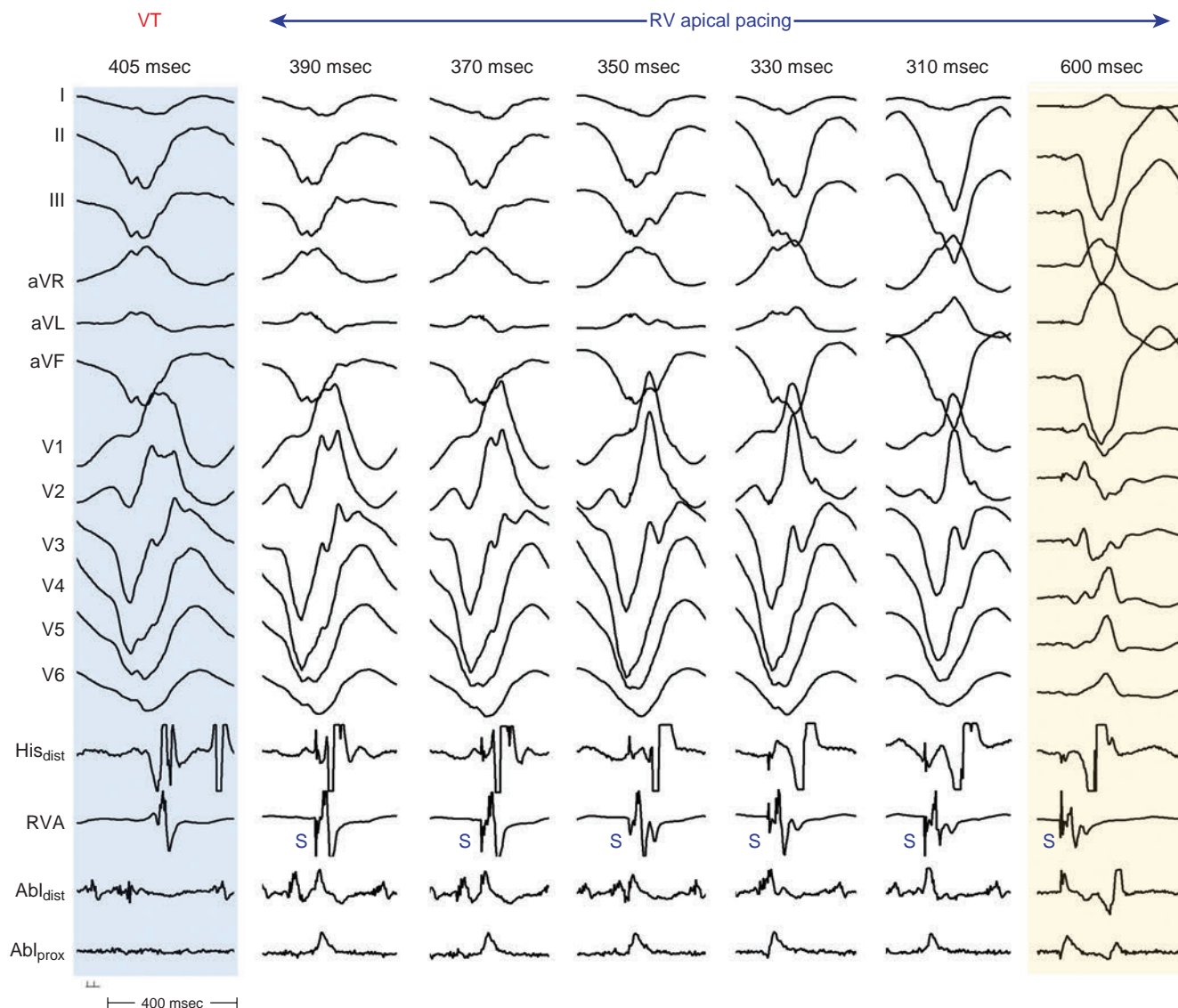


Fig. 22.14 Fusion With Ventricular Pacing During Macroreentrant Postinfarction Ventricular Tachycardia (VT). VT with a right bundle branch block pattern and right superior axis is shown at left (cycle length [CL], 405 milliseconds, in blue shading). In the panels at right, pacing during VT over a range of CLs from the right ventricular (RV) apex (with a left bundle branch block pattern and left superior axis) is shown. Pure RV pacing during sinus rhythm at CL of 600 milliseconds is shown at far right (yellow shading). It is evident that while pacing during VT, QRS complexes at each paced CL are different from both VT and pure pacing, indicating contribution of both the VT and paced wavefronts to the QRS complexes (fusion, most evident in leads III, aVL, aVF, and V₁ and V₂). *Abl_{dist}*, Distal ablation site; *Abl_{prox}*, proximal ablation site; *His_{dist}*, distal His bundle; *RVA*, right ventricular apex.

measured at the site of the presystolic electrogram, exceeds the PCL (see later).

Entrainment with concealed fusion. Entrainment with concealed fusion (sometimes referred to as “concealed entrainment” or “exact entrainment”) is defined as entrainment with orthodromic capture and a surface ECG complex identical to that of the tachycardia (Fig. 22.16).⁶⁹ Entrainment with concealed fusion suggests that the pacing site is within a protected isthmus inside the reentrant circuit or outside but attached to the circuit (i.e., the pacing site can be in, attached to, or at the entrance to a protected isthmus that forms the diastolic pathway of the circuit). In this setting, transient entrainment is achieved when the stimulated wavefront propagating orthodromically resets the tachycardia, while the stimulated wavefront propagating antidromically

collides with the tachycardia wavefront in or near the reentry circuit and fails to exit the slow conduction zone. Only the tissue near the pacing site within the critical isthmus is antidromically activated; hence, there is no evidence of fusion. Compared with the intrinsic tachycardia, this antidromic capture can result in earlier intracardiac recordings from bipole sites located adjacent to the pacing region. The morphological appearance of the ECG, however, is the same during entrainment as during the tachycardia.

It should be emphasized that entrainment with concealed fusion can occur not only when pacing at the critical isthmus of the reentry circuit, but also during pacing at bystander pathways (such as a blind alley, alternate pathway, or inner loop) that are not critical to the maintenance of reentry. In the latter situation, activation propagates from

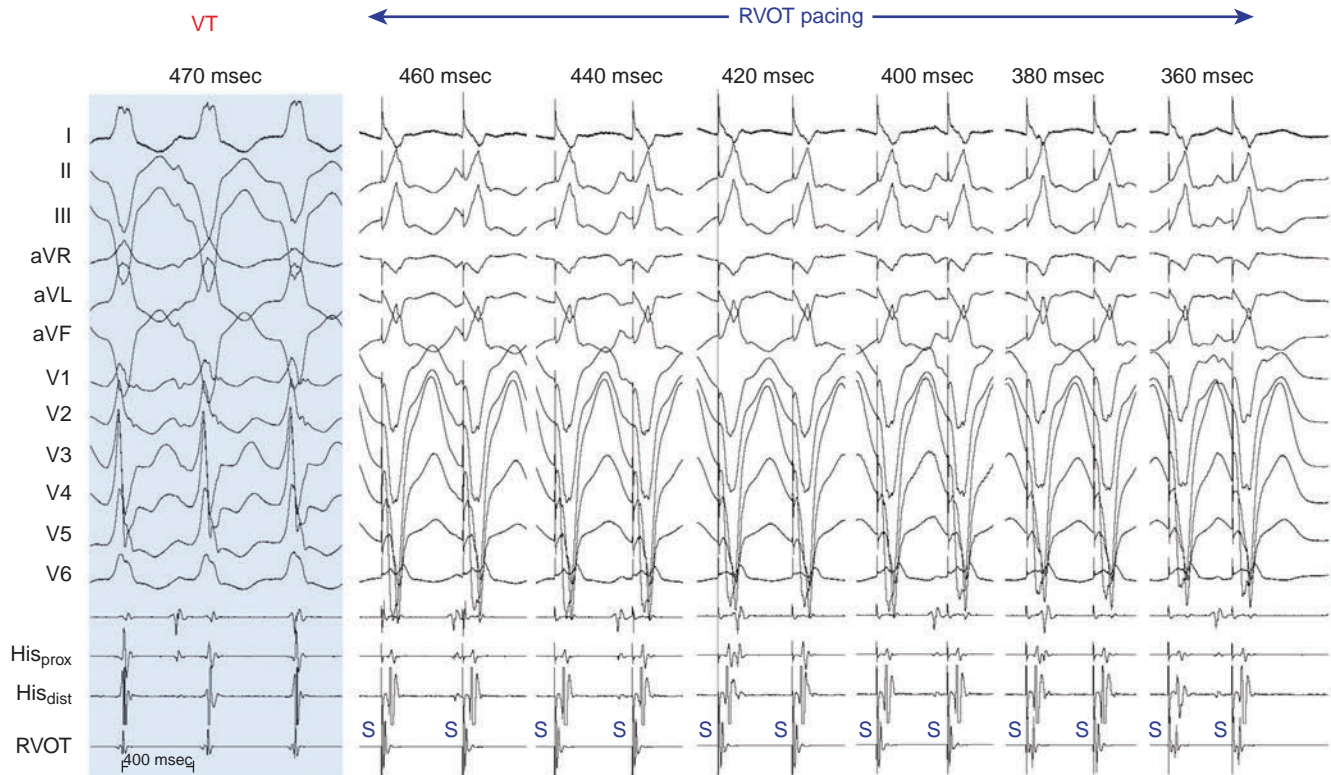


Fig. 22.15 Lack of Fusion With Ventricular Pacing During Focal Ventricular Tachycardia (VT). VT with a right bundle branch block pattern and left superior axis is shown at left in blue shading (cycle length [CL], 470 milliseconds). In the panels at right, pacing during VT over a range of CLs from the right ventricular outflow tract (RVOT, with a left bundle branch block pattern and right inferior axis) is shown. It is clear that while pacing during VT, all QRS complexes are identical, indicating no contribution of the VT to the QRS complexes (thus no fusion). *His_{dist}*, Distal His bundle; *His_{prox}*, proximal His bundle.

the main circuit loop but is constrained by block lines having the shape of a cul-de-sac; ablation at these sites does not terminate reentry.^{69,70,72}

Occasionally, one of the first few stimuli of a drive train intended to entrain VT terminates VT without propagation. Subsequent stimuli often result in QRS complexes that do not resemble VT, leading the operator to conclude that the site is far from the isthmus. Review of the first few stimuli of pacing may show that the site actually was very attractive for ablation (eFig. 22.9).

Entrainment with antidromic capture. When pacing is performed at a PCL significantly shorter than the TCL, the paced impulse can penetrate the circuit retrogradely (antidromically) to capture the presystolic electrogram (within the protected isthmus prior to the exit site). As a result, the tachycardia wavefront cannot exit from the reentrant circuit and, thus, cannot contribute to myocardial activation. Therefore the surface QRS during entrainment appears fully paced. When pacing is stopped, the impulse that conducts antidromically also conducts orthodromically to reset the reentrant circuit with orthodromic activation of the presystolic electrogram. When antidromic (retrograde) capture of the local presystolic electrogram occurs, the return cycle, even when measured at the site of the presystolic electrogram, will exceed the PCL by the difference in time between when the electrogram is activated retrogradely (i.e., preexcited antidromically) and when it would have been activated orthodromically (see Fig. 5.17).⁷⁰

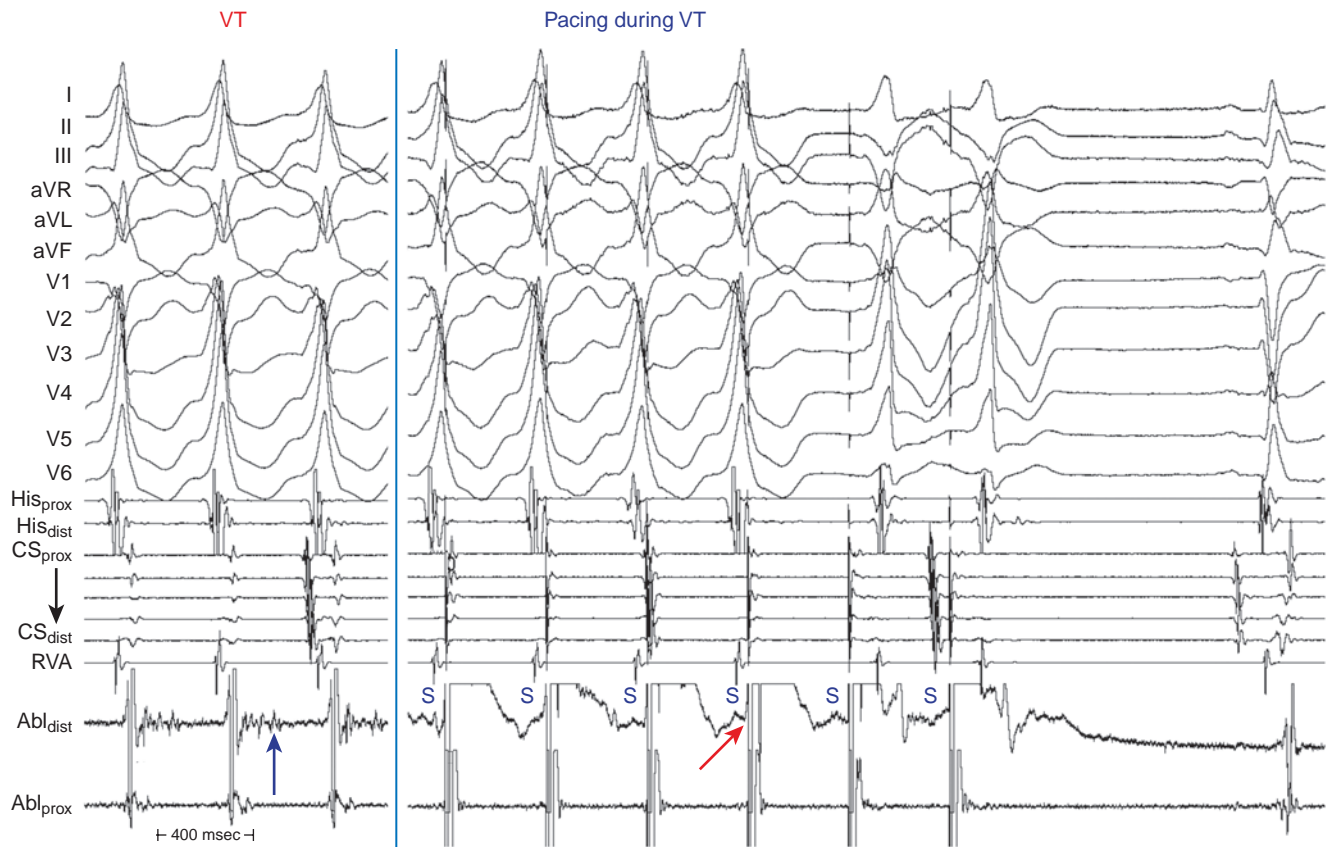
Tachycardia termination. The ability to terminate SMVT by rapid ventricular pacing or VES is influenced most importantly by the TCL (about 50% of VTs with TCLs less than 300 milliseconds will require electrical cardioversion), but also by the local ERP at the pacing site,

conduction time from the stimulation site to the site of origin of the VT, duration of the excitable gap, and presence of antiarrhythmic agents.

Failure of rapid ventricular pacing or VES to terminate VT has several potential explanations: (1) the reentrant circuit being a protected focus; (2) inability of VES to access the reentrant circuit because of local myocardial refractoriness; (3) absence of an accessible excitable gap; (4) termination of VT followed by reinitiation by a subsequent pacing impulse in the same pacing drive; or (5) failure of conduction block to occur within the reentrant circuit, despite accelerating the VT to the faster pacing rate.

Factors influencing termination of VT can be modified. Refractoriness at the site of stimulation can be overcome by the use of multiple VESs or a higher pacing current. The distance and conduction time from the site of stimulation to the VT site can be modified by changing the site of stimulation. The TCL can be increased by antiarrhythmic agents, but the response is unpredictable. Nonetheless, two problems are frequently encountered in attempts to terminate VT—acceleration of the VT by overdrive pacing and the appearance of multiple distinct uniform VT morphologies.

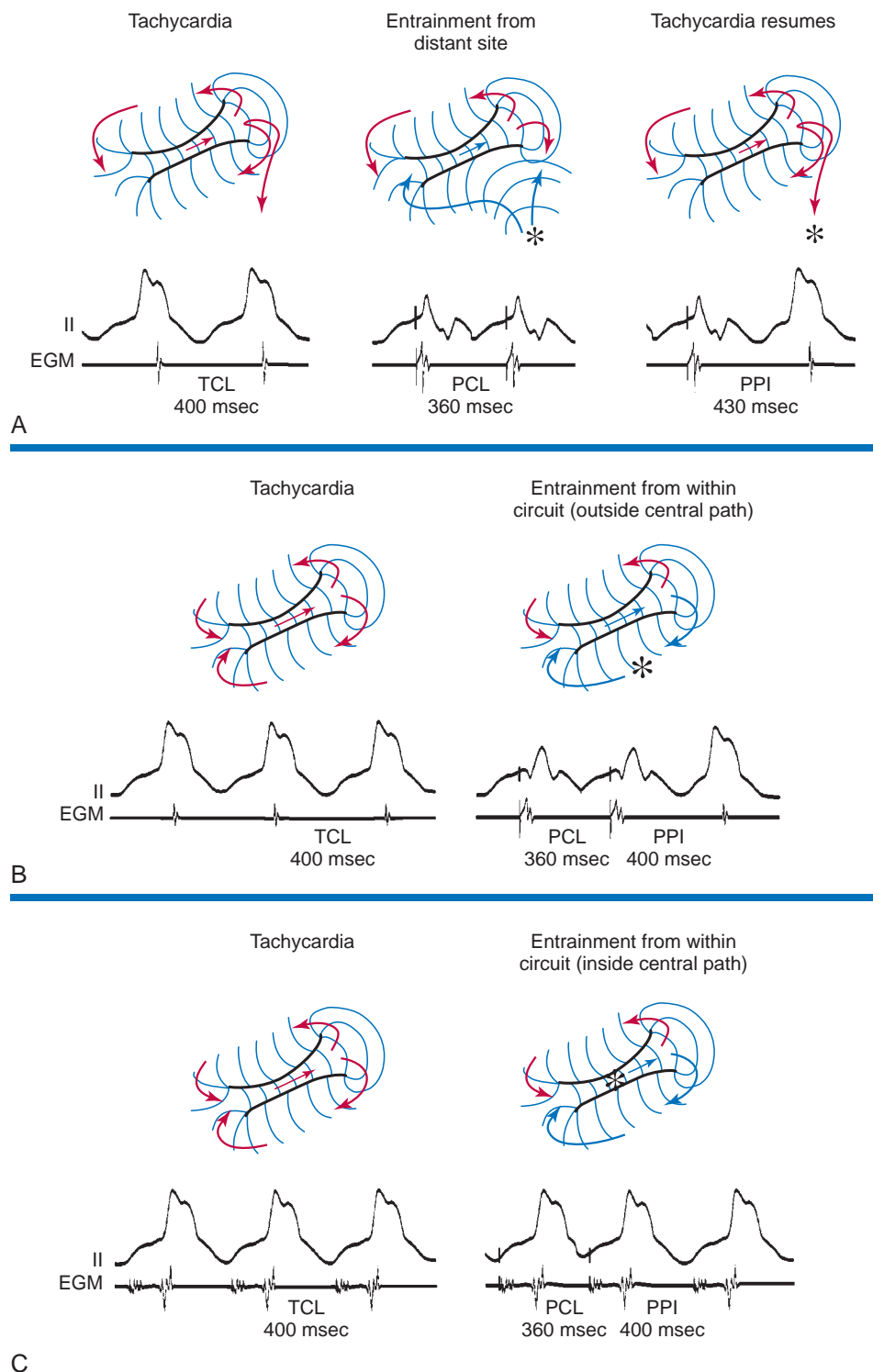
When tachycardia termination occurs, it is usually abrupt (regardless of the mode of stimulation used), which distinguishes reentrant VTs from triggered VTs. In reentrant VTs, termination must occur when an impulse penetrates the circuit and blocks in both directions. Rapid ventricular pacing is the most efficacious way of VT termination, regardless of the TCL. Approximately 80% of VTs terminated by a single VES have a TCL longer than 400 milliseconds. All VTs terminated by single or double VESs can also be terminated by ventricular pacing.



eFig. 22.9 Nonpropagated Ventricular Tachycardia (VT) Termination During Attempted Entrainment. VT is shown with a diastolic potential (*blue arrow*); during attempted stimulation at this site during VT, the first several stimuli (*S*) have no effect but the fifth stimulus (*red arrow*) results in VT termination without propagation of the impulse (no subsequent QRS). Subsequent stimuli capture the site but result in a very different QRS configuration. *Abl_{dist}*, Distal ablation site; *Abl_{prox}*, proximal ablation site; *CS_{dist}*, distal coronary sinus; *CS_{prox}*, proximal coronary sinus; *His_{dist}*, distal His bundle; *His_{prox}*, proximal His bundle; *RVA*, right ventricular apex.

Fig. 22.16 Entrainment Mapping of Ventricular Tachycardia (VT).

(A) Entrainment of VT from a distant site. Diagrammatic representation of a figure-of-8 VT circuit at left, with an electrogram recorded at a site remote from critical circuit elements. At center, during entrainment pacing, the paced wavefront from this remote site (*) interacts with the circuit by colliding with a VT wavefront that has exited the diastolic corridor while also entering the diastolic corridor at the opposite end. This results in fusion (part of the ventricle depolarized by the VT wavefront, part by the paced wavefront). For as long as pacing continues, this fusion of ventricular activation remains stable. With cessation of pacing (*right figure*), the last paced wavefront enters the diastolic corridor as on other cycles, but there is no subsequent paced wavefront to collide with the wavefront that is exiting the corridor; thus the first return cycle complex is entrained, but not fused. The PPI measured at the site of pacing reflects the time it takes to make one complete revolution around the circuit plus any time required to get from the pacing site to the circuit and back from the circuit to the pacing site. (B) Entrainment of VT from a site within the circuit. The pacing site (*) is within the circuit but outside the diastolic corridor. As a result, the entrained QRS complex shows fusion and the PPI equals the TCL. (C) Entrainment of VT from a site within the critical isthmus. The pacing site (*) is within the circuit and inside the diastolic corridor, recording the mid-diastolic electrogram. As a result, the entrained QRS complex shows no fusion and the PPI equals the TCL. The S-QRS interval equals the electrogram-to-QRS interval during VT. This is the ideal ablation site. EGM, Intra-cardiac electrogram; PCL, pacing cycle length; PPI, postpacing interval; TCL, tachycardia cycle length.



Termination is less likely to occur when the VT cannot be reset with very premature VES (i.e., the VES coupling interval is more than 75% of the TCL).

A single VES delivered during entrainment of VT can facilitate termination of VT by allowing easier access to the excitable gap. Even when a single VES alone or overdrive pacing alone fails to terminate the VT, the combination of both can be successful. Overdrive pacing ensures stable resetting of the VT circuit, allowing a single VES to interact with the circuit much more prematurely than it could in the absence

of entrainment. Overdrive pacing also shortens the excitable gap of tissue in the reset circuit, making it possible for a single VES to terminate the VT. This technique avoids the need for multiple VESs, which can increase the heterogeneity of conduction and refractoriness in the intervening tissue and produce polymorphic VT, and the need for rapid pacing, which might induce acceleration of the VT. This method is especially helpful in VTs that were accelerated by rapid pacing and especially in those VTs for which antiarrhythmic agents have made the tachycardia more difficult to terminate.

Response to Antiarrhythmic Drugs

Class I agents are the most uniformly successful drugs for slowing or terminating SMVT. These drugs can also facilitate the induction of SMVT in patients in whom SMVT cannot be induced by the standard programmed electrical stimulation protocol and in patients with CAD and nonsustained VT. Occasionally, class I agents produce incessant SMVT in patients who, before therapy, only had paroxysmal events. This phenomenon, almost always associated with a slower VT and prolongation of conduction by the agent, would not be expected if the mechanism were triggered activity or abnormal automaticity. Adenosine, beta-blockers, and calcium channel blockers are ineffective for termination of post-MI VT.

Exclusion of Other Arrhythmia Mechanisms

Exclusion of Triggered-Activity Ventricular Tachycardia

Stimulation site specificity. The site of ventricular stimulation should have no effect on the initiation of triggered-activity VT as long as the impulse reaches the focus of the VT. Reentrant VT, on the other hand, can demonstrate absolute or relative site specificity for initiation.

Inducibility with programmed electrical stimulation. Ventricular stimulation can initiate triggered-activity VT in less than 65% of cases. Rapid ventricular pacing to initiate triggered VT should be more effective than VES. Multiple VESs during NSR or following a drive train of fewer than 8 to 10 beats usually fail to initiate triggered-activity VT. Most episodes of triggered-activity VT induced by ventricular stimulation are usually nonsustained. Induction of triggered-activity VT with atrial pacing is not uncommon. In contrast, VES is more effective than rapid pacing at initiating reentrant VT.

Reproducibility of initiation. Reproducibility of triggered-activity VT induction using all methods is less than 50%. Reproducibility is markedly affected by quiescence. Once a triggered rhythm is initiated, a period of quiescence is necessary to reinstate the rhythm. Thus the ability to initiate, terminate, and reinstate a sequence is uncommon, in contrast to reentrant VT.

Relationship of ventricular stimulus to the onset of VT. Typically, both the initial cycle of the triggered-activity VT (the return cycle) and the TCL following cessation of pacing bear a direct relationship to the PCL (and a direct relationship to the coupling interval of the VES, when used). Thus the shorter the initiating ventricular PCL, or the shorter the initiating VES coupling interval, the shorter the interval to the first VT beat and the shorter the initial TCL. Occasionally, with early VESs, a jump in the interval to the onset of the VT complex occurs, so that it is approximately twice the interval to the onset of the VT initiated by later coupled VESs. This is secondary to failure of the initial DAD to reach the threshold while the second DAD reaches the threshold. Thus, in triggered-activity VTs caused by DADs, the coupling interval of the initial VT complex shortens or suddenly increases in response to progressively premature VES. It would not be expected to demonstrate an inverse or gradually increasing relationship, in contrast to reentrant VT. Only with the addition of very early VESs or, occasionally, very rapid ventricular pacing (PCL < 300 milliseconds) can a sudden jump in the interval to the first VT complex be observed. Furthermore, ventricular PCLs longer or shorter than the critical CL window fail to induce triggered-activity VT. This critical window may shift with changing autonomic tone.

Effects of catecholamines. Inducibility of triggered-activity VT is facilitated by catecholamines, whereas in the setting of reentrant VT, isoproterenol facilitates VT induction in only 5% of cases. However, induction of triggered-activity VT can be inconsistent and is exquisitely sensitive to the immediate autonomic status of the patient. Therefore noninducibility during a single EP study is not enough evidence to attribute the arrhythmia to a nontriggered activity mechanism.

Response to antiarrhythmic drugs. Triggered-activity VTs respond favorably to calcium channel blockers and beta-blockers. Conversely, those drugs fail to terminate the vast majority of VTs associated with CAD.

Diastolic electrical activity. In reentrant VT, electrical activity occurs throughout the TCL. Thus, during diastole, conduction is extremely slow and in a small enough area that it is not recorded on the surface ECG. Demonstration that the VT initiation is dependent on a critical degree of slow conduction, manifested by fragmented electrograms spanning diastole, and that maintenance of the VT is associated with repetitive continuous activity is consistent with a reentrant mechanism.

Exclusion of Bundle Branch Reentrant Ventricular Tachycardia

His bundle–ventricular interval. BBR should be suspected when the His potential precedes ventricular activation and the HV interval during VT is longer than that during NSR. In other VTs, the His potential is usually recorded immediately before or after, or obscured within the local ventricular electrogram. Occasionally, the His potential can precede the onset of the QRS in post-MI VT; however, in contrast to BBR VT, the HV interval in those VTs is shorter than that during NSR.

Oscillation of TCL. Spontaneous or induced changes in the V-V intervals during BBR VT are dictated and preceded by similar changes in the H-H intervals. These changes can be demonstrated by ventricular stimulation during VT or can occur spontaneously following initiation. In other VTs, in contrast to BBR VT, the V-V interval variation usually dictates the subsequent H-H interval changes.

Activation sequence. In the common type of BBR VT (LBBB pattern), the activation wavefront travels retrogradely up the LB to the HB and then anterogradely down the RB, with subsequent ventricular activation. This sequence is reversed in BBR VT with an RBBB pattern. Unfortunately, RB and LB potentials are not routinely recorded, so that the typical activation sequences (LB-HB-RB-V or RB-HB-LB-V) are not available for analysis. Even if either sequence is present, the HPS (usually the LB) could be activated passively in the retrograde fashion to produce an HB-RB-V sequence during an intramyocardial VT with an LBBB pattern without reentry requiring the LB. In these cases, other diagnostic criteria for BBR VT should be used.

Exclusion of Supraventricular Tachycardia

SVT with aberrancy. If VT exhibits 1:1 ventriculoatrial (VA) conduction, it can mimic SVT with aberrancy. Surface QRS morphology usually helps distinguish SVT with typical RBBB or LBBB from VT.⁷³ Furthermore, in VT, the atrium is not part of the tachycardia circuit and can be dissociated by atrial pacing. Also, the HV interval in aberrantly conducted SVT is always equal to or longer than that during NSR, which is in contrast to intramyocardial VTs. In addition, tachycardia response to VES and atrial pacing can be useful for distinguishing SVT from VT, as discussed in detail in **Chapter 21**.

Preexcited SVT. Differentiation between VT and preexcited SVT (i.e., SVT with anterograde conduction over an AV BT) is particularly difficult on the surface ECG because ventricular activation begins outside the normal intraventricular conduction system in both tachycardias. As a result, many of the standard criteria cannot discriminate between preexcited SVT and VT. The HV interval is usually short or negative in both preexcited SVT and VT, and does not help in the differential diagnosis.

Because the atrium is not part of the VT circuit, the ability to dissociate the atrium (with rapid atrial pacing) without influencing the TCL (V-V interval) or QRS morphology suggests VT and excludes preexcited SVTs. Other pacing maneuvers used for differential diagnosis are discussed in **Chapter 21**.

MAPPING

Preprocedural Evaluation

Evaluation and treatment of potential ischemia and heart failure decompensation, which could contribute to instability during the ablation procedure, is necessary. Cardiac imaging studies may be used to identify the size and location of the infarct that potentially contains the arrhythmogenic substrate. These tests also help exclude the presence of LV thrombus, which can increase the risk of embolization during mapping. Patients with post-MI VT should also be evaluated for comorbidities that can alter the approach to mapping and ablation. In patients with suspected peripheral vascular disease and valvular heart disease, evaluation of the presence of severe disease is warranted, because it can affect the approach to LV access (atrial transseptal vs. retrograde transaortic vs. epicardial). In addition, assessment of the risks for sedation and anesthesia must be performed prior to the procedure because these patients are likely to require deep sedation or general anesthesia.

Optimization of Cardiac Function

Treatment of congestive heart failure and myocardial ischemia should be optimized. Coronary revascularization should be considered in patients with reversible ischemia because substantial ischemic burden can often be aggravated by the potential induction of prolonged periods of tachycardia or hemodynamically unstable arrhythmias during the ablation procedure. In patients with frequent or incessant VT, however, catheter ablation may be required on an urgent basis before the assessment for CAD in order to gain prompt control of the ventricular arrhythmia.

Evaluation for Intracardiac Thrombi

Assessment of LV intracavitary thrombi is an important part of the preprocedural workup. The presence of LV thrombi can increase the risk of thromboembolism due to catheter manipulation, and can also prevent endocardial access to “critical” portions of the arrhythmia circuit. The incidence of LV thrombus after acute MI has diminished in the era of PCI but has been reported in up to 5% to 15%, especially in patients with anterior MI, LVEF less than 35%, and apical dyskinesia or aneurysm. Contrast transthoracic echocardiography (TTE), transesophageal echocardiography (TEE), cardiac computed tomography, and CMR may be used to exclude the presence of intracardiac thrombi. Although CMR is the gold standard, contrast TTE is a readily available tool with reliable positive and negative predictive value (93% and 91%, respectively). A recent report found intracardiac echocardiography (ICE) to be superior to TTE for the detection of LV thrombi. Another advantage of ICE is that it enables intraprocedural visualization of thrombus margins and guide catheter placement in relation to the LV thrombus.⁷⁴

The risk of embolic episodes is high in the presence of soft, mobile, and protruding LV thrombi, and less for chronic, organized, mural thrombi. Assessment of thrombus chronicity can be challenging. Laminated appearance of the thrombus is highly suggestive of an organized thrombus; however, specific criteria indicating thrombus chronicity are lacking. Furthermore, it is often difficult to reliably exclude acute-on-chronic thrombus layering.⁷⁵ The presence of a *mobile* thrombus is an absolute contraindication to endocardial catheter ablation. Conversely, the presence of a laminated thrombus per se is not a perceived contraindication if the patient has been therapeutically anticoagulated with warfarin for at least 4 weeks prior to ablation; however, the thrombus is very likely to reside in an area where mapping would be important (scar/aneurysm) and thus catheter movement in this area is generally inadvisable.

Similarly, the presence of intraatrial clots should be excluded in patients with inadequately anticoagulated persistent AF to reduce the risk of thromboembolism in the event of AF termination following

electrical shocks for termination of unstable ventricular arrhythmias, or transseptal access to the LV.

Imaging the Arrhythmogenic Substrate

In patients with ventricular dysfunction, tissue heterogeneity with inexcitable myocardial fibrous scar and surviving myocardium provides a potential substrate for reentry circuits. Several noninvasive methodologies have been used to assess the substrate and identify patients at high risk for ventricular arrhythmias.

Ventriculography. Left ventriculography provides valuable information about LV function and ventricular thrombi. In addition, regions of wall motion abnormalities and aneurysms can be identified that likely harbor the VT substrate.

Echocardiography. TTE is routinely performed to evaluate LV systolic function, LVEF, and wall motion abnormalities that may contain the potential VT substrate. TTE also serves as a reliable tool to rule out ventricular thrombi before LV procedures. In addition, it helps to identify relatively infrequent cardiomyopathies associated with VT such as arrhythmogenic right ventricular cardiomyopathy and hypertrophic cardiomyopathy. Although echocardiography can provide anatomical and contractile parameters, it cannot provide relevant clinical information about transmural extent and intramycocardial location of the scar.

TEE can be used in patients with AF or atrial flutter (AFL) to detect thrombi within the left atrium (LA) and LA appendage to prevent thromboembolic events when a transseptal access to the LV or cardioversion is required. Severe atheroma in the aorta detected on TEE may encourage the operator to avoid the retrograde approach to the LV.

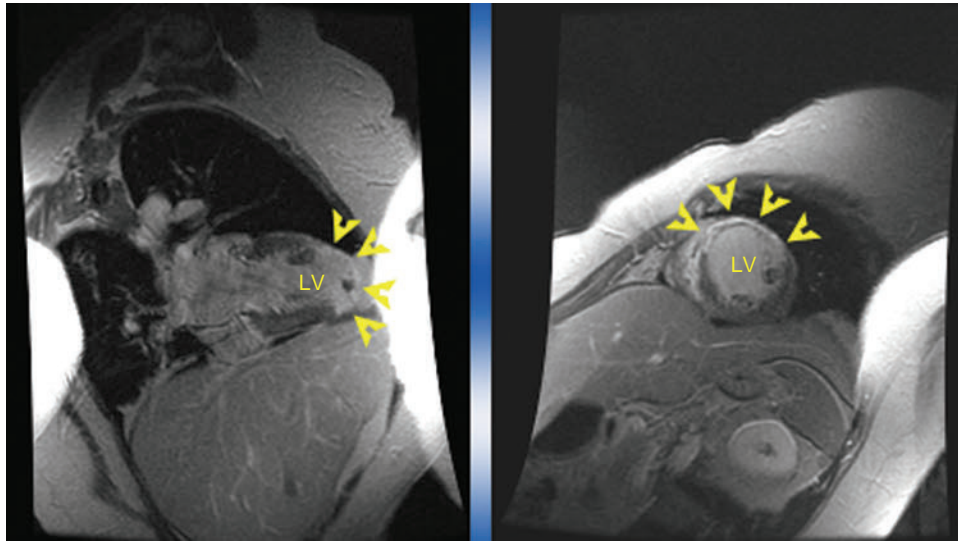
ICE applied from the right atrium (RA) and the right ventricle (RV) has been used for real-time imaging during VT ablation procedures. ICE provides both an anatomical and a functional assessment of the LV, allowing for real-time identification of wall motion abnormalities. ICE also allows for visualization of scarred tissue and thus may help to identify the VT substrate and facilitate mapping and ablation (see later).⁷⁶

Cardiac magnetic resonance. CMR is currently the noninvasive gold standard for quantification of cardiac anatomy and function, with a unique ability to differentiate and characterize tissues. CMR has been shown to detect myocardial fibrosis and necrosis and delineate regions of scar tissue potentially forming part of the arrhythmia substrate in patients with ischemic cardiomyopathy.^{30,31}

CMR is extremely valuable for assessing viable and nonviable myocardium in infarcted and poorly contracting myocardial areas, and enables the depiction of transmural and nontransmural infarctions with high spatial resolution and better accuracy than scintigraphic techniques (eFig. 22.10). Assessing the characteristics and distribution of myocardial scar by CMR can potentially help identify patients at high risk of VT. In patients with ischemic cardiomyopathy; the non-transmural hyperenhanced areas, but not the transmural hyperenhanced areas, were found to predict higher risk of sustained VT.

In addition, visualizing scar topography and transmural extent on delayed enhancement CMR helps focus mapping and ablation to the culprit regions and can potentially predict the approach required for successful VT ablation (endocardial vs. epicardial).^{77,78}

Furthermore, registration of preacquired CMR images with real-time electroanatomical mapping has successfully been used to facilitate and guide catheter navigation and ablation in the LV. Visualization of ventricular anatomy and obstacles to procedural success, for example, epicardial fat in the case of epicardial mapping approaches, and the possibility of navigation and ablation in the ventricular chambers have the potential to reduce procedure time, decrease the rate of complications, and increase success rates.



eFig. 22.10 Magnetic Resonance Scans of the Left Ventricle (LV) in a Patient With an Old Anterior Myocardial Infarction. Long axis (*at left*) and short axis (*at right*) views of the LV show a dense anteroapical scar (*arrowheads*), which can be visualized as a white thin area of the LV wall.

One potential disadvantage concerns the safety and quality of CMR imaging in patients with implanted cardiac devices. Nonetheless, recent studies have consistently demonstrated the feasibility and safety of CMR in patients with cardiac devices, and evolving technologies have further improved the CMR imaging compatibility of some devices. Importantly, the device hardware introduces significant artifacts, especially in the basal anterior free LV wall, which degrades the image quality and often limit interpretation of CMR in VT patients. However, the interventricular septum, and the LV lateral and inferior walls are mostly free of artifact in most patients. Recently, a wideband late gadolinium enhanced CMR technique has been reported to reduce hyperintense artifacts from the ICD generator.^{77,79}

Positron emission tomography. Currently, positron emission tomography (PET) is considered the gold standard for tissue viability assessment. In patients with scar-related VT, PET can accurately detect myocardial scar within the LV and provide additional tissue characterization by displaying metabolic and morphological information of the VT substrate. Its spatial resolution of 4 to 6 mm can delineate scar in any wall segment, with good correlation between areas of endocardial voltage less than 0.5 mV and PET-defined myocardial scar.⁸⁰

Because PET scans alone do not provide the necessary anatomical information required for integration with electroanatomic maps, computed tomography (CT) angiography scan is required to provide an anatomical skeleton onto which the physiological information acquired from the PET scan would be superimposed on its precise anatomical location. Fusion of multimodality imaging sets derived from PET/CT allows accurate, simultaneous display of LV anatomy and myocardial scar and can facilitate an image-guided approach to substrate-based VT ablations.⁸⁰

Cardiac CT. Contrast-enhanced cardiac CT enables a detailed and comprehensive evaluation of LV myocardium using multimodality imaging based on anatomical, dynamic, and perfusion parameters to identify abnormal substrate (myocardial scar and border zone) with high spatial (≤ 1 mm) and temporal resolution. Areas of CT hypoperfusion and ventricular wall thinning correlate best with areas of abnormal voltage (less than 1.5 mV) rather than scar alone (less than 0.5 mV). Perfusion imaging from CT can indicate scar transmural and intramyocardial scar location.^{78,81}

The ability of contrast-enhanced CT to characterize the transmural extent and intramyocardial location of scar tissue and to visualize surviving mid- and epicardial myocardium at sites of endocardial scar can potentially help identify areas involved in myocardial reentry representing appropriate ablation targets and help to overcome one of the significant limitations of endocardial voltage mapping. In addition, the presence of an epicardial VT substrate can facilitate planning of VT ablations, such as for a combined endocardial and epicardial approach. When compared with contrast-enhanced CMR, absolute sizes of early hypoperfused and late hyperenhanced regions were similar on contrast-enhanced CT and contrast-enhanced CMR.

In addition, the three-dimensional (3-D) CT-defined image of abnormal myocardium can be accurately extracted and embedded in clinical mapping systems displaying areas of abnormal anatomical, dynamic, and perfusion parameters for substrate-guided VT ablations.

Left Ventricular Access

The LV is generally accessed through the retrograde transaortic approach, usually via a femoral arterial access. An atrial transseptal approach can also be used, although accessing the entire LV is then more difficult. Both transseptal and retrograde approaches can be used concomitantly, so when a particular region of the LV cannot be mapped using one approach, it can be mapped using the other approach. Anticoagulation (with IV heparin) is started once the LV is accessed (or, more commonly,

before) to maintain the activated clotting time (ACT) between 250 and 350 seconds. Certain electrode arrays with high thrombogenicity may require an ACT of at least 300 seconds.

The presence of severe arterial disease, severe aortic stenosis, or mechanical aortic prosthesis prohibits the retrograde transaortic access to the LV. On the other hand, the presence of mechanical mitral valve precludes an atrial access to the LV. In addition, the presence of a *mobile* thrombus is an absolute contraindication to endocardial catheter ablation, and the epicardial approach should be considered.

Hemodynamic Support

Post-MI VT is often associated with hemodynamic instability that precludes detailed entrainment and activation mapping techniques. Furthermore, repetitive inductions of short periods of unstable VT, or even prolonged episodes of otherwise hemodynamically tolerated arrhythmia, can have a detrimental cumulative effect and expose patients to progressive hemodynamic compromise, myocardial ischemia, and exacerbation of heart and renal failure, affecting patient morbidity and clinical outcomes.⁸²

In some patients undergoing VT ablation, particularly those with severely depressed LVEF or preexisting significant heart failure, and in those in whom the induced VT is only marginally tolerated, circulatory support can be achieved with an IV infusion of dopamine, dobutamine, or phenylephrine; intraaortic balloon counterpulsation; extracorporeal membrane oxygenation (ECMO); or LV assist devices (Impella microcirculatory axial blood flow pump, Abiomed, Danvers, MA; and TandemHeart, Cardiac Assist, Pittsburgh, PA, United States). In addition, IV procainamide (infused with a maximal loading dose of 15 mg/kg at a rate of 50 mg/min, followed by a continuous infusion at a maximal rate of 0.11 mg/kg per minute) can help slow and stabilize the VT rate.⁸²⁻⁸⁴

Although intraaortic balloon pumps augment diastolic pressure and diminish afterload during periods of sinus rhythm, they do not provide a significant level of hemodynamic support during VT. Intraaortic balloon pumps require synchronization with the cardiac cycle, which is not feasible during fast ventricular arrhythmias. Conversely, temporary percutaneous LV assist devices are generally capable of providing greater hemodynamic stability and maintaining cardiac output and vital organ perfusion in the setting of unstable VT.⁸⁴ ECMO can be of particular advantage when the use of percutaneous LV assist devices is limited by the presence of mechanical aortic valves or LV thrombosis.⁸⁵

In addition to the potential benefit in reducing the risk of acute heart failure after the procedure, the improved hemodynamic support provided by percutaneous LV assist devices can permit sustaining VT for longer durations and, hence, allow more detailed entrainment and activation mapping during VT, ultimately yielding a greater number of VT terminations with ablation. Even in the setting of hemodynamically stable VT, mechanical hemodynamic support can help reduce intracardiac filling pressures, ventricular wall stress, and myocardial oxygen consumption, which can potentially reduce the risk of cardiac stunning due to multiple VT inductions for mapping and during ablation.

Percutaneous LV assist devices have been used as a “rescue” intervention in patients who develop periprocedural acute hemodynamic decompensation or when mapping and ablation of hemodynamically unstable VT is needed. More recently, several centers have reported potential benefits of the preemptive use of mechanical hemodynamic support in high-risk patients undergoing VT ablation. Predictors of periprocedural acute hemodynamic decompensation include advanced age, ischemic cardiomyopathy, severely reduced LVEF, presentation with VT storm, New York Heart Association (NYHA) functional class III/IV, chronic obstructive pulmonary disease, diabetes, and the use of

general anesthesia.⁸⁶ However, in recent studies, this did not necessarily translate into improved short-term procedural success or greater long-term freedom from VT. Furthermore, several potential risks of using those devices should be considered, including complications related to vascular access and thromboembolism. Therefore these devices are used selectively, and their potential risks should be balanced against the expected added value for the mapping and ablation strategy utilized in the individual patient. Although some interference from these devices with electroanatomic mapping may be observed, it is generally not detrimental to ablation success.^{54,84,87}

Importantly, the volume status and fluid balance should be closely monitored during the ablation procedure, especially when utilizing open-irrigated ablation catheters. In some patients, administration of diuretics and utilization of decreased irrigation rates or closed-irrigation ablation catheters need to be considered. When the transeptal approach is utilized for LV access, monitoring LA pressure can help assess volume status.

Electroanatomic Mapping

The main goal of VT mapping is the identification of the site of origin of the VT. The site of origin of the tachycardia is the source of electrical activity producing the QRS. Although this is a discrete site of impulse formation in focal rhythms, during macroreentrant VT it represents the exit site from the diastolic pathway (i.e., from the critical isthmus of the reentrant circuit) to the myocardium giving rise to the QRS complex. During macroreentrant VT, the critical isthmus is typically formed by a corridor of conductive myocardial tissue bounded by non-conductive tissues (barriers) through which the depolarization wavefront must propagate to perpetuate the tachycardia. These barriers can be anatomical (e.g., scar areas, mitral annulus) or functional (present only during tachycardia, but not in sinus rhythm) obstacles (Fig. 22.17).

Activation and entrainment mapping are used to identify the critical isthmus of the VT and guide ablation. When multiple VTs are inducible, it is recommended that all mappable VTs be completely mapped and targeted. However, some recommend targeting only the clinical VT, especially in very ill patients in whom the goal is to decrease the frequency of ICD shocks and improve the quality of life. It is important to have a 12-lead ECG of the clinical VTs available, if possible, for review at the time of the EP procedure. This information can be used to focus on the exit region suggested by the VT morphology to help limit the extent of detailed mapping, particularly when the clinical VT is hemodynamically unstable. In patients with ICDs, VT is usually terminated promptly and a 12-lead ECG is often not available. Nonetheless,

comparing the TCL and ICD electrogram morphology during spontaneous and induced VTs can be helpful, particularly when trying to limit ablation and target only the presumptive clinical VT.

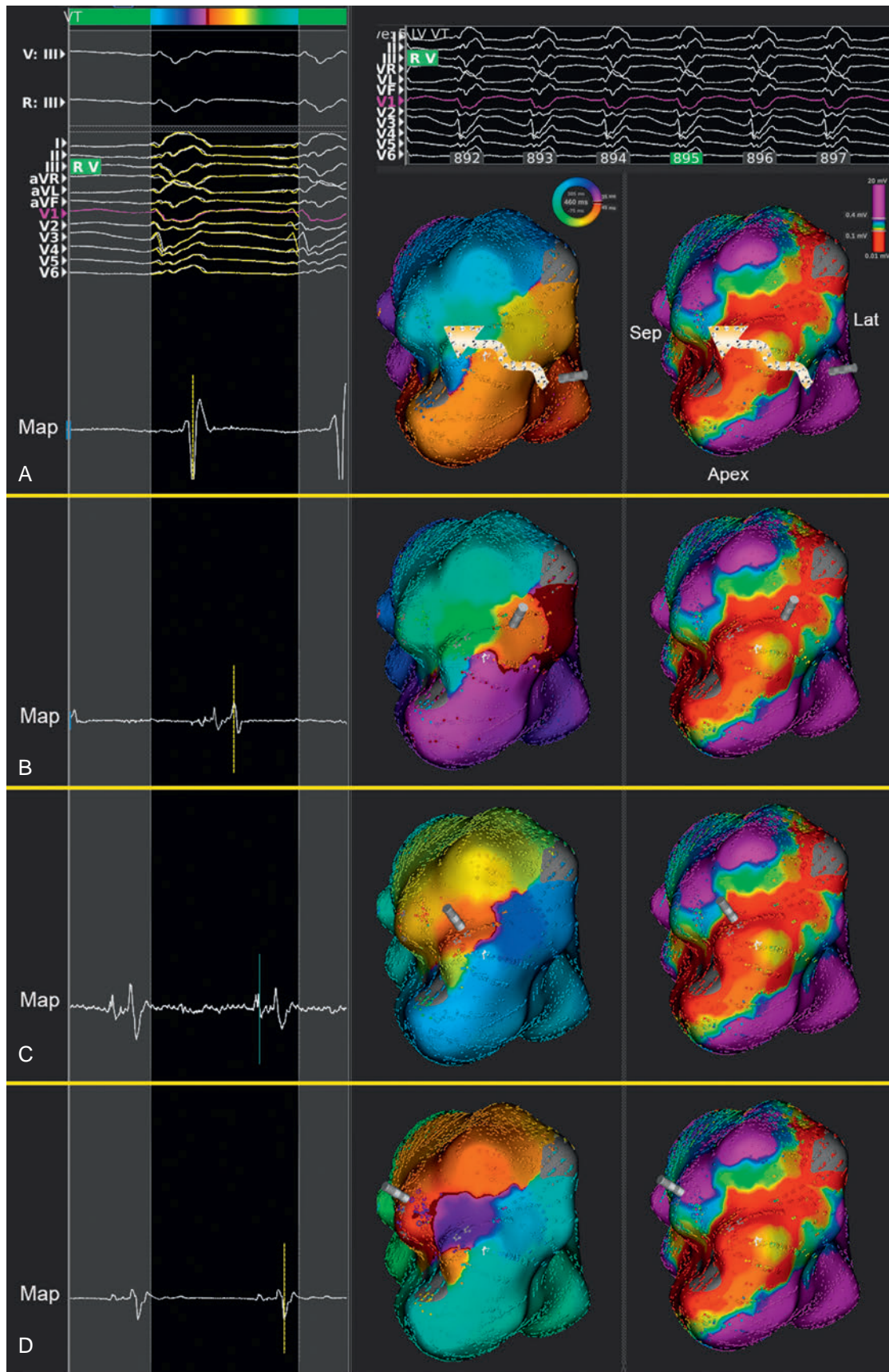
However, mapping of VT circuits and identification of critical isthmuses are often challenging, and require reproducibly inducible SMVT that is hemodynamically stable. The abnormal area of scarring, where the isthmus is located, is often large and contains false isthmuses (bystanders) that confuse mapping. Although in the majority of cases a portion of the VT isthmus is located in the subendocardium, where it can be ablated, in some cases the isthmuses or even the entire circuits are deep in the myocardium or even in the epicardium and cannot be identified or ablated from the endocardium. In addition, multiple potential reentry circuits are frequently present, giving rise to multiple different monomorphic VTs in a single patient. Ablation in one area may abolish more than one VT or leave VT circuits in other locations intact.

Substrate mapping has evolved as an adjunct to activation and entrainment mapping to help identify potential circuit isthmuses during NSR, which can then be targeted by entrainment and activation mapping techniques during VT. Substrate mapping becomes the main strategy to guide ablation when SMVT is not reproducibly inducible or not hemodynamically tolerated. This approach reduces or eliminates the need for mapping during prolonged periods of VT.

Using conventional mapping techniques, it is difficult to conceive the 3-D orientation of cardiac structures because these techniques use a limited number of recording electrodes guided by fluoroscopy. Although catheters using multiple electrodes to acquire data points are available, the exact location of an acquired unit of EP data is difficult to ascertain because of inaccurate delineation of the location of anatomical structures. The inability to associate the intracardiac electrogram accurately with a specific endocardial site also limits the reliability with which the roving catheter tip can be placed at a site that was previously mapped. This results in limitations when the creation of long linear lesions is required to modify the substrate, and when multiple isthmuses, or channels, are present. This inability to identify, for example, the site of a previous ablation increases the risk of repeated ablation of areas already dealt with and the likelihood that new sites can be missed.

Therefore electroanatomic mapping using CARTO (Biosense Webster, Diamond Bar, CA, United States), ESI-NavX (St. Jude Medical, St. Paul, MN, United States), or Rhythmia (Boston Scientific, Cambridge, MA, United States) is generally utilized for mapping and ablation of post-MI VT. Electroanatomic mapping can help in the precise description of VT reentrant circuits, sequence of ventricular activation during the VT, rapid visualization of the activation wavefront, and identification of a

Fig. 22.17 Electroanatomic Activation and Voltage Mapping of Postinfarction Ventricular Tachycardia (VT). A series of electroanatomic (Rhythmia) activation and voltage maps of VT originating from the anteroapical region of the left ventricle (LV). Top panel, window of interest includes the QRS complex template (*left, white*) with overlay of the acquired QRS complex (*yellow*), and continuous recording during VT (*top right*). Panels A through D each include: (1) recorded local electrogram (*left*) with timing annotation; (2) activation map (*middle*) with leading propagation wavefront in red and tail in purple and roving electrode icon denoting the anatomical location of annotated local electrogram; (3) voltage map (*right*) and identical location of the roving electrode icon as that in the corresponding activation map. Red on the voltage map indicates local electrogram amplitudes of <0.1 mV; purple indicates electrogram amplitudes >0.4 mV. (A) The activation wavefront arrives at the lateral aspect of the anteroapical scar, where local electrogram occurs at the end of the QRS complex. The arrow shows the likely path of wavefront propagation during diastole. (B) The wavefront is propagating transversely through the scar; the local recording exhibits mid-diastolic fractionated electrogram, likely corresponding to the diastolic pathway of the reentry circuit. (C) The wavefront continues propagating toward the septal aspect of the scar, and the corresponding local activation time is late diastolic. (D) The propagating wavefront arrives at the septal scar border, where the local activation timing is presystolic, likely denoting the exit site. *Lat*, Lateral LV wall; *Sep*, septal LV wall.



slow-conducting pathway. These systems also help navigation of the ablation catheter, planning of ablation lines, and cataloging sites of interest (e.g., sites with favorable entrainment or pace mapping findings), which can then be revisited with precision. In addition, the use of electroanatomic mapping systems is essential for substrate-based approaches to mapping and ablation of post-MI VT.

A quadripolar mapping-ablation catheter is typically utilized for point-by-point mapping. Poles 1 to 3 (distal) and 2 to 4 (proximal) of the ablation catheter are used for recording, and poles 1 to 3 are used for stimulation. High-density mapping can be facilitated by the use of a 20-pole catheter (PentaRay, Biosense-Webster) or mini-basket catheter (Orion, Boston Scientific).^{88–90}

Activation Mapping

In post-MI VT, the goal of activation mapping is to seek sites with continuous activity spanning diastole or with an isolated mid-diastolic potential, presumably representing the diastolic pathway (critical isthmus) of the reentrant circuit. Unlike focal tachycardias, a presystolic electrogram preceding the tachycardia complex by 10 to 40 milliseconds is not adequate in defining the ablation target of a macroreentrant tachycardia.

Activation mapping of post-MI VT has several prerequisites, including inducibility of VT at the time of EP testing, hemodynamic stability of the VT (which usually requires a relatively slow VT rate), and stability of the VT reentry circuit (i.e., stable VT morphology and TCL). If the tachycardia is not stable (morphologically or hemodynamically), mapping can still be performed in some cases by starting and stopping the VT after data acquisition at each site, assuming reinitiation of the same VT. In addition, poorly tolerated rapid VTs can sometimes be slowed by antiarrhythmic drugs to allow for mapping. Generally, antiarrhythmic drugs do not alter the sequence of activation, despite slowing of the VT and widening of the QRS and, although the electrogram at the site of origin can widen, its relationship to the onset of the QRS remains unchanged. Furthermore, as discussed previously, the use of IV vasopressors and external hemodynamic support devices can potentially provide hemodynamic support and allow mapping of otherwise unstable VT.^{82–84} The use of 20-pole catheter (PentaRay; 2–6–2 mm interelectrode spacing, 1 mm electrodes), the mini-basket catheter (Orion), and noncontact mapping can also provide large amounts of activation mapping data during nonsustained or unstable VT.

Technique of Activation Mapping

During electroanatomic activation mapping, the electrical reference is generally chosen as a morphologically stable and regular electrogram obtained from an endocardial (e.g., RV apical electrogram) or surface lead (e.g., surface ECG lead with a QRS complex during VT demonstrating a sharp apex and a strong positive or negative deflection). The width of the window of interest is adjusted to approximate, usually 20 milliseconds less than, the TCL. The middle of the window of interest is selected to coincide with the electrical reference or with mid-diastole on the ECG.

Point-by-point activation mapping or high-density multielectrode or mini-basket catheter mapping is performed by moving the mapping catheter over the endocardium of the region of interest to sample local electrogram morphology and activation timing. Initially, one should seek the general region of the origin of the tachycardia as indicated by the surface ECG and preablation imaging studies localizing the infarct region that possibly harbors the arrhythmogenic substrate (see Fig. 22.17).

Typically, bipolar electrogram recordings are used for activation mapping as they provide an improved signal-to-noise ratio and more clearly defined high-frequency components. Unipolar recordings in

scar areas, on the other hand, have very low amplitudes with a poor signal-to-noise ratio and distant electrical activity can be difficult to separate from local electrograms. This is especially true when recording from areas of prior MI, where the QS potentials are ubiquitous, and it is often impossible to select a rapid negative dV/dt when the entire QS potential is of low amplitude and/or slowly inscribed. Therefore unipolar electrograms are typically filtered at comparable settings to those of bipolar electrograms (30 to 300 Hz or more) when scar-related VT is studied. Filtering gives reasonably clean signals; however, the signal is often of very low amplitude. Therefore bipolar recordings are preferred for activation mapping; filtered unipolar electrograms can be used to help ensure that the tip electrode, which is the ablation electrode, is responsible for the early component of the bipolar electrograms.

The local activation time for each endocardial position under the mapping catheter is calculated as the interval between the electrical reference and the onset of the high-frequency bipolar electrogram as it leaves the baseline. Infarct regions are sought first and more data points are acquired around these areas, as identified by low-amplitude potentials, with diastolic electrograms, or double potentials. In regions of myocardial scar, electrode catheters often record multiple potentials separated in time, some of which are far-field potentials that are caused by depolarization of adjacent myocardium. Therefore it is important to carefully interrogate the recorded electrogram and assign activation timing only to the local electrogram. Assignment of an incorrect time of activation that can render activation sequence maps misleading.

The resulting reentrant circuit is considered to be the spatially shortest route of unidirectional activation encompassing a full range of mapped activation times (greater than 90% of the TCL) and returning to the site of earliest activation (see Fig. 22.17). Contact is critical when standard quadripolar catheters are used. The degree of contact can be assessed by pacing threshold or impedance measurements at the recording electrode pair. Use of ICE and contact force catheters can also help ensure adequate catheter contact.⁹¹

Continuous Activity

Theoretically, if reentry is the mechanism of VT, electrical activity should occur throughout the VT cycle. Thus, during diastole, conduction should be extremely slow and in a small enough area that it is not recorded on the surface ECG. Demonstration that VT initiation is dependent on a critical degree of slow conduction, manifested by fragmented electrograms spanning diastole, and that maintenance of the VT is associated with repetitive continuous activity, would be compatible with reentry.

In post-MI VT, continuous activity, when observed, invariably occurs at sites that demonstrate markedly abnormal electrograms during NSR (Fig. 22.18). However, continuous diastolic activity can be recorded in only 5% to 10% of post-MI VTs with detailed mapping using standard equipment. The ability to record continuous activity depends on the spatial and geometric arrangement of the involved tissue, the position of the catheter, and the interelectrode distance. Thus continuous diastolic activity is likely to be recorded only if a bipolar pair records a short isthmus. If a longer isthmus is recorded (i.e., the isthmus is larger than the recording area of the catheter or the catheter is not covering it completely), a nonholodiastolic electrogram will be recorded. In such VTs, when nonholodiastolic electrical activity is recorded at the isthmus, repositioning of the catheter to other sites can allow recording of the bridging of diastole (electrical activity in these adjacent sites spans diastole) (Fig. 22.19). Failure to record continuous activity is not surprising because catheter and intraoperative VT mapping suggest that most post-MI VTs incorporate a diastolic pathway 1 to 3 cm long and a few millimeters to 1 cm wide, with a circuit area probably larger than 4 cm².

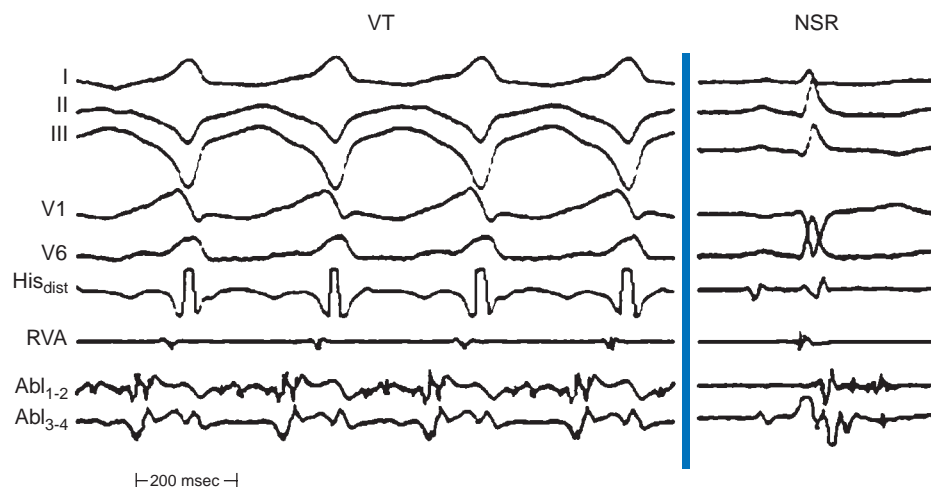


Fig. 22.18 Continuous Diastolic Electrical Activity During Reentrant Ventricular Tachycardia (VT). VT is shown with almost continuous electrical activity in the distal ablation recording. During sinus rhythm (*right*), the electrogram is very fragmented and outlasts the surface QRS complex. *NSR*, Normal sinus rhythm.

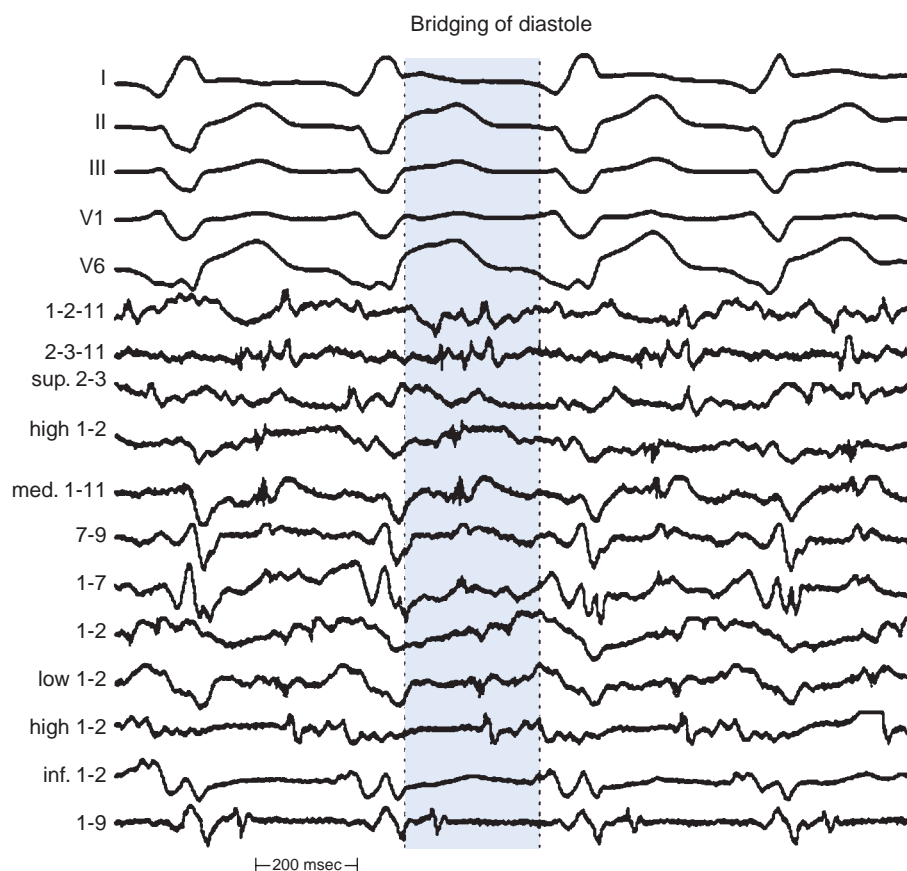


Fig. 22.19 Bridging of Diastole During Reentrant Ventricular Tachycardia (VT). Shown is the compilation of numerous mapping sites around the left ventricular apical region during VT; diastole is shaded, showing progression of activation from early to mid to late diastole.

Not all areas from which diastolic activity is recorded are necessarily part of the reentrant circuit. Such sites can represent late activation and may not be related to the VT critical isthmus. Analysis of the response of these electrograms to spontaneous or induced changes in TCL is critical in deciding their relationship to the VT circuit. Electrical signals that come and go throughout diastole should not be considered

continuous. For continuous activity to be consistent with reentry, the following must be demonstrated: (1) VT initiation is dependent on continuous activity (i.e., broadening of electrograms that span diastole); (2) VT maintenance is dependent on continuous activity, so that termination of continuous activity, either spontaneously or following stimulation, without affecting the VT would exclude such continuous

activity as requisite for sustaining the VT; (3) the recorded continuous diastolic activity is not just a broad electrogram whose duration equals the diastolic interval, which can be verified by analyzing the local electrogram while pacing during sinus rhythm at a PCL comparable to the TCL—if pacing produces continuous diastolic activity in the absence of VT, the continuous electrogram has no mechanistic significance; (4) motion artifact should be excluded (this is easiest because such electrograms are recorded only in infarcted areas and never from moving, contractile normal areas); (5) the continuous activity should be recorded from a circumscribed area; and (6) if possible, ablation of the area from which continuous activity is recorded will terminate the VT.

Mid-Diastolic Activity

An isolated mid-diastolic potential is defined as a low-amplitude, high-frequency diastolic potential separated from the preceding and subsequent ventricular electrograms by an isoelectric segment (see Fig. 22.17; eFig. 22.11). It is likely that isolated mid-diastolic potentials that cannot be dissociated from the VT are generated in segments of the zone of slow conduction or critical isthmus, which are integral components of the reentry circuit. The earliest presystolic electrogram closest to mid-diastole is the most commonly observed indicator of an isthmus site in a VT circuit; however, continuous diastolic activity or bridging of diastole at adjacent sites or mapping a discrete diastolic pathway would be most consistent with a reentrant circuit (see Fig. 22.18).

In post-MI reentrant VT, the earliest presystolic electrogram is invariably abnormal and frequently fractionated or split, regardless of the QRS morphology of the VT or the location of the isthmus. Thus a normal presystolic bipolar electrogram (amplitude greater than 3 mV, duration less than 70 milliseconds) should prompt further search for earlier activity. The earliest electrogram in post-MI VT not infrequently has diastolic and systolic components separated by an isoelectric component, representing activation of different pieces of tissue separated by a barrier of scar (see eFig. 22.11). Detailed mapping will usually reveal more than one site of diastolic activity. It is therefore essential to demonstrate that the diastolic site recorded is in fact the earliest site. This can be done by demonstrating that sites surrounding the assumed earliest site are activated later than the index site, even though they may be diastolic in timing. If, after very detailed mapping, the earliest recorded site is not at least 50 milliseconds presystolic, this suggests that either the map is inadequate (most common) or the VT isthmus is deeper than the subendocardium, in the midmyocardium, or even incorporating the subepicardium.

It is important to recognize that mid-diastolic sites can also be part of a larger area of abnormal slow conduction unrelated to the VT circuit (i.e., a dead-end pathway), and can be recorded from a bystander site attached to the isthmus. Therefore, regardless of where in diastole the presystolic electrogram occurs (early, mid, or late), its appearance on initiation of VT and diastolic timing, although necessary, does not confirm its relevance to the VT mechanism. One must always confirm that the electrogram cannot be dissociated from the VT and is required for VT maintenance (see eFig. 5.2). This can be verified by demonstrating that the electrogram (regardless of its position in diastole) maintains a fixed relationship to the subsequent QRS (and not the preceding QRS) during induced or spontaneous changes in the TCL.

In general, local activation at post-MI VT exit sites precedes the onset of the surface QRS complex by 40 to 80 milliseconds (see Fig. 22.17). Sites with local activation occurring at less than 20 milliseconds before the QRS are considered “post-exit” sites. At sites with presystolic potentials, the time interval between the recorded near-field diastolic and far-field systolic potentials can help confirm whether those sites with presystolic potentials truly represent the exit of the VT circuit versus being merely bystander sites. Short intervals (approximately 25

milliseconds) are suggestive of an exit site, whereas longer intervals are more compatible with either a bystander site or a more proximal location within the isthmus.⁹²

Limitations of Activation Mapping

Standard transcatheter endocardial mapping as performed in the EP laboratory is limited by the number, size, and types of electrodes that can be placed within the heart. Because these methods cover only a small portion of the endocardial surface, time-consuming point-by-point maneuvering of the catheter is required to trace the origin of an arrhythmic event and its activation sequence in the neighboring areas.

The success of roving point mapping is predicated on the sequential beat-by-beat stability of the activation sequence being mapped and the ability of the patient to tolerate the sustained arrhythmia. Therefore it can be difficult to perform activation mapping in the setting of poorly inducible VT at the time of EP testing, hemodynamically unstable VT, and unstable VT morphology.

Although activation mapping is adequate for defining the site of origin of focal tachycardias, it is deficient by itself in defining the critical isthmus of macroreentrant tachycardias. Adjunctive mapping modalities (e.g., entrainment mapping, pace mapping) are required for this.

Entrainment Mapping

Focal ablation of multiple sites defined as being in the reentrant circuit may not result in elimination of VT; that instead requires ablation of an isthmus bordered by barriers on either side, which is critical to the reentrant circuit. Because the circuit incorporates sites outside this critical isthmus, ablation of these external sites will not eliminate VT. Entrainment mapping during reentrant VT is used to verify whether a site recording diastolic activity (regardless of where in diastole it occurs, its position, and appearance on initiation of VT) is functionally involved in the VT circuit, which helps in focusing ablation efforts in areas likely to eliminate VT (see Fig. 22.16).

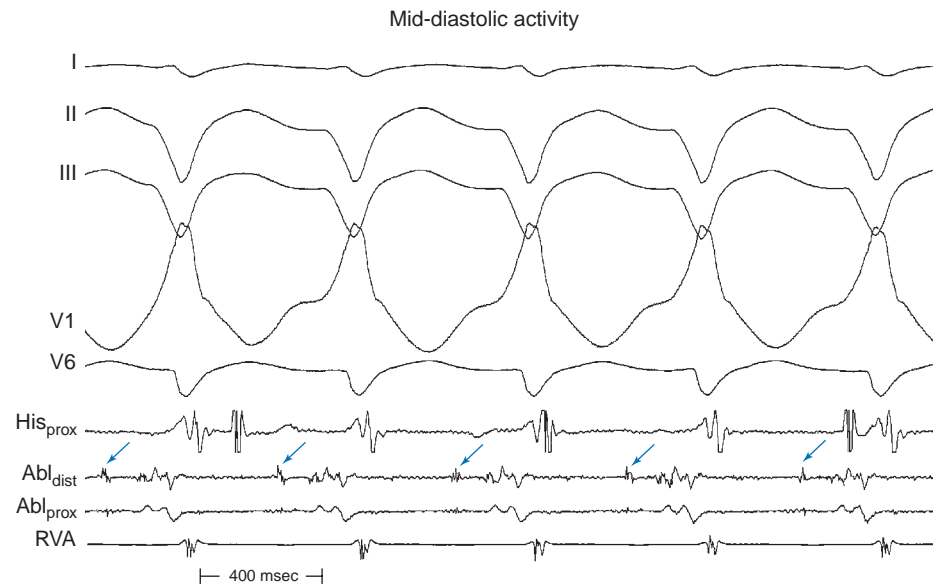
Technique of Entrainment Mapping

Entrainment mapping is directed to sites identified by other mapping modalities, such as activation and pace mapping, as potentially related to the reentrant circuit. These include areas of slow conduction (manifest as fractionated electrograms), sites with mid-diastolic electrograms, or those displaying long delays between the pacing stimulus and the captured surface ECG complex.

Entrainment mapping can be reliably carried out only if one can record and stimulate from the same area (e.g., for 2-5-2-mm spacing catheters, record from the second and fourth poles and stimulate from the first and third poles). Pacing is usually started at a PCL just shorter (10 to 30 milliseconds) than the TCL. Pacing should be continued for a long enough duration to allow for entrainment; short pacing trains are usually not helpful.

After cessation of each pacing drive, the presence of entrainment should be verified, employing the entrainment criteria discussed previously (see Figs. 5.17 and 5.19). The mere acceleration of the tachycardia to the pacing rate and then resumption of the original tachycardia after cessation of pacing does not establish the presence of entrainment, and evaluation of the postpacing interval (PPI) or other criteria is meaningless when the presence of true entrainment has not been verified. Moreover, it is important to verify the absence of termination and reinitiation of the tachycardia during the same pacing train.^{69,70}

Once the presence of entrainment is verified, several criteria can be used to indicate the relation of the pacing site to the reentrant circuit. The first entrainment criterion to be sought is concealed fusion. Entrainment with concealed fusion indicates that the pacing site is in a protected isthmus located within or attached to the reentrant circuit. Whether



eFig. 22.11 Mid-Diastolic Electrical Activity During Reentrant Ventricular Tachycardia (VT). VT is shown with small mid-diastolic potentials (*arrows*) on the ablation recording. *Abl_{dist}*, Distal ablation site; *Abl_{prox}*, proximal ablation site; *His_{prox}*, proximal His bundle; *RVA*, right ventricular apex.

this protected isthmus is crucial to the reentrant circuit or is just a bystander site needs to be verified by other criteria, mainly comparing the PPI to the TCL and comparing the stimulus-exit interval to the electrogram-exit interval. Furthermore, the ratio of the stimulus-exit interval to the TCL can provide information regarding the location of the pacing site within the diastolic pathway of the reentry circuit. Long (51% to 70% of TCL), intermediate (31% to 50% of TCL), and short ($\leq 30\%$ of TCL) stimulus-exit intervals are observed during pacing from the entrance, central isthmus, and exit site of the reentry circuit, respectively. Features of entrainment when pacing from different sites are listed in Box 22.2 (Fig. 22.20; and see Fig. 5.16).⁷²

BOX 22.2 Entrainment Mapping Reentrant Ventricular Tachycardia

Pacing From Sites Outside Ventricular Tachycardia Circuit

- Manifest fusion on surface ECG and/or intracardiac recordings
- PPI – TCL > 30 msec
- S-QRS interval > local electrogram to QRS interval

Pacing From Sites Inside Ventricular Tachycardia Circuit but Outside Protected Isthmus

- Manifest fusion on surface ECG and/or intracardiac recordings
- PPI – TCL < 30 msec
- S-QRS interval = local electrogram-to-QRS interval

Pacing From Protected Isthmus Outside Ventricular Tachycardia Circuit

- Concealed fusion
- PPI – TCL > 30 msec
- S-QRS interval > local electrogram to QRS interval

Pacing From Protected Isthmus Inside Ventricular Tachycardia Circuit

- Concealed fusion
- PPI – TCL < 30 msec
- S-QRS interval = local electrogram to QRS interval (± 20 msec)

ECG, Electrocardiogram; PPI, postpacing interval; S, stimulus; TCL, tachycardia cycle length; VT, ventricular tachycardia.

Entrainment With Concealed Fusion

Entrainment with concealed fusion (sometimes also referred to as “concealed entrainment” or “exact entrainment”) is defined as entrainment with orthodromic capture and a QRS complex on all 12 surface ECG leads identical to that of the VT, and it suggests that the pacing site is within, attached to, or at the entrance to a protected isthmus that forms the diastolic pathway of the circuit (see Figs. 22.16 and 22.21). However, the positive predictive value of entrainment with concealed fusion in identifying effective ablation sites is only 50% to 60%, indicating that entrainment with concealed fusion can often occur at sites that are not critical to the maintenance of reentry (i.e., bystander pathways), such as a blind alley, alternate pathway, or nondominant inner loop. Even when such sites are believed to reside within the reentrant circuit isthmus, ablation can fail if lesions are too small to interrupt the circuit completely. Other mapping criteria can be helpful in increasing the probability of identifying an effective site for ablation of VT in combination with entrainment with concealed fusion (Table 22.3).

1. PPI equal to the TCL (± 30 milliseconds)
2. Electrogram-QRS interval is equal to the S-QRS interval (this criterion improves the positive predictive value for successful ablation to approximately 80%).
3. Ratio of the S-QRS interval to the TCL less than 70% (this criterion improves the positive predictive value for successful ablation to approximately 70%).
4. An isolated mid-diastolic potential that cannot be dissociated from VT (this criterion increases the positive predictive value for identifying an effective ablation site to approximately 90%).

Postpacing Interval

The PPI is the interval from the last pacing stimulus that entrained the tachycardia to the next recorded local electrogram at the pacing site (see Fig. 22.16). The PPI remains relatively stable when entrainment of VT is performed at the same site, regardless of the length of the pacing drive. This is in contrast to overdrive suppression seen in automatic arrhythmias, which would be associated with progressive delay of the first tachycardia beat return cycle with progressively longer overdrive pacing drives.

Assessment of the PPI helps differentiate early presystolic electrical activity from late diastolic activity, which can be unrelated to the tachycardia circuit (see Fig. 22.21). During entrainment from sites within

TABLE 22.3 Sensitivity, Specificity, and Predictive Values of Analyzed Mapping Criteria in Association With Concealed Entrainment for Effective Ablation Sites

Mapping Criterion	Sensitivity (%)	Specificity (%)	Positive Predictive Value (%)	Negative Predictive Value (%)
Concealed entrainment	—	—	54	—
IMDP				
Overall	40	76	67	53
Not dissociable from VT	32	95	89	54
PPI = TCL	58	19	45	29
S-QRS/TCL < 0.7	96	52	71	92
S-QRS = EGM-QRS				
Excluding IMPD	32	86	73	51
Including IMPD	56	86	82	62

EGM, Electrogram; IMPD, isolated mid-diastolic potential; PPI, postpacing interval; S-QRS, stimulus-to-QRS interval; TCL, tachycardia cycle length; VT, ventricular tachycardia.

From Bogun F, Bahu M, Knight BP, et al. Comparison of effective and ineffective target sites that demonstrate concealed entrainment in patients with coronary artery disease undergoing radiofrequency ablation of ventricular tachycardia. *Circulation*. 1997;95:183.

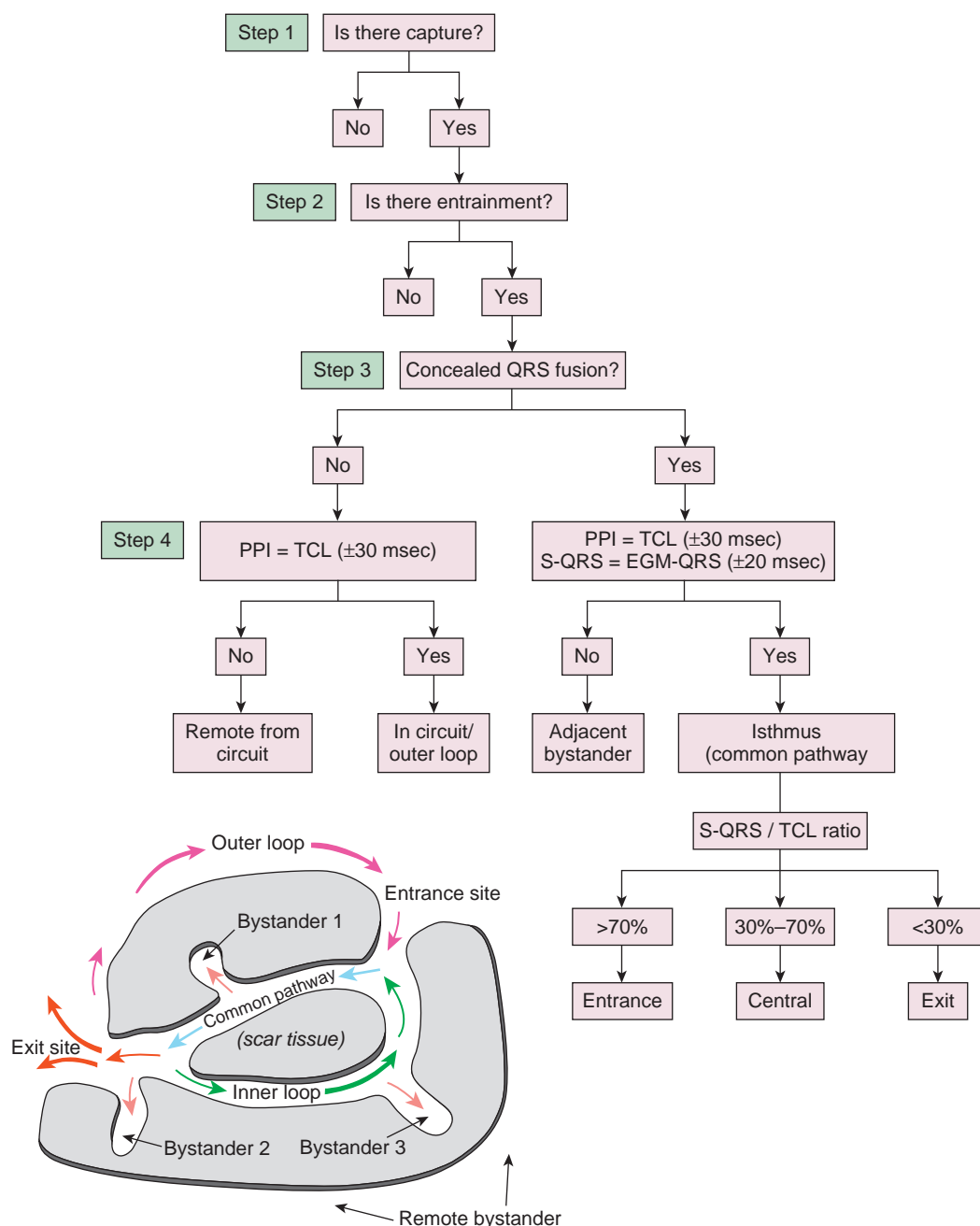


Fig. 22.20 An Algorithmic Approach to Entrainment in Ventricular Tachycardia. The accompanying illustration is a schematic representation of a macroreentrant ventricular tachycardia circuit, showing a common diastolic pathway (critical isthmus), entrance and exit sites, inner and outer loops, and bystander dead-end paths in three locations. *EGM*, Electrogram; *PPI*, postpacing interval; *S*, stimulus; *TCL*, tachycardia cycle length.

the reentrant circuit, the orthodromic wavefront from the last stimulus propagates through the reentry circuit and returns to the pacing site following the same path as the circulating reentry wavefront. The conduction time required is the revolution time through the circuit. Thus the PPI, measured from the pacing site recording, should be equal (± 30 milliseconds) to the TCL. At sites distant from the circuit, stimulated wavefronts propagate to the circuit, then through the circuit, and finally back to the pacing site. Thus the PPI should be equal to the TCL (representing one complete revolution through the reentry circuit) plus the time required for the stimulus to propagate from the pacing site to the

tachycardia circuit and back (see Fig. 22.20). The greater the difference between the PPI and the TCL, the longer the conduction time and distance between the pacing site and the reentry circuit. The PPI – TCL value is highly reproducible during repeated entrainment attempts at the same PCL.^{72,93}

The PPI should be measured to the near-field potential that indicates depolarization of tissue at the pacing site (see Figs. 22.16 and 22.21). Far-field potentials (caused by depolarization of adjacent myocardium) are common during mapping of infarct-related VT and can confound interpretation of the PPI. Measurement of the PPI to a far-field potential

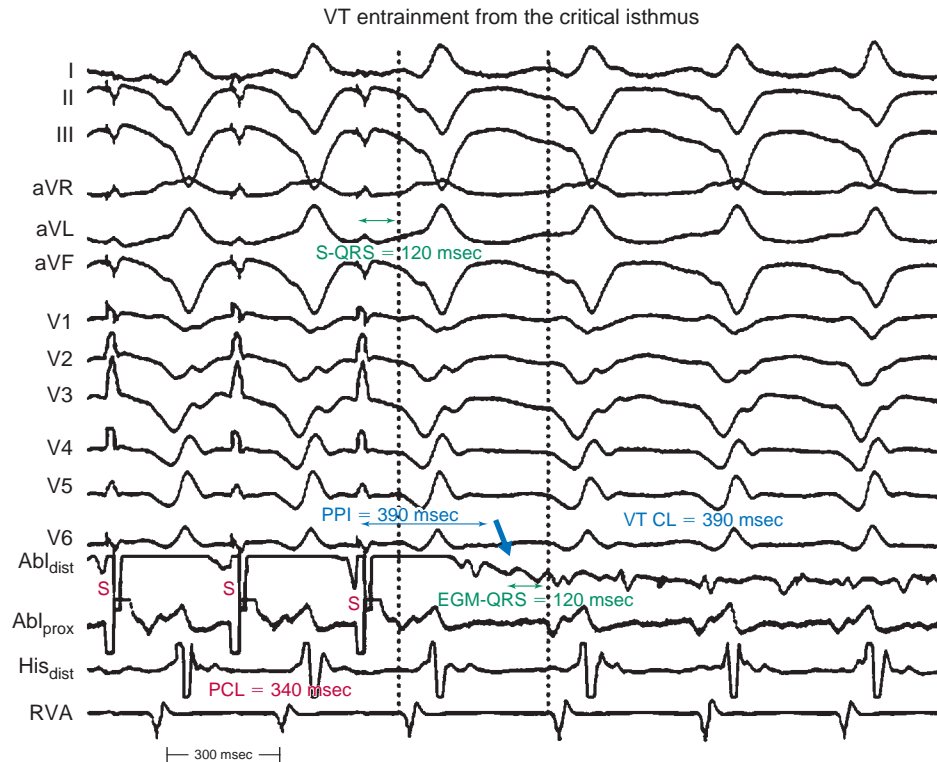


Fig. 22.21 Entrainment During Post-Myocardial Infarction Ventricular Tachycardia (VT) From the Critical Isthmus. The mid-diastolic potential (arrow) is present at the pacing site. Dashed lines denote QRS onset. Each stimulated complex is identical to that of VT at right (entrainment with concealed fusion). This, and findings that the stimulus-QRS (S-QRS) interval with pacing equals the electrogram-QRS (EGM-QRS) interval in VT and that the PPI equals the TCL, indicates that pacing is from the protected diastolic corridor. Radio-frequency delivery at this site terminated VT in 4 seconds. Abl_{dist}, distal ablation site; Abl_{prox}, proximal ablation site; CL, cycle length; His_{dist}, distal His bundle; PCL, pacing cycle length; PPI, postpacing interval; RVA, right ventricular apex.

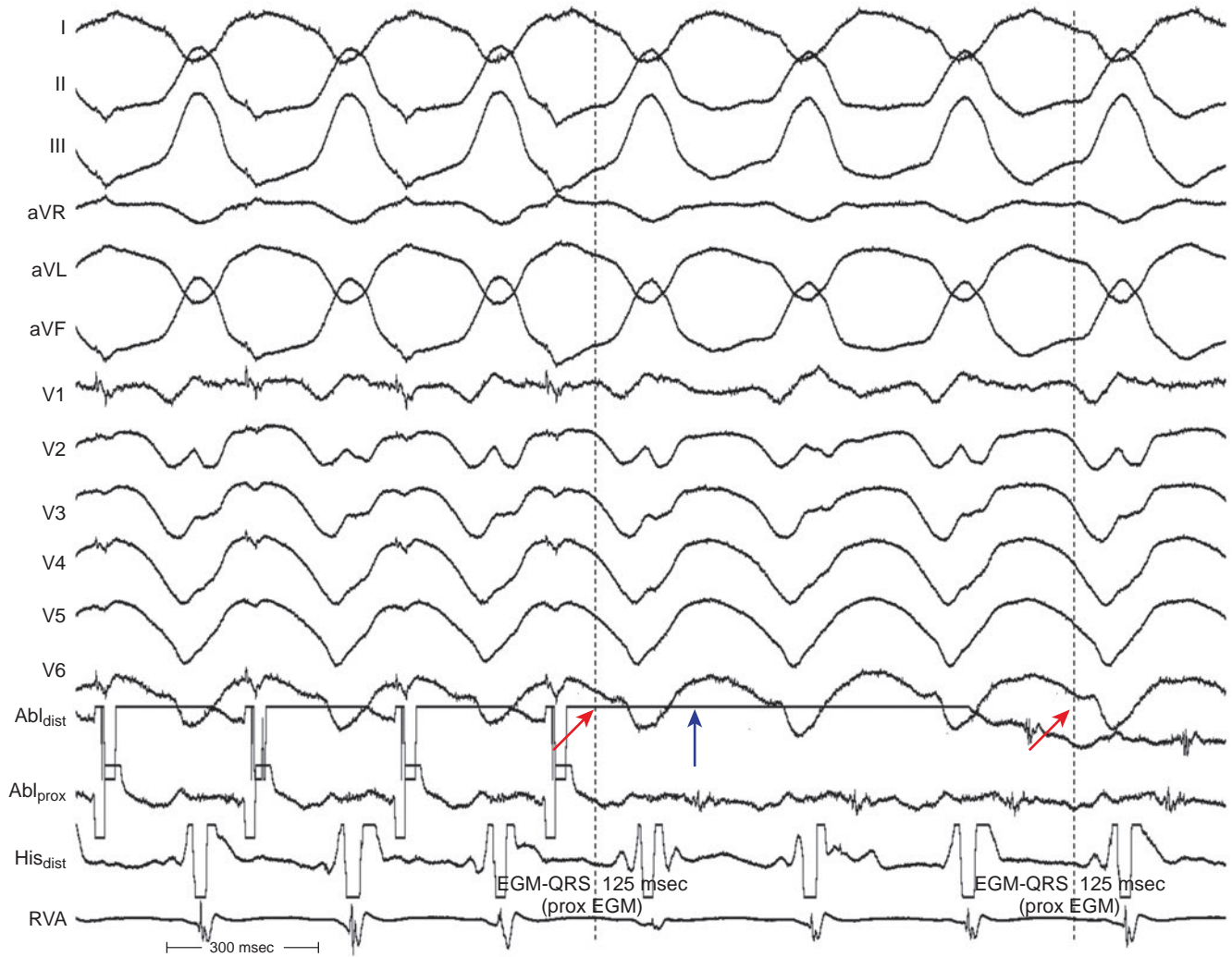
introduces an error, the magnitude of which is related to the conduction time between the pacing site and the source of the far-field potential (Fig. 22.22). When the PPI appears to be shorter than the TCL, the potential used for measurement is likely a far-field potential. Analysis of the potentials recorded during entrainment often allows identification of the far-field potential so that it can be excluded from activation maps and the PPI measurement and, hence, improves the accuracy of mapping scar-related arrhythmias. The stimulus artifact obscures the potential produced in the tissue immediately at the stimulation site (i.e., near-field potentials). Thus the local potential is not visible during pacing, but reappears after the last entrained QRS complex. On the other hand, far-field potentials usually fall sufficiently late after the pacing stimulus to be visible, and remain undisturbed during entrainment (see Fig. 22.22). These far-field potentials are accelerated to the pacing rate, but are not changed in morphology compared with those observed during tachycardia. The far-field potentials often precede the next stimulus by a short interval so that the tissue generating the far-field potential is probably refractory at the time of the next stimulus. Hence, the stimulus is not directly depolarizing the tissue generating the far-field potential. That these potentials are distant from the distal recording electrode is further supported by the lack of effect of RF ablation on the far-field potential.^{69,94,95}

The validity of the difference between the PPI and TCL (PPI – TCL) is based on the assumption that the recorded electrogram represents depolarization at the pacing site. Ideally, electrograms are recorded from the mapping catheter electrodes used for stimulation, but this is

sometimes difficult. Electrical noise introduced during pacing can obscure the electrograms at the stimulating electrodes, and some recording systems do not allow recording from the pacing site. When the electrograms from the pacing site are not discernible because of stimulus artifact, relating the timing of the near-field potential to a consistent intracardiac electrogram or surface ECG wave can be used to determine the PPI. A reasonable alternative is to calculate the PPI from electrograms recorded by electrodes adjacent to those used for pacing (i.e., from the proximal electrodes of the mapping catheter), provided such electrograms are also present in the distal electrode recordings (eFig. 22.12). However, this does introduce potential error, particularly if low-amplitude local electrograms present at the pacing site are absent at the proximal recording site. A more accurate alternative is assessment of the (PPI – TCL) value from the conduction time between the last pacing stimulus that entrains tachycardia and the second beat after the stimulus (the N + 1 beat) by comparing this interval with the electrogram timing at the pacing site in any following beat (Fig. 22.23). Additional errors can also be introduced by the decremental conduction properties of the zone of slow conduction that might cause a rate-dependent lengthening of the PPI.^{94,95}

Electrogram-to-QRS Interval Versus Stimulus-to-QRS Interval

This criterion is helpful in differentiating a critical component of the zone of slow conduction from a blind alley or noncritical alternate (bystander) pathway, in a manner analogous to that of the (PPI – TCL) method (see Fig. 5.16). During entrainment with concealed fusion, an



eFig. 22.12 Using the Proximal Electrogram Recording as a Surrogate for the Distal Electrogram. Entrainment of ventricular tachycardia (VT) is shown. The postpacing interval cannot be directly assessed owing to saturation of the distal ablation electrode (*Abl_{dist}*) recording (*blue arrow*). The interval from the proximal ablation electrode (*Abl_{prox}*) recording electrogram to QRS can be compared with the same interval during VT (*red arrows*) to serve as a surrogate for the distal ablation recording electrogram, as long as there is minimal disparity in the timing of these two recordings. *EGM*, electrogram; *His_{dist}*, distal His bundle; *RVA*, right ventricular apex.

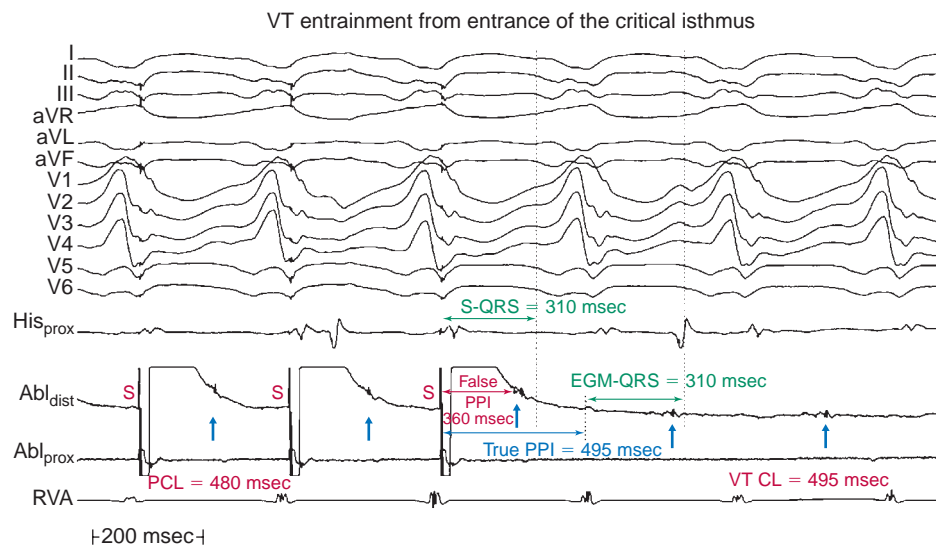


Fig. 22.22 Entrainment During Postmyocardial Infarction Ventricular Tachycardia (VT) at a Site With Both Systolic and Late Diastolic (Arrows) Potentials. Stimulation (S) entrains VT with an identical QRS configuration (concealed fusion) and a very long S-QRS interval, suggesting pacing at the entrance of the protected isthmus. The sharp electrogram (arrows) at this site is present and accelerated to the PCL, suggesting that the tissue generating this potential is not directly depolarized by the pacing stimulus and is, therefore, a far-field potential. The PPI measured from the last stimulus to this far-field potential is falsely short. The local potential (red arrow) is not discernible during pacing, consistent with direct capture, but reappears after the last stimulus. The true PPI is measured from the last stimulus to this local potential. *Abl_{dist}*, Distal ablation site; *Abl_{prox}*, proximal ablation site; *CL*, cycle length; *EGM*, electrogram; *His_{prox}*, proximal His bundle; *PCL*, pacing cycle length; *PPI*, postpacing interval; *RVA*, right ventricular apex.

electrogram-QRS interval equal to the S-QRS interval (± 20 milliseconds) suggests that the pacing site lies within the reentry circuit and not in a dead-end bystander pathway attached to the circuit (see Figs. 22.21 and 22.22).

During entrainment of reentrant tachycardia, the interval between the pacing stimulus and the onset of the QRS complex reflects the conduction time from the pacing site to the exit of the reentrant circuit (S-QRS interval), regardless of whether the pacing site is inside or outside the reentrant circuit. This is because activation starts at the pacing site and propagates in sequence to the circuit exit site. Pacing from the outer loop and remote bystander sites generates very short stimulus-exit intervals because the myocardium outside the circuit is directly activated by the pacing stimulus. In contrast, pacing from protected sites, such as the diastolic pathway (isthmus) of the reentry circuit or attached bystander or inner loop sites (communicating with the isthmus of the circuit and sharing the same exit), produces longer S-QRS intervals that reflect the conduction time from the pacing site through the protected pathway to the exit site of the circuit.

On the other hand, during tachycardia, the interval between the local electrogram at a given mapping site and circuit exit site (electrogram-QRS interval) can reflect the true conduction time between those two sites if they are activated in sequence (as occurs when the mapping site is located directly within the reentrant pathway), or it can be shorter than the true conduction time if those two sites are activated in parallel (which occurs when the mapping site is located outside the reentrant circuit).^{69,72} Consequently, when mapping along the diastolic pathway of the reentry circuit, the electrogram-QRS interval becomes progressively shorter as the mapping catheter is sequentially moved from the entrance toward the central isthmus and then the exit site of the circuit. Electrograms from the isthmus are generally fractionated and low amplitude, and occur during diastole resulting in early- (entrance), mid- (central), and late- (exit) diastolic (or presystolic) potentials. In

contrast, mapping sites located at bystander sites attached to the isthmus of the circuit are activated in parallel with the exit site, resulting in a shortened electrogram-QRS interval (i.e., a “pseudo-interval” that does not represent a true conduction time between the two locations).

Because a diastolic electrogram is not specific for the isthmus and can be recorded from bystander sites, comparing the S-QRS interval during entrainment to the electrogram-QRS interval (measured at the pacing site) during tachycardia can help distinguish the isthmus sites from attached bystander and inner loop sites. At isthmus sites, activation from those sites to the exit of the circuit follow the same pathway during both tachycardia and entrainment. In contrast, attached bystander and inner loop sites are activated in parallel with the exit site during tachycardia but in sequence during entrainment, resulting in a significantly shorter (more than 20 milliseconds) electrogram-QRS interval than S-QRS interval. On the other hand, at any given pacing site, an electrogram-QRS interval that is equal (± 20 milliseconds) to the S-QRS interval indicates that the pacing site lies within the reentry circuit and excludes the possibility that the site is a dead-end pathway attached to the circuit (i.e., not a bystander).

This method requires that the stimulated orthodromic wavefronts exit from the circuit at the same site as the tachycardia wavefronts (i.e., presence of entrainment with concealed fusion). Any degree of QRS fusion indicates that the stimulated wavefronts could be exiting from another route, invalidating this analysis. However, QRS fusion is often difficult to detect when less than 22% of the QRS is fused, which poses a major limitation to the S-QRS method.⁷¹ To avoid this limitation, a modification of the S-QRS interval method has been proposed whereby the S-QRS interval is measured to the second beat, which unquestionably results from a wavefront that has emerged from the tachycardia circuit and is not fused. The QRS complex and electrogram inscribed during or immediately after the pacing stimulus are defined as QRS(N) and electrogram(N), respectively; the following QRS and electrogram

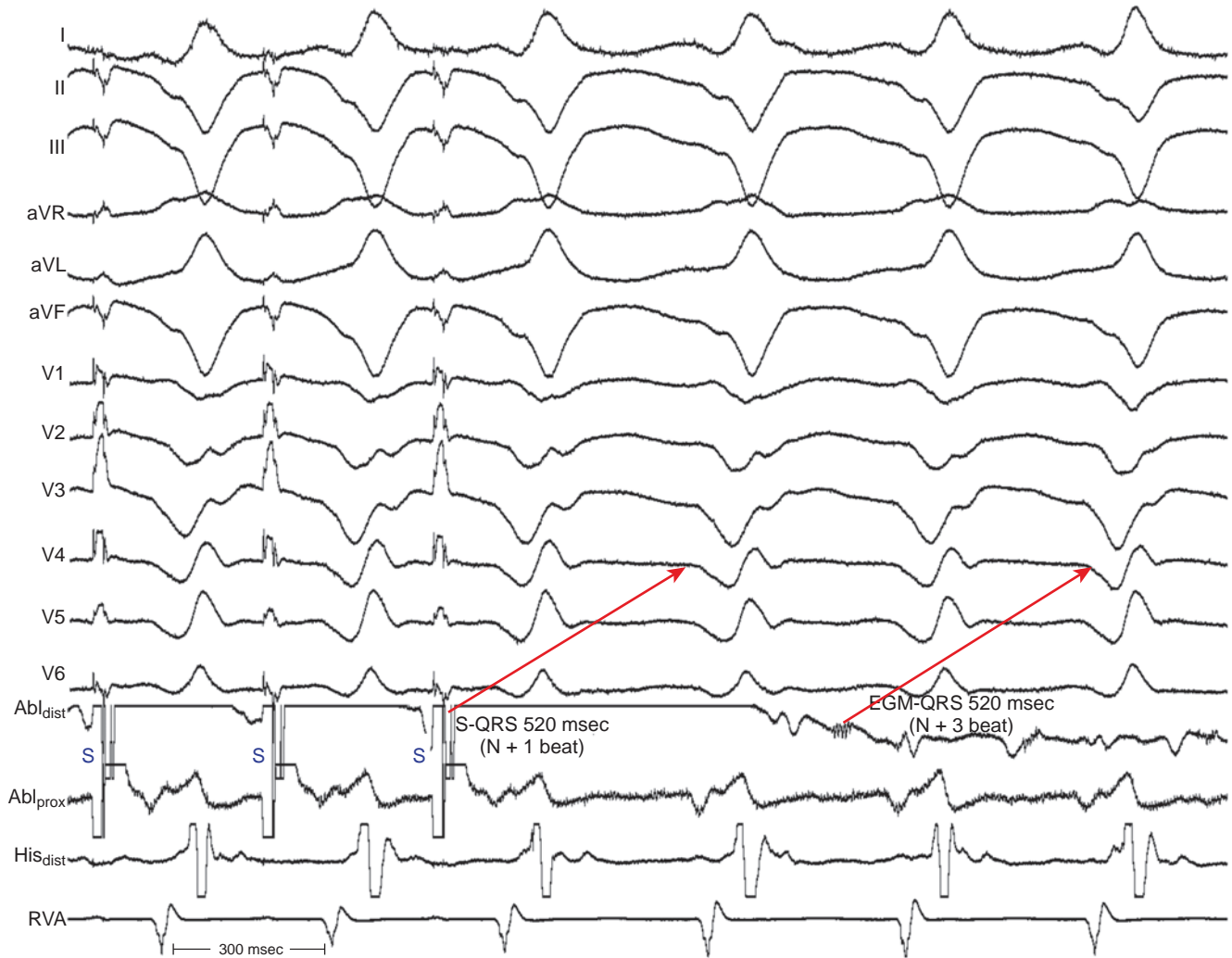


Fig. 22.23 The $N + 1$ Rule. Entrainment of ventricular tachycardia (VT) is shown. The postpacing interval cannot be directly assessed because of saturation of the distal ablation electrode (Abl_{dist}) recording. The interval from stimulus (S) to the next VT complex ($N + 1$) can be compared with the interval from the electrogram after it is again visible, to a subsequent VT complex ($N + 3$ in this case). If the difference between these intervals is less than 20 milliseconds, the site of stimulation is likely in the circuit. Abl_{prox} , Proximal ablation site; EGM, electrogram; His_{dist} , distal His bundle; RVA , right ventricular apex.

are defined as $QRS(N+1)$ and $electrogram(N+1)$, respectively. The $S-QRS(N+1)$ interval and $electrogram(N+1)-QRS(N+2)$ interval are then determined; the difference between these two intervals is defined as the $N+1$ difference. Because the $S-QRS(N+1)$ interval is not influenced by QRS fusion during entrainment, an endocardial electrogram that is remote from the pacing site can potentially be used as the timing reference, instead of the QRS onset. Often, the endocardial recording is more precise and easily used for the fiducial point.

The $S-QRS$ criterion increases the positive predictive value of successful ablation outcome at sites demonstrating entrainment with concealed fusion to 80% (see Table 22.3). However, the electrogram-QRS interval may not be equal to the $S-QRS$ interval at sites within the reentrant circuit. Several factors can explain this. Decremental conduction properties of the zone of slow conduction can potentially lengthen the $S-QRS$ interval during pacing, and stimulus latency in an area of diseased tissue can also account for a delay in the $S-QRS$ interval compared with the electrogram-QRS interval. In addition, failure of the

recording electrodes to detect low-amplitude depolarizations at the pacing site can account for a mismatch of the $S-QRS$ and electrogram-QRS intervals (Fig. 22.24).⁷²

Ratio of Stimulus-to-QRS Interval to Tachycardia Cycle Length

Some investigators have proposed that critical areas of slow conduction within the reentrant circuit could be identified by overdrive pacing from LV sites associated with prolonged conduction times from the pacing site to the exit from the infarct scar, as reflected by the $S-QRS$ interval. Although sites requisite for the reentrant circuit that exhibit slow conduction can behave in this manner, the mere presence of prolonged conduction from the $S-QRS$ interval does not prove that the slow conduction is part of a reentrant circuit pathway. Multiple areas within the infarct zone can exhibit fractionated or abnormal electrograms and reduced excitability, which are associated with increased $S-QRS$ intervals, yet may have nothing to do with the VT circuit itself.

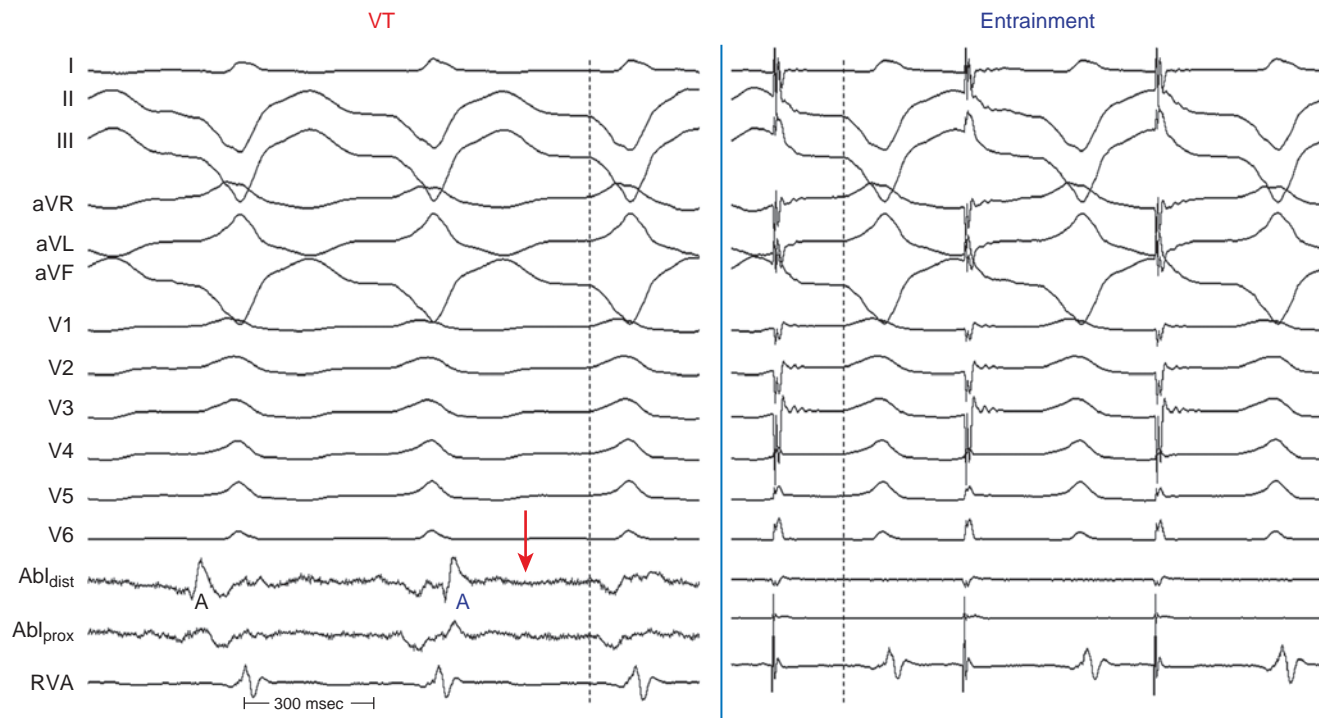


Fig. 22.24 Pacing Capture During Inferobasal Postinfarct Ventricular Tachycardia (VT) Without Recorded Electrogram. At left is VT during which the distal ablation electrode (Abl_{dist}) recording shows no clear diastolic activity; however, stimulation at this site readily captures the ventricle. The red arrow shows the timing during VT equal to the stimulus-QRS interval during pacing. A, Atrial recording; Abl_{prox} , proximal ablation site; RVA, right ventricular apex.

Other investigators have used a prolonged stimulus-to-local electrogram time during entrainment to identify pathways containing slow conduction. This again does not prove that the electrogram at the recording site has anything to do with the VT because slow conduction involved in the orthodromic capture of this electrogram can occur inside or outside the circuit. In fact, whenever ECG fusion occurs, some electrograms outside the circuit (i.e., those activated after leaving the exit that is part of the VT wavefront) will be orthodromically activated and will fulfill the requirements for entrainment. For the same reason, termination with block before this orthodromically entrained electrogram does not mean that it was a critical component of the circuit.

On the other hand, during entrainment with concealed fusion, the S-QRS interval is an approximate indication of the location of the pacing site relative to the reentry circuit exit. A short S-QRS interval (less than 30% of the TCL) suggests a site near the exit. Long S-QRS intervals (greater than 70% of the TCL) suggest bystander sites rather than a critical isthmus. Therefore, at sites demonstrating entrainment with concealed fusion, an S-QRS interval-to-TCL ratio of 70% or less suggests that the sites lie within the common pathway (isthmus) of the reentrant circuit, and sites at which the ratio is more than 70% are considered to lie outside the common pathway (see Fig. 22.20). This criterion improves the positive predictive value of entrainment with concealed fusion to approximately 70%. Moreover, the negative predictive value of this criterion is 92%, indicating that ablation at sites with entrainment with concealed fusion at which the S-QRS interval-to-TCL ratio is more than 70% is unlikely to be successful (see Table 22.3).

Limitations of Entrainment Mapping

There are several limitations to the entrainment mapping technique. Entrainment requires the presence of sustained, hemodynamically well-

tolerated tachycardia of stable morphology and TCL. Furthermore, overdrive pacing can result in termination, acceleration, or transformation of the index tachycardia into a different one, making further mapping challenging. In addition, pacing and recording from the same area is required for entrainment mapping. This is usually satisfied by pacing from electrodes 1 and 3 and recording from electrodes 2 and 4 of the mapping catheter. However, this technique has its own limitations. Differences, albeit slight, exist in the area from which electrodes 2 and 4 record as compared with electrodes 1 and 3, as do differences in the relationship of the site of stimulation from poles 1 and 3 to the recorded electrogram from poles 2 and 4 (i.e., proximal or distal to the recording site). Also, the total area affected by the pacing stimulus can exceed the local area, especially when high currents (more than 10 mA) are required for stimulation, in addition to the fact that the pacing artifact can obscure the early part of the captured local electrogram.⁹⁴

Pace Mapping

In the setting of post-MI VT, pace mapping serves only as a corroborative method of localizing the VT circuit. It can be used to identify the presumptive exit or isthmus region of the VT circuit, but is not sufficiently specific or sensitive to be the sole guide for ablation. Pace mapping can also be used in conjunction with substrate mapping when other mapping techniques are not feasible, so that it can provide information on where ablation can be directed.⁹⁶

Technique of Pace Mapping

Pace mapping in NSR after VT termination is attempted at potential isthmus sites (as identified by activation and entrainment mapping during VT). Either bipolar or unipolar pacing can be used; however, pace mapping is preferably performed with unipolar stimuli (10 mA,

2 milliseconds) from the distal electrode of the mapping catheter (cathode) and an electrode in the inferior vena cava (IVC; anode). Although bipolar pacing produces a smaller stimulus artifact, there is the possibility of capture at the proximal ring electrode and at the tip electrode, which may reduce accuracy, particularly if larger interelectrode distances (8 to 10 mm) and high-current strength are used (Fig. 22.25). Pacing only slightly above the threshold is likely to improve accuracy. The PCL is usually in the range of 500 to 700 milliseconds, which is faster than the sinus rate and slower than the rate of the induced VTs.

The resulting 12-lead ECG morphology is compared with that of the VT. ECG recordings should be reviewed at the same gain and filter settings and at a paper-sweep speed of 100 mm/s. It is often helpful to have a split-screen display of the target VT in one panel, and to compare this with all 12 leads of the paced QRS complexes in another panel,

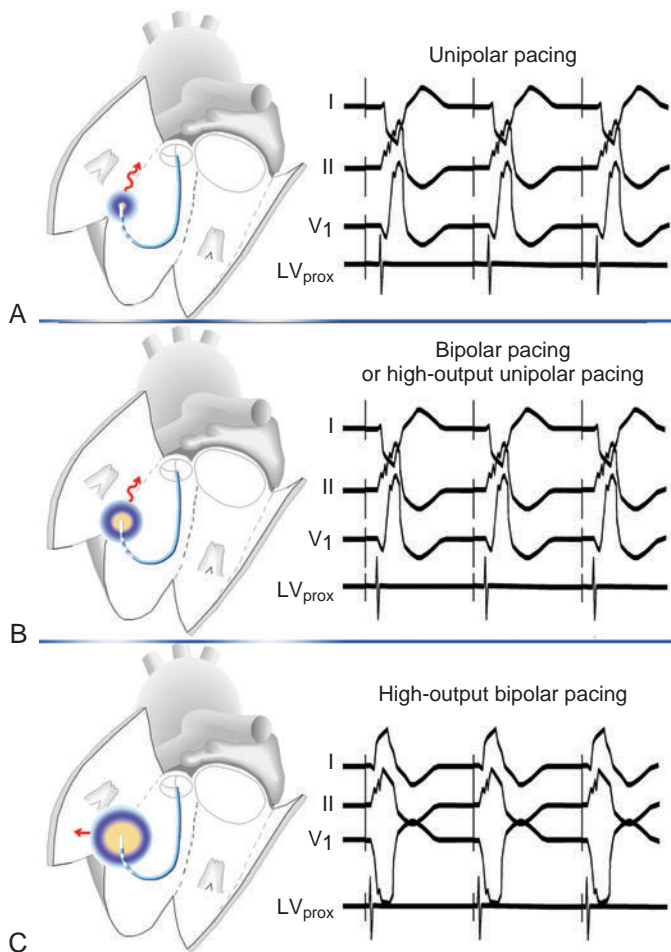


Fig. 22.25 Effect of Bipolar and High-Output Stimulation on the Paced QRS Complex Morphology in Scarred Myocardium. The diagram illustrates a catheter stimulating a site within scar tissue on the left ventricular (LV) anterior septum. (A) With low-output unipolar pacing, a relatively small zone is captured (*blue halo*) resulting in a long stimulus (S)-QRS interval because the impulse must travel through scar until it encounters enough tissue to generate a QRS complex. (B) Bipolar or higher-output unipolar pacing captures a larger area, resulting in a shorter S-QRS but using the same path, resulting in the same QRS morphology as at lower output unipolar pacing. (C) High-output bipolar pacing captures a much larger area and can now activate normal myocardium directly, bypassing the slow conduction zone in scar tissue. This results in a very short S-QRS and a very different QRS complex morphology than previously, despite pacing at the same site.

and with regular printed 12-lead ECGs for side-by-side comparison on paper. Also, automated pace map matching is now available in some recording and electroanatomic mapping systems (see Figs. 5.25 and 5.26). The greater the degree of concordance between the morphology during pacing and tachycardia, the closer the catheter is to the exit zone of the VT isthmus (see Fig. 5.24).

Evaluation of the S-QRS is also of value. The S-QRS interval is measured to the onset of the earliest QRS on the 12-lead ECG. Sites from which pace mapping produces the same QRS as that of the initial isthmus site with different S-QRS delays are identified in an attempt to trace the course of the VT isthmus (see Figs. 5.16, 5.23, and 22.20).

QRS Morphology During Pacing Versus Tachycardia

When ventricular activation originates from a point-like source (e.g., during focal VT or during pacing from an electrode catheter), the QRS configuration recorded in the surface ECG is determined by the sequence of ventricular activation, which is largely determined by the initial site of ventricular depolarization. Analysis of specific QRS configurations in multiple leads allows estimation of the pacing site location to within several square centimeters (see Fig. 5.24 and eFig. 5.5). Therefore comparing the paced QRS configuration with that of VT is particularly useful for locating a small arrhythmia focus in a structurally normal heart (e.g., idiopathic RVOT VT).

On the other hand, reentry circuits in healed infarct scars often extend over several square centimeters and can have a variety of configurations. In many circuits, the excitation wavefront circulates through surviving myocytes within the scar, the depolarization of which is not detectable on the standard surface ECG. The QRS complex is then inscribed after the reentry wavefront exits the scar and propagates across the ventricles. Consequently, QRS morphology during pacing in NSR at sites in the vicinity of the VT circuit depends on where the paced wavefront exits the scar region to activate the larger myocardium. A 12-lead QRS morphology during pacing that matches that during VT suggests proximity to the exit or isthmus of the VT reentry circuit (see Fig. 5.23). Pace mapping at sites more proximally located in the isthmus can also produce a similar QRS complex, but with a longer S-QRS interval (due to the delay of conduction of the paced wavefront to the exit site). The S-QRS interval lengthens progressively as the pacing site is moved along the isthmus, consistent with pacing progressively farther from the exit (see Fig. 5.23). Conversely, a poor pace map is typically observed during pace mapping at sites located closer to the entrance zone of the VT isthmus. As noted above, using all 12 ECG leads for comparison of paced versus VT morphologies is critical.

However, it is important to recognize that pace mapping has been less useful for guiding the ablation of post-MI VT. Paced QRS configurations that are different from VT morphology can be observed even when pacing in the vicinity of the VT isthmus, and match paced and VT morphologies can be observed when pacing from bystander sites that are not optimal targets for ablation (see later).⁹⁶

Stimulus-to-QRS Interval During Pace Mapping

Pacing in normal myocardium is associated with an S-QRS interval of less than 40 milliseconds. Longer S-QRS intervals suggest that the pacing site is located within a protected zone, forcing the paced wavefront to propagate slowly within the scar before exiting at remote scar borders to activate the larger myocardium, causing the latency between myocardial capture and the onset of surface QRS. These sites are typically associated with abnormal fractionated electrograms during NSR. In the setting of post-MI VT, it is likely that pacing sites with long S-QRS delays identify slowly conducting channels that traverse dense scar and can potentially form VT isthmuses. However, although such sites often are located *within the vicinity of putative isthmuses of clinical VT*, they

can be part of the reentrant circuit (i.e., critical isthmus) or just a bystander (see Figs. 5.16 and 5.18), and other mapping maneuvers are required for confirming the role of such sites in the clinical VT circuit. Creating a latency map using an electroanatomic mapping system to represent the regions of S-QRS latency graphically can also be a useful method for initially screening sites during NSR (see Fig. 5.23).

Parts of VT reentry circuit isthmuses can be traced during NSR by combining both the QRS morphology and the S-QRS delay during pace mapping in anatomical maps. The reentry circuit exit, which is more likely to be at the border of the infarct and close to the normal myocardium, often has no delay during pace mapping in NSR, even though it can be reasonable to target for ablation. Sites with long S-QRS intervals can be more proximal in the isthmuses; therefore they are more likely to be associated with propagation of the paced wavefront in the antidromic direction away from the reentry circuit, producing a QRS different from that of the VT (see Fig. 5.23). Sites with prolonged S-QRS intervals during pace mapping are frequently associated with other markers of reentry circuit sites; however, this can be a somewhat limited mapping guide. Approximately 25% of likely reentry circuit sites have short S-QRS intervals during pace mapping, and more than 20% of sites with long S-QRS intervals do not appear to be in the reentry circuit.

Limitations of Pace Mapping

In infarct-related VT, pace mapping has significant limitations in its ability to identify the critical isthmus of the VT circuit. A paced QRS configuration different from that during VT does not reliably indicate that the pacing site is distant from the reentry circuit. In fact, it is rather uncommon to have similar or even almost identical morphology result from pacing from a known isthmus determined by mapping.

During VT, the wavefront propagates in one direction (i.e., orthodromically) within the reentry circuit. Similarly, during entrainment of the tachycardia from sites within the critical isthmus, the paced wavefront propagates in the orthodromic direction along the VT isthmus, while collision with the previous tachycardia wavefront prevents its antidromic propagation, resulting in a QRS morphology that is identical to that of the VT. Conversely, during pace mapping in NSR (when there is no preexisting orthodromic wavefront propagating along the VT isthmus), the paced wavefront (even when pacing from the critical

isthmus) can potentially propagate in at least two directions—orthodromic and antidromic (relative to the direction of VT propagation) and, hence, exit the scar region at different sites, resulting in different QRS morphology. This pattern of activation during pace mapping can vary depending on the proximity of the pacing site relative to the entrance and exit sites along the critical isthmus. During pacing at sites closer to the entrance zone, the stimulated antidromic wavefront leaves the protected isthmus at the entrance before the orthodromic wavefront reaches the exit site. As a result, myocardial activation results predominantly from the antidromic wavefront, producing a QRS morphology that is significantly different from that of the VT (see Fig. 5.23). If the orthodromic wavefront reaches the exit, a fusion QRS is produced that includes depolarization from both the antidromic and orthodromic wavefronts.⁹⁶

In addition, the presence of functional block during VT but not during NSR further limits the value of pace mapping. Functional block can be critical in defining a protected channel for conduction that allows reentry. Such block can vary or be absent during NSR when pace mapping is performed and, as a consequence, the paced wavefront (even when pacing from the critical isthmus) may not be forced to follow the same path as that of the VT wavefront (Fig. 22.26). This is further exaggerated by the fact that pace mapping is usually performed at rates slower than the VT to avoid VT induction during the mapping process, which can reduce the likelihood of development of a line of functional block.

Furthermore, the area over which the current is delivered, especially where high current is required for relatively inexcitable tissue, can influence the pattern of subsequent ventricular activation, presumably by capturing more distant (i.e., far-field) tissue. When this occurs, it can indicate pacing in a region of a protected isthmus, where pacing at low output would capture only the isthmus, whereas pacing at a higher output can capture both the isthmus and far-field tissue, resulting in different QRS morphologies and S-QRS intervals (Fig. 22.27).

On the other hand, pacing during NSR from sites attached to the reentrant circuit but not part of the circuit can occasionally produce QRS morphology identical to that of the VT because the stimulated wavefront can be physiologically forced to follow the same route of activation as the VT as long as pacing is carried out between the entrance and exit of the protected isthmus. Although this strategy can result in

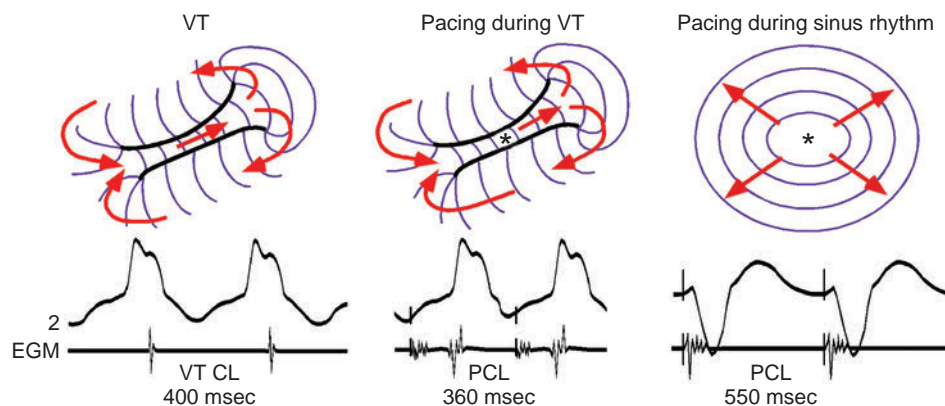


Fig. 22.26 Functional Block During Ventricular Tachycardia (VT). At left, VT propagates through a diastolic corridor maintained by lines of block. At center, pacing during VT within the diastolic corridor (asterisk) propagates in the same manner as VT because of maintenance of lines of block. At right, pacing during sinus rhythm at the same site results in a completely different activation pattern and QRS complex if the lines of block during VT were functionally, rather than anatomically, determined. EGM, Intracardiac electrogram; PCL, pacing cycle length.

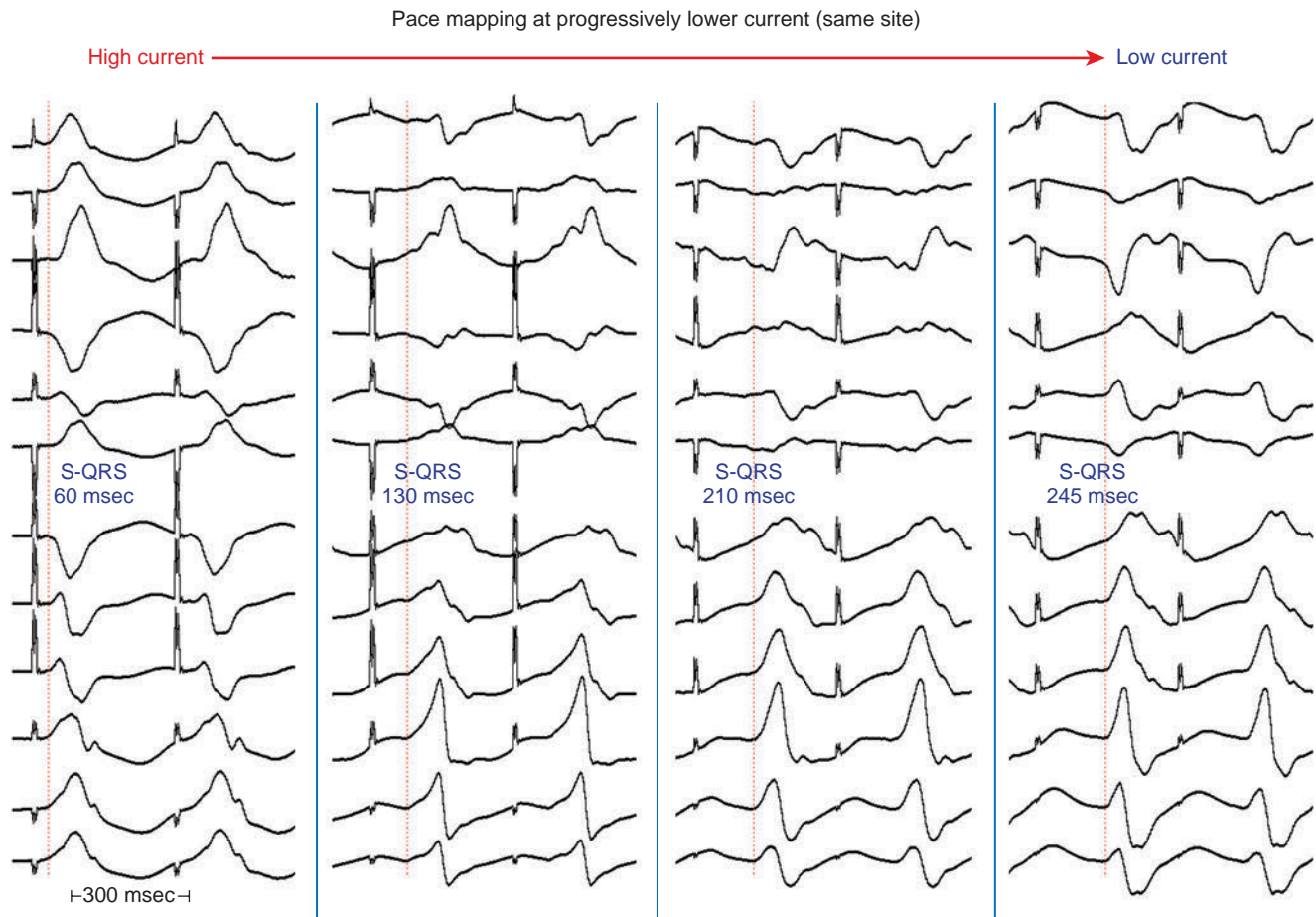


Fig. 22.27 Effect of Stimulus Strength on QRS Complex and Stimulus (S)-QRS During Pace Mapping. QRS complexes resulting from pacing from the same site, but at different current strength, are shown from higher (left) to lower (right) output. Note the dramatic changes in QRS configuration as well as the progressively longer S-QRS interval. This was easily reproducible; increasing output reversed the electrocardiogram and S-QRS interval findings, and lowering output again recapitulated the data shown here.

the identification of irrelevant inner loop and adjacent bystander sites as well as the desired isthmus sites, it can still be helpful in gross identification of the region of the VT circuit.

At best, a pace map that matches the VT would only identify the exit site to the normal myocardium, which can be distant from the critical sites of the circuit required for ablation. Thus pace mapping remains only a corroborative method of localizing reentrant VT.

Substrate Mapping During Baseline Rhythm

Substrate mapping refers to delineation of the infarcted myocardium and portions of the myocardial scar that likely support the VT reentry circuit (called conducting channels). Conducting channels represent isolated bundles of viable myocardium embedded within areas of dense fibrosis. Conduction through these bundles is typically slow and anisotropic, resulting in low-amplitude, multipotential, fractionated bipolar electrograms. Further, when these bundles form isolated regions deep within confluent scar areas, local activation can become delayed, occurring much later than the surrounding larger myocardium, and resulting in late or isolated near-field potentials recorded after the far-field potential and after the offset of the QRS complex. These channels can potentially form protected diastolic isthmuses necessary to support VT.

Substrate mapping is performed during baseline rhythm (NSR, AF, or ventricular pacing) and aims to identify: (1) abnormal local elec-

trogram amplitude (voltage mapping); (2) electric unexcitability with high-output pacing; (3) abnormal local electrogram configuration (fractionated electrograms, multipotential electrograms, late potentials, or electrograms with isolated delayed components); and (4) local pacing capture with a long S-QRS interval.

Post-MI VTs can be unstable or unsustainable and therefore not approachable by conventional point-by-point activation mapping and entrainment maneuvers. Therefore mapping during the baseline rhythm rather than during VT is of significant value. Substrate mapping also facilitates ablation of multiple and pleomorphic VTs. Even in well-tolerated SMVTs, substrate mapping is also of value, because it can help focus activation and entrainment mapping efforts on a small region harboring the VT substrate and, therefore, minimize the duration during which the patient is actually in VT. In these patients, prolonged periods of sustained VT during the mapping procedure can induce ischemia or exacerbation of heart and renal failure.

Voltage (Scar) Mapping

In post-MI VT, the diastolic pathway (isthmus) of the circuit is typically located within areas of scar, while the circuit exit is often located in the scar border zone. Voltage mapping helps identify the infarct and infarct border zones, which are likely to harbor the tachycardia circuit (see Fig. 22.17).⁵⁴

Bipolar voltage mapping has been correlated with dense scar defined by histopathology and CMR. Electrical scarring is defined by low amplitude of local electrograms and tissue unexcitability during high-output pacing. Although the true range of normal electrogram amplitude is often difficult to define, endocardial ventricular bipolar electrogram amplitude less than 1.5 mV has been accepted as an abnormally low voltage, and a cutoff of 0.5 mV as the signal amplitude that best defines the anatomical region of dense infarct scar. The border zone at the margins of confluent postinfarct scarring tend to have relatively more preserved voltages (in the range from 0.5 to 1.5 mV). The distinction between normal and abnormal bipolar signals in most patients with prior MI tends to be very discrete and dramatic.⁵⁴

A more rigid voltage cutoff criterion is used during epicardial bipolar voltage mapping to limit the influence of epicardial fat and coronary vasculature. Normal epicardial electrogram amplitude is defined as greater than 1.0 mV. As epicardial fat overlying normal myocardium insulates the underlying tissue, attenuated low-amplitude signals can be mistaken for abnormal myocardial tissue. Dense scar is defined as confluent areas with bipolar electrogram amplitude less than 0.5 mV, and border zone in regions with bipolar electrogram amplitude between 0.5 and 1.0 mV. Because epicardial fat can decrease signal amplitude, low-voltage areas during epicardial mapping should also show abnormal electrogram configuration.⁵⁴

Importantly, bipolar recordings have a limited field of view such that the amplitude of the bipolar electrogram is primarily driven by local tissue activity, while far-field activity is subtracted out. Although voltage properties of the endocardium are well represented in the bipolar signal, intramural or epicardial scar that can potentially harbor the arrhythmogenic substrate can be missed by purely endocardial bipolar voltage mapping. In contrast, unipolar electrograms reflect the voltage difference between the exploring electrode in contact with myocardium and a second electrode that is distant from the heart (usually the Wilson central terminal). Thus the unipolar electrode has a wide field of view, and unipolar electrogram amplitude primarily represents more remote, far-field tissue depolarization.⁹⁷ Therefore unipolar voltage mapping has recently been proposed to improve myocardial sensing with a wider field of view to detect the presence of midmyocardial and epicardial scar. A voltage cutoff of 8.3 mV is used to distinguish normal from abnormal LV unipolar endocardial electrogram amplitude.⁵⁴

Pacing provides complementary information to electrogram amplitude; only 2% of sites with amplitude more than 0.5 mV have a pacing threshold more than 10 mA, whereas a substantial number of very low-amplitude sites have high pacing thresholds, and many sites in reentry circuit isthmuses have very low amplitudes. A dense scar is defined by the lack electrical excitability during high-output pacing.

Identification of areas of scar and scar border zones by voltage mapping is frequently not adequate to guide ablation. In patients with post-MI VT, the low-voltage infarct areas are relatively large (average area, 39 ± 35 cm²; range, 6 to 205 cm²), so that complete encirclement with RF ablation lesions is likely to be difficult. Therefore an important goal of substrate mapping is to also identify conducting channels within the infarct region, which are relatively small bundles of viable tissue compared with the scar areas. This helps focus the diagnostic techniques and ablation on defined areas that potentially harbor the VT substrate. Relative voltage preservation within denser regions of scar is a hallmark of central conducting channels that may form anatomically constrained diastolic isthmuses during VT, and adjusting the voltage representation on the isopotential map can help visualize these zones. Analysis of electrogram morphology and pace mapping can help identify potential channels within low-voltage regions.

Technique of voltage mapping. The LV is mapped during baseline rhythm (NSR or ventricular pacing) to construct a color-coded

voltage map displaying peak-to-peak bipolar electrogram amplitude sampled at each site and is measured automatically by the mapping system. The color range is set between 0.5 and 1.5 mV, so that all areas of viable myocardium are given the same color code and the scar can be differentiated further into different zones according to the local voltage.

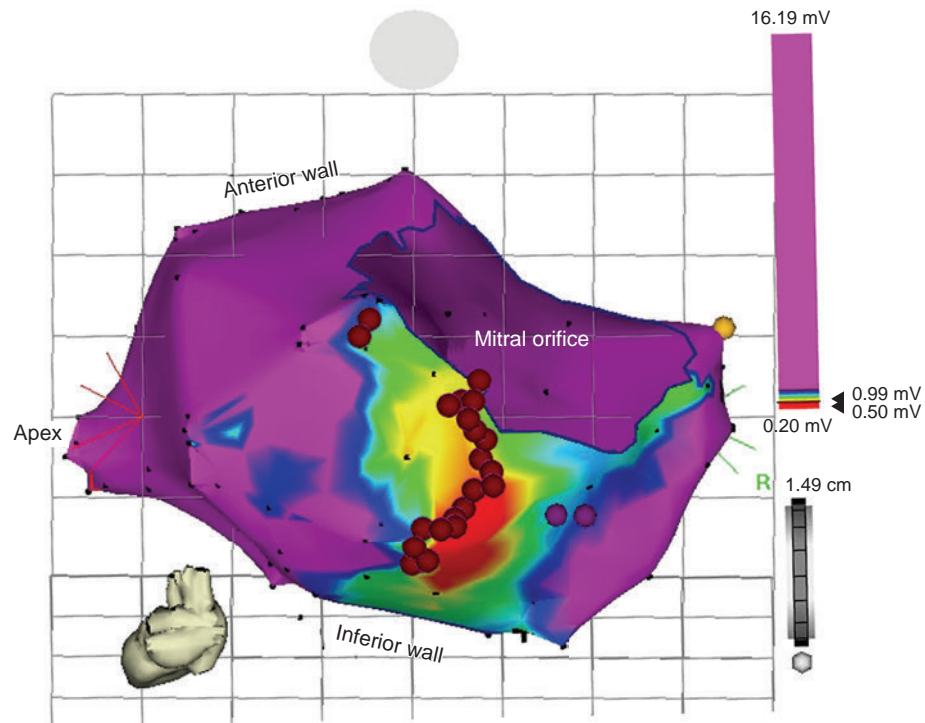
Higher-density points are obtained around areas of scar, focusing on the scar border and electrograms within the scar. All scar borders need to be clearly defined. During the mapping process, areas of fractionated or late potentials (irrespective of the voltage obtained) are tagged on the electroanatomic map. At low-amplitude (less than 0.5 mV) sites, pacing is performed with 10-mA, 2-millisecond pulse width stimuli. A pacing threshold greater than 10 mA has been used to define unexcitable scar, provided electrode-tissue contact is adequate. In addition, sites with long S-QRS intervals during pacing need to be tagged.⁶⁶

A color-coded voltage map is then created and superimposed on the anatomical model to show the amplitudes of all selected points (eFig. 22.13).⁵⁴ Careful step-by-step manual adjustment of voltage upper and lower limits on the color-coded electroanatomic voltage map (scar thresholding) can help maximize the color contrast between adjacent myocardium with different electrogram voltage levels within the 0.5-mV scar and, thus, unmask channels of viable myocardium within a dense scar. For example, resetting the voltage limits to 0.3 to 0.5 mV as the upper limit and to 0.1 mV as the lower, may be required for the identification of viable myocardium and conducting channels within the scar area (see Figs. 22.17 and 22.28; eFig. 22.14). Conducting channels on the electroanatomic voltage map are identified corridors of voltage preservation (voltage channels) within denser regions of scar or corridors between a dense scar and a valvular annulus.⁶⁶ Recent evidence, however, has questioned the value of this method for identification of conducting channels. This technique likely has limited sensitivity and specificity. In comparison, mapping techniques utilizing electrogram morphology and late potentials are more capable at identifying a higher proportion of conducting channels that serve as the substrate for VTs. This may not be surprising because voltage mapping incorporates the larger far-field signals commonly present at sites recording smaller near-field late potentials.

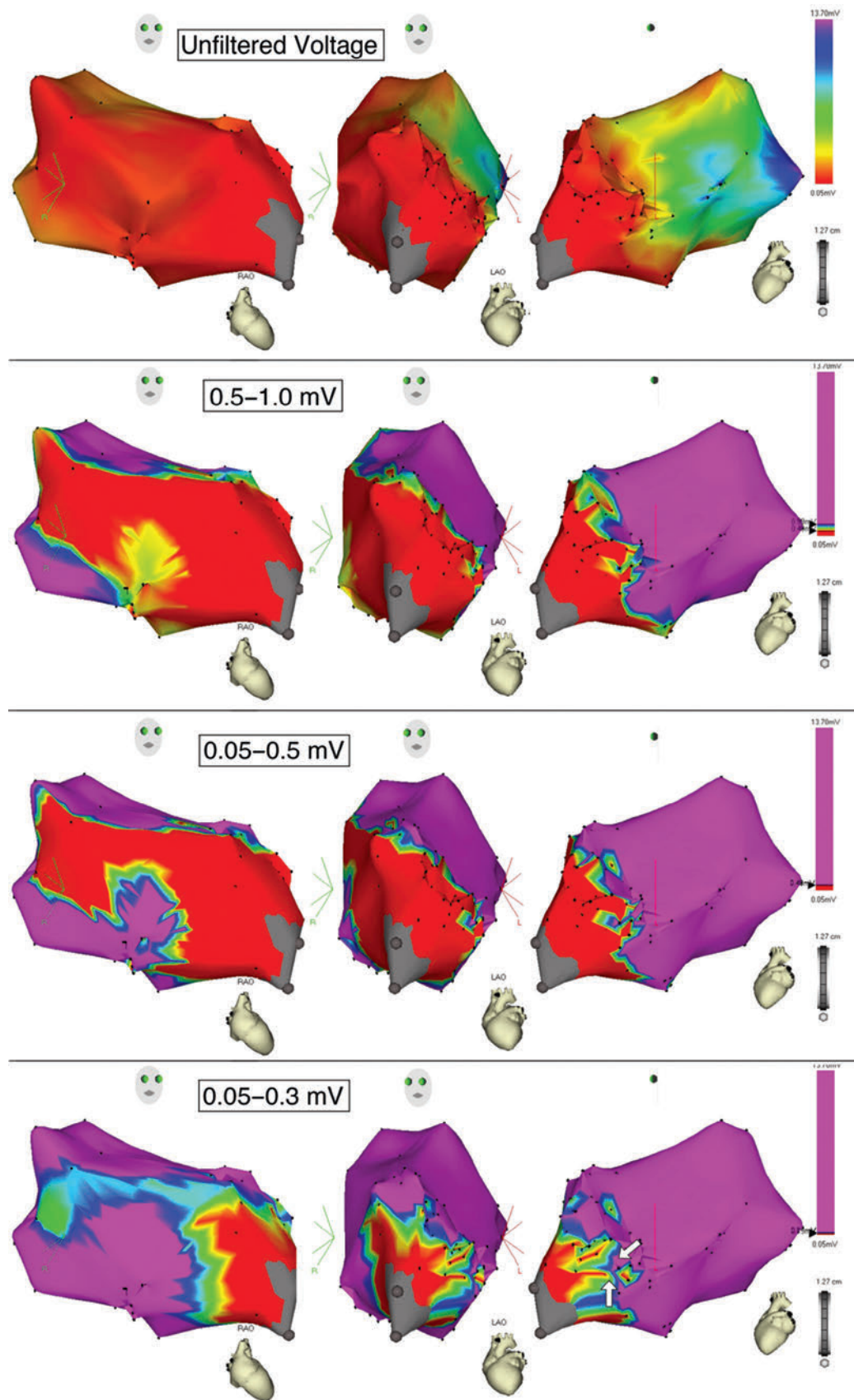
Abnormal Local Ventricular Electrograms

The vast majority of post-MI VTs occur at sites that have abnormal or late electrograms during NSR (see Fig. 22.18). Infarct regions are well delineated as areas of low-amplitude abnormal electrograms. However, abnormal low-voltage electrograms can be recorded throughout extensive areas of scar that are not sufficiently specific for the components of the reentrant circuit and, hence, cannot be used as the sole guide for ablation. Therefore additional electrogram characteristics have been proposed to improve the accuracy of substrate mapping, including electrogram fractionation and late potentials.⁹⁸

Local abnormal ventricular activity. Conduction through the reentry circuit isthmus or at its entrance or exit is often slow and non-uniformly anisotropic because of the transverse uncoupling of myocytes by fibrosis. Therefore electrogram fractionation (i.e., electrograms with three or more sharp spikes, either separated by very low-amplitude signals or an isoelectric interval) is a common finding in areas of scar and VT substrate. In addition, during NSR, a typical local electrogram in the border of an infarct has a low voltage but is adjacent to more normal myocardium in the border, causing a multipotential electrogram that has markedly different amplitudes, with a large rounded potential (reflecting a far-field signal from activation of the large mass of surrounding tissue) and a small sharp potential (reflecting local depolarization of a small mass of fibers in the infarct). These abnormal electrograms (the so-called local abnormal ventricular activity [LAVA])



eFig. 22.13 Electroanatomic Voltage Map of Scar-Based Ventricular Tachycardia (VT) in a Patient With a Prior Inferior Wall Myocardial Infarction (Posterior View). The scale at right shows bipolar voltage; the red area denotes a very low-voltage (<0.5 mV) infarct zone with a small isthmus of higher voltage between this area and the mitral annulus. Red dots indicate a line of radiofrequency applications to transect this isthmus (additional *red dots* denote ablation at other sites that terminated the VT).



eFig. 22.14 Filtering Voltage Maps to Expose Conduction Channels. Right and left anterior oblique (RAO and LAO, respectively) and left lateral views of endocardial left ventricular voltage maps are shown (higher, normal voltages are *purple*, low voltages *red*; dense scar is *gray*). At top is the “raw,” unfiltered voltage. Successive panels beneath show different bandwidths of filtering as indicated at the top of each panel, revealing possible “channels” of viable tissue coursing with scar areas (*white arrows* in bottom panel). Ablation lines to transect these channels (which would not otherwise be evident) can then be performed.

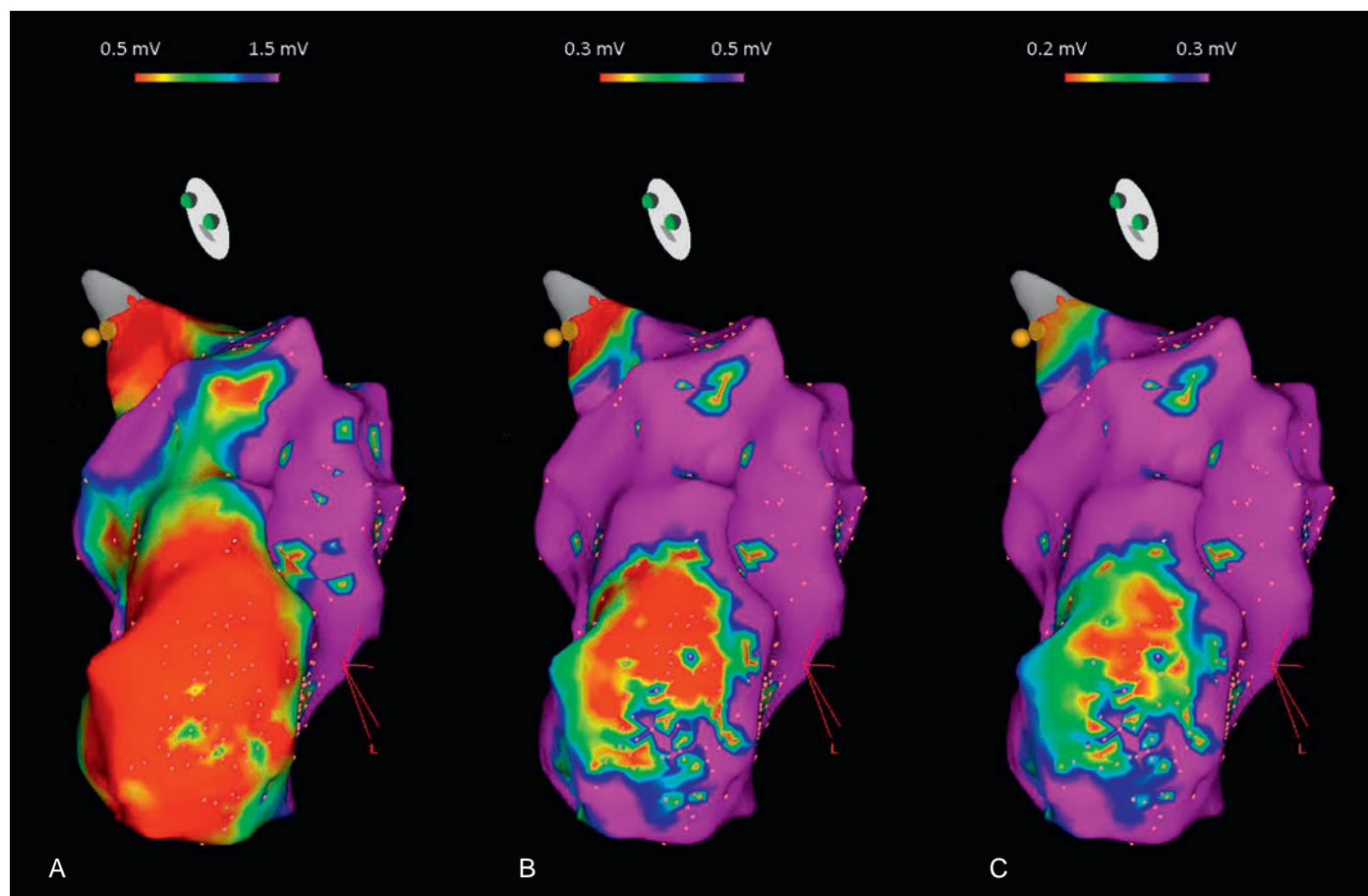


Fig. 22.28 Voltage Channels. Bipolar voltage map of the left ventricle (modified anterior view) in a patient with ventricular tachycardia and prior anterior wall infarction. (A) Large inferior wall scar is obtained when the cut-off value is set at <0.5 mV (red area), and the border zone is set at 0.5 to 1.5 mV. (B) By modifying the color scale ("voltage scanning" or "scar thresholding"), different areas within the scar can be identified: very-low-voltage areas (<0.3 mV) corresponding to true scar (border zone is set at 0.3 to 0.5 mV) and corridors between them with slightly greater voltage (in green and yellow) constituting voltage channels and potential circuit isthmuses. (C) Further voltage scanning is performed, with red color corresponding to voltages <0.2 mV, and the border zone is set at 0.2 to 0.3 mV.

are common in the infarct region, but can be found throughout the scar and are not specific for the critical isthmus of the reentry circuit.^{89,99}

Late potentials. A bipolar electrogram is defined as "late" if any component is recorded after the end of the QRS complex on the surface ECG. Electrograms with isolated delayed components are defined as electrograms with double or multiple components separated by a very low-amplitude signal or an isoelectric interval of more than 50 milliseconds in duration. These electrograms can reflect local depolarization of surviving muscle bundles that are well insulated by dense scar, where local activation is recorded late, well after the higher-amplitude far-field electrogram and often well after the end of the surface QRS complex or T wave.^{89,99,100}

Late potentials are present in about two-thirds of post-MI patients with larger and more solid scars. Most critical isthmus sites display broad (greater than 200 milliseconds in duration) or isolated diastolic potentials during NSR (see Fig. 22.18). However, although sites with late potentials can be markers of an anatomically constrained, slowly conducting diastolic isthmus during VT and have been used to guide substrate-based ablation strategies, the sensitivity remains modest, likely due to the low amplitude of local signals and the direction of wavefront propagation obscuring isolated potentials. In one report, late potentials

during NSR were absent in 29% of central VT reentrant circuits and in 46% of VT termination sites. Furthermore, isolated potential mapping is limited by the imperfect specificity, and is unable to differentiate the central isthmus from bystander cul-de-sacs or nonspecific slowed conduction.^{100–102}

Nevertheless, this type of electrogram can help refine the area of interest. The areas demonstrating such electrograms are relatively small compared with scar areas; therefore this method permits a focus on the diagnostic techniques and ablation in defined areas. Furthermore, recording of these electrograms before and during VT induction serves to relate them and VT within seconds, provided that the isolated diastolic component of the electrogram precedes the first VT beat and then becomes mid-diastolic. In addition, pacing at these sites may capture the local potential and conduct slowly out of the scar, resulting in a long S-QRS interval and, if sharing an exit of a targeted VT, producing a good or excellent pace map. The ablation of all sites demonstrating electrograms with isolated diastolic components can overcome the lack of specificity of the selection of a single site as an ablation target when entrainment mapping criteria are not fulfilled. Ablation of these electrograms can also eliminate the substrate for different VTs otherwise not ablated by limited, conventional strategies.^{100–102}

During substrate mapping, sites recording abnormal electrograms are tagged on the electroanatomic map. Late potential conducting channels are defined as a path of more than two adjacent late potentials connecting with healthy tissue. Further, studies suggested a sequential activation pattern from the border of the scar through conducting channels. Late potentials are classified as being an entrance or an inner part of a given conducting channel, depending on the local activation time of the near-field component. The entrance of a conducting channel is tagged as sites within the border zone (i.e., voltage zone of 0.5 to 1.5 mV) recording the earliest late potential, that is, late potentials with the shortest delay between the far-field component of healthy/border zone myocardium (low frequency, usually high voltage) and the near-field component (delayed, high frequency, usually fractionated, and low voltage) corresponding to the local activation of myocardial fibers in the scar. Sites with longer delays likely reside farther along the conducting channel within the dense scar. The method involves high-density mapping of channels of activation of late potentials.^{102,103} Multielectrode catheters with small and closely spaced electrodes (PentaRay) or the mini-basket catheter (Orion) offer improved mapping resolution within the low-voltage areas and allow identifying channels of surviving myocardial bundles, otherwise considered dense scar by standard linear catheters.¹⁰⁴

In addition, 3-D electroanatomic late potential maps can be constructed, whereby the *terminal* portion of every local electrogram is manually marked during the mapping procedure (“isochronal late activation maps”). The lower time threshold of the color-coded map is set to the difference between the reference and end of the surface QRS complex. The isochronal late activation maps can be superimposed on voltage maps to further delineate their relationship to scar distribution.¹⁰⁵ Of note, late potentials in the latest isochrone of activation during NSR appear to be mostly bystander sites, and are infrequently correlated with successful ablation sites for VT. On the other hand, slow conduction regions with isochronal crowding propagating into the latest zone of activation were found to be better markers to guide substrate-based VT ablation.⁹⁸

The discrimination between far-field from near-field potentials is critical for substrate mapping approaches. Late potentials typically are of low amplitude and are often obscured by larger far-field electrograms produced by activation of the surrounding larger mass of myocardium outside the infarct region. Verification that a recorded electrogram is far-field rather than near-field can be achieved by pacing at the local site. When the recorded electrogram is near-field, capture of the pacing stimulus results in capturing the tissue generating all components of the electrogram, so that no clear electrogram component is identifiable during pacing. Conversely, when the recorded electrogram is far-field, pacing may not capture (due to dense scar) or, when it captures local tissue, the far-field electrograms remain discernable during pacing (because they reflect activation of myocardium adjacent to the pacing site). Furthermore, changing the direction of depolarization approaching the mapping site (e.g., sinus rhythm vs. RV pacing) and VES (causing decremental conduction) can help unmask some areas of block and slow conduction, expose late potentials, and separate local (near-field) from far-field potentials (Fig. 22.29).⁹⁹

Substrate Image Integration

LV scar and its border zone represent the target of “substrate modification” for VT ablations; therefore an exact anatomical delineation is critical. As noted, the current gold standard of voltage mapping has several limitations. Many of those limitations can be overcome by integrating scar imaging into the VT ablation. Multiple imaging modalities detailing the LV substrate in a 3-D format can be visualized and displayed simultaneously with the electroanatomic 3-D LV voltage map. These imaging approaches can be used to correctly predict abnormal voltage locations in advance of the mapping procedure, which allows the electrophysiologist to concentrate on areas of likely myocardial scar, obviate the need to perform a complete point-by-point voltage mapping, identify falsely low-voltage recordings in areas of normal perfusion due to sub-optimal catheter contact, and reduce procedure time and radiation exposure. In addition, some imaging modalities are able to characterize the transmural extent and intramyocardial location of scar tissue, which

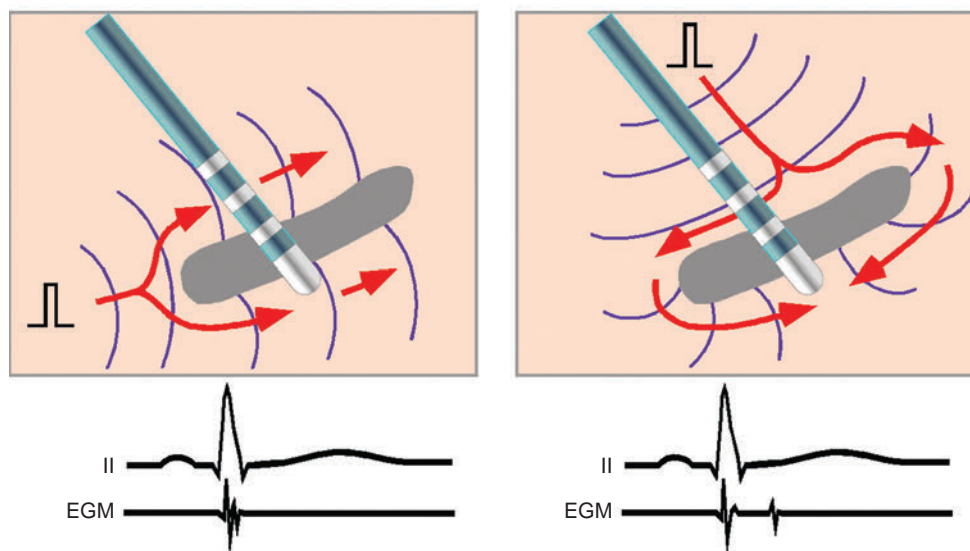


Fig. 22.29 Effect of Direction of Wavefront Propagation on Electrogram (EGM) Configuration. A catheter is recording over an island of scar surrounded by normal tissue. At *left*, a wavefront arriving from the left side is split by the scar, but tissue on each side of the scar is activated at about the same time, resulting in a relatively normal EGM. At *right*, a wavefront arriving from right angles to the prior one is split by the scar, with tissue on the near side activated early and that on the opposite side activated much later, resulting in a markedly split recording.

can potentially help identify intramural and epicardial arrhythmia substrate, overcoming a limitation of endocardial voltage mapping.⁹⁰

PET-CT. Because PET scans alone do not provide the necessary anatomical information required for integration with electroanatomic maps, a CT angiography scan is required to provide an anatomical skeleton onto which the biological information acquired from the PET scan would be superimposed on its precise anatomical location.

Both PET and CT images can be spatially aligned using an automatic registration algorithm. All regions in the PET image with uptake greater than a threshold (50% of maximal uptake) are overlaid at the corresponding location on the CT image. Thus a fused image can be created having accurate anatomical information at the spatial resolution of the original CT with accurate metabolic information for the LV myocardium from the registered PET. The regions in the fused image showing [¹⁸F] fluorodeoxyglucose (FDG) uptake represent nonscarred myocardium, and regions with no uptake indicate scarred myocardium. Myocardial scar is displayed as an area of absent voxels (“hole in the wall”) within the reconstructed LV wall to indicate scar location and size. The use of PET 3-D reconstructions at multiple metabolic thresholds allows the characterization of the scar border zone and simultaneous 3-D display of myocardial scar and border zone embedded in the LV anatomy as well as the display of detailed scar anatomy, which can be targeted during the VT ablation.

The fused “anatomical-metabolic” PET-CT image is imported into the electroanatomic mapping system. To merge the PET-CT image, landmark points at the coronary ostia, coronary cusps, LV apex, coronary sinus (CS), and mitral annulus are usually acquired (guided by ICE; see later). The corresponding points are matched on the fused PET-CT image. Once the 3-D voltage map is created, surface registration is performed. Alternatively, multiple points can be acquired at different planes of the aorta as the catheter is dragged along the descending aorta, arch, and ascending aorta. Using an automated program available in the mapping system, the electroanatomic map and the fused PET-CT image are then aligned. After primary registration, the registered model is refined using a second set of fiducial points placed in stepwise fashion to further align both surfaces at sites of local mismatch.⁷⁸

CMR. The spatial resolution of PET/CT imaging is limited to 4 to 6 mm, which does not allow for determination of complex scar anatomy and mural location. Epicardial scar can have a low PET signal, but normal endocardial voltage. In contrast, delayed-enhancement CMR imaging provides excellent detail and is quickly becoming the gold standard for scar determination and is currently the only modality that can assess the transmural extent of the infarct (i.e., can determine whether the scar is endocardial, intramyocardial, or epicardial).⁷⁷ The CMR image can be merged with the 3-D electroanatomic voltage map employing landmark and surface registration (as discussed previously).

Contrast-enhanced CT. Cardiac contrast-enhanced CT scanning enables a comprehensive three-modality characterization (anatomical, dynamic, and perfusion) of LV scar from a single contrast-enhanced CT with high spatial (≤ 1 mm) and temporal resolution. Areas of CT hypoperfusion correlate best with areas of abnormal voltage (less than 1.5 mV) rather than scar alone (less than 0.5 mV). Perfusion imaging from CT can indicate scar transmural extent and intramyocardial scar location. The 3-D CT scan can be integrated into clinical mapping systems to guide VT ablation. Primary registration is performed with landmark points and visual alignments, as previously discussed.

Intracardiac ultrasound. Although preacquired CMR, PET, and CT images have been used to define LV scar and guide mapping and ablation in post-MI VT, registration is often difficult and can be imprecise. In addition, images obtained on different days can confound registration if LV geometry changes because of loading conditions.

Real-time ICE images can provide accurate chamber geometries and scar boundaries of the LV. Scar zones (identified on endocardial voltage maps) were found to have increased tissue echogenicity on ICE compared to myocardial areas without scar in ischemic and nonischemic patients. Border zones were found to have more heterogeneous signal intensities than normal myocardium.⁷⁶ Also, ICE provides both an anatomical and a functional assessment of the LV, allowing for real-time identification of wall motion abnormalities. Unlike PET/CT and CMR imaging, ICE imaging does not require potentially toxic contrast agents, nor does it expose the patient to ionizing radiation.

In addition, ICE can be used to guide catheter navigation. Real-time monitoring of the endocardial-catheter interface helps direct the catheter to the important anatomical structures that can be critical to the VT circuit, such as crypts and trabeculations, which may otherwise be missed. ICE can also be used as a facilitator of CT/MR image integration.

The CARTOSound image integration module (Biosense Webster) incorporates the electroanatomic map into a map derived from ICE and allows for 3-D reconstruction of the LV from real-time 2-D ICE images, facilitating interventional navigation within the LV. ICE imaging is performed using a phased-array transducer-catheter incorporating a navigation sensor (SoundStar; Biosense Webster), which records individual 90-degree sector image planes of the cardiac chamber of interest, including their location and orientation, to the CARTO workspace. A 3-D volume rendered image is created by obtaining ECG-gated ICE images of the endocardial surface of the LV.⁷⁶

To create the CARTOSound volume map of the LV, the ICE catheter is manipulated in the RA, RV, and RVOT to visualize all parts of the LV. The left ventricular outflow tract (LVOT), the aortic root, and the mitral valve are mapped with the probe positioned in the RA, whereas the body of the LV is mapped with the probe positioned in the RV, against the interventricular septum. The latter position provides a longitudinal view of the LV cavity. Lateral tilt allows base-to-apex scanning through the body of the LV with deeper insertion, withdrawal, or rotation of the probe used as necessary to complete the map. Short-axis cross-sectional views of the LV can be obtained with the ICE probe positioned in the RVOT. Images are acquired in end expiration and gated to the R wave or the pacing spike. Ultrasound imaging in which the wall segment is well visualized can reliably identify scar both by wall thickness and motion, a process that does not require wall contact. Akinetic and thinned wall segments are marked in a separate volume and labeled as scar on the ultrasound volume map. Normal or hypokinetic segments are labeled as nonscar. Separate geometries (scar and nonscar) are made of the LV and each of the papillary muscles. Once the ultrasound map is completed, a distinct CARTO voltage map is created (as described previously).

Limitation of Substrate Mapping

Voltage mapping relies heavily on consistent catheter contact. If catheter contact is suboptimal and falsely low voltage measurements are recorded, the voltage map will erroneously suggest a scar. The use of ICE and contact force catheters can help ensure adequate catheter contact. In addition, low mapping density is associated with significant interpolation of data between sampled points. The use of multielectrode catheters enables rapid high-density voltage mapping through simultaneous multiple-point acquisition, which reduces interpolation of data between points and improves mapping accuracy.¹⁰⁶

It is also important to note that, although an electrogram amplitude of 0.5 mV has been used to identify electrical scars, a minimal amplitude that distinguishes excitable tissue from unexcitable scar has not been established. Because different catheters with various electrode sizes and interelectrode spacings are becoming available, individualized validation

is required, and catheter-specific thresholds are needed to improve scar characterization.

Electrogram amplitude is annotated to the electrogram peak. In regions of scar, far-field signals are frequently of larger amplitude than local electrograms. Voltage annotation of the larger far-field electrograms can introduce errors in the voltage map. Manual tagging of abnormal potentials or manual annotation of near-field electrogram voltage can help improve the map accuracy, but this can be challenging with high-density point acquisition.

Bipolar electrogram amplitude is influenced by multiple variables that can affect the accuracy and resolution of the voltage map, including mapping electrode size, interelectrode distance, conduction velocity between the bipolar electrodes, vector of activation, the angle at which the electrode engages the tissue, and signal filtering. The spatial resolution of the standard mapping catheter is limited due to the large electrode surface area and wide interelectrode spacing. Although voltage mapping likely identifies large unexcitable areas of scar, small strands of fibrosis, which may still create important conduction block, may escape detection amid the background of high-amplitude far-field signals. Similarly, small strands of surviving myocardium within an area of dense scar may not be detected during voltage mapping. Mapping catheters with smaller electrodes and shorter interelectrode spacing (e.g., PentaRay, Orion) record signals from smaller tissue mass and are subjected to less signal averaging and cancellation effects, and minimal far-field signals and background noise. As a result, data acquisition with smaller electrodes allows for accurate detection of very small amplitude signals and improves the resolution of the voltage map. This can be of particular advantage in the low-voltage zones and areas of heterogeneous scar distribution.^{106–108}

The vector of propagation of the activation wavefront in relation to the two recording electrodes, and orientation of the recording electrode relative to the tissue influences the degree of signal cancellation and therefore the resultant bipolar signal amplitude. Therefore voltage mapping during more than one activation sequence (e.g., during NSR and ventricular pacing) can potentially increase the sensitivity to detect arrhythmogenic substrate. Dense scar appears to be less sensitive to wavefront changes compared with mixed scars, likely due to lesser available mass of normal far-field myocardium to contribute to the electrogram signal within the field of view of the mapping catheter.¹⁰⁹

Even when conducting channels within the scar area can be identified by substrate mapping, their functional contribution to the VT circuit remains to be assessed by other mapping methods (e.g., entrainment mapping). Substrate mapping does not distinguish abnormal bystander areas that are not involved in a VT circuit from clinically relevant channels. In one report, only 30% of “channels” identified with electroanatomic mapping contained a clinical VT isthmus, and only 44% of mappable VTs were associated with any identifiable channel. The presence of isolated late potentials within a channel, however, increases the likelihood that the channel will be important for maintaining VT.¹¹⁰

Furthermore, substrate mapping during NSR depends on the assumption that the arrhythmogenic substrate responsible for the reentry circuit is limited to fixed myocardial scar and anatomical barriers. It is now well known that functional lines of block (present during VT but not in NSR) play an important role in arrhythmogenesis, and these barriers cannot be detected by substrate mapping performed in NSR. Therefore the correlation between channels developing during arrhythmias and surrogates of channels identified by substrate mapping in NSR may not correspond.¹⁰

It is also important to recognize that the transmural distribution of the scar may not be reliably represented by voltage mapping from

either the endocardial or epicardial surface. In particular, identifying septal or midmyocardial substrates can be challenging.⁵⁴

Noncontact Mapping

When VT is short-lived, hemodynamically unstable, or cannot be reproducibly initiated, simultaneous multisite data acquisition using a noncontact mapping system (EnSite 3000; St. Jude Medical) can help localize the VT site of origin. The system has been shown to reliably identify presystolic endocardial activation sites (potential exits) for reentrant VTs and thus starting points for conventional mapping. It can also potentially help identify VT isthmuses and guide ablation.

The noncontact mapping system records electrical potentials from a multielectrode array (MEA) surrounding a 7.5-mL balloon within the LV cavity. Electrical potentials at the LV endocardial surface some distance away are calculated. Sites of mid-diastolic endocardial activity, which are likely adjacent to reentry circuit exits, are usually identifiable; in some cases, isthmuses can be identified (eFig. 22.15).

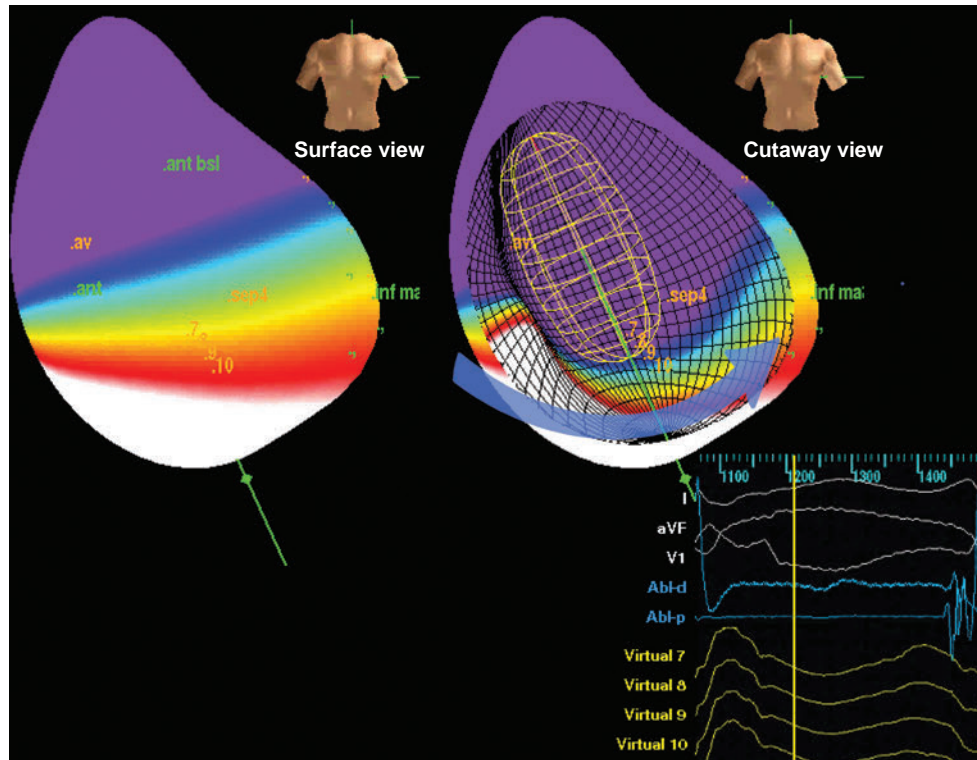
Voltages are displayed as a colored isopotential map on the virtual endocardium. The color scale is adjusted to create a binary display, with negative unipolar potentials in white on a purple background, producing a unipolar activation map. Diastolic depolarization is defined as activity on the isopotential map that can be continuously tracked back in time from VT exit sites, and is defined on the map as synchronous with the QRS onset. Diastolic activity and exit sites are then marked on the virtual endocardium, and the mapping catheter is navigated to them by the locator.

The noncontact mapping technology also enables substrate mapping based on scar or diseased tissue, which can be particularly helpful when the VT is not inducible during the procedure. Dynamic substrate mapping allows the creation of voltage maps from a single cardiac cycle and provides the ability to identify low-voltage areas, as well as fixed and functional block, on the virtual endocardium through noncontact methodology. The dynamic substrate mapping algorithm allows the creation of unipolar noncontact voltage maps from a single cardiac cycle, defined as the percentages of the maximal voltage recorded in the entire chamber. Until further studies define the correct dynamic substrate mapping percentage that can be compared with the scar and scar border zone defined by contact mapping, areas having values less than 50% may be defined as “abnormal myocardium.”

Technique of Noncontact Mapping

The EnSite 3000 system requires a 9 Fr MEA and a 7 Fr conventional (roving) deflectable mapping-ablation catheter. A standard ablation catheter is placed in the LV by a retrograde transaortic route. Using a separate arterial access site, the MEA catheter is advanced to the LV apex over a 0.032-inch J-tipped guidewire. Fluoroscopy is used to assess the correct position of the balloon catheter, placed parallel to the long axis and with the pigtail end as close as possible to the LV apex. The guidewire is then withdrawn and the balloon inflated with a contrast-saline mixture. The balloon is positioned in the center of the LV and does not come in contact with the LV wall. Care is taken to have a distance between the MEA catheter and the region of interest less than 40 mm; if necessary the catheter can be repositioned.

Construction of the virtual endocardium model is preliminarily obtained during sinus rhythm by moving the ablation catheter along the LV endocardial surface to collect a series of geometric points during NSR or VT. Using this geometric information, the computer creates a model of the LV. After the LV geometry is reconstructed, 5 seconds of NSR is recorded by the system, and the substrate map is superimposed on the anatomy. High-pass filters are adjusted at the lowest value that minimizes the shift of the isoelectric baseline to avoid confusing depolarization with repolarization.



eFig. 22.15 Use of Multipolar Electrode Array for Ventricular Tachycardia (VT) Mapping. Maps from the EnSite system are shown in a patient with inferior wall infarction. At left is a snapshot of the activation wavefront projected on the endocardial surface (*white* = activation). At right is the same instant of activation in a cutaway view, showing the wireframe of the endocardial balloon-based electrode array. At bottom right are contact and virtual electrograms from the array during VT; the wavefront propagates from left to right, along the mitral annulus (*curved blue arrow*).

Subsequently, VT is induced by programmed stimulation and mapping of the arrhythmia can begin. A 5- to 10-second segment of any induced VT is recorded with the noncontact system and the VT may then be terminated by overdrive pacing or electrical shock. The data acquisition process is performed automatically by the system, and all data for the entire LV are acquired simultaneously.

VT circuit exit points and potential ablation targets can be identified as sites where a QS unipolar electrogram morphology is recorded, which, on the color-coded isopotential map, corresponded to the site of earliest activation followed by a rapid activation wavefront. Projection of the virtual endocardial electrograms over this area is performed at different high-pass filter settings (1, 2, 4, 8, 16, and 32 Hz) to avoid misinterpretation with repolarization waveforms. This region is searched starting from the abnormal myocardium defined by dynamic substrate mapping and is considered a good target site for ablation when confirmed by EP criteria (contact activation mapping, entrainment mapping, and/or pace mapping).

The locator technology is used to guide the ablation catheter to the proper location in the heart. The system allows the operator to create linear ablation lesions that transect critical regions and then return precisely to areas of interest, visualizing lines of ablation as they are being created and performing the ablation during NSR.

Limitations of Noncontact Mapping

The most important shortcoming of the noncontact mapping system is the deterioration in the accuracy of noncontact electrograms for distances greater than 40 mm between the MEA catheter and the recording site, which can occur in dilated ventricles. Very low-amplitude signals may not be detected, particularly if the distance between the center of the balloon catheter and endocardial surface exceeds 40 mm, limiting the accurate identification of diastolic signals.

Because the geometry of the cardiac chamber is contoured at the beginning of the study during NSR, changes in chamber size and in contraction pattern during tachycardia can adversely affect the accuracy of the location of the endocardial electrograms. In addition, detection and display of activation from two adjacent structures, such as the papillary muscle and subjacent myocardium, is problematic.

Moreover, because isopotential maps are predominantly used, ventricular repolarization must be distinguished from atrial depolarization and diastolic activity. Early diastole can be especially challenging to map during VT. Care has to be taken to confirm that the virtual electrogram is related to local activation and not baseline drift or repolarization.

Because of the potential for thrombus formation, the use of this system requires the maintenance of a greater degree of anticoagulation (ACT >350 seconds) while the mapping balloon is in place than is generally required for the point-by-point mapping techniques. In addition, positioning of the MEA catheter in the LV can be difficult in the setting of atherosclerotic aorta or tortuous peripheral arteries, requiring a transseptal approach. The mapping sheath is 9 Fr in diameter; femoral hematomas and pseudoaneurysms are the most frequently encountered complications.

Mapping Postinfarction Premature Ventricular Complexes

In the majority of post-MI patients with frequent PVCs, the origin of the PVCs is mapped to sites of low voltage corresponding to the infarct location, similar to patients with post-MI VT. In addition, in patients with ischemic cardiomyopathy and VT that matches the PVC morphology, both types of arrhythmias have critical target sites within areas of low voltage, and the site of origin of PVCs often corresponds with the exit site of the VT reentrant circuit. Furthermore, as is the case with

VT, late potentials can be detected during diastole at the site of origin of most of the PVCs. The late potentials follow the ventricular electrogram during sinus rhythm and precede the ventricular electrogram during PVCs. Slight differences in morphology between PVCs and VT may be observed and may be rate related.

Possible mechanisms of PVCs in post-MI patients include reentry, triggered activity, and abnormal automaticity. Because of several features in common with post-MI VT, reentry may play a principal role in post-MI PVCs; however, this has not been confirmed by high-resolution mapping. Nevertheless, in a small percentage of patients, PVCs do not originate from scar tissue. In those patients, the PVCs can be due to triggered activity or abnormal automaticity, similar to idiopathic PVCs.

Because post-MI PVCs and VT often share critical areas, mapping of the PVCs can be used as a surrogate for mapping of the VT. Ablation of frequent PVCs can potentially eliminate VT in these patients. However, the sensitivity and specificity of this approach in an unselected population are not known, nor is the prevalence of PVCs indicating VT exit sites. If this concept is confirmed in larger series, PVC mapping can be used to identify exit sites of PVCs and to search for diastolic potentials prior to PVCs that may indicate areas of slow conduction relevant for the VT. Targeting the PVCs alone may be sufficient to eliminate the VTs that had an exit site near or at the PVC site of origin, obviating the need for induction of VT, which can be of great value in patients with unstable or unmappable VTs. Voltage mapping in these patients can be helpful in focusing the mapping procedure on the low-voltage areas because this area contains the arrhythmogenic substrate in most patients.¹¹¹

Furthermore, in post-MI patients with frequent PVCs, catheter ablation of the PVCs can potentially result in an improvement in the LVEF. It may be appropriate to screen patients with ischemic cardiomyopathy for frequent PVCs with a 24-hour Holter monitor before implanting an ICD for primary prevention of SCD. Ablation of the frequent PVCs may improve the LVEF such that the patient no longer meets the LVEF criterion for an ICD.

In addition, in patients with recurrent polymorphic VT or VF that are triggered by PVCs of consistent QRS morphology, ablation of the arrhythmia trigger (PVCs), rather than the substrate, is often successful in reducing the burden of those arrhythmias.^{1,4,14}

Mapping of Epicardial Circuits

The infarct scar is primarily located in the subendocardium and extends to the epicardium depending on the patient's specific coronary artery distribution. Therefore unlike VT substrates in patients with nonischemic cardiomyopathy, the arrhythmogenic tissue can be accessed from the endocardium in the majority of post-MI patients. Even in the presence of an epicardial substrate, endocardial ablation can often eliminate the overlying epicardial targets through thinned scar, minimizing the need for epicardial ablation.¹¹²

Nonetheless, VT originating from the subepicardium remains an important cause of failure of endocardial ablation approaches. In tertiary centers, epicardial ablation has been required in approximately 10% to 25% of post-MI VTs, and seems to be more common with inferior than anterior wall infarctions.¹¹³ Epicardial access, however, frequently is not feasible for patients who have undergone prior cardiac surgery (which is present in up to 55% of patients undergoing VT ablation).¹¹⁴

Currently, there are no consensus criteria to guide the need and appropriate timing of an epicardial approach in post-MI VT substrate ablation procedures. An epicardial approach is typically perused when extensive endocardial mapping or ablation fails in achieving the desired procedural endpoint. During endocardial mapping of post-MI VT, inability to identify the reentry circuit isthmus on the endocardium can suggest that the isthmus is epicardial or intramural. In these cases,

endocardial activation mapping can demonstrate a focal point of earliest endocardial activation where entrainment indicates a potential exit or outer loop site, but ablation fails to interrupt VT, suggesting that there is an epicardial or intramural circuit with a broad endocardial exit. In addition, endocardial unipolar (rather than bipolar) voltage mapping can predict the presence of and more closely approximate the greater extent of epicardial bipolar signal abnormalities, which can potentially serve as a substrate for VT.

Although various ECG characteristics have traditionally been used to predict whether an epicardial approach may be required based on the VT morphology, the surface ECG alone is not reliably predictive of the need for epicardial access and mapping for any given VT. QRS morphology is related solely to the VT exit site and this does not imply that some other component of the circuit (such as the critical isthmus or entrance site) cannot be ablated from the endocardium, even when an epicardial exit is implied by the ECG characteristics.

On the other hand, infarct transmuralities appear to predict epicardial arrhythmic substrate and the need for the epicardial approach to improve ablation outcome. Transmurality of the myocardial scar can be assessed by preprocedural cardiac imaging techniques (CMR, echocardiography, CT, and single photo emission CT), and can potentially help select post-MI VT patients in whom a combined endocardial-epicardial approach is appropriate as a first-line approach.^{103,115} Also, a large endocardial dense scar area on a bipolar voltage map (exceeding 10% area of endocardial surface area) was found to predict scar transmuralities.¹⁰⁰

The approach to epicardial mapping is essentially the same as for endocardial ablation, including activation mapping, entrainment mapping, substrate mapping, and pace mapping, and is discussed in detail in **Chapter 27**.

Practical Approach to Ventricular Tachycardia Mapping

The main goal of VT mapping is identification of the critical isthmus of the VT by activation and entrainment mapping techniques. Initially, substrate mapping is performed during NSR to delineate infarcted myocardium and the conducting channels within the myocardial scar that likely support the VT reentry circuit. This helps refine the area of interest and identify potential targets for further activation and entrainment mapping and, hence, minimize the time spent in sustained VT (**Box 22.3**).

When the VT is unstable or unsustainable, it may not be approachable by conventional point-by-point activation mapping and entrainment maneuvers. In this setting, substrate-based mapping becomes the main strategy to guide ablation by identifying the portions of the infarct region that most likely harbor the isthmuses of the clinical VT (**Fig. 22.30**).

Electroanatomic mapping is usually used to aid mapping and ablation. A standard 4-mm or 8-mm tip or, preferably, an irrigated-tip ablation catheter is used. High-density mapping can be facilitated by the use of a 20-pole catheter (PentaRay) or mini-basket catheter (Orion).⁸⁹

Identification of the Tachycardia Substrate

The majority of post-MI VTs are caused by macroreentry involving the dense myocardial scar interspersed with branching and merging bundles of viable myocytes with poor intercellular coupling and abnormal conduction properties. Buried in the arrhythmogenic substrate is the common central pathway (critical isthmus), which is a narrow path of tissue with abnormal conduction properties, causing slowing of impulse propagation and allowing reentry to occur. The isthmus itself can be surrounded by dead ends or branches that do not participate in the common pathway of the main reentrant circuit (bystander).¹⁰

BOX 22.3 Approach to Mapping of Postinfarction Ventricular Tachycardia

Identification of the Tachycardia Substrate

- Preprocedural substrate imaging:
 - Echocardiography, CT, or CMR.
 - Substrate mapping during baseline rhythm (sinus rhythm, or ventricular pacing).
 - Identification of scar location and distribution:
 - Dense scar: bipolar voltage <0.5 mV and electric unexcitability (pacing threshold >10 mA).
 - Border zone: bipolar voltage between 0.5 and 1.5 mV.
 - Identification of conducting channels within the scar region:
 - Voltage channels on the electroanatomic voltage map.
 - Local abnormal ventricular activity (amplitude \leq 0.5 mV; duration \geq 60 msec).
 - Late potentials.
 - Long (>40 msec) S-QRS interval during pacing.
- Pace mapping during sinus rhythm:
 - Identification of potential exit sites at the infarct border zone:
 - Paced QRS morphology matching that of the VT.
 - Long S-QRS interval.

Identification of the Critical Isthmus

- Activation mapping during VT:
 - Identification of sites with isolated mid-diastolic potentials or continuous activity spanning diastole.
 - Verification that the diastolic electrograms cannot be dissociated from the VT.
- Entrainment mapping during VT:
 - Confirmation of the presence of entrainment.
 - Entrainment criteria consistent with isthmus location:
 1. Concealed QRS fusion.
 2. PPI = TCL (\pm 30 msec).
 3. Electrogram-QRS interval = S-QRS interval (\pm 20 msec).
 4. Ratio of the S-QRS interval to the TCL less than 70%.

CMR, Cardiac magnetic resonance; CT, computed tomography; PCL, pacing cycle length; PPI, postpacing interval; S, stimulus; TCL, tachycardia cycle length; VT, ventricular tachycardia.

Substrate mapping is performed during baseline rhythm (NSR, AF, or ventricular pacing) and aims to identify: (1) scar location and distribution (as identified by low electrogram voltage and electric unexcitability); and (2) conducting channels within the scar region that can potentially serve as isthmuses for reentrant VTs (as identified by LAVA, late potentials, and long S-QRS interval during pacing).^{89,99}

Step 1: preprocedural substrate imaging. Echocardiography, CT, PET, or CMR imaging may be used to identify the size, location, and transmuralities of the infarct scar that potentially contains the arrhythmogenic substrate (see **eFig. 22.10**). Also, ICE can be of value for real-time identification of scar regions. In addition, integration of those imaging modalities into the 3-D electroanatomic mapping system can help visualize and display the LV substrate in a 3-D format and focus initial mapping efforts in those regions.

Step 2: scar mapping during sinus rhythm. Electrical scar is defined by low-amplitude local electrograms and tissue unexcitability during high-output pacing. Voltage mapping is utilized to identify the infarct and infarct border zones, which are likely to harbor the VT circuit. Bipolar voltage mapping is performed using a 3-D mapping system to identify areas of abnormal low-amplitude local electrograms during NSR or ventricular pacing.⁵⁴

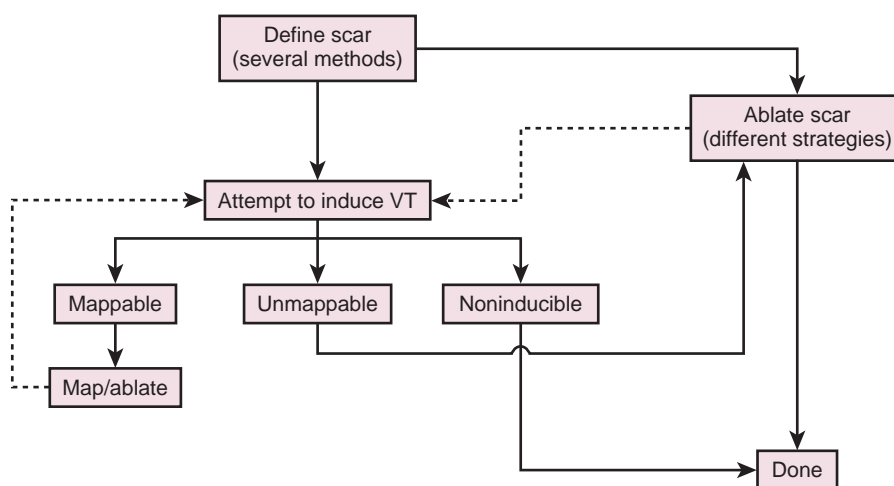


Fig. 22.30 An Algorithmic Approach to Treatment of Scar-Based Ventricular Tachycardia (VT), Consisting of an Iterative Process. See text for details.

Conventionally, bipolar electrogram amplitude less than 0.5 mV defines dense scar, with signal amplitudes between 0.5 and 1.5 mV representing the infarct border zone. Endocardial electrogram voltage exceeding 1.5 mV generally defines normal myocardium (a voltage cutoff of 1.0 mV is used for normal epicardial bipolar electrograms). The LV is mapped during baseline rhythm to construct a voltage map displaying peak-to-peak bipolar electrogram amplitude, with the color range set between 0.5 and 1.5 mV. Higher-density points are obtained around areas of scar, focusing on the scar border and electrograms within the scar. All scar borders need to be clearly defined. A color-coded voltage map is then created and superimposed on the anatomical model to show the amplitudes of all selected points (see eFig. 22.13).⁵⁴

At low-amplitude (less than 0.5 mV) sites, pacing is performed with 10-mA, 2-millisecond pulse width stimuli. A pacing threshold greater than 10 mA has been used to define unexcitable scar, provided electrode-tissue contact is adequate.

Step 3: identification of conducting channels during sinus rhythm. In patients with post-MI VT, the areas of electrical scar identified by voltage mapping are relatively large; therefore identification of the conducting channels within the infarct region, which are relatively small bundles of viable tissue compared with the scar areas, helps refine the area that potentially supports the VT circuit.

Conducting channels within the scar region can be identified by: (1) voltage channels; (2) late potentials; and (3) S-QRS latency during pacing. During the voltage mapping, areas of fractionated or late potentials (irrespective of the voltage obtained) and sites with long S-QRS intervals during pacing are tagged on the electroanatomic map.^{66,103}

Voltage channels. Conducting channels on the electroanatomic voltage map are identified corridors of voltage preservation (voltage channels) within denser regions of scar or corridors between a dense scar and the mitral annulus. Careful step-by-step manual adjustment of voltage upper and lower limits on the color-coded electroanatomic voltage map can help maximize the color contrast between adjacent myocardium with different electrogram voltage levels within the 0.5-mV scar and, thus, unmask channels of viable myocardium within a dense scar (see eFig. 22.14).⁶⁶

Late potentials. Low-amplitude, high-frequency, fractionated electrograms with multiple components of prolonged duration and late potentials (defined as bipolar electrogram with any component is recorded after the offset of the QRS complex on the surface ECG) can

reflect local depolarization of surviving muscle bundles that are well insulated by dense scar.^{54,89,99,100}

Sites recording abnormal electrograms are tagged on the electroanatomic map. Conducting channels are defined as a path of more than two adjacent late potentials connecting with healthy tissue. Further, late potentials are classified as being an entrance or an inner part of a given conducting channel, depending on the local activation time of the near-field component. The entrance of a conducting channel is tagged as sites within the border zone (i.e., voltage zone of 0.5 to 1.5 mV) recording late potentials with the shortest delay between the far-field component of healthy/border zone muscle (low frequency, usually high voltage) and the near-field component (delayed, high frequency, usually fractionated and low voltage) corresponding to the local activation of myocardial fibers in the scar. Sites with longer delays likely reside farther along the conducting channel within the dense scar. Once a specific sequence of late potential activation has been identified, focal ablation of the earliest late potential is delivered with the endpoint of eliminating a consecutive series of late potentials. The method involves reconstruction with high-density mapping of channels of activation of late potentials.^{102,103}

In addition, 3-D electroanatomic late potential maps may be constructed, whereby the *terminal* portion of every local electrogram is manually marked during the mapping procedure. The lower time threshold of the color-coded map is set to the difference between the reference and end of the surface QRS complex. Late potential maps can be superimposed on voltage maps to further delineate their relationship to scar distribution.¹⁰⁵

Unmasking late potentials and distinguishing between local and far-field signals are critical for the accuracy of substrate mapping. This can require mapping pacing at the local site (to confirm local electrogram capture), changing the direction of depolarization approaching the mapping site (e.g., sinus rhythm vs. RV pacing), and VES (causing decremental conduction) to separate far-field from near-field potentials (see Fig. 22.29).⁹⁹

S-QRS intervals. Pacing during NSR at sites with low-amplitude electrograms can help identify potential conducting channels within low-voltage regions. S-QRS intervals longer than 40 milliseconds suggest that the pacing site is located within a protected zone, forcing the paced wavefront to propagate slowly before exiting this zone to activate the larger myocardium, causing the latency between myocardial capture and the onset of surface QRS. These sites are typically associated with

abnormal fractionated electrograms during NSR. In the setting of post-MI VT, it is likely that pacing sites with long S-QRS delays identify slowly conducting channels that traverse dense scar and can potentially form VT isthmuses.¹⁰³

Identification of the Critical Isthmus

Identification of the critical isthmus of macroreentrant VT employs activation and entrainment mapping techniques, which have several prerequisites, including inducibility of VT at the time of EP testing, hemodynamic stability of the VT (which usually requires a relatively slow VT rate), and stability of the VT reentry circuit (i.e., stable VT morphology and TCL).

When hemodynamic compromise during the VT is the main limitation for conventional activation and entrainment mapping methods, inductions of brief episodes of VT (with the mapping catheter at the optimal site, as identified by substrate and pace mapping approaches) can allow assessment of the relationship of the abnormal electrograms to the VT circuit. This can also allow entrainment maneuvers to be performed at those sites to help distinguish sites critical to the VT circuit from bystander sites. VT is then quickly terminated before significant hemodynamic compromise ensues. In addition, poorly tolerated rapid VTs can sometimes be slowed by antiarrhythmic drugs to allow for mapping. Furthermore, the use of IV vasopressors and external hemodynamic support devices can potentially provide hemodynamic support and allow mapping of otherwise unstable VT.^{82–84} The use of a 20-pole catheter (PentaRay), the mini-basket catheter (Orion), and noncontact mapping can also provide large amounts of activation mapping data during nonsustained or unstable VT.

Activation mapping during tachycardia. After complete substrate mapping, electrical stimulation is used to induce VT and to ascertain the ease of inducibility for subsequent testing, unless the VT is incessant.

During electroanatomic activation mapping, the electrical reference is generally chosen as a morphologically stable and regular electrogram obtained from an endocardial (e.g., RV apical electrogram) or surface lead (e.g., surface ECG lead with a QRS complex during VT demonstrating a sharp apex and a strong positive or negative deflection). The width of the window of interest is adjusted to approximate, usually 20 milliseconds less than, the TCL. The middle of the window of interest is selected to coincide with the electrical reference. In general, bipolar electrogram recordings are used for activation mapping because they provide an improved signal-to-noise ratio and more clearly defined high-frequency components. The local activation time for each endocardial position under the mapping catheter is calculated as the interval between the electrical reference and the onset of the high-frequency bipolar electrogram as it leaves the baseline.

Care is taken to annotate only true near-field diastolic activity based on sharp near-field electrograms. Filtered unipolar electrograms can help ensure that the tip electrode, which is the ablation electrode, is responsible for the early component of the bipolar electrograms. In addition, demonstration of a fixed relationship of the diastolic electrograms to the subsequent VT QRS, despite spontaneous or induced oscillations of the TCL, is important to exclude the possibility that those electrograms do not reflect late activation from unrelated dead-end pathways.

Activation mapping during VT is then carried out, initially focusing mapping on regions of VT substrate as identified during substrate mapping.⁶⁶ Particular sites of interest identified by activation mapping include: (1) sites with an abnormal local bipolar electrogram (amplitude ≤ 0.5 mV; duration ≥ 60 milliseconds); (2) sites at which the local electrogram precedes the QRS complex by at least 50 milliseconds (activation times are taken from the onset of the bipolar electrogram); (3) sites with the earliest local activation closest to mid-diastole (isolated

mid-diastolic potentials); (4) sites with continuous activity spanning diastole; and (5) adjacent sites with electrical activity spanning diastole (bridging of diastole). The resulting reentrant circuit is considered to be the spatially shortest route of unidirectional activation encompassing a full range of mapped activation times (greater than 90% of the TCL) and returning to the site of earliest activation.

It is important to recognize that mid-diastolic sites can also be part of a larger area of abnormal slow conduction unrelated to the VT circuit (i.e., a dead-end pathway), and can be recorded from a bystander site attached to the isthmus. Therefore, regardless of where in diastole the presystolic electrogram occurs (early, mid, or late), it is important to confirm that the electrogram cannot be dissociated from the VT and is required for VT maintenance (see eFig. 5.2).

Entrainment mapping during tachycardia. Entrainment mapping during reentrant VT is used to verify whether a site recording diastolic activity (regardless of where in diastole it occurs, its position, and its appearance on initiation of VT) is functionally involved in the VT circuit.

Entrainment mapping is directed to sites identified by other mapping modalities (such as activation, substrate, and pace mapping) as potentially related to the reentrant circuit. These include areas of slow conduction (manifest as fractionated electrograms), sites with mid-diastolic electrograms, or those displaying long S-QRS intervals.

Pacing is performed at a PCL just shorter (10 to 30 milliseconds) than the TCL, and is continued for a long enough duration to allow for entrainment. After cessation of each pacing drive, the presence of entrainment and resumption of the same tachycardia morphology should be verified.^{69,70}

Once the presence of entrainment is verified, several criteria can be used to indicate the relation of the pacing site to the reentrant circuit. The first entrainment criterion to be sought is concealed fusion. Entrainment with concealed fusion indicates that the pacing site is in a protected isthmus located within or attached to the reentrant circuit. Whether this protected isthmus is crucial to the reentrant circuit or is just a bystander site needs to be verified by other entrainment criteria including the PPI versus the TCL and the local electrogram-QRS interval during VT versus the S-QRS interval.⁷²

The following four criteria are used to define the critical isthmus and predict the success of RF application in elimination of the VT: (1) there is entrainment with concealed fusion; (2) the PPI is equal to the TCL (± 30 milliseconds); (3) the electrogram-QRS interval is equal to the S-QRS interval; and (4) the ratio of the S-QRS interval to the TCL is less than 70%.⁹⁴

Pace mapping during sinus rhythm. Pace mapping can be used to complement activation and entrainment mapping findings, although it may not always be necessary, especially when several criteria localizing the VT isthmus have been identified. In the setting of post-MI VT, pace mapping serves only as a corroborative method to identify the presumptive exit or isthmus region of the VT circuit, but is not sufficiently specific or sensitive to be the sole guide for ablation.

Pace mapping during NSR is performed at the border zone between scar and normal tissue to approximate the exit site of each inducible VT and at isthmus sites defined during VT. Preferably, pace mapping is performed with unipolar stimuli (10 mA, 2 milliseconds) from the distal electrode of the mapping catheter (cathode) and an electrode in the IVC (anode). The same PCL is usually used for each site in an individual patient (500 to 700 milliseconds), slightly faster than the sinus rate and slower than the rate of the induced VTs.

Pacing at each site is evaluated for two criteria: paced QRS morphology matching that of the VT and long S-QRS interval. The greater the degree of concordance between the morphology during pacing and tachycardia, the closer the catheter is to the exit site of the tachycardia

isthmus. Pace mapping at sites more proximally located in the isthmus can also produce a similar QRS complex, but with a longer S-QRS interval (due to the delay of conduction of the paced wavefront to the exit site). The S-QRS interval lengthens progressively as the pacing site is moved along the isthmus, consistent with pacing progressively farther from the exit (see Fig. 5.23).⁹⁶ It is important to recall that pace mapping at an isthmus may not produce a QRS identical to VT for reasons discussed previously.

ABLATION

Target of Ablation

Approaches for ablation include selective targeting of the critical isthmus that supports the development and maintenance of VT (as identified by activation, entrainment, and pace mapping techniques), more extensive substrate modification to reduce the arrhythmogenicity of a scar without any specific arrhythmia targeting, or a hybrid of both techniques.^{54,66,116,117}

Identification and ablation of the critical isthmus of the VT circuit is the gold standard for macroreentrant VT. This approach provides focused, high-yield ablation, and avoids unnecessary ablation at bystander sites. However, this strategy may not be feasible when the VT is not reproducibly inducible or poorly tolerated. Even in the setting of stable SMVT, this approach can be time-consuming and expose the patient to the detrimental hemodynamic consequences of prolonged periods of sustained tachycardia, especially when multiple VTs are targeted.¹¹⁷

On the other hand, substrate-based ablation approaches aim at modifying the potential arrhythmogenic substrate without requiring mapping during VT. These strategies involve more extensive, nonselective ablation, frequently involving nonarrhythmogenic regions of the scar. Although substrate-based ablation strategies offer the ability of performing the ablation during NSR and, hence, maintaining hemodynamic stability, these approaches typically require extensive ablation given the less precise localization of the reentry circuit. Furthermore, a purely substrate-based mapping and ablation strategy may not address the focal mechanism of VT that can be observed in patients with structural heart disease.¹¹⁷

Selective Ablation of the Critical Isthmus of the Reentrant Circuit

The reentrant VT wavefront rotates around the isthmus boundaries and propagates slowly through the critical isthmus, which harbors diastolic potentials. Focal ablation of multiple sites defined as in the reentrant circuit may not eliminate post-MI VT. Elimination requires ablation of an isthmus bordered by barriers on either side. These isthmuses are usually found at the border zone of the infarct and are defined as conductive myocardial tissue delineated by nonconductive tissue. The nonconductive tissue can be a scar area or an anatomical obstacle, such as the mitral annulus.

VT isthmuses measure, on average, approximately 30 mm long by 16 mm wide. The axis of a critical isthmus is typically oriented parallel to the mitral annulus plane in perimitral circuits and perpendicular to the mitral annulus plane in other circuits. Successful ablation of post-MI VT is achieved by selectively targeting the critical isthmus where the circuit can be interrupted with linear RF lesions transecting the isthmus. The isthmuses are the preferred targets for VT ablation because they are usually narrow and critical parts of the VT reentry circuit, allowing ablation with a small set of RF lesions.¹⁰

Results of ablation of infarct-related VTs have been improving over the past decade because of better understanding and selection of ablation sites. Initial attempts at ablation targeted early presystolic potentials, followed by targeting mid-diastolic potentials; both approaches yielded

unsatisfactory results. Presystolic potentials were found to be nonspecific, because they might be in an area of scar tissue—for example, inner loop, bystander (inner sites attached to the central pathway), and not related to the VT circuit. Mid-diastolic potentials that cannot be dissociated from the VT during entrainment can be related to a bystander site. Demonstration of entrainment of VT with concealed fusion as a guide to VT ablation has increased ablation success rates. However, entrainment with concealed fusion alone to guide VT ablation has only a 50% positive predictive value for terminating VT because concealed entrainment can be observed during pacing from bystander sites connected to, but not integral parts of, the reentrant circuit. Multiple criteria activation and mapping criteria have been suggested, alone or in combination, to improve identification of the critical zone of the VT. These criteria have a different sensitivity and specificity with variable positive predictive values whenever they are used in different combinations (see Table 22.3).

For stable VTs, reentry circuit isthmuses are defined by activation and entrainment mapping as sites with: (1) continuous activity or isolated mid-diastolic potentials that cannot be dissociated from the tachycardia; (2) entrainment with concealed fusion; (3) a PPI equal to the TCL (± 30 milliseconds); (4) an S-QRS interval equal to electrogram-to-QRS interval (± 20 milliseconds); and (5) a ratio of S-QRS interval of the TCL between 30% to 70%. These criteria have the highest ablation success rates, with a positive predictive value of 100% and negative predictive value of 96% (see Box 22.3).^{54,116}

In addition, there are other criteria that can identify the location of the critical isthmus. Reproducible alteration of the TCL or termination of VT by subthreshold or nonpropagated pacing stimuli is also an indication that the pacing site is in a circuit isthmus (see eFig. 22.9). The stimulus likely captures local myocardium, but the propagated impulse blocks before exiting the scar region and creates bidirectional conduction block in the reentry circuit. Alternatively, the stimulus prolongs refractoriness at the site through an electrotonic effect. This finding is specific for predicting a successful ablation site, but is observed infrequently, with a sensitivity of only 16%. Furthermore, mild mechanical trauma caused by the mapping catheter occasionally terminates the VT and may render the tachycardia noninducible for a variable period of time, preventing further mapping. This event suggests that the vulnerable region for the VT is small and superficial, and ablation at the site can be successful. Empiric thermal mapping (RF application for 10 seconds to assess VT termination) can also help confirm sites within the VT isthmus. VT termination during short RF applications without induction of PVCs suggests an isthmus location. When RF application fails to terminate the VT at a site that appears to be in the circuit, catheter-tissue contact may be inadequate, the site may be a bystander, or the isthmus may consist of a broad band.

The inability to find the appropriate target site can be caused by: (1) inadequate density of mapping points; (2) the presence of a large amount of scar tissue; (3) intramyocardial or epicardial location of the VT isthmus; (4) technical difficulty in catheter manipulation; or (5) acceleration, termination, or changing of VT to a different arrhythmia during attempts at entrainment limiting mapping of the VT.

Substrate-Based Ablation

Over the past three decades, two effective surgical strategies have been developed for treatment of post-MI VT. Subendocardial resection, guided by the presence of the endocardial scar and involving removal of the subendocardial layer containing the arrhythmogenic tissue, is associated with a 70% to 80% arrhythmia cure rate. Such surgical therapy is performed when uniform sustained VT cannot be initiated at the time of surgery. The second technique is encircling endocardial ventriculotomy, whereby circumferential surgical lesions are placed through the border

zone, presumably interrupting potential VT circuits. This experience was critical in establishing the concepts on which substrate-based ablation is based; the arrhythmogenic substrate is predominantly located in the subendocardium and resides, at least partly, in the border zone between densely infarcted or fibrotic tissue and normal tissue. This substrate has distinguishing electrogram characteristics, and removal or interruption of this arrhythmogenic tissue can abolish the VT.⁵⁴

Substrate-based approaches to ablation of post-MI VT, guided by delineation of the infarct region from sinus rhythm electrograms, have dramatically improved ablation outcomes in patients with complex substrates. These approaches often allow successful ablation to be performed during NSR without the need for detailed mapping of the critical isthmus of the VT circuit. Although substrate-based ablation was initially proposed for the treatment of unstable or noninducible VT, it has recently emerged as an effective primary ablation strategy for any type of scar-related VT. The added value of VT induction and activation mapping has recently been challenged.¹¹⁶

Strategies for substrate ablation range from a thorough ablation of the entire abnormal substrate harboring abnormal electrograms (e.g., ablation of late potentials and fragmented electrograms, and scar homogenization) to more selective ablation approaches such as linear ablation, “scar dechanneling,” and “core isolation” (Fig. 22.31). These different strategies have not been directly compared and differences in outcomes are not apparent in the literature. Further, the optimal targets and sequence of ablation when combined with mapping during VT are uncertain and continue to evolve. Variations in anatomy may also influence the effectiveness of the different methods. In many patients, a combination of these techniques is needed for successful identification and ablation of critical sites of the reentrant circuit.^{54,90,102,116}

Scar homogenization. This approach aims to completely eliminate all the abnormal electrograms (fragmented electrograms and late potentials) within the scar defined by bipolar voltage mapping (Fig. 22.32).

Extensive RF ablation is performed throughout the entire scar based on the substrate and targeting all sites with abnormal electrograms in NSR. Ablation is continued until abnormal and late potentials are extinguished, as confirmed by reduction of electrogram amplitude to the noise level and electrical unexcitability in response to high-output pacing (20 mA at 10 milliseconds).

However, the infarct size or area of low-voltage electrograms is usually large (averaging 21 cm in circumference in one study), necessitating extensive and transmural ablation lesions, which is difficult to achieve using the current catheter-based ablative techniques and can result in increased risk of complications, including damage to functioning myocardium. Therefore ablation over the entire infarct region is often not feasible, nor necessarily desirable.^{54,66,102}

Scar dechanneling. Scar dechanneling involves RF ablation of all conducting channels within the scar as identified by substrate mapping. This strategy attempts to limit the extent of ablation required to achieve scar homogenization by preferentially targeting the entrance sites to the conducting channels. Ablation at the entrance of these channels can result in disappearance of conduction downstream in the channel and its ramifications, as confirmed by elimination of a consecutive series of late potentials within the conducting channel (Fig. 22.33).

Conducting channel entrances are identified by substrate mapping as sites within the border zone (i.e., zone with 0.5 to 1.5 mV voltage) recording the earliest late potential, that is, late potentials with the shortest delay between the far-field component (low frequency, usually high voltage) and the near-field local ventricular activity (typically delayed, high frequency, fractionated, and low voltage). This is in contrast to the inner points of conducting channels within the dense scar, which are characterized by longer delays between the local and far-field electrogram components.

The endpoint of this ablation strategy is conducting channel entrance conduction block, manifesting as the disappearance of the

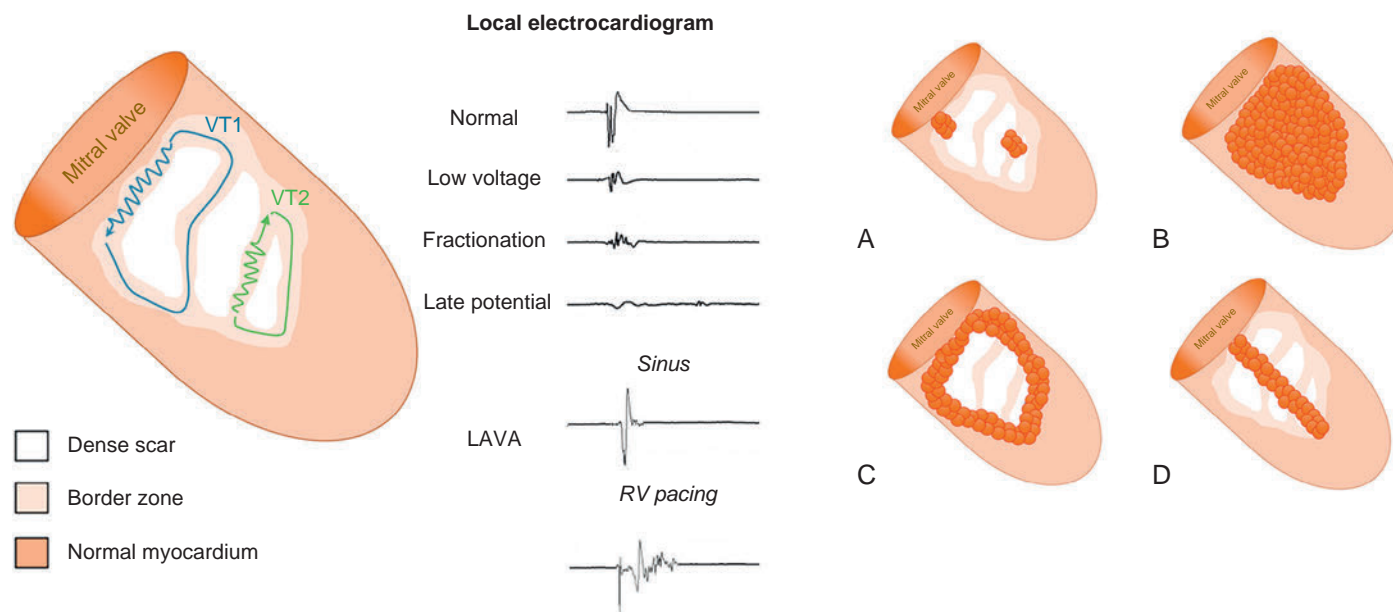


Fig. 22.31 Substrate-Based Ablation Strategies. (A) Isthmus ablation. (B) Scar homogenization. (C) Ablation lines applied parallel to the scar border within the low-voltage area encompassing the exit region. (D) Ablation lines placed perpendicular to all defined isthmuses between islands of unexcitable segment or extend perpendicular to the scar border from the area of dense scar, across the border zone and connecting out to normal myocardium or anatomical barrier (e.g., mitral valve). RV, Right ventricular. (From Tanawuttiwat T, Nazarian S, Calkins H. The role of catheter ablation in the management of ventricular tachycardia. *Eur Heart J*. 2016;37:594–609.)

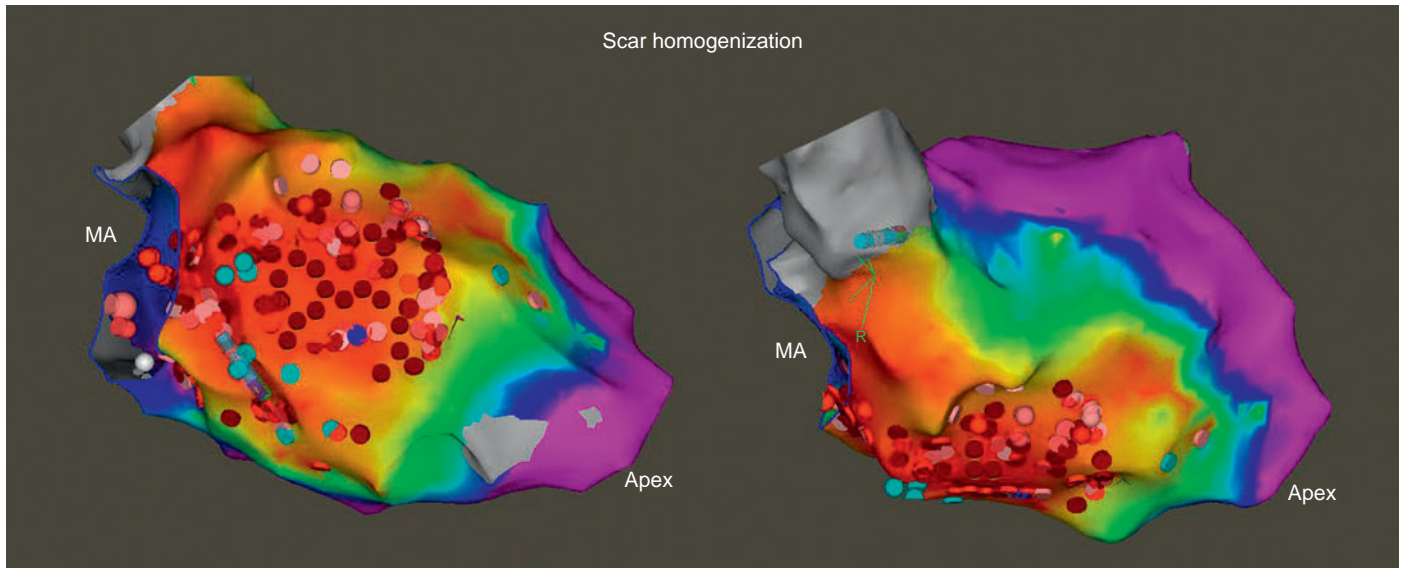


Fig. 22.32 Scar Homogenization. A voltage map of the left ventricle (posteroinferior [left] and right anterior oblique [right] views) is shown in a patient with prior inferior wall infarction. A large inferior wall scar (bipolar electrogram amplitude <0.5 mV, red area). Substrate-based ablation (tagged as red dots) is performed to achieve extensive scar homogenization. Ablation targets included fragmented electrograms and late potentials. Blue dots denote sites of good pace mapping. MA, Mitral annulus.

inner point of the conducting channels or delayed activation of conducting channel inner points, usually with the activation sequence in reverse order.^{54,102,103,118,119}

Core isolation. Core isolation refers to circumferential ablation around all critical or “core” areas of the scar containing the putative VT circuit elements or around the dense scar (voltage less than 0.5 mV) when VT is not inducible. The putative VT circuit elements are defined by conventional mapping techniques, including conducting channels identified on voltage mapping (voltage channels), sites with late potentials, sites with good pace maps and long S-QRS intervals, and isthmus sites defined by entrainment mapping. Once the critical area is identified, contiguous ablation lesions are delivered all around that area or using anatomical anchors (when present) to minimize the amount of ablation necessary (Fig. 22.34).^{54,102,119}

The goal of core isolation is electrically isolating the segment of low-voltage scar confirmed by the demonstration of exit block from the core of the scar (i.e., failure of global ventricular capture during high-output pacing from multiple, discrete sites inside the core that had previously demonstrated capture). In addition, entrance block can be demonstrated by dissociated fragmented electrical activity inside the core. Core isolation obviates the need for extensive ablation within the scar as proposed by scar homogenization.^{120,121}

Linear ablation. Linear ablation targeting the VT substrate is also widely used.⁵⁴ Linear RF lesions are placed using one of several guiding principles:

- Ablation lines extending perpendicular to all potential isthmuses (i.e., conducting channels identified on substrate mapping) within the scar areas or between islands of unexcitable segments within the infarct (identified as a region of relatively larger voltage bordered by low voltage within the scar and abnormal electrograms during NSR).
- Ablation lines extending parallel to the scar edge at the scar border zone (voltage 0.5 to 1.0 mV) encompassing all approximate exit sites identified by pace mapping.¹⁰²
- Ablation lines extending perpendicular to the scar border, from the area of dense scar (i.e., voltage less than 0.5 mV) across the border

zone and connecting out to normal myocardium (i.e., voltage greater than 1.5 mV) or to anatomical barriers (e.g., mitral annulus).¹⁰²

Multiple Inducible Ventricular Tachycardias

In patients referred for post-MI VT ablation, an average of three to four VTs is commonly inducible by programmed electrical stimulation. When multiple VTs are inducible during EP testing, several investigators have targeted the predominant morphology of VT. Ablation that focused on the clinical VT but did not target other inducible VTs successfully abolished the clinical VT in 71% to 76% of cases. However, during follow-up, approximately one-third of patients with acutely successful ablation of the clinical VT had arrhythmia recurrences, some of which occurred because of a VT different from that initially targeted for ablation. Furthermore, there are several difficulties with selecting a dominant, clinical VT for ablation. Often, it is not possible to determine which VT is the one that has occurred spontaneously. Only a limited recording of one or a few ECG leads may be available. In patients with an ICD, the device typically terminates VT before an ECG is obtained, and VT is documented only on intracardiac recordings. Even if one VT is identified as predominant, other VTs that are inducible can subsequently occur spontaneously. An alternative approach is to attempt ablation of all inducible VTs that are sufficiently tolerated to allow mapping. The 3-year risk of recurrent VT after such an approach is 33%.

At present, the clinical endpoint for VT ablation remains unclear. Targeting of all inducible SMVTs is a prevalent strategy because recordings of all VTs before ablation often are not reliably obtainable to define clinically relevant VTs. Nonetheless, the level of aggressiveness to achieve this endpoint must be weighed against hemodynamic stability, volume shifts, and prolonged anesthesia in tenuous patients.⁶⁶ Therefore the goal(s) of ablation should be individualized. In patients undergoing ablation because of frequent ICD shocks or tachycardia-induced cardiomyopathy, elimination of problematic VT morphologies is appropriate. On the other hand, elimination of all inducible VTs should be considered especially for patients who cannot undergo or decline ICD implantation.¹¹⁶

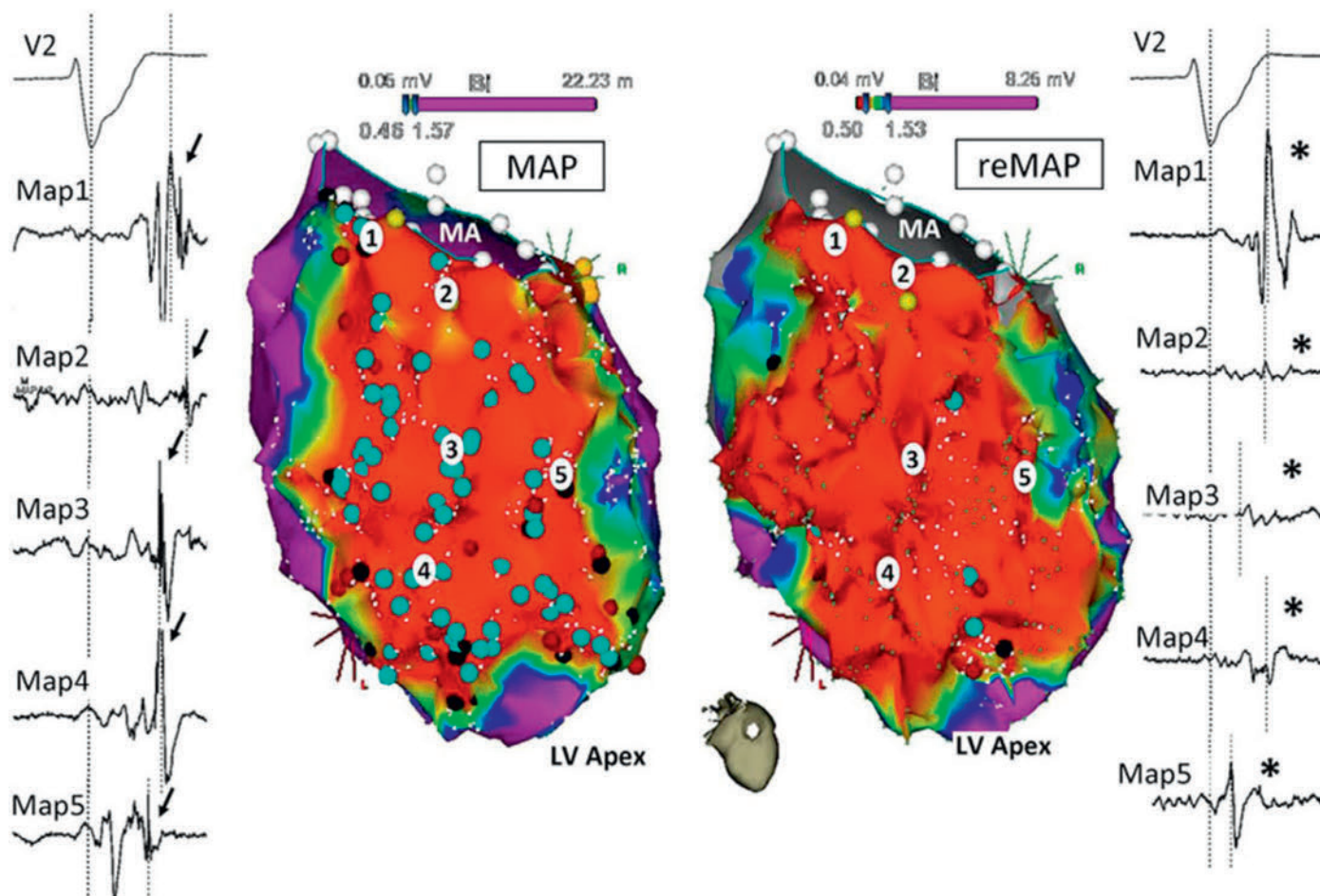


Fig. 22.33 Scar Dechanneling. Inferior view of left ventricular (LV) bipolar voltage electroanatomic substrate maps during sinus rhythm before (MAP) and after (reMAP) scar dechanneling in a patient with healed myocardial infarction. Electrograms recorded as conducting channel entrances are labeled with black dots and inner sites with blue dots. Examples of bipolar electrograms at entrances (1 and 5) and inner parts (2–4) are shown (left). Delayed components of the electrograms are highlighted with arrows. Electrogram aspect after elimination of the delayed component (asterisks) in the same sites after scar dechanneling is shown (left). MA, mitral annulus. (From Berruezo A, Fernández-Armenta J, Andreu D, et al. Scar dechanneling: new method for scar-related left ventricular tachycardia substrate ablation. *Circ Arrhythm Electrophysiol*. 2015;8:326–336.)

Ablation Technique

Catheter ablation of scar-related VT usually requires relatively extensive tissue injury to abolish the arrhythmia substrate, which can be facilitated by the use of larger electrodes or irrigated electrodes. In general, irrigated RF electrodes are preferred to large (8-mm)-tip electrodes. Cooled RF ablation allows increased power delivery, deeper lesions in myocardial scar, and potentially improved outcomes. In contrast, increasing the size of the electrode both reduces the spatial resolution of mapping and increases the disparity in temperatures across the surface of the electrode such that hot regions can lead to coagulum formation despite relatively low temperatures recorded from the electrode. On the other hand, external irrigation involves administration of potentially large amounts of IV saline, which can cause acute heart failure. Internal irrigation catheters, large-tip catheters, or external irrigation catheter designs employing lower irrigation flow rates (e.g., ThermoCool SF, Biosense Webster) should be considered if intravascular volume administration will be difficult to manage, as in patients with renal failure or severe heart failure.

The external irrigation system (ThermoCool; Biosense Webster) uses an 8 Fr catheter that has an electrode 3.5 mm in length with six holes in the tip through which saline flows at 30 mL/min during RF application. In the internal irrigation system (Chilli; Boston Scientific, Natick, MA), saline flows at 36 mL/min through the electrode and returns through a second lumen to be discarded outside the patient. For both cooled RF systems, RF application is initiated at a power output of 20 to 30 W; the power is gradually increased to achieve a fall in impedance of 5 to 10 Ω or a maximal measured electrode tip temperature of 40°C to 45°C. Energy application is continued for 30 to 120 seconds. RF current application is discontinued if measured impedance increases by more than 10 Ω , the catheter changes position, or VT fails to terminate after 30 to 60 seconds.

Alternatively, RF current can be delivered generally during VT from a mapping catheter with a solid 8-mm tip. RF energy is delivered in a temperature-controlled mode for 60 to 120 seconds at each ablation target site, with a maximal temperature target of 60°C to 70°C and 50 to 70 W of maximal power delivered. Impedance is monitored during RF delivery. In case of an impedance rise, the ablation catheter is removed

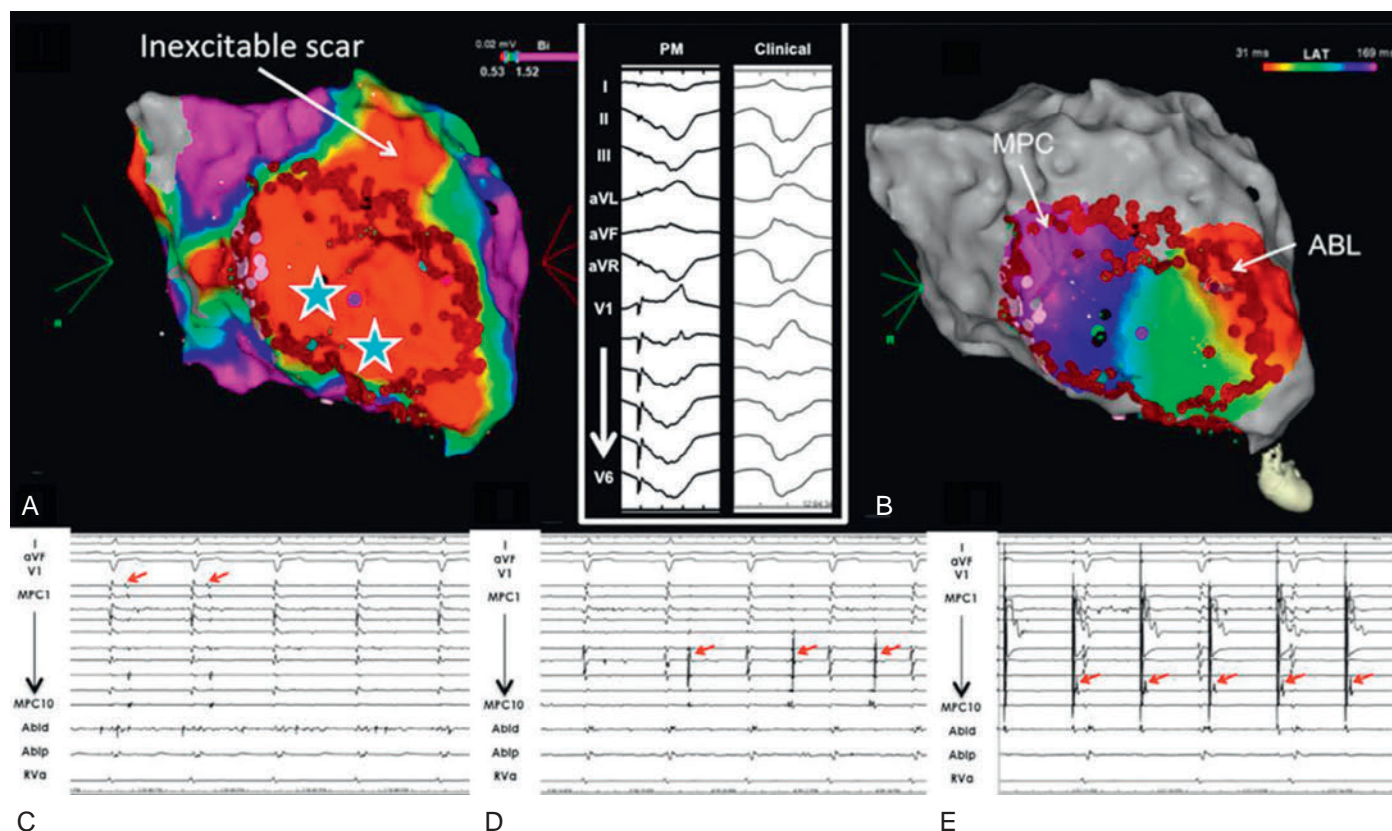


Fig. 22.34 Core Isolation. (A) Endocardial voltage map (anteroposterior view) in a patient with ventricular tachycardia (VT) and a large anterior myocardial infarction. The VT circuit core was defined by good pace map (PM) sites (stars depict examples), as defined in the text and was isolated by contiguous ablation at the junction between dense scar and border zone or regions without pacing capture at baseline. (B) Late potential activation map performed after core isolation identifying a single site of endocardial breakthrough within the isolated area. A multipolar catheter (MPC) was positioned within the core isolation area, and the ablation catheter (ABL) at the site of endocardial breakthrough. (C) Ablation at the earliest breakthrough results in core isolation, with entrance block demonstrated by disappearance of near-field late potentials from the MPC during ablation (arrows). (D) After core isolation, dissociated potentials were recorded (arrows). (E) After isolation, pacing from the MPC shows local myocardial capture (arrows) with exit block. (From Tzou WS, Frankel DS, Hegeman T, et al. Core isolation of critical arrhythmia elements for treatment of multiple scar-based ventricular tachycardias. *Circ Arrhythm Electrophysiol.* 2015;8:353–361.)

from the body and the distal electrode is wiped clean of the coagulum before continuing with the procedure.

At isthmus sites identified by entrainment, successful ablation sites usually result in VT termination within 5 to 15 seconds of the RF application. A second RF application is typically given at successful target sites if VT cannot immediately be reinitiated and the catheter has not moved. If there is no termination of VT after 30 seconds of RF application, it is suggested to discontinue RF energy delivery to decrease the likelihood of ablation of noninvolved myocardial tissue, with potential impairment of LV function. However, assuring adequate catheter-tissue contact is important before abandoning what appeared to be a good target site.

Application of RF energy at successful exit, central, or entry VT isthmus sites usually results in termination of the VT within a mean time of 10 ± 11 seconds. When RF application at other sites terminates the VT, the average time to termination is 19 ± 16 seconds, which suggests that a larger region must be heated for interruption of reentry. Persistence of inducibility of VT after successful termination with a

single RF application, despite further applications of RF energy at the same site, is probably secondary to inadequate lesion size because of a wide isthmus, epicardial location, or the presence of significant fibrosis, thrombus, or calcification. In some cases, lack of consistent electrode-tissue contact can result from dislodgment of the electrode when a sudden change in rhythm occurs (such as VT termination).

When RF application fails to terminate the VT at a site that appears to be in the circuit, the site may be a bystander. Failure of ablation has been attributed to a number of factors, including inaccurate mapping because of failure to apply appropriate criteria for localizing a protected isthmus and/or inability to find such a site, and also to inadequate lesion size produced by the RF application. Occasionally, successful termination of VT is achieved with RF application at a site at which failure is predicted. This may occur if the site is not at the isthmus region but in the nearby vicinity, with good conduction of temperature to the isthmus.

For ablation of unstable VT, RF energy is delivered during NSR. A series of ablation lesions are made to transect the critical isthmus in

the most convenient area, targeting the narrowest portion of the isthmus when allowed by catheter positioning and stability. To join the isthmus boundaries, RF lines are usually drawn perpendicular to the mitral annulus plane in perimitral circuits (see eFig. 22.13) and parallel to the mitral annulus plane in all other circuits. RF lesions are applied to the region until pacing with 10-mA, 2-millisecond strength stimuli fails to capture, or reversal of ventricular electrograms in CS recordings occurs (eFig. 22.16). After completion of each set of RF lesions, programmed electrical stimulation is repeated.

For intramural circuits, catheter ablation from both sides of the scar (epicardially and endocardially) may be necessary. Midseptal circuit can require high-energy RF ablation at the endocardial breakthrough sites from the right and left sides of the interventricular septum, but can be associated with increased risk of AV block. RF delivery within a perforator vein of the great cardiac vein may be considered in some cases. RF ablation of midseptal targets frequently result in acute tachycardia termination, but persistent inducibility later during the procedure as well as high recurrence of clinical tachycardias during follow-up. Alternative ablation modalities have been described, including bipolar RF, high-intensity focused ultrasound, needle ablation, or intracoronary ethanol injection, but currently these modalities are not available for routine clinical application.⁵⁸

Endpoints of Ablation

Noninducibility of All Sustained Monomorphic Ventricular Tachycardias

Noninducibility of any VT (excluding ventricular flutter, polymorphic VT, and VF) is the preferred and recommended endpoint of the ablation procedure. In a meta-analysis and a large-scale, multicenter cohort, elimination of inducibility of all SMVTs was found to be associated with a significant reduction in both mortality and recurrence of VT/VF events. However, the mortality benefit has not been consistent across different studies.^{54,91,119,122,123}

For verification of VT inducibility, the entire programmed electrical stimulation protocol should be performed and should include up to three VESs delivered from at least two ventricular sites, with the shortest coupling intervals of 180 to 200 milliseconds or to refractoriness. If the initial stimulation protocol required additional LV pacing sites or catecholamine infusion to induce VT, then that protocol should be repeated following ablation. The complete protocol of programmed electrical stimulation is again repeated after a 30-minute waiting period, unless such aggressive stimulation places the patient at risk of cardiopulmonary deterioration.

However, while noninducibility of VT is considered an ideal endpoint of the ablation procedure, it has several limitations. VT may not be inducible at baseline. In addition, the inducibility of some VTs may not be reproducible. Furthermore, an aggressive ventricular stimulation protocol at the conclusion of a long procedure in marginally stable patients can potentially lead to hemodynamic compromise. Importantly, the predictive value of noninducibility for VT recurrence is limited; VT recurs in 26% to 44% of patients who were rendered noninducible by catheter ablation. On the other hand, more than 50% of patients who remained inducible for a previously undocumented (nonclinical) VT do not experience VT recurrences on short-term follow-up, suggesting that pursuing elimination of nonclinical VTs can lead to overtreatment in a large proportion of patients. Finally, it is important to recognize that noninducibility of all SMVTs may not be achievable in a relatively large proportion of patients despite aggressive ablation attempts.^{56,122,123}

Noninducibility of All Clinical Ventricular Tachycardias

“VT modification” is defined as noninducibility of all clinical VTs (i.e., all inducible VTs that are known to have the same 12-lead ECG QRS

morphology and approximate TCL as spontaneous VTs), but with other SMVTs remaining inducible. Following ablation of one or more reentry circuits, the remaining inducible VTs are often faster, suggesting that regions of slow conduction have been ablated; the remaining circuits that can form have a shorter revolution time. Thus the arrhythmia substrate appears to have been modified. Modification of the reentry substrate is a common outcome of ablation, and is usually associated with a favorable outcome and a decrease of the arrhythmia burden in most patients.¹²³

When clinical or presumed clinical VTs have been adequately documented previously and can be induced at the outset of the procedure, the minimal endpoint of ablation should be to eliminate the induction of that VT during postprocedure programmed stimulation. On the other hand, the mere change in the “intensity” of stimulation required to induce VT (greater number of extrastimuli and alternative stimulation sites) is not a reliable endpoint. Nevertheless, in patients who present with incessant VT, restoration of stable sinus rhythm may represent a reasonable clinical endpoint, irrespective of the outcome of subsequent programmed stimulation.¹²³

This endpoint, however, does not apply in the majority of patients in whom morphology of the spontaneous VTs have not been documented on a 12-lead ECG prior to the ablation procedure.^{116,123}

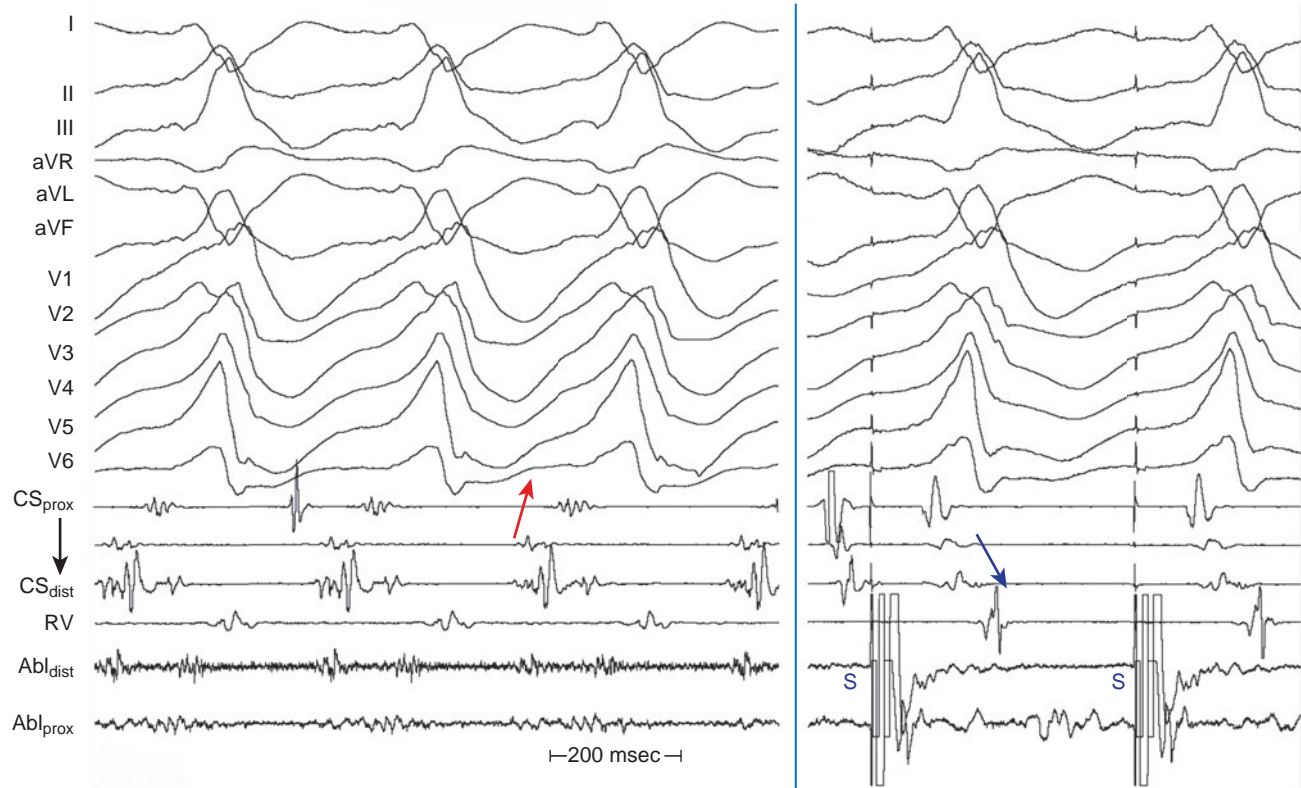
Elimination of the Arrhythmogenic Substrate

Complete elimination of all fragmented and late potentials, scar homogenization, scar dechanneling, or core isolation (as described previously) may also be utilized as alternative procedural endpoints, especially in patients in whom VT is not reproducibly inducible at baseline. Furthermore, even in patients with inducible VTs, some reports suggested an improvement in outcome (reduction in VT recurrence cardiac mortality) when these substrate-based endpoints are combined with VT noninducibility. As noted, noninducibility of VT is not a perfect endpoint; the rate of VT recurrence remains relatively high even in patients whose VT is rendered noninducible after ablation. Substrate-based endpoints can potentially improve outcome by eliminating the arrhythmogenic substrate and reducing the risk of developing new VTs or preexisting VTs that were not inducible during the ablation procedure. However, achieving substrate-based endpoints is more challenging than noninducibility of a given VT and typically requires more extensive, nonselective ablation.^{120,122,123}

Management After Ablation

Following successful catheter ablation, antiarrhythmic drugs may be discontinued in some patients. Nonetheless, because of the relatively high risk of VT recurrence and the progressive nature of the VT substrate, antiarrhythmic drug therapy is often continued in most patients following VT ablation. In some cases, cessation of antiarrhythmic drugs that had suppressed some VTs may allow them to occur. Therefore freedom from antiarrhythmic drugs may not be a reasonable goal of ablation; instead, dose reduction may be an important goal, particularly for amiodarone, for which the incidence of side effects is closely related to daily dose. In various trials, dose reduction of amiodarone has been feasible following ablation. Reduction of amiodarone dose may be attempted in a progressive manner starting within the first 3 to 6 months post ablation in patients who remain free of VT/VF.

Within the first 3 months post ablation in the LV, there may be a risk of systemic thromboembolism, particularly if extensive ablation lesions were applied. Antiplatelet agents (aspirin, clopidogrel, or both) are typically used in all patients with ischemic heart disease. In addition, short-term (6 to 12 weeks) warfarin therapy may be considered for higher-risk patients (documented thrombus, previous stroke or transient ischemic attack, AF, severe LV dysfunction), especially those



eFig. 22.16 Mitral Isthmus Block in Inferior Wall Postinfarction Ventricular Tachycardia (VT). During VT, shown in the left panel (as well as sinus rhythm and right ventricular pacing [data not shown]), ventricular electrograms in the coronary sinus (CS) recordings propagate from distal to proximal (*red arrow*). After ablation to the mitral annulus, pacing from a coronary vein branch distal to the ablation line (*right panel*) shows propagation now from proximal to distal CS (*blue arrow*), indicating conduction block in the mitral isthmus. *Abl_{dist}*, Distal ablation site; *Abl_{prox}*, proximal ablation site; *RV*, right ventricular.

patients who received extensive ablation over large areas (e.g., several centimeters).

Outcome

Success and Recurrence

Clinical studies have demonstrated the superiority of catheter ablation compared with medical therapy in controlling recurrent post-MI VT. However, long-term freedom from VT remains an issue, with reported long-term success rates of only 35% to 60%.⁶⁶ Nonetheless, in patients with drug-refractory post-MI VT, catheter ablation generally results in improved arrhythmia control, reduced frequency of ICD therapies, and significant reduction in the use of antiarrhythmic drug therapy in the majority (50% to 83%) of patients, even when occasional recurrences of VT persist during follow-up. Reductions in VT episodes and ICD shocks lead to a decrease in hospitalizations as well as improvements in anxiety and depression.^{116,124}

Ablation targeting critical isthmuses for stable VTs is successful in abolishing the inducible “targeted” or “clinical” VT in 71% to 93% of selected patients. During average follow-ups ranging from 9 to 42 months, noninducibility of the clinical VT immediately postprocedure is associated with a lower risk of VT recurrence and nonfatal VT (13% to 46%), compared with persistent inducibility of the clinical VT (up to 80%); the risk of SCD is low (0% to 6%), reflecting the common use of ICDs for patients felt to be at risk. Substrate-based ablation has been used as an adjunctive or an alternative approach, and appears to further reduce the risk of recurrence of any VT at follow-up when compared with ablation targeting only mappable VTs.⁶⁶ However, in the largest three prospective studies, complete elimination of VT inducibility as a procedural endpoint was achieved in 40% to 75%, whereas elimination of “clinical” VT was achieved in 72% to 93% of patients. In addition, a recent meta-analysis failed to show superiority of either approach in terms of acute procedural success (noninducibility of the targeted VT), procedural complications, VT recurrence, or mortality.¹²⁵

In patients with a single stable spontaneous VT morphology well documented prior to the procedure, the persistent induction of “non-clinical” VTs that are faster than the targeted VT was reported to have little influence on subsequent spontaneous recurrence rates. Although the occasional spontaneous occurrence of these “nonclinical” VTs during follow-up is well documented, ablation of only the clinical VT (but not necessarily all VTs) can be associated with a lower incidence of electrical storm and cardiac death, despite a high likelihood of sporadic VT recurrence. On the other hand, complete elimination of VT inducibility at the conclusion of the ablation procedure is associated with improved survival and reduced long-term risk of VT recurrence.

In patients with incessant VT or VT storm, catheter ablation can be life-saving with an acute success rate of VT ablation of 72%, recurrence rate of 6%, and procedure-related mortality rate of 0.6%.⁵⁴ Although single episodes of VT recur in approximately one-third of patients, 74% to 92% remain free of incessant VT or VT storm.

Procedural success, long-term prognosis, and procedure-related mortality and complications appear to be better in patients who undergo the ablation procedure early in the course of disease. Successful VT ablation may have benefit beyond arrhythmia control, and was found to be strongly associated with improved transplant-free survival, independent of heart failure severity.¹²⁶ Two small randomized controlled trials examined catheter ablation as primary treatment for VT in patients with prior MI. In the Ventricular Tachycardia Ablation in Coronary Heart Disease (VTACH) trial, 110 patients with ischemic cardiomyopathy who were receiving an ICD for hemodynamically stable SMVT were randomly assigned to undergo VT ablation before ICD implantation or to a control group receiving no additional intervention. In the Substrate Mapping and Ablation in Sinus Rhythm to Halt Ventricular

Tachycardia (SMASH-VT) trial, 128 patients with ischemic cardiomyopathy who had hemodynamically unstable VT and an ICD were randomly assigned to undergo substrate-guided VT ablation or no ablation. Both studies showed that catheter ablation significantly reduced arrhythmia recurrence but had no impact in mortality (likely due to the fact that ICDs were implanted in both study groups). The rate of complications was 5% and no periprocedural mortality was observed.⁵⁴

A more recent study (the Ventricular Tachycardia Ablation versus Escalated Antiarrhythmic Drug Therapy in Ischemic Heart Disease [VANISH] trial) examined the value of catheter ablation versus escalation of antiarrhythmic drug therapy (usually in terms of increasing the dose of amiodarone or adding mexiletine) in patients with ischemic cardiomyopathy and an ICD, who had recurrent VT despite first-line antiarrhythmic drug therapy. The rate of the composite outcome of death at any time or VT storm or appropriate ICD shock after 30 days was lower in the ablation group than among patients who received escalated antiarrhythmic drug therapy. In addition, sustained VT at a rate below the detection limit of the ICD and adverse events that were attributed to treatment were more frequent among patients in the escalated-therapy group. This trial provides evidence supporting the consideration of catheter ablation in patients with recurrent VT refractory to an initial regimen of antiarrhythmic drug therapy, in preference to an escalating antiarrhythmic drug regimen.¹²⁷

In contrast, short- and long-term outcome remains poor (mainly driven by VT recurrences and heart failure–related death) in patients with severe LV systolic dysfunction undergoing ablation for recurrent VT as a last resort (after failure of multiple antiarrhythmic medications), independent of the acute outcome of the procedure. Induction of multiple morphologies of VT and unstable VT at baseline appear to be associated with a higher risk of VT recurrence. Although possibly affected by selection bias, an early intervention with VT ablation aiming at noninducibility seems to be appropriate.^{54,56}

Importantly, recurrence of VT after ablation is an independent predictor of all-cause mortality. The prognostic impact of VT recurrence after ablation appears to be time dependent; early recurrences (within the first month post ablation) are associated with the highest risk of adverse prognosis, and the risk decreases gradually with later recurrences.¹²⁸

Causes of Arrhythmia Recurrence

The causes of recurrent VT after an acutely successful ablation procedure are speculative. Recurrence of the patient’s initial spontaneous VT is usually presumed to occur if the 12-lead ECG demonstrates the same VT morphology as the initial VT, or the TCL as recorded from the ICD is within 20 milliseconds of the initial TCL (if there has been no change in antiarrhythmic drug therapy). When the clinical VT recurs, it generally has a longer TCL. This occurs because (1) the RF lesion might have produced slowing of conduction, and not block, in the critical isthmus, possibly because the width of the isthmus exceeds the size of the ablation lesion; (2) the RF lesion might have increased the length of the central common pathway by increasing the barrier around which the impulse circulated, without changing the circuit exit; or (3) the RF lesion might actually have been successful in eliminating the critical isthmus of the VT circuit, but an inner loop, which was present and not part of the primary reentry circuit, became an active participant in a new longer circuit that had the same exit site as the original VT.¹¹⁴

The majority of VTs recurring after prior ablation display morphologies not seen or targeted at the initial procedure.⁵ This likely reflects different exit sites or different potential reentrant circuits in the vicinity of prior ablation lesions. Long-term evolution and progression of underlying myocardial and coronary disease and continued infarct remodeling can potentially lead to the formation of new VT circuits. Patients with

VT recurrence tend to have more extensive scarring than those without recurrent VT. In addition, lack of inducibility at the time of ablation likely account, at least in part, for the inability to identify areas participating in the arrhythmogenic substrate, which can become manifest much later or after withdrawal of antiarrhythmic drug therapy.^{54,91,96}

The acute failure of catheter ablation to terminate an inducible SMVT often reflects inaccurate mapping or inadequate RF lesion size due to poor tissue contact or a deep intramural or epicardial circuit. Furthermore, ablation can be hindered by the proximity of the ablation target to the HB, coronary artery, or phrenic nerve, or by anatomical obstacles that preclude access to the ablation target (e.g., mechanical aortic and mitral valves or epicardial adhesions).^{54,96}

Complications

Patients with post-MI VT typically have depressed LV function and multiple comorbidities. Ablation is often a late attempt at controlling refractory arrhythmias, sometimes after significant hemodynamic compromise has developed. Therefore significant complications (e.g., worsened heart failure, stroke, transient ischemic attack, MI, cardiac perforation, or heart block) occur in approximately 3% to 10% of patients. Procedure-related mortality ranges from 0% to 3%. Vascular access complications (large hematomas or arterial pseudoaneurysms, arteriovenous fistula) occur in more than 2% of patients. Strokes and transient ischemic attacks occur in approximately 1%, and cardiac tamponade in 1%.

In one series, acute hemodynamic decompensation (i.e., persistent hypotension despite vasopressors and requiring mechanical support or procedure discontinuation) occurred in 11% of patients during 24 ablation procedures, and was associated with increased mortality over follow-up. This is likely related to prolonged times of reduced cardiac output, myocardial stunning with VT and long anesthesia times, and target organ hypoperfusion occurring before and during the procedure.¹²⁹

Exacerbation of heart failure can develop in the acute phase post ablation. Extensive ablation in viable myocardium, injury to the aortic or mitral valves during LV catheter manipulation, repeated hemodynamically unstable VT episodes, and saline administration from externally irrigated ablation catheters are procedural factors that can potentially exacerbate heart failure and myocardial ischemia. Therefore it is prudent to restrict ablation lesions to areas of infarction, as identified from low-amplitude electrograms in regions observed to have little contractility on echocardiography or ventriculography. Of note, coronary artery injury is not common during endocardial RF application of post-MI VT. Larger coronary vessels are less susceptible to injury than small vessels, likely due to the greater cooling effect of blood flow. In addition, ablation in infarct-related areas is likely to involve territories of occluded infarct arteries. Of 215 patients in one series, only a single patient suffered MI from occlusion of a marginal artery.

Although ablation guided by substrate mapping avoids the hemodynamic consequences of prolonged mapping during VT, the lack of a precise reentry circuit target is compensated by extensive ablation lesion sets, which increases the potential for complications. In a multicenter study, major complications including worsening heart failure were observed in 7.3% of patients, and 3.0% died within 7 days of ablation.

Importantly, many of the patients with prior MI and VT undergoing ablation have very severe heart disease and, despite good arrhythmia control with catheter ablation, the overall mortality remains high, exceeding 10% per year in some studies, mainly driven by progressive heart failure.^{5,54}

Predictors of periprocedural complications include advanced age, depressed LVEF, NYHA class III/IV, presentation with VT storm, anemia, chronic obstructive pulmonary disease, renal insufficiency, operator


experience, and use of general anesthesia.^{54,130,131} In addition, failure to eliminate clinical VT during ablation, the need for intraoperative intraaortic balloon pump insertion for hemodynamic support, and procedure duration are associated with hospital mortality. In one report, recurrent VT accounted for 46% of hospital deaths, and 85% of patients with hospital deaths presented with VT storm.^{131,132} In patients with multiple risk markers, prophylactic mechanical hemodynamic support and adoption of substrate-based ablation approaches (without inducing VT) need to be considered to minimize the risk of hemodynamic decompensation.¹²⁹

VIDEOS

The following videos accompany this chapter:

Video 22.1. Ventricular Fibrillation Triggered by Coronary Artery Spasm 

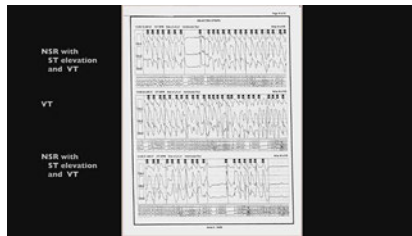
See Video 3.1. Reentrant Ventricular Tachycardia: Optical Mapping

Video 22.2. Postinfarction Ventricular Tachycardia: Rhythmia Activation, Propagation, and Voltage Maps 

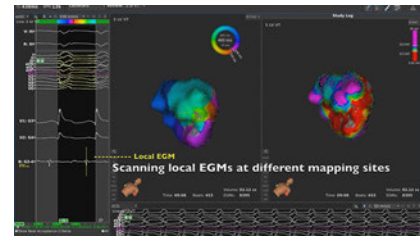
See Video 6.5. CARTO-Sound: Mapping of Ventricular Tachycardia

REFERENCES

1. Peachey H, et al. EHRA/HRS/APHS expert consensus on ventricular arrhythmias. *Heart Rhythm*. 2014;11:e166–e196.
2. Natale A, et al. Venice chart international consensus document on ventricular tachycardia/ventricular fibrillation ablation: special article. *J Cardiovasc Electrophysiol*. 2010;21:339–379.
3. Liang JJ, Prasad A, Cha Y-M. Temporal evolution and implications of ventricular arrhythmias associated with acute myocardial infarction. *Cardiol Rev*. 2013;21:289–294.
4. Gorenk B, et al. Cardiac arrhythmias in acute coronary syndromes: position paper from the joint EHRA, ACCA, and EAPCI Task Force. *EuroIntervention*. 2015;10:1095–1108.
5. Haqqani HM, Callans DJ. Ventricular tachycardia in coronary artery disease. *Card Electrophysiol Clin*. 2014;6:525–534.
6. Shenthar J, Deora S, Rai M, et al. Prolonged Tpeak-end and Tpeak-end/QT ratio as predictors of malignant ventricular arrhythmias in the acute phase of ST-segment elevation myocardial infarction: a prospective case-control study. *Heart Rhythm*. 2015;12:484–489.
7. Hsieh CHC, et al. Evolution of ventricular tachycardia and its electrophysiological substrate early after myocardial infarction: an ovine model. *Circ Arrhythm Electrophysiol*. 2013;6:1010–1017.
8. Liuba I, et al. Scar progression in patients with nonischemic cardiomyopathy and ventricular arrhythmias. *Heart Rhythm*. 2014;11:755–762.
9. Piers SRD, et al. Contrast-enhanced MRI-derived scar patterns and associated ventricular tachycardias in nonischemic cardiomyopathy implications for the ablation strategy. *Circ Arrhythm Electrophysiol*. 2013;6:875–883.
10. Proietti R, et al. A historical perspective on the role of functional lines of block in the re-entrant circuit of ventricular tachycardia. *Pacing Clin Electrophysiol*. 2016;39:490–496.
11. Haqqani HM, et al. Fundamental differences in electrophysiologic and electroanatomic substrate between ischemic cardiomyopathy patients with and without clinical ventricular tachycardia. *J Am Coll Cardiol*. 2009;54:166–173.
12. Das MK, Scott LR, Miller JM. Focal mechanism of ventricular tachycardia in coronary artery disease. *Heart Rhythm*. 2010;7:305–311.
13. Aldhoun B, et al. Nonischemic cardiomyopathy substrate and ventricular tachycardia in the setting of coronary artery disease. *Heart Rhythm*. 2013;10:1622–1627.
14. Priori SG, Blomström-Lundqvist C, Mazzanti A. 2015 ESC Guidelines for the management of patients with ventricular arrhythmias and the prevention of sudden cardiac death. *Eur Heart J*. 2015;8:746–837.



Video 22.1 Ventricular Fibrillation Triggered by Coronary Artery Spasm. Ambulatory cardiac monitor (Holter) recordings in a patient with recurrent syncope and presyncope. There was no evidence of structural heart disease on echocardiogram and cardiac stress testing. During the monitored period, patient developed several episodes of ST elevation (indicative of acute myocardial injury) associated with a high burden of PVCs. The last episode of ST elevation triggered sustained VT that degenerated into VF. The arrhythmia terminated spontaneously within less than 3 minutes, followed by AIVR and then NSR with resolution of ST elevation. The patient was found to have coronary artery spasm, which was treated medically with resolution of symptoms and arrhythmias. *AIVR*, Accelerated idioventricular rhythm; *NSR*, normal sinus rhythm; *PVCs*, premature ventricular complexes; *VF*, ventricular fibrillation; *VT*, ventricular tachycardia.



Video 22.2 Postinfarction Ventricular Tachycardia: Rhythmia Activation, Propagation, and Voltage Maps. Electroanatomic (rhythmia) maps of the left ventricle are acquired during sustained ventricular tachycardia in a patient with a previous large anteroapical infarction. Voltage scanning (scar thresholding) involves careful step-by-step manual adjustment of voltage upper and lower limits on the color-coded electroanatomic voltage map can help maximize the color contrast between adjacent myocardium with different electrogram voltage levels within the 0.5-mV scar and, thus, unmask channels of viable myocardium within a dense scar. Local electrograms at different sites of the electroanatomic map (as indicated by the catheter tip icon) are also shown. Ablation at the isthmus of the tachycardia circuit resulted in elimination of the tachycardia. *EGM*, Electrogram; *LV*, left ventricle.

15. Kusumoto FM, et al. HRS/ACC/AHA expert consensus statement on the use of implantable cardioverter-defibrillator therapy in patients who are not included or not well represented in clinical trials. *J Am Coll Cardiol*. 2014;64:1143–1177.
16. Piccini JP, et al. Sustained ventricular tachycardia and ventricular fibrillation complicating non-ST-segment-elevation acute coronary syndromes. *Circulation*. 2012;126:41–49.
17. van der Weg K, et al. Prospective evaluation of where reperfusion ventricular arrhythmia “bursts” fit into optimal reperfusion in STEMI. *Int J Cardiol*. 2015;195:136–142.
18. Majidi M, et al. Implications of ventricular arrhythmia ‘bursts’ with normal epicardial flow, myocardial blush, and ST-segment recovery in anterior ST-elevation myocardial infarction reperfusion: a biosignature of direct myocellular injury ‘downstream of downstream’. *Eur Heart J Acute Cardiovasc Care*. 2015;4:51–59.
19. Bui AH, et al. Relationship between early and late nonsustained ventricular tachycardia and cardiovascular death in patients with acute coronary syndrome in the Platelet Inhibition and Patient Outcomes (PLATO) trial. *Circ Arrhythm Electrophysiol*. 2016;9:e002951.
20. Fordyce CB, et al. Long-term post-discharge risks in older survivors of myocardial infarction with and without out-of-hospital cardiac arrest. *J Am Coll Cardiol*. 2016;67:1981–1990.
21. Dagres N, Hindricks G. Risk stratification after myocardial infarction: is left ventricular ejection fraction enough to prevent sudden cardiac death? *Eur Heart J*. 2013;34:1964–1971.
22. Lerma C, Gorelick A, Ghanem RN, et al. Patterns of ectopy leading to increased risk of fatal or near-fatal cardiac arrhythmia in patients with depressed left ventricular function after an acute myocardial infarction. *Europace*. 2013;15:1304–1312.
23. Deyell MW, Krahn AD, Goldberger JJ. Sudden cardiac death risk stratification. *Circ Res*. 2015;116:1907–1918.
24. Epstein AE, et al. 2012 ACCF/AHA/HRS focused update incorporated into the ACCF/AHA/HRS 2008 guidelines for device-based therapy of cardiac rhythm abnormalities: a report of the American College of Cardiology Foundation/American Heart Association Task Force on Practice Guide. *Circulation*. 2013;127:e283–e352.
25. Verrier RL, et al. Elevated T-Wave alternans predicts nonsustained ventricular tachycardia in association with percutaneous coronary intervention in st-segment elevation myocardial infarction (STEMI) patients. *J Cardiovasc Electrophysiol*. 2013;24:658–663.
26. Au-Yeung WTM, et al. SCD-HeFT: use of R-R interval statistics for long-term risk stratification for arrhythmic sudden cardiac death. *Heart Rhythm*. 2015;12:2058–2066.
27. Disertori M, et al. Heart rate turbulence is a powerful predictor of cardiac death and ventricular arrhythmias in postmyocardial infarction and heart failure patients: a systematic review and meta-analysis. *Circ Arrhythm Electrophysiol*. 2016;9:e004610.
28. Rosengarten JA, Scott PA, Morgan JM. Fragmented QRS for the prediction of sudden cardiac death: a meta-analysis. *Europace*. 2015;17:969–977.
29. Jain R, Singh R, Yamini S, et al. Fragmented ECG as a risk marker in cardiovascular diseases. *Curr Cardiol Rev*. 2014;10:277–286.
30. Yalin K, et al. Infarct characteristics by CMR identifies substrate for monomorphic VT in post-MI patients with relatively preserved systolic function and NS-VT. *Pacing Clin Electrophysiol*. 2014;37:447–453.
31. El Aidi H, et al. Cardiac magnetic resonance imaging findings and the risk of cardiovascular events in patients with recent myocardial infarction or suspected or known coronary artery disease: a systematic review of prognostic studies. *J Am Coll Cardiol*. 2014;63:1031–1045.
32. Reinstadler SJ, Thiele H, Eitel I. Risk stratification by cardiac magnetic resonance imaging after ST-elevation myocardial infarction. *Curr Opin Cardiol*. 2015;30:681–689.
33. Al-Ahmad A, Shenasa M, Shenasa H, et al. Incessant ventricular tachycardia and fibrillation: electrical storms. *Card Electrophysiol Clin*. 2014;6:613–621.
34. Remo BF, et al. Safety and efficacy of renal denervation as a novel treatment of ventricular tachycardia storm in patients with cardiomyopathy. *Heart Rhythm*. 2014;11:541–546.
35. Vaseghi M, et al. Cardiac sympathetic denervation in patients with refractory ventricular arrhythmias or electrical storm: intermediate and long-term follow-up. *Heart Rhythm*. 2014;11:360–366.
36. Nedios S, et al. Electrical storm in patients with implantable cardioverter-defibrillator in the era of catheter ablation: implications for better rhythm control. *Heart Rhythm*. 2015;12:2419–2425.
37. Santangeli P, et al. Comparative effectiveness of antiarrhythmic drugs and catheter ablation for the prevention of recurrent ventricular tachycardia in patients with implantable cardioverter defibrillators: a systematic review and meta-analysis of randomized controlled trials. *Heart Rhythm*. 2016;13:1552–1559.
38. Nair GM, Nery PB, Redpath CJ, et al. Ventricular arrhythmias in patients with heart failure secondary to reduced ejection fraction. *Curr Opin Cardiol*. 2014;29:152–159.
39. Al-Khatib SM, et al. 2017 AHA/ACC/HRS guideline for management of patients with ventricular arrhythmias and the prevention of sudden cardiac death. *Heart Rhythm*. 2017 Oct 26. [Epub ahead of print].
40. Mondesert B, et al. Impact of revascularization in patients with sustained ventricular arrhythmias, prior myocardial infarction and preserved left ventricular ejection fraction. *Heart Rhythm*. 2016;13:1221–1227.
41. Poole JE. Present guidelines for device implantation: clinical considerations and clinical challenges from pacing, implantable cardiac defibrillator, and cardiac resynchronization therapy. *Circulation*. 2014;129:383–394.
42. Russo AM, et al. ACCF/HRS/AHA/ASE/HFSA/SCAI/SCCT/SCMR 2013 appropriate use criteria for implantable cardioverter-defibrillators and cardiac resynchronization therapy. *J Am Coll Cardiol*. 2013;61:1318–1368.
43. Guerra F, et al. Implantable cardioverter-defibrillator programming and electrical storm: results of the OBSERVational registry On long-term outcome of ICD patients (OBSERVO-ICD). *Heart Rhythm*. 2016;13:1987–1992.
44. Katritsis DG, et al. Effect of left ventricular ejection fraction and QRS duration on the survival benefit of implantable cardioverter-defibrillators: meta-analysis of primary prevention trials. *Heart Rhythm*. 2013;10:200–206.
45. Epstein AE, et al. Wearable cardioverter-defibrillator use in patients perceived to be at high risk early post-myocardial infarction. *J Am Coll Cardiol*. 2013;62:2000–2007.
46. Singh M, et al. Utility of the wearable cardioverter-defibrillator in patients with newly diagnosed cardiomyopathy: a decade-long single-center experience. *J Am Coll Cardiol*. 2015;66:2607–2613.
47. Kron J, Ellenbogen KA. Life vest: sink or swim. *Circ Arrhythm Electrophysiol*. 2013;6:5–6.
48. Chung MK. The role of the wearable cardioverter defibrillator in clinical practice. *Cardiol Clin*. 2014;32:253–270.
49. Aliot EM, et al. EHRA/HRS expert consensus on catheter ablation of ventricular arrhythmias. Developed in a partnership with the European Heart Rhythm Association (EHRA), a Registered Branch of the European Society of Cardiology (ESC), and the Heart Rhythm Society (HRS); in collaboration with the American College of Cardiology (ACC) and the American Heart Association (AHA). *Heart Rhythm*. 2009;6:886–933.
50. Bunch TJ, et al. Patients treated with catheter ablation for ventricular tachycardia after an ICD shock have lower long-term rates of death and heart failure hospitalization than do patients treated with medical management only. *Heart Rhythm*. 2014;11:533–540.
51. Liang JJ, et al. Amiodarone discontinuation or dose reduction following catheter ablation for ventricular tachycardia in structural heart disease. *JACC Clin Electrophysiol*. 2017;3:503–511.
52. Patel D, et al. Catheter ablation for ventricular tachycardia (VT) in patients with ischemic heart disease a systematic review and a meta-analysis of randomized controlled trials. *J Interv Card Electrophysiol*. 2016;45:111–117.
53. Delacrétaez E, et al. Catheter ablation of stable ventricular tachycardia before defibrillator implantation in patients with coronary heart disease

- (VTACH): an on-treatment analysis. *J Cardiovasc Electrophysiol.* 2013;24:525–529.
54. Tanawuttiwat T, Nazarian S, Calkins H. The role of catheter ablation in the management of ventricular tachycardia. *Eur Heart J.* 2016;37:594–609.
 55. Dinov B, et al. Early referral for ablation of scar-related ventricular tachycardia is associated with improved acute and long-term outcomes: results from the Heart Center of Leipzig Ventricular Tachycardia Registry. *Circ Arrhythm Electrophysiol.* 2014;7:1144–1151.
 56. De Riva M, et al. Reassessing noninducibility as ablation endpoint of post-infarction ventricular tachycardia. *Circ Arrhythm Electrophysiol.* 2015;8:853–862.
 57. Kuck K-H, et al. Impact of substrate modification by catheter ablation on implantable cardioverter–defibrillator interventions in patients with unstable ventricular arrhythmias and coronary artery disease. *Circ Arrhythm Electrophysiol.* 2017;10:e004422.
 58. Kumar S, et al. Role of alternative interventional procedures when endo- and epicardial catheter ablation attempts for ventricular arrhythmias fail. *Circ Arrhythm Electrophysiol.* 2015;8:606–615.
 59. Kumar S, Tedrow UB, Stevenson WG. Adjunctive interventional techniques when percutaneous catheter ablation for drug refractory ventricular arrhythmias fail: a contemporary review. *Circ Arrhythm Electrophysiol.* 2017;10:e003676.
 60. De Riva M, Watanabe M, Zeppenfeld K. Twelve-lead ECG of ventricular tachycardia in structural heart disease. *Circ Arrhythm Electrophysiol.* 2015;8:951–962.
 61. Miller JM, Marchlinski FE, Buxton AE, et al. Relationship between the 12-lead electrocardiogram during ventricular tachycardia and endocardial site of origin in patients with coronary artery disease. *Circulation.* 1988;77:759–766.
 62. Segal OR, et al. A novel algorithm for determining endocardial VT exit site from 12-lead surface ECG characteristics in human, infarct-related ventricular tachycardia. *J Cardiovasc Electrophysiol.* 2007;18:161–168.
 63. Yokokawa M, et al. Automated analysis of the 12-lead electrocardiogram to identify the exit site of postinfarction ventricular tachycardia. *Heart Rhythm.* 2012;9:330–334.
 64. Martinek M, Stevenson WG, Inada K, et al. QRS characteristics fail to reliably identify ventricular tachycardias that require epicardial ablation in ischemic heart disease. *J Cardiovasc Electrophysiol.* 2012;23:188–193.
 65. Fernandez-Armenta J, Berrueto A. How to recognize epicardial origin of ventricular tachycardias? *Curr Cardiol Rev.* 2014;10:246–256.
 66. Di Biase L, et al. Ablation of stable VTs versus substrate ablation in ischemic cardiomyopathy: the VISTA Randomized Multicenter Trial. *J Am Coll Cardiol.* 2015;66:2872–2882.
 67. Josephson ME. Programmed stimulation for risk stratification for postinfarction sudden cardiac arrest: why and how? *Pacing Clin Electrophysiol.* 2014;37:791–794.
 68. Zaman S, et al. Significance of inducible very fast ventricular tachycardia (cycle length 200–230 ms) after early reperfusion for ST-segment-elevation myocardial infarction. *Circ Arrhythm Electrophysiol.* 2013;6:884–890.
 69. Josephson ME, Almendral J, Callans DJ. Resetting and entrainment of reentrant ventricular tachycardia associated with myocardial infarction. *Heart Rhythm.* 2014;11:1239–1249.
 70. Almendral J, Caulier-Cisterna R, Rojo-Álvarez JL. Resetting and entrainment of reentrant arrhythmias: part I: concepts, recognition, and protocol for evaluation: surface ECG versus intracardiac recordings. *Pacing Clin Electrophysiol.* 2013;36:508–532.
 71. Almendral J. Resetting and entrainment of reentrant arrhythmias: part II: informative content and practical use of these responses. *Pacing Clin Electrophysiol.* 2013;36:641–661.
 72. Deo R, Berger R. The clinical utility of entrainment pacing. *J Cardiovasc Electrophysiol.* 2009;20:466–470.
 73. Vereckei A, Duray G, Szénási G, et al. New algorithm using only lead aVR for differential diagnosis of wide QRS complex tachycardia. *Heart Rhythm.* 2008;5:89–98.
 74. Peichl P, Wichterle D, Cihak R, et al. Catheter ablation of ventricular tachycardia in the presence of an old endocavitary thrombus guided by intracardiac echocardiography. *Pacing Clin Electrophysiol.* 2016;39:581–587.
 75. Rao HB, et al. Ventricular tachycardia ablation in the presence of left ventricular thrombus: safety and efficacy. *J Cardiovasc Electrophysiol.* 2016;27:453–459.
 76. Hussein A, et al. Assessment of ventricular tachycardia scar substrate by intracardiac echocardiography. *Pacing Clin Electrophysiol.* 2014;37:412–421.
 77. Njeim M, et al. Value of cardiac magnetic resonance imaging in patients with failed ablation procedures for ventricular tachycardia. *J Cardiovasc Electrophysiol.* 2016;27:183–189.
 78. Komatsu Y, et al. Regional myocardial wall thinning at multidetector computed tomography correlates to arrhythmogenic substrate in postinfarction ventricular tachycardia: assessment of structural and electrical substrate. *Circ Arrhythm Electrophysiol.* 2013;6:342–350.
 79. Stevens SM, et al. Device artifact reduction for magnetic resonance imaging of patients with implantable cardioverter-defibrillators and ventricular tachycardia: late gadolinium enhancement correlation with electroanatomic mapping. *Heart Rhythm.* 2014;11:289–298.
 80. Duell J, Dilsizian V, Smith M, et al. Nuclear imaging guidance for ablation of ventricular arrhythmias. *Curr Cardiol Rep.* 2016;18:1–7.
 81. Yamashita S, et al. Myocardial wall thinning predicts transmural substrate in patients with scar-related ventricular tachycardia. *Heart Rhythm.* 2017;14:155–163.
 82. Miller MA, et al. Percutaneous hemodynamic support with Impella 2.5 during scar-related ventricular tachycardia ablation (PERMIT 1). *Circ Arrhythm Electrophysiol.* 2013;6:151–159.
 83. Reddy YM, et al. Percutaneous left ventricular assist devices in ventricular tachycardia ablation multicenter experience. *Circ Arrhythm Electrophysiol.* 2014;7:244–250.
 84. Miller MA, Reddy VY. Percutaneous hemodynamic support during scar-ventricular tachycardia ablation is the juice worth the squeeze? *Circ Arrhythm Electrophysiol.* 2014;7:192–194.
 85. Baratto F, et al. Extracorporeal membrane oxygenation for hemodynamic support of ventricular tachycardia ablation. *Circ Arrhythm Electrophysiol.* 2016;9:e004492.
 86. Mathuria N, et al. Outcomes of pre-emptive and rescue use of percutaneous left ventricular assist device in patients with structural heart disease undergoing catheter ablation of ventricular tachycardia. *J Interv Card Electrophysiol.* 2017;48:27–34.
 87. Aryana A, et al. Procedural and clinical outcomes after catheter ablation of unstable ventricular tachycardia supported by a percutaneous left ventricular assist device. *Heart Rhythm.* 2014;11:1122–1130.
 88. Anter E, Li J, Tschabrunn CM, et al. Mapping of a postinfarction left ventricular aneurysm-dependent macroreentrant ventricular tachycardia. *Heart Rhythm Case Rep.* 2015;1:472–476.
 89. Nayyar S, et al. High-density mapping of ventricular scar: a comparison of ventricular tachycardia (VT) supporting channels with channels that do not support VT. *Circ Arrhythm Electrophysiol.* 2014;7:90–98.
 90. Yamashita S, et al. Impact of new technologies and approaches for post-myocardial infarction ventricular tachycardia ablation during long-term follow-up. *Circ Arrhythm Electrophysiol.* 2016;9:e003901.
 91. Yokokawa M, et al. Reasons for recurrent ventricular tachycardia after catheter ablation of post-infarction ventricular tachycardia. *J Am Coll Cardiol.* 2013;61:66–73.
 92. Das M, et al. Temporal-component analysis of diastolic electrograms in ventricular tachycardia differentiates non-vulnerable regions of the circuit. *Heart Rhythm.* 2015;12:1737–1744.
 93. Derejko P, et al. Effect of the restitution properties of cardiac tissue on the repeatability of entrainment mapping response. *Circ Arrhythm Electrophysiol.* 2014;7:497–504.
 94. Wong KCK, Rajappan K, Bashir Y, et al. Entrainment with long postpacing intervals from within the flutter circuit: what is the mechanism? *Circ Arrhythm Electrophysiol.* 2012;5:e90–e92.
 95. Asirvatham SJ, Stevenson WG. Mapping reentry. *Circ Arrhythm Electrophysiol.* 2016;9:e003609.

96. Tokuda M, et al. Characteristics of clinical and induced ventricular tachycardia throughout multiple ablation procedures. *J Cardiovasc Electrophysiol.* 2016;27:88–94.
97. Berte B, et al. Characterization of the left-sided substrate in arrhythmogenic right ventricular cardiomyopathy. *Circ Arrhythm Electrophysiol.* 2015;8:1403–1412.
98. Irie T, et al. Relationship between sinus rhythm late activation zones and critical sites for scar-related ventricular tachycardia: systematic analysis of isochronal late activation mapping. *Circ Arrhythm Electrophysiol.* 2015;8:390–399.
99. Baldinger SH, et al. Electrogram analysis and pacing are complimentary for recognition of abnormal conduction and far-field potentials during substrate mapping of infarct-related ventricular tachycardia. *Circ Arrhythm Electrophysiol.* 2015;8:874–881.
100. Tsiachris D, et al. Electroanatomical voltage and morphology characteristics in postinfarction patients undergoing ventricular tachycardia ablation. *Circ Arrhythm Electrophysiol.* 2015;8:863–873.
101. Komatsu Y, et al. Electrophysiologic characterization of local abnormal ventricular activities in postinfarction ventricular tachycardia with respect to their anatomic location. *Heart Rhythm.* 2013;10:1630–1637.
102. Santangeli P, Marchlinski FE. Substrate mapping for unstable ventricular tachycardia. *Heart Rhythm.* 2016;13:569–583.
103. Acosta J, et al. Infarct transmural as a criterion for first-line endo-epicardial substrate-guided ventricular tachycardia ablation in ischemic cardiomyopathy. *Heart Rhythm.* 2016;13:85–95.
104. Tschabrunn CM, et al. High-resolution mapping of ventricular scar. *Circ Arrhythm Electrophysiol.* 2016;9:e003841.
105. Silberbauer J, et al. Noninducibility and late potential abolition: a novel combined prognostic procedural end point for catheter ablation of postinfarction ventricular tachycardia. *Circ Arrhythm Electrophysiol.* 2014;7:424–435.
106. Anter E, Josephson ME. Bipolar voltage amplitude: what does it really mean? *Heart Rhythm.* 2016;13:326–327.
107. Josephson ME, Anter E. Substrate mapping for ventricular tachycardia assumptions and misconceptions. *JACC Clin Electrophysiol.* 2015;1:341–352.
108. Gianni C, Natale A. Voltage mapping for ventricular tachycardia ablation: we can work it out. *Heart Rhythm.* 2016;13:2003.
109. Tung R, Josephson ME, Bradfield JS, et al. Directional influences of ventricular activation on myocardial scar characterization: voltage mapping with multiple wavefronts during ventricular tachycardia ablation. *Circ Arrhythm Electrophysiol.* 2016;9.
110. Mountantonakis SE, et al. Relationship between voltage map ‘channels’ and the location of critical isthmus sites in patients with post-infarction cardiomyopathy and ventricular tachycardia. *J Am Coll Cardiol.* 2013;61:2088–2095.
111. Makimoto H, et al. Clinical impact of mapping strategies for treatment of ventricular tachycardias in patients with structural heart disease. *Pacing Clin Electrophysiol.* 2015;38:630–640.
112. Komatsu Y, et al. Endocardial ablation to eliminate epicardial arrhythmia substrate in scar-related ventricular tachycardia. *J Am Coll Cardiol.* 2014;63:1416–1426.
113. Yoshiga Y, et al. Correlation between substrate location and ablation strategy in patients with ventricular tachycardia late after myocardial infarction. *Heart Rhythm.* 2012;9:1192–1199.
114. Kosmidou I, et al. Role of repeat procedures for catheter ablation of postinfarction ventricular tachycardia. *Heart Rhythm.* 2011;8:1516–1522.
115. Izquierdo M, et al. Endo-epicardial versus only-endocardial ablation as a first line strategy for the treatment of ventricular tachycardia in patients with ischemic heart disease. *Circ Arrhythm Electrophysiol.* 2015;8:882–889.
116. Marchlinski FE, et al. Long-term success of irrigated radiofrequency catheter ablation of sustained ventricular tachycardia: post-approval THERMOCOOL VT trial. *J Am Coll Cardiol.* 2016;67:674–683.
117. Tung R, Kottkamp H. A moving target for catheter ablation of ventricular tachycardia ablation of scar or arrhythmia? *J Am Coll Cardiol.* 2015;66:2883–2885.
118. Berrueto A, et al. Scar dechanneling: new method for scar-related left ventricular tachycardia substrate ablation. *Circ Arrhythm Electrophysiol.* 2015;8:326–336.
119. Santangeli P, Frankel DS, Marchlinski FE. End points for ablation of scar-related ventricular tachycardia. *Circ Arrhythm Electrophysiol.* 2014;7:949–960.
120. Tzou WS, et al. Core isolation of critical arrhythmia elements for treatment of multiple scar-based ventricular tachycardias. *Circ Arrhythm Electrophysiol.* 2015;8:353–361.
121. Proietti R, Roux J-F, Essebag V. Recent advances in ablation of ventricular tachycardia associated with structural heart disease. *Curr Opin Cardiol.* 2016;31:64–71.
122. Ghanbari H, et al. Noninducibility in postinfarction ventricular tachycardia as an end point for ventricular tachycardia ablation and its effects on outcomes a meta-analysis. *Circ Arrhythm Electrophysiol.* 2014;7:677–683.
123. Yokokawa M, et al. Predictive value of programmed ventricular stimulation after catheter ablation of post-infarction ventricular tachycardia. *J Am Coll Cardiol.* 2015;65:1954–1959.
124. Kumar S, et al. Long-term outcomes after catheter ablation of ventricular tachycardia in patients with and without structural heart disease. *Heart Rhythm.* 2016;13:1957–1963.
125. Kumar S, et al. Substrate-based ablation versus ablation guided by activation and entrainment mapping for ventricular tachycardia: a systematic review and meta-analysis. *J Cardiovasc Electrophysiol.* 2016;27:1437–1447.
126. Tung R, et al. Freedom from recurrent ventricular tachycardia after catheter ablation is associated with improved survival in patients with structural heart disease: an International VT Ablation Center Collaborative Group study. *Heart Rhythm.* 2015;12:1997–2007.
127. Sapp JL, et al. Ventricular tachycardia ablation versus escalation of antiarrhythmic drugs. *N Engl J Med.* 2016;275:111–121.
128. Siontis KC, et al. Prognostic impact of the timing of recurrence of infarct-related ventricular tachycardia after catheter ablation. *Circ Arrhythm Electrophysiol.* 2016;9:e004432.
129. Santangeli P, et al. Acute hemodynamic decompensation during catheter ablation of scar-related ventricular tachycardia: incidence, predictors, and impact on mortality. *Circ Arrhythm Electrophysiol.* 2015;8:68–75.
130. Santangeli P, et al. Acute hemodynamic decompensation during catheter ablation of scar-related ventricular tachycardia: incidence, predictors, and impact on mortality. *Circ Arrhythm Electrophysiol.* 2015;8:68–75.
131. Katz DF, et al. Safety of ventricular tachycardia ablation in clinical practice. *Circ Arrhythm Electrophysiol.* 2015;8:362–370.
132. Yu R, et al. Catheter ablation of scar-based ventricular tachycardia: relationship of procedure duration to outcomes and hospital mortality. *Heart Rhythm.* 2015;12:86–94.

Idiopathic Focal Ventricular Tachycardia

OUTLINE

Pathophysiology, 816

- Mechanism of Focal Idiopathic Ventricular Tachycardia, 818
- Mechanism of Premature Ventricular Complex-Induced Cardiomyopathy, 818

Anatomical Considerations, 818

- Right Ventricular Outflow Tract, 818
- Pulmonary Root, 820
- Left Ventricular Outflow Tract, 820
- Aortic Root, 820
- Aortomitral Continuity, 822
- Left Ventricular Summit, 822
- Left Ventricular Papillary Muscles, 822
- Cardiac Crux, 823

Epidemiology and Natural History, 823

Clinical Presentation, 823

Initial Evaluation, 824

- Electrocardiography, 824
- Ambulatory Cardiac Monitoring, 824
- Exercise Electrocardiography, 824
- Cardiac Magnetic Resonance, 824

Differential Diagnosis, 825

- Arrhythmogenic Right Ventricular Cardiomyopathy, 825
- Dilated Cardiomyopathy, 825
- Idiopathic Ventricular Fibrillation, 826
- Other Arrhythmia Mechanisms, 826

Principles of Management, 826

- Acute Management, 826
- Chronic Management, 826

Electrocardiographic Localization of Focal Ventricular Tachycardia, 827

- Precordial Transition, 827
- Frontal Plane Horizontal Axis, 828
- Frontal Plane Vertical Axis, 828

Electrophysiological Testing, 836

- Induction of Tachycardia, 836
- Tachycardia Features, 837
- Diagnostic Maneuvers During Tachycardia, 837

Mapping, 837

- Activation Mapping, 837
- Pace Mapping, 840
- Electroanatomic Mapping, 841
- Noncontact Mapping, 842
- Basket Catheter Mapping, 843

Ablation, 843

- Target of Ablation, 843
- Ablation Technique, 843
- Endpoints of Ablation, 854
- Outcome, 854
- Cryoablation, 854

PATHOPHYSIOLOGY

Ventricular tachycardia (VT) is usually associated with structural heart disease—most commonly coronary artery disease and cardiomyopathy. However, about 10% of patients who present with VT have no obvious structural heart disease (idiopathic VT). Absence of structural heart disease is usually suggested if the electrocardiogram (ECG) (except in Brugada syndrome and long QT syndrome), echocardiogram, and coronary arteriogram collectively are normal.

Nevertheless, cardiac magnetic resonance (CMR) may demonstrate mild structural abnormalities and subtle areas of diminished wall motion in some patients with idiopathic VT, even if all other test results are normal. In addition, focal dysautonomia in the form of localized sympathetic denervation has been reported in patients with VT and no other obvious structural heart disease. However, there is no conclusive evidence that such structural abnormalities are causally related to idiopathic ventricular arrhythmias (VAs). Of note, idiopathic VAs can also occur in patients with apparent structural heart disease, in whom the structural cardiac abnormalities are not related to the VAs. Furthermore, frequent or incessant idiopathic VAs can be a cause of cardiomyopathy.

Several distinct types of idiopathic VTs have been recognized and classified with respect to the chamber of origin of the VT (right ventricle [RV] vs. left ventricle [LV]), VT morphology (left bundle branch block [LBBB] vs. right bundle branch block [RBBB] pattern), response to exercise testing, response to pharmacological agents (adenosine-sensitive versus verapamil-sensitive vs. propranolol-sensitive VT), and behavior of VT (repetitive salvos vs. sustained).

A prototype of an idiopathic focal VAs is outflow tract (OT) VAs. Approximately 90% of OT VAs are caused by one of two phenotypic forms of adenosine-sensitive VT. Repetitive monomorphic VT is the most common form (60% to 90%) and is characterized by frequent isolated monomorphic premature ventricular complexes (PVCs), couplets, or salvos of nonsustained VT, interrupted by brief periods of normal sinus rhythm (NSR; Fig. 23.1). This form of VT usually occurs at rest or following a period of exercise, and typically decreases during exercise, but can be incessant. On the other hand, paroxysmal exercise-induced VT is characterized by sustained episodes of VT precipitated by exercise or emotional stress, separated by long intervals of NSR with infrequent PVCs (Fig. 23.2). Evidence has suggested that both types represent polar ends of the spectrum of idiopathic VT caused by triggered activity, and there is considerable overlap between the two types. Furthermore, this

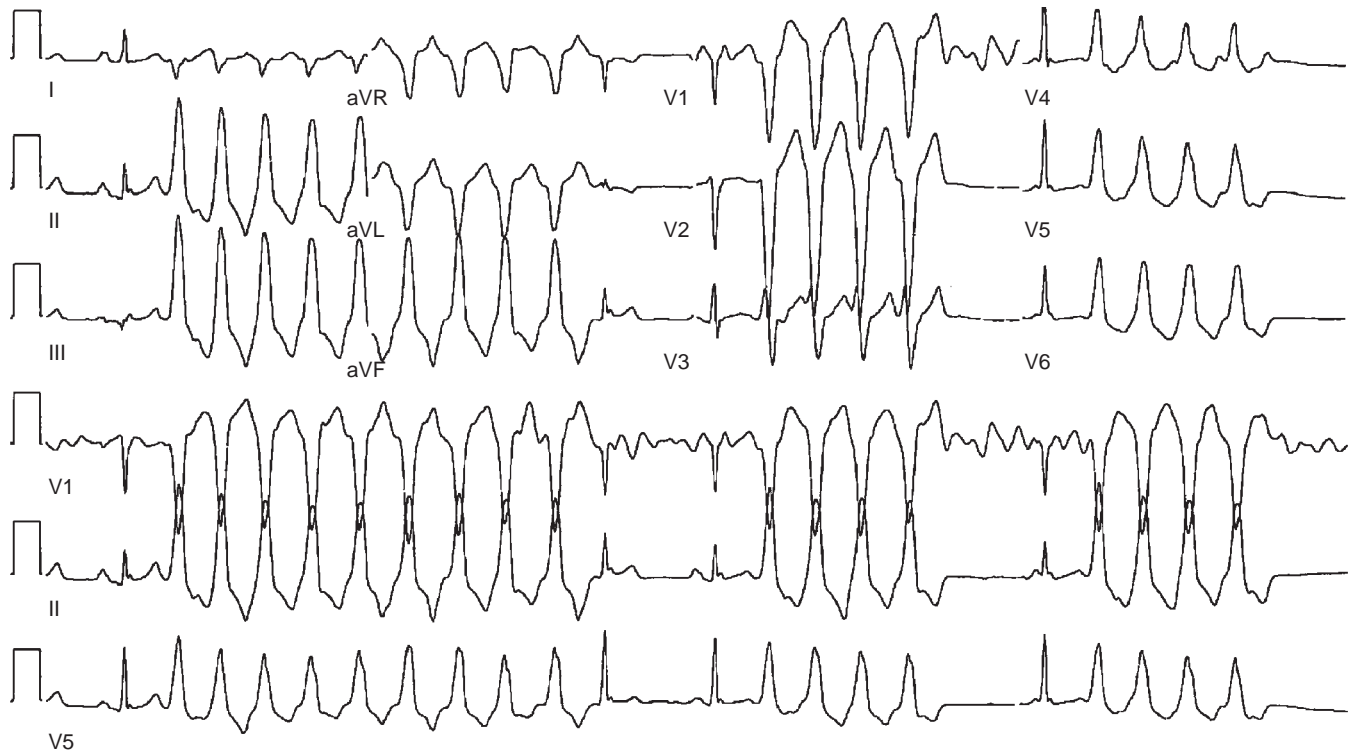


Fig. 23.1 Surface Electrocardiogram of Repetitive Monomorphic Right Ventricular Outflow Tract Tachycardia. Repetitive bursts of ventricular tachycardia are present, with occasional sinus complexes.

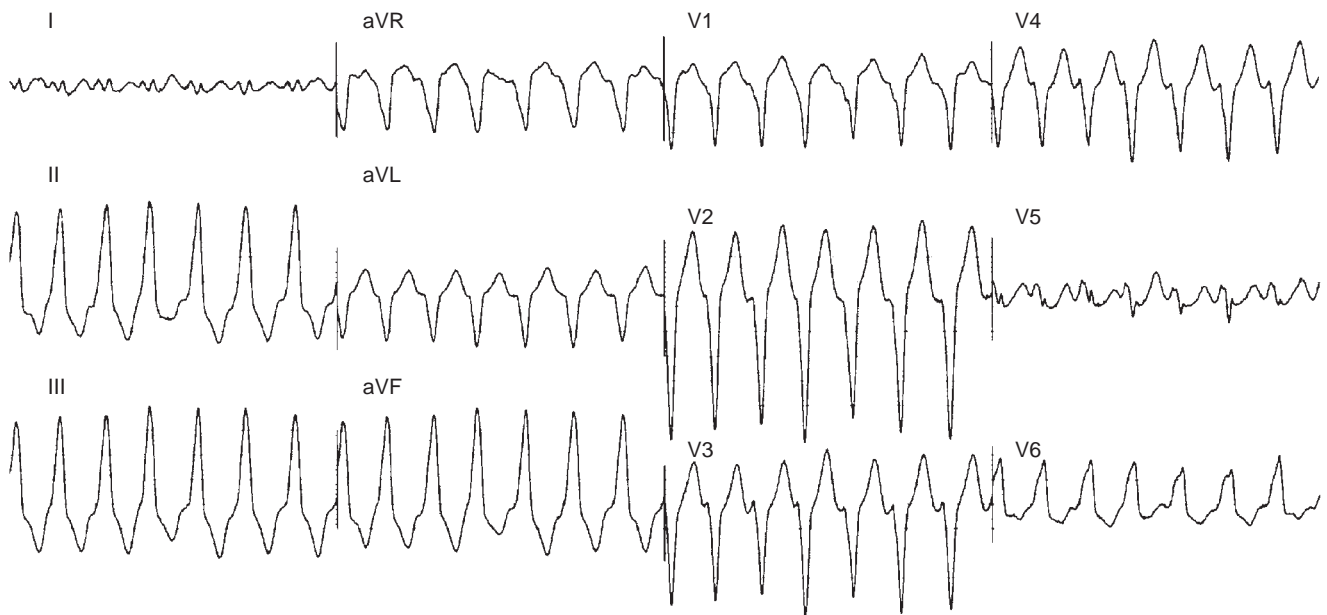


Fig. 23.2 Surface Electrocardiogram of Sustained Right Ventricular Outflow Tract Tachycardia.

subtype classification, although useful, is not necessarily precise and depends on the means and duration of rhythm recordings. Patients are typically categorized based on their presenting or index arrhythmia. Prolonged telemetry and long-term ambulatory ECG recordings have demonstrated that most patients with one subtype of OT VAs show

evidence for at least one other subtype with an identical morphology. Almost all patients with nonsustained VT have high-density repetitive runs and frequent PVCs. In patients who present with repetitive PVCs, nonsustained VT can also be observed in approximately 70%; however, only 20% of these patients develop runs of more than five beats.

Mechanism of Focal Idiopathic Ventricular Tachycardia

Idiopathic VT comprises multiple discrete subtypes that are best differentiated by their mechanism, QRS morphology, and site of origin.¹ Most forms of focal idiopathic VAs are adenosine-sensitive and are thought to be caused by catecholamine-induced, cyclic adenosine monophosphate (cAMP)–mediated delayed afterdepolarizations (DADs) and triggered activity. Several features of idiopathic VAs support triggered activity as the underlying mechanism (see Chapter 3). Heart rate acceleration facilitates VT initiation. This can be achieved by catecholamine infusion or rapid pacing from either the ventricle or the atrium. In addition, termination of the VT is dependent on direct blockade of the dihydropyridine receptor by calcium channel blockers or by agents or maneuvers that lower cAMP levels (e.g., by activation of the M₂ muscarinic receptor with edrophonium or vagal maneuvers, inhibition of the beta-adrenergic receptor with beta-blockers, or activation of the A₁ adenosine receptor with adenosine). Furthermore, a direct relationship exists between the coupling interval of the initiating ventricular extra-stimulus (VES) or ventricular pacing cycle length (CL) and the coupling interval of the first VT beat. In addition, VT initiation is CL-dependent; pacing cycle lengths (PCLs) longer or shorter than a critical CL window fail to induce VT. This critical window can shift with changing autonomic tone. Notably, a small proportion (11%) of VAs are insensitive to adenosine.²

A subset of idiopathic focal VAs arises from the Purkinje system in either ventricle. Focal Purkinje VTs (classified as “propranolol-sensitive automatic VTs”) are typically provoked by exercise and catecholamines and are suppressed by beta-blockers (but not verapamil). Furthermore, programmed electrical stimulation fails to induce or terminate those arrhythmias. Purkinje VTs are transiently suppressed by adenosine and with overdrive pacing. These characteristics suggest abnormal automaticity as the underlying mechanism of focal Purkinje VTs, in contrast to the reentrant verapamil-sensitive fascicular VT. Purkinje VAs can manifest as monomorphic VT or PVCs, or as an accelerated idioventricular rhythm that competes with and can be suppressed by NSR.³

Other subtypes of idiopathic VAs include verapamil-sensitive, reentrant fascicular VT (see Chapter 24), and idiopathic polymorphic VT and ventricular fibrillation (VF; see Chapter 31). Those arrhythmias are discussed in elsewhere in this book. In this chapter, focal idiopathic monomorphic PVCs and VT are collectively referred to as “idiopathic ventricular arrhythmias (VAs).”

Mechanism of Premature Ventricular Complex-Induced Cardiomyopathy

Frequent idiopathic nonsustained VT or PVCs can precipitate a reversible form of dilated cardiomyopathy. The mechanisms of how frequent PVCs cause LV systolic dysfunction have yet to be elucidated. Potential mechanisms include (1) dyssynchronous ventricular contraction caused by abnormal ventricular activation during PVCs (similar to LBBB or ventricular pacing); (2) alterations in intracellular calcium handling and membrane ionic currents (caused by short PVC coupling intervals and post-extrasystolic potentiation of contractility); (3) abnormal ventricular filling (due to the postextrasystolic pause); (4) myocardial and peripheral vascular autonomic dysregulation; and (5) alterations in heart rate dynamics and hemodynamic parameters. Although PVC-induced cardiomyopathy was originally thought to be a type of tachycardia-induced cardiomyopathy, tachycardia is an unlikely mechanism, since the overall heart rates in patients with frequent PVCs have remained within the normal range due to the usual compensatory pause following the PVC. Interpolated PVCs can increase the overall heart rate.^{4–6}

The most prominent predictor of cardiomyopathy in patients with frequent PVCs appears to be the daily burden of PVCs. However, the

PVC burden necessary to induce LV dysfunction is not yet clearly defined.⁷ Although a PVC burden as low as 4% to 10% can be associated with cardiomyopathy, a PVC burden of more than 13% to 24% appears to be more likely to cause PVC-induced cardiomyopathy.

Nonetheless, it is well recognized that considerable variability exists in susceptibility to PVC-related cardiomyopathy, even among patients with high PVC burden. Multiple other factors were linked to the development of PVC-induced cardiomyopathy, including (1) lack of symptoms (with the consequent delay of diagnosis and treatment); (2) broader PVC-QRS duration (>140 or >153 milliseconds, likely due to more pronounced mechanical dyssynchrony); (3) longer PVC coupling interval (due to more pronounced LV dyssynchrony); (4) percent PVC interpolation; (5) non-OT site of origin of PVCs (in particular papillary muscle and epicardial foci); (6) presence of retrograde P waves following PVCs (likely related to worsened hemodynamics caused by simultaneous atrial and ventricular contraction); and (7) constant PVC burden throughout the day and night (i.e., less circadian fluctuation in PVC frequency). However, it is important to recognize that there is inconsistent evidence as to whether these factors represent independent predictors of PVC-induced cardiomyopathy. In fact, different studies arrived at different conclusions regarding the association of the different factors with developing LV dysfunction. Furthermore, a significant overlap in these parameters usually exists between groups with and without PVC-induced cardiomyopathy, limiting their prognostic utility.^{6,8–13}

ANATOMICAL CONSIDERATIONS

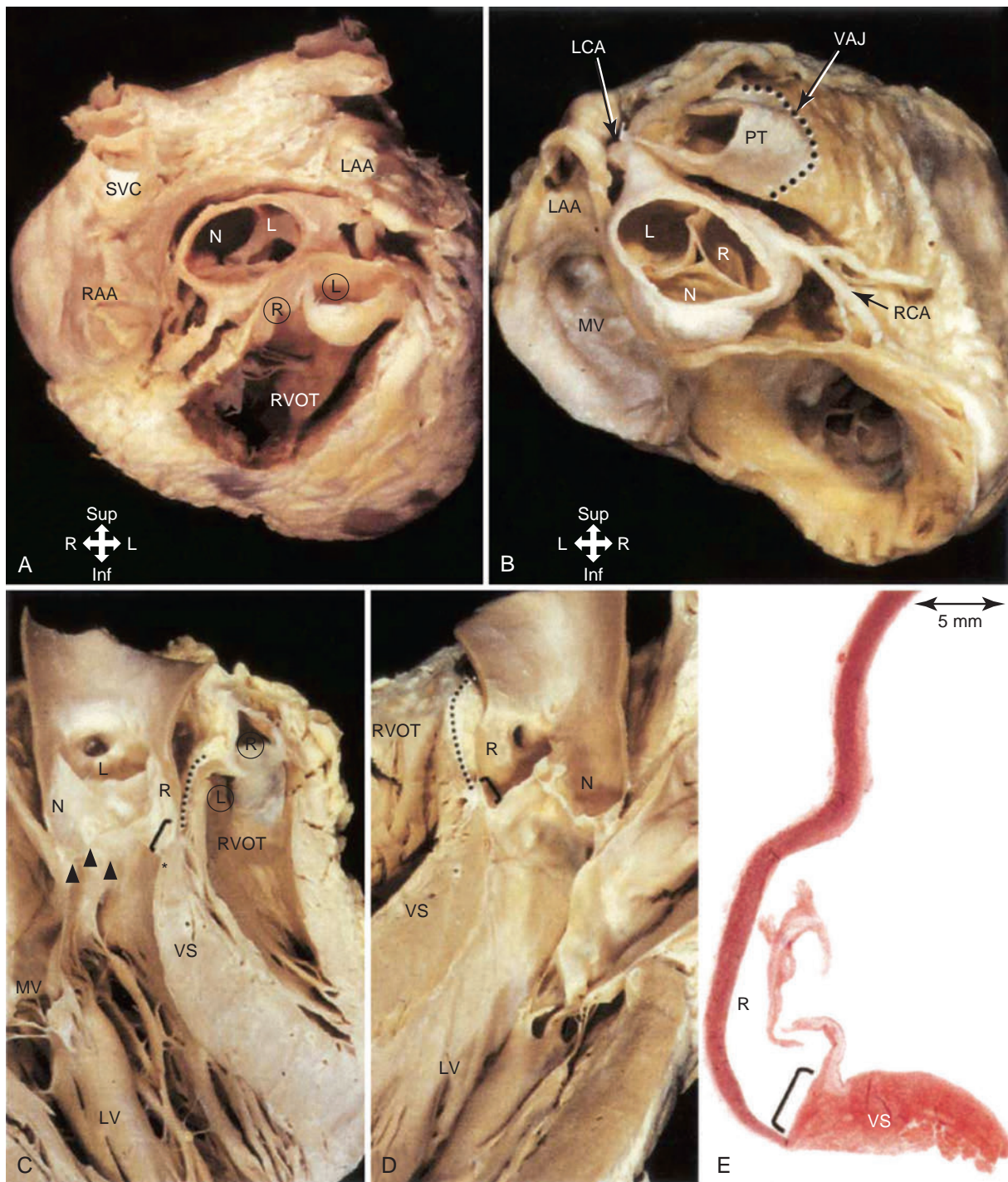
Most idiopathic VAs originate from the OT region of either ventricle (most frequently from the right ventricular outflow tract [RVOT]). Other variants of OT VAs (with similar underlying electrophysiology [EP] mechanism) include VAs arising from the aortic sinuses of Valsalva, pulmonary artery, mitral or tricuspid inflow tracts, papillary muscles, and epicardial foci in close proximity to the coronary venous system (in the LV summit or cardiac crux). The thorough knowledge of the unique and complex anatomical relationships of the OTs is of utmost importance for analyzing the ECG and mapping findings during OT VAs, as well as for safe catheter maneuvering and ablation.

Right Ventricular Outflow Tract

The RVOT is the tube-like portion of the RV cavity above the supra-ventricular crest, and is defined superiorly by the pulmonic valve and inferiorly by the RV inflow tract and the top of the tricuspid annulus (the region of the His bundle [HB] and proximal right bundle branch). The RVOT passes cephalad in a posterior and slightly leftward direction. The lateral aspect of the RVOT region is the RV free wall. The medial aspect is formed by the anterior interventricular septum at the base of the RVOT and RV musculature opposite to the anterior left ventricular outflow tract (LVOT; as a cephalad continuation of the interventricular septum) and the root of the aorta (immediately adjacent to the right aortic sinus of Valsalva) at the region just inferior to the pulmonic valve (eFig. 23.1).

Although the medial aspect of the RVOT is frequently referred to as the “septal” wall, it should be noted that the OT per se is not part of the interventricular septum, and the septum is a component only of the most proximal (inferior) part of the RVOT at the branch point of the septomarginal trabeculation. Above this area, the RVOT curves to pass anterior and cephalad to the LVOT, and, therefore, any perforation in the “septal” part is more likely to go outside the heart than into the LV (Fig. 23.3).

From the coronal view above the pulmonic valve, the RVOT region is seen wrapping around the LVOT and the root of the aorta and extending leftward (see eFig. 23.1). Whereas the inflow portion of the RV lies



eFig. 23.1 Anatomy of the Outflow Tracts and Aortic Sinuses. These heart specimens illustrate the anatomical arrangement between the right ventricular outflow tract (RVOT) and the aortic sinuses. (A) Supero-anterior view shows that the RVOT passes leftward and superior to the aortic valve. (B) The superoposterior view shows the left (L) and right (R) coronary aortic sinuses adjacent to the pulmonary infundibulum. The noncoronary (N) aortic sinus is remote from the RVOT but is related to the mitral valve (MV) and central fibrous body. The dotted line marks the ventriculoarterial junction (VAJ) between the wall of the pulmonary trunk (PT) and right ventricular muscle. Note the cleavage plane behind the pulmonary infundibulum and in front of the aortic root. (C) and (D) These simulated parasternal long-axis sections show two halves of the same heart and display the left and right coronary orifices. The right- and left-facing pulmonary sinuses (R and L in circles, respectively) are situated superior to the aortic sinuses. The fibrous continuity between the aortic and mitral valves (arrowheads in C) lies between the noncoronary leaflet and the posterior part of the left coronary leaflet, to a greater or lesser extent. The posterior part of the right coronary aortic sinus is adjacent to the central fibrous body (asterisk in C), which carries within it the penetrating His bundle. The dotted line marks the epicardial aspect of the subpulmonary infundibulum in the so-called "septal" area (as illustrated in E). *Inf*, Inferior; *LAA*, left atrial appendage; *LCA*, left coronary artery; *LV*, left ventricle; *RAA*, right atrial appendage; *RCA*, right coronary artery; *SVC*, superior vena cava; *Sup*, superior; *TV*, tricuspid valve; *VS*, ventricular septum. (From Ouyang F, Fotuhi P, Ho SY, et al. Repetitive monomorphic ventricular tachycardia originating from the aortic sinus cusp: electrocardiographic characterization for guiding catheter ablation. *J Am Coll Cardiol*. 2002;39:500.)

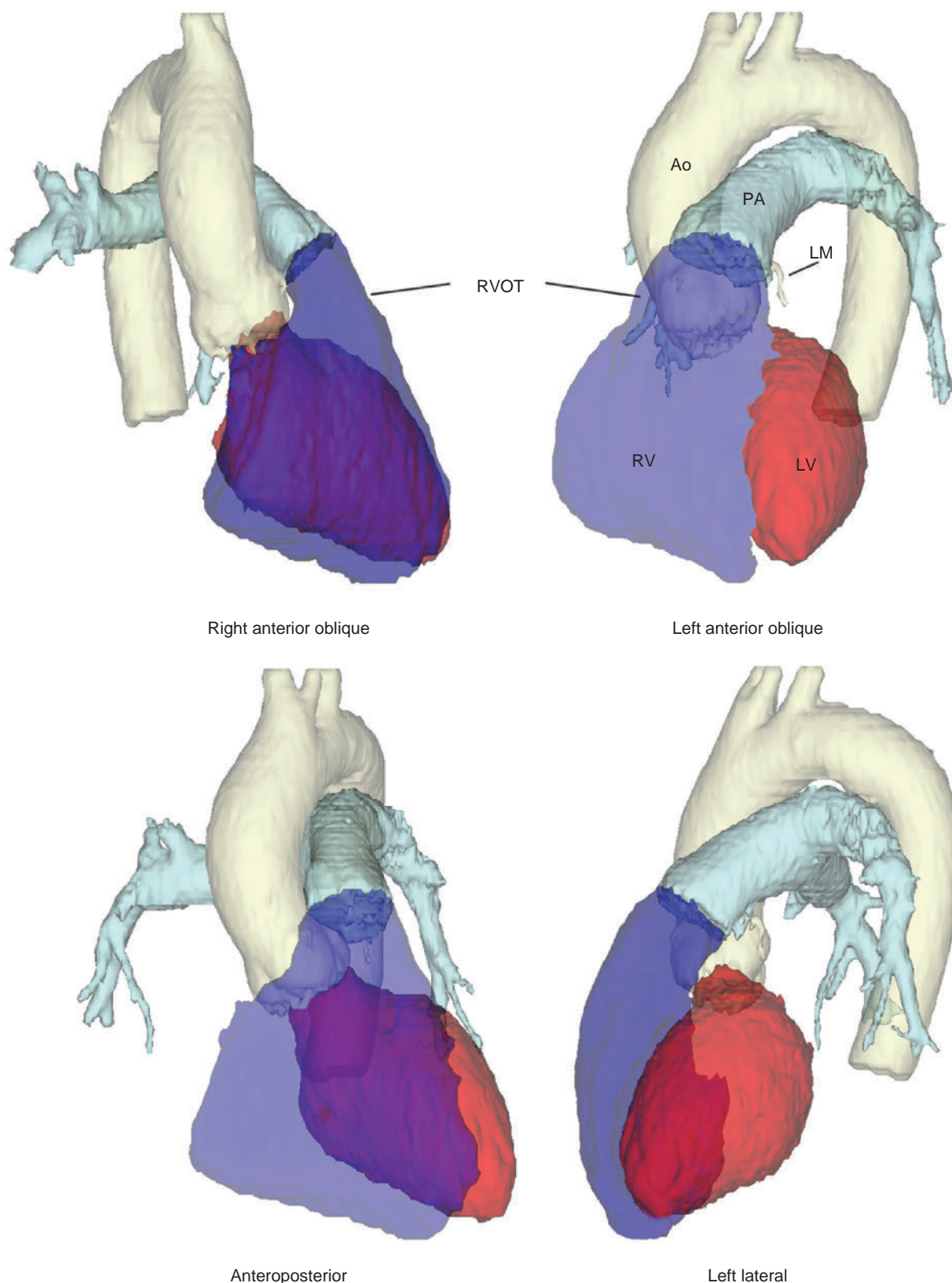


Fig. 23.3 Anatomical Relationships for Ablation of Outflow Tract Ventricular Tachycardia (VT). Most right ventricular outflow tract (RVOT) VTs arise from just proximal to the pulmonic valve; note that the RVOT in this region is all free wall (not septal wall) and the leftward aspect of the RVOT is very near the left main coronary artery (LM), making it vulnerable to injury. Note also the close relationships among RVOT, aortic sinuses of Valsalva, and subaortic left ventricle (LV), explaining why VTs from this general region can have similar electrocardiographic morphologies. Ao, Aorta; PA, pulmonary artery; RV, right ventricle.

to the right and anterior to the inflow portion of the LV, the RVOT courses anterior to the LVOT such that the distal RVOT and pulmonic valve are located to the left of the aortic valve and the distal LVOT. The pulmonic valve is typically placed approximately 1 to 2 cm cephalad and to the left of the aortic valve and offset 90 degrees from the aortic valve in the horizontal plane. Hence the supra-ventricular portion of the aorta lies in immediate proximity to the portions of the pulmonic valve. Immediately anterior to the aortic valve is the posterior muscular infundibular portion of the RVOT.¹⁴

The top of the RVOT can be convex or crescent-shaped, with the posteromedial region directed rightward and the anterolateral region directed leftward. The anteromedial aspect of the RVOT actually is located in close proximity to the LV epicardium, adjacent to the anterior interventricular vein and in proximity to the left anterior descending coronary artery. The aortic sinuses of Valsalva sit squarely within the crescent-shaped posterior region of the RVOT and are inferior to the pulmonic valve (see eFig. 23.1). The most posterior aspect of the RVOT is adjacent to the region of the right sinus of Valsalva, and the posteromedial (leftward) surface is adjacent to the anterior margin of the right sinus of Valsalva or the medial aspect of the left sinus of Valsalva.

The thickness of the RVOT wall is variable, ranging from approximately 3 to 6 mm, and is thinnest in the rightward, anterior, and subpulmonic valve portions, and thickest in the posterior infundibular part that is adherent to the anterior LVOT as a cephalad continuation of the interventricular septum. Of note, despite the absence of epicardial connections, subendocardial fibers connect the RVOT and LVOT across the infundibular septum.¹⁵

Pulmonary Root

The pulmonic and aortic valves are not at the same level (see eFig. 23.1). The pulmonic valve, the most superiorly situated of the cardiac valves, lies at the level corresponding to the third left costal cartilage at its junction with the sternum. The transverse plane of the aortic valve slopes inferiorly, away from the plane of the pulmonic valve, such that the orifice of the aortic valve faces rightward at an angle of at least 45 degrees from the median plane.

Because of its anterior and leftward location, only the posterior and rightward parts of the pulmonary artery have important relations with other cardiac structures. Of the three cusps of the pulmonic valve, the septal (right) pulmonic cusp lies at variable distances from and sometimes adjacent to the distal portions of the right atrial (RA) appendage. The left pulmonic cusp, being the most superficial, lies immediately beneath the pericardium and has no other cardiac structures related to it. The posterior pulmonary cusp overlies in the proximal portion of the left main coronary artery and the distal portions in the LA appendage. The supra-ventricular portion of the aorta lies close to and in some cases adjacent to the junction and surrounding parts of the right and posterior pulmonic cusps.

The pulmonary sinuses are not as prominent as the aortic sinuses. Nonetheless, owing to the semilunar configuration of the valvular leaflets, the hinge line of each leaflet crosses the ventriculo-arterial junction at two points. Consequently, there are always small segments of the infundibular myocardium at the nadirs of the three sinuses. Between adjacent sinuses, the wall comprises small triangles of fibrous tissue that become incorporated into the RV when the valve closes. On the epicardial aspect, the ventriculo-arterial junction is not always a sharply defined line. Sleeves of ventricular myocardium extend above the semilunar valves for a variable distance (a few millimeters and up to more than 2 cm).

The subpulmonary infundibulum is an entirely muscular funnel that supports in uniform fashion the leaflets of the pulmonic valve. As a result, all three pulmonary sinuses are continuous with myocardium of the RVOT.¹⁶ The muscular fibers typically extend circumferentially

around the pulmonic valve between and above all three cusps just above the annulus; more distally the extension is patchy and generally asymmetrical. The presence of fibrosis and fatty tissue among these muscular sleeves may create a possible substrate for VAs.¹⁷ In studies using pulmonary arteriography or intracardiac echocardiography (ICE) to accurately identify the location of the pulmonic valve, up to 50% of “RVOT” arrhythmia foci were actually localized beyond the pulmonic valve.^{18–20}

Left Ventricular Outflow Tract

Unlike the RV, the inflow and outflow regions of the LV are at an acute angle to one another. Although commonly referred to as the LVOT, there is no tubular muscular “tract” in the LV outflow region. The LVOT consists of both muscular and fibrous portions. This contrasts with the RVOT, which is composed entirely of myocardium. The central location of the aortic valve places the LVOT between the mitral valve and the ventricular septum. The curvature of the ventricular septum forms the anterosuperior wall of the LVOT, and this continues smoothly into the LV wall. The major portion of the septal component is primarily muscular, but also includes the membranous portion of the ventricular septum. Adjoining the membranous septum is the fibrous half of the LVOT that makes up the posterior wall. This is formed by the area of fibrous continuity between the aortic valve and the anterior leaflet of the mitral valve. The mitral leaflet hangs like a curtain between the inflow and OTs of the LV.²¹ The extremities of the fibrous continuity are the left and right fibrous trigones, the right trigone forming the central fibrous body. The LVOT passes underneath the RVOT in a rightward and cephalad direction pointing toward the right shoulder (see Fig. 23.3).²²

The atrioventricular node (AVN), located in the wall of the right atrium at the apex of the triangle of Koch, is relatively distant from the aortic root. As the conduction axis penetrates through the central fibrous body, however, it is positioned at the base of the interleaflet triangle between the noncoronary and right aortic sinuses (eFig. 23.2).²³

Aortic Root

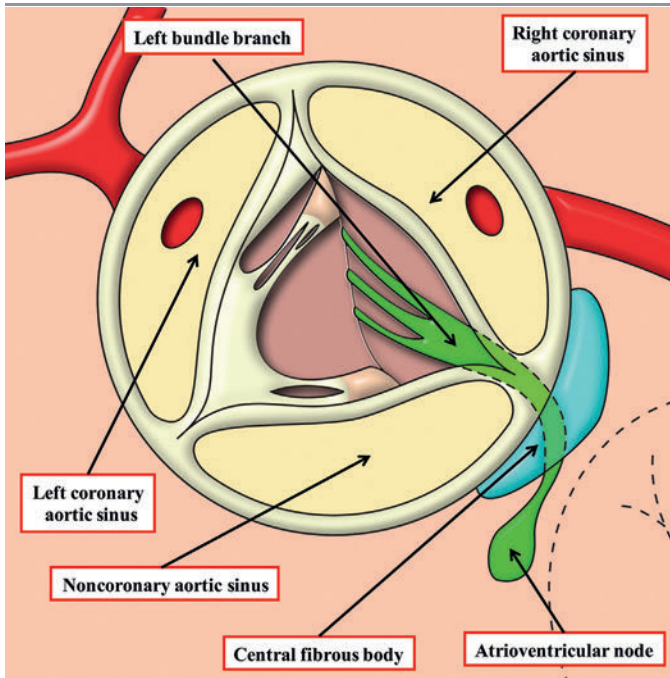
The aortic root is the portion of the LV outlet that supports the leaflets of the aortic valve and represents the interface between the LV and the ascending aorta. The aortic root extends from the sinotubular junction in the aorta to the plane defined by the bases of the aortic valve leaflets attaching to the crown shaped aortic annulus. Within these boundaries, the aortic root is composed of the aortic valve leaflets, the sinuses of Valsalva, and the interleaflet triangles (eFig. 23.3).

Sinotubular Junction

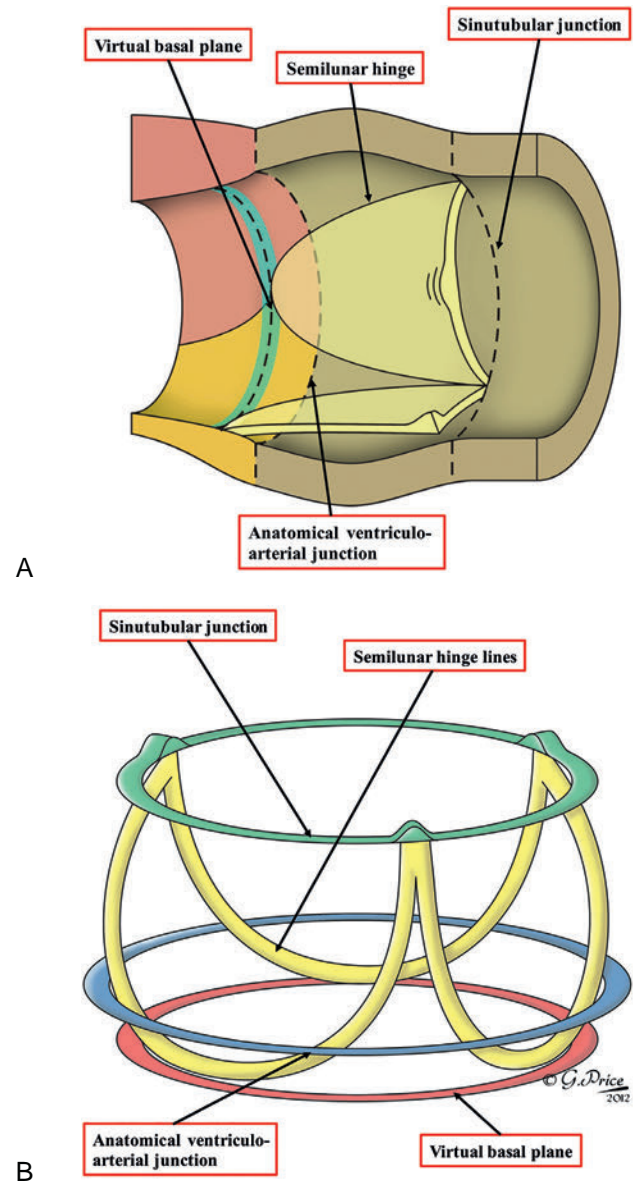
The sinotubular junction marks the junction of the sinuses and the aorta proper. On the innermost aspect of the aortic wall, the sinotubular junction forms a slightly raised ridge of thickened aortic wall (known as the sinotubular ridge or supra-aortic ridge) at the upper margin of each sinus.²³

Aortic Valve

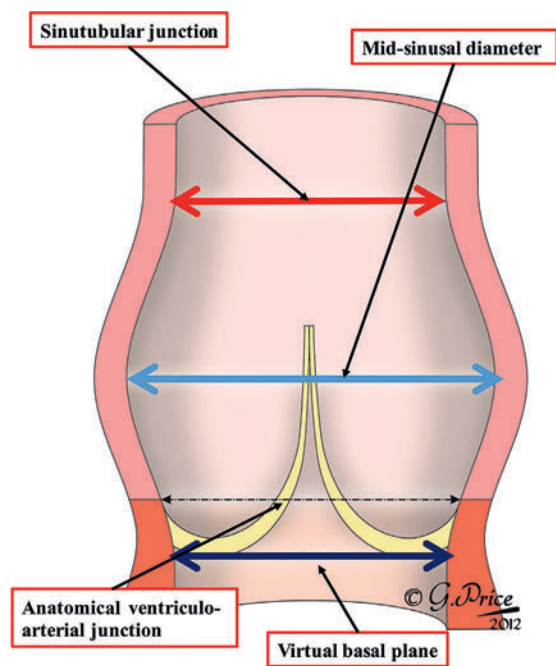
The aortic valve is normally composed of three symmetrical, semilunar-shaped leaflets (cusps). Each aortic cusp has (1) a functional hinge point where it attaches to the aortic root, (2) a body of the semilunar valve, and (3) a coaptation surface of the leaflet with a thickened central nodule (nodule of Arantius). The hinge points of the aortic leaflets attach to the fibrous skeleton within the aortic root in a semilunar fashion, instead of the traditional sense of a ring-like, annular valvular attachment. Therefore the hinge line of the attachment of the aortic valvular leaflets actually forms a crown-like structure (the annulus fibrosus) with the tips right at the sinotubular junction and the nadirs within the LVOT (see eFig. 23.3). The apices of the leaflets attaching to the annulus fibrosus



eFig. 23.2 Schematic Illustration of Aortic Root Anatomy in Relation to the Atrioventricular Conduction Axis. The cartoon shows the location of the atrioventricular conduction axis as it would be seen by a surgeon looking down through the aortic root. (Reproduced by kind permission of Professor Robert H. Anderson. Mrs. Gemma Price retains the intellectual copyright in the drawings used.)



eFig. 23.3 Schematic Illustration of Aortic Root Anatomy. (A) The cartoon shows a bisected aortic root, and illustrates how the semilunar attachment of the valvar leaflets incorporates aortic wall in the interleaflet triangles, and ventricular tissues at the base of each of the coronary aortic sinuses. (B) The cartoon shows an idealized aortic root. The attachments of the valvar leaflets, shown in red, extend through the entire length of the root, from the sinotubular junction, in blue, to the virtual basal ring, shown in green, and produced by joining together the basal attachments of the leaflets. The crown-like attachments of the leaflets cross the anatomical ventriculo-aortic junction, shown in yellow. (C) The cartoon shows a longitudinal section across the aortic root. (Reproduced by kind permission of Professor Robert H. Anderson. Mrs. Gemma Price retains the intellectual copyright in the drawings used.)



C

eFig. 23.3—cont'd

attach to the sinotubular junction. The bases of the aortic leaflets attach to the annulus at or below the anatomical ventriculo-arterial junction. The semilunar hinge lines of adjacent leaflets meet at the level of the sinotubular junction, forming the commissures.²¹

Aortic Sinuses

Corresponding with each of the three valvular leaflets, the aortic root is expanded forming the three aortic “sinuses of Valsalva.” The aortic sinuses of Valsalva are defined inferiorly by the attachments of the aortic valve leaflets and superiorly by the sinotubular junction (see eFig. 23.3). Three equally spaced sites of minimal tethering within the aortic root mark the junctions of the sinuses of Valsalva. Each sinus is associated with a leaflet of the aortic valve, whereas the junctions between the adjacent sinuses are aligned with the commissures between the aortic valve leaflets. Two of the aortic sinuses give rise to the left and right coronary arteries, and these sinuses are termed right and left coronary sinuses (CS), respectively (see eFig. 23.2). Usually no vessels arise from the third sinus, which is then termed the noncoronary aortic sinus. In anatomical descriptions, however, the aortic sinuses (and cusps) are named anterior (for right coronary), left posterior (for left coronary), and right posterior (for noncoronary). In attitudinal orientation, however, the sinuses are in anterior, left posterolateral, and right posterolateral positions, respectively (see eFig. 23.1).²¹

Interleaflet Triangles

Because of the semilunar nature of the attachments of the valvular leaflets, there are three triangular extensions of the LVOT that reach to the level of the sinotubular junction. Therefore, when considered as a whole, the aortic root is divided by the semilunar attachment of the aortic leaflets (i.e., leaflet annulus) into supra- and subvalvular components. The supra- and subvalvular components, the aortic sinuses, are primarily aortic in structure, but contain structures of ventricular origin at their base. The supporting subvalvular parts (the interleaflet triangles) are primarily ventricular (eFig. 23.4). However, these triangles are formed not of ventricular myocardium but of the thinned fibrous walls of the aorta between the expanded sinuses of Valsalva.^{16,18}

Ventriculo-Aortic Junction

Unlike the tricuspid and pulmonic valves that occupy opposite ends of the banana-shaped RV, the aortic and mitral valvular orifices are fitted alongside each other (with no muscle in between) within the elliptical ostium of the LV. As a result, the leaflets of the aortic valve are attached only in part to the muscular walls of the LV. About half of the circumference of the lower part of the aortic root is connected to the muscular ventricular septum, with the remaining half in fibrous continuity with the anterior leaflet of the mitral valve.^{16,21,23}

The “anatomical” ventriculo-aortic junction is a circular locus within the aortic root, marking the interface between the ventricular structures and the fibro-elastic walls of the aortic sinuses. This discrete ring, however, is markedly discordant with the morphology of the semilunar attachment of the leaflets of the aortic valve (the annulus fibrosus) that form the “hemodynamic” junction between the LV and the aorta. Indeed, ventriculo-aortic junction is crossed at several points by the hinge lines of the valvular leaflets. As a result, a crescent of ventricular musculature is incorporated at the base of each of the right and left aortic sinuses. In contrast, there is no muscular crescent at the base of the noncoronary sinus, since this sinus has exclusively fibrous walls, the basal part beneath the anatomical ventriculo-aortic junction being part of the aortomitral continuity (see eFig. 23.4).²³

Furthermore, sleeves (isolated strands) of ventricular myocardium extend beyond the aortic valve attachments for variable distances (analogous to atrial myocardial extensions in the pulmonary veins [PVs]).

Myocardial extensions can be seen in the aortic wall, in the valve leaflet itself, or in the intercuspular region. The myocardial extensions within the aortic sinuses are mostly asymmetrical and do not exceed more than a few millimeters above the basal valvar attachment. Whereas the right sinus of Valsalva and the anterior portions of the left sinus of Valsalva frequently exhibit these myocardial sleeves (given their anatomical contact with ventricular myocardium), the posterior portions of the left sinus and the entire noncoronary sinus of Valsalva, particularly in relation to the aortomitral continuity, are exclusively fibrous and do not come in direct contact with the LV myocardium. The noncoronary cusp at its junction with the right sinus of Valsalva may have sleeves of ventricular myocardium, and at present, it is not clearly known whether myocardial extensions into the noncoronary sinus represent atrial or ventricular myocardium.^{16,23}

Approximately 10% to 15% of idiopathic VAs require ablation within the aortic root. The left sinus of Valsalva is the most common source, followed by the right sinus, and then the left-right sinus junction. The substrate of this VT likely originates from the strands of ventricular myocardium present at the bases of those sinuses. In contrast, the base of the noncoronary sinus of Valsalva is composed of fibrous tissue and, thus, is an extremely rare site of origin of VT (7% of the idiopathic aortic root VAs). However, the nature of the actual substrate being ablated has not been clearly defined. For example, the ablation electrode placed in the depth of the right sinus of Valsalva may be mapping and ablating a focus arising from the supra- and subvalvular extension into the cusp, LVOT myocardium, or a deeper posterior RVOT myocardium.^{22,24}

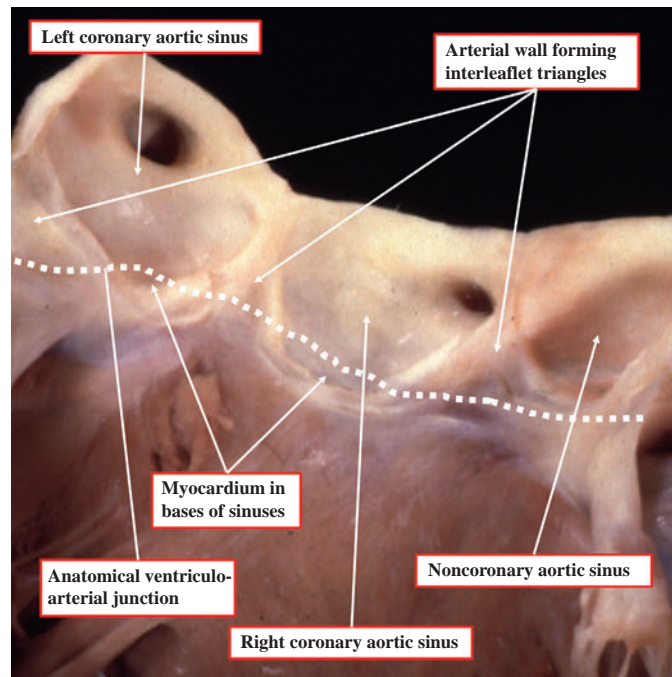
Anatomical Relationships

The aortic valve is the cardiac centerpiece; it lies in contact or continuity with all four cardiac chambers and shares important proximate relationships with each of the other cardiac valves (see Fig. 9.1). It comes into contact with the RA, LA, interatrial septum, RVOT, mitral valve (aortomitral continuity), pulmonic valve, tricuspid valve, and conduction system (see eFig. 23.1). The aortic valve plane tilts rightward (at about 30 to 45 degrees) in the horizontal plane as it is joined to the LV ostium. This positions the noncoronary sinus of Valsalva as the most inferior of the aortic sinuses, the left sinus of Valsalva as the most superior, and the right sinus of Valsalva as the most anterior. The degree of tilt is determined by the axis of the LV and can vary substantially among different individuals. As the LV axis flattens horizontally, the right and noncoronary sinuses are displaced inferiorly relative to the left sinus.¹⁴ The aortic root is inferior, posterior, and somewhat rightward compared with the RVOT. The posterior subpulmonic valve portions of the RVOT are immediately anterior and more proximally continuous with the anterior myocardial subaortic LVOT and more distally to the right sinus (eFig. 23.5). The lateral and more distal portions of the left sinus of Valsalva lie immediately subjacent to the peripulmonic valve portions of the RVOT.^{16,23}

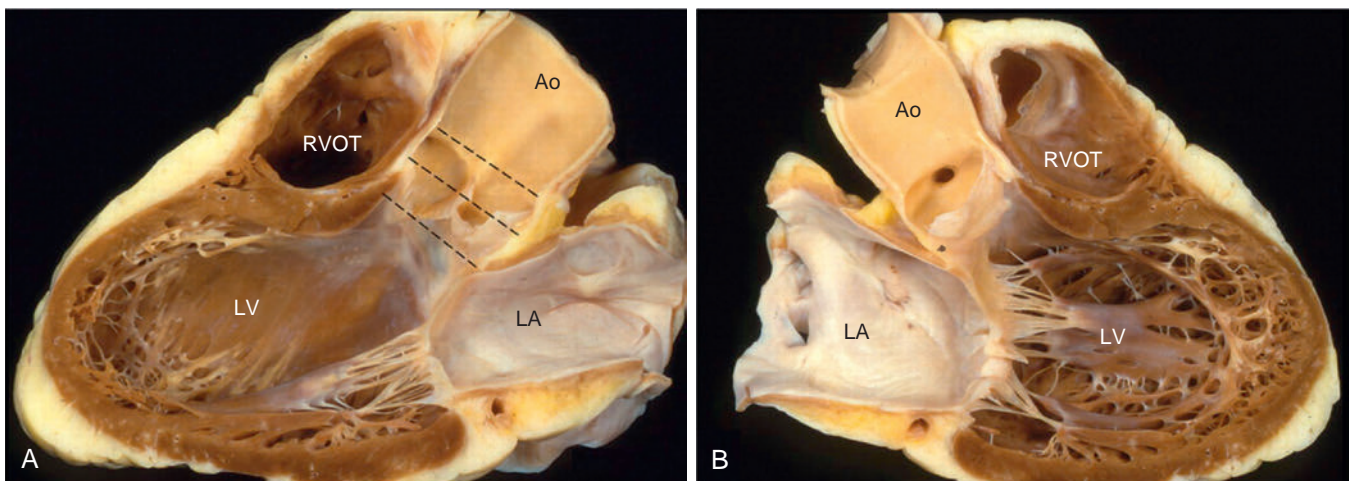
The triangle between the noncoronary and left sinuses is part of the aortomitral fibrous continuity. The triangle between the noncoronary and the right sinuses is directly continuous with the membranous part of the ventricular septum. The triangle between the left and right sinuses is the least extensive of the three, and abuts the muscular sub-pulmonary infundibulum (see Fig. 9.1).^{16,23}

Left Aortic Sinus of Valsalva

The left sinus of Valsalva lies to the left of the right sinus and is related to the posterior wall of the RVOT (see Fig. 9.1). The anterior part of the left sinus and the commissure between the right and left sinuses lie just posterior to the distal RVOT and are close but caudal to the posterior pulmonic valve annulus. The rest of the left sinus (more leftward



eFig. 23.4 Anatomy of the Ventriculo-Aortic Junction. The aortic root has been opened from behind and spread apart, so that the full width of the cylinder can be seen. The aortic valvar leaflets have then been removed, revealing the semilunar nature of their attachments. The purple dotted line shows the anatomical ventriculo-aortic junction, which is the union between the ventricular musculature and the aortic wall at the bases of the left and right coronary aortic valvar sinuses, but between the aortic wall and fibrous continuity with the mitral valve at the base of the noncoronary sinus. Note how the semilunar attachments incorporate muscle at the base of the right and left coronary aortic sinuses, but fibrous tissue within the ventricle as the hinge lines extend distally to reach the sinotubular junction. (Reproduced by kind permission of Professor Robert H. Anderson.)



eFig. 23.5 Anatomy of the Aortic Root and Left Ventricular Outlet. (A) and (B) are two halves of the same heart sectioned longitudinally through the left ventricle (LV), left atrium (LA), and aorta (Ao) to show the mitral leaflet between inflow and outflow regions in the LV. This section replicates the parasternal long axis echocardiographic cut. Note that the aortic root is the centerpiece of the heart. The right ventricular outflow tract (RVOT) is anterosuperior to the LV outlet. The three broken lines mark the levels of the aortic root at the sinotubular junction, at the sinuses, and at the bases of the aortic leaflets. (From Ho SY. Structure and anatomy of the aortic root. *Eur J Echocardiogr.* 2009;10:3–10.)

and posteriorly) lies in fibrous continuity with the anterior leaflet of the mitral valve (namely, the aortomitral continuity). Adjacent to this site lies the peripulmonic valve myocardium and, more laterally, the posterior lobe of the LA appendage (when present). Rightward tilting of the aortic root causes the left sinus to be situated higher than the right and noncoronary sinuses. The right sinus of Valsalva and anterior part of the left sinus are connected with the ventricular musculature at their bases because the semilunar leaflets are hinged superiorly to the aortic wall but inferiorly to muscle.²²

Right Aortic Sinus of Valsalva

The right aortic sinus is the most anterior sinus relative to the sternum, and it lies immediately posterior to the relatively thick posterior infundibular portion of the RVOT (see Fig. 9.1). Caudally, there is continuity with the anterior LVOT, and at the level of valve insertion there is either physical continuity or very close proximity between the myocardium that extends above this sinus, the LVOT, and the posterior RVOT (see eFig. 23.1). The posterior part of the right sinus of Valsalva is adjacent to the central fibrous body, which carries within it the penetrating portion of the HB. Anteriorly, the right sinus is related to the bifurcating AV bundle and the origin of the left bundle branch (see eFig. 23.2). The right sinus does not have a direct relationship with either atrium, but lateral to the commissure with the noncoronary sinus lies the RA appendage, trunk of the right coronary artery, and a variable amount of fat (eFig. 23.6).

Noncoronary Aortic Sinus of Valsalva

The noncoronary sinus of Valsalva is the most posterior, inferior, and medial of the aortic cusps. The noncoronary sinus lies immediately anterior to the interatrial septum and superior to the central fibrous body and has the RA and LA as the posterior right and left relations, respectively (see eFigs. 23.2 and 23.6). Because of this relationship to the atria, some atrial tachycardias (ATs) arising from the roof of the interatrial septum can be ablated only within the noncoronary sinus. For most of its anatomical course, the noncoronary sinus is attached to the anterior leaflet of the mitral valve from its most leftward extent in continuity with the left sinus commissure. Only the most anterior and rightward extension of the noncoronary sinus comes into contact with the interventricular septum near its junction with the right sinus of Valsalva. The commissure between the noncoronary and the right sinuses is located immediately adjacent to the commissure of the anterior and septal leaflets of the tricuspid valve (see Fig. 9.1). The joining of these commissures forms the membranous portion of the interventricular septum and is the location of the penetrating HB. The compact AVN itself is located more posteriorly and inferiorly to this commissure. The membranous septum is crossed on its right side by the hinge of the tricuspid valve, which divides the septum into *atrioventricular* and *interventricular* components. The membranous septum and anterior mitral leaflet almost completely separate the noncoronary sinus from the LV myocardium. Because of this limited relationship to the ventricle, VAs originating from the noncoronary sinus are very rare (7% of the idiopathic aortic root VAs).^{22,24}

Aortomitral Continuity

The cardiac skeleton consists of four rings of dense connective tissue that surround the AV canals (mitral and tricuspid) and extends to the origins of the aorta and the pulmonary trunk. The aortic valve occupies the central position with the other valve rings attached to it or nearby (pulmonic). The right fibrous trigone is formed by the triangular formation between the aortic valve and the medial parts of the tricuspid and mitral valves, and it represents the largest thickening and strongest portion of the cardiac skeleton. Together with the membranous

septum, the right fibrous trigone constitutes the central fibrous body (see Fig. 9.1).

Another junction between the mitral annulus and aortic valvular ring occurs at the left fibrous trigone, anchoring the anteromedial aspect of the mitral annulus to the base of the left aortic sinus of Valsalva. The left fibrous trigone is less substantial than the right fibrous trigone. Between the left and right fibrous trigones, a rigid and broad fibrous curtain (often referred to as the aortic curtain) extends across the anterior leaflet of the mitral valve and supports the aortic valve leaflets. The aortomitral continuity refers to a fibrous continuity of the medial part of the noncoronary and left sinuses and the anterior mitral leaflet.²²

The membranous interventricular septum is an inferior extension of the central fibrous body that attaches to the muscular interventricular septum. The membranous septum is crossed on its right aspect by the attachment of the tricuspid valve, dividing the septum into atrioventricular and interventricular components. As a result, the membranous septum separates the LVOT from both the RV and RA; the line of attachment of the tricuspid annulus determines the line of division between the RV and RA.²⁶ The penetrating HB runs through the portion of the membranous interventricular septum at the commissure where the right sinus of Valsalva meets the noncoronary sinus (see Fig. 9.1).

Although the aortomitral continuity is a fibrous structure, catheter ablation in this region can successfully eradicate VAs arising in this vicinity. The exact origin of arrhythmias ablated from this fibrous region is still uncertain.

Left Ventricular Summit

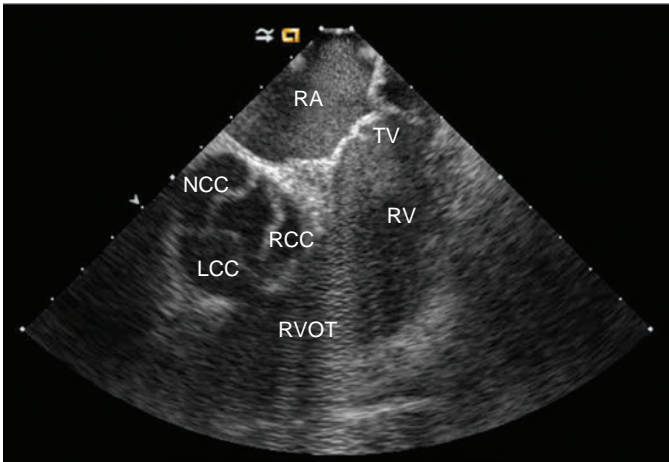
The LV summit refers to the most superior portion of the LV epicardium, which lies on the basal portion of the LV ostium next to the septum and the anterior mitral annulus, abutting on the left aortic sinus of Valsalva superiorly, laterally, and anteriorly.²⁷

The LV summit represents the triangular region in the epicardial LVOT with its apex at the bifurcation of the left main coronary artery (between the left anterior descending and the circumflex coronary arteries) and its base formed by an arc connecting the first septal perforator branch of the left anterior descending coronary artery and the circumflex coronary artery (eFig. 23.7). The left main coronary artery arises cranial to the left sinus of Valsalva (about 15 to 20 mm above the nadir of the cusp). The aortomitral continuity and LV summit face each other, with the superior end of the LV muscle between them.²⁹

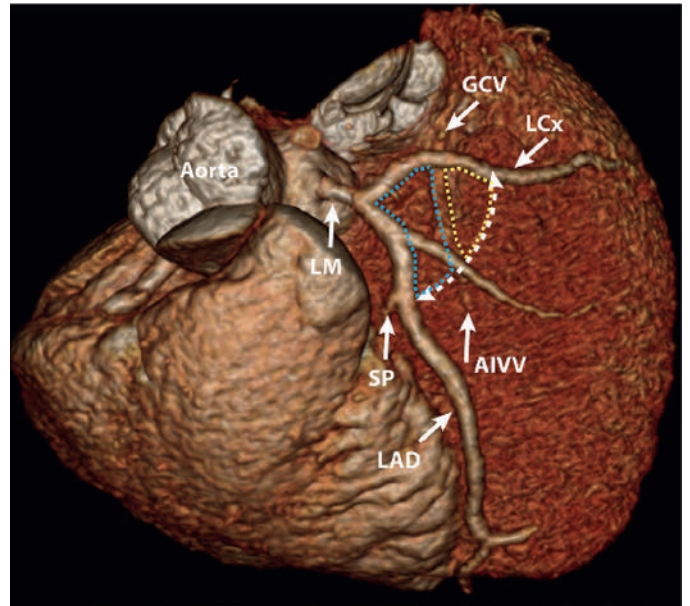
The great cardiac vein bisects the LV summit into superior (closer to the apex of the summit) and inferior regions. Approximately 12% of VAs from the LV are estimated to occur from the LV summit. While the inferior portion of the summit is usually accessible to epicardial catheter ablation, successful ablation in the superior region is frequently limited by the close proximity of the coronary arteries and the thick layer of epicardial fat that overlies the proximal portion of these vessels.²²

Left Ventricular Papillary Muscles

The anterolateral (or anterior) and posteromedial (or posterior) LV papillary muscles are thick, finger-like processes attached to the ventricular wall at one end and to the mitral leaflets by multiple tendons (chordae tendineae) on the other end (Fig. 23.4). The anterior papillary muscle originates from the middle to apical region of the LV ventral wall, lies on the anterolateral free wall, and provides chordae to the anterolateral half of the anterior and posterior mitral leaflets. The posterior papillary muscle arises from the inferoseptal wall of the LV, lies between the LV septum and posterior free wall, and provides chordae to the posteromedial half of both leaflets. The anterior papillary muscle typically has a single head, while the posterior papillary muscle often has two heads.³¹ Focal VAs generally originate from the base of the papillary muscle.³¹



eFig. 23.6 Intracardiac Echocardiography (ICE) Cross-Sectional Image of the Aortic Valve. The image is acquired with the ICE catheter positioned at the His bundle region of the right ventricle (RV) septum. LCC, Left coronary cusp; NCC, noncoronary cusp; RA, right atrium; RCC, right coronary cusp; RVOT, right ventricular outflow tract; TV, tricuspid valve.



eFig. 23.7 Cardiac Computed Tomography Reconstruction Depicting the Anatomy of the Left Ventricular (LV) Summit. The LV summit is a triangular region of the LV epicardium with the apex at the bifurcation between the left anterior descending (LAD) and left circumflex (LCx) coronary arteries, and the base formed by an arc connecting the first septal perforator branch (SP) of the LAD with the LCx (white dotted line and arrows). The LV summit is bisected by the great cardiac vein (GCV) in 2 regions: (1) closer to the apex of the triangle (blue dotted line, inaccessible area), and (2) more lateral toward the base of the triangle (yellow dotted line, accessible area). AIVV, Anterior interventricular vein; LM, left main coronary artery. (From Santangeli P, Lin D, Marchlinski FE. Catheter ablation of ventricular arrhythmias arising from the left ventricular summit. *Card Electrophysiol Clin*. 2016;8:99–107.)

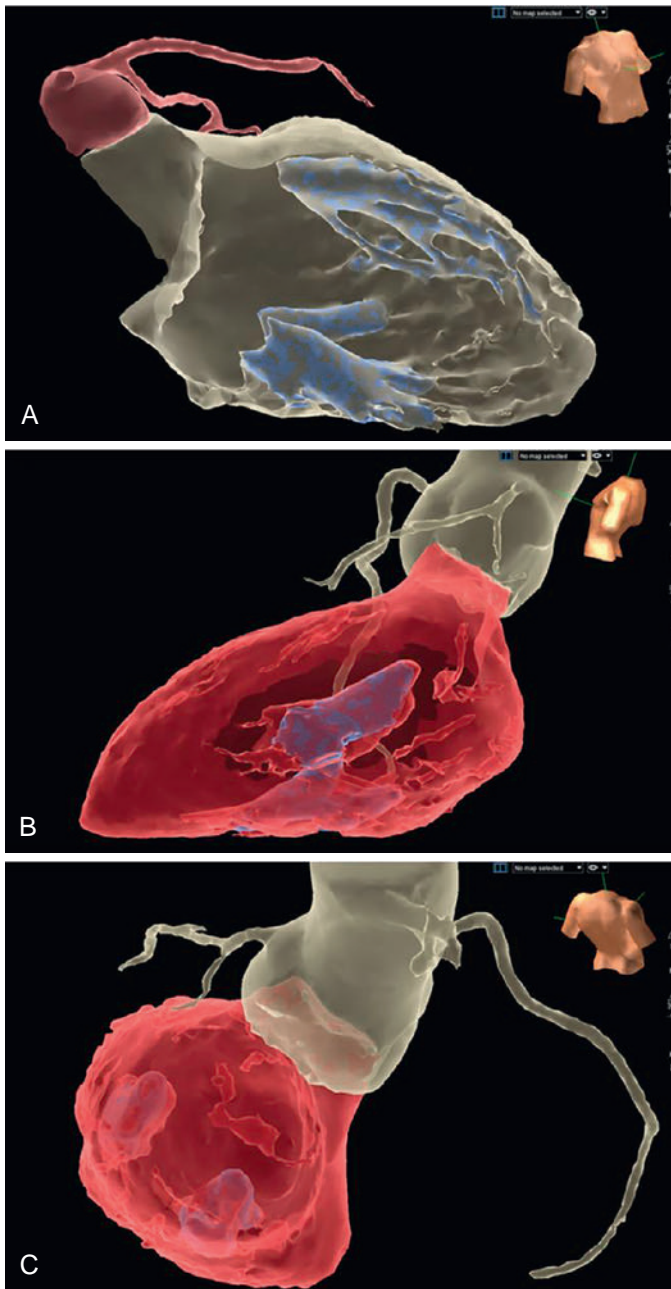


Fig. 23.4 Anatomy of the Left Ventricular (LV) Papillary Muscles. (A) Three-dimensional reconstruction of the cardiac multidetector computed tomography and integration to the mapping system guided by intracardiac echocardiography. This corresponds to a lateral view of the endocardial aspect of the LV. The papillary muscles are depicted in blue, whereas the aortic root and left coronary artery are depicted in red. (B) Left lateral view of the LV and aortic root. The anterior papillary muscle in blue and the rest of the LV in red. (C) Posterior view of the LV (red) and aortic root (gray). Notice the anterior and posteromedial papillary muscles in blue. (From Rivera S, Ricapito Mde L, Tomas L, et al. Results of cryoenergy and radiofrequency-based catheter ablation for treating ventricular arrhythmias arising from the papillary muscles of the left ventricle, guided by intracardiac echocardiography and image integration. *Circ Arrhythm Electrophysiol.* 2016;9:1–9.)

The peripheral Purkinje network extends to the surface of the papillary muscles. Free-running false tendons traverse the ventricular chamber and reattach at the free wall myocardium, projecting predominantly toward the papillary muscles. The left anterior fascicle crosses the antero-basal LV region toward the anterior papillary muscle and terminates in the Purkinje system of the anterolateral LV wall. The left posterior fascicle fans out extensively toward the posterior papillary muscle and terminates in the Purkinje system of the posteroinferior LV wall. The close relationship that exists between the Purkinje fiber and papillary muscles has caused some difficulties in distinguishing arrhythmias from the two structures. Furthermore, VAs originating from the body of the papillary muscle can exhibit multiple QRS morphologies caused by variable exit sites from an intramural focus or its attachment to false chordae.^{31,32}

Cardiac Crux

The cardiac crux (crux cordis, from Latin “crux” meaning “cross”) is the posteroseptal region (the diaphragmatic aspect) of the heart where the atrioventricular, interventricular, and interatrial grooves form a roughly cross-shaped intersection. This four-sided pyramidal space represents the confluence of all four cardiac chambers and the CS in their nearest proximity. The “basal” crux area lies in proximity to the ostium of middle cardiac vein, whereas the “apical” crux area lies near the posterior interventricular artery, more inferior and epicardial as compared with the basal crux area.³³ Hence the apical crux is often not accessible from the proximal CS or the middle cardiac vein, and a transcutaneous subxiphoid epicardial approach is typically required.³⁴

EPIDEMIOLOGY AND NATURAL HISTORY

Idiopathic VT comprises 10% of all patients referred for evaluation of VT. Idiopathic VAs are not evenly distributed, but have a predilection for originating from certain anatomical regions of the ventricles and aortic and pulmonary roots. Approximately 60% to 80% of idiopathic VAs arise from the ventricular outflow regions, including myocardium around the aortic and pulmonic cusps, as well as the summit of the LV. Although the RVOT has been the most common site of origin of OT VAs, a significant proportion (20% to 50%) arise from the LVOT and adjacent structures.²

Age at presentation is usually 30 to 50 years (range, 6 to 80 years). Women are more commonly affected, although LVOT VAs are more frequently observed in men. The clinical course is benign and the prognosis is excellent. Sudden cardiac death is rare. Spontaneous remission of the VT occurs in 5% to 20%. However, very frequent idiopathic nonsustained VT or PVCs can precipitate a potentially reversible form of LV systolic dysfunction (observed in about 5% to 7% of patients with a PVC burden >10%). The relationship between the LV dysfunction and VT may not be initially recognized, and those patients can present with heart failure symptoms and become diagnosed with idiopathic dilated cardiomyopathy, and may even undergo prophylactic implantation of a defibrillator, which unfortunately often results in the delivery of inappropriate shocks triggered by frequent nonsustained episodes of idiopathic VT. Rarely, monomorphic focal PVCs can trigger idiopathic polymorphic VT or VF in patients with no apparent structural heart disease.³⁵

CLINICAL PRESENTATION

When present, symptoms are mild in many of patients, but they can be disabling in some individuals. Most symptomatic patients present with palpitations, 50% develop lightheadedness, and a minority (<10%)

present with syncope. Symptoms can be attributed to the PVC, the subsequent compensatory pause, the hypercontractile sinus beat following the pause, or a combination of all. A sensation that the heart has “stopped” or pulsation in the head or neck can be noted.³⁶

Not infrequently, initial presentation can be related to effort intolerance due to fatigue and dyspnea, as a result of decreased effective cardiac function. Some patients can be completely asymptomatic and present with ectopy detected incidentally by an irregular pulse or on cardiac recordings obtained for other clinical reasons. Other patients present because of “low pulse rates,” which is related to ineffective ventricular contraction during PVCs with insufficient pressure to allow opening of the aortic valve.^{7,37}

Most commonly, patients present with frequent PVCs or short runs of repetitive nonsustained VT. Less frequently, paroxysmal sustained VT is observed. Idiopathic VAs are usually provoked by emotional or physical stress and stimulants such as caffeine. Not infrequently, however, VAs become quiescent during exercise and arise only during the recovery phase or during rest. In females, the burden of arrhythmia tends to increase during periods of hormonal variations (premenstrual and perimenopausal).

Frequent idiopathic nonsustained VT or PVCs can precipitate a reversible form of LV systolic dysfunction, and present with heart failure symptoms. Such arrhythmias may also exacerbate preexisting LV dysfunction and is a cause of loss of effective biventricular pacing in heart failure patients treated with cardiac resynchronization therapy. At the first clinical encounter, patients often present with both PVCs and LV dysfunction. In this setting, it can be difficult to determine the onset of frequent PVCs relative to the onset of LV dysfunction and whether the cardiomyopathy is PVC-induced or PVC-worsened.^{7,38}

INITIAL EVALUATION

The diagnosis of idiopathic VT is one of exclusion; structural heart disease, cardiomyopathy, and coronary artery disease should be excluded, usually by cardiac stress testing and echocardiography. Coronary angiography may be warranted, especially in those with LV systolic dysfunction and coronary risk factors.

Diagnostic features of idiopathic VAs include (1) structurally normal heart; and (2) QRS morphology consistent with site of origin from typical locations of idiopathic VAs (in particular, the RVOT or LVOT). The echocardiogram is normal in most patients. Slight RV enlargement is observed rarely.

Electrocardiography

The surface ECG during NSR is usually normal. Up to 10% of patients have complete or incomplete RBBB. Other ECG abnormalities may be observed when idiopathic VAs coexist with structural heart disease.

Idiopathic focal VAs are characterized by frequent monomorphic PVCs, couplets, or salvos of nonsustained VT, interrupted by brief periods of NSR (see Fig. 23.1). Paroxysmal exercise-induced VT is characterized by sustained episodes of VT precipitated by exercise or emotional stress (see Fig. 23.2). The tachycardia rate is frequently rapid (CL <300 milliseconds), but can be highly variable. A single morphology for the VT or PVCs is characteristic. QRS morphology during VAs on the surface ECG is discussed later in this chapter.

Ambulatory Cardiac Monitoring

Holter monitors can assess the burden of VAs and their correlation to symptoms. Cardiac event monitors are more appropriate when symptoms occur less frequently.

Several characteristics of idiopathic VAs can be observed on ambulatory cardiac monitoring. Idiopathic VAs typically occur at a critical

range of heart rates (CL dependence). The coupling interval of the first PVC is relatively long (approximately 60% of the baseline sinus CL). A positive correlation exists between the sinus rate preceding the VT and the VT duration. In addition, the VT occurs in clusters, and is most prevalent on waking and during the morning and later afternoon hours. Catecholamines increase during waking hours and nocturnal decrease in catecholamine levels, and predominance of vagal tone might account for the differences in the circadian PVC burden. The largest change in PVC burden is observed in the transition from the sleeping hours to the morning waking hours. Notably, the lack of circadian fluctuation in PVCs frequency has been correlated with increased risk of PVC-induced cardiomyopathy.

Idiopathic focal VAs are very sensitive to autonomic influences, resulting in poor day-to-day reproducibility. Therefore a single 24-hour recording may not reflect the true PVC burden. When frequent PVCs are strongly suspected, it may be necessary to obtain extended Holter recordings of 48 to 72 hours or several 24-hour Holter recordings.⁷

Exercise Electrocardiography

Exercise stress testing is recommended for evaluation of patients with exercise-related symptoms, but may not be clinically helpful in those in whom the arrhythmias have already been documented on ambulatory recordings.¹¹

Exercise testing can reproduce patients' clinical VT 25% to 50% of the time. Exercise-provoked VT usually manifests as nonsustained or, less often, sustained VT. In those with isolated PVCs, the frequency of PVCs tends to increase during exercise. The VT can be initiated either during the exercise test or during the recovery period. Both scenarios likely represent examples of the dependence of VT on a critical window of heart rates for induction. This window can be narrow and only transiently present during exercise, resulting in induction of VT only during recovery. In some patients with repetitive monomorphic VT, the VT can become suppressed during exercise. The response of VAs to exercise can be helpful in planning the strategy for arrhythmia induction during an ablation procedure.³⁹

Catecholaminergic polymorphic ventricular tachycardia (CPVT), also exercise dependent, can be distinguished by the alternating QRS axis with 180-degree rotation on a beat-to-beat basis (bidirectional VT) or polymorphic VT, which can degenerate into VF.¹¹

Cardiac Magnetic Resonance

CMR is of value when structural heart disease is suspected despite a normal echocardiogram. CMR can help exclude arrhythmogenic right ventricular cardiomyopathy (ARVC), amyloidosis, and sarcoidosis, among other diseases. CMR can also evaluate the presence and extent of myocardial fibrosis in patients with LV dysfunction.¹¹

It is important to recognize that CMR can reveal concealed myocardial structural abnormalities involving the RV and the LV among patients with apparently *idiopathic* VAs, including subepicardial or midmyocardial foci of fibrosis, acute inflammation, and focal fatty infiltration. Of note, the morphology of VAs appears to be related to the presence of such abnormalities on CMR. In contrast to the infrequent abnormalities noted among patients with VAs of LBBB pattern, CMR detected myocardial structural abnormalities (mainly involving the LV inferior and lateral wall) in a sizable proportion (41%) of patients with unexplained VAs with RBBB configurations (consistent with an LV origin). Whether these abnormalities are causally related to the observed VAs is uncertain; however, the presence of myocardial structural abnormalities on CMR seems to predict spontaneous sustained arrhythmias among patients presenting with apparently idiopathic VAs of LV origin.⁴⁰

DIFFERENTIAL DIAGNOSIS

It is important to differentiate idiopathic VT from other potentially malignant forms of VT that may also arise from the OT region, including VT in ARVC, CPVT, Brugada syndrome, and idiopathic polymorphic VT and VF. A Brugada ECG pattern, findings of reduced LV or RV function, polymorphic VT, multiple monomorphic VT morphologies, a history of recurrent syncope, or a family history of sudden cardiac death mandate further detailed evaluation.

Arrhythmogenic Right Ventricular Cardiomyopathy

RVOT VAs should, in particular, be distinguished from ARVC, a disorder with a more serious clinical outcome (see Chapter 29). Although RVOT VAs are associated with a benign prognosis with no familial basis, it can be extremely difficult to distinguish from the concealed phase of ARVC, in which typical ECG and imaging abnormalities are absent. The VT in ARVC also affects young adults, is commonly catecholamine-facilitated, and can originate from the RVOT. The distinction between the two entities has important prognostic and therapeutic implications.

Electrocardiogram During Sinus Rhythm

Although the VT in ARVC can have morphological features similar to RVOT VAs (LBBB with inferior axis), several ECG criteria during VT can help distinguish between the two arrhythmias. Longer QRS duration in lead I (≥ 120 milliseconds), late precordial transition (at lead V_5 or V_6), and the presence of notching in the QRS in multiple leads all favor ARVC over idiopathic RVOT VAs. In addition, the presence of an LBBB morphology with a superior axis is very unlikely in idiopathic RVOT VAs. Also, VAs in ARVC patients generally have lower QRS amplitude and more fragmentation, but these are qualitative differences and not always present.

In ARVC, the resting 12-lead ECG in NSR typically shows inverted T waves in the right precordial leads. When present, RV conduction delay with an epsilon wave (best seen in leads V_1 and V_2) is helpful in the diagnosis of ARVC. The resting surface ECG in NSR is typically normal in patients with idiopathic VT, with no epsilon wave, QRS widening or fragmentation, or other markers of delayed activation of the RV. Patients with idiopathic VT also have a normal signal-averaged ECG in NSR.

Nevertheless, the ECG can also be normal in up to 40% to 50% of patients with ARVC at presentation, but in almost no patient 6 years after initial diagnosis. Furthermore, approximately 10% of patients with idiopathic VT can have complete or incomplete RBBB during NSR.

Electrocardiogram During Ventricular Tachycardia

In general, patients with idiopathic VT typically present with a single-morphology VT. The presence of multiple VT morphologies and RV sites of origin of the VT that are inconsistent with idiopathic RVOT VT (e.g., LBBB with superior axis) should prompt the consideration of ARVC. Nonetheless, it should be recognized that patients with several idiopathic VT morphologies have been reported, and patients with ARVC can initially present with only one VT morphology consistent with an RVOT origin.⁴¹

During VTs with LBBB and inferior axis, certain features of the QRS complex favor ARVC over RVOT VT, including (1) late precordial transition (at V_5 or later); (2) QRS notching in at least two leads (in particular, leads I and aVL); and (3) QRS duration in lead I longer than 120 to 125 milliseconds. The most specific finding was late precordial transition (100% specificity at lead V_6 and 90% specificity at lead V_5 or later), and the most sensitive was duration of QRS in lead I exceeding

120 milliseconds, followed by the presence of any notching on the QRS complex. QRS notching and the longer QRS duration in ARVC reflect the abnormal myocardial substrate underlying the VT, which is lacking in idiopathic RVOT VT.^{42–44}

Invasive Electrophysiology Testing

An invasive EP study is usually not necessary to establish a diagnosis, although it can help exclude other forms of tachyarrhythmias in selected patients. The response of VT during EP testing can be helpful in distinguishing idiopathic RVOT VAs from ARVC. Reentry is the mechanism of VT in most ARVC patients, whereas RVOT VT almost always displays features of triggered activity. The repetitive initiation of these VAs by programmed ventricular stimulation suggests a reentrant mechanism, and is much more common in ARVC than idiopathic OT VAs (93% vs. 3%). In addition, recording fractionated diastolic electrograms during VT or NSR at the site of origin of VT or other RV sites is very rare with idiopathic RVOT VAs, but is typical for ARVC. As noted, the induction of VAs with different QRS morphologies is common in ARVC (observed in 73% of patients in one report) and is rare with RVOT VT. Furthermore, the VT in ARVC does not terminate with adenosine.⁴¹

In addition, electroanatomic voltage mapping can help distinguish early or concealed ARVC from idiopathic VT by detecting RV electroanatomical scars that correlate with the histopathological features pathognomonic of ARVC.

Isoproterenol Testing

An arrhythmogenic response to high-dose intravenous (IV) isoproterenol (45 $\mu\text{g}/\text{min}$ for 3 minutes, regardless of heart rate) can potentially help diagnose ARVC, particularly in the early stages of the disease. The occurrence of polymorphic VAs (PVCs and sustained and nonsustained VT) with predominant LBBB morphology (with features that are not typical for an RVOT origin) during isoproterenol testing (during isoproterenol infusion or within 10 minutes after the cessation of the infusion) is highly suggestive of ARVC (sensitivity, 91%; negative predictive value, 99%). In contrast, a sustained monomorphic RVOT VT response during isoproterenol testing is considered a negative response.⁴⁵

Cardiac Imaging

Patients with idiopathic VT have normal imaging studies (echocardiography, CMR, contrast ventriculography) of RV size and function. The presence of RV dilation or aneurysm is consistent with ARVC.

Dilated Cardiomyopathy

It is important to recognize that, in some patients, idiopathic VAs can coexist with structural heart disease, including cardiomyopathy, in which setting the VAs may not be related to the cardiac disease. On the other hand, very frequent idiopathic nonsustained VT or PVCs can precipitate dilated cardiomyopathy that can improve or completely resolve after elimination of the VAs. Therefore in patients who present with a dilated cardiomyopathy of unclear etiology and who have frequent PVCs or nonsustained VT, it is important to assess the contribution of VAs to LV systolic dysfunction. Failure to recognize a causal relationship between the arrhythmia and LV dysfunction can have important consequences. These patients can be misdiagnosed with “idiopathic” dilated cardiomyopathy and may not be offered therapeutic measures to reduce the PVC burden (e.g., catheter ablation), which can significantly impact LV systolic function and long-term outcome.

A reversible form of dilated cardiomyopathy precipitated by idiopathic VAs should be suspected when frequent PVCs or nonsustained VT are observed on a 24-hour Holter recording, especially when the QRS morphology is monomorphic and is suggestive of origin from typical locations of idiopathic VAs.

The diagnosis of PVC-induced cardiomyopathy is one of exclusion and often retrospective based on recovery of LV function after elimination of the arrhythmia, typically by catheter ablation. Although pharmacological suppression of the PVCs, such as by amiodarone therapy, may help evaluate the relationship between the arrhythmia and cardiomyopathy, the usefulness of this approach and duration of therapy required have not been defined.

Predictors of reversibility of LV systolic dysfunction in patients with PVC-induced cardiomyopathy include the absence of myocardial scar (on CMR), a large PVC burden baseline, and effective long-lasting elimination of PVCs. Although no single cutoff value of PVC burden completely discriminates reversible from irreversible LV dysfunction, a burden of $\geq 13\%$ at baseline was shown to predict recovery of left ventricular ejection fraction (LVEF) following ablation of PVCs.⁴⁶ Of note, early improvement in LVEF (at 1-week follow-up) post PVC ablation was shown to predict complete recovery of LV systolic function.⁴⁷ One report suggested that patients with PVC QRS duration of 170 milliseconds or longer are unlikely to normalize their LV function after ablation of the PVCs, suggesting that PVC QRS duration can be a marker of the presence and severity of underlying structural heart disease.^{12,38}

Given the large magnitude of potential improvement in LV systolic function that could be achieved by elimination of frequent PVCs (regardless of whether the cardiomyopathy is in fact PVC-induced or PVC-worsened), evaluation for the presence of frequent PVCs (by 24- or 48-hour Holter monitoring) needs to be considered in all patients with depressed LVEF. This is particularly important in patients who meet criteria for primary prevention implantable cardioverter-defibrillator (ICD) implantation, as the recovery of LVEF following ablation can potentially remove the ICD indication.⁴⁷

Idiopathic Ventricular Fibrillation

Idiopathic monomorphic focal VAs, although generally considered “benign,” can also trigger polymorphic VT and VF in some patients with idiopathic VF and no apparent structural heart disease (see Fig. 31.20). Hence, for patients presenting with idiopathic VF, it is imperative to pay special attention to recording potential monomorphic PVC “triggers,” since catheter ablation of those foci can potentially prevent further episodes of VF or reduce the burden of arrhythmias. Also, patients with polymorphic VT and VF should be carefully evaluated for underlying channelopathies.^{3,34,48}

Even in patients with no prior history of VF, it is also particularly important to distinguish the “malignant” from “benign” forms of idiopathic monomorphic VAs because the malignant form often leads to unexpected sudden cardiac death. Identification of patients presenting with idiopathic focal VAs carrying some risk for VF remains challenging. Malignant VAs should be suspected in patients with known idiopathic focal VAs who present with syncope. Patients with idiopathic VF frequently (57%) experience syncopal episodes before presenting with cardiac arrest.²

Several ECG parameters have been suggested as markers of malignant OT VAs. However, the diagnostic value of these ECG parameters is inconsistent and their clinical utility is limited. Although idiopathic VF and polymorphic VT can arise from triggers located in the RVOT and LVOT, PVCs arising from the Purkinje network, RV moderator band, papillary muscles, and apical cardiac crux, due to unclear mechanism, appear to be particularly prone to induce sustained VT and VF, leading to syncope or cardiac arrest. Therefore VAs with QRS morphology suggestive of those sites of origin should be carefully scrutinized.²

The prognostic implications of the coupling intervals of clinical PVCs have been debated. Although no absolute coupling interval cutoff identifies potentially “malignant” PVCs, shorter coupling interval to the preceding QRS complex, and a shorter CL during monomorphic

VT were found to predict the coexistence of VF or polymorphic VT in patients with idiopathic RVOT VT/PVCs; however, significant overlap exists. In contrast, one report showed that the prematurity index (defined as the ratio of the coupling interval of the first VT beat or isolated PVC to the preceding R-R interval of the sinus cycle just before the VT or isolated PVC), but not the coupling interval, was the only independent predictor for polymorphic VT. A more recent report found that the second coupling interval of nonsustained VT was significantly shorter in malignant OT VT than in benign OT VT. A second coupling interval of nonsustained VT of less than 317 milliseconds could predict a malignant OT VT with modest diagnostic accuracy (sensitivity 58%, specificity 87.5%). However, prospective validation of these criteria is yet to be tested in a larger population.⁴⁹

Other Arrhythmia Mechanisms

Idiopathic OT VT should be differentiated from other forms of VT with an LBBB pattern, including bundle branch reentrant VT (see Chapter 26), reentrant VT following surgical repair of congenital heart disease (see Chapter 30), and postinfarction VT originating from the LV septum (see Chapter 22). In addition, antidromic AVRT using an atriofascicular BT also presents with wide complex tachycardia with an LBBB pattern (see Chapter 18). Often the diagnosis of these VTs can be established without difficulty, given the frequently associated structural heart disease. Nevertheless, idiopathic focal VT also can occur in patients with unrelated structural heart disease, and the distinction of those “ablatable” VTs has important prognostic and therapeutic implications.

PRINCIPLES OF MANAGEMENT

Acute Management

Acute termination of most forms of idiopathic VT can be achieved by vagal maneuvers or IV administration of adenosine. IV verapamil is an alternative, provided the patient has adequate blood pressure and has a previously established diagnosis of a VT that is sensitive to verapamil. Hemodynamic instability warrants emergency cardioversion.

Chronic Management

Conservative Management

Given the generally benign long-term prognosis, reassurance and counseling, with no pharmacological therapy, are the preferred treatment for patients with idiopathic VAs who are asymptomatic or only mildly symptomatic and have normal LV function. Annual follow-up with ambulatory ECG monitoring and echocardiography is recommended in those with frequent PVCs ($>10,000$ PVCs per 24 hours) to monitor for possible development of cardiomyopathy, which should prompt the initiation of therapy.^{8,11,50}

Importantly, many patients with frequent PVCs do not complain of palpitations and present primarily with occult cardiac symptoms, such as weakness, fatigue, and effort intolerance. Such complaints should not be dismissed as “unrelated,” and those patients should not be labeled “asymptomatic.” Treatment to reduce the burden of PVCs should be considered to alleviate symptoms.^{11,37,51}

Although frequent PVCs can precipitate LV systolic dysfunction in some patients who are otherwise asymptomatic, there is currently no risk stratification model to reliably identify patients at risk. Therefore prophylactic PVC elimination for the sole purpose of preventing PVC-induced cardiomyopathy is not recommended.⁵¹

Pharmacological Therapy

Medical therapy can be considered in symptomatic patients. Beta-blockers, verapamil, and diltiazem are the first-line treatment. However,

these medications have a modest efficacy rate (only 10% to 15% of patients achieve $\geq 90\%$ PVC suppression), and they may not be well tolerated by the generally young patient population. Although class I and III antiarrhythmic drugs (sotalol, flecainide, mexiletine, propafenone, amiodarone) are more effective in reducing the burden of PVCs, they are not optimal as first-line therapy, given the potential for proarrhythmic risk and a greater side-effect profile.^{11,52–54}

Catheter Ablation

Catheter ablation is the treatment of choice for significantly symptomatic patients in whom long-term drug therapy is unsuccessful, not tolerated, or not desired. In addition, catheter ablation should be strongly considered in patients with “malignant” forms of idiopathic VAs, such as those with short-coupled PVCs and syncope or cardiac arrest, or in whom the PVCs were found to trigger polymorphic VT or VF.^{51–55}

Catheter ablation is also recommended for patients with frequent PVCs or nonsustained VT when they are presumed to be contributing to a cardiomyopathy or worsening of preexisting LV dysfunction, even in otherwise asymptomatic patients. Effective elimination of PVCs (reduction of PVC burden is by $>80\%$ or to <5000 PVCs per 24 hours) with ablation has been shown to improve LVEF, ventricular dimensions, mitral regurgitation, and functional status. A recent meta-analysis estimated a mean improvement of 12% in LVEF after PVC ablation, which was observed in the whole population of patients with frequent PVC and LV dysfunction. The magnitude of improvement is superior to that achieved by other heart failure treatments. Although improvement in LVEF after PVC ablation was initially described in patients with suspected PVC-induced cardiomyopathy, recent studies showed a comparable benefit in patients with previously diagnosed cardiomyopathy and therefore considered to have a “PVC-worsened” cardiomyopathy.³⁸ Importantly, the recurrence of PVCs (after initially successful ablation and subsequent normalization of LVEF) can again result in a decline of LVEF. Therefore long-term follow-up and reassessment of the PVC burden are recommended in these patients, particularly those whose PVCs were asymptomatic or pleomorphic.^{46,56,57}

Radiofrequency (RF) ablation now has cure rates of over 90%, which makes it a preferable option, given the young age of most patients with idiopathic VAs. Late recurrence (few months after an acutely successful ablation) of frequent PVCs (from the same area where the original predominant PVCs originated or from a different focus) can be observed in approximately 15% of the patients. Risk of recurrent PVCs after ablation is higher in patients who originally had multiple PVC morphologies, likely suggesting that nondominant PVCs can become dominant PVCs over time. Also, the risk of recurrence seems to be higher in patients in whom the PVCs originated from the papillary muscles.^{46,57}

Implantable Cardioverter-Defibrillator

ICD implantation is recommended in patients with prior cardiac arrest. ICD therapy also should be considered for patients with “malignant” idiopathic VAs that are found to trigger polymorphic VT or VF, especially those presenting with syncope and in whom the PVC trigger cannot be completely eliminated by catheter ablation.

Importantly, for patients presenting with frequent PVCs and LV systolic dysfunction (PVC-induced or PVC-worsened cardiomyopathy) who have a primary prevention indication for ICD implantation, it is advisable to consider therapeutic measures to reduce the PVC burden (such as catheter ablation) before implanting a prophylactic ICD. Elimination of PVCs with ablation has been shown to improve LVEF within a few months in the majority of these patients (especially those with PVC burden of $\geq 13\%$ at baseline) such that the patients no longer qualify for an ICD. Prophylactic ICD implantation in these patients

unfortunately often results in delivery of inappropriate shocks triggered by frequent nonsustained episodes of idiopathic VT. Therefore withholding the ICD and reevaluating within the first 6 months of ablation seems to be an appropriate and safe strategy.^{38,51}

ELECTROCARDIOGRAPHIC LOCALIZATION OF FOCAL VENTRICULAR TACHYCARDIA

Of all idiopathic VAs, approximately 70% arise from the ventricular OTs, more commonly in the RVOT. Up to 20% to 50% originate in the LV. For LV VAs, the aortic root (the right and left aortic sinuses of Valsalva or the commissure between the two sinuses) is the most common site of origin (70%). The LV summit accounts for 12%, while the LV ostium (septal para-Hisian, aortomitral continuity, and the mitral annulus) accounts for about 5% to 10%.^{58,59} Other less frequent sites of origin include the LV and RV papillary muscles, the moderator band, and cardiac crux (Table 23.1).^{3,22}

Due to the focal nature of most idiopathic VAs, the surface ECG is often very valuable for localizing the site of origin of the VT. Using the surface ECG to predict the site of origin of the OT VAS has important implications in preprocedural planning of the appropriate anatomical and cardiac access approach for mapping and ablation, and for counseling patients appropriately regarding anticipated procedural risks and outcome.

Importantly, the criteria for ECG localization of the site of origin of OT VAs utilize surface ECG electrodes accurately placed in standard anatomic positions. Even minor displacements of surface ECG electrodes can significantly alter the QRS morphology and adversely affect the diagnostic accuracy of surface ECG for localizing the VT focus. In particular, superior deviation of leads V_1 and V_2 in VAs originating from the LVOT can result in reduced R wave amplitude and R/S ratio, erroneously suggesting an RVOT origin, while inferior deviation of those leads in VAs of RVOT origin can result in increased R wave amplitude and R/S ratio, erroneously suggesting an LVOT origin. In addition, anterior displacement of the upper limb leads from shoulders to lateral chest wall (torso) can significantly reduce the R wave amplitude and reverse the QRS polarity in lead I, falsely suggesting a more anterior/leftward origin of RVOT VAs. Therefore verifying accurate positioning of the surface ECG leads is important, especially in the EP laboratory, where other patches on the chest frequently affect usual ECG lead placement.⁶⁰

Understanding the attitudinal anatomical relationships of the OTs and adjacent structures is critical for analyzing the ECG and predicting expected changes in QRS morphology when moving from one structure to the next. It is helpful to maintain a mental three-dimensional representation of the anatomical relationships as it lies within the chest (“attitudinally correct orientation”) while interrogating the ECG. With this in mind, R wave progression in precordial leads, and QRS frontal plane horizontal and vertical axis, are valuable for predicting the site of origin of OT VA.¹⁴

It is also important to note that while the ECG helps localize the region from which activation spreads across the ventricles, it does not necessarily identify the site of successful ablation. This is relevant, especially given the close anatomical relationship of the cardiac structures of the ventricular OT region.⁶¹

Precordial Transition

Lead V_1 is a unipolar lead positioned at the right anterior chest wall. Therefore VAs originating from anterior structures are expected to produce a predominantly negative deflection (i.e., LBBB pattern), whereas more posterior sites of origin produce more positive deflections (RBBB pattern). Since the RVOT and pulmonary artery are the most anterior cardiac structures, all VAs originating from these regions have an LBBB

TABLE 23.1 Common Sites of Origin for Idiopathic Ventricular Tachycardia

Sites of Origin	Prevalence	Mechanism	ECG Findings
1. Outflow tract VT RVOT	70%–80% of idiopathic VT	DAD-related triggered activity	LBBB inferior axis <ul style="list-style-type: none"> • Delayed R wave transition (at or after V₃ or later than sinus rhythm) • V₂ transition ratio^a <0.6
LVOT, aortic cusps, AMC	16% of outflow tract VT	DAD-related triggered activity	LBBB inferior axis <ul style="list-style-type: none"> • Early R wave transition • V₂ transition ratio ≥0.6 • Sometimes presents with >1 morphology
2. Fascicular VT Verapamil-sensitive VT	10%–15% of idiopathic VT	Macroreentry	Relatively narrow QRS <ul style="list-style-type: none"> • LPF: RBBB, LAD • LAF: RBBB, RAD
Focal Purkinje VT (Propranolol-sensitive automatic VT)	Rare	Enhanced automaticity	Relatively narrow QRS. <ul style="list-style-type: none"> • Depending on origin: LBBB (from RV distal Purkinje) or RBBB (from LV distal Purkinje)
3. Intracavity VT papillary muscle	2.4%–5.2% of idiopathic VT	Enhanced automaticity vs. DAD-related triggered activity	APM: RBBB (q in V ₁), inferior axis <ul style="list-style-type: none"> • PPM: RBBB (q in V₁), left superior axis. • RVPM: LBBB, more variable
Moderator band	2.5% of idiopathic VT	Enhanced automaticity vs. DAD-related triggered activity	LBBB with precordial transition later than V ₄ or later than sinus rhythm <ul style="list-style-type: none"> • Left superior axis • Relatively narrow QRS
4. Perivalvular VT tricuspid annulus	8% of idiopathic VT	Enhanced automaticity vs. DAD-related triggered activity	LBBB <ul style="list-style-type: none"> • R or r in lead I, R in V₆ • A negative component (QS, qs, Qr, or qr pattern) in lead aVR
Mitral annulus	5% of idiopathic VT	Enhanced automaticity vs. DAD-related triggered activity	RBBB <ul style="list-style-type: none"> • S (or s) wave in V₆ • Precordial transition in V₁ or between V₁ and V₂
5. Epicardial VT	1.8%–9.2% of idiopathic VT	Enhanced automaticity vs. DAD-related triggered activity	LBBB, early transition <ul style="list-style-type: none"> • R in V₆ • MDI^b >0.55 • AIV/GCV: inferior axis, abrupt loss of R waves in V₂ • Crux: left superior axis, positive concordance V₂–V₆

^aV₂ transition ratio = R/(R + S)_{VT} 4 R/(R + S)_{sinus} of V₂.

^bMDI = interval from earliest ventricular activation to the peak of the largest amplitude deflection/QRS duration.

AIV, Anterior interventricular vein; AMC, aortomitral continuity; APM, anterior papillary muscle; DAD, delayed afterdepolarization; ECG, electrocardiogram; GCV, greater cardiac vein; LAD, left-axis deviation; LAF, left anterior fascicle; LBBB, left bundle branch block; LPF, left posterior fascicle; LV, left ventricle; LVOT, left ventricular outflow tract; MDI, maximum deflection index; PPM, posterior papillary muscle; RAD, right-axis deviation; RBBB, right bundle branch block; RV, right ventricle; RVOT, right ventricular outflow tract; RVPM, right ventricular papillary muscle; VT, ventricular tachycardia.

From Tanawuttivat T, Nazarian S, Calkins H. The role of catheter ablation in the management of ventricular tachycardia. *Eur Heart J*. 2016;37:594–609.

configuration, with rare exceptions. Similarly, VAs originating from the anterior aspect of the LVOT (e.g., the right aortic sinus of Valsalva) typically exhibit an LBBB pattern. As the site of VT origin shifts progressively more posteriorly from the RVOT free wall toward the lateral mitral annulus (i.e., left aortic sinus, aortomitral continuity, LV summit, and lateral mitral annulus), the precordial transition (i.e., the first precordial lead where the R wave amplitude exceeds the S wave amplitude) becomes sequentially earlier, thereby transforming the precordial QRS morphology from a late transition LBBB pattern to a positively concordant RBBB pattern.¹⁴

Frontal Plane Horizontal Axis

Lead I primarily reflects the horizontal axis. Structures closer to the left axilla will produce a deeply negative complex in lead I (i.e., rightward axis); conversely, structures closer to the right axilla are strongly positive in lead I (i.e., leftward axis). Furthermore, leads II/aVL and III/aVR also have net leftward and rightward vectors, respectively. Hence, as the

site of origin of the VT moves progressively to the left (progressively from most rightward to leftward aspects of the RVOT, to the left aortic sinus, LV summit, and lateral mitral annulus), the QRS assumes progressively less positive/more negative deflection in lead I, a taller R wave in lead III than in lead II, and a larger S wave in lead aVL compared with lead aVR.¹⁴

Frontal Plane Vertical Axis

The inferior leads (II, III, and aVF) reflect the vertical axis. Given the high anatomical location of the left and right OTs in relation to the rest of the ventricles, all OT VAs exhibit positive deflections in the inferior leads (vertical axis). However, the magnitude of the inferiorly directed vector diminishes as the site of origin shifts from superior to inferior regions of the OT (such as from the subpulmonic region to the para-Hisian region). In addition, leads aVL and aVR exhibit QS complexes in the vast majority of OT VAs, as these two leads are not only leftward and rightward but also are superior leads. Therefore VAs

originating from the superior aspect of the ventricles produce negative deflection in leads aVL and aVR, whereas VAs arising from more apical locations exhibit positive deflections.

Right Ventricular Outflow Tract Tachycardias

VAs originating from the RVOT typically display LBBB morphology with a precordial QRS transition that begins no earlier than lead V₃ and more typically occurs in lead V₄. The frontal plane axis, precordial R/S transition, QRS width, and complexity of the QRS morphology in the inferior leads can more precisely indicate the origin of VT within the RVOT. For practical considerations, the RVOT can be viewed as two opposing crescentic surfaces: (1) an anterolateral or “free wall” surface and (2) a posteromedial (“septal”) surface. Both the free wall and posteromedial surfaces have leftward and rightward extensions. The RVOT free wall surface is the more anterior surface and will therefore give rise to VAs with a later precordial transition (V₄ or V₅); VAs from the “septal” surface transition earlier (typically V₃ or V₄).¹⁴

Most RVOT VAs originate from the anterosuperior aspect of the leftward (“septal”) aspects, just under the pulmonic valve. These tachycardias produce a characteristic surface ECG appearance with tall positive QRS complexes in leads II, III, and aVF, and large negative complexes in leads aVR and aVL (Fig. 23.5). The QRS morphology in lead I typically is multiphasic and has a net QRS vector of zero or is only modestly positive (see Fig. 23.2).

It is important to recognize that the prediction of the precise origin of OT VAs can still be challenging because of the close anatomical relationship of the different anatomical compartments of the OT region. For example, an R/S transition zone in precordial lead V₃ is common in patients with OT VAs, with a prevalence of up to 58%. The prevalence of R/S transition in lead V₃ in RVOT VAs is not statistically different from those originating outside the RVOT; therefore the predictive value for this ECG criterion is low. Approximately 50% of OT VAs with an R/S transition in V₃ could be successfully ablated from the RVOT, while other anatomical approaches can be required in other patients (including the LV, the aortic sinus of Valsalva, the CS, the pulmonary artery, and the epicardium via a percutaneous pericardial puncture).

Posteromedial versus free wall RVOT. QRS duration less than 140 milliseconds, monophasic R wave without notching (i.e., no RR' or Rr') in leads II and III, and early precordial transition (by lead V₄) suggest a posteromedial (“septal”) origin. On the other hand, the triphasic RR' or Rr' waves in leads II and III in VT of free wall origin probably reflect the longer QRS duration and the phased excitation from the RV free wall to the LV (see Fig. 23.5).

Left (anteromedial) vs. right (posterolateral) aspect of the RVOT. In general, a QS complex in lead I is generated from sites at or near the anteromedial aspect of the RVOT (the most leftward portion of the RVOT in the supine anteroposterior orientation). As the site of origin moves rightward, on either the posterior or the anterior wall, R waves appear in lead I and become progressively dominant and the QRS axis becomes more leftward. Similarly, a QS amplitude in aVL greater than that in aVR suggests an origin in the left side of the RVOT; a QS amplitude in aVR greater than that in aVL suggests an origin in the right side (see Fig. 23.5).

Superior vs. inferior aspect of the RVOT. The R wave amplitude tends to be larger in leads V₁ and V₂ at superior and leftward locations. As the site of origin shifts to the right or inferiorly, there is a trend toward lower right precordial R wave amplitude and a shift in the precordial transition zone to the left. Furthermore, R wave amplitude in lead V₂ or “r” wave amplitude in leads V₁ and V₂ greater than 0.2 mV suggests a superior origin. In addition, the closer the origin to the pulmonic valve, the more rightward and inferior the axis (i.e., R wave taller in lead III than in lead II) because of the anatomical leftward

location of the pulmonic valve and lead III being an inferior and rightward lead; the more posterior and inferior the origin, the more leftward the axis (see Fig. 23.5). Also, lead aVL (being a left-sided lead) becomes isoelectric or slightly positive as the site of origin moves inferiorly (close to the HB region), whereas aVR (being a right-sided lead) remains negative.

Suprapulmonic vs. subpulmonic RVOT. Because of the superior and leftward location of these sites, VAs arising above the pulmonic valve (particularly from the left pulmonic cusp) are associated with a small but definite vector toward the right, resulting in a small initial R wave in lead V₁. In addition, suprapulmonic origins exhibit a strong right inferior frontal plane axis (QS or rS wave in lead I, large R waves in leads II, III, aVF, and deep QS complexes in leads aVR and aVL, with the R wave being taller in lead III than in lead II and the S wave being deeper in aVL than in aVR). Those VAs also tend to display an R/S ratio in lead V₂ and R wave amplitude in inferior leads that are larger than those observed in subpulmonic RVOT VAs. However, moderate overlap exists between VAs originating above the pulmonic valve and RVOT VAs, and because the RVOT is the exit site of VT arising from the pulmonary artery, discriminating between the two groups using ECG parameters can be difficult.^{19,20}

Right Versus Left Ventricular Outflow Tract Tachycardias

Because of the close anatomical relationship between the RVOT and LVOT, VAs arising from the LVOT/aortic root can have similar ECG morphology to those originating from the RVOT. However, the presence of a prominent R wave in leads V₁ and V₂, and RS transition in leads V₁ or V₂ are characteristic of an LVOT origin (because of the posterior location of LVOT relative to the anterior precordial leads), whereas the absence of an R wave in lead V₁ and precordial transition zone in lead V₄, V₅, or V₆ predicts an RVOT origin (see Fig. 23.5). However, it is important to recognize that about 20% of VAs with arising from the aortic sinuses of Valsalva show a late QRS transition after lead V₃, and approximately 25% of the VAs with an aortic sinus of Valsalva origin had a preferential localized breakout site in the RVOT, which may also explain the difficulty in using ECG algorithms for accurate localization of VT arising in the aortic cusps.¹⁷

Given the continuity between the posterior RVOT and the anterior LVOT/aortic root, a very similar R wave in lead V₃ may be seen with arrhythmia that originates in either structure, and R/S transition in lead V₃ is not specific.¹⁴ In the latter setting, several algorithms using the ECG characteristics, especially the QRS transition in the precordial leads, have been proposed to help distinguish origins from the LVOT/aortic root versus RVOT, including the R wave duration index, R/S wave amplitude index, transitional zone index, V₂ transition ratio, and V₂S/V₃R index (Table 23.2; Fig. 23.6).

R wave duration index. R wave duration in leads V₁ or V₂ is determined from the onset of the QRS complex to the transition point between the R wave and the isoelectric line. The R wave duration index is calculated as a percentage by dividing the total QRS complex duration by the longer R wave duration in lead V₁ or V₂ (see Fig. 23.6). An R wave duration index of ≥50% suggests an aortic cusp origin in patients with a typical LBBB morphology and an inferior axis.⁶²

R/S wave amplitude index. The R/S wave amplitude ratio in leads V₁ and V₂ is measured from the QRS complex peak or nadir to the isoelectric line, expressed as a percentage. The R/S wave amplitude index is defined as the greater value of the R/S wave amplitude ratio in lead V₁ or V₂ (see Fig. 23.6). An R/S wave amplitude index ≥30% suggests an aortic cusp origin in patients with a typical LBBB morphology and an inferior axis.⁶²

V₂ transition ratio. The V₂ transition ratio compares the R wave amplitude divided by total QRS amplitude (i.e., R/[R + S]) in lead V₂

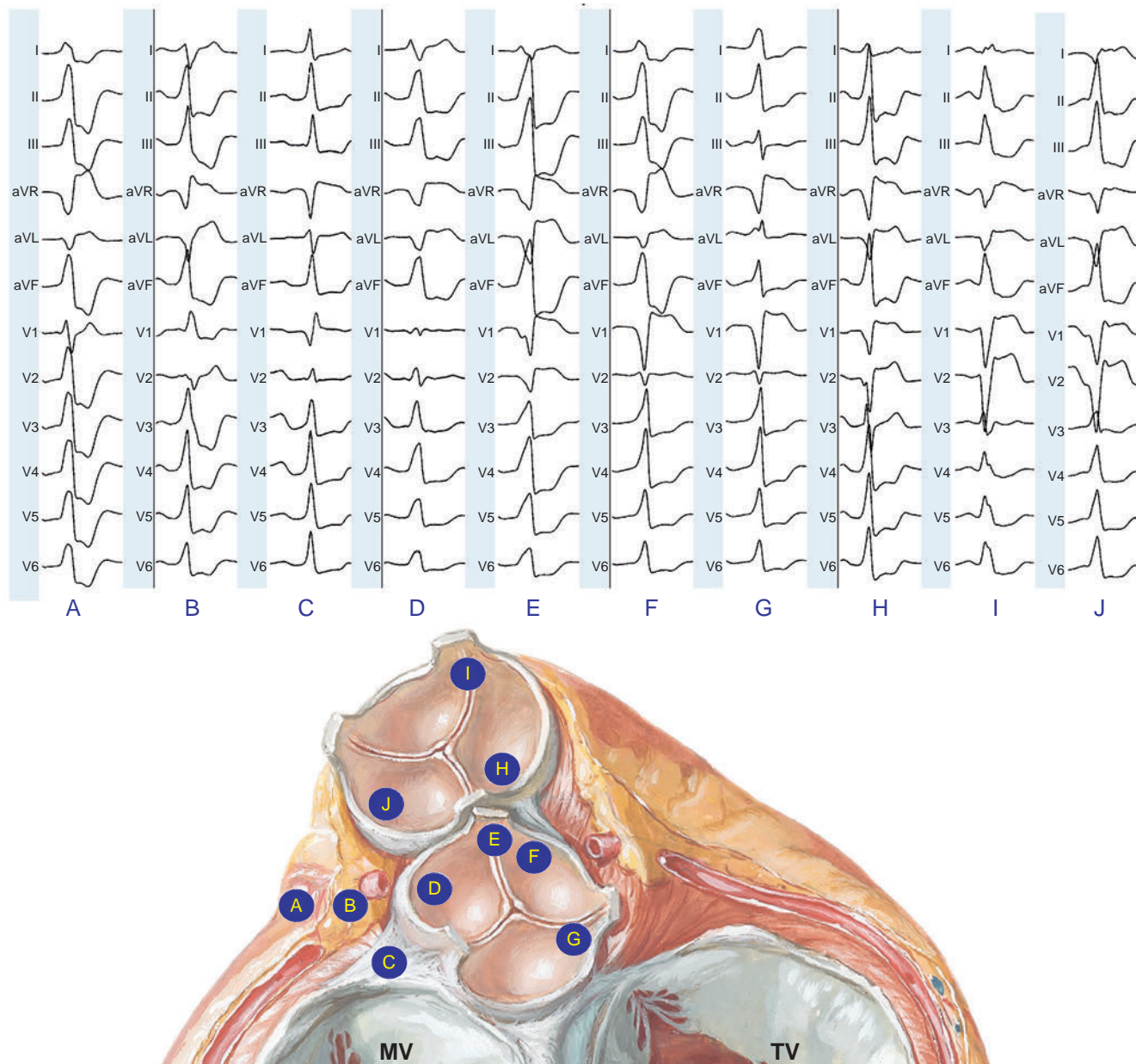


Fig. 23.5 Surface Electrocardiogram (ECG) QRS Morphology of Premature Ventricular Complexes (PVCs) Originating from the Ventricular Outflow Regions. Representative surface 12-lead ECG of QRS morphology during PVCs (*top panels*) with the corresponding location of the successful ablation site on an anatomical illustration (*bottom*). (A) Inferior mitral annular; (B) Lateral mitral annular; (C) Anterior mitral annular; (D) Left ventricular summit; (E) Aortomitral continuity; (F) Right para-Hisian; (G) Anterior tricuspid annular; (H) Lateral anterior tricuspid annular; (I) Posterolateral anterior tricuspid annular; (J) Inferior tricuspid annular. Schematic illustration of tricuspid valve (TV) and mitral valve (MV) is shown at the bottom. (From Netter Images [www.netterimages.com] with permission.)

during VT with that during NSR (see Fig. 23.6). The V_2 transition ratio can help distinguish between LVOT and RVOT origins in patients with lead V_3 precordial transition. A transition ratio ($R/[R + S]_{VT} \div R/[R + S]_{NSR}$) of ≥ 0.60 is highly suggestive of an LVOT origin (with a sensitivity of 95% and a specificity of 100%).^{14,63}

V_2S/V_3R index. The V_2S/V_3R index is defined as the S-wave amplitude in lead V_2 divided by the R-wave amplitude in lead V_3 during the OT-VT (see Fig. 23.6). The V_2S/V_3R index is significantly smaller for LVOT origins than RVOT origins. An index of ≤ 1.5 predicted an LVOT origin with a sensitivity of 89% and specificity of 94%. In

the area under the curve and accuracy, the V_2S/V_3R index was found superior to other previously proposed ECG criteria in an analysis of all OT VAs.⁶⁴

Transitional zone index. Approximately 35% of patients with OT VAs present a shift of the precordial transitional zone during NSR. Cardiac rotation can result in a similar shift in the precordial transitional zone also during VT. The transitional zone index corrects the transitional zone to cardiac rotation (comparing the R/S transitional zone in precordial leads during VT with that during NSR) and can be useful for differentiating RVOT from aortic cusp origin with high sensitivity and

TABLE 23.2 Comparison of the Accuracy Among the ECG Criteria for Predicting the LVOT Origin of VT

	Sensitivity	Specificity	PPV	NPV
All Patients (n = 207)				
V ₂ S/V ₃ R index ≤1.5	89%	94%	84%	96%
Transitional zone index <0	83%	93%	80%	94%
R/S wave amplitude index ≥30%	79%	86%	66%	92%
R wave duration index ≥50%	45%	92%	67%	83%
Patients With a Lead V₃ Precordial Transition (n = 77)				
V ₂ S/V ₃ R index ≤1.5	94%	78%	79%	94%
Transitional zone index <0	78%	88%	85%	82%
V ₂ transition ratio	81%	61%	64%	78%
R/S wave amplitude index ≥30%	78%	68%	68%	78%
R wave duration index ≥50%	36%	88%	72%	61%

ECG, Electrocardiographic; LVOT, left ventricular outflow tract; NPV, negative predictive value; PPV, positive predictive value; VT, ventricular tachycardia.

From Yoshida N, Yamada T, McElderry HT, et al. A novel electrocardiographic criterion for differentiating a left from right ventricular outflow tract tachycardia origin: the V₂S/V₃R index. *J Cardiovasc Electrophysiol*. 2014;25:747–753.

specificity, regardless of cardiac rotation. The transitional zone score is graded with 0.5-point increments according to the site of the R wave transition. If the amplitudes of the R and S waves are equal (i.e., R/S-wave amplitude ratio is between 0.9 and 1.1) in any precordial lead (V₁ to V₆), the transitional zone score is the same as the lead number (e.g., transitional zone in V₂ = 2-point, transitional zone between V₂ – V₃ = 2.5-point, V₃ = 3-point, and V₃ – V₄ = 3.5-point). The transitional zone index is defined as transitional index score during VT minus transitional zone score during NSR (Fig. 23.7). When the transitional zone during VT occurs in one or more precordial leads earlier than during NSR (i.e., transitional zone index <0), an aortic cusp origin is favored, even when the transitional zone during VT occurs later than lead V₂.⁶⁵

Aortic Root Ventricular Tachycardias

The ECG discrimination characteristics between VAs originating from the RVOT and LVOT/aortic sinus of Valsalva regions are discussed above. For LVOT VAs, the presence of an S wave in leads V₅ or V₆ suggests an infravalvular origin. In addition, the presence of an R wave in lead aVL argues against an origin in the aortic sinuses of Valsalva.

Interestingly, the behavior of idiopathic VAs can potentially suggest the site of origin. PVCs occur at relatively fixed coupling intervals from the preceding normal QRS complex in most patients. A recent report found that highly variable coupling intervals from the prior QRS complex characterize foci in the aortic cusps and great cardiac vein compared with PVCs from other regions. It was postulated that PVCs originating from sites within narrow, relatively isolated muscle fibers such as the aortic cusps and great cardiac vein may behave more like a modulated parasystolic focus than a more typical PVC focus, and that this behavior may explain the differences in the coupling intervals. Lacking large amounts of surrounding myocardium to provide electrotonic inhibition,

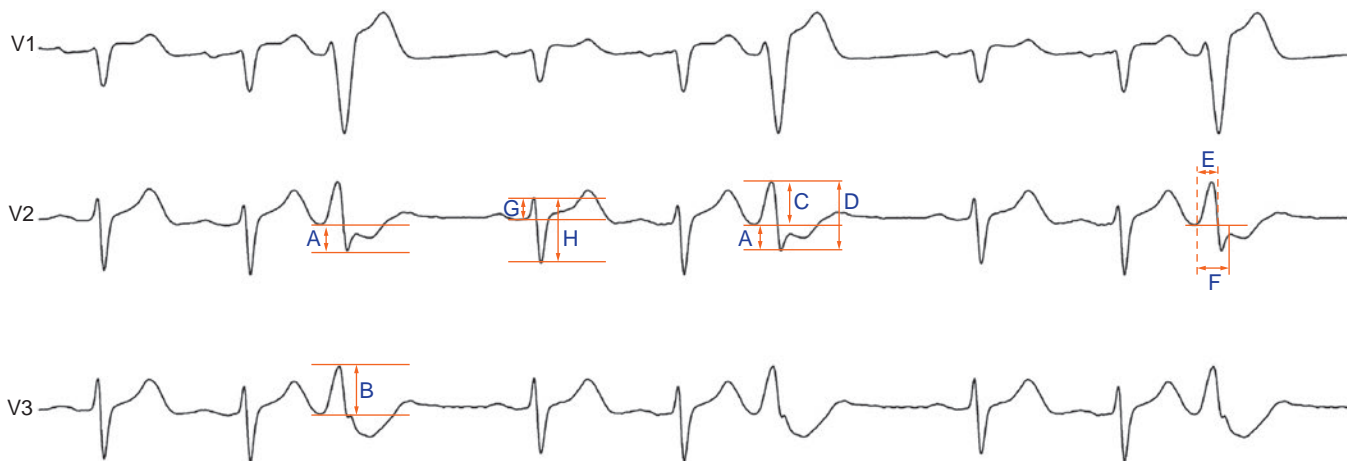


Fig. 23.6 Electrocardiogram (ECG) Criteria for Predicting the Left Ventricular Origin of Outflow Tract Ventricular Tachycardia. Surface ECG leads V₁ to V₃ showing normal sinus rhythm with frequent premature ventricular complexes (PVCs) originating from the ventricular outflow tract. The measurements are as follows:

- A = S-wave amplitude (during PVC) in lead V₂ (mV).
- B = R-wave amplitude (during PVC) in lead V₃ (mV).
- C = R-wave amplitude (during PVC) in lead V₂ (mV).
- D = Total QRS amplitude (during PVC) in lead V₂ (mV).
- E = R-wave duration (during PVC) in lead V₂ (mV).
- F = Total QRS duration (during PVC) in lead V₂ (mV).
- G = R-wave amplitude (during sinus rhythm) in lead V₃ (mV).
- H = Total QRS amplitude (during sinus rhythm) in lead V₂ (mV).

ECG criteria are calculated as follows:

- V₂S/V₃R index = A/B.
- V₂ transition ratio = C/D ÷ G/H.
- R wave duration index = E/F.
- R/S wave amplitude index = C/A.

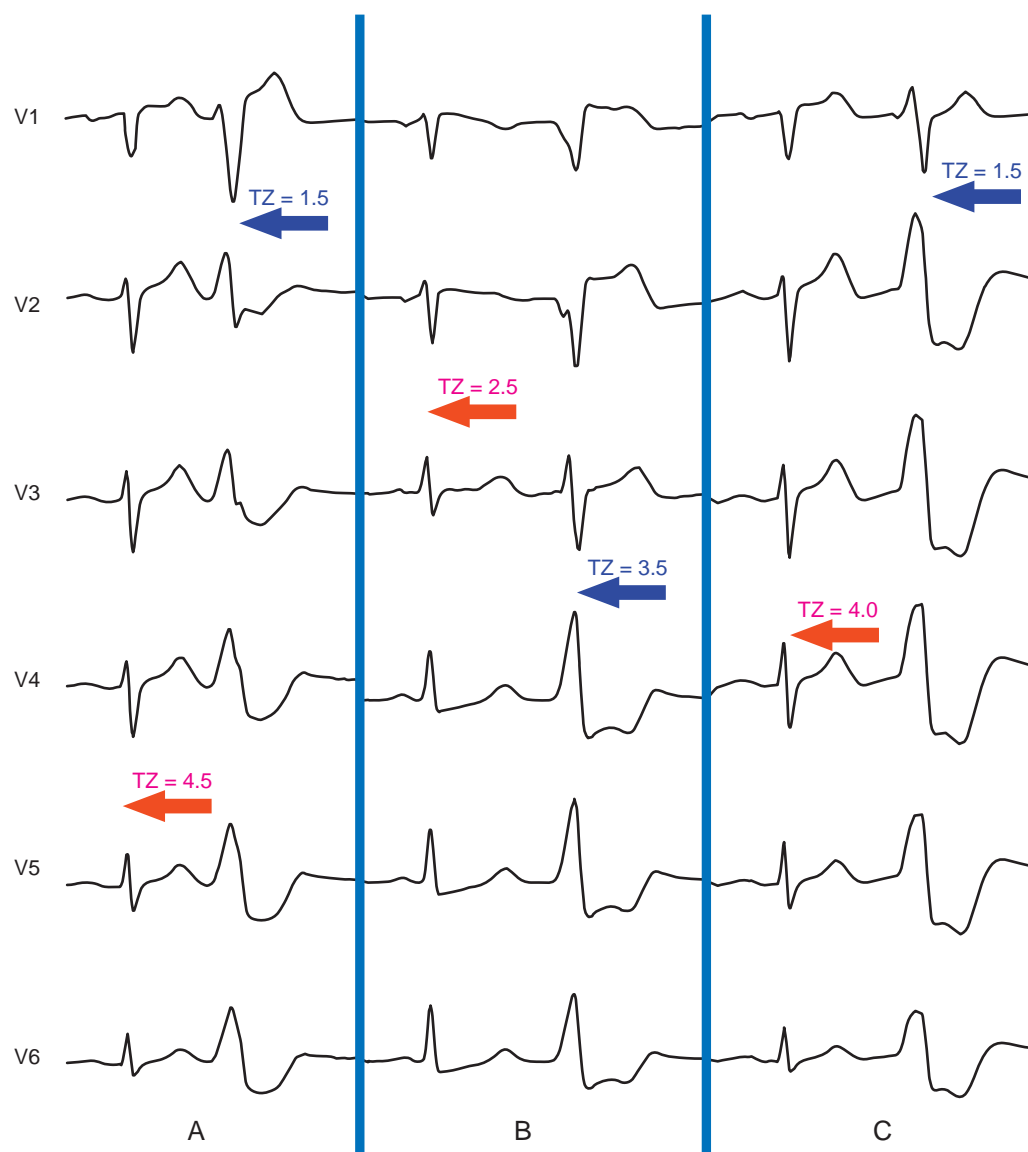


Fig. 23.7 Example of Calculating the Transitional Zone (TZ) Score and TZ Index. Red arrows indicate TZ scores during normal sinus rhythm (NSR). Blue arrows indicate the TZ scores of outflow tract premature ventricular complexes (PVCs). TZ index is calculated according to the following formula: TZ score of PVC minus TZ score of NSR. TZ index is -3 in (A) 1.0 in (B) and -2.5 in (C).

the narrow muscle strands in the aortic cusps and extending along the great cardiac vein may be more prone to partial entrance block, providing relative isolation and protection from the PVC focus from the modulation by the sinus rhythm.⁶⁶

Right aortic sinus of Valsalva. The right sinus of Valsalva lies directly posterior to the midposterior “septal” aspect of the RVOT; thus the VAs originating from both regions frequently appear similar. In fact, VAs originating from the aortic sinus of Valsalva often (25%) show preferential conduction to the RVOT, which can render some algorithms using the ECG characteristics less reliable. Approximately 20% of the VAs with an aortic sinus of Valsalva origin in that report showed a late QRS transition after V₃ (see Fig. 23.5). Nonetheless, the ECG criteria discussed above can help distinguish between VAs originating from the RVOT and LVOT/aortic sinus of Valsalva regions.^{67,68}

Left aortic sinus of Valsalva. Relative to the right sinus of Valsalva, the left sinus is positioned leftward, posteriorly, and more cranially

(superiorly). As such, when compared with the right sinus of Valsalva, VAs originating from the left sinus exhibit less positive (and often negative) deflection in lead I, larger R waves in the inferior leads, and taller R wave amplitude in lead III compared with lead II.¹⁴ In the precordial leads, the QRS is predominantly positive by lead V₁ or V₂ with VT from the left aortic cusp. Also, left aortic sinus of Valsalva VAs initially depolarize the LV and typically have a multiphasic QRS complex such as an M or W pattern in lead V₁, suggesting transseptal activation (see Fig. 23.5). A simple qR complex or a monophasic R wave in lead V₁ suggests an origin near the aortomitral continuity. In young patients with a vertical heart, the QRS complex in lead I can be negative in and around both the left and right aortic sinus of Valsalva regions. In patients with a horizontal heart, the area surrounding the aortic valve will be directed rightward relative to the LV apex–lateral wall, and a positive QRS complex in lead I can be seen. In general, when comparing origins from the right versus the left sinuses of Valsalva, RBBB morphology in lead V₁

argues against origins from the right sinus of Valsalva. In addition, the ratio of the R wave amplitude ratio in leads III/II is significantly greater (>0.9) for VAs with a left sinus of Valsalva origin than for those with a right sinus of Valsalva origin.^{14,67}

Right-left aortic sinus commissure. A common site of origin is the junction between the right and left aortic sinuses (which abuts the midposterior “septal” aspect of the RVOT). Because of the anatomical location, VAs with this origin seem to be associated with ECG findings that are between those of left and right sinus morphologies. This site of origin is often recognized by a QS complex with notching of the downstroke in lead V_1 with an intermediate precordial transition (relative to the right and left sinuses of Valsalva; see Fig. 23.5). A qRS pattern in leads V_1 to V_3 is very helpful for predicting an origin in the junction between the right and left sinuses.

Noncoronary aortic sinus of Valsalva. VAs originating from the noncoronary sinus of Valsalva tend to have similar QRS morphology to those originating from the right sinus of Valsalva, including an LBBB pattern, left superior or inferior axis, upright R wave in lead I, and frequent presence of S wave in lead III (see Fig. 23.5). However, several other ECG characteristics can help predict an origin from the noncoronary sinus, including a narrower QRS duration (typically <150 milliseconds), smaller lead III/II ratio (typically <0.65), a bifid QRS in lead V_1 , early precordial transition, and a negative QRS complex in aVL. Of note, foci from the noncoronary cusp predominantly exhibit VT rather than PVCs.^{24,69–71}

Basal Left Ventricular Tachycardias

The LV base includes the subaortic septal para-Hisian region, aortomitral continuity, as well as ventricular regions in close proximity to the mitral annulus. The majority of these VAs originate from the aortomitral continuity, and less commonly from the lateral, posterior, or posteroseptal mitral annulus. VAs arising from the left septal para-Hisian region typically exhibit a relatively narrow QRS duration with LBBB pattern, an early precordial transition (at or before lead V_3), and predominantly positive vector in lead I. More laterally, the aortomitral continuity produces VAs with a signature qR pattern (i.e., a fusion between LBBB and RBBB patterns) with broad monophasic R waves across the precordial leads (see Fig. 23.5). As the site of origin moves laterally (superolateral and lateral mitral annulus), the initial vector is directed away from lead V_1 , resulting in RBBB pattern (monophasic R waves or Rs complexes) in lead V_1 , and either no precordial transition or a late appearing s wave (in lead V_5 or V_6 ; for inferolateral basal LV sites). Posterior annular VAs display a dominant R in lead V_1 , whereas posteroseptal annular foci are characterized by a negative QRS component in lead V_1 (qR, qr, rs, rS, or QS; Fig. 23.8).

Lead I polarity transitions from predominantly positive for septal (anterior or posterior) annular foci to predominantly negative for lateral annular locations.¹⁴ Also wider QRS durations and notching in the late phase of the QRS in the inferior leads characterize the lateral free wall as compared with more medial/septal annular locations.

QRS polarity in the inferior leads is positive in VAs originating from the anterior/anterolateral annular locations, and negative during VAs arising from the posterior and posteroseptal mitral annulus. In addition, lead III/II R wave amplitude ratio becomes greater as sites of origin move from antero-septal to lateral annular locations. Also, lead III/II Q wave amplitude ratio is greater in posteroseptal VAs than in posterior annular VAs.

In LVOT VAs, an abrupt loss of the R wave in lead V_2 compared to leads V_1 and V_3 suggests an origin close to the anterior interventricular sulcus (anatomically opposite to lead V_2), which is the septal aspect of the LV summit, and in close proximity to the left anterior descending coronary artery (see Fig. 23.5).⁷²

Left Ventricular Summit Tachycardias

The LV summit is the most superior aspect of the “epicardial” LVOT. Hence VAs originating from this region exhibit the classic slower spread of activation from a focus on the epicardial surface relative to the endocardium and delayed global ventricular activation resulting from later engagement of the His-Purkinje network. Several ECG characteristics can help distinguish epicardial idiopathic VAs from endocardial arrhythmias, including (1) slurring of the initial portion of the QRS complex (pseudo-delta wave ≥ 34 milliseconds), (2) long R-wave peak time (i.e., the interval from the beginning of the QRS complex to the time of initial downstroke of the R wave after it has peaked [previously known as the intrinsicoid deflection] ≥ 85 milliseconds) in lead V_2 , and (3) shortest precordial RS complex of greater than 120 milliseconds. The degree of initial QRS slurring, as measured by the *maximal deflection index* (defined as the quotient of the time from QRS onset to maximal deflection [i.e., the largest positive or negative amplitude deflection] in precordial leads divided by the total QRS duration), can help identify epicardial LV summit VAs. A delayed shortest precordial maximal deflection index (≥ 0.55) discriminates LV summit VAs from those originating within the aortic cusps.¹⁴ Similarly, a peak deflection index (determined in the inferior lead presenting the tallest R wave by dividing the time from the QRS onset to the peak QRS deflection by a total QRS duration) of greater than 0.6 predicts an epicardial LV summit origin.⁷³

VAs arising from the LV summit exhibit either LBBB or, less frequently, RBBB pattern in lead V_1 . As noted, VAs arising from the aortomitral continuity display a characteristic qR pattern, whereas VAs originating from more posterior and lateral structures (e.g., proximal segment of the great cardiac vein, superior/lateral mitral annulus) generally exhibit an RBBB pattern (see Fig. 23.8). As the site of origin moves toward the distal part of the great cardiac vein, closer to the antero-septal myocardium (near junction of the great cardiac and anterior interventricular veins), the initial vector is directed away from V_1 , resulting in RBBB morphology. However, the precordial transition of the arrhythmia will invariably be earlier than that of the sinus rhythm QRS. VAs originating more distally along the anterior interventricular vein as it courses apically within the interventricular groove exhibit an LBBB pattern with a later precordial transition (generally after V_2).¹⁴

Because of its superior location in the LV, VAs originating from the LV summit uniformly exhibit larger R wave amplitudes in the inferior leads. However, R wave amplitude ratio in leads III/II can vary according to the location of VT focus within the LV summit. As the site of origin shifts progressively more laterally (from the superior region of the summit toward the inferior region then toward the lateral mitral annulus), R wave amplitude becomes progressively larger in lead III as compared to lead II (concurrent with progressively more steeply negative complexes in lead I). R wave amplitude ratio in leads III/II ratio of greater than 1.25 can predict the requirement of a pericardial approach for VT ablation (i.e., origins from the inferior aspect of the LV summit).^{14,74}

Similarly, the aVL/aVR Q-wave ratio was strongly correlated with the anatomical distance between the successful ablation site and the apex of the LV summit; the longer distance away from the apex of the LV summit, the larger the aVL/aVR Q-wave ratio. This indicates that the ECG vectors would shift laterally and inferiorly if the distance between the VT and the apex of the LV summit increased. Also, the aVL/aVR Q-wave ratio was found to predict the approach to successful ablation; the aVL/aVR Q-wave ratio was significantly higher for VAs requiring an epicardial approach, followed by VAs arising from the coronary venous system, subvalvular area, and aortic cusp. An aVL/aVR Q-wave ratio of less than 1.45 predicted successful ablation from

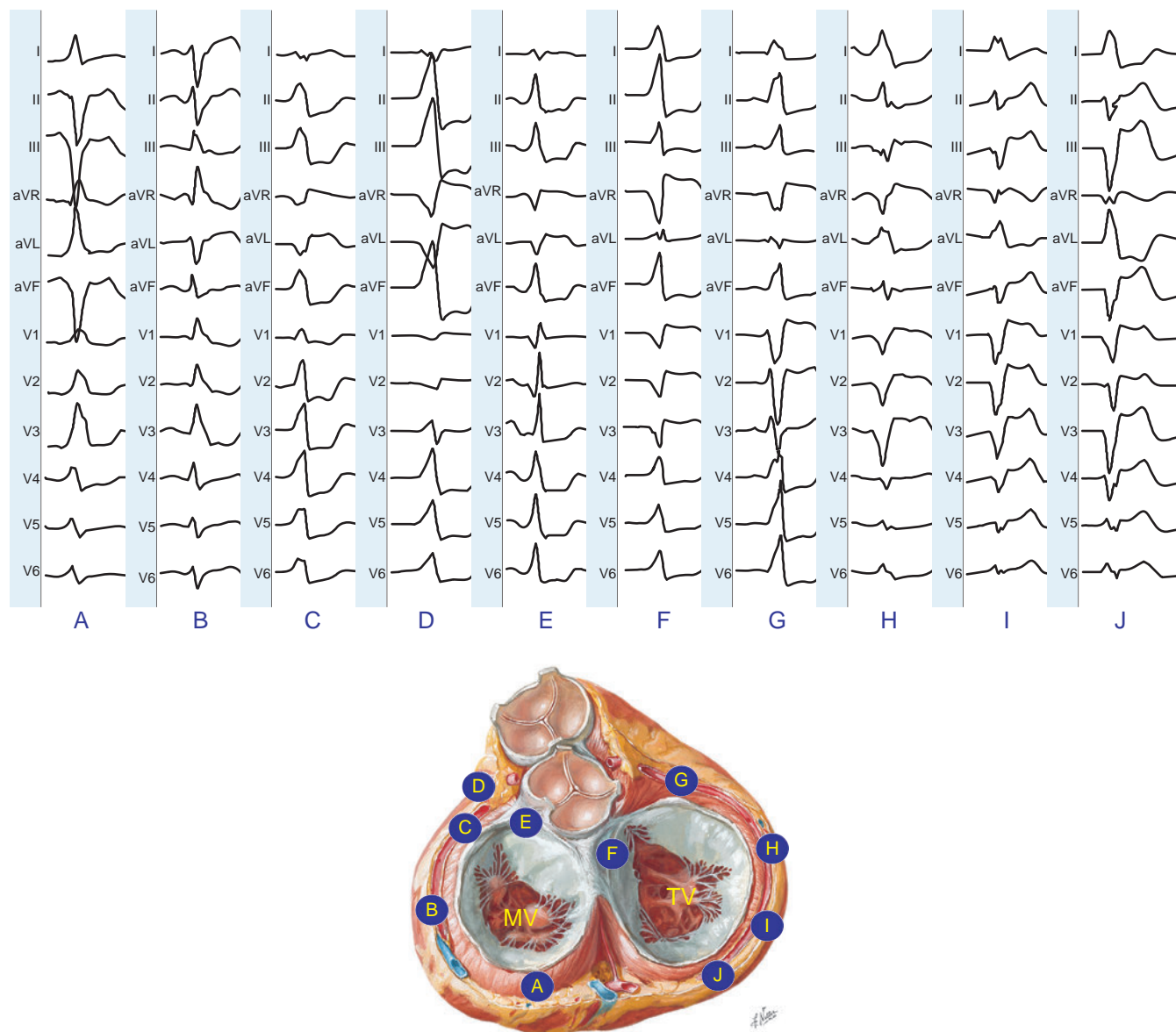


Fig. 23.8 Surface Electrocardiogram (ECG) QRS Morphology of Premature Ventricular Complexes (PVCs) Originating from the Perivalvular Regions. Representative surface 12-lead ECG of QRS morphology during PVCs (*top panels*) with the corresponding location of the successful ablation site on an anatomical illustration (*bottom*). (A) Left ventricular (LV) summit; (B) Septal aspect of the LV summit; (C) Aortomitral continuity; (D) Left sinus of Valsalva; (E) Commissure between the left and right sinuses; (F) Right sinus of Valsalva; (G) Noncoronary sinus of Valsalva; (H) Posterolateral right ventricular outflow tract (RVOT); (I), RVOT free wall; (J) Posteromedial RVOT. Anatomical illustration of valvular annuli is shown at the bottom MV, Mitral valve; TV, tricuspid valve. (From Netter Images [www.netterimages.com] with permission.)

aortic sinus of Valsalva or subvalvular approaches, whereas an aVL/aVR Q-wave ratio of greater than 1.75 indicated the need for a pericardial approach (see [Fig. 23.8](#)).^{28,75}

Because of its superior location in the LV, VAs originating from the superior region of the LV summit (the “inaccessible region” close to the apex of the summit) typically exhibit an LBBB pattern, larger R wave amplitudes in the inferior leads, and absence of an S wave in leads V₅ to V₆.¹⁴ When LV summit VAs exhibit an RBBB pattern, a transition zone earlier than lead V₁, aVL/aVR amplitude ratio of greater than 1.1, and S waves in V₅ to V₆, those VAs are likely to be cured by catheter ablation within the great cardiac or anterior interventricular veins. When LV summit VAs exhibit a lead III/II amplitude ratio of greater than

1.25 and lead aVL/aVR amplitude ratio of greater than 1.75, those VAs are likely to require a pericardial approach for ablation.^{22,74,76}

Left Ventricular Papillary Muscle Tachycardias

VAs can arise from the posterior or, less commonly, anterior LV papillary muscles. VAs from the papillary muscles exhibit a RBBB pattern in lead V₁ and RS transition at leads V₃ to V₅. VAs from the anterior papillary muscle demonstrate a rightward inferior axis (negative in leads I and aVL, positive in lead aVR) and frequently inferior lead discordance (negative in lead II, positive in lead III), whereas VAs from the posterior papillary muscle demonstrate left superior axis (negative in leads II and III).³¹

Of note, the ECG morphology of VAs originating from the LV papillary muscle can mimic that of fascicular VAs. Nonetheless, papillary muscle VT has a broader QRS complex than that of fascicular VT (150 ± 15 milliseconds vs. 127 ± 11 milliseconds). In addition, the presence of an rsR' pattern in lead V_1 (with r smaller than R') favors fascicular over papillary muscle foci; papillary muscle VAs typically exhibit qR or R in lead V_1 . The shorter QRS duration and lead V_1 morphology (mimicking typical RBBB pattern) likely reflect the proximal exit of fascicular VAs from the His-Purkinje system (HPS) and early engagement of the Purkinje system in the depolarization of the LV. Furthermore, spontaneous variations in QRS morphology occur relatively frequently during VAs originating from the LV papillary muscles, a feature that can help distinguish these VAs from fascicular VT, the latter being a reentrant tachycardia with a consistent QRS morphology. Unlike fascicular VTs, papillary muscle foci are less likely to present as sustained VT.^{34,77}

Compared with papillary muscle and fascicular foci, VAs originating close to the mitral annulus exhibit positive precordial concordance because of the more basal location of those foci. An R/S ratio ≤ 1 in lead V_6 for VAs in the LV anterolateral region also suggests papillary muscle VT.⁷⁷

Cardiac Crux Ventricular Tachycardias

Cardiac crux VAs exhibit a left superior axis and QS pattern in the inferior leads. A prominent R wave ($R > S$) in lead V_2 is observed in the majority of cases. Additional ECG features include those of other “epicardial” VAs, including a pseudo-delta wave ≥ 34 milliseconds and precordial maximum deflection index (i.e., the interval from QRS onset to the peak of the largest amplitude deflection in each precordial lead, taking the lead with the shortest time, divided by QRS duration) of ≥ 0.55 .³³

Basal crux VAs exhibit a left superior axis and an LBBB pattern with either negative or isoelectric pattern in lead V_1 and $R > S$ in lead V_6 . In contrast, apical crux VAs exhibit a deep S or rS wave in lead V_6 , $R > S$ in lead aVR , and either an RBBB or an LBBB pattern in lead V_1 . Those with an RBBB pattern display a prominent R wave in lead V_1 with transition to rS or qS in lead V_6 . VAs with an LBBB pattern exhibit early precordial transition (in lead V_2) with late transition to rS or qS in lead V_6 , (resulting in a characteristic R wave in lead V_2 that is taller than in leads V_1 or V_3). Occasionally, the QRS morphology in lead V_1 changes spontaneously and abruptly from RBBB to LBBB pattern.³³

Basal crux VT should be distinguished from VAs originating from posteroseptal tricuspid or mitral annular regions. While basal crux VT exhibits a QS pattern in lead II, tricuspid annular VT shows an rS or RS wave in lead II. In addition, the R wave in lead V_2 is taller, and QRS duration is longer in basal crux VT as compared with tricuspid annular VT. On the other hand, mitral annular VT shows an rS wave in lead II and a variable pattern including (R , qR , and rS) in lead V_1 , in contrast with the QS pattern in lead V_1 characteristic of basal crux VT.³³

Apical crux VAs exhibiting an RBBB pattern can mimic VAs originating from the LV papillary muscle or left posterior fascicle. The apical crux is located more inferiorly compared with other LV posteroseptal locations such as papillary muscle or left posterior fascicle, and a combination of QS pattern or R/S ratio of less than 0.15 in lead V_6 , and a monophasic R in lead aVR can distinguish apical crux VAs from other adjacent sites. Of note, patients with arrhythmias originating from apical crux or left posterior fascicle are more likely to present with sustained or nonsustained VT rather than only PVCs compared with those with papillary muscle VAs. Also, patients with apical crux VAs more frequently present with syncope or cardiac arrest compared with patients with other VT origins.³⁴

Right Ventricular Papillary Muscle Tachycardias

RV papillary muscle VAs display an LBBB pattern with a QS or rS pattern in lead V_1 and a wider QRS complex and more prevalent notching than in RVOT VA. VAs arising from the anterior and posterior papillary muscles are frequently associated with a superior axis and a late R wave transition in the precordial leads (later than lead V_4), whereas septal papillary muscle VAs more often display an earlier precordial transition (in lead V_4 or earlier) and an inferior axis (due to the more basal insertion of the septal compared with the anterior and posterior papillary muscles). More than one PVC or VT morphology can be present in a significant proportion of patients with papillary muscle VAs. Compared with origins from the septum, VAs from the free wall exhibit longer QRS duration and deeper S waves in leads V_2 and V_3 .

Focal Purkinje Ventricular Tachycardias

Idiopathic focal VAs can arise from the Purkinje system in either ventricle. Focal Purkinje VTs (classified as “propranolol-sensitive automatic VTs”) can present as an accelerated idioventricular rhythm or VT and display chronotropic properties. Importantly, PVCs arising from the Purkinje system are particularly prone to induce polymorphic VT and VF (due to unclear mechanism). Hence patients presented with idiopathic VF can benefit from special attention to recording PVCs that suggest a Purkinje origin as a potential ablation target.³

Focal Purkinje VAs arising from the left HPS exhibit an RBBB pattern with either left- or right-axis deviation, and can be difficult to distinguish from fascicular VT (Fig. 23.9).

VTs originating from the right bundle (RB) and RV moderator band have been recently reported. The moderator band is a muscular structure that crosses from the septum to the RV free wall and supports the anterior papillary muscle of the tricuspid valve. The moderator band contains bundles of Purkinje fibers that cross subendocardially from the interventricular septum, through the moderator band (with no connection to the surrounding myocardium), and spread after the moderator band joins the anterior papillary muscle to the RV free wall, supplying the subendocardial ventricular plexus. VAs originating from the RB exhibit a classic LBBB morphology with sharp downstroke of the S wave and short rS duration (<70 milliseconds) in leads V_1 and V_2 , and late precordial transition (typically after V_4 or V_5).⁷⁸ VAs originating from the moderator band exhibit an LBBB pattern in lead V_1 with a late precordial transition pattern (typically after V_4) that is always later than that during NSR (see Fig. 23.9). Other ECG characteristics include a left superior frontal plane axis, a sharp downstroke of the QRS in the precordial leads, and a relatively narrow QRS width (due to the proximity to the right bundle and early incorporation of the HPS). Nonetheless, wide variations exist in the morphology and insertion sites of the moderator band, which results in a variety of ECG morphologies of VT originating from this structure. Within the RV, the late precordial transition and superior axis differentiate moderator band VAs from those originating in the RV base or septum, although moderator band VAs tend to display a later precordial transition than VAs originating from the septal RV papillary muscle. However, discrimination of anterior papillary muscle origin VAs is challenging, likely because of the similar insertion on the RV free wall and highly variable anatomy.³

Tricuspid Annular Ventricular Tachycardias

VAs arising from the tricuspid annulus demonstrate LBBB morphology and positive QRS polarity in leads V_5 and V_6 (see Fig. 23.8). Septal annular VAs exhibit early precordial transition (at lead V_3), narrower QRS complexes, and Qs in lead V_1 , whereas lateral annular foci have later precordial transition. Also, as the site of origin moves from medial/septal to lateral locations along the tricuspid annulus, the precordial

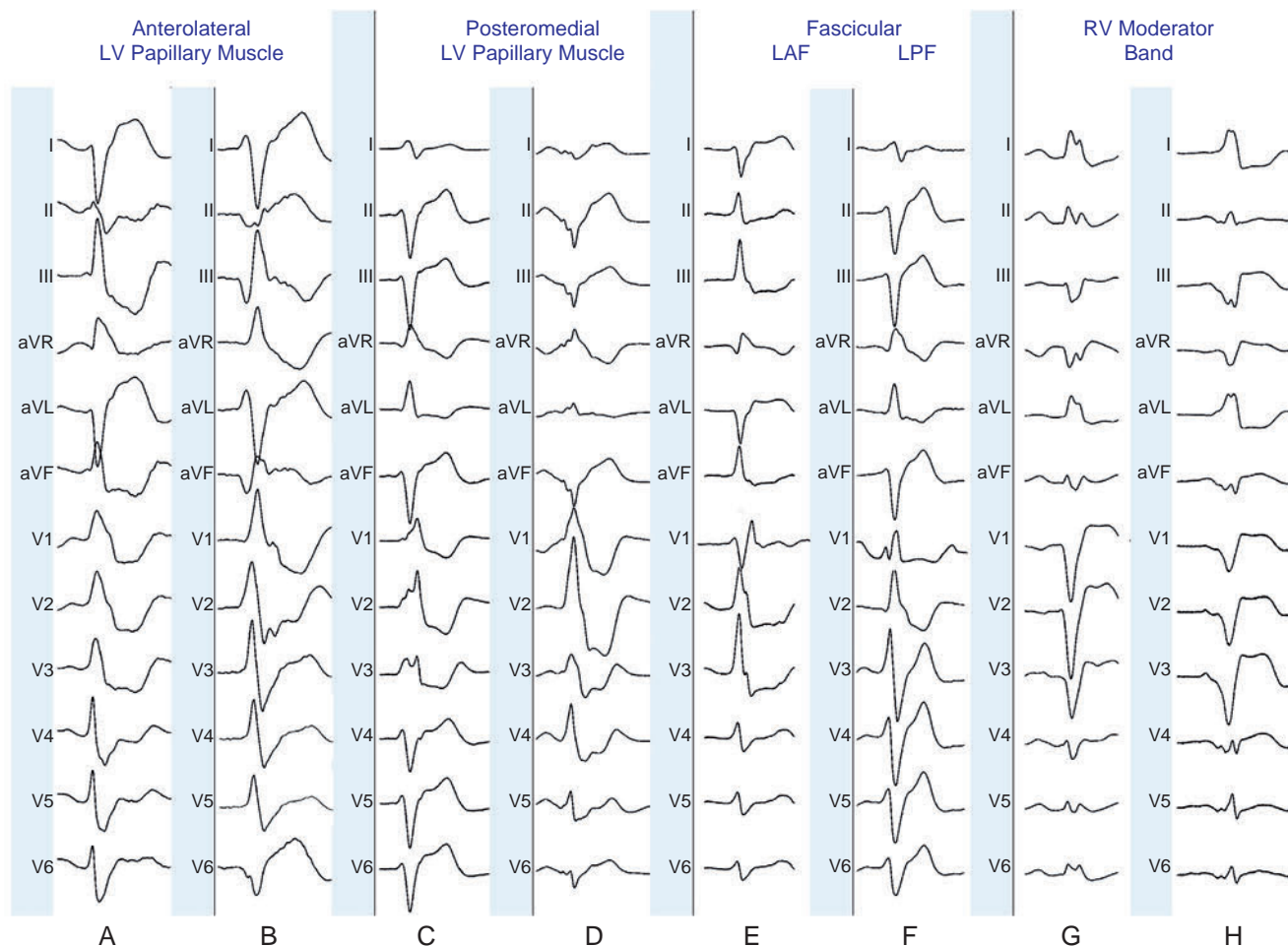


Fig. 23.9 Surface Electrocardiogram (ECG) QRS Morphology of Intracavitary Premature Ventricular Complexes (PVCs). Representative surface 12-lead ECG of QRS morphology during PVCs originating from the left ventricular (LV) anterolateral papillary muscle (A and B), posteromedial papillary muscle (C and D), left anterior fascicle (LAF, E), and left posterior fascicle (LPF, F), and right ventricular (RV) moderator band (G and H).

transition becomes later (at lead V_3 in septal locations, and after lead V_3 in free wall locations), the QRS becomes wider, Q wave amplitude becomes larger in anterior precordial leads (V_1 to V_3), and notching in the inferior leads becomes more prevalent and prominent.

VAs arising from the tricuspid annulus have an rS or QS pattern in lead aVR, just as those arising from the RVOT; however, the QRS polarity in lead aVL is positive in almost all VAs arising from the annulus (89%), unlike those arising from the RVOT. In addition, annular VAs typically display a large R wave (with no negative component) in lead I. QRS polarity in the inferior leads is positive in anterior annular VAs, and negative in posterior and posteroseptal annular VAs.⁷⁹

VAs originating in the vicinity of the HB share many of the same ECG features as those originating from the RVOT (including an LBBB pattern in lead V_1 with an inferior axis and an R wave in lead I), the right or noncoronary aortic sinuses adjacent to the membranous septum, or the subaortic LV septum. However, para-Hisian VAs are characterized by a narrower QRS width (due to the rapid ventricular activation caused by early engagement of the HPS), a higher R wave amplitude in lead I, a lower R wave amplitude in the inferior leads, and a higher R wave amplitude ratio in leads II/III. In addition, a prominent R wave in lead aVL is observed in VAs arising from the RV para-Hisian region.

Given its rightward and inferior location, this is the only site of origin in the RVOT that does not exhibit a completely negative deflection in lead aVL.^{59,80}

Discrimination between LV versus RV septal para-Hisian VAs can be difficult, given the close anatomical relationship and rapid transseptal conduction from both locations. Although an early QRS transition (before lead V_3) predicts VAs with an origin in the subvalvular LVOT or aortic root, and a late QRS transition (after lead V_3) predicts those with an origin in the RV para-Hisian region, the sensitivity of these ECG features is limited.

ELECTROPHYSIOLOGICAL TESTING

Induction of Tachycardia

Not infrequently, idiopathic VAs foci can become inactive in the EP laboratory environment, likely due to sedative medications or deviation from daily routine activities (e.g., exercise or caffeine intake) that can affect VT activity. Thus, in preparation for the ablation procedure, antiarrhythmic drugs should be withheld for at least five half-lives before the EP study and minimal sedation should be used throughout the procedure, if possible. In addition, it may be appropriate to monitor

the patient in the EP laboratory initially without sedation. If no spontaneous tachycardia is observed, isoproterenol is administered. If no VAs could be induced during isoproterenol administration or during the washout phase, a single quadripolar catheter may be placed in the RV, and programmed electrical stimulation is performed. If VT focus remains quiescent, the procedure may be aborted and retried at a future date. If the clinical VAs are inducible at any step, the full EP catheter arrangement and EP study are undertaken.

Several pharmacological agents may be used to enhance inducibility of idiopathic VAs. Isoproterenol infusion (targeting a 20% to 30% increment in heart rate) is the first choice. Importantly, VAs may develop (with and without programmed electrical stimulation) only during the washout phase after discontinuation of isoproterenol (analogous to VAs occurring during the recovery phase postexercise). If needed, IV atropine and aminophylline may be sequentially administered (with and without programmed electrical stimulation) to attenuate the potential antiarrhythmic effects of endogenous acetylcholine and adenosine, which inhibit cAMP. Calcium infusion can also facilitate arrhythmia induction. Occasionally, epinephrine or phenylephrine can be more effective than isoproterenol.

Ventricular stimulation can initiate the VAs in less than 65% of patients and, in contrast to reentrant VT, rapid ventricular pacing is usually more effective than VES. Induction of sustained VT is less common in patients with repetitive monomorphic VT than in those with paroxysmal sustained VT. In one report, sustained VT was inducible during EP testing in 78% of patients who presented clinically with sustained VT, in 48% of patients who presented with nonsustained VT, and in 4% of those with PVCs only. Most episodes of triggered activity VT induced by ventricular stimulation are usually nonsustained. Reproducibility of VT induction using all methods is less than 50%, whereas reproducibility of induction with single or double VESs is approximately 25%. Induction with atrial pacing is not uncommon. Of note, in contrast to reentrant VT, initiation of OT VAs does not require associated ventricular conduction delay or block for initiation.

Typically the initial cycle of the VT bears a direct relationship to the PCL (whether or not VESs are delivered following the pacing drive). Thus the shorter the initiating PCL, the shorter the interval to the first VT beat and the shorter the initial VT CL. Similarly, the initial cycle of the VT bears a direct relationship to the coupling interval of the VES initiating the VT. Occasionally, with the addition of very early VESs or with very rapid ventricular pacing (PCL <300 milliseconds), a sudden jump in the interval to the first VT complex may be observed, such that it is approximately twice the interval to the onset of the VT initiated by later coupled VESs. This can be caused by failure of the initial DAD to reach threshold, whereas the second DAD reaches threshold. Thus in triggered activity VAs caused by DADs, the coupling interval of the initial VT complex either shortens or suddenly increases in response to progressively premature VES; it usually does not demonstrate an inverse or gradually increasing relationship (in contrast to reentrant VT).

Of note, successful induction of VAs can be linked to a critical window of heart rates. Ventricular PCLs longer or shorter than the critical CL window may fail to induce VT. This critical window can shift with changing autonomic tone. Therefore it is important to perform ventricular pacing at a wide spectrum of CLs to define the range of CLs most successful in inducing the VAs. The site of ventricular stimulation has no effect on the initiation of triggered activity VT as long as the paced impulse reaches the focus of the VT (in contrast to reentrant VT).

VT induction can be inconsistent. Induction is exquisitely sensitive to the immediate autonomic status of the patient. Therefore noninducibility during a single EP study is not enough evidence to attribute the arrhythmia to a nontriggered activity mechanism.

Tachycardia Features

Idiopathic focal VAs can manifest in the form of sustained VT or, more commonly, frequent monomorphic PVCs, couplets, and salvos of non-sustained VT. When sustained, the VT rate is frequently rapid (CL <300 milliseconds) but can be highly variable.

During VT, the His potential follows the onset of the QRS (i.e., negative HV interval) and is usually buried inside the local ventricular electrogram. Ventriculoatrial conduction may or may not be present. The VT is very sensitive to adenosine, Valsalva maneuvers, carotid sinus massage, edrophonium, verapamil, and beta-blockers.

Diagnostic Maneuvers During Tachycardia

Idiopathic focal VT cannot be entrained by overdrive ventricular pacing (i.e., no QRS fusion demonstrable). Notably, rapid ventricular pacing during the VT can result in acceleration of the VT. In addition, a direct relationship exists between the overdrive PCL and the coupling interval and CL of the VT resuming after cessation of pacing, characteristic of DAD-related triggered activity. VES results in a decreasing resetting response curve characteristic of DAD-related triggered activity.

MAPPING

The prediction of the precise origin of OT VAs based on surface ECG can be challenging, given the close anatomical relationship of the different compartments of the OT region. Therefore it is important to be prepared for mapping and ablation in the different cardiac compartments, including the CS, the aortic retrograde approach, and occasionally, the percutaneous pericardial approach. In addition, angiography of the CS and coronary arteries might be necessary for ablation in specific regions, and the required equipment for these procedures needs to be readily available.

In general, a multielectrode catheter positioned as far as possible in the CS (into the great cardiac vein) and a catheter positioned at the HB region in the RV can be very useful in mapping of OT VAs.

When the ECG QRS morphology strongly suggests a site of origin (e.g., RVOT, LVOT, LV summit, papillary muscle), that region is the initial target for mapping. On the other hand, when the ECG does not provide conclusive criteria to guide localization of the VT focus in the OT region, a stepwise mapping procedure has been proposed. Because most VAs originate from the RVOT, mapping is started there, and if that fails to identify the origin of the VT, mapping is extended to involve the pulmonary artery. If activation mapping and pace mapping suggest a focus outside the RVOT, mapping the CS can add useful information as to whether a left-sided epicardial origin is present. When the transvenous approach is unsuccessful, mapping the LVOT and aortic cusps via a retrograde arterial access is usually the next step. Finally, if all previous anatomical accesses are unsuccessful, epicardial mapping via a percutaneous pericardial access can be considered.

Activation Mapping

Activation mapping can be performed by point-by-point mapping with a standard mapping/ablation catheter, a high-density multielectrode mapping catheter (e.g., PentaRay, Biosense Webster, Diamond Bar, CA, United States), or multielectrode arrays. In idiopathic focal VAs, activation mapping is typically performed in conjunction of electroanatomic mapping.

The goal of activation mapping is to identify the site of origin (focus) of VT/PVCs, defined as the site with the earliest bipolar recording preceding the surface QRs (typically more than 20 to 25 milliseconds presystolic) in which the distal tip shows the earliest intrinsic deflection and QS unipolar electrogram configuration.

Initially, one should seek the general region of the origin of VAs as indicated by the surface ECG. All 12 leads should be inspected, and the lead showing the earliest and most discernible onset of the QRS during VT or PVCs should be selected as the reference point for subsequent mapping. Subsequently, the mapping catheter is moved under the guidance of fluoroscopy into the RVOT, and the bipolar signals are sampled from several endocardial sites. It is important to record examples of VT or PVCs prior to inserting catheters because the catheters can cause ectopic complexes that resemble the target VT or PVCs (Fig. 23.10).

Activation times are generally measured from the onset or the first rapid deflection of the bipolar electrogram to the earliest onset of the QRS on the surface ECG during VT or PVCs. The distal pole of the mapping catheter should be used to search for the earliest activation site, because it is the pole through which RF energy is delivered. Once an area of relatively early local activation is found, small movements of the catheter tip in that region are undertaken until the site is identified with the earliest possible local activation relative to the tachycardia complex.

Bipolar electrograms at the site of origin are modestly early (preceding the surface QRS by 10 to 45 milliseconds) and have high-amplitude and rapid slew rates. Fractionated complex electrograms and mid-diastolic potentials are not typically observed at sites of origin of idiopathic VAs.

Once the site with the earliest bipolar signal is identified, the unipolar signal from the distal ablation electrode should be used to supplement

conventional bipolar mapping (Fig. 23.11). The unfiltered (0.05 to >300 Hz) unipolar electrogram morphology should show a monophasic QS complex with a rapid negative deflection. Although this electrogram configuration is very sensitive for successful ablation sites, it is not specific (70% of unsuccessful ablation sites also manifest a QS complex). In fact, a QS configuration can be observed with unipolar recordings from a relatively large area (exceeding 10 mm in diameter and significantly larger than the VT focus), since the entirety of the heart is directed away from most locations in the ventricular OT region. The timing of the unipolar electrograms recorded at those sites distant from the VT focus, however, is later than that at the site of origin of the VT. Thus a QS complex should not be the only mapping finding used to guide ablation (see Fig. 23.11). Nonetheless, successful ablation is unusual at sites with an RS complex because these are generally distant from the VT focus.

The timing of the unipolar electrograms is also important. Concordance of the timing of the onset of the bipolar electrogram with that of the filtered or unfiltered unipolar electrogram, with the rapid downslope of the S wave of the unipolar QS complex coinciding with the initial peak of the bipolar signal, helps ensure that the tip electrode, which is the ablation electrode, is responsible for the early component of the bipolar electrogram (see Fig. 23.11). In addition, the presence of slight ST elevation on the unipolar recording and the ability to capture the site with unipolar pacing are used to indicate good electrode contact.

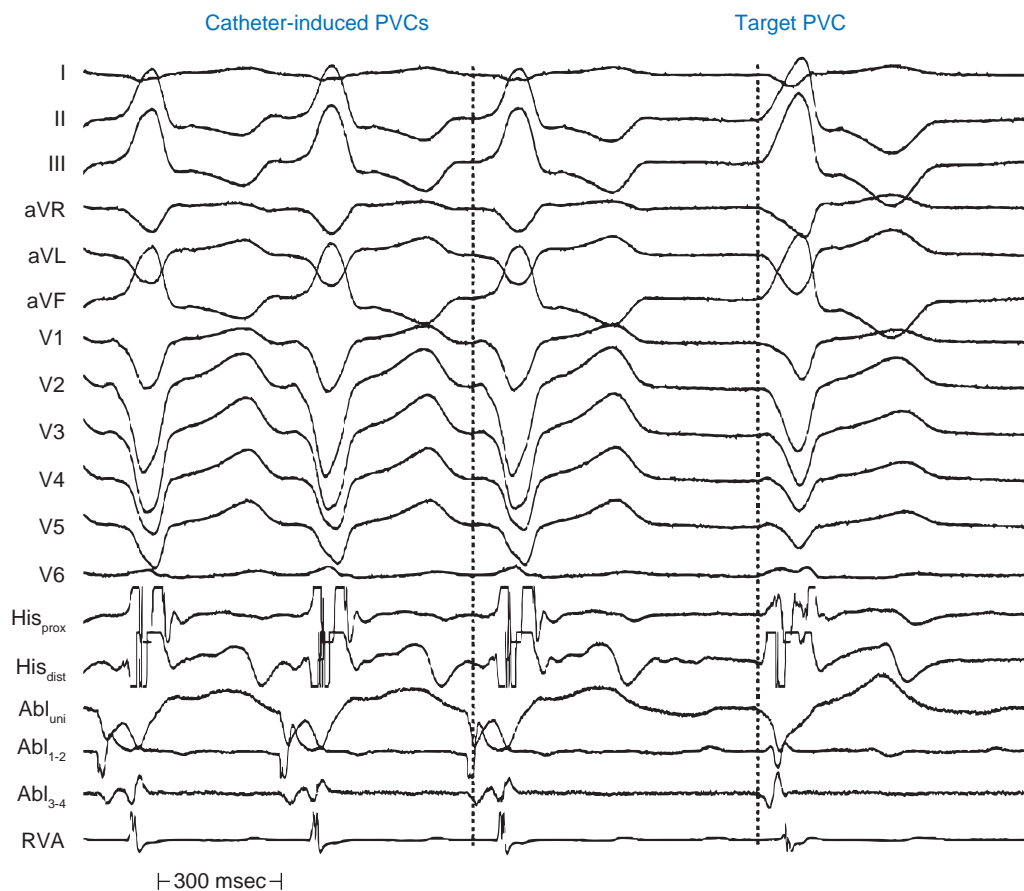


Fig. 23.10 Catheter-Induced Premature Ventricular Complexes (PVCs) Versus Target Spontaneous PVCs. Three complexes of catheter-induced PVCs are seen at left, during which both unipolar and bipolar signals are very early (as would be expected, because catheter tip irritation is causing these complexes). During the actual target PVC, however, this site is not early at all. This illustrates the need to be certain of the characteristics of the target PVC or ventricular tachycardia complex before beginning mapping. *Abl_{uni}*, Unipolar ablation; *His_{dist}*, distal His bundle; *His_{prox}*, proximal His bundle; *RVA*, right ventricular apex.

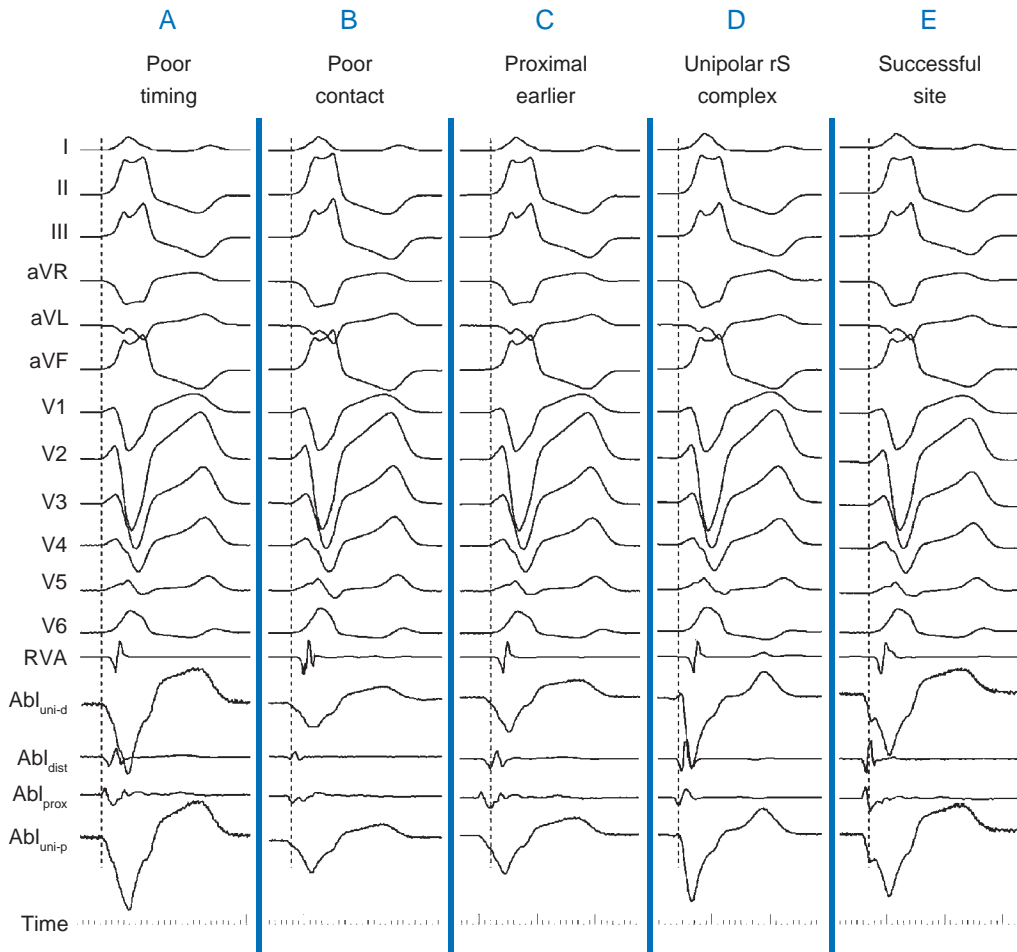


Fig. 23.11 Activation Mapping of Idiopathic Ventricular Tachycardia (VT). Activation mapping results from five sites are shown with 12 leads of a single VT complex, as well as intracardiac recordings from the right ventricular apex, proximal and distal ablation electrode bipolar recordings, and unipolar recordings from the tip electrode (*uni-d*) and the second electrode (*uni-p*). A vertical dashed line denotes QRS onset. Sites A to D are suboptimal ablation sites for the reasons noted. Site E was where ablation terminated VT. *Abl_{dist}*, Distal ablation; *Abl_{prox}*, proximal ablation; *RVA*, right ventricular apex.

In addition to the electrogram temporal relationship assessment, a negative concordance in the initial forces (first 20 milliseconds) of both unipolar and bipolar electrograms further improves the accuracy of conventional mapping to localize the site of origin of PVCs. In a recent report, the presence of this criterion (at sites fulfilling other conventional criteria used to guide focal PVC ablation) highly predicted the acute success rate of RF ablation with a sensitivity and specificity of 94% and 95%, respectively. Furthermore, its positive predictive value was significantly superior to the those of all other conventional criteria (76% vs. 33% to 43%).⁸¹

Careful catheter manipulation during mapping should seek to avoid mechanical trauma that can transiently abolish the arrhythmia. Importantly, catheter manipulation frequently induces PVCs that can closely mimic target PVCs. The findings on the mapping catheter during these catheter-induced PVCs are invariably excellent (e.g., substantial presystolic activation time, sharp QS on the unipolar recording). These complexes must be analyzed and carefully compared with prerecorded VT or PVC complexes to avoid the delivery of RF energy to sites with no relevance to actual VT.

It is important to recognize that some myocardial fibers in the RVOT can potentially be in continuity with those in the LVOT. Consequently,

when mapping is confined to the RVOT, the endocardial site with the earliest presystolic activation time does not necessarily indicate the focus of the tachycardia. This can be observed especially in tachycardias originating in the supraaortic sinuses of Valsalva, whereby the activation wavefront after leaving the focus exits both to the infravalvular LVOT myocardium and to the posterolateral subpulmonic RVOT. Then, mapping in the RVOT merely localizes the breakthrough site, where ablation would not eliminate the arrhythmia.

When mapping above the aortic or pulmonic valve, near- and far-field potentials are typically recorded. The exact nature and cause of these spikes are unknown but are thought to be analogous to PV potentials—that is, they represent electrical activation of myocardial sleeves distal to valve attachment. Because of the overlapping nature of the OT and supraaortic region, when two potentials are seen, only the near-field potential should be used for activation timing. In addition to noting the actual timing of activation, the timing of the near-field electrogram relative to the far-field electrogram should be evaluated. Typically, in sinus rhythm, the near-field potential (representing local supraaortic myocardial activation) is recorded after the far-field ventricular electrogram (likely representing OT activation) separated by an isoelectric period (presumably from conduction delay across the

site of valve insertion). If the sequence of activation is reversed during VT or PVC—that is, the near-field electrogram precedes the far-field electrogram by a similar or greater isoelectric period duration—an etiological role for the supraventricular myocardium can be inferred. This finding alone, however, does not suggest that ablation at this particular site will be successful because other supraventricular locations may show earlier activation than the site being mapped. On the other hand, if the near-field electrogram still succeeds the far-field ventricular electrogram during VT or PVC, then the supraventricular tissue, although present, is a bystander being passively activated during arrhythmia originating in the OT myocardium below the valve. In some cases, the near-field electrogram is fused with the far-field electrogram during tachycardia. This suggests an origin of arrhythmia exactly at the sinus of Valsalva or passive activation from a true distant site of origin to both the supraventricular and infraventricular myocardium.⁸

Pace Mapping

Given the focal nature of idiopathic VAs, comparing the paced QRS configuration with that of VT/PVC is particularly useful for locating the arrhythmia focus in a structurally normal heart. Pace mapping is used to confirm the results of activation mapping, but also can be of great value as the primary mapping technique when the VAs are scarcely inducible. Although there are some limitations to this technique, several studies have demonstrated efficacy using pace mapping to choose ablation target sites for idiopathic VT. However, the spatial resolution of pace mapping remains inferior to that of activation mapping.

Technique

Pace mapping during VT (at PCL 20 to 40 milliseconds shorter than the PCL) is preferable whenever possible because it facilitates rapid comparison of VT and paced QRS complexes at the end of a pacing train in simultaneously displayed 12-lead ECGs. If only nonsustained VT or PVCs are inducible, pacing is performed during NSR. In this setting, the PCL and coupling intervals of the VES should match those of spontaneous ectopy. Pace mapping is preferably performed with unipolar stimuli (≤ 10 mA, 2 milliseconds) from the distal electrode of the mapping catheter (cathode) and an electrode in the inferior vena cava (IVC) (anode). Unipolar pacing, however, causes a large stimulus artifact in the surface ECG. Bipolar pacing from the closely spaced distal electrodes of the mapping catheter is more commonly used. Although the possibility for capture at either the distal or proximal bipolar electrodes can reduce spatial accuracy, this does not appear to be a major limitation. Using the minimum stimulus amplitude required for consistent capture should improve accuracy by limiting the size of the virtual electrode in the tissue and preventing capture of myocardium distant from the pacing site. Pacing thresholds exceeding 5 to 10 mA typically indicate insufficient electrode-tissue contact or electrically inexcitable tissue.¹⁴

Interpretation

The greater the degree of concordance between the morphology during pacing and that during VT/PVC, the closer the catheter will be to the site of origin of the tachycardia. Pace maps with identical or nearly identical matches of the tachycardia morphology in all 12 surface ECG leads can be indicative of the site of origin of the tachycardia or breakout site to the myocardium (see Fig. 5.24).

ECG recordings should be reviewed at the same gain and filter settings and at a paper-sweep speed of 100 mm/s. It is often helpful to have a split-screen display of the target VT in one panel, comparing this with all 12 leads of the paced QRS complexes brought into another panel, as well as with printed regular 12-lead ECGs for side-by-side

comparison on paper. Differences in the QRS morphology between pacing and spontaneous VT in a single lead can be critical. Pacing at a site 5 mm from the index pacing site can result in minor differences in QRS configuration (notching, new small component, change in amplitude of individual component, or overall change in QRS shape) in at least one lead in most patients. In contrast, if only major changes in QRS morphology are considered, pacing sites separated by as much as 15 mm can appear similar.

Although qualitative comparison of the 12-lead ECG morphology between a pace map and VT is frequently performed, there are few objective criteria for quantifying the similarity between two 12-lead ECG waveform morphologies. Such comparisons are frequently completely subjective or semiquantitative, such as a “10/12 lead match.” Discrepancies in ablation outcome can result, in part, from subjective differences in opinion regarding the closeness of a pace map match to the clinical VT. In addition, a common human error in analyzing a pace map is not appreciating subtle amplitude or precordial lead transition differences between two ECG patterns. To overcome these limitations, template matching software is currently available and integrated into some EP recording systems (e.g., LabSystem PRO™ EP recording system, Boston Scientific, Boston, MA, United States; see Fig. 5.25) or 3-D mapping systems (e.g., CARTO, PaSo, Biosense Webster; see Fig. 5.26). This software processes digital images to match the target QRS complex (template signal) and the paced QRS complex (test signal), and provides a score according to the similarity between the two QRS morphologies. The software “slides” the reference over the incoming data until the best local match is found by using a correlation calculation. For each lead-to-lead comparison, both the polarity and the amplitude of the QRS complexes play an important role as to the resulting value of the percentage of correlation calculated by the software. The site that yields the highest average correlation (value toward 99% to 100%) across all of ECG leads means a perfect match between two 12-lead ECG morphologies. In general, an average template-matching score above 90% is considered sensitive for the identification of successful versus unsuccessful ablation sites.^{82,83}

Pitfalls

Current strengths up to 10 mA have little effect on unipolar-paced ECG configuration. In contrast, bipolar pacing can introduce some variability in the paced ECG; a significantly large amount of local myocardium is captured, which, combined with varying degrees of anodal capture, can be detrimental to mapping accuracy. This can be minimized by low pacing outputs and small interelectrode distance (≤ 5 mm). In addition, the morphology of single-paced QRS complexes can vary depending on coupling interval, and the QRS morphology during overdrive pacing is affected by the PCL. Therefore the coupling interval or CL of the template arrhythmia should be matched during pace mapping; otherwise, rate-dependent changes in QRS morphology independent of the pacing site can confound mapping results. Similarly, spontaneous couplets from the same focus may have slight variations in QRS morphology that must be considered when seeking a pace match. Of note, isoproterenol infusion has no significant effect on the QRS configuration.¹⁴ More rapid tachycardias (and sometimes relatively slower ones) can potentially show slight beat-to-beat variations in QRS morphology; depending on which beat is chosen for a template, achieving a perfect “match” to that one with pacing may not be feasible, and yet the paced QRS matches a different VT beat. Similarly, rapid pacing can result in slight changes in QRS morphology from beat to beat.

Importantly, the rapid electrical propagation within the RVOT limits the spatial resolution of pace mapping. In one report, the spatial resolution of a good pace map for targeting RVOT VAs was about 1.8 cm² and was inferior to that of an activation map.⁸⁴

Pace mapping can be particularly difficult to perform above the semilunar valves (in the aortic sinuses of Valsalva or pulmonary artery) and can require high pacing current strengths. Because of the close anatomical proximity of the various structures in the supraventricular region, high-output pacing may reproduce the ECG of clinical arrhythmia, even when the origin is in a different cardiac chamber. For example, high-output pace mapping from the right aortic sinus of Valsalva may reproduce the ECG morphology of VAs originating from the posterior RVOT or subvalvular anterior LVOT. On the other hand, supraventricular arrhythmia origin may exit to the ventricular myocardium below the valve, and pacing at the exit site can potentially produce perfect pace maps. For example, if pace mapping is performed at a breakthrough site on the posterior RVOT to try to match VT that originate in an aortic sinus of Valsalva VT, a perfect result (despite supraaortic origin) will be obtained. Yet ablation energy delivered there typically fails to terminate the arrhythmia and may result in a change in VT morphology, resulting now from a different exit of the sinus of Valsalva arrhythmogenic focus.¹⁷

It is also important to recognize that in a significant minority of patients, pace mapping at the successful ablation site produced a poor pace map, likely due to an intramural site of origin or secondary to conduction through preferential fibers connecting the site of origin to the myocardium.

Electroanatomic Mapping

Centrifugal propagation of activation during RVOT VAs is very rapid, with $3.0 \pm 1.6 \text{ cm}^2$ of the endocardium being activated within the first 10 milliseconds (ranging up to 6.4 cm^2). Therefore minor differences between adjacent sites become difficult to detect, leading to a large number of sites with clinically indistinguishable activation times when examined on a site-by-site basis. However, when displayed simultaneously on a spatially precise electroanatomical reconstruction, the centers of the early activation area and the presumed site of VT origin become easy to identify (Fig. 23.12). Electroanatomic 3-D mapping (CARTO mapping system [Biosense Webster], EnSite NavX system [St. Jude Medical, St. Paul, MN, United States], or Rhythmia [Boston Scientific, Cambridge, MA, United States]) permits spatial discrimination between sites separated by less than 1 mm.

Initially, a stable reference electrogram is selected. This is the fiducial marker on which the entire mapping procedure is based. Preferably, a QRS on the surface ECG (with a well-defined narrow R wave peak) is selected as the reference signal. Alternatively, an intracardiac electrogram (e.g., RV apex) can be selected as the reference point, in which case care must be taken to avoid dislodging this catheter, because if it moves, timing of mapping catheter activations will not be comparable to previously mapped sites. Following selection of the reference electrogram, positioning of the anatomical reference, and determination of the window of interest, the mapping catheter is positioned in the RVOT under fluoroscopic guidance.

At the outset, the plane of the HB location and pulmonic valve are defined and tagged to outline the superior and inferior limits of the RVOT. The mapping catheter is advanced superiorly in the RVOT until no discrete bipolar electrograms are seen in the distal electrode pair. The catheter then is retracted until electrograms in the distal electrode pair reappear and pacing results in capture of the RVOT endocardium. This marks the level of the pulmonic valve. At least three points are acquired and tagged to construct the pulmonic valve. Next, a detailed electroanatomic activation map of the RVOT is constructed by acquiring multiple points during PVCs or VT. The local activation time at each site is determined from the intracardiac bipolar electrogram and is measured in relation to the fixed reference electrogram (surface QRS or intracardiac electrogram). Points are added to the map only if

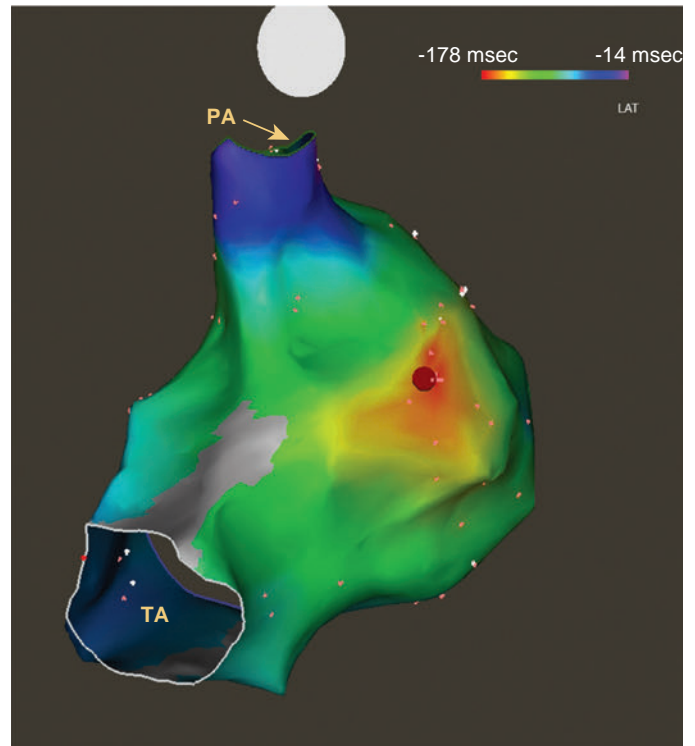


Fig. 23.12 Electroanatomic Activation Mapping of Ventricular Ectopy Originating From the Right Ventricular Outflow Tract (RVOT). CARTO 3 activation map (posterior view) is shown. The site of impulse origin during ectopy was in the posterolateral aspect of the RVOT (red area), at which point ablation eliminated the ventricular tachycardia (red dot). PA, Pulmonic valve annulus; TA, tricuspid annulus.

stability criteria in space and local activation time are met. The end-diastolic location stability criterion is less than 2 mm, and the local activation time stability criterion is less than 2 milliseconds. Activation maps display the local activation time by a color-coded overlay on the reconstructed 3-D geometry (see Fig. 23.12). The electroanatomic maps of focal VT demonstrate radial spreading of activation, from the earliest local activation site in all directions (a well-defined early activation site surrounded by later activation sites).

The principles used for conventional activation mapping discussed above are also used here to define the site of origin of VT. Although the traditional single-catheter mapping of the region of interest is still required, the ability to use the catheter localization system to steer precisely back to previously obtained sites of earliest activation greatly facilitates the ablation process. Display of activation times facilitates comparison of data from nearby sites, overcoming the imprecision of assigned activation times at single points, and permits rapid identification of a putative site of origin. The activation map can also be used to catalog sites at which pacing maneuvers are performed during assessment of the tachycardia (e.g., sites with a good pace map).

Current iterations of electroanatomic mapping systems allow the construction of high-resolution electroanatomic maps through catheters with multiple electrodes, as well as automated data acquisition. The EnSite NavX system can utilize any multielectrode catheter for data acquisition. The multipolar Lasso, PentaRay, DecaNav catheters (Biosense Webster) are equipped with the electromagnetic sensor and can be used with the CARTO system. The Rhythmia system utilizes a minibasket catheter (Orion; see Fig. 6.7). These techniques can significantly facilitate

the mapping procedure, especially in the presence of infrequent or scarcely inducible VAs.

The CARTO system incorporates an automated template-matching software (PaSo). The ECG waveform of each paced signal is compared to the VT waveform, and correlation is scored between 0 and 1. An automated isochronal pace map is collected by pacing at different sites. This helps eliminate operator subjectivity and provide a visual reference of all the sites visited on the map.⁸²

In addition, ICE imaging can facilitate mapping by visualization of the ablation catheter in the context of the complex anatomy of the OT region. ICE imaging can be coupled with electroanatomic mapping (CARTOSound), which can facilitate tagging anatomic landmarks (on the anatomical model).⁸⁵

When using a 3-D electroanatomic mapping system, it is important to understand that a change in rhythm during the mapping procedure can alter cardiac geometry to the extent that anatomical points acquired during one rhythm cannot be relied on after a change in rhythm. This is relevant during mapping of isolated PVCs or nonsustained VT, because locations assigned to early activation sites during the PVC on the electroanatomic map can potentially be spatially displaced (up to 10 mm) from the same anatomical locations when assigned during normal rhythm (e.g., at the time of RF delivery after tachycardia termination; see Fig. 6.19). Therefore, after termination of the arrhythmia, “revisiting” the site of early activation tagged during PVCs may not be feasible or even misleading as a target for ablation. To mitigate this problem, it might be helpful to assign the location of the identified site of origin of the tachycardia during the PVC (or the location of best pace map acquired during ventricular pacing) and also during sinus beats, while the mapping catheter is maintained at the same location (tagged as “location only” during sinus beats). This technique allows navigating to the site of interest, whether during tachycardia or during NSR.⁸⁶

Noncontact Mapping

The spatial and temporal resolution of point-by-point activation mapping is limited by the number of contact electrodes and the time required. When VT is hard to induce or the PVCs are infrequent, simultaneous multisite data acquisition can help map the VT focus. The biggest advantage of noncontact endocardial mapping is its ability to recreate the endocardial activation sequence from simultaneously acquired multiple data points over a few (theoretically one) tachycardia beats, without requiring sequential point-to-point acquisitions. More detailed mapping, however, is necessary to find the precise site to ablate.⁸⁷

The EnSite 3000 noncontact mapping system (St. Jude Medical) consists of a noncontact catheter (9 Fr) with a multielectrode array surrounding a 7.5-mL balloon mounted at the distal end. To create a map, the balloon catheter is advanced over a 0.035-inch guidewire under fluoroscopic guidance and positioned in the RVOT. The balloon is then deployed; it may be filled with contrast dye, permitting it to be visualized fluoroscopically (eFig. 23.8). The balloon is positioned in the center of the RVOT and does not come in contact with the endocardial walls being mapped. Systemic anticoagulation is critical to prevent thromboembolic complications; intravenous heparin is usually administered to maintain the ACT at 250 to 300 seconds.

A conventional (roving) deflectable mapping catheter is also positioned in the RVOT and used to collect geometry information. The tricuspid annulus, HB, and pulmonic valve are initially tagged, and a detailed 3-D geometry of the RVOT (“virtual” endocardium) is reconstructed by moving the mapping catheter around the RVOT.

The multielectrode array simultaneously acquires multiple data points over a few tachycardia beats or PVCs. The system then reconstructs more than 3360 unipolar electrograms simultaneously and superimposes

them onto the computer-generated model of the RVOT, producing isopotential maps with a color range representing voltage amplitude. The highest chamber voltage is at the site of origin of the electrical impulse. Color settings are adjusted so that the color range matches 1 to 1 with the millivolt range of the electrogram deflection of interest. The color scale for each isopotential map is set so that white indicates the most negative potential and blue indicates the least negative potential. Activation can be tracked on the isopotential map throughout the cycle to the onset of the tachycardia beat. Wavefront propagation can be displayed as a user-controlled 3-D movie (eFig. 23.9).

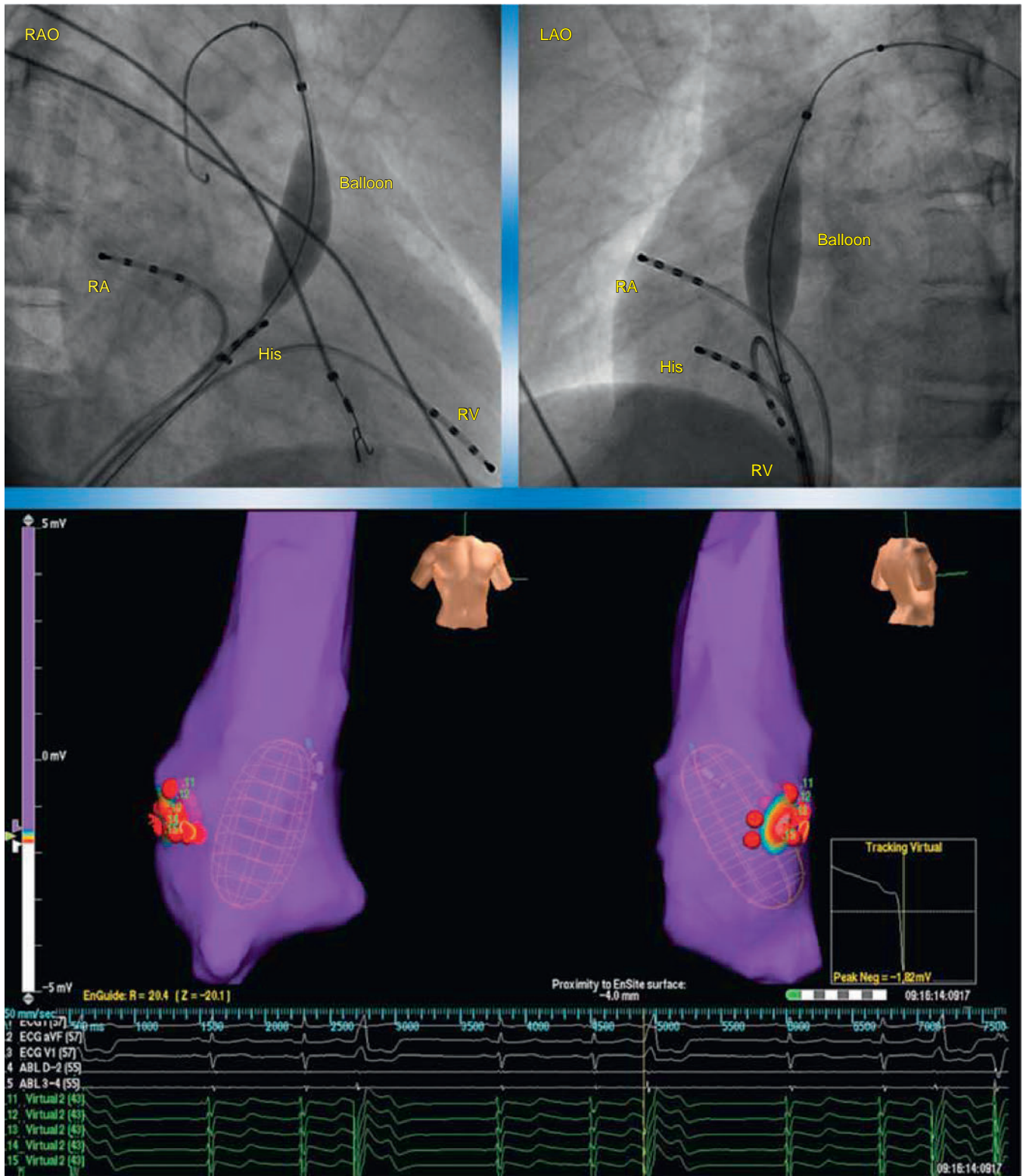
In addition, the system can simultaneously display as many as 32 electrograms as waveforms. Unipolar or bipolar electrograms (virtual electrograms) are then reconstructed at sites of earliest activation on the isopotential maps to look for a unipolar QS pattern (see Fig. 6.20). The origin of VT is defined as the earliest site showing a single spot of isopotential mapping and a QS pattern of the noncontact unipolar electrogram. Isochronal maps can also be created, which represent the progression of activation throughout the chamber relative to a user-defined electrical reference timing point.

Contact mapping using the conventional ablation catheter is then performed at sites of interest to supplement noncontact mapping findings, and color-coded contact activation maps can be displayed on the same 3-D geometry. Once the earliest activation is identified, the site is labeled on the 3-D map and the locator signal is used to navigate the ablation catheter to it in real time during tachycardia or during normal rhythm when sustained tachycardia is not inducible.

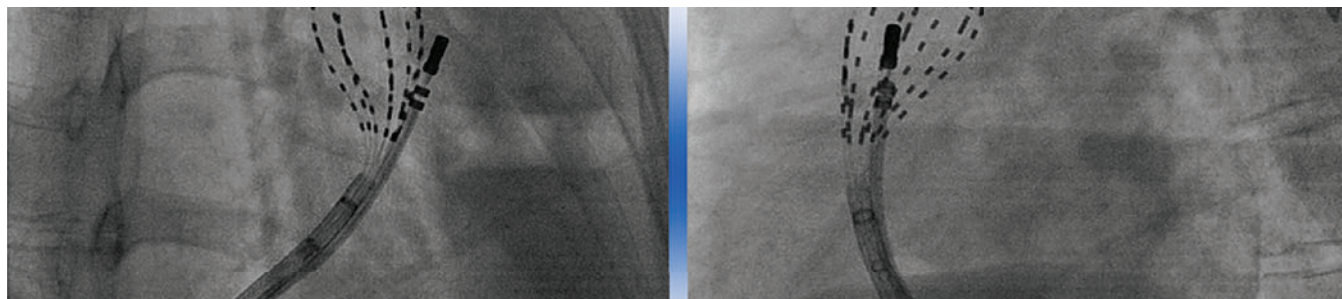
When analyzing noncontact activation map data to locate the site of origin of RVOT VAs, two distinct sites can be marked at the onset of electrical activity: earliest activation and breakout sites. The earliest activation site is defined as the site with the earliest unipolar deflection from baseline during VT/PVCs, forming a single spot on the isopotential map, as well as characterized by a QS pattern of noncontact unipolar electrogram. The breakout site is marked as the site along the depolarization pathway identified by the color-coded activation map where rapid centrifugal electrical propagation originated from and local unipolar electrograms exhibited the maximum negative dV/dt. For the identification of earliest activation and breakout sites, a broad color band setting is used with color high (defined as unipolar electrogram baseline) at -0.1 mV and color low at -2 mV. The virtual unipolar high-pass filter is set to 4 Hz. While earliest activation and breakout sites appear to be associated with similar pace map scores and endocardial bipolar activation prematurity in relation to QRS onset, one study found that the earliest activation site was a more sensitive marker for the true site of origin of the VT/PVC, as evident by the greater likelihood of achieving acute ablative success.⁸⁴

It was speculated that the distance between earliest activation and breakout sites could be affected by the subendocardial depth of the foci and/or the presence of preferential routes of conduction. Electrical propagation from deeper foci results in a larger endocardial area being activated simultaneously. By using unipolar mapping, this would appear like a wide earliest activation and breakout area (with r waves on unipolar signals, rather than QS complexes), and by using bipolar mapping, this would appear like a wide area of early activation. Within the earliest activation and breakout area, small differences in local activation time would result in the earliest activation site appearing to activate milliseconds earlier than breakout sites. The alternative explanation is that there are preferential routes of activation from these subendocardial sites to the endocardial surface, resulting in variable distances between earliest activation and breakout sites.⁸⁴

The EnSite 3000 noncontact mapping system is not commonly used because of several limitations. Manipulation of the array into the RVOT can be difficult, and contact of some portions of the area with



eFig. 23.8 Noncontact Mapping of Idiopathic Right Ventricular Outflow Tract (RVOT) Ventricular Tachycardia. Upper panel, Fluoroscopic (right anterior oblique [RAO] and left anterior oblique [LAO]) views of the EnSite balloon catheter positioned in the RVOT. Middle panel, Color-coded isopotential map of RVOT activation during a single premature ventricular complex (PVC). The inset shows a virtual electrogram at the site of earliest activation (note the QS pattern). Red dots indicate radiofrequency applications. Further detailed mapping using a standard mapping catheter localized the PVC focus to a site adjacent to the site, with the earliest local activation identified by the balloon catheter. Lower panel, Surface electrocardiogram and intracardiac contact (ABL) and virtual noncontact (green) electrograms are shown during mapping of PVCs. His, His bundle; RA, right atrium; RV, right ventricle.



eFig. 23.9 Noncontact Isopotential Maps During a Premature Ventricular Complex (PVC) Originating From the Right Ventricular Outflow Tract. Wavefront propagation spreads radially from a small focus (from *left to right*). The insets show a virtual electrogram with the bar indicating the timing of activation during the PVC.

myocardium may induce PVCs that appear similar to clinical PVCs or VT and confuse mapping efforts. In addition, this mapping tool is appropriate mostly for idiopathic VAs originating from the RVOT. Since the exact site of origin cannot be accurately predicted based on ECG morphology, there will be a significant proportion of patients who will require mapping outside the RVOT (e.g., aortic root or CS) utilizing conventional mapping techniques, in which setting the multielectrode array would not be beneficial.

Basket Catheter Mapping

Basket catheters have been used successfully to guide ablation of idiopathic VAs arising from the RVOT, and are of particular interest in patients with infrequent arrhythmia that limits mapping. This mapping catheter consists of an open-lumen catheter shaft with a collapsible, basket-shaped distal end, which is composed of 64 electrodes mounted on eight flexible, self-expanding, equidistant metallic splines (each spline carrying eight ring electrodes; see Fig. 4.3). The electrodes are equally spaced 4 or 5 mm apart, depending on the size of the basket catheter used (with diameters of 48 or 60 mm, respectively). Each spline is identified by a letter (from A to H) and each electrode by a number (from 1 to 8), with electrode 1 having the distal position on the splines. The size of the RV is initially evaluated (usually with echocardiography) to help select the appropriate size of the basket catheter. The collapsed basket catheter is advanced under fluoroscopic guidance through an 11 Fr long sheath into the RV; the basket is then expanded. After basket catheter deployment, the conventional catheters are introduced and positioned in standard positions (eFig. 23.10). Several observations can help determine electrical-anatomical relations of the basket catheter electrodes, including fluoroscopically identifiable markers (spline A has one marker and spline B has two markers located near the shaft of the basket catheter) and electrical signals recorded from certain electrodes (e.g., ventricular, atrial, or HB electrograms), which can help identify the location of those particular splines.

From the 64 electrodes, 64 unipolar signals and 32 to 56 bipolar signals can be recorded, by combining 1–2, 3–4, 5–6, 7–8, or by combining 1–2, 2–3, until 7–8 electrodes are on each spline. The color-coded animation images simplify the analysis of multielectrode recordings and help establish the relation between activation patterns and anatomical structures. The degree of resolution is lower than that in 3-D mapping systems but appears satisfactory for clinical purposes.

The concepts of conventional activation mapping discussed above are then used to determine the site of origin of the tachycardia. The ablation catheter is placed in the region of earliest activity and is used for more detailed mapping of the site of origin of the VT. The Astronomer navigation system (Boston Scientific, Natick, MA) permits precise and reproducible guidance of the ablation catheter tip electrode to targets identified by the basket catheter. Without the use of this navigation system, it can be difficult to identify the alphabetical order of the splines by fluoroscopic guidance. The capacity of pacing from most basket electrodes allows the evaluation of activation patterns and pace mapping.

Basket catheter mapping is not commonly used because of several limitations. Most basket catheters are difficult, if not impossible, to steer; thus positioning in the RVOT can be challenging. In addition, firm contact with the tip of the basket and RVOT myocardium can induce ectopic complexes that mimic spontaneous VT or PVCs. Spatial sampling is limited by the interspline and interelectrode distances, and endocardial contact is often limited because of the complex geometry of the ventricles. A second catheter is still required to be manipulated to the site identified for more precise localization of the target for ablation, as well as RF energy delivery.

ABLATION

Target of Ablation

The ablation target site is defined as the site where the earliest local activation time during VT or PVCs (bipolar recording preceding the surface QRS typically by more than 20 to 25 milliseconds, and the distal tip recoding the earliest intrinsic deflection and QS unipolar electrogram configuration) and exact or best pace map matches can be obtained. Activation mapping and pace mapping are highly correlated techniques, and both methods are typically used in conjunction to select ablation sites (see Fig. 23.11).

RF delivery at successful ablation sites often results in an early “flurry” of PVCs or acceleration of VT (likely due to stimulatory effect of RF energy in proximity to the arrhythmia focus), followed by gradual slowing and complete resolution of the arrhythmia within 10 to 15 seconds (Fig. 23.13). At these sites, RF application is usually continued for 30 to 60 seconds. The inability to eliminate the PVCs or terminate VT after 20 seconds of RF application should prompt cessation of RF energy delivery and additional mapping to look for a better target site. Of note, late arrhythmia suppression during RF is more commonly seen with ablation of LVOT and LV summit VAs, and likely suggest a site of origin remote from the site of ablation (most commonly seen with intramural foci).¹⁴

Occasionally, following several RF applications, the first VT/PVC morphology is no longer seen, but a second, slightly different one is now observed. This can be caused by an actual second focus near the first or, more likely, by modification of the exit site from the first focus (Fig. 23.14). In this situation, ablation within 1 to 2 cm of the first site frequently eliminates the second VT morphology.

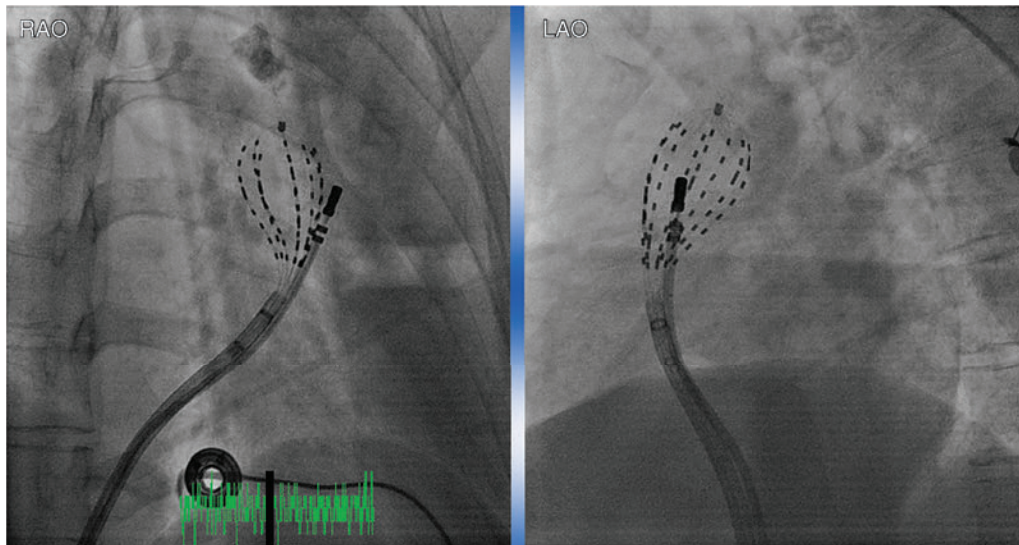
Ablation Technique

Ventricular Tachycardias Originating in the Right Ventricular Outflow Tract

To map the RVOT via the femoral vein, the mapping catheter is advanced into the mid-RV. From there, a sharp clockwise torque directs the catheter toward the anterior portion of the RVOT. The mapping catheter is then advanced into the proximal pulmonary artery and slowly withdrawn into the RVOT until the first local endocardial electrogram is recorded. This site is just below the pulmonic valve, and is at the level where most RVOT VAs originate. It is important to avoid trying to advance the catheter when its tip is perpendicular to the RVOT because this can result in perforation and cardiac tamponade. Torque is applied to the catheter for circumferential mapping of the RVOT within 1 cm of the pulmonic valve. The plane of the septum in the left anterior oblique (LAO) view is nearly perpendicular to the imaging plane. Delineating the boundaries within which mapping will be carried out is useful, rather than discovering after several minutes of mapping that more tissue lies in one direction or another from where efforts had previously been concentrated.

For mapping of the posterior portion of the RVOT, the catheter needs to be flexed posteriorly and counterclockwise torque applied. Such application of counterclockwise torque, however, will tend to pull the electrodes back into the RV inflow portion. Using a long guiding sheath in the RV may offer adequate catheter stability. In addition, mapping of the posterior RVOT wall can be facilitated by advancing the mapping catheter retrogradely into the right aortic sinus (see below), which lies immediately anterior to the RVOT (see eFig. 23.1).

VAs originating from the RVOT typically have local presystolic activation of more than 20 milliseconds and produce a near perfect pace map match. If very thorough mapping in the RVOT fails to localize the VT focus, mapping is extended into the pulmonary artery. It is important to resist the temptation to ablate the earliest site in a given chamber



eFig. 23.10 Basket Catheter Mapping During a Premature Ventricular Complex Originating From the Right Ventricular Outflow Tract (RVOT). Fluoroscopic (right anterior oblique and left anterior oblique) views of a basket catheter positioned in the RVOT. A second catheter is used for further mapping and ablation.



Fig. 23.13 Ablation (ABL) of Idiopathic Ventricular Tachycardia (VT). Radiofrequency (RF) energy delivery is started during sustained VT originating from the right ventricular outflow tract (RVOT). Acceleration of the VT is observed within a few seconds, followed by slowing and termination of the VT.

unless all of the different chambers have been mapped or unless the unipolar electrogram displays a QS morphology concordant with the earliest bipolar electrogram and the pace map at the site of earliest activation matches perfectly.

In some VAs originating from the aortic sinuses of Valsalva, a preferential conduction to the RVOT can render activation and pace mapping misleading. In fact, in one report, 27% of patients with VAs with an aortic sinus of Valsalva origin had the local ventricular activation in the RVOT preceding the QRS onset during VT/PVCs. Therefore it is important to carefully analyze the electrogram at the site of early activation on the RVOT to investigate whether the early electrogram recorded represents a far-field signal. Mapping the supra-ventricular aortic sinus of Valsalva should be considered if the earliest signal is far field in character near the posterior portion of the pulmonic valve. Also, when early presystolic activation from the RVOT is accompanied with a poor pace map match or when RF ablation at a seemingly good RVOT target site fails to permanently suppress the arrhythmia, mapping should be extended to the right aortic sinus of Valsalva. Similarly, RVOT sites displaying good pace maps but not particularly early local activation should prompt consideration for aortic sinus of Valsalva mapping.¹⁴

For catheter ablation in the RVOT, a nonirrigated 4-mm-tip ablation catheter is usually used. Idiopathic VAs are focal in nature and usually superficial toward the RVOT endocardium; therefore, extensive tissue injury is usually not necessary for successful ablation. RF applications at moderate temperatures (target temperature, 55°C) and a maximal power output of 30 to 40 W seem to be safe and effective. The high flow within the RVOT enhances the cooling effect and facilitates adequate RF power delivery. The duration of energy application should not exceed 30 to 60 seconds. Rarely, if ever, does one need more than 50 W or use of irrigated or large-tip electrodes to ablate RVOT VAs successfully, and

it is preferable to avoid those ablation approaches to prevent perforation of the thin free wall of the RVOT.

Ventricular Tachycardias Originating in the Pulmonary Cusps

The pulmonic valve can be defined on electroanatomic mapping by using ICE or by voltage mapping. A cutoff value of 1.9 mV likely discriminates between subvalvular and supra-ventricular positions with 90% sensitivity and 96% specificity. Therefore the level of pulmonic valve may be defined by color-coded voltage map adjustment of the lower and upper thresholds at 1.9 and 1.91 mV, respectively.¹⁵

The ablation target within the pulmonary artery is typically identified by the earliest ventricular activation, with simultaneous activation in bipolar and unipolar recordings. Discrete potentials, representing myocardial extensions into the pulmonary artery, are useful in guiding ablation of VAs arising from pulmonary cusps. Two components at the site with the earliest local activation can be observed: During NSR, the first potential is far-field (representing subvalvular RVOT myocardial activation), and the second potential is near-field (representing local supra-ventricular activation). During VT/PVC originating from the supra-ventricular RVOT, reversal of the two potentials is observed. Of note, RF application during VAs originating from the pulmonary cusps can occasionally lead to a change in QRS morphology, likely caused by interruption of conduction from the PVC focus over one of the myocardial extensions to the subvalvular myocardium, resulting in detouring the activation impulse.¹⁹

Ventricular Tachycardias Originating in the Left Ventricular Outflow Tract

Anatomically, successful catheter ablation sites of LVOT VAs include the aortic root, endocardium underneath the aortic valve (the aorto-mitral continuity), and epicardial surface of the LV (LV summit).²⁹

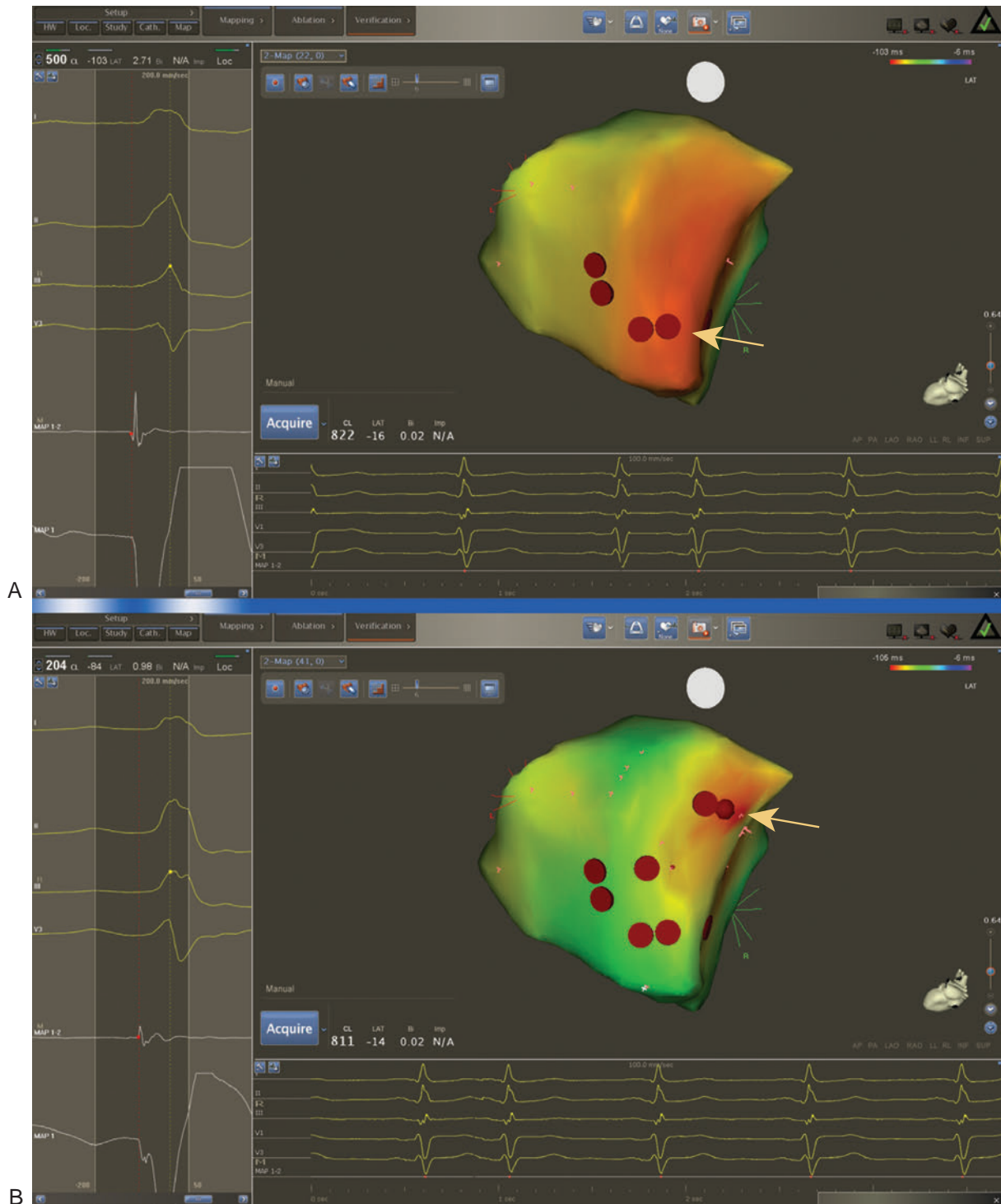


Fig. 23.14 Ablation of Premature Ventricular Complexes (PVCs) Originating From the Right Ventricular Outflow Tract (RVOT). Electroanatomic (CARTO) activation map (posterior views) of PVCs originating from the RVOT. Left panels show (in order from top to bottom) surface electrocardiogram (ECG) leads (I, II, III, V₁) and bipolar and unipolar recording of the distal ablation electrodes during the PVCs. (A) The site of impulse origin during ectopy is in the posterolateral aspect of the RVOT (red area, arrow), at which intracardiac recordings show early bipolar electrogram concordant with a QS-unipolar electrogram; ablation (red dots) at this site eliminated VT. (B) PVCs with slightly different QRS morphology (note the notching in the QRS in ECG leads II and III) emerged after initial ablation. Mapping revealed the focus of the latter PVCs (note intracardiac recordings) at a close but different location from the site targeted by initial ablation, at which ablation (red area, arrow) eliminated all PVCs.

Mapping is initially performed at the medial (“septal”) aspect of the RVOT and via the coronary venous system. LV and aortic root mapping is performed when the surface ECG strongly suggest an LV origin (e.g., VAs with RBBB configuration), when very thorough mapping and ablation in the RVOT and pulmonary artery fail to localize or terminate the tachycardia, or when recordings from distal CS or great cardiac or anterior interventricular veins suggest an LV origin.

LV and aortic root mapping is performed retrogradely via the femoral artery. Anticoagulation (IV heparin) should be started once the LV is accessed to maintain the ACT above 250 seconds. Importantly, catheter stability in the LVOT below the aortic valve is often challenging using the retrograde transaortic approach. The moving aortic valve leaflets can limit catheter manipulation and prevent stable tissue contact. The use of a long sheath (e.g., SL0 or SL1; 81 cm; St. Jude Medical), with the tip of the sheath placed through the aortic valve into the LV, can facilitate catheter stability and limit catheter dislodgement out of the LV.²⁹

Also, the catheter tip may be looped within the LV and then withdrawn so that the tip of the mapping catheter points upward underneath the aortic valve. The catheter loop may be rotated and partially released to optimized tissue contact while avoiding the disturbance from the movements of the aortic leaflets.²²

Mapping and ablation of the subaortic LVOT endocardium is performed to identify the arrhythmia focus as described for RVOT mapping. Standard or irrigated ablation catheters may be used for LVOT VAs. Some operators prefer irrigated ablation for left-sided idiopathic focal VT because of perceived higher risk of coagulum formation and thromboembolic complications compared with ablation in the RV.

Ventricular Tachycardias Originating in the Aortic Sinuses of Valsalva

Mapping and ablation are generally performed under the guidance of fluoroscopy and 3-D mapping. ICE imaging or contrast aortography can be required to facilitate comprehensive mapping of the supraventricular region (Fig. 23.15). ICE allows direct visualization of the ablation catheter tip, aortic sinuses of Valsalva, left and right coronary artery ostia, and surrounding anatomy, and can potentially eliminate the need for angiography. For catheter ablation in the aortic sinuses of Valsalva, the ICE catheter is positioned in the RV inflow region, just past the tricuspid valve. Longitudinal views are best to appreciate the relationship of the RVOT and LVOT and for identifying the ostia of the coronary arteries. A cross-sectional view is of most value in identifying the sinuses themselves (Fig. 23.16). Once the three sinuses are visualized, the interatrial septum will be seen in immediate relationship to the noncoronary sinus. Rightward and anterior to the noncoronary sinus and immediately behind the RVOT lies the right sinus of Valsalva. Another landmark for the right sinus is that the septal and anterior leaflets of the tricuspid valve will meet at the junction between the right and noncoronary sinuses. The left sinus of Valsalva is identified as being leftward and anterior to the noncoronary sinus and in close relation to the anterior leaflet of the mitral valve. In addition, integration of 3-D electroanatomic mapping and ICE (CARTOSound, Biosense Webster) can facilitate tagging anatomical landmarks (coronary ostia) on the anatomical model. Doppler color flow can be used to determine the degree of aortic regurgitation before and after ablation.^{14,85}

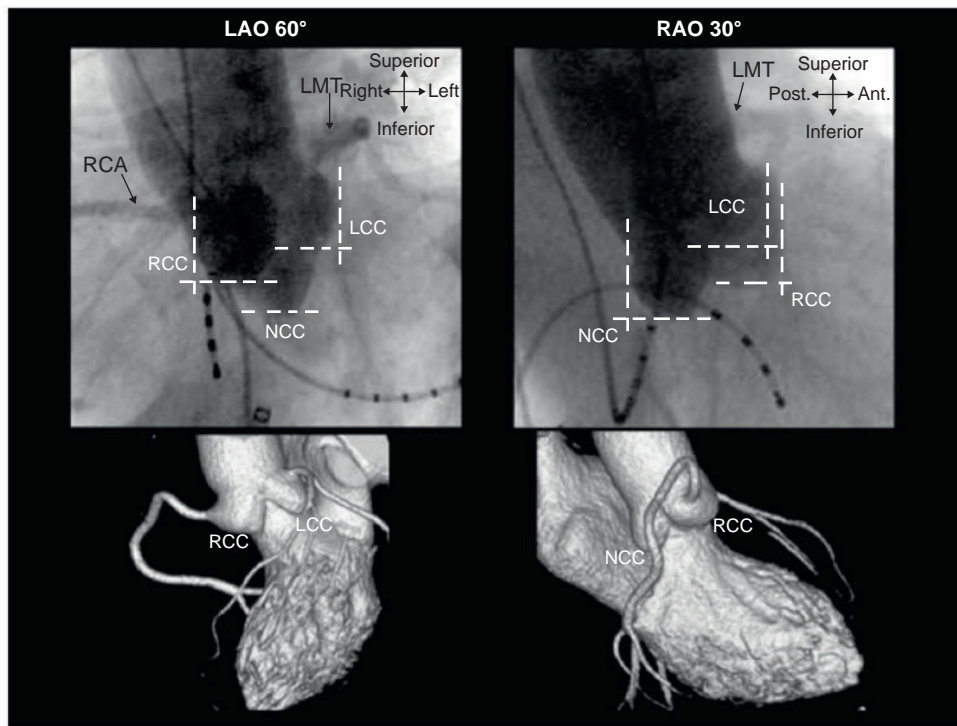


Fig. 23.15 Aortography and Multidetector Computed Tomography of the Aortic Sinuses of Valsalva. Relative positions among each sinus of Valsalva are viewed in the right anterior oblique (RAO) 30-degree, left anterior oblique (LAO) 60-degree projections. Ant., Anterior; LCC, left sinus of Valsalva; LMT, left main trunk; NCC, noncoronary sinus of Valsalva; Post., posterior; RCA, right coronary artery; RCC, right sinus of Valsalva. (From Sasaki T, Hachiya H, Hirao K, et al. Utility of distinctive local electrogram pattern and aortographic anatomical position in catheter manipulation at coronary cusps. *J Cardiovasc Electrophysiol*. 2011;22:521–529.)

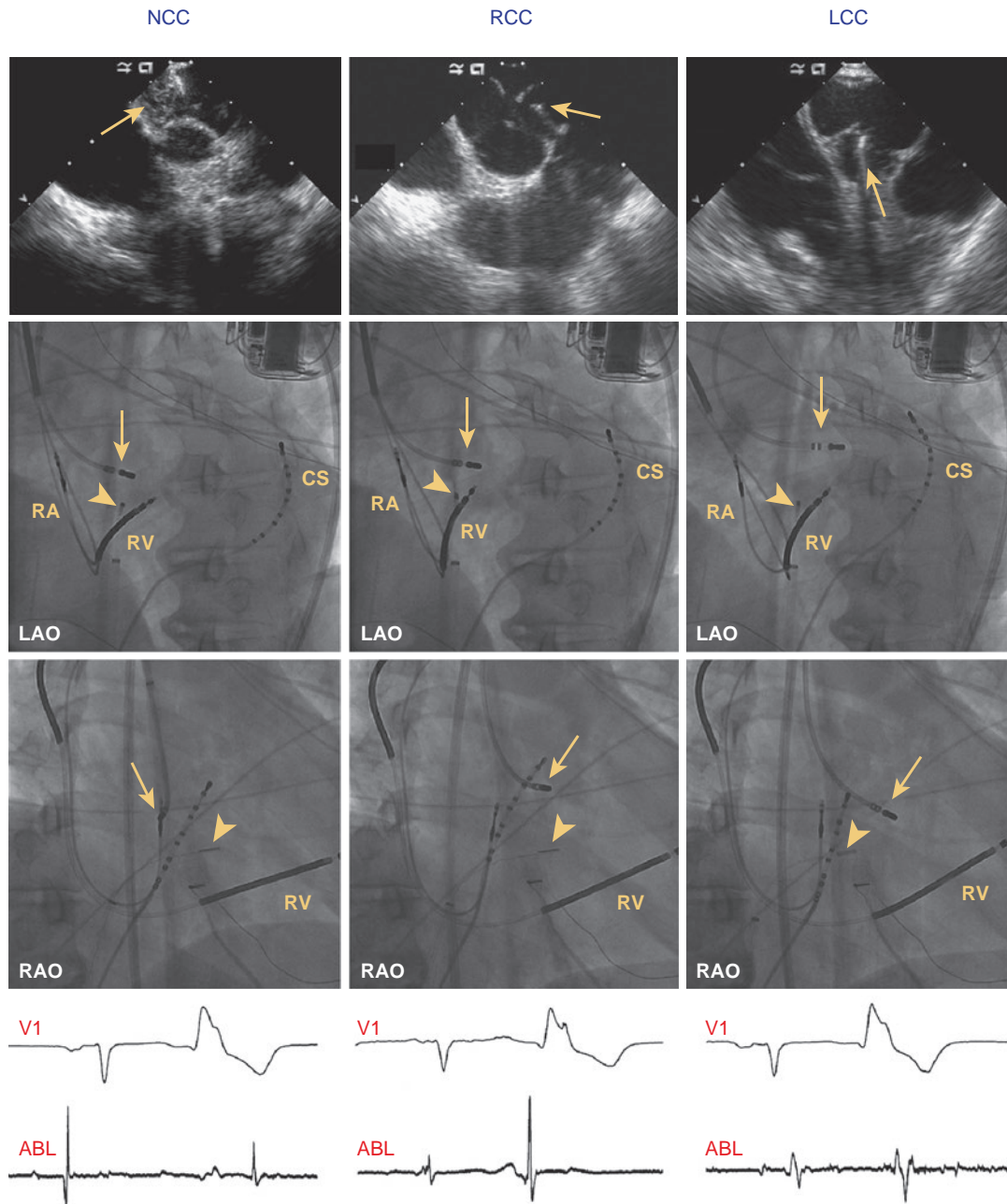


Fig. 23.16 Catheter Ablation in the Aortic Root. Top, Intracardiac echocardiography (ICE) images (*top row*) and left anterior oblique (LAO) and right anterior oblique (RAO) fluoroscopic views (*middle and bottom rows*, respectively). Bottom, Intracardiac recordings. Images and recordings were obtained during mapping in the noncoronary cusp (NCC, *left panels*), right coronary cusp (RCC, *middle panels*), and left coronary cusp (LCC, *left panels*). The ablation catheter tip on ICE and fluoroscopic images is marked by yellow arrows. Cross-sectional ICE images of the aortic valve were obtained with the ICE catheter (*arrowheads*) positioned at the His bundle region of the right ventricular (RV) septum. Right atrial (RA) and RV leads of an implantable cardioverter-defibrillator and a decapolar catheter positioned in the coronary sinus (CS) are marked. In the NCC, large near-field atrial and small far-field ventricular electrograms are recorded by the ablation (ABL) catheter tip. The recorded electrograms from the RCC show a large ventricular electrogram and far-field atrial electrogram. In the LCC, large ventricular and small, far-field atrial electrograms are recorded.

When mapping the aortic sinuses of Valsalva, it is important to consider the entire surface of each of the sinus regions (at the valve level and up to 2 cm above the valve), as well as the corresponding area just beneath the valve, as distinct activation times and pace maps might be obtained from each point. The aortic sinuses of Valsalva are not flat surfaces, and mapping the floor of each sinus often requires rotation

as well bending of the catheter tip. Also, moving the mapping catheter from one sinus to another typically requires withdrawing the catheter tip back toward the ascending aorta out of the recess of the sinus and then reorienting the catheter tip before advancing it into the recess of a neighboring sinus.¹⁴ In addition, myocardial extensions can exist between the right and left sinuses, and mapping and ablation of these

sites usually require the catheter prolapsed below the valve and flexed onto the aortic wall for contact and then gently pulled up into this commissural region.⁸⁸

The earliest endocardial activation time during VT or PVCs should be sought. In a subset (26%) of patients, meticulous mapping within the aortic root can uncover a discrete prepotential with an activation time preceding the QRS onset by more than 50 milliseconds, separated from the ventricular electrogram by an isoelectric interval. Such finding can predict a successful ablation site.⁸⁹

Notably, pace mapping may not be feasible within the aortic sinuses of Valsalva due to the inability to capture the ventricle. Pacing at high output can result in “remote” capture of ventricular myocardium with or without capture of local myocardial sleeves. Therefore pace mapping from the aortic sinuses of Valsalva can potentially produce a poor pace map, even when pacing from the site of origin of the VT, and hence it

is often of limited value to determine the site of origin of VAs arising in the aortic root.¹⁴ Pacing at the junction of left and right sinuses of Valsalva may produce different QRS configurations, due to varying exits from the site (Fig. 23.17). Multiple QRS configurations of VT or PVCs from this site, with multiple exits from a focus, have been described that can be eliminated with a single RF application.

A catheter positioned at the HB region in the RV can be very useful in mapping and ablation of aortic sinus of Valsalva VAs. The HB catheter can be used as a landmark for mapping within the noncoronary and right sinuses, where the proximity to the HB should be kept in mind to avoid inadvertent damage to the AV conduction system. Not infrequently, early far-field ventricular electrograms (reflecting aortic sinus activation) can be recorded preceding the later near-field electrograms reflecting activity of the RV HB region.²⁴ In addition, the local ventricular activation time relative to the QRS onset at the HB region

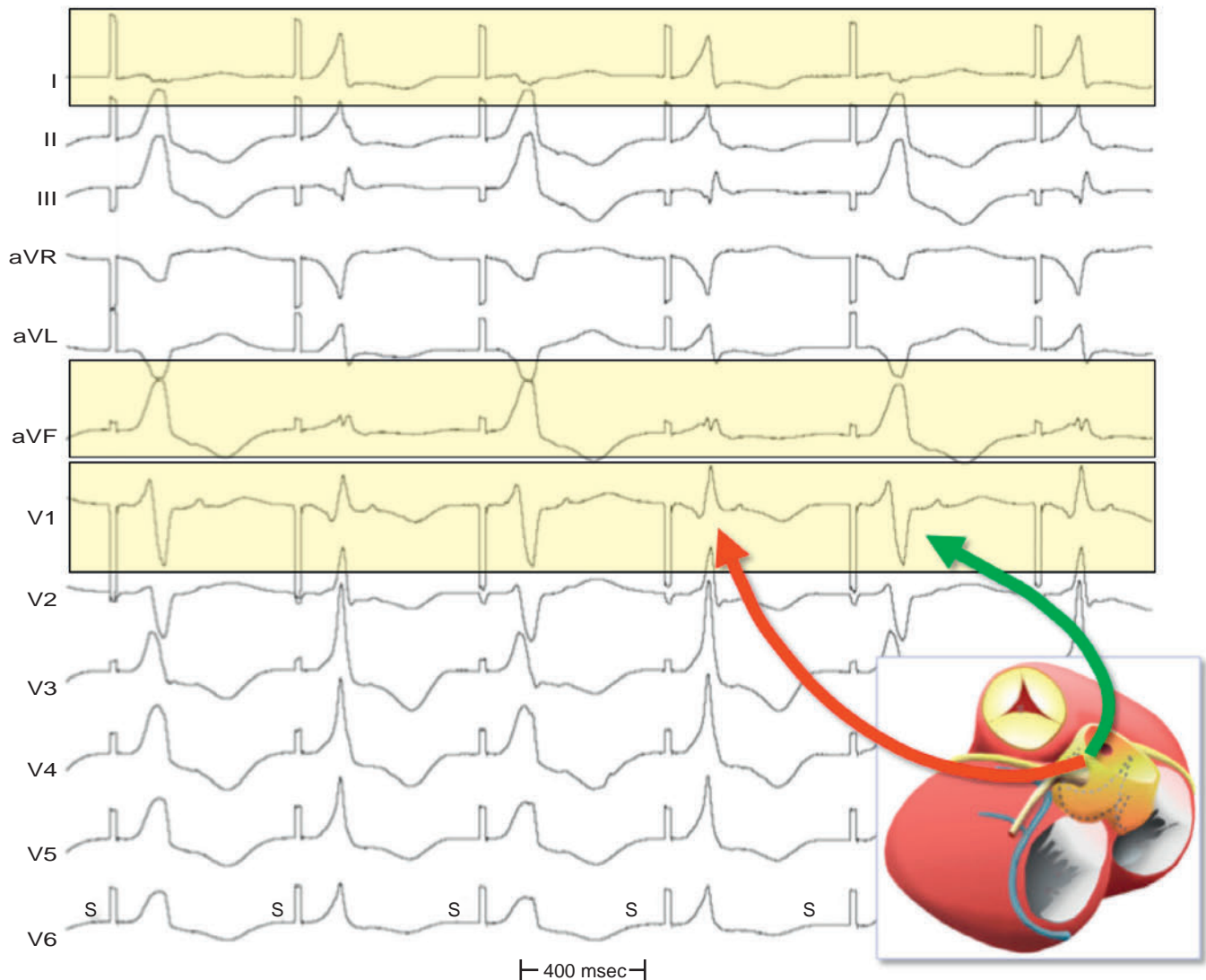


Fig. 23.17 Multiple Electrocardiogram (ECG) Configurations When Pacing From Left-Right Aortic Leaflet Commissure. All 12 ECG leads are shown during continuous pacing at a consistent site and output. Note wide differences in QRS configurations (left vs. right axis [lead I]; degrees of inferior axis [lead aVF]; left vs. right bundle branch block [lead V₁]). Diagram at bottom right is a cartoon of the aortic root showing possible paths of activation from the same source in the root, spreading in different directions around the right ventricular outflow tract to yield the ECG patterns shown.

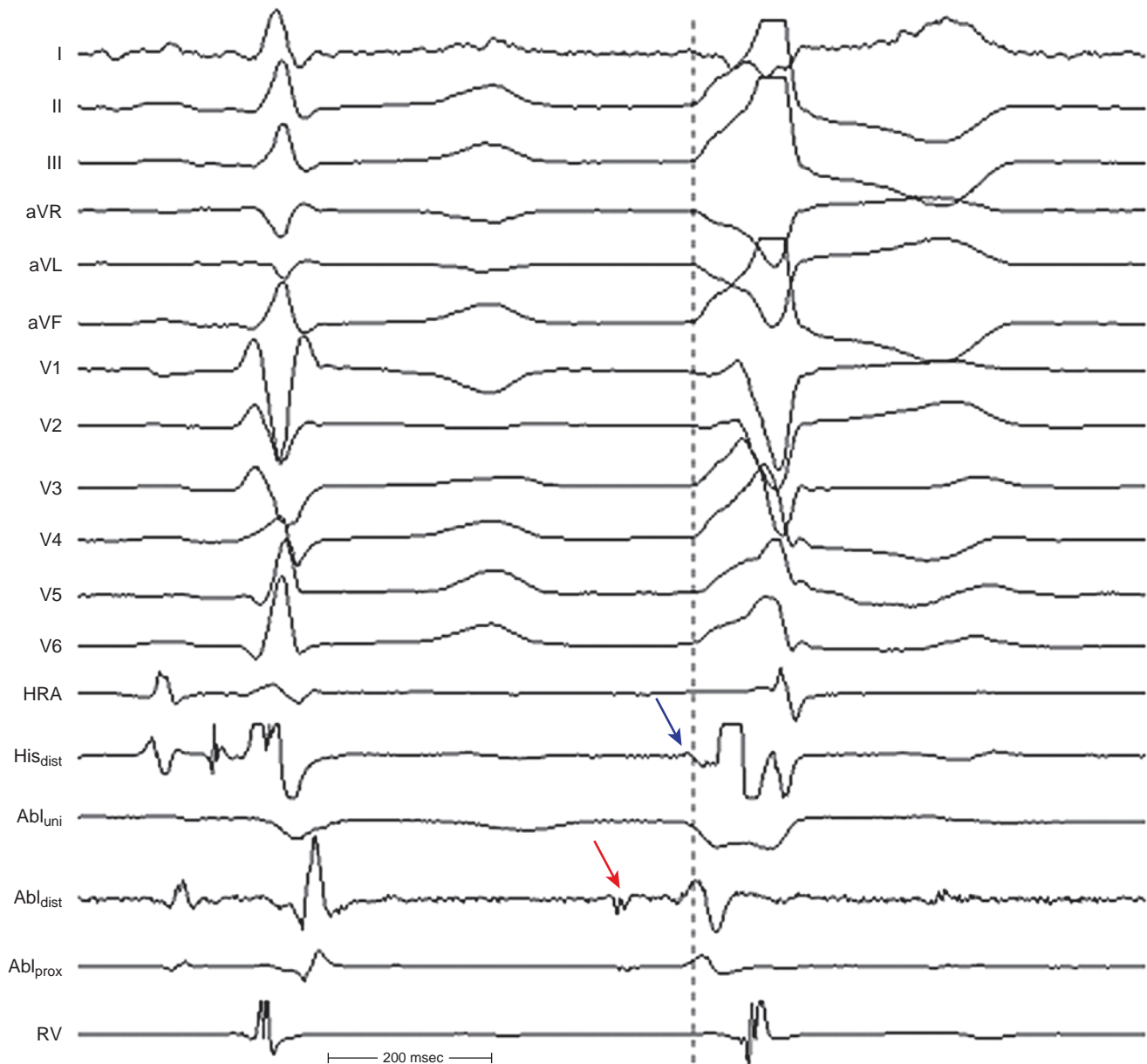


Fig. 23.18 Recordings From a Patient With Premature Ventricular Complexes (PVCs) Originating From the Right Aortic Sinus of Valsalva. A sinus rhythm complex as well as the PVC is shown; the vertical line denotes the onset of the PVC QRS. The blue arrow shows that the His bundle ventricular electrogram is slightly presystolic, whereas the red arrow shows the electrogram at the site of origin of the PVC in the sinus of Valsalva, occurring about 100 milliseconds prior to the QRS onset. *Abl_{dist}*, Distal ablation; *Abl_{prox}*, proximal ablation; *Abl_{uni}*, unipolar ablation; *His_{dist}*, distal His bundle; *HRA*, high right atrium; *RV*, right ventricle.

in the RV can be an important clue for differentiating VT origins in the aortic root. The activation time in the HB region is usually significantly earlier during PVCs originating from the right versus the left aortic sinus, suggesting that the activation from the right sinus of Valsalva may propagate to the ventricular septum and RV before the LV free wall, whereas that from the left sinus may do so after part of the LV free wall activates (Fig. 23.18). The local ventricular activation time relative to the QRS onset at the RV HB region typically is significantly later for the VAs with origins from the left sinus of Valsalva and the junction of the right and left sinuses than for those from the noncoronary and right sinuses. Not infrequently, early far-field ventricular electrograms

(reflecting aortic sinus of Valsalva activation) can be recorded preceding the later near-field electrograms reflecting activity of the RV HB region.²⁴

Before performing catheter ablation within the aortic sinuses of Valsalva, it is critical to ensure a safe distance (more than 5 to 10 mm) between the ablation target site and the ostia of the coronary arteries. This can be accomplished by aortic root angiography or selective angiography of the coronary arteries, performed with the ablation catheter positioned at the desired location (via separate arterial access). If the origin of VT is in the left sinus of Valsalva, cannulation the left main coronary artery with a 4 to 5 Fr left Judkin catheter can be utilized as

a marker and for protection of the left main coronary artery in case of ablation catheter dislodgment during RF application. Alternatively, a combination of electroanatomic mapping and ICE imaging (usually appreciated in the longitudinal view of the LVOT) can be used to confirm anatomical location, catheter tip position and contact, and distance to coronary vasculature and to monitor RF delivery. Longitudinal views are best to appreciate the relationship of the RVOT and LVOT and for identifying the ostia of the coronary arteries. For ablation performed in the left sinus of Valsalva or at the left-right sinus junction, the left main coronary ostium is easily visualized at approximately 6 o'clock of the cross-sectional view of the aortic root. Once the left main ostium is visualized, the catheter is rotated or advanced to locate the catheter tip to determine the distance from the coronary ostium. If the catheter tip is seen in the same plane as the coronary ostia, or the catheter tip cannot be clearly visualized, coronary angiography is performed. For ablation performed in the right sinus of Valsalva, a long-axis view of the aortic root is obtained. If the catheter tip is located at the level of the aortic cusp leaflets, a safe distance from the right coronary ostium can be assumed. If the catheter tip is at a level higher than the aortic sinus of Valsalva, above the sinotubular junction, aortic or coronary angiography is performed.⁸⁵

Irrigated or nonirrigated RF ablation catheters may be used for ablation of VAs arising in the aortic root. RF energy delivery in the aortic sinuses is preferably started at a low power output. Using a standard 4-mm-tip catheter, RF power is typically started at 15 to 20 W and then slowly titrated up to achieve a target temperature of 50°C to 55°C and an impedance drop of approximately 10 Ω . For irrigated ablation, RF energy delivery is preferably started at a 15 to 20 W and gradually increased to no more than 30 to 35 W. Occasionally powers of up to 50 W may be used for intramyocardial or epicardial foci targeted from the aortic root. The impedance drop should be carefully observed and power discontinued at any sign of a rise in impedance. It is advisable to apply RF energy during continuous fluoroscopy to observe for catheter dislodgment; RF application should be discontinued in case of even minimal dislodgment from the site showing the best mapping findings. When an acceleration or reduction in the frequency of the VT or PVCs is observed during the first 10 seconds of the application, RF delivery is continued for 30 to 60 seconds. Otherwise, RF delivery is terminated, and additional mapping is performed.²⁴ Coronary angiography is often performed immediately after the ablative procedure to exclude coronary artery spasm, dissection, or thrombus.

Right aortic sinus of Valsalva. Analysis of the electrogram is helpful for identifying the correct positioning of the mapping-ablation catheter at the aortic sinuses of Valsalva during the ablation procedure. The recorded electrogram from the right sinus of Valsalva typically shows a large ventricular electrogram, which represents activation of the overlying relatively thick posterior wall of the RVOT infundibulum (see Fig. 23.16). Because this tissue is immediately adjacent to the anterior portion of the right sinus, the electrogram may appear near field, and the site of early activation can be difficult to distinguish between arrhythmia origination from the myocardium extending above this cusp. Nonetheless, during PVCs originating from the right sinus of Valsalva itself, a smaller and relatively fragmented but near-field electrogram will be observed to precede the large ventricular electrogram and results from activation of the small myocardial sleeve extending into the sinus.

A far-field atrial electrogram may also be recorded in the right sinus of Valsalva, particularly at more posterior locations (closer to the noncoronary sinus), and it usually represents atrial activation of the antero-septal tricuspid annulus or the RA appendage.¹⁴

On fluoroscopy, a catheter positioned in the right sinus of Valsalva (using the retrograde approach) will point rightward in the LAO projection and anterior in the right anterior oblique (RAO) projection.

When the fluoroscopic view appears to suggest right sinus position but a large atrial electrogram is noted, the catheter should be manipulated with clockwise torque to see whether the atrial electrogram becomes larger. If so, the catheter is likely to be in the noncoronary sinus and the fluoroscopic images are misleading, perhaps because of atrial enlargement or counterclockwise rotation of the heart. In this setting, withdrawal of the catheter followed by application of counterclockwise torque and then advancing the catheter again will move the catheter from the noncoronary sinus to the right sinus of Valsalva.

Left aortic sinus of Valsalva. Electrograms obtained in the left sinus of Valsalva are the most variable of the aortic sinuses of Valsalva, but typically the ventricular electrogram amplitude is larger than that of the atrial electrogram. More anteriorly close to the commissure with the right sinus, a large ventricular electrogram, again originating in the posterior RVOT, can be recorded (see Fig. 23.16). More leftward and posteriorly, however, because of the aortomitral continuity, recorded ventricular electrograms are small and far field in nature. In the RAO fluoroscopic view, as the catheter is rotated counterclockwise in the left sinus, a relatively larger but usually far-field atrial electrogram is located representing LA activation close to the antero-septal mitral annulus.

A distinct potential preceding the QRS complex (prepotential) is often recorded at successful ablation sites during VAs originating from the left sinus of Valsalva. When the left sinus site appears early but ablation is unsuccessful, mapping should be extended to the posterior supraventricular pulmonary artery region and the transitional zone from the great cardiac vein to the anterior interventricular vein (LV summit).

Noncoronary aortic sinus of Valsalva. A large near-field atrial electrogram (much larger than the ventricular electrogram amplitude) is typically recorded in the noncoronary sinus of Valsalva, which represents activation of the thick myocardium of the interatrial septum located immediately posterior to the midportion of the noncoronary sinus (see Fig. 23.16). When the catheter is rotated leftward and rightward from the interatrial septum, electrograms from the LA and RA, respectively, are recorded. A far-field ventricular electrogram may also be recorded from the noncoronary sinus, and depending on the exact catheter location, this smaller electrogram may reflect ventricular activation of the posterior LVOT, antero-septal tricuspid annulus, or supraventricular myocardial activation.

On fluoroscopy, a catheter positioned in the noncoronary sinus of Valsalva will point posteriorly in the RAO projection. In the LAO projection, however, the noncoronary sinus can be difficult to distinguish from the left sinus of Valsalva because both appear to be somewhat leftward. When counterclockwise torque is applied and a large near-field atrial electrogram is seen, catheter location in the noncoronary sinus is verified.

The most inferior portions of the noncoronary and right sinuses of Valsalva are in contact with the membranous portion of the inter-ventricular septum, where it comes in close apposition to the penetrating HB. Because of this close proximity, a catheter recording HB activation across the tricuspid annulus typically records an early ventricular activation during VAs originating from the noncoronary and right sinuses of Valsalva. However, as compared with right sinus origins, noncoronary sinus VAs tend to have earlier ventricular activation in the HB region (typically preceding QRS onset by >25 milliseconds), and a larger atrial to ventricular electrogram amplitude ratio, as well as a narrower QRS duration (typically <150 milliseconds), and a smaller lead III/II ratio (typically <0.65).²⁴

In addition, because of the anatomical proximity to the HB, ablation within the noncoronary sinus of Valsalva can result in injury to the HB and AVN. Therefore, before RF energy application, it is important to carefully investigate the presence of His potential during sinus beats at the ablation target site. In addition, monitoring AV conduction and

applying RF energy output in an incremental fashion may help avoid such a complication.

Epicardial Idiopathic Ventricular Tachycardias

Idiopathic focal VAs requiring epicardial ablation (via the coronary venous system or transpericardial approach) are observed in up to 14% of patients. These VAs typically arise in close proximity to the coronary venous system in the LV summit and cardiac crux, including the anterior interventricular vein (which runs in the anterior interventricular sulcus parallel to the left anterior descending coronary artery), the great cardiac vein (which runs in the left AV groove parallel to the left circumflex coronary artery and forms the CS once it is joined by the left atrial oblique vein of Marshall and the posterolateral vein of the LV), the junction of the anterior interventricular and great cardiac veins (near the bifurcation of the left coronary artery), and less commonly the middle cardiac vein (which runs with the posterior descending coronary artery in the posterior interventricular groove).

An epicardial approach typically is not required for VAs originating in the RVOT. The anterior and lateral portions of the RVOT are fairly thin; thus ablation from the endocardium is usually effective, even when VT foci occur on the epicardial surface. The posterior RVOT (infundibulum) is much thicker, but the epicardial surface of the posterior infundibulum is the LVOT, and thus ablation may be effective from either the LVOT or the RVOT for arrhythmias arising deep in the myocardium of the posterior RVOT. For the supraaortic region there is no true epicardial location because the RVOT lies anterior to the right and left sinuses of Valsalva and the atria lie posterior to the noncoronary sinus.

Mapping findings suggestive of epicardial origin include suboptimal pace maps generated from the ventricular endocardial surface, absence of sharp potentials earlier than 15 milliseconds prior to QRS onset, low-amplitude far-field potentials at the earliest endocardial sites, the occurrence of a very slurred upstroke and wide QS complex, and a large area of equally (and minimally) presystolic sites on the activation map.

Ventricular Tachycardias Originating in the Left Ventricular Summit

The LV summit is the most common site of idiopathic epicardial LV arrhythmias. LV summit VAs are most commonly ablated within the great cardiac or anterior interventricular veins. CS venography can help delineate coronary venous anatomy and evaluate feasibility of access to the target area via the CS. Mapping can be facilitated by using small (2.5 Fr), flexible, multipolar electrode catheters introduced through a guiding catheter positioned at the coronary sinus ostium (CS os). Once the ablation catheter is positioned at the target site, and before RF energy delivery, coronary arteriography is performed to outline the spatial relationship between the target vein and the adjacent coronary artery (Fig. 23.19). Although the minimal safe distance between ablation sites and coronary arteries is not clear, ablation is not performed within 5 mm of a coronary artery. Coronary arteriography is also performed after ablation to rule out damage to coronary arteries. In addition, pacing from the distal ablation electrode should be performed at an output of 20 mA. If diaphragmatic capture can be demonstrated, then ablation should not be attempted to avoid phrenic nerve injury.

Although the coronary venous approach can be successful in more than half of patients with LV summit VAs, it is often technically limited. Currently available ablation catheters often are difficult to advance beyond the distal great cardiac vein or the proximal portions of the middle cardiac vein because of the tortuosity, sharp angulation, and small caliber of the distal veins. Also, the coronary veins offer only a limited access to parts of LV summit immediately adjacent to those

veins. In addition, proximity to within 5 mm of a coronary artery (as defined by coronary angiography) can be observed in about three quarters of patients, prohibiting RF ablation because of the potential risk of coronary injury. Furthermore, RF energy delivery is often limited because of impedance and temperature rise (due to limited cooling from surrounding blood flow). It is recommended to use irrigated catheters when ablating within the coronary veins. Cryoablation may also be considered because it is not limited by high impedance and is likely facilitated by low blood flow. Freezing also seems less likely to damage adjacent coronary arteries. However, the cryocatheter can be difficult to maneuver in the coronary venous system.^{14,75,90-92}

When the great cardiac vein is of sufficient size to allow adequate RF energy applications, the elimination of VT can be achieved in most patients. When this approach is not feasible or is unsuccessful, ablation can be attempted at the best identifiable endocardial sites in the LV (immediately below the aortic valve) or in the left aortic sinus. Not infrequently, RF application at the site closest to the early great cardiac vein site can produce a lesion of sufficient transmural to suppress VAs originating from the LV summit, despite a later local activation time (~10 milliseconds) and a poorer pace map at the successful ablation site compared with the best coronary venous site. A close anatomical distance (<13.5 mm) and a Q wave ratio of less than 1.45 in leads aVL/aVR may help identify the most appropriate cases for an ablation attempt from the left sinus of Valsalva or the adjacent LV endocardium in this setting. Also, a recent report found that all successful ablation sites had VAs with an initial r wave in lead I and local activation time within 7 milliseconds of the earliest activation site within the great cardiac vein.^{14,90,91}

When endocardial ablation and ablation from within the coronary venous system is not feasible or unsuccessful, the percutaneous trans-thoracic epicardial approach needs to be considered. The percutaneous epicardial approach, required in about 20% to 30% of patients with LV summit VAs, provides access to the entire epicardial surface and allows the deployment of a greater range of ablation catheters and energy sources (see Chapter 27 for a detailed discussion). However, in addition to the increased risk of complications, the transthoracic epicardial approach has significant limitations. Sedation and anesthesia as is generally used for transpericardial procedures can suppress arrhythmias. In addition, the close proximity of the coronary arteries and the thick layer of epicardial fat that overlies the proximal portion of these vessels ("the inaccessible area" in the superior aspect of the LV summit) often prohibit successful ablation in a significant proportion of these patients. In fact, LV summit foci account for the majority of ablation failures for OT VAs in the present era.^{14,74,75,90,91}

When epicardial ablation within the coronary veins or via the transpericardial approach is anticipated, an irrigated ablation catheter is preferred, giving the frequent occurrence of high tip temperatures limiting power delivery via nonirrigated catheters. Power output is typically started at 20 W with an irrigation flow rate of 30 mL/min. RF power output is increased gradually (up to 30 W within the coronary venous system, and 50 W within the pericardium), with a goal of impedance drop of impedance of 8 to 10 Ω . Precautions should be undertaken to avoid injuring the coronary arteries during ablation, as discussed above for ablation within the aortic root. RF ablation should never be performed within 5 mm of a coronary artery.

Ventricular Tachycardias Arising From the Cardiac Crux

VAs originating from the basal crux of the heart can be ablated via the middle cardiac vein, whereas ablation of apical crux VAs often requires the percutaneous subxiphoid epicardial approach. The use of thin multielectrode catheters can facilitate mapping distally in the middle cardiac vein.^{33,34}

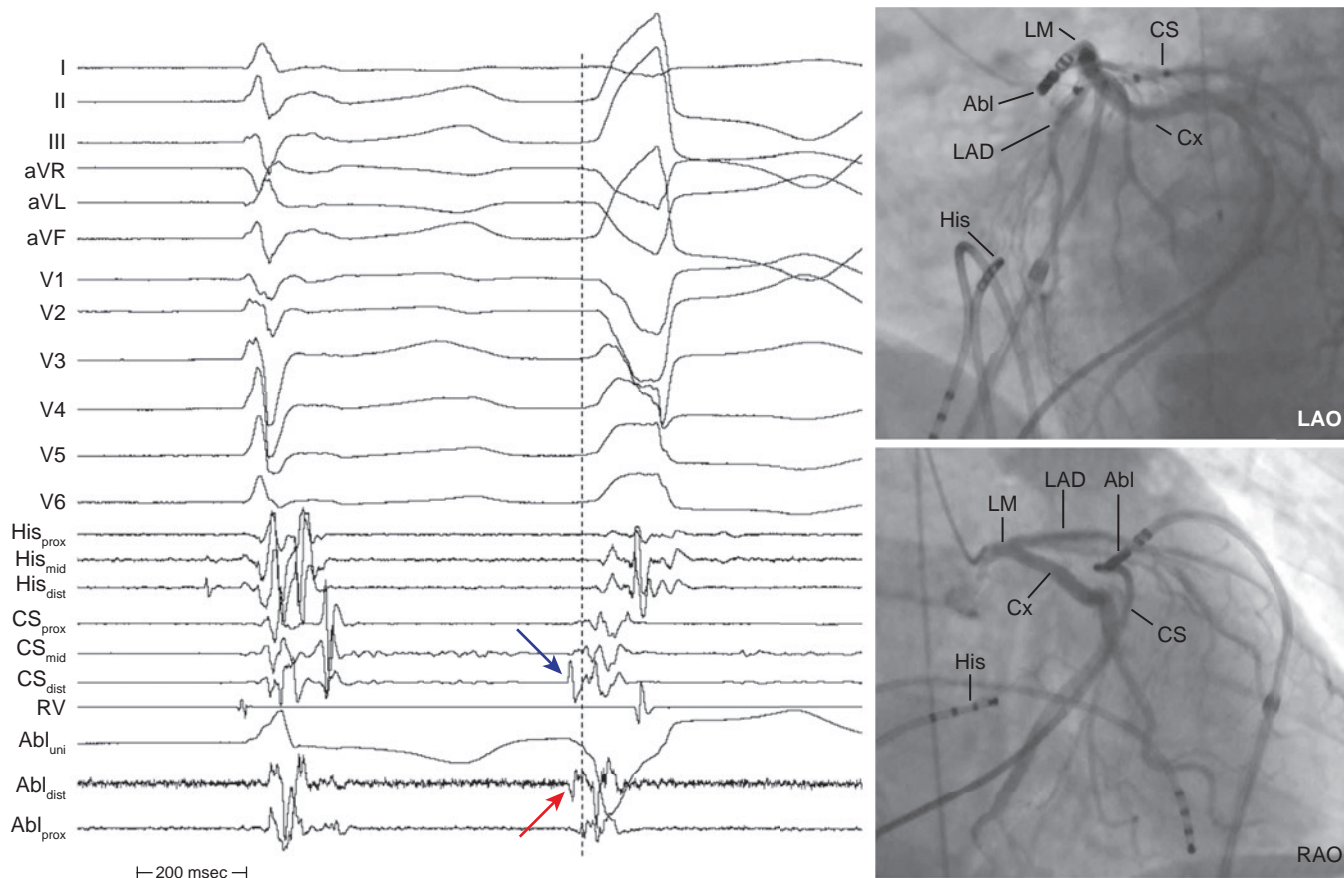


Fig. 23.19 Recordings From a Patient With Premature Ventricular Complexes (PVCs) Originating on the Left Ventricular (LV) Summit. The dashed line denotes the onset of the PVC QRS complex. Note that the distal coronary sinus electrogram (CS_{dist}) (blue arrow) occurs well before the onset of the QRS, similar to the ablation catheter recording in the pericardial space (red arrow); the location is shown in the fluoroscopic views at right (Abl). Abl_{dist}, Distal ablation; Abl_{prox}, proximal ablation; Abl_{uni}, unipolar ablation; Cx, circumflex coronary artery; CS_{prox}, proximal coronary sinus; His_{dist}, distal His bundle; His_{prox}, proximal His bundle; LAD, left anterior descending artery; LAO, left anterior oblique; LM, left main coronary artery; RAO, right anterior oblique; RV, right ventricle.

Ventricular Tachycardias Originating From the Left Ventricular Papillary Muscles

RF catheter ablation of these VAs is particularly challenging, likely secondary to the complex structure of the papillary muscles as well as the relatively deep intramural VT origins within the thick muscle. In addition, maintaining an adequate and stable catheter tip contact with the papillary muscle during ablation can be challenging because of the vigorous motion associated with normal papillary muscle contraction. Furthermore, induction of mechanical and thermally provoked ectopy can complicate catheter stability and hinder activation mapping.

While the retrograde transaortic approach to the LV usually is adequate for mapping and ablation of VAs originating from the posterior papillary muscle, the transseptal approach often provides added advantage for access and catheter stability to the anterior papillary muscle. The use of a long sheath can enhance catheter manipulation and stability. With the retrograde transaortic approach, a long SL0 or SL1 sheath (81 cm, St. Jude Medical) is often used with the tip of the sheath placed through the aortic valve into the LV. With the transseptal approach, a deflectable sheath with a large curve (Agilis, St. Jude Medical) is preferred with the tip positioned near the mitral annulus. In addition, ICE can help facilitate catheter navigation and positioning

and visualize direct contact with the papillary muscle (Fig. 23.20).⁹³ Ablation catheters with contact force capabilities can be of significant benefit in these procedures.^{30,31}

Sites with the earliest endocardial activation and matching pace maps are targeted by ablation. Purkinje potentials often (in 40% of patients) can be observed at successful ablation sites. Importantly, pace mapping alone is usually insufficient to guide successful ablation. The site of origin of VT can be located deep within the muscle and away from the exit site at the base of the papillary muscle. The latter sites can exhibit perfect pace maps but are not good targets for ablation.³¹

Use of high RF power delivered from an irrigated ablation catheter and RF lesions in a relatively wide area and, not infrequently, on both sides of the papillary muscle often are required to achieve successful ablation. For deep intramural arrhythmia sources, circumferential ablation at the base of the targeted papillary muscle (aiming for exit block) can overcome the anatomical limitations and improve the ablation outcome.^{31,34,94}

Of note, in up to 50% of patients, LV papillary muscle VAs exhibit variable QRS morphologies spontaneously or after the initial RF ablation lesions, likely related to different directions of propagation of the wavefront exiting the papillary muscle.

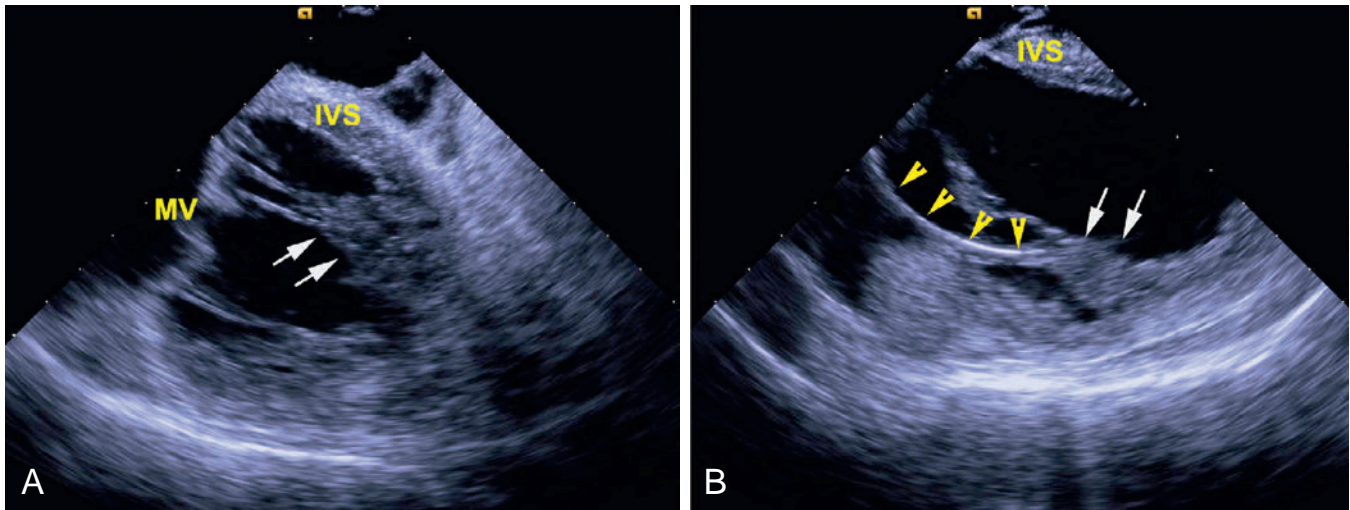


Fig. 23.20 Intracardiac Echocardiography (ICE) for Ablation of Arrhythmias Rising From Left Papillary Muscles. The ICE transducer is positioned in the right ventricle, across the tricuspid valve, abutting the interventricular septum (IVS). (A) The left posteromedial papillary muscle is visualized (white arrows). (B) The left anterolateral papillary muscle is visualized (white arrows) as well as the ablation catheters (yellow arrowheads) which was advanced across the mitral valve (via the atrial transseptal approach). ICE allows confirmation of catheter contact with the anterolateral muscles. MV, Mitral valve.

When catheter stability remains an issue, cryoablation can be considered. Cryoadhesion helps ensure constant contact of the ablation catheter to the target tissue on the mobile papillary muscle during ablation. The lack of catheter motion (as well as the lack of tissue heating) also limits mechanical and thermally induced ectopy, which can impede catheter stability. However, cryoablation may not result in sufficiently deep lesions to eliminate foci within the papillary muscle.³⁰

Para-Hisian Ventricular Tachycardias

If the earliest ventricular activation was observed close to the HB region (i.e., the area near the HB and within 10 mm of the largest His potential recording site) in the RV during the VT or PVCs, mapping should be extended to the aortic root and subaortic LV septum before attempting ablation in the RV His region. The most inferior portion of the non-coronary and right sinuses of Valsalva are in contact with the membranous portion of the interventricular septum where it comes in close apposition to the penetrating HB (see Fig. 9.1). Because of this close proximity, VAs originating from those two sinuses can be associated with early activation recorded from a catheter in the para-Hisian position across the tricuspid annulus, which likely represents a breakout point into the RV myocardium.

Ablation at the para-Hisian region carries a risk of AV block. To minimize this risk, it is recommended to use a standard, nonirrigated 4-mm tip ablation catheter and start RF energy application at low power output (10 to 20 W) with gradual titration up to the target output. RF application should be discontinued immediately if accelerated junctional rhythm or AV block is observed. It is also advisable to avoid ablation immediately over the proximal HB (as indicated by an A:V electrogram amplitude ratio above 1:1 with His potential).⁵⁹ Cryoablation can also potentially limit the risk of injury to the AV conduction system.

When ablation at the RV para-Hisian region causes a change in the QRS morphology during VT/PVCs, an aortic sinus of Valsalva focus should be suspected, since ablation in the RV region can potentially alter the connection from the sinus of Valsalva to the RV myocardium, which in turn precipitates the change in ventricular activation pattern.¹⁷

Intramural Ventricular Tachycardias

Diagnosis of an intramural VT/PVC foci is challenging and is often made only after extensive mapping of the left and RVs and related endocardial and epicardial anatomical areas. Clues for an intramural site of origin include (1) the earliest local activation sites on both sides of ventricular wall share a similar activation timing (within less than 10 milliseconds) and neither produce a satisfactory pace map; (2) far-field ventricular potentials preceding near-field local electrograms can be recorded in the endocardial and epicardial sites during VAs; (3) RF ablation at the site of the earliest local ventricular activation or best pace map (from the endocardial or epicardial side) results in either only transient suppression or no effect on the arrhythmia.^{29,95}

For intramural LVOT foci, RF ablation can be performed in a sequential manner from the endocardium followed by the epicardium (via the coronary venous system), or vice versa. For refractory cases, RF ablation can be performed simultaneously from two ablation catheters positioned on the endocardial and epicardial LVOT. The latter approach typically entails the application of irrigated unipolar RF current to the distal electrodes of two ablation catheters using two RF generators at the same sites. In intramural LVOT foci, this ablation approach was most successful when the distance between the endocardial and epicardial ablation sites was more than 8 mm and the local ventricular activation time relative to the QRS onset during the VAs earlier than -30 milliseconds was recorded in the aortomitral continuity or great cardiac vein. RF current can also be applied in a bipolar configuration from the distal electrode of the two ablation catheters. However, bipolar RFCA may not be effective when there is an impedance mismatch between the aortomitral continuity and coronary venous system, as the higher impedance of either electrode will limit the current that can be applied to both electrodes. An intramural needle ablation catheter has been developed to create an intramural RF lesion, but this catheter is not yet commercially available.^{29,95}

The region of the interventricular septum between the RVOT and LVOT can be mapped by using thinner multielectrode catheters advanced via the septal perforating venous tributaries of the great cardiac vein

that give direct access to intramural locations.⁹⁶ When this is not feasible, a recent report described the utility of infusing cold saline into those veins for the diagnosis of intramural foci. An irrigated-tip catheter is positioned in the distally in the great cardiac vein close to the origin of the anterior interventricular vein. During ongoing ventricular ectopy, cold saline is infused via catheter the ablation catheter at a rate of 60 mL/min for 10 seconds. Reproducible suppression of PVCs by cold saline infusion suggests an intramural PVC site of origin in the territory of the anterior interventricular vein. For intramural septal foci, several reports described the value of sequential or simultaneous irrigated RF ablation at the sites directly across the myocardial wall (right and left sides of the interventricular septum).^{97,98}

Endpoints of Ablation

Successful ablation is defined as the lack of spontaneous or inducible PVCs and VT, with and without isoproterenol administration (using the best method for induction documented before ablation), at least 30 minutes after ablation.

Outcome

The acute success rate of ablation of idiopathic VAs ranges from 75% to more than 90%.¹¹ The recurrence rate after an acutely successful ablation is approximately 15%. Of these, 40% recur during the first 24 to 48 hours after the ablation procedure. Recurrence of VT beyond the first year post ablation is rare. The acute success of ablation largely depends on the presence of spontaneous or inducible VT or PVCs at the time of the procedure, as well as on the anatomical site of origin of the arrhythmia. Predictors of recurrences include poor pace map, late activation at target sites, reliance on pace mapping alone, and termination of VT inducibility with mechanical trauma by the mapping-ablation catheter before RF delivery. Success rates are highest for RVOT VAs, but are more modest for VAs arising from the LV summit, papillary muscles, and intramural foci. Late (after few months of initially successful ablation) recurrences of PVCs can also be observed, especially in patients who had pleomorphic PVCs at baseline. Successful ablation of the dominant PVC focus can be followed by increasing frequency of previously nondominant foci.^{57,99}

Complications are very infrequent. RBBB develops in 2%, and cardiac tamponade is rare. Systemic thromboembolism and damage to the aortic valve (causing aortic regurgitation) can occur during ablation of LVOT or aortic sinus of Valsalva VAs.

The potential for acute coronary artery occlusion is a major risk consideration with catheter ablation within the aortic cusps. Damage to the coronary arteries can result from catheter manipulation and ablation in the aortic root, secondary to RF energy delivery in close proximity to the ostia of the right or left coronary arteries, as well as inadvertent catheter engagement of the left main coronary artery when ablating in the left aortic sinus of Valsalva. Damage to the left coronary artery and its branches can also complicate epicardial ablation via the coronary venous system or the percutaneous pericardial approach. It is also important to recognize the potential risk of coronary artery damage when ablating in the RVOT and pulmonary artery. The right coronary artery is typically 4 to 5 mm away from the proximal part of the RVOT near the free wall, and is separated by a variable amount of fat. In addition, the cephalocaudal separation of the pulmonic and aortic valve results in close proximity of the pulmonic valve to the origin of the right coronary artery, and the left main coronary artery lies in immediate posterior proximity to the subvalvular RVOT near the pulmonic valve as well as the supra-ventricular pulmonary artery; in fact, an ablation catheter at this site is closer to the left main coronary artery than a catheter at the floor of the left aortic sinus of Valsalva. Thus when concern exists about possibly damaging the artery, the

ablation catheter should be kept where energy delivery is to be given, and a root aortogram, coronary angiography, or careful ICE imaging should be performed.

Catheter ablation at the right or left para-Hisian region can cause AV block. Furthermore, the penetrating HB lies at the membranous septum formed in part by the commissure between the right and non-coronary sinuses, and ablation at this region can potentially damage the HB. Typically the HB electrogram can be recorded from the right sinus of Valsalva posteriorly, the noncoronary sinus anteriorly, and when the electrode has been prolapsed below the plane of the semilunar valve in between these two sinuses. However, during VT, the His potential can be inscribed within the ventricular electrogram because of retrograde activation to the HB, and hence may not be easily recognizable. Therefore, when ablating in the depths of the noncoronary sinus of Valsalva, particularly toward the junction with the right sinus, monitoring for fast pathway damage (AH interval prolongation, junctional beats) is advisable.²⁴

Cryoablation


Focal ablation of idiopathic VAs can be performed using an 8-mm cryoablation catheter (Freezor MAX 3, Medtronic, Minneapolis, MN, United States). A major advantage of cryoablation is the virtual absence of pain, which makes the use of analgesia unnecessary. Moreover, reasonable fluoroscopy and procedure times can be achieved by an experienced investigator. Stability of the catheter during cryoablation can be advantageous because monitoring of catheter position by fluoroscopy is not necessary. Adhesion of the catheter, however, requires precise positioning before the start of cryoablation. Slight dislocations, as may easily occur with breathing, can delay ablation success. Furthermore, brushing of the catheter within a small, defined area, as often observed with RF ablations, cannot occur; therefore repositioning of the catheter to adjust for a dislocation is not possible during cryoablation. The cryocatheter differs substantially in size and rigidity from standard RF catheters and requires some experience in handling.

Complete disappearance of the arrhythmia is typically observed within 20 seconds of freezing. Therefore cryoablation is stopped after 60 seconds if no positive effect is observed.

Given the high success rate and low risk of RF ablation of idiopathic VAs, it may be difficult to demonstrate a clinical advantage of cryoablation over RF ablation. Nonetheless, cryoablation can be of value in difficult or atypical sites when a maximal stability of the catheter is necessary—for example, to avoid dislodgment of the catheter into the coronary arteries during ablation of idiopathic VAs originating from the aortic sinuses of Valsalva. In addition, cryoablation may be considered for elimination of epicardial VAs from within the coronary venous system, when RF energy delivery is limited. Cryoablation may have a role in para-Hisian PVCs to reduce the risk of AV block. Also, the absence of pain during ablation may render the procedure more comfortable for the patient, especially when the use of sedative medications suppresses inducibility of the VT.¹⁰⁰


VIDEOS

The following videos accompany this chapter:

See Video 6.22. Cardiac Anatomy (Segmented Computed Tomography) 

See Video 6.19. Intracardiac Echocardiography Imaging of the Left Ventricle and Aortic Valve 

See Video 6.20. Intracardiac Echocardiography for Visualization of the Papillary Muscle 

Video 23.1. Ablation of Ventricular Tachycardia Originating From the Aortic Root: Guided by Intracardiac Echocardiography 

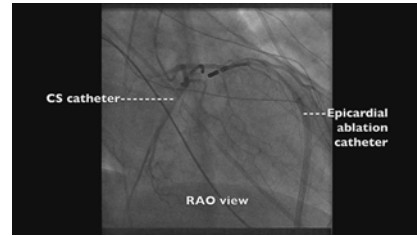
- ▶ **Video 23.2.** Epicardial Ablation of Focal Ventricular Tachycardia Originating From the Left Ventricular Summit
- ▶ **See Video 6.16.** Outflow Tract Ventricular Tachycardia: Noncontact Mapping

REFERENCES

- Mittal S. 'Focal' ventricular tachycardia: insights from catheter ablation. *Heart Rhythm*. 2008;5:S64–S67.
- Maury P, Rollin A, Mondoly P, et al. Management of outflow tract ventricular arrhythmias. *Curr Opin Cardiol*. 2015;30:50–57.
- Sadek MM, et al. Idiopathic ventricular arrhythmias originating from the moderator band: electrocardiographic characteristics and treatment by catheter ablation. *Heart Rhythm*. 2015;12:67–75.
- Potfay J, et al. Abnormal left ventricular mechanics of ventricular ectopic beats: insights into origin and coupling interval in premature ventricular contraction induced cardiomyopathy. *Circ Arrhythm Electrophysiol*. 2015;8:1194–1200.
- Wang Y, et al. Cellular mechanism of premature ventricular contraction-induced cardiomyopathy. *Heart Rhythm*. 2014;11:2064–2072.
- Sadron Blaye-Felice M, et al. Premature ventricular contraction-induced cardiomyopathy: related clinical and electrophysiologic parameters. *Heart Rhythm*. 2016;13:103–110.
- Cha YM, Lee GK, Klarich KW, et al. Premature ventricular contraction-induced cardiomyopathy: a treatable condition. *Circ Arrhythm Electrophysiol*. 2012;5:229–236.
- Lee YH, et al. Frequency, origin, and outcome of ventricular premature complexes in patients with or without heart diseases. *Am J Cardiol*. 2014;114:1373–1378.
- Carballeira Pol L, et al. Ventricular premature depolarization QRS duration as a new marker of risk for the development of ventricular premature depolarization-induced cardiomyopathy. *Heart Rhythm*. 2014;11:299–306.
- Ban J-E, et al. Electrocardiographic and electrophysiological characteristics of premature ventricular complexes associated with left ventricular dysfunction in patients without structural heart disease. *Europace*. 2013;15:735–741.
- Bas HD, et al. Effect of circadian variability in frequency of premature ventricular complexes on left ventricular function. *Heart Rhythm*. 2015;13:98–102.
- Deyell MW, et al. Predictors of recovery of left ventricular dysfunction after ablation of frequent ventricular premature depolarizations. *Heart Rhythm*. 2012;9:1465–1472.
- Hamon D, et al. A new combined parameter to predict premature ventricular complexes induced cardiomyopathy: impact and recognition of epicardial origin. *J Cardiovasc Electrophysiol*. 2016;27:10–12.
- Hutchinson MD, Garcia FC. An organized approach to the localization, mapping, and ablation of outflow tract ventricular arrhythmias. *J Cardiovasc Electrophysiol*. 2013;24:1189–1198.
- Acosta J, et al. Impact of earliest activation site location in the septal right ventricular outflow tract for identification of left vs right outflow tract origin of idiopathic ventricular arrhythmias. *Heart Rhythm*. 2015;12:726–734.
- Anderson R. Clinical anatomy of the aortic root. *Heart*. 2000;84:670–673.
- Motonaga KS, Ceresnak SR, Hsia HH. Unusual outflow tract ventricular tachycardia. *Card Electrophysiol Clin*. 2016;8:79–88.
- Hai JJ, Lachman N, Syed FF, et al. The anatomic basis for ventricular arrhythmia in the normal heart: what the student of anatomy needs to know. *Clin Anat*. 2014;27:885–893.
- Liao Z, et al. Idiopathic ventricular arrhythmias originating from the pulmonary sinus cusp. *J Am Coll Cardiol*. 2015;66:2633–2644.
- Liu CF, et al. Ubiquitous myocardial extensions into the pulmonary artery demonstrated by integrated intracardiac echocardiography and electroanatomic mapping changing the paradigm of idiopathic right ventricular outflow tract arrhythmias. *Circ Arrhythm Electrophysiol*. 2014;7:691–700.
- Ho SY. Structure and anatomy of the aortic root. *Eur J Echocardiogr*. 2009;10:3–10.
- Ouyang F, et al. Ventricular arrhythmias arising from the left ventricular outflow tract below the aortic sinus cusps: mapping and catheter ablation via transseptal approach and electrocardiographic characteristics. *Circ Arrhythm Electrophysiol*. 2014;7:445–455.
- Anderson RH. The surgical anatomy of the aortic root. *Multimed Man Cardiothorac Surg*. 2007;2007:mmcts.2006.002527.
- Yamada T, et al. Prevalence and clinical, electrocardiographic, and electrophysiologic characteristics of ventricular arrhythmias originating from the noncoronary sinus of Valsalva. *Heart Rhythm*. 2013;10:1605–1612.
- Deleted in review.
- Faletra FF, Ho SY, Auricchio A. Anatomy of right atrial structures by real-time 3D transesophageal echocardiography. *JACC Cardiovasc Imaging*. 2010;3:966–975.
- Enriquez A, et al. How to map and ablate left ventricular summit arrhythmias. *Heart Rhythm*. 2017;14:141–148.
- Deleted in review.
- Yamada T, et al. Radiofrequency catheter ablation of idiopathic ventricular arrhythmias originating from intramural foci in the left ventricular outflow tract: efficacy of sequential versus simultaneous unipolar catheter ablation. *Circ Arrhythm Electrophysiol*. 2015;8:344–352.
- Deleted in review.
- Enriquez A, Supple GE, Marchlinski FE, et al. How to map and ablate papillary muscle ventricular arrhythmias. *Heart Rhythm*. 2017;14:1721–1728.
- Naksuk N, Kapa S, Asirvatham SJ. Spectrum of ventricular arrhythmias arising from papillary muscle in the structurally normal heart. *Card Electrophysiol Clin*. 2016;8:555–565.
- Kawamura M, et al. Idiopathic ventricular arrhythmia originating from the cardiac crux or inferior septum epicardial idiopathic ventricular arrhythmia. *Circ Arrhythm Electrophysiol*. 2014;7:1152–1158.
- Kawamura M, et al. Clinical and electrocardiographic characteristics of idiopathic ventricular arrhythmias with right bundle branch block and superior axis: comparison of apical crux area and posterior septal left ventricle. *Heart Rhythm*. 2015;12:1137–1144.
- Sirichand S, et al. Incidence of idiopathic ventricular arrhythmias. *Circ Arrhythm Electrophysiol*. 2017;10:e004662.
- Luebbert J, Auberson D, Marchlinski F. Premature ventricular complexes in apparently normal hearts. *Card Electrophysiol Clin*. 2016;8:503–514.
- van Huls van Taxis CFB, et al. Fatigue as presenting symptom and a high burden of premature ventricular contractions are independently associated with increased ventricular wall stress in patients with normal left ventricular function. *Circ Arrhythm Electrophysiol*. 2015;8:1452–1459.
- Penela D, et al. Ablation of frequent PVC in patients meeting criteria for primary prevention ICD implant: safety of withholding the implant. *Heart Rhythm*. 2015;12:2434–2442.
- Peachey H, et al. EHRA/HRS/APHRS Expert consensus on ventricular arrhythmias. *Heart Rhythm*. 2014;11:e166–e196.
- Nucifora G, et al. Prevalence and prognostic value of concealed structural abnormalities in patients with apparently idiopathic ventricular arrhythmias of left versus right ventricular origin: a magnetic resonance imaging study. *Circ Arrhythm Electrophysiol*. 2014;7:456–462.
- Hoffmayer KS, Scheinman MM. Electrocardiographic characteristics of ventricular tachycardia in arrhythmogenic right ventricular dysplasia. *Card Electrophysiol Clin*. 2014;6:595–601.
- Hoffmayer KS, et al. Electrocardiographic comparison of ventricular arrhythmias in patients with arrhythmogenic right ventricular cardiomyopathy and right ventricular outflow tract tachycardia. *J Am Coll Cardiol*. 2011;58:831–838.
- Ren L, et al. Electrocardiographic difference between ventricular arrhythmias from the right ventricular outflow tract and idiopathic



Video 23.1 Ablation of Ventricular Tachycardia Originating From the Aortic Root: Guided by Intracardiac Echocardiography. *Part 1:* Intracardiac echocardiography (ICE) of the aortic valve. A cross-section image of the aortic valve is obtained with the ICE catheter positioned in the mid right atrium (RA) with slight anterior deflection. Clockwise torque of the ICE catheter brings its tip closer to the aortic root (His bundle region) and better visualizes the interatrial septum and left atrium (LA). *Part 2:* With the ICE catheter in the mid RA, anterior and clockwise deflection of the catheter tip to the medial aspect of the tricuspid annulus allows a long-axis view of the left ventricle (LV), LV outflow region and mitral valve (MV), and LA. From that position, counterclockwise torque of the catheter brings more of the RA in view as well as the TV, RV, and cross-section of the aortic valve. *Part 3:* A cross-sectional view of the aortic valve with the tip of the ablation catheter (Abl) visualized in the NCC. *Part 4:* A cross-sectional view of the aortic valve with the tip of the ablation catheter visualized in the RCC. *Part 5:* A cross-sectional view of the aortic valve with the tip of the ablation catheter visualized in the LCC. *Part 6:* A long-axis view of the aortic root with the tip of the ablation catheter visualized in the LCC. LCC, Left coronary cusp; NCC, noncoronary cusp; RCC, right coronary cusp; RV, right ventricle; TV, tricuspid valve.



Video 23.2 Epicardial Ablation of Focal Ventricular Tachycardia Originating From the Left Ventricular Summit. Right anterior oblique (RAO) and left anterior oblique (LAO) fluoroscopic views during selective left coronary angiography with the ablation catheter positioned at the site of origin of focal ventricular tachycardia (VT) originating from the left ventricle (LV) summit. The ablation catheter is positioned epicardially via the subxiphoid percutaneous approach. Note the proximity of the ablation catheter to the left anterior descending coronary artery. CS, Coronary sinus.

- right ventricular arrhythmias. *Pacing Clin Electrophysiol.* 2014;37:1658–1664.
44. Hoffmayer KS, et al. An electrocardiographic scoring system for distinguishing right ventricular outflow tract arrhythmias in patients with arrhythmogenic right ventricular cardiomyopathy from idiopathic ventricular tachycardia. *Heart Rhythm.* 2013;10:477–482.
 45. Denis A, et al. Diagnostic value of isoproterenol testing in arrhythmogenic right ventricular cardiomyopathy. *Circ Arrhythm Electrophysiol.* 2014;7:590–597.
 46. El Kadri M, et al. Effect of ablation of frequent premature ventricular complexes on left ventricular function in patients with nonischemic cardiomyopathy. *Heart Rhythm.* 2015;12:706–713.
 47. Penela D, et al. Neurohormonal, structural, and functional recovery pattern after premature ventricular complex ablation is independent of structural heart disease status in patients with depressed left ventricular ejection fraction: a prospective multicenter study. *J Am Coll Cardiol.* 2013;62:1195–1202.
 48. Van Herendael H, et al. Catheter ablation of ventricular fibrillation: importance of left ventricular outflow tract and papillary muscle triggers. *Heart Rhythm.* 2014;11:566–573.
 49. Kim YR, et al. Second coupling interval of nonsustained ventricular tachycardia to distinguish malignant from benign outflow tract ventricular tachycardias. *Heart Rhythm.* 2014;11:2222–2229.
 50. Yokokawa M, et al. Relation of symptoms and symptom duration to premature ventricular complex-induced cardiomyopathy. *Heart Rhythm.* 2012;9:92–95.
 51. Gopinathannair R, et al. Arrhythmia-induced cardiomyopathies mechanisms, recognition, and management. *J Am Coll Cardiol.* 2015;66:1714–1728.
 52. Ling Z, et al. Radiofrequency ablation versus antiarrhythmic medication for treatment of ventricular premature beats from the right ventricular outflow tract prospective randomized study. *Circ Arrhythm Electrophysiol.* 2014;7:237–243.
 53. Zhong L, et al. Relative efficacy of catheter ablation vs antiarrhythmic drugs in treating premature ventricular contractions: a single-center retrospective study. *Heart Rhythm.* 2014;11:187–193.
 54. Lamba J, et al. Radiofrequency catheter ablation for the treatment of idiopathic premature ventricular contractions originating from the right ventricular outflow tract: a systematic review and meta-analysis. *Pacing Clin Electrophysiol.* 2014;37:73–78.
 55. Tanawuttiwat T, Nazarian S, Calkins H. The role of catheter ablation in the management of ventricular tachycardia. *Eur Heart J.* 2016;37:594–609.
 56. Hasdemir C, et al. Time course of recovery of left ventricular systolic dysfunction in patients with premature ventricular contraction-induced cardiomyopathy. *Pacing Clin Electrophysiol.* 2013;0:1–6.
 57. Baser K, et al. Recurrence of PVCs in patients with PVC-induced cardiomyopathy. *Heart Rhythm.* 2015;12:1519–1523.
 58. Wasmer K, et al. Ventricular arrhythmias from the mitral annulus: patient characteristics, electrophysiological findings, ablation, and prognosis. *Heart Rhythm.* 2013;10:783–788.
 59. Yamada T, McElderry HT, Doppalapudi H, et al. Catheter ablation of ventricular arrhythmias originating in the vicinity of the His bundle: significance of mapping the aortic sinus cusp. *Heart Rhythm.* 2008;5:37–42.
 60. Anter E, Frankel DS, Marchlinski FE, et al. Effect of electrocardiographic lead placement on localization of outflow tract tachycardias. *Heart Rhythm.* 2012;9:697–703.
 61. Asirvatham SJ, Stevenson WG. Similia similibus curantur. *Circ Arrhythm Electrophysiol.* 2013;6:85–86.
 62. Ouyang F, et al. Repetitive monomorphic ventricular tachycardia originating from the aortic sinus cusp: electrocardiographic characterization for guiding catheter ablation. *J Am Coll Cardiol.* 2002;39:500–508.
 63. Betensky BP, et al. The V(2) transition ratio: a new electrocardiographic criterion for distinguishing left from right ventricular outflow tract tachycardia origin. *J Am Coll Cardiol.* 2011;57:2255–2262.
 64. Yoshida N, et al. A novel electrocardiographic criterion for differentiating a left from right ventricular outflow tract tachycardia origin: the V2S/V3R index. *J Cardiovasc Electrophysiol.* 2014;25:747–753.
 65. Yoshida N, et al. Novel transitional zone index allows more accurate differentiation between idiopathic right ventricular outflow tract and aortic sinus cusp ventricular arrhythmias. *Heart Rhythm.* 2011;8:349–356.
 66. Bradfield JS, Homsy M, Shivkumar K, et al. Coupling interval variability differentiates ventricular ectopic complexes arising in the aortic sinus of Valsalva and great cardiac vein from other sources: mechanistic and arrhythmic risk implications. *J Am Coll Cardiol.* 2014;63:2152–2158.
 67. Lin D, et al. Twelve-lead electrocardiographic characteristics of the aortic cusp region guided by intracardiac echocardiography and electroanatomic mapping. *Heart Rhythm.* 2008;5:663–669.
 68. Yamada T, et al. Idiopathic ventricular arrhythmias originating from the aortic root. Prevalence, electrocardiographic and electrophysiologic characteristics, and results of radiofrequency catheter ablation. *J Am Coll Cardiol.* 2008;52:139–147.
 69. Yamada T, et al. Electrocardiographic characteristics of ventricular arrhythmias originating from the junction of the left and right coronary sinuses of Valsalva in the aorta: the activation pattern as a rationale for the electrocardiographic characteristics. *Heart Rhythm.* 2008;5:184–192.
 70. Bala R, et al. Electrocardiographic and electrophysiologic features of ventricular arrhythmias originating from the right/left coronary cusp commissure. *Heart Rhythm.* 2010;7:312–322.
 71. Alasady M, Singleton CB, McGavigan AD. Left ventricular outflow tract ventricular tachycardia originating from the noncoronary cusp: electrocardiographic and electrophysiological characterization and radiofrequency ablation. *J Cardiovasc Electrophysiol.* 2009;20:1287–1290.
 72. Hayashi T, et al. Outcomes of catheter ablation of idiopathic outflow tract ventricular arrhythmias with an R wave pattern break in lead V2: a distinct clinical entity. *J Cardiovasc Electrophysiol.* 2017;28:504–514.
 73. Daniels DV, et al. Idiopathic epicardial left ventricular tachycardia originating remote from the sinus of Valsalva: electrophysiological characteristics, catheter ablation, and identification from the 12-lead electrocardiogram. *Circulation.* 2006;113:1659–1666.
 74. Yamada T, et al. Idiopathic ventricular arrhythmias originating from the left ventricular summit anatomic concepts relevant to ablation. *Circ Arrhythm Electrophysiol.* 2010;3:616–623.
 75. Lin CY, et al. Radiofrequency catheter ablation of ventricular arrhythmias originating from the continuum between the aortic sinus of Valsalva and the left ventricular summit: electrocardiographic characteristics and correlative anatomy. *Heart Rhythm.* 2015;13:111–121.
 76. Yamada T, Doppalapudi H, Litovsky SH, et al. Challenging radiofrequency catheter ablation of idiopathic ventricular arrhythmias originating from the left ventricular summit near the left main coronary artery. *Circ Arrhythm Electrophysiol.* 2016;9:e004202.
 77. Al'Aref SJ, et al. Differentiation of papillary muscle from fascicular and mitral annular ventricular arrhythmias in patients with and without structural heart disease. *Circ Arrhythm Electrophysiol.* 2015;8:616–624.
 78. Chen M, et al. Idiopathic accelerated idioventricular rhythm or ventricular tachycardia originating from the right bundle branch: unusual type of ventricular arrhythmia. *Circ Arrhythm Electrophysiol.* 2014;7:1159–1167.
 79. Li T, et al. Combined approach improves the outcomes of catheter ablation of idiopathic ventricular arrhythmias originating from the vicinity of tricuspid annulus. *Pacing Clin Electrophysiol.* 2014;37:624–629.
 80. Ban JE, et al. Idiopathic ventricular arrhythmia originating from the para-Hisian area: prevalence, electrocardiographic and electrophysiological characteristics. *J Arrhythmia.* 2014;30:48–54.
 81. Sorgente A, et al. Negative concordance pattern in bipolar and unipolar recordings: an additional mapping criterion to localize the site of origin of focal ventricular arrhythmias. *Heart Rhythm.* 2016;13:519–526.
 82. Luther V, Qureshi N, Kanagaratnam P, et al. Automated activation and pace-mapping to guide ablation within the outflow tract. *J Cardiovasc Electrophysiol.* 2015;27:127–128.

83. Lüker J, et al. Automated template matching correlates with earliest activation during mapping of idiopathic premature ventricular contractions. *Int J Cardiol Heart Vessel*. 2014;4:25–29.
84. Zhang F, et al. Noncontact mapping to guide ablation of right ventricular outflow tract arrhythmias. *Heart Rhythm*. 2013;10:1895–1902.
85. Hoffmayer KS, et al. Safety of radiofrequency catheter ablation without coronary angiography in aortic cusp ventricular arrhythmias. *Heart Rhythm*. 2014;11:1117–1121.
86. Andreu D, et al. Displacement of the target ablation site and ventricles during premature ventricular contractions: relevance for radiofrequency catheter ablation. *Heart Rhythm*. 2012;9:1050–1057.
87. Miyazawa K, et al. Rapid mapping and differentiation in ventricular outflow tract arrhythmia using non-contact mapping. *J Interv Card Electrophysiol*. 2017;49:41–49.
88. Sasaki T, et al. Utility of distinctive local electrogram pattern and aortographic anatomical position in catheter manipulation at coronary cusps. *J Cardiovasc Electrophysiol*. 2011;22:521–529.
89. Hachiya H, et al. Discrete prepotential as an indicator of successful ablation in patients with coronary cusp ventricular arrhythmia. *Circ Arrhythm Electrophysiol*. 2013;6:898–904.
90. Nagashima K, et al. Ventricular arrhythmias near the distal great cardiac vein challenging arrhythmia for ablation. *Circ Arrhythm Electrophysiol*. 2014;7:906–912.
91. Jauregui Abularach ME, et al. Ablation of ventricular arrhythmias arising near the anterior epicardial veins from the left sinus of Valsalva region: ECG features, anatomic distance, and outcome. *Heart Rhythm*. 2012;9:865–873.
92. Mountantonakis SE, et al. Ventricular arrhythmias from the coronary venous system: prevalence, mapping, and ablation. *Heart Rhythm*. 2015;12:1145–1153.
93. Proietti R, et al. Intracardiac echo-facilitated 3D electroanatomical mapping of ventricular arrhythmias from the papillary muscles: assessing the ‘fourth dimension’ during ablation. *Europace*. 2016;19:euw099.
94. Wo H-T, et al. Circumferential ablation at the base of the left ventricular papillary muscles: a highly effective approach for ventricular arrhythmias originating from the papillary muscles. *Int J Cardiol*. 2016;220:876–882.
95. Yamada T, et al. Prevalence and electrocardiographic and electrophysiological characteristics of idiopathic ventricular arrhythmias originating from intramural foci in the left ventricular outflow tract. *Circ Arrhythm Electrophysiol*. 2016;9:e004079.
96. Chen H, et al. Intramural outflow tract ventricular tachycardia anatomy, mapping, and ablation. *Circ Arrhythm Electrophysiol*. 2014;7:978–981.
97. Yokokawa M, Morady F, Bogun F. Injection of cold saline for diagnosis of intramural ventricular arrhythmias. *Heart Rhythm*. 2015;13:78–82.
98. Yokokawa M, et al. Intramural idiopathic ventricular arrhythmias originating in the intraventricular septum mapping and ablation. *Circ Arrhythm Electrophysiol*. 2012;5:258–263.
99. Latchamsetty R, et al. Multicenter outcomes for catheter ablation of idiopathic premature ventricular complexes. *JACC Clin Electrophysiol*. 2015;1:116–123.
100. McDonnell K, Rhee E, Srivathsan K, et al. Novel utility of cryoablation for ventricular arrhythmias arising from the left aortic cusp near the left main coronary artery: a case series. *Heart Rhythm*. 2014;11:34–38.

Fascicular Ventricular Tachycardia

OUTLINE

Pathophysiology, 858

Tachycardia Circuit, 858

Anatomy of the Left Fascicular System, 858

Epidemiology, 859

Clinical Presentation, 859

Initial Evaluation, 859

Principles of Management, 860

Acute Management, 860

Chronic Management, 860

Electrocardiographic Features, 860

Electrocardiogram During Normal Sinus Rhythm, 860

Electrocardiogram During Ventricular Tachycardia, 860

Electrophysiological Testing, 860

Induction of Tachycardia, 860

Diagnostic Maneuvers During Tachycardia, 861

Exclusion of Other Arrhythmia Mechanisms, 861

Mapping, 861

Activation Mapping, 861

Entrainment Mapping, 863

Pace Mapping, 863

Electroanatomic Mapping, 864

Noncontact Mapping, 864

Ablation, 864

Target of Ablation, 864

Ablation Technique, 866

Endpoints of Ablation, 867

Outcome, 867

Empirical Ablation of Noninducible Ventricular Tachycardia, 867

PATHOPHYSIOLOGY

The His-Purkinje system plays an important role in the genesis of cardiac arrhythmias. The mechanisms of several types of monomorphic ventricular tachycardias (VTs) have been directly linked to the Purkinje system, including bundle branch reentrant VT, interfascicular reentrant VT, fascicular VT, and focal Purkinje VT. A subset of polymorphic VTs and ventricular fibrillation has also been linked to triggers originating from the Purkinje system. Most of those arrhythmias occur in patients with underlying structural heart disease; however, fascicular VT and a subset of focal Purkinje VTs are idiopathic, occurring in the absence of apparent cardiac disease.^{1,2}

Idiopathic fascicular VT is a reentrant tachycardia involving the left fascicular Purkinje system. The reentry circuit is most commonly (90%) located in the territory of the left posterior fascicle (LPF), infrequently (5% to 10%) in the region of the left anterior fascicle (LAF), and rarely arise from fascicular locations high in the septum. Fascicular VT is also referred to as “verapamil-sensitive” VT, given its tendency to slow or terminate with intravenous verapamil.^{3,4}

Tachycardia Circuit

In the most common form (LPF-VT), the tachycardia circuit incorporates the LPF serving as one limb and abnormal Purkinje tissue with slow, decremental conduction serving as the other limb. The anterograde limb may be associated with longitudinal dissociation within the LPF or contiguous tissue that is directly coupled to the LPF (such as a false tendon) or, alternatively, has ventricular myocardium interposed. The zone of slow conduction appears to depend on the slow inward calcium current because the degree of slowing of tachycardia cycle length (TCL) in response to verapamil is entirely attributed to its negative dromotropic effects on the area of slow conduction.^{5,6}

The entrance site to the slow conduction zone is thought to be located closer to the base of the left ventricle (LV) septum. From there,

activation propagates anterogradely (from basal to apical segments along the LV septum) over the abnormal Purkinje tissue with decremental conduction properties and verapamil sensitivity, which serves as the anterograde limb of the circuit and appears to be insulated from the nearby ventricular myocardium. The lower turnaround point of the reentrant circuit is located in the lower third of the septum, where the wavefront captures the fast conduction Purkinje tissue from or contiguous to the LPF, and retrograde activation occurs over the LPF from the apical to basal septum forming the retrograde limb of the reentrant circuit. In addition, at the lower turnaround point, anterograde activation occurs down the septum to break through (at the exit of the tachycardia circuit) in the posterior septal myocardium. The upper turnaround point of the reentrant circuit occurs over a zone of slow conduction located close to the main trunk of the left bundle branch (LB) in the basal interventricular septum (Fig. 24.1). The estimated distance between the entrance and exit of the circuit is approximately 2 cm.^{5,6}

Anatomy of the Left Fascicular System

The LB arises from the His bundle (HB) as numerous fine, intermingling fascicles that leave the left margin of the branching HB through most of its course along the crest of the muscular ventricular septum. The predivisional portion of the LB penetrates the membranous portion of the interventricular septum under the aortic ring and then divides under the septal endocardium into two branches: the LAF and the LPF. An estimated 65% of individuals have a third fascicle of the LB, the left median fascicle (LMF). The fascicles cascade down the LV septum in a fan-like configuration with extensive interconnections. Unlike the cord-like right bundle branch, the LB and its divisions are diffuse, fan-like structures that quickly arborize just beyond their origin. The LAF represents the superior (anterior) division of the LB, the LPF represents the inferior (posterior) division, and the LMF represents the septal (median) division.

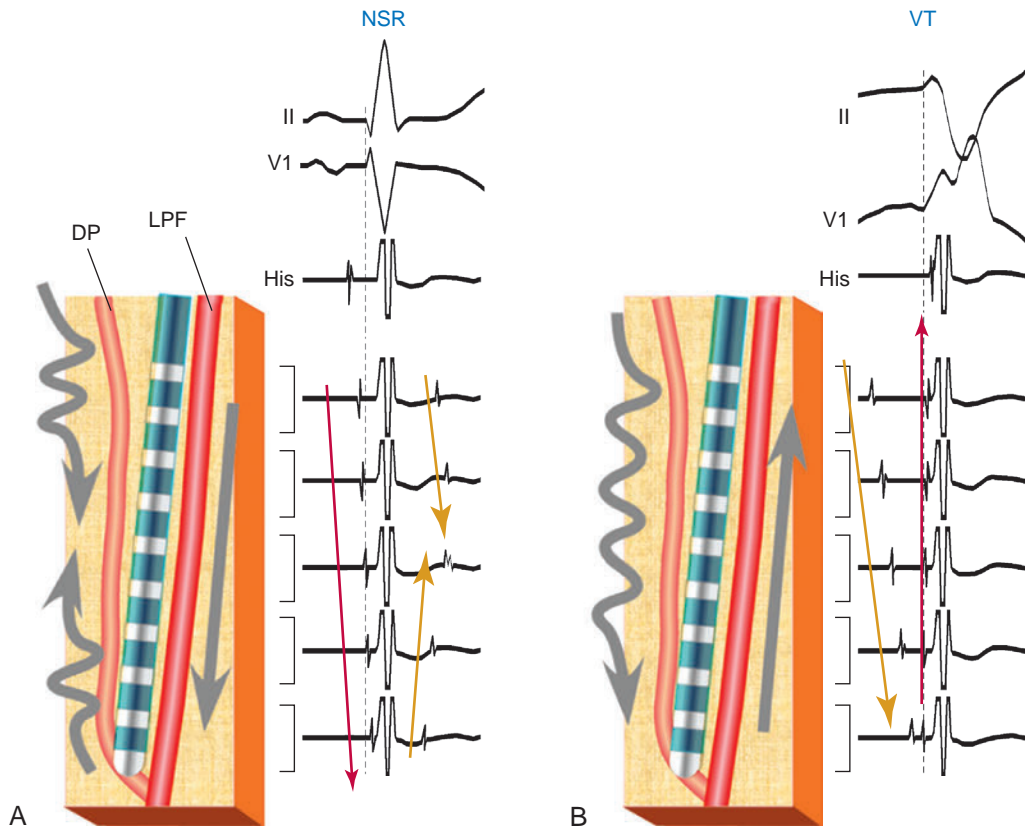


Fig. 24.1 Schematic Illustration of the Reentrant Circuit in Fascicular Ventricular Tachycardia (VT). A block of the LV septum is depicted with the left posterior fascicle (LPF) and diastolic pathway (DP) running in parallel until they intersect at the bottom. A 10-pole catheter is shown recording between pathways; electrograms from each pair are shown along with surface electrocardiogram leads and His bundle recordings. (A) Activation sequence is shown during normal sinus rhythm (NSR), the dashed line denotes QRS onset. Note the direction and speed of propagation over the LPF while the DP is activated after the QRS and in both directions (arrows). (B) During VT complex, the DP is activated anterogradely and the LPF retrogradely (arrows). See text for discussion.

The LB subdivisions extend to the midportion of the septum before they detach from the underlying endocardium and form free-running false tendons that traverse the ventricular chamber, projecting predominantly toward the papillary muscles. The fascicles become ramified in the ventricular apex and extend back along the ventricular walls toward the cardiac base.⁷

The thin LAF crosses the anterobasal LV region toward the anterolateral papillary muscle and terminates in the Purkinje system of the anterolateral LV wall. The LPF appears as an extension of the main LB and is broad in its initial course. It then fans out extensively toward the posterior papillary muscle and terminates in the Purkinje system of the posteroinferior LV wall. The LMF runs to the interventricular septum; it arises in most cases from the LPF, less frequently from the LAF, or from both fascicles, and in a few cases it has an independent origin from the central part of the main LB at the site of its bifurcation.²

EPIDEMIOLOGY

Fascicular VT accounts for 10% to 15% of all idiopathic VTs. Age at presentation is typically 15 to 40 years (unusual after 55 years). Males are more commonly affected (60% to 80%). The clinical course is generally benign, and the prognosis is excellent. Sudden cardiac death is very rare. Tachycardia-induced cardiomyopathy precipitated by incessant

VT can be observed in 6% of patients. Spontaneous remission of the VT can occur with time.⁸

CLINICAL PRESENTATION

Most patients present with mild to moderate symptoms of palpitations and lightheadedness. Occasionally, symptoms are debilitating and include fatigue, dyspnea, and presyncope. Syncope and cardiac arrest are rare. The VT is typically paroxysmal and can last for minutes to hours. Although fascicular VT can occur at rest, it is sensitive to catecholamines and often occurs during physical or emotional stress. Rarely, the VT can become incessant, sustained for a long period (days) and does not revert spontaneously to normal sinus rhythm (NSR). When incessant, fascicular VT can precipitate tachycardia-induced cardiomyopathy and heart failure.⁸

INITIAL EVALUATION

The diagnosis of fascicular VT is based on: (1) VT morphology on the surface electrocardiogram (ECG) (right bundle branch block [RBBB] with left or, less commonly, right axis deviation); (2) VT sensitivity to verapamil; and (3) absence of structural heart disease. Invasive electrophysiology (EP) testing is required to confirm the diagnosis. Evaluation

to exclude structural heart disease is necessary and typically includes echocardiographic examination (that may show one or more prominent false tendons), stress testing, and coronary arteriography, depending on patient age and risk factors.⁸

PRINCIPLES OF MANAGEMENT

Acute Management

Electrical cardioversion is required for VT termination in hemodynamically unstable patients. For stable patients with an established diagnosis of verapamil-sensitive fascicular VT, intravenous verapamil is the first-line treatment and is very successful in acutely terminating the VT. Intravenous verapamil slows the rate of VT progressively and then terminates it. Diltiazem is equally effective. Nonsustained VT may continue to occur for a while after termination.³

Response of VT to lidocaine, procainamide, amiodarone, sotalol, and beta-blockers is less consistent, and these drugs are usually ineffective. Carotid sinus massage and Valsalva maneuvers have no effect on the VT. Fascicular VT is generally unresponsive to adenosine; however, when catecholamine stimulation (isoproterenol infusion) is required for the initiation of VT (in the EP laboratory), the VT can become adenosine sensitive.^{8,9}

Chronic Management

Oral verapamil or diltiazem is useful in mild cases; however, long-term efficacy is variable and the benefit of these drugs in management of patients with severe symptoms is often limited. Catheter ablation is highly effective (success rate of 85% to 90%) and is recommended for patients in whom drug therapy is not successful, not tolerated, or not preferred.^{3,8,9}

ELECTROCARDIOGRAPHIC FEATURES

Electrocardiogram During Normal Sinus Rhythm

The resting ECG is usually normal. Symmetrical inferolateral T wave inversion can be observed after termination of the VT (cardiac memory).

Electrocardiogram During Ventricular Tachycardia

Fascicular VT is characterized by relatively narrow QRS duration (127 ± 11 milliseconds) and short RS interval (the duration from the beginning of the QRS to the nadir of the S wave) in the precordial leads (60 to 80 milliseconds). The shorter QRS duration reflects the proximal exit of fascicular VTs from the His-Purkinje system (HPS). In addition, during fascicular VT, the interventricular septum is activated early with a left-to-right direction, resulting in an initial “r” waves in lead V_1 and small “q” waves in leads I and aV_L (similar to classic RBBB pattern). In addition, the rapid activation of the LV via the Purkinje system results in unopposed late activation of the right ventricular outflow tract (RVOT), leading to a large R' amplitude in lead V_1 (and $r < R'$).^{8,10}

The VT rate is approximately 150 to 200 beats/min (range, 120 to 250 beats/min). Alternans in the TCL is frequently noted; otherwise, the VT rate is stable.

According to the fascicular territory involved and, consequently, the QRS morphology, fascicular VTs are classified into three subtypes: (1) LPF VT (with the reentrant circuit exit in the inferoposterior septum) exhibits an RBBB and superior axis configuration (most common form); (2) LAF VT (with the reentrant circuit exit in the anterolateral wall of the LV) exhibits RBBB and right-axis deviation configuration; and (3) upper septal fascicular VT with a narrow QRS and normal axis configuration (rare form). In the most common form (LPF-VT), the QRS during VT typically has RBBB with LAF block configuration. The R/S ratio is less than 1 in leads V_5 and V_6 (Fig. 24.2). VTs arising more toward the middle at the region of the posterior papillary muscle have a left superior axis and RS in leads V_5 and V_6 , whereas those arising closer to the apex have a right superior axis with a small “r” and deep S (or even QS) in leads V_5 and V_6 .^{1,8}

ELECTROPHYSIOLOGICAL TESTING

Induction of Tachycardia

Given the reentrant mechanism of fascicular VT, the arrhythmia is usually inducible by programmed electrical stimulation. In fact, fascicular

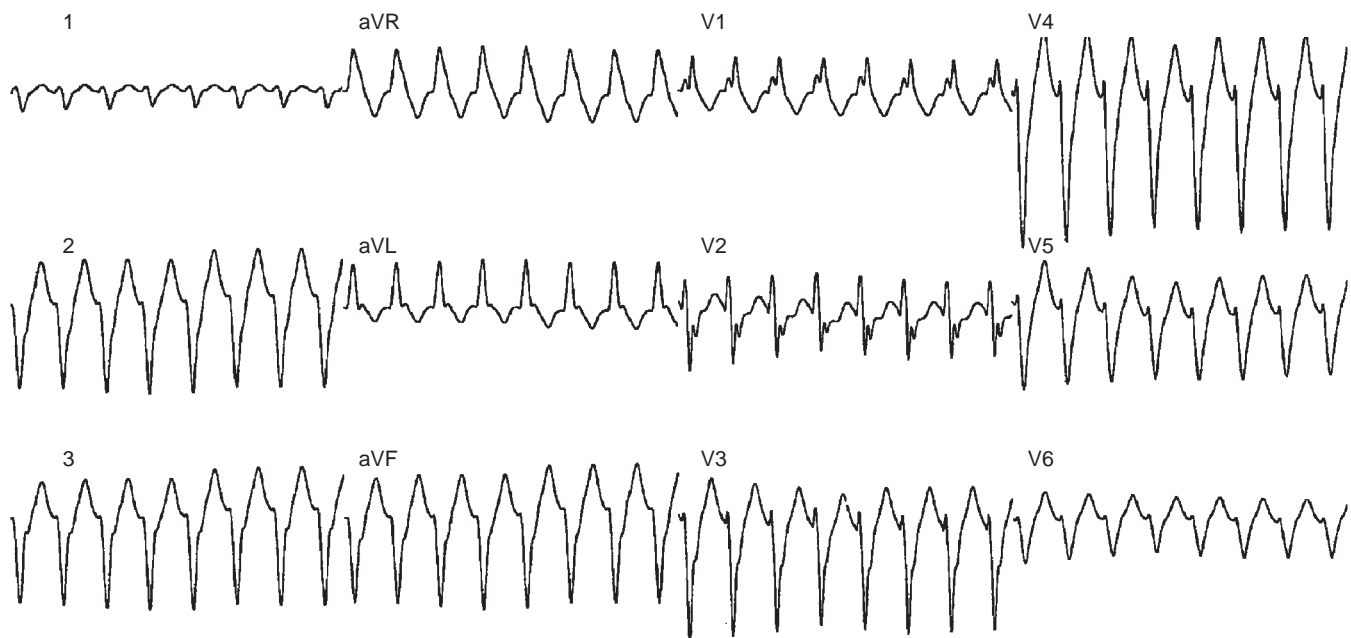


Fig. 24.2 Surface Electrocardiogram of Fascicular Ventricular Tachycardia (VT). Note the right bundle branch block and left anterior fascicle block pattern characteristic of these VTs.

VT is characterized by its reproducible initiation and termination not just by ventricular stimulation but also by atrial pacing. Often, isoproterenol infusion facilitates VT induction. Consistent with a reentry mechanism, an inverse relationship is observed between the coupling interval of the initiating ventricular extrastimulation (VES) or ventricular pacing cycle length (PCL) and the first VT beat.⁶

Diagnostic Maneuvers During Tachycardia

Entrainment

Entrainment of fascicular VT can usually be demonstrated with ventricular pacing at a PCL approximately 10 to 30 milliseconds shorter than the TCL. Manifest entrainment is more frequently achieved when pacing is performed from the RVOT because the RVOT is closer to the entrance site of the area of slow conduction in the reentrant circuit, located near the base of the LV septum. On the other hand, pacing from the RV apex is less likely to demonstrate entrainment and, when it does, it is unlikely to demonstrate manifest fusion because of the larger distance from the entrance site of the circuit and because of the narrow excitable gap of the reentrant circuit.

Resetting

Fascicular VT can be reset by VES, with an increasing or mixed resetting response (characteristic of reentrant circuit with an excitable gap).

Termination

VT can be reproducibly terminated with programmed atrial or ventricular stimulation.

Exclusion of Other Arrhythmia Mechanisms

The differential diagnosis of fascicular VT includes interfascicular VT, supraventricular tachycardia (SVT) with aberrant conduction, and VT originating from the LV papillary muscles.

Interfascicular Ventricular Tachycardia

Interfascicular VT has several characteristic features (see Chapter 26): (1) bifascicular block QRS morphology during VT, which is identical to that during NSR; (2) reversal of activation sequence of the HB and LB during VT; and (3) spontaneous oscillations in the TCL caused by changes in the LB-LB interval that precede and drive the TCL. Interfascicular VT terminates with VES or radiofrequency (RF) ablation that produces block in LAF or LPF.

Supraventricular Tachycardia

When fascicular VT is associated with a 1:1 VA conduction and because of its responsiveness to verapamil and inducibility by atrial pacing, it can be misdiagnosed as SVT with bifascicular block aberrancy. During SVT (similar to NSR), the HB is activated in an anterograde direction with sequential activation of the HB and ventricles (see Chapter 21). In contrast, during fascicular VT, the HB is activated retrogradely, with parallel activation of the HB and ventricle. Thus the HV interval during SVT with aberrancy is equal to or slightly longer than that during NSR. On the other hand, the HV interval during fascicular VT is frequently negative (i.e., His potential is recorded after onset of the QRS). The His potential can also precede the QRS onset during fascicular VT (especially during upper septal fascicular VT); however, the HV interval during VT will be shorter than that during NSR. In addition, unlike fascicular VT, aberrantly conducted SVTs are typically responsive to adenosine, beta-blockers, and Valsalva maneuvers.

Papillary Muscle Ventricular Tachycardia

Papillary muscle VTs typically manifest as premature ventricular complexes (PVCs) rather than sustained monomorphic VT and are more

likely to occur in older patients with structural heart disease. VTs arising from the LV papillary muscles exhibit a QRS morphology that can mimic fascicular VT. However, compared with fascicular VT, papillary muscle VTs have a broader QRS complex (150 ± 15 milliseconds vs. 127 ± 11 milliseconds). In addition, VTs originating from the papillary muscles (which are farther away from the septum) lack the rsR' pattern in lead V₁; rather, those VTs often have a qR pattern (or, less commonly, a monophasic R wave) in lead V₁. Furthermore, spontaneous variations in QRS morphology occur relatively frequently during VTs originating from the LV papillary muscles, a feature that can help distinguish these VTs from LV fascicular VT; the latter being a reentrant tachycardia with a consistent QRS morphology.^{8,10} Unlike patients with fascicular VAs, papillary muscle VAs are typically not inducible with programmed electrical stimulation, which is consistent with a nonreentrant mechanism of papillary muscle VTs.

Focal Purkinje Ventricular Tachycardia

Idiopathic focal VTs can arise from the Purkinje system in either ventricle and can present as PVCs, accelerated idioventricular rhythm, or VT. Focal Purkinje VTs arising from the left Purkinje network exhibit an RBBB pattern with either left- or right-axis deviation and can be difficult to distinguish from fascicular VT. In contrast to the reentrant idiopathic fascicular VT, focal Purkinje VTs are most likely related to abnormal automaticity. These VTs are sensitive to autonomic tone and frequently display chronotropic properties. Focal Purkinje VTs are typically induced by exercise and catecholamines and slowed or terminated by beta-blockers (and hence classified as "propranolol-sensitive" VTs) and lidocaine. Unlike fascicular VT, focal Purkinje VTs are not responsive to verapamil and cannot be induced or terminated by programmed electrical stimulation. In addition, these VTs are transiently suppressed by adenosine and with overdrive pacing.¹¹

MAPPING

Activation Mapping

Activation mapping is performed during sustained VT and is specifically directed toward sites with His or Purkinje potentials (PPs) extending from LV basal septal sites with HB recordings to most apical sites with presystolic PPs. Activation mapping is used to identify sites with the earliest ventricular activation and earliest presystolic PPs, as well as late diastolic potentials (LDPs).^{6,8} Mapping is performed along the LV inferior septum (for LPF VT), along the anterolateral LV (for LAF VT), or the basal LV septum (for left upper septal VT). Strategies for mapping and ablation of LPF VT, the most common type of fascicular VT, are discussed here in detail. The same principles can be applied for the two other types of fascicular VT.

When the VT is not inducible or not sustained, mapping can be performed during NSR to record the PPs along the posterior aspect of the LV septum, identifying the course of the LPF.

Site of Earliest Ventricular Activation

The site of earliest ventricular activation during VT (which represents the exit of the reentrant circuit) is in the region of the LPF (inferoposterior LV septum) in 90% of fascicular VTs (explaining the RBBB–superior axis configuration of the QRS), and in the region of the LAF (anterosuperior LV septum) in 5% to 10% of fascicular VTs (explaining the RBBB–right axis configuration of the QRS). In most cases, ventricular electrograms at the site of earliest activation are discrete during both NSR and VT. The HB is not a component of the reentrant circuit; in fact, a retrograde His potential is often recorded 20 to 40 milliseconds after the earliest ventricular activation (Fig. 24.3).¹²

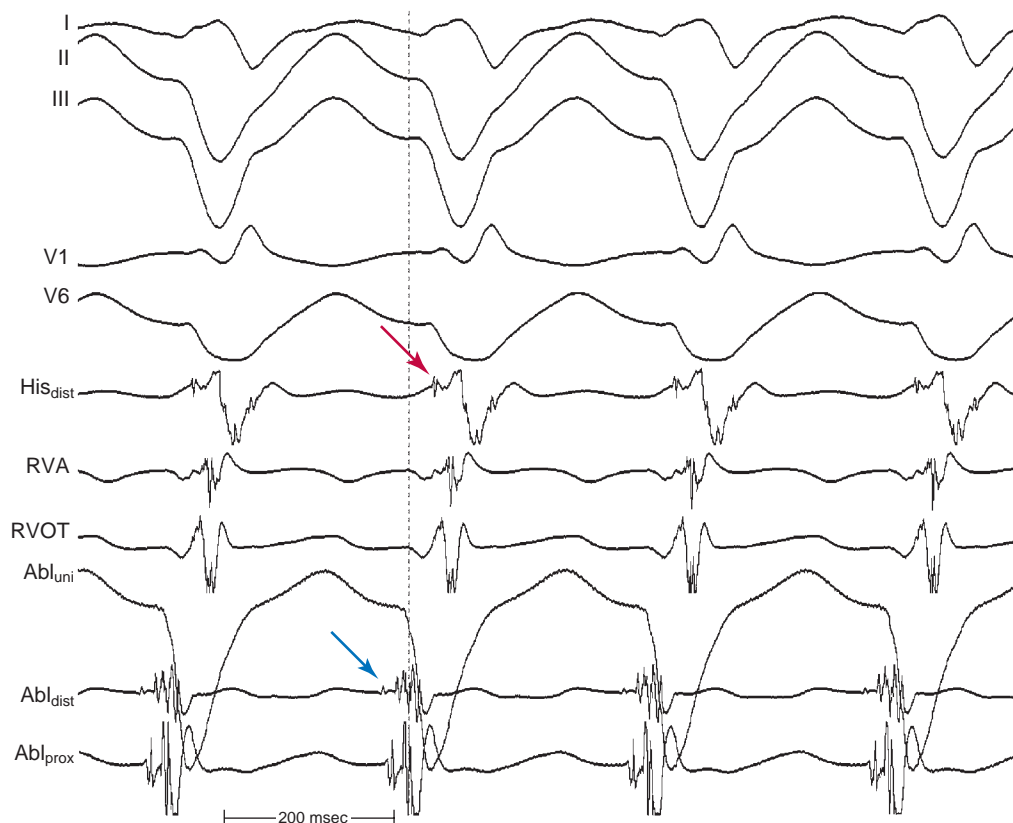


Fig. 24.3 Idiopathic Fascicular Ventricular Tachycardia. The blue arrow shows late diastolic small potential, 45 milliseconds prior to QRS onset. Distinct Purkinje-like potentials (*blue arrow*) are evident before the dotted line denoting QRS onset, as well as in the proximal ablation electrogram. The red arrow indicates retrograde His potential. Note the unipolar QS configuration just coinciding with QRS onset. *Abl_{dist}*, Distal ablation; *Abl_{prox}*, proximal ablation; *Abl_{uni}*, unipolar ablation; *His_{dist}*, distal His bundle; *RVA*, right ventricular apex; *RVOT*, right ventricular outflow tract.

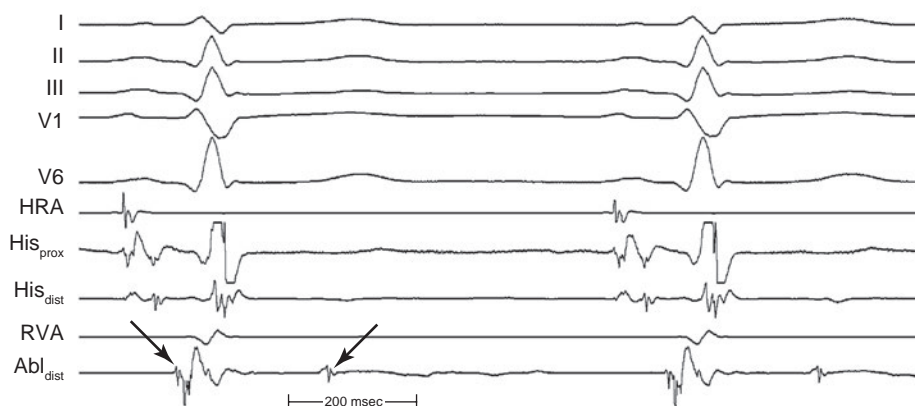


Fig. 24.4 Sinus Rhythm Recordings at a Successful Ablation Site for Fascicular Ventricular Tachycardia. The left arrow points to a Purkinje-like potential just prior to the local electrogram (also slightly preceding the onset of the QRS); the right arrow shows a sharp, delayed diastolic potential, purportedly from the slow-conducting limb of the circuit. *Abl_{dist}*, Distal ablation; *His_{dist}*, distal His bundle; *His_{prox}*, proximal His bundle; *HRA*, high right atrium; *RVA*, right ventricular apex.

Purkinje Potential

The PP (also referred to as “P2” in literature) is a discrete, high-frequency potential that precedes the site of earliest ventricular activation by 15 to 42 milliseconds and is recorded in the posterior third of the IV septum during VT, as well as during NSR (see Figs. 24.3 and 24.4). Because this

potential also precedes ventricular activation during NSR, it is believed to originate from activation of a segment of the LPF and to represent the lower turnaround point in the reentrant circuit. The earliest ventricular activation site (exit) during VT is identified more distally (apically) in the septum than the region with the earliest recorded PP.¹²

Late Diastolic Potential

The LDP, also referred to as “P₁” or “pre-PP,” is a discrete potential that precedes the PP during VT and is recorded at the basal, middle, or apical LV septum. During NSR, the LDP is inscribed after the QRS. The LDP is thought to originate from activation at the entrance to the abnormal Purkinje tissue (the specialized, verapamil-sensitive zone), which is thought to serve as the anterograde limb of the reentrant circuit and is isolated from surrounding muscle (allowing it to have a discrete diastolic activation time). The LDP differs in morphology from the PP and has a relatively small amplitude and low-frequency component. The area with LDP recording is confined to a small region (0.5 to 1.0 cm²) and is included in the larger area where the PP is recorded (2 to 3 cm²); hence the LDP often is recorded simultaneously with the PP by the same electrode. The LDP is recorded within an area proximal to the earliest PP recording site and is activated from the basal to apical septum toward the earliest PP site. The relative activation times of the LDP, PP, and local ventricular potential at the LDP recording site to the onset of QRS complex are -50.4 ± 18.9 , -15.2 ± 9.6 , and 3.0 ± 13.3 milliseconds, respectively (see Fig. 24.3). The earliest ventricular activation site (exit) during VT is identified at the posteroapical septum and is more apical in the septum than the region with LDP.¹²

Ventricular Activation Sequence

During NSR, conduction propagates anterogradely (proximal to distal or basal to apical) and rapidly down the LPF, generating an anterograde PP followed by ventricular activation (see Fig. 24.1). In parallel, the impulse slowly conducts anterogradely over the abnormal Purkinje tissue, and such slow conduction (or block) in the proximal segment allows the anterograde wavefront traveling rapidly over the LPF to conduct retrogradely up the slow pathway, resulting in fusion of delayed (late) ascending and descending potentials that follow (or are buried in) local ventricular depolarization, which likely represent the LDPs recorded during VT (see Fig. 24.4). Those late potentials have been found only in patients with fascicular VT but not in control subjects and have been recorded in the midinferior septum within or contiguous to the LPF.

During ventricular pacing, the LPF is activated retrogradely, generating a retrograde PP. In parallel, the impulse produces bidirectional activation of the abnormal Purkinje pathway in a manner similar but in reverse direction to that during NSR.

During VT, activation propagates anterogradely (from the basal to the apical site of the LV septum) over the abnormal Purkinje tissue, giving rise to an anterograde LDP; hence the earliest LDP is seen in the basal septum and the latest LDP is seen in the apical septum. The reentrant wavefront then turns around in the lower third of the septum and activates the fast conduction Purkinje fibers along the LPF, generating a retrograde PP. From the lower turnaround point, the wavefront propagates anterogradely down the septum to exit the reentrant circuit and activate the posterior septal myocardium, and retrogradely over the LPF from apical to basal septum, forming the retrograde limb of the tachycardia, with an upper turnaround point of the reentrant wavefront occurring over a zone of slow conduction (between LDP and PP areas) located close to the main trunk of the LB (see Fig. 24.1).

For a VES to initiate VT, retrograde block must occur in the abnormal Purkinje tissue, and the paced wavefront is retrogradely conducted up the LPF (generating a retrograde PP) with some delay and then down the abnormal Purkinje tissue (generating an anterograde LDP) to initiate reentry. Thus, during VT, the LDP precedes PP, which in turn precedes ventricular activation.

Verapamil significantly prolongs the TCL, LDP-PP interval, and PP-LDP interval during VT. However, the interval from PP to the onset of the QRS complex remains unchanged.

Entrainment Mapping

Analysis of entrainment from different ventricular sites helps to identify the relationship of those sites to the VT circuit (Box 24.1). Entrainment with concealed fusion and a PPI that approximates the TCL helps to identify the diastolic slow zone (isthmus) of the reentrant circuit. Notably, because of the overlap between the fascicular tissue and the ventricular myocardium, pacing from the isthmus of the VT circuit may not produce concealed fusion, because pacing frequently results in local myocardial capture outside that region, producing manifest fusion.¹³

During entrainment, the LDP (representing the entrance of the circuit) is orthodromically captured and, as the pacing rate is increased, the LDP-PP interval (representing an area of decremental Purkinje tissue) prolongs, whereas the stimulus-to-LDP and PP-QRS intervals typically remain constant.¹²

Pace Mapping

Pace mapping is not very reliable in identifying the optimal target site for ablation of fascicular VT. Pace mapping during NSR that matches the QRS morphology during VT can help to identify the exit site (i.e., the myocardial breakthrough site) of the VT circuit, but the exit site does not represent an effective ablation target. Pacing at successful ablation sites (within the slow diastolic zone of the VT circuit) often captures both the Purkinje fiber system and adjacent local myocardial tissue (away from the exit of the reentrant circuit) and also result in antidromic

BOX 24.1 Entrainment Mapping of Verapamil-Sensitive Left Ventricle Ventricular Tachycardia

Pacing From Sites Outside VT Circuit (RV Apex or RVOT)

- Manifest ventricular fusion on the surface ECG (fixed fusion at a single PCL and progressive fusion on progressively shorter PCLs) or fully paced QRS morphology
- PPI – TCL > 30 ms
- Interval between stimulus artifact to onset of QRS on surface ECG is greater than the interval between local ventricular electrogram on pacing lead to onset of QRS on surface ECG

Pacing From Sites Inside VT Circuit (Posteroinferior LV Septum)

- Manifest ventricular fusion on the surface ECG (fixed fusion at a single PCL and progressive fusion on progressively shorter PCLs)
- PPI – TCL < 30 ms
- Interval between stimulus artifact to onset of QRS on surface ECG equals the interval between local ventricular electrogram on pacing lead to onset of QRS on surface ECG (± 20 ms)

Pacing From Protected Isthmus Inside VT Circuit (Site Where Both PP and LDP Are Recorded)

- Concealed ventricular fusion (i.e., paced QRS is identical to the VT QRS)
- PPI – TCL < 30 ms
- Interval between stimulus artifact to onset of QRS on surface ECG equals the interval between PP to onset of QRS on surface ECG (± 20 ms)
- Stimulus-to-LDP interval is long, and LDP is orthodromically captured from proximal to distal sites during activation

CL, Cycle length; ECG, electrocardiogram; LDP, late diastolic potential; LV, left ventricle; PP, Purkinje potential; PPI, post-pacing interval; RV, right ventricle; RVOT, right ventricular outflow tract; VT, ventricular tachycardia.

activation of the isthmus of the VT circuit, generating a QRS morphology that can be significantly different from the VT morphology.^{1,8}

Electroanatomic Mapping

Electroanatomic three-dimensional (3-D) mapping (CARTO mapping system [Biosense Webster, Diamond Bar, CA, United States] or EnSite NavX system [St. Jude Medical, St. Paul, MN, United States]) can facilitate mapping of the left fascicular system and is of particular value when mapping is performed during NSR. After the LV geometry is created, activation mapping is performed during NSR along the LV septum to trace the conduction system from the site of recording of His potential just under the aortic valve and moving progressively distally (apically) until no fascicular/PP can be recorded. These sites, as well as the sinus breakout point, are tagged as special landmarks on the electroanatomic map to help identify ablation targets (Fig. 24.5). Once sustained VT is induced, activation mapping is performed during VT, with particular attention to sites with earliest ventricular activation, sites with presystolic PPs, as well as sites with LDPs. These sites are tagged on the electroanatomic map to identify the different components of the reentry circuit in relation to the fascicular system identified during NSR.^{14,15}

Noncontact Mapping

The EnSite 3000 noncontact mapping system (St. Jude Medical) may be used to identify the sinus breakout point (i.e., the LV site with the earliest local activation during NSR), and that point has been used to guide linear ablation perpendicular to the conduction direction of LPE. Particular attention is paid to the geometric detail in the areas of the HB, septum, and apex of the LV. After the ventricular geometry has been generated, the system can then calculate electrograms from more than 3000 endocardial points simultaneously by reconstructing far-field

signals to create the isopotential map of sinus rhythm using a single cardiac cycle. The HB, LB, fascicles, and sinus breakout point are tagged as special landmarks in the geometry. The sinus breakout point is located in the midposterior septum and the local virtual electrogram presents with QS morphology (Fig. 24.6). Virtual electrograms at points from the HB down to the sinus breakout point show a sharp, low-amplitude potential preceding the ventricular potential. The interval between these two potentials becomes progressively shorter as the activation propagates from the HB to the sinus breakout point, until the two potentials finally fuse together at the sinus breakout point.¹⁶

ABLATION

Target of Ablation

Definition of the appropriate ablation target has evolved with better understanding of the anatomical substrate of fascicular VT. Initially, the ablation target site was defined as the site where the earliest endocardial ventricular activation time and the best pace map could be obtained during VT (which represents the exit of the reentrant circuit). Subsequently, in combination with pace mapping, the earliest PP preceding QRS onset during VT (considered to be the lower turnaround point of the reentrant circuit) in the posterior third of the LV septum was reported to be a marker for successful ablation. Successful ablation is achieved at sites where PP is recorded 30 to 40 milliseconds before QRS onset (Fig. 24.7). Entrainment mapping at this location helps to confirm the relationship to the reentrant circuit. Of note, this area is located more basally than the LV area that shows the earliest ventricular activation during VT (the exit point of the circuit into the ventricular septum), suggesting that the location of the earliest ventricular activation during tachycardia is not an ideal site for ablation of this arrhythmia. Later on, the LDP recorded during VT, which likely reflects

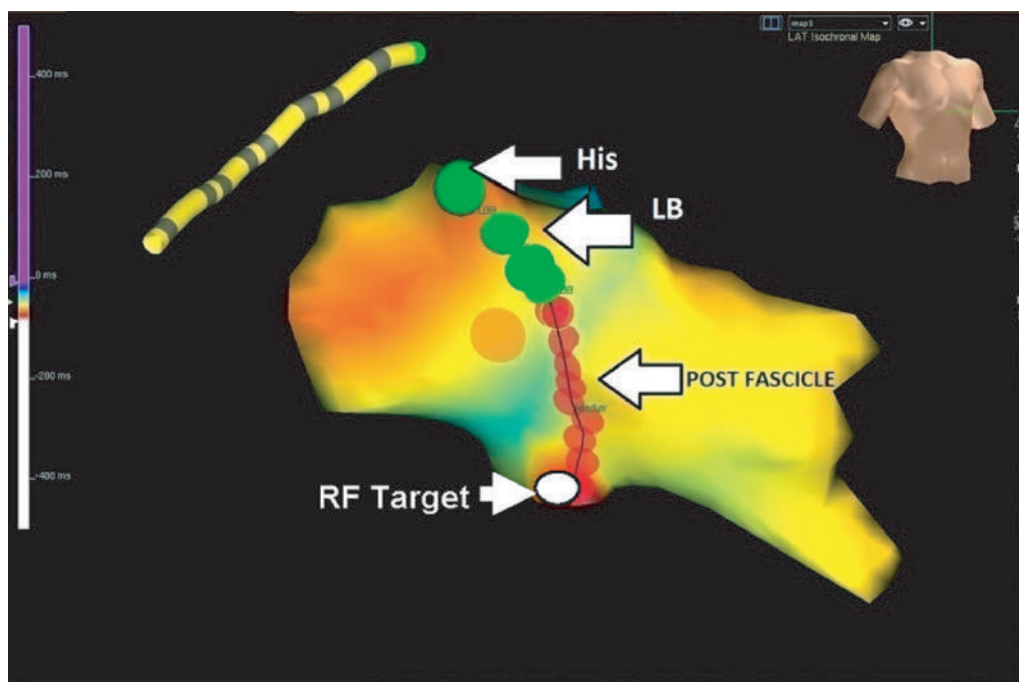


Fig. 24.5 Three-dimensional Electroanatomic (ESI NavX) Map of the Left Ventricle With Its Conduction System Obtained During Sinus Rhythm. Green markers denote His bundle and left bundle branch (LB) recording site; red markers denote posterior fascicle and Purkinje potential recording site; white marker denotes target for radiofrequency (RF) catheter ablation. (From Kataria V, Yaduvanshi A, Kumar M, Nair M. Demonstration of posterior fascicle to myocardial conduction block during ablation of idiopathic left ventricular tachycardia: an electrophysiological predictor of long-term success. *Heart Rhythm*. 2013;10:638–645.)

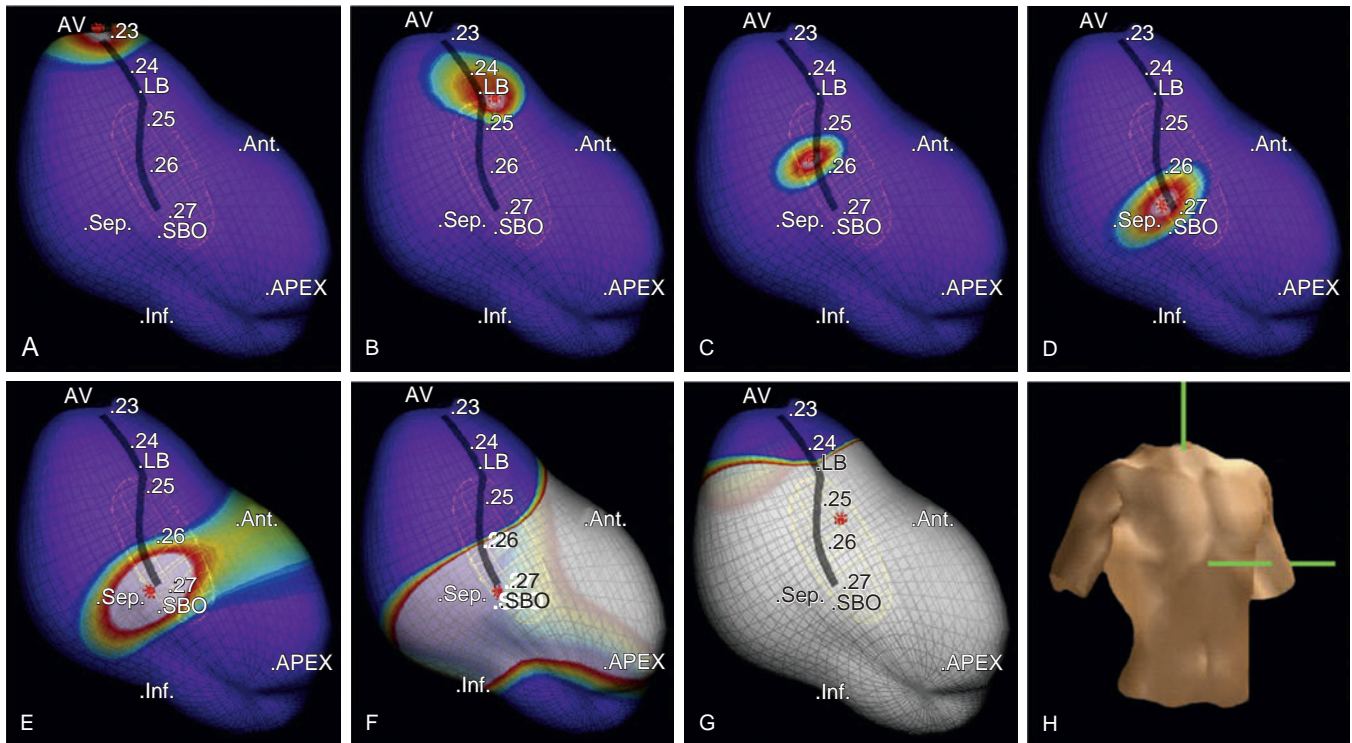


Fig. 24.6 Noncontact Mapping During Normal Sinus Rhythm (NSR). Shown is an animated propagation map of the left ventricle (LV) from frames A to G in the right anterior oblique view during NSR. Note that the sinus activation propagates down from the His bundle (AV) to the left bundle branch (LB) and then bifurcates into left anterior and left posterior fascicles before the entire LV is finally activated. The activation breakout point is at the midposterior septum and marked sinus breakout point (SBO) on the map. The thick black line indicates the propagation direction of the wavefronts from AV down to SBO. (H) Right anterior oblique orientation of the images. Ant., Anterior; Inf., inferior; Sep., septal. (From Chen M, Yang B, Zou J, et al. Non-contact mapping and linear ablation of the left posterior fascicle during sinus rhythm in the treatment of idiopathic left ventricular tachycardia. *Europace*. 2005;7:138.)

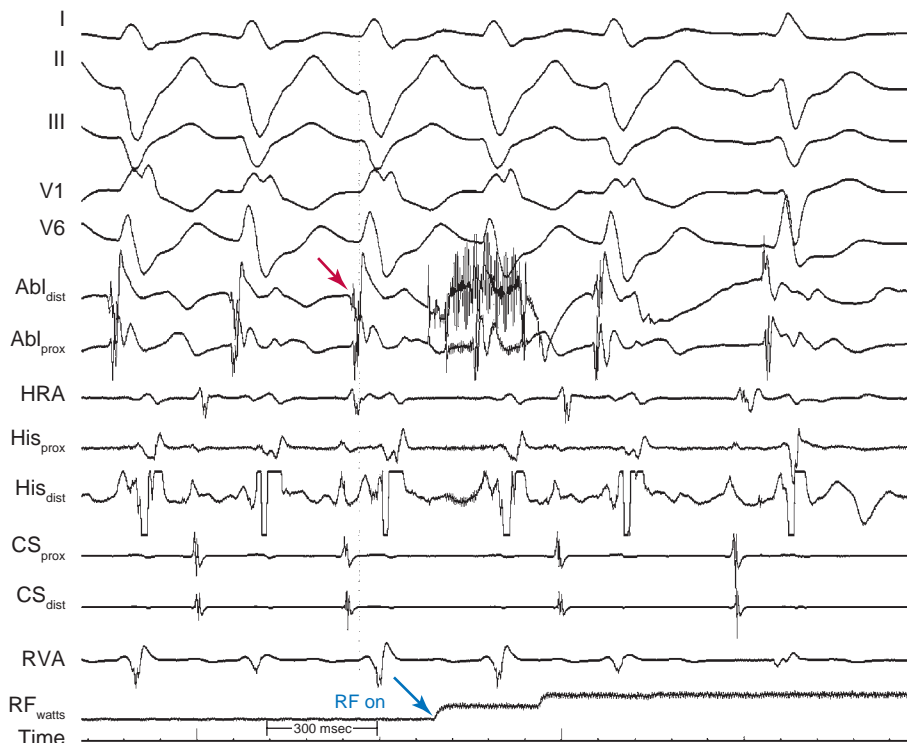


Fig. 24.7 Ablation of Idiopathic Fascicular Ventricular Tachycardia. Radiofrequency (RF) delivery is begun (blue arrow) at the site of the diastolic Purkinje potential during fascicular ventricular tachycardia. Within less than 1 second, the tachycardia terminates. The red arrow indicates probable Purkinje potentials. Abl_{dist}, Distal ablation; Abl_{prox}, proximal ablation; CS_{prox}, proximal coronary sinus; CS_{dist}, distal coronary sinus; His_{dist}, distal His bundle; His_{prox}, proximal His bundle; HRA, high right atrium; RF_{watts}, radiofrequency watts; RVA, right ventricular apex.

the excitation within the critical slow conduction area participating in the reentry circuit, was reported to be a useful marker in guiding successful ablation.

Currently, ablation is targeted to a site over the middle or inferoapical portion of the LV septum where the earliest PP and LDP are recorded (Fig. 24.8). Verification of these sites can be achieved with entrainment mapping demonstrating concealed fusion and progressive prolongation of the LDP-PP interval with increasing pacing rate. In addition, pressure applied to the catheter tip at the LDP region occasionally results in VT termination with conduction block between LDP and PP. Pace mapping can also be used as an adjunct to verify this site but, because of poor sensitivity, is less helpful than in focal VTs. It is important to recognize that successful ablation is not necessarily predicted by targeting the earliest (most proximal) LDP. Success can be achieved by ablating an LDP distal to the earliest potential (within the apical third of the septum). This approach is preferred to help reduce the risk of damaging the trunk of the LB. If such an LDP cannot be detected, the site with the earliest PP may then be targeted by ablation.^{1,6}

One report showed a high success rate of an ablation strategy targeting the distal most fascicular potentials of the LPF, close to the Purkinje-myocardial interface, as guided by electroanatomic mapping of the left fascicular system. Ablation is extended progressively distal linearly to the surrounding myocardium until conduction block is achieved between the LV myocardium and the distal posterior fascicle/Purkinje network. At successful ablation sites, the fascicular potential typically preceded the local ventricular electrogram by an interval of 12 ± 1.7 milliseconds, which is less presystolic than the earliest PP targeted in other ablation

strategies. Myocardium-fascicular conduction block during NSR was defined as the prolongation of the interval between the local ventricular electrogram and the fascicular/PP just proximal to the ablation site (duration of >100 milliseconds) or a higher degree of myocardium-fascicular block is recorded. Notably, this ablation approach did not result in LPF block or left axis deviation given the site of ablation being distal to LPF itself.¹⁴

Ablation Technique

Ablation is usually performed through the retrograde transaortic approach using a standard 4-mm-tip catheter. The catheter is advanced by prolapsing into the LV and directed to the LV septum. Mapping is initially concentrated at the inferoapical septum. If an ideal site is not found in this area, the ablation catheter is moved upward to the mid-septal area. It is important to move the catheter slowly and carefully to avoid mechanical trauma to the circuit. Endocardial activation mapping and entrainment mapping are performed to define the target site of ablation.¹

Once the target site is identified, a test RF current is applied during VT for 20 seconds with an initial power of 20 to 35 W, targeting a temperature of 60°C. If the VT is terminated or slowed within 15 seconds, additional current is applied for another 60 to 120 seconds and power is increased up to 40 W to reach the target temperature if necessary. If the test RF current is ineffective despite adequate catheter contact, ablation is directed to another site after additional mapping, usually targeting a more proximal site with the earlier LDP. This approach helps to limit RF damage to the area of LPF and LB. Rarely, if ever, does one need

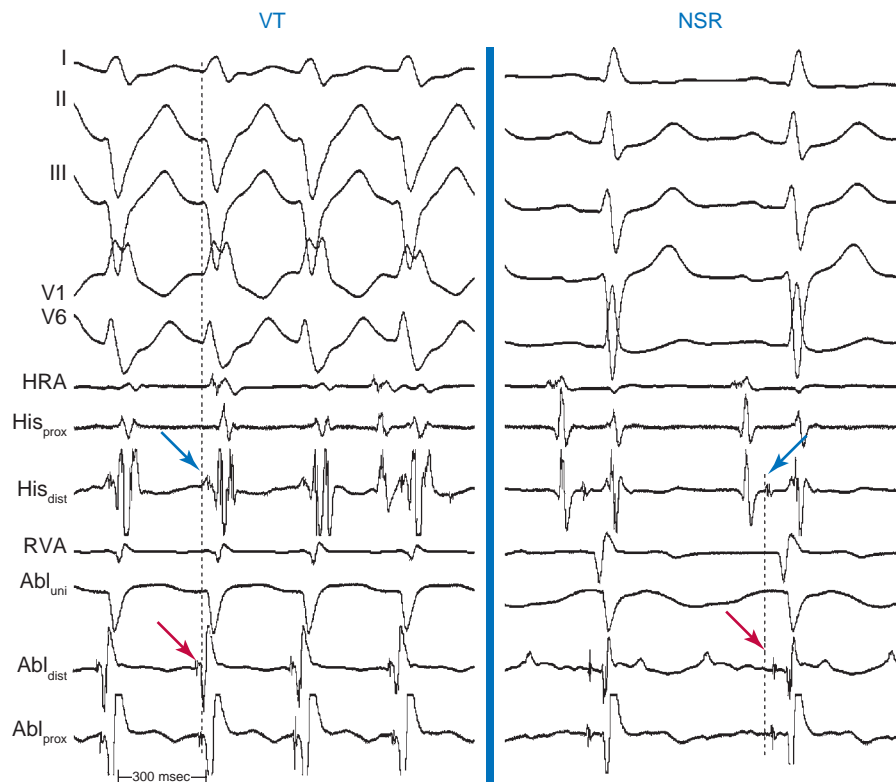


Fig. 24.8 Ablation of Fascicular Ventricular Tachycardia (VT). Shown are recordings during VT (left) and normal sinus rhythm (NSR; right) from a successful ablation site for idiopathic left ventricular tachycardia. Red arrows indicate probable Purkinje potentials, activated distal-to-proximal during VT and proximal-to-distal during sinus. Blue arrows show His potentials, occurring after QRS onset during VT. *Abl_{dist}*, Distal ablation; *Abl_{prox}*, proximal ablation; *Abl_{uni}*, unipolar ablation; *His_{dist}*, distal His bundle; *His_{prox}*, proximal His bundle; *HRA*, high right atrium; *RVA*, right ventricular apex.

more than 50 W or the use of irrigated or large-tip electrodes to ablate these VTs successfully.¹

During the RF application, successful ablation sites often display progressive prolongation of the LDP-PP interval, with termination of VT coincident with conduction block between the two potentials. After successful ablation, the LDP can no longer be recorded during NSR.

Endpoints of Ablation

Successful ablation is defined as the lack of inducibility of VT, with and without isoproterenol administration (using the best method for induction documented before ablation), at least 30 minutes after ablation. Importantly, creation of LPF block is not an effective endpoint for ablation and does not prevent arrhythmia recurrence.

Outcome

The acute success rate is more than 90%, even when different mapping methods and ablation strategies are used. The recurrence rate is approximately 7% to 15%, with most recurrences occurring in the first 24 to 48 hours after the ablation procedure. Arrhythmia recurrences after an initially successful ablation are caused most commonly by recurrent fascicular VT involving the same fascicle and by new onset of upper septal VT in one third of patients. Of note, the development of new LPF block after fascicular VT ablation was associated with more basal ablations and did not protect against VT recurrence.⁶

Complications are rare and include different degrees of fascicular block (most likely because of inadvertent collateral damage to the LPF, particularly when ablation is delivered more basally), LBBB, cardiac tamponade, aortic regurgitation, and mitral regurgitation caused by torn chordae that may result from entrapment of the ablation catheter in a chorda of the mitral leaflet.¹⁷

Empirical Ablation of Noninducible Ventricular Tachycardia

Conventional activation mapping, guided by either the earliest PP or the LDP, although effective, depends on the inducibility of sustained and hemodynamically stable fascicular VT. However, the VT may not be inducible in the EP laboratory. In addition, the critical substrate of

fascicular VT is vulnerable to mechanical injury because of catheter manipulation, which can render the tachycardia noninducible. In these cases, substrate mapping and ablation during NSR have been suggested to eradicate fascicular VT.^{1,8}

Three approaches have been used for substrate-based ablation during sinus rhythm: (1) ablation of the slow conduction zone adjacent to the LPF; (2) anatomical linear ablation to transect the middle to distal portion of the LPF; and (3) ablation of the most distal LPF fibers at the Purkinje-myocardial interface.¹⁸

The first approach involves identifying areas of the slow conduction zone that is adjacent to the LPF, which might represent the anterograde limb of the VT reentry circuit. The location of this region is suggested by recording low-amplitude electrograms visible after the sinus QRS complex (presumably resulting from delayed retrograde activation of abnormal Purkinje fibers) in conjunction with more prominent PP (which is generated by anterograde conduction down the LPF). At these locations the low-amplitude signals occur 15 to 45 milliseconds after the PP, and the PP precedes the QRS onset by a relatively short interval (13 ± 8 milliseconds). A major limitation of this ablation strategy is the inability to identify the low-amplitude signals in a sizable proportion of patients. In addition, in another subset of patients, similar non-specific low-amplitude signals are recorded over a sizeable area of the septum; targeting all those regions would increase the risk of injury to the conducting system.⁸

The second approach involves creation of an ablation line perpendicular to the activation direction of LPF and 1 cm above the sinus breakout point, as defined by electroanatomic or noncontact mapping during NSR (Fig. 24.9). The ablation line typically extends for approximately 2.0 ± 0.4 cm in the region of the mid to midinferior LV septum and is guided by recording a small PP preceding the ventricular activation at its starting and ending points. A significant rightward shift of the QRS axis in the surface limb leads can be observed after the ablation procedure.¹⁶

The third approach involves targeting the distal most fascicular potentials of the LPF, close to the Purkinje-myocardial junction, as described previously. This approach can be used both for inducible or noninducible VT cases.¹⁴

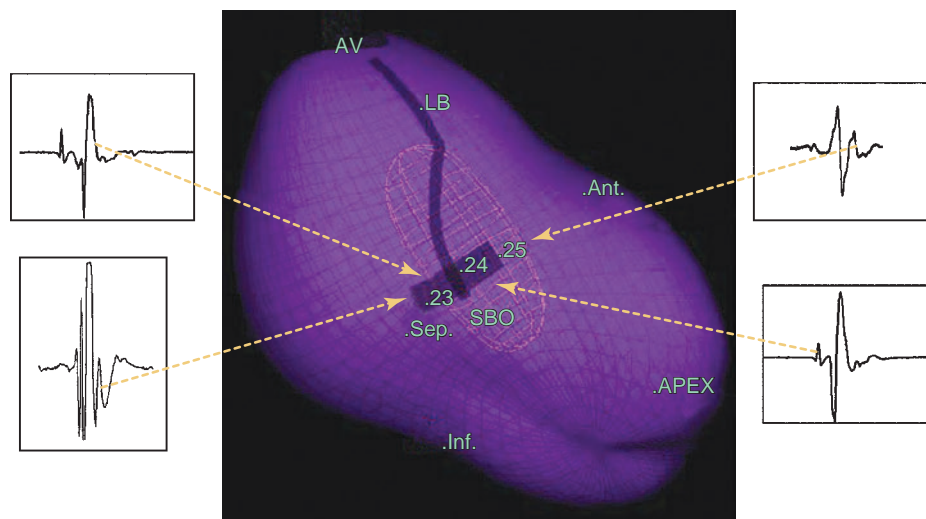


Fig. 24.9 Noncontact Mapping of Fascicular Ventricular Tachycardia During Normal Sinus Rhythm. A linear ablation lesion was created perpendicular to the wavefront propagation direction and 1 cm above the sinus breakout point (SBO). Both the starting and ending lesion points have a small Purkinje potential preceding the ventricular activation. Ant., Anterior; AV, His recording area; Inf., inferior; LB, left bundle branch; Sep., septal. (From Chen M, Yang B, Zou J, et al. Non-contact mapping and linear ablation of the left posterior fascicle during sinus rhythm in the treatment of idiopathic left ventricular tachycardia. *Europace*. 2005;7:138.)

REFERENCES

1. Nogami A. Purkinje-related arrhythmias. *J. Arrhythmia*. 2011;27:6–27.
2. Scheinman MM. Role of the His-Purkinje system in the genesis of cardiac arrhythmia. *Heart Rhythm*. 2009;6:1050–1058.
3. Tsuchiya T, et al. Effects of verapamil and lidocaine on two components of the re-entry circuit of verapamil-sensitive idiopathic left ventricular tachycardia. *J Am Coll Cardiol*. 2001;37:1415–1421.
4. Talib AK, et al. Verapamil-sensitive upper septal idiopathic left ventricular tachycardia prevalence, mechanism, and electrophysiological characteristics. *JACC Clin Electrophysiol*. 2015;1:369–380.
5. Nogami A, et al. Demonstration of diastolic and presystolic Purkinje potentials as critical potentials in a macroreentry circuit of verapamil-sensitive idiopathic left ventricular tachycardia. *J Am Coll Cardiol*. 2000;36:811–823.
6. Liu Y, et al. Catheter ablation of fascicular ventricular tachycardia: long-term clinical outcomes and mechanisms of recurrence. *Circ Arrhythmia Electrophysiol*. 2015;8:1443–1451.
7. Dobrzynski H, et al. Structure, function and clinical relevance of the cardiac conduction system, including the atrioventricular ring and outflow tract tissues. *Pharmacol Ther*. 2013;139:260–288.
8. Latchamsetty R, Bogun F. Fascicular tachycardia. *Card Electrophysiol. Clin*. 2014;6:567–579.
9. Collins KK, et al. Fascicular and nonfascicular left ventricular tachycardias in the young: an international multicenter study. *J Cardiovasc Electrophysiol*. 2013;24:640–648.
10. Al'Aref SJ, et al. Differentiation of papillary muscle from fascicular and mitral annular ventricular arrhythmias in patients with and without structural heart disease. *Circ Arrhythmia Electrophysiol*. 2015;8:616–624.
11. Sadek MM, et al. Idiopathic ventricular arrhythmias originating from the moderator band: electrocardiographic characteristics and treatment by catheter ablation. *Heart Rhythm*. 2015;12:67–75.
12. Sung RK, et al. Diagnosis and ablation of multiform fascicular tachycardia. *J Cardiovasc Electrophysiol*. 2013;24:297–304.
13. Ma W, et al. Mapping and ablation of ventricular tachycardia from the left upper fascicle: how to make the most of the fascicular potential? *Circ Arrhythmia Electrophysiol*. 2013;6:47–51.
14. Kataria V, Yaduvanshi A, Kumar M, et al. Demonstration of posterior fascicle to myocardial conduction block during ablation of idiopathic left ventricular tachycardia: an electrophysiological predictor of long-term success. *Heart Rhythm*. 2013;10:638–645.
15. Zhan XZ, et al. A new electrophysiologic observation in patients with idiopathic left ventricular tachycardia. *Heart Rhythm*. 2016;13:1460–1467.
16. Chen M, et al. Non-contact mapping and linear ablation of the left posterior fascicle during sinus rhythm in the treatment of idiopathic left ventricular tachycardia. *Europace*. 2005;7:138–144.
17. Li D, Guo J, Xu Y, et al. The surface electrocardiographic changes after radiofrequency catheter ablation in patients with idiopathic left ventricular tachycardia. *Int J Clin Pract*. 2004;58:11–18.
18. Chen H, et al. A novel method to identify the origin of ventricular tachycardia from the left fascicular system. *Heart Rhythm*. 2016;13:686–694.

Ventricular Tachycardia in Nonischemic Dilated Cardiomyopathy

OUTLINE

Pathophysiology, 869

- Molecular Genetics, 869
- Ventricular Arrhythmias, 870

Epidemiology and Natural History, 871

- Initial Evaluation, 871

Risk Stratification, 872

- Left Ventricular Ejection Fraction, 872
- Syncope, 872
- Nonsustained Ventricular Tachycardia, 872
- Electrophysiological Testing, 872
- Electrocardiographic Markers, 872
- Autonomic Testing, 872
- Microvolt T Wave Alternans, 873
- Cardiac Magnetic Resonance Imaging, 873
- Genetic Testing, 873

Principles of Management, 873

- Pharmacological Therapy, 873
- Implantable Cardioverter-Defibrillator, 873
- Catheter Ablation, 876

Electrocardiographic Features, 876

- Anteroseptal Versus Inferolateral Ventricular Tachycardia, 876
- Apical Ventricular Tachycardia, 876
- Septal Ventricular Tachycardia, 876
- Epicardial Ventricular Tachycardia, 876

Mapping, 877

- Preprocedural Evaluation, 878
- Left Ventricular Access, 878

Hemodynamic Support, 878

- Induction of Tachycardia, 878
- Substrate Mapping, 878
- Activation Mapping, 882
- Entrainment Mapping, 882
- Pace Mapping, 882
- Epicardial Mapping, 883

Ablation, 883

- Target of Ablation, 883
- Ablation Technique, 884
- Endpoints of Ablation, 884
- Outcome, 885

Cardiac Sarcoidosis, 885

- Pathophysiology, 885
- Epidemiology and Natural History, 886
- Clinical Presentation, 886
- Initial Evaluation, 886
- Risk Stratification, 888
- Management, 888

Chagas Cardiomyopathy, 889

- Pathophysiology, 889
- Epidemiology and Natural History, 890
- Clinical Presentation, 892
- Initial Evaluation, 892
- Risk Stratification, 893
- Management, 893

PATHOPHYSIOLOGY

Cardiomyopathies are traditionally defined on the basis of structural and functional phenotypes, notably dilated, hypertrophic, and restrictive. The dilated cardiomyopathy (DCM) phenotype is the most common and is often viewed as a “final common pathway” of numerous types of cardiac injuries.¹

The diagnosis of nonischemic DCM is established by the absence of significant (greater than 75% stenosis) coronary artery disease and prior myocardial infarction (MI). Nonischemic DCM is not a single disease entity. Valvular heart disease, hypertension, Chagas disease, sarcoidosis, amyloidosis, infections, hypothyroidism, thiamine deficiency, pregnancy (postpartum cardiomyopathy), vasculitides (e.g., Kawasaki disease and Churg-Strauss syndrome), and toxins (e.g., alcohol, anthracyclines, tyrosine kinase inhibitors), among others, need to be considered as possible etiologies. An underlying etiology for adult DCM is found in only 50% of patients. The remaining 50% are considered idiopathic. Idiopathic DCM is characterized by an increase in myocardial mass and a reduction in ventricular wall thickness. The heart assumes a

globular shape, and there is a pronounced ventricular chamber dilation and atrial enlargement.

Molecular Genetics

There is increasing evidence that a significant portion (30% to 50%) of idiopathic DCM is familial. Familial DCM is clinically and genetically heterogeneous and exhibits various patterns of hereditary transmission, including autosomal dominant with variable penetrance (the predominant pattern of transmission, accounting for about 90% of cases), X-linked (5% to 10%), autosomal recessive (rare), and maternal transmission through mitochondrial DNA (rare). It is also likely that many sporadic DCM cases can be due to genetic mutations. Although usually nonsyndromic, DCM can be included in syndromic disease involving various organ systems, most commonly skeletal muscle disease (muscular dystrophies).

To date, more than 40 genes have been linked to nonsyndromic familial DCM. Notably the frequencies of DCM mutations in any one gene are low (less than 1% to 8%), and a genetic cause is identified in only 35% to 40% of familial DCM cases. Most patients with familial

TABLE 25.1 Associated Clinical Features Which Are Present in a Minority of Patients With Familial Dilated Cardiomyopathy

Associated Phenotype	Clinical Features	Comment	Associated Gene ^a
Conduction disease	Sinus arrest Atrioventricular block Interventricular block	May precede DCM	<i>DES</i> <i>DMD</i> <i>EMD</i> <i>LMNA</i> <i>SCN5A</i>
Supraventricular arrhythmia prior to DCM	Premature atrial contraction Atrial fibrillation	Often with slow ventricular response	<i>EMD</i> <i>LMNA</i> <i>SCN5A</i>
Skeletal myopathy	Limb girdle Emery-Dreifuss Myotonic dystrophy Duchenne/Becker Myofibrillar myopathy	Proximal muscle weakness Contractures, skeletal myopathy and wasting Myotonia, weakness, baldness and cataracts Progressive X-linked proximal myopathy Slowly progressive proximal and distal weakness	<i>LMNA</i> <i>EMD</i> , <i>LMNA</i> <i>ZNF9</i> , <i>DMPK1</i> <i>DMD</i> <i>DES</i>
Hearing loss	Sensorineural hearing loss	Hearing loss typically occurs in the 1st and 2nd decade of life	<i>EVA</i>
Palmoplantar keratoderma	Increased thickness of the palms and soles with woolly or excessively curly hair	May precede cardiac involvement	<i>DSP</i>

^aSelected, incomplete list of associated disease genes.

DCM, Dilated cardiomyopathy.

From Lakdawala NK, Winterfield JR, Funke BH. Dilated cardiomyopathy. *Circ Arrhythmia Electrophysiol.* 2013;6:228–237.

DCM have isolated heart muscle disease; however, a minority of patients also manifest extracardiomyopathic phenotypes, including conduction system disease, supraventricular arrhythmias, sensorineural hearing loss, and skeletal myopathy (Table 25.1).¹ Clinical phenotypes and outcome in patients with DCM often vary according to the disease gene, penetrance, age, and type of mutation. At least four phenotypes are generally recognized: isolated DCM, DCM with cardiac conduction disease, DCM with concomitant skeletal myopathy (with or without conduction disease), and DCM with sensorineural deafness.

Familial forms of DCM can be due to mutations in cytoskeletal, sarcomeric, Z-disk, nuclear envelope, sarcolemmal, and intercalated disc protein genes. Several gene mutations have been identified in the autosomal form of familial DCM, including those encoding Z-disc proteins (alpha-actin-2, muscle LIM protein, titin-cap), costameres, adherens junctions, desmosomes, intermediate filaments, sarcomere proteins (cardiac alpha-actin, beta-myosin heavy chain, cardiac troponin T, alpha-tropomyosin, titin), sarcoplasmic reticulum proteins (phospholamban), and ion channel (SUR2A). Of note, different mutations in the sarcomere genes can cause hypertrophic cardiomyopathy (HCM). Mutations in the *LMNA* gene (which encodes Lamin A/C, a nuclear envelope protein) are involved in 8% of familial DCM and in 2% of sporadic DCM. Mutations in Lamin A/C also cause Emery-Dreifuss muscular dystrophy. Autosomal dominant DCM can exhibit either a pure DCM phenotype or DCM with cardiac conduction system disease. X-linked familial DCM is usually caused by mutations in the dystrophin gene and is typically associated with skeletal muscle involvement (Duchenne and Becker muscular dystrophy). The infantile form of X-linked DCM or Barth syndrome typically affects male infants (characterized by neutropenia and growth retardation). Mitochondrial cytopathies and inherited metabolic disorders such as hemochromatosis can also be associated with DCM.¹

Compared with sporadic cases of idiopathic DCM, familial DCM patients are younger and tend to have higher left ventricular ejection fraction (LVEF) and more significant myocardial fibrosis. In patients with idiopathic DCM, the proposed diagnostic criteria for the familial

form of the disease are the existence of two or more affected family members, or of one first-degree relative with a documented history of unexplained sudden death before 35 years of age. In most cases, proof of a genetic cause of a cardiomyopathy has limited impact on the treatment of the index patient, but can have important implications in regard to family screening and genetic counseling. DCM in patients who do not have a known family history may also have a genetic basis.¹

A new nomenclature system (the MOGE[S]) was recently developed for the description of familial DCM. This system proposes a nosology that addresses five attributes of cardiomyopathies, including morpho-functional characteristic (M), organ involvement (O), genetic or familial inheritance pattern (G), and an explicit etiological annotation (E) with details of the genetic defect or underlying disease/cause, allowing complete description of the disease and precise communication among physicians.²

Ventricular Arrhythmias

Patients with DCM can develop any variety of ventricular arrhythmias, including premature ventricular complexes (PVCs), nonsustained ventricular tachycardia (VT), sustained monomorphic VT, polymorphic VT, and ventricular fibrillation (VF). Cardiac arrest is usually precipitated by polymorphic VT or monomorphic VT degenerating to VF. Nonetheless, asystolic arrest and pulseless electric activity are common modes of death, particularly in patients with end-stage heart failure (HF).

Sustained monomorphic VT is less common in DCM than in patients with prior MI. In contrast to ischemic heart disease, the electrophysiological (EP) substrate for sustained monomorphic VT in patients with nonischemic DCM is not clearly defined. Although bundle branch reentry (BBR) VT is identified as the VT mechanism in a significant percentage of patients with monomorphic VT in the setting of nonischemic DCM, the majority (80%) of VTs appear to originate from the myocardium and are due to scar-related reentry rather than BBR. BBR VT is discussed separately in Chapter 26.

On the other hand, PVCs and nonsustained VTs induced by programmed electrical stimulation or occurring spontaneously in patients

with idiopathic DCM initiate primarily in the subendocardium by a focal mechanism without evidence of macroreentry. The nature of the focal mechanism remains unknown; triggered activity arising from early or delayed afterdepolarizations seems to be more likely than microreentry.

Myocardial fibrosis, myocyte disarray, and membrane abnormalities are important factors in the substrate, causing VT in patients with DCM. Sustained VT is associated with more extensive myocardial fibrosis and nonuniform anisotropy involving both the endocardium and epicardium, compared with patients without sustained reentry. The reentry circuits are typically associated with regions of low-voltage electrograms, consistent with scar. Catheter mapping studies of patients with nonischemic DCM point to reentry around scar deep in the myocardium, near the ventricular base and in the perivalvular region, as the underlying mechanism for VT. Studies of explanted hearts with nonischemic DCM have found unexcitable fibrosis creating regions of conduction block and surviving myocardium, providing the substrate for potential reentry circuits. Slow conduction through muscle bundles separated by interstitial fibrosis can cause a zigzag path and promote reentry. Furthermore, patients with nonischemic DCM who have predominance of scar distribution involving 26% to 75% of wall thickness (as quantified by cardiac magnetic resonance [CMR]) are more likely to have inducible VT. Delayed-enhancement CMR typically reveals nontransmural scar areas often distributed in the basal portion of the ventricular free wall or basal to midportion of the septum. Sustained VTs are observed more frequently in patients having a greater extent of fibrosis detected on CMR, and nontransmural scar tissue is observed at the VT circuit exit site in the majority of patients.

The cause of fibrosis in nonischemic DCM is not well defined. Scattered foci of myocyte necrosis and replacement fibrosis are commonly seen at autopsy (evident histologically in 35% of sections of the right ventricle [RV] and in 57% of sections of the left ventricle [LV]), but grossly visible confluent regions of scar are not common (observed in only 14% of subjects). The unique propensity for abnormal basal endocardial voltage and VT site of origin in patients with nonischemic DCM remains unexplained. Low-voltage areas have also been observed during electroanatomic mapping in patients with focal VT and BBR VT, although the scar areas appeared to be smaller.

The scar and fibrosis resulting from nonischemic etiologies are distinctly different from post-MI scar; hence the reentrant circuit may have different anatomical and functional properties that affect propagation. Compared with post-MI VT, the scar in DCM tends to be smaller and less confluent, the total number of the transmural scar segments is significantly smaller, and there is less endocardial involvement. Whereas ischemia produces a predictable wavefront of necrosis progressing from subendocardium to epicardium (and scar areas larger endocardially than epicardially), usually confined to a specific coronary vascular territory, scars in nonischemic DCM have been shown to have a predilection for the midmyocardium and epicardium. In contrast to the dense post-MI scar with isolated surviving myocardial bundles, scar in nonischemic DCM is patchy with fewer fixed boundaries and protected channels or isthmuses. In addition, the myopathic process in DCM can be dynamic and progressive over time, resulting in increasing myocardial fibrosis and, as a result, progressively worsening LV dilatation and systolic dysfunction, as well as the development of new VTs.^{3,4}

Nonetheless, several similarities of the arrhythmia substrate exist in myocardial reentry VT in patients with nonischemic DCM compared with that in post-MI patients. Low-voltage areas are observed in all patients, and the regions of scar are frequently adjacent to a valve annulus, as is often the case in VT after inferior wall MI. The annulus often seems to form a border for an isthmus in the reentry path, which suggests the formation of a long channel, or isthmus, along an annulus contributing to the formation of reentry circuits that can support VT.

Other factors may serve as triggers for ventricular arrhythmias, including electrolyte abnormalities (e.g., hypokalemia, hypomagnesemia), ischemia caused by small vessel disease, inflammation, heightened sympathetic tone, and stretch-induced shortening of the ventricular refractory period.

EPIDEMIOLOGY AND NATURAL HISTORY

The incidence of nonischemic DCM in adults in Western countries varies from 5 to 8 per 100,000 person-years, with a prevalence of 36 to 40 per 100,000 individuals. DCM accounts for 30% to 40% of all HF cases and is the most common indication for heart transplantation.

Although nonischemic DCM is regarded as a largely progressive disorder, the natural history of individual patients is highly variable. The 5-year mortality for DCM has been estimated at 20%, with sudden cardiac death (SCD) accounting for approximately one-third (8% to 51%) of deaths. Among all cardiomyopathy patients, nonischemic DCM patients likely represent a relatively low arrhythmic death risk subgroup. While the likelihood of death from progressive pump failure rather than SCD increases with the severity of HF symptoms, the absolute likelihood of SCD (presumed arrhythmic death) increases with the severity of HF.³

Ventricular arrhythmias, both symptomatic and asymptomatic, are common in patients with nonischemic DCM, and the frequency of arrhythmias increases with the severity of HF. PVCs (often multifocal) are observed in up to 90% of patients. In addition, nonsustained VT can be observed in 40% to 60% of patients, but its incidence decreases significantly after the optimization of HF medical treatment. Sustained monomorphic VT is less common in DCM than in patients with prior MI; DCM accounts for about one-fifth of patients undergoing catheter ablation for drug-refractory VT because of structural heart disease.⁵

Nonischemic DCM is the second leading cause of SCD in the United States. Syncope and SCD are infrequent initial manifestations of the disease. The incidence of SCD is highest among patients with indicators of more advanced cardiac disease who are also at highest risk of all-cause mortality. Although VT and VF are considered the most common mechanism of SCD, bradycardia, pulmonary embolism, electromechanical dissociation, and other causes account for up to 50% of SCDs in patients with advanced HF.⁵

Initial Evaluation

Transthoracic echocardiography is the usual modality for diagnosis of DCM. Cardiac stress testing or coronary angiography is typically performed in patients with coronary risk factors and those with new-onset ventricular arrhythmias to exclude the presence of obstructive coronary artery disease.

Ambulatory cardiac monitoring is required for patients with symptoms suggestive of arrhythmias (e.g., palpitations, dizziness, syncope), but not for screening purposes.

CMR provides accurate assessment of ventricular chamber size, wall thickness, and systolic function. Furthermore, CMR is a useful tool to detect and assess the characteristics and heterogeneous distribution of scar tissue and its composition of the wall layer, as well as its precise location within the ventricle. CMR can also help determine the underlying etiology of cardiomyopathy in some patients, such as myocarditis, sarcoidosis, and arrhythmogenic right ventricular cardiomyopathy (ARVC). In addition, the findings on CMR can potentially have prognostic implications; the extent of myocardial fibrosis is associated with HF-related hospitalization and death, and is a powerful predictor of VT/VF.^{1,6}

Genetic testing can be considered in selected patients when familial DCM is suspected. This can be of particular value when the clinical

management is influenced by the results of genetic testing (e.g., in patients with suspected cardiac sarcoidosis vs. familial DCM). Also, identification of a causative mutation can facilitate screening of family members. The likelihood of identifying a pathogenic mutation is less likely in older patients (older than 40 years) with nonfamilial disease.¹

RISK STRATIFICATION

Risk stratification in DCM is difficult. Although SCD occurs less frequently in patients with less advanced cardiac disease, the proportion of SCD to all-cause death is higher in this group.

Predictors of overall outcome (such as LVEF, end-diastolic LV volume, older age, hyponatremia, pulmonary capillary wedge pressure, systemic hypotension, atrial fibrillation [AF]) also predict SCD and generally reflect the severity of disease. Unfortunately these findings do not specifically predict arrhythmic death and are not useful in the patient with less severe disease.

Left Ventricular Ejection Fraction

LVEF remains the most studied and the most useful predictor of SCD despite limitations (see below) and is the primary method currently used in clinical decisions for the prevention of SCD in patients with HF. Depressed LVEF is also a powerful predictor of cardiac mortality. On the basis of the results of large studies, in clinical practice an LVEF $\leq 35\%$ has become the primary criterion used for prophylactic implantable cardioverter-defibrillator (ICD) placement.⁷

However, the use of LVEF as the predominant risk stratifier has serious limitations because it lacks both sensitivity and specificity for prediction of SCD. There is no evidence of any direct mechanistic link between low LVEF and mechanisms responsible for ventricular tachyarrhythmias, and no study has demonstrated that reduced LVEF is specifically related to SCD. Although low LVEF predicts total mortality (SCD and heart failure death), its value in predicting benefit from ICD implantation is limited. In these patients, ICD may reduce the risk of SCD but total mortality may not be modified. Even a very low LVEF (less than 20%) may not have a high positive predictive value for SCD. Many DCM patients who die from SCD have only a moderately depressed LVEF. Furthermore, the arrhythmic mechanisms underlying DCM and the risk of SCD can be different in different etiologies and clinical situations. Clinical factors such as functional class, symptomatic HF, nonsustained VT, age, LV conduction abnormalities, inducible sustained VT, and AF influence the risk of arrhythmic death and total mortality, and hence potentially influence the prognostic value of a depressed LVEF. Therefore patients with an LVEF greater than 30% and other risk factors may have a higher mortality and a higher risk of SCD than those with an LVEF less than 30% but no other risk factors.⁸

Another limitation is that methods of LVEF determination lack precision. Different imaging modalities can produce significantly different LVEF values, and the accuracy of techniques varies among laboratories and institutions, and there is evidence that prognosis, and hence risk, depends on the method by which the LVEF is measured. Clinically, when a patient has multiple LVEF measurements over time, it raises the question of which of the many measurements should be used—the most recent, the average, or the lowest.^{5,9} In cases in which frequent atrial or ventricular ectopic complexes or AF is present, sampling of representative contractions for the estimation of LVEF is especially problematic.

Syncope

Syncope has been associated with a higher risk of SCD and mortality (exceeding 30% at 2 years) regardless of the proven etiology of the syncope. Further, ICD recipients with syncope experience a high fre-

quency of appropriate ICD therapy at a rate comparable to a secondary prevention cohort.⁵

Nonsustained Ventricular Tachycardia

PVCs and nonsustained VT correlate with the severity of cardiac disease and occur in the majority of patients with severe LV dysfunction. Although the negative predictive value of these arrhythmias is high (greater than 90%), the positive predictive value is relatively low (20% to 50%), which limits the usefulness of ventricular arrhythmias as risk stratifiers. In addition, the presence and characteristics (frequency, length, and rate) of nonsustained VT do not appear to predict increased risk of subsequent life-threatening ventricular arrhythmias in patients with severe LV impairment receiving optimal medical treatment.¹

Nevertheless, it has been suggested that the presence of nonsustained VT may be more specific in patients with only mild to moderate LV systolic dysfunction. Nonsustained VT significantly increases the risk of malignant ventricular arrhythmias in the subgroup with LVEF greater than 35%. In these patients, even without worsening LV systolic function and symptoms, survival free from malignant ventricular arrhythmias is similar to that of patients with LVEF less than 35% with or without nonsustained VT.¹

Electrophysiological Testing

In contrast to patients with ischemic cardiomyopathy, invasive EP testing with programmed ventricular stimulation to assess inducibility of sustained ventricular arrhythmias did not prove to be useful for SCD risk stratification in patients with DCM. EP testing was found to offer low VT inducibility (13% sustained monomorphic ventricular tachycardia [SMVT], 6% ventricular flutter, 9% polymorphic VT/VF), low reproducibility, and poor predictive value of induced VT. Also, failure to induce SMVT during programmed electrical stimulation can be associated with high rates of arrhythmia recurrence and SCD, although at lower incidence rates than in patients with inducible VT.⁸ A recent study in patients with idiopathic DCM found that, among ICD recipients, induction of sustained ventricular arrhythmias during invasive EP testing was associated with significantly higher rates of appropriate ICD therapies (73% vs. 18%).^{1,10}

Electrocardiographic Markers

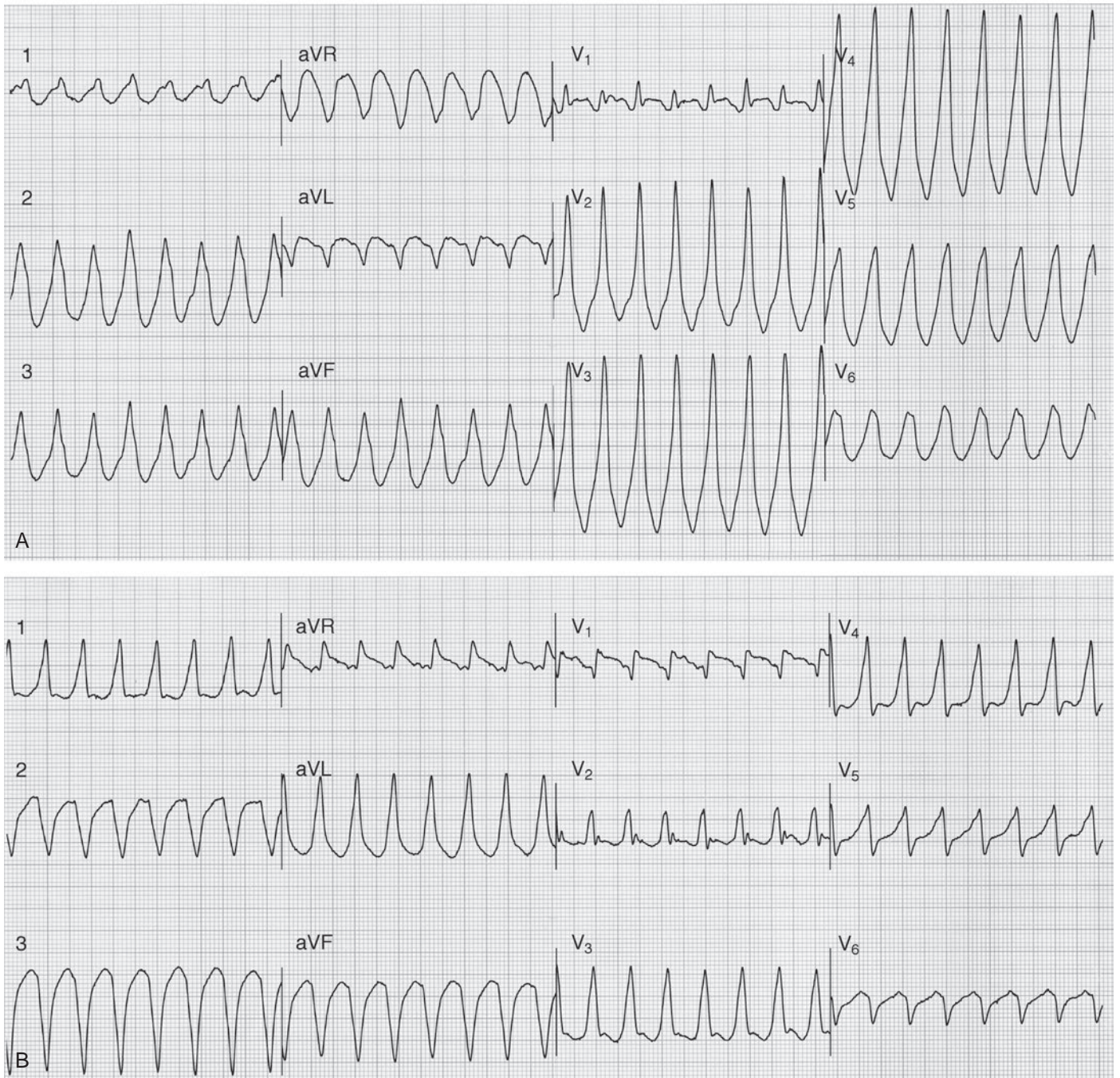
DCM patients typically have wide QRS complexes during the baseline rhythm, often with left bundle branch block (LBBB) or nonspecific intraventricular conduction defect. Prolonged QRS duration has been associated with increased mortality in HF patients, but association with SCD has not been proven.

Fragmentation of the QRS complex on the 12-lead surface electrocardiogram (ECG; filter range, 0.15 to 100 Hz; AC filter, 60 Hz, 25 mm/s, 10 mm/mV) has been found to potentially predict increased risk of appropriate ICD therapies as well as a higher combined endpoint of ICD therapy and mortality in nonischemic DCM patients who received an ICD for primary and secondary prevention. The usefulness of this parameter needs further evaluation. During VT, QRS complexes are typically very wide and fragmented; most patients have multiple QRS morphologies of VT (eFig. 25.1).

Prolongation of the QT interval, QT dispersion, and QT variability have had mixed predictive results with limited clinical applicability at present. The role of signal-averaged ECG is controversial.^{8,11}

Autonomic Testing

The prognostic value of autonomic tests, such as heart rate turbulence, heart rate variability, and baroreflex sensitivity, in DCM patients is questionable, and currently those parameters have little clinical application for risk stratification for SCD.¹¹



eFig. 25.1 Surface 12-Lead Electrocardiograms of Two Different Ventricular Tachycardias Configurations in a Patient With Dilated Cardiomyopathy. QRS morphology is suggestive of origin from basal septal left ventricular substrate. (A) Right bundle branch block morphology, positive precordial concordance, and inferior axis. (B) Left bundle branch block morphology, early precordial transition (leads V₂), and inferior axis.

Microvolt T Wave Alternans

Microvolt T wave alternans provides a quantitative assessment of temporal and spatial heterogeneity of repolarization, which are linked to cellular arrhythmia mechanisms. Microvolt T wave alternans was found to have relatively modest (0.22) positive predictive value for SCD in patients with DCM, largely due to the high rates of abnormal results (37% to 51%) and the low event rate within a short follow-up period. Previous studies suggested a high negative predictive value for primary prevention of SCD, and T-wave alternans was hypothesized to be a useful tool to differentiate between patients who would benefit from ICD implantation and those who would not. However, results from subsequent studies failed to support this hypothesis and strongly suggested that a negative microvolt T-wave alternans result should not be used to withhold ICD therapy among patients who meet standard criteria.^{8,11}

Cardiac Magnetic Resonance Imaging

Late gadolinium enhancement on contrast CMR reflects myocardial fibrosis, which represents a potential substrate for ventricular arrhythmias. Fibrosis detected by CMR is evident in 40% to 50% of DCM patients. On average, regions of hyperenhancement indicative of fibrosis account for up to 10% to 12% of the ventricular mass.^{1,6}

The presence of myocardial scar, as assessed by late gadolinium enhancement CMR, has been reported to be an independent predictor of appropriate ICD therapies, SCD, and all-cause mortality in patients with nonischemic DCM. The pattern and extent of myocardial fibrosis was found to be a predictor of both inducible and spontaneous VT, independent of LVEF, and appear to be a stronger predictor of monomorphic VT than of polymorphic VT/VF. In addition, larger scar extent in basal LV segments, higher maximal signal intensity, and increased scar transmural extent further indicate a predisposition for monomorphic VT. On the other hand, the absence of myocardial fibrosis on CMR was associated with a very low risk of arrhythmic events (0% to 3% per year).^{12,13}

It is likely that late gadolinium enhancement on CMR can contribute to risk stratification in patients with DCM. However, its utility for selecting DCM patients to receive an ICD has yet to be demonstrated.^{8,12–14}

Genetic Testing

Some familial forms of DCM are associated with a particularly high risk of arrhythmias and SCD, including LMNA, TNNT2, SGCD, RBM20, and CHRM2 mutations, whereas other forms (such as X-linked DCM related to dystrophin gene mutations) were found to have a high risk of severe HF but a lower risk of malignant ventricular arrhythmias. However, large studies documenting the correlation between individual genotypes and arrhythmogenicity are lacking, and current guidelines do not advise the use of genetic testing for SCD risk stratification in patients with DCM.^{1,7}

PRINCIPLES OF MANAGEMENT

Pharmacological Therapy

Drug therapy, such as beta-blockers, angiotensin-converting enzyme inhibitors, and mineralocorticoid receptor antagonists, improves overall mortality in patients with HF and reduces the risk of SCD. In contrast, the use of antiarrhythmic drugs for primary prevention in patients with nonischemic DCM does not improve survival and is not recommended.¹⁵

In patients with symptomatic ventricular arrhythmias, amiodarone is generally the preferred antiarrhythmic agent because of the absence of significant negative hemodynamic effects and low proarrhythmic potential, but controlled comparative trials of drugs are not available.

Antiarrhythmic drug therapy can help improve quality of life in ICD patients receiving frequent appropriate shocks and those with incessant VT. Although amiodarone can potentially improve mortality and reduce the incidence of SCD in patients with nonischemic DCM, it is inferior to ICD therapy for secondary prevention of VT and VF. Treatment of asymptomatic PVCs or nonsustained VT with antiarrhythmic drug therapy has not been shown to improve survival and is not recommended.¹⁵

Implantable Cardioverter-Defibrillator Secondary Prevention

The benefit of ICD therapy in secondary prevention of SCD in nonischemic DCM has been well established and is superior to amiodarone or any other drug therapy. ICD implantation is recommended in patients with prior cardiac arrest or sustained VT—even in those undergoing catheter ablation of the VT or responding to antiarrhythmic therapy (Table 25.2; Fig. 25.1).^{5,15–17}

Primary Prevention

The benefit of ICD treatment in nonischemic DCM for primary prevention of SCD remains uncertain. Several randomized studies arrived at contradictory conclusions. Whereas prophylactic ICD implantation is of significant benefit in ischemic cardiomyopathy patients, the magnitude of absolute benefit in those with nonischemic DCM is relatively small (1.4% per year; cumulative, 7% over 5 years) at best. Nevertheless, a pooled analysis of six randomized primary prevention trials (2967 patients with nonischemic DCM) demonstrated that the use of prophylactic ICD is associated with a significant 22% reduction in total mortality and 54% reduction in arrhythmia-related death as compared with control (eFig. 25.2). These findings reflect the fact that nonischemic DCM patients have a better prognosis and a lower rate of SCD than patients with ischemic cardiomyopathy.^{5,15,17–21}

Vigorous efforts have been made in developing noninvasive stratification methods to identify the subgroup of nonischemic DCM patients at high risk for SCD. However, the best approach to identifying patients and the value of various risk stratification tools are not entirely clear. Currently there is no coherent strategy for intervention based on data integrating the results of these techniques. Many of the identified risk factors are also associated with increased risk for nonsudden death.^{5,15}

At the present time, LVEF remains the single most important risk stratification tool to identify individuals with a high risk of SCD, again emphasizing that it predicts all-cause mortality and not necessarily arrhythmic risk. Despite some uncertainty regarding ICD benefit for nonischemic DCM patients without HF, regardless of LVEF, the cumulative information available from clinical trials and observational data, in conjunction with opinions of experts in the field, support prophylactic ICD therapy among the subgroup of patients with nonischemic DCM and LVEF $\leq 35\%$ who remain in New York Heart Association (NYHA) functional class II or III HF on optimal medical therapy (provided that a reversible cause of transient LV function has been excluded and their response to optimal medical therapy has been assessed), and for those with a history of syncope and documented significant LV dysfunction (see Table 25.2; Fig. 25.1). Furthermore, cardiac resynchronization with an ICD was found to significantly reduce all-cause mortality compared with pharmacological therapy alone in patients with DCM, QRS prolongation, and mild-to-severe HF symptoms (Box 25.1).^{5,15,17}

The value of ICD therapy in primary prophylaxis in asymptomatic DCM patients with NYHA functional class I has not been adequately tested and remains unanswered. Nevertheless, since this patient population has a relatively low mortality rate, the benefit of ICD therapy probably is modest at best. In addition, ICD therapy is not recommended in DCM with advanced HF and NYHA functional class IV who are not

TABLE 25.2 AHA/ACC/HRS Recommendations for Prevention of SCD in Patients With Nonischemic Cardiomyopathy**Secondary Prevention**

- In patients who either survive SCA due to VT/VF or experience hemodynamically unstable VT or stable VT not due to reversible causes, an ICD is recommended if meaningful survival >1 year is expected. Class I
- In patients who experience syncope presumed to be due to ventricular arrhythmias and who do not meet indications for a primary prevention ICD, an ICD or an electrophysiological study for risk stratification for SCD can be beneficial if meaningful survival >1 year is expected. Class IIa
- In patients who survive a cardiac arrest, have sustained VT, or have symptomatic ventricular arrhythmias who are ineligible for an ICD (due to a limited life expectancy and/or functional status or lack of access to an ICD), amiodarone may be considered for prevention of SCD. Class IIb

Primary Prevention

- In patients with NYHA class II–III symptoms and an LVEF of $\leq 35\%$ despite GDMT, an ICD is recommended if meaningful survival of >1 year is expected. Class I
- In patients with nonischemic cardiomyopathy due to a Lamin A/C mutation who have 2 or more risk factors (NSVT, LVEF <45%, non-missense mutation, and male sex), an ICD can be beneficial if meaningful survival of >1 year is expected. Class IIa
- In patients with Emery-Dreifuss and limb-girdle type IB muscular dystrophies with progressive cardiac involvement, an ICD is reasonable if a meaningful survival of >1 year is expected. Class IIa
- In patients with NYHA class I symptoms and an LVEF of $\leq 35\%$ despite GDMT, an ICD may be considered if meaningful survival of >1 year is expected. Class IIb
- In patients with myotonic dystrophy type 1 with an indication for a permanent pacemaker, an ICD may be considered to minimize the risk of SCA from VT if meaningful survival of >1 year is expected. Class IIb
- In patients with medication-refractory NYHA class IV heart failure who are not also candidates for cardiac transplantation, an LVAD, or a CRT defibrillator that incorporates both pacing and defibrillation capabilities, an ICD should not be implanted. Class III

ACC, American College of Cardiology; AHA, American Heart Association; CRT, cardiac resynchronization therapy; GDMT, guideline-directed management and therapy; HRS, Heart Rhythm Society; ICD, implantable cardioverter-defibrillator; LVAD, left ventricular assist device; LVEF, left ventricular ejection fraction; NSVT, nonsustained ventricular tachycardia; NYHA, New York Heart Association; SCA, sudden cardiac arrest; SCD, sudden cardiac death; VF, ventricular fibrillation; VT, ventricular tachycardia.

From Al-Khatib SM, Stevenson WG, Ackerman MJ, et al. 2017 AHA/ACC/HRS guideline for management of patients with ventricular arrhythmias and the prevention of sudden cardiac death: a report of the American College of Cardiology/American Heart Association Task Force on Clinical Practice Guidelines and the Heart Rhythm Society. *Heart Rhythm*. 2017 Oct 26. [Epub ahead of print]

BOX 25.1 Heart Rhythm Society Recommendations for Cardiac Resynchronization Therapy in Patients With Cardiomyopathy

Class I: CRT is indicated for:

- Patients who have LVEF $\leq 35\%$; sinus rhythm; LBBB with a QRS duration ≥ 150 msec; and NYHA class II, III, or ambulatory IV; symptoms on GDMT

Class IIa: CRT is reasonable for:

- Patients who have LVEF $\leq 35\%$, sinus rhythm; LBBB with a QRS duration 120–149 msec; and NYHA class II, III, or ambulatory IV symptoms on GDMT
- Patients who have LVEF $\leq 35\%$, sinus rhythm; a non-LBBB pattern with a QRS duration ≥ 150 msec; and NYHA class III/ambulatory class IV symptoms on GDMT
- Patients with atrial fibrillation and LVEF $\leq 35\%$ on GDMT if (a) the patient requires ventricular pacing or otherwise meets CRT criteria and (b) AVN ablation or pharmacological rate control will allow near 100% ventricular pacing with CRT
- Patients on GDMT who have LVEF $\leq 35\%$ and are undergoing new or replacement device placement with anticipated requirement for significant (>40%) ventricular pacing

Class IIb: CRT may be considered for:

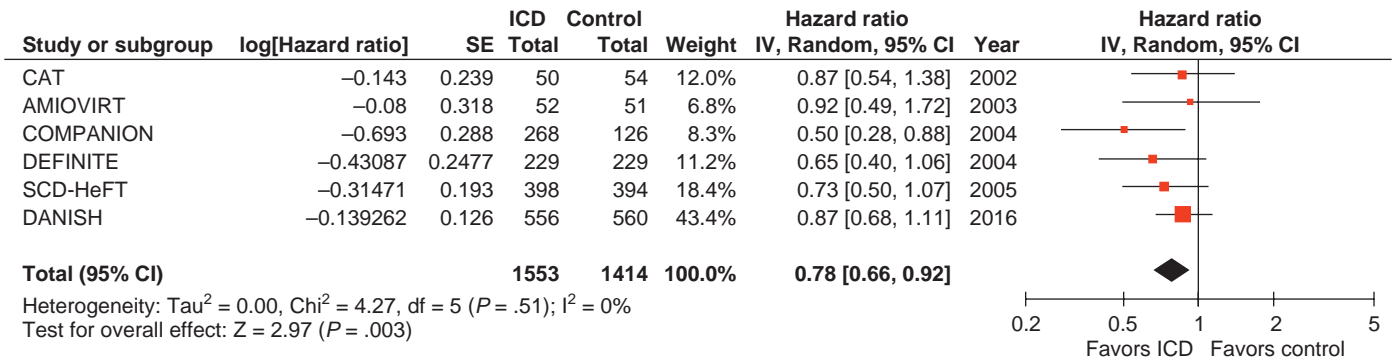
- Patients who have LVEF $\leq 30\%$, ischemic etiology of heart failure, sinus rhythm, LBBB with a QRS duration ≥ 150 msec, and NYHA class I symptoms on GDMT
- Patients who have LVEF $\leq 35\%$, sinus rhythm, a non-LBBB pattern with QRS duration 120–149 msec, and NYHA class III/ambulatory class IV on GDMT
- Patients who have LVEF $\leq 35\%$, sinus rhythm, a non-LBBB pattern with a QRS duration ≥ 150 msec, and NYHA class II symptoms on GDMT.

Class III: CRT is not recommended for:

- Patients with NYHA class I or II symptoms and non-LBBB pattern with QRS duration <150 msec
- Patients whose comorbidities and/or frailty limit survival with good functional capacity to <1 year

AVN, Atrioventricular node; CRT, cardiac resynchronization therapy; GDMT, guideline-directed medical therapy; LBBB, left bundle branch block; LVEF, left ventricular ejection fraction; NYHA, New York Heart Association.

Modified from Epstein AE, DiMarco JP, Ellenbogen KA, et al. 2012 ACCF/AHA/HRS focused update incorporated into the ACCF/AHA/HRS 2008 guidelines for device-based therapy of cardiac rhythm abnormalities: a report of the American College of Cardiology Foundation/American Heart Association Task Force on Practice Guide. *Circulation*. 2013;127:e283–e352.



eFig. 25.2 The Benefit of Implantable Cardioverter Defibrillator (ICD) Treatment in Nonischemic Cardiomyopathy. Forest plot of study-specific and pooled risk ratio and 95% confidence interval for the end-point of total mortality among patients assigned to ICD versus control. *AMIOVIRT*, Randomized trial in patients with nonischemic dilated cardiomyopathy and asymptomatic nonsustained ventricular tachycardia; *CAT*, cardiomyopathy trial; *CI*, confidence interval; *COMPANION*, comparison of medical therapy, pacing, and defibrillation in heart failure trial; *DANISH*, the Danish study to assess the efficacy of ICDs in patients with nonischemic systolic heart failure on mortality; *DEFINITE*, defibrillators in nonischemic cardiomyopathy treatment evaluation; *IV*, intravenous; *SCD-HeFT*, the sudden cardiac death in heart failure trial. (From Stavrakis S, Asad Z, Reynolds D. Implantable cardioverter defibrillators for primary prevention of mortality in patients with nonischemic cardiomyopathy: a meta-analysis of randomized controlled trials. *J Cardiovasc Electrophysiol*. 2017;28:659–665.)

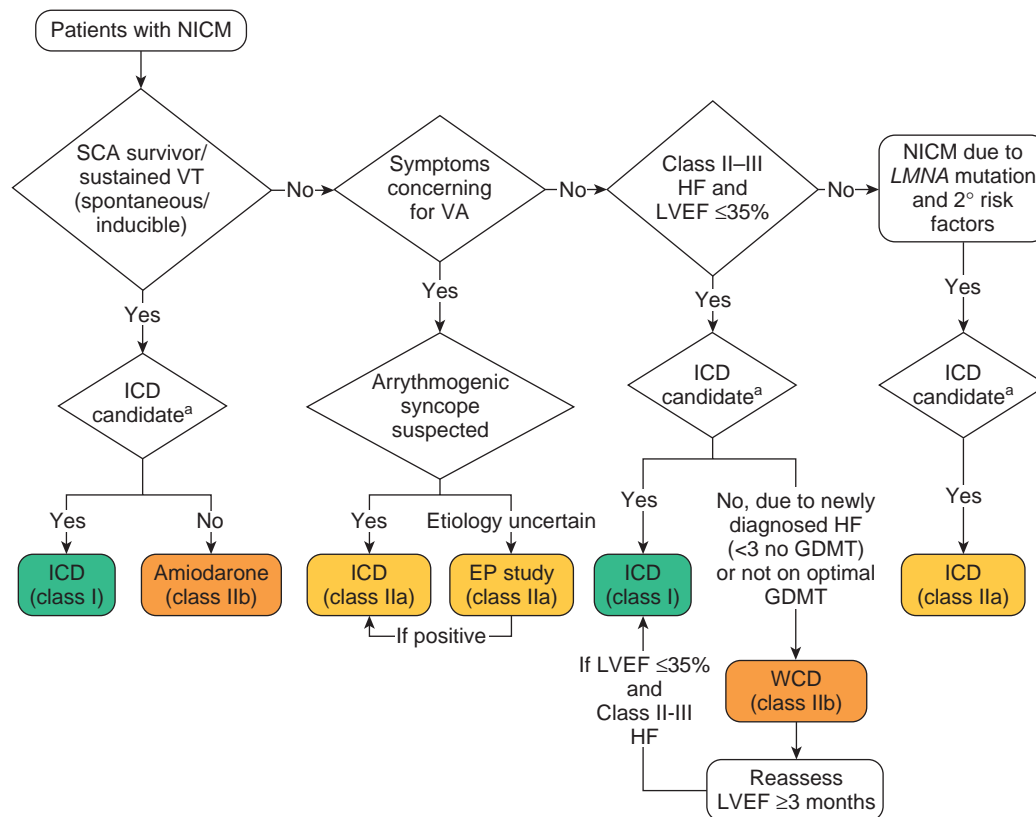


Fig. 25.1 American Heart Association/American College of Cardiology/Heart Rhythm Society Recommendations for Secondary and Primary Prevention of Sudden Cardiac Death in Patients With Nonischemic Cardiomyopathy. ^aImplantable cardioverter-defibrillator (ICD) candidacy as determined by functional status, life expectancy, or patient preference. 2°, Secondary; EP, electrophysiological; GDMT, guideline-directed management and therapy; HF, heart failure; LVEF, left ventricular ejection fraction; NICM, nonischemic cardiomyopathy; SCA, sudden cardiac arrest; VA, ventricular arrhythmia; VT, ventricular tachycardia; WCD, wearable cardiac-defibrillator. (From Al-Khatib SM, Stevenson WG, Ackerman MJ, et al. 2017 AHA/ACC/HRS guideline for management of patients with ventricular arrhythmias and the prevention of sudden cardiac death: a report of the American College of Cardiology/American Heart Association Task Force on Clinical Practice Guidelines and the Heart Rhythm Society. *Heart Rhythm*. 2017 Oct 26. [Epub ahead of print])

candidates for cardiac resynchronization therapy. This group of patients has a high mortality rate driven mainly by progressive HF, and recurrent VT/VF can be a sign of progression of the impaired LV function. Therefore, in these patients, ICD therapy may shift the mode of death from SCD to HF death rather than reduce total mortality.^{5,8}

The appropriate timing to perform ICD implantation in DCM remains controversial. In general, implantation of an ICD for primary prevention is not recommended within the first 3 months after initial diagnosis of DCM.^{7,15} It is important to understand that medical management with angiotensin-converting enzyme inhibitors and beta-blockers (with or without aldosterone antagonists) has proven mortality benefit in these patients and should be optimized as much as possible before ICD placement. Furthermore, improvements of LVEF have been observed in about 50% of patients with recent onset DCM after a period of 3 to 9 months on guideline-directed medical therapy. Many of these patients may be excluded as candidates for an ICD after optimization of medical treatment.^{22–24} The deleterious effects of residual ventricular scarring, despite improvement in overall LV function, is unknown.

At initial evaluation, predicting the course of LV dysfunction is difficult. In one report, a smaller LV end-diastolic diameter, higher systolic blood pressure, and an acute inflammatory process identified at biopsy were associated with an increased likelihood of recovery of LV function. Conversely, black race and higher NYHA functional class

were associated with a lower LVEF at follow-up. Furthermore, DCM due to cardiac sarcoidosis, giant cell myocarditis, or certain genetic mutations is unlikely to improve with medical therapy. On the other hand, peripartum cardiomyopathy, myocarditis, acute drug-induced cardiomyopathy, tachycardia-, or PVC-induced cardiomyopathy have higher likelihood of improvement with optimal medical therapy and elimination of underlying etiology, if possible.

There is no evidence that early ICD implantation benefits patients with newly diagnosed nonischemic DCM. Data suggest that the impact of defibrillators on reducing SCD in patients during the first 90 days on optimal medical therapy is low, and in most studies, ICD benefit did not become apparent for more than a year. Furthermore, a recent retrospective study reported a low incidence of appropriate ICD shocks in patients who received an ICD before mandated waiting periods were complete.²⁵ Therefore, for patients with a new diagnosis of DCM, it is prudent to treat with optimal HF medications for at least 3 months and reassess for recovery of ventricular function before consideration of prophylactic ICD therapy, unless there are high-risk features such as sarcoidosis, giant cell myocarditis, or familial cardiomyopathy, known to be associated with malignant ventricular arrhythmias.⁷

On the other hand, ICD implantation can be considered in patients with recent (less than 3 months) diagnosis of nonischemic DCM who also require nonelective permanent pacing, develop sustained (or

hemodynamically significant) ventricular tachyarrhythmia, present with syncope that is thought to be due to a ventricular tachyarrhythmia (by clinical history, documented nonsustained ventricular tachycardia [NSVT], or EP study), or are listed for heart transplant or implanted with a LV assist device.^{7,26}

To mitigate the risk of arrhythmic SCD during the 90-day waiting period on optimal medical therapy before reevaluation of LV function, wearable cardioverter defibrillators are frequently prescribed for patients with newly diagnosed nonischemic DCM. However, data to support such a practice are lacking. Observation studies demonstrated that the risk of SCD in this patient population is very low, and the utility of wearable cardioverter defibrillators is very limited and unlikely to be cost effective.²⁵

Catheter Ablation

While ICD therapy reduces the risk of arrhythmic death, it does not prevent the recurrence of symptomatic VT. Further, antiarrhythmic drug therapy has limited success rate for control of VT (approximately 40% of cases), leaving a significant proportion of patients with symptomatic VT or ICD shocks. Catheter ablation of VT in patients with nonischemic DCM is typically considered in those with incessant VT or with frequent ICD discharges (or electrical storm) refractory to antiarrhythmic drug therapy (see Box 22.1). However, because of the future risk of life-threatening VT due to progression of the myopathic process, catheter ablation is not a substitute for an ICD, even when excellent short-term results are achieved.²⁷

In addition, limited data found that catheter ablation (in conjunction with ICD implantation) earlier in the course of treatment of VT or as a primary therapy (i.e., before antiarrhythmic drug therapy), with the goal of avoiding future ICD shocks, was associated with better acute procedural success as compared with delayed ablation. However, evidence for the efficacy and safety of such an approach in patients with nonischemic DCM remains limited.^{28,29}

The success rate for catheter ablation of VT in DCM is lower than that for ischemic VT, and depends on VT substrate location, which can be endocardial, intramural, or epicardial. An epicardial ablation approach is necessary in a large proportion of patients and is associated with higher complication rates. In experienced centers, catheter ablation is associated with acute success rates of up to 71%. VT recurs in 50% to 60% during the first year post ablation, although VT burden can be significantly reduced. Alcohol septal ablation can be particularly useful in patients with intramural septal VTs refractory to catheter ablation.³⁰

Furthermore, catheter ablation also should be considered for patients with BBR VT or interfascicular VT, and those with frequent PVCs, nonsustained VT, or sustained VT that is presumed to cause ventricular dysfunction. Box 22.1 lists the recommendation of ablation for VT in structural heart disease, in accordance with the published guidelines for management of patients with ventricular arrhythmias.^{15,31}

ELECTROCARDIOGRAPHIC FEATURES

The site of origin of VT is the source of electrical activity producing the VT QRS complex. Although this is a discrete site of impulse formation in automatic and triggered (i.e., focal) rhythms, during reentrant VT it represents the exit site from the diastolic pathway (isthmus) to the myocardium giving rise to the QRS.

Although the surface ECG during VT can help predict the location of the arrhythmogenic substrate in patient with DCM, it is important to recognize its limitations. The pattern of ventricular activation and hence the resultant QRS depends on how the wavefront propagates from the site of origin to the remainder of the heart, which (because of scar-related alterations of propagation) can be totally different during

VT than during pacing from the same site in normal sinus rhythm (NSR). Furthermore, the 12-lead ECG provides information about the VT exit site from the scar border and not about the site to be targeted by ablation. Ablation of scar-related VTs targets the critical isthmus of the reentrant circuit, which can be removed from the exit site indicated by the surface ECG. In addition, the overall QRS morphology during scar-related VT is determined not just by the site of origin of the VT, but also by scar extent and distribution in the rest of the ventricle. Therefore the presence of large confluent myocardial scars can limit the accuracy of the 12-lead ECG to localize the VT.³²

Anteroseptal Versus Inferolateral Ventricular Tachycardia

The VT substrate in patients with nonischemic DCM is often located in the basal LV, clustering around the mitral and aortic annuli, with variable extension toward the LV apex. Two predominant scar patterns account for the arrhythmogenic substrate in the majority of these patients: anteroseptal LV scar and inferolateral LV scar. VT morphologies consistent with anteroseptal substrate include (1) right bundle branch block (RBBB) morphology, positive precordial concordance, and inferior axis VTs; and (2) LBBB morphology, early precordial transition (leads V₁ to V₃), and inferior axis (see eFig. 25.1). In contrast, RBBB morphology, late precordial transition, and right (superior or inferior) axis during VT are consistent with an inferolateral scar (Fig. 25.2).²⁷

Apical Ventricular Tachycardia

An apical VT origin is suggested by (1) LBBB morphology with late precordial transition (leads V₅ to V₆) to a dominant positive QRS complex; or (2) RBBB morphology and early precordial transition (leads V₁ to V₃) to a dominant negative QRS complex.

Septal Ventricular Tachycardia

In the setting of isolated septal substrates, VT morphologies can vary but predominantly exhibit RBBB, with either superior or inferior axis. About 40% of those VTs exhibit one of two particular configurations. The first is characterized by a precordial “transition pattern break” in lead V₂ with qR/Rs morphology in leads V₁ and V₃ but reversal of this in lead V₂, usually in the presence of an inferior-axis RBBB configuration. The second is characterized by an inferior limb lead discordance, usually LBBB configuration with a net positive vector in II, negative in III, and positive in aVL.³³

Epicardial Ventricular Tachycardia

For VTs originating from the LV and having RBBB pattern, some findings on the surface ECG suggest an epicardial origin. These ECG characteristics, which generally rely on the late engagement of rapidly conducting His-Purkinje fibers by tachycardia circuit exits on the epicardium, include the following: (1) a pseudo-delta wave (measured from the earliest ventricular activation to the earliest fast deflection in any precordial lead) of 34 milliseconds or more (sensitivity, 83%; specificity, 95%); (2) a QRS duration exceeding 200 milliseconds; (3) a long R-wave peak time in lead V₂ (i.e., an interval from the beginning of the QRS complex to the time of initial downstroke of the R wave after it has peaked [previously known as the *intrinsicoid deflection*]) of at least 85 milliseconds (sensitivity, 87%; specificity, 90%); and (4) a shortest RS complex duration (measured from the earliest ventricular activation to the nadir of the first S wave in any precordial lead) of 121 milliseconds or more (sensitivity, 76%; specificity, 85%).³⁴

Importantly, ECG criteria for identifying an epicardial origin of VT appear to be region and substrate specific. ECG interval criteria that identify slow conduction in the initial portion of the QRS do not appear to be equally accurate among all LV regions and are not as reliable for

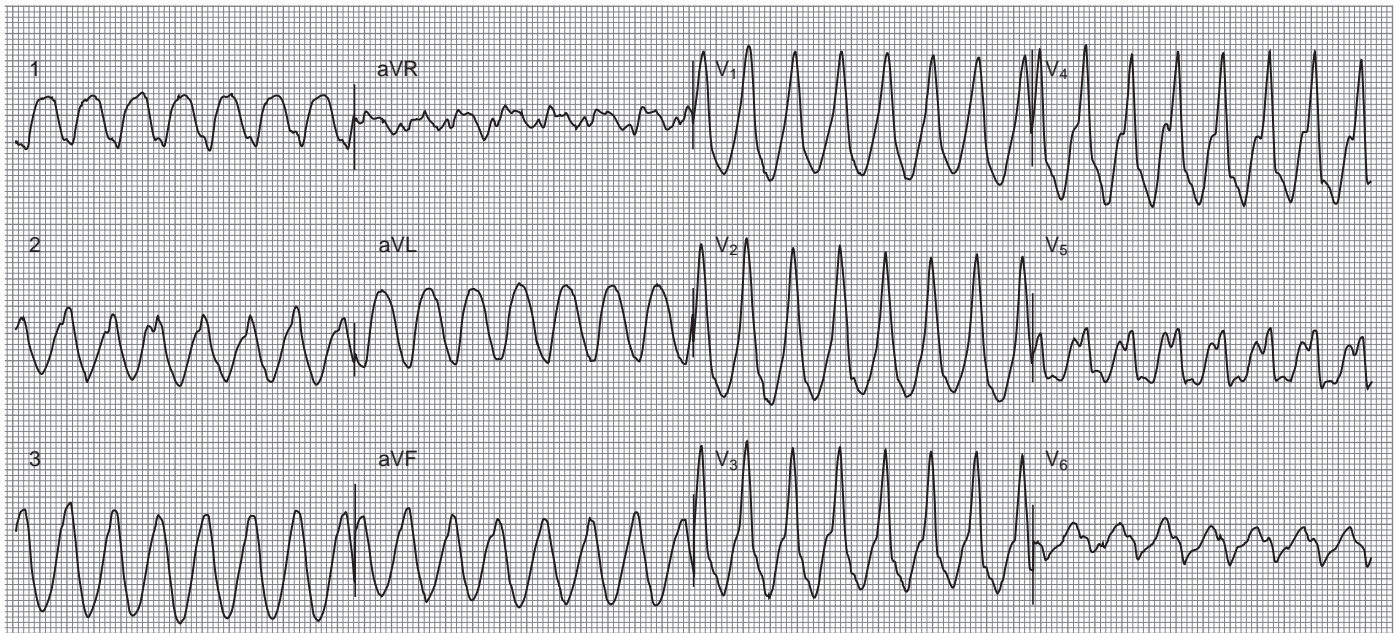


Fig. 25.2 Surface Electrocardiogram of Ventricular Tachycardias in a Patient With Dilated Cardiomyopathy. QRS morphology is suggestive of origin from inferolateral left ventricular substrate. Right bundle branch block morphology, late precordial transition (leads V_6), and right inferior axis.

consistently identifying the endocardial versus epicardial origin in the setting of nonischemic DCM, despite their proven value in patients without structural heart disease.^{34,35}

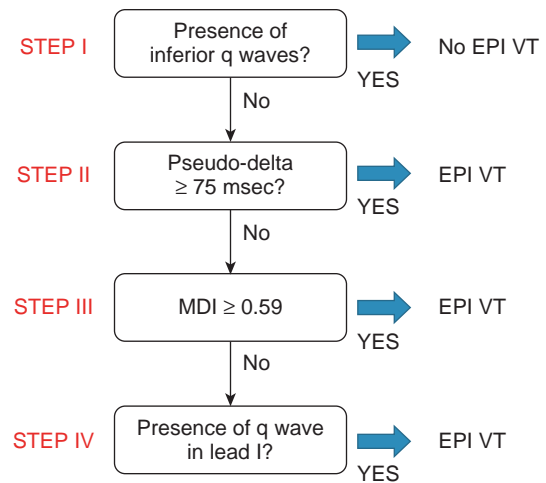
Given the limited predictive value of ECG criteria when applied individually, a multistep algorithm that incorporates several criteria (two morphology criteria and two adjusted interval criteria) was proposed to predict the site of origin of VTs from the basal-superior/lateral epicardium in patients with nonischemic DCM (Fig. 25.3). The criteria included, in a stepwise fashion, (1) the absence of Q waves in inferior leads; (2) a pseudo-delta wave of at least 75 milliseconds; (3) a maximum deflection index of 0.59 or more; and (4) the presence of a Q wave in lead I. The maximum deflection index is defined as the shortest time to maximal deflection in the precordial leads, divided by the total QRS duration—that is, the interval measured from the earliest ventricular activation (or from the stimulation artifact) to the peak of the largest amplitude deflection in each precordial lead (taking the lead with shortest time), divided by the QRS duration.³⁵

This four-step algorithm had a 95% specificity and at least 20% sensitivity for identifying basal-superior/lateral epicardial origin of VTs in nonischemic cardiomyopathy. The morphological criteria (presence of a q wave in lead I and absence of q waves in the inferior leads) appear to be the most specific criteria. In particular, the presence of a q wave in lead I is a very specific (88%) and also a very sensitive criterion (88%) for identifying an epicardial site of origin.³⁵

MAPPING

Scar-related macroreentry is the dominant mechanism of VT in DCM. Therefore mapping techniques for these VT are similar to those used for post-MI VT (see Chapter 22 for detailed discussion).

There are two strategies for VT ablation: (1) identification of the critical isthmus of the tachycardia circuit; and (2) identification of the potential arrhythmogenic substrate. Identification of the critical isthmus of the VT by activation and entrainment mapping techniques is the gold standard for VT mapping. However, this goal may not be achiev-



SN = 96% SP = 93%

Fig. 25.3 Four-Step Algorithm to Identify an Epicardial (EPI) Left Ventricular Ventricular Tachycardia (VT) Site of Origin From the Basal Superior and Lateral Left Ventricle in Patients With Nonischemic Cardiomyopathy. The cutoff values of the pseudo-delta wave and maximum deflection index (MDI) were modified to increase its individual predictive value. The three top steps have a high specificity and the last step is the most accurate. The total sensitivity (SN) and specificity (SP) of the algorithm in the study population for pace map localization reach 96% and 93%, respectively. (From Vallès E, Bazan V, Marchlinski FE. ECG criteria to identify epicardial ventricular tachycardia in nonischemic cardiomyopathy. *Circ Arrhythmia Electrophysiol.* 2010;3:63–71.)

able in patients with noninducible or poorly tolerated VTs. Therefore it is a common practice to utilize substrate mapping during NSR as an initial strategy to delineate the potential arrhythmogenic substrate and refine the area of interest, and then attempt focused activation and entrainment mapping after VT induction, if feasible. When the VT is

unstable or unsustainable, substrate-based mapping becomes the main strategy to guide ablation. Substrate mapping during NSR as the sole strategy to guide ablation has also been employed successfully to guide ablation without attempting mapping during VT, even in patients with inducible VTs (see Fig. 22.30).³⁶

When VT mapping is the goal of the procedure, it is recommended that isthmuses of all mappable VTs be identified and selectively targeted, with an ultimate goal of elimination of all those VTs. On the other hand, when multiple VTs are inducible during EP testing, some investigators recommend targeting only the clinical VT, especially in very ill patients in whom the goal is to decrease the frequency of ICD shocks.³⁶

However, there are several difficulties with selecting a dominant clinical VT for ablation. Often it is not possible to determine which VT is the one that has occurred spontaneously. Only a limited recording of one or a few ECG leads may be available. In patients with an ICD, VT is usually terminated promptly and a 12-lead ECG often is not available. Even if one VT is identified as predominant, other VTs that are inducible can subsequently occur spontaneously. Nonetheless, comparing the tachycardia cycle length (TCL) and ICD electrogram morphology during spontaneous and induced VTs can be helpful, particularly when trying to limit ablation and target only the presumptive clinical VT.

Electroanatomic mapping systems have become an essential tool for mapping and ablation of scar-related VT. Electroanatomic mapping can help in the precise description of VT reentrant circuits, sequence of ventricular activation during the VT, rapid visualization of the activation wavefront, and identification of slow-conducting pathways and appropriate sites for entrainment mapping. These systems also help navigation of the ablation catheter, planning of ablation lines, and cataloging sites of interest (e.g., sites with favorable entrainment or pace mapping findings), which can then be revisited with precision. In addition, the use of electroanatomic mapping systems is essential for substrate-based approaches to mapping and ablation of post-MI VT.

A quadripolar mapping-ablation catheter is typically utilized for point-by-point mapping. High-density mapping can be facilitated by the use of a 20-pole catheter (PentaRay, Biosense-Webster, Diamond Bar, CA, United States) or the Orion minibasket catheter (Boston Scientific, Cambridge, MA, United States).^{37,38} Multielectrode catheters with small and closely spaced electrodes offer improved mapping resolution, especially when mapping in areas of heterogeneous scar distribution, where they allow identification of distinct diastolic activity that may not be seen with standard linear catheters.³⁹

Preprocedural Evaluation

Preprocedural optimization of HF and hemodynamic status is necessary. Echocardiography, computed tomographic (CT), or CMR imaging may be used to identify the size, location, and transmural extent of the myocardial scar that potentially contains the arrhythmogenic substrate. This information can potentially predict the approach required for successful VT ablation (endocardial vs. epicardial) and help focus initial mapping strategies to the area of interest within the ventricle. Furthermore, registration of preacquired CT or CMR images with real-time electroanatomic mapping has successfully been used to facilitate and guide catheter navigation and VT ablation (see eFig. 6.8).^{40,41}

These tests also help exclude the presence of LV thrombus, which can increase the risk of embolization during mapping. Organized thrombus can overlie the area of interest for ablation and prevent effective energy delivery to target sites.⁴

Left Ventricular Access

The LV is accessed through the retrograde transaortic approach, the atrial transseptal approach, the subxiphoid epicardial mapping, or a combination of these approaches.

VT mapping and ablation in patients with DCM often is challenging, more so than post-MI VT, partly because of the frequent intramural and subepicardial location of the arrhythmogenic substrate. Two scar patterns (basal anteroseptal and inferolateral) account for arrhythmogenic substrates in the majority of patients. Basal anteroseptal scars are most effectively approached from the endocardial retrograde transaortic approach, and are usually not well accessible from the epicardium. Mapping and ablation of midseptal circuits requires a biventricular endocardial approach. In patients with inferolateral scars, an epicardial approach is frequently required.⁴

Hemodynamic Support

Not infrequently, hemodynamic instability during sustained VT precludes conventional mapping approaches (entrainment and activation mapping), especially in patients with severe LV dysfunction. In some patients, hemodynamic support can be achieved by the use of intravenous (IV) vasopressors (dopamine, dobutamine, or phenylephrine), partial or complete cardiopulmonary bypass, or percutaneous LV assist devices. In addition, IV procainamide can help slow and stabilize the VT rate.^{42–44}

Percutaneous LV assist devices (Impella microcirculatory axial blood flow pump [Abiomed, Danvers, MA, United States] and TandemHeart [Cardiac Assist, Pittsburgh, PA, United States]) generally provide greater hemodynamic stability during sustained VT than intraaortic balloon pumps. Although the ability to maintain sustained VT without hemodynamic compromise allows for more detailed mapping to identify the critical isthmus of the VT circuit, the use of these devices has not been proven to improve outcome. Therefore the potential benefits of these approaches should be weighed against the risk of vascular and thromboembolic complications in the individual patient.^{44–46}

Importantly, the volume status and intake and output should be closely monitored during the ablation procedure, especially when utilizing open-irrigated ablation catheters. In some patients, administration of diuretics and utilization of decreased irrigation rate or closed-irrigation ablation catheters need to be considered. In addition, when the transseptal approach is utilized for LV access, monitoring left atrial (LA) pressure can help assess volume status.

Induction of Tachycardia

Typically the stimulation protocol applies pacing output at twice the diastolic threshold and a pulse width of 1 to 2 milliseconds. Single ventricular extrastimuli (VESs) during NSR and at pacing drive CLs of 600 and 400 milliseconds are delivered, first from the RV apex and then from the right ventricular outflow tract (RVOT). The prematurity of extrastimuli is increased until refractoriness or induction of sustained VT is achieved. If these measures fail to induce VT, double and then triple VESs are used in the same manner. If VT still cannot be induced, rapid ventricular pacing is started at a pacing cycle length (PCL) of 400 milliseconds, gradually decreasing the PCL until 1:1 ventricular capture is lost or a PCL of 220 milliseconds is reached. Repeating the protocol at other pacing drive CLs, at other RV sites, or after administration of isoproterenol is then attempted.²⁹ Short-long-short coupling intervals may be helpful in initiating BBR-VT.

Substrate Mapping

The majority of VTs in patients with DCM are caused by scar-related macroreentry. Substrate mapping aims at identification of the areas of scar (as identified by low-amplitude electrograms and electrical unexcitability), as well as delineation of conducting channels within or adjacent to the scar regions that can potentially support the VT circuit (as identified by voltage channels and local abnormal ventricular activity [LAVA]).

Substrate mapping during NSR often is employed as an initial mapping strategy to help identify potential isthmuses that support the VT circuit, and narrow the area of interest for further activation and entrainment mapping maneuvers required to confirm the target for ablation. This approach helps minimize the duration spent in sustained VT that can potentially result in exacerbation of cardiac and renal failure. On the other hand, when the VT is not approachable by conventional point-by-point activation mapping and entrainment maneuvers (because of hemodynamic intolerance, inconsistent induction, altering QRS morphology, or nonsustained duration), substrate mapping approaches become the primary strategy to guide VT ablation.

Preprocedural Substrate Imaging

CT or CMR imaging can be used to identify the size, location, and transmural extent of the scar that potentially contains the arrhythmogenic substrate. In addition, registration of those imaging modalities in the three-dimensional (3-D) electroanatomic mapping system can help visualize the LV substrate and focus the mapping procedure to the region of interest. In addition, CMR is able to characterize the transmural extent and intramyocardial location of scar tissue, which can potentially help identify intramural and epicardial arrhythmia substrate, overcoming a limitation of endocardial voltage mapping.⁴⁷

Scar Mapping

While substrate mapping techniques are similar to those describe for post-MI VT, it is important to note that the VT substrate in DCM exhibits more complicated morphology and distribution patterns compared with the substrate in post-MI VT, given the propensity for intramural, epicardial, and patchy scar morphologies characteristic of DCM. In addition, the scar in DCM tends to be smaller and less confluent, and more diffuse, necessitating high-density mapping of the entire ventricular surface.

Electrical scar is defined by low amplitude of local electrograms and tissue unexcitability during high-output pacing. Voltage mapping is performed during sinus rhythm, atrial pacing, or ventricular pacing. During bipolar voltage mapping, endocardial scar is defined as areas with peak-to-peak electrogram amplitude less than 0.5 mV. A low-voltage “border zone” is defined as endocardial bipolar voltages between 0.5 and 1.5 mV. At low-amplitude (less than 0.5 mV) sites, pacing is performed with 10-mA, 2-millisecond pulse width stimuli. A pacing threshold greater than 10 mA has been used to define unexcitable scar, provided electrode-tissue contact is adequate. The use of intracardiac echocardiography (ICE) and contact force catheters can help ensure adequate catheter contact, an essential prerequisite for reliable voltage mapping. The voltage map is displayed in a color-coded manner, with the color range set between 0.5 and 1.5 mV, and superimposed on the on the electroanatomical model.^{45,48}

In general, endocardial sites with evidence of slow conduction (e.g., late potentials, fragmented electrograms, and long S-QRS intervals during pacing) correspond to areas with more than 75% scar transmural or patchy scar.^{45,49}

Because of the predilection of nonischemic scar for the midwall and epicardium, low-voltage areas on endocardial electroanatomic mapping are smaller in patients with nonischemic scar-related VTs compared with patients with post-MI VTs. Frequently the VT substrate can be solely or predominantly intramural or epicardial and hence might not be detected during bipolar voltage mapping. In this setting, unipolar voltage mapping (with threshold of 8.3 mV for detection of LV scar and 5.5 mV for RV scar) can be used effectively to identify substrates deeper to the endocardial recording site, such as intramural, midseptal, and epicardial scar. Low unipolar voltages indicate regions of epicardial involvement with high positive and negative predictive values in patients

with no or minimal endocardial changes evident on bipolar electrogram analysis (Fig. 25.4). In addition, if VT circuits within the interventricular septum are suspected, the RV side of the septum should be mapped.^{45,49,50}

Voltage mapping in patients with DCM typically demonstrates a modest-sized area of endocardial electrogram abnormalities (ranging from 6% to 48% of the LV endocardial surface, but uncommonly involving more than 25% of the total endocardial surface area) located near the LV base and lateral aspect, frequently surrounding the aortic and mitral valve region and then extending apically. The amount of dense scar (electrogram amplitude less than 0.5 mV) accounts for approximately $27\% \pm 20\%$ (range, 0% to 64%) of the overall abnormal low-voltage endocardial substrate. The exit site of a VT circuit corresponds to these basal electrogram abnormalities.

The electroanatomical substrate abnormalities in DCM are often found in the LV basal and perivalvular regions with a predilection for the midmyocardial and epicardial layers (Fig. 25.5). Two predominant scar patterns account for the arrhythmogenic substrate in the majority of these patients: anteroapical LV scar and inferolateral LV scar. VT originating from the inferolateral scar often requires epicardial ablation, in contrast to VT originating from an anteroapical scar that more frequently appear to have an intramural origin requiring ablation from the aortic root or the anteroapical LV endocardium, but not from the epicardium.²⁷

In addition, the interventricular septum is a frequent location for the VT substrate, which can escape detection by bipolar voltage mapping. Unipolar voltage mapping on both sides of the septum and preprocedural CMR, as well as delayed transseptal activation time and patterns, can help identify midseptal scar.²⁷

Identification of Conducting Channels

Diastolic isthmuses during VT are typically composed of relatively small bundles of viable myocardium embedded within or between dense scar regions. Abnormal low-voltage electrograms can be recorded throughout extensive areas of scar that are not sufficiently specific for the components of the reentrant circuit. Therefore identification of the conducting channels within the low voltage zones helps refine the area that potentially supports the VT circuit. Those channels can be identified by voltage channels or, more reliably, as sites with late potentials embedded within dense scar.⁵¹ It is important to recognize, however, that the assessment of the relationship between conducting channels identified in NSR and those detected by entrainment mapping during tachycardia has been limited.⁵²

Voltage channels. Conducting channels can be visualized on the electroanatomic voltage map as corridors of voltage preservation (voltage channels) within denser regions of scar or corridors between a dense scar and a valvular annulus. Careful step-by-step manual adjustment of voltage upper and lower limits on the color-coded electroanatomic voltage map (i.e., the voltage limits are reset to 0.3 to 0.5 mV as the upper limit and to 0.1 mV as the lower, representing dense scar) can help maximize the color contrast between adjacent myocardium with different electrogram voltage levels within the 0.5-mV scar and thus unmask channels of viable myocardium within a dense scar (Fig. 25.6).^{51,53}

Recent evidence, however, has questioned the value of this method (voltage scanning) for the identification of conducting channels. This technique likely has limited sensitivity and specificity. The technique utilizing late potentials identifies a higher proportion of conducting channels and, more importantly, most conducting channels that serve as the substrate for VTs. This may not be surprising since voltage mapping incorporates the larger far-field signals commonly present at sites recording smaller near-field late potentials.

Late potentials. The majority of VT isthmus sites are associated with the presence of multipotential and fractionated electrograms (i.e.,

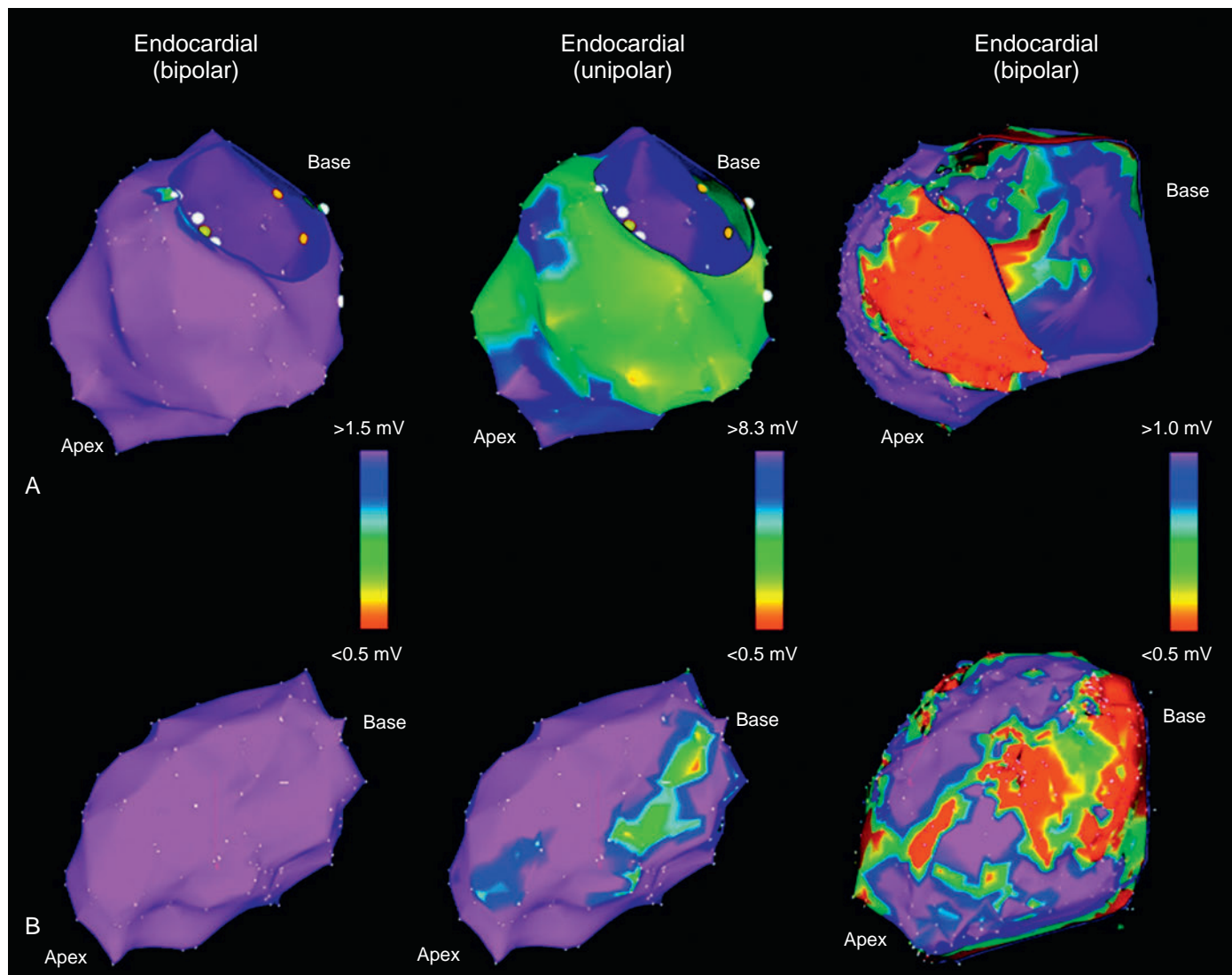


Fig. 25.4 Voltage Mapping in Nonischemic Dilated Cardiomyopathy. Left ventricular (LV) endocardial (bipolar and unipolar) and epicardial bipolar voltage maps are shown in two different patients. (A) Maps are shown in the posterior-anterior projection. The LV endocardial bipolar voltage map (*left*) is normal, whereas the endocardial unipolar voltage map (*middle*) shows extensive low voltage involving the lateral and inferior LV walls. There is a large region of corresponding LV epicardial bipolar low voltage (*right*) seen corresponding spatially with the endocardial unipolar abnormality. (B) Maps are shown in the lateral projection. The LV endocardial bipolar voltage map (*left*) is normal, whereas the endocardial unipolar voltage map (*middle*) shows two confluent low voltage regions at the basal-mid lateral and apical LV segments, which correspond to the low voltage zone identified on the corresponding LV epicardial bipolar voltage map (*right*). (From Hutchinson MD, Gerstenfeld EP, Desjardins B, et al. Endocardial unipolar voltage mapping to detect epicardial ventricular tachycardia substrate in patients with nonischemic left ventricular cardiomyopathy. *Circ Arrhythmia Electro-physiol.* 2011;4:49–55.)

electrograms with three or more sharp spikes, either separated by an isoelectric interval or continuous) and/or late potentials (i.e., low-voltage electrograms with a single-component or multiple continuous delayed electrical components separated from the higher-amplitude component of the local ventricular electrogram by at least 20 milliseconds and recorded after the end of the surface QRS). Electrogram fractionation reflects slow and nonuniform anisotropic conduction, while late potentials can reflect local depolarization of surviving muscle bundles that are well insulated by dense scar, where local activation is recorded late, well after the higher amplitude far-field electrogram and often well after the end of the surface QRS complex or T wave.^{38,54,55} In DCM, late

potentials are recorded more frequently in association with the infero-lateral than antero-septal scar subtypes. When recorded endocardially, abnormal local ventricular activity usually suggests the presence of a transmural scar.⁴⁹

However, local abnormal electrical activity is limited by imperfect specificity due to bystander cul-de-sacs or nonspecific slowed conduction, as well as imperfect sensitivity due to low-amplitude local signals or the direction of wavefront propagation obscuring isolated potentials. Nevertheless, late potentials can help refine the area of interest. The areas demonstrating such electrograms are relatively small compared with scar areas; therefore this method permits a focus on the diagnostic

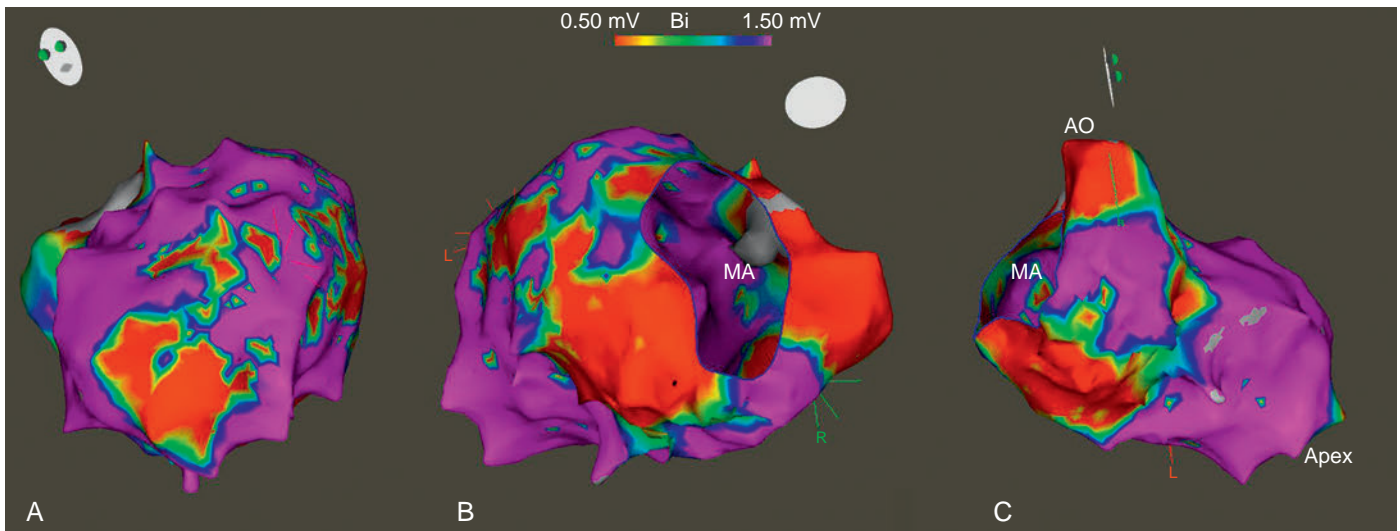


Fig. 25.5 Scar Distribution in Nonischemic Dilated Cardiomyopathy. Bipolar voltage map of the left ventricle in a patient with ventricular tachycardia and nonischemic dilated. Scar cutoff value is set at <0.5 mV (red area), and border zone is set at 0.5 to 1.5 mV. (A) Apical view. (B) Posterior view. (C) Right lateral view. Note predilection of scar distribution to the left ventricular basal and perivalvular regions, and the patchy nature of the scar. AO, Aorta; MA, mitral annulus.

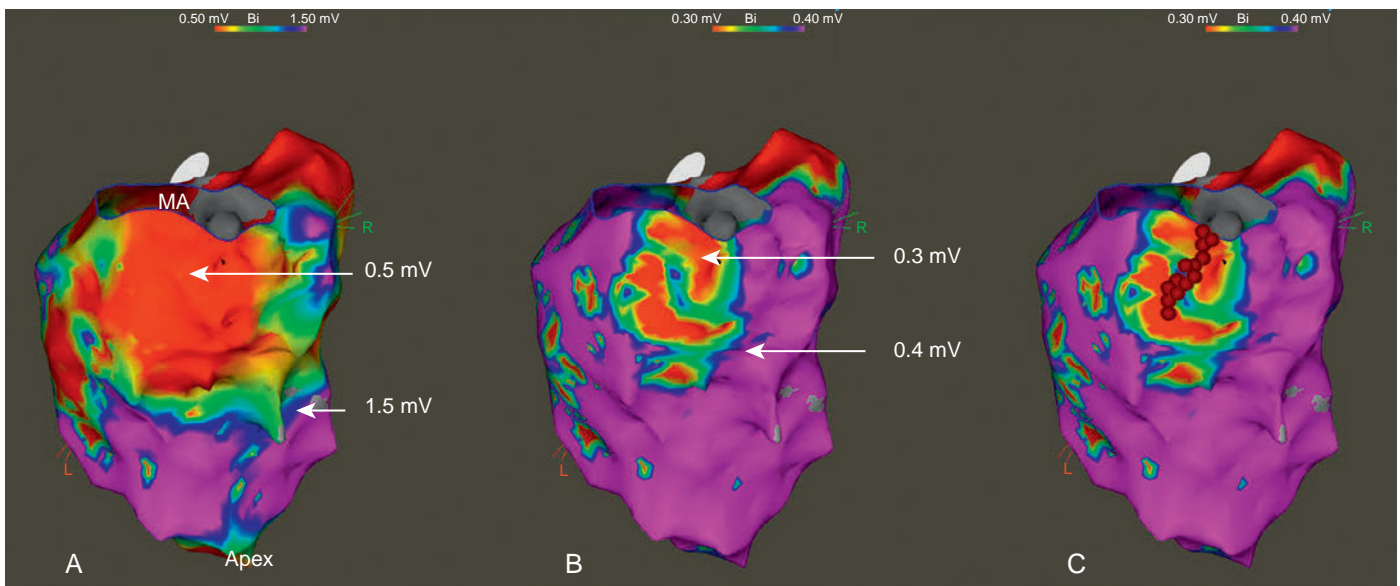


Fig. 25.6 Voltage Channels. Bipolar voltage map of the left ventricle (*inferior view*) in a patient with ventricular tachycardia and nonischemic dilated. (A) Large basal inferior wall scar is obtained when the cutoff value is set at <0.5 mV (red area), and border zone is set at 0.5 to 1.5 mV. (B) By modifying the color scale, different areas within the scar can be identified: very low voltage areas (<0.3 mV) corresponding to true scar (border zone is set at 0.3 to 0.4 mV) and corridors between them with slightly greater voltage (in green and yellow) constituting voltage channels and potential circuit isthmuses. (C) Catheter ablation (red dots) is performed to transect the voltage channels. MA, Mitral annulus.

techniques and ablation in defined areas. Furthermore, recording these electrograms before and during VT induction serves to relate them and VT within seconds, provided that the isolated diastolic component of the electrogram precedes the first VT beat and then becomes mid-diastolic. In addition, pacing is systematically attempted at these sites looking for morphology match with any induced VT and for latency between the stimulus and the QRS. The paced wavefront at those sites usually propagates slowly out of the scar, resulting in a long S-QRS

interval (greater than 40 milliseconds) and, if sharing an exit of a targeted VT, a good or excellent pace map.

Late potentials typically are low-amplitude and often are obscured by larger far-field electrograms produced by activation of the surrounding myocardium outside the scar region. Changing the direction of depolarization approaching the mapping site (e.g., sinus rhythm vs. RV pacing) and premature ventricular stimulation (causing decremental conduction) can help separate local (near-field) from far-field potentials.

Furthermore, pacing at the local site can help distinguish far-field from near-field signals. When the recorded electrogram is near-field, capture of the pacing stimulus results in capturing the tissue generating all components of the electrogram, so that no clear electrogram component is identifiable during pacing. Conversely, when the recorded electrogram is far-field, pacing may not capture (due to dense scar) or, when it captures local tissue, the far-field electrograms remain discernible during pacing (since they reflect activation of myocardium adjacent to the pacing site).⁵⁴

Sites recording abnormal electrograms are tagged and superimposed on voltage maps to further delineate their relationship to scar distribution. Late potential conducting channels are defined as a path of more than two adjacent late potentials connecting with healthy tissue. Further, late potentials are classified as being an entrance or an inner part of a given conducting channel, depending on the local activation time of the near-field component. The entrance of a conducting channel is tagged as sites within the border zone (i.e., voltage zone of 0.5 to 1.5 mV) recording late potentials with the shortest delay between the far-field component (low frequency, usually high voltage) and the near-field, local component (delayed, high frequency, usually fractionated and low voltage). Sites with longer delays likely reside farther along the conducting channel within the dense scar.^{49,56}

Activation Mapping

After construction of an endocardial voltage map during the baseline rhythm, VT is induced by programmed ventricular stimulation. VT activation mapping has several prerequisites, including inducibility of VT by programmed stimulation, hemodynamic stability of the VT, and stability of the VT reentry circuit (i.e., stable VT morphology and TCL). If the tachycardia is not stable (morphologically or hemodynamically), mapping can still be performed by starting and stopping the VT after data acquisition at each site. In addition, poorly tolerated rapid VTs sometimes can be slowed by antiarrhythmic drugs to allow for mapping. Furthermore, the use of intravenous vasopressors and external hemodynamic support devices can potentially provide hemodynamic support and allow mapping of otherwise unstable VT.^{42–44} The use of 20-pole catheter (PentaRay; 2–6–2 mm interelectrode spacing, 1 mm electrodes), the mini-basket catheter (Orion), and noncontact mapping can also provide large amounts of activation mapping data during nonsustained or unstable VT.

Activation mapping aims to identify with continuous activity spanning diastole or with an isolated mid-diastolic potential, presumably representing the diastolic pathway (critical isthmus) of the reentrant circuit. Unlike focal tachycardias, a presystolic electrogram preceding the tachycardia complex by 10 to 40 milliseconds is not adequate in defining the site of origin of a macroreentrant tachycardia (eFig. 25.3). The earliest presystolic electrogram closest to mid-diastole is the most commonly observed indicator of an isthmus site in a VT circuit; however, continuous diastolic activity and/or bridging of diastole at adjacent sites or mapping a discrete diastolic pathway would be most consistent with a reentrant circuit.

Initially one should seek the general region of the origin of the tachycardia guided by VT morphology on the surface ECG, as well the findings on substrate mapping and preprocedural substrate imaging studies localizing the arrhythmogenic substrate. In particular, activation mapping during VT should first be directed to conducting channels and sites with late potentials identified during NSR. Most reentrant circuits in DCM cluster around the basal anteroseptal and inferolateral LV.

Once identified, the relationship of sites with mid-diastolic activity to the VT should be verified. One must always confirm that the diastolic electrical activity (early, mid, or late) cannot be dissociated from the VT and is required for VT maintenance. Thus during spontaneous

changes in the TCL or those produced by programmed electrical stimulation, the electrogram, regardless of its position in diastole, should show a fixed relationship to the subsequent QRS and not the preceding QRS. The ability to dissociate diastolic electrical activity from the VT indicates that those sites are parts of areas of abnormal slow conduction unrelated to the VT circuit (i.e., a dead-end pathway) or bystander sites attached to the VT isthmus. Entrainment mapping (see later) can help establish the relationship of those sites to the tachycardia circuit.

If, after very detailed mapping, the earliest recorded site is not at least 50 milliseconds presystolic, this suggests that either the map is inadequate (most common) or the VT arises deeper in the midmyocardium or subepicardium.

Entrainment Mapping

Entrainment mapping during reentrant VT is used to verify whether a site recording diastolic activity (regardless of where in diastole it occurs, its position, and appearance on initiation of VT) is functionally involved in the VT circuit.

Entrainment mapping is directed to sites identified by other mapping modalities, such as activation and pace mapping, as potentially related to the reentrant circuit. These include areas of slow conduction (manifest as fractionated electrograms), sites with mid-diastolic electrograms, or those displaying long delays between the pacing stimulus and the captured surface ECG complex. Pacing is performed during VT at a PCL 10 to 30 milliseconds shorter than the TCL, at sites identified during activation mapping, demonstrating continuous activity or isolated mid-diastolic potentials.

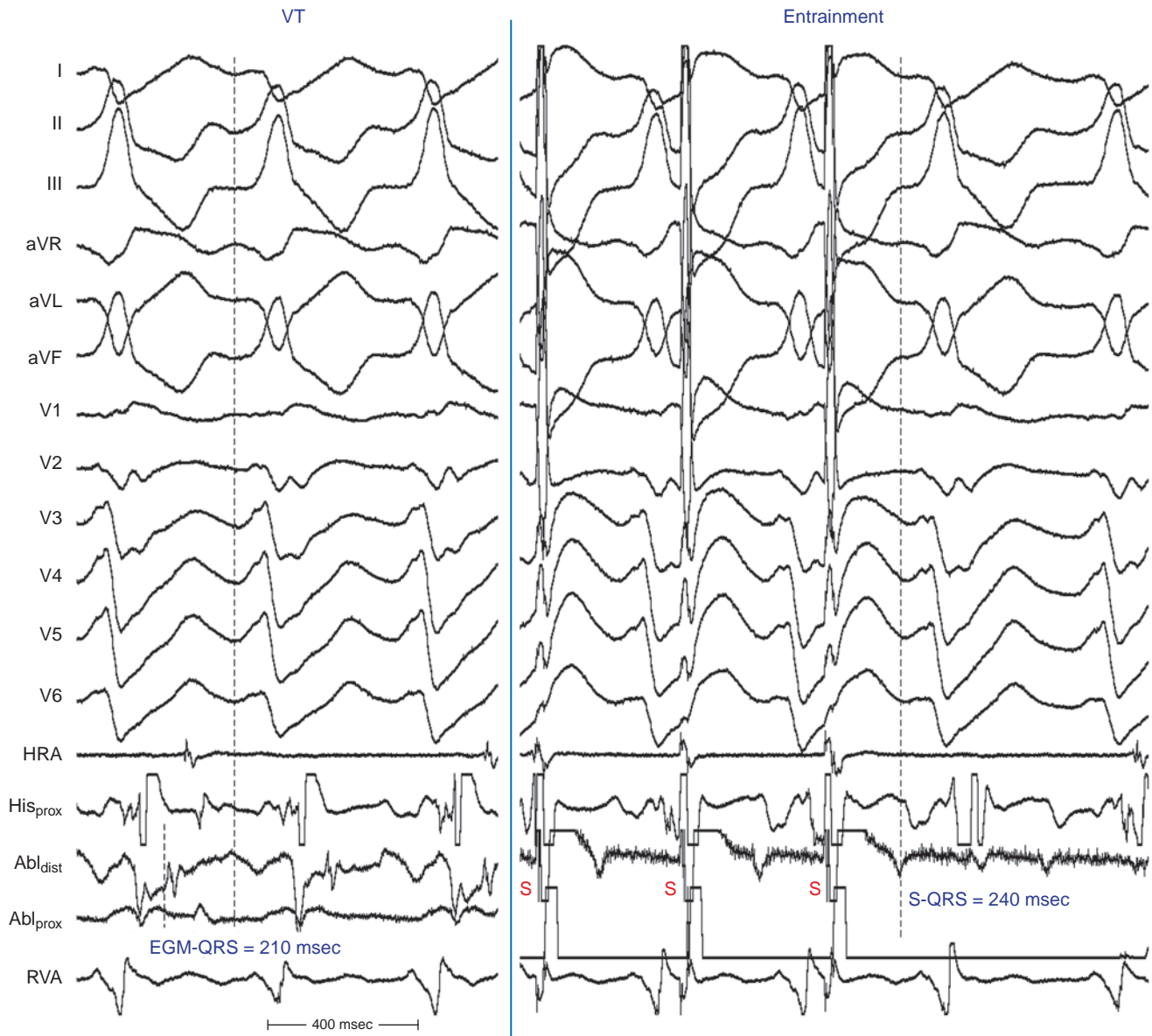
Once the presence of entrainment is verified, several criteria can be used to indicate the relation of the pacing site to the reentrant circuit. The first entrainment criterion to be sought is concealed fusion. Entrainment with concealed fusion indicates that the pacing site is in a protected isthmus located within or attached to the reentrant circuit. Whether this protected isthmus is crucial to the reentrant circuit or is just a bystander site needs to be verified by other entrainment criteria including the postpacing complex (PPI) versus the TCL and the local electrogram-QRS interval during VT versus the S-QRS interval (see Fig. 22.20).⁵⁷

For stable SMVTs, the following three criteria are used to define the critical isthmus and predict the success of radiofrequency (RF) application in termination of the VT: (1) entrainment with concealed fusion; (2) PPI equal to the TCL (± 30 milliseconds); (3) and S-QRS interval equal to the local electrogram-to-QRS interval (± 20 milliseconds; see eFig. 25.3). Other predictors of successful ablation sites include S-QRS interval-to-VT CL ratio less than 70%, long S-QRS interval, and alteration of the TCL or VT termination by subthreshold or nonpropagated stimuli.⁵⁸

As noted, when hemodynamic compromise during the VT is the main limitation for conventional activation and entrainment mapping methods, inductions of brief episodes of VT (with the mapping catheter at the optimal site, as identified by substrate and pace mapping approaches) can allow assessment of the relationship of the abnormal electrograms to the VT circuit. This can also allow entrainment maneuvers to be performed at those sites to help distinguish sites critical to the VT circuit from bystander sites. VT is then quickly terminated before significant hemodynamic compromise ensues. This approach can be facilitated by hemodynamic support with the use of IV vasopressors, LV assist devices, or both. This approach, however, requires being able to induce the same VT reproducibly.

Pace Mapping

Pace mapping has been shown to be an effective corroborative method to regionalize the VT circuit and define potential exit sites along the



eFig. 25.3 Entrainment Mapping of Ventricular Tachycardia (VT) in Dilated Nonischemic Cardiomyopathy. VT is shown at left, with the ablation catheter at a site with an early diastolic recording; entrainment at this site has a stimulus-QRS interval similar to that of the electrogram-QRS during VT, with a perfect pace match. Ablation at this site eliminated VT. *Abl_{dist}*, Distal ablation; *Abl_{prox}*, proximal ablation; *EGM*, electrogram; *His_{prox}*, proximal His bundle; *HRA*, high right atrium; *RVA*, right ventricular apex.

border zone of any low-voltage region. Pace mapping in NSR is attempted after VT termination at potential isthmus sites (as identified by activation and entrainment mapping during VT as well as substrate mapping during NSR). Pace mapping is preferably performed with unipolar stimuli (10 mA, 2 milliseconds) from the distal electrode of the mapping catheter (cathode) and an electrode in the inferior vena cava (anode), at a PCL around 600 milliseconds.

The resulting 12-lead ECG morphology is compared with that of the VT. The greater the degree of concordance between the morphology during pacing and tachycardia, the closer the catheter is to the exit zone of the VT isthmus (see Fig. 5.23). In addition, pace mapping can identify regions of slow conduction with a stimulus-QRS interval (S-QRS) greater than 40 milliseconds and a pace map match consistent with the exit region from an isthmus. Pace mapping at sites more proximally located in the isthmus can also produce a similar QRS complex, but with a longer S-QRS interval (due to the delay of conduction of the paced wavefront to the exit site). The S-QRS interval lengthens progressively as the pacing site is moved more proximally along the isthmus, consistent with pacing progressively farther from the exit (see Fig. 5.23). Sites from which pace mapping produces the same QRS as that of the initial isthmus site with different S-QRS delays are identified in an attempt to trace the course of the VT isthmus (see Figs. 5.16 and 5.23).

Importantly, pace mapping has significant limitations in its ability to identify the critical isthmus of the VT circuit. A poor pace map does not reliably indicate that the pacing site is distant from the reentry circuit, since the VT wavefront is forced by fixed and functional conduction barriers to follow an orthodromic direction through the diastolic pathway of the tachycardia circuit, whereas the paced wavefront can follow different directions that are not constrained by functional barriers present during tachycardia but absent during NSR. In fact, it is rather uncommon to have an identical morphology result from pacing from a known isthmus determined by mapping. On the other hand, pacing during NSR from sites attached to the reentrant circuit but not part of the circuit can occasionally produce QRS morphology identical to that of the VT, because the stimulated wavefront can be physiologically forced by fixed conduction barriers to follow the same route of activation as the VT, as long as pacing is carried out between the entrance and exit of the protected isthmus.⁵⁹

Therefore, in the setting of scar-related macroreentrant VT, pace mapping serves only as a corroborative method of localizing the VT circuit. It can be used to identify the presumptive exit or isthmus region of the VT circuit, but is not sufficiently specific or sensitive to be the sole guide for ablation. Pace mapping can also be used in conjunction with substrate mapping when other mapping techniques are not feasible, so that it can provide information on where ablation can be directed.⁵⁹

Epicardial Mapping

Because of the propensity for epicardial scar in DCM, an endocardial mapping strategy often is limited. Therefore an epicardial approach should be considered early in the mapping process, especially in patients with limited endocardial substrate and those with failed or late VT termination with endocardial RF delivery. In addition, unipolar voltage mapping from the endocardium may be used for evaluation of epicardial scar. Endocardial unipolar (rather than bipolar) voltage mapping can predict the presence of and more closely approximate the extent of epicardial involvement and hence the need for the epicardial approach.⁶⁰

Some studies have shown that a combined endocardial-epicardial mapping and ablation as a first-line strategy in patients with DCM, and especially in those with failed prior endocardial ablation, could improve the procedure results and midterm outcomes. Furthermore, if there are clues on the ECG that suggest an epicardial VT or if there is documentation by CMR imaging of largely epicardial scar, a simultaneous

endocardial and epicardial mapping approach should be considered in the initial ablation procedure, whereby percutaneous epicardial access is obtained as the first step (before the administration of heparin).

The approach to epicardial mapping is essentially the same as for endocardial ablation, including activation mapping, entrainment mapping, substrate mapping, and pace mapping, and is discussed in detail in Chapter 27.

ABLATION

Target of Ablation

There are two strategies for ablation of scar-related VT: (1) selective targeting the critical isthmus that supports the development and maintenance of VT (as identified by activation, entrainment, and pace mapping techniques); and (2) extensive substrate modification to reduce the arrhythmogenicity of a scar without any specific arrhythmia targeting (see Fig. 22.31).^{36,45,61–63}

Selective Ablation of the Critical Isthmus of the Reentrant Circuit

Identification and ablation of the critical isthmus of the VT circuit is the gold standard for macroreentrant VT. This approach provides focused, high-yield ablation, and avoids unnecessary ablation at bystander sites. However, this strategy may not be feasible when the VT is not reproducibly inducible or is poorly tolerated. Even in the setting of stable SMVT, this approach can be time-consuming and expose the patient to the detrimental hemodynamic consequences of prolonged periods of sustained tachycardia, especially when multiple VTs are targeted.⁶³

For each induced stable SMVT, reentry circuit isthmuses are the target of ablation and are defined by activation and entrainment mapping as sites with: (1) continuous activity or isolated mid-diastolic potentials that cannot be dissociated from the tachycardia; (2) entrainment with concealed fusion; (3) PPI equal to the TCL (± 30 milliseconds); (4) S-QRS interval equal to electrogram-to-QRS interval (± 20 milliseconds); and (5) ratio of S-QRS interval of the TCL between 30% and 70%. Alteration of the TCL or termination of VT by subthreshold or non-propagated stimuli, and repeated VT termination occurring with catheter manipulation or pacing at the site, also suggest an isthmus location. These findings are consistent with a central/proximal isthmus site.³⁶

When the critical isthmuses of the reentrant circuit(s) can be identified, linear ablation lesions are delivered to sever those isthmuses. Terminating VT by targeting this area during ablation provides confirmatory evidence that it is a critical site for the arrhythmia. Isthmuses can be relatively broad and require transection with linear ablation lesions, usually connecting two regions of scar, or scar and an anatomical barrier, such as the mitral annulus.

Substrate-Guided Ablation

Substrate-based ablation approaches aim to ablate surrogate markers of the VT circuit during NSR without the need for detailed mapping of the critical isthmus of the VT circuit. Although substrate-based ablation was initially proposed for the treatment of unstable or noninducible VT, it has been increasingly adopted in clinical practice as a primary ablation strategy for any type of scar-related VT. The added value of VT induction and activation mapping has recently been challenged.^{36,62} However, given the less precise localization of the reentry circuit, these strategies involve more extensive, nonselective ablation, frequently involving nonarrhythmogenic regions of the scar. Furthermore, a purely substrate-based mapping and ablation strategy may not address a focal mechanism of VT that can be observed in patients with structural heart disease.^{27,63}

Strategies for substrate ablation are modeled after the technique used for post-MI VT, and range from a thorough ablation of the entire

abnormal substrate harboring abnormal electrograms (scar homogenization) to more selective ablation approaches such as “scar dechanneling” and “core isolation.” The comparative efficacy and safety between those different ablation strategies and their impact on ablation outcome have not been systematically studied. Variations in anatomy often influence the effectiveness of the different methods, and in many patients, a combination of these techniques is employed.^{36,45,49,62}

Scar homogenization. This approach involves extensive RF ablation throughout the entire scar (as defined by substrate mapping) to completely eliminate all the abnormal electrograms (fragmented electrograms and late potentials) within the scar region, without verifying their relationship to the targeted VT (see Fig. 22.32). Ablation is continued until abnormal and late potentials are eliminated, as confirmed by reduction of electrogram amplitude to the noise level and electrical unexcitability in response to high-output pacing (20 mA at 10 milliseconds).^{45,49,61}

Importantly, this approach frequently requires extensive ablation, and complete elimination of abnormal ventricular activity often requires epicardial ablation, especially given the high propensity of epicardial locations of those abnormal electrograms and in areas without ventricular wall thinning (unlike the substrate in post-MI patients), rendering endocardial ablation along ineffective in eliminating epicardial targets.^{60,64}

Scar dechanneling. Scar dechanneling involves RF ablation of all conducting channels within the scar as identified by substrate mapping (see earlier). If feasible, ablation is preferentially performed at the entrance of the conducting channels to eliminate conduction downstream along the channel and its ramifications while obviating the need for extensive ablation through the scar region (see Fig. 22.33). Those targets are identified by substrate mapping as sites within the border zone (i.e., zone with 0.5 to 1.5 mV voltage) recording late potentials with the shortest delay between the far-field and near-field signals. This is in contrast to the inner points of conducting channels within the dense scar, which are characterized by longer delays between the far-field electrogram and local components of the recorded electrogram. The endpoint of this ablation strategy is conducting channel entrance block, manifest as the disappearance of the inner point of the conducting channels or delayed activation of conducting channel inner points, usually with the activation sequence in reverse order.^{45,49,56,65}

Core isolation. This approach involves ablation with contiguous RF lesions placed circumferentially all around the “core” area of the scar containing the putative VT circuit elements (defined by conventional mapping techniques, including voltage channels, sites with late potentials, sites with good pace maps and long S-QRS intervals, as well as isthmus sites defined by entrainment mapping; see Fig. 22.34). The goal of core isolation is electrically isolating the segment of low voltage scar confirmed by the demonstration of exit block from the core of the scar (i.e., failure of global ventricular capture during high-output pacing from multiple, discrete sites inside the core that had previously demonstrated capture). In addition, entrance block can be demonstrated by dissociated fragmented electrical activity inside the core. Core isolation obviates the need for extensive ablation within the scar, as proposed by scar homogenization.^{45,49,66,67}

Linear ablation. This approach entails applying linear RF lesions using one of several guiding principles: (1) ablation lines extending perpendicular to all defined isthmuses (channels of surviving myocardium) within the scar areas or between islands of unexcitable segments within the infarct (identified as a region of relatively larger voltage bordered by low voltage within the scar and abnormal electrograms during NSR); (2) ablation lines extending parallel to the scar edge at the scar border zone (voltage 0.5 to 1.0 mV) encompassing all approximate exit sites identified by pace mapping; or (3) ablation lines extending perpendicular to the scar border, from the area of dense scar (i.e.,

voltage less than 0.5 mV) across the border zone and connecting out to normal myocardium (i.e., voltage greater than 1.5 mV) or to anatomical barriers (e.g., mitral annulus; see Fig. 22.31).^{45,49}

Ablation Technique

Ablation may be performed with an 8-mm-tip (maximal temperature of 65°C and maximal power of 75 W), or an irrigated-tip catheter (maximal temperature of 40°C to 45°C and maximal power of 40 to 50 W). Irrigated RF ablation is generally preferred for scar-related VT, as it allows increased power delivery, deeper lesions in myocardial scar, and potentially improved outcomes. However, external irrigation involves administration of potentially large amounts of IV saline, which can exacerbate HF. Therefore close monitoring volume status is important, and administration of IV diuretics may be required. Internal irrigation catheters or large-tip nonirrigated catheters may be considered if IV fluid administration will be difficult to manage, as in patients with renal failure or severe HF.

When selective ablation is performed during stable VT, RF application is usually maintained for 60 to 120 seconds at the site where the tachycardia is terminated. Application of RF energy at narrow critical isthmuses can terminate VT within 1 to 15 seconds. Wider isthmuses require multiple contiguous ablation lesions transecting the isthmus. Failure of RF ablation to terminate the tachycardia at a site that appears to be in the circuit suggests that the ablated site is a bystander and should prompt reexamination of mapping findings. Persistence of inducibility of VT after successful termination with RF application is probably secondary to inadequate lesion size because of a wide isthmus, poor tissue contact, intramural or epicardial location, or the presence of significant fibrosis, thrombus, or calcification. In some cases, abrupt termination of VT during ablation results in displacement of the ablation electrode from the target tissue. In such instances, entraining VT with RV pacing at the same rate will allow continued energy delivery without catheter movement, since the ventricular rate remains constant even after VT termination.

Patients with an inferolateral scar distribution pattern frequently require epicardial ablation. RF ablation, however, can be hindered by the close proximity of coronary arteries or the left phrenic nerve. Intramural circuits can require sequential ablation on both the endocardial and epicardial aspects of the ventricular free wall. On the other hand, in patients with an anteroseptal scar subtype, the arrhythmia substrate is often intramural and can be difficult to eliminate. High-energy RF ablation at the endocardial breakthrough sites from the right and left sides of the interventricular septum can be necessary, which increases the risk of atrioventricular (AV) block. RF delivery within a perforator vein of the great cardiac vein may be considered in some cases. RF ablation of midseptal targets frequently result in acute tachycardia termination, but persistent inducibility later during the procedure as well as high recurrence of clinical tachycardias during follow-up. Transcatheter alcohol ablation can be useful in targeting basal septal or intramural substrates. For refractory intramural circuits, alternative ablation modalities have been described, including bipolar RF, high-intensity focused ultrasound, or retractable needle ablation.⁶⁸

Endpoints of Ablation

The procedural endpoints for VT ablation in patients with DCM is not well defined, and have largely been based on data derived from studies of post-MI VT ablation.²⁹

Noninducibility of All Monomorphic Ventricular Tachycardias

Noninducibility of any VT (excluding very fast [TCL <240 milliseconds] nonclinical VT, polymorphic VT, and VF), using the entire programmed

electrical stimulation protocol, is the preferred endpoint of the ablation procedure. In small, observational studies, complete VT noninducibility was found to be associated with reduced risk of VT recurrence and improved all-cause mortality in patients with DCM.^{45,69}

However, elimination of all inducible monomorphic VTs can be challenging and may not be achievable in a significant proportion of patients. In addition, achieving this endpoint typically requires extensive mapping and ablation and repetition of aggressive ventricular stimulation, which can potentially lead to hemodynamic compromise. Furthermore, the predictive value of noninducibility for VT recurrence remains limited; the rate of VT recurrence remains relatively high even in patients whose VT is rendered noninducible after ablation. Therefore, while it is reasonable to attempt modification of the arrhythmogenic substrate to achieve a complete VT noninducibility, the benefits of such approach should be weighted carefully against the risks of extensive and prolonged ablation procedure.^{45,69}

Noninducibility of All Clinical Ventricular Tachycardias

Elimination of inducibility of all clinical VTs (i.e., all inducible VTs that are known to have the same 12-lead ECG QRS morphology and approximate CL as spontaneous VTs), using the entire programmed stimulation protocol, can be an acceptable procedural endpoint, even when other “nonclinical” SMVTs remain inducible. Elimination of clinical VTs is usually associated with a favorable outcome and a decrease of the arrhythmia burden and ICD shocks in most patients (especially in patients presenting with frequent ICD shocks or incessant VT) while obviating excessive mapping and ablation and prolonged procedure duration that may not be well tolerated.⁶⁹

However, this endpoint does not apply in the majority of patients in whom recordings of all VTs before ablation often are not reliably obtainable to define clinical or presumed clinical VTs or when the clinically relevant VTs are not reproducibly inducible at the outset of the procedure.

Modification of the Arrhythmogenic Substrate

Complete elimination of all fragmented and late potentials, scar homogenization, scar dechanneling, or core isolation (as described previously) may also be utilized as alternative procedural endpoints, especially in patients in whom VT is not reproducibly inducible at baseline. Furthermore, even in patients with inducible VTs, some reports suggested an improvement in outcome (reduction in VT recurrence cardiac mortality) when these substrate-based endpoints are combined with VT noninducibility, likely by eliminating the arrhythmogenic substrate and reducing the risk of developing new VTs or preexisting VTs that were not inducible during the ablation procedure.^{66,70,71}

Outcome

The acute success rates of catheter ablation of VT in DCM (i.e., achieving VT noninducibility as an endpoint) remain modest (50% to 75%) and lower than those for post-MI VT. This might be related to differences in scar distribution between the two pathologies. Unlike post-MI patients, combined endocardial-epicardial ablation is required in a large proportion of DCM patients.

VTs recur following ablation in DCM patients at a higher rate (23% to 77%) than in patients with post-MI VT. Nonetheless, the burden of VT and the frequency of ICD shocks are reduced in the majority of patients.^{27,45,72} The higher VT recurrence rates among DCM patients is likely related, at least in part, to disease progression; the majority of recurrent VTs appear to result from new circuits, representing a changing substrate. Incomplete procedural success, lower LVEF, VT storm, higher number of clinical VTs, and a higher number of failed antiarrhythmic drugs appear to predict increased risk of VT recurrence.²⁹

CARDIAC SARCOIDOSIS

Pathophysiology

Sarcoidosis is multisystem infiltrative, granulomatous disease of unknown etiology. The pathological hallmark of sarcoidosis is the formation of noncaseating granulomas composed of epithelioid and multinucleated giant cells. Sarcoidosis is thought to represent a T cell–mediated immune process in response to an unidentified antigenic trigger. Infectious, organic, and inorganic agents have been proposed as putative antigens. Regardless of the trigger, the disease progresses through three successive histopathological stages: (1) inflammation and edema with the infiltration of leukocytes, (2) noncaseating (necrotizing) epithelioid cell granuloma formation, and (3) fibrosis leading to post-inflammatory scarring.⁷³

The clinical course and prognosis of sarcoidosis are largely dependent on the location of granulomatous infiltration. The main organ systems involved by sarcoidosis are the lungs and thoracic lymph nodes, although virtually no organ systems are spared, including the central nervous system and the skin. Intrathoracic involvement occurs in more than 90% of patients.

Among patients with extracardiac sarcoidosis, clinical cardiac involvement occurs in approximately 5%, whereas subclinical cardiac involvement was reported in more than 25% on autopsy and in up to 55% on cardiac imaging studies. Only 40% to 50% of patients with cardiac sarcoidosis at necropsy had clinical evidence of myocardial involvement during their lifetime. Importantly, extracardiac involvement can be minimal or even clinically absent, whereby extensive cardiac sarcoid can be present as the only disease manifestation.

Cardiac sarcoidosis can affect the interventricular septum, RV and LV free walls, and atria. Involvement of the basal septum by scar tissue, granulomas, or the involvement of the nodal artery can lead to various degrees of AV block and intraventricular conduction abnormalities. A recent study primarily implicated inflammation-induced edema in the interventricular septum, rather than fibrosis, in the pathophysiology of AV block. Focal inflammation in the septum (as detected on CMR and positron emission tomography [PET]) was significantly associated with complete AV block, while septal fibrosis and scarring were not.⁷⁴

Atrial involvement is common but tends to be less extensive as compared with ventricular involvement. Atrial disease can precipitate atrial arrhythmias (AF and AT are the most common) as well as sinus node dysfunction (SND).⁷⁵

Involvement of the ventricular myocardium can lead to LV and RV dysfunction and DCM. Two patterns of regional wall motion abnormalities are frequently observed, involving the basal free wall and the anteroapical septum. Mitral valve abnormalities, papillary muscle dysfunction, LV aneurysm formation, and pericardial effusions are also seen. The inflammatory process in cardiac sarcoidosis often is initiated in the myocardium, creating lesions (granulomas) that then extend to the epicardium, endocardium, or both.^{75,76}

Early inflammation and late fibrosis participate in ventricular arrhythmogenesis, one of the hallmarks of cardiac sarcoidosis. Sustained monomorphic VTs are predominantly due to scar-related macroreentry. RV involvement seems to be particularly arrhythmogenic, as the VT substrate preferentially involves confluent regions of endocardial and, more predominantly, epicardial RV scarring. Although some studies suggested predilection of the peritricuspid region or RV apex, a recent report found no predilection for any particular RV region. In contrast to the confluent RV scarring, LV scarring in patients with clinical VTs tends to be patchy, with less epicardial predominance, and with a predilection for the basal septum, anterior wall, and perivalvular regions. The diffuse and heterogeneous ventricular infiltration in cardiac sarcoidosis provides

a substrate potentially capable of sustaining a large number of reentrant VT circuits, explaining the common occurrence of multiple monomorphic VTs and pleomorphic VT in cardiac sarcoidosis. In a small proportion of patients, monomorphic sustained VT seemed to be secondary to a reentrant or nonreentrant mechanism closely associated with a diseased Purkinje system in either ventricle, including bundle branch reentry.⁷⁵⁻⁷⁷

Myocardial inflammation also plays a role in arrhythmogenesis in cardiac sarcoidosis. Triggered activity and abnormal automaticity secondary to inflammation are the likely mechanisms of frequent PVCs in these patients. Further, active inflammation can potentially promote macroreentrant VT either by increasing the frequency of triggers (i.e., PVCs) or by slowing conduction in diseased tissue within granulomatous scar.^{75,79}

Epidemiology and Natural History

The estimated annual incidence of sarcoidosis is about 5 to 64 per 100,000. The incidence varies greatly by ethnicity and region, with the highest rates occurring in northern Europeans and African Americans, particularly in women. Sarcoidosis occurs at all ages, with peak incidence in young adults (25 to 45 years).^{75,80}

Patients with cardiac sarcoidosis have a much worse prognosis than patients without cardiac involvement. In fact, progressive HF and malignant ventricular arrhythmias account for up to 77% of deaths due to sarcoidosis. However, the prognosis in cardiac sarcoidosis is highly variable, with 5-year survival rates ranging from 60% to 90%. Prior to the use of ICDs, SCD accounted for approximately 25% to 65% of deaths caused by cardiac sarcoidosis. LV dysfunction and deterioration in HF symptoms were found to be independent predictors of mortality.⁷⁵ The prognosis of clinically silent cardiac sarcoidosis has not been well defined. Progression to end-stage HF or intractable ventricular arrhythmias is observed in some patients despite optimal therapy. Ventricular assist devices or cardiac transplantation may be required.

Clinical Presentation

Clinical manifestations of cardiac sarcoidosis are highly variable and dependent on the location, extent, and activity of the disease. Patients with cardiac sarcoidosis can present with (1) AV and intraventricular conduction abnormalities, (2) ventricular arrhythmias, (3) supraventricular arrhythmias, (4) congestive HF, and (5) sudden death.⁷³

Biventricular HF is the most common clinical feature of cardiac sarcoidosis. Papillary muscle involvement can result in severe mitral regurgitation. Complete AV block can be observed in up to 30% of patients, whereas various types of intraventricular conduction disturbances (IVCDs) occur in up to 61%. Approximately 50% of patients with cardiac sarcoidosis require treatment for ventricular arrhythmias. These patients usually have multiple monomorphic VTs, with either RBBB or LBBB morphology.⁷⁵ Atrial arrhythmias can be observed in up to one-third of patients with clinical cardiac sarcoidosis, with AF and AT being the most common. Both reentrant and nonreentrant ATs can be observed.

In some patients, cardiac symptoms can be the first presentation of sarcoidosis from any organ. Studies have found that up to 19% of young adults (less than 55 years old) presenting with AV block of unknown etiology, and up to 28% of patients presenting with unexplained monomorphic VT (without idiopathic VT, ischemic VT, or known sarcoidosis) had cardiac sarcoidosis. AV block was observed in the majority of that latter cohort of patients.⁸¹ Furthermore, cardiac sarcoidosis has been reported to represent 5% to 17% of unexplained nonischemic cardiomyopathy patients referred for management of ventricular arrhythmias.⁸²

Initial Evaluation

The diagnosis of cardiac sarcoidosis should be considered in patients with biopsy-proven extracardiac sarcoidosis, with or without cardiac symptoms. Initial evaluation includes ECG and echocardiography. The presence of suggestive cardiac symptoms or abnormal findings on ECG or echocardiography should prompt additional cardiac studies (CMR and PET).⁷⁵

In the absence of previous diagnosis of extracardiac sarcoidosis, screening for cardiac sarcoidosis should be considered in young patients (less than 60 years) with unexplained Mobitz II or third-degree AV block, in those with unexplained monomorphic VT, and in those with unexplained nonischemic cardiomyopathy presenting with ventricular arrhythmias (Box 25.2).^{75,82} Initial testing typically includes a computed tomographic scan of the chest for pulmonary sarcoid and advanced cardiac imaging (CMR or PET). Abnormal findings on those tests should prompt definitive histological diagnosis.⁷³

Electrocardiography

The sinus rhythm surface ECG commonly exhibits BBB (RBBB in particular), QRS complex fragmentation, atrial or ventricular ectopy, or some degree of AV block. Unexplained pathological Q waves (pseudo-infarct patterns) can be observed in localized myocardial infiltration.⁷⁵

The QRS morphology during monomorphic VT varies according to the origin of the tachycardia. The majority of VTs in cardiac sarcoidosis originate from the RV and hence manifest a LBBB pattern on

BOX 25.2 Heart Rhythm Society Expert Consensus Recommendations on Criteria for Diagnosis of Cardiac Sarcoidosis

There are two pathways to a diagnosis of CS:

1. Histological diagnosis from myocardial tissue

CS is diagnosed in the presence of noncaseating granuloma on histological examination of myocardial tissue with no alternative cause identified (including negative organismal stains, if applicable).

2. Clinical diagnosis from invasive and noninvasive studies

It is probable that there is CS if:

a. There is a histological diagnosis of extracardiac sarcoidosis

and

b. One or more of the following is present:

1. Steroid ± immunosuppressant-responsive cardiomyopathy or heart block
2. Unexplained LVEF <40%
3. Unexplained sustained (spontaneous or induced) ventricular tachycardia
4. Mobitz type II second- or third-degree heart block
5. Patchy uptake on dedicated cardiac FDG-PET (in a pattern consistent with CS)
6. LGE on CMR (in a pattern consistent with CS)
7. Positive gallium uptake (in a pattern consistent with CS)

and

c. Other causes for the cardiac manifestation(s) have been reasonably excluded

CMR, Cardiovascular magnetic resonance; CS, cardiac sarcoidosis; FDG-PET, fluorodeoxyglucose-positron emission tomography; LGE, late gadolinium enhancement; LVEF, left ventricular ejection fraction.

From Birnie DH, Nery PB, Ha AC, Beanlands RSB. Cardiac sarcoidosis. *J Am Coll Cardiol*. 2016;68:411-421.

the surface ECG. When VT is the first manifestation of sarcoidosis, VT morphology on the surface ECG can mimic VTs observed in patients with ARVC. One report suggested that a reduced LVEF should raise suspicion of cardiac sarcoidosis, even if ARVC diagnostic criteria are fulfilled. As compared with patients with ARVC, patients with cardiac sarcoidosis tend to have a significantly lower mean LVEF, significantly wider QRS complexes, and more different morphologies of inducible monomorphic VT, which originated more commonly in the apical region of the RV.^{83,84}

In addition, VT in cardiac sarcoidosis can occur in the absence of structural heart disease on echocardiography, in which case it can be misdiagnosed as idiopathic VT. Unlike idiopathic VT, significant variations in the TCL and pleomorphism (i.e., VT with more than one morphologically distinct QRS complex occurring during the same episode of VT, but the QRS not continuously changing) is commonly (in about 50% of cases) observed in cardiac sarcoidosis. Although pleomorphic VT is not pathognomonic of cardiac sarcoidosis and can be observed in other structural heart diseases (e.g., MI, HCM, DCM, ARVC), it is rare in idiopathic VT. Therefore the presence of this feature in a structurally normal heart on echocardiogram and in the absence of coronary artery disease should raise the suspicion for cardiac sarcoidosis.⁸⁵

Echocardiography

About 14% to 56% of the patients with cardiac sarcoidosis have detectable abnormalities on echocardiogram, such as LV or RV systolic dysfunction, wall-motion abnormalities (often in a noncoronary distribution), ventricular aneurysm, or basal septum thinning. Early stages of the disease may not be detected.⁷⁵

Cardiac Magnetic Resonance

CMR is very valuable in the diagnosis of cardiac sarcoidosis. CMR has a high sensitivity (100%) and specificity (78%) for myocardial scar detection in patients with sarcoidosis, with positive and negative predictive values of 55% and 100%, respectively, and an overall accuracy of 83%.⁷³

CMR findings are not pathognomonic for cardiac sarcoidosis, and can vary depending on the stage of the pathological process. Early gadolinium enhancement of sarcoid granulomas in CMR T2-weighted images suggests the presence of acute inflammation-induced edema, whereas delayed enhancement can assess the presence, extent, and distribution of myocardial fibrosis or scar (Fig. 25.7). CMR imaging with delayed enhancement can sometimes detect the granular cells, which resemble clumps of sand or salt grains, and help regionalize the disease process. Patchy regions of myocardial fibrosis are the most common findings on CMR, but confluent areas of scar (mimicking MI) can occasionally be observed.⁷⁵

Positron Emission Tomography

The uptake of fluorine-18 fluoro-2-deoxyglucose (18-FDG) PET appears to detect the inflammatory activity in cardiac sarcoidosis with a slightly higher sensitivity than CMR, but with a slightly lower specificity. In addition, PET can be particularly useful in patients with a pacemaker or ICD who are unable to undergo CMR. PET and CMR imaging allow visualization of different aspects of cardiac sarcoidosis and can have a complementary role (see Fig. 25.7). Cardiac sarcoidosis typically manifests with focal (patchy) uptake either in isolation or on a background of mild diffuse uptake with or without resting perfusion defects and

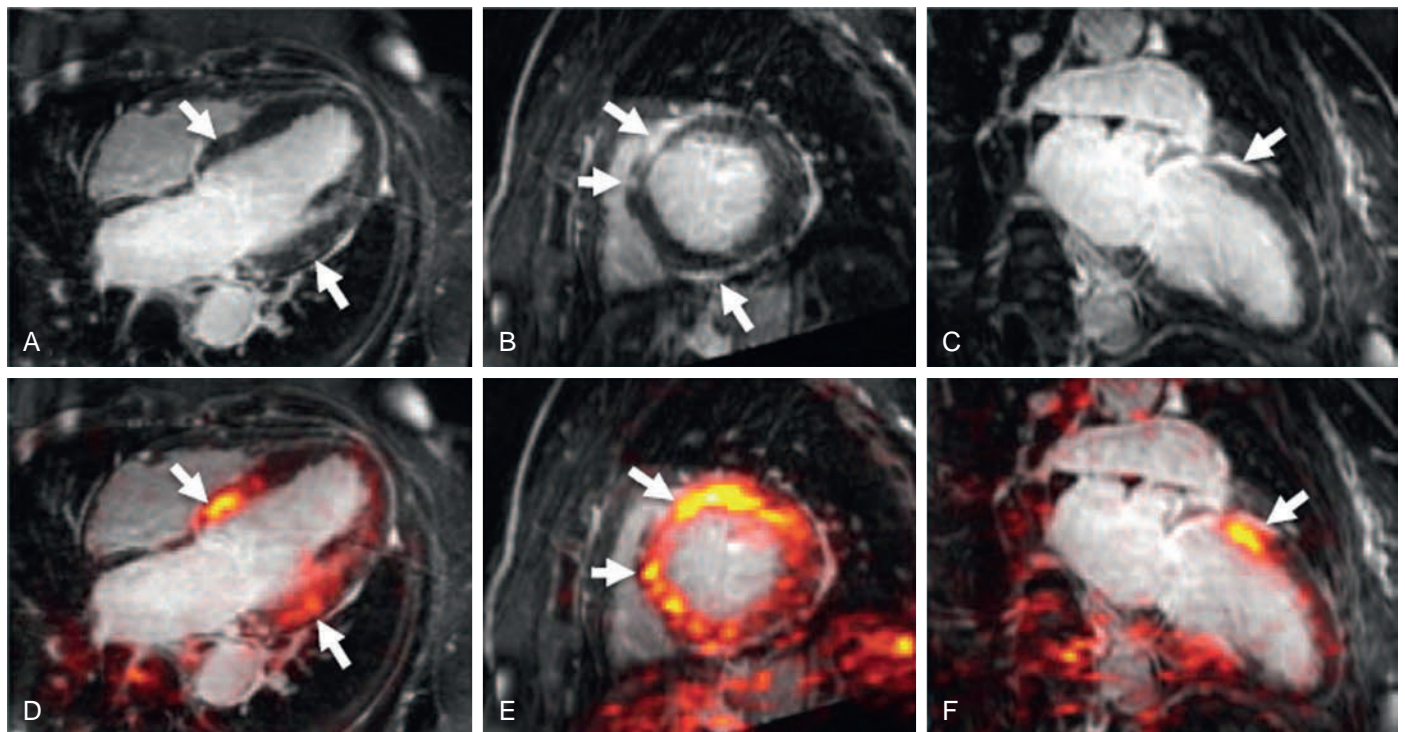


Fig. 25.7 Cardiac Magnetic Resonance (CMR) and Positron Emission Tomography (PET) Imaging in Cardiac Sarcoidosis. Top row, CMR images in 4-chamber (A), short-axis (B), and 2-chamber (C) orientations showing three-dimensional (3-D) late gadolinium enhancement (LGE) scar imaging. Arrows indicate regions of abnormal LGE, consistent with mature scar. Bottom row (D–F), shows 3-D LGE images with fusion of fluorodeoxyglucose-PET signal, suggestive of active inflammation surrounding regions of established scar. (From Birnie DH, Nery PB, Ha AC, Beanlands RS. Cardiac sarcoidosis. *J Am Coll Cardiol*. 2016;68:411–421.)

wall motion abnormalities. Importantly, PET findings are not pathognomonic for cardiac sarcoidosis, and should be interpreted in the appropriate clinical context.⁷⁵

Histological Examination

Cardiac sarcoidosis can only be confirmed by histological examination of cardiac tissue. However, endomyocardial biopsy is generally not required, and myocardial involvement can be diagnosed by noninvasive cardiac imaging, if sarcoidosis has already been demonstrated histologically in another organ and other causes for the cardiac manifestations have been reasonably excluded. Nevertheless, tissue examination showing noncaseating granulomas (in the absence of any other identifiable cause such as tuberculosis) is required in those patients with features suggestive of cardiac sarcoidosis but no prior diagnosis of pulmonary/systemic sarcoidosis.⁷⁵

Biopsies should first be obtained from the most accessible lesion that appears to be affected (e.g., cutaneous lesions or palpable lymph nodes), and then lung or intrathoracic lymph nodes are typically targeted if radiographic and CT abnormalities are detected. In cases of isolated cardiac sarcoidosis or negative extracardiac biopsy, endomyocardial biopsy may be considered to confirm the diagnosis. However, endomyocardial biopsy has very limited sensitivity (less than 25%) due to the focal and patchy nature of cardiac sarcoidosis. To increase the yield, low voltage areas on electroanatomic voltage mapping or affected myocardial segments identified on PET or CMR are targeted by the biopsy.^{73,75}

Electrophysiological Testing

EP testing may be considered in patients with documented or suspected cardiac arrhythmias, when catheter ablation is contemplated. EP study may also be considered in patients with syncope and those with first-degree AV block or fascicular block to define levels of conduction system disease and guide pacing therapy. EP testing may also be of value for SCD risk stratification.⁷⁵

Risk Stratification

Left Ventricular Ejection Fraction

Reduced LVEF is an independent predictors of mortality and appropriate ICD therapy in ICD recipients for primary or secondary prevention. Even mild degrees of LV systolic dysfunction (LVEF of 35% to 49%) predict a substantial risk of arrhythmia. In one study, a large proportion of primary and secondary prevention ICD recipients who received appropriate ICD therapies had an LVEF of greater than 35%. In contrast, none of the primary prevention ICD recipients with normal RV and LV function received an appropriate therapy.⁷⁵

Electrophysiological Testing

Invasive EP testing with programmed ventricular stimulation to assess inducibility of sustained ventricular arrhythmias can potentially provide prognostic information in asymptomatic patients with cardiac sarcoidosis. In small series, VT inducibility was associated with increased risk for clinical arrhythmic events (ICD shocks or death), as well as with progressive deterioration of LVEF, especially in patients with reduced LVEF at baseline. A negative EP study appears to predict a benign course within the first several years after diagnosis. Until more data become available, EP testing may be considered for risk stratification in patients with LVEF greater than 35%, despite optimal medical therapy and a period of immunosuppression (if there is active inflammation).⁷⁵

Cardiac Magnetic Resonance

Late gadolinium enhancement on contrast CMR reflects myocardial fibrosis, which represents a potential substrate for ventricular arrhyth-

mias. Fibrosis detected by CMR is evident in 20% to 30% of patients with extracardiac sarcoidosis. Several studies showed a direct correlation between the presence of myocardial scar and arrhythmic events, with a high negative predictive value in patients with cardiac sarcoidosis; however, these findings have not been consistent in all studies. Despite the limitations of the current data, CMR may be considered for the purpose of SCD risk stratification, particularly in patients chronic LVEF above 35%.⁷⁵

Positron Emission Tomography

Small studies correlated the presence and extent of active myocardial inflammation identified on PET with increased risk of SCD and sustained VT, likely related to disease activity and increased risk of progression. However, the utility of PET for SCD risk stratification is still uncertain.

Syncope

Syncope in patients with cardiac sarcoidosis can be a clinical marker for either ventricular arrhythmias or bradyarrhythmias, and was found to predict higher risk of arrhythmic events (ICD shocks) in ICD recipients.⁸⁶

Complete Heart Block

Advanced AV block was found to be a significant predictor of appropriate ICD therapy. Advanced conduction disease is likely to be a surrogate marker for more extensive myocardial involvement and hence higher risk of ventricular arrhythmias.⁸⁶

Management

Immunosuppression

Although data are limited, immunosuppressive therapy is commonly utilized in patients with active cardiac sarcoidosis. Early initiation of therapy to control inflammation, before the development of advanced clinical manifestations, can potentially help prevent extensive fibrosis, retard disease progression, and improve survival. However, the true benefit of immunosuppressive therapy on the disease course and outcome remains to be evaluated. Also, the timing, dose, and duration of treatment remain uncertain.⁸⁰

Corticosteroids are the primary immunosuppressive therapy, with gradual tapering over a period of months until establishing a minimum effective maintenance dose. Other immunosuppressants (e.g., infliximab, methotrexate, azathioprine) are frequently utilized to help reduce the dose or duration of steroid therapy.⁷³

Management of Conduction Abnormalities

In addition to the conventional recommendations for management of AV block (discussed in **Chapter 9**), pacemaker implantation can be useful in patients with cardiac sarcoidosis with an indication for pacing even if the AV block reverses transiently. In these patients, since AV block likely signifies extensive cardiac disease and portends a higher risk of future ventricular arrhythmias, implantation of an ICD implantation (for the primary prevention of SCD) instead of a pacemaker needs to be considered, regardless of LVEF or prior occurrence of ventricular arrhythmias.^{74,75,86}

Immunosuppression results in improvement in AV conduction in almost half of patients with cardiac sarcoidosis presenting with advanced AV block. Focal inflammation (detected on CMR and PET) with preserved wall thickness in the interventricular septum (suggesting the lack of significant scarring) might predict recovery of AV conduction after corticosteroid therapy. However, even in the setting of positive response to medical therapy, ICD or pacemaker implantation is recommended because reversibility is unpredictable. Since immunosuppression

can potentially increase the risk of device infection and impair wound healing, it may be prudent to postpone immunosuppression until after device implantation and complete wound healing.⁷⁵

Management of Atrial Arrhythmias

For patients with symptomatic AF, beta-blockers, calcium-channel blockers, sotalol, dofetilide, and amiodarone can be considered. Also, a trial of immunosuppression can be useful in some. Given the frequent presence of myocardial scarring, class I agents are not recommended. Anticoagulation is recommended in patients with cardiac and AF if there is sufficiently high risk, as determined by CHA₂DS₂-VASc score. The role of catheter ablation has not been well defined. On the other hand, catheter ablation may be considered in patients with focal or reentrant ATs. These arrhythmias are typically related to atrial scarring identified on electroanatomic mapping.⁷⁵

Management of Ventricular Arrhythmias

Pharmacological therapy. Active inflammation can precipitate frequent PVCs and promote VT and exacerbation of electrical storm. Thus a trial of immunosuppression therapy with corticosteroids, alone or in combination with antiarrhythmic drug therapy, is often utilized to suppress symptomatic ventricular arrhythmias or electrical storm. Immunosuppression is likely to be beneficial for ventricular arrhythmias in the early (inflammatory) phase of cardiac sarcoidosis or when active inflammation is observed on cardiac imaging studies. When antiarrhythmic drug therapy is required, amiodarone and sotalol are the most widely utilized. Ventricular arrhythmias can be refractory to a combination of steroids and antiarrhythmic drugs in about 35% to 50% of patients.^{77,86}

Catheter ablation. Catheter ablation is typically considered in patients with incessant VT, electrical storm, or frequent ICD discharges refractory to immunosuppressive and antiarrhythmic therapy. Ablation can be effective in eliminating or markedly reducing VT burden, with success rates ranging from 25% to 70%, depending on the location of the reentrant circuit. Efficacy is more limited in patients with advanced LV dysfunction. Importantly, because of the future risk of life-threatening arrhythmias, catheter ablation is not a substitute for an ICD, even when excellent short-term results are achieved.^{76,77,87}

Sustained monomorphic VTs in patients with cardiac sarcoidosis are predominantly secondary to scar-related macroreentry involving confluent regions of RV endocardial and epicardial scarring (with no predilection for any particular RV region) and patchy endocardial LV scarring (with a predilection for the septum, anterior wall, and perivalvular regions; Fig. 25.8). The techniques for mapping and ablation of VT in these patients are similar to those described for patients with nonischemic DCM. QRS morphology during VT can be used to regionalize the site of origin of the VT. Most VTs are commonly localized to the scar areas in the RV. Since the scar formation in cardiac sarcoidosis is patchy and can be intramural or epicardial, both endocardial as well as epicardial approaches to ablation may be required. Multiple, monomorphic VTs are commonly observed in cardiac sarcoidosis.⁷⁶ Preprocedural evaluation of the extent and distribution of myocardial scarring by CMR can be of particular value.⁷⁵⁻⁷⁷

In a small proportion of patients, monomorphic sustained VT can be secondary to a reentrant or nonreentrant mechanism closely associated with a diseased Purkinje system in either ventricle (including bundle branch reentry), as evidenced by the finding that Purkinje potentials were observed during sinus rhythm and always preceded VT-QRS onset by at least 20 milliseconds at the successful ablation site. Those VTs tend to have shorter QRS duration (less than 170 milliseconds) as compared with scar-related VT originating elsewhere in the ventricle.⁷⁷

ICD implantation. ICD implantation is recommended for secondary prevention in patients with cardiac sarcoidosis and spontaneous sustained ventricular arrhythmias, including prior cardiac arrest (Fig. 25.9). In addition, prophylactic ICD implantation is recommended in those with LVEF less than 36%, despite optimal medical therapy and a period (3 to 9 months) of immunosuppression (if there is active inflammation). Furthermore, ICD implantation can be useful for primary prevention in patients with LVEF greater than 35% and (1) unexplained syncope or near-syncope, felt to be arrhythmic in etiology; (2) inducible sustained monomorphic or polymorphic VT or clinically relevant VF; or (3) an indication for permanent pacemaker implantation. Prophylactic ICD implantation may also be considered in patients with late gadolinium enhancement on CMR (even if LVEF is normal). In the latter group, invasive EP testing may be of value for further risk stratification.⁷⁵

When clinically feasible, it is prudent to perform ICD implantation when immunosuppressive therapy is at the lowest possible maintenance dose or temporarily withheld.⁷⁵

Cardiac sarcoidosis patient cohorts appear to have more frequent appropriate ICD therapies (approximately 15% per year) than other populations, not only in patients with secondary prevention devices but also in those with an ICD implanted for primary prevention. The annual rate of inappropriate ICD shocks (most commonly secondary to atrial arrhythmias) is about 4.1% to 5.7%.^{75,88,89}

CHAGAS CARDIOMYOPATHY

Pathophysiology

Chagas disease is caused by a unicellular parasite, *Trypanosoma cruzi*. Chronic Chagas heart disease, the most serious manifestation of Chagas disease, is an inflammatory form of DCM. Although the mechanism of the chronic myocarditis remains uncertain, parasite persistence in cardiac tissue, immune-mediated myocardial injury, and microvascular disturbances likely play a role.⁹⁰

The panmyocarditis of Chagas heart disease progressively involves the various cardiac tissues and results in extensive myocardial fibrosis. When the extent of myocardial damage is severe, the disease manifests as myocardial dysfunction that may be segmental, typically a ventricular aneurysm, or global, resembling a DCM. The LV is generally affected more frequently and earlier than the RV.⁹¹

Myocardial damage can occur in various areas of both ventricles, but the inferolateral segment of the LV is the most commonly involved site, with frequently observed wall motion abnormalities. Apical, septal, and inferoapical aneurysms can be observed in 8.5% of asymptomatic patients with mild cardiac damage and in 45% of patients with LV systolic dysfunction and HF. The classic lesion of Chagas disease is a localized aneurysm of the LV apex, with relatively normal surrounding wall motion. This results in a narrow neck when visualized by echocardiography or ventriculography; when present, this can usually distinguish an aneurysm of Chagas heart disease from one due to coronary artery disease.⁹¹

On histological examination, chronic chagasic cardiomyopathy is characterized by a focal, diffuse inflammatory process that results in cell death and severe reparative fibrosis. Myocardial fibrosis is focal and diffuse, predominantly subepicardial, interspersed with viable but often damaged myocardial fibers. VT can arise from various regions in both ventricles, but LV inferolateral scar is the main source of sustained VT reentrant circuits. In these areas, endocardial mapping frequently shows fragmented and late potentials during sinus rhythm, as well as continuous or diastolic activity during VT. Epicardial VT reentrant circuits occur frequently in Chagas cardiomyopathy; approximately 70% of VTs have epicardial sources.⁹¹

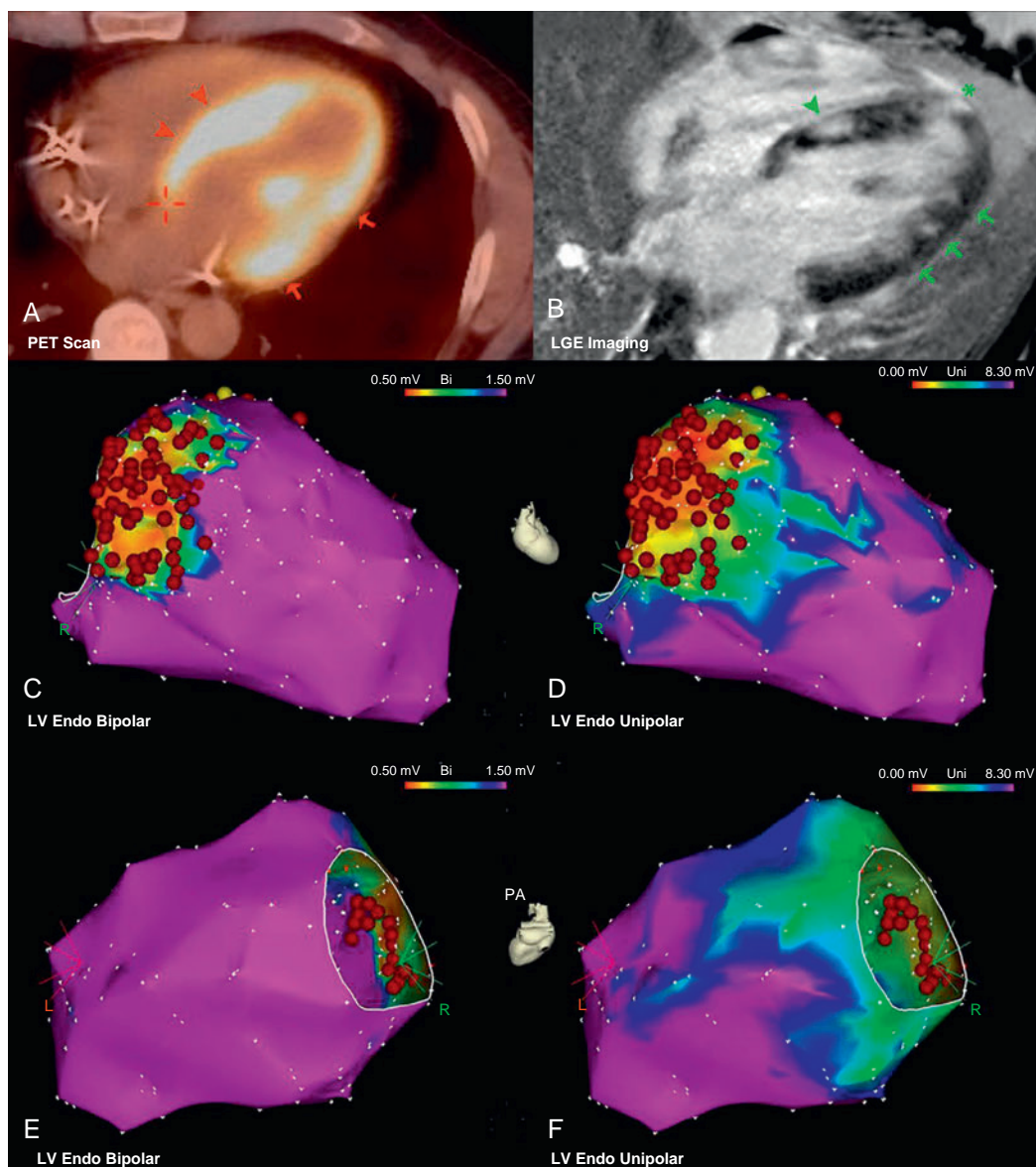


Fig. 25.8 Catheter Ablation of Scar-Related Ventricular Tachycardia in Cardiac Sarcoidosis. (A) Positron emission tomographic (PET) scan showing active inflammation of the whole inferior septum (red arrowheads) and anterolateral wall (red arrows). (B) Contrast-enhanced magnetic resonance imaging of the same patient showing diffuse myocardial scar involving the basal inferior septum (green arrowhead), the septal apex (asterisk), and the anterolateral wall (green arrows). (C–F) Left ventricular (LV) endocardial (Endo) electroanatomic map (EAM) showing a low bipolar voltage area (≤ 1.5 mV) on the basal septum (C, right anterior oblique [RAO] view; E, modified posteroanterior view) and a more diffuse area of low unipolar voltage (≤ 8.3) on the midbasal septum and anterolateral wall (D, RAO view; F, modified posteroanterior [PA] view). EAM shows areas of abnormal voltage largely superimposable with both scar and inflammation particularly at midbasal wall level. Red dots represent ablation lesions. LGE, Late gadolinium enhancement. (From Muser D, Santangeli P, Pathak RK, et al. Long-term outcomes of catheter ablation of ventricular tachycardia in patients with cardiac sarcoidosis. *Circ Arrhythm Electrophysiol.* 2016;9:e004333.)

Diffuse fibrosis of the conduction system often results in bundle branch and fascicular block, different grades of AV block, and SND.⁹² Chagas disease is also associated with cardiac autonomic denervation secondary to inflammation and autoantibodies against cholinergic and adrenergic receptors, which can potentially promote arrhythmogenesis.⁹¹

Epidemiology and Natural History

Chagas disease (American trypanosomiasis) is a vector-borne infection that is endemic in 21 continental Latin American countries (from

southern United States to the north of Argentina and Chile), where 10 to 20 million people are infected and nearly 100 to 120 million are at risk of contracting the disease. The prevalence of Chagas disease in endemic areas is in the range of 1% to 6%, with 300,000 new cases being reported each year.⁹⁰

Chagas disease had attracted little attention outside endemic areas, and many cases of Chagas cardiomyopathy likely remain undiagnosed or are misdiagnosed as idiopathic DCM. However, recent patterns of emigration from endemic countries have drastically altered the

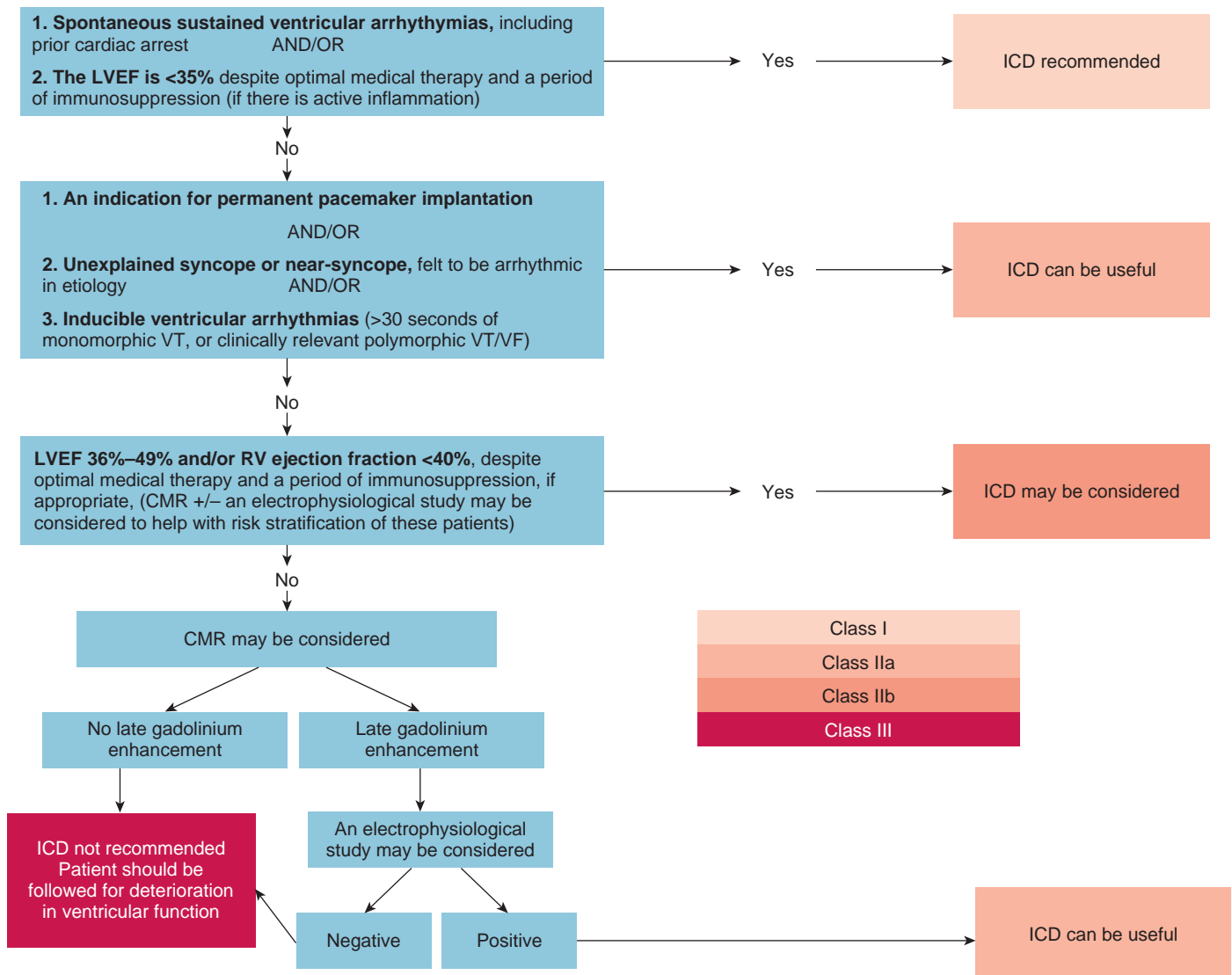


Fig. 25.9 Heart Rhythm Society Expert Consensus Recommendations for Implantable Cardioverter-Defibrillator (ICD) Implantations in Patients Diagnosed With Cardiac Sarcoidosis. *CMR*, Cardiovascular magnetic resonance; *LVEF*, left ventricular ejection fraction; *RV*, right ventricle; *VF*, ventricular fibrillation; *VT*, ventricular tachycardia. (From Birnie DH, Sauer WH, Bogun F, et al. HRS expert consensus statement on the diagnosis and management of arrhythmias associated with cardiac sarcoidosis. *Heart Rhythm*. 2014;11:1305–1323.)

epidemiology of this disease in the United States and other nonendemic regions. It is estimated that there are more than 300,000 immigrants living in the United States infected with *T. cruzi*. Of these, 30,000 to 45,000 have clinical manifestations of Chagas cardiomyopathy, and the estimated index of underdiagnosis is around 95%.^{90,91,93}

In endemic areas, *T. cruzi* infection is acquired most commonly during childhood and young adulthood, primarily through parasite-laden secretions from bloodsucking insects (triatomine). The triatomine vectors are only found in the Americas. Oral transmission through food or drink contaminated with triatomine feces also has been described. Other modes of transmission that do not involve insect vectors include transfusion of contaminated blood products, organ transplantation, and vertical transmission (from mother to child at birth). The non-vectorial modes of transmission are most prominent in nonendemic countries.

The natural history of Chagas disease is characterized by successive stages of disease progression. The acute phase of Chagas disease is most often asymptomatic but can manifest nonspecific symptoms and signs (e.g., fever, inflammation at the inoculation site, lymphadenopathy, and hepatosplenomegaly). Less than 1% to 5% of patients develop acute myocarditis, pericardial effusion, or meningoencephalitis, which can be fatal in some cases.

The acute phase usually resolves spontaneously within a few weeks, and most patients, if left untreated, enter into a lengthy “indeterminate” form of Chagas disease that is defined by the presence of positive serologic tests but no clinical evidence of heart or visceral involvement. The indeterminate phase persists indefinitely in about half of infected patients and does not adversely impact prognosis or life expectancy. However, 30% to 40% of infected patients ultimately develop chronic symptomatic disease (cardiac or digestive), which typically develops 10

BOX 25.3 Clinical Stages of Chronic Chagasic Cardiomyopathy

Stage A

- Patients with “indeterminate form,” without present or previous symptoms of heart failure, without structural heart disease (normal ECG and chest x-ray). As long as the patient remains in this form of the disease, prognosis is not compromised.

Stage B

- Patients with structural heart disease, who have never had signs or symptoms of heart failure. This stage is divided into:
 - B1: Patients with ECG changes (arrhythmias or conduction disorders) may have mild echocardiographic abnormalities (such as abnormalities of regional contractility), but global ventricular function is normal
 - B2: Patients with global ventricular dysfunction (decreased LV ejection fraction)

Stage C

- Patients with LV dysfunction and prior or current symptoms of heart failure (NYHA I, II, III, and IV)

Stage D

- Patients with symptoms of heart failure at rest, refractory to maximized medical therapy (NYHA IV), requiring specialized and intensive interventions

ECG, Electrocardiogram; LV, left ventricle; NYHA, New York Heart Association.

From Andrade JP, Marin Neto JA, Paola AA, et al. I Latin American Guidelines for the diagnosis and treatment of Chagas' heart disease: executive summary. *Arq Bras Cardiol.* 2011;96:434–442.

to 30 years after acute infection. New ECG abnormalities or evidence of definite cardiomyopathy develop in 1.8% to 5% of patients each year. Cardiac and gastrointestinal involvement seldom (in 5% to 20% of patients) present together. A direct progression from acute infection to any clinical form of Chagas disease occurs in just 5% of cases.⁹¹

The natural history and the type of cardiac involvement can vary widely in patients with Chagas disease. Patients with Chagas cardiomyopathy have worse long-term outcomes than patients with non-Chagas cardiomyopathy. Chagas cardiomyopathy results in approximately 50,000 deaths per year. Of these, 60%, 25%, and 15% are related to SCD, HF, and stroke, respectively.

Chagasic damage to the myocardium is generally a progressive process and has been classified into clinical stages (Box 25.3). Importantly, SCD can occur at any time during the evolution of the disease and can be related to ventricular arrhythmia, AV block, stroke, or refractory HF.⁹³

Clinical Presentation

Patients with Chagas cardiomyopathy can present with a wide variety of clinical manifestations; the most important of these are ventricular arrhythmias, sudden death, congestive HF, thromboembolism, and AV block.

The most common initial manifestations include ECG abnormalities (RBBB, LAF block, PVCs) and echocardiographic abnormalities (segmental ventricular wall motion abnormalities, diastolic dysfunction). Disease progression is associated with worsening conduction system abnormalities (AV block, SND), LV systolic dysfunction (DCM, congestive HF, ventricular aneurysms), complex ventricular arrhythmias, and thromboembolism.⁹²

Thromboembolic events, including cardioembolic stroke, are relatively common in Chagas cardiomyopathy, with an annual incidence of 1% to 2%. The incidence is higher in patients with advanced HF,

apical aneurysm, and LV mural thrombosis. Also, pulmonary thromboembolism can occur, predominantly in patients with HF and those with mural thrombosis in the right heart chambers.

VT in Chagas disease can have heterogeneous presentations. SCD, usually due to VF and VT, is the most common cause of death, occurring more often than in other types of DCM, with an incidence ranging from 51% to 65%. Frequently the arrhythmic episodes are clustered in short periods, causing electrical storms (“chagasic storm”). Ventricular ectopy is remarkably frequent in all stages of the disease, even when there is no other evidence of cardiac involvement.

Initial Evaluation

Electrocardiography

ECG abnormalities are often the first indicator of Chagas heart disease. RBBB and LAF block are the most common ECG findings. In fact, the pattern of RBBB and LAFB in patients with cardiomyopathy of unknown etiology and epidemiologic risk factors should raise the possibility of Chagas disease and prompt specific diagnostic testing. Unlike other types of DCM, LBBB and left posterior fascicular block are rare in Chagas cardiomyopathy. PVCs, repolarization abnormalities, abnormal Q waves, various degrees of AV block, SND, and low QRS voltage can be observed on the surface ECG.

Ambulatory Cardiac Monitoring

On Holter monitoring, the burden of PVCs is usually high and temporally unvarying, with patients often having tens of thousands of ectopic beats per day. Nonsustained VT is observed on ambulatory monitoring in 10% of patients with mild wall motion abnormalities, in 56% of those with severe wall motion abnormalities or aneurysms without HF, and in 87% of those with advanced congestive HF. Ambulatory cardiac monitoring may also reveal varying degree AV block, sinus bradycardia, and sinus pauses.^{93,94}

Echocardiography

Echocardiography allows evaluating ventricular systolic and diastolic function, chamber size, and wall motion, as well as the presence of aneurysms or cavity thrombus. Echocardiographic findings can vary depending on the stage of the pathological process. Early evidence of cardiac involvement can manifest as isolated segmental inferior or apical LV wall motion abnormalities (with preserved global systolic function). Ventricular dilatation with diffuse hypokinesia and mitral and tricuspid insufficiency are observed in advanced stages. Ventricular aneurysms (predominantly LV apical) are observed in approximately half of patients with moderate to severe cardiac impairment, but also may be present in up to 9% of asymptomatic patients.^{91,93}

Cardiac Magnetic Resonance

CMR is valuable for evaluating chamber size and function. Furthermore, CMR with delayed enhancement can assess the presence and extent of myocardial fibrosis, which correlates well with disease stage and prognosis. Myocardial fibrosis on CMR is observed in 20% of patients without clinical cardiac involvement, 85% of those with clinical cardiac involvement, and 100% of those with VT. Furthermore, the extent of fibrosis increases across the three groups (0.9%, 16%, and 25% of LV mass, respectively). CMR allows early detection of myocardial involvement unrecognized by ECG and echocardiography.⁹¹

Serologic Testing

Diagnosis of chronic infection relies on serological testing based on detection of antibodies against the *T. cruzi*. Given the low parasitemia in the chronic phase of the disease, parasitological examinations are not routinely used.⁹³

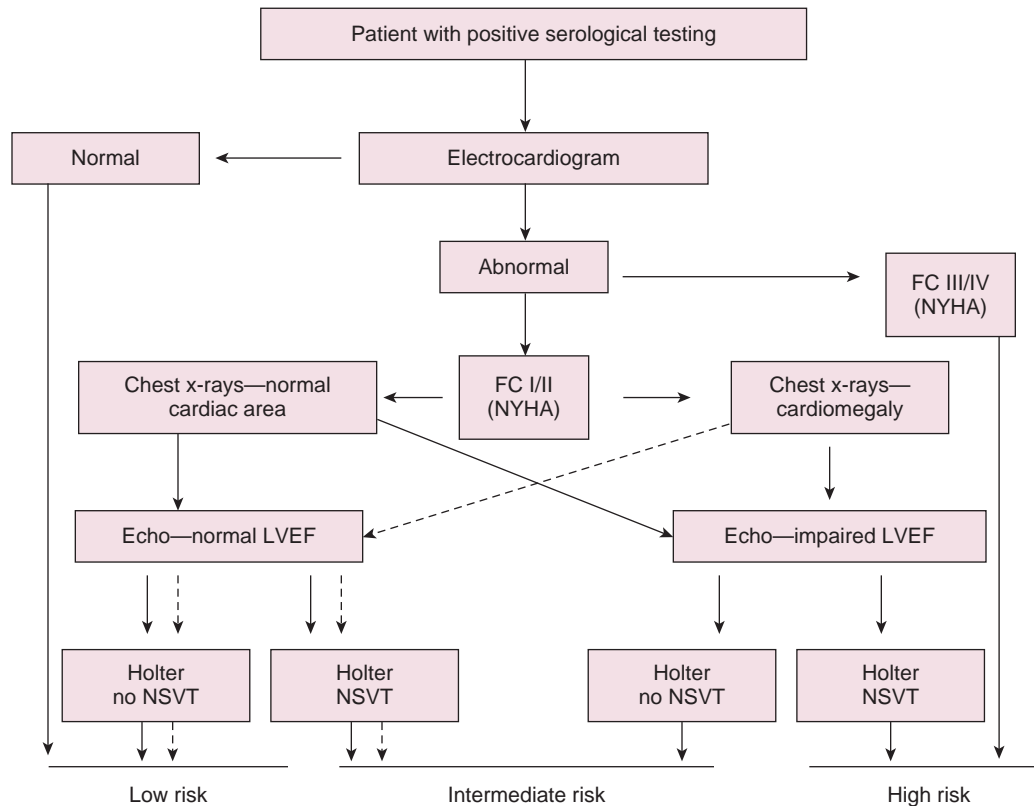


Fig. 25.10 Algorithm for Risk Stratification in the Chronic Phase of the Chagas Disease. FC, Functional class; LVEF, left ventricular ejection fraction; NSVT, nonsustained ventricular tachycardia; NYHA, New York Heart Association. (From Andrade JP, Marin Neto JA, Paola AA, et al. I Latin American Guidelines for the diagnosis and treatment of Chagas' heart disease: executive summary. *Arq Bras Cardiol.* 2011;96:434–442.)

Electrophysiological Testing

Invasive EP testing can be considered in patients with documented or suspected cardiac arrhythmias, when catheter ablation is contemplated. Sustained VT is inducible with programmed ventricular stimulation in most patients who present with sustained ventricular arrhythmias and in half of those who have symptomatic nonsustained VT. EP testing in asymptomatic patients with cardiac involvement has shown that SND is present in 18%, pacing-induced AV block in 41%, and multiple sites of conducting system dysfunction often coexist.⁹³

Risk Stratification

Predictors of poor prognosis include LV systolic dysfunction, NYHA class III/IV, and cardiomegaly on chest x-ray. In patients with LV dysfunction or HF, the presence of NSVT on Holter monitoring also predicts a higher risk for sudden death (Fig. 25.10). Aneurysms are predictors of mural thrombus and stroke; however, their association with the risk of death is uncertain.⁹³

Management

The treatment of Chagas disease involves (1) parasite-specific therapy; (2) HF management; and (3) management of cardiac arrhythmias.

Antiparasitic therapy is indicated for patients with acute infection. The value of antitrypanosomal treatment in the management of chronic disease remains uncertain; however, current evidence indicates no apparent benefit from treating patients with established Chagas cardiomyopathy.⁹⁵

Management of Chagas cardiomyopathy and HF follows the standard recommendations for treatment of HF due to other conditions. Cardiac transplantation is considered in patients with advanced HF.

Ventricular tachyarrhythmias in the setting of Chagas disease are very difficult to treat. Antiarrhythmic drug therapy is frequently ineffective. Limited data exist on the catheter ablation of VTs associated with Chagas cardiomyopathy. Success rates are limited when only endocardial mapping and ablation techniques are used. Epicardial ablation has been shown to improve outcome and should be considered in these cases, perhaps as the initial ablation strategy. Despite the lack of strong evidence, the recommendations for ICD implantation for primary and secondary prevention follow criteria extrapolated from those used for patients with idiopathic DCM. Of note, the incidence of appropriate ICD therapies and sustained ventricular tachyarrhythmias in Chagas patients with ICDs (for primary or secondary prevention indications) is higher than in those with non-Chagas cardiomyopathy.^{96,97}

Similarly, the indications of pacing therapy for symptomatic bradyarrhythmias follow the same guidelines as for non-Chagas patients with AV block or SND.

Because of the high incidence of thromboembolic phenomena, oral anticoagulants are recommended for patients with AF, previous embolism, and apical aneurysm with thrombus.

REFERENCES

1. Lakdawala NK, Winterfield JR, Funke BH. Dilated cardiomyopathy. *Circ Arrhythm Electrophysiol.* 2013;6:228–237.

2. Arbustini E, et al. The MOGE(S) classification for a phenotype-genotype nomenclature of cardiomyopathy endorsed by the World Heart Federation. *J Am Coll Cardiol*. 2013;62:2046–2072.
3. Liuba I, et al. Scar progression in patients with nonischemic cardiomyopathy and ventricular arrhythmias. *Heart Rhythm*. 2014;11:755–762.
4. Piers SRD, et al. Contrast-enhanced MRI-derived scar patterns and associated ventricular tachycardias in nonischemic cardiomyopathy implications for the ablation strategy. *Circ Arrhythm Electrophysiol*. 2013;6:875–883.
5. Epstein AE, et al. 2012 ACCF/AHA/HRS focused update incorporated into the ACCF/AHA/HRS 2008 guidelines for device-based therapy of cardiac rhythm abnormalities: a report of the American College of Cardiology Foundation/American Heart Association Task Force on Practice Guide. *Circulation*. 2013;127:e283–e352.
6. Memon S, Ganga HV, Kluger J. Late gadolinium enhancement in patients with nonischemic dilated cardiomyopathy. *Pacing Clin Electrophysiol*. 2016;39:731–747.
7. Kusumoto FM, et al. HRS/ACC/AHA expert consensus statement on the use of implantable cardioverter-defibrillator therapy in patients who are not included or not well represented in clinical trials. *J Am Coll Cardiol*. 2014;64:1143–1177.
8. Disertori M, et al. The need to modify patient selection to improve the benefits of implantable cardioverter-defibrillator for primary prevention of sudden death in non-ischaemic dilated cardiomyopathy. *Europace*. 2013;15:1693–1701.
9. Schliamser JE, et al. Significance of follow-up left ventricular ejection fraction measurements in the Defibrillators in Non-Ischemic Cardiomyopathy Treatment Evaluation trial (DEFINITE). *Heart Rhythm*. 2013;10:838–846.
10. Gatzoulis KA, et al. Primary prevention of sudden cardiac death in a nonischemic dilated cardiomyopathy population reappraisal of the role of programmed ventricular stimulation. *Circ Arrhythmia Electrophysiol*. 2013;6:504–512.
11. Pezawas T, et al. Multiple autonomic and repolarization investigation of sudden cardiac death in dilated cardiomyopathy and controls. *Circ Arrhythmia Electrophysiol*. 2014;7:1101–1108.
12. Piers SRD, et al. Myocardial scar predicts monomorphic ventricular tachycardia but not polymorphic ventricular tachycardia or ventricular fibrillation in nonischemic dilated cardiomyopathy. *Heart Rhythm*. 2015;12:2106–2114.
13. Perazzolo Marra M, et al. Impact of the presence and amount of myocardial fibrosis by cardiac magnetic resonance on arrhythmic outcome and sudden cardiac death in nonischemic dilated cardiomyopathy. *Heart Rhythm*. 2014;11:856–863.
14. Di Marco A, et al. Late gadolinium enhancement and the risk for ventricular arrhythmias or sudden death in dilated cardiomyopathy. *JACC Heart Fail*. 2017;5:28–38.
15. Priori SG, Blomström-Lundqvist C, Mazzanti A. 2015 ESC guidelines for the management of patients with ventricular arrhythmias and the prevention of sudden cardiac death. *Eur Heart J*. 2015;36:2253–2367.
16. Katz DF, et al. Survival after secondary prevention implantable cardioverter-defibrillator placement. *JACC Clin Electrophysiol*. 2017;3:20–28.
17. Al-Khatib SM, et al. 2017 AHA/ACC/HRS guideline for management of patients with ventricular arrhythmias and the prevention of sudden cardiac death. *Heart Rhythm*. 2017;[Epub ahead of print].
18. Betts TR, et al. Absolute risk reduction in total mortality with implantable cardioverter defibrillators: analysis of primary and secondary prevention trial data to aid risk/benefit analysis. *Europace*. 2013;15:813–819.
19. Køber L, et al. Defibrillator implantation in patients with nonischemic systolic heart failure. *N Engl J Med*. 2016;375:1221–1230.
20. Luni FK, et al. Mortality Effect of ICD in primary prevention of nonischemic cardiomyopathy: a meta-analysis of randomized controlled trials. *J Cardiovasc Electrophysiol*. 2017;28:538–543.
21. Stavrakis S, Asad Z, Reynolds D. Implantable cardioverter defibrillators for primary prevention of mortality in patients with nonischemic cardiomyopathy: a meta-analysis of randomized controlled trials. *J Cardiovasc Electrophysiol*. 2017;28:659–665.
22. Poole JE. Present guidelines for device implantation: clinical considerations and clinical challenges from pacing, implantable cardiac defibrillator, and cardiac resynchronization therapy. *Circulation*. 2014;129:383–394.
23. Voskoboinik A, Bloom J, Taylor A, et al. Early implantation of primary prevention implantable cardioverter defibrillators for patients with newly diagnosed severe nonischemic cardiomyopathy. *Pacing Clin Electrophysiol*. 2016;39:992–998.
24. Losurdo P, et al. Early arrhythmic events in idiopathic dilated cardiomyopathy. *JACC Clin Electrophysiol*. 2016;2:535–543.
25. Singh M, et al. Utility of the wearable cardioverter-defibrillator in patients with newly diagnosed cardiomyopathy a decade-long single-center experience. *J Am Coll Cardiol*. 2015;66:2607–2613.
26. Russo AM, et al. ACCF/HRS/AHA/ASE/HFSA/SCAI/SCCT/SCMR 2013 appropriate use criteria for implantable cardioverter-defibrillators and cardiac resynchronization therapy. *J Am Coll Cardiol*. 2013;61:1318–1368.
27. Betensky BP, Marchlinski FE. Outcomes of catheter ablation of ventricular tachycardia in the setting of structural heart disease. *Curr Cardiol Rep*. 2016;18:68.
28. Dinov B, et al. Early referral for ablation of scar-related ventricular tachycardia is associated with improved acute and long-term outcomes: results from the heart center of Leipzig ventricular tachycardia registry. *Circ Arrhythmia Electrophysiol*. 2014;7:1144–1151.
29. Piers SR, et al. Outcome of ventricular tachycardia ablation in patients with nonischemic cardiomyopathy: the impact of noninducibility. *Circ Arrhythm Electrophysiol*. 2013;6:513–521.
30. Muser D, et al. Long-term outcome after catheter ablation of ventricular tachycardia in patients with nonischemic dilated cardiomyopathy. *Circ Arrhythm Electrophysiol*. 2016;9:e004328.
31. Aliot EM, et al. EHRA/HRS Expert Consensus on Catheter Ablation of Ventricular Arrhythmias. Developed in a partnership with the European Heart Rhythm Association (EHRA), a Registered Branch of the European Society of Cardiology (ESC), and the Heart Rhythm Society (HRS). *Heart Rhythm*. 2009;9:886–933.
32. De Riva M, Watanabe M, Zeppenfeld K. Twelve-lead ECG of ventricular tachycardia in structural heart disease. *Circ Arrhythmia Electrophysiol*. 2015;8:951–962.
33. Haqqani HM, et al. Isolated septal substrate for ventricular tachycardia in nonischemic dilated cardiomyopathy: incidence, characterization, and implications. *Heart Rhythm*. 2011;8:1169–1176.
34. Haqqani HM, Callans DJ. Ventricular tachycardia in coronary artery disease. *Card Electrophysiol Clin*. 2014;6:525–534.
35. Vallès E, Bazan V, Marchlinski FE. ECG criteria to identify epicardial ventricular tachycardia in nonischemic cardiomyopathy. *Circ Arrhythmia Electrophysiol*. 2010;3:63–71.
36. Makimoto H, et al. Clinical impact of mapping strategies for treatment of ventricular tachycardias in patients with structural heart disease. *Pacing Clin Electrophysiol*. 2015;38:630–640.
37. Anter E, Li J, Tschabrunn CM, et al. Mapping of a postinfarction left ventricular aneurysm-dependent macroreentrant ventricular tachycardia. *Heart Case Reports*. 2015;1:472–476.
38. Nayyar S, et al. High-density mapping of ventricular scar: a comparison of ventricular tachycardia (VT) supporting channels with channels that do not support VT. *Circ Arrhythmia Electrophysiol*. 2014;7:90–98.
39. Tschabrunn CM, et al. High-resolution mapping of ventricular scar. *Circ Arrhythmia Electrophysiol*. 2016;9:e003841.
40. Njeim M. Value of cardiac magnetic resonance imaging in patients with failed ablation procedures for ventricular tachycardia. *J Cardiovasc Electrophysiol*. 2016;27:183–189.
41. Komatsu Y, et al. Regional myocardial wall thinning at multidetector computed tomography correlates to arrhythmogenic substrate in postinfarction ventricular tachycardia: assessment of structural and electrical substrate. *Circ Arrhythmia Electrophysiol*. 2013;6:342–350.
42. Miller MA, et al. Percutaneous hemodynamic support with Impella 2.5 during scar-related ventricular tachycardia ablation (PERMIT 1). *Circ Arrhythmia Electrophysiol*. 2013;6:151–159.

43. Reddy YM, et al. Percutaneous left ventricular assist devices in ventricular tachycardia ablation multicenter experience. *Circ Arrhythmia Electrophysiol.* 2014;7:244–250.
44. Miller MA, Reddy VY. Percutaneous hemodynamic support during scar-ventricular tachycardia ablation is the juice worth the squeeze? *Circ Arrhythmia Electrophysiol.* 2014;7:192–194.
45. Tanawuttawat T, Nazarian S, Calkins H. The role of catheter ablation in the management of ventricular tachycardia. *Eur Heart J.* 2016;37:594–609.
46. Aryana A, et al. Procedural and clinical outcomes after catheter ablation of unstable ventricular tachycardia supported by a percutaneous left ventricular assist device. *Heart Rhythm.* 2014;11:1122–1130.
47. Desjardins B, et al. Characteristics of intramural scar in patients with nonischemic cardiomyopathy and relation to intramural ventricular arrhythmias. *Circ Arrhythmia Electrophysiol.* 2013;6:891–897.
48. Berrueto A, et al. Combined endocardial and epicardial catheter ablation in arrhythmogenic right ventricular dysplasia incorporating scar dechanneling technique. *Circ Arrhythmia Electrophysiol.* 2012;5:111–121.
49. Santangeli P, Marchlinski FE. Substrate mapping for unstable ventricular tachycardia. *Heart Rhythm.* 2016;13:569–583.
50. Hutchinson MD, et al. Endocardial unipolar voltage mapping to detect epicardial ventricular tachycardia substrate in patients with nonischemic left ventricular cardiomyopathy. *Circ Arrhythmia Electrophysiol.* 2011;4:49–55.
51. Fernández-Armenta J, et al. Sinus rhythm detection of conducting channels and ventricular tachycardia isthmus in arrhythmogenic right ventricular cardiomyopathy. *Heart Rhythm.* 2014;11:747–754.
52. Proietti R, et al. A historical perspective on the role of functional lines of block in the re-entrant circuit of ventricular tachycardia. *Pacing Clin Electrophysiol.* 2016;39:490–496.
53. Kumar P, Mounsey JP, Chung EH. Adjusting voltage criteria can unmask conducting channels in a patient with arrhythmogenic right ventricular cardiomyopathy and ventricular tachycardia. *Heart Case Reports.* 2015;1:275–278.
54. Baldinger SH, et al. Electrogram analysis and pacing are complimentary for recognition of abnormal conduction and far-field potentials during substrate mapping of infarct-related ventricular tachycardia. *Circ Arrhythmia Electrophysiol.* 2015;8:874–881.
55. Tsiachris D, et al. Electroanatomical voltage and morphology characteristics in postinfarction patients undergoing ventricular tachycardia ablation. *Circ Arrhythmia Electrophysiol.* 2015;8:863–873.
56. Acosta J, et al. Infarct transmural as a criterion for first-line endo-epicardial substrate-guided ventricular tachycardia ablation in ischemic cardiomyopathy. *Heart Rhythm.* 2016;13:85–95.
57. Deo R, Berger R. The clinical utility of entrainment pacing. *J Cardiovasc Electrophysiol.* 2009;20:466–470.
58. Wong KCK, et al. Entrainment with long postpacing intervals from within the flutter circuit: what is the mechanism? *Circ Arrhythm Electrophysiol.* 2012;5:e90–e92.
59. Tokuda M, et al. Characteristics of clinical and induced ventricular tachycardia throughout multiple ablation procedures. *J Cardiovasc Electrophysiol.* 2016;27:88–94.
60. Komatsu Y, et al. Endocardial ablation to eliminate epicardial arrhythmia substrate in scar-related ventricular tachycardia. *J Am Coll Cardiol.* 2014;63:1416–1426.
61. Di Biase L, et al. Ablation of stable VTs versus substrate ablation in ischemic cardiomyopathy the VISTA randomized multicenter trial. *J Am Coll Cardiol.* 2015;66:2872–2882.
62. Marchlinski FE, et al. Long-term success of irrigated radiofrequency catheter ablation of sustained ventricular tachycardia: post-approval THERMOCOOL VT trial. *J Am Coll Cardiol.* 2016;67:674–683.
63. Tung R, Kottkamp H. A moving target for catheter ablation of ventricular tachycardia ablation of scar or arrhythmia? *J Am Coll Cardiol.* 2015;66:2883–2885.
64. Gökoğlu Y, et al. Scar homogenization versus limited-substrate ablation in patients with nonischemic cardiomyopathy and ventricular tachycardia. *J Am Coll Cardiol.* 2016;68:1990–1998.
65. Berrueto A, et al. Scar dechanneling: new method for scar-related left ventricular tachycardia substrate ablation. *Circ Arrhythmia Electrophysiol.* 2015;8:326–336.
66. Tzou WS, et al. Core isolation of critical arrhythmia elements for treatment of multiple scar-based ventricular tachycardias. *Circ Arrhythmia Electrophysiol.* 2015;8:353–361.
67. Proietti R, Roux J-F, Essebag V. Recent advances in ablation of ventricular tachycardia associated with structural heart disease. *Curr Opin Cardiol.* 2016;31:64–71.
68. Kumar S, et al. Role of alternative interventional procedures when endo- and epicardial catheter ablation attempts for ventricular arrhythmias fail. *Circ Arrhythmia Electrophysiol.* 2015;8:606–615.
69. Dinov B, et al. Catheter ablation of ventricular tachycardia and mortality in patients with nonischemic dilated cardiomyopathy: can noninducibility after ablation be a predictor for reduced mortality? *Circ Arrhythmia Electrophysiol.* 2016;8:598–605.
70. Ghanbari H, et al. Noninducibility in postinfarction ventricular tachycardia as an end point for ventricular tachycardia ablation and its effects on outcomes a meta-analysis. *Circ Arrhythmia Electrophysiol.* 2014;7:677–683.
71. Yokokawa M, et al. Predictive value of programmed ventricular stimulation after catheter ablation of post-infarction ventricular tachycardia. *J Am Coll Cardiol.* 2015;65:1954–1959.
72. Tzou WS, et al. Outcomes after repeat ablation of ventricular tachycardia in structural heart disease: an analysis from the International VT Ablation Center Collaborative Group. *Heart Rhythm.* 2017;14:991–997.
73. Birnie DH, et al. Cardiac sarcoidosis. *J Am Coll Cardiol.* 2016;68:411–421.
74. Oriti M, et al. Comparison of cardiac MRI and 18 F-FDG positron emission tomography manifestations and regional response to corticosteroid therapy in newly diagnosed cardiac sarcoidosis with complete heart block. *Heart Rhythm.* 2015;12:2477–2485.
75. Birnie DH, et al. HRS expert consensus statement on the diagnosis and management of arrhythmias associated with cardiac sarcoidosis. *Heart Rhythm.* 2014;11:1305–1323.
76. Kumar S, et al. Ventricular tachycardia in cardiac sarcoidosis: characterization of ventricular substrate and outcomes of catheter ablation. *Circ Arrhythm Electrophysiol.* 2015;8:87–93.
77. Naruse Y, et al. Systematic treatment approach to ventricular tachycardia in cardiac sarcoidosis. *Circ Arrhythm Electrophysiol.* 2014;7:407–413.
78. Deleted in review.
79. Segawa M, et al. Time course and factors correlating with ventricular tachyarrhythmias after introduction of steroid therapy in cardiac sarcoidosis. *Circ Arrhythmia Electrophysiol.* 2016;9:e003353.
80. Nery PB, Leung E, Birnie DH. Arrhythmias in cardiac sarcoidosis: diagnosis and treatment. *Curr Opin Cardiol.* 2012;27:181–189.
81. Nery PB, et al. Prevalence of cardiac sarcoidosis in patients presenting with monomorphic ventricular tachycardia. *Pacing Clin Electrophysiol.* 2014;37:364–375.
82. Tung R, et al. Incidence of abnormal positron emission tomography in patients with unexplained cardiomyopathy and ventricular arrhythmias: the potential role of occult inflammation in arrhythmogenesis. *Heart Rhythm.* 2015;12:2488–2498.
83. Decherer DG, et al. Electrophysiological characteristics of ventricular tachyarrhythmias in cardiac sarcoidosis versus arrhythmogenic right ventricular cardiomyopathy. *Heart Rhythm.* 2013;10:158–164.
84. Philips B, et al. Arrhythmogenic right ventricular dysplasia/cardiomyopathy and cardiac sarcoidosis: distinguishing features when the diagnosis is unclear. *Circ Arrhythmia Electrophysiol.* 2014;7:230–236.
85. Panda S, et al. Pleomorphism during ventricular tachycardia: a distinguishing feature between cardiac sarcoidosis and idiopathic VT. *Pacing Clin Electrophysiol.* 2015;38:694–699.
86. Kron J, et al. Efficacy and safety of implantable cardiac defibrillators for treatment of ventricular arrhythmias in patients with cardiac sarcoidosis. *Europace.* 2013;15:347–354.

87. Muser D, et al. Long-term outcomes of catheter ablation of ventricular tachycardia in patients with cardiac sarcoidosis. *Circ Arrhythm Electrophysiol*. 2016;9:e004333.
88. Zipse MM, Sauer WH. Cardiac sarcoidosis. *Curr Cardiol Rep*. 2014; 16:514.
89. Betensky BP, et al. Long-term follow-up of patients with cardiac sarcoidosis and implantable cardioverter-defibrillators. *Heart Rhythm*. 2012;9:884–891.
90. Pérez-Molina JA, Molina I. Chagas disease. *Lancet*. 2018;391:82–94.
91. Healy C, Viles-gonzalez JF, Sáenz LC, et al. Arrhythmias in Chagasic cardiomyopathy. *Card Electrophysiol Clin*. 2015;7:251–268.
92. Nunes MCP, Dones W, Morillo CA, et al. Chagas disease: an overview of clinical and epidemiological aspects. *J Am Coll Cardiol*. 2013;62:767–776.
93. Andrade JP, et al. I Latin American Guidelines for the diagnosis and treatment of Chagas' heart disease: executive summary. *Arq Bras Cardiol*. 2011;96:434–442.
94. Cardoso R, et al. The prevalence of atrial fibrillation and conduction abnormalities in Chagas' disease: a meta-analysis. *J Cardiovasc Electrophysiol*. 2016;27:161–169.
95. Benznidazole for chronic Chagas' cardiomyopathy. *N Engl J Med*. 2016; 374:188–190.
96. Pereira FT, et al. Long-term follow-up of patients with chronic Chagas disease and implantable cardioverter-defibrillator. *Pacing Clin Electrophysiol*. 2014;37:751–756.
97. Barbosa MP, et al. Efficacy and safety of implantable cardioverter-defibrillators in patients with Chagas disease. *Europace*. 2013;15:957–962.

Bundle Branch Reentrant Ventricular Tachycardia

OUTLINE

- Pathophysiology, 897**
- Epidemiology, 897**
- Clinical Presentation, 898**
- Initial Evaluation, 898**
- Principles of Management, 898**
- Electrocardiographic Features, 898**
 - Baseline Electrocardiogram, 898
 - Electrocardiogram During Ventricular Tachycardia, 898
- Electrophysiological Testing, 898**
 - Baseline Observations During Normal Sinus Rhythm, 898
 - Induction of Tachycardia, 898
 - Tachycardia Features, 900
 - Diagnostic Maneuvers During Tachycardia, 902
 - Exclusion of Other Arrhythmia Mechanisms, 902
- Ablation, 903**
 - Target of Ablation, 903
 - Ablation Technique, 903
 - Endpoints of Ablation, 905
 - Outcome, 905
- Interfascicular Reentrant Ventricular Tachycardia, 905**

PATHOPHYSIOLOGY

Bundle branch reentrant (BBR) ventricular tachycardia (VT) is a reentrant VT with a well-defined reentry circuit, incorporating the right bundle branch (RB) and left bundle branch (LB) as obligatory limbs of the circuit, connected proximally by the His bundle (HB) and distally by the ventricular septal myocardium (Fig. 26.1). Fascicular reentry is very uncommon (see below). The QRS during BBR VT can display either left bundle branch block (LBBB) or right bundle branch block (RBBB) when anterograde ventricular activation occurs over the RB or LB, respectively. The vast majority of BBR VTs exhibit LBBB configuration (“counterclockwise” BBR), whereby the reentrant wavefront propagates anterogradely down the RB, crosses the septum, and then travels retrogradely up the LB. In clockwise BBR, the reentrant wavefront propagates in the opposite direction, and ventricular activation occurs via anterograde conduction over the LB, resulting in a RBBB pattern.^{1,2}

Single BBR beats can be induced in up to 50% of patients with normal intraventricular conduction undergoing electrophysiological (EP) study. The QRS during BBR typically exhibits LBBB pattern, although an RBBB pattern (clockwise BBR) can rarely be induced by right ventricular (RV) pacing; the latter condition requires that the effective refractory period of the LB be longer than that of the RB, or that retrograde conduction over the RB be resumed after an initial bilateral block in the His-Purkinje system (HPS; i.e., gap phenomenon). Left ventricular (LV) pacing does not seem to increase the yield of induction of BBR with RBBB morphology.^{1,2}

In patients with normal intraventricular conduction, BBR is a self-limited phenomenon. The rapid conduction and long refractory period of the HPS prevent sustained BBR in normal hearts. Spontaneous termination of BBR most commonly occurs in the retrograde limb between the ventricular muscle and the HB. Sometimes, anterograde block can also occur, making refractoriness in the RB-Purkinje system the limiting factor. Continuation of BBR as a tachycardia is critically dependent on the interplay between conduction velocity and recovery of the tissue ahead of the reentrant wavefront. Two changes from normal physiology

must occur for BBR to become sustained: (1) an anatomically longer reentrant pathway caused by a dilated heart, providing sufficiently longer conduction time around the HPS; and (2) slow conduction in the HPS caused by HPS disease. These two factors are responsible for sufficient prolongation of conduction time to permit expiration of the refractory period of the HPS ahead of the propagating reentrant wavefront.¹⁻³

Rarely, self-terminating BBR can occur with a narrow QRS during ventricular extrastimulation (VES) in the setting of normal intraventricular conduction. After retrograde conduction via the left anterior fascicle (LAF) or left posterior fascicle (LPF), anterograde propagation occurs over the RB and the remaining LB fascicle, resulting in a narrow QRS with either LAF or LPF block.

EPIDEMIOLOGY

Sustained BBR VT usually occurs in patients with structural heart disease, especially dilated cardiomyopathy. Idiopathic dilated cardiomyopathy is the anatomical substrate for BBR VT in 45% of cases, and BBR VT accounts for up to 13% to 41% of all inducible sustained VTs in this population. BBR VT can also be associated with cardiomyopathy secondary to valvular or ischemic heart disease, and has been reported with Ebstein anomaly, hypertrophic cardiomyopathy, and even in patients without structural heart disease other than intraventricular conduction abnormalities (and even normal baseline QRS configuration in rare cases).⁴

In patients with spontaneous sustained monomorphic VT, the incidence of inducible BBR VT ranges from 4.5% to 6% in patients with ischemic heart disease to 16.7% to 41% in patients with nonischemic cardiomyopathy. BBR VT accounts for up to 6% of all forms of induced sustained monomorphic VT. Importantly, additional myocardial VTs occur in about 25% of patients presenting with BBR VT.⁵ Of note, BBR VT is more frequently found in patients with VT clusters (up to 12.5%) than in patients with less frequent episodes of VT.⁶ Because the incidence of BBR VT is not trivial, and is imminently curable, it is important for the electrophysiologist to consider it as a possible cause of VT.

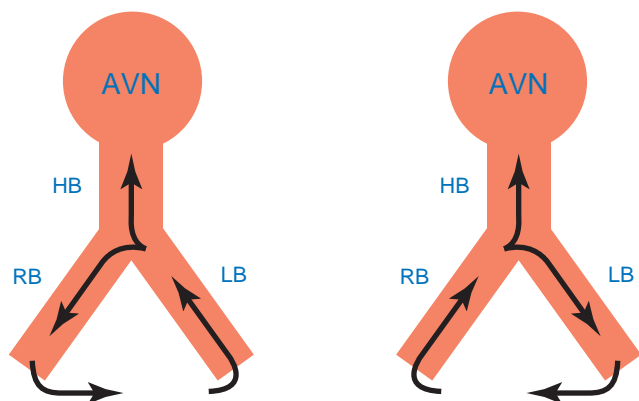


Fig. 26.1 Schematic Illustration of the Two Types of Bundle Branch Reentry (BBR) Circuits. At left is the most commonly seen type of BBR ventricular tachycardia (VT). Retrograde conduction occurs via the left bundle branch (LB) and anterograde conduction occurs via the right bundle branch (RB). This yields a VT in which the QRS has a left bundle branch block pattern. At right is the uncommon type of BBR VT. Retrograde conduction occurs via the RB and anterograde conduction occurs via the LB, which yields a VT in which the QRS has an RBBB pattern. AVN, Atrioventricular node; HB, His bundle.

CLINICAL PRESENTATION

Sustained BBR VT is typically unstable secondary to very rapid ventricular rates (often 200 to 300 beats/min) and poor underlying ventricular function; 75% of patients present with syncope or cardiac arrest.

INITIAL EVALUATION

BBR VT should be suspected in the presence of typical QRS morphology on the surface electrocardiogram (ECG) during normal sinus rhythm (NSR) and VT (see later), especially in a patient with dilated cardiomyopathy. Echocardiographic examination and coronary arteriography are required in most patients to evaluate for structural heart disease.

PRINCIPLES OF MANAGEMENT

Pharmacological antiarrhythmic therapy is usually ineffective for BBR VT. On the other hand, RF catheter ablation of a bundle branch (typically the RB) is very successful in eliminating BBR VT and hence is currently regarded as first-line therapy.

As noted, associated myocardial VT occurs in approximately 25% of patients post ablation of BBR VT, and these patients continue to be at a high risk of sudden cardiac death. Therefore implantable cardioverter-defibrillator (ICD) therapy is indicated for secondary prevention, and additional antiarrhythmic therapy is required for some patients. ICD implantation will also provide backup pacing, which is frequently required post ablation secondary to the development of AV block or an excessively prolonged His bundle–ventricular (HV) interval. Implantation of a dual-chamber or biventricular ICD should be considered in these patients.

Because BBR VT has a limited response to antiarrhythmic drugs and can be an important cause of repetitive ICD therapies, catheter ablation of the arrhythmia should always be considered as an important adjunct to the device therapy.

EP testing should be considered in patients with repetitive episodes of VT and dilated cardiomyopathy, history of cardiac valve repair or replacement, or QRS morphology during VT similar to sinus rhythm

QRS. If sustained BBR VT is inducible during programmed stimulation, catheter ablation is recommended.⁶

ELECTROCARDIOGRAPHIC FEATURES

Baseline Electrocardiogram

The baseline rhythm is usually NSR or AF. Almost all patients with BBR VT demonstrate intraventricular conduction abnormalities. The most common ECG abnormality is nonspecific intraventricular conduction defect (IVCD) with an LBBB pattern and PR interval prolongation (Fig. 26.2). Complete RBBB is rare but does not preclude BBR as the mechanism of VT. Although total interruption of conduction in one of the bundle branches would theoretically prevent occurrence of BBR, an ECG pattern of complete BBB may not be an accurate marker of *complete* conduction block; a similar QRS configuration can be caused by conduction delay, rather than block, in the bundle branch. In addition, anterograde block can be present with retrograde conduction. Occasionally, complete AV block may be observed.

Electrocardiogram During Ventricular Tachycardia

Twelve-lead ECG documentation of BBR VT is usually unavailable because the VT is rapid and hemodynamically unstable. The VT rate is usually 200 to 300 beats/min. QRS morphology during VT is a typical BBB pattern and can be identical to that in NSR. BBR VT with an LBBB pattern is the most common VT morphology, and it usually has normal or left axis deviation (see Fig. 26.2). In contrast to VT of myocardial origin, BBR with an LBBB pattern characteristically shows a rapid intrinsicoid deflection in the right precordial leads, suggesting that initial ventricular activation occurs through the HPS and not ventricular muscle. BBR VT with an RBBB pattern usually has a leftward axis, but it can have a normal or rightward axis, depending on which fascicle is used for anterograde propagation.⁴

ELECTROPHYSIOLOGICAL TESTING

Baseline Observations During Normal Sinus Rhythm

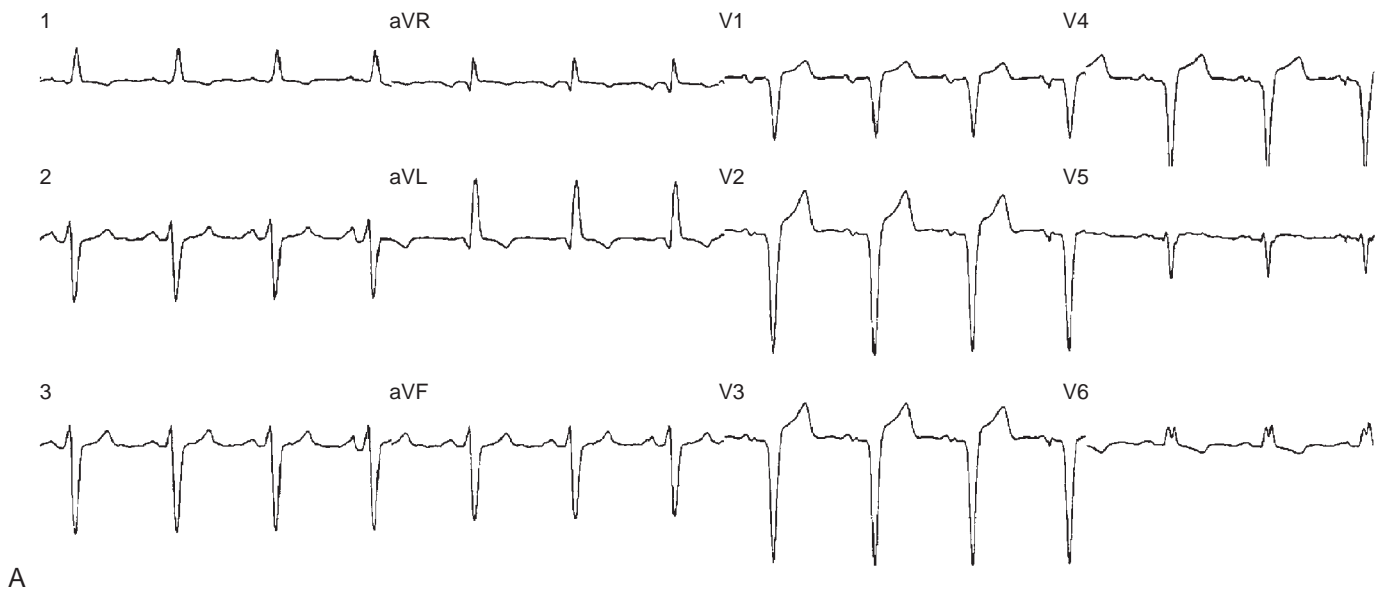
Conduction abnormalities in the HPS are almost invariably present and are a critical prerequisite for the development of sustained BBR, regardless of the underlying anatomical substrate (Fig. 26.3). The average HV interval is about 80 milliseconds (range, 60 to 110 milliseconds). Although some patients can have the HV interval in NSR within normal limits, functional HPS impairment in these patients manifests as HV interval prolongation or split HB potentials, commonly becoming evident during atrial programmed stimulation or burst pacing. Nonspecific IVCD with an LBBB pattern and PR interval prolongation are the most common abnormalities.

Induction of Tachycardia

VES from the RV apex is the usual method used to induce BBR with an LBBB pattern. Induction is consistently dependent on the achievement of a critical conduction delay in the HPS (i.e., critical ventricular–His bundle [VH] interval) following the VES.

During RV pacing at a constant PCL and during introduction of VES at relatively long coupling intervals, retrograde conduction to the HB occurs via the RB. At shorter VES coupling intervals, retrograde delay and block occur in the RB when its relative and effective refractory periods are encountered, respectively. When retrograde block occurs in the RB, the impulse propagates across the septum and retrogradely up the LB to the HB, producing a long V₂–H₂ interval. The LB would still be capable of retrograde conduction because of its shorter refractoriness and because of the delay associated with transeptal propagation. Further shortening of the coupling intervals is associated with increasing

Sinus rhythm



Bundle branch reentrant VT

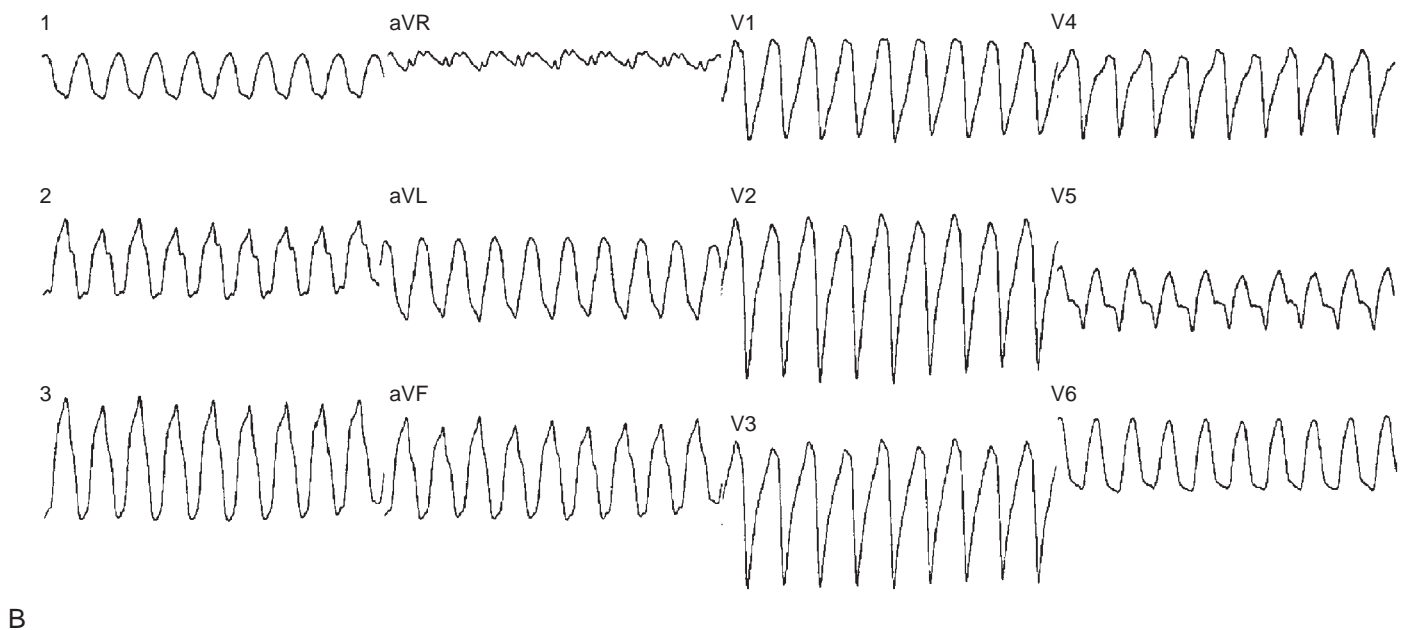


Fig. 26.2 Electrocardiogram of Bundle Branch Reentrant (BBR) Ventricular Tachycardia (VT). (A) Normal sinus rhythm baseline with intraventricular conduction delay resembling left bundle branch block. (B) BBR VT. Note typical-appearing complete left bundle branch block in this rapid VT.

delay in LB conduction (i.e., increasing V_2 - H_2 interval). Within a certain range of coupling intervals, increasing retrograde LB delay allows for the recovery of anterograde conduction via the RB, and another ventricular activation ensues, displaying a wide QRS with an LBBB pattern. This beat is called the “BBR beat” or “ V_3 phenomenon.”

An inverse relationship exists between retrograde conduction delay in the LB (V_2 - H_2 interval) and the time of anterograde conduction in the RB (H_2 - V_3 interval). This is because the faster the impulse propagates

transseptally and up the LB, the more likely it will reach the RB while it is still refractory from the previous retrograde activation (concealment) by the VES, resulting in slower anterograde conduction down the RB.

BBR is more likely to occur when the VES is delivered following pacing drives incorporating long to short CL changes as compared with constant CL drives, because of CL dependency of the HPS refractoriness. An abrupt change in CL (i.e., long to short) can result in a

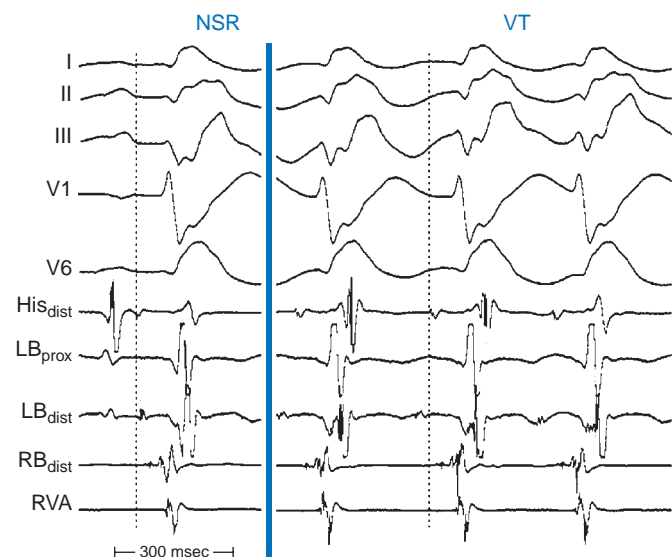


Fig. 26.3 Bundle Branch Reentrant (BBR) Ventricular Tachycardia (VT) Versus Normal Sinus Rhythm (NSR). Sinus and BBR VT with His, left bundle branch (LB), and right bundle branch (RB) recordings in a patient with a prior septal myocardial infarction. Dashed lines mark the onset of His deflection. During NSR, the His potential is followed first by the LB potential; RB activation is further delayed. The fact that left bundle branch block (LBBB) is present on the electrocardiogram (ECG) suggests that, although the LB is activated prior to the RB, delay is encountered more distally in the left ventricular His-Purkinje system such that LBBB is evident on the ECG. During BBR VT, activation propagates in an LB-His-RB sequence. Retrograde LB activation is very delayed, most likely because of the same factors responsible for the ECG in NSR. *His_{dist}*, Distal His bundle; *LB_{dist}*, distal left bundle branch; *LB_{prox}*, proximal left bundle branch; *RB_{dist}*, distal right bundle branch; *RVA*, right ventricle apical.

more distal site of retrograde block, and less concealment, along the myocardium-Purkinje-RB axis, which can allow sufficient recovery of excitability in the anterograde limb of the circuit (i.e., the RB-Purkinje-myocardium axis) for reentry to develop. In addition, earlier recovery of excitability along this axis, because of the more distal site of block and less concealment, is associated with a shorter H_2 - V_3 interval in this reentrant beat.

Procainamide (which increases conduction time within the HPS, especially in the diseased HPS), and potentially isoproterenol can facilitate induction of sustained BBR. In some patients, the arrhythmia can be inducible only with atrial pacing.

Tachycardia Features

BBR VT can only be definitively diagnosed using intracardiac recordings (Box 26.1); most particularly, HB recordings are essential. Many electrophysiologists do not use a HB recording catheter during VT diagnostic studies and will thus likely miss diagnosing some cases of BBR. AV dissociation is typically present, during the tachycardia, but 1:1 VA conduction can occur. BBR VT is characterized by inscription of the His potential before the QRS complex, with the HV interval during BBR with LBBB pattern generally being similar to or longer than that during baseline rhythm (the HV interval is usually 55 to 160 milliseconds; see Fig. 26.3).¹

The relative duration of the HV interval recorded during VT as compared with NSR would depend on two factors: the balance between anterograde and retrograde conduction times from the upper turnaround point of the reentry circuit, and the site of HB recording relative to the

BOX 26.1 Diagnostic Criteria of Bundle Branch Reentrant Ventricular Tachycardia

- The QRS morphology of the tachycardia shows a typical RBBB or LBBB pattern.
- The onset of ventricular depolarization is preceded by HB and either RB or LB potentials with an appropriate sequence of H-RB-LB activation and relatively stable HV, RB-V, or LB-V intervals.
- Spontaneous variations in V-V intervals are preceded by similar changes in H-H/RB-RB/LB-LB intervals, but the HV interval remains constant.
- The induction of tachycardia during programmed stimulation is consistently dependent on achieving a critical conduction delay in the HPS.
- Tachycardia termination is preceded by a spontaneous or pacing-induced block in the HPS.
- The HV interval during tachycardia is equal to or longer than HV interval during sinus rhythm.
- BBR is noninducible after successful ablation of the RB.
- Entrainment from the RV apex results in manifest fusion and a (PPI – TCL) difference <30 msec.

BBR, Bundle branch reentry; *HB*, His bundle; *HPS*, His-Purkinje system; *HV*, His bundle ventricular; *LB*, left bundle branch; *LBBB*, left bundle branch block; *LB-V*, left bundle ventricular; *PPI*, postpacing interval; *RB*, right bundle branch; *RBBB*, right bundle branch block; *RV*, right ventricular; *RVRB-V*, right bundle-ventricular; *TCL*, tachycardia cycle length.

upper turnaround point (i.e., the HB catheter electrode positioned at the proximal versus distal HB). Conduction delay in the bundle branch used as the anterograde limb of the circuit tends to prolong the HV interval during VT, whereas retrograde conduction delay to the HB recording site, as well as the use of a relatively proximal HB recording site (far from the turnaround point), tend to shorten the HV interval.^{1,2} During NSR, activation of the HB and activation of the bundle branch occur in sequence; hence the HV interval represents a true conduction time from HB depolarization, through the bundle branches, to ventricular myocardium. In contrast, during BBR VT, the HB is activated in the retrograde direction concurrently (in parallel) with the proximal part of the bundle branch serving as the anterograde limb of the reentry circuit. Therefore the HV interval during BBR represents the difference in local activation timing of two points (the HB and the ventricle) being activated in parallel by the reentry wavefront, rather than an actual conduction time from sequential activation of the HB, bundle branch, and ventricle.^{1,2}

Although the HV interval during BBR VT is intuitively expected to be falsely abbreviated and shorter than the “true” HV interval during NSR, this occurs only in rare cases of BBR VT. Two possible mechanisms can potentially explain the longer HV interval during BBR VT: (1) rate-related decremental conduction in the bundle branch used as the anterograde limb of the BBR circuit, and (2) anisotropic conduction in the upper turnaround between the LB and the RB. Both mechanism can result in prolongation of the anterograde conduction times from the upper turnaround point of the reentry circuit to the ventricle, resulting in a longer HV interval during tachycardia than NSR. Furthermore, the recorded His potential might in fact be a RB potential, and hence the measured HV interval actually represents the right bundle-ventricular (RB-V) interval. The RB and ventricle are activated sequentially during both NSR and counterclockwise BBR VT; thus the RB-V interval during BBR VT must always be longer (due to the decremental conduction in the RB during tachycardia) than that during NSR.^{1,7}

Of note, the HV interval during clockwise BBR (RBBB pattern) can be significantly longer than that during NSR (the HV interval is usually

65 to 250 milliseconds). During NSR, the HV interval is usually determined by conduction over whichever bundle branch conducts most rapidly, whereas during BBR with RBBB pattern, it is determined by anterograde conduction over the typically diseased LB.

In the common type of BBR VT (LBBB pattern), the activation wavefront propagates retrogradely up the LB to the HB and then anterogradely down the RB, with subsequent ventricular activation. This sequence is reversed in BBR with an RBBB pattern (Fig. 26.4). The HV and RB-V (during VT with LBBB morphology) or left bundle–ventricular (LB-V) intervals (during VT with RBBB morphology) are relatively stable.¹

During BBR VT, spontaneous variations in the V-V intervals are preceded and dictated by similar changes in the H-H (and RB-RB or LB-LB) intervals. In other words, the tachycardia cycle length (TCL) is affected by variation in the V-H (V-RB or V-LB) intervals. These changes can occur spontaneously, most commonly immediately after induction of the VT, or be demonstrated by ventricular stimulation during VT. However, oscillations in the V-V intervals can occasionally precede those of the H-H intervals during BBR VT because of conduction variations in the anterograde, rather than the retrograde, conducting bundle branch.⁵

Because the breakout of the RBB is near the RV apex, an electrode catheter at this site should record an electrogram very close to the onset of the QRS in BBR VT and serve as a good site for entrainment. Thus an effort should be made to place the RV catheter close to the apex. In patients who have an ICD with an RV apical lead position, a clue to the diagnosis of BBR VT is that (1) the timing of the bipolar ventricular electrogram during VT is similar to the onset of the far-field shock electrogram (an analog of the QRS complex); and (2) both bipolar and shock electrograms in VT should have a very similar appearance to those during sinus rhythm (Fig. 26.5).

Recording from both sides of the septum can help identify the BBR mechanism. Documentation of a typical H-RB-V-LB activation sequence (during VT with LBBB morphology), or of an H-LB-V-RB activation sequence (during VT with RBBB morphology), supports the diagnosis of BBR (see Fig. 26.3). Unfortunately, the RB and LB potentials are not always recorded, so that the typical activation sequences (LB-H-RB-V or RB-H-LB-V) are not available for analysis. Even if either activation sequence is present, the HPS (usually the LB) could be activated passively in a retrograde fashion to produce an H-RB-V sequence during a VT with LBBB pattern without reentry requiring the LB. In these

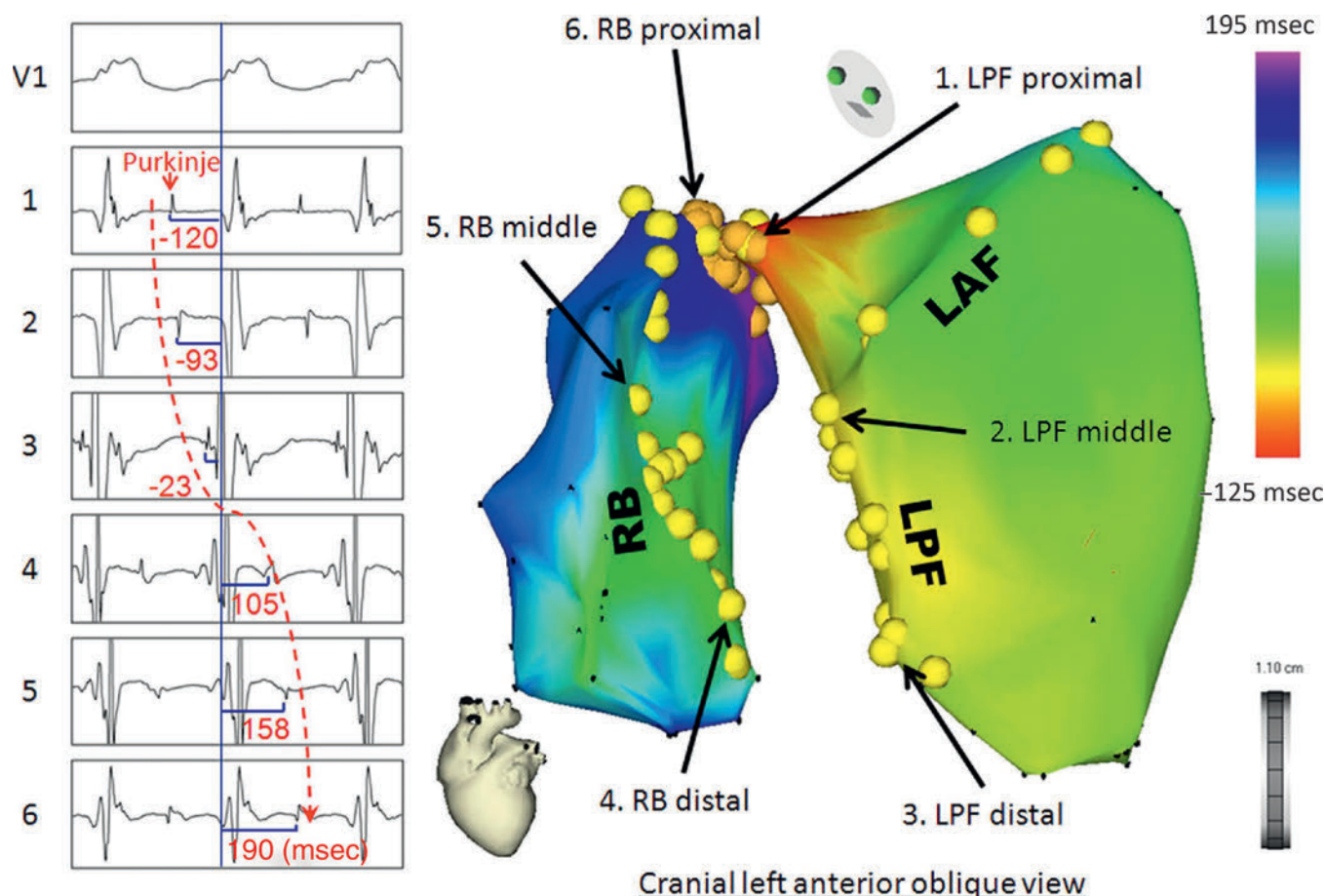


Fig. 26.4 Electroanatomic Three-dimensional (CARTO) Activation Map of the Bundle Branch Reentrant Ventricular Tachycardia. The left posterior fascicle (LPF) serves as the descending limb and the right bundle branch (RB) serves as the ascending limb of the reentry circuit. The earliest activation displayed in red (LPF proximal) and the latest in violet (RB proximal). The yellow dots and the numbered sites with arrows indicate the fascicular potentials and local activations of the His-Purkinje system (left boxes), respectively. The sequential activations of the local His-Purkinje system accounted for the entire tachycardia cycle length. (From Machino T, Tada H, Sekiguchi Y, Aonuma K. Three-dimensional visualization of the entire reentrant circuit of bundle branch reentrant tachycardia. *Heart Rhythm*. 2013;10:459–460.)

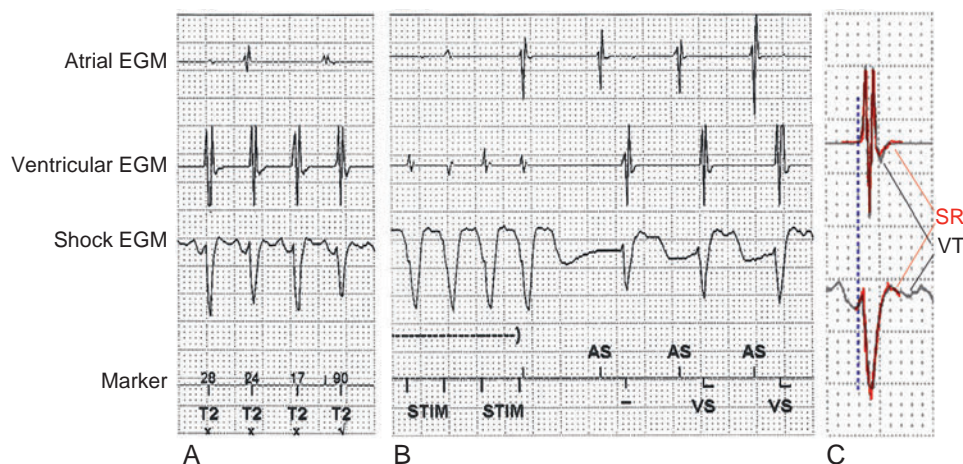


Fig. 26.5 Implantable Cardioverter-Defibrillator Recordings During Bundle Branch Reentrant Ventricular Tachycardia (VT). Panels show stored electrograms as labeled. (A) VT is shown. The timing of the near-field bipolar electrogram is similar to the onset of the far-field shock electrogram (a rough correlate of the QRS complex; dashed blue line in C). (B) The last few complexes of antitachycardia pacing are shown after which sinus rhythm (SR) ensues. The SR ventricular electrogram is very similar to that during VT as shown in C (SR electrogram in red superimposed on VT electrogram). AS, Atrial sensed event; EGM, electrogram; STIM, antitachycardia ventricular stimulation; VS, ventricular sensed event.

cases, other diagnostic criteria for BBR should be used. In addition, during VT with LBBB morphology, RV activation must precede the LV activation. The opposite is true for the VT with RBBB morphology.

BBR can be terminated by block in the HPS—spontaneous, pacing-induced, secondary to catheter trauma, or caused by ablation.

Diagnostic Maneuvers During Tachycardia

Pacing maneuvers can be extremely helpful to establish the diagnosis of BBR; however, application of these maneuvers during BBR is often not feasible because of the hemodynamic compromise commonly associated with these VTs.

Entrainment

BBR VT can be entrained by ventricular pacing. Entrainment from the protected isthmuses within the BBR circuit (i.e., the LB and RB) results in concealed fusion (i.e., QRS morphology during entrainment resembles the tachycardia) and a short postpacing interval (PPI), with a (PPI – TCL) difference of less than 30 milliseconds. Entrainment from the RV apex (within the BBR circuit, but not within a protected isthmus) results in a (PPI – TCL) difference of less than 30 milliseconds but with manifest fusion. Importantly, a (PPI – TCL) difference of more than 30 milliseconds during entrainment of VT performed from the RV apex excludes a BBR mechanism, provided that the RV apex catheter is correctly positioned. The greater this value is, the more reliable is the certainty of exclusion.¹

Entrainment of BBR VT with concealed QRS fusion can also occur during atrial pacing. This approach, however, demands that the patient not be in AF and usually requires the infusion of atropine or isoproterenol to avoid AV block during rapid atrial pacing. The combination of entrainment with concealed QRS fusion during atrial pacing and entrainment with manifest QRS fusion during ventricular pacing (outside the HPS) has been recently proposed as a useful diagnostic criterion for BBR VT with LBBB QRS morphology.

Resetting

VES can reset the VT by advancing the HB or bundle branch potential. Even a late-coupled VES can reset the VT when pacing is performed

from sites within or close to the BBR circuit (RB, LB, RV apex). In addition, VES can reverse the direction of impulse propagation during BBR. Theoretically this requires double VESs, with the first VES producing block and the second initiating the reentry in the opposite direction.¹

Other Pacing Maneuvers

The ability to dissociate the HB or, particularly, a bundle branch (RB or LB) potential strongly argues against a BBR mechanism. An AES that blocks below the HB deflection should terminate BBR. In addition, simultaneous LV and RV pacing should prevent BBR.

Exclusion of Other Arrhythmia Mechanisms

Myocardial Ventricular Tachycardias

Myocardial VTs can have 1:1 VH relation during tachycardia with passive retrograde activation of the HB. However, myocardial VTs are rarely associated with classic LBBB (or RBBB) QRS morphology, as is expected with BBR VT. In addition, in myocardial VTs, the His potential is often obscured within the local ventricular electrogram. Occasionally, the His potential can precede the onset of the QRS, thus resembling BBR VT; however, the HV interval in myocardial VTs is usually shorter than that during NSR. In contrast to BBR VT, spontaneous or induced TCL variations during myocardial VTs usually precede and dictate H-H interval changes.⁵

Entrainment with concealed QRS fusion during atrial pacing excludes myocardial VT and should be expected in BBR VT. When entrainment with concealed fusion can be demonstrated by pacing at the LB or RB, BBR VT is very likely. In addition, a (PPI – TCL) difference of less than 30 milliseconds after entrainment of the VT from the RV apex is suggestive of BBR VT; in contrast, in myocardial VTs, the (PPI – TCL) difference is greater than 30 milliseconds, unless the VT originates in (exits from) the apex.¹

Idiopathic (Fascicular) Left Ventricular Tachycardia

The QRS and HV interval are normal during NSR in patients with fascicular VT. In contrast, BBR VT is rare in the absence of baseline HPS conduction abnormalities. In addition, the His potential falls within

or before the QRS in fascicular VT, producing a negative or short HV interval, and HB activation follows activation of the left fascicles, which is inconsistent with RBBB-type BBR VT.

Supraventricular Tachycardia With Aberrancy

BBR VT typically exhibits AV dissociation, which excludes atrial tachycardia (AT) and atrioventricular reentrant tachycardia (AVRT). Occasionally, BBR VT can be associated with 1:1 VA conduction, and it can then mimic supraventricular tachycardia (SVT) with aberrancy.

Multiple HB recordings, using a hexapolar or octapolar catheter, can help demonstrate the direction of HB depolarization—anterograde during SVT and retrograde during BBR VT. Also, recording LB and RB potentials in addition to the HB potential can be helpful; activation of the HB occurs anterogradely via the atrioventricular node (AVN) during SVT and precedes the RB potential by an interval equal to or longer than that during NSR.

The atrium is not part of the circuit in the BBR VT and can be dissociated by atrial pacing, which excludes AT and AVRT as the mechanism of wide complex tachycardia. Moreover, during entrainment from the RV apex, a (PPI – TCL) difference greater than 30 milliseconds excludes a BBR mechanism. Conversely, a (PPI – TCL) difference less than 30 milliseconds excludes atrioventricular nodal reentrant tachycardia (AVNRT). In addition, entrainment with manifest fusion during ventricular pacing excludes AVNRT and AT, and should be expected in BBR VT. Furthermore, the ability to terminate or reset the tachycardia with a VES introduced when HB is refractory excludes AT and AVNRT.

Antidromic Atrioventricular Reentrant Tachycardia Using an Atriofascicular Bypass Tract

Several findings can help distinguish antidromic AVRT from BBR VT. During antidromic AVRT, the impulse propagates retrogradely over the RB to the HB, a sequence inconsistent with the common type of BBR VT (LBBB pattern). The timing of a HB recording during the arrhythmia also differs: with antidromic atriofascicular reentry, the HB is typically recorded just after the onset of the QRS (or near the end of the QRS, in the presence of RBBB), whereas in BBR, the HB is recorded well before (in LBBB BBR) or after (in RBBB BBR) the QRS complex. In addition, the AV relationship is always 1:1 during AVRT and rarely so during BBR VT. Because the atrium is not part of the circuit in BBR VT, it can be dissociated by atrial pacing, which excludes AVRT. Moreover, resetting the tachycardia with an AES from the right atrial (RA) free wall, timed when the AV junctional atrium is refractory, excludes VT. Similarly, the ability of an AES to terminate the tachycardia without conduction to the ventricle or to retard (delay) the following ventricular activation excludes VT (see Figs. 18.41 and 19.5).¹

ABLATION

Target of Ablation

The ablation target is either the RB or the LB; RB ablation is easier and usually is the method of choice. However, in most patients with BBR VT, although diffuse conduction system disease is present, the conduction abnormality in the LB is more severe than that in the RB. Nonetheless, preserved slow conduction over the LB can be demonstrated in the majority of patients, and the LB can still maintain 1:1 AV conduction during NSR following ablation of the RB. For the occasional patients in whom anterograde conduction down the LB is known to be inadequate for maintaining 1:1 AV conduction, ablation of the RB will commit the patient to a permanent pacemaker. Therefore ablation of the LB in these patients is preferable because it can prevent BBR and still preserve anterograde conduction.^{5,8}

The mere presence of LBBB on the surface ECG does not mean complete block in the LB. Signs that can indicate that conduction down the LB may be inadequate in maintaining 1:1 AV conduction and favor ablation of the LB over the RB include: (1) development of high-grade AV block below the HB on transient RBBB that can occur secondary to RV catheter manipulation, and (2) observation of an LB potential following the ventricular electrogram either intermittently or during every sinus beat.

Importantly, the HB is not an essential component of the BBR circuit; hence ablating the HB rather than the RB would not adequately eliminate the arrhythmia.

Ablation Technique

Ablation of the Right Bundle Branch

The HB divides at the junction of the fibrous and muscular boundaries of the intraventricular septum into the RB and LB. The RB is a long, thin, discrete structure that travels as the extension of the HB after the origin of the LB. The RB courses down the right side of interventricular septum near the endocardium in its upper third, deeper in the muscular portion of the septum in the middle third, and then again near the endocardium in its lower third. The RB does not divide throughout most of its course, and begins to ramify as it approaches the base of the right anterior papillary muscle, with fascicles going to the septal and free walls of the RV.

A quadripolar catheter is positioned at the HB region and maintained as a reference. The ablation catheter is initially positioned in the HB region and the area of the septum at which the largest His potential is recorded. The catheter is then advanced gradually (in the right anterior oblique [RAO] view) superiorly and to the patient's left side, with clockwise torque to ensure adequate catheter tip contact with the septum and RB and continuous adjustment of the catheter's curvature until the RB potential is recorded. Attempts should be made to obtain the distal RB recording to ensure that the catheter tip is away from the HB and LB.

The RB potential can be distinguished from the HB potential by the absence of or minimal atrial electrogram on the recording and presence of a sharp deflection inscribed at least 10 to 15 milliseconds later than the His potential (Fig. 26.6). Notably, the RB-V interval can be abnormally prolonged (more than 30 milliseconds) due to the frequently prevalent RB conduction disease in these patients.

When there is RB conduction delay at baseline, the RB potential can become hidden within the ventricular electrogram, and it may be impossible to map during NSR, especially when the surface ECG shows complete or incomplete RBBB. However, the RB potential should be readily observed during BBR beats induced by RV stimulation or during BBR VT. In this setting, anatomically guided lesions or a linear ablation perpendicular to the axis of the RB distal to the HB recording can be effective.

A 4-mm-tip ablation catheter is typically used for RB ablation. RF application is usually started at low levels (5 W) and gradually increased every 10 seconds, targeting a temperature of 60°C. In general, RBBB develops at 15 to 20 W. Successful ablation will result in clear development of RBBB in lead V₁ (see Figs. 26.6 and 26.7). Occasionally, an accelerated rhythm from the RB is observed during ablation (analogous to accelerated junctional rhythm with HB ablation; see Fig. 26.7).

Ablation of the Left Bundle Branch

Whereas the RB is anatomically a continuation of the HB, the LB arises as a broad band of fibers from the HB in a perpendicular direction toward the inferior septum. The main LB penetrates the membranous portion of the interventricular septum under the aortic ring and then divides into several fairly discrete branches. The LPF, which arises more

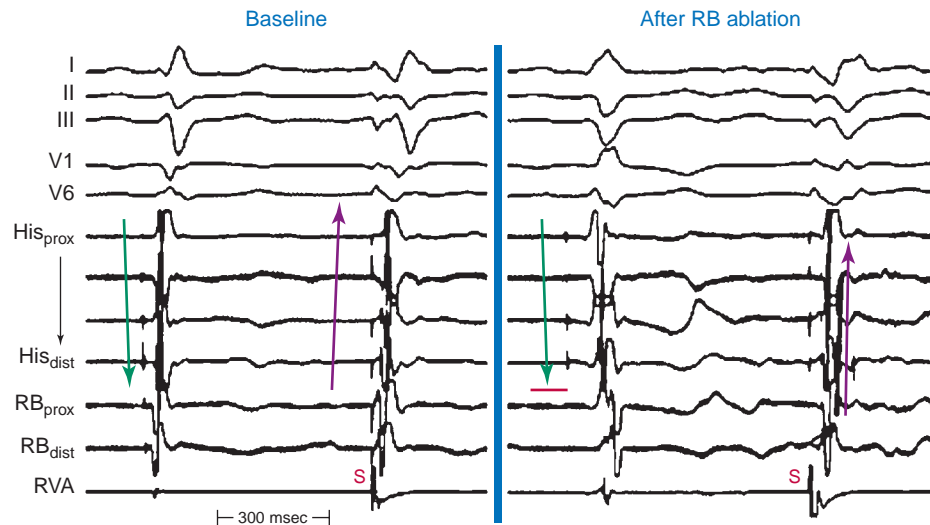


Fig. 26.6 Ablation of Bundle Branch Reentry (BBR). Sinus and right ventricular apical paced complexes from before (left) and after (right) catheter ablation of the right bundle branch (RB) in a patient with BBR ventricular tachycardia (VT). Four bipolar recordings from a catheter at the His position and RB are shown. Prior to RB ablation, propagation along the His-RB axis is linear, antegrade during sinus rhythm (green arrow), and retrograde during RV pacing (purple arrow). After RB ablation, antegrade propagation is interrupted (green arrow, red line) and retrograde activation of the His electrograms occurs after the local ventricular electrogram (purple arrow), indicating block in the RB with transseptal propagation, then up the left bundle. *His_{dist}*, distal His bundle; *His_{prox}*, proximal His bundle; *RB_{dist}*, distal right bundle branch; *RB_{prox}*, proximal right bundle branch; *RVA*, right ventricle apical.

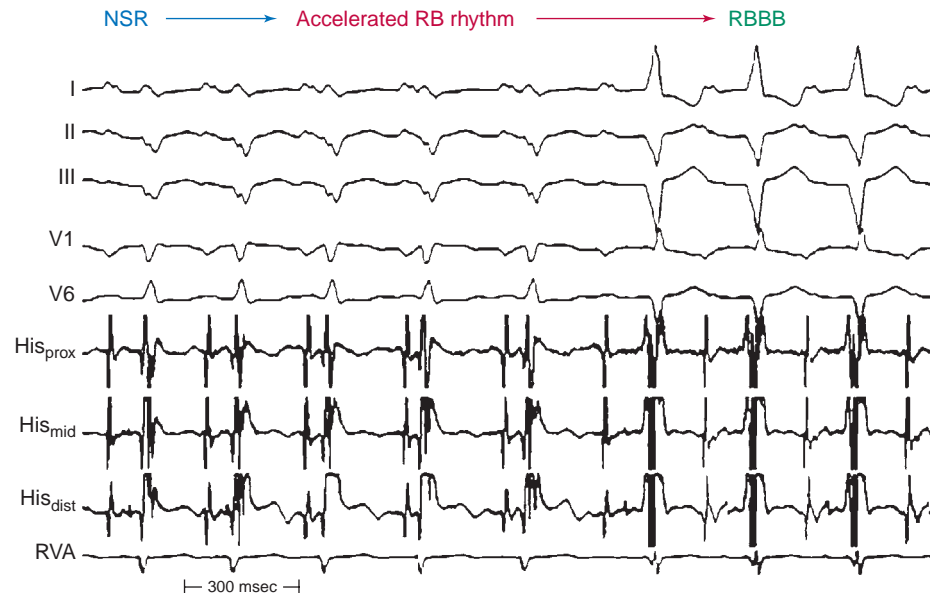


Fig. 26.7 Right Bundle Branch (RB) Ablation. During RB ablation, delivery of radiofrequency current causes accelerated rhythm from the RB until complete block occurs (note lead V1). The His bundle–ventricular interval after ablation is 145 milliseconds (baseline, 80 milliseconds). *His_{dist}*, Distal His bundle; *His_{mid}*, middle His bundle; *His_{prox}*, proximal His bundle; *NSR*, normal sinus rhythm; *RBBB*, right bundle branch block; *RVA*, right ventricle apical.

proximally than the LAF, appears as an extension of the main LB, and is large in its initial course. The LPF then fans out extensively posteriorly toward the papillary muscle and inferoposteriorly to the free wall of the LV. The LAF crosses the LV outflow region and terminates in the Purkinje system of the anterolateral wall of the LV. In the RAO view, the LPF extends from the HB region toward the inferior diaphragmatic

wall and the LAF extends toward the apex of the heart. However, considerable variability exists.

The mapping catheter is placed via a retrograde aortic approach into the LV. The inferoapical septum is a starting point. The catheter is then gradually withdrawn toward the HB until a discrete LB potential is recorded. The LB-V interval should be less than 20 milliseconds, and

the AV electrogram amplitude ratio should be less than 1:10. At this position, the tip of the catheter typically is 1 to 1.5 cm inferior to the optimal HB recording site near the distal portion of the common LB.

Because the LB is a broad band of fibers (typically 1 to 3 cm long and 1 cm wide), it can be difficult to ablate with a single RF application. Furthermore, the fascicles can diverge proximally; thus ablation of the LB can be difficult without harming the HB. In these situations, it may be necessary to deliver several lesions along the left side of the septum in an arc distal to the HB, extending from the anterior superior septum (a point near the RB in the RAO view) to the inferior basal septum to transect both fascicles. Nevertheless, the disease process that results in LBBB in patients with BBR probably leaves only a remnant of conducting tissue that may be more readily ablated than a normal LB would be.

It is more difficult to monitor the progress of LB ablation during RF delivery. Most patients will already have some IVCD localized to the LB system. As opposed to the usually clear development of RBBB in lead V₁ during RB ablation, LB ablation can produce relatively subtle ECG changes, primarily manifesting as widening of the QRS and changes in the QRS axis. One can also monitor the presence of retrograde conduction during VES after each RF application. Elimination of the retrograde V₂-H₂ conduction that was present before ablation is a good indication that sufficient ablation of the LB has been achieved to eliminate BBR.

Endpoints of Ablation

Endpoints of RB ablation include the development of an RBBB pattern (see Fig. 26.7), noninducibility of BBR, and reversal of the direction of HB and RB activation during RV pacing. Prior to ablation, HB electrodes are depolarized during RV pacing from distal to proximal (RB-HB); after RB ablation, HB activation is delayed and reversed (HB-RB; see Fig. 26.6).

Endpoints of LB ablation include elimination of retrograde conduction of VESs over the LB and noninducibility of BBR.

After ablation, aggressive ventricular stimulation should be performed to evaluate the inducibility of VT. Also, decremental atrial pacing should be performed to evaluate the conduction properties of the HPS and the propensity for infra-Hisian AV block. It is advisable to stress the HPS with intravenous procainamide and ensure that anterograde conduction is preserved.

Outcome

The acute success rate of BBR VT approaches 100%, and tachycardia recurrence after successful ablation is extremely rare. However, myocardial VTs can be induced in up to 60% of these patients, and the risk of SCD remains high. Therefore ICD implantation is indicated for secondary prevention in such cases.

The reported incidence of clinically significant conduction system impairment requiring implantation of a permanent pacemaker varies from 10% to 30%. Pacemaker implantation is indicated when infra-Hisian AV block is demonstrated with atrial pacing, or when the postablation HV interval is 100 milliseconds or greater.

INTERFASCICULAR REENTRANT VENTRICULAR TACHYCARDIA

Of the two types of macroreentry in the HPS (i.e., BBR and interfascicular reentry), BBR is by far the most common mechanism of VT. VT secondary to interfascicular reentry is extremely rare; when it does occur, it is most commonly seen in patients with coronary artery disease, specifically those with anterior MI with LAF or LPF block. In these patients, RBBB is usually complete and bidirectional; hence true BBR cannot occur. In addition, there is slow conduction in the apparently

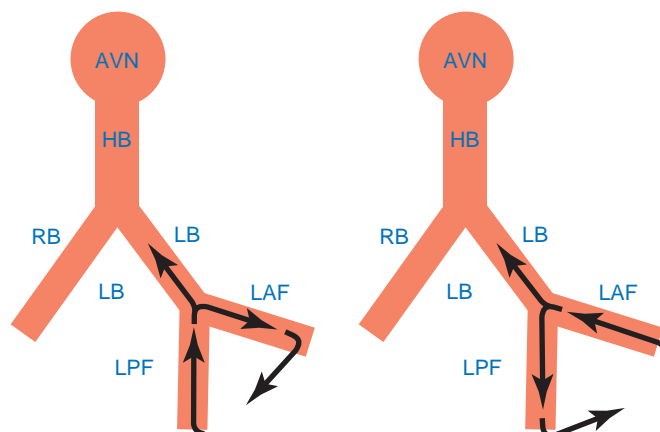


Fig. 26.8 Schematic Illustration of the Two Types of Interfascicular Ventricular Tachycardia (VT) Circuits. *Left*, The interfascicular reentrant VT uses the left posterior fascicle (LPF) as the retrograde limb of the reentrant circuit and the left anterior fascicle (LAF) as the anterograde limb. *Right*, The interfascicular reentrant VT uses the LAF as the retrograde limb of the reentrant circuit and the LPF as the anterograde limb. In both types, because the ventricle is activated via the left bundle branch (LB), the QRS has right bundle branch block morphology. The QRS axis will depend on which fascicle serves as the anterograde route of ventricular activation. The right bundle branch (RB) is activated in a bystander fashion and is not necessary for sustaining the tachycardia. AVN, Atrioventricular node; HB, His bundle.

blocked fascicle. Of note, interfascicular reentrant VT can develop in patients following ablation of the RB for the treatment of BBR VT.⁹

Interfascicular reentry incorporates the LAF and LPF as obligatory limbs of the circuit, connected proximally by the main trunk of the LB and distally by the ventricular myocardium (Fig. 26.8). The tachycardia usually has RBBB morphology. The orientation of the frontal plane axis is variable and depends on the direction of propagation in the reentrant circuit. Anterograde activation over the LAF and retrograde through the LPF would be associated with right axis deviation, whereas the reversed activation sequence shows left axis deviation.¹⁰

In contrast to BBR VT, the HV interval during interfascicular VT is usually shorter (by more than 40 milliseconds) than that recorded in NSR. This is because the upper turnaround point of the circuit, the distal end of the LB bifurcation point, is relatively far from the retrogradely activated HB. In addition, the LB potential is inscribed before the His potential during interfascicular VT. Contrariwise, during BBR VT with RBBB morphology, the His potential usually precedes the LB potential, although the reverse is theoretically possible if the retrograde conduction time to the HB recording point is significantly prolonged. Interfascicular reentry also demonstrates variations in the V-V interval preceded by similar changes in the H-H interval.¹

Atrial pacing, AES, VES, and ventricular pacing can initiate interfascicular reentry by producing transient anterograde block in the slowly conducting fascicle (LAF or LPF), with subsequent impulse anterograde conduction over the healthy fascicle, giving rise to a QRS morphology identical to that during NSR, and then retrogradely in the initially blocked fascicle to initiate reentry. Compared with BBR VT, interfascicular VT can be more difficult to induce by ventricular pacing, because of the inability to create the necessary EP conditions for this type of reentry during ventricular stimulation (i.e., retrograde block in the distal LAF and slow conduction via the LPF, or vice versa), although this may occur during anterograde penetration of the HPS by supra-ventricular impulses (i.e., anterograde block in the LPF and slow conduction in the LAF, or vice versa).⁹

Successful ablation of the arrhythmia can be performed by targeting the diseased fascicle (LAF or LPF), guided by fascicular potentials. When interfascicular reentry occurs in the setting of an anterior MI, complete cure by ablation is usually not possible because other myocardial VTs are almost always present, and the LV ejection fraction is usually poor, thereby mandating ICD implantation for improved survival. When interfascicular reentry occurs without coronary artery disease, in association with degenerative disease of the conduction system, LV systolic function is usually normal and cure of the VT is possible by ablation of the diseased fascicle, although implantation of a permanent pacemaker will likely be required.¹⁰

REFERENCES

1. Nayyar S, Young GD, Sanders P, et al. Paradoxical ventricular activation sequence and paraHisian entrainment response: do they challenge the diagnosis? *Circ Arrhythm Electrophysiol*. 2013;6:e1–e6.
2. Asirvatham SJ, Stevenson WG. Bundles branch reentry. *Circ Arrhythm Electrophysiol*. 2013;6:e92–e94.
3. Roberts JD, et al. Bundle branch re-entrant ventricular tachycardia. *JACC Clin Electrophysiol*. 2017;3:276–288.
4. Reithmann C, Herkommer B, Remp T, et al. Atypical surface ECG complicating the diagnosis of bundle branch reentry tachycardia. *Pacing Clin Electrophysiol*. 2017;40:191–198.
5. Balasundaram R, Rao HB, Kalavakolanu S, et al. Catheter ablation of bundle branch reentrant ventricular tachycardia. *Heart Rhythm*. 2008;5:S68–S72.
6. Sakata T, Tanner H, Stuber T, et al. His-Purkinje system re-entry in patients with clustering ventricular tachycardia episodes. *Europace*. 2008;10:289–293.
7. Machino T, Tada H, Sekiguchi Y, et al. Three-dimensional visualization of the entire reentrant circuit of bundle branch reentrant tachycardia. *Heart Rhythm*. 2013;10:459–460.
8. Schmidt B, et al. Left bundle branch–Purkinje system in patients with bundle branch reentrant tachycardia: lessons from catheter ablation and electroanatomic mapping. *Heart Rhythm*. 2009;6:51–58.
9. Blanck Z, Sra J, Akhtar M. Incessant interfascicular reentrant ventricular tachycardia as a result of catheter ablation of the right bundle branch: case report and review of the literature. *J Cardiovasc Electrophysiol*. 2009;20:1279–1283.
10. Okishige K, et al. The radio frequency catheter ablation of inter-fascicular reentrant tachycardia: new insights into the electrophysiological and anatomical characteristics. *J Interv Card Electrophysiol*. 2014;41:39–54.

Epicardial Ventricular Tachycardia

OUTLINE

Electrophysiological Substrate, 907

- Ischemic Cardiomyopathy, 907
- Arrhythmogenic Right Ventricular Cardiomyopathy, 908
- Nonischemic Dilated Cardiomyopathy, 908
- Idiopathic Ventricular Tachycardia, 908

Electrocardiographic Features, 908

- Ventricular Tachycardia in Nonischemic Dilated Cardiomyopathy, 909
- Ventricular Tachycardia in Arrhythmogenic Cardiomyopathy, 909
- Idiopathic Ventricular Tachycardia, 909
- Postinfarction Ventricular Tachycardia, 910

Clinical Considerations, 910

- Anticoagulation, 911
- Contrast-Enhanced Magnetic Resonance Imaging, 911
- Contrast-Enhanced Computed Tomography, 912

Navigating the Pericardial Space, 912

- Anatomical Considerations, 912
- Technical Considerations, 912

Pericardial Adhesions, 914

Epicardial Fat, 914

Transthoracic Epicardial Mapping, 915

- Activation Mapping, 915
- Entrainment and Pace Mapping, 915
- Electroanatomic Substrate Mapping, 916

Transthoracic Epicardial Ablation, 916

- Radiofrequency Ablation, 916
- Cryoablation, 918
- Complications of Transthoracic Epicardial Ablation, 918
- Outcome, 920

Transvenous Epicardial Mapping and Ablation, 920

- Anatomical Considerations, 920
- Technical Considerations, 922
- Outcome, 922

Ventricular tachycardia (VT) originating from the subepicardium is an important cause of failure of endocardial VT ablation approaches. Mapping arrhythmia foci or circuits that are deep within the myocardium or in the epicardium can be attempted via the coronary sinus (CS) or pericardial space. However, the CS approach has important limitations. Catheter manipulation is limited by the anatomical distribution of the cardiac veins, and epicardial circuits may be identified only when the vessel cannulated happens to be in the region of the circuit. An alternative epicardial approach involves inserting an introducer sheath percutaneously into the pericardial space in the manner used for pericardiocentesis. The subxiphoid approach to the epicardial space allows extensive and unrestricted mapping of the epicardial surface of both ventricles (assuming no areas of pericardial adhesions), and has been used most commonly for VT mapping and ablation (far less so for supraventricular arrhythmias). Nevertheless, mapping within the CS and accessible coronary venous branches can be performed prior to the percutaneous epicardial approach to look for clues of an epicardial origin of the VT circuit, and has been particularly useful in idiopathic focal VTs.

ELECTROPHYSIOLOGICAL SUBSTRATE

Mapping and ablation of arrhythmogenic substrates have traditionally been performed via the endocardial approach. Often, however, the site of origin of a focal tachycardia or a portion of the critical isthmus or even the entire circuit of a macroreentrant VT is located intramurally or in the subepicardium and cannot be identified or ablated from the

endocardium. In these settings, the epicardial approach to mapping and ablation can be a valuable strategy for elimination of the arrhythmia.

The importance of epicardial VT circuits was first highlighted in Chagas disease, which classically results in an epicardial involvement in approximately 70% of patients. Epicardial substrates also have been increasingly recognized in the setting of scar-related VT in patients with nonischemic dilated cardiomyopathy (DCM), arrhythmogenic right ventricular cardiomyopathy (ARVC), post-myocardial infarction (MI) VT, as well as in patients with idiopathic VT. Among patients with VT, an arrhythmogenic substrate requiring epicardial ablation is seen more commonly in patients with nonischemic DCM (25% to 50%), ARVC (30% to 40%), and less frequently in ischemic cardiomyopathy (10% to 16%).^{1,2}

Ischemic Cardiomyopathy

MI produces a predictable wavefront of necrosis progressing from subendocardium to epicardium, resulting in a wedge-shaped, primarily subendocardial scar with variable epicardial extension (depending on the transmural extent of the infarction), usually confined to a specific coronary vascular territory. Therefore, unlike VT substrates in patients with nonischemic cardiomyopathy, the arrhythmogenic tissue can be accessed from the endocardium in the majority of post-MI patients. Even when the arrhythmogenic substrate is located epicardially, elimination of the overlying epicardial substrate is often successful by endocardial ablation through the thinned transmural scar, minimizing the need for epicardial ablation in this population. Nonetheless, VT originating from the subepicardium remains an important cause of failure of endocardial ablation

approaches. In tertiary centers, epicardial ablation has been required in approximately 10% to 25% of post-MI VTs, and seems to be more common with inferior than anterior wall MI.³ However, epicardial access frequently is not feasible for patients who have undergone prior cardiac surgery (which is the case in more than half of post-MI patients undergoing VT ablation).^{1,2,4}

Arrhythmogenic Right Ventricular Cardiomyopathy

In ARVC, fibrofatty replacement usually begins in the subepicardium or midmural layers and progresses to the subendocardium. Thus the arrhythmogenic substrate in patients with ARVC is more extensive epicardially, predominantly located in the subtricuspid and right ventricular outflow tract (RVOT) regions. Although epicardial ablation is required in a significant proportion of these patients, the often-thinned right ventricular (RV) wall often allows for successful elimination of the epicardial substrate by endocardial ablation.

Nonischemic Dilated Cardiomyopathy

Myocardial scarring in nonischemic DCM has been shown to have a predilection for the midmyocardium and epicardium. The epicardial left ventricular (LV) scar areas in nonischemic DCM are typically larger than the endocardial scar and have a typical distribution similar to that for endocardial LV scars, usually located in basal lateral areas of the LV adjacent to the mitral valve annulus. Often, the epicardial substrate can exist with no significant endocardial scarring or ventricular wall thinning (unlike the substrate in post-MI and ARVC patients), rendering endocardial ablation alone ineffective in eliminating epicardial targets. As a result, epicardial ablation is needed more often in patients with VT associated with nonischemic DCM than in patients with prior MI.^{1,2}

Idiopathic Ventricular Tachycardia

Idiopathic focal VTs requiring epicardial ablation are observed in up to 14% of patients, and they typically arise in close proximity to the coronary venous system in the LV summit and cardiac crux. On the other hand, the anterior and lateral portions of the RVOT are fairly thin; thus ablation from the endocardium is usually effective, even when VT foci occur on the epicardial surface. The posterior RVOT (infundibulum) is much thicker, but the epicardial surface of the posterior infundibulum is the left ventricular outflow tract (LVOT), and thus ablation may be effective from either the LVOT or the RVOT for arrhythmias arising deep in the myocardium of the posterior RVOT. For the supraaortic region there is no true epicardial location because the RVOT lies anterior to the right and left coronary cusps and the atria lie posterior to the noncoronary cusp.

For epicardial idiopathic VT, a combined approach from the coronary venous system and adjacent anatomical sites has been most effective, with a success rate around 70%. The outcome of the subxiphoid epicardial ablation is poor in the majority of cases due to the close proximity of the coronary arteries and the thick layer of epicardial fat that overlies the ablation targets.

ELECTROCARDIOGRAPHIC FEATURES

Various electrocardiogram (ECG) characteristics have been used to predict whether an epicardial approach may be required based on the VT morphology (Box 27.1). Those ECG methods are mainly based on the concept that when ventricular activation starts at the epicardial level, the initial part of the wavefront progresses slowly through the myocardial wall until reaching the Purkinje system, which is located only at the subendocardium. This slow transmural activation is reflected as slurred onset of the QRS on the surface ECG. Furthermore, propagation of ventricular activation from the epicardial surface results in

BOX 27.1 Electrocardiographic Characteristics Suggesting an Epicardial Origin of Ventricular Tachycardia

LV VT in Nonischemic Dilated Cardiomyopathy

- Pseudo-delta wave >34 msec
- Long R-wave peak time (≥ 85 msec) in lead V_2
- Shortest precordial RS complex duration >120 msec
- QRS duration >200 msec
- The presence of a Q wave in lead I (for basal superior and apical superior VTs)
- The absence of a Q wave in any of the inferior leads (for basal superior VTs)
- The presence of a Q wave in the inferior leads (for basal inferior and apical inferior VTs)
- Maximum deflection index ≥ 0.59 (for basal-superior/lateral VTs)

RV VT in Arrhythmogenic Cardiomyopathy

- The presence of an initial Q wave in lead I and QS in lead V_2 (for anterior sites in the RV).
- The presence of an initial Q wave in leads II, III, and aVF (for inferior sites in the RV)

LV Summit Idiopathic VT

- Pseudo-delta wave >34 msec
- Long R-wave peak time (≥ 85 msec) in lead V_2
- Shortest precordial RS complex duration >120 msec
- Delayed shortest precordial maximal deflection index (≥ 0.55)
- Peak deflection index >0.6
- R wave amplitude ratio in leads III/II ratio of >1.25
- R wave amplitude ratio in leads aVL/aVR >1.75

LV, Left ventricle; RV, right ventricle; VT, ventricular tachycardia.

a QS pattern in the ECG leads over that region. This is in contrast to endocardial VT exit sites, which produce an initial “r” wave in the corresponding ECG leads, reflecting transmural ventricular activation in an endocardial-to-epicardial direction (towards the overlying ECG lead).

It is important to understand that in the setting of scar-related VT, the QRS morphology is related solely to the VT exit site and this does not imply that some other component of the circuit (such as the critical isthmus or entrance site) cannot be ablated from the endocardium, even when an epicardial exit is indicated by the ECG characteristics. Therefore it is unlikely that the surface ECG by itself will ever be entirely predictive of the need for epicardial access for mapping and ablation for any given VT. In addition, large areas of conduction delay often present in patients with myocardial scar can produce misleading activation sequences and confound ECG prediction.

Furthermore, ECG criteria for identifying an epicardial origin of VT appear to be region and substrate specific. The published ECG criteria have very limited accuracy (40% to 60%) for differentiating epicardial from endocardial VT sites of origin when applied indiscriminately to all ventricular locations. The development of region-specific criteria has significantly improved the sensitivity and specificity (up to the 90% range). However, these criteria were validated only for a single region in the heart and only for patients with nonischemic cardiomyopathy.⁵

A computerized algorithm was recently reported to improve ECG utility for identifying epicardial sites of origin of VT, with an accuracy of 80%. The algorithm has been validated for all regions of the

endocardium and epicardium in patients with and without structural heart disease, and it performed better in most regions than previously described criteria. However, this will require further validation in large clinical studies.⁵

Ventricular Tachycardia in Nonischemic Dilated Cardiomyopathy

Several ECG findings can suggest an epicardial origin of the LV VT with right bundle branch block (RBBB)-like configuration, and all generally rely on the late engagement of the rapidly conducting His-Purkinje fibers by exits on the epicardium, resulting in intramyocardial delay of conduction and a slurred initial part of the QRS complex. These ECG criteria include: (1) pseudo-delta wave (so called because of its similarity to the slurred upstroke delta wave observed during ventricular preexcitation) greater than 34 milliseconds (measured from the earliest ventricular activation to the earliest fast deflection in any precordial lead), which has a sensitivity of 83% and a specificity of 95%; (2) long R-wave peak time in lead V₂ (i.e., interval from the beginning of the QRS complex to the time of initial downstroke of the R wave after it has peaked [previously known as the *intrinsicoid deflection*]) greater than 85 milliseconds, which has a sensitivity of 87% and a specificity of 90%; (3) shortest RS complex duration (measured from the earliest ventricular activation to the nadir of the first S wave in any precordial lead) greater than 120 milliseconds, which has a sensitivity of 76% and a specificity of 85%; and (4) QRS duration greater than 200 milliseconds (see Fig. 22.11).⁶ However, all of these interval criteria suffer from being absolute numbers, which can be modified by effects of antiarrhythmic drugs; that is, an unmedicated patient's pseudo-delta interval of 28 milliseconds (i.e., not epicardial) may be nonspecifically prolonged to 38 milliseconds (i.e., epicardial) by the effect of a sodium channel blocking antiarrhythmic drug. Morphological criteria and the maximum and peak deflection indices (see below) are not subject to this limitation.

However, these criteria do not seem to apply uniformly to all LV regions or to VTs originating from the RV. Other site-specific criteria have been suggested for identifying an epicardial origin for LV VTs: (1) the presence of a Q wave in lead I for basal superior and apical superior VTs; (2) the absence of a Q wave in any of the inferior leads for basal superior VTs; and (3) the presence of a Q wave in the inferior leads for basal inferior and apical inferior VTs. Also, measurement of the *maximal deflection index* (defined as the time from QRS onset to maximal deflection in precordial leads divided by the QRS duration) can help identify epicardial VT originating in the LVOT region.

Given the limited predictive value of ECG criteria when applied individually, a multistep algorithm that incorporates several criteria (two morphology criteria and two adjusted interval criteria) was proposed to predict the site of origin of VTs from the basal-superior/lateral epicardium in patients with nonischemic DCM. The criteria included, in a stepwise fashion: (1) the absence of Q waves in inferior leads; (2) a pseudo-delta wave greater than or equal to 75 milliseconds; (3) maximum deflection index (defined as the interval measured from the earliest ventricular activation [or from the stimulation artifact] to the peak of the largest amplitude deflection in each precordial lead [taking the lead with shortest time] divided by the QRS duration) greater than or equal to 0.59; and (4) the presence of a Q wave in lead I. This four-step algorithm had a 95% specificity and at least 20% sensitivity for identifying basal-superior/lateral epicardial origin of VTs in nonischemic cardiomyopathy. The morphological criteria (presence of a q wave in lead I and absence of q waves in the inferior leads) appear to be the most specific criteria. In particular, the presence of a q wave in lead I is a very specific (88%) and a very sensitive criterion (88%) for identifying an epicardial site of origin.⁷

Ventricular Tachycardia in Arrhythmogenic Cardiomyopathy

Ventricular ectopy in ARVC usually arises from the "triangle of dysplasia" in the RV and therefore has a left bundle branch block (LBBB) pattern with superior, inferior, or indeterminate axis. Most sustained VTs arise from the RV free wall, and most VTs display LBBB configuration with poor R-wave progression in the precordial leads. Nonetheless, VT with RBBB morphology can be observed in patients with LV disease or when advanced structural RV disease distorts normal ventricular geometry within the thorax (see Fig. 29.7).⁸ For VTs originating from the RV, the presence of an initial Q wave in lead I and QS in lead V₂ for anterior sites in the RV strongly predicts an epicardial origin. Similarly, an initial Q wave in leads II, III, and a VF is observed with pace mapping from the inferior epicardial locations in the RV.⁹

Idiopathic Ventricular Tachycardia

The LV summit is the most superior aspect of the "epicardial" LVOT. Hence, VTs originating from this region exhibit the classic slower spread of activation from a focus on the epicardial surface relative to the endocardium and delayed global ventricular activation resulting from later engagement of the His-Purkinje network. Several ECG characteristics can help distinguish epicardial idiopathic VTs from endocardial arrhythmias, including: (1) pseudo-delta wave ≥ 34 milliseconds, (2) long R-wave peak time (≥ 85 milliseconds) in lead V₂, and (3) shortest precordial RS complex of greater than 120 milliseconds.

Furthermore, the degree of initial QRS slurring, as measured by the *maximal deflection index* (defined as the product of the time from QRS onset to maximal deflection [i.e., the largest positive or negative amplitude deflection] in precordial leads divided by the total QRS duration), can help identify epicardial LV summit VTs. A delayed shortest precordial maximal deflection index (≥ 0.55) discriminates LV summit VTs from those originating within the aortic sinuses of Valsalva.¹⁰ Similarly, a peak deflection index (determined in the inferior lead presenting the tallest R wave by dividing the time from the QRS onset to the peak QRS deflection by a total QRS duration) of greater than 0.6 predicts an epicardial LV summit origin.¹¹ This observation is consistent with slower spread of activation from a focus on the epicardial surface relative to the endocardium and delayed global ventricular activation resulting from later engagement of the His-Purkinje network.

Because of its superior location in the LV, VTs originating from the LV summit uniformly exhibit large R wave amplitudes in the inferior leads. However, R wave amplitude ratio in leads III/II can vary according to the location of VT focus within the LV summit. As the site of origin shifts progressively more laterally (from the superior region of the summit towards the inferior region, then towards the lateral mitral annulus), R wave amplitude becomes progressively larger in lead III compared to lead II (concurrent with progressively more steeply negative complexes in lead I). R wave amplitude ratio in leads III/II ratio of greater than 1.25 can predict the requirement of a pericardial approach for VT ablation (i.e., origins from the inferior aspect of the LV summit).^{10,12}

Similarly, the aVL/aVR Q-wave ratio was strongly correlated with the anatomical distance between the successful site and the apex of the LV summit; the longer distances away from the apex of the LV summit the larger the aVL/aVR Q-wave ratio. This indicates that the ECG vectors would shift laterally and inferiorly if the distance between the VT and the apex of the LV summit increased. Also, the aVL/aVR Q-wave ratio was found to predict the approach to successful ablation; the aVL/aVR Q-wave ratio was significantly higher for VTs requiring an epicardial approach, followed by VTs arising from the coronary venous system, subvalvular area, and aortic sinuses of Valsalva. An aVL/aVR Q-wave

ratio of less than 1.45 predicted successful ablation from aortic sinuses of Valsalva or subvalvular approaches, whereas an aVL/aVR Q-wave ratio of greater than 1.75 indicated the need for a pericardial approach.^{13,14}

VTs originating from the superior region of the LV summit (the “inaccessible region” close to the apex of the summit) typically exhibit LBBB pattern, larger R wave amplitudes in the inferior leads, and absence of an S wave in leads V₅ to V₆.¹⁰ When LV summit VTs exhibit an RBBB pattern, transition zone earlier than lead V₁, aVL/aVR amplitude ratio of greater than 1.1, and S waves in V₅ to V₆, those VTs are likely to be cured by catheter ablation within the great cardiac or anterior interventricular veins. As noted, when LV summit VTs exhibit lead III/II amplitude ratio of greater than 1.25 and lead aVL/aVR amplitude ratio of greater than 1.75, those VTs are likely to require a pericardial approach for ablation.^{12,15}

Postinfarction Ventricular Tachycardia

The proposed 12-lead ECG features for differentiation of epicardial versus endocardial VT exit sites were assessed in patients without MI, and their utility for localization of post-MI VTs has not been validated. In fact, in a recent report, those QRS characteristics failed to reliably identify post-MI VTs requiring epicardial ablation. Slow initial forces can be present during tachycardia at the MI scar region and, hence, are not specific for epicardial origins. Furthermore, the presence of typical Q waves in the VT ECGs of patients with previous MI precludes the use of morphological ECG criteria, and when present in the precordial leads, Q waves can interfere with the measurement of all interval criteria.^{6,16–18}

As noted earlier, epicardial VT exits are uncommon in post-MI VT because of the subendocardial nature of the underlying substrate. Furthermore, the VT 12-lead ECG provides information about the VT exit site from the scar border, which generally is not the target of ablation. The critical isthmus of the VT circuit, which constitutes the ablation target, often is complex, and can have an endocardial and epicardial trajectory permitting successful ablation from the endocardium (especially in the presence of wall thinning caused by the infarct scar) even in the setting of VT with an epicardial exit. Therefore endocardial mapping should be the first approach to catheter ablation for VTs in patients with ischemic heart disease, even when the surface ECG suggests an epicardial origin of the tachycardia.^{17,18}

CLINICAL CONSIDERATIONS

Catheter ablation from the epicardium is often required for elimination of VTs due to nonischemic cardiomyopathy and is occasionally useful for VTs in a variety of other diseases, as well as some idiopathic VTs. In addition, epicardial mapping and ablation is necessary in patients in whom endocardial ablation cannot be performed (e.g., LV thrombus, mechanical aortic and mitral valve prosthesis). However, there are several conditions that can significantly limit the feasibility of percutaneous epicardial mapping and ablation. Previous cardiac surgery or pericarditis usually results in significant pericardial fibrosis, and the pericardial space is often, but not always, virtually replaced by fibrotic adhesions. In this setting, percutaneous cannulation of the pericardial sac is very difficult; even when percutaneous cannulation is successful, manipulation of the instruments can be extremely limited.^{19,20}

The need for epicardial ablation, however, is often difficult to determine at the beginning of a procedure. Although percutaneous epicardial VT ablation frequently is pursued after extensive endocardial mapping or ablation fails in achieving the desired procedural endpoint, the epicardial approach should be considered early in the procedure in patients known to have high propensity of epicardial substrates (including those with DCM and ARVC).

Combined endocardial and epicardial mapping during the initial procedure is increasingly being utilized in selected VT patients. Such an approach allows for performing pericardial puncture before initiating systemic anticoagulation and offers a better chance to map and ablate all inducible VTs during the index procedure (eFig. 27.1).²¹ However, this strategy inevitably leads to unnecessary pericardial punctures in some patients. In fact, in a recent study employing simultaneous endocardial and epicardial mapping, the endocardium was ultimately thought to be a better target than the epicardium in up to 21% of patients. Therefore epicardial access should be obtained at the beginning of a procedure only when an epicardial origin of the VT circuit is strongly suspected based on a thorough preprocedural assessment.

Several preprocedural clues can potentially help select VT patients in whom a combined endocardial-epicardial approach is appropriate as a first-line approach (Box 27.2), including: (1) the presence of a predominantly epicardial underlying disease substrate (e.g., nonischemic DCM, ARVC, Chagas disease); (2) previously failed endocardial ablation; (3) predominantly epicardial location of myocardial scar on preprocedural cardiac imaging studies (cardiac magnetic resonance [CMR] or computed tomography [CT]); or (4) ECG criteria suggesting an epicardial VT exit site. As noted previously, while ECG characteristics can help predict an epicardial exit site, they alone are not reliably predictive of the need for epicardial access and mapping for any given VT. QRS morphology is related solely to the VT exit site and this does not imply that the critical isthmus of the VT circuit cannot be ablated from the endocardium, even when an epicardial exit is implied by the ECG characteristics.^{22–25}

During endocardial VT mapping and ablation, several findings should prompt early consideration of the epicardial approach: (1) the inability to identify the reentry circuit isthmus on the endocardium; (2) endocardial activation mapping demonstrating a focal point of earliest

BOX 27.2 Factors Predicting the Need for an Epicardial Approach for Ventricular Tachycardia Ablation

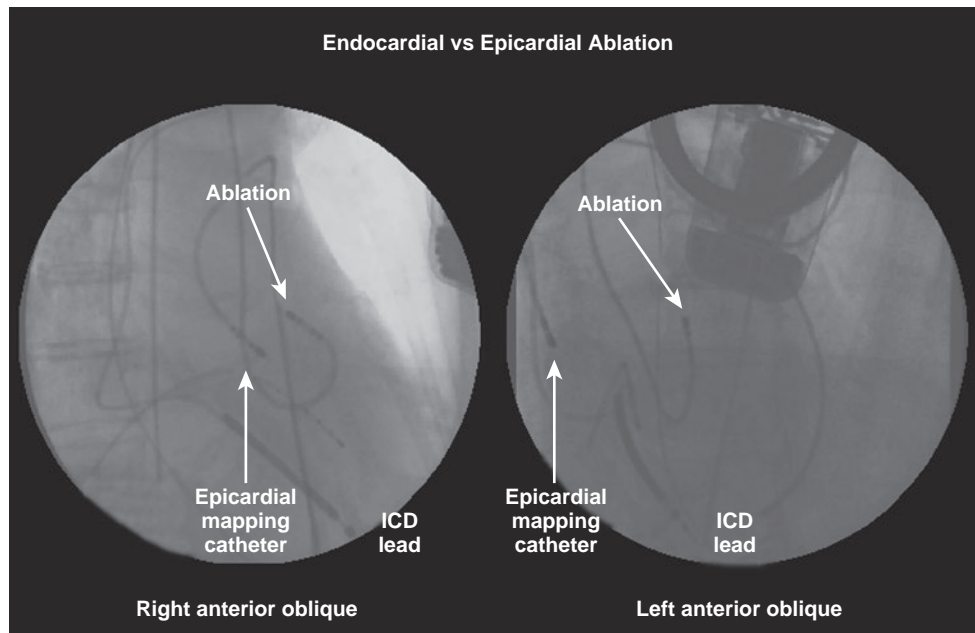
Preprocedural Factors

- Intracavitary thrombus
- Mechanical aortic and mitral valves
- Prior failed endocardial ablation
- Predominantly epicardial underlying disease substrate (nonischemic cardiomyopathy or arrhythmogenic right ventricular cardiomyopathy)
- Predominantly epicardial scar on preprocedural cardiac magnetic resonance
- Electrocardiographic criteria suggesting an epicardial VT exit site

Intraprocedural Factors

- Inability to identify the reentry circuit isthmus on the endocardium
- Failed or late VT termination with endocardial radiofrequency ablation
- Endocardial activation mapping demonstrating a focal point of earliest endocardial activation with unfavorable results of entrainment or pace mapping
- Endocardial activation mapping demonstrating diffusely endocardial area of equally earliest activation, with unfavorable unipolar electrogram characteristics or paced mapping results
- Endocardial bipolar voltage mapping demonstrating small areas of abnormalities
- Abnormal endocardial unipolar voltage mapping suggestive of greater extent of epicardial scar

VT, Ventricular tachycardia.



eFig. 27.1 Combined Endocardial and Epicardial Mapping of Ventricular Tachycardia (VT) in Dilated Nonischemic Cardiomyopathy. Shown are fluoroscopic views of endocardial and epicardial ablation catheter positions. VT was eventually eliminated with endocardial ablation at the site shown (basal left ventricle). ICD, Implantable cardioverter-defibrillator.

endocardial activation with unfavorable results of entrainment or pace mapping techniques; or (3) large endocardial area ($>2 \text{ cm}^2$ region) of equally earliest activation, with no single site showing favorable unipolar electrogram characteristics or paced mapping results; (4) failed or late VT termination with endocardial radiofrequency (RF) energy application; (5) limited endocardial substrate, as indicated by endocardial bipolar voltage mapping demonstrating small areas of abnormalities; and (6) endocardial unipolar voltage mapping is suggestive of greater extent of epicardial bipolar signal abnormalities compared to the bipolar voltage abnormalities.^{23,26–28}

On the other hand, it is probably more appropriate to defer epicardial intervention in patients with ischemic cardiomyopathy and those anticipated difficult epicardial access (due to prior cardiac surgery) until an endocardial approach has failed ablation.^{1,2}

Anticoagulation

Epicardial access is generally avoided in patients on therapeutic doses of oral or IV anticoagulation. In patients requiring both endocardial and epicardial LV mapping, the pericardial access is typically obtained before endocardial mapping and before administering anticoagulation. When the decision to proceed to the epicardial approach is made after the patient has already received IV heparin during endocardial LV mapping, reversal of anticoagulation effects of heparin with protamine is generally recommended prior to pericardial puncture to reduce the risk of intrapericardial or access-related bleeding. Heparin may be started (if additional endocardial LV mapping is required) after safe epicardial access has been obtained without significant bleeding complications.

Of note, a recent report found that percutaneous pericardial access could be performed safely in anticoagulated patients. This approach obviates the need for temporary reversal of systemic anticoagulation (and potential difficulties in reestablishing therapeutic anticoagulation following protamine administration) in patients who already had endocardial LV ablation, which can potentially increase the risk of systemic thromboembolism. Furthermore, this approach obviates obtaining epicardial access until its value is confirmed based on findings of endocardial mapping.²⁹

Contrast-Enhanced Cardiac Magnetic Resonance

Delayed contrast-enhanced CMR delineates regions of scar tissue potentially forming part of the arrhythmia substrate in patients with ischemic and nonischemic cardiomyopathy, and enables the depiction of transmural and nontransmural scars with high spatial resolution, allowing determination of whether the scar is endocardial, intramyocardial, or epicardial (Fig. 27.1).^{30,31}

The suspicion of an epicardial VT substrate can facilitate planning of VT ablations, such as for a combined endocardial and epicardial approach, especially given the fact that visualization of epicardial or intramyocardial scar on preprocedure-delayed enhancement CMR was found to be predictive of failure of the endocardial approach and of the need for the epicardial approach for VT ablation.^{32,33}

CMR can also help determine the underlying etiology of nonischemic cardiomyopathy in some patients, such as myocarditis, sarcoidosis, and ARVC, which can be associated with a higher susceptibility for epicardial VTs. Furthermore, in patients undergoing epicardial mapping and ablation procedures, the registration of preacquired CMR images with real-time electroanatomic mapping allows visualization of the ventricular anatomy and obstacles to procedural success, such as epicardial fat, which can be helpful during the mapping procedure in differentiating the cause of low epicardial voltages (fat vs. scar).

One potential disadvantage concerns the safety and quality of CMR imaging in patients with implanted cardiac devices. However, recent studies have consistently demonstrated the feasibility and safety of CMR in patients with pacemakers and defibrillators, and evolving technologies have further improved the CMR imaging compatibility of some devices. Also, the device hardware introduces significant artifacts, especially in the basal anterior free LV wall, which degrades the image quality and often limit interpretation of CMR in VT patients. Nonetheless, the interventricular septum, and the LV lateral and inferior walls are mostly free of artifact in most patients. Recently, a wideband late gadolinium enhanced CMR technique has been reported to reduce hyper-intense artifacts from the cardiac device generator.^{30,34} When CMR cannot be obtained, cardiac CT may be used for scar and fat imaging.

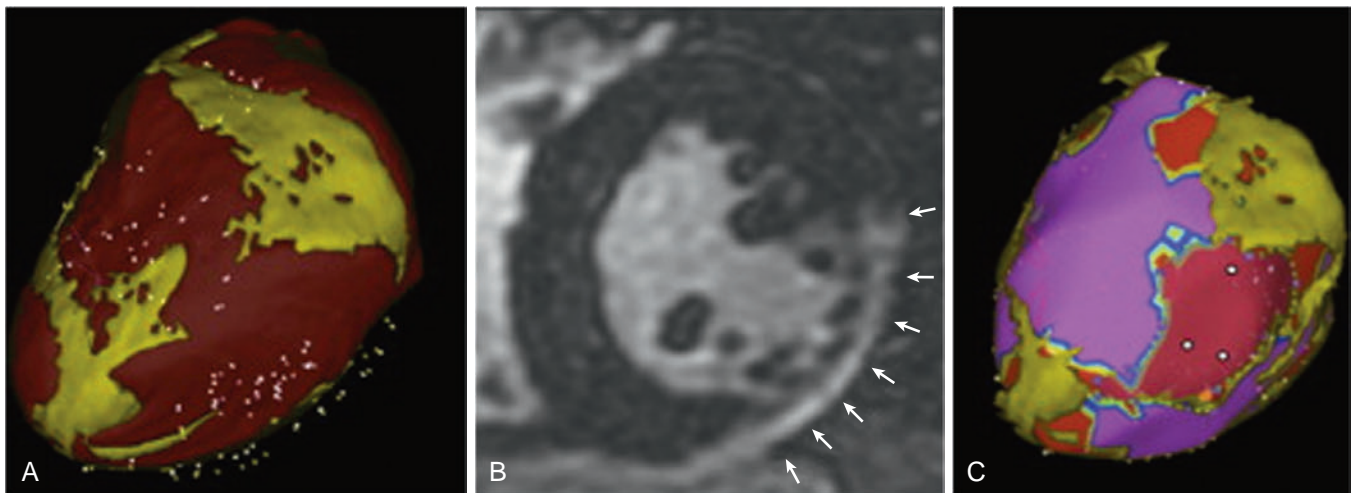


Fig. 27.1 Epicardial Fat and Scar. (A) Extracted epicardial fat (yellow) together with the epicardium (dark red) in a patient with nonischemic cardiomyopathy. (B) Short-axis magnetic resonance imaging indicates an epicardial scar in the inferolateral left ventricular area (arrows). (C) Voltage map in the same patient, indicating an area of low voltage extending from the basolateral free wall of the left ventricle to the left ventricular apex. The epicardial fat (yellow) is merged with the electroanatomic voltage map. The low-voltage area projects on the left ventricular epicardium that is devoid of fat. (From Desjardins B, Morady F, Bogun F. Effect of epicardial fat on electroanatomical mapping and epicardial catheter ablation. *J Am Coll Cardiol*. 2010;56:1320–1327.)

Contrast-Enhanced Computed Tomography

Contrast-enhanced CT scanning enables detailed and comprehensive evaluation of LV myocardium using triple multimodality imaging based on anatomical, dynamic, and perfusion parameters to identify abnormal substrate (myocardial scar and border zone) with high spatial (≤ 1 mm) and temporal resolution. Areas of CT hypoperfusion correlate best with areas of abnormal voltage (<1.5 mV) rather than scar alone (<0.5 mV). Perfusion imaging from CT enables characterization of the transmural extent and intramyocardial location of scar tissue and visualization of surviving mid- and epicardial myocardium in the regions of the scar, which can help identify areas potentially involved in the VT substrate. Such preprocedural information can help the operator to plan an appropriate mapping and ablation strategy, and better inform the patient about the risks, benefits, and chances of procedural success.

The three-dimensional (3-D) CT-defined abnormal myocardium can be accurately extracted and embedded in clinical mapping systems displaying areas of abnormal anatomical, dynamic, and perfusion parameters for substrate-guided VT ablations. In addition, CT epicardial fat imaging can be used to characterize the extent of fat tissue by extracting and integrating epicardial fat information into the 3-D electroanatomic voltage map, thereby helping to distinguish epicardial fat from scar tissue.

NAVIGATING THE PERICARDIAL SPACE

Anatomical Considerations

The pericardium is a double-walled sac that contains the heart and the roots of the great arteries, the superior vena cava (SVC), and pulmonary veins (PVs). By separating the heart from its surroundings—the descending aorta, lungs, diaphragm, esophagus, trachea, and tracheobronchial lymph nodes—the pericardial space allows complete freedom of cardiac motion within this sac.^{35,36}

The pericardium consists of two sacs intimately connected with one another: an outer fibrous envelope (the fibrous pericardium) and an inner serous sac (the serous pericardium). The fibrous pericardium (0.8 to 2.5 mm in thickness) consists of fibrous tissue and forms a flask-shaped bag, the neck of which is closed by its fusion with the adventitia of the great vessels, while its base is attached by loose fibroareolar tissue to the central tendon and to the muscular fibers of the left side of the diaphragm. The fibrous pericardium is also attached to the posterior sternal surface by the superior and inferior sterno-pericardial ligaments. These attachments are essential to maintain the normal cardiac position in relation to the surrounding structures, to restrict the volume of the thin-walled cardiac chambers (right atrium [RA] and ventricle), and to serve as direct protection against injuries.

The fibrous pericardium extends up to 5 to 6 cm along the great vessels, including the aorta, the SVC, the right and left pulmonary arteries, and the four PVs. The inferior vena cava (IVC) enters the pericardium through the central tendon of the diaphragm and receives no covering from the fibrous pericardium.³⁷ Nerve fibers from the parietal layer of the pericardium transmitted by the phrenic nerve are sensitive to pain (e.g., during pericarditis). In contrast, the visceral pericardial layer on the cardiac surface is insensitive to pain.³⁸

The serous pericardium is a delicate membrane that lies within the fibrous pericardium and lines its walls; it is composed of two layers: the parietal pericardium and the visceral pericardium. The parietal pericardium is fused to and inseparable from the fibrous pericardium. On the other hand, the visceral pericardium, which is composed of a single layer of mesothelial cells, is part of the epicardium (i.e., the layer immediately outside the myocardium) and covers the heart and the great vessels except for a small area on the posterior wall of the atria.

The visceral layer extends to the beginning of the great vessels, and is reflected from the heart onto the parietal layer of the serous pericardium along the great vessels in tube-like extensions. This happens at two areas: where the aorta and pulmonary trunk leave the heart and where the SVC, IVC, and PVs enter the heart.

At the pericardial reflections and at the posterior wall between the great vessels, the pericardial space is divided up into a contiguous network of recesses and sinuses (eFig. 27.2). There are three sinuses in the pericardial space: superior, transverse, and oblique. The two pericardial space sinuses that can be accessed in electrophysiological (EP) procedures are the transverse and oblique sinuses. The superior sinus (superior aortic recess), which lies anterior to the upper ascending aorta and main pulmonary artery, is irrelevant to the EP procedure.¹⁹

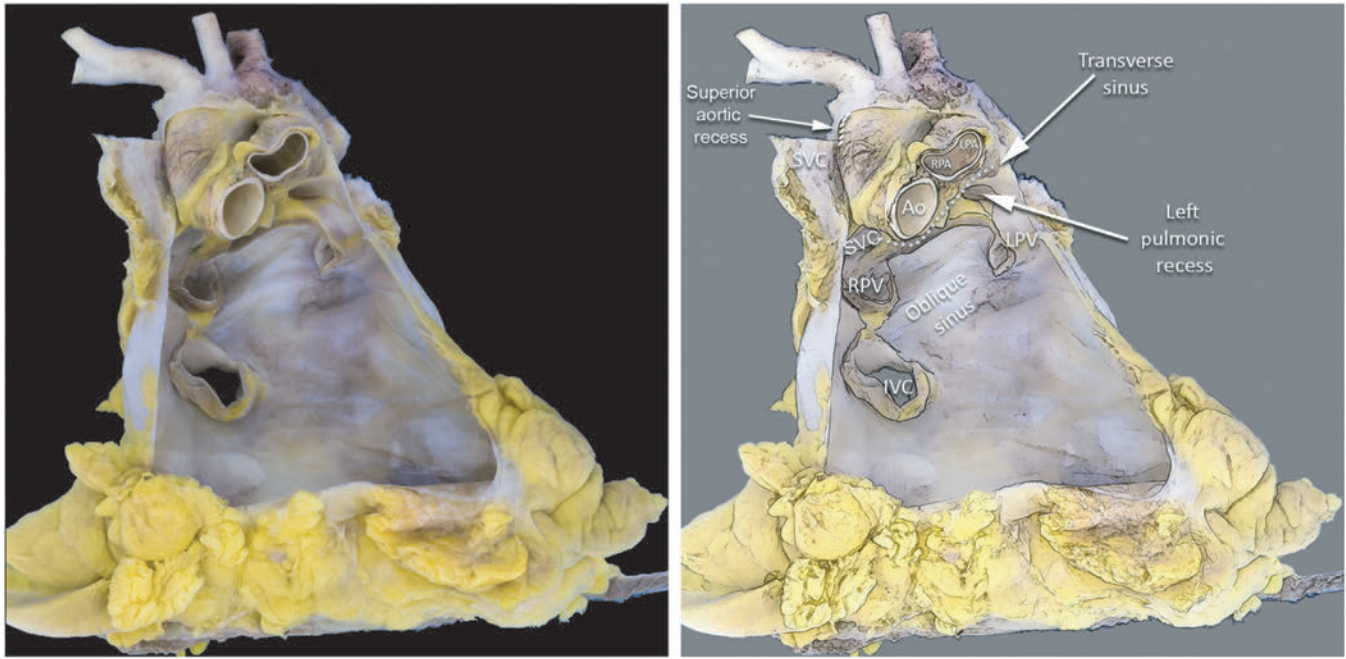
The oblique sinus is a cul-de-sac located posterior to the atria (particularly the left atrium [LA] in the region between the four PVs) and anterior to the esophagus and descending aorta. The oblique sinus is an inverted U-shaped pericardial reflection bordered by the right PVs and IVC on the right side, the left PVs on the left side, and the right and left PVs superiorly (Fig. 27.2). The right and left PV recesses extend from the oblique sinus between the upper and lower PVs on each side.^{19,35–37}

The tunnel-shaped transverse sinus lies posterior to the ascending aorta and pulmonary trunk, anterior to the SVC and superior PVs (eFig. 27.3). The roof of the transverse sinus is formed in parts by the aortic arch, the floor of the right pulmonary artery, and a part of the main pulmonary artery. Inferiorly, the transverse sinus is bound by the LA roof and by the pericardial reflection between the right and left superior PVs (which separates the transverse sinus from the oblique sinus below). The transverse sinus contains the right pulmonary artery and the inferior aortic recess (between the ascending aorta and the LA).³⁷ Catheter exploration of the sinus allows access to the anterior portion of the LA, the area of Bachman's bundle, and via the inferior aortic recess, the noncoronary and right coronary aortic sinuses of Valsalva.^{19,39} The transverse sinus can be accessed by a catheter passed posteriorly around the lateral wall of the LV and LA, and then under the pulmonary arteries.^{35,36}

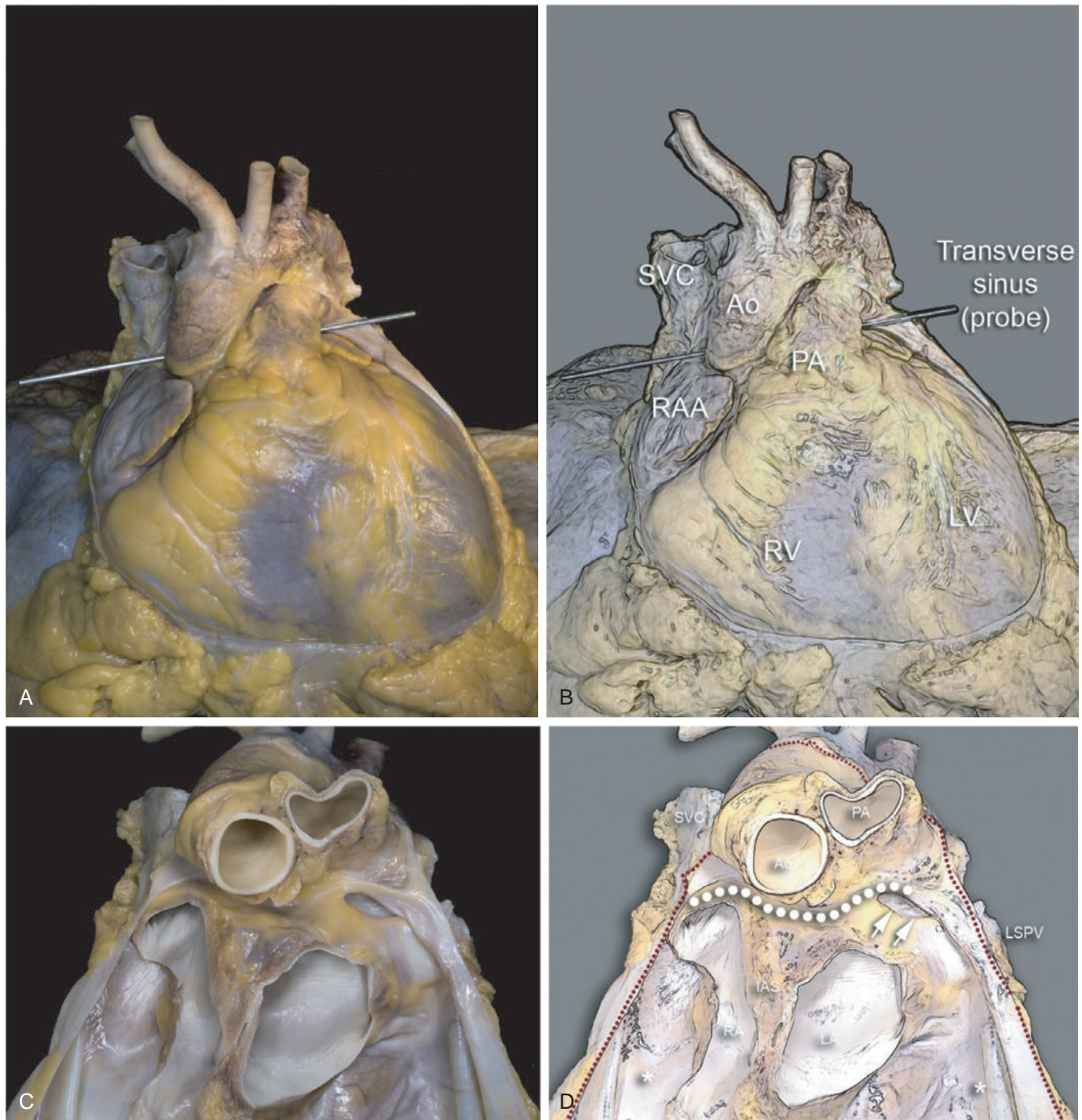
The pericardial cavity or sac is a continuous virtual space that lies between the parietal and visceral layers of serous pericardium. The heart invaginates the wall of the serous sac from above and behind, and practically obliterates its cavity, the space being merely a potential one. The sac normally contains 20 to 40 mL of clear fluid that occupies the virtual space between the two layers. Although pericardial reflections can become anatomical obstacles for catheter navigation, all those reflections are located basally in relation to the great vessels; thus most of the epicardial surface is freely accessible from the pericardial space, except for the atrial and ventricular septa (which are not in direct contact with the pericardium) and the atrioventricular (AV) grooves and interventricular sulci (which are separated from the visceral pericardium by epicardial fat). Unlike the endovascular approach, the pericardial space is notable for the absence of obstacles and the relative ease with which catheter manipulation can be performed. By the same token, achieving firm, stable contact with the catheter tip at the target site can be difficult.¹⁹

Technical Considerations

A thorough understanding of the clinical anatomy of the epicardial space and the reflections and recesses of the pericardium is necessary for the mapping procedure. In addition, contrast pericardiography, once the epicardial access is obtained, can help delineate the anatomy and assess for the presence of adhesions, which can limit catheter navigation.³⁸ Techniques of obtaining pericardial access are discussed in Chapter 4.



eFig. 27.2 Anatomy of Pericardial Sinuses and Recesses. Anterior view of the sinuses and recesses of the pericardium. Ventral aspect of the pericardium with the anterior portion of the pericardial sac and the heart removed to show the great vessels at the base of the heart. The aorta (Ao) and pulmonary artery (PA) have been transected to show the path of the transverse sinus (*dotted line*) that separates the arteries from the venae cavae and pulmonary veins (PVs). The pericardial reflection extends to the proximal aortic arch and the recess between the aorta and the superior vena cava (SVC) is called the superior aortic recess (*dotted line*). The left lateral extension of the transverse sinus is the left pulmonic recess bordered by the left PA and left superior PV. The oblique sinus is the cul-de-sac behind the left atrium and bound by the pericardial reflection over the inferior PVs and the inferior vena cava (IVC). Note the abundance of adipose tissue between the pericardium and diaphragm. LPA, Left pulmonary artery; LPV, left pulmonary veins; RPA, right pulmonary artery; RPV, right pulmonary veins. (From Rodriguez ER, Tan CD. Structure and anatomy of the human pericardium. *Prog Cardiovasc Dis.* 2017;59:327–340.)



eFig. 27.3 The Transverse Sinus of the Pericardium. (A) and (B) The transverse sinus is shown in this anterior view (probe). The transverse sinus is the pericardial space delimited by the superior vena cava (SVC) and anterior surfaces of the right atrium (RA) and left atrium (LA) dorsally. The ventral surface of the transverse sinus is formed by the posterior aspect of the ascending aorta and the inferior-posterior surface of the right and left pulmonary arteries before they emerge from the pericardial sac. (C) and (D) In this anterior view, most of the heart and the anterior portion of the pericardial sac have been removed. Only the dorsal segments of the RA, interatrial septum and LA remain. The red dots delineate the cut border of the pericardial sac. The asterisks below the atria mark the pericardial space. The white dots delineate the transverse sinus as it spans from right to left. The pericardial space bounded by the cephalad surface of the left superior pulmonary vein and inferior-posterior surface of the left pulmonary artery (PA) is designated the left pulmonary recess (double arrows). Ao, Aorta; IAS, interatrial septum; LSPV, left superior pulmonary vein; LV, left ventricle; RAA, right atrium appendage; RV, right ventricle. (From Rodriguez ER, Tan CD. Structure and anatomy of the human pericardium. *Prog Cardiovasc Dis*. 2017;59:327–340.)

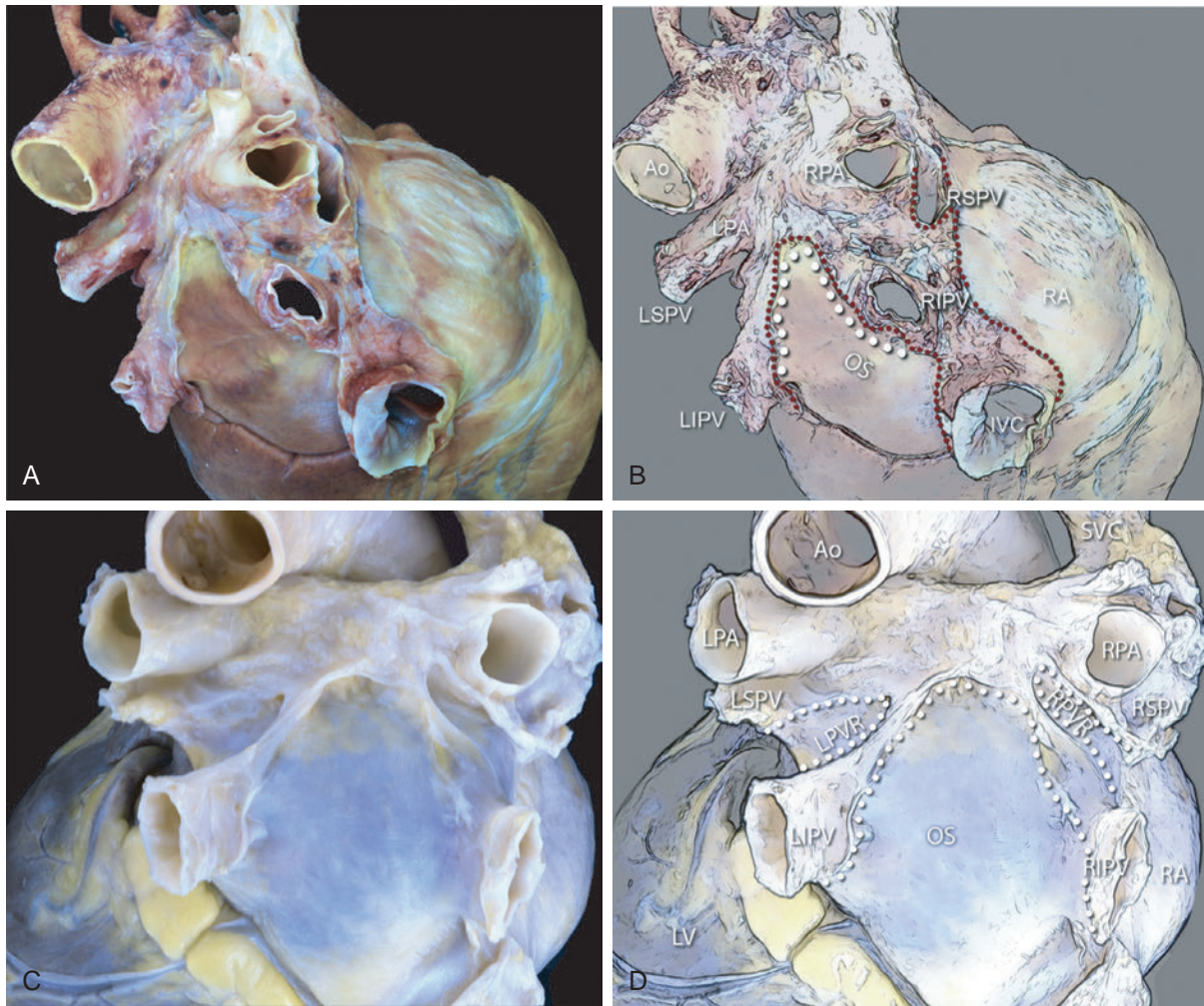


Fig. 27.2 The Oblique Sinus of the Pericardium. (A) and (B) The oblique sinus of the pericardium is the space flanked by the reflections of the pericardium below the inferior pulmonary veins (PVs). A and B show a slightly right cephalad-dorsal view of the left and right atria. The four PVs are shown as they drain into the left atrium (LA). The pericardial sac has been almost entirely removed. The cut border of the remaining pericardial sac is shown delineated by red dots. The white dots mark the contour of the oblique sinus. (C) and (D) A slightly left cephalad-dorsal view of the LA, PVs, and pulmonary arteries. The pericardial recesses above the inferior PVs on the right and the left sides of the LA, as well as the oblique sinus are delineated by the white dots. Ao, Aorta; IVC, inferior vena cava; LIPV, left inferior pulmonary vein; LPA, left pulmonary artery; LPVR, left pulmonary venous recess; LSPV, left superior pulmonary vein; LV, left ventricle; OS, oblique sinus; RA, right atrium; RIPV, right inferior pulmonary vein; RPA, right pulmonary artery; RSPV, right pulmonary venous recess; SVC, superior vena cava. (From Rodriguez ER, Tan CD. Structure and anatomy of the human pericardium. *Prog Cardiovasc Dis.* 2017;59:327–340.)

Once the introducer sheath and catheter are in place, the mapping catheter can be moved freely in the pericardial sac, constrained only by the reflections of the pericardial membrane located around the PVs and great vessels. Mapping of the atrial surface can be limited by the normal pericardial reflections and by the atrial irregular atrial anatomy (right and left atrial appendages). In the absence of pericardial adhesions, the epicardial surfaces of the RV and LV free walls are devoid of reflections, allowing unrestricted navigation of the mapping catheter.³⁹ The inferior and anterior approach taken during percutaneous epicardial access allows for easier access to the respective surfaces of the heart. Importantly, whereas the anterior aspects of the RVOT are easily accessible epicardially, the LVOT is bounded anteriorly by the RVOT and posteriorly by mitral valve and LA, prohibiting access via the percutaneous epicardial approach.^{35,40}

The use of a deflectable sheath can facilitate catheter navigation and improve contact with the epicardium. Careful catheter manipulation and sheath management are imperative to help avoid aspiration of air into the epicardial space and to avoid laceration of the epicardial vessels. When using stiff sheaths in the epicardial space, it is recommended to lead with a wire or ablation catheter before advancing or moving the curl of the sheath. Also, it is recommended not to leave a large sheath in the pericardial space without a catheter in place because the edges of the sheath can potentially lacerate epicardial vessels or the myocardium itself.^{41,42}

During manipulation of the sheath, small amounts of air can reach the pericardial space, which can be easily detected by fluoroscopy. The presence of air can induce instability to the catheter secondary to the lack of contact between the parietal and visceral membranes of the

pericardial sac. Aspiration of air will restore contact characteristic of the pericardial space.

Pericardial Adhesions

Percutaneous pericardial access can be obtained in more than 90% of patients who have not had prior cardiac surgery or clinical pericarditis, even in those who required repeated epicardial procedures. However, the presence of pericardial adhesions between the parietal and visceral serosal surfaces (e.g., following pericarditis, prior cardiac surgery, or previous epicardial instrumentation-induced pericarditis) can severely limit percutaneous access to the pericardium, and have been the primary reason of failure of epicardial instrumentation (Fig. 27.3). Whereas the pericardial adhesions in postpericarditis patients are often diffusely distributed, adhesions in postsurgical patients are mostly concentrated in the anterior portion of the heart (the area where the pericardial sac was opened during sternotomy). This allows subxiphoid epicardial access to the inferolateral LV (via posterior approach) in a large proportion of postsurgical patients.

Importantly, even when epicardial access is possible, the presence of pericardial adhesions can significantly limit catheter maneuverability within the pericardial space.⁴¹ Some reports described the feasibility of disruption of some adhesions with meticulous and gentle blunt dissection of the adhesions by advancing the curve of a deflected ablation and a steerable epicardial sheath. This technique can help increase the epicardial areas accessible for mapping and ablation. Flow of intrapericardial contrast dye on repeat injection helps assess effective disruption of the adhesions. Care must be taken to avoid cardiac perforation with the catheter tip in these cases. Furthermore, in patients with prior coronary bypass surgery, dense adhesions typically occupy the area of the coronary graft, hindering epicardial access to that region. In these patients, it is important to perform coronary native vessel and graft angiography to define anatomy and avoid graft disruption by catheter manipulation. It is also important to note that, in patients with coronary artery occlu-

sion, disruption of pericardial adhesions with blunt catheter dissection can potentially disrupt natural bypasses (collaterals) that form between the parietal pericardial vessels and the visceral myocardium.^{42–44}

However, in some patients, the presence of dense adhesions can produce compartmentalization of the pericardial space, which is resistant to blunt catheter dissection. In these cases, a hybrid procedure involving surgical access with a subxiphoid pericardial window or a limited anterior or lateral thoracotomy, and manual dissection and lysis of the adhesions can facilitate access to the epicardial region of interest. However, access to other areas may still be limited.⁴² However, this technique should be reserved for specific patients with recurrent VT refractory to endocardial ablation and antiarrhythmic medications, in whom a high degree of confidence exists as to the origin of the arrhythmia.^{43,44}

Epicardial Fat

Epicardial fat is the adipose tissue located between the visceral pericardium and the myocardium. Epicardial fat covers 80% of the heart surface, with a mean thickness of the fat layer of 5.3 ± 1.6 mm and variable distribution, being more abundant in the AV and interventricular grooves, and the RV lateral wall. There is a broad individual variation in the amount and distribution of epicardial fat. Epicardial fat seems to increase with age, obesity, diabetes, and female gender.^{19,45}

Epicardial fat is an important consideration as it presents two unique challenges for mapping and ablation of VT. First, interposed between the mapping catheter and myocardium, epicardial fat dampens recorded electrogram amplitude as well as the ventricular stimulation threshold, hindering activation and pace mapping techniques and making it difficult to differentiate fat from true scar. Second, interposed fat impairs the efficacy of RF ablation.¹⁹

Preprocedural CMR and CT imaging can accurately define epicardial fat thickness and distribution. Those images can be registered on the electroanatomic map and help the interpretation of mapping findings and anticipate the success of RF ablation.^{19,45}

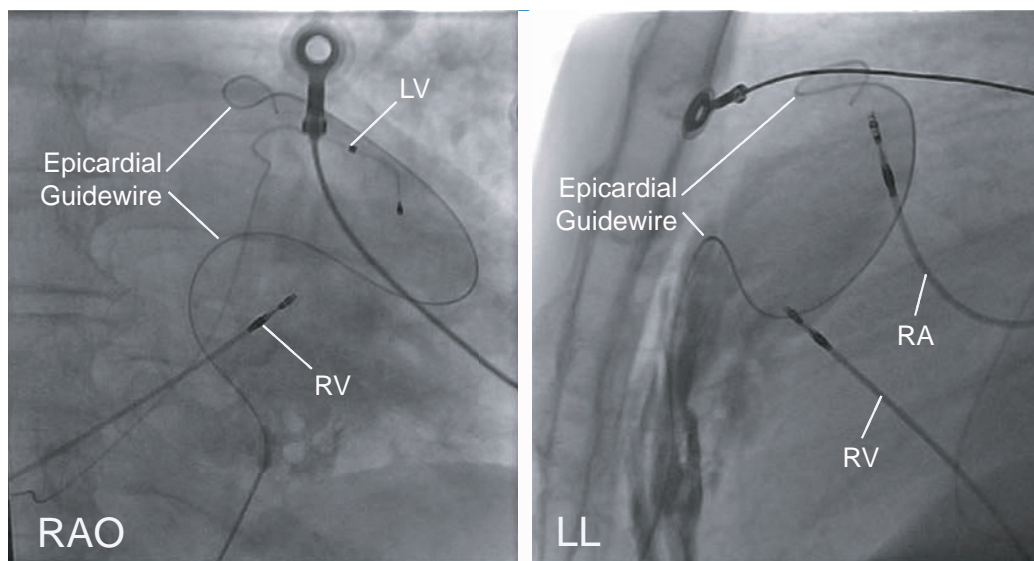


Fig. 27.3 Pericardial Adhesions. Pericardial access is performed (anterior approach) in a patient with biventricular pacemaker and prior episode of pericarditis. Right anterior oblique (RAO) and left lateral (LL) fluoroscopy views are shown during advancing the pericardial guidewire via the pericardial access needle. Note that the contrast dye injected initially via the pericardial access needle remained stagnant at the anterior aspect of the heart, and the guidewire coiled in the same region, due to compartmentalization of the pericardial space secondary to pericardial adhesions. Right atrial (RA), right ventricular (RV), and left ventricular (LV) pacemaker leads are visualized.

TRANSTHORACIC EPICARDIAL MAPPING

The approaches to epicardial mapping are essentially the same as for endocardial ablation, including activation mapping, entrainment mapping, substrate mapping, and pace mapping. Those techniques are discussed in detail in **Chapter 22**. The following discussion highlights certain peculiarities pertaining to the percutaneous epicardial approach to mapping.

Activation Mapping

In scar-related VTs, inability to identify the reentry circuit isthmus on the endocardium can suggest that the isthmus is epicardial or intramural. In these cases, endocardial activation mapping can demonstrate a focal point of earliest endocardial activation where entrainment mapping indicates a potential exit or outer loop site, but ablation fails to interrupt VT, suggesting that there is an epicardial or intramural circuit with a broad endocardial exit.

During focal VTs originating from the epicardium, a focal origin may be identifiable during endocardial mapping, typically at a point of earliest endocardial breakthrough. However, local activation timing at that location is not particularly early. Sometimes, electrical propagation from epicardial foci results in a diffuse, broad endocardial area ($>2 \text{ cm}^2$) being activated simultaneously (**eFig. 27.4**), with no single site showing favorable unipolar electrogram characteristics or paced mapping results. Other clues suggest the presence of an endocardial far-field electrogram preceding the sharp near-field electrogram in the

region of early activation (**Fig. 27.4**), and an inability to capture the far-field component of the earliest endocardial electrogram or replicate VT morphology on the surface ECG during pace mapping at the earliest endocardial activation site.²⁶

If an appropriate target site for VT ablation cannot be identified despite extensive endocardial and epicardial mapping, an epicardial or intramural VT circuit or focus should be suspected. Epicardial mapping of local activation timing and electrogram morphology employs principles similar to those of endocardial mapping. However, because of the presence of epicardial fat, low electrogram amplitude may not have the same implications as those during endocardial mapping (see below).

Entrainment and Pace Mapping

Entrainment and pace mapping maneuvers are usually difficult to perform using bipolar pacing because of a very high epicardial stimulation threshold ($>15 \text{ mA}$) in the majority (approximately 70%) of cases, and are likely related to the presence of epicardial fat and poor catheter contact due to freedom of catheter movement in the pericardial space. With unipolar pacing, the pacing threshold generally is less than 10 mA at 2 milliseconds in normal tissue. Epicardial fat of less than 5 mm in thickness interposed between the ablating catheter and the epicardium usually does not modify the epicardial ventricular stimulation threshold. Of note, ablation with irrigated RF generally increases the pacing threshold secondary, in part, to the introduction of irrigant fluid into the pericardial space, which can potentially result in decreased physical contact between the electrode and the epicardial surface.

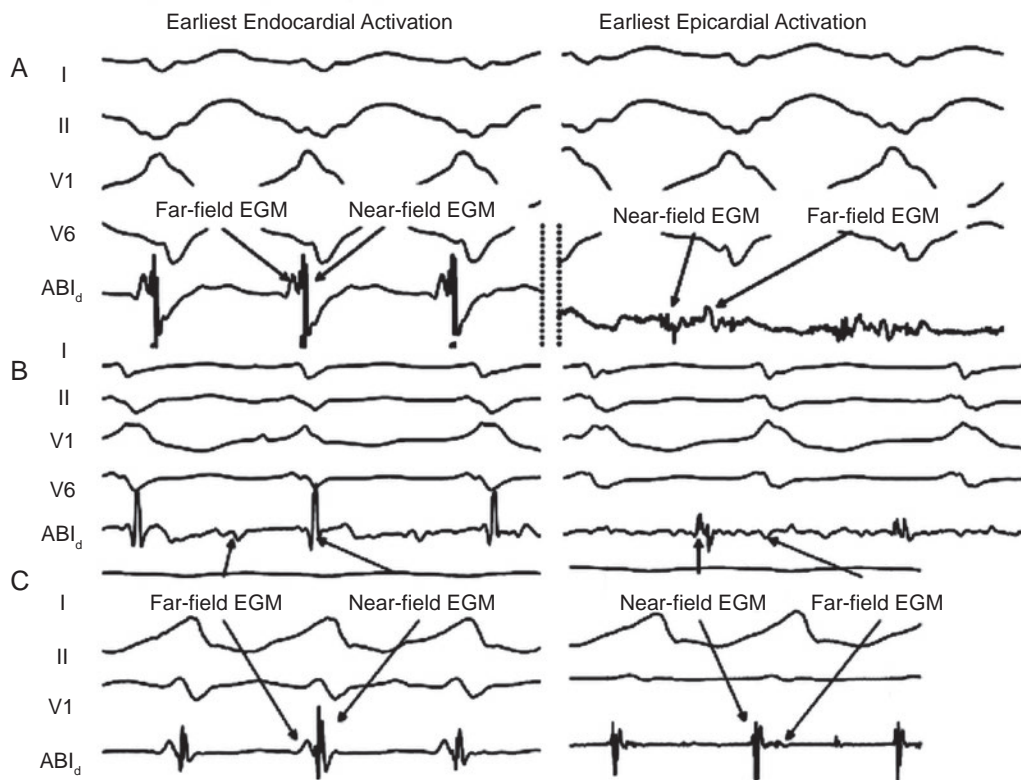
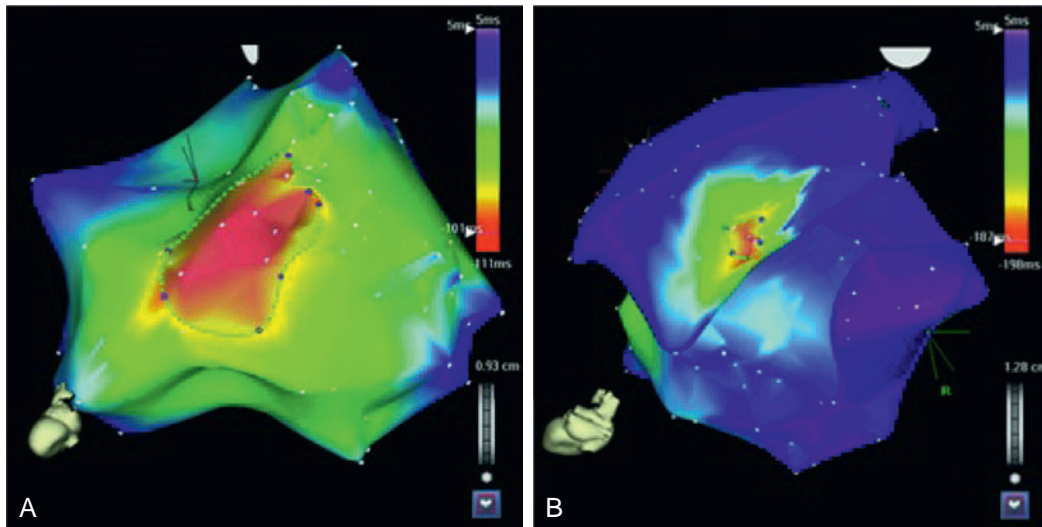


Fig. 27.4 Endocardial Versus Epicardial Activation Mapping. The panels depict representative electrograms (EGMs) from earliest endocardial activation (*left*) and earliest epicardial activation (*right*) during VT from three patients (A, B, and C) with nonischemic cardiomyopathy. A typical bipolar activation sequence pattern was observed reproducibly at the earliest endocardial site, with a far-field EGM preceding the near-field EGM. The sequence is reversed on the epicardium. ABL_d, Distal ablation. (From Tzou WS, Nguyen DT, Aleong RG, et al. Endocardial electrogram characteristics of epicardial ventricular arrhythmias. *J Cardiovasc Electrophysiol*. 2013;24:649–654.)



eFig. 27.4 Endocardial Versus Epicardial Electroanatomic Activation Mapping. A representative example of endocardial (A) and epicardial (B) electroanatomic activation maps is shown from a patient nonischemic cardiomyopathy. A significantly wider endocardial area of early activation is observed compared to epicardial activation. (From Tzou WS, Nguyen DT, Aleong RG, et al. Endocardial electrogram characteristics of epicardial ventricular arrhythmias. *J Cardiovasc Electrophysiol.* 2013;24:649–654.)

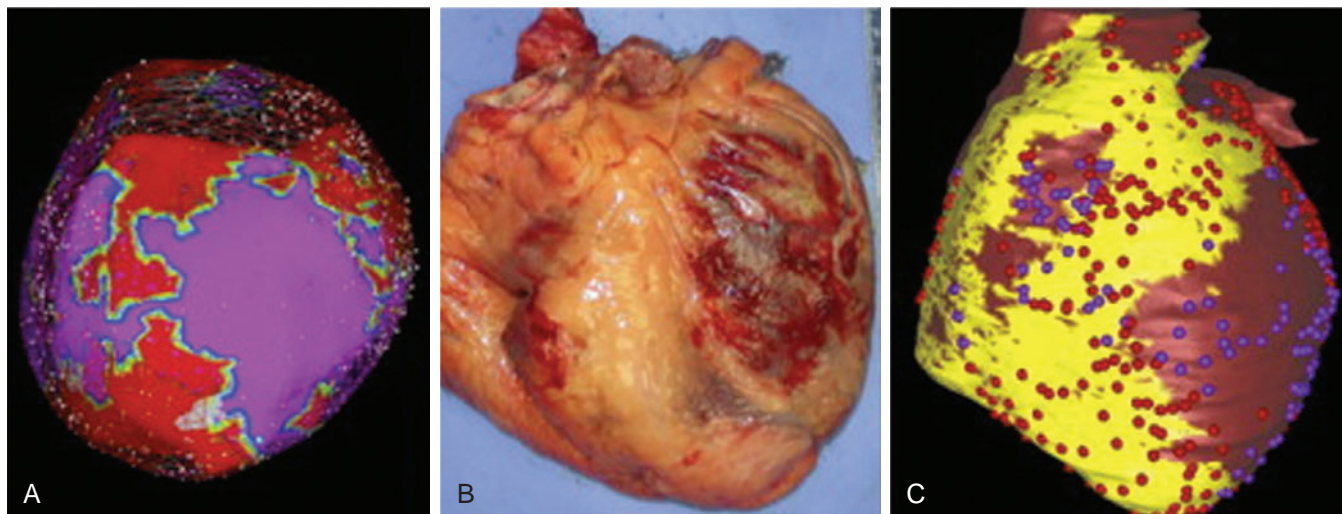


Fig. 27.5 Distribution of Epicardial Fat and Electroanatomic Mapping. (A) Epicardial voltage map of a patient with nonischemic cardiomyopathy. The voltage map shows surface reconstruction of the anterior surface of the heart. There is a low-voltage area (red) extending from the right ventricular outflow tract to the apex and following the lateral inferior margin to the base of the right ventricle. (B) Gross pathology of the same heart after cardiac transplantation illustrating that the area of low voltage on the left largely corresponds to an area of epicardial fat. (C) The extracted epicardial fat from the computed tomography data in this patient is shown in yellow. The remaining epicardial surface (dark red) is devoid of fat. The three-dimensional epicardial fat map was integrated with the voltage map. Low-voltage points are bright red and normal voltage points are purple. (From Desjardins B, Morady F, Bogun F. Effect of epicardial fat on electroanatomical mapping and epicardial catheter ablation. *J Am Coll Cardiol.* 2010;56:1320–1327.)

Electroanatomic Substrate Mapping

Substrate VT mapping approaches are similar to those described for the endocardium. Areas of infarction or scar have low-amplitude electrograms similar to findings during endocardial mapping. However, epicardial fat, which is concentrated along the coronary sulcus and the interventricular grooves, can cause low-amplitude electrograms, falsely suggesting scar in voltage maps. Normal epicardial electrograms demonstrate bipolar signal amplitude typically above 0.94 to 1.5 mV, whereas signal amplitude associated with fat or large vessel coronary anatomy might demonstrate significantly lower amplitude.

As noted, epicardial fat of less than 5 mm in thickness interposed between the ablating catheter and the epicardium usually does not modify the amplitude or duration of the bipolar epicardial electrogram. However, in areas with a layer of epicardial fat greater than 5 mm in thickness, the amplitude of the recorded bipolar epicardial electrogram can decrease, which may confound the ability to discriminate between fat and scar. Importantly, despite the lower electrogram amplitude, epicardial fat will not produce “abnormal” (fractionated and split) electrograms. Therefore to avoid a misclassification of low-voltage areas due to epicardial fat or major coronary vasculature as abnormal, it is important to analyze the location and extent of the confluent voltage abnormality as well as the electrogram morphology characteristics. The presence of abnormal electrograms (fractionated, split, or late potentials) is usually a more reliable indicator of scarring. Thus during epicardial bipolar voltage mapping, an amplitude cutoff of 1.0 mV combined with an abnormal electrogram morphology is used to identify the low voltage zone.

The registration of preacquired CT or CMR images detailing the LV substrate with the real-time 3-D electroanatomic voltage map allows the visualization of regions of scar tissue and can potentially facilitate mapping and ablation (see Fig. 27.1). CMR and CT imaging also can

be used to characterize the extent of fat tissue by extracting and integrating epicardial fat information into the electroanatomic voltage maps, thereby helping to distinguish epicardial fat from scar tissue and to identify areas that are difficult to penetrate because of extensive epicardial fat (Fig. 27.5).

Endocardial unipolar voltage mapping can be beneficial to indicate the presence of intramural or epicardial scar (Fig. 27.6). While endocardial bipolar mapping is capable of assessing local electrograms originating from tissue adjacent to the recording electrodes (i.e., sub-endocardium), the broader field of view of unipolar mapping enables the recording of deeper tissue layers and the identification of nonendocardial scar located intramurally or epicardially. A reduction in endocardial unipolar electrogram amplitude (<8.3 mV in the LV and <5.5 mV in the RV), even in the absence of endocardial bipolar voltage abnormalities, has been shown to identify the presence of epicardial scar.¹

TRANSTHORACIC EPICARDIAL ABLATION

Radiofrequency Ablation

The ablation target is selected exactly the same way as the endocardial target. RF energy remains the primary ablative energy source for epicardial ablation. During standard RF energy application in the pericardial space, heating to the point of thrombus formation and charring is of less concern, because there is no potential for arterial embolization from the epicardial space; therefore higher temperatures ($>60^{\circ}\text{C}$) can be tolerated. However, standard RF ablation may not be as effective when delivered to the epicardium compared with lesions delivered to the endocardium. The lack of convective cooling of the ablation electrode in the epicardium (as opposed to convective cooling provided by the circulating blood during endocardial RF ablation) results in high electrode temperatures at low-power settings (≤ 10 W), limiting power delivery in the pericardial space and impairing lesion formation. In

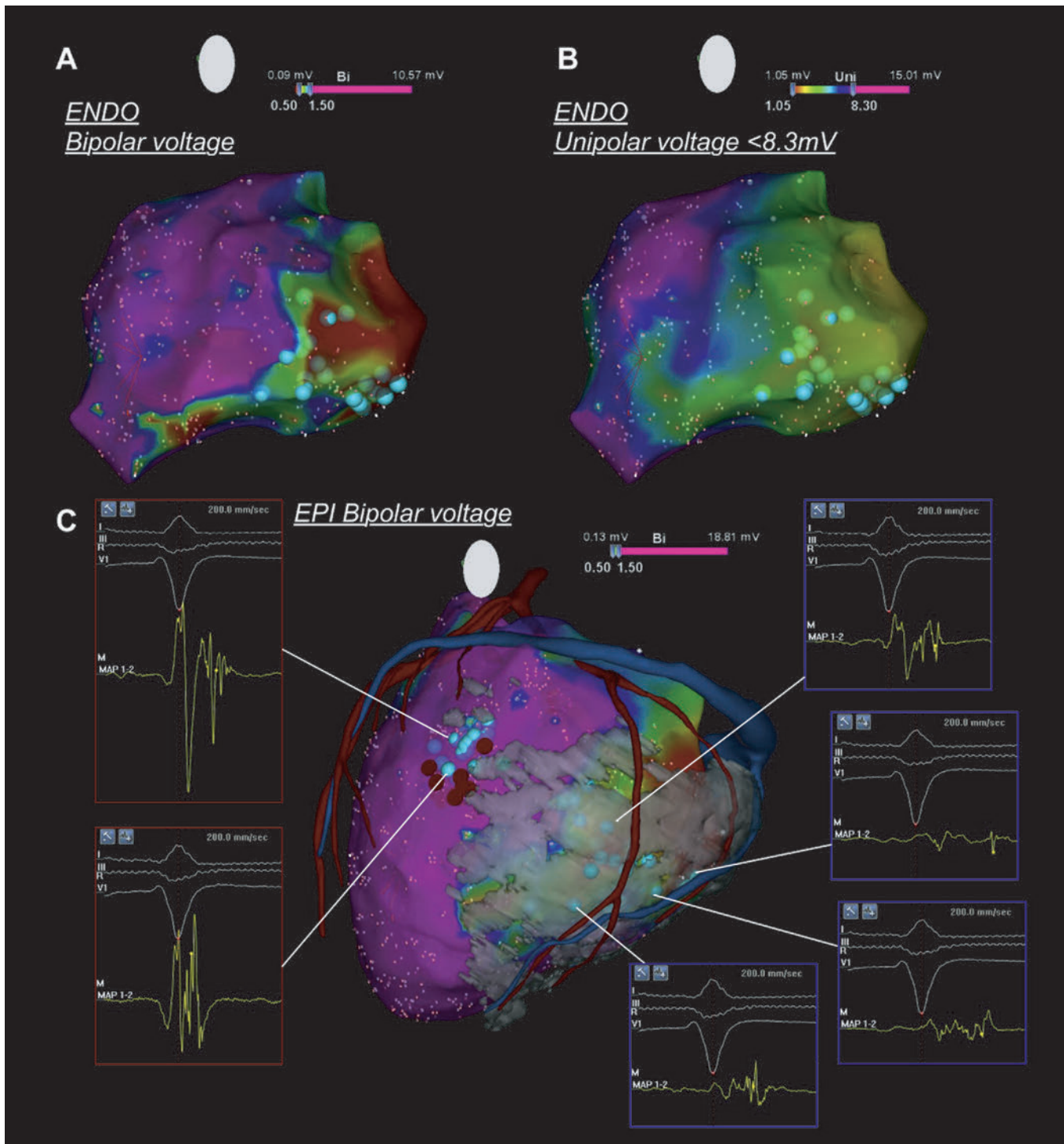


Fig. 27.6 Endocardial (ENDO) and Epicardial (EPI) Voltage Map With Wall Thinning Segmentation in Patient With Ischemic Cardiomyopathy. (A) Endocardial bipolar voltage map shows low voltage with the presence of local abnormal ventricular activity (LAVA, light blue dots) at the basal posterolateral left ventricle. A peak-to-peak bipolar amplitude less than 1.5 mV is defined as low voltage, and less than 0.5 mV is defined as dense scar. (B) Endocardial unipolar voltage map is shown. A unipolar amplitude of less than 8.3 mV is defined as abnormal voltage. (C) Epicardial bipolar voltage map merged with the multidetector computed tomography model shows the location of low-voltage area and LAVA corresponding to the wall thinning segmentation (white area). Endocardial ablation successfully eliminated the posterolateral LAVA (in blue box), which had the following characteristics: low bipolar amplitude; location within the wall thinning segmentation; opposite endocardial low unipolar voltage; and presence of LAVA at the opposite endocardium. On the contrary, epicardial LAVA located mid-anteriorly (in red box) could not be eliminated by endocardial ablation and needed to be ablated epicardially. They were of higher bipolar voltage (>1.5 mV), located outside the wall thinning segmentation, and opposite endocardium with higher unipolar amplitude. (From Komatsu Y, Daly M, Sacher F, et al. Endocardial ablation to eliminate epicardial arrhythmia substrate in scar-related ventricular tachycardia. *J Am Coll Cardiol*. 2014;63:1416–1426.)

addition, the presence of epicardial fat (≥ 3.5 to 10 mm in thickness) between the ablation catheter and the targeted area can also represent an important obstacle to the effectiveness of ablation.⁴⁰

On the other hand, open and closed loop irrigated catheters allow the delivery of energy at power settings capable of creating larger and deeper (up to 5 mm) epicardial lesions than standard RF ablation, even in the absence of circulating blood in the pericardial space. Nonetheless, the presence of epicardial fat interposed between the catheter tip and the myocardial tissue only moderately attenuates the efficacy of cooled-tip ablation.

Optimal parameters for RF power titration and irrigation are not completely defined. With external irrigation, it is desirable to use lower flow rates than those used during endocardial mapping and ablation, to control fluid accumulation in the pericardial space. Commonly, the flow rate is set at 0 to 1 mL/min during mapping and at 10 to 17 mL/min during ablation, and is titrated as required to maintain the electrode temperature at less than 50°C. RF energy is commonly delivered at a power output of 30 to 50 W for 60 to 120 seconds. Monitoring for an impedance fall is commonly used to assess adequacy of power delivery.⁴¹

With open irrigation, an obligatory fluid volume will enter the pericardial sac and, unless intermittently or continuously evacuated, it gradually results in cardiac tamponade (as well as allowing the catheter to “float” in the fluid as opposed to maintaining contact with target epicardial tissue). Therefore intrapericardial fluid must be periodically drained after every few RF applications or every 15 to 20 minutes. This can be accomplished by intermittently removing the ablation catheter to allow aspiration from the pericardial sheath or placing a second pericardial catheter for drainage purposes. Alternatively, using a single sheath that is larger than the ablation catheter allows aspiration of fluid around the catheter from the side port, either intermittently or continuously (via attaching the side port to a suction bottle or gravity drain) without withdrawing the ablation catheter. Internally cooled RF ablation is an attractive choice for pericardial ablation as no fluid is infused and one need not worry about monitoring pericardial fluid throughout the ablation procedure.¹

At the completion of the mapping-ablation procedure, the ablation catheter is replaced by a pigtail catheter, which is gently aspirated to remove excess intrapericardial fluid, and to confirm the absence of bleeding. Evaluation of the pericardial space can be performed by intracardiac or transthoracic echocardiography, and by injecting 2 to 3 mL of contrast under fluoroscopy, to confirm complete drainage before removing the sheath. Methylprednisolone at 0.5 to 1.0 mg can be injected into the pericardial space prior to removal of the pigtail catheter to decrease the likelihood of postprocedure pericarditis. Generally, no major reaccumulation of pericardial fluid is observed following postprocedure draining of the pericardial fluid. The pigtail catheter and ablation sheath may be removed at the end of the procedure if there is no residual pericardial fluid, or kept inside the pericardial sac for as long as it is considered necessary. After controlling the bleeding, monitoring the patient with serial transthoracic echocardiography over the following 24 hours is recommended. Antibiotic therapy is administered postprocedure and as long as a drain is left in the pericardial space.

Cryoablation

Cryoablation has two potential advantages over RF ablation in the pericardial space: (1) the absence of cooling blood flow in the pericardial space enhances the formation of the cryolesion; and (2) cryoablation is less prone to cause coronary artery injury in experimental studies. However, human experience is limited, and more studies are needed to assess safety and efficacy. Cryoablation did not produce significantly larger lesions than irrigated RF in an animal model. Cryoablation is

commonly used in the operating room. Surgical cryoablation with hand-held surgical probes achieves much lower temperatures (less than -150°C) and generates larger lesions than small EP catheters.⁴⁰

Complications of Transthoracic Epicardial Ablation

Acute complications related to the epicardial approach have been reported in about 9% of cases at experienced centers, and can be related to the pericardial access procedure or to catheter manipulation or ablation within the pericardial space.^{21,46,47}

Pericardial Bleeding

Bleeding into the pericardial space is the most common complication, with pericardial bleeding of more than 80 mL observed in up to 7%, although cardiac tamponade and severe bleeding are infrequent.^{21,46,47}

Pericardial bleeding related to the epicardial access procedure is most commonly related to RV puncture. The coronary arteries are covered by epicardial fat along the AV groove and the interventricular septum, located away from the typical path of the access needle and, therefore, are less vulnerable to injury. Occasionally, disruption of epicardial fat can result in limited bleeding. Pericardial bleeding also can develop later during the mapping and ablation procedure. Laceration of the myocardium or epicardial vessels can occur during manipulation of the pericardial sheath or catheter, or as a result of RF ablation.

Several precautions are important to reduce the risk of pericardial bleeding. The epicardial access is the most important part of the procedure, and it is critical to employ extreme caution to avoid RV puncture and to promptly recognize such a complication before introducing the pericardial sheath.⁴¹ The use of the “needle-in-needle” technique can help reduce the risk of significant bleeding in the setting of inadvertent RV puncture.^{48,49} When the curved-tip Tuohy needle is used, directing the needle bevel away from the myocardium can help minimize the risk of cardiac perforation.³⁹ In addition, systemic anticoagulation is generally deferred (or reversed) at the time of epicardial access, and may be restarted only after verifying the absence of continued pericardial bleeding. Furthermore, careful catheter manipulation leading with a wire or ablation catheter before maneuvering the curl of the pericardial sheath can help reduce the risk of damage to the myocardium and epicardial vessels.^{41,49,50}

Approximately 10% to 20% of patients experience pericardial bleeding, particularly if inadvertent RV puncture has occurred. RV puncture is usually benign if only the needle or guidewire has entered the chamber in a patient who is not anticoagulated. The amount of blood drained from the pericardial space usually ranges from 20 to 300 mL. Thus, most of the time, the occurrence of hemopericardium does not preclude the continuation of the procedure, although repeated aspiration of the pericardial space may be required throughout the procedure.³⁹ However, major pericardial bleeding remains the most common complication (4.5%), occasionally requiring surgical intervention. Therefore precautions must be in place for managing severe bleeding, including the availability of appropriate surgical expertise.³⁹

When intrapericardial bleeding continues at the end of the epicardial procedure, a pericardial drain is left in place to allow for prompt management of effusion. The drain may be removed once the absence of reaccumulating effusion is verified on echocardiographic examinations over a 24-hour period.⁴¹ Importantly, late (within 1 to 2 days) pericardial effusions and cardiac tamponade requiring pericardiocentesis can develop in up to 5% of patients after removal of the pericardial sheath. Therefore leaving a pericardial drain in place for several hours also may be considered even in patients with no evidence of pericardial effusion or intrapericardial bleeding at the end of the procedure. However, such a practice should be balanced against the risk of pericarditis, infection, and patient discomfort associated with a persistent drain.⁵¹

Coronary Artery Injury

Coronary artery injury (laceration, intimal hyperplasia, intravascular thrombus formation, or vasospasm) can occur during epicardial mapping and RF ablation. The anterior and posterior septal and basal ventricular areas, where coronary arteries and veins are known to traverse, are the more dangerous zones. Coronary artery spasm has been reported during mapping in the pericardial space and can be induced by RF energy delivery close to the artery. Extrinsic compression of a coronary artery can also result from edema caused by nearby ablation.

Laceration of a coronary vessel manifests as intrapericardial bleeding. Acute occlusion of a coronary artery (by spasm or thrombosis) can manifest as chest discomfort (in nonanesthetized patients) or acute ST-T segment changes on the surface ECG.³⁷ Importantly, delayed (chronic) coronary damage may develop in the absence of detectable acute injury, and should be suspected in patients presenting with new ischemic symptoms following a prior epicardial ablation procedure.⁴¹

Prior to the delivery of RF energy, direct visualization of the relation between the ablation site and adjacent coronary arteries must be obtained, usually by coronary angiography performed with the ablation catheter at the target site. An absolute safe distance between the ablation site and epicardial artery has not been defined, and likely varies depending on the RF energy applied; the coronary artery diameter and flow; and the presence of overlying fat. Larger vessels are less susceptible to RF-induced injury due to the enhanced cooling effect of the greater blood flow. Based on available data and experience, a distance of at least 5 mm between the coronary artery and the ablating electrode (at any point of the cardiac cycle during coronary angiography and in at least two projections) is commonly accepted. Registering preprocedural CMR or CT images of the epicardial coronary arteries or contrast coronary angiographic images acquired during the procedure on the electroanatomic map can help anticipate the risk of coronary injury during the procedure. Close monitoring of the ST-T segment on the surface ECG is important for early detection of acute coronary spasm or occlusion.^{37,39}

Cryoablation appears to have less risk of coronary injury in animal models, but can still create occlusion and intimal damage when in close proximity, particularly to small vessels. Further confirmatory studies are warranted.

Phrenic Nerve Injury

The left phrenic nerve is susceptible to injury along its epicardial course adjacent to the lateral LV wall. The left phrenic nerve descends behind the left brachiocephalic vein and passes over the aortic arch, pulmonary trunk, and then with the pericardium over the LA appendage. From there it descends either anteriorly or anterolaterally along the fibrous pericardium over the LV to insert into the diaphragm behind the cardiac apex (eFig. 27.5). The left phrenic nerve frequently passes laterally over the obtuse margin of the LV (between the fibrous pericardium and the mediastinal pleural layers), close to the lateral vein and the left marginal artery and, in only a small percentage of cases, close to the left main coronary artery and great cardiac vein.^{37,39}

Often, the phrenic nerve courses through sites that might be considered appropriate ablation target sites, potentially limiting the safety and efficacy of ablation. Proximity to the phrenic nerve can be detected by high-output pacing (20 mA, pulse width of 2 milliseconds) to detect diaphragmatic stimulation on fluoroscopy, allowing its course to be marked on a 3-D map. The phrenic nerve can branch over the LV; thus simply noting sites at which phrenic capture occurred does not necessarily delineate the course of all branches. Further, the pacing output that would indicate a safe distance for epicardial ablation is not known. Also, it is important to recognize that detection by phrenic nerve capture

is prevented by the use of paralytic agents during general anesthesia. However, these drugs are typically used during the induction of anesthesia, and their effects have dissipated by the time ablation is being performed.⁴¹

Catheter ablation should be avoided at sites adjacent to the phrenic nerve. Alternatively, interposing a balloon, saline, or air in the pericardium between the ablation catheter and the phrenic nerve can allow safe RF ablation (see Chapter 32 for detailed discussion). Mechanical separation of the phrenic nerve from adjacent structures, using a large balloon, involves insertion of a wire through one of the existing pericardial sheaths to the vicinity of the ablation catheter positioned at the target epicardial site. Another method is to introduce a combination of saline and air into the pericardium to achieve a “controlled” hydro-pneumopericardium to increase the distance between the phrenic nerve and the ablation target area. The lack of phrenic nerve capture still should be confirmed to ensure sufficient separation, and monitoring of diaphragmatic movement on fluoroscopy during RF energy application remains important, even when no phrenic nerve capture is observed during pacing. Alternative energy sources, such as cryoenergy, have been used to prevent phrenic nerve injury. Cryomapping uses reversible phrenic nerve injury to determine when to avoid full cryoablation. However, data on the success of cryoablation in the pericardial space are limited.^{39,41}

Pericarditis

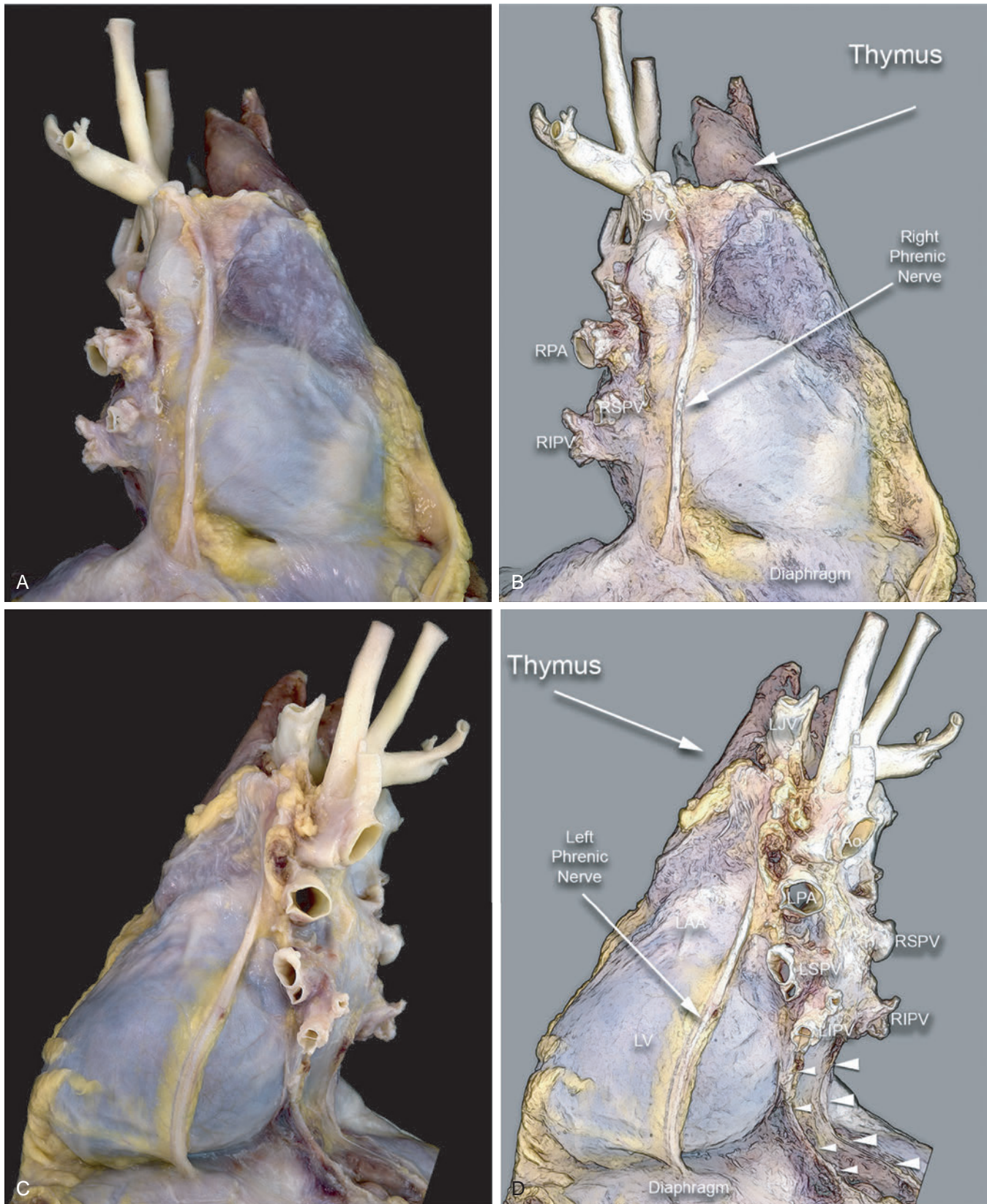
Pericarditis is the most common complication of epicardial ablation, occurring in the majority of the patients, and typically manifesting as precordial discomfort and friction rub. Postprocedural pericarditis often is mild and self-limiting, and resolves within a few days with oral nonsteroidal antiinflammatory agents. The degree of severity of pericardial inflammation appears to be related to procedural duration and the extent of epicardial RF ablation, as well as individual susceptibility to develop postprocedure pericarditis. Colchicine and oral steroids may be considered for the treatment of refractory cases. Of note, pericarditis can develop even when no epicardial ablation has been performed (i.e., only pericardial access and epicardial mapping).

It is important to note that inflammatory pericarditis can render the epicardial space percutaneously inaccessible for repeat procedures because of the development of adhesions. Several measures have been suggested to help reduce the severity of pericardial inflammation: (1) injection of steroids (e.g., 0.5 to 1.0 mg/kg of methylprednisolone or 2.0 mg/kg of triamcinolone) into the pericardial space at the conclusion of the procedure has been shown in animal models to be effective in reducing postprocedural pericarditis and adhesion formation; (2) postprocedural use of colchicine has been shown in small series to reduce postsurgical pericardial inflammation; (3) the administration of antibiotic therapy as long as the pericardial drain is in place; and (4) the removal of all pericardial sheaths and drains at the end of the procedure, except in cases of continued bleeding.^{39,41,52}

Intraabdominal Bleeding

Hemoperitoneum is a rare complication of epicardial ablation (<1%), and usually results from injury to the subdiaphragmatic vessels (e.g., epigastric artery) or abdominal viscera (liver and colon). The risk is higher when the angle of the needle is too steep (during the posterior approach to pericardial access), when the subxiphoid entry site is too caudal, and in the presence of hepatomegaly, gastric or colon distension, or left diaphragmatic paralysis.^{39,41,52}

Recognition of this complication can be difficult and requires a high index of suspicion. Abdominal pain (in nonanesthetized patients), rebound tenderness, progressive hypotension in the absence of a pericardial effusion, and unexplained decrease in hemoglobin should prompt



eFig. 27.5 Anatomical Course of the Right and Left Phrenic Nerves. (A) and (B) A right lateral view showing the right phrenic nerve just anterior to the superior vena cava (SVC). It follows an almost vertical path on the right border of the heart until it reaches the diaphragm. (C) and (D) A left lateral view of the heart and pericardium showing the left phrenic nerve emerging just behind the adipose tissue in front of the left pulmonary artery. It follows a roughly vertical direction and moves slightly anteriorly as it courses over the contour of the “obtuse margin” of the left lateral ventricular wall, and it moves slightly posterior as it reaches the diaphragm. The arrowheads delineate the pericardiovertebral ligaments in the posterior aspect of the pericardium. Ao, Aorta; LIPV, left inferior pulmonary vein; LJV, left jugular vein; LPA, left pulmonary artery; LSPV, left superior pulmonary vein; LV, left ventricle; RIPV, right inferior pulmonary vein; RPA, right pulmonary artery; RSPV, right superior pulmonary vein. (From Rodriguez ER, Tan CD. Structure and anatomy of the human pericardium. *Prog Cardiovasc Dis*. 2017;59:327–340.)

evaluation with abdominal ultrasound or (in hemodynamically stable patients) CT imaging.

Adequate palpation of the xiphoid process, manual pressure over the epigastrium to push away the liver from the path of the needle—using a shallow needle angle and avoiding sideways movements of the needle—can help prevent injury to subdiaphragmatic structures. Also, avoiding general anesthesia at the time of epicardial access can help early recognition of this complication as it can manifest as abdominal pain.^{39,41,52}

Pneumopericardium

Air can be introduced into the pericardial space during the exchange of sheaths and catheters. Although pericardial air can rarely cause cardiac tamponade, it can increase the transthoracic defibrillator threshold, which can be highly detrimental given the frequent need for electrical cardioversion of ventricular arrhythmias during those procedures. Air in the pericardial space tends to stay around the cardiac apex (which is located most anteriorly in the supine position) and is easily detected on fluoroscopy. Once detected, pericardial air should be evacuated, especially before the induction of ventricular arrhythmias that may require electrical cardioversion.³⁹ Careful sheath management is important to prevent air aspiration.⁴¹

Pleuritis

Symptomatic pleuritis (dyspnea, chest pain, and a pleural friction rub) is uncommon (1.5% in one case series), and usually responds well to antiinflammatory agents.^{39,41}

Outcome

Percutaneous access to the pericardial space has improved the outcome of catheter ablation in patients with scar-related VT. Percutaneous pericardial access can be obtained in more than 90% of patients who have not had prior cardiac surgery or clinical pericarditis, even in those who required repeated epicardial procedures. However, pericardial adhesions after cardiac surgery often prevent percutaneous access, although limited access is possible in some patients. A direct surgical approach to the pericardial space via a subxiphoid pericardial window or thoracotomy can achieve access in most patients.

In several reports, arrhythmia control with epicardial ablation was achieved in 63% to 78% of patients. The acute outcome is highly dependent on the target area. Epicardial ablation has a low yield (10%) in idiopathic VTs. Success rates are highest for VTs originating in the RV in patients with ARVC.^{46,47} However, it is important to note that these findings reflect practices at centers that specialize in arrhythmia management and may not be applicable to less experienced operators or centers. Careful patient selection is important, and the procedure should be performed by experienced operators with surgical backup.

The main reason for procedural failure is the inability to access or adequately map the epicardium, which is usually because of the presence of pericardial adhesions in patients with prior cardiac surgery or previous pericarditis. Even after successful epicardial access, RF ablation can be limited by close proximity to a coronary artery or the left phrenic nerve. In addition, failure to identify an epicardial target, or the presence of a thick layer of pericardial fat precluding adequate RF lesion formation, account for a significant proportion of procedural failures.

TRANSVENOUS EPICARDIAL MAPPING AND ABLATION

Coronary veins provide endovascular access to certain epicardial regions of the ventricles, and have been used for mapping and ablation of

arrhythmia foci or circuits that are deep within the myocardium or in the epicardium without having to access the epicardium percutaneously. Access through the great cardiac and anterior interventricular veins allows mapping over a wide area of the anterolateral LV wall, whereas access through the middle cardiac vein allows mapping over the inferior wall of the ventricles and posterior aspect of the interventricular septum. Up to 14% of patients with idiopathic VT or premature ventricular complexes (PVCs) have an epicardial site of origin identified within the coronary venous system, most often in the great cardiac vein.

Anatomical Considerations

Cardiac Venous System

The myocardium drains mainly by three groups of veins: (1) the CS and its tributaries, which return blood from almost the whole heart; (2) the anterior cardiac veins, which primarily drain the anterior regions of the RV and the right cardiac border, ending principally in the RA; and (3) the Thebesian venous network (*venae cordis minimae*), which is the smaller cardiac venous system and is composed of small venous branches made primarily of endothelial cells that are continuous with the lining of the cardiac chambers. The Thebesian veins drain the sub-endocardium and open directly into any of the four chambers but are more prominent on the right and, to a lesser extent, the LA and sometimes the LV.⁵³

Normally, the CS has five first-order tributaries: the great cardiac vein, the middle cardiac vein, the small cardiac vein, the posterior cardiac vein of the LV, and the oblique vein of the LA (oblique vein of Marshall) (Fig. 27.7). These tributaries then branch into second- and third-order tributaries. The CS returns the blood to the RA from the whole heart (including its septa) except the anterior region of the RV and small, variable parts of both atria and the LV.³⁵

The CS is a short trunk that begins as a continuation of the great cardiac vein, extending from the valve of Vieussens (which often marks the junction of the CS with the great cardiac vein) to the ostium of the CS as it terminates in the RA. The length of the CS varies from 15 to 55 mm and its diameter varies from 6 to 16 mm in its middle portion (depending on the loading conditions and the presence of underlying cardiac disease or prior cardiac surgery).⁵⁴

The CS invariably lies in the posterior aspect of the AV groove in the sulcus between the LA and LV and opens into the RA. The coronary sinus ostium (CS os) is 5 to 15 mm in diameter and is located on the posterior interatrial septum anterior to the eustachian ridge and valve and posterior to the tricuspid annulus. The CS os is guarded by the highly variable, crescent-shaped Thebesian valve, which can be grossly identified in approximately two-thirds of hearts. When present, the valve is located on the posterior aspect of the CS os and extends to the superior aspect in about half the cases. The orientation of the Thebesian valve favors cannulation of the CS from an anterior (ventricular) and inferior approach. Occasionally, the Thebesian valve nearly completely cover the CS os, with formation of fenestrations, and can hinder cannulation of the CS.^{54,55}

The anterior interventricular vein is the largest and most consistent of the cardiac veins. It drains a significant portion of the LV anterior wall and the interventricular septum, begins at the cardiac apex, and ascends toward the base of the heart in the anterior interventricular sulcus, parallel to the left anterior descending coronary artery. The phrenic nerve may lie close to the lateral branches of this vein. The anterior interventricular vein is the most anterior vein seen in the right anterior oblique (RAO) projection. At the base of the heart, near the bifurcation of the left coronary artery, the anterior interventricular vein turns laterally and becomes the “great cardiac vein,” which courses along the left AV groove (parallel to the left circumflex coronary artery) and wraps around the left side of the heart.⁵⁴

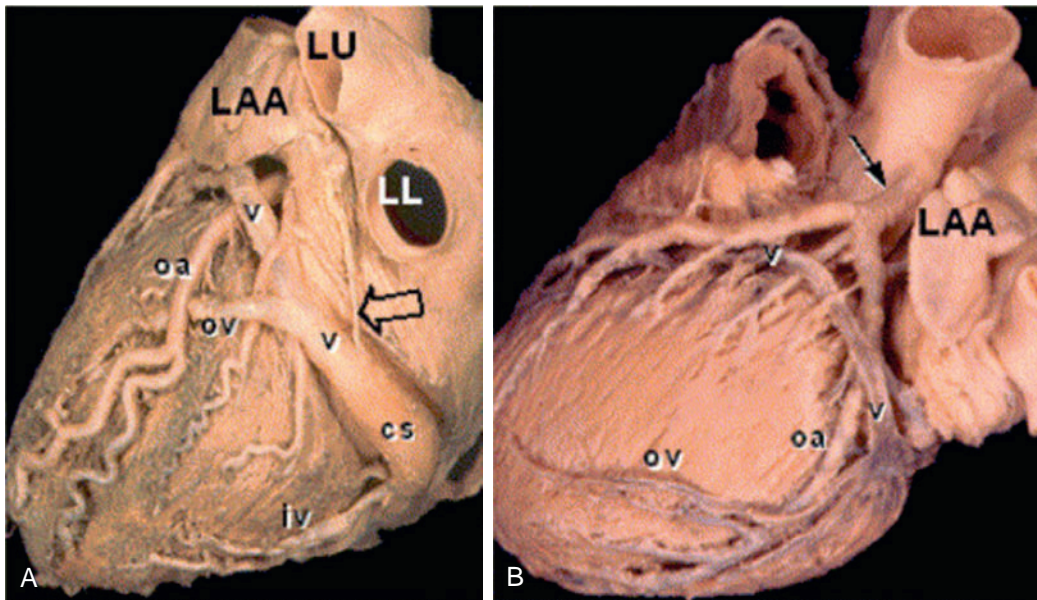


Fig. 27.7 Anatomy of the Coronary Venous System. (A) Posterior view of the heart showing the coronary sinus (CS) and its major venous tributaries. Note the cross-overs between veins and arteries. The obtuse marginal artery (oa) passes underneath the great cardiac vein (v) and then over the left obtuse marginal vein (ov). An inferior left ventricular vein (iv) ascends to enter the CS. Note the course of the ligament of Marshall (arrow) passing between the left atrial appendage (LAA) and the left upper and lower pulmonary veins (LU and LL). (B) Left lateral view of the heart showing the obtuse margin demonstrates the course of the v relative to the main branches of the left coronary artery. The arrow indicates the main stem of the left coronary artery. The oa passes underneath the v and is then crossed superficially by the ov. (From Ho SY, Sánchez-Quintana D, Becker AE. A review of the coronary venous system: a road less travelled. *Heart Rhythm*. 2004;1: 107–112.)

The great cardiac vein is joined by the LA oblique vein of Marshall and the posterolateral vein of the LV to form the CS (see Fig. 27.7). In addition to several smaller tributaries from the LA and ventricles, the great cardiac vein receives two main branches; namely, the large left marginal vein (along the lateral border of the heart), and the posterior cardiac vein of the LV (also known as the posterolateral vein).

The middle (or “posterior interventricular”) cardiac vein is the largest proximal tributary of the CS and is present in nearly all hearts. This vein drains the inferior walls of both ventricles and interventricular septum and courses with the posterior descending coronary artery in the posterior interventricular groove, joining the CS close to the RA orifice or, rarely, entering the RA directly.

The small cardiac vein receives blood from the back of the RA and RV, runs in the coronary sulcus between the RA and RV parallel to the right coronary artery, and empties into either the CS, the middle cardiac vein, or the RA.

Of all the branches of the coronary venous system, the anterior interventricular and middle cardiac veins are the two most consistently present branches. Unlike the middle cardiac vein, the great cardiac vein varies considerably in its course. Lateral and posterior venous branches together are seen in approximately 50% of human hearts, unlike the anterior interventricular and middle cardiac veins, which are seen in more than 90%.⁵⁶

The venous valves can hinder catheter access within the coronary venous system, especially the Thebesian valve, which may completely cover the CS os in a variety of forms or be imperforate. Other venous valves, like the valve of Vieussens, are often present at the entrances of the ventricular veins into the great cardiac vein, or at the entrance of a smaller vein into a larger vein. These tend to be flimsy endothelial

ridges but can present some resistance on probing or when trying to pass a catheter.

Left Ventricular Summit

The LV summit, the most superior portion of the LV myocardium, lies on the anterior mitral annulus epicardially, abutting on the left CS of Valsalva superiorly, laterally, and anteriorly. The LV summit represents the triangular region in the epicardial LVOT with its apex at the bifurcation of the left main coronary artery (between the left anterior descending and the circumflex coronary arteries) and its base formed by an arc connecting the first septal perforator branch of the left anterior descending coronary artery and the circumflex coronary artery (Fig. 27.8). The great cardiac vein bisects by the LV summit into superior (closer to the apex of the summit) and inferior regions.

The LV summit is the most common site of idiopathic epicardial LV arrhythmias, accounting for about 12% of idiopathic LV VTs. LV summit VTs are most commonly ablated within the great cardiac or anterior interventricular veins. However, while the inferior portion of the summit is usually accessible to epicardial catheter ablation, successful ablation in the superior region is frequently limited by the close proximity of the coronary arteries and the thick layer of epicardial fat that overlies the proximal portion of these vessels.¹⁵

Cardiac Crux

The cardiac crux is the posteroseptal region (the diaphragmatic aspect) of the heart where the AV, interventricular, and interatrial grooves form a roughly cross-shaped intersection, which represents the confluence of all four cardiac chambers with the CS in their nearest proximity. The “basal” crux area lies in proximity to the ostium of middle cardiac

vein, whereas the “apical” crux area lies near the posterior interventricular artery, which is more inferior and epicardial compared with the basal crux area. Hence, the apical crux is often not accessible from the proximal CS or the middle cardiac vein. VTs originating from the basal crux of the heart can be ablated via the middle cardiac vein, whereas ablation of apical crux VAs often requires the percutaneous subxiphoid epicardial approach.^{57,58}

Technical Considerations

Baseline CS venography is typically required to help delineate its anatomy and guide ablation. The great cardiac and the anterior interventricular

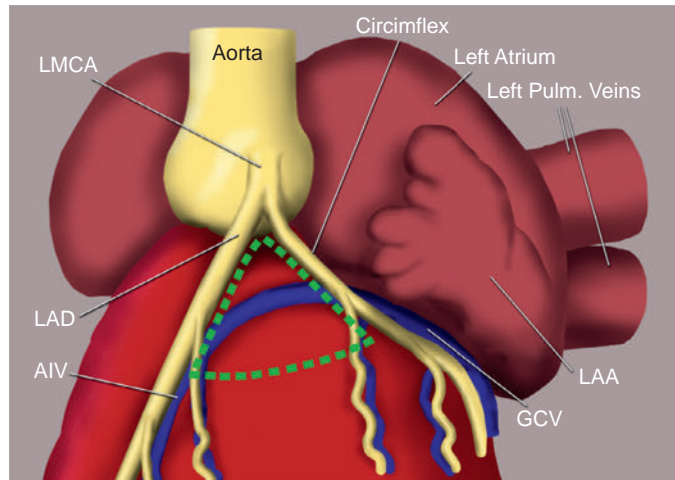


Fig. 27.8 Diagrammatic Representation of Left Ventricular Summit. The heart is viewed from a cranially angulated left anterior oblique perspective. The aorta is shown from which the left main coronary artery (LMCA) arises, branching to the left anterior descending (LAD) and circumflex arteries with their respective branches. The great cardiac vein (GCV) leaves the atrioventricular groove to become the anterior interventricular vein (AIV) that parallels the LAD. The LV summit is outlined by green dashes and is roughly bisected by the AIV. LAA, Left atrial appendage.

veins allow epicardial access to the anterior basal ventricular surface. The middle cardiac vein allows epicardial access to the inferior ventricular surface.

Mapping can be facilitated using small (2.5 Fr), flexible, multipolar electrode catheters introduced through a guiding catheter positioned at the CS os. The catheter can be positioned in different coronary venous branches to map different regions of the epicardial surface of the ventricles.

Once the ablation catheter is positioned at the target site, and before RF energy delivery, coronary arteriography is performed to outline the spatial relationship between the target vein and the adjacent coronary artery (see Fig. 23.19). Although the minimal safe distance between ablation sites and coronary arteries is not clear, ablation is not performed within 5 mm of a coronary artery (Fig. 27.9). In addition, pacing from the distal ablation electrode should be performed at an output of 20 mA. If diaphragmatic capture can be demonstrated, then ablation should not be attempted unless phrenic nerve injury can be avoided by physical displacement, as discussed earlier.

RF ablation within the coronary venous system is usually performed with a 3.5-mm open-irrigated-tip catheter at a power output of 15 to 25 W (with an irrigation flow rate of 30 mL/min) for up to 60 seconds (eFig. 27.6). If this catheter cannot be maneuvered to the ablation target site, a 5 Fr, 6 Fr, or 7 Fr ablation catheter may be used. For nonirrigated-tip catheters, the target temperature is usually set to 55°C to 60°C with a power output of 15 to 30 W. Impedance should be monitored during RF applications, and RF energy delivery should be stopped if impedance rises significantly.^{10,13,59,60}

Cryoablation can also be considered because it is not limited by high impedance. In fact, formation of the cryolesion is likely facilitated by the low blood flow in the coronary venous system. Freezing also seems less likely to damage adjacent coronary arteries. However, the cryocatheter often is difficult to maneuver in the coronary venous system.

Outcome

The outcome of the ablation procedure is a function of the proximity of the ideal target site to accessible portions of the coronary venous system as well as the ability to deliver an effective amount of ablative

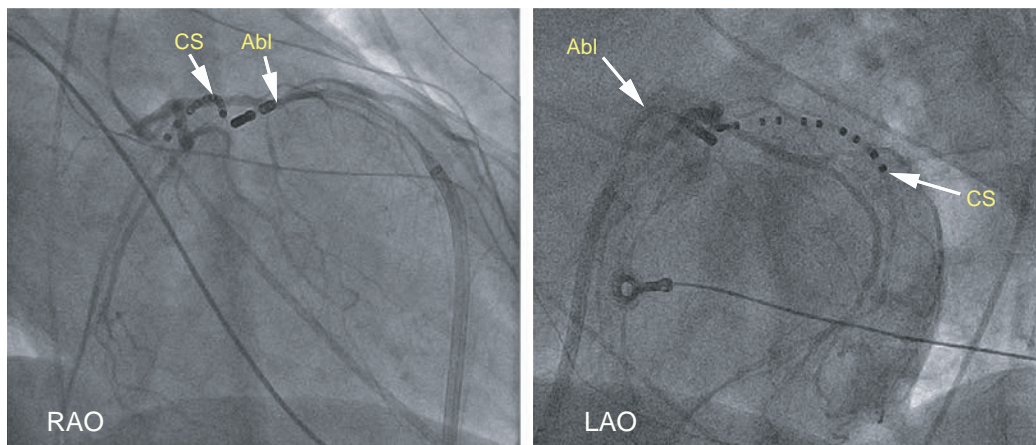
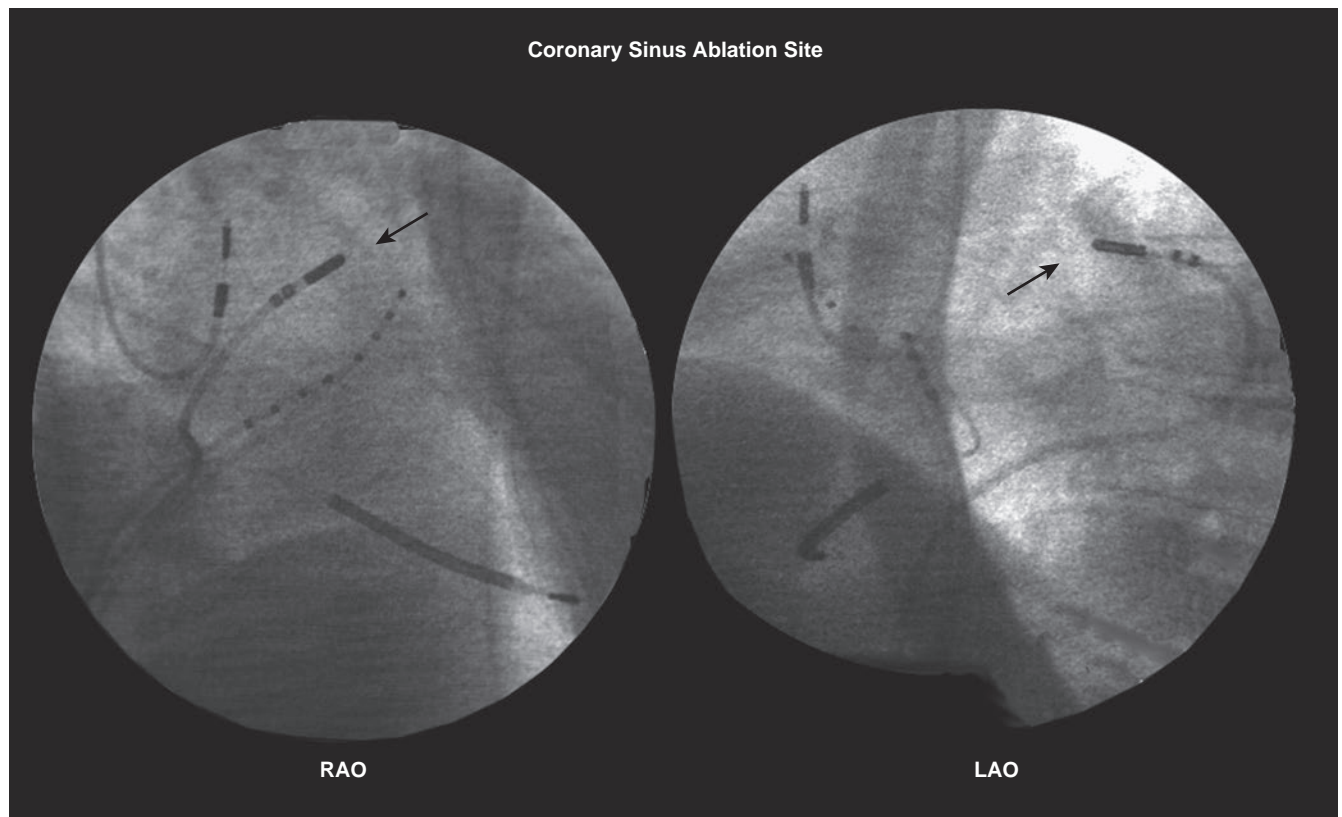
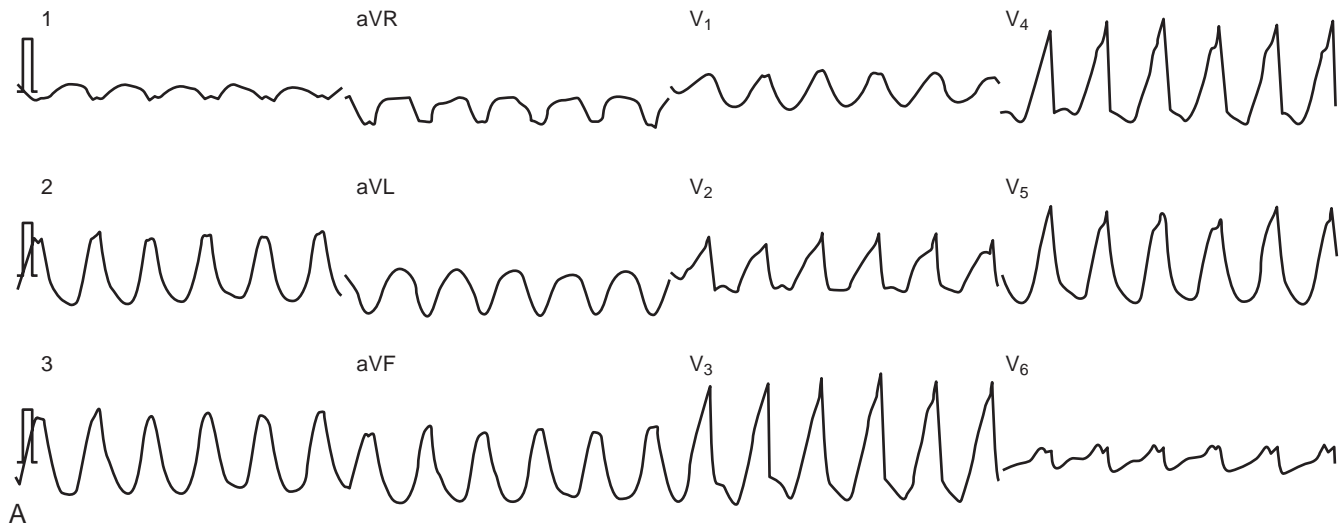


Fig. 27.9 Idiopathic Ventricular Tachycardia (VT) Originating From the Left Ventricular Summit. Right anterior oblique (RAO) and left anterior oblique (LAO) fluoroscopic views during selective left coronary angiography with the ablation (Abl) positioned at the site of origin of focal VT originating from the left ventricular summit. The ablation catheter is positioned epicardially via the subxiphoid percutaneous approach. Note the proximity of the ablation catheter to the coronary sinus (CS) catheter. Ablation from the CS failed in terminating the VT. Ablation via the epicardial approach was not feasible due to the proximity of epicardial coronary arteries.



B

eFig. 27.6 Idiopathic Epicardial Ventricular Tachycardia (VT). (A) Surface electrocardiogram of a slow VT that was ablated from the coronary sinus (CS) after both endocardial and epicardial mapping failed to eliminate the VT. (B) Right anterior oblique (RAO) and left anterior oblique (LAO) fluoroscopic views of catheter location for VT ablation from the CS.

energy to the target site. When the VT substrate can be accessed via the coronary venous system and the cardiac vein is of sufficient size to allow adequate RF energy applications, elimination of VT can be achieved in most patients.

However, epicardial mapping and ablation via the coronary venous system has important limitations. Epicardial VT sites of origin can be identified only when the cannulated vessel happens to be in the region of the VT origin. In addition, catheter manipulation is limited by the anatomical distribution and size of these vessels. Currently available ablation catheters often are difficult to advance beyond the distal great cardiac vein or the proximal portions of the middle cardiac vein because of the tortuosity, sharp angulation, and small caliber of the distal veins. Furthermore, a conventional ablation catheter can potentially completely occlude a branch of the CS, preventing cooling of the ablation electrode and resulting in high impedance when RF energy is delivered. This markedly reduces the amount of power that can be delivered and may result in adherence of the ablation electrode to the wall of the vein. In fact, delivery of more than 10 to 15 W seldom is possible. An external saline-cooled ablation catheter allows more consistent delivery of RF energy, with less heating at the electrode-tissue interface.³⁵ RF energy delivery in a small venous branch can cause thrombotic occlusion or severe stenosis, such that it may be impossible, subsequently, to maneuver the catheter tip more distally in the vessel; thus ablation should not be performed unless the more distal portion of the vessel has been explored (or been shown to be too narrow to advance the catheter) and shown to have less attractive electrogram ablation site characteristics.

Coronary artery injury is an ever-present risk, especially near the proximal part of the anterior interventricular vein. Arterial injury, including thrombosis, medial necrosis, and hyperplasia, is inversely proportional to vessel diameter; there is little evidence of injury when vessel diameter exceeds 0.5 to 1.0 mm. Similar findings were reported for cryoablation. As noted, coronary angiography should be performed before delivering RF energy near or within a branch of the CS to determine whether there are any branches of the right or left coronary artery in proximity to the ablation site. Unfortunately, proximity to within 5 mm of a coronary artery (as defined by coronary angiography) can be observed in about three-quarters of patients, prohibiting RF ablation.^{10,12,13,59–61}

Despite the anatomical constraints, ablation of LV summit VTs via the coronary venous system has yielded success rates of approximately 70%. Using the coronary venous system for mapping and ablation can potentially result in a lower complication rate than the percutaneous pericardial approach because damage to the RV or extracardiac structures is less likely to occur. When endocardial ablation and ablation from within the coronary venous system is not feasible or unsuccessful, the percutaneous transthoracic epicardial approach may be considered. However, the latter approach to epicardial idiopathic VTs has very limited success rates. The close proximity of the coronary arteries and the thick layer of epicardial fat that overlies the proximal portion of coronary veins (“the inaccessible area” in the superior aspect of the LV summit) often prohibit successful ablation in a significant proportion of these patients. Also, the percutaneous epicardial approach often requires deeper levels of sedation, which can suppress idiopathic VT and hinder the mapping and ablation procedure.^{10,12,13,59,60,62}

VIDEOS

The following videos accompany this chapter:

See **Video 4.8**. Pericardial Access: Technique

See **Video 23.2**. Epicardial Ablation of Focal Ventricular Tachycardia Originating From the Left Ventricular Summit

REFERENCES

1. Komatsu Y, et al. Endocardial ablation to eliminate epicardial arrhythmia substrate in scar-related ventricular tachycardia. *J Am Coll Cardiol*. 2014; 63:1416–1426.
2. Sarkozy A, et al. Epicardial ablation of ventricular tachycardia in ischemic heart disease. *Circ Arrhythm Electrophysiol*. 2013;6:1115–1122.
3. Yoshiga Y, et al. Correlation between substrate location and ablation strategy in patients with ventricular tachycardia late after myocardial infarction. *Heart Rhythm*. 2012;9:1192–1199.
4. Kosmidou I, et al. Role of repeat procedures for catheter ablation of postinfarction ventricular tachycardia. *Heart Rhythm*. 2011;8:1516–1522.
5. Yokokawa M, et al. Computerized analysis of the 12-lead electrocardiogram to identify epicardial ventricular tachycardia exit sites. *Heart Rhythm*. 2014;11:1966–1973.
6. Haqqani HM, Callans DJ. Ventricular tachycardia in coronary artery disease. *Card Electrophysiol Clin*. 2014;6:525–534.
7. Valles E, Bazan V, Marchlinski FE. ECG criteria to identify epicardial ventricular tachycardia in nonischemic cardiomyopathy. *Circ Arrhythm Electrophysiol*. 2010;3:63–71.
8. Zhang L, Liu L, Kowey PR, et al. The electrocardiographic manifestations of arrhythmogenic right ventricular dysplasia. *Curr Cardiol Rev*. 2014;10: 237–245.
9. Haqqani HM, Marchlinski FE. Electroanatomic mapping and catheter ablation of ventricular tachycardia in arrhythmogenic cardiomyopathy. *Card Electrophysiol Clin*. 2011;3:299–310.
10. Hutchinson MD, Garcia FC. An organized approach to the localization, mapping, and ablation of outflow tract ventricular arrhythmias. *J Cardiovasc Electrophysiol*. 2013;24:1189–1197.
11. Daniels DV, et al. Idiopathic epicardial left ventricular tachycardia originating remote from the sinus of Valsalva: electrophysiological characteristics, catheter ablation, and identification from the 12-lead electrocardiogram. *Circulation*. 2006;113:1659–1666.
12. Yamada T, et al. Idiopathic ventricular arrhythmias originating from the left ventricular summit: anatomic concepts relevant to ablation. *Circ Arrhythm Electrophysiol*. 2010;3:616–623.
13. Lin CY, et al. Radiofrequency catheter ablation of ventricular arrhythmias originating from the continuum between the aortic sinus of Valsalva and the left ventricular summit: electrocardiographic characteristics and correlative anatomy. *Heart Rhythm*. 2015;13:111–121.
14. Santangeli P, Lin D, Marchlinski FE. Catheter ablation of ventricular arrhythmias arising from the left ventricular summit. *Card Electrophysiol Clin*. 2016;8:99–107.
15. Ouyang F, et al. Ventricular arrhythmias arising from the left ventricular outflow tract below the aortic sinus cusps: mapping and catheter ablation via transseptal approach and electrocardiographic characteristics. *Circ Arrhythm Electrophysiol*. 2014;7:445–455.
16. De Riva M, Watanabe M, Zeppenfeld K. Twelve-lead ECG of ventricular tachycardia in structural heart disease. *Circ Arrhythm Electrophysiol*. 2015; 8:951–962.
17. Martinek M, Stevenson WG, Inada K, et al. QRS characteristics fail to reliably identify ventricular tachycardias that require epicardial ablation in ischemic heart disease. *J Cardiovasc Electrophysiol*. 2012;23: 188–193.
18. Fernandez-Armenta J, Berrueto A. How to recognize epicardial origin of ventricular tachycardias? *Curr Cardiol Rev*. 2014;10:246–256.
19. Garikipati NV, Paruchuri V, Mittal S. How to learn epicardial intervention techniques in electrophysiology. *Card Electrophysiol Clin*. 2010;2:35–43.
20. Soejima K, et al. Epicardial catheter ablation of ventricular tachycardia in no entry left ventricle: mechanical aortic and mitral valves. *Circ Arrhythm Electrophysiol*. 2015;8:381–389.
21. Bradfield JS, Tung R, Boyle NG, et al. Our approach to minimize risk of epicardial access: standard techniques with the addition of electroanatomic mapping guidance. *J Cardiovasc Electrophysiol*. 2013; 24:723–727.
22. Berte B, et al. Characterization of the left-sided substrate in arrhythmogenic right ventricular cardiomyopathy. *Circ Arrhythm Electrophysiol*. 2015;8:1403–1412.

23. Fernandez-Armenta J, et al. Sinus rhythm detection of conducting channels and ventricular tachycardia isthmus in arrhythmogenic right ventricular cardiomyopathy. *Heart Rhythm*. 2014;11:747–754.
24. Acosta J, et al. Infarct transmuralty as a criterion for first-line endo-epicardial substrate-guided ventricular tachycardia ablation in ischemic cardiomyopathy. *Heart Rhythm*. 2016;13:85–95.
25. Izquierdo M, et al. Endo-epicardial versus only-endocardial ablation as a first line strategy for the treatment of ventricular tachycardia in patients with ischemic heart disease. *Circ Arrhythm Electrophysiol*. 2015;8:882–889.
26. Tzou WS, et al. Endocardial electrogram characteristics of epicardial ventricular arrhythmias. *J Cardiovasc Electrophysiol*. 2013;24:649–654.
27. Philips B, et al. Outcomes and ventricular tachycardia recurrence characteristics after epicardial ablation of ventricular tachycardia in arrhythmogenic right ventricular dysplasia/cardiomyopathy. *Heart Rhythm*. 2015;12:716–725.
28. Pisani CF, Lara S, Scanavacca M. Epicardial ablation for cardiac arrhythmias: techniques, indications and results. *Curr Opin Cardiol*. 2014;29:59–67.
29. Page SP, et al. Epicardial catheter ablation for ventricular tachycardia in heparinized patients. *Europace*. 2013;15:284–289.
30. Njeim M. Value of cardiac magnetic resonance imaging in patients with failed ablation procedures for ventricular tachycardia. *J Cardiovasc Electrophysiol*. 2016;27:183–189.
31. Komatsu Y, et al. Regional myocardial wall thinning at multidetector computed tomography correlates to arrhythmogenic substrate in postinfarction ventricular tachycardia: assessment of structural and electrical substrate. *Circ Arrhythm Electrophysiol*. 2013;6:342–350.
32. Yalin K, et al. Infarct characteristics by CMR identifies substrate for monomorphic VT in post-MI patients with relatively preserved systolic function and NS-VT. *Pacing Clin Electrophysiol*. 2014;37:447–453.
33. El Aidi H, et al. Cardiac magnetic resonance imaging findings and the risk of cardiovascular events in patients with recent myocardial infarction or suspected or known coronary artery disease: a systematic review of prognostic studies. *J Am Coll Cardiol*. 2014;63:1031–1045.
34. Stevens SM, et al. Device artifact reduction for magnetic resonance imaging of patients with implantable cardioverter-defibrillators and ventricular tachycardia: late gadolinium enhancement correlation with electroanatomic mapping. *Heart Rhythm*. 2014;11:289–298.
35. Syed F, et al. The pericardial space: obtaining access and an approach to fluoroscopic anatomy. *Card Electrophysiol Clin*. 2010;2:9–23.
36. Rodriguez ER, Tan CD. Structure and anatomy of the human pericardium. *Prog Cardiovasc Dis*. 2017;59:327–340.
37. Ernst S, Sanchez-Quintana D, Ho SY. Anatomy of the pericardial space and mediastinum: relevance to epicardial mapping and ablation. *Card Electrophysiol Clin*. 2010;2:1–8.
38. Boyle NG, Shivkumar K. Epicardial interventions in electrophysiology. *Circulation*. 2012;126:1752–1769.
39. Lim HS, et al. Safety and prevention of complications during percutaneous epicardial access for the ablation of cardiac arrhythmias. *Heart Rhythm*. 2014;11:1658–1665.
40. Yamada T. Transthoracic epicardial catheter ablation. *Circ J*. 2013;77:1672–1680.
41. Yamada T, Kay GN. Recognition and prevention of complications during epicardial ablation. *Card Electrophysiol Clin*. 2010;2:127–134.
42. D'Avila A, Koruth JS, Dukkipati S, et al. Epicardial access for the treatment of cardiac arrhythmias. *Europace*. 2012;14:13–18.
43. Killu AM, et al. Percutaneous epicardial access for mapping and ablation is feasible in patients with prior cardiac surgery, including coronary bypass surgery. *Circ Arrhythm Electrophysiol*. 2015;8:94–101.
44. Tschabrunn CM, et al. Percutaneous epicardial ventricular tachycardia ablation after noncoronary cardiac surgery or pericarditis. *Heart Rhythm*. 2013;10:165–169.
45. Bertaso AG, Bertol D, Duncan BB, et al. Epicardial fat: definition, measurements and systematic review of main outcomes. *Arq Bras Cardiol*. 2013;101:e18–e28.
46. Baldinger SH, et al. Epicardial radiofrequency ablation failure during ablation procedures for ventricular arrhythmias: reasons and implications for outcomes. *Circ Arrhythm Electrophysiol*. 2015;8:1422–1432.
47. Tung R, et al. Epicardial ablation of ventricular tachycardia: an institutional experience of safety and efficacy. *Heart Rhythm*. 2013;10:490–498.
48. Kumar S, et al. “Needle-in-needle” epicardial access: preliminary observations with a modified technique for facilitating epicardial interventional procedures. *Heart Rhythm*. 2015;12:1691–1697.
49. Gunda S, et al. Differences in complication rates between large bore needle and a long micropuncture needle during epicardial access. *Circ Arrhythm Electrophysiol*. 2015;8:890–895.
50. Swale M, et al. Epicardial access: patient selection, anatomy, and a stepwise approach. *J Innov Card Rhythm Manag*. 2011;2:239–249.
51. Killu AM, et al. Pericardial effusion following drain removal after percutaneous epicardial access for an electrophysiology procedure. *Pacing Clin Electrophysiol*. 2015;38:383–390.
52. Killu AM, et al. Atypical complications encountered with epicardial electrophysiological procedures. *Heart Rhythm*. 2013;10:1613–1621.
53. Loukas M, Bilinsky S, Bilinsky E, et al. Cardiac veins: a review of the literature. *Clin Anat*. 2009;22:129–145.
54. Randhawa A, Saini A, Aggarwal A, et al. Variance in coronary venous anatomy: a critical determinant in optimal candidate selection for cardiac resynchronization therapy. *Pacing Clin Electrophysiol*. 2013;36:94–102.
55. Noheria A, et al. Anatomy of the coronary sinus and epicardial coronary venous system in 620 hearts: an electrophysiology perspective. *J Cardiovasc Electrophysiol*. 2013;24:1–6.
56. Spencer JH, Larson AA, Drake R, et al. A detailed assessment of the human coronary venous system using contrast computed tomography of perfusion-fixed specimens. *Heart Rhythm*. 2014;11:282–288.
57. Kawamura M, et al. Idiopathic ventricular arrhythmia originating from the cardiac crux or inferior septum epicardial idiopathic ventricular arrhythmia. *Circ Arrhythm Electrophysiol*. 2014;7:1152–1158.
58. Kawamura M, et al. Clinical and electrocardiographic characteristics of idiopathic ventricular arrhythmias with right bundle branch block and superior axis: comparison of apical crux area and posterior septal left ventricle. *Heart Rhythm*. 2015;12:1137–1144.
59. Nagashima K, et al. Ventricular arrhythmias near the distal great cardiac vein challenging arrhythmia for ablation. *Circ Arrhythm Electrophysiol*. 2014;7:906–912.
60. Jauregui Abularach ME, et al. Ablation of ventricular arrhythmias arising near the anterior epicardial veins from the left sinus of Valsalva region: ECG features, anatomic distance, and outcome. *Heart Rhythm*. 2012;9:865–873.
61. Garabelli PJ, Stavakis S, Po SS. A case series and review of the literature regarding coronary artery complications associated with coronary sinus catheter ablation. *HeartRhythm Case Rep*. 2015;1:315–319.
62. Nazer B, et al. Importance of ventricular tachycardia induction and mapping for patients referred for epicardial ablation. *Pacing Clin Electrophysiol*. 2015;38:1333–1342.

Arrhythmias in Hypertrophic Cardiomyopathy

OUTLINE

Pathophysiology, 925

- Ventricular Hypertrophy, 925
- Diastolic Dysfunction, 925
- Left Ventricular Outflow Obstruction, 925
- Myocardial Ischemia, 926
- Ventricular Arrhythmias, 926
- Molecular Genetics, 926

Epidemiology and Natural History, 927

Clinical Presentation, 929

- Heart Failure, 929
- Left Ventricular Outflow Obstruction, 929
- Myocardial Ischemia, 929
- Syncope, 929
- Atrial Fibrillation, 929
- Ventricular Arrhythmias, 929

Initial Evaluation, 930

- Electrocardiography, 930
- Ambulatory Cardiac Monitoring, 930
- Echocardiography, 930

Exercise Testing, 930

- Electrophysiological Testing, 930
- Cardiac Magnetic Resonance, 930
- Genetic Testing, 931

Differential Diagnosis, 932

- Phenocopies of Hypertrophic Cardiomyopathy, 932
- Athlete's Heart, 933

Risk Stratification, 935

- Established Risk Markers, 935
- Possible Risk Modifiers, 936
- Conventional Risk Stratification Model, 937
- "HCM Risk-SCD" Model, 937

Principles of Management, 938

- Treatment of Heart Failure and Left Ventricular Outflow Obstruction, 938
- Treatment of Atrial Fibrillation, 938
- Treatment of Ventricular Arrhythmias, 938
- Family Screening, 940
- Genotype-Positive/Phenotype-Negative Patients, 940

PATHOPHYSIOLOGY

Hypertrophic cardiomyopathy (HCM) is characterized by a thickened but nondilated left ventricle (LV) in the absence of any other cardiac or systemic condition capable of producing the magnitude of hypertrophy evident (e.g., aortic valve stenosis, systemic hypertension, some expressions of athlete's heart, infiltrative or storage disorders), independent of whether obstruction to the left ventricular outflow tract (LVOT) is present.¹

Ventricular Hypertrophy

HCM is characterized by myocyte disarray. Cardiomyocytes in HCM become hypertrophied, enlarged, and distorted, which leads to disorientation of adjacent cells and arrangement in chaotic disorganized patterns (instead of the normal parallel cellular arrangement), forming circles or whorls around foci of connective tissue. Although the disorganized architecture is evident in the majority (95%) of patients dying from HCM, it is not specific to HCM, and it occurs in other syndromic causes of LV hypertrophy such as Noonan syndrome and Friedreich ataxia, congenital heart disease, hypertension, and aortic stenosis. Nevertheless, myocyte disarray in HCM is typically more extensive, occupying more than 5% of the total myocardium (including substantial portions of hypertrophied as well as nonhypertrophied LV myocardium), 33% of the ventricular septum, and 25% of the free wall.¹

Changes in myocyte architecture, myocyte hypertrophy, and expanded extracellular matrix composed of interstitial and replacement fibrosis lead to ventricular hypertrophy (Fig. 28.1). The degree and distribution

of LV hypertrophy vary markedly. LV hypertrophy can be asymmetrical or symmetrical. Asymmetrical septal hypertrophy is the most common variant and is associated with thickening of the basal anterior septum, which bulges beneath the aortic valve and causes narrowing of the LVOT region. However, isolated segmental hypertrophy can affect the LV apex (apical HCM) or any portion of the LV. The symmetrical form accounts for more than one-third of cases and is characterized by concentric thickening of the LV with small ventricular cavity dimensions. The morphological pattern of LV hypertrophy is not closely predictive of the severity of symptoms or prognosis.²

Diastolic Dysfunction

Diastolic dysfunction is a major pathophysiological abnormality in HCM. Myocardial hypertrophy, LVOT obstruction, myocardial ischemia, replacement scarring, extracellular fibrosis, and disorganized cellular architecture, as well as abnormal cellular energetics and calcium handling, all contribute to increased LV stiffness, reduced compliance, impaired relaxation, and diastolic dysfunction.³

Left Ventricular Outflow Obstruction

In the majority of patients, LVOT obstruction is precipitated by prolapse of the anterior leaflet of the mitral valve into the LVOT. This is related to systolic anterior motion (SAM) of the leaflet caused by systolic flow against the abnormally positioned mitral valve apparatus, independent of the presence of septal hypertrophy. Morphological abnormalities of the mitral valve (elongation of leaflets or accessory tissue), as well as papillary muscle abnormalities (hypertrophy, displacement, direct

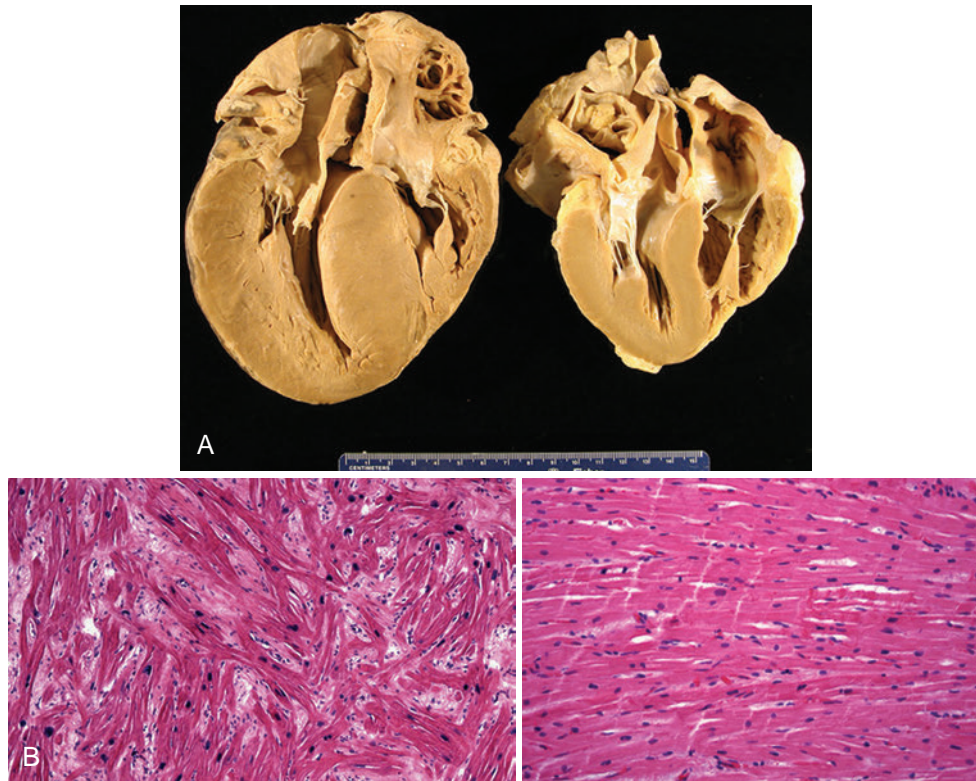


Fig. 28.1 Pathological Features of Hypertrophic Cardiomyopathy (HCM). (A) Gross pathology showing markedly increased left ventricular wall thickness associated with HCM (*left*) as compared with normal cardiac morphology (*right*). (B) Histological sections stained with hematoxylin and eosin demonstrate myocyte disarray, where myocytes are oriented at bizarre and variable angles to each other, and increased myocardial fibrosis (*left*), the pathognomonic features of HCM. In contrast, normal myocardium demonstrates a very orderly arrangement of myocytes (*right*). Images are shown at $\times 10$ magnification. (From Ho CY. Hypertrophic cardiomyopathy. *Heart Fail Clin*. 2010;6:141–159.)

insertion into the anterior leaflet of the mitral valve), contribute to LVOT obstruction. In addition, septal hypertrophy can cause narrowing of the LVOT and promote obstruction caused by SAM. Almost always, SAM results in failure of normal leaflet coaptation and eccentric mitral regurgitation, with the jet directed laterally and posteriorly and predominating during mid and late systole.⁴ In addition, LVOT obstruction can result in reduced forward cardiac output, impaired LV relaxation, increased LV diastolic pressure, and myocardial ischemia.

In a minority of patients, obstruction occurs at the mid LV cavity level, caused by systolic apposition of hypertrophied (abnormally positioned) papillary muscle and LV wall. This form of obstruction may be associated with LV apical aneurysm (in up to 25% of patients).

LVOT obstruction is dynamic and is typically aggravated by maneuvers that decrease LV preload or afterload or increase contractility or heart rate. By convention, LVOT obstruction is defined as an instantaneous peak Doppler LVOT pressure gradient of 30 mm Hg or more at rest or during physiological provocation such as Valsalva maneuver, standing, and exercise. A gradient of 50 mm Hg or more is usually considered to be the threshold at which LVOT obstruction becomes hemodynamically important.

Myocardial Ischemia

Severe myocardial ischemia and even infarction can occur in HCM and is frequently unrelated to atherosclerotic epicardial coronary artery disease. Microvascular ischemia can be induced by a supply-demand mismatch. Increased demand is usually related to increased muscle mass, as well as increased wall stress due to elevated diastolic pressures.

Reduced supply can be precipitated by impaired vasodilator reserve, myocardial bridging and compression of intramural vessels, LVOT obstruction, abnormalities in intramural coronary arterioles, reduced capillary density relative to the myocardial mass, and microvascular dysfunction.¹ Bursts of focal myocardial ischemia result in repeated cycles of myocyte death with consequent replacement fibrosis and occasionally extensive scarring.

Ventricular Arrhythmias

The arrhythmogenic substrate responsible for ventricular tachycardia (VT) occurrence in HCM has not been completely defined. Myofibrillar disarray, as well as diffuse interstitial myocardial fibrosis or replacement scar (likely caused by focal ischemia), which potentially predispose to disordered conduction patterns and increased dispersion of electrical depolarization and repolarization, have been suggested as factors contributing to reentry and ventricular arrhythmogenesis.

Molecular Genetics

HCM is familial in approximately half of the cases and sporadic in the other half. The disease is transmitted as an autosomal dominant trait with variable expressivity and age-related (incomplete) penetrance. Sporadic cases can be due to *de novo* (new) mutations present in the proband (and absent in the parents), which then initiates a new familial disease. Furthermore, apparently sporadic cases can arise because of incomplete penetrance (absence of clinical expression despite the presence of a mutation) in a parent, inaccurate family history, or, less commonly, autosomal recessive inheritance.^{1,5}

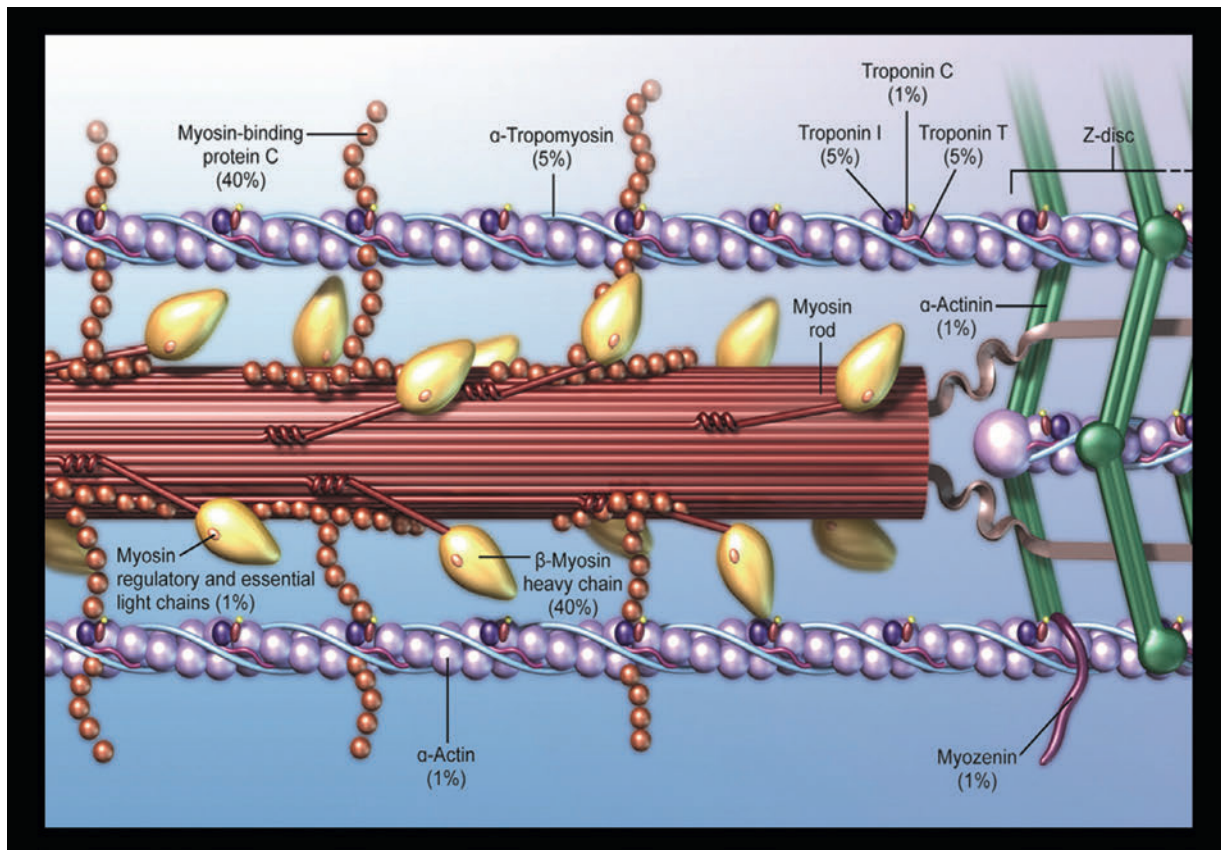


Fig. 28.2 Cardiac Sarcomere Showing the Location of Known Hypertrophic Cardiomyopathy (HCM) Disease-Causing Genes. Prevalence for each of the 11 genes derived from studies in unrelated HCM probands with positive genotyping are shown in parentheses. Not shown are genes previously linked to HCM, but with lesser evidence for pathogenicity: alpha-myosin heavy chain, titin, muscle LIM protein, telethonin, vincalin/metavinculin, junctophilin 2. (From Maron BJ, Omman SR, Semsarian C, Spirito P, Olivetto I, Maron MS. Hypertrophic cardiomyopathy: present and future, with translation into contemporary cardiovascular medicine. *J Am Coll Cardiol.* 2014;64:89–99.)

There is a substantial diversity in the genetic causes of HCM. To date, more than 1500 disease-causing mutations have been identified in genes that encode proteins of the thick and thin contractile myofibrillar components of the cardiac sarcomere or the adjacent Z-disc (Fig. 28.2).⁶ These mutations have been localized to 11 sarcomere genes, 6 Z-disc genes, and 2 calcium-handling genes. Among these genes, mutations in *MYH7* (encoding beta-myosin heavy chain) and *MYBPC3* (encoding cardiac myosin binding protein-C) are the most common, each accounting for one-quarter to one-third of all cases (Fig. 28.3). Other sarcomeric mutations (including genes encoding troponin T, troponin I, alpha-tropomyosin, actin, regulatory light chain, and essential light chain) are less common. For each gene, several different mutations have been identified. Approximately 5% of patients with HCM have two or more mutations in the same gene or different genes.^{1,2} The vast majority of those mutations are missense (whereby a single normal amino acid is replaced for another). Frameshift mutations (insertion or deletion of one or more nucleic acids) are less common.

HCM is a complex and clinically heterogeneous disease that demonstrates remarkable diversity in disease course, age of onset, severity of symptoms, LVOT obstruction, and risk for sudden cardiac death (SCD). The characteristic diversity of the HCM phenotype is attributable to the *intergenetic* heterogeneity (with a variety of mutations encoding protein components of the cardiac sarcomere) and the *intra-genetic* heterogeneity (with multiple different mutations identified in each gene),

as well as the potential influence of modifier genes and environmental factors. Of note, no definitive genotype-phenotype relationships have been established between individual sarcomere mutations and the type or extent of morphological expression in HCM. The clinical outcome may not be predicted based on individual mutations, and the extent and distribution of LV hypertrophy can be dramatically different among relatives with the same disease-causing sarcomere mutation.⁷

EPIDEMIOLOGY AND NATURAL HISTORY

HCM is the most common genetic cardiovascular disease, with a prevalence of approximately 0.2% of the general population for the disease phenotype (i.e., LV hypertrophy recognized by echocardiography). Some investigators suggested that the combined prevalence of clinically expressed HCM and gene carriers (at risk for developing the disease phenotype) is likely higher and estimated that up to 0.6% of the population may carry disease-causing sarcomere mutations. However, this estimate has been debated.^{2,6,8,9}

The major causes of death in HCM are SCD, heart failure, and stroke. SCD accounts for approximately half of total mortality in patients with HCM. Progressive heart failure is responsible for the death of one-third of patients, usually after middle age (more than 55 years), and atrial fibrillation (AF)-associated stroke is responsible for the death of 13% of the patients at a higher age, usually older than 65 years.

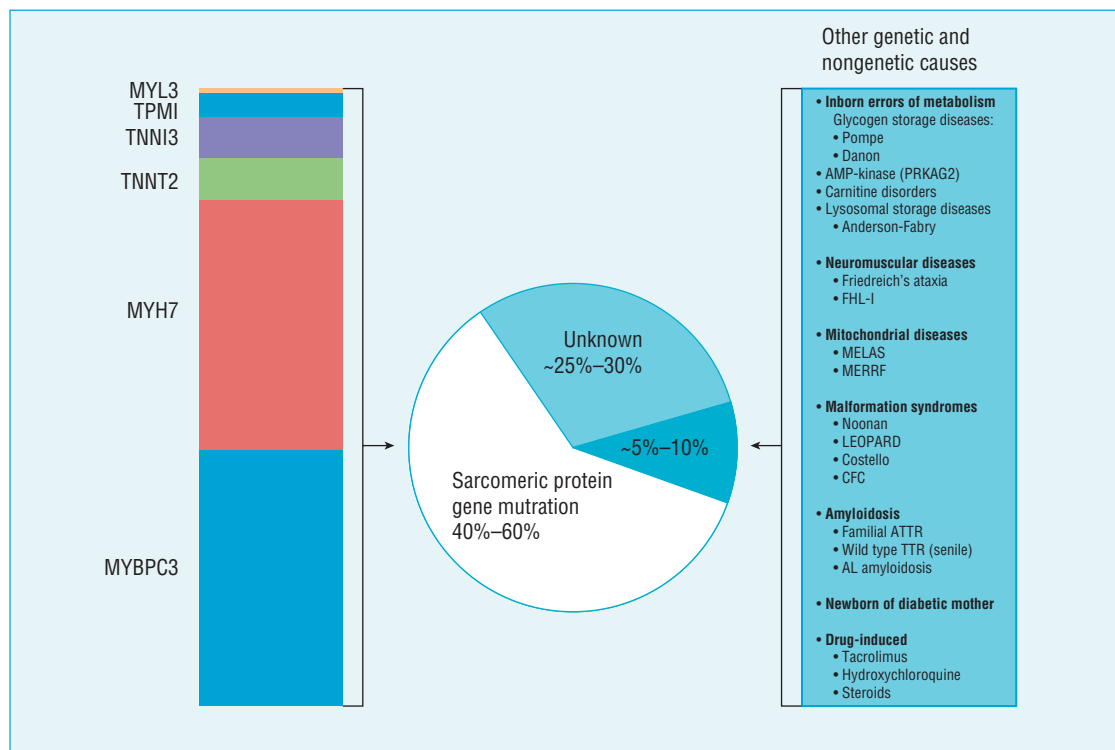


Fig. 28.3 Diverse Etiology of Hypertrophic Cardiomyopathy. The majority of cases in adolescents and adults are caused by mutations in sarcomere protein genes. *AL*, Amyloid light chain; *ATTR*, amyloidosis, transthyretin type; *CFC*, cardiofaciocutaneous; *FHL-I*, four-and-a-half LIM domains protein I; *LEOPARD*, lentigines, electrocardiographic abnormalities, ocular hypertelorism, pulmonary stenosis, abnormal genitalia, retardation of growth, and sensorineural deafness; *MELAS*, mitochondrial myopathy, encephalopathy, lactic acidosis, and stroke-like episodes; *MERRF*, myoclonic epilepsy with ragged red fibers; *MYBPC3*, myosin-binding protein C, cardiac-type; *MYH7*, myosin, heavy chain 7; *MYL3*, myosin light chain 3; *TNNI3*, troponin I, cardiac; *TNNT2*, troponin T, cardiac; *TPM1*, tropomyosin I alpha chain; *TTR*, transthyretin. (From Elliott PM, Anastakis A, Borger MA, et al. 2014 ESC guidelines on diagnosis and management of hypertrophic cardiomyopathy: the task force for the diagnosis and management of hypertrophic cardiomyopathy of the European Society of Cardiology [ESC]. *Eur Heart J*. 2014;35:2733–2779.)

Approximately 10% to 20% of individuals with HCM have a lifetime-increased risk for SCD, most likely resulting from VT and ventricular fibrillation (VF). SCD can be the first manifestation of the disease. HCM is the most common cause of SCD in the young and is the leading single cause of SCD in competitive athletes in the United States, accounting for approximately one-third of athletic field deaths in high school and college students engaged in organized sports. Although SCD occurs most often in adolescents or adults younger than 35 years, it can occur at any age. However, SCD is uncommon in young children and very uncommon in patients older than 60 years, even among those with established risk factors.²

Individuals with HCM who are at the highest risk can have a greater than 3% to 5% annual rate of SCD. However, studies on broader-based populations suggest that the prognosis is typically more favorable and most affected individuals probably achieve a normal life expectancy with little functional disability. Individuals in the general HCM population have 0.5% to 1% annual risk of SCD and 1.4% annual total cardiovascular mortality.²

Compared with patients with LVOT obstruction, HCM patients without the capacity to physiologically generate LVOT obstruction appear to have a more favorable prognosis, with lower risk for developing most HCM-related complications, including progressive heart failure, SCD, or embolic stroke, and with an HCM-related mortality rate of 0.5% per year.¹⁰

Approximately 2% to 9% of HCM patients progress to end-stage (or “burned-out”) phase of the disease, marked by LV systolic dysfunction (ejection fraction less than 50%) and occasionally progressive LV dilatation and wall thinning. Progression to end-stage disease is likely related to extensive myocardial scarring, and it can occur at a young age (approximately 50% of the patients are less than 40 years of age). The only known predictor of end-stage HCM is a family history of end-stage disease. The transition to end-stage HCM carries an ominous prognosis; over a 3-year interval, approximately two-thirds of these patients die secondary to severe heart failure or SCD or require cardiac transplantation. Posttransplantation survival is favorable (75% at 5 years; 60% at 10 years).²

Contemporary medical and invasive management strategies, including implantable cardioverter-defibrillator (ICD) implantation and septal reduction procedures, as well as heart transplantation, have significantly altered the natural history of HCM, currently resulting in an annual disease-related total mortality rate of only 0.5%.¹¹

Men are overrepresented in published HCM patient cohorts, suggesting a higher penetrance of HCM-causing mutations in male patients. Moreover, at the time of diagnosis, women were on average 9 years older than men. In addition, the extent of myocardial fibrosis is higher in male patients; nonetheless, diagnosed women tend to be more symptomatic, more likely to have LVOT obstruction, and fare worse than men. There appears to be no gender impact on the risk of

SCD or the incidence of atrial or ventricular arrhythmias in patients with HCM.³

CLINICAL PRESENTATION

The clinical presentation of HCM is characterized by extreme variability in disease course, age of onset, severity of symptoms, and risk for SCD. Many patients are either asymptomatic or mildly symptomatic, and the diagnosis is frequently made as a result of family screening, detection of a murmur during routine examination, or the identification of an abnormal electrocardiogram (ECG). The majority of patients present during adolescence or young adulthood, but symptoms can develop at any age. Symptoms can be related to LV diastolic dysfunction, LVOT obstruction, myocardial ischemia, cardiac arrhythmias, or a combination of those mechanisms. Nonetheless, there is no predictable correlation between clinical symptoms and the presence or severity of LVOT obstruction or the extent of LV hypertrophy. The extent of LV hypertrophy does not typically change once early adulthood is reached.

Heart Failure

Variable degrees of heart failure occur in more than 50% of HCM patients. Shortness of breath, particularly exertional, is the most common symptom of HCM. The most common mechanism of heart failure is LVOT obstruction, but diastolic LV dysfunction can precipitate heart failure symptoms even in the absence of LVOT obstruction. Although left ventricular ejection fraction (LVEF) is typically preserved or even hyperdynamic, a minority of patients can progress to the end-stage phase of HCM, marked by LV systolic dysfunction and occasionally progressive LV dilatation and wall thinning. These patients can develop advanced heart failure symptoms of pulmonary and systemic venous congestion (orthopnea, paroxysmal nocturnal dyspnea, edema), which can become refractory to medical therapy and require cardiac transplantation.

Left Ventricular Outflow Obstruction

Approximately 20% to 30% of individuals with HCM demonstrate LVOT obstruction at rest, and a similar proportion exhibit LVOT obstruction only in response to maneuvers that decrease LV preload or afterload or increase contractility or heart rate ("dynamic" LVOT obstruction). LVOT obstruction is the most common cause of heart failure symptoms (dyspnea) in HCM patients but can also precipitate chest pain and syncope. LVOT gradients and related symptoms can be aggravated by exercise, dehydration, low blood volume, large meals, excess alcohol intake, and certain drugs (such as vasodilators, diuretics, digoxin). On physical examination, LVOT obstruction can manifest as a dynamic ejection systolic murmur (with increasing intensity in response to Valsalva maneuver, during or immediately after exercise, or on standing), mitral regurgitation murmur, and an arterial pulse with bisferiens contour. Squatting reduces the LVOT gradient and intensity of the systolic murmur.

Myocardial Ischemia

Exertional chest discomfort occurs in 25% to 30% of patients with HCM, usually in the setting of a normal coronary arteriogram, and likely is related to microvascular angina caused by supply/demand mismatch. Some patients also experience atypical chest pain, frequently precipitated or worsened by heavy meals. A subset of patients can also have obstructive epicardial coronary artery disease, which heralds an adverse outcome.

Syncope

Syncope occurs in 15% to 25% of patients with HCM. Another 20% complain of presyncope. Different mechanisms can precipitate syncope

in HCM patients, including arrhythmias (VT or AF), neurocardiogenic syncope, and hypotension during exercise caused by LVOT obstruction or by abnormal vascular responses. Changes in LV loading conditions during exercise, heavy meals, and dehydration often provoke symptoms.^{12,13}

Syncope typically occurs in younger patients with small LV end-diastolic volume. Syncope during exertion is more common in patients with LVOT obstruction than in patients without obstruction, whereas unexplained syncope at rest and neurally mediated syncope do not appear to be related to LVOT obstruction.

Neurocardiogenic syncope is characterized by classic prodromal symptoms, including lightheadedness, warmth, nausea, and tunnel vision. Individuals tend to slump to the ground rather than drop suddenly. Syncope is brief, and patients awake nauseous and exhausted. On the other hand, syncope during exertion, or immediately following palpitation or chest pain, suggests a cardiac mechanism. Ventricular arrhythmias are an uncommon cause of syncope but should be suspected when loss of consciousness occurs suddenly, without a prodrome, particularly when it occurs at rest or on minimal effort. Occasionally, paroxysmal atrial arrhythmias with rapid ventricular rates can precipitate syncope, particularly in patients with preserved atrial function and high filling pressures.

Atrial Fibrillation

AF is the most common arrhythmia observed in HCM, with an annual incidence of approximately 1% to 2% and a prevalence of approximately 20% to 25%.¹⁴ The incidence of AF increases with age, occurring most frequently after the age of 55 years (but approximately 10 years earlier than in the general population), and is very uncommon in patients younger than 25 years. The high incidence of AF in HCM is likely related to increased left atrium (LA) atrial pressure and size, caused by LV diastolic dysfunction. In fact, LA size is one of the most important determinants of AF occurrence. In addition, the extent of LV myocardial fibrosis (as determined by cardiac magnetic resonance [CMR]) and interatrial conduction delay (as reflected by longer P wave duration) seem to correlate with higher incidence of AF. Furthermore, certain HCM mutations appear to predispose to AF, possibly by causing intrinsic atrial myopathy.³ Notably, the presence or severity of LVOT obstruction does not appear to be associated with an increased incidence of AF.

Due to the underlying ventricular hypertrophy and impaired relaxation, rapid ventricular rates and loss of atrial contribution to ventricular filling during AF are usually poorly tolerated. In fact, paroxysmal episodes of AF can precipitate acute clinical deterioration, resulting in syncope or acute heart failure, particularly in patients with severe diastolic dysfunction and LVOT obstruction. In addition, AF in HCM is associated with increased risk of stroke and thromboembolic complications (eightfold increase in risk compared with HCM patients without AF), with a prevalence and annual incidence of 27.1% and 3.8%, respectively.¹⁵ AF is associated with a fourfold increase in HCM-related mortality, predominantly driven by the higher occurrence of heart failure and stroke-related death. Of note, AF does not appear to be associated with an increased risk of SCD.

Ventricular Arrhythmias

The predominant arrhythmia syndrome associated with HCM is sudden cardiac arrest, presumably due to polymorphic VT or VF. SCD occurs with an annual rate of approximately 6% in referral-based populations and 1% in community-based studies. However, certain patient subgroups can have much higher rates, surpassing the American College of Cardiology/American Heart Association (ACC/AHA) guideline definition of high risk for SCD ($\geq 2\%$ annual risk).

HCM is the most common cause of SCD in young people, including competitive athletes, in the United States. SCD occurs throughout life,

with a peak in adolescence and young adulthood (less than 35 years of age), and can be the initial disease presentation. Although SCD occurs most commonly during mild exertion or sedentary activities, an important proportion of such events is associated with vigorous exertion. In HCM patients with ICDs, more than half of the ventricular arrhythmias identified and appropriate ICD therapies were associated with moderate or competitive physical activity.¹⁶

Ambulatory cardiac monitoring frequently reveals premature ventricular complexes (PVCs) (in more than 80% of patients) and nonsustained VT (25% to 30%). Nonsustained VT is associated with severity of LV hypertrophy and symptom class. Stable sustained monomorphic VT is rare but has been observed particularly in patients with LV apical aneurysms. Among ICD recipients for primary or secondary prevention, appropriate ICD therapies in response to ventricular arrhythmias occur in approximately 5.5% of HCM patients per year.¹

INITIAL EVALUATION

The initial evaluation is aimed at establishing the diagnosis of HCM, excluding other potential causes of LV hypertrophy, assessing the extent of the disease, and evaluating the underlying mechanisms of symptoms (e.g., chest pain, syncope), as well as risk stratification for SCD.

Clinically, HCM in adults is defined by a wall thickness ≥ 15 mm in one or more LV myocardial segments (as measured by echocardiograph or CMR), in the absence of an identifiable hemodynamic cause (such as coronary artery disease, valvular heart disease, hypertension, or congenital heart disease) capable of producing the observed myocardial abnormality (Fig. 28.4). With borderline wall thickness (13 to 14 mm), the diagnosis of HCM requires evaluation of other features including family history, noncardiac symptoms and signs, ECG abnormalities, laboratory tests, and multimodality cardiac imaging.

It is important to understand that any degree of wall thickness is compatible with the presence of the HCM genetic substrate. Because of the age-dependent and incomplete penetrance, many mutation carriers may not exhibit phenotypic expression (i.e., LV hypertrophy). These individuals are usually referred to as being “genotype positive/phenotype negative” or as having “subclinical HCM.”¹

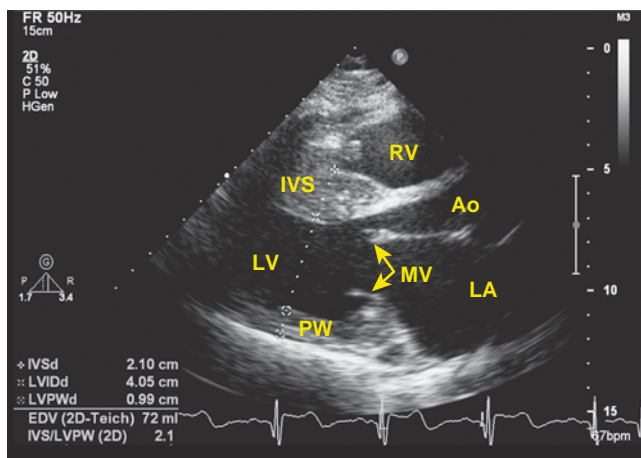


Fig. 28.4 Echocardiographic Appearance of Hypertrophic Cardiomyopathy (HCM). Parasternal long-axis view from a patient with HCM demonstrating asymmetrical septal hypertrophy. The interventricular septum (marked by arrow) measures 2.1 cm, the posterior wall measures 0.99 cm. Ao, Aorta; IVS, interventricular septum; LA, left atrium; LV, left ventricle; MV, mitral valve; PW, posterior wall; RV, right ventricle.

Electrocardiography

The ECG is abnormal in more than 90% of patients with HCM and in 75% of asymptomatic relatives. An abnormal ECG in the young is a sensitive—although nonspecific—marker of early disease expression.¹

The surface ECG in HCM patients can show a wide variety of abnormal patterns; however, ECG abnormalities do not correlate with severity or pattern of LV hypertrophy, and no particular ECG pattern is characteristic or predictive of future events. LA enlargement, repolarization abnormalities (ST-T changes including marked T wave inversion), and deep and narrow Q waves (mimicking myocardial infarction, most commonly in the inferolateral leads) are the most frequent ECG findings and may precede manifest evidence of LV hypertrophy (Fig. 28.5). Voltage criteria for LV hypertrophy alone are nonspecific and are often seen in normal young adults. Giant negative T waves in the midprecordial leads are characteristic of hypertrophy confined to the LV apex.

Ambulatory Cardiac Monitoring

Ambulatory 24-hour (Holter) cardiac monitoring is recommended as part of the initial evaluation for asymptomatic and symptomatic HCM patients because the detection of ventricular tachyarrhythmias is important for risk stratification. PVCs occur during ambulatory ECG monitoring in the vast majority of patients, nonsustained VT in 25% to 30%, and paroxysmal supraventricular arrhythmias in 38%. It is reasonable to perform serial 24-hour Holter monitoring every 1 to 2 years in patients who are stable and had no VT on previous evaluation.¹ Reevaluation with ambulatory cardiac monitoring is also recommended to evaluate patients with palpitations, lightheadedness, or syncope.

Echocardiography

Echocardiography is central to the diagnosis of HCM (see Fig. 28.4). Comprehensive transthoracic echocardiography should be performed in the initial evaluation of all patients with suspected HCM, as well as during follow-up, particularly when there is a change in the clinical status or symptoms. Echocardiography can help assess the nature, distribution, and extent of hypertrophy, systolic and diastolic function, LVOT obstruction, and identify apical aneurysms.¹

Exercise Testing

Exercise testing can help assess blood pressure responses to exercise. In addition, combining exercise testing with Doppler echocardiography is useful for determining the presence of dynamic LVOT obstruction. Metabolic stress testing (i.e., determination of maximum oxygen consumption) may be considered when a more precise assessment of functional capacity is clinically required.¹

Electrophysiological Testing

Invasive electrophysiological (EP) testing is indicated in patients with documented or suspected supraventricular or ventricular arrhythmias when catheter ablation is being considered. However, programmed ventricular stimulation to evaluate inducibility of ventricular arrhythmias has little predictive value for SCD in HCM and is not recommended for SCD risk stratification. Similarly, the routine use of EP study for evaluation of patients with syncope is not recommended.¹

Cardiac Magnetic Resonance

CMR should be considered when the echocardiogram is inconclusive or suboptimal. CMR also can provide valuable additional information in the diagnosis of HCM, including more precise LV wall thickness measurements, defining extent and location of myocardial scars, and identification of regional wall hypertrophy and LV apical aneurysms.

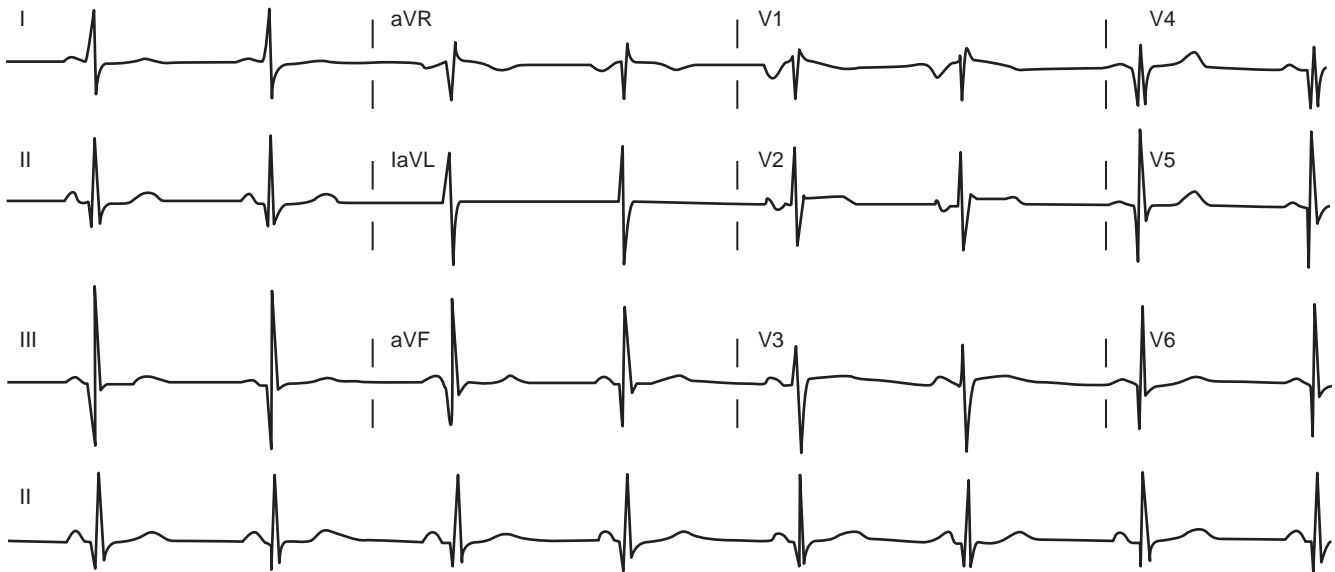


Fig. 28.5 Surface Electrocardiogram in a Patient With Hypertrophic Cardiomyopathy. Note the deep narrow Q waves in the inferolateral leads.

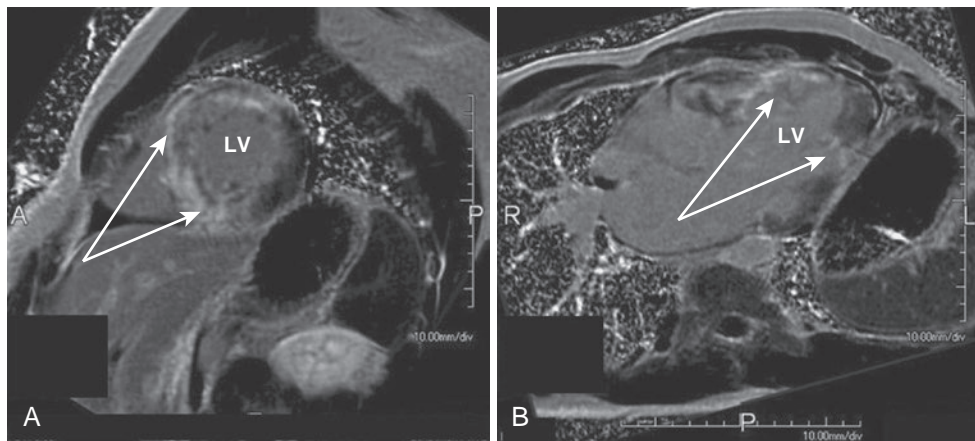


Fig. 28.6 Cardiac Magnetic Resonance Images in Obstructive Hypertrophic Cardiomyopathy (HCM). Delayed hyperenhancement magnetic resonance images from a patient with symptomatic obstructive HCM demonstrating areas of extensive scarring in the basal interventricular septum (A, arrow). Notice also the areas of patchy scarring in the posterior wall (B, arrow). The image on the left is a short-axis view, and the image on the right is a three-chamber view. LV, Left ventricle. (From Kwon DH, Smedira NG, Rodriguez ER, et al. Cardiac magnetic resonance detection of myocardial scarring in hypertrophic cardiomyopathy: correlation with histopathology and prevalence of ventricular tachycardia. *J Am Coll Cardiol.* 2009;54:242–249.)

In addition, CMR can help differentiate apical HCM from LV noncompaction.² Furthermore, late gadolinium enhancement on contrast CMR can help to define the presence, severity, and distribution of myocardial fibrosis (Fig. 28.6). Late gadolinium enhancement is present in 65% of HCM patients, typically in a patchy mid-wall pattern in areas of hypertrophy. More extensive late gadolinium enhancement can be associated with more severe disease and worse prognosis.¹⁷

Genetic Testing

Given the lack of strong evidence of specific genotype-phenotype associations, the knowledge of the underlying gene and mutation has a limited role in risk stratification and management of the individual patient. Nonetheless, genetic testing is recommended for patients with established clinical diagnosis of HCM in whom mutation-specific confirmatory testing would help to confirm or exclude the diagnosis in

at-risk family members. Similarly, postmortem genetic analysis should be considered in deceased patients with pathologically confirmed HCM, to enable cascade genetic screening of their relatives.^{1,5}

Genetic analysis should include the most commonly implicated sarcomere protein genes. Overall, the yield of genetic testing in probands with HCM is approximately 60% because some genes causing HCM have not yet been identified and are absent from testing panels. The likelihood of finding a causal mutation depends on patient selection, being highest in patients with familial disease and lowest in older patients and individuals with nonclassical features.⁵

Genetic testing is not recommended as a diagnostic test of HCM in patients with nondiagnostic clinical features (e.g., athletes and those with hypertension) because the absence of a sarcomere mutation cannot rule out familial HCM. Furthermore, finding variants of uncertain significance are difficult to interpret.

Genetic counseling is recommended for all patients with HCM, to explain the potential risks and benefits and enhance understanding of the medical and familial implications of test results. Even when genetic testing is not undertaken, genetic counseling about the potential for familial transmission of HCM is medically important.^{1,5}

DIFFERENTIAL DIAGNOSIS

Phenocopies of Hypertrophic Cardiomyopathy

LV hypertrophy is a relatively nonspecific phenotype that may reflect the final common pathway for a number of different disease processes. It does not indicate etiology or reveal underlying pathophysiology. In infants, older children, and young adults, LV hypertrophy mimicking sarcomeric HCM is often associated with congenital malformations and syndromes (e.g., Noonan, LEOPARD, and Costello syndromes), inherited metabolic storage disorders (e.g., Anderson-Fabry disease, Danon disease, PRKAG2 syndrome, Pompe disease, Forbes disease), mitochondrial cytopathies (e.g., MELAS, MERRE, LHON), and neuro-

muscular diseases (e.g., Friedreich ataxia). These clinical entities are distinct from HCM caused by sarcomere protein mutations, despite the shared feature of LV hypertrophy (Table 28.1).^{5,18}

The incidence of phenocopy in patients with the clinical diagnosis of HCM is estimated at 5% to 10%. The distinction between sarcomeric HCM and its phenocopies is important, given the differences in the inheritance pattern, natural history, prognosis, and, in some cases, management strategies. Both cardiac and extracardiac traits contribute to clinical recognition of phenocopies. A phenocopy should be suspected when an atypical feature of classic HCM or multiorgan involvement is present. HCM can be distinguished from these disorders by dysmorphological examination, neuromuscular examination, metabolic screening, family history, and genetic testing (Table 28.1).

It is recommended to limit the use of the term *hypertrophic cardiomyopathy* or *HCM* to those patients in whom overt disease expression (with LV hypertrophy) appears to be confined to the heart and the definitive mutation is either one of a gene encoding proteins of the cardiac sarcomere or alternatively when the genotype is unresolved using

TABLE 28.1 Hypertrophic Cardiomyopathy Phenocopies

Associated Phenotype	Gene	Protein	Inheritance	Frequency in Patients With HCM Phenocopy Diseases	Common Clinical Features	Diagnosis	Treatment
PRKAG2 syndrome	<i>PRKAG2</i>	AMP-activated protein kinase γ 2 regulatory subunit	• Autosomal dominant	<1%	<ul style="list-style-type: none"> • LV hypertrophy • Ventricular preexcitation • SND • AVB 	<ul style="list-style-type: none"> • Genetic testing 	<ul style="list-style-type: none"> • Nonspecific, supportive
Anderson-Fabry disease	<i>GLA</i>	Alpha-galactosidase A	• X-linked	<5%	<ul style="list-style-type: none"> • LV hypertrophy • AVB, IVCD • Atrial and ventricular arrhythmias • Aortic and mitral regurgitation • Aortic root dilatation • Renal failure • Stroke • Skin manifestations: telangiectasias, angiokeratomas 	<ul style="list-style-type: none"> • Enzyme assay (alpha-galactosidase) • Endomyocardial biopsy • Genetic testing 	<ul style="list-style-type: none"> • Enzyme replacement with recombinant α-galactosidase A
Pompe disease (glycogen storage disease type IIa, acid maltase deficiency)	<i>GAA</i>	Acid alpha-1,4-glucosidase	• Autosomal recessive	Rare	<ul style="list-style-type: none"> • LV hypertrophy • Ventricular preexcitation • Skeletal myopathy • Hepatomegaly • Macroglossia 	<ul style="list-style-type: none"> • Enzyme assay (Acid alpha-1,4-glucosidase) • Genetic testing • Tissue biopsy (skeletal muscle, skin) • Increased serum creatine kinase 	<ul style="list-style-type: none"> • Enzyme replacement with alglucosidase alfa
Danon disease	<i>LAMP2</i>	Lysosomal-associated membrane protein 2	• X-linked	Rare	<ul style="list-style-type: none"> • LV hypertrophy • Ventricular preexcitation • Skeletal myopathy • Mental retardation • Ophthalmological manifestations 	<ul style="list-style-type: none"> • Elevated creatine kinase • Muscle biopsy • Genetic testing 	<ul style="list-style-type: none"> • Nonspecific, supportive • Cardiac transplant

TABLE 28.1 Hypertrophic Cardiomyopathy Phenocopies—cont'd

Associated Phenotype	Gene	Protein	Inheritance	Frequency in Patients With HCM Phenocopy Diseases	Common Clinical Features	Diagnosis	Treatment
Mitochondrial cytopathies (MELAS, MERRF, LHON)	Various mitochondrial genes (e.g., <i>MTTG</i> , <i>MTT1</i>)	Protein-encoding mitochondrial ribosomal and transfer RNA (respiratory chain protein complexes)	<ul style="list-style-type: none"> Autosomal recessive Autosomal dominant X-linked Maternal inheritance 	Rare	<ul style="list-style-type: none"> LV hypertrophy Dilated cardiomyopathy LV noncompaction AVB, IVCD Skeletal myopathy Optic atrophy Pigmentary retinopathy CNS features Neuropathy 	<ul style="list-style-type: none"> Genetic testing Tissue biopsy (heart, skeletal muscle) 	<ul style="list-style-type: none"> Nonspecific, supportive
Noonan syndrome	<ul style="list-style-type: none"> <i>PTPN11</i> <i>SOS1</i> <i>RAF1</i> 	RAS/RAF/MEK/ERK signal transduction pathway	<ul style="list-style-type: none"> Autosomal dominant 	Rare	<ul style="list-style-type: none"> LV hypertrophy Pulmonic stenosis Short stature Learning problems Pectus excavatum Facial abnormalities (hypertelorism, down-slanting eyes, webbed neck) 	<ul style="list-style-type: none"> Genetic testing 	<ul style="list-style-type: none"> Nonspecific, supportive
Friedreich ataxia	<i>FXN</i>	Frataxin	<ul style="list-style-type: none"> Autosomal recessive 	Rare	<ul style="list-style-type: none"> LV hypertrophy Atrial fibrillation Skeletal myopathy Ataxia Vision impairment Hearing impairment Scoliosis High plantar arches Diabetes 		<ul style="list-style-type: none"> Nonspecific, supportive

AMP, adenosine monophosphate; AVB, Atrioventricular block; CNS, central nervous system; IVCD, intraventricular conduction defect; LHON, Leber hereditary optic neuropathy; LV, left ventricular; MELAS, mitochondrial myopathy, encephalopathy, lactic acidosis, and stroke-like episodes; MERRF, myoclonus epilepsy associated with ragged-red fibers; SND, sinus node dysfunction.

current genetic testing. On the other hand, LV hypertrophy that occurs in the context of multisystem disorders or nonsarcomeric genetic diseases is considered a phenocopy of the sarcomeric HCM and is described as “LV hypertrophy” rather than “hypertrophic cardiomyopathy.”¹

Athlete's Heart

Intensive and long-term athletic training can lead to constellation of physiological cardiovascular adaptations, including increased LV wall thickness and cavity size. Such remodeling, termed *athlete's heart*, permits enhanced filling of the LV in diastole and augmentation of stroke volume, allowing generation of a large and sustained cardiac output even at rapid heart rates. Compared with nonathletes, athletes have 15% to 20% greater LV wall thickness and 10% to 15% larger LV size. However, the absolute increases in LV wall thickness are usually modest and fall within the normally accepted range for the general population.^{19,20}

A minority (approximately 2%) of adult male athletes, predominantly those involved in endurance sports, demonstrate extreme physiological adaptation with LV wall thickness measurements of 13 to 15 mm, which overlaps with measurements observed in morphologically mild HCM. Although the majority of individuals with HCM have a mean LV wall thickness of 18 to 20 mm, 8% have milder degrees of LV hypertrophy,

especially in the setting of incomplete phenotypic expression of HCM during periods of rapid growth.¹⁹

The distinction between physiological LV hypertrophy and HCM is critical; an incorrect diagnosis has far-reaching implications. A false-positive diagnosis can potentially lead to erroneous disqualification from competition, whereas a false-negative diagnosis may result in devastating SCD, especially when one considers that HCM is the most common cause of exercise-related SCD in young athletes.

In the majority of athletes, differentiating physiological from pathological LV hypertrophy is possible using ECG and echocardiography. If the diagnosis is still uncertain, CMR, cardiopulmonary exercise testing, and genetic testing can provide further information (Table 28.2).^{19,21}

Demographics

The magnitude of expected LV wall thickening varies with age, gender, ethnicity, body surface area, and degree and type of athletic training. Athletes participating ultra-endurance sport with a high isotonic and isometric component such as rowing, canoeing, swimming, cycling, and ultra-endurance running exhibit the greatest increases in LV wall thickness. On the other hand, athletes participating in pure isometric sports (such as weightlifting or wrestling) rarely exhibit LV wall thickness

TABLE 28.2 Differences Between Hypertrophic Cardiomyopathy and Athlete's Heart

	Favors Athlete's Heart	Favors HCM
Age	—	<16 years
Sex	Male	Female
Ethnicity	Black	—
Type of sport	High-intensity endurance sport	Low-intensity sport
Family history of HCM or SCD	Absent	Present
Symptoms	Absent	Dyspnea, chest pain, presyncope, syncope, palpitations, fatigue
Physical examination	Unremarkable	Dynamic systolic murmur
Electrocardiogram	No abnormalities	Pathological Q waves
	Isolated LVH criteria	ST-segment depression
		T-wave inversions in anterolateral leads
		LBBB
LV hypertrophy	Symmetrical, uniform	Asymmetric
		LVWT >15 mm
		LVWT >13 mm in female and adolescent athletes
Echocardiogram	Normal or improved LV diastolic function	LV diastolic dysfunction
	LVEDD >55 mm	LVEDD <45 mm
	Balanced RV dilation	LVOT obstruction
		Disproportionate LA dilatation
Cardiopulmonary exercise testing	VO _{2max} >45 mL/kg/min	VO _{2max} lower than predicted
	VO _{2max} >120% of predicted	
Gadolinium-enhanced CMR	Absence of late enhancement or nonspecific pattern	Typical late enhancement
Deconditioning	Reduction in LVWT by 2–5 mm	No reduction in LVWT
Genetic testing	Negative	Positive for HCM-causing sarcomere mutation

CMR, Cardiac magnetic resonance; HCM, hypertrophic cardiomyopathy; LA, left atrium; LBBB, left bundle branch block; LV, left ventricular; LVEDD, left ventricular end-diastolic diameter; LVH, left ventricular hypertrophy; LVOT, left ventricular outflow tract; LVWT, left ventricular wall thickness; RV, right ventricle; SCD, sudden cardiac death.

exceeding 12 mm. In addition, an athlete's body surface area of more than 2.0 m² increases the probability of identification of LV hypertrophy.

Black male athletes appear to be more prone to develop greater degrees of physiological LV hypertrophy than are white athletes. In one report, 18% of black athletes exhibited LV wall thickness exceeding 12 mm compared with only 4% of white athletes of similar age, size, and sporting caliber. In addition, 3% of the black athletes, but none of the whites, exhibited LV wall thickness of 15 to 16 mm.²² In another report, LV wall thickness exceeding 12 mm was observed in 3.3% black female athletes (all 12 to 13 mm), but none of their white counterparts had LV wall thickness exceeding 11 mm.

Furthermore, LV wall thickening exceeding 12 mm is extremely rare in female or adolescent athletes. Athletes with LV wall thickness of more than 12 mm are invariably males older than 16 years, and the identification of such degrees of LV hypertrophy in a female athlete, any adolescent athlete aged younger than 16 years, or any athlete participating in low-intensity endurance sports is highly suggestive of HCM.

Electrocardiography

The ECG changes that develop as part of the cardiovascular adaptation in an endurance athlete include sinus bradycardia, increased QRS voltage, tall peaked T wave, J point elevation, and U waves. However, pathological Q waves, left axis deviation, and T wave inversion strongly favor a diagnosis of HCM.²¹

Although both LV hypertrophy and HCM are associated with large QRS complexes in LV leads, *isolated* QRS voltage criteria for LV hypertrophy are commonly observed in athletes but occur in only 2% of individuals with HCM. In contrast, pathological Q waves, ST segment depression, deep T wave inversions (greater than 0.2 mV), and left bundle branch block (LBBB) are highly suggestive of HCM.

Echocardiography

Physiological LV hypertrophy is homogeneous and associated with concomitant LV dilation and normal indexes of diastolic function. In contrast, individuals with HCM often show asymmetrical patterns of LV hypertrophy, small chamber size, abnormal indexes of LV diastolic filling, and impaired relaxation, independent of whether heart failure or outflow obstruction is present. LVOT obstruction and SAM of mitral valve leaflets are inconsistent with athlete's heart and strongly suggest HCM.²⁰

LV cavity size is the single most important discriminator between physiological LV hypertrophy and HCM. More than 90% of athletes with physiological LV hypertrophy have concomitant enlargement of the LV cavity (LV end-diastolic dimension of 55 to 65 mm). In contrast, the majority of patients with HCM have a small LV cavity (LV end-diastolic dimension less than 45 mm).²¹

Cardiac Magnetic Resonance

CMR provides accurate characterization of the severity, extent, and distribution of myocardial hypertrophy, particularly of apical LV segments. In addition, the identification of myocardial fibrosis (as indicated by late gadolinium enhancement) favors the diagnosis of HCM.²¹

Cardiopulmonary Exercise Testing

Elite athletes have efficient LV filling and stroke volume augmentation during exercise. Consequently, during cardiopulmonary exercise testing, athletes achieve high peak oxygen consumption (VO₂) values that exceed normal levels. In contrast, patients with HCM have low peak VO₂ (irrespective of symptoms) secondary to impaired myocardial relaxation and failure to augment stroke volume effectively during exercise. Thus a peak VO₂ of more than 50 mL/kg per minute or more than 120% of

that predicted for age and size favors physiological LV hypertrophy over HCM. Of note, cardiopulmonary exercise parameters were found to reliably distinguish HCM from endurance athletes (middle/long distance runners) but not from strength trained athletes (weightlifters).²¹

Genetic Testing

Genetic analysis has a high positive predictive value but a low negative predictive value. The identification of a disease-causing sarcomere mutation in an athlete with a maximal LV wall thickness in the “gray zone” establishes the diagnosis of HCM. However, there is significant potential for false-negative test results in which a HCM diagnosis cannot be excluded.²¹

Deconditioning

Deconditioning (detraining) can help to differentiate physiological from pathological LV hypertrophy. Elite athletes with LV hypertrophy may show regression in wall thickness measurements (of approximately 2 to 5 mm) on serial echocardiography or CMR over short periods (approximately 3 months) of deconditioning. In one report, complete normalization of LV wall thickness occurred in elite athletes after 5.6 ± 3.8 years of deconditioning. Reverse LV remodeling (wall thickness reduction) with detraining is inconsistent with pathological hypertrophy of HCM. Compared with echocardiography, CMR can be more accurate for comparison of serial LV wall thickness measurements.^{20,21}

RISK STRATIFICATION

The incidence of SCD in an unselected HCM patient population is approximately 0.7% per year. However, certain subgroups of patients can have a greater than 3% to 5% annual risk for SCD. Because ICD implantation offers the only effective means of preventing SCD, it is critical to identify high-risk patients who are appropriate for prophylactic ICD therapy. Risk stratification models currently used to guide ICD implantation in HCM patients are based on observational, retrospective cohort studies that have determined the relationship between clinical characteristics and prognosis. Randomized trials or statistically validated prospective prediction models are lacking.^{1,5}

Established Risk Markers

Cardiac Arrest/Sustained Ventricular Arrhythmias

Patients who survived a cardiac arrest or experienced an episode of spontaneous sustained VT have the highest risk for subsequent cardiac events (approximately 10% per year), with 41% risk of SCD or ICD-discharge in 5 years and 33% mortality in 7 years. Nonetheless, some of these patients may have no recurrence of cardiac events for years or decades.^{1,5}

Stable sustained monomorphic VT is rare but can occur particularly in patients with midventricular obstruction or apical LV aneurysms. The recurrence rate of VT in HCM patients is relatively high (56%), and electrical storm can occur.

Importantly, inducibility of ventricular arrhythmias with programmed ventricular stimulation has little predictive value for SCD in HCM and has no advantage over the traditional noninvasive risk stratification.

Nonsustained Ventricular Tachycardia

Ambulatory cardiac monitoring frequently reveals PVCs (in more than 80% of patients) and nonsustained VT (25% to 30%). Nonsustained VT is more frequent in patients with pronounced LV hypertrophy, LVOT obstruction, LA enlargement, and AF. Nonsustained VT appears to be associated with severity of hypertrophy and symptom class.

The predictive value of nonsustained VT detected on 24-hour ambulatory monitors or during stress testing remains controversial. Some

studies demonstrated that nonsustained VT is associated with an eightfold increase in SCD risk, but with a low (26%) positive predictive value. Rare, isolated brief episodes of nonsustained VT, especially in patients older than 30 years, do not appear to predict SCD risk. On the other hand, prolonged (greater than 7 to 10 beats), fast (greater than 200 beats/min), or repetitive episodes of nonsustained VT, particularly in younger patients (less than 30 years), may predict a high arrhythmogenic substrate for SCD. Until more data are available, it is probably more appropriate to consider duration, rate, and frequency of nonsustained VT, rather than just the presence or absence of the arrhythmia, although this strategy has not been validated.^{1,5,23}

Family History of Sudden Death

SCD events tend to cluster in families. However, there has not been a universal agreement regarding the prognostic implications of a positive family history of SCD. A single SCD is seen in up to 25% of HCM families, and it seems to have a low positive predictive value. Nonetheless, a family history of SCD (presumably caused by HCM) is considered more significant when the SCD has occurred in one or more first-degree relatives younger than 40 years (with or without a diagnosis of HCM) or in a first-degree relative at any age with an established diagnosis of HCM. Of note, families with multiple SCD under the age of 40 years are uncommon (approximately 5%). Family history is most useful when considered within the context of the overall risk profile.¹

Syncope

As noted, syncope occurs in 15% to 25% of patients with HCM. Syncope can be related to arrhythmias (VT or AF), neurocardiogenic syncope, and hypotension during exercise caused by LVOT obstruction or by abnormal vascular responses. However, in the majority of cases, no likely mechanism can be identified despite extensive investigation.

Syncopal episode of unexplained origin (i.e., not neurally mediated) or thought to be consistent with ventricular arrhythmias is often regarded as a marker of high risk for SCD. The occurrence of unexplained syncope is associated with a 1.8-fold higher probability of SCD; however, the prognostic significance of syncope is influenced by timing of the syncope event and patient's age. Patients with a recent (within 6 months before initial evaluation) episode of unexplained syncope had a fivefold relative risk of SCD higher than patients without syncope and an eightfold relative risk if they were younger than 18 years. In contrast, remote (greater than 5 years before initial evaluation) episodes of syncope in patients older than 40 years showed no association with SCD. Prognostic implications of syncopal events occurring within the time frame between recent and remote syncope are not clear. Therefore assessment should be individualized, depending on the patient's overall clinical profile.^{1,5,12}

The prognostic value of syncope in HCM patients is further supported by the fact that patients who received ICDs with unexplained syncope as the sole risk marker had a 5% annual rate of appropriate interventions compared with an annual rate of 3.5% in the overall study group with primary prevention ICDs.

Extreme Left Ventricular Hypertrophy

Marked hypertrophy (wall thickness ≥ 30 mm) in any part of the LV is an independent risk factor for SCD (particularly in patients younger than 18 years). Up to 10% of HCM patients exhibit this severe degree of LV hypertrophy, and those patients exhibit a threefold higher risk of SCD compared with those with less severe hypertrophy. Importantly, the risk of SCD increases in a linear fashion with increasing LV wall thickness. Therefore it may not be appropriate to use the 30-mm threshold in a binary manner (i.e., as either greater than 30 mm or less than

30 mm) in all cases; rather, the complete individual risk profile should be considered.^{1,5}

Abnormal Blood Pressure Response to Exercise

Approximately 20% to 40% of the patients with HCM exhibit an abnormal blood pressure response during exercise (defined as either a failure of systolic blood pressure to rise more than 20 mm Hg or a fall in systolic blood pressure during effort). Often these patients are younger than 40 years and have a small LV cavity. The mechanism of this abnormal blood pressure response is either inability to increase stroke volume in response to exercise (secondary to dynamic LVOT obstruction) or inappropriate drop in systemic vascular resistance (mediated by extensive systemic vasodilatation). Autonomic dysregulation can potentially underlie an abnormal reflex response (hypotension and bradycardia) to LVOT obstruction.¹ The prognostic significance of abnormal blood pressure response during exercise is not clearly defined but is likely more important in patient younger than 40 years and those with a family history of premature SCD.¹

Possible Risk Modifiers

End-Stage Hypertrophic Cardiomyopathy

End-stage HCM (characterized by LV ejection fraction less than 50%, wall thinning, and chamber enlargement) is observed in 2% to 9% of patients, with an annual incidence of less than 1%. The transition to end-stage HCM carries an ominous prognosis; within 3 years from the time of diagnosis, two-thirds of patients with end-stage HCM die from heart failure or SCD or require heart transplantation. Patients awaiting heart transplantation have a substantial arrhythmia-related event rate of 10% per year.^{1,11}

Left Ventricular Apical Aneurysm

LV apical aneurysms occur in 2% of HCM patients, particularly those with midventricular hypertrophy or, less commonly, apical hypertrophy. In small series, patients with LV apical aneurysms were found to exhibit a substantial (up to 10%) annual event rate, including SCD, progressive heart failure, evolution into the end-stage phase, stroke, and cardiovascular mortality. Therefore LV aneurysms may warrant consideration in SCD risk-assessment strategies, but prophylactic ICD implantation is not recommended in the absence of other clinical features that suggest an increased risk of SCD.^{1,11}

Previous Alcohol Septal Ablation

Percutaneous alcohol septal ablation appears to augment the risk of SCD in patients with HCM. Alcohol septal ablation typically creates a sizable transmural scar occupying on average 30% of the ventricular septum and 10% of the overall LV mass. Alcohol-induced infarcts can potentially compound preexisting myocardial electrical instability, resulting in increased arrhythmogenicity and higher risk of malignant ventricular arrhythmias.

The results of studies regarding the effect of alcohol septal ablation on long-term prognosis are conflicting. Several studies have documented the occurrence of sustained ventricular arrhythmias and SCD following septal ablation in approximately 10% to 20% of patients with or without SCD risk factors. Long-term outcome and survival following alcohol ablation is fourfold less favorable compared with myotomy/myectomy (which leaves no intramyocardial septal scar), and the rate of appropriate ICD therapy among alcohol ablation patients with primary prevention ICDs is threefold more frequent than in other patients (10.3% per year vs. 3.6% per year). On the contrary, other studies have shown no increase in the risk of SCD or ICD discharges after alcohol ablation. Therefore previous septal alcohol ablation is not currently considered an independent prognostic factor for SCD in HCM.

Extensive Late Gadolinium Enhancement

Late gadolinium enhancement on contrast CMR reflects myocardial fibrosis, which represents a potential substrate for ventricular arrhythmias. In fact, studies have demonstrated a linear correlation between the extent of late gadolinium enhancement and the risk of ventricular arrhythmias. HCM patients with evidence of late gadolinium enhancement on CMR tend to have more markers of risk of SCD, as well as higher mortality, than do patients without late gadolinium enhancement. Late gadolinium enhancement of 15% or more of LV mass showed a twofold increase in SCD event risk. However, available data are currently insufficient to consider late gadolinium enhancement as an independent risk marker of SCD. Nonetheless, late gadolinium enhancement can serve an arbitrator in HCM. When the level of SCD risk remains uncertain after standard stratification, the presence of extensive late gadolinium enhancement supports the benefit of ICD implantation, whereas minimal or only focal late gadolinium enhancement suggests low risk.^{5,11,24}

Left Ventricular Outflow Obstruction

Up to two-thirds of HCM patients demonstrate either resting or provokable LVOT obstruction. Although LVOT obstruction is a determinant of progressive heart failure and increased overall cardiovascular mortality, it does not specifically predict arrhythmic death. Furthermore, reduction of obstruction by septal myectomy or alcohol ablation is not considered a primary strategy for mitigating SCD risk. Similarly, the severity of clinical symptoms such as dyspnea, chest pain, and effort intolerance has not been correlated with increased risk of SCD. It is important to note that it can be challenging to use the LVOT gradient as a risk marker in individual patients, given the dynamic nature of the obstruction, characterized by spontaneous variability on a day-to-day (or even hourly) basis and influenced by factors that alter myocardial contractility and loading conditions. The 2011 ACC/AHA guidelines include marked LVOT obstruction only as a potential SCD risk modifier to be considered in borderline situations. In contrast, the 2014 European Society of Cardiology (ESC) guidelines on HCM consider LVOT obstruction as a major clinical feature associated with increased risk of SCD.^{1,5}

Genetic Testing

Adult patients with HCM and an established pathogenic mutation have worse long-term prognosis (cardiovascular mortality, stroke, and severe heart failure) compared with genotype-negative HCM patients. However, genetic testing appears to have little clinical application for risk stratification for SCD. Although certain mutations (e.g., some beta-myosin heavy chain and troponin T mutations) responsible for HCM can be associated with a higher risk for SCD compared with other mutations, there is substantial overlap between different disease gene groups, and exceptions are common. Hence the prognostic value of disease-causing mutations in HCM for risk stratification remains questionable.

On the other hand, the presence of more than one HCM-associated sarcomere mutation appears to be associated with greater disease severity and malignant ventricular arrhythmia, as well as SCD. Thus the identification of double to triple mutations on genetic testing can potentially be considered for risk stratification.

Age at Diagnosis

In HCM the risk of SCD is greatest in patients younger than 30 years and decreases thereafter. HCM patients older than 60 years appear to have low annual event rate (0.6% disease-related mortality and 0.2% SCD), despite the fact that 30% of patients have one or more risk factors for SCD. Hence the prognostic implications of the traditional SCD risk markers are of greater significance in young and middle-aged patients than in older patients with HCM.

Conventional Risk Stratification Model

The traditionally acknowledged noninvasive risk stratification strategy for primary prevention uses five clinical markers that have been defined in several retrospective and observational studies (Box 28.1). These primary prevention risk factors (applicable to HCM patients without prior cardiac arrest) are: (1) premature SCD (presumably caused by HCM) in one or more relatives; (2) unexplained syncope (particularly if recent and in young patients); (3) nonsustained VT on ambulatory (Holter) monitoring (particularly when the bursts of VT are multiple, repetitive, or prolonged); (4) severe LV hypertrophy (maximal wall thickness ≥ 30 mm); and (5) abnormal blood pressure response during exercise.¹

The relative weight that can be assigned to each of the traditional risk markers has not been defined. Although the absence of risk factors identifies a low-risk group (negative predictive value of 85% to 95%), the positive predictive value of any single risk factor is limited (approximately 10% to 20%). Risk for SCD is increased in proportion to the absolute number of risk factors.

It is also important to recognize that the absence of all risk factors does not convey immunity to SCD; the traditional risk stratification strategy in HCM remains imprecise, and a few SCDs have been reported in young patients judged to be at low risk without any of the acknowledged risk predictors.

Age is an important factor in considering patients at risk. The risk associated with each of the established risk factors is greatest in adults younger than 50 years. This risk stratification model is not easily translated to children, although a marked degree of LV hypertrophy or syncope have proven the most reliable markers in this age group. Similarly, this model may not apply to adults older than 50 years. HCM patients who have achieved an age of 60 years or more are at very low risk for disease-related adverse events, including SCD, even in the presence of conventional risk factors. However, it is important to note that even achieving this measure of longevity does not confer immunity to SCD.

In unselected HCM patient populations, approximately 60% of the patients have none of the five conventional risk factors, 20% have one risk factor, 14% have two, 3.5% have three, and 3.5% had four risk factors.

Surprisingly, in one study, neither the nature nor the number of risk factors predicted appropriate ICD therapies among ICD recipients

for primary prevention. Approximately 35% of patients with appropriate ICD interventions for VT/VF had undergone implantation for only a single risk factor, and the likelihood of appropriate discharge was similar in patients with 1, 2, or 3 or more risk markers. However, in another study, during an average of 3.6 years of follow-up, the rate of SCD was 3%, 5%, 17%, and 57%, when 1, 2, 3, or 4 risk factors were present, respectively. It is also important that during the same period only 3% of the patients without any risk factor displayed SCD. Nonetheless, it is reasonable to assume that SCD risk increases according to the number of risk factors, and risk stratification based on incorporation of multiple risk factors, as well as other “nonconventional” potential risk modifiers (Box 28.1), would likely improve positive predictive accuracy and better guide clinical decisions regarding prophylactic ICD implantation, particularly in patients in the “gray zone” of risk stratification.¹ The recognition that SCD can occur in the absence of classic risk factors should prompt the continuing search of other, unexplored risk markers.

“HCM Risk-SCD” Model

The ESC has incorporated a new, mathematical approach to risk stratification (the “HCM Risk-SCD” model) into their 2014 guidelines (Table 28.3). Instead of the conventional model that is based on the sum of the established risk factors, the “HCM Risk-SCD” model calculates individual 5-year SCD risk estimates. The algorithm is based on a Cox proportional hazards model based on data obtained from a retrospective, multicenter, longitudinal cohort study involving 3675 consecutively presenting patients.^{5,25}

The biggest changes in the HCM Risk-SCD model, compared with the risk stratification models proposed by the older guidelines, are the following: (1) abnormal blood pressure response during exercise is no longer included in the risk stratification; (2) increasing age is a protective factor; (3) LV wall thickness is no longer regarded as dichotomous, but as a continuous variable; and (4) LA diameter and LVOT gradient are added as continuous risk factors.^{5,26}

The seven continuous or binary risk factors (Table 28.3) are used to stratify patients into one of three groups based on 5-year risks of SCD (the ESC calculator is available at <http://www.doc2do.com/hcm/webHCM.html>). If the 5-year risk was calculated at less than 4%, an ICD would not be recommended; if the calculated risk is in the range 4% to 6%, it would be contingent; and if greater than 6%, ICD

BOX 28.1 Risk Factors for Sudden Death in Hypertrophic Cardiomyopathy

Established Risk Factors

1. Massive left ventricular hypertrophy (maximal wall thickness ≥ 30 mm)
2. Unexplained syncope in the past 6 months
3. Family history of premature sudden death in a first-degree relative <50 years of age
4. Nonsustained ventricular tachycardia (multiple, repetitive)
5. Abnormal blood pressure response on exercise

Possible Risk Factors or Arbitrators

1. End-stage hypertrophic cardiomyopathy (left ventricular ejection fraction <50%)
2. Left ventricular apical aneurysm
3. Extensive late gadolinium enhancement on cardiac magnetic resonance
4. Significant left ventricular outflow tract gradient at rest
5. Multiple sarcomere mutations
6. Previous alcohol septal ablation
7. Modifiable factors (intensive exercise, coronary artery disease)

TABLE 28.3 Prespecified Predictor Variables Assessed at Baseline Evaluation

Predictor Variable	Coding
Age	Continuous, years
History of SCD in one or more first-degree relatives <40 years of age or SCD in a first-degree relative with confirmed HCM at any age	Binary (yes = 1/no = 0)
Maximal LV wall thickness	Continuous, mm
LA diameter (determined by M-mode or 2-D echocardiography in the parasternal long axis plane)	Continuous, mm
Maximal LVOT gradients determined at rest and with Valsalva provocation	Continuous, mm Hg
Nonsustained ventricular tachycardia	Binary (yes = 1/no = 0)
Unexplained syncope	Binary (yes = 1/no = 0)

2-D, Two-dimensional; HCM, hypertrophic cardiomyopathy; LA, left atrial; LVOT, left ventricular outflow tract; SCD, sudden cardiac death.

implantation would be recommended. So far, two studies have examined how the guidance would have performed in their patients and arrived to opposing conclusions, emphasizing the need for new methods to identify patients at risk of SCD.^{5,25}

PRINCIPLES OF MANAGEMENT

No treatments to prevent or modify disease progression currently exist. Therefore current treatment focuses on symptom management, assessment for risk of SCD, and family screening.

Treatment of Heart Failure and Left Ventricular Outflow Obstruction

Pharmacological Therapy

In patients with LVOT obstructive symptoms or heart failure, beta-blockers are the mainstay of pharmacological therapy. The negative chronotropic and inotropic effects of beta blockade help alleviate symptoms related to diastolic dysfunction, LVOT obstruction, and myocardial ischemia. Verapamil or diltiazem can be used as an alternative or in conjunction with beta-blocker therapy. For refractory cases, disopyramide (a class IA antiarrhythmic agent with negative inotropic properties) can potentially reduce both resting and provokable gradients and may be added to beta-blockers or verapamil therapy. The initiation of disopyramide requires in-hospital cardiac monitoring for potential arrhythmias and QT prolongation.²

It is also important to avoid factors that exacerbate the degree of LVOT obstruction such as dehydration (e.g., aggressive diuresis) and arterial and venous dilator drug therapy (including nitrates and phosphodiesterase type 5 inhibitors).

Treatment of patients with end-stage disease (with LVEF $\leq 50\%$) is similar to that of other types of heart failure with LV systolic dysfunction (including angiotensin-converting enzyme inhibitors, angiotensin receptor blockers, beta-blockers, and other indicated drugs).

Septal Reduction Therapy

Septal reduction therapy is recommended for severely symptomatic patients who have substantial LVOT gradients (greater than 50 mm Hg at rest or provoked) and are refractory to medical therapy. Surgical septal myectomy is generally preferred when septal reduction is indicated. Alcohol septal ablation (eFig. 28.1) may be considered in patients with serious comorbidities or when surgery is contraindicated or not preferred. Following alcohol septal ablation, the annual mortality rate is 2.4%, whereas the risk of SCD is 1% per year.²⁷

Importantly, AV and intraventricular conduction abnormalities often complicate septal reduction procedures. Right bundle branch block (RBBB) develops in 36% of patients following alcohol septal ablation. Complete heart block requiring pacemaker implantation develops in 10% to 15%. In addition, LBBB develops in approximately 40% of patients undergoing surgical septal myectomy, and 3% develop complete heart block.^{2,27,28}

Permanent Pacing

RV pacing modifies the LV excitation pattern by changing the depolarization synchrony of LV contraction and can potentially reduce LVOT gradient and improve symptoms. Although the initial observational studies in patients with HCM showed promising results, subsequent randomized clinical studies failed to show a significant benefit of permanent pacing, and there are currently no data available to support the contention that pacing alters the clinical course of the disease or improves survival or long-term quality of life. Hence routine implantation of dual-chamber pacemakers is no longer recommended, except in a subset of symptomatic patients who have substantial LVOT gradients

refractory to medical therapy and are suboptimal candidates for surgical myectomy or alcohol septal ablation (eFig. 28.2).¹ A trial of dual-chamber pacing may also be considered for the relief of symptoms attributable to LVOT obstruction in HCM patients who already have dual-chamber cardiac devices implanted (pacemakers or defibrillators).

When permanent pacing is used, it is recommended to position the pacing lead in the RV apex, to promote excitation of the interventricular septum prior to the remainder of the LV. In addition, an atrial-synchronous ventricular pacing mode is selected, and the AV delay is optimized (usually in the range of 100 to 120 milliseconds) to shorten the ventricular peak filling time and reduce the preload. In addition, increasing the heart rate (using the DDD pacing mode with a lower rate of 60 to 70 beats/min) can help to further reduce LVOT gradient. Further adjustments of pacing parameters in the individual patient and assessment of the therapeutic effects using echocardiography will need to be considered to maximize the benefit of pacing therapy.²⁹

Treatment of Atrial Fibrillation

For patients with AF, the goal is to restore and maintain sinus rhythm because the loss of AV synchrony can precipitate or worsen symptoms. Amiodarone is the most effective. Disopyramide can also be considered, given its negative inotropic effects and additional potential benefit in reducing LVOT obstruction. Sotalol, dofetilide, and dronedarone are second line agents but may be considered as initial therapy in patients with ICDs. Flecainide and propafenone are not recommended. Catheter ablation can be considered in patients with drug-refractory AF. Surgical ablation can also be performed in AF patients undergoing surgical myectomy for LVOT obstruction. Anticoagulation is recommended in all HCM patients with AF (regardless of the CHA₂DS₂-VASc score), because of the high risk for thromboembolic complications in this patient population.

Treatment of Ventricular Arrhythmias

Pharmacological Therapy

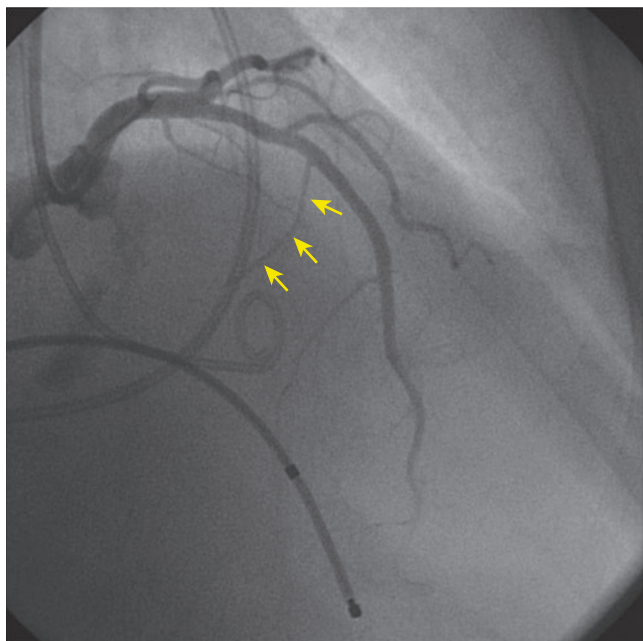
There is currently no indication for any medication for primary prevention of SCD in HCM patients. Similarly, pharmacological therapy is not recommended in patients with asymptomatic PVCs or nonsustained VT for the purpose of arrhythmia suppression. However, beta-blockers, sotalol, and amiodarone may be considered as adjunctive therapy in ICD patients who experience frequent symptoms or device discharges triggered by ventricular arrhythmias.^{1,2}

Catheter Ablation

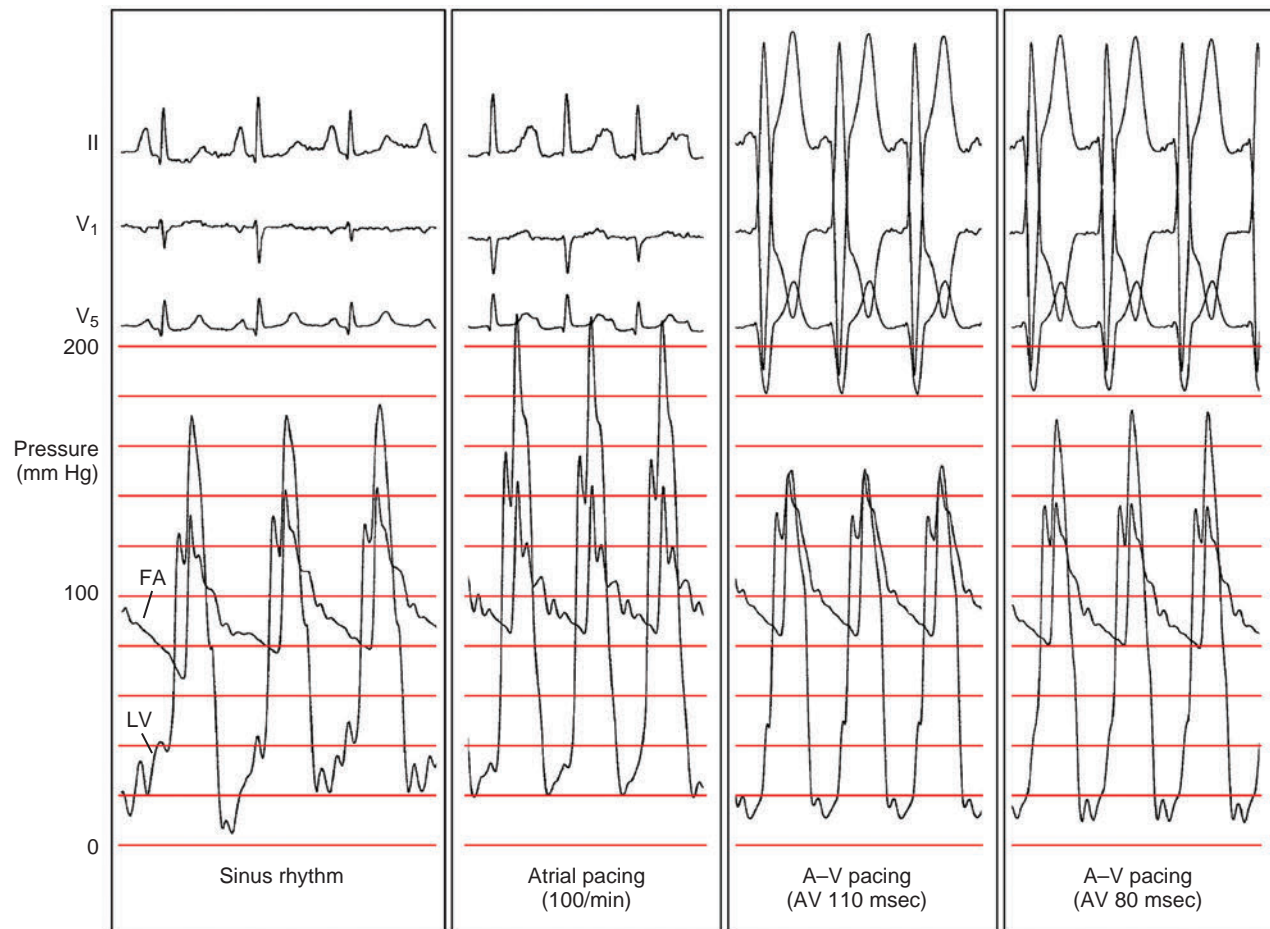
Sustained monomorphic VT is highly unusual in HCM patients and is more likely to occur in patients with LV apical aneurysms. In those patients the VT exhibits RBBB and superior axis on the surface ECG. Catheter ablation can be considered in patients with frequently recurring or incessant VT that is refractory to antiarrhythmic drug therapy. Macroreentry is the likely mechanism of VT, and catheter ablation techniques similar to those described for postinfarction VT can be used. Preprocedural CMR is helpful to identify the apical aneurysm, as well as areas of myocardial scarring that can potentially harbor the substrate for VT. Of note, an epicardial approach can be warranted in a significant proportion of patients.^{1,2}

Implantable Cardioverter-Defibrillator

ICD therapy is the most effective and reliable approach for reduction of the risk of SCD in patients with HCM, both for primary and secondary prevention. On the other hand, prophylactic pharmacological treatment alone (amiodarone, beta-blockers, or verapamil) does not offer HCM patients reliable protection against SCD and is generally not indicated. Of note, the interval from ICD implantation to first appropriate



eFig. 28.1 Left Coronary Angiography in a Patient With Asymmetrical Septal Hypertrophic Cardiomyopathy. A right lateral oblique view is shown. The septal perforator branch (marked by *arrows*) of the left anterior descending artery is the target for alcohol septal ablation. A temporary pacing wire is positioned in the right ventricle and a pigtail catheter is positioned in the left ventricle.



eFig. 28.2 Reduction of Left Ventricular (LV) Outflow Obstruction by Ventricular Pacing. The four panels show electrocardiogram and hemodynamics (femoral arterial [FA] and LV) under different conditions in a patient with hypertrophic cardiomyopathy and dynamic LV outflow obstruction. *Panels from left to right:* Baseline sinus rhythm showing a peak LV-FA gradient of almost 40 mm Hg. During atrial pacing at 100/min, the gradient increases to 50 mm Hg. With addition of right ventricular pacing at 100/min and an atrioventricular (AV) interval of 110 milliseconds, the gradient is almost eliminated; finally, when the AV interval is shortened, the gradient increases again to approximately 30 mm Hg.

device intervention is quite variable and often of considerable length. Even ICD recipients for secondary prevention after a cardiac arrest can survive for many years without the aid of ICD therapies. Previous reports found that ICD shocks occur randomly during the day without defined circadian periodicity, often unassociated with physical activity and sometimes during sleep.² However, in a recent report of HCM patients with ICDs, more than half of appropriate ICD interventions occurred during moderate to strenuous physical activity.¹⁶

ICD implantation is recommended for secondary prevention in patients with prior cardiac arrest or sustained VT, because of the relatively high recurrence rates in this subgroup. ICD implantation is also recommended for primary prevention in patients with (1) massive LV thickness (≥ 30 mm), (2) family history of SCD (including appropriate ICD therapy for ventricular tachyarrhythmias), or (3) personal history of recent unexplained syncope (Fig. 28.7). For those with nonsustained VT or abnormal blood pressure response to exercise, management decisions should be individualized, taking into consideration other markers of disease severity, as well as the desires of the fully informed patient and family. In these patients, other less-established risk factors (including LVOT obstruction, late gadolinium enhancement on CMR,

LV apical aneurysm, presence of multiple genetic mutations) may be used as arbitrators and to help resolve otherwise uncertain ICD decision making.¹

Appropriate ICD discharges in HCM patients occur annually in 10% to 14% of ICD recipients for secondary prevention after cardiac arrest and in 2.6% to 4% of ICD recipients for primary prevention. The incidence of appropriate ICD therapy does not increase with the aggregation of risk factors. Of note, arrhythmogenic events do not necessarily portend other adverse clinical outcomes. Specifically, appropriate ICD discharges do not appear to predict the occurrence of heart failure or the need for other invasive therapies (e.g., surgical myectomy or septal ablation).^{30–32}

The absence of risk factors for SCD accurately identifies a cohort of patients with a low risk of SCD. Nevertheless, regular periodic (every 12 to 24 months) reassessment of low-risk adults with Holter monitoring, exercise testing, and echocardiography is recommended. In addition, changes in symptoms, particularly sustained palpitations or syncope, at any age, should prompt urgent reevaluation.

It is important to recognize that ICD implantation is an invasive measure and carries a definite rate of complications, as well as the need

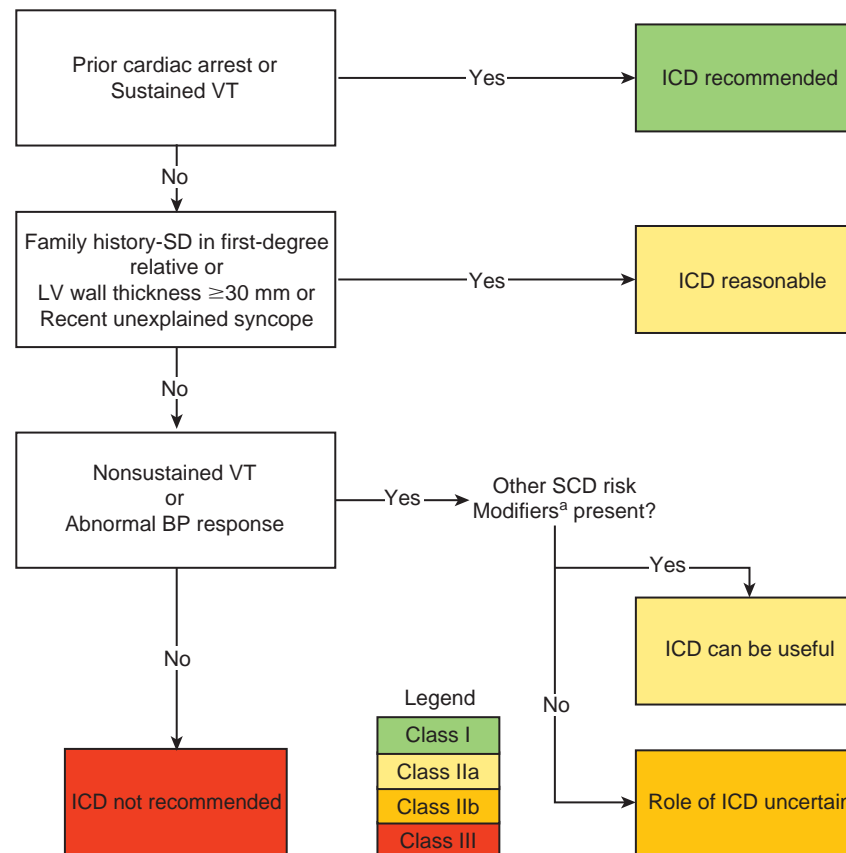


Fig. 28.7 Guidelines for Implantation of Implantable Cardioverter-Defibrillators (ICDs) in Patients With Hypertrophic Cardiomyopathy. ^aSudden cardiac death (SCD) risk modifiers include established risk factors and emerging risk modifiers (see text). Regardless of the level of recommendation put forth in these guidelines, the decision for placement of an ICD must involve prudent application of individual clinical judgment, thorough discussions of the strength of evidence, the benefits, and the risks (including but not limited to inappropriate discharges, lead and procedural complications) to allow active participation of the fully informed patient in ultimate decision making. BP, Blood pressure; LV, left ventricular; SD, sudden death; VT, ventricular tachycardia. (From Gersh BJ, Maron BJ, Bonow RO, et al. 2011 ACCF/AHA Guideline for the Diagnosis and Treatment of Hypertrophic Cardiomyopathy: a report of the American College of Cardiology Foundation/American Heart Association Task Force on Practice Guidelines. Developed in collaboration with the American As. *J Am Coll Cardiol.* 2011;58:e212–e260.)

for recurring device service and generator changes. Furthermore, inappropriate ICD shocks are common, occurring in up to 28% of HCM patients (5.3% per year), particularly in younger patients and those with AF. The negative psychological impact of an implanted device and inappropriate shocks should not be underestimated. Therefore the benefit of ICD implantation should be carefully weighed against the risks of such a procedure in this young patient population.

Of note, in a recent report of HCM patients with ICDs, ventricular tachyarrhythmias were more commonly monomorphic VT or ventricular flutter than VF, and antitachycardia pacing ICD therapies was successful in arrhythmia termination in two-thirds of episodes, thereby avoiding the need for delivery of ICD shocks. Therefore programming the ICD to deliver antitachycardia pacing therapy, even for those arrhythmias with rapid rates, can potentially reduce the risk of appropriate ICD shocks. Furthermore, these data suggest that transvenous ICD systems are likely preferable subcutaneous ICDs for HCM patients because subcutaneous ICDs do not possess antitachycardia pacing capability.¹⁶

Exercise Restriction

The physical and metabolic stresses associated with intense exercise (including catecholamine surge, hyperpyrexia, dehydration, electrolyte imbalances) can serve as triggers of fatal arrhythmias in patients with HCM. In fact, engagement in intense competitive sports is itself an acknowledged risk factor in these patients. However, this is a modifiable risk factor and by itself is not considered an indication for prophylactic ICD implantation. ICD indications for competitive athletes with HCM should not differ from those in other HCM patients, and using ICDs for the explicit purpose of allowing organized sports participation is inadvisable.^{31,33}

Therefore it is recommended that patients with HCM not participate in intense competitive sports, even when conventional markers are absent, and regardless of age, sex, race, magnitude of LV hypertrophy, presence or absence of LVOT obstruction, presence or absence of myocardial fibrosis on CMR, prior septal reduction therapy, and even in patients with ICDs.

In a recent report of HCM patients with ICDs, the majority of appropriate (and inappropriate) ICD therapies occurred during moderate to strenuous physical activity. Importantly, the increased risk for ventricular arrhythmias during exercise and high adrenergic tone can be coupled with the potential for failure of arrhythmia termination with appropriate device therapy, presenting an argument against participation of HCM patients with ICDs in competitive sports.¹⁶ Nonetheless, exclusion from competitive sports is not absolute; the ultimate decision should be made by the fully informed athletes and their families in concert with their physician and third-party interests.^{16,33}

Participation in low-intensity competitive sports (e.g., golf and bowling) and recreational sporting activities (of lesser intensity than that of competitive sports) is reasonable and should be tailored to the individual’s desires and abilities. In general, aerobic exercise is preferred to isometric exercise. It is also prudent to avoid activities associated with abrupt increase in heart rate or during extreme environmental conditions.³³

Family Screening

All HCM patients and relatives should have access to some form of genetic counseling. As expected in an autosomal dominant disease, every offspring has a 50% chance of inheriting the disease-causing mutation. However, because of the age-dependent penetrance, many mutation carriers may not exhibit phenotypic expression early in life, and many others may express the phenotype but remain asymptomatic and hence remain undiagnosed unless screened.

When the causative mutation in the index patient is identified, all first-degree relatives should first be genetically tested and then clinically evaluated if they are found to carry the same mutation. Genetic testing can have particular advantages over clinical screening because ECG and echocardiographic abnormalities may be absent or subtle, or develop late in life. Furthermore, genetic testing affords permanent reassurance to those family members who test gene-negative. Mutation-negative family members and their descendants have no risk for developing HCM and do not need further evaluation.^{2,5}

When genetic testing is not performed in the proband, or when genetic analysis fails to identify a definite disease-causing mutation (or reveals one or more genetic variants of unknown significance), it is recommended that all first- and second-degree genetically related family members of patients with HCM should undergo clinical screening with detailed history and physical examination, 12-lead ECG, and echocardiogram. CMR may also be considered for screening, particularly if the ECG is abnormal. As noted, because penetrance is age dependent, many family members may not express the phenotype at the time of examination and may be falsely considered “unaffected.” Thus periodic evaluation of the “unaffected” family members is necessary because some may develop HCM later in life. Annual screening should be considered in adolescents and young adults (ages 12 to 20 years), in athletes, and in those with a family history of early-onset disease. Screening every 3 to 5 years in other individuals may be adequate because of the rare possibility of adult-onset hypertrophy and phenotypic conversion later in life between 20 and 50 years of age (Table 28.4).^{2,5}

Individuals who have nondiagnostic clinical features consistent with early disease (e.g., ECG abnormalities, increased LVEF, delayed myocardial relaxation, or myocardial fibrosis on CMR) should be followed initially at intervals of 6 to 12 months and then less frequently if there is no progression. In addition, those who develop new cardiac symptoms should be reevaluated promptly.

Genotype-Positive/Phenotype-Negative Patients

Family members testing positive for pathogenic (disease-causing) sarcomere mutations (i.e., genotype-positive) should undergo a comprehensive cardiac evaluation and risk stratification similar to patients with known HCM, even in the absence of clinical evidence of LV hypertrophy on echocardiography and CMR (i.e., phenotype-negative). The clinical expression of HCM in this population is unpredictable. When

TABLE 28.4 Clinical Family Screening Strategies for Detection of HCM Phenotype

Age of Family Member	Screening Strategy
<12 year old	Screening optional unless: <ul style="list-style-type: none">• Family history of premature HCM-related death or other adverse complications• Competitive athlete in an intense training program• Onset of symptoms• Other clinical suspicion of early left ventricular hypertrophy
12 to 18–21 year old	Every 12–18 months
>18–21 year old	<ul style="list-style-type: none">• At onset of symptoms or at least every 5 years through midlife• More frequent intervals with a family history of late-onset HCM and/or malignant clinical course

HCM, Hypertrophic cardiomyopathy.

LV hypertrophy develops, it typically manifests between 12 and 20 years of age and much less frequently later in life. ECG abnormalities, increased LVEF, delayed myocardial relaxation, or myocardial fibrosis on CMR can precede the onset of LV hypertrophy and indicate early emergence of clinical disease.^{2,5}

Genotype-positive/phenotype-negative individuals should also undergo periodic screening (with clinical examination, ECG, echocardiogram, or CMR) for detecting development of clinical disease with LV hypertrophy. The frequency of screening is similar to that described for clinical family screening (Table 28.4). Exercise stress testing or Holter monitoring to screen for ventricular arrhythmias may also be considered in individuals of families with high risk for SCD.

At present, there is no compelling evidence to suggest an increased risk for SCD in asymptomatic, genotype-positive/phenotype-negative HCM patients; therefore participation in competitive athletics is not prohibited, particularly in the absence of a family history of HCM-related SCD.³³

Prophylactic pharmacological therapy in asymptomatic carriers of HCM genes is ineffective and not recommended.

REFERENCES

- Gersh BJ, et al. 2011 ACCF/AHA guideline for the diagnosis and treatment of hypertrophic cardiomyopathy: a report of the American College of Cardiology Foundation/American Heart Association Task Force on Practice Guidelines. *J Am Coll Cardiol*. 2011;58:e212–e260.
- Maron BJ, et al. Hypertrophic cardiomyopathy: present and future, with translation into contemporary cardiovascular medicine. *J Am Coll Cardiol*. 2014;64:89–99.
- Nijenkamp LLAM, Güçlü A, Appelman Y, et al. Sex-dependent pathophysiological mechanisms in hypertrophic cardiomyopathy: implications for rhythm disorders. *Heart Rhythm*. 2015;12:433–439.
- Popescu BA, Rosca M, Schwammenthal E. Dynamic obstruction in hypertrophic cardiomyopathy. *Curr Opin Cardiol*. 2015;30:468–474.
- Elliott PM, et al. 2014 ESC guidelines on diagnosis and management of hypertrophic cardiomyopathy: the Task Force for the Diagnosis and Management of Hypertrophic Cardiomyopathy of the European Society of Cardiology (ESC). *Eur Heart J*. 2014;35:2733–2779.
- Semsarian C, Ingles J, Maron MS, et al. New perspectives on the prevalence of hypertrophic cardiomyopathy. *J Am Coll Cardiol*. 2015;65:1249–1254.
- Sherid MV, Arabadjian M, Koulova A. Thin-filament mutations, hypertrophic cardiomyopathy, and risk*. *J Am Coll Cardiol*. 2014;64:2601–2604.
- Baudhuin LM, Kotzer KE, Kluge ML, et al. What is the true prevalence of hypertrophic cardiomyopathy? *J Am Coll Cardiol*. 2015;66:1845–1846.
- Maron MS, Hellawell JL, Lucove JC, et al. Occurrence of clinically diagnosed hypertrophic cardiomyopathy in the United States. *Am J Cardiol*. 2016;117:1651–1654.
- Maron MS, et al. Contemporary natural history and management of nonobstructive hypertrophic cardiomyopathy. *J Am Coll Cardiol*. 2016;67:1399–1409.
- Maron BJ, et al. Hypertrophic cardiomyopathy in adulthood associated with low cardiovascular mortality with contemporary management strategies. *J Am Coll Cardiol*. 2015;65:1915–1928.
- Spirito P, et al. Syncope and risk of sudden death in hypertrophic cardiomyopathy. *Circulation*. 2009;119:1703–1710.
- Williams L, Frenneaux M. Syncope in hypertrophic cardiomyopathy: mechanisms and consequences for treatment. *Europace*. 2007;9:817–822.
- Wille I, et al. High incidence of de novo and subclinical atrial fibrillation in patients with hypertrophic cardiomyopathy and cardiac rhythm management device. *J Cardiovasc Electrophysiol*. 2016;27:779–784.
- Guttmann OP, Rahman MS, O'Mahony C, et al. Atrial fibrillation and thromboembolism in patients with hypertrophic cardiomyopathy: systematic review. *Heart*. 2014;100:465–472.
- Link MS, et al. Ventricular tachyarrhythmias in patients with hypertrophic cardiomyopathy and defibrillators: triggers, treatment, and implications. *J Cardiovasc Electrophysiol*. 2017;28:531–537.
- Greulich S, et al. Incremental value of late gadolinium enhancement for management of patients with hypertrophic cardiomyopathy. *Am J Cardiol*. 2012;110:1207–1212.
- Wahbi K, et al. Long-term cardiac prognosis and risk stratification in 260 adults presenting with mitochondrial diseases. *Eur Heart J*. 2015;36:2886–2893.
- Chandra N, Bastiaenen R, Papadakis M, et al. Sudden cardiac death in young athletes. *J Am Coll Cardiol*. 2013;61:1027–1040.
- Wasfy MM, Weiner RB. Differentiating the athlete's heart from hypertrophic cardiomyopathy. *Curr Opin Cardiol*. 2015;30:1.
- Rawlins J, Bhan A, Sharma S. Left ventricular hypertrophy in athletes. *Eur J Echocardiogr*. 2009;10:350–356.
- Basavarajaiah S, et al. Ethnic differences in left ventricular remodeling in highly-trained athletes relevance to differentiating physiologic left ventricular hypertrophy from hypertrophic cardiomyopathy. *J Am Coll Cardiol*. 2008;51:2256–2262.
- Wang W, et al. Prognostic implications of nonsustained ventricular tachycardia in high-risk patients with hypertrophic cardiomyopathy. *Circ Arrhythm Electrophysiol*. 2017;10:1–8.
- McLellan AJ, et al. Diffuse ventricular fibrosis on cardiac magnetic resonance imaging associates with ventricular tachycardia in patients with hypertrophic cardiomyopathy. *J Cardiovasc Electrophysiol*. 2016;27:571–580.
- Vriesendorp PA, et al. Validation of the 2014 ESC guidelines risk prediction model for the primary prevention of sudden cardiac death in hypertrophic cardiomyopathy. *Circ Arrhythm Electrophysiol*. 2015;8:829–835.
- Fraiche A, Wang A. Hypertrophic cardiomyopathy: new evidence since the 2011 American Cardiology of Cardiology Foundation and American Heart Association Guideline. *Curr Cardiol Rep*. 2016;18:70.
- Veselka J, et al. Long-term clinical outcome after alcohol septal ablation for obstructive hypertrophic cardiomyopathy: results from the Euro-ASA registry. *Eur Heart J*. 2016;37:1517–1523.
- Maron BJ, et al. Low operative mortality achieved with surgical septal myectomy. *J Am Coll Cardiol*. 2015;66:1307–1308.
- Yue-Cheng H, et al. Long-term follow-up impact of dual-chamber pacing on patients with hypertrophic obstructive cardiomyopathy. *Pacing Clin Electrophysiol*. 2013;36:86–93.
- Maron BJ, et al. Prevention of sudden cardiac death with implantable cardioverter-defibrillators in children and adolescents with hypertrophic cardiomyopathy. *J Am Coll Cardiol*. 2013;61:1527–1535.
- Maron BJ, Maron MS. Contemporary strategies for risk stratification and prevention of sudden death with the implantable defibrillator in hypertrophic cardiomyopathy. *Heart Rhythm*. 2016;13:1155–1165.
- Thavikulwat AC, Tomson TT, Knight BP, et al. Appropriate implantable defibrillator therapy in adults with hypertrophic cardiomyopathy. *J Cardiovasc Electrophysiol*. 2016;27:953–960.
- Maron BJ, et al. Eligibility and disqualification recommendations for competitive athletes with cardiovascular abnormalities: Task Force 3: hypertrophic cardiomyopathy, arrhythmogenic right ventricular cardiomyopathy and other cardiomyopathies, and myocarditis. *J Am Coll Cardiol*. 2015;66:2362–2371.

Ventricular Tachycardia in Arrhythmogenic Right Ventricular Cardiomyopathy

OUTLINE

Pathophysiology, 942

- Molecular Genetics, 942
- Pathogenesis, 943
- Pathology, 945

Epidemiology and Natural History, 945

Clinical Presentation, 946

- Phases of Clinical Disease Expression, 946
- Ventricular Arrhythmias, 946
- Supraventricular Arrhythmias, 946
- Thromboembolism, 946

Initial Evaluation, 946

- Diagnostic Criteria, 946
- Endomyocardial Biopsy, 948
- Genetic Testing, 948
- Invasive Electrophysiological Testing, 948

Differential Diagnosis, 948

- Idiopathic Right Ventricular Outflow Tract Tachycardia, 948
- Cardiac Sarcoidosis, 949
- Dilated Cardiomyopathy, 950
- Athlete's Heart, 950
- Exercise-Induced Arrhythmogenic Right Ventricular Cardiomyopathy, 950

Risk Stratification, 950

Principles of Management, 950

- Pharmacological Therapy, 950
- Catheter Ablation, 952
- Implantable Cardioverter-Defibrillator, 952
- Participation in Sports, 953
- Family Screening, 953

Electrocardiographic Features, 954

- Electrocardiogram During Sinus Rhythm, 954
- Electrocardiogram During Ventricular Tachycardia, 957

Electrophysiological Features, 957

- Induction of Tachycardia, 957
- Tachycardia Features, 957

Mapping, 959

- Activation Mapping, 959
- Entrainment Mapping, 959
- Pace Mapping, 960
- Substrate Mapping, 960
- Epicardial Mapping, 962

Ablation, 962

- Target of Ablation, 962
- Ablation Technique, 964
- Endpoints of Ablation, 964
- Outcome, 964

PATHOPHYSIOLOGY

Arrhythmogenic right ventricular cardiomyopathy (ARVC), also referred to as “arrhythmogenic cardiomyopathy,” is an inherited desmosomal cardiomyopathy with incomplete penetrance and variable expressivity. ARVC is characterized by ventricular arrhythmias and structural abnormalities of the right ventricle (RV) (and left ventricle [LV] more manifest during the latter stages of the disease). The hallmark pathological findings are progressive myocyte loss and fibrofatty (fibrous and adipose) tissue replacement, with a predilection for the RV, but the LV also can be affected. Fibrofatty replacement of the myocardium produces “islands” of scar that can lead to reentrant ventricular tachycardias (VTs) and increased risk of sudden cardiac death (SCD).^{1–3}

Molecular Genetics

Familial disease occurs in approximately 30% to 60% of cases of ARVC. The remainder of patients with ARVC have undiscovered genetic abnormalities or have the disease *de novo*. Two patterns of inheritance have been described: autosomal dominant disease with incomplete penetrance (most common) and autosomal recessive disease (rare). Autosomal recessive forms of ARVC include Naxos disease (also known as familial palmoplantar keratosis and “mal de Meleda” disease) and Carvajal syndrome (a disorder of LV cardiomyopathy), both of which are associated with skin and hair abnormalities.⁴

The autosomal dominant nonsyndromic ARVC-1 to ARVC-12 as well as the two rare recessive forms (Naxos disease and Carvajal syndrome) have been mapped to 12 genetic loci, with mutations in eight gene loci identified (Table 29.1). Although some identified gene mutations such as ryanodine receptor 2 (RYR2) may be phenocopies of ARVC, a common theme of *desmosomal protein mutations* has been emerging. In fact, five of the eight gene loci encode desmosomal proteins (plakophilin-2 [PKP2], desmoglein-2 [DSG2], desmoplakin [DSP], desmocollin-2 [DSC2], and junctional plakoglobin [JUP]) have been found in association with the ARVC phenotype in up to 50% of cases. Among genotype-positive probands, mutations in PKP2 appear to be the most common causes of ARVC, accounting for approximately 73% to 79% of cases. Mutations in DSG2 and DSP account for approximately 10% to 14% and 3% to 8% of cases, respectively. Therefore ARVC is currently considered to be, at least in a subset, a disease of the cardiac desmosome.^{2,5}

The majority of disease-causing mutations are insertion/deletion or nonsense mutations, which are expected to cause premature termination of the encoded proteins. Data from the North American ARVC registry showed that 86% of patients had a single heterozygous gene mutation, 7% showed compound heterozygosity, 7% had digenic heterozygosity, and 1% had homozygous mutation. Patients with multiple mutations seem to have early disease onset and a worse arrhythmic course.⁶ Mutations can be inherited from a parent or can be the result

TABLE 29.1 Known Genetic Loci for Arrhythmogenic Right Ventricular Cardiomyopathy-Dysplasia

Locus Name	Causative Gene	Mode of Inheritance	% of Mutations
ARVC-1	Transforming growth factor- β_3	Autosomal dominant	
ARVC-2	Cardiac ryanodine receptor (RYR2)	Autosomal dominant	
ARVC-3	Unknown	Autosomal dominant	
ARVC-4	Unknown	Autosomal dominant	
ARVC-5	Transmembrane protein-43	Autosomal dominant	
ARVC-6	Unknown	Autosomal dominant	
ARVC-7	Unknown	Autosomal dominant	
ARVC-8	Desmoplakin (DSP)	Autosomal dominant	3%–8%
ARVC-9	Plakophilin-2 (PKP2)	Autosomal dominant	73%–79%
ARVC-10	Desmoglein-2 (DSG2)	Autosomal dominant	10%–14%
ARVC-11	Desmocollin-2	Autosomal dominant	
ARVC-12	Plakoglobin (JUP)	Autosomal dominant	
Naxos disease	Plakoglobin (JUP)	Autosomal recessive	Rare
Carvajal syndrome	Desmoplakin (DSP)	Autosomal recessive	Rare

ARVC, Arrhythmogenic right ventricular cardiomyopathy;
JUP, junctional plakoglobin.

of a new mutation. Approximately 20% to 30% of patients with ARVC have a family history of ARVC or of SCD.

Mutations in several nondesmosome genes have also been reported to cause ARVC: Transmembrane protein 43 (*TMEM43*), transforming growth factor-beta3 (*TGF β 3*), desmin (*DES*), lamin A/C (*LMNA*), titin (*TTN*), and phospholamban (*PLN*). A mutation in *TMEM43*, encoding a transmembrane protein with ties to an adipogenic transcription factor, was reported as the cause for ARVC-5, a subtype of ARVC with prominent LV involvement.

Furthermore, mutations in *RYR2*, encoding the cardiac ryanodine receptor (the major calcium release channel of the sarcoplasmic reticulum in cardiomyocytes, also implicated in familial catecholaminergic polymorphic ventricular tachycardia [CPVT]), result in a form of arrhythmogenic cardiomyopathy (ARVC-2) characterized by exercise-induced polymorphic VT that does not appear to have a reentrant mechanism, occurring in the absence of significant structural abnormalities. Patients do not develop characteristic features of ARVC on the 12-lead electrocardiogram (ECG) or signal-averaged ECG, and global RV function remains unaffected. ARVC-2 shows a closer resemblance to familial CPVT in both etiology and phenotype, and its inclusion under the umbrella term of ARVC remains controversial.^{7–9}

Genotype–phenotype studies have identified an association of genotype with clinical course and disease expression, including the onset of overt disease, LV involvement, and the severity of heart failure. In a multicenter study, 80% of individuals had a single copy of a *PKP2* mutation whereas 4% of individuals carried two or more pathogenic mutations. *PKP2* mutation carriers are more likely to experience an earlier onset of both symptoms and arrhythmias. *PLN* mutation carriers presented at a significantly older age yet had worse long-term prognosis, with more LV dysfunction and heart failure. Also, individuals harboring DSP were considerably more likely to develop heart failure and more

prominent LV involvement, and are more likely to present with SCD rather than other mutation carriers.¹⁰

Carriers of single pathogenic mutations in any of the genes appear to exhibit a similar high risk of developing a life-threatening arrhythmia, with no significant differences in survival from life-threatening VT/ventricular fibrillation (VF) among the different genes. Conversely, patients with more than one mutation have considerably worse clinical course with a significantly earlier onset of symptoms and first sustained VT or VF, a greater chance of developing sustained VT or VF, and a fivefold increase in the risk of developing LV dysfunction and heart failure than those carrying a single mutation.^{6,10}

Pathogenesis

Cardiac desmosomes are specialized, multiprotein complexes in the intercalated disks that anchor intermediate filaments to the cytoplasmic membrane in adjacent cardiomyocytes, thereby forming a three-dimensional (3-D) scaffolding and providing mechanical strength and cohesion of cardiomyocytes in the beating heart (Fig. 29.1). Cardiac desmosomes are also responsible for regulating the transcription of genes involved in adipogenesis and apoptosis as well as maintaining proper electrical conductivity through the regulation of gap junctions and calcium homeostasis.

Cardiac desmosomes are composed of three groups of proteins: the cadherin family, the Armadillo family, and the plakin family. The cadherin family is composed of three desmocollins and three desmogleins, which are primarily responsible for anchoring the structure to the membrane. The Armadillo family is composed of plakoglobin and three plakophilins, which form the core structure and possess signaling capabilities. The plakin family is composed of DSP, envoplakin, periplakin, plectin, and pinin, which are responsible for the attachment of the desmosomes to intermediary filaments.

The mechanisms by which the affected desmosomes cause myocyte apoptosis, fibrogenesis, adipogenesis, and slow ventricular conduction, thus leading to impaired RV function and increased arrhythmogenicity, remain to be determined. Mutations in desmosomal genes alter the number or integrity of desmosomes and thereby lead to impaired mechanical coupling and the failure of cell-to-cell adhesion structures during exposure to physical strain, resulting in cardiomyocyte detachment and degeneration, with subsequent inflammation and replacement by fibrofatty tissue. This course may be triggered or aggravated by inflammatory processes (superimposed myocarditis), autonomic dysfunction, or mechanical stretch of the myocardium (e.g., during intense exercise) and lead to myocardial damage, inflammation, and cell death.^{2,11} The reason behind the preferential involvement of the RV in ARVC remains elusive; nonetheless, several factors can make the RV particularly vulnerable to impaired mechanical cellular coupling, more so than the LV, including thinner RV free wall, high distensibility, and variations in preload and stretch. These factors expose the RV to disproportionately greater strain during exercise compared with the LV.^{12,13}

Fibrofatty replacement is a nonspecific repair process also observed in the muscular dystrophies. The architecture of thin surviving myocardial bundles within the fibrofatty tissue creates lengthened conduction pathways, conduction slowing at pivotal points, and conduction block, creating an electrophysiological (EP) substrate for reentry and VT. Furthermore, fibrofatty replacement of the myocardium results in abnormal structure, morphology, geometry, and wall motion of the ventricle.¹¹

In addition, impaired desmosomal structure and function can affect other cell-to-cell contact structures in the myocardium. Mutations in desmosomal proteins can impair the expression of interacting proteins at the intercalated disk (e.g., gap junction or sodium channel proteins), giving rise to the impairment of intercellular conductance and promoting ventricular arrhythmogenesis, even in the absence of fibrofatty tissue

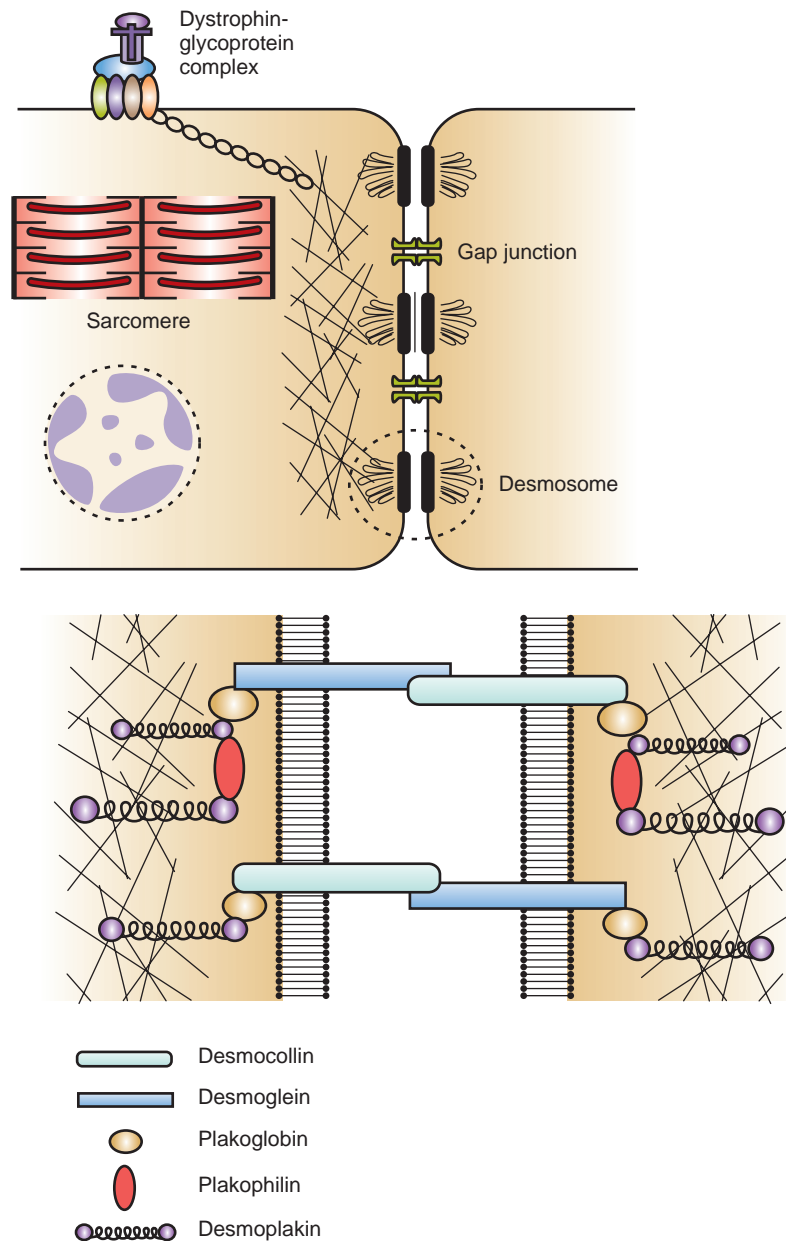


Fig. 29.1 Molecular Structure of the Cardiac Desmosome. The desmosomal cadherins desmocollin and desmoglein form classic homotypic and heterotypic interactions between cells. These membrane-bound proteins are linked through the Armadillo family members, plakoglobin, and plakophilin to the intermediate filament-binding protein desmoplakin. This complex anchors the desmosome to the cytoskeleton of the cell, and thus indirectly to the sarcomere, the nuclear membrane, and the dystrophin-associated glycoproteins. (From Ellinor PT, MacRae CA, Thierfelder L. Arrhythmogenic right ventricular cardiomyopathy. *Heart Fail Clin.* 2010;6:161–177.)

replacement. In particular, connexin-43 (Cx43) remodeling in the gap junctions, which contributes to delayed conduction and ventricular arrhythmogenesis, is often observed in ARVC patients. Also, a reduction in Cx43 protein can potentially lead to reduced sodium channel expression and function. Abnormal electrical coupling and ion channel dysfunction, leading to electrical instability, can promote arrhythmias and predispose patients to a high risk of SCD, even in the early disease stages, prior to the development of significant ventricular dysplasia and scarring.^{14–16}

In the early disease phase, VF likely reflects acute ventricular electrical instability secondary to acute myocyte death and reactive

inflammation, which is often characterized by dynamic T wave inversion, ST segment elevation, and myocardial enzyme release.² In later disease stages of ARVC, fibrofatty replacement of RV myocardium creates scar regions that provide the arrhythmogenic substrate for VT. In fact, scar-related macroreentry in areas of abnormal myocardium (similar to that observed in the post-myocardial infarction [MI] setting) is the most common mechanism of VT in ARVC patients. Most reentrant circuits cluster around the tricuspid annulus and the right ventricular outflow tract (RVOT). The critical isthmus contained in these reentry circuits often is a narrow path of tissue with abnormal conduction properties, typically bounded by two approximately

parallel conduction barriers that consist of scar areas, the tricuspid annulus, or both.

Of note, among ARVC patients with frequent premature ventricular complexes (PVCs) at baseline, a high degree of association has been reported between induced sustained VT and the clinical PVCs. VT in these patients exhibited features suggestive of a focal mechanism. The site of origin of those catecholamine-facilitated VTs was uniformly the border region of scar, typically in the RVOT and RV basal regions.¹⁷

Pathology

The most striking morphological feature of ARVC is the diffuse or regional loss (atrophy) of myocardium with subsequent replacement by fibrofatty tissue, leading to localized ventricular wall thinning, sacculations, aneurysms (eFig. 29.1), and segmental hypokinesia. Fibrofatty replacement usually begins in the subepicardium or midmural layers and progresses to the subendocardium. Patchy inflammatory infiltrates can be present in areas of myocardial damage. Myocarditis can reflect an active phase of ARVC during which worsening of ventricular systolic function or ventricular arrhythmia can develop.¹⁸

In ARVC, the muscle cells affected initially are primarily in the RV, but the LV can be involved later in the course of ARVC or occasionally be an early or predominant site of the disease. The sites of involvement can be localized, and in early disease they are often confined to the so-called triangle of dysplasia—namely, the RVOT, RV apex, and inferolateral wall near the tricuspid valve (which is considered a pathognomonic feature of ARVC, although it is not necessarily present in all cases). More recent evidence suggests that, unlike the other two areas, the RV apex is usually not involved in arrhythmogenesis; histopathologically, myocardium at the apex is often thin and replaced by fat (but not fibrosis) in older persons without ARVC. Thus some of the early reports of ARVC probably included patients with age-related apical thinning and fatty replacement that was mistaken for apical involvement with the disease.

RV trabeculae are not primarily affected by the atrophic process and tend to show a compensatory hypertrophy, resulting in an aspect of increased trabeculation and fissuring of the RV walls. Involvement of the interventricular septum is minimal. In more advanced stages of ARVC, diffuse myocardial involvement leads to global RV dilation and dysfunction.¹¹ End-stage disease typically exhibits biventricular involvement, usually with multiple aneurysms and a parchment-like appearance of the ventricular free wall. Although several hypotheses have been put forth, currently there is no unifying hypothesis that explains the patchy, yet predictable pattern of RV involvement in ARVC.

Although the dysplastic tissue predominantly involves the RV, the increasing use of advanced imaging studies (cardiac magnetic resonance [CMR]) revealed that LV involvement is common from the early disease stage, but is often clinically subtle.¹⁹ The fibrofatty pattern exhibits a predilection for the LV posteroseptal and posterolateral areas, typically extending from the epicardium to the mid-myocardium, with sparing of the endocardium. In a recent report in a cohort of genetically confirmed ARVC patients, regional cardiac involvement in ARVC mutation carriers had a characteristic pattern involving the RV basal inferior wall, the RV basal anterior wall, and the LV posterolateral wall. RV apical involvement was only observed in advanced cases of ARVC, typically as a part of global RV disease.²⁰ These findings support the adoption of the broader term “arrhythmogenic cardiomyopathy.”²¹ Furthermore, the ARVC phenotype can vary depending on the desmosomal component affected by the primary mutation. Genotype–phenotype correlations have shown “nonclassical” clinical variants in genetically predisposed ARVC patients exhibiting early and more extensive LV involvement, which may either parallel (“biventricular” variant) or exceed (“left dominant” variant) the severity of RV disease.^{19,22}

In ARVC, the regions of abnormal myocardium do not always follow the pattern of dense scar surrounded by a ring of abnormal myocardium, which is often referred to as the scar border zone. Sometimes, abnormal voltages are found alone without a dense scar defining the regions. This is because ARVC is a different process from scarring caused by MI. Infarction causes dense scar surrounded by a border zone because of the ischemic penumbra that surrounds the infarcted territory. However, in ARVC, the process is patchy and can cause inhomogeneous scarring in anatomically disparate areas. Nonetheless, previous data have shown that it is still possible to identify well-demarcated borders around these abnormal regions.

EPIDEMIOLOGY AND NATURAL HISTORY

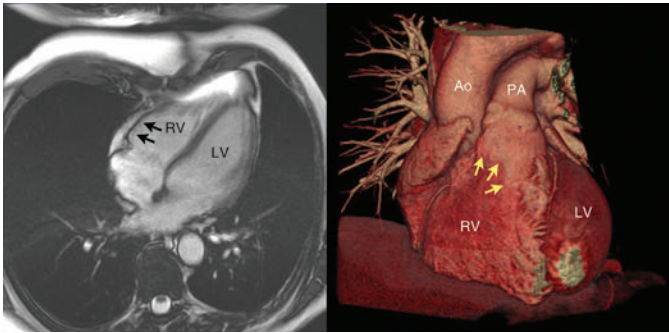
The incidence and prevalence of ARVC are uncertain. The prevalence of the disease in the general population is estimated at 0.02%, but it varies geographically. In certain regions of Italy (Padua, Venice) and Greece (the island of Naxos), a prevalence as high as 0.4% to 0.8% for ARVC has been reported.³ Approximately 50% of affected patients have a positive family history. ARVC exhibits incomplete penetrance (i.e., not all carriers of the pathogenic mutation will develop a phenotypic expression) and limited phenotypic expression, which probably account for the underestimation of the prevalence of familial disease.³

ARVC occurs in young adults; about 80% of familial ARVC patients are younger than 50 years, and the mean age at diagnosis is 31 years. The disease is almost never diagnosed in infancy and rarely before the age of 10 years.²³ The high risk of life-threatening arrhythmias in patients with ARVC spans from adolescence to advanced age, reaching its peak (4.0 per 100 person-years) between the ages of 21 and 40 years.²⁴ Of note, the phenotypic first presentation with SCD or VF appears to occur at a significantly younger age (median 23 years) than presentation with sustained monomorphic VT (median 36 years).¹⁰ Late clinical presentation is not uncommon and does not confer a benign prognosis; about 21% of all ARVC patients present after 50 years of age, predominantly with sustained VT.²⁵

Because ARVC is an autosomal-dominant disease, an equal number of men and women are genetically affected. However, a predominance of male gender exists in phenotypically affected individuals. In worldwide cohorts, men seem more likely to develop a more severe disease phenotype, present with SCD, be symptomatic at presentation, and have worse long-term prognosis.¹⁰ However, in the North American ARVC Registry, no gender differences were found in the clinical expression of ARVC.²⁶ In one study of patients with sporadic ARVC, men had a significantly higher risk of VT/VF, whereas women had a significantly higher risk of heart failure death or heart transplantation. However, the other clinical manifestations, including ECG findings and LV and RV function, as well as total cardiac mortality, were comparable in both genders.²⁷

Some patients are asymptomatic and ARVC is only suspected by the finding of ventricular ectopy and other abnormalities on routine ECG or other testing because of a positive family history. In one report, 10% of those initially unaffected subjects developed structural signs of disease on echocardiography during a mean follow-up of 8.5 years; almost 50% had symptomatic ventricular arrhythmias. Progression from mild to moderate disease occurred in 5% of patients, and progression from moderate to severe disease occurred in 8%.

The estimated overall mortality rate in ARVC patients varies among different studies, ranging from 0.08% to 3.6% per year.² Mortality is predominantly related to arrhythmic SCD, mostly in young people and athletes, which is the first clinical manifestation of ARVC in 50% of afflicted individuals. In fact, up to 5% of SCDs in young adults in the United States are attributed to ARVC. In northeast Italy, ARVC is



eFig. 29.1 Right Ventricular (RV) Aneurysm. This cardiac computed tomography angiogram shows thinning and aneurysmal dilation of the RV anterior wall and outflow tract (*arrows*) in a patient with arrhythmogenic right ventricular cardiomyopathy and ventricular tachycardia. Ao, Aorta; LV, left ventricle; PA, pulmonary artery; RV, right ventricle.

responsible for 22% of SCDs in young athletes and 8% of SCDs in nonathletes. In advanced disease, progressive RV or biventricular heart failure contributes to poor outcome.¹

CLINICAL PRESENTATION

The clinical presentation varies widely because ARVC includes a spectrum of different conditions rather than a single entity. Different pathological processes can manifest a diversity of symptoms. In addition, ARVC can have a temporal progression and, hence, present differently according to the time of presentation.

Phases of Clinical Disease Expression

Four clinicopathological stages of ARVC can be considered: (1) “concealed” phase, (2) “overt electrical disorder,” (3) phase of “RV failure,” and (4) phase of “biventricular failure.” Although ARVC is a genetically transmitted disease, it is associated with a long asymptomatic lead time and individuals in their teens may not have any characteristics of ARVC clinically or on screening tests. Early ARVC is often asymptomatic (the “concealed” phase), and is occasionally associated with minor ventricular arrhythmias and subtle RV structural changes. Nonetheless, these patients are still at risk of SCD, especially during intense physical exertion.

With disease progression, the “overt electrical disorder” typically causes symptomatic ventricular arrhythmia (manifesting as palpitations, effort-induced syncope, or cardiac arrest) and more obvious morphological abnormalities detectable by cardiac imaging. Further disease extension results in RV dilation and dysfunction (the “phase of RV failure”), precipitating symptoms and signs of right heart failure. Unless SCD occurs, progressive impairment of cardiac function can result in biventricular heart failure late in the evolution of ARVC, usually within 4 to 8 years after typical development of complete right bundle branch block (RBBB). End-stage disease is often indistinguishable from dilated cardiomyopathy and manifests with congestive heart failure, atrial fibrillation (AF), and an increased incidence of thromboembolic events. Overall, judging the accurate position of the patient on the time scale of the spectrum can be difficult, and some patients can remain stable in the same phase of the disease for several decades.²

Ventricular Arrhythmias

ARVC is one of the most arrhythmogenic human heart diseases known. Unlike other cardiomyopathies, electrical instability is present at the very early stages of ARVC; ventricular arrhythmias and SCD are often presenting symptoms before the development of any overt myocardial dysfunction. Ventricular arrhythmias range from isolated ectopy to sustained VT or VF. Approximately 50% of patients with ARVC present with symptomatic ventricular arrhythmias, most commonly sustained and nonsustained monomorphic VT, which are manifested by palpitations, dizziness, or syncope. Importantly, unlike other forms of cardiomyopathies and channelopathies, most syncopal episodes in ARVC are attributable to ventricular arrhythmias (rather than vasovagal or nonarrhythmic causes) and are associated with a poor prognosis. In fact, unexplained syncope is an independent predictor of SCD, with a sensitivity of 40% and a specificity of 90%.

The frequency of ventricular arrhythmias in ARVC varies with the severity of the disease, ranging from 23% in patients with mild disease to almost 100% in patients with severe disease. Ventricular arrhythmias characteristically occur during exercise; up to 50% to 60% of patients with ARVC develop monomorphic VT during exercise testing.^{2,14}

One of the unfortunate features of ARVC is SCD, which is the first clinical manifestation of ARVC in 50% of afflicted individuals. In most patients, the mechanism of SCD in ARVC is the acceleration of VT,

with ultimate degeneration into VF. In addition, RV failure and LV dysfunction are independently associated with cardiovascular mortality.²¹

Supraventricular Arrhythmias

Supraventricular arrhythmias are observed in approximately 14% of patients with ARVC, and in up to 25% of those referred for treatment of ventricular arrhythmias. In decreasing order of frequency, supraventricular tachyarrhythmias in these patients include AF, atrial tachycardia (AT), and atrial flutter (AFL). The presence of atrial arrhythmias is associated with increasing disease severity and heart failure. Often, atrial arrhythmias in this population can be asymptomatic, detected only on implantable cardioverter-defibrillator (ICD) interrogation or following an inappropriate ICD shock.²⁸

Thromboembolism

Thromboembolic complications occur in approximately 0.5% of ARVC patients annually, and are likely related to thrombus formation in ventricular aneurysms and sacculations, or global ventricular dilatation.²

INITIAL EVALUATION

ECG, Holter monitoring, signal-averaged ECG (if available), echocardiography, and CMR provide optimal clinical evaluation of patients suspected of having ARVC. Electrical abnormalities often precede structural changes in ARVC, and therefore ECG, signal-averaged electrocardiogram (SAECG), exercise stress testing, and Holter monitoring may have more diagnostic utility than CMR in the early stages of ARVC. If noninvasive work-up is suggestive but not diagnostic of ARVC, further testing should be considered to establish the diagnosis, including RV angiography, endomyocardial biopsy, and invasive EP testing.^{11,21}

The noninvasive diagnosis of ARVC can be exceedingly difficult. Several factors, including marked phenotypic variation, incomplete and low (30%) penetrance, and age-related disease development and progression contribute to the complexity of the clinical diagnosis. Particularly problematic is recognition of the early stages of ARVC when overall RV function may be normal, with local or regional wall-motion abnormalities that are difficult to quantify; nonetheless, the absence of clinical features does not necessarily confer low risk.

Diagnostic Criteria

There is no single test that is conclusively diagnostic (gold standard) of ARVC in the disease's early stages. At initial presentation, the ECG can be normal in up to 50% of ARVC patients. Furthermore, up to 36% of ARVC patients presenting with a history of sustained ventricular arrhythmias or cardiac arrest exhibit no major or minor criteria on cardiac imaging (CMR or echocardiogram).

Therefore the diagnosis of ARVC is currently guided by the modified task force criteria, a composite of clinical, imaging, pathological, and ECG features (Table 29.2). According to this scheme, the diagnosis of ARVC is fulfilled by the presence of (1) two major or one major and two minor criteria, or by four minor criteria (definite diagnosis); (2) one major and one minor or three minor criteria (borderline diagnosis); or (3) one major or two minor criteria from different categories (possible diagnosis).²⁹

Echocardiography, CMR, and angiography are the current imaging modalities incorporated into the modified task force criteria. Because ARVC is a rare disease, when performing and analyzing these studies it is important to recognize the importance of expert interpretation of the complex-shaped RV and the need for quantitation of RV structure and function, as well as specific protocols for optimal evaluation. Referral to centers with expertise in this field should be considered.²⁹

TABLE 29.2 Revised Task Force Criteria for the Diagnosis of ARVC

Major Criteria	Minor Criteria
I. Imaging By 2-D echo: Regional RV akinesia, dyskinesia, or aneurysm And 1 of the following (end diastole): PLAX RVOT ≥ 32 mm (corrected for body size [PLAX/BSA] ≥ 19 mm/m ²) PSAX RVOT ≥ 36 mm (corrected for body size [PSAX/BSA] ≥ 21 mm/m ²) Fractional area change $\leq 33\%$ By CMR: Regional RV akinesia or dyskinesia or dyssynchronous RV contraction And one of the following: Ratio of RV end-diastolic volume to BSA ≥ 110 mL/m ² (male) or ≥ 100 mL/m ² (female) RV ejection fraction $\leq 40\%$ By RV angiography: Regional RV akinesia, dyskinesia, or aneurysm	By 2-D echo: Regional RV akinesia or dyskinesia And 1 of the following (end diastole): PLAX RVOT ≥ 29 to <32 mm (corrected for body size [PLAX/BSA] ≥ 16 to <19 mm/m ²) PSAX RVOT ≥ 32 to <36 mm (corrected for body size [PSAX/BSA] ≥ 18 to <21 mm/m ²) Fractional area change $>33\%$ to $\leq 40\%$ By CMR: Regional RV akinesia or dyskinesia or dyssynchronous RV contraction And one of the following: Ratio of RV end-diastolic volume to BSA ≥ 100 to <110 mL/m ² (male) or ≥ 90 to <100 mL/m ² (female) RV ejection fraction $>40\%$ to $\leq 45\%$
II. Endomyocardial Biopsy Residual myocytes (60% by morphometric analysis or 50% if estimated), with fibrous replacement of the RV free wall myocardium in ≥ 1 sample, with or without fatty replacement of tissue on endomyocardial biopsy	Residual myocytes (60% to 75% by morphometric analysis or 50% to 65% if estimated), with fibrous replacement of the RV free wall myocardium in ≥ 1 sample, with or without fatty replacement of tissue on endomyocardial biopsy
III. Repolarization Abnormalities Inverted T waves in right precordial leads (V ₁ , V ₂ , and V ₃) or beyond in individuals >14 years of age (in the absence of complete RBBB QRS ≥ 120 msec)	Inverted T waves in leads V ₁ and V ₂ in individuals >14 years of age (in the absence of complete RBBB) or in V ₄ , V ₅ , or V ₆ Inverted T waves in leads V ₁ , V ₂ , V ₃ , and V ₄ in individuals >14 years of age in the presence of complete RBBB
IV. Depolarization/Conduction Abnormalities Epsilon wave (reproducible low-amplitude signals between end of QRS complex to onset of the T wave) in the right precordial leads (V ₁ to V ₃)	Late potentials by SAECD in ≥ 1 of 3 parameters in the absence of a QRS duration of ≥ 110 msec on the standard ECG Filtered QRS duration (fQRS) ≥ 114 msec Duration of terminal QRS <40 μ V (low-amplitude signal duration) ≥ 38 msec Root mean square voltage of terminal 40 msec ≤ 20 μ V Terminal activation duration of QRS ≥ 55 msec measured from the nadir of the S-wave to the end of the QRS, including R', in V ₁ , V ₂ , or V ₃ , in the absence of complete RBBB
V. Arrhythmias Nonsustained or sustained ventricular tachycardia of left bundle-branch morphology with superior axis (negative or indeterminate QRS in leads II, III, and aVF and positive in lead aVL)	Nonsustained or sustained ventricular tachycardia of RV outflow configuration, LBBB morphology with inferior axis (positive QRS in leads II, III, and aVF and negative in lead aVL), or of unknown axis >500 ventricular extrasystoles per 24 h (Holter)
VI. Family History ARVC confirmed in a first-degree relative who meets current TFC ARVC confirmed pathologically at autopsy or surgery in a first-degree relative Identification of a pathogenic mutation categorized as associated or probably associated with ARVC in the patient under evaluation	History of ARVC in a first-degree relative in whom it is not possible or practical to determine whether the family member meets current TFC Premature sudden death (<35 years of age) due to suspected ARVC in a first-degree relative ARVC confirmed pathologically or by current TFC in a second-degree relative

Diagnostic terminology: definite diagnosis: two major or one major and two minor criteria, or four minor from different categories; borderline: one major and one minor or three minor criteria from different categories; possible: one major or two minor criteria from different categories. 2-D, 2-Dimensional; ARVC, arrhythmogenic right ventricular cardiomyopathy; BSA, body surface area; CMR, cardiac magnetic resonance; ECG, electrocardiogram; echo, echocardiography; LBBB, left bundle branch block; PLAX, parasternal long-axis view; PSAX, parasternal short-axis view; RBBB, right bundle branch block; RV, right ventricle/ventricular; RVOT, right ventricular outflow tract; SAECD, signal averaged electrocardiogram; TFC, task force criteria.

From Etom Y, Govindapillai S, Hamilton R, et al. Importance of CMR within the task force criteria for the diagnosis of ARVC in children and adolescents. *J Am Coll Cardiol*. 2015;65:987–995.

Endomyocardial Biopsy

Definitive diagnosis of ARVC requires histological confirmation. A myocardial biopsy showing myocyte loss (<45% residual myocytes) with fibrosis and fatty infiltration (>40% fibrous tissue and >3% fat) confirms the diagnosis. However, myocardial biopsy lacks sufficient sensitivity (67% in one report) owing to the patchy nature of the disease. For safety reasons, the biopsy is performed mostly in the interventricular septum, which is histopathologically rarely involved in the disease process. Biopsy sampling performed on the RV free wall may improve the ability to diagnose ARVC. However, because of the frequently observed wall thinning with aneurysms or diverticula, free wall sampling is associated with risk of cardiac perforation, particularly when performed at random sites. Therefore the role of endomyocardial biopsy in the diagnosis of ARVC remains controversial.

Electroanatomic voltage mapping, which seems to be an effective technique to detect RV low-voltage regions reflecting fibrofatty myocardial atrophy in ARVC patients, has been shown to improve the diagnostic accuracy of myocardial biopsy by reducing the sampling errors. Endomyocardial biopsies are obtained from low-voltage areas, preferably from the border zone, to minimize the risk of perforation.

Immunohistochemical analysis of conventional biopsy samples to detect a change in the distribution of desmosomal proteins can also improve the sensitivity and specificity of endomyocardial biopsy. Reduced immunoreactive signal levels of plakoglobin at intercalated discs were found to be a consistent feature in patients with ARVC. Nonetheless, more recent studies revealed that sarcoidosis and giant cell myocarditis can cause similar patterns.³⁰

Genetic Testing

Molecular genetic analysis can potentially facilitate timely diagnosis, guide interpretation of borderline investigations, and corroborate clinical suspicion of disease in an index case. Although the patient with an established clinical diagnosis of ARVC may not personally benefit from genetic testing (since the presence or absence of a gene defect would not alter the treatment), genetic testing is still recommended because it can enable cascade screening of relatives and the early identification of asymptomatic carriers who must be considered at risk, because the disease is progressive and can appear later, due to the age-related penetrance.^{6,31}

However, sequence analysis of the known desmosomal ARVC-related genes only identifies a responsible mutation in approximately 50% of ARVC probands. Nevertheless, recent studies support the use of genetic testing as a new diagnostic tool in ARVC and suggest a prognostic impact, as the severity of the disease appears different according to the underlying gene or the presence of multiple mutations. Importantly, genetic testing is not recommended for patients with only a single minor criterion according to the 2010 task force criteria.

In a significant proportion of probands, more than one disease-causing mutation can be found (mostly in different genes). Therefore it is recommended that all desmosome genes be tested simultaneously in the proband. Whenever a pathogenic mutation is identified, it becomes possible to establish a presymptomatic diagnosis of the disease among family members and to provide them with genetic counseling to monitor the development of the disease and to assess the risk of transmitting the disease to offspring.³²

Invasive Electrophysiological Testing

The value of invasive EP testing with programmed ventricular stimulation for the diagnosis and risk stratification in ARVC patients appears to be limited and, hence, is rarely indicated. The inducibility of VT or VF in an EP study was not found to reliably predict arrhythmic events or appropriate ICD therapies.

Nonetheless, electroanatomic voltage mapping can help identify and quantify an electroanatomical scar area (which correlates with fibrofatty myocardial replacement), and was found to be more sensitive than CMR in identifying an RV scar.³³ The extent of RV low-voltage areas appear to predict increased risk of arrhythmic events.²⁴ In addition, this technique has been shown to be especially useful in distinguishing subclinical ARVC from idiopathic RVOT VT.²¹ Substrate mapping can also be used to guide and improve the diagnostic accuracy of myocardial biopsy. Therefore EP testing may be considered in individual patients, but it is not recommended as a routine diagnostic tool.

Importantly, an arrhythmogenic response to high-dose intravenous (IV) isoproterenol (45 µg/min for 3 minutes, regardless of heart rate) can potentially help diagnose ARVC, particularly in the early stages of the disease. The occurrence of polymorphic ventricular arrhythmias (PVCs and sustained and nonsustained VT) with predominant left bundle branch block (LBBB) morphology (different from the typical pattern observed in RVOT VT) during isoproterenol testing (during or within 10 minutes after the cessation of isoproterenol infusion) is highly suggestive of ARVC in the absence of other structural heart disease (sensitivity, 91%; negative predictive value, 99%). In contrast, a sustained monomorphic RVOT VT response during isoproterenol testing is considered a negative response.³⁴

DIFFERENTIAL DIAGNOSIS

Differential diagnosis of ARVC include idiopathic RVOT VT, dilated cardiomyopathy (DCM), cardiac sarcoidosis, Brugada syndrome, myocarditis, RV infarction, and congenital heart disease, and pulmonary hypertension. In addition, other forms of VT with an LBBB pattern need to be considered, including bundle branch reentry (BBR) VT, reentrant VT following surgical repair of congenital heart disease, and postinfarction VT originating from the LV septum, as well as AVRT using an atriofascicular bypass tract (BT).

Idiopathic Right Ventricular Outflow Tract Tachycardia

In clinical practice, the disease that most frequently mimics ARVC is idiopathic RVOT VT. Although RVOT VT is associated with a benign prognosis with no familial basis, it can be extremely difficult to distinguish from the concealed phase of ARVC, in which typical ECG and imaging abnormalities are absent. Similar to RVOT VT, the VT in ARVC also affects young adults, is commonly catecholamine-facilitated, and can originate from the RVOT. The distinction between the two entities has important prognostic and therapeutic implications (Box 29.1).

Electrocardiogram During Sinus Rhythm

In ARVC, the resting 12-lead ECG in normal sinus rhythm (NSR) typically shows characteristic depolarization and repolarization abnormalities (see below). In contrast, the resting ECG in NSR is typically normal in patients with idiopathic RVOT VT, with no epsilon wave, QRS widening or fragmentation, or other markers of delayed activation of the RV. Patients with idiopathic VT also have a normal SAECG in NSR.

Nevertheless, the ECG also can be normal in up to 50% of patients with ARVC at presentation, but in almost no patients 6 years after initial diagnosis. Furthermore, approximately 10% of patients with idiopathic RVOT VT can have complete or incomplete RBBB during NSR.

Electrocardiogram During Ventricular Tachycardia

Patients with idiopathic RVOT VT typically present with a single-morphology VT. The presence of multiple VT morphologies and RV sites of origin of the VT that are inconsistent with idiopathic RVOT VT (e.g., LBBB with superior axis) should prompt the consideration of ARVC. Nonetheless, it should be recognized that patients with several

BOX 29.1 Findings Favoring Arrhythmogenic Right Ventricular Cardiomyopathy Over Idiopathic Right Ventricular Outflow Tract Ventricular Tachycardia

Electrocardiogram During Sinus Rhythm

- Depolarization abnormalities: epsilon waves, RBBB, QRS fragmentation, localized QRS widening, and terminal S wave prolongation in right precordial leads
- Repolarization abnormalities: T wave inversion in the right precordial leads

Electrocardiogram During Ventricular Tachycardia

- Multiple VT morphologies and RV sites of origin
- LBBB with superior axis
- QRS duration in lead I ≥ 120 msec
- Late precordial transition (at lead V₅ or V₆)
- Notching in the QRS in multiple leads (especially in leads I and aVL)
- LBBB morphology with a superior axis is very unlikely in idiopathic RVOT VT

Signal-Averaged Electrocardiogram

- Late potentials and fragmented electrical activity

Isoproterenol Testing

- Inducibility of polymorphic ventricular arrhythmias (PVCs, sustained or non-sustained VT) with predominant LBBB morphology (different from the typical pattern observed in RVOT VT) during high-dose isoproterenol testing

Invasive Electrophysiological Testing

- Reproducible initiation of VT by programmed stimulation
- Lack of response of VT to adenosine
- Induction of VTs with different QRS morphologies
- Fractionated diastolic electrograms recorded during VT or sinus rhythm at the VT site of origin
- Electroanatomical scars on voltage mapping

Cardiac Imaging

- RV dilation, aneurysm, or systolic dysfunction

LBBB, Left bundle branch block; *PVCs*, premature ventricular complexes; *RBBB*, right bundle branch block; *RV*, right ventricle; *RVOT*, right ventricular outflow tract; *VT*, ventricular tachycardia.

idiopathic VT morphologies have been reported, and patients with ARVC can initially present with only one VT morphology consistent with an RVOT origin.³⁵

During VTs with LBBB and inferior axis, certain features of the QRS complex favor ARVC over RVOT VT including: (1) later precordial transition (at lead V₅ or V₆); (2) QRS notching in at least two leads (in particular, leads I and aVL); and (3) QRS duration in lead I exceeding 120 to 125 milliseconds. The most specific finding was late precordial transition (100% specificity at lead V₆ and 90% specificity at lead V₅ or later), and the most sensitive was the duration of QRS in lead I exceeding 120 milliseconds, followed by the presence of any notching on the QRS complex. QRS notching and longer QRS duration in ARVC reflect the abnormal myocardial substrate underlying the VT, which is lacking in idiopathic RVOT VT.^{36–38}

Invasive Electrophysiological Testing

The response during EP testing is also helpful in distinguishing idiopathic RVOT VT from ARVC. Reentry is the mechanism of VT in the

majority of the ARVC patients, whereas RVOT VT almost always displays features of triggered activity. The repetitive initiation of VT by programmed stimulation suggests a reentrant mechanism. In one report, programmed electrical stimulation induced VT in all but 1 of 15 patients with ARVC compared with only 2 patients with idiopathic RVOT VT (93% vs. 3%). Unlike RVOT VT, the VT in ARVC does not terminate with adenosine. Furthermore, the induction of VT with different QRS morphologies is common in ARVC (observed in 73% of patients in one report) and is very rare with RVOT VT (except for minor variations in QRS axis). In addition, fractionated diastolic electrograms recorded during VT or NSR at the VT site of origin or other RV sites, or late potentials in NSR, are inconsistent with idiopathic RVOT VT but are typical for ARVC.³⁵

In addition, electroanatomic voltage mapping can help distinguish early or concealed ARVC from idiopathic VT by detecting RV electroanatomical scars that correlate with the histopathological features pathognomonic of ARVC.

Isoproterenol Testing

As noted earlier, the inducibility of polymorphic ventricular arrhythmias with predominant LBBB morphology (not typical for RVOT VT) during high-dose isoproterenol testing favors ARVC over RVOT VT (sensitivity, 91%; and negative predictive value, 99%). Induction of a single monomorphic VT morphology favors RVOT VT.³⁴

Cardiac Imaging

Patients with idiopathic VT have normal imaging studies (echocardiography, CMR, contrast ventriculography) of RV size and function. The presence of RV dilation or aneurysm is consistent with ARVC.

Cardiac Sarcoidosis

In the absence of a previous diagnosis of extracardiac sarcoidosis, sarcoid heart disease can present a diagnostic challenge and can mimic the clinical presentation of ARVC with respect to arrhythmic, ECG, and structural cardiac findings. In fact, cardiac sarcoid patients often fulfill the revised task force diagnostic criteria for ARVC (63% in one report). Furthermore, cardiac sarcoidosis is diagnosed in about 15% of patients who are initially suspected to have ARVC.³⁵

Several similarities exist between sarcoid heart disease and ARVC. Cardiac sarcoidosis is associated with the replacement of myocytes with noncaseating granulomas. RV involvement (with confluent regions of endocardial and, more predominantly, epicardial RV scarring) is common and appears to be particularly arrhythmogenic. Multiple scar-related monomorphic VTs (predominantly due to scar-related macroreentry) are frequent, and commonly originate from the RV and, hence, exhibit LBBB morphology. The surface ECG during NSR commonly exhibits RBBB, QRS fragmentation, T wave inversion in the right precordial leads, and PVCs. Epsilon waves can be observed with a similar frequency in both ARVC and cardiac sarcoidosis. Furthermore, about 14% to 56% of the patients with cardiac sarcoidosis have detectable abnormalities on echocardiogram, such as LV or RV systolic dysfunction, wall-motion abnormalities, ventricular aneurysm, or basal septum thinning.^{39,40} In contrast to ARVC, a disorder largely confined to the RV free wall, cardiac sarcoidosis typically spares the free wall and involves the septum.

One report suggested that a reduced left ventricular ejection fraction (LVEF) should raise suspicion of cardiac sarcoidosis even if ARVC diagnostic criteria are fulfilled. Compared to patients with ARVC, those with cardiac sarcoidosis tend to have a significantly lower LVEF, significantly wider QRS complexes, and more different morphologies of inducible monomorphic VT, which originate more commonly in the apical region of the RV.^{35,41} In addition, screening for cardiac sarcoidosis should be considered in young patients (<60 years) with unexplained

Mobitz II or third-degree AV block, in those with unexplained monomorphic VT, and in those with unexplained nonischemic cardiomyopathy presenting with ventricular arrhythmias.^{39,42} Initial testing typically includes computed tomography (CT) scan of the chest for pulmonary sarcoid and advanced cardiac imaging (CMR or positron emission tomography [PET]). Abnormal finding on those tests should prompt definitive histological diagnosis.⁴³

Dilated Cardiomyopathy

ARVC is distinguished from DCM by the greater degree of arrhythmogenicity. Although ventricular arrhythmia is a relatively common finding in DCM, it is rare in the absence of significant ventricular dysfunction, and SCD is seldom the mode of presentation. In contrast, ARVC is associated with a propensity toward ventricular arrhythmias even in the absence of significant ventricular dysfunction. SCD is the first clinical manifestation of the disease in more than 50% of ARVC probands. In addition, regional involvement and aneurysm formation, which are characteristic of ARVC, argue against the diagnosis of DCM.

Athlete's Heart

The term *athlete's heart* refers to a constellation of electrical and structural cardiac adaptations in response to intensive and long-term athletic training. Such physiological cardiac remodeling allows the generation of a large and sustained cardiac output even at rapid heart rates. Although athletic adaptation of the left side of the heart has been well recognized, recent evidence revealed that the athlete's RV undergoes structural and functional adaptation in synergy with the LV. Physiological remodeling of the RV can manifest electrical and structural changes that mimic those observed in ARVC, including RV enlargement (typically in conjunction with LV enlargement and normal ventricular wall motion), anterior precordial T wave inversion (typically biphasic T wave morphology with preceding convex ST segment elevation), and PVCs of RV origin.^{44,45}

Distinguishing physiological remodeling of the athlete's RV (generally considered benign and nonarrhythmogenic) from ARVC (which is responsible for as many as 22% of SCDs in young athletes in Europe) has important management and prognostic implications. A false-positive diagnosis can potentially lead to erroneous disqualification from competition, whereas a false-negative diagnosis can result in devastating SCD.

RV dilatation in conjunction with convex ST segment elevation and biphasic anterior T wave inversion, and concomitant enlargement of the left and right sides of the heart with normal wall motion, appear to be benign findings and should not trigger further evaluation for ARVC in asymptomatic athletes without an adverse family history (Fig. 29.2). Conversely, the presence of symmetrical anterior T wave inversion that extends beyond lead V₁, preceded by isoelectric or downsloping ST segments, depolarization abnormalities (e.g., Epsilon waves or terminal QRS activation delay), reduced limb lead voltages, PVCs with LBBB morphology and superior axis, and global RV systolic dysfunction or regional wall motion abnormalities, should prompt careful investigation to exclude ARVC.^{44,45}

Exercise-Induced Arrhythmogenic Right Ventricular Cardiomyopathy

A relationship has been postulated between intense endurance exercise and an "acquired" ARVC-like phenotype without an identifiable genetic predisposition (sometimes referred to as "exercise-induced ARVC"). In favor of this hypothesis is the lower than expected prevalence of desmosomal gene mutations (13% vs. 50%) identified in endurance athletes with complex ventricular arrhythmias of RV origin and definite or suspected ARVC diagnosis according to the revised task force criteria. Furthermore, 3% of black and 0.3% of white athletes were found to

meet the criteria for ARVC, but further investigation did not detect any pathological findings.^{14,46–49}

Intense endurance exercise is associated with increased hemodynamic load (increased afterload, wall stress, work, and oxygen demand), which is proportionally greater for the RV than for the LV, and can result in transient exercise-induced RV dysfunction. Consecutive bouts of RV dilatation and dysfunction can potentially alter the RV interstitial matrix and lead to chronic RV remodeling, generating a substrate for serious arrhythmias in the absence of a known genetic predisposition.^{14,47,48}

Uncertainty exists regarding why a small fraction of athletes develop this profound degree of nonphysiological, arrhythmogenic RV remodeling. Impaired balance between cellular stress and repair and a milder degree of yet unidentified genetic predisposition have been hypothesized.^{47–49}

RISK STRATIFICATION

Once the diagnosis of ARVC is established, evaluation should be directed to assessing the patient's risk of arrhythmic events and SCD. Those deemed at low risk at initial evaluation should undergo periodic evaluation (every 1 to 2 years or whenever clinical symptoms develop or worsen) with ECG, echocardiography, 24-hour Holter monitoring, and exercise testing to reassess the risk of SCD and to optimize the treatment.

Factors identifying ARVC patients at risk for SCD have not yet been defined in large prospective studies focusing on survival. Nonetheless, three categories of risk for SCD (high, intermediate, and low) have been determined by consensus based on observational studies or registries of ARVC patients (Box 29.2).^{2,26,50–52}

The *high-risk* category (estimated annual rate of malignant arrhythmic events >10%) includes patients who experienced cardiac arrest due to VF or sustained VT, or those with severe RV dysfunction (RV fractional area change ≤17% or RV EF ≤35%) or LV dysfunction (LVEF ≤35%). This group of patients has an estimated annual rate of life-threatening arrhythmic events >10%.^{24,52–54}

The *intermediate-risk* category (estimated annual rate of malignant arrhythmic events 1% to 10%) includes patients with one or more of the risk factors recognized by consensus experts. Those risk factors are classified as either "major" or "minor." Major risk factors include a syncopal episode of unexplained origin (i.e., not neurally mediated) or thought to be consistent with ventricular arrhythmia, nonsustained ventricular tachycardia (NSVT), and moderate RV dysfunction (RV fractional area change of 17% to 24% or right ventricular ejection fraction [RVEF] of 36% to 40%) or LV dysfunction (LVEF of 36% to 45%). The prognostic implications of minor risk factors remain uncertain.^{2,21,52}

The *low-risk* category (estimated annual rate of malignant arrhythmic events <1%) includes ARVC patients and relatives without risk factors as well as healthy gene carriers. Of note, family history of arrhythmic events does not appear to influence risk in other family members.

PRINCIPLES OF MANAGEMENT

Pharmacological Therapy

Beta-Blockers

The current consensus recommends the use of beta-blockers (titrated to the maximally tolerated dose) in most patients diagnosed with ARVC, given the multiple potential benefits in this patient population. First, the inhibition of sympathetic activity can potentially reduce the risk of effort-induced ventricular arrhythmias. Second, beta-blockers can reduce the risk of inappropriate ICD therapies triggered by sinus tachycardia or supraventricular arrhythmias. Third, beta-blockers have a proven benefit in heart failure management. Another potential value

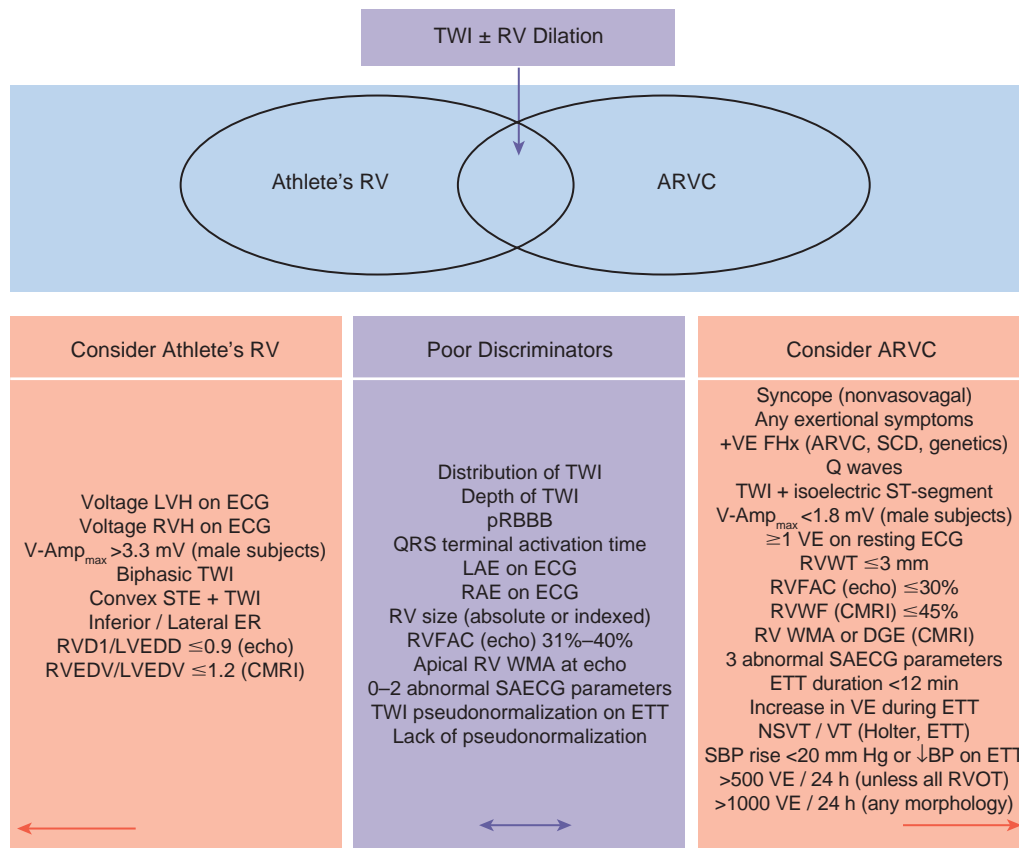


Fig. 29.2 Proposed Clinical Indicators to Assist in the Differentiation Between Athletic Right Ventricle (RV) Remodeling and Arrhythmogenic Right Ventricular Cardiomyopathy (ARVC). BP, Blood pressure; CMRI, cardiac magnetic resonance imaging; DGE, delayed gadolinium enhancement; ECG, electrocardiogram; ER, early repolarization; ETT, exercise tolerance test; FHx, family history; LAE, left atrial enlargement; LVEDD, left ventricular end-diastolic dimension; LVEDV, left ventricular end-diastolic volume; LVH, left ventricular hypertrophy; NSVT, nonsustained ventricular tachycardia; pRBBB, partial right bundle branch block; RAE, right atrial enlargement; RVD1, right ventricular basal dimension; RVEDV, right ventricular end-diastolic volume; RVEF, right ventricular ejection fraction; RVFAC, right ventricular fractional area change; RVH, right ventricular hypertrophy; RVOT, right ventricular outflow tract; RV WMA, right ventricular wall motion abnormality; RVWT, right ventricular wall thickness; SAECD, signal-averaged electrocardiogram; SBP, systolic blood pressure; SCD, sudden cardiac death; STE, ST segment elevation; TWI, T-wave inversion; V-Amp_{max}, maximal QRS amplitude in precordial leads; VE, ventricular extrasystole; VT, ventricular tachycardia; WMA, wall motion abnormality. (From Zaidi A, Sheikh N, Jongman JK, et al. Clinical differentiation between physiological remodeling and arrhythmogenic right ventricular cardiomyopathy in athletes with marked electrocardiographic repolarization anomalies. *J Am Coll Cardiol*. 2015;65:2702–2711.)

of beta-blocker therapy is retarding the progression of disease in individuals who are asymptomatic (by lowering RV wall stress); however, this has not been proven. Importantly, there is no proof that beta-blocker therapy confers protection against SCD.^{2,3,55}

Antiarrhythmic Drugs

Although antiarrhythmic drug therapy does not lower the risk of SCD in ARVC, it is indicated to reduce the frequency of symptomatic ventricular arrhythmias (PVCs, sustained and nonsustained VT) and as an adjunct therapy to ICD to reduce the frequency of ventricular arrhythmias in patients with unacceptably frequent ICD therapies. Antiarrhythmic agents can also be considered as an adjunct therapy to catheter ablation without a back-up ICD in patients with recurrent, hemodynamically stable VT. Prophylactic antiarrhythmic drug therapy alone (without ICD implantation) in asymptomatic ARVC patients does not offer reliable protection against SCD and is generally not indicated.^{2,24}

Amiodarone, alone or in combination with beta-blockers, is the most effective drug for preventing symptomatic ventricular arrhythmias.² Sotalol can also be considered; however, evaluation of its efficacy with programmed electrical stimulation or with cardiac monitoring needs to be considered.^{55,56}

Heart Failure Therapy

For patients with RV or biventricular heart failure, standard pharmacological treatment with angiotensin-converting-enzyme inhibitors, angiotensin II receptor blockers, beta-blockers, and diuretics is recommended. Although angiotensin-converting enzyme inhibitors are well known for slowing progression in other cardiomyopathies, their value in ARVC patients is yet to be proven.

Anticoagulation Therapy

Long-term oral anticoagulation is generally indicated for secondary prevention in patients with documented intracardiac clots or venous

BOX 29.2 Risk Categories for Sudden Cardiac Death in ARVC**High Risk**

- Prior sustained ventricular arrhythmias
- Severe dysfunction of RV, LV, or both (EF $\leq 35\%$)
- Aborted sudden cardiac death

Intermediate Risk**Major Risk Factors**

- Syncope
- NSVT
- Moderate dysfunction of RV, LV, or both (RV fractional area change between 24% and 17% or RVEF between 40% and 36% and/or LV EF between 45% and 36%)

Minor Risk Factors

- Young age
- Male gender
- Complex genotype

Minor Risk Factors—cont'd

- Presence of more than one mutation
- Compound or digenic heterozygosity of desmosomal-gene mutations
- Desmoplakin mutation
- Proband status
- Inducible VT/VF
- Extent of RV scar on electroanatomic mapping
- Fragmented electrograms on electroanatomic mapping
- Extent of TWI across precordial leads or in inferior leads
- QRS fragmentation
- Precordial QRS amplitude ratio
- CMR abnormalities
- Heart failure/transplantation

Low Risk

- No risk factors
- Healthy gene carriers

The high-risk category includes patients with prior sustained ventricular arrhythmias, severe dysfunction of RV, LV, or both (ejection fraction $\leq 35\%$), or aborted sudden cardiac death. The estimated rate of life-threatening arrhythmic events is greater than 10% per year, and therefore ICD implantation is considered a class I indication in this group. The low-risk group includes probands and relatives without risk factors and healthy gene carriers who have a less than 1% per year life-threatening arrhythmic event rate. These patients do not require ICD implantation (class III). The intermediate group had an estimated annual event rate between 1% and 10% and was composed of ARVC patients with one risk factor. There was general agreement that patients with one major risk factor, which includes syncope, NSVT, and moderate ventricular dysfunction (RVEF between 36% and 40% or LVEF between 36% and 45%) should undergo prophylactic ICD implantation (class IIa).

ARVC, Arrhythmogenic right ventricular cardiomyopathy; CMR, cardiac magnetic resonance; EF, ejection fraction; ICD, implantable cardioverter-defibrillator; LV, left ventricle; LVEF, left ventricular ejection fraction; NSVT, nonsustained ventricular tachycardia; RV, right ventricle; RVEF, right ventricular ejection fraction; TWI, T wave inversion; VF, ventricular fibrillation; VT, ventricular tachycardia.

From Philips B, Cheng A. 2015 Update on the diagnosis and management of arrhythmogenic right ventricular cardiomyopathy. *Curr Opin Cardiol.* 2015;31:1.

or systemic thromboembolism. However, prophylactic anticoagulation for primary prevention of thromboembolism on the basis of ventricular dilatation or dysfunction, either global or regional, is not recommended.²

Catheter Ablation

Endocardial catheter ablation of monomorphic VT has a 60% to 80% acute success rate in patients with ARVC, but long-term recurrences are frequent (50% to 70%). Additional antiarrhythmic drug therapy and repeated ablation procedures are frequently required to provide clinical control of VT. Some reports show that epicardial catheter ablation is substantially more effective acutely, and has better long-term success than endocardial ablation. At present, catheter ablation of VT is considered palliative rather than curative, and is recommended mainly for patients with recurrent VT causing frequent ICD shocks and for those with VT storm or incessant VT refractory to antiarrhythmic drug therapy.²

Importantly, VT ablation does not appear to reduce the risk of SCD in ARVC. Therefore catheter ablation should not be considered as an alternative to ICD therapy in ARVC patients with VT. Nonetheless, catheter ablation may be considered as first choice therapy without a back-up ICD for selected patients with drug-refractory, hemodynamically stable, single-morphology VT (class IIb indication).^{2,21,57}

Implantable Cardioverter-Defibrillator

ICD therapy is the most effective and reliable approach for reduction of the risk of SCD in ARVC patients, both for primary and secondary prevention, with an estimated 24% to 35% mortality reduction at 36 months of follow-up. ICD implantation is recommended for secondary prevention in patients with prior cardiac arrest or sustained VT because of the relatively high recurrence rates in this subgroup.

Candidates for primary prevention ICDs are categorized into high-risk, intermediate-risk, and low-risk groups (Box 29.2; Fig. 29.3). Prophylactic ICD implantation is recommended in patients with high risk factors (severe RV dysfunction [RV fractional area change $\leq 17\%$ or RVEF $\leq 35\%$] or LV dysfunction [LVEF $\leq 35\%$]) irrespective of arrhythmias. Conversely, prophylactic ICD implantation is not recommended in asymptomatic ARVC patients with no risk factors, or healthy gene carriers. Among patients in the intermediate-risk group, ICD implantation should be considered in patients with “major” risk factors such as unexplained syncope, NSVT, or moderate RV dysfunction (RV fractional area change of 17% to 24% or RVEF of 36% to 40%) or moderate LV dysfunction (LVEF of 36% to 45%). The value of ICD therapy in those with “minor” risk factors is not well established, but may be considered after a careful discussion of the long-term risks and benefits of ICD implantation in the individual patient and considering the desires of the fully informed patient and family.⁵⁵

The rate of appropriate ICD therapy is high (24% to 78%) in the first few years after implantation, with an annualized rate of about 9.5%. Multiple ICD discharges and VT storm are not uncommon. Of note, the interval from ICD implantation to first appropriate device intervention is quite variable, and typically exceeds 1 year in a large proportion of patients.²

It is important to recognize that ICD implantation is an invasive measure and carries a definite rate of complications as well as the need for recurring device service and generator changes. In particular, lead-related adverse events are relatively common in this patient population. More than 6% of patients experience major complications requiring the revision of the implant over a 7-year follow-up period.²⁴ The thin RV wall can predispose to lead perforation. In addition, the progressive loss of myocardium with fibrofatty replacement can result in suboptimal

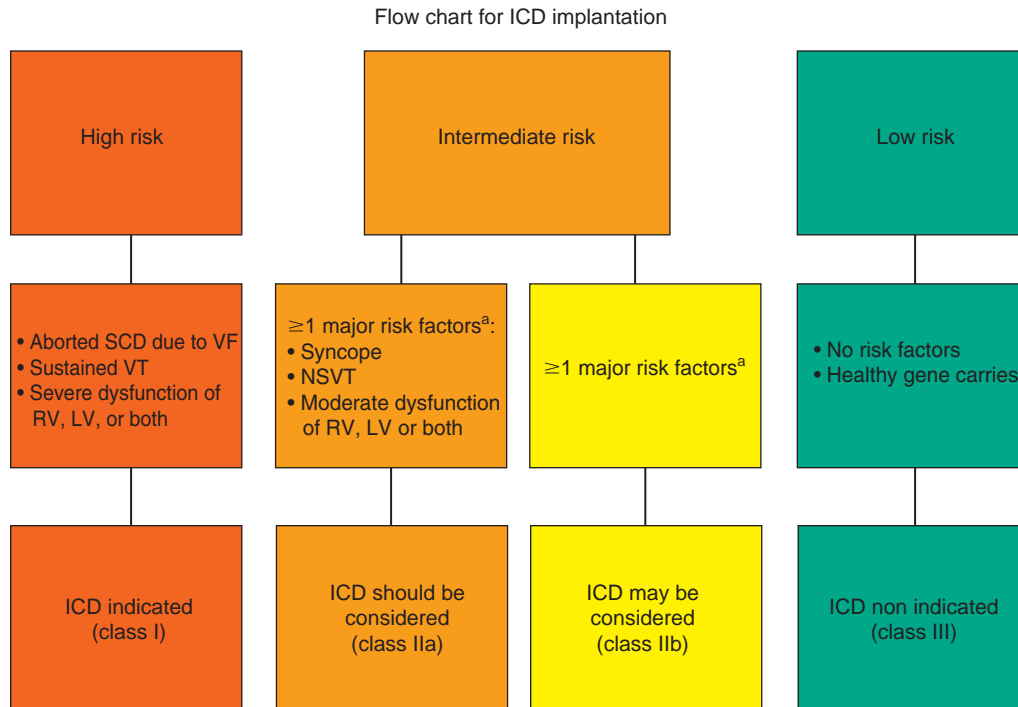


Fig. 29.3 Risk Stratification and Indications of Implantable Cardioverter-Defibrillator (ICD) Implantation in Arrhythmogenic Right Ventricular Cardiomyopathy. Based on the available data on annual mortality rates associated with specific risk factors, the estimated risk of major arrhythmic events in the high-risk category is greater than 10% per year, in the intermediate ranges from 1 to 10% per year, and in the low-risk category is less than 1% per year. Indications to ICD implantation were determined by consensus taking into account not only the statistical risk, but also the general health, socioeconomic factors, the psychological impact, and the adverse effects of the device. ^aSee the text for distinction between *major* and *minor* risk factors. LV, Left ventricle; NSVT, nonsustained ventricular tachycardia; RV, right ventricle; SCD, sudden cardiac death; VF, ventricular fibrillation; VT, ventricular tachycardia. (From Corrado D, Wichter T, Link MS, et al. Treatment of arrhythmogenic right ventricular cardiomyopathy/dysplasia: an international task force consensus statement. *Eur Heart J*. 2015;36:3227–3237.)

ventricular sensing and pacing functions, especially for RV apical lead placement. Septal positioning of the RV lead appears to improve long-term lead performance.⁵⁸

Furthermore, inappropriate ICD interventions occur in 10% to 25% of ARVC patients (annualized rate of about 3.7%), mostly at a young age, and are usually caused by sinus tachycardia or atrial tachyarrhythmia.²¹ Strategic ICD programming can help reduce the incidence of inappropriate interventions.⁵⁹ The vast majority of ventricular arrhythmias in ARVC patients are monomorphic VTs, which can be successfully terminated by antitachycardia pacing therapy. Therefore ICDs should be programmed for antitachycardia pacing therapy, even for rapid VT.⁵² In addition, beta-blocker therapy can help prevent excessive sinus tachycardia and rapid ventricular rates during atrial arrhythmias. Dual-chamber devices can improve the discrimination of ventricular from supraventricular arrhythmias but at the expense of additional potential complications of adding an atrial lead.^{2,59,60}

Therefore the benefit of ICD implantation should be carefully weighed against the risks of such a procedure in this young patient population. The negative psychological impact of an implanted device and inappropriate shocks should not be underestimated.⁵⁹

Participation in Sports

Intense exercise can serve as a trigger for fatal arrhythmias and has been shown to double the risk of SCD in adolescent and young adults with ARVC, likely related to acute volume overload with RV stretching and adrenergic stimulation during exercise. Further, mechanical stress

can potentially promote the development and progression of the ARVC phenotype.²⁴

In fact, sports disqualification *per se* is a life-saving measure. Therefore individuals with a definite, borderline, or possible diagnosis of ARVC should not participate in most competitive sports, with the possible exception of low-intensity class 1A sports.⁶¹ Furthermore, any activity, competitive or not, that causes symptoms of palpitations, presyncope, or syncope should be avoided. Although the restriction of moderate- to high-intensity-level recreational activities is generally recommended, a recent report suggested that recreational sport participation was not associated with the earlier presentation of symptoms or the increased risk of ventricular arrhythmias or death when compared with inactive ARVC probands.¹³

The issue of exercise restriction is challenging in family members of ARVC patients. Restriction from competitive sports activity is reasonable in healthy gene carriers without symptoms or overt clinical disease.^{2,62} For family members of probands without an identified mutation, the benefit of exercise restriction is uncertain. Exercise stress testing (to evaluate for exertional ventricular arrhythmias) can potentially help guide exercise prescription. In those preferring to participate in competitive sports, frequent screening for ARVC should be considered.⁶³

Family Screening

Since ARVC is primarily caused by an autosomal dominant genetic defect, every offspring has a 50% chance of inheriting the disease-causing mutation. However, because of the age-dependent penetrance, many

mutation carriers may not exhibit phenotypic expression early in life, and many others may express the phenotype but remain asymptomatic and, hence, remain undiagnosed unless screened.²⁴

When the causative mutation in the index patient is identified, genetic testing is recommended in all first-degree relatives. Mutation-negative family members and their descendants have no risk for developing ARVC and do not need further evaluation.⁶ Family members who test positive for an ARVC genetic mutation may not exhibit clinical manifestations of the disease, given the lack of association of the genotype with the phenotypic expression of the disease. Therefore cardiac evaluation is required in mutation-positive patients to identify those with the disease. Clinical evaluation may start at the age of 10 to 12 years; clinical expression of the disease and SCD are extremely rare at less than 10 years of age.^{4,64} Due to the age-related penetrance of ARVC, healthy gene carriers should also be offered repeat clinical assessment (every 2 to 3 years), especially during adolescence and young adulthood.

When genetic testing is not performed in the proband, or when genetic analysis fails to identify a definite disease-causing mutation (or reveals one or more genetic variants of unknown significance), genetic testing in the related family members is not recommended. Instead, it is recommended that all first-degree genetically related family members undergo clinical screening with detailed history and physical examination, 12-lead ECG, echocardiography, Holter monitoring, and CMR imaging. Given the low penetrance observed in most families, screening should be extended throughout the kindred to at least one generation beyond the last affected individual. Importantly, no single test is capable of excluding the diagnosis of ARVC. Therefore a full baseline evaluation remains necessary in determining an at-risk individual's phenotype. Approximately, one-third of at-risk relatives fulfill diagnostic 2010 task force criteria for ARVC at the first evaluation.^{4,64}

Asymptomatic family members with a normal comprehensive evaluation are less likely to experience life-threatening arrhythmias during short-term (4 years) follow-up, and are less likely to have inherited the gene defect. Nevertheless, these individuals should undergo follow-up at regular intervals until definitive diagnostic tools are available.⁵⁰ It is suggested that clinical screening be performed every 2 to 3 years between the ages of 10 and 20 years, and every 5 years after the age of 20 years. Screening may be stopped at the age of 50 to 60 years because the disease uncommonly presents after that. Importantly, the overall rate of progression in relatives of ARVC probands is typically slow, and only minimal changes may be observed on any single testing modalities between baseline and last follow-up. Electrical progression on ECG, Holter monitoring, or SAECG is observed to a much greater extent than structural progression on CMR.^{4,6,64}

Among family members of ARVC patients, approximately one-third eventually develop disease, and 10% develop sustained ventricular arrhythmias. The risk is higher in genotype-positive family members, who have double the risk of developing ARVC and an eightfold increased risk of developing sustained ventricular arrhythmias in comparison to family members of probands without a desmosomal mutation.

ELECTROCARDIOGRAPHIC FEATURES

Electrocardiogram During Sinus Rhythm

ECG abnormalities are present in the majority of patients with ARVC and often precede structural abnormalities. Although a normal ECG can be present in up to 40% of ARVC patients at presentation, by 6 years, almost all patients have one or more of several characteristic findings on ECG during NSR. Significant differences exist in most ECG features among ARVC patients according to the degree of RV involvement, and they are more prevalent in diffuse ARVC than in the localized form of the disease.³⁵

ECG abnormalities during ARVC can be subdivided into abnormalities of repolarization or depolarization. Depolarization abnormalities are caused by cellular uncoupling and altered tissue architecture due to fibrofatty infiltration, and typically manifest on the ECG as epsilon waves, RBBB, QRS fragmentation, localized QRS widening, and terminal S wave prolongation in right precordial leads (Fig. 29.4). Repolarization abnormalities typically manifest as T wave inversion in the right precordial leads.^{65,66}

Repolarization Abnormalities

Repolarization abnormalities are the most common ECG features, with T wave inversion in leads V₁ through V₃ observed in 87% of patients with ARVC (prevalence has been reported as 55% to 94% in different series). T wave inversion in ARVC is likely secondary to the regional conduction delay and RV dilatation, rather than a primary repolarization abnormality. The extent of right precordial T wave inversion relates to the degree of RV involvement, and was found to predict an increased risk of arrhythmic events.^{35,51,67}

T wave inversion in leads V₁ through V₃ or beyond (in the absence of complete RBBB) in individuals older than 14 years is considered a major diagnostic criterion for ARVC. On the other hand, inverted T waves *only* in leads V₁ and V₂ (in the absence of complete RBBB) or in leads V₁ through V₄ (in the presence of RBBB) in individuals older than 14 years are considered as minor diagnostic criteria for ARVC.⁶⁸ The absence of negative T waves beyond lead V₁ characterizes a low-risk subgroup of ARVC patients with a more favorable clinical course because of a low rate of arrhythmic events.⁶⁹

However, T wave inversion in the right precordial leads is non-specific and can be observed in a multitude of conditions such as athlete heart, Brugada syndrome, and occasionally in the normal adult female.^{68,70}

Depolarization Abnormalities

Epsilon wave. The epsilon wave, the hallmark feature of ARVC, is a marker of delayed activation of the RV free wall and outflow tract and is considered a major diagnostic criterion for ARVC. The epsilon wave has the appearance of a reproducible distinct wave (low-amplitude small deflections) between the end of QRS complex to the onset of the T wave in the right precordial leads, particularly in lead V₁ (Figs. 29.5 and 29.6).^{70,71}

Epsilon waves represent low-amplitude potentials caused by delayed excitation of islands of surviving cardiomyocytes bordered by or embedded in interstitial fibrous and fatty tissue of some portion of the RV. Epsilon waves appear to be associated with significant endocardial scarring in addition to an epicardial scar, thus signifying extensive disease. Of note, the timing of epsilon waves on the surface ECG correlated with electrical activation of in the RV inflow and perivalvular regions (rather than RVOT or the RV apex).⁶⁶

The bipolar Fontaine precordial ECG leads I to III may be also used to enhance the recording of epsilon waves by applying placement of the right arm electrode on the manubrium, the left arm electrode on the xiphoid, and the left leg lead in V₄ location. The sensitivity of recording epsilon waves by using the Fontaine lead positions can be further accentuated when the ECG is taken at double paper speed and sensitivity, and a filter setting of 40 Hz.⁷⁰

Although the epsilon wave has been considered highly specific for ARVC, ECG markers that reflect ventricular conduction delay in ARVC (including the epsilon wave) are frequently observed in subjects with a spontaneous or drug-induced type 1 ECG pattern of Brugada syndrome and in association with diseases that involve the RV (such as RV infarction or sarcoidosis). In addition, this criterion is of limited sensitivity, observed in only 10% to 37% of ARVC patients when

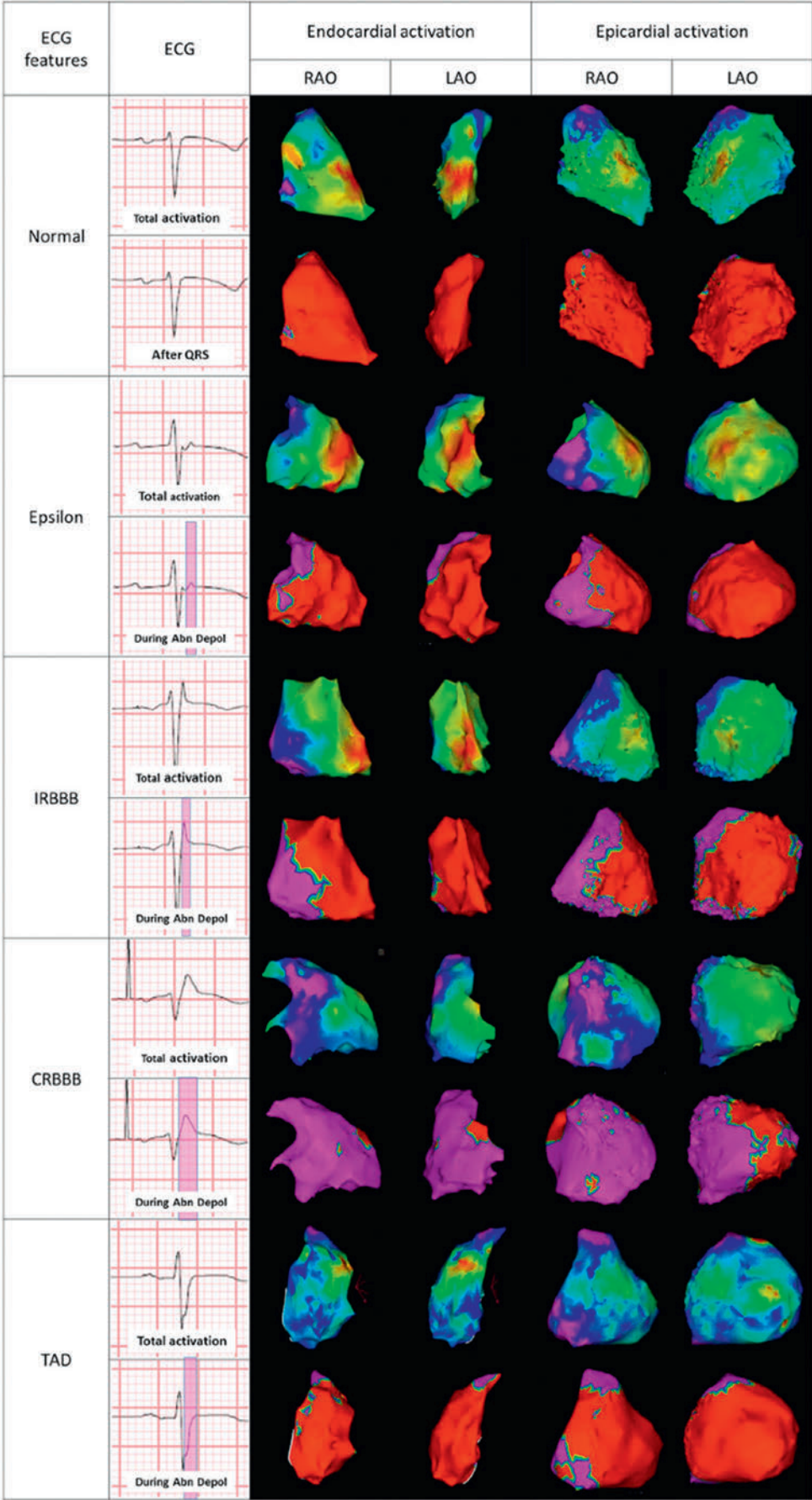


Fig. 29.4 Representative of Total Endocardial and Epicardial Bipolar Activation and the Area of Activation During the Delayed Depolarization Period of QRS Complex in Different Electrocardiographic (ECG) Features in Arrhythmogenic Right Ventricular Cardiomyopathy Patients. The gradual color-coded model showed the sequence activation patterns of each ECG features. The two-color coded model with red for the activation before the abnormal depolarization and purple for activation during abnormal depolarization showed the area of activation during abnormal depolarization. *Abn*, Abnormal; *CRBBB*, complete right bundle branch block; *Depol*, depolarization; *ECG*, electrocardiogram; *IRBBB*, incomplete right bundle branch block; *LAO*, left anterior oblique view; *RAO*, right anterior oblique view; *TAD*, terminal activation duration. (From Tanawuttiwat T, Te Riele AS, Philips B, et al. Electroanatomic correlates of depolarization abnormalities in arrhythmogenic right ventricular dysplasia/cardiomyopathy. *J Cardiovasc Electrophysiol*. 2016;27:443–452.)

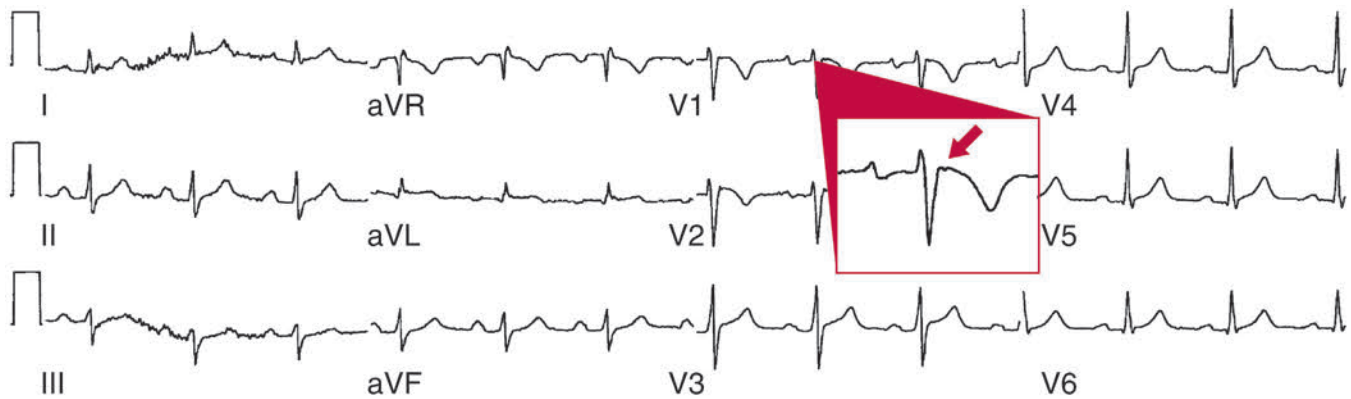


Fig. 29.5 Epsilon Wave. Surface electrocardiogram of sinus rhythm in a patient with arrhythmogenic right ventricular dysplasia-cardiomyopathy. *Inset:* Magnified view of a single complex in V_1 showing epsilon waves (arrow).

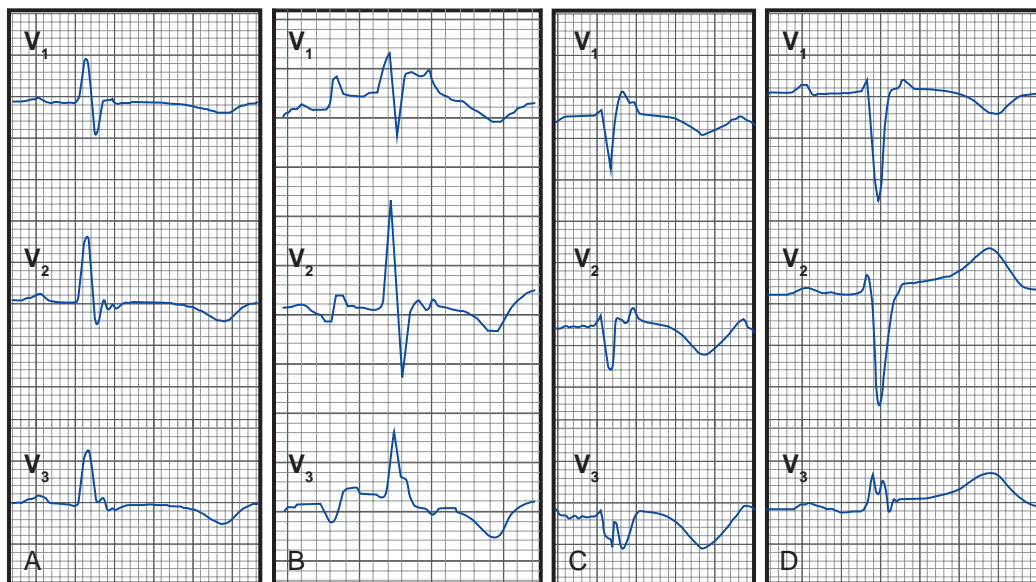


Fig. 29.6 Examples of Epsilon Waves in Patients With Arrhythmogenic Right Ventricular Cardiomyopathy. (A–D) Right precordial surface electrocardiographic leads obtained from four different patients. (From Platonov PG, Calkins H, Hauer RN, et al. High interobserver variability in the assessment of epsilon waves: implications for diagnosis of arrhythmogenic right ventricular cardiomyopathy/dysplasia. *Heart Rhythm*. 2016;13:208–216.)

evaluated by standard ECG. The use of highly amplified (20 mV) precordial leads and modified limb leads can increase the detection of epsilon potentials to 75%, but is rarely utilized.^{14,35}

Right bundle branch block. Incomplete or complete RBBB can be observed in 18% and 15% of patients, respectively. Epicardial mapping suggests that these patterns are usually caused by parietal block (due to the irregular and delayed propagation of activation in the zones of dysplasia), rather than by disease of the bundle branch itself. In the presence of an RBBB pattern, selective prolongation of the QRS duration in leads V_1 to V_3 compared with lead V_6 (>25 milliseconds, parietal block) is an important hallmark of ARVC (sensitivity of 52% to 64%). Increased QT dispersion (i.e., interlead variability of the QT interval) has been observed in ARVC.⁷⁰

Localized prolongation of QRS duration. Localized QRS widening (>110 milliseconds) in the right precordial leads can indicate an activation delay in the diseased region of the RV. QRS duration greater than 110 milliseconds in lead V_1 has a sensitivity of 26% to 75% and a

specificity of 100% in patients suspected of having ARVC based on historical features. To discriminate localized QRS prolongation from RBBB, the ratio of the sum of the QRS durations in leads $(V_1 + V_2 + V_3)/(V_4 + V_5 + V_6)$ is calculated. A ratio of ≥ 1.2 is considered abnormal and has a sensitivity of 35% to 98%.^{68,70}

Prolongation of S wave upstroke. Prolongation of the upstroke of the S wave (≥ 55 milliseconds from the nadir of the S wave to the isoelectric line) in leads V_1 through V_3 in the absence of RBBB was found in the original report to be a very sensitive ECG criterion for ARVC (present in all cases with diffuse ARVC and in 90% in the localized form of the disease). However, the sensitivity of this criterion was less than 60% in several other reports. This measurement has the highest diagnostic usefulness for differentiating the localized form of ARVC from idiopathic RVOT VT, correlates with the degree of RV involvement, and is an independent predictor of VT induction. It is recognized that a prolonged S wave upstroke directly relates to the QRS width in the right precordial leads; nonetheless, it is superior to localized QRS

prolongation in distinguishing the mild form of ARVC from idiopathic RVOT VT.^{35,68}

Prolonged terminal activation duration. Another ECG marker of abnormal depolarization in ARVC is the “terminal activation delay.” This parameter is measured from the nadir of the S wave to the end of all depolarization deflections, thereby including not only the S wave upstroke but also both late fractionated signals and epsilon waves, to the completion of the QRS complex. This criterion is only applicable in the absence of complete RBBB. A prolonged terminal activation delay (≥ 55 milliseconds) was observed in 71% of ARVC patients and only 4% of controls.⁶⁸

QRS fragmentation. QRS fragmentation in standard ECG leads is defined as deflections (slurs or notches) at the beginning of the QRS complex, on top of the R wave or in the nadir of the S wave, or as total QRS complex having four or more spikes. QRS fragmentation presenting in multiple leads is likely pathological, reflecting regional delay in ventricular depolarization. QRS fragmentation is highly prevalent in ARVC, especially when using amplified and modified ECG recording techniques (including the use of the Fontaine Leads System), with a sensitivity of 61% to 85%.³⁵ However, QRS fragmentation is not specific for ARVC and is prevalent in other types of cardiomyopathy, both ischemic and nonischemic.⁷⁰

QRS fragmentation can be of value in the stratification of the high-risk ARVC patients for arrhythmic events. In one report, the presence of QRS fragmentation in three or more of the standard 12-lead ECG predicted arrhythmic events with a sensitivity of 56% and a specificity of 99.7%.

Furthermore, a recent study found a strong correlation between QRS fragmentation on the surface ECG and the extent and anatomical distribution of abnormal RV endocardial and epicardial scarring (as identified on electroanatomic substrate mapping) in patients with ARVC.⁷²

Late potentials. “Late potentials” refer to the low-amplitude, high-frequency, and altered frequency components in the terminal QRS complex. These signals are too small to be visible on the surface ECG, but can be detected by high resolution SAECG. The SAECG is a highly amplified and signal-processed ECG that can detect microvolt-level electrical potentials. Late potentials, which reflect the slow conduction in the ventricular myocardium and electrical potentials that extend beyond the activation time of normal myocardium, typically arise from scarred myocardium, an anatomical substrate potentially responsible for reentrant ventricular arrhythmias.^{67,70}

The SAECG and its three components (filtered QRS duration, low-amplitude signal duration, and root-mean-square voltage of the last 40 milliseconds of the QRS) are highly associated with the diagnosis of ARVC. Late potentials and fragmented electrical activity can be detected by SAECG in 50% to 80% of patients with ARVC.^{67,70}

Although there are no guidelines for abnormal SAECG in patients with ARVC, it is common practice to categorize the SAECG as abnormal if two or more of these parameters are abnormal. In one report, the sensitivity of using SAECG for the diagnosis of ARVC was increased from 47% using two of the three criteria to 69% by using any one of the three criteria, while maintaining a high specificity of 90% to 95%. Abnormal SAECG was strongly associated with dilated RV volumes and decreased RV ejection fraction detected by CMR. SAECG abnormalities did not vary with clinical presentation, and had limited correlation with ECG findings. In addition, SAECG abnormalities appear to correlate with the presence of low-voltage areas selectively in the RVOT as observed during electroanatomic voltage mapping, whereas surface ECG abnormalities are associated with a more diffuse RV involvement. However, the value of SAECG for predicting inducible VT in ARVC remains uncertain.⁶⁷

Electrocardiogram During Ventricular Tachycardia

Ventricular ectopy in ARVC usually arises from the basal peri-valvular region in the RV and therefore has an LBBB pattern with superior, inferior, or indeterminate axis. Most sustained VTs arise from the RV free wall, most VTs display LBBB configuration with poor R-wave progression in the precordial leads. Nonetheless, VT with RBBB morphology can be observed in patients with LV disease or when advanced structural RV disease distorts normal ventricular geometry within the thorax (Fig. 29.7). The QRS axis during VT is typically between -90 and $+110$ degrees; an extreme rightward direction of the QRS axis is uncommon.⁷⁰

Leads I and aVR can help localize the VT exit site within the RV. The QRS complex is typically positive in lead I during VTs originating from the RV basal regions, but is isoelectric or negative in VTs with more apical sites of origins. Inferior RV exit sites exhibit a positive QRS in lead aVR, usually with a superior axis. Furthermore, the presence of a Q wave or QS configuration in leads I and V_2 (anterior RV epicardial sites) or Q waves leads II, III, or aVF (inferior RV epicardial sites) on the surface ECG during VT suggests the presence of an epicardial source of VT.⁷³

Importantly, patients with ARVC frequently demonstrate the presence of more than one VT morphology, either spontaneously (64%) or during an EP study (88%).

ELECTROPHYSIOLOGICAL FEATURES

Induction of Tachycardia

The most commonly used stimulation protocol applies pacing output at twice the diastolic threshold current and a pulse width of 1 to 2 milliseconds. Single ventricular extrastimuli (VESs) during NSR and at pacing drive cycle lengths (CLs) of 600 and 400 milliseconds are delivered, first from the RV apex and then from the RVOT. The prematurity of extrastimuli is increased until refractoriness or induction of sustained VT is achieved. If these measures fail to induce VT, double and then triple VESs are used in the same manner. If VT still cannot be induced, rapid ventricular pacing is started at a pacing cycle length (PCL) of 400 milliseconds, gradually decreasing the PCL until 1:1 ventricular capture is lost or a PCL of 220 milliseconds is reached. Repeating the protocol at other pacing drive CLs, at other RV sites, or after administration of isoproterenol is then attempted.

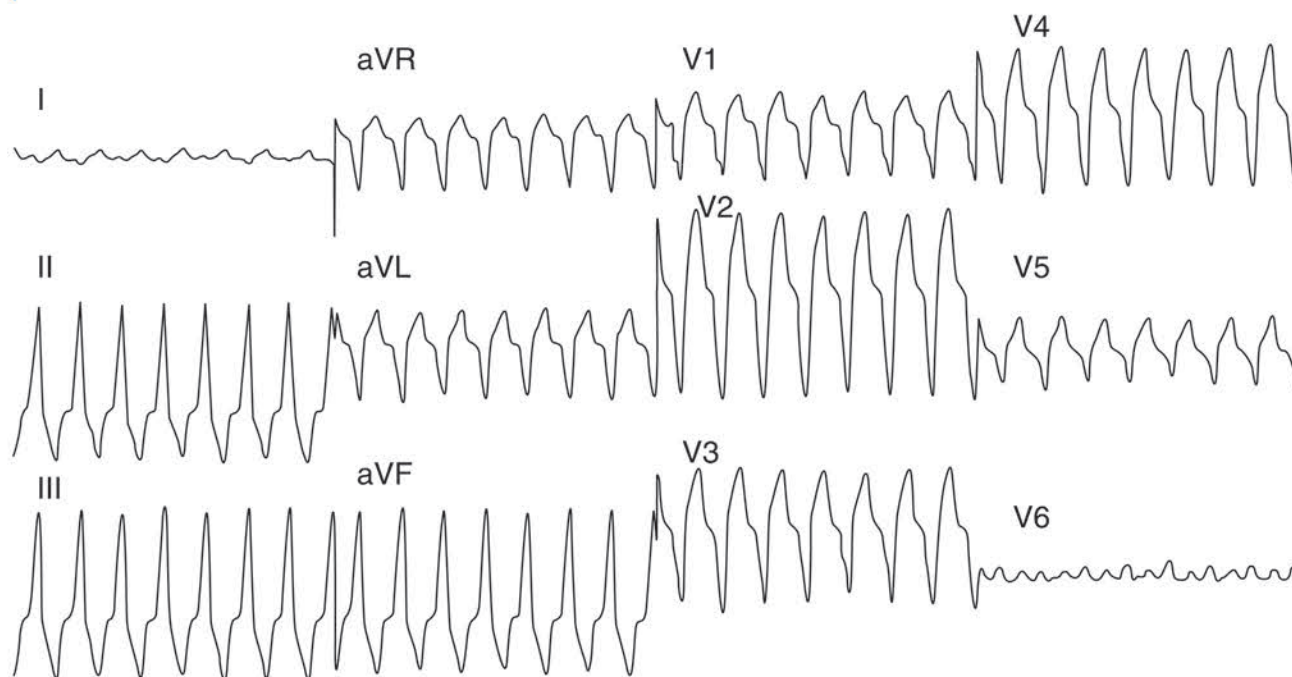
VT can be induced with programmed electrical stimulation in the majority of ARVC patients with clinical VT. Isoproterenol infusion facilitates VT induction in many patients. In patients with frequent PVCs at baseline, induction of VT with identical morphology to the clinical PVCs has been reported and frequently requires high-dose isoproterenol (up to 30 $\mu\text{g}/\text{min}$) combined with ventricular burst pacing. In these patients, salvos of nonsustained monomorphic VT may precede the emergence of sustained monomorphic ventricular tachycardia (SMVT) with an identical morphology.¹⁷

Tachycardia Features

Reentry in areas of abnormal myocardium is the most common mechanism of VT in ARVC. Most reentrant circuits cluster around the tricuspid annulus and the RVOT. Multiple morphologies of inducible VT are common. A variety of different reentry circuit sites can be identified with entrainment mapping. A single region can give rise to multiple VT morphologies. The VT burden is exceptionally high in this patient population, with a median of four distinct VTs (clinical and inducible) per patient.⁷⁴

The response of VT to programmed stimulation and resetting and entrainment maneuvers, is consistent with macroreentry, similar to post-MI VT (see Chapter 22 for detailed discussion).

VT-1



VT-2

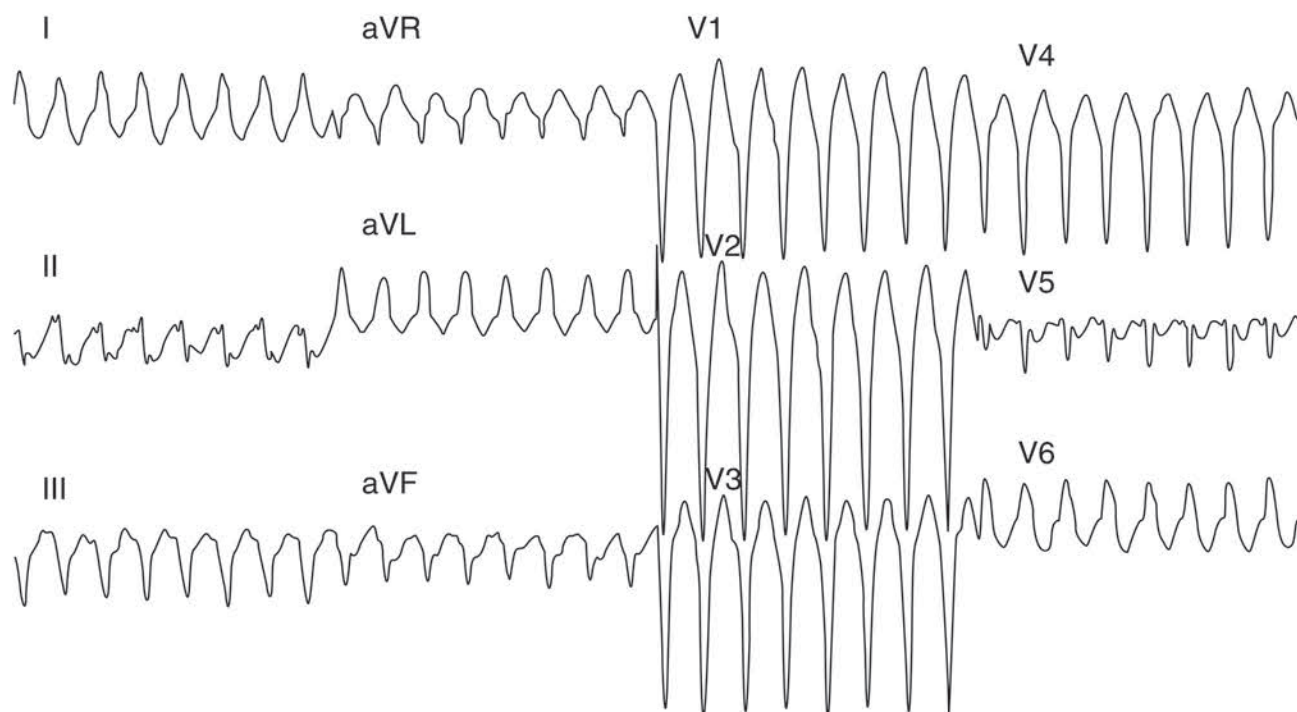


Fig. 29.7 Surface Lead Electrocardiograms of Ventricular Tachycardia (VT) in a Patient With Arrhythmogenic Right Ventricular Cardiomyopathy. Both VTs have left bundle branch block-type morphology but with very different frontal axes.

A focal mechanism of VT has been observed in a minority of ARVC patients. Among patients with frequent PVCs at baseline, a high degree of association has been reported between catecholamine-facilitated induced sustained VTs and the clinical PVCs. VT in these patients exhibited features suggestive of a focal mechanism and had a QRS morphology identical to that of clinical PVCs. The site of origin of those VTs was mapped to the border region of the scar, typically in the RVOT and RV basal regions.¹⁷

MAPPING

VTs in ARVC share many features observed in post-MI VTs. First, the tachycardias typically are monomorphic and have a macroreentrant mechanism. Second, the circuits are composed of zones of abnormal conduction, characterized by low-amplitude abnormal electrograms, with identifiable exit regions to the surrounding myocardium. Third, outer loops, which can be broad portions of the reentry circuit in communication with the surrounding myocardium, have also been observed. Fourth, the ablation targets in post-MI VT (critical isthmus) are similar to those in ARVC. Therefore mapping techniques for ARVC-related VT are similar to those used for post-MI VT (see Chapter 22 for detailed discussion).

Electroanatomic mapping with CARTO (Biosense Webster, Diamond Bar, CA, United States), ESI-NavX (St. Jude Medical, St. Paul, MN, United States), or Rhythmia (Boston Scientific, Cambridge, MA, United States) is generally used for the mapping and ablation of VT associated with ARVC. Electroanatomic 3-D mapping can help in the precise description of VT reentrant circuits, the rapid visualization of the sequence of ventricular activation during the VT, and the identification of slow-conducting pathways and appropriate sites for entrainment mapping. Local activation times are assigned according to the onset of the bipolar electrogram registered at the tip of the mapping catheter, and are color-coded. These systems also help in the navigation of the ablation catheter, the planning of ablation lines, and the maintaining a log of sites of interest (e.g., sites with favorable entrainment or pace mapping findings), which can then be revisited with precision. In addition, voltage (scar) mapping is a helpful feature of some of the electroanatomic mapping systems (see later).

Activation Mapping

Most reentrant circuits cluster around the inferolateral tricuspid annulus, the RVOT, and less commonly the RV apex, which are the typical areas of fibrous and fatty infiltration in ARVC. Hence, these areas are targeted first by activation mapping. Because the VT circuit is composed of zones of abnormal conduction, which are characterized by low-amplitude abnormal electrograms with identifiable exit regions to the surrounding myocardium, endocardial activation mapping during VT typically detects abnormal fragmented or split low-voltage electrograms, with diastolic potentials (eFig. 29.2).

During activation mapping, particular sites of interest include: (1) sites with abnormal local bipolar electrogram (amplitude, ≤ 0.5 mV; duration, ≥ 60 milliseconds); (2) sites at which the local electrogram precedes the QRS complex by at least 50 milliseconds (activation times are taken from the onset of the bipolar electrogram); and (3) sites with the earliest local activation closest to mid-diastole, isolated mid-diastolic potentials, or continuous activity. Once identified, these sites are targeted by entrainment mapping (see later) to establish their relationship to the tachycardia circuit.

Detailed mapping will usually reveal more than one site of presystolic activity. Therefore it is essential to demonstrate that the presystolic site recorded is in fact the earliest site. A normal presystolic bipolar electrogram (amplitude, >3 mV; duration, <70 milliseconds) should prompt

further search for earlier activity. If, after very detailed mapping, the earliest recorded site is not at least 50 milliseconds presystolic, this suggests that either the map is inadequate (most common) or the VT arises deeper than the subendocardium, in the midmyocardium, or even incorporating the subepicardium. VTs in patients with ARVC exhibiting a focal activation pattern have also been described; however, an epicardial reentrant circuit with a defined endocardial exit may explain a focal activation pattern of the RV endocardium.

An isolated mid-diastolic potential is defined as a low-amplitude, high-frequency diastolic potential separated from the preceding and subsequent ventricular electrograms by an isoelectric segment. It is likely that isolated mid-diastolic potentials that cannot be dissociated from the VT are generated in segments of the zone of slow conduction or common pathway (isthmus), which are integral components of the reentry circuit. It is important to recognize that not all presystolic activity recorded during VT is related to the mechanism; it could represent delayed activity not related to the tachycardia mechanism, dead-end pathways, or even an artifact. Therefore it is important to confirm that presystolic activity is related to the reentrant circuit. Demonstration of a fixed relationship of the diastolic electrograms to the subsequent VT QRS, despite spontaneous or induced oscillations of the tachycardia cycle length (TCL), helps exclude the possibility that those electrograms reflect late activation from unrelated dead-end pathways.

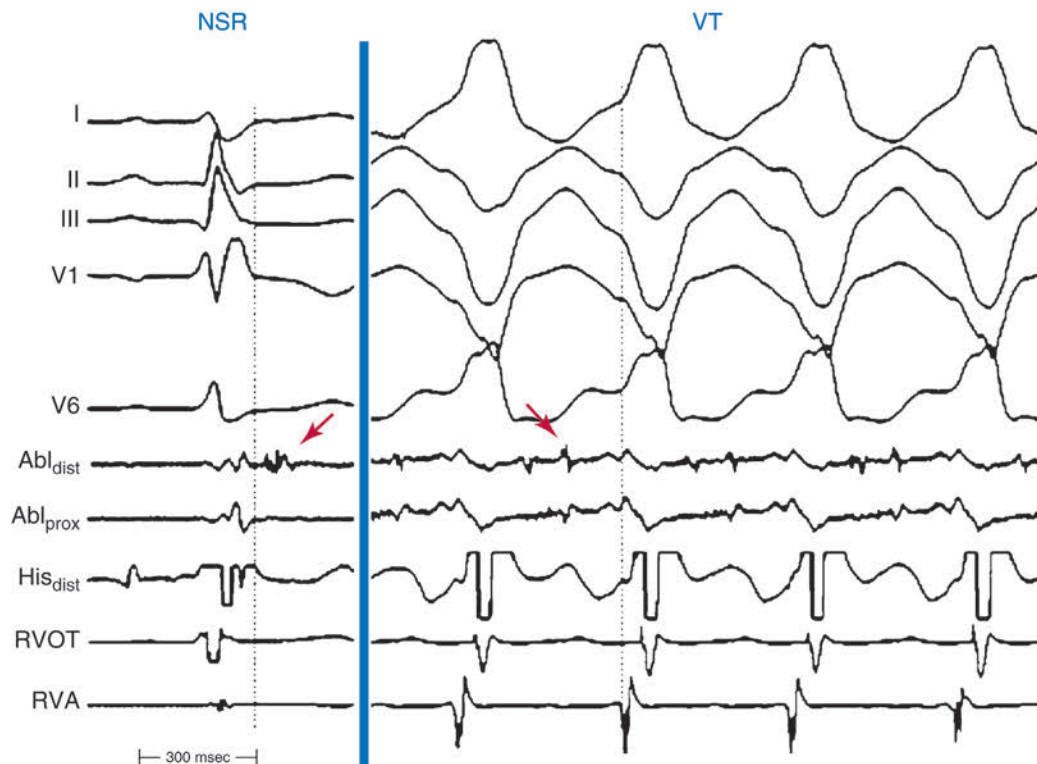
Successful activation mapping of VT has several prerequisites, including the inducibility of VT at the time of EP testing, hemodynamic stability of the VT (which usually requires a relatively slow VT rate), and stability of the VT reentry circuit (i.e., stable VT morphology and TCL). If the tachycardia is not stable (morphologically or hemodynamically), mapping can still be performed by starting and stopping the VT after data acquisition at each site. In addition, poorly tolerated rapid VTs sometimes can be slowed by antiarrhythmic drugs to allow for mapping. The use of 20-pole catheter (PentaRay; 2-6-2 mm interelectrode spacing, 1 mm electrodes; Biosense-Webster), the mini-basket catheter (Orion, Boston Scientific), and noncontact mapping can also provide large amounts of activation mapping data during nonsustained or unstable VT. The use of percutaneous LV assist devices is unlikely to be beneficial in ARVC patients, given the generally preserved LV function.⁷³

Entrainment Mapping

Entrainment mapping during reentrant VT is used to verify whether a site recording diastolic activity (regardless of where in diastole it occurs, its position, and its appearance on initiation of VT) is functionally involved in the VT circuit. Pacing is performed during VT at a PCL 10 to 30 milliseconds shorter than the VT CL, at RV sites identified during activation mapping, demonstrating continuous activity or isolated mid-diastolic potentials.^{75,76}

Once the presence of entrainment is verified, several criteria can be used to indicate the relation of the pacing site to the reentrant circuit. The first entrainment criterion to be sought is concealed fusion. Entrainment with concealed fusion indicates that the pacing site is in a protected isthmus located within or attached to the reentrant circuit. Whether this protected isthmus is crucial to the reentrant circuit or is just a bystander site needs to be verified by other entrainment criteria including the postpacing interval (PPI) versus the TCL and the local electrogram-QRS interval during VT versus the S-QRS interval (see Fig. 22.20).⁷⁷

For stable SMVTs, the following three criteria are used to define the critical isthmus and predict the success of radiofrequency (RF) application in termination of the VT: (1) entrainment with concealed fusion; (2) PPI equal to the TCL (± 30 milliseconds); (3) and S-QRS interval equal to the local electrogram-to-QRS interval (± 20 milliseconds). Other



eFig. 29.2 Electrocardiogram and Intracardiac Recordings During Normal Sinus Rhythm (NSR) and Ventricular Tachycardia (VT) in a Patient With Arrhythmogenic Right Ventricular Cardiomyopathy. During NSR (*left*), a late potential is present (*arrow*); the same potential occurs during mid-diastole during VT (*right*). Abl, Ablation; RVA, right ventricular apex; RVOT, right ventricular outflow tract.

predictors of successful ablation sites include S-QRS interval-to-VT CL ratio less than 70%, long S-QRS interval, and alteration of the TCL and/or termination by subthreshold or nonpropagated stimuli. However, because of the diffuse nature of the disease in ARVC, isthmuses may sometimes be wide, and good entrainment maps can be obtained from a rather large area. In this case, linear RF applications across the diastolic pathway may be necessary.⁷⁸

When hemodynamic compromise during the VT is the main limitation for conventional activation and entrainment mapping methods, inductions of brief episodes of VT (with the mapping catheter at the optimal site, as identified by substrate and pace mapping approaches) can allow assessment of the relationship of the abnormal electrograms to the VT circuit. This can also allow entrainment maneuvers to be performed at those sites to help distinguish sites critical to the VT circuit from bystander sites. VT is then quickly terminated before significant hemodynamic compromise ensues. This approach can be facilitated by hemodynamic support with the use of IV vasopressors. However, it requires being able to reproducibly induce the same VT morphology.

Pace Mapping

Pace mapping can be used to complement activation and entrainment mapping findings and to confirm ablation target sites. At isthmus sites defined during VT, pace mapping during NSR is attempted after VT termination, with the mapping catheter being kept at the same location. Pace mapping is preferably performed with unipolar stimuli (10 mA, 2 milliseconds) from the distal electrode of the mapping catheter (cathode) and an electrode in the inferior vena cava (IVC) (anode).

The resulting 12-lead ECG paced morphology is compared with that of the tachycardia. ECG recordings should be reviewed at the same gain and filter settings. The greater the degree of concordance between the morphology during pacing and tachycardia, the closer the catheter is to the exit site of the tachycardia.

At best, a pace map that matches the VT would only identify the exit site to the normal myocardium, and can be distant from the critical sites of the circuit to be targeted by ablation. Thus pace mapping remains only a corroborative method of localizing VT. It can be used to focus initial mapping to regions likely to contain the reentrant circuit exit or abnormal conduction but is not sufficiently specific or sensitive to be the sole guide for ablation.

Pace mapping can also be used in conjunction with substrate mapping when other mapping techniques are not feasible, so that it can provide information on where ablation can be directed. The VT circuit's exit site is approximated by the site of pace mapping that generates QRS complexes similar to those of VT. From that point, evaluation of the S-QRS interval (measured to the onset of the earliest QRS on the 12-lead ECG) can help trace the course of the VT isthmus. Sites along the VT isthmus are associated with good pace maps but with progressively longer S-QRS intervals.

Substrate Mapping

In a subset of ARVC patients, conventional activation and entrainment mapping during VT can be limited by the changing multiple morphologies, the nonsustainability of the tachycardia, or the hemodynamic instability. Substrate-based voltage mapping during sinus rhythm can be used in these cases to identify regions of scar and abnormal myocardium and guide—in conjunction with pace mapping—the ablation of linear lesions to connect or encircle the abnormal regions.

The majority of VTs in ARVC patients are caused by macroreentry involving the dense myocardial scar interspersed with branching and merging bundles of viable myocytes with poor intercellular coupling and abnormal conduction properties. Buried in the arrhythmogenic substrate is the common central pathway (critical isthmus), which is a

narrow path of tissue with abnormal conduction properties, causing the slowing of impulse propagation and allowing reentry to occur. The isthmus itself can be surrounded by dead ends or branches that do not participate in the common pathway of the main reentrant circuit (bystander).⁷⁹

The dysplastic regions can be identified, quantified, and differentiated from healthy myocardium by the presence of electrograms with low amplitudes and longer durations, reflecting replaced myocardial tissue. Substrate mapping is performed during NSR and aims to identify: (1) scar location and distribution (as identified by voltage mapping and electric unexcitability); and (2) conducting channels within the scar, between two confluent scar areas, or between a scar and the tricuspid annulus that can potentially serve as isthmuses for reentrant VTs (as identified by local abnormal ventricular activity, late potentials, and long S-QRS interval during pacing).^{80,81}

Preprocedural Substrate Imaging

CT or CMR imaging can be used to identify the size, location, and transmural extent of the scar that potentially contains the arrhythmogenic substrate. In addition, integration of those imaging modalities into the 3-D electroanatomic mapping system can help visualize and display the LV substrate in a 3-D format and focus initial mapping efforts to those regions.

Scar Mapping

An electrical scar is defined by low-amplitude of local electrograms and tissue inexcitability during high-output pacing. Voltage mapping is performed during sinus rhythm, atrial pacing, or ventricular pacing. The peak-to-peak signal amplitude of the bipolar electrogram is measured automatically. RV endocardial regions with a bipolar electrogram amplitude greater than 1.5 mV are defined as normal, and dense scar areas are defined as those with an amplitude less than 0.5 mV. Abnormal myocardium is defined as an area of contiguous recordings with a bipolar electrogram amplitude between 0.5 and 1.5 mV. Of note, for the epicardium, normal myocardium is defined as regions with bipolar electrogram amplitude greater than 1.0 mV (to limit the influence of epicardial fat and coronary vasculature), and dense scar as regions with bipolar electrogram amplitude less than 0.5 mV. Because epicardial fat can decrease signal amplitude, low-voltage areas during epicardial mapping should also show abnormal electrogram configuration. At low-amplitude (<0.5 mV) sites, pacing is performed with 10-mA, 2-millisecond pulse width stimuli. A pacing threshold greater than 10 mA has been used to define unexcitable scar, provided electrode-tissue contact is adequate. A color-coded voltage map is then created (with the color range set between 0.5 and 1.5 mV) and superimposed on the anatomical model to show the amplitudes of all selected points.^{82,83}

As noted, in ARVC, the normal myocardium is replaced by fatty and then fibrous tissue, causing thinning and scarring, predominantly in the RV. Studies have found that regions of abnormal voltage suggestive of scar were observed in all ARVC patients. The endocardial bipolar voltage abnormalities tend to be perivalvular and, although predominantly affecting the RV free wall, involve some aspect of the septum in most patients (76%). This pattern is consistent with pathological studies demonstrating a predilection for scar to occur in these particular areas in ARVC. Whether an extensive perivalvular fibrotic process is specific for patients who present with sustained monomorphic VT in the setting of ARVC is yet to be determined. In contrast to the post-MI pattern of dense scar surrounded by a border zone, the regions of abnormal myocardium in ARVC are commonly patchy and inhomogeneous, occurring in anatomically disparate areas. Consequently, low-voltage identification in ARVC is less useful as a marker for ablation because it is very widespread. Nonetheless, evaluating the existence of different voltage areas

within the 0.5 mV scar (i.e., the voltage limits are reset to 0.3 to 0.5 mV as the upper limit and to 0.1 mV as the lower, representing dense scar) can potentially help visualize channels of slow conduction within scar tissue. The critical isthmus of each of the reentrant circuit typically is bounded by an area of low-voltage scar on one side and an anatomical barrier (tricuspid annulus) on the other side, or by two parallel lines of double potentials.

Importantly, fibrofatty replacement in ARVC typically begins in the subepicardium or midmural layers and progresses to the subendocardium. This contrasts with the VT substrate in post-MI patients, whereby the wave of necrosis progresses from subendocardium to epicardium, producing larger scar areas endocardially rather than epicardially, and intramural or epicardial substrate abnormalities are almost always associated with endocardial scar. Therefore bipolar voltage mapping from the endocardial surface likely underestimates the degree of abnormal

myocardium in ARVC patients (eFig. 29.3). Endocardial *unipolar* voltage mapping (with a cutoff of 5.5 mV for RV free wall scar detection, and 7.5 mV for the RV septum) can potentially provide a more global assessment of myocardial voltage and more closely approximate the degree and location of epicardial bipolar voltage abnormalities that serve as a substrate for VT in ARVC patients with no or limited endocardial bipolar voltage abnormalities. Endocardial unipolar voltage mapping was found to accurately predict the location and extent of epicardial involvement and may help in decision making related to proceeding to epicardial substrate mapping and ablation (eFig. 29.4).^{83,84}

Identification of Conducting Channels

Identification of the conducting channels within the scar region helps refine the area that potentially supports the VT circuit. Those channels can be identified by voltage channels, late potentials, or both. Recent

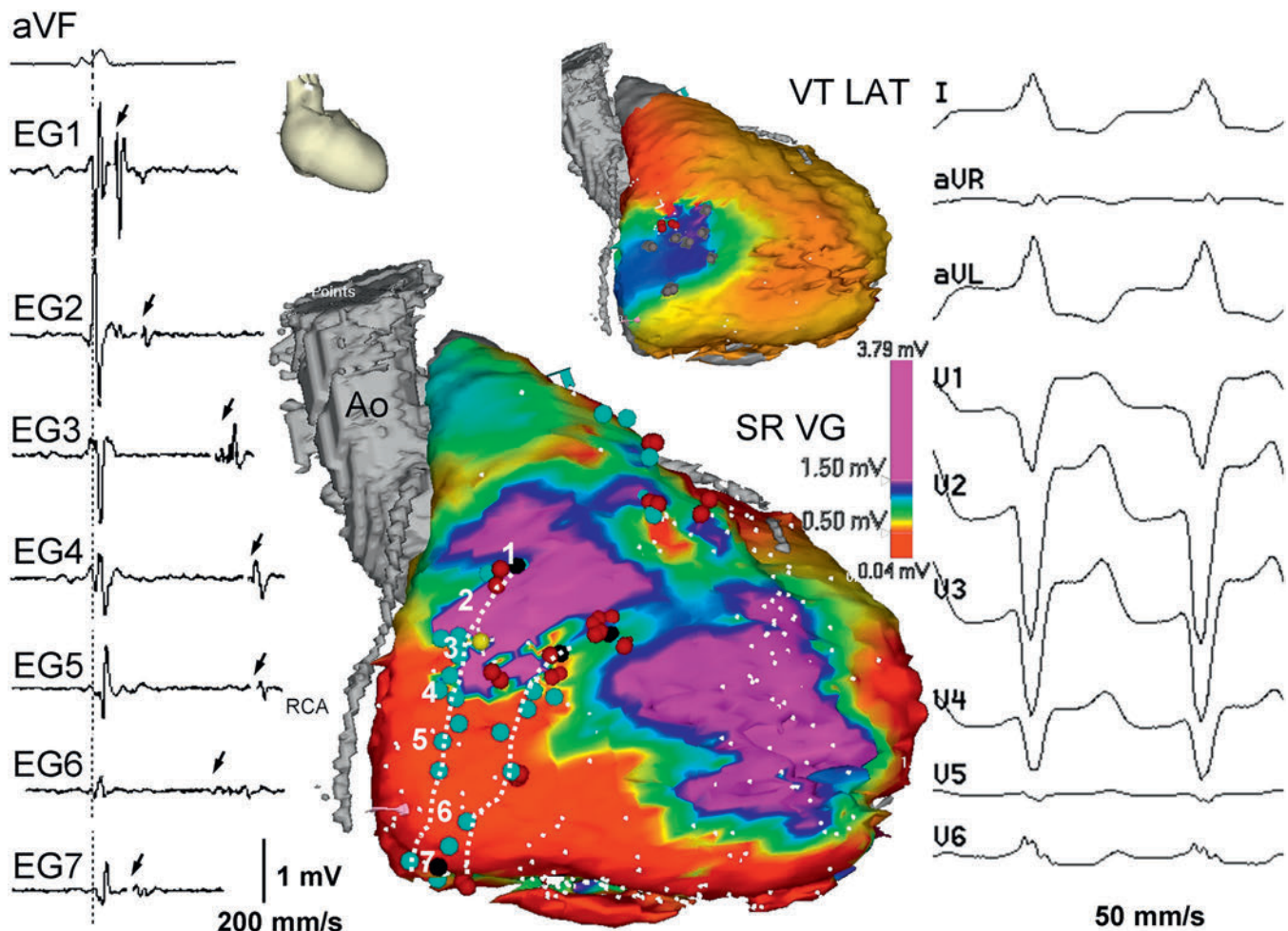
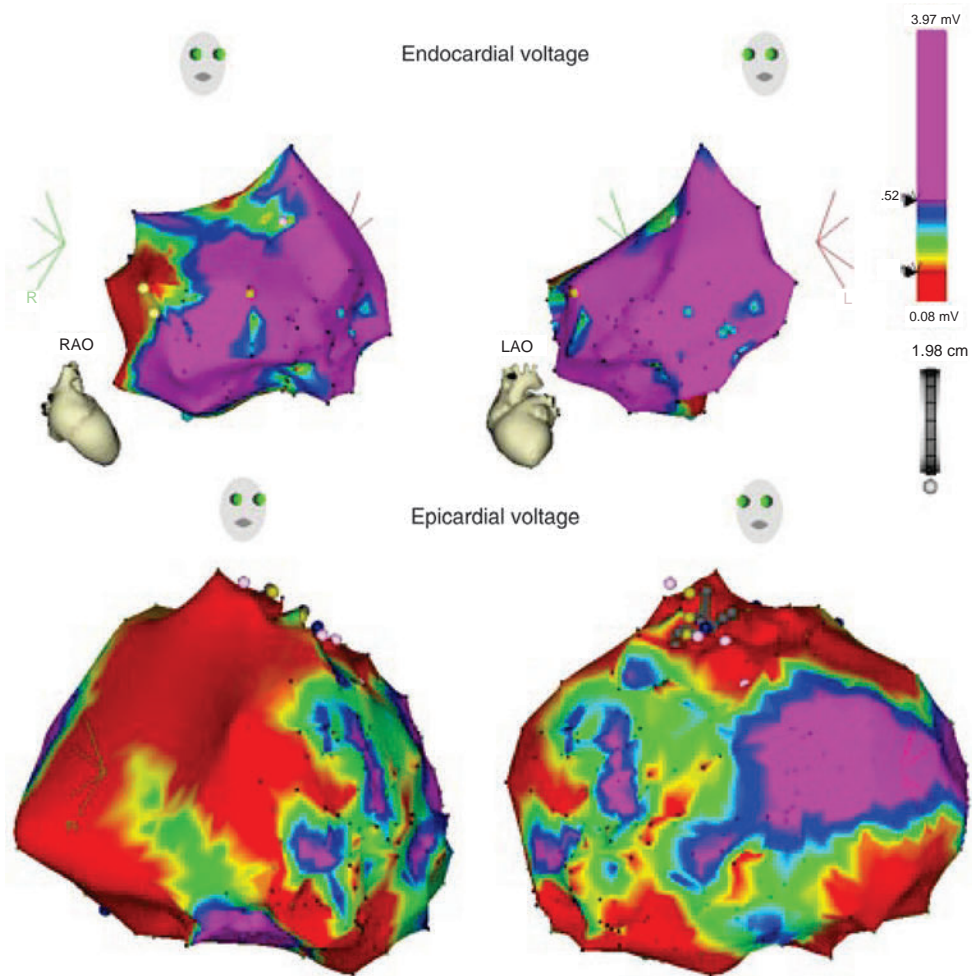
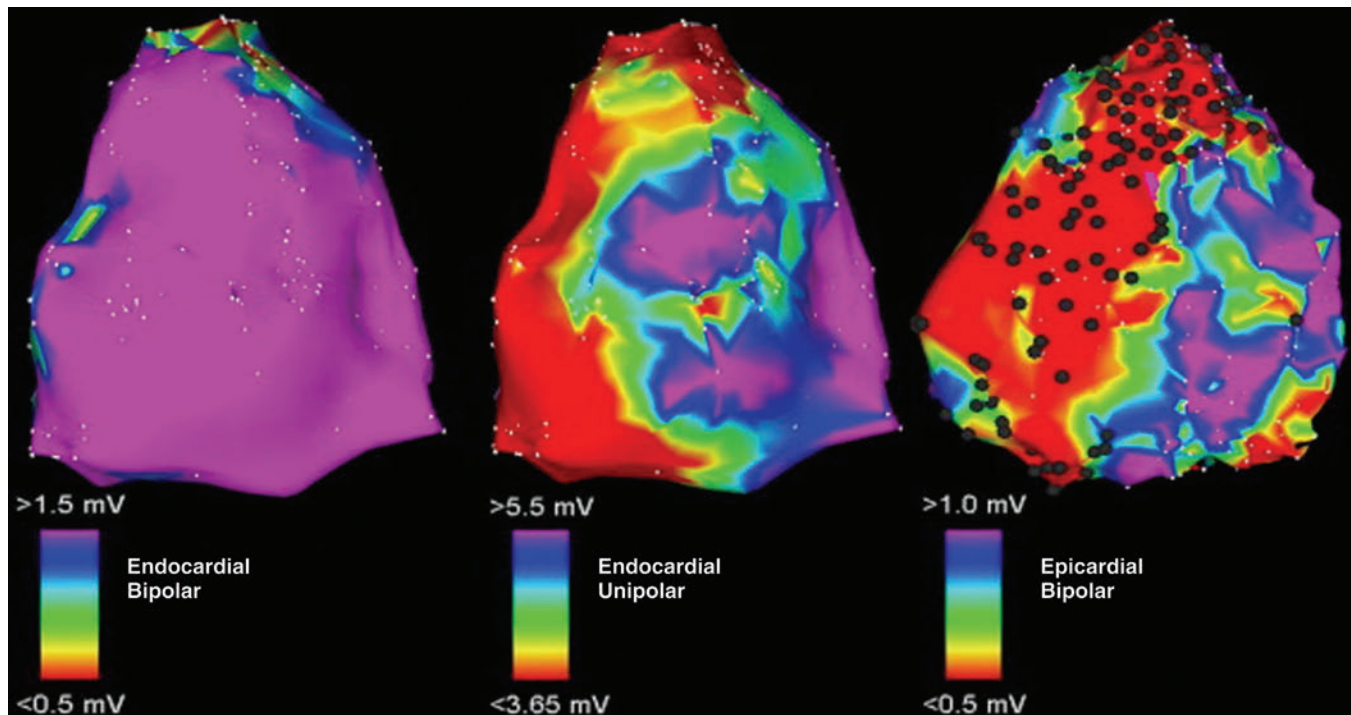


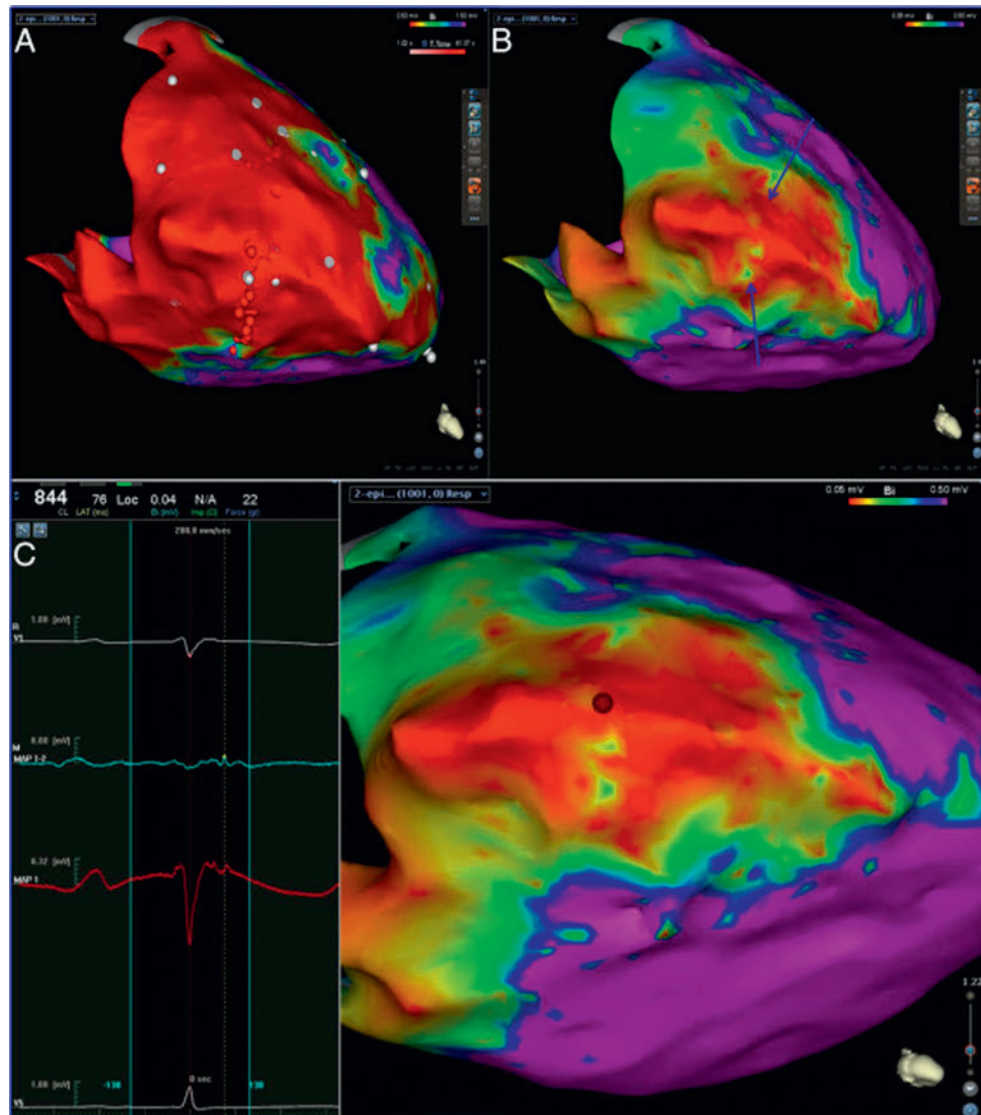
Fig. 29.8 Late Potential Conducting Channel Containing a Ventricular Tachycardia (VT) Isthmus Site. Epicardial bipolar voltage map during sinus rhythm (SR VG) from a patient with arrhythmogenic right ventricular cardiomyopathy and a low-voltage area in the epicardial right ventricular free wall. Two late potential channels are highlighted with white dotted lines. Electrograms (EGs) during sinus rhythm in the more basal channel are shown on the left. Epicardial activation mapping (VT LAT) and electrocardiogram of the clinical ventricular tachycardia are shown. The VT isthmus site (exit site) was identified by activation mapping during VT. This exit site is located in the transition from blue to red colors in the VT LAT map and could also be recognized because from this location to red dots marks the precise location of the radiofrequency delivery. This VT isthmus exit site is projected over the SR VG map (highlighted with a yellow dot) and coincides with the conducting channel-entrance electrogram identified during sinus rhythm. Ao, Ascending aorta; RCA, right coronary artery. (From Fernandez-Armenta J, Andreu D, Penela D, et al. Sinus rhythm detection of conducting channels and ventricular tachycardia isthmus in arrhythmogenic right ventricular cardiomyopathy. *Heart Rhythm*. 2014;11:747–754.)



eFig. 29.3 Voltage Mapping in Arrhythmogenic Right Ventricular Cardiomyopathy (ARVC). Right and left anterior oblique electroanatomic endocardial (*top*) and epicardial (*bottom*) voltage maps in a patient with ARVC. Red areas denote low voltage/scar. On the endocardial map, only a small area shows abnormal voltage (near lateral tricuspid valve, *red area*); however, on the epicardial map, substantially larger areas show abnormal low voltage. LAO, Left anterior oblique; RAO, right anterior oblique.



eFig. 29.4 Bipolar and Unipolar Voltage Mapping in Arrhythmogenic Right Ventricular Cardiomyopathy (ARVC). Unipolar endocardial voltage mapping identifies the location and greater extent of epicardial bipolar electrogram abnormalities in a patient with ARVC. Endocardial bipolar voltage map demonstrates a paucity of low-voltage regions (*left*). Endocardial unipolar voltage mapping reveals a much greater burden of abnormal myocardium (<5.5 mV) extending from the lateral tricuspid valve up to the pulmonic valve region and inferiorly across the right ventricular free wall (*center*). Epicardial bipolar voltage map confirms the extensive area of abnormal epicardium (*right*). Black dots represent wide, split, and/or late epicardial electrograms and help to identify low-voltage areas consistent with scar versus fat. (From Polin GM, Haqqani H, Tzou W, et al. Endocardial unipolar voltage mapping to identify epicardial substrate in arrhythmogenic right ventricular cardiomyopathy/dysplasia. *Heart Rhythm*. 2011;8:76–83.)



eFig. 29.5 Voltage Channels. Epicardial voltage map during sinus rhythm showing extensive scarring of the right ventricular free wall. (A) Voltage map with standard voltage threshold of 0.5 to 1.5 mV showing uniform extensive scarring of the right ventricular free wall. (B) Unmasked channel of relatively higher voltage (blue arrows) after the voltage threshold was reduced to 0.05 to 0.5 mV. (C) Unipolar and bipolar recordings from the epicardium with ablation catheter during sinus rhythm in the area of the channel (red tag) showing late potential. (From Kumar P, Mounsey JP, Chung EH. Adjusting voltage criteria can unmask conducting channels in a patient with arrhythmogenic right ventricular cardiomyopathy and ventricular tachycardia. *Heart Rhythm Case Rep.* 2015;1:275–278.)

evidence has shown that the technique using late potentials identifies a higher proportion of conducting channels and, more importantly, most conducting channels that serve as the substrate for VTs. Using only the bipolar voltage adjustment, more than 70% of the conducting channels and 60% of the VT isthmuses would not be identified.⁸⁵

Voltage channels. Conducting channels on the electroanatomic voltage map are identified corridors of voltage preservation (voltage channels) within denser regions of scar or corridors between a dense scar and the tricuspid annulus. Careful step-by-step manual adjustment of voltage upper and lower limits on the color-coded electroanatomic voltage map can help maximize the color contrast between adjacent myocardium with different electrogram voltage levels within the 0.5 mV scar and, thus, unmask channels of viable myocardium within a dense scar (eFig. 29.5).^{85,86}

Late potentials. Fractionated electrograms (i.e., near-field signals with three or more sharp spikes, either separated by an isoelectric interval or continuous) and late potentials (defined as bipolar electrogram with any component is recorded after the offset of the QRS complex on the surface ECG) can reflect local depolarization of surviving muscle bundles that are well insulated by dense scar. Sites recording abnormal electrograms are tagged on the electroanatomic map.^{83,85}

Late potential conducting channels are defined as a path of more than two adjacent late potentials connecting with healthy tissue (Fig. 29.8). Further, late potentials are classified as being an entrance or an inner part of a given conducting channel, depending on the local activation time of the near-field component. The entrance of a conducting channel is tagged as sites within the border zone (i.e., zone with 0.5 to 1.5 mV voltage) recording late potentials with the shortest delay between the far-field component of healthy/border zone muscle (low frequency, usually high voltage) and the near-field component (delayed, high frequency, usually fractionated and low voltage) corresponding to the local activation of myocardial fibers in the scar. Sites with longer delays likely reside farther along the conducting channel within the dense scar.⁸⁵

Often, late potentials are obscured by larger far-field electrograms. Therefore verification that a recorded electrogram is far-field rather than near-field is important and can be achieved by pacing at the local site. When the recorded electrogram is near-field, capture of the pacing stimulus results in capturing the tissue generating all components of the electrogram, so that no clear electrogram component is identifiable during pacing. Conversely, when the recorded electrogram is far-field, pacing may not capture local tissue (due to dense scar) or, when capture occurs, the far-field electrograms remain discernable during pacing (since they reflect activation of myocardium adjacent to the pacing site). Furthermore, changing the direction of depolarization approaching the mapping site (e.g., sinus rhythm vs. RV pacing) and premature

ventricular stimulation (causing decremental conduction) can help unmask some areas of block and slow conduction, expose late potentials by separating the local (near-field) from the far-field potentials.

Epicardial Mapping

As noted, the arrhythmogenic substrate in ARVC is more extensive epicardially. Several studies demonstrated that the scar and conducting channels supporting the VT circuit are more prevalent on epicardial compared to endocardial mapping, and are predominantly located in the subtricuspid region, followed by the RVOT region. This limits the success of purely endocardial mapping and ablation, since wall thickness in involved areas can be 1 cm or more.

Therefore patients with limited endocardial substrate (as demonstrated on voltage mapping), those with late VT termination with endocardial RF delivery, and certainly those with persistent VT despite aggressive endocardial ablation should be considered for an epicardial approach. In addition, unipolar voltage mapping from the endocardium can be used for evaluation of epicardial scar. Endocardial unipolar (rather than bipolar) voltage mapping can predict the presence of and more closely approximate the extent of epicardial involvement and, hence, the need for the epicardial approach. RV endocardial unipolar voltages less than 5.5 mV identify extensive RV epicardial bipolar abnormalities (eFig. 29.4).^{85,87}

Some studies have shown that a combined endocardial-epicardial mapping and ablation as a first-line strategy in patients with ARVC, and especially in those with failed prior endocardial ablation, can improve procedural success and mid-term outcomes.^{19,85} Furthermore, the presence of a Q wave or QS configuration in leads I and V₂ (anterior RV epicardial sites) or Q waves leads II, III, or aVF (inferior RV epicardial sites) on the surface ECG during VT suggests the presence of an epicardial source of VT, and can be helpful in identifying patients who should be considered for an epicardial approach with the initial procedure.

The approach to epicardial mapping is essentially the same as for endocardial ablation, including activation mapping, entrainment mapping, substrate mapping, and pace mapping, and is discussed in detail in Chapter 27.

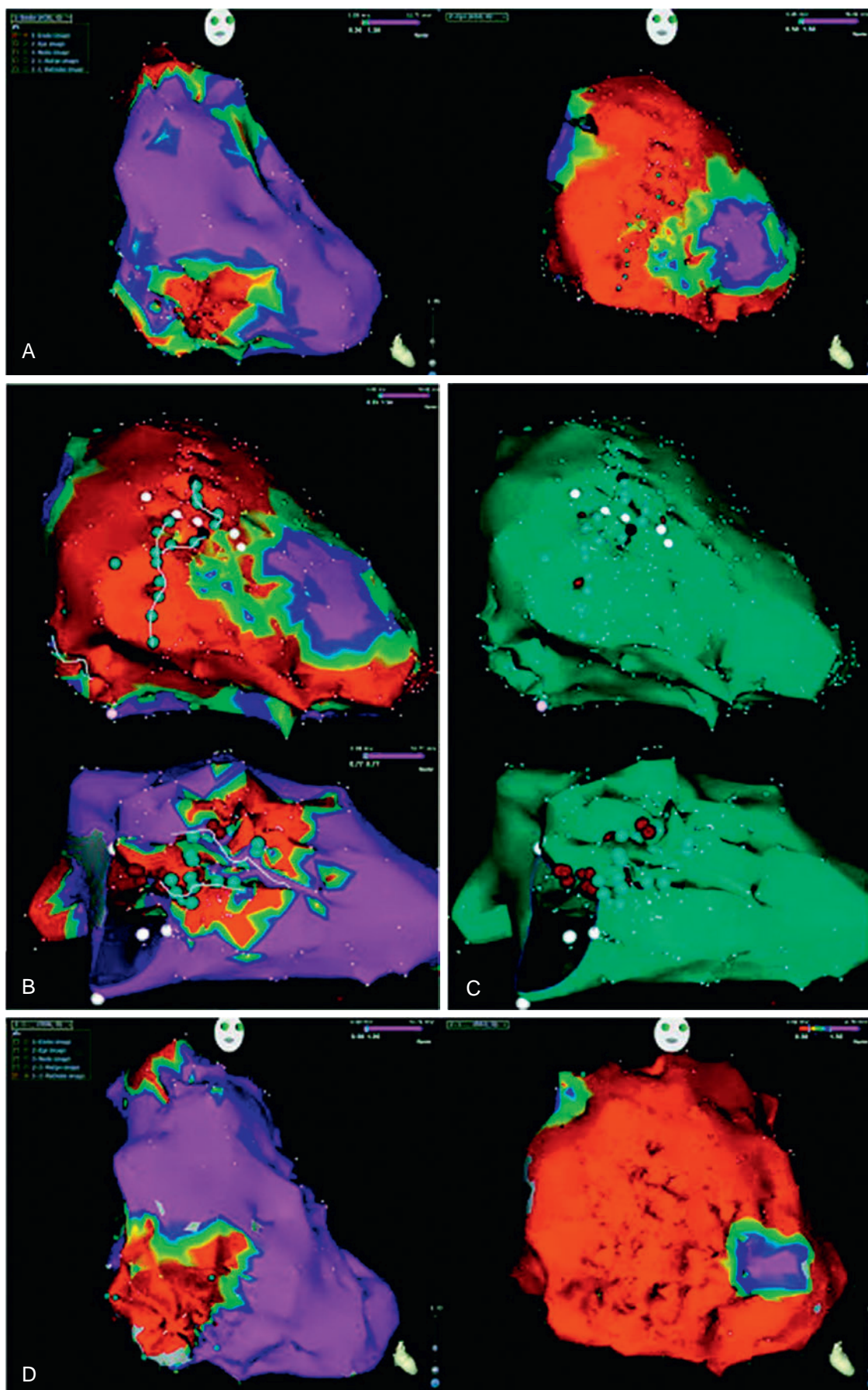
ABLATION

Target of Ablation

Selective Ablation of the Critical Isthmus of the Reentrant Circuit

For each induced stable SMVT, reentry circuit isthmuses are the target of ablation and are defined by activation and entrainment mapping as sites with: (1) continuous activity or isolated mid-diastolic potentials

Fig. 29.9 Scar Dechanneling. (A) Endocardial (*left*) and epicardial (*right*) substrate voltage maps, before scar dechanneling. (B) In this patient, three conducting channels (CCs) were identified: (1) one long and branched late potential channel localized at the right ventricular free wall (*top*); (2) one voltage channel parallel to the tricuspid annulus (*bottom*); and (3) another short late potential channel perpendicular to the tricuspid annulus (*bottom*). (C) A low number of radiofrequency (RF) lesions at the CC entrance (*black dots*) were necessary to eliminate all the channels as follows: (1) RF applications were delivered at the right ventricular free wall CC entrance and required two additional RF applications in the scar core to be completely eliminated (*top*); (2) RF was delivered at the CC entrance to eliminate the voltage CC parallel to the tricuspid annulus (*bottom*); and (3) RF was delivered to eliminate the CC perpendicular to the tricuspid annulus (*bottom*). (D) An increase in the epicardial scar area can be observed in the postablation remaps. Of note, despite a very wide epicardial scar after the ablation, endocardial electrograms opposite these areas are normal in sites outside of the initial endocardial scar. (From Berruezo, A, Fernández-Armenta J, Mont L, et al. Combined endocardial and epicardial catheter ablation in arrhythmogenic right ventricular dysplasia incorporating scar dechanneling technique. *Circ Arrhythmia Electrophysiol.* 2012;5:111–121.)



that cannot be dissociated from the tachycardia; (2) entrainment with concealed fusion; (3) PPI equal to the TCL (± 30 milliseconds); (4) S-QRS interval equal to electrogram-to-QRS interval (± 20 milliseconds); and (5) ratio of S-QRS interval of the TCL between 30% to 70%. Alteration of the TCL or termination of VT by subthreshold or nonpropagated stimuli, and repeated VT termination occurring with catheter manipulation or pacing at the site, also suggest an isthmus location (eFig. 29.6). These findings are consistent with a central/proximal isthmus site.

For hemodynamically unstable VTs, substrate mapping during sinus rhythm followed by brief inductions of VT (with the mapping catheter at the optimal site, as identified by substrate and pace mapping) can allow assessment of the relationship of the abnormal electrograms to the VT circuit. This can also allow entrainment maneuvers to be performed at those sites to help distinguish sites critical to the VT circuit from bystander sites. VT is then quickly terminated before significant hemodynamic compromise ensues. This approach, however, requires being able to induce the same VT reproducibly. The use of noncontact mapping can be of value in these cases.

When the critical isthmuses of the reentrant circuit(s) can be identified, linear ablation lesions are delivered to sever those isthmuses. Terminating VT by targeting this area during ablation provides confirmatory evidence that it is a critical site for the arrhythmia. Isthmuses can be relatively broad and require transection with linear ablation lesions, usually connecting two regions of scar, or scar and an anatomical barrier, such as the tricuspid annulus.⁸⁸

Substrate-Based Ablation

Often, several VT morphologies are inducible in an individual patient, and usually only a minority of induced VTs are mappable using the conventional activation and entrainment mapping techniques. For unmappable VTs (due to poor inducibility, changing VT morphology or hemodynamic instability), RF ablation can be performed as linear lesions targeting potential exit sites and isthmuses of VT circuits based on the location of the best pace map, the location of valvular anatomical boundaries, and the conducting channels defined by substrate mapping. Typically, linear lesions are created over target regions by sequential point lesions designed to: (1) connect scar or abnormal myocardium to a valve continuity (e.g., tricuspid annulus); (2) connect scar or abnormal myocardium to another scar; or (3) encircle the scar or abnormal region, depending on the scar location and size.^{85,87}

In addition, “scar dechanneling” with combined endocardial and epicardial RF ablation of all conducting channels within the scar, has been reported to improve short- and long-term success rates. This strategy preferentially targets the entrance sites to the conducting channels, which are identified by substrate mapping as sites within the border zone recording late potentials with the shortest delay between the far-field component (low frequency, usually high voltage) component and the near-field local ventricular activity (typically delayed, high frequency, fractionated, and low voltage). The endpoint of this ablation strategy is conducting channel entrance conduction block, manifest as the disappearance of the inner point of the conducting channels or delayed activation of conducting channel inner points, usually with the activation sequence in reverse order (Fig. 29.9).⁸²

Given the high burden of clinical and inducible VTs in ARVC patients, a strategy that incorporates extensive substrate-based ablation (linear ablation or scar dechanneling) in addition to selective ablation of the critical isthmus of the clinical VT may be reasonable to improve the long-term outcome.^{74,82,85,89}

Ablation of Premature Ventricular Complexes

In ARVC patients with frequent PVCs whose morphology is identical to that of the clinical or induced VT, an ablation strategy selectively

targeting the focus of the PVCs (typically at the border region of scar in the RVOT and RV basal regions) has been reportedly successful in eliminating the VT.¹⁷

Ablation Technique

Ablation may be performed with a 4-mm-tip catheter (maximal target temperature of 60°C and maximal power of 50 W), an 8-mm-tip catheter (maximal temperature of 65°C and maximal power of 75 W), or an irrigated-tip catheter (maximal temperature of 40°C to 45°C and maximal power of 40 to 50 W). Irrigated RF ablation catheters are preferred because power delivery can otherwise be limited in the trabeculated and annular regions where cooling from circulating blood flow is low (as well as the epicardial surface where there is no passive blood pool cooling). However, careful attention to power titration and monitoring impedance is necessary to reduce the risk of perforation when ablating in the free wall of the RV. Ablation is usually maintained for 60 to 120 seconds at the site where the tachycardia is terminated (while ablating during stable VT) or at each point along the linear ablation. The use of a deflectable sheath can help catheter manipulation in the RV.^{74,82,85}

Endpoints of Ablation

Successful VT ablation is defined as noninducibility of any VT (excluding very fast [TCL <240 milliseconds] nonclinical VTs) using the entire programmed electrical stimulation protocol. When the VT is scarcely inducible at baseline, the endpoint of substrate-based scar dechanneling involves conducting channel entrance conduction block, as described earlier. When linear ablation is performed, conduction block across the ablation line needs to be verified.^{74,82,85}

Outcome

Ablation of VT in ARVC remains a clinical challenge and should be viewed as a potentially palliative, rather than curative, procedure in selected patients. Although VT ablation has been reported to successfully eliminate inducible VT acutely in up to 60% to 80% of patients, the recurrence rates during long-term follow-up of 3 to 5 years are as high as 50% to 70%, even following extensive or repeated ablation attempts. Recurrences usually manifest as nonsustained VT, a slower monomorphic sustained VT, or a new monomorphic VT.²

The discrepancy between the good acute results and the unfavorable long-term outcome may be related to the progressive nature of ARVC, which predisposes to the occurrence of new and malignant arrhythmogenic substrates over time.^{2,89} Furthermore, multiple morphologies, hemodynamic instability, or noninducibility can limit the success of VT ablation. In addition, ARVC can create a large number of potential circuits; an empirical approach may not eliminate all the possible pathways. Achieving adequate energy delivery also can be a problem, especially in regions difficult to access by catheter; in particular, abnormal regions along the tricuspid annulus, which can require the use of 8-mm-tip or irrigation-tip ablation catheters to achieve effective lesions underneath the tricuspid valve. It is necessary to emphasize that caution must be taken when using irrigated-tip ablation in patients with very thin ventricular walls, although thick fibrous tissue is present in many areas. The risk of creating deeper lesions in thin walls of the RV body or apex potentially increases the risk of perforation. Although the magnitude of this risk is not well known, it seems to be infrequent.

Furthermore, recent studies have shown a high prevalence of epicardial isthmuses in ARVC. Epicardial mapping and ablation, and combined endocardial/epicardial substrate-based ablation approaches have yielded a significant improvement in short- and long-term ablation efficacy (VT free survival in up to 71% of patients over a mean follow-up of 56 months). Therefore it is reasonable to begin mapping endocardially, but be prepared to move to epicardial mapping following



eFig. 29.6 Ablation of Ventricular Tachycardia in Arrhythmogenic Right Ventricular Cardiomyopathy (ARVC). Shown is radiofrequency (RF) energy delivery in the basal lateral right ventricle in a patient with ARVC. Note the mid-diastolic potential (red arrow) 130 milliseconds prior to QRS onset and almost immediate cessation of ventricular tachycardia on RF delivery. The blue arrow marks initiation of RF energy delivery. Abl, Ablation; RVA, right ventricular apex; RVOT, right ventricular outflow tract.

pericardial puncture if endocardial mapping and ablation do not quickly yield good results. Combined endocardial-epicardial mapping and ablation strategy also may be considered as an initial strategy, especially in patients with VT recurrences after prior endocardial ablation.^{2,74,82,85}

REFERENCES

- Basso C, Corrado D, Bauce B, et al. Arrhythmogenic right ventricular cardiomyopathy. *Circ Arrhythmia Electrophysiol*. 2012;5:1233–1246.
- Corrado D, et al. Treatment of arrhythmogenic right ventricular cardiomyopathy/dysplasia: an international task force consensus statement. *Eur Heart J*. 2015;36:3227–3237.
- Corrado D, Link MS, Calkins H. Arrhythmogenic right ventricular cardiomyopathy. *N Engl J Med*. 2017;376:61–72.
- Marcus F, Mestroni L. Family members of patients with ARVC: who is at risk? At what age? When and how often should we evaluate to determine risk? *J Am Coll Cardiol*. 2014;64:302–303.
- Lorenzon A, et al. Homozygous desmocollin-2 mutations and arrhythmogenic cardiomyopathy. *Am J Cardiol*. 2015;116:1245–1251.
- Marcus FI, Edson S, Towbin JA. Genetics of arrhythmogenic right ventricular cardiomyopathy: a practical guide for physicians. *J Am Coll Cardiol*. 2013;61:1945–1948.
- Roux-Buisson N, et al. Prevalence and significance of rare RYR2 variants in arrhythmogenic right ventricular cardiomyopathy/dysplasia: results of a systematic screening. *Heart Rhythm*. 2014;11:1999–2009.
- Hodgkinson KA, et al. Long-term clinical outcome of arrhythmogenic right ventricular cardiomyopathy in individuals with a p.S358L mutation in *TMEM43* following implantable cardioverter defibrillator therapy. *Circ Arrhythmia Electrophysiol*. 2016;9:e003589.
- Thiene G. The research venture in arrhythmogenic right ventricular cardiomyopathy: a paradigm of translational medicine. *Eur Heart J*. 2015;36:837–846.
- Bhonsale A, et al. Impact of genotype on clinical course in arrhythmogenic right ventricular dysplasia/cardiomyopathy-associated mutation carriers. *Eur Heart J*. 2015;36:847–855.
- Wichter T, Indik JH, Paul M. Ventricular angiography in arrhythmogenic cardiomyopathy. *Card Electrophysiol Clin*. 2011;3:255–267.
- Cruz FM, et al. Exercise triggers ARVC phenotype in mice expressing a disease-causing mutated version of human plakophilin-2. *J Am Coll Cardiol*. 2015;65:1438–1450.
- Ruwaldo AC, et al. Association of competitive and recreational sport participation with cardiac events in patients with arrhythmogenic right ventricular cardiomyopathy: results from the North American multidisciplinary study of arrhythmogenic right ventricular cardiomyopathy. *Eur Heart J*. 2015;36:1735–1743.
- Sawant AC, Calkins H. Relationship between arrhythmogenic right ventricular dysplasia and exercise. *Card Electrophysiol Clin*. 2015;7:195–206.
- Shaw RM. Reduced sodium channels in human ARVC. *Heart Rhythm*. 2013;10:420–421.
- Noorman M, et al. Remodeling of the cardiac sodium channel, connexin43, and plakoglobin at the intercalated disk in patients with arrhythmogenic cardiomyopathy. *Heart Rhythm*. 2013;10:412–419.
- Philips B, et al. High prevalence of catecholamine-facilitated focal ventricular tachycardia in patients with arrhythmogenic right ventricular dysplasia/cardiomyopathy. *Circ Arrhythmia Electrophysiol*. 2013;6:160–166.
- Lopez-Ayala JM, et al. Genetics of myocarditis in arrhythmogenic right ventricular dysplasia. *Heart Rhythm*. 2015;12:766–773.
- Berte B, et al. Characterization of the left-sided substrate in arrhythmogenic right ventricular cardiomyopathy. *Circ Arrhythmia Electrophysiol*. 2015;8:1403–1412.
- Te Riele ASJM, et al. Mutation-positive arrhythmogenic right ventricular dysplasia/cardiomyopathy: the triangle of dysplasia displaced. *J Cardiovasc Electrophysiol*. 2013;24:1311–1320.
- Philips B, Cheng A. 2015 Update on the diagnosis and management of arrhythmogenic right ventricular cardiomyopathy. *Curr Opin Cardiol*. 2015;31:1.
- Groeneweg JA, et al. Left-dominant arrhythmogenic cardiomyopathy in a large family: associated desmosomal or nondesmosomal genotype? *Heart Rhythm*. 2013;10:548–559.
- Te Riele ASJM, et al. Arrhythmogenic right ventricular dysplasia/cardiomyopathy in the pediatric population. *JACC Clin Electrophysiol*. 2015;1:551–560.
- Migliore F, et al. Prognostic value of endocardial voltage mapping in patients with arrhythmogenic right ventricular cardiomyopathy/dysplasia. *Circ Arrhythmia Electrophysiol*. 2013;6:167–176.
- Bhonsale A, et al. Cardiac phenotype and long-term prognosis of arrhythmogenic right ventricular cardiomyopathy/dysplasia patients with late presentation. *Heart Rhythm*. 2016;14:883–891.
- Choudhary N, et al. Clinical presentation and outcomes by sex in arrhythmogenic right ventricular cardiomyopathy: findings from the North American ARVC Registry. *J Cardiovasc Electrophysiol*. 2016;27:555–562.
- Kimura Y, et al. Potentially lethal ventricular arrhythmias and heart failure in arrhythmogenic right ventricular cardiomyopathy: what are the differences between men and women? *JACC Clin Electrophysiol*. 2016;2:546–555.
- Camm CF, et al. Prevalence of atrial arrhythmias in arrhythmogenic right ventricular dysplasia/cardiomyopathy. *Heart Rhythm*. 2013;10:1661–1668.
- Etoom Y, et al. Importance of CMR within the task force criteria for the diagnosis of ARVC in children and adolescents. *J Am Coll Cardiol*. 2015;65:987–995.
- Asimaki A, et al. A new diagnostic test for arrhythmogenic right ventricular cardiomyopathy. *N Engl J Med*. 2009;360:1075–1084.
- Sen-Chowdhry S, Syrris P, Quarta G, et al. Clinical impact of genetics in arrhythmogenic cardiomyopathy. *Card Electrophysiol Clin*. 2011;3:205–215.
- Groeneweg JA, et al. Functional assessment of potential splice site variants in arrhythmogenic right ventricular dysplasia/cardiomyopathy. *Heart Rhythm*. 2014;11:2010–2017.
- Marra MP, et al. Imaging study of ventricular scar in arrhythmogenic right ventricular cardiomyopathy: comparison of 3D standard electroanatomical voltage mapping and contrast-enhanced cardiac magnetic resonance. *Circ Arrhythmia Electrophysiol*. 2012;5:91–100.
- Denis A, et al. Diagnostic value of isoproterenol testing in arrhythmogenic right ventricular cardiomyopathy. *Circ Arrhythmia Electrophysiol*. 2014;7:590–597.
- Hoffmayer KS, Scheinman MM. Electrocardiographic characteristics of ventricular tachycardia in arrhythmogenic right ventricular dysplasia. *Card Electrophysiol Clin*. 2014;6:595–601.
- Hoffmayer KS, et al. Electrocardiographic comparison of ventricular arrhythmias in patients with arrhythmogenic right ventricular cardiomyopathy and right ventricular outflow tract tachycardia. *J Am Coll Cardiol*. 2011;58:831–838.
- Ren L, et al. Electrocardiographic difference between ventricular arrhythmias from the right ventricular outflow tract and idiopathic right ventricular arrhythmias. *Pacing Clin Electrophysiol*. 2014;37:1658–1664.
- Hoffmayer KS, et al. An electrocardiographic scoring system for distinguishing right ventricular outflow tract arrhythmias in patients with arrhythmogenic right ventricular cardiomyopathy from idiopathic ventricular tachycardia. *Heart Rhythm*. 2013;10:477–482.
- Birnie DH, et al. HRS expert consensus statement on the diagnosis and management of arrhythmias associated with cardiac sarcoidosis. *Heart Rhythm*. 2014;11:1305–1323.
- Kumar S, et al. Ventricular tachycardia in cardiac sarcoidosis: characterization of ventricular substrate and outcomes of catheter ablation. *Circ Arrhythmia Electrophysiol*. 2015;8:87–93.
- Decherer DG, et al. Electrophysiological characteristics of ventricular tachyarrhythmias in cardiac sarcoidosis versus arrhythmogenic right ventricular cardiomyopathy. *Heart Rhythm*. 2013;10:158–164.
- Tung R, et al. Incidence of abnormal positron emission tomography in patients with unexplained cardiomyopathy and ventricular arrhythmias: the potential role of occult inflammation in arrhythmogenesis. *Heart Rhythm*. 2015;12:2488–2498.

43. Philips B, et al. Arrhythmogenic right ventricular dysplasia/cardiomyopathy and cardiac sarcoidosis: distinguishing features when the diagnosis is unclear. *Circ Arrhythmia Electrophysiol.* 2014;7:230–236.
44. Zaidi A, et al. Clinical differentiation between physiological remodeling and arrhythmogenic right ventricular cardiomyopathy in athletes with marked electrocardiographic repolarization anomalies. *J Am Coll Cardiol.* 2015;65:2702–2711.
45. Zaidi A, et al. Clinical significance of electrocardiographic right ventricular hypertrophy in athletes: comparison with arrhythmogenic right ventricular cardiomyopathy and pulmonary hypertension. *Eur Heart J.* 2013;34:3649–3656.
46. La Gerche A, et al. Lower than expected desmosomal gene mutation prevalence in endurance athletes with complex ventricular arrhythmias of right ventricular origin. *Heart.* 2010;96:1268–1274.
47. Zaidi A, et al. Physiological right ventricular adaptation in elite athletes of African and Afro-Caribbean origin. *Circulation.* 2013;127:1783–1792.
48. La Gerche A, Heidbuchel H. Exercise-induced arrhythmogenic right ventricular cardiomyopathy. *Card Electrophysiol Clin.* 2013;5:97–105.
49. La Gerche A, et al. Exercise-induced right ventricular dysfunction is associated with ventricular arrhythmias in endurance athletes. *Eur Heart J.* 2015;36:1998–2010.
50. Te Riele ASJM, et al. Approach to family screening in arrhythmogenic right ventricular dysplasia/cardiomyopathy. *Eur Heart J.* 2016;37:755–763.
51. Bhonsale A, et al. Risk stratification in arrhythmogenic right ventricular dysplasia/cardiomyopathy-associated desmosomal mutation carriers. *Circ Arrhythmia Electrophysiol.* 2013;6:569–578.
52. Link MS, et al. Ventricular arrhythmias in the North American multidisciplinary study of ARVC: predictors, characteristics, and treatment. *J Am Coll Cardiol.* 2014;64:119–125.
53. Kikuchi N, Yumino D, Shiga T, et al. Long-term prognostic role of the diagnostic criteria for arrhythmogenic right ventricular cardiomyopathy/dysplasia. *JACC Clin Electrophysiol.* 2016;2:107–115.
54. Brun F, et al. Risk stratification in arrhythmic right ventricular cardiomyopathy without implantable cardioverter-defibrillators. *JACC Clin Electrophysiol.* 2016;2:558–564.
55. Priori SG, Blomström-Lundqvist C, Mazzanti A. 2015 ESC guidelines for the management of patients with ventricular arrhythmias and the prevention of sudden cardiac death. *Eur Heart J.* 2015;36:2551–2661.
56. Ermakov S, Gerstenfeld EP, Svetlichnaya Y, et al. Use of flecainide in combination antiarrhythmic therapy in patients with arrhythmogenic right ventricular cardiomyopathy. *Heart Rhythm.* 2016;14:564–569.
57. Müssigbrodt A, et al. Should all patients with arrhythmogenic right ventricular dysplasia/cardiomyopathy undergo epicardial catheter ablation? *J Interv Card Electrophysiol.* 2017;48:193–199.
58. Herman ARM, et al. Long-term right ventricular implantable cardioverter-defibrillator lead performance in arrhythmogenic right ventricular cardiomyopathy. *Heart Rhythm.* 2016;13:1964–1970.
59. Schinkel AFL. Implantable cardioverter defibrillators in arrhythmogenic right ventricular dysplasia/cardiomyopathy: patient outcomes, incidence of appropriate and inappropriate interventions, and complications. *Circ Arrhythmia Electrophysiol.* 2013;6:562–568.
60. Mugnai G, et al. Implantable cardioverter-defibrillators in patients with arrhythmogenic right ventricular cardiomyopathy: the course of electronic parameters, clinical features, and complications during long-term follow-up. *J Interv Card Electrophysiol.* 2014;41:23–29.
61. Maron BJ, et al. Eligibility and disqualification recommendations for competitive athletes with cardiovascular abnormalities: Task Force 3: hypertrophic cardiomyopathy, arrhythmogenic right ventricular cardiomyopathy and other cardiomyopathies, and myocarditis. *J Am Coll Cardiol.* 2015;66:2362–2371.
62. Sawant AC, et al. Safety of American Heart Association-recommended minimum exercise for desmosomal mutation carriers. *Heart Rhythm.* 2016;13:199–207.
63. Perrin MJ, et al. Exercise testing in asymptomatic gene carriers exposes a latent electrical substrate of arrhythmogenic right ventricular cardiomyopathy. *J Am Coll Cardiol.* 2013;62:1772–1779.
64. Te Riele ASJM, et al. Yield of serial evaluation in at-risk family members of patients with ARVD/C. *J Am Coll Cardiol.* 2014;64:293–301.
65. Te Riele ASJM, et al. Malignant arrhythmogenic right ventricular dysplasia/cardiomyopathy with a normal 12-lead electrocardiogram: a rare but underrecognized clinical entity. *Heart Rhythm.* 2013;10:1484–1491.
66. Tanawuttiwat T, et al. Electroanatomic correlates of depolarization abnormalities in arrhythmogenic right ventricular dysplasia/cardiomyopathy. *J Cardiovasc Electrophysiol.* 2016;27:443–452.
67. Bae MH, et al. Changes in follow-up ECG and signal-averaged ECG in patients with arrhythmogenic right ventricular cardiomyopathy. *Pacing Clin Electrophysiol.* 2014;37:430–438.
68. Hauer RNW, Cox MGPJ. Twelve-lead ECG in arrhythmogenic cardiomyopathy. *Card Electrophysiol Clin.* 2011;3:237–244.
69. Zorzi A, et al. Electrocardiographic predictors of electroanatomic scar size in arrhythmogenic right ventricular cardiomyopathy: implications for arrhythmic risk stratification. *J Cardiovasc Electrophysiol.* 2013;24:1321–1327.
70. Zhang L, Liu L, Kowey PR, et al. The electrocardiographic manifestations of arrhythmogenic right ventricular dysplasia. *Curr Cardiol Rev.* 2014;10:237–245.
71. Platonov PG, et al. High interobserver variability in the assessment of epsilon waves: implications for diagnosis of arrhythmogenic right ventricular cardiomyopathy/dysplasia. *Heart Rhythm.* 2016;13:208–216.
72. Tschabrunn CM, Haqqani HM, Santangeli P, et al. 12-lead electrocardiogram to localize region of abnormal electroanatomic substrate in arrhythmogenic right ventricular cardiomyopathy. *JACC Clin Electrophysiol.* 2017;3:654–665.
73. Haqqani HM, Marchlinski FE. Electroanatomic mapping and catheter ablation of ventricular tachycardia in arrhythmogenic cardiomyopathy. *Card Electrophysiol Clin.* 2011;3:299–310.
74. Santangeli P, et al. Long-term outcome with catheter ablation of ventricular tachycardia in patients with arrhythmogenic right ventricular cardiomyopathy. *Circ Arrhythmia Electrophysiol.* 2015;8:1413–1421.
75. Josephson ME, Almendral J, Callans DJ. Resetting and entrainment of reentrant ventricular tachycardia associated with myocardial infarction. *Heart Rhythm.* 2014;11:1239–1249.
76. Almendral J, Caulier-Cisterna R, Rojo-Álvarez JL. Resetting and entrainment of reentrant arrhythmias: part I: concepts, recognition, and protocol for evaluation: surface ECG versus intracardiac recordings. *Pacing Clin Electrophysiol.* 2013;36:508–532.
77. Deo R, Berger R. The clinical utility of entrainment pacing. *J Cardiovasc Electrophysiol.* 2009;20:466–470.
78. Wong KCK, Rajappan K, Bashir Y, et al. Entrainment with long postpacing intervals from within the flutter circuit: what is the mechanism? *Circ Arrhythmia Electrophysiol.* 2012;5:e90–e92.
79. Proietti R, et al. A historical perspective on the role of functional lines of block in the re-entrant circuit of ventricular tachycardia. *Pacing Clin Electrophysiol.* 2016;39:490–496.
80. Nayyar S, et al. High-density mapping of ventricular scar: a comparison of ventricular tachycardia (VT) supporting channels with channels that do not support VT. *Circ Arrhythmia Electrophysiol.* 2014;7:90–98.
81. Baldinger SH, et al. Electrogram analysis and pacing are complimentary for recognition of abnormal conduction and far-field potentials during substrate mapping of infarct-related ventricular tachycardia. *Circ Arrhythmia Electrophysiol.* 2015;8:874–881.
82. Berruezo A, et al. Combined endocardial and epicardial catheter ablation in arrhythmogenic right ventricular dysplasia incorporating scar dechanneling technique. *Circ Arrhythmia Electrophysiol.* 2012;5:111–121.
83. Tanawuttiwat T, Nazarian S, Calkins H. The role of catheter ablation in the management of ventricular tachycardia. *Eur Heart J.* 2016;37:594–609.
84. Santangeli P, Marchlinski FE. Substrate mapping for unstable ventricular tachycardia. *Heart Rhythm.* 2016;13:569–583.
85. Fernandez-Armenta J, et al. Sinus rhythm detection of conducting channels and ventricular tachycardia isthmus in arrhythmogenic right ventricular cardiomyopathy. *Heart Rhythm.* 2014;11:747–754.

86. Kumar P, Mounsey JP, Chung EH. Adjusting voltage criteria can unmask conducting channels in a patient with arrhythmogenic right ventricular cardiomyopathy and ventricular tachycardia. *Heart Case Reports*. 2015;1:275–278.
87. Philips B, et al. Outcomes and ventricular tachycardia recurrence characteristics after epicardial ablation of ventricular tachycardia in arrhythmogenic right ventricular dysplasia/cardiomyopathy. *Heart Rhythm*. 2015;12:716–725.
88. Lerman BB. Eliminating ventricular tachycardia by targeting premature ventricular contractions in arrhythmogenic right ventricular dysplasia/cardiomyopathy: innocent bystander or heart of the matter? *Circ Arrhythmia Electrophysiol*. 2013;6:7–9.
89. Berte B, et al. VT recurrence after ablation: incomplete ablation or disease progression? A multicentric European study. *J Cardiovasc Electrophysiol*. 2016;27:80–87.

Ventricular Arrhythmias in Adults With Congenital Heart Disease

OUTLINE

Pathophysiology, 968

Epidemiology and Natural History, 968

Initial Evaluation, 969

Risk Stratification, 969

Noninvasive Risk Stratification, 969

Electrophysiological Testing, 970

Principles of Management, 970

Implantable Cardioverter-Defibrillator, 970

Antiarrhythmic Drug Therapy, 970

Surgical Repair and Ablation, 971

Catheter Ablation, 971

Electrocardiographic Features, 971

Mapping, 972

Vascular and Cardiac Access, 972

Identification of Barriers and Potential Lines of Block, 972

Identification of the Critical Isthmus, 972

Ablation, 973

Target of Ablation, 973

Ablation Technique, 974

Endpoints of Ablation, 974

Outcome, 974

PATHOPHYSIOLOGY

In general, patients with congenital heart disease (CHD) are prone to two forms of ventricular tachyarrhythmias: (1) macroreentrant monomorphic ventricular tachycardia (VT) related to scar or prosthetic materials used during surgical repair, such as that observed in patients with repaired tetralogy of Fallot, ventricular septal defects repaired through a ventriculotomy incision, and Ebstein anomaly; and (2) polymorphic VT and ventricular fibrillation (VF) (with the risk of sudden cardiac death [SCD]) which occur in the setting of a generalized ventricular myopathic process related to chronic pressure and volume overloads that ultimately result in advanced degrees of hypertrophy, fibrosis, and ventricular dilation. The latter type can be observed in patients with transposition of the great arteries after Mustard or Senning operations, congenital aortic outflow obstruction, tetralogy of Fallot, unrepaired ventricular septal defect (VSD) with Eisenmenger syndrome, and univentricular hearts with Fontan circulation.¹

Most information concerning patients with monomorphic VT and CHD pertains to tetralogy of Fallot, as compared with other forms of CHD. Tetralogy of Fallot is the most common cyanotic congenital cardiac malformation. The core lesion is an underdeveloped subpulmonary infundibulum, which is superiorly and anteriorly displaced, resulting in the well-known tetrad of pulmonic stenosis, ventricular septal defect, aortic override, and right ventricular (RV) hypertrophy. Correction of the anomaly involves patch closure of the ventricular septal defect and relief of right ventricular outflow tract (RVOT) obstruction, which typically requires resection of a large amount of RV muscle. When the procedure was first performed, it was not done through the tricuspid valve but required a ventriculotomy. The pulmonic valve annulus is usually small, and repair with a transannular patch leads to chronic pulmonic insufficiency, which can be severe if associated with downstream obstruction caused by pulmonary arterial stenosis, and can eventually precipitate RV dilatation and dysfunction.²

Macroreentry is the most common mechanism for sustained ventricular arrhythmias in adults with repaired tetralogy of Fallot. The

sites of the diastolic activation and delayed conduction along the reentrant circuit have been shown to have significant abnormalities such as interstitial or replacement fibrosis, adiposis, and degeneration of the myocardium.³ The scattered surviving myocyte islets embedded in the extensive adiposis or fibrosis can form an electrical maze around the ventriculotomy incision and patch repairs, resembling the histological findings in the border zone of infarcted myocardium. Furthermore, RV remodeling induced by pressure overload (caused by inadequate relief of obstruction) and volume overload (secondary to severe pulmonic regurgitation) promotes hypertrophy and fibrosis, which can potentially result in slow conduction, providing the link between impaired hemodynamics and VT.⁴

Using intraoperative mapping, monomorphic VT after surgical correction of tetralogy of Fallot has been classified into two types: (1) VT originating from the RVOT, which is considered to be related to prior right ventriculotomy or reconstruction of the RVOT (Fig. 30.1); and (2) VT originating from the RV inflow tract septum, which is thought to be related to closure of the ventricular septal defect. Reentry circuit isthmuses are located within anatomically defined pathways bordered by unexcitable tissue.^{4,5}

EPIDEMIOLOGY AND NATURAL HISTORY

CHD is the most common form of birth defect, with an estimated 0.5% to 1% of live newborns afflicted by moderate or severe types. Currently, more than 1 million adults are living with CHD in the United States, and this group now outnumbers children with CHD, reflecting the marked improvements in the early diagnosis and surgical and medical management of CHD. Ventricular arrhythmias late after repair of CHD are an increasingly common finding, predominantly in patients with tetralogy of Fallot, and contribute to mortality and morbidity in this population.

The incidence of SCD in the general CHD population is relatively low (less than 0.1% per year), but it accounts for 20% to 25% of all late deaths in adults with CHD.⁶ The risk of SCD is higher in patients

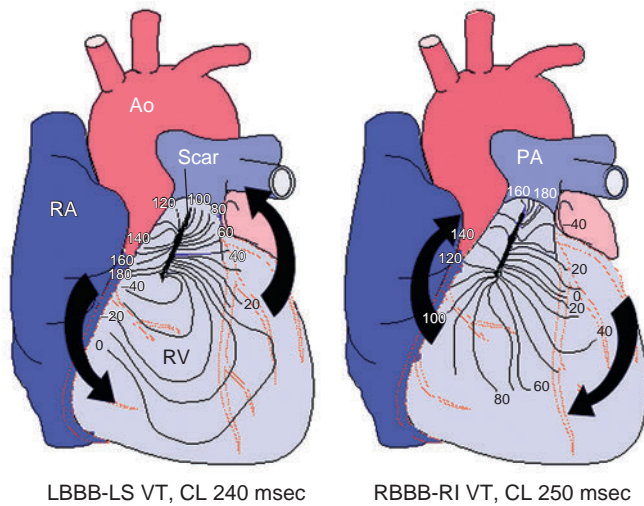


Fig. 30.1 Ventricular Tachycardia (VT) Postsurgical Repair of Tetralogy of Fallot Illustrated is scar-based reentry in surgically repaired tetralogy of Fallot with a right ventriculotomy. The incision heals as a nonconductive scar, leaving a small rim of muscle between the pulmonic valve annulus and scar. This is the diastolic corridor for rotation in either direction as shown, giving rise to VT with left bundle branch block–like QRS morphology and left superior axis or, in the opposite direction of rotation, right bundle branch block–like QRS morphology and right inferior axis. Ao, Aorta; CL, cycle length; LBBB, left bundle branch block; LS, left superior; PA, pulmonary artery; RA, right atrium; RI, right inferior; RV, right ventricle.

with complicated hemodynamic lesions, including tetralogy of Fallot (0.2% to 0.3% per year), D-transposition of the great arteries with Mustard or Senning baffles, congenitally corrected transposition of the great arteries, left-sided obstructive lesions, Eisenmenger syndrome, and Ebstein anomaly.^{6,7}

Although ventricular ectopy and nonsustained VT are relatively common, sustained monomorphic VT is rare in the general adult CHD population, with an annual incidence of 0.1% to 0.2%.⁶ Notably, the incidence of arrhythmias increases as the patient ages. In patients with tetralogy of Fallot, serious ventricular arrhythmias are rare during the first 10 to 15 years following corrective surgery. This quiescent period is followed by a steady increase in the incidence of ventricular arrhythmias, primarily monomorphic VT, which are prevalent in 15% of adult patients late after surgery. By 35 years of follow-up, the incidence of VT is 11.9%, with an 8.3% risk of SCD.^{6,8–11} Since the mid-1990s, surgical repair of the tetralogy of Fallot has usually been performed using a combined approach through the RA and the pulmonary artery. In these cases, there is no incision in the RV free wall around which reentry can occur, although reentry around the ventricular septal defect patch can still take place. In addition, a limited RV incision may still be needed when patch augmentation for the RVOT or pulmonary annulus is necessary.

Tetralogy of Fallot is the most common substrate for sustained VT and is typically cited as the archetypal lesion when VT in the adult CHD patient population is discussed. Nonetheless, serious ventricular arrhythmias can also develop in other types of congenital heart malformations, even in the absence of direct surgical scarring to ventricular muscle, including congenital aortic stenosis, transposition of the great arteries when the RV supports the systemic circulation, severe Ebstein anomaly, certain forms of single ventricle, and ventricular septal defect with pulmonary arterial hypertension. The appearance of ventricular

arrhythmias in these cases commonly coincides with deterioration in overall hemodynamic status.^{6,7}

INITIAL EVALUATION

Patients with CHD presenting with symptoms suggestive of ventricular arrhythmias, such as palpitations, dizziness, and syncope, require careful evaluation to help document cardiac rhythm during clinical symptoms. This is typically achieved by ambulatory cardiac monitoring or implantation of a loop recorder. Electrophysiological (EP) testing can also be considered when the index of suspicion is high.

Importantly, new-onset or worsening ventricular arrhythmias can herald deterioration of the hemodynamic status, which requires a thorough evaluation of ventricular function and residual lesions. In addition, detailed evaluation of cardiac function and anatomy and knowledge of the congenital anomaly and previous surgical procedures are very important. This evaluation can require transthoracic or transesophageal echocardiography, right or left heart catheterization, angiography of the desired cardiac chamber, and cardiac magnetic resonance imaging.

RISK STRATIFICATION

Noninvasive Risk Stratification

Some subgroups of patients with CHD are recognized as being at risk for life-threatening ventricular arrhythmias and SCD, including those with large scars from a prior ventriculotomy (e.g., tetralogy of Fallot repair) and those who develop advanced degrees of ventricular dysfunction from longstanding hemodynamic burdens (e.g., congenital aortic stenosis, single ventricle).

Although controversy still exists, several noninvasive risk factors for VT and SCD have been identified in the CHD patient population. Tetralogy of Fallot is the one condition for which such data are fairly extensive. QRS duration exceeding 180 milliseconds, left ventricular (LV) systolic dysfunction (ejection fraction less than 50 %), and LV diastolic dysfunction (LV end-diastolic pressure ≥ 12 mm Hg) have consistently predicted adverse outcome. In addition, symptomatic nonsustained VT and atrial arrhythmias are associated with increased SCD risk. Asymptomatic nonsustained VT has been associated with inducible sustained VT by programmed ventricular stimulation and with clinical ventricular tachyarrhythmias in implantable cardioverter-defibrillator (ICD) recipients, but its value for SCD risk prediction is limited. Several other clinical characteristics, such as RV pressure overload and RV systolic dysfunction, have been proposed as risk factors for SCD but with inconsistent validation in the literature.^{2,8,9,12} A risk score to predict appropriate ICD shocks in tetralogy patients with ICDs for primary prevention indications was derived from six clinical variables (surgical, hemodynamic, electrocardiographic, and EP factors) identified by multivariate analyses (Table 30.1). Patients with fewer than 3 points (low risk) experienced no appropriate shocks. In patients with 3 to 5 points (intermediate risk) and more than 5 points (high risk), the annual rates of appropriate shocks were 3.8% and 17.5%, respectively. Although these risk-stratification schemes can provide reasonable sensitivity, they have suboptimal specificity for patients at high risk because of the small population size and the relatively low incidence of SCD in CHD patients (approximately 2% per decade of follow-up in patients with repaired tetralogy of Fallot repair).¹³

For congenital malformations other than tetralogy of Fallot, SCD risk predictors have not been clearly defined. Severely impaired systolic function of the systemic ventricle (ejection fraction $\leq 35\%$) has been associated with ventricular arrhythmias and SCD; however, QRS duration has been inconsistently noted to predict SCD. Recurrent unexplained syncope in the presence of ventricular dysfunction may also identify a

TABLE 30.1 Risk Score for Appropriate Defibrillator Shocks in Primary Prevention in Patients With Tetralogy of Fallot

Variable	Exponential Values of Beta Coefficients	Points Attributed
Prior palliative shunt	3.2	2
Inducible sustained ventricular tachycardia	2.6	2
QRS duration ≥ 180 msec	1.4	1
Ventriculotomy incision	3.4	2
Nonsustained ventricular tachycardia	3.7	2
Left ventricular end-diastolic pressure ≥ 12 mm Hg	4.9	3
Total points		0–12

high-risk group. Factors such as nonsustained VT, prior palliative shunt, ventriculotomies, and atrial tachyarrhythmias have been proposed, but uncertainty remains as to their true prognostic significance. Notably, among ICD recipients, adults with non-tetralogy of Fallot congenital lesions are significantly less likely to receive appropriate ICD therapy than those with tetralogy of Fallot (11.5% vs. 27.3%).^{6,14}

Electrophysiological Testing

In patients with repaired tetralogy of Fallot, inducible monomorphic or polymorphic sustained VT by programmed ventricular stimulation is independently associated with a nearly fivefold higher rate of clinical VT or SCD on follow-up. Sustained VT is inducible in approximately 35% of this patient population, which is similar to that reported in patients with prior myocardial infarction (MI) and LV ejection fractions less than 40% and spontaneous nonsustained VT. Independent risk factors for inducible sustained VT include: (1) age older than 18 years at the time of testing, (2) history of palpitations, (3) prior palliative surgery, (4) frequent or complex ventricular ectopy or nonsustained VT, and (5) cardiothoracic ratio of greater than 0.6 on chest radiograph. The diagnostic value of EP testing (sensitivity, 77%; specificity, 80%; diagnostic accuracy, 79%) and prognostic significance (relative ratio, 4.7 for subsequent clinical VT or SCD) compares favorably with programmed ventricular stimulation in post-MI patients. However, the yield of EP testing remains too imperfect and too impractical to be recommended as a general screening tool and the timing and frequency of testing remain to be elucidated. Nonetheless, EP testing may be considered in selected patients with concerning symptoms (e.g., palpitations, dizziness, or unexplained syncope) or Holter findings, when VT is suspected but not yet proven. In addition, the subpopulation of patients deemed at intermediate risk of SCD based on a combination of other parameters may benefit most from risk stratification with an EP study.^{8,10,12}

For congenital malformations other than tetralogy of Fallot, the value of programmed ventricular stimulation in risk stratification remains uncertain. Inducibility of sustained VT at EP study does not appear to predict clinical VT or SCD in patients with transposition of the great arteries and Mustard or Senning baffles.⁶

PRINCIPLES OF MANAGEMENT

Implantable Cardioverter-Defibrillator

ICDs play an important role in the primary and secondary prevention of SCD in patients with CHD. In a prevalence study, ICDs were implanted in 10% of the adult population with repaired tetralogy of Fallot for

either primary (59%) or secondary (41%) prevention indications. Both groups experienced high rates of appropriate therapies.

Secondary Prevention

ICD implantation is recommended in patients who have survived cardiac arrest or an episode of spontaneous sustained VT. The most common anatomical diagnosis among ICD recipients is tetralogy of Fallot, followed by transposition of the great arteries and aortic stenosis. The rate of appropriate therapies for VT or VF events in this patient population averages 9.8% per year, and approximately 35% over a follow-up period of 5 years, with the median time to first shock less than 1 year.^{8,9,13,15}

Primary Prevention

Recent data support the benefit of ICD implantation for primary prevention in patients deemed to be at high risk for SCD. Up to 44% of patients with repaired tetralogy of Fallot repair who received prophylactic ICDs experience sustained ventricular tachyarrhythmias, with an annual rate of appropriate ICD therapies of 7.7%. These annual rates are comparable with those of other high-risk populations, including patients with primary prevention ICDs for ischemic, dilated, or hypertrophic cardiomyopathy.^{8,9}

As noted, multiple risk factors for VT and SCD in CHD patients have been identified in an effort to better define which are most likely to benefit from a primary prevention ICD; however, at present, there is no generally accepted scheme for rhythm surveillance in asymptomatic CHD patients.^{8,10} Box 30.1 lists the current recommendations for ICD therapy in adults with CHD.

Even in patients considered at risk for malignant ventricular arrhythmias, the benefit of ICD implantation should be carefully weighed against the risks of such a procedure in this unique group of patients. Transvenous implantation of the ICD may not be feasible in patients with the more complex varieties of CHD, necessitating epicardial insertion of the ICD leads with the added morbidity of a sternotomy or thoracotomy for epicardial electrodes. Even when transvenous implantation procedures are feasible, they can be very challenging in patients with distorted anatomy, requiring that the implanting physician be well acquainted with the details of congenital heart lesions and the types of surgical repairs. Because of the considerable variation in surgical techniques and individual anatomy, careful review of detailed operative reports is essential in these cases. In addition, the ICD lead failure rate from both insulation breaches and conductor breaks is high in this patient population, exceeding 20% over 5 years (likely due to the young age and high activity level of this patient group), which results in added morbidity of corrective procedures. Moreover, the negative psychological impact of an implanted device and inappropriate shocks (occurring in more than 20%, predominantly caused by supraventricular tachycardias and lead failures) in a relatively young patient should not be underestimated. Programming ICD treatment zones with faster VT detection rates and longer detection times can help to reduce the rate of inappropriate shocks.¹⁶

For all these reasons, ICD decisions in CHD patients should be individualized, taking into account the various risk factors, all of which must then be viewed in the context of the individual patient's history and general hemodynamic status to refine the selection process.^{8,13,15}

Antiarrhythmic Drug Therapy

Similar to patients with post-MI VT, antiarrhythmic agents are generally not a stand-alone therapy in CHD patients with sustained ventricular arrhythmias or cardiac arrest but can be considered in two main settings: (1) as adjunctive therapy in patients with an ICD, and (2) as preventive therapy in patients who do not want or are not candidates for an ICD. ICD patients who experience frequent symptoms or device

BOX 30.1 Recommendations for ICD Therapy in Adults With CHD**Class I**

1. Cardiac arrest due to VF or hemodynamically unstable VT of nonreversible etiology
2. Spontaneous sustained VT
3. Systemic LV ejection fraction $\leq 35\%$, biventricular physiology, and NYHA class II or III symptoms

Class IIa

1. ICD therapy is reasonable in selected adults with tetralogy of Fallot and multiple risk factors for SCD, such as LV systolic or diastolic dysfunction, nonsustained VT, QRS duration ≥ 180 msec, extensive RV scarring, or inducible sustained VT at EP study

Class IIb

1. CHD and a single or systemic RV ejection fraction $<35\%$, particularly in the presence of additional risk factors such as complex ventricular arrhythmias, unexplained syncope, NYHA functional class II or III symptoms, QRS duration ≥ 140 msec, or severe systemic AV valve regurgitation
2. CHD and a systemic ventricular ejection fraction $<35\%$ in the absence of overt symptoms (NYHA class I) or other known risk factors

3. CHD and syncope of unknown origin with hemodynamically significant sustained VT or VF inducible at EP study
4. Nonhospitalized adults with CHD awaiting heart transplantation
5. Syncope and moderate or complex CHD in whom there is a high clinical suspicion of ventricular arrhythmia and in whom thorough invasive and non-invasive investigations have failed to define a cause

Class III

1. Life expectancy with an acceptable functional status <1 year
2. Incessant VT or VF
3. Significant psychiatric illness that may be aggravated by ICD implantation or preclude systematic follow-up
4. Patients with drug-refractory NYHA class IV symptoms who are not candidates for cardiac transplantation or cardiac resynchronization therapy
5. Advanced pulmonary vascular disease (Eisenmenger syndrome)
6. Endocardial leads are generally avoided in adults with CHD and intracardiac shunts. Risk assessment regarding hemodynamic circumstances, concomitant anticoagulation, shunt closure prior to endocardial lead placement, or alternative approaches for lead access should be individualized

AV, Atrioventricular; CHD, congenital heart disease; EP, electrophysiology; ICD, implantable cardioverter-defibrillator; LV, left ventricle; NYHA, New York Heart Association; RV, right ventricle; SCD, sudden cardiac death; VF, ventricular fibrillation; VT, ventricular tachycardia. Modified from Khairy P, Van Hare GF, Balaji S, et al. PACES/HRS Expert Consensus Statement on the Recognition and Management of Arrhythmias in Adult Congenital Heart Disease: developed in partnership between the Pediatric and Congenital Electrophysiology Society (PACES) and the Heart Rhythm Society (HRS). *Heart Rhythm*. 2014;11:e102–e165.

discharges triggered by ventricular arrhythmias may benefit from adjunctive drug therapy. When antiarrhythmic drug therapy is required, beta-blockers and sotalol are commonly used. Amiodarone can carry a significant long-term risk of adverse events given the young age of the patient population. The efficacy of dofetilide and dronedarone has not been adequately evaluated in this group.¹⁰

Surgical Repair and Ablation

Surgical interventions to improve cardiac status and alleviate residual hemodynamic problems (such as valve replacement, closure of septal defect, or relief of conduit stenosis) can play a role in reducing arrhythmia risk in certain carefully selected CHD patients, especially those with new-onset or worsening arrhythmias. However, the impact of surgery on modifying the risk for SCD remains controversial. In patients with clinical monomorphic VT who require cardiac surgery, mapping and ablation of the arrhythmia can be performed intraoperatively at the time of the surgery.^{1,8,10,12}

In tetralogy of Fallot patients, replacement of the pulmonary valve is frequently required later in life after the initial repair, but it does not appear to reduce the risk of SCD. In these patients, empirical intraoperative ablation the RVOT appears to be safe and may be protective and may be considered in patients with preoperative syncope, nonsustained or sustained VT, or inducible VT during previous EP study. In these patients, ablation lesions are performed to connect the superior aspect of the ventricular septal defect patch to the pulmonary annulus or to connect the ventriculotomy to the pulmonary or tricuspid annulus.

Catheter Ablation

Catheter ablation for VT in repaired tetralogy of Fallot generally is not considered a stand-alone therapy, given the potential risk of recurrences of the same or new ventricular arrhythmias, and is primarily performed in patients with recurrent sustained monomorphic VT that is causing frequent ICD shocks or significant symptoms. Catheter ablation may

also be considered in patients with symptomatic spontaneous sustained monomorphic VT in whom ICD implantation is not recommended or not feasible.

However, catheter ablation can be considered as isolated VT therapy in a selected group of patients presenting with hemodynamically stable monomorphic VT in the absence of residual lesions and with a preserved ventricular function, and in whom ablation successfully eliminated inducibility of all monomorphic VTs. Even then, follow-up EP studies need to be considered to ensure that the same or different circuits cannot be induced before dismissing the need for an ICD.

Furthermore, tetralogy of Fallot patients with a history of syncope and induced monomorphic VT during EP testing may be considered for either ICD placement or an attempt at catheter ablation of the VT with or without back-up ICD implantation.^{5,10}

ELECTROCARDIOGRAPHIC FEATURES

During normal sinus rhythm (NSR), QRS widening after tetralogy of Fallot repair is probably the result of a combined effect of the surgical injury to the myocardium and the right bundle branch and from the RV enlargement. Therefore a prolonged QRS duration cannot be considered the specific expression of delayed intraventricular conduction from an arrhythmogenic substrate but a nonspecific marker of electrical instability.

The VT in CHD patients is most commonly monomorphic and macroreentrant, rotating clockwise or counterclockwise around myotomy scars or surgical patches. QRS morphology during VT is determined by the pattern of ventricular activation around the scar. Most commonly, left or right bundle branch block with right inferior axis morphology is seen during clockwise rotation around the scar. Less commonly, left bundle branch block with left axis morphology is observed (Fig. 30.2). Right bundle branch block–like morphology can be present if the tachycardia exits on the septal aspect of the RV free wall.

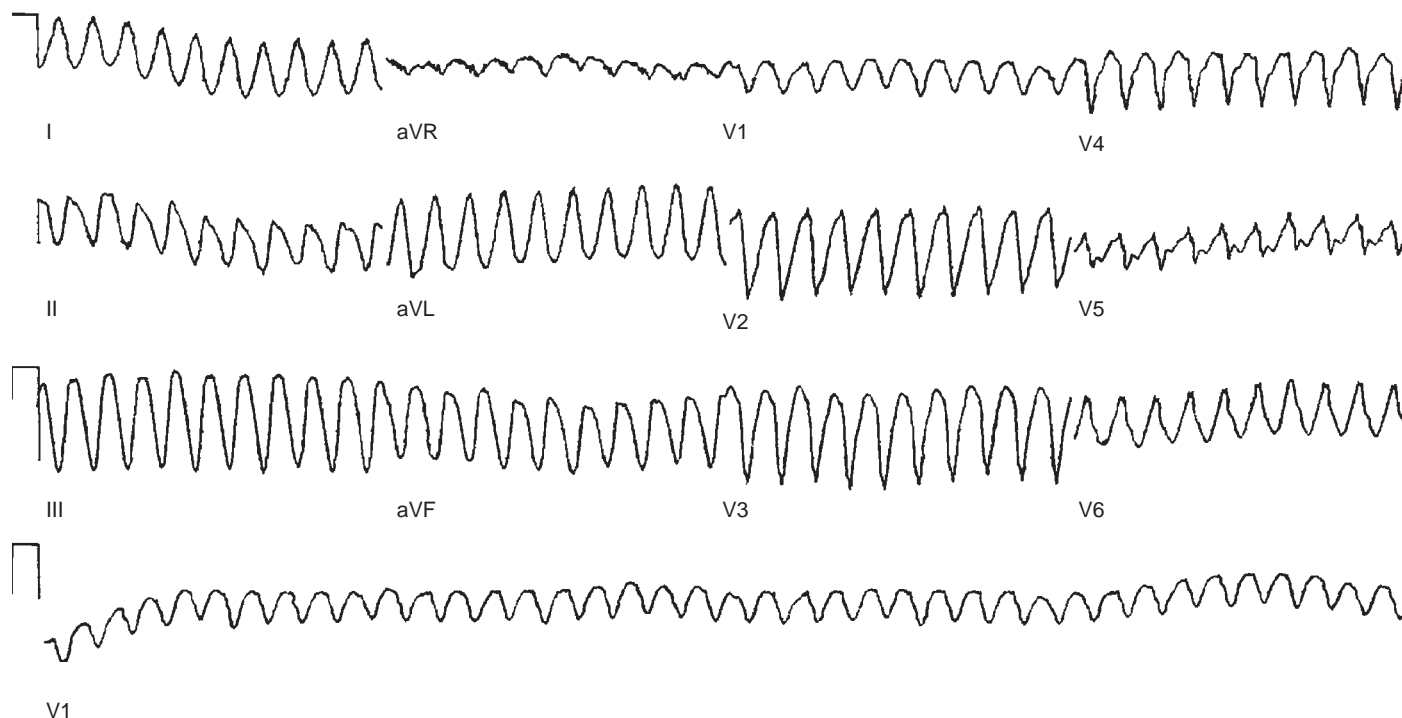


Fig. 30.2 Surface Electrocardiogram of Ventricular Tachycardia Postsurgical Repair of Tetralogy of Fallot. Note the left bundle branch block pattern and left superior axis morphology characteristic of clockwise macroreentry around the right ventriculotomy scar.

MAPPING

Detailed knowledge of the congenital and surgical anatomy, including all available operative reports, is essential before ablation. Transthoracic and transesophageal echocardiography, angiography of the chamber of interest, computed tomography, and/or magnetic resonance imaging should be considered to clarify the anatomical landmarks for mapping.⁶

Vascular and Cardiac Access

Feasibility and adequacy of vascular access must be confirmed in advance. In the CHD patient population, several conditions can pose vascular or cardiac chamber access challenges. There is often limited opportunity to place the standard number of diagnostic electrode catheters due to access issues. A superior vena cava (SVC) approach (via the internal jugular or subclavian veins) or, in rare instances, transhepatic approach can be required in some patients. In addition, in some cases, access to the target ventricle can require nonconventional approaches. For example, in patients who have had a Mustard or Senning procedure for D-transposition of the great arteries, access to the RV (the systemic ventricle) is accomplished via the retrograde aortic approach.

Identification of Barriers and Potential Lines of Block

As noted, in patients with repaired tetralogy of Fallot, the mechanism of VT is scar-based macroreentry involving the RV, either at the site of anterior right ventriculotomy or at the site of a ventricular septal patch. Hence three-dimensional (3-D) electroanatomic substrate (voltage) mapping is initially performed before VT induction to identify RV anatomical landmarks and conduction barriers (such as the ventricular septal defect patch, ventriculotomy scar, and RVOT patch).^{1,2,4} These systems also allow for good reconstruction of a 3-D anatomical shell of the often distorted cardiac chamber and integration of the created chamber geometry with preacquired cardiac CT or CMR images or

with intraprocedural intracardiac echocardiography or rotational angiography images.

Most VT circuits use the anatomical isthmus between the RVOT free wall scar or patch and the tricuspid annulus or pulmonic valve, and/or the septal scar or patch and either the tricuspid annulus or the pulmonic valve. Identification of those anatomical isthmuses by substrate mapping helps to guide subsequent mapping and ablation strategies. Confluent of electrically silent areas (defined as having a ventricular potential amplitude less than 0.05 mV and the absence of ventricular capture at 20 mA, provided that catheter contact is verified) can localize scar tissue and patches. Lines of block (manifest as double or split potentials separated by a clearly discernible isoelectric period) are tagged for easy identification because they can serve as boundaries for a subsequent design of ablation strategies.

Identification of the Critical Isthmus

The clinical monomorphic VT can be induced by programmed ventricular stimulation in the majority of patients after repair of CHD. Once sustained and stable monomorphic VT is induced, endocardial activation mapping and entrainment mapping are performed to identify the critical isthmus of the reentry circuit. Initial mapping efforts are focused on potential reentry isthmuses identified by substrate mapping. Activation mapping during VT is used to identify sites with mid-diastolic activity. Electrograms recorded within the critical isthmus can exhibit long, fractionated, low-amplitude potentials, but that is not uniformly observed.

Entrainment mapping is performed in a manner analogous to that used for post-MI VT and is used to characterize the relationship of ventricular sites to the reentrant circuit and to verify that a diastolic electrogram, regardless of where in diastole it occurs and its position and appearance on initiation of VT, is part of the VT circuit. Entrainment with concealed fusion should be sought; this indicates that the

pacing site is in a protected isthmus located within or attached to the reentrant circuit. Whether the protected isthmus is crucial to the reentrant circuit or just a bystander site needs to be verified by comparing the postpacing interval (PPI) with the tachycardia cycle length (TCL) and the stimulus-to-QRS (S-QRS) interval with the electrogram-QRS interval. A difference between the PPI and TCL not exceeding 30 milliseconds and S-QRS interval not exceeding 70% of the TCL helps to identify the critical isthmus of the reentrant circuit to be targeted by catheter ablation.

For VTs that are not mappable because of hemodynamic instability or termination during catheter manipulation or entrainment mapping, pace mapping during sinus rhythm is used to identify exit sites of the reentrant circuit, as guided by voltage mapping. Reentry circuit isthmuses can be approximated by pace mapping at sites where the QRS morphology matches that of the VT with an S-QRS interval of at least 40 milliseconds. If the VT can be briefly tolerated, the catheter is moved to the presumed isthmus site during NSR, and the VT is reinduced to confirm the position within the circuit either by entrainment mapping or by termination during radiofrequency (RF) energy application.⁴

When VT is short-lived, hemodynamically unstable, or cannot be reproducibly initiated, simultaneous multisite data acquisition using a noncontact mapping system (EnSite 3000; St. Jude Medical, St. Paul, MN, United States) can help to localize the VT site of origin. Propaga-

tion of activation within the RV can be traced throughout the whole tachycardia cycle by analyzing color-coded isopotential maps to identify the protected zone of the reentrant circuit between surgical barriers, anatomic barriers, or both. In addition, dynamic substrate mapping allows the creation of voltage maps from a single cardiac cycle and provides the ability to identify low-voltage areas, as well as fixed and functional block, on the virtual endocardium through noncontact methodology.¹⁷

ABLATION

Target of Ablation

The critical isthmus of the VT circuit is the usual target of ablation. A good pace map and entrainment with concealed QRS fusion and a prolonged S-QRS interval indicate more precisely an adequate site for ablation. Linear ablation lesions can also be performed using data obtained from substrate mapping to target anatomical isthmuses between surgical and structural lines of block.

In tetralogy of Fallot patients, four discrete anatomical isthmuses that often support macroreentrant VT have been identified (Fig. 30.3): (1) the isthmus between the superior aspect of the tricuspid annulus and ventriculotomy scar/patch in the free wall of the RVOT, (2) the isthmus between the pulmonic valve annulus and RV free wall scar (in

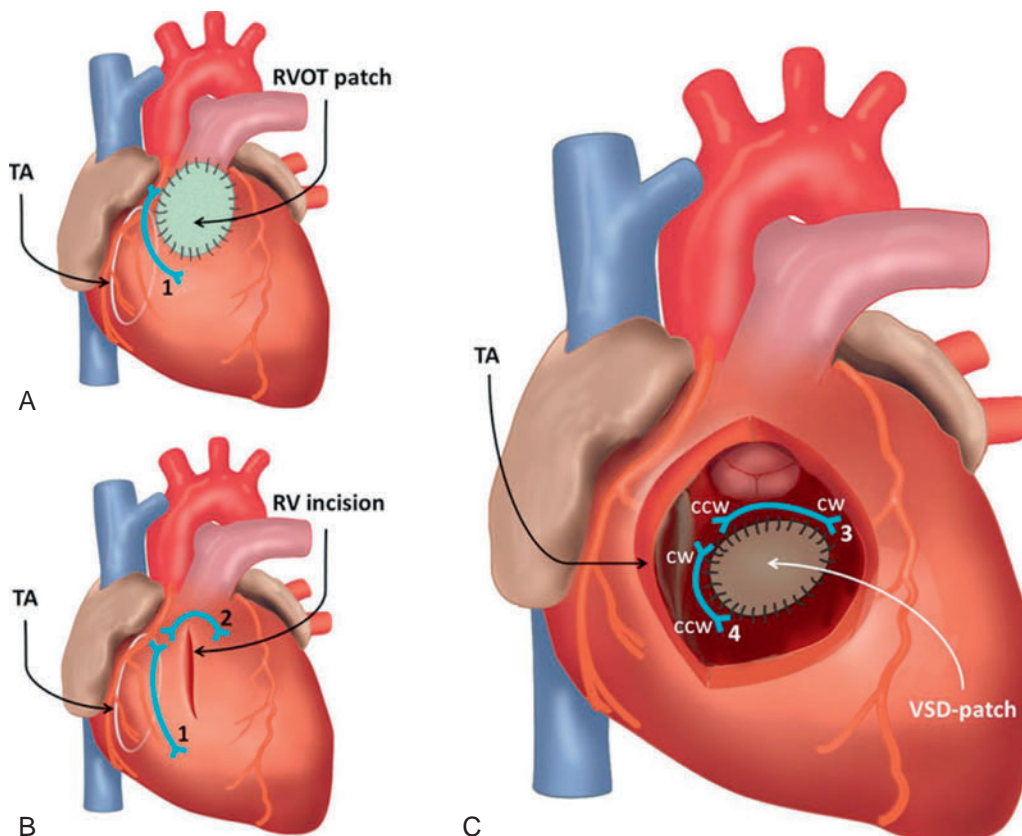


Fig. 30.3 Anatomical Isthmuses for Ventricular Tachycardia (VT) in Repaired Tetralogy of Fallot (rTOF). Anatomical isthmus 1 is located between the tricuspid annulus (TA) and a right ventricular (RV) incision/ RV outflow tract (RVOT) patch (A and B), and anatomical isthmus 2 is located between a RV incision and pulmonary valve (PV; B). Anatomical isthmus 3, located between the PV and ventricular septal defect (VSD) patch, and anatomical isthmus 4, located between the VSD patch and TA (C), are bordering on the septum. ccw, Counterclockwise; cw, clockwise. (From Kapel GF, Reichlin T, Wijnmaalen AP, et al. Left-sided ablation of ventricular tachycardia in adults with repaired tetralogy of Fallot a case series. *Circ Arrhythm Electrophysiol*. 2014;7:889–897.)

the absence of a transannular patch), (3) the isthmus between pulmonic valve annulus and the ventricular septal patch, and (4) the isthmus between the tricuspid annulus and ventricular septal patch through the region of the ventriculo-infundibular fold. Significant variation exists in the frequency of the presence and involvement of these isthmuses in the VT circuit, as well as variability in the anatomical characteristics of these isthmuses. In general, the isthmus between the superior aspect of the tricuspid annulus and unexcitable scar/patch in the free wall of the RVOT is the most common isthmus incorporated in the VT circuit, and frequently it is the isthmus with the greatest overall dimensions in terms of length and wall thickness.³

Ablation lines transecting these anatomical isthmuses eliminate the VT in most patients, even when conventional mapping is not feasible because of poorly tolerated or noninducible tachycardia. Typically, linear ablation should be continued to span the entire width of the VT isthmus, connecting two anatomical boundaries, even when partial isthmus ablation results in termination or noninducibility of the VT. This ablation approach is comparable to ablation of the cavotricuspid isthmus-dependent for typical atrial flutter.^{3, 4, 5, 17, 18}

Although VT in tetralogy of Fallot patients is primarily RV in origin, a left-sided approach can be required for ablation of some anatomical isthmuses bordering on the infundibular septum. The hypertrophied septal myocardium, the overlying pulmonary homograft, and overlying ventricular septal defect patch can potentially prohibit complete ablation of those isthmuses via the RV.^{18, 19}

When the isthmus between the superior aspect of the tricuspid annulus and unexcitable scar/patch in the free wall of the RVOT is the ablation target, achieving complete isthmus block can be challenging due to its length and thickness. In these situations, ablation of the nearby, smaller isthmus (between the ventriculotomy incision and the ventricular septal defect patch) in combination with ablation of the isthmus between the septal patch and tricuspid annulus can potentially serve as an alternate ablation strategy to create a line of block between the RVOT scar/patch and tricuspid annulus.³

Ablation Technique

RF ablation is usually performed with an irrigated-tip ablation catheter (power limit, 50 W) or an 8-mm-tip catheter (power limit, 70 W). Ablation is performed during VT when possible. Slowing or termination of the VT during RF application should prompt additional lesions being placed to connect the adjoining anatomical boundaries across the VT circuit isthmus, as defined by voltage mapping and pace mapping techniques, and RF lesions being placed during NSR until unipolar pacing fails to capture.⁴ Because manipulating catheters in the often-distorted chambers is challenging, the use of long, preformed or deflectable vascular sheaths can help to augment the reach of the ablation catheter and ensure adequate and stable catheter-tissue contact.

Endpoints of Ablation

Tachycardia Termination

When ablation is performed during sustained VT, termination of VT during RF application suggests that the lesion has affected a critical isthmus, and that site should be targeted for additional lesions. However, VT termination is not an adequate endpoint because VT can terminate spontaneously by partial, rather than complete, ablation of the critical isthmus.¹⁷

Noninducibility of Tachycardia

Noninducibility of the clinical VT is an important endpoint of the procedure. In addition, noninducibility of any sustained monomorphic VT should be verified, especially when ICD implantation is not preferred. It is important to carefully assess VT inducibility at baseline and use

the best method of reproducible induction of the VT for postablation testing. In the setting of easy inducibility prior to ablation, one can consider the lack of inducibility as an indicator of successful ablation. Noninducibility of the arrhythmia is not applicable if the original arrhythmia either is noninducible at baseline or was inadvertently terminated mechanically.¹⁷

Documentation of a Line of Block

Termination and noninducibility of VT can be the result of conduction delay in the critical isthmus and not stable block and hence may not represent adequate procedural endpoints. Achievement of complete and stable conduction block across the anatomical isthmus of the VT circuit is the most objective endpoint for successful ablation. The demonstration of a continuous corridor of widely split double potentials recorded during sinus rhythm along the entire length of the ablation line confirms the presence of block. In addition, differential ventricular pacing can help to verify conduction block across the ablation line. Ventricular pacing is performed at two separate sites on the same side of the ablation line, one site very close to the ablation line and the second site 10 to 20 mm farther away. Local activation time is recorded on the contralateral side of the ablation line. In the presence of conduction block across the ablation line, moving the pacing site away from the ablation line shortens the conduction time to the contralateral side and shortens the distance between the double potentials straddling the ablation line. Withdrawal of the pacing site farther away from the ablation line results in a delay of the first component of the double potentials (which represents activation on the side of the ablation line ipsilateral to the pacing site). In contrast, the second component of the double potentials (which represent activation on the contralateral side of the ablation line) becomes activated earlier because the length of the detour the wavefront has to travel around the line of block is shortened by the new site of pacing. Consequently, the separation of double potentials decreases. On the other hand, in the setting of incomplete block, both components of the double potentials are the result of sequential activation by the same paced wavefront propagating across the ablation line. Therefore withdrawal of the pacing site farther away from the ablation line causes a similar degree of delay of the timing of both components of the electrogram (relative to the pacing stimulus), so that the interval between the double potentials remains constant.¹⁷

Outcome

The experience with catheter ablation of VT in CHD is limited. Several reports have described single-center experiences spanning several eras of technological advances. The limited acute and long-term success rates are related to the complexity of the underlying congenital defect and surgical repair and the complexity of the reentry circuits. In a report of 20 patients with VT and CHD, 50% of patients were unable to undergo ablation because of VT noninducibility, hemodynamic instability, access or anatomical problems, or proximity of the ablation target to the His bundle. The acute success rate for mappable VTs was 83%, with a long-term recurrence rate of 40%. Other studies reported procedural success rates ranging from 74% to 94%.^{4, 17, 18}

REFERENCES

1. Sherwin ED, Triedman JK, Walsh EP. Update on interventional electrophysiology in congenital heart disease: evolving solutions for complex hearts. *Circ Arrhythmia Electrophysiol.* 2013;6:1032–1040.
2. Walsh EP. Interventional electrophysiology in patients with congenital heart disease. *Circulation.* 2007;115:3224–3234.
3. Moore JP, et al. Characterization of anatomic ventricular tachycardia isthmus pathology after surgical repair of tetralogy of Fallot. *Circ Arrhythmia Electrophysiol.* 2013;6:905–911.

4. Zeppenfeld K, et al. Catheter ablation of ventricular tachycardia after repair of congenital heart disease: electroanatomic identification of the critical right ventricular isthmus. *Circulation*. 2007;116:2241–2252.
5. Khairy P, Stevenson WG. Catheter ablation in tetralogy of Fallot. *Heart Rhythm*. 2009;6:1069–1074.
6. Khairy P, et al. PACES/HRS expert consensus statement on the recognition and management of arrhythmias in adult congenital heart disease: developed in partnership between the Pediatric and Congenital Electrophysiology Society (PACES) and the Heart Rhythm Society (HRS). *Heart Rhythm*. 2014;11:e102–e165.
7. Roos-Hesselink JW, Karamermer Y. Significance of postoperative arrhythmias in congenital heart disease. *Pacing Clin Electrophysiol*. 2008;31:2–6.
8. Khairy P, et al. Implantable cardioverter-defibrillators in tetralogy of Fallot. *Circulation*. 2008;117:363–370.
9. Khairy P, et al. Arrhythmia burden in adults with surgically repaired tetralogy of Fallot: a multi-institutional study. *Circulation*. 2010;122:868–875.
10. Le Gloan L, Khairy P. Management of arrhythmias in patients with tetralogy of Fallot. *Curr Opin Cardiol*. 2011;26:60–65.
11. Wu M-H, et al. Arrhythmic burdens in patients with tetralogy of Fallot: a national database study. *Heart Rhythm*. 2015;12:604–609.
12. Sabate Rotes A, et al. Ventricular arrhythmia risk stratification in patients with tetralogy of Fallot at the time of pulmonary valve replacement. *Circ Arrhythmia Electrophysiol*. 2015;8:110–117.
13. Walsh EP. Practical aspects of implantable defibrillator therapy in patients with congenital heart disease. *Pacing Clin Electrophysiol*. 2008;31(suppl 1):S38–S40.
14. Kella DK, Merchant FM, Veledar E, et al. Lesion-specific differences for implantable cardioverter defibrillator therapies in adults with congenital heart disease. *Pacing Clin Electrophysiol*. 2014;37:1492–1498.
15. Tomaske M, Bauersfeld U. Experience with implantable cardioverter-defibrillator therapy in grown-ups with congenital heart disease. *Pacing Clin Electrophysiol*. 2008;31:35–37.
16. Garnreiter JM, Pilcher TA, Etheridge SP, et al. Inappropriate ICD shocks in pediatrics and congenital heart disease patients: risk factors and programming strategies. *Heart Rhythm*. 2015;12:937–942.
17. Kriebel T, Saul JP, Schneider H, et al. Noncontact mapping and radiofrequency catheter ablation of fast and hemodynamically unstable ventricular tachycardia after surgical repair of tetralogy of Fallot. *J Am Coll Cardiol*. 2007;50:2162–2168.
18. Kapel GFL, et al. Re-entry using anatomically determined isthmuses: a curable ventricular tachycardia in repaired congenital heart disease. *Circ Arrhythm Electrophysiol*. 2015;8:102–109.
19. Tedrow UB, et al. Left-sided ablation of ventricular tachycardia in adults with repaired tetralogy of Fallot: a case series. *Circ Arrhythm Electrophysiol*. 2014;7:889–897.

Ventricular Arrhythmias in Inherited Channelopathies

OUTLINE

Long QT Syndrome, 976

- Genetics of the Long QT Syndrome, 977
- Pathophysiology of the Long QT Syndrome, 980
- Epidemiology, 983
- Clinical Presentation and Natural Course, 983
- Electrocardiographic Features, 985
- Diagnosis of the Long QT Syndrome, 989
- Differential Diagnosis: Acquired Long QT Syndrome, 992
- Risk Stratification, 994
- Principles of Management, 996

Brugada Syndrome, 1000

- Genetics of the Brugada Syndrome, 1000
- Pathophysiology of the Brugada Syndrome, 1002
- Epidemiology, 1004
- Clinical Presentation, 1004
- Electrocardiographic Features, 1005
- Diagnosis of the Brugada Syndrome, 1008
- Differential Diagnosis, 1009
- Risk Stratification, 1011
- Principles of Management, 1013

Short QT Syndrome, 1017

- Genetics of the Short QT Syndrome, 1017
- Pathophysiology of Short QT Syndrome, 1018
- Epidemiology, 1018
- Clinical Presentation, 1018
- Electrocardiographic Features, 1018
- Diagnosis of the Short QT Syndrome, 1019
- Differential Diagnosis, 1019
- Risk Stratification, 1019
- Principles of Management, 1019

Catecholaminergic Polymorphic Ventricular Tachycardia, 1020

- Genetics of Catecholaminergic Polymorphic Ventricular Tachycardia, 1020
- Pathophysiology of Catecholaminergic Polymorphic Ventricular Tachycardia, 1020
- Epidemiology, 1022
- Clinical Presentation, 1022
- Electrocardiographic Features, 1022
- Diagnosis of Catecholaminergic Polymorphic Ventricular Tachycardia, 1022
- Differential Diagnosis, 1024
- Risk Stratification, 1024
- Principles of Management, 1024

Idiopathic Ventricular Fibrillation, 1025

- Genetics of Idiopathic Ventricular Fibrillation, 1025
- Pathophysiology of Idiopathic Ventricular Fibrillation, 1026
- Epidemiology, 1026
- Clinical Presentation, 1026
- Electrocardiographic Features, 1026
- Diagnosis of Idiopathic Ventricular Fibrillation, 1026
- Principles of Management, 1028

Early Repolarization Syndromes, 1029

- Genetics of Early Repolarization Syndrome, 1029
- Pathophysiology of Early Repolarization Syndromes, 1030
- Epidemiology, 1031
- Clinical Presentation, 1031
- Electrocardiographic Features, 1031
- Diagnosis of Early Repolarization Syndrome, 1034
- Differential Diagnosis, 1034
- Risk Stratification, 1034
- Principles of Management, 1037

Sudden cardiac death (SCD) is a major contributor to population mortality, with an overall incidence in the United States estimated to be between 0.1% and 0.2%, resulting in approximately 300,000 to 350,000 deaths annually. Ventricular fibrillation (VF) or pulseless ventricular tachycardia (VT) is the initial rhythm recorded in 25% to 36% of witnessed cardiac arrests occurring at home, but in a much higher proportion (38% to 79%) of witnessed cardiac arrests occurring in a public setting. The majority of SCD events are associated with structural heart disease, with coronary artery disease and its complications being involved in up to 60% to 80% of cases, followed by other cardiomyopathies. However, in 10% to 20% of SCDs, no cardiac structural abnormalities are detectable. The lack of an apparent cause in many of those cases initially led to the classification as “sudden unexplained death syndrome” (SUDS) or “sudden infant death syndrome” (SIDS). Many of these are caused by primary electrical disorders, including long QT syndrome

(LQTS), catecholaminergic polymorphic VT (CPVT), Brugada syndrome, and short QT syndrome (SQTS), as well as cases identified as “idiopathic VF” when the underlying cause often remains unknown.¹

LONG QT SYNDROME

The LQTS is an uncommon inherited cardiac channelopathy that is associated with an abnormally prolonged QT interval and an increased propensity for life-threatening ventricular arrhythmias in the presence of a structurally normal heart.

In 1957, Anton Jervell and Fred Lange-Nielsen published the first report on a familial (autosomal recessive) disorder (“Jervell and Lange-Nielsen syndrome”) characterized by the presence of a striking prolongation of the QT interval, congenital deafness, and a high incidence of SCD at a young age. Subsequently, Romano and Ward independently

identified an almost identical, but autosomal dominant, disorder that is not associated with deafness (“Romano-Ward syndrome”). A genetic relationship between the two was then proposed and the two syndromes were considered variants of one disease under the unifying name of “LQTS.” In the contemporary literature, Romano-Ward syndrome is used interchangeably with LQTS, but is now less commonly used in favor of the LQT1 to LQT17 scheme according to the underlying genetic mutation (see later).

The initial molecular studies suggested that all genes linked to the LQTS phenotype encode for various subunits of cardiac ion channels. Subsequent findings, however, revealed that LQTS could also be caused by mutations of gene coding for channel-associated cellular structural proteins as well. Nonetheless, the concept that LQTS genes ultimately affect cardiac ion currents, either directly (ion channel mutations) or indirectly (modulators), still holds true.

Genetics of the Long QT Syndrome

To date, more than 600 mutations of 17 different genes responsible for a hereditary form of LQTS have been identified (LQT1–17) (Table 31.1; Fig. 31.1), with the majority (more than 90%) of the known mutations located in the first three genes: LQT1 (*KCNQ1*) mutations account for 40% to 55% of genetically positive LQTS, LQT2 (*KCNH2*) for 30% to 45%, and LQT3 (*SCN5A*) for 5% to 10%.

Overall, nine of these genes encode ion channel subunits that are specifically involved in cardiac action potential generation. LQT4, LQT9, LQT11, LQT12, and LQT14–LQT17 are caused by mutations in a family of versatile membrane adapters other than ion channel subunits.

The majority of LQTS cases are inherited in an autosomal dominant fashion. Conversely, Jervell and Lange-Nielsen syndrome, which is inherited in an autosomal recessive fashion, is very rare, affecting less than 1% of LQTS cases.

Genetic analysis reveals two or more mutations in 8% to 11% of LQTS patients with clinical phenotypes of autosomal dominant Romano-Ward syndrome. These compound mutations (so-called “double hits”)

appear to be associated with a more severe phenotype than that associated with a single hit.

Most reported LQTS genetic mutations occur in coding regions, although noncoding mutations (resulting in the loss of allele expression) have also been described. Most LQTS families have their own mutations, which are often termed “private” mutations.

Several genetic mechanisms have been implicated in the development of LQTS including abnormalities in protein synthesis (transcription, translation), posttranslational protein processing resulting in abnormal transport to the cell surface membrane (protein trafficking, folding, assembly of subunits, glycosylation), ion channel gating (biophysical and kinetic properties), or permeation (ion selectivity, unitary conductance).

The majority of LQTS cases are caused by heterozygous disease; thus mutations causing abnormalities in channel coassembly or trafficking result in up to 50% maximal reduction in the number of functional channels (haplotype insufficiency), because the gene product from the healthy allele remains intact. On the other hand, mutations that abolish channel function while preserving subunit assembly can result in dominant-negative suppression of the healthy allele as well, causing a more severe reduction (up to 94%) of the total amount of functional protein (dominant-negative effect) and favoring a more severe clinical course and a higher frequency of arrhythmia-related cardiac events.

Mutations Related to the Potassium Current

Mutations related to the slowly activating delayed rectifier potassium current. Slowly activating delayed rectifier potassium current (I_{Ks}) contributes to human atrial and ventricular repolarization, particularly during action potentials of long duration, and plays an important role in determining the rate-dependent shortening of the cardiac action potential. Mutations in LQT1, LQT5, and LQT11 result in attenuation of I_{Ks} and, as a consequence, prolongation of repolarization, action potential duration and QT interval. LQT1 is caused by loss-of-function mutations of

TABLE 31.1 Molecular Basis of the Congenital Long QT Syndrome

Disease	Gene	Protein	Functional Effect	Frequency
LQT1	<i>KCNQ1 (KvLQT1)</i>	K _v 7.1	↓ I_{Ks}	40%–55%
LQT2	<i>KCNH2 (HERG)</i>	K _v 11.1	↓ I_{Kr}	30%–45%
LQT3	<i>SCN5A</i>	Na _v 1.5	↑ I_{Na}	5%–10%
LQT4 (Ankyrin-B syndrome)	<i>ANKB</i>	Ankyrin-B	Aberrant ion channel/transporter localization	<1%
LQT5	<i>KCNE1</i>	MinK	↓ I_{Ks}	<1%
LQT6	<i>KCNE2</i>	MiRP1	↓ I_{Kr}	<1%
LQT7 (Andersen-Tawil syndrome)	<i>KCNJ2</i>	Kir2.1	↓ I_{K1}	<1%
LQT8 (Timothy syndrome)	<i>CACNA1C</i>	Ca _v 1.2	↑ I_{CaL}	<1%
LQT9	<i>CAV3</i>	Caveolin 3	↑ I_{Na}	<1%
LQT10	<i>SCN4B</i>	Na _v β4	↑ I_{Na}	<1%
LQT11	<i>AKAP9</i>	Yotiao	↓ I_{Ks}	<1%
LQT12	<i>SNTA1</i>	Syntrophin-α1	↑ I_{Na}	<1%
LQT13	<i>KCNJ5</i>	Kir3.4 (GIRK4)	↓ I_{KACH}	<1%
LQT14	<i>CALM1</i>	Calmodulin 1	↑ I_{CaL}	1%–2%
LQT15	<i>CALM2</i>	Calmodulin 2	↑ I_{CaL}	<1%
LQT16	<i>CALM3</i>	Calmodulin 3	↑ I_{CaL}	<1%
LQT17 (Triadin knockout syndrome)	<i>TRDN</i>	Triadin	↑ I_{CaL}	2%
JLN1	<i>KCNQ1 (KvLQT1)</i>	K _v 7.1	↓ I_{Ks}	Very rare
JLN2	<i>KCNE1</i>	MinK	↓ I_{Ks}	Very rare

I_{CaL} , L-type Ca^{2+} current; I_{K1} , inward rectifier K^{+} current; I_{KACH} , acetylcholine-activated inward rectifier K^{+} current; I_{Kr} , rapidly activating delayed rectifier K^{+} current; I_{Ks} , slowly activating delayed rectifier K^{+} current; I_{Na} , Na^{+} current; JLN1 and JLN2, Jervell and Lange-Nielsen syndrome types 1 and 2, respectively; LQT1 to LQT17, long QT syndrome types 1 to 17, respectively.

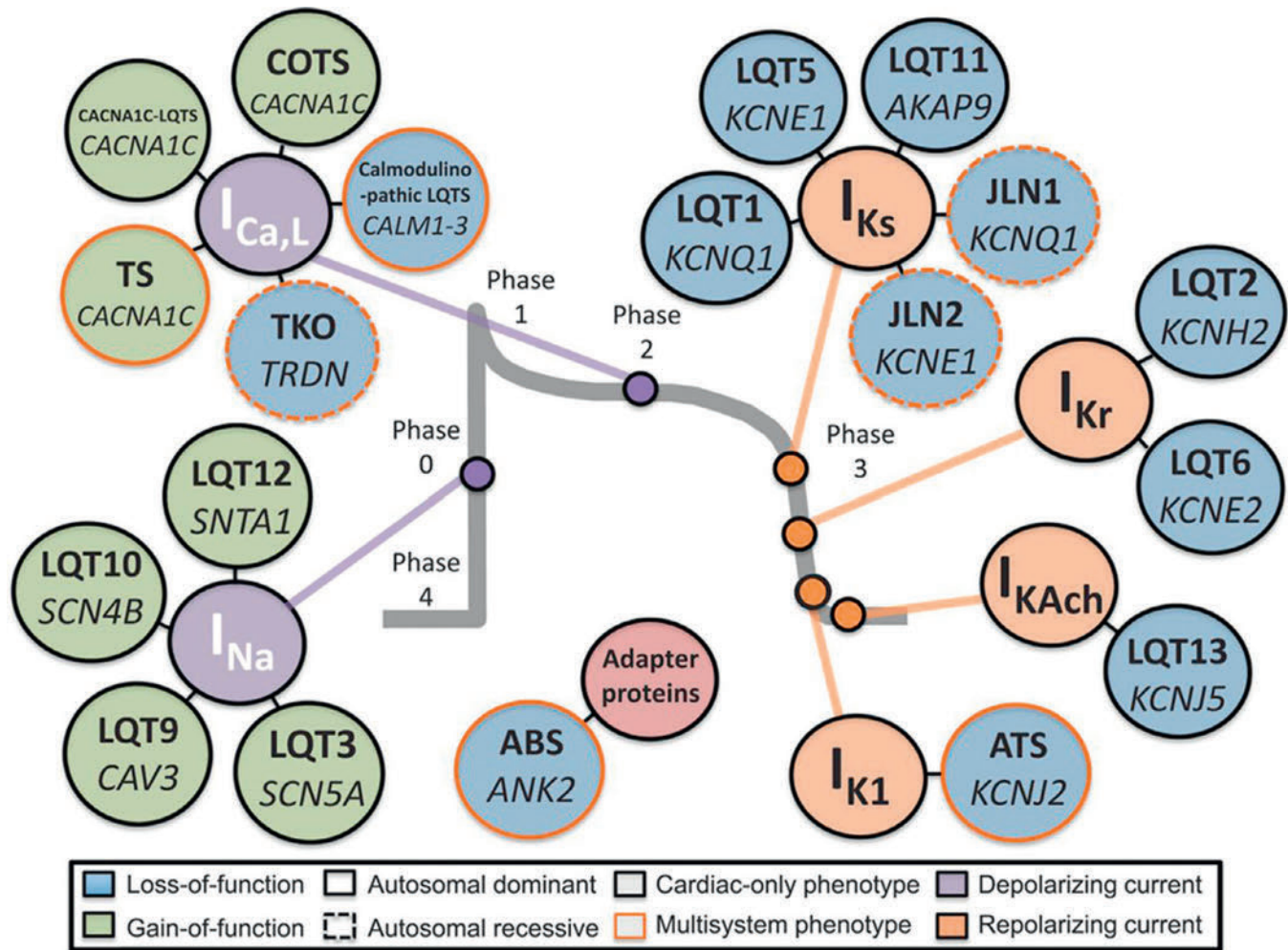


Fig. 31.1 Current-Centric Classification of Long QT Syndrome (LQTS) Genotypes. The clinical phenotypes resulting from the abnormal ventricular cardiac action potential depolarization (purple) or repolarization (orange) are grouped according to the specific current perturbed by an underlying genetic defect. Blue circles represent mutations that confer a loss of function to the specified current, whereas green circles confer a gain of function. Solid lines indicate those disorders that are autosomal dominant, whereas dashed lines indicate those disorders that are autosomal recessive. Solid black outlines indicate nonsyndromic genotypes and solid orange outlines represent multisystem genotypes. ABS, Ankyrin-B syndrome; COTS, cardiac-only Timothy syndrome; JLN1, Jervell and Lange-Nielsen syndrome; $I_{Ca,L}$, L-type calcium current; I_{K1} , inwardly rectifying potassium current; I_{KACh} , G-protein-coupled inwardly rectifying potassium current; I_{Kr} , rapid component of the delayed rectifier potassium current; I_{Ks} , slow-component of the delayed rectifier potassium current; I_{Na} , cardiac sodium current; TKO, triadin knockout syndrome. (From Giudicessi JR, Ackerman MJ. Calcium revisited. *Circ Arrhythmia Electrophysiol.* 2016;9:e002480.)

the *KCNQ1* (*KvLQT1*) gene, which encodes the α subunit ($K_v7.1$) of the inward I_{Ks} . More than 170 mutations of this gene have been reported, comprising many Romano-Ward (autosomal dominant) syndromes and accounting for approximately 40% to 55% of all genotyped LQT families. Of note, mutations involving the transmembrane domain of *KCNQ1* result in more severe disease compared with C-terminal mutations. LQT5 is caused by loss-of-function mutations of the *KCNE1* gene, which encodes the β -subunit (MinK) that modulates I_{Ks} .

Homozygous or compound heterozygous loss-of-function mutations of either the *KCNQ1* or *KCNE1* genes cause the autosomal recessive form of LQTS (the Jervell and Lange-Nielsen syndrome). Patients with *KCNQ1* mutations (type 1 Jervell and Lange-Nielsen syndrome) have an almost sixfold greater risk of arrhythmic events, whereas patients with *KCNE1* mutations (type 2 Jervell and Lange-Nielsen syndrome)

appear to be at lower risk. Although the Jervell and Lange-Nielsen syndrome is the most severe among the major variants of LQTS, the parents of Jervell and Lange-Nielsen syndrome patients are generally less symptomatic than other LQT1 patients, despite the fact that they all are heterozygous for the same gene. This is likely related to the observation that most of the LQT1 genetic variants are missense mutations exerting a dominant-negative effect, whereas most (74%) Jervell and Lange-Nielsen mutations of *KCNQ1* are frame-shift/truncating mutations that are unable to cause dominant-negative suppression but are likely to interfere with subunit assembly. Jervell and Lange-Nielsen syndrome accompanies complete loss of I_{Ks} in hair cells and endolymph of the inner ear, which results in congenital deafness.

LQT11 is caused by loss-of-function mutations of the *AKAP9* gene, which encodes an A-kinase anchoring protein (Yotiao), shown to be

an integral part of the I_{Ks} macromolecular complex. The presence of Yotiao is necessary for the physiological response of the I_{Ks} to beta-adrenergic stimulation. LQT11 mutations reduce the interaction between Yotiao and the I_{Ks} channel ($K_{0.7.1}$), preventing the functional response of I_{Ks} to cyclic adenosine monophosphate (cAMP) and adrenergic stimulation and causing an attenuation of I_{Ks} .

Mutations related to the rapidly activating delayed rectifier potassium current. Rapidly activating delayed rectifier potassium current (I_{Kr}) presents the principal repolarizing current at the end of the plateau phase in most cardiac cells and plays an important role in governing the cardiac action potential duration and refractoriness. Mutations in LQT2 and LQT6 result in attenuation of I_{Kr} and cause a decrease in the K^+ outward current and prolongation of repolarization, action potential duration, and QT interval.

LQT2 is caused by loss-of-function mutations of the *KCNH2* (*HERG*) gene, which encodes the α -subunit ($K_{0.11.1}$) of the inward I_{Kr} . LQT2 syndrome accounts for almost 30% to 45% of all genotyped congenital LQTS cases. Approximately 200 mutations in this gene have been identified, which result in rapid closure of the hERG channels and decrease the normal rise in I_{Kr} , leading to delayed ventricular repolarization and QT prolongation. Mutations involving the pore region of the hERG channel are associated with a significantly more severe clinical course than nonpore mutations; most pore mutations are missense mutations with a dominant-negative effect.

LQT6 is caused by loss-of-function mutations of the *KCNE2* gene, which encodes the accessory β -subunit (MiRP1) of the hERG channel. LQT6 displays clinical resemblance to LQT2.

Mutations related to the inward rectifier potassium current. Inward rectifier potassium current (I_{K1}) contributes to the terminal portion of phase 3 repolarization. Andersen-Tawil syndrome (LQT7) is caused by loss-of-function mutations of the *KCNJ2* gene, which encodes the voltage-dependent K^+ channel (Kir2.1) that contributes to the inward I_{K1} . Kir2.1 channels are expressed primarily in skeletal muscle, heart, and brain. The majority of mutations exert a dominant-negative effect on channel current.

Disruption of the I_{K1} function can potentially lead to prolongation of the terminal repolarization phase and QT interval, which can predispose to the generation of early afterdepolarizations (EADs) and delayed afterdepolarizations (DADs) causing ventricular arrhythmias. However, unlike other types of LQTS, where the afterdepolarizations arise from reactivation of L-type Ca^{2+} channels, the EADs/DADs generated in LQT7 are likely secondary to Na^+ - Ca^{2+} exchanger-driven depolarization. It is believed that the differential origin of the triggering beat is responsible for the observed discrepancy in arrhythmogenesis and the clinical features compared with other types of LQTS. In addition, it is likely that prolongation of the action potential duration in LQT7 is somewhat homogeneous across the ventricular wall (i.e., transmural dispersion of repolarization is less prominent than in other types of LQTS), which can potentially explain the low frequency of torsades de pointes. Flaccid paralysis results from failure to propagate action potentials in the skeletal muscle membrane as a result of sustained membrane depolarization.

Mutations related to the acetylcholine-activated potassium current. LQT13 is caused by loss-of-function mutations of the *KCNJ5* gene, which encodes the α subunit (Kir3.4, GIRK4) of the inward acetylcholine-activated potassium current (I_{KACH}). Kir3.4 mutations exert dominant-negative effects on Kir3.1/Kir3.4 channel complexes by disrupting membrane targeting and stability of Kir3.4.

Mutations Related to the Sodium Current

LQT3 is caused by gain-of-function mutations of the *SCN5A* gene, which encodes the α subunit ($Na_v1.5$) of the cardiac voltage-gated Na^+

channel that is responsible for the sodium content (I_{Na}). LQT3 accounts for approximately 5% to 10% of genotype-positive LQTS cases. More than 200 mutations have been identified in the *SCN5A* gene, with the majority being missense mutations mainly clustered in $Na_v1.5$ regions that are involved in fast inactivation, or in regions that stabilize fast inactivation.

Several mechanisms have been identified to underlie ionic effects of *SCN5A* mutations in LQT3. Most of the *SCN5A* mutations cause a gain of function through disruption of fast inactivation of the Na^+ channel, allowing repeated reopening during sustained depolarization and resulting in an abnormal, small but functionally important sustained (or persistent) noninactivating Na^+ current (I_{sus}) during the action potential plateau that acts to slow repolarization and prolong the action potential duration (eFig. 31.1). Other, less common mechanisms (eFig. 31.2) include increased window current, which results from delayed inactivation of mutant Na^+ channels, occurring at more positive potentials and widening the voltage range during which the Na^+ channel may reactivate without inactivation. In addition, some mutations cause slower inactivation, which allows longer channel openings, and causes a slowly inactivating Na^+ current (the late Na^+ current, I_{NaL}).

Regardless of the mechanism, increased Na^+ current (I_{sus} , window current, I_{NaL} , or peak I_{Na}) upsets the balance between depolarizing and repolarizing currents in favor of depolarization. Gain-of-function LQT3 mutations often increase I_{NaL} two- to fourfold. Because the general membrane conductance is small during the action potential plateau, the presence of a persistent inward Na^+ current, even of small amplitude, can potentially have a major impact on the plateau duration and can be sufficient to prolong repolarization and QT interval. The resulting delay in the repolarization process triggers EADs (i.e., reactivation of the L-type Ca^{2+} channel during phase 2 or 3 of the action potential), especially in Purkinje fiber myocytes where action potential durations are intrinsically longer. Also, increased influx of Na^+ (via the enhanced I_{NaL}) can stimulate the Na^+ - Ca^{2+} exchanger in the reverse mode (3 Na^+ ions out, one Ca^{2+} ion in), with consequent intracellular Ca^{2+} overload and DADs. QT prolongation and the risk of developing arrhythmia is more pronounced at slow heart rates, when the action potential duration is longer, allowing more Na^+ current to enter the cell.²

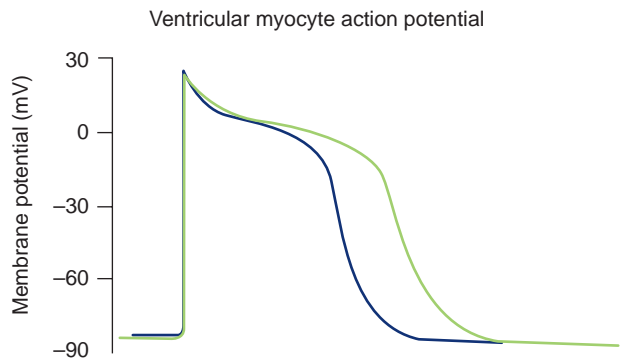
LQT9 is caused by gain-of-function mutations of the *CAV3* gene, which encodes caveolin-3, a plasma membrane scaffolding protein that interacts with $Na_v1.5$ and plays a role in compartmentalization and regulation of channel function. Mutations in caveolin-3 induce kinetic alterations of the Na^+ channel that result in persistent late Na^+ current (I_{sus}) and have been reported in cases of SIDS.

LQT10 is caused by gain-of-function mutations of the *SCN4B* gene, which encodes the β -subunit ($Na_v\beta_4$) of the $Na_v1.5$ ion channel. To date, only a single mutation in one patient has been described, which resulted in a shift in the inactivation of the Na^+ current toward more positive potentials, but did not change the activation. This resulted in increased window currents at membrane potentials corresponding to phase 3 of the action potential.

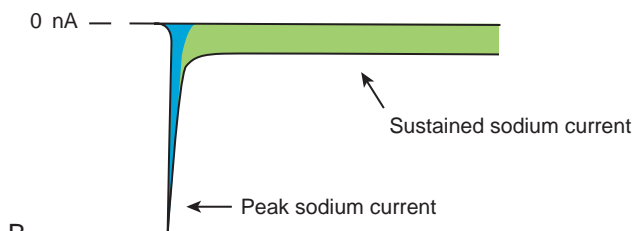
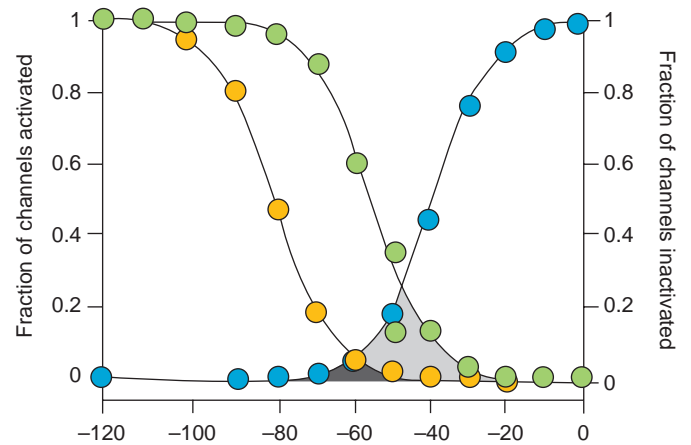
LQT12 is caused by mutations of the *SNTA1* gene, which encodes $\alpha 1$ -syntrophin, a cytoplasmic adaptor protein that enables the interaction between $Na_v1.5$, nitric oxide synthase, and sarcolemmal Ca^{2+} adenosine triphosphatase (ATPase) complex that appears to regulate ion channel function. By disrupting the interaction between $Na_v1.5$ and sarcolemmal calcium ATPase complex, *SNTA1* mutations cause increased $Na_v1.5$ nitrosylation with consequent reduction of channel inactivation and increased I_{sus} densities.

Mutations Related to the Calcium Current

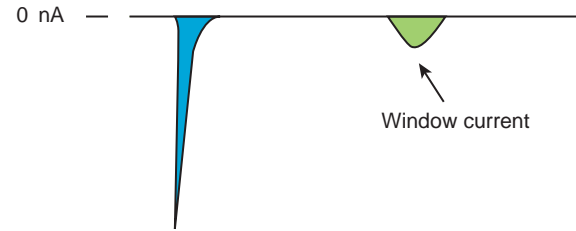
Mutations related to the L-type calcium current. Timothy syndrome (LQT8) is caused by gain-of-function mutations of the *CACNA1C*



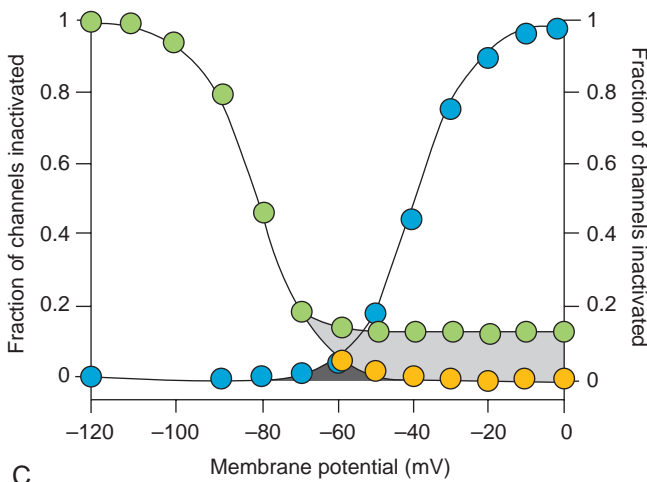
A



B

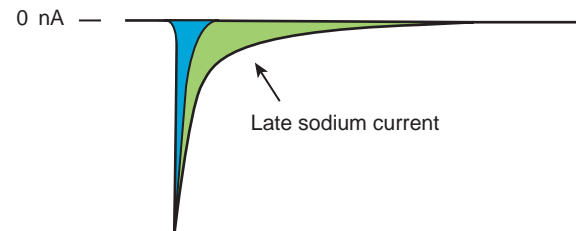


A

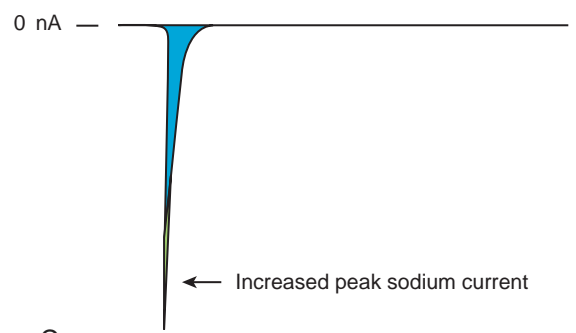


C

eFig. 31.1 Mechanism of Long QT Syndrome Type 3 (LQT3). (A) QT interval prolongation results from delayed repolarization of ventricular action potentials. (B) Delayed repolarization in LQT3 is often due to the presence of abnormal sustained non-inactivating sodium current (green area). (C) Sustained current results from incomplete inactivation of the sodium channels (green circles). (From Amin AS, Asghari-Roodsari A, Tan HL. Cardiac sodium channelopathies. *Pflügers Arch Eur J Physiol.* 2010;460:223–237.)



B



C

eFig. 31.2 Alternative Mechanisms of Sodium Channel Gain-of-Function in Long QT Syndrome Type 3. (A) Increased window current due to delayed inactivation of cardiac sodium channels (green circles). Increased window current is carried at potentials corresponding to phases 2 and 3 of the ventricular action potential (green area), remote from the peak sodium current during phase 0 (blue area). (B) Slower inactivation creates a late sodium current (green area). (C) Increased peak sodium current. (From Amin AS, Asghari-Roodsari A, Tan HL. Cardiac sodium channelopathies. *Pflügers Arch Eur J Physiol.* 2010;460:223–237.)

gene, which encodes the α subunit ($\text{Ca}_v1.2$) of the voltage-dependent L-type Ca^{2+} channel that contributes to L-type calcium current (I_{CaL}).

Recently, multiple nonsyndromic LQTS-causative mutations in *CACNA1C* were described in LQTS patients with isolated QT prolongation and propensity to ventricular arrhythmias in the absence of congenital heart defects and extracardiac manifestations that define Timothy syndrome clinically (nonsyndromic LQT8).³ Other *CACNA1C* mutations were found to cause cardiac-only Timothy syndrome (COTS), characterized by the concomitant but variably expressed phenotypes of LQTS (QT prolongation), hypertrophic cardiomyopathy, congenital heart defects, and SCD in the absence of any extracardiac symptoms.^{3,4}

The inward I_{CaL} sustains depolarization and gives rise to the plateau phase essential for excitation-contraction coupling. Gain-of-function mutations of *CACNA1C* result in near complete elimination of voltage-dependent inactivation of $\text{Ca}_v1.2$ channels, leading to inappropriate continuation of the depolarizing I_{CaL} and lengthening of the plateau phase, predisposing to the generation of EADs. In addition, augmentation of I_{CaL} leads to intracellular Ca^{2+} overload, which promotes spontaneous ectopic Ca^{2+} release from sarcoplasmic reticulum and the generation of potentially arrhythmogenic DADs.³

The exact pathophysiology of hypertrophic cardiomyopathy, congenital heart defects, and extracardiac manifestations of Timothy syndrome and their relation to *CACNA1C* mutations remain unclear.

Mutations related to calmodulin (calmodulinopathy). Calmodulin is a small cytoplasmic Ca^{2+} -binding protein with ubiquitous expression. Calmodulin is involved, directly and indirectly, in modulation of several ion channels, including Na^+ , K^+ , L-type Ca^{2+} , and RYR2 channels. The main binding partner of calmodulin in cardiac cells is RyR2, which regulates Ca^{2+} release from the sarcoplasmic reticulum. Acting as an intracellular Ca^{2+} sensor, Ca^{2+} -saturated calmodulin binds RYR2 to inhibit Ca^{2+} release by stabilizing the RyR2 channel closed state.

Three different genes (*CALM1–3*) in the human genome encode exactly the same calmodulin protein. Recent genetic studies have identified several calmodulin mutations associated with CPVT, LQTS, and idiopathic VF. Defective calmodulin–RyR2 binding results in impaired calmodulin inhibition of RyR2 function with consequent dysregulation of sarcoplasmic reticulum Ca^{2+} release. Further, de novo mutations in *CALM1*, *CALM2*, or *CALM3* genes were found to disrupt Ca^{2+} -dependent inactivation of the cardiac L-type Ca^{2+} channel ($\text{Ca}_v1.2$), which leads to augmentation of I_{CaL} , prolongation of the plateau phase of action potential, and LQTS phenotype (LQT14–16).^{5,6}

Mutations related to triadin: triadin knockout syndrome. *TRDN* encodes triadin, a sarcoplasmic reticulum protein functionally and physically related to the RYR2. Homozygous or compound heterozygous loss-of-function mutations in *TRDN* likely reduce triadin-mediated negative feedback on the L-type Ca^{2+} channel, resulting in augmentation of I_{CaL} , prolonged action potential duration, and the recessively inherited LQTS phenotype (LQT17). Intracellular Ca^{2+} overload and increases in spontaneous sarcoplasmic reticulum Ca^{2+} release, particularly in the setting of beta-adrenergic stimulation, result in ventricular arrhythmias.

LQT17 is characterized by extensive T wave inversions in the precordial leads V_1 through V_4 , with either persistent or transient QT prolongation, exercise-induced cardiac arrest in early childhood (2 to 6 years of age), and mild-to-moderate proximal skeletal muscle weakness. Because all *TRDN*-null patients display a strikingly similar phenotype, it has been proposed that either triadin knockout syndrome or *TRDN*-mediated autosomal-recessive LQTS should be used rather than LQT17.^{3,7}

Mutations in the Ankyrin-B Gene: Ankyrin-B Syndrome

LQT4 is caused by loss-of-function mutations of the *ANK2* gene, which encodes ankyrin-B, a structural membrane adapter protein that anchors

ion channels to specific domains in the plasma membrane. Functionally, ankyrins bind to several ion channel proteins, targeting these proteins to specialized membrane domains, such as the anion exchanger (chloride-bicarbonate exchanger), Na^+ - K^+ ATPase, I_{Na} , the Na^+ - Ca^{2+} exchanger ($I_{\text{Na-Ca}}$), and Ca^{2+} release channels (including those mediated by the receptors for inositol triphosphate [IP_3] or RyR2). Hence, *ANK2* mutations can potentially result in improper localization and activity of ion-conducting proteins.

Mutations of the *ANK2* gene have been reported to lead to increased intracellular concentration of Ca^{2+} and, sometimes, fatal arrhythmia. However, QT interval prolongation is not a consistent feature in patients with ankyrin-B dysfunction, and the clinical phenotypes often extend beyond the typical LQTS, including sinus node dysfunction (SND), atrioventricular (AV) block, and atrial fibrillation (AF), in addition to idiopathic VF, exercise-induced, polymorphic VT, and SCD. Therefore ankyrin-B dysfunction is now regarded as a clinical entity distinct from classic LQTS (referred to as the “ankyrin-B syndrome”).

Pathophysiology of the Long QT Syndrome

Mechanism of QT Interval Prolongation

Any factor that evokes lengthening of the action potential duration holds the potential of causing an LQTS phenotype, especially if it does it heterogeneously. Electrophysiologically, prolongation of the action potential duration and QT interval can arise from either a decrease in the outward repolarizing current (K^+ currents: I_{Kr} , I_{Ks} , I_{K1} , I_{KACh}) or an increase in inward depolarizing membrane current (I_{Na} , I_{CaL}) during phases 2 and 3 of the action potentials (Fig. 31.2).

Most commonly, QTc prolongation is produced by delayed repolarization due to attenuation of I_{Ks} (LQT1, LQT5, LQT11), I_{Kr} (LQT2, LQT6), I_{K1} (LQT7), or I_{KACh} (LQT13). Less commonly, QT prolongation results from prolonged depolarization due to an increase in I_{Na} (LQT3, LQT4, LQT9, LQT10, LQT12) or I_{CaL} (LQT8, LQT14–17).

Mechanism of Dispersion of Repolarization

LQTS is caused by an excessive and heterogeneous prolongation of the repolarization phase of the ventricular action potential. In the normal ventricle, there are heterogeneous cell types with different action potential morphologies and durations, mainly attributed to cell-specific and regional variability in the functional expression of different populations of ion channels (transient outward K^+ channels [I_{to}], I_{Ks}) and the Na^+ window current (I_{Na}), and their accessory proteins. Some experimental studies proposed the presence of three irregular cell layers in the ventricular wall with distinct electrical properties: endocardial, midmyocardial (putative M cells), and epicardial cells. Overall, the midmyocardial cells (which have a smaller I_{Ks} , a larger late I_{Na} , and a larger Na^+ - Ca^{2+} exchange current [$I_{\text{Na-Ca}}$]) appear to generate longer action potential durations that are more susceptible to modification compared with the endocardium and epicardium. The epicardial cells have the shortest action potential durations because of a prominent I_{to} . Repolarization of endocardial cells usually occurs between repolarization of the epicardial and midmyocardial cells. Notably, factors that prolong the action potential appear to elicit a disproportionate prolongation of the action potential duration in midmyocardial cells. As a result, dispersion of the action potential duration becomes irregularly exaggerated across the ventricular wall, yielding an increase in the action potential duration heterogeneity.

Conditions leading to a reduction in I_{Kr} (e.g., LQT2) or augmentation of late I_{Na} (e.g., LQT3) produce a preferential prolongation of the midmyocardial cell action potential. Consequently, QT interval prolongation is accompanied by a dramatic increase in transmural dispersion of repolarization. In contrast, conditions leading to a reduction in I_{Ks} alone (e.g., LQT1) result in a homogeneous prolongation of action

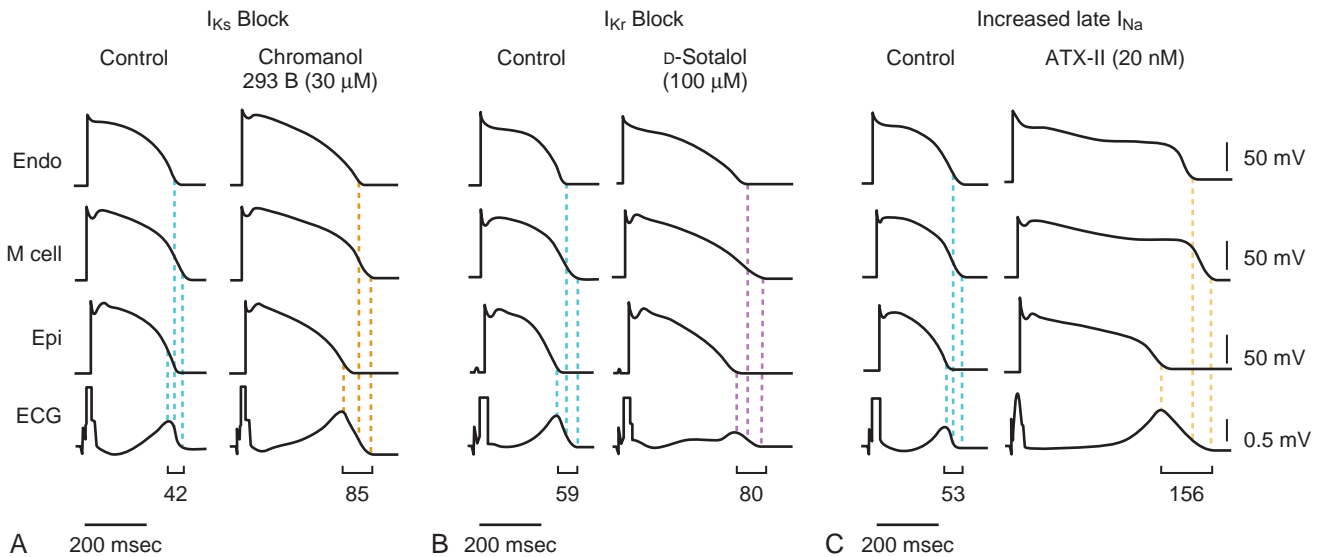


Fig. 31.2 Pathophysiology of Long QT Syndrome. Transmembrane action potentials and transmural electrocardiogram (ECG) traces in control and after I_{Ks} block (A), I_{Kr} block (B), and increase in late I_{Na} (C), in arterially perfused canine left ventricular wedge preparations. (A) to (C) depict action potentials simultaneously recorded from endocardial (Endo), M cell, and epicardial (Epi) sites, together with a transmural ECG trace. Basic cycle length, 2000 milliseconds. In all cases, the peak of the T wave in the ECG is coincident with the repolarization of the epicardial action potential, whereas the end of the T wave is coincident with the repolarization of the M cell action potential. Repolarization of the endocardial cell is intermediate between that of the M cell and epicardial cell. Transmural dispersion of repolarization across the ventricular wall, defined as the difference in the repolarization time between M and epicardial cells, is denoted below the ECG traces. ATX-II, Sea anemone toxin; I_{Na} , sodium current; I_{Kr} , rapidly activating delayed rectifier K⁺ current; I_{Ks} , slowly activating delayed rectifier potassium current. (From Antzelevitch C. Drug-induced channelopathies. In: Zipes DP, Jalife J, eds. *Cardiac Electrophysiology: From Cell to Bedside*. 5th ed. Philadelphia: WB Saunders; 2009:195–203.)

potential duration across the ventricular wall with little increase in transmural dispersion of repolarization. However, concurrent beta-adrenergic stimulation (e.g., exercise, isoproterenol) results in abbreviation of epicardial and endocardial action potential duration with little or no change in the midmyocardial cell action potential, resulting in marked augmentation of transmural dispersion of repolarization and arrhythmogenesis (see Fig. 31.2).

Mechanism of Torsades de Pointes

The excessive increase in the spatial and/or temporal heterogeneity of the duration of the action potential favors the generation of EADs caused by reactivation of L-type Ca^{2+} channels, and on some occasions the late I_{Na} or Na^{+} - Ca^{2+} exchanger. EADs can cause premature ventricular complexes (PVCs) (predominantly arising from the Purkinje network) that can potentially infringe on the underlying substrate of heterogeneous repolarization to initiate polymorphic reentrant VT. Excessive transmural heterogeneity of the action potential duration provides the substrate for unidirectional block and functional reentry circuits to perpetuate torsades de pointes. Although controversy still exists, it is likely that the propagation of torsades de pointes is facilitated by intramural reentrant mechanisms giving rise to one or more intramural rotors that impose a rapid ectopic ventricular rhythm (typically 150 to 300 beats/min) while migrating inside the ventricular wall. Hence, with each new cycle the principal depolarization focus migrates accordingly, resulting in a progressive change of the electrical axis, typically rotating 180 degrees in approximately 10 to 12 cycles. This results in a polymorphic VT with the characteristic sinusoidal “twisting of the points” pattern on the 12-lead electrocardiogram (ECG).⁸

Notably, although the atrium seems to be resistant to generating EADs in response to agents that prolong repolarization, atrial EADs

and “atrial torsades de pointes” have been reported in some LQTS patients as well as cesium-treated dogs.

Mechanism of Exercise-Induced QT Interval Changes

Arrhythmic events in LQTS are strongly associated with triggers linked to inappropriate QT adaptation to changes in heart rate. Patients with LQT1 and LQT2 genotypes have differing patterns of QT adaptation during beta-adrenergic stimulation (e.g., during stress, exercise, or epinephrine infusion). LQT1 patients appear to have less repolarization reserve during exercise as evidenced by a progressive or persistent pattern of QTc prolongation at faster heart rates, compared with patients with LQT2, in whom maximal QTc prolongation occurs at submaximal heart rates in the early phase of sympathetic stimulation with subsequent fall toward baseline values at faster heart rates.

I_{Ks} is an important determinant of rate-dependent shortening of the cardiac action potential and QT interval. As heart rate increases, I_{Ks} increases because channel deactivation is slow and incomplete during the shortened diastole. This allows I_{Ks} channels to accumulate in the open state during rapid heart rates and contribute to the faster rate of repolarization. Furthermore, I_{Ks} is markedly enhanced by beta-adrenergic stimulation through G-protein/cAMP-mediated channel phosphorylation by protein kinase A (PKA) (requiring AKAP9 [Yotiao]) and PKC (requiring MinK). Importantly, I_{Ks} is functionally upregulated when other repolarizing currents (such as I_{Kr}) are reduced, potentially serving as a “repolarization reserve” and a safeguard against loss of repolarizing power, especially when beta-adrenergic stimulation is present. LQT1 subjects have compromised I_{Ks} channels that are not as responsive to sympathetic stimulation, and phase 3 repolarization in these individuals is retarded. Consequently, during beta-adrenergic stimulation, there are relatively more unopposed depolarizing forces via the L-type Ca^{2+}

channel and the $\text{Na}^+\text{-Ca}^{2+}$ exchanger that prolong the action potential duration and the QT interval.

In contrast, subjects with LQT2 have dysfunctional I_{Kr} channels, which represent a smaller fraction of the K^+ channels responsible for phase 3 repolarization and are not as sympathetically responsive as I_{Ks} channels. Therefore, in LQT2 patients, the QT fails to shorten at the intermediate heart rates in the early phase of exercise or epinephrine infusion because of attenuation of I_{Kr} . This is followed by recruitment of I_{Ks} (“repolarization reserve”) at faster heart rates during continuing exercise or epinephrine infusion, with concomitant appropriate abbreviation of the action potential duration and QT shortening, which persists into the recovery phase. This consequently leads to an exaggerated QT difference between the exercise and recovery QT/R-R curves that is manifested as increased QT hysteresis, which appears to be a characteristic feature of the LQT2 phenotype.

The LQT3 phenotype is characterized by a constant reduction of the action potential duration with epinephrine because of stimulation of the intact I_{Ks} channel and augmentation of the late inward I_{Na} . In fact, LQT3 patients may have supernormal QT adaptation in response to exercise compared with control subjects. *SCN5A* mutations in LQT3 cause a gain of function through disruption of fast channel inactivation, allowing repeated reopening during sustained depolarization and resulting in a small but functionally important enhancement of the I_{Na} during action potential plateau. As a consequence, the risk of developing arrhythmia will be expected to be particularly high at slow heart rates, when the action potential duration is longer, allowing more Na^+ current to enter the cell.

The differences in the dynamic response of ventricular repolarization to sympathetic stimulation may explain the epidemiological observation that patients with LQT1 are more likely to have life-threatening events during sympathetic activation compared with patients with other genotypes and also may underlie the responsiveness of LQT1 patients to beta-blocker therapy.⁹

Mechanism of Genotype-Phenotype Variability

The LQTS is a complex and multifactorial disorder characterized by significant phenotypic heterogeneity. The clinical phenotype (QTc values, arrhythmia-related symptoms, and outcomes) is highly variable, with a broad continuous spectrum of clinical or subclinical phenotypes, not only between families carrying different pathogenic mutations, but also among family members carrying an identical mutation. One end of this spectrum is concealed LQTS (silent carriers of disease-causing mutations), whereby no QT prolongation or related symptoms are observed. At the other end of the spectrum are the severe symptomatic LQTS patients, who often represent the index cases easily identified in families. In between are patients with different degrees of QT prolongation and different levels of severity of arrhythmias.

A multitude of genetic and acquired interacting factors (some defined but many still unknown) influence the pathophysiology and clinical course of each LQTS subject and ultimately determine a spectrum of phenotypes. Among these factors is the fact that action potential generation is a polygenic process; different LQTS genes affect different ion current mechanisms. Even mutations in the same gene can affect gene expression levels and ionic current activity to different extents and via different mechanisms. As noted above, mutations located in the transmembrane segment (for LQT1) or pore region (for LQT2) of the ion channel generally result in more malignant disease compared with mutations in other locations. Similarly, mutations causing a dominant-negative effect (e.g., missense mutations involving the pore region of the channel) result in more profound channel dysfunction and more severe clinical disease than those associated with haplotype insufficiency (e.g., mutations causing coassembly or trafficking abnormalities).

The “repolarization reserve” concept can underlie, at least in part, the phenotypic heterogeneity in LQTS. Cardiac muscle repolarization has built-in redundancy, or reserve, such that perturbation of one ion current does not necessarily result in excessive repolarization changes because other currents can compensate. Hence, there exists an inherent variability of arrhythmic response to QT interval prolongation with the relationship between perturbations of one ion channel in relation to the sum total of repolarizing currents. This concept implies that often multiple “hits” to repolarization are required to compromise repolarization and surpass the threshold for developing clinical QT prolongation and torsades de pointes. In this setting, a mutation in one of the LQT-linked genes causing an attenuation of a cardiac ionic current may result in only a limited disruption of the repolarization process, which can be clinically concealed and become unmasked (manifesting as QT prolongation and arrhythmias) only when accompanied by another insult to the same or a different ionic current (e.g., drugs or electrolyte abnormalities). In fact, it has been suggested that some cases of acquired LQTS represent inadvertent “unmasking” of subclinical congenital LQTS.^{10,11}

Adding to the complexity is the “double-hit” phenomenon, secondary to either two mutations in the same gene (compound heterozygosity) or mutations in two different LQT genes (digenic heterozygosity). Double hits occur in 5% to 10% of LQTS patients and the resulting phenotype is more severe than with a single hit.

Genetic factors are also involved in the control of cardiac repolarization at the population level. The heritability of the QTc interval has been estimated as being between 25% and 52%. Ventricular action potential is under the joint control of multiple ionic currents, and the activity and expression levels of the channels underlying each of these currents establish a subtle equilibrium between depolarizing and repolarizing currents determining the action potential duration in each individual. Common genetic variants differing from the ancestor sequence by one nucleotide (i.e., single nucleotide polymorphism) in genes coding for proteins that are known or suggested to affect ion channel function appear to influence this equilibrium even via weak effects on activity and/or expression level of channel subunits and can potentially play a role in determining cardiac repolarization duration and QTc length in healthy individuals. Therefore apart from the known LQT-linked genetic mutations, allelic variation elsewhere in the genome, most often single nucleotide polymorphisms, in the same disease-causing gene or in other genes, can amplify otherwise subclinical disturbances of the repolarization into overt LQTS and potentially contribute to the variable penetrance and clinical phenotype heterogeneity.

Furthermore, the resultant intrinsic risk for arrhythmias can be modulated by a variety of intrinsic or extrinsic environmental factors, including age, gender, heart rate, sympathetic tone, electrolyte balance, presence of QT-prolonging drugs, as well as inherited and acquired pathological conditions such as LV hypertrophy, and heart failure.

In summary, the interaction of the underlying LQTS genetic mutation with other genetic factors in the same gene or elsewhere in the host genome (“modifier genes”), as well as with multiple superimposed acquired risk determinants (“disease modifiers”), has a substantial impact on the expressivity of the phenotype of the LQT genotype.¹²

Mechanism of Gender Effects

In the healthy population, QTc intervals are longer in women than in men, a difference that becomes apparent only after puberty. This is associated with a higher susceptibility to drug-induced LQTS and torsades de pointes; women account for 70% of cases of drug-induced QT prolongation and torsades de pointes. In healthy volunteers, drug-induced QT interval prolongation is greatest during the menses and ovulation phases and least during the luteal phase. Age-dependent

gender-related differences also exist among patients with congenital LQTS. Although the risk of cardiac events is higher in boys with LQTS as compared with girls during childhood and early adolescence, a gender risk reversal occurs after the onset of puberty. LQT1 and LQT2 women of childbearing age have longer QT intervals and higher risk for polymorphic VT and SCD than men. The extent of QT prolongation and the risk of cardiac events appear to be more pronounced during periods with high estradiol and low progesterone levels (e.g., during the follicular phase of the menstrual cycle) and mildly reduced during periods with higher progesterone/estradiol ratio (e.g., during the luteal phase of the menstrual cycle, and during pregnancy). The arrhythmogenic risk markedly increases immediately postpartum (especially among women with the LQT2 genotype), when serum progesterone concentrations abruptly decline.^{13–15}

The mechanisms underlying these gender-related differences are poorly understood. Environmental (increased physical activity), hormonal, and genetic factors (modifier genes not shared by boys and girls) have been proposed. Current evidence supports the role of sex hormones as a significant contributor to the action potential duration. Recent studies suggest that the duration of ventricular repolarization and QTc interval are influenced by complex interactions between sex steroid hormones and gonadotropins depending on gender, rather than on one single hormone. In general, testosterone in men and an increased progesterone/estradiol ratio in women shorten repolarization, whereas follicle-stimulating hormone prolongs repolarization in both genders.^{15,16}

The effect of sex hormones on the QT interval and arrhythmogenesis in LQTS can partly be explained by direct and indirect interaction with the ion channel. Experimental studies suggest that estrogen suppresses I_{Kr} and increases I_{CaL} , Na^+-Ca^{2+} exchanger activity, RyR2 leakiness, and α_1 - and β_2 -adrenoceptor responsiveness. Estradiol also enhances the sensitivity of I_{Kr} channels to their specific antagonist and predisposes to greater drug-induced QT prolongation. Conversely, testosterone enhances the outward currents (I_{Kr} , I_{Ks} , I_{K1}) and reduces the inward current (I_{CaL}). Progesterone, a testosterone precursor, enhances I_{Ks} and reduces I_{CaL} . Thus estradiol can potentially exert a proarrhythmic effect

in LQTS patients, whereas testosterone and progesterone shorten QT duration and exert an antiarrhythmic effect with a reduced susceptibility to sympathetic stimuli.^{14,15,17} In fact, a recent study demonstrated potential benefit of oral progesterone for the prevention of drug-induced QT interval prolongation.¹⁸

Epidemiology

There are no systematic studies on LQTS prevalence in the general population. A recent estimate of the prevalence of LQTS is 1:2000 live births, based on the results of genetic screening in families and the incidence of compound heterozygotes (i.e., persons with two mutations). However, the clinical disease is less common (approximately 1 in 5000) because most mutation carriers remain asymptomatic. The usual mode of inheritance is autosomal dominant, with the exception of the autosomal recessive Jervell and Lange-Nielsen type and triadin knockout syndrome (LQT17).

LQT1, LQT2, and LQT3 comprise more than 90% of all genotyped LQTS cases. LQT1 is the most frequent genetic form of LQTS, accounting for 40% to 55% of genotyped LQTS cases. LQT2 and LQT3 account for 30% to 45% and 5% to 10% of genotyped LQTS cases, respectively (Table 31.2). The remaining 14 types (LQT4 to LQT17) make up less than 5% of the genotype-identified LQTS. Although LQT3 is infrequent among adolescents and adults with LQTS, it constitutes the most common genetic form associated with LQTS-related perinatal and early-infancy mortality.

LQTS exhibits incomplete penetrance (i.e., not all carriers of the pathogenic mutation will develop a phenotypic expression) and variable expressivity (i.e., the level of phenotypic expression varies among affected patients).

Clinical Presentation and Natural Course

Romano-Ward Syndrome

Most information regarding the clinical features of LQTS have been derived from analysis of data from large series of LQTS patients, the largest of which is the International LQTS Registry. LQTS probands

TABLE 31.2 Common Types of the Long QT Syndrome

	LQT1	LQT2	LQT3
Pathophysiology			
Gene	<i>KCNQ1 (Kv LQT1)</i>	<i>KCNH2 (HERG)</i>	<i>SCN5A</i>
Protein	Kv7.1	Kv11.1	Na _v 1.5
Ionic current	Decreased I_{Ks}	Decreased I_{Kr}	Increased late I_{Na}
Clinical Presentation			
Incidence of cardiac events	63%	46%	18%
Incidence of SCD	4%	4%	4%
Arrhythmia triggers	Emotional/physical stress (swimming, diving)	Emotional stress, arousal (alarm clock, telephone), rest	Sleep/rest
Electrocardiogram	Broad-based T wave	Low-amplitude, bifid T wave	Long isoelectric ST segment
QT response to exercise	Attenuated QTc shortening and an exaggerated QTc prolongation during early and peak exercise	Normal QT during exercise but with exaggerated QT hysteresis	Supernormal QT shortening
Management			
Exercise restriction	+++	++	?
Response to beta-blockers	+++	+++	?
Potassium supplement	+	++	+
Left cervicothoracic sympathectomy	++	++	++
Response to mexiletine	+	+	++

I_{Kr} , Rapidly activating delayed rectifier K⁺ current; I_{Ks} , slowly activating delayed rectifier potassium current; I_{Na} , sodium current; QTc, corrected QT interval; SCD, sudden cardiac death.

are diagnosed at an average age of 21 years. The clinical course of patients with LQTS is variable, and is influenced by age, gender, genotype, environmental factors, therapy, and possibly other modifier genes. At least 37% of individuals with the LQT1 phenotype, 54% with the LQT2 phenotype, and 82% with the LQT3 phenotype remain asymptomatic and many are referred for evaluation because of the diagnosis of LQTS of a family member or the identification of a long QT interval on a surface ECG obtained for unrelated reasons.

Symptomatic patients can present with palpitations, presyncope, syncope, or cardiac arrest. Syncope is the most frequent symptom, occurring in 50% of symptomatic probands by the age of 12 years, and in 90% by the age of 40 years. The incidence of syncope in LQTS patients is approximately 5% per year, but can vary depending on the LQTS genotype. Syncope in patients with LQTS is generally attributed to polymorphic VT (torsades de pointes), but can also be precipitated by severe bradycardia in some patients with LQT3. Cardiac arrest and SCD are usually due to VF. Recurrent syncope can mimic primary seizure disorders.

The incidence of SCD is much lower, approximately 1.9% per year. Nonfatal events (syncope and aborted cardiac arrest) in LQTS patients remain the strongest predictors of subsequent LQTS-related fatal events. The overall risk of subsequent SCD in an LQTS patient who has experienced a previous episode of syncope is approximately 5% per year. Of individuals who die of complications of LQTS, SCD is the first sign of the disorder in an estimated 10% to 15%. The risk for SCD from birth to age 40 years has been reported as approximately 4% in each of the phenotypes.

Risk and lethality of cardiac events among untreated individuals are strongly influenced by the genotype. The frequency of cardiac events is significantly higher among LQT1 (63%) and LQT2 (46%) patients than among patients with the LQT3 genotype (18%). However, the likelihood of dying during a cardiac event is significantly higher among LQT3 patients (20%) than among those with the LQT1 (4%) or the LQT2 (4%) genotype. Overall, LQT3 is to be considered a severe LQTS variant; the first cardiac event is more likely to be lethal and seems to occur later in childhood, during or after puberty.¹⁹

Cardiac events (syncope, cardiac arrest, SCD) in LQTS patients do not occur at random; the factors precipitating cardiac events seem to

be specific for each genetic variant. LQT1 patients present an increased risk during physical or emotional stress (90%), and only 3% of the arrhythmic episodes occur during rest or sleep. Swimming and diving appear as highly specific triggers in LQT1 patients. LQT2 patients are at higher risk for lethal events during arousal (44%), but are also at risk during sleep and at rest (43%). Only 13% of cardiac events occur during exercise. Cardiac events in LQT2 patients are characteristically associated with arousal and auditory stimulation. In fact, the triggering of events by startling, sudden awakening, or sudden loud noises (such as a telephone or alarm clock ring) is virtually diagnostic of LQT2. Notably, individual factors such as gender, location and type of mutation, and QTc prolongation appear to be associated with trigger-specific events; female adolescents with LQT2 appear to experience a greater than ninefold increase in the risk for arousal-triggered cardiac events compared with male adolescents in the same age group. In contrast, gender does not seem to be a significant risk factor for exercise-triggered events among carriers of the same genotype (Fig. 31.3).

On the other hand, LQT3 patients experience cardiac events largely while asleep or at rest (65%) without emotional arousal, and only occasionally during exercise (4%). Notably, the majority of patients continue to experience their cardiac events under conditions similar to their first classified event.²⁰

The effect of gender on outcome is age dependent, with boys being at higher risk than girls during childhood and early adolescence, but no significant difference in gender-related risk being observed between 13 and 20 years. The gender-related risk reverses afterward, and female patients maintain higher risk than male patients throughout adulthood.

The genotype can potentially affect the clinical course of the LQTS and modulate the effects of age and gender on clinical manifestations. Although the three major LQTS genotypes (LQT1, LQT2, or LQT3) are associated with similar risks for life-threatening cardiac events in children and adolescents after adjustment for clinical risk factors (including gender, QTc duration, and time-dependent syncope), the risk for cardiac events is augmented in LQT2 women aged 21 to 40 years and in LQT3 patients greater than 40 years of age. The risk of syncope and SCD decreases during pregnancy but increases in the postpartum period, especially among LQT2 women.

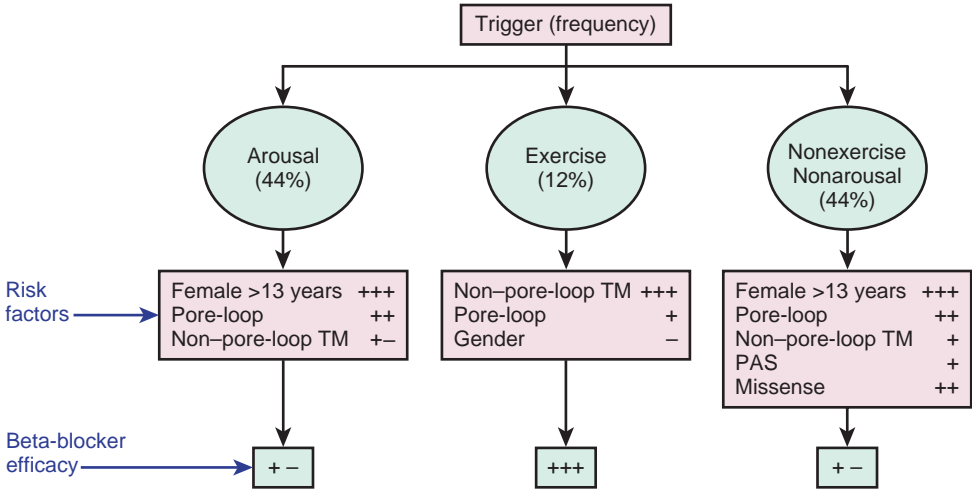


Fig. 31.3 Trigger-Specific Risk Factors and Response to Therapy in Long QT Syndrome Type 2 (LQT2). Plus and minus signs are approximate representations of the risk/response based on the hazard ratios and associated *P* values from the multivariate models. PAS, Per-Arnt-Sim domain of the hERG channel; TM, transmembrane. (Reproduced with permission from Kim JA, Lopes CM, Moss AJ, et al. Trigger-specific risk factors and response to therapy in long QT syndrome type 2. *Heart Rhythm*. 2010;7:1797–1805.)

Jervell and Lange-Nielsen Syndrome

The Jervell and Lange-Nielsen syndrome is the recessive variant of the LQTS, characterized by congenital deafness and cardiac phenotype (QT prolongation, ventricular arrhythmias, and SCD). The Jervell and Lange-Nielsen syndrome is caused by two homozygous or compound heterozygous mutations of one of the two genes (*KCNQ1* and *KCNE1*) that encode components of the I_{Ks} channel.

Patients with Jervell and Lange-Nielsen syndrome have a more severe cardiac phenotype than those with Romano-Ward syndrome. Patients begin to experience cardiac events very early in life; 15% suffer a cardiac event during the first year of life, 50% by age 3 years, and 90% by age 18 years. In untreated patients, approximately 50% die of ventricular arrhythmias by the age of 15 years. Furthermore, SCD occurs in more than 25% of patients despite medical therapy. In addition, complete loss of I_{Ks} in hair cells and endolymph of the inner ear results in congenital bilateral sensorineural deafness.

The conditions that trigger the cardiac events are, overall, very similar to those described for LQT1. Up to 95% of events occur during sympathetic activation (exercise and emotions), and only 5% of the events occur at rest or during sleep.

Andersen-Tawil Syndrome

Andersen-Tawil syndrome (LQT7) is a rare autosomal dominant disorder caused by mutations of the gene *KCNJ2*, which encodes the inward rectifier potassium channel, Kir2.1. This syndrome is characterized by a triad of a cardiac phenotype, a skeletal muscle phenotype (periodic paralysis caused by abnormal muscle relaxation), and distinctive craniofacial and skeletal dysmorphic features (low-set ears, ocular hypertelorism, small mandible, fifth-digit clinodactyly, syndactyly, short stature, scoliosis, and a broad forehead).

Although Andersen-Tawil syndrome is classified as LQTS (LQT7), QT prolongation is more related to a prominent U wave (i.e., prolonged “QTUc interval”) rather than a QTc prolongation. Further, unlike other types of LQTS, cardiac arrhythmias in Andersen-Tawil syndrome are characterized by high burden of asymptomatic PVCs, ventricular bigeminy, or nonsustained VT, with a predominantly benign course and very rare degeneration into hemodynamically compromising rhythms like torsades de pointes. In addition, a specific type of polymorphic VT, bidirectional VT, is observed in Andersen-Tawil syndrome, similar to that observed in CPVT patients. Beta-blockers, Ca^{2+} channel blockers, and flecainide have been utilized for suppression of ventricular arrhythmias in these patients, but the efficacy of these drugs is yet to be proven.²¹

Patients with Andersen-Tawil syndrome present initially with periodic paralysis or cardiac symptoms (palpitations, syncope, or both) in the first or second decade of life. Intermittent weakness occurs spontaneously, or can be triggered by prolonged rest or rest following exertion; however, the frequency, duration, and severity of symptoms are variable between and within affected individuals, and are often linked to fluctuations in plasma K^+ levels. Mild permanent weakness is common.

There is a high degree of variability in penetrance and phenotypic expression. Approximately 60% of affected individuals manifest the complete triad and up to 80% express two of the three cardinal features.

Timothy Syndrome

Timothy syndrome (LQT8) is an extremely rare multisystem disorder caused by mutations of the *CACNA1C* gene, which encodes the L-type Ca^{2+} channel ($Ca_v1.2$), and is characterized by syndactyly, QT prolongation, congenital heart disease, cognitive and behavioral problems, musculoskeletal diseases, immune dysfunction, and more sporadically, autism.

Timothy syndrome is a severe form of LQTS, characterized by a remarkable prolongation of the QTc interval (QTc often exceeding 550 to 600 milliseconds), functional 2:1 AV block (observed in up to 85% of patients, and likely caused by the extremely prolonged ventricular repolarization and refractory periods), and macroscopic T wave alternans (positive and negative T waves alternating on a beat-to-beat basis). In addition, congenital heart defects are observed in approximately 60% of patients and include patent ductus arteriosus, patent foramen ovale, ventricular septal defect, tetralogy of Fallot, and hypertrophic cardiomyopathy. Timothy syndrome is highly malignant; the majority of patients seldom survive beyond 3 years of age. Polymorphic VT and VF occur in 80% of patients (commonly triggered by an increase in sympathetic tone) and are the leading cause of death, followed by infection and complications of intractable hypoglycemia.³

Extracardiac features include cutaneous syndactyly (variably involving the fingers and toes), which is observed in almost all patients. Facial findings (observed in approximately 85% of individuals) include low-set ears, flat nasal bridge, thin upper lip, small upper jaw, small, misplaced teeth, and round face. Neuropsychiatric involvement occurs in approximately 80% of individuals and includes global developmental delays and autism spectrum disorders.

In general, the diagnosis of Timothy syndrome is made within the first few days of life based on the markedly prolonged QT interval and 2:1 AV block. Occasionally, the diagnosis is suspected prenatally because of fetal distress secondary to AV block or bradycardia.

Although LQT8 (Timothy syndrome) is associated with gain-of-function in I_{CaL} , reduction of I_{CaL} influx by Ca^{2+} channel blockade (such as verapamil) failed to shorten QTc or prevent ventricular arrhythmias. A recent report suggested a potential antiarrhythmic benefit of ranolazine (an antianginal agent with inhibitory effects on multiple ion channels) in patients with Timothy syndrome.

Electrocardiographic Features

Abnormal prolongation of the QT interval on the surface ECG, reflecting delayed ventricular repolarization, is the hallmark of LQTS. In addition, T wave abnormalities are encountered in the majority of patients.

QT Interval Measurement

The QT interval is the body surface representation of the duration of ventricular depolarization and subsequent repolarization. Any deviation or dispersion of depolarization (e.g., bundle branch block) or repolarization (e.g., prolongation or dispersion of the action potential duration) results in prolongation of the QT interval.

An accurate measurement of the QT interval is important for the diagnosis of LQTS. A 12-lead ECG tracing at a paper speed of 25 mm/s at 10 mm/mV is usually adequate to make accurate measurements of the QT interval. The QT interval is measured as the interval from the onset of the QRS complex, that is, the earliest indication of ventricular depolarization, to the end of the T wave, that is, the latest indication of ventricular repolarization. The QT interval is measured in all ECG leads where the end of the T wave can be clearly defined (preferably leads II and V_5 or V_6), with the longest value being used. The end of the T wave is the point at which the descending limb of the T wave intersects the isoelectric line. Three to five consecutive cardiac cycles are taken to derive average values for R-R, QRS, and QT intervals.²²

When the end of the T wave is indistinct, or if a U wave is superimposed or inseparable from the T wave, it is recommended that the QT be measured in the leads not showing U waves (often leads aVR and aVL) or that the downslope of the T wave be extended by drawing a tangent to the steepest proportion of the downward limb of the T wave until it crosses the baseline (i.e., the T-P segment) (Fig. 31.4).

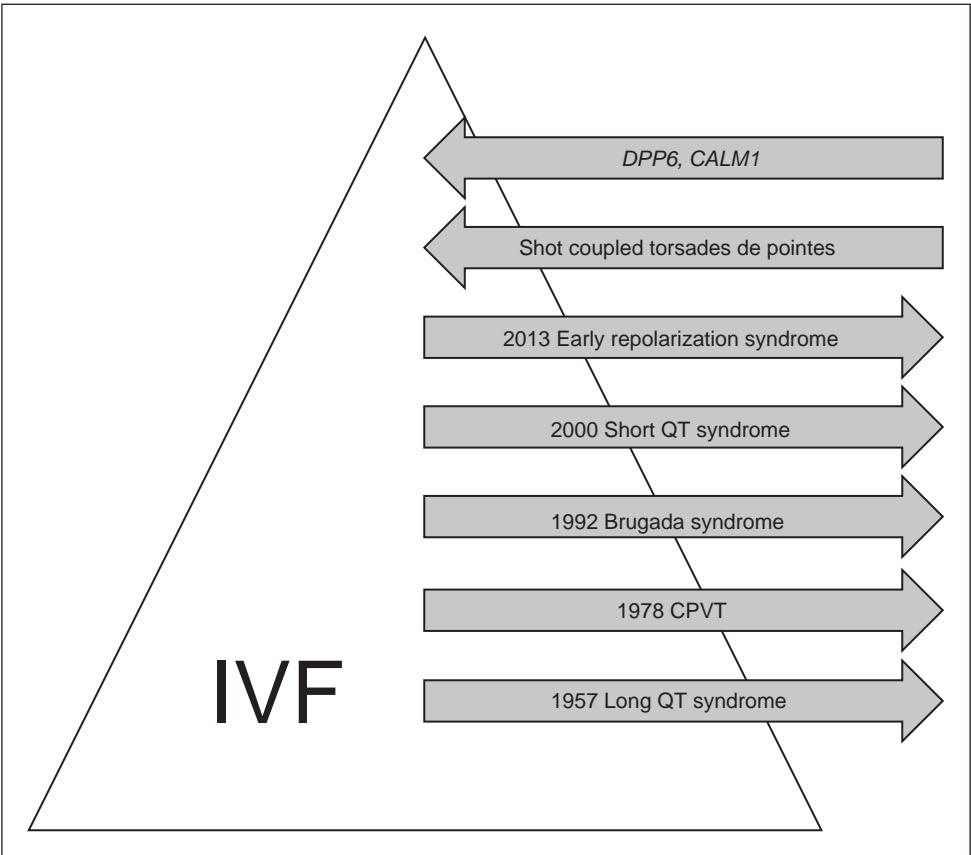


Fig. 31.4 Schematic illustration of the use of the tangent method to define the end of the T wave in normal and abnormal TU-wave morphologies. CPVT, Catecholaminergic polymorphic ventricular tachycardia; IVF, idiopathic ventricular fibrillation. (From Postema PG, Wilde AAM. The measurement of the QT interval. *Curr Cardiol Rev.* 2014;10:287–294.)

However, it should be recognized that defining the end of the T wave in these ways can potentially underestimate the QT interval. Some investigators advocate measurement of both the QT interval and the QTU interval (with the latter measurement taken to the end of the U wave as it intersects the isoelectric line) because the QTU interval probably reflects the total duration of ventricular depolarization.

The highest diagnostic and prognostic value in LQTS families has been observed for QTc in leads II and V₅ of the 12-lead ECG. Thus QTc should be obtained in one of these leads if measured in only a single ECG lead. However, other leads were found to offer similar diagnostic (aVR) or prognostic (V₂/V₃) value alone, and, in general, the lead with the longest QT interval is used for measurement.

The QT interval should ideally be measured at a heart rate closest to 60 beats/min and definitely less than 100 beats/min. The use of beta-blockers or long-term ECG monitoring need to be considered to obtain optimal measurements.

QT Interval Correction for Gender

The QT interval shortens after puberty in males but not in females, resulting in a longer QT in women than in men. The reported gender difference in various studies varies from 6 to 10 milliseconds in older age groups and from 12 to 15 milliseconds in younger adults. Overall, the gender difference in the QTc interval becomes small after 40 years of age and practically disappears in older men and women. Separate gender- and age-specific QT adjustment formulas have been proposed to accommodate these differences.

TABLE 31.3 Formulas for Heart Rate Correction of the QT Interval	
Bazett	QTcB = QT/(R-R interval) ^{1/2} (all intervals in seconds)
Framingham-Sagie	QTcFa = QT + 154(1 – 60/HR)
Fridericia	QTcFi = QT/(R-R interval) ^{1/3}
Hodges	QTcH = QT + 1.75(HR – 60)
Nomogram-Karjalainen	QTcN = QT + nomogram correction factor
Rautaharju	QTcRa = QT – 155 × (60/HR – 1) – 0.93 × (QRS – 139) + k (k = –22 msec for men, and –34 msec for women)

HR, Heart rate.

QT Interval Correction for Heart Rate

Because the heart rate (R-R cycle length) is the primary modifier of ventricular action potential, QT interval measurements must be corrected (QTc) for the baseline R-R interval to allow for comparisons. Various correction formulas have been developed (Table 31.3), the most widely used being the formula derived by Bazett in 1920 from a graphic plot of measured QT intervals in 39 young subjects. The Bazett correction, however, performs less well at high and low heart rates (under-corrects at fast heart rates and overcorrects at slow heart rates).

In addition to the Bazett formula, many other correction formulas, such as the Framingham-Sagie, Fridericia, Hodges, and Nomogram-Karjalainen formulas, have been proposed. In a study comparing the accuracy of those five different QT correction formulas for determining drug-induced QT interval prolongation, the Bazett correction formula provided the most marked QTc variations at heart rates distant from 60 beats/min. The Fridericia formula was found to overestimate QTc at faster heart rates, being more reliable at slower heart rates. Conversely, the Hodges, Nomogram, and Framingham formulas demonstrated less QTc variability over the whole range of the investigated heart rates and seemed to be similarly satisfactory at heart rates of up to 100 beats/min. Among them, the Hodges method, followed by the Nomogram-Karjalainen method, appeared to be the most accurate in determining the correct QTc and subsequently in guiding clinical decisions.²²

Nonetheless, the Bazett formula remains the one most commonly used to measure the QT interval for the diagnosis of LQTS. However, when a prolonged QTc is observed during faster heart rates (greater than 90 beats/min), it is important to repeat the ECG once the heart rate slows down, to minimize the error that can potentially be introduced by heart rate correction formulas.

Importantly, there exists a substantial interindividual variability of the relationship between QT duration and heart rate (the QT/R-R relationship). In contrast, a high intraindividual stability of the QT/R-R pattern has been demonstrated, suggesting that a genetic component might partly determine individual QT length. Therefore population-based and averaged QT correction cannot accurately predict a normal QT interval at a given R-R interval in a *given* patient. Individual-specific QT/R-R hysteresis correction in combination with individualized heart rate correction can potentially reduce intraindividual QTc variability.

QT Interval Correction to QRS Duration

The QT interval prolongs in ventricular conduction defects, mainly due to a delay in depolarization (i.e., prolongation of the QRS duration) and not in repolarization. Most QT correction formulae do not take bundle branch block into consideration. Only a few formulae (such as the Rautaharju formula, the Bogossian formula, and the JT index) are designed to include bundle branch blocks in their calculations, but none of them have been widely adopted in clinical practice.

A widely used approach is to apply the Bazett formula to the uncorrected QT interval and accept a longer QTc as the upper limit of acceptable (550 milliseconds rather than 500 milliseconds). Another method to adjust the QT measurement after the development of a bundle branch block is to subtract the difference in QRS widths before and after the block (when such information is available). A third method is to measure the JT interval from the end of the QRS complex to the end of the T wave. Unlike the QTc interval which describes both cardiac depolarization and repolarization, the JTc interval is independent of the QRS duration and thus represents only repolarization ($JTc = QTc - QRS$). If the JT interval is chosen, normal standards established specifically for the JT interval should be used. QT and JT adjustment formulas have recently been introduced for use in the setting of prolonged ventricular conduction. With confirmation, they may be incorporated into automated algorithms to provide appropriate correction factors.^{23,24} However, because of delay in depolarization in left bundle branch block (LBBB), repolarization begins before the end of the QRS complex (i.e., before the J point); hence, the JT interval likely underestimates the duration of repolarization, particularly when QRS duration was very prolonged (greater than 175 milliseconds).²⁵

A recent study in a series of patients with intermittent LBBB found that the net increase in QRS duration contributes to 92% of the extra time in measured QT in LBBB, and a new formula (the Wang formula) was developed to calculate the true QT: True QT interval = measured

QT in LBBB – $(0.86 * QRS \text{ in LBBB} - 71)$. The QT so derived can then be corrected using the Bazett or other standard formulation.²⁵

QT Interval Measurement During Right Ventricular Pacing

Reliable estimation of the QT interval in ventricular paced rhythm is challenging. It has been demonstrated that the Rautaharju formula (see Table 31.3) yields QTc values during ventricular pacing that are closest with the non-paced QTc interval values; however, this formula is complex to apply and exhibits significant interaction with heart rate changes.

The Framingham and Nomogram correction methods were found to offer the most optimal balance for assessing the QTc interval, including minimal interaction between pacing mode and heart rate. The use of the Bazett formula significantly exaggerates the QTc rate dependency during ventricular pacing and, therefore, is less reliable.²⁶

A recent study suggested the use of the Framingham and Nomogram methods to calculate the corresponding nonpaced intrinsic QTc interval from the measured ventricular paced QTc interval (regardless of heart rate) by subtracting 43 milliseconds in normal-QTc patients, and 37 milliseconds (for the Framingham method) or 36 milliseconds (for the Nomogram method), in prolonged-QT patients.²⁶

Another study found that RV pacing causes prolongation of the QT due to a paced LBBB without prolongation of the JT interval, and that QT prolongation caused by ventricular pacing constitutes about 50% of the QRS width. The Bogossian formula subtracts this value from the measured ventricular paced QT interval ($QT \text{ in LBBB} = \text{measured QT interval} - 50\% * QRS \text{ duration}$).²³ Although this formula can provide a simple method for estimating the nonpaced intrinsic QT interval, it tends to overcorrect the QT interval, that is, making the QT shorter than it should be.

The paced JTc interval was found to more accurately represent ventricular repolarization (as compared to the paced QTc interval) and mirror repolarization changes observed during nonpaced rhythm. However, as noted previously, the sensitivity of the JT interval in identifying patients with delayed ventricular repolarization decreases with increasing QRS duration, and that can artificially shorten the calculated QT interval. Therefore the JT interval appears ineffective in predicting delayed repolarization in patients with a very wide QRS.^{24,25}

QT Interval Prolongation

The diagnosis of QT interval prolongation can be challenging because of the difficulty in defining the “end” of the T wave and the need for correction for heart rate, age, and gender. This is further complicated by the lack of linear behavior of the Bazett formula at slower and faster heart rates as well as the arbitrary definition of the gender-based diagnostic cutoff values that define an abnormally prolonged QTc (QTc of 450 milliseconds for men and QTc of 460 milliseconds for women; Table 31.4).

TABLE 31.4 Suggested Bazett-Corrected QT Interval Values for Diagnosis of QT Prolongation

Rating	1–15 Years	Adult Man	Adult Woman
Normal	<440	<430	<450
Borderline	440–460	430–450	450–470
Prolonged	>460	>450	>470

Values given in milliseconds.

From Goldenberg I, Moss AJ. Long QT syndrome. *J Am Coll Cardiol*. 2008;51:2291–2300.

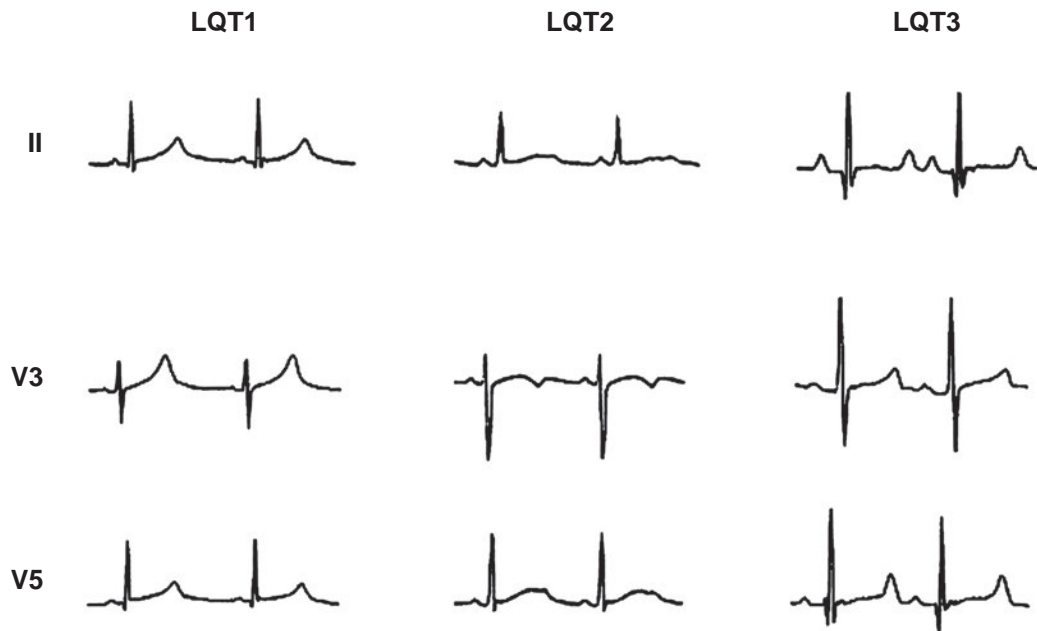


Fig. 31.5 Electrocardiogram Recordings From Leads II, V₃, and V₅ in Three Patients From Families With Long QT Syndrome (LQTS). The typical morphology of LQT3 with straight ST segment and small T wave is shown in the right panel. (From Ruan Y, Liu N, Bai R, Priori SG, Napolitano C. Congenital long QT syndrome type 3. *Card Electrophysiol Clin*. 2014;6:705–713.)

Furthermore, no single QTc value separates all LQTS patients from healthy controls. In fact, LQTS cannot be excluded merely by the presence of a normal QTc interval. The QT interval is subject to large variations even in healthy individuals, and substantial overlap exists with QTc values obtained from LQTS mutation carriers in the range between 410 and 470 milliseconds. In up to 40% of LQTS patients, QTc intervals fall in the normal range. On the other hand, QTc values greater than 470 milliseconds in men and greater than 480 milliseconds in women are practically not observed among healthy individuals (especially when their heart rate is 60 to 70 beats/min). Therefore unless excessive QTc prolongation (greater than 500 milliseconds, corresponding to the upper quartile among affected genotyped individuals) is present, the QTc interval should always be evaluated in conjunction with the other diagnostic criteria.

Of note, a considerable variability in QTc interval duration can be observed in patients with LQTS when serial ECGs are recorded during follow-up. This time-dependent change in QTc duration is an important determinant of the phenotypic expression of the disease. Up to 40% of patients with LQTS will have QTc greater than 500 milliseconds at least once during long-term follow-up, but only 25% will have that degree of QT prolongation during their initial evaluation. The maximal QTc duration measured at any time before age 10 years was shown to be the most powerful predictor of cardiac events during adolescence, regardless of baseline, mean, or most recent QTc values. In addition, the QT interval may normally exhibit individual variations during the day. Therefore in the case of borderline QTc prolongation, serial ECG and 24-hour Holter recordings can potentially assist in establishing QT prolongation.

T Wave Morphology

ST-T wave abnormalities are common among LQTS patients, and some of the ST-T changes are characteristic for a certain genotype. Specifically, “broad,” “notched,” and “late” T waves are associated with LQT1,

LQT2, and LQT3, respectively, although these features are often subtle and inconsistently observed (Fig. 31.5).²⁷

Patients with LQT1 commonly exhibit a smooth, broad-based T wave that is present in most leads, and particularly evident in the precordial leads. The T wave generally has a normal to relatively high amplitude and often no distinct onset. LQT2 patients generally present with low-amplitude T waves, which are notched or bifid in approximately 60% of carriers. The bifid T wave can be confused with a T-U complex; however, unlike the U waves, the bifid T waves are usually present in most of the 12 ECG leads. LQT3 patients often show late-onset, narrow, peaked, and/or biphasic T waves with a prolonged isoelectric ST segment. Occasionally, the T wave is peaked and asymmetrical with a steep downslope. These ST-T wave patterns can be seen in 88% of LQT1 and LQT2 carriers and in 65% of LQT3 carriers.

No specific T wave pattern has been suggested in the LQT5 and LQT6 syndromes. T-U wave abnormalities such as biphasic T waves following long pauses like those found in the LQT2 syndrome are commonly observed in the LQT4 syndrome. Enlarged U waves separated from the T wave are reported to be characteristic ECG features in the LQT7 syndrome. Severe QT interval prolongation and macroscopic T wave alternans can be observed in LQT8.

Despite the initial enthusiasm in achieving a genotype-phenotype correlation for specific LQT-associated genes, this approach failed to provide a high diagnostic yield because of the frequent exceptions in T wave morphology presentation. Furthermore, the T wave pattern can vary with time, even in the same patient with a specific mutation. Therefore other T wave parameters, such as duration, amplitude, asymmetry, and flatness, as well as the interval from the peak of the T wave to the end of the T wave (Tp-e), have been used as highly specific quantitative descriptors (see later).

Of note, quantitative analysis of T wave morphology in lead V₆ was found in a recent report to be capable of distinguishing patients with genetically proven LQTS from matched controls and even permits

identification of over 80% of patients with LQTS, despite having a normal resting QTc. The potential implications of this tool for universal screening for LQTS warrant further investigation.²⁸

Torsades de Pointes

Torsades de pointes is a polymorphic VT occurring in the setting of QT interval prolongation (acquired or congenital LQTS) and is characterized by a progressive change of the electrical axis, typically rotating 180 degrees in approximately 10 to 12 cycles. This results in the characteristic sinusoidal twisting of the peaks of the QRS complexes around the isoelectric line of the recording; hence, the name *torsades de pointes* or “twisting of the points.” However, this characteristic pattern may not be evident in all ECG leads. Also, during a very fast VT, periodic decrease in the amplitude of the entire QRS-T complex can be observed with less distinct shifts in the QRS axis. Occasionally, a polymorphic QRS configuration is observed without displaying those characteristics. Of note, different patterns can be seen in different VT episodes from the same patient.²⁹

The VT is frequently preceded by a variable period of bigeminal rhythm caused by one or two PVCs coupled to the prolonged QT interval of the preceding basic beat. The tachycardia rate is typically in the range of 150 to 300 beats/min. In many cases, torsades de pointes is a self-limiting arrhythmia that spontaneously dies out after a few tens of cycles; however, most patients experience multiple episodes of the VT occurring in rapid succession. Only in a minority of cases does torsades de pointes degenerate into VF, which almost without exception leads to SCD if immediate rescue intervention, including defibrillation, is not performed.

Dispersion of Repolarization

Prolongation of the action potential duration (and QT interval) per se is not pathogenic, as evidenced by the fact that a homogeneous action potential duration prolongation (such as occurs following amiodarone therapy) fails to generate reentry. As demonstrated in experimental models of the LQTS, prolonged repolarization, transmural dispersion of repolarization, and EADs are the three electrophysiological (EP) components linked to the genesis of torsades de pointes. Transmural dispersion of repolarization arises from repolarization heterogeneity that exists between the epicardial and putative midmyocardial (M) cells that lie toward the endocardium of the LV wall. These midmyocardial cells are especially sensitive to a repolarization challenge and exhibit significant prolongation of the action potential duration compared with other transmural cell types. Several ECG indices have been proposed in recent years as noninvasive surrogates for transmural dispersion of repolarization, including the T wave peak to T wave end (Tp-e) interval, QT interval dispersion, and ratio of the amplitudes of the U and T waves.

Tp-e interval. Although controversy exists, some experimental models suggest that the peak of the T wave coincides with the end of epicardial repolarization (the shortest action potentials), whereas the end of the T wave coincides with the end of repolarization of the M cells (the longest action potentials). Hence, the Tp-e interval in each surface ECG lead has been proposed as an index of transmural repolarization. However, subsequent investigations using intact hearts have challenged this concept and suggested that, in vivo, the Tp-e interval is a measure of “global” dispersion of repolarization of the whole ventricle rather than “transmural” dispersion.

Because increased dispersion of repolarization promotes reentry and enhances arrhythmogenesis, prolongation of the Tp-e interval has been proposed as a more sensitive predictor of risk for arrhythmic events than the QT interval; the latter represents the total duration of electrical ventricular activation and not necessarily the dispersion of

transmural repolarization. In fact, a prolonged Tp-e interval has been shown to be a marker of increased arrhythmogenic risk in patients with Brugada syndrome, hypertrophic cardiomyopathy, and structural heart disease, as well as in certain populations.

Although changes in the Tp-e interval can potentially show the dynamicity of the dispersion of repolarization in clinical settings in LQTS patients, the role of measuring the Tp-e interval in these patients has yet to be clearly defined. In fact, the normal value of the Tp-e interval on the ECG has not been established. Nonetheless, an interval of more than 100 milliseconds is uncommon in normal subjects compared with that in patients with LQTS (9% vs. 55%).

On ambulatory monitoring, LQT2 exhibits a larger-degree of dispersion of repolarization, as measured by the Tp-e interval, compared with LQT1 and normal hearts. In fact, the Tp-e interval has been proposed as a diagnostic criterion in differentiation between LQT2 and LQT1 patients. Also, LQT1 patients exhibit abrupt increases in Tp-e intervals at elevated heart rates, whereas LQT2 patients exhibit increases in dispersion of repolarization at a much wider range of rates. In addition, beta-adrenergic stimulation (exercise or epinephrine infusion) increases dispersion of repolarization in both LQTS models, transiently in LQT2 and persistently in LQT1.

QT interval dispersion. An alternate approach to determine repolarization heterogeneity is provided by the dispersion of the QT interval. The QT dispersion index is obtained by the difference between the maximal and minimal QT intervals (QT_{max} – QT_{min}) measured on a 12-lead ECG. The QT dispersion index reflects the spatial heterogeneity of myocardial refractoriness more accurately than single QT values. Visualization of the differences in QT interval in the different ECG leads can be facilitated by the display of temporally aligned simultaneous ECG leads with a slight separation on the amplitude scale.

Importantly, QT interval dispersion measurements are subject to similar shortcomings encountered with the QT interval assessment, as a large overlap between affected and healthy individuals is observed. Further, accurate measurement on the scalar ECG at a paper speed of 25 mm/s is difficult. The same caveat applies to measuring the Tp-e interval.

U wave-to-T wave amplitude ratio. The ratio of the amplitudes of the U and T waves has been suggested as the clinical counterpart of EADs, and a progressive increase in this ratio was found to precede the onset of torsades de pointes in an experimental model of LQTS. In addition, the increment in U wave amplitude after a PVC has been suggested as a marker for arrhythmia risk in “pause-dependent” LQTS.

In patients with bifid T waves, some investigators used the late component of the T wave, rather than the U wave. The diurnal maximal ratio between late and early T wave peak amplitude was found to correlate with a history of LQTS-related symptoms better than the baseline QTc interval in both LQT1 and LQT2 patients, and the diurnal distributions of maximal T2-to-T1 wave amplitude ratios were similar to those of cardiac events.

Diagnosis of the Long QT Syndrome

According to the most recent consensus statement, LQTS can be diagnosed in individuals testing positive for an unequivocally pathogenic mutation in one of the LQTS genes. In the absence of a pathogenic mutation, and in the absence of a secondary cause for QT prolongation, the diagnosis of LQTS requires the presence of one of the following: (1) QTc interval of at least 500 milliseconds (using the Bazett formula) on repeated 12-lead ECGs; (2) QTc interval between 480 and 499 milliseconds on repeated 12-lead ECGs in conjunction with unexplained syncope; or (3) Schwartz score of at least 3.5 points (see later).

In addition, LQTS can be suspected in individuals with QTc values exceeding 450 milliseconds for men and exceeding 460 milliseconds

for women; the probability for LQTS increases if these subjects also have a history of syncope and familial SCD. On the other hand, LQTS is very unlikely among men with QTc less than 390 milliseconds and among women with QTc less than 400 milliseconds.

It is important to note that the LQTS is largely a clinical diagnosis, primarily based on the clinical presentation, personal and family history, and ECG findings. A detailed family history of syncope and SCD is essential, not only in first-degree relatives (mother, father, siblings, children), but also in more distant relatives. Also, the family history should also be investigated for other potential manifestations of malignant arrhythmias that might not have been classified as cardiac in origin, such as drowning, death while driving, epileptic seizures, and SIDS. Data on comorbidities in evaluated individuals or family members (such as congenital deafness) should also be acquired. Clinical features such as triggers of syncope and specific QT morphological attributes in patients in whom the clinical diagnosis has been made can suggest the affected gene in 70% to 90% of patients.

Importantly, a significant proportion (20% to 40%) of patients with genetically proven LQTS have normal or borderline QTc measurements at rest ("concealed" LQTS). It has been reported that these silent mutation carriers account for 36% of LQT1 patients, 19% of LQT2 patients, and 10% of LQT3 patients. Therefore the diagnosis of LQTS should not be excluded based solely on a QTc interval in the normal range (400 to 450 milliseconds), and additional testing is indicated whenever the clinical history requires exclusion of LQTS. In this setting, obtaining a resting ECG periodically and ambulatory ECG monitoring can sometimes uncover abnormal prolongation of the QTc interval, given the considerable day-to-day variability in QTc of patients with LQTS. In addition, reviewing the ECGs of all family members can be valuable because some family members can have obvious QT prolongation. The probability of LQTS in an index subject can be augmented if one of those family members has QTc prolongation.

Several provocative tests have been used to unmask LQTS patients with normal QTc on resting ECG. These include QT measurement upon abrupt standing, in the recovery phase of exercise testing, or during infusion of epinephrine. Also, genetic testing is recommended in patients with a strong clinical index of suspicion for LQTS. Although these diagnostic tools can all contribute to identifying patients with LQTS, a gold standard diagnostic tool is still lacking. Invasive EP testing is generally not useful in the diagnosis of LQTS.¹

Clinical Scoring Systems

When the diagnosis of LQTS is suspected but uncertain, a clinical scoring system (Schwartz score) has been developed to enhance the diagnostic reliability of clinical parameters and to estimate the probability of LQTS. The most recent (2011) update of the Schwartz score incorporates ECG features in combination with personal clinical history and family history. Scores were arbitrarily divided into three probability categories, providing a quantitative estimate of the risk for LQTS (Table 31.5). A score of 3.5 or higher makes the diagnosis of LQTS very likely and should compel further investigation, including genetic testing when available. Among patients with suspected LQTS (based on QTc interval prolongation or clinical history), "high probability" of LQTS (score greater than or equal to 3.5) using the Schwartz criteria identified LQTS mutation carriers with a sensitivity of 89% and a specificity of 82%. Further testing is required in the group with "intermediate probability" of LQTS to confirm or exclude the diagnosis, including serial ECGs, Holter recordings, and provocative testing.^{30,31}

Ambulatory Cardiac Monitoring

Holter monitoring is not sufficiently well standardized to serve in the primary assessment for ventricular repolarization analysis, and only

TABLE 31.5 Diagnostic Criteria for the Long QT Syndrome

			Points
Electrocardiographic Findings^a			
A	QTc ^b	≥480 msec	3
		460–479 msec	2
		450–459 (male) msec	1
B	QTc ^b fourth minute of recovery from exercise stress test	≥480 msec	1
C	Torsade de pointes ^c		2
D	T wave alternans		1
E	Notched T wave in three leads		1
F	Low heart rate for age ^d		0.5
Clinical History			
A	Syncope ^e	With stress	2
		Without stress	1
B	Congenital deafness		0.5
Family History			
A	Family members with definite LQTS ^e		1
B	Unexplained sudden cardiac death younger than age 30 among immediate family members ^e		0.5

Score: ≤1 point: low probability of LQTS. 1.5–3 points: intermediate probability of LQTS. ≥3.5 points high probability.

^aIn the absence of medications or disorders known to affect these electrocardiographic features.

^bQTc calculated by the Bazett formula where QTc = QT/√RR.

^cMutually exclusive.

^dResting heart rate below the second percentile for age.

^eThe same family member cannot be counted in A and B. (From Di Fusco SA, Palazzo S, Colivicchi F, Santini M. The influence of gender on heart rhythm disease. *Pacing Clin Electrophysiol.* 2014;37:650–657.)

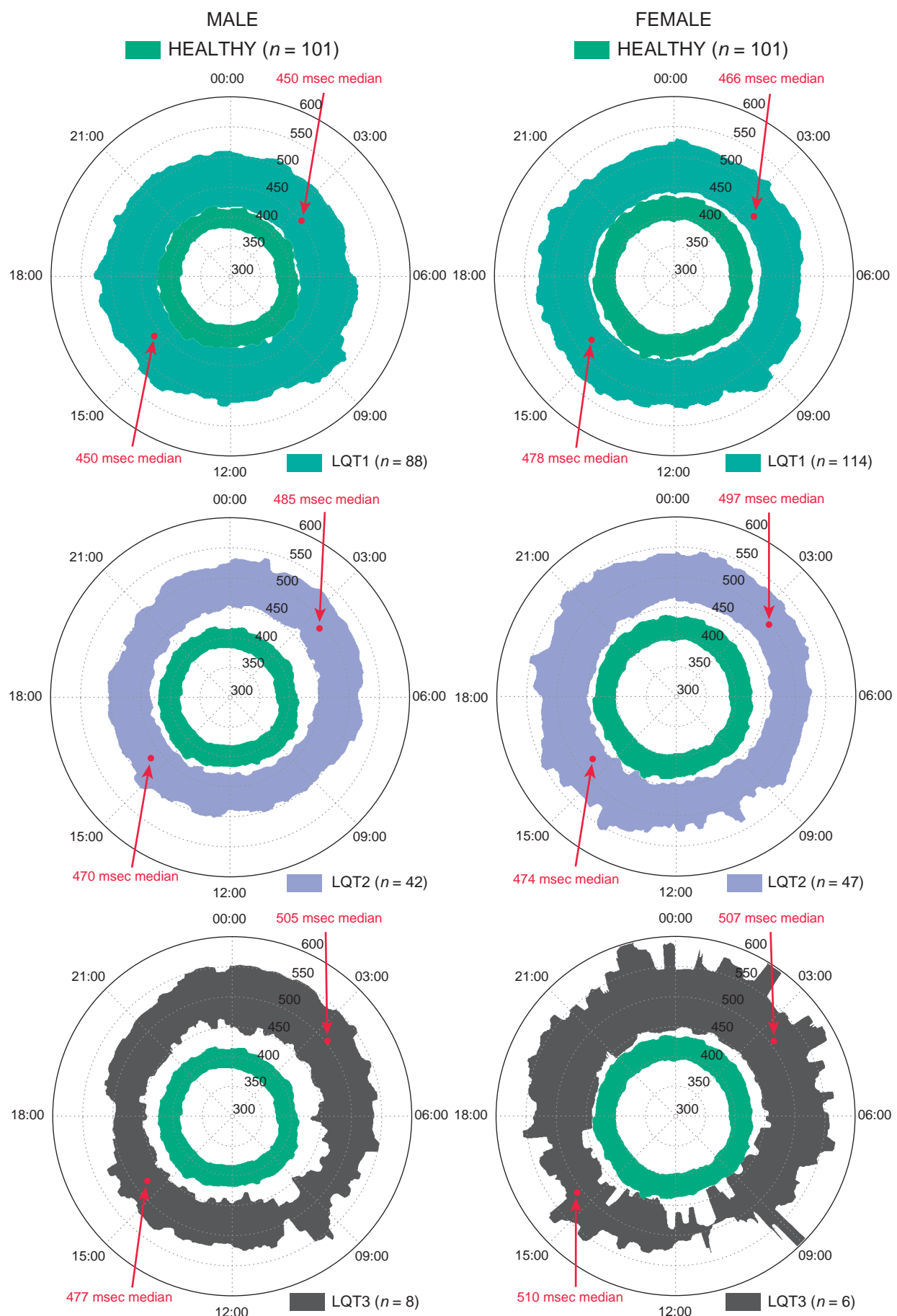
From Schwartz PJ, Crotti L. QTc behavior during exercise and genetic testing for the long-QT syndrome. *Circulation.* 2011;124:2181–2184.

rarely will show spontaneous arrhythmias in LQTS patients. However, this method can sometimes be used for the detection of extreme QT interval events that occur infrequently during the day. An important value of Holter recordings lies in showing T wave changes characteristic of LQTS, which can become evident especially during sleep or following post-extrasystolic pauses.³²

A recent study described a novel computer algorithm that measures QTc in a beat-to-beat manner during 24-hour Holter monitoring. The QTc measurements for a population or for an individual patient are displayed on a plot ("QTc clock" plot) to illustrate QT dynamics and characterize the extent and duration of QT prolongation. Using this technology, unique patterns of QT prolongation were observed in patients with LQT1 and LQT2. LQT1 patients were more likely to have diagnostic QTc prolongation during the daytime hours than during the night, likely correlating with the level of sympathetic activity (eFig. 31.3). Conversely, LQT2 patients showed more QT prolongation during the night. Whether these observations can be used to distinguish between the different LQTS genotypes or to predict arrhythmogenic risk requires further investigation.³³

QT Interval Response to Abrupt Standing

The brief tachycardia associated with abrupt standing can potentially uncover patients with insufficient QT adaptation abilities and poor



eFig. 31.3 QTc Clock. QTc clock plots for long QT syndrome type 1 (*LQ1*) males and females (top left and right panels, respectively), *LQ2* males and females (middle left and right panels, respectively), and *LQ3* males and females cohorts (bottom left and right panels, respectively). Each area is defined by the middle 68th percentile of QTc values, that is, same percentage as ± 1 SD, measured across all Holter recordings, for each 1-minute slice. The dark green area represents the expected range of QTc variations in our healthy cohort. The figure highlights the changes in QT prolongation in *LQ2* and *LQ3* cohorts during the night. This phenomenon is expressed as graph asymmetry in which the area corresponding to *LQ2*/*LQ3* cohort stretches away from the normal value during the night (22:00–08:00). Arrows indicate median QTc between two periods of the day: 3:00–4:00 a.m. and 3:00–4:00 p.m. Note that the *LQ3* ranges are computed from only six female and eight male patients. (From Page A, Aktas MK, Soyata T, Zareba W, Couderc J-P. “QT clock” to improve detection of QT prolongation in long QT syndrome patients. *Heart Rhythm*. 2016;13:190–198.)

repolarization reserve, which characterize LQTS. Initially, an ECG is obtained in the supine position; then, the patient is asked to stand up briskly and a second ECG is obtained.

In one report, postural-induced QTc prolongation was more than 30 milliseconds in 68% of patients with “concealed” LQTS. Also, a QTc cutoff value of 490 milliseconds yielded a sensitivity of 89% and a specificity of 87% for the diagnosis of LQTS in patients with no excessive prolongation of the supine QT intervals (i.e., less than 480 milliseconds for females, less than 470 milliseconds for males).²² Postural QTc prolongation can be attenuated with beta-blockade.

Furthermore, T wave morphology changes exposed by quick standing are useful for diagnosing LQTS. The diagnosis of LQTS can be made with a higher degree of confidence when QT prolongation is accompanied by abnormal T wave morphology. The value of postural changes of T wave morphology for determining the specific LQTS genotype is modest, being most useful for LQT2, less useful for LQT1, and least useful for LQT3.³⁴

QT Interval Response to Exercise

Exercise testing can be useful to assess QT adaptation to heart rate, a measure of the integrity of the I_{Ks} channels. Changes in QTc duration and prolonged QT hysteresis during exercise testing can be helpful in identifying patients with LQTS and even in predicting the genotype. Gradual supine bicycle testing can help minimize signal artifact from upper body motion observed during treadmill exercise.

In particular, the QTc at 4 minutes of recovery after maximal exercise discriminates between patients with LQTS and healthy subjects. In one study of patients with normal or borderline QTc intervals at baseline (i.e., less than 480 milliseconds for females, less than 470 milliseconds for males), a QTc greater than or equal to 480 milliseconds during the fourth minute of recovery identified LQTS patients with a sensitivity of 94% and a specificity of 90%. However, these diagnostic strategies have not been meticulously studied in an unselected population suspected of LQTS.²²

In addition, a gene-specific QTc interval behavior during exercise has been reported. Genetic mutations in LQT1 result in reduction of the amplitude of I_{Ks} , one of the dominant K^+ currents responsible for repolarization especially at rapid heart rates. Attenuation of I_{Ks} results in failure of the QT to adapt (i.e., failure to shorten) in response to increasing heart rate. A maladaptive, paradoxical prolongation of the QTc interval during the recovery phase (QTc greater than 470 milliseconds or a Δ QTc [QTc at 3 minutes of recovery minus the baseline supine QTc] greater than 30 milliseconds) was found to distinguish patients with manifest or concealed LQT1 from normal subjects and those with LQT2 and LQT3 genotypes.

In contrast, patients with LQT2 mutations have normal QT shortening or minimal QTc prolongation during exercise, but they characteristically demonstrate an exaggerated QT hysteresis compared with LQT1 patients and normal subjects. QT hysteresis is normally measured by comparing the QT intervals during exercise versus the recovery period at comparable heart rates (e.g., when the heart rate accelerates to approximately 100 beats/min during early exercise, and when the heart rate decelerates to approximately 100 beats/min during the recovery phase). In LQT2 patients, the QT fails to shorten at these intermediate heart rates in early exercise because of attenuated I_{Kr} (a so-called I_{Kr} zone). This is followed by recruitment of the unimpaired, sympathetically responsive I_{Ks} , resulting in appropriate QT shortening at faster heart rates through to peak exercise, which persists into the recovery phase. This leads to increased QT hysteresis, that is, the QT interval is significantly longer during exercise than during recovery at comparable heart rates.

The LQT3 phenotype is characterized by a constant shortening of the QT interval with exercise because of stimulation of the intact I_{Ks}

channel and augmentation of a late inward Na^+ current. In fact, the QT interval in LQT3 patients shortens during exercise much more in LQT1 and LQT2 patients and even more than in healthy controls.

In addition, exercise treadmill testing can reveal the characteristic T wave morphology in patients with LQT1 and LQT2 syndromes.

Exercise-induced QTc prolongation and QT hysteresis can be attenuated with beta-blockade; therefore beta-blocker therapy should be discontinued before exercise testing.

Importantly, induction of arrhythmias during exercise is very rare in LQTS patients. Exercise-induced ventricular ectopy exceeding isolated PVCs is observed in less than 10% of patients. The presence of exercise-induced ventricular ectopy beyond single, isolated PVCs must prompt intense evaluation because it was found to have a positive predictive value exceeding 90% for the presence of significant cardiac pathology. However, CPVT, rather than LQTS, is the far more likely diagnosis.³²

Epinephrine QT Stress Test

Catecholamine provocation testing can help diagnose patients with concealed LQT1, with a positive predictive value approaching 75% and a negative predictive value of 96%. Furthermore, epinephrine provocation testing was found to be a powerful test to predict the genotype of LQT1, LQT2, and LQT3 syndromes.

Two major protocols have been developed for epinephrine infusion. Using the “escalating-dose infusion protocol,” epinephrine infusion is initiated at 0.025 μ g/kg per minute and then increased sequentially every 10 minutes to 0.05, 0.1, and 0.2 μ g/kg per minute. The 12-lead ECG is continuously recorded during sinus rhythm under baseline conditions and during epinephrine infusion. The QT interval is measured 5 minutes after each dose increase. Epinephrine infusion should be stopped for systolic blood pressure greater than 200 mm Hg, sustained or nonsustained VT, frequent PVCs (greater than 10 per minute), T wave alternans, or patient intolerance. A paradoxical QT interval response (prolongation of the absolute QT interval of greater than or equal to 30 milliseconds) during low-dose epinephrine infusion provides a presumptive clinical diagnosis of LQT1, with a positive predictive value of 75%. The diagnostic accuracy can be reduced in patients receiving beta-blockers.

Using the “bolus and infusion protocol,” an epinephrine bolus (0.1 μ g/kg) is administered and immediately followed by continuous infusion (0.1 μ g/kg per minute) for 5 minutes. The QT interval is measured 1 to 2 minutes after the start of epinephrine infusion when the R-R interval is the shortest (which represents the peak epinephrine effect) and 3 to 5 minutes after the start of epinephrine infusion (which represents the steady-state epinephrine effect). During the epinephrine test, patients with LQT1 manifest prolongation of the QTc at the peak of the epinephrine effect, which is maintained under steady-state conditions of epinephrine. In contrast, epinephrine prolongs the QTc more dramatically at the peak of epinephrine infusion in LQT2 patients, but the QTc returns to baseline levels under steady-state conditions. A much milder prolongation of QTc at the peak of epinephrine has been described in LQT3 patients and in healthy subjects, and it returns to the baseline levels under steady-state conditions. A subject is considered to have an LQT1 response if the QTc increase in the peak phase is greater than 35 milliseconds and is maintained throughout the steady-state phase (Fig. 31.6). LQT2 response is likely if the peak QTc increase of greater than 80 milliseconds is not maintained in the steady-state phase. In one report, the sensitivity and specificity of the epinephrine test to differentiate LQT1 from LQT2 were 97% and 96%, those from LQT3 were 97% and 100%, and those from healthy subjects were 97% and 100%, respectively, when Δ QTc greater than 35 milliseconds at steady state was used. The sensitivity and specificity to differentiate LQT2 from

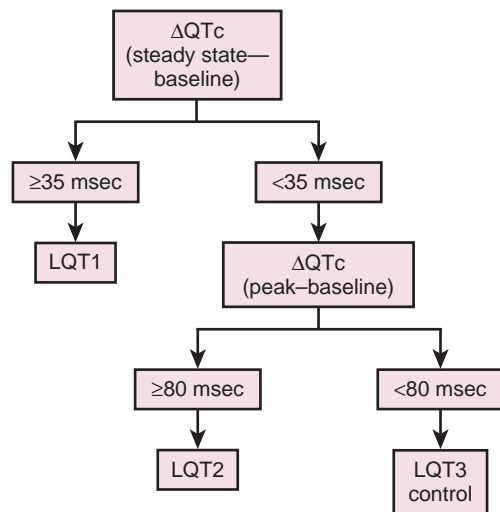


Fig. 31.6 Epinephrine Provocative Testing for the Diagnosis of Long QT Syndrome (LQTS). Control, Normal subjects; LQT, long QT syndrome genotype; QTc, corrected QT interval.

LQT3 or healthy subjects were 100% and 100%, respectively, when Δ QTc greater than 80 milliseconds at peak was used.

The escalating-dose infusion protocol is generally better tolerated by the patient and carries a lower incidence of false-positive responses. On the other hand, the bolus and infusion protocol offers the ability to monitor the temporal course of the epinephrine response at peak dose (during the bolus) and during steady state (during the infusion), which is particularly important in individuals with LQT2 in whom transient prolongation of the uncorrected QT interval can occur, followed by subsequent shortening.

Genetic Testing

Although the diagnosis of LQTS can frequently be certain based on clinical diagnostic measures, genetic testing can still be of value; identification of the specific disease-causing mutation can potentially guide therapeutic choice, enhance risk stratification, and facilitate the identification of affected family members and implementation of lifestyle adjustment and presymptomatic treatment. Furthermore, genetic testing may be important in the identification of concealed LQTS, because a significant proportion (25% to 50%) of individuals with genetically proven LQTS can have a nondiagnostic QTc.

However, genetic testing remains expensive. Depending on the stringency of clinical phenotype assessment, the yield for positive genetic results in LQTS ranges from 50% to 78%, and is highest among tested individuals with the highest clinical probability (i.e., those with longer QTc intervals and more severe symptoms). The remaining probands with a strong clinical probability of LQTS will have a negative genetic test result, probably because of technical difficulties with genotyping, noncoding variants, or as yet unidentified disease-associated genes. Therefore a negative genetic test in a subject with clinical LQTS (i.e., genotype-negative/phenotype-positive LQTS) does not provide a basis to exclude the diagnosis. Nonetheless, a negative genetic test renders the diagnosis of LQTS very unlikely in those patients with low to moderate pretest probability based on clinical findings.³²

There is also the potential for false-positive results; genetic testing may identify novel mutations of unclear significance, which could represent normal variants, and require validation and further analysis (e.g., linkage within a family or in vitro studies).

Currently, comprehensive or targeted (LQT1, LQT2, and LQT3) genetic testing is recommended for symptomatic patients with a strong

clinical index of suspicion for LQTS (Schwartz score greater than or equal to 3.5 points) and for asymptomatic patients with QT prolongation (QTc greater than or equal to 480 milliseconds [prepuberty] or greater than or equal to 500 milliseconds [adults]) in the absence of other clinical conditions that might prolong the QT interval. In addition, LQTS genetic testing may be considered for the asymptomatic subject with a QTc greater than or equal to 470 milliseconds on serial ECGs but with negative family history.³²

Differential Diagnosis: Acquired Long QT Syndrome

It is important to distinguish acquired factors that result in QT interval prolongation from the inherited form of LQTS. Acquired LQTS is far more prevalent than the congenital form. However, the occurrence of torsade de pointes is far less common than that of QT prolongation. Nonetheless, there is an increased risk for torsade de pointes whenever the QTc interval exceeds 500 milliseconds and whenever the QTc interval increases by more than 60 milliseconds from baseline, especially when the increase occurs rapidly.

In contrast to the most common types of congenital LQTS (LQT1 and LQT2), a short-long-short pattern of R-R cycles constitutes the typical pattern of initiation of torsades de pointes in acquired LQTS. The long pause exaggerates the QT interval prolongation, and the short-long-short sequence is thought to promote torsades de pointes by increasing transmural dispersion of repolarization. The short-long R-R interval is usually caused by a short-coupled PVC followed by a compensatory pause and then another PVC occurring during the T wave. However, because of the underlying QT interval prolongation, this R-on-T PVC does not have the short coupling interval that is characteristic of idiopathic VF. Torsades de pointes can also occur in association with bradycardia or frequent pauses (sometimes referred to as “pause-dependent LQTS”).³⁵

Etiology

Acquired causes of abnormal prolongation of the QT interval include myocardial ischemia, cardiomyopathies, electrolyte abnormalities (hypokalemia, hypomagnesemia, and hypocalcemia), autonomic influences, drugs, hypothyroidism, hypothermia, pheochromocytoma, intracranial bleeding, and bradycardia.

Hypokalemia causes prolongation of the action potential duration because of reductions in multiple K^+ currents including I_{Kr} , I_{K1} , and I_{to} . Low extracellular K^+ levels accelerate fast inactivation of the hERG channel and further decrease I_{Kr} .^{36,37}

Acquired LQTS is also observed in the setting of extreme bradycardia, in particular, bradycardia complicating acquired AV block (spontaneous or iatrogenic). In fact, the original description of torsade de pointes, the hallmark arrhythmia of the LQTS, was entirely based on patients with LQTS complicating atrioventricular block. It is important to note that QT prolongation in patients with complete AV block is more pronounced than that in response to similar degrees of sinus bradycardia, and it is the magnitude of this QT prolongation in response to bradycardia, rather than the bradycardia per se, that determines the risk of torsade de pointes. It has been proposed that a change in QRS morphology, commonly observed in the setting of complete AV block but not during SND, leads to T wave changes associated with cardiac memory, which contributes to excessive QT prolongation. In one report, patients who developed a change in QRS morphology at the time of AV block had a sevenfold higher incidence of torsades de pointes and a change in the QRS axis seemed to be associated with an even greater incidence. These observations suggest that repolarization changes influenced by cardiac memory play a role in arrhythmia risk during AV block. Also, premature beats that lead to short-long-short cycles can foster the development of torsade de pointes.^{10,38}

By far, the most common environmental stressor resulting in acquired LQTS is drug therapy, including antiarrhythmic drugs, some antihistamines, antipsychotics, and antibiotics (www.qtdrugs.org). Noncardiovascular drugs that can potentially precipitate QT interval prolongation and arrhythmias comprise approximately 2% to 3% of total prescribed medications. Indeed, the risk of acquired LQTS is the most common cause of withdrawal or restriction of drugs that have already been marketed. For specific drugs, the incidence of torsade de pointes is difficult to quantify, and ranges from extremely low for many of the macrolide antibiotics, to 0.5% to 1% for drugs such as sotalol and azimilide, to 1.5% to 9% for quinidine.^{36,39}

The vast majority of drugs associated with the acquired form of LQTS are known to interact with the hERG channel (which mediates I_{Kr}), likely because of unique structural properties rendering this channel unusually susceptible to blockade by a wide range of different drugs. Compared with other cardiac K^+ channels, the hERG channel has a large, funnel-like vestibule that allows many small-sized molecules to enter and block the channel (see Chapter 2). The more spacious inner cavity is due to the lack of the Pro-X-Pro sequence motif in the S6 segment (which is present in most other voltage-gated K^+ channels and is believed to induce a sharp bend in the inner S6 helices of voltage-gated K^+ channels, reducing the inner vestibule), presumably facilitates access of drugs to the pore region from the intracellular side of the channel to block the channel current. In addition, the hERG channel contains two aromatic sites inside its pore (not present in most other K^+ channels), which provide high-affinity binding sites for aromatic moieties of a wide range of structurally diverse compounds. Interaction of these compounds with the channel's pore causes functional alteration of its biophysical properties, occlusion of the permeation pathway, or both.

Other mechanisms underlying drug-induced LQTS have been recently described, including disruption of hERG channel protein trafficking, with consequent reduction of surface membrane expression of otherwise functional channels (e.g., pentamidine), or folding and assembly of channel subunits. The accessory β -subunit (MiRP1, *KCNE2*) of the hERG channel also determines the drug sensitivity.

Risk Factors of Drug-Induced Long QT Syndrome

Several factors can potentially increase the susceptibility to drug-induced LQTS, including female gender (70% of patients with drug-induced torsades de pointes are women), advanced age, hypokalemia, hypomagnesemia, hypocalcemia, bradycardia, congestive heart failure, LV hypertrophy, recent conversion from AF, and the presence of QT interval prolongation on baseline ECG. Other risk factors include high drug doses (with the exception of quinidine), rapid IV infusion, and concurrent use of other drugs that prolong the QT interval or promote other QT-prolonging factors (such as bradycardia or electrolyte abnormalities). Also, conditions leading to accumulation of QT-prolonging drugs in plasma, such as from drug-drug interactions, are in general risk factors for torsades de pointes. These include the presence of renal or hepatic failure and the concomitant use of drugs that slow drug metabolism or impair drug excretion.¹⁰ In addition, genetically determined variability in pharmacodynamics (e.g., polymorphisms and mutations of the cytochrome system) can be responsible for significant variations in drug response. Most patients with drug-induced torsades de pointes have one or more risk factors.^{10,37,40}

Hospitalized patients appear to be at greater risk of drug-induced QT interval prolongation and torsades de pointes than outpatients, likely due to a greater preponderance of risk factors, including structural heart disease, advanced age, electrolyte abnormalities, bradycardia, or renal or hepatic disease.⁴¹ A risk score was developed for predicting the risk of developing acquired LQTS in hospitalized patients in cardiac care units (Table 31.6). The risk score effectively distinguished hospital-

TABLE 31.6 Calculation of Risk Score for QTc Interval Prolongation

Risk Factor Points	
Age ≥ 68 years	1
Female sex	1
Loop diuretic	1
Serum potassium ≤ 3.5 mEq/L	2
Admission QTc ≥ 450 msec	2
Acute myocardial infarction	2
≥ 2 QTc-prolonging drugs	3
Sepsis	3
Heart failure	3
One QTc-prolonging drug	3
Maximum Risk Score	21

From Tisdale JE, Jaynes HA, Kingery JR, et al. Development and validation of a risk score to predict QT interval prolongation in hospitalized patients. *Circ Cardiovasc Qual Outcomes*. 2016;6:479–487.

ized patients at moderate or high risk for QTc interval prolongation from those at low risk. The occurrence of drug-induced torsades de pointes is an extremely rare event in patients without any risk factors. Over 90% of patients who develop torsades de pointes have at least one, and 71% of patients have at least two risk factors.^{42,43}

Genetics

Evidence suggests that drug-induced LQTS can represent a “forme fruste” of congenital LQTS in a significant proportion of patients, whereby drug challenge merely exposes the presence of the congenital form of the syndrome. This is likely related to a redundancy in repolarizing currents; normal repolarization is accomplished by multiple ion channels, providing a safety reserve for repolarization (the concept of “repolarization reserve”), which is genetically determined and compensates for any factor (e.g., drugs or genetic mutation) that might either decrease repolarizing or increase depolarizing currents during the action potential. As a result, a mutation or polymorphism in one of the LQTS genes can be clinically inapparent until another insult to repolarization, such as a drug, hypokalemia, or hypomagnesemia, is superimposed.³⁶

Mutations of ion channel genes responsible for LQTS have been implicated as a risk factor. In fact, previously unrecognized congenital LQTS, of any subtype, can be identified in as many as 36% to 40% of drug-induced LQTS patients. In addition, polymorphisms (i.e., common genetic variations present in greater than 1% of the population) in cardiac ion channels can potentially increase the risk for the development of drug-induced torsades de pointes. In a recent study, drug-induced LQTS patients had a greater burden of amino acid coding variants (missense, nonsynonymous, or frameshift), than the control subjects, suggesting that multiple rare variants, notably across congenital LQTS genes, predispose to drug-induced LQTS.⁴⁴

In a large cohort of acquired LQTS subjects, the QTc interval remained prolonged (although to a milder degree than that observed in congenital LQTS carriers) in a significant proportion of patients even after the QT-prolonging factors are removed (withdrawal of culprit drugs or correction of serum electrolytes), suggesting that acquired LQTS could represent at least in part a latent genetic predisposition. Further, 28% of acquired LQTS subjects were found to harbor mutations in one of the major LQTS-related genes (most commonly in the *KCNH2* gene). Even among the “true” acquired LQTS, i.e., those with normal QT interval outside the triggering episode, 23% had congenital LQTS-causing

TABLE 31.7 Predictors of the Probability of Being Mutation Carriers in Acquired Long QT Syndrome

	OR (95% CI)	P Value
Age, <40 vs. ≥40 years	2.5 (1.2–5.3)	0.020
QTc, >440 vs. ≤440 msec	5.2 (2.2–12.2)	<0.001
Clinical status, symptomatic vs. asymptomatic	10.6 (1.3–83.5)	0.025

CI, Confidence interval; OR, odds ratio.

From Itoh H, Crotti L, Aiba T, et al. The genetics underlying acquired long QT syndrome: impact for genetic screening. *Eur Heart J*. 2016; 37:1456–1464

mutations. Predictors for carrying a pathogenic mutation in acquired LQTS included (1) age less than 40 years, (2) baseline QTc interval exceeding 440 milliseconds, and (3) history of symptoms at the time of acquired LQTS diagnosis (Table 31.7). Of the acquired LQTS patients carrying a mutation, 88% had two or more of those predictors, while only 3% of patients with one or none of those risk factors had a mutation. Therefore some investigators have proposed genetic screening in acquired LQTS subjects with two or more of the risk factors to enable “cascade screening” in their family members and thereby prevent avoidable risks of life-threatening arrhythmias.⁴⁵

Management

First-line treatment approaches to torsades de pointes include removal of the offending causes, the use of IV magnesium, maintenance of high-normal serum K⁺ level, and avoidance of QT-prolonging agents. In some refractory cases, isoproterenol infusion or temporary transvenous overdrive pacing may be required to increase heart rate, which can shorten the QT interval and suppress torsades de pointes.

Magnesium suppresses torsades de pointes without shortening the QT interval, presumably by suppressing the EADs that trigger torsades de pointes. EAD suppression by magnesium has been attributed to its Ca²⁺ channel-blocking effects but may also be mediated by a reduction of the late component of the sodium current (I_{NaL}). The value of acute K⁺ repletion is less well documented than that of IV magnesium for the acute treatment of drug-induced torsades de pointes. Normal levels of both potassium and magnesium should be maintained aggressively in hospitalized patients at risk.⁴⁶

Recent studies suggested that mexiletine (a strong I_{NaL} blocker) may be an effective treatment for acute termination of torsades de pointes in several acquired causes of QT interval prolongation. Although torsades de pointes often responds to a lidocaine bolus, arrhythmias tend to recur despite continuous infusions. In contrast, ranolazine (an I_{NaL} blocker), flecainide (a strong I_{Na} blocker), and verapamil (a strong I_{CaL} blocker) also block I_{Kr}, thus limiting their use in patients with drug-induced LQTS.³⁵ Of note, a recent report demonstrated potential benefit of oral progesterone for the prevention of drug-induced QT interval prolongation.¹⁸

Risk Stratification

The clinical course in LQTS patients is not uniform and is influenced by many factors, including age, gender, genotype, environmental factors, therapy, and possibly other modifier genes.

Clinical Markers of Risk

Syncope. Nonfatal events (syncope and aborted cardiac arrest) in LQTS patients remain the strongest predictor of subsequent LQTS-

related fatal events, and the overall risk of subsequent SCD in an LQTS patient who has experienced a previous episode of syncope is approximately 5% per year.

The risk of subsequent syncope episodes can be reduced with beta-blocker therapy; however, patients experiencing syncope while receiving beta-blockers are at high risk of subsequent cardiac events, a risk similar to that observed in patients who are not treated with beta-blockers.

Both the timing and frequency of syncopal events are related to the subsequent risk of cardiac events. Patients with recent (within the past 2 years) syncope and a higher number of syncopal events during this period carry a higher risk of subsequent cardiac events.

However, it is important to distinguish between suspected arrhythmogenic and nonarrhythmogenic causes of syncope, especially given the fact that neurocardiogenic syncope is not uncommon in this patient population and its occurrence does not impact the prognosis negatively. A detailed clinical history in LQTS patients presenting with syncope is imperative, since clinical features (in particular, the occurrence of prodromes and the presence of specific triggers) can allow distinction between suspected arrhythmogenic and nonarrhythmogenic etiologies in a large proportion of cases.

Family history. The incomplete penetrance and variable expressivity in LQTS preclude predicting severity of symptoms in relatives of a symptomatic LQTS patient. In fact, SCD of a sibling (at any age) does not seem to contribute to increased personal risk of LQTS-related life-threatening cardiac events. Instead, the risk of adverse events in relatives appears to be determined more by the individual's own risk factors (QTc duration, personal history of syncope, and gender).

Gender. The effect of gender on outcome is age dependent, with boys exhibiting a significant (71% to 85%) increase in risk for syncope, aborted cardiac arrest, or SCD as compared with girls during childhood and early adolescence. However, a gender risk reversal occurs after age 14 years, in which girls exhibit an 87% increase in the risk of cardiac events compared with boys among probands and a 3.3-fold increase in the risk among affected family members. When only life-threatening cardiac events (aborted cardiac arrest or SCD) are considered, the onset of gender risk reversal occurs at a later age. The cumulative probability of a first life-threatening cardiac event from age 1 to 12 years is 5% in boys compared with only 1% among girls, whereas in the age range of 12 to 20 years, there is no significant gender difference in risk. Risk reversal for the endpoint of aborted cardiac arrest or SCD occurs after the age of 20 years, and women maintain higher risk than men throughout adulthood.

Importantly, the effect of gender on outcome appears to be genotype dependent. Among those younger than 15 years, male LQT1 patients exhibit the highest risk of cardiac events; female LQT1 patients had intermediate risk; and both male and female LQT2 patients had the lowest risk. No significant gender-related difference in risk was shown among LQT2 and LQT3 children. In contrast, in the 15- through 40-year-old age group, the risk is highest among LQT2 women, intermediate among LQT1 women, and lowest among LQT1 and LQT2 men.¹⁹

Age. Risk factors in LQTS are time dependent and age specific (Table 31.8). LQTS patients who experience an aborted cardiac arrest during the first year of life are at a very high risk for subsequent life-threatening cardiac events during the first decade of life. The risk factors for a cardiac event in LQTS infants also include a QTc of at least 500 milliseconds, a heart rate not exceeding 100 beats/min, and female gender.

In LQTS children, risk factors for life-threatening cardiac events include male gender, a history of syncope at any time during childhood, and a QTc duration greater than 500 milliseconds.

Among adolescent patients with suspected LQTS, recent episodes of syncope (in particular within the past 2 years) and QTc greater than

TABLE 31.8 Age-Specific Risk Factors for Life-Threatening Cardiac Events in Long QT Syndrome Patients^a

Age Group	Risk Factor	Hazard Ratio (P Value)	Beta-Blocker Efficacy, % Reduction (P Value)
Childhood (1–12 years)	Male gender	3.96 (<0.001)	73% (0.002)
	QTc >500 msec	2.12 (0.02)	
	Prior syncope		
	Recent (>2 years)	14.34 (<0.001)	
	Remote (≥2 years)	6.45 (<0.001)	
Adolescence (10–20 years)	QTc >530 msec	2.3 (<0.001)	64% (0.01)
	Syncopal events		
	≥2 syncopal events in past 2 years	18.1 (<0.001)	
	1 syncopal event in past 2 years	11.7 (<0.001)	
	≥2 syncopal events in past 2–10 years	5.8 (<0.001)	
	1 syncopal events in past 2–10 years	2.7 (<0.001)	
Adulthood (18–40 years)	Female gender	2.68 (<0.05)	60% (<0.01)
	QTc duration		
	QTc ≥500 msec	6.35 (<0.01)	
	QTc = 500–549 msec	3.34 (<0.01)	
	Prior syncope	5.10 (<0.01)	
Adulthood (41–60 years) ^b	Recent syncope (<2 years)	9.92 (<0.001)	42% (0.40) ^c
	QTc > 530 msec	1.68 (0.06)	
	LQT3 genotype	4.76 (0.02)	

^aFindings are from separate multivariable Cox models in each age group for the endpoint of aborted cardiac arrest or sudden cardiac death.

^bBecause long QT syndrome (LQTS)-related events are more difficult to delineate in the older age group, the endpoint in the 41- to 60-year-old age group comprised aborted cardiac arrest or death from any cause.

^cLack of a statistically significant beta-blocker effect in this age group may relate to the broad endpoint of death from any cause.

QTc, Corrected QT interval.

From Goldenberg I, Moss AJ. Long QT syndrome. *J Am Coll Cardiol*. 2008;51:2291–2300.

530 milliseconds predict increased risk of LQTS-related cardiac events. Although LQT1 genotype predicts higher risk in patients not more than 14 years of age (especially boys), the risk is higher for LQT2 in patients 15 years of age or older (especially women).

In adult patients, predictors of worse outcome include a QTc greater than 500 milliseconds, female gender, and history of syncope before age 18 years. In addition, patients with LQT2 mutations appear to be at a greater risk for a cardiac event than patients with LQT1 or LQT3 genotypes.

Beyond 40 years of age, recent syncope (within the past 2 years) appears to be the predominant risk factor in affected subjects, and those with a positive mutation had a significantly higher mortality, particularly those with an LQT3 mutation. Furthermore, women with a QTc greater than 470 milliseconds are at a higher risk of LQTS-related cardiac events, whereas in men, event rates are similar in the various QTc categories. After the age of 60 years, the risk of death due to LQTS competes with other disease entities that may lead to death.

Electrocardiographic Markers of Risk

QT interval prolongation. The QTc interval is the best prognostic ECG parameter in LQTS families. A QTc interval of at least 470 milliseconds is a predictor for increased risk for symptoms, whereas a QTc of at least 500 milliseconds predicts an increased risk of life-threatening cardiac events. Although there is no threshold of QTc prolongation at which torsades de pointes is certain to occur, a gradual increase in risk for torsades de pointes is observed as the QTc interval increases. Each 10-millisecond increase in QTc contributes approximately a 5% to 7% additional increase in risk for torsades de pointes. Therefore a patient with a QTc of 540 milliseconds has a 63% to 97% higher risk of

developing torsades de pointes than a patient with a QTc of 440 milliseconds.

Importantly, considerable time-dependent variability and instability of ventricular repolarization exist in LQTS. Thus risk stratification should take into account the risk associated with variability in the duration of the QTc interval in the individual LQTS patient during follow-up. In fact, it has been shown that the maximum QTc duration measured at any time before age 10 was the most powerful predictor of cardiac events during adolescence, regardless of baseline, mean, or most recent QTc values.

Furthermore, a considerable variability in the duration of the QTc interval exists among LQTS patients with identical mutations. Evidence suggests that mutation-specific QTc variability (defined as QTc standard deviation [QTcSD] among all carriers of a specific mutation) provide incremental prognostic information for risk stratification that is independent of those related to the individual's own QTc. A greater degree of repolarization instability associated with specific LQTS mutations (manifesting as a high mutation-specific QTcSD) was identified as an independent risk predictor even in high-risk patients with long QTc durations. It has been reported that every 20-millisecond increment in mutation-specific QTcSD resulted in a 33% increased risk for cardiac events after adjustment for the patient-specific QTc, and patients who had mutations with QTcSD of 45 milliseconds or more experienced a significant 48% increase in the risk of cardiac events compared with patients who had mutations with QTcSD less than 45 milliseconds. These findings emphasize the importance of checking mutation-specific effects in various genetic backgrounds to identify mutations that are more susceptible to intrinsic or extrinsic modifying factors. It is important to note that the prognostic implications of QTcSD appear to be

genotype specific; the risk associated with a higher QTcSD was pronounced among patients with LQT1, whereas in patients with LQT2, no significant association of QTcSD with cardiac events was found.⁴⁷

T-U wave morphology. The ratio of the amplitude of the U wave to that of the T wave has been suggested as the clinical counterpart of EADs; a progressive increase in the ratio of the U wave to the T wave preceded the onset of torsades de pointes in an experimental model of LQTS. In addition, the increment in U wave amplitude after a PVC has been suggested as a marker for arrhythmia risk in “pause-dependent” LQTS.

In patients with bifid T waves, the diurnal maximal ratio between late and early T wave peak amplitude was found to correlate with a history of LQTS-related symptoms better than the baseline QTc interval in both LQT1 and LQT2 patients, and can potentially be used to assess the risk of symptoms in asymptomatic patients with known type 1 or 2 LQTS genotype. In LQT1 patients, a ratio of at least three suggests a high probability of being symptomatic whereas a ratio not exceeding two suggests a low probability. Among LQT2 patients, ratios suggestive of being symptomatic or asymptomatic are, respectively, at least 2.4 and not more than 1.5.

Of note, the presence of macroscopic T wave alternans (bidirectional beat-to-beat changes in T wave polarity) indicates electrical instability and high acute risk of ventricular arrhythmias.

Genetic Markers of Risk

The genotype is an important predictor of LQTS-related cardiac events. The risk of cardiac events has been shown to be significantly higher in LQT1 and LQT2 when compared with LQT3, with events occurring at a younger age. The cumulative mortality, however, appears to be similar regardless of the genotype, since patients with LQT3 develop arrhythmias less often, but these are more likely to be lethal when they ultimately occur.

LQT1 patients exhibit a 49% increase in the risk of cardiac events as compared with LQT2 patients. However, in the 15- through 40-year-old age group, the risk of a first cardiac event is significantly higher among LQT2 patients (67% increase in the risk as compared with LQT1 patients). Among LQTS patients receiving beta-blocker therapy, the LQT2 and LQT3 genotypes are associated with increased risk of arrhythmic events as compared with LQT1.

In addition to identifying the LQT genotype, knowing the specific mutation and its biophysical function can help improve risk stratification. For LQT1, patients with mutations in the transmembrane domain of the KCNQ1 channel had more frequent cardiac events (syncope, aborted cardiac arrest, or SCD) and a greater risk of the first cardiac event occurring at a younger age than did patients with C-terminal mutations. For LQT2, pore mutations have a more severe clinical course and a higher frequency of arrhythmic events occurring at a younger age when compared with nonpore mutations. In particular, missense mutations in the transmembrane pore (S5-loop-S6) region appear to be associated with the highest risk of clinical arrhythmia.

Preliminary data for LQT3 patients also suggest that the location and biophysical function of the mutation can play a role in determining the severity of the clinical phenotype. Mutations with a dominant-negative effect on ion channel function (greater than 50% reduction in function) have a more severe phenotype compared with mutations exhibiting haploinsufficiency (less than or equal to 50% reduction in function).

Jervell and Lange-Nielsen syndrome and the Timothy syndromes (LQT8) have a highly malignant course with poor prognosis, and are less likely to respond to beta-blocker therapy alone. In contrast, the Andersen-Tawil syndrome has a generally more benign clinical course in terms of arrhythmic death.

The presence of multiple mutations (the so-called “double hits,” observed in 8% to 11% of patients with LQTS) is associated with a significantly higher risk for life-threatening cardiac events as compared with patients with a single mutation. Also, among patients with multiple mutations, a double hit in a single gene (compound heterozygosity) was associated with a greater risk for life-threatening cardiac events than a double hit in different genes (digenic heterozygosity).^{48,49}

Principles of Management

The main therapeutic modalities for the prevention of life-threatening cardiac events include beta-blockers, left (sometimes bilateral) cervicothoracic sympathetic denervation, and implantable cardioverter-defibrillator (ICD) implantation. In nongenotyped patients, beta-blockers comprise the mainstay therapy, whereas cervicothoracic sympathetic denervation and ICD implantation are therapeutic options in high-risk LQTS patients who experience recurrent cardiac events despite beta-blocker therapy (Table 31.9). Renal sympathetic denervation may play a future role.

Pharmacological Therapy

Treatment with beta-blockers is associated with a significant (53% to 64%) reduction in risk of LQTS-related life-threatening events (syncope, cardiac arrest, and SCD), regardless of age (see Table 31.8). The benefit appears to be most substantial in patients at highest risk for cardiac events. On the other hand, very low-risk patients (no history of syncope, QTc less than 500 milliseconds, girls younger than 14 years, LQT2 men of any age, and LQT1 women older than 14 years) have such a small frequency of events that beta-blockers may not provide a substantial benefit.⁵⁰

Genetic data can be used to guide the therapeutic management plan. Given the critical role of catecholamines in precipitating arrhythmias in LQT1, beta-blocker therapy is particularly effective for this group of patients; approximately 90% of LQT1 patients treated with beta-blockers remained free from syncope and cardiac arrest after a mean follow-up time of 5.4 years and showed a total mortality rate of 1%. Although beta-blockers were generally considered to have lower efficacy in LQT2 patients as compared with LQT1 patients, recent data argue for a similar magnitude of risk reduction in LQT2 patients (beta-blocker therapy decreased cardiac events from 58% to 23% after an average follow-up of 4.9 years on therapy). The higher residual event rate in LQT2 patients while receiving beta-blocker therapy is likely due to a higher overall event rate in patients with this genotype, rather than to an attenuated efficacy of medical therapy in this high-risk population. Of note, a trigger-specific response to beta-blocker therapy exists within the LQT2 population; beta-blockers appear to be more protective against exercise-triggered cardiac events than arousal- or non-exercise-related events (see Fig. 31.3).

On the other hand, the value of beta-blocker therapy in LQT3 patients is debated. These patients continue to experience high rates of cardiac events despite beta-blocker therapy. Among LQT3 patients receiving beta-blocker therapy, the adjusted risk for a cardiac event is fourfold higher than among LQT1 patients. However, when excluding LQT3 patients with the most severe phenotype (i.e., patients who had suffered a cardiac event during infancy and those with QTc greater than 600 milliseconds), beta-blocker therapy appears to be beneficial in LQT3. It is important to note, however, that prolongation of the QT intervals is aggravated at slow heart rates; thus a reduction in heart rate with beta-blockers can potentially pose a therapeutic problem in these patients.¹⁹

Currently, beta-blockers are considered the mainstay therapy for the prevention of life-threatening cardiac events and, given the approximately 12% risk of SCD as the first manifestation of LQTS, they should

TABLE 31.9 Expert Consensus Recommendations on Long QT Syndrome (LQTS) Therapeutic Interventions

Class I	<ol style="list-style-type: none"> The following lifestyle changes are recommended in all patients with a diagnosis of LQTS: <ol style="list-style-type: none"> Avoidance of QT-prolonging drugs (www.qtdrugs.org) Identification and correction of electrolyte abnormalities that may occur during diarrhea, vomiting, metabolic conditions, or imbalanced diets for weight loss. Beta-blockers are recommended for patients with a diagnosis of LQTS who are: <ol style="list-style-type: none"> Asymptomatic with QTc ≥ 470 msec <i>and/or</i> Symptomatic for syncope or documented ventricular tachycardia/ventricular fibrillation (VT/VF). Left cardiac sympathetic denervation (LCSD) is recommended for high-risk patients with a diagnosis of LQTS in whom: <ol style="list-style-type: none"> Implantable cardioverter-defibrillator (ICD) therapy is contraindicated or refused <i>and/or</i> Beta-blockers are not effective in preventing syncope/arrhythmias, not tolerated, not accepted, or contraindicated. ICD implantation is recommended for patients with a diagnosis of LQTS who are survivors of a cardiac arrest. All LQTS patients who wish to engage in competitive sports should be referred to a clinical expert for evaluation of risk.
Class IIa	<ol style="list-style-type: none"> Beta-blockers can be useful in patients with a diagnosis of LQTS who are asymptomatic with QTc ≤ 470 msec. ICD implantation can be useful in patients with a diagnosis of LQTS who experience recurrent syncope events while on beta-blocker therapy. LCSD can be useful in patients with a diagnosis of LQTS who experience breakthrough events while on therapy with beta-blockers/ICD. Sodium channel blockers can be useful, as add-on therapy, for LQT3 patients with a QTc > 500 msec who shorten their QTc by > 40 msec following an acute oral drug test with one of these compounds.
Class III	<ol style="list-style-type: none"> Except under special circumstances, ICD implantation is not indicated in asymptomatic LQTS patients who have not been tried on beta-blocker therapy.

From Priori SG, Wilde AA, Horie M, et al. HRS/EHRA/APHRS expert consensus statement on the diagnosis and management of patients with inherited primary arrhythmia syndromes. *Heart Rhythm*. 2013;10:1932–1963.

be considered the first-line measure in all nongenotyped patients and in patients with LQT1 or LQT2 genotypes, regardless of their symptomatic or risk status (Fig. 31.7). Possible exceptions could include very low-risk LQTS patients (based on clinical and ECG parameters) in whom beta-blocker therapy may be considered on an individual basis. That said, it is important to understand that all these recommendations are based on observational studies and not randomized clinical trials.

Propranolol and nadolol are the beta-blockers most widely used. Limited data exist regarding the effectiveness of other beta-blockers in preventing cardiac events in patients with LQTS, although some evidence suggests the superiority of nadolol and propranolol as compared to metoprolol in LQT1 and LQT2 patients. Long-acting medications are preferred to improve compliance and avoid wide fluctuations in blood levels. The nonselective beta-blocker nadolol (which has strong negative chronotropic effect and long half-life [20 to 24 hours]) is the most preferred first-choice therapy in patients with LQTS. Propranolol is probably the preferred beta-blocker in LQT3 patients, given its direct late Na⁺ current blocking properties.^{32,51}

The protective effect of beta-blockers is related to their adrenergic blockade, which diminishes the risk of cardiac arrhythmias; hence, the goal of beta-blocker therapy is to blunt the maximal heart rate during exercise, and the adequacy of beta-blockade should be assessed by exercise testing or ambulatory monitoring. It is recommended to start at a low dose and slowly up-titrate the dose (over several weeks, especially in asymptomatic patients) to help improve patient tolerance and compliance, which can potentially lead to otherwise unnecessary ICD implantation. Of note, beta-blockers do not substantially shorten the QT interval.^{1,52,53}

Despite the beneficial effects of beta-blockers, a high rate of residual cardiac events has been reported in patients receiving beta-blocker therapy, occurring in 10%, 23%, and 32% of LQT1, LQT2, and LQT3 patients, respectively, after a mean follow-up time of 5.4 years. Therefore

patients who remain symptomatic despite treatment with beta-blockers should be considered for other therapeutic modalities. Interestingly, it has been reported that noncompliance is an important cause of events occurring during beta-blocker treatment in LQT1 patients.

Implantable Cardioverter-Defibrillator

ICD therapy is highly effective to prevent SCD in high-risk LQTS patients (mortality of 1.3% in high-risk ICD patients compared with 16% in non-ICD patients during a mean follow-up time of 8 years). Therefore ICD implantation should be considered for secondary prevention in patients with prior cardiac arrest and for primary prevention in those who experience unexplained syncope or ventricular tachyarrhythmias while receiving beta-blocker therapy (Fig. 31.8).⁵³

Although prophylactic ICD therapy used to be considered for LQTS patients with risk factors for SCD (see Table 31.8) regardless of medical therapy, recent data suggest that high-risk LQT1 and LQT2 patients should be considered for prophylactic ICD implantation only if they develop recurrent cardiac events (e.g., syncope or torsades de pointes) despite beta-blocker therapy or when compliance with or intolerance to medical therapy is a concern. Using this approach, most patients with LQTS do not need an ICD. Clear understanding by the patient and family of the relative merits of each strategy is essential. Although beta-blocker therapy significantly reduces the risk of SCD in this population, it is not completely protective, and residual cardiac events still occur. On the other hand, data suggest that syncopal episodes almost always precede cardiac arrest in patients receiving beta-blockers, allowing for institution of other therapeutic modalities, such as ICD implantation. In addition, ICD therapy is not without complications; infection, lead malfunction, inappropriate shocks, psychological sequelae, as well as the need for periodic device or lead revisions, have to be taken into consideration. This is especially important in children and young adults in whom the initial decision to implant an ICD carries decades-long implications, such as multiple procedures for generator replacements

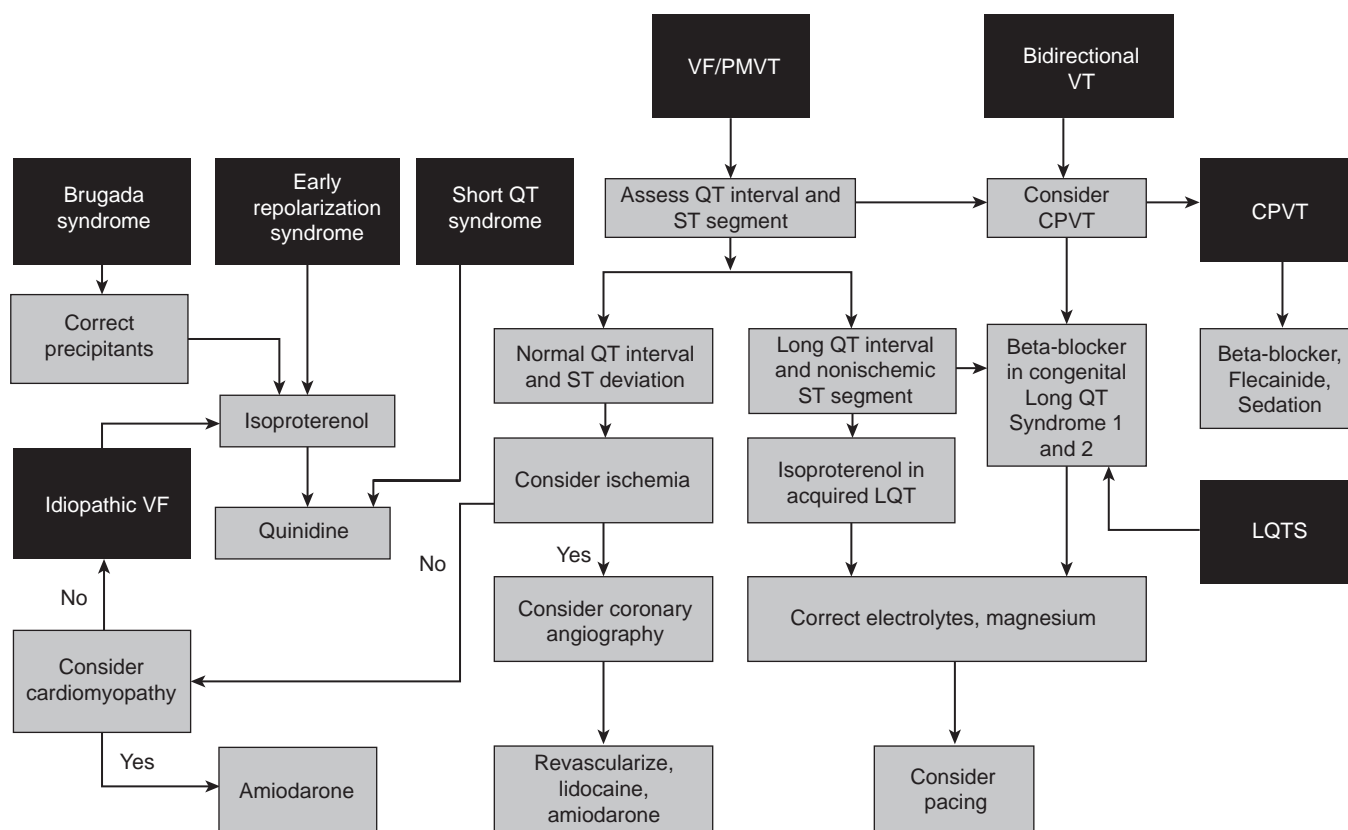
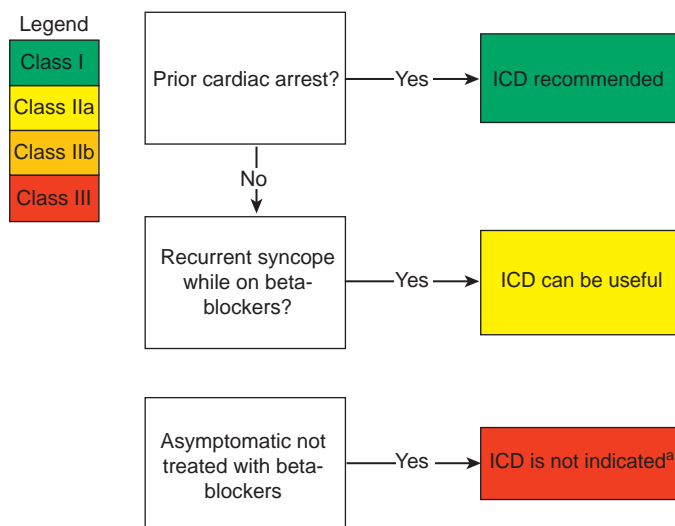


Fig. 31.7 An Algorithm for Acute Pharmacological Treatment of Arrhythmias in Suspected Channelopathies. CPVT, Catecholaminergic polymorphic ventricular tachycardia; LQTS, long QT syndrome; PMVT, polymorphic ventricular tachycardia; VF, ventricular fibrillation. (From Obeyesekere MN, Antzelevitch C, Krahn AD. Management of ventricular arrhythmias in suspected channelopathies. *Circ Arrhythmia Electrophysiol.* 2015;8:221–231.)



^aExcept under special circumstances, ICD implantation is not indicated in asymptomatic patients who have not been tried on beta-blocker therapy.

Fig. 31.8 Consensus Recommendations for Implantable Cardioverter-Defibrillators (ICDs) in Patients Diagnosed With Long QT Syndrome. (From Priori SG, Wilde AA, Horie M, et al. HRS/EHRA/APHS expert consensus statement on the diagnosis and management of patients with inherited primary arrhythmia syndromes. *Heart Rhythm.* 2013;10:1932–1963.)

and lead extractions, increasing the lifetime risks of morbidity and mortality.⁵³

Because ICD therapy does not prevent the occurrence of arrhythmias, concurrent treatment with beta-blockers is recommended for symptomatic and high-risk patients. Furthermore, careful programming of the ICD arrhythmia detection settings is recommended to reduce the risk of inappropriate shocks. This usually involves programming a single VF zone of more than 220 beats/min with or without a monitoring zone of more than 180 beats/min.¹

The European registry of 233 LQTS patients with ICDs showed that 28% received appropriate ICD therapies, and that future appropriate ICD therapies could be predicted by four variables: (1) age younger than 20 years at implantation; (2) QTc greater than 500 milliseconds; (3) prior cardiac arrest; and (4) cardiac events despite therapy. The M-FACT scoring system (Table 31.10), based on those clinical variables, was developed to identify in advance those patients with the highest and lowest probability of receiving appropriate shocks, which might represent the justification for the ICD implantation. Within 7 years, appropriate ICD therapies did not occur in any patients who had none of these factors and did occur in 70% of patients with all four clinical factors. Patients with an M-FACT score of 0 are unlikely to benefit from ICD implantation.^{32,54}

In addition, prophylactic ICD therapy should be considered in very-high-risk patients, including symptomatic patients with two or more gene mutations, including those with the Jervell and Lange-Nielsen syndrome variant with congenital deafness.¹

TABLE 31.10 M-FACT Risk Score

	Points
Event-free on therapy for >10 years	−1
QTc	
501–550 msec	1
>550 msec	2
Age at implantation ≤20 years	1
Prior aborted cardiac arrest	1
Events on therapy	1

*Acronym derived from M (minus 1 point for being free of cardiac events while on therapy for >10 years), F (500- and 550-msec QTc), A (age ≤20 years at implantation), C (cardiac arrest), and T (events on therapy).

Left Cervicothoracic Sympathectomy

Left cervicothoracic sympathectomy, which involves resection of the lower half of the left stellate ganglion and the first two to four thoracic ganglia (T1–T4), is another antiadrenergic therapeutic option for patients with LQTS. Care must be taken to not damage the top half of the ganglia to avoid Horner syndrome.

Currently, left cervicothoracic sympathectomy is recommended for the management of high-risk LQTS patients in whom drug therapy may not be sufficiently protective when ICD therapy is refused or not feasible (e.g., small infants) and when beta-blockers are not effective, not tolerated, or contraindicated.^{1,32}

Although cardiac sympathetic denervation provides a significant long-term reduction in the frequency of aborted cardiac arrest and syncope (more effective in patients with LQT1 than in those with other types of LQTS), it is not completely protective against SCD. Studies of LQTS patients who have undergone left cervicothoracic sympathectomy demonstrated a residual mortality rate of 5% at 5 years. Furthermore, about 50% of high-risk LQTS patients have experienced one or more cardiac events, and patients with extremely malignant LQTS might not be responsive to cardiac sympathetic denervation. Hence, left cervicothoracic sympathectomy must not be viewed as curative or as an ICD alternative for high-risk patients.⁵⁵

Importantly, postoperative morbidity is common in patients undergoing left cervicothoracic sympathectomy. A large proportion of patients experience left-sided dryness, unilateral facial flush with exercise, contralateral hyperhidrosis, differential hand temperatures, transient and permanent ptosis, and left arm paresthesia. Nonetheless, postoperative satisfaction is generally high and patients feel safer following the procedure, despite the side effects.^{56,57}

Permanent Pacemaker

Cardiac pacing, in conjunction with beta-blocker therapy, can potentially reduce the risk of bradycardia-dependent QT prolongation, decrease heart-rate irregularities (eliminating short-long-short sequences), and reduce repolarization heterogeneity. Permanent pacemakers can be of value, especially in patients who continue to be symptomatic despite beta-blocker therapy or those in whom bradycardia or AV block limits the use of such therapy. In particular, patients with documented pause- or bradycardia-induced torsades de pointes and those with the LQT3 genotype may derive significant benefit from cardiac pacing.⁵⁸

Nevertheless, the high mortality in patients with recurrent symptoms (syncope or torsades de pointes) while receiving beta-blocker therapy is not adequately attenuated by the addition of cardiac pacing. Therefore

if cardiac pacing is being considered, the use of an ICD is more logical because it provides protection from SCD as well as the benefit of cardiac pacing. However, when ICD implantation is associated with an extremely high rate of adverse events (such as in small infants), an atrial pacemaker in combination with beta-blocker therapy can potentially serve as a bridge to ICD placement.⁵⁸

When cardiac pacing is employed, atrial pacing is preferred, at a rate that shortens the QTc to less than 440 milliseconds. It is recommended to minimize ventricular pacing as possible because it can potentially increase the heterogeneity of ventricular repolarization. However, in patients with AV block, ventricular pacing is important to maintain AV synchrony and elimination of ventricular pauses and long-short cycles.

Catheter Ablation

In LQTS patients, frequent episodes of torsades de pointes are occasionally triggered by focal, monomorphic PVCs. In this setting, catheter ablation of the focus of the PVCs can be valuable in reducing the burden of arrhythmias and the frequency of ICD therapies.

Lifestyle Modifications

Education and lifestyle changes for the prevention of arrhythmias are critical in patients with LQTS. Patients should avoid drugs that prolong the QT interval (www.qtdrugs.org) or reduce their serum potassium or magnesium levels, and they should consult with their physician before taking any medications or over-the-counter supplements. Furthermore, patients need to be educated on conditions that can lead to potentially dangerous electrolyte abnormalities (e.g., dehydration, diarrhea, vomiting, imbalanced diets for weight loss).¹

In addition, the importance of compliance with medical therapy should be emphasized. Beta-blocker noncompliance and use of QT-prolonging drugs account for the vast majority of life-threatening events in LQT1 patients. Preventive measures in LQTS patients in general and LQT2 patients in particular include avoidance of unexpected auditory stimuli (such as alarm clocks, doorbells, and telephones), especially during rest or sleep. Families with LQTS may also consider basic life support training and operation of an automated external defibrillator.

Participation in Sports

Physical activity and stress-related emotions frequently trigger cardiac events in patients with LQTS, especially patients with LQT1 or LQT2. Therefore all competitive sports (except those in the class IA category, such as billiards, bowling, cricket, and golf) should be restricted in symptomatic LQTS patients (regardless of the QTc duration or underlying genotype) as well as asymptomatic patients with baseline QT prolongation (QTc greater than or equal to 470 milliseconds in men, greater than or equal to 480 milliseconds in women). Swimming is particularly hazardous in LQT1 patients and should therefore be limited or performed under appropriate supervision, even in subjects with genotype-positive/phenotype-negative LQT1.

Because many first cardiac events occur before the age of 15 years in male patients, particularly those with the LQT1 genotype, whereas female patients may experience first cardiac events after the age of 20 years, LQT1 male patients require stricter exercise restriction before the age of 15.

Recent data suggests that sports participation is safer than previously recognized, and the restriction limiting participation to class IA activities may be liberalized for the asymptomatic patient with genetically proven LQT3 genotype and those with genotype-positive/phenotype-negative LQTS (especially patients genotyped as non-LQT1 and no family history of multiple SCDs), assuming that appropriate disease-specific

treatments are in place. In addition, automated external defibrillators and personnel trained in basic life support should be readily available. Furthermore, precautionary measures should be undertaken to avoid exercise-related dehydration, heat exhaustion, and electrolyte abnormalities.^{1,59}

Sports participation may also be carefully considered in LQTS patients with QT prolongation and those rendered asymptomatic after institution of treatment. These decisions, however, should be deliberated carefully by an LQTS expert to ensure that the athletes and their family members have been well informed, well risk stratified, and well treated.⁶⁰

Other considerations include the acquisition of a personal automatic external defibrillator as part of the athlete's personal sports safety gear, and establishment of an emergency action plan with the appropriate training facility and team officials.

Gene-Specific Therapy

The standard therapeutic options for LQTS (including beta-blockers, cardiac sympathetic denervation, ICD) rely on genotype to only a minor degree, yet are quite effective. Nevertheless, beta-blockers and left cervicothoracic sympathectomy have some degree of genotype specificity, being quite effective in LQT1 and LQT2 and less effective in LQT3. Similarly, lifestyle modification and exercise restriction are most helpful in LQT1 and LQT2. For practical purposes, however, this apparent genotype specificity influences therapy decisions in only a very small number of patients.

Several gene-specific LQTS therapies are being evaluated, including Na⁺ channel blockers, K⁺ channel activators, alpha-adrenergic receptor blockers, protein-kinase inhibitors, and atropine. However, current experience with these drugs is limited.

LQT3. Currently, LQT3 is the only LQTS variant for which a gene-specific therapy is recommended by current guidelines (see Table 31.9). Given the fact that augmentation of the late Na⁺ inward current (I_{NaL}) underlies the prolongation of the QT interval in patients with the LQT3 genotype, Na⁺ channel blockers have been successfully used in these patients. Mexiletine, a class IB Na⁺ channel blocker, was shown to shorten the QT interval and reduce the occurrence of arrhythmic events in LQT3 patients.⁶¹

Until prospective clinical trials confirm the effectiveness of mexiletine, it should be used in LQT3 patients with a QTc exceeding 500 milliseconds only in conjunction with beta-blockers or with the backup of an ICD. In addition, some investigators recommend testing the effectiveness of mexiletine by the administration of half the daily dose during continuous ECG monitoring. Only if the QTc is shortened by more than 40 milliseconds within 90 minutes of drug administration (when the peak plasma concentration is reached) should mexiletine be added to beta-blocker therapy.

Flecainide, a class IC Na⁺ channel blocker, was shown to shorten the QT interval in LQT3 patients with a specific mutation (D1790G) in the *SCN5A* gene. However, flecainide is reported to elicit a Brugada phenotype in some LQT3 patients; therefore this drug should not be used in LQT3 patients except for those with this specific *SCN5A* mutation.

The antianginal agent ranolazine has unique EP properties. Unlike other Na⁺ channel blockers, which reduce both the early (peak) and late components of the Na⁺ current (I_{Na} and I_{NaL} , respectively), ranolazine preferentially reduces I_{NaL} . Moreover, ranolazine reduces Ca²⁺ overload of myocardial cells and suppresses EAD-triggered arrhythmias in animal models of LQT3. Ranolazine was shown to shorten the QT interval without widening the QRS complex in LQT3 patients, and can potentially offer a therapeutic benefit in these patients.⁶²

LQT2. Potassium supplements can be of value, especially in LQT2 patients, who are particularly sensitive to low K⁺ levels because the

conductance of KCNH2 channels is directly related to extracellular K⁺ concentrations. Therefore efforts should be made to maintain a serum K⁺ level greater than 4 mEq/L in patients with this genotype. Acute treatment with IV potassium can be effective in suppressing torsades de pointes. Furthermore, long-term oral potassium supplements, even in patients with normal K⁺ levels at baseline, can potentially reduce repolarization abnormalities in LQT2. Increasing extracellular K⁺ concentrations enhances IKr, at least partially compensates for the loss of IKr in LQT2, and can potentially limit the development of an arrhythmogenic substrate under long QT conditions. Whether these effects translate into clinical benefit in reduction of the risk of cardiac events remains to be proven.

Family Screening

Timely (often presymptomatic) identification of disease carriers is important because preventive measures and therapies can effectively avert SCD. Therefore when a patient is diagnosed with LQTS, ECGs should be obtained on all first-degree family members (i.e., parents, siblings, offspring) to determine whether others are affected. Unexplained sudden death in a young individual should trigger a similar evaluation to determine if LQTS is present in the family.

When the causal mutation has been identified in the proband, first-degree relatives should be offered genetic screening, even those with a negative clinical and ECG phenotype. Genotyping of family members can help exclude the diagnosis in some persons, and identify silent mutation carriers and allow prophylactic treatment. However, detailed genetic counseling is warranted before proceeding to this testing, particularly for asymptomatic persons for whom the option of not testing must also be recognized.

BRUGADA SYNDROME

The Brugada syndrome is an autosomal dominant inherited channelopathy characterized by typical ECG changes (ST segment elevation or J waves) in the right precordial leads. Described in 1992, the syndrome is associated with a high incidence of SCD secondary to polymorphic VT or VF in the absence of structural heart disease.⁶³

Genetics of the Brugada Syndrome

The Brugada syndrome is a channelopathy that causes current dysfunction in multiple channels participating in the generation of the cardiac action potential. To date, mutations in 19 genes have been identified as associated with the Brugada phenotype (Table 31.11) with an autosomal dominant mode of transmission. These include genes related to the Na⁺ current (I_{Na}) and genes that affect L-type Ca²⁺ channels (I_{CaL}) or transient outward K⁺ channels (I_{to}). These channelopathies cause Brugada syndrome phenotype by attenuating I_{Na} , attenuating I_{CaL} , or enhancing I_{to} , resulting in an outward shift in the balance of current active during the early phases of the action potential in the right ventricular outflow tract (RVOT). The relationships between genotype and phenotype are not always predictive. Mutations in different genes can express similar Brugada syndrome phenotypes. Conversely, mutations in the same gene can lead to different syndromes.^{64,65}

More than 65% of Brugada syndrome probands remain genetically undetermined, which suggests that unknown mutations or pathophysiological cellular regulations (such as posttranslational modulations, phosphorylation, glycosylation) may also cause similar ion current defects and clinical manifestations.⁶⁶

Mutations Related to the Sodium Current

Most cases of the Brugada syndrome are attributable to loss-of-function mutations in the cardiac Na⁺ channel resulting in a reduction of the

TABLE 31.11 Molecular Basis of the Brugada Syndrome

	Gene	Protein	Functional Effect	% of Probands
BrS1	<i>SCN5A</i>	Na _v 1.5	↓ I _{Na}	11%–28%
BrS2	<i>GPD1L</i>	G3PD1L	↓ I _{Na}	Rare
BrS3	<i>CACNA1C</i>	Ca _v 1.2	↓ I _{CaL}	6.6%
BrS4	<i>CACNB2B</i>	Ca _v β2	↓ I _{CaL}	4.8%
BrS5	<i>SCN1B</i>	Na _v β1	↓ I _{Na}	1.1%
BrS6	<i>KCNE3</i>	MiRP2	↑ I _{to}	Rare
BrS7	<i>SCN3B</i>	Na _v β3	↓ I _{Na}	Rare
BrS8	<i>KCNJ8</i>	Kir6.1	↑ I _{KATP}	2%
BrS9	<i>CACNA2D1</i>	Ca _v α2δ1	↓ I _{CaL}	1.8%
BrS10	<i>KCND3</i>	K _v 4.3	↑ I _{to}	Rare
BrS11	<i>RANGRF</i>	MOG1, Na _v 1.5 cofactor	↓ I _{Na}	Rare
BrS12	<i>SLMAP</i>	Sarcolemmal-associated protein	↓ I _{Na}	Rare
BrS13	<i>ABCC9</i>	SUR2A	↑ I _{KATP}	Rare
BrS14	<i>SCN2B</i>	Na _v β2	↓ I _{Na}	Rare
BrS15	<i>PKP2</i>	Plakophilin-2	↓ I _{Na}	Rare
BrS16	<i>FGF12</i>	FHF-1	↓ I _{Na}	Rare
BrS17	<i>SCN10A</i>	Na _v 1.8	↓ I _{Na}	5%–16.7%
BrS18	<i>HEY2</i>	Transcriptional factor	↑ I _{Na}	Rare
BrS19	<i>SEMA3A</i>	Semaphorin	↑ I _{to}	Rare

BrS, Brugada syndrome; FHF-1, fibroblast growth factor homologous factor-1; I_{CaL}, L-type Ca²⁺ current; I_{KACH}, acetylcholine-activated inward rectifier K⁺ current; I_{KS}, slowly activating delayed rectifier K⁺ current; I_{Na}, Na⁺ current; I_{to}, transient outward K⁺ current.

Modified from Antzelevitch C, Yan GX, Ackerman MJ, et al. J-wave syndromes expert consensus conference report: emerging concepts and gaps in knowledge. *Heart Rhythm*. 2016;13:e295–e324.

inward Na⁺ current (I_{Na}). I_{Na} initiates the ventricular action potential, thereby controlling cardiac excitability and electric conduction velocity.

SCN5A is the first gene to be linked to Brugada syndrome. Loss-of-function mutations in the *SCN5A* gene (encoding the α subunit of the cardiac voltage-gated Na⁺ channel [Na_v1.5]) account for the vast majority (greater than 75%) of genotype-positive Brugada syndrome cases (but only 11% to 28% of total Brugada syndrome probands). A higher incidence of *SCN5A* mutations has been reported in familial than in sporadic cases.^{66,67}

So far, more than 300 Brugada syndrome-associated mutations have been described in the *SCN5A* gene. Some of these mutations result in loss of function due to impaired channel trafficking to the cell membrane, disrupted ion conductance, or altered gating function. Most of the mutations are missense mutations, whereby a single amino acid is replaced by a different amino acid. Missense mutations commonly alter the gating properties of mutant channels. Because virtually all reported *SCN5A* mutation carriers are heterozygous, mutant channels with altered gating can result in an up to 50% reduction of I_{Na}. Different *SCN5A* mutations can cause different degrees of I_{Na} reduction and, hence, different levels of severity of the clinical phenotype of the Brugada syndrome.⁶⁶

SCN5A loss-of-function mutations have also been linked to patients with progressive cardiac conduction system disease (Lev-Lenègre disease). Mutated *SCN5A* can also impede the closure (gain of function) of the Na⁺ channel, leading to type 3 LQTS (LQT3). It was reported that all three syndromes (Brugada syndrome, LQT3, and Lev-Lenègre disease)

occurred within a single family because of a single mutated *SCN5A* gene. Approximately 65% of mutations identified in the *SCN5A* gene are associated with the Brugada syndrome phenotype.

Compared with Brugada patients without an *SCN5A* mutation, those with *SCN5A* mutations generally exhibit longer and progressive conduction delays (PQ, QRS, and HV intervals), frequent occurrences of fragmented QRS complex, and ventricular arrhythmias of extra-RVOT origin.

In addition to *SCN5A* mutations, reduction in I_{Na} can be caused by mutations in *SCN1B* (encoding the β1- and β1b-subunits of the Na⁺ channel [Na_v1.5]), *SCN2B* (encoding the β2-subunit of the Na⁺ channel), and *SCN3B* (encoding the β3-subunit of Na_v1.5), resulting in the clinical phenotype of the Brugada syndrome.⁶⁶ Recently, *SCN10A* (which encodes Na_v1.8, a neuronal Na⁺ channel, which appears to play a role in the heart) was identified as a major susceptibility gene for Brugada syndrome (identified in 16.7% of probands). Loss of function mutations in *SCN10A* lead to significant reduction in I_{Na}. The majority of patients with *SCN10A* Brugada syndrome present with mixed phenotypes, the most common of which is progressive cardiac conduction system disease.⁶⁴

Furthermore, mutations in *GPD1L* (which encodes the protein glycerol-3-phosphate dehydrogenase 1-like [G3PD1L] protein) affect the trafficking of the cardiac Na⁺ channel to the cell surface, resulting in reduction of I_{Na} and Brugada syndrome. The Brugada phenotype associated with *GPD1L* mutations is characterized by progressive conduction disease, low sensitivity to procainamide, and a relatively good prognosis.⁶⁴

Mutations in several other genes have been reported to cause reduction in I_{Na} and lead to the Brugada phenotype, including *HEY2* (encoding the transcriptional factor HEY2), *FGF12* (encoding for a fibroblast growth factor homologous factor-1, which exerts modulatory effects on cardiac Na⁺ and Ca²⁺ channels), *PKP2* (encoding the desmosomal protein plakophilin-2, a known susceptibility gene for arrhythmogenic right ventricular cardiomyopathy [ARVC]), *RANGRF* (encoding MOG1, a protein known to modulate the Na⁺ channel), and *SLMAP* (encoding the sarcolemmal membrane-associated protein, SLMAP, a component of T-tubules and sarcoplasmic reticulum).⁶⁴

Mutations Related to the Calcium Current

Approximately 13% of cases of the Brugada syndrome are attributable to loss-of-function mutations in the cardiac Ca²⁺ channel resulting in a reduction of the depolarizing I_{CaL}. These include *CACNA1C* (which encodes the pore-forming α1C-subunit [Ca_v1.2] of the L-type voltage-gated Ca²⁺ channel), *CACNB2* (which encodes for the regulatory β2-subunit [Ca_vβ2] of Ca_v1.2, which modifies gating of I_{CaL}), and *CACNA2D1* (which encodes the regulatory α2δ-subunit of Ca_v1.2). In this setting, the mechanism of Brugada syndrome involves a reduction of the depolarizing I_{CaL}. Loss of function mutations in these genes are also reported to contribute to SQTs, idiopathic VF, and early repolarization syndrome.⁶⁵

Mutations Related to the Potassium Current

Gain-of-function mutations in *KCNE3* (which encodes the auxiliary β-subunit [MiRP2] of the transient outward K⁺ channel [K_v4.3]) and *KCND3* (which encodes the α-subunit of K_v4.3) result in an increase in I_{to} density and causes Brugada syndrome.

Furthermore, gain-of-function mutations in *SCN1B* (which encodes the auxiliary β1-subunit of the Na⁺ channel), in addition to reducing I_{Na}, can also increase I_{to}. In addition, mutations in *KCNJ8* (which encodes Kir6.1) can augment I_{KATP}, resulting in accentuation of the action potential notch as well as depression of the plateau, leading to Brugada syndrome phenotype. These mutations can also result in shortening of action potential duration and SQTs phenotype. Recently, mutations in *ABCC9*

(which encodes SUR2A, the adenosine triphosphate [ATP]-binding cassette transporter of the I_{KATP} channel) has been reported to cause Brugada phenotype by augmenting I_{KATP} , likely due to reduced channel sensitivity to the inhibitory effects of ATP.⁶⁴

Other Candidate Genes

New susceptibility genes recently proposed and awaiting confirmation include the transient receptor potential melastatin protein-4 gene (*TRPM4*, which encodes a calcium-activated nonselective cation channel) and the *KCND2* gene (which encodes the voltage-gated potassium channel subfamily D, $K_{4.2}$).⁶⁵

Other genetic variants were found to be capable of modulating, but not necessarily causing, the expression of Brugada syndrome by increasing I_{to} (*KCNE5*, which encodes one of the regulatory β -subunits of the I_{to} and I_{Ks} channels), or by increasing I_{Kr} (*KCNH2*, which encodes the α -subunit of the rapid delayed rectifier potassium channel [hERG]). Further, loss-of-function mutations in *HCN4* (encoding the hyperpolarization-activated cyclic nucleotide-gated channel 4 protein of the human cardiac pacemaker channel) can lead to reduction in the pacemaker current (I_f) and bradycardia, which can accentuate or unmask the Brugada syndrome phenotype.⁶⁴

Pathophysiology of the Brugada Syndrome

The mechanisms underlying the ECG changes and arrhythmogenesis in Brugada syndrome patients remain incompletely understood. Two hypotheses have been proposed: (1) the repolarization disorder hypothesis, based on transmural dispersion in repolarization of the RVOT; and (2) the depolarization disorder hypothesis, based on activation delay in the RVOT subepicardium. It is likely that a combination of the two mechanisms plays a role in the genesis of the ECG pattern and arrhythmogenicity and that both may coexist. Also, both hypotheses recognize a central role for the RVOT as a critical arrhythmogenic substrate in Brugada syndrome.⁶⁴

Repolarization Hypothesis

The ST-T wave changes in Brugada syndrome likely reflect a profound change in the process of ventricular repolarization, particularly in the relationship between the endocardial and epicardial repolarization processes. The cellular basis for this phenomenon is thought to be the result of loss of function of Na^+ channels (reduced I_{Na}) that differentially alters the action potential morphology in epicardial versus endocardial cells.

I_{to} is a prominent repolarizing current; it partially repolarizes the membrane, shaping rapid (phase 1) repolarization of the action potential, setting the height of the initial plateau (phase 2), and resulting in a pronounced action potential notch and, in combination with depolarizing Ca^{2+} currents, in a “spike-and-dome” action potential morphology. I_{to} channel densities are heterogeneously distributed across the myocardial wall and in different regions of the heart, being much higher in the right ventricle (RV) than in the left ventricle (LV), in the epicardium than in the endocardium, and nearer the base than the apex of the ventricles. These regional differences are responsible for the shorter duration, the prominent phase 1 notch, and the “spike and dome” morphology of RV epicardial and midmyocardial action potentials compared with endocardium and LV. A prominent I_{to} -mediated action potential notch in ventricular epicardium but not endocardium produces a transmural voltage gradient during early ventricular repolarization that registers as a J wave or J point elevation on the ECG (Fig. 31.9).^{68,69}

Na^+ channel malfunction and reduction of I_{Na} associated with the Brugada syndrome accentuate the notch produced by I_{to} , leading to partial or complete loss of the action potential dome, premature repolarization, and significant action potential shortening, presumably by

deactivation or voltage modulation that reduces I_{CaL} . These changes occur predominantly in regions where I_{to} is abundant (such as RVOT epicardium). In contrast, endocardial cells display a much smaller I_{to} and, consequently, I_{Na} reduction would not significantly affect action potential morphology and duration. This is likely to manifest on the ECG as an early repolarization pattern consisting of a J point elevation, slurring of the terminal part of the QRS, and mild ST segment elevation. A further increase in net repolarizing current can result in complete loss of the action potential dome in the RVOT epicardium, leading to more pronounced dispersion of repolarization (epicardial repolarization precedes repolarization in endocardial regions) and a transmural voltage gradient that manifests as greater ST segment elevation.^{68,69}

Depolarization Hypothesis

A growing body of evidence suggests that depolarization abnormalities related to ionic channelopathy and structural abnormalities in the RVOT contribute to the arrhythmogenic substrate underlying the Brugada syndrome.

The reduction in I_{Na} observed in Brugada syndrome linked to an *SCN5A* mutation leads to a reduction in the upstroke velocity of action potential phase 0, and, as a result, slowing in atrial and ventricular electrical conduction. This is often reflected by prolongation in AV and intraventricular conduction intervals (PR interval and QRS duration) on the ECGs of Brugada syndrome patients with an *SCN5A* mutation. Conduction slowing preferentially involves the RVOT, likely combined with ultrastructural abnormalities of the RVOT epicardium (interstitial fibrosis and altered expression of gap junction proteins). These depolarization abnormalities likely contribute to ST elevation, thus increasing the transmural gradient of the membrane potential.^{68,69}

The depolarization hypothesis is indirectly supported by several histological, imaging, ECG, and EP observations, including the presence of late potentials and fragmented electrograms recorded from the RVOT epicardium on high-density electroanatomical mapping, signal-averaged ECG, and body surface potential maps. Catheter ablation of these epicardial sites significantly reduced the arrhythmia vulnerability and ECG manifestation of the disease.^{68,69}

Mechanism of Ventricular Arrhythmias

The excessive increase in transmural dispersion of repolarization (between epicardium and endocardium) facilitates reentrant excitation waves between depolarized endocardium and prematurely repolarized epicardium. A significant outward shift in current can cause a prominent action potential notch causing more negative potentials during phase 1 of the action potential and loss of activation of I_{CaL} . As a consequence, loss of the action potential dome and marked abbreviation of the action potential develop in regions where I_{to} is prominent (epicardium) but not in other locations. The dome can then propagate from regions where it is maintained to regions where it is lost, giving rise to a very closely coupled extrasystole (phase 2 reentry) that in turn can initiate polymorphic VT or VF (Fig. 31.10).

Although the repolarization abnormalities facilitate the onset of polymorphic VT, it may be the depolarization disturbance (conduction slowing leading to wave break of the reentrant wave) that allows the VT to become sustained and to degenerate to VF. Because the RVOT is the critical area associated with depolarization and repolarization abnormalities, it is a frequent origin of VT and VF in the setting of Brugada syndrome.⁶⁴

Mechanism of Age and Gender Effects

The effects of age and gender on the Brugada syndrome phenotype (being more prevalent in adult males) may be due to intrinsic differences in Na^+ channel expression between men and women (e.g., higher

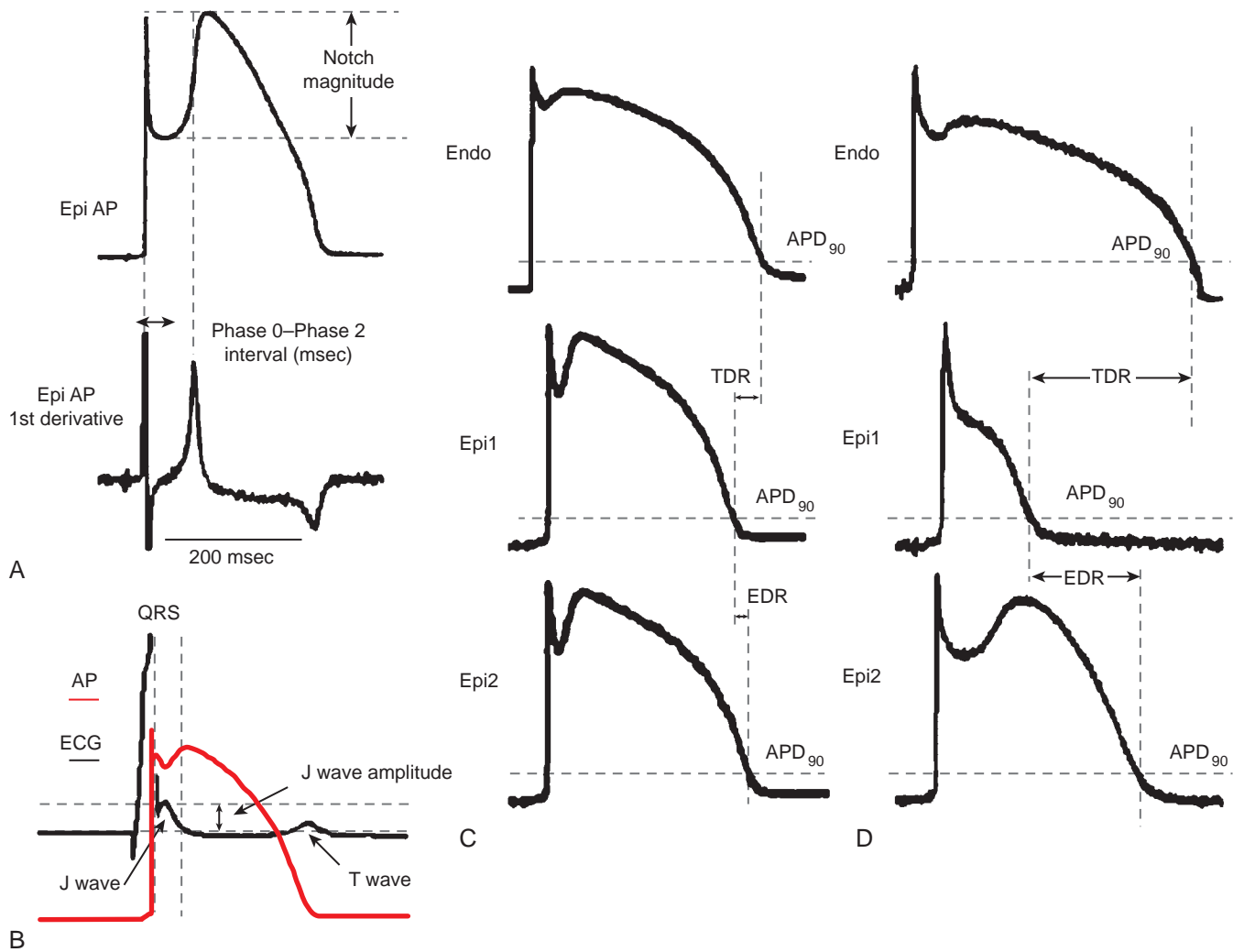


Fig. 31.9 Dispersion of Action Potential (AP) Repolarization in J Wave Syndromes. (A and B) Quantitation dispersion of AP and J wave parameters. (C) Measurement of dispersion of AP repolarization. (D) Measurement of dispersion of repolarization when the AP dome is lost at 1 epicardial (Epi) site but not the other. APD₉₀, Action potential duration at 90% repolarization; ECG, electrocardiogram; EDR, epicardial dispersion of repolarization; Endo, endocardial; TDR, transmural dispersion of repolarization. (From Gurabi Z, Koncz I, Patocskaï B, Nesterenko VV, Antzelevitch C. Cellular mechanism underlying hypothermia-induced ventricular tachycardia/ventricular fibrillation in the setting of early repolarization and the protective effect of quinidine, cilostazol, and milrinone. *Circ Arrhythmia Electrophysiol.* 2014;7:134–142.)

I_{to} densities in men) or due to differences in hormone levels (e.g., higher testosterone levels in men). The concentration of testosterone is reportedly higher in men with Brugada syndrome than in controls, and regression of the Brugada ECG pattern after castration in men with prostate neoplasia has been reported.

The phase 1 notch potentially mediates the effects of sex hormones on the phenotypic expressions of Na^+ channel dysfunction, thus contributing to the male predominance of Brugada syndrome. Estrogen suppresses the expression of the $K_v4.3$ channel, resulting in reduced I_{to} and a shallow phase 1 notch, whereas testosterone enhances the outward currents (I_{Kr} , I_{Ks} , I_{K1}) and reduces the inward current (I_{CaL}), thus deepening the phase 1 notch.

Mechanism of Temperature Sensitivity

Fever-induced Brugada is the term used to describe the aggravation of clinical and/or ECG characteristics of this syndrome during febrile states in susceptible individuals. In fact, fever has been reported to be

the precipitating factor of ventricular arrhythmias in 18% of cases in a large series of Brugada patients presenting with cardiac arrest. In one report, the prevalence of a type I Brugada ECG pattern in patients with fever was 20 times higher than in afebrile patients, emphasizing the potency of fever in uncovering this ECG phenomenon.⁷⁰

The exact mechanism by which fever triggers arrhythmias in Brugada syndrome remains unknown. It is possible that high temperatures result in worsening of the biophysical properties of the defective Na^+ channels, leading to further reduction of I_{Na} . Alternatively, fever-induced arrhythmias may be mediated by the effect of temperature on the normal (unaffected) channels. According to this model, normal Na^+ channels are less efficient at high temperatures, but this slight loss of function becomes clinically significant only in the presence of other factors that reduce the repolarization or depolarization reserve (e.g., heterozygosity with loss-of-function mutations). Of note, fever does not appear to prolong the PR interval or QRS duration as drug challenge does.⁷¹

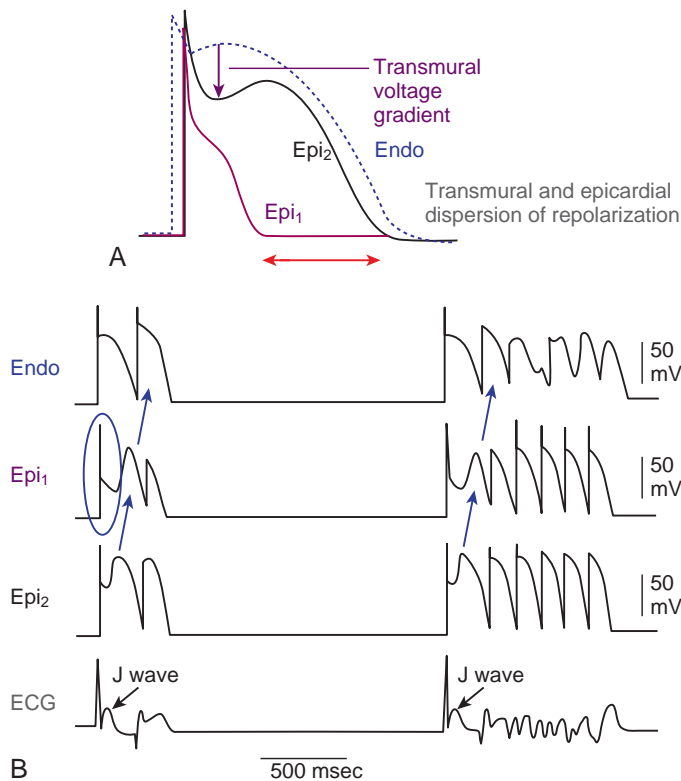


Fig. 31.10 Potential Mechanism for Arrhythmogenesis in the Brugada and Early Repolarization Syndromes. (A) With enhanced repolarization in regions with prominent transient outward current (I_{to}), all-or-none repolarization can occur, creating a substrate for arrhythmias. (B) Simultaneous action potentials from two epicardial sites (Epi_1 and Epi_2) and one endocardial site ($Endo$), and surface electrocardiogram (ECG). A loss of the action potential dome in Epi_1 , but not in Epi_2 , leads to apparent propagation of the dome from Epi_2 to Epi_1 , inducing reentry. (From Benito B, Guasch E, Rivard L, Nattel S. Clinical and mechanistic issues in early repolarization of normal variants and lethal arrhythmia syndromes. *J Am Coll Cardiol*. 2010;56:1177–1186.)

Mechanism of Exercise-Induced Changes

Exercise can aggravate the ECG abnormalities in the Brugada syndrome, but does not appear to induce ventricular arrhythmia in these patients. The mechanisms underlying the ECG responses in the Brugada syndrome to exercise are complex, which may be related to different molecular-genetic mutations underlying the Brugada syndrome phenotype.

Brugada syndrome-linked loss-of-function mutations in *SCN5A* reduce I_{Na} more during tachycardia, likely secondary to accumulation of mutant Na^+ channels in the slow inactivated state. Na^+ channels activate on depolarization and inactivate within milliseconds thereafter. Before reopening, channels must recover from inactivation during diastole. At fast heart rates, the diastolic interval becomes too short for mutant channels to completely recover from the slow inactivated state, resulting in decreased availability of open channels and, as a consequence, accentuation of Na^+ channel loss of function produced by *SCN5A* mutations. Besides tachycardia associated with exercise, other factors (e.g., autonomic nervous system, ion current imbalances) also play a role.

Mechanism of Drug Effects

Pharmacological agents that primarily block I_{Na} but not I_{to} (flecainide, ajmaline, and procainamide) can further diminish I_{Na} that is already reduced by the Brugada mutations. This may explain the use of Na^+

channel blockers to unmask concealed forms of the Brugada syndrome and the potential proarrhythmic adverse effects of these and other pharmacological agents. In contrast, quinidine, in addition to blocking I_{Na} , has a relatively strong effect in blocking I_{to} . Hence, quinidine can effectively suppress ST elevation and ventricular arrhythmias in patients with the Brugada syndrome.

Beta-adrenergic stimulation augments the inward I_{CaL} and attenuates the excess of outward current, resulting in reduction of ST segment elevation in right precordial leads and potentially underlying the therapeutic benefit observed for isoproterenol infusion for prevention of ventricular arrhythmias in Brugada syndrome patients with electrical storm. In contrast, acetylcholine facilitates the loss of the action potential dome by suppressing I_{CaL} and/or augmenting K^+ current.

Epidemiology

The prevalence of the Brugada ECG pattern in an apparently healthy population varies depending on the demographics of the patient population studied, ranging from 0.017% in Europe and 0.005% to 0.1% in North America to 0.15% to 0.27% in Japan and 0.18% in the Philippines. However, because the Brugada ECG pattern can be intermittently present or concealed, it is difficult to estimate the true prevalence of the disease in the general population. For unclear reasons, the Brugada syndrome is either more prevalent or more penetrant in Eastern countries (mainly in Southeast Asia), where the disease occurs endemically and is the leading cause of death in men younger than 40 years.

The Brugada syndrome exhibits an autosomal dominant pattern of transmission with incomplete penetrance (i.e., the pathogenic mutation is inherited by 50% of the offspring, but not all will develop the disease). In up to 60% of patients the disease can be sporadic, that is, absent in parents and other relatives. A family history of unexplained SCD is present in approximately 20% to 40% of Brugada probands in Western countries and in a lower percentage of probands (15% to 20%) in Japan.⁶⁵

Although the disease is inherited as an autosomal dominant trait and the prevalence of gene carriers among males and females is similar, the vast majority of patients who actually develop symptoms are male (ratio of men to women, 8:1).

The age of onset of clinical manifestations (syncope or cardiac arrest) is the third to fourth decade of life (mean age of SCD occurrence, 41 ± 15 years). Brugada syndrome is rare in children and the elderly, but cases have been diagnosed in infancy and in patients in their 80s.^{64,72}

The prognosis of Brugada syndrome varies widely among patients with this disorder, ranging from benign to malignant. Patients with a history of cardiac arrest are at the highest risk of recurrent events (7.7% to 13.5% per year) in the absence of drug therapy.⁷³ The arrhythmic risk is intermediate (0.6% to 1.2% per year) for patients with “malignant” syncope, and small, but not trivial (0.5% per year) in asymptomatic patients.⁷⁴

Clinical Presentation

There are three main clinical presentations of the Brugada syndrome: (1) cardiac arrest secondary to polymorphic VT/VF; (2) syncope; and (3) no symptoms. Less frequently, patients can present with symptoms secondary to SND, AV conduction abnormalities, or supraventricular arrhythmias.

In contemporary practice, the majority (more than 60%) of Brugada syndrome patients are asymptomatic at the time of diagnosis, often discovered during routine evaluation (preoperative or before sports participation), family screening, or upon the observation of the abnormal ECG pattern during a febrile illness. Only a minority (less than 10% to 20%) of Brugada syndrome patients diagnosed today have a history of cardiac arrest, and about one-third present with syncope.⁶⁴

Symptoms associated with Brugada syndrome are related to polymorphic VT, VF. Cardiac arrest is often the first manifestation of arrhythmias in the Brugada syndrome. When the arrhythmia terminates spontaneously, patients can present with syncope, agonal respirations, nocturnal labored respiration with agitation, or “seizures.” About 25% of patients suffering from SCD had already experienced a syncopal episode.⁶⁵

The Brugada syndrome is a leading cause of SCD in men younger than 40 years of age, particularly in countries in which the syndrome is endemic. The Brugada syndrome is believed to be responsible for 4% to 12% of all SCDs, and at least 20% of those occurring in patients with structurally normal hearts. The Brugada syndrome has even been described as responsible for SIDS and sudden unexplained nocturnal death syndrome (SUNDS; also known as SUDS). Nevertheless, the majority of Brugada syndrome patients do not manifest life-threatening events; approximately 10% to 15% of clinically affected patients experience one or more cardiac arrests before age 60. In a meta-analysis of prognostic studies, patients with a Brugada ECG pattern have an approximately 10% risk of SCD, syncope, or ICD shock at an average follow-up time of 2.5 years, or approximately 3.8% per year. More recent data suggest a lower annual event rate (approximately 1.5%); the discrepancy is likely due to selection bias, as initial reports included patients at higher risk.⁶⁵

Cardiac arrhythmia and death in the Brugada syndrome seem to occur largely in the early morning hours during sleep and in the setting of bradycardia. Circadian variation of sympathovagal balance, hormones, and other metabolic factors are likely to contribute to this circadian pattern. Bradycardia resulting from altered autonomic balance or other factors likely contributes to the initiation of arrhythmia.

Some episodes of syncope or SCD can be triggered by large meals (gastric distention), alcohol and cocaine toxicity, drugs, and fever. In

fact, it now appears that many previously described episodes of “febrile seizures” may in fact represent bouts of polymorphic VT in patients with temperature-sensitive mutations. Some patients with the Brugada syndrome experience an electrical storm of VF, but with no obvious precipitating factors.

Syncope is common (28%) in patients with Brugada syndrome; however, a large proportion of those patients have nonarrhythmic (often vasovagal) causes of syncope. Clinical features allow distinction between suspected arrhythmogenic and nonarrhythmogenic causes of syncope in 70% of cases. The absence of prodromes, brief (less than 1 minute) loss of consciousness, and absence of specific triggers (e.g., hot and crowded surroundings, pain or other emotional stress, seeing blood, or prolonged standing) are suggestive of an arrhythmic etiology. Of note, palpitations are very common in patients with suspected nonarrhythmic syncope, likely because of the pronounced postural tachycardia occurring before an actual faint.⁷⁵

Approximately 20% of patients with Brugada syndrome develop supraventricular arrhythmias. AF is the most common, observed in 10% to 20% of patients, especially in those with more advanced disease. Atrioventricular nodal reentrant tachycardia and Wolff-Parkinson-White syndrome have also been reported.⁷⁶

The identification of concomitant AV and intraventricular conduction defects have been shown to correlate with the presence of *SCN5A* mutations. Therefore all *SCN5A*-positive patients should be closely monitored for the onset of conduction block.

Electrocardiographic Features

Brugada Electrocardiogram Patterns

Previously, three ECG repolarization patterns in the right precordial leads were recognized (Fig. 31.11). Type 1 is characterized by ST segment

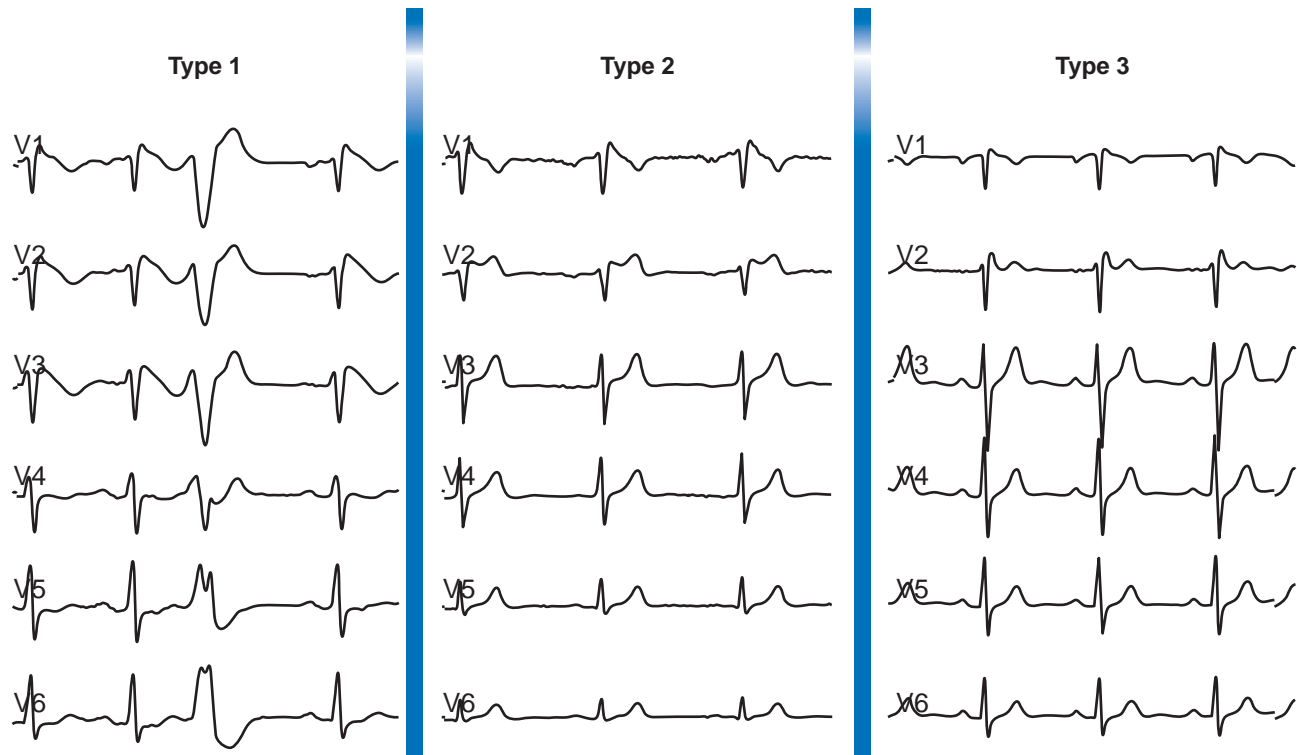


Fig. 31.11 Brugada Electrocardiogram (ECG) Patterns. Note the ventricular ectopic beat in the left panel with a QRS morphology consistent with origin from the right ventricular outflow tract. See text for discussion.

elevation of at least 2 mm (0.2 mV) with a coved (downward convex) morphology, associated with an incomplete or complete right bundle branch block (RBBB) pattern and followed by a descending negative T wave, with little or no isoelectric separation. The type 2 pattern has a “saddleback” appearance with a high take-off ST segment elevation of at least 2 mm, a trough displaying an ST elevation greater than or equal to 1 mm, and then either a positive or biphasic T wave. The type 3 pattern has either a saddleback or coved appearance with an ST segment elevation of less than 1 mm. These three patterns can be observed spontaneously in serial ECG tracings from the same patient or after the introduction of specific drugs. Only the type 1 ECG pattern is diagnostic of the Brugada syndrome, with type 2 and type 3 ECG patterns being suggestive but not specific.⁶⁵

The most recent consensus statement recommended that only two Brugada ECG patterns be considered: type 1 (coved type) and type 2 (saddleback type). Given the minimal morphological differences between type 2 and 3 Brugada patterns and the lack of impact on prognosis and risk stratification, the new type 2 ECG pattern definition encompasses patterns 2 and 3 of the previous consensus. Type 1 remains identical to the classic type 1 described previously, but with some new measurements that may also help to quantify the difference in the r' wave morphology (Box 31.1; Table 31.12).^{77,78}

The ECG Brugada pattern type 1 with the above criteria is easily recognized; and when found in a patient without apparent structural heart disease, it is very specific and strongly supports the diagnosis of Brugada syndrome (see Box 31.1). The infrequent cases with a coved-type pattern that present a high takeoff of QRS-ST between 0.1 and 0.2 mV, but with negative T wave in leads V_1 - V_2 , have been considered suggestive of the type 1 Brugada pattern, and should be evaluated

with complementary ECG criteria testing to confirm the diagnosis (see Table 31.12).^{77,78}

Electrocardiogram Electrode Locations

The use of more cephalad placement of the right precordial (in the third or second intercostal spaces) can increase the sensitivity for detecting the Brugada ECG pattern (both in the presence or absence of a drug challenge), likely with no reduction in the specificity of the diagnosis. In fact, it has been reported that the superior displacement of V_1 - V_2 leads could reveal more than 20% of new Brugada syndrome cases. This is likely related to the normal projection of the RVOT (which harbors the abnormalities underlying the ECG changes) onto the anterior chest surface.^{79,80}

Therefore the standard position of leads V_1 - V_2 in the fourth intercostal space is not sufficient to exclude the presence of a Brugada ECG pattern; ECG recordings need to be obtained with the V_1 - V_2 electrodes positioned in the second and third intercostal spaces in all patients. Also, those electrodes should be positioned in the same diagnostic location when serial recordings are performed to allow comparative assessments.⁷⁹

Dynamicity of the Brugada Pattern

The ECG changes associated with the Brugada pattern can be dynamic, intermittent, and are sometimes concealed. In fact, it is rare for patients to present with uniformly diagnostic tracings. Therefore serial ECGs can be necessary for diagnostic evaluation in high-risk patients. Continuous Holter monitoring also can help assess ST segment elevation at night because such changes can be modified by autonomic tone.⁷⁷

BOX 31.1 ECG Alterations in Brugada Syndrome

ECG Diagnostic Criteria in Precordial Leads

- **Brugada pattern:** (usually, the pattern is seen only in leads V_1 - V_2 ; but in some cases, it is recorded only in V_1 or V_2 ; and, in others, it is observed from V_1 to V_3).
- **Type 1 Brugada pattern (coved pattern):** Initial ST elevation ≥ 2 mm, slowly descending and concave or rectilinear with respect to the isoelectric baseline, with negative symmetric T wave (see other characteristics in Table 31.12).
- **Type 2 Brugada pattern (saddleback pattern):** The high take-off terminal positive wave (r') is ≥ 2 mm with respect to the isoelectric line and is followed by ST elevation; convex with respect to the isoelectric baseline (saddleback pattern) with elevation ≥ 0.05 mV with positive/flat T wave in lead V_2 , and variable (mildly positive, flat, or mildly negative) T wave in lead V_1 . If there is some doubt (i.e., $r' < 2$ mm), it is necessary to record the ECG in the second and third intercostal space (see other characteristics in Table 31.12).
- New ECG criteria:
 - Corrado index (2010): The ratio between the peak height of the take-off of QRS-ST to the height of ST segment at 80 msec later in leads V_1 - V_2 is >1 (because the ST is downsloping). In athletes, the ST especially in lead V_2 is upsloping; hence, the index is <1 . The end of QRS (J point) often does not coincide with the high take-off of QRS-ST as was suggested by Corrado. However, using the high takeoff of QRS-ST for the application of the Corrado index is valid for discriminating the Brugada pattern and other conditions mimicking the Brugada pattern.

- The β angle formed by ascending S and descending r' is >58 degrees in the type 2 Brugada pattern (in athletes, it is much lower) (sensitivity, 79%; specificity, 84%).
- Duration of the base triangle of r' at 5 mm from the high takeoff is more than 3.5 mm in the type 2 Brugada pattern (sensitivity, 81%; specificity, 82%). This measurement is much shorter in healthy athletes with incomplete RBBB.

Other ECG Findings

- QT generally is normal but can be prolonged in right precordial leads.
- Conduction disorders: Sometimes, prolonged PR interval (long HV interval). The conduction delay located in the RV explains the r' and longer QRS duration in right precordial leads compared with mid/left precordial leads.
- Supraventricular arrhythmias. Mostly atrial fibrillation.
- Some other ECG findings may be seen: the presence of r' wave in lead aVR >3 mm, early repolarization pattern in inferior leads, fractioned QRS, alternans of T wave after ajmaline injection, etc.

Other ECG Techniques

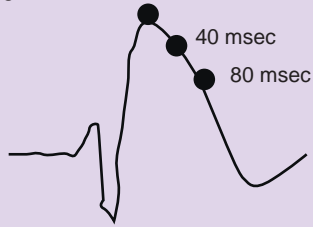
- In some occasions, it is necessary or convenient to find some new diagnostic clues with exercise testing, late potentials, and impaired QT dynamics studied by Holter. Electrophysiological studies remain controversial for diagnosis and for risk stratification.

ECG, Electrocardiogram; RBBB, right bundle branch block; RV, right ventricle.

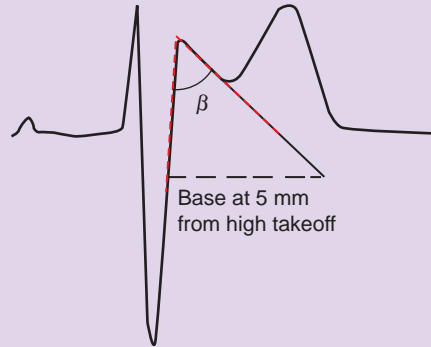
Modified from Bayés De Luna A, Brugada J, Baranchuk A, et al. Current electrocardiographic criteria for diagnosis of Brugada pattern: a consensus report. *J Electrocardiol*. 2012;45:433-442.

TABLE 31.12 Brugada Electrocardiogram Patterns in Leads V_1 - V_2 **Type 1: Coved Pattern**

High takeoff

Characteristics of the typical coved pattern in leads V_1 - V_2 :

- At the end of QRS, an ascending and quick slope with a high takeoff ≥ 2 mm followed by concave or rectilinear downsloping ST. There are few cases of coved pattern with a high takeoff between 1 and 2 mm.
- There is no clear r' wave.
- The high takeoff often does not correspond with the J point.
- At 40 msec of high takeoff, the decrease in amplitude of ST is ≤ 4 mm (≤ 0.4 mV). This is much less than the decrease observed in right bundle branch block because the downslope is slower.
- ST at high takeoff $>$ ST at 40 msec $>$ ST at 80 msec.
- ST is followed by negative and symmetric T wave
- QRS duration "mismatch:" The QRS duration is longer in V_1 - V_2 than in mid/left precordial leads (because of evidence of RV conduction delay), although this is sometimes difficult to determine.

Type 2: Saddleback PatternCharacteristics of the typical saddleback pattern in leads V_1 - V_2 :

- High takeoff of r' (that often does not coincide with J point) ≥ 2 mm.
- Descending arm of r' coincides with beginning of ST (often is not well seen).
- Minimum ST ascent ≥ 0.5 mm
- ST is followed by positive T wave in lead V_2 (Tpeak $>$ ST minimum > 0) and of variable morphology in lead V_1 .
- The characteristics of triangle formed by r' allow definition of different criteria useful for diagnosis.
 - β angle > 58 degrees
 - Duration of the base of the triangle of r' at 5 mm from the high takeoff greater than 3.5 mm
- The duration of QRS is longer in the type 2 Brugada pattern than in other cases with r' in lead V_1 , and there is a mismatch between V_1 and V_6 .

From Bayés De Luna A, Brugada J, Baranchuk A, et al. Current electrocardiographic criteria for diagnosis of Brugada pattern: a consensus report. *J Electrocardiol.* 2012;45:433–442.

When concealed, the ECG manifestations of the Brugada syndrome can be unmasked by stress, fever, various vagal stimuli (including gastric distention), vagotonic agents, a combination of glucose and insulin, electrolyte abnormalities (e.g., hyperkalemia, hypokalemia, hypercalcemia, hyponatremia), alcohol and cocaine toxicity, class I antiarrhythmic medications, and a number of other noncardiac medications.⁸¹

Furthermore, the ECG phenotype in the Brugada syndrome can be modified by autonomic changes. Adrenergic stimulation attenuates whereas acetylcholine accentuates the ECG abnormalities in affected individuals. Clinically, this correlates well with the propensity for cardiac events to occur at rest or during sleep.

QT Interval Prolongation

A slight prolongation of the QT interval is sometimes observed in association with ST segment elevation in patients with the Brugada syndrome. The QT interval is prolonged more in the right precordial leads than it is in the left leads, presumably because of a preferential prolongation of action potential duration in RV epicardium secondary to accentuation of the action potential notch.⁷⁸

QRS Fragmentation

In addition to the repolarization abnormality, the Brugada syndrome is associated with depolarization abnormalities and conduction disturbances. Fragmentation of the QRS complex (manifesting as multiple small spikes within the QRS complex) can be observed in 40% of patients with the Brugada syndrome and in the majority (85%) of those who had VF episodes. It has been proposed that the multiple

spikes within the fragmented QRS complex suggest the presence of an arrhythmogenic substrate that has multiple areas of conduction slowing, and can potentially predict a high risk of life-threatening ventricular arrhythmias. Notably, fragmentation of the QRS occurs preferentially in the right precordial leads, especially in the higher intercostal spaces, suggesting a localized conduction abnormality within the RVOT region. The use of a low-pass filter with a low cutoff frequency (greater than 25 Hz), as commonly employed to remove the electromyogram signal, can eliminate the QRS fragmentation. Thus a low-noise amplifier and a relatively high cutoff low-pass filter frequency (150 Hz) need to be used.⁷⁸

Of note, epsilon-like waves and localized prolongation of the QRS complex in the right precordial leads have been observed in some patients with a spontaneous or drug-induced type 1 Brugada ECG pattern, likely reflecting RV activation delay.

Conduction Abnormalities

Depolarization abnormalities, including prolongation of P wave duration, PR interval, and QRS duration, are frequently observed, particularly in patients with *SCN5A* mutations. PR interval prolongation likely reflects infranodal conduction delay. Of note, loss-of-function *SCN5A* mutations can also lead to isolated cardiac conduction defects or Lev-Lenègre disease, characterized by disturbances in any part of the conduction system without QT interval prolongation or Brugada ST segment elevation. In addition, prolonged sinus node recovery time and sinoatrial conduction time, slowed atrial conduction, and atrial standstill have been reported in association with the Brugada syndrome.⁷⁸

Diagnosis of the Brugada Syndrome

The 2013 consensus report recommended that Brugada syndrome is definitively diagnosed when a type 1 ECG pattern is observed, either spontaneously or after provocative drug testing (with IV administration of a sodium channel blocker such as ajmaline, flecainide, pilsicainide, or procainamide), in at least one right precordial lead (V_1 or V_2), placed in a standard or a superior position (i.e., in the fourth, third, or second intercostal space) (Fig. 31.12).^{1,82}

Although symptoms are no longer mandatory for diagnosis according to the consensus report, several investigators have suggested that when a type 1 ECG pattern is unmasked using a sodium channel blocker, a definitive diagnosis of Brugada syndrome should require that the patient also present with either symptoms (cardiac arrest, agonal nocturnal respiration, documented polymorphic VT or VF, or unexplained syncope) or positive family history (unexplained SCD at age younger than 45 years or diagnosed Brugada syndrome in a first-degree relative). Inducibility of VT/VF with 1 or 2 ventricular extrastimuli (VESs) at EP study supports the diagnosis of Brugada syndrome under these circumstances.^{65,77,82}

The type 2 Brugada ECG pattern is suspicious, but not diagnostic for Brugada syndrome, and requires further investigation. A drug challenge test to unmask a type 1 Brugada ECG pattern is recommended in those individuals only when the type 2 ECG pattern is accompanied by symptoms or positive family history, as specified above.⁶⁵

A diagnostic score system for Brugada syndrome (the Shanghai Brugada syndrome score, (Table 31.13) has been proposed based on the available literature, but validation by large-scale trials is lacking.⁶⁵

Provocative Drug Testing

Provocative testing with Na^+ channel blockers is used to unmask a Brugada ECG pattern in nondiagnostic cases (e.g., unexplained cardiac

arrest, unexplained syncope, or family screening). Up to 30% to 50% of the patients are diagnosed with Brugada syndrome after a positive drug challenge. Provocative drug testing is generally not performed if a patient displays an intermittently spontaneous type 1 ECG because the test does not offer additional diagnostic or prognostic value in these patients, and it is not devoid of risk for provoking arrhythmic events. It is also important to recognize that a negative provocative drug test does not exclude a latent form of Brugada syndrome.

The drug challenge test involves administration of ajmaline, flecainide, procainamide, or pilsicainide (Table 31.14) under close cardiac monitoring and in a setting that is fully equipped for resuscitation. The drug challenge test is terminated when (1) the diagnostic type 1 ST segment elevation develops (Fig. 31.13), (2) the ST segment elevation in the type 2 ECG pattern increases by at least 2 mm, (3) PVCs or other arrhythmias develop, or (4) the QRS widens by 30% or more.

Although the drug challenge test is considered safe if performed in a controlled environment, it can potentially precipitate malignant cardiac arrhythmias or advanced AV block, particularly in patients with pre-existing AV or intraventricular conduction abnormalities. Ventricular arrhythmias during or shortly after drug challenge have been reported in 0.3% to 15% of the tests, but are predominantly nonsustained and self-terminating. Sustained ventricular arrhythmias occur in about 1.8% of the patients during ajmaline challenge. Notably, such an occurrence in patients with Brugada syndrome does not appear to identify a category at higher risk of spontaneous arrhythmic events. Isoproterenol and sodium lactate can be effective antidotes in this setting.

The different Na^+ channel blockers exhibit different efficacies in unmasking the Brugada pattern ECG, mostly secondary to the different potency of inhibition of I_{to} and I_{Na} . Data suggest that ajmaline (a class IA Na^+ channel blocker) is the most efficacious and is likely safer than others because of its shorter half-life and stronger rate-dependent Na^+ channel blocking effects. In *SCN5A*-positive subjects with Brugada

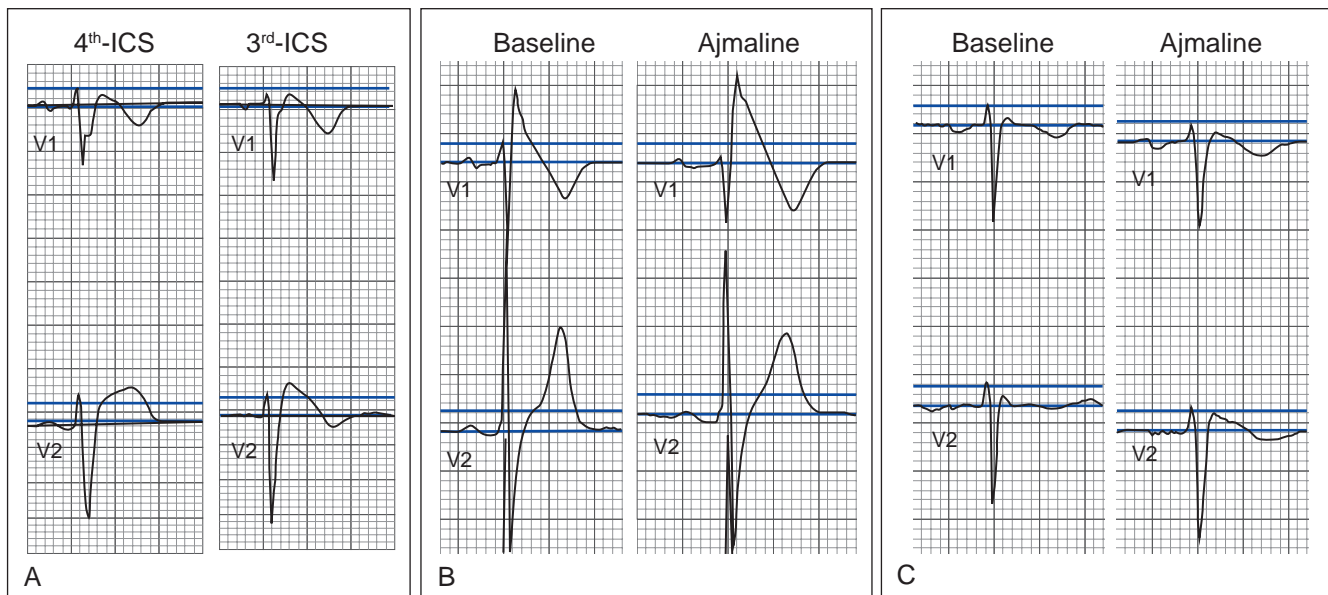


Fig. 31.12 Diagnosis of the Brugada Electrocardiogram (ECG) Patterns. ECG leads V_1 and V_2 are shown. (A) Single-lead covered-type ECG exceeding 2 mm only in the third intercostal space (ICS). (B) Single-lead covered-type ECG exceeding 2 mm only at baseline and further accentuated upon 1 mg/kg ajmaline; in (A) and (B) Brugada syndrome can be diagnosed according to 2013 criteria. (C) Incomplete right bundle branch block with minimal ST segment abnormalities at baseline that are converted to a coved pattern after ajmaline, but ST segment elevation remains less than 2 mm. In this case the challenge is considered negative. Horizontal blue lines represent 2 mm. (From Curcio A, Mazzanti A, Bloise R, et al. Clinical presentation and outcome of Brugada syndrome diagnosed with the new 2013 criteria. *J Cardiovasc Electrophysiol*. 2016;27:937–943.)

TABLE 31.13 Proposed Shanghai Score System for Diagnosis of Brugada Syndrome

	Points
I. ECG (12-Lead/Ambulatory)	
A. Spontaneous type 1 Brugada ECG pattern at nominal or high leads	3.5
B. Fever-induced type 1 Brugada ECG pattern at nominal or high leads	3
C. Type 2 or 3 Brugada ECG pattern that converts with provocative drug challenge	2
<i>Only award points once for highest score within this category. One item from this category must apply.</i>	
II. Clinical History	
A. Unexplained cardiac arrest or documented VF/polymorphic VT	3
B. Nocturnal agonal respirations	2
C. Suspected arrhythmic syncope	2
D. Syncope of unclear mechanism/unclear etiology	1
E. Atrial flutter/fibrillation in patients <30 years without alternative etiology	0.5
<i>Only award points once for highest score within this category.</i>	
III. Family History	
A. First- or second-degree relative with definite BrS	2
B. Suspicious SCD (fever, nocturnal, Brugada aggravating drugs) in a first- or second-degree relative	1
C. Unexplained SCD <45 years in first- or second-degree relative with negative autopsy	0.5
<i>Only award points once for highest score within this category.</i>	
IV. Genetic Test Result	
A. Probable pathogenic mutation in BrS susceptibility gene	0.5
Score (requires at least one ECG finding)	
≥3.5 points: Probable/definite BrS	
2–3 points: Possible BrS	
<2 points: Nondiagnostic	

BrS, Brugada syndrome; ECG, electrocardiogram; SCD, sudden cardiac death; VF, ventricular fibrillation; VT, ventricular tachycardia. From Antzelevitch C, Yan GX, Ackerman MJ, et al. J-wave syndromes expert consensus conference report: emerging concepts and gaps in knowledge. *Heart Rhythm*. 2016;13:e295–e324.

TABLE 31.14 Drugs Used to Unmask Brugada Electrocardiogram Pattern

Drug	Dose
Ajmaline	1 mg/kg IV infusion over 10 min
Flecainide	2 mg/kg IV infusion over 10 min, maximum 150 mg; or 200–300 mg oral
Procainamide	10 mg/kg IV infusion over 10 min
Pilsicainide	1 mg/kg IV infusion over 10 min

IV, Intravenous.

syndrome and their relatives, ajmaline was reported to have a sensitivity of 80% and a specificity of 94%. Flecainide has been shown to have a lower efficacy compared with ajmaline, likely due to a greater inhibition of I_{to} . Pilsicainide, a pure class IC drug, is believed to be more potent than flecainide. The class IA Na^+ channel blocker procainamide is traditionally regarded as the least potent, likely due to a more rapid dissociation of the drug from the Na^+ channels resulting in comparatively less inhibition of I_{Na} . The choice of Na^+ channel blocker used, however,

is usually based on availability. Procainamide remains the only choice for IV pharmacological induction protocols in the United States.^{83,84}

Of note, the response to flecainide infusion exhibits time-dependent variability of ECG patterns and intervals. Although most of the induced type I ECG patterns are observed during the first 30 minutes of the initiation of provocative testing, a recent study showed that extended periods of recording time (100 to 120 minutes) increased the percentage of positive testing from 12% to 19%.⁸⁵

Signal-Averaged Electrocardiography

Signal-averaged ECG demonstrates late potentials in approximately 60% to 70% of clinically affected Brugada syndrome patients. In this setting, late potentials can be a clinical marker of the disease, representing the delayed second upstroke of the epicardial action potential, a local phase 2 reentry (failing to trigger transmural reentry), or an intraventricular conduction delay.⁶⁴

Exercise Testing

Treadmill exercise testing can potentially aggravate the ECG abnormalities in the Brugada syndrome, including widening of the QRS, prolongation of the QTc duration, and augmentation of precordial peak ST segment elevation (which reaches its maximal amplitude during the early phase of recovery from exercise). Nonetheless, exercise was not found to induce ventricular arrhythmias in Brugada patients.⁸⁶

Genetic Testing

Genetic testing is recommended to support the diagnosis in patients manifesting the clinical phenotype of the Brugada syndrome. Although the knowledge of a specific mutation may not provide guidance for determining prognosis or treatment in the index patient, identification of a disease-causing mutation in the family can lead to genetic identification of at-risk family members who are clinically asymptomatic and who may have a normal ECG. However, it is important to remember that a negative result of genetic testing does not exclude the presence of the disease and, therefore, only a positive genetic diagnosis is informative. Genetic screening of *SCN5A* in unselected patients with a diagnosis of Brugada syndrome has low yield (less than 30%) and may not be cost-effective. The yield of genotyping increases substantially in patients with type 1 Brugada ECG pattern and prolonged PR interval, suggesting that this subset of patients with Brugada syndrome should be screened.⁶⁴

Genetic testing is not recommended in the setting of an isolated type 2 Brugada ECG pattern. It is important to recognize that genetic testing can produce “false-positive” results. Although *SCN5A* mutations are the most common genetic cause of Brugada syndrome, *SCN5A* genetic testing is complicated by an approximately 3% to 5% “benign” variant frequency in the general population.⁶⁵

Electrophysiological Testing

In patients with Brugada syndrome, EP testing may be considered for: (1) risk stratification to guide ICD implantation decisions in patients who have no history of cardiac arrest (including asymptomatic patients and those presenting with syncope); (2) evaluation of the efficacy of quinidine to suppress inducibility of VF in patients with inducible VF who do not prefer ICD therapy; and (3) assessment of sinus node function, conduction disturbances, and inducibility of supraventricular arrhythmias in patients with syncope.⁸⁷

Differential Diagnosis

Acquired Brugada Phenotype

ECG patterns identical to the type 1 or type 2 Brugada pattern can be seen in the absence of known genetic factors and family history. Some

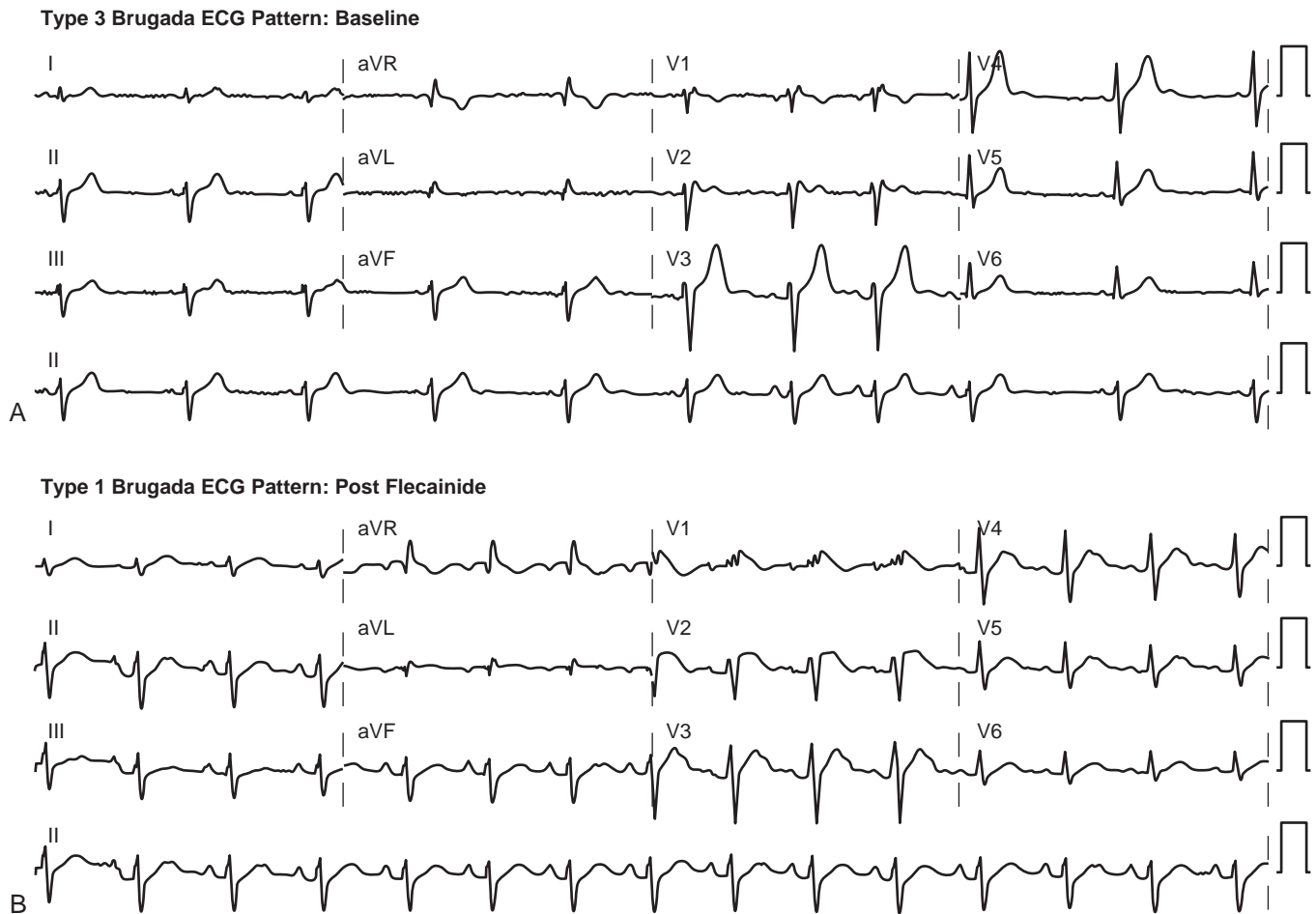


Fig. 31.13 Provocative Drug Testing to Unmask Brugada Electrocardiogram (ECG) Pattern. (A) ECG showing type 3 Brugada ECG pattern at baseline. (B) Type 1 Brugada ECG pattern developed post administration of flecainide.

investigators have labeled these “phenocopies,” indicating that they mimic the phenotype without a genetic predisposition. These acquired forms of Brugada phenotype can be elicited by a variety of pathological and physiological conditions (e.g., acute ischemia, pericarditis, myocarditis, pulmonary embolism, metabolic disorders, acidosis, ionic abnormalities, cocaine ingestion, some drugs, surgical RVOT manipulation) and disappear upon resolution of the underlying condition (Box 31.2). Characteristically, these patients lack symptoms, medical history, and family history suggestive of the true Brugada syndrome. Also, the ECG returns to normal upon resolution of the inciting environmental factors.²⁰

In some doubtful cases of type 2 Brugada pattern, provocative testing with a Na^+ channel blocker is recommended, which is typically negative in Brugada phenocopies.⁷⁷ Genetic testing may also be considered to rule out true Brugada syndrome, although it should be recognized that a negative genetic test result does not exclude the congenital Brugada syndrome.⁷⁸

Drug-Induced Brugada Electrocardiogram Pattern

A variety of pharmacological agents have been implicated in drug-induced Brugada ECG phenotype, although the likelihood of arrhythmias is unclear. In general, factors that increase outward currents (e.g., I_{to} , I_{KATP} , I_{Kr} , I_{Ks}) or decrease inward currents (e.g., I_{Na} , I_{CaL}) at the end of phase 1 of the action potential can potentially accentuate or unmask ST segment elevation similar to the ECG pattern observed in patients with the Brugada syndrome.³⁹

Among antiarrhythmic drugs, class IC agents (flecainide, propafenone, pilsicainide) and class IA drugs (ajmaline and procainamide) most effectively amplify or unmask ST segment elevation. On the other hand, class IB antiarrhythmic drugs (lidocaine, mexiletine) block fast I_{Na} primarily at fast heart rates (because of the rapid dissociation of these drugs from Na^+ channels). Therefore these drugs have little or no effect on fast I_{Na} at moderate or slow heart rates.³⁹

Several noncardiac drugs can potentially induce a Brugada-like ECG pattern secondary to block of I_{Na} , including psychotropic drugs, lithium, and cocaine. In addition, verapamil, H1 antihistamines, propofol, alcohol intoxication, vagomimetic agents, and beta-blockers and potentially nitrates can induce a Brugada-like ECG pattern (Table 31.15). Drug-induced Brugada syndrome from noncardiac drugs occurs predominantly in adult males, is frequently due to drug toxicity, and occurs late after the onset of therapy. However, the likelihood of drug-induced Brugada syndrome is difficult to predict in routine clinical practice.⁸⁸

Na^+ channel blocker provocation testing, family screening for Brugada syndrome, and possibly genetic analysis may be performed in a subject with an acquired form of Brugada ECG phenotype by noncardiac agents. Subjects with drug-induced Brugada syndrome by noncardiac agents should be advised to avoid the majority of class I and class III antiarrhythmic agents as well as beta-blockers and calcium channel blockers. Rigorous treatment of fever, a well-known trigger of arrhythmic events in Brugada syndrome, is also advised in subjects with an acquired Brugada syndrome ECG pattern by noncardiac agents.⁸⁹

BOX 31.2 Conditions Associated With Brugada-Like Electrocardiogram Pattern

Acute Conditions

- Acute pericarditis/myocarditis
- Acute myocardial ischemia or infarction (especially of the right ventricle)
- Pulmonary thromboembolism
- Prinzmetal angina
- Dissecting aortic aneurysm
- Hypothermia
- Postdefibrillation electrocardiogram
- Metabolic disorders
- Electrolyte abnormalities

Persistent Conditions

- Atypical right bundle branch block
- Left ventricular hypertrophy
- Early repolarization
- Athlete's heart
- Central and autonomic nervous system abnormalities
- Duchenne muscular dystrophy
- Friedreich ataxia
- Spinobulbar muscular atrophy
- Myotonic dystrophy
- Arrhythmogenic right ventricular dysplasia
- Chagas disease
- Mechanical compression of the right ventricular outflow tract (e.g., pectus excavatum, mediastinal tumor, hemopericardium)

Modified from Antzelevitch C, Yan GX, Ackerman MJ, et al. J-wave syndromes expert consensus conference report: emerging concepts and gaps in knowledge. *Heart Rhythm*. 2016;13:e295–e324.

TABLE 31.15 Drug-Induced Brugada Electrocardiogram Pattern

Drug Group	Example(s)
Class IC antiarrhythmic drugs	Flecainide, propafenone, pilsicainide
Class IA antiarrhythmic drugs	Ajmaline, procainamide, disopyramide
Calcium channel blockers	Verapamil, diltiazem, nifedipine
Beta-blockers	Propranolol
H1-Antihistamines	Dimenhydrinate
Tricyclic antidepressants	Amitriptyline, nortriptyline, desipramine
Tetracyclic antidepressants	Maprotiline
Selective serotonin reuptake inhibitors	Fluoxetine
Phenothiazines	Perphenazine, trifluoperazine
Local anesthetics	Bupivacaine
Other drugs	Lithium, nitrates, propofol

Whether the “acquired” form of Brugada syndrome unmasks clinically inapparent Brugada syndrome (“forme fruste”) or merely represents one end of a broad spectrum of responses to Na⁺ channel blockers is not known. The prognosis for asymptomatic patients with a drug-induced Brugada ECG pattern, but without a family history of SCD, appears to be benign once the offending agent is discontinued, provided the full-blown Brugada syndrome is not uncovered.⁸²

Conditions Associated With Right Precordial ST Elevation

A variety of pathophysiological conditions are associated with distinct right precordial abnormalities on the ECG that need to be distinguished

from the type 1 or type 2 Brugada ECG pattern. These include RBBB, LV hypertrophy, early repolarization, athlete's heart, and ARVC.

Right bundle branch block. Complete RBBB and the type 1 Brugada pattern are characterized by the presence of positive terminal deflections of the QRS and negative T waves in leads V₁-V₂. It is possible to distinguish between the two entities on the basis of the following^{77,78}:

1. The positive terminal r' wave is peaked in RBBB (β angle less than 58 degrees). Conversely, the high takeoff of r' in the Brugada pattern is rounded, wide, and usually of relatively low voltage, with a gradual slope of the descending arm of r'.
2. The terminal wave (r' or R') in RBBB observed in leads V₁-V₂ is synchronous with the broad S wave observed in leads I and V₆, and the QRS complex duration in leads V₁-V₂ is identical to that observed in lead V₆. In contrast, the QRS duration in the Brugada syndrome is longer in leads V₁-V₂ than in mid/left precordial leads (“QRS duration mismatch”) because the terminal deflection observed in lead V₁ (the r' wave overlying the RVOT) is not recorded by the V₆ electrode.
3. The ST segment in RBBB is not elevated in the right precordial leads.

Healthy athletes. Although lead V₁ in athletes can exhibit an r' wave, this wave is usually peaked and sharp (β angle less than 58 degrees) with no or only mild ST elevation (less than 1 mm), and the ST segment starts after the clear end of QRS and is often followed by a negative and sometimes deep T wave in lead V₁. Furthermore, the ST segment elevation observed in healthy athletes is upsloping, especially in lead V₂ (Corrado index less than or equal to 1).^{77,78}

Pectus excavatum. Mechanical compression of the RVOT in the setting of pectus excavatum can produce right precordial ECG abnormalities mimicking the Brugada pattern. The ECG pattern observed in pectus excavatum usually presents a narrow, very well defined r' wave in lead V₁, followed by a slight ST segment elevation. The T wave is usually negative or positive/negative in lead V₁ and positive in lead V₂.⁷⁸

Arrhythmogenic right ventricular cardiomyopathy. ARVC can produce repolarization and depolarization ECG abnormalities than can occasionally mimic the Brugada pattern. The depolarization abnormalities are caused by cellular uncoupling and altered tissue architecture due to fibrofatty infiltration, and typically manifest on the ECG as epsilon waves, RBBB, QRS fragmentation, localized QRS widening, and terminal S wave prolongation in right precordial leads. Repolarization abnormalities typically manifest as T wave inversion in the right precordial leads. T wave inversion in ARVC is observed in several precordial leads (V₁ to V₃-V₅), and not limited to leads V₁-V₂ as seen in the Brugada syndrome. In addition, the ECG pattern in ARVC is always fixed, in contrast to the dynamic Brugada pattern.⁷⁸

Although positive late potentials can be observed on signal-averaged ECG in both Brugada syndrome and ARVC, the prevalence is much higher in ARVC, and wavelet analysis demonstrates that the frequency level is higher in ARVC.^{77,78}

Risk Stratification

As noted, the risk of arrhythmic events varies widely among patients with Brugada syndrome, and is highest in patients with a history of cardiac arrest and intermediate in those with syncope. The risk of life-threatening arrhythmic events in patients who are asymptomatic when diagnosed is small, but not trivial (0.5% to 1.5% per year); therefore these patients are the main target of risk stratification strategies. However, risk stratification in these patients remains difficult because the event rate is low but the presenting symptom is often cardiac arrest.⁷⁴

Several criteria have been proposed for selecting asymptomatic patients with Brugada syndrome prone to a significant risk of malignant ventricular arrhythmias (Box 31.3). Gender, multiple ECG parameters,

BOX 31.3 Established and Potential Markers of Risk in Brugada Syndrome

Clinical Markers

- Aborted SCD
- Documented VT/VF
- Syncope likely due to VT/VF
- Nocturnal agonal respiration
- Male gender

Electrocardiogram Markers

- Spontaneous type 1 Brugada ECG pattern
- Early repolarization pattern in the inferolateral leads
- Increased Tpeak-Tend interval
- Fragmented QRS
- Prominent R wave in lead aVR
- Prominent S wave in lead I
- QRS duration ≥ 90 msec in lead V_6
- r-J interval ≥ 90 msec in lead V_2
- QRS duration ≥ 120 msec in lead V_2
- Late potentials on epicardial bipolar electrogram or signal-averaged ECG

Electrophysiological Markers

- Inducible VT/VF
- Short ventricular refractory period < 200 msec

ECG, Electrocardiogram; SCD, sudden cardiac death; VF, ventricular fibrillation; VT, ventricular tachycardia.

and VT/VF inducibility by programmed electrical stimulation have been reported to be useful in identifying high-risk patients; however, individual prediction performances of these parameters are limited. The presence of multiple independent risk factors likely provides additive prognostic information. Nevertheless, it is important to recognize that risk stratification in asymptomatic patients with Brugada syndrome has been a matter of continuous controversy.^{74,73}

Cardiac Arrest

Patients with a history of cardiac arrest are at the highest risk of recurrent events (35% at 4 years, 44% at 7 years, and 48% at 10 years). In a meta-analysis, the annual rate of arrhythmic events or SCD in these patients was estimated at 13.5%. The mean time from presentation to VF recurrence is 1.5 to 2 years, but late recurrence (5 years after the initial event) also can happen.⁷³

Syncope

Unexplained syncope (presumed to be of arrhythmogenic etiology, based on clinical characteristics) is considered a risk marker in patients with a spontaneous type I ECG at baseline (without conditions known to unmask the signature sign, i.e., drugs and fever).¹ In these patients, the risk of arrhythmic events during follow-up appears to be intermediate: about four times higher than the risk of asymptomatic patients but four times lower than that of patients presenting with cardiac arrest. In contrast, “nonarrhythmogenic” syncope (such as neurocardiogenic syncope, which is relatively common in Brugada patients) does not predict an increased arrhythmic risk. Therefore it is important to obtain a detailed clinical history because clinical features allow distinction between suspected arrhythmogenic and nonarrhythmogenic causes of syncope in 70% of cases.⁷⁵ Current guidelines state that ICD implantation can be useful in patients with a spontaneous type I ECG who have a history of syncope presumed to be of arrhythmic origin.⁷³

Gender

Male gender has consistently been shown to be associated with more arrhythmic events. However, male predominance is also observed in asymptomatic patients, which leads to a nonsignificant association with SCD.⁷³

Family History

Familial forms of the Brugada syndrome do not appear to be associated with a worse prognosis than are sporadic cases. In other words, a positive family history of Brugada syndrome does not predict outcome. Similarly, a positive family history for SCD is not a reliable predictor for poor outcome in asymptomatic patients with Brugada syndrome.

Genotype

Large registries have not found an association between specific genetic mutations and the risk of VF. Therefore genetic testing is not recommended for the sole purpose of risk stratification.⁷³

Invasive Electrophysiological Testing

The value of inducibility of ventricular arrhythmias by programmed stimulation as a predictor of poor outcome has been debated and remains unresolved. VF or sustained polymorphic VT can be induced in approximately 50% to 70% of Brugada patients during EP testing. Although large registries agree that VT/VF inducibility at EP study is greatest among Brugada syndrome patients with previous cardiac arrest or syncope, different studies arrived at different conclusions regarding the value of the EP testing for risk stratification in asymptomatic patients. These discrepancies are likely the result of differences in patient characteristics, subtle differences in the diagnostic criteria, and the use of nonstandardized or noncomparable stimulation protocols.

It is important to recognize that VF can be induced by programmed electrical stimulation in 6% to 9% of apparently healthy individuals and can represent a false-positive and nonspecific response, particularly when aggressive stimulation protocols are used. Limiting programmed ventricular stimulation to a maximum of two extrastimuli (while disregarding the induction of VF with three extrastimuli) delivered only from the RV apex (while avoiding pacing from the RVOT) has been suggested to increase the specificity of EP testing in Brugada patients. Although a negative study is a sign of good prognosis, the yield of a positive study remains controversial. Current guidelines consider the use of ventricular arrhythmia inducibility at EP study as an indication for ICD implantation in asymptomatic patients a class IIb indication.^{73,90}

In one report, a short ventricular effective refractory period (less than 200 milliseconds) was found to be a significant risk marker, but its use for clinical decision making awaits corroboration by further studies.

Electrocardiographic Parameters

Type 1 Brugada ECG pattern. In asymptomatic patients, spontaneous type 1 Brugada ECG pattern (recorded in whichever intercostal space) is a risk marker for fatal arrhythmias (0.5% to 0.8% per year), while the event rate of patients with drug-induced type 1 ECG is much lower (less than or equal to 0.35% per year). This observation is true for asymptomatic patients and for patients presenting with syncope.⁷³

A recent report found that the presence of a type 1 ECG pattern conferred a 3.5-fold increased risk of arrhythmic events in previously asymptomatic subjects. Because the Brugada ECG pattern is highly variable over time, it is imperative to obtain serial 12-lead ECG Holter recordings (at the fourth, third, and second intercostal spaces) to detect a spontaneous ECG pattern in asymptomatic subjects.⁷³

The risk of arrhythmic events in patients with fever-induced type 1 ECG pattern appears to be affected by the clinical presentation: the

annual event rate was 3.0% in patients with a history of VF, 1.3% in patients with a history of syncope, and 0.9% in asymptomatic patients.

Type 2 Brugada ECG pattern. Patients with a type 2 ECG pattern that did not convert to type 1 during drug challenge testing were found to have a good prognosis. However, in a recent report, the prognosis of probands with a type 2 Brugada ECG pattern (even after challenge with a Na⁺ channel blocker) was similar to that of patients with spontaneous or drug-induced type 1 ST elevation. Patients presenting with aborted cardiac arrest had a grim prognosis (annual rate of arrhythmic events of 10.6%), whereas those presenting with syncope or no symptoms had an excellent prognosis (annual rate of arrhythmic events less than or equal to 1.2%) irrespective of their ECG pattern (that is, type 1 vs. non-type 1). Also, a family history of SCD at an age younger than 45 years and coexistence of early repolarization in the inferolateral leads (observed in 8% to 11% of Brugada patients) were predictors of poor outcome. In contrast, VT/VF inducibility during programmed stimulation was not a predictor of outcome. Furthermore, men with a spontaneous type 1 ECG recorded only at the higher leads V₁ and V₂ showed a prognosis similar to that of men with a type 1 ECG when using standard leads.

Early repolarization. The prevalence of early repolarization in inferolateral leads is relatively high (11% in one report) among Brugada patients, and it appears to be associated with a worse outcome in both symptomatic and asymptomatic patients. The location of J waves in the inferior and lateral leads and horizontal ST segment morphology after the J wave may be related to a highly arrhythmogenic substrate in patients with Brugada syndrome.

Interval between the peak and the end of the T wave. The time interval between the peak and the end of the T wave (Tp-e interval) is thought to represent the difference in repolarization times between subendocardial and subepicardial myocardial cells and has been proposed as an ECG marker of transmural dispersion of repolarization when measured in the precordial leads. An increased Tp-e interval in the precordial leads has been shown to identify patients at higher risk of malignant arrhythmic events in various settings.⁹¹

The Tp-e interval was shown to be significantly longer from lead V₁ to V₄ in patients with Brugada syndrome presenting with malignant ventricular arrhythmia or syncope than in asymptomatic patients. A maximum Tp-e interval of at least 100 milliseconds in the precordial leads has been found to be highly and independently related to arrhythmic events in a large series of unselected patients with Brugada syndrome.⁹²

Furthermore, Tp-e interval dispersion (defined as the difference between the maximum and the minimum value of the Tp-e interval in leads V₁-V₆) has been reported to be useful in identifying high-risk patients.⁷⁴

S wave in lead I. The presence of a deep (greater than 0.1 mV) and/or large (greater than 40 milliseconds) S wave in lead I was found to be an independent predictor of arrhythmic events during follow-up. The S wave in lead I is generated by the terminal vector of ventricular activation, which is directed upward and somewhat to the right and backward. This vector is determined by electrical activation of the basal region of both ventricles and by depolarization of the RVOT. A prominent S wave in lead I is typically observed in cases of congenital heart disease, valvular heart disease, and cor pulmonale, which cause RV enlargement and fibrosis.

Of note, a large and prominent S wave in leads I and V₆ in adults is also a diagnostic criterion for RBBB, whereas an S_IS_{II}S_{III} pattern (i.e., an S wave is present in all three leads I, II, and III) and an S_IR_{II}R_{III} pattern with a QRS interval of less than 120 milliseconds can be produced by RV enlargement or zonal RV block. In the setting of Brugada syndrome, the presence of a prominent S wave in lead I could be related

to conduction delay over the RVOT and could be used to identify high-risk patients.⁶⁸

aVR sign. A prominent R wave in lead aVR (denoted “aVR sign”), defined as an R wave equal to or greater than or equal to 0.3 mV or an R/q ratio greater than or equal to 0.75 in lead aVR, has been suggested to reflect RV conduction delay. This association has not been confirmed in large studies.

Other ECG markers. QRS duration greater than or equal to 90 milliseconds in lead V₆, r-J interval greater than or equal to 90 milliseconds in lead V₂, QRS duration greater than or equal to 120 milliseconds in lead V₂, and fragmented QRS (defined as greater than or equal to 2 spikes within the QRS complex in leads V₁-V₃) have been reported to be useful in identifying high-risk patients.^{73,74,93}

Signal-Averaged Electrocardiogram

The presence of late potentials on signal-averaged ECG (which reflect ventricular conduction delay) has been reported to predict arrhythmic events during follow-up on univariate analysis; however, this finding remains unconfirmed.⁷³

Principles of Management

Implantable Cardioverter-Defibrillator

Currently, an ICD is the most effective treatment modality for the prevention of SCD in patients with Brugada syndrome. There is general consensus that ICD implantation is recommended in patients with type 1 Brugada ECG (either spontaneously or after Na⁺ channel blockade) and a history of aborted SCD (class I indication) (Fig. 31.14). The cumulative efficacy of ICD therapy (at least one appropriate defibrillation) in these patients is 18%, 24%, 32%, 36%, and 38% at 1, 2, 3, 4, and 5 years of follow-up, respectively.^{64,94}

In addition, ICD therapy is considered useful in Brugada patients with syncope, seizure, or nocturnal agonal respiration judged to be likely caused by ventricular tachyarrhythmias (class IIa indication). This group of patients, however, requires a thorough clinical assessment to exclude noncardiac causes of these symptoms before recommending ICD implantation. This is particularly important given the fact that most cases of syncope in Brugada patients have a nonarrhythmic mechanism, in whom the risk of life-threatening arrhythmic events is not higher than that in completely asymptomatic patients.

On the other hand, there is no similar consensus regarding the management of asymptomatic patients with the Brugada syndrome. Although some experts advocate close follow-up, others propose the evaluation of VT/VF inducibility by programmed stimulation for risk stratification in patients with spontaneous type 1 Brugada ECG. ICD implantation in those with inducible VT/VF is controversial and has a class IIb indication. For asymptomatic patients with normal baseline ECG and those with spontaneous type 1 Brugada ECG but noninducible VT/VF during programmed stimulation, a conservative approach (i.e., general precautions and follow-up) and reassurance are adequate management.⁸²

It is important to recognize that ICD therapy is not without complications, and the decision to implant an ICD prophylactically in asymptomatic patients must be examined in the context of the low rate of cardiac events (0.5% per year) and the high long-term risk of device-related complications (16%). This is relevant given that Brugada patients enjoy extended longevity post ICD implantation, and because of younger age and more activity, they have a greater propensity for lead fractures, require multiple generator exchanges over a lifetime, and experience quality-of-life issues from inappropriate shocks.⁹⁵

Inappropriate shocks are among the most important adverse effects of ICD therapy, occurring 2.5 times more frequently than appropriate shocks. In one report, inappropriate shocks at 10-years post ICD

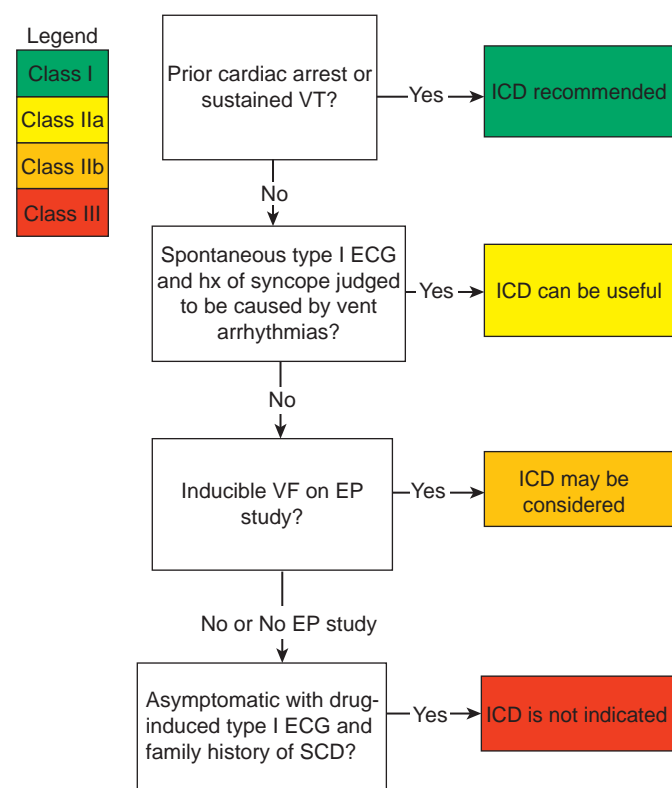


Fig. 31.14 Consensus Recommendations for Implantable Cardioverter-Defibrillators in Patients Diagnosed With Brugada Syndrome. ECG, Electrocardiogram; ICD, implantable cardioverter defibrillator; SCD, sudden cardiac death; VF, ventricular fibrillation; VT, ventricular tachycardia. (From Priori SG, Wilde AA, Horie M, et al. HRS/EHRA/APHS expert consensus statement on the diagnosis and management of patients with inherited primary arrhythmia syndromes. *Heart Rhythm*. 2013;10:1932–1963.)

implantation were observed in 37% of ICD recipients. Inappropriate ICD therapies are usually triggered by supraventricular arrhythmias, lead fracture, and T wave oversensing. Several strategies can potentially reduce the frequency of inappropriate shocks, such as adding an atrial lead (for better discrimination between ventricular and supraventricular arrhythmias), modifying the arrhythmia detection settings (programming a single VF zone of more than 210 beats/min with or without a monitoring zone of more than 180 beats/min), and aggressive treatment of supraventricular arrhythmias. Of note, high rates of inappropriate shock have been reported even after careful device programming.^{1,95}

Catheter Ablation

In Brugada patients with frequent episodes of VT/VF, monomorphic PVCs originating predominantly in the RVOT or RV Purkinje network are often the trigger for VT, and focal radiofrequency (RF) ablation of the PVCs can be valuable in reducing the burden of arrhythmias and ICD therapies (Fig. 31.15). Furthermore, recent studies suggest that extensive ablation of the epicardial arrhythmogenic substrate in the RVOT and RV anterior wall can significantly reduce arrhythmia vulnerability and ECG manifestation of the disease in most patients. Ablation targets include sites displaying late potentials and low-voltage, fractionated bipolar electrograms, potentially representing depolarization abnormalities or concealed phase 2 reentry secondary to heterogeneous repolarization. Na⁺ channel blockade challenge (e.g., with flecainide, ajmaline, or procainamide) has been used to delineate the arrhythmic

substrate before ablation, and to ensure complete substrate elimination post ablation (Fig. 31.16).^{96,97}

The mechanism of the ameliorative effects of epicardial ablation in the setting of Brugada syndrome remains uncertain; nonetheless, recent experimental studies suggest that catheter ablation abolishes the cells with the most prominent action potential notch, thus eliminating sites of abnormal repolarization and the substrate for ventricular arrhythmias.⁹⁸

Catheter ablation therapy can be lifesaving in patients with refractory arrhythmias or those in whom ICD implantation is not feasible or not desired. The most recent expert consensus guidelines recommend ablation (class IIb) for patients with Brugada syndrome and frequent appropriate ICD shocks due to recurrent electrical storms (see Fig. 31.15).⁹⁶ Importantly, despite normalization of the spontaneous type 1 Brugada ECG pattern after epicardial ablation, VT/VF recurrence was observed in 27% of patients in one report, suggesting that ICD remains the cornerstone therapy for Brugada syndrome patients.⁹⁹

Pharmacological Therapy

Several pharmacological agents have been used for treatment and prevention of ventricular arrhythmias in patients with Brugada syndrome (see Fig. 31.15). Because of the critical role of I_{to} and I_{CaL} in the arrhythmogenesis in the Brugada syndrome, drugs such as quinidine that inhibit I_{to} or augment I_{CaL} have been shown to have a therapeutic value. Both groups of drugs can potentially restore the RV epicardial action potential dome, thus normalizing the ST segment and preventing phase 2 reentry and ventricular arrhythmias in the Brugada syndrome. Of note, amiodarone and beta-blockers are ineffective. Also, class IC (flecainide, propafenone) and some class IA antiarrhythmic agents (procainamide) with predominant Na⁺ channel blocking effects are contraindicated, as they can worsen ST elevation and arrhythmogenesis.

I_{to} blockade. No cardioselective I_{to}-specific blockers are currently available. Nonetheless, quinidine, a class IA Na⁺ channel blocker, has a relatively strong effect in blocking I_{to} and has been found effective in suppressing arrhythmia inducibility on EP testing in up to 76% of Brugada syndrome patients and in preventing the occurrence of spontaneous arrhythmias. In particular, quinidine has been extraordinarily effective in the treatment of VF storms in Brugada patients. Doses between 600 and 900 mg are recommended, if tolerated, but even lower doses can be beneficial.¹⁰⁰

The use of quinidine is recommended as adjunctive chronic treatment in ICD patients with frequent appropriate ICD therapies, and in patients with electrical storm. Also, quinidine should be considered in high-risk Brugada patients in whom ICD implantation is not feasible or not desired. Although quinidine has been proposed as a preventative measure in asymptomatic patients displaying a spontaneous type 1 ECG pattern, this has not been evaluated in large clinical trials.

Nonrandomized clinical studies suggest that EP-guided therapy with quinidine (or alternatively disopyramide) that effectively suppresses the induction of VF by programmed electrical stimulation can potentially be used as an alternative to ICD therapy under certain circumstances, especially in those patients who do not prefer device implantation. This approach requires that sustained polymorphic VT or VF is induced during EP testing, and that arrhythmia inducibility is eliminated by drug therapy despite aggressive stimulation protocol (less than or equal to 3 extrastimuli, less than or equal to 5 diastolic threshold, 2 RV sites, 2 pacing drive cycle lengths [CLs]). This strategy also requires tolerance and compliance to long-term drug therapy.^{100–102}

The experience with disopyramide (a class IA Na⁺ channel blocker) is much more limited but its efficacy seems to be acceptable. More recently, bepridil was shown to suppress VT/VF, mainly through I_{to} inhibition and I_{Na} augmentation. Tedisamil, an experimental potent I_{to}

blocker without the relatively strong inward current-blocking actions of quinidine, may become a therapeutic option.

I_{CaL} augmentation. Several drugs that augment I_{CaL} can potentially be effective for the treatment of ventricular arrhythmias associated with the Brugada syndrome. Beta-adrenergic agonists, such as isoproterenol, denopamine, and orciprenaline, have been shown to be useful. Isoproterenol infusion (dose titrated to achieve a 20% increase in heart rate), alone or in combination with quinidine, has been successfully used to decrease ST elevation and suppress repetitive episodes of VF in patients presenting with electrical storms (see Fig. 31.7). Before consideration of isoproterenol therapy, however, it is critical that the diagnosis of Brugada syndrome be clearly established as the underlying etiology of VF storm. Isoproterenol infusion can be devastating in patients with VF due to other mechanisms, especially CPVT. This is especially important to recognize because a Brugada-like ST segment elevation can occasionally appear for a brief period in a patient successfully defibrillated from VF.

The phosphodiesterase III inhibitors cilostazol and milrinone are other promising agents for suppressing ST elevation and arrhythmogenesis in Brugada syndrome, likely by augmenting I_{CaL} and by reducing I_{to} secondary to an increase in cAMP and heart rate.

I_{Na} augmentation. Agents that augment I_{Na} , including bepridil and dimethyl lithospermate B, have also been suggested to be of value in the pharmacological approach to therapy of Brugada syndrome. As noted, the antiarrhythmic effects of bepridil are likely mediated by inhibition of I_{to} as well as augmentation of peak and late I_{Na} .

Lifestyle Modifications

Education and lifestyle changes for the prevention of arrhythmias are critical in patients with Brugada syndrome (see Fig. 31.15). Patients need to be educated about the importance of seeking medical attention during febrile illnesses to ensure the rapid and aggressive treatment of pyrexia (often with cardiac monitoring in place). In addition, several drugs have been reported to exacerbate the ECG pattern of ST segment elevation in the Brugada syndrome and to trigger arrhythmias (as outlined at www.brugadadrugs.org), and should be avoided. Family members may consider basic life support training and operation of an automated external defibrillator for home use.

Participation in Sports

Currently available data are insufficient to make definitive recommendations for participation of asymptomatic Brugada patients in competitive sports. A clear association between exercise and SCD has not been established. Given the fact that the risk of an arrhythmic event in asymptomatic patients with Brugada syndrome is small and that malignant ventricular arrhythmias are usually unrelated to physical activity, participation of asymptomatic athletes with Brugada syndrome in competitive sports is not prohibited.¹⁰³

Competitive sports participation may also be considered for an athlete with previously symptomatic Brugada syndrome assuming appropriate disease-specific treatments are in place and that the athlete has been asymptomatic on treatment for at least 3 months.¹⁰³

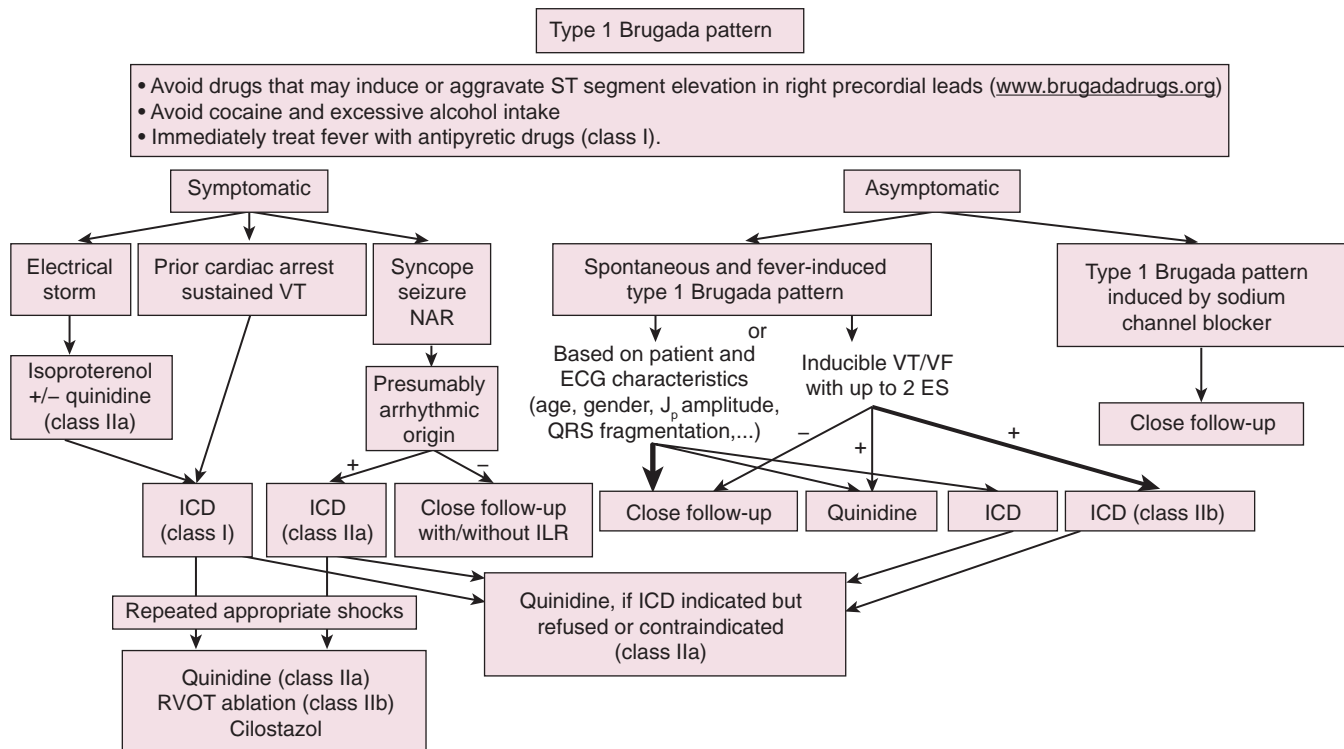


Fig. 31.15 Indications for Therapy of Patients With Brugada Syndrome. Recommendations with class designations are taken from Priori et al.¹ and Priori and Blomström-Lundqvist.¹⁵⁴ Recommendations without class designations are derived from expert consensus. ECG, Electrocardiogram; ES, extrastimuli at right ventricular apex; ICD, implantable cardioverter-defibrillator; ILR, implantable loop recorder; NAR, nocturnal agonal respiration; RVOT, right ventricular outflow tract; VF, ventricular fibrillation; VT, ventricular tachycardia. (From Antzelevitch C, Yan GX, Ackerman MJ, et al. J-wave syndromes expert consensus conference report: emerging concepts and gaps in knowledge. *Heart Rhythm*. 2016;13:e295–e324.)

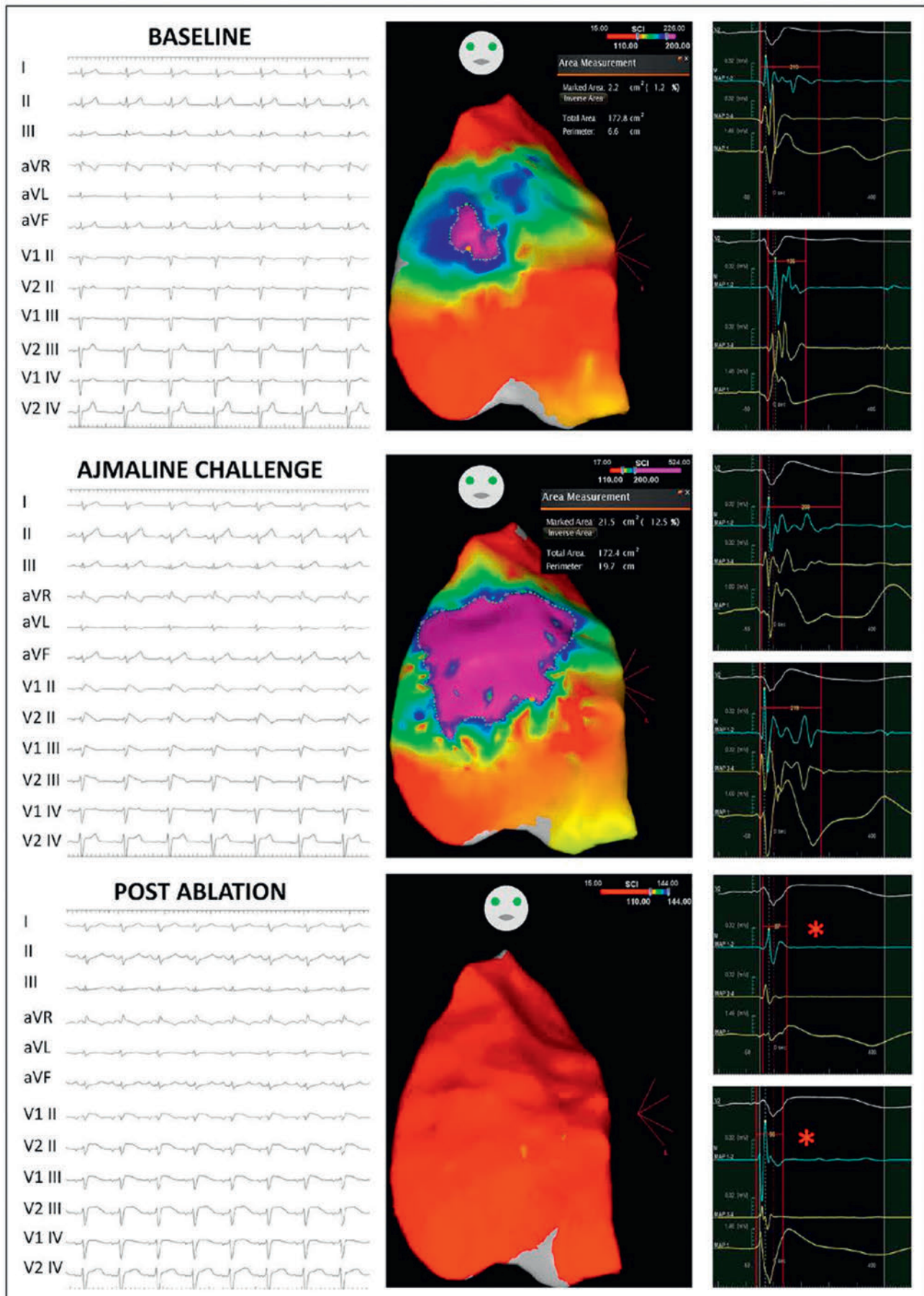


Fig. 31.16 Brugada Syndrome (BrS) Phenotype Abolition by Epicardial Substrate Ablation. *Top*, Baseline BrS electrocardiogram (ECG) pattern and epicardial color-coded duration CARTO maps. A saddleback pattern is evident in V₂ (II intercostal space) with a corresponding small (2.2 cm²) purple area of abnormally prolonged potentials (210 msec in the example). The border-zone area (green/blue area >110 msec and <200 msec) shows potentials with relatively shorter duration (136 msec). *Middle*, BrS ECG pattern and color-coded duration maps after ajmaline. After type 1 ajmaline-induced ECG pattern, the abnormal purple area significantly increased to 21.5 cm². Examples of abnormal and prolonged electrograms found in the purple area after ajmaline test are shown beside the map (289 and 219 msec). *Bottom*, BrS ECG pattern and color-coded duration maps after radiofrequency ablation of epicardial substrate. After ajmaline rechallenge at the end of the procedure, the ECG showed a horizontal and ascendant ST segment elevation, with minimal intraventricular conduction delay characterized by slight QRS broadening with a more pronounced S wave in leads I and II and qR morphology in aVR. Abnormally prolonged fragmented and delayed electrograms disappeared (87 and 96 msec, light blue color). The two examples of ventricular electrograms were recorded from the previously abnormal area, and the red asterisks indicate disappearance of the late components. Electrogram panels are from the CARTO system and show ECG lead V₂ (white), distal (light blue), and proximal bipolar (yellow) and unipolar signals (yellow) at 200 mm/s speed, from top to bottom, respectively. Of note, in the middle, lead V₂ shows a typical coved-type pattern, which after ablation was modified into a horizontal and at ST segment elevation. (From Pappone C, Brugada J, Vicedomini G, et al. Electrical substrate elimination in 135 consecutive patients with Brugada syndrome. *Circ Arrhythmia Electrophysiol.* 2017;10:e005053.)

Importantly, appropriate precautionary measures should be undertaken to avoid exercise-related hyperthermia, dehydration, and electrolyte abnormalities, which can potentially trigger ventricular arrhythmias in Brugada patients. Also, athletes should be aware of the potential impact of postexercise increase in vagal tone on triggering cardiac events. Other considerations include the acquisition of a personal automatic external defibrillator as part of the athlete's personal sports safety gear, and establishment of an emergency action plan with the appropriate training facility and team officials.¹⁰³

Family Screening

Most individuals diagnosed with the Brugada syndrome have inherited the disease-causing mutation from a parent. Although a proband with the Brugada syndrome may have the disorder as the result of a *de novo* gene mutation, this is very rare (approximately 1%). Because the disease is caused by an autosomal dominant genetic defect, every offspring has a 50% chance of inheriting the disease-causing mutation. Nonetheless, the family history may appear to be negative because of failure to recognize the disorder in family members, low penetrance, early death of the parent before the onset of warning symptoms, or late onset of symptoms in the affected parent. Therefore the lack of a family history does not rule out a heritable disease.

When the causative mutation in the index patient is identified, genetic testing is recommended in all first-degree relatives. Family members who test positive for the familial mutation should receive baseline ECG and annual ECG screening examinations, and should be instructed to avoid medications that can induce ventricular arrhythmias and to seek medical attention immediately on occurrence of symptoms. On the other hand, mutation-negative family members and their descendants have no risk for developing the disease and do not need further evaluation. Genetic testing also can be used for prenatal diagnosis. All patients who undergo genetic testing should receive pretest and posttest genetic counseling to understand the implications of testing.

When genetic testing is not performed in the proband, or when genetic analysis fails to identify a definite disease-causing mutation (or only reveals one or more genetic variants of unknown significance), genetic testing in the related family members is not recommended. In this setting, it is recommended that at-risk individuals with a family history of Brugada syndrome should undergo ECG monitoring every 1 to 2 years. The presence of type 1 ST elevation should be further investigated.

TABLE 31.16 Molecular Basis of the Short QT Syndrome

	Gene	Protein	Functional Effect
SQT1	<i>KCNH2 (HERG)</i>	K _v 11.1	↑I _{Kr}
SQT2	<i>KCNQ1 (KvLQT1)</i>	K _v 7.1	↑I _{Ks}
SQT3	<i>KCNJ2</i>	Kir2.1	↑I _{K1}
SQT4	<i>CACNA1C</i>	Ca _v 1.2	↓I _{CaL}
SQT5	<i>CACNB2B</i>	Ca _v β2b	↓I _{CaL}
SQT6	<i>CACNA2D1</i>	Ca _v α2δ1	↓I _{CaL}

I_{CaL}, L-type Ca²⁺ current; I_{K1}, inward rectifier K⁺ current; I_{Kr}, rapidly activating delayed rectifier K⁺ current; I_{Ks}, slowly activating delayed rectifier K⁺ current; SQT1 to SQT6, short QT syndrome types 1 to 6, respectively.

SHORT QT SYNDROME

The SQTs, first described in 2000, is a highly arrhythmogenic inherited channelopathy occurring in young individuals with structurally normal hearts. Affected patients are characterized by constantly short QT intervals associated with AF, syncope, and/or SCD.¹⁰⁴

Genetics of the Short QT Syndrome

To date, mutation analysis has implicated six distinct genes in the etiology of a proportion of patients diagnosed with SQTs, although the majority of diagnosed cases do not have reported genetic associations. It is expected that further genes will be identified. Genetic studies reveal a genetically heterogeneous disease with gain-of-function mutations of voltage-gated K⁺ channel genes (Table 31.16). Loss-of-function mutation in the L-type Ca²⁺ channel genes have also been linked to SQTs, but in some cases might represent a clinical spectrum of Brugada or early repolarization syndromes. These mutations cause either an increase in the outward repolarizing K⁺ currents or a decrease in the inward depolarizing Ca²⁺ currents, leading to shortening of the action potential duration, the QT interval, and the effective refractory period.

Mutations Related to the Potassium Current

SQT1, the most common genotype, is caused by mutations of the *KCNH2* gene (*HERG*, encoding the α-subunit K_v11.1 of the I_{Kr}). A

gain-of-function mutation on *KCNH2* causes a shift of voltage dependence of inactivation of I_{Kr} by +90 mV out of the range of the action potential, which results in a significant increase in I_{Kr} during the action potential plateau. The resulting I_{Kr} augmentation achieved by altered gating hastens repolarization, thereby shortening the action potential duration and QT interval and facilitating reentrant excitation waves to induce atrial and/or ventricular arrhythmias. Of note, loss-of-function mutations in the *KCNH2* gene are responsible for LQT2.

SQT2 is caused by mutations of the *KCNQ1* gene (*KvLQT1*, encoding the α -subunit $K_{v7.1}$ of the I_{Ks}). A gain-of-function mutation of *KCNQ1* causes a shift in the voltage dependence of I_{Ks} activation by -20 mV and acceleration of activation kinetics, leading to enhancement of I_{Ks} and shortening of the action potential duration and QT interval. Of note, loss-of-function mutations in the *KCNQ1* gene are responsible for LQT1.

SQT3 is caused by a mutation in the *KCNJ2* gene (encoding the strong inwardly rectifying channel protein Kir2.1 of the I_{K1}). A gain-of-function mutation causes a significant increase in the outward I_{K1} at potentials between -75 and -45 mV, leading to shortening of the QT interval and asymmetrical T waves, with a normal ascending component and a rapid descending terminal phase. On the other hand, loss-of-function mutations in the *KCNJ2* gene, identified in patients with the Andersen syndrome, generate prolongation of the QT intervals (LQT7).

Because I_{Kr} , I_{Ks} , and I_{K1} each contribute differentially to cardiac repolarization, gene-specific mutations will differentially influence repolarization and the susceptibility to arrhythmia. However, detailed information regarding the genotype-phenotype correlation is currently limited by the rare nature of this disorder.

Mutations Related to the Calcium Current

SQT4-6 is caused by mutations in the *CACNA1C*, *CACNB2*, and *CACNA2D1* genes, encoding the $\alpha 1C$ -, $\beta 2b$ -, and $\alpha 2\delta 1$ -subunits of the cardiac L-type Ca^{2+} channel $Ca_v1.2$, respectively. Loss-of-function mutations of those genes result in major attenuation in I_{CaL} amplitude, leading to shortening of the action potential duration, and are associated with asymmetrical T waves, an attenuated QT-heart rate relationship, and AF. Three patients reported to harbor these mutations had a Brugada type 1 phenotype. In addition, loss-of-function mutations of the *CACNA1C* and *CACNB2* genes have recently been linked to a sudden death syndrome that combines the features of Brugada syndrome, including the characteristic ECG pattern, and a short QT interval. It was speculated that these mutations cause Brugada syndrome by aggravating transmural voltage gradients. Of note, loss-of-function mutations in L-type Ca^{2+} channel proteins can also, in certain cases, cause early repolarization syndromes. Conversely, a gain-of-function mutation of the L-type Ca^{2+} channel is known to generate the LQT8 (Timothy syndrome).¹⁰⁴

Pathophysiology of Short QT Syndrome

Reduced wavelength of activation and heterogeneous shortening of action potential duration (preferentially more in epicardial and endocardial layers, causing increased transmural dispersion of repolarization), predispose to functional reentry and play a role in the increased atrial and ventricular susceptibility to premature stimulation, leading to AF and VF.^{1,104}

Epidemiology

SQTS has been described in very few families worldwide; therefore all the information available is based on small numbers of cases. The majority (more than 75%) of affected subjects have been men, suggesting a sex-dependent penetrance (similar to the Brugada syndrome). Nonetheless, the prevalence of cardiac arrest appears equal in both genders,

suggesting that females should not be regarded at a lower risk for malignant arrhythmias. The age of presentation is quite variable, ranging from infancy to the eighth decade of life, with a mean age of 20 to 30 years. There seems to exist an age dependency in the susceptibility to arrhythmias, with a peak in the occurrence of cardiac arrest in the first year of life (incidence, 4% per year) and a second peak between 20 and 40 years of age (incidence, 1.3% per year). Up to 72% of patients with SQTS have a family history of SQTS or SCD.^{105,106}

Clinical Presentation

More than 60% of the subjects have symptoms at presentation, with cardiac arrest being the most frequent symptom, representing the first clinical manifestation in one-third of patients. Syncope is observed as a first clinical presentation less frequently (14%). AF has been documented in approximately 30% of patients with SQTS. No information is available on whether specific triggers precipitate cardiac events, and the majority of cardiac events appear to occur under resting conditions or during sleep.¹⁰⁷

Electrocardiographic Features

A short QT interval is the hallmark of SQTS. However, the definition of the lower limit of a "normal" QT interval and the diagnostic criteria sufficient to establish the diagnosis of SQTS remain to be determined unequivocally. Based on ECG analysis of 14,379 healthy individuals, some investigators proposed that a QTc interval less than 350 milliseconds (which is less than 88% of the mean predicted value, or less than 2 standard deviations below the mean) be considered short, and a QTc interval less than 320 milliseconds (which is less than 80% of the mean predicted value) be considered abnormally short. The prevalence of a QTc interval less than 88% of the mean was 2.5% and that of a QTc interval less than 80% of the mean was 0.03%.¹⁰⁴

Importantly, the mere presence of a short QT interval on the surface ECG does not necessarily translate into an increased risk of arrhythmias. In fact, in a study in a middle-aged Finnish population ($n = 10,822$) followed up for 29 ± 10 years, the prevalence of QTc less than 320 milliseconds (using the Bazett formula) was 0.1% and that of QTc less than 340 milliseconds was 0.4%. There was no difference in the all-cause or cardiovascular mortality between subjects with a very short QTc (less than or equal to 320 milliseconds) or short QTc (less than or equal to 340 milliseconds) and those subjects with a normal QTc interval (360 to 450 milliseconds). On the other hand, in a recent epidemiological study of a cohort of 1.7 million persons with 6.4 million ECGs, a QTc of 300 milliseconds or less was extraordinarily rare (0.7 per 100,000 ECGs) and was associated with significant ECG abnormalities and a 2.6-fold increased risk of death.¹⁰⁸

Of note, the physiological shortening of the QT interval during exercise-induced tachycardia can be blunted in patients with SQTS. This is relevant because impaired QT adaptation to heart rate changes makes the correction formulas such as those of Bazett or Fredericia inappropriate or of limited value in SQTS patients with heart rates above 100 beats/min or below 60 beats/min. The poor performance of correction formulas, in addition to the lack of a universal diagnostic cutoff value for an SQTS, makes it difficult to establish a diagnosis in cases of borderline shortened QT intervals.

Several other ECG markers can potentially be helpful to support the diagnosis of SQTS especially in patients with borderline QTc intervals (QTc intervals 330 to 370 milliseconds). In addition to constantly short QTc intervals, affected patients have in common a short or even absent ST segment, with the T wave initiating immediately from the S wave. Extreme abbreviation of the Jpoint-Tpeak interval (less than 120 milliseconds) can help distinguish patients with SQTS from healthy subjects with an apparent abbreviation of the ST segment and shortened QT

intervals (mean Jpoint-Tpeak interval of 188 ± 11 milliseconds). Furthermore, the increase in dispersion of repolarization in patients with SQTs results in increased Tp-e interval and ratio of Tp-e/QT.

In addition, high-amplitude, narrow, and symmetrical T waves in the precordial leads are frequently observed in SQTs patients; but asymmetrical T waves also can be observed, especially in SQT3 patients. Another ECG characteristic observed in most (81%) SQTs patients is PQ segment depression (greater than or equal to 0.05 mV), likely caused by heterogeneous shortening of atrial repolarization.¹⁰⁹

Diagnosis of the Short QT Syndrome

A diagnostic scoring system to facilitate the diagnosis of SQTs was proposed in 2011 by Gollob et al., based on a comprehensive review of 61 reported cases of the SQTs. The Gollob score incorporates ECG findings, clinical history, family history, and genotype findings (Table 31.17). In this system, all patients should have a QTc interval (using the Bazett formula) of no more than 370 milliseconds. Clinical events (cardiac arrest, nonsustained polymorphic VT or VF, syncope, AF) must occur in the absence of other identified clinical pathologies. Although these diagnostic criteria can potentially facilitate evaluation in suspected cases of SQTs, their value for evaluation of family members can poten-

tially be limited because of incomplete disease penetrance. Importantly, treatment considerations should be reserved for subjects receiving a high-probability score, whereas medical surveillance or expert opinion should be considered for intermediate- or low-probability cases.

More recently, in 2013, an expert consensus recommended that SQTs is diagnosed in the presence of a QTc of 330 milliseconds or less. SQTs also can be diagnosed in the presence of a QTc between 330 and 360 milliseconds in conjunction with at least one additional criterion including: (1) a pathogenic mutation, (2) family history of SQTs, (3) family history of SCD below age 40, or (4) survival of a VT/VF episode in the absence of heart disease.¹

Electrophysiology Testing

The role of EP study in diagnosis and risk stratification is not yet fully defined. During EP testing, atrial and ventricular effective refractory periods are significantly shortened, and VT/VF is inducible in 60% to 91% of patients. However, inducibility of ventricular arrhythmias does not appear to be predictive of adverse clinical outcome.

Genetic Testing

Genetic analysis may be considered for patients with a strong clinical index of suspicion for SQTs based on the personal and family history and the ECG phenotype. A mutation in genes related to SQTs is observed in 23% of probands, with SQTs1 being the most common. Genetic testing can help identify silent carriers of SQTs-related mutations; however, the risk of cardiac events in genetically affected individuals with a normal ECG is currently not known. Similarly, given the limited number of patients with SQTs so far identified, genetic analysis at present does not contribute to risk stratification.

Differential Diagnosis

Shortening of the QT interval can be encountered in a variety of pathophysiological states, including hyperkalemia, hypercalcemia, hyperthermia, acidosis, digitalis overdose, androgen use, increased vagal tone, administration of acetylcholine and catecholamines, and carnitine deficiency (an autosomal recessive disorder due to a defective transport of carnitine into the cell).^{104,110}

Risk Stratification

The optimal strategy for risk stratification of asymptomatic SQTs patients remains uncertain. SQTs patients with prior cardiac arrest are considered at high risk for SCD. However, no independent risk factors for life-threatening arrhythmias have been identified in asymptomatic patients. The degree of shortening of the QT interval at faster heart rates has not been found to be a prognostic indicator in asymptomatic patients. Although mutation carriers exhibited a significantly shorter QTc interval compared with noncarriers, this finding did not correlate with a different outcome. As noted, inducibility of ventricular arrhythmia during EP testing was found ineffective for predicting cardiac arrest (sensitivity of 37% and a negative predictive value of 58%). Also, the Gollob score was not a predictor of adverse cardiac events in this patient population.¹⁰⁶

Principles of Management

Implantable Cardioverter-Defibrillator

At present, ICD implantation is the therapy of choice for the prevention of SCD in symptomatic SQTs patients (survivors of cardiac arrest and those with spontaneous VT). The role of ICD therapy for primary prevention is uncertain, although ICD implantation may be reasonable in asymptomatic SQTs patients with a strong family history of SCD (class IIb). Importantly, patients with SQTs are potentially susceptible to inappropriate shocks because of oversensing of the tall, narrow T

TABLE 31.17 Diagnostic Criteria of the Short QT Syndrome

QTc	
• <370 msec	1
• <350 msec	2
• <330 msec	3
• Jpoint-Tpeak interval <120 msec	1
Clinical History	
• History of sudden cardiac arrest	2
• Documented polymorphic VT or VF	2
• Unexplained syncope	1
• Atrial fibrillation	1
Family History	
• First- or second-degree relative with high-probability SQTs	2
• First- or second-degree relative with autopsy-negative sudden cardiac death	1
• Sudden infant death syndrome	1
Genotype	
• Genotype positive	2
• Mutation of undetermined significance in a culprit gene	1

Notes:

- High-probability SQTs, ≥ 4 points; intermediate-probability SQTs, 3 points; low-probability SQTs, ≤ 2 points.
- Electrocardiogram: Must be recorded in the absence of modifiers known to shorten the QT.
- Jpoint-Tpeak interval must be measured in the precordial lead with the greatest amplitude T wave.
- Clinical history: Events must occur in the absence of an identifiable etiology, including structural heart disease.
- Points cannot be combined for the following three markers: cardiac arrest, documented polymorphic VT, and unexplained syncope.
- Family history: Points can only be received once in this section.
- A minimum of 1 point must be obtained in the electrocardiographic section to obtain additional points.

QTc, Corrected QT interval; SQTs, short QT syndrome; VF, ventricular fibrillation; VT, ventricular tachycardia.

waves and the high prevalence of AF. Therefore appropriate programming of the ICD is necessary.¹

Pharmacological Therapy

Of the pharmacological agents tested to date, quinidine seems the most effective at prolonging the QT interval in patients with SQTs. Quinidine was shown to prolong the QT interval, normalize atrial and ventricular effective refractory periods, and prevent inducibility of ventricular arrhythmias during EP testing in patients with SQT1, with a weaker and variable effect in the non-SQT1 patients. In a recent report, the incidence of arrhythmic events during follow-up was 4.9% per year in the patients without pharmacological prophylaxis, whereas no arrhythmic events occurred in those receiving hydroquinidine (even if previously symptomatic).

Hence, quinidine can potentially serve as an adjunct to ICD therapy in the treatment of paroxysmal AF or recurrent ventricular tachyarrhythmias in this subgroup of patients or as an alternative option to ICD in patients who cannot receive it (small children) or who decline the implant. Quinidine may also be considered primary prevention of cardiac arrest in asymptomatic SQTs patients with a family history of SCD.¹

Other drugs, including class III agents (e.g., sotalol), are not effective in prolonging the QTc interval in SQT1 patients, and efficacy in the other subtypes is unknown.¹

Participation in Sports

Until the phenotype of SQTs is better understood, a universal restriction from competitive sports, with the possible exception of class IA activities, seems to represent the most prudent recommendation.

CATECHOLAMINERGIC POLYMORPHIC VENTRICULAR TACHYCARDIA

CPVT, also known as familial polymorphic VT, is a rare but highly malignant inherited arrhythmia disorder characterized by exercise- and stress-induced polymorphic or bidirectional VT. CPVT is an important cause of syncope and SCD in individuals with a structurally normal heart.¹¹¹

Genetics of Catecholaminergic Polymorphic Ventricular Tachycardia

Mutations in genes that encode for four key Ca^{2+} regulatory proteins are currently implicated in the pathogenesis of CPVT (Table 31.18).

TABLE 31.18 Molecular Basis of Catecholaminergic Polymorphic Ventricular Tachycardia

Disease	Gene	Protein	Inheritance	% Probands
CPVT1	<i>RyR2</i>	Ryanodine receptor 2	Autosomal dominant	50%–55%
CPVT2	<i>CASQ2</i>	Calsequestrin	Autosomal recessive	2%–5%
CPVT3	<i>Unknown</i>	Unknown	Autosomal recessive	Rare
CPVT4	<i>CALM1</i>	Calmodulin	Autosomal dominant	<1%
CPVT5	<i>TRDN</i>	Triadin	Autosomal recessive	1%–2%

CPVT, Catecholaminergic polymorphic ventricular tachycardia.

CPVT1 is the most common genetic variant and is caused by mutations in the *RyR2* gene. *RyR2* is the major calcium release channel of the sarcoplasmic reticulum, mediating excitation-contraction coupling. Approximately 50% to 70% of patients with CPVT harbor *RyR2* mutations. CPVT mutant *RyR2*s typically show gain-of-function defects following channel activation by PKA phosphorylation (in response to beta-adrenergic stimulation or caffeine), resulting in uncontrolled Ca^{2+} release from the sarcoplasmic reticulum during electrical diastole, which facilitates the development of DADs and triggered arrhythmias.

Of note, missense mutations in *RyR2* have also been linked to a form of arrhythmogenic cardiomyopathy (ARVC-2) characterized by exercise-induced polymorphic VT that does not appear to have a reentrant mechanism, occurring in the absence of significant structural abnormalities. Patients do not develop characteristic features of ARVC on the 12-lead ECG or signal-averaged ECG, and global RV function remains unaffected. ARVC-2 shows a closer resemblance to familial CPVT in both etiology and phenotype; its inclusion under the umbrella term of ARVC remains controversial.

CPVT2 is much less common (accounting for less than 5% of CPVT index cases), and is associated with homozygous mutations in the *CASQ2* gene. Heterozygous carriers of one *CASQ2* mutation are usually healthy. Although *CASQ2* mutations are typically identified in consanguineous families, compound heterozygosity has been observed in nonconsanguineous families. *CASQ2* is a sarcoplasmic reticulum Ca^{2+} buffering protein associated with *RyR2*. *CASQ2* plays an active role in the control of Ca^{2+} release from the sarcoplasmic reticulum to the cytosol. Although some of *CASQ2* mutations are thought to compromise *CASQ2* synthesis and result in reduced expression or complete absence of *CASQ2* in the heart, other mutations seem to cause expression of defective *CASQ2* proteins with abnormal regulation of cellular Ca^{2+} homeostasis.

CPVT3 is caused by a mutation mapped to chromosome 7. The exact gene has not yet been identified. CPVT4 is caused by a mutation of the *CALM1* gene (encoding calmodulin). Calmodulin is a Ca^{2+} -binding protein that directly interacts with and regulates *RyR2* and L-type Ca^{2+} channels. Like CPVT1, CPVT4 is autosomal dominant. Of note, three genes (*CALM1–3*) in the human genome encode exactly the same calmodulin protein. Mutations in *CALM1–3* have also been linked to LQTS. In addition, mutations in *CALM1* were identified in a family with idiopathic VF.

CPVT5 is caused by mutations of the *TRDN* gene (encoding triadin). Triadin is a transmembrane sarcoplasmic reticulum anchoring protein of calsequestrin to the ryanodine channel. CPVT2, CPVT3, and CPVT5 are autosomal recessive.

Recently, three novel loss-of-function mutations of the *KCNJ2* gene (encoding for the strong inwardly rectifying channel Kir2.1 of the I_{K1}) have been found in patients with CPVT, and may represent a CPVT phenocopy. These patients had prominent U waves, ventricular ectopy, and polymorphic VT, but no dysmorphic features or skeletal muscle abnormalities. I_{K1} reduction may trigger arrhythmia by allowing inward currents, which are no longer counterbalanced by the strong outward I_{K1} , to gradually depolarize the membrane potential during phase 4. Membrane depolarization during phase 4 induces arrhythmia by facilitating spontaneous excitability.

Pathophysiology of Catecholaminergic Polymorphic Ventricular Tachycardia

Mechanism of Ventricular Arrhythmias

Abnormalities in the control of sarcoplasmic reticulum Ca^{2+} release constitute the central pathogenic abnormality in CPVT, although considerable controversy exists about the molecular mechanisms causing these defects. *RyR2* and *CASQ2* are both critically involved in the regulation of cardiac excitation-contraction coupling. Ca^{2+} influx via the

L-type Ca^{2+} channels in the cell membrane during the action potential plateau triggers more massive Ca^{2+} release (Ca^{2+} transients) from the sarcoplasmic reticulum into the cytosol via activation of RyR2. This amplifying process, termed calcium-induced calcium release (CICR), causes a rapid increase in cytosolic Ca^{2+} concentration to a level required for optimal binding of Ca^{2+} to troponin C and induction of contraction. During diastole, most of the surplus Ca^{2+} in the cytosol is resequestered into the sarcoplasmic reticulum by the sarcoplasmic/endoplasmic reticulum calcium ATPase (SERCA), the activity of which is controlled by the phosphoprotein phospholamban. In addition, some of the Ca^{2+} is extruded from the cell by the Na^{+} - Ca^{2+} exchanger to balance the Ca^{2+} that enters with the Ca^{2+} current. Recurring Ca^{2+} release-uptake cycles provide the basis for periodic elevations of the cytosolic Ca^{2+} concentration and contractions of myocytes, and hence for the orderly beating of the heart (see Fig. 1. 7).

The molecular mechanisms by which RyR2 mutations alter the physiological properties and function of RyR2 are not completely defined. It has been suggested that CPVT mutations in RyR2 reduce the binding affinity of RyR2 for the regulatory protein FKBP12.6 (calstabin-2), which stabilizes the closed conformational state of the RyR2 channel, thus enabling the channel to close completely during diastole (at low intracellular Ca^{2+} concentrations) and preventing aberrant Ca^{2+} leakage from the sarcoplasmic reticulum, ensuring muscle relaxation. PKA phosphorylation (induced by beta-adrenergic stimulation) of the mutant channels results in further worsening of the binding affinity of FKBP12.6 for the mutant RyR2, thus increasing the probability of an open state at diastolic Ca^{2+} concentrations. As a consequence, the mutant RyR2 channel fails to completely close during diastole, resulting in diastolic Ca^{2+} leak from the sarcoplasmic reticulum during stress or exercise.

An alternative hypothesis is that RyR2 mutations sensitize the channel to luminal (within the sarcoplasmic reticulum) Ca^{2+} such that under baseline conditions, where sarcoplasmic reticulum load is normal, there is no Ca^{2+} leak. Under beta-adrenergic (sympathetic) stimulation, sarcoplasmic reticulum Ca^{2+} concentration becomes elevated above the reduced threshold, causing Ca^{2+} to leak out of the sarcoplasmic reticulum. A third hypothesis is that mutations in RyR2 impair the intermolecular interactions between discrete RyR2 domains necessary for proper folding of the channel and self-regulation of channel gating.¹¹²

Calsequestrin is the most important Ca^{2+} storage protein in the sarcoplasmic reticulum and it forms a part of a large quaternary complex with RyR2, triadin, and junctin; together, these proteins play a major role in regulating intracellular Ca^{2+} . Calsequestrin represents a high-capacity, low-affinity Ca^{2+} -binding protein that is able to bind luminal Ca^{2+} (40 to 50 Ca^{2+} ions per molecule) during diastole, buffering Ca^{2+} within the sarcoplasmic reticulum and preventing diastolic Ca^{2+} release via RyR2 into the cytosol. CASQ2 mutations result in disruption of the control of RyR2s by luminal Ca^{2+} required for effective termination of sarcoplasmic reticulum Ca^{2+} release and prevention of spontaneous Ca^{2+} release during diastole, leading to diminished Ca^{2+} signaling refractoriness and generation of arrhythmogenic spontaneous Ca^{2+} releases (eFig. 31.4).¹¹²

Dysregulation of RyR2 likely underlies the disease mechanisms of calmodulin mutation-associated CPVT. Calmodulin is a small cytoplasmic Ca^{2+} -binding protein that regulates, directly or indirectly, the activity of proteins that play a key role in excitation-contraction coupling, and in particular, those responsible for the release and subsequent sequestration of cytosolic Ca^{2+} into the sarcoplasmic reticulum. The main binding partner of calmodulin in cardiac cells is the RyR2, which regulates Ca^{2+} release from the sarcoplasmic reticulum. Calmodulin inhibits RyR2 channel open probability. CPVT-linked calmodulin mutations result in defective calmodulin-RyR2 binding and impaired

calmodulin inhibition of RyR2 function. This can lead to excessive Ca^{2+} release from RyR2 channels, primarily from insufficient termination of RyR2-mediated Ca^{2+} release.^{5,6}

DADs and triggered activity have been proposed as the arrhythmogenic mechanism in CPVT because the bidirectional ECG pattern of this VT closely resembles the arrhythmias associated with intracellular Ca^{2+} overload and the DADs observed during digitalis toxicity. CPVT-related mutations lead to cytosolic Ca^{2+} overload, which results in activation of the Na^{+} - Ca^{2+} exchanger, which in turn generates a net inward current (the so-called transient inward current [I_{ti}]). I_{ti} underlies DADs, which may reach the threshold for Na^{+} channel activation and trigger abnormal beats.

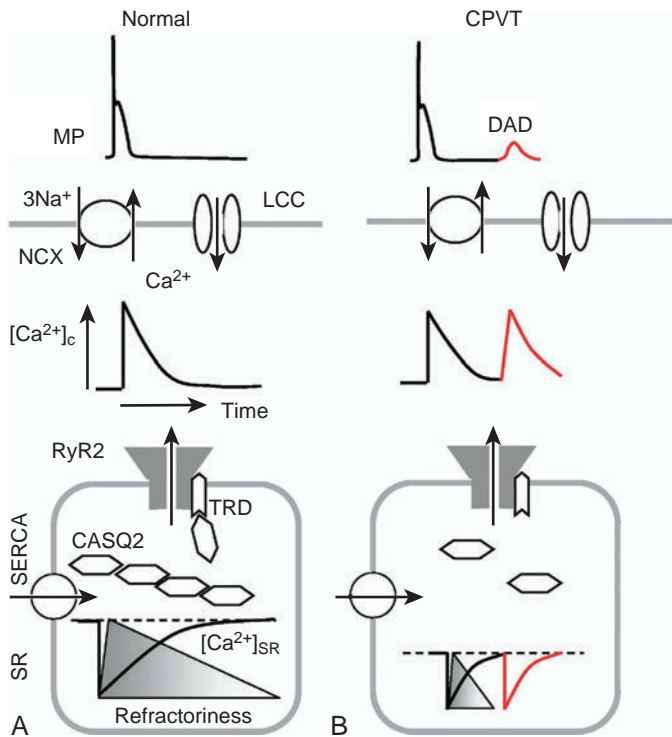
When the DADs are of low amplitude, they are usually not apparent or clinically significant. Probably the most important influence that causes subthreshold DADs to reach threshold is a decrease in the initiating cycle length; fast heart rates increase both the amplitude and rate of the DADs. In addition, catecholamines can facilitate the development of DADs via several mechanisms, including (1) increasing the L-type Ca^{2+} current through stimulation of beta-adrenergic receptors and increasing cAMP, which results in an increase in transsarcolemmal Ca^{2+} influx and intracellular Ca^{2+} overload; (2) enhancing the activity of the Na^{+} - Ca^{2+} exchanger, thus increasing the likelihood of DAD-mediated triggered activity; (3) enhancing the uptake of Ca^{2+} by the sarcoplasmic reticulum, leading to increased Ca^{2+} stored in the sarcoplasmic reticulum and the subsequent release of an increased amount of Ca^{2+} from the sarcoplasmic reticulum during contraction; and (4) increasing the heart rate. These effects underlie the increased susceptibility to ventricular arrhythmias in CPVT patients during exercise and emotional stress associated with increased sympathetic stimulation and increased heart rates.

Importantly, in the setting of digitalis poisoning, the abnormal RyR2 behavior leading to spontaneous Ca^{2+} release and DADs is secondary to the elevation of the sarcoplasmic reticulum Ca^{2+} content (store overload-induced Ca^{2+} release, SOICR). In CPVT, on the other hand, spontaneous Ca^{2+} release and DADs can occur without Ca^{2+} overload. Mutations in RyR2 or CASQ2 lead to defective Ca^{2+} signaling that reduces the sarcoplasmic reticulum Ca^{2+} threshold for spontaneous Ca^{2+} release below the normal baseline level ("perceived" Ca^{2+} overload). A similar mechanism may underlie triggered arrhythmias in other disease conditions, including heart failure and ischemic heart disease, in which sarcoplasmic reticulum Ca^{2+} release regulation is compromised because of acquired defects in components of the RyR2 channel complex.

As expected with DAD-mediated triggered activity, a positive direct correlation has been observed between the coupling interval of ventricular arrhythmias and the preceding R-R interval. This observation can also suggest that supraventricular arrhythmias commonly observed prior to the onset of ventricular arrhythmias during exercise in CPVT patients may act as a trigger for the development of DADs and triggered activity in the ventricle.

Mechanism of the Bidirectional Morphology of Ventricular Tachycardia

The EP mechanisms leading to the characteristic bidirectional morphology of the VT are not clear. Changes in conduction direction from a single ventricular focus with every other beat, VT originating from one focus that triggers another focus, and double ventricular foci (from the right and left apical portions of the heart) are some of the proposed mechanisms. The QRS morphology of bidirectional VT is inconsistent in the same recording lead, suggesting that the focus of the arrhythmia can vary to some extent. Some investigators suggested that CPVT starts from a single focus or double foci, usually originating from the RVOT, whereas the ensuing beats tend to originate from the LV. Others found



eFig. 31.4 Calcium Cycling in Normal Myocytes and Myocytes Harboring Catecholaminergic Polymorphic Ventricular Tachycardia (CPVT) Calsequestrin (CASQ2) Mutations. (A) In normal myocytes, Ca^{2+} influx through L-type Ca^{2+} channels (LCC) during the action potential activates ryanodine receptor type 2s (RyR2s) and initiates the release of Ca^{2+} stored in the sarcoplasmic reticulum (SR) on CASQ2 polymers. SR Ca^{2+} release terminates when the drop in intra-SR $[\text{Ca}^{2+}]$ causes RyR2s to close because of inhibition by CASQ2 monomers at reduced $[\text{Ca}^{2+}]_{\text{SR}}$. The RyR2s stay refractory until $[\text{Ca}^{2+}]_{\text{SR}}$ is restored by sarco-plasmic/endoplasmic reticulum calcium ATPase (SERCA). The rate of $[\text{Ca}^{2+}]_{\text{SR}}$ recovery and thus the rate of restitution from luminal Ca^{2+} -dependent refractoriness depends on both SERCA activity and the Ca^{2+} -binding capacity of CASQ2. Ca^{2+} signaling refractoriness prevents spontaneous Ca^{2+} release during diastole. (B) Arrhythmogenic CASQ2 mutations disrupt Ca^{2+} handling through either one or a combination of decreased CASQ2 expression, reduced CASQ2 Ca^{2+} binding capacity (via disruption of CASQ2 polymerization), and impaired CASQ2 interaction with the RyR2 complex (via triadin [TRD]). Alterations in CASQ2 abundance and/or behavior result in diminished and shortened Ca^{2+} signaling refractoriness after each release through accelerating recovery of $[\text{Ca}^{2+}]_{\text{SR}}$, altering RyR2 gating dependency on $[\text{Ca}^{2+}]_{\text{SR}}$, or both. PKA-mediated stimulation of SERCA (via PLB) further accelerates SR refilling, accounting for the dependency of CPVT on adrenergic stimulation. Compromised RyR2 refractoriness results in spontaneous SR Ca^{2+} release, which in turn elicits delayed afterdepolarizations (DADs) through stimulation of Na^+ - Ca^{2+} exchange (NCX). PKA, Protein kinase A; PLB, phospholamban. (Reproduced with permission from Györke S. Molecular basis of catecholaminergic polymorphic ventricular tachycardia. *Heart Rhythm*. 2009;6:123–129.)

that a left posterior inferior origin accounts for the majority of cases. In addition, the Purkinje network has been suggested as the site of origin of bidirectional VT, with alternating firing from the right and left branches of the Purkinje fibers.

A recent experimental model suggested a “ping-pong” mechanism may underlie ventricular arrhythmias in CPVT, whereby DAD-induced triggered activity develops at different heart rate thresholds in different regions of the His-Purkinje system (HPS) or ventricles. First, once the heart rate exceeds a certain threshold, ventricular bigeminy develops from a single site in the HPS or ventricular myocardium. The shortened R-R cycle length due to ventricular bigeminy induces DAD-triggered beats from a second focus within the HPS, with the latter reciprocally activating PVCs from the first focus; a process that is repeated back and forth, in a ping-pong pattern. “Reciprocating bigeminy” from the two sites produces the bidirectional VT characteristic of CPVT. Polymorphic VT results when three or more sites concurrently develop bigeminy, whereas monomorphic VT develops when repetitive DADs generate a run of triggered activity from a single site.

Mechanism of Drug Effects

As noted, activation of the adrenergic nervous system exerts profound effects on Ca^{2+} handling, and it is often the initiator of Ca^{2+} -mediated arrhythmogenesis. Hence, beta-adrenergic blockade plays an important role in the management of CPVT. It is likely that beta-blocker therapy inhibits the increase of Ca^{2+} content of the sarcoplasmic reticulum with reduced propensity to aberrant Ca^{2+} leakage from the sarcoplasmic reticulum during diastole. Also, beta-blockers attenuate the effect of adrenergic stimulation induced by exercise or emotion. In addition, because the amplitude of DADs is directly related to heart rate, the bradycardia induced by beta-blockers reduces the probability that a DAD would reach the threshold for triggering PVCs. Accordingly, the lower the heart rate achieved with beta-blocker therapy, the higher the probability of preventing malignant arrhythmias.

Flecainide (a Na^+ channel blocker) has recently been demonstrated to prevent lethal ventricular arrhythmias in CPVT. The mechanisms mediating those effects are still debated. It has been speculated that flecainide suppresses spontaneous sarcoplasmic reticulum Ca^{2+} release events via direct blockade of RyR2 channels, reducing Ca^{2+} spark amplitude. An alternative hypothesis is that flecainide prevents the development of abnormal threshold potentials through the inhibition of the Na^+ - Ca^{2+} exchange pump that contributes to the formation of premature and arrhythmogenic Ca^{2+} waves. The negative chronotropic effects of flecainide can also reduce ventricular arrhythmias during exercise by keeping the heart rate below the threshold of PVC initiation.

Epidemiology

The prevalence of CPVT has been roughly estimated at 1:10,000. Despite the low prevalence, CPVT is an important cause of sudden cardiac arrest in young individuals, and cardiac event rates as high as 80% before the age of 40 years have been reported if left untreated. The mean age at clinical presentation is between 7 and 9 years, although later onset has been reported. Approximately 30% of probands have a family history of stress-related syncope, seizure, or SCD before age 40 years. There is a high level of penetrance of the *RYR2*-related disease (75% to 80%); therefore asymptomatic individuals with *RYR2*-related CPVT are a minority.¹

Clinical Presentation

CPVT patients typically present with syncope triggered by exercise or emotion, and a distinctive pattern of reproducible, stress-related, bidirectional VT in the absence of structural heart disease or QT interval prolongation.

CPVT is one of the most malignant forms of ventricular arrhythmia. The majority of untreated CPVT patients develop symptoms (syncope, VT or VF) by age 40 and overall mortality is 30% to 50%. SCD can be the first manifestation of the disease in a significant proportion of cases.

Electrocardiographic Features

The resting ECG of patients with CPVT is often normal, without prolongation or shortening of the QT interval, atrioventricular and intraventricular conduction defects, or Brugada-like ST elevation. Sinus bradycardia and prominent U waves can be observed in some patients.

“Bidirectional VT,” the hallmark of CPVT, is characterized by an alternating QRS axis with 180-degree rotation on a beat-to-beat basis (Fig. 31.17). The typical bidirectional VT, however, is not present in all patients. In one report, bidirectional VT was documented in only 35% of probands, whereas other patients showed polymorphic VT or VF. Single PVCs during an exercise test can be the only finding recorded in some CPVT patients. Importantly, the morphology of VT, which is polymorphic or bidirectional, is strongly dependent on the ECG recording lead. When the maximal QRS vector changes in one lead during bidirectional VT, the axis perpendicular to the former lead shows polymorphic VT. However, unlike other polymorphic VTs, such as torsades de pointes, the QRS morphology is not chaotic but has some regularity.

A characteristic feature of CPVT is the progressive worsening of arrhythmias with increasing exercise workload. Ventricular arrhythmias during exercise stress testing appear quite consistently at a heart rate of 110 to 130 beats/min. Initially, monomorphic PVCs appear, which become polymorphic with continued exercise. Typically, the PVCs in CPVT are late-coupled and can exhibit an LBBB pattern with an inferior axis or RBBB pattern with a superior axis. Notably, PVC morphologies are usually reproducible in an individual patient. With increasing heart rates, ventricular bigeminy, ventricular couplets, and nonsustained VT develop. If exercise is not promptly discontinued, bidirectional VT may degenerate into polymorphic VT and VF. On termination of exercise, arrhythmias progressively diminish in terms of VT rate and VT duration until they disappear. Isolated premature atrial complexes (PACs), nonsustained SVT, and short runs of AF are usually observed during exercise, with an onset at a range of heart rates similar to or slower than that of ventricular arrhythmias.¹¹³

PVCs also can be observed in healthy subjects in response to exercise testing. Certain features of PVCs during an exercise test can potentially assist in distinguishing CPVT from healthy controls, including a larger number of PVCs, first appearance at higher workload, an LBBB pattern and an inferior axis, bigeminy or trigeminy at peak stress, QRS duration of more than 120 milliseconds, a coupling interval of more than 400 milliseconds, and disappearance in the first minute of the recovery.¹¹⁴

Diagnosis of Catecholaminergic Polymorphic Ventricular Tachycardia

A clinical diagnosis of CPVT is made based on symptoms (syncope or aborted SCD), family history, and unexplained exercise or catecholamine-induced bidirectional VT or polymorphic PVCs or VT in an individual (especially those younger than 40 years), in the presence of a structurally normal heart and normal baseline ECG. Ventricular arrhythmias can be observed (using a combination of Holter monitoring, exercise testing, and drug provocation) in more than 80% of patients.¹

In patients presenting with syncope or cardiac arrest, the CPVT diagnosis is frequently missed or delayed, unless exercise stress testing or ambulatory cardiac monitoring is performed to document ventricular arrhythmias. Not infrequently, syncopal episodes are considered as vasovagal in origin, and no further workup is performed. If the loss of consciousness is associated with convulsions, it can be misdiagnosed as epileptic seizures if a prolonged circulatory arrest resulted in brain

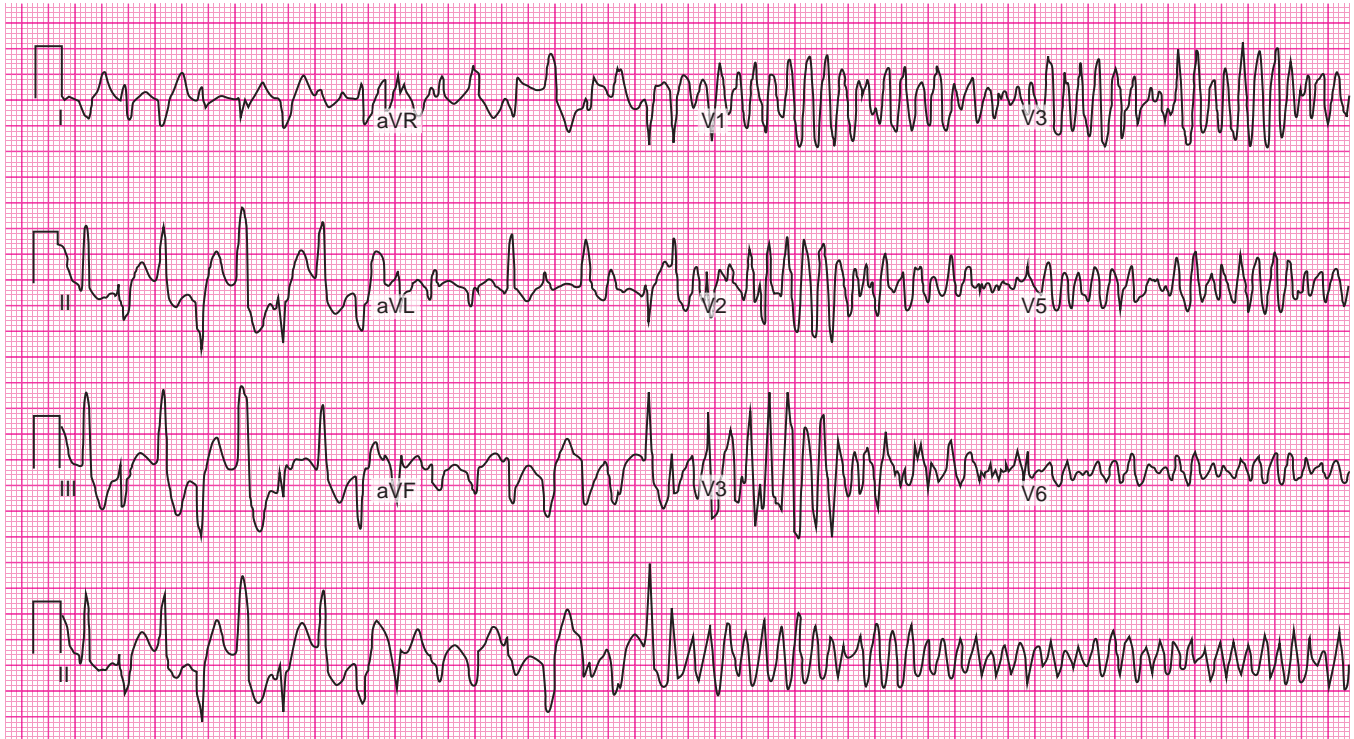


Fig. 31.17 Ventricular Arrhythmias in Catecholaminergic Polymorphic Ventricular Tachycardia (CPVT). This 12-lead electrocardiogram from a 9-year-old boy with ryanodine-positive CPVT shows a transition from bidirectional ventricular tachycardia followed by brief polymorphic ventricular tachycardia to ventricular fibrillation. (From Roses-Noguer F, Jarman JWE, Clague JR, Till J. Outcomes of defibrillator therapy in catecholaminergic polymorphic ventricular tachycardia. *Heart Rhythm*. 2014;11:58–66.)

ischemia. Unexplained cardiac arrest is also frequently misdiagnosed as idiopathic VF.

CPVT should be suspected when a syncopal episode induced by exercise or emotion occurs in a child or in a young patient with a normal resting ECG and no structural heart disease. In addition, CPVT should be considered in all cases of idiopathic VF and unexplained cardiac arrest (normal coronary arteries, normal ventricular function, and normal ECG), especially if an adrenergic trigger is present.¹¹⁵

Exercise Stress Testing

A standardized exercise stress test is the most important step for diagnosis of CPVT. In at least 80% of CPVT patients, exercise stress testing induces ventricular arrhythmias, which typically appear when the sinus rate exceeds an individual threshold rate (usually at 110 to 130 beats/min). The progressive worsening of arrhythmias during exercise is highly reproducible and is a diagnostic marker of CPVT. Sometimes, the exercise-provoked arrhythmias can be demonstrated only after a delay of months or more after the first syncopal episode has occurred, emphasizing the necessity of repeated exercise stress tests when there is a high suspicion of CPVT.

Ambulatory Cardiac Monitoring

Continuous ambulatory monitoring can reveal arrhythmias typical for CPVT if the sinus rate of the patient exceeds the individual arrhythmia-inducing threshold during monitoring. Ambulatory monitoring can be very useful in young children, whenever performing a maximal exercise stress test is difficult. Implantation of a loop recorder can also be valuable in some cases.

Provocative Drug Testing

Catecholamine provocation testing can help diagnose patients with concealed CPVT. Progressive ventricular arrhythmias can also be provoked by IV infusion of isoproterenol or epinephrine. The protocol for epinephrine infusion is similar to that described for LQTS. The test is considered positive for CPVT if epinephrine provoked three or more beats of polymorphic VT or bidirectional VT and borderline if polymorphic couplets, PVCs, or nonsustained monomorphic VT is induced.

Electrophysiological Testing

Invasive EP testing is of no value in the diagnosis or risk stratification in patients with CPVT. Arrhythmias are seldom inducible by programmed electrical stimulation.

Genetic Testing

Genetic testing is recommended in all probands with definitive clinical diagnosis of CPVT and is also considered in subjects with idiopathic VF when an adrenergic trigger is identified. Using a comprehensive screening approach, the percentage of successfully genotyped CPVT patients is approximately 55% to 60%. Mutations in *RYR2* are identified in approximately 60% of patients with a strong CPVT phenotype. The yield of *RYR2* genetic testing drops to 5% to 38% in patients with a possible clinical diagnosis in CPVT. Of note, because the *RyR2* gene (which underlies the most common form of CPVT) is one of the largest genes in the human genome, genetic testing can be time-consuming and costly. Genetic screening for disease-causing mutations in the calsequestrin (*CASQ2*) and triadin (*TRDN*) genes, which underlie the

autosomal recessive form of CPVT, is advisable in all pedigrees compatible with a recessive pattern of inheritance but also in all apparently sporadic CPVT cases with negative *RyR2* screening even in the absence of parental consanguinity.

Differential Diagnosis

Other inherited arrhythmogenic cardiac disorders that can cause malignant ventricular tachyarrhythmias should also be excluded. A QTc interval less than 320 milliseconds should raise a suspicion of SQTS. On the other hand, a prolonged QTc suggests LQTS. Although the onset of clinical symptoms of LQTS is often around puberty, the first syncopal events in CPVT patients tend to occur during childhood. Importantly, induction of arrhythmias during exercise is very rare in LQTS patients. Furthermore, LQTS patients develop torsades de pointes (characterized by the twisting of the points of the QRS complexes), in contrast to CPVT patients who manifest with the typical bidirectional VT with a beat-to-beat 180-degree rotation of the QRS complex.

Bidirectional VT can also occur in patients with LQT7 (Andersen-Tawil syndrome) linked to mutations in the *KCNJ2* gene, which may be considered a CPVT phenocopy, particularly in patients with Andersen-Tawil syndrome having borderline QT interval prolongation and lacking the extracardiac features of the syndrome (e.g., periodic paralysis, facial and limb dysmorphism). Distinguishing between LQT7 and CPVT is important; patients with Andersen-Tawil syndrome show a much more benign course than those with other forms of CPVT, and SCD is rare among Andersen-Tawil syndrome patients and *KCNJ2* mutation carriers.

Ankyrin-B syndrome can also manifest with catecholamine-mediated ventricular arrhythmias. Loss-of-function mutations in the *ANK2* gene (encoding cardiac ankyrin-B, a structural membrane adapter protein) result in increased intracellular concentration of Ca^{2+} and, sometimes, fatal arrhythmia. Although this syndrome has been categorized under LQTS (LQT4), the inconsistent QT interval prolongation and the varying degrees of cardiac dysfunction and arrhythmias observed (including bradycardia, sinus arrhythmia, idiopathic VF, adrenergically mediated VT, and SCD) distinguishes ankyrin-B syndrome as a clinical entity distinct from classic LQTS.

Exercise-provoked arrhythmias also can develop in ARVC, but the typical ECG pattern of ARVC and the structural abnormalities of the RV distinguish ARVC from CPVT. The typical arrhythmia in ARVC, monomorphic VT with an LBBB pattern, is clearly different from the polymorphic PVCs or VT in CPVT.

In contrast to CPVT, patients with Brugada syndrome do not manifest polymorphic PVCs on physical effort; rather, arrhythmias in Brugada syndrome usually appear at rest or during sleep. Furthermore, the absence of ST segment elevation in the precordial ECG leads at baseline and after provocation testing with Na^+ channel blockers helps distinguish CPVT from Brugada syndrome.

Risk Stratification

CPVT is one of the most malignant forms of ventricular arrhythmias, with a high mortality rate. CPVT patients with prior cardiac arrest and those in whom symptoms are not completely suppressed by pharmacological therapy are considered at high risk for SCD. Also, diagnosis in childhood is a predictor of adverse outcome. However, the optimal strategy for risk stratification for SCD in asymptomatic CPVT patients or mutation carriers remains uncertain. Programmed electrical stimulation typically fails in inducing ventricular arrhythmias, and is of no value for risk stratification. Furthermore, the predictive value of inducibility of ventricular arrhythmias by catecholamine infusion or exercise for risk stratification has not been demonstrated.¹

Principles of Management

Pharmacological Therapy

Beta-blockers. Beta-blockers without intrinsic sympathomimetic activity combined with exercise restriction are the first line of treatment for CPVT and should be promptly initiated to prevent occurrence of ventricular tachyarrhythmias (see Fig. 31.7). Because of the poor prognosis of untreated CPVT, drug therapy is indicated for all clinically diagnosed patients and usually also for all silent carriers of a CPVT mutation.

Differences in the pharmacodynamics and pharmacokinetics of the various beta-blockers (including their beta-1 selectivity, half-life, and lipophilicity) appear to be relevant. Studies found nadolol superior to beta-1 selective (cardioselective) beta-blockers (e.g., metoprolol succinate and bisoprolol) in preventing arrhythmias in patients with CPVT. This may be explained, at least in part, by a stronger negative chronotropic effect as well as the longer half-life (20 to 24 hours) of nadolol, which reduces the risk of breakthrough symptoms during potential drug noncompliance. Nonetheless, other mechanisms, such as membrane-stabilizing effects of nadolol, have been speculated. The efficacy of other nonselective beta-blockers (such as propranolol and carvedilol) has not been investigated.

Presently, there is a strong consensus that the nonselective beta-blocker nadolol (1 to 2.5 mg/kg per day) is the preferred antiarrhythmic, antiadrenergic therapy for CPVT patients. When nadolol is not available or not tolerated, the choice should be guided by the ability of the beta-blocker to suppress ventricular ectopy on the exercise test. Propranolol (3 to 4 mg/kg per day) has been widely used in these situations. IV propranolol is the treatment of choice for acute management of CPVT.^{52,116,117}

Exercise stress testing and Holter monitoring can help determine the adequate beta-blocker dosage for arrhythmia control. It should be noted, however, that the absence of exercise-provoked arrhythmias does not completely exclude the risk of arrhythmia recurrence, and the maximal tolerated dose of beta-blockers should be prescribed to maximize control of arrhythmias with a goal to avoid the heart rate exceeding the threshold rate for CPVT. Furthermore, compliance with regular therapy is extremely important because missing even a single dose can potentially lead to arrhythmias and increase the risk of SCD. In fact, in one report, poor adherence contributed to 48% of arrhythmic events in children with CPVT.

It should be recognized that the efficacy of beta-blockers in CPVT is not sufficiently protective and appears to be lower than that seen in patients with LQT1. The annual rate of arrhythmic events on beta-blocker therapy ranges between 3% and 11% per year (27% over 8 years).¹ Of note, recent reports found that beta-blocker therapy was unable to modify the arrhythmic pattern during exercise testing in 30% to 43% of patients, especially those with less severe arrhythmias.¹¹³

Flecainide. Recent studies show that the addition of flecainide to beta-blocker therapy can effectively reduce exercise-induced ventricular arrhythmias in CPVT patients not controlled by beta-blocker therapy alone. Thus flecainide should be regarded as the first addition to beta-blockers when control of arrhythmias seems incomplete.¹ Flecainide monotherapy may be considered in selected CPVT patients truly intolerant of beta-blockade.¹¹⁸

Verapamil. Limited data suggest that verapamil (an inhibitor of *RyR2*) can be an alternative option for treatment of CPVT. Also, verapamil can potentially provide additional protection when used in combination with beta-blockers. However, because of the small number of patients and the limited follow-up in these studies, there is no conclusive evidence for recommending verapamil alone or in combination with beta-blockers, and its impact on prognosis remains unknown.¹

Implantable Cardioverter-Defibrillator

Given that no drugs can be effective in providing complete protection from SCD, ICD therapy is recommended for CPVT patients who have survived a cardiac arrest and those who continue to have symptoms (syncope or sustained or hemodynamically unstable VT) despite adequate beta-blocker therapy.¹¹⁵

Patients with CPVT experience a high rate of appropriate ICD therapies; approximately half of ICD recipients experience an appropriate shock to terminate VT during 2 years of follow-up. Importantly, the efficacy of ICD therapy in CPVT patients depends on the mechanism of the arrhythmia treated. VF episodes are almost always terminated by ICD shocks; in contrast, ICD discharges nearly always fail to terminate polymorphic and bidirectional VT.^{115,119,120} Therefore it is important to maintain the maximal tolerated dose of beta-blockers in ICD patients to help reduce the risk of arrhythmic storms and ICD shocks.

The risks and benefits of ICD therapy in patients with CPVT should be carefully considered before device implantation, particularly for primary prevention. Inappropriate shocks, electrical storm, and ICD complications are common. Inappropriate ICD therapy is often triggered by supraventricular arrhythmias or spontaneous termination of a ventricular arrhythmia before the ICD discharge. Also, it is important to note that ICDs can potentially have proarrhythmic effects in patients with CPVT. The stress and catecholamine surge caused by the painful ICD shocks (whether appropriate or inappropriate) can evoke an electrical storm.¹¹⁵

Careful device programming can help improve effectiveness of ICD therapies and decrease related comorbidities. Extending detection intervals and altering reconfirmation rates (to avoid therapy delivery in response to frequent PVCs and spontaneously terminating arrhythmias), as well as adjusting ICD detection rates to shorter CLs (for detection of VF rather than VT) can potentially improve outcomes for CPVT patients.¹²⁰

Catheter Ablation

When ventricular arrhythmias are triggered by monomorphic PVCs, catheter ablation of the focus of PVCs can be attempted to help reduce the frequency and burden of arrhythmias and ICD shocks. Not infrequently, the initiating beat of VT exhibits an LBBB–inferior axis pattern, suggestive of a ventricular outflow tract origin.

Left Cervicothoracic Sympathectomy

Left cervicothoracic sympathectomy involves resection of the lower half of the left stellate ganglion and the first two to four thoracic ganglia (T1 to T4). In recent reports, left cardiac sympathetic denervation successfully reduces major arrhythmic events by almost 90%, including cardiac arrest and SCD, in CPVT patients. Therefore left cardiac sympathetic denervation can be considered in patients with recurrent symptoms despite pharmacological therapy or those experiencing frequent ICD shocks or intractable arrhythmic storms.¹²¹

Although left cervicothoracic sympathectomy can be associated with frequent side effects (including left-sided dryness, unilateral facial flush with exercise, contralateral hyperhidrosis, and ptosis), generally these symptoms are fairly tolerated and patient satisfaction with surgical outcome remains high.^{56,57}

Participation in Sports

Symptomatic CPVT patients and asymptomatic patients (detected as part of familial screening) with documented exercise- or isoproterenol-induced VT should refrain from all competitive sports with the possible exception of minimal contact, class IA activities. A less restrictive approach may be possible for the genotype-positive/phenotype-negative (asymptomatic, no provokable VT) athlete.

Family Screening

Given the severe clinical manifestations and poor prognosis of CPVT, once CPVT diagnosis is made in a proband, it is essential to expand the evaluation to both first- and second-degree relatives to find other potential CPVT patients. Exercise testing and Holter monitoring are used for screening family members. Importantly, some CPVT patients may not have arrhythmias during exercise testing during early childhood, but a change in the phenotype occurs later in life. Therefore regular follow-up with repeated exercise stress tests is indicated, for example, for younger siblings of a CPVT patient.

Screening of family members by genetic testing is recommended when a gene mutation has been identified in the proband. Considering the early age of manifestation of CPVT and its association with SIDS, confirmatory genetic testing should be performed at birth. Genetic evaluation facilitates diagnosis in silent carriers and allows implementation of preventive pharmacological therapy and reproductive risk assessment. Approximately 50% of *RYR2* mutation-carrying relatives identified by cascade screening have a CPVT phenotype.

It is suggested that genetically positive family members without clinical manifestations of CPVT (concealed mutation-positive patients) should receive beta-blockers, even after a negative exercise test, although the natural history of these individuals and the efficacy of beta-blockers on their prognosis have not been studied.¹

IDIOPATHIC VENTRICULAR FIBRILLATION

Idiopathic VF is a rare primary arrhythmia syndrome of unknown genetic origin.¹²² The 2013 expert consensus on inherited arrhythmia defined idiopathic VF as “a resuscitated cardiac arrest victim, preferably with documentation of VF, in whom known cardiac, respiratory, metabolic and toxicological etiologies have been excluded through clinical evaluation.”¹

Genetics of Idiopathic Ventricular Fibrillation

Three familial forms of idiopathic VF have recently been linked to the *DPP6* gene (encoding dipeptidyl-peptidase 6), the *CALM1* gene (encoding calmodulin), and the *RYR2* gene (encoding ryanodine receptor).

In several Dutch families heavily affected by SCD attributed to familial idiopathic VF, the arrhythmic events were associated with a risk haplotype on chromosome 7 harboring the arrhythmia gene *DPP6* gene as a founder effect (i.e., the families are descendants of the same ancestor). Higher *DPP6* expression in *DPP6* risk haplotype-positive individuals was proposed as a likely pathogenetic mechanism. *DPP6* is a putative regulatory β -subunit of the transient outward current (I_{to}) channel complex in the heart. The arrhythmia syndrome typically occurs between the age of 20 and 60 years, with an autosomal dominant inheritance. The penetrance of idiopathic VF is high: 50% of the male *DPP6* haplotype carriers experienced (aborted) SCD before the age of 58 years. Importantly, despite comprehensive cardiac evaluation, no relevant differences between haplotype-positive and haplotype-negative individuals were observed, and no clinical parameters could be linked to SCD risk other than their genetic predisposition.¹²³

Another familial form of idiopathic VF was linked to mutations in the *CALM1* gene, with autosomal dominant transmission. Calmodulin is a Ca^{2+} -binding protein with ubiquitous expression that has a regulatory function for numerous calcium-dependent processes. Calmodulin inhibits *RyR2* channel open-state probability. Defective calmodulin–*RyR2* binding results in impaired calmodulin inhibition of *RyR2* function and consequent dysregulation of sarcoplasmic reticulum Ca^{2+} release. Calmodulin mutations have been previously described in LQTS and CPVT4.^{5,6}

Recently, two different heterozygous mutations in the *RYR2* gene have been identified in a family with multiple idiopathic VF victims. Those mutations resulted in a phenotype distinct from classic *RYR2*-related CPVT.^{124,125}

Pathophysiology of Idiopathic Ventricular Fibrillation

The mechanism(s) underlying idiopathic VF remain to be elucidated. Monogenic mutations have been identified in a small subset of patients with idiopathic VF. Polygenic mutations (i.e., mutations involving two or more genes) and subclinical structural abnormalities currently undetectable with the available diagnostic modalities, have also been speculated. Those underlying substrates can be silent and manifest with VF only during particular pathophysiological processes (e.g., minimal electrolyte disturbances).

Recent evidence suggests that the Purkinje network and the RVOT play a pivotal role in both the initiation and perpetuation of VF. PVCs with short-coupled intervals (i.e., R-on-T phenomenon) originating from the RVOT or HPS have been frequently implicated as the trigger of VF or torsades de pointes, at least in a subset of patients with idiopathic VF. The short-coupled PVCs can cause phase 2 reentry and thereby elicit VF. It is likely that idiopathic VF is initiated by an interaction between triggering PVCs and a susceptible ventricular substrate that is prone to transmural reentry.^{123,126}

The exact arrhythmogenic mechanism of how DPP6 overexpression causes idiopathic VF is uncertain. Idiopathic VF associated with the DPP6 risk haplotype is predominantly elicited by monomorphic short-coupled PVCs from the RV apex or inferior free wall. It has been hypothesized that DPP6 overexpression in DPP6 risk haplotype-positive individuals significantly alters the inactivation kinetics of both $K_{4.2}$ and $K_{4.3}$ channels and preferably increases I_{to} in the Purkinje network more so than in ventricular cardiomyocytes, resulting in a more negative phase 1 and an abnormal plateau phase of the Purkinje action potentials. Because the I_{to} only increases in the Purkinje fibers, a strong local repolarization gradient is created with the adjacent ventricular myocardium that results in local ectopy and short-coupled PVCs. DPP6 overexpression does not result in discernible ECG changes, as Purkinje activity is not recorded on the surface ECG.¹²²

Dysregulation of RyR2 likely underlies the disease mechanisms of *RYR2* and *CAM1* mutation-associated CPVT. These mutations can lead to excessive Ca^{2+} release from RyR2 channels and DADs.^{5,6}

Epidemiology

Idiopathic VF accounts for up to 10% of victims of SCD, mainly in the young. The proportion of “unexplained” or “idiopathic” VF among victims of cardiac arrest has been declining, thanks to the advances in genetic testing and cardiac imaging techniques, and the expanding recognition of new disease entities, which improved the ability to diagnose distinct primary inherited arrhythmia syndromes, thereby excluding idiopathic VF (Fig. 31.18).^{122,127}

The mean age at presentation is approximately 35 to 45 years, and two-thirds of patients are men. A family history of SCD or idiopathic VF is present in up to 20% of patients, suggesting that at least a subset of idiopathic VF is hereditary.

Clinical Presentation

Idiopathic VF manifests as syncope or cardiac arrest that is typically not related to physical or emotional stress. VF often occurs at night, when heart rate is slower and vagal tone is augmented. The recurrence of VF in patients with idiopathic VF is approximately 30%, and the proportion of patients presenting with cardiac arrest as opposed to syncope appears to be much higher in idiopathic VF than in other channelopathies, suggesting that ventricular arrhythmias in other chan-

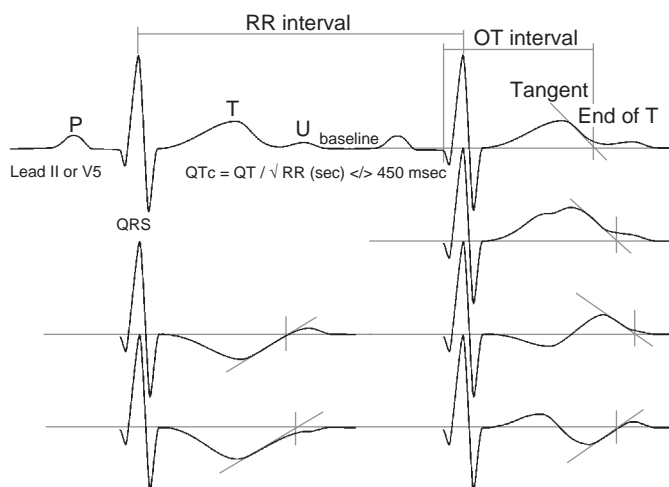


Fig. 31.18 Schematic Illustration of the Evolution of the Diagnosis Idiopathic Ventricular Fibrillation (IVF). *CALM1*, Calmodulin 1 gene mutation; *CPVT*, catecholaminergic polymorphic ventricular tachycardia; *DPP6*, Dutch DPP6 risk haplotype associated with sudden cardiac death. (From Visser M, van der Heijden JF, Doevendans PA, Loh P, Wilde AA, Hassink RJ. Idiopathic ventricular fibrillation: the struggle for definition, diagnosis, and follow-up. *Circ Arrhythm Electrophysiol*. 2016;9:e003817.)

nelopathies are more likely to terminate spontaneously, whereas idiopathic VF tends to be sustained. Electrical storm occurs in approximately 10% of patients.

Electrocardiographic Features

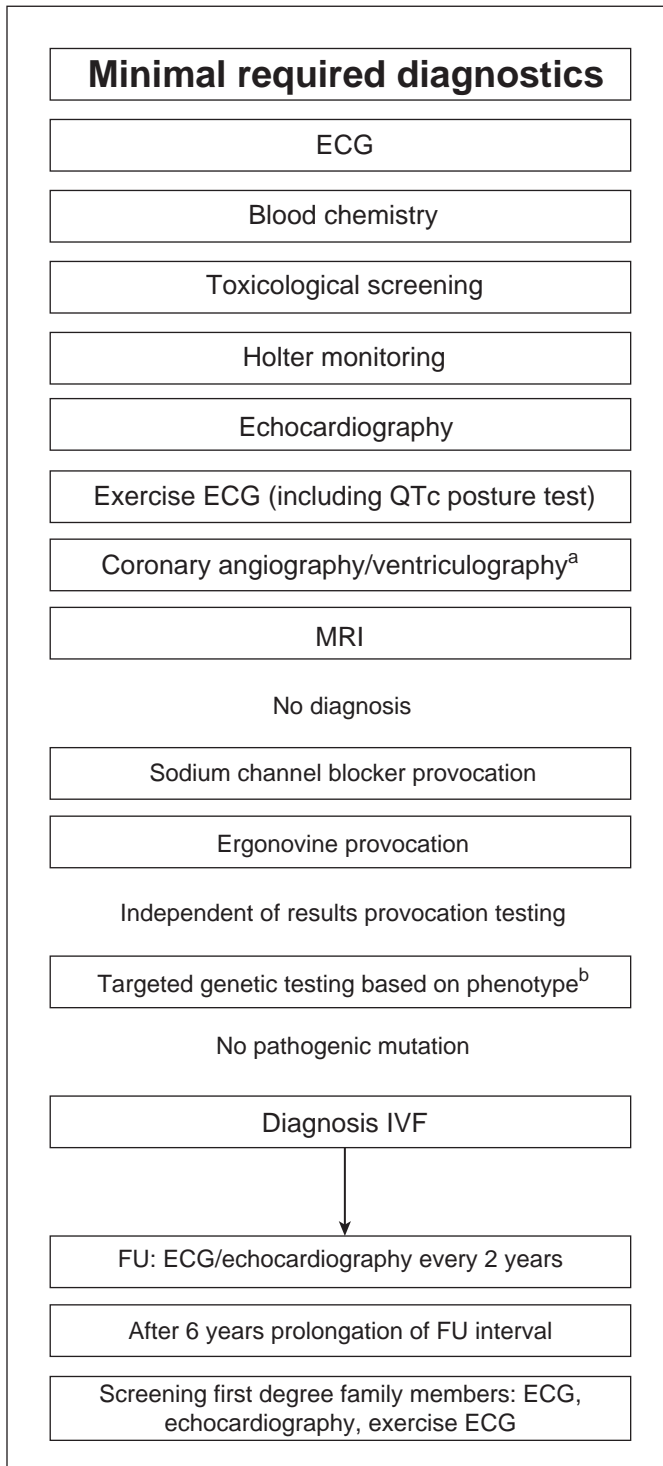
Typically, the resting ECG of patients with idiopathic VF is normal, without prolongation or shortening of the QT interval, AV and intra-ventricular conduction defects, or Brugada-like ST elevation. Nonetheless, VF storms in idiopathic VF patients appear to be associated with J waves that show augmentation prior to VF onset. The J waves disappear during follow-up. However, the early repolarization pattern in patients with idiopathic VF does not fulfill the criteria for “early repolarization syndrome,” which is considered a separate disease entity with a distinctive phenotype.¹²⁸ VF onset is not related to bradycardia or preceding ventricular pauses.¹²²

Arrhythmic events in idiopathic VF frequently occur at rest or during sleep (similar to Brugada and early repolarization syndromes). A circadian pattern of VF occurrence has been observed in idiopathic VF patients, with two peaks: early morning and late evening. J waves also exhibit circadian rhythmicity, with nocturnal augmentation, likely a result of enhanced vagal activity or slowing of the heart rate.^{126,129}

Characteristically, idiopathic VF is triggered by short-coupled PVCs predominantly originating from the HPS or from the RVOT. Short-coupled PVCs may elicit torsades de pointes or immediate VF. PVCs originating from the RVOT display an inferior axis with an LBBB pattern. PVCs originating in the right Purkinje system display relatively uniform ECG morphologies and typically have an LBBB pattern with a left superior axis and a relatively short QRS duration. On the other hand, PVCs arising in the left Purkinje system produce more variable 12-lead ECG patterns, and generally exhibit a positive vector in lead V_1 and a relatively narrow QRS duration (less than 120 milliseconds).

Diagnosis of Idiopathic Ventricular Fibrillation

The diagnosis of idiopathic VF is based on exclusion of an underlying structural or primary electrical heart disease, and exclusion of respiratory, metabolic, and toxicological causes (Fig. 31.19). Therefore the



diagnosis of idiopathic VF requires extensive diagnostic testing. Systematic advanced testing allows determination of a specific diagnosis in approximately half of initially unexplained cardiac arrest patients, with the majority (more than two-thirds) having a potentially inherited mechanism of disease.¹³⁰ Differentiation from structural cardiac disease and other primary arrhythmia syndromes is critical to provide targeted medical treatment and prevention of arrhythmic events in the proband and to identify other potentially treatable cases in family members.¹

Fig. 31.19 Proposed Flowchart for the Diagnosis and Follow-up (FU) of Patients With Idiopathic Ventricular Fibrillation (IVF). ^aIn young patients (less than 45 years) without risk factors for coronary artery disease, coronary computed tomography (CT) angiography is an alternative diagnostic tool to exclude coronary artery disease. The sensitivity is 85% and 99%, respectively, the specificity is 90% and 64%, respectively, the positive predictive value is 91% and 86%, respectively, and the negative predictive value is 83% and 90%, respectively. Coronary CT angiography has a higher sensitivity compared with MRI in detecting coronary stenosis; therefore CT is a better alternative for coronary angiography. ^bProposed genetic testing consists of a basic panel of *SCN5A*, the most common LQTS genes (*KCNQ1* and *KCNH2*), *RyR2*, and *CALM1* in patients with exercise-induced VF. In patients with a negative phenotype, *SCN5A*, *KCNQ1*, and *KCNH2* screening is recommended. ECG, Electrocardiogram. (From Visser M, van der Heijden JF, Doevendans PA, Loh P, Wilde AA, Hassink RJ. Idiopathic ventricular fibrillation: the struggle for definition, diagnosis, and follow-up. *Circ Arrhythm Electrophysiol.* 2016;9:e003817.)

Exclusion of Structural Heart Disease

Echocardiography, stress testing, coronary angiography, and cardiac magnetic resonance (CMR) need to be considered to exclude structural cardiac disease, such as coronary artery disease, congenital coronary anomalies, dilated or hypertrophic cardiomyopathy, ARVC, cardiac sarcoidosis, myocarditis, and left apical ballooning. In addition, ergonovine or acetylcholine provocation can be necessary to exclude coronary artery spasm. Metabolic disorders, electrolyte abnormalities, and drug intoxication also need to be excluded.^{1,122}

Exclusion of Primary Arrhythmia Syndromes

A thorough clinical and family history is critical; subtle information regarding the triggers and circumstances of arrhythmic events can point to distinct arrhythmia syndromes. Also, careful analysis of the surface 12-lead ECG is mandatory to exclude primary electrical heart disease. Abnormal shortening or prolongation of the QT interval can suggest SQTs or LQTS, respectively. Repolarization abnormalities in the right precordial leads can suggest the Brugada syndrome. The presence of ventricular preexcitation can suggest preexcited supraventricular tachyarrhythmias, usually AF with very rapid ventricular rates, as the underlying cause of VF. It is important to understand that all these disorders can manifest with minor or borderline ECG abnormalities, and recording serial ECGs, recording of modified precordial leads (such as in the Brugada ECG pattern), recording the ECG during exercise or after drug challenge, and/or continuous ambulatory cardiac monitoring can be necessary to unmask diagnostic ECG abnormalities. Pharmacological drug challenge to exclude the Brugada syndrome, and exercise stress testing or catecholamine infusion to exclude CPVT, should be considered.¹²²

Given the variable penetrance among gene carriers in the same family, some studies have suggested a role for family screening with ECG and echocardiogram as a diagnostic tool when conventional tests, including pharmacological tests, have not identified the cause of unexplained cardiac arrest in the proband.¹³¹

Electrophysiological Testing

Invasive EP testing may be considered, especially when SND, AV conduction abnormalities, or the presence of a bypass tract (BT) is suspected. However, routine invasive EP testing is not currently recommended for the diagnosis and risk stratification of idiopathic VF. Inducibility of VF with programmed electrical stimulation is associated with limited sensitivity and specificity (43% and 64% respectively).¹²²

Genetic Testing

The role of extensive genetic testing in patients with idiopathic VF is uncertain. Currently, the routine screening of large gene panels is not recommended because of the relatively low yield (about 15%) and the frequent detection of variants of uncertain clinical significance, which can potentially lead to unnecessary treatment and anxiety among patients. Nonetheless, targeted genetic testing is recommended when certain electrical syndromes are suspected based on clinical evaluation of the patient or family members. Testing for idiopathic VF-related mutations is only recommended in the presence of a strong family history of idiopathic VF or unexplained SCD. It should be recognized, however, that a negative genetic test result does not exclude concealed primary arrhythmia syndromes or a genetic origin of idiopathic VF.^{1,122,127}

Certain clinical information can help guide targeted genetic testing. For example, arrhythmic events (VF or prior syncope episodes) triggered by exercise should point to CPVT or LQT1, whereas those triggered by emotion suggest CPVT or LQT2. Arrhythmic events occurring during sleep suggest Brugada syndrome or LQTS. Fever-associated arrhythmias favor Brugada syndrome. Furthermore, polymorphic PVCs on Holter monitoring or exercise test suggest CPVT. The concomitant potentially arrhythmogenic drugs should raise the suspicion of LQTS and Brugada syndrome.¹³¹

Principles of Management

Pharmacological Therapy

Data from controlled trials or experimental studies are largely lacking. Preliminary clinical experience with quinidine (a class IA antiarrhythmic agent with potent inhibition of I_{to}) is promising. Beta-adrenergic agonists are beneficial in idiopathic VF, particularly for arrhythmic storm. Amiodarone has limited efficacy. Beta-blockers, lidocaine, mexiletine, and verapamil are generally not beneficial (see Fig. 31.7).¹

Acceleration of the heart rate (up to 120 beats/min) by isoproterenol infusion or by atrial or ventricular pacing can be very effective for the acute control of ventricular arrhythmias. Deep sedation may also be considered in refractory cases.

Implantable Cardioverter-Defibrillator

ICD implantation is recommended in patients with prior cardiac arrest due to VF given the high risk of recurrence of ventricular arrhythmias (11% to 45% mean follow-up of 3.2 to 5.3 years) and the fact that neither medical therapy nor catheter ablation provides absolute protection from SCD.^{1,122,127}

In patients with ICDs and frequent nonsustained ventricular arrhythmias or recurrent sustained arrhythmias precipitating frequent ICD therapies, adjuvant antiarrhythmic therapy with quinidine can be helpful. Of note, patients with VF and early repolarization have shown a higher risk of VF recurrence than those without early repolarization (43% vs. 23% during 5 years of follow-up). ICD recipients also experience a high rate of inappropriate shocks (14% to 44%; mean follow-up, 1.9 to 8.8 years), frequently precipitated by AF.^{1,122,127}

In view of the lack of specific risk factors and the absence of abnormalities on the ECG or imaging studies in patients with idiopathic VF, identification of at-risk asymptomatic subjects is currently not possible. In addition, the optimal management of asymptomatic family relatives and mutation carriers is uncertain. Nonetheless, ICD implantation may be considered in the presence of unexplained syncope in a first-degree relative of an idiopathic VF victim, but only after careful work-up of the cause of syncope and patient counseling.^{1,123}

Catheter Ablation

Recent evidence suggests an important role of specific triggers for initiation of idiopathic VF (Fig. 31.20). Distal Purkinje fibers have been recognized as the most frequent site of VF-triggering PVCs occurring during the vulnerable period of cardiac repolarization. The culprit PVCs have also been demonstrated to originate from sites other than the HPS, including the RVOT, LVOT, and papillary muscles.¹³²

PVCs originating from the RVOT, although generally considered “benign,” can initiate polymorphic VT and VF in some patients with idiopathic VF. Distinguishing between the “malignant” forms and the benign form of RVOT PVCs is often challenging. Data suggest that shorter CLs during monomorphic VT, short coupling intervals

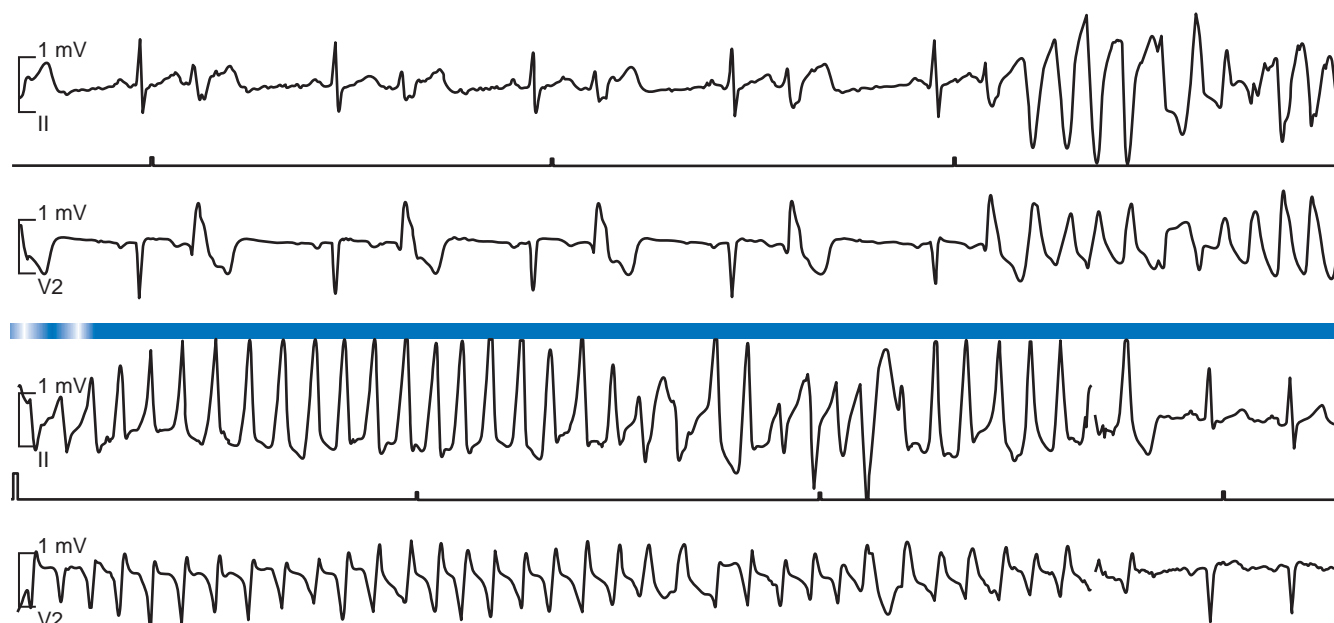


Fig. 31.20 Polymorphic Ventricular Tachycardia (VT) Triggered by Premature Ventricular Complexes (PVCs). The telemetry rhythm strips show normal sinus rhythm with PVCs that trigger an episode of polymorphic VT. Note that the morphology of the triggering PVCs is similar to that of the isolated PVC.

of the PVCs, and a history of syncope with malignant characteristics, can potentially predict the coexistence of VF or polymorphic VT in patients with idiopathic RVOT VT/PVCs. However, significant overlap exists.

When ventricular arrhythmias are triggered by monomorphic PVCs, catheter ablation of the PVC focus can potentially prevent further episodes of VF or reduce the burden of arrhythmias. In the setting of PVCs arising from the Purkinje network, a presystolic low-amplitude and high-frequency signal (Purkinje potential) is typically recorded at the successful ablation site, whereby the Purkinje potential precedes and is closely coupled with the ventricular signal of the culprit PVC (eFig. 31.5). Abolition of the local Purkinje potentials and suppression of the targeted PVCs have been shown in a small series to significantly reduce the frequency of VF.¹³²

The presence of frequent PVCs during the ablation procedure can significantly improve the success of ablation. Not infrequently, the optimal time for ablation is at the time of an arrhythmic storm when the PVCs tend to be frequent. When the PVCs are absent at the time of the procedure, provocative maneuvers (including the use of isoproterenol or programmed electrical stimulation) are not usually helpful. Pace mapping can be used in cases of monomorphic ventricular ectopy when a clear 12-lead recording of the clinical PVCs initiating VF has been obtained (eFigs. 31.6 and 31.7).¹³²

Catheter ablation of focal PVCs may be considered especially in patients with frequent episodes of syncope or repeated ICD shocks refractory to drug therapy. Nonetheless, ablation therapy is not a substitute for ICD therapy because of the risk of recurrence of VF (in 18% of patients) triggered by PVCs either from the original focus or from new foci.¹

It is worth noting that recent studies found a concordance between the site of origin of VF-triggering PVCs and the location of the early repolarization pattern on the surface ECG. Patients with early repolarization recorded in inferior leads alone had PVCs originating from the inferior LV wall, whereas those with early repolarization recorded in both inferior and lateral leads had PVCs originating from multiple regions.

Participation in Sports

Restriction from competitive sports is appropriate in patients with idiopathic VF.⁶⁰

Periodic Evaluation

Importantly, the initial diagnosis of idiopathic VF can change during follow-up, despite comprehensive clinical investigation at the time of the index event. Phenotypic findings of other primary electric diseases or latent structural causes are often dynamic and may not be present at initial evaluation.¹³⁰ In fact, 11% to 38% of patients initially diagnosed with idiopathic VF reveal a specific disease (e.g., ARVC or Brugada syndrome) during follow-up. Therefore the diagnosis of idiopathic VF should be periodically reassessed with clinical history, physical examination, ECG, and possibly other tests, as guided by clinical suspicion. An annual assessment including an ECG is recommended, with repeat imaging, ambulatory monitoring, and exercise testing every 2 to 3 years, and with any change in arrhythmia burden.^{127,133}

Family Screening

Unlike other arrhythmia syndromes, such as Brugada syndrome and LQTS, no cardiac abnormalities are observed in idiopathic VF patients, apart from the early repolarization ECG pattern, which is also not infrequently observed in the general population. Hence, family members who may be at risk cannot be identified and the penetrance of idiopathic VF cannot be assessed on the basis of an ECG phenotype.¹²²

As noted, phenotype penetrance of inherited arrhythmogenic syndromes can vary among gene carriers in the same family; hence, it is recommended to evaluate first-degree relatives of all idiopathic VF victims with resting ECG, exercise stress testing, and echocardiography.¹³¹ In addition, Holter monitoring, and signal-averaged ECGs, CMR, and provocative testing with class IC antiarrhythmic drugs and epinephrine infusion may also be considered, especially in relatives with unexplained syncope. Furthermore, even when the initial assessment is normal, periodic clinical assessment is indicated in young family members of idiopathic VF victims (as young patients may only manifest symptoms or signs of the disease at an older age and certain diseases have age-related penetrance) and in all family members whenever additional suspicious sudden deaths are identified in the family.¹

The recent identification of mutations of the *DPP6* and *CALM1* genes as a potential familial component in idiopathic VF may allow presymptomatic identification of individuals at risk. Cascade family screening should be considered when a pathogenic mutation is found (e.g., *DPP6* or *CALM1*) or a specific diagnosis is revealed.¹²²

EARLY REPOLARIZATION SYNDROMES

Early repolarization ECG patterns, consisting of a distinct J wave or J point elevation, or a notch or slur of the terminal part of the QRS, are predominantly found in healthy young men and have traditionally been viewed as totally benign, “normal variants.” However, this concept has been challenged by several recent studies, which demonstrated that early repolarization patterns in apparently healthy subjects could represent a marker of increased dispersion of repolarization and arrhythmogenesis, and of the presence of a relationship between certain repolarization patterns and some cases of unexplained VF and SCD.^{65,134}

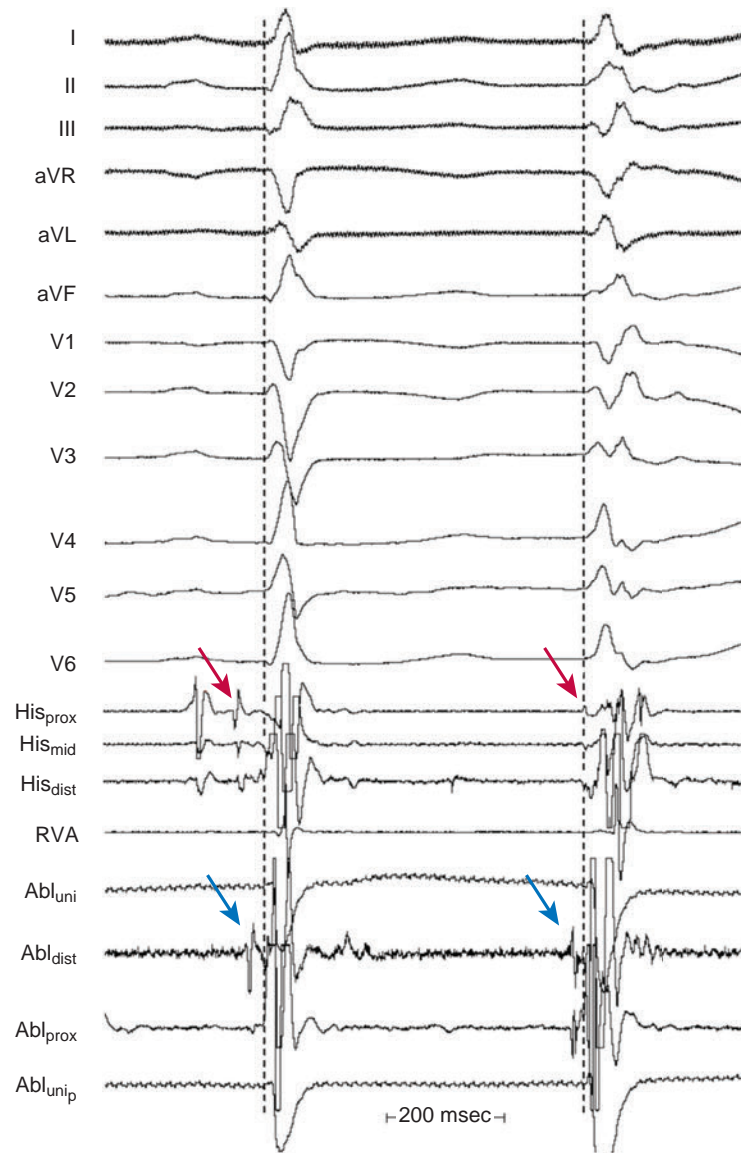
Genetics of Early Repolarization Syndrome

Several studies have suggested the early repolarization pattern is a heritable phenotype. Familial early repolarization has been reported to have an autosomal dominant inheritance pattern with incomplete penetrance. Variants in genes encoding cardiac ion channels have been identified in individuals and families with early repolarization syndrome (Table 31.19). Gain-of-function mutations in *KCNJ8* and *ABCC9* genes (encoding the pore-forming and ATP-sensing subunits of the I_{K-ATP} channel) and the *KCNE5* gene (encoding the I_{to} channel) have been reported in patients with early repolarization syndrome. Loss-of-function variations in the $\alpha 1$, $\beta 2$, and $\alpha 2\delta$ subunits of the cardiac L-type Ca^{2+} channel (encoded respectively by the *CACNA1C*, *CACNB2*, and *CACNA2D1* genes) and the $\alpha 1$ subunit of $Na_v1.5$ and $Na_v1.8$ (*SCN5A*, *SCN10A*) have been reported in patients with early repolarization syndrome.

TABLE 31.19 Molecular Basis of the Early Repolarization Syndrome

	Gene	Protein	Functional Effect	% of Probands
ERS1	KCNJ8	Kir6.1	$\uparrow I_{K-ATP}$	
ERS2	CACNA1C	$Ca_v1.2$	$\downarrow I_{CaL}$	4.1%
ERS3	CACNB2B	$Ca_v\beta 2b$	$\downarrow I_{CaL}$	8.3%
ERS4	CACNA2D1	$Ca_v\alpha 2\delta$	$\downarrow I_{CaL}$	4.1%
ERS5	ABCC9	SUR2A	$\uparrow I_{K-ATP}$	Rare
ERS6	SCN5A	$Na_v1.5$	$\downarrow I_{Na}$	Rare
ERS7	SCN10A	$Na_v1.8$	$\downarrow I_{Na}$	

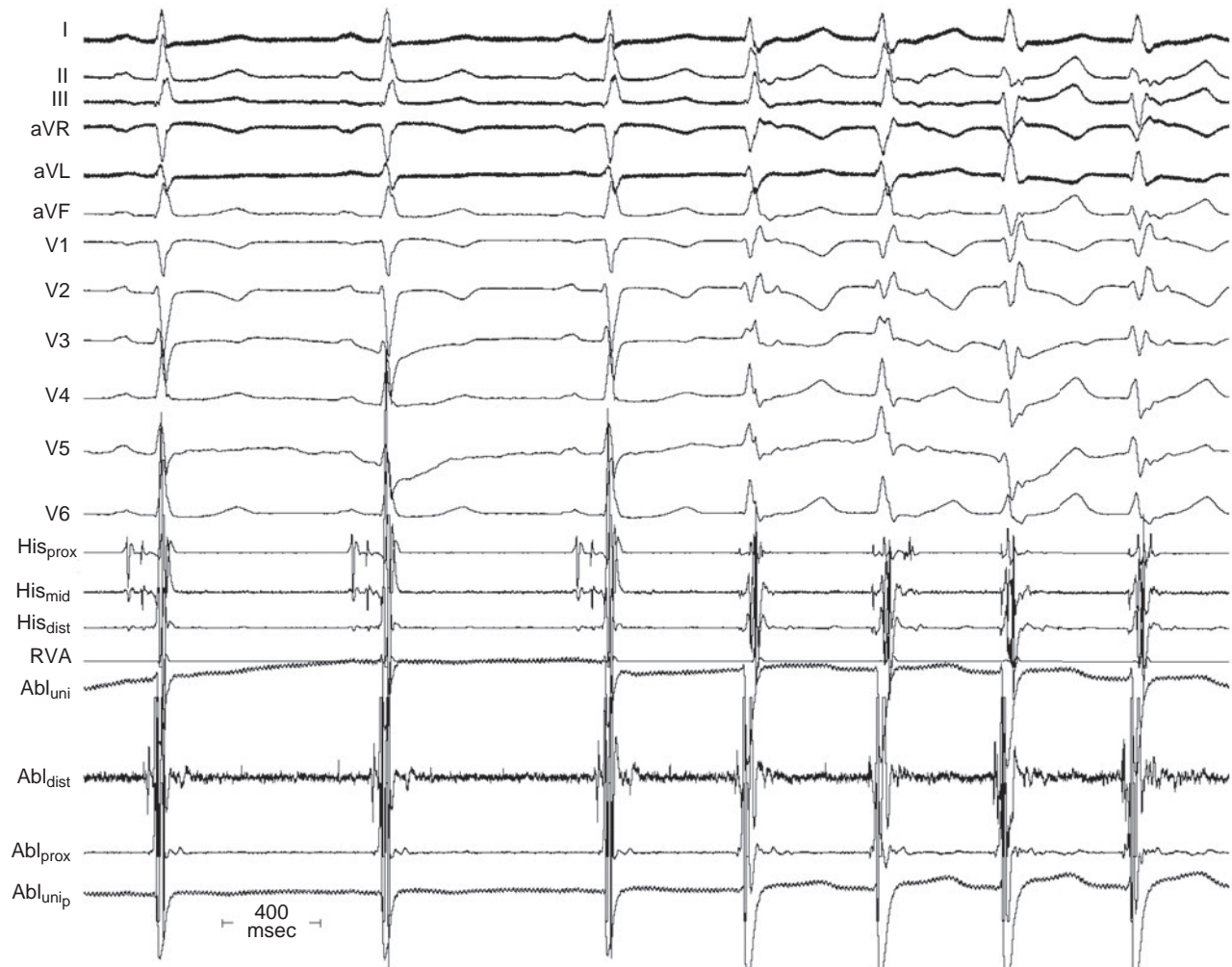
I_{CaL} , L-type Ca^{2+} current; I_{K-ATP} , ATP-activated inward rectifier K^+ current; I_{Na} , Na^+ current; ERS1 to ERS7, early repolarization syndrome types 1 to 7, respectively.



eFig. 31.5 Sinus Rhythm (*Left*) and Premature Ventricular Complexes (PVCs, *Right*) in a Patient With Idiopathic Ventricular Fibrillation. Dashed lines denote the onset of QRS complexes. Blue arrows indicate Purkinje potentials, and red arrows indicate His potentials. During sinus rhythm, His potentials precede Purkinje potentials, the sequence of which is reversed in the PVCs.



eFig. 31.6 Pace Mapping of Premature Ventricular Complexes (PVCs) in a Patient With Idiopathic Ventricular Fibrillation. *Left*, Sinus rhythm (SR) and a PVC in a patient with idiopathic ventricular fibrillation are shown. *Right*, Pacing at the PVC site of origin closely mimics the PVC.



eFig. 31.7 Catheter Ablation of Premature Ventricular Complexes (PVCs) in a Patient With Idiopathic Ventricular Fibrillation. Three seconds after the onset of radiofrequency energy delivery at the site of PVC origin, a burst of ectopy occurs having the same QRS configuration as the spontaneously occurring PVC (see eFigs. 31.5 and 31.6).

Recently, gain-of-function mutations in the genes encoding the major channel subunits of I_{to} , *KCNQ2* and *KCNQ3*, have been described in Brugada syndrome and an atypical anterior J wave syndrome associated with SCD.^{134–136}

Pathophysiology of Early Repolarization Syndromes

Mechanism of Early Repolarization and J Waves

The exact ionic and cellular mechanisms for the J wave and early repolarization pattern are still under investigation. Heterogeneity in the distribution of I_{to} channels across the myocardial wall, being more prominent in ventricular epicardium than endocardium, results in the shorter duration, prominent phase 1 notch, and “spike and dome” morphology of the epicardial action potential as compared with the endocardial action potential. The resultant transmural voltage gradient during the early phases (phases 1 and 2) of the action potential is thought to be responsible for the inscription of the J wave on the surface ECG (see Fig. 31.9).^{137,138}

An outward shift of currents, secondary to a decrease in the inward currents (I_{Na} and I_{CaL}), an increase in the outward K^+ currents (I_{to} , I_{Kr} , I_{Ks} , I_{KACH} , I_{KATP}), or both, can cause accentuation of the action potential notch, leading to augmentation of the J wave or the appearance of ST segment elevation on the surface ECG. An outward shift of currents that extends beyond the action potential notch not only can accentuate the J wave, but also lead to partial or complete loss of the dome of the action potential, leading to a protracted transmural voltage gradient that manifests as greater ST segment elevation and gives rise to J wave syndromes. The type of ion current affected and its regional distribution in the ventricles determines the particular phenotype (including the Brugada syndrome, early repolarization syndrome, hypothermia-induced ST segment elevation, and infarction-induced ST segment elevation).¹³⁹ Male predominance can potentially result from larger epicardial I_{to} density versus that in women.¹³⁵

It should be mentioned that not all investigators are in complete agreement about the EP basis of J waves and whether the mechanism responsible for abnormal J waves is related to depolarization abnormalities (i.e., slow impulse conduction) rather than repolarization abnormalities.¹³⁵ However, while there is evidence that depolarization abnormalities are involved in the formation of a Brugada-type ECG (i.e., conduction delay to the RVOT) and ischemia-related early repolarization (conduction delay through ischemic myocardial zones) and contribute to the arrhythmias in those diseases, there is less evidence for depolarization abnormalities in patients with inferolateral early repolarization and hypothermia-related early repolarization.¹⁴⁰

Mechanism of Arrhythmogenesis

The exact relationship of an early repolarization pattern and malignant ventricular arrhythmias remains unclear. It is likely that the increased transmural heterogeneity of ventricular repolarization (i.e., dispersion of repolarization between epicardium and endocardium), which is responsible for J point elevation and the early repolarization pattern on the surface ECG, is also responsible for the increased vulnerability to ventricular tachyarrhythmias. A significant outward shift in current can cause partial or complete loss of the dome of the action potential in regions where I_{to} is prominent (epicardium), with the consequent loss of activation of I_{CaL} . The dome of the action potential can then propagate from regions where it is preserved (midmyocardium and endocardium) to regions where it is lost (epicardium), giving rise to phase 2 reentry, which can generate short-coupled PVCs (falling on the descending limb of the T wave: the R-on-T phenomenon) that interacts with a susceptible ventricular substrate to trigger transmural reentry and polymorphic VT or VF (see Fig. 31.10). This phenomenon is also observed during “ischemic VF,” Brugada syndrome, and idiopathic

VF. J wave appearance represents an initial response to acute ischemia, resulting from the loss of the transient outward potassium current–mediated epicardial action potential dome triggering VF. This might explain why early repolarization is a marker for increased arrhythmic mortality across a heterogeneous clinical spectrum.^{139,141,142}

Notably, this pathophysiology is analogous to the mechanism operative in the Brugada syndrome. Although the ECG location of early repolarization in Brugada syndrome is thought to be secondary to the presence of increased transmural dispersion of repolarization in the RVOT mediated by increased epicardial I_{to} , the location of early repolarization and associated J waves involving inferolateral leads caused by heterogeneity in action potential morphology and duration across the LV wall. Higher intrinsic levels of I_{to} in the inferior LV wall likely accounts for the greater vulnerability of this region for developing VF.¹³⁴

Importantly, the J wave in early repolarization syndrome increases markedly just before arrhythmic events, an occurrence which is now recognized as a hallmark of the disease. J wave amplitude is augmented by slow heart rate and increased vagal activity, which can potentially explain why VF in these patients often occurs during sleep or at a low level of physical activities.¹³⁴

Modulation of Early Repolarization Pattern

Patients with early repolarization syndrome can display dynamic J point elevation. Factors that influence the kinetics of I_{to} or the other repolarization currents (including heart rate, heart rhythm, autonomic tone, and drugs) can modify the manifestation of the J wave on the ECG. J wave amplitude increases during slow heart rates as well as a short-long-short sequence and a pause, which is likely related to augmentation of I_{KACH} and IK-A P (secondary to increased vagal tone) as well as augmentation of I_{to} (facilitated by bradycardia). It is important to note that during episodes of high vagal tone, a degree of elevation of the J point can be a physiological finding in normal individuals. In patients with early repolarization syndrome, however, bradycardia-mediated J point elevation is markedly amplified. On the other hand, acceleration of the heart rate, which is associated with reduction of I_{to} (because of the slow recovery of I_{to} from inactivation), results in a decrease in the magnitude of the J wave.¹⁴³ Circadian variation of the J-wave amplitude is also known to occur, and its augmentation is in concordance with a vagal tone.

J waves can be augmented or induced by hypothermia and fever; however, the development of arrhythmias in early repolarization syndrome is much more sensitive to hypothermia, whereas arrhythmogenesis in Brugada syndrome appears to be promoted only by fever.

Quinidine, which inhibits both I_{to} and I_{Na} , reduces the magnitude of the J wave and normalizes ST segment elevation. Quinidine was found to be effective in partially reversing the repolarization abnormalities, thus restoring electric homogeneity and abolishing the arrhythmogenic substrate.^{135,144}

Na^+ channel blockers (ajmaline, procainamide, pilsicainide, propafenone, flecainide, and disopyramide), which reduce the inward I_{Na} , unmask or accentuate J wave manifestation in Brugada syndrome but attenuate the J wave amplitude in early repolarization patients. Although this differential effect of Na^+ channel blockers initially invoked a potentially different pathophysiology of early repolarization from that of the Brugada syndrome, a recent study demonstrated that J waves recorded with unipolar LV epicardial leads introduced into the left lateral coronary vein in early repolarization syndrome patients were indeed augmented, even though J waves recorded in the lateral precordial leads were diminished, principally because of engulfment of the surface J wave by the widened QRS. Na^+ channel blockade results in slowing of conduction and delay of the terminal ventricular activation whereby the S waves superimpose the J waves. These S waves represent an opposing force

to the J waves and depending on their amplitude and duration, can decrease or completely obscure the J waves.^{144,145}

Via beta-adrenergic stimulation, isoproterenol augments I_{CaL} by increasing the mean channel open time and probability of channel opening. In addition, because of slow recovery from inactivation, I_{to} is rate dependent with decreasing current magnitude at higher heart rates, and isoproterenol decreases I_{to} via an acceleration of heart rate. The combined effect of increasing Ca^{2+} influx (via I_{CaL} augmentation) and reducing K^+ efflux (via I_{to} inhibition) counteracts some of the primary mechanisms thought to underlie the formation of J waves and early repolarization. The observed effects of isoproterenol are most compatible with the repolarization disorder hypothesis for early repolarization. Depolarization abnormalities are expected to worsen, rather than improve, at faster heart rates.

Cilostazol and milrinone inhibit the activity of phosphodiesterase III, increasing the intracellular concentrations of cAMP, which in turn results in augmentation of I_{CaL} . Milrinone has much greater potency than cilostazol, possibly because milrinone blocks both phosphodiesterase III and phosphodiesterase IV.^{138,144}

Bepridil is a Ca^{2+} channel antagonist with lidocaine-like rapid kinetic blocking effects of Na^+ channels. Bepridil also blocks most types of K^+ currents, including I_{to} . Bepridil can decrease the number of VF episodes in patients with idiopathic VF (including those with Brugada syndrome).

Epidemiology

The prevalence of the early repolarization pattern in the general population varies from 1% to 13%, depending on age (predominant in children and young adults), race (highest among African-Americans and Southeast Asians), gender (predominant in men), and the criterion for J point elevation (0.05 mV vs. 0.1 mV).¹ The prevalence of an early repolarization pattern is several-fold higher in athletes (ranging from 10% to 90%) than in the general population. In athletes, this ECG pattern is thought to be related, at least in part, to heightened vagal tone.¹⁴⁶

Early repolarization is more frequent in patients with idiopathic VF than in control subjects, occurring in 15% to 70% of the idiopathic VF cases. Further, the prevalence of inferolateral J point elevation is higher in the family members of sudden arrhythmic death syndrome probands compared with the general population (23% vs. 11%). Importantly, among patients with idiopathic VF, those with early repolarization are more likely to have a history of syncope or SCD than those without early repolarization. Moreover, the presence of an early repolarization pattern, especially in the inferior or inferolateral leads, has recently been recognized as associated with vulnerability to VF and a 1.7 relative risk for SCD. In the 35- to 45-year-old age range of maximal early repolarization-related SCD incidence, a J wave is estimated to increase idiopathic VF risk from 3.4 per 100,000 to 11 per 100,000.^{135,146}

However, it is important to recognize that although early repolarization is a common entity, idiopathic VF itself is very rare. Therefore the incidental discovery of a J wave on routine screening should not be interpreted as a marker of “high risk” for SCD because the odds for this fatal disease would still be approximately 0.01% (and well less than 0.1% among asymptomatic individuals with J waves with the most “malignant” morphology), which is significantly less than the estimated 1% annual risk of spontaneous VF among asymptomatic adults with a type I Brugada ECG.¹

In addition to reports of SCD in otherwise healthy patients, the presence of early repolarization on the ECG appears to be a modulator of arrhythmic risk in patients with other cardiac disorders. An early repolarization ECG pattern has been associated with an increased risk of malignant arrhythmias and SCD in patients with Brugada syndrome, acute myocardial infarction (MI), chronic ischemic heart disease, heart failure, and hypothermia.¹³⁴

Early repolarization appears to be a heritable phenotype; offspring of early repolarization-positive parents have a 2.5-fold increased risk of presenting with early repolarization on the surface ECG. In addition, genetic contributions to SCD-associated early repolarization are suggested by common familial SCD histories in symptomatic early repolarization patients. Several reports demonstrated a high familial aggregation of sudden death in early repolarization syndrome patients; a family history of sudden death is reported in about one-fifth of patients with VF and early repolarization. Geographic differences in distribution have also been described, with early repolarization-related SCD being particularly prevalent among Southeast Asians.¹³⁶

Clinical Presentation

The vast majority of individuals with an early repolarization ECG pattern remain asymptomatic, and are usually found to have an early repolarization pattern as an incidental finding. Idiopathic VF patients (e.g., survivors of unexplained cardiac arrest) who are found to have clear ECG evidence of early repolarization are now defined as early repolarization syndrome patients. Early repolarization syndrome is extremely rare, but these patients have a high risk of recurrent cardiac events. Life-threatening arrhythmias are often the first and unexpected manifestation of early repolarization syndrome, and usually occur at a young age (typically less than 40 years).^{1,135}

Electrocardiographic Features

There has been considerable variation in the use of the terms “early repolarization” and “J point.” Historically, the term “early repolarization” was used to describe two ECG phenomena: (1) an upward deflection of the J point (or terminal part of the QRS complex) termed “J point elevation” or “J wave” and (2) ST segment elevation not associated with pathological conditions such as MI. More recently, after the emergence of reports associating early repolarization with idiopathic VF, most studies used the term “early repolarization” to describe an elevation of the QRS-ST segment junction (J point) greater than or equal to 0.1 mV in greater than or equal to 2 contiguous inferolateral leads (I, II, III, aVL, aVF, and V_4 to V_6), excluding right precordial leads. The morphology of the J point can be slurring (a smooth transition from the QRS segment to the ST segment) or notching (a positive J deflection inscribed on the S wave). Also, there is a consensus that the pattern of end-QRS notching and slurring may, on occasion, be due to late depolarization rather than early repolarization. Therefore some investigators suggest that the term “early repolarization” should be replaced by “J waves.”^{135,147}

Terminology

An expert consensus report published in 2015 proposed a standardized terminology and definition of ECG manifestations of early repolarization. It is recommended that the peak of an end-QRS notch and/or the onset of an end-QRS slur be designated as Jp, and that the onset of the end-QRS notch or J wave be designated as Jo and the end of a notch or slur as Jt. In the case of a slur, Jo and Jp are electrocardiographically the same point (Fig. 31.21).^{65,147}

The pattern of ST segment elevation after the J point can be classified as horizontal or downward sloping (if the amplitude of the ST segment 100 milliseconds after Jt is less than or equal to the amplitude at Jt) or upward sloping (if the amplitude of the ST segment 100 milliseconds after Jt is greater than the amplitude at Jt). ST segment elevation in the absence of a slur or notch should not be reported as early repolarization.^{65,147}

Definition

Early repolarization is present if all of the following criteria are met:^{65,147}

1. There is an end-QRS notch or slur on the downslope of a prominent R wave (with and without ST segment elevation). If there is a notch,

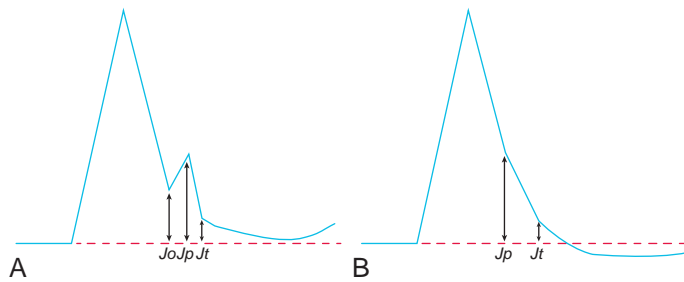


Fig. 31.21 Standardized Terminology and Definition of Electrocardiogram Manifestations of Early Repolarization. (A) In case of an end-QRS notch, the peak of the notch is designated as J_p , the onset of the notch is designated as J_o , and the end of a notch as J_t . (B) In the case of an end-QRS slur, J_o and J_p are electrocardiographically the same point. (Modified from MacFarlane PW, Antzelevitch C, Haissaguerre M, et al. The early repolarization pattern: a consensus paper. *J Am Coll Cardiol.* 2015;66:470–477.)

it should lie entirely above the baseline. The onset of a slur must also be above the baseline.

2. The peak of the notch or J wave (J_p) is greater than or equal to 0.1 mV in more than two contiguous leads of the 12-lead ECG, excluding leads V_1 to V_3 .
3. QRS duration (measured in leads in which a notch or slur is absent) is less than 120 milliseconds.

If the ST segment is upward sloping and followed by an upright T wave, the pattern should be described as “early repolarization with an ascending ST segment.” If the ST segment is horizontal or downward sloping, the pattern should be described as “early repolarization with a horizontal or descending ST segment.”

Right precordial leads (V_1 to V_3) have been excluded from the new definition of early repolarization to avoid confusion with the Brugada pattern.

An end-QRS notch is a notch that occurs on the final 50% of the downslope of an R wave occurring as the final segment of the QRS complex; that is, it links with the ST segment of the waveform (Fig. 31.22A). It should be distinguished from a notch midway on the downslope of an R wave (see Fig. 31.22B) because this may be due to

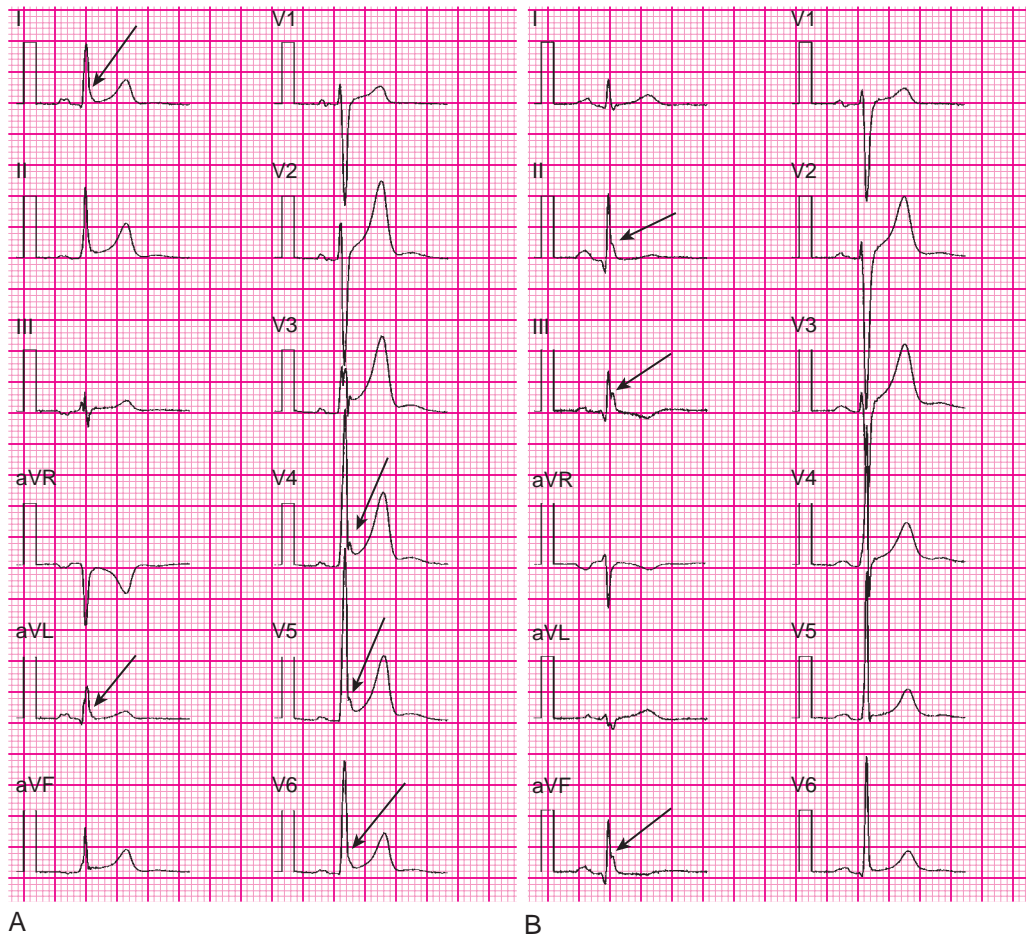


Fig. 31.22 QRS Notching and Slurring. (A) Electrocardiographic leads showing end-QRS notching in lead V_4 progressing to end-QRS slurring in lead V_6 . End-QRS slurring is also present in leads I and aVL. The arrows localize the notching or slurring. (B) Leads III and aVF show notching. In lead III, the notch peak is greater than 50% of the R wave amplitude and could be regarded as fragmentation. In lead II, appearances on the R wave downslope take the form of a slur, and there is also a notch in lead aVF. They are most probably due to the same underlying physiological process. The arrows indicate the location of the notches and slur. (From MacFarlane PW, Antzelevitch C, Haissaguerre M, et al. The early repolarization pattern: a consensus paper. *J Am Coll Cardiol.* 2015;66:470–477.)

fragmentation. Similarly, an end-QRS slur is an apparent slowing of the inscription of the waveform at the end of the QRS complex that merges with the ST segment of the complex. Likewise, a slur should occur in the final 50% of the R wave downslope.¹⁴⁷

Importantly, ST segment elevation is not a required criterion (Fig. 31.23). In the absence of any end-QRS notching or slurring, it is recommended that the finding of ST segment elevation be described as nonspecific ST segment elevation and not described as early repolarization (Fig. 31.24).¹⁴⁷

The early repolarization pattern can vary in response to autonomic tone and heart rate. Bradycardia and increased vagal tone (e.g., during sleep) accentuate ST segment elevation. Contrariwise, tachycardia and adrenergic stimulation (e.g., exercise testing or the infusion of isoproterenol) suppress J wave amplitude and ST segment elevation. In addition, hypothermia can induce prominent J waves (“Osborn waves”).

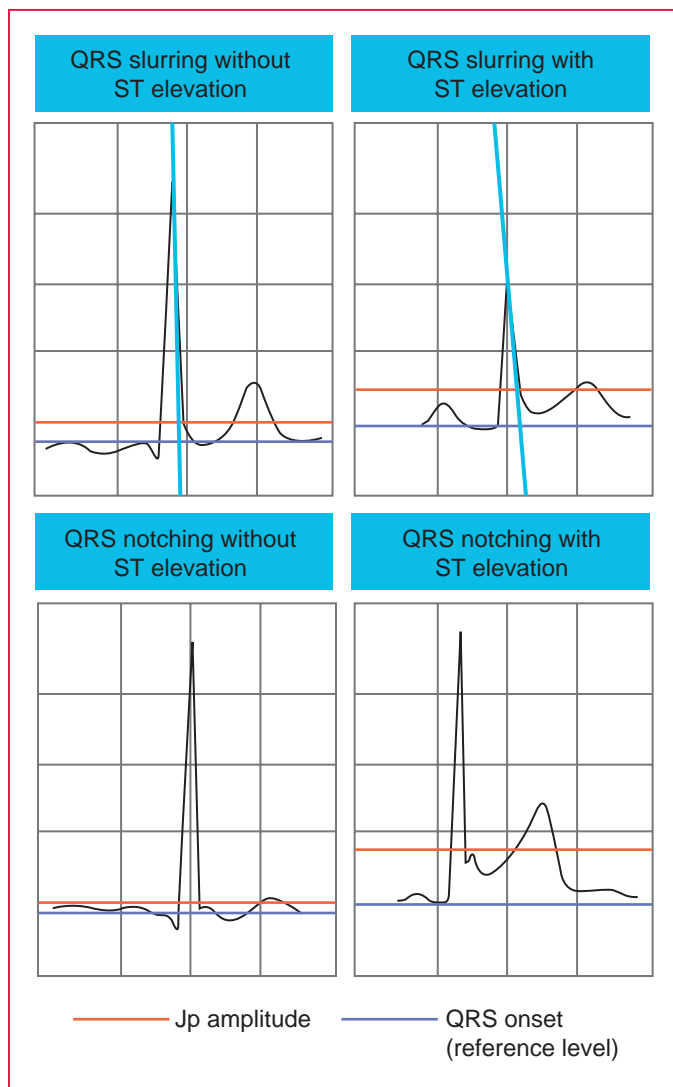


Fig. 31.23 End-QRS Notching and Slurring With and Without ST Segment Elevation. The upper salmon line indicates the notch or slur amplitude, J peak (Jp), while the lower purple line indicates the baseline used as a reference with respect to which amplitudes should be measured. The blue lines indicate tangents to the initial component of the R wave downslope. All of these waveforms are illustrations of the early repolarization pattern. (From MacFarlane PW, Antzelevitch C, Haissaguerre M, et al. The early repolarization pattern: a consensus paper. *J Am Coll Cardiol.* 2015;66:470–477.)

Localization of Early Repolarization

Based on the localization of the early repolarization pattern on the 12-lead ECG and its potential association with risk for life-threatening arrhythmias, some investigators classified early repolarization patterns into three types¹³⁴:

Type 1: The early repolarization pattern manifests predominantly in the lateral precordial leads (V₄–V₆). This pattern is rarely seen in cases of idiopathic VF, is highly prevalent among healthy young adults and athletes, and is thought to be associated with a relatively low level of risk for arrhythmic events.

Type 2: The early repolarization pattern is localized to the inferior or inferolateral leads. This pattern is less common in the general

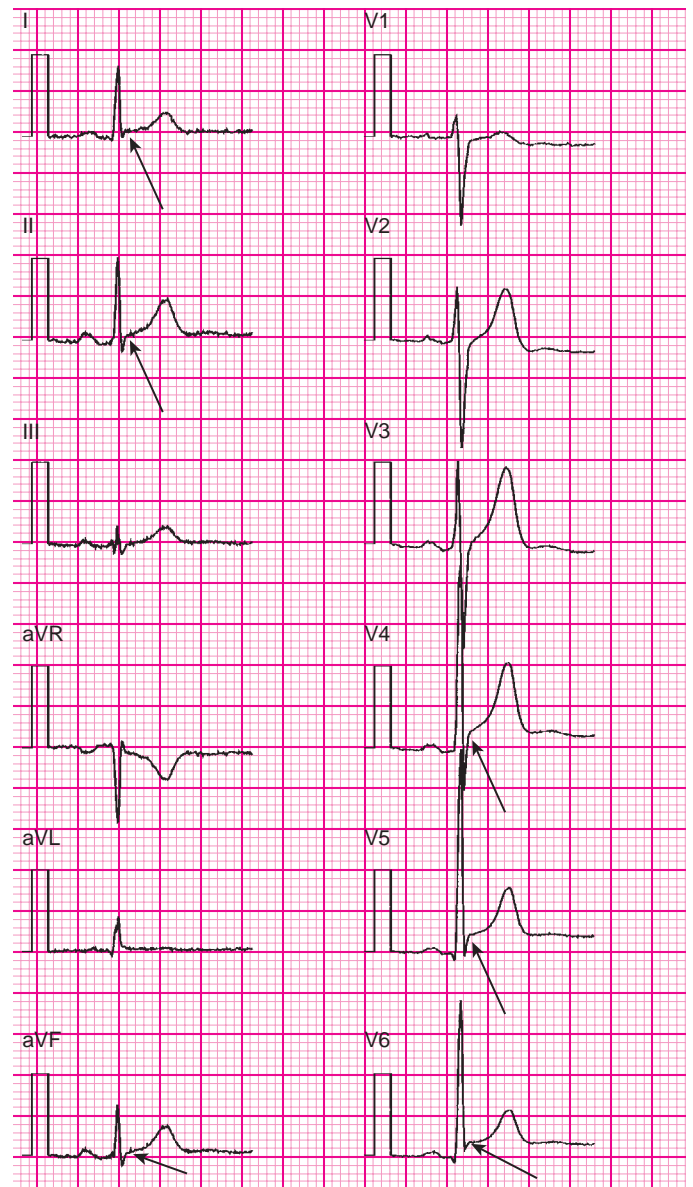


Fig. 31.24 Nonspecific ST Segment Elevation. An illustration of an electrocardiogram showing moderate ST segment elevation in leads I, II, and aVF and more marked ST segment elevation in leads V₄–V₆, in the absence of any end-QRS notching or slurring. It is recommended that this finding not be described as early repolarization. The arrows indicate the points of ST segment elevation. (From MacFarlane PW, Antzelevitch C, Haissaguerre M, et al. The early repolarization pattern: a consensus paper. *J Am Coll Cardiol.* 2015;66:470–477.)

population, but is observed in approximately 50% of cases of idiopathic VF. Early repolarization in the inferior leads is also associated with an increased risk of cardiovascular death from any cause.

Type 3: Early repolarization is more global, involving the inferior, lateral, and right precordial leads. This pattern is the rarest and carries the highest risk of malignant ventricular arrhythmias.

Diagnosis of Early Repolarization Syndrome

According to a recent expert consensus, an “early repolarization pattern” can be diagnosed in the presence of J point elevation greater than or equal to 1 mm in more than two contiguous inferior and/or lateral leads of a standard 12-lead ECG. An “early repolarization syndrome” is diagnosed in the presence of early repolarization pattern in a patient resuscitated from otherwise unexplained VF/polymorphic VT or in an SCD victim with a negative autopsy and medical chart review.¹

A scoring system (the Shanghai Score) has been proposed for the diagnosis of early repolarization syndrome (Table 31.20). This system is based on evidence available in the literature to date, but is yet to be validated in future studies.

TABLE 31.20 Shanghai Score System for Diagnosis of Early Repolarization Syndrome

	Points
I. Clinical History	
A. Unexplained cardiac arrest, documented VF or polymorphic VT	3
B. Suspected arrhythmic syncope	2
C. Syncope of unclear mechanism/unclear etiology	1
<i>Only award points once for highest score within this category.</i>	
II. Twelve-Lead ECG	
A. ER >0.2 mV in >2 inferior and/or lateral ECG leads with horizontal/descending ST segment	2
B. Dynamic changes in J point elevation (≥0.1 mV) in ≥2 inferior and/or lateral ECG leads	1.5
C. ≥0.1 mV J point elevation in at least 2 inferior and/or lateral ECG leads	1
<i>Only award points once for highest score within this category.</i>	
III. Ambulatory ECG Monitoring	
A. Short-coupled PVCs with R on ascending limb or peak of T wave	2
IV. Family History	
A. Relative with definite ERS	2
B. ≥2 first-degree relatives with a II.A. ECG pattern	2
C. First-degree relative with a II.A. ECG pattern	1
D. Unexplained sudden cardiac death <45 years in a first- or second-degree relative	0.5
<i>Only award points once for highest score within this category.</i>	
V. Genetic Test Result	
A. Probable pathogenic ERS susceptibility mutation	0.5
Score (requires at least one ECG finding)	
≥5 points: Probable/definite ERS	
3–4.5 points: Possible ERS	
<3 points: Nondiagnostic	

ECG, Electrocardiogram; ER, early repolarization; ERS, early repolarization syndrome; PVC, premature ventricular contraction; VF, ventricular fibrillation; VT, ventricular tachycardia.

From Antzelevitch C, Yan GX, Ackerman MJ, et al. J-wave syndromes expert consensus conference report: emerging concepts and gaps in knowledge. *Heart Rhythm*. 2016;13:e295–e324.

Importantly, the diagnosis of “early repolarization syndrome” in survivors of cardiac arrest requires a complete evaluation to exclude underlying structural or other primary electrical heart disease, and exclusion of respiratory, metabolic, and toxicological etiologies. This typically necessitates extensive diagnostic testing, as discussed previously for idiopathic VF.¹ Furthermore, other causes of J point elevation (ischemia, hypokalemia, hypercalcemia, hypothermia) need to be excluded. Genetic testing for early repolarization syndrome is still of questionable benefit and, until validated in future studies, is considered investigational.^{1,135,147}

No consensus exists regarding the evaluation of asymptomatic individuals incidentally found to have an early repolarization pattern on the surface ECG. Currently, in the absence of syncope or a strong family history of juvenile SCD, the finding of the early repolarization pattern does not merit further investigation.^{1,135,147}

Differential Diagnosis

Early repolarization ECG patterns can be observed in a spectrum of acquired and congenital disorders, collectively referred to as “J wave syndromes,” which include the Brugada syndrome, hypothermia, and acute myocardial ischemia, in addition to the early repolarization syndrome. Those syndromes appear to share similar pathophysiology and arrhythmogenic mechanisms characterized by polymorphic VT or VF triggered by short-coupled PVCs.^{134,140}

In hypothermia (including therapeutic hypothermia), J waves (Osborne waves) can manifest diffusely in all leads or be confined to selected leads. Rarely, hypothermia can induce ECG changes that mimic those of Brugada syndrome.¹⁴⁰

The early repolarization syndrome shares a number of features with Brugada syndrome (Table 31.21). Both syndromes are associated with vulnerability to polymorphic VT and VF in young adults without apparent structural heart disease. However, in the Brugada syndrome, the region most affected by the disease is the anterior RVOT, and ST segment elevation is limited to the right precordial leads. Of note, a Brugada pattern on the surface ECG can be missed in patients with an inferolateral early repolarization pattern unless appropriate ECG recordings from the high intercostal space region are obtained. The presence of the Brugada ECG pattern was found to be a marker of poor outcome in patients with early repolarization; similarly, the presence of an inferolateral early repolarization ECG pattern was found to be a marker of poor outcome in patients with Brugada syndrome.^{134,148}

In addition, several cardiac and noncardiac conditions can produce ECG changes that can potentially thus masquerade as a J wave (Box 31.4).

Risk Stratification

Despite the reports linking early repolarization with sudden death, only a very small minority (1:10,000) of patients with this pattern on the ECG will have sudden cardiac arrest, while the majority remain asymptomatic. The identification of this minority of patients before they experience sudden death continues to be a challenge.

Currently, the identification of the “malignant” variant of the early repolarization pattern relies on several parameters, including the amplitude, distribution, and dynamicity of J point elevation, as well as the morphology of the ST segment, pause-dependent augmentation of J point elevation, and the presence of short-coupled PVCs, among others. However, the sensitivity and specificity of these parameters remain limited. Although the presence of those markers is predicted to progressively augment the cumulative risk of SCD (Fig. 31.25), the absolute risk conferred for an asymptomatic patient remains too small to justify an aggressive approach in the absence of symptoms. Nonetheless, the presence of early repolarization should attract careful attention in certain groups of patients.

TABLE 31.21 Similarities and Differences Between BrS and ERS and Possible Underlying Mechanisms

	BrS	ERS	Possible Mechanism(s)
Similarities Between BrS and ERS			
Male predominance	Yes (>75%)	Yes (>80%)	Testosterone modulation of ion currents underlying the epicardial AP notch
Average age of first event	30–50	30–50	
Associated with mutations or rare variants in <i>KCNJ8</i> , <i>CACNA1C</i> , <i>CACNB2</i> , <i>CACNA2D</i> , <i>SCN5A</i> , <i>ABCC9</i> , <i>SCN10A</i>	Yes	Yes	Gain of function in outward currents (I_{K-ATP}) or loss of function in inward currents (I_{Ca} or I_{Na})
Relatively short QT intervals in subjects with Ca channel mutations	Yes	Yes	Loss of function of I_{Ca}
Dynamicity of ECG	High	High	Autonomic modulation of ion channel currents underlying early phases of the epicardial AP
VF often occurs during sleep or at a low level of physical activity	Yes	Yes	Higher level of vagal tone and higher levels of I_{to} at the slower heart rates
VT/VF trigger	Short-coupled PVC	Short-coupled PVC	Phase 2 reentry
Ameliorative response to quinidine and bepridil	Yes	Yes	Inhibition of I_{to} and possible vagolytic effect
Ameliorative response to isoproterenol, denopamine and milrinone	Yes	Yes	Increased I_{Ca} and faster heart rate
Ameliorative response to cilostazol	Yes	Yes	Increased I_{Ca} , reduced I_{to} and faster heart rate
Ameliorative response to pacing	Yes	Yes	Reduced availability of I_{to} due to slow recovery from inactivation
Vagally mediated accentuation of ECG pattern	Yes	Yes	Direct effect to inhibit I_{Ca} and indirect effect to increase I_{to} (due to slowing of heart rate)
Effect of sodium channel blockers on unipolar epicardial electrogram	Augmented J waves	Augmented J wave	Outward shift of balance of current in the early phases of the epicardial AP
Fever	Augmented J waves	Augmented J waves (rare)	Accelerated inactivation of I_{Na} and accelerated recovery of I_{to} from inactivation.
Hypothermia	Augmented J waves mimicking BrS	Augmented J waves	Slowed activation of I_{Ca} leaving I_{to} unopposed. Increased phase 2 reentry but reduced pVT due to prolongation of APD. ³⁵⁸
Differences Between BrS and ERS			
Region most involved	RVOT	Inferior LV wall	Higher levels of I_{to} and/or differences in conduction
Leads affected	V_1 – V_3	II, II a, VF, V_4 , V_5 , V_6 ; I, aVL, Both: inferolateral	
Regional difference in prevalence			Europe: BrS = ERS Asia: BrS > ERS
Incidence of late potential in signal-averaged ECG	Higher	Lower	
Prevalence of atrial fibrillation	Higher	Lower	
Effect of sodium channel blockers on surface ECG	Increased J wave manifestation	Reduced J wave manifestation	Reduction of J wave in the setting of ER is thought to be due largely to prolongation of QRS. Accentuation of repolarization defects predominates in BrS, whereas accentuation of depolarization defects predominates in ERS.
Structural changes, including mild fibrosis and reduced expression of Cx43 in RVOT or fibrofatty infiltration in cases of arrhythmogenic right ventricular cardiomyopathy. Imaging studies have also revealed wall motion abnormalities and mild dilation in the region of the RVOT.	Higher in some forms of the syndrome	Unknown	Some investigators have hypothesized that some of these changes may be the result of, rather than the cause of, the BrS substrate, which may create a hibernation-like state due to loss of contractility in the RVOT secondary to loss of the AP dome.

AP, Action potential; APD, action potential duration; BrS, Brugada syndrome; ECG, electrocardiogram; ERS, early repolarization syndrome; RVOT, right ventricular outflow tract; PVC, premature ventricular contraction; pVT, polymorphic ventricular tachycardia; VF, ventricular fibrillation; VT, ventricular tachycardia.

From Antzelevitch C, Yan GX, Ackerman MJ, et al. J-wave syndromes expert consensus conference report: emerging concepts and gaps in knowledge. *Heart Rhythm*. 2016;13:e295–e324.

J Wave Amplitude

Evidence suggests that the height of J point elevation, rather than its mere presence, can potentially provide important risk stratification information. A slurred or notched J point elevation greater than 0.2 mV in the inferior leads predicts a 2.9-fold increase in SCD risk, whereas

an elevation of at least 0.1 mV predicts a more modest (1.4-fold) increase in risk of arrhythmic death. A similar phenomenon was also observed in survivors of primary VF. It is worth noting that J point elevation greater than 0.2 mV seems to be rare (0.3% to 0.7%) in the normal population, but was observed in 16% of patients with idiopathic VF.^{1,139}

BOX 31.4 Differential Diagnosis of Early Repolarization Pattern

- Juvenile ST pattern
- Pericardial disease (pericarditis, pericardial cyst, pericardial tumor)
- Hypothermia
- Hyperthermia
- Myocardial tumor (lipoma)
- Hypertensive heart disease
- Athlete's heart
- Myocardial ischemia
- ST segment elevation myocardial infarction
- Fragmented QRS (terminal notching)
- Hypocalcemia
- Hyperkalemia
- Thymoma
- Aortic dissection
- Arrhythmogenic right ventricular cardiomyopathy
- Takotsubo cardiomyopathy
- Neurological causes (intracerebral bleeding, acute brain injury)
- Myocarditis
- Chagas disease
- Cocaine use

From Antzelevitch C, Yan GX, Ackerman MJ, et al. J-wave syndromes expert consensus conference report: emerging concepts and gaps in knowledge. 2016;13, e295–e324.

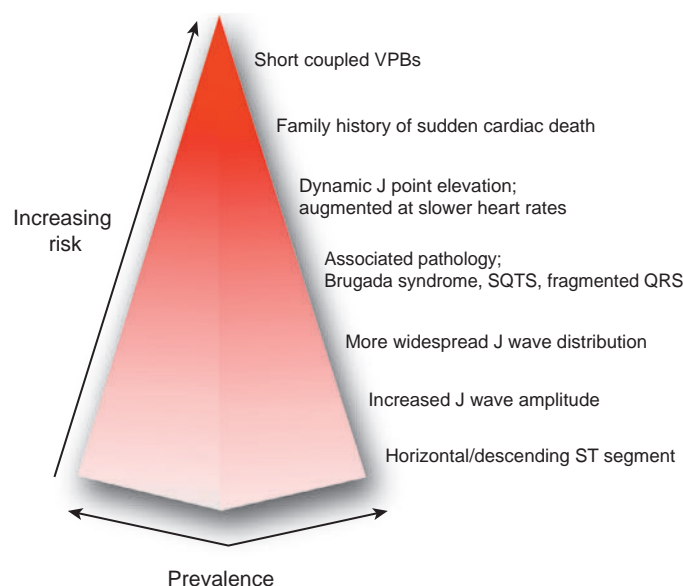


Fig. 31.25 Risk Stratification of Patients With Early Repolarization. The highest risk corresponds to the top of the pyramid, whereas the lowest risk is at the bottom. The estimated prevalence of the risk factor corresponds to the width of the pyramid. *SQTS*, Short QT syndrome; *VPBs*, ventricular premature beats. (From Mahida S, Derval N, Sacher F, et al. History and clinical significance of early repolarization syndrome. *Heart Rhythm*. 2015;12:242–249.)

J Wave Distribution

The distribution of J waves has been reported to influence the risk of sudden death in early repolarization patients. Several studies demonstrated that a lateral distribution of early repolarization portends the lowest risk, whereas an inferior and combined inferior and lateral J

wave distribution confers a progressively increased risk of arrhythmic death. Also, in asymptomatic individuals, early repolarization is most prominent in midprecordial leads (V_2 to V_4), a pattern that is especially predominant among athletes and is thought to confer a more benign prognosis.¹³⁹

J Wave Morphology

A recent report suggested a potential role of J wave duration and slope as markers of an increased arrhythmic risk. A delayed and prolonged J wave, a marker of a transmural dispersion of repolarization, may represent a new discriminant able to distinguish between benign and malignant early repolarization.¹⁴⁹

J Wave Amplitude Fluctuation

Although the pattern of J point elevation on baseline measurement remains constant during long-term follow-up in the majority of subjects, the magnitude of J point elevation can fluctuate even without drug provocation or exercise. Marked spontaneous accentuation of J wave amplitude, bradycardia- or pause-dependent dynamicity of the J wave, and spontaneous beat-to-beat fluctuation in the morphological pattern of early repolarization are frequently observed during periods of electrical storm (including frequent PVCs and episodes of VF). Transient and marked augmentation of J wave amplitude can potentially portend a high risk for VF in patients with early repolarization.^{135,139}

ST Segment and T Wave Morphology

For early repolarization patterns in the inferior or lateral leads, the presence of horizontal or downward-sloping ST segments after the J point predicts an increased risk for arrhythmic death, especially if accompanied by a high-amplitude (greater than 0.2 mV) J point elevation. In contrast, the presence of rapidly upsloping ST segments after the J point, followed by an upright T wave (which is the most common pattern observed in young athletes) is associated with a benign prognosis.^{134,147}

The rapidly ascending ST segment variant is universal in populations with benign prognosis (such as athletes); in contrast, cohorts with increased arrhythmic risk (such as patients with ischemic VF or idiopathic VF) have J waves predominantly followed by a horizontal ST segment without ST segment elevation.

A recent study reported that in patients with idiopathic VF, the prominent J wave is followed not only by a flat ST segment but also by a low-amplitude T wave (defined as T waves in leads I, II, or V_4 – V_6 that were inverted, biphasic, or smaller than 1 mm), and a low T wave-to-R wave amplitude ratio (in lead II or V_5). In fact, a low-amplitude ratio (T wave amplitude less than or equal to 10% of the R wave amplitude in the same lead) performed superior to J wave amplitude and ST segment pattern in differentiating malignant from benign inferolateral early repolarization.¹⁵⁰

Short-Coupled Premature Ventricular Complexes

The presence of frequent and short-coupled PVCs (which can potentially act as a trigger of polymorphic VT or VF) on ECG or during cardiac monitoring confers a significantly increased arrhythmic risk in early repolarization patients.

Syncope

More than one-third of early repolarization syndrome patients with SCD have experienced a previous episode of syncope. However, the presence of syncope has a low specificity in predicting future events and, although syncope is common in the early repolarization population, sudden death is a rare event. Nonetheless, a history of syncope in a patient with early repolarization merits detailed evaluation. The

presence of unexplained syncope, especially when occurring at rest or agonal respiration while sleeping, especially in a patient with a strong family history of sudden death, may identify a subset of early repolarization patients who are at high risk for arrhythmic events.

Family History

A number of studies have reported familial clustering of early repolarization syndrome and SCD. Approximately one-fifth of early repolarization syndrome patients with VF have a family history of sudden death. However, there is currently insufficient evidence to quantify the risk conferred by a positive family history in asymptomatic individuals.

Coexisting Arrhythmia Syndromes

In the presence of other cardiac conditions, the EP substrate leading to early repolarization and J wave formation can potentially reduce the threshold for malignant ventricular arrhythmias. Besides idiopathic VF, recent studies showed that the presence of a J wave was associated with a higher incidence of malignant ventricular arrhythmias in patients with Brugada syndrome and SQTs.¹⁴⁸

Furthermore, the presence of early repolarization (especially early repolarization in the inferior leads and without ST segment elevation) appears to increase the vulnerability to fatal arrhythmia risk in patients with structural cardiac disease, and was found to be a predictor of increased VT/VF or sudden death in patients with chronic ischemic heart disease, acute and subacute MI, vasospastic angina, heart failure (regardless of the etiology), noncompaction cardiomyopathy, and Takotsubo cardiomyopathy.^{151,152}

Exercise Testing

Exercise suppresses the early repolarization pattern both in symptomatic and asymptomatic subjects, especially early repolarization patterns in the lateral leads or those with an ascending ST segment. Therefore exercise testing does not seem to provide prognostic information.¹⁴⁵

Invasive Electrophysiological Testing

Invasive EP testing is not helpful for risk stratification. VF induction by programmed ventricular stimulation has been found to be a poor predictor of arrhythmic risk in symptomatic and asymptomatic patients with early repolarization. Patients with early repolarization do not exhibit significantly higher inducibility with programmed ventricular stimulation than those without early repolarization. Furthermore, VF is inducible during EP testing in only 22% to 34% of the patients with a clinical history of cardiac arrest secondary to VF. In addition, VF inducibility is not correlated with known risk factors, such as the degree of J point elevation, the distribution of J waves, or the ST segment morphology on the surface ECG.¹³⁶

Genetic Screening

The early repolarization pattern is associated with sudden death and has been shown to be heritable. Genetic contributions to SCD-associated early repolarization are suggested by common familial SCD histories in symptomatic early repolarization patients. As noted, several genes have been associated with early repolarization. However, so far, the genetic markers to differentiate benign and arrhythmic forms of early repolarization have not been identified, and the clinical benefit of genetic testing in these patients is currently questionable.

Principles of Management

Patients With Early Repolarization Syndrome

ICD implantation is recommended for secondary prevention in survivors of cardiac arrest or those with documented sustained ventricular arrhythmias and early repolarization pattern. Quinidine is considered an alter-

native therapy when an implanted ICD is not feasible or not preferred. A proposed algorithm for an approach to patients with early repolarization is shown in Fig. 31.26.^{1,135,147}

For acute suppression of ventricular arrhythmias in a patient with an electrical storm, acceleration of the heart rate (20% increase in heart rate or an absolute heart rate greater than 90 beats/min) by isoproterenol infusion or by atrial or ventricular pacing can be very effective. Deep sedation may also be considered in refractory cases (see Fig. 31.7).^{1,134}

For long-term suppression of VF in patients with recurrent arrhythmias or frequent ICD therapies, quinidine has been shown to ameliorate the early repolarization pattern and prevent VF recurrence. The combination therapy of cilostazol and bepridil may be considered an alternative therapy when quinidine is not available or not tolerated.¹³⁵

Syncope Patients With Early Repolarization Pattern

Management decisions for patients with syncope and family history of SCD in the context of early repolarization can be problematic, and should be individualized. The underlying etiology of syncope should be thoroughly investigated. Vasovagal syncope is not uncommon in patients with early repolarization patterns. When etiology of syncope is equivocal, ambulatory cardiac monitoring and loop recorder implantation should be considered. If malignant arrhythmias are highly suspected, ICD implantation may be considered in the patient with a strong family history of SCD.^{1,135,146,147}

Asymptomatic Patients With Early Repolarization Pattern

There is not yet a clear consensus on the specific risk factors that identify asymptomatic early repolarization subjects in whom the probability of SCD is sufficiently high to warrant an ICD for primary prevention. Pending further research, the finding of the early repolarization pattern in the absence of syncope or a strong family history of juvenile SCD does not merit further investigation, regardless of J wave amplitude or ST segment slope. With a strong family history for juvenile SCD, ICD implantation may be considered in subjects with high-risk ECG features of early repolarization.^{1,135,147}

Participation in Sports

Restriction from competitive sports is appropriate in patients with idiopathic VF. However, no information is available about lifestyle modification in asymptomatic patients with early repolarization ECG pattern. Given the high prevalence of early repolarization patterns (especially in leads V₂ to V₆) in athletes, occurring in 20% of noncompetitive athletes and in up to 90% of high-performance athletes, and because the midprecordial location of early repolarization is generally believed to be benign, and in the absence of reliable risk-stratifying parameters, a universal restriction from competitive sports does not seem warranted in asymptomatic athletes with early repolarization and a negative family history of SCD.¹⁴⁶

Nonetheless, certain restrictions may be considered in highly active patients with resting bradycardia and prominent early repolarization patterns localized to the inferior or inferolateral leads and a strong family history of SCD, although definitive guidelines are still lacking.¹⁴⁶

Family Screening

No consensus exists concerning the screening of families of individuals with symptomatic or asymptomatic early repolarization pattern. There are no established provocative tests to diagnose a concealed early repolarization ECG pattern in family members of early repolarization syndrome patients, although preliminary observations suggest that the Valsalva maneuver can potentially assist in identifying concealed early repolarization cases.

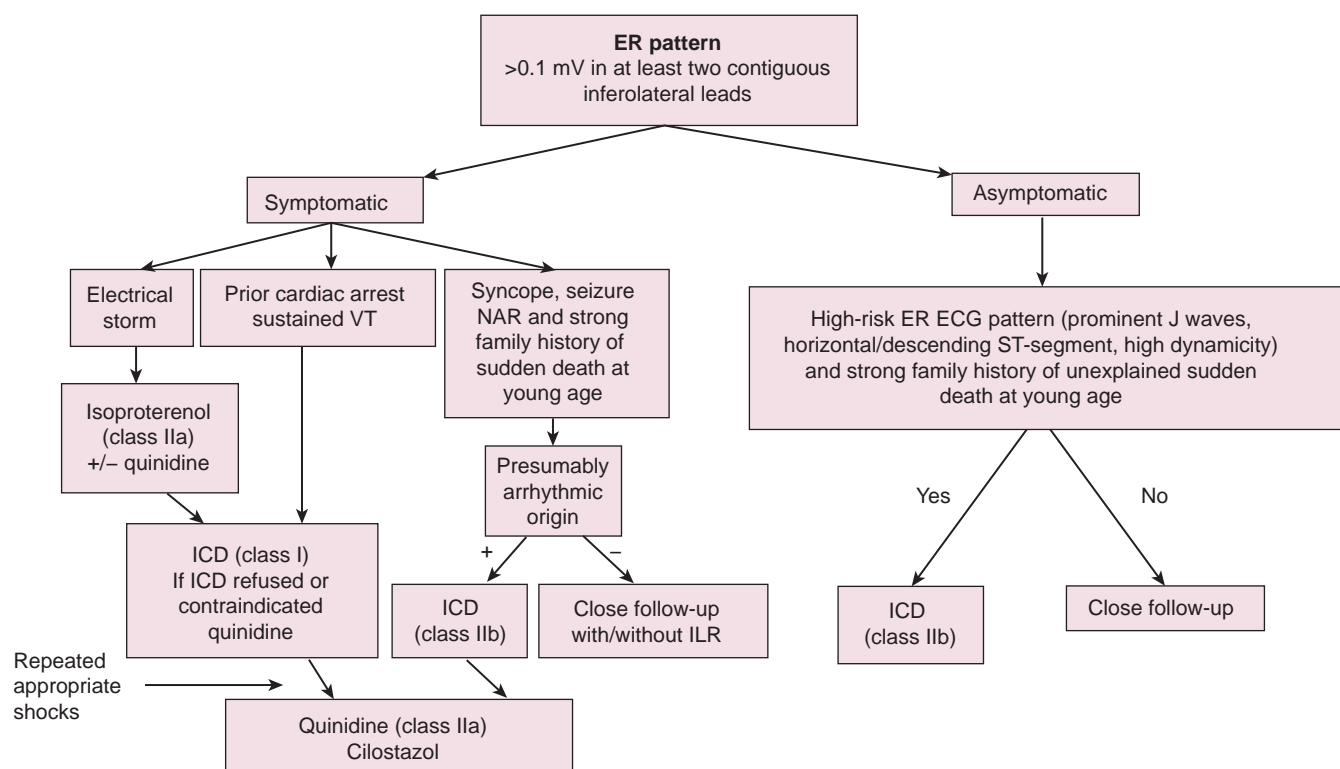


Fig. 31.26 Indications for Therapy of Patients With Early Repolarization Syndrome. ECG, Electrocardiogram; ER, early repolarization; ICD, implantable cardioverter-defibrillator; NAR, nocturnal agonal respiration; VT, ventricular tachycardia. (From Antzelevitch C, Yan GX, Ackerman MJ, et al. J-wave syndromes expert consensus conference report: emerging concepts and gaps in knowledge. *Heart Rhythm*. 2016;13:e295–e324.)

A number of drugs also have been tested as potential provocative agents, including verapamil, epinephrine, ATP, cibenzoline, and pilsicainide, and have been reported to have a minimal effect on the degree of J point elevation. In contrast to the Brugada syndrome, Na⁺ channel blockers result in a paradoxical attenuation, rather than accentuation, of J point elevation in early repolarization syndrome patients.^{139,145}

VIDEOS

The following video accompanies this chapter:

▶ See **Video 22.1**. Ventricular Fibrillation Triggered by Coronary Artery Spasm

REFERENCES

- Priori SG, et al. HRS/EHRA/APHRS Expert consensus statement on the diagnosis and management of patients with inherited primary arrhythmia syndromes. *Heart Rhythm*. 2013;10:1932–1963.
- Belardinelli L, Giles WR, Rajamani S, et al. Cardiac late Na⁺ current: proarrhythmic effects, roles in long QT syndromes, and pathological relationship to CaMKII and oxidative stress. *Heart Rhythm*. 2015;12:440–448.
- Giudicessi JR, Ackerman MJ. Calcium revisited. *Circ Arrhythm Electrophysiol*. 2016;9:e002480.
- Boczek NJ, et al. Identification and functional characterization of a novel CACNA1C-mediated cardiac disorder characterized by prolonged QT intervals with hypertrophic cardiomyopathy, congenital heart defects, and sudden cardiac death. *Circ Arrhythm Electrophysiol*. 2015;8:1122–1132.
- Nomikos M, et al. Altered RyR2 regulation by the calmodulin F90L mutation associated with idiopathic ventricular fibrillation and early sudden cardiac death. *FEBS Lett*. 2014;588:2898–2902.
- Søndergaard MT, et al. Arrhythmogenic calmodulin mutations affect the activation and termination of cardiac ryanodine receptor-mediated Ca²⁺ release. *J Biol Chem*. 2015;290:26151–26162.
- Altmann HM, et al. Homozygous/compound heterozygous triadin mutations associated with autosomal-recessive long-QT syndrome and pediatric sudden cardiac arrest: elucidation of the triadin knockout syndrome. *Circulation*. 2015;131:2051–2060.
- Kim JJ, Némec J, Li Q, et al. Synchronous systolic subcellular Ca²⁺ elevations underlie ventricular arrhythmia in drug-induced long QT type 2. *Circ Arrhythm Electrophysiol*. 2015;8:703–712.
- Wu J, et al. A molecular mechanism for adrenergic-induced long QT syndrome. *J Am Coll Cardiol*. 2013;63:819–827.
- McCauley M, Vallabhajosyula S, Darbar D. Proarrhythmic and torsadogenic effects of potassium channel blockers in patients. *Card Electrophysiol Clin*. 2016;8:481–493.
- Nguyen TP, Singh N, Xie Y, et al. Repolarization reserve evolves dynamically during the cardiac action potential: effects of transient outward currents on early afterdepolarizations. *Circ Arrhythm Electrophysiol*. 2015;8:694–702.
- Earle N, et al. Single nucleotide polymorphisms in arrhythmia genes modify the risk of cardiac events and sudden death in long QT syndrome. *Heart Rhythm*. 2014;11:76–82.
- Abelsira G, et al. Complex influence of gonadotropins and sex steroid hormones on QT interval duration. *J Clin Endocrinol Metab*. 2016;101:2776–2784.
- Odening KE, Koren G. How do sex hormones modify arrhythmogenesis in long QT syndrome? Sex hormone effects on arrhythmogenic substrate and triggered activity. *Heart Rhythm*. 2014;11:2107–2115.

15. Di Fusco SA, Palazzo S, Colivicchi F, et al. The influence of gender on heart rhythm disease. *Pacing Clin Electrophysiol*. 2014;37:650–657.
16. Salem J-E, Alexandre J, Bachelot A, et al. Influence of steroid hormones on ventricular repolarization. *Pharmacol Ther*. 2016;167:38–47.
17. Lang CN, et al. Electro-mechanical dysfunction in long QT syndrome: role for arrhythmogenic risk prediction and modulation by sex and sex hormones. *Prog Biophys Mol Biol*. 2016;120:255–269.
18. Tisdale JE, et al. Influence of oral progesterone administration on drug-induced QT interval lengthening. *JACC Clin Electrophysiol*. 2016;2:765–774.
19. Wilde AAM, et al. Clinical aspects of type 3 long-QT syndrome: an international multicenter study. *Circulation*. 2016;134:872–882.
20. Peters CH, Abdelsayed M, Ruben PC. Triggers for arrhythmogenesis in the Brugada and long QT 3 syndromes. *Prog Biophys Mol Biol*. 2016;120:77–88.
21. Miyamoto K, et al. Efficacy and safety of flecainide for ventricular arrhythmias in patients with Andersen-Tawil syndrome with KCNJ2 mutations. *Heart Rhythm*. 2015;12:596–603.
22. Postema PG, Wilde AAM. The measurement of the QT interval. *Curr Cardiol Rev*. 2014;10:287–294.
23. Bogossian H, et al. New formula for evaluation of the QT interval in patients with left bundle branch block. *Heart Rhythm*. 2014;11:2273–2277.
24. Tsai SF, et al. QTc compared to JTc for monitoring drug-induced repolarization changes in the setting of ventricular pacing. *Heart Rhythm*. 2014;11:485–491.
25. Wang B, et al. A new formula for estimating the true QT interval in left bundle branch block. *J Cardiovasc Electrophysiol*. 2017;28:684–689.
26. Chiladakis JA, et al. Facilitating assessment of QT interval duration during ventricular pacing. *Europace*. 2013;15:907–914.
27. Ruan Y, Liu N, Bai R, et al. Congenital long QT syndrome type 3. *Card Electrophysiol Clin*. 2014;6:705–713.
28. Sugrue A, et al. Identification of concealed and manifest long QT syndrome using a novel T wave analysis program. *Circ Arrhythm Electrophysiol*. 2016;9:e003830.
29. El-Sherif N, et al. Electrophysiological basis of ECG characteristics of torsades de pointes in long QT syndrome. *Card Electrophysiol Clin*. 2014;6:433–444.
30. Schwartz PJ, Crotti L. QTc behavior during exercise and genetic testing for the long-QT syndrome. *Circulation*. 2011;124.
31. Hayashi K, et al. Impact of updated diagnostic criteria for long QT syndrome on clinical detection of diseased patients. *JACC Clin Electrophysiol*. 2016;2:279–287.
32. Schwartz PJ, Ackerman MJ. The long QT syndrome: a transatlantic clinical approach to diagnosis and therapy. *Eur Heart J*. 2013;34:3109–3116.
33. Page A, Aktas MK, Soyata T, et al. “QT clock” to improve detection of QT prolongation in long QT syndrome patients. *Heart Rhythm*. 2016;13:190–198.
34. Chorin E, et al. Diagnostic value of T-wave morphology changes during ‘QT stretching’ in patients with long QT syndrome. *Heart Rhythm*. 2015;12:2263–2271.
35. Badri M, et al. Mexiletine prevents recurrent torsades de pointes in acquired long QT syndrome refractory to conventional measures. *JACC Clin Electrophysiol*. 2015;1:315–322.
36. Eijkemans MJC, et al. Predicting the unpredictable. *Anesthesiology*. 2010;112:41–49.
37. Algalarrondo V, Nattel S. Potassium channel remodeling in heart disease. *Card Electrophysiol Clin*. 2016;8:337–347.
38. Rosso R, et al. Long QT syndrome complicating atrioventricular block: arrhythmogenic effects of cardiac memory. *Circ Arrhythm Electrophysiol*. 2014;7:1129–1135.
39. Risgaard B, et al. Sudden cardiac death. *JACC Clin Electrophysiol*. 2017;3:473–481.
40. Roden DM. Pharmacogenetics of potassium channel blockers. *Card Electrophysiol Clin*. 2016;8:385–393.
41. Tisdale JE, et al. Effectiveness of a clinical decision support system for reducing the risk of QT interval prolongation in hospitalized patients. *Circ Cardiovasc Qual Outcomes*. 2014;7:381–390.
42. Tisdale JE, et al. Development and validation of a risk score to predict QT interval prolongation in hospitalized patients. *Circ Cardiovasc Qual Outcomes*. 2013;6:479–487.
43. Yu H, et al. Acquired long QT syndrome in hospitalized patients. *Heart Rhythm*. 2017;14:974–978.
44. Weeke P, et al. Exome sequencing implicates an increased burden of rare potassium channel variants in the risk of drug-induced long QT interval syndrome. *J Am Coll Cardiol*. 2014;63:1430–1437.
45. Itoh H, et al. The genetics underlying acquired long QT syndrome: impact for genetic screening. *Eur Heart J*. 2016;37:1456–1464.
46. Drew BJ, et al. Prevention of torsade de pointes in hospital settings. *J Am Coll Cardiol*. 2010;55:934–947.
47. Mathias A, et al. Prognostic implications of mutation-specific QTc standard deviation in congenital long QT syndrome. *Heart Rhythm*. 2013;10:720–725.
48. Mullally J, et al. Risk of life-threatening cardiac events among patients with long QT syndrome and multiple mutations. *Heart Rhythm*. 2013;10:378–382.
49. Amin AS, Wilde AAM. Genetic control of potassium channels. *Card Electrophysiol Clin*. 2016;8:285–306.
50. Koponen M, et al. Follow-up of 316 molecularly defined pediatric long-QT syndrome patients. *Circ Arrhythm Electrophysiol*. 2015;8:815–823.
51. Obeyesekere MN, Antzelevitch C, Krahn AD. Management of ventricular arrhythmias in suspected channelopathies. *Circ Arrhythm Electrophysiol*. 2015;8:221–231.
52. Ackerman MJ, et al. Beta-blocker therapy for long QT syndrome and catecholaminergic polymorphic ventricular tachycardia: are all beta-blockers equivalent? *Heart Rhythm*. 2016;14:e41–e44.
53. Gaba P, et al. Implantable cardioverter-defibrillator explantation for overdiagnosed or overtreated congenital long QT syndrome. *Heart Rhythm*. 2016;13:879–885.
54. Schwartz PJ, et al. Who are the long-QT syndrome patients who receive an implantable cardioverter-defibrillator and what happens to them? Data from the European Long-QT Syndrome Implantable Cardioverter-Defibrillator (LQTS ICD) Registry. *Circulation*. 2010;122:1272–1282.
55. Bos JM, Bos KM, Johnson JN, et al. Left cardiac sympathetic denervation in long QT syndrome: analysis of therapeutic nonresponders. *Circ Arrhythm Electrophysiol*. 2013;6:705–711.
56. Waddell-Smith KE, et al. Physical and psychological consequences of left cardiac sympathetic denervation in long-QT syndrome and catecholaminergic polymorphic ventricular tachycardia. *Circ Arrhythm Electrophysiol*. 2015;8:1151–1158.
57. Antiel RM, et al. Quality of life after videoscopic left cardiac sympathetic denervation in patients with potentially life-threatening cardiac channelopathies/cardiomyopathies. *Heart Rhythm*. 2016;13:62–69.
58. Früh A, Siem G, Holmström H. The Jervell and Lange-Nielsen syndrome; atrial pacing combined with β -blocker therapy, a favorable approach in young high-risk patients with long QT syndrome? *Heart Rhythm*. 2016;13:2186–2192.
59. Aziz PF, et al. Sports participation in genotype positive children with long QT syndrome. *JACC Clin Electrophysiol*. 2015;1:62–70.
60. Zipes DP, et al. Eligibility and disqualification recommendations for competitive athletes with cardiovascular abnormalities: Task Force 9: arrhythmias and conduction defects: a scientific statement from the American Heart Association and American College of Cardiology. *Circulation*. 2015;132:e315–e325.
61. Mazzanti A, et al. Gene-specific therapy with mexiletine reduces arrhythmic events in patients with long QT syndrome type 3. *J Am Coll Cardiol*. 2016;67:1053–1058.
62. Chorin E, et al. Ranolazine for congenital long-QT syndrome type III: experimental and long-term clinical data. *Circ Arrhythm Electrophysiol*. 2016;9:e004370.

63. Curcio A, Santarpia G, Indolfi C. The Brugada syndrome—from gene to therapy. *Circ J*. 2017;81:290–297.
64. Antzelevitch C, Patocskaï B. Brugada syndrome: clinical, genetic, molecular, cellular, and ionic aspects. *Curr Probl Cardiol*. 2016;41:7–57.
65. Antzelevitch C, et al. J-wave syndromes expert consensus conference report: emerging concepts and gaps in knowledge. *Heart Rhythm*. 2016;13:e295–e324.
66. Hu D, et al. Mutations in SCN10A are responsible for a large fraction of cases of Brugada syndrome. *J Am Coll Cardiol*. 2014;64:66–79.
67. Varga Z, et al. Direct measurement of cardiac Na⁺ channel conformations reveals molecular pathologies of inherited mutations. *Circ Arrhythm Electrophysiol*. 2015;8:1228–1239.
68. Calò L, et al. A new electrocardiographic marker of sudden death in Brugada syndrome. *J Am Coll Cardiol*. 2016;67:1427–1440.
69. Guillem MS, et al. Spatiotemporal characteristics of QRS complexes enable the diagnosis of Brugada syndrome regardless of the appearance of a type 1 ECG. *J Cardiovasc Electrophysiol*. 2016;27:563–570.
70. Adler A, et al. Fever-induced Brugada pattern: how common is it and what does it mean? *Heart Rhythm*. 2013;10:1375–1382.
71. Mizusawa Y, et al. The prognostic significance of fever-induced Brugada syndrome. *Heart Rhythm*. 2016;13:1515–1520.
72. Kitamura T, et al. Clinical characteristics and long-term prognosis of senior patients with Brugada syndrome. *JACC Clin Electrophysiol*. 2017;3:57–67.
73. Adler A, et al. Risk stratification in Brugada syndrome: clinical characteristics, electrocardiographic parameters, and auxiliary testing. *Heart Rhythm*. 2016;13:299–310.
74. Kawazoe H, et al. Risk stratification of ventricular fibrillation in Brugada syndrome using noninvasive scoring methods. *Heart Rhythm*. 2016;13:1947–1954.
75. Nordkamp LRAO, et al. Syncope in Brugada syndrome: prevalence, clinical significance, and clues from history taking to distinguish arrhythmic from nonarrhythmic causes. *Heart Rhythm*. 2015;12:367–375.
76. Giustetto C, et al. Atrial fibrillation in a large population with Brugada electrocardiographic pattern: prevalence, management, and correlation with prognosis. *Heart Rhythm*. 2014;11:259–265.
77. Bayés De Luna A, et al. Current electrocardiographic criteria for diagnosis of Brugada pattern: a consensus report. *J Electrocardiol*. 2012;45:433–442.
78. de Luna AB, et al. New electrocardiographic features in Brugada syndrome. *Curr Cardiol Rev*. 2014;10:175–180.
79. Savastano S, et al. A comprehensive electrocardiographic, molecular, and echocardiographic study of Brugada syndrome: validation of the 2013 diagnostic criteria. *Heart Rhythm*. 2014;11:1176–1183.
80. Curcio A, et al. Clinical presentation and outcome of Brugada syndrome diagnosed with the new 2013 criteria. *J Cardiovasc Electrophysiol*. 2016;27:937–943.
81. Casado-Arroyo R, et al. Long-term trends in newly diagnosed Brugada syndrome implications for risk stratification. *J Am Coll Cardiol*. 2016;68:614–623.
82. Adler A. Brugada syndrome: diagnosis, risk stratification, and management. *Curr Opin Cardiol*. 2016;31:37–45.
83. Greene EA. Universal ECG changes in pediatric patients undergoing procainamide challenge. *Pacing Clin Electrophysiol*. 2014;37:1106–1111.
84. Somani R, et al. Procainamide infusion in the evaluation of unexplained cardiac arrest: from the Cardiac Arrest Survivors with Preserved Ejection Fraction Registry (CASPER). *Heart Rhythm*. 2014;11:1047–1054.
85. Calvo D, Rubín JM, Pérez D, et al. Time-dependent responses to provocative testing with flecainide in the diagnosis of Brugada syndrome. *Heart Rhythm*. 2015;12:350–357.
86. Subramanian M, et al. The utility of exercise testing in risk stratification of asymptomatic patients with type 1 Brugada pattern. *J Cardiovasc Electrophysiol*. 2017;28:677–683.
87. Belhassen B, Michowitz Y. Arrhythmic risk stratification by programmed ventricular stimulation in Brugada syndrome. *Circ Arrhythm Electrophysiol*. 2015;8:757–759.
88. Königstein M, et al. Drug-induced Brugada syndrome: clinical characteristics and risk factors. *Heart Rhythm*. 2016;13:1083–1087.
89. Letsas KP, et al. Drug-induced Brugada syndrome by noncardiac agents. *Pacing Clin Electrophysiol*. 2013;36:1570–1578.
90. Sieira J, et al. Prognostic value of programmed electrical stimulation in Brugada syndrome. *Circ Arrhythm Electrophysiol*. 2015;8:777–784.
91. Tse G, et al. The T peak 2 T end interval as an electrocardiographic risk marker of arrhythmic and mortality outcomes: a systematic review and meta-analysis. *Heart Rhythm*. 2017;14:1131–1137.
92. Maury P, et al. Increased Tpeak-Tend interval is highly and independently related to arrhythmic events in Brugada syndrome. *Heart Rhythm*. 2015;12:2469–2476.
93. Tokioka K, et al. Electrocardiographic parameters and fatal arrhythmic events in patients with Brugada syndrome: combination of depolarization and repolarization abnormalities. *J Am Coll Cardiol*. 2014;63:2131–2138.
94. Sieira J, Brugada P. Management of Brugada syndrome 2016: should all high risk patients receive an ICD? All high-risk patients should receive an implantable cardiac defibrillator. *Circ Arrhythm Electrophysiol*. 2016;9:e004195.
95. Conte G, et al. Implantable cardioverter-defibrillator therapy in Brugada syndrome. *J Am Coll Cardiol*. 2015;65:879–888.
96. Brugada J, Pappone C, Berrueto A, et al. Brugada syndrome phenotype elimination by epicardial substrate ablation. *Circ Arrhythm Electrophysiol*. 2015;8:1373–1381.
97. Pappone C, et al. Electrical substrate elimination in 135 consecutive patients with Brugada syndrome. *Circ Arrhythm Electrophysiol*. 2017;10:e005053.
98. Patocskaï B, Yoon N, Antzelevitch C. Mechanisms underlying epicardial radiofrequency ablation to suppress arrhythmogenesis in experimental models of Brugada syndrome. *JACC Clin Electrophysiol*. 2016;3:353–363.
99. Zhang P, Tung R, Zhang Z, et al. Characterization of the epicardial substrate for catheter ablation of Brugada syndrome. *Heart Rhythm*. 2016;13:2151–2158.
100. Andorin A, et al. The QUIDAM study: hydroquinidine therapy for the management of Brugada syndrome patients at high arrhythmic risk. *Heart Rhythm*. 2017;14:1147–1154.
101. Belhassen B. Management of Brugada syndrome 2016: should all high risk patients receive an ICD? Alternatives to implantable cardiac defibrillator therapy for Brugada syndrome. *Circ Arrhythm Electrophysiol*. 2016;9:e004185.
102. Sieira J, et al. Asymptomatic Brugada syndrome clinical characterization and long-term prognosis. *Circ Arrhythm Electrophysiol*. 2015;8:1144–1150.
103. Levine BD, et al. Eligibility and disqualification recommendations for competitive athletes with cardiovascular abnormalities: Task Force 1: classification of sports: dynamic, static, and impact: a scientific statement from the American Heart Association and American College of Cardiology. *Circulation*. 2015;132:e262–e266.
104. Khera S, Jacobson JT. Short QT syndrome in current clinical practice. *Cardiol Rev*. 2015;24:1–17.
105. Guerrier K, et al. Short QT interval prevalence and clinical outcomes in a pediatric population. *Circ Arrhythm Electrophysiol*. 2015;8:1460–1464.
106. Mazzanti A, et al. Novel insight into the natural history of short QT syndrome. *J Am Coll Cardiol*. 2014;63:1300–1308.
107. Villafañe J, et al. Long-term follow-up of a pediatric cohort with short QT syndrome. *J Am Coll Cardiol*. 2013;61:1183–1191.
108. Iribarren C, et al. Short QT in a cohort of 1.7 million persons: prevalence, correlates, and prognosis. *Ann Noninvasive Electrocardiol*. 2014;19:490–500.
109. Tülümen E, et al. PQ segment depression in patients with short QT syndrome: a novel marker for diagnosing short QT syndrome? *Heart Rhythm*. 2014;11:1024–1030.
110. Roussel J, et al. Carnitine deficiency induces a short QT syndrome. *Heart Rhythm*. 2016;13:165–174.
111. Imberti JF, Underwood K, Mazzanti A, et al. Clinical challenges in catecholaminergic polymorphic ventricular tachycardia. *Heart Lung Circ*. 2016;25:777–783.

112. Györke S. Molecular basis of catecholaminergic polymorphic ventricular tachycardia. *Heart Rhythm*. 2009;6:123–129.
113. Steriotes AK, et al. Follow-up with exercise test of effort-induced ventricular arrhythmias linked to ryanodine receptor type 2 gene mutations. *Am J Cardiol*. 2012;109:1015–1019.
114. Blich M, et al. Electrocardiographic comparison of ventricular premature complexes during exercise test in patients with CPVT and healthy subjects. *Pacing Clin Electrophysiol*. 2015;38:398–402.
115. Roston TM, et al. Catecholaminergic polymorphic ventricular tachycardia in children: analysis of therapeutic strategies and outcomes from an international multicenter registry. *Circ Arrhythm Electrophysiol*. 2015;8:633–642.
116. Van Der Werf C, Lieve KV. Beta-blockers in the treatment of catecholaminergic polymorphic ventricular tachycardia. *Heart Rhythm*. 2016;13:441–442.
117. Leren IS, et al. Nadolol decreases the incidence and severity of ventricular arrhythmias during exercise stress testing compared with β 1-selective β -blockers in patients with catecholaminergic polymorphic ventricular tachycardia. *Heart Rhythm*. 2016;13:432–440.
118. Padfield GJ, et al. Flecainide monotherapy is an option for selected patients with catecholaminergic polymorphic ventricular tachycardia intolerant of β -blockade. *Heart Rhythm*. 2016;13:609–613.
119. Roses-Noguer F, Jarman JWE, Clague JR, et al. Outcomes of defibrillator therapy in catecholaminergic polymorphic ventricular tachycardia. *Heart Rhythm*. 2014;11:58–66.
120. Miyake CY, et al. Efficacy of implantable cardioverter defibrillators in young patients with catecholaminergic polymorphic ventricular tachycardia: success depends on substrate. *Circ Arrhythm Electrophysiol*. 2013;6:579–587.
121. De Ferrari GM, et al. Clinical management of catecholaminergic polymorphic ventricular tachycardia: the role of left cardiac sympathetic denervation. *Circulation*. 2015;131:2185–2193.
122. Visser M, et al. Idiopathic ventricular fibrillation: the struggle for definition, diagnosis, and follow-up. *Circ Arrhythm Electrophysiol*. 2016;9:e003817.
123. Ten Sande JN, et al. Detailed characterization of familial idiopathic ventricular fibrillation linked to the DPP6 locus. *Heart Rhythm*. 2016;13:905–912.
124. Marsman RE, et al. A mutation in CALM1 encoding calmodulin in familial idiopathic ventricular fibrillation in childhood and adolescence. *J Am Coll Cardiol*. 2014;63:259–266.
125. Paech C, et al. Ryanodine receptor mutations presenting as idiopathic ventricular fibrillation: a report on two novel familial compound mutations, c.6224T>C and c.13781A>G, with the clinical presentation of idiopathic ventricular fibrillation. *Pediatr Cardiol*. 2014;35:1437–1441.
126. Murakoshi N, Aonuma K. Catheter ablation for ventricular tachyarrhythmia in patients with channelopathies. *J Arrhythm*. 2016;32:404–410.
127. Visser M, et al. Long-term outcome of patients initially diagnosed with idiopathic ventricular fibrillation: a descriptive study. *Circ Arrhythm Electrophysiol*. 2016;9:e004258.
128. Aizawa Y, et al. Electrical storm in idiopathic ventricular fibrillation is associated with early repolarization. *J Am Coll Cardiol*. 2013;62:1015–1019.
129. Aizawa Y, et al. Circadian pattern of fibrillatory events in non-Brugada-type idiopathic ventricular fibrillation with a focus on J waves. *Heart Rhythm*. 2014;11:2261–2266.
130. Herman ARM, et al. Outcome of apparently unexplained cardiac arrest: results from investigation and follow-up of the prospective Cardiac Arrest Survivors With Preserved Ejection Fraction Registry. *Circ Arrhythm Electrophysiol*. 2016;9:e003619.
131. Jiménez-Jáimez J, et al. Diagnostic approach to unexplained cardiac arrest (from the FIVI-Gen study). *Am J Cardiol*. 2015;116:894–899.
132. Shah AJ, et al. Polymorphic ventricular tachycardia/ventricular fibrillation and sudden cardiac death in the normal heart. *Card Electrophysiol Clin*. 2016;8:581–591.
133. Conte G, et al. True idiopathic ventricular fibrillation in out-of-hospital cardiac arrest survivors in the Swiss Canton Ticino: prevalence, clinical features, and long-term follow-up. *Europace*. 2017;19:259–266.
134. Antzelevitch C, Yan GX. J-wave syndromes: Brugada and early repolarization syndromes. *Heart Rhythm*. 2015;12:1852–1866.
135. Adler A, Gollob MH. A practical guide to early repolarization. *Curr Opin Cardiol*. 2015;30:8–16.
136. Mahida S, et al. Role of electrophysiological studies in predicting risk of ventricular arrhythmia in early repolarization syndrome. *J Am Coll Cardiol*. 2015;65:151–159.
137. Yan G-X, Lankipalli RS, Burke JF, et al. Ventricular repolarization components on the electrocardiogram: cellular basis and clinical significance. *J Am Coll Cardiol*. 2003;42:401–409.
138. Patocskaï B, et al. Cellular and ionic mechanisms underlying the effects of cilostazol, milrinone, and isoproterenol to suppress arrhythmogenesis in an experimental model of early repolarization syndrome. *Heart Rhythm*. 2016;13:1326–1334.
139. Mahida S, et al. History and clinical significance of early repolarization syndrome. *Heart Rhythm*. 2015;12:242–249.
140. Harhash A, Gussak I, Cassuto J, et al. Clinical significance of J waves in patients undergoing therapeutic hypothermia for out-of-hospital cardiac arrest. *Pacing Clin Electrophysiol*. 2017;40:154–161.
141. Benito B, Guasch E, Rivard L, et al. Clinical and mechanistic issues in early repolarization of normal variants and lethal arrhythmia syndromes. *J Am Coll Cardiol*. 2010;56:1177–1186.
142. Zhang J, et al. The electrophysiological substrate of early repolarization syndrome: noninvasive mapping in patients. *JACC Clin Electrophysiol*. 2017;3:894–904.
143. Aizawa Y, et al. Tachycardia-dependent augmentation of ‘notched J waves’ in a general patient population without ventricular fibrillation or cardiac arrest: not a repolarization but a depolarization abnormality? *Heart Rhythm*. 2015;12:376–383.
144. Gurabi Z, Koncz I, Patocskaï B, et al. Cellular mechanism underlying hypothermia-induced ventricular tachycardia/ventricular fibrillation in the setting of early repolarization and the protective effect of quinidine, cilostazol, and milrinone. *Circ Arrhythm Electrophysiol*. 2014;7:134–142.
145. Mellor G, et al. The prevalence and significance of the early repolarization pattern in sudden arrhythmic death syndrome families. *Circ Arrhythm Electrophysiol*. 2016;9:e003960.
146. Aagaard P, Baranowski B, Aziz P, et al. Early repolarization in athletes: a review. *Circ Arrhythm Electrophysiol*. 2016;9:1–8.
147. MacFarlane PW, et al. The early repolarization pattern: a consensus paper. *J Am Coll Cardiol*. 2015;66:470–477.
148. Kamakura T, et al. Significance of electrocardiogram recording in high intercostal spaces in patients with early repolarization syndrome. *Eur Heart J*. 2016;37:630–637.
149. Cristoforetti Y, et al. J-wave duration and slope as potential tools to discriminate between benign and malignant early repolarization. *Heart Rhythm*. 2016;13:806–811.
150. Roten L, et al. Benign vs malignant inferolateral early repolarization: focus on the T wave. *Heart Rhythm*. 2016;13:894–902.
151. Naruse Y, et al. Early repolarization increases the occurrence of sustained ventricular tachyarrhythmias and sudden death in the chronic phase of an acute myocardial infarction. *Circ Arrhythm Electrophysiol*. 2014;7:626–632.
152. Naruse Y, et al. J waves are associated with the increased occurrence of life-threatening ventricular tachyarrhythmia in patients with nonischemic cardiomyopathy. *J Cardiovasc Electrophysiol*. 2016;27:1448–1453.
153. Amin AS, Asghari-Roodsari A, Tan HL. Cardiac sodium channelopathies. *Pflugers Arch*. 2010;460:223–237.
154. Priori SG, Blomström-Lundqvist C. 2015 European Society of Cardiology Guidelines for the management of patients with ventricular arrhythmias and the prevention of sudden cardiac death summarized by co-chairs. *Eur Heart J*. 2015;36:2757–2759.

Complications of Catheter Ablation of Cardiac Arrhythmias

OUTLINE

Local Vascular Complications, 1042

- Incidence, 1042
- Detection and Management, 1042
- Prevention, 1043

Cardiac Perforation, 1043

- Incidence, 1043
- Mechanism, 1044
- Detection, 1044
- Management, 1045

Thromboembolism, 1046

- Mechanism, 1046
- Prevention, 1046

Air Embolism, 1047

- Mechanism, 1047
- Clinical Presentation, 1047
- Detection, 1047
- Prevention, 1047
- Management, 1047

Coronary Artery Injuries, 1048

- Mechanism, 1048
- Clinical Presentation, 1048
- Prevention, 1048

Iatrogenic Cardiac Arrhythmias, 1049

- Atrioventricular Block, 1049
- Macroreentrant Atrial Tachycardias, 1049
- Ventricular Arrhythmias, 1049
- Abnormal Sinus Node Function, 1049

Valvular Damage, 1050

Phrenic Nerve Injury, 1051

- Clinical Presentation, 1051
- Prevention, 1051

Pulmonary Vein Stenosis, 1054

- Incidence, 1054
- Mechanism, 1055
- Clinical Presentation, 1056
- Detection, 1056
- Prevention, 1056
- Management, 1056

Esophageal Injury, 1056

- Incidence, 1056
- Mechanism, 1057
- Clinical Presentation, 1057
- Detection, 1058
- Management, 1058
- Prevention, 1058

Radiation Exposure, 1062

- Biological Effects of Ionizing Radiation, 1062
- Nomenclature of Radiation Quantities and Units, 1062
- Exposure to Ionizing Radiation During Electrophysiology Procedures, 1063
- Clinical Presentation, 1063
- Prevention, 1064

Reported rates of major complications following contemporary catheter ablation procedures vary by as much as five- to eightfold between various types of ablation procedures, ranging from 0.8% for supraventricular tachycardia (SVT), 3.4% for idiopathic ventricular tachycardia (VT), 5.2% for atrial fibrillation (AF), and 6.0% for VT associated with structural heart disease. Death is a rare complication of catheter ablation, occurring in 0.11% to 0.30% of patients with regular SVT, and in 0.31% of those with VT. Transseptal catheterization appears to contribute to the cause of death in 0.2% of procedures.

LOCAL VASCULAR COMPLICATIONS

Incidence

Complications related to vascular access are among the most common problems observed following catheter ablation procedures, and these complications directly impact patient morbidity and increase health care costs. The reported incidence of local vascular complications varies between different studies because of differences in definition of minor and major complications, different types of procedures performed, and

different patient population characteristics. The risk of local vascular complications is higher among females, older adults, obese patients, and those with preexisting peripheral vascular disease. In addition, the risk is related to the type of procedure performed (right or left heart catheterization), the size and number of sheaths used during the procedure, as well as the associated periprocedural use of anticoagulant or antiplatelet therapy. The rates of complications related to the site of vascular access are higher following catheter ablation of AF (1% to 13%) and VT (0.7% to 4.7%) compared with ablation of SVT (0.4%).¹

Detection and Management

Hematomas

Bleeding is the most common vascular complication. Acute bleeding generally can be controlled with prolonged manual compression. Vascular laceration can cause large hematomas in the groin and thigh. Groin hematomas usually resolve in 1 to 2 weeks if ongoing bleeding is stopped. Large hematomas can require blood transfusion, but surgical repair is rarely required. Arteriovenous fistulas and pseudoaneurysms need to be excluded in the setting of large or continually expanding

hematomas. Retroperitoneal hematomas are often the result of arterial puncture above the inguinal ligament, allowing bleeding and hematoma to extend to the retroperitoneal space. Retroperitoneal hematomas should be suspected in the setting of a marked drop in hematocrit or unexplained hypotension or flank pain. Abdominal computed tomography (CT) scanning or ultrasound is required to confirm the diagnosis. Retroperitoneal bleeds are generally managed conservatively (bed rest, blood transfusion). Catheter or surgical interventions, however, can occasionally be required.

Pseudoaneurysms

Femoral artery pseudoaneurysms form when a hole through all the layers of the artery at the puncture site fails to seal, allowing persistent blood flow outside the vessel into a space contained by the surrounding tissue. This is in contrast to a hematoma, which has clotted blood outside the vessel with absence of flow. Pseudoaneurysms lack a fibrous wall and are contained by a surrounding shell of hematoma and the overlying soft tissues. Risk factors for pseudoaneurysm development include the use of large vascular sheaths, potent postprocedure anticoagulation, inadequacy of initial effort at hemostasis after removal of sheaths, and punctures of the femoral artery that are too distal—that is, at the level of bifurcation of the femoral artery or below. In addition, multiple attempts at vascular access (arterial or venous) with inadvertent arterial puncture appear to increase the risk for pseudoaneurysm formation; repeated damage to the arterial wall may result in weakening that leads to pseudoaneurysm development.

A pseudoaneurysm typically manifests as a painful pulsatile mass with a systolic bruit or thrill, and the diagnosis is confirmed by duplex ultrasonography. Pseudoaneurysms can be complicated by rupture or distal embolization. Pseudoaneurysms that are less than 2 cm in size and not enlarging often resolve without intervention, and serial imaging is recommended to confirm spontaneous resolution. On the other hand, pseudoaneurysms that are enlarging or are greater than 2 cm in size can be treated by ultrasound-guided compression of the “neck,” connecting the pseudoaneurysm with the vessel or by percutaneous thrombin injection. Occasionally, surgical repair is required, especially for large pseudoaneurysms with a wide connection to the parent artery.

Arteriovenous Fistulas

Femoral arteriovenous fistulas commonly result when bleeding from the arterial puncture tracks into the adjacent venous puncture. Arteriovenous fistulas are more likely to arise when arterial and venous punctures are performed on the same side or when femoral venous puncture is performed below the common femoral artery, where several superficial branches of the femoral artery overlie the femoral vein. The diagnosis is made on examination with the finding of a continuous “to and fro” bruit, and is confirmed by ultrasound. Many of the iatrogenic arteriovenous fistulas are small and close spontaneously within 1 year, but ultrasound-guided compression or surgical repair can be necessary. Because cardiac volume overload and limb damage are highly unlikely with persistent arteriovenous fistulas, conservative management for at least 1 year is reasonable.

Vascular Thromboembolism

Deep venous thrombosis and pulmonary embolism are rare but can result from venous injury, especially during prolonged procedures requiring multiple venous lines, or in the setting of venous compression by a large arterial hematoma. Femoral arterial thrombosis is rare and occurs more commonly in the setting of a small vessel lumen, the use of a large-diameter sheath, preexisting peripheral vascular disease, diabetes mellitus, female gender, and occasionally with vascular closure devices.

Prevention

Accurate vascular puncture and effective initial control of bleeding after sheath removal are the best measures to prevent local vascular complications. Early diagnosis and management of local access site complications are essential to reduce morbidity and improve outcome.

Traditionally, vessel puncture has relied upon an anatomical landmark technique using palpation of local arterial and bony landmarks. However, significant heterogeneity exists in the anatomical relationship of the femoral vein and artery. Overlap of the femoral artery and the common femoral vein occurs along some portion of their course in two-thirds of patients. In addition, high bifurcation of the common femoral artery at the level of the mid femoral head is not uncommon. Such anatomical variation cannot be appreciated using the anatomical landmark techniques, predisposing to accidental puncture of the artery during intended venous cannulation, and increasing the risk of pseudoaneurysm and AV fistula formation.²

Real-time ultrasound guidance allows direct visualization of femoral vein size and location relative to the femoral artery, and identification of anatomical variations in arterial and venous spatial relationships, minimizing the risk of inadvertent arterial puncture. Ultrasound also allows easy identification of venous bifurcations, which are unsuitable targets for vascular access. Further, visualization of the vein and of the needle tip trajectory during the puncture allows directing the needle tip into the center of the vein and avoidance of a glancing approach toward the periphery of the vessel.

Although evidence on the value of ultrasound guidance is more robust for internal jugular vein cannulation, several recent nonrandomized studies have found the use of ultrasound to guide femoral venous cannulation in the electrophysiological (EP) laboratory to significantly (by more than 60%) reduce the risk of major and minor vascular access complications, decrease cannulation times, and reduce both the number of unsuccessful attempts and the number of unintended arterial punctures. Using micropuncture needle kits has also decreased vascular complications to a degree, especially in the event of inadvertent arterial access (that resolves more quickly after small-needle entry than with a larger needle).^{1,3}

CARDIAC PERFORATION

Incidence

Previous studies reported the incidence of cardiac perforation with catheter-based interventions as follows: 0.8% for all procedures, 1.5% to 4.7% for valvuloplasty, 0.5% to 0.8% for angioplasty-atherectomy, 0.01% for diagnostic catheterization, 0.1% to 0.2% for EP studies, 0.2% for SVT ablation, 0.4% to 2.7% for VT ablation, and 0.5% to 4.0% for left atrium (LA) ablation.

The incidence of procedure-related cardiac tamponade has increased with the increasing number of catheter ablation procedures for the treatment of AF, which typically involves one or more atrial septal punctures, extensive intracardiac catheter manipulation and ablation within the thin-walled LA, and the need for high levels of systemic anticoagulation during the procedure.⁴

Bleeding into the pericardial space is the most common complication of epicardial ablation procedures using the subxiphoid percutaneous approach. While approximately 10% to 20% of patients experience pericardial bleeding, particularly if inadvertent right ventricular (RV) puncture has occurred, pericardial bleeding of more than 80 mL is observed in up to 7%, though cardiac tamponade and severe bleeding are infrequent. Pericardial bleeding related to the epicardial access procedure is most commonly related to RV puncture. The proximal coronary arteries are covered by epicardial fat along the atrioventricular (AV)

groove and the interventricular septum, located away from the typical path of the access needle and thus are less vulnerable to injury. Occasionally disruption of epicardial fat can result in limited bleeding. Pericardial bleeding also can develop later during the mapping and ablation procedure. Laceration of the myocardium or epicardial vessels can occur during manipulation of the pericardial sheath or catheter or as a result of radiofrequency (RF) ablation.⁵⁻⁸

Mechanism

Cardiac perforation can be caused by mechanical trauma secondary to catheter manipulation, myocardial tissue rupture due to RF ablation, or inadvertent injury during atrial septal puncture. Extensive catheter manipulation, especially in areas with thin walls such as the LA roof, RV free wall, right ventricular outflow tract (RVOT), RV apex, and atrial appendages, can cause mechanical tear of the chamber wall. Cardiac perforation can also occur away from the area of mapping and ablation, usually caused by penetration of an unattended RV catheter in the setting of rapid and vigorous heart action because of high-dose isoproterenol infusion. Inadvertent puncture of the right atrium (RA) free wall or lateral LA wall can occur during atrial transseptal puncture.

High RF power application can cause excessive tissue heating and boiling of water within the tissue under the electrode. As a result, evaporation and rapid steam expansion can occur intramurally, and a gas bubble can develop in the tissue under the ablation electrode. Continuous application of RF energy causes the bubble to expand and its pressure to increase, which can lead to eruption of the gas bubble (causing a popping sound) through the path with the least mechanical resistance that leaves behind a gaping hole (the so-called steam pop). This often occurs toward the heat-damaged endocardial surface (leading to crater formation) or, infrequently, across the myocardial wall (resulting in myocardial perforation). Steam pops are often associated with a sudden, although small (<10 Ω) impedance rise and a sudden drop in electrode temperature. When steam pops burst toward the endocardial surface, an intense shower of microbubbles is often detected on intracardiac echocardiography (ICE). The risk of steam pops is relatively low with temperature-controlled standard 4-mm-tip RF catheter ablation, since the electrode temperature, which approximates tissue temperature, is limited to a safe level. However, when there is significant discrepancy between tissue and electrode temperature, due to passive or active electrode cooling, tissue temperature can reach the boiling point without being detected by the monitoring electrode temperature.

Detection

Prompt recognition and management of cardiac perforation are critical to prevent the development of cardiac tamponade and potentially life-threatening hemodynamic collapse. Although the presentation often is dramatic with abrupt hypotension, it is often insidious, with a more gradual fall in blood pressure. Continuous blood pressure monitoring using an arterial line can help detect early hemodynamic compromise. Sinus tachycardia is common in the setting of cardiac tamponade that gradually develops. Nonetheless, the absence of tachycardia does not exclude cardiac tamponade; in fact, sinus bradycardia is often observed secondary to a vagal reflex in the setting of a rapidly developing cardiac tamponade, and patients who are dependent on ventricular pacing will not show this. Any chest pain that persists beyond the completion of an ablation lesion, especially if associated with hypotension and diaphoresis, should alert the operator to the possible development of pericardial effusion.

Assessment of the cardiac silhouette fluoroscopically can provide the first clue, especially if a similar assessment was made at baseline. Decreased excursion of the lateral heart border on fluoroscopy in the left anterior oblique (LAO) projection, indicating accumulating pericardial

effusion, usually can be seen well before a drop in blood pressure and prior to progression to cardiac tamponade. Cineangiography often reveals a double layer in which the epicardial fat can be visualized separate from the outer pericardial shadow. Some operators obtain a baseline LAO cine image at the onset of a procedure to serve as a reference for comparison during the procedure, followed by intermittent evaluation of the same fluoroscopic projection during the procedure.⁹

Transthoracic echocardiography is the most definitive method for confirming the development of pericardial effusion. ICE, commonly used to guide transseptal puncture for LA procedures, can enable early detection of pericardial effusions before the emergence of tamponade physiology. Most of the pericardial space is not visualized from the RA imaging perspective used to visualize the interatrial septum; advancing the ICE catheter into the RV and rotating the transducer against the interventricular septum can readily identify pericardial effusions (Fig. 32.1).

Perforation without tamponade can occur during placement of diagnostic catheters, or while accessing the LA by transseptal catheterization. Detection of pericardial effusion at this time can prevent progression to tamponade but requires a high index of suspicion. Several clues should alert the operator to the possibility of cardiac perforation, including a ventricular catheter that reaches the edge of the cardiac silhouette, high pacing thresholds at sites despite normal electrograms and apparent good tissue contact on fluoroscopy, right bundle branch block pattern during “RV” pacing, and a catheter tip position discordant from where it should be (i.e., an RV catheter too far leftward with intended RV apical location; eFig. 32.1).

With atrial septal puncture for accessing the left heart chambers, the aorta can be inadvertently entered; if only the needle enters the aorta and this is recognized before advancing the dilator and sheath, the needle can be withdrawn and the patient monitored for stability of vital signs and with echocardiography. The procedure can be continued if there is no accumulation of pericardial fluid after 15 to 30 minutes of monitoring. If the dilator and sheath have been advanced into the aortic root before the error is recognized, it is imperative that the sheath not be removed at this time, as this can result in immediate and perhaps irreversible hemodynamic collapse due to intractable bleeding into the pericardial space. A cardiothoracic surgeon should be consulted immediately, who can then remove the sheath and repair the defect in the aortic wall under direct vision.

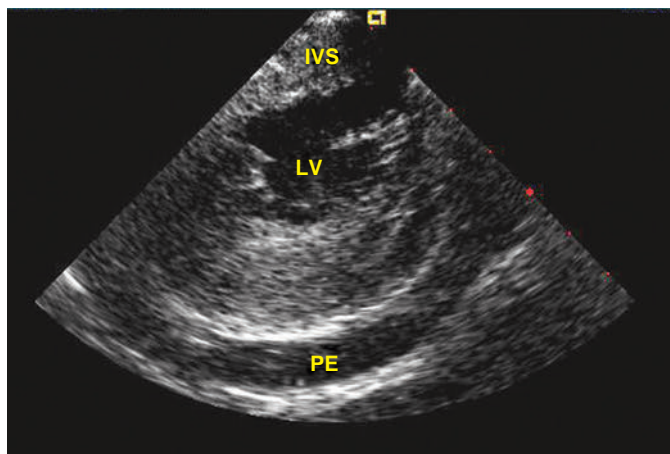
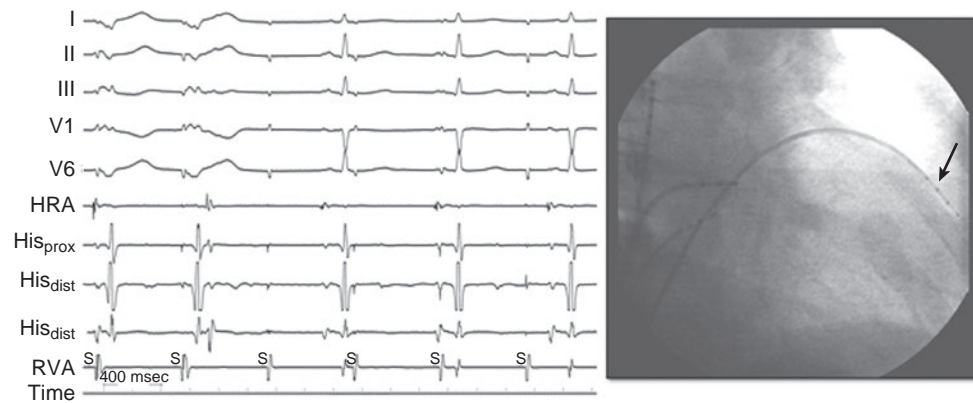


Fig. 32.1 Intracardiac Echocardiography (ICE) Imaging of Pericardial Effusion. The phased-array ICE transducer is positioned in the right ventricle, showing a short-axis view of the left ventricle (LV) and a moderate pericardial effusion (PE). IVS, Interventricular septum.



eFig. 32.1 Cardiac Perforation During Electrophysiological Study. Surface electrocardiogram and intracardiac recordings from a patient who was undergoing electrophysiological study. Recordings show poor capture from a catheter intended for the right ventricular apex (*RVA*); captured complexes have a right bundle branch block pattern. These features are explained by the accompanying right anterior oblique fluoroscopic image showing that the *RVA* catheter (*arrow*) has perforated the RV anterior wall and is pacing the anterolateral left ventricular epicardium. *His_{dist}*, Distal His bundle; *His_{prox}*, proximal His bundle; *HRA*, high right atrium.

In addition, during attempted atrial septal puncture, the needle and dilator can climb higher on the right atrial septal wall, where puncture of the free wall occurs, and with continued advancement of the trans-septal apparatus, it immediately enters the LA, at which time a left atrial pressure tracing will be observed and fluoroscopic and ICE appearance shows stable LA placement. Only when the sheath is removed later in the procedure does pericardial bleeding occur. Similarly, other catheters (RV, coronary sinus [CS]) may perforate at the time of initial placement and “plug their own hole” until the end of the procedure when they are removed, allowing bleeding into the pericardium.

Management

Cardiac tamponade is the most dramatic complication observed during catheter ablation procedures and can be associated with increased mortality if not managed promptly.

The management of pericardial effusion is largely determined by its relative size and hemodynamic effect. Trivial pericardial effusions, if recognized early during the procedure, should be monitored continuously but do not warrant termination of the procedure. For larger effusions, the procedure should be terminated and anticoagulation, if administered, should be reversed. Protamine is used to reverse the effects of heparin, idarucizumab for dabigatran, four-factor prothrombin complex concentrate for direct factor Xa inhibitors, and activated factor VII, fresh frozen plasma, and vitamin K can be used in patients with therapeutic anticoagulation with warfarin. IV fluids, vasopressors, and transfusion of blood products can be required, depending on the extent of the effusion and the severity of hemodynamic decompensation. IV atropine can be of value in patients with increased vagal tone.¹⁰

If perforation without tamponade is recognized, an echocardiogram should be obtained as a baseline. If the offending catheter is a standard 5 or 6 Fr shaft, it can often be withdrawn back into the heart while monitoring the echocardiogram for accumulation of pericardial fluid. Most often, there will be no further bleeding into the pericardial space and the procedure can be continued. If systemic anticoagulation is planned for left-sided catheterization, the operator must decide how important it is to continue the procedure with the risk of bleeding into the pericardium. If a larger catheter or large vascular sheath has been inadvertently placed in the pericardial space, echocardiography should be obtained along with immediate cardiothoracic surgical consultation. In many if not most cases, the sheath can be safely withdrawn into the heart without adverse consequences, but the team must be ready to transport the patient to an operating room for repair of a hole or tear in the wall of the affected heart chamber. In some cases, especially when the patient is fully anticoagulated, it may be prudent to transport the patient to the operating room and prepare for urgent sternotomy before removing the catheter/sheath, so as to be able to rapidly enter the chest if hemodynamic collapse occurs.

Although pericardiocentesis typically is required for large pericardial effusions and for smaller effusions manifesting signs of cardiac tamponade, and can effectively restore hemodynamic function, it carries the potential risk of cardiac chamber laceration, inadvertent puncture of the RV, pneumothorax, and infection. In a subset of patients (especially older female patients with a small to moderate amount of pericardial effusion who are not anticoagulated), a conservative approach incorporating administration of IV fluids and vasopressors to address the hemodynamic consequences of cardiac tamponade was found in a recent report to be a reasonable initial strategy and could obviate the need for emergency pericardiocentesis.

Pericardiocentesis

Pericardiocentesis should be performed promptly when indicated because there is usually a narrow therapeutic time window for intervention

before critical hemodynamic compromise ensues. The procedure can be performed under fluoroscopic guidance. Echocardiography can also be used to guide pericardiocentesis. When echocardiography is not readily available, fluoroscopy is usually adequate to establish the diagnosis and guide a safe procedure, and reliance on transthoracic echocardiography should not lead to unnecessary delay in diagnosis or therapy. The technique of percutaneous pericardial access via the sub-xiphoid approach is discussed in **Chapter 4**.

Some investigators have proposed the insertion of two drains in the pericardial sac to allow for faster evacuation of blood, followed by continuous aspiration with negative pressure manual suction. This technique can potentially allow the pericardium to abut and oppose the perforation site and “seal” of the bleeding source. Furthermore, rapid evacuation of the pericardial effusion can help prevent the formation of an intrapericardial thrombus (Fig. 32.2).⁹

Autotransfusion of blood removed from the pericardial space can be of value in patients with persistent bleeding, and is best done using an autologous blood recovery system (Cell Saver) because direct autotransfusion can result in a systemic inflammatory response.⁹

Complete drainage of pericardial effusion can be confirmed by ICE, transthoracic echocardiography, or contrast injection into the pericardium. In most patients, an indwelling catheter is required for a short interval after initial drainage to confirm that the bleeding has stopped and that no effusion is reaccumulating. Traditionally the drain is left in the pericardial space for approximately 12 to 24 hours, although recent reports suggest that early removal of drains (within 1 to 4 hours of ensuring cessation of bleeding) is a safe practice and is associated with less patient discomfort and shorter hospitalization.¹¹ Of note, coagulation of the pericardial blood and intrapericardial thrombus formation can impede effective pericardial drainage and cause restrictive effects on cardiac chamber filling; if this is even a moderate volume, urgent surgical exploration can be warranted, since any additional bleeding that can further compromise the circulation may be difficult to detect and impossible to evacuate with percutaneous drainage. High-dose protamine, especially when combined with prothrombin complex concentrate, can potentially be thrombogenic.¹⁰

Early pericarditis after cardiac perforation is common. In one report, 53% of patients with cardiac perforation had persistent chest pain (suggestive of pericardial inflammation) after effusion evacuation and removal of the pericardial catheter. Subacute reaccumulation of pericardial fluid (suggestive of post cardiac injury syndrome or inflammatory pericarditis) can also occur, requiring repeat pericardiocentesis. Several measures have been suggested to help reduce the severity of pericardial inflammation: (1) injection of steroids (e.g., 0.5 to 1.0 mg/kg of methylprednisolone or 2.0 mg/kg of triamcinolone) into the pericardial space at the conclusion of the procedure has been shown in animal models to be effective in reducing postprocedural pericarditis and adhesion formation; (2) postprocedural use of colchicine has been shown in small series to reduce postsurgical pericardial inflammation; (3) an administration of antibiotic therapy as long as the pericardial drain is in place; and (4) early removal of pericardial drains.^{8,12,13} Some patients have persistent mild hypotension and bradycardia for 1 to 2 days after drainage of blood from the pericardial space, causing concern for fluid reaccumulation. This may be due to a prolonged vagal reaction and typically resolves spontaneously.

Surgical Repair

There is currently no consensus on the threshold for surgical exploration and repair of cardiac perforation. Even large effusion (up to 2 L) can be managed with percutaneous pericardiocentesis without surgical intervention. However, continuing intrapericardial bleeding and rapid reaccumulation of pericardial effusion after initial evacuation can suggest

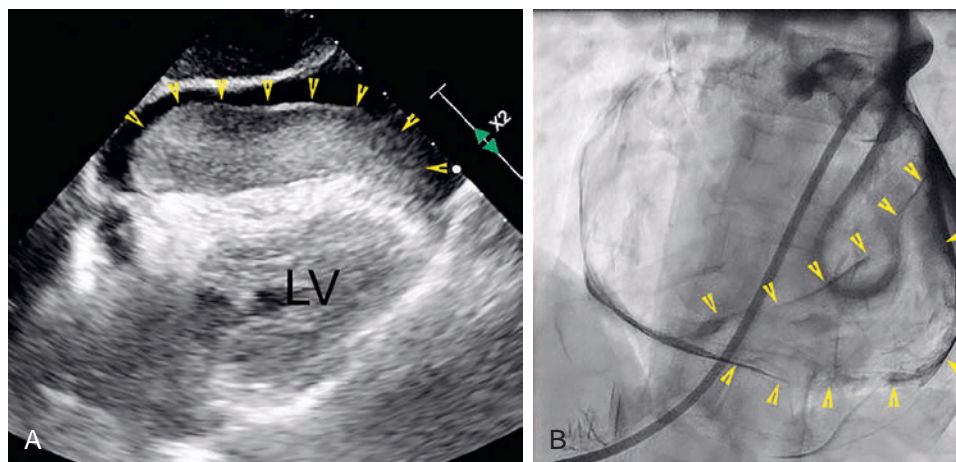


Fig. 32.2 Intrapericardial Thrombus. Transthoracic echocardiography (A) and contrast pericardiography (B) in a patient who developed cardiac perforation and hemopericardium following catheter ablation of atrial fibrillation. Reversal of heparin effects with protamine and pericardiocentesis was performed via the subxiphoid pericardial access approach. A pigtail catheter pericardial drain was inserted in the pericardial space, and pericardiography was performed by contrast injection through the drain. Note the large intrapericardial thrombus (arrowheads) overlying the left ventricle (LV).

cardiac chamber wall laceration rather than microperforation, and should prompt consideration of immediate surgical exploration. Up to 16% of LA perforations during AF ablation require surgical closure.⁹

It is often helpful to identify the potential site of cardiac perforation to guide appropriate surgical exploratory approach. This can often be indicated by the techniques used during the procedure and cardiac chambers being catheterized. However, cardiac perforation caused by a catheter remote from the site of ablation should also be considered.⁹

Measurement of oxygen saturation of aspirated pericardial blood can be helpful diagnostically to assess for venous (right-sided) versus arterial (left-sided) bleed. In addition, the location of the effusion or superimposed thrombus within the intrapericardial space sometimes can suggest the site of cardiac perforation (e.g., posterior effusion in the setting of LA perforation, and anterior effusion in the setting of RV perforation).⁹

THROMBOEMBOLISM

Systemic thromboembolism can complicate EP procedures in the left side of the heart. The rate of thromboembolic events is 0.4% to 2.1% for AF ablation and up to 2.8% for ablation of VT originating in the LV. In patients undergoing AF ablation, a history of a prior cerebrovascular event is the most potent individual risk factor for postablation cerebrovascular events and is associated with a ninefold increased risk of periprocedural stroke. In addition, the incidence of periprocedural stroke increases in a stepwise fashion with an increasing CHADS2 score.

Mechanism

Potential sources of emboli include thrombus formation on high-profile wires, catheters, and sheaths inserted in the LA or LV, char formation at the tip of the ablation catheter or at the site of ablation, thrombi or air passing through a patent foramen ovale or transseptal puncture, and dislodgment of a preexistent LA or LV thrombus by catheter manipulation. In addition, new LA appendage thrombi can develop in patients with persistent AF after planned or inadvertent conversion to normal sinus rhythm (NSR), especially in the setting of insufficient levels of anticoagulation before, during, or after ablation. Furthermore, endocardial disruption from the ablation lesions can potentially become a

nidus for thrombus formation. Also, aortic atheroembolism can occur during retrograde transaortic LV access for ablation of VTs or AV bypass tracts (BTs), and it tends to be associated with difficulty in the manipulation of catheters within a severely diseased aorta.

Thromboembolic events typically occur within 24 hours of the ablation procedure, with the high-risk period extending for the first 2 weeks following ablation. Cerebral thromboembolism is most common, but emboli can also involve the coronary, abdominal, or peripheral vascular circulations. In addition, recent studies demonstrated a high incidence of asymptomatic cerebral emboli (detected on brain magnetic resonance imaging [MRI] in up to 50% of patients) in the first 24 to 48 hours following AF ablation. The pathogenesis and clinical significance of these lesions remain uncertain.¹

Prevention

Prevention remains the best strategy in minimizing cerebrovascular events during left heart mapping and ablation, and this may be achieved by the following: (1) exclusion of intracardiac thrombi with preprocedural transesophageal echocardiography (TEE) in patients with AF (and transthoracic echocardiography in patients with ischemic VT and cardiomyopathy); (2) aggressive intraprocedural anticoagulation, including early heparin administration (preferably before catheterization of the left heart), followed by continuous infusion to maintain the activated clotting time at greater than 300 seconds; (3) meticulous attention to sheath management, including constant infusion of heparinized saline and air filters; (4) minimizing char formation during lesion creation by regulating power delivery to prevent abrupt impedance rise; and (5) using ICE during AF ablation for early detection of intracardiac thrombi and accelerated bubble formation consistent with endocardial tissue disruption with RF application.

Open-irrigation RF ablation or cryoablation, compared with standard 4- or 8-mm solid tip or closed irrigation electrodes, can potentially decrease the formation of char and thrombus at the tip of the ablation catheter. Administration of large doses of protamine on completion of the ablation procedure to reverse heparin abruptly can potentially promote thrombogenesis and warrants further evaluation to confirm its safety. Also, an uninterrupted oral anticoagulation strategy at the time of AF ablation eliminates a period of inadequate anticoagulation immediately

following the ablation procedure, a critical period for thromboembolic risk because of the inflammation and irritation inherently associated with ablation. In patients with severe disease of the aorta, using a long vascular sheath to advance the ablation catheter directly into the LV can potentially reduce the risk of aortic atheroembolism.

AIR EMBOLISM

Vascular air embolism is a potentially life-threatening event that can occur during left and right heart procedures. Because many cases of venous air embolism go unnoticed, the true incidence of this complication is unknown. Air embolism has been reported in the interventional radiology literature at an incidence of 0.13%.

Mechanism

Small amounts of air embolized in the venous circulation are generally broken up in the pulmonary capillary bed and absorbed from the circulation without significant sequelae. Embolization of large volumes of air (>5 mL/kg) can cause severe complications (shock or cardiac arrest). However, complications have been reported with as little as 20 mL of air. On the other hand, embolization of as little as 2 or 3 mL of air into the arterial circulation can be fatal.

Paradoxical air embolization into the arterial circulation can occur through direct passage of air into the arterial system via anomalous structures such as an atrial or ventricular septal defect, a patent foramen ovale, or pulmonary arterial-venous malformations. Direct arterial air embolism is caused by the introduction of air into the LA via the transeptal sheath, as well as via long vascular sheaths occasionally used for catheter stabilization during transaortic mapping and ablation in the LV.

With the patient in the supine position, large volumes of air rapidly entering the venous circulation typically lodge in the RVOT or pulmonary artery, and can cause RVOT obstruction, marked reduction of cardiac output, and potentially hemodynamic collapse. Also, air embolization can lead to serious inflammatory changes in the pulmonary vessels, including direct endothelial damage and accumulation of platelets and fibrin. Air in the systemic circulation can induce ischemia by various mechanisms, such as obstruction of the blood flow, vasospasm, and thrombus formation because of platelet activation.

Clinical Presentation

Most cases of venous air embolism are subclinical and do not result in untoward outcomes, and even when symptomatic, they go unrecognized because of the nonspecific nature of clinical presentation that can mimic other cardiac, pulmonary, and neurological dysfunctions. Therefore, a high index of suspicion is necessary to establish the diagnosis.

The outcome of venous air embolism is directly related to the amount of air and the rate at which it enters the vein. Spontaneously breathing patients can experience more serious consequences than those under controlled positive-pressure ventilation because they generate negative intrathoracic pressure during the respiratory cycle, facilitating air entrainment. Awake patients typically manifest shortness of breath, continuous coughing, chest pain, and a sense of “impending doom.” Jugular venous distention, hypotension, tachycardia, and electrocardiogram (ECG) signs of right heart strain (ST-T wave abnormalities) can be observed. Severe cases are characterized by cardiovascular collapse.

Arterial air emboli can distribute to almost any organ and can have devastating clinical sequelae. Direct cerebral air embolism can be associated with altered mental status, seizures, and focal neurological signs. A common presentation of air embolism during LA mapping and ablation is acute inferior ischemia, heart block, or both (eFig. 32.2). This reflects preferential downstream migration of air emboli into the right

coronary artery (ostium of the right coronary artery is located more superiorly than that of the left coronary artery in the supine patient). Importantly, atrial-esophageal fistula should be ruled out if air embolism is documented days or weeks after the ablation procedure.

Detection

Routine diagnostic modalities to identify air embolism in the terminal arterial circulations lack sensitivity, and diagnosis is typically based on the appropriate clinical scenario, with possible air identified in cardiac chambers. Air in the RV or pulmonary artery can be visualized on fluoroscopy as well as transthoracic echocardiography. TEE is currently the most sensitive monitoring device for venous air embolism. Prompt CT or MRI obtained before the intravascular air is absorbed can show multiple serpiginous hypodensities representing air in the cerebral vasculature, with or without acute infarction, but imaging later in the course of the disease shows diffuse acute infarcts (eFig. 32.3).

Prevention

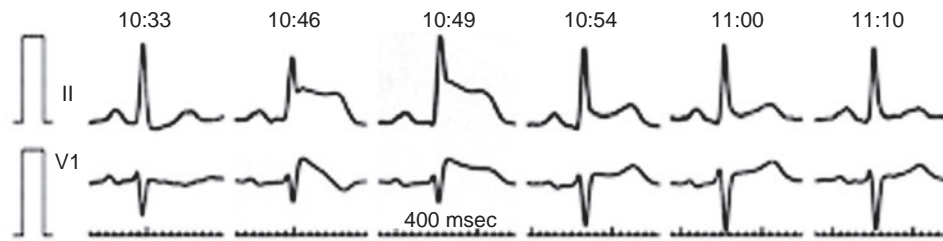
The optimal management of air embolism is prevention. Careful sheath management, including constant infusion of heparinized saline and air filters, should be observed. Although air can be introduced through the infusion line, it can also occur with suction when catheters are removed. Therefore whenever catheters are removed, they need to be withdrawn slowly to minimize suction effects, and the fluid column within the sheath should be aspirated simultaneously. The sheath should then be aspirated and irrigated to ascertain that neither air nor blood has collected in the sheath. Importantly, the entire volume of the sheath should be aspirated after initial deployment as well as after each time a catheter is removed and reinserted, to ensure that a continuous column of fluid is present in the sheath and disallowing the possibility of trapped air that could otherwise be introduced when a catheter is advanced through the sheath. Testing to ascertain the sheath's capacity prior to insertion is a good practice. This is especially important when inserting and removing balloon catheters through large sheaths.

Management

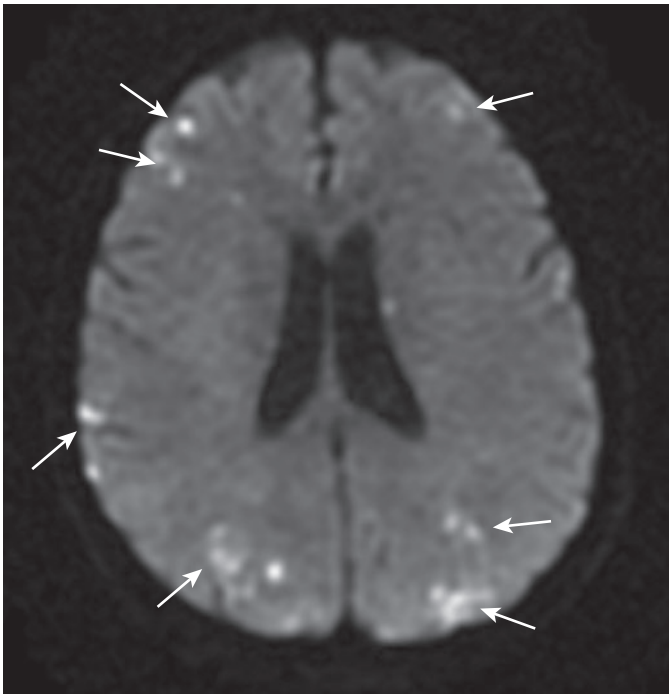
Initially it is essential to take all measures necessary to prevent further air embolization. For venous air embolism, placing the patient in the left lateral decubitus and Trendelenburg position helps air remain in the RA, where it will not contribute to an “air lock” in the RVOT. In addition, direct extraction of air from the venous circulation if localized in the RA or RV can be attempted by aspiration from a central venous or pulmonary artery catheter. Air aspiration should be performed with the patient supine or in a Trendelenburg position while holding his or her breath at the end of inspiration or during a Valsalva maneuver.

Administration of intravenous (IV) fluids and vasopressors may be necessary for hemodynamic support. Supplemental 100% oxygen therapy can reduce the size of the air embolus by increasing the rate of nitrogen absorption from air bubbles. Because gas bubbles are not buoyant enough to counteract arterial blood flow, these measures are more suitable for treating venous and RV air emboli. Supportive care usually results in complete resolution of symptoms and signs within minutes. Suspected coronary arterial air embolism should be investigated with coronary arteriography, especially if ST segments changes persist beyond 2 to 3 min, to exclude spasm or true thrombus.

When cerebral air embolism is suspected, it is important to maximize cerebral perfusion by administration of fluids and supplemental oxygen. Hyperbaric oxygen therapy is regarded as the treatment of choice in patients with cerebral air embolism, and prompt transfer to a hyperbaric oxygen therapy center should be considered. When started within a few hours, hyperbaric oxygen therapy can potentially compress the existing bubbles, speed resolution of bubbles by establishing a high



eFig. 32.2 Coronary Air Embolism. Leads II and V₁ are shown from a patient with a left-sided bypass tract who suffered air embolism during transseptal catheterization and catheter advancement into the left atrium. Snapshots of electrocardiograms taken at the designated times show the baseline (10:33) normal findings, dramatic ST elevation immediately following transseptal catheterization (10:46), and progressive resolution over the next 25 minutes. Time scale and 10-mV calibration marks are shown.



eFig. 32.3 Cerebral Air Embolism. A transverse section of a magnetic resonance image of the brain in a patient who sustained cerebral air embolism during ablation of atrial fibrillation, showing many areas of diffusion restriction scattered throughout both hemispheres, representing acute infarcts.

diffusion gradient, improve oxygenation of ischemic tissues, and reduce endothelial thrombo-inflammatory injury.

CORONARY ARTERY INJURIES

The incidence of coronary artery injuries during ablation procedures is extremely low (0.06% to 0.1%), despite the close proximity of coronary arteries to common sites of ablation. The low incidence is likely due, at least in part, to the protective effect of convective cooling conferred by the high-velocity blood flow within the epicardial coronary arteries.^{14,15}

The potential for acute coronary artery occlusion is a significant risk consideration with catheter ablation within the aortic sinuses of Valsalva. Damage to the coronary arteries can result from catheter manipulation and ablation in the aortic root, secondary to RF energy delivery in close proximity to the ostium of the right or left coronary artery, as well as inadvertent catheter engagement of the left main coronary artery when ablating in the left sinuses of Valsalva.

It is also important to recognize the potential risk of coronary artery damage when ablating in the RVOT and pulmonary artery. The right coronary artery is typically 4 to 5 mm away from the proximal part of the RVOT near its rightward free wall, and is separated by a variable amount of fat. In addition, the cephalocaudal separation of the pulmonic and aortic valves results in close proximity of the pulmonic valve to the origin of the right coronary artery, and the left main coronary artery lies in immediate posterior proximity to the subvalvular RVOT near the pulmonic valve as well as the supra-ventricular pulmonary artery.

Because of the proximity of the right coronary artery to the cavotricuspid isthmus (CTI) and the left circumflex artery to the lateral mitral annulus, coronary artery injury can potentially occur during ablation at mitral or tricuspid annuli. Transient inferior ST segment elevation and acute occlusion of the right coronary artery have been reported following ablation of the CTI, and left circumflex artery injury has been reported following ablation of left-sided AV BTs. Also, late stenosis of the right coronary artery has been observed in children with Ebstein anomaly of the tricuspid valve who undergo ablation of a right-sided AV BT, and coronary injury or infarction has occurred during ablation of posterior septal BTs ablated within the CS or middle cardiac vein.

Percutaneous epicardial ablation probably poses a greater risk of coronary artery injury (laceration, intimal hyperplasia, intravascular thrombus formation, or vasospasm), especially in the anterior and posterior septal and the basal ventricular areas, where coronary arteries and veins are known to traverse. The CS and its branches are also in close relation to the distal circumflex and the posterolateral branches of the right coronary artery, and ablation within the coronary venous system (for AV BTs, lateral mitral isthmus, and VT) can cause coronary injuries.

Mechanism

RF ablation-induced acute coronary artery injury can be mediated by vasospasm, intravascular thrombus formation, or direct vessel trauma. Transient thermal irritability resulting in coronary spasm appears to be the most common mechanism. Acute or subacute thrombosis can result from RF-induced functional and morphological damage to the coronary artery media and endothelium. Thermally induced denaturation of collagen fibers can develop in the vessel wall, leading to intimal hyperplasia and subsequent vessel narrowing. In addition, an inflammatory mechanism can result in delayed medial necrosis and intimal hyperplasia causing late stenosis. During epicardial ablation, coronary injury can result from direct disruption of the arterial wall or coronary laceration.¹⁴

In general, the susceptibility of coronary arteries to thermal damage is inversely proportional to the electrode-to-artery distance. Arterial injury is inversely proportional to vessel diameter; there is little evidence of injury when vessel diameter exceeds 0.5 to 1.0 mm. High RF power delivery in small hearts, such as in pediatric patients, or in direct contact with the vessel can increase the risk of coronary arterial injury.¹⁴

The high-velocity blood flow within the epicardial coronary arteries confer a protective effect against RF-induced thermal injury by allowing these vessels to act as a heat sink. Substantive heating of vascular endothelium is prevented by heat dissipation in the coronary blood flow (convective cooling), even when the catheter is positioned close to the vessel. Convective cooling likely accounts for the low incidence of coronary artery complications following RF ablation. The protection conferred by convective cooling during RF ablation, however, can be limited by reduction in coronary blood flow, as can be seen in small caliber vessels and in arteries with preexisting stenosis.

Clinical Presentation

Acute occlusion of a coronary artery (by spasm or thrombosis) can manifest as chest discomfort (in nonanesthetized patients) or acute ST-T segment changes on the surface ECG. A high index of suspicion is warranted, since the clinical presentation of acute coronary injury (e.g., chest discomfort and elevation in cardiac troponin levels) can easily be misdiagnosed as pericardial irritation or myocardial injury secondary to RF ablation. Monitoring surface ECG leads for ST changes during an ablation at high-risk sites is imperative to detect acute coronary injury. Also, obtaining a 12-lead ECG immediately after ablation is a critical step that can diagnose ST changes while still treatable and possibly prevent dramatic complications.^{15,16}

Importantly, RF ablation frequently (in 25% to 100% of cases) causes significant elevations in cardiac troponin levels that are not related to coronary arterial injury, with mean peak levels of 0.13 to 6 ng/mL for troponin I, and 0.20 to 2.41 ng/mL for troponin T. In contrast to acute coronary syndromes, troponin elevations observed following RF ablation typically peak early (2 to 8 hours vs. 18 to 24 hours) and normalize early. The levels of troponin elevation correlate with the number of RF lesions applied, the site of lesions (ventricular more than atrial more than annular), and the approach to the left side (transaortic more than transseptal). Ablation of focal lesions (atrioventricular nodal reentrant tachycardia [AVNRT], atrioventricular reentrant tachycardia) causes less frequent (in 25% to 88% of cases) elevation of troponin levels as compared with linear lesion ablation (atrial flutter, AF, and VT), where all patients are expected to have an increase in troponin levels. The prognostic significance of asymptomatic elevations of troponin I remains unclear.¹⁷

Prevention

Several precautions are important to avoid injury to coronary arteries during percutaneous epicardial ablation, ablation via the coronary venous system, and ablation in the aortic sinuses of Valsalva. Prior to ablation, direct visualization of the relation between the ablation site and adjacent coronary arteries must be obtained, usually by coronary angiography (or ICE imaging) performed with the ablation catheter positioned at the target site. Although an absolute safe distance between the ablation site and epicardial artery has not been defined, a distance of at least 5 mm between the ablation catheter and an epicardial artery is commonly accepted. It is also important to ensure that the catheter is not touching the vessel at any point of the cardiac cycle during angiography.^{8,16,18–22}

When ablation in the aortic sinus of Valsalva is planned, aortic root angiography may be considered to visualize the aortic root and the ostia of the right and left coronary arteries. Also, when selective

angiography of the coronary arteries is performed, a 5 Fr coronary angiography catheter may be left at the ostium of the coronary artery to serve as a marker and for protection of the artery in case of ablation catheter dislodgment during RF application. Alternatively, a combination of electroanatomic mapping and ICE imaging can be used to confirm anatomic location, catheter tip position and contact, and distance to coronary vasculature, and to monitor RF delivery.

In addition, RF energy output should be minimized during ablation in close proximity to coronary arteries, especially in the presence of small-caliber or diseased vessels. RF application should also be stopped as soon as it is evident that the ablation lesion is not successful in achieving the desired EP effect. Furthermore, ablation is often performed during continuous fluoroscopy to observe for catheter dislodgment, and energy delivery should be discontinued when even minimal dislodgment from the site showing the best mapping findings. Coronary angiography is often performed immediately after the ablation procedure to exclude coronary artery spasm, dissection, or thrombus.²³

Of note, experimental studies suggest a potential benefit of intracoronary irrigation with chilled saline for coronary protection from heat-induced damage during epicardial RF ablation. The safety and efficacy of this technique in clinical practice, however, have not been evaluated. Also, cryoablation appears to have less risk of coronary injury in animal models, but can still create occlusion and intimal damage when in close proximity, particularly to small vessels.¹⁴

IATROGENIC CARDIAC ARRHYTHMIAS

Atrioventricular Block

AV block is the most important complication of AVNRT ablation, occurring in about 0.2% to 0.8% of slow pathway ablation. AV block generally occurs during RF delivery or within the first 24 hours postablation, and is almost always preceded by junctional ectopy with VA block. The level of block is usually in the atrioventricular node (AVN). Predictors of AV block include proximity of the anatomical ablation site to the compact AVN, occurrence of fast junctional tachycardia (cycle length [CL] <350 milliseconds) during RF application, occurrence of junctional rhythm with VA block, the number of RF applications (related to the amount of tissue damage), and significant worsening of anterograde AV conduction during the ablation procedure. The anterior approach for AVNRT ablation is associated with a higher risk of inadvertent complete AV block (approximately 10%, but ranging from 2% to 20%). During ablation of AVNRT, careful monitoring of AV conduction during RF application and prompt discontinuation of energy delivery on evidence of AV block are the keys to minimize the incidence of AV block. RF delivery should be immediately discontinued when the following occur: (1) the impedance rises suddenly (>10 Ω); (2) the PR interval (during NSR or atrial pacing) prolongs; (3) AV block develops; (4) retrograde conduction block is observed during junctional ectopy; or (5) fast junctional tachycardia (tachycardia cycle length <350 milliseconds) occurs, which can herald imminent heart block.

AV block can also occur when ablating along the interventricular septum in the close vicinity of the compact AVN or His bundle (HB), including ablation of superoparaseptal and midseptal AV BTs or ATs, as well as para-Hisian VTs. In addition, because the penetrating HB lies at the membranous septum formed in part by the commissure between the right coronary and noncoronary sinuses of Valsalva, ablation of VTs originating in this region can potentially damage the HB (Fig. 32.3).

When a His potential is detectable at the ablation catheter location, titrated RF energy output and RF application for a short duration should be used, coupled with overdrive atrial pacing to monitor AV

conduction in case accelerated junctional rhythm occurs. Alternatively, cryoablation can be used in this region, with its slightly better safety margin for AV conduction.

In some patients, mechanical trauma from the catheter induces temporary AV block. Also, catheter manipulation in the RV or LV can cause mechanical bundle branch block (often transient), which can potentially cause complete AV block in patients with preexisting block in the contralateral bundle branch. Furthermore, ablation of the right bundle branch in patients with bundle branch reentrant VT is commonly followed by complete AV block (in up to 30%) because of preexisting severe disease in the left bundle branch.

Macroreentrant Atrial Tachycardias

Whereas the occurrence of new arrhythmias following focal RF ablation has not been a clinical problem, linear ablation lesions, if incomplete, can promote reentry propagating through the gaps in the ablation lines. Even when conduction block across the ablation lines is verified, the ablation lines commonly performed in the LA for ablation of AF can still facilitate reentry by providing conduction obstacles and protected isthmuses with adjacent anatomical structures in the atrium. In fact, LA macroreentry is a relatively common complication of catheter ablation of AF, occurring in up to 50% of cases. The incidence of ATs seems to be lower following segmental ostial pulmonary vein (PV) isolation (<5%) compared with circumferential PV isolation, and much higher following circumferential or linear LA ablation. Targeting complex fractionated atrial electrograms without linear lesions or PV isolation is associated with a moderate risk for postablation ATs. Following stepwise approaches of catheter ablation incorporating extensive lesions in the LA and RA to terminate persistent AF, ATs can be observed in more than 50% of patients. Although ATs can occur at variable time intervals after AF ablation procedures, the most common timing appears to be 1 to 2 months postablation.

Ventricular Arrhythmias

Malignant ventricular arrhythmias and sudden cardiac death (SCD) have been observed in the early phase following AV junction ablation. Polymorphic VTs are related to electrical instability caused by an initial prolongation and then slow adaptation of repolarization caused by changes in the heart rate and activation sequence. Most polymorphic VTs, ventricular fibrillation, and torsades de pointes that have been reported seem to be consistent with a pause or bradycardia-dependent mechanism. To reduce the risk of these arrhythmias, routine pacing at 80 beats/min has been recommended following AV junction ablation for some period of time. Patients with high-risk factors for arrhythmias, such as congestive heart failure or impaired LV function, may require pacing at higher rates (e.g., at 90 beats/min for 1 to 3 months), as well as in-hospital monitoring for at least 48 hours. Adjustment of the pacing rate, although rarely to less than 70 beats/min, is usually undertaken after 1 week in most patients, preferably after an ECG evaluation for repolarization abnormalities at the lower rate.²⁴

Abnormal Sinus Node Function

Inappropriate sinus tachycardia can occur in some patients after posteroseptal BT or AVN ablation, suggesting disruption of the parasympathetic input and/or sympathetic input into the sinus node and AVN. This typically resolves within 3 months following ablation. Some patients have severe sinus bradycardia or arrest after AF ablation; this may be due to sinus node remodeling after long periods of AF (months), but has also been observed in patients with normal sinus node function prior to ablation. In these cases, damage to the sinoatrial node artery can occur when it originates from the circumflex artery (and courses over the LA roof), and an LA roof ablation line interrupts the sinus

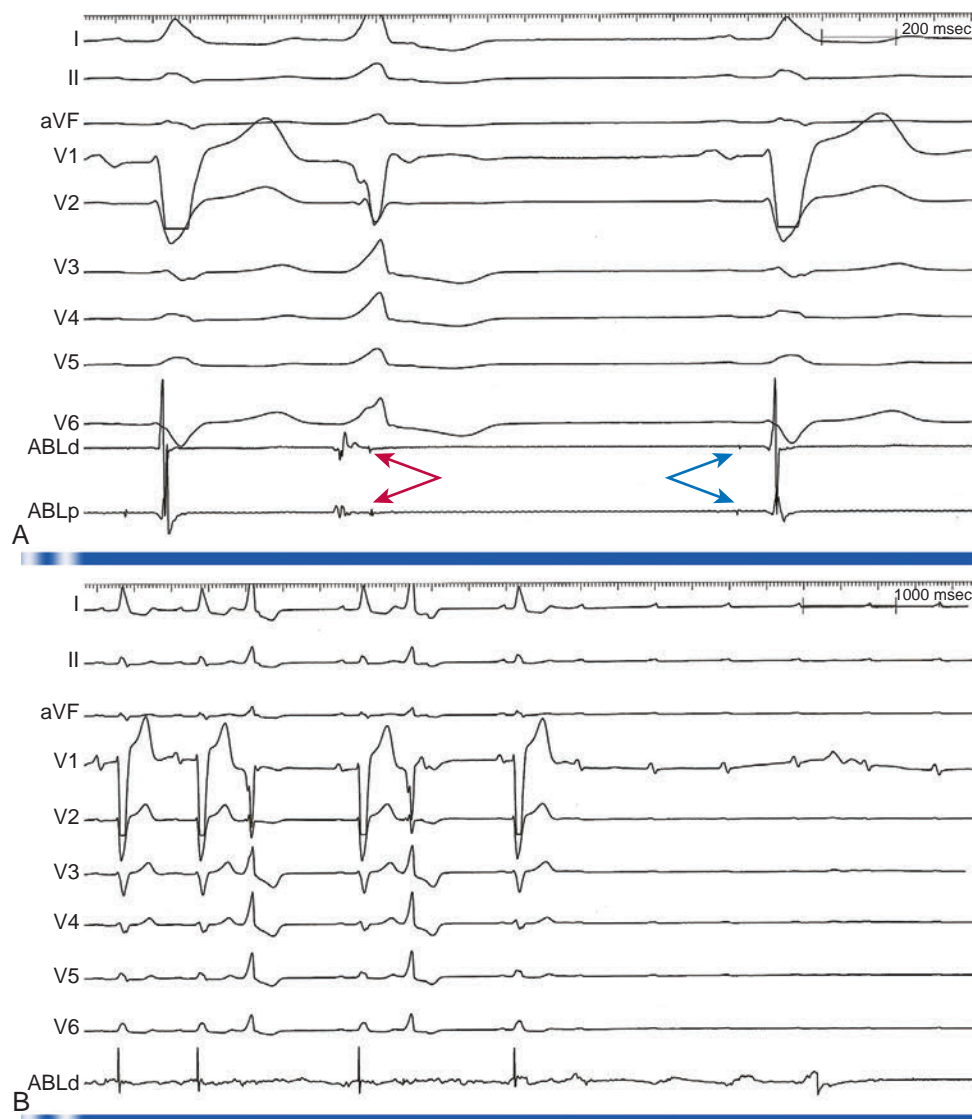


Fig. 32.3 Atrioventricular (AV) Block Complicating Catheter Ablation of Premature Ventricular Complexes (PVCs) Originating From the Para-Hisian Region. In A, note the presence of anterograde His potentials on the proximal and distal ablation electrodes (ABLp and ABLd, respectively) during sinus rhythm (blue arrows) and retrograde His potentials during PVCs (red arrows) at the site of earliest ventricular activation during PVCs. In B, radiofrequency energy delivery results in complete AV block secondary to injury to the His bundle.

node artery. This often resolves but may take over a week, and some patients have had permanent pacemaker implantation.

VALVULAR DAMAGE

The aortic valve can be damaged during retrograde crossing of the ablation catheter for retrograde ablation of LV VTs and left-sided BTs. To prevent leaflet damage or perforation, the straight catheter tip must never be used to cross the aortic valve; instead, a tight J curve is formed with the catheter tip before passage to the aortic root. Ablation of arrhythmias originating from the aortic cusp can also result in valvular damage, and limiting RF power output and duration is necessary. If standard methods of prolapsing the catheter into the LV are unsuccessful after several attempts, consideration should be given to introducing a long vascular sheath into the LV over a guidewire or a pigtail catheter (usually with easier valve crossing). Though somewhat cum-

bersome, this is preferable to struggling to cross the aortic valve with the ablation catheter by itself, only to have the catheter fall back into the aortic root and needing to re-cross the valve.

Damage to the mitral valve can result from entanglement of the ablation catheter within the mitral valve apparatus during transaortic or transseptal ablation procedures, but serious damage is unlikely. The risk of valvular damage (occasionally requiring thoracic surgery and valve replacement) is higher following entrapment of catheters with multiple splines or circular mapping catheters in the valvular apparatus (e.g., during AF ablation), which can be particularly difficult to free. Forcible traction of the catheter should be avoided, as it can potentially damage the valve and ultimately lead to mitral valve replacement. To prevent injury to the papillary muscles or chordae tendineae, prior to pulling on the catheter, one may consider instead advancing the catheter toward the LV apex. Advancing the sheath over the catheter and withdrawing the catheter into the sheath followed by withdrawal of the

whole assembly can facilitate the effort further. When gentle manipulation and moderate traction are unsuccessful, removing the catheter by thoracic surgery may be preferable; in this way the valve can potentially be spared significant damage.

PHRENIC NERVE INJURY

Phrenic nerve damage and consequent diaphragmatic paralysis have been a long-recognized complication during endocardial ablation in the RA or LA, as well as during percutaneous epicardial ablation procedures.

The right phrenic nerve descends between the parietal pericardium and parietal pleura along the lateral side of the RA between the right superior PV and SVC. This course renders the phrenic nerve vulnerable to injury from endocardial ablation during sinus node modification or ablation of ATs arising in the vicinity of the crista terminalis, SVC, or right superior PV. Right phrenic nerve injury has become more frequent with the increasing number of AF ablation procedures that involve electrical isolation of the SVC, as well as ablation around the right superior PV, especially when balloon ablation catheters are used. Right phrenic nerve injury is rare after isolation of the right-sided (mostly superior) PV (up to 0.48%) or isolation of the SVC (2.1%) using RF energy. The incidence of right phrenic nerve injury is significantly higher in the setting of cryoballoon PV isolation, occurring in more than 11% with first-generation cryoballoon. Using second-generation cryoballoon, transient (intraprocedural only) and persistent right phrenic nerve injury has been observed in 9.0% and 3.0% of patients, respectively. The epicardial approach to sinus node modification also carries the risk of right phrenic nerve damage.^{25–29}

The left phrenic nerve descends behind the left brachiocephalic vein and passes over the aortic arch, pulmonary trunk, and then with the pericardium over the LA appendage. From there it descends (between the fibrous pericardium and the mediastinal pleural layers) over the LV and frequently passes laterally over the obtuse margin of the LV, close to the lateral vein and the left marginal artery and, in only a small percentage of cases, close to the left main coronary artery and great cardiac vein. Left phrenic nerve injury can occur during endocardial ablation AF or AT in the region of the proximal roof of the LA appendage, during ablation of left posterolateral BTs, ablation within the distal CS or persistent left SVC, as well as during percutaneous epicardial VT ablation adjacent to the lateral LV wall.^{8,16,28,30}

The use of a non-RF source of energy is unlikely to prevent this complication because phrenic nerve injury has been reported with ultrasound, laser, and cryotherapy. Of note, diaphragmatic paralysis may develop 1 to 2 days after the procedure despite normal function at the end of the ablation protocol; this may reflect inflammation rather than direct injury to the phrenic nerve.

Clinical Presentation

Phrenic nerve injury can be asymptomatic in about a third of cases. The most frequent symptom is dyspnea. Other symptoms or clinical findings are cough or hiccup during ablation, and the development of postablation pneumonia or pleural effusion. In asymptomatic patients, the diagnosis is made on physical examination or a routine chest x-ray (Fig. 32.4) with hemidiaphragm paresis or paralysis (hemidiaphragm elevation with paradoxical movement on exhalation and inhalation x-ray). There is no active treatment known to aid phrenic nerve healing. Complete or partial recovery of diaphragmatic function can be observed in 66% and 17% of patients, respectively, sometimes not realized until several weeks or even months later.

Prevention

Several strategies are used to minimize the risk of phrenic nerve injury. The best strategy is to avoid ablation at sites close to the phrenic nerve. However, this is not always feasible. Therefore, careful monitoring of phrenic nerve function during ablation at high-risk sites is important to terminate energy delivery before the development of frank phrenic nerve palsy. Occasionally, displacement of the phrenic nerve from the ablation target site needs to be considered to facilitate the ablation procedure.³¹

Avoiding Ablation in Close Proximity to the Phrenic Nerve

In areas at high risk of phrenic nerve injury (RA free wall, posteroseptal part of the SVC, inferoanterior aspect of the right PV ostium, and proximal roof of the LA appendage, lateral LV epicardium) that require ablation, high-output (20 to 25 mA at 1.0 to 2.0 milliseconds) pacing should be performed before energy delivery. The ability to capture the phrenic nerve should prompt attempts to find a slightly different site or, if this is not possible, applying RF energy at low power and/or for short duration. This technique can be combined with electroanatomic mapping of the RA, SVC, LA, and right PVs to reconstruct the anatomical

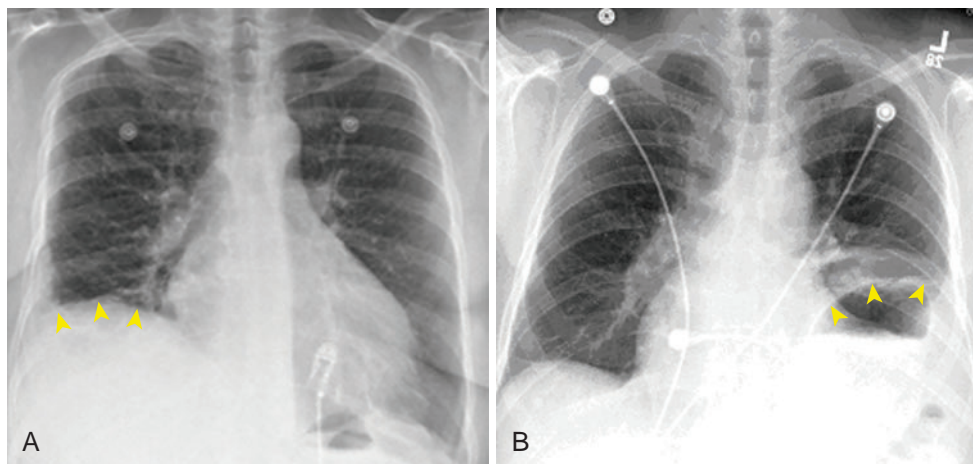


Fig. 32.4 Hemidiaphragmatic Paralysis Secondary to Phrenic Nerve Injury. Chest x-rays (posteroanterior views) showing right hemidiaphragmatic paralysis (arrowheads) caused by right phrenic nerve injury (A), and left hemidiaphragmatic paralysis caused by left phrenic nerve injury (B) during catheter ablation of atrial fibrillation.

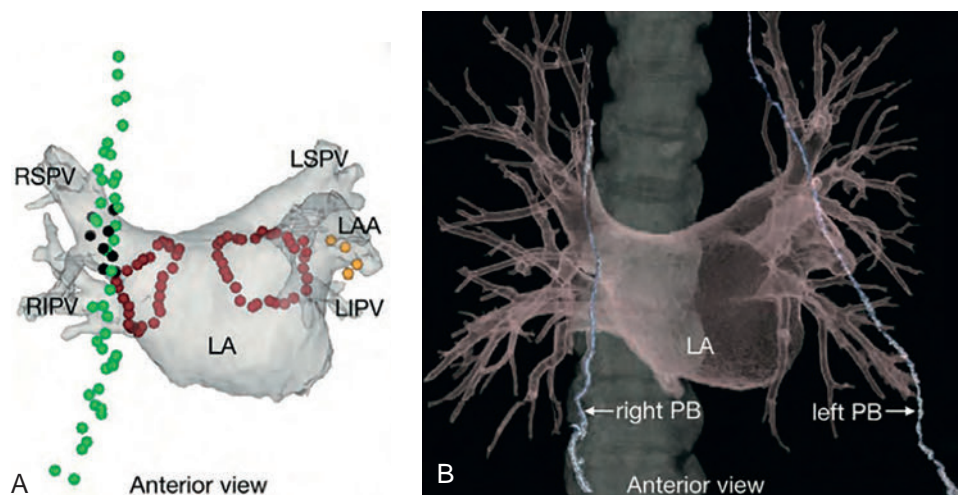


Fig. 32.5 Three-Dimensional (3-D) Computed Tomography (CT) Imaging and Mapping of the Phrenic Nerve (PN). A comparison of the right and left PN pace map generated by CARTO and the 3-D CT of the pericardio-phrenic bundles (PBs). Panel A shows a PN pace map. Point tags are superimposed on the CT of the left atrium (LA). Red tags show ablation sites. Green, black, and yellow dots indicate PN-capture sites by electrical pacing from the superior vena cava-right atrium, RSPV, and LAA, respectively. Panel B shows a clear image of the PBs reconstructed from CT data in the same patient as panel A. The running course of the right PN and the right PB are in close accordance. LAA, Left atrial appendage; LIPV, left inferior pulmonary vein; LSPV, left superior pulmonary vein; RIPV, right inferior pulmonary vein; RSPV, right superior pulmonary vein. (From Fukumoto K, Takatsuki S, Jinzaki M, et al. Three-dimensional imaging and mapping of the right and left phrenic nerves: relevance to interventional cardiovascular therapy. *Europace*. 2013;15:937–943.)

course of the right phrenic nerve. This approach provides a guide to phrenic nerve position relative to potential ablation targets (Fig. 32.5).³¹

Monitoring Phrenic Nerve Function During Ablation

When ablation is performed at high-risk sites, monitoring of phrenic nerve function is necessary to prevent permanent damage, even when the phrenic nerve cannot be captured by high-output pacing at the site targeted by ablation. This approach entails continuous pacing of the phrenic nerve (at a site superior to the ablation target site) during energy application with simultaneous monitoring ipsilateral diaphragmatic contractility. Studies have indicated that transient phrenic nerve injury occurs early and uniformly before permanent injury; thus early recognition of impending phrenic nerve injury during energy delivery allows immediate interruption of the energy delivery prior to the onset of permanent injury, which is associated with the rapid recovery of phrenic nerve function.³¹

It is important to recognize that detection by phrenic nerve capture is prevented by the use of paralytic agents during general anesthesia. Therefore when the procedure is performed under general anesthesia, it is important to avoid paralytic agents or use short-acting paralytic agents only at the time intubation and allow sufficient time for the paralytic effect to fade away before ablation or use a reversal agent (e.g., neostigmine).^{12,32,33}

For monitoring right phrenic nerve function, a diagnostic catheter is positioned at the anterolateral aspect of the SVC at a site above the level of ablation where the phrenic nerve can be consistently captured. Pacing output is adjusted at twice the nerve capture threshold; higher pacing outputs can potentially overcome early nerve injury and thus delay necessary interruption of energy application. In addition, it is important to achieve a stable catheter position and consistent phrenic nerve capture; loss of phrenic nerve capture due to catheter movement can mimic phrenic nerve injury and lead to unnecessary interruption of ablation.³¹

Successful phrenic nerve capture is confirmed when contraction of the right hemidiaphragm can be observed both under fluoroscopy or ICE and with manual palpation of the right subcostal region. Phrenic nerve capture can also be monitored by diaphragmatic electromyography. Diaphragmatic compound motor activation potential (CMAP) of the right diaphragm can be recorded using two chest wall standard surface ECG electrodes; one electrode is positioned 5 cm above the xiphoid process and the second electrode positioned 16 cm away along the right costal margin (Fig. 32.6). These electrodes are connected to the EP recording system, where bipolar electromyography signals are amplified and band-pass filtered between 1 and 50 Hz. SVC catheter positioning is optimized during right phrenic nerve pacing to obtain the highest amplitude diaphragmatic CMAP signals. Diaphragmatic CMAPs can also be recorded via a standard EP catheter placed in a subdiaphragmatic hepatic vein (see Fig. 32.6). Although the latter technique attenuates respiratory variations in CMAP amplitude observed with surface electrode CMAP recording, it necessitates an additional venous puncture and EP catheter. A decrease in diaphragmatic CMAP amplitude is the earliest sign of detectable injury to the phrenic nerve; studies showed that a 30% reduction in diaphragmatic CMAP amplitude presaged impending hemidiaphragmatic paralysis by approximately 30 seconds, making it a valuable method for monitoring phrenic nerve function.^{32,33}

Impending phrenic nerve injury can be indicated by diminishing diaphragmatic excursion (on palpation, fluoroscopy, or ICE), or a reduction of the maximal diaphragmatic CMAP amplitude by more than 30% (Table 32.1). Palpation of the strength of diaphragmatic excursion is a simple method, but tactile feedback is inadequate as the sole technique for monitoring phrenic nerve injury. Continuous or intermittent fluoroscopy is more accurate, but it increases radiation exposure to the patient and operator. ICE (with the transducer positioned at the level of the diaphragm and pointed at the liver) may also be used to continuously visualize hepatic movement from the diaphragmatic excursion.

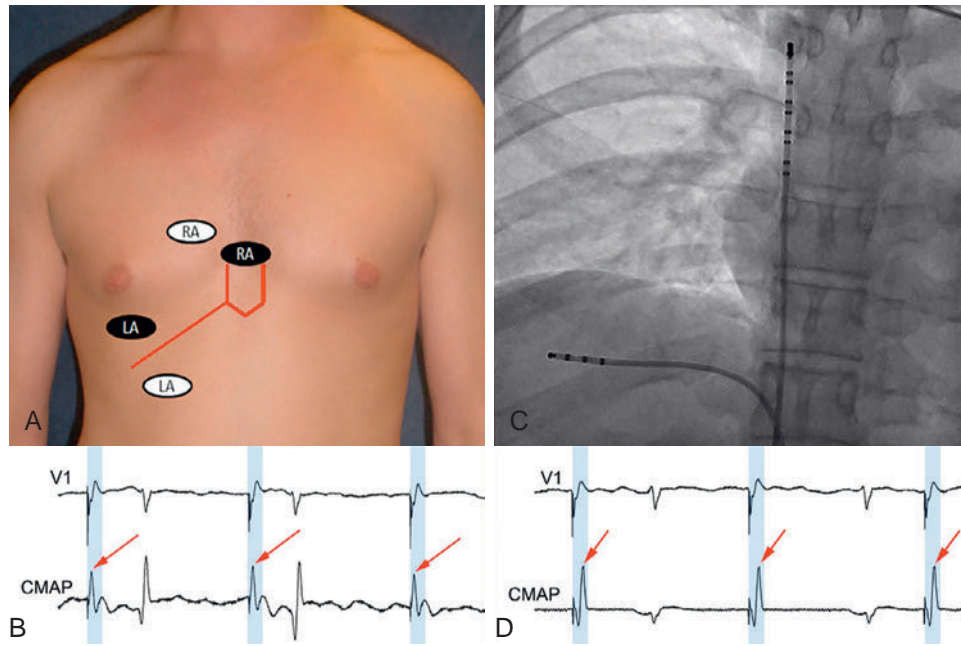


Fig. 32.6 Diaphragmatic Compound Motor Action Potential (CMAP). *Left panel*, Configuration of surface electrodes for recording diaphragmatic CMAP on modified lead I. (A) The right arm (RA black oval) surface electrode is placed 5 cm above the xiphoid, the left arm (LA black oval) surface electrode is placed 16 cm from the xiphoid along the costal margin. In some instances, the leads must be modified because of the patient's body habitus (e.g., in an obese patient) by moving the leads to the right and more separated (white ovals) to obtain the optimal CMAP amplitude (lower recording). (B) Surface electrocardiogram (ECG) lead V₁ and a diaphragmatic CMAP tracing (arrows) obtained by modified lead I. *Right panel*, CMAP tracing obtained by a quadripolar catheter in the right hepatic vein. (C) Anteroposterior fluoroscopic view centered on the diaphragm showing catheter position for phrenic CMAP recording. A quadripolar catheter is positioned in a hepatic vein to record phrenic CMAP. A decapolar catheter is placed in the superior vena cava to pace the right phrenic nerve. (D) Surface ECG lead V₁ and a diaphragmatic CMAP tracing obtained by quadripolar catheter in the right hepatic vein. This technique attenuates respiratory variations in CMAP amplitude observed with surface electrode CMAP recording (modified lead I). (A, Modified from Kowalski M, Ellenbogen KA, Koneru JN. Prevention of phrenic nerve injury during interventional electrophysiologic procedures. *Heart Rhythm*. 2014;11:1839–1844.)

TABLE 32.1 Pros and Cons of Various Phrenic Nerve Monitoring Strategies

Method	Description	Advantages	Disadvantages
Fluoroscopy	Direct visualization of diaphragmatic motion	Sensitive method for monitoring diaphragmatic motion	Additional radiation exposure to patient and operator Does not predict PNI
Palpation	Palpation of diaphragmatic excursion	Reliable and practical method for monitoring diaphragmatic motion	Requires additional staff member Palpable strength of diaphragmatic excursion may vary with respiration
Electromyography	Recording of diaphragmatic CMAP by 2 standard surface electrodes positioned across the diaphragm or by advancing a quadripolar catheter in the right hepatic vein during PN pacing	Earliest detection of PNI Simple, reliable, and easily applicable Only technique that predicts PNI	CMAP signals might be susceptible to respiratory variations Baseline amplitude must be adequate Affected by paralytic agents
Auditory cardiocardiography	Decrescendo pitch on fetal heart monitor (placed across patient's chest that can detect diaphragmatic contractions)	Auditory cue to the operator May portend PNI before palsy	Extra equipment needed Difficult to record in obese patients
Intracardiac echocardiography	Direct visualization of diaphragmatic excursion	Minimal radiation exposure to patient and operator	Requires additional venous access and intracardiac ultrasound

CMAP, Compound motor action potential; PN, phrenic nerve; PNI, phrenic nerve injury.

From Kowalski M, Ellenbogen KA, Koneru JN. Prevention of phrenic nerve injury during interventional electrophysiologic procedures. *Heart Rhythm*. 2014;11:1839–1844.

Furthermore, auditory monitoring of diaphragmatic contraction can be provided by an external fetal heart Doppler monitor placed at the costal margin. A change in the pitch of the diaphragmatic contraction is used to indicate reduction of the strength of the diaphragmatic contraction.³¹

Percutaneous Displacement of the Phrenic Nerve

During percutaneous epicardial ablation, proximity to the phrenic nerve can be detected by high-output pacing (typically at >10 mA) to detect diaphragmatic stimulation on fluoroscopy, allowing its course to be marked on the electroanatomic map. The nerve can branch over the LV; thus simply noting sites at which phrenic nerve capture occurs does not necessarily delineate the course of all branches. Further, the pacing output that would indicate a safe distance for epicardial ablation is not known.

If proximity to the phrenic nerve prohibits ablation at desired endocardial sites, interposing a balloon, saline, or air in the pericardium between the ablation catheter and the phrenic nerve can allow safe RF ablation. Mechanical separation of the phrenic nerve from adjacent structures, using a large balloon, entails insertion of a wire through one of the existing pericardial sheaths to the vicinity of the ablation catheter positioned at the target epicardial site. A 25 mm × 40 mm peripheral vascular angioplasty balloon (or esophageal balloon) is advanced over the wire to these locations. The balloon is inflated using an insufflator and contrast until complete inflation is seen on fluoroscopy. This technique can be limited by the inability to steer the balloon catheter and position it in the desired epicardial location. Not infrequently, a deflectable sheath is required to direct the balloon to the appropriate location and provide additional support and stability.^{31,34,35}

Another method is to introduce a combination of saline and air into the pericardium to achieve a “controlled hydropneumopericardium” to increase the distance between the phrenic nerve and the ablation target area. This involves using a 20-mL syringe to introduce saline and air alternately in 20-mL increments under careful monitoring of arterial pressure and fluoroscopy. At each step, epicardial pacing is performed to assess phrenic nerve capture and diaphragmatic stimulation. Instillation of air and saline is performed slowly until phrenic nerve capture is lost or severe hypotension develops. Although cardiac tamponade can develop secondary to sudden accumulation of fluid or air in the pericardial space, controlled and progressive introduction of fluid and air with careful hemodynamic monitoring usually allows separation of

the phrenic nerve from the epicardial surface without causing clinically significant tamponade. The combination of air and saline appears to be more successful in preventing phrenic nerve injury during epicardial ablation than injecting air alone or fluid alone. The combination of air and fluid allows the injection of a higher volume in the pericardial space with a lower impact on blood pressure than using fluid alone. With air only, a significant resistance can be felt in most patients after injections of more than 300 mL despite stable blood pressure. Of note, air is a poor conductor of electricity, and its presence in the pericardial space can increase the defibrillation threshold, requiring evacuation if defibrillation is anticipated (e.g., before induction of ventricular arrhythmias). In addition, ablation catheter contact with the epicardial surface is more problematic with a volume of fluid and/or air in the space.^{8,26,27,31}

PULMONARY VEIN STENOSIS

Incidence

PV stenosis is one of the most serious complications of AF ablation. A wide range of incidence (0% to 40%) of postablation PV stenosis has been reported, depending on the ablation strategy employed, methodology used for estimating PV ostial size and location, and intensity of surveillance. Focal ablation inside the PV carries the highest risk for PV stenosis, with rates of up to 33% to 42%. With PV isolation techniques, the incidence of severe PV stenosis is approximately 1% to 5%, with the highest risk in patients undergoing ostial PV isolation. Circumferential antral LA ablation, with ablation limited to atrial tissue outside the PV orifice, has a significantly lower rate of PV stenosis.³⁶

The severity of PV stenosis is generally categorized as mild (<50% decrease in diameter), moderate (50% to 70%), or severe (>70%). Late progression of PV stenosis to severe stenosis or even complete occlusion has been observed (Figs. 32.7 and 32.8), particularly in the smaller PVs. Of note, stenosis seems to be more common in the left-sided PVs. In a recent report, mild, moderate, and severe PV stenosis was observed (on cardiac magnetic resonance [CMR] or CT) in 31%, 4%, and 1% of patients who underwent RF antral PV isolation, respectively. Symptomatic PV stenosis necessitating intervention occurred in only 1 patient (0.1%).³⁶ Similar rates of PV stenosis have been reported following cryoballoon PV isolation.^{37,38} Significant PV stenosis (>50% diameter decrease) appears to be exceedingly rare following laser balloon PV isolation; however, the experience with this technology is still limited.^{39,40}

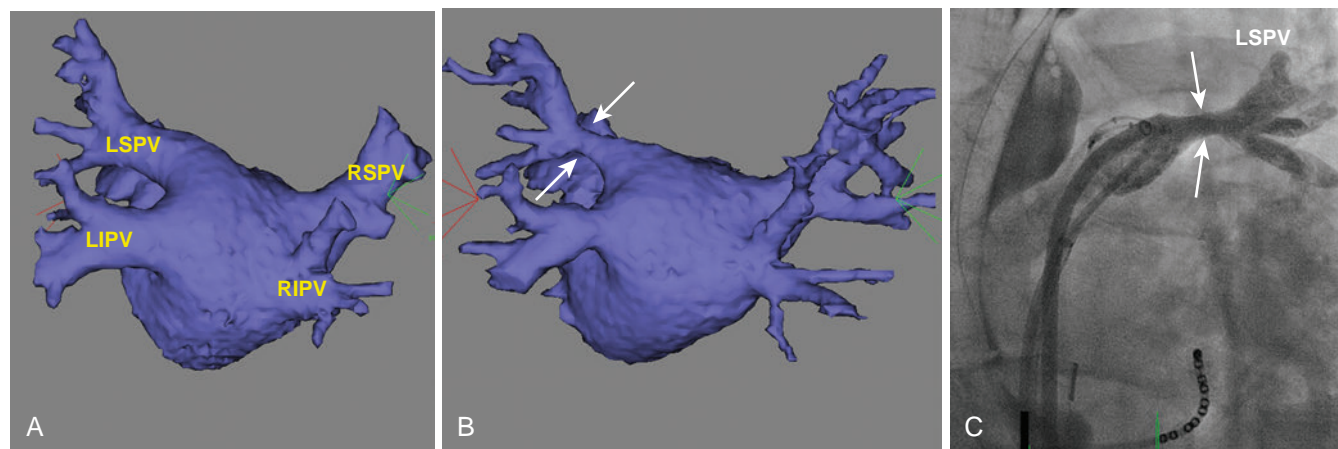


Fig. 32.7 Pulmonary Vein (PV) Stenosis. (A) Computed tomography (CT) image of the left atrium and PVs at baseline before segmental ostial PV isolation. (B) CT image 3 months after the ablation procedure, showing moderate stenosis of the left superior PV (LSPV; arrows) and mild stenosis of the left inferior PV (LIPV). (C) Angiogram (left anterior oblique view) of the LSPV, showing a moderate degree of stenosis (arrows). RIPV, Right inferior PV; RSPV, right superior PV.

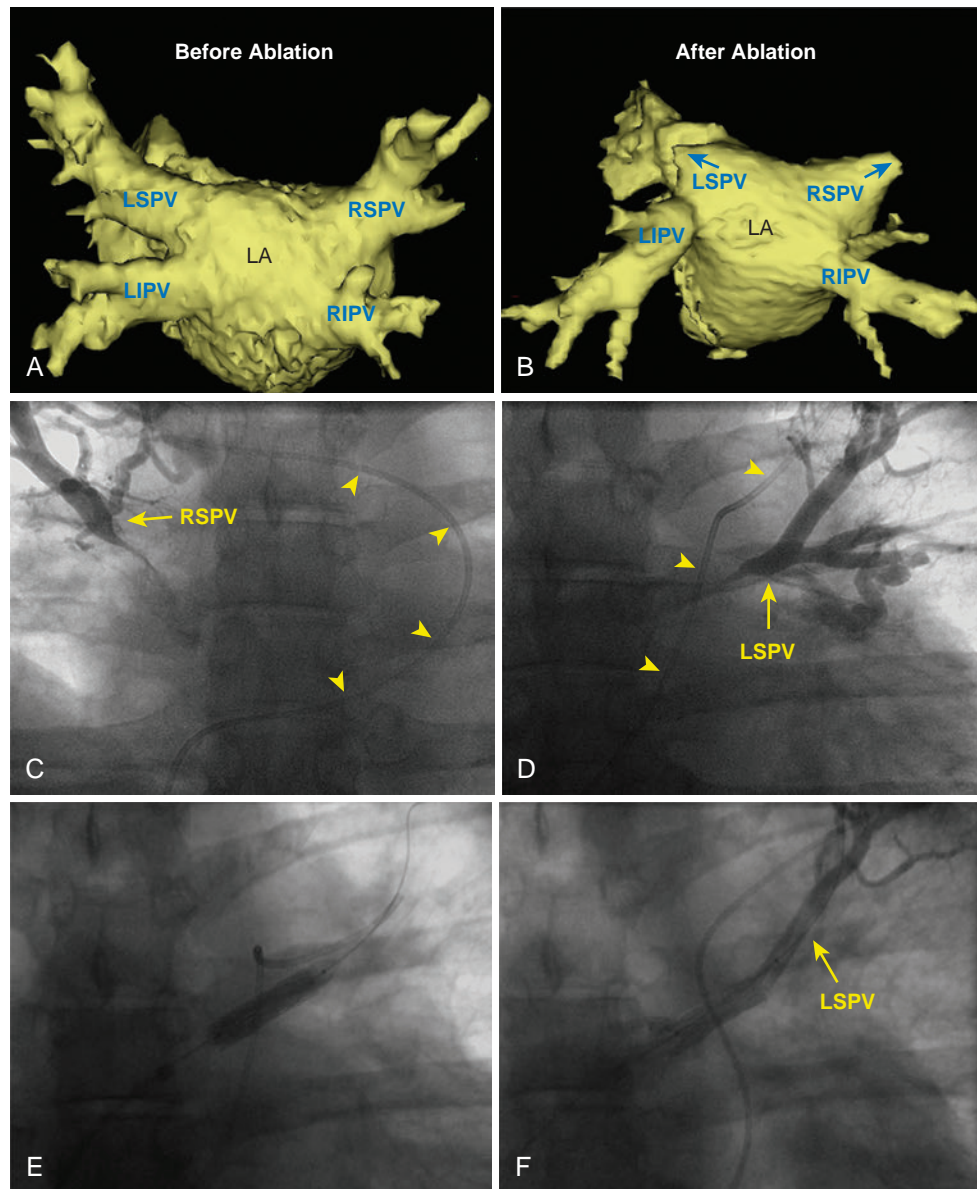


Fig. 32.8 Pulmonary Vein (PV) Occlusion. *Upper panels,* Computed tomography (CT) image of the left atrium (LA) and PVs at baseline before segmental PV isolation (A) and 5 months after ablation (B). Following ablation complete occlusion of both superior PVs is observed. *Middle panels,* Fluoroscopic (antero-posterior) views during angiography of the right superior PV (RSPV) (C) and left superior PV (LSPV) (D), showing severe stenosis-occlusion of both PVs at the ostia. PV angiography was performed with contrast injection via a catheter positioned in the pulmonary artery (arrowheads). *Lower panels,* Fluoroscopic (antero-posterior) views during stenting of the LSPV: (E) Angioplasty balloon is inflated for stent deployment in the LSPV; (F) angiogram of the left superior PV following stenting. LIPV, Left inferior PV; RIPV, right inferior PV.

Mechanism

The mechanism of the development of PV stenosis remains unclear. Several mechanisms have been implicated, including reversible edema, endothelial disruption with platelet activation and later neointimal proliferation, and thermally induced collagen denaturation and shrinkage, leading to tissue contracture. The occurrence and degree of PV stenosis correlate with the amount of energy delivered and the proportion of the PV circumference ablated.

Cryothermal ablation is distinguished from hyperthermic injury by the lesser degree of endothelial disruption and collagen denaturation

or contracture, which helps preserve tissue ultrastructural integrity, and matrix architecture tensile strength. These characteristics were expected to translate into a reduction in PV stenosis as compared with RF ablation; nonetheless, cryoballoon ablation for PV isolation still can lead to PV stenosis. The true mechanism of the PV narrowing following cryoballoon PV isolation remains uncertain.³⁷

Severe stenosis or occlusion of a PV (especially when it develops suddenly) can potentially result in gradual decline and then cessation of the arterial flow to the affected lung segment, caused by a decline in the arteriovenous gradient as well as compression by the developing tissue edema. The resulting alveolar ischemia and surrounding edema

lead to atelectasis, infarction, or susceptibility to infections. Furthermore, with the resulting alterations in pulmonary hemodynamics, redistribution of blood flow occurs with the opening of vascular channels or neovascularization in which tissue hypoxia is known to play a role. Hence the venous drainage of the affected segment becomes mainly dependent on the ipsilateral veins draining the healthy lobes. If the ipsilateral vein(s) is also stenosed, the impedance to the pulmonary flow increases, adding to the hemodynamic burden. Symptoms attributable to PV stenosis are typically not seen unless the perfusion of the affected lobe falls below 20% or the perfusion of the entire lung on the affected side falls below 25%.

Clinical Presentation

PV stenosis after ablation is frequently asymptomatic, especially when a mild or moderate degree of PV stenosis is present or a single vein is involved. The severity of symptoms is related not only to the degree of stenosis, but also to the number of affected PVs. Severe PV stenosis can be associated with various respiratory symptoms that frequently mimic more common lung diseases, such as asthma, pneumonia, lung cancer, and pulmonary embolism. Therefore, a high degree of suspicion is necessary to avoid performing misleading diagnostic procedures and to allow proper and prompt management. The onset of symptoms is usually several months following ablation. The initial manifestation is generally dyspnea on exertion, which typically evolves over the course of 1 to 3 months. Persistent cough is a common symptom. Pleuritic chest pain and hemoptysis occur infrequently, and are likely related to complete vessel or branch occlusion.

Symptoms can potentially improve spontaneously over time in a significant percentage of patients. In one report, this improvement occurred in 50% of patients and was always related to improvement in the radiological abnormalities previously detected, although other hemodynamic compensatory mechanisms (e.g., development of collaterals) can also play a role.

Detection

Several imaging modalities have been used for detecting PV stenosis, including CT imaging, MRI, perfusion scans, TEE, and pulmonary venography. To date, it remains unclear which is the best and most cost-effective noninvasive modality for detecting PV stenosis after ablation, and no single imaging modality has been able to assess all relevant aspects of PV stenosis. Therefore complementary methods such as TEE and CT scanning are most commonly used (see Fig. 32.7). Although many investigators recommend routine follow-up CT or MR imaging for detection of asymptomatic PV stenosis 3 to 4 months after AF ablation, it is unknown whether early diagnosis and treatment of asymptomatic PV stenosis provide any long-term benefit to the patient. Nevertheless, it is recommended that follow-up PV imaging be performed to screen for PV stenosis during the initial experience with a new AF ablation technique for quality control purposes.

CT and CMR imaging of the PVs are readily available and are the most widely used for initial evaluation for PV stenosis. Although both imaging modalities can identify the location and extent of PV stenosis (see Fig. 32.7), their sensitivity and specificity need further evaluation. Also, the diagnosis of PV occlusion cannot be made reliably using CT or MR imaging, and pulmonary artery wedge angiography is the only method for confirming the diagnosis.

TEE provides adequate visualization of the superior PVs, but imaging of the right and left inferior PVs is inconsistent. Hence TEE is not typically used as a first-line imaging study for routine screening. Nonetheless, TEE provides additional functional data regarding the significance of PV stenosis. On TEE, PV stenosis is usually indicated by an increased maximal PV Doppler flow velocity, or by the presence of turbulence

and deformity of the flow signal, as defined by a minimal flow between systolic and diastolic peak flow of 60% of the mean of both peaks. ICE allows straightforward imaging of all PVs and provides a good view into the first 1 to 3 cm of the vein. Color flow contrast imaging is also useful for identifying the location of the orifice of the most tightly stenotic vessels.

Blood gas assessment and pulmonary function testing do not seem to be useful as screening measures for early PV stenosis. Radiographic findings in PV stenosis are nonspecific. Chest radiography often reveals parenchymal consolidation, pleural effusion, or both. Ventilation/perfusion scanning can characterize the functional significance of the stenosis; in the presence of significant PV stenosis, perfusion abnormalities are usually marked and appear similar to the changes seen in pulmonary embolism.

Prevention

The best strategy to manage PV stenosis is to avoid it. Limiting RF ablation to the extraostial portion of the PV or PV antrum and using electroanatomic mapping and ICE to accurately define the PV orifice and guide the positioning of the ablation catheter are important measures to achieve this goal.

With cryoablation, it is imperative to avoid mismatch between the cryoballoon size and the PV ostial dimensions. In addition, several measures can be undertaken to avoid distal positioning of the cryoballoon within the PV. Further, very low balloon temperatures (below -55°C to -60°C) can potentially indicate a distal balloon position, and should prompt interruption of the freezing cycle.

Management

PV intervention is recommended in symptomatic patients. PV stenting appears to be associated with a lower restenosis rate compared with angioplasty. For asymptomatic patients with severe PV stenosis, some investigators have also suggested interventional therapy, because lesions can progress and eventually lead to total occlusion, precluding dilation and potentially resulting in hemodynamic compromise (see Fig. 32.8). Others have proposed regular clinical follow-up, with intervention considered only when symptoms develop. However, it is important to understand that patients can become symptomatic only after the long-term sequelae of PV occlusion become manifest, at which time intervention may not be technically feasible or, even when successful, may not be associated with significant improvement in perfusion of the affected lung segments. It is also important to consider the age, functional capacity, and associated comorbidities, as well as anatomical and technical factors pertaining to the stenotic vein when deciding about interventional treatment in asymptomatic patients.

TEE or ICE can facilitate accurate stent placement by reliably identifying the orifice of the tightly stenotic vein. Unfortunately, both in-stent and in-segment restenosis can recur in up to 60% of patients, and repeat intervention is warranted in symptomatic patients. Stenosis within the body of the stent is likely caused by neointimal hyperplasia and fibrosis. Out-of-stent restenosis is usually observed at bifurcation points beyond the stent into the vessel, also suggesting the progression of PV pathology, despite stent placement. There is no experience to date with the use of drug-eluting stents in this setting, but such a high restenosis rate makes a strong case for the investigation of those devices and larger diameter stents.

ESOPHAGEAL INJURY

Incidence

The development of esophagus-related collateral damage, such as esophageal injury and periesophageal vagal nerve injury, remains a rare but

important complication of AF ablation procedures, regardless of the energy source.⁴¹

Esophageal mucosal changes consistent with thermal injury have been reported in up to 48% of the patients following AF RF ablation, and clinically silent esophageal ulcerations confirmed by esophagogastroscopy or capsule endoscopy can be observed in 14% to 18%.⁴²

Esophageal perforation can develop with or without fistula formation. Fistulas can develop connecting the esophageal lumen to either the LA or pericardium. In a recent survey, about a quarter of patients with esophageal perforation presented without fistula or with pericardial-esophageal fistula, and the prognosis of these patients was significantly better than that of patients presenting with atrioesophageal fistula.⁴¹

The true incidence of atrioesophageal fistula after RF catheter ablation is unknown, but has been estimated to be between 0.01% and 0.25%, although underreporting is likely. Despite its rarity, atrioesophageal fistula remains a devastating complication associated with high mortality (more than 60%), and accounts for 16% of cases with fatal outcome (the second leading cause of death post AF ablation, following cardiac tamponade).

Cryoballoon ablation commonly causes significant decreases in esophageal temperature, especially during cryoablation of the inferior PVs, resulting in esophageal injury. Esophageal ulcerations have been observed following cryoballoon ablation at rates similar to those seen with RF ablation. In a recent study, esophageal thermal lesions with the second-generation cryoballoon were detected by endoscopy in 20% of patients at a mean of 1.5 days after ablation. Nevertheless, the occurrence of atrioesophageal fistula following cryoballoon ablation of AF is very rare (0.009% to 0.014%), and the risk seems less than that following RF ablation.⁴³

Excessive esophageal heating, esophageal ulcerations, and atrioesophageal fistula formation have been observed post PV isolation using high-intensity focused ultrasound (HIFU). In one report, elevated esophageal temperature prompting cessation of HIFU energy delivery occurred in 9% of PVs. Despite use of the safety algorithm, the occurrence of esophageal thermal damage and lethal atrioesophageal fistula could not be prevented, occurring in 1 of 28 patients. This safety concern led to a halt of the clinical use of HIFU for PV isolation.⁴⁴

Mechanism

The precise mechanism of atrioesophageal fistula formation has not yet been determined. The most likely mechanism involves direct thermal injury of the esophageal wall in immediate proximity to the posterior LA wall. A second proposed mechanism is ablation-related injury to the esophageal vasculature with late esophageal wall ischemia and necrosis. The latter mechanism likely explain the deferred development of atrioesophageal fistula.^{42,45,46}

The esophagus is located at the center of the posterior mediastinum and runs in close proximity to the posterior LA wall for about 5 cm of its course. In that region, the esophagus is separated from the LA only by the pericardial sac (the oblique sinus), which insinuates itself between the openings of the right and left PVs, and in some patients a thin fat pad. The LA posterior wall thickness is approximately 2 to 4 mm, and the thickness of the esophageal wall is 2 to 3 mm in cross section at the LA-esophageal area of contact.

The esophagus does not have a serosal layer, and it is fixed primarily in the pharynx and gastroesophageal junction. In the mediastinum, the esophageal position is dynamic because of peristalsis. In fact, the esophagus often shifts sideways by 2 cm or more in most patients undergoing catheter ablation for AF under conscious sedation. In addition, the position of the esophagus in relation to the LA and PV demonstrates high variability. In many cases, the esophagus is very close to the ostia of the PVs and lies only a short distance from the LA wall.

In most subjects (90%), the esophagus courses down beside the ostia of the left PVs with a mean distance of 10 mm to the left superior PV and 3 mm to the left inferior PV. Therefore anatomical localization of the esophagus can be critical before or during AF ablation to prevent atrioesophageal fistula, especially as there is a need for transmural atrial lesions.

During RF catheter ablation, the risk of esophageal injury likely is enhanced by increasing the magnitude and duration of local tissue heating (i.e., the total ablation energy delivered to cardiac tissue near the esophagus), which is related to catheter tip size, contact pressure, catheter orientation, and power output and duration. In fact, all reported cases of atrioesophageal fistulas have in common attempts to perform deep RF lesions on the LA posterior wall. In addition, ablation strategies incorporating extensive ablation in the LA posterior wall and the type of AF (persistent more than paroxysmal AF, possibly due to the additional linear ablation lesions) have been associated with an increased rate of esophageal ulcerations. A short LA-to-esophagus distance, the use of nasogastric tubes, and general anesthesia are other potential risk factors for esophageal injury during RF ablation.⁴⁷

The potential mechanisms of esophageal injury during cryoablation are similar to those with RF ablation: direct effect of thermal ablation on esophageal tissue or thermal-related injury to esophageal vasculature with subsequent esophageal wall ischemic necrosis. Factors associated with ulcerations include the mean nadir and the cumulative decrease of luminal esophageal temperature. During cryoballoon PV isolation, extracardiac damage can result from deeper positioning of the balloon within the PV, which reduces exposure of the balloon surface area to the convective warming effects by the circulating blood in the atria and, as a result, leads to an increased freezing area and greater ice formation. If the esophagus is in contact with the pericardium at the site of the ice formation, the freezing area will extend into esophageal tissues. A distal position of the cryoballoon within a PV can be indicated by a rapid decline in balloon temperatures to less than -40°C within 30 seconds of ablation or nadir temperatures of -60°C or lower during ablation. To date, all documented cases of cryoballoon-associated atrioesophageal fistulas have been in relation to the left PVs—particularly the left inferior PV. The esophagus appears more vulnerable to injury during cryoballoon ablation of the left inferior PV; the ostium of the left inferior PV has the closest relationship to the esophagus, and inflation of the cryoballoon in this vein, especially when positioned deep into the vein and forward pressure is applied on the balloon for stability, exerts posteriorly directed forces that brings the balloon closer to the esophagus. There is some evidence that gastric acid refluxing into the esophagus is a component of the injury process as well.^{46,48}

Clinical Presentation

Mild esophageal injury, manifesting as mucosal changes or ulceration, is predominantly asymptomatic, but can cause epigastric or retrosternal pain or discomfort and dysphagia.

The leading symptom of esophageal perforation is high fever or severe chest or epigastric pain. Esophago-pericardial fistulas are characterized by chest or epigastric pain resulting from pericardial effusion and pericarditis accompanied by signs of infection (fever and leukocytosis).⁴⁹

Patients with atrioesophageal fistulas can also present with hematemesis, odynophagia, sepsis, and stroke (secondary to air embolization). Furthermore, hematemesis or hemorrhagic shock can occur secondary to bleeding in the esophagus. The clinical course of atrioesophageal fistula formation varies in the mode and timing of presentation, and mostly is manifest after patient discharge from the hospital. In a recent report, the mean interval between the procedure and presentation of 20 ± 12 days (range, 2 to 60 days).^{41,49}

Detection

Leukocytosis is the earliest and most sensitive laboratory marker in patients with atrioesophageal fistulas. Thoracic CT or CMR imaging is the most valuable diagnostic examination (Figs. 32.9 and 32.10). The dramatic neurological complications occur with a delay of at least a few hours after the first symptoms.

The sensitivity of barium swallow studies for detection of a fistula is limited. Endoscopy is a diagnostic modality that should be avoided because insufflation of the esophagus with air can force air from the esophagus into the LA and result in a devastating cerebrovascular accident and death secondary to a large air embolus. The use of CO₂ instead of air for insufflation appears to present a lower risk.

Management

Although the prevalence of atrioesophageal fistula post-AF ablation is low, the fatality rate is high, reported between 67% and 100%, and traditionally it has been attributed to the lack of recognition and late presentation of this complication. The prognosis of patients who survive to obtain an accurate diagnosis and receive corrective surgical intervention is unknown, but the morbidity and mortality associated remain high despite surgical repair.

The window from symptom onset to neurological injury is often short; therefore a high index of suspicion is crucial to establish the diagnosis and implement immediate intervention. Delayed diagnosis (after the onset of neurological symptoms because of air embolism and sepsis) dramatically worsens prognosis, and delayed treatment is unlikely to prevent permanent disability or death. Because fistula tracts develop over the first 2 to 4 weeks after the procedure, when the patient is already home and recovering in other regards, it is important that patients be aware of and report symptoms of dysphagia, fever, stroke-like symptoms, new chest discomfort, or gastrointestinal bleeding. Early diagnosis of atrioesophageal fistula is critical to give the best chance for survival and recovery.

Immediate surgical repair of atrioesophageal fistula (within a few hours after the first symptoms) can potentially prevent neurological complications and possibly improve survival rate. Esophageal stenting can be sufficient in patients with esophageal perforation without fistula formation. Esophageal stenting in conjunction with pericardial drainage has also been described for the treatment of esophageal-pericardial fistulas once esophageal-atrial communication is excluded. However, it is important to recognize that although esophageal stenting can quickly establish a barrier that minimizes air and solid material embolism without the risks of esophageal surgery, this approach can be detrimental when an undiagnosed atrioesophageal fistula is also present. Fatal complications can result from air insufflation during upper gastrointestinal endoscopy or stent dislocation. Therefore an early surgical approach to esophageal perforation should be strongly considered, even when the formation of atrioesophageal fistula has not been established.^{41,49}

Prevention

Various strategies may be used to try to avoid the development of an atrioesophageal fistula. However, because of the rarity of this complication,

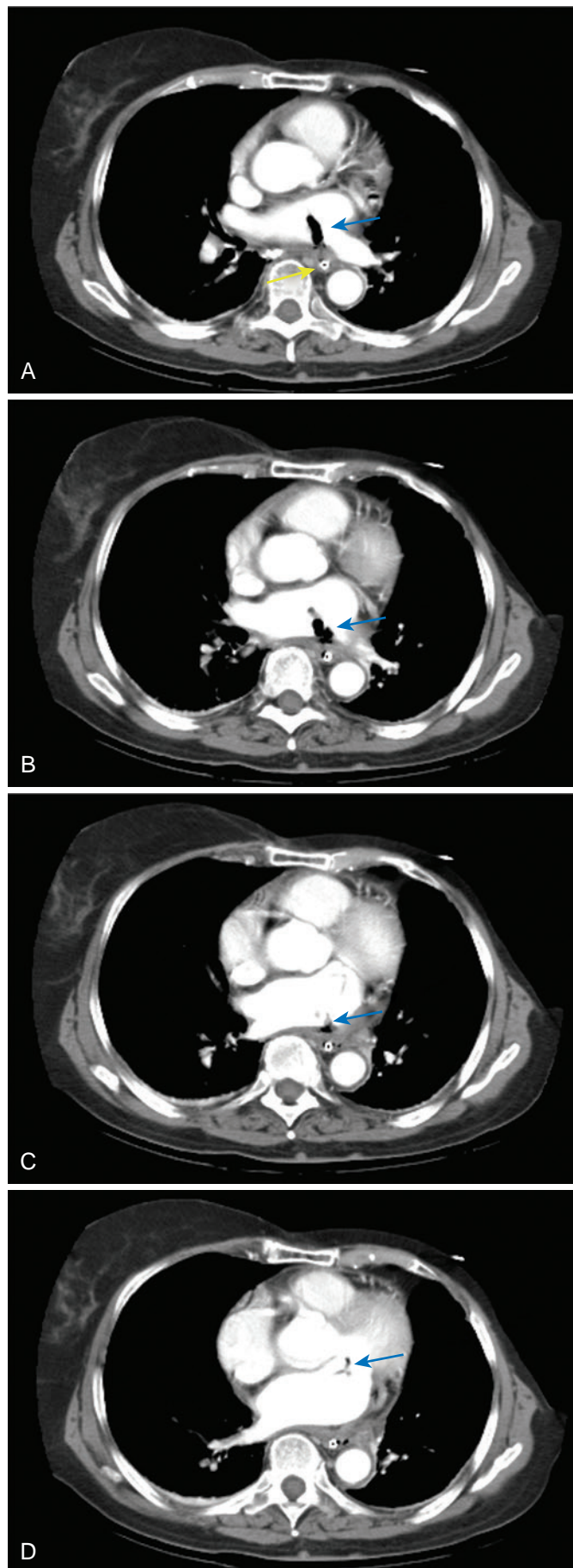


Fig. 32.9 Atrioesophageal Fistula Postablation of Atrial Fibrillation. Multiple transverse sections of a chest computed tomography scan, revealing air bubbles (blue arrows) in the superior aspect of the left atrium (A–C) and at the level of the mitral valve (D). Note that air appears to originate from the anterior esophageal wall (B and C). Nasogastric tube is visualized in the esophagus (yellow arrow).

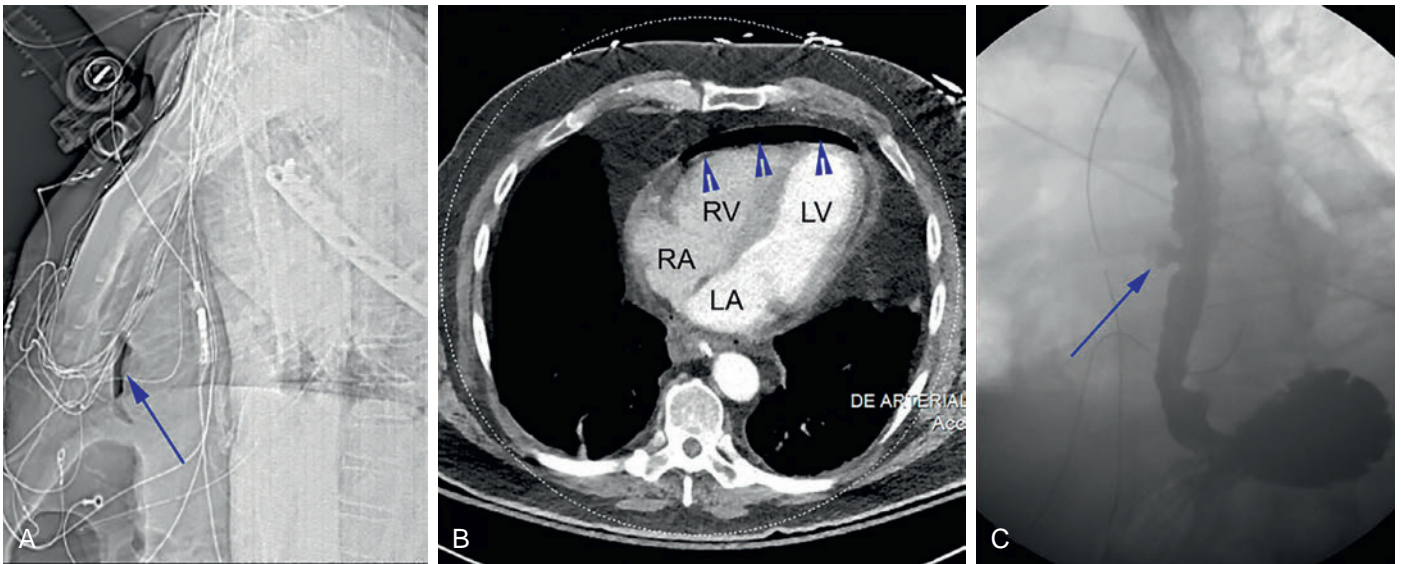


Fig. 32.10 Esophageal-Pericardial Fistula. A 62-year-old patient presented with chest pain 21 days following ablation of atrial fibrillation, and was diagnosed with esophageal-pericardial fistula. (A) Chest x-ray (left lateral projection) obtained in supine position showing air accumulation (arrow) anterior to the cardiac silhouette. (B) Computed tomographic scan showing pneumopericardium (arrowheads). The free air wraps around the anterior right ventricle (RV) extending across the apex of the left ventricle (LV). No air is observed within the cardiac chambers. (C) Gastrografin esophagogram showing focal out-pouching from the esophageal wall (arrow) at the junctions of the middle and distal thirds of the esophagus representing local ulceration or sinus tract. LA, Left atrium; RA, right atrium.

it remains unproven whether the use of these approaches lowers or eliminates the risk of esophageal perforation or fistula formation, and the optimal technique has not yet been determined. Therefore it appears prudent to apply a combination of these preventive techniques during AF ablation.

Avoiding Ablation in the Vicinity of the Esophagus

The most effective measure to prevent atrioesophageal fistula formation is to avoid ablation in the LA posterior wall at sites close to the esophagus. However, effective treatment of AF and PV isolation typically require ablation at those sites, and complete avoidance of the LA posterior wall usually is not feasible. Nonetheless, inclusion of a linear lesion connecting the PV encirclements in the posterior LA wall is no longer advised. If such a connection is thought to be clinically necessary, it should be performed superiorly in the dome of the LA instead of the posterior wall.

Assessment of Esophageal Location

The precise understanding of the real-time esophageal location and anatomical characteristics is critical for the prevention of ablation-induced esophageal injury. Newer imaging techniques have been used to visualize the anatomical relationship between the esophagus and the LA during AF catheter ablation. Esophageal imaging is not part of the usual CT or CMR of the LA and PVs. Visualization of the esophagus can be achieved during the CT angiography using barium sulfate or Gastrografin (with swallowing instructions to help the contrast substance to lodge in the middle and distal esophagus, rather than in the stomach (Fig. 32.11)). Visualization of the esophagus during CMR can be achieved by combining the barium sulfate paste with gadolinium diglutamate. The barium cream helps the gadolinium lodge in the esophagus. However, these approaches have several limitations. The esophagus is a mobile structure, and CT and CMR scans of the esophagus are static and not real-time images, acquired on a previous session; therefore these images

may be an unreliable guide to the position of the esophagus during the ablation procedure. This may be particularly true for procedures performed while the patient is under conscious sedation, when esophageal peristalsis is likely to occur. Furthermore, the image of the esophagus is obtained with a barium sulfate paste, and the real dimensions of the esophagus depend on the volume of contrast media injected. During ablation, the esophagus is empty, and the real dimension and probably the exact location can be misinterpreted.

The use of 3-D mapping systems that allow the integration of pre-acquired 3-D CT scans or CMR of the LA, PVs, and esophagus provides a visualization tool that permits a rapid understanding of complex cardiac anatomical relationships. In addition, 3-D rendering of the esophagus can be generated during the procedure using an electroanatomic mapping system; esophageal location can be marked by advancing a diagnostic EP catheter into the esophagus and tagging its location (see Fig. 32.11). It is important to recognize, however, that the catheter used for tagging can be positioned eccentrically in the esophageal lumen, thus providing potentially misleading information.

Phased-array ICE can provide rapid real-time identification of esophageal location in relation to the posterior LA wall. The location of the esophagus determined by ICE during the ablation procedure was found to correlate well with the location determined by CMR before the procedure. This technique has the advantage of providing real-time information on the location of the esophagus, especially when movement occurs.

Another strategy to limit the risk of esophageal injury is real-time imaging of the anatomical course of the esophagus during the ablation procedure by placement of a radiopaque esophageal monitoring probe or use of a viscous radiopaque contrast paste. Orally administered barium provides a simple, inexpensive, and safe way to keep track of the esophagus accurately during an ablation procedure (see Fig. 32.11). In most patients, barium paste coats the wall of the esophagus, and residual barium often allows visualization of the esophagus for 1 to 2 hours

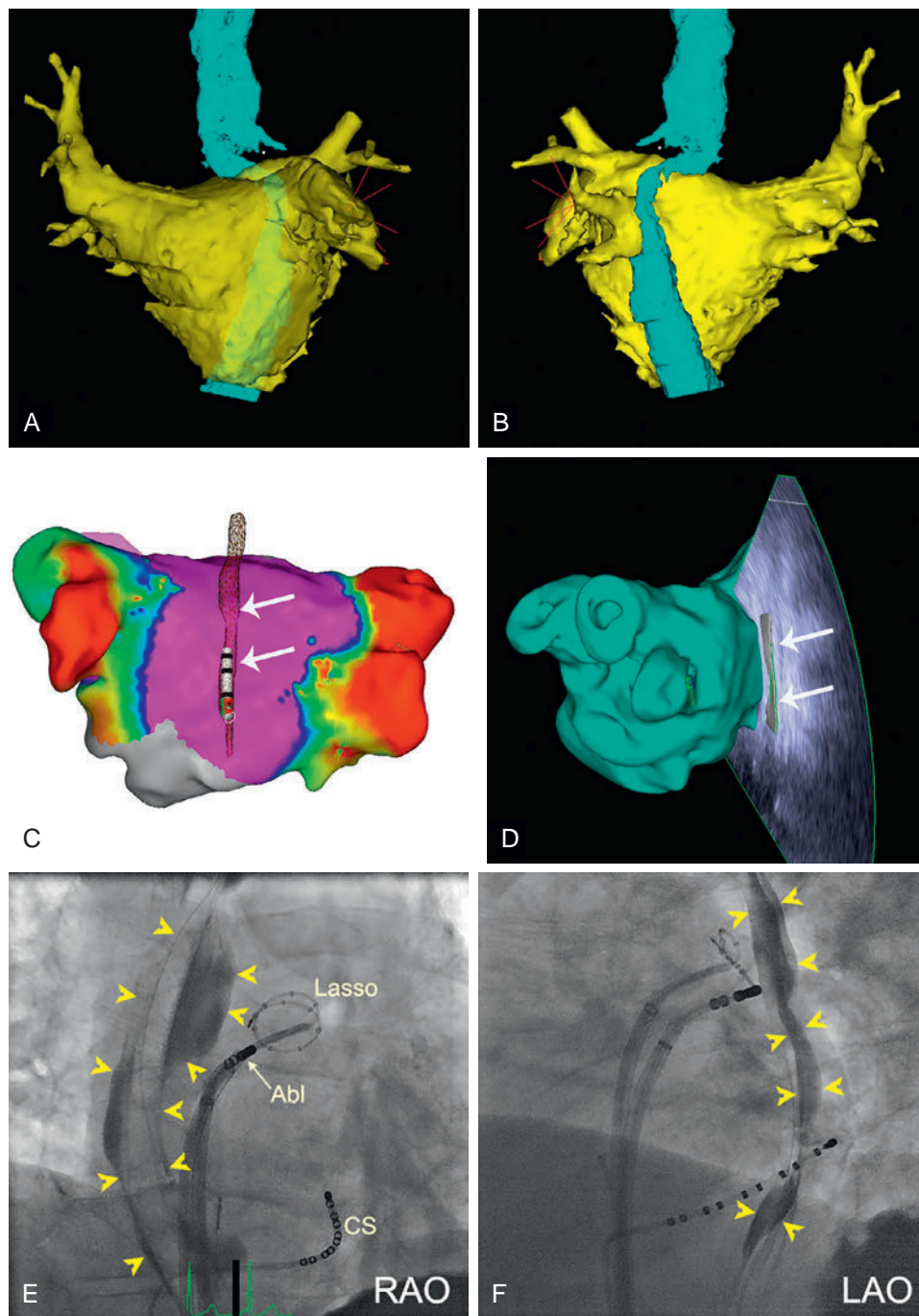


Fig. 32.11 Assessment of Esophageal Location During Catheter Ablation of Atrial Fibrillation. (A and B) Anteroposterior and posteroanterior (PA) views of a computed tomography (CT) image of the left atrium (LA), pulmonary veins (PVs) and esophagus. The esophagus is visualized during CT scanning by the use of Gastrografin (contrast medium). Note that the real dimensions of the mid-segment are not very clear because of peristaltic movements and inadequate filling of the esophagus. (C) Electroanatomic (CARTO) map of the LA and PVs (PA view) incorporating reconstruction of the esophagus (*arrows*). The esophageal mapping catheter can also be visualized. (D) Electroanatomic (CARTO) map of the LA and PVs (left posterior oblique view). Intracardiac echocardiography is used to visualize the esophagus (*arrows*) and incorporate its location in the electroanatomic map (CARTO-Sound). (E and F) Fluoroscopic (right anterior oblique [RAO] and left anterior oblique [LAO]) views of the esophagus during catheter ablation of atrial fibrillation. Barium paste was given to the patient just before initiation of sedation for real-time visualization of the esophagus (*arrowheads*) during the ablation procedure. The ring (*Lasso*) and ablation (*Abl*) catheters are positioned at the ostium of the left superior PV. CS, Coronary sinus.

after the initial barium swallow. However, to avoid the risk of aspiration, patients should receive little or no sedation before swallowing the barium. The ablation procedure can also be performed with the patient under general anesthesia with orotracheal intubation and esophagography during the procedure. General anesthesia guarantees enough esophageal immobilization because the swallow reflex is abolished. Placement of an orogastric tube to allow esophageal localization is carried out before anticoagulation to avoid any risk of trauma and bleeding. At the end of the procedure, the contrast is totally removed. This technique allows visualization of the esophagus position in real time. However, the use of nasogastric tubes can potentially increase the risk of esophageal injury by pressing the anterior esophageal wall against the LA posterior wall.

Mechanical Displacement of the Esophagus

When ablation cannot be performed in certain LA regions because of proximity of the ablation site to the esophagus, mechanical displacement of the esophagus to the contralateral side from the ablation catheter by an endoscope has been suggested to facilitate safe energy delivery. However, the risk of esophageal perforation by the endoscope should be recognized, and the safety of this strategy needs to be determined before implementation into general clinical practice. Furthermore, apparent displacement of the esophagus with an endoscope can potentially represent mere distortion rather than anatomical displacement. In addition, the presence of the endoscope probe can increase the diameter of the esophagus and increase its contact with the posterior LA wall, rendering it more vulnerable to injury.

Luminal Esophageal Temperature Monitoring

Thermal monitoring of the esophagus during ablation is the most widely applied method for prevention of esophageal injury. Measurement of esophageal temperature involves the placement of a monotherm temperature probe, which is advanced under fluoroscopy guidance to the lower third of the esophagus directly posterior to the LA. This technique requires general anesthesia to allow tolerability of the esophageal probe. Adjustment of the position of the temperature probe during ablation to keep the probe in close vicinity to the ablation catheter tip is crucial to obtain reliable information on the real current esophageal temperature. The use of a multithermocouple temperature probe requires less manipulation since it can monitor a broader area of the esophagus simultaneously.

The role of esophageal temperature monitoring remains controversial. Discrepancies between the temperatures of the external and internal esophagus and thermal latency in heat transfer from the atrium to the esophagus can limit the utility of esophageal temperature monitoring. In addition, if the temperature sensor is not in contact with the esophageal wall, temperature changes may not be accurately detected. Also, because the esophagus is broad, a lateral position of the temperature probe may not align with the ablation electrode. The possibility of heating of the esophageal wall without recording a change in central luminal esophageal temperature can be harmful by providing a false sense of safety. In fact, atrioesophageal fistula formation occurred in the absence of changes in luminal esophageal temperature in the majority of patients in which temperature monitoring was reported. This can be confounded by the possibility that esophageal injury may be precipitated by injury to the esophageal vasculature with consequent remote esophageal necrosis, rather than direct thermal injury, which may not be heralded by monitoring of the luminal esophageal temperature.^{45,47}

Although studies demonstrated the absence of esophageal lesions in patients with a maximal esophageal luminal temperature lower than 41.8°C, the safety zone of temperature rise from baseline has not been

validated. It is also important to note that esophageal temperature can continue to increase for several seconds after discontinuation of RF delivery; thus energy application must be stopped as soon as there is any increase in esophageal temperature.

Despite monitoring of esophageal temperatures, esophageal lesions can occur in 10% to 30% of cases. It is worth noting that esophageal temperature monitoring of some form was performed in the vast majority of published cases of esophageal perforation, suggesting that the use of esophageal monitoring alone is insufficient for prevention of this complication.^{41,49}

Even more alarming, some studies have suggested that luminal esophageal temperature monitoring by itself might contribute to thermal injury of the esophagus during RF ablation. The metal thermistor electrodes of the esophageal temperature probes can potentially interact with the RF current and act as secondary antennas during RF energy delivery, so that inductive heating of stainless steel thermocouples of the esophageal probe itself can result in thermal injury to esophageal tissue.⁴²

Luminal esophageal temperature monitoring has also been utilized during cryoballoon PV isolation. In animal studies, evidence of esophageal injury was seen only below 10°C. Several studies showed that interrupting cryoapplication if the intraesophageal temperature falls to less than 12°C to 15°C was associated with the lowest incidence of esophageal injury, given that the esophageal temperature probe is positioned as close as possible to the inflated cryoballoon. In addition, rapid decline in luminal temperature when the esophagus is located in immediate proximity to the left inferior PV probably should prompt the termination of cryoenergy delivery. However, it is important to know that thermal esophageal injury, including atrioesophageal fistula formation, has been observed despite luminal esophageal temperatures higher than 20°C. Therefore a clear cutoff for a luminal esophageal temperature beyond which thermal damage can be prevented remains uncertain. Furthermore, some reports found that the use of esophageal temperature probes was associated with increased the risk of subclinical esophageal lesions on routine endoscopy following cryoballoon ablation.^{43,48,50}

Limiting Ablation Energy

Modifying RF application parameters at sites close to the esophagus is the most widely used strategy to avoid atrioesophageal fistula formation. Limiting the power and duration of RF applications, particularly in the posterior LA, even if a significant reduction in bipolar electrogram amplitude is not recorded, can be the most important safety consideration for avoidance of fistula formation. Although no data exist on which to make specific recommendations, there is widespread agreement that prolonged RF applications in the posterior LA are to be avoided, and that low power settings should be used. When standard RF energy is to be applied close to the esophagus, the RF power is typically reduced to 20 to 30 W and 55°C for no more than 20 seconds. When using open-irrigated RF ablation, lower energy outputs (15 W compared with 25 W) were found to be associated with a decreased rate of esophageal ulcerations. Also, direct perpendicular orientation of the ablating electrode and forward pressure against the posterior LA wall are better avoided, particularly if an 8-mm or irrigated electrode is used. It is preferable to maintain frequent movements of the ablation catheter when RF energy is applied at the posterior LA wall in the vicinity of the esophagus. The impact of using contact force-sensing ablation catheters is not known, but it is worth noting that the number of reported atrioesophageal fistula cases has increased since the introduction of contact force technology. The optimal contact force setting and energy output in the posterior wall of the LA to help maximize safety while enhancing long-term efficacy of AF ablation procedures is yet to be determined.⁴⁷

The value of limiting the duration of RF application without energy output reduction for prevention of ulcerations remains to be evaluated. Although many investigators recommend using lower power settings for longer periods of time (25 W for 20 to 30 seconds), some investigators suggest that short RF applications (for 2 to 5 seconds) at a higher power (50 W, irrigation rate 30 mL/min, maximum temperature 43°C) result in momentarily higher LA tissue temperatures and allow the tip to be set at a high power to injure the superficial tissue while minimizing time-dependent deep heating through excessive heat transfer. The latter approach can compromise lesion efficacy because the time-dependent variable of “total heat transferred” is decreased. Typically the ablation catheter is dragged continuously in small increments every 2 to 5 seconds during continuous RF delivery, and ablation is repeated at each site, if required, for many times throughout the procedure until the local atrial electrogram is completely eliminated. It is probably reasonable to allow at least 2-minute time intervals before returning to ablate a previously ablated site to allow for heat dissipation and complete cooling of potential esophageal heating.

Of note, using light conscious sedation during the procedure can allow the use of pain as an indicator for potential esophageal injury; RF application should be interrupted promptly and the catheter moved to a different site on the development of significant or sharp pain during energy delivery.

During cryoballoon ablation, it is recommended to terminate cryoapplication if excessive freezing is observed, as indicated by rapid descent to less than -40°C within 30 seconds of freezing or nadir temperatures less than -55°C during ablation. Limiting the maximal cryoapplication time to 180 seconds may also help reduce the risk of esophageal injury.

Prophylactic Proton Pump Inhibitors

The value of routine prophylactic administration of proton pump inhibitors after AF ablation to reduce the risk of fistula formation is unknown. However, this therapy is commonly offered to patients in whom esophageal lesions are detected by endoscopy or capsule endoscopy following the procedure.

RADIATION EXPOSURE

Ionizing radiation (such as x-ray) is radiation that has enough energy to remove electrons from atoms or molecules when it passes through matter. The loss of an electron causes the atom (or molecule) to become positively charged (ionized). In contrast, the energy of microwave, infrared, and ultraviolet radiation is not enough to remove electrons and, thus, those types radiation are considered nonionizing.

Biological Effects of Ionizing Radiation

The biological effects of ionizing radiation can be described in terms of *deterministic* (tissue damage) and *stochastic* effects (genetic changes and resultant carcinogenesis).

The *stochastic* effects are effects for which the probability of occurring is proportional to the dose of radiation exposure but there is no identifiable threshold for producing the effect, and its severity is independent of the dose (i.e., nonthreshold function of the dose; eFig. 32.4). Radiation-related malignancy is a stochastic risk, and can occur even with minimum dose of radiation, but likelihood of occurring increases with increasing radiation dose. The stochastic mechanism represents an unpredictable, unrepaired radiation damage to the DNA of a limited, potentially single, number of viable cells.

The *deterministic* effect is a dose-dependent direct biological effect of radiation, typically associated with a threshold dose above which tissue damage occurs and the severity increases with increasing dose (see eFig. 32.4). Below the threshold radiation exposure, the probability

of causing harm is zero. The deterministic effect occurs when a significant, predictable number of existing cells are sufficiently damaged to cause a directly observable injury. Radiation-induced skin injury (threshold, 2 to 3 Gy) is a deterministic effect.^{51,52}

Nomenclature of Radiation Quantities and Units

Modern radiographic imaging systems provide several measurements of the amount of radiation exposure during procedures. The radiation dose is related to the damage inflicted on the body and is usually described in terms of the following parameters: the absorbed dose, the equivalent dose, the effective dose, or the collective dose.

Fluoroscopy Time

Fluoroscopy time (in minutes) is the time during a procedure that fluoroscopy is used, but does not include cine acquisition imaging. In addition, patient body habitus has a dramatic effect on actual dose (see below) despite similar values of simple fluoroscopy time. Therefore fluoroscopy time alone is not a useful descriptor of patient radiation dose.

Air Kerma

Air kerma represents the “kinetic energy released per unit mass” when an x-ray beam is traveling through air at a specific point, and it is how the intensity (strength) of the x-ray beam is characterized. Air kerma is expressed in grays (Gy). The total air kerma is the procedural cumulative air kerma, and is used to monitor patient dose burden as it is associated with threshold-dependent deterministic skin effects. Air kerma does not address the extent (area) of the x-ray beam.

The “kerma area product” (KAP), also known as the “dose area product” (DAP), is reported in $\text{Gy}\cdot\text{cm}^2$, as the average air kerma (in Gy) multiplied by the corresponding x-ray beam cross-sectional area (in cm^2). The KAP can be used to estimate organ doses, effective doses, and the total energy deposited in the patient and is therefore directly related to the total patient stochastic risk. Converting KAP into accurate patient dose estimates requires explicit information on the x-ray beam quality, the size and age of the exposed patient, and data on the body region exposed and exposure geometry (projections and field sizes).

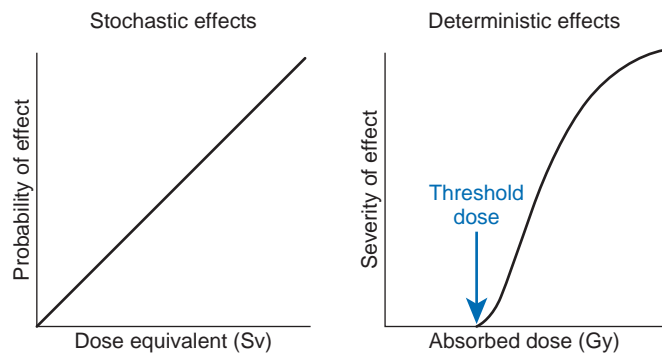
Peak Skin Dose

Peak skin dose (in Gy) is the maximum radiation dose received by any local patient skin area. Both the probability and severity of skin effects increases as peak skin dose increases. Peak skin dose is highly dependent upon instantaneous dose rate, and the duration that the x-ray is directed at a specific body area. There is no currently available method to measure peak skin dose, but it can be estimated (by a physicist) when the air kerma and x-ray geometry details are known.

Absorbed Dose

The absorbed dose is the radiation energy absorbed per unit mass of an organ or tissue. The absorbed dose describes the intensity of the energy deposited in any small amount of tissue located anywhere in the body, and is used to assess the potential for damage to a particular organ or tissue. The unit is joule per kilogram (J/kg), which is assigned the special name “Gray” (Gy), thus replacing the units of “rad” (short for “radiation absorbed dose”). One hundred rad equals 1 joule/kilogram (J/kg), which also equals 1 Gy.

The absorbed dose is a measure of the actual energy deposited in the irradiated tissue and can be used to compare against deterministic effects, but it is not satisfactory for comparing the stochastic radiological risk. To estimate the stochastic risk, the type of radiation and the sensitivity of the irradiated tissues must be considered. The dose quantities *equivalent dose* and *effective dose* were devised to calculate the biological effect of an absorbed dose.



eFig. 32.4 Risk of Deterministic and Stochastic Effects of Ionizing Radiation.

Equivalent Dose

The equivalent dose addresses the impact that the type of radiation has on that tissue, and is defined as the absorbed radiation dose in an organ or tissue corrected by a radiation weighting factor. The equivalent dose takes into account the different probability of effects that occur when the same amount of absorbed dose is delivered by different types of radiation (alpha particles, electrons, and photons). This correction factor is numerically 1 for x-rays, and the unit is J/kg and is given the special name “Sievert” (Sv), which replaced the units of “rem” (short for “roentgen equivalent in man”; 1 Sv = 100 rem).

The equivalent dose is used to assess how much biological damage is expected from the absorbed dose of certain type of radiation. Because all radiation used in diagnostic medicine has the same low-harm potential, the equivalent dose in Sv is numerically equal to the absorbed dose in Gy.

Effective Dose

The effective dose takes three factors into account: (1) the absorbed dose to all organs or tissues of the body; (2) the relative harm level of the radiation; and (3) the radiosensitivity of each organ or tissue. As different organs or tissues exhibit different sensitivities to radiation, the equivalent dose is multiplied by the appropriate tissue weighting factors (i.e., the sensitivity factors assigned to specified tissues and organs). The tissue weighting factors summate to 1.0, so that if an entire body is radiated with uniformly penetrating external radiation, the effective dose for the entire body is equal to the equivalent dose for the entire body. When only part of the body is irradiated, then only those regions are used to calculate the effective dose. The sum of effective doses to all organs and tissues of the body represents the effective dose for the whole body.

The *effective dose* is used to assess patient stochastic risk (i.e., the long-term risk of radiation-induced cancer and genetic effects). The effective dose is not intended as a measure of *deterministic* health effects, which is measured by the quantity *absorbed dose*. Further, the effective dose is not intended to apply to a specific patient; rather, it relates to the overall long-term risk to a person from a procedure and is useful for comparing risks from different procedures. This unit is widely used to estimate the ionizing radiation exposure to patients and staff during procedures. The unit is the joule per kilogram (J/kg) and is given the special name sievert (Sv).⁵³

Exposure to Ionizing Radiation During Electrophysiology Procedures

Ionizing radiation exposure related to natural sources is relatively minimal, whereas nowadays, medicine-related exposure is considered a major exposure source. Fluoroscopic guidance remains the standard tool for catheter visualization in interventional cardiac and EP procedures, and cardiologists are among the leading users of medical radiation. In fact, interventional cardiology accounts for almost 40% of the entire cumulative radiation dose to the US population from all medical sources, excluding radiotherapy. Moreover, data suggest that the occupational radiation exposure to interventional cardiologists and cardiac electrophysiologists is the greatest registered by any medical staff exposed to x-rays.⁵¹

Radiation exposures during the different cardiac interventional procedures are highly variable. In general, the average radiation exposure to patients is estimated at 2.5 mSv for diagnostic cardiac catheterization, 6.4 mSv for percutaneous coronary interventions, 3.2 mSv for diagnostic EP study, and 4.4 mSv for SVT ablation. Catheter ablation of complex cardiac arrhythmias, including AF, macroreentrant ATs, and reentrant VTs, can be associated with markedly prolonged fluoroscopy durations and radiation exposure (Table 32.2). In addition, the same patient often

TABLE 32.2 Exposure to Ionizing Radiation During Electrophysiology Procedures

Type of Electrophysiology Procedure	Exposure to Patient in mSv: Median (Range)
Diagnostic electrophysiology study	3.2 (1.3–23.9)
Supraventricular tachycardia (AVNRT, AVRT, AT) ablation procedure	4.4 (1.6–25)
Atrial fibrillation ablation	16.6 (6.6–59.6)
Ventricular tachycardia ablation	12.5 (3 to >45)
CIED pacemaker or ICD implant	4 (1.4–17)
CRT-CIED implant	7 (2.0–16)

AT, Atrial tachycardia; AVNRT, atrioventricular nodal reentrant tachycardia; AVRT, atrioventricular reentrant tachycardia; CIED, cardiac implantable electronic device; CRT, cardiac resynchronization therapy; ICD, implantable cardioverter defibrillator.

From Nair GM, Nery PB, Redpath CJ, Sadek MM, Birnie DH.

Radiation safety and ergonomics in the electrophysiology laboratory: update on recent advances. *Curr Opin Cardiol*. 2016;31:11–22.

requires different or repeated procedures, increasing the radiation exposure and risk. The use of CT scanning before and after AF ablation procedures further increases patient exposure to radiation. Typical effective dose estimates are 7.0 mSv for a standard chest CT, 16 mSv for cardiac CT, and 0.1 mSv for a chest x-ray.

Compared with patients, operators and laboratory staff get exposed to much smaller amounts of radiation during each procedure, but are exposed repeatedly, resulting in potentially substantial lifetime occupational radiation doses. In fact, the occupational radiation exposure to interventional cardiologists is estimated at 5 mSv (which is equivalent to 250 chest x-rays), which is two to three times higher than that of diagnostic radiologists. Operator exposure is expressed as equivalent dose for organ-specific exposure and effective dose for whole-body exposure. The effective dose represents the sum of equivalent doses from different tissues, adjusted to the radiation sensitivity of each tissue.^{51,54}

Clinical Presentation

Exposure to ionizing radiation can adversely impact both the patient and the medical personnel and expose them to an increased risk of radiation-related injuries. Even low doses appear to be potentially harmful, particularly in women, children, and young adults.

Radiation-Induced Skin Injury

In EP procedures, the patient tissue receiving the greatest radiation dose is the skin area of the back at the entrance point of the x-ray beam, and skin injuries are well-recognized complications for catheter ablation procedures.

The response of the skin to radiation is dose related. The thresholds for dose or time of appearance of radiation-induced skin changes are variable, depending on the individual patient's radiosensitivity. Several conditions can increase radiation sensitivity, including autoimmune and connective tissue disorders, obesity, hyperthyroidism, diabetes, ataxia telangiectasia, and a number of drugs (e.g., doxorubicin, 5-fluorouracil, and methotrexate).⁵³

For most patients, the lowest dose that may produce a noticeable skin changes is 2 Gy, which can manifest transient skin erythema and epilation, which usually occurs within hours of exposure and fades after 24 hours. When the absorbed skin dose exceeds 6 Gy, a second



Fig. 32.12 Acute Radiation-Induced Skin Injury (Erythema) 2 to 3 Weeks Following Radiofrequency Ablation of Atrial Fibrillation Using Biplane Fluoroscopy. The affected areas have well-defined borders congruent with the entrance of the x-ray beam.

hyperemic phase (main erythema) can develop after several days and fade away over a period of weeks. This usually manifests as erythematous and edematous skin, with burning, tenderness, and itching (Fig. 32.12). At higher doses, progressively more severe dose-dependent skin damage can manifest as hyperpigmentation, dry desquamation, skin blisters, and ischemic dermal necrosis. Chronic radiation injury manifests months to years after exposure and presents clinically as permanent erythema, dermal atrophy, and ulceration. Of note, skin cancer directly related to radiation from an interventional procedure has not been reported.

The diagnosis of radiation-induced skin injury is often delayed. Acute radiation-induced skin injury (characterized by erythema with vesiculation, erosion, and pain) can be misdiagnosed as contact dermatitis, viral or bacterial infection, or insect bite, and the history of fluoroscopy often is overlooked or considered irrelevant. Therefore a high index of suspicion is required. Characteristically, fluoroscopy-induced skin injuries affect an area congruent to the entrance of the x-ray beam that typically has well-defined borders (see Fig. 32.12), which occur when the beam is not moved or resized during prolonged fluoroscopy over one site. It is important to alert patients who have undergone prolonged procedures, or are known to have received a high skin radiation dose, to examine themselves about 2 to 3 weeks after the procedure to look for skin changes, contacting the physician if any are observed.

Skin biopsy usually is not necessary and not recommended, especially given the potential risk of a nonhealing ulcer at the site of biopsy in the radiation-damaged skin area. Furthermore, the findings on skin biopsy generally are not specific for radiation injury.

Radiation-Induced Cataract

The lens is a highly radiosensitive tissue, and an association between cataracts and radiation exposure has been well established and has been demonstrated among staff involved in interventional procedures using x-rays.

Ionizing radiation typically causes posterior subcapsular cataract formation. This type of cataract is uncommon but can also develop secondary to diabetes or systemic corticosteroids. Age-related cataracts, in contrast, are cortical or nuclear. Cataracts cause impairment of visual acuity, sensitivity to glare, and slow light-dark adaptation.

Radiation-induced cataractogenesis has traditionally been considered a deterministic tissue reaction and thus requires a threshold radiation dose (0.5 Gy) and damage to multiple cells. However, recent evidence suggests that cataracts may form stochastically, without a threshold dose.^{55,56}

Radiation-Induced Cardiovascular Disease

Cardiovascular radiation effects include focal myocardial degeneration and fibrosis and accelerated arterial atherosclerosis, which can lead to ischemic heart disease and cardiomyopathy. Although uncertainty remains, cardiovascular radiation effects have been reported to occur at doses greater than 0.5 Gy.⁵⁵

Radiation-Induced Carcinogenesis

The absolute risk of fatal cancer increases by 0.05% for every 10 mSv of exposure over and above the background fatal cancer risk of 20%. An effective dose of 15 mSv is associated with an excess cancer risk of 1 per 750 men older than 50 years, with half the cancers being fatal. The risk of stochastic effects is not a great concern for older patients because of the latency period (10 years or more) for the development of most cancers. The risk, however, is fourfold higher in children, who have longer life expectancies.⁵⁷

Ionizing radiation is one of the few established causes of brain tumors. Increased risk of skin cancer, breast cancer, and leukemias had been linked to high occupational doses before 1950, when knowledge of the effects of radiation exposure was still developing and before modern radiation safety practices were common.^{55,58}

Prevention

Reduction of Radiation Exposure

Radiation safety is the responsibility of all health care professionals working in an x-ray producing environment. Understanding adverse effects of radiation exposure and formal education and training on radiation safety and management are essential for minimizing the adverse impact of radiation exposure on patients as well as medical personnel. A policy to reduce exposure to ionizing radiation to a level that is “as low as reasonably achievable” (ALARA) for medical necessity has recently been adopted by occupational health groups. No amount of radiation can be considered safe; thus there should not be any exposure to ionizing radiation without the expectation of an overall benefit from the activity causing the exposure.^{51,58,59}

An important step to reduce fluoroscopy exposure is to optimize setting of the fluoroscopy system, such as x-ray beam collimation, frame rate, protocol setting, and system angulation, detector sensitivity and distance, and signal filtering. In addition, optimizing permanent and temporary shielding, correct use of personal protective equipment, optimal positioning of both the patient and the operator, and operator behavior modification during the procedure are essential for reducing exposure to ionizing radiation. Several strategies have been recommended to optimize patient radiation dose and to minimize occupational injury to staff in the EP laboratory (Boxes 32.1 and 32.2).^{54,57}

Recent technologies, such as low-exposure radiographic imaging, improved radiographic imaging protection systems, nonfluoroscopic navigation and mapping systems, contact force-sensing catheters, and remote navigation systems have allowed for a marked reduction in ionizing radiation exposure in the EP laboratory. With the assistance of novel technologies, strategies to perform EP procedures zero or near-zero fluoroscopy are being increasingly adopted.^{51,60–62}

Radiation Dosimetry

Personal dosimetry for all staff employed is required for radiation surveillance in an area utilizing ionizing radiation, including the EP

BOX 32.1 Practical Advice to Reduce Patient Radiation Exposure

- Use a low-dose-rate fluoroscopy mode when possible.
- Use a low-pulse-rate fluoroscopy mode when possible.
- Remove the grid when performing procedures on small children.
- Use the lowest-dose mode for image (cine) acquisition that is compatible with the required image quality.
- Minimize fluoroscopy time: use fluoroscopy only to guide devices and observe motion.
- Use the last-image-hold image for review when possible, instead of using fluoroscopy.
- When possible, store a fluoroscopy loop instead of performing a cine run.
- If available, use a stored fluoroscopy loop for review instead of using fluoroscopy.
- Minimize the number of cine series.
- Minimize the number of frames per cine series.
- Never use cine as a substitute for fluoroscopy.
- Collimate the radiation beam to the area of interest.
- Use virtual collimation if it is available.
- Use wedge filters when they are appropriate.
- Keep the image detector (image intensifier or flat detector) as close as possible to the patient.
- Keep the patient as far as possible from the x-ray tube.
- Try to avoid steeply angulated projections (especially left anterior oblique cranial).
- Try to vary the C-arm angulation slightly to avoid concentrating the radiation dose at a single site on the patient's skin.
- Use magnification only when necessary.
- Remember that for large patients, and also for steeply angulated projections, the dose to the patient increases substantially.
- Pay attention to the patient radiation dose display in the procedure room.
- If the patient has had previous similar procedures, try to obtain information about the previous radiation doses to optimize subsequent procedures.

From Cousins C, Miller DL, Bernardi G, et al. ICRP publication 120: radiological protection in cardiology. *Ann ICRP*. 2013;42:1–125.

laboratory. The International Commission on Radiological Protection (ICRP) recommendations suggest two personal dosimeters: one worn under the personal protective lead garment at the level of the waist and the second worn at the thyroid collar outside the protective garment that provides information regarding radiation exposure to the brain and eye.⁵⁴

Periodic audits and feedback to operators, along with review of EP laboratory radiation protection equipment, are mandated. The World Health Organization recommends investigation of high occupational dose whenever the effective operator dose exceeds 0.5 mSv/month, the lens equivalent dose exceeds 5 mSv/month, or the extremity equivalent dose exceeds 15 mSv/month. ICRP has established a 100 mSv 5-year limit of whole-body effective dose and a 50 mSv limit in any single year. Dose equivalents should not exceed 20 mSv per year for the lens (averaged over 5 consecutive years) and 500 mSv per year for skin, hands, and feet.⁵⁴

A clear dose limit for exposure has not been applied to patients undergoing procedures. In general, the radiation dose for an individual patient should not be a reason to terminate a procedure. However, high values of patient doses (DAP >500 Gy·cm², total air kerma >5 Gy, or fluoroscopy time >60 minutes) should prompt surveillance for skin injuries. Appropriate actions should be taken to inform the patient and provide him with follow-up instructions to notify the operator or a

BOX 32.2 Practical Advice to Reduce Staff Radiation Exposure

- Increase your distance from the patient (the source of scatter radiation) whenever possible. This is obviously only possible when angiographic runs are not performed by hand. Scatter radiation levels decrease drastically with increased distance from the irradiated volume of the patient.
- Try to position yourself in a low scatter area. Scattered radiation is higher at the x-ray-tube side of the gantry and lower on the side of the image receptor.
- Use a ceiling-suspended shield, a table-suspended screen, and other protective shielding (e.g., a lead apron, thyroid collar, and leaded glasses with side shields) whenever possible.
- The ceiling-suspended shield should be placed as close to the patient as possible.
- If biplane systems are used, proper use of lateral shields is very important for eye protection.
- When appropriate, use a dose reduction pad or drape at the catheter entrance site to reduce your hand dose.
- Minimize the use of fluoroscopy and use low-dose fluoroscopy modes (e.g., low-dose-rate pulsed fluoroscopy) when possible.
- Minimize the number of cine series and the number of frames in each cine series.
- Use magnification as little as possible.
- Collimate the x-ray beam as tightly as possible.
- Avoid direct exposure of the hands to primary radiation.
- Obtain appropriate training in radiation management and radiation protection.
- Wear your dosimeters and know your own dose.
- In addition, a final general concept: reduce the patient's radiation dose and you will also reduce your own dose.

From Cousins C, Miller DL, Bernardi G, et al. ICRP publication 120: radiological protection in cardiology. *Ann ICRP*. 2013;42:1–125.

medical physicist if deterministic effects to the irradiated skin area are noted during self-examination.⁵⁴

VIDEOS

The following videos accompany this chapter:

Video 32.1. Pericardiocentesis: Guided by Fluoroscopy

Video 32.2. Pericardiocentesis: Guided by Echocardiography

Video 32.3. Intrapericardial Thrombus: Fluoroscopy and Echocardiography

See Video 15.5. Right Superior Pulmonary Vein Occlusion: Transesophageal Echocardiography (TEE) Before and After Stenting

See Video 15.6. Right Superior Pulmonary Vein Occlusion: Computed Tomography (CT) Before and After Stenting

See Video 15.7. Pulmonary Vein Stenting

See Video 15.8. Atrioesophageal Fistula: Computed Tomography (CT)

See Video 15.9. Pneumopericardium: Computed Tomography Scan of the Chest

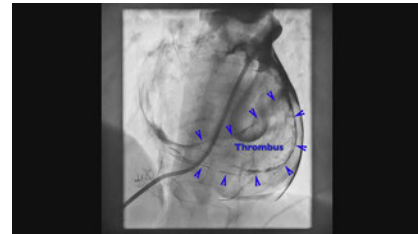
REFERENCES

1. Sharma PS, Padala SK, Gunda S, et al. Vascular complications during catheter ablation of cardiac arrhythmias: a comparison between vascular ultrasound guided access and conventional vascular access. *J Cardiovasc Electrophysiol*. 2016;27:1160–1166.

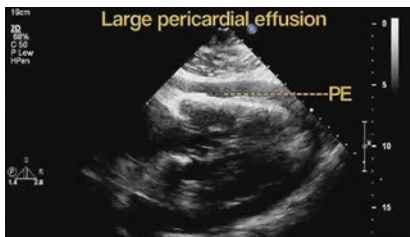




Video 32.1 Pericardiocentesis: Guided by Fluoroscopy. Sequence of events in a patient who developed a large pericardial effusion during ablation of atrial fibrillation. Fluoroscopy at baseline (left anterior oblique [LAO] projection) demonstrates normal cardiac silhouette motion in the absence of pericardial effusion. Normal excursion of the lateral cardiac border is also visualized immediately after atrial septal puncture. Decreased excursion of the lateral cardiac border becomes evident later in the procedure secondary to development of a large pericardial effusion. Pericardiocentesis is performed under fluoroscopy guidance. The pericardial needle is advanced in the subxiphoid region toward the inferior cardiac border in the LAO fluoroscopic projection. Injection of contrast through the needle confirms the location of the tip in the pericardial space, as evident with layering of the contrast within the pericardial effusion. A pigtail catheter is inserted in the pericardial space. Contrast injection via this catheter demonstrates the size of the pericardial effusion. Note that cardiac border movement is now evident within the standstill silhouette of the pericardial effusion.



Video 32.3 Intrapericardial Thrombus: Fluoroscopy and Echocardiography. Pericardiocentesis via the subxiphoid approach is performed in a patient with cardiac perforation during catheter ablation, resulting in large pericardial effusion and cardiac tamponade. Contrast pericardiography is performed via the pericardial drain, demonstrating a large pericardial effusion and a large thrombus. Transthoracic echocardiography revealed a large intrapericardial thrombus overlying the left ventricle (LV).



Video 32.2 Pericardiocentesis: Guided by Echocardiography. Transthoracic echocardiography is utilized to guide pericardiocentesis in a patient who developed a large pericardial effusion (PE) during ablation of atrial fibrillation. A moderately large PE is visualized on the four-chamber apical and long-axis echocardiographic view. The pericardiocentesis needle (not visualized) is advanced from the precordial region under the guidance of transthoracic echocardiography. Access to the pericardial space is confirmed by injection of agitated saline through the needle, which is visualized on echocardiography as a dense shower of bubbles. After pericardiocentesis, only a trivial pericardial effusion is observed.

2. Wiles BM, Child N, Roberts PR. How to achieve ultrasound-guided femoral venous access: the new standard of care in the electrophysiology laboratory. *J Interv Card Electrophysiol*. 2017;49:3–9.
3. Brass P, Hellmich M, Kolodziej L, et al. Ultrasound guidance versus anatomical landmarks for subclavian or femoral vein catheterization. *Cochrane Database Syst Rev*. 2015;(1):CD011447.
4. Michowitz Y, et al. Effects of sex on the incidence of cardiac tamponade after catheter ablation of atrial fibrillation results from a worldwide survey in 34943 atrial fibrillation ablation procedures. *Circ Arrhythm Electrophysiol*. 2014;7:274–280.
5. Baldinger SH, et al. Epicardial radiofrequency ablation failure during ablation procedures for ventricular arrhythmias: reasons and implications for outcomes. *Circ Arrhythm Electrophysiol*. 2015;8:1422–1432.
6. Bradfield JS, Tung R, Boyle NG, et al. Our approach to minimize risk of epicardial access: standard techniques with the addition of electroanatomic mapping guidance. *J Cardiovasc Electrophysiol*. 2013;24:723–727.
7. Tung R, et al. Epicardial ablation of ventricular tachycardia: an institutional experience of safety and efficacy. *Heart Rhythm*. 2013;10:490–498.
8. Lim HS, et al. Safety and prevention of complications during percutaneous epicardial access for the ablation of cardiac arrhythmias. *Heart Rhythm*. 2014;11:1658–1665.
9. Macias C, Shivkumar K, Tung R. Novel approach to intraprocedural cardiac tamponade: dual-site drainage with continuous suction. *Heart Rhythm*. 2016;13:2091–2094.
10. Gianni C, et al. Management of periprocedural and early pericardial effusions with tamponade following ablation of atrial fibrillation with uninterrupted factor Xa inhibitors: a case series. *J Cardiovasc Electrophysiol*. 2016;27:399–403.
11. Pedersen MEF, et al. Management of tamponade complicating catheter ablation for atrial fibrillation. *JACC Clin Electrophysiol*. 2016;3:367–373.
12. Yamada T, Kay GN. Recognition and prevention of complications during epicardial ablation. *Card Electrophysiol Clin*. 2010;2:127–134.
13. Killu AM, et al. Atypical complications encountered with epicardial electrophysiological procedures. *Heart Rhythm*. 2013;10:1613–1621.
14. Castao A, Crawford T, Yamazaki M, et al. Coronary artery pathophysiology after radiofrequency catheter ablation: review and perspectives. *Heart Rhythm*. 2011;8:1975–1980.
15. Garabelli PJ, Stavarakis S, Po SS. A case series and review of the literature regarding coronary artery complications associated with coronary sinus catheter ablation. *HeartRhythm Case Rep*. 2015;1:315–319.
16. Ernst S, Sanchez-Quintana D, Ho SY. Anatomy of the pericardial space and mediastinum: relevance to epicardial mapping and ablation. *Card Electrophysiol Clin*. 2010;2:1–8.
17. Reichlin T, et al. Early release of high-sensitive cardiac troponin during complex catheter ablation for ventricular tachycardia and atrial fibrillation. *J Interv Card Electrophysiol*. 2016;47:69–74.
18. Yamada T, et al. Idiopathic ventricular arrhythmias originating from the left ventricular summit anatomic concepts relevant to ablation. *Circ Arrhythm Electrophysiol*. 2010;3:616–623.
19. Lin CY, et al. Radiofrequency catheter ablation of ventricular arrhythmias originating from the continuum between the aortic sinus of Valsalva and the left ventricular summit: electrocardiographic characteristics and correlative anatomy. *Heart Rhythm*. 2015;13:111–121.
20. Hutchinson MD, Garcia FC. An organized approach to the localization, mapping, and ablation of outflow tract ventricular arrhythmias. *J Cardiovasc Electrophysiol*. 2013;24:1189–1197.
21. Nagashima K, et al. Ventricular arrhythmias near the distal great cardiac vein challenging arrhythmia for ablation. *Circ Arrhythm Electrophysiol*. 2014;7:906–912.
22. Jauregui Abularach ME, et al. Ablation of ventricular arrhythmias arising near the anterior epicardial veins from the left sinus of Valsalva region: ECG features, anatomic distance, and outcome. *Heart Rhythm*. 2012;9:865–873.
23. Chugh A, et al. Manifestations of coronary arterial injury during catheter ablation of atrial fibrillation and related arrhythmias. *Heart Rhythm*. 2013;10:1638–1645.
24. Chatterjee NA, et al. Atrioventricular nodal ablation in atrial fibrillation: a meta-analysis and systematic review. *Circ Arrhythm Electrophysiol*. 2012;5:68–76.
25. Johnsrude C. Cryoablation of focal tachycardia originating from the right atrial free wall during upstream phrenic pacing to avoid phrenic nerve injury. *Pacing Clin Electrophysiol*. 2015;38:120–128.
26. Jacobson JT, Kraus A, Lee R, et al. Epicardial/endocardial sinus node ablation after failed endocardial ablation for the treatment of inappropriate sinus tachycardia. *J Cardiovasc Electrophysiol*. 2014;25:236–241.
27. Rubenstein JC, Kim MH, Jacobson JT. A novel method for sinus node modification and phrenic nerve protection in resistant cases. *J Cardiovasc Electrophysiol*. 2009;20:689–691.
28. Fukumoto K, et al. Three-dimensional imaging and mapping of the right and left phrenic nerves: relevance to interventional cardiovascular therapy. *Europace*. 2013;15:937–943.
29. Ichihara N, et al. Prevalence and pre-procedural predictors associated with right phrenic nerve injury in electromyography-guided, second-generation cryoballoon ablation. *JACC Clin Electrophysiol*. 2016;2:508–514.
30. Huemer M, Wutzler A, Parwani AS, et al. Mapping of the left-sided phrenic nerve course in patients undergoing left atrial catheter ablations. *Pacing Clin Electrophysiol*. 2014;37, 1141–1149.
31. Kowalski M, Ellenbogen KA, Koneru JN. Prevention of phrenic nerve injury during interventional electrophysiologic procedures. *Heart Rhythm*. 2014;11:1839–1844.
32. Mondésert B, et al. Clinical experience with a novel electromyographic approach to preventing phrenic nerve injury during cryoballoon ablation in atrial fibrillation. *Circ Arrhythm Electrophysiol*. 2014;7:605–611.
33. Franceschi F, et al. Electromyographic monitoring for prevention of phrenic nerve palsy in second-generation cryoballoon procedures. *Circ Arrhythm Electrophysiol*. 2015;8:303–307.
34. Kumar S, et al. Epicardial phrenic nerve displacement during catheter ablation of atrial and ventricular arrhythmias. *Circ Arrhythm Electrophysiol*. 2015;8:896–904.
35. Ibarra-Cortez SH, et al. Strategies for phrenic nerve preservation during ablation of inappropriate sinus tachycardia. *Heart Rhythm*. 2016;13:1238–1245.
36. Teunissen C, et al. Incidence of pulmonary vein stenosis after radiofrequency catheter ablation of atrial fibrillation. *JACC Clin Electrophysiol*. 2017;3:589–598.
37. Narui R, et al. Incidence and factors associated with the occurrence of pulmonary vein narrowing after cryoballoon ablation. *Circ Arrhythm Electrophysiol*. 2017;10:e004588.
38. Matsuda J, et al. Pulmonary vein stenosis after second-generation cryoballoon ablation. *J Cardiovasc Electrophysiol*. 2017;28:298–303.
39. Dukkupati SR, et al. Pulmonary vein isolation using the visually guided laser balloon a prospective, multicenter, and randomized comparison to standard radiofrequency ablation. *J Am Coll Cardiol*. 2015;66:1350–1360.
40. Kumar N, et al. Pulmonary vein stenosis after laser balloon ablation for atrial fibrillation. *JACC Clin Electrophysiol*. 2015;1:220–221.
41. Barbhuiya CR, et al. Global survey of esophageal injury in atrial fibrillation ablation. *JACC Clin Electrophysiol*. 2016;2:143–150.
42. Müller P, et al. Higher incidence of esophageal lesions after ablation of atrial fibrillation related to the use of esophageal temperature probes. *Heart Rhythm*. 2015;12:1464–1469.
43. Fürnkranz A, et al. Reduced incidence of esophageal lesions by luminal esophageal temperature-guided second-generation cryoballoon ablation. *Heart Rhythm*. 2015;12:268–274.
44. Neven K, Metzner A, Schmidt B, et al. Two-year clinical follow-up after pulmonary vein isolation using high-intensity focused ultrasound (HIFU) and an esophageal temperature-guided safety algorithm. *Heart Rhythm*. 2012;9:407–413.
45. Syed FF, Oral H. Esophageal temperature and atrioesophageal fistula: ‘If you cannot measure it, you cannot control it’. *Heart Rhythm*. 2016;13:2201–2202.

46. Halbfass P, et al. Progression from esophageal thermal asymptomatic lesion to perforation complicating atrial fibrillation ablation: a single-center registry. *Circ Arrhythm Electrophysiol*. 2017;10:1–11.
47. Black-Maier E, et al. Risk of atrioesophageal fistula formation with contact force-sensing catheters. *Heart Rhythm*. 2017;14:1328–1333.
48. John RM, Kapur S, Ellenbogen KA, et al. Atrio-esophageal fistula formation with cryo-balloon ablation is most commonly related to the left inferior pulmonary vein. *Heart Rhythm*. 2016;14:184–189.
49. Eitel C, et al. Successful nonsurgical treatment of esophagopericardial fistulas after atrial fibrillation catheter ablation: a case series. *Circ Arrhythm Electrophysiol*. 2013;6:675–681.
50. Miyazaki S, et al. Gastric hypomotility after second-generation cryoballoon ablation—unrecognized silent nerve injury after cryoballoon ablation. *Heart Rhythm*. 2017;14:670–677.
51. Gaita F, Guerra PG, Battaglia A, et al. The dream of near-zero x-rays ablation comes true. *Eur Heart J*. 2016;37:2749–2755.
52. Badawy MK, Deb P, Chan R, et al. A review of radiation protection solutions for the staff in the cardiac catheterisation laboratory. *Heart Lung Circ*. 2016;25:961–967.
53. Nair GM, Nery PB, Redpath CJ, et al. Radiation safety and ergonomics in the electrophysiology laboratory: update on recent advances. *Curr Opin Cardiol*. 2016;31:11–22.
54. Christopoulos G, et al. Optimizing radiation safety in the cardiac catheterization laboratory. *Catheter Cardiovasc Interv*. 2016;87:291–301.
55. Elmaraezy A, et al. Risk of cataract among interventional cardiologists and catheterization lab staff: a systematic review and meta-analysis. *Catheter Cardiovasc Interv*. 2017;90:1–9.
56. Seals KF, Lee EW, Cagnon CH, et al. Radiation-induced cataractogenesis: a critical literature review for the interventional radiologist. *Cardiovasc Intervent Radiol*. 2016;39:151–160.
57. Cousins C, et al. ICRP publication 120: radiological protection in cardiology. *Ann ICRP*. 2013;42:1–125.
58. Parikh JR, et al. Potential radiation-related effects on radiologists. *AJR Am J Roentgenol*. 2017;208:595–602.
59. Nof E, et al. Reducing radiation exposure in the electrophysiology laboratory: it is more than just fluoroscopy times! *Pacing Clin Electrophysiol*. 2015;38:136–145.
60. Giaccardi M, et al. Near-zero x-ray in arrhythmia ablation using a 3-dimensional electroanatomic mapping system: a multicenter experience. *Heart Rhythm*. 2016;13:150–156.
61. Voskoboinik A, Kalman ES, Savicky Y, et al. Reduction in radiation dose for atrial fibrillation ablation over time: a 12-year single centre experience of 2344 patients. *Heart Rhythm*. 2017;14:810–816.
62. Lerman BB, et al. Fluoroless catheter ablation of atrial fibrillation. *Heart Rhythm*. 2017;14:928–934.

INDEX

A

Aberrancy, supraventricular tachycardia with, 779
versus in bundle branch reentrant ventricular tachycardia, 903

Aberration, 286. *see also* Bundle branch block
 acceleration-dependent, 290*f*
 persistence of, 292–293, 292*f*
 alternation during atrial bigeminy, 293, 288.e1*f*
 due to Ashman phenomenon, 287–289, 288*f*
 due to concealed conduction, 292–293
 due to concealed transseptal conduction, 291–293
 due to heart rate acceleration, 289
 due to premature excitation, 287, 287*f*
 phase 3, 286
 phase 4, 289
 premature ventricular complexes, 289.e1*f*
 in supraventricular tachycardia, persistence of, 291, 292*f*
 during tachyarrhythmias, perpetuation of, 291, 292*f*
 tachycardia-dependent, 289*f*

Ablation
 of atrial flutter, 359–372
 anticoagulation for, 359–361
 catheter positioning for, 361–362, 362*f*
 complications of, 371
 cryoablation, 364
 difficult cavotricuspid isthmus in, 363–364
 endpoints for, 364–365
 maximum voltage-guided technique, 363
 outcome of, 371–372
 radiofrequency, 360*f*, 362
 role of electroanatomic mapping systems, 363
 target of, 359, 361*f*
 technique for, 359–364
 of atrial tachycardia macroreentrant, 397–404
 of anterior mitral isthmus, 402, 405*f*
 atrial fibrillation after, 399
 endpoints for, 400
 left atrial macroreentry, 399
 of mitral isthmus, 399.e1*f*
 of mitral isthmus block, 402–404, 403*f*–404*f*, 402.e1*f*
 outcome of, 404
 overdrive suppression, 388
 perimitral left atrial macroreentry, 399
 perimitral macroreentrant, 401–404, 399.e1*f*
 of posterior mitral isthmus, 401–402
 right atrial macroreentry and, 398–399
 target of, 397–399
 technique of, 399–400
 termination of, 388
 transformation to different loop/tachycardia in, 388
 of atrioventricular nodal reentrant tachycardia, 591–597
 anatomical approach in, 591–593, 592*f*
 atrioventricular block after, 596

Ablation(Continued)

electroanatomic approach in, 591, 593, 593*f*, 593.e1*f*
 endpoints of, 595
 junctional rhythm after, 594–595, 594*f*–595*f*
 palpitations, 596
 radiofrequency energy delivery in, 593–594
 slow pathway, 596–597
 target of, 591
 technique of, 591–595
 of bypass tract, 660–674
 anterosseptal (superoparaseptal), 667–670
 electrophysiological criteria of, 663*b*
 endpoints of, 662–663
 epicardial, 672–673
 failed, causes of, 673–674, 673.e1*f*, 674.e1*f*
 left free-wall, 663–666
 midseptal, 667–670
 outcome of, 674
 posteroseptal (inferoparaseptal), 670–672
 right free-wall, 666–667
 target of, 660–661
 technique for, 661–662, 664*f*
 catheter. *see also* Catheter ablation
 of focal atrial tachycardia, 333
 of focal atypical tachycardia, 310–311
 for idiopathic focal ventricular tachycardia, 827
 of congenital heart disease, 973–974, 973*f*
 energy sources for, 206–237
 of focal atrial tachycardia, 333–337
 endpoints for, 335–337
 outcome of, 337
 of para-Hisian atrial tachycardias, 333–335, 335*f*
 target of, 333
 technique of, 333, 334*f*
 in idiopathic focal ventricular tachycardia, 843–854
 cryoablation, 854
 endpoints, 854
 outcomes of, 854
 target, 843, 844*f*
 technique, 843–854, 845*f*
 phrenic nerve function during, 1052–1054, 1053*f*, 1053*t*
 surgical, of atrial fibrillation, 454, 455*f*
 in ventricular tachycardia, 805–812
 complications of, 812
 of critical isthmus, of reentrant circuit, 805
 endpoints of, 810–811
 management after, 810–811
 in multiple inducible, 807
 outcome of, 811–812
 substrate-based, 805–807
 success and recurrence of, 811
 target of, 805–807
 technique for, 808–810, 810.e1*f*

Absolute refractory period, 9, 110

Absorbed dose, for radiation energy, 1062

Accelerated ectopic automatic rhythms, 57

Accelerated idioventricular rhythm, epidemiology and natural history of, 752

Acceleration, atrial overdrive pacing and, in paroxysmal supraventricular tachycardia, 714

Acceleration-dependent aberration, 290*f*

persistence of, 292–293, 292*f*

Acetylcholine-activated potassium current, 24*t*, 32–33, 26.e1*f*

in long QT syndrome, 979

Action potentials

amplitude of, 10

atrioventricular heterogeneity of, 7

definition of, 2–8

duration of, sodium channels in, 17

excitability and, 8

excitation-contraction coupling and, 12–13, 13*f*

fast response, 3–8

phases

early repolarization, 6

final rapid repolarization, 7

plateau, 6–7

rapid depolarization, 6

resting, 3–6

phases of

fast response potential, 3–8

reentry and, 67

slow response potential, 8

prolongation of, early afterdepolarizations and, 60–61

propagation of, 10–12. *see also* Conduction

gap junctions in, 48

potassium channels in, 19

safety factor for, 12

sodium channels in, 18

refractoriness and, 9

regional differences in, 3, 5*t*

regional heterogeneity of, 7

resting, 3–6

slow response, 8

phases of

diastolic depolarization, 8

slow depolarization, 8

triggered, 58–63, 58*f*. *see also* Triggered activity

ventricular regional heterogeneity of, 7–8

Activation mapping, 125–135

in arrhythmic right ventricular

cardiomyopathy (ARVC), 959, 959.e1*f*

of atrial flutter, 356

bipolar recordings in, 126–127

direction of local activation in, 127, 127.e1*f*

timing of local activation in, 126–127, 126*f*

catheters for, 129, 131*f*

in circumferential left atrial ablation, 496

direction of local activation in

from bipolar recordings, 127, 127.e1*f*

reference point for, 128, 130*f*

from unipolar recordings, 125, 126*f*

electrical reference point in, selection of, 128

electroanatomic, 161–169

activation map in, 166–167, 167*f*

anatomical reference in, 161

data acquisition in, 165–166

electrical reference in, 161–162

entrainment map in, 167–169, 168*f*

isochronal map, 167

- Activation mapping (*Continued*)
 limitations of, 169
 local activation time in, 162–165
 propagation map in, 167, 168*f*
 window of interest, 162, 163*f*–165*f*
 endocardial, 128–129
 epicardial, 128–129
 of fascicular ventricular tachycardia, 861–863
 filtering in, 125, 127*f*
 of focal atrial tachycardia, 330
 of focal tachycardias, 128–132, 130*f*, 132*f*–133*f*
 fundamental concepts of, 125–127
 goal of, defining, 128, 130*f*
 in idiopathic focal ventricular tachycardia, 837–840, 838*f*–839*f*
 in inappropriate sinus tachycardia, 553
 limitations of, 135
 of macroreentrant atrial tachycardia, 388, 396
 of macroreentrant tachycardias, 128, 130*f*, 132–135, 134*f*
 continuous electrical activity in, 134, 134.*elf*
 critical isthmuses in, 133, 143, 152
 mid-diastolic activity, 134–135, 134*f*
 in nonischemic dilated cardiomyopathy, 882
 P wave onset in, 128, 130*f*, 326.*elf*
 prerequisites, 127
 procedure for, 127–135
 QRS wave onset, 128, 130*f*
 timing of local activation in
 from bipolar recordings, 126–127, 126*f*, 128*f*–129*f*
 from unipolar recordings, 125, 126*f*
 unipolar recordings in, 125–126
 advantages of, 125
 direction of local activation in, 125, 126*f*
 disadvantages of, 126
 timing of local activation in, 125, 126*f*
 in ventricular tachycardia, 784–786, 804
 continuous activity of, 784–786, 785*f*
 limitations of, 786
 mid-diastolic activity of, 786, 786.*elf*
 technique of, 782*f*–783*f*, 784
- Activation sequence. *see* Atrial activation sequence
- AcuNav catheter, 194–195
- Acute anterior myocardial infarction, atrioventricular block and, 259
- Acute Coronary Artery Disease Defibrillator in Acute Myocardial Infarction Trial (DINAMIT), 755*t*–756*t*
- Acute inferior myocardial infarction, atrioventricular block and, 259
- Acute treatment, of atrial flutter, 344*f*
- Adenosine
 for atrial flutter, 348.*elf*
 automaticity and, 55
 challenge, for atrial flutter ablation, 364–365
 termination with, in paroxysmal supraventricular tachycardia, 713, 714*f*
- Adenosine testing, in bypass tract ablation, 663
- Adenosine-sensitive posterior septal atrioventricular (AV) bypass tract, 679.*elf*
- ADP-activated potassium current, 33
- Advanced Catheter Location Technology, 156
- Advanced mapping and navigation modalities, 155–205
 electroanatomic mapping as, 156–176
- AES mapping, during supraventricular tachycardia, 686
- AF. *see* Atrial fibrillation
- AFL. *see* Atrial flutter
- Afterdepolarizations
 definition of, 58
 delayed, 58–63, 58*f*–59*f*
 in arrhythmogenesis, 59–60
 ionic basis of, 58–59, 59*f*
 properties of, 60
 early, 58*f*, 60
 in arrhythmogenesis, 62–63
 ionic basis of, 60–62, 61*f*, 62.*elf*
 properties of, 63
- Age
 atrial fibrillation and, 434
 at diagnosis, of hypertrophic cardiomyopathy, 936
- AH interval. *see* Atrial-His bundle (AH) interval
- AH/HA ratio
 in fast-slow atrioventricular nodal reentrant tachycardia, 565
 in slow-fast atrioventricular nodal reentrant tachycardia, 564
 in slow-slow atrioventricular nodal reentrant tachycardia, 566
- Air embolism, 1047–1048
 arterial, 1047
 after atrial fibrillation ablation of, 524
 cerebral, 1047–1048, 1047.*elf*
 coronary, 1047.*elf*
 after transseptal puncture, 95
 venous, 1047
- Air kerma, for radiation energy, 1062
- Ajmaline
 in bypass tract, 608
 provocation, in Brugada syndrome, 1008, 1008*f*, 1009*t*, 1010, 1011*t*
- AKAP9, in long QT syndrome, 977*t*, 978–979
- Alcohol
 atrial fibrillation and, 438
 septal ablation, previous, in hypertrophic cardiomyopathy, 936
- Almokalant, 28
- Alternating bundle branch block, 299, 300*f*–301*f*
 during atrial bigeminy, 299
- Ambulatory cardiac monitoring
 for Chagas cardiomyopathy, 892
 for hypertrophic cardiomyopathy, 930
 for idiopathic focal ventricular tachycardia, 824
- Ambulatory electrocardiographic monitoring
 for catecholaminergic polymorphic VT, 1023
 in long QT syndrome, 990
 in sinus node dysfunction, 242–243
- Aminophylline, mechanism of action of, 33
- 4-Aminopyridine, mechanism of action of, 25
- Amiodarone
 for atrial fibrillation, 450, 452
 postoperative, 457
 for atrial flutter, 344–345
 atrioventricular block and, 258
 mechanism of action of, 28, 30, 33
 for nonischemic dilated cardiomyopathy, 873
 sinus node response to, 250
 for sustained ventricular tachycardia, 757
- Amplatzer Cardiac Plug, 535–537
 deployment of, 535, 535.*elf*
 outcome of, 535–537
 postoperative management of, 535
- Amplatzer Cardiac Plug (*Continued*)
 sizing of, 535
 specifications of, 535, 536*f*
- AN cells, 257
- Anatomical approach, in ablation, of
 atrioventricular nodal reentrant tachycardia, 591–593, 592*f*
- Anatomical course, of atriofascicular pathway, 687*f*
- Andersen-Tawil syndrome, 32, 258, 977*t*, 979, 985.
see also Long QT syndrome
 bidirectional VT in, 1024
versus catecholaminergic polymorphic VT, 1024
- Angiography
 pulmonary vein, 466, 466.*elf*
 three-dimensional rotational, 202–203
 clinical implications of, 203
 fundamental concepts of, 202
 imaging technique, 202–203
 integration of, 202, 202.*elf*
 limitations of, 203
- Anisotropic reentry, 66, 76–78
 cellular coupling and, 77
 gap junctions and, 77
 myocyte packing and tissue geometry and, 77
 unidirectional block and, 78–79
 uniform *versus* nonuniform anisotropy in, 77–78, 77*f*
- Ankyrin-B, in long QT syndrome, 977*t*, 980
- Ankyrin-B syndrome, 977*t*, 980
versus catecholaminergic polymorphic VT, 1024
- Anterior myocardial infarction, acute, atrioventricular block and, 259
- Anterior myocardial infarction ventricular tachycardias, 767
- Anterior septum atypical tachycardia, 314, 314.*e2f*
- Anterograde bypass tract conduction, earliest activation site during, 655, 655*f*, 655.*elf*
- Anterograde conduction
 in fast-slow atrioventricular nodal reentrant tachycardia, 564
 in slow-fast atrioventricular nodal reentrant tachycardia, 564
 in slow-slow atrioventricular nodal reentrant tachycardia, 565
- Anterograde dual atrioventricular nodal physiology, 570–573
- Anteroseptal (superoparaseptal) bypass tracts, 623
 ablation of, 667–670
 anatomical considerations for, 667–668
 cryoablation and, 669–670
 advantages of, 670
 outcome of, 670
 cryomapping and, 669–670
 electrocardiographic considerations for, 668
 technical considerations for, 668–669, 669*f*
- Antiarrhythmics
 for arrhythmogenic right ventricular cardiomyopathy (ARVC), 951
 for atrial fibrillation, 463
 for atrial flutter, 341–342, 346–347
 for atrial tachyarrhythmias, in congenital heart disease, 412
 for atrioventricular block, 258
 for Brugada ST segment elevation, 1010
 for Brugada syndrome, 1015
 for bypass tract conduction block, 608
 for Chagas disease, 893

- Antiarrhythmics (*Continued*)
 class I
 classification of, 19
 mechanism of action of, 18
 potassium channels and, 19
 sodium channels and, 18
 for congenital heart disease, 970–971
 for early repolarization syndromes, 1030
 for idiopathic ventricular fibrillation, 1030
 long QT syndrome due to, 993
 mechanism of action of
 potassium channels and, 19
 sodium channels and, 18
 for nonischemic dilated cardiomyopathy, 873
 sinus node response to, 250
 for triggered-activity ventricular tachycardia, 779
 for ventricular tachycardia, 779
 for Wolff-Parkinson-White syndrome, 609
- Anticoagulation
 for arrhythmogenic right ventricular cardiomyopathy (ARVC), 951–952
 for atrial fibrillation
 periprocedural, 463–464
 in prevention, 447–448
 for cardiac sarcoidosis, 889
 for electrophysiological testing, 83–84, 88
 for pericardial effusion, 1046
 periprocedural, of atrial flutter, 359–361
 for thromboembolism, prevention of, 1046
- Antidromic capture, entrainment with, 141–142
 in ventricular tachycardia, 777
- Antidromic resetting, 71
- Antiparasitic therapy, for Chagas disease, 893
- Antiplatelet therapy, for atrial fibrillation, 445
- Aortic atheroembolism, 1046
- Aortic cusps, ablation in, valvular damage in, 1050
- Aortic puncture, after transseptal puncture, 94–95
- Aortic root, anatomy of, 820–822, 821.e1f, 820.e1f
- Aortic sinus of Valsalva
 noncoronary, 318, 336f–337f
 from ventricular tachycardia, 846–851, 846f–849f
- Aortic sinuses, anatomy of, 821
- Aortic valve, 255–256
 anatomy of, 820–821
 damage of, 1050
- Apical ventricular tachycardia, in nonischemic dilated cardiomyopathy, 876
- Argon laser, 231. *see also* Laser ablation
- Arousal-related triggers, in long QT syndrome, 984, 984f
- Arrhythmias
 associated with Wolff-Parkinson-White syndrome, 603–606
 iatrogenic cardiac, 1049–1050
- Arrhythmogenic cardiomyopathy, ventricular tachycardia in, 909
- Arrhythmogenic right ventricular cardiomyopathy (ARVC)
 in epicardial ventricular tachycardia, 908
 idiopathic focal ventricular tachycardia, 825
 ventricular tachycardia in, 942–967
 ablation of, 962–965
 endpoints of, 964
 outcome of, 964–965
 target of, 962–964
 technique of, 964
 clinical presentation of, 946
- Arrhythmogenic right ventricular cardiomyopathy (ARVC) (*Continued*)
 differential diagnosis of, 948–950
 athlete's heart, 950
 cardiac sarcoidosis, 949–950
 dilated cardiomyopathy, 950
 exercise-induced arrhythmogenic right ventricular cardiomyopathy in, 950
 idiopathic right ventricular outflow tract tachycardia, 948–949, 949b
 electrocardiographic features of, 954–957
 during sinus rhythm, 954–957, 955f
 during ventricular tachycardia, 957, 958f
 electrophysiological features of, 957–959
 epidemiology of, 945–946
 initial evaluation of, 946–948
 diagnostic criteria in, 946, 947t
 endomyocardial biopsy in, 948
 genetic testing in, 948
 invasive electrophysiological testing in, 948
 mapping in, 959–962
 activation, 959, 959.e1f
 entrainment, 959–960
 epicardial, 962
 pace, 960
 substrate, 960–962
 natural history of, 945–946
 pathophysiology of, 942–945
 molecular genetics in, 942–943, 943t
 pathogenesis of, 943–945, 944f
 pathology of, 945, 945.e1f
 principles of management of, 950–954
 catheter ablation of, 952
 family screening in, 953–954
 implantable cardioverter-defibrillator, 952–953, 953f
 pharmacological therapy of, 950–952
 sports in, 953
 risk stratification in, 950, 951f, 952b
- Arrhythmogenic right ventricular cardiomyopathy-dysplasia, *versus* catecholaminergic polymorphic VT, 1024
- Arrhythmogenic substrate
 elimination of, 810
 imaging, 780–781
- Arterial air embolism, 1047
- Arteriovenous fistulas, femoral, 1043
- ARVC. *see* Arrhythmogenic right ventricular cardiomyopathy
- Ashman phenomenon, 287–289
- Aspirin, for atrial fibrillation, 445
- Astronomer, in basket catheter mapping, 180
- Atheroembolism. *see also* Embolism
 aortic, 1046
- Athletes
 atrioventricular block in, 260
 Brugada syndrome in, 1011
- Athlete's heart, 933–935, 950
 cardiac magnetic resonance in, 934
 cardiopulmonary exercise testing in, 934–935
 deconditioning in, 935
 demographics of, 933–934
 differences between hypertrophic cardiomyopathy, 934t
 echocardiography in, 934
 electrocardiography in, 934
 genetic testing in, 935
- ATP-sensitive potassium current, 24f, 33–35, 34f–35f
- Atria. *see* Atrium
- ATRIA (Anticoagulation and Risk Factors in Atrial Fibrillation) score, in atrial fibrillation
 for bleeding risk, 443, 444t
 for stroke risk, 442, 443t
- Atrial ablation. *see* Atrial fibrillation, catheter ablation of
- Atrial activation sequence, 320, 587
 in antidromic atrioventricular reentrant tachycardia, 640
 during atrial pacing, 365–367, 366f–368f, 366.e1f
 in atrioventricular nodal reentrant tachycardia, 578
 in orthodromic atrioventricular reentrant tachycardia, 637
 in para-Hisian pacing, during sinus rhythm, 631
 in paroxysmal supraventricular tachycardia
 in programmed ventricular stimulation
 retrograde, 705
 programmed ventricular stimulation in, 705
 ventricular overdrive pacing in, 710, 716
 ventricular pacing in, 723
 in permanent junctional reciprocating tachycardia, 639, 640f
- Atrial appendage, left, electrical isolation of, 515
- Atrial arrhythmias
 management of, in cardiac sarcoidosis, 889
 sinus node dysfunction and, 241
- Atrial bigeminy, alternation of aberration during, 293
- Atrial defibrillators, 455. *see also* Implantable cardioverter-defibrillator
- Atrial electrogram. *see* Intracardiac electrograms
- Atrial electrogram polarity reversal, during
 retrograde bypass tract conduction, 656–657
- Atrial electrogram sequence, following cessation, 585
- Atrial entrainment
 in orthodromic atrioventricular reentrant tachycardia, 641, 641f
 in programmed atrial stimulation, 581
- Atrial extrastimulation/pacing, 112–115, 589, 590f
 atrial response to
 in premature pacing, 115
 in rate-incremental pacing, 113–114
 repetitive, 115
 normal response to
 atrial, 113–115
 atrioventricular node, 113–115, 115.e1f
 with premature stimulation, 114–115
 with rate-incremental pacing, 112–114
 sinus node, 112, 114, 114f
 premature, 114–115
 atrial response to, 115
 atrioventricular node response to, 114–115, 115.e1f
 sinus node response to, 114, 114f
 ramp, 112
 rate-incremental, 112–114
 atrial response to, 113–114
 atrioventricular node response to, 113, 113f
 sinus node response to, 112
 repetitive atrial responses to, 115, 116f
 sites of, 112
 during tachycardia, 714
 technical aspects of, 112

- Atrial fibrillation (AF), 421–548
 aberration in, 288
 Ashman phenomenon and, 288
 atrial antitachycardia pacing for, 455, 455.e1f
 atrial fibrosis and, 428
 atrial flutter
 interrelationship of, 341–342, 342f–343f
 management of coexistent, 347
 atrial remodeling in, 429–430
 atrial stretch and, 428
 autonomic nervous system in, 430
 catheter ablation of, 453–454, 453f, 462–466, 462f
 air embolism after, 524
 antiarrhythmic drug therapy in, 463
 atrial flutter after, 520–522
 atrial tachycardia after, 520–522, 522f
 atrioesophageal fistula after, 523
 atrioventricular junction, 526–530
 atrioventricular nodal modification, 530–531, 530f
 cardiac tamponade in, 523
 catheter entrapment in mitral valve in, 524
 circumferential left atrial, 494–497
 of complex fractionated atrial electrograms, 504–507
 complications of, 522–525
 controversies in, 525–526
 evolution of, 462–463
 focal, of pulmonary vein triggers, 462
 focal impulse and rotor mapping in, 504–507
 left atrial access for, 466
 linear atrial, 497–501
 of nonpulmonary vein triggers, 509–515
 outcome and efficacy of, 516–525
 pericarditis after, 525
 peri-esophageal vagal nerve injury in, 524–525
 periprocedural anticoagulation in, 463–464
 phrenic nerve injury in, 524
 pulmonary vein catheterization in, 466
 pulmonary vein denervation in, 507–509
 pulmonary vein identification in, 466
 pulmonary vein isolation in. *see* Pulmonary vein isolation
 pulmonary vein stenosis after, 522–523
 recommendations for, 525–526
 sedation during, 465–466
 segmental ostial pulmonary vein isolation, 471–483
 sinus bradycardia after, 525
 stiff left atrial syndrome after, 525
 substrate modification in, 462–463, 525–526
 thromboembolism after, 523–524
 classification of, 422–423, 422t, 423.e1f
 clinical presentation of, 439–441
 concealed conduction in, 120
 in congenital heart disease, 408
 device-detected, 440–441, 440.e1f
 drug-induced, 438
 electrocardiographic features of, 457–461
 atrial activity in, 457–458, 458f, 458.e1f
 atrioventricular conduction in, 458–460, 459f–460f
 digitalis toxicity in, 459–460
 QRS morphology in, 461, 461f
 right ventricular rate in, 459
 ventricular preexcitation in, 459, 460f
- Atrial fibrillation (AF) (*Continued*)
 electrocardiography of, 457–461, 614, 617f–618f
 atrial activity in, 457–458, 458f, 458.e1f
 atrioventricular conduction in, 458–460, 459f–460f
 digitalis toxicity in, 459–460
 QRS morphology in, 461, 461f
 right ventricular rate in, 459
 ventricular preexcitation in, 459, 460f
 electrophysiological features of, 428
 epidemiology of, 433–439
 familial, 20t, 22
 SCN1B mutations in, 20t, 22
 SCN2B mutations in, 20t, 22
 SCN5A mutations in, 20t, 22
 genetics in, 433
 in hypertrophic cardiomyopathy, 929
 treatment of, 938
 inflammation in, 428–429
 initial evaluation of, 444–445
 diagnostic cardiac testing in, 444–445
 electrophysiological testing in, 445
 laboratory testing in, 445
 other diagnostic tests, 445
 screening in, 445
 initiation of, 423–425, 424f–425f
 left atrial appendage and
 anatomy of, 532, 532f
 catheterization of, 534
 device closure for, percutaneous, 531–537
 electrical isolation of, 515
 imaging of, 532–534, 533f
 ligation of, percutaneous, 537–540, 539f
 surgical exclusion of, 540–541, 541.e1f
 longstanding persistent, 422
 after macroreentrant atrial tachycardia, 399
 maintenance of, 425–427
 localized source hypothesis of, 426
 multiple wave reentry hypothesis of, 425–426
 normal sinus rhythm in, 450–452, 451f, 451t
 management of, 445–457
 mapping of, 426–427, 427f, 426.e1f–426.e2f
 mechanism of, 423–427, 423f
 mutations in
 KCNJ2 mutations in, 32
 KCNQ1 mutations in, 30
 potassium channel, 29–30, 32
 SCN1B/SCN2B, 20t, 22
 SCN5A, 20t, 22
 noninducibility of
 in circumferential antral pulmonary vein isolation, 493
 in circumferential left atrial ablation, 496–497
 nonparoxysmal, ablation of, 518
 nonpulmonary vein triggers in, 509–515
 in coronary sinus, 513–514, 514.e1f
 in left atrial appendage, 515
 in ligament of Marshall, 510–512, 511f–512f, 511.e1f, 510.e1f
 mapping of, 509–510
 rationale for, 509
 in superior vena cava, 512–513, 513f–514f, 512.e1f, 513.e1f
 paroxysmal, ablation of, 518
 pathophysiology of, 422–433
 permanent, 422
 postoperative, 439
 management of, 457
- Atrial fibrillation (AF) (*Continued*)
 preexcited, 608–609
 premature ventricular complexes during, 289.e1f
 prevention of systemic embolization in, 445–448
 anticoagulation in, 447–448
 antithrombotic drug therapy in, 445–446
 long-term stroke prevention, 447, 447t
 nonpharmacological interventions in, 446, 447b
 pulmonary veins in, 430–433
 anatomy of, 431, 432f–433f
 catheterization of, 466
 denervation of, 507–509
 electrophysiology of, 431
 focal ablation of, 462, 467–471
 identification of, 466
 imaging of, 465
 isolation of, 462, 525
 all *versus* only arrhythmogenic, 471
 circumferential antral, 483–494
 electrical, 471
 segmental ostial, 471–483
 in tachycardia *versus* fibrillation, 431–433
 rate control in, 448–449
 atrioventricular junction ablation, 448–449
 pharmacologic therapy for, 448
 recurrence of, 519–520, 520f
 reversion to normal sinus rhythm in, 449–450
 rhythm control in, 449–455
 other nonpharmacological approaches for, 455
 rate control *versus*, 452–453
 risk factors of, 434–438, 435t
 management for, 456–457, 456f
 modifiable, 435–438
 unmodifiable, 434–435
 risk prediction, 434
 silent, 440
 sinus node dysfunction in, 240
 with slow ventricular rate
 atrioventricular block and, 276–277, 277f
 sinus node dysfunction in, 244–245, 245f
 substrate for, 427–429
 surgical ablation of, 454, 455f
 symptom scales, 440, 440t
 symptomatic, 439–440
 systemic embolization prevention in, 445–448
 anticoagulation in, 447–448
 antithrombotic drug therapy in, 445–446
 long-term stroke prevention, 447, 447t
 nonpharmacological interventions in, 446, 447b
 thromboembolism and, 441–444
 bleeding risk stratification and, 443–444, 444t
 stroke risk stratification and, 442–443, 442t–443t, 443f
 transesophageal echocardiography of, 464–465, 465f, 465.e1f
 triggers of
 nonpulmonary vein, 425
 pulmonary vein, 424–425
 upstream therapy for, 455–456
 ventricular response during, 608
 in Wolff-Parkinson-White syndrome, 603–605, 605f
- Atrial fibrosis, atrial fibrillation and, 428

Atrial flutter (AFL)

- ablation of, 359–372
 - anticoagulation for, 359–361
 - catheter positioning for, 361–362, 362f
 - complications of, 371
 - cryoablation, 364
 - difficult cavotricuspid isthmus in, 363–364
 - endpoints for, 364–365
 - maximum voltage-guided technique, 363
 - outcome of, 371–372
 - radiofrequency, 360f, 362
 - role of electroanatomic mapping systems, 363
 - target of, 359, 361f
 - technique for, 359–364

acceleration of, 355–356

acute treatment of, 344f

antiarrhythmics for, 341–342

atrial extrastimulation during tachycardia, 353

after atrial fibrillation ablation, 520–522

bipolar electrogram polarity of, 370–371

circuits in, 339

clinical presentation of, 343

clockwise, 339

counterclockwise, 339, 375

definition of, 305, 339, 375

diagnostic maneuvers during tachycardia, 353

differential pacing of, 369–370, 369f, 370.e1f

double potentials of, 368–369

double-wave reentry in, 342

electrical cardioversion of, 346

electroanatomic mapping of, 371, 372f, 371.e1f

electrocardiography of, 347–348, 614

atrioventricular conduction in, 348, 352f–354f

flutter waves, 347–348, 348f–351f, 347.e1f

QRS morphology in, 348

electrophysiological testing in, 348–356

entrainment of, 353–355

epidemiology of, 343

incremental pacing of, 370, 370.e2f

induction of tachycardia, 351, 355f

initial evaluation of, 343–344

interrelationship of atrial fibrillation, 341–342, 342f–343f

maintenance of sinus rhythm, 346–347

mapping of, 356–359

activation, 356

electroanatomic, 358–359, 361f

entrainment, 356–358, 356b, 357f–358f

noncontact, 359, 359.e1f

mitral annulus, 379

natural history of, 343

ongoing management of, 345f

overdrive pacing for, 346

overdrive suppression of, 355

pathophysiology of, 339–342

pharmacological cardioversion of, 346

prevention of thromboembolism, 347

principles of management of, 344–347

maintenance of sinus rhythm, 346–347

management of coexistent and atrial

fibrillation, 347

prevention of thromboembolism, 347

rate control of, 344–345

restoration of sinus rhythm of, 345–346

restoration of sinus rhythm of, 345–346

right atrial anatomy of, 339–340

sinus node dysfunction in, 241

tachycardia features of, 351–353

Atrial flutter (AFL) (*Continued*)

termination of, 355, 355.e1f

transformation of, 356

trans-isthmus conduction interval of, 368

typical, 339–374

circuit, 340–341, 341f

cryoablation for, 230–231

unipolar electrogram morphology of, 370

waves, 347–348, 348f–351f, 347.e1f

in Wolff-Parkinson-White syndrome, 605

Atrial fusion, in paroxysmal supraventricular

tachycardia, manifest

atrial extrastimulation in, 714

atrial overdrive pacing in, 714

Atrial overdrive pacing, during tachycardia,

714–715

Atrial pacemakers, 54

Atrial pacing

cycle length, 572–573

during tachycardia, 589–590

at tachycardia cycle length, 323, 586, 648

in paroxysmal supraventricular tachycardia, 722–723

Atrial rate, in paroxysmal supraventricular

tachycardia, 702

Atrial remodeling, in atrial fibrillation, 429–430

Atrial resetting, during transition zone, 720

Atrial response, to atrial extrastimulation

in premature pacing, 115

in rate-incremental pacing, 113–114

repetitive, 115

Atrial septal defect

in congenital heart disease, 409

transseptal puncture and, 94, 94.e1f

Atrial septal puncture, complications of, 1044

Atrial sites, in bypass tract localization, 649

Atrial standstill, 245, 245.e1f

Atrial stimulation, programmed

in atrioventricular nodal reentrant tachycardia

initiation by, 575–576

during sinus rhythm, 570–573

during tachycardia, 580–582

in paroxysmal supraventricular tachycardia

initiation of, 710

during sinus rhythm, 704

Atrial stimulus, shortest, to delta (S-V) interval,

mapping of, 685–686

Atrial stretch, atrial fibrillation and, 428

Atrial tachyarrhythmias

atrioventricular block and, 276

in congenital heart disease. *see also* Tetralogy of

Fallot

ablation of, 417–420

end-point of, 419–420

outcome of, 420

target of, 417–418, 418f

technique, 418–419

clinical presentation of, 411

electrocardiographic features of, 412

epidemiology of, 410–411

after Fontan procedure, 407, 410

initial evaluation of, 411

management of, 411–412

maintenance of sinus rhythm in, 412

prevention of systemic embolization in,

412

rate control in, 411

restoration of sinus rhythm in, 411

Atrial tachyarrhythmias (*Continued*)

mapping of, 412–417

approach, 415

exclusion of cavotricuspid isthmus

dependence in, 415–416

identification of barriers and potential lines

of block in, 416, 416f

identification of complete reentrant circuit

in, 416–417

identification of critical isthmus in, 417,

417.e1f–417.e2f

vascular and cardiac access, 413–415, 413t

natural history of, 410–411

pathophysiology of, 407–410

atrial fibrillation in, 408

atrial septal defect in, 409

early postoperative atrial tachycardia in,

408–409

focal atrial tachycardia in, 408

great arteries, dextro-transposition of, 410

macroreentrant atrial tachycardias in,

407–408, 408f–409f

tetralogy of Fallot in, 409

univentricular hearts with Fontan palliation

in, 410

sinus node dysfunction in, 241

Atrial tachycardia (AT)

after atrial fibrillation ablation of, 520–522, 522f

atrioventricular nodal reentrant tachycardia and,

587, 587b, 603

automatic, 320f, 322

classification of, 305, 306t

in congenital heart disease

early postoperative, 408–409

focal, 408

macroreentrant, 407–408, 408f–409f

electrocardiography of, 614

exclusion of, 650b

focal, 305–338

ablation of, 333–337

catheter, 333

endpoints for, 335–337

outcome of, 337

of para-Hisian atrial tachycardias, 333–335,

335f

target of, 333

technique of, 333, 334f

anatomical locations of, 307–308, 307f

atrial activation sequence of, 320

atrial-ventricular relationship, 320

automatic, 305

bundle branch block and, 320

classification of, 306t

clinical presentation of, 309

crystal, 314, 317f

diagnostic maneuvers during, 321–324

electrocardiographic features of, 311–318

P wave morphology in, 311, 312f–314f,

311.e1f

P/QRS relationship in, 311, 315f

QRS morphology in, 311

electrophysiological testing in, 318–324

baseline observations during sinus rhythm,

318

epidemiology of, 309

exclusion of other arrhythmia mechanisms,

324, 325t

incessant, 307, 309

Atrial tachycardia (AT) (*Continued*)

- initial evaluation of, 309
- initiation by programmed atrial stimulation, 318–320
- intracardiac echocardiography in, 333, 333.e2f
- left atrial, 317–318, 318.e1f
 - appendage, 318
- versus* macroreentrant atrial tachycardia, 326t
- mapping of, 324–333
 - activation, 324–328, 325.e1f
 - electroanatomic, 330–332
 - local activation time, 326–328, 327f
 - nonsustained, 332–333
 - pace, 328–329, 329f
 - postpacing intervals, 329–330
 - reference electrogram, 325–326
 - right atrial *versus* right superior pulmonary vein foci, 328
 - right *versus* left atrial foci, 328
 - tachycardia transformation, 328
 - technique, 330
- mechanism of, 305
- noncoronary aortic sinus of Valsalva, 318, 336f–337f
- versus* orthodromic atrioventricular reentrant tachycardia, 325t
- oscillation of tachycardia cycle length, 320, 321f
- pathophysiology of, 305–309, 306t
- principles of management of, 309–311
 - acute, 309–310, 310f
 - chronic, 310–311, 310f
 - long-term, 310
- programmed atrial stimulation during tachycardia, 321–322
- programmed ventricular stimulation during tachycardia, 322–323, 323f–325f
- pulmonary veins, 308, 319f, 318.e2f
- repetitive, 309
- right atrial, 314–317, 317f, 314.e1f
- right *versus* left, 311–314
- site of, localization of, 311–318, 316f
- tachycardia features in, 320–321
- tachycardia induction, 318–320, 318b
- termination and response to physiological and pharmacological maneuvers, 320–321
- variability in postpacing intervals, 322
- ventriculoatrial linking and, 322

localized reentry in, 305–306

macroreentrant, 375–406

- ablation of, 397–404
 - of anterior mitral isthmus, 402, 405f
 - atrial fibrillation after, 399
 - endpoints for, 400
 - left atrial macroreentry, 399
 - of mitral isthmus block, 402–404, 403f–404f, 402.e1f, 399.e1f
 - outcome of, 404
 - overdrive suppression, 388
 - perimitral left atrial macroreentry, 399
 - perimitral macroreentrant, 401–404, 399.e1f
 - of posterior mitral isthmus, 401–402
 - right atrial macroreentry and, 398–399
 - target of, 397–399
 - technique of, 399–400
 - termination of, 388
 - transformation to different loop/tachycardia in, 388

Atrial tachycardia (AT) (*Continued*)

- after ablation of atrial fibrillation, 399
- atrial extrastimulation/pacing for, 382
- catheter ablation, macroreentrant atrial tachycardia after, 398f
- cavotricuspid isthmus in, 377–378, 377f, 396
 - intra-isthmus reentry, 378
 - lower loop reentry, 377–378
- circuits in, 375–377
- clinical presentation of, 381
- clockwise, 375
- dual-loop reentry in, 375
- electroanatomic mapping of, 388–392
- electrocardiographic features of, 381–382
- electrophysiological testing in, 382–388
- entrainment of, 384–386, 396
 - with concealed fusion, 387–388
 - criteria, 384
 - with fusion, 384–386
 - with inapparent fusion, 387
 - with manifest fusion, 386–387, 387f
- epidemiology of, 380–381
- identification of critical isthmus, 391–392
- initial evaluation of, 381
- left atrial, 378–380, 382
 - in absence of previous surgery or ablation, 380
 - circuits involving pulmonary veins, 379
 - incisional, 378–379
 - left septal circuits, 379–380
 - perimitral, 379, 382
 - postablation of atrial fibrillation, 379, 379f
- left septal circuits in, 382, 382.e1f
- lesional right atrial, 375
- localized reentry of, 375–377, 376f
- lower loop reentry in, 375, 382
- mapping of, 388–397
 - activation, 389–391, 390f–391f
 - cycle length variations in, 396
 - electrocardiographic findings of, 396
 - entrainment, 392–395, 393b
 - exclusion of isthmus dependence in, 396
 - identification of barriers and lines of block in, 397
 - identification of complete reentrant circuit in, 397
 - identification of critical isthmus, 397
 - localization of reentrant circuit chamber in, 389, 390f
 - noncontact, 395–396
 - practical approach to, 396–397
 - technique, 388–389
- P waves in, 381
- pathophysiology of, 375–380
 - macroreentry, 375
- perimitral, 380f
- principles of management, 381
- pulmonary vein circuits in, 382
- QRS complex in, 395
- right atrial, 381–382
 - in absence of previous surgery, 378
 - incisional, 378, 381–382
 - intra-isthmus reentry, 382
 - isthmus-dependent, 377–378, 377f
 - noncavotricuspid isthmus-dependent, 378
 - upper loop reentry, 378

Atrial tachycardia (AT) (*Continued*)

- tachycardia
 - atrial extrastimulation, 383
 - atrial pacing during, 384–388
 - diagnostic maneuvers during, 383–388
 - documentation of line of block, 400
 - features of, 382–383, 383f–384f
 - induction of, 382, 383b
 - noninducibility of, 400
 - termination, 400
 - upper loop reentry, 378, 382
- macroreentrant, classification of, 306t
- microreentrant, 321–322
- multifocal, 308–309, 308f
- P wave morphology in, 348
- paroxysmal, 309
- pulmonary vein, 308
- triggered-activity, 322

Atrial-His bundle

- interval, 109
- interval jump, 572, 572.e1f
- intervals during normal sinus rhythm, 572–573

Atrial-His bundle (AH) interval, in paroxysmal

- supraventricular tachycardia
- atrial overdrive pacing in, 714
- atrial pacing at tachycardia cycle length, 722–723

Atrial-ventricular relationship

- in antidromic atrioventricular reentrant tachycardia, 640
- in atrioventricular nodal reentrant tachycardia, 578–579
- in orthodromic atrioventricular reentrant tachycardia, 637–638, 638f
- in paroxysmal supraventricular tachycardia, 703, 710–711
- in permanent junctional reciprocating tachycardia, 640

Atriosophageal fistula, after atrial fibrillation

- ablation, 523

Atriofascicular bypass tracts, 677–688, 680f

- ablation in, 687f, 688
- endpoints of, 688
- outcome of, 688
- target of, 688
- technique in, 688
- arrhythmias associated with, 678
- comparison of atrioventricular pathway to, 682f
- differential diagnosis of, 684, 684f, 685b–686b
- electrocardiographic features of, 678–679
- electrophysiologic testing in, 679–684
 - baseline observations during sinus rhythm, 679
 - diagnostic maneuvers during tachycardia, 683–684
 - features of tachycardia, 682–683
 - induction of tachycardia, 679–681
- long decrementally conducting, 677–678
- mapping in, 684–688
 - of atrial insertion site, 685–686
 - of bypass tract potential, 686
 - of sites of mechanically induced loss of preexcitation, 686–688
 - of ventricular insertion sites, 686

Atrio-Hisian bypass tracts, 599, 692–695

- electrophysiologic testing for, 695
- programmed atrial stimulation, 695
- programmed ventricular stimulation, 695
- response to pharmacologic maneuvers, 695

- Atrio-Hisian bypass tracts (*Continued*)
 general considerations in, 692–695, 694f, 694t
 supraventricular tachycardias in, 695
 with enhanced atrioventricular node conduction, 695
- Atrionodal bypass tracts, 599
- Atrionodal cells, 257
- Atrionodal region, 561
- Atrioventricular block
 after ablation, of atrioventricular nodal reentrant tachycardia, 596
 in ablation, 337
 acquired, 258–261
 in athletes, 260
 atrial fibrillation with slow ventricular rate and, 276–277, 277f
 atrial tachyarrhythmias and, 276
 atrioventricular dissociation and, 275–276, 276f
 bundle branch block and, 299.e1f
 causes of, 261
 concealed junctional ectopy and, 274–275, 275.e1f
 congenital, 257–258, 263
 diagnosed in utero, 264
 permanent pacing for, 279, 279b
 defined, 257
 echo beats and, 276
 first-degree
 permanent pacing for, 277–278
 site of, 273
 hereditary cardiac conduction disease and, 258
 high-grade, 270, 270f
 iatrogenic, 260–261
 permanent pacing for, 278–279
 in iatrogenic cardiac arrhythmias, 1049, 1050f
 nonconducted premature atrial complexes and, 274, 274f–275f
 pacemaker device and mode selection for, 280–281, 281b
 paroxysmal, 261–262
 differential diagnosis of, 262t
 idiopathic, 262, 263f
 intrinsic, 261–262, 261f
 vagally mediated, 261
 permanent pacing for, 279, 280f
 in paroxysmal supraventricular tachycardia, 711, 711f
 pathophysiology of, 257–262
 pseudoblock, 113, 113f
 second-degree, 265–270
 Mobitz type 1 (Wenckebach), 113, 265–267
 atypical, 113
 site of block in, 267
 in ventricular pacing, 117
 Mobitz type 2, 267–268, 268f, 267.e1f
 permanent pacing for, 277
 sinus node dysfunction, 242
 site of, localization of, 272–274
 third-degree, 270, 271f
 permanent pacing for, 277
 ventriculophasic sinus arrhythmia and, 277
- Atrioventricular bypass tracts (AV BTs), 599–677.
see also Bypass tracts
- ablation in, 687f, 688
 endpoints of, 688
 outcome of, 688
 target of, 688
 technique in, 688
- Atrioventricular bypass tracts (AV BTs) (*Continued*)
 arrhythmias associated with, 678
 comparison of atriofascicular pathway and, 682f
 differential diagnosis of, 684, 684f, 685b–686b
 electrocardiographic features of, 678–679
 baseline observations during sinus rhythm, 679
 diagnostic maneuvers during tachycardia, 683–684
 features of tachycardia, 682–683
 induction of tachycardia, 679–681
 electrophysiologic testing in, 679–684
 long decrementally conducting, 677–678
 mapping in, 684–688
 of atrial insertion site, 685–686
 of bypass tract potential, 686
 of sites of mechanically induced loss of preexcitation, 686–688
 of ventricular insertion sites, 686
 multiple, 601
 electrophysiological findings in, 652b
 pathophysiology of, 601–602, 602f
 retrograde, electrophysiological findings in, 649b
 short decrementally conducting, 678
 in supraventricular tachycardia, 649b
 electrophysiological findings in, 649b
- Atrioventricular conduction
 in atrial fibrillation, 458–460, 459f
 in atrial flutter, 348, 352f–354f
 normal, 272, 273f
- Atrioventricular conduction abnormalities, 255–285
 atrioventricular block in, pathophysiology of, 257–262
 clinical presentation of, 262–263
 diagnostic evaluation of, 264
 autonomic modulation in, 264, 264f
 electrocardiography in, 264
 electrophysiological testing in, 264
 exercise testing in, 264
 electrocardiographic features of, 264–270
 electrophysiological testing of, 270–277
 exclusion of other phenomena in, 274–277
 localization of the site of atrioventricular block in, 272–274
 normal atrioventricular conduction in, 272, 273f
 role of, 270–272
 management of, 277–282
 pacemaker device and mode selection in, 280–281, 281b
 permanent pacing in, 277–279, 278b–279b
 ventricular pacing site in, 281–282
 natural history of, 263–264
 prognosis for, 264
- Atrioventricular delay, in atrioventricular block, first-degree, 264–265, 265f
 site of block in, 265
- Atrioventricular dissociation
 atrioventricular block and, 275–276, 276f
 in wide complex tachycardias, 732–733, 735f–737f
- Atrioventricular echo beats
 nodal
 in programmed atrial stimulation, for paroxysmal supraventricular tachycardia, 704
 in programmed ventricular stimulation, for paroxysmal supraventricular tachycardia, 707
 in programmed atrial stimulation, for paroxysmal supraventricular tachycardia, 704
 in programmed ventricular stimulation, for paroxysmal supraventricular tachycardia, 707
- Atrioventricular junction
 ablation of, 448–449, 526–530
 endpoints of, 528
 outcome of, 528–530
 rationale for, 526–527
 target of, 527
 technique of, 527–528, 527f–529f
 anatomy and physiology of, 255–257
 atrioventricular node in, 257
 central fibrous body in, 255–256, 256f
 His bundle in, 257
 internodal and interarterial conduction in, 255
 triangle of Koch in, 256, 256f
- Atrioventricular junctional pacemakers, 54
- Atrioventricular nodal modification, 530–531
 ablation endpoints in, 531
 ablation target in, 530, 530f
 outcome of, 531
 rationale for, 530
 technique of, 531
- Atrioventricular nodal reentrant tachycardia (AVNRT), 560–598
 ablation of, 591–597
 anatomical approach in, 591–593, 592f
 atrioventricular block after, 596
 electroanatomic approach in, 591, 593, 593f, 593.e1f
 endpoints of, 595
 junctional rhythm after, 594–595, 594f–595f
 palpitations, 596
 radiofrequency energy delivery in, 593–594
 slow pathway, 596–597
 target of, 591
 technique of, 591–595
 acute management of, 567, 567f
 anatomy and physiology of, 560–562
 atrionodal region, 561
 atrioventricular node, 560–562
 nodal region, 561–562
 nodal-His region, 562
 triangle of Koch, 560, 561f
 atrial activation sequence in, 578
 atrial tachycardia and, 603
 atrial-ventricular relationship in, 578–579
 atypical, 579f
 fast-slow, 564–565
 slow-slow, 565–566
 bundle branch block in, 579, 579.e1f
 catheter ablation for, 568
 chronic management of, 567–569, 568f
 cryoablation for, 230

- Atrioventricular nodal reentrant tachycardia (AVNRT) (*Continued*)
- electrocardiography of, 569–570, 614
 - P wave morphology in, 569–570, 571f
 - P-QRS relationship in, 570, 571f
 - PR intervals in, 569, 569f–570f
 - QRS morphology in, 570
 - rapid ventricular rates in, 569
 - single supraventricular beat in, 569
 - electrophysiological testing for, 570–590
 - baseline observations during sinus rhythm in, 570–575
 - diagnostic maneuvers during sinus rhythm after tachycardia termination, 586–587
 - diagnostic maneuvers during tachycardia, 580–586
 - exclusion of other arrhythmia mechanism, 587–590
 - induction of tachycardia, 575–578
 - programmed stimulation protocol for, 570, 572b
 - tachycardia features in, 578–580
 - exclusion of, 650b–651b
 - induction of, 578f
 - initial evaluation of, 567
 - pathophysiology of, 562–567
 - clinical presentation of, 567
 - epidemiology of, 566–567
 - tachycardia circuit, 562–563
 - types, 563–566, 564t
 - pharmacological therapy for, 568–569
 - physiological and pharmacological maneuvers in, 579
 - preexcited, antidromic atrioventricular reentrant tachycardia and, differentiation between, 651b
 - tachycardia cycle length, oscillation in, 579
 - typical (slow-fast), 564
 - videos for, 597
- Atrioventricular node (AVN), 257, 339, 560–562
- atrioventricular block in, 265, 265f
 - first-degree, 273
 - second-degree
 - Mobitz type 1, 267, 273
 - Mobitz type 2, 268
 - 2:1, 269–270, 269f
 - third-degree, 270, 273–274, 274f
 - response to atrial pacing in
 - premature, 114–115, 115.e1f
 - rate-incremental, 113, 113f
- Atrioventricular node echo beats, in atrial stimulation, 115, 116f
- Atrioventricular node (AVN)-His-Purkinje system (HPS), 599
- Atrioventricular reentrant tachycardia (AVRT), 602–603, 603f, 678, 682–683. *see also* Bypass tracts; Wolff-Parkinson-White syndrome
- antidromic, 603, 603f–604f, 603.e1f
 - atrial activation sequence in, 640
 - atrioventricular relationship in, 640
 - bundle branch block in, 640–641
 - cycle length of, oscillations in, 640
 - electrocardiography of, 614
 - features of, 640–641
 - physiological and pharmacological maneuvers, termination and response to, 641
 - preexcited atrioventricular nodal reentrant tachycardia, differentiation between, 651b
- Atrioventricular reentrant tachycardia (AVRT) (*Continued*)
- programmed atrial stimulation during, 634–635, 642, 643f
 - programmed ventricular stimulation during, 637, 648
 - atrioventricular nodal reentrant tachycardia and, 587, 588b
 - atrioventricular relationship in, 683
 - changes in TCL and, 683
 - clinical presentation of, 607
 - cycle length of
 - atrial pacing at, 648
 - ventricular pacing at, 648–649
 - diagnostic maneuvers during, 641–648
 - electrophysiological testing in, 623–649
 - baseline observations, during sinus rhythm, 623–633
 - goals of, 623b
 - induction of, 633–637
 - for initial evaluation, 608
 - tachycardia features and, 637–641
 - management of, 608–612
 - acute, 608–609
 - chronic, 609–612
 - nodal, 603
 - orthodromic, 603, 603f–604f
 - atrial activation sequence of, 637
 - atrial entrainment in, 641, 641f
 - atrial resetting, during transition zone, 647, 647f
 - atrial-ventricular relationship in, 637–638, 638f
 - bidirectional atrioventricular bypass tract in, 633–634, 633f
 - bundle branch block in, 638, 639f, 652
 - concealed atrioventricular bypass tract in, 634, 634f–635f
 - differential-site right ventricular entrainment in, 646
 - electrocardiography of, 614, 615f–616f
 - exact and paradoxical capture in, 642–643
 - features of, 637–641
 - management of, 609, 610f
 - manifest ventricular fusion in, 645, 645f
 - oscillations, in tachycardia cycle length, 638–639
 - pacing drive, required for entrainment, 646–647
 - physiological and pharmacological maneuvers, termination and response to, 639
 - postpacing interval in, 646
 - preexcitation index in, 642
 - programmed atrial stimulation during, 641–642
 - programmed ventricular stimulation during, 635–636, 636f–637f, 642–647
 - QRS alternans in, 639
 - resetting and entrainment with manifest atrial fusion in, 641–642
 - resetting in, 641–642, 644f
 - termination in, 641, 643–645
 - VA interval in, 645
 - ventricular entrainment in, 645, 652–655, 654f
 - ventricular extrastimulation, during His bundle refractoriness, 642
 - ventriculoatrial linking in, 642
- Atrioventricular reentrant tachycardia (AVRT) (*Continued*)
- para-Hisian pacing during, 648
 - physiological and pharmacological maneuvers, termination and response to, 641
 - preexcited atrioventricular nodal reentrant tachycardia, differentiation between, 651b
 - response to drugs of, 683
 - response to RBBB of, 683
 - site of earliest ventricular activation in, 682
 - VH interval and, 682
- Atrium
- action potentials in, 5t, 7
 - atrioventricular block in, 265, 265.e1f
 - first-degree, 273
 - left, confirming position in, 90–91
 - right, anatomy of, 339.e1f
- Atropine, sinus node response to, 250–251
- Atypical bypass tracts, 600
- Atypical tachycardia
- anterior septum, 314, 314.e2f
 - midseptum, 314
 - posterior septum, 314
- Auditory stimuli, in long QT syndrome, 984, 999
- Autodecremental pacing, 110
- Automatic atrial tachycardia, 320f, 322
- Automatic mode switching, 253
- Automaticity, 51–58
- abnormal, 51, 55–56, 54.e1f
 - arrhythmias caused by, 57–58
 - overdrive suppression of, 56–57
 - reduced membrane potential and, 55, 54.e1f
 - arrhythmias caused by, 57–58
 - definition of, 51
 - enhanced normal, 52f
 - adenosine and, 55
 - digitalis and, 55
 - mechanoelectric feedback and, 55
 - pacemaker hierarchy and, 53–54
 - pacemaker mechanisms and, 51–53
 - pacemaker regulation in, 54–55, 54.e1f
 - parasympathetic activity and, 54
 - in sinus node, 51, 53f
 - subsidiary pacemakers and, 54
 - sympathetic activity and, 54–55
 - ionic currents in, funny (pacemaker), 42, 52
 - overdrive suppression of, 56–57, 56f
- Autonomic blockade, sinus node response to, 250
- Autonomic evaluation, in inappropriate sinus tachycardia, 551
- Autonomic imbalance, measures of, 756–757
- Autonomic modulation
- in atrioventricular block, 264, 264f
 - in sinus node dysfunction, 243
- Autonomic testing, for nonischemic dilated cardiomyopathy, 872
- AV search hysteresis (AVSH) algorithm, 252
- AVN. *see* Atrioventricular node
- AVNRT. *see* Atrioventricular nodal reentrant tachycardia
- AVR algorithm, in wide complex tachycardias, 741, 741f
- AVRT. *see* Atrioventricular reentrant tachycardia
- Azimidilide, mechanism of action of, 28

- B**
- Barium, as Kir channel blocker, 32
- Baseline rhythm, substrate mapping during, 795–800, 802
- Basket catheter mapping, 180–182
in circumferential antral pulmonary vein isolation, 484, 484.e1f
clinical implications of, 181
fundamental concepts, 180–181
in idiopathic focal ventricular tachycardia, 843, 843.e1f
limitations of, 181–182
multielectrode, of focal atrial tachycardia, 332–333, 333.e1f
in segmental ostial pulmonary vein isolation, 479, 479f, 479.e1f
technology application, 181, 181f, 180.e1f
- Bayesian algorithm, in wide complex tachycardias, 740
- BBB. *see* Bundle branch block
- Benzodiazepines, mechanism of action of, 30
- Bepridil, for Brugada syndrome, 1015
- Beta-blockers
for arrhythmogenic right ventricular cardiomyopathy (ARVC), 950–951
for atrial flutter, 344
for catecholaminergic polymorphic VT, 1024
for long QT syndrome, 994
for postoperative atrial fibrillation, 457
for ventricular arrhythmias, 757
- Bidirection conduction block, bypass tract, 662–663
- Bidirectional atrioventricular bypass tract, in orthodromic atrioventricular reentrant tachycardia, 633–634, 633f
- Bidirectional isthmus block
for atrial flutter ablation, 364
confirmation of, 365–371, 365t
- Bidirectional ventricular tachycardia, 749
in catecholaminergic polymorphic VT, 1021–1022, 1024
differential diagnosis of, 1024
- Bifascicular block, 295, 297f, 299, 304b
- Bipolar electrogram amplitude, 800
- Bipolar electrogram polarity, of atrial flutter, 370–371
- Bipolar voltage mapping, 796
- Biventricular pacing, for atrioventricular block, 281–282
- Bleeding, pericardial, in percutaneous left atrial appendage ligation, 540
- Blood pressure
abnormal, response to exercise, in hypertrophic cardiomyopathy, 936
monitoring, during electrophysiological testing, 83
- Blood supply, of bundle branch block, 294
- Body surface potential mapping, 188–190, 190f
clinical implications of, 190
defined, 188
fundamental concepts of, 188–190
limitations of, 190
- Both Ischemic and Nonischemic Cardiomyopathy Sudden Cardiac Death in Heart Failure Trial (SCD-HeFT), 755t–756t
- Bradycardia
sinus
causes of, 241–242
electrocardiographic features of, 243
in tachycardia-bradycardia syndrome, 244
- Bradycardia-dependent block, 289–291, 291f
- Brechenmacher fiber, 600t
- Bridging of diastole, 134
- Brookenbrough needle, for transeptal catheterization, 87
- Brugada criteria, for wide complex tachycardias, 739–740, 740f, 742f
- Brugada pattern, 1005f, 1006–1007, 1007f, 1007t, 1010f
- Brugada syndrome, 1000–1017, 1006b
age and, 1002–1003
arrhythmia types in, 1005–1006
versus catecholaminergic polymorphic VT, 1024
clinical presentation of, 1004–1005
depolarization hypothesis in, 1002
diagnosis of, 1008–1009, 1008f, 1009t
differential diagnosis of, 1009–1011, 1011b
drug effects in, mechanism of, 1004
drug-induced, 1010–1011, 1011t
early repolarization in, 1002, 1004f
versus early repolarization syndromes, 1034
electrocardiographic features of, 1005–1007, 1005f
conduction abnormalities, 1007
dynamicity of Brugada pattern, 1006–1007
electrocardiogram electrode locations, 1006
electrocardiogram patterns, 1005–1006
QRS fragmentation, 1007
QT interval prolongation, 1007
ST segment elevation, 1011
electrocardiographic parameters in, 1012–1013
epidemiology of, 1004
exercise-induced changes, 1004
exercise testing in, 1009
family screening for, 1017
gender and, 1002–1003, 1012
genetic aspects of, 1000–1002, 1001t
genotype in, 1012
versus idiopathic ventricular fibrillation, 1026
invasive electrophysiological testing for, 1012
M cells in, 7–8
management of, 1013–1017
catheter ablation in, 1014, 1016f–1017f
implantable cardioverter-defibrillator in, 1013–1014, 1014f
lifestyle modifications in, 1015, 1015f
pharmacological therapy in, 1014–1015
mutations in
in calcium channel, 41
in potassium channels, 25
in sodium channels, 20t, 21
pathophysiology of, 1002–1004
provocative drug testing in, 1008–1009, 1009t
repolarization hypothesis in, 1002, 1003f
right bundle branch block in, 296–297, 1011
risk stratification for, 1011–1013, 1012b
sports participation in, 1015–1017
ST segment elevation in, 1011
sudden cardiac death in, 1000
temperature sensitivity in, 1003
ventricular arrhythmias in, 1002
- BTs. *see* Bypass tracts
- Bundle
His, 293, 293.e1f
left, 293–295
Purkinje fibers, 294
right, 293–294
- Bundle branch
electrophysiological testing for, diagnostic maneuvers, 301–303
pacing
atrial, 302, 302f
His bundle, 302, 302.e1f
ventricular, 302–303, 303f
- Bundle branch block (BBB)
alternating, 299, 300f–301f
during atrial bigeminy, 293, 288.e1f
in antidromic atrioventricular reentrant tachycardia, 640–641
atrial extrastimulation/pacing for, 301
in atrioventricular nodal reentrant tachycardia, 579, 579.e1f
blood supply of, 294
bradycardia-dependent, 289–291, 291f
chronic, 293–295
clinical significance of, 295
complete heart block, 300
electrocardiography of, 295–298, 296b
baseline intervals for, 300–301, 300.e1f
electrophysiological testing for, 300–303
focal atrial tachycardia and, 320
HV interval in, 300, 302f
intermittent, 299–300
left, 297–298, 897, 898f
anatomy and physiology of, 293–294
atypical, 298
electrocardiography of, 295–298, 296b
electrophysiological testing in, 301
in epicardial ventricular tachycardia, 909
incomplete, 298, 298f
localization of, 301
in nonischemic dilated cardiomyopathy, 872, 872.e1f
masquerading, 299
in orthodromic atrioventricular reentrant tachycardia, 638, 639f, 652
in paroxysmal supraventricular tachycardia, 712, 713f
pause-dependent, 289–291, 290f
in permanent junctional reciprocating tachycardia, 640
procainamide challenge for, 303
right, 897, 898f
anatomy and physiology of, 293
atypical, 296
in Brugada syndrome, 296, 1011
electrophysiological testing in, 300–301
incomplete, 296–297
localization of, 300–301, 302f
in nonischemic dilated cardiomyopathy, 872.e1f
role of electrophysiological testing, 303
tachycardia-dependent, 289f
transient, 286–293
acceleration-dependent, 286–289, 287f
phase 3 block, 286
phase 4 block, 289
trifascicular, pacing for, 299
in ventricular pacing, 116, 118.e1f

- Bundle branch block (BBB) (*Continued*)
 in ventricular tachycardia, 764, 765f–766f
 left, 764, 767
 right, 764–767
- Bundle branch reentrant beats, in programmed ventricular stimulation, for paroxysmal supraventricular tachycardia, 707
- Bundle branch reentrant ventricular tachycardia, 897–906
 ablation of, 903–905
 endpoints of, 905, 905f
 of left bundle branch, 903–905
 outcome of, 905
 of right bundle branch, 903, 904f
 target of, 903
 technique of, 903–905
- activation sequence in, 901–902
- versus* antidromic atrioventricular reentrant tachycardia, 903
- clinical presentation of, 898
- diagnostic criteria of, 900b
- diagnostic maneuvers in, 902
- electrocardiographic features of, 898, 899f
- electrophysiological testing in, 898–903
 in induction, 898–900
 during normal sinus rhythm, 898, 899f–900f
- entrainment of, 902
- epidemiology of, 897
- exclusion of, 779
- HV interval in, 898
- idiopathic (fascicular) left ventricular tachycardia, 902–903
- initial evaluation for, 898
- management of, 898
- versus* myocardial ventricular tachycardias, 902
- pathophysiology of, 897
- reentry circuit in, 897, 898f
- resetting, 902
- supraventricular tachycardia with aberrancy, 903
- tachycardia features in, 900–902, 901f
- ventricular extrastimulation in, induction of, 898
- Bundle branch reentry, 897
 self-limited, 897
 sustained. *see* Bundle branch reentrant ventricular tachycardia
- Bundle branch reentry beats, 118–120, 119f
- Bundle branch reentry (BBR) circuits, 898f
- Bundle branches, type 1 second-degree atrioventricular block in, 273
- Bundle of Kent, 599
- Burns, from radiofrequency ablation, 207, 207.e1f
- Burst pacing, 109
- Bypass tract bidirection conduction block, 662–663
- Bypass tract potential, direct recording of, 657–658, 659f–660f
- Bypass tracts (BTs). *see also* Preexcitation ablation of, 660–674
 anteroseptal (superoparaseptal), 667–670
 electrophysiological criteria of, 663b
 endpoints of, 662–663
 epicardial, 672–673
 failed, causes of, 673–674, 673.e1f, 674.e1f
 left free-wall, 663–666
 midseptal, 667–670
- Bypass tracts (BTs) (*Continued*)
 outcome of, 674
 posteroseptal (inferoparaseptal), 670–672
 right free-wall, 666–667
 target of, 660–661
 technique for, 661–662, 664f
- anteroseptal, 623
- arrhythmia mechanisms, exclusion of, 649, 649b–652b, 652f–653f
- associated cardiac abnormalities and, 606
- atrio-Hisian, 599
- atrionodal, 599
- atrioventricular, 599
- atypical, 600, 677–696
 atriofascicular, 677–688
 ablation in, 688
 arrhythmias associated with, 678
 differential diagnosis of, 684, 684f, 685b–686b
 electrocardiographic features of, 678–679
 electrophysiologic testing in, 679–684
 long decrementally conducting, 677–678
 mapping in, 684–688
- atrio-Hisian, 692–695
 general considerations in, 692–695, 694t
 supraventricular tachycardias in, 695
- atrioventricular, 677
 ablation in, 688
 arrhythmias associated with, 678
 differential diagnosis of, 684, 684f, 685b–686b
 electrocardiographic features of, 678–679
 electrophysiologic testing in, 679–684
 long decrementally conducting, 677–678
 mapping in, 684–688
 short decrementally conducting, 678
- fasciculoventricular, 690–692
 electrocardiographic features of, 690, 691f–692f
 electrophysiologic testing for, 690–692
 features of, 690b
 general considerations in, 690
- Mahaim fibers and, 677
- Mahaim tachycardia and, 677
- nodofascicular, 688–690
 ablation in, 690
 arrhythmias associated with, 688
 electrocardiographic features of, 689
 electrophysiologic testing for, 689–690
 mapping in, 690
- nodoventricular, 688–690
 ablation in, 690
 arrhythmias associated with, 688
 electrocardiographic features of, 689
 electrophysiologic testing for, 689–690
 mapping in, 690
- types of, 678f
- concealed, 600
- epidemiology and natural history of, 607
- orthodromic atrioventricular reentrant tachycardia, 634, 634f–635f
- symptomatic patients with
 acute management, 608, 609f
 chronic management, 609, 610f
- conduction block, in antiarrhythmic agents, 608
- cryoablation for, 230, 230.e1f
- Bypass tracts (BTs) (*Continued*)
 definition of, 599
- electrocardiography of
 features of, 612–623
 localization of, 614–623
 using delta wave, 616–623, 619b, 619f–622f
 using polarity of the retrograde P wave morphology, 623, 624f
- electrophysiological testing in, 608
- frontal plane horizontal axis in, 618–620
- frontal plane vertical axis in, 620
- left *versus* right free-wall, 620–621
- left-sided, 621
- localization of, 649–660
 atrial electrogram polarity reversal, during retrograde bypass tract conduction, 656–657
 direct recording of bypass tract potential, 657–658, 659f–660f
 earliest ventricular activation site during antegrade bypass tract conduction, 655, 655f, 655.e1f
 during retrograde bypass tract conduction, 655–656, 656f–658f
 electrophysiological maneuvers for, 653b
- local atrioventricular interval, 658–660, 661f–662f
- orthodromic atrioventricular reentrant tachycardia
 bundle branch block during, 652
 ventricular entrainment during, 652–655, 654f
- pacing from multiple atrial sites in, 649
- preexcitation index in, 649
- manifest
 asymptomatic patients with, chronic management of, 609–612
 symptomatic patients with
 acute management of, 608
 chronic management of, 609
- midseptal, 623
- posteroseptal, 623
- precordial transition in, 618
- refractory period, evaluation of, 607–608
- right-sided, 621
- types of, 599–600
 historic description of, 600t

C

CACNA1C

- in Brugada syndrome, 41, 1001, 1001t
 in long QT syndrome, 41, 977t, 979–980
 in short QT syndrome, 41, 1017t, 1018

CACNB2

- in Brugada syndrome, 41, 1001, 1001t
 in short QT syndrome, 41, 1017t, 1018

Caffeine, atrial fibrillation and, 438

Calcium

- intracellular
 delayed afterdepolarizations and, 58
 early afterdepolarizations and, 60–61, 61f
 intracellular cycling of, pacemaker activity and, 52–53

Calcium channel blockers

- atrioventricular block and, 258
 for inappropriate sinus tachycardia, 552–553

- Calcium channels, 37–42
 delayed afterdepolarizations and, 58, 59f
 early afterdepolarizations and, 60–61, 61f
 L-type, 39–41
 in Brugada syndrome, 1001
 in long QT syndrome, 977t, 979–980
 in short QT syndrome, 1018
 RyR2, 12
 structure and physiology of, 37–38, 38f
 $\alpha 1$ subunit, 38
 $\alpha 2\delta$ subunit, 38–39
 β subunit, 38
 γ subunit, 39
 T-type, 41–42
- Calcium release channels, RyR2, in myocyte contraction, 12
- Calcium-calmodulin-dependent protein kinase II, RyR2 channels and, 45
- Calcium-induced calcium release (CICR), in myocyte contraction, 12
- Calmodulin, RyR2 channels and, 45–46
- Calsequestrin
 in catecholaminergic polymorphic VT, 1021, 1021.e1f
 RyR2 channels and, 45–46
- CaMKII, RyR2 channels and, 45
- cAMP-mediated triggered activity, 58, 59f
- Canadian Cardiovascular Society Severity in Atrial Fibrillation (CCS-SAF) symptom scale, 440, 440t
- Carbon dioxide monitoring, during electrophysiological testing, 83
- Carbonization, in basket catheter mapping, 182
- Carcinogenesis, radiation-induced, 1064
- Cardiac access, in congenital heart disease, 972
- Cardiac action potentials. *see* Action potentials
- Cardiac arrest. *see also* Sudden cardiac death
 in Brugada syndrome, 1012
 in hypertrophic cardiomyopathy, 935
 in long QT syndrome, 984
 in Romano-Ward syndrome, 984
 in short QT syndrome, 1018
- Cardiac catheterization. *see* Catheterization
- Cardiac cells, excitability of, 8–9
 action potential propagation and, 10
 refractoriness and, 9
- Cardiac conduction disease, hereditary, atrioventricular block and, 258
- Cardiac crux
 and transvenous epicardial mapping and ablation, 921–922
 ventricular tachycardia from, 851
- Cardiac death. *see* Sudden cardiac death
- Cardiac electrical activity, molecular mechanisms of, 1–14
 action potentials and, 2–8
 fast response, 3–8
 slow response, 8
 excitability and, 8–9, 9f
 excitation-contraction coupling and, 12–13, 13f
 ionic equilibrium and, 1
 propagation and, 10–12
 refractoriness and, 9–10, 9f–10f
 transmembrane potentials and, 1–2, 2t
- Cardiac electrograms. *see* Intracardiac electrograms
- Cardiac gap junctions. *see* Gap junction
- Cardiac ion channels, 15–50
 calcium. *see* Calcium channels
 classification of, 15
 gap junction, 46–49
 overview of, 15
 pacemaker, 42–43
 potassium. *see* Potassium channels
 selectivity of, 15
 sodium. *see* Sodium channels
 subunits of, 15
- Cardiac magnetic resonance imaging
 of athlete's heart, 934
 for cardiac sarcoidosis, 887
 for Chagas cardiomyopathy, 892
 for hypertrophic cardiomyopathy, 930–931, 931f
 for idiopathic focal ventricular tachycardia, 824
 for nonischemic dilated cardiomyopathy, 873
- Cardiac mapping. *see* Mapping
- Cardiac myocytes, contraction of, 12, 13f
- Cardiac pacemaker. *see also* Pacemaker
 current, 42–43
 in acquired disease, 43
 function of, 42–43
 in inherited channelopathies, 43
 pharmacology of, 43
 regulation of, 43
 structure and physiology of, 42
- Cardiac perforation, 1043–1046
 detection of, 1044–1045, 1044f, 1044.e1f
 incidence of, 1043–1044
 management of, 1045–1046
 mechanism of, 1044
 after transseptal puncture, 94
- Cardiac repolarization, measures of, 756
- Cardiac sarcoidosis, 885–889
 arrhythmogenic right ventricular cardiomyopathy (ARVC) and, 949–950
 cardiac magnetic resonance for, 887, 887f
 clinical presentation of, 886
 echocardiography for, 887
 electrocardiography for, 886–887
 electrophysiological testing for, 888
 epidemiology and natural history of, 886
 histological examination for, 888
 initial evaluation for, 886–888, 886b
 management of, 888–889
 pathophysiology of, 885–886
 positron emission tomography for, 887–888
 risk stratification for, 888
- Cardiac surgery, atrioventricular block and, 260
- Cardiac tamponade, 1044
 in atrial fibrillation ablation, 523
 in cooled radiofrequency ablation, 223
 in sinus node ablation, 558
- Cardiac troponin, in ablation, 1048
- Cardiac venous system, in transvenous epicardial mapping and ablation, 920–921, 921f
- Cardiomyocytes, coupling of, 47
- Cardiomyopathy
 BBR VT in, 897
 Chagas, 889–893. *see also* Chagas cardiomyopathy
 infiltrative, atrioventricular block and, 260
 sinus node dysfunction and, 241
 ventricular, incessant tachycardia and, 309
- Cardiopulmonary exercise testing, in athlete's heart, 934–935
- Cardiovascular disease, radiation-induced, 1064
- Cardioversion
 for atrial fibrillation
 electrical of, 449–450
 pharmacological, 450
 timing of, 449
 for atrial flutter, 344
 in electrophysiological testing, 82
- Cardioverter-defibrillator. *see* Implantable cardioverter-defibrillator
- Carotid sinus hypersensitivity, 245, 245.e1f
- Carotid sinus massage, for wide complex tachycardia, 732
- CARTO electroanatomic mapping system, 156–158, 157f, 176, 782–784. *see also* Electroanatomic mapping
 activation maps in, 330, 331f
 Advanced Catheter Location Technology, 156
 advantages of, 330
 anatomical reference in, 161
 CARTO-3, 156, 157f–158f, 176
 CARTO-Merge, 156–157, 158f
 CARTO-Sound, 157–158, 159f, 196–197
 CARTO-Univ, 157
 data acquisition in, 165
 Fast Anatomical Mapping (FAM) in, 156
 high-resolution, 171–172
 integration of, with CT/MRI, 156–157, 158f
 limitations of, 330–332, 395
 of macroreentrant right atrial (RA) tachycardia, 388.e1f
 voltage maps in, 388
- CARTOSound image integration module, in substrate image integration, 799
- CASQ2, in catecholaminergic polymorphic VT, 1020, 1021.e1f
- Cataract, radiation-induced, 1064
- Catecholaminergic polymorphic ventricular tachycardia, 1020–1025
 versus arrhythmogenic right ventricular cardiomyopathy-dysplasia, 1024
 bidirectional morphology in, 1021–1022
 catheter ablation for, 1025
 clinical presentation of, 1022
 diagnosis of, 1022–1024
 diastolic membrane depolarizations in, 1020
 differential diagnosis of, 1024
 drug effects in, 1022
 electrocardiographic features of, 1022, 1023f
 electrophysiological testing for, 1023
 epidemiology of, 1022
 family screening for, 1025
 genetic aspects of, 1020, 1020t
 implantable cardioverter-defibrillator for, 1025
 left cervicothoracic sympathectomy for, 1025
 management of, 1024–1025
 mutations in, potassium channel, 32
 pathophysiology of, 1020–1022
 provocative drug testing for, 1023
 risk stratification for, 1024
 sports participation and, 1025
 ventricular arrhythmias in, 1023f
- Catecholamines
 delayed afterdepolarizations and, 60
 in triggered-activity ventricular tachycardia, 779
- Catheter ablation
 of atrial fibrillation, 453–454, 453f, 462–466, 462f
 air embolism after, 524
 antiarrhythmic drug therapy in, 463

Catheter ablation (*Continued*)

atrial flutter after, 520–522
 atrial tachycardia after, 520–522, 522f
 atrioesophageal fistula after, 523
 atrioventricular junction, 526–530
 atrioventricular nodal modification, 530–531, 530f
 cardiac tamponade in, 523
 catheter entrapment in mitral valve in, 524
 circumferential left atrial, 494–497
 of complex fractionated atrial electrograms, 504–507
 complications of, 522–525
 controversies in, 525–526
 evolution of, 462–463
 focal, of pulmonary vein triggers, 462
 focal impulse and rotor mapping in, 504–507
 left atrial access for, 466
 linear atrial, 497–501
 of nonpulmonary vein triggers, 509–515
 outcome and efficacy of, 516–525
 pericarditis after, 525
 peri-esophageal vagal nerve injury in, 524–525
 periprocedural anticoagulation in, 463–464
 phrenic nerve injury in, 524
 pulmonary vein catheterization in, 466
 pulmonary vein denervation in, 507–509
 pulmonary vein identification in, 466
 pulmonary vein isolation in. *see* Pulmonary vein isolation
 pulmonary vein stenosis after, 522–523
 recommendations for, 525–526
 sedation during, 465–466
 segmental ostial pulmonary vein isolation, 471–483
 sinus bradycardia after, 525
 stiff left atrial syndrome after, 525
 substrate modification in, 462–463, 525–526
 thromboembolism after, 523–524
 of atrial flutter
 maintenance of sinus rhythm, 346
 restoration of sinus rhythm, 346
 for atrioventricular nodal reentrant tachycardia, 568
 for Brugada syndrome, 1014, 1016f–1017f
 for bypass tract, 609
 for cardiac sarcoidosis, 889, 890f
 of catecholaminergic polymorphic VT, 1025
 complications of, 1042–1067
 air embolism, 1047–1048, 1047.e1f
 in atrial fibrillation, 522–525
 air embolism as, 524
 atrioesophageal fistula as, 523
 cardiac tamponade as, 523
 catheter entrapment in mitral valve as, 524
 pericarditis as, 525
 peri-esophageal vagal nerve injury as, 524–525
 phrenic nerve injury as, 524
 pulmonary vein stenosis as, 522–523
 sinus bradycardia as, 525
 stiff left atrial syndrome as, 525
 thromboembolism as, 523–524
 cardiac perforation, 1043–1046, 1044f, 1044.e1f
 coronary artery injuries, 1048–1049
 esophageal injury in, 1056–1062

Catheter ablation (*Continued*)

iatrogenic cardiac arrhythmias, 1049–1050, 1050f
 local vascular, 1042–1043
 phrenic nerve injury, 1051–1054
 pulmonary vein stenosis, 1054–1056, 1054f–1055f
 radiation exposure and, 1062–1065
 thromboembolism, 1046–1047
 valvular damage, 1050–1051
 for congenital heart disease, 412, 417–420, 971
 atrial activation sequence of, 419
 differential pacing of, 419–420
 double potentials of, 419
 endpoint of, 419–420
 line of block, documentation of, 419–420
 noninducibility of tachycardia in, 419
 tachycardia termination in, 419
 outcome of, 420
 target of, 417–418, 418f
 technique, 418–419
 energy sources for, 206–237
 for focal atrial tachycardia, 333
 for focal atypical tachycardia, 310–311
 for idiopathic focal ventricular tachycardia, 827
 for idiopathic ventricular fibrillation, 1028–1029, 1028f
 for inappropriate sinus tachycardia, 553
 of ligament of Marshall, 510–512, 511f–512f, 511.e1f, 510.e1f
 linear atrial, 497–501
 in long QT syndrome, 999
 of mitral isthmus, 401f, 404
 for paroxysmal supraventricular tachycardia, 701
 radiofrequency, 206–225
 for ventricular tachycardia, 760–762
 recommendations on, 762b
 Catheter-induced atrial beats, in programmed
 atrial stimulation, for paroxysmal
 supraventricular tachycardia, 704
 Catheterization. *see also* Catheters
 in electrophysiological testing
 complications of, 122–123
 iatrogenic problems in, 123
 risks of, 122
 transaortic, 87, 87.e1f
 transcaval, 85–87
 transseptal, 87–95
 alternative methods for, 93–94
 anatomical considerations of, 87–88, 87f–88f
 in atrial septal defect repair, 94, 94.e1f
 complications of, 94–95
 fluoroscopic guidance for, 88–91, 89f–90f
 intracardiac echocardiography-guided, 91–93, 92f–93f
 radiofrequency puncture in, 93–94
 Catheters
 cryoablation, 225–226, 228f, 230
 electrode, 84
 ablation, 84, 215, 84.e1f, 215.e1f
 basket, 84, 85f
 complications of, 122–123
 coronary sinus, 85f–86f, 86–87
 Cournand, 84.e1f
 Damato, 84.e1f
 decapolar, 84, 84f
 deflectable, 84, 84.e1f

Catheters (*Continued*)

duodecapolar, 84, 84f
 epicardial, 95–101
 Halo, 84, 84f
 His bundle, 86
 iatrogenic problems in, 123
 Josephson, 84.e1f
 lasso, 84, 84f
 positioning of, 84–85
 quadripolar, 84, 84f
 right atrial, 85, 85f
 right ventricular, 85, 85f
 transaortic, 87, 87.e1f
 transcaval, 85–87
 transseptal, 87–95
 types of, 84, 84f, 84.e1f
 for high-frequency ultrasound, 233.e1f
 for mapping, 129, 131f
 high-density, 330
 open-irrigation, radiofrequency ablation and, 210f, 223
 CAV3 mutations, in long QT syndrome, 977t, 979
 Cavotricuspid isthmus (CTI), 305
 ablation of, pseudo-block and pseudo-conduction during, 368f
 in atrial flutter, 339, 357f–358f
 bidirectional, confirmation of, 369f, 371f
 confirmation of, 367f
 counterclockwise, 368f
 dependence, in atrial tachyarrhythmias, in
 congenital heart disease, 415–416
 electroanatomic mapping of, 372f
 intra-isthmus reentry, 378
 line ablation, 500–501
 lower loop reentry of, 377–378
 in macroreentrant atrial tachycardia, 377–378, 377f
 Central fibrous body, 255–256, 256f
 Cerebral air embolism, 1047–1048, 1047.e1f
 Cerebral thromboembolism, 1046
 CHA2DS2-VASc scoring system, 442, 442t–443t
 CHADS2 scoring system, 442, 442t
 Chagas cardiomyopathy, 889–893
 clinical presentation of, 892, 892b
 epidemiology and natural history of, 890–892
 initial evaluation for, 892–893
 management of, 893
 pathophysiology of, 889–890
 risk stratification for, 893, 893f
 Chagas disease
 atrioventricular block and, 260
 in epicardial ventricular tachycardia, 907
 Chemical gradient, in ionic equilibrium, 1
 Chronic ischemic heart disease, atrioventricular block and, 259
 Chronic kidney disease, atrial fibrillation and, 437
 Chronic oral beta-blocker, for Wolff-Parkinson-White syndrome, 609
 Chronotropic incompetence, sinus node
 dysfunction and, 241–244, 244f
 CICR. *see* Calcium-induced calcium release
 Cilobradine, 43
 Cilostazol, for Brugada syndrome, 1015
 Circumferential antral pulmonary vein isolation, 483–494
 ablation endpoints in, 493
 ablation target in, 485–487

- Circumferential antral pulmonary vein isolation (*Continued*)
 computed tomography in, 485
 cryoballoon ablation in, 487–491, 489f–490f, 490.e1f, 488.e1f
 identification of pulmonary vein antra in, 483–485
 intracardiac echocardiography in, 485
 laser ablation in, 491–493, 491f–492f
 magnetic resonance imaging in, 485
 mapping in
 basket catheter, 484, 484.e1f
 electroanatomic, 484–485, 486f
 ring catheter, 484
 outcome of, 493–494
 radiofrequency ablation in, conventional, 487
 rationale for, 483, 484f
 technique of, 487–493
- Circumferential left atrial ablation, 494–497
 endpoints of, 496–497
 mapping in
 activation, 496
 electroanatomic, 494–495
 voltage, 496
 noninducibility of atrial fibrillation in, 496–497
 organized atrial arrhythmias in, 496
 outcome of, 497
 pulmonary vein isolation in, 496
 rationale for, 494
 target of, 495, 495f
 technique of, 495–496
 termination of persistent atrial fibrillation in, 496
- Clinical disease expression, phases of, in arrhythmogenic right ventricular cardiomyopathy (ARVC), 946
- Clinical ventricular tachycardias, noninducibility of, ablation in, 810
- Clonidine, mechanism of action of, 43
- Closed-loop irrigation catheters, for radiofrequency ablation, 210, 210f
- Coagulum formation
 prevention of, 217
 radiofrequency ablation and, 212
- Color-coded voltage map, 796, 796.e1f
- Complete heart block
 bundle branch block and, 300
 cardiac sarcoidosis and, 888
- Complete reentrant circuit, in atrial tachyarrhythmias, in congenital heart disease, 416–417
- Complex fractionated atrial electrograms
 ablation of, 504–507
 endpoints of, 506
 outcome of, 507
 rationale for, 504
 target of, 506
 technique of, 506
 mapping of, 504–506, 505f, 506.e1f
- Computed tomography (CT), 197–202
 cardiac, in arrhythmogenic substrate, 781
 in circumferential antral pulmonary vein isolation, 485
 clinical implications of, 199–201, 200f–201f, 200.e1f
- Computed tomography (CT) (*Continued*)
 fundamental concepts of, 197–198
 image acquisition in, 197
 image integration technique for, 198–199
 using CARTO-Merge, 156–157, 158f, 198
 using CARTO-Sound, 198
 using fluoroscopy, 199
 using NavX fusion, 198–199, 199f
 image registration in, 197–198
 accuracy of, 201–202
 image segmentation in, 197, 197.e1f
 integration of, in EnSite NavX Electroanatomic mapping system, 156–157
 limitation of, 201–202
 overlay in, 198–199
- Concealed bypass tracts, 600
 epidemiology and natural history of, 607
 orthodromic atrioventricular reentrant tachycardia, 634, 634f–635f
 symptomatic patients with
 acute management, 608, 609f
 chronic management, 609, 610f
- Concealed conduction, 120–121
 in atrial fibrillation, 120
 in supraventricular tachycardia, 121, 121f
 unexpected facilitation of conduction and, 120–121
 unexpected prolongation/failure of conduction and, 120
- Concealed fusion, 141, 143
 entrainment mapping with, 787, 787t, 789f
 entrainment with, in ventricular tachycardia, 776–777, 778f, 777.e1f
- Concealed junctional ectopy, atrioventricular block and, 274–275, 275.e1f
- Concealed perpetuation, in ventricular tachycardia, 771, 771.e1f
- Concertina preexcitation, 613
- Conducting channels, 170
- Conduction
 action potential propagation and, 10
 anisotropic, 11, 66, 11.e1f. *see also* Anisotropic reentry
 assessment of, 110
 atrioventricular, in atrial fibrillation, 458–460, 459f
 isotropic, 66
 limitations of, 112
 in programmed electrical stimulation, 110
 safety factor for, 12
 supernormal, 122
 unexpected facilitation of, 120–121
- Conduction velocity, 10
 measurement of, 110
- Congenital heart disease
 atrial fibrillation and, 436
 atrial tachyarrhythmias in. *see also* Tetralogy of Fallot
 ablation of, 417–420
 endpoint of, 419–420
 outcome of, 420
 target of, 417–418, 418f
 technique, 418–419
 clinical presentation of, 411
 electrocardiographic features of, 412
 epidemiology of, 410–411
 after Fontan procedure, 407, 410
 initial evaluation of, 411
- Congenital heart disease (*Continued*)
 management of, 411–412
 maintenance of sinus rhythm in, 412
 prevention of systemic embolization in, 412
 rate control in, 411
 restoration of sinus rhythm in, 411
 mapping of, 412–417
 approach, 415
 exclusion of cavotricuspid isthmus dependence in, 415–416
 identification of barriers and potential lines of block in, 416, 416f
 identification of complete reentrant circuit in, 416–417
 identification of critical isthmus in, 417, 417.e1f–417.e2f
 vascular and cardiac access, 413–415, 413t
 natural history of, 410–411
 pathophysiology of, 407–410
 atrial fibrillation in, 408
 atrial septal defect in, 409
 early postoperative atrial tachycardia in, 408–409
 focal atrial tachycardia in, 408
 great arteries, dextro-transposition of, 410
 macroreentrant atrial tachycardias in, 407–408, 408f–409f
 tetralogy of Fallot in, 409
 univentricular hearts with Fontan palliation in, 410
 atrioventricular block and, 260, 263
 diagnosed in utero, 264
 permanent pacing for, 279, 279b
 sinus node dysfunction and, 241
 ventricular arrhythmias in, 968–975
 ablation of, 973–974, 973f
 electrocardiographic features of, 971, 972f
 epidemiology of, 968–969
 initial evaluation of, 969
 mapping of, 972–973
 natural history of, 968–969
 pathophysiology of, 968, 969f
 principles of management of, 970–971
 risk stratification for, 969–970
- Congenital sick sinus syndrome, SCN5A mutations in, 20t, 22
- Congestive heart failure, HCN2/HCN4 in, 43
- Connexins, 47
- Connexons, 47
- Contact force monitoring, catheter-tissue contact and, 219–222, 220f–221f
- Continuous activity, in activation mapping, 784–786, 785f
- Contractile remodeling, in atrial fibrillation, 429–430
- Contrast-enhanced CT, in substrate image integration, 799
- Conventional risk stratification model, in hypertrophic cardiomyopathy, 937, 937b
- Core isolation, 807, 809f
- Coronary air embolism, 1047.e1f
- Coronary Artery Bypass Graft (CABG) Patch Trial, 755t–756t
- Coronary artery disease
 atrial fibrillation and, 436
 implantable cardioverter-defibrillator therapy in, 755t–756t

- Coronary artery injury, 1048–1049
in transthoracic epicardial ablation, 919
- Coronary sinus
atrial tachycardias arising in, 318
electrical isolation of, 513–514, 514.e1f
- Coronary sinus catheter, 85f–86f, 86–87
- Coronary sinus electrogram, 107, 108f
- Correlation coefficient (CORR), in pace mapping, 149
- Cox-maze procedure, for atrial fibrillation, 454
- Crista terminalis
anatomy of, 339.e1f
of atypical tachycardia, 314
- Cristal atrial tachycardia, 317f
- Critical isthmus
ablation of, 805
in atrial tachyarrhythmias, in congenital heart disease, 417, 417.e1f–417.e2f
in congenital heart disease, 972–973
identification of, 391–392, 394, 804–805
in the reentry circuit, 145–146
of macroreentrant tachycardias, 133, 143, 152
- Cromakalim, mechanism of action of, 35
- Cryoablation, 225–231. *see also* Catheter ablation
of atrial flutter, 364
biophysics of cryothermal energy in, 225–226, 228f
clinical advantages of, 230
clinical applications of, 230–231
on atrioventricular nodal reentrant tachycardia, 230
on bypass tracts, 230, 230.e1f
on focal atrial tachycardia, 231
on pulmonary vein isolation, 231
on typical atrial flutter, 230–231
on ventricular tachycardia, 231
- esophageal injury in, 1057
- in idiopathic focal ventricular tachycardia, 854
- lesion formation by, pathophysiology of, 226–228
chronic cryogenic lesion formation in, 228
extracellular ice formation (solution effect injury) in, 226–227
intracellular ice formation in, 227–228
vascular-mediated tissue injury, 228
- lesion size, determinants of, 228–229, 228t
- of slow pathway, in atrioventricular nodal reentrant tachycardia, 596–597
advantages of, 597
cryomapping in, 596
endpoints of, 597
outcome of, 597
target of, 596
technique for, 596–597
- of superoparaseptal and midseptal bypass tracts, 669–670
- technical aspects of, 229, 229.e1f
cryoballoon ablation in, 229, 229f
cryomapping, 229
- Cryoadherence effect, 230
- Cryoballoon ablation, 229, 229f
in circumferential antral pulmonary vein isolation, 487–491, 489f–490f, 490.e1f, 488.e1f
- Cryolesions, 230
- Cryomapping, 229
of superoparaseptal and midseptal bypass tracts, 669–670
- Cryothermal energy
application of, 230–231
biophysics of, 225–226, 228f
- CTI. *see* Cavotricuspid isthmus
- Cyclic adenosine monophosphate-mediated triggered activity, 58, 59f
- D**
- Dabigatran, for atrial fibrillation, 446
- Damato catheter, 84.e1f
- Decapolar catheter, 84, 84f
- Deconditioning, in athlete's heart, 935
- Decremental conduction, 601–602
- Decremental pacing, 109
- Deep venous thrombosis, 1043. *see also* Thromboembolism
- Defibrillation. *see* Implantable cardioverter-defibrillator
- Defibrillator pads, for electrophysiological testing, 83
- Deflectable catheters, 84, 84.e1f
- Degenerative diseases
atrioventricular block and, 259
sinus node dysfunction and, 240
- Delta wave, 600–601
in localization, of bypass tract, 616–623, 619b, 619f–622f
- Denopamine, for Brugada syndrome, 1015
- Depolarization, 2. *see also* Membrane depolarization
abnormalities, in arrhythmogenic right ventricular cardiomyopathy (ARVC), 954–957
- Desmosomes, 46
- Deterministic effect, of ionizing radiation, 1062, 1062.e1f
- Dextro-transposition, of great arteries, in congenital heart disease, 410
- Diabetes mellitus
atrial fibrillation and, 437
management of, 456
neonatal, Kir6.2 subunit mutations in, 35
- Diaphragmatic electromyography, 1052
- Diaphragmatic paralysis, 1051. *see also* Phrenic nerve injury
in sinus node ablation, 558
- Diastolic dysfunction, in hypertrophic cardiomyopathy, 925
- Diastolic electrical activity, in triggered-activity ventricular tachycardia, 779
- Diastolic membrane depolarization, in catecholaminergic polymorphic VT, 1020
- Dielectric heating, 233
- Differential pacing, of atrial flutter, 369–370, 369f, 370.e1f
- Differential-site pacing, for focal atrial tachycardia, 322
- Differential-site right ventricular entrainment, 584–585
in orthodromic atrioventricular reentrant tachycardia, 646
in paroxysmal supraventricular tachycardia, 719–720
- Differential-site right ventricular pacing, 575, 629–631, 630f
in programmed ventricular stimulation, for paroxysmal supraventricular tachycardia, 705–706
- Digitalis
automaticity and, 55
delayed afterdepolarizations and, 60
- Digoxin
arrhythmia due to, 731
for atrial fibrillation, 608–609
for atrial flutter, 344
for atrioventricular block, 258
sinus node response to, 250
- Dilated cardiomyopathy
arrhythmogenic right ventricular cardiomyopathy (ARVC) and, 950
BBR VT in, 897
familial, 869, 870t
idiopathic focal ventricular tachycardia, 825–826
nonischemic. *see* Nonischemic dilated cardiomyopathy
potassium channel defects in, 26
SCN5A mutations in, 20t, 22
- Diltiazem
for inappropriate sinus tachycardia, 552–553
sinus node response to, 250
for Wolff-Parkinson-White syndrome, 609
- Diode laser, 231
- Dipyridamole, mechanism of action of, 33
- Direct thrombin inhibitors, for atrial fibrillation, 446
- Disopyramide
for atrial fibrillation, 452
Brugada ST segment elevation and, 1011t, 1014–1015
mechanism of action of, 19
- Distal fascicular insertion site, mapping of, 686
- Distal ventricular insertion site, mapping of, 686
- Dofetilide, 28
for atrial fibrillation, 450, 452
for atrial flutter, 346
- Double-loop reentry, 66, 66f
- DPP6, in idiopathic ventricular fibrillation, 1026
- Dronedaron
for atrial fibrillation, 452
atrioventricular block and, 258
- Drugs
atrioventricular block and, 258
delayed afterdepolarizations and, 60
early afterdepolarizations and, 62
- Dual atrioventricular nodal physiology
anterograde, 570–573, 572b
electrocardiographic manifestations of, 569
prevalence of, 573
in programmed atrial stimulation, for paroxysmal supraventricular tachycardia, 704
retrograde, 573–575
- Dual-chamber pacing, for atrioventricular block, 280
- Dual-chamber sequential extrastimulation, during sinus rhythm, 633
in paroxysmal supraventricular tachycardia, 709–710
- Duodecapolar catheter, 84, 84f
- E**
- E-4031, 28
- Early repolarization syndromes, 1029–1038
clinical presentation of, 1031
diagnosis of, 1034, 1034t

- Early repolarization syndromes (*Continued*)
 differential diagnosis of, 1034, 1036*b*
 electrocardiographic features of, 1031–1034, 1032*f*–1033*f*
 electrophysiological testing in, 1037
 epidemiology of, 1031
 exercise testing in, 1037
 genetic aspects of, 1029–1030, 1029*t*
 genetic screening in, 1037
 invasive electrophysiological testing for, 1037
 J waves in, 1030, 1035*t*
 amplitude of, 1035
 distribution of, 1036
 fluctuation of, 1036
 morphology of, 1036
 localization of, 1033–1034
 management of, 1037–1038, 1038*f*
 mutations in
 calcium channel, 41
 sodium channels, 20*t*, 21
 pathophysiology of, 1030–1031
 pattern, modulation of, 1030–1031
 risk stratification for, 1034–1037, 1036*f*
 sports participation in, 1037
 ST segment in, 1036
 syncope in, 1036–1037
- Echo beats
 atrioventricular block and, 276
 atrioventricular node, 115, 116*f*
 ventricular, 120, 120*e1f*
- Echocardiography
 for arrhythmogenic substrate, 780
 of athlete's heart, 934
 for cardiac sarcoidosis, 887
 for Chagas cardiomyopathy, 892
 for hypertrophic cardiomyopathy, 930
 intracardiac, 193–197
 in circumferential antral pulmonary vein isolation, 485
 of pulmonary vein, 466
 transesophageal, of atrial fibrillation, 464–465, 465*f*, 465*e1f*
 in transseptal catheterization, 91–93, 92*f*–93*f*
 transthoracic, for pericardial effusion, 1044, 1044*f*
- Ectopic automatic rhythms
 accelerated, 57
 escape, 57
- Effective dose, for radiation energy, 1063
- Effective refractory period, 9, 111
- Electrical activity. *see* Cardiac electrical activity
- Electrical cardioversion, for ventricular tachycardia, 757
- Electrical gradient, in ionic equilibrium, 1
- Electrical potential, membrane. *see* Membrane potential
- Electrical remodeling, in atrial fibrillation, 429
- Electrical scar, 169, 802
- Electrical storm, in Brugada syndrome, 1015
- Electroanatomic approach, in ablation, of
 atrioventricular nodal reentrant tachycardia, 591, 593, 593*f*, 593*e1f*
- Electroanatomic mapping, 156–176
 activation mapping and, 161–169
 anatomical mapping in, 172–174
 limitations of, 174, 175*f*
 of atrial flutter, 358–359, 361*f*, 371, 372*f*, 371*e1f*
 ablation, 363
- Electroanatomic mapping (*Continued*)
 CARTO, 156–158, 157*f*, 176
 activation maps in, 330, 331*f*
 advantages of, 330
 limitations of, 330–332, 395
 of macroreentrant right atrial (RA) tachycardia, 388*e1f*
 voltage maps in, 388
 choice of, 175–176
 circuit exit site, 393–394
 in circumferential antral pulmonary vein isolation, 484–485, 486*f*
 in circumferential left atrial ablation, 494–495
 clinical implications of, 174–175
 color-coded mapping of postpacing intervals, 394–395
 conduction time from pacing site to circuit exit site, 393–394
 EnSite NavX, 158–160, 160*f*, 162*f*, 176
 EnSite noncontact, 176–177, 176*e1f*
 in fascicular ventricular tachycardia, 864, 864*f*
 focal impulse and rotor mapping and, 182
 fundamental concepts of, 156–161
 high-resolution, 171–172
 in idiopathic focal ventricular tachycardia, 841–842, 841*f*
 limitations of, 395
 use of, 392
 localization of reentry circuit, 394, 394*f*
 of macroreentrant atrial tachycardia, 388–392
 of nonischemic dilated cardiomyopathy, 878
 postpacing interval of, 393
 propagation, 392
 of pulmonary vein, 466
 Rhythmia, 160–161, 161*f*, 176, 782–784
 stimuli needed to entrain, 393
 substrate
 of macroreentrant atrial tachycardia, 396
 of nonischemic dilated cardiomyopathy, 878–882
 tachycardia transformation of, 392, 392*e1f*
 of ventricular tachycardia, 782–784, 782*f*–783*f*
 voltage, 169–171, 169*t*, 170*e1f*, 169*e1f*
 in CARTO electroanatomic mapping, 392
 limitation of, 171, 172*f*
 resolution of, factors influencing, 170
- Electroanatomic catheter localization, catheter-tissue contact in, 219
- Electrocardiographic features
 of atrial tachyarrhythmias, in congenital heart disease, 412
 of focal atrial tachycardia, 311–318
 P wave morphology in, 311, 312*f*–314*f*, 311*e1f*
 P/QRS relationship in, 311, 315*f*
 QRS morphology in, 311
- Electrocardiographic fusion. *see* Fusion
- Electrocardiographic mapping, 190–193, 191*f*
 clinical implications of, 192–193
 components of, 190
 fundamental concepts of, 190–191
 limitations of, 193
 modes of display in, 192
 technology application of, 191–192, 192*f*, 192*e1f*
- Electrocardiography
 ambulatory, in long QT syndrome, 990
 for antidromic atrioventricular reentrant tachycardia, 614
 of athlete's heart, 934
- Electrocardiography (*Continued*)
 for atrial fibrillation, 614, 617*f*–618*f*
 for atrial flutter, 614
 for atrial tachycardia, 614
 for atrioventricular block, 264
 for atrioventricular nodal reentrant tachycardia, 614
 for atrioventricular reentrant tachycardia
 antidromic, 614
 orthodromic, 614, 615*f*–616*f*
 for Brugada syndrome, 295–298, 296*b*, 1009, 1013
 for bundle branch block, 295–298, 296*b*
 of bypass tract, localization of, 614–623
 for cardiac sarcoidosis, 886–887
 for Chagas cardiomyopathy, 892
 features of, 612–623
 for hypertrophic cardiomyopathy, 930, 931*f*
 for idiopathic focal ventricular tachycardia, 824
 for idiopathic ventricular fibrillation, 1026, 1026*f*
 localization, of pulmonary vein ectopy, in atrial fibrillation, 467, 470*f*
 monitoring, postprocedural, for atrial fibrillation, 465
 for permanent junctional reciprocating tachycardia, 614, 616*f*
 of preexcitation, 612–613, 612*f*, 613*e1f*
 signal-averaged, in Brugada syndrome, 1009
 for sinus node dysfunction, 242–243
- Electrode catheters. *see* Catheters, electrode
- Electrodes
 in body surface potential mapping, 188
 size of, voltage mapping and, 170, 171*f*
- Electrograms. *see* Intracardiac electrograms
- Electrogram-to-QRS interval, stimulus-to-QRS interval *versus*, 789–791, 792*f*
- Electromyography, diaphragmatic, 1052
- Electronic Phased-Array Catheter Sector Imaging System, 193
- Electrophysiological mechanisms, of cardiac arrhythmias, 51–80
 automaticity and, 51–58. *see also* Automaticity
 reentry, 63–79. *see also* Reentry
 triggered activity and, 58–63. *see also* Triggered activity
- Electrophysiological testing, 81–124, 623–649
 anesthesia for, 82–83
 effects of, 83
 general, 82–83
 local, 82
 antiarrhythmic drugs for, 83
 anticoagulation for, 83–84, 88
 for atrial flutter, 348–356
 atrial stimulation in, 112–115. *see also* Atrial extrastimulation/pacing
 for atrioventricular block, 264
 for atrioventricular conduction abnormalities, 270–277
 exclusion of other phenomena in, 274–277
 localization of the site of atrioventricular block in, 272–274
 normal atrioventricular conduction in, 272, 273*f*
 role of, 270–272
 baseline intervals in, 107–109
 baseline observations, during sinus rhythm, 623–633
 for Brugada syndrome, 1009

- Electrophysiological testing (*Continued*)
 for bundle branch block, 300–303, 300.e1f
 carbon dioxide monitoring for, 83
 catheters for
 complications of, 122–123
 positioning of, 84–85
 types of, 84–101, 84f, 84.e1f
 for Chagas cardiomyopathy, 893
 complications of, 122–123
 concealed conduction in, 120–121. *see also* Concealed conduction
 for conduction velocity measurement, 110
 for congenital heart disease, 970
 consent for, 81–82
 defibrillator pads for, 83
 for early repolarization syndromes, 1037
 epicardial approach in, 95–101
 anatomical considerations of, 95–96, 96.e1f
 anterior *versus* posterior, 98–100, 100f
 pericardial access, complications of, 100–101
 technical considerations of, 96–100
 for fascicular ventricular tachycardia, 860–861
 femoral access in, 85
 for focal atrial tachycardia, 318–324
 gap phenomenon in, 121–122, 122f
 goals of, 623b
 for hypertrophic cardiomyopathy, 930
 iatrogenic problems in, 123
 for idiopathic ventricular fibrillation, 1027
 for inappropriate sinus tachycardia, 551
 indications for, 81
 induction of, 633–637
 for initial evaluation, 608
 intracardiac electrograms in, 103–107. *see also* Intracardiac electrograms
 invasive, in risk stratification, 756
 jet ventilation in, 83
 miscellaneous electrophysiological phenomena in, 120–122
 modified Seldinger technique in, 85
 oxygen saturation monitoring for, 83
 pacing techniques in, 109–110. *see also* Pacing
 periprocedural management of, 81–84
 preprocedure evaluation for, 81
 processing of, 101–103
 programmed electrical stimulation in, 109–112.
 see also Programmed electrical stimulation
 in refractory period measurement, 111
 risks of, 122
 sedation for, 82–83
 conscious, 82
 deep, 82
 for short QT syndrome, 1019
 signal acquisition of, 101–103
 for sinus node dysfunction, 243, 246–250
 supernormality in, 122
 tachycardia features and, 637–641
 transaortic approach in, 87, 87.e1f
 transcaval approach in, 85–87
 transseptal approach in, 87–95
 alternative methods for, 93–94
 anatomical considerations of, 87–88, 87f–88f
 in atrial septal defect repair, 94, 94.e1f
 complications of, 94–95
 fluoroscopic guidance for, 88–91, 89f–90f
 intracardiac echocardiography-guided, 91–93, 92f–93f
 radiofrequency puncture in, 93–94
- Electrophysiological testing (*Continued*)
 urinary problems in, 83
 ventricular, 115–120. *see also* Ventricular
 extrastimulation/pacing
 for ventricular arrhythmias, 753
- Electroporation, 235
 irreversible, 235
 membrane, 235
 reversible, 235
- Elevated pacing threshold, endpoints of ablation, 337
- Embolism, 1043. *see also* Thromboembolism
 air, 1047–1048
 arterial, 1047
 after atrial fibrillation ablation of, 524
 cerebral, 1047–1048, 1047.e1f
 coronary, 1047.e1f
 venous, 1047
 pulmonary, 1043
 atrial fibrillation and, 437
- Emotional triggers, in long QT syndrome, 984, 984f, 999
- Endocardial access, in percutaneous left atrial
 appendage ligation, 537–538, 539f
- Endocardial activation mapping, in atrial
 fibrillation, 467–470
- Endocardial mapping system, with basket catheter, 181
- Endocarditis, infective, atrioventricular block and, 260
- Endocardium, action potentials in, 7
- End-stage hypertrophic cardiomyopathy, in
 hypertrophic cardiomyopathy, 936
- Enhanced atrioventricular node conduction
 programmed atrial stimulation in, 695
 programmed ventricular stimulation in, 695
 response to pharmacologic and physiologic
 maneuvers in, 695
 supraventricular tachycardias in, 695
- Enoxaparin, for atrial flutter ablation, 359–361
- EnSite NavX electroanatomic mapping system, 158–160, 160f, 162f
 anatomical reference in, 161, 176
 data acquisition in, 165
 high-resolution, 171–172
 propagation map in, 167, 168f
- EnSite noncontact mapping system, 176–180. *see also* Noncontact mapping
 clinical implications of, 179f, 180
 fundamental concepts, 176–177, 176.e1f
 limitations of, 180
 procedure for, 332
 technology application in, 177–180, 178f–179f
- Entrainment, 73–74, 135, 384–388, 385f–386f. *see also* Reentrant tachycardia, resetting
 activation wavefronts, 138
 with antidromic capture, 141–142
 of atrial flutter, 353–355
 of bundle branch reentrant ventricular
 tachycardia, 902
 with concealed fusion, 387–388
 conduction time for, 142
 criteria for, 138, 138b, 384
 definition of, 73
 diagnostic criteria of, 74
 in fascicular ventricular tachycardia, 861
 with fusion, 72, 384–386, 72.e1f
- Entrainment (*Continued*)
 fusion during, 138–142, 139f–140f
 concealed, 141, 143
 fixed, 139
 inapparent, 141, 142f
 manifest, 141
 with inapparent fusion, 387
 last entrained interval and, 73
 with manifest fusion, 386–387, 387f
 pacing for
 constant rate, 138
 overdrive, 73, 138, 139.e1f
 sites in, 143
 conduction time and, 142
 cycle length and, 74
 in paroxysmal supraventricular tachycardia
 atrial overdrive pacing and, 714
 para-Hisian, 722
 ventricular overdrive pacing and, 716–719
 length of, 720, 721f, 720.e1f
 postpacing interval, 142–143, 142.e1f
 principles of, 73
 response curves for, 73–74
 during tachycardia, 684
 transient, 73
 in ventricular tachycardia, 775–777
 with antidromic capture, 777
 with concealed fusion, 776–777, 778f, 777.e1f
 criteria of, 775
 with fusion, 775, 776f–777f
 with inapparent fusion, 775–776
 with manifest fusion, 775
- Entrainment mapping, 135–146
 in arrhythmogenic right ventricular
 cardiomyopathy (ARVC), 959–960
 clinical implications of, 144–146
 color-coded 3-D, 169
 in electroanatomic activation map, 167–169, 168f
 fundamental concepts of, 135–144, 136f–137f
 fusion in, 72, 72.e1f
 graphical representation of, 144
 limitations of, 146
 of macroreentrant atrial tachycardia, 392–395, 393b
 of nonischemic dilated cardiomyopathy, 882, 882.e1f
 pacing sites in, 143
 recording site and, 141
 of ventricular tachycardia, 786–792, 804
 with concealed fusion, 787, 787t, 789f
 limitations of, 792
 postpacing interval in, 787–789, 790f–791f, 789.e1f
 stimulus-to-QRS interval in
 electrogram-to-QRS interval *versus*, 789–791, 792f
 ratio of, to tachycardia cycle length, 791–792
 technique of, 786–787, 787b, 788f
- EpiAccess Smart Needle, 98, 98f–99f
- Epicardial ablation, transthoracic, 916–920
 complications of, 918–920
 coronary artery injury as, 919
 intraabdominal bleeding as, 919–920
 pericardial bleeding as, 918
 pericarditis, 919
 phrenic nerve injury as, 919, 919.e1f

- Epicardial ablation, transthoracic (*Continued*)
 pleuritis as, 920
 pneumopericardium as, 920
 cryoablation, 918
 outcome of, 920
 radiofrequency, 916–918
- Epicardial access, in percutaneous left atrial
 appendage ligation, 537
- Epicardial action potentials, 7
- Epicardial bypass tracts, ablation of, 672–673
- Epicardial circuits, mapping of, 801–802
- Epicardial idiopathic ventricular tachycardias, 851
- Epicardial mapping
 activation, 128–129
 in arrhythmogenic right ventricular
 cardiomyopathy (ARVC), 962
 of nonischemic dilated cardiomyopathy, 883
 transthoracic, 915–916
 activation, 915, 915f, 915.e1f
 electroanatomic, 916
 electroanatomic substrate, 916, 916f–917f
 entrainment, 915
 pace, 915
 transvenous, 920–923
 anatomical considerations in, 920–922, 921f
 outcome of, 922–923
 technical considerations of, 922, 922f, 922.e1f
 907–924
 clinical consideration in, 910–912, 910b, 910.e1f
 anticoagulation in, 911
 contrast-enhanced computed tomography in,
 912
 contrast-enhanced magnetic resonance
 imaging in, 911, 911f
 electrocardiographic features of, 908–910, 908b
 in arrhythmogenic cardiomyopathy, 909
 in idiopathic ventricular tachycardia, 909–910
 idiopathic ventricular tachycardia in, 909–910
 in nonischemic dilated cardiomyopathy, 909
 postinfarction ventricular tachycardia, 910
 electrophysiological substrate of, 907–908
 in nonischemic dilated cardiomyopathy,
 876–877, 877f
 pericardial space in, 912–914
 anatomical considerations in, 912, 913f,
 912.e1f–912.e2f
 epicardial fat and, 914
 pericardial adhesions in, 914, 914f
 technical considerations in, 912–914
- Epicardial window, 762
- Epinephrine
 provocation, in long QT syndrome, 991–992, 992f
 sinus node response to, 250
- Epsilon wave, in arrhythmogenic right ventricular
 cardiomyopathy (ARVC), 954–956, 956f
- Equilibrium, ionic, 1
- Equilibrium potential, 1
- Equivalent dose, for radiation energy, 1063
- Escape ectopic automatic rhythms, 57
- ESI-NavX, in electroanatomic mapping, 782–784
- Esophageal injury, 1056–1062
 clinical presentation of, 1057
 detection of, 1058
 incidence of, 1056–1057
 management of, 1058
 mechanism of, 1057
 prevention of, 1058–1062, 1058f–1060f
- Esophagus
 ablation and, 1059
 location of, 1059–1061, 1060f
 mechanical displacement of, 1061
 temperature, luminal, monitoring of, 1061
- Eustachian ridge, 339–340
 prominent, of atrial flutter, 364
- Exacerbation, of heart failure, in ablation, 812
- Exact capture, in orthodromic atrioventricular
 reentrant tachycardia, 642–643
- Excitability, of cardiac cells, 8–9
 action potential propagation and, 10
 refractoriness and, 9
- Excitable gaps, 68–69, 69f
 resetting zone and, 70–71
- Excitation-contraction coupling, 12–13, 13f
- Exercise. *see also* Sports, participation
 atrial fibrillation and, 437–438
 in Brugada syndrome, 1015–1017
 in long QT syndrome, 981–982, 999–1000
- Exercise electrocardiography, for idiopathic focal
 ventricular tachycardia, 824
- Exercise testing
 in atrioventricular block, 264
 in Brugada syndrome, 1009
 for catecholaminergic polymorphic VT, 1023
 in early repolarization syndromes, 1037
 in hypertrophic cardiomyopathy, 930
 in inappropriate sinus tachycardia, 551
 in long QT syndrome, 991
 in sinus node dysfunction, 243
- Exercise-induced arrhythmogenic right ventricular
 cardiomyopathy, arrhythmogenic right
 ventricular cardiomyopathy (ARVC) and, 950
- Exit block, sinoatrial, 243
- Extensive late gadolinium enhancement, in
 hypertrophic cardiomyopathy, 936
- External irrigation system, 808
- Extra beats
 atrial, in programmed atrial stimulation, for
 paroxysmal supraventricular tachycardia,
 704
 ventricular
 in programmed ventricular stimulation, for
 paroxysmal supraventricular tachycardia,
 707
 in ventricular stimulation, 120
- Extrastimulation
 atrial, 589, 590f
 in paroxysmal supraventricular tachycardia
 atrial, 714
 ventricular
 programmed ventricular stimulation in,
 705
 during tachycardia, 715–716
- Extrastimulus pacing, 110. *see also* Atrial
 extrastimulation/pacing; Ventricular
 extrastimulation/pacing
- Extreme left ventricular hypertrophy, in
 hypertrophic cardiomyopathy, 935–936
- F**
- Factor Xa inhibitors, for atrial fibrillation, 446
- FAM. *see* Fast Anatomical Mapping
- Familial atrial fibrillation. *see* Atrial fibrillation,
 familial
- Familial dilated cardiomyopathy, 869, 870t
- Familial progressive cardiac conduction disease,
 SCN5A/SCN1B mutations in, 20t, 21–22
- Familial Wolff-Parkinson-White syndrome,
 606–607
- Family screening. *see also* Genetic screening
 in hypertrophic cardiomyopathy, 940, 940t
- Fascia adherens, 46
- Fascicular block, 298–299
 left anterior, 298–299
 left median, 293
 left posterior, 293
- Fascicular ventricular tachycardia, 858–868
 ablation of, 864–867
 empirical, 867, 867f
 endpoints of, 867
 outcome of, 867
 target of, 864–866, 865f–866f
 technique of, 866–867
 activation sequence in, 863
 clinical presentation of, 859
 diagnostic maneuvers during, 861
 electroanatomic mapping in, 864, 864f
 electrocardiographic features of, 860
 during normal sinus rhythm, 860
 during ventricular tachycardia, 860, 860f
 electrophysiological testing in, 860–861
 entrainment in, 861
 entrainment mapping in, 863, 863b
 epidemiology of, 859
 focal Purkinje ventricular tachycardia *versus*, 861
 initial evaluation for, 859–860
 interfascicular ventricular tachycardia *versus*, 861
 late diastolic potential in, 863
 mapping in, 861–864
 noncontact mapping in, 864, 865f
 pace mapping in, 863–864
 papillary muscle ventricular tachycardia *versus*,
 861
 pathophysiology of, 858–859
 principles of management for, 860
 Purkinje potential in, 862
 resetting of, 861
 site of earliest ventricular activation in, 861, 862f
 supraventricular tachycardia *versus*, 861
 tachycardia circuit in, 858, 859f
 termination of, 861
- Fasciculoventricular bypass tracts, 690–692, 693f
 electrocardiographic features of, 690, 691f–692f
 electrophysiologic testing for, 690–692
 baseline observations during sinus rhythm,
 690
 programmed atrial stimulation, 691, 693f
 programmed His bundle stimulation, 691–692
 response to pharmacologic maneuvers, 692
 features of, 690b
 general considerations in, 690
- Fasciculoventricular fibers, 677
- Fast Anatomical Mapping (FAM), 156
- Fast pathways, in atrioventricular nodal reentrant
 tachycardia, 562
 differences between slow and, 562
- Fast response potential. *see* Action potentials, fast
 response
- Fast-slow atrioventricular nodal reentrant
 tachycardia, 564–565
 AH/HA ratio in, 565
 anterograde conduction in, 564
 induction of, 576f

- Fast-slow atrioventricular nodal reentrant tachycardia (*Continued*)
 lower common pathway in, 565
 retrograde conduction in, 564–565, 565f
 tachycardia features of, 579–580, 579f
- Femoral arteriovenous fistulas, 1043
- Femoral artery pseudoaneurysms, 1043
- Fever, in Brugada syndrome, 1003
- Fibrosis, atrioventricular block and, 259
- Fiducial point, 162
- Field Scaling, EnSite NavX electroanatomic mapping system and, 159–160, 160f, 173–174
- Figure-of-eight reentry, 66, 66f
- Fistula
 atrioesophageal, after atrial fibrillation ablation, 523
 femoral arteriovenous, 1043
- Fixed fusion, 139
- Fixed-rate pacing, 369
- FK506-binding protein, RyR2 channels and, 45
- Flat response curves, in reentrant rhythms, 72
- Flcainide
 for atrial fibrillation, 450, 452
 Brugada ST segment elevation and, 1008, 1009t, 1010
 for catecholaminergic polymorphic VT, 1024
 for long QT syndrome, 1000
 mechanism of action of, 19
 potassium channels and, 25
- Flufenamic acid, 29
- Fluoroscopy, 155
 catheter-tissue contact and, 219
 of pulmonary vein, 466
 time, for radiation energy, 1062
- Flutter waves, of atrial flutter, 347–348, 348f–351f, 347.e1f
- Focal atrial tachycardia. *see also* Atrial tachycardia, focal
 in congenital heart disease, 408
 cryoablation for, 231
- Focal impulse and rotor mapping, 182, 501–504
 ablation endpoints in, 502–503
 ablation target in, 501
 clinical implications of, 182
 limitations of, 182
 modulation in, 501, 502f, 501.e1f
 outcome of, 503–504
 rationale for, 501
 technique of, 501–502, 503f
 technology application in, 182, 183f
- Focal junctional tachycardia
 atrioventricular nodal reentrant tachycardia and, 587–590
 electrocardiographic features of, 587
 electrophysiological features of, 587–590, 589f
 exclusion of, 588b
 management of, 590
- Focal Purkinje ventricular tachycardia, fascicular ventricular tachycardia *versus*, 861
- Focal tachycardias
 activation mapping of, 128–132, 130f, 132f–133f
 technique for, 131–132
 electroanatomic maps of, 166, 167f
- Focal ventricular tachycardia, 749
 idiopathic, 816–857
 ablation in, 843–854
 cryoablation, 854
 endpoints, 854
- Focal ventricular tachycardia (*Continued*)
 outcomes of, 854
 target, 843, 844f
 technique, 843–854, 845f
- anatomical considerations in, 818–823
 aortic root in, 820–822
 aortomitral continuity in, 822
 cardiac crux in, 823
 left ventricular outflow tract in, 819f, 820, 818.e1f
 left ventricular papillary muscles in, 822–823, 823f
 left ventricular summit, 822, 822.e1f
 pulmonary root in, 820
 right ventricular outflow tract in, 818–820, 819f, 818.e1f
- arrhythmogenic right ventricular cardiomyopathy, 825
 clinical presentation of, 823–824
 diagnostic maneuvers in, 837
 differential diagnosis of, 825–826
 electrocardiographic localization of, 827–836, 828t
 aortic root ventricular tachycardias in, 831–833
 basal left ventricular tachycardias in, 833
 cardiac crux ventricular tachycardias in, 835
 focal Purkinje ventricular tachycardias in, 835, 836f
 frontal plane vertical axis in, 828–836
 left ventricular outflow tract tachycardias in, 829–831, 831f–832f, 831t
 left ventricular papillary muscle tachycardias in, 834–835
 left ventricular summit tachycardias in, 833–834, 834f
 precordial transition in, 827–828
 right ventricular outflow tract tachycardias in, 829, 830f
 right ventricular papillary muscle tachycardias in, 835
 tricuspid annular ventricular tachycardias, 835–836
 electrophysiological testing for, 836–837
 epidemiology of, 823
 features of, 837
 idiopathic ventricular fibrillation and, 826
 induction of, 836–837
 initial evaluation for, 824
 mapping in, 837–843
 activation, 837–840, 838f–839f
 basket catheter, 843, 843.e1f
 CARTO system, 842
 electroanatomic, 841–842, 841f
 noncontact, 842–843, 842.e1f–842.e2f
 pace, 840–841
 mechanism of, 818
 natural history of, 823
 pathophysiology of, 816–818, 817f
- Fontan palliation, univentricular hearts with, in congenital heart disease, 410
- Force-time integral, 221
- Fossa ovalis
 confirming position at, 90
 engaging, 89–90
- Frontal plane horizontal axis, in bypass tract, 618–620
- Frontal plane vertical axis, in bypass tracts, 620
- Functional refractory period, 111, 111t
- Funny current, 42, 52
- Fusion, 72, 72.e1f
 concealed, 141, 143
 entrainment with, in ventricular tachycardia, 775, 776f–777f
 fixed, 139
 inapparent, 141, 142f
 manifest, 141
- ## G
- Gap junction, 46–49
 in acquired diseases, 48–49
 altered distribution and number of, 77
 anisotropy and, 77
 function of, 47–48
 in inherited channelopathies, 48
 intercellular coupling and, 77
 pharmacology of, 48
 regulation of, 48
 remodeling, 75–76
 structure and physiology of, 46–47, 47f
- Gender, atrial fibrillation and, 434
- Genetic mutations, delayed afterdepolarizations and, 60
- Genetic screening
 for early repolarization syndromes, 1037
 for long QT syndrome, 1000
- Genetic testing
 of athlete's heart, 935
 for Brugada syndrome, 1009
 for catecholaminergic polymorphic VT, 1025
 for hypertrophic cardiomyopathy, 931–932, 936
 for idiopathic ventricular fibrillation, 1028
 for long QT syndrome, 992, 997t, 1000
 for short QT syndrome, 1019
- Genetics, in atrial fibrillation, 433, 435
- Genotype-positive/phenotype-negative patients, in hypertrophic cardiomyopathy, 940–941
- GPD1L mutations, in Brugada syndrome, 20t, 21, 1001, 1001t
- Great arteries, dextro-transposition of, in congenital heart disease, 410
- Griffith algorithm, for wide complex tachycardia, 740
- Groin hematomas, 1042–1043
- Guidewires, in percutaneous left atrial appendage ligation, 538
- ## H
- HA interval
 in paroxysmal supraventricular tachycardia, ventricular pacing at tachycardia cycle length, 723
 in ventricular pacing, 586, 586f
- Halo catheter, 84, 84f
- HAS-BLED bleeding risk score, 443, 444t
- HCM Risk-SCD model, in hypertrophic cardiomyopathy, 937–938, 937t
- HCN channel blockers, 42
- HCN channels, 42
- HCN4 mutations, 43
- Heart disease, ischemic
 atrioventricular block and, 258–259
 chronic, atrioventricular block and, 259
 sinus node dysfunction and, 240

- Heart failure
 - in acquired disease, 22
 - atrial fibrillation and, 435–436
 - exacerbation of, in ablation, 812
 - in hypertrophic cardiomyopathy, 929
 - treatment of, 938, 938.e1f–938.e2f
 - potassium channel defects in, 37
 - Heart failure therapy, for arrhythmogenic right ventricular cardiomyopathy (ARVC), 951
 - Heart valve, mitral, catheter entrapment in, in atrial fibrillation ablation, 524
 - Hematomas, 1042–1043
 - in complications of catheter ablation, 1042–1043
 - Hemodynamic support, in mapping, of ventricular tachycardia, 781–782
 - HEMORR2HAGES score, 443, 444t
 - Heparin. *see also* Anticoagulation
 - for atrial flutter ablation, 359
 - for transseptal puncture, 84, 87
 - Hereditary cardiac conduction disease,
 - atrioventricular block and, 258
 - HERG channels, 24t, 27
 - in long QT syndrome, 977t, 979
 - in short QT syndrome, 1017t
 - High-frequency ultrasound
 - balloon catheter for, 233.e1f
 - radiofrequency ablation and, 222
 - High posterolateral myocardial infarction
 - ventricular tachycardias, 767
 - High-resolution electroanatomic mapping, 171–172
 - His bundle, 257, 293, 293.e1f
 - type 1 second-degree atrioventricular block in, 273
 - His bundle activation, in ventricular tachycardia, 770–771, 770.e1f
 - His bundle-atrial intervals, in para-Hisian pacing, during sinus rhythm, 631–633
 - His bundle catheters, 86
 - His bundle electrogram, 106–107, 107f
 - His bundle pacing
 - for atrioventricular block, 282, 282f–283f
 - for bundle branch block, 302, 302.e1f
 - His bundle refractoriness, ventricular
 - extrastimulation during, 628, 629f, 642
 - His bundle-ventricular (HV) interval, 898
 - in bundle branch block, 300, 302f
 - in bundle branch reentrant ventricular tachycardia, 779
 - measurement of, 107f, 109, 272
 - His potential
 - measurement of, 109
 - retrograde, in ventricular stimulation, 117, 118f
 - His-Purkinje system
 - anatomy and physiology of, 293–294
 - atrioventricular block in, 265, 265f
 - first-degree, 273
 - second-degree
 - type 1, 267, 267f
 - type 2, 268, 268f, 273, 274f, 273.e1f–273.e2f
 - third-degree, 270, 272f, 274
 - pathophysiology of, 294–295
 - Holter monitoring
 - in inappropriate sinus tachycardia, 550–551, 551f
 - in long QT syndrome, 990
 - in sinus node dysfunction, 244
 - Hyperkalemia, wide complex tachycardia and, 732, 732.e1f
 - Hyperpolarization, 2
 - Hypertension, atrial fibrillation and, 435
 - management of, 456
 - Hyperthermia, in Brugada syndrome, 1003
 - Hyperthyroidism, atrial fibrillation and, 437
 - Hypertrophic cardiomyopathy, arrhythmias in, 925–941
 - clinical presentation of, 929–930
 - differential diagnosis of, 932–935
 - epidemiology of, 927–929
 - initial evaluation of, 930–932, 930f
 - ambulatory cardiac monitoring for, 930
 - cardiac magnetic resonance for, 930–931, 931f
 - echocardiography for, 930
 - electrocardiography for, 930, 931f
 - electrophysiological testing for, 930
 - exercise testing for, 930
 - genetic testing for, 931–932
 - natural history of, 927–929
 - pathophysiology of, 925–927
 - diastolic dysfunction, 925
 - left ventricular outflow obstruction, 925–926
 - molecular genetics in, 926–927, 927f–928f
 - myocardial ischemia, 926
 - ventricular arrhythmias, 926
 - ventricular hypertrophy, 925, 926f
 - phenocopies of, 932–933, 932t–933t
 - principles of management of, 938–941
 - of atrial fibrillation, 938
 - family screening, 940, 940t
 - genotype-positive/phenotype-negative patients, 940–941
 - of heart failure and left ventricular outflow obstruction, 938, 938.e1f–938.e2f
 - of ventricular arrhythmias, 938–940, 939f
 - risk stratification of, 935–938
 - conventional risk stratification model, 937, 937b
 - established risk markers, 935–936
 - HCM Risk-SCD model, 937–938, 937t
 - possible risk modifiers, 936
 - Hypervagotonia, sinus node dysfunction and, 241
 - Hypokalemia
 - long QT syndrome and, 992, 1000
 - wide complex tachycardia and, 732
 - Hypothermia, early repolarization and, 1031, 1035t
- I**
- Iatrogenic atrioventricular block, 260–261
 - permanent pacing for, 278–279
 - Iatrogenic cardiac arrhythmias, 1049–1050
 - Ibutilide, 28
 - for atrial fibrillation, 450
 - for atrial flutter, 346
 - ICD. *see* Implantable cardioverter-defibrillator
 - ICE. *see* Intracardiac echocardiography
 - Ice formation
 - extracellular, 226–227
 - intracellular, 227–228
 - Idiopathic focal ventricular tachycardia, 816–857
 - ablation in, 843–854
 - cryoablation, 854
 - endpoints, 854
 - outcomes of, 854
 - Idiopathic focal ventricular tachycardia
 - (*Continued*)
 - target, 843, 844f
 - technique, 843–854, 845f
 - anatomical considerations in, 818–823
 - aortic root in, 820–822
 - aortomitral continuity in, 822
 - cardiac crux in, 823
 - left ventricular outflow tract in, 819f, 820, 818.e1f
 - left ventricular papillary muscles in, 822–823, 823f
 - left ventricular summit, 822, 822.e1f
 - pulmonary root in, 820
 - right ventricular outflow tract in, 818–820, 819f, 818.e1f
 - arrhythmogenic right ventricular cardiomyopathy, 825
 - clinical presentation of, 823–824
 - diagnostic maneuvers in, 837
 - differential diagnosis of, 825–826
 - electrocardiographic localization of, 827–836, 828t
 - aortic root ventricular tachycardias in, 831–833
 - basal left ventricular tachycardias in, 833
 - cardiac crux ventricular tachycardias in, 835
 - focal Purkinje ventricular tachycardias in, 835, 836f
 - frontal plane vertical axis in, 828–836
 - left ventricular outflow tract tachycardias in, 829–831, 831f–832f, 831t
 - left ventricular papillary muscle tachycardias in, 834–835
 - left ventricular summit tachycardias in, 833–834, 834f
 - precordial transition in, 827–828
 - right ventricular outflow tract tachycardias in, 829, 830f
 - right ventricular papillary muscle tachycardias in, 835
 - tricuspid annular ventricular tachycardias, 835–836
 - electrophysiological testing for, 836–837
 - epidemiology of, 823
 - features of, 837
 - idiopathic ventricular fibrillation and, 826
 - induction of, 836–837
 - initial evaluation for, 824
 - mapping in, 837–843
 - activation, 837–840, 838f–839f
 - basket catheter, 843, 843.e1f
 - CARTO system, 842
 - electroanatomic, 841–842, 841f
 - noncontact, 842–843, 842.e1f–842.e2f
 - pace, 840–841
 - mechanism of, 818
 - natural history of, 823
 - pathophysiology of, 816–818, 817f
- Idiopathic (fascicular) left ventricular tachycardia, *versus* bundle branch reentrant ventricular tachycardia, 902–903
- Idiopathic right ventricular outflow tract tachycardia, arrhythmogenic right ventricular cardiomyopathy (ARVC) and, 948–949, 949b
 - cardiac imaging in, 949
 - electrocardiogram during sinus in, 948

- Idiopathic right ventricular outflow tract tachycardia, arrhythmogenic right ventricular cardiomyopathy (ARVC) and (*Continued*) electrocardiogram during ventricular tachycardia, 948–949
invasive electrophysiological testing in, 949
isoproterenol testing in, 949
- Idiopathic ventricular fibrillation, idiopathic focal ventricular tachycardia, 826
- Idiopathic ventricular tachycardia, 909–910
epicardial ablation in, 908
- I_K -decay theory, 51–52
- Immediate Risk Stratification Improves Survival Study (IRIS), 755t–756t
- Immunosuppression, for cardiac sarcoidosis, 888
- Implantable cardioverter-defibrillator (ICD)
for Brugada syndrome, 1013–1014, 1014f
for bundle branch reentrant ventricular tachycardia, 898, 902f
for cardiac sarcoidosis, 889, 891f
for catecholaminergic polymorphic VT, 1025
for congenital heart disease, 970, 971b
for coronary artery disease, 755t–756t
for idiopathic focal ventricular tachycardia, 827
for idiopathic ventricular fibrillation, 1028
for long QT syndrome, 997–998, 998f, 999t
for nonischemic dilated cardiomyopathy, 873–876, 874b, 874t, 875f, 874.e1f
for short QT syndrome, 1019–1020
for ventricular arrhythmias, 758–760
antiarrhythmic drug therapy with, 758
in primary prevention, 759–760, 761f
in secondary prevention, 758–759, 759t, 760f
for wide complex tachycardia, 731
- Inadequate radiofrequency energy delivery, of atrial flutter, 363
- Inapparent fusion, 141, 142f
entrainment with, in ventricular tachycardia, 775–776
- Inapparent preexcitation, 613
- Inappropriate sinus tachycardia (IST), 549–559
ablation of, 554–558
endpoints of, 555–558
outcome of, 558
target of, 554, 554.e1f
technique of, 554–555, 556f–557f, 555.e1f–555.e2f
clinical presentation of, 550
differential diagnosis of, 551–552
postural orthostatic tachycardia syndrome and, 551–552, 552t
supraventricular tachycardias and, 552
electrophysiological testing in, 553–554, 554f
epidemiology and natural history of, 550
initial evaluation of, 550–551, 550b
autonomic evaluation in, 551
exercise testing in, 551
Holter monitoring in, 550–551, 551f
isoproterenol provocation in, 551
management of, 552–553
catheter ablation in, 553
pharmacological therapy in, 552–553
surgical ablation in, 553
pathophysiology of, 549–550
tachycardia in
features of, 553–554
induction of, 553
- Incessant ventricular tachycardia, 749
- Incisional right atrial macroreentrant tachycardia, 378
- Incremental pacing, 109, 370, 370.e2f
of atrial flutter, 370, 370.e2f
- Indapamide, mechanism of action of, 30
- Inducibility, of paroxysmal supraventricular tachycardia
programmed atrial stimulation in, 710
programmed ventricular stimulation in, 710
- Infectious diseases, atrioventricular block and, 260
- Infective endocarditis, atrioventricular block and, 260
- Inferior myocardial infarction, acute, atrioventricular block and, 259
- Inferior myocardial infarction ventricular tachycardia, 764–767, 767f
- Inferior vena cava (IVC), anatomy of, 339
- Infiltrative processes, atrioventricular block and, 260
- Inflammation, in atrial fibrillation, 428–429
- Inherited channelopathies
potassium channel
 I_{K1} defects in, 32
 I_{KACH} defects in, 33
 I_{KATP} defects in, 35
 I_{Kr} defects in, 29
 I_{Ks} defects in, 30
 I_{Kur} defects in, 27
 I_{to} defects in, 25–26
sodium channels, 19–22, 20t. *see also* Sodium channels
sudden cardiac death in, 976
ventricular arrhythmias in, 976–1041
in Brugada syndrome, 1000–1017
in catecholaminergic polymorphic VT, 1020–1025
in early repolarization syndromes, 1029–1038
in idiopathic ventricular fibrillation, 1025–1029
in long QT syndrome, 976–1000
in short QT syndrome, 1017–1020
- Interarterial conduction, 255
- Interatrial conduction, 108
- Interatrial shunt, after transseptal puncture, 95
- Intercellular propagation, 10–11
- Interfascicular ventricular tachycardia, fascicular ventricular tachycardia *versus*, 861
- Interleaflet triangles, anatomy of, 821
- Intermittent preexcitation, 607, 613, 613f
- Internal irrigation system, 808
- Internodal atrial myocardium, 255
- Internodal conduction, 255
- Intraabdominal bleeding
as complications of pericardial access, 101
in transthoracic epicardial ablation, 919–920
- Intraatrial reentrant beats
in atrial stimulation, 115
in programmed atrial stimulation, for paroxysmal supraventricular tachycardia, 704
- Intracardiac echocardiography (ICE), 193–197. *see also* Electrocardiography
AcuNav catheter for, 194–195
in CARTO-Sound, 157
catheter design in, 193
catheter-tissue contact and, 219, 222
in circumferential antral pulmonary vein isolation, 485
- Intracardiac echocardiography (ICE) (*Continued*)
clinical implications of, 195–197
electronic phased-array catheter sector imaging system in, 193
in focal atrial tachycardia ablation, 333, 333.e2f
imaging technique for, 193–195
interatrial septum in, 194–195
left and right ventricular targets in, 195, 196f
left atrial structures in, 195, 195f
mechanical radial intracardiac echocardiographic catheter for, 193, 194f
mechanical ultrasound catheter radial imaging system, 193
practical uses for, 196, 197f
of pulmonary vein, 466
right atrial targets in, 194, 194f
- Intracardiac electrograms, 103–107
amplification of, 101
atrial, complex fractionated, 504–507
clipping of, 101–102, 102f
coronary sinus, 107, 108f
His bundle, 106–107, 107f
overdrive pacing for, 109
recording of
analog *versus* digital, 101
bipolar, 104f
unipolar, 103–104, 104f
right atrial, 105
right ventricular, 107
signal filtering for, 102–103
band-pass, 103
high-pass, 102–103
low-pass, 103
notch, 103
surface and intracardiac signal selection for, 105–107, 106f
timing of local events and, 105
- Intracardiac fusion, 141
- Intracardiac mapping. *see* Mapping
- Intracardiac thrombi, evaluation for, 780
- Intracardiac ultrasound, in substrate image integration, 799
- Intracellular “calcium clock,” 52–53
- Intracellular propagation, 10
- Intramural ventricular tachycardias, 853–854
- Intraventricular conduction abnormalities, 286–304
- Intraventricular conduction disturbances (IVCDs), 286
bifascicular block, 295
electrophysiological testing, 303b
nonspecific, 295
transient bundle branch block, 286–293
trifascicular block, 299
- Intraventricular reentrant beats, 120
in programmed ventricular stimulation, for paroxysmal supraventricular tachycardia, 707
- Intrinsic heart rate, sinus node response to, 250
- Intrinsicoid deflection, 741, 909
- Inwardly rectifying potassium (K^+) current (I_{KACH}), 257
- Ion channel clock, 52
- Ion channels, 1
action potentials and, 2–8
heterogeneity of, 67

- Ion channels (*Continued*)
 membrane polarization and, 2
 regional differences in, 3, 5*t*
 transmembrane potentials and, 1–2, 2*t*. *see also* Action potentials
- Ionic currents. *see also* Ion channels
 action potential and, 2–8, 4*f*–5*f*
 fast response, 3–8
 slow response, 8
 funny (pacemaker), 8, 42, 52
 Kir, 3, 23, 23*f*, 24*t*
 net transmembrane, 2–3
 potassium, 22–37. *see also* Potassium currents
 regional differences in, 3, 5*t*
- Ionic equilibrium, 1
- Ischemic cardiomyopathy, in epicardial ventricular tachycardia, 907–908
- Ischemic Cardiomyopathy Multicenter Automatic Defibrillator Implantation Trial (MADIT), 755*t*–756*t*
- Ischemic heart disease. *see also* Myocardial ischemia
 atrioventricular block and, 258–259
 chronic, atrioventricular block and, 259
 sinus node dysfunction and, 240
 ventricular arrhythmias in, 748–815
- Isochronal map, in electroanatomic activation mapping, 167
- Isoproterenol
 for Brugada syndrome, 1015
 during electrophysiological testing, 611
 provocation, in inappropriate sinus tachycardia, 551
 sinus node response to, 250–251
 in ventricular tachycardia, induction of, 769
- Isotropic conduction, 66
- IST. *see* Inappropriate sinus tachycardia
- Isthmus. *see* Critical isthmus; Mitral isthmus
- I_{to} channels, 24–27, 24*t*, 26*t*
- IV ibutilide, for atrial flutter, 346
- Ivabradine, 43
 for inappropriate sinus tachycardia and, 553
- IVCDs. *see* Intraventricular conduction disturbances
- J**
- J waves, in early repolarization syndromes, 25–26, 1030, 1035*t*. *see also* Early repolarization syndromes
 amplitude of, 1035
 distribution of, 1036
 fluctuation of, 1036
 morphology of, 1036
- James fiber, 600*t*
- Jervell and Lange-Nielsen syndrome, 30, 976–978, 985. *see also* Long QT syndrome
- Joule-Thomson effect, 225
- JTV-519, 45–46
- Junctional rhythm, after ablation, of
 atrioventricular nodal reentrant tachycardia, 594–595, 594*f*–595*f*
- K**
- K_{2P} potassium channels, 23, 24*t*, 36
- K201, 45–46
- KCNA5, 27
- KCNE1
 in acquired diseases, 30–31
 in long QT syndrome, 30, 977*t*, 978
- KCNE2, in long QT syndrome, 977*t*, 979
- KCNE3, 25
 in Brugada syndrome, 1001, 1001*t*
- KCNJ2, mutations in
 in catecholaminergic polymorphic VT, 32, 1020
 in familial atrial fibrillation, 32
 in long QT syndrome, 32, 977*t*, 979
 in short QT syndrome, 32, 1017*t*, 1018
- KCNJ5, in long QT syndrome, 977*t*, 979
- KCNQ1
 in acquired diseases, 30–31
 mutations in
 in familial atrial fibrillation, 30
 in long QT syndrome, 30, 977*t*
 in short QT syndrome, 30, 1017*t*, 1018
- Kent bundles, 599, 600*t*
- Kir channel, 3
- Kir6.2 subunit, 35
 in atrial fibrillation, 35
 in heart failure, 35
 in neonatal diabetes mellitus, 35
- L**
- LAF. *see* Left anterior fascicle
- Laplace's equation, 190
- Lariat system/procedure, in percutaneous left atrial appendage ligation, 537, 539*f*
- Laser ablation. *see also* Catheter ablation
 in circumferential antral pulmonary vein isolation, 491–493, 491*f*–492*f*
- Laser energy, 231–232
 argon, 231
 biophysics of, 231, 231*f*
 clinical applications of, 231–232
 diode, 231
 Nd:YAG, 231
- Lasso catheter, 84, 84*f*
- Last entrained interval, 73
- Late potentials
 in abnormal local ventricular electrograms, 797–798, 798*f*
 in arrhythmogenic right ventricular cardiomyopathy (ARVC), 961*f*, 962
 in conducting channels, during sinus rhythm, 803
- Lateral mitral isthmus line ablation, 498–500
- LAVA. *see* Local abnormal ventricular activity
- Leading circle concept, 65–66
- Left anterior fascicle (LAF), 293
- Left anterior fascicular block, 298–299
 electrocardiography of, 296*b*
- Left atrial appendage
 anatomy of, 532, 532*f*
 catheterization of, 534
 device closure for, percutaneous, 531–537
 Amplatzer Cardiac Plug, 535–537
 Watchman device, 534–535
 electrical isolation of, 515
 imaging of, 532–534, 533*f*
 ligation of, percutaneous, 537–540
 device specification for, 537
 endocardial access in, 537–538, 539*f*
 epicardial access in, 537
 guidewires in, 538
- Left atrial appendage (*Continued*)
 imaging in, 537
 outcome of, 538–540
 postoperative management of, 538
 snaring in, 538
 surgical exclusion of, 540–541, 541*e1f*
- Left atrial posterior wall isolation, 498, 499*f*–500*f*, 498*e1f*
- Left atrial roof line ablation, 497–498
- Left bundle. *see also* Bundle branch
 anatomy of, 293–294
- Left cervicothoracic sympathectomy
 for catecholaminergic polymorphic VT, 1025
 for long QT syndrome, 999
- Left fibrous trigone, 256
- Left free-wall bypass tracts, 620–621
 ablation of, 663–666
 anatomical considerations for, 663–665, 665*e1f*
 technical considerations for, 665–666
 transaortic (retrograde) approach in, 665
 transeptal approach in, 665–666, 666*e1f*
- Left median fascicle, 293
- Left median fascicular block, 299
- Left posterior fascicle (LPF), 293
- Left posterior fascicular block, 299
 electrocardiography of, 299
- Left septal circuits, 382, 382*e1f*
- Left ventricular access, 781
- Left ventricular apical aneurysm, in hypertrophic cardiomyopathy, 936
- Left ventricular ejection fraction (LVEF)
 in nonischemic dilated cardiomyopathy, 872
 in risk stratification, of ventricular arrhythmias, 754–756, 755*t*–756*t*, 754*e1f*
- Left ventricular outflow obstruction, in
 hypertrophic cardiomyopathy
 clinical presentation of, 929
 pathophysiology of, 925–926
 as possible risk modifiers, 936
 treatment of, 938, 938*e1f*–938*e2f*
- Left ventricular outflow tract, ventricular tachycardia from, 844–846
- Left ventricular papillary muscle, ventricular tachycardia from, 852–853, 853*f*
- Left ventricular summit
 and transvenous epicardial mapping and ablation, 921, 922*f*
 ventricular tachycardia from, 851, 852*f*
- Left-sided bypass tracts, 621
- Lenègre disease, atrioventricular block and, 259
- Lev disease, atrioventricular block and, 259
- Lidocaine
 for atrial fibrillation, 608–609
 mechanism of action of, 19
 for sustained ventricular tachycardia, 757
- Ligament of Marshall, mapping and ablation of, 510–512, 511*f*–512*f*, 511*e1f*, 510*e1f*
- Limitations, in programmed ventricular stimulation, for paroxysmal supraventricular tachycardia, 705–706, 706*f*
- Linear ablation, 807
- Linear atrial ablation, 497–501
 cavotricuspid isthmus line ablation, 500–501
 lateral mitral isthmus line, 498–500
 left atrial posterior wall isolation, 498, 499*f*–500*f*, 498*e1f*
 left atrial roof line, 497–498

- Lines of block, in congenital heart disease
documentation, 974
identification of, 972
- Local abnormal ventricular activity (LAVA),
796–797
- Local atrioventricular interval, 658–660, 661f–662f
- Local fusion, 141, 142f
- Local ventricular electrograms, abnormal, 796–798
late potentials in, 797–798, 798f
LAVA in, 796–797
- Localized source hypothesis, 426
- Long QT syndrome, 976–1000
age and, 984, 994, 995t
ankyrin-B mutations in, 977t, 980
atrioventricular block and, 258
beta-blockers for, 994
calcium channel mutations in, 977t, 979–980
clinical presentation of, 983–985
concealed, 990
congenital type 1, 30
congenital type 3, 19–20, 20t
congenital type 5, 30
congenital type 7, 32
congenital type 9, 20t, 21
congenital type 10, 20t, 21
congenital type 11, 30
congenital type 12, 20t, 21
course of, 983–985
diagnosis of, 989–992, 990t
ambulatory cardiac monitoring in, 990
clinical scoring systems for, 990
epinephrine QT stress test in, 991–992, 992f
genetic testing in, 992
QT interval response to abrupt standing,
990–991
differential diagnosis of, 992–994
dispersion of repolarization in, 980–981, 989
drug-induced, 993
early afterdepolarizations and, 62–63
electrocardiographic features of, 985–989, 988f
QT interval prolongation in, 981–982,
987–988, 987t, 993
epidemiology of, 983
exercise and, 981–982, 991, 997
family screening, 1000
gender and, 982–984, 994
genetic aspects of, 977–980, 977t, 978f, 993–994,
994t, 1000
genotype-phenotype variability in, 982
hypokalemia and, 992
management of, 996–1000
catheter ablation in, 999
gene-specific therapy in, 997t, 1000
implantable cardioverter-defibrillator in,
997–998, 998f, 999t
left cervicothoracic sympathectomy in, 999
lifestyle modification in, 999
participation in sports in, 999–1000
permanent pacing in, 999
pharmacological, 996–997, 998f
mutations in
Andersen-Tawil syndrome, 32
calcium channel, 41, 41t
potassium channel, 29–30, 32
Romano-Ward syndrome, 30
Timothy syndrome, 41
pathophysiology of, 980–983, 981f
potassium channel mutations in, 977–979, 977t
- Long QT syndrome (*Continued*)
QT interval in
correction for gender, 986
correction for heart rate, 986–987, 986t
correction for QRS duration, 987
measurement of, 985–986, 986f
prolongation of, 981–982, 987–988, 987t,
995–996
during right ventricular pacing, 987
QTc clock, 990, 990.e1f
risk stratification for, 994–996
age in, 994, 995t
clinical markers in, 994–995
electrocardiographic markers in, 995–996
family history in, 994
gender in, 994
genetic markers in, 996
syncope in, 994
sodium channel mutations in, 19–21, 20t, 977t,
979, 979.e1f
sports participation in, 999–1000
stress and, 981, 984f, 991–992, 999
syncope in, 984
beta-blockers for, 994
as risk marker, 994
T wave in, 988–989
torsades de pointes in, 981, 988–989
triggers in, 984f, 993–994, 999
T-U wave in, 996
types of, 983, 983t
Andersen-Tawil syndrome, 985
Jervell and Lange-Nielsen syndrome, 30,
985
Romano-Ward syndrome, 983–984
Timothy syndrome, 985
- Lower common pathway
in fast-slow atrioventricular nodal reentrant
tachycardia, 565
in slow-fast atrioventricular nodal reentrant
tachycardia, 564
in slow-slow atrioventricular nodal reentrant
tachycardia, 566
- Lower turnaround point, 563
- Lown-Ganong-Levine syndrome, 600
- LPF. *see* Left posterior fascicle
- LVEF. *see* Left ventricular ejection fraction
- Lyme disease, atrioventricular block and, 260
- M**
- M cells, 7–8
- Macroreentrant atrial tachycardias (MRATs)
in congenital heart disease, 407–408, 408f–409f
in iatrogenic cardiac arrhythmias, 1049
- Macroreentrant tachycardias
activation mapping of, 128, 130f, 132–135, 134f
continuous electrical activity in, 134, 134.e1f
mid-diastolic activity, 134–135, 134f
critical isthmuses in, 133, 143
electroanatomic activation map in, 167
pace mapping of, 152
ventricular, 130f
bridging of diastole, 134
- Macroreentry circuits, 749
- MADIT-II. *see* Multicenter Automatic Defibrillator
Implantation Trial II
- Magnetic navigation system. *see* Stereotaxis
magnetic navigation system
- Magnetic resonance imaging, 197–202
cardiac
in arrhythmogenic substrate, 780–781, 780.e1f
in substrate image integration, 799
in ventricular arrhythmias, 757
in circumferential antral pulmonary vein
isolation, 485
fundamental concepts of, 197–198
image acquisition in, 197
image integration technique for, 198–199
clinical implications of, 199–201, 200f–201f,
200.e1f
limitation of, 201–202
using CARTO-Merge, 198
using CARTO-Sound, 198
using fluoroscopy, 199
using NavX fusion, 198–199, 199f
image registration in, 197–198
accuracy of, 201–202
image segmentation in, 197, 197.e1f
- Mahaim fibers, 600t, 677
- Mahaim tachycardia, 677
- Mahaim variant of preexcitation, 600
- Managed ventricular pacing (MVP) algorithm, 252
- Manifest atrial fusion, in paroxysmal
supraventricular tachycardia
atrial extrastimulation in, 714
atrial overdrive pacing in, 714
- Manifest bypass tracts
asymptomatic patients with, chronic
management of, 609–612, 610f, 611b
symptomatic patients with
acute management of, 608
chronic management of, 609, 610f
- Manifest fusion, 141
entrainment with, in ventricular tachycardia, 775
- Manifest perpetuation, in ventricular tachycardia,
771
- Manifest ventricular fusion, in paroxysmal
supraventricular tachycardia
ventricular extrastimulation in, 715
ventricular overdrive pacing in, 717
- Mapping, 125–154
access challenges in, 413–415, 413t
to arrhythmia substrate and cavotricuspid
isthmus, 413, 414f
to coronary sinus and atrioventricular node,
413, 414f
to pulmonary venous atrium, 414–415, 415f
to systemic venous atrium, 413
in arrhythmogenic right ventricular
cardiomyopathy (ARVC), 959–962
activation, 959, 959.e1f
entrainment, 959–960
epicardial, 962
pace, 960
substrate, 960–962
- of atrial flutter, 356–359
activation, 356
electroanatomic, 358–359, 361f
entrainment, 356–358, 356b, 357f–358f
noncontact, 359, 359.e1f
- of atrial tachycardia, macroreentrant, 388–397
activation, 389–391, 390f–391f
cycle length variations in, 396
electrocardiographic findings of, 396
entrainment, 392–395, 393b
exclusion of isthmus dependence in, 396

- Mapping (*Continued*)
- identification of barriers and lines of block in, 397
 - identification of complete reentrant circuit in, 397
 - identification of critical isthmus, 397
 - localization of reentrant circuit chamber in, 389, 390f
 - noncontact, 395–396
 - practical approach to, 396–397
 - technique, 388–389
 - of congenital heart disease, 972–973
 - endocardial, with basket catheter, 181
 - endocardial activation, 467–470
 - EnSite NavX, 158–160
 - EnSite noncontact mapping system, 176–180
 - of focal atrial tachycardia, 324–333
 - activation, 324–328, 330, 325.e1f
 - electroanatomic, 330–332
 - local activation time, 326–328, 327f
 - nonsustained, 332–333
 - pace, 328–329, 329f
 - postpacing intervals, 329–330
 - reference electrogram, 325–326
 - right atrial *versus* right superior pulmonary vein foci, 328
 - right *versus* left atrial foci, 328
 - tachycardia transformation, 328
 - technique, 330
 - in focal ventricular tachycardia, idiopathic, 837–843
 - activation, 837–840, 838f–839f
 - basket catheter, 843, 843.e1f
 - CARTO system, 842
 - electroanatomic, 841–842, 841f
 - noncontact, 842–843, 842.e1f–842.e2f
 - pace, 840–841
 - intracardiac echocardiography, 193–197
 - three-dimensional rotational angiography, 202–203
 - of ventricular tachycardia, 780–805
 - activation, 784–786
 - electroanatomic, 782–784, 782f–783f
 - entrainment, 786–792
 - hemodynamic support in, 781–782
 - left ventricular access in, 781
 - noncontact, 800–801, 800.e1f
 - pace, 792–795
 - postinfarction premature ventricular complexes, 801
 - practical approach to, 802–805, 802b, 803f
 - preprocedural evaluation of, 780–781
 - substrate, 795–800
 - voltage (scar), 795–796, 795f
- Maximal deflection index, 909
- Maximum voltage-guided technique, of atrial flutter, 363
- Mean absolute deviation, in pace mapping, 149, 149.e1f
- Mechanical Ultrasound Catheter Radial Imaging System, 193
- Mechanoelectric feedback, automaticity and, 55
- MediGuide navigation systems, 187–188
 - clinical implications of, 188
 - fundamental concepts of, 187, 188f
 - limitations of, 188
 - technology application of, 187, 189f
- Membrane capacitance, 1–2
- Membrane conductance, 1
- Membrane depolarization, 2. *see also* Action potentials
 - action potentials and, 2–8, 4f
 - fast response, 3–8
 - slow response, 8
 - delayed afterdepolarizations and, 58–63, 58f–59f
 - diastolic, in catecholaminergic polymorphic VT, 1020
 - early afterdepolarizations and, 58f, 60, 62.e1f
 - triggered activity and, 58–63
- Membrane electroporation, 235
- Membrane excitability, reduced, 75
- Membrane hyperpolarization, 2
- Membrane permeability, 3
- Membrane potential
 - action potentials and, 2–8. *see also* Action potentials
 - reduced, abnormal automaticity and, 55, 54.e1f
 - resistance and, 1
 - resting, 3–6, 3t
 - regional differences in, 3, 5t
 - restoration of, 7
 - trans, 1–2
- Membrane repolarization
 - early, 6
 - final rapid, 7
 - rapid, 6
- Membrane resistance, 1
- Mexiletine
 - for Brugada syndrome, 1010
 - for long QT syndrome, 1000
 - mechanism of action of, 19
 - sinus node response to, 250
- Microbubbles, in radiofrequency ablation, 222
- Microreentrant atrial tachycardia, 321–322
- Microvolt T-wave alternans, 756
 - in nonischemic dilated cardiomyopathy, 873
- Microwave, 234
 - defined, 233
- Microwave ablation, 233–234. *see also* Catheter ablation
 - biophysics of microwave energy and, 233–234
 - clinical applications of, 234
 - effectiveness of, 233–234
 - lesion formation by, pathophysiology of, 234
- Microwave energy
 - biophysics of, 233–234
 - delivery of, 234
 - radiofrequency energy and, 234
- Mid-diastolic activity, in activation mapping, 786, 786.e1f
- Midseptal bypass tracts, 623
 - ablation of, 667–670
 - anatomical considerations for, 667–668
 - cryoablation and, 669–670
 - advantages of, 670
 - outcome of, 670
 - cryomapping and, 669–670
 - electrocardiographic considerations for, 668
 - technical considerations for, 668–669, 669f
- Midseptum atypical tachycardia, 314
- Mitral annulus
 - atrial flutter arising from, 379, 380f
 - atrial tachycardia arising from, 318
- Mitral isthmus, ablation of, 399.e1f
- Mitral valve
 - catheter entrapment in, in atrial fibrillation ablation, 524
 - damage to, 1050–1051
- Mixed response curves, in reentrant rhythms, 72
- MK-499, 28
- Mobitz block
 - type 1 (Wenckebach), 113, 258
 - atypical, 113
 - site of block in, 267
 - in ventricular pacing, 117
 - type 2, 258–259, 267–268, 268f
- Modified European Heart Rhythm Association symptom scale, 440, 441t
- Modified Seldinger technique, in electrophysiological testing, 85
- Molecular genetics
 - cardiomyopathy, 869–870
 - in hypertrophic cardiomyopathy, 926–927, 927f–928f
- Monomorphic ventricular tachycardia, 748, 749f
- MRATs. *see* Macroreentrant atrial tachycardias
- Multi-Array Ablation Catheter, 223–224, 224f
- Multi-Array Septal Catheter, 223–224, 224f
- Multicenter Automatic Defibrillator Implantation Trial II (MADIT-II), 755t–756t
- Multicenter Unsustained Tachycardia Trial (MUSTT), 755t–756t
- Multifocal atrial tachycardia, 308–309, 308f
- Multiple atrioventricular bypass tracts, 601
 - electrophysiological findings in, 652b
- Multiple atrioventricular nodal pathways, 573
- Multiple inducible ventricular tachycardias, ablation in, 807
- Multiple monomorphic ventricular tachycardia, 748
- Multiple wave reentry hypothesis, 425–426
- MUSTT. *see* Multicenter Unsustained Tachycardia Trial
- Myocardial conduction disorders, measures of, 757
- Myocardial fibrosis, in nonischemic dilated cardiomyopathy, 871
- Myocardial infarction
 - acute
 - anterior, atrioventricular block and, 259
 - atrioventricular block after, permanent pacing for, 278, 279b
 - inferior, atrioventricular block and, 259
 - potassium channel defects in
 - I_{Kr}, 29
 - I_{to}, 26
- Myocardial ischemia
 - acute phase of, 750
 - delayed afterdepolarizations and, 60
 - evaluation of, 753
 - genetic testing in, 757
 - in hypertrophic cardiomyopathy
 - clinical presentation of, 929
 - pathophysiology of, 926
 - potassium channel defects in, 26
 - subacute phase of, 750
- Myocardial ventricular tachycardia, *versus* bundle branch reentrant ventricular tachycardia, 902–903
- Myocardium
 - action potentials in, 7
 - internodal atrial, 255
- Myocytes, contraction of, 11

- N**
- N cells, 257
- Nadolol, for long QT syndrome, 997
- Narrow QRS complex, 730
- Narula method, for sinoatrial conduction time, 250
- Navigation systems
- Astronomer, 180
 - MediGuide, 187–188
 - Navigant, 184
 - Sensei robotic, 186–187
 - stereotaxis magnetic, 183–186
- Nd:YAG laser, 231
- Needle
- advancing, 96
 - intrapercardial position of, 96–97, 97f
- “Needle-in-needle” technique, 98
- Neonatal lupus, congenital atrioventricular block and, 258
- Nernst potential, 1
- Neuromyopathies, atrioventricular block and, 258
- NH cells, 257
- Niflumic acid, 29
- Niobe MNS, 183
- nMARQ ablation system, 225, 227f
- NOACs. *see* Non-vitamin K antagonist oral anticoagulants
- Nodal cells, 257
- Nodal-His cells, 257
- Nodal-His region, 562
- Nodal region, 561–562
- Nodofascicular bypass tracts, 688–690
- ablation in, 690
 - arrhythmias associated with, 688
 - electrocardiographic features of, 689
 - electrophysiologic testing for, 689–690
 - baseline observations during sinus rhythm, 689 - diagnostic maneuvers, during tachycardia, 689–690, 689b
 - tachycardia features, 689
 - mapping in, 690
- Nodoventricular bypass tracts, 688–690
- ablation in, 690
 - arrhythmias associated with, 688
 - electrocardiographic features of, 689
 - electrophysiologic testing for, 689–690
 - baseline observations during sinus rhythm, 689 - diagnostic maneuvers, during tachycardia, 689–690, 689b
 - tachycardia features, 689
 - mapping in, 690
- Nonapical right ventricular pacing, for atrioventricular block, 281
- Nonconducted premature atrial complexes, atrioventricular block and, 274, 274f–275f
- Noncontact mapping
- of atrial flutter, 359
 - in idiopathic focal ventricular tachycardia, 842–843, 842.e1f–842.e2f
 - limitations of, 396
 - of macroreentrant atrial tachycardia, 395–396
 - substrate, of macroreentrant atrial tachycardia, 396
 - in ventricular tachycardia, 800–801, 800.e1f
 - limitations of, 801
 - technique of, 800–801
- Noncoronary aortic sinus of Valsalva, 318, 336f–337f
- Nondihydropyridine calcium-channel blockers (verapamil and diltiazem), for atrial flutter, 344
- Noninducibility of tachycardia
- in congenital heart disease, 974
 - endpoints of ablation, 335–337
- Noninvasive risk stratification, in congenital heart disease, 969–970
- Nonischemic dilated cardiomyopathy, 869–896
- ablation of, 883–885
 - endpoints of, 884–885
 - outcome of, 885
 - target of, 883–884
 - technique of, 884 - autonomic testing for, 872
 - cardiac magnetic resonance imaging for, 873
 - cardiac sarcoidosis, 885–889
 - Chagas, 889–893
 - electrocardiographic features of, 876–877
 - electrocardiographic markers of, 872
 - electrophysiologic testing for, 872
 - entrainment mapping of, 882
 - epicardial mapping of, 883
 - epidemiology of, 871–872
 - genetic testing for, 873
 - implantable cardioverter-defibrillator for, 873–876, 874b, 874t, 875f, 874.e1f
 - initial evaluation for, 871–872
 - management of, 873–876
 - mapping of, 877–883
 - activation, 882
 - hemodynamic support in, 878
 - induction of tachycardia in, 878
 - left ventricular access in, 878
 - pace, 882–883
 - preprocedural evaluation for, 878
 - substrate, 878–882 - microvolt T-wave alternans in, 873
 - molecular genetics of, 869–870
 - natural history of, 871–872
 - nonsustained ventricular tachycardia in, 872
 - pathophysiology of, 869–871
 - pharmacological therapy for, 873
 - risk stratification in, 872–873
 - syncope in, 872
 - ventricular arrhythmias and, 870–871
 - in ventricular tachycardia, 876, 877f, 909
 - epicardial, 908
- Nonprimary ventricular fibrillation, 752
- Nonpulmonary vein triggers, in atrial fibrillation, 509–515
- in coronary sinus, 513–514, 514.e1f
 - in left atrial appendage, 515
 - in ligament of Marshall, 510–512, 511f–512f, 511.e1f, 510.e1f
 - mapping of, 509–510
 - rationale for, 509
 - in superior vena cava, 512–513, 513f–514f, 513.e1f, 512.e1f
- Nonspecific intraventricular conduction defects, 299
- Nonsustained ventricular tachycardia, 749
- epidemiology and natural history of, 752
 - in hypertrophic cardiomyopathy, 935
 - pharmacological therapy for, 757
 - risk stratification in, 754
- Non-vitamin K antagonist oral anticoagulants (NOACs), for atrial fibrillation, 446
- Normal sinus rhythm, in atrioventricular and atriofascicular bypass tracts, 678–679
- O**
- Obesity, atrial fibrillation and, 437
- Obstructive sleep apnea
- atrial fibrillation and, 436–437
 - management of, 456
 - sinus node dysfunction and, 242
- Open-irrigation catheters, radiofrequency ablation and, 210f, 223
- Oral dofetilide, for atrial flutter, 346
- ORBIT score, 443, 444t
- Orion Mini-Basket Catheter, 161, 161f
- continuous data acquisition mode in, 161
- Orthodromic atrioventricular reentrant tachycardia, 603, 603f–604f
- atrial activation sequence of, 637
 - atrial entrainment in, 641, 641f
 - atrial resetting, during transition zone, 647, 647f
 - atrial-ventricular relationship in, 637–638, 638f
 - bidirectional atrioventricular bypass tract in, 633–634, 633f
 - bundle branch block in, 638, 639f, 652
 - concealed atrioventricular bypass tract in, 634, 634f–635f
 - cycle length of, oscillations in, 638–639
 - differential-site right ventricular entrainment in, 646
 - electrocardiography of, 614, 615f–616f
 - exact and paradoxical capture in, 642–643
 - features of, 637–641
 - management of, 609, 610f
 - manifest ventricular fusion in, 645, 645f
 - pacing drive, required for entrainment, 646–647
 - physiological and pharmacological maneuvers, termination and response to, 639
 - postpacing interval in, 646
 - preexcitation in, 642
 - programmed atrial stimulation during, 641–642
 - programmed ventricular stimulation during, 635–636, 636f–637f, 642–647
- QRS alternans in, 639
- resetting and entrainment with manifest atrial fusion in, 641–642
 - resetting in, 641–642, 644f
 - termination in, 641, 643–645
 - VA interval in, 645
 - ventricular entrainment in, 645, 652–655, 654f
 - ventricular extrastimulation, during His bundle refractoriness, 642
 - ventriculoatrial linking in, 642
- Orthodromic resetting, 71, 73
- Oscillations
- in antidromic atrioventricular reentrant tachycardia, 640
 - in bundle branch reentrant ventricular tachycardia, 779
 - in orthodromic atrioventricular reentrant tachycardia, 638–639
 - in permanent junctional reciprocating tachycardia, 640

- Overdrive acceleration, 60
- Overdrive pacing
for atrial flutter, 346
for entrainment, 73, 138, 139.e1f
for intracardiac electrograms, 109
during tachycardia
atrial, 714–715
ventricular, 716–722, 717f–718f
triggered activity and, 60
- Overdrive suppression, 56–57, 56f
atrial overdrive pacing and, in paroxysmal
supraventricular tachycardia, 714
in ventricular tachycardia, 774
- Oxygen saturation monitoring, during
electrophysiological testing, 83
- P**
- P cells, 238
- P wave, in macroreentrant atrial tachycardia, 381
- P wave-atrial interval, 107–108
- P wave morphology
in atrioventricular nodal reentrant tachycardia,
569–570, 571f
in focal atrial tachycardia, 311, 312f–314f,
311.e1f
in paroxysmal supraventricular tachycardia,
702–703
- P wave onset, in activation mapping, 128, 130f,
326.e1f
- Pace mapping, 146–152
in arrhythmogenic right ventricular
cardiomyopathy (ARVC), 960
clinical implications of, 152
of focal atrial tachycardia, 328–329, 329f
fundamental concepts, 146–151, 147f, 146.e1f
in idiopathic focal ventricular tachycardia,
840–841
limitations of, 152, 153f
mapping procedure in, 152
matching in, 148–151, 148f, 151f
in nonischemic dilated cardiomyopathy,
882–883
QRS complex in, 146
stimulus-QRS interval during, 151, 151.e1f
in ventricular tachycardia, 792–795, 804–805
limitations of, 794–795, 794f–795f
QRS morphology, during pacing *versus*
tachycardia, 793
stimulus-to-QRS interval during, 793–794
technique of, 792–793, 793f
waveform comparison algorithm for, 149–151,
149f–150f
- Pacemaker. *see also* Automaticity
hierarchy of, 53–54
intracellular Ca^{2+} cycling and, 52–53
ionic mechanisms of, 51–53. *see also* Pacemaker
(funny) current
primary, 51. *see also* Sinus node
regulation of, 54–55
sodium channels and, 18
subsidiary, 54
atrial, 54
AV junctional, 54
hierarchy of, 53–54
overdrive suppression of, 56–57, 56f
ventricular, 54
- Pacemaker (funny) current, 42, 52
- Pacemaker device and mode selection, for sinus
node dysfunction, 251–253, 252b
minimizing right ventricular pacing in, 252–253
mode switch algorithms in, 253
rate adaptive programming in, 253
- Pacemaker implantation, for atrial
tachyarrhythmias, in congenital heart disease,
412
- Pacemaker syndrome, 252
atrioventricular block and, 281
- Pacing
atrial, 302. *see also* Atrial extrastimulation/pacing
antitachycardia, for atrial fibrillation, 455,
455.e1f
atrial activation sequence during, 365–367,
366f–368f, 366.e1f
at tachycardia cycle length, 323
trans-isthmus conduction interval, 368
autodecremental, 110
burst, 109
cycle length and, 109
decremental, 109
differential, 369–370, 369f, 370.e1f
differential-site, for focal atrial tachycardia, 322
in electrophysiological testing, 109–110
for entrainment, 73
extrastimulus, 110
fixed-rate, 369
His bundle, for bundle branch block, 302,
302.e1f
incremental, 109, 370, 370.e2f
stepwise rate, 110
for long QT syndrome, 999
overdrive. *see* Overdrive pacing
ramp, 110
 S_1 - S_1 drive stimuli and, 110
 S_1 - S_N drive stimuli and, 110
stepwise rate-incremental, 110
during tachycardia, for atrial flutter, 353
trains and, 110
ultraprapid train stimulation, 110
ventricular, 115–120. *see also* Ventricular
extrastimulation/pacing
for bundle branch block, 302–303, 303f
at tachycardia cycle length, 323
wide complex tachycardias due to, 731
- Pacing drive, length of, in programmed ventricular
stimulation, 585
- Pacing drive CL, in ventricular tachycardia,
induction of, 769
- Pacing output, 109
- Pacing rate, 109
- Pacing threshold, 109
- Paladino fiber, 600t
- Palpitations, in ablation, of atrioventricular nodal
reentrant tachycardia, 596
- Paradoxical capture, in orthodromic
atrioventricular reentrant tachycardia,
642–643
- Para-Hisian atrial tachycardias, ablation of,
333–335, 335f
- Para-Hisian pacing
in paroxysmal supraventricular tachycardia
overdrive, 722
during sinus rhythm, 707–709
concept of, 707
interpretation of results of, 709
limitations of, 709
- Para-Hisian pacing (*Continued*)
response to, 707–709, 708b
technique of, 707
during tachycardia, 722
during sinus rhythm, 575, 631–633, 631f–632f
during tachycardia, 585–586, 648
- Para-Hisian ventricular tachycardias, 853
- Parasympathetic nervous system, in automaticity,
54
- Parasystole, 57–58
- Parietal pericardium, puncturing, 96, 97f
- Paroxysmal atrial tachycardia, 309
- Paroxysmal atrioventricular block, 261–262
differential diagnosis of, 262t
idiopathic, 262, 263f
intrinsic, 261–262, 261f
vagal mediated, 261
permanent pacing for, 279, 280f
- Paroxysmal supraventricular tachycardia, 607,
697–729
acute management of, 698f–699f, 699–701
catheter ablation for, 609
chronic management of, 701–702, 701f
clinical presentation of, 698
electrocardiographic features of, 702–703
atrial activity, 702–703
effects of interventions in, 703
P/QRS relationship, 703
QRS morphology, 703
regularity of tachycardia in, 702, 702f
electrophysiological diagnosis of, practical
approach to, 723–728
algorithm, 724f
overdrive atrial pacing, 727
overdrive ventricular pacing, 727
programmed electrical stimulation during
sinus rhythm, 726t–727t
programmed electrical stimulation during
tachycardia, 725t–726t
tachycardia features, 724t
ventricular extrastimulation, 727
- electrophysiological testing for, 703–723
baseline observations during tachycardia, 704
diagnostic maneuvers during sinus rhythm,
722–723
diagnostic maneuvers during tachycardia,
714–722
induction of tachycardia, 710
programmed electrical stimulation during
sinus rhythm, 704–710
tachycardia features, 710–714
- epidemiology of, 697–698
initial evaluation of, 699
natural history of, 697–698
pharmacological maneuvers in, 713–714
pharmacological therapy for, 701–702
physiological maneuvers in, 713–714
proportion of, mechanism by age, 698f
- Peak skin dose, for radiation energy, 1062
- Pectinate muscles, prominent, of atrial flutter,
364
- Pericardial adhesions, 100
- Pericardial bleeding
as complications of pericardial access, 100–101
in transthoracic epicardial ablation, 918–920
- Pericardial effusion, 1044, 1044f
- Pericardiocentesis, for cardiac perforation, 1045,
1046f

- Pericarditis
 after atrial fibrillation ablation, 525
 after cardiac perforation, 1045, 1046f
 in percutaneous left atrial appendage ligation, 540
 in transthoracic epicardial ablation, 919
- Perimitral macroreentrant atrial tachycardia, 380f
- Periodic vagal bursting, 240
- Permanent junctional reciprocating tachycardia (PJRT), 603
 atrial activation sequence in, 639, 640f
 atrial-ventricular relationship in, 640
 bundle branch block in, 640
 clinical presentation of, 607
 cycle length, oscillations in, 640
 electrocardiography of, 614, 616f
 features of, 639–640
 physiological and pharmacological maneuvers, termination and response to, 640
 programmed atrial stimulation in, 634, 634.e1f
 programmed ventricular stimulation in, 636–637, 648
- Permanent pacing, for atrioventricular block, 277–279, 278b–279b
- PET-CT. *see* Positron emission tomography-computed tomography
- Pharmacologic maneuvers, response to, in atrioventricular and atriofascicular bypass tracts, 679
- Pharmacological therapy
 for atrioventricular nodal reentrant tachycardia, 568–569
 of focal atypical tachycardia, 311
- Phenocopies, of hypertrophic cardiomyopathy, 932–933, 932t–933t
- Phrenic nerve injury
 in ablation, 1051–1054, 1051f–1053f, 1053t
 of atrial fibrillation, 524
 of focal atrial tachycardia, 337
 prevention of, in cryoballoon ablation, 490
 in transthoracic epicardial ablation, 919, 919.e1f
- Physical activity. *see* Exercise; Sports, participation
- Physiologic maneuvers, response to, in atrioventricular and atriofascicular bypass tracts, 679
- Pilsicainide provocation, in Brugada syndrome, 1008, 1009t, 1010
- Pinacidil, mechanism of action of, 35
- PJRT. *see* Permanent junctional reciprocating tachycardia
- Pleomorphic ventricular tachycardia, 749
- Pleuritis, in transthoracic epicardial ablation, 920
- Pneumopericardium
 as complications of pericardial access, 101
 in transthoracic epicardial ablation, 920
- Polymorphic ventricular tachycardia, 748, 749f
 epidemiology and natural history of, 752
 induction of, 770
- Positron emission tomography
 in arrhythmogenic substrate, 781
 cardiac sarcoidosis and, 888
- Positron emission tomography-computed tomography (PET-CT), in substrate image integration, 799
- Posterior septum atypical tachycardia, 314
- Posteroseptal (inferoparaseptal) bypass tracts, 623
 ablation of, 670–672
 anatomical considerations for, 670
 electrocardiographic considerations for, 670–671
 technical considerations for, 671–672, 671t, 672f
- Postinfarction premature ventricular complexes, mapping, 801
- Postinfarction ventricular tachycardia, 910
 electrocardiogram localization of, 763–767
- Postpacing interval (PPI), 355
 in entrainment, 142–143
 in entrainment mapping, 787–789, 790f–791f, 789.e1f
 in orthodromic atrioventricular reentrant tachycardia, 646
 in paroxysmal supraventricular tachycardia, 718–719, 719f
 programmed ventricular stimulation in, 710
 in programmed ventricular stimulation, 582, 584f
 variability in, 322
- Postrepolarization refractoriness, 9–10
- Postural orthostatic tachycardia syndrome (POTS), inappropriate sinus tachycardia *versus*, 551–552, 552t
- Potassium, supplemental, for long QT syndrome, 1000
- Potassium channel blockers
 for Brugada syndrome, 1002
 I_{K1} , 31–32
 I_{KACH} , 32–33
 I_{KATP} , 33–35
 I_{Kr} , 27–29
 I_{Ks} , 29–31
 I_{Kur} , 27
 I_{to} , 24–27, 24t, 26t
- Potassium channels, 22–37
 activation/inactivation of, 23
 alpha subunits of, 22, 23f, 24t, 25
 antiarrhythmics and, 19
 beta subunits of, 24t
 classification of, 23, 24t
 expression of, 23
 function of, 24
 HERG, 24t, 27
 I_{K1} , 24t, 31–32, 31f, 26.e1f
 I_{KACH} , 24t, 32–33, 26.e1f
 I_{KATP} , 24t, 33–35, 34f–35f
 I_{Kr} , 24t, 27–29
 I_{Ks} , 24t, 29–31
 I_{Kur} , 24t, 26t, 27, 26.e1f
 I_{to} , 24–27, 24t, 26t
 Kir, 23, 23f, 24t
 ligand-gated, 22–23
 structure and physiology of, 22–24, 23f
 TASK, 24t, 36
 TREK, 36
 two-pore, 24t, 36
 voltage-gated, 22–23, 24t
- Potassium currents
 acetylcholine-activated (I_{KACH}), 24t, 32–33, 979, 26.e1f
 ADP-activated, 33
 ATP-sensitive (I_{KATP}), 24t, 33–35, 34f–35f
 in Brugada syndrome, 1001–1002
 in early repolarization syndromes, 1030
- Potassium currents (*Continued*)
 inward rectifying (I_{K1}), 24t, 31–32, 31f, 26.e1f
 in long QT syndrome, 977t, 979
 rapidly activating delayed outward rectifying (I_{Kr}), 24t, 27–29
 in long QT syndrome, 977t, 979
 in short QT syndrome, 1017–1018
 slowly activating delayed outward rectifying (I_{Ks}), 24t, 29–31
 in long QT syndrome, 977–979, 977t
 transient outward (I_{to}), 24–27, 24t, 26t
 two-pore (K_{2P}), 24t, 36
 ultrarapidly activating delayed outward rectifying (I_{Kur}), 24t, 26t, 27, 26.e1f
- Potassium imbalance
 long QT syndrome and, 992, 1000
 prolonged QT interval and, 992
- POTS. *see* Postural orthostatic tachycardia syndrome
- PPI. *see* Postpacing interval
- P/QRS relationship
 in atrioventricular nodal reentrant tachycardia, 570, 571f
 in focal atrial tachycardia, 311, 315f
 in paroxysmal supraventricular tachycardia, 711, 712f
- PR intervals
 in atrioventricular nodal reentrant tachycardia, 569, 569f–570f
 longer than RR interval, 572
- Precordial concordance, in ventricular tachycardia, 764
- Precordial transition, 618
- Preexcitation. *see also* Bypass tracts
 alternans, 613
 in atrial fibrillation, 603–605, 605f
 in atrial flutter, 605
 in atrial tachycardia, 603
 in atrioventricular nodal reentrant tachycardia, 603
 concertina, 613
 delta wave characteristics during, according to bypass tract location, 619b
 electrocardiography of, 612–613, 612f, 613.e1f
 inapparent, 613
 intermittent, 607, 613, 613f
 loss of, during exercise, 607–608
 to transesophageal atrial stimulation, 608
 ventricular, in atrial fibrillation, 459, 460f
- Preexcitation index
 in bypass tract localization, 649
 in orthodromic atrioventricular reentrant tachycardia, 642
 in ventricular extrastimulation, in paroxysmal supraventricular tachycardia, 715
- Preexcitation syndromes, 600. *see also* Wolff-Parkinson-White pattern
 clinical presentation of, 607
 epidemiology and natural history of, 606–607
 Mahaim variant of, 600
 pathophysiology of, 600–606
 types of, 600
- Preexcited atrial fibrillation, 608–609
- Preexcited atrioventricular nodal reentrant tachycardia, antidromic atrioventricular reentrant tachycardia and, differentiation between, 651b

- Preexcited QRS morphology, in atrioventricular and atriofascicular bypass tracts, 679
- Preexcited supraventricular tachycardia, 779
- Premature atrial complexes, atrioventricular block and, 261–262
- Premature excitation, aberration caused by, 287, 287f
- during atrial fibrillation, 288t
- Premature ventricular complexes (PVCs)
- ablation of, in arrhythmogenic right ventricular cardiomyopathy (ARVC), 964
- epidemiology and natural history of, 752
- idiopathic ventricular fibrillation and, 1028f, 1029.e1f–1029.e3f
- pharmacological therapy for, 757
- repetitive complex, 754
- short-coupled, in early repolarization syndromes, 1036
- Premature ventricular complex-induced cardiomyopathy, 818
- Premature ventricular contractions, 261–262, 261f
- Preprocedural substrate imaging, 802
- for arrhythmogenic right ventricular cardiomyopathy (ARVC), 960
- Primary ventricular fibrillation, 752
- PRKAG2 gene, 258
- Procainamide
- in bundle branch reentrant ventricular tachycardia, 900
- in bypass tract, 608
- mechanism of action of, 19
- RyR2 channels and, 46
- sinus node response to, 250
- for sustained ventricular tachycardia, 757
- Procainamide provocation
- in Brugada syndrome, 1008, 1009t, 1010
- in bundle branch block, 303
- Programmed atrial stimulation
- in atrio-Hisian bypass tracts, 695
- in atrioventricular nodal reentrant tachycardia
- initiation by, 575–576
- during sinus rhythm, 570–573
- during tachycardia, 580–582
- in fasciculoventricular bypass tracts, 691, 693f
- initiation of, 633–635, 679–681
- in paroxysmal supraventricular tachycardia
- initiation of, 710
- during sinus rhythm, 704
- during sinus rhythm, 679, 681f
- during tachycardia, 641–642, 683–684
- Programmed electrical stimulation, 109–112
- atrial, 112–115. *see also* Atrial extrastimulation/pacing
- conduction in, 110
- endpoints of, 769–770
- inducibility with, in triggered-activity ventricular tachycardia, 779
- pacing in, 109–110. *see also* Pacing
- refractoriness in, 110–111, 111t–112t
- stimulators for, 109
- ventricular, 115–120. *see also* Ventricular extrastimulation/pacing
- Programmed His bundle stimulation, in fasciculoventricular bypass tracts, 691–692
- Programmed ventricular stimulation
- atrio-Hisian bypass tracts in, 695
- in atrioventricular nodal reentrant tachycardia
- initiation by, 576–578
- during sinus rhythm, 573–575
- during tachycardia, 582–585
- initiation of, 320, 681
- in paroxysmal supraventricular tachycardia
- initiation of, 710
- during sinus rhythm, 704–707
- during sinus rhythm, 679
- during tachycardia, 684
- Progressive cardiac conduction disease
- atrioventricular block and, 259
- SCN5A/SCN1B mutations in, 20t, 21–22
- Propafenone
- for atrial fibrillation, 450, 452
- Brugada ST segment elevation and, 1010
- mechanism of action of, 19
- potassium channels and, 25
- Propagation mapping
- in CARTO electroanatomic mapping, 394
- in electroanatomic activation mapping, 167, 168f
- Prophylactic proton pump inhibitors, in esophageal injury, after ablation, 1062
- Propranolol
- for long QT syndrome, 997
- sinus node response to, 250
- Protein kinase A, RyR2 channels and, 45
- Protein kinase C, sodium channels and, 18
- PR-RP intervals, in paroxysmal supraventricular tachycardia, 710–711
- Pseudoaneurysms, femoral artery, 1043
- Pseudo-atrial-atrial-ventricular response, 721, 721.e1f
- Pseudo-A-V response, 721–722
- Pulmonary cusps, ventricular tachycardia from, 844
- Pulmonary embolism, 1043
- atrial fibrillation and, 437
- Pulmonary root, anatomy of, 820
- Pulmonary Vein Ablation Catheter, 224f, 226f
- Pulmonary vein atrial tachycardia, 308
- Pulmonary vein ectopy. *see* Pulmonary veins, arrhythmogenic
- Pulmonary vein fibrillation, pulmonary vein tachycardia *versus*, 431–433
- Pulmonary vein isolation
- cryoablation for, 231
- ultrasound energy for, 233
- Pulmonary vein potentials
- circumferential mapping of, 471–479
- identification using pacing maneuvers, 472–474, 474f–477f
- organization of, 478, 478f
- Pulmonary vein stenosis, 1054–1056
- clinical presentation of, 1056
- detection of, 1056
- incidence of, 1054, 1054f–1055f
- management of, 1056
- mechanism of, 1055–1056
- prevention of, 1056
- Pulmonary vein tachycardia
- intermittent, in atrial fibrillation, 474–478
- pulmonary vein fibrillation *versus*, 431–433
- Pulmonary vein triggers, focal ablation of, 467–471
- arrhythmogenic vein identification in, 467
- endpoints of, 470
- mapping in, 467–470, 469f, 467.e1f
- Pulmonary vein triggers, focal ablation of (Continued)
- outcome of, 470–471
- rationale for, 467, 468f
- target of, 470
- technique of, 470
- Pulmonary veins
- anatomy of, 431, 432f–433f
- angiography of, 466, 466.e1f
- arrhythmogenic
- definition of, 467
- identification of, 467, 469f
- mapping of, 467–470, 469f, 467.e1f
- provocation for, 467
- catheterization of, 466
- denervation of, 507–509
- ablation target in, 508, 508f
- endpoints for, 509
- localization of ganglionated plexuses in, 507–508, 507f
- outcome of, 509
- rationale for, 507
- technique of, 508–509, 509.e1f
- electrical disconnection of
- in circumferential antral pulmonary vein isolation, 493, 493.e1f
- in segmental ostial pulmonary vein isolation, 480–481, 482f, 480.e1f–480.e2f
- fluoroscopy of, 466
- identification of, 466
- imaging of, 465
- intracardiac echocardiography of, 466
- isolation of, 462. *see also* Atrial fibrillation, catheter ablation of
- all *versus* only arrhythmogenic, 471
- circumferential antral, 483–494
- in circumferential left atrial ablation, 496
- cryoballoon, 494
- electrical, 471
- laser balloon, 494
- radiofrequency, 493
- segmental ostial, 471–483
- macroreentrant atrial tachycardia arising from, 382
- mapping of
- electroanatomic, 466
- endocardial activation, 467–470
- in focal ablation of triggers, 467–470, 469f, 467.e1f
- postablation stenosis of, 522–523
- Pulseless ventricular tachycardia, sudden cardiac death and, 976
- Purkinje fibers, 294
- PV ostia, 307–308
- PVCs. *see* Premature ventricular complexes

Q

- QRS alternans, in orthodromic atrioventricular reentrant tachycardia, 639
- QRS axis
- in ventricular tachycardia, 764
- in wide complex tachycardia, 733b, 734, 734f
- QRS complex
- in arrhythmogenic right ventricular cardiomyopathy (ARVC)
- duration, localized prolongation of, 956
- fragmentation, 957

- QRS complex (*Continued*)
 in atrial flutter, 348
 fragmentation of, in Brugada syndrome, 1007
 in macroreentrant atrial tachycardia, 381
 in nonischemic dilated cardiomyopathy, 872, 872.e1f
 in ventricular tachycardia, 763–764
 in wide complex tachycardia
 atrioventricular dissociation in, 732–733, 734f, 737f
 duration of, 733
 morphology of, 734–738, 737f
 precordial concordance, 734
- QRS morphology
 in atrial fibrillation, 461, 461f
 in atrioventricular nodal reentrant tachycardia, 570
 in focal atrial tachycardia, 311
- QS complexes, in ventricular tachycardia, 764
- QT prolongation. *see also* Long QT syndrome
 acquired causes of, 992
 in Brugada syndrome, 1007
 HCN4 mutations and, 43
 measurement of, 987–988, 987t
- QTc interval
 in long QT syndrome, 993t
 in short QT syndrome, 1018
- Quadripolar catheter, 84, 84f
- Quadripolar mapping-ablation catheter, 784
- Quinidine
 for Brugada syndrome, 1014
 mechanism of action of, 19
 potassium channels and, 25
 for short QT syndrome, 1020
 sinus node response to, 250
- Quinine, mechanism of action of, gap junctions in, 48
- R**
- Race, atrial fibrillation and, 434
- Radiation dosimetry, 1064–1065
- Radiation exposure, 1062–1065
 clinical presentation of, 1063–1064
 during electrophysiology procedures, 1063, 1063t
 prevention of, 1064–1065, 1065b
 reduction of, 1064
- Radiofrequency, definition of, 206
- Radiofrequency ablation, 155, 206–225
 biophysics of, 206–210
 radiofrequency energy delivery in, 206–208
 burns from, 207, 207.e1f
 catheter tip temperature in, 209–210
 monitoring of, 216
 catheter-tissue contact in, optimization of, 218–221, 219t
 contact force monitoring and, 219–221, 220f–221f
 electroanatomic catheter localization, 219
 fluoroscopy in, 219
 impedance monitoring in, 219
 intracardiac echocardiography in, 219
 record electrograms in, 218
 tactile feedback in, 219
 temperature monitoring in, 219
 cellular effects of, 211
- Radiofrequency ablation (*Continued*)
 clinical applications of, 222
 coagulum formation, 212
 complications of, phrenic nerve injury, 337
 convective cooling in, 209, 209f, 215
 cooled
 biophysics of, 210–211, 211f
 clinical applications of, 222–223
 energy titration in, 217–218
 potential advantages of, 223
 electrodes for
 dispersive, 206
 features of, comparison of, 223t
 flexibility of, 215
 length of, 212–214, 214f
 material of, 213
 orientation of, 210–211, 214
 position of, 207
 size of, 207
 temperature of, 208–209, 213, 222
 monitoring of, 216–217
 electrogram-gated, 221
 electrophysiologic effects of, 217
 healing in, 211
 lesion formation in
 monitoring of, 215–217
 pathophysiology of, 211–212
 lesion size in, 210
 blood flow and, 215
 determinants of, 212–215, 213t
 duration of, 213
 electrode material and, 213
 electrode tip temperature and, 209–210
 electrode-tissue contact in, 213–214
 length of, 212–214, 214f
 orientation and, 210–211, 214
 radiofrequency system polarity and, 215
 reference patch electrode location and size in, 215
 limitation of, 222
 monitoring in
 contact force, 219–222, 220f–221f
 impedance, 216, 219, 222
 temperature, 216–217, 219
 nMARQ system for, 225, 227f
 phased, 223–225, 224f–225f
 radiofrequency systems for
 bipolar, 207–208, 207f–208f
 unipolar, 206–207, 207f
 steam pop in, 212
 prevention of, 221–222, 221t
 ablation electrode temperature, 222
 contact force monitoring in, 222
 high-frequency ultrasound and, 222
 impedance monitoring in, 222
 intracardiac echocardiography, 222
 power output in, 222
 tissue effects of, 211–212, 211.e1f
 tissue heating in, 208–209
 temperature monitoring and, 217, 222
 titration of energy in, 217
- Radiofrequency energy
 delivery, in ablation, of atrioventricular nodal reentrant tachycardia, 593–594
 microwave energy and, 234
 titration of
 cooled, 217–218
 standard, 217
- Ramp pacing, 110
 atrial, 112
 ventricular, 115–116
- Ranolazine, for long QT syndrome, 1000
- Rapid ventricular rates, in atrioventricular nodal reentrant tachycardia, 569
- Rapidly activating delayed outward rectifying current (I_{Kr}), 24t, 27–29
 in long QT syndrome, 977t, 979
- Rate adaptive programming, 253
- Rate control, in management of AT, 411
- Real-time ICE images, in substrate image integration, 799
- Recreational drugs, atrial fibrillation and, 438
- Reentrant beats
 intraventricular, 120
 in programmed atrial stimulation, for paroxysmal supraventricular tachycardia
 intraatrial, 704
 in programmed ventricular stimulation, for paroxysmal supraventricular tachycardia
 intraventricular, 707
- Reentrant circuit chamber, localization of, 396
 activation sequence in coronary sinus, 396
 electrocardiographic findings, 396
- Reentrant circuits, 63–64
 anatomical, 63–65, 63f
 components of, 135, 136f
 excitable gaps and, 68–69, 69f
 resetting zone and, 70–71
 functional, 63–68, 63f
 slow conduction in, 74–76
 reduced cellular coupling and, 75–76, 76f
 reduced membrane excitability and, 74–75, 75f
 tissue structure/geometry and, 76, 79
 unidirectional block in, 63, 78–79
 anisotropy and, 78–79
 membrane excitability/refractoriness and, 78, 78f
 tissue structure/geometry and, 79
- Reentrant tachycardia. *see also* Reentry
 bundle branch ventricular
 ablation of
 endpoints of, 905, 905f
 of left bundle branch, 903–905
 outcome of, 905
 of right bundle branch, 903, 904f
 target of, 903
 technique of, 903–905
 electrophysiological testing in
 in induction, 898–900
 during normal sinus rhythm, 898, 899f–900f
 definition of, 63
 orthodromic, resetting of, 71
 overdrive pacing for, 73
 resetting, 69–73, 70f, 135–137
 antidromic, 71
 bundle branch ventricular, 902
 definition of, 69
 with diverse mechanisms, 72–73
 entrainment of, 73–74, 135, 144b
 excitable gaps and, 70–71
 with fusion, 72, 72.e1f
 orthodromic, 71, 73
 resetting zone and, 70–71
 response curves in, 71–72, 71f

- Reentrant tachycardia (*Continued*)
 return cycle and, 71
 site specificity of, 72
 sinus node, 309
 inappropriate sinus tachycardia and, 554, 555f
 synonyms for, 63
- Reentry, 63–79. *see also* Reentrant circuits;
 Reentrant tachycardia
 anatomical, 63–65, 63f
 anisotropic, 66, 76–78
 cellular coupling and, 77
 gap junctions and, 77
 myocyte packing and tissue geometry and, 77
 unidirectional block and, 78–79
 uniform *versus* nonuniform anisotropy in, 77–78, 77f
 circuit, localization of, 394, 394f
 diagnostic criteria for, 63, 63b
 double-loop, 66, 66f
 excitable gaps and, 68–69, 69f
 figure-of-eight, 66, 66f
 functional, 63–68, 63f
 initiation of, 65
 leading circle concept and, 65–66
 ordered, 65
 phase 2, 67
 principles of, 63
 reflection, 63f, 67
 requisites for, 63–65
 area of slow conduction, 64–65
 central area of block, 64
 critical tissue mass, 65
 initiating trigger, 65
 substrate, 63–64
 unidirectional conduction, 64
 scar-related
 nonischemic, 870
 in nonischemic dilated cardiomyopathy, 870
 spiral wave (rotor) activity and, 67–68, 68f
 wavelength and, 68–69
 in Wolff-Parkinson-White syndrome, 64f
- Reflection, 63f, 67
- Refractoriness, in programmed stimulation, 110–111
- Refractory period
 absolute, 9, 110
 cycle length responsiveness of, 111–112
 definition of, 111
 effective, 9, 111
 functional, 111, 111t
 limitations of, 112
 measurements of, 111
 movements of, 111
 normal values for, 112
 in programmed electrical stimulation, 110–111
 relative, 9, 111
- Relative refractory period, 9, 111
- Reperfusion arrhythmias, epidemiology and
 natural history of, 752
- Repetitive complex premature ventricular
 complexes, 754
- Repolarization, membrane
 early, 6
 final rapid, 7
 rapid, 6
- Repolarization abnormalities, in arrhythmogenic
 right ventricular cardiomyopathy (ARVC), 954
- Resetting. *see also* Entrainment; Reentrant
 tachycardia, resetting
 atrial, during transition zone, 585
 in paroxysmal supraventricular tachycardia
 atrial, during transition zone, 720
 atrial extrastimulation in, 714
 para-Hisian, 722
 ventricular extrastimulation in, 715–716
 with delay of atrial activation, 715
 with different atrial activation sequence, 715
 failure of, 715
 during His bundle refractoriness, 715–716
 without atrial activation, 715
 in programmed atrial stimulation, 580–581, 580f–581f
 in programmed ventricular stimulation, 582, 583f
 during tachycardia, 683–684, 683f
 in ventricular tachycardia, 771–774, 773f, 771.e1f
- Resetting response curve
 in paroxysmal supraventricular tachycardia, 714
 in ventricular stimulation, of ventricular
 tachycardia, 772
- Respiratory sinus arrhythmia, 245
- Response curves, in resetting, 71–72, 71f
 decreasing, 72
 flat, 72
 increasing, 72
 mixed, 72
- Resting membrane potential, 3–6, 3t
 regional differences in, 3, 5t
 restoration of, 7
- Restitution, 289
- Retrograde atrial activation sequence, 627–628, 627f–628f
 in programmed ventricular stimulation, for
 paroxysmal supraventricular tachycardia, 705
- Retrograde atrioventricular bypass tract,
 electrophysiological findings in, 649b
- Retrograde bypass tract conduction
 atrial electrogram polarity reversal during, 656–657
 earliest activation site during, 655–656, 656f–658f
- Retrograde conduction
 in fast-slow atrioventricular nodal reentrant
 tachycardia, 564–565, 565f
 in slow-fast atrioventricular nodal reentrant
 tachycardia, 564, 565f–566f
 in slow-slow atrioventricular nodal reentrant
 tachycardia, 565–566
- Retrograde dual atrioventricular nodal physiology, 573–575
 in programmed ventricular stimulation, for
 paroxysmal supraventricular tachycardia, 705
- Retrograde P wave morphology, polarity of,
 localization using, 623, 624f
- Retrograde right bundle branch block
 in programmed ventricular stimulation, for
 paroxysmal supraventricular tachycardia, 706–707
 during ventricular extrastimulation, 628–629
- Retrograde ventriculoatrial conduction, 624–627
 in programmed ventricular stimulation, for
 paroxysmal supraventricular tachycardia, 704–705
- Retroperitoneal hematomas, 1042–1043
- Return cycle, in ventricular stimulation, of
 ventricular tachycardia, 772
- Reversal potential, 1
- Rheumatic diseases, atrioventricular block and, 259
- Rhythmia electroanatomic mapping system,
 160–161, 161f, 176, 782–784
 anatomical reference in, 161
 data acquisition in, 165
 high-resolution, 172
- Right atrial appendage atypical tachycardia, 317
- Right atrial catheter, 85, 85f
- Right atrial electrogram, 105
- Right bundle. *see also* Bundle branch
 anatomy of, 293
- Right bundle branch block, in arrhythmogenic
 right ventricular cardiomyopathy (ARVC), 956
- Right fibrous trigone, 255–256
- Right free-wall bypass tracts, 620–621
 ablation of, 666–667
 anatomical considerations for, 666
 technical considerations for, 666–667, 667f
- Right lateral atrioventricular bypass tract,
 adenosine in, 679.e1f
- Right-sided bypass tracts, 621
- Right ventricular apical local activation time, 771
- Right ventricular apical pacing, for atrioventricular
 block, 281–282
- Right ventricular cardiomyopathy, arrhythmogenic,
 942–967
 ablation of, 962–965
 endpoints of, 964
 outcome of, 964–965
 target of, 962–964
 technique of, 964
 clinical presentation of, 946
 differential diagnosis of, 948–950
 athlete's heart, 950
 cardiac sarcoidosis, 949–950
 dilated cardiomyopathy, 950
 exercise-induced arrhythmogenic right
 ventricular cardiomyopathy in, 950
 idiopathic right ventricular outflow tract
 tachycardia, 948–949, 949b
 electrocardiographic features of, 954–957
 during sinus rhythm, 954–957, 955f
 during ventricular tachycardia, 957, 958f
 electrophysiological features of, 957–959
 induction of tachycardia, 957
 tachycardia features, 957–959
 epidemiology of, 945–946
 initial evaluation of, 946–948
 diagnostic criteria in, 946, 947t
 endomyocardial biopsy in, 948
 genetic testing in, 948
 invasive electrophysiological testing in, 948
 mapping in, 959–962
 activation, 959, 959.e1f
 entrainment, 959–960
 epicardial, 962
 pace, 960
 substrate, 960–962
 natural history of, 945–946
 pathophysiology of, 942–945
 molecular genetics in, 942–943, 943t
 pathogenesis of, 943–945, 944f
 pathology of, 945, 945.e1f

- Right ventricular cardiomyopathy, arrhythmogenic (*Continued*)
 principles of management of, 950–954
 catheter ablation of, 952
 family screening in, 953–954
 implantable cardioverter-defibrillator, 952–953, 953f
 pharmacological therapy of, 950–952
 sports in, 953
 risk stratification in, 950, 951f, 952b
- Right ventricular catheter, 85, 85f
- Right ventricular electrogram, 107
- Right ventricular outflow tract, ventricular tachycardia from, 843–844
- Ring catheter. *see also* Lasso catheter
 mapping
 in circumferential antral pulmonary vein isolation, 484
 in segmental ostial pulmonary vein isolation, 471–472, 472f, 471.e1f
- Ring of fire, 307
- Ripple mapping, 172, 173f–174f
- Romano-Ward syndrome, 30, 983–984. *see also* Long QT syndrome
- Rotor activity, 67–68, 68f
- RP-PR interval ratio, in paroxysmal supraventricular tachycardia, 703
- Ryanodine, 46
- RyR2 channels, 43–46, 1020
 in acquired diseases, 46
 in arrhythmogenic right ventricular cardiomyopathy-dysplasia, 1023–1024
 in catecholaminergic polymorphic VT, 1020–1021
 function of, 44–45, 1021
 in inherited channelopathies, 46, 1021
 in myocyte contraction, 12
 pharmacology of, 45–46
 regulation of, 45
 structure and physiology of, 43–44, 44f
- S**
- S wave upstroke, prolongation of, in arrhythmogenic right ventricular cardiomyopathy (ARVC), 956–957
- S₁-S₁ drive stimuli, 110
- S₁-S_N drive stimuli, 110
- SafeSept Transseptal Guidewire, 93
- Safety factor, for conduction, 12
- SAMe-TT2R2 score, 447, 447t
- Sarcoidosis, cardiac, 885–889
 cardiac magnetic resonance for, 887, 887f
 clinical presentation of, 886
 echocardiography for, 887
 electrocardiography for, 886–887
 electrophysiological testing for, 888
 epidemiology and natural history of, 886
 histological examination for, 888
 initial evaluation for, 886–888, 886b
 management of, 888–889
 pathophysiology of, 885–886
 positron emission tomography for, 887–888
 risk stratification for, 888
- Scar dechanneling, 806–807, 808f
- Scar homogenization, 806, 807f
- Scar mapping, 795–796. *see also* Electroanatomic mapping, voltage
 for arrhythmogenic right ventricular cardiomyopathy (ARVC), 960–961, 961.e1f
 for nonischemic dilated cardiomyopathy, 879, 881f
 during sinus rhythm, 802–803
 technique of, 796, 797f, 796.e1f–796.e2f
- Scar-related reentrant ventricular tachycardia, 749
- Scar-related reentry, in nonischemic dilated cardiomyopathy, 870
- SCD. *see* Sudden cardiac death
- Schwartz score, in long QT syndrome, 990
- Sclerosis, atrioventricular block and, 259
- SCN1B mutations
 in Brugada syndrome, 20t, 21, 1001, 1001t
 in familial atrial fibrillation, 20t, 22
 in long QT syndrome, 977t
 in progressive cardiac conduction disease, 20t, 21–22
- SCN2B mutations, in familial atrial fibrillation, 20t, 22
- SCN3B mutations, in Brugada syndrome, 1001, 1001t
- SCN4B mutations, in long QT syndrome, 977t, 979
- SCN5A gene, 258
- SCN5A mutations
 in Brugada syndrome, 20t, 21, 1001t, 1009
 in congenital sick sinus syndrome, 20t, 22
 in dilated cardiomyopathy, 20t, 22
 in familial atrial fibrillation, 20t, 22
 in long QT syndrome, 20–21, 20t, 977t, 979
 in overlap syndrome, 20t, 22
 in progressive cardiac conduction disease, 20t, 21–22
 in sudden infant death syndrome, 20t, 22
- Screening
 for Brugada syndrome, 1017
 for catecholaminergic polymorphic VT, 1025
 for early repolarization syndromes, 1037–1038
 for idiopathic ventricular fibrillation, 1029
 for long QT syndrome, 1000
- Sedation
 during atrial fibrillation ablation, 465–466
 for electrophysiological testing, 82–83
- Seebeck effect, 209–210
- Segmental ostial pulmonary vein isolation, 471–483
 ablation endpoints in, 480–483, 482f, 482.e1f, 480.e1f, 480.e2f
 ablation target in, 480
 sites in, 474, 477f–478f
 of all *versus* only arrhythmogenic veins, 471
 mapping in
 during atrial fibrillation, 474–478
 basket catheter, 479, 479f, 479.e1f
 during normal sinus rhythm, 472–474, 473f
 ring catheter, 471–472, 472f, 471.e1f
 outcome of, 483
 rationale for, 471
 technique of, 480, 481f
- Seizures, febrile, Brugada syndrome and, 1005
- Selective ablation, in arrhythmogenic right ventricular cardiomyopathy (ARVC), 962–964, 964.e1f
- Sensei robotic navigation system, 186–187
 clinical implications of, 186–187
 fundamental concepts of, 186
- Sensei robotic navigation system (*Continued*)
 limitation of, 187
 technology application of, 186
- Septal ventricular tachycardia, in nonischemic dilated cardiomyopathy, 876
- Septum, puncturing, 90
- Serologic testing, for Chagas cardiomyopathy, 892
- Short QT syndrome, 1017–1020
versus catecholaminergic polymorphic VT, 1022
 clinical presentation of, 1018
 diagnosis of, 1019, 1019t
 differential diagnosis of, 1019
 electrocardiographic features of, 1018–1019
 epidemiology of, 1018
 genetic aspects of, 1017–1018, 1017t
 management of, 1019–1020
 mutations in, calcium channel, 41
 pathophysiology of, 1018
 potassium channel mutations in, 29–30, 32
 pharmacological therapy for, 1020
 risk stratification in, 1019
 sports participation in, 1020
- SIDS. *see* Sudden infant death syndrome
- Single atrial impulse, ventricular responses to, 572, 573f–574f
- Single-chamber ventricular pacing, for atrioventricular block, 280–281
- Single-lead atrioventricular pacing, for atrioventricular block, 280
- Single supraventricular beat, in atrioventricular nodal reentrant tachycardia, 569
- Sinoatrial conduction time, 248–250, 248f
 measurement of
 direct recordings as, 248
 Kirkorian-Touboul method of, 250
 Narula method for, 250
 Strauss technique for, 248–250, 249f
 in patients with sinus node dysfunction, 250
- Sinoatrial exit block, 243
- Sinotubular junction, anatomy of, 820
- Sinus arrest, 243
- Sinus arrhythmia, 245–246
 ventriculophasic, 246, 246f
 atrioventricular block and, 277
- Sinus bradycardia
 after atrial fibrillation ablation, 525
 causes of, 241–242
 electrocardiographic features of, 243
 HCN4 mutations and, 43
- Sinus cycle length, sinus node recovery time and, 247
- Sinus node
 anatomy and physiology of, 238–240, 239f, 549
 blood supply in, 239
 histology in, 238
 innervation of, 239–240
 inappropriate discharge, 57
 overdrive suppression of, 56
 pacemaker activity in, 51, 53f. *see also* Pacemaker response to atrial pacing
 premature, 114, 114f
 rate-incremental, 112
- Sinus node dysfunction, 238–254
 in ablation, 337
 ambulatory monitoring of, 242–243
 anatomy of, 238, 239f
 autonomic modulation in, 243
 causes of, 240b

- Sinus node dysfunction (*Continued*)
 clinical presentation of, 242
 diagnostic evaluation of, 238–254
 drugs and, 241, 250
 electrocardiogram for, 242–243
 electrocardiographic features of, 243–246
 electrophysiological testing in, 246–250
 sinoatrial conduction time, 248–250, 248f
 sinus node recovery time, 246–248, 247f
 endpoints of ablation, 337
 epidemiology and natural history of, 242, 242f
 excessive vagal tone in, 241
 extrinsic, 241–242
 familial, 241
 hypervagotonia, 241
 intrinsic, 240–241
 management of, 251–253
 acute, 251
 chronic, 251, 251b
 pacemaker device and mode selection in, 251–253, 252b
 pathophysiology of, 240–242
 sinoatrial conduction time in, 250
- Sinus node recovery time, 246–248, 247f
 corrected, 247
 definition of, 247
 limitations of, 247
 maximum, 247
 measurement of, 247
 in patients with sinus node dysfunction, 247–248
 secondary pauses in, 247
 technique for, 246–247
 total recovery time, 247
- Sinus node reentrant tachycardia, 309
 inappropriate sinus tachycardia and, 554, 555f
- Sinus of Valsalva
 left aortic, 821–822
 noncoronary aortic, 822, 822.e1f
 right aortic, 822
- Sinus pauses, 243f, 244
- Sinus rhythm
 baseline observations during, 623–633
 diagnostic maneuvers during, 648–649
 dual-chamber sequential extrastimulation during, 633
 identification of conducting channels during, 803–804
 maintenance of, 346–347
 in management of AT
 maintenance of, 412
 restoration of, 411
 para-Hisian pacing during, 631–633, 631f–632f
 programmed atrial stimulation during, 623–624, 625f–626f, 624.e1f
 programmed ventricular stimulation during, 624–631
 restoration of, 345–346
 scar mapping during, 802–803
- Sinus tachycardia, inappropriate, 549–559
 ablation of, 554–558
 endpoints of, 555–558
 outcome of, 558
 target of, 554, 554.e1f
 technique of, 554–555, 556f–557f, 555.e1f–555.e2f
- Sinus tachycardia, inappropriate (*Continued*)
 clinical presentation of, 550
 differential diagnosis of, 551–552
 postural orthostatic tachycardia syndrome and, 551–552, 552t
 supraventricular tachycardias and, 552
 electrophysiological testing in, 553–554, 554f
 epidemiology and natural history of, 550
 in iatrogenic cardiac arrhythmias, 1049–1050
 initial evaluation of, 550–551, 550b
 autonomic evaluation in, 551
 exercise testing in, 551
 Holter monitoring in, 550–551, 551f
 isoproterenol provocation in, 551
 management of, 552–553
 catheter ablation in, 553
 pharmacological therapy in, 552–553
 surgical ablation in, 553
 pathophysiology of, 549–550
 tachycardia in
 features of, 553–554
 induction of, 553
- Six-step protocol, in ventricular tachycardia, induction of, 768
- Skin injury, radiation-induced, 1063–1064, 1064f
- Slow-fast atrioventricular nodal reentrant tachycardia, 564
 AH/HA ratio in, 564
 anterograde conduction in, 564
 initiation
 by programmed atrial stimulation, 575–576
 by programmed ventricular stimulation, 576–578, 577f–578f
 lower common pathway in, 564
 retrograde conduction in, 564, 565f–566f
 tachycardia features of, 578–579
- Slow pathways, in atrioventricular nodal reentrant tachycardia, 562–563
 ablation of, 596–597
 conduction, elimination of, 595
 differences between fast and, 562
- Slow response potential. *see* Action potentials, slow response
- Slowly activating delayed outward rectifying current (I_{Ks}), 24t, 29–31
 in long QT syndrome, 977–979, 977t
- Slow-slow atrioventricular nodal reentrant tachycardia, 565–566
 AH/HA ratio in, 566
 anterograde conduction in, 565
 lower common pathway in, 566
 retrograde conduction in, 565–566
- Small-conductance calcium-activated potassium channels, 36–37, 26.e1f
- Smoking, atrial fibrillation and, 438
- SNTA1* mutations, in long QT syndrome, 20t, 21, 977t, 979
- Sodium channel blockers, for Brugada syndrome, 1008
- Sodium channels, 16–22
 activation/inactivation of, 16
 antiarrhythmics and, 18
 early afterdepolarizations and, 60–61
 function of, 18
 inactivation of, reentry and, 75
- Sodium channels (*Continued*)
 mutations affecting
 in acquired heart disease, 22
 in inherited channelopathies, 19–22, 20t
 Brugada syndrome, 20t, 21, 1000–1001
 congenital sick sinus syndrome, 20t, 22
 dilated cardiomyopathy, 20t, 22
 early repolarization syndrome, 20t, 21
 familial atrial fibrillation, 20t, 22
 long QT syndrome, 19–21, 20t, 979, 979.e1f
 overlap syndrome, 20t, 22
 progressive cardiac conduction disease, 20t, 21–22
 sudden infant death syndrome, 20t, 22
 pharmacology of, 18–19
 regulation of, 18, 19f
 structure and physiology of, 16–18, 16f
 subunits of, 16, 17f
 glycosylation of, 18
- Solution effect injury, 226–227
- Sotalol, 28
 for atrial fibrillation, 452
 postoperative, 457
- Sound, defined, 232
- Source-sink relationships, 11–12, 12f
- Spiral wave (rotor) activity, 67–68, 68f
- Spontaneous termination, in paroxysmal supraventricular tachycardia, 713
- Sports
 participation. *see also* Exercise
 in Brugada syndrome, 1015–1017
 in catecholaminergic polymorphic VT, 1025
 in early repolarization syndromes, 1037
 in idiopathic ventricular fibrillation, 1029
 in long QT syndrome, 999–1000
 in short QT syndrome, 1020
 Wolff-Parkinson-White patients and, 612
- S-QRS intervals, 803–804
- Steam pop, 212
 prevention of, 221–222, 221t
 ablation electrode temperature, 222
 contact force monitoring in, 222
 high-frequency ultrasound and, 222
 impedance monitoring in, 222
 intracardiac echocardiography, 222
 power output in, 222
- Stenosis, pulmonary vein, 1054–1056
 clinical presentation of, 1056
 detection of, 1056
 incidence of, 1054, 1054f–1055f
 management of, 1056
 mechanism of, 1055–1056
 prevention of, 1056
- Stepwise rate-incremental pacing, 110
- Stereotaxis magnetic navigation system, 183–186
 claustrophobia and, 185
 clinical implications of, 185
 fundamental concepts of, 183–184, 184f, 183.e1f
 limitations of, 185–186
 morbid obesity, 185
 technology application of, 184–185
- Stiff left atrial syndrome, after atrial fibrillation ablation, 525
- Stimulation protocols, in ventricular tachycardia, induction of, 768–769
- Stimulation site specificity, in triggered-activity ventricular tachycardia, 779
- Stimulators, 109–112

- Stimulus-to-QRS interval
 entrainment mapping
 electrogram-to-QRS interval *versus*, 789–791, 792f
 ratio of, to tachycardia cycle length, 791–792
 pace mapping, 151, 793–794, 151.e1f
- Stochastic effects, of ionizing radiation, 1062, 1062.e1f
- Straight pacing. *see* Overdrive pacing
- Strauss technique, for sinoatrial conduction time, 248–250, 249f
- Stress, long QT syndrome and, 981, 984f, 991–992, 999
- Stress test, epinephrine, in long QT syndrome, 984f, 991–992
- Stroke, periprocedural, 1046
- Structural heart disease, early afterdepolarizations and, 63
- Structural remodeling, in atrial fibrillation, 429–430
- Sub-eustachian pouches, of atrial flutter, 364
- Substrate-based ablation, 805–807
 in arrhythmogenic right ventricular cardiomyopathy (ARVC), 962f–963f, 964
 core isolation in, 807, 809f
 linear ablation and, 807
 scar dechanneling in, 806–807, 808f
 scar homogenization in, 806, 807f
 strategies for, 806, 806f
- Substrate-guided ablation, in nonischemic dilated cardiomyopathy, 883–884
- Substrate image integration, 798–799
- Substrate mapping. *see also* Electroanatomic mapping, substrate
 in arrhythmogenic right ventricular cardiomyopathy (ARVC), 960–962
 during baseline rhythm, 795–800, 802
 limitation of, 799–800
- Sudden cardiac death (SCD). *see also* Cardiac arrest
 in Brugada syndrome, 1000
 in catecholaminergic polymorphic VT, 1020
 causes of, 976
 in early repolarization syndromes, 1029
 epidemiology and natural history of, 752
 in idiopathic ventricular fibrillation, 1025
 in inherited channelopathies, 976
 in ischemic heart disease, prevention of, 759t
 in Jervell and Lange-Nielsen syndrome, 985
 in long QT syndrome, 984. *see also* Long QT syndrome
 risk stratification for, 994
 nocturnal, in Brugada syndrome, 1005
 in Romano-Ward syndrome, 984
 in short QT syndrome, 1017–1020
 unexpected, 976
 in Wolff-Parkinson-White syndrome, 605–606
 epidemiology and natural history of, 606
- Sudden death, in hypertrophic cardiomyopathy, 935, 937b
- Sudden infant death syndrome (SIDS)
 in Brugada syndrome, 1005
 genetic factors in, 20t, 22
- Sudden unexplained nocturnal death syndrome (SUNDS), in Brugada syndrome, 1005
- Superior vena cava (SVC)
 anatomy of, 339
 electrical isolation of, 512–513, 513f–514f, 513.e1f, 512.e1f
- Supernormal conduction, 122
- Supernormal excitability, 9
- Supraventricular arrhythmias, in arrhythmogenic right ventricular cardiomyopathy (ARVC)
 clinical presentation of, 946
- Supraventricular tachyarrhythmias, associated with Wolff-Parkinson-White syndrome, 614
- Supraventricular tachycardia (SVT)
 aberrantly conducted, persistence of, 291, 292f
 AES mapping during, 686
 in atrio-Hisian bypass tracts, 695
 in atrioventricular and atriofascicular bypass tracts, 679
 atrioventricular bypass tract in,
 electrophysiological findings in, 649b
 exclusion of, 779
 inappropriate sinus tachycardia *versus*, 552
 not requiring bypass tract, for initiation and maintenance, 678
 paroxysmal, 697–729
 acute management of, 698f–699f, 699–701
 chronic management of, 701–702, 701f
 clinical presentation of, 698
 electrocardiographic features of, 702–703
 atrial activity, 702–703
 effects of interventions in, 703
 P/QRS relationship, 703
 QRS morphology, 703
 regularity of tachycardia in, 702, 702f
 electrophysiological diagnosis of, practical
 approach to, 723–728
 algorithm, 724f
 overdrive atrial pacing, 727
 overdrive ventricular pacing, 727
 programmed electrical stimulation during
 sinus rhythm, 726t–727t
 programmed electrical stimulation during
 tachycardia, 725t–726t
 tachycardia features, 724t
 ventricular extrastimulation, 727
 electrophysiological testing for, 703–723
 baseline observations during tachycardia, 704
 diagnostic maneuvers during sinus rhythm, 722–723
 diagnostic maneuvers during tachycardia, 714–722
 induction of tachycardia, 710
 programmed electrical stimulation during
 sinus rhythm, 704–710
 tachycardia features, 710–714
 epidemiology of, 697–698
 initial evaluation of, 699
 natural history of, 697–698
 proportion of, mechanism by age, 698f
 requiring bypass tract, for initiation and maintenance, 678
 ventricular tachycardia *versus*, 742, 742f
- Supraventricular tachycardia with aberrancy, *versus* bundle branch reentrant ventricular tachycardia, 903
- Surgery, for congenital heart disease. *see* Congenital heart disease
- Surgical ablation
 of atrial fibrillation, 454, 455f
 of atrial tachyarrhythmias, in congenital heart disease, 412
 in inappropriate sinus tachycardia, 553
- Surgical repair
 and ablation, for congenital heart disease, 971
 for cardiac perforation, 1045–1046
- Sustained monomorphic VT, in congenital heart disease, 969
- Sustained ventricular arrhythmias, in hypertrophic cardiomyopathy, 935
- Sustained ventricular tachycardia, 749
 monomorphic
 clinical, induction of, 769
 epidemiology and natural history of, 752–753
 multiple, induction of, 769–770
 noninducibility of, ablation in, 810
 pharmacological therapy for, 757
 risk stratification in, 754
- SVC. *see* Superior vena cava
- SVC syndrome, in sinus node ablation, 558
- SVT. *see* Supraventricular tachycardia
- Sympathetic denervation, for catecholaminergic polymorphic VT, 1025
- Sympathetic nervous system, in automaticity, 54–55
- Syncope
 in Andersen-Tawil syndrome, 985
 in Brugada syndrome, 1012
 cardiac sarcoidosis and, 888
 in catecholaminergic polymorphic VT, 1020
 in early repolarization syndromes, 1036–1037
 in hypertrophic cardiomyopathy, 929
 as established risk markers, 935
 in long QT syndrome, 984
 beta-blockers for, 994
 as risk marker, 994
 in nonischemic dilated cardiomyopathy, 872
 in risk stratification, of ventricular arrhythmias, 754
 in Romano-Ward syndrome, 984
 in short QT syndrome, 1018
 sinus node dysfunction and, 242
- Systemic embolism, after transeptal puncture, 95
- Systemic embolization, prevention of, 412
- T**
- T tubules, 12, 13f
- T wave, in long QT syndrome, 988–989
- T wave alternans (TWA), microvolt-level, 756
- Tachycardia
 atrial, macroreentrant
 atrial extrastimulation, 383
 atrial pacing during, 384–388
 diagnostic maneuvers during, 383–388
 documentation of line of block, 400
 features of, 382–383, 383f–384f
 induction of, 382, 383b
 noninducibility of, 400
 termination, 400
 cristal atrial, 317f
 macroreentrant tachycardias, mapping of, 128, 130f, 132–135, 134f
 continuous electrical activity in, 134, 134.e1f
 mid-diastolic activity, 134–135, 134f
 pace mapping of, 152
 noninducibility of, 595
 endpoints of ablation, 335–337
 para-Hisian atrial, ablation of, 333–335, 335f
 programmed ventricular stimulation during, 322–323, 323f–325f

- Tachycardia (*Continued*)
 reentrant, sinus node, 309
 sinus node reentrant, 309
 wide complex, 730–747. *see also* Wide complex tachycardias
- Tachycardia-bradycardia syndrome, 244, 245f, 251
- Tachycardia cycle length
 atrial pacing, 586
 oscillation of, 320, 321f
 in paroxysmal supraventricular tachycardia
 atrial pacing at, 722–723
 oscillation in, 711–712
 ventricular pacing at, 723
 ventricular pacing, 586–587
- Tachycardia-dependent block, 289f
- Tachycardia elimination, for atrial flutter ablation, 364
- Tachycardia termination
 in congenital heart disease, 974
 endpoints of ablation, 335
 in paroxysmal supraventricular tachycardia, 713–714
- Tactile feedback, catheter-tissue contact in, 219
- Tamponade. *see* Cardiac tamponade
- TAVR. *see* Transcatheter aortic valve replacement
- Tedisamil, for Brugada syndrome, 1014–1015
- Tendon of Todaro, 256
- Terminal activation duration, prolonged, in arrhythmogenic right ventricular cardiomyopathy (ARVC), 957
- Termination
 in paroxysmal supraventricular tachycardia
 atrial extrastimulation in, 714
 atrial overdrive pacing in, 714
 ventricular extrastimulation in, 716, 716f
 ventricular overdrive pacing in, 722
 in programmed atrial stimulation, 581
 in programmed ventricular stimulation, 582
- Tetralogy of Fallot, in congenital heart disease, 409, 969, 970t
- Theophylline, mechanism of action of, 33
- Thermistors, 209–210
- Thermocouples, 209–210
- Thiopentone, mechanism of action of, 30
- Three-dimensional rotational angiography, 202–203
 clinical implications of, 203
 fundamental concepts of, 202
 imaging technique, 202–203
 integration of, 202, 202.e1f
 limitations of, 203
- Thromboembolism, 1046–1047
 in arrhythmogenic right ventricular cardiomyopathy (ARVC)
 clinical presentation of, 946
 atrial fibrillation and, 441–444
 bleeding risk stratification and, 443–444, 444t
 postablation, 523–524
 stroke risk stratification and, 442–443, 442t–443t, 443f
 in catheter ablation, 1043
 prevention of, 347
 vascular, 1043
- Thrombus formation
 laser energy and, 231–232
 in percutaneous left atrial appendage ligation, 540
- Timothy syndrome, 41, 977t, 979–980, 985. *see also* Long QT syndrome
- Tocainide, mechanism of action of, 19
- Torsades de pointes, 748
 differential diagnosis of, 992
 drug-induced, 731, 993
 HCN4 mutations and, 43
 in long QT syndrome, 981, 989
- Trains, 110
- Transaortic (retrograde) approach, in ablation of left free-wall bypass tracts, 665
- Transcatheter aortic valve replacement (TAVR), atrioventricular block and, 260–261
- Transcoronary ethanol ablation, 762
- Transesophageal atrial stimulation, preexcitation to, 608
- Transesophageal echocardiography. *see also* Echocardiography
 of atrial fibrillation, 464–465, 465f, 465.e1f
- Transient outward potassium current (I_{to}), 24–27, 24t, 26t
- Trans-isthmus conduction interval, 368
- atrial pacing, 368
- Transitional cells, 238, 257
- Transitional zone index, 830–831
- Transmembrane potential. *see* Membrane potential
- Transseptal approach, in ablation of left free-wall bypass tracts, 665–666, 666.e1f
- Transseptal puncture, 1044
 atrial septal defect and, 94, 94.e1f
 complications of, 94–95
 second, 91
- Transthoracic echocardiography. *see also* Echocardiography
 for pericardial effusion, 1044, 1044f
- Transthoracic epicardial ablation, 916–920
 complications of, 918–920
 coronary artery injury as, 919
 intraabdominal bleeding as, 919–920
 pericardial bleeding as, 918
 pericarditis, 919
 phrenic nerve injury as, 919, 919.e1f
 pleuritis as, 920
 pneumopericardium as, 920
 cryoablation, 918
 outcome of, 920
 radiofrequency, 916–918
- Transthoracic epicardial mapping, 915–916
 activation, 915, 915.e1f
 electroanatomic, 916
 substrate, 916, 916f–917f
 entrainment, 915
 pace, 915
- Transvenous epicardial mapping, 920–923
 anatomical considerations in, 920–922, 921f
 outcome of, 922–923
 technical considerations of, 922, 922f, 922.e1f
- Transverse (T) tubules, 12, 13f
- Treadmill testing. *see* Exercise testing
- Triadin, RyR2 channels and, 46
- Triangle of Koch, 256, 256f, 560, 561f
- Tricuspid annular atrial tachycardia, 314–317
- Tricuspid annulus atypical tachycardia, 314–317
- Triggered activity, 58–63
 automaticity *versus*, 58
 cAMP-mediated, 58–59, 59f
 definition of, 58
 delayed afterdepolarizations and, 58–63
- Triggered activity (*Continued*)
 early afterdepolarizations and, 60–62
 overdrive pacing and, 60
 reentry and, 62
- Triggered-activity atrial tachycardia, 322
- Triggered-activity ventricular tachycardia, exclusion of, 779
- Troponin, in ablation, 1048
- TRPM4 gene, 258
- T-type calcium current, 41–42
- T-U wave, in long QT syndrome, 996
- TWA. *see* T wave alternans
- TWIK-related potassium channels, 24t
- Two-pore (K_{2P}) potassium channels, 24t, 36
- Typical atrial flutter
 ablation of, 359–372
 anticoagulation for, 359–361
 catheter positioning for, 361–362, 362f
 complications of, 371
 cryoablation, 364
 difficult cavotricuspid isthmus in, 363–364
 endpoints for, 364–365
 maximum voltage-guided technique, 363
 outcome of, 371–372
 radiofrequency, 360f, 362
 role of electroanatomic mapping systems, 363
 target of, 359, 361f
 technique for, 359–364
 clinical presentation of, 343
 electrocardiographic features of, 347–348
 atrioventricular conduction in, 348, 352f–354f
 flutter waves, 347–348, 348f–351f, 347.e1f
 QRS morphology in, 348
 electrophysiological testing, 348–356
 acceleration of, 355–356
 diagnostic maneuvers during tachycardia, 353
 induction of tachycardia, 351, 355f
 overdrive suppression of, 355
 tachycardia features of, 351–353
 termination of, 355, 355.e1f
 transformation of, 356
 epidemiology of, 343
 initial evaluation of, 343–344
 mapping of, 356–359
 activation, 356
 electroanatomic, 358–359, 361f
 entrainment, 356–358, 356b, 357f–358f
 noncontact, 359, 359.e1f
 natural history of, 343
 pathophysiology of, 339–342
 principles of management of, 344–347
 maintenance of sinus rhythm, 346–347
 management of coexistent and atrial fibrillation, 347
 prevention of thromboembolism, 347
 rate control of, 344–345
 restoration of sinus rhythm of, 345–346
- U**
- Ultra ICE catheter, 193
- Ultrarapidly activating delayed outward rectifying (I_{Kur}), 24t, 26t, 27, 26.e1f
- Ultrasound energy, 232–233
 biophysics of, 232
 clinical applications of, 233, 233.e1f

- Ultrasound energy (*Continued*)
 lesion formation in, pathophysiology of, 232–233
 transmission of, 232
- Unidirectional block, in reentrant circuits, 63–64, 78–79
 anisotropy and, 78–79
 membrane excitability/refractoriness and, 78, 78f
 tissue structure/geometry and, 79
- Unipolar electrogram morphology, of atrial flutter, 370
- Univentricular hearts, with Fontan palliation, in congenital heart disease, 410
- Upper turnaround point, 563
- V**
- V₂ transition ratio, 829–830
- V₂S/V₃R index, 830
- VA interval
 in orthodromic atrioventricular reentrant tachycardia, 645
 in paroxysmal supraventricular tachycardia, atrial overdrive pacing in, 717–718
 in programmed ventricular stimulation, 582
- Vagal maneuvers
 for focal atrial tachycardia, 309
 termination with, in paroxysmal supraventricular tachycardia, 713–714
- Vagal nerve injury, peri-esophageal, in atrial fibrillation ablation, 524–525
- Vagal tone, excessive, sinus node dysfunction and, 241
- Valvular heart disease, atrial fibrillation and, 436
- Vascular access, in congenital heart disease, 972
- Vascular complications, of catheter ablation, 1042–1043
- Vascular-mediated tissue injury, cryoablation and, 228
- Vascular thromboembolism, 1043
- Vena cava. *see* Inferior vena cava; Superior vena cava
- Venous air embolism, 1047
- Ventricular arrhythmias
 alternative interventional treatment for, 762
 in arrhythmogenic right ventricular cardiomyopathy (ARVC), clinical presentation of, 946
 catheter ablation for, 760–762
 recommendations on, 762b
 clinical presentation of, 753
 in congenital heart disease, 968–975
 ablation of, 973–974, 973f
 electrocardiographic features of, 971, 972f
 epidemiology of, 968–969
 initial evaluation of, 969
 mapping of, 972–973
 natural history of, 968–969
 pathophysiology of, 968, 969f
 principles of management of, 970–971
 risk stratification for, 969–970
 epidemiology and natural history, 751–753
 accelerated idioventricular rhythm in, 752
 nonsustained ventricular tachycardia in, 752
 polymorphic ventricular tachycardia in, 752
 premature ventricular complexes in, 752
 reperfusion arrhythmias in, 752
 sudden cardiac death in, 752
- Ventricular arrhythmias (*Continued*)
 sustained monomorphic ventricular tachycardia in, 752–753
 ventricular fibrillation in, 752
 exclusion of, 779
 in hypertrophic cardiomyopathy
 clinical presentation of, 929–930
 pathophysiology of, 926
 treatment of, 938–940, 939f
 in iatrogenic cardiac arrhythmias, 1049
 implantable cardioverter-defibrillator for, 758–760
 in primary prevention, 759–760, 761f
 in secondary prevention, 758–759, 759t, 760f
 initial evaluation of, 753
 electrophysiological testing in, 753
 myocardial ischemia and, 753
 triggers of, 753
 type and burden of, 753
 in ischemic heart disease, 748–815
 management of, 757–762
 in cardiac sarcoidosis, 889
 mechanisms of
 associated with acute ischemia, 749–750, 750.e1f
 associated with healed infarction, 750–751
 in nonischemic dilated cardiomyopathy, 870–871
 pathophysiology of, 749–751
 pharmacological therapy for, 757–758
 acute therapy in, 757–758
 chronic therapy in, 758
 recurrence of, causes of, 811–812
 risk stratification for, 754–757
 autonomic imbalance in, 756–757
 cardiac magnetic resonance imaging in, 757
 cardiac repolarization in, 756
 early postinfarction, 757
 genetic testing in, 757
 invasive electrophysiological testing in, 756
 left ventricular ejection fraction in, 754–756, 755t–756t, 754.e1f
 myocardial conduction disorders in, 757
 syncope in, 754
- Ventricular beats, echo, in ventricular stimulation, 120, 120.e1f
- Ventricular block, 595
- Ventricular cardiomyopathy. *see also* Cardiomyopathy
 incessant tachycardia and, 309
- Ventricular echo beats, 120, 120.e1f
- Ventricular electrogram sequence, following cessation, 585
- Ventricular entrainment
 in orthodromic atrioventricular reentrant tachycardia, 645
 in programmed ventricular stimulation, 582–585
- Ventricular extrastimulation/pacing, 115–120
 for bundle branch block, 302–303, 303f
 during His bundle refractoriness, 628, 629f, 642
 normal response to
 with premature stimulation, 117–118, 118.e1f
 with rate-incremental pacing, 117, 118f
 in paroxysmal supraventricular tachycardia
 programmed ventricular stimulation in, 705
 during tachycardia, 715–716
- Ventricular extrastimulation/pacing (*Continued*)
 premature stimulation, normal response to, 117–118, 118.e1f
 ramp, 115–116
 rate-incremental, normal response to, 117, 118f
 repetitive ventricular responses to, 118–120
 bundle branch reentry beats, 118–120, 119f
 intraventricular reentrant beats, 120
 ventricular echo beats, 120, 120.e1f
 retrograde His potential in, 117, 118f
 retrograde right bundle branch block during, 628–629
 during tachycardia, 590
 at tachycardia cycle length, 323, 586–587, 648–649
 in paroxysmal supraventricular tachycardia, 723
 technical aspects of, 115–117, 117f, 118.e1f
 during ventricular tachycardia, 774–778
- Ventricular extrastimulus (VES), in ventricular tachycardia, induction of, 768–769
- Ventricular fibrillation (VF), 749, 749f
 in Brugada syndrome, 1014
 epidemiology and natural history of, 752
 hypothermia-mediated, 1034, 1035t
 in iatrogenic cardiac arrhythmias, 1049
 idiopathic, 1025–1029, 1029.e1f–1029.e3f
 clinical presentation of, 1026
 diagnosis of, 1026–1028, 1027f
 early repolarization in, 1031
 electrocardiographic features of, 1026
 electrophysiological testing for, 1027
 epidemiology of, 1026, 1026f
 genetic aspects of, 1025–1026
 pathophysiology of, 1026
 periodic evaluation in, 1029
 primary arrhythmia syndromes and, 1024–1025
 sports participation in, 1029
 structural heart disease and, 1027
 triggers for, 1028f, 1030
 in J wave syndromes, 1035t
 nonprimary, 752
 primary, 752
 in sudden unexplained death syndrome, 976
 in Timothy syndrome, 985
 in Wolff-Parkinson-White syndrome, 605–606
- Ventricular fibrillation storm, in Brugada syndrome, 1014
- Ventricular flutter, 749, 749f
- Ventricular fusion
 in orthodromic atrioventricular reentrant tachycardia, 645, 645f
 in paroxysmal supraventricular tachycardia
 ventricular extrastimulation in, 715
 ventricular overdrive pacing in, 717
 in programmed ventricular stimulation, 582–583
- Ventricular hypertrophy, in hypertrophic cardiomyopathy, 925, 926f
- Ventricular overdrive pacing, during tachycardia, 716–722, 717f–718f
- Ventricular pacemakers, 54
- Ventricular preexcitation, 600, 601f
 in programmed atrial stimulation, for paroxysmal supraventricular tachycardia, 704

- Ventricular stimulation
programmed
in atrioventricular nodal reentrant tachycardia
initiation by, 576–578
during sinus rhythm, 573–575
during tachycardia, 582–585
in paroxysmal supraventricular tachycardia
initiation of, 710
during sinus rhythm, 704–707
in ventricular tachycardia
acceleration in, 774–775
concealed perpetuation in, 771, 771.e1f
entrainment in, 775–777, 776f–778f, 777.e1f
induction of, 769
manifest perpetuation in, 771
overdrive suppression in, 774
resetting in, 771–774, 773f, 771.e1f
response to antiarrhythmic drugs, 779
in termination, 774, 774f, 777–778
transformation in, 775
ventricular pacing and, 774–778
- Ventricular stimulus (VES)
onset of ventricular tachycardia and, 771
in triggered-activity ventricular tachycardia, 779
- Ventricular tachyarrhythmias, classification of, 748–749
- Ventricular tachycardia (VT)
ablation in, 805–812
complications of, 812
of critical isthmus, of reentrant circuit, 805
endpoints of, 810–811
management after, 810–811
in multiple inducible, 807
outcome of, 811–812
substrate-based, 805–807
target of, 805–807
technique for, 808–810, 810.e1f
acceleration of, 774–775
anterior myocardial infarction, 767
anteroseptal and inferolateral, in nonischemic dilated cardiomyopathy, 876, 877f
aortic sinuses of Valsalva from, 846–851, 846f–849f
in arrhythmogenic right ventricular cardiomyopathy (ARVC), 942–967
ablation of, 962–965
endpoints of, 964
outcome of, 964–965
target of, 962–964
technique of, 964
clinical presentation of, 946
differential diagnosis of, 948–950
athlete's heart, 950
cardiac sarcoidosis, 949–950
dilated cardiomyopathy, 950
exercise-induced arrhythmogenic right ventricular cardiomyopathy in, 950
idiopathic right ventricular outflow tract tachycardia, 948–949, 949b
electrocardiographic features of, 954–957
during sinus rhythm, 955f
during ventricular tachycardia, 957, 958f
electrophysiological features of, 957–959
induction of tachycardia, 957
tachycardia features, 957–959
epidemiology of, 945–946
- Ventricular tachycardia (VT) (*Continued*)
initial evaluation of, 946–948
diagnostic criteria in, 946, 947t
endomyocardial biopsy in, 948
genetic testing in, 948
invasive electrophysiological testing in, 948
mapping in, 959–962
activation, 959, 959.e1f
entrainment, 959–960
epicardial, 962
pace, 960
substrate, 960–962
natural history of, 945–946
pathophysiology of, 942–945
molecular genetics in, 942–943, 943t
pathogenesis of, 943–945, 944f
pathology of, 945, 945.e1f
principles of management of, 950–954
catheter ablation of, 952
family screening in, 953–954
implantable cardioverter-defibrillator, 952–953, 953f
pharmacological therapy of, 950–952
sports in, 953
risk stratification in, 950, 951f, 952b
bidirectional, 749
bundle branch block pattern in, 764, 765f–766f
left, 764, 767
right, 764–767
bundle branch reentrant, 897–906
ablation of, 903–905
versus antidromic atrioventricular reentrant tachycardia, 903
clinical presentation of, 898
diagnostic criteria of, 900b
diagnostic maneuvers in, 902
electrocardiographic features of, 898, 899f
electrophysiological testing in, 898–903
entrainment of, 902
epidemiology of, 897
idiopathic (fascicular) left ventricular tachycardia, 902–903
initial evaluation for, 898
management of, 898
versus myocardial ventricular tachycardias, 902
pathophysiology of, 897
reentry circuit in, 897, 898f
resetting, 902
supraventricular tachycardia with aberrancy, 903
tachycardia features in, 900–902, 901f
cardiac function in, optimization of, 780
catecholaminergic polymorphic, 32, 1020–1025
classification of, 748–749
according to duration, 749
according to mechanism, 749
according to morphology, 748–749
according to QRS morphology, in lead V₁, 749
clinical, noninducibility of, 885
clinical presentation of, 753
cryoablation for, 231
definition of, 748
diagnostic maneuvers during, 771–779
electrocardiographic features of, 762–768, 763f–764f
clues to the underlying substrate, 762–763
postinfarction, localization of, 763–767
- Ventricular tachycardia (VT) (*Continued*)
electrophysiological testing in, 768–779
epicardial, 767–768, 768f, 907–924
clinical consideration in, 910–912, 910b, 910.e1f
anticoagulation in, 911
contrast-enhanced computed tomography in, 912
contrast-enhanced magnetic resonance imaging in, 911, 911f
electrocardiographic features of, 908–910, 908b
in arrhythmogenic cardiomyopathy, 909
in idiopathic ventricular tachycardia, 909–910
idiopathic ventricular tachycardia in, 909–910
in nonischemic dilated cardiomyopathy, 909
postinfarction ventricular tachycardia, 910
electrophysiological substrate of, 907–908
pericardial space in, 912–914
anatomical considerations in, 912, 913f, 912.e1f–912.e2f
epicardial fat and, 914
pericardial adhesions in, 914, 914f
technical considerations in, 912–914
exclusion of
bundle branch reentrant, 779
supraventricular, 779
triggered-activity, 779
familial polymorphic, 1020
features of, 770–771
focal, 749
high posterolateral myocardial infarction, 767
His bundle activation in, 770–771
no visible His potential, 770
visible His potential, 770–771, 770.e1f
hypothermia-mediated, 1034, 1035t
idiopathic focal, 816–857
ablation in, 843–854
cryoablation, 854
endpoints, 854
outcomes of, 854
target, 843, 844f
technique, 843–854, 845f
anatomical considerations in, 818–823
aortic root in, 820–822
aortomitral continuity in, 822
cardiac crux in, 823
left ventricular outflow tract in, 819f, 820, 818.e1f
left ventricular papillary muscles in, 822–823, 823f
left ventricular summit, 822, 822.e1f
pulmonary root in, 820
right ventricular outflow tract in, 818–820, 819f, 818.e1f
arrhythmogenic right ventricular cardiomyopathy, 825
clinical presentation of, 823–824
diagnostic maneuvers in, 837
differential diagnosis of, 825–826
electrocardiographic localization of, 827–836, 828t
aortic root ventricular tachycardias in, 831–833
basal left ventricular tachycardias in, 833

- Ventricular tachycardia (VT) (*Continued*)
- cardiac crux ventricular tachycardias in, 835
 - focal Purkinje ventricular tachycardias in, 835, 836f
 - frontal plane vertical axis in, 828–836
 - left ventricular outflow tract tachycardias in, 829–831, 831f–832f, 831t
 - left ventricular papillary muscle tachycardias in, 834–835
 - left ventricular summit tachycardias in, 833–834, 834f
 - precordial transition in, 827–828
 - right ventricular outflow tract tachycardias in, 829, 830f
 - right ventricular papillary muscle tachycardias in, 835
 - tricuspid annular ventricular tachycardias, 835–836
 - electrophysiological testing for, 836–837
 - epidemiology of, 823
 - features of, 837
 - idiopathic ventricular fibrillation and, 826
 - induction of, 836–837
 - initial evaluation for, 824
 - mapping in, 837–843
 - activation, 837–840, 838f–839f
 - basket catheter, 843, 843.e1f
 - CARTO system, 842
 - electroanatomic, 841–842, 841f
 - noncontact, 842–843, 842.e1f–842.e2f
 - pace, 840–841
 - mechanism of, 818
 - natural history of, 823
 - pathophysiology of, 816–818, 817f
 - implantable cardioverter-defibrillator for, 758–760
 - incessant, 749
 - induction of, 768–770
 - of clinical SMVT, 769
 - endpoints of, 769–770
 - isoproterenol in, 769
 - of multiple SMVT, 769–770
 - pacing current output in, 769
 - pacing drive CL, 769
 - of polymorphic, 770
 - recommended stimulation protocols in, 768–769
 - reproducibility of, 769
 - ventricular stimulation, site of, 769
 - of very fast, 770
 - VEs in, number of, 768–769
 - inferior myocardial infarction, 764–767, 767f
 - macroreentrant, 128, 130f, 132–135, 134f
 - bridging of diastole, 134
 - continuous electrical activity in, 134, 134.e1f
 - critical isthmuses in, 133, 143, 152
 - entrainment mapping of, 145f
 - mid-diastolic activity, 134–135, 134f
 - pace mapping of, 152
 - ventricular, 130f
 - management of, 757–762
 - mapping of, 780–805
 - activation, 784–786
 - electroanatomic, 782–784, 782f–783f
 - entrainment, 786–792
 - hemodynamic support in, 781–782
 - left ventricular access in, 781
 - noncontact, 800–801, 800.e1f
- Ventricular tachycardia (VT) (*Continued*)
- pace, 792–795
 - postinfarction premature ventricular complexes, 801
 - preprocedural evaluation of, 780–781
 - substrate, 795–800
 - voltage (scar), 795–796, 795f
 - monomorphic, 748, 749f
 - noninducibility of, 884–885
 - multiple monomorphic, 748
 - nonsustained, 749. *see also* Nonsustained ventricular tachycardia
 - pathophysiology of, 749–751
 - pleomorphic, 749
 - polymorphic, 748, 749f. *see also* Polymorphic ventricular tachycardia
 - precordial concordance in, 764
 - preexcited supraventricular tachycardia *versus*, 742, 742f
 - QRS axis in, 764
 - QRS duration in, 763–764
 - QS complexes in, 764
 - reentrant circuit in, 135, 136f
 - identification of critical isthmus in, 145–146
 - location of, approximation of, 145, 146f
 - right ventricular apical local activation time in, 771
 - scar-related reentrant, 749
 - sustained, 749. *see also* Sustained ventricular tachycardia
 - ventricular extrastimulation during, 771–774
 - acceleration in, 774–775
 - concealed perpetuation in, 771, 771.e1f
 - entrainment in, 775–777, 776f–778f, 777.e1f
 - manifest perpetuation in, 771
 - overdrive suppression in, 774
 - resetting in, 771–774, 773f, 771.e1f
 - response to antiarrhythmic drugs, 779
 - in termination, 774, 774f, 777–778
 - transformation in, 775
 - ventricular pacing and, 774–778
 - ventricular stimulus and, 771
 - very fast, induction of, 770
 - in Wolff-Parkinson-White syndrome, 606
- Ventriculo-aortic junction, anatomy of, 821, 821.e1f
- Ventriculoatrial block, 586–587
 - in paroxysmal supraventricular tachycardia in atrial-ventricular relationship, 711
 - in ventricular pacing, 723
- Ventriculoatrial dissociation, in paroxysmal supraventricular tachycardia, 716
- Ventriculoatrial interval
 - in para-Hisian pacing, during sinus rhythm, 631–633
 - in programmed ventricular stimulation, for paroxysmal supraventricular tachycardia, 705
- Ventriculoatrial linking
 - atrial overdrive pacing and, in paroxysmal supraventricular tachycardia, 714–715
 - in orthodromic atrioventricular reentrant tachycardia, 641f, 642
 - in programmed atrial stimulation, 581–582
- Ventriculography, in arrhythmogenic substrate, 780
- Ventriculophasic sinus arrhythmia, 246, 246f
 - atrioventricular block and, 277
- Verapamil
 - for catecholaminergic polymorphic VT, 1024
 - for inappropriate sinus tachycardia and, 552–553
 - sinus node response to, 250
 - for Wolff-Parkinson-White syndrome, 609
- Verapamil-sensitive ventricular tachycardia
 - ablation of, 864–867
 - empirical, 867, 867f
 - endpoints of, 867
 - outcome of, 867
 - target of, 864–866, 865f–866f
 - technique of, 866–867
 - activation sequence in, 863
 - clinical presentation of, 859
 - diagnostic maneuvers during, 861
 - electroanatomic mapping in, 864, 864f
 - electrocardiographic features of, 860
 - during normal sinus rhythm, 860
 - during ventricular tachycardia, 860, 860f
 - electrophysiological testing in, 860–861
 - entrainment in, 861
 - entrainment mapping in, 863, 863b
 - epidemiology of, 859
 - focal Purkinje ventricular tachycardia *versus*, 861
 - initial evaluation for, 859–860
 - interfascicular ventricular tachycardia *versus*, 861
 - late diastolic potential in, 863
 - mapping in, 861–864
 - noncontact mapping in, 864, 865f
 - pace mapping in, 863–864
 - papillary muscle ventricular tachycardia *versus*, 861
 - pathophysiology of, 858–859
 - principles of management for, 860
 - Purkinje potential in, 862
 - resetting of, 861
 - site of earliest ventricular activation in, 861, 862f
 - supraventricular tachycardia *versus*, 861
 - tachycardia circuit in, 858, 859f
 - termination of, 861
- Vereckei algorithm, in wide complex tachycardias, 740–741, 741f
- Vernakalant, for atrial fibrillation, 450
- Very fast ventricular tachycardia, induction of, 770
- VES. *see* Ventricular extrastimulus
- VF. *see* Ventricular fibrillation
- Vitamin K antagonists, for atrial fibrillation, 445–446
- Voltage channels
 - in arrhythmogenic right ventricular cardiomyopathy (ARVC), 962, 961.e2f–961.e3f
 - in nonischemic dilated cardiomyopathy, 879, 880f–881f
 - during sinus rhythm, 803
- Voltage mapping, 795–796. *see also*
 - Electroanatomic mapping, voltage
- in circumferential left atrial ablation, 496
- electroanatomic, 169–171, 169t, 170.e1f, 169.e1f
- bipolar, 169
- limitation of, 171, 172f
- resolution of, factors influencing, 170
- electrode size in, 170, 171f
 - mapping density in, 170
 - tissue contact in, 170
 - vector of activation in, 170
- during sinus rhythm, 802–803
- technique of, 796, 797f, 796.e1f–796.e2f

Voltage-guided substrate modification, 515–516
 ablation endpoint in, 516
 ablation target in, 515
 outcome of, 516
 rationale for, 515
 technique of, 515–516, 516f–517f

W

Wandering atrial pacemaker, sinus node
 dysfunction and, 246, 246.e1f
 Warfarin, for atrial fibrillation, 445
 Warm-up, in programmed atrial stimulation, of
 paroxysmal supraventricular tachycardia, 710
 Watchman device, 534–535
 deployment of, 534
 outcome of, 535
 postoperative management of, 534
 sizing of, 534
 specifications of, 534
 Wavelength, in reentry, 68–69
 Wenckebach block, 113
 atypical, 113
 focal atypical tachycardia and, 311, 315f
 macroreentrant atrial tachycardia and, 383
 in ventricular pacing, 117
 Wenckebach periodicity, 265–266, 266f, 266.e1f
 Wide complex tachycardias, 730–747
 age and, 730
 atrial activation sequence in, 743
 atrial extrastimulation in, 744
 atrial pacing in, 745, 746f
 atrioventricular dissociation in, 732–733,
 735f–737f
 atrioventricular relationship in, 743, 744f
 aVR algorithm, 741, 741f
 Bayesian algorithm, 740
 Brugada criteria for, 739–740, 740f, 742f
 capture beats in, 733
 causes of, 730, 731f, 731t
 clinical considerations in, 730–732
 clinical history in, 730–731

Wide complex tachycardias (*Continued*)
 diagnostic maneuvers during, 744–747
 differential diagnosis of, 739f
 dissociated P waves in, 733
 duration of, 730
 effects of adenosine on, 743
 electrocardiographic diagnosis
 algorithm of, 738–742
 limitations of, 742, 743t
 electrocardiographic features of, 732–742,
 733b
 electrophysiological testing for, 742–747
 fusion beats in, 733
 Griffith algorithm for, 740
 His bundle-right bundle electrogram sequence,
 743
 His bundle-ventricular interval in, 743
 laboratory testing for, 732
 lead II R wave peak time in, 740
 left bundle branch block pattern, 735–738, 738f
 medications and, 731
 oscillation in, 743, 745f
 pacemaker or implantable cardioverter-
 defibrillator implantation and, 731
 physical examination in, 731–732
 QRS in
 axis of, 734
 duration of, 733
 morphology of, 734–738, 737f
 precordial concordance in, 734
 variation in, 738
 rate of, 732
 regularity of, 732
 right bundle branch block pattern, 734–735
 supraventricular tachycardia as, 730
 symptoms of, 730
 tachycardia features in, 743
 underlying heart disease and, 730
 ventricular extrastimulation in, 745
 ventricular pacing in, 747, 747.e1f
 ventricular tachycardia as, 730, 732–738, 732.e1f
 Vereckei algorithm, 740–741, 741f

Wolff-Parkinson-White pattern, 600, 601f
 electrocardiogram, 602f
 epidemiology and natural history of, 606
 initial evaluation for, 607–608
 Wolff-Parkinson-White syndrome, 600
 antidromic atrioventricular reentrant
 tachycardia in, 603, 603f–604f, 603.e1f
 asymptomatic patients with, management for,
 609, 610f
 atrial fibrillation in, 603–605, 605f
 atrial flutter in, 605
 atrial tachycardia in, 603, 603f
 atrioventricular bypass tracts in, 601–602,
 602f
 atrioventricular nodal reentrant tachycardia in,
 603, 603f
 atrioventricular reentry in, 602–603, 603f
 catheter ablation for, 609
 clinical presentation of, 607
 epidemiology and natural history of, 606
 familial, 606–607
 life-threatening events in, 609, 611b
 orthodromic atrioventricular reentrant
 tachycardia in, 603, 603f–604f
 other arrhythmias associated with, 603–606
 pathophysiology of, 600–601, 601f–602f
 permanent junctional reciprocating tachycardia
 in, 603
 sports participation and, 612
 sudden cardiac death in, 605–606
 supraventricular tachyarrhythmias associated
 with, 614
 ventricular fibrillation in, 605–606
 ventricular tachycardia in, 606

Y

Yotiao, 30

Z

Zatebradine, 43